ANGEWANDTE CHEMIE

International Edition in English

Volume 27 · Number 1
January 1988
Pages 5–39

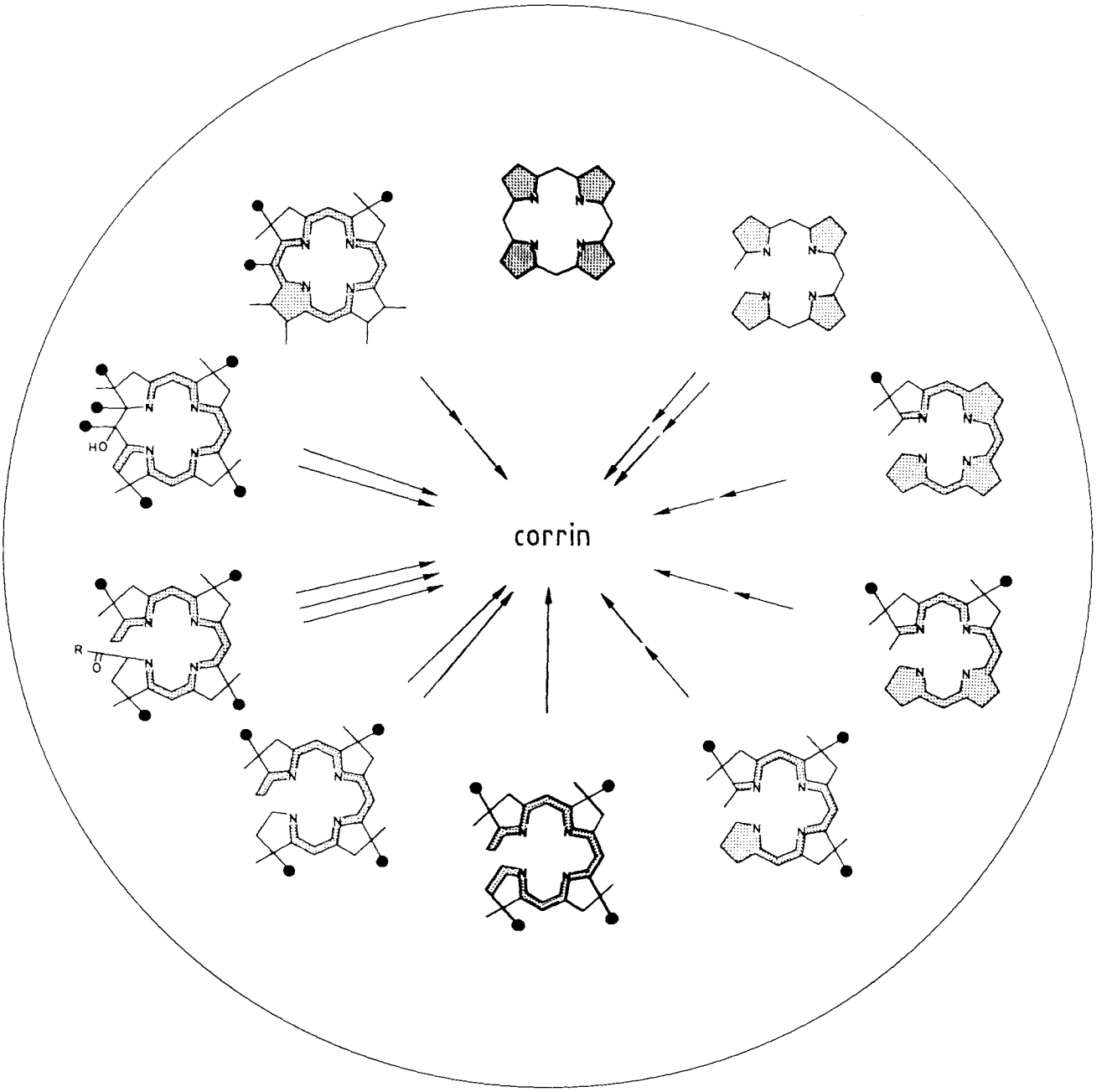

Albert Eschenmoser

Vitamin B_{12}: Experiments Concerning the Origin of Its Molecular Structure

 © VCH Verlagsgesellschaft mbH, D-6940 Weinheim, 1988 *0570-0833/88/0101-0005 $ 02.50/0*

Vitamin B_{12}: Experiments Concerning the Origin of Its Molecular Structure**

By Albert Eschenmoser*

Following the chemical synthesis of vitamin B_{12}, a search was begun for a potentially biomimetic "dark" variant of the photochemical A/D-secocorrin → corrin cycloisomerization, the central ring-closure step in one of the two cobyric acid syntheses. Significantly, not just one but a whole family of such variants was discovered. According to what is currently known, one of these variants can indeed be regarded as a chemical model for the reaction path followed by Nature in the biosynthetic construction of the corrin ring. These chemical studies of vitamin B_{12} biosynthesis had revealed that the A/D-ring junction, regarded as the main obstacle to a chemical vitamin B_{12} synthesis at the outset, is in fact a structural element that is formed readily and in a variety of ways from structurally appropriate precursors. More recent investigations have shown that the same holds for other specific structural elements of the vitamin B_{12} molecule, including the characteristic arrangement of double bonds in the corrin chromophore, the special dimension of the macrocyclic ring of the corrin ligand, the specific attachment of the nucleotide loop to the propionic acid side chain of ring D, and the characteristic constitutional arrangement of the side chains around the ligand periphery (which vitamin B_{12} shares with all uroporphinoid cofactors). All these outwardly complex structural elements are found to "self-assemble" with surprising ease under structurally appropriate preconditions; the amount of "external instruction" required for their formation turns out to be surprisingly small in view of the complexity and specificity of these structural elements. We view these findings as steps on the way toward a chemical rationalization of the vitamin B_{12} structure. The goal is to arrive experimentally at a perception of the biomolecule's intrinsic potential for structural self-assembly. This potential, together with the specific type of reactivity related to the biological function, is considered to be responsible for the biomolecule having been chosen by natural selection. The chemical rationalization of the structure of biomolecules is an objective of organic natural product chemistry. The field of natural product synthesis provides appropriate conceptual and methodological tools to approach this objective experimentally.

1. Introduction: Concerning the Origin of Cofactors and the Emergence of Biosynthetic Pathways

The (organic) cofactors occupy an exquisite position with respect to structure and function among the low-molecular-weight natural products. Their diverse and sometimes quite unusual structures, often occurring in families, are distinguished by their disposition to special types of reactivity. In partnerships between cofactors and specific proteins these dispositions are expressed and functionally exploited to a high degree of perfection with respect to both efficiency and selectivity. This perfection may seem natural to biologists, but it never ceases to surprise and amaze chemists to whom it represents a source of permanent challenge. Hardly anything reveals the state and limits of our chemical knowledge and skills so clearly as the level of performance of these systems. For a chemist, the functional partnerships between cofactors and proteins represent one of those incredible accomplishments of biomolecular evolution.

[*] Prof. Dr. A. Eschenmoser
Laboratorium für Organische Chemie der
Eidgenössischen Technischen Hochschule, ETH-Zentrum
Universitätstrasse 16, CH-8092 Zürich (Switzerland)

[**] The preceding page shows Figure 11 of this article.

The challenge referred to above has many aspects. The focus of current interest has been on molecular structure and dynamics, that is, on the mechanism of functional interaction between substrates, cofactors, and proteins. However, alternative objectives focus on chemical rationales for the cofactors' structures, questions concerning the relationship between structure and function, the chance or necessity of their occurrence, and questions concerning their origin. Such questions are motivated not the least by the extraordinary fact that important cofactors have remained structurally unchanged over the entire course of biological evolution for which evidence is available to us. The cofactor structures appear to represent optimal molecular solutions to specific biological tasks, the "institutionalization" of which apparently occurred at an early evolutionary phase. Can experiments aimed at a deeper understanding of the molecular structure of cofactors tell us something about that early phase of biological evolution?

According to the Darwinian paradigm of molecular evolution,[1-3] the structure of functional biomolecules is the result of a process of *selection* (as opposed to a "Lamarkian" process where instructions from the environment would guide molecular construction). Selection of a particular chemical structure presumes its "*preformation*," either as a product of a biotic process or (in the extreme)

as a product of a prebiotic process. Biotic preformation schemes might include both reactions catalyzed (fortuitously) by enzymes and nonenzymic (endogenous as well as exogenous) reaction sequences. A molecular structure can—irrespective of the preformation route—be regarded as being biologically selected once the enzymic control over its biological function is genetically fixed. Involvement of an enzyme in a biotic preformation sequence implies genetic fixation of at least one step of the biosynthetic pathway. In such a case, enzymic control over the (original) synthesis of the biomolecule can be older than enzymic control over its biological function. In other variants of preformation, particularly the prebiotic ones, the opposite holds: genetic fixation of function precedes the appearance (and thus the genetic fixation) of the biosynthetic pathway.

Such efforts to classify possible ways in which biomolecules might have emerged take for granted a principle of operation of biological systems that—although this is a truism to biologists—must be mentioned here, as it is fundamental to any picture of the emergence of biochemical pathways: the synthesis of protein biocatalysts proceeds exclusively via a coding process. This not only guarantees a faithful *reproduction* of the structure of the protein itself, but also implies a *preregistration* of the protein structure. The constitution of a given protein is registered (and thus potentially fixed genetically) *before* it is formed. If a new protein, arising as the result of a mutation, fortuitously turns out to be a catalyst, lasting genetic fixation of the newly discovered catalyst requires in principle no further instruction but only replication by reproduction. Preregistration is a fundamental aspect in the ability of evolving systems to develop biosyntheses; without it, an emergence of biosynthetic pathways would be inconceivable.

In the functioning of such machinery, it is helpful to differentiate between two types of fortuitous, mutually *independent* steps which determine the route by which a biosynthetic pathway arises: the preformation step and the step at which enzymic control takes over. The latter includes the two mutually dependent processes of mutation and expression and has as a prerequisite the fortuitous catalytic activity of the protein. In the case of enzymically induced preformation, the takeover of enzymic control may coincide with the preformation step. Chemists engaged in natural product synthesis are probably in the best position to grasp the vast number as well as the nature of lucky prerequisites that must be fulfilled for a multistep biosynthesis of a complex natural product to emerge. It seems inescapable to suppose that genetic fixation in the sense of preregistration can be maintained through steps involving nonfunctional (intermediate) products before the fixation becomes final through reproduction feedback after a functional (end) product has been reached. In terms of this model, the classical suggestion of *Horowitz*[4] that biosyntheses emerge "from back to front" represents an extreme case.

If the question is posed as to which factors have determined the molecular structure of a functional biomolecule, the type of answer usually given is: the molecular structure of a biomolecule is the result of biological selection processes directed toward the optimization of the molecule's biological function. Functional optimizations occur via mutation steps and reproduction feedback, the structures of the substrates lying within the boundaries delimited by the preformation steps. Although preformation steps, whether nonenzymic or enzymic, must be determined in part by chance, they are also directed by structural factors intrinsic to the substrate molecules themselves. To this extent, these steps are amenable to chemical rationalization. The structural changes involved occur along reaction channels in what is in principle a predetermined structural "landscape." In addition to a structure-function analysis, the mapping of this landscape is the goal to be aspired to in attempting a chemical rationalization of a biomolecular structure. Chemical synthesis provides an empirical, but suitable, instrument for mapping these landscapes; indeed, we should regard such mapping as one of the objectives of natural product synthesis. In fact, ever since *Stanley Miller*'s classical experiment,[5] the mapping of such structural landscapes of potentially prebiotic organic matter has been one of the goals of prebiotic chemistry.

In principle, the structural landscapes could only be referred to as "predetermined" if we were allowed to ignore the world of catalysts. Catalysts become part of the structural landscapes in the regions of the reaction channels. Our lack of knowledge of the catalysts that may have participated in preformation steps sets stringent limits to a chemical rationalization of biomolecular structures, in addition to the limits already set by the role of chance. However, these very limitations point to an important objective that can and should be studied with the tools of natural product synthesis, namely, the systematic delimitation of the boundary separating the reactivity of biomolecules (or their precursors) from structural changes for which *structured* catalysis is a prerequisite. Such questions become particularly pertinent as one attempts to proceed ever further backward along the axis of biochemical evolution, from the region where enzymic preformation steps (presumably) dominated to the region where these steps become (necessarily) increasingly nonenzymic in nature, until finally one reaches that dark area beyond which the questions posed belong to the realm of prebiotic chemistry. Ultimately, the problems referring to that dark area are equally and primarily related to the phenomenon of catalysis; after all, the major prerequisite for self-reproduction of a (macro)molecular system is its ability to act as a specific catalyst for its own synthesis.

In chemistry and biology today the experimentally[2] and theoretically[3] supported view[1] prevails that the molecular building blocks of proteins and nucleic acids are of prebiotic origin. This view refers to the (simpler) α-amino acids, the nucleic acid bases, and the (simpler) carbohydrates. The question arises[6] whether this should also hold for the molecular structures of cofactors. Should one regard these molecules as biosynthetic "inventions" of organisms that existed early in evolutionary history, or is it more reasonable to consider the basic patterns of their structures as being of prebiotic origin? Did biological systems originally take up these structures from the environment as "vitamins" (in the original sense of the word), use them as catalysts, fix their function genetically, later under selection pressure copy them biosynthetically and, finally,

optimize them structurally? Although it would be better to pose such a question not in general terms but rather for each cofactor individually, much is in favor of the idea that emerging biological systems have been heterotrophic with respect to organic (low-molecular-weight) catalysts. It must be advantageous to a system in its critical stage of development when it can take enzymic control over a catalyst's function without having to cumulate this task with the one of first "discovering" its structure via an enzymic synthesis. Although today cofactors carry out their biological function exclusively in concert with specific proteins, many are known[7] to be catalysts themselves; in the present context, this is a pertinent property. Modern biosynthetic pathways to most cofactors appear hopelessly complex when we look at them in the context of the problem of their origin. Although it may be true that present-day biosynthetic pathways could be quite different from their archaic predecessors, the argument is best illustrated by using adenine as an example. Along with *Miller*'s experiment on the origin of α-amino acids,[5] the perception of the structure of adenine as a pentamer of HCN and the discovery of its direct formation from HCN by *Oró*[8] as well as, subsequently, of its photochemical formation by *Ferris* and *Orgel*[9] represent true milestones of prebiotic chemistry (Fig. 1). The structural self-assembly of the adenine molecule from HCN contrasts starkly with the complex network of enzymic reactions,[10] which Nature was, so to speak, forced to evolve for its biosynthesis. From a chemosynthetic point of view, the structure of adenine is of utmost simplicity whereas it is quite complex from the point of view of its biosynthesis; the structure is "simple" with respect to its derivation from HCN and "complex" with respect to its construction from those precursors that present-day organisms are directed to use in their biosyntheses.

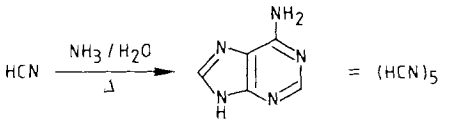

Fig. 1. Adenine, a pentamer of HCN (*J. Oró* (1960) [8]).

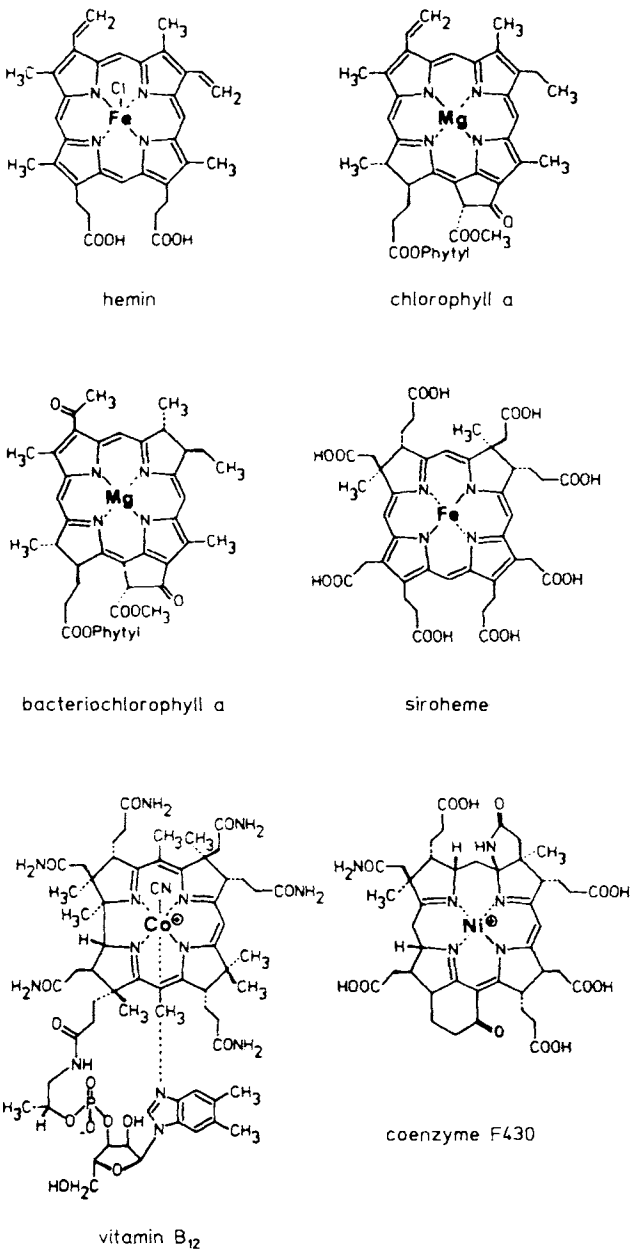

Fig. 2. Family of uroporphinoid cofactors.

The example of adenine refutes the opinion that an inquiry into the origin of cofactor structures is futile since it would be a priori impossible to draw conclusions or to study the problem experimentally. Were cofactors of prebiotic (or of otherwise nonenzymic) origin, then structural complexity of such molecules would be an apparent complexity; straightforward pathways of structural self-assembly of these structures would have to exist, and these pathways would be detectable experimentally.

The possibility that cofactor structures might be of prebiotic origin has been discussed several times in the literature.[2,6,11] In contrast to the extensive prebiotic chemistry of protein and nucleic acid building blocks,[2,11,12] however, only meager experimental results regarding potentially prebiotic routes to cofactors are available.[13]

The uroporphinoid family shown in Figure 2 occupies a special position among cofactors. Varying a single structural theme, that of uroporphyrinogen, Nature has selected a rich variety of magnificent structures which exhibit a diversity of fundamental biological functions in all kinds of organism, from microorganisms and plants to man. The diversity of form and function existing in this family is the result of selection processes for which two dimensions of structural variation were available, the central coordinated metal ion and the ligand sphere. Figure 3 indicates in abstract form the essential features, the central ion and the oxidation state of the ligand system. There is the fully unsaturated (oxidized) chromophore of the protoporphyrin iron complexes, which, in a variety of forms, are in charge of the biochemistry of molecular oxygen. Then there are the chlorin ligands of the chlorophylls, less oxidized than the porphyrins, absorbing at longer wavelength, and containing in their center a "harmless" metal ion, which, however, fulfills the crucial condition of being compatible with the ligand system's photochemistry. Finally, we have the

reduced ligand systems of the corrin of vitamin B_{12} and the (tetrahydro)corphin of coenzyme F430, whose coordination centers, cobalt and nickel, respectively, have been selected by Nature in order to gain access to the unique reactivity potential of organometallic compounds. The latter two cofactors, in particular, appear to represent exceptional examples of Nature's fine-tuning porphinoid ligands to an optimum of a cofactor's biological function; this is achieved by the appropriate choice of the size of the macrocycle, the constitution of the ligand chromophore, and the nature of the chromophore's substituents. Vitamin B_{12} is a particularly suitable target for attempting a chemical rationalization of a biomolecule's structure and for inquiring about its origin. The fact that the compound is the structurally most complex member of the uroporphinoid family should not present an obstacle; quite the opposite is true, the more complex a molecular structure, the greater the wealth of information it can potentially provide.

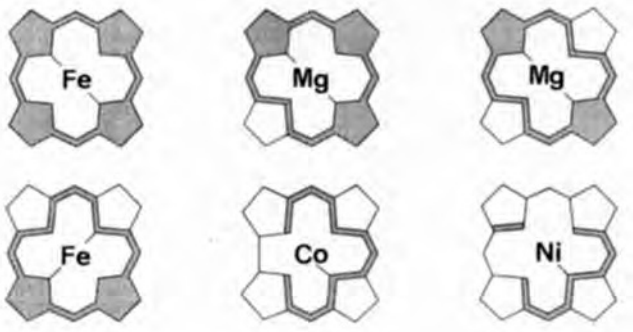

Fig. 3. Structural variability within the family of uroporphinoid cofactors (see text). The chromophore systems are indicated in grey.

The ubiquitous biological roles of uroporphinoids, together with the finding that the key step in their biosynthesis, the tetramerization of the monopyrrolic precursor porphobilinogen to give the macrocyclic uroporphyrinogens, not only occurs enzymically but also takes place under proton catalysis with great ease[14, 15] (see also Section 3.4), have already led earlier authors[16] to raise the question of a prebiotic origin of the uroporphinoid type of structure. Microbiologists[17] have expressed the opinion that corrinoids, which—according to current knowledge—are biosynthesized exclusively by microorganisms, might be functionally older than the porphyrins, since strictly anaerobic bacteria are reported to exist that produce corrinoids but apparently no porphyrins. Furthermore, it has been pointed out[17] that the corrinoid's biological task is exclusively the catalysis of biosynthetic steps, that they are not involved in energy metabolism, as the porphyrins and chlorins are.

In our laboratory, the question as to the origin of the corrin structure emerged as a consequence of our chemical studies on vitamin B_{12} biosynthesis, carried out subsequent to our work on its chemical synthesis. The next section summarizes the stages and developments that these studies have gone through.

2. From the Chemical Synthesis of Vitamin B_{12} to the Question as to the Origin of the Corrin Structure

When we look back from today's perspective at the chemical synthesis of vitamin B_{12}, we are inclined to regard that work as what would now be called "hard chemistry," in the sense that the planning and execution of these syntheses did not take into consideration at all the question as to the natural, structurally appropriate route of formation of the natural product. This means de facto, and probably rightfully so, that these syntheses were not designed in a biomimetic fashion, but this is not what is actually meant. What is meant is the more basic question concerning the structurally intrinsic reaction channels that are ultimately responsible for the very existence of a given type of natural product structure, and which often deter-

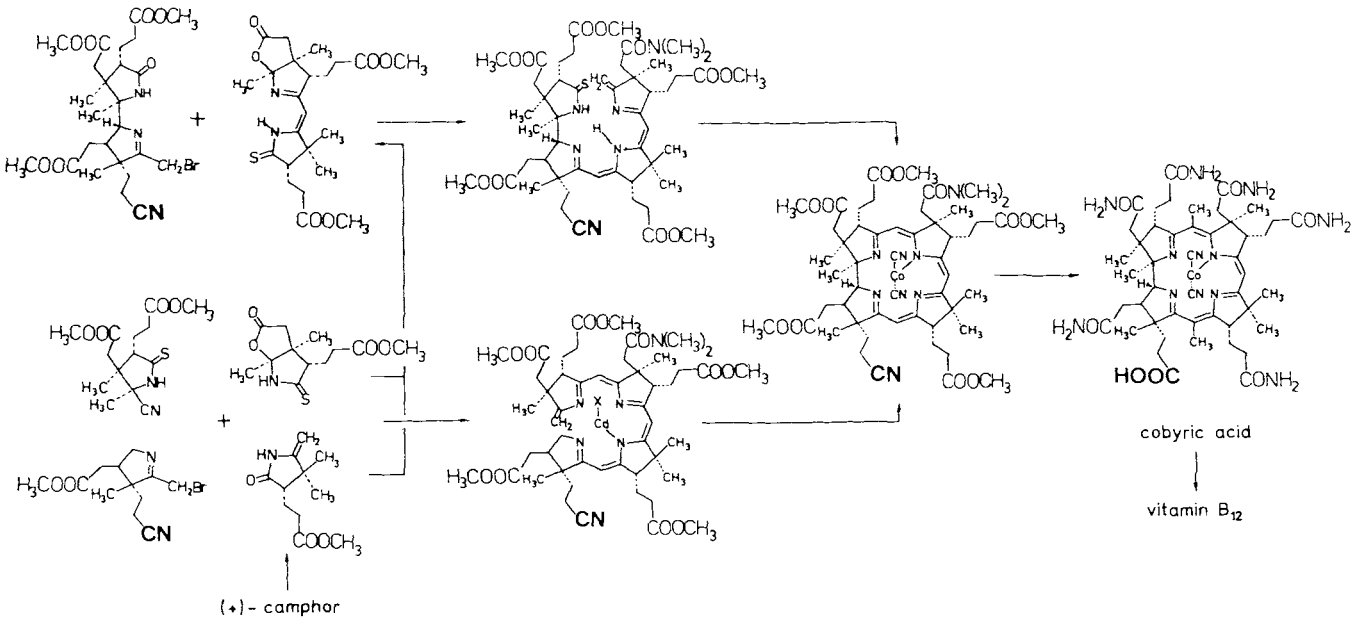

Fig. 4. Overview of the two variants for the synthesis of cobyric acid [18, 19].

mine its biosynthetic pathway (but not always, as demonstrated by the example of adenine). Nonetheless, the work on vitamin B_{12} provides an example of how research on the synthesis of a natural product, carried out originally from a chemically "hard" point of view, can lead in unexpected ways to the very questions with which this article is concerned.

The two syntheses of cobyric acid that have so far been realized are delineated schematically in Figure 4.[18,19] At the time when the Harvard group pursued the original strategy of solving the A/D-ring junction problem at the beginning of the synthesis, the Woodward–Hoffmann rules were discovered.[20] Out of the new perspective of these rules emerged at ETH the concept of a photochemical variant of the cobyric acid synthesis, the key step of which is the photoinduced ring closure of an A/D-secocorrinoid cadmium complex. The direct coupling of rings A and D was thereby accomplished in one step with high diastereoselectivity in the final phase of the synthesis (Fig. 5).[19,21] In retrospect, this photochemical A/D-secocorrin→corrin cycloisomerization proved to be the tailored solution to the problem of the A/D-ring coupling, which, for its part, had given birth to the discovery of the Woodward–Hoffmann rules.

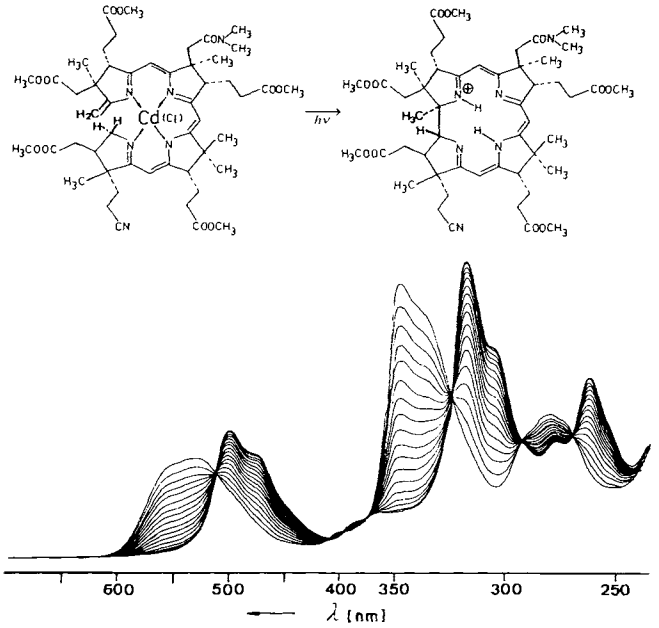

Fig. 5. Above: The A/D-secocorrin→corrin cycloisomerization step in the photochemical variant of the cobyric acid synthesis [19]. Conditions: visible *hv*, 200 W, 25 cm; in CH_3OH/HOAc/NaOAc, under argon; RT; $c \approx 10^{-4}$ mol L^{-1}. Under these conditions the cyclized cadmium(II) complex demetalates spontaneously. Below: Course of the reaction monitored by UV/VIS spectroscopy (from *W. Fuhrer* [154]).

Could there exist a dark variant of the photochemical ring-closure reaction, which might provide us with an insight into the process used by Nature to construct the corrin framework during the (in any case non-photochemical) biosynthesis of the vitamin? It was this question that directed our work for several years after completion of our studies on the chemical synthesis of vitamin B_{12}. Not just one but a whole family of such dark variants was the result of work carried out on synthetic model compounds. An overview of these reactions is presented in Figure 6.[22]

The act of photoexcitation in the photocycloisomerization of a 1-methylidene-1,19-secocorrin (e.g., cadmium, zinc, or magnesium) complex can be successfully replaced, in the case of the corresponding nickel(II) complex, by a reaction sequence consisting of (one-electron) electrochemical oxidation followed by direct reduction of the meanwhile isomerized radical cation (oxidoreductive variant, 1976[23]). The corrin complex can also be formed, however, starting from a 18,19-didehydro-1,19-secocorrin nickel(II) complex by electrochemical (two-electron) reduction in a protonating medium (reductive variant, 1975[24]). Thermal decarboxylation of the 19-carboxy derivative of a 1-methylidene-1,19-secocorrin nickel(II) complex in nonpolar medium also results in the formation of the corrin complex (decarboxylative variant, 1976[22,25]). Finally, the corresponding 19-formylsecocorrin derivative readily undergoes cyclization in the simultaneous presence of proton donors and acceptors (e.g., acetic acid/triethylamine 4 : 1 in benzene at room temperature) to give the 19-formylcorrin complex, which, in turn, undergoes smooth deformylation upon treatment with potassium hydroxide (tautomerization variant, 1977[25]). All these ring-closure variants are members of a common family of reactions; they all involve intermediates having the same type of constitution (see Fig. 6). The last two variants were worked out following the then surprising discovery of *Shemin* et al.[26] and *Scott* et al.[27] that the *meso* carbon atom between rings A and D of the uroporphyrinogen precursor is extruded during the biosynthesis of vitamin B_{12} (Fig. 7a). The cyclization of the formyl derivative demonstrated for the first time how the extrusion of a single carbon-atom equivalent from the ring-A/D region can serve a specific function in the A→D ring-coupling process and how, from a chemical standpoint, the B_{12} biosynthesis can occur in principle by transformation of a porphyrinogen-type structure to a corrin-type structure without the use of an external reducing agent (but instead by extrusion of a *meso* carbon as a carboxyl carbon).

A decisive impulse in our further search for a chemical model for the natural route of formation of the A/D-ring junction of vitamin B_{12} was imparted by a completely unexpected and very important result obtained in the laboratories of *Battersby*,[28] *G. Müller*,[29] and *Scott*.[29] In the third methylation step along the biosynthetic pathway leading from uroporphyrinogen to cobyric acid, the methyl group is introduced at the *meso* position between rings A and D, that is, at just that carbon center that is going to be extruded during subsequent biosynthetic steps. The *meso* carbon is thus extruded as a C_2 fragment along with the previously introduced methyl group, instead of as a C_1 fragment (see Fig. 7b). This discovery gave rise in our laboratory to the concept of a dihydrocorphinol→corrin rearrangement, the last variant of corrin formation shown in Figure 6. In this process, the macrocycle of a 1,20-dihydro-20-hydroxy-20-methylcorphin derivative undergoes contraction to give the macrocycle of a 19-acetylcorrin derivative (ring contraction variant, 1980[30–32]). The experimental observations are summarized in greater detail in Figure 8. It is, in particular, the stepwise reaction pathway leading

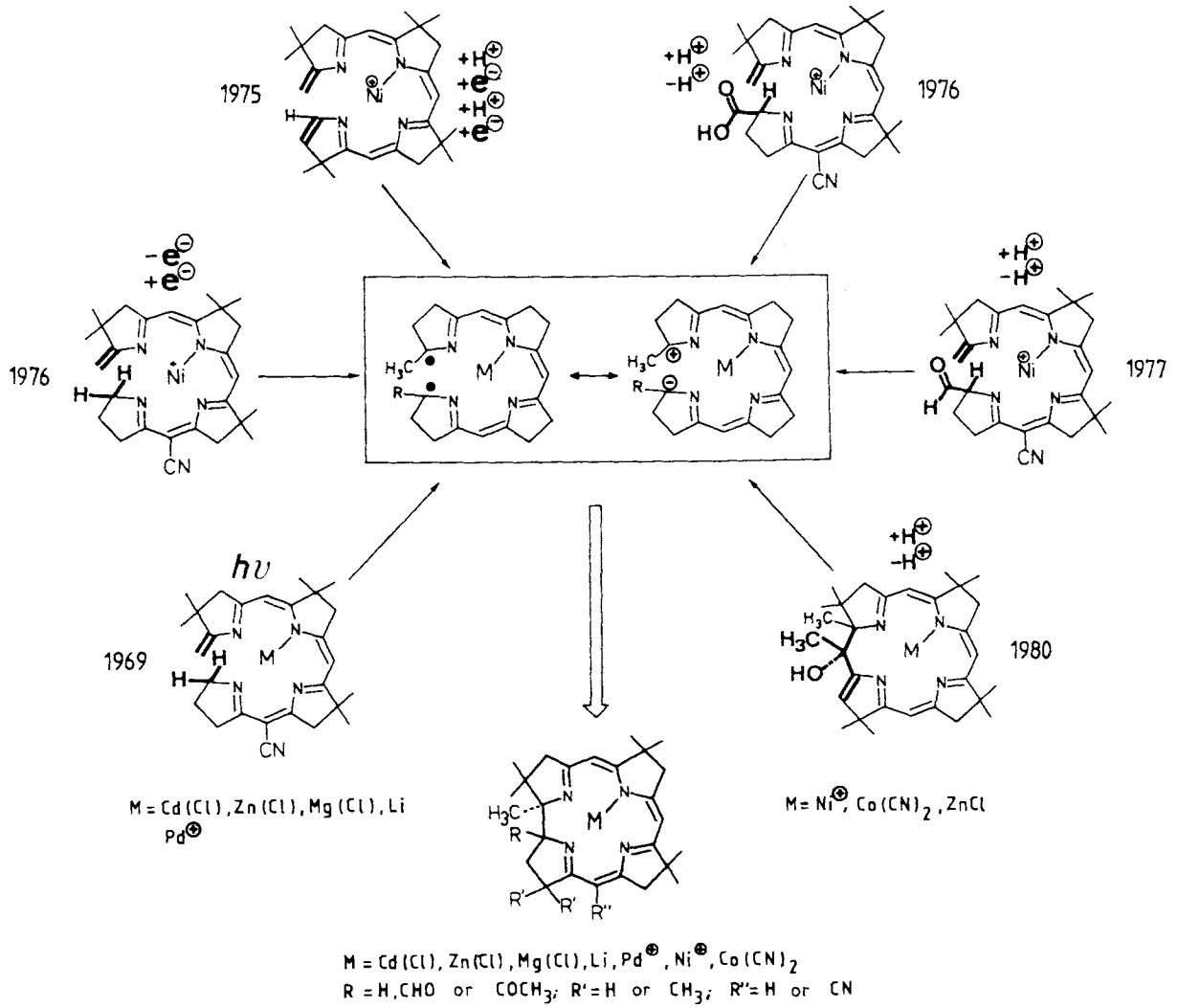

Fig. 6. Oxidoreductive [23], reductive [24], decarboxylative [25], tautomerization [25], and ring-contraction [30] variants of the photochemical A/D-secocorrin→corrin cycloisomerization [21] in synthetic model systems.

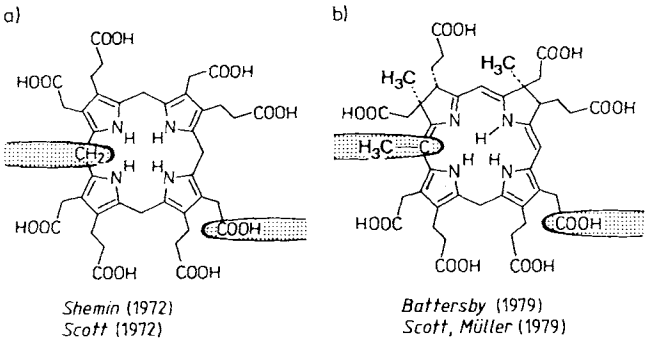

Fig. 7. Extrusion of carbon centers in the biosynthesis of vitamin B_{12} from uroporphyrinogens of type III [26–29]. For a, b see text.

to ring contraction[31] that reveals how closely related this type of corrin formation indeed is to the previously discussed cyclization of a 19-formylsecocorrin and thus to the original photochemical A/D-secocorrin→corrin cycloisomerization.

As a type of structural change, the dihydrocorphinol→corrin rearrangement is regarded in current B_{12} research[33,34] (compare Fig. 49, Section 4) as a valid model for the process by which Nature accomplishes the crucial step in the formation of the corrin system of vitamin B_{12}. In the laboratories of *Arigoni*[35] and *Battersby*[36] it has been shown experimentally that the C_2 fragment extruded during the course of biosynthesis is an acetic acid equivalent.

Thus, by transient methylation of the *meso* position between rings A and D, Nature makes use of a reaction channel leading to ring contraction, which, via intramolecular shift of π-oxidation equivalents of the chromophore system, allows the formation of the (more reduced) corrin system without the necessity of employing an external reducing agent. Among biosyntheses of low-molecular-weight natural products, the acrobatics of this sequence of reactions is probably unique. It is just such kinds of molecular complexity in the course of the biosynthesis that offer us clues as to the origin of the vitamin B_{12} structure, particularly when we study and compare the autochthonous reactivity of the type of structures that occur along the pathway leading from uroporphyrinogen to cobyric acid.

An interesting example of such autochthonous reactivity is provided by the finding made in a study of the behavior of a model dihydrocorphinol derivative lacking the critical

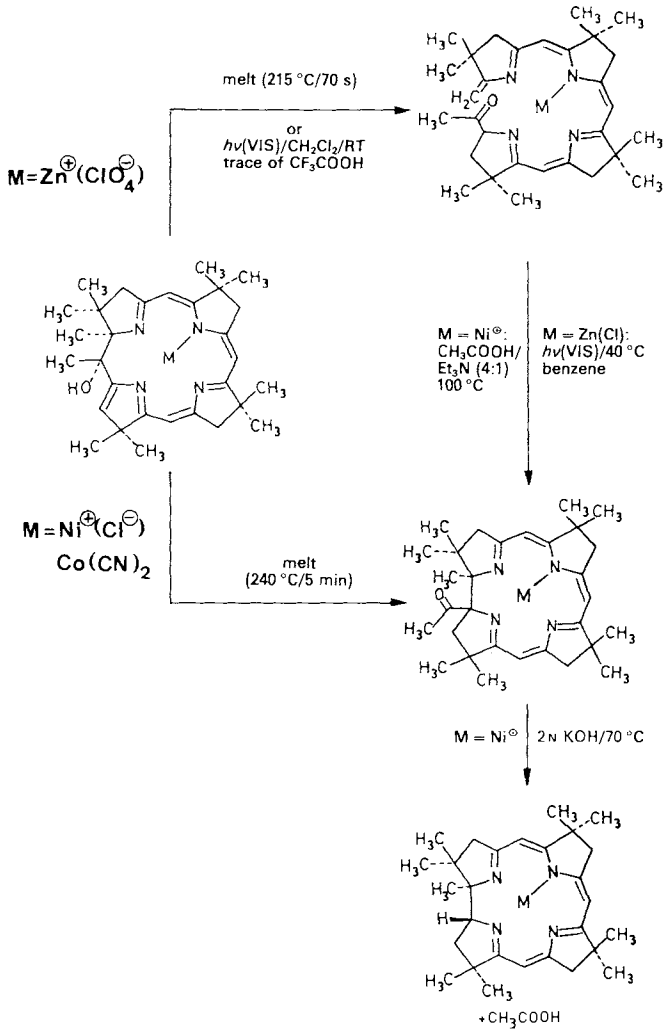

Fig. 8. The dihydrocorphinol→corrin rearrangement: synthetic model for the ring-contraction step in the biosynthesis of the corrin ring of vitamin B_{12} (*V. Rasetti* et al. [30, 31], *K. Hilpert* [32]) (cf. Fig. 27).

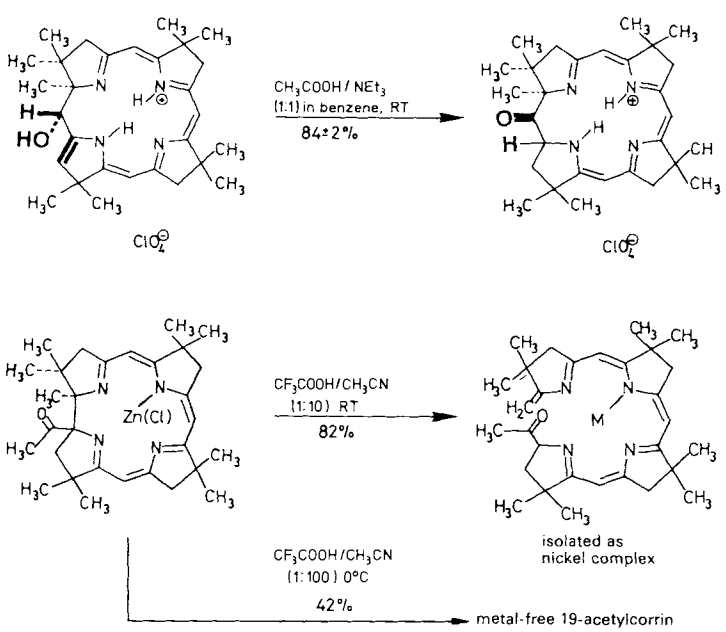

Fig. 9. Observations made in model studies on corrin biosynthesis [31] (cf. *A. Fässler* [37] and *K. Hilpert* [32]).

C-methyl group at the *meso* position between rings A and D (see Fig. 9). In contrast to the corresponding *tertiary alcohol, such a secondary* alcohol apparently has little chance to undergo the kind of ring contraction shown in Figure 8, since, under very mild reaction conditions, it undergoes irreversible tautomerization to give the 20-oxotetrahydrocorphin derivative.[31,37] This finding provides a worthy comment on the question of why Nature found it useful to transiently *C*-methylate the critical *meso* position between rings A and D in the course of developing the biosynthetic pathway to vitamin B_{12}.

The model studies on the dihydrocorphinol→corrin rearrangement have resulted in a further noteworthy finding in this connection. As also shown in Figure 9, it is the extraordinary lability of metal-free 19-acetylcorrins toward proton-induced opening of the macrocycle between rings A and D, first observed during attempted acidolytic decomplexation of a zinc(II) 19-acetylcorrin complex.[31,32] In contrast, synthetic metal-free corrins having a hydrogen atom in place of the acetyl group at position C-19 are completely stable toward such a ring opening.[38] This contrasting behavior is understandable in terms of the mechanism of ring opening in the 19-acetyl derivative. The biosynthesis of the corrin system is believed to proceed via a (potential) 19-acetyl derivative; however, it does not stop there but removes the acetyl group at position C-19 and replaces it by a proton. This fact conforms well to the above-mentioned finding.

The search for a dark variant of the photochemical A/D-secocorrin→corrin cycloisomerization led to the discovery of an entire family of alternative routes of corrin formation; the family is portrayed in Figure 6. Moreover, it led to the realization that the corrin-specific A/D-ring junction, which, at the start of the vitamin B_{12} work, had to be considered the most imposing obstacle to any chemical synthesis of vitamin B_{12}, is in fact a structural element that can form itself very readily and in a variety of ways under structurally appropriate preconditions.

In this connection, *A. W. Johnson*'s discovery[39] in the mid-1960s of the oxidative A→D cyclization of dehydrobilin derivatives to corrols and octadehydrocorrins deserves special mention.[40] We now recognize that this A→D ring-closure concept, first realized in these highly dehydrogenated systems, is relevant to the vitamin B_{12} structure in an even more comprehensive way than the pioneer of the A→D cyclization may ever have imagined. The gap in oxidation level between *Johnson*'s cyclization to octadehydrocorrins and the photochemical cyclization of A/D-secocorrins to corrins has meanwhile been bridged in our laboratory[41,42] and in that of *Montforts*.[43] The results, summarized in Figure 10, show that it is possible to carry out A→D cyclizations for a total of five different corrinoid oxidation states. These findings document the extraordinarily broad constitutional and mechanistic scope of approaches to the carbon/nitrogen skeleton of the corrin structure via A→D ring closure.

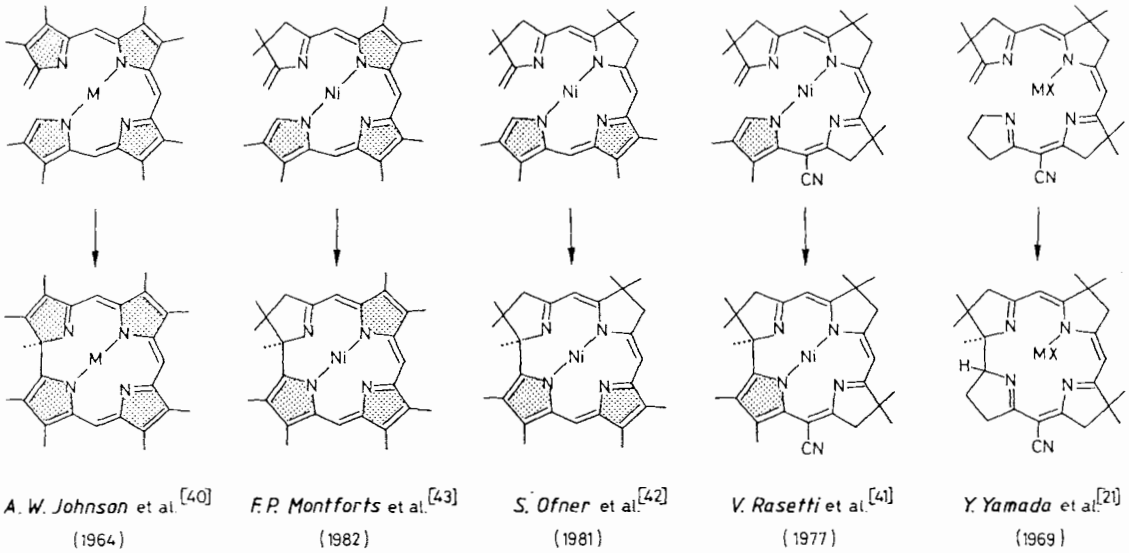

Fig. 10. A→D cyclizations to corrinoids in model systems whose ligand systems exhibit different degrees of dehydrogenation and methylation.

Figure 11 is an attempt to summarize schematically all reported cases in which an A→D cyclization was used in order to transform synthetic substrates into products having a corrinoid structure.[44] The direct coupling of two rings can be accomplished under diverse reaction conditions, largely independent of both the degree of methylation of the ligand periphery and the degree of dehydrogenation of the chromophore. *This schematic diagram might well be said to symbolize the demystification of the vitamin B_{12} structure by chemical synthesis.* The corrin-specific A/D-ring junction of the vitamin B_{12} molecule is a structural element that, under appropriate preconditions, self-assembles so to speak in a preprogramed way.

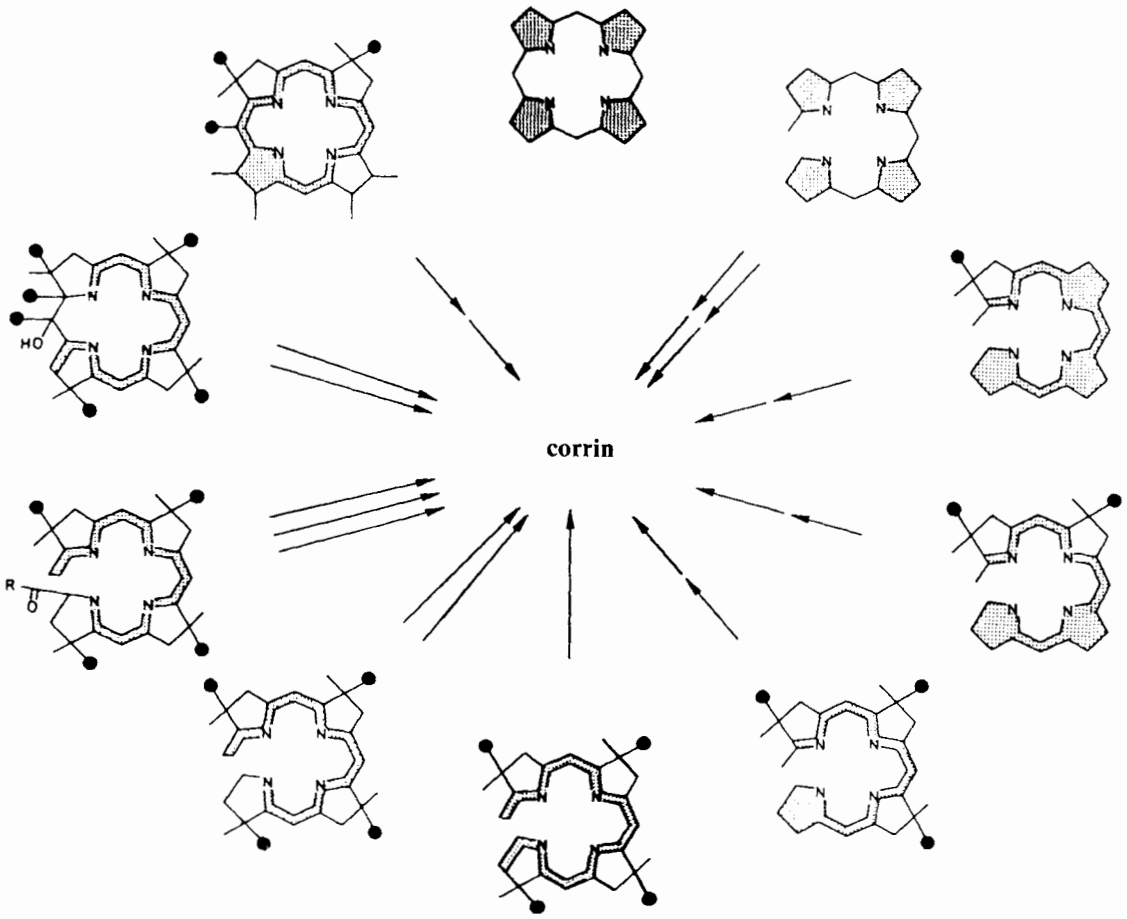

Fig. 11. Overview of the types of A→D cyclizations to corrinoids so far realized [44].

Are other structural elements of vitamin B_{12} similar to the A/D-ring junction in this respect? Do, for example, the characteristic arrangement of double bonds in the corrin chromophore, the pattern of *C*-methylation of the ligand periphery, the configuration of the ligand periphery, and the specific attachment of the nucleotide chain to the corrin ligand also represent structural elements that readily form under structurally appropriate preconditions? Or, in other words, is the outward complexity of the vitamin B_{12} molecule only a deceptive appearance?

The incisive change in our attitude toward the vitamin B_{12} structure evidenced by questions of this kind has led us to go as far as to envisage the extreme possibility of a prebiotic origin of the corrin structure.[45] Do reaction conditions exist that will, via a self-directing sequence of reactions (e.g., tautomerization, complexation, ring-opening, and ring-closing), convert a porphyrinogen into a corrin complex? Such a question (see Fig. 12) presupposes the occurrence of *reversible* protonation steps, which would have to replace the *irreversible* (but regioselective) *C*-methylation steps of B_{12} biosynthesis; electrophilic *C*-methylations (by adenosylmethionine) and *C*-protonations are isoelectronic processes. Possible intermediates would be metal complexes in which the double bonds of the chromophore system are arranged in a corrinoid (or corphinoid) fashion, with the carbon/nitrogen skeleton still being unchanged (see Fig. 12). The target product would be a corrin complex, one among constitutional and stereochemical isomers, which would correspond in constitution and configuration to cobyrinic acid with protons replacing the *C*-methyl groups around the periphery (a "protocobyrinic acid").

It was the pursuit of this question that ultimately led us to the experiments discussed in the next section.

3. Synthetic Analysis of Specific Structural Elements of the Vitamin B_{12} Molecule

This four-part section deals with experimental results and insights that we regard as way stations along the road toward a chemical rationalization of the structure of vitamin B_{12}. Some of the structural elements characteristic of vitamin B_{12} are found to be self-assembling in the sense that the amount of "external instruction" required for their formation under structurally appropriate preconditions is surprisingly small in view of the complexity and specificity of these structural elements. The investigations carried out so far have focused on the characteristic arrangement of double bonds in the corrin chromophore, the special dimension of the corrin macrocycle, the specific attachment of the nucleotide loop to the propionic acid side chain of ring D, and the arrangement of side chains around the ligand periphery. Most of these investigations have been carried out on synthetic model systems.

3.1. The Corrin Chromophore: Its Specific Arrangement of Double Bonds

At the start of this work, virtually nothing was known about the reaction behavior of porphyrinogen-type structures with respect to the problems raised in Figure 12.[46] The use of a fully symmetric model substrate in the exploratory investigations was therefore deemed advisable; the model of choice was the readily accessible octaethylporphyrinogen.

Our earlier work on the synthesis of corphin derivatives[47] provided us with a background of experience that proved to be crucial in designing and carrying out these investigations. *Corphins* are hexahydroporphinoid ligands

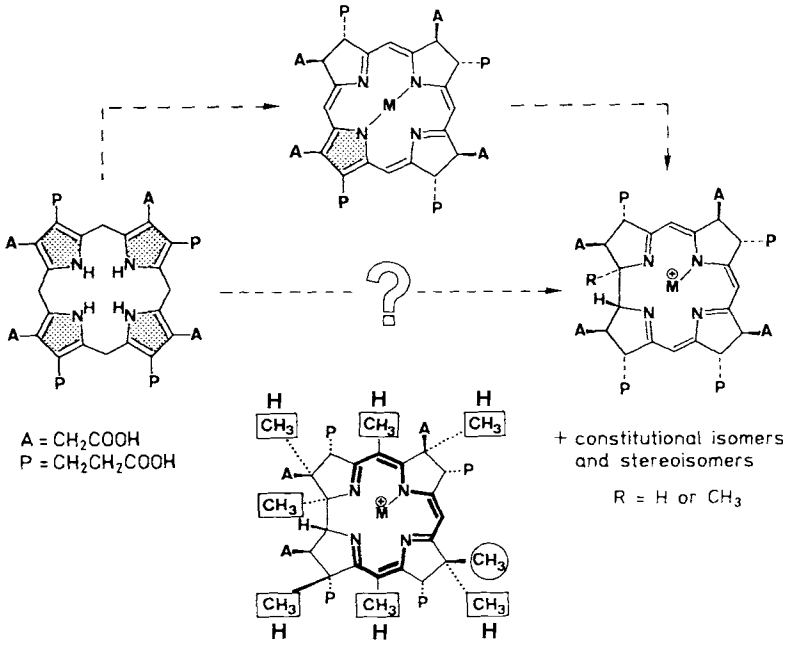

Fig. 12. Do reaction conditions exist that would transform uroporphyrinogens into (peripherally nonmethylated) corrin complexes?

which have a corrin-like chromophore but possess the carbon/nitrogen skeleton of the porphins (see Fig. 13). They form transition-metal complexes whose stabilities are similar to those of the corrins;[47,48] this gave rise to the expectation that complexes of their monopyrrolic tautomers, the *pyrrocorphins*,[49] might exist as the corresponding *C*-protonated corphin complexes in protonating media.

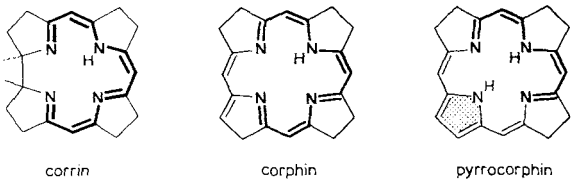

Fig. 13. Three types of chromophores.

The translation of the overall problem formulated in Figure 12 into a less demanding but experimentally more directly accessible question is depicted in Figure 14. What is the position of the tautomeric equilibrium between the tetrapyrrolic arrangement of double bonds in a porphyrinogen and the arrangement in its corphinoid (quasi-corrinoid) counterpart? Does it lie on the side of the tetrapyrrole in the absence of metal ions and on the side of the corphinic (quasi-corrinic) ligand in their presence? In other words, is it possible to force a porphyrinogen-type structure to undergo transformation to a corphin-type (or pyrrocorphin-type) structure by imposing on it a complexing metal ion?

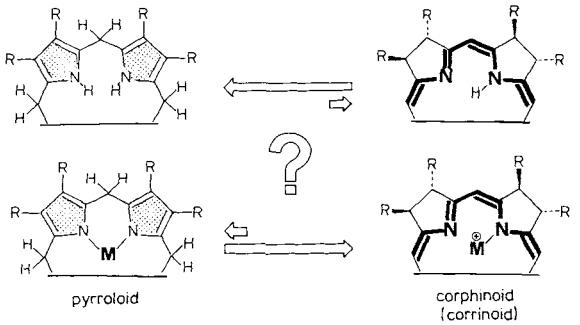

Fig. 14. Can a porphyrinogen be transformed into a corphin by imposing on the system a complexing metal ion?

The answer to this question followed a tortuous road.[50-53] This was due above all to the fact that both octaethylporphyrinogen and its tautomers are extremely prone to undergo autooxidative dehydrogenation upon exposure to oxygen, especially in basic medium. Success was finally achieved by the use of a basic and, insofar as possible, nonpolar medium—rather than a protonating medium, as originally thought. Figure 15 summarizes what we regard as the most advanced accomplishments; they were achieved following exploratory experiments with zinc(II),[50] cobalt(II),[51] and nickel(II).[52] Reaction of octaethylporphyrinogen with a mixture of 1,5,7-triazabicyclo[4.4.0]dec-5-ene ("TBD") and its iodomagnesium salt in a nonpolar solvent such as xylene in a sealed tube with strict exclusion of air resulted in tautomerization and complexation to afford a mixture of diastereomeric magnesium pyrrocorphinate complexes in nearly quantitative yield. Careful demetalation of the products with acetic acid gave the mixture of octaethylpyrrocorphins represented by HPLC 1 in Figure 15.[54-56] A ternary mixture of the three thermodynamically most stable diastereomers *ttttt*, *tttct*, and *tctct*[54] can be obtained by incorporation of an equilibration step (short treatment with magnesium bromide in moist benzene) between the tautomerization/complexation step and the demetalation step (compare HPLC 2). If the entire mixture of diastereomeric, metal-free pyrrocorphins (HPLC 1) is subjected to tautomerizing conditions (pyridine/acetic acid) with strict exclusion of air, (nearly) complete tautomerization back to octaethylporphyrinogen occurs.[53,56]

From a preparative viewpoint the discovery of the porphyrinogen→pyrrocorphin tautomerization opened up a simple and direct approach to the new type of structure represented by this hexahydroporphyrin.[56,57] The configuration of the majority of the diastereomeric octaethylpyrrocorphins appearing in the HPLCs of Figure 15 has been elucidated (X-ray structure analysis, usually of the nickel(II) complex;[58,59] autooxidative dehydrogenation to nickel(II) isobacterio- and nickel(II) bacteriochlorinates[56,57]). By metalation of metal-free pyrrocorphins it is possible to obtain nickel(II) pyrrocorphinates as well as the corresponding cobalt(II), iron(II), and copper(II) complexes, without epimerization.[56,57] Nickel(II) pyrrocorphinates may also be obtained directly by complexation-tautomerization of octaethylporphyrinogen with nickel(II) acetate and TBD in xylene.[53]

The experimental answer to the question as to the relative thermodynamic stability of the pyrrocorphin ligand system versus the tetrapyrrolic porphyrinogen is summarized in Figure 16. In the absence of complexing metal ions, the porphyrinogen is thermodynamically more stable than the pyrrocorphin; in the presence of a complexing metal ion and a base, on the other hand, the equilibrium

porphyrinogen + metal salt + base ⇌
pyrrocorphinate complex + salt

lies on the side of the pyrrocorphinate. Isolation of the unstable metal-free pyrrocorphin by demetalation of the magnesium(II) pyrrocorphinate is only successful because, in this special case, the acidolytic decomplexation can be achieved under *kinetic control*.

Pyrrocorphinate complexes undergo reversible protonation by protic acids in nonpolar medium to give the corresponding corphinate complexes, which are easily detected by UV/VIS spectroscopy (see, e.g., Fig. 17[56]). The regioselectivity of this C-protonation is associated with the specific formation of a (complexed) chromophore system, which, in the region of the five-membered rings, is identical with the (complexed) chromophore system of a corrin. Since the tautomeric equilibrium between a *metal-free pyrrocorphin* and a *metal-free corphin* lies on the side of the pyrrocorphin, the corphin too is thermodynamically less stable than its porphyrinogen tautomer.

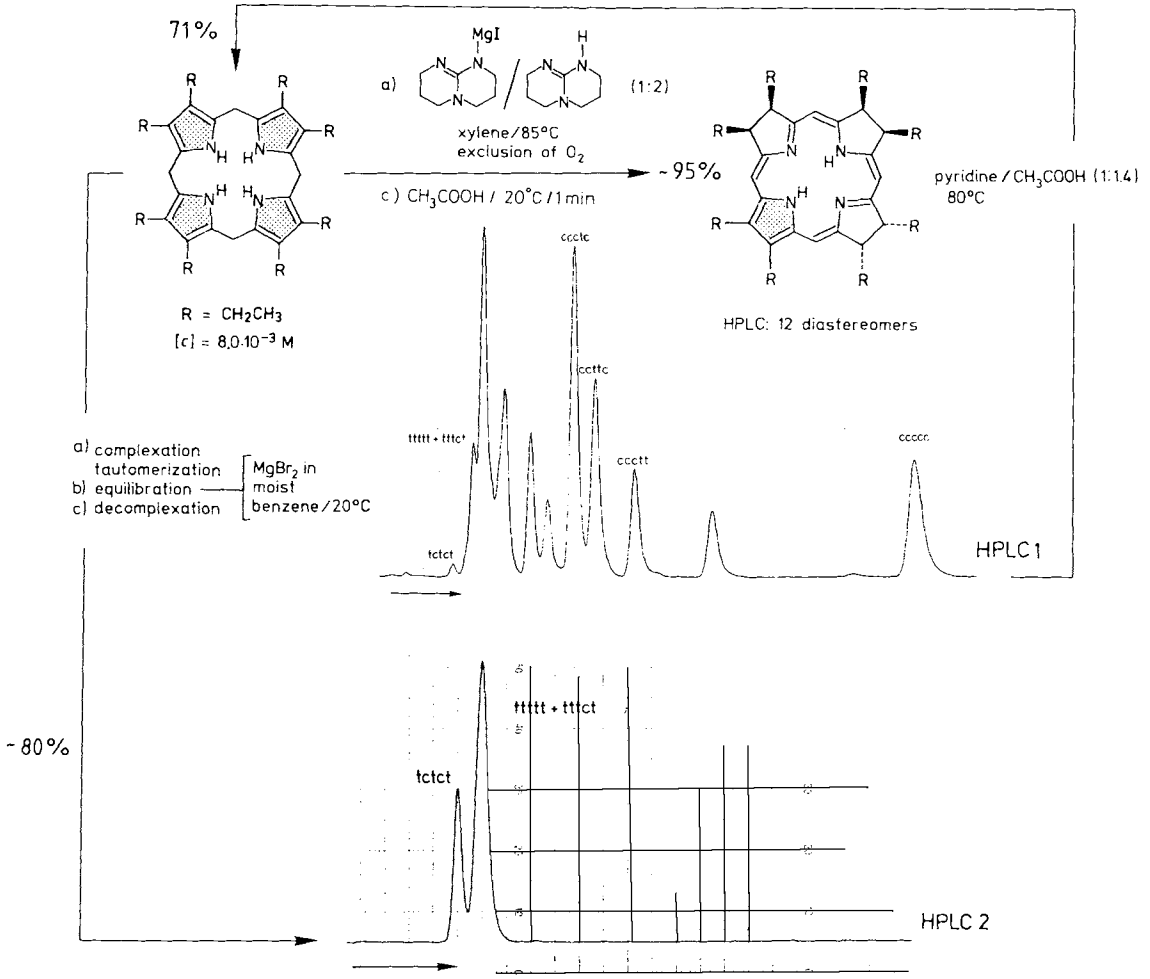

Fig. 15. The porphyrinogen→pyrrocorphin tautomerization [53, 54] (cf. *C. Angst* [50], *R. Waditschatka* [56]). Configurational designation of diastereomers: starting at ring A (above left) and proceeding in a clockwise direction (*c*=*cis*, *t*=*trans*).

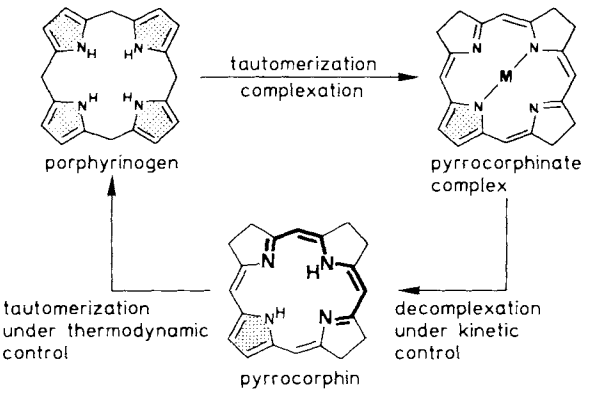

Fig. 16. In the absence of metal ions, a porphyrinogen is thermodynamically more stable than the corresponding pyrrocorphin (and corphin).

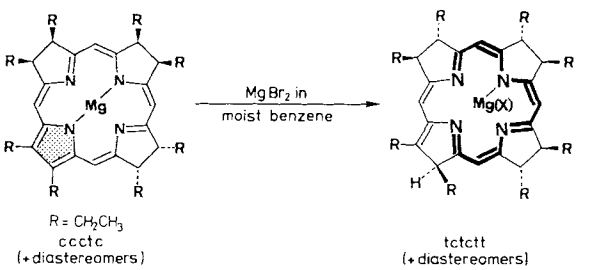

Fig. 17. In protonating medium, pyrrocorphin complexes are present as corphin complexes [56].

In the context of a chemical rationalization of the vitamin B_{12} structure, the experimentally established connection between the porphyrinogen-type structure and the isomeric hexahydroporphinoid ligand systems of pyrrocorphins and corphins affords an insight into the thermodynamic status of the corrin chromophore: *Within the family of hexahydroporphinoid ligand systems, the corphinic (or corrinic) arrangement of double bonds in the chromophore corresponds to a thermodynamically favored arrangement if the ligand is present in complexed form* (Fig. 18). The corrin chromophore is not a complex structural element that presupposes correspondingly complex pathways of formation. Quite to the contrary, the specific arrangement of double bonds in the macrocycle is in a sense a self-constituting structural element since it can form spontaneously under structurally appropriate preconditions.

How can the arrangement of double bonds in a tetrapyrrolic porphyrinogen be transformed into the thermodynamically less stable corphinic arrangement without complexation? An answer is provided by the biosynthesis of vitamin B_{12}: by electrophilic *C*-methylation of one periph-

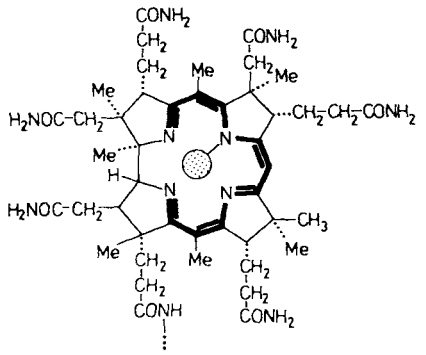

Fig. 18. "Within the family of hexahydroporphinoid ligand systems, the corphinic (or corrinic) arrangement of double bonds in the chromophore corresponds to a thermodynamically favored arrangement if the ligand is present in complexed form."

eral position of each of the four pyrrole rings! Of the eight biosynthetic methylation steps, the sequence of the six crucial ones is now known, as a result of important experimental studies carried out in the laboratories of *Battersby*[60,61] and *Scott* and *G. Müller*.[62] This sequence reveals that the biosynthetic pathway involves intermediates that are pyrrocorphins and corphins, respectively,[33,34,61] or at least very close tautomers thereof (compare Fig. 49, Section 4). Chemically, interesting parallels indeed exist between the two strategies, the biosynthetic pathway on the one hand and the porphyrinogen→pyrrocorphin tautomerization induced by complexation on the other; both achieve the transformation of a porphyrinogen to the thermodynamically less stable corphin.

The relationship of *C*-protonation and electrophilic *C*-methylation as isoelectronic processes is not only relevant in terms of classification, but it also has a counterpart in the actual chemistry of pyrrocorphins: Treatment of magnesium(II), zinc(II), or even nickel(II) complexes with methyl iodide results in regioselective *C*-methylation on the periphery of the pyrrolic ring to give the corresponding corphinate complexes.[56,63-65] Thus, pyrrocorphinates have emerged as substrates that make the (long sought[39,66]) *biomimetic* *C*-methylation of hydroporphinoids possible.

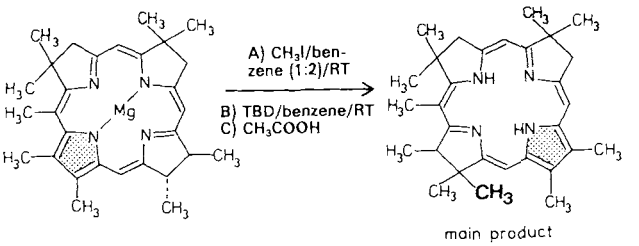

Fig. 19. Peripheral *C*-methylation of a magnesium pyrrocorphinate [67] (cf. *C. Leumann* [65]).

Figure 19 shows an example in which a synthetic model, a pyrrocorphinate bearing a methyl group at the *meso* position between rings A and D, was used to study the effect of this methyl group on the course of peripheral *C*-methylation.[32,65,67] Later, it was found that pyrrocorphinates, although the most reactive, are not necessarily the only type of substrate capable of undergoing biomimetic *C*-methylation. In general, systems containing a mixed pyrrolic-vinamidinic[68] chromophore that is not macrocyclically conjugated can undergo this type of reaction with high and predictable regioselectivity. Figure 20 shows an example involving the synthetic model of a type of chromophore that is assumed to occur along the biosynthetic pathway

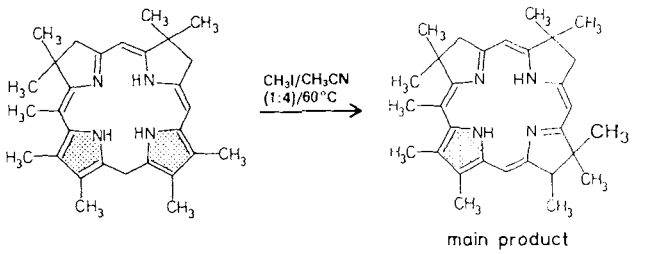

Fig. 20. Biomimetic *C*-methylation of a metal-free dipyrrolic pyrrocorphin tautomer [67] (cf. *C. Leumann* [65]).

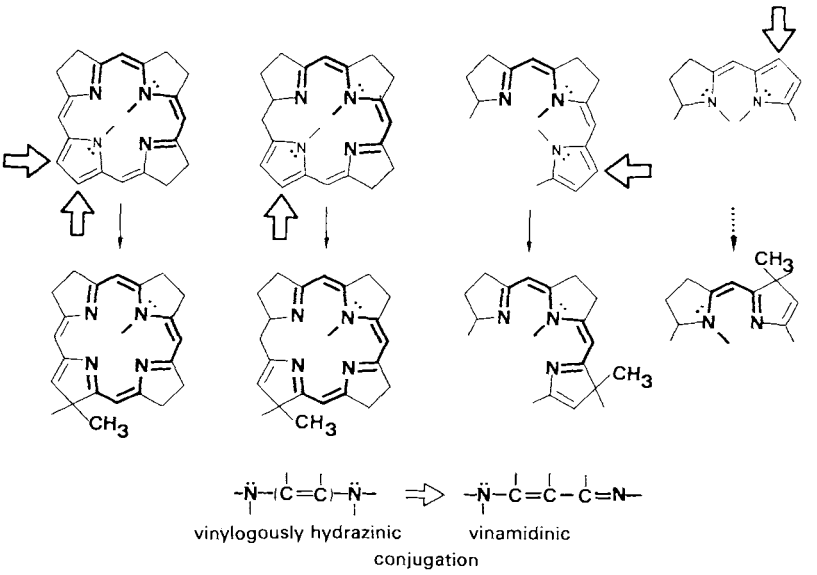

Fig. 21. Constitutional criteria related to the regioselectivity of the C-methylation of pyrrolic-vinamidinic chromophore systems [67].

leading to cobyric acid.[69] Common to all successfully tested chromophores is the presence of two NH electron pairs belonging to the π system and mutually conjugated in a vinylogously hydrazinic (i.e., potentially destabilizing) fashion. *C*-methylation results in the transformation of this system to one displaying vinamidinic (i.e., stabilizing) conjugation, in which an NH electron pair is linearly conjugated with an electrophilic ketimine group. This argument provides a way of interpreting the course of the reaction and allows predictions to be made concerning its regioselectivity. A schematic illustration is presented in Figure 21.[67]

3.2. The Corrin Ring: Its Contracted Dimension Compared with the Corphin Ring

In connection with our experiments aimed at finding a porphyrinogen→pyrrocorphin transformation in the presence of nickel(II) salts, *C. Kratky* (Institut für Physikalische Chemie, Universität Graz) carried out for us X-ray structure analyses of two diastereomeric nickel(II) hexahydroporphinates in order to confirm their constitution and determine their configuration. This work led to the discovery of an unexpected phenomenon, namely, the conformational coupling of the hydropyrrolic rings in these complexes.[52] After the existence of this phenomenon was confirmed for two diastereomeric nickel(II) isobacteriochlorinates of known structure,[70] we pursued systematic investigations in close collaboration with *C. Kratky*. The experimental data and insights thereby obtained are of general importance for the chemistry of hydroporphinoid metal complexes.[59] In particular, we believe that these insights contribute to a deeper understanding of the structure of vitamin B_{12}.

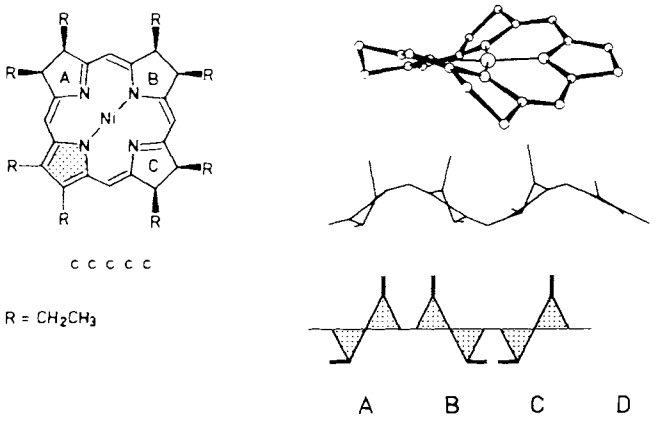

Fig. 22. X-ray structure analysis of nickel(II) *ccccc*-octaethylpyrrocorphinate (*C. Kratky* et al. [59]). Ruffling of the ligand system [71] and conformational coupling of the hydropyrrolic rings.

Figure 22 shows the X-ray crystal structure of nickel(II) *ccccc*-octaethylpyrrocorphinate, which is representative of all available crystal structures of tetra- and hexahydroporphinoid nickel(II) complexes.[55,59] The ligand system of the planar-tetracoordinated, diamagnetic nickel(II) complex is not planar but instead exhibits a saddle-shaped deformation ("ruffling") with approximate S_4 symmetry. Each of the four *meso* carbon atoms lies, on the average, 0.74 Å alternatingly above and below an equatorial plane roughly defined by the four nitrogen centers and the metal coordination center. The three hydropyrrolic five-membered rings are in half-chair conformations, resulting in quasi-equatorial and quasi-axial positions for the peripheral substituents of these rings, as revealed by the cylindrical projection[71] of the structure. The three half-chairs are conformationally coupled with each other in the sense that their puckering alternates in such a way as to parallel the wave form of the saddle-shaped ligand periphery (W conformation of the half-chair ensemble,[59] see Figs. 22 and 29.)

The phenomenon of ligand ruffling in this system is by no means the result of crystal packing factors. This is documented in Figure 23, in which the cylindrical projections of the crystal structures of nickel(II) pyrrocorphinates, structurally isomeric hexahydroporphinates, isobacteriochlorinates, and a nickel(II) bacteriochlorinate are compared.[59] Moreover, the saddle-shaped conformation is not an intrinsic property of the ligands but rather a consequence of their coordination to the central ion, as shown by the X-ray structure data for a metal-free octaethylpyrrocorphin and two octaethylisobacteriochlorins.[59] The ligand system of nickel(II) *ccccc*-octaethylpyrrocorphinate has been shown to exhibit an S_4-like deformation in solution (CS_2) as well. The conformational heterotopicity of constitutionally homotopic *meso* vinyl protons, which results from the saddle-shaped conformation, can be observed in the ^{1}H-NMR spectrum below -40 °C.[55]

Ligand ruffling was first observed by *Meyer*[72] in an X-ray structure analysis of one of the two dimorphic forms of nickel(II) octaethylporphinate and was first interpreted by *Hoard*[73] for this example. More recently, it has also been studied intensively by *Ibers* and his co-workers[74] for nickel(II) di- and tetrahydroporphinates. *Ibers'* data and our own results reveal the following correlation: the "steepness" of the ligand ruffling increases with decreasing Ni–N bond lengths. This finding is in accord with the idea of a nickel(II) ion that seeks to satisfy its electrophilicity in the square-planar environment by drawing the four nitrogen centers in the coordination plane closer to it, thereby increasing the strengths of the bonds involved in this coordination. The ligand system, in particular that of hexahydroporphinoids, whose flexibility is greater than that of porphyrins, tolerates this process by ruffling, thereby allowing the size of the inner coordination hole to be diminished. The increase in coordination bonding energy is viewed to be balanced by the increase in the strain energy of the ligand system.

The ligand ruffling process is schematically depicted by the geometric model in Figure 24.[75] Coplanar, concentric circles of constant circumference undergo deformation, forming saddle-shaped surfaces of *increasing steepness* and, at the same time, resulting in the *increasing convergence* of four equidistant points (representing the four nitrogen centers) toward the center (representing the coordination center) of the original circle, the points remaining in a common plane.

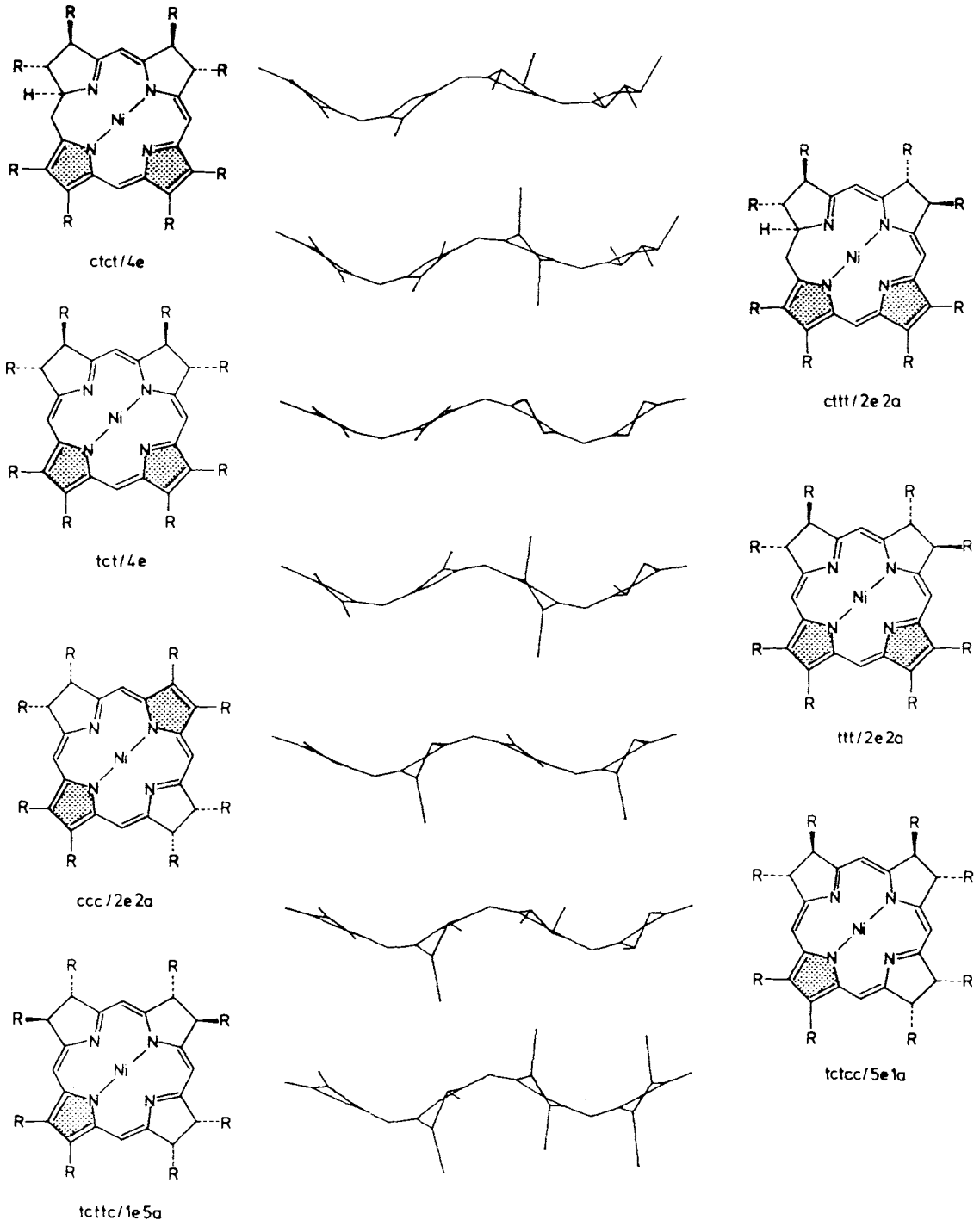

Fig. 23. X-ray structure analyses (cylindrical projections [71]) of hexahydro- and tetrahydroporphinoid nickel(II) complexes (*C. Kratky* et al. [59]).

The relationship between the "steepness" of ligand ruffling and metal-nitrogen bond length is clearly documented by comparison of the structural data for the pyrrocorphinate complexes of nickel(II), cobalt(II), and copper(II) (Fig. 25). The conspicuous inverse relationship between the steepness of the ligand ruffling and the mean length of the four M–N bonds is of significance because the chromophores in the three complexes are identical. Of particular interest is the finding that the pyridinato cobalt(II) pyrrocorphinate complex, despite its additional axial ligands, still exhibits appreciable ligand ruffling.[56,59]

According to all the structural data currently available to us, the (square-planar-complexed) nickel(II) ion (and, similarly, the cobalt(II) ion) is too small-sized for the coordination hole of hydroporphinoid ligand systems. On the other hand, the coordination hole of corrinoid ligands appears to conform well to the spatial demands of the nickel(II) ion, as clearly shown, for example, by the X-ray structure data in Figure 26. The two complexes in Figure 26 have identical chromophore systems; they differ only in the dimensions of their coordination holes. In the case of the (tetradehydro)corrinoid complex, hardly any ligand

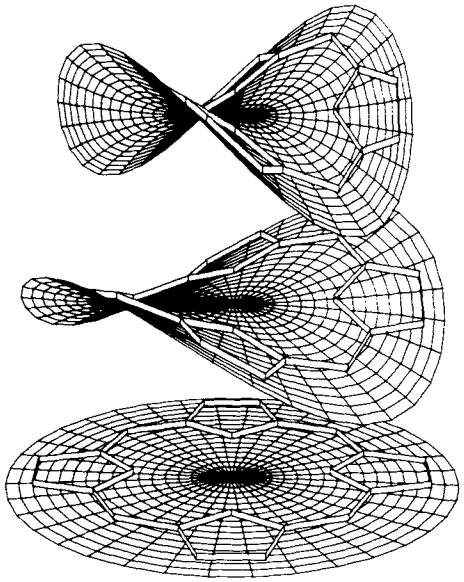

Fig. 24. Geometric model of the ruffling of the ligand periphery of hydroporphinoid nickel(II) complexes by nickel(II)-induced contraction of the inner coordination hole (*C. Kratky* et al. [59], cf. footnote [75]).

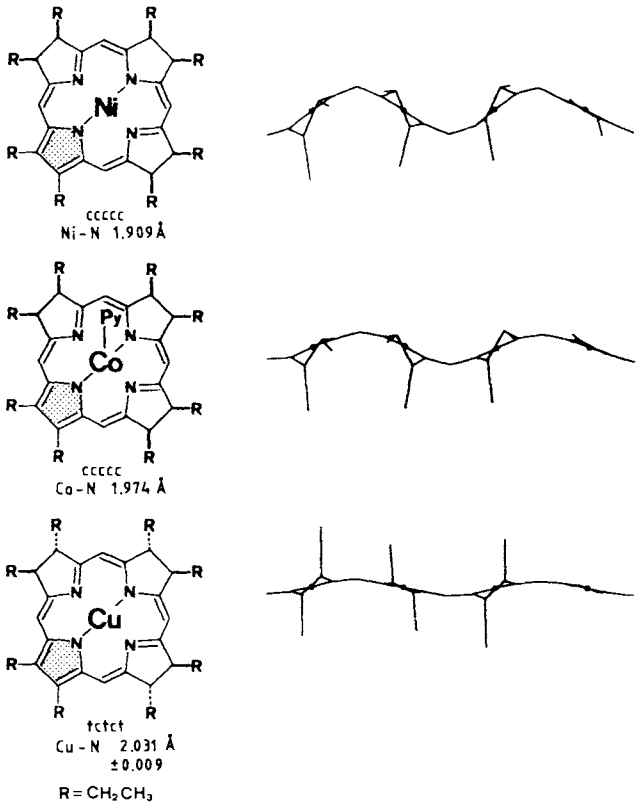

Fig. 25. Increasing "steepness" of the ligand ruffling in pyrrocorphinates is associated with decreasing metal-nitrogen bond lengths [56, 59]. Py in the cobalt complex signifies pyridine; Co-N(Py) 2.161 Å, Co is located 0.09 Å above the plane defined by the four N atoms.

ruffling is apparent, whereas it is appreciable for the hexahydroporphinate. The mean value of the four Ni–N bond lengths in the corrinoid complex is less than the statistical value (1.88 Å[159]) of Ni–N bond lengths in nickel(II) complexes exhibiting square-planar coordination, whereas the mean value of the four Ni–N bond lengths of all hydroporphinoid nickel(II) complexes so far investigated lies above this value. The corresponding value for a synthetic nickel(II) corrinate complex[76] is 1.874 Å.[77]

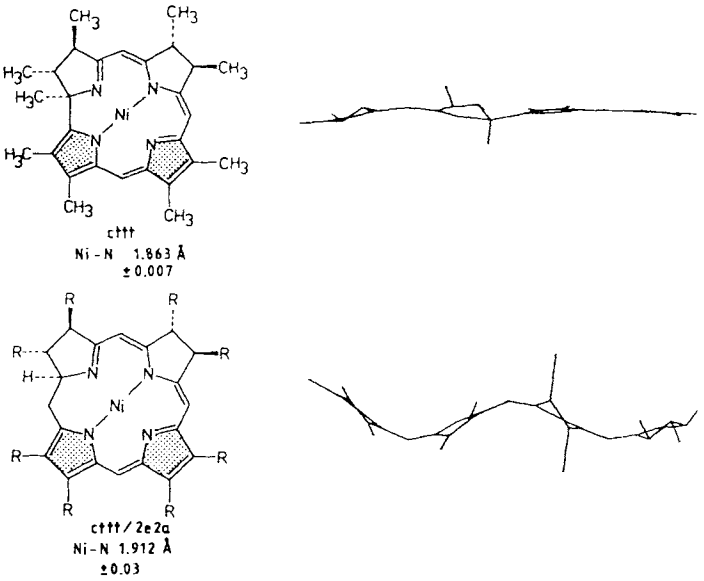

Fig. 26. The ligand system of a *corrinoid* nickel(II) complex exhibits no ruffling [50, 59]. R = ethyl.

If the interpretation of the structural data determined for hydroporphinoid and corrinoid complexes and their thermodynamic implications are correct, then a corphinoid nickel(II) complex should be expected to rearrange to a corrinoid complex, provided that a reaction pathway is made available. This, in fact, has been done in the case of the biosynthetic model discussed in Section 2, the dihydrocorphinol→corrin rearrangement (see Fig. 8). In one of the variants (Fig. 27), the crystalline complexes of both nickel(II) and dicyanocobalt(III) undergo ring contraction upon melting to give the corresponding 19-acetylcorrin complexes. Even though the difference in overall bonding energy due to the change in functional groups alone might favor product formation, the two ring contractions provide a fitting chemical illustration for the thermodynamic interpretation of the structural data.[78]

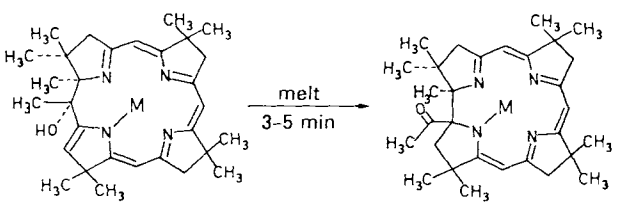

Fig. 27. Thermally induced ring contraction of corphinoid complexes to the corresponding corrin complexes (*Rasetti* et al. [30], cf. also Fig. 8).

Not only the constitution of the corrin chromophore, but also the specific size of the macrocyclic ring in corrin complexes is recognized to be a thermodynamically fa-

vored structural element: *The coordination hole in the (ring-contracted) corrin ligand is spatially better suited for the optimal coordination of metal ions such as nickel(II) and cobalt(II) than the (too large) coordination hole of corphin ligands* (Fig. 28). Apart from the importance that the specific dimension of the corrin ring has for the functional properties of the vitamin B_{12} structure (cf. Section 5), the fitting size of this ring for complexation is certainly responsible for the ease with which corrinoid structures form (see Fig. 11).

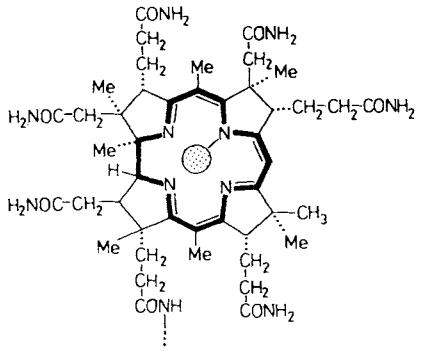

Fig. 28. In terms of the coordination of the metal ion by the macrocyclic ligand system, nickel(II) and cobalt(II) corrin complexes are thermodynamically more stable than the corresponding corphin complexes.

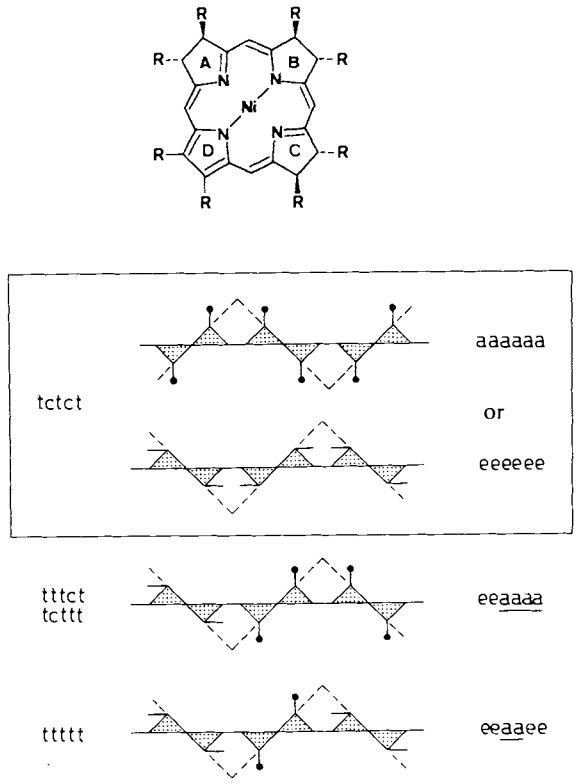

Fig. 29. As a result of the conformational coupling of the hydropyrrolic rings, the *tctct* configuration of substituents on the ligand periphery represents, of all possible configurations, the thermodynamically most stable configuration for nickel(II) pyrrocorphinates. R = ethyl.

If the ligand ruffling and the accompanying increase in coordination bond strength amounts to a stabilization of a hydroporphinoid nickel(II) complex, then the W-form conformation of the half-chair ensemble of hydropyrrolic rings (paralleling the wave form of the saddle-shaped periphery) must correspond to the energetically favored conformation, insofar as it permits maximal contraction of the coordination hole. This implies, in turn, that, of the three diastereomers of a constitutionally symmetrical pyrrocorphinate having a *trans* arrangement of all vicinal substituents (*ttttt*, *tttct*, and *tctct*; cf. Fig. 15), the *tctct* diastereomer must be the thermodynamically most stable one. The reason for this is that in the W conformation of the ring ensemble, all ring substituents exist in a uniform quasi-equatorial conformation (or a uniform quasi-axial conformation) when these substituents are in the *tctct* configuration (see Fig. 29). A variety of experimental findings are available which confirm this remarkable control of the configuration at the ligand periphery by the central nickel(II) ion; they indirectly contribute to the coherence of the interpretation given above. Two of these experiments will be briefly discussed below.

In equilibrium mixtures of octaethylpyrrocorphins or their metal complexes, the three diastereomers *ttttt*, *tttct*,[79] and *tctct* should be present in the statistical ratio of 1 : 2 : 1, since, in contrast to substituents in vicinal positions, there is no mutual steric interaction between substituents on neighboring rings flanking a common *meso* position. Indeed, this was essentially observed to be the case in product mixtures of porphyrinogen→pyrrocorphin tautomerization experiments that included the equilibration step (cf. Fig. 15). On the other hand, Figure 30 shows the result of an experiment[80] in which the pure *tttct* diastereomer[56] of nickel(II) octaethylpyrrocorphinate was subjected to configurational equilibration (occurring via double C-protonation). The product distribution, as determined by HPLC, reveals an 87% predominance of the *tctct* diastereomer. The analogous experiment performed with the palladium(II) complex led to a product mixture in which the *tctct* diastereomer predominated to a lesser extent. This result is plausible since the "larger" palladium(II) ion is expected to induce ligand ruffling only weakly, if at all.[56,57,59]

The other experiment involves the recently discovered coenzyme F430 from methogenic bacteria,[81] the corphinoid structure of which was elucidated in our laboratory together with *Pfaltz* and *Jaun* in collaboration with *Thauer* (Marburg).[82] It was known that this coenzyme undergoes structural change upon extraction from the bacteria at raised temperature, whereas no change occurs upon extraction at 0 °C in the presence of neutral salts.[83] This phenomenon has been studied[84] and Figure 31 presents the results. Upon heating in a neutral buffer solution, pure coenzyme F430 undergoes equilibration to afford a ternary mixture of products, in which the diastereomer of the natural coenzyme that is doubly epimerized in ring C predominates to the extent of 88%. Model considerations require (owing to steric hindrance of the quasi-equatorial position of the propionic acid chain by the neighboring carbonyl group) and ^{1}H-NMR analyses confirm that the two substituents in ring C affected by the double epimerization adopt the quasi-diaxial conformation, both in the natural coenzyme and in its 12-*epi*-13-*epi* diastereomers—a very

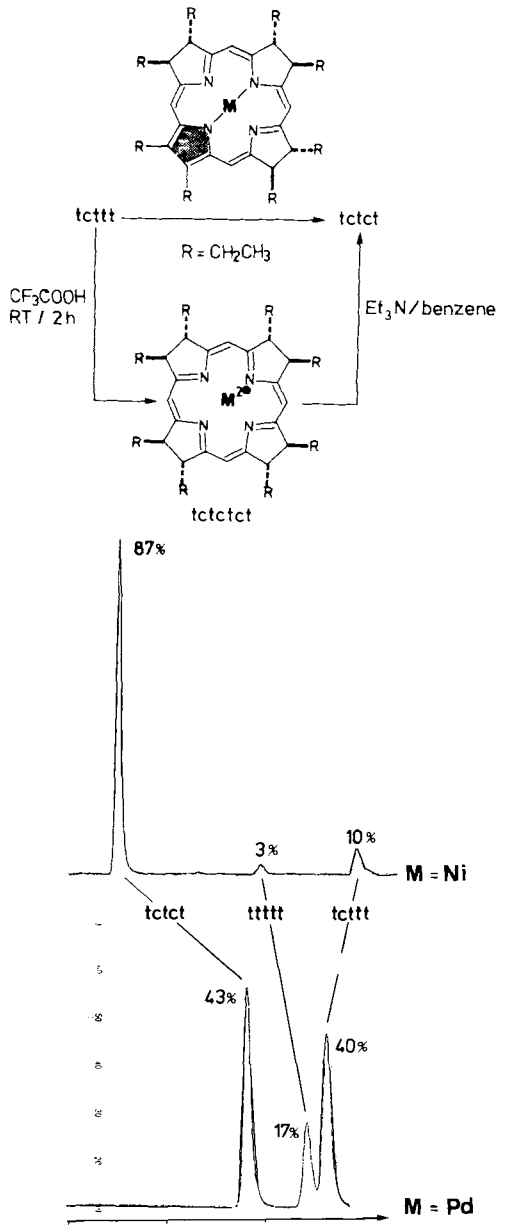

Fig. 30. Acid-catalyzed isomerization of nickel(II) *tcttt*-octaethylpyrrocorphinate to the *tctct* diastereomer [59] (*R. Waditschatka* [56]).

unusual situation, indeed. However, ^{1}H-NMR spectroscopy also reveals that the ensemble conformation of the hydropyrrolic five-membered rings present in the natural coenzyme clearly disobeys the W-form rule, which was established for hydroporphinoid nickel(II) complexes (see above). This rule is broken because the two substituents on ring C are not allowed (for the steric reasons already discussed) to occupy quasi-diequatorial positions. The double epimerization of these two substituents resolves the dilemma: since the two ring-C substituents have to remain quasi-diaxial, the epimerization induces an inversion of the half-chair of ring C and thereby generates the W conformation of the ring ensemble.

In light of the above interpretation, the configurational instability of coenzyme F430 provides a superb example of the importance of the spatial coordination demands of the central ion in influencing the configuration of substituents on the periphery of a hydroporphinoid ligand system.

3.3. The Nucleotide Ligand: Its Specific Attachment to Ring D of the Corrin Ligand

To discover that the A/D-ring junction and the ring size of the corrin ligand as well as the specific arrangement of the double bonds of its chromophore are all thermodynamically favored and largely self-assembling structural elements had come as an inspiring experience to us. Otherwise, we would probably never have dared to invest time and energy in seeking to answer a question such as that posed in this section.

In the vitamin B_{12} molecule, a nucleotide ligand forms a 19-membered loop on the bottom side of the corrin plane extending from cobalt, via the building blocks 5,6-dimethylbenzimidazole, α-D-ribose-3-phosphate, and D-1-amino-2-propanol, to the carboxyl function on the propionic acid side chain of ring D[85] (cf., e.g., Fig. 2). Constitutionally similar propionamide side chains are found on the bottom side of the vitamin B_{12} molecule on each of the four hydropyrrolic five-membered rings. Thus, the specific attachment of the nucleotide chain to ring D represents a

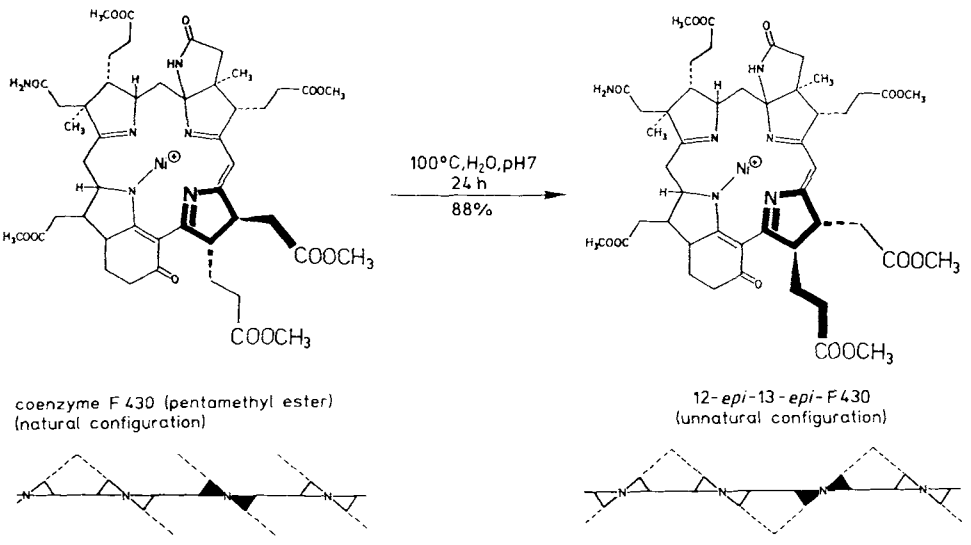

Fig. 31. The diepimerization of coenzyme F430 on the periphery of ring C is a consequence of the contraction of the coordination hole induced by the nickel(II) ion (*A. Pfaltz* et al. [84]).

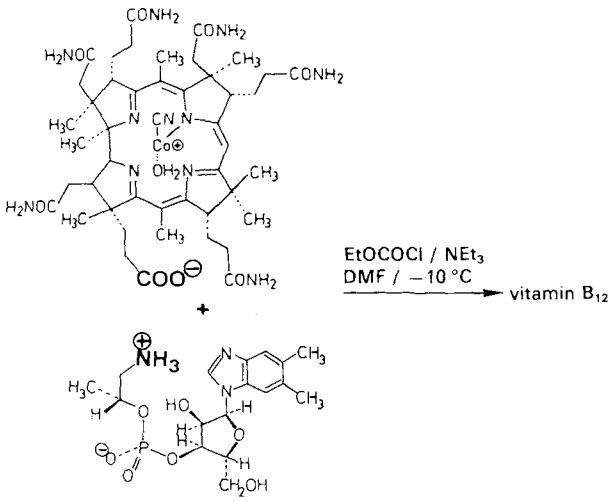

Fig. 32. Transformation of cobyric acid to vitamin B_{12} in the chemical semisynthesis [86] and total synthesis [18].

structural element whose formation ought to require a corresponding external "instruction." Indeed, at the time the chemical synthesis of vitamin B_{12} was planned, it was clear from the very beginning and in both laboratories then involved that this particular carboxyl function on ring D (=f-carboxyl function) had to be present in a constitutional form that is different from the other six carboxyl functions throughout the entire course of the synthesis (as the nitrile; cf. Fig. 4). Only in this way would it be possible to reach cobyric acid, the compulsive intermediate along the synthetic road leading to vitamin B_{12} (cf. Fig. 32 and Ref. [86]). In an undifferentiated derivative (e.g., the heptamethyl ester of cobyrinic acid or "cobester"), it would no longer be possible to attack selectively the f-carboxyl function by reaction with an external nucleophile. This was experimentally confirmed later, for example by the results obtained in the partial ammonolysis of cobester[87] (see Fig. 33).

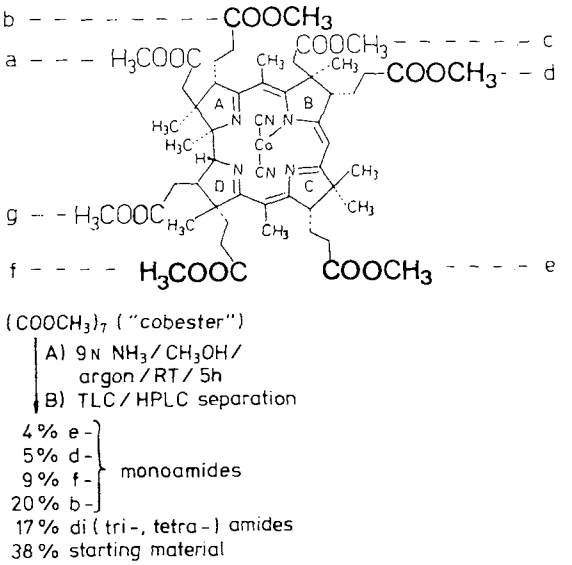

Fig. 33. Product mixture from the partial ammonolysis of the heptamethyl ester of cobyrinic acid ("cobester") (*H. Maag* [87]).

Out of the change in attitude toward the vitamin B_{12} structure came a question that (unfortunately) was totally beyond our conceptual horizon at the time the vitamin B_{12} synthesis was planned: *Is the specific attachment of the nucleotide ligand to ring D also a potentially self-assembling structural element of vitamin B_{12}?*

Once this question is posed, it is easy to recognize a unique possibility of how the nucleotide chain could be linked selectively to the f-carboxyl function, without the necessity of having this carboxyl function exist in a form different from all others. This possibility is illustrated in Figure 34.

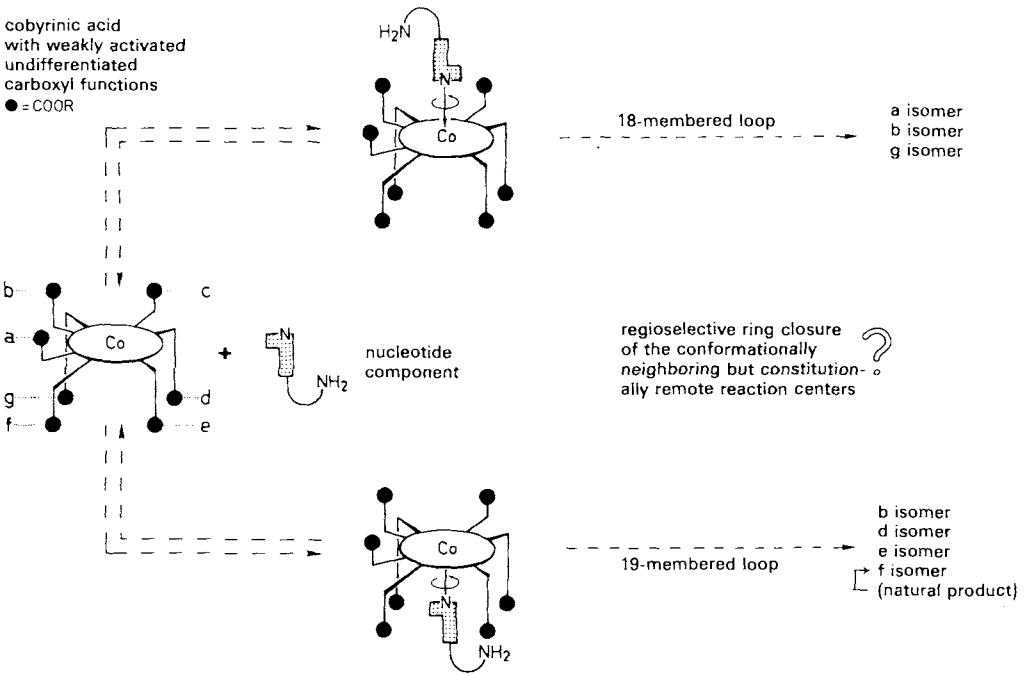

Fig. 34. Working hypothesis for the nucleotide-attachment reactions of cobyrinic acid derivatives containing undifferentiated carboxyl functions.

Consider a solution of the free nucleotide building block and a suitably activated (undifferentiated) cobyrinic acid derivative in which an equilibrium is established between the respective components of two pairs of isomeric cobalt/nucleotide complexes. In one pair, the nucleotide NH_2 group is complexed to the cobalt from either above or below the corrin plane; in the other pair (see Fig. 34), the free nitrogen of benzimidazole is the complexing ligand center. Whereas the first pair possesses no opportunities for undergoing intramolecular reactions, this is not true for the pair having a complexed imidazole nitrogen. In the component with the imidazole complexed from below, there exists a 19-membered precyclic relationship between the (free) NH_2 group of the nucleotide chain and each of the four propionic acid side chains; in principle, intramolecular amide formation can take place with each of them. An analogous (albeit 18-membered) relationship exists in the other component between the NH_2 group and the three acetic acid carboxyl functions.

If one assumes that the natural nucleotide loop (that is, the one attached to the f-carboxyl function) is the most stable one among the four (or seven) constitutionally isomeric loops, and if one further assumes that this stability maximum is due to an optimal conformation along the chain of the 19-membered nucleotide loop, then the conformation adopted by the f-propionic acid chain and the nucleotide chain in the corresponding precyclic complex should be similar to that in the cyclized complex. The nucleotide NH_2 group and the f-carboxyl function in the precyclic complex should statistically be in spatial proximity (Fig. 35), and the kinetics of the ring closures might reflect the thermodynamics of the isomeric nucleotide loops. An experimental observation of such regioselective amide formation due to the conformational neighborhood of reaction centers would, however, require a specially balanced activation of the (seven) carboxyl groups: this activation should be strong enough for *intramolecular* (conformationally assisted) amide formation to proceed, but, at the same time, it should be weak enough so that *intermolecular* (and therefore nonselective) amide formation does not occur.

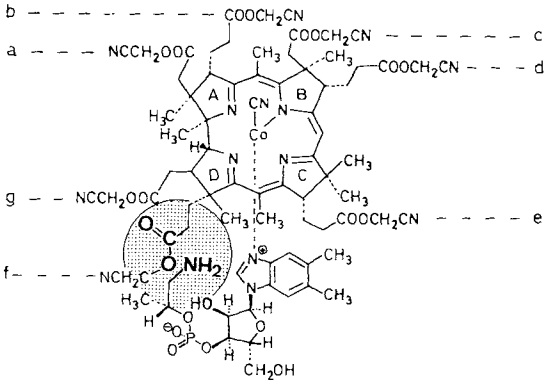

Fig. 35. Does the amino group of the nucleotide component in this complex of the heptakis(cyanomethyl) ester of cobyrinic acid react most rapidly with the f-carboxyl function?

The actual experiments fulfilled these expectations to an extent that was surprising to us (see Figs. 36–39).[88] Since this work has not yet been published, it will be described here in somewhat greater detail.

The question as to a suitable form of activation for the seven carboxyl functions of cobyrinic acid (so as not to differentiate them) happened to be solved straightaway by the use of the heptakis(cyanomethyl) ester of cobyrinic

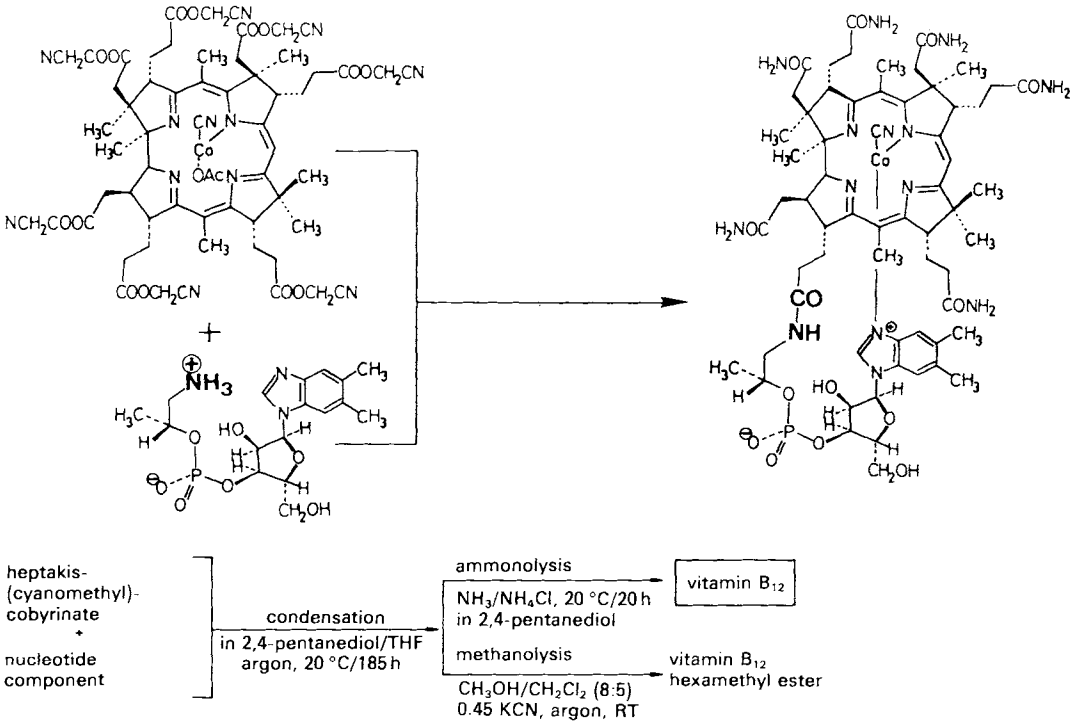

Fig. 36. The nucleotide-attachment reaction of the heptakis(cyanomethyl)ester of cobyrinic acid and direct subsequent ammonolysis (or methanolysis) leads selectively to vitamin B_{12} (or the hexamethyl ester of vitamin B_{12}) (*G. Bartels* et al. [88]).

acid,[89] after it was realized that the reactivity of the simple heptamethylester was insufficient. In order to render the cobalt(III) coordination center reactive (capable of undergoing rapid ligand exchange), the acetato-cyano form of the complex was prepared; it was obtained as an α/β mixture of diastereomers by treatment of the dicyano cobalt(III) form (which does not readily exchange ligands) with acetic acid. Later in the work, it was realized that the two diastereomers are just sufficiently stable to allow their chromatographic separation and thereby their use as pure epimers in nucleotide-attachment experiments.

When ca. 0.04 M degassed solutions of the heptakis(cyanomethyl) ester of (β or α)-acetato-(α or β)-cyanocobalt(III) cobyrinic acid and 1.5 molar equivalents of the free nucleotide component[90] (Fig. 36) in pentane-2,4-diol/tetrahydrofuran (1:1) (molecular sieves, argon, room temperature) were allowed to stand for one week, ca. 50% conversion took place, leading, after immediately following ammonolysis of the reaction mixtures, to products that, according to HPLC (see Fig. 37), mainly consisted of roughly equal amounts of only two components, vitamin B_{12} and the starting material (in the form of its ammonolysis product, the heptamide of cobyrinic acid). In the experiment corresponding to Figure 37, the product (neutral at pH 2.5) was first separated from the (positively charged) heptamide of the starting material, then purified by reversed-phase chromatography, and finally, after crystallization, identified as vitamin B_{12} by comparison of its HPLC behavior as well as its UV/VIS, CD, IR, and ^{1}H-NMR spectra with those of authentic material. In another experiment, in which the heptakis(cyanomethyl) ester of configurationally pure α-acetato-β-cyano cobalt(III) cobyrinic acid (ca. 50 μmol) was used and the mixture of starting material and product obtained by ammonolysis was not separated electrophoretically but rather by reversed-phase chromatography,[91] spectroscopically pure, crystalline vitamin B_{12} was isolated in 41% yield (Fig. 36).

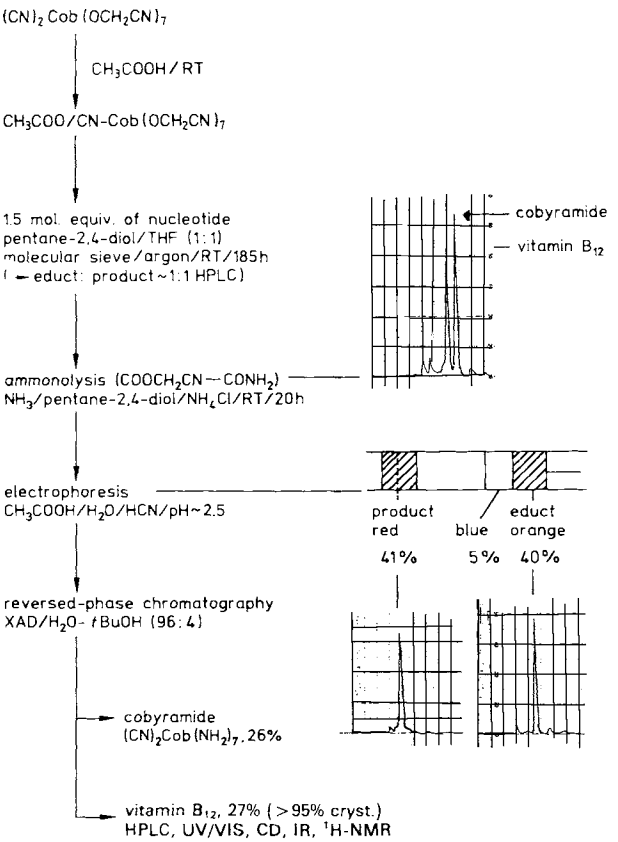

Fig. 37. Nucleotide-attachment reaction of the heptakis(cyanomethyl) ester of cobyrinic acid: HPLC of a crude product (after ammonolysis) and HPLC [91] of the two main components after separation of the crude products by electrophoresis [88].

In order to have an easier access to the information of whether and to what extent isomeric nucleotide-attachment products are formed under such reaction conditions, experiments were carried out in which the (sensitive) cyanomethyl esters of the reaction mixture components were not trapped by ammonolysis but rather by (cyanide-catalyzed) methanolysis. Both the product and the starting material components were thereby obtained as stable methyl esters (instead of amides), which are both soluble in organic solvents and readily crystallizable. Figure 38a shows the result of such an experiment starting from an α,β-diastereomeric mixture of starting materials. The two HPLCs reveal the composition of the reaction mixture immediately before and after the methanolysis. The two methanolysis products are the heptamethyl ester of cobyrinic acid[92] and the previously unknown vitamin B_{12} hexamethyl ester (cf. Fig. 36). Both products were obtained in crystalline form after chromatographic separation and repurification[93] and identified spectroscopically. For direct comparison, authentic B_{12} hexamethyl ester was prepared by semisynthesis starting from cobyrinic f-acid hexamethyl ester.[94] The minor fraction appearing after the product peak in the (second) HPLC of Figure 38a was thoroughly checked to determine whether the isomeric B_{12} hexamethyl esters might also be present. The material turned out to consist of a complex mixture[95] in which the e-iso-B_{12} hexamethyl ester (nucleotide chain on the ring-C propionic acid chain) was present, if at all, in an amount corresponding to less than 1% yield.[96]

Figure 38b shows an experiment that provides simple and convincing proof for the validity of the expectation that the regioselective attachment of the nucleotide chain takes place intramolecularly after precomplexation. The two chromatograms show the results (after methanolysis) of two nearly identical parallel experiments[97] that differed in only one respect; one of the two reaction solutions was in vapor contact with a solution of acetone cyanohydrin in acetonitrile (a source of trace amounts of gaseous HCN). The color of this reaction solution changed within ca. 10 min from red (acetato-cyano form of the starting complex) to violet (dicyano form), whereas the color of the other reaction solution remained unchanged. As revealed by a comparison of the HPLCs of the two reaction mixtures (see Fig. 38b), the presence of trace amounts of HCN results in nearly complete suppression of product formation,[98] the dicyano form of the starting complex being stable toward ligand exchange under the reaction conditions.

The regioselectivity of the nucleotide attachment can be observed most clearly during the first half of reaction, after which the rate of conversion markedly decreases. If the reaction is pushed beyond this first stage, side reactions

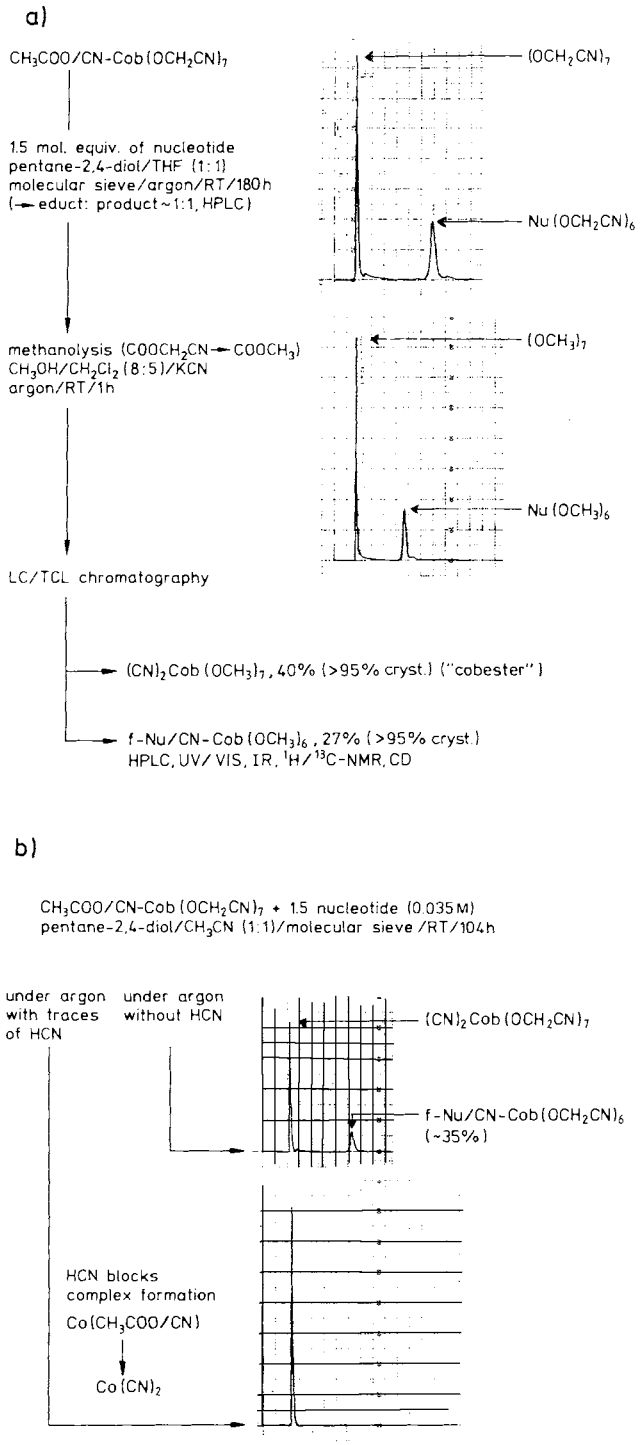

Fig. 38. Nucleotide-attachment reaction of the heptakis(cyanomethyl) ester of cobyrinic acid: a) HPLC of the crude product before and after methanolysis. b) HPLC of the crude product (before methanolysis) of a reaction in the absence and in the presence of HCN in the reaction mixture [88].

begin to become important. It was initially thought that the $\alpha \rightarrow \beta$ exchange of the axial ligands in the acetato-cyano complex (originally postulated to occur rapidly) may take place too slowly under the conditions of the nucleotide attachment. However, experiments with the two configurationally uniform complexes provided only partial support for this interpretation: although the starting material/product ratios turned out to be complementary, e.g., 1:2 (starting from the α-acetato diastereomer) and 2:1 (from the β-acetato diastereomer), an all-or-none result was obtained in none of the experiments. The factors limiting both the conversion and the uniformity of the reaction course include, besides oxidations and disproportionations, the great propensity of the seven (or six) reactive cyanomethyl ester groups in both starting material *and* product to undergo transesterification with hydroxyl-containing components of the reaction medium or hydrolysis with traces of water.[95]

We interpret the kinetic regioselectivity of the nucleotide-attachment reaction of the heptakis(cyanomethyl) ester of cobyrinic acid, in the sense of the original working hypothesis, by the assertion that *the nucleotide loop to the propionic acid side chain of ring D of the vitamin B_{12} structure represents, of all possible regioisomers, the thermodynamically most stable loop* (Fig. 39). This statement has also been subjected (subsequently) to direct experimental test. By means of potentiometric pH measurements, *Kräutler*[99] determined the equilibrium constants for the intramolecular nucleotide complexation of the four iso-B_{12} hexamethyl esters (b, d, e, and f isomers, prepared by semisynthesis) and found the highest value for the f isomer. Furthermore, in a (preliminary) molecular modeling study, *K. Müller*[100] concluded that, of the four vitamin B_{12} isomers, the natural f isomer is expected to be the lowest in energy.

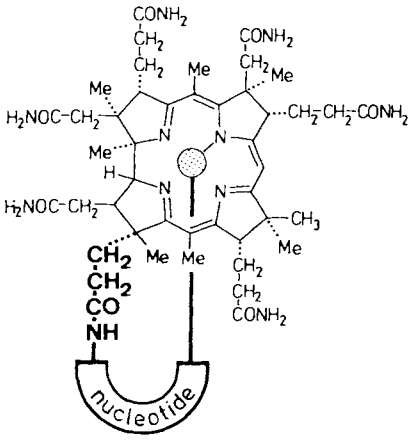

Fig. 39. The nucleotide loop in vitamin B_{12} containing the propionic side chain of ring D is the thermodynamically most stable nucleotide loop of all (four or seven) isomeric possibilities.

The findings discussed here teach us not to view the nucleotide loop of the vitamin B_{12} structure exclusively from a functional point of view. It is as though the vitamin B_{12} structure possessed an intramolecular code capable of directing the formation of a linkage between the corrin nucleus and the nucleotide chain selectively to the propionacyl group of ring D without need for external instruction. Also this structural element of the vitamin B_{12} molecule, the ring-D attachment of the nucleotide chain, is capable of self-assembly.

The present-day biosynthesis of vitamin B_{12} apparently makes no use of this capability. According to present knowledge,[101] the construction of the nucleotide loop occurs via a multistep sequence of reactions, in which the f-propionic acid side chain is converted into its 2-hydroxy-

propyl amide form and thus differentiated constitutionally from all the other carboxyl functions. This should not be surprising, since such a differentiation may well be the simplest solution for enzymes.

3.4. The Ligand Periphery: The Thermodynamic Favoring of the Type-III Arrangement of Substituents in Uroporphyrinogen-Type Structures

An analysis of the structure of vitamin B_{12} as attempted in this article should not omit a discussion of the uroporphyrinogen structures. One of these uroporphyrinogens, namely, type III, is the parent compound involved in the biosynthesis of all known porphinoid cofactors[102] (Fig. 40). Furthermore, the route via porphyrinogens is also chemically an efficient and structurally appropriate approach to the chromophore systems of these biomolecules (see Section 3.1). The central process of all porphinoid biosyntheses, the "tetrameroidization"[103] of the monopyrrolic precursor porphobilinogen, is what we might call a

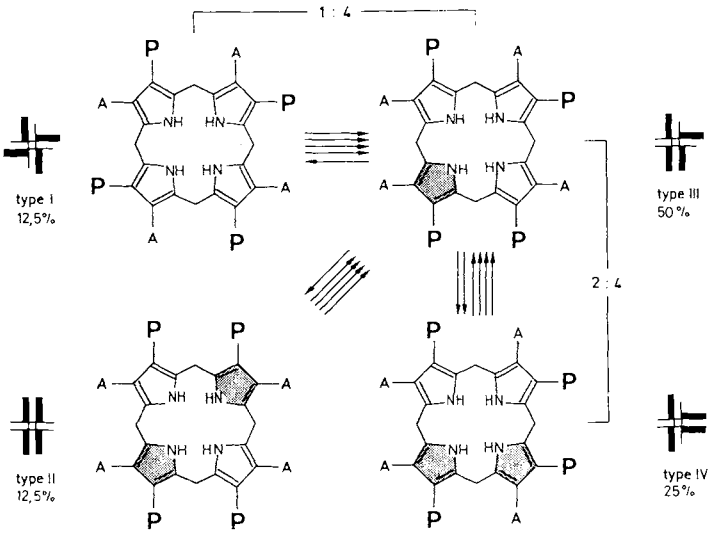

Fig. 41. Statistical favoring of the type-III constitution in the ensemble of the four isomeric uroporphyrinogens [14, 15, 106]. The arrangement of substituents in the grey regions deviates from type I.

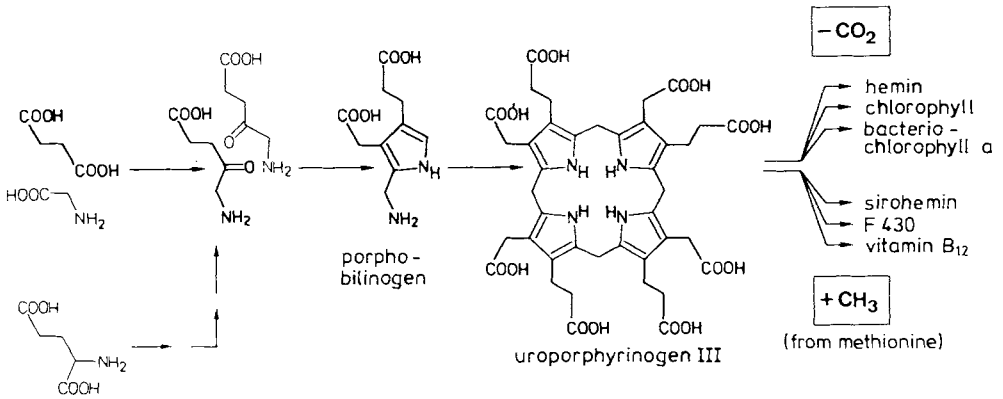

Fig. 40. Overview of the early stages in the biosynthesis of uroporphinoids [102, 104].

typical "chemomimetic" biosynthetic step insofar as such coupling of four porphobilinogen building blocks can also take place nonenzymically in the presence of acids with great ease.[14, 15] The salient feature of the *enzymically* controlled process is the diversion of the reaction sequence toward the selective formation of uroporphyrinogen type III.[104] This deviation from the straight reaction path to uroporphyrinogen type I (Fig. 41) is mechanistically complex, requiring an additional enzyme. The *nonenzymic* process most rapidly produces the type-I structure, but, under the influence of acids, the reaction course readily becomes thermodynamically controlled through isomerizations of the carbon framework to form a mixture of the four constitutionally isomeric uroporphyrinogens (types I–IV) in roughly the statistically expected ratio[14, 15, 106] of 1 : 1 : 4 : 2 (see *Mauzerall*'s[15] indirect analysis of such a reaction mixture[105]).

The statistical distribution of the four uroporphyrinogen isomers in equilibrium presupposes the (plausible) enthalpic equivalence of the isomers; the distribution is due to the isomers' differences in molecular symmetry, as visualized in Figure 41.[106] The equilibration can proceed via numerous reaction pathways, which are mechanistically related to one another. The diversity of pathways is due to the reversibility of a group of reactions, the prototype of which is the acid-catalyzed, electrophilic α-hydroxyalkylation of pyrroles by aldehydes.

The statistically favored isomer present in greatest amount in the equilibrium mixture of the four uroporphyrinogens is the biological isomer. A coincidence? Although this question is one of those that produce interpretations and not answers, this biomimetic chemosynthesis, or "chemomimetic" biosynthesis, of the uroporphyrinogen-type structure is a provocative phenomenon. Nature's enzymic acrobatics for selectively constructing the uroporphyrinogen (type-III) structure would certainly fit the idea of a biosynthesis that had to adapt itself to the structure of a nonenzymically preformed cofactor that was functionally already under enzymic control. This picture implies that the biological function was established for the *major product* (or a biologically functional derivative thereof) derived from a uroporphyrinogen mixture preformed under statistical control. Such a rationalization[16, 107] for the existence of the type-III structure of natural porphinoids would seem acceptable if, from a chemical perspective, the idea of a prebiotic origin of the uroporphyrinogen-type struc-

ture could be given "the green light." Experimentally, there is little experience that would be relevant in this connection apart from the finding that the nonenzymic simulation of the self-condensation of aminolevulinic acid was shown to proceed mainly in the wrong direction, leading only to a very small extent to porphobilinogen.[108, 109] Recently, however, as part of an extensive investigation of the chemistry of α-amino nitriles, a study was carried out in our laboratory that deals directly with potentially prebiotic routes to uroporphyrinogens. The results of this study, recently reported in detail,[110] are summarized in Figures 42 to 44.

A remarkably close structural connection exists between the nitrile form of glutamic acid and the monopyrrole derivative desaminomethylporphobilinogen, a connection that

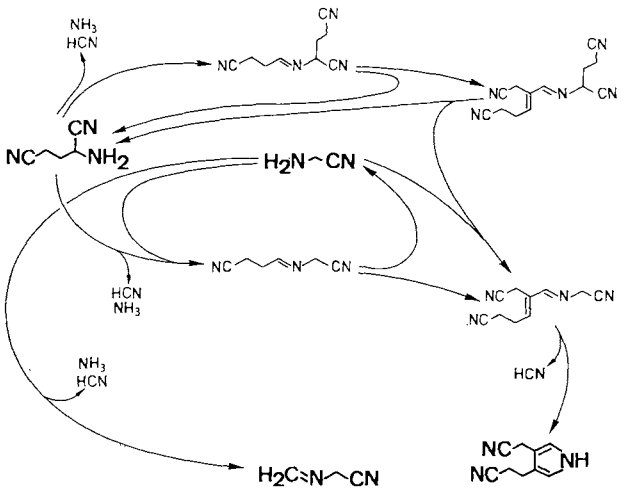

Fig. 42. General scheme for the formation of desaminomethylporphobilinogendinitrile from glutaminedinitrile and glycinenitrile [110] (cf. *G. Bold* [155]).

is evidenced in the existence of experimentally established reaction pathways linking glutaminedinitrile, glycinenitrile, and the dinitrile form of the pyrrole derivative. These reaction pathways exist as a consequence of the ability of α-amino nitriles to react as aldehyde imine derivatives; they are thereby capable of undergoing thermal coupling (with loss of HCN and NH_3) to give dimeroid or mixed imine derivatives. In the presence of weak bases in nonaqueous medium, such imine derivatives of glutaminedinitrile readily undergo condensation reactions analogous to aldol reactions. The condensation product formed from one glycine and two glutamine building blocks can thermally eliminate HCN to give (via electrocyclic ring closure of a carbenoid or ylidic intermediate) the pyrrole derivative. When this product is heated together with the trimer of *N*-methylideneglycinenitrile in acetonitrile with strict exclusion of oxygen in the presence of, for example, montmorillonite as catalyst, a mixture of the four isomeric uroporphyrinogenoctanitriles (types I–IV) is formed in high yield. The HPLC of the *crude product* of such a reaction (Fig. 43) reveals the statistical ratio of 1 : 1 : 4 : 2 for the four isomers. The efficiency of this complex reaction process is indeed extraordinary; even at a starting material concentration of 10^{-6} M (corresponding to 1 mg in ca. 5 L of acetonitrile!), the distribution is still detectable by HPLC.[111]

The nitrile forms of the four uroporphyrinogens show up in this study as a consequence of the imposed constraints decided upon in carrying out our investigation on α-amino nitriles. These not only include the exclusion of molecular oxygen[1,2] but also of water. Much of the specific reactivity of α-amino nitriles is obviated by the presence of water—insofar as this leads to hydrolysis of the nitrile group. The chemistry of α-amino nitriles has been largely unexplored, despite the fact that the *Strecker* α-am-

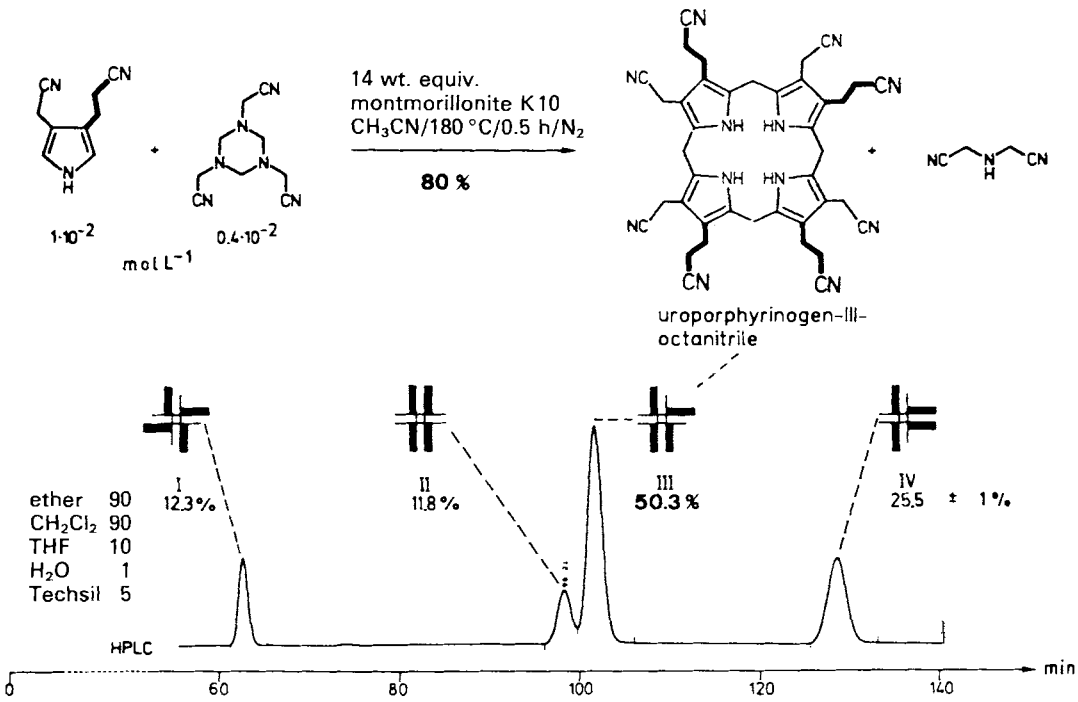

Fig. 43. "Tetrameroidization" of desaminomethylporphobilinogendinitrile with trimeric *N*-methylideneglycinenitrile in the presence of montmorillonite: HPLC of the crude product [110] (cf. *C. Lehmann* [111]).

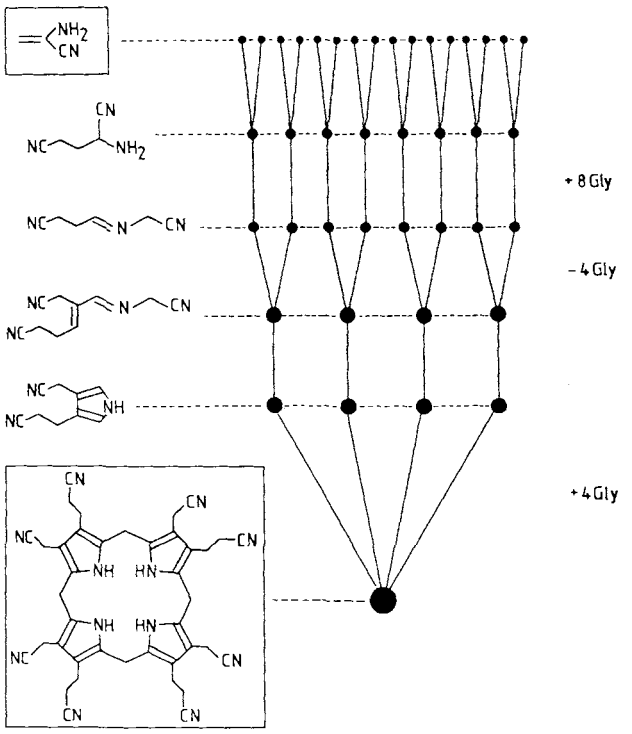

Fig. 44. Overview of the formation of uroporphyrinogenoctanitrile (type III) from 2-aminopropenenitrile (*G. Ksander* et al. [110]).

ino acid synthesis[112] has been carried out for over one hundred years and *Miller*'s experiments on the potentially prebiotic formation of α-amino acids[5] were first performed over three decades ago. In both cases, the primary interest relates to the hydrolysis products, the α-amino acids, and not to the unstable amino nitrile intermediates.

Figure 44 emphasizes the oligomeroidization aspect of the reaction sequence leading from glutaminedinitrile (or a photochemical precursor thereof[113]) all the way to uroporphyrinogenoctanitrile. This aspect is also characteristic for the biosynthesis of uroporphyrinogen (Fig. 40[102, 114]). In molecular synthesis, an oligomeroidization route is quite generally the strategy of choice if large molecules are to be built with a minimum number of precursors and steps. Not only biopolymers but also uroporphinoids provide examples.

With the ensembles of starting materials and reaction types outlined in Figures 42–44, alternative pathways undoubtedly exist that will lead to uroporphyrinogenoctanitrile percursors (including the nitrile form of porphobilinogen). In the "amino nitrile pathway" studied so far, glutaminedinitrile appears as the "natural" precursor of the uroporphyrinogen structure. The fact that one of the two known biosynthetic pathways to aminolevulinic acid starts from glutamic acid[115, 116] is noteworthy in this context.

To achieve the porphyrinogen→pyrrocorphin tautomerization (see Section 3.1) with uroporphyrinogenoctanitriles is somewhat more difficult than with the model octaethylporphyrinogen, because, under the reaction conditions found to be effective (see Fig. 45), not only the correspond-

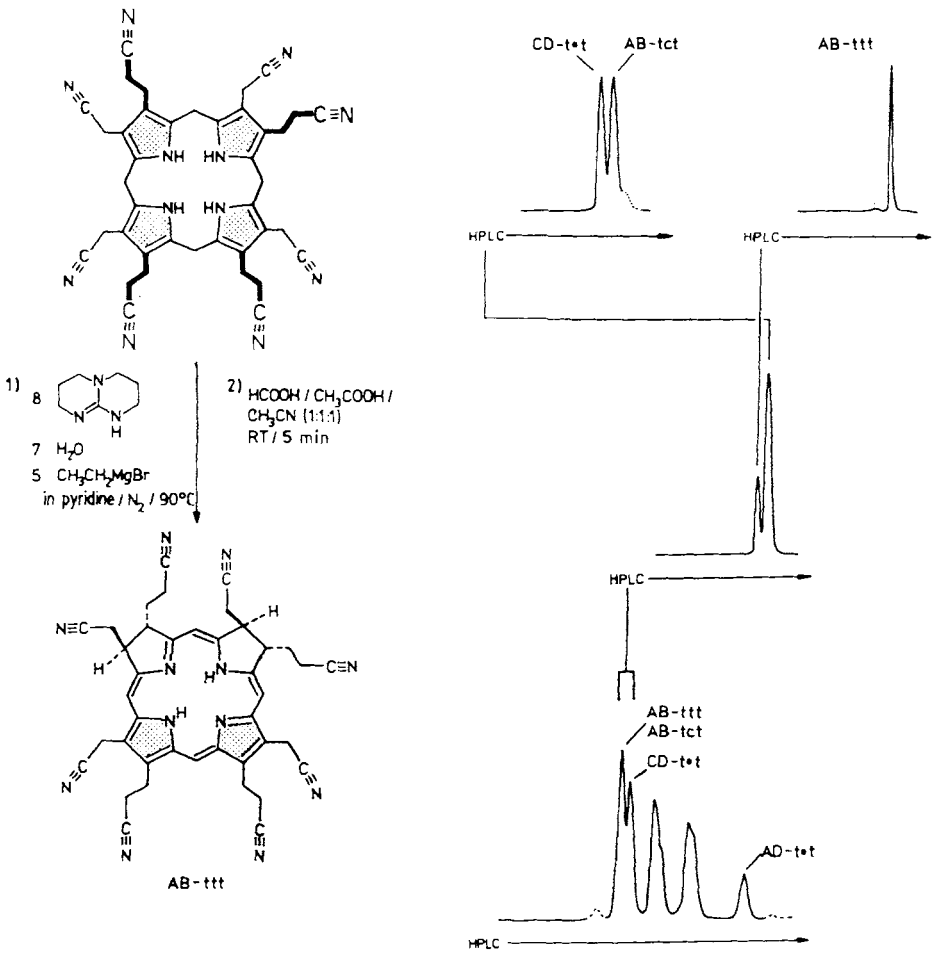

Fig. 45. One-step formation of 2,7-bis(desmethyl)sirohydrochlorinoctanitrile from uroporphyrinogenoctanitrile (*T. Früh* [117]). Conditions of HPLC (top to bottom): CH_2Cl_2/THF/H_2O (500:40:1), Techsil (SiO_2); ether/THF/H_2O (200:100:3), Partisil 10; AcOEt/pentane/H_2O (350:200:3), Techsil (SiO_2). AB-*ttt* was obtained in crystalline form and characterized by ^{1}H-NMR, UV/VIS, and FAB-MS data.

ing pyrrocorphins but also the corresponding isobacteriochlorins are formed (in roughly equal amounts), the latter by didehydrogenation. For the special case of the uroporphyrinogenoctanitrile type III, we undertook the isolation and spectroscopic identification of the constitutionally and configurationally pure AB-*ttt* isobacteriochlorin derivative; the isolation out of the complex mixture of isobacteriochlorin isomers was achieved by means of a three-step HPLC procedure[117] (see Fig. 45). We were motivated by the fact that this particular isomer corresponds to the ligand system of the natural sirohydrochlorin with respect to both its constitution and its configuration (see Fig. 46). The constitutional difference, apart from the nitrile form, lies in rings A and B, which bear protons in the places where the natural product has methyl groups. The iron(II) complex of sirohydrochlorin is the cofactor of sulfite and nitrite reductases[118] and, as a dihydro derivative, sirohydrochlorin is an intermediate in the biosynthesis of vitamin B_{12}.[69] *Thus, it is possible to reach the chromophore type of the simplest of the porphinoid coenzymes, starting from glutaminedinitrile and glycinenitrile, by means of a reaction sequence comprising a total of only five steps.*[119]

Too few of the experiments that seem desirable (both within and beyond the framework of constraints referred to above) have been carried out for making a concluding comment on the question as to whether—from the point of view of chemistry—the proposal of a prebiotic origin of the uroporphyrinogen-type structure is justified. However, in our opinion, the results shown in Figures 42 to 46 mean that we are given a "green light" to further thinking in this direction. Therefore, a chemical rationalization of the vitamin B_{12} structure must include—whatever the preformation steps between uroporphyrinogen and vitamin B_{12} may have been—the following statement concerning the specific constitution of the ligand periphery: *The arrangement of (modified) acetic acid and propionic acid side chains around the periphery of the vitamin B_{12} structure (as well as of all other uroporphinoid cofactor structures) corresponds to the thermodynamically favored arrangement in the structure type of the four isomeric uroporphyrinogens* (Fig. 47).

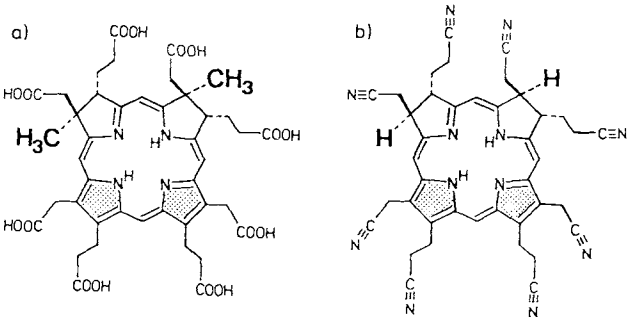

Fig. 46. a) Sirohydrochlorin; b) rac. "proto-sirohydrochlorinoctanitrile," formed in five steps from glutaminedinitrile.

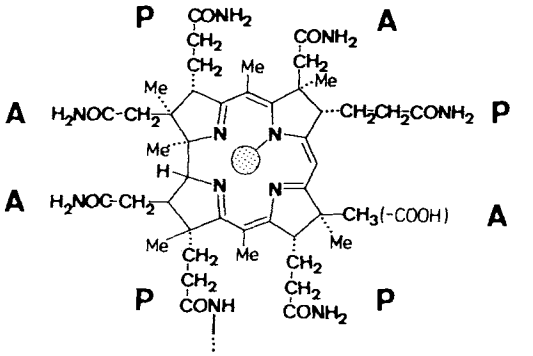

Fig. 47. The constitution of the ligand periphery of vitamin B_{12} reflects the statistically favored arrangement of the peripheral substituents for the four isomeric uroporphyrinogens.

4. Structure and Function

In the previous sections, we have dealt with synthetic aspects of the vitamin B_{12} structure, that is, essentially with preformation "chances," and omitted consideration of its function, the ultimately decisive criterion for its biological selection. The biological part of the function, its effect on and importance to the network of metabolic reactions, cannot be treated here. Instead, questions concerning the relationships between structure and molecular function for this cofactor will be dealt with—albeit in a fragmentary way. Despite the diversity of its enzymic reactions,[120] as an object of structure/function analysis, coenzyme B_{12} may well represent a lucky case among all the other coenzymes. As *Halpern*[121] was probably the first to point out clearly (see quotation in Fig. 48), the diverse molecular functions of coenzyme B_{12} can be summarized in terms of one generalized function, which consists in the coenzyme structure serving as a molecular reservoir for the dissociative generation of an alkyl radical (the 5′-adenosyl radical). The prevailing view at present is that this radical is the true catalytically active species in the B_{12}-catalyzed rearrangement reactions.[120-122] The cobalt-carbon bond of adenosylcobalamine (dissociation enthalpy of approximately 31 kcal mol^{-1} in ethylene glycol[121,123-125]) is evidently sufficiently strong for the coenzyme to be stable in the absence of light, but, at the same time, sufficiently weak that acceleration of dissociation by several orders of magnitude is possible merely by association of the coenzyme with B_{12}-enzyme proteins and with substrates.[126] It is this protein- and substrate-controlled acceleration of the reversible homolysis of the cobalt-carbon bond, that—above all other properties—a structure/function analysis of the coenzyme B_{12} structure must explain.

This problem has been recently approached by several research groups using theoretical,[127] kinetic,[121] spectroscopic,[128] and structural[129] methods. At present, attempts to interpret the phenomenon focus on an allegedly specific conformational flexibility of the corrin ligand, which should enable it to modulate, in a protein- and substrate-induced manner, the dissociation enthalpy of the cobalt-carbon bond. In reply to their question, "Why does Nature not use the porphyrin ligand in vitamin B_{12}?," *Halpern* et al.[130] have given the answer, supported by experimental data, that such flexibility is lacking in the porphyrin ligand.

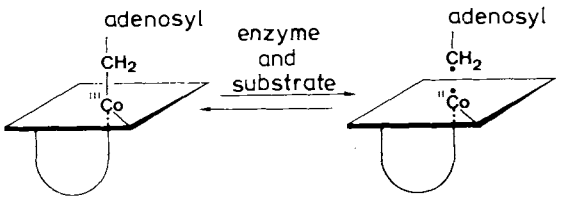

Fig. 48. Quotation from *J. Halpern* [121]: "Coenzyme B_{12} fulfills its biochemical role by serving as a *free radical reservoir* from which 5'-deoxyadenosyl radicals are reversibly released, just as oxyhemoglobin serves as a reservoir for the storage and reversible release of oxygen."

What alternative cofactor structures should be considered in analyzing the functional optimization of the vitamin B_{12} structure? The biosynthesis of vitamin B_{12} points to a clear answer. The structure type of a *corphinic* coenzyme B_{12} analogue stands out among all others. In terms of their charge and π-bond structure, corrins and corphins are (essentially) isoelectronic ligand systems. Nonetheless, B_{12} biosynthesis, in proceeding via a corphin intermediate (or a very close relative thereof)[33, 34] to cobyric acid (Fig. 49), involves a complex series of enzymic processes for the sake of transforming the 16-membered macrocycle of a (potential) corphin ligand system into the 15-membered ring of the corrin system. Such an additional investment of biosynthetic reaction steps must have functional reasons, quite apart from the aspects treated in Sections 2 and 3.2. An analysis of the cofactor structure should reveal these reasons.

A specific opportunity for our laboratory to make an experimental contribution to this problem consists in directly comparing the structural and chemical properties of cobalt

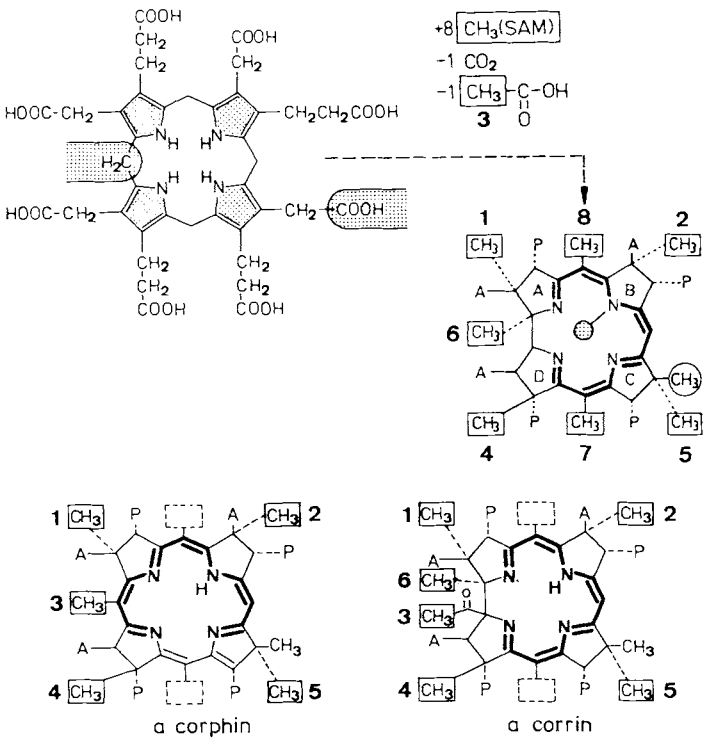

Fig. 49. Overview of the sequence of C-methylation steps in the biosynthesis of vitamin B_{12} (*A. R. Battersby* et al. [33, 60, 61], *I. A. Scott, G. Müller* et al. [34, 62]). SAM = *S*-adenosylmethionine.

complexes of the synthetic corrin and corphin models displayed in Figure 50, which we had prepared for other purposes in the course of earlier work.[47, 48, 76, 131] In addition, our investigations on hydrocorphinoid nickel(II) complexes have proved to be especially informative; we recently carried out such studies in connection with our work on the chemistry of coenzyme F430 (see Figure 54).[37, 132, 133] In fact, the discovery of this uroporphinoid nickel-containing cofactor with its unique hydrocorphinoid structure[81, 82] has in many respects stimulated our efforts and deepened our insight into the ligand-specific properties of corrin complexes.

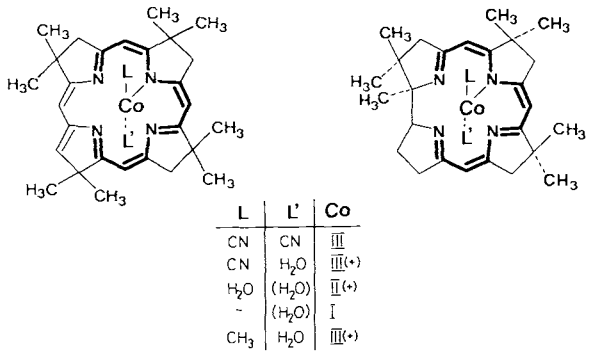

L	L'	Co
CN	CN	III
CN	H_2O	III(+)
H_2O	(H_2O)	II(+)
-	(H_2O)	I
CH_3	H_2O	III(+)

Fig. 50. Synthetic model complexes for comparison of the properties of cobalt(III,II,I) complexes of corphin [47, 48] and corrin [76, 131] (*K. Zimmermann* et al. [140]).

Since the very start of our work on the synthesis of corrins[76, 134] and during all phases of this investigation, nickel(II) corrin complexes have served as model systems in developing the methodology of synthetic corrin chemistry. The reason has been the recurring experience that corrin complexes of divalent nickel exhibit an especially "simple chemistry." They resist decomplexation by all common demetalation methods (including reaction with KCN); they are stable toward light; they are always monocationic and tetracoordinated regardless of the counterion; they are diamagnetic in common solvents (including the relatively nucleophilic ones, such as acetonitrile and methanol) and are therefore accessible to normal ^{1}H- and ^{13}C-NMR spectroscopy, and their UV/VIS spectra are largely solvent independent. All findings indicate that the electrophilicity of the nickel(II)ion in corrin complexes is "saturated" by the equatorial coordination and that there is no observable residual electrophilicity in an axial direction. In contrast, the nickel(II) (hexafluorophosphate or perchlorate) complex shown in Figure 51, which was synthesized as a model of coenzyme F430,[37, 132] is a prime example of a corphinoid nickel(II) complex containing an electrophilically unsaturated nickel ion. Although the complex is diamagnetic (tetracoordinated) in dichloromethane, it is paramagnetic in the nucleophilic solvents acetonitrile and methanol. The nickel(II) ion is electrophilic in the axial direction, a property that is reflected preparatively in the finding that the complex reacts smoothly with potassium thiocyanate to give a neutral, covalent isothiocyanato complex, whose nickel(II) ion is pentacoordinated in (highly dilute) dichloromethane solution and hexacoordinated in the crystal

(Fig. 51). The X-ray crystal structure analysis of the isothiocyanato complex reveals a noteworthy structure, namely, a centrosymmetric (racemic) dimer in which the ligand-bound nitrile group of a given molecule serves as a sixth ligand for the nickel ion of an enantiomorphic partner molecule[133] (Fig. 51).

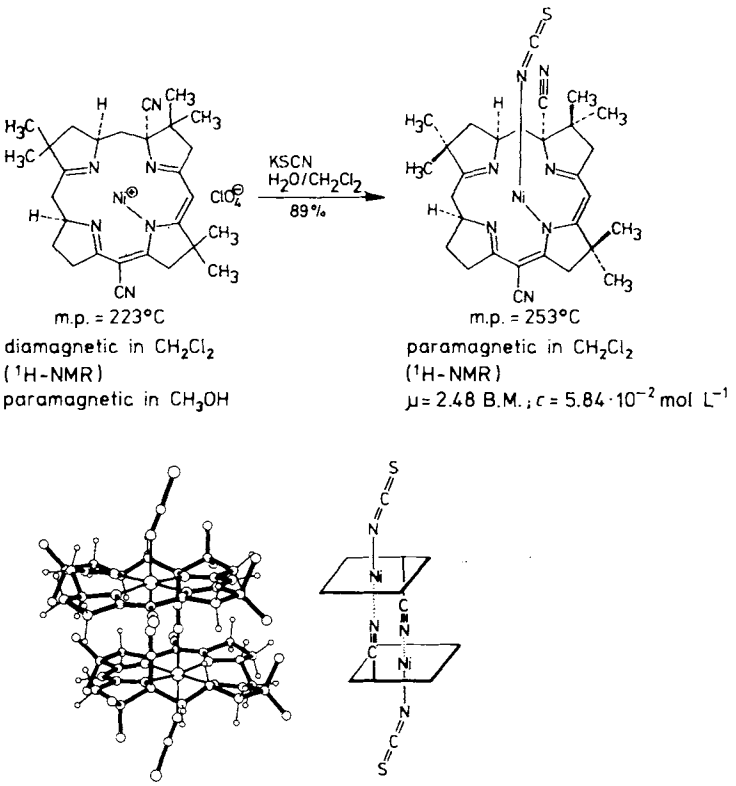

Fig. 51. Synthetic model for the coenzyme F430 from methanogenic bacteria; reactivity of the nickel(II) ion in the direction of axial coordination [132] (cf. *A. Fässler* [37] (see text).

In terms of the analysis presented in Section 3.2 concerning the structure of corphinoid nickel(II) complexes, there can be no doubt that an important cause of the difference in electrophilicity of nickel in corrin and (hydro)corphin complexes lies in the difference in the dimension of the coordination hole in the two types of ligand. A contracted, steeply ruffled ligand conformation is to be assumed for the tetracoordinated complex of Figure 51 in dichloromethane solution[135] and the strain energy due to this ruffling is to be assumed to take part in causing the residual axial electrophilicity of the nickel ion. The coherence of this qualitative picture is further confirmed by the structural data of Figure 52. Hexacoordination suppresses the propensity of the nickel(II) ion to contract the coordination hole and thereby to increase the strength of its equatorial coordination. Correspondingly, the conformation of the ligand reveals no sign of ruffling.[132]

In addition to the spatial factor, also the nitrile group attached to the chromophore contributes to the electrophilicity of the nickel ion in the F430 model complex. This nitrile group stands for the acyl substituent sitting at the corresponding position of the natural coenzyme. The effect of such a chromophore-bonded nitrile group is illustrated by the trends observed in the magnetic and electrochemical data obtained for the nickel(II) complexes shown in Figure 53. The nitrile group is evidently capable of causing a (dihydro)corphin complex, but not a corrin complex, to undergo hexacoordination (in methanolic solution). The A/D-secocorrin complex also shown provides, for comparison, a nickel complex whose central ion is not subject to the spatial coordination constraints of a macrocycle.

Of all corrinic and corphinic nickel(II) model complexes whose electrochemical reduction potentials have been determined in our laboratory by *Kräutler*[23b, 133] and *Jaun*,[133] the F430 model undergoes reduction most readily (compare the reduction in tetrahydrofuran, a solvent of low nucleophilicity). Recently, *Jaun* and *Pfaltz*[136] were able to show by ESR spectroscopy that the one-electron reduction of coenzyme F430 (in the form of its pentamethyl ester) is not ligand-centered—as suggested for the nickel(II) corrin complex[23b]—but metal-centered; i.e., it leads to the nickel(I) complex of F430. More recently, these authors, in studying the reductive chemistry of the pentamethyl ester of coenzyme F430, discovered a F430-catalyzed, reductive cleavage of *S*-methylsulfonium salts to give methane.[137] All this evidence points strongly to a central biological function of the nickel(I) form of coenzyme F430.

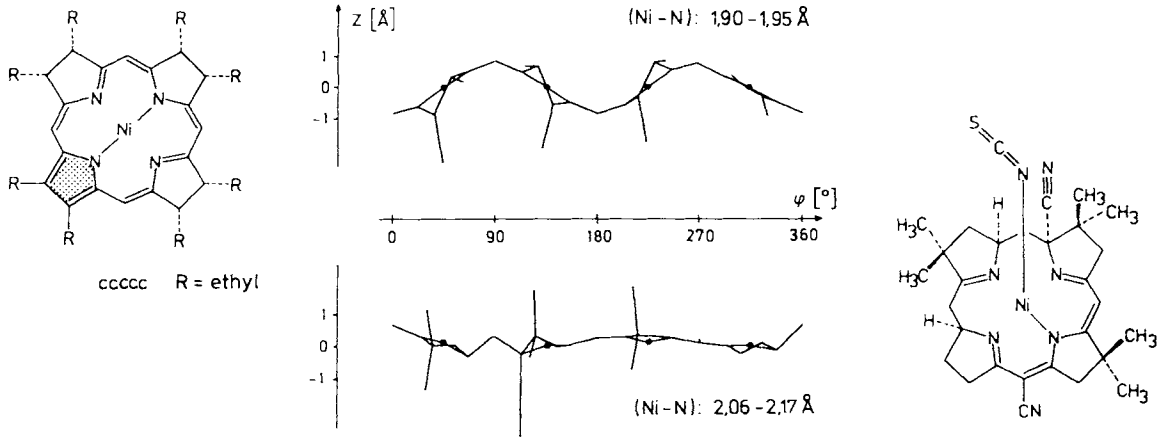

Fig. 52. The absence of coordination-hole contraction in the hexacoordinated (dimeric) F430 model complex (*C. Kratky* et al. [133]).

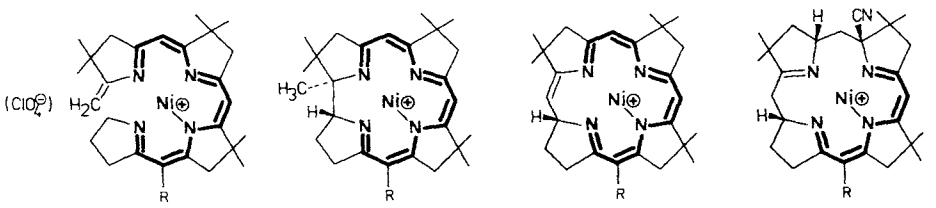

R	CN	H	CN	H	CN	CN
μ(B.M) CH_2Cl_2	dia	dia	dia	dia	dia	dia
CH_3CN	dia	dia	dia	dia	dia	para (2.73)
CH_3OH	dia	dia	dia	dia	para(2.27)	para (2.50)
$E_{1/2}$ (V) CH_3CN	-0.97	-1.47	-1.19	-1.20	-1.05	-1.05
NBu_4ClO_4	-0.86(CH_2Cl_2)					-0.51(THF)
Hg/0.1 NCE						
0.1 V s^{-1}						

Fig. 53. Magnetic properties and redox potentials of synthetic nickel(II) complexes containing corrinoid and corphinoid ligands [133]. NCE = normal calomel electrode.

That a nickel(II) ion should be at the coordination center of a porphinoid cofactor that fulfills a coenzymic function in Nature was, at the time of its discovery, a surprise for us, because we had been conditioned by years of experience with chemically totally inert nickel(II) corrin complexes and by the sharp contrast between the chemically "boring" tetracoordinated nickel ion and the "so interesting" hexacoordinated cobalt ion. From our present standpoint, however, it is just this nickel coenzyme from methanogenic bacteria that has afforded—through its novel ligand structure—a deeper insight into the structure/function relationship of coenzyme B_{12} (Fig. 54). A monovalent, tetrahydrocorphinoid ligand system, whose coordination hole is too large for a (monocationic) nickel(II) ion and whose chromophore system is further substituted with an (electrophilic) acyl group (Fig. 54) is Nature's answer to the problem of selecting a cofactor structure from among uroporphinoid ligands that contains a firmly (macrocyclically) coordinated and yet electrophilic nickel(II) ion.[138] What particular property of the cobalt ion was selected for in the case of the corrin system? Taking the F430 structure as a reference may well facilitate answering this question. Figure 55 indicates how.

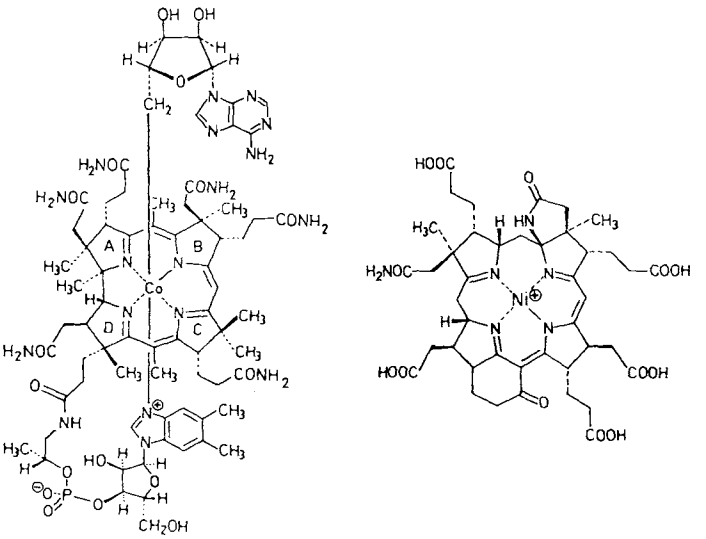

Fig. 54. Coenzyme B_{12} (left) and coenzyme F430 (right).

Extending the trend observed for the coordination number of nickel(II) complexes[139] (see Fig. 53) to the uniformly hexacoordinated cobalt(III) complexes leads to the following expectation: The binding energy of axial ligands in cobalt(III) *corrinate* complexes (ceteris paribus) should be weaker than that in cobalt(III) *corphinate* complexes and a dissociative ligand exchange via pentacoordinated cobalt(III) should occur more rapidly in *corrinate* complexes than in *corphinate* complexes. Ligand exchange occurring with a change in valence state via pentacoordi-

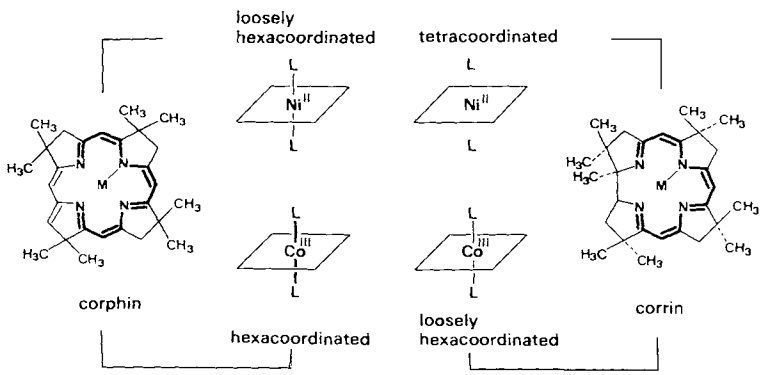

Fig. 55. A prognosis concerning the properties of axial ligands in cobalt(III) complexes of corphin and corrin.

nated cobalt(II) (e.g., the reversible homolysis of a cobalt–carbon bond) is more difficult to assess, but—compare the saddle-shaped ligand conformation of the pyridinato cobalt(II) pyrrocorphinate in Figure 25—should also be faster for *corrinates*.

The results obtained in a current study concerning the chemistry of synthetic model systems, e.g., the octamethylcorphinates and heptamethylcorrinates shown in Figure 50,[140] are only of a qualitative nature so far: The dicyanocobalt(III) *corphinate* is more stable toward acidolytic decyanidation (e.g., by silica gel during thin layer chromatography) than the dicyanocobalt(III) *corrinate*. The methylcobalt(III) corphinate complex is more difficult to prepare by Co^{I} methylation than the corresponding corrin complex; this is, first and foremost, due to the fact that the method of initial $Co^{III} \rightarrow Co^{I}$ reduction, e.g., with $NaBH_4$, which is so unproblematic with corrins, leads, in the case of corphinates, primarily to reduction of the ligand chromophore. Methylcobalt corphinate (perchlorate) eventually could be prepared under carefully controlled conditions by electrochemical $Co^{II} \rightarrow Co^{I}$ reduction in the presence of CH_3I;[141] it is—like the corresponding corrinate—a very sensitive compound. The methyl-transfer[142] equilibrium

$$CH_3Co^{III}(H_2O)\text{–corphinate} + Co^{II}(H_2O)\text{–corrinate} \rightleftharpoons Co^{II}(H_2O)\text{–corphinate} + CH_3Co^{III}(H_2O)\text{–corrinate}$$

(in methanol, 27 °C, exclusion of air and light[143]) favors the methylcobalt corphinate by a ratio of ca. 3:1. Noteworthy for the cobalt(II)(aquo) complexes is the observation that, in contrast to corrinates (and in analogy to the nickel(II) complexes), the UV/VIS spectrum of the Co^{II} corphinate is solvent dependent. Co^{II} corphinates are apparently hexacoordinated in nucleophilic solvents, whereas Co^{II} corrinates are pentacoordinated.[144]

Even these few qualitative observations concerning the properties of cobalt in a corphinate ligand indicate that the expectations depicted in Figure 55 are generally valid, but that one should not expect a significantly higher dissociation energy for a cobalt-alkyl bond in a corphinate compared with a corrinate. Of great interest would be a systematic comparison of corphins and corrins with respect to the kinetics of the ligand exchange reaction of cobalt(III) complexes proceeding dissociatively via cobalt(III), -(II), or -(I); the high rate of ligand exchange of vitamin B_{12} derivatives[145] may be a pertinent property in this connection. To get to the heart of the problem, it would seem desirable to construct a corphinic analogue of coenzyme B_{12} (including the nucleotide loop) derived from uroporphyrinogen (type III) via a chemical or a biosynthetic route.

5. Outlook

The experimental findings discussed in the four parts of Section 3 indicate that four characteristic structural elements of the vitamin B_{12} molecule represent thermodynamically favored structural fragments. However, a central goal of the investigation, namely, to discover reaction conditions under which a porphyrinogen transforms itself into a corrin (see Fig. 12), has not yet been attained. The important first hurdle along this way, the porphyrinogen → pyrrocorphin transformation, has been taken, and, moreover, a model for the final step, namely, the dihydrocorphinol → corrin ring contraction, has been found; however it has so far not been possible to connect the two. The outcome of extensive model studies makes us believe that it may be indispensable to carry out the search in the uroporphyrinogen series itself rather than in oversimplified model systems. In this context, an aspect emerges that must be considered to be part of the task of rationalizing the vitamin B_{12} structure: to give a rationale for the specific *site* of the corrinic direct ring junction. Rings A and D are the site of this direct ring junction, not the ring pairs A/B, B/C, or C/D (Fig. 56). This structural feature is just as specific for the vitamin B_{12} molecule as the corrin ring itself. Should we consider this feature as being merely fortuitous, or as related to function, or as a consequence of the preformation process? The contention upon which the chemical rationalization of cofactor structures is based would tend to disconnect this feature from the role of chance and does not rule out a priori a dependence on function, but, above all, assumes that this feature of the B_{12} structure is a specific consequence of structurally intrinsic factors. Once this point of view is taken, an attractive and, moreover, experimentally accessible possibility appears (Fig. 56): *Is the site of direct ring junction related to the fact that, in the uroporphyrinogen (type III), only the meso position between rings A and D has two flanking acetic acid side chains?*

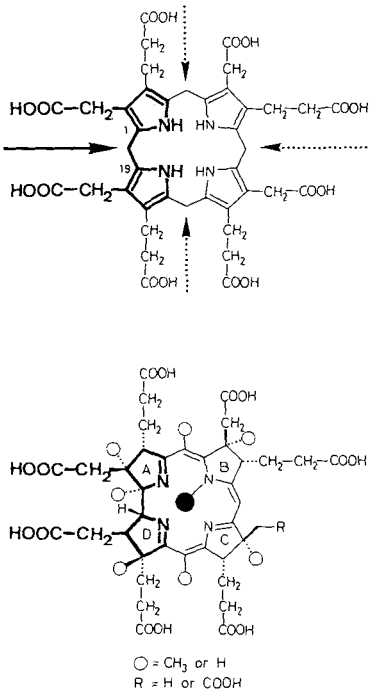

Fig. 56. Is there a relationship between the site of direct ring junction in the corrin ligand of vitamin B_{12} and the fact that in uroporphyrinogen (type III) only the *meso* position between rings A and D has two flanking acetic acid side chains?

Addressing this question experimentally is the next task in our synthetic analysis of the structure of vitamin B_{12}. The underlying working hypothesis, namely, the structural element in question is to be related to the preformation process and is therefore amenable to chemical rationalization, is typical of the overall approach used in this analysis. In each step, this approach can justify itself again and again only by producing experimental results that create a deeper insight into the architecture of the vitamin B_{12} molecule. The porphyrinogen→pyrrocorphin tautomerization and the regioselective nucleotide attachment reaction provide pertinent examples.

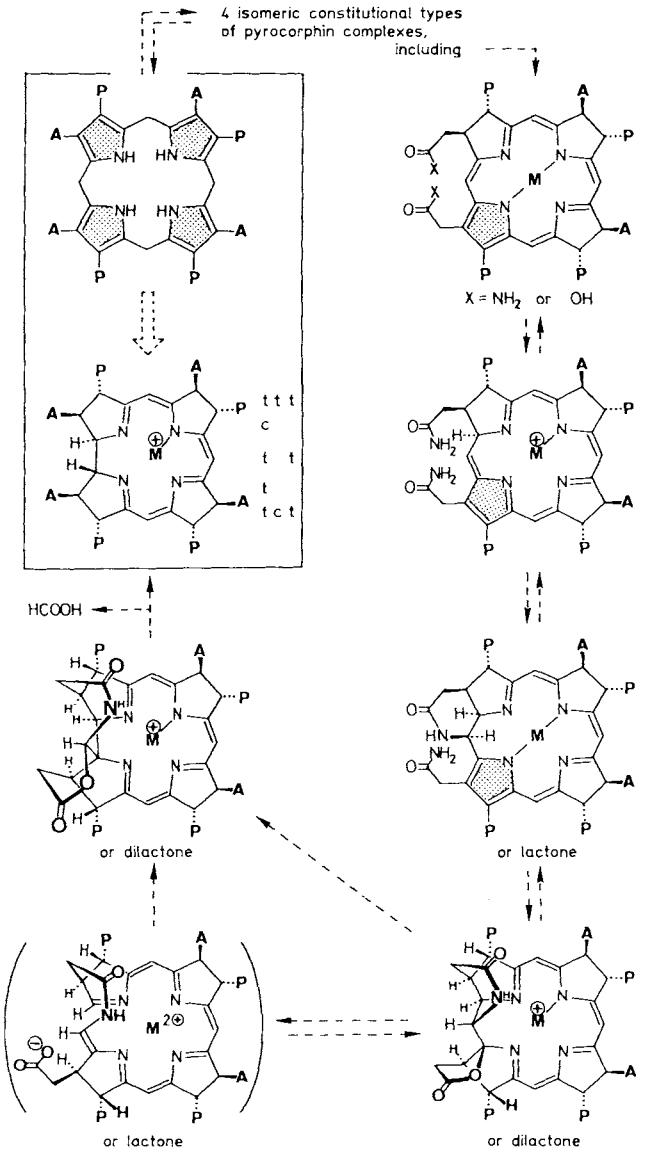

Fig. 57. Hypothesis for a regio- and stereoselective pathway from uroporphyrinogen (type III) to a proton analogue of cobyrinic acid.

Figure 57 summarizes a detailed *working hypothesis*. It integrates the wealth of observations made in our model studies (see Sections 2, 3.1, and 3.2), especially on the dihydrocorphinol→corrin transformation (Fig. 8). The proposed sequence of steps is believed to correspond to a reaction channel that connects uroporphyrinogen type III with proton analogues (Fig. 56) of cobyrinic acid regioselectively as well as diastereoselectively, and might require, in addition to a metal ion, only (unstructured) acid/base catalysis for this transformation. All steps of the reaction sequence prior to the ring-contraction step are expected to be reversible, thus making regioselection of the A/D structural region feasible. A (reversible) key step is the functionalization of the *meso* position between rings A and D by formation of a six-membered ring lactam (or lactone) group after protonation of the angular position C-1[146] (or C-19) of a pyrrocorphinate that has a pyrrolic ring D (or ring A). The ring-contraction step[30] is envisaged to occur as a dyotropic[147] 1,2-migration of antiperiplanar groups within a corphinoid lactam-lactone (or dilactone) to give the corrinoid isomer. The six-membered lactam (or lactone) ring thereby serves as a "*clamp*" which prevents a dissociative reaction course[31] or makes such a process reversible. As in the model of the dihydrocorphinol→19-acetylcorrin rearrangement (Fig. 27), the driving force for the ring contraction is supposed to be the contracting influence of a centrally coordinated metal ion (Section 3.2).

The hypothesis not only aims at a possible rationalization of the *topical* but also of the *configurational* aspect of the direct ring junction of the vitamin B_{12} structure. The steric course of the overall reaction occurring in the A/D region is viewed to be directed by the constitutional and configurational constraints of the (concerted) contraction step[148] and corresponds in all respects (protons in place of methyl groups!) to the specific configuration of vitamin B_{12} in the region of rings A and D (*trans-cis-trans-trans-trans*). If the substituents in the *peri* positions of the A/B, B/C, and C/D regions of the macrocycle are allowed to have the *trans* or *cis* configuration[149] but the vicinal substituents only the thermodynamically more stable *trans* arrangement (cf. Fig. 15), then, from among a total of 2048 racemic variants (4 constitutional types, each with 512 diastereomers), the reaction sequence formally selects eight diastereomers of one single constitution, all of which display the corrinic direct ring junction specifically between rings A and D.[150]

The numerous questions that we would very much like to address experimentally to an "urocorrin complex" such as the one shown in Figure 57 include the following one: Of the two acetic acid side chains in rings B and C, is it the latter—as would seem mechanistically reasonable[151]—that could be selectively decarboxylated? This question refers to a structural element of the vitamin B_{12} molecule not considered in our analysis of the cofactor structure so far.

The *biosynthesis* of cobyrinic acid from uroporphyrinogen (type III) occurs via a reaction sequence that, instead of (reversible) *C*-protonations, involves isoelectronic (irreversible) *C*-methylations, the sequence of which[60-62] does not correspond, however, to the protonation steps postulated in the hypothetical reaction scheme of Figure 57. Nonetheless, the way in which the two flanking acetic acid carboxyl functions can be integrated into the reaction pathway of the ring contraction prompts the question as to whether both these groups might be involved in the ring-

contraction process of vitamin B_{12} biosynthesis in a way not previously considered.[152] The course of the biosynthetic ring contraction has so far been traced only indirectly; the current notions concerning the details of this process[33,34,61,62] are mainly based on the chemical model, the dihydrocorphinol→19-acetylcorrin ring contraction.[30,31] With the structural formulas of Figure 58, we would like to indicate a way in which that ring-contraction principle might be realized in the biosynthesis.[153]

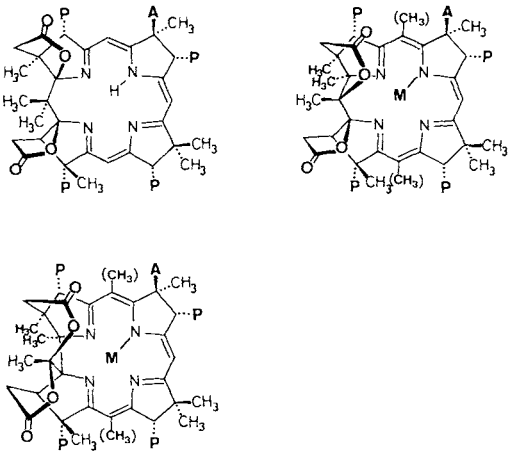

Fig. 58. Hypothetical intermediates along the route of ring contraction in the biosynthesis of vitamin B_{12}. M = H or metal ion.

The project of "chemically rationalizing the vitamin B_{12} structure" aims ultimately at providing chemical reasons for the fact that this specific molecular structure has been biologically selected as a cofactor. The search for relationships between structure and function represents one part, the mechanistic one, of this endeavor. It does not need to be further emphasized that this part will require consideration of the structure of the proteins involved in exercising this function. The other part, the synthetic one so to say, is to arrive experimentally at a perception of the biomolecule's intrinsic potential for structural self-assembly, the attempt to identify the structural factors that played a part in determining the course of its preformation steps—regardless of whether they ultimately were prebiotic or biotic. Whether, to what extent, and in what manner the prerequisites of steps leading to such a self-assembly include the assistance of enzymic catalysis is part of the overall problem. The challenge posed by the complexity of this cofactor's structure has caused two directions of research to come together and to complement each other in a synergistic manner, namely, the systematic mapping of the biosynthetic pathway on the one side, and the chemical search for the structure's potential for self-assembly on the other. The way in which this convergence takes place in this special case should perhaps be considered as a guide to how it may be possible—in concert with studies on structure/function relationships—to arrive at rational concepts concerning the origin of cofactor structures. Regardless of how far away one is from valid concepts of this kind, whatever their form and significance might assume or demand, the path leading in that direction along strictly experimental grounds is bound to result in a deeper understanding of the structures of biomolecules. Research in natural product synthesis is of crucial importance in following this path. The ultimate goal is an insight into the principles that govern the molecular architecture of biomolecules and a chemically founded view regarding the nature and extent of their structural predestination.

The following doctoral and postdoctoral researchers (in chronological order) have taken part, since the mid-1970s, in the work described here or in related work: Bernhard Kräutler, Andreas Pfaltz, Reinhard Neier, René Nordmann, Vittorio Rasetti, Christof Angst, Silvio Ofner, Beat Zehnder, René Lattmann, Kurt Hilpert, Alexander Fässler, Rudolf Waditschatka, Rolf Nussberger, Guido Bold, Christian Leumann, Thomas Früh, Christian Lehmann, Ulrich Kämpfen, Fritz Kreppelt, André Kobelt, Wlodzimierz Iwanowski, Kaspar Zimmermann (Doktoranden); Franz-Peter Montforts, Paul Naab, Masuhiro Kajiwara, Engelbert Zass, James Rigby, Gary Ksander, Reinhard Schwesinger, Jon Eigill Johansen, Mitsunori Ono, Virginia Piermattie, Günter Bartels, John Norman Lewis, Katsuhiko Inomata, Anthony Davis, Douglas Livingston, Karl Grubmayr, Jean-Christophe Plaquevent, Susan Thomas, Sundeep Dugar, Wolf-Ulrich Nickel, Michael Göbel, Jerome Hayes (Postdoktoranden).

I would like to express my deep appreciation and gratitude to all my former and present collaborators. Their contributions and achievements, their knowledge and skills, and their enthusiasm have often greatly inspired me. I would like to extend my special thanks to my scientific colleague and friend Dr. Jakob Schreiber, a member of our research group since the beginning, without whose autochthonous genius in experimental and instrumental matters our work would have been much more difficult if not impossible. I express my gratitude to Dorothee Felix, the "good spirit" of our group, for her continual help and faithful cooperation. I would also like to emphasize the names of my former Doktoranden and current Privatdozenten Bernhard Kräutler and Andreas Pfaltz, whose special competence in the areas of corrin and corphin chemistry have decisively enriched the research of our group. Our group has been particularly lucky to have as members the married couple Dr. Engelbert and Hermine Zass-Gächter; I would like to express to both my high opinion of their work as well as my gratitude. The numerous X-ray structure analyses that have been so crucial in our work were all performed in the laboratory of Privatdozent Dr. Christoph Kratky (Institut für Physikalische Chemie der Universität Graz); I owe him thanks for a very fruitful collaboration.

Our work was generously supported by the Schweitzerischer Nationalfonds zur Förderung der wissenschaftlichen Forschung, by Ciba-Geigy AG in Basel, and by Firmenich & Co. in Geneva.

Received: September 14, 1987 [A 647 IE]
German version: *Angew. Chem. 100* (1988) 5

[1] A. I. Oparin: "*The Origin of Life*" (English translation of the Russian first edition published in 1924) in J. D. Bernal: *The Origin of Life*, Weidenfeld & Nicolson, London 1967, p. 197; J. B. S. Haldane: "*The Origin of Life*" in *Ration. Annu. 148* (1929) 3 (reprinted in J. D. Bernal, op. cit., p. 242).

[2] S. L. Miller, L. E. Orgel: *The Origins of Life on the Earth*, Prentice-Hall, Englewood Cliffs, NJ (USA) 1974.

[3] M. Eigen, P. Schuster, *Naturwissenschaften 64* (1977) 541; *65* (1978) 7, 341; H. Kuhn, *ibid. 63* (1976) 68.

[4] N. H. Horowitz, *Proc. Natl. Acad. Sci. USA 31* (1945) 153.

[5] S. L. Miller, *Science 117* (1953) 528; *J. Am. Chem. Soc. 77* (1955) 2351; *Biochim. Biophys. Acta 23* (1957) 480.

[6] R. E. Eakin, *Proc. Natl. Acad. Sci. USA 49* (1963) 360; H. B. White, *J. Mol. Evol. 7* (1976) 101; G. A. M. King, *BioSystems 13* (1980) 23; C. M. Visser, *Bioorg. Chem. 9* (1980) 411; *Origins Life 12* (1982) 165; H. B. White III in J. Everse, B. Anderson, K.-S. You (Eds.): *The Pyridine Nucleotide Coenzymes*, Academic Press, New York 1982, p. 1.

[7] The following two, preparatively important examples are taken from the extensive literature on catalytic properties of cofactor-type structures: The electrochemical C-C coupling reactions in the presence of vitamin B_{12} as catalyst (R. Scheffold, *Chimia 39* (1985) 203); the Stetter-Breslow reactions inspired by the biochemical function of thiamine (H. Stetter, H. Kuhlmann, *Angew. Chem. 86* (1974) 589; *Angew. Chem. Int. Ed. Engl. 13* (1974) 539; R. Breslow, *J. Am. Chem. Soc. 80* (1958) 3719).

[8] J. Oró, *Biochem. Biophys. Res. Commun. 2* (1960) 407; J. Oró, B. P. Kimball, *Arch. Biochem. Biophys. 94* (1961) 217; *96* (1962) 293; review: J. P. Ferris, W. J. Hagan, Jr., *Tetrahedron 40* (1984) 1093.

[9] J. P. Ferris, L. E. Orgel, *J. Am. Chem. Soc. 88* (1966) 1074.

[10] See, for example, S. Dagley, D. E. Nicholson: *An Introduction to Metabolic Pathways*, Blackwell, Oxford 1970; T. Kosluk, I. D. Spenser, *J. Am. Chem. Soc. 109* (1987) 4698.

[11] J. P. Ferris, D. A. Usher in G. Zubay (Ed.): *Biochemistry*, Addison-Wesley, Reading, MA (USA) 1983, p. 1191.

[12] R. Shapiro: *Origins, a Sceptic's Guide to the Creation of Life on Earth*, Summit Books, New York 1986.

[13] These results refer to derivatives of nicotinic acid: cf. M. J. Dowler, W. D. Fuller, L. E. Orgel, R. A. Sanchez, *Science 169* (1970) 1320; N. Friedmann, S. L. Miller, R. A. Sanchez, *ibid. 171* (1971) 1026; see also the important observations on riboflavin made by T. Patterson, H. C. F. Wood, *J. Chem. Soc. Perkin Trans. I 1972*, 1051.

[14] G. H. Cookson, C. Rimington, *Biochem. J. 57* (1954) 476.

[15] D. Mauzerall, *J. Am. Chem. Soc. 82* (1960) 2601, 2605.

[16] See, for example, D. Mauzerall in D. Dolphin (Ed.): *The Porphyrins, Vol. II, Part B*, Academic Press, New York 1978, p. 91.

[17] a) K. Decker, K. Jungermann, R. K. Thauer, *Angew. Chem. 82* (1970) 153; *Angew. Chem. Int. Ed. Engl. 9* (1970) 138; J. De Ley, K. Kersters, *Compr. Biochem. 29B* (1975) 1, 29; S. R. Dickmann, *J. Mol. Evol. 10* (1977) 251; b) N. H. Georgopapadakou, A. I. Scott, *J. Theor. Biol. 69* (1977) 381.

[18] R. B. Woodward, *Pure Appl. Chem. 17* (1968) 519; *25* (1971) 283; *33* (1973) 145; R. B. Woodward in B. Zagalak, W. Friedrich (Eds.): *Vitamin B_{12}*, de Gruyter, Berlin 1979, p. 37.

[19] A. Eschenmoser, *Q. Rev. Chem. Soc. 24* (1970) 366; *23rd Congr. Pure Appl. Chem. 2* (1971) 69; *Naturwissenschaften 61* (1974) 513; A. Eschenmoser, C. Wintner, *Science 196* (1977) 1410.

[20] R. B. Woodward, *Spec. Publ. Chem. Soc. 21* (1967) 217.

[21] Y. Yamada, D. Miljkovic, P. Wehrli, B. Golding, P. Löliger, R. Keese, K. Müller, A. Eschenmoser, *Angew. Chem. 81* (1969) 301; *Angew. Chem. Int. Ed. Engl. 8* (1969) 343.

[22] See also A. Eschenmoser, *Chem. Soc. Rev. 5* (1976) 377.

[23] a) B. Kräutler, A. Pfaltz, R. Nordmann, K. O. Hodgson, J. D. Dunitz, A. Eschenmoser, *Helv. Chim. Acta 59* (1976) 924; b) B. Kräutler: *Eine elektrochemische Redox-Simulation der lichtinduzierten A/D-Secocorrin→Corrin-Cycloisomerisierung, Dissertation No. 5877*, ETH Zürich 1977.

[24] A. Pfaltz, B. Hardegger, P. M. Müller, S. Farooq, B. Kräutler, A. Eschenmoser, *Helv. Chim. Acta 58* (1975) 1444.

[25] A. Pfaltz, N. Bühler, R. Neier, K. Hirai, A. Eschenmoser, *Helv. Chim. Acta 60* (1977) 2653; A. Pfaltz: *Nicht-photochemische A/D-Ringschlüsse zu Corrin-Komplexen. Dissertation No. 6184*, ETH Zürich 1978.

[26] C. E. Brown, J. J. Katz, D. Shemin, *Proc. Natl. Acad. Sci. USA 69* (1972) 2585; C. E. Brown, D. Shemin, J. J. Katz, *J. Biol. Chem. 248* (1973) 8015.

[27] A. I. Scott, C. A. Townsend, K. Okada, M. Kajiwara, P. J. Whitman, R. J. Cushley, *J. Am. Chem. Soc. 94* (1972) 8267; A. I. Scott, C. A. Townsend, K. Okada, M. Kajiwara, R. J. Cushley, P. J. Whitman, *ibid. 96* (1974) 8069.

[28] A. R. Battersby, G. W. J. Matcham, E. McDonald, R. Neier, M. Thompson, W.-D. Woggon, V. Ya. Bykhovsky, H. R. Morris, *J. Chem. Soc. Chem. Commun. 1979*, 185.

[29] G. Müller, K. D. Gneuss, H.-P. Kriemler, A. I. Scott, A. J. Irwin, *J. Am. Chem. Soc. 101* (1979) 3655.

[30] V. Rasetti, A. Pfaltz, C. Kratky, A. Eschenmoser, *Proc. Natl. Acad. Sci. USA 78* (1981) 16.

[31] V. Rasetti, K. Hilpert, A. Fässler, A. Pfaltz, A. Eschenmoser, *Angew. Chem. 93 (1981) 1108*; *Angew. Chem. Int. Ed. Engl. 20* (1981) 1058.

[32] K. Hilpert: *Synthetische Untersuchungen zur Biosynthese des Corrinsystems, Dissertation No. 7390*, ETH Zürich 1983.

[33] A. R. Battersby, *Ann. N. Y. Acad. Sci. 471* (1986) 138; *Acc. Chem. Res. 19* (1986) 147.

[34] A. I. Scott, *Ann. N. Y. Acad. Sci. 471* (1986) 174.

[35] L. Mombelli, C. Nussbaumer, H. Weber, G. Müller, D. Arigoni, *Proc. Natl. Acad. Sci. USA 78* (1981) 11.

[36] A. R. Battersby, M. J. Bushell, C. Jones, N. G. Lewis, A. Pfenninger, *Proc. Natl. Acad. Sci. USA 78* (1981) 13.

[37] A. Fässler: *Synthese und Eigenschaften von Modellkomplexen des Coenzyms F430, Dissertation No. 7799*, ETH Zürich 1985, pp. 82, 204.

[38] A. Fischli, A. Eschenmoser, *Angew. Chem. 79* (1967) 865; *Angew. Chem. Int. Ed. Engl. 6* (1967) 866; N. J. Lewis, A. Pfaltz, A. Eschenmoser, *ibid. 95* (1983) 743 and *22* (1983) 735.

[39] A. W. Johnson, *Chem. Br. 3* (1967) 253; *Chem. Soc. Rev. 4* (1975) 1; *9* (1980) 125.

[40] A. W. Johnson, I. T. Kay, *Proc. Chem. Soc. 1964*, 89; *J. Chem. Soc. 1965*, 1620; D. Dolphin, R. L. N. Harris, A. W. Johnson, I. T. Kay, *Proc. Chem. Soc. 1964*, 359; D. Dolphin, R. L. N. Harris, J. L. Huppatz, A. W. Johnson, I. T. Kay, *J. Chem. Soc. C1966*, 30; I. D. Dicker, R. Grigg, A. W. Johnson, H. Pinnock, K. Richardson, P. van den Broek, *ibid. 1971*, 536.

[41] V. Rasetti, B. Kräutler, A. Pfaltz, A. Eschenmoser, *Angew. Chem. 89* (1977) 475; *Angew. Chem. Int. Ed. Engl. 16* (1977) 459; V. Rasetti: *Synthese eines Nickel(II)-$\Delta^{18,19}$-dehydrocorrinats und eines Isobakteriochlorins, Dissertation No. 6462*, ETH Zürich 1979, p. 74.

[42] S. Ofner, V. Rasetti, B. Zehnder, A. Eschenmoser, *Helv. Chim. Acta 64 (1981) 1431*; S. Ofner: *Synthese eines Isobakteriochlorins und eines C,D-Tetradehydrocorrins, Dissertation No. 6939*, ETH Zürich 1981, p. 285.

[43] F.-P. Montforts, *Angew. Chem. 94* (1982) 208; *Angew. Chem. Int. Ed. Engl. 21* (1982) 214; F.-P. Montforts, J. W. Bats, *Helv. Chim. Acta 70* (1987) 402.

[44] One-step arrows correspond to cyclization steps that lead directly to corrins or corrin complexes; two-step arrows stand for reaction sequences in which the cyclization step results in the formation of a dehydro derivative of a corrin, which then is (or would have to be) subjected to reduction (or hydrogenation) to give the corrin. Parallel arrows indicate that several variants of the reaction are known. The literature quotations for the types of cyclization included in the figure are presented in the text, with the exception of the first variant at the above left (C. Leumann, A. Eschenmoser, *J. Chem. Soc. Chem. Commun. 1984*, 583); see also C. Angst, C. Kratky, A. Eschenmoser, *Angew. Chem. 93* (1981) 275; *Angew. Chem. Int. Ed. Engl. 20* (1981) 263.

[45] A. Eschenmoser, *Jahrb. Akad. Wiss. Göttingen*, Vandenhoeck und Ruprecht, Göttingen 1977, p. 29; A. Eschenmoser in B. Zagalak, W. Friedrich (Eds.): *Vitamin B_{12}*, de Gruyter, Berlin 1979, p. 89; A. Eschenmoser: *Über organische Naturstoffsynthese: Von der Synthese des Vitamins B_{12} zur Frage nach dem Ursprung der Corrinstruktur (Nova Acta Leopold. 55* (1982) No. 247).

[46] An exception is provided by the observation reported by *H. W. Whitlock, Jr.*, and *D. H. Buchanan* (*Tetrahedron Lett. 1969*, 3711) that, in CH_3COOD, the hydrogen atoms of all four *meso*-methylene groups of octaethylporphyrinogen are rapidly replaced by deuterium. *U. Eisner* (*J. Chem. Soc. 1957*, 3461) assigned a reduction product obtained from iron(II) octaethylchlorinate to a pyrrocorphin-type constitution; however, subsequent work in our laboratory proved this assignment to be incorrect [50, 52]. The sole characterized derivative having a pyrrocorphinate structure was a palladium(II) complex prepared by *N. Müller* and *H. H. Inhoffen* (unpublished results, cf. N. Müller, *Dissertation*, Technische Universität Braunschweig 1969).

[47] A. P. Johnson, P. Wehrli, R. Fletcher, A. Eschenmoser, *Angew. Chem. 80* (1968) 622; *Angew. Chem. Int. Ed. Engl. 7* (1968) 623; P. M. Müller, S. Farooq, B. Hardegger, W. S. Salmond, A. Eschenmoser, *ibid. 85* (1973) 954 and *12* (1973) 914; A. Eschenmoser, *Ann. N. Y. Acad. Sci. 471* (1986) 108.

[48] P. M. Müller: *Corphin, ein neuartiges porphinoid-corrinoides Ligandsystem, Dissertation No. 5135*, ETH Zürich 1973.

[49] For the first use of this term, see R. Schwesinger, R. Waditschatka, J. Rigby, R. Nordmann, W. B. Schweizer, E. Zass, A. Eschenmoser, *Helv. Chim. Acta 65 (1982)* 600.

[50] C. Angst: *Neue hexahydroporphinoide Ligandsysteme, Dissertation No. 6783*, ETH Zürich 1981.

[51] C. Angst, M. Kajiwara, E. Zass, A. Eschenmoser, *Angew. Chem. 92* (1980) 139; *Angew. Chem. Int. Ed. Engl. 19* (1980) 140.

[52] J. E. Johansen, C. Angst, C. Kratky, A. Eschenmoser, *Angew. Chem. 92* (1980) 141; *Angew. Chem. Int. Ed. Engl. 19* (1980) 141.

[53] J. E. Johansen, V. Piermattie, C. Angst, E. Diener, C. Kratky, A. Eschenmoser, *Angew. Chem. 93* (1981) 273; *Angew. Chem. Int. Ed. Engl. 20* (1981) 261.

[54] R. Waditschatka, A. Eschenmoser, *Angew. Chem. 95* (1983) 639; *Angew. Chem. Int. Ed. Engl. 22* (1983) 630.

[55] R. Waditschatka, C. Kratky, B. Jaun, J. Heinzer, A. Eschenmoser, *J. Chem. Soc. Chem. Commun. 1985*, 1604.

[56] R. Waditschatka: *Die Porphyrinogen ⇌ Pyrrocorphin-Tautomerisierung, Dissertation No. 7707*, ETH Zürich 1985.

[57] C. Angst, R. Waditschatka, J. E. Johansen, V. Piermattie, J. C. Plaquevent, C. Kratky, J. Schreiber, E. Zass, A. Eschenmoser, manuscript in preparation.

[58] C. Kratky, manuscript in preparation.

[59] C. Kratky, R. Waditschatka, C. Angst, J. E. Johansen, J. C. Plaquevent, J. Schreiber, A. Eschenmoser, *Helv. Chim. Acta 68* (1985) 1312.

[60] H. C. Uzar, A. R. Battersby, *J. Chem. Soc. Chem. Commun. 1982*, 1204; *1985*, 585.

[61] H. C. Uzar, A. R. Battersby, T. A. Carpenter, F. J. Leeper, *J. Chem. Soc. Perkin Trans. 1 1987*, 1689.

[62] A. I. Scott, N. E. Mackenzie, P. J. Santander, P. E. Fagerness, G. Müller, E. Schneider, R. Sedlmeier, G. Wörner, *Bioorg. Chem. 12* (1984) 356.

[63] R. Waditschatka, E. Diener, A. Eschenmoser, *Angew. Chem. 95* (1983) 641; *Angew. Chem. Int. Ed. Engl. 22* (1983) 631.

[64] C. Leumann, T. Früh, M. Göbel, A. Eschenmoser, *Angew. Chem. 99* (1987) 273; *Angew. Chem. Int. Ed. Engl. 26* (1987) 261.

[65] C. Leumann: *Biomimetische C-Methylierungsreaktionen an Corphinderivaten, Dissertation No. 8064*, ETH Zürich 1986.

[66] A. W. Johnson in H. C. Heinrich (Ed.): *Vitamin B_{12} and Intrinsic Factor*. Enke-Verlag, Stuttgart 1962, p. 1; K. Hosaka, A. P. Johnson, A. W. Johnson, *Tetrahedron Lett. 1978*, 2959.

[67] C. Leumann, K. Hilpert, J. Schreiber, A. Eschenmoser, *J. Chem. Soc. Chem. Commun. 1983*, 1404; cf. [44], and references cited therein.

[68] "Vinamidine" = vinylogous amidine, cf. D. Lloyd, H. McNab, *Angew. Chem. 88* (1976) 496; *Angew. Chem. Int. Ed. Engl. 15* (1976) 459.

[69] A. R. Battersby, K. Frobel, F. Hammerschmidt, C. Jones, *J. Chem. Soc. Chem. Commun. 1982*, 455.

[70] C. Kratky, C. Angst, J. E. Johansen, *Angew. Chem. 93* (1981) 204; *Angew. Chem. Int. Ed. Engl. 20* (1981) 211.

[71] For the construction of the cylindrical projections shown here, see footnote 4 in [59].

[72] E. F. Meyer, Jr., *Acta Crystallogr. Sect. B28* (1972) 2162; D. L. Cullen, E. F. Meyer, Jr., *J. Am. Chem. Soc. 96* (1974) 2095.

[73] J. L. Hoard, *Ann. N. Y. Acad. Sci. 206* (1973) 18; *Science 174* (1971) 1295.

[74] L. J. Pace, J. Martinsen, A. Ulman, B. M. Hoffman, J. A. Ibers, *J. Am. Chem. Soc. 105* (1983) 2612; F. W. Kutzler, P. N. Swepston, Z. Berkovitch-Yellin, D. E. Ellis, J. A. Ibers, *ibid. 105* (1983) 2996; M. P. Suh, P. N. Swepston, J. A. Ibers, *ibid. 106* (1984) 5164.

[75] We thank Dr. *Christoph Kratky* for the construction of this model. For the construction data, see footnote 5 in [59].

[76] E. Bertele, H. Boos, J. D. Dunitz, F. Elsinger, A. Eschenmoser, I. Felner, H. P. Gribi, H. Gschwend, E. F. Meyer, M. Pesaro, R. Scheffold, *Angew. Chem. 76* (1964) 393; *Angew. Chem. Int. Ed. Engl. 3* (1964) 490; A. Eschenmoser, R. Scheffold, E. Bertele, M. Pesaro, H. Gschwend, *Proc. R. Soc. London A 288* (1965) 306.

[77] J. D. Dunitz, E. F. Meyer, *Helv. Chim. Acta 54* (1971) 77.

[78] Attempts to carry out an analogous ring contraction with the palladium(II) complex failed.

[79] *tttct* and *tcttt* isomers are identical when the ligand periphery is symmetrically substituted.

[80] In contrast to the free ligands, the nickel (II) complexes of the *tttct* and *ttttt* diastereomers of octaethylpyrrocorphins are separable by HPLC [56].

[81] R. P. Gunsalus, R. S. Wolfe, *FEMS Microbiol. Lett. 3* (1978) 191; G. Diekert, B. Klee, R. K. Thauer, *Arch. Microbiol. 124* (1980) 103; W. B. Whitman, R. S. Wolfe, *Biochem. Biophys. Res. Commun. 92* (1980) 1196.

[82] A. Pfaltz, B. Jaun, A. Fässler, A. Eschenmoser, R. Jaenchen, H. H. Gilles, G. Diekert, R. K. Thauer, *Helv. Chim. Acta 65* (1982) 828; D. A. Livingston, A. Pfaltz, J. Schreiber, A. Eschenmoser, D. Ankel-Fuchs, J. Moll, R. Jaenchen, R. K. Thauer, *ibid. 67* (1984) 334; A. Fässler, A. Kobelt, A. Pfaltz, A. Eschenmoser, C. Bladon, A. R. Battersby, R. K. Thauer, *ibid. 68* (1985) 2287.

[83] G. Diekert, U. Konheiser, K. Piechulla, R. K. Thauer, *J. Bacteriol. 148* (1981) 459.

[84] A. Pfaltz, D. A. Livingston, B. Jaun, G. Diekert, R. K. Thauer, A. Eschenmoser, *Helv. Chim. Acta 68* (1985) 1338.

[85] D. Crowfoot-Hodgkin, J. Kamper, J. Lindsey, M. MacBay, J. Pickworth, J. H. Robertson, C. K. Shoemaker, J. G. White, R. J. Prosen, K. N. Trueblood, *Proc. R. Soc. London A 242* (1957) 228.

[86] W. Friedrich, G. Gross, K. Bernhauer, P. Zeller, *Helv. Chim. Acta 43* (1960) 704.

[87] H. Maag: *Totalsynthese von Vitamin B_{12}: Dicyano-Co(III)-cobyrinsäure-hexamethylester-f-amid, Dissertation No. 5173*, ETH Zürich 1973, p. 226.

[88] G. Bartels, R. Nussberger, F. Kreppelt, J. Schreiber, A. Eschenmoser, manuscript in preparation.

[89] Cyanomethyl esters behave as mildly activated carboxylic acid derivatives upon aminolysis: cf. R. Schwyzer, B. Iselin, M. Feurer, *Helv. Chim. Acta 38* (1955) 69.

[90] Prepared according to an unpublished procedure by hydrazinolysis of vitamin B_{12} (hydrazine hydrate, hydrazine sulfate, 65 °C, 15 h) [88].

[91] Conditions: XAD-2, H_2O–*t*BuOH (96 : 4 → 4 : 1).

[92] R. Keese, L. Werthemann, A. Eschenmoser; work published in L. Werthemann: *Untersuchungen an Cobalt(II)- und Cobalt(III)-Komplexen des Cobyrinsäure-heptamethylesters, Dissertation No. 4097*, ETH Zürich 1968.

[93] Yields 37 and 27%; the yield of crystalline B_{12} hexamethyl ester was 40% (along with 23% of cobester) in a preparative run carried out under optimized isolation conditions.

[94] B. Kräutler, C. Caderas, unpublished, cf. C. Caderas: *Aufbau von binuklearen und überbrückten Cobyrinsäurederivaten, Dissertation No. 7822*, ETH Zürich 1987. The constitution of the f-monoacid was established by conversion to authentic f-monoamide [19, 87].

[95] FAB mass spectroscopic data obtained in other runs indicated the presence of, among other products, derivatives of the starting material and of the product containing one and two carboxyl functions esterified with pentane-2,4-diol.

[96] In collaboration with *B. Kräutler* (ETH), the three isomeric b-, d-, and e-iso-B_{12} hexamethyl esters were prepared by semisynthesis from hexamethyl esters of the corresponding cobyrinic monoacids [94]; in this way, it was possible to determine their chromatographic behavior and to estimate the maximum (possible) amount of individual isomers present in the nucleotide-attachment mixtures.

[97] Ca. 5 μmol, in pentane-2,4-diol/acetonitrile, RT, 104 h (conversion ca. 35%).

[98] The amount of nucleotide-attachment product in the reaction mixture in one of the experiments was 36%, in the other, 0.3%.

[99] B. Kräutler, unpublished results. I wish to thank Priv.-Doz. Dr. *B. Kräutler* (ETH) for permission to mention his results here.

[100] K. Müller, unpublished results. I wish to thank Priv.-Doz. Dr. *K. Müller* (Hoffmann-La Roche AG, Basel) for permission to mention his results here.

[101] Review: F. M. Huennekens, K. S. Vitols, K. Fujii, D. W. Jacobsen in D. Dolphin (Ed.): *B_{12}, Vol. 1*, Wiley, New York 1982, p. 145.

[102] Review: L. Bogorad in D. Dolphin (Ed.): *The Porphyrins, Vol. VI, Part A*, Academic Press, New York 1979, p. 125; F. J. Leeper, *Nat. Prod. Rep. 2* (1985) 561.

[103] The term "oligomeroid" refers to reaction products that, in contrast to true oligomers, are not identical in elemental composition with the ensemble of starting materials.

[104] Review: A. R. Battersby, C. J. R. Fookes, G. W. J. Matcham, E. McDonald, *Nature (London) 285* (1980) 17.

[105] Method of analysis [15]: Conversion of the mixture of ^{14}C-labeled uroporphyrinogens to a mixture of the four uroporphyrins and the four coproporphyrins, respectively, followed by radiometric determination of the amounts of types I, II, and (as a mixture) III/IV in zones obtained by paper chromatography.

[106] H. von Dobeneck, B. Hansen, E. Vollmann, *Z. Naturforsch. B 27* (1972) 922.

[107] R. B. Woodward: Comment in *„Further Perspectives in Organic Chemistry"* (*Ciba Found. Symp. 53* (1978) 43); see also [17b].

[108] J. J. Scott, *Biochem. J. 62* (1956) 6p.

[109] C. A. Townsend, A. I. Scott, unpublished results; cf. C. A. Townsend, *Dissertation*, Yale University 1974; cf. also A. I. Scott, C. A. Townsend, K. Okada, M. Kajiwara, *Trans. N. Y. Acad. Sci. 35* (1973) 72.

[110] G. Ksander, G. Bold, R. Lattmann, C. Lehmann, T. Früh, Y.-B. Xiang, K. Inomata, H.-P. Buser, J. Schreiber, E. Zass, A. Eschenmoser, *Helv. Chim. Acta 70* (1987) 1115.

[111] C. Lehmann: *Untersuchungen über Uroporphyrinogen-octanitrile, Dissertation No. 8215*, ETH Zürich 1987.

[112] A. Strecker, *Ann. Chem. Pharm. 75* (1850) 27.

[113] Glutaminedinitrile is, for example, the reaction product obtained from the triplet-sensitized photochemical [2+2] dimerization (followed by base treatment) of 2-aminopropenenitrile [110]. It is also the product obtained by Strecker α-amino nitrile synthesis performed on the 1,4 adduct obtained from acrolein and HCN [110] and, as such, an accepted prebiotic precursor for glutamic acid [2].

[114] B. Franck, *Angew. Chem. 91* (1979) 453; *Angew. Chem. Int. Ed. Engl. 18* (1979) 429.

[115] S. I. Beale, *Philos. Trans. R. Soc. London B273* (1976) 99; J. D. Weinstein, S. I. Beale, *Plant Physiol. 74* (1984) 146.

[116] B. Franck, M. Bruse, J. Dahmer, *Angew. Chem. 96* (1984) 1000; *Angew. Chem. Int. Ed. Engl. 23* (1984) 998.

[117] T. Früh: *Zur Chemie der Uroporphyrinogen-octanitrile, Dissertation No. 8054*, ETH Zürich 1986.

[118] L. M. Siegel in T. P. Singer, R. N. Ondarza (Eds.): *Mechanisms of Oxidizing Enzymes*. Elsevier, New York 1978, p. 201.

[119] In carrying out the reaction sequence experimentally (Figs. 42–45), the intermediate products were also prepared by preparatively more effective, alternative methods (cf. Ref. [110]). The direct transformation of uroporphyrinogen(III)octanitrile to the iron(II) complex of the "protosirohydrochlorinoctanitrile" (porphyrinogen → pyrrocorphinate or porphyrinogen → isobacteriochlorinate transformation) in the presence of

iron(II), although presumably possible, was not attempted, since the isolation of the pure iron(II) complex free of isomers would certainly be very difficult.

[120] R. H. Abeles, D. Dolphin, *Acc. Chem. Res. 9* (1976) 114.

[121] J. Halpern, *Science 227* (1985) 869.

[122] B. M. Babior, *Acc. Chem. Res. 8* (1975) 376; B. T. Golding in D. Dolphin (Ed.): *B_{12}, Vol. 1*, Wiley, New York 1982, p. 543.

[123] J. Halpern, S.-H. Kim, T. W. Leung, *J. Am. Chem. Soc. 106* (1984) 8317.

[124] B. P. Hay, R. G. Finke, *J. Am. Chem. Soc. 108* (1986) 4820.

[125] In contrast to the values determined in water (26 kcal mol^{-1} [122] and 30 ± 2 kcal mol^{-1} [123]), those determined in ethylene glycol are in aggreement (cf. comment 14 in [121]).

[126] J. M. Pratt, *Chem. Soc. Rev. 14* (1985) 161.

[127] D. W. Christianson, W. N. Lipscomb, *J. Am. Chem. Soc. 107* (1985) 2682.

[128] A. Bax, L. G. Marzilli, M. F. Summers, *J. Am. Chem. Soc. 109* (1987) 566.

[129] V. P. Pett, M. N. Liebman, P. Murray-Rust, K. Prasad, J. P. Glusker, *J. Am. Chem. Soc. 109* (1987) 3207; L. Randaccio, N. Bresciani-Pahor, P.-J. Toscano, L. G. Marzilli, *ibid. 102* (1980) 7372.

[130] M. K. Geno, J. Halpern, *J. Am. Chem. Soc. 109* (1987) 1238.

[131] I. Felner, A. Fischli, A. Wick, M. Pesaro, D. Bormann, E.-L. Winnacker, A. Eschenmoser, *Angew. Chem. 79* (1967) 863; *Angew. Chem. Int. Ed. Engl. 6* (1967) 864; E.-L. Winnacker: *Ligandreaktivität synthetischer Kobalt(III)-corrin-Komplexe, Dissertation No. 4177*, ETH Zürich 1968.

[132] A. Fässler, A. Pfaltz, B. Kräutler, A. Eschenmoser, *J. Chem. Soc. Chem. Commun. 1984*, 1365.

[133] C. Kratky, A. Fässler, A. Pfaltz, B. Kräutler, B. Jaun, A. Eschenmoser, *J. Chem. Soc. Chem. Commun. 1984*, 1368; see also J. A. Shelnutt, *J. Am. Chem. Soc. 109* (1987) 4169.

[134] A. Eschenmoser, *Pure Appl. Chem. 7* (1963) 297.

[135] Unfortunately, an X-ray structure analysis of neither the hexafluorophosphate nor the perchlorate complex is available. On the other hand, one is available for the 3,5-dinitrobenzoate (C. Kratky), which is a tetracoordinated complex in CH_2Cl_2 solution according to its UV/VIS spectrum. In the crystal, however, the nickel ion is again hexacoordinated [37].

[136] B. Jaun, A. Pfaltz, *J. Chem. Soc. Chem. Commun. 1986*, 1327.

[137] Private communication from Dr. *B. Jaun* (ETH).

[138] In this connection, compare the concept of the "entactic state" used by *R. J. P. Williams* (*Proc. Natl. Acad. Sci. USA 59* (1968) 498).

[139] Nickel(II) octamethylcorphinate (in contrast to the corrinate) is paramagnetic in methanolic solution [48].

[140] K. Zimmermann, W.-U. Nickel, B. Kräutler, B. Jaun, A. Eschenmoser, unpublished.

[141] The successful electrochemical solution to the problem of preparing methylcobalt corphinate is due to *B. Kräutler*. A comparative study of the redox potentials of cobalt(II) corphinates and cobalt(II) corrinates in a variety of solvents is in progress in collaboration with *B. Kräutler*.

[142] B. Kräutler, M. Hughes, C. Caderas, *Helv. Chim. Acta 69* (1986) 1571; B. Kräutler, *ibid. 70* (1987) 1268.

[143] The equilibrium position was determined for the corresponding trideuteriomethyl derivatives by ^{2}H-NMR spectroscopy after workup of the equilibrium mixtures with methanolic HCN in the presence of air ($Co^{II} \rightarrow Co^{III}(CN)_2$).

[144] The following cobalt(II) corrinate complexes investigated by X-ray analysis display pentacoordination at the cobalt(II) ion. The heptamethyl ester of iodocobalt(II) cobyrinic acid [92]: E. Edmond, D. Crowfoot Hodgkin (details not published), *cf. D. Crowfoot Hodgkin in* B. Zagalak, W. Friedrich (Eds.): *Vitamin B_{12}*, de Gruyter, Berlin 1979, p. 19, and review by J. P. Glusker in D. Dolphin (Ed.): *B_{12}, Vol. 1*, Wiley, New York 1982, p. 23. The heptamethyl ester of aquacobalt(II) cobyrinic acid perchlorate: B. Kräutler, W. Keller, M. Hughes, C. Caderas, C. Kratky, *J. Chem. Soc. Chem. Commun. 1987*, 1678. Cobalt(II) cobalamine: personal communication Priv.-Doz. Dr. *B. Kräutler*.

[145] Cf. P. Schulthess, D. Ammann, W. Simon, C. Caderas, R. Stepánek, B. Kräutler, *Helv. Chim. Acta 67* (1984) 1026.

[146] Compare the complexation/tautomerization of octaethylporphyrinogen to a hexahydroporphinate complex, the formation of which presupposes a protonation of the C-1 position of the chromophore system [50, 52].

[147] M. Reetz, *Angew. Chem. 84* (1972) 161; *Angew. Chem. Int. Ed. Engl. 11* (1972) 129.

[148] Only when (assuming the β configuration of the acetic acid chain at C-2) the protonation at C-1 (ring A) occurs in the α position is a six-membered lactam (or lactone) ring formed on the β side, and only when the proton at C-18 (ring D) likewise enters from the α side does the acyloxy function of the five-membered lactone ring (in the β position) end up antiperiplanar to the C–C bond migrating on ring contraction. Under thermodynamic control, vicinal substituents (e.g., in pyrrocorphinates, Fig. 15) always exhibit the *trans* configuration. The subsequent deformylation step leads to a 1,19-*trans*-corrin complex [30] (cf. Fig. 8); 1,19-*cis*-corrin complexes are unknown; the synthesis of such a complex had been attempted at the time (A→B ring-closure method [76]), but was unsuccessful (M. Roth, *Dissertation No. 4668*, ETH Zürich 1971, p. 116–123).

[149] The following finding [51] is relevant for this question: The complexation/tautomerization (occurring with dehydrogenation) of octaethylporphyrinogens in the presence of cobalt(II) ions has afforded mainly two diastereomeric isobacteriochlorins (*ttt* and *tct*) with the *ttt* isomer as the major product (ca. 2:1).

[150] All vicinal substituents in *trans* arrangement, A/D configuration sequence *tctt* or *tttct*; under these preconditions, the *peri*-configuration sequence only can be either *ttc*, *tct*, *ctt*, or *ccc*.

[151] Of all the positions allylic to the chromophore system in a corrin complex, the positions *C-8* (ring B) and *C-12* (ring C) are most easily deprotonated (cf. D. Bormann, A. Fischli, R. Keese, A. Eschenmoser, *Angew. Chem. 79* (1967) 867; *Angew. Chem. Int. Ed. Engl. 6* (1967) 868.

[152] *Uzar* and *Battersby* [60] have considered a different kind of involvement of the ring-D acetic acid chain.

[153] Figure 58 implies that the C-1 methyl group would be introduced via a prior α-methylation of the *meso* position C-20. This methylation mode corresponds to the (nucleophilic) reactivity expected for a corphin chromophore. The dyotropic migration of the methyl group to the C-1 position would convert a 1,19-*cis*-homocorrinate into a (presumably more stable, cf. [37] pp.82–86) 1,19-*trans*-homocorrinate and thereby create the configurational preconditions for a subsequent ring contraction via dyotropic migration.

[154] W. Fuhrer: *Totalsynthese von Vitamin B_{12}: Der photochemische Weg, Dissertation No. 5158*, ETH Zürich 1973.

[155] G. Bold: *Zur Chemie des 2-Amino-propennitrils, Dissertation No. 7702*, ETH Zürich 1984.

ANGEWANDTE CHEMIE

International Edition in English

Volume 27 · Number 1
January 1988
Pages 41–62

Horst Baumann, Matthias Bühler, Heinz Fochem, Frank Hirsinger, Hans Zoebelein, and Jürgen Falbe

Natural Fats and Oils—Renewable Raw Materials for the Chemical Industry

© VCH Verlagsgesellschaft mbH, D-6940 Weinheim, 1988

0570-0833/88/0101-0041 $ 02.50/0

Natural Fats and Oils—Renewable Raw Materials for the Chemical Industry

By Horst Baumann, Matthias Bühler, Heinz Fochem, Frank Hirsinger, Hans Zoebelein, and Jürgen Falbe*

Since last century, the supply of raw materials for the chemical industry has undergone a radical change. Whereas at the beginning of the nineteenth century the demand for basic chemicals was satisfied entirely by renewable raw materials, from about 1850 the chemical industry came to rely increasingly upon coal. In the 1940's, mineral oil started to become increasingly important, and during the past thirty years it has remained by far as the most important source of raw materials. Renewable raw materials are likely to become important again in the future, as the choice of raw materials is now of great significance not only for economic reasons by influencing competitiveness, but also because this choice largely determines the properties of the derivatives produced and their ecological effects. Following the two oil crises of the 1970's, there is also now a growing awareness of the limits of raw material resources, and against the continuing background of agricultural surpluses, chemists are again showing an increasing interest in renewable raw materials. Since the end of the seventies, the Bundesministerium für Forschung und Technologie (Ministry of Research and Technology of the Federal Republic of Germany) has supported research projects on renewable raw materials in universities and in industry. For the chemical industry the use of natural products as raw materials opens up a wider spectrum of synthetic methods and finished products, some of which are not accessible by petrochemical routes.

1. Introduction

Mineral oil is at present the most important source of raw materials for the chemical industry. Natural gas, coal and renewable raw materials are used to a much lesser extent for this purpose. However, in the future this situation will change quite significantly. Natural products which are already processed by the chemical industry and used in many fields of application include in particular sugar, starch, cellulose, proteins and natural fats and oils. Many of the products thus obtained cannot be produced economically by petrochemical routes.

Table 1 gives a summary of the present consumption of renewable raw materials. The largest share is taken up by oils and fats of vegetable and animal origin. These alone have a wide range of chemical applications (Table 2) which is scarcely less than that of petrochemicals.

2. Economic Aspects

2.1. Demand

World production of oils and fats in 1985 was about 68.2 million tonnes, of which only 9.5 million tonnes (14%) was used for chemicals. 80% of the world production was used in foodstuffs and 6% in animal feeds. Taking the consumption of oils and fats in the EEC countries in 1985 as an example, an analysis of the market structure shows that, of

Table 1. Present consumption of biological raw materials by the chemical industry (estimated).

Raw material	German Federal Republic	EEC	World
	k tonnes/yr		
Sugar	15	65	800
Starch	115	390	1750
Cellulose	220	600	5014
Oils and fats	700	2700	9500

Table 2. Areas of application of oils and fats in the chemical industry.

Fatty acids and derivatives	→	Plastics; metal soaps; washing and cleaning agents; soaps; cosmetics; alkyd resins; dyestuffs; textile, leather and paper industries; rubbers; lubricants
Methyl esters of fatty acids	→	Cosmetics; washing and cleaning agents
Glycerol and derivatives	→	Cosmetics; toothpastes; pharmaceuticals; foodstuffs; lacquers; plastics; synthetic resins; tobacco; explosives; cellulose processing
Fatty alcohols and derivatives	→	Washing and cleaning agents; cosmetics; textile, leather and paper industries; mineral oil additives
Fatty amines and derivatives	→	Fabric conditioners; mining; road-making; biocides; textile and fiber industries; mineral oil additives
Drying oils	→	Lacquers; dyestuffs; varnishes; linoleum
Neutral oil derivatives	→	Soaps

[*] Prof. Dr. J. Falbe, Dr. H. Baumann, Dr. M. Bühler, H. Fochem, Dr. F. Hirsinger, Dr. H. Zoebelein
Henkel KGaA
Postfach 1100, D-4000 Düsseldorf (FRG)

[**] The figure on the preceding page shows some examples of renewable raw materials (clockwise from top center): soybeans, rapeseeds, castor beans, linseed, jojoba seeds, and sunflower seeds; the center of the picture shows part of a coconut palm with fruit.

the total consumption of 2.7 million tonnes, about 2.2 million tonnes (80%) consisted of raw materials which contain fatty acids with 16, 18 or higher numbers of carbon atoms. In this latter class, animal fats accounted for about 1.4 million tonnes (64%) consisting mainly of tallow and other non-edible animal fats, which find valuable applications with the help of chemistry.

Vegetable oils and fats with a chain length of at least C_{16} accounted for a further 800000 tonnes. These were mainly imported directly from third world countries. For example, rapeseed oil and castor oil came from Eastern Europe, Brazil and India. Other raw materials were imported in the form of oil fruits or seeds (linseed, soybean) from Canada, the USA, Brazil and Argentina. From EEC sources came sunflower oil and rapeseed oil with a low erucic acid content, the estimated total of these being almost 300000 tonnes.

For animal products the share coming from EEC sources was only 300000–400000 tonnes. The main sources of imports were the USA, Canada, Australia and New Zealand. Oils and fats with shorter chains, e.g. C_{12} and C_{14}, are nearly all imported in the form of coconut and palm kernel oil from South East Asian countries.

The present agricultural surpluses also lead to the possibility of using EEC butter as a raw material in the chemical industry. However, the particular distribution of fatty acids in butter calls for new process technologies, and appropriate research programs have already been started. Olive oil is also a surplus product, especially since the entry of Spain and Portugal into the EEC, and here, too, there are interesting possible industrial uses. However, butter and olive oil can only be introduced as chemical raw materials if they continue to be available at moderate costs over a long period.

2.2. Price Variations

Oils and fats are traded as commodities in international raw materials markets such as those in Chicago and Kuala Lumpur and are consequently subject to daily price fluctuations. The chemical process industry attempts to average out these fluctuations by its policies of buying and storing materials. As examples of market price trends for natural oils and fats, Figure 1 shows prices covering the period 1962 to 1987 for the US tallow "Bleachable Fancy" and for coconut oil, compared with naphtha as an example of a petrochemical raw material. Despite a few marked price jumps, the average annual rates of increase over the past 25 years (based on prices in DM) for coconut oil (2.20%/yr) and tallow (2.15%/yr) are below the overall rate of inflation, and are much lower than the average rate of increase for petrochemical products. These trends are likely to continue.

3. Raw Materials for the Oleochemical Industry

3.1. Animal Oils and Fats

Animal oils and fats have already been used for many years as raw materials in the oleochemical industry. Figure 2 summarizes the fatty acids composition of pork fat, beef fat and butter. It can be seen that animal oils and fats are made up chiefly of saturated and mono-unsaturated C_{16} and C_{18} fatty acids. Butter also contains some fatty acids with shorter chain lengths.

Under EEC regulations with regard to waste disposal (which are incorporated into the waste disposal regulations of the Federal Republic of Germany), tallow products arise unavoidably from abattoir wastes, and are used

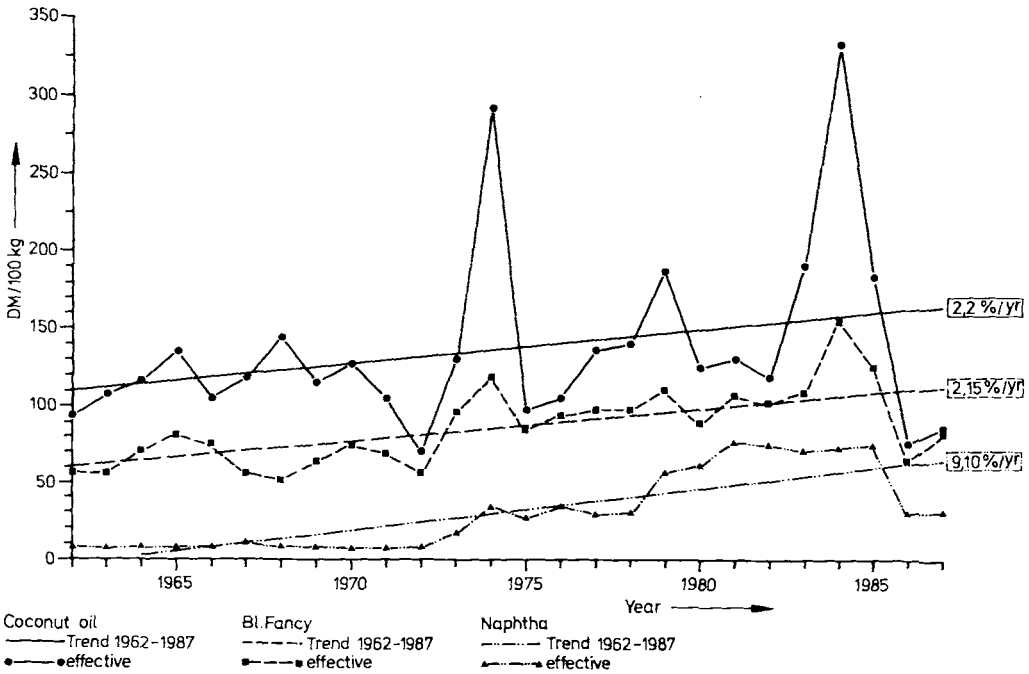

Fig. 1. Variation in price of coconut oil, US tallow ("Bleachable Fancy), and naphtha (1962-1987).

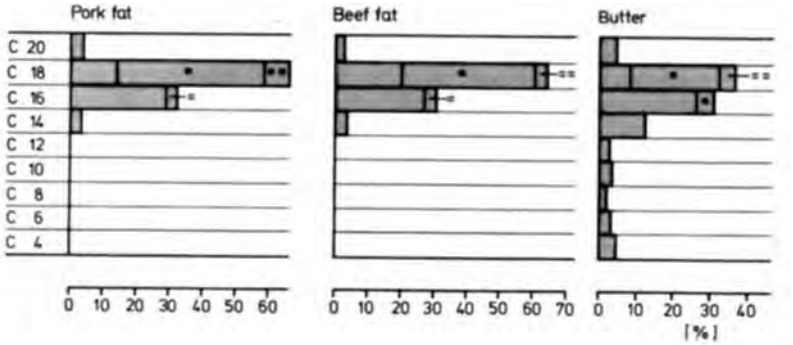

= Number of double bonds in the fatty acid chain

Fig. 2. Fatty acid composition of some animal fats.

profitably in animal feeds and in the soap and oleochemical industry.

Figure 3 summarizes the world production of individual types of animal oils and fats and also the use of tallow divided into edible and non-edible products.

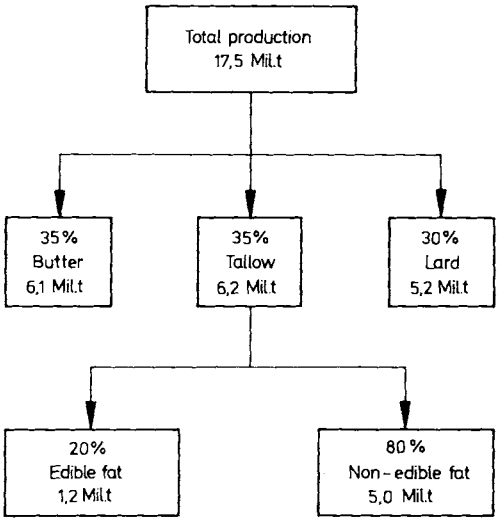

Fig. 3. World production of animal fats and oils (1985).

Because tallows unsuitable for human consumption are comparatively cheap and fairly consistent in their fatty acids composition, which is important for chemical derivatization processes, animal oils and fats now constitute the largest share of renewable raw materials used industrially.

$CH_3-(CH_2)_{14}-COOH$ **1**

$CH_3-(CH_2)_{16}-COOH$ **2**

$CH_3-(CH_2)_7-\underset{cis}{CH=CH}-(CH_2)_7-COOH$ **3**

Lard and tallow are the principal sources of the saturated and mono-unsaturated fatty acids palmitic **1**, stearic **2** and oleic acids **3**. However, vegetable oils and fats are also becoming increasingly important in this area (cf. Section 3.3.1).

3.2. Marine Animal Oils and Fats

Oils and fats from marine animals contain, in addition to C_{16} and C_{18} fatty acids, larger quantities of polyunsaturated C_{20} and C_{22} fatty acids (see Fig. 4). Up to the 1970's, sperm whale oil was of considerable importance for certain areas in which oleochemicals are used. However, as a result of legislation to protect endangered species, it has no longer been permissible, since January 1, 1982, to import these types of oils into the EEC.[1]

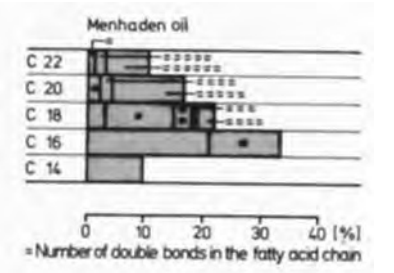

Fig. 4. Fatty acid composition of menhaden oil as an example of marine animal fats and oils.

3.3. Vegetable Oils and Fats

3.3.1. Sources and Importance

World production of vegetable oils and fats in 1985 was 49.4 million tonnes, which represents almost a fourfold increase since 1950. By contrast, world production of animal oils and fats increased by a factor of only two during the same period (Table 3).

Table 3. World production of natural oils and fats in M tonnes.

Year	Vegetable oils and fats	Animal oils and fats (including marine animal oils)	Total
1950	13.9	9.3	23.2
1960	18.6	13.6	32.2
1970	26.2	13.9	40.1
1980	43.2	17.3	60.5
1985	49.4	18.8	68.2

Figure 5 shows the countries which are most important as exporters of vegetable oils and fats. Soya is grown chiefly in the USA, Brazil and China, while palm oil comes

	Soybeans		Cotton seeds		Castor beans
	Rapeseeds		Copra		Tallow & other animal fats
	Sunflower seeds		Palm fruits / Palm kernels		Marine animal oils
	Ground nuts		Linseed		Olives

Fig. 5. Chief exporters of renewable fat raw materials.

mainly from Indonesia, Malaysia and other South East Asian countries. Table 4 gives an overview.

The data given in Table 5 for the predicted future production of important vegetable oils and fats indicate that the greatest increase is expected for palm oil. The predictions are based on the areas of existing plantations, planned areas for further cultivation, and maximization of the oil content of the crops through breeding. For soybean oil a rapid growth in production is also expected up to 1995 taking into account the EEC's declared intention of achieving increased crop production in the EEC as well as in Brazil and Argentina.

Table 4. Production of renewable raw materials in M tonnes listed according to products and countries (1985).

Product	Important producers	Amount
Soybeans	USA/Brazil/China	14.7
Rape/rape-seed	India/Canada/Europe/China	5.5
Sunflower seeds	East & South Europe/Central & South America	6.2
Groundnuts	India/China/West Africa/USA	3.2
Cottonseed	USSR/USA/China/India/Brazil	3.7
Copra	East Asia (Philippines/Indonesia)	2.6
Palm fruits	East Asia/West Africa	6.7
Palm kernels	East Asia/West Africa	0.9
Linseed	North & South America/USSR/India	0.7
Castor beans	Brazil/India/USSR	0.4
Tallow & other animal fats	USA/Europe/Australia/New Zealand	17.5 [a]
Marine animal oils	North & South America/Europe/Japan	1.3
Olives	Mediterranean countries	1.8
Sesame, maize, safflower, babassu etc.		3.0
Total		68.2

[a] For subdivision according to products, see Fig. 3.

Table 5. Production and prospective production of selected fats and oils (world production) in M tonnes.

Year	Soybean oil	Palm oil	Coconut oil	Rape oil
1981	11.8	4.9	3.7	3.5
1985	14.7	6.7	3.2	5.2
1990	15.5	11.2	4.7	7
1995	19	18	6	8.2

3.3.2. Composition and Biogenesis of Vegetable Oils and Fats

The storage of oils and fats in plants occurs mainly in seeds and fruits. Table 6 summarizes the broad spectrum of vegetable fatty acids.

There is no indication that evolution has led to the preferential formation of one or another particular fatty acid in a certain species of plants. Within a species the pattern of fatty acids shows little variation. Consequently, the fatty acid composition of seeds has assumed great taxonomic importance for classifying plant species and families.[2]

Table 6. Fatty acids contents [%] in the seed oil of common oil crops. The column headings "m : n" signify: m = number of carbon atoms, n = number of double bonds. 18 : 1 = oleic acid **3** (+isomers); 18 : 2 = linoleic acid **13** (+isomers); 22 : 1 = erucic acid (+isomers).

	10 : 0	12 : 0	14 : 0	16 : 0	18 : 0	18 : 1	18 : 2	18 : 3	20 : 1	22 : 1
Normal oil crops										
Rape (old variety)	—	—	0.5	2	1	15	15	7	7	50
Ground nut	—	—	—	10	3	50	30	—	3	—
Safflower (old variety)	—	—	—	5	1	15	79	—	—	—
Poppy	—	—	—	10	2	11	72	5	—	—
Sunflower (old variety)	—	—	—	6	3	28	61	—	—	—
Linseed	—	—	—	5	3	22	17	52	—	—
Olive	—	—	—	14	2	64	16	2	—	—
Coconut	7	48	17	9	2	7	1	—	—	—
Oil palm/palm kernel	5	50	15	7	2	15	1	—	—	—
Palm oil	—	—	2	42	5	41	10	—	—	—
Oil-bearing plants modified by breeding										
Rape (new)	—	—	0.5	4	1	60	20	9	2	2
Safflower (new)	—	—	—	4	1	82	13	—	—	—
Sunflower ("Hioleic" variety)	—	—	—	4	4	85	7	—	—	—

Extensive studies by *Pohl* and *Wagner*[3] have established certain well-defined trends in the formation of fat reserves in plants. In the Bacteriophyta there is a strong preference for fatty acids with C_{14} and C_{16} chains. In the Rhodophyta, on the other hand, a preponderance of C_{20} fatty acids has been established in the course of their evolution. Lastly, in the Spermatophyta one finds a preference for C_{18} fatty acids. This evolutionary trend in the biosynthesis of fatty acids is also reflected in the phylogenesis of plants, e.g. in the maturing seeds of soybean and rapeseed.[4,5]

According to *Röbbelen* and *Thies*,[6] the evolutionary strategy in plant biosynthesis of fatty acids is directed towards the biochemical necessity of keeping the melting points of the oils as low as possible, sometimes by introducing double bonds or by conversion into the *cis* isomers (see Fig. 6). This strategy also appears to be one of the reasons why plants, in contrast to animals, have developed such a great variety in the formation of unusual fatty acids (see Fig. 7).

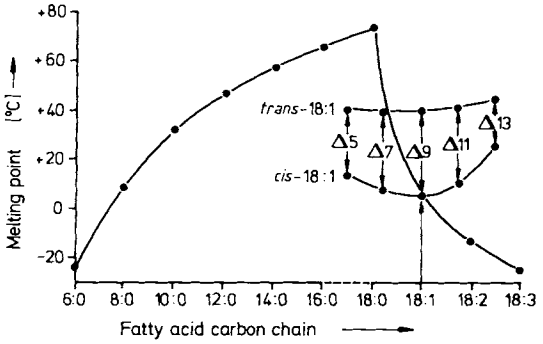

Fig. 6. Dependence of the melting points of synthetic triglycerides on the structure of their constituent fatty acids. The increase in melting point with increasing length of the carbon chain can be compensated by the incorporation of double bonds. *Cis*-isomers have lower melting points than *trans*-isomers (according to data quoted by *Gunstone* (1979) and Henkel KGaA (1971) and cited by *Röbbelen* and *Thies* [6]).

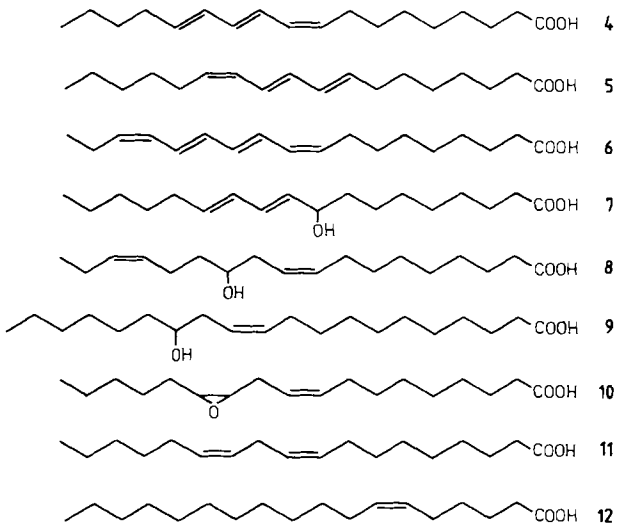

Fig. 7. Unusual fatty acids in the seed oil of one year old plants (after [19]). **4**: α-elaeostearic acid from *Centranthus macrosiphon* Boiss; **5**: calendulic acid from *Calendula officinalis* L.; **6**: α-parinaric acid from *Impatiens balsamina* L.; **7**: dimorphecolic acid from *Dimorphotheca pluvialis* (L.); **8**: densipolic acid from *Lesquerella lescurii* (Gray) Wats.; **9**: lesquerolic acid from *Lesquerella gracilis* (Hook.) Wats.; **10**: vernolic acid from *Euphorbia lagascae* Spreng.; **11**: crepenic acid from *Crepis alpina* L.; **12**: petroselinic acid from *Coriandrum sativum* L.

3.3.3. New Sources of Vegetable Oils

Extensive crop research programs have been undertaken to meet the increase in demand for renewable resources as well as to improve existing products. For this, both conventional breeding techniques and newer biotechnological methods are being used. Some of the most important characteristics typically aimed at in such work are as follows:

- consistent germination,
- predictable growth pattern,
- growth little affected by length of day (neutral photoperiodicity),
- consistent ripening,
- resistance to plant diseases and pests,
- a fatty acid distribution of interest for oleochemistry,

- oils and fats with functional groups,
- a high content of a single fatty acid,
- waxes in vegetable oils and fats.

3.3.3.1. Breeding Work with Existing Oil Crops

Plant breeding programs are able to increase the productivity of oil crops, in both a quantitative and a qualitative sense, through mutation, selection and recombination of appropriate phenotypes. In both annual and perennial plants, plant breeding has succeeded in increasing the oil yields by raising the harvest index (introduction of dwarf types) or by using the heterosis effect (production of hybrid varieties). Examples of such successes are the introduction of hybrid varieties of sunflowers and the development of short-stemmed varieties of linseed and dwarf types of coconut palm.

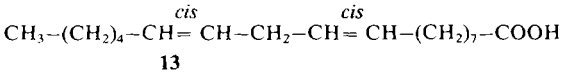

13

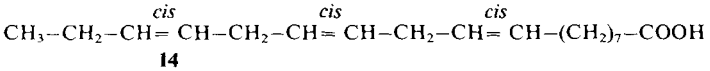

14

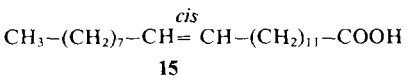

15

Table 7. Oil content and oil yield for various oil plants.

Species	Oil content [%]	Oil yield kg oil/ha/year
Oil palm	25	3000
Olive	15	800
Soybean	18	400
Groundnut	50	600
Rape	38	950

Table 8. Fatty acids content in the seed oil of various genotypes of safflower.

Genotype	18 : 1 [%]	18 : 2 [%]
F F	10-15	75-80
F f*	15-20	70-75
F f	18-35	60-75
f f*	35-50	42-54
f* f*	55-63	30-40
f f	64-83	12-30

Nevertheless, different oil crops vary widely in their productivity as measured by their oil yields (see Table 7). For example, the oil palm produces almost three times as much oil per hectare as does rape. The quality of the oil, too, which is determined by the chain lengths and degree of saturation of the fatty acids, varies between individual types of oil crops. In annual plants C_{18} fatty acids with one, two or three double bonds dominate. Groundnut oil and olive oil contain chiefly oleic acid **3**, while in sunflower oil and poppy seed oil the dominant acid is linoleic acid **13**, in flax seed (linseed) oil it is linolenic acid **14**, and in rapeseed oil it is normally erucic acid **15** (Table 6).

It has been possible through selective breeding to change the fatty acid pattern of rapeseed oil so that the erucic acid content nowadays is reduced to 3%. Doubts expressed from the standpoint of nutritional physiology concerning the unlimited use of rapeseed oil in human nutrition have thereby been overcome. The reduction in the content of erucic acid was caused by a spontaneous mutation resulting in genetic blocking of the uptake of two additional C_2 units by oleic acid.[7] Rape of low erucic acid content known in North America as canola quality has been grown worldwide since 1975.

In other plants, too, the quality of the oil has been improved. In safflower, for example, experimental mutagenesis has succeeded in altering the genes so that the mutant produces 80% of oleic acid instead of normally 80% of linoleic acid (Tables 6 and 8).

A further example indicating how oil quality in plants can be altered is given by new sunflower varieties recently selected for high contents of oleic acid. In such new varieties an enzymatic system normally responsible for the desaturation of oleic acid to linoleic acid is genetically blocked, resulting in an oleic acid content of up to 90% (Table 6).[8,9]

3.3.3.2. New Oil-Bearing Plants

Table 9 lists a selection of oil crops which might be used as new sources of raw materials. None of these has gained greater commercial importance. Most of them were identified in extensive screening studies carried out by the United States Department of Agriculture (USDA) at the Northern Regional Research Center, Peoria, Illinois, in the course of which the seed composition of about 8000 plant species was analyzed.[9-11]

Although the chemical analysis of the seeds was a comparatively simple task, the agricultural and economic eval-

Table 9. Fatty acid contents [%] in the seed oil of new types of oil-bearing plants.

	8 : 0	10 : 0	12 : 0	14 : 0	16 : 0	18 : 0	18 : 1	18 : 2	18 : 3	20 : 1	22 : 1	22 : 2
Cuphea painteri	65	24	—	1	3	—	3	4	—	—	—	—
C. paucipetala	1	87	2	1	2	—	2	4	—	—	—	—
C. parsonsia	—	8	74	4	1	—	1	6	—	—	—	—
C. palustris	20	1	2	64	7	—	3	3	—	—	—	—
Euphorbia lathyris	—	—	—	—	6	2	84	4	3	—	—	—
E. lagascae	—	—	—	—	4	2	20 + 62 [a]	12	—	—	—	—
Coriandrum sativum	—	—	—	—	4	—	3 + 80 [b]	13	—	—	—	—
Calendula officinalis	—	—	—	—	6	2	4	20	55 [c]	—	—	—
Limnanthes alba	—	—	—	—	1	—	2	1	—	62	13	20
Crambe	—	—	—	—	1	11	5	4	1	5	60	—
Jojoba	—	—	—	—	—	—	12	—	—	70	14	—

[a] 62% vernolic acid **10**. [b] 80% petroselinic acid **12**. [c] 55% calendulic acid **5**.

uation of these potential new raw materials encountered considerable problems, since it was often necessary to take into account complex factors, e.g. the plants' architecture, indehiscence of seed, and the possible toxicity of by-products. Some new oil-bearing plants useful for the oleochemical industry and the composition of their oils are described below.

Cuphea: Various species of *Cuphea* have been recognized since the late 1950's as potential oil crops.[12] Investigations on the cultivation and economics of these plants were started in 1975,[13-15] but practical methods for growing them as a large scale crop have not yet been successfully developed. *Cuphea* is especially attractive for oleochemistry, as this annual plant is suitable for cultivation in the southern countries of the temperate zone. It has an almost ideal fatty acids composition. Several species of *Cuphea* contain large amounts of different medium chain fatty acids in the oil of their seeds. These substances could be useful for the oleochemical industry as tailored raw materials;[12] they can be obtained from *Cuphea* in a purity and quality previously unknown and could find uses in all those areas of application where coconut oil and palm oil are now being used. The presence of high fractions of C_8 and C_{10} fatty acids also offers possibilities in the oleochemical industry for synthesizing molecules based on C_8 units, e.g. dioctyl phthalate.

Euphorbia lathyris: This plant of the spurge family has been considered mainly as a possible source of industrial hydrocarbons.[16, 17] Its use as an oil-bearing plant is a comparatively recent development.[18] Its oil content of 50% is exceptionally high, with also an unusually high proportion of oleic acid (80–90%). It also satisfies the main economic criteria for a future agricultural crop.

Euphorbia lagascae: This plant is gaining increasing importance[19] because the oil from its seeds contains a large amount (60–80%) of epoxy fatty acids. It therefore provides a completely new type of oil raw material, which could open up many new applications.

Coriandrum sativum: This is a well known herb of the Umbelliferae family which synthesizes up to about 80% of petroselinic acid in the oil of its seeds.[19] This acid can be transformed by ozonolysis into lauric and adipic acid (see Section 4.2.1.2).

Calendula: The oil from the seeds of the well known ornamental *Calendula officinalis* (marigold) contains up to 55% of calendulic acid,[18] a C_{18} fatty acid with three conjugated double bonds.

Limnanthes alba: Meadowfoam, a new oil-bearing plant from the north western USA,[20, 21] contains in the oil of its seeds about 95% of long chain fatty acids, of which about 62% is $C_{20:1}$. These fatty acids have potential uses in the manufacture of cosmetics, e.g. as substitutes for sperm whale oil.

Crambe: Crambe abyssinica, a wild species of the *Cruciferae* family which comes from Ethiopia, has already been cultivated over large areas in the southern states of the USA and in Canada. The erucic acid (**15**) content is about 60%. Cultivation experiments in the Federal Republic of Germany indicate that *Crambe* can be used as an alternative to rapeseed with high erucic acid content. This could provide an answer to the problem of genetic impurities caused by inadequate isolation of rapeseed strains with high and low erucic acid contents.[22-24]

Jojoba: Jojoba wax, which already has many uses, mainly in cosmetics, is obtained from the nuts of the jojoba scrub *Simmondsia chinensis*, a native perennial of the desert regions of north western Mexico and the south western USA. Throughout the world there exist about 20000 ha of jojoba plantations.[25] The oil from the seeds is a liquid wax similar to sperm whale oil.

3.3.3.3. Biotechnological Methods for Producing New Oil Raw Materials

Conventional plant breeding methods are limited by the extent of the gene pool achievable by cross-breeding within a plant species. The methods of biotechnology now make it possible to introduce new genetic material across the natural barriers of plant species.

Plant cell cultures: For many species of plants it is possible by techniques similar to those used for microorganisms, to grow sterile pieces of tissue on a culture medium containing phytohormones (cytokinins, auxins) giving an undifferentiated growth of cells (callus culture). By this means one can propagate and grow the genetically defined tissue of the original plant. By suitably modifying the hormone treatment the formation of branching nodules can be induced and the entire plant can thus be regenerated.[26-28] It is also possible to cultivate plant cells in liquid media.[29] Regenerable plant tissue cultures can be used both for transformation experiments with isolated DNA and for the selection of mutants. Following exposure to chemical or physical mutagens, appropriate selection methods can be used to recognize cells with the desired properties. Thus, by adding a herbicide to the tissue culture medium, cells with resistance to this herbicide can be selected which then can be regenerated to intact plants.[30] Hence it is possible to shorten breeding programs by many years.

Tissue culture techniques have already been used in breeding programs on oil palms.[31, 32] A ten-year breeding program using plant tissue cultures has resulted in about 10000 oil palms being grown from these for palm oil production in Malaysia. Initial studies have already shown that the oil yield per hectare from these plantations is 30% higher than previously, and there is an increase in the amounts of oleic, linoleic or palmitic acids present depending on the different cell lines used.[33]

Protoplast fusion: If plant tissue is treated in a suitable environment with cell wall degrading enzymes such as cellulases, hemicellulases or pectinases, round single cells surrounded only by the cell membrane, so-called protoplasts, are formed which can be used to regenerate whole plants by suitable treatment.[34]

Under the influence of high frequency alternating fields,[35] or in the presence of polyethylene glycol[36] or dimethyl sulfoxide,[37] it is possible to fuse protoplasts of different species which cannot be cross-bred by conventional methods. In cases where these methods succeed, the cell nuclei can not only be caused to fuse, but combination between other information carriers (plastides and mitochondria) which are present in the cells can also be ef-

fected. However, despite the high hopes held out for these techniques, they have so far failed to achieve a breakthrough in plant breeding, as the few hybrid varieties successfully regenerated have proved to be infertile.[38,39]

Specific gene transfer methods: Many different methods are available for specifically transferring genetic material into plant cells. These include the direct transformation of plant cell protoplasts using isolated DNA,[40,41] and the use of gene vectors such as genetically modified Ti plasmids from *Agrobacterium tumefaciens*[42] or plant-pathogenic DNA viruses.[43] Such techniques have already been used successfully to obtain resistance to herbicides[44,45] and viruses[46] in plants. Other proposed applications of genetic manipulation techniques in plant breeding are to control plant physiological processes such as photosynthesis or photorespiration, to influence nitrogen fixation by plants, or to cause changes in the type and proportions of substances present in plants.

Specific gene transfer methods are now being used to alter the content and the distribution patterns of fatty acids in oil-bearing plants.[47] The similarity between the biosynthetic routes for fatty acids in these plants and in prokaryotic microorganisms has turned out to be an advantage. The biosynthesis is catalyzed by seven enzymes, all of which can be isolated.[48,49] The individual concentrations of these enzymes can in principle be altered by way of genetic engineering techniques. However, the details of how the enzymatic steps are regulated are not yet fully understood. Furthermore, the various reactions take place in different plant compartments, and no method is yet known whereby specific genetic information can be expressed in a distinct part of the plant. The use of molecular genetics to modify oil-bearing plants or other types of plants is therefore a rather long-term prospect for the future.[50]

3.4. Oils and Fats from Microorganisms

3.4.1. Microbial Oils (Single Cell Oils)

The methods of biotechnology not only play an important part in developing new sources of vegetable oils as raw materials, but are also used in optimizing the amounts and composition of fatty acids present in fat-storing microorganisms. The ability to store fat is especially common in eukaryotic microorganisms such as yeasts, molds and algae, and its possible application as a basis for oil production was considered as early as the 1940's.[51] The fat content can be as much as 70% of the cells' dry weight. Its distribution pattern of fatty acids is generally similar to that found in commonly used raw materials such as soybean oil and tallow.[52-56]

The production process is similar to those generally used for manufacturing bakers' yeast or single cell protein. This is followed by a further step to separate the fat by solvent extraction.[57] However, the efficiency of the overall biotransformation from the carbohydrate fermentation feedstock to fat, a highly reduced substance, is relatively low (about 20%). Consequently the economic viability of processes of this kind is limited by the cost of the feedstock.[58] Up to now, there have been few reports of fat-storing microorganisms which can grow on cheap feedstocks such as methane or methanol. The higher the value of the end product, the less important is the price of the feedstock as a determining factor for the economics of the process. This is shown in the case of an oil rich in γ-linolenic acid, a potential raw material for the pharmaceutical industry. Its manufacture by the fermentation of purified glucose-containing substrates using the mold *Mucor sp.* was recently started on a production scale of 220 m^3.[59]

3.4.2. Waxes

Microbial and enzymatic systems have been described which can be used in the biotechnical synthesis of waxes, i.e. esters of long chain fatty acids with fatty alcohols, as substitutes for sperm whale oil and jojoba wax. Using the algal species *Euglena gracilis*, the change from aerobic to anaerobic growth conditions leads to a wax content of up to 50% of the cells' dry weight.[60,61] In the manufacture of substitutes for sperm whale oil using the bacterium *Acinetobacter sp.*, the effects of substrate chain length and concentration on the degree of saturation and chain length distribution in the product has been investigated in detail.[62-64]

Waxes can also be produced enzymatically by using lipases for esterifying fatty alcohols with fatty acids. This must be carried out under conditions which favor the synthesis and inhibit the hydrolysis (see Section 4.3.1). Isolated enzymes and also dried cell material can be used in such processes.[65,66]

3.4.3. Unusual Microbial Lipids

Archaebacteria which survive under extreme conditions (e.g. 60°C and pH values of 2) synthesize membrane lipids which have so far not been found in other microorgan-

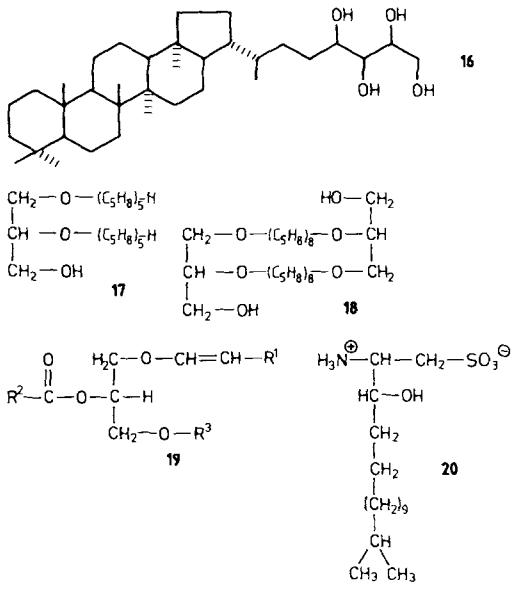

Fig. 8. Structures of unusual microbial lipids. **16**: tetrahydroxybacteriohopan (THBH) [70]; **17**: glycerol dialkyl ether (C_5H_8: isoprene unit); **18**: cyclic diglycerol dialkylene tetraether (C_5H_8: isoprene unit) [68]; **19**: alkenyl ether lipid (R^1, R^2 = alkyl, R^3 = phosphatidyl) [72]; **20**: capnin (sulfolipid) [73].

isms.[67-69] These glycerol ethers (cf. **17**-**19**) consist basically of polyisoprene chains with terminal ether linkages to either one or two glycerol molecules. Other substances found in archaebacteria include hopanoids, bacterial derivatives of steroids such as **16**, which are currently the object of intensive studies (see Fig. 8).[69-71]

The alkenyl ether lipids **19**[72] found in anaerobic organisms and the sulfolipid capnin **20** from the bacterium *Capnocytophaga*[73] (see Fig. 8) may offer hints to new types of surfactants (biosurfactants[74]) or to new applications.

4. Reactions of Oils and Fats

The limitations of oils and fats as chemical feedstocks have up to now been regarded as unavoidable. Factors contributing to these limitations are:

- the predominance of unsaturated fatty acids with chain lengths in the range C_{16} to C_{22}, and especially of C_{18}, combined with the absence of unsaturated C_8 to C_{14} fatty acids in natural sources, and
- the fact that a mixture of fatty acids is usually present, necessitating separation processes.

Due to these limitations, more than 90% of oleochemical reactions have been those occurring at the fatty acid carboxy groups, while less than 10% have involved rearrangements of the acid chain.[75] However, future progress will be along the lines of these latter types of reactions with their potential for considerably extending the range of compounds obtainable from oils and fats. Such progress is essential for a growth in the use of oils and fats as renewable raw materials.

Industrial and academic research in oleochemistry is becoming increasingly directed towards demonstrating new possibilities for reactions involving the hydrocarbon chains of fatty acids, especially at the CC double bonds in unsaturated fatty acids. In the following discussion, emphasis is put on reactions involving fatty acid hydrocarbon chains including biotechnological processes. "Classical" oleochemical reactions at the fatty acid carboxy group and the products which result from them are described only briefly as an introduction to this survey.

4.1. Reactions at the Carboxy Function of Oils and Fats

4.1.1. Hydrolysis and Methanolysis of Fats

Hydrolysis by steam[76] or transesterification with methanol transforms oils and fats into the basic compounds of oleochemistry, i.e. the fatty acids or their methyl esters and glycerol. The hydrolysis is carried out in continuously operating reaction columns at 250 °C and pressures between 2×10^6 and 6×10^6 Pa (20-60 bar). In the countercurrent flow method, the glycerol which is formed is extracted continuously from the equilibrium mixture using water, yielding 98% hydrolysis in a single pass. No catalyst is needed (Scheme 1).

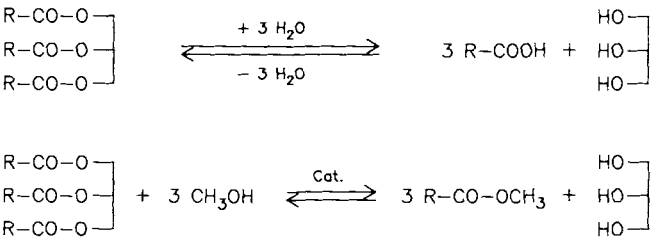

Scheme 1. Equilibria in the hydrolysis and methanolysis of fats. Cat. = catalyst.

The alkaline hydrolysis of fats to give alkali soaps, which historically marked the beginning of industrial fats chemistry, is now only of minor importance. It is now preferred to make soaps by neutralization of the fatty acids.[77]

The alkali-catalyzed transesterification of oils and fats with methanol to give fatty acid methyl esters and glycerol is likewise carried out in continuously operating reaction columns, at 240 °C and 10^7 Pa (100 bar)[78] (Scheme 1).

As an alternative to this, alkali-catalyzed esterification of fatty acids with methanol is carried out at 250 °C and about 10^6 Pa (10 bar) in counter-flow reaction columns.

4.1.2. High-Pressure Hydrogenation of Fatty Acid Methyl Esters, Fatty Acids and Fats

Methyl esters of fatty acids are chiefly significant as intermediate products. Their most important downstream reaction is high pressure hydrogenation to form fatty alcohols, i.e. linear primary aliphatic alcohols with chain lengths C_8 to C_{22}. Fatty acid methyl esters are hydrogenated at temperatures of 200-250 °C and hydrogen pressures of 2.5×10^7 to 3×10^7 Pa (250-300 bar) using solid mixed metal oxide catalysts. By choosing mixed catalysts of suitable composition the reaction can be controlled so that the double bond in unsaturated fatty acid esters is not hydrogenated. Catalysts containing copper (e.g. copper chromite) give saturated fatty alcohols, while special catalysts containing zinc preserve the double bonds in the starting compounds and give unsaturated fatty alcohols such as oleyl alcohol[78] (Scheme 2).

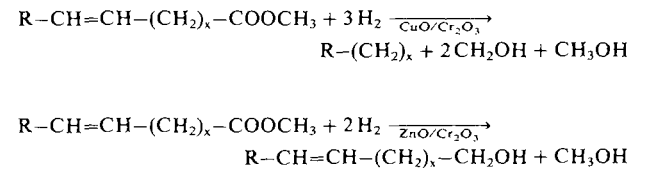

Scheme 2. Catalytic hydrogenation of fatty acid methyl esters to fatty alcohols.

Whereas long chain saturated alcohols can also be manufactured industrially from petrochemical feedstocks (by Ziegler synthesis,[79] oxo reactions,[80] oxidation of paraffins[80] or Fischer-Tropsch synthesis[81]), this is not possible for unsaturated fatty alcohols. High-pressure hydrogenation of unsaturated fatty acid methyl esters is the only

technically feasible route for synthesizing these compounds.

Fatty alcohols can be produced under certain conditions by high-pressure hydrogenation of fatty acids[78,82] and triglycerides.[83] The direct hydrogenation of fats to fatty alcohols appears attractive as a short route. Instead of glycerol as the co-product 1,2-propanediol is formed in this reaction.

Glycerol which arises as the co-product (10–15%) in the hydrolysis or transesterification of fats finds uses either as such or in the form of derivatives—mainly glycerol esters and polyglycerol esters of inorganic or carboxylic acids.

4.1.3. Synthesis of Fatty Amines

Another important class of basic oleochemicals are the fatty amines. They are obtained by reacting fatty acids with ammonia, which gives the amides and the nitriles as intermediates; the latter are then hydrogenated with a nickel catalyst to the fatty amines.[84] By adding ammonia or a secondary amine during the hydrogenation of the nitriles, the reaction can be controlled to give primary, secondary or tertiary amines (Scheme 3).

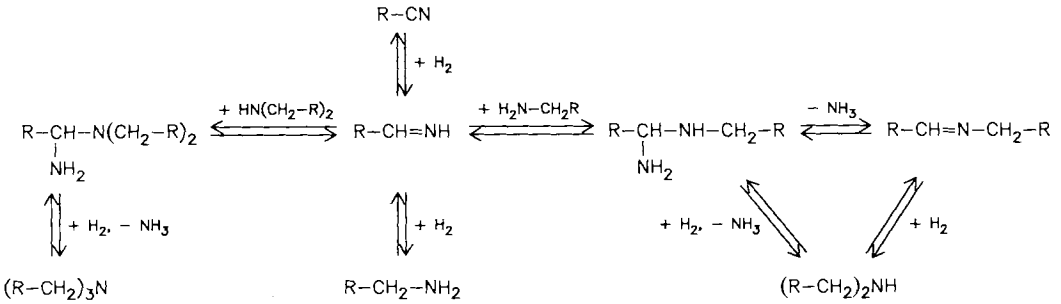

Scheme 3. Fatty amines from fatty acids via the fatty acid amides and fatty acid nitriles.

A more recent method makes possible the production of the nitriles in a single step directly from the fat also using ammonia.[85] Fatty amines are also formed in a one-step process from fatty acids or their methyl esters, using ammonia or lower amines under hydrogenating conditions with a hydrogen pressure of 2.5×10^7 Pa (250 bar) and with oxide catalysts.[86]

Another industrial process for producing fatty amines starts with fatty alcohols which are reacted with ammonia or short chain alkyl or dialkyl amines at 210–280 °C in the presence of dehydrogenation catalysts (Scheme 4).[87]

The oleochemicals mentioned above provide the basis for manufacturing a wide range of fat derivatives. The most important of these are listed in Table 10 (see overleaf).

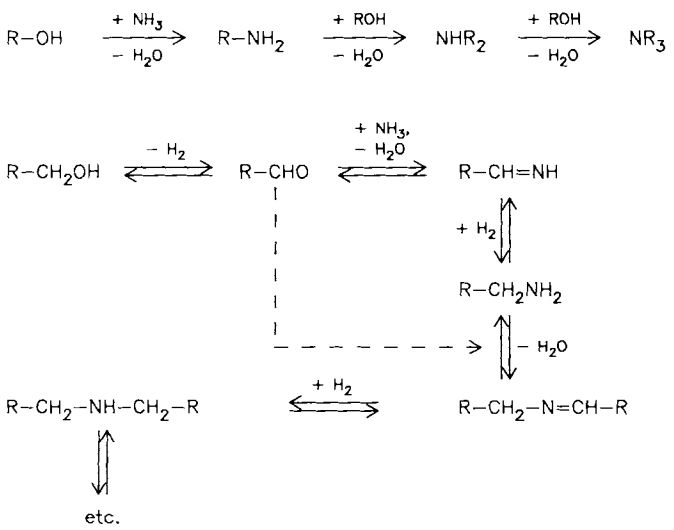

Scheme 4. Fatty amines from fatty alcohols.

4.2. Reactions Involving the Fatty Acid Hydrocarbon Chain

As has already been mentioned, in addition to reactions at the carboxy group, rearrangements in the hydrocarbon chain of fatty acids are becoming increasingly important in oleochemistry. Through these the spectrum of chemical products that are based on raw materials from renewable sources is being greatly widened. Table 11 (see overleaf) gives a survey of the many reactions that are possible, only a fraction of which have yet been studied scientifically. Of those reactions which have been investigated in detail, the following account includes only the ones of greatest importance in oleochemistry with indications concerning any still unresolved problems.

4.2.1. Reactions of Unsaturated Fatty Acid Chains

Because of their high reactivity the double bonds in unsaturated fatty acids offer a favorable position of attack for reactions in the fatty acid chain.

4.2.1.1. Hydrogenation

The nickel-catalyzed hydrogenation of the double bonded positions in unsaturated fatty substances is used extensively in industry to improve stability and color and to raise the melting point of unsaturated fat derivatives.[88,89]

The problem of achieving selective hydrogenation in unsaturated fatty acids with several double bonds has so far only been partly solved. An example is the conversion of linolenic **14** and linoleic acids **13** to oleic acid **3**, without unwanted positional or *cis-trans* isomerizations occurring at the same time. Heterogeneous metal catalysts whose use

Table 10. Important fat derivatives and products made from fatty acids contained in new oil-bearing plants.

Starting material	Reaction (Reactants)	Derivative
Fatty acids	Amidation (NH_3, alkanolamines)	Fatty acid (alkanol)amides
	Esterification (long-chain alcohols, glycerol, polyols)	Fatty acid esters ("wax esters", partial glycerides, polyolesters)
	Ethoxylation, propoxylation	Fatty acid polyglycol esters
Fatty acid methyl esters	Amidation (NH_3, alkanolamines)	Fatty acid (alkanol)amides
	Ester rearrangement (long-chain alcohols, glycerol, polyols)	Fatty acid esters ("wax esters", partial glycerides, polyesters)
Fatty alcohols	Ethoxylation, propoxylation	Fatty alcohol polyglycol ethers [a]
	Formation of sulfates	Fatty alcohol sulfates
	Production of phosphates (P_2O_5 or (poly-)phosphoric acid)	Alkyl phosphates
Fatty amines	Ethoxylation, propoxylation	Fatty amine polyglycol ethers
	Alkylation (CH_3Cl or dimethyl sulfate)	Quaternary ammonium compounds
	Alkylation ($ClCH_2COOH$)	Betaines (amphoteric surfactants)
	Oxidation	Fatty amine oxides

[a] Products: Sulfation to fatty alcohol polyglycol ether sulfates; reaction with P_2O_5 or (poly-)phosphoric acid to give fatty alcohol polyglycol ether phosphates; reaction with $ClCH_2COOH$ to give alkyl ether carboxylic acids; reaction with alkyl chlorides to give polyalkylene glycol dialkyl ethers.

is preferred in technical processes have not yet led to satisfactory results.[90,91] Homogeneous catalysts based on complexes of precious metals could offer a solution to the problem, if a method could be found for recovering and recycling these expensive catalysts. Possibilities which have been investigated are immobilization of the homogeneous catalyst on a support or the use of microdispersed catalyst systems such as colloids, clusters, or soluble polymer chelates; the last of these seems to offer good prospects.[92]

The olefin reactions that are described in the following sections are found to proceed with little or no formation of by-products only if starting materials of technically consistent quality are available including sufficiently pure oleic acid obtained by optimal selective hydrogenation. Oleic acid which is obtained from fatty acid mixtures by physical separation methods[93,94] contains only about 70% of *cis*-9-octadecenoic acid.

An alternative method for producing pure alkenecarboxylic acids is by catalytic dehydrogenation of saturated fatty acids. However, no suitable process has yet been developed for carrying this out on an industrial scale. Biotechnology may provide a solution to this problem.

The selective dehydrogenation of saturated fatty acids could extend the spectrum of available unsaturated fatty acids beyond the narrow range occurring naturally (mainly C_{18} and C_{22} acids) thereby providing a broader foundation for olefin chemistry based on syntheses from alkenecarboxylic acids.

Table 11. Reactions of unsaturated and saturated fatty acid chains.

Type of reaction	Reaction products	Topics for further research
Unsaturated chain:		
Hydrogenation	Saturated fatty acids	Selective hydrogenation of fatty acids with several double bonds
Epoxidation	Epoxyacids	—
Hydroformylation	Aldehyde carboxylic acids	Improving selectivity and linearity
Hydrocarboxylation	Dicarboxylic acids	Improving selectivity and linearity
Koch synthesis	Highly branched dicarboxylic acids	—
Metathesis	Mono- and dicarboxylic acids	Catalyst optimization, increasing the proportion of substrate to catalyst
Oxidative scission	Mono- and dicarboxylic acids	Oxidizing agents other than ozone
Diels-Alder reaction	Cyclic di- and tricarboxylic acids	Use of non-activated dienophiles
Ene reaction	Branched di- and tricarboxylic acids	Use of non-activated enophiles
Ane reaction	Branched fatty acids	Not yet investigated for fatty acids
Dimerization	Long-chain di- and tricarboxylic acids	Catalyst optimization, elucidation of the reaction mechanism and structure of reaction products
Scission of ricinoleic acid		Access to other fatty acids with the β-hydroxyalkene structure
- by alkalis - thermally	Sebacic acid, 2-octanol 10-Undecenoic acid, n-heptanal	
Hydrozirconation	ω-Substituted fatty acids	Optimization of catalyst system
Saturated chain:		
Chlorination	Chloroacids	(Regio-)selectivity
Sulfochlorination	Sulfoacids	(Regio-)selectivity
Sulfoxidation	Sulfoacids	(Regio-)selectivity
Catalytic oxidation	Hydroxyacids, oxoacids	Reaction so far unsuccessful
Catalytic dehydrogenation	Unsaturated fatty acids	
Sulfonation	α-Sulfoacids	—
Guerbet reaction	α-Alkylalkanols	Optimization of the catalyst
Claisen condensation	α-Alkyl-β-oxoesters	—

4.2.1.2. *Oxidative Scission*

The double bond in unsaturated fatty acids provides a point of attack for oxidative scission. In the ozonolysis of unsaturated fatty acids, which is a highly selective reaction, ozonides are formed initially.[95] These can undergo scission either reductively to mono- and dialdehydes, or oxidatively to mono- and dicarboxylic acids.[96]

By the oxidative route, oleic acid **3** gives nonanoic acid (pelargonic acid) and nonane-1,9-dioic acid (azelaic acid **21**, n = 7), while erucic acid **15** gives pelargonic acid and brassylic acid (tridecane-1,13-dioic acid) **21**, n = 11 (Scheme 5). Petroselinic acid **12**, which constitutes about

80% of coriander oil (see Section 3.3.2), can be split by this route to give lauric acid and adipic acid.[97]

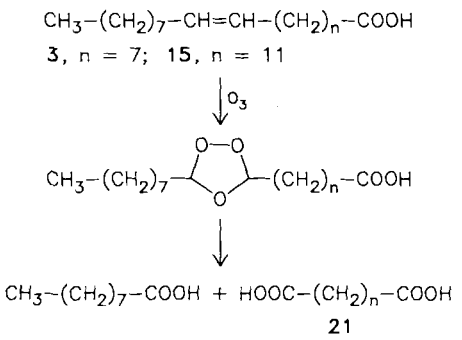

Scheme 5. Ozonolysis of unsaturated fatty acids (**3**: oleic acid; **15**: erucic acid).

The only industrial application of ozonolysis up to now is in the large scale production of azelaic acid from oleic acid;[98] azelaic acid is used in the textile fiber and plastics industries. Wider use of ozonolysis is still hindered by a number of technical and economic problems. Although some important advances have been made in this respect in recent years,[96] the alternative processes which have so far been investigated, involving diols or hydroxyoxo acids as intermediates have not succeeded in replacing the ozonolysis route.[99-101] Metal complex catalyzed direct oxidation methods, using ruthenium complexes for example, offer another possible approach to this problem.[101]

4.2.1.3. Epoxidation

Epoxidation is one of the most important addition reactions occurring at the double bond in unsaturated fatty compounds. The best method for unsaturated fatty acid esters is the *in situ* performic acid process. Scheme 6 shows

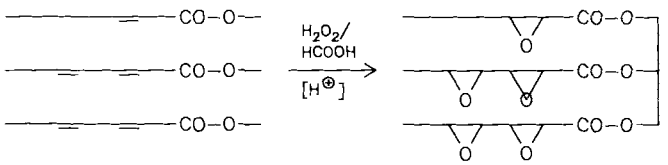

Scheme 6. Epoxidation of unsaturated fatty materials.

the application to a triglyceride. Methyl oleate is allowed to react in an analogous fashion to this to give 9,10-epoxystearic acid methyl ester.[102] The oxirane groups in epoxidated fatty compounds react readily with nucleophilic reagents. Opening up the epoxide ring leads to a large number of products, as summarized in Table 12. In particular, detailed studies have been carried out on ring opening in epoxyesters of fatty acids and in epoxyalcohols using mono-alcohols or polyols; by means of these reactions a wide range of alkoxy alcohols (fatty ether alcohols) and corresponding polyols can be synthesized. These are especially suitable for manufacturing polyurethane foams and molding resins with interesting properties for technological applications.[103]

Table 12. Reactions possible with fatty acids having an epoxy group.

HX	Name of partial structure
H_2	Alcohol
H_2O	Diol
ROH	Alkoxy alcohol ("ether alcohol")
RCOOH	Hydroxy ester ("ester alcohol")
$RCONH_2$	*N*-hydroxyalkylamide
H_2S	Mercapto alcohol
R_2NH	Amino alcohol
HCN	Hydroxynitrile
HCl	Chlorohydrin
$NaHSO_3$	Sodium hydroxysulfonate

4.2.1.4. Carboxylation

The three types of reactions which are most suitable for the addition of carbon monoxide at the double bond in unsaturated fat derivatives are hydroformylation (oxo synthesis),[80] hydrocarboxylation (Reppe reaction)[80, 104, 105] and the Koch synthesis (Scheme 7).[80]

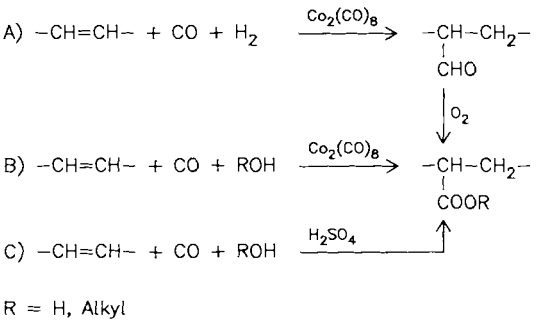

Scheme 7. Production of carboxylic acids by carbonylation reactions. A: hydroformylation with oxidation; B: hydrocarboxylation; C: Koch reaction.

Hydroformylation using transition metal complexes forms a formyl group which can then be hydrogenated to give a hydroxy group or oxidized to a carboxy group. In protonic solvents such as water or methanol, the carbonyl group is added as a carboxy function. By this hydrocarboxylation reaction, carboxylic acids or their derivatives are formed.[80, 106] Hydroformylation and hydrocarboxylation are catalyzed by $Co_2(CO)_8$ and carbonyl hydrides of metals of the eighth subgroup. These catalysts favor isomerization at the double bond. Because of this, the products of this reaction are mixtures of the various chain positional isomers. However, these reactions can be controlled by the addition of suitable complex ligands. Thus, for example, methyl oleate reacts with carbon monoxide and water in the presence of rhodium triphenylphosphane to give exclusively products hydroformylated at the 9 and 10 positions[107, 108], whereas hydrocarboxylation of the methyl esters of oleic or erucic acids using cobalt/4-picoline as the catalyst yields up to 50-60% of linear C_{19} or C_{23} dicarboxylic acid diesters (Scheme 8).[109] In the Koch synthesis, strong acids are used as catalysts. The carbonium ions formed as the primary reaction products isomerize very rapidly, with the results that the carbon chain undergoes

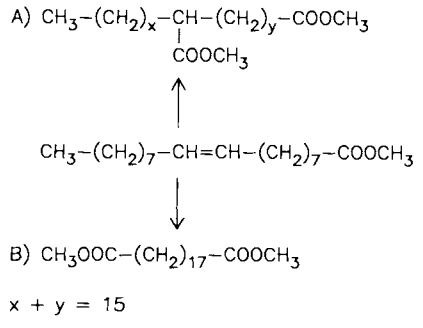

Scheme 8. Hydrocarboxymethylation of methyl oleate. A: in the presence of rhodium/triphenylphosphane. B: in the presence of cobalt/4-picoline.

rearrangement, yielding a mixture of isomers with a high proportion of α-branched dicarboxylic acids.[80]

4.2.1.5. *Olefin Metathesis*

Olefin metathesis is a bond rearrangement reaction catalyzed by certain transition metal compounds (molybdenum, tungsten or rhenium).[110] The reaction can also be applied to unsaturated fatty acid esters.[111] The self-metathesis of methyl oleate, carried out by means of the catalyst system tungsten(VI) chloride/tetramethyltin results in the highly selective formation of 9-octadecene **22** and 9-octadecene-1,18-dicarboxylic acid dimethyl ester **23**, in an equilibrium mixture with the starting ester (Scheme 9). Co-

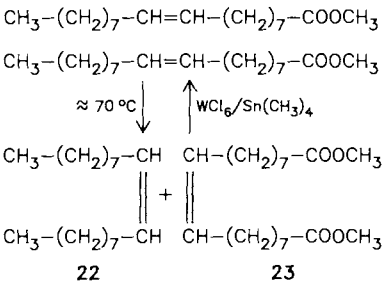

Scheme 9. Self-metathesis of methyl oleate.

metathesis of the methyl esters of oleic or erucic acids with short-chain olefins such as ethene or 2-butene results in the synthesis of unsaturated fatty acid methyl esters with chain lengths C_{10} to C_{15} and the corresponding olefins (Scheme 10).[112] Industrial application of this interesting oleochemical reaction path is at present still hindered by the poor efficiency of the expensive catalyst. At present the

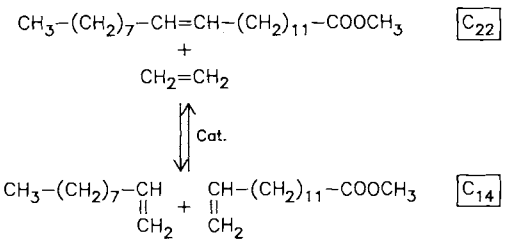

Scheme 10. Metathesis of erucic acid methyl ester and ethene. Cat. = catalyst (see text).

conversion of 150 mol of ester needs 1 mol of the tungsten compound used as catalyst. For this reason it is essential to look for new catalyst systems which are more effective.

4.2.1.6. *Diels–Alder and Ene Reactions*

Addition reactions of isolated and conjugated double bond systems are also often used for introducing ring systems or alkyl branching groups into fatty acids. Unsaturated fatty acids with two double bonds, such as linoleic acid **13**, undergo Diels–Alder reactions with appropriately substituted dienophiles after isomerizing to a conjugated fatty acid. Thus, isomerized linoleic acid, at temperatures above 100 °C, forms adducts with maleic anhydride, fumaric acid, acrylic acid and other dienophiles with activated double bonds (Scheme 11).[113–118] In order to synthe-

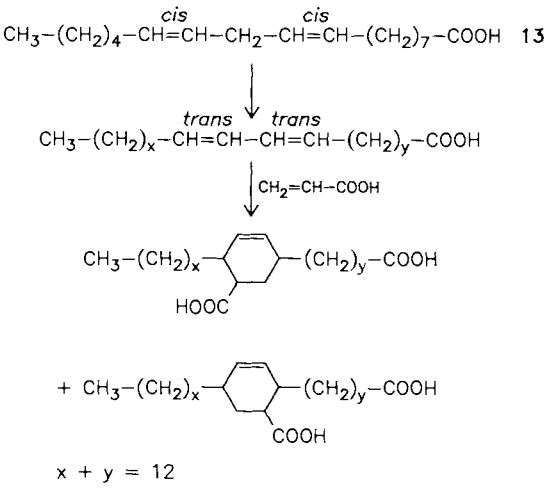

Scheme 11. Diels–Alder reaction of isomerized linoleic acid ("conjugated fatty acid") and acrylic acid.

size Diels–Alder adducts the conjugated double bonds must be in the *trans,trans* form.[119] The desired configuration of the double bonds can be induced by means of an isomerization catalyst, e.g. iodine or sulfur.

Unsaturated fatty acids such as oleic acid can undergo an ene reaction at temperatures above 220 °C with maleic anhydride or other compounds having activated double bonds (Scheme 12).[120, 121] It is suitable for introducing

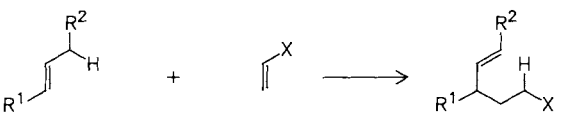

Scheme 12. Ene reaction of oleochemical compounds.

side chains containing hetero functions such as –COOR or –CN into unsaturated fatty compounds with retention of the double bond shifted across a carbon atom. Only a few examples are known so far of Diels–Alder and ene reactions of unsaturated fatty acids with unactivated dienophiles and enophiles.

4.2.1.7. *Fatty Acid Dimerization*

C_{18} fatty acids with one or more double bonds undergo dimerization at 210–250°C in the presence of layer silicate catalysts such as montmorillonite, giving a complex mixture of C_{36} dicarboxylic acids (Scheme 13).[122] This fatty

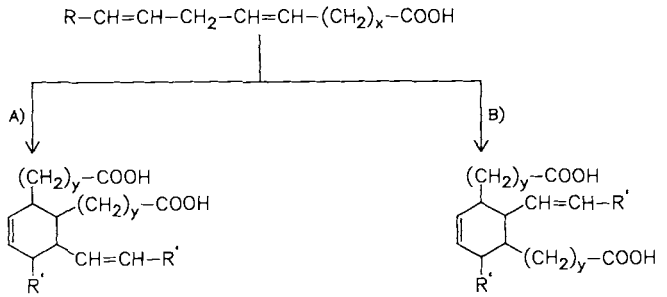

Scheme 13. Dimerization of C_{18} fatty acids by Diels–Alder reaction, schematic. For conditions see text. A: head/head reaction; B: head/tail reaction. In the products $y = x$, $R' = RCH_2$ or $y = x + 1$, $R' = R$.

acid dimerization is assumed to result from a Diels–Alder addition of oleic acid to linoleic acid. The conjugate linoleic acid dimerizes with formation of a cyclohexene ring. However, from the fact that acyclic aliphatic structures also appear it can be inferred[123] that ene reactions and reactions through carbocation intermediates also occur. An industrially important application of dimer acids is the manufacture of hot melts, printing inks and curing agents for epoxy resins.

4.2.1.8. *Free Radical Reactions*

Alkanes add to olefins at temperatures of about 400°C in a thermally initiated free radical reaction, e.g. cyclohexane adds to acrylic acid esters or to 1-octene (Scheme 14).[124, 125] This "direct substituting addition" reaction

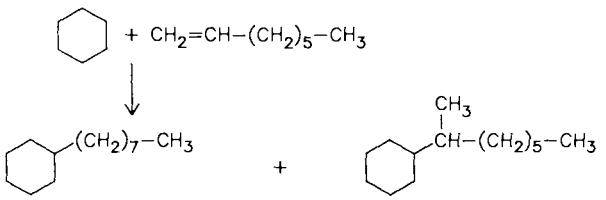

Scheme 14. "Ane reaction" of cyclohexane with 1-octene. By-products are 2-, 3-, and 4-octene.

is called an "ane reaction" by analogy with the ene reaction to which it is related. Its extension to fatty acids offers a potentially interesting topic for research.

4.2.1.9. *Scission and Rearrangement Reactions*

The β-hydroxyalkene structure exemplified by *cis*-12-hydroxy-9-octadecenoic acid (ricinoleic acid) **24**, which is the principal fatty acid in castor oil, can undergo a variety of scission and rearrangement reactions. Heating ricinoleic acid to 250–280°C with excess alkali under oxidizing conditions in the presence of catalytic amounts of calcium or lead compounds causes scission, with formation of sebacic acid (decane diacid) and 2-octanol (Scheme 15).[126–129] Sebacic acid is an important starting material in the manufacture of plasticizers, lubricants, polyesters, and polyamides.

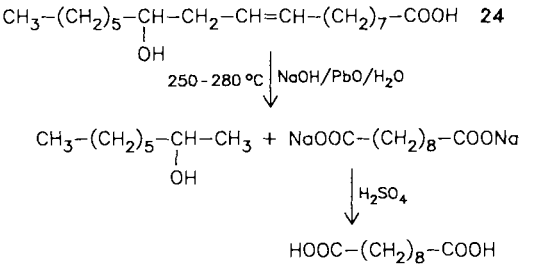

Scheme 15. Synthesis of sebacic acid by alkaline cleavage of ricinoleic acid **24**.

Thermal scission of ricinoleic acid methyl ester at 500–600°C produces 10-undecenoic acid (undecylene acid) **25** and heptanal (enanthaldehyde) (Scheme 16).[130] This scission reaction is of general validity for β-hydroxyolefins in which the OH group is free to interact unhindered with the π-electrons of the double bond. 10-Undecenoic acid is valuable as a starting material for the manufacture of Nylon 11 ("Rilsan") which proceeds via 11-bromoundecanoic acid and 11-aminoundecanoic acid as intermediates.[131]

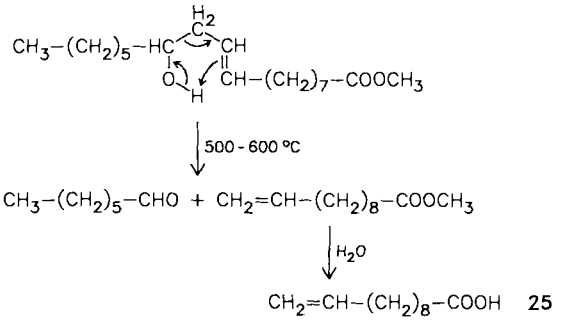

Scheme 16. Synthesis of 10-undecenoic acid **25** by thermal cleavage of methyl ricinoleate.

Ricinoleic acid undergoes rearrangement at 250°C over a palladium contact catalyst to give 12-oxostearic acid by shifting of the double bond and the formation of an enol structure as an intermediate.[132] In the presence of manganese salts as catalysts, 12-oxostearic acid can be made to undergo oxidative scission to mono- and dicarboxylic acids.[133]

4.2.2. *Substitution Reactions in the Alkyl Chain of Saturated Aliphatic Fatty Acids*

Whereas in unsaturated fatty acids the double bonds, because of their high reactivity, allow specific reactions to be carried out on the fatty acid hydrocarbon chain, this is not the case for saturated fatty acid chains. Here the methylene groups—apart from that at the α position—have

little reactivity and the differences in reactivity from one methylene group to another are small. Consequently, the substituents that are introduced are randomly distributed along the entire fatty acid chain. Substitution reactions of this type include the free radical chlorination, sulfochlorination and sulfoxidation of fatty acids and their esters.

The light-induced chlorination of fatty acids and fatty acid esters leads to an essentially uniform distribution of chlorine substituents in the methylene groups of the fatty acid chain. However, α and ω substitutions occur only to a small extent or not at all.[134] The same is also true for the sulfochlorination (reaction with sulfur dioxide and chlorine leading to the introduction of SO_2Cl groups)[135] and the sulfoxidation of fatty acids and fatty acid esters (reaction with sulfur dioxide and oxygen with introduction of SO_3H groups).[136, 137]

Success in finding methods for carrying out selective substitution reactions on the alkyl chain of fatty acids would considerably widen the spectrum of compounds available through fats chemistry and with it the range of uses. Possibilities to be considered include electrostatic alignment of reagent molecules relative to protonated fatty acid molecules[138-143] and partial shielding by adsorption on inert surfaces or retention in zeolites.[143]

Except for α substitution, which can be achieved easily, only a few starting points have so far been found which offer approaches to selective substitution.[138-146] The utilization of a strongly acidic medium and the addition of a free radical trapping agent have the effect of directing chlorination predominantly into the α position.[147] This reaction is an extension of the well-known Hell-Volhard-Zelinsky reaction for α-bromination of fatty acids. Adsorbing fatty acids on aluminum oxide produces an orientation of their molecules resulting in preferential chlorination at the last and penultimate carbon atoms of the fatty acid chain.[141, 142] The chlorination of fatty acids by *N*-haloamines using a free radical initiator occurs with high selectivity at the penultimate carbon atom of the fatty acid chain.[138, 148-152] Specific substitution at the end carbon atom can also be achieved by hydrozirconation.[153] In this reaction, zirconium hydrides in the form of complexes are added at the double bond position of unsaturated fatty acids; by a repeated process of elimination and reattachment of the zirconium hydride, the zirconium substituent migrates to the ω position, where it can be replaced by any desired electrophilic reagent.[154]

Substitution of saturated fatty acids and fatty acid esters at the α position is, by contrast, relatively easy and specific. Some examples of this are the following:

- The ionic sulfonation of fatty acid methyl esters using SO_3, leading to α-sulfonated esters ("ester sulfonates") (Scheme 17A).[155-157] Ester sulfonates represent an oleochemical alternative to the petrochemicals-based surfactant alkylbenzene sulfonate.
- The Guerbet reaction,[158, 159] i.e. the alkali-catalyzed self-condensation of two molecules of a fatty alcohol to form a molecule of an α-alkyl branched dimeric alcohol (the Guerbet alcohol). This reaction probably takes place via an aldol condensation of the aldehyde formed as an intermediate (Scheme 17B).[160]
- The Claisen condensation of two molecules of a fatty acid methyl ester, which leads to the formation of an α-alkyl-β-oxoester of the fatty acid (Scheme 17C).[161]

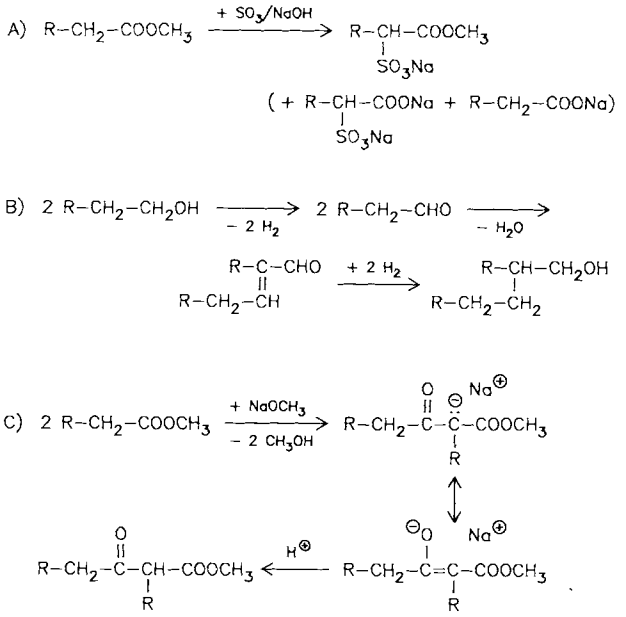

Scheme 17. Reactions of the saturated fatty acid chain: A: sulfoxidation; B: Guerbet reaction; C: Claisen condensation of fatty acid methyl esters.

Most of the reactions discussed in this connection are typical of those on which industrial oleochemistry is based. Reactions such as these are essential for the manufacture of chemical products from renewable raw materials.

4.3. Biologically Catalyzed Reactions

Biochemical reactions provide pathways for carrying out already known chemical rearrangements such as hydrolysis or esterification under mild conditions, thus saving energy and preventing the products from thermal deterioration. Additionally, biochemical processes give rise to possibilities for the manufacture of new oleochemical products.

4.3.1. Reactions Involving the Ester Group

During the past few years the applications of enzymatic catalysis and bioreactor technology to the basic reactions of oleochemistry, namely hydrolysis, esterification and transesterification have been intensively studied.[162, 163]

As is predicted by thermodynamic calculations, the hydrolysis of triglycerides has an exceptionally small reaction enthalpy with the result that the splitting of fat as an equilibrium reaction (Scheme 1) is easily reversed under suitable reaction conditions to ester synthesis or transesterification.[164] Such reactions are catalyzed by enzymes of the ester hydrolases class (E.C. 3.1.1), namely the lipases. The enzymes act preferentially on substrates insoluble in water, so that the reaction occurs at the interface between the lipophilic and hydrophilic phases.[165]

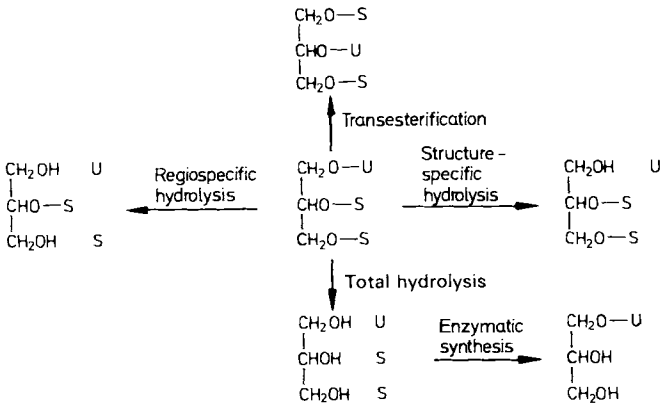

Fig. 9. Enzymatic fat splitting, transesterification, and ester synthesis. U = *cis*-9-alkenoic acid ("Δ^9-unsaturated fatty acid"), S = saturated fatty acid.

Lipases are technically available from animal, plant and microbial sources. They have different specificities with regard to the structure or chain length of the fatty acids undergoing splitting or esterification, or with regard to the position of the hydrolyzed or formed ester bond of the glycerol molecule[166, 167] (Fig. 9). They are therefore particularly suitable for the synthesis of optically active compounds and for isolating specific fatty acids. However, chemical reactions such as intramolecular exchange of acyl groups and the interfacial properties of the substrates and reaction products can interfere with these enzymatic specificities.

4.3.1.1. Enzymatic Splitting of Fats

It was suggested as long ago as the beginning of this century that castor bean seeds might be used industrially for the hydrolysis of fats and oils.[168] It is only recently, however, that interest has again grown in the lipase-catalyzed splitting of fats.[162]

A lipase for use in an industrial splitting process should act nonselectively on the ester bonds in the triglyceride causing hydrolysis of each of them with approximately equal reaction rates. Furthermore, it should be thermally stable. An enzyme which meets these requirements quite well is obtained from *Candida cylindracea*. Other lipases suitable for this purpose, with particular regard to their thermal stability, have been investigated.[169]

Various experimental reactor devices for the enzymatic splitting of fats have been described such as stirred tank reactors,[162] tubular reactors,[170] and membrane reactors.[171] Approximate cost calculations for a stirred tank reactor process show that the catalyst accounts for the greatest share of the costs. The product-specific costs of the catalyst can be considerably reduced by using more efficient manufacturing techniques and by stabilization and recovery of the lipase after the reaction. Even so, enzymatic splitting of fats cannot yet compete with conventional methods, despite the possibility of saving energy.

Enzymatic processes can be expected to show the greatest advantage when a complete breakdown of the material is not necessary or when the objective is to produce special fatty acids making use of the specificity or selectivity of lipases. In Japan, about 8000 tonnes of fatty acids have been produced enzymatically each year since 1983 for the manufacture of soap. A process which has been used in Japan since 1985 for producing unsaturated fatty acids on a tonnage scale with a purity of up to 99% combines enzymatic splitting with special procedures for product recovery.[172] The highly purified fatty acids are under investigation for applications in the cosmetic, pharmaceutical, and electronic fields.

4.3.1.2. Transesterification

In contrast to chemical methods, the use of lipases with regiospecificity for the 1 and 3 positions allows defined exchanges of the fatty acids in triglycerides. By this means, fats with a specified melting behavior can be synthesized, as is required for the manufacture of cocoa butter substitutes, margarine, butterfat and cooking fat.[173, 174] It is also possible to increase the half-life of the enzymes by immobilization techniques, thus reducing catalyst costs.[175]

4.3.1.3. Ester Synthesis

The reversibility of the enzyme-catalyzed hydrolysis of fats was demonstrated as early as 1900 by esterifying butyric acid and ethanol with a lipase-containing pancreas extract.[176] There has been further detailed development work on the enzymatic synthesis of esters during the past two decades. The ability of the various lipases to catalyze esterification reactions varies very widely for different reactants.[163, 177] Whereas tertiary alcohols and sugar alcohols undergo little or no reaction, it has been possible to synthesize the corresponding esters from many different terpene alcohols, giving products which are important in perfumery. The esterification of 2-methylpentanoic acid with prenyl alcohol has been found to give 98% conversion (Scheme 18). Enzymatic syntheses of wax-type esters and ester oligomers from dicarboxylic acids and diols also gave up to 90% conversion.[178] Sugar esters can also be obtained by enzymatic catalysis in aqueous and organic media. They are used as emulsifiers for foodstuffs.[179, 180]

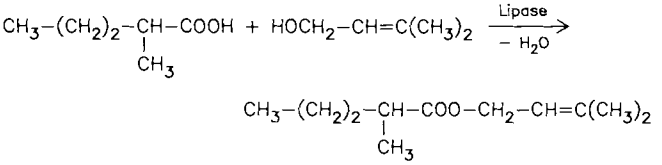

Scheme 18. Lipase-catalyzed synthesis of 2-methylpentanoic acid prenyl ester.

In recent years, the synthetic potential of lipases has been broadened by using them in non-aqueous and nonpolar solvents. They are increasingly used for synthesizing chiral esters (Scheme 19),[181, 182] which are potential intermediates for fine chemicals and pharmaceuticals.

Another possible area of application for lipase-catalyzed esterifications is in the production of pure monoglycerides, which are important emulsifiers and stabilizers used in foodstuffs, pharmaceuticals and cosmetics.[183]

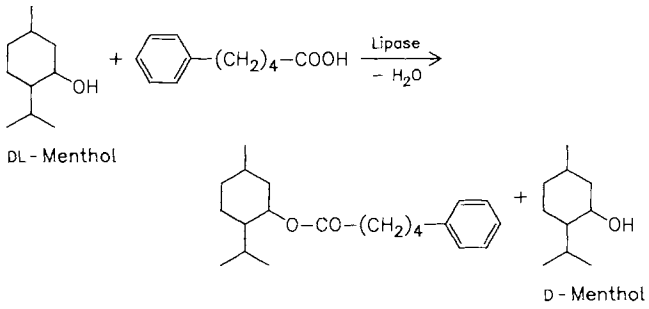

Scheme 19. Stereoselective esterification of DL-menthol with 5-phenylpentanoic acid: only L-menthol is converted into the ester. D-Menthol remains behind.

Of the several possible reaction pathways for obtaining fatty acid glycerides, namely the partial hydrolysis of triglycerides, the transesterification of triglycerides with alcohols, the glycerolysis of triglycerides and the synthesis from glycerol and fatty acids, only the last two are useful for preparing pure monoglycerides.[163] The main enzymatic method which has been studied is the esterification of fatty acids with glycerol. Continuous reaction in a membrane bioreactor using lipases adsorbed onto membranes gave mixtures of mono- and diglycerides.[184] A mixture of glycerides containing 95% of the monooleate and 5% of the dioleate was successfully synthesized in the presence of a lipase obtained from *Penicillium cyclopium* with 50% conversion of oleic acid.[185]

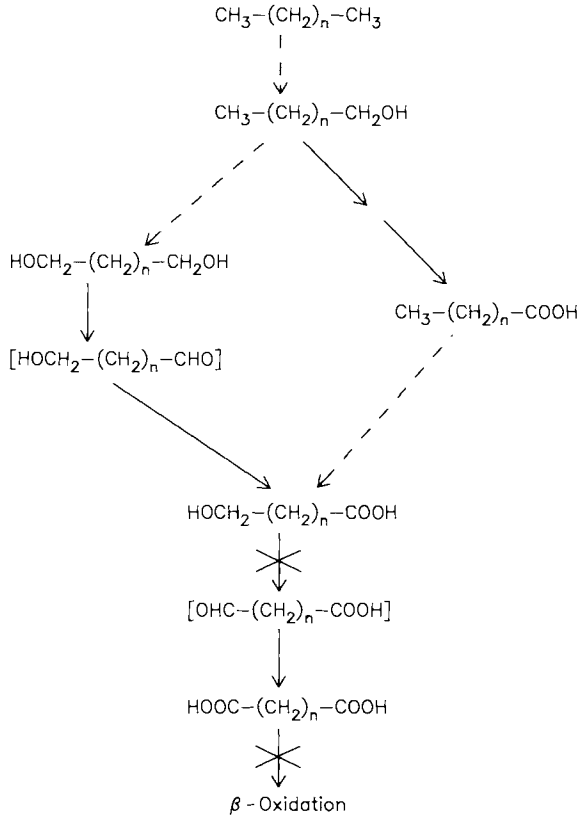

Scheme 20. Microbial transformation of alkanes to dicarboxylic acids [50]. Catalysis by oxygenases (---) or dehydrogenases (——); hypothetical intermediates in square brackets; x: block mutants of technical interest.

4.3.2. *Biotransformations of Fatty Acids*

Besides the reactions involving the carboxy group, biotechnical processes also open up possibilities for carrying out specific reactions at non-activated positions in the fatty acid chain. Here the biotechnological use of isolated enzyme systems is of only limited importance, owing to the complex structure of enzymic redox systems compared with hydrolytic systems.

4.3.2.1. *Oxidative Transformations*

Oxidation of fatty acids at the terminal position leads to dicarboxylic acids, which are technically important as monomers for polymer manufacture and as intermediates for making bleaching agents. The diterminal microbial oxidation of unbranched alkanes and alkenes to give mono- and dicarboxylic acids using bacteria and especially yeasts has been thoroughly investigated. The metabolic pathway of this transformation proceeds via fatty acids and ω-hydroxyacids as intermediates. Subsequently, breakdown of fatty acids by β-oxidation can occur (Scheme 20).[186]

Whereas it has been possible to obtain yields of dicarboxylic acids at concentrations up to 140 g/L of fermentation liquid from alkanes using yeast, the yields of dicarboxylic acids from fatty acids have been considerably less up to now.[188] In order to develop an economical process, whether by fermentation or in the bioreactor after immobilization of the cells, highly efficient microorganisms are required in which the ability to break down fatty acids by β-oxidation has been eliminated as far as possible. A fermentation process for producing tridecane-1,13-dioic acid (brassylic acid **21**, n = 11) by terminal oxidation of tridecane is already being used on an industrial scale in Japan.[189]

The oxidation reactions that are described below have not yet been carried out on a technical scale, but they indicate the potential of microbial fatty acid transformations. Subterminal oxidation of one or more of the methylene groups in *n*-alkanes gives secondary alcohols and the corresponding ketones, which then undergo further metabolization to fatty acids (Scheme 21). Transformations of this kind have been described for a wide variety of bacteria, yeasts and molds.[190]

Hydroxylation as the initial enzymatic step can be catalyzed in these reactions as in terminal oxidation by monooxygenases, which are enzyme systems based on cytochrome P450.[186] Hydroxylation can also be achieved by addition of water to double bonds. Such reactions using various bacteria under anaerobic conditions have been described for Δ^9-unsaturated fatty acids and fatty alcohols.[191–193]

Unsaturated fatty acids containing a *cis,cis*-1,4-pentadienyl group undergo specific oxidation by the enzyme lipoxygenase, with a regiospecificity and/or stereospecificity which differs according to the source of the enzyme, in the presence of oxygen, to yield *cis,trans* conjugated monohydroperoxides (Scheme 22).[194, 195] The compounds thus obtained lead in turn to a range of further products and

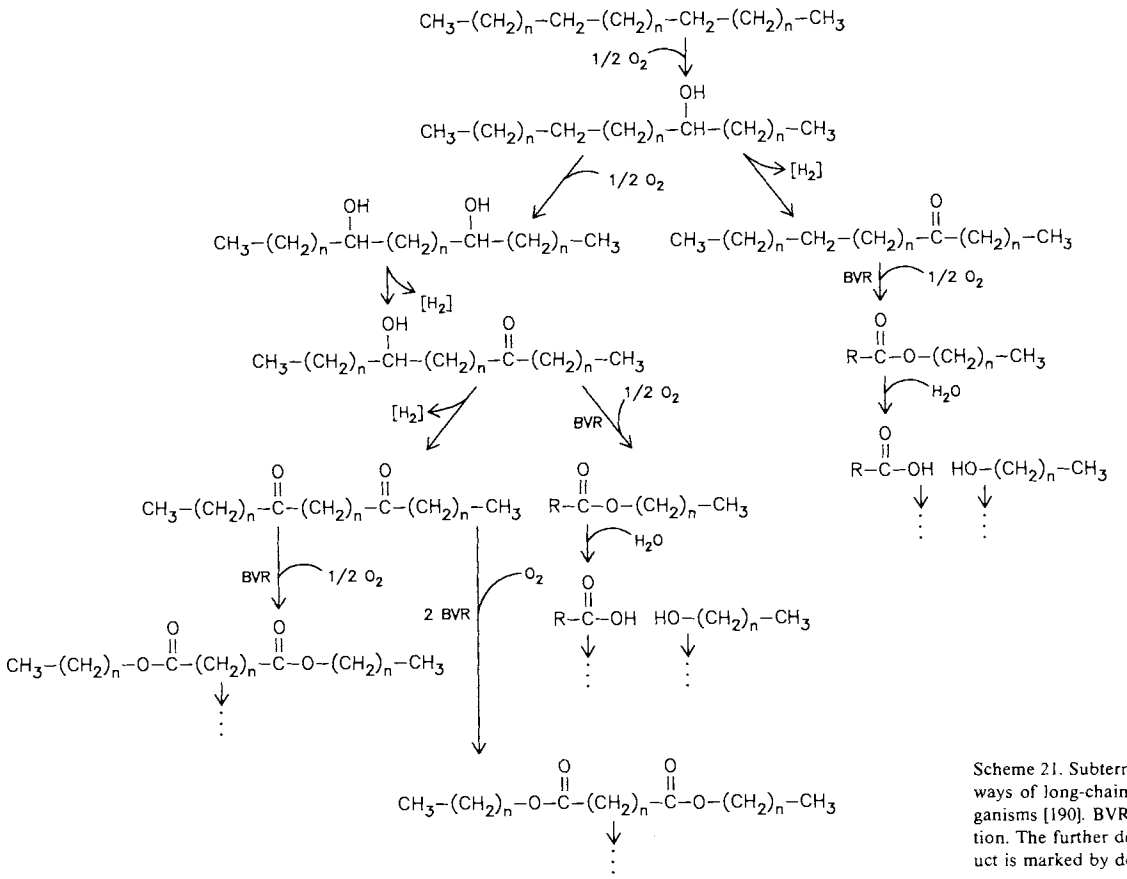

Scheme 21. Subterminal degradation pathways of long-chain *n*-alkanes by microorganisms [190]. BVR = Baeyer-Villiger reaction. The further degradation of the product is marked by dots.

are of considerable interest for synthesizing prostaglandins and prostaglandin precursors.[196-198] The lipoxygenase for such reactions can be provided either as the crude product obtained by roasting soybean meal or as the immobilized enzyme.[199]

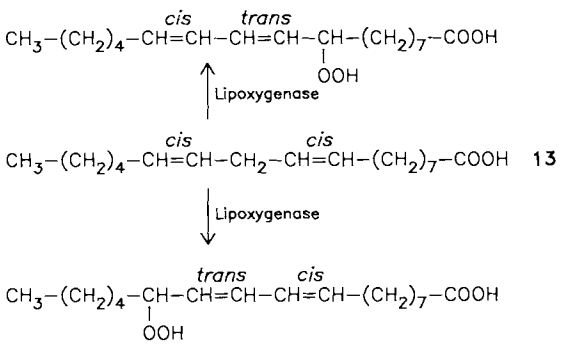

Scheme 22. Oxidation of linoleic acid **13** by lipoxygenase. The product composition—9- and/or 13-hydroperoxide—varies with the source of the enzyme.

Desaturation of fatty acids in microorganisms and in higher organisms has been investigated in detail.[200] In eukaryotic organisms, the reaction is catalyzed by a membrane-associated enzyme system.[201]

4.3.2.2. *Reductive Transformations*

Fatty alcohols are widely distributed in nature as components of waxes. Their biosynthesis involves the reduction of activated fatty acids in several steps by cofactor-dependent enzyme systems which are usually attached to membranes.[202] Consequently, technical processes for the bioreduction of fatty acids to fatty alcohols can only be carried out using intact microorganisms, as it is still uneconomic at present to use isolated enzymes for complex reaction sequences with the necessary regeneration of cofactors. A quantitative study of the use of enriched isolated enzyme material derived from various microorganisms and plants indicated that the biochemical potential of this conversion process is probably insufficient.[50]

The hydrogenation of unsaturated fatty acids using anaerobic microorganisms has only been demonstrated qualitatively in most cases so far.[203] Linoleic acid has been converted to *trans*-11-octadecenoic acid using several different bacterial strains.[204] By using a rumen bacterium, linolenic and linoleic acids were converted to *cis*-15-octadecenoic acid and stearic acid respectively, with yields of 85%.[205] Up to now there has been little or no investigation of the enzyme systems involved.[206]

4.3.3. *Biotransformations of Other Fat Components*

Biotransformations of glycerol, the co-product from the splitting and transesterification of fats, and the use of sterols which occur as minor components of fats with considerable economic potential, will be only briefly discussed here.

4.3.3.1. Glycerol

Glycerol can often replace glucose or other carbohydrates as a carbon and energy source in fermentation processes. Numerous fermentation products obtained from glycerol have been reported, such as bioemulsifiers,[207] flocculating agents,[208] and celluloses.[209]

Glycerol has been converted on a laboratory scale into various products of higher added value such as dihydroxyacetone,[210] glycerol-2,3-dihydroxypropylaldehyde,[211] 1,3-propanediol,[212] 3-hydroxypropylaldehyde and 3-hydroxypropionic acid[213] using in some cases bioreactors with immobilized cells.[214] For dihydroxyacetone yields of up to 149 g per liter of culture medium have been reported.

4.3.3.2. Sterols

Sterols are obtained from oils and fats used in industry, which contain up to about 0.35% of sterols.[215] With an annual consumption of 9.5 million tonnes of oils and fats in the chemical industry, the potential supply of raw materials in the form of sterols is therefore about 33 000 tonnes. Sterols are used mainly in manufacturing steroid derivatives, especially corticosteroids, for pharmaceutical purposes.[216-223]

5. Future Prospects

Oils and fats of plant and animal origin offer possibilities for providing chemistry with a wealth of reaction products which will be of great value in the future. Successful applications in this field will reduce the present over-dependence on petrochemical feedstocks and will give rise to new synthetic routes. The chemical possibilities of renewable oils and fats are still very far from being fully exploited. Interdisciplinary collaboration involving chemistry, biotechnology, plant breeding and agriculture is necessary to extend the successful applications of this technology.

The authors wish to acknowledge the contributions by Dr. G. Lück, Mr. K. Siekmann, and Dr. K. Schumann to this work.

Received: July 16, 1987 [A 645 IE]
German version: *Angew. Chem. 100* (1988) 41
Translated by Dr. *J. K. Becconsall*, Northwich (UK)

[1] *Official Bulletin, EG, No. 121/5* May 20, 1980.
[2] S. A. Graham, F. Hirsinger, G. Röbbelen, *Am. J. Bot. 68* (1981) 908.
[3] P. Pohl, H. Wagner, *Fette, Seifen, Anstrichm. 74* (1972) 424, 541.
[4] G. Grimmer, J. Jacob, D. Düvel, *Beitr. Biol. Pflanz. 46* (1969) 223.
[5] D. B. Fowler, R. K. Downey, *Can. J. Plant Sci. 50* (1970) 233.
[6] G. Röbbelen, W. Thies in S. Tsunoda, K. Hinata, C. Gomez-Campo (Eds.): *Brassica Crops and Wild Allies*, Japan Science Society Press, Tokyo 1980, p. 253.
[7] D. G. Dorrel, R. K. Downey, *Can. J. Plant Sci. 44* (1964) 499.
[8] G. N. Fick, *J. Am. Oil Chem. Soc. 60* (1983) 1252.
[9] G. N. Fick, US-Pat. 4627192 (1986), Sigco Research.
[10] I. A. Wolff, Q. Jones, *Chemurg. Dig. 17* (1958) 4.
[11] L. H. Princen, *Econ. Bot. 37* (1983) 478.
[12] T. L. Wilson, T. K. Miwa, C. R. Smith, *J. Am. Chem. Soc. 37* (1960) 675.
[13] F. Hirsinger, *Fette, Seifen, Anstrichm. 82* (1980) 385.
[14] F. Hirsinger, *J. Am. Oil Chem. Soc. 62* (1985) 76.
[15] A. E. Thompson, *Hort. Science 19* (1984) 352.
[16] M. Calvin, *Naturwissenschaften 67* (1980) 525.
[17] L. Ayerbe, J. L. Tenorio, P. Ventas, E. Fuenes, L. Mellado, *Biomass 4* (1984) 283; *5* (1985) 37.
[18] W. Hondelmann, W. Radatz, *Fette, Seifen, Anstrichm. 84* (1982) 73.
[19] H. Meyer zu Beerentrup, *Dissertation*, Universität Göttingen 1986.
[20] G. D. Jolliff, I. J. Tinsley, W. Calhoun, J. M. Cranee, *Oregon Agricultural Experimental Station Bulletin 648*, Corvallis 1981.
[21] G. D. Jolliff, W. Calhoun, J. M. Crane, *Crop Sci. 24* (1984) 369.
[22] R. K. Downey, *J. Am. Oil Chem. Soc. 48* (1971) 718.
[23] H. J. Nieschlag, I. A. Wolff, *J. Am. Oil Chem. Soc. 48* (1971) 723.
[24] K. J. Lessman, W. P. Anderson in W. R. Fehr, H. H. Hadley (Eds.): *Hybridization of Crop Plants*, American Society of Agronomy, Crop Science Society of America, Madison, WI (USA) 1980, p. 339.
[25] D. M. Yermanos (Ed.): *Proceedings of the 3rd International Conference on Jojoba*, University of California at Riverside 1978, p. 387.
[26] a) I. K. Vasil (Ed.): *Cell Culture and Somatic Cell Genetics of Plants, Vol. 1*, Academic Press, New York 1984; b) F. Constabel in [26a], p. 27.
[27] H. Binding, G. Krumbiegel-Schroeren in [26a], p. 43.
[28] P. Eckes, G. Donn, F. Wengenmeyer, *Angew. Chem. 99* (1987) 392; *Angew. Chem. Int. Ed. Engl. 26* (1987) 382.
[29] M. W. Fowler, *Prog. Ind. Microbiol. 16* (1982) 207.
[30] S. R. Singer, C. N. McDaniel, *Plant Physiol. 78* (1985) 411.
[31] L. H. Jones, *Biologist 30* (1983) 181.
[32] A. T. James, *AOCS Monogr. 11* (1984) 1.
[33] C. Ratledge, *Fette, Seifen, Anstrichm. 86* (1984) 379.
[34] O. L. Gamborg, P. J. Bottino, *Adv. Biochem. Eng. 19* (1981) 239.
[35] U. Zimmermann, *Biochim. Biophys. Acta 694* (1982) 227.
[36] K. N. Kao, M. R. Michayluk, *Planta 120* (1974) 215.
[37] L. Menczel, K. Wolfe, *Plant Cell Rep. 3* (1984) 196.
[38] G. Melchers, M. D. Sacristan, A. A. Holder, *Carlsberg Res. Commun. 43* (1978) 203.
[39] Y. Y. Gelba, F. Hoffmann, *Planta 149* (1980) 112.
[40] I. Potrykus, R. D. Shillito, M. W. Saul, J. Paszkowski, *Plant Mol. Biol. Rep. 3* (1985) 117.
[41] J. P. Freeman, J. Draper, M. R. Davey, E. C. Cocking, K. M. A. Gartland, K. Harding, D. Pental, *Plant Cell. Physiol. 25* (1984) 1353.
[42] M. R. Davey, E. C. Cocking, J. Freeman, N. Pearce, J. Tudor, *Plant Sci. Lett. 18* (1980) 307.
[43] J. Takebe in [26a], p. 492.
[44] D. M. Shah, R. B. Horsch, H. J. Klee, G. M. Kishore, J. A. Winter, N. E. Tumer, C. M. Hironaka, P. R. Sanders, C. S. Gasser, S. Aykent, N. R. Siegel, S. G. Rogers, R. T. Fraley, *Science (Washington D.C.) 233* (1986) 478.
[45] L. Comai, D. Facciotti, W. R. Hiatt, G. Thompson, R. E. Rose, D. M. Stalke, *Nature (London) 317* (1985) 741.
[46] P. P. Abel, R. S. Nelson, B. De, N. Hoffmann, S. G. Rogers, R. T. Fraley, R. N. Beachy, *Science (Washington D.C.) 232* (1986) 738.
[47] V. C. Knauf, *Trends Biotechnol. 5* (1987) 40.
[48] P. K. Stumpf, *New Compr. Biochem. 7* (1984) 155.
[49] P. K. Stumpf, M. R. Pollard in J. K. G. Kramer, F. D. Sauer, W. J. Pigden (Eds.): *High and Low Erucic Acid Rapeseed Oils*, Academic Press, New York 1983, p. 131.
[50] R. D. Schmid, *Fette, Seifen, Anstrichm. 88* (1986) 555.
[51] H. Damm, *Chem.-Ztg. 67* (1943) 47.
[52] J. F. T. Spencer, D. M. Spencer, *Annu. Rev. Microbiol. 37* (1983) 121.
[53] C. Ratledge, *Prog. Ind. Microbiol. 16* (1982) 119.
[54] C. Ratledge, *AOCS Monogr. 11* (1984) 119.
[55] N. S. Shifrin, *AOCS Monogr. 11* (1984) 145.
[56] B. A. Glatz, E. G. Hammond, K. H. Hsu, L. Baehman, N. Bati, W. Bednarski, D. Brown, M. Floetenmeyer, *AOCS Monogr. 11* (1984) 163.
[57] J. Litchfield, *Adv. Appl. Microbiol. 22* (1977) 267.
[58] C. Ratledge, *Econ. Microbiol. 2* (1978) 263.
[59] K. W. Sinden, *Enzyme Microb. Technol. 9* (1987) 124.
[60] H. Inui, K. Miyatake, Y. Nakano, S. Kitaoka, *FEBS Lett. 150* (1982) 89.
[61] H. Inui, K. Miyatake, Y. Nakano, S. Kitaoka, *Agric. Biol. Chem. 47* (1983) 2669.
[62] S. De Witt, J. L. Ervin, D. Howes-Orchison, D. Dalietos, S. L. Neidleman, *J. Am. Oil Chem. Soc. 59* (1982) 69.
[63] S. L. Neidleman, J. Geigert, *J. Am. Oil Chem. Soc. 61* (1984) 290.
[64] J. Geigert, S. L. Neidleman, S. K. De Witt, *J. Am. Oil Chem. Soc. 61* (1984) 1747.
[65] C. W. Seo, Y. Yamada, H. Okada, *Agric. Biol. Chem. 46* (1982) 405.
[66] J. D. E. Patterson, J. A. Blain, C. E. L. Shaw, R. Todd, G. Bell, *Biotechnol. Lett. 1* (1979) 211.
[67] H. Egge in F. Paltauf (Ed.): *Ether Lipids: Biochemical and Biomedical Aspects*, Academic Press, New York 1983, p. 141.
[68] M. De Rosa, A. Gambacorta, B. Nicolaus, B. Chappe, P. Albrecht, *Biochim. Biophys. Acta 753* (1983) 249.

[69] M. Kates in R. T. Holman (Ed.): *Progress in the Chemistry of Fats and Other Lipids*, Pergamon Press, Oxford 1979, p. 301.
[70] K. Poralla, *Forum Mikrobiol. 5* (1982) 176.
[71] E. Kannenberg, A. Blume, R. N. McElhaney, K. Poralla, *Chem. Phys. Lipids 39* (1986) 145.
[72] W. O. Thiele, J. Oulevey, H. Bahl, *Fette, Seifen, Anstrichm. 87* (1985) 551.
[73] W. Godchaux, E. R. Leadbetter, *J. Biol. Chem. 259* (1984) 2982.
[74] J. Schindler, R. D. Schmid in J. Falbe (Ed.): *Surfactants in Consumer Products*, Springer, Berlin 1987, p. 118.
[75] H. J. Richtler, J. Knaut, *J. Am. Oil Chem. Soc. 61* (1984) 160.
[76] N. O. V. Sonntag, *J. Am. Oil Chem. Soc. 59* (1982) 795A.
[77] U. Ploog, G. Reese, *Chem.-Ztg. 97* (1973) 342.
[78] U. R. Kreutzer, *J. Am. Oil Chem. Soc. 61* (1984) 343.
[79] K. Weissermel, H.-J. Arpe: *Industrielle Organische Chemie*, Verlag Chemie, Weinheim 1978, p. 73; M. F. Gautreaux, W. T. Davis, E. D. Travis in: *Kirk-Othmer, Encyclopedia of Chemical Technology, Vol. 1*, Wiley, New York 1978, p. 716; D. G. Demianiv in: *Kirk-Othmer, Encyclopedia of Chemical Technology, Vol. 16*, Wiley, New York 1981, p. 485; H. Weber in: *Ullmanns Encyklopädie der technischen Chemie, Bd. 14*, Verlag Chemie, Weinheim 1977, p. 664; B. Fell, *Tenside Deterg. 12* (1975) 3.
[80] J. Falbe: *Synthesen mit Kohlenmonoxid*, Springer, Berlin 1967; J. Falbe: *Carbon Monoxide in Organic Synthesis*, Springer, Berlin 1970; J. Falbe: *New Syntheses with Carbon Monoxide*, Springer, Berlin 1980.
[81] J. Falbe: *Chemierohstoffe aus Kohle*, Georg Thieme Verlag, Stuttgart 1977; C. D. Frohning, H. Kölbel, M. Ralck, W. Rattig, F. Schnur, H. Schulz in J. Falbe (Ed.): *Chemical Feedstocks from Coal*, Wiley, New York 1982, p. 309.
[82] T. Voeste, H. Buchold, *J. Am. Oil Chem. Soc. 61* (1984) 350.
[83] J. Pohl, F.-J. Carduck, J. Falbe, T. Fleckenstein, DAS 3624812 (1986), Henkel.
[84] S. Billenstein, G. Blaschke, *J. Am. Oil Chem. Soc. 61* (1984) 353.
[85] S. Billenstein, B. Kukla, H. Stühler, US-Pat. 4234509 (1980), Farbwerke Hoechst.
[86] H. Rutzen, H. Schütt, DBP 1543676 (1966), Henkel; H. Rutzen, US-Pat. 3579585 (1968), Henkel.
[87] P. H. Moss, E. L. Yeakey, G. P. Speranza, Br. Pat. 1074603 (1967), Jefferson Chemical.
[88] Joint project of the Deutschen Gesellschaft für Fettforschung (DGF), 67. Mitteilung, *Fette, Seifen, Anstrichm. 78* (1976) 385.
[89] J. Baltes, B. Cornils, C. D. Frohning, *Chem.-Ing.-Tech. 47* (1975) 522.
[90] M. Singer, *Seifen, Öle, Fette, Wachse 105* (1979) 589; *110* (1984) 227.
[91] E. Draguez de Hault, A. Demoulin, *J. Am. Oil Chem. Soc. 61* (1984) 195.
[92] E. Bayer, Eur. Pat. 0008407 (1979), Heyl & Co.; E. Bayer, DBP 3226865 (1982), Heyl & Co.; E. Bayer, W. Schumann, *J. Chem. Soc. Chem. Commun. 1986*, 949.
[93] L. D. Myers, V. J. Muckerheide, US-Pat. 2298501 (1942), Emery Industries; R. L. Demmerle, *Ind. Eng. Chem. 39* (1947) 126.
[94] W. Stein, *J. Am. Oil Chem. Soc. 45* (1968) 471; H. Hartmann, W. Stein, DBP 970292 (1953), Henkel.
[95] R. Criegee, *Angew. Chem. 87* (1975) 765; *Angew. Chem. Int. Ed. Engl. 14* (1975) 745.
[96] a) *Schriftenreihe des Fonds der Chemischen Industrie, Heft 26: Fette und Öle*, VCI, Frankfurt 1986; b) M. Witthaus in [96a], p. 19.
[97] L. H. Princen, J. A. Rothfus, *J. Am. Oil Chem. Soc. 61* (1984) 281.
[98] C. G. Goebel, A. C. Brown, H. F. Oehlschlaeger, R. P. Rolfes, US-Pat. 2813113 (1957), Emery Industries.
[99] R. G. Kadesch, *J. Am. Oil Chem. Soc. 56* (1979) 845A.
[100] U. Zeidler, H. Lepper, W. Stein, *Fette, Seifen, Anstrichm. 76* (1974) 260.
[101] P. H. J. Carlsen, T. Katsuki, V. S. Martin, K. B. Sharpless, *J. Org. Chem. 46* (1981) 3936.
[102] E. C. Ladd, H. Sargent, US-Pat. 2485100 (1949), Rohm & Haas; A. Bezard, A. Jacot-Guillarmod, DBP 1042562 (1955), Rohm & Haas.
[103] B. Gruber, R. Höfer, H. Kluth, A. Meffert, *Fat Sci. Technol. 89* (1987) 147.
[104] E. N. Frankel, E. H. Pryde, *J. Am. Oil Chem. Soc. 54* (1977) 873A.
[105] E. T. Roe, D. Swern, *J. Am. Oil Chem. Soc. 37* (1960) 661.
[106] W. Reppe, H. Kröper, *Justus Liebigs Ann. Chem. 582* (1933) 38.
[107] E. H. Pryde, *J. Am. Oil Chem. Soc. 61* (1984) 419.
[108] J. P. Friedrich, *J. Am. Oil Chem. Soc. 53* (1976) 125.
[109] B. Gruber, M. Biermann, *Fette, Seifen, Anstrichm. 87* (1985) 400.
[110] R. L. Banks, G. C. Bailey, *Ind. Eng. Chem. Prod. Res. Dev. 3* (1964) 170.
[111] C. Boelhouwer, J. C. Mol, *J. Am. Oil Chem. Soc. 61* (1984) 425.
[112] M. Biermann in [96a], p. 26.
[113] M. J. Danzig, J. L. O'Donnell, E. W. Bell, J. C. Cowan, H. M. Teeter, *J. Am. Oil Chem. Soc. 34* (1957) 136.
[114] H. M. Teeter, J. L. O'Donnell, W. J. Schneider, L. E. Gast, M. J. Danzig, *J. Org. Chem. 2* (1957) 512.
[115] H. M. Teeter, E. W. Bell, J. L. O'Donnell, M. J. Danzig, J. C. Cowan, *J. Am. Oil Chem. Soc. 35* (1958) 238.
[116] G. S. R. Sastry, B. G. K. Murthy, J. S. Aggarwal, *J. Am. Oil Chem. Soc. 48* (1971) 686.
[117] B. F. Ward, US-Pat. 3753968 (1973), Westvaco Corp.; J. R. Powers, C. Miller, US-Pat. 4081462 (1976), Westvaco Corp.
[118] B. F. Ward, C. G. Force, A. M. Bills, *J. Am. Oil Chem. Soc. 52* (1975) 219.
[119] K. Alder, R. Kuth, *Justus Liebigs Ann. Chem. 609* (1957) 19.
[120] K. Holenberg, J. A. Johansson, *Acta Chem. Scand. Ser. B36* (1982) 481.
[121] A. E. Rheineck, T. H. Khoe, *Fette, Seifen, Anstrichm. 71* (1969) 644.
[122] E. C. Leonhard, *J. Am. Oil Chem. Soc. 56* (1979) 782A.
[123] M. J. den Otter, *Fette, Seifen, Anstrichm. 72* (1970) 667, 875.
[124] J. O. Metzger, J. Hartmanns, P. Köll, *Tetrahedron Lett. 22* (1981) 1891.
[125] J. Hartmanns, K. Klenke, J. O. Metzger, *Chem. Ber. 119* (1986) 488.
[126] W. Stein, DBP 867090 (1950), Henkel.
[127] F. C. Naughton, P. C. Daidone, US-Pat. 2851491, 2851492, 2851493 (1958), Baker Castor Oil.
[128] M. Grimberg, *Seifen, Öle, Fette, Wachse 89* (1963) 771.
[129] K. T. Achaya, *J. Am. Oil Chem. Soc. 48* (1971) 758.
[130] P. F. C. Gregory, M. Genas, O. Kostelitz, Fr. Pat. 952985 (1949), Société Organico; G. Wetroff, G. d'Ivacheff, J. Khaldij, Fr. Pat. 1120247 (1955), Société Organico.
[131] M. Genas, *Angew. Chem. 74* (1962) 535.
[132] T. R. Steadmann, J. O. H. Peterson, US-Pat. 2847432 (1958).
[133] D. A. O'Brien, Eur. Pat. 0153522 (1984), Procter & Gamble.
[134] J. O. O. Korhonen, J. N. J. Korvola, *Acta Chem. Scand. Ser. B35* (1981) 673.
[135] A. Commichau, *Dissertation*, Technische Hochschule Aachen 1965.
[136] M. Biermann, Paper presented at a GDCh specialist group conference on detergents chemistry. Würzburg 1985.
[137] F. Asinger, B. Feil, A. Commichau, *Tetrahedron Lett. 1966*, 3095.
[138] N. C. Deno, W. E. Billups, R. Fishbein, C. Pierson, R. Whalen, J. C. Wyckoff, *J. Am. Chem. Soc. 93* (1971) 438.
[139] G. A. Olah, D. G. Parker, N. Yoneda, *Angew. Chem. 90* (1978) 962; *Angew. Chem. Int. Ed. Engl. 17* (1978) 909.
[140] B. Westrup, *Diplomarbeit*, Universität Münster 1978.
[141] N. C. Deno, R. Fishbein, C. Pierson, *J. Am. Chem. Soc. 92* (1970) 1451.
[142] C. Eden, Z. Shaked, *Isr. J. Chem. 13* (1975) 1.
[143] B. Dors, *Diplomarbeit*, Universität Münster 1975.
[144] N. C. Deno, P. E. J. Jedziniak, L. A. Messer, M. D. Meyer, S. G. Stroud, E. S. Tomezsko, *Tetrahedron 33* (1977) 2503.
[145] F. R. Hewgill, G. M. Proudfoot, *Aust. J. Chem. 29* (1976) 637.
[146] M. A. Winnik, D. S. Saunders, *J. Chem. Soc. Chem. Commun. 1976*, 156.
[147] R. J. Crawford, *J. Org. Chem. 48* (1983) 1364.
[148] F. Minisci, R. Galli, A. Galli, *Tetrahedron Lett. 1967*, 2207.
[149] F. Minisci, G. P. Gardini, F. Bertini, *Can. J. Chem. 48* (1970) 544.
[150] N. C. Deno, R. Fishbein, J. C. Wyckoff, *J. Am. Chem. Soc. 93* (1971) 2065.
[151] D. A. Konen, R. J. Maxwell, L. S. Silbert, *J. Org. Chem. 44* (1979) 3594.
[152] N. C. Deno, E. J. Jedziniak, *Tetrahedron Lett. 1976*, 1259.
[153] J. Schwartz, J. A. Labinger, *Angew. Chem. 88* (1976) 402; *Angew. Chem. Int. Ed. Engl. 15* (1976) 333.
[154] J. Alvhäll, S. Gronowitz, A. Hallberg, R. Svenson, *J. Am. Oil Chem. Soc. 61* (1984) 430.
[155] W. Stein, H. Weiss, O. Koch, P. Neuhausen, H. Baumann, *Fette, Seifen, Anstrichm. 72* (1970) 956.
[156] W. Stein, H. Baumann, *J. Am. Oil Chem. Soc. 52* (1975) 323.
[157] K. H. Schmid, H. Baumann, W. Stein, H. Dolhaine, *Kongressberichte, Welt-Tensid-Kongreß, Vol. II*, München 1984, p. 105.
[158] H. Machemer, *Angew. Chem. 64* (1952) 213.
[159] S. Veibel, J. I. Nielsen, *Tetrahedron 23* (1967) 1723.
[160] H. J. Krause, A. Syldatk, *Fette, Seifen, Anstrichm. 87* (1985) 386.
[161] H. J. Krause, *Fette, Seifen, Anstrichm. 86* (1984) 293.
[162] M. Bühler, C. Wandrey, *Fat Sci. Technol. 89* (1987) 156.
[163] a) A. R. Baldwin (Ed.): *Proceedings of the World Conference on Emerging Technologies in the Fats and Oils Industry*, AOCS, Illinois 1986; b) G. Lazar, A. Weiss, R. D. Schmid in [163a], p. 346.
[164] A. Sturzenegger, H. Sturm, *Ind. Eng. Chem. 43* (1951) 510.
[165] H. L. Brockmann in B. Borgström, H. L. Brockmann (Eds.): *Lipases*, Elsevier, New York 1984, p. 4.
[166] Y. Tsujisaka, M. Iwai, *Kagaku to Kogyo (Osaka) 58* (1984) 60; *Chem. Abstr.* 100:205378 j.
[167] A. R. Macrae in W. M. Fogarty (Ed.): *Microbial Enzymes and Biotechnology*, Applied Science Publ., Barking 1983, p. 225.

[168] W. Connstein, E. Hoyer, H. Wartenberg, *Ber. Dtsch. Chem. Ges. 35* (1902) 3988.
[169] F. Taylor, C. C. Panzer, J. C. Craig, Jr., D. J. O'Brien, *Biotechnol. Bioeng. 28* (1986) 1318.
[170] S. Ishida in [163a], p. 359.
[171] M. M. Hoq, T. Yamane, S. Shimizu, *J. Am. Oil Chem. Soc. 62* (1985) 1016.
[172] J. Falbe, R. D. Schmid, *Fette, Seifen, Anstrichm. 88* (1986) 203.
[173] A. R. Macrae, *Stud. Org. Chem. (Amsterdam) 22* (1985) 195.
[174] T. Nielsen, *Fette, Seifen, Anstrichm. 87* (1985) 15.
[175] T. T. Hansen, P. Eigtved in [163a], p. 365.
[176] J. H. Kastle, A. S. Loevenhart, *Am. Chem. J. 24* (1900) 491.
[177] S. Okumura, M. Iwai, Y. Tsujisaka, *Biochim. Biophys. Acta 575* (1979) 156.
[178] G. Lazar, *Fette, Seifen, Anstrichm. 87* (1985) 394.
[179] H. Seino, T. Uchibori, T. Nishitani, S. Inamasu, *J. Am. Oil Chem. Soc. 61* (1984) 1761.
[180] M. Therisod, A. M. Klibanov, *J. Am. Chem. Soc. 108* (1986) 5638.
[181] G. Kirchner, M. P. Scollar, A. M. Klibanov, *J. Am. Chem. Soc. 107* (1985) 7072.
[182] S. Koshiro, K. Sonomoto, A. Tanaka, S. Fukui, *J. Biotechnol. 2* (1985) 47.
[183] G. Schuster, W. F. Adams in G. Schuster (Ed.): *Emulgatoren für Lebensmittel*, Springer, Berlin 1985, p. 72.
[184] M. M. Hoq, H. Tagami, T. Yamane, S. Shimizu, *Agric. Biol. Chem. 49* (1985) 335.
[185] S. Yamaguchi, T. Mase, S. Asada, Eur. Pat. 0191217 (1986), Amano Pharmaceutical Co.
[186] M. Bühler, J. Schindler in H.-J. Rehm, G. Reed (Eds.): *Biotechnology, Vol. 6a*, Verlag Chemie, Weinheim 1984, p. 329.
[187] N. Uemura, *Ferment. Ind. (Tokyo) 43* (1985) 436.
[188] R. Uchio, I. Shiio, *Agric. Biol. Chem. 36* (1972) 1169.
[189] *CEER, Chem. Econ. Eng. Rev. 17* (1985) 37.
[190] H.-J. Rehm, J. Reif, *Adv. Biochem. Eng. 19* (1981) 175.
[191] P. J. Thomas, *Gastroenterology 62* (1972) 430.
[192] L. L. Wallen, E. N. Davies, Y. V. Wu, W. K. Rohwedder, *Lipids 6* (1971) 745.
[193] G. J. Schroepfer, Jr., W. G. Niehaus, Jr., *J. Biol. Chem. 245* (1970) 3798.
[194] J. F. G. Vliegenthart, G. A. Veldink in W. A. Pryor (Ed.): *Free Radicals in Biology, Vol. 5*, Academic Press, New York 1982, p. 29.
[195] H. Kühn, R. Wiesner, V. Z. Lankin, A. Nekrasov, L. Alder, T. Schewe, *Anal. Biochem. 160* (1987) 24.
[196] S. Shak, H. D. Perez, I. M. Goldstein, *J. Biol. Chem. 258* (1983) 14948.
[197] B. Samuelsson, *Science (Washington D.C.) 220* (1983) 568.
[198] T. J. Ahern, *J. Am. Oil Chem. Soc. 61* (1984) 1754.
[199] J. Laakso, *Lipids 17* (1982) 667.
[200] a) P. K. Stumpf, E. E. Conn (Eds.): *The Biochemistry of Plants, Vol. 4*, Academic Press, New York 1980; b) P. K. Stumpf in [200a], p. 177.
[201] H. A. Dailey, P. Strittmatter, *J. Biol. Chem. 255* (1980) 5184.
[202] P. E. Kolattukudy in [200a], p. 617.
[203] C. G. Harfoot in W. W. Christie (Ed.): *Lipid Metabolism in Ruminant Animals*, Pergamon Press, New York 1981, p. 1.
[204] P. E. Hughes, S. B. Tove, *J. Biol. Chem. 255* (1980) 4447.
[205] P. Kemp, R. W. White, O. J. Lander, *J. Gen. Microbiol. 90* (1975) 100.
[206] P. E. Hughes, W. J. Hunter, S. B. Tove, *J. Biol. Chem. 257* (1982) 3643.
[207] C. Syldatk, U. Matulovic, F. Wagner, *Z. Naturforsch. C40* (1985) 61.
[208] P. Rapp, C. A. Beck, F. Wagner, *Eur. J. Appl. Microbiol. Biotechnol. 7* (1979) 67.
[209] K. Ramamurti, G. L. Morrison, C. F. Crumpton, *Biotechnol. Bioeng. 24* (1982) 2267.
[210] S. Yamada, K. Nabe, N. Izuo, M. Wada, I. Chibata, *J. Ferment. Technol. 57* (1979) 215.
[211] T. Uwajima, Y. Shimizu, O. Terada, *J. Biol. Chem. 259* (1984) 2748.
[212] H. Schütz, F. Radler, *Syst. Appl. Microbiol. 5* (1984) 169, B102; P. J. Slininger, R. J. Bothast, *Appl. Environ. Microbiol. 50* (1985) 1444.
[213] M. Sobolov, K. L. Smiley, *J. Bacteriol. 79* (1960) 261.
[214] N. Izuo, K. Nabe, S. Yamada, I. Chibata, *J. Ferment. Technol. 58* (1980) 221.
[215] B. W. Werdelmann, R. D. Schmid, *Fette, Seifen, Anstrichm. 84* (1982) 436.
[216] K. Kieslich, *Econ. Microbiol. 5* (1980) 370.
[217] V. S. Malik, *Z. Allg. Mikrobiol. 22* (1982) 261.
[218] P. Atrat, *Z. Allg. Mikrobiol. 22* (1982) 723.
[219] F. Hill, J. Schindler, R. D. Schmid, R. Wagner, W. Voelter, *Eur. J. Appl. Microbiol. Biotechnol. 15* (1982) 25.
[220] W. Preuss, Eur. Pat. 0041612 (1981), Henkel.
[221] P. Atrat, E. Hüller, C. Hörhold, M. J. Bucher, A. Y. Arinbasarova, K. A. Koschtschejenko, *Z. Allg. Mikrobiol. 20* (1980) 159.
[222] K. Sonomoto, M. Hoq, A. Tanaka, S. Fukui, *J. Ferment. Technol. 59* (1981) 465.
[223] S. Ohlson, P. O. Larsson, K. Mosbach, *Biotechnol. Bioeng. 20* (1978) 1267.

ANGEWANDTE CHEMIE

International Edition in English

Volume 27 · Number 1
January 1988
Pages 63–78

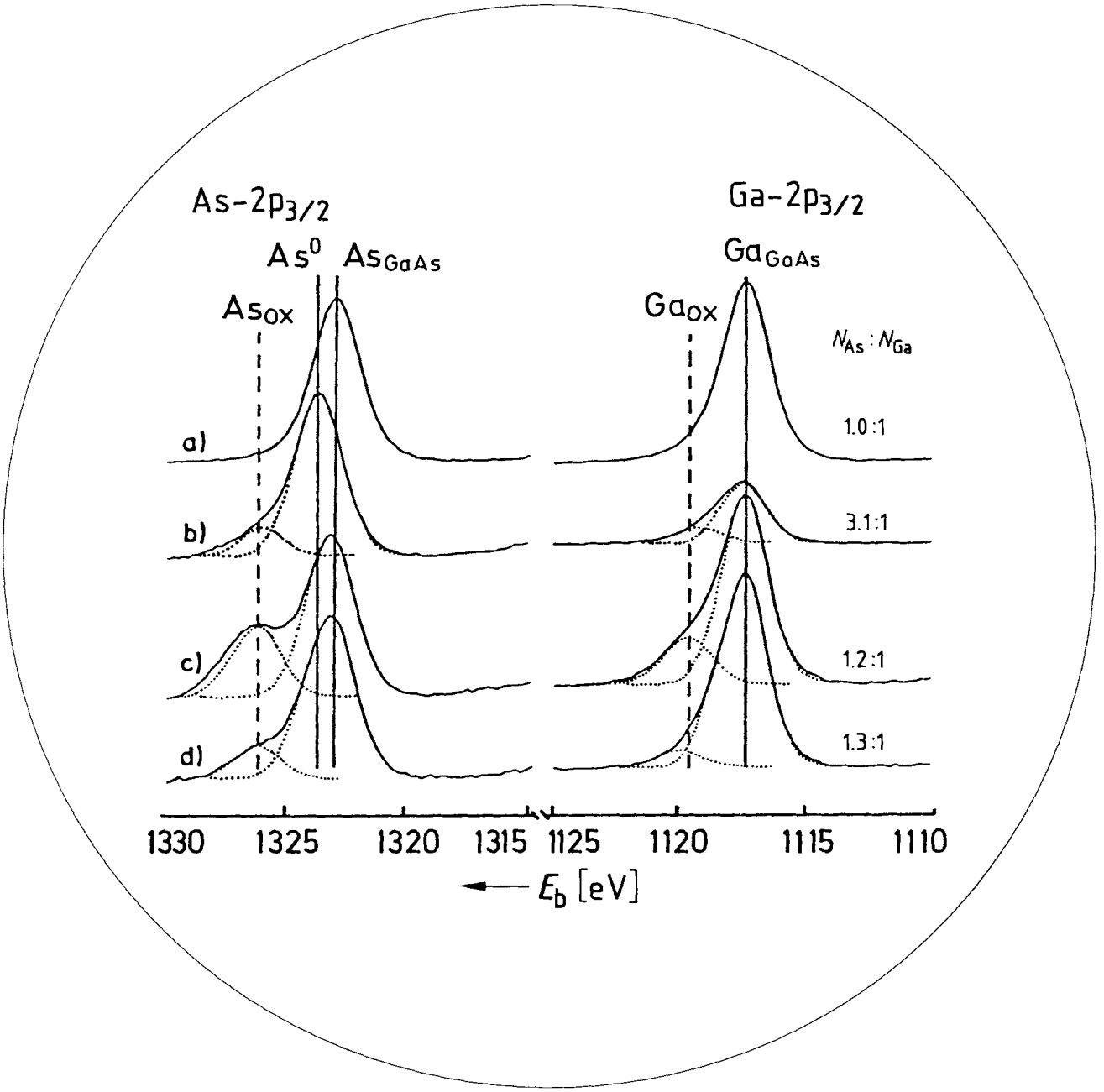

Heinz Gerischer

The Use of Light in the Study of Interfacial Electrochemical Reactions

The Use of Light in the Study of Interfacial Electrochemical Reactions

Heinz Gerischer*

Spectroscopic analysis techniques have become particularly important in the study of interfacial electrochemical processes since it has become possible to increase their sensitivity to the extent where changes occurring in the absorption of light by fractions of monolayers can be detected. At the same time the development of new techniques in surface physics, though most of these can only be used in ultra-high vacuum, has also had a considerable influence on electrochemistry since it has enabled studies to be carried out on electrodes after transfer to UHV. The availability of well-defined semiconductors in which photocurrents can be generated by the absorption of light has led to the development of photoelectrochemical methods that can be used for the study of electrode reactions at semiconductors or at metal surfaces which are covered with a semiconducting film. Finally, it has been observed during the study of semiconductor electrodes that redox reactions at an electrode can result in the generation of luminescence. This, in turn, can lead to important information on the mechanism of the charge transfer process. These recent developments are reviewed in the present article.

1. Introduction

Classical investigation techniques in electrochemistry have usually depended on the analysis of quantitative and time-dependent relationships between current and potential to characterize equilibrium conditions and reaction rates of electrode processes. The kinetics of many processes could be deduced from the response of parameters measured in amplitude and time during a modulation of one of these variables. Relatively little information, however, can be obtained in this way about the influence of structural factors, intermediate products, or changes in the electrode that occur during such a reaction. Insight into the structural properties of surfaces and their behavior or into molecular processes can only be attained by the use of spectroscopic methods. Since the quantitative changes that occur on a surface are minute when measured on an absolute scale, the use of such spectroscopic techniques only became possible with the development of instrumentation with exceedingly high sensitivities. This problem is common both to electrochemistry and to surface studies performed in vacuum or in the gas phase. The development of new measurement techniques in surface physics has thus made a considerable contribution to the fact that the use of spectroscopic methods has today become indispensable in the characterization of electrochemical processes. The presence of a liquid phase at the electrode surface, however, causes severe restrictions in the use of such techniques since the majority of them involve the use of ultra-high vacuum or very low gas pressures. Many of these new techniques can consequently be used only in ex-situ measurements, which necessitates that the conditions at the electrode surface be stable on transfer to UHV.

[*] Prof. Dr. H. Gerischer
Fritz-Haber-Institut der Max-Planck-Gesellschaft
Faradayweg 4-6, D-1000 Berlin 33

[**] The previous page shows Figure 10 of this article.

The use of semiconductors and insulators as electrode materials gave a new impetus to the application of light to electrochemical processes. The absorption of light by these materials can lead to dramatic changes in their electronic properties which also influence their electrochemical reactivity. Photocurrents are produced, whose intensities and spectral dependences provide information on the relationships between the electronic properties of the solid and the electrochemical reactions. This article will attempt to describe these techniques together with a series of examples without, however, attempting to be completely comprehensive. The choice of examples is a personal selection taken largely from work carried out in the institute in which the author has worked for the past two decades.

2. Principles of the Usage of Light as an Analytic Tool

As in classical spectroscopy, the absorption of light at electrodes can be used to detect any changes occurring therein. Since most electrode materials possess metallic properties and themselves absorb light very strongly, one must normally work in the reflection mode, in which the reflected light intensity is dependent upon the angle of incidence and the direction of polarization of the incoming light. It is therefore necessary to be able to recognize the reflection from the "pure" surface and to derive information from the changes in this reflection. Historically, this was first achieved in ellipsometry,[1] where the thicknesses of light-transparent films were measured from the changes in phase and amplitude of polarized light reflected by the metal. This method, which can be used in-situ, achieves even today an unsurpassable accuracy in the determination of thin transparent layers, if their optical properties are well known.[2-4] On the other hand, for films which are less well characterized or which are absorbing, the method is extremely tedious and the analysis very time-consuming,

especially in cases where the optical properties of a film are not homogeneous. The less exact, but rather quicker method of direct measurement of absorption of reflected light is therefore more frequently used.

Considerable advances have recently been made in the measurement of absorption of IR light. Many metals have an extremely high reflectivity in the infrared region; thus, despite the low extinction coefficients of molecular vibrational excitation, one can observe the production and presence of adsorbed molecules in the reflection mode even at very low coverages. The excitation must, however, occur at a frequency where the solution is transparent and the extinction coefficient of the adsorbed species must not be too low.[5,6] The sensitivities of such optical methods may be increased by orders of magnitude if the absorption wavelength or the surface coverage is dependent upon the field strength and thus enables the absorption to be reproducibly modulated by periodic variation of the electrode potential. In the visible and UV regions, for which very sensitive detectors are available, changes in reflectivity of even 10^{-6} can be measured with the help of the lock-in technique.[7,8] At these wavelengths, the reflectivity of metal surfaces can be altered by the electrode potential due to the modification of the electron density at the surface.[9,10]

Another technique that can, however, achieve high sensitivity only on certain metals, is that of increased Raman scattering by rough metal surfaces, first observed at electrodes by *Fleischmann, Hendra* et al.[11] With the help of surface-enhanced Raman effects molecules adsorbed on the metals gold, silver and copper have been detected in very low concentrations,[12] which would not have been possible with normal Raman scattering.

At wavelengths where the electrolyte precludes the use of these methods due to its own absorption properties, information can, instead, be obtained by transferring the electrode to a vacuum (ex-situ methods[13,14,15]). Electron diffraction techniques and photoelectron spectroscopic methods from surface physics using X-rays, synchrotron radiation or electron beams may then be employed in the surface analysis provided that no alterations are made to the structure or composition of the surface by the transfer to an ultra-high vacuum.

Absorption of light can also lead to variations of the electrochemical behavior of the electrode itself. This can be seen in metals when excited electrons attain enough energy to enter a neighboring phase (photoelectron emission[16,17]). Such reactivity resulting from absorption of light is even more marked in the case of semiconductors.[18,19] Here, the oxidation or reduction properties which these materials possess as a result of the production of minority electronic carriers, i.e. electron holes in n-type semiconductors or conduction electrons in p-type semiconductors, are changed to such an extent that new charge transfer processes become possible at the phase boundary with the electrolyte. These may be detected by the appearance of photocurrents whose intensities and spectral behavior yield information regarding the properties of the electrode and the processes occurring at the phase boundary. It may be added that semiconductor electrodes also allow redox reactions of excited molecules adsorbed at the phase boundary to be studied (spectral sensitization[20]), a procedure which has been used for more than a hundred years in photography.[21]

Finally, the emission of light may also occur as a consequence of an electrochemical reaction, when such a reaction gives rise to electronically excited states. One example of this is the electroluminescence of semiconductor electrodes which is produced by the injection of minority carriers.[22-24] From such observations, information concerning energetic relationships during electron transfer processes can be acquired. Such data have recently even been obtained from light emitted by metal electrodes.[25]

3. Spectroscopic Methods

The spectroscopic determination of reaction products in solution which have been produced by electrode reactions is one of the most important analytical techniques. For the investigation of short-lived intermediates thin-layer cells with transparent electrodes have been developed. The electrodes are generally composed of either thin evaporated metal layers or transparent, heavily doped oxide layers (tin or indium oxides, for example, or a mixture of these components). However, only those methods which yield direct information on processes occurring at the surface of an electrode will be considered here. In the case of compact electrodes which are not transparent to light these measurements are carried out in the reflection mode. These types of investigations may be carried out in-situ if the electrolyte is transparent to light in the particular region of the spectrum used. Otherwise, the electrode must be removed from the electrolyte and transferred to a vacuum or to an inert gas atmosphere (ex-situ methods). Examples of both procedures will be given in the following.

3.1. Infrared Reflectance Spectroscopy

IR spectroscopy has only recently begun to be used in electrochemistry. This is largely due to the disturbing absorptions of the electrolyte layers next to the electrode and the relatively low sensitivity of previous IR detectors. *Bewick, Pons* et al. were the first to overcome these difficulties, using very thin electrolyte layers between the electrode and an IR-transparent window together with a modulation of the electrode potential by periodic potential stepping.[26] This procedure is called "Electrochemically Modulated Infra Red Spectroscopy (EMIRS)". By changing the potential, either a change in coverage is induced or, as is often the case, the absorption frequency of a vibrational excitation is shifted to other wavelengths as a result of the electric field produced at the electrode and the corresponding change in bond strength. Thus, a modulation of the reflected light intensity as a result of variation in absorption can, with the help of the lock-in amplifier technique, be detected with very high accuracy. The relative change in reflectivity, $\Delta R/R$, is usually measured during this process. With the help of Fourier transform spectroscopy it has become possible to record spectra in the IR region relatively quickly[27,28] and, by averaging over many repetitions, to considerably improve the signal-to-noise ra-

tio, thereby allowing difference spectra to be constructed at various potentials. This procedure is referred to as "Subtractively Normalized Interfacial FTIR Spectroscopy (SNIFTIRS)".

Since the electric vector of the light parallel to the surface of metallic conductors in the IR region goes to zero, the selection rule valid in reflectance spectroscopy in the IR region is that only vibrations with an electric moment normal to the surface can be excited. Only for such vibrations can the change of the electric field in the Helmholtz double layer influence the bond strength involved and hence the position of the absorption maximum. For this reason, linearly polarized light with a vector normal to the surface, i.e. p-polarized light, with an angle of incidence between 45° and 70° is used for such measurements. From a comparison between the reflection of p- and s-polarized light one can determine which signals are due to adsorbed molecules, since molecules in the solution, being uniformly distributed in orientation, absorb both polarizations to the same degree. By modulating the polarization angles between s and p the signal originating from the surface can be separated from the background absorption of the electrolyte. This procedure can be carried out with a dispersive monochromator or by using a Fourier transform system.[29,30]

The principles of such a system are shown schematically in Figure 1. The sensitivity of IR reflectance spectroscopy is limited by the sensitivity of the detectors. Changes in reflectivity in the order of 10^{-3} are necessary to obtain a measurable effect. This implies that one largely detects materials that adsorb in rather high coverages on the electrode. These need not necessarily be the species that dictate the reaction mechanism—they can also, of course, be by-products that only slowly undergo further reaction and thus play no decisive role in determining the overall reaction rate.

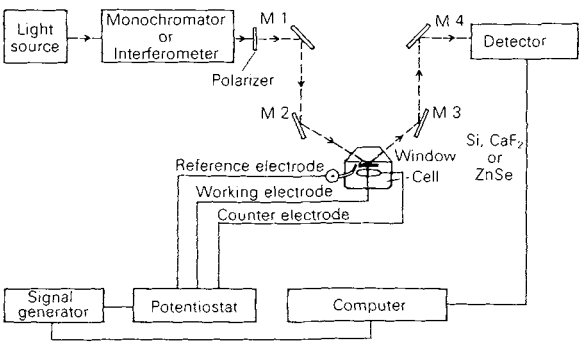

Fig. 1. Block diagram of the system used for measuring the spectra of reflected light at a given or modulated electrode potential. M = mirror.

As an example let us consider the oxidation of methanol, formaldehyde and formic acid at noble metal electrodes. From cyclic current-potential curves it was concluded that an intermediate product was produced which was very strongly adsorbed at the electrode surface. This intermediate blocks the course of the reaction until at higher anodic potentials it can be displaced by chemisorbed oxygen and thus oxidized to CO_2. It was believed to be either the COH or the HCO radical.[31,32] Spectroscopically, however, only adsorbed CO was detected on these noble metal

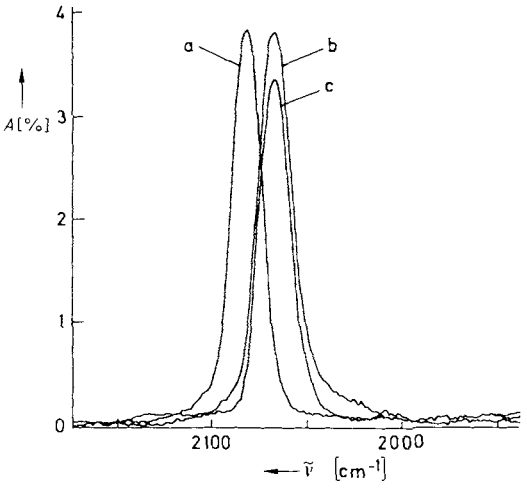

Fig. 2. IR absorption spectra of CO adsorbed on platinum at 86% coverage (Θ) in 0.5 M H_2SO_4: a) solution saturated with CO; b) + 1 M CH_3OH at $U = 0.4$ V; c) + 0.1 M HCOOH at $U = 0.3$ V; after *Kunimatsu* [34]. A = absorption. U measured versus a reversible hydrogen electrode (RHE) in the same electrolyte.

electrodes.[33,34] Figure 2 shows spectra measured for a platinum electrode that has been in contact for a certain length of time with methanol or formic acid at a specific anodic potential. For comparison, the spectrum of directly adsorbed CO is also shown. Aside from a slight shift in the position of the absorption band, indicative of the fact that the molecule is in a different environment, it has exactly the same profile and almost the same intensity as the above. This absorption band can be attributed to linearly adsorbed CO.[35] Figure 3 shows the changes occurring in the spectrum with increasing CO coverage, the CO being generated as an intermediate in the oxidation of CH_3OH.[34]

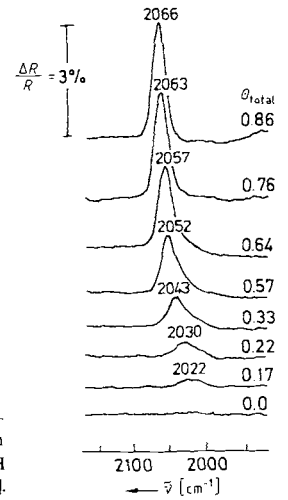

Fig. 3. Absorption spectra for various coverages (Θ) of CO adsorbed on platinum and formed during the oxidation of CH_3OH at $U = 0.4$ V (RHE); after *Kunimatsu* [34].

Other techniques have shown, however, that an intermediate is produced on the surface which blocks three adsorption sites, whereas adsorbed CO needs only one adsorption site. With the help of mass spectroscopic techniques it has recently been conclusively shown that the COH radical is present as an intermediate.[36] This discrepancy could be due to the fact that the mass spectroscopic

experiment was carried out at rather lower methanol concentrations, where sufficient adsorption sites were available for the COH radical, which requires three sites.[37] CO is preferentially produced at higher concentrations of CH_3OH. The spectroscopic evidence for adsorbed COH has still to be demonstrated.

IR spectroscopy of electrodes is still in the process of further development and one can certainly expect that significant information on reaction mechanisms will be acquired with the use of this technique.

3.2. Reflectance Spectroscopy in the Visible and Ultraviolet Regions

Very sensitive detectors are available for measurements in the UV and visible regions of the spectrum. Changes in reflectivity in the order of $\Delta R/R = 10^6$ can be measured. The first experiments of this nature were carried out by *Koch* and *Scaife*, who recorded spectra at various potentials during the growth of an oxide layer on Pt.[38] The introduction of modulation spectroscopy with the electrode potential as the modulated parameter, a technique first applied by *Seraphin* to the study of semiconductor band structure,[39] significantly increased the sensitivity that could be obtained. These techniques even allow the behavior of electrons at a metal surface in the electric field of the Helmholtz double layer and the interaction of this field with various ions or solution molecules in the double layer to be studied.[8,40,41]

Some processes in which the origins of the changes in reflectivity are easily recognized will be given here as examples. Figure 4 shows the changes occurring in the reflectance spectra of a single crystal silver surface which occur as a result of the development of a surface complex with molecules from the solution.[42,43] A repetitive anodic polarization of the silver surface is used to generate this complex, during each pulse of which a monolayer of silver chloride is built up in the chloride-containing electrolyte. On reduction, this leaves behind active silver atoms on the surface. These silver atoms form very stable surface complexes with pyridine or pyrazine which cannot be destroyed any more by reduction over a wide potential range. Figure 4 shows the difference spectrum obtained by subtraction of the reflectance spectrum taken before the cycling treatment. It is clear that a broad absorption band is visible for each of the complexes generated in this way. One knows that the complexes formed between these molecules and the silver ions in solution are transparent to light at these wavelengths. The new absorption band arises as a result of a charge transfer process between the molecular complex and the metal electronic levels. The change in reflectivity is in the order of a few per cent. This extraordinarily large amount for a single monolayer can only be explained by assuming that in this optical transition a strong interaction with the metal occurs.

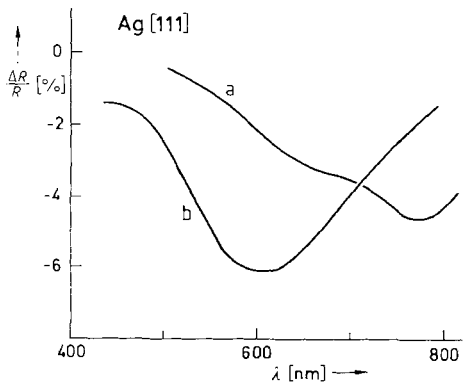

Fig. 4. Normalized electroreflectance spectra using p-polarized light for (a) pyridine and (b) pyrazine adsorbed on an activated single crystal silver surface. Modulation potential 0.5 V; after *Kolb* et al. [42, 43].

A further example demonstrating the high sensitivity that can be achieved by potential modulation is given in Figure 5a.[44] In this figure is shown the electroreflectance spectrum of *p*-nitroaniline which is strongly adsorbed on a platinum surface. The considerable difference between s- and p-polarized light may clearly be seen. In the case of s-polarized light, with the electric field vector parallel to the surface, there is no change in reflectivity on modulating the potential by ±50 mV, whereas for p-polarized light two clear maxima are produced. These maxima are not produced at the absorption maxima of the molecules in question. The maximum at 436 nm lies on the shoulder of the *p*-nitroaniline absorption band. The absorption band is considerably shifted by the change in the electric field in

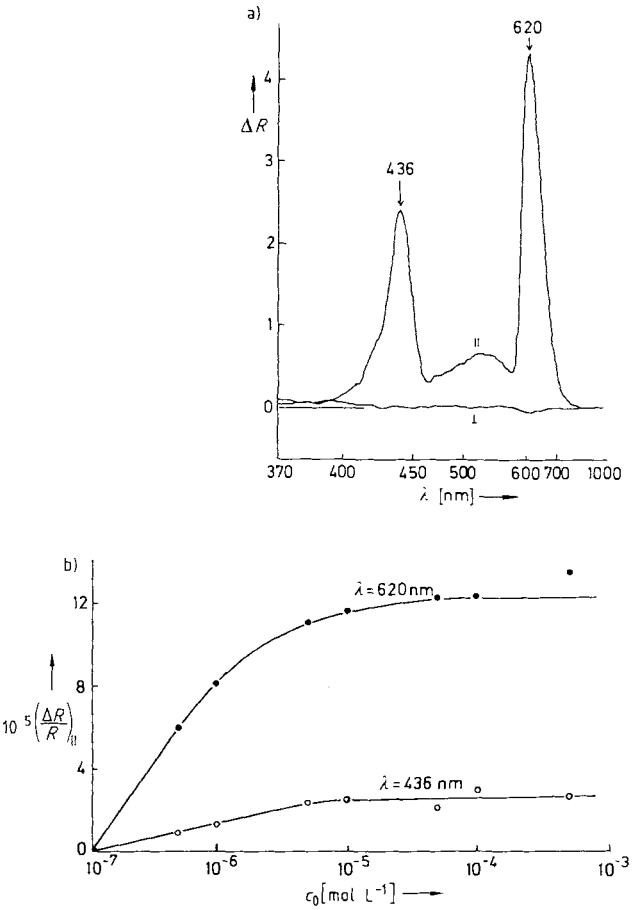

Fig. 5. a) Electroreflectance spectra of *p*-nitroaniline on a Pt electrode in 0.5 M Na_2SO_4 + 5×10^{-5} M $H_2NC_6H_4NO_2$ for p(||)- and s(⊥)-polarized light. Modulation potential: 0.1 V. ΔR in relative units ($\Delta R/R$ approximately 10^{-5} per unit). b) Normalized electroreflectance intensities of the two maxima in (a) as a function of the concentration (c_0) of *p*-nitroaniline in the solution; after *Plieth* et al. [44].

the Helmholtz double layer as a result of the fact that these electronic transitions in the molecules have an electric moment normal to the surface (Stark Effect). The maximum at 620 nm may be attributed to the build-up of aggregates of molecules on the surface. As shown in Figure 5b adsorption isotherms may be obtained from the intensity of these signals measured as a function of the concentration of molecules in the solution.

Very marked effects are observed when a second metal is deposited onto a metal electrode. The optical constants of the metal surface are, in this case, dramatically changed. Of particular interest are those systems in which adsorption of the first monolayer yields an ordered phase structure, a situation often observed on single crystal surfaces. This occurs at potentials which are more positive than the actual deposition potential of the bulk metal (underpotential deposition).[45] From the reflection spectra, one can also see how the bulk properties of a new phase are developed on deposition of successive monolayers. As an example of this, measurements made for the deposition of silver on a Cu[111] single crystal surface are presented in Figure 6.[46] The potential dependent reflectance spectrum with a potential modulation of 300 mV in a specific potential region is shown first for the pure copper and then for deposition of various thicknesses of silver. Of the changes which occur in the reflectance spectrum, the minimum occurring at 3.8 eV which first becomes visible at coverages of more than three monolayers is especially interesting.

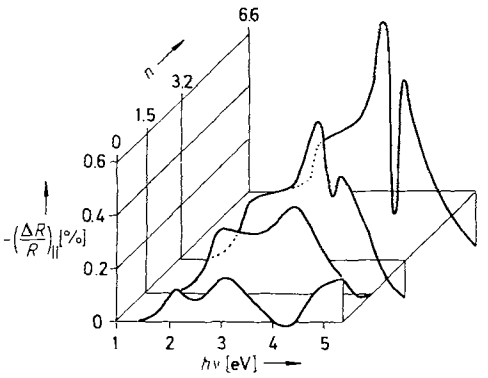

Fig. 6. Electroreflectance spectra of p-polarized light from a copper[111] surface before and after the deposition of various amounts of silver in 0.5 M H_2SO_4. Modulation potential 0.3 V (after *Kolb* et al. [46]). n = Number of atomic layers.

This minimum is typical of the excitation of bulk plasmons in the silver and shows that at these thicknesses the electronic system of the silver film already begins to show the properties of bulk silver. At thicknesses of over six monolayers the deposited layer exhibits practically the properties of the bulk metal.

3.3. Raman Reflectance Spectroscopy

Since the normal Raman effect is extremely weak, the observation of Raman lines for adsorbed molecules appeared at first rather a hopeless expectation. As already mentioned, an enhancement of Raman scattering from the surface rendering this effect measurable was first observed by *Fleischmann* and *Hendra* et al.[111] This enhancement can be up to 10^6 times greater than the original signal.[112] This phenomenon is termed "Surface Enhanced Raman Spectroscopy (SERS)" and is observed in this magnitude on only a few metals, e.g. silver, gold and copper. It occurs in connection with a plasmon resonance in the electronic systems of these metals at wavelengths at which strong absorption does not yet occur. This leads to a substantial increase in the electronic field strength on the surface under the influence of the electromagnetic field of the light. Since an excitation of this resonance is not allowed on a smooth surface, a surface roughening either by cyclic dissolution/deposition of the metal or by formation of metal clusters must precede. There must also be a very strong interaction between the adsorbed molecule and the surface, if the observed enhancement is to be explained.[47] The SERS effect is very clearly visible on colloid particles of the above mentioned metals.[48,49]

The origin of this phenomenon is, in fact, not fully understood in detail. Its restriction to only a few metals unfortunately prohibits general application, and detailed structural information on the positions of adsorbed molecules on the surface is also lost as a result of the necessary surface roughening involved. The possibility that a vibration-spectroscopic method of molecule characterization with visible light may become possible with this technique is, however, exceedingly attractive and lends impetus to the undertaking of further intensive research in this area.

The classical system in which this phenomenon has been thoroughly investigated in detail is the adsorption of pyridine at silver surfaces. Figure 7 shows a comparison between two Raman spectra, one taken from molecules in solution (Fig. 7a), the other from molecules adsorbed at a silver surface (Fig. 7b).[42] The topmost spectrum taken from pyridine in solution is recorded from ca. 6×10^{13} molecules, i.e. from that amount of pyridine to be found in the volume of solution through which the laser beam is passed. The lower Raman spectrum is taken from a single crystal silver surface, which, in order to produce an adsorbed complex of the type described above, was subjected to five oxidation-reduction cycles, thus generating activated silver atoms. If one assumes that a monolayer of pyridine molecules exists on the surface, then in this case only 10^{11} molecules should be affected by the laser beam. This difference and a comparison of the signal intensities indicate that the Raman scattering from the molecules adsorbed on the surface is a factor of 10^4 times greater than that from the molecules in the solution. One must also take into consideration the fact that in all probability not all of the molecules to be found on the surface take part in this scattering phenomenon. Furthermore, the surface roughening can be increased to such an extent that an increase in the Raman signal by as much as two more orders of magnitude can be achieved.[42]

Complementary experiments performed on colloid particles have also produced very informative results.[50] It has been observed here that fluorescence from adsorbed molecules can be almost totally repressed and the energy involved transferred to Raman scattering. This has the advantage that individual vibration lines, which otherwise would not be recognized in the broad fluorescence spec-

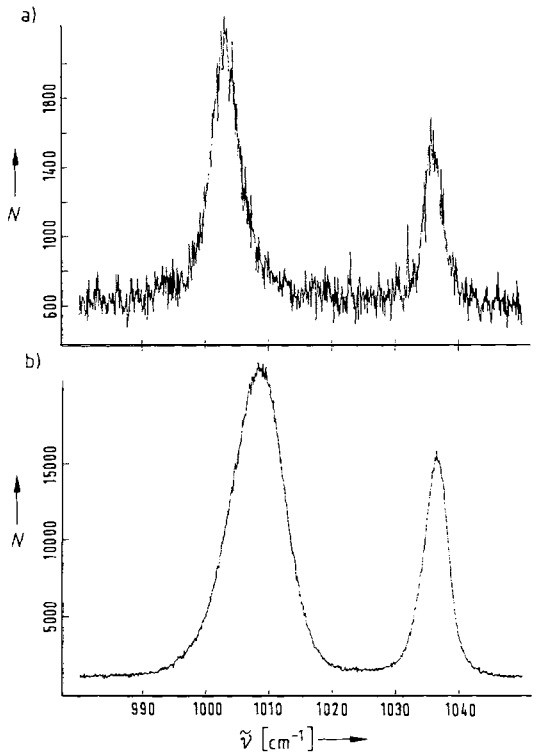

Fig. 7. Raman spectra of pyridine. a) From a solution of 0.05 M pyridine + 1 M KCl. b) After adsorption at an Ag[111] surface, activated by five oxidation/reduction cycles (after *Pettinger* et al. [42]). N = intensity, $\tilde{\nu}$ = Raman frequency.

trum, now become visible. A very sensitive technique is thus obtained for the characterization of specific molecules, a technique which looks especially promising for the study of biological molecules.[51]

3.4. Photoelectron Spectroscopy

As mentioned above, the most important spectroscopic methods used in surface physics, which deal with the energy spectrum of reflected electrons or electrons emitted from the surface, can only be used ex-situ. The electrode must therefore be transferred from the electrochemical system to a vacuum chamber. Figure 8 shows one type of setup which allows transfer in either direction to be carried out with a minimum of delay.[52] Such systems have been used to determine changes occurring in the surface structure as a result of adsorption or reaction with the electrolyte. Two examples of this will be given in the following.

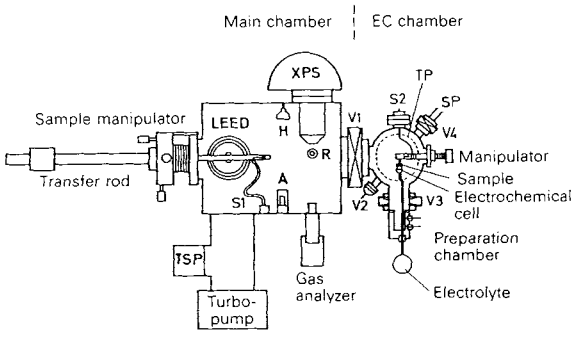

Fig. 8. Sketch of the apparatus used for investigation of electrodes in ultra-high vacuum by LEED or XPS [52]. A = ion source, H = halogen lamp, X = X-ray tube, S = sample support, V = valve, SP = sorption pump, TSP = thermosorption pump.

It has long been known from capacitance measurements carried out on electrodes in the absence of Faradaic currents that certain ions specifically adsorb on metal surfaces and can thus considerably alter the structure of the double layer. This is especially true of the halide ions, which can become strongly bonded to many metal surfaces through a partial transfer of electrons. These adsorbed ions can be directly detected with the help of photoelectron spectroscopy. The results of ion adsorption from a cesium bromide solution on gold electrodes will be discussed as an example. The electrolyte flows almost completely away from a very smooth gold electrode when the electrode is taken out of the solution. Only those ions bound by chemical or electrostatic forces to the surface remain attached. When such a surface is transferred to a ultra-high vacuum and exposed to X-rays of specific wavelength, electrons whose energies may be analyzed by detectors are released into the vacuum. From their kinetic energy and the excitation energy of the X-rays, which is well known, the energy levels from which the electrons originate can be calculated.

Figure 9 shows the concentration of the adsorbed bromide and cesium ions which remain on the electrode surface as a function of the potential at which the electrodes are taken out of the electrolyte. It may be seen that at very negative potentials only cesium is adsorbed whereas on going towards more positive potentials, bromide is adsorbed in ever increasing amounts. The point of zero charge, U_0, and the $Cs^{\oplus}$ coverage in an electrolyte in which specific adsorption of the anion does not occur are also shown in the diagram. This point of zero charge is the potential at which no excess charge would normally be found on the surface. It should be noted that the bromide adsorption first begins at quite negative potentials relative to U_0 and

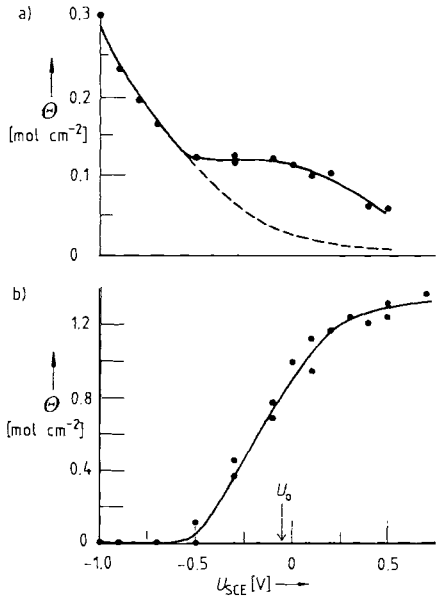

Fig. 9. Ions [a) $Cs^{\oplus}$; b) $Br^{\ominus}$] present in the electric double layer of a gold electrode after withdrawal at various potentials from a 0.01 M CsBr solution (XPS of the Cs $3d_{5/2}$ and Br $3p_{3/2}$ electrons). Dashed curve: amount of $Cs^{\oplus}$ measured using a 0.005 M Cs_2SO_4 solution; U_0 = point of zero charge in the sulfate solution (after *Kolb* et al. [53]).

that cesium ions may still be found on the surface even when it is positively charged. The bromide ions are attached to the surface not only by electrostatic forces but also by additional chemical interactions. The increase in concentration of bromide ions at the surface results in a coadsorption of cesium ions. The picture that had previously been indirectly built up from thermodynamic investigations is thus confirmed analytically.

A second example is given to illustrate the changes in chemical composition that occur in a solid during oxidation. Figure 10 shows photoelectron spectra taken from a

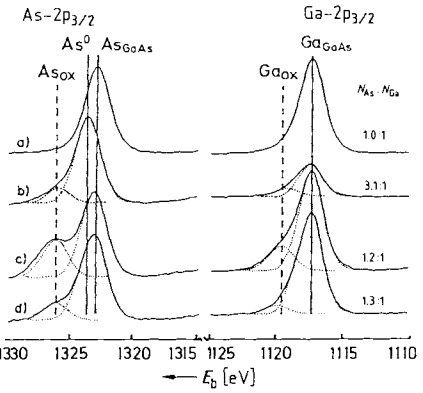

Fig. 10. Photoelectron spectra of [110] n-GaAs electrodes after various treatments [54]; AlK_α radiation; E_b = bonding energy. a) Well defined surface after tempering in UHV. b)–d) After passing 60 mC/cm² in 0.1 M NH_4BF_4 at anodic potentials of 0.7 V (vs. Ag/AgCl) under illumination: b) at pH 2 (addition of $HClO_4$); c) at pH 10 (addition of NH_4OH); d) at pH 13 (addition of NaOH).

gallium arsenide single crystal before and after oxidation.[52,54] The photoelectron spectra of the 2p-core electrons from As and Ga in the solid state after various methods of pretreatment are shown. The spectra taken from a well-defined surface after tempering (Fig. 10a) show the position of the electron energy levels, E_b, and their corresponding intensities, N, in a well-ordered crystal lattice. A spectrum obtained after oxidation in an acidic medium shows a considerable difference in the intensity ratio between the Ga and As signals (Fig. 10b). The As signal is also shifted towards higher binding energies for electrons, which may be attributed to the presence of As–As bonds in elementary As. (In gallium arsenide, arsenic has an excess negative charge which somewhat reduces the binding energy.) It therefore can be concluded that in acidic media the arsenic content is increased whereas the gallium is preferentially oxidized forming a soluble complex. This is a result of the lower electron affinity of the gallium in this bond. Figure 10c shows the spectra obtained after treatment in a weakly alkaline medium. In this case no change is observed in the gallium:arsenic ratio. Both materials are apparently oxidized to more or less the same extent. On removal of the electrolyte from the electrode, however, a part of the oxidized material remains in an oxidized state on the surface. This can be seen from the shift of both signals towards higher binding energies. Clearly the difference in electron affinity observed in the experiments described above is compensated for in alkaline solutions by the strong tendency of arsenic to form acidic compounds with oxygen.[54]

It was also observed that the oxidation of arsenic could be promoted in acidic solutions by the application of high anodic potentials which then lead to only a slight increase of the As concentration at the surface. A more careful analysis of various core level spectra has shown that the As enrichment is not limited only to the topmost layer of the metal but rather also stretches into the bulk of the crystal, so that a porous coverage of clusters of arsenic atoms is obtained.[54] Such processes are extremely important in the surface treatment of semiconductor devices.

The entire range of analytical techniques in surface physics may, of course, be applied to the electrode surface when the electrode may first be transferred to a ultra-high vacuum. For instance, EXAFS may be used to determine interatomic distances in noncrystalline ordered regions or to determine the position of adsorbed atoms or molecules on a surface.[55] Such information may also be obtained from the X-ray fluorescence seen when standing waves are generated on a surface with the use of synchrotron radiation.[56] Many new developments are taking place in this field from which one can expect to obtain very detailed information about bonding on surfaces in the future.

4. Photocurrents as a Means of Detection

Photocurrents may be observed when the absorption of light leads either to the setting free of mobile charge carriers in a solid or to ionization of atoms or molecules. In a metallic conductor where a great many mobile charge carriers already exist, the effect of absorption of light is almost impossible to detect, especially since the lifetime of the excited state is extremely short. Only when they lead to electron emission to a neighboring phase from which the charge carriers may be extracted can photocurrents be observed. Quite another situation exists in the case of semiconductors and insulators. The lifetime of an excited state is much longer here because of the existence of a band gap in their electronic systems. In addition to this, electric fields can exist in the bulk of these materials which can hinder the recombination of excited electrons with vacant energy states, the so-called electron holes or "holes", by spatially separating the two species. An analogous situation occurs for the ionization of atoms or molecules if these come under the influence of an electric field, as often happens at an interface.

If light having a quantum energy greater than the band gap energy, E_{gap}, of the semiconductor is absorbed in its bulk, pairs of conducting electrons and electron holes are generated. This is shown in Figure 11, in the energy band diagram of an n-type semiconductor. If an anodic potential is applied to the semiconductor, i.e. an excess positive charge is present, then in an n-type semiconductor a depletion layer of electrons is produced generating an electric field just under the surface. The holes formed have a specific lifetime during which they can diffuse toward the interface so long as this is within their average diffusion range. On reaching the space charge layer they are drawn to the surface by the electric field there, shown in Figure

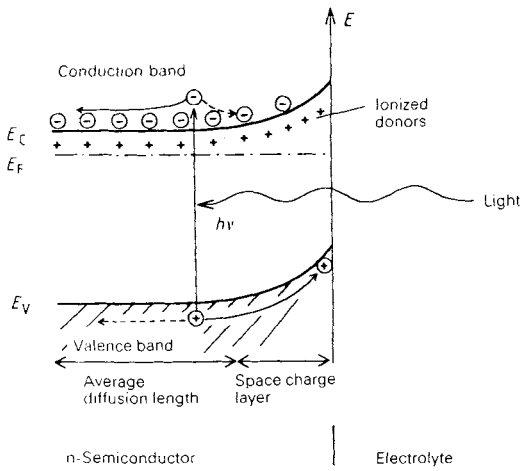

Fig. 11. Energy diagram showing the generation of photocurrents in an n-type semiconductor on application of a positive potential. E_C, E_V = position of the conduction and valence bands, resp.; E_F = Fermi level. The electric field at the interface is shown as a bending of the band edges. ⊖ = conduction electron; ⊕ = hole (defect electron).

11 as a band bending, whereas the conduction electrons are held at a distance from the surface. In this way recombination of the two species is prevented and measurable photocurrents are thus generated in semiconductors. The quantum yield obtained depends upon the properties of the solid, in particular its absorption coefficient of light and the average diffusion length of the holes. At sufficiently high anodic potentials it can reach a maximum quite close to unity.[57-59] In the following, some examples will be given of processes which have been detected by means of photocurrents.

4.1. Photooxidation of Semiconductors

It has been shown that oxidative dissolution of semiconductors occurs as a result of an enrichment of holes at the interface with an electrolyte.[60] Electron holes are simply bonding quantum states of the solid state lattice from which electrons are missing. They therefore weaken the bond strength between neighboring atoms. If such a hole reaches the surface of a solid, it acts as an ideal reaction partner for nucleophilic reagents. Consequently, p-type conductors in contact with an aqueous electrolyte are very easily oxidized on application of an anodic potential since not only nucleophilic reagents such as anions but also water molecules are present in such electrolytes. In the case of n-type conductors, exposure to light is necessary in order to form such holes. On application of anodic potentials they are drawn towards the surface, and the photocurrent observed can be taken as a measure of the decomposition rate.

Certain peculiarities are observed in the quantum yields of the photocurrents measured for germanium and silicon electrodes which provide further information on the mechanisms of these reactions. It can be shown that with these materials, the photocurrent produced can be higher than the quantum yield for production of holes would permit. In the case of silicon, which will be considered here in more detail, this increase in the quantum yield in aqueous electrolytes is only observed when $F^{\ominus}$ ions are present,[61-63] as shown in Figure 12a. In the presence of fluoride, the species $[SiF_6]^{2\ominus}$ is produced as a soluble reaction product.

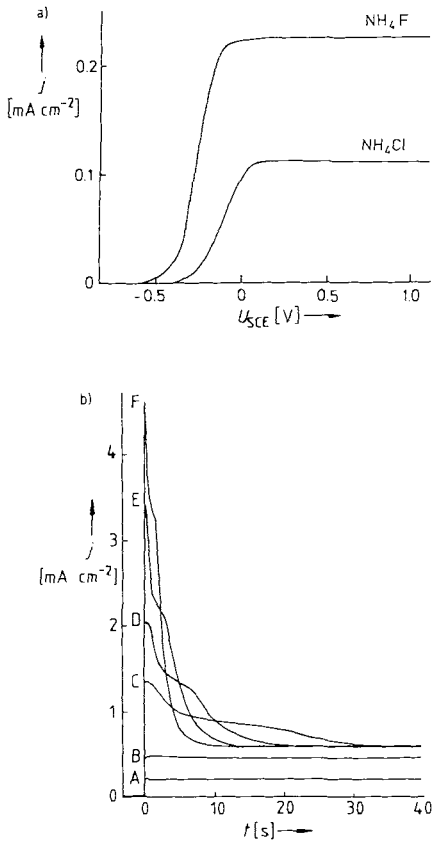

Fig. 12. (a) Photocurrent-potential curves for an n-type silicon electrode in 1 M NH_4F and 1 M NH_4Cl (pH 4.5); j = photocurrent density. b) Time decay of the photocurrents in an n-type silicon electrode in 0.13 M NH_4F (pH 4) at various light intensities: A) 0.3 mW; B) 0.7 mW; C) 2.2 mW; D) 3.6 mW; E) 6 mW; F) 8.8 mW.

In all other electrolytes, films of sparingly soluble or insoluble oxides are formed. When the silicon can react directly with the fluoride ions, the quantum yield is twice as great as in the presence of the oxide (see Fig. 12a). This is also visible in the behavior of the photocurrent when the light intensity is increased to such an extent that the rate of formation of the fluoride complex is no longer rate-determining. The photocurrent-time curves for various light intensities at constant potential in a fluoride-containing solution illustrate this effect (Fig. 12b). At higher intensities a decrease in current is observed after a short period of time, at first to about half of the original value and then to lower values. When the oxide layer reaches a certain limiting thickness the current is only limited by the dissolution rate of the oxide. A more detailed analysis has shown that, at lower light intensities and at the start of the experiment, the photocurrent is twice as great as would be generated exclusively by the transport of holes to the surface. This may be explained by assuming that of the four oxidation steps leading from Si^0 to Si^{IV}, only two are dependent on the presence of a hole as reaction partner for $F^{\ominus}$ ions. The other two steps result from interactions of surface atoms with $F^{\ominus}$ ions in which electrons are injected into the conduction band from the previously produced intermediates

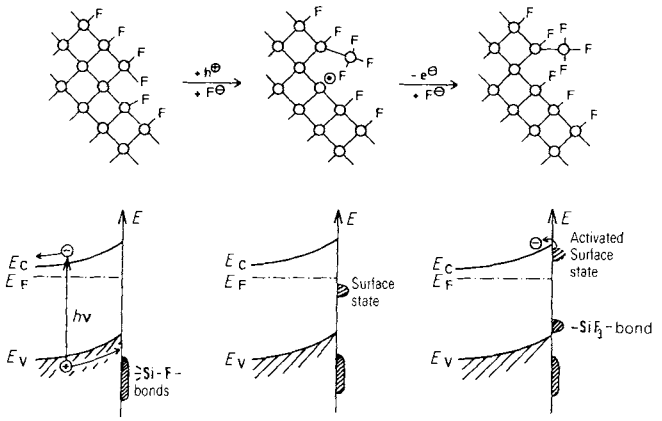

Fig. 13. Oxidation of a silicon electrode in fluoride solution. Top: reaction profile in a 2-dimensional bond scheme. Bottom: the corresponding electron energy terms in an energy band diagram [63]. $h^{\oplus}$ = Defect electron.

which contain an unpaired electron. The reaction path for the two steps is illustrated in Figure 13 (top). The bottom half of the figure also shows how the injection of an electron from the energy level of the unpaired electron in the intermediate product can be explained. An analogous mechanism may be described for the two subsequent steps, which lead to the formation of SiF_4.[63]

If the surface is covered with an oxide layer so that the $F^{\ominus}$ ions can no longer come into direct contact with the Si surface, then further growth of the oxide requires four holes. In the case of germanium, where the oxide is more soluble in acidic and alkaline solutions and the band gap is smaller, this two-step oxidation mechanism with electron injection into the conduction band can even be observed in its reaction with $OH^{\ominus}$ ions.[64] In the case of semiconductors with larger band gaps such as GaAs, GaP, CdS, and ZnO, electron injection from intermediate states is not observed, since in these materials the electrons are so strongly bound even in the radical-like intermediates that the electron cannot be excited to the level of the conduction band by thermal activation.[57]

4.2. Photooxidation of Organic Compounds

Electrons in the conduction band and holes in the valence band have a particular energy value with respect to an electrolyte. Their reactivity towards an electrolyte can thus be described energetically by a type of redox potential. Redox potentials are a measure of the electron affinity of a redox system. The more positive their value, the greater the affinity for, and hence the greater the tendency to take up, electrons, or the lower the tendency to give up electrons. The redox potential may be correlated with the work function involved in taking an electron from a solid phase to a vacuum; the higher the work function, then the greater the electron affinity. The unoccupied states in the valence band of a semiconductor, i.e. the holes, have, therefore, a much greater electron affinity than the unoccupied states in the conduction band. With the help of various techniques, which will not be described in detail here, it is possible to relate the band edges of a semiconductor to the scale of redox potentials of electrolytes.[17-19,65,66]

Figure 14 shows such a scheme for a series of semiconductors. The list of redox potentials—all referred to the normal hydrogen electrode (NHE)—is given in reverse order to that normally used in electrochemistry in order to show that we are concerned here with a thermodynamic scale for electron affinities. If the zero on this scale is put equal to the vacuum then it would lie at about −4.5 V (cf. the right-hand scale in Fig. 14). It can clearly be seen that electronic levels in the conduction and valence bands of various semiconductors have very different redox potentials. The lower down the valence band lies, the more oxidizing are its holes. The higher the level of the conduction band, then the greater the reducing strength of the electrons it contains. On the other hand, extraction of electrons from the valence band, i.e. injection of holes, requires the presence of a redox system with a redox potential lower than the band edge of the valence band and similarly, injection of electrons into the conduction band can only occur from a redox system whose redox potential lies higher than the edge of the conduction band.

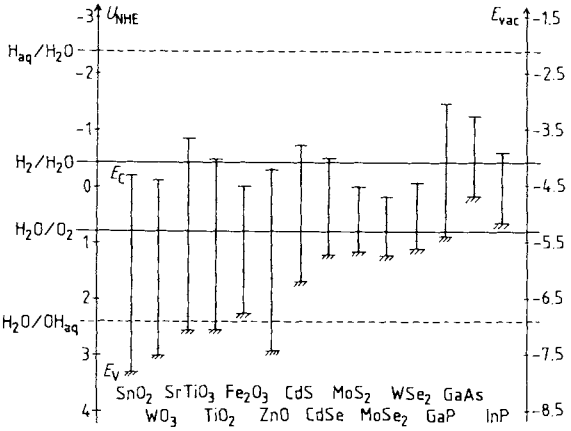

Fig. 14. Positions of the band edges of various semiconductors (at pH 7) in the scale of redox potentials, referred to the NHE (left), and to the vacuum level over the electrolyte (right).

From the position of the valence band edges of the semiconductors shown in Figure 14, it can be seen that holes in the valence band have, in general, a very strong oxidizing capability. This constitutes the energetic explanation for the photodecomposition of semiconductors considered above. If, however, species are present in the electrolyte which react with holes, i.e. which can be oxidized by them, then these reactions compete with the decomposition process and in some cases can completely prevent its occurrence. This is one of the most important factors in the operation of photoelectrochemical solar cells.[67-69]

It is therefore not surprising that organic materials can be oxidized by contact with semiconductors in which holes are generated. If it is desired to measure the competition between the oxidation of a redox system and the anodic decomposition of a semiconductor, however, then it is necessary to carry out analysis of the reaction products in the electrolyte and to determine the weight loss in the semiconductor. Such questions will not be dealt with in detail here but instead, a peculiarity in the photocurrent magnitude will be considered, which gives some insight into the

mechanism of the particular reaction. An increase in the quantum yield of the photocurrent measured in the oxidation of some organic materials analogous to that seen in the previously described oxidation of silicon (Section 4.1) was observed here. This has been found in the case of organic acids, aldehydes and alcohols.[70–72]

As an example, we will consider the oxidation of formic acid on the n-type semiconductor, ZnO. Figure 15 shows that the photocurrent, which reaches a constant value at the anodic potentials applied, increases even further on addition of formic acid. The oxidation of formic acid also occurs in two steps. The $HCOO^{\odot}$ radical is first produced with loss of a proton. An electron hole is necessary for this to occur. The radical can be further oxidized by donation of an electron to the conduction band, thereby doubling the value of the quantum yield. An increase of a factor of two is not quite achieved in Figure 15. This is because the competing photoreactions, such as oxidation of water which also require holes, cannot be completely prevented.

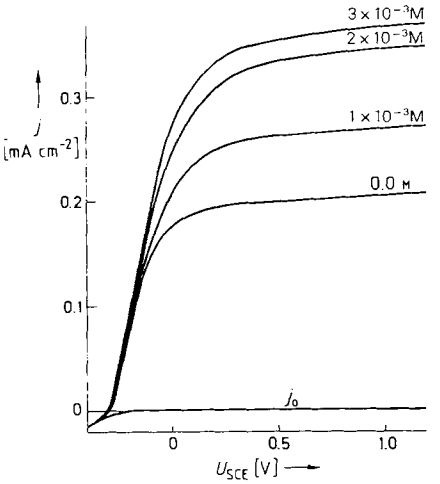

Fig. 15. Photocurrent-potential curves from n-ZnO electrodes in 0.5 M $NaClO_4$ (pH 4) with and without the addition of formic acid in three different concentrations. The dark current density j_0 was chosen as the zero point of the current density scale.

Comparison of the energetic relationships in the redox reactions of the individual steps with the redox properties of the electrons in the valence and conduction bands clearly indicates that the loss of an electron in the second step is, energetically, highly probable. The redox potential of the net reaction with two charge transfers is well known. The first oxidation step, which leads to production of the radical, requires a greater amount of energy and has, thus, a correspondingly higher, i.e. more positive, redox potential. This extra energy required is released again in the second stage, which has, therefore, a more negative redox potential. The redox potentials for the net and partial reactions of formic acid, formaldehyde and methanol are shown in Figure 16 relative to the position of the band edge of ZnO. The redox potentials for the partial reactions which are not known have been deduced from thermodynamic data on the formation energy of the radical in the gas phase. Despite the inaccuracies involved, the resulting picture clearly shows that generation of a hole is required

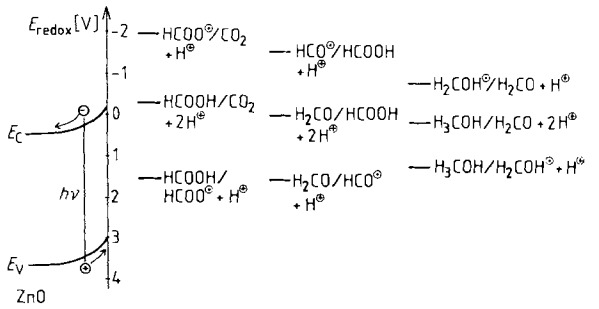

Fig. 16. Positions of the redox potentials for the total and partial reactions of the oxidation of formic acid, formaldehyde, and methanol.

for initiation of the first step, but that the intermediate product possesses enough excess energy to complete the oxidation reaction. The second step, having a redox potential near the conduction band can subsequently take place by the faster electron injection process. A similar explanation may be given for the analogous results obtained for the oxidation of methanol and formaldehyde.[70, 71, 73]

The extraordinary oxidizing properties of holes in semiconductors whose valence bands lie very far down on the redox potential scale shown in Figure 14 have, indeed, practical consequences. They yield, for instance, an explanation as to why pigments, such as TiO_2, may very easily photooxidize and decompose organic materials, such as binding species on exposure to light.

4.3. Passivating Films on Metals

Passivation of metals towards corrosion is a result of the formation of protective films on the metal, usually oxides, which prevent or slow down further attack by the oxidizing agent. These layers possess semiconductor properties and are, sometimes, insulators. When light is absorbed by these films under simultaneous application of an electric potential, photocurrents may be produced. Since they are often very thin, only a fraction of the light is usually absorbed. The transmitted light is partially reflected from the metal and can also contribute to the photocurrent. As a result of the very small film thickness, only a limited space charge is developed in layers of low conductivity, and the electric field extends over the entire film. Even when the film is an insulator, photocurrents can be produced by application of an electric potential, if mobile charge carriers are set free by the absorption of light. Figure 17 shows the conditions necessary for this to occur, by mean of an energy band di-

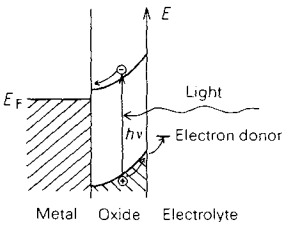

Fig. 17. Electron energy diagram showing the generation of a photocurrent in a semiconducting or an insulating film on a metal.

agram. In this diagram the electric field strength in the film corresponds to the slope of the band edges. A positive slope, in this scheme, implies a negative field. The photocurrent spectrum which may be determined can be used as a means of characterizing the film.[74-76]

As one of the many examples of such phenomena, measurements on tin will be described here.[77] Corrosion of tin in alkaline solution is only partially prevented by the formation of an oxide layer. The photocurrent which is observed is superimposed on a large dark current and must therefore be distinguished from the latter with the use of modulated illumination and the lock-in technique. In spite of this, the technique allows very high sensitivities to be achieved.

A continuous cyclic current-potential curve is shown in Figure 18a alongside the corresponding photocurrents recorded at constant wavelengths. Both the nature and the thickness of the layer are altered during the potential cycle, as is the current density. The dark current shows a large hysteresis. The photocurrent, on the other hand, has a completely different potential dependence from that of the dark current. It indicates the presence of two potential regions in each of which the film shows different properties. This is most clearly seen when the photocurrent is observed in only a particular region during a potential cycle after the electrode has reached a steady state. Curves B and C of Figure 18a illustrate this. The onset of the photocurrent occurs at different potentials.

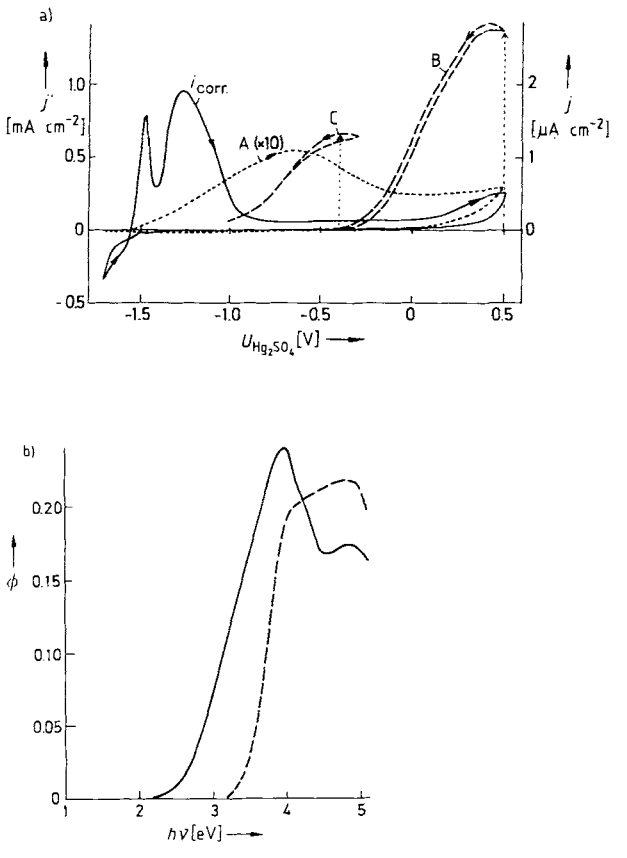

Fig. 18. a) Cyclic current-potential curves for a tin electrode in 1 M KOH solution. Full curve: current measured in the dark; dashed curves: photocurrents measured under illumination by light with a wavelength of $\lambda = 350$ nm A) cycling between -1.6 and $+0.5$ V (vs. Hg/Hg_2SO_4, 1 N H_2SO_4; B) cycling from $+0.5$ V to -0.5 V from an initial potential of $+0.5$ V; C) cycling between -0.4 V and -1.0 V from an initial potential of -0.4 V; [77]. j = photocurrent density; j' = corrosion current density. b) Photocurrent spectra as function of the irradiating energy. Full curve: in the presence of a passivating film on Sn, produced at $+0.5$ V; dashed curve: from an SnO_2 layer produced by chemical vapor deposition on steel at 400 °C. ϕ = Quantum yield.

The photocurrent spectra are also different from one potential region to the other, though the differences are not so marked and indicate only differences in the amount of hydroxide and the number of defects in the films, both of which are dependent on the formation conditions. Figure 18b shows the photocurrent spectrum of a film produced at 0.5 V (corresponding to curve B of Fig. 18a). For comparison, the photocurrent spectrum of an SnO_2 layer produced by chemical vapor deposition is also shown. This layer, produced at 400 °C, has a more well ordered structure and absorption first begins at much higher quantum energy values of the light. The large shift towards longer wavelengths, for the absorption edge of the passive layer, is indicative of the large number of electronic defects in the less well ordered structure.

The information obtainable from such photocurrent spectra is, however, limited. For a more exact chemical and electron-energy analysis of the film it is necessary to use techniques taken from surface physics, which can only be used ex-situ, as already described in Section 3.4.

4.4. Sensitization of Semiconductors

A semiconductor can be made sensitive to light at wavelengths at which it does not usually absorb light by the adsorption of certain substances at its surface. If these species can transfer charge to the semiconductor from an excited state and an electric field is present at the interface, which prevents a back-reaction occurring, then photocurrents are generated whose spectra illustrate the absorption properties of these adsorbed materials.[20,78,79] Dyes are frequently used for this purpose since the quantum yield with respect to incoming light reaches higher values only when the adsorbate has a high extinction coefficient. Ideal substrates are those semiconductors which are transparent to visible light, such as ZnO[80] or TiO_2.[81] Figure 19 illustrates the principles of this type of charge transfer in the energy diagram of a semiconductor on whose surface such molecules are adsorbed. It is assumed here that in the excited state an electron is present in what was formerly the lowest unoccupied level of the unexcited molecule (LUMO) and that the level now unoccupied is that which was previously the highest occupied molecular orbital

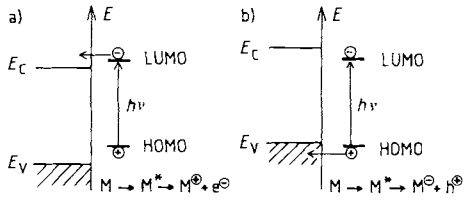

Fig. 19. Energy correlations for the charge transfer occurring between electronically excited molecules and semiconductors: a) electron injection in the conduction band; b) removal of electrons from the valence band = injection of holes.

(HOMO). Figure 19 shows the two possible mechanisms by which the semiconductor may be made responsive to light. In Figure 19a is illustrated the most common case, where the LUMO lies above the edge of the conduction band and a photooxidation is therefore possible by electron injection. A more infrequent mechanism is shown in Figure 19b in which the HOMO now lies below the valence band edge thus enabling a photoreduction of the adsorbed molecule to occur by injection of holes. In order to measure the photocurrent the semiconductor must be polarized in the reverse direction since otherwise the dyes could be either oxidized or reduced in the dark period, or a fast recombination reaction could take place. This means that in case (a) an n-type conductor and in case (b) a p-type conductor is necessary for the charge injection.

The silver halides are also semiconductors in their electronic behavior, though their conductivity in the dark is due to the mobility of the silver ions in the crystal lattice. This property introduces difficulties in the measurement of the electronic photocurrents but the use of the lock-in technique has helped to alleviate this, and has made sensitization measurements on silver halide crystals possible.[82,83] Figure 20 shows a comparison between the sensitized photocurrent spectrum of a thin AgCl single crystal sheet and that of the absorption spectrum of the dye used. The photocurrent spectrum is quite similar to the absorption spectrum but somewhat broader and shifted towards longer wavelengths. The latter is a result of the interaction between the electronically excited molecule and the crystal. Without going into detail, this example is intended to show that this phenomenon, which plays such an important role in the field of photography, can also be observed with electrochemical techniques. The quantum yield in photography is, admittedly, generally rather higher than that obtained in electrochemical experiments since in photographic emulsions the electrons injected from silver ions are very quickly captured on interstitial sites. The silver atoms thus produced form the nuclei necessary for photographic development by grouping together in clusters. This process cannot, however, be seen in a photocurrent since the current is interrupted by the capture of the electrons. Photoelectrochemical measurements are therefore carried out with crystals that have been doped and which have no silver ions in interstitial sites but only silver-ion vacancies.[83] This enables various dyes to be tested for their energetic position and their effectiveness in charge transfer without the need to involve the complicated photographic developing process.

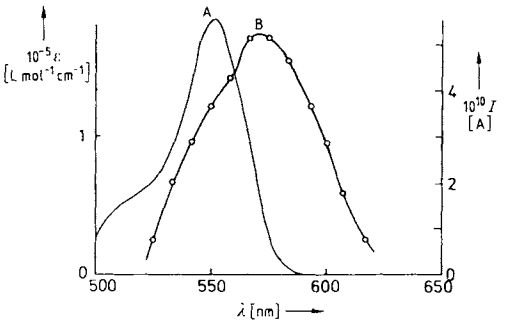

Fig. 20. A) Absorption spectrum (ε) of rhodamine B in 0.1 M $NaClO_4$ and B) the sensitized photocurrent I from a rhodium β-sensitized AgCl crystal (doped with $CdCl_2$) [83].

5. Luminescence as a Means of Detection

When a redox reaction takes place very far from equilibrium, i.e. at very high overpotentials, excited electronic states can be generated by the electron transfer. The consequent dissipation of energy is usually radiationless as the excess energy is transferred to vibrational energy or other heat sinks. In some cases, however, radiation of energy does occur. This may be seen particularly clearly at semiconductor electrodes if an excited state is produced by injection of minority carriers.[22-24] Visible light has, however, also recently been observed to radiate from metal electrodes when the corresponding redox reaction occurs at very high overpotentials.[25]

5.1. Luminescence at Semiconductor Electrodes

From the energy correlations made for photooxidation at semiconductors (see Fig. 14 in Section 4.2) it is clear that an oxidizing species can inject holes only when its redox potential is similar to or more positive than that of the redox potential of the valence band edge. In the same way, a reducing species can only inject electrons if its redox potential is the same or more negative than the redox potential of the conduction band edge. What would happen then if a hole were injected into an n-type conductor? As long as the n-type conductor remains anodically polarized, its conducting electrons are kept at a distance from the surface. The injection of holes into the surface then leads to corrosion of the semiconductor, usually without a current flowing. A reduction current can normally first be observed when the applied potential no longer keeps the electrons away from the surface or actually leads to accumulation of electrons on the surface. Thermodynamically speaking, the reduction then takes place at a very high overpotential, which is higher the bigger the band gap of the semiconductor. There are, thus, two possible mechanisms for the reduction process; these are shown in Figure 21.

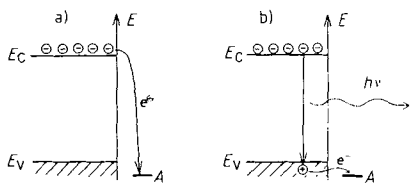

Fig. 21. Two possible mechanisms for the reduction of an electron acceptor at a semiconductor. When the acceptor A injects holes (case b), luminescence can occur.

a) The electrons can be directly transferred to the acceptor in the electrolyte. The excess energy is taken up by the acceptor and the surrounding solution mainly as vibrational energy and subsequently dissipated as heat. The rate

of electron transfer is then determined by the Franck-Condon factors governing the excitation of these vibrations.
b) Despite the presence of electrons at the surface, holes may still be injected which can then recombine with the electrons. This recombination normally takes place as a radiationless process at the interface. It can, however, also result in a radiative emission of the excess energy, which in the case of semiconductors can be observed under illumination as photoluminescence.

Experiments on n-type conductors for which photoluminescence is known to occur has shown that luminescence is very often observed when very strongly oxidizing redox systems are reduced.[22-24] Figure 22a illustrates an example of this. In the upper region the current-potential curve for the reduction of $Fe(CN)_6^{3\ominus}$ at n-gallium phosphide is given.[84] Also shown is the variation of the luminescence with applied potential. Figure 22b shows the spectrum of the luminescent light. The potential, U_{fb}, at which there is no excess charge on the semiconductor is indicated; this is the so-called flat band potential. At this potential the concentration of electrons at the surface is equal to that in the bulk. At more positive potentials electrons are prevented from reaching the surface; at more negative potentials the surface is enriched with electrons. It may be seen that the reduction current flows before this potential is actually reached. Thus, despite the potential barrier, electrons are able to reach the surface in sufficient numbers, and recombine there with injected holes. Luminescence can, however, only be seen close to the flat band potential, U_{fb}, and increases rapidly beyond this potential.

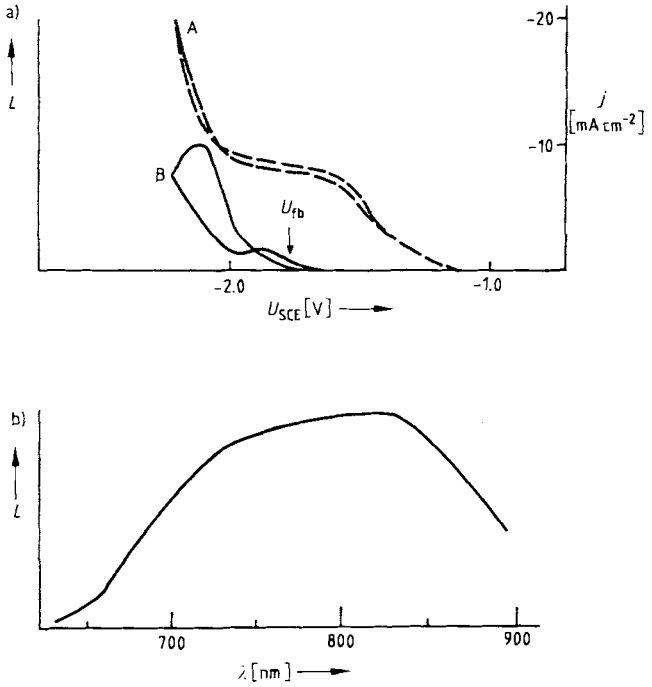

Fig. 22. The reduction of $[Fe(CN)_6]^{3\ominus}$ at an n-GaP electrode in 1 M KOH. a) Current-potential curve and potential dependence of the luminescence ina 0.1 M $[Fe(CN)_6]^{3\ominus}$ solution (the hysteresis is attributed to a chemical change taking place on the surface). b) Corresponding luminescence spectrum [84]. L = luminescence in relative units.

Recombination at the surface is apparently radiationless. When, however, holes can diffuse into the interior of the semiconductor before they are captured by recombination at the surface, luminescence results. At potentials more cathodic than the flat band potential, electrons accumulate at the surface. An electric field is thereby generated which draws the holes towards the bulk of the semiconductor and the intensity of the luminescence is further increased. The luminescence spectrum thus observed corresponds to that of the luminescence produced when the semiconductor is exposed to light of an energy which is absorbed by its bulk.[84]

This indicates that the mechanism of electron transfer is that described in case (b) above (cf. Fig. 21b), which is in agreement with the theoretical assumption that electron transfer occurs preferentially between energy levels of equal energy.[85-87] The increase in luminescence in the potential region cathodic of the flat band potential shows this very clearly; despite the increasing concentration of electrons at the surface which should facilitate mechanism (a), the luminescence continues to increase since more holes can diffuse into the bulk.

5.2. Luminescence from Metal Electrodes

There is no gap in the upper energy bands of a metal where conduction occurs; they overlap each other. Because of this, excited electronic states have a very short lifetime. A recombination involving radiation is, therefore, highly improbable. A radiation of excess energy can, however, be observed in experiments with injection of electrons to the metal from vacuum—the so-called inverse photoemission.[88] The injection currents in these experiments are small. Much larger currents can be achieved in electrochemical reactions. The question, then, is whether such luminescence can also be observed at electrochemical electrodes at sufficiently high overpotentials.

Since the overpotentials that can be reached are limited by the decomposition potentials of the solution involved, water is not an ideal medium for such experiments. They are therefore usually carried out in nonaqueous electrolytes. It has been shown that emission of light does actually occur during oxidation of a redox system with a very negative redox potential at very positive potentials[89] and during reduction of a redox system with a very positive redox potential at very negative potentials.[90,91] Such experiments can usually only be carried out with noble metal electrodes which do not corrode at the very high redox potentials necessary. They show that the electron transfer between metal and redox system at very high overpotentials leads to excited electronic states in the metal which correspond either to electrons in energy levels far above the Fermi level or to holes far below it. These states can release their excess energy as radiation. Figure 23 illustrates these possibilities in an energy diagram. On the right-hand side is shown the energy distribution of the electron levels of the compound to be oxidized (Fig. 23a) or reduced (Fig. 23b) and on the left-hand side the energy levels in the metal that are occupied or vacated in the electron transfer. The dissipation of energy after electron transfer takes place to an overwhelming extent by a radiationless elec-

tron-electron or electron-phonon interaction; the experiment shows, however, that transitions involving radiation of energy also occur.

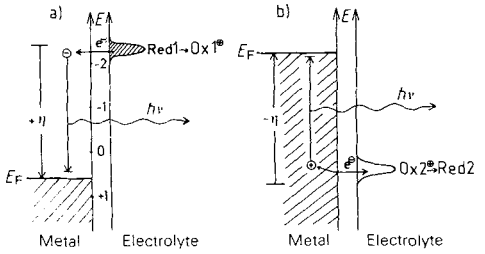

Fig. 23. Principles of the generation of luminescence by (a) electron injection and (b) hole injection when a redox reaction takes place at a metal electrode at high overpotentials. η = Energy difference between the redox potential—of the compound to be oxidized or reduced—and the Fermi level of the electrode metal.

Figure 24 shows spectra corresponding to the light radiated at various potentials in the experiment shown in Figure 23a.[92] It may be seen that, as predicted by this model, the radiation is shifted to shorter wavelengths, i.e. higher energies, as the overpotential is increased. The model of equipotential electron transfer is thus also experimentally established for metal electrodes.

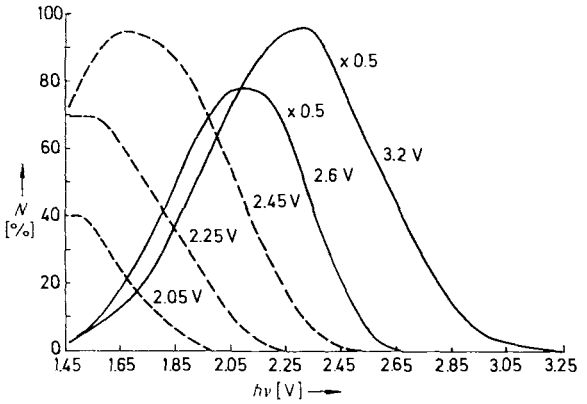

Fig. 24. Luminescence spectra produced on injection of electrons from the reduced *trans*-stilbene (0.02 M) in a solution of acetonitrile and 0.2 M $(C_4H_9)_4NPF_6$ at the indicated potentials. Full curves are for gold electrodes, dashed curves for silver electrodes (after *McIntyre* [92]). N = Intensity.

6. Future Trends

The results obtained with the spectroscopic methods described above have made a significant contribution to the understanding of both the mechanistic pathways of electrochemical processes and the influence exerted by the electronic properties of the electrode in these reactions. Another equally important factor in the understanding of electrode properties is the role played by their surface structures. To obtain information on this topic it is necessary to carry out experiments on well-defined single crystal surfaces. The development of UHV techniques and the methods of analysis made possible with their use has allowed considerable progress also to be made in this field. The structure of electrode surfaces may be determined on transfer to UHV by electron diffraction techniques such as LEED (Low Energy Electron Diffraction) or RHEED (Reflective High Energy Electron Diffraction).[15,93] The separation between individual atoms and their nearest neighbors can be determined with the help of EXAFS (Extended X-ray Absorption Fine Structure). This can even be carried out on electrodes in-situ.[94] The X-ray fluorescence from atoms in an adsorbed film on a well-prepared single crystal surface can be used to determine their exact separation from the surface and their exact position on the electrode surface. The adsorbed layer is made to fluoresce in the field of an X-ray standing wave which can be produced with the use of synchrotron radiation. This technique may also be applied in-situ.[56] Finally, great hopes are held for the use of scanning tunneling microscopy (STM) in the determination of the surface structure of electrodes, particularly if it is possible to apply this technique in-situ, i.e. with the electrode still in the electrolyte. Such studies are at present being carried out in various laboratories.

Despite all the complications of the electrochemical system, the use of interdisciplinary techniques as described above indicates the direction which should be taken to achieve a deeper understanding of reaction routes on an atomic or molecular level. This should also prove extremely fruitful for the many complex technical applications of electrochemistry.

The author wishes to express his thanks to Dr. Teresa A. Twomey, at present a Alexander-von-Humboldt fellow at the Fritz-Haber-Institut der Max-Planck-Gesellschaft in Berlin, for translating the original German text into English.

Received: August 12, 1987 [A 650 IE]
German version: *Angew. Chem. 100* (1988) 63

[1] L. Tronstad, *Z. Phys. Chem. Abt. A 142* (1929) 241; *Trans. Faraday Soc. 29* (1933) 235.
[2] R. H. Müller in P. Delahay, C. W. Tobias (Eds.): *Advances in Electrochemistry and Electrochemical Engineering, Vol. 9*, Wiley, New York 1973, p. 167.
[3] B. D. Cahan, *Surf. Sci. 56* (1976) 354.
[4] D. E. Aspnes, A. A. Studna, *Phys. Rev. B 27* (1983) 985.
[5] A. Bewick, S. Pons in R. J. H. Clark, R. E. Hester (Eds.): *Advances in Infrared and Raman Spectroscopy, Vol. 12*, Wiley, New York 1985, p. 1.
[6] J. K. Foley, C. Korzeniewski, J. L. Daschbach, S. Pons in A. J. Bard (Ed.): *Electroanalytical Chemistry, Vol. 14*, Dekker, New York 1986, p. 309.
[7] J. D. E. McIntyre in P. Delahay, C. W. Tobias (Eds.): *Advances in Electrochemistry and Electrochemical Engineering, Vol. 9*, Wiley, New York 1973, p. 61.
[8] D. M. Kolb in R. J. Gale (Ed.): *Spectroelectrochemistry*, Plenum, New York 1987, p. 8.
[9] W. N. Hansen, A. Prostak, *Phys. Rev. 174* (1968) 500.
[10] J. D. E. McIntyre, *Surf. Sci. 37* (1973) 658.
[11] M. Fleischmann, P. J. Hendra, A. J. McQuillan, *J. Chem. Soc. Chem. Commun. 1973*, 80; *Chem. Phys. Lett. 26* (1974) 163.
[12] Summary reports in R. K. Chang, T. E. Furtak (Eds.): *Surface Enhanced Raman Scattering*, Plenum, New York 1982.
[13] J. S. Hammond, N. Winograd, *J. Electroanal. Chem. Interfacial Electrochem. 80* (1977) 123.
[14] D. M. Kolb, W. N. Hansen, *Surf. Sci. 79* (1979) 205.
[15] D. M. Kolb, *Z. Phys. Chem. Munich 154* (1987) 179.
[16] G. C. Barker, *Ber. Bunsenges. Phys. Chem. 75* (1971) 728.
[17] Yu. Ya. Gurevich, Yu. V. Pleskov, Z. A. Rotenberg: *Photoelectrochemistry*, Consultants Bureau - Plenum, New York 1980.
[18] H. Gerischer in P. Delahay, C. W. Tobias (Eds.): *Advances in Electrochemistry and Electrochemical Engineering, Vol. 1*, Wiley, New York 1961, p. 139.
[19] Yu. V. Pleskov, Yu. Ya. Gurevich: *Semiconductor Photoelectrochemistry*, Consultants Bureau - Plenum, New York 1986.
[20] H. Gerischer, F. Willig, *Top. Curr. Chem. 61* (1976) 31.

[21] W. West, *Photogr. Sci. Engin. 18* (1974) 35.
[22] K. H. Beckmann, R. Memming, *J. Electrochem. Soc. 116* (1969) 368.
[23] B. Pettinger, H.-R. Schöppel, H. Gerischer, *Ber. Bunsenges. Phys. Chem. 80* (1976) 849.
[24] A. B. Ellis in R. B. Hall, A. B. Ellis (Eds.): *Chemistry and Structure at Interfaces: New Laser and Optical Techniques*, VCH Verlagsgesellschaft, Weinheim/VCH Publishers, Deerfield Beach, FL (USA) 1986, p. 245.
[25] R. McIntyre, J. K. Sass, *J. Electroanal. Chem. Interfacial Electrochem. 196* (1985) 199.
[26] A. Bewick, K. Kunimatsu, S. Pons, *Electrochim. Acta 25* (1980) 465.
[27] H. Neugebauer, G. Nauer, N. Brinda-Konopik, G. Gidaly, *J. Electroanal. Chem. Interfacial Electrochem. 122* (1982) 381.
[28] T. Davidson, S. Pons, A. Bewick, P. P. Schmit, *J. Electroanal. Chem. Interfacial Electrochem. 125* (1981) 237.
[29] W. G. Golden, K. Kunimatsu, H. Seki, *J. Phys. Chem. 88* (1984) 1275.
[30] J. W. Russel, J. Overend, K. Scanlon, M. Severson, A. Bewick, *J. Phys. Chem. 86* (1982) 3066; *87* (1983) 293.
[31] V. S. Bagotski, Yu. B. Vassiliev, O. A. Khazova, *J. Electroanal. Chem. Interfacial Electrochem. 81* (1977) 229.
[32] J. Willsau, O. Wolter, J. Heitbaum, *J. Electroanal. Chem. Interfacial Electrochem. 185* (1985) 163.
[33] B. Beden, C. Lamy, A. Bewick, K. Kunimatsu, *J. Electroanal. Chem. Interfacial Electrochem. 121* (1981) 343.
[34] K. Kunimatsu, *J. Electroanal. Chem. Interfacial Electrochem. 213* (1986) 149.
[35] N. Sheppard, T. T. Nguyen in R. J. H. Clar, R. E. Hester (Eds.): *Advances in Infrared and Raman Spectroscopy, Vol. 5*, Heyden, London 1978, p. 67.
[36] T. Iwasita, W. Vielstich, E. Santos, *J. Electroanal. Chem. Interfacial Electrochem. 229* (1987) 367.
[37] S. Wilhelm, W. Vielstich, H. W. Buschmann, T. Iwasita, *J. Electroanal. Chem. Interfacial Electrochem. 229* (1987) 377.
[38] D. F. A. Koch, D. E. Scaife, *J. Electrochem. Soc. 113* (1966) 302.
[39] B. O. Seraphin in A. Beer (Ed.): *Semiconductors and Semimetals, Vol. 1X*, Academic Press, New York 1972, p. 1.
[40] R. Adžić, E. Yeager, B. D. Cahan, *J. Electroanal. Chem. Interfacial Electrochem. 85* (1977) 267.
[41] W. J. Plieth, *Isr. J. Chem. 18* (1979) 105.
[42] B. Pettinger, U. Wenning, D. M. Kolb, *Ber. Bunsenges. Phys. Chem. 82* (1978) 1326.
[43] J. Schneider, D. M. Kolb, A. Otto, unpublished.
[44] R. M. Schmidt, W. J. Plietz, *J. Electroanal. Chem. Interfacial Electrochem. 201* (1986) 163.
[45] D. M. Kolb in H. Gerischer, C. W. Tobias (Eds.): *Advances in Electrochemistry and Electrochemical Engineering, Vol. 11*, Wiley, New York 1978, p. 125.
[46] R. Kötz, D. M. Kolb, *Surf. Sci. 97* (1980) 575.
[47] R. K. Chang, *Ber. Bunsenges. Phys. Chem. 91* (1987) 296.
[48] J. A. Creighton, C. G. Blatchford, M. G. Albrecht, *J. Chem. Soc. Faraday Trans. 2 75* (1979) 790.
[49] M. Kerker, D.-S. Wang, H. Chow, O. Siiman, L. A. Bumm in R. K. Chang, T. E. Furtak (Eds.): *Surface Enhanced Raman Scattering*, Plenum, New York 1982, p. 109.
[50] B. Pettinger, A. Gerolymatou, *Ber. Bunsenges. Phys. Chem. 88* (1984) 359.
[51] P. Hildebrand, M. Stockburger, *J. Phys. Chem. 90* (1986) 6017.
[52] T. Solomun, W. Richtering, H. Gerischer, *Ber. Bunsenges. Phys. Chem. 91* (1987) 412.
[53] D. M. Kolb, L. Rath, R. Wille, W. N. Hansen, *Ber. Bunsenges. Phys. Chem. 87* (1983) 1108.
[54] W. Richtering, *Dissertation*, Technische Universität Berlin 1987.
[55] J. Stöhr, R. Jaeger, *Phys. Rev. B 26* (1982) 4111.
[56] G. Materlik, M. Schmäh, J. Zegenhagen, W. Uelhoff, *Ber. Bunsenges. Phys. Chem. 91* (1987) 292.
[57] W. Gärtner, *Phys. Rev. 116* (1959) 84.
[58] H. Reiss, *J. Electrochem. Soc. 125* (1978) 937.
[59] J. Reichman, *Appl. Phys. Lett. 36* (1980) 574.
[60] H. Gerischer, W. Mindt, *Electrochim. Acta 13* (1968) 1329.
[61] R. Memming, G. Schwandt, *Surf. Sci. 4* (1966) 109.
[62] M. Matsumura, S. R. Morrison, *J. Electroanal. Chem. Interfacial Electrochem. 144* (1983) 113; *147* (1983) 157.
[63] H. Gerischer, M. Lübke, *Ber. Bunsenges. Phys. Chem. 91* (1987) 394.
[64] H. Gerischer, F. Beck, *Z. Phys. Chem. Frankfurt 24* (1960) 378.
[65] H. Gerischer in H. Eyring, D. Henderson, W. Jost (Eds.): *Physical Chemistry, Vol. 9A*, Academic Press, New York 1970, p. 463.
[66] R. Memming in B. E. Conway (Ed.): *Comprehensive Treatise of Electrochemistry, Vol. 7*, Plenum, New York 1983, p. 529.
[67] H. Gerischer, *Top. Appl. Phys. 31* (1979) 115.
[68] A. Heller (Ed.): *Semiconductor Liquid-Junction Solar Cells, Proceedings 77-3*, The Electrochemical Society, Princeton 1977.
[69] M. Grätzel (Ed.): *Energy Resources through Photochemistry and Catalysis*, Academic Press, New York 1983.
[70] W. P. Gomes, T. Freund, S. R. Morrison, *J. Electrochem. Soc. 115* (1968) 818.
[71] E. C. Dutoit, F. Cardon, W. P. Gomes, *Ber. Bunsenges. Phys. Chem. 80* (1976) 1285.
[72] Y. Maeda, A. Fujishima, K. Honda, *J. Electrochem. Soc. 128* (1981) 1781.
[73] H. Gerischer, unpublished.
[74] J. F. McAleer, L. M. Peter, *Faracay Discuss. R. Soc. Chem. 70* (1980) 67.
[75] U. Stimming, *Electrochim. Acta 31* (1986) 415.
[76] L. M. Peter, *Ber. Bunsenges. Phys. Chem. 91* (1987) 419.
[77] T. D. Burleigh, H. Gerischer, unpublished.
[78] D. Möbius in H. Gerischer, J. J. Katz (Eds.): *Light-Induced Charge Separation in Biology and Chemistry (Dahlem Workshop Reports Life Sc. 12)*, Verlag Chemie, Weinheim 1979, p. 171.
[79] R. Memming in S. G. Davison (Ed.): *Progress in Surface Science, Vol. 17*, Pergamon, New York 1984, p. 7.
[80] H. Gerischer, H. Tributsch, *Ber. Bunsenges. Phys. Chem. 72* (1968) 437; *73* (1969) 251.
[81] T. Takizawa, T. Watanabe, K. Honda, *J. Phys. Chem. 82* (1978) 1391.
[82] H. Gerischer, H. Selzle, *Electrochim. Acta 18* (1973) 799.
[83] H. Gerischer, B. Bressel, *Ber. Bunsenges. Phys. Chem. 89* (1985) 1083.
[84] B. Smandek, H. Gerischer, *Electrochim. Acta 30* (1985) 1101.
[85] R. A. Marcus, *J. Chem. Phys. 24* (1956) 966; *43* (1965) 679.
[86] H. Gerischer, *Z. Phys. Chem. Frankfurt 26* (1960) 233; *27* (1961) 48.
[87] V. G. Levich in P. Delahay, C. W. Tobias (Eds.): *Advances in Electrochemistry and Electrochemical Engineering, Vol. 4*, Wiley, New York 1966, p. 249.
[88] V. Dohse, *Progr. Surf. Sci. 13* (1983) 225.
[89] R. McIntyre, J. K. Sass, *Phys. Rev. Lett. 56* (1986) 651.
[90] R. McIntyre, D. K. Roe, J. K. Sass, H. Gerischer, *Ber. Bunsenges. Phys. Chem. 91* (1987) 488.
[91] J. Ouyang, A. J. Bard, *J. Phys. Chem. 91* (1987) 4058.
[92] R. McIntyre, unpublished.
[93] M. S. Zei, G. Qiao, G. Lehmpfuhl, D. M. Kolb, *Ber. Bunsenges. Phys. Chem. 91* (1987) 349.
[94] L. Blum, H. D. Abruña, J. White, J. G. Gordon II, G. L. Borges, M. G. Samant, O. R. Melroy, *J. Chem. Phys. 85* (1986) 6732.

ANGEWANDTE CHEMIE

International Edition in English

Volume 27 · Number 1
January 1988
Pages 79–88

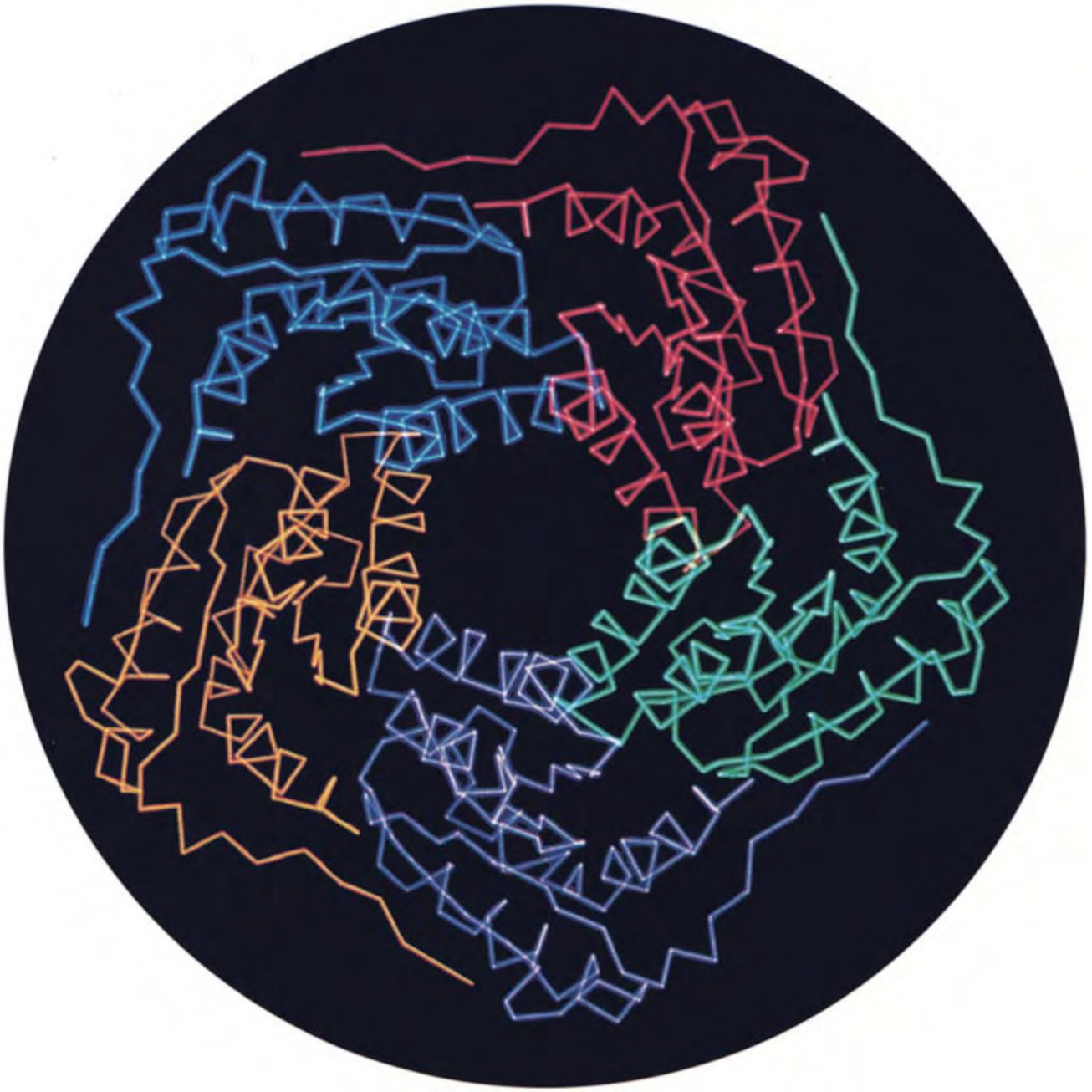

Robert Huber

Flexibility and Rigidity of Proteins and Protein–Pigment Complexes

 © VCH Verlagsgesellschaft mbH, D-6940 Weinheim, 1988 *0570-0833/88/0101-0079 $ 02.50/0*

Flexibility and Rigidity of Proteins and Protein-Pigment Complexes**

By Robert Huber

Proteins may be rigid or flexible to various degrees as required for optimal function. Flexibility of large parts of a protein, which rearrange or move, is particularly interesting and will be discussed in this article. We differentiate between several categories, although the boundaries between them are diffuse: flexibility of peptide segments, order-disorder transitions of spatially contiguous regions, and domain motions. The domains may be flexibly linked to allow rather unrestricted motions or the motions may be constrained to certain modes. The various categories of large-scale flexibility will be illustrated with the following examples: (1) Small protein proteinase inhibitors are rather rigid molecules which provide binding surfaces complementary to their cognate proteases but show also limited segmental flexibility and adaptation. (2) Large plasma proteinase inhibitors exhibit large conformational changes after interaction with proteases probably for regulatory purposes. (3) Pancreatic serine proteases employ a disorder-order transition of their activation domain as a means to regulate enzymic activity. (4) Immunoglobulins show rather unrestricted and also hinged domain motions in different parts of the molecule probably to allow binding to antigens in different arrangements. (5) Citrate synthase adopts open and closed forms by a hinged domain motion to bind substrates and release products and to perform the catalytic condensation reaction, respectively. (6) Riboflavin synthase, a bifunctional multienzyme complex, catalyzes two consecutive reactions by means of two subunits, α and β. The β-subunits form a shell, in which the α-subunits are enclosed. Diffusional motion of the catalytic intermediates is therefore restricted. In addition, rearrangement of the *N*-terminal segment occurs during the assembly of the β-subunit. In contrast, rigidity is dominant in the structures of the light-harvesting complexes and the photosynthetic reaction centers involved in photosynthetic light reactions. These are large protein-pigment complexes in which the proteins serve as matrices to hold the pigments in the appropriate conformation and relative arrangement. Since motion would contribute to deactivation of the photoexcited states of the pigments and diminish the efficiency of light-energy and electron transfer, the functional role of rigidity is easy to rationalize for these proteins.

1. Introduction

The term molecular flexibility is not well-defined but is picturesque and used often in reference to vibrations, disorder, or structural adaptation of molecules. These are quite diverse physical phenomena, but all are determined by the nature and three-dimensional arrangement of the atoms of the molecules and the force field in which the atoms move.

Many physical and chemical properties of molecules depend on their dynamic properties, which have been studied by a variety of theoretical and experimental approaches. Such studies have led to a very detailed understanding of structure and dynamics of many small molecules. However, theoretical approaches to understanding the flexibility of proteins by analysis of the normal modes of vibrations or by molecular dynamics suffer from both fundamental and computational problems, owing to the very large number of atoms and internal vibrational degrees of freedom, the lack of precise knowledge of the potential energy for displacement from the equilibrium atomic positions, and the breakdown of the harmonic approximation in normal-mode analysis. In addition, the effects of the solvent cannot be neglected and add to the complexity of the system. Despite these limitations, some useful information about macromolecules has been obtained by theoretical approaches.[1-5]

Similarly, experimental approaches in the case of complex protein molecules provide usually only partial and approximate insights. These are nevertheless most welcome in view of the importance of dynamic properties for protein function. It seems likely that essentially any interaction of proteins with small or large ligands involves some structural adaptation: be it enzymic reactions, where chemical bonds are formed or broken or groups of atoms transferred, be it rearrangements of domains in proteins or of subunits in oligomeric proteins occurring in a cycle of reactions, motion is essential. Even in structural proteins, such as viral capsid proteins, flexibility of parts is important for the assembly process.[6]

On the other hand, the constituent groups of atoms are as densely packed in protein molecules as in crystals, indicating quasi-crystallinity and rigidity. Steric complementarity intimately related to rigidity is indeed the basis for precise protein-ligand interaction. Thus it is important to recognize that both flexibility and rigidity are general

[*] Prof. Dr. R. Huber
Max-Planck-Institut für Biochemie
D-8033 Martinsried (FRG)

[**] The preceding page shows Figure 8c of this article.

properties of protein molecules and that one or the other apparently dominates in each particular case.

To illustrate this, a number of proteins with various kinds and degrees of flexibility, as well as their functional significance and the underlying structural features, will be discussed and compared with particularly rigid proteins. The selection of examples and aspects is somewhat arbitrary but will emphasize flexibility involving the movement or rearrangement of large parts of proteins. Small-scale flexibility at the level of amino acid side chains is also functionally important but occurs universally and seems less interesting in an attempt to document the versatility of proteins.

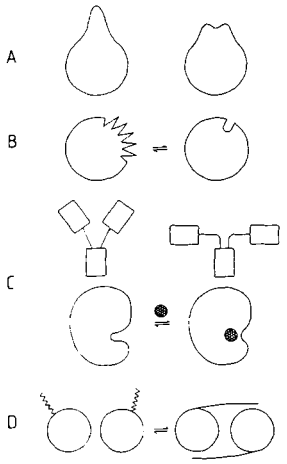

Fig. 1. Types of large-scale flexibility: A) segmental flexibility; B) order-disorder transition; C) free and hinged domain motion; D) rearrangement in subunits during assembly.

Figure 1 illustrates the various kinds of flexibility observed in proteins and discussed in the examples below. Flexibility occurs at the level of amino acid side chains, polypeptide segments, or domains. Flexibility of large parts of a protein might serve a regulatory purpose, allow binding to epitopes in different geometric arrangements, generate an active site, or stabilize oligomeric association.

2. Segmental Flexibility

Small protein proteinase inhibitors are particularly stable protein molecules by a variety of criteria. Basic pancreatic trypsin inhibitor (BPTI), a representative of this class of proteins, is thermally very stable and a high proportion of the main-chain amide hydrogen atoms do not undergo exchange in D_2O as shown by ^{1}H-NMR[7,8] and neutron diffraction studies.[9] However, NMR studies have also shown that BPTI undergoes very substantial structural fluctuations as revealed by the observation of flipping of aromatic amino acid side chains located in the interior of the protein molecule.[10] This is a process requiring high activation energies and activation volumes and indicates that large fluctuations of energy and void volume occur in the protein even at room temperature.

X-ray diffraction techniques are unable to provide information about such activated processes, which are rare and very fast and do not measurably influence the crystal structure observed as an average in time and space. However, X-ray diffraction data do bear information on the positions and the temperature factors (or, better, disorder factors) of the atoms. The latter are measures of the average deviation from the equilibrium positions. They help to differentiate rigid and "flexible" parts of a protein, but do not distinguish between the quite different physical phenomena of thermal mobility and static disorder. In addition to temperature factors, the analysis of different crystal forms of the same protein may help to define flexible parts, since, in contrast to the rigid parts, they are readily distorted by crystal lattice forces (Fig. 2).

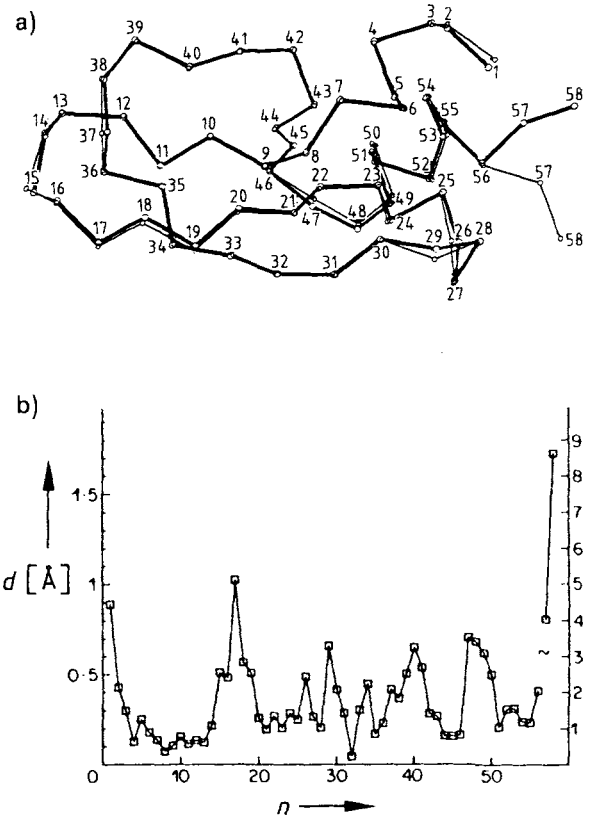

Fig. 2. Comparison of two different crystal forms of BPTI. a) Overlay of the C^α atomic positions; b) their positional deviations [11]. n = position, d = deviation (the right ordinate refers to residues 56, 57).

In the case of BPTI, both experiments, the analysis of temperature factors and the comparison of different crystal forms[11] showed enhanced flexibility of the segment around lysine 18. This segment is involved in binding to proteases and undergoes slight rearrangements upon complex formation to improve the stereochemical fit of the interacting surfaces (see Fig. 10 in Ref. [12]). Segmental flexibility is functionally relevant in this case. Similar phenomena have been found in the family of ovomucoids and secretory inhibitors.[13,14] It has been observed that the segment of the inhibitor buried in the complex shows much lower temperature factors in the complex than in the free state (see Fig. 11a in Ref. [13] and Fig. 5 in Ref. [14]).

The structural adaptations upon complex formation are small and not at variance with the notion of preformed

steric complementarity between small protease inhibitors and their cognate proteases. In accord with this notion, all inhibitors of serine proteases, even those with unrelated polypeptide chain folds show a closely similar conformation of the protease binding segment.[15, 16]

The consistent picture of structure and function of small protein inhibitors of serine proteases does not hold for α_1 protease inhibitor, the major serine protease inhibitor in mammalian blood. It is a much larger molecule and functions differently in at least one respect: proteases specifically cleave the susceptible peptide bonds in both small and large inhibitors, but the cleaved species are active only in the small inhibitors, where the new chain ends remain in close proximity as recent crystal structure analyses of cleaved ovomucoid inhibitors have shown (Fig. 3a).[17] In-

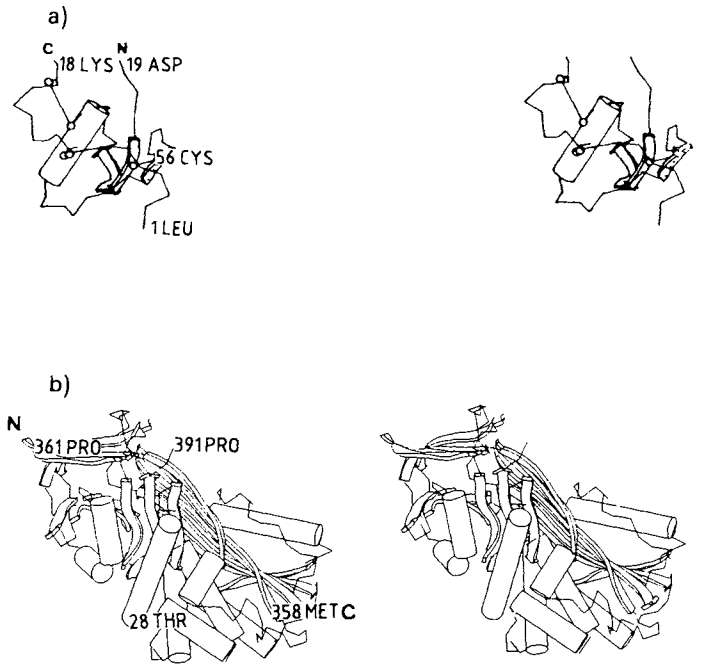

Fig. 3. a) Stereodrawing of the cleaved form of Japanese quail ovomucoid inhibitor OMJPQ. The new *N*- and *C*-termini (N and C) at residues 18 and 19 produced by proteolytic cleavage remain in close proximity [17]. b) Stereodrawing of the cleaved form of α_1 protease inhibitor. The new chain ends (N and C) at residues 359 and 358 are located on opposite ends of the molecule [19].

teraction of the cleaved species with proteases leads to resynthesis of the susceptible peptide bond.[18] In contrast, the cleaved species of α_1 protease inhibitor is inactive. An analysis of the crystal and molecular structure of α_1 protease inhibitor has provided an interpretation in molecular terms.[19] The structure of α_1 protease inhibitor cleaved at Met358–Ser359 showed a compact molecule with a very high proportion of well-ordered secondary structure. Surprisingly, the new chain termini Met358 and Ser359 were found on opposite ends of the molecule, separated by about 70 Å and incorporated in two β-sheets (Fig. 3b). Although the structure of the intact α_1 protease inhibitor is not yet known, it is clear that it is rather different since Met358 and Ser359 are covalently bonded in this species. In accord with this notion, a number of observations suggest that cleavage of the Met358–Ser359 bond is accompanied by very substantial alterations in structure, stability,

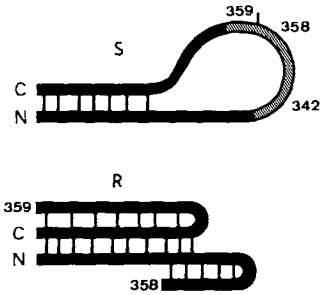

Fig. 4. In the intact form of the α_1 protease inhibitor, the segment around 358–359 is believed to be exceptionally exposed and in a strained conformation (S). Upon limited proteolysis, the molecule relaxes to the crystallographically observed compact form (R), shown in Fig. 3b.

and physiological properties (Fig. 4).[20] The intact protein species may be regarded as a strained form (S), which relaxes after limited proteolysis to form R. Conformational strain may accumulate in the Met358–Ser359 peptide bond and lead to exceptional affinity toward serine proteases.

α_1 protease inhibitor is a member of a large family of proteins to which serine protease inhibitors in serum and other proteins with quite different functions belong.[21] Other members of this family, at least those with inhibitor function, probably have similar structures and functional properties. Conformational strain may also apply to α_2 macroglobulin, another plasma protease inhibitor, though unrelated to α_1 protease inhibitor.[22] It may explain the unusual proteolytic susceptibility of a particular segment, the bait region.

3. Order–Disorder Transition

The target molecules of the natural serine protease inhibitors, the serine proteases, show a different kind of flexibility. Serine proteases are synthesized as proenzymes, which are activated by limited proteolysis.[23, 24] The corresponding structural, thermodynamic, and kinetic data have been analyzed in great detail.[25] Figure 5a summarizes the results obtained through comparison of the structures of trypsinogen, trypsin, and their complexes with BPTI. In the proenzyme trypsinogen a part of the molecule, called the activation domain, is disordered. It becomes ordered upon conversion to trypsin. The trigger for this event is the formation of a salt linkage between an aspartate residue and the *N*-terminus liberated by the activation cleavage. The activation domain is involved in substrate binding, which requires an ordered state. The catalytic inefficiency of trypsinogen is therefore due to inefficient substrate binding. Very strong ligands like BPTI are able to bind to trypsinogen and induce a disorder–order transition of the activation domain without activation cleavage at the expense of a part of the energy of interaction.

Other systems involving biological macromolecules that show an order–disorder transition have been characterized at the atomic level although in less detail than the serine protease system. Similar to the serine proteases there is a disorder–order transition that occurs when prophospholipase is converted into the active enzyme phospholipase.[26] A substantial part of the C_H2 domain (one of the constant domains of the heavy (H) chain) of the *C*-terminal frag-

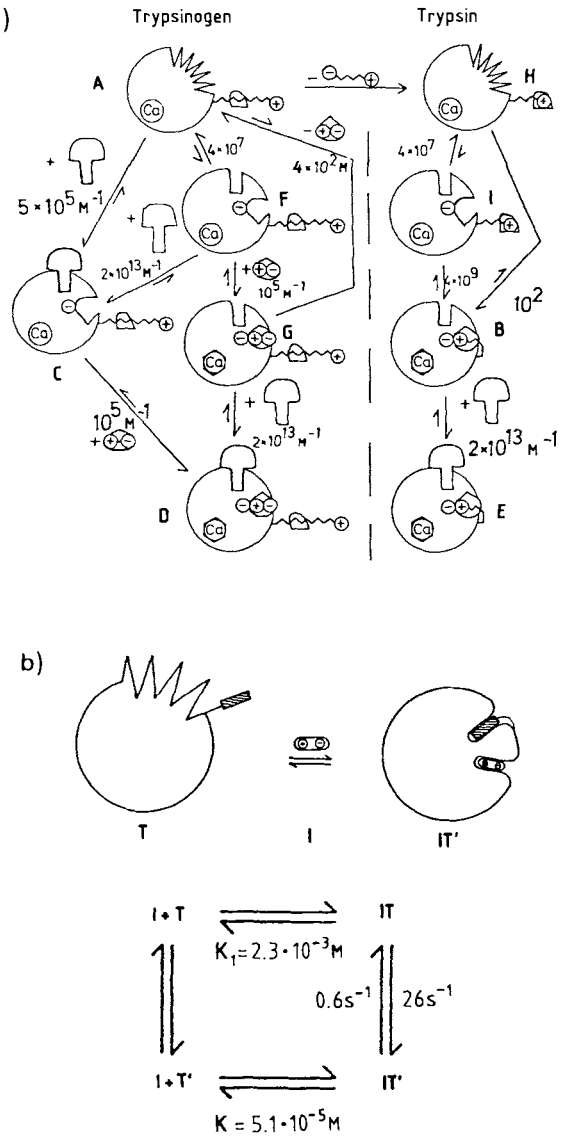

Fig. 5. Schemes of the structures and thermodynamics of the system trypsinogen/trypsin/BPTI/activation peptide. a) In trypsinogen the activation domain is disordered (**A**), but becomes ordered (**B**) after cleavage of the *N*-terminal peptide (**A**→**H**). The newly liberated *N*-terminus interacts strongly with the trypsin moiety (**B**). **B** forms a very strong complex with BPTI (**E**). Trypsinogen also forms a complex with BPTI (**C**) in which the activation domain is ordered. This complex is much weaker than **E** but is strongly stabilized by interaction with an exogenous peptide simulating the *N*-terminus of trypsin (**D**). States **A**–**E** have been crystallographically observed and the corresponding association or equilibrium constants have been characterized (large numbers). The other states and corresponding association and equilibrium constants are hypothetical (small numbers) [25]. b) The simple system of trypsinogen with covalently linked *p*-guanidinobenzoate (**T**). The activation domain becomes ordered and the binding pocket for the ligand *p*-guanidinobenzoate is formed in the presence of the exogenous peptide (**I**). Structure, thermodynamics, and kinetics of this system have been analyzed [25, 71]. These data indicate a relatively slow isomerization step with a rate constant of 26 s^{-1} from a loose **IT** complex to the stable **IT'** species; this step is probably associated with the rigidification process.

ment (Fc) of immunoglobulins is disordered.[27] It has been suggested that some of the disordered segments in immunoglobulins are involved in effector functions. In tobacco mosaic virus (TMV), the polypeptide chain in contact with the ribonucleic acid (RNA) is ordered in the intact virus[28] but disordered in the empty protein disk[29] suggesting that a disorder–order transition of this region of the coat protein accompanies the process of viral assembly. The disorder–order transition of flexible *N*-terminal "arm" regions of selected coat-protein subunits also seems to be involved in the assembly of tomato bushy stunt virus and other small icosahedral viruses.[30]

So far the unspecific term "disorder" has been used to describe the state of the activation domain in trypsinogen, indicating only that this region does not contribute significantly to the X-ray diffraction pattern of the crystal. This behavior could be caused by either "static" or "dynamic" disorder, which break the perfect arrangement of the crystalline lattice. Static disorder may be defined by the existence of different conformers of the molecule located at different sites in the crystal lattice, while dynamic disorder would imply a single conformer with large thermal fluctuations. The temperature dependence of these two models is expected to be quite different, so that a series of diffraction experiments at different temperatures may discriminate between them. Low-temperature diffraction studies of protein crystals are difficult but have been carried out with trypsinogen crystals.[31] These show that even at the temperature of liquid nitrogen the activation domain of trypsinogen does not contribute to X-ray scattering. This suggests that static disorder is predominant. We conclude that the activation domain exists in a number of different conformations of comparable stability. Transitions between these conformers may occur readily at room temperature, and the equilibrium of the conformers may be shifted by weak external forces like crystal packing, one conformer being thereby selectively stabilized. This is indeed the case in α-chymotrypsinogen, a serine protease proenzyme related to trypsinogen. Two different crystal forms have been analyzed, one of which was found to have two independent molecules in the asymmetric unit.[32–34] All three molecules experience different crystal packing forces, which have little effect on the rigid parts of the molecular structures but distort the flexible activation domain and stabilize different conformers. These studies confirm the general conclusions drawn from the studies on trypsinogen and reveal another facet of the enigmatic term disorder. A deeper understanding of the physical basis of the experimental findings may be brought to light by molecular dynamics calculations of the trypsinogen–trypsin system which are currently in progress.[35]

X-ray crystallographic experiments at different temperatures are able to differentiate between dynamic and static disorder in the above-mentioned sense and in the latter case to define a lower limit for the number of conformers. However, the term "static disorder" is somewhat confusing, since transitions between the conformers may occur depending on temperature. Diffraction experiments cannot reveal rates and energies of dynamic processes. This is the domain of spectroscopy. In the case of trypsinogen, perturbed angular γ-correlation spectroscopy has been applied and, indeed, has shown transitions in the nanosecond range at room temperature which are frozen at low temperature.[36,37] The conclusion drawn from the crystallographic and spectroscopic experiments is that the activation domain fluctuates rapidly at room temperature between conformers of nearly equal stability. In addition to this motion, the atoms vibrate about their equilibrium positions in the different conformers. Such properties are

characteristic of liquids but surely apply only to disordered regions of a protein (for a critical general discussion see Ref. [38]).

4. Domain Motion

So far structural and functional aspects of flexibility and disorder in relatively small parts of proteins have been discussed. We now turn to proteins where very large parts (domains) move relative to others as rigid bodies. The changes in conformation that accompany or allow such motions are usually limited to short segments or single peptide units, called hinges. Glycine amino acid residues are very common in hinge regions, possibly because the absence of a side chain imposes less restrictions on conformation. Similarly, glycine residues very often mark the boundaries between ordered and disordered segments in the protein systems discussed in Section 3.

Probably the best-defined example of a protein with rather unrestricted domain motions is the immunoglobulin molecule. Immunoglobulins of the class G (IgG) are symmetrical dimers of two heavy chains (H) and two light chains (L). Amino acid sequence studies had suggested long before crystal structures became available that the H and L chains are linear arrangements of four and two, respectively, structurally related domains. Consistent with this notion were the observations that the segments connecting the domains are preferentially cleaved by proteolytic enzymes to liberate stable fragments which retain partial functions of the intact molecule.

Hydrodynamic, spectroscopic, and electron microscopic studies provided evidence for extensive flexibility of the immunoglobulin molecule,[39-42] but it required crystallographic studies to confirm the domain motif of immunoglobulin structure and to reveal the potential modes of motion at the atomic level (Fig. 6).[43] It was found that closely related IgG fragments analyzed in different crystal forms differ in the relative arrangement of the pairs of domains (modules). The arrangement of the (V_H-V_L) module (V domains are variable domains) relative to the (C_H1-C_L) module within the arms of the antigen-binding fragment (Fab) shows variations up to 60° in elbow angle. The relative orientation of the Fab arms is even more variable, from maximal extension (T-shape) to almost parallel arrangement, as suggested by electron micrographs. The structure of the Fc fragment, the stem part of the immunoglobulin molecule is more constant, but the orientations of the C_H2 domain relative to the C_H3 domain vary by 5° to 10° in different crystalline environments. In a fortunate case, crystallographic experiments allowed direct observation of flexibility between Fab and Fc, because crystals of an intact immunoglobulin and its $(Fab)_2$ fragment, which lacks Fc, were available.[44] Both crystals show a very similar distribution of X-ray diffraction intensities even at low resolution. This observation proves disorder of the Fc part in the crystalline state and shows that it is predominantly static as defined above. If the Fc part were dynamically disordered, oscillating about a single equilibrium position, the diffraction patterns of intact IgG and the $(Fab)_2$ fragment should be different, at least at low resolution.

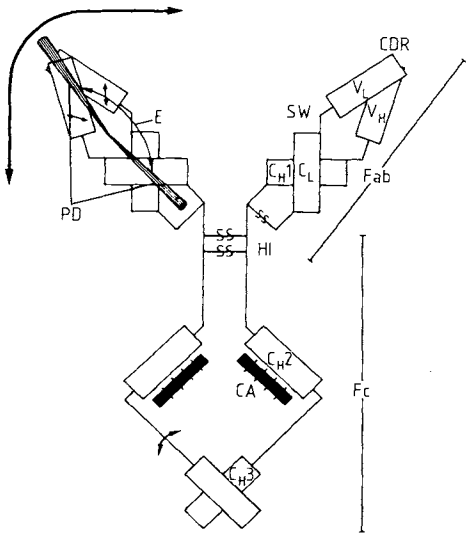

Fig. 6. Scheme of an immunoglobulin molecule of the IgG class. It is a symmetrical dimer assembled from two heavy and two light chains, which are folded into four and two domains, respectively. The V_H-V_L module forms the antigen-combining site by its complementarity-determining regions (CDR). There is flexibility in the relative arrangement of modules and domains. The extent is indicated by the lengths of the double headed arrows. E = elbow, HI = hinge, SW = switch, CA = carbohydrate, PD = pseudo diads.

A flexible linkage of the Fab parts to the Fc stem has functional importance as shown by IgG variants in which the hinge segment linking Fab and Fc is shortened by a deletion. These are defective in some of the biological functions associated with the Fc part (for a review of these functions see Ref. [44b]). This relates to the interesting issue of cooperation between the different functions of the Fab and Fc parts, namely, antigen binding and effector functions, respectively. The covalent association of Fab and Fc links these functions in space, while the relative flexibility of these segments imposes little restrictions on the reactivity of Fab and Fc with other macromolecules. Flexibility is impaired in the hingeless IgG variants, and binding sites on Fc might be concealed by the Fab part. There are no functional data that support the existence of cooperative effects other than those mentioned. Structural flexibility is inconsistent with the idea of signal transmission between Fab and Fc unless a conformer with a rigid arrangement of the Fab and Fc parts exists.[45] However, signal transmission between the (V_H-V_L) and (C_H1-C_L) modules within the Fab part has been shown by a number of experiments. The (V_H-V_L) and (C_H1-C_L) modules are separated by the switch peptides, which allow elbow bending and the formation or breakage of longitudinal V_H–C_H1 noncovalent interactions. The recently suggested distortion of the V_H-V_L module by antigen binding could act as a trigger, altering the elbow angle and the contact with the C_H1-C_L module.[46]

A number of other proteins are known which have covalently but flexibly linked domains, including protein A[27,47] and ovomucoid protease inhibitors.[14,18] Structural studies have been performed on proteolytic fragments of these proteins. These studies and the functional properties of the fragments indicate that the fragments retain their structure and thermal stability in the intact molecules and suggest a lack of significant interaction between the do-

mains. As deduced from repeating amino acid sequences it is likely that a similar scheme of construction holds for the main protein components of the cytoskeleton (spectrin)[48] and the extracellular matrix (fibronectin and laminin).[49] These proteins form a network of domains which have specific binding sites for other cellular components and may serve to organize these components in space.

Motion of the Fab parts of immunoglobulins relative to each other and to the Fc part is quite free, since the long extended connecting segments impose little steric restrictions. Elbow bending within the Fab parts is more restricted owing to the double linkage of (V_H-V_L) and (C_H-C_L) modules. This latter type of domain motion leads to flexibility in some enzymes, where domains oscillate through a small angular range.

Citrate synthase, the condensing enzyme, is a well-characterized example in structural and functional terms.[50-52] Citrate synthase is a dimeric molecule. Each subunit is folded into a large and a small domain as shown by crystal structural studies of liganded and unliganded enzyme forms. The unliganded enzyme form has a deep cleft between the large and small domains. The small domain is folded from a contiguous chain segment and doubly linked to the large domain. In the molecular form having bound product, i.e., citrate and coenzyme A (CoA), the cleft between the large and the small domain is closed, enclosing the product molecules (Fig. 7). A very similar closed form is found when the substrate and a co-substrate analogue, i.e., oxaloacetate and acetonyl-CoA, are bound. The difference between open and closed forms may, to a first approximation, be described by a rigid body rotation of about 18° of the small domain relative to the large domain. The right packing of the closed form of the enzyme suggests that it represents a stable conformation which prevails also in solution. However, an ensemble of open forms may exist in solution of which the one seen in the crystals is favored by crystal packing. From a detailed analysis of the structures it appears most likely that catalysis proceeds in the closed form, while substrate uptake and product release occur in the open form, where the substrate binding site is accessible to solvent. It is not surprising that the condensation reaction between oxaloacetate and acetyl-CoA is favored in the solvent-free environment of the closed form of citrate synthase where both substrates are in close proximity. In addition to this general effect of proximity and desolvation, there are specific residues involved in catalysis, of which His274 deserves special mention. It is adjacent to Gly275, which is at the domain rotation axis and undergoes a dramatic change in conformation between open and closed form. It appears that the interaction of His274 with the substrate might trigger the conformational transition to the closed form which is then stabilized by a multitude of substrate-protein interactions. The presence of a glycine residue at the domain boundary is in line with previously discussed cases. When the two closed forms of citrate synthase, which have product and substrate bound, respectively, are compared, numerous differences in the internal structure of the small domains are observed. The enzyme structure responds evidently to the state of the catalytic reaction and the binding requirements of the reaction intermediates. This type of flexibility

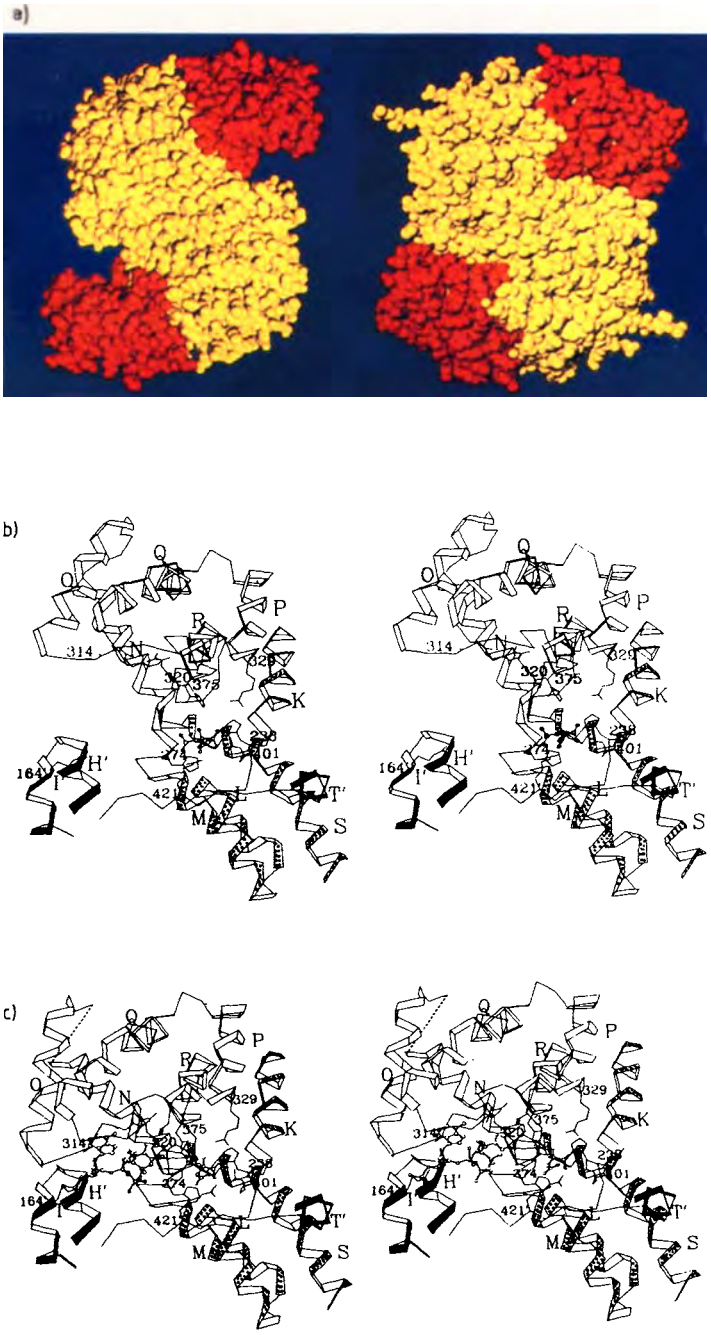

Fig. 7. a) Space-filling representation of open (left) and closed (right) forms of citrate synthase. The small and large domains are red and yellow, respectively. b) Stereodrawings of the open form of citrate synthase in the vicinity of the ligand citrate. c) Stereodrawing of the closed form with product citrate and coenzyme A bound. The binding site of coenzyme A is generated in the closed form by residues of the small domain (open ribbon) and the large domains of both subunits (dotted and filled ribbons). The filled ribbons represent diad-related subunits [50-52]).

is related to the subtle conformational changes seen in small protease inhibitors when bound to proteases.

A domain motion generating the open and closed forms seen in citrate synthase has been found and defined in detail in a few other proteins, aspartate aminotransferase,[53,54] alcohol dehydrogenase,[55] hexokinase,[56] and adenylate kinase[57] and is likely to occur in arabinose binding protein[58] and glyceraldehydephosphate dehydrogenase.[59]

5. Flexibility in Subunit Assembly

It is not surprising that flexibility plays an important role not only in the interaction of protein domains of a single polypeptide chain but also in the assembly of oligomers. The development of favorable contacts between the subunits drives the association. Polypeptide segments exposed in the isolated subunits become buried in the aggregate and will respond to this dramatic change in environment. One type of response we have already seen in the disorder-order transition in TMV assembly, where direct observations of both states, the empty disc and the intact virus, have been possible. Another type of response is seen in the spherical viruses, where the chemically identical protein subunits are in not exactly identical positions in the icosahedral capsid.[60] In an icosahedron sixty units may occupy equivalent positions. In $T=3$ particles the 3×60 protein subunits are arranged in equivalent triples of quasi-equivalent molecules. Quasi-equivalence is reflected in distinct differences in the protein subunits, namely in the form of the relative arrangement of two globular domains. They may adopt one of two different relative orientations depending on the subunit's location with respect to the icosahedral symmetry.

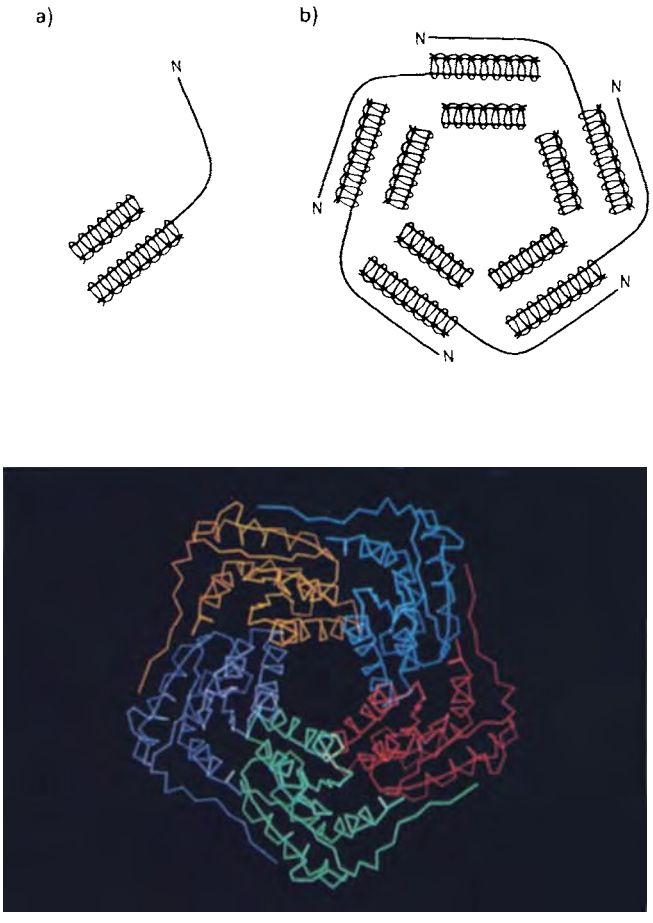

Fig. 8. a) Folding of a β-subunit of heavy riboflavin synthase. It consists of a four-stranded central β-sheet flanked on either side by two α-helices. Only the upper pair of α-helices is shown. b) The *N*-terminal segment projects away, but is attached to the β-sheet of a neighboring subunit in the pentamer. c) The observed C$^{\alpha}$ carbon position in the pentamer [61, 62]. The five subunits are color-coded.

In other cases polypeptide segments project away from the globular part of a protein subunit but are associated with a neighboring subunit in the aggregate. It is likely that these segments are disordered or in an alternative conformation in the isolated subunits. The arm segments of the icosahedral viruses described earlier are one example of this type of flexibility. A recent example is the bifunctional multienzyme complex riboflavin synthase.[61,62]

Riboflavin synthase consists of two chemically different subunits. Sixty β-subunits form a capsid with icosahedral symmetry. Three α-subunits occupy the central cavity. The β-subunit is folded into a globular body consisting of a four-stranded β-sheet and four α-helices, two on either side of the β-sheet. The *N*-terminal segment of about ten residues stretches away from the globule and is attached as the outer fifth strand to the β-sheet of a neighboring subunit in the pentamer. This occurs in a cyclic manner (Fig. 8). Although the structure of the isolated subunit is unknown, it is likely that the *N*-terminal segment is flexible, since its conformation is not supported by secondary structural interactions. Assembly of the subunits in the pentamer therefore involves rearrangement and stabilization of the *N*-terminal polypeptide strand.

6. Rigidity

I now close the circle in the discussion of the dual aspects of flexibility and rigidity in proteins. We might have lost sight of the fact that proteins provide a spatial framework to bind ligands, turn over substrates, and accommodate prosthetic groups and pigments. These functions require a quite precise geometrical arrangement of the interacting groups. To demonstrate this, any of the examples presented under the aspect of flexibility could have been chosen, since, in all cases, well-defined complementary surfaces play an important role in the interaction with ligands or macromolecules. Yet these surfaces often require some flexibility to adapt to the desolvation and change in environment. However, there exists a class of proteins where rigidity is dominant and flexibility would lead to wasteful side reactions. These are protein-pigment complexes involved in the transfer of light energy and electrons in photosynthesis. Their substrates and products are massless or very small (photons and electrons) and the reactions are intramolecular. I have therefore chosen two examples from this system to emphasize the functional significance of rigidity.

Light collection and light energy transfer in the peripheral light-harvesting complexes (phycobilisomes) of cyanobacteria occurs by a three-dimensional array of open-chain tetrapyrrole (bilin) chromophores.[63,64] The excitation energy is funneled into the photosynthetic membrane where it is trapped and converted into an electron flow across the membrane by the reaction centers of the photosystems. The energy transfer within the light-harvesting complexes, taking place by an inductive resonance mechanism, is very fast and occurs with minimal loss of energy and a quantum efficiency close to one. The electromagnetic coupling of the chromophores and the energy-transfer times are governed by distances and orientations. Motion would interfere with efficient coupling and slow down the energy

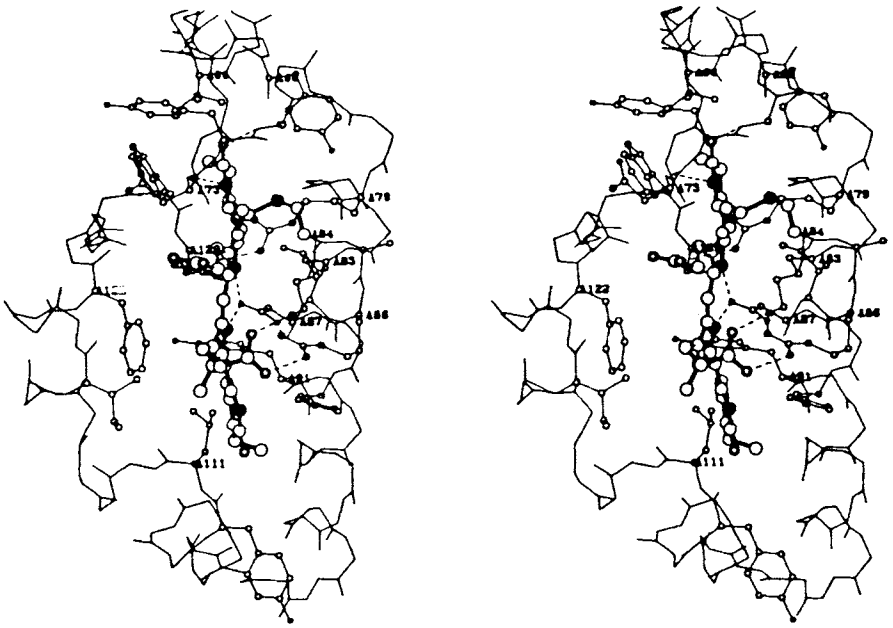

Fig. 9. Stereodrawing of the dihydrobiliverdin chromophore A84 and its environment in C-phycocyanin. Polar and charge-charge interactions of Asp A87 with the central pyrrolic nitrogens and of Arg A79, Lys A83, and Arg A86 with the propionic acid side chains form a network of bonds sequestering the chromophore in the protein matrix [65-67].

transfer, so that loss of the excitation energy by fluorescence emission could occur. In the intact complexes the energy-transfer time is several orders of magnitude shorter than the intrinsic fluorescence lifetime. Another mechanism of deexcitation would involve photochemical rearrangements of the excited chromophores. Open-chain tetrapyrrole systems indeed have this capacity and undergo photochemical isomerization as pigments in the plant photoreceptor phytochrome. In the phycobilisome components the pigments are rigidly held by hydrogen bonding interactions with charged groups of the proteins (Fig. 9). These forces are strongly directed and oppose motions leading to weaker coupling and to isomerizations.[65-67]

Similar considerations apply to the very fast electron transfer steps in the reaction centers of the photosystem, in which the excitation energy provided by the light-harvesting systems drives electrons from a primary donor to a primary acceptor.[68] Detailed structural data are available for the reaction center of a purple bacterium, *Rhodopseudomonas viridis*.[69,70] A special pair of bacteriochlorophyll chromophores is excited and ejects an electron, which is transferred to a primary electron acceptor, a quinone, via a chain of bacteriochlorophyll and bacteriopheophytin pigments. As in the light-harvesting systems, the quantum efficiency of this process is close to one. Processes such as deexcitation by fluorescence emission do not occur to a significant extent, because the electron transfer is orders of magnitude faster owing to the appropriate overlap of the electronic orbitals of the electron-conducting elements. To achieve this, the molecules must be held precisely by the

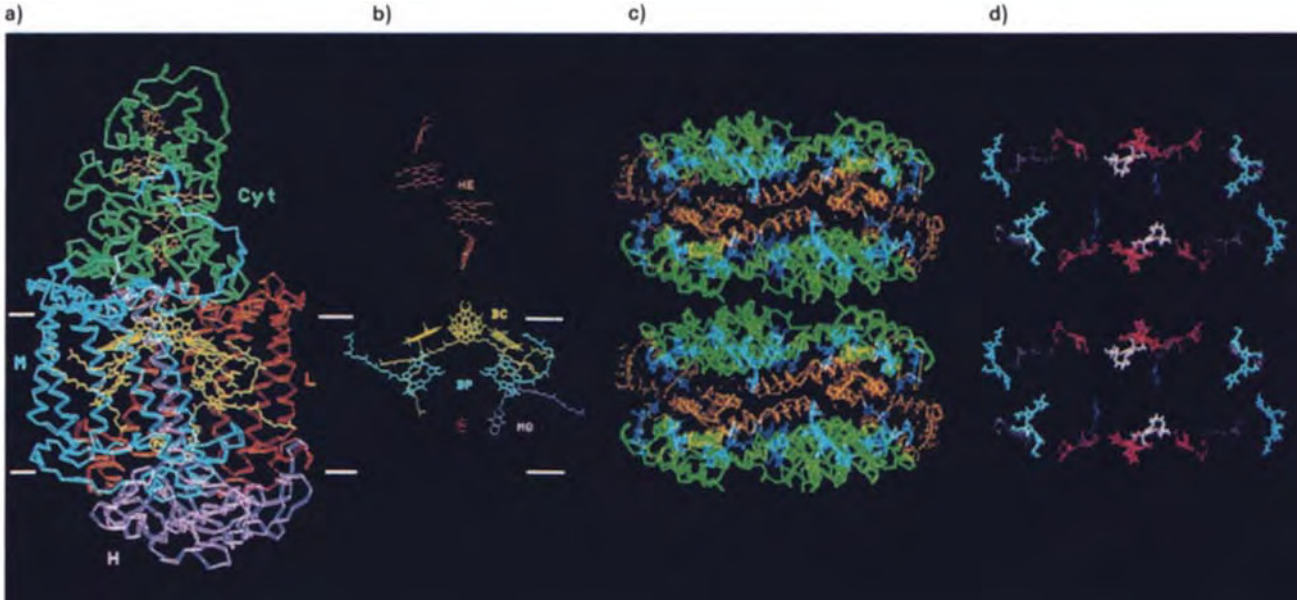

Fig. 10. a) C$^{\alpha}$-chain ribbon drawing of the reaction center protein-pigment complex. The four protein components are color-coded: green, cytochrome (Cyt); blue, M-subunit; brown, L-subunit; violet, H-subunit; yellow, pigments. b) The isolated pigments of the protein-pigment complex: brown, hemes; yellow, special pair of bacteriochlorophylls and accessory bacteriochlorophyll; blue, bacteriopheophytin; violet, menaquinone-9 (MQ); red, Fe. The presumable position of the photosynthetic membrane is indicated [69, 70]. c, d) For a comparison of sizes, three stacked hexamers of C-phycocyanin and the associated tetrapyrrole pigments are shown. This aggregate resembles an antenna of a phycobilisome organelle. The protein components of C-phycocyanin are color-coded: brown, α-subunit; green, β-subunit; blue and violet, different tetrapyrrole chromophores.

protein matrix. Photochemical isomerizations as a mechanism of deexcitation are unlikely in the cyclic bacteriochlorophyll systems, in contrast to the tetrapyrrole systems in the light-harvesting complexes. But the electron transfer might be retarded through the drag of a moving electron exerted on ions or dipolar mobile molecules, in particular water. The fast electron transfer steps indeed occur remote from water by carriers embedded in a hydrophobic protein matrix which is integrated in a membrane (Fig. 10). The energy of activation of the electron-transfer processes is very low and they are even faster at low temperatures, proving that nuclear motions are not required.

The cyclic electron transfer of photosynthesis also involves a number of slower steps not considered in this context, which require nuclear motions, rearrangements, and diffusional processes and therefore activation energy.

7. Conclusion

It was the intention of this article to point out certain aspects of rigidity and flexibility with respect to structure and function of a number of protein systems and to demonstrate the dual nature of proteins as passive, rigid matrices and as active, mobile participants in chemical reactions, respectively. The kinds of flexibility are as diverse and complex as the chemical reactions themselves. It was not and could not be the intention to describe the selected systems in detail. Instead, the article represents a selective view and the interested reader is referred to the original publications for further information.

Dr. W. S. Bennett made valuable suggestions to improve the manuscript in form and substance.

Received: July 28, 1987 [A 651 IE]
German version: *Angew. Chem. 100* (1988) 79

[1] S. Krimm, J. Bandekar, *Adv. Protein Chem. 38* (1986) 181.
[2] M. Karplus, J. A. McCammon, *CRC Crit. Rev. Biochem. 9* (1981) 293.
[3] M. Levitt, *Annu. Rev. Biophys. Bioeng. 11* (1982) 251.
[4] W. L. Peticolas, *Methods Enzymol. 61* (1979) 425.
[5] A. Cooper, *Prog. Biophys. Mol. Biol. 44* (1984) 181.
[6] W. S. Bennett, R. Huber, *CRC Crit. Rev. Biochem. 15* (1984) 291.
[7] G. Wagner, K. Wüthrich, *J. Mol. Biol. 134* (1979) 75.
[8] K. Wüthrich, G. Wagner, *Trends Biochem. Sci. 9* (1984) 152.
[9] A. Wlodawer, J. Walter, R. Huber, L. Sjölin, *J. Mol. Biol. 180* (1984) 301.
[10] R. Hetzel, K. Wüthrich, J. Deisenhofer, R. Huber, *Biophys. Struct. Mech. 2* (1976) 159.
[11] A. Wlodawer, J. Deisenhofer, R. Huber, *J. Mol. Biol. 193* (1987) 145.
[12] W. Bode, P. Schwager, R. Huber in D. W. Ribbons, K. Brew (Eds.): *Proteolysis and Physiological Regulation, Miami Winter Symposia*, Academic Press, New York 1976, p. 43.
[13] M. Bolognesi, G. Gatti, E. Menegatti, M. Guarneri, M. Marquart, E. Papamokos, R. Huber, *J. Mol. Biol. 162* (1982) 839.
[14] E. Papamokos, E. Weber, W. Bode, R. Huber, M. W. Empie, I. Kato, M. Laskowski, Jr., *J. Mol. Biol. 158* (1982) 515.
[15] W. Bode, E. Papamokos, D. Musil, U. Seemüller, H. Fritz, *EMBO J. 5* (1986) 813.
[16] R. J. Read, M. N. G. James in A. J. Barrett, J. Salvesen (Eds.): *Proteinase Inhibitors*, Elsevier, Amsterdam 1986, p. 301.
[17] D. Musil, *Dissertation*, Technische Universität München 1987.
[18] M. Laskowski, Jr., I. Kato, *Annu. Rev. Biochem. 49* (1980) 593.
[19] H. Loebermann, R. Tokuoka, J. Deisenhofer, R. Huber, *J. Mol. Biol. 177* (1984) 531.
[20] R. Carrell, *Nature (London) 312* (1984) 14.
[21] S. C. Bock, K. Skriver, E. Nielsen, H.-C. Thogersen, B. Wiman, V. H. Donaldson, R. L. Eddy, J. Marrinan, E. Radziejewska, R. Huber, T. B. Shows, S. Magnusson, *Biochemistry 25* (1986) 4292.
[22] L. Sottrup-Jensen, H. F. Hansen, S. B. Mortensen, T. E. Peterssen, S. Magnusson, *FEBS Lett. 123* (1981) 145.
[23] H. Neurath, E. Davie, *J. Biol. Chem. 212* (1955) 515.
[24] P. Desnuelle, C. Fabre, *Biochem. Biophys. Acta 18* (1955) 49.
[25] R. Huber, W. Bode, *Acc. Chem. Res. 11* (1978) 114.
[26] B. W. Dijkstra, G. J. H. van Nes, K. H. Kalk, N. P. Brandenburg, W. G. J. Hol, J. Drenth, *Acta Crystallogr. Sect. B 38* (1982) 793.
[27] J. Deisenhofer, *Biochemistry 20* (1981) 2361.
[28] G. Stubbs, S. Warren, K. C. Holmes, *Nature (London) 267* (1977) 216.
[29] a) J. N. Champness, A. C. Bloomer, G. Bricogne, P. J. G. Butler, A. Klug, *Nature (London) 259* (1976) 20; b) A. C. Bloomer, J. N. Champness, G. Bricogne, R. Staden, A. Klug, *ibid. 276* (1978) 362.
[30] S. C. Harrison, *Adv. Virus Res. 28* (1983) 175.
[31] J. Walter, W. Steigemann, T. P. Singh, H. Bartunik, W. Bode, R. Huber, *Acta Crystallogr. Sect. B 38* (1982) 1462.
[32] D. Wang, W. Bode, R. Huber, *J. Mol. Biol. 185* (1985) 595.
[33] J. Kraut in R. D. Boyer (Ed.): *The Enzymes, Vol. 3*, 3rd ed., Academic Press, New York 1971, p. 165-183.
[34] H. T. Wright, *J. Mol. Biol. 79* (1973) 13.
[35] A. Brünger, R. Huber, M. Karplus, *Biochemistry 26* (1987) 5153.
[36] Review: A. Lerf, T. Butz, *Angew. Chem. 99* (1987) 113; *Angew. Chem. Int. Ed. Engl. 26* (1987) 110.
[37] T. Butz, A. Lerf, R. Huber, *Phys. Rev. Lett. 48* (1982) 890; *Hyperfine Interact. 15/16* (1983) 869.
[38] W. Bialek, M. F. Goldstein, *Biophys. J. 48* (1985) 1027.
[39] M. E. Noelken, C. A. Nelsen, C. E. Buckley, C. Tanford, *J. Biol. Chem. 240* (1965) 218.
[40] J. Yugerabide, H. G. Epstein, L. Stryer, *J. Mol. Biol. 51* (1970) 573.
[41] V. N. Schumaker, G. W. Seegan, C. A. Smith, S. K. Ma, J. D. Rodwell, M. F. Schumaker, *Mol. Immunol. 17* (1980) 413.
[42] R. C. Valentine, N. M. Green, *J. Mol. Biol. 27* (1967) 615.
[43] R. Huber, *Behring Inst. Mitt. 76* (1984) 1.
[44] a) M. Marquart, J. Deisenhofer, R. Huber, W. Palm, *J. Mol. Biol. 141* (1980) 369; b) M. L. Morgan, W. O. Weigle, *Adv. Immunol. 40* (1987) 61.
[45] R. Huber, J. Deisenhofer, P. M. Colman, M. Matsushima, W. Palm, *Nature (London) 264* (1976) 415.
[46] P. M. Colman, W. G. Laver, J. N. Varghese, A. J. Baker, P. A. Tulloch, G. M. Air, R. G. Webster, *Nature (London) 326* (1987) 358.
[47] J. Deisenhofer, T. A. Jones, R. Huber, J. Sjödahl, J. Sjöquist, *Hoppe Seylers Z. Physiol. Chem. 359* (1978) 975.
[48] D. W. Speicher, J. S. Morrow, W. J. Knowles, V. T. Marchesi, *J. Biol. Chem. 257* (1982) 9093.
[49] J. Engel, E. Odermatt, A. Engel, J. A. Madri, H. Furthmayr, H. Rohde, R. Timpl, *J. Mol. Biol. 150* (1981) 97.
[50] S. Remington, G. Wiegand, R. Huber, *J. Mol. Biol. 158* (1982) 111.
[51] G. Wiegand, S. Remington, J. Deisenhofer, R. Huber, *J. Mol. Biol. 174* (1984) 205.
[52] G. Wiegand, S. Remington, *Annu. Rev. Biophys. Biophys. Chem. 15* (1986) 97.
[53] G. C. Ford, G. Eichele, J. N. Jansonius, *Proc. Natl. Acad. Sci. USA 77* (1980) 2559.
[54] A. Arnone, P. D. Briley, P. H. Rogers, C. C. Hyde, C. M. Metzler, D. M. Metzler in J. F. Griffin, W. L. Duax (Eds.): *Molecular Structure and Biological Activity*, Elsevier, New York 1982, p. 57.
[55] H. Eklund, J. P. Samama, L. Wallen, C. I. Bränden, Å. Åkeson, T. A. Jones, *J. Mol. Biol. 146* (1981) 561.
[56] W. S. Bennett, T. A. Steitz, *J. Mol. Biol. 140* (1980) 211.
[57] U. Egner, A. G. Tomasselli, G. E. Schulz, *J. Mol. Biol. 195* (1987) 649.
[58] M. A. Saper, F. A. Quiocho, *J. Biol. Chem. 258* (1983) 11057.
[59] A. G. W. Leslie, A. S. Wonnacott, *J. Mol. Biol. 178* (1984) 743.
[60] L. Liljas, *Prog. Biophys. Mol. Biol. 48* (1986) 1.
[61] R. Ladenstein, B. Meyer, R. Huber, H. Labischinski, K. Bartels, H.-D. Bartunik, L. Bachmann, H. C. Ludwig, A. Bacher, *J. Mol. Biol. 187* (1986) 87.
[62] R. Ladenstein, A. Bacher, R. Huber, *J. Mol. Biol. 195* (1987) 751.
[63] H. Zuber, *Trends Biochem. Sci. 11* (1986) 414.
[64] A. N. Glazer, *Annu. Rev. Biophys. Biophys. Chem. 14* (1985) 47.
[65] T. Schirmer, W. Bode, W. Sidler, R. Huber, H. Zuber, *J. Mol. Biol. 184* (1985) 257.
[66] T. Schirmer, R. Huber, M. Schneider, W. Bode, M. Miller, M. L. Hackert, *J. Mol. Biol. 188* (1986) 651.
[67] T. Schirmer, W. Bode, R. Huber, *J. Mol. Biol. 196* (1987) 677.
[68] Reviews: a) J. Deisenhofer, H. Michel, R. Huber, *Trends Biochem. Sci. 10* (1985) 243, and references cited therein; b) J. Deisenhofer, R. Huber, H. Michel, *Nachr. Chem. Tech. Lab. 34* (1986) 416, and references cited therein.
[69] J. Deisenhofer, O. Epp, K. Miki, R. Huber, H. Michel, *J. Mol. Biol. 180* (1984) 385.
[70] J. Deisenhofer, O. Epp, K. Miki, R. Huber, H. Michel, *Nature (London) 318* (1985) 618.
[71] H. J. Nolte, E. Neumann, *Biophys. Chem. 10* (1979) 253.

ANGEWANDTE CHEMIE

International Edition in English

Volume 27 · Number 1
January 1988
Pages 89–112

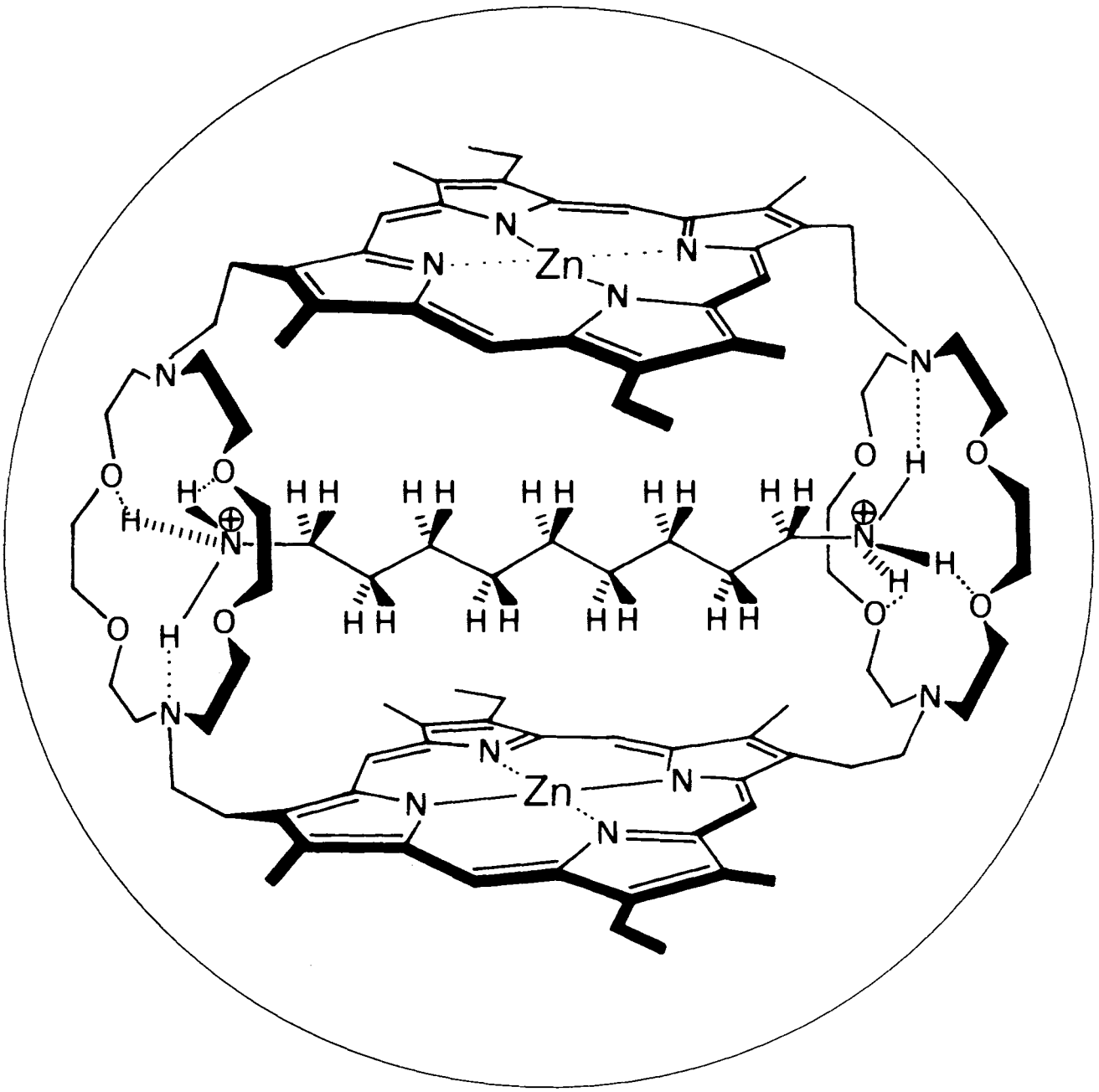

Jean-Marie Lehn

Supramolecular Chemistry—Scope and Perspectives
Molecules, Supermolecules, and Molecular Devices (Nobel Lecture)

© VCH Verlagsgesellschaft mbH, D-6940 Weinheim, 1988

0570-0833/88/0101-0089 $ 02.50/0

Supramolecular Chemistry—Scope and Perspectives Molecules, Supermolecules, and Molecular Devices (Nobel Lecture)**

By Jean-Marie Lehn*

Supramolecular chemistry is the chemistry of the intermolecular bond, covering the structures and functions of the entities formed by association of two or more chemical species. Molecular recognition in the supermolecules formed by receptor-substrate binding rests on the principles of molecular complementarity, as found in spherical and tetrahedral recognition, linear recognition by coreceptors, metalloreceptors, amphiphilic receptors, and anion coordination. Supramolecular catalysis by receptors bearing reactive groups effects bond cleavage reactions as well as synthetic bond formation via cocatalysis. Lipophilic receptor molecules act as selective carriers for various substrates and make it possible to set up coupled transport processes linked to electron and proton gradients or to light. Whereas endoreceptors bind substrates in molecular cavities by convergent interactions, exoreceptors rely on interactions between the surfaces of the receptor and the substrate; thus new types of receptors, such as the metallonucleates, may be designed. In combination with polymolecular assemblies, receptors, carriers, and catalysts may lead to molecular and supramolecular devices, defined as structurally organized and functionally integrated chemical systems built on supramolecular architectures. Their recognition, transfer, and transformation features are analyzed specifically from the point of view of molecular devices that would operate via photons, electrons, or ions, thus defining fields of molecular photonics, electronics, and ionics. Introduction of photosensitive groups yields photoactive receptors for the design of light-conversion and charge-separation centers. Redox-active polyolefinic chains represent molecular wires for electron transfer through membranes. Tubular mesophases formed by stacking of suitable macrocyclic receptors may lead to ion channels. Molecular self-assembling occurs with acyclic ligands that form complexes of double-helical structure. Such developments in molecular and supramolecular design and engineering open perspectives towards the realization of molecular photonic, electronic, and ionic devices that would perform highly selective recognition, reaction, and transfer operations for signal and information processing at the molecular level.

1. From Molecular to Supramolecular Chemistry

Molecular chemistry, the chemistry of the covalent bond, is concerned with uncovering and mastering the rules that govern the structures, properties, and transformations of molecular species.

Supramolecular chemistry may be defined as "chemistry beyond the molecule," bearing on the organized entities of higher complexity that result from the association of two or more chemical species held together by intermolecular forces. Its development requires the use of all resources of molecular chemistry combined with the designed manipulation of noncovalent interactions so as to form supramolecular entities, supermolecules possessing features as well defined as those of molecules themselves. One may say that supermolecules are to molecules and the intermolecular bond what molecules are to atoms and the covalent bond.

Basic concepts, terminology, and definitions of supramolecular chemistry were introduced earlier[1-3] and will only be summarized here. Section 2.3 provides a brief account of the origins and initial developments of our work which led to the formulation of supramolecular chemistry. Molecular associations have been recognized and studied for a long time[4] and the term "Übermoleküle," i.e., supermolecules, was introduced already in the mid-1930s to describe entities of higher organization resulting from the association of coordinatively saturated species.[5] The partners of a supramolecular species have been named *molecular receptor* and *substrate*,[1,2,65] the substrate being usually the smaller component whose binding is being sought. This terminology conveys the relation to biological receptors and substrates for which *Paul Ehrlich* stated that molecules do not act if they are not bound ("Corpora non agunt nisi fixata"). The widely employed term of *ligand* seemed less appropriate in view of its many unspecific uses for either partner in a complex.

Molecular interactions form the basis of the highly specific recognition, reaction, transport, regulation, etc. pro-

[*] Prof. J.-M. Lehn
Institut Le Bel, Université Louis Pasteur
4, rue Blaise Pascal, F-67000 Strasbourg (France)
and
Collège de France
11 Place Marcelin Berthelot, F-75005 Paris (France)

[**] Copyright © The Nobel Foundation 1988.—We thank the Nobel Foundation for permission to print this lecture. The figure on the preceding page shows a supermolecule formed from a heterotopic metallocoreceptor and a diammonium substrate; metal ions and an organic molecule are bound simultaneously. For further details see Section 4.4 (structure taken from Ref. [100]).

cesses that occur in biology, such as substrate binding to a receptor protein, enzymatic reactions, assembling of protein-protein complexes, immunological antigen-antibody association, intermolecular reading, translation and transcription of the genetic code, signal induction by neurotransmitters, and cellular recognition. The design of artificial, abiotic receptor molecules capable of displaying processes of highest efficiency and selectivity requires the correct manipulation of the energetic and stereochemical features of the noncovalent, intermolecular forces (electrostatic interactions, hydrogen bonding, van der Waals forces, etc.) within a defined molecular architecture. In doing so, the chemist may find inspiration in the ingenuity of biological events and encouragement in the demonstration that such high efficiencies, selectivities, and rates can indeed be attained. However, chemistry is not limited to systems similar to those found in biology, but is free to create novel species and to invent processes.

Emphasis will bear on conceptual framework, classes of compounds, and types of processes. Considering the vast literature that has developed, the topics of various meetings and symposia, etc., there is no possibility here to do justice to the numerous results obtained, all the more to provide an exhaustive account of this field of science. Supramolecular chemistry, the designed chemistry of the intermolecular bond, is rapidly expanding at the frontiers of molecular science with physical and biological phenomena.

2. Molecular Recognition

2.1. Recognition, Information, Complementarity

Molecular recognition has been defined as a process involving *both binding* and *selection* of substrate(s) by a given

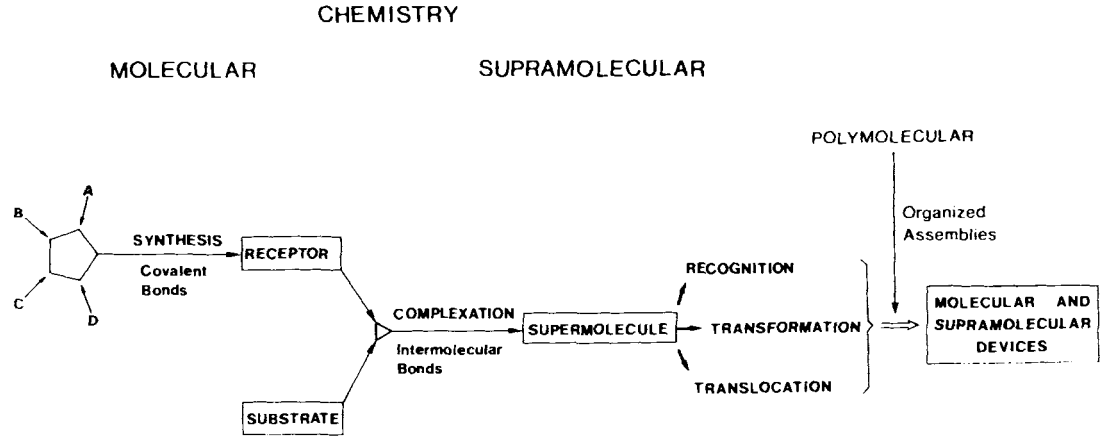

Scheme 1. From molecular to supramolecular chemistry: molecules, supermolecules, molecular and supramolecular devices.

Binding of a substrate σ to its receptor ρ yields the supermolecule ρσ and involves a molecular recognition process. If, in addition to binding sites, the receptor also bears reactive functions, it may effect a chemical transformation on the bound substrate, thus behaving as a supramolecular reagent or catalyst. A lipophilic, membrane-soluble receptor may act as a carrier effecting the translocation of the bound substrate. Thus, *molecular recognition, transformation,* and *translocation* represent the basic functions of supramolecular species. More complex functions may result from the interplay of several binding subunits in a polytopic coreceptor. In association with organized polymolecular assemblies and phases (layers, membranes, vesicles, liquid crystals, etc.), functional supermolecules may lead to the development of *molecular devices.* This article describes these various aspects of supramolecular chemistry (see Scheme 1) and sketches some lines of future development (for earlier general presentations see Refs. [1-3, 6-9]). The results discussed here, taken mainly from our own work, have been completed by references to other studies, in order to draw a broader picture of this rapidly evolving field of research.

receptor molecule, as well as possibly a specific *function.*[11] Mere binding is not recognition, although it is often taken as such. One may say that recognition is binding with a purpose, like receptors are ligands with a purpose. It implies a structurally well-defined pattern of intermolecular interactions.

Binding of σ to ρ forms a supermolecule characterized by its thermodynamic and kinetic stability and selectivity, i.e., by the amount of energy and of information brought into operation. Molecular recognition thus is a question of *information storage* and *read out* at the supramolecular level. Information may be stored in the architecture of the ligand, in its binding sites (nature, number, arrangement) and in the ligand layer surrounding bound σ; it is read out at the rate of formation and dissociation of the supermolecule. Molecular recognition thus corresponds to optimal information content of ρ for a given σ.[11] This amounts to a generalized *double complementarity principle* extending over energetical (electronic) as well as geometrical features, the celebrated "lock and key," steric fit concept enunciated by *Emil Fischer* in 1894.[10] Enhanced recognition beyond that provided by a single equilibrium step may

be achieved by multistep recognition and coupling to an irreversible process.[11]

The ideas of molecular recognition and of receptor chemistry have been penetrating chemistry more and more over the last fifteen years, namely in view of their bioorganic implications, but more generally for their significance in intermolecular chemistry and in chemical selectivity.[1-3,6-9,12-21]

2.2. Molecular Receptors—Design Principles

Receptor chemistry, the chemistry of artificial receptor molecules, may be considered a generalized coordination chemistry, not limited to transition-metal ions but extending to all types of substrates: cationic, anionic, or neutral species of organic, inorganic, or biological nature.

In order to achieve high recognition it is desirable that receptor and substrate be in contact over a large area. This occurs when ρ is able to wrap around its guest so as to establish numerous noncovalent binding interactions and to sense its molecular size, shape, and architecture. It is the case for receptor molecules that contain intramolecular cavities into which the substrate may fit, thus yielding an inclusion complex, a *cryptate*. In such concave receptors the cavity is lined with binding sites directed towards the bound species; they are endopolarophilic[1] and *convergent*, and may be termed *endoreceptors* (see also Section 7).

Macropolycyclic structures meet the requirements for designing artificial receptors: they are large (macro) and may therefore contain cavities and clefts of appropriate size and shape; they possess numerous branches, bridges, and connections (polycyclic) that allow the construction of a given architecture endowed with desired dynamic features; they allow the arrangement of structural groups, binding sites, and reactive functions.

The balance between rigidity and flexibility is of particular importance for the dynamic properties of ρ and of σ. Although high recognition may be achieved with rigidly organized receptors, processes of exchange, regulation, cooperativity, and allostery require a built-in flexibility so that ρ may adapt and respond to changes. Flexibility is of great importance in biological receptor–substrate interactions, where adaptation is often required for regulation to occur. Such designed dynamics are more difficult to control than mere rigidity, and recent developments in computer-assisted molecular design methods, allowing the exploration of both structural and dynamical features, may greatly help.[22] Receptor design thus covers both static and dynamic features of macropolycyclic structures.

The stability and selectivity of σ binding result from the set of interaction sites in ρ and may be structurally translated into *accumulation* (or collection) and *organization* (or orientation), i.e., bringing together binding sites and arranging them in a suitable pattern. Model computations on $(NH_3)_n$ clusters of different geometries have shown that collection involves appreciably larger energies than changes in orientation.[23] One may note that these intersite repulsions are built into a polydentate ligand in the course of synthesis.

We have studied receptors belonging to various classes of macropolycyclic structures (macrocycles, macrobicycles, cylindrical and spherical macrotricycles, etc.), expanding progressively our initial work on macrobicyclic cationic cryptates into the investigation of the structures and functions of supermolecules presenting molecular recognition, catalysis, and transport processes.

2.3. Initial Studies. Spherical Recognition in Cryptate Complexes

The simplest recognition process is that of spherical substrates; these are either positively charged metal cations (alkali, alkaline-earth, lanthanoid ions) or the negative halide anions.

During the last 20 years, the complexation chemistry of alkali cations developed rapidly with the discovery of several classes of more or less powerful and selective ligands: natural[24] or synthetic[25,26] macrocycles (such as valinomycin, [18]crown-6, and spherands) as well as macropolycyclic cryptands and cryptospherands.[1,6,9,26,27] It is the design and study of alkali-metal cryptates that started our work which developed into supramolecular chemistry.

It may be suitable at this stage to recount briefly the *origins of our work*, trying to trace the initial motivations and the emergence of the first lines of research. In the course of the year 1966, my interest for the processes occurring in the nervous system led me to wonder how a chemist might contribute to the study of these highest biological functions. The electrical events in nerve cells rest on changes in the distributions of sodium and potassium ions across the membrane. This seemed a possible entry into the field, since it had just been shown that the cyclodepsipeptide valinomycin,[24c] whose structure and synthesis had been reported,[24d] was able to mediate potassium ion transport in mitochondria.[24e] These results[24d,e] made me think that suitably designed synthetic cyclopeptides or analogues could provide means of monitoring cation distribution and transport across membranes. Such properties were also displayed by other neutral antibiotics[24f] of the enniatin and actin[24g] groups, and were found to be due to selective complex formation with alkali-metal cations,[24h-l] thus making these substances *ionophores*.[24m] However, since cation complexation might also represent a means of increasing the reactivity of the counteranion (anion activation),[6,35] it became desirable to envisage molecules which would be chemically less reactive than cyclic peptides.[*] Thus, when the cation binding properties of macrocyclic polyethers (crown ethers) were reported by *Charles Pe-*

[*] Earlier observations had suggested that polyethers interact with alkali cations. See, for instance, H. C. Brown, E. J. Mead, P. A. Tierney, *J. Am. Chem. Soc. 79* (1957) 5400; J. L. Down, J. Lewis, B. Moore, G. Wilkinson, *J. Chem. Soc. 1959*, 3767; suggestions had also been made for the design of organic ligands, see R. J. P. Williams, *The Analyst (London) 78* (1953) 586; *Q. Rev. Chem. Soc. 24* (1970) 331.

[**] To name this new class of chemical entities, a term rooted in Greek and Latin, which would also be equally suggestive in French, English, German, and possibly (!) other languages, was sought; "cryptates" appeared particularly suitable for designating a complex in which the cation was contained inside the molecular cavity, the crypt, of the ligand termed "cryptand."

dersen,[25a] these substances were perceived as combining the complexing ability of the macrocyclic antibiotics with the chemical stability of ether functions. Meanwhile, it had also become clear that compounds containing a three-dimensional, spheroidal cavity, surrounding entirely the bound ion, should form stronger complexes than the rather flat macrocycles; thus emerged the idea of designing macrobicyclic ligands.

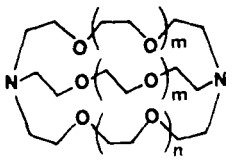

1 = [2.1.1]: m=0, n=1
2 = [2.2.1]: m=1, n=0
3 = [2.2.2]: m=n=1

Work started in October 1967 yielded the first such ligand **3** ("[2.2.2]") in the fall of 1968; its very strong binding of potassium ions was noted at once and a cryptate structure was assigned to the complex obtained, allowing us also to envisage its potential use for anion activation and for cation transport.[29a][**] Other ligands such as **1** and **2** and larger ones were synthesized and numerous cryptates were obtained.[29b] Their structure was confirmed by crystal structure determinations of a number of complexes, such as the rubidium cryptate of **3**, **4b**,[29c] and their stability constants were measured.[28]

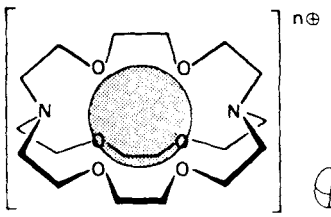

4a

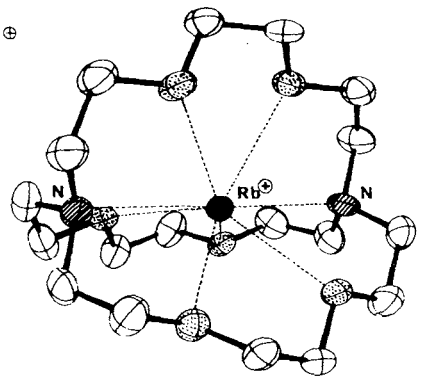

4b

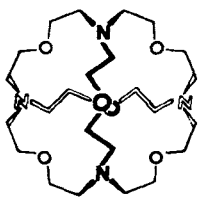

5

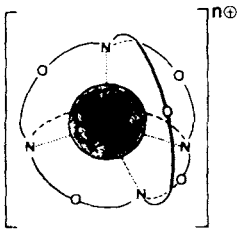

6

The problem of spherical recognition is that of selecting a given spherical ion from among a collection of different spheres of same charge. Thus, the macrobicyclic cryptands **1**–**3** form highly stable and selective cryptates $[M^{n\oplus} \subset (\text{cryptand})]$ **4a**, such as **4b**, with the cation whose size is complementary to the size of the cavity; i.e., $Li^{\oplus}$, $Na^{\oplus}$, and $K^{\oplus}$ for **1**, **2**, and **3**, respectively.[28a, 29a] Others display high selectivity for alkali versus alkaline-earth cations.[28b] Thus, recognition features equal to or higher than those of natural macrocyclic ligands may be achieved. The spherical macrotricyclic cryptand **5** binds strongly and selectively the larger spherical cations, giving a strong $Cs^{\oplus}$ complex, as in **6**.[30]

Anion cryptates are formed by the protonated polyamines **7**[31] and **5**[32] with the spherical halide anions $F^{\ominus}$ and $Cl^{\ominus}$, respectively. **5**-4 $H^{\oplus}$ binds $Cl^{\ominus}$ very strongly and very selectively compared with $Br^{\ominus}$ and other types of anions, giving the $[Cl^{\ominus} \subset (\mathbf{5}\text{-}4H^{\oplus})]$ cryptate **8**. Quaternary ammonium derivatives of such type of macrotricycles free of oxygen also bind spherical anions.[33]

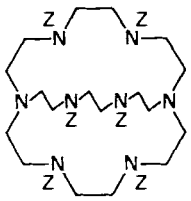

7, Z=H

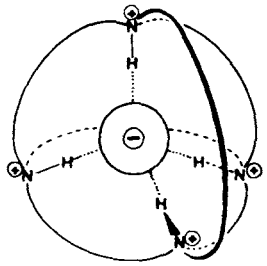

8

Thus, cryptands **1**–**3** and **5** as well as related compounds display *spherical recognition* of appropriate cations and anions. Their complexation properties result from their macropolycyclic nature and define a *cryptate effect* characterized by high stability and selectivity, slow exchange rates, and efficient shielding of the bound substrate from the environment.

As a consequence of these features, cryptate formation strongly influences physical properties and chemical reactivity. Numerous effects have been brought about and studied in detail, such as stabilization of alkalides and electrides,[34] dissociation of ion pairs, anion activation, isotope separation, and toxic metal binding. These results will not be described here and reviews may be found in Refs. [6, 35–38].

2.4. Tetrahedral Recognition

Selective binding of a tetrahedral substrate requires the construction of a receptor molecule possessing a tetrahedral recognition site, as realized in the macrotricycle **5**, which contains four nitrogen and six oxygen binding sites located, respectively, at the corners of a tetrahedron and of an octahedron.[30] Indeed, **5** forms an exceptionally stable and selective cryptate $[NH_4^{\oplus} \subset \mathbf{5}]$ **9**, with the tetrahedral $NH_4^{\oplus}$ cation, due to the high degree of structural and energetical complementarity. $NH_4^{\oplus}$ has the size and shape for fitting into the cavity of **5** and forming a tetrahedral array of $^{\oplus}N-H\cdots N$ hydrogen bonds with the four nitrogen sites.[39] As a result of its very strong binding, the pK_a of the $NH_4^{\oplus}$ cryptate is about six units higher than that of free $NH_4^{\oplus}$, indicating how much strong binding may affect the properties of the substrate. It also indicates that similar effects exist in enzyme active sites and in biological receptor-substrate binding.

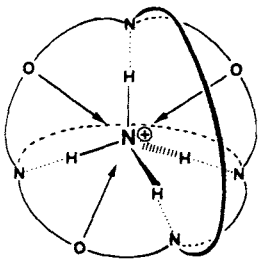

9

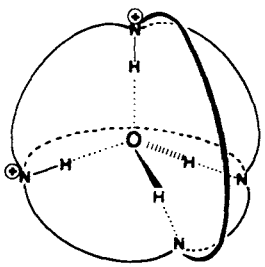

10

The unusual protonation features of **5** in aqueous solution (high pK_a for double protonation, very slow exchange) and ^{17}O-NMR studies led to the formulation of a water cryptate $[H_2O \subset (\mathbf{5}\text{-}2H^{\oplus})]$ **10** with the diprotonated macrotricycle.[2,6,40] The facilitation of the second protonation of **5** represents a *positive cooperativity*, in which the first proton and the effector molecule water set the stage both structurally and energetically for the fixation of a second proton.

Considering together the three cryptates $[NH_4^{\oplus} \subset \mathbf{5}]$ **9**, $[H_2O \subset (\mathbf{5}\text{-}2H^{\oplus})]$ **10**, and $[Cl^{\ominus} \subset (\mathbf{5}\text{-}4H^{\oplus})]$ **8**, it is seen that the spherical macrotricycle **5** is a molecular receptor possessing a *tetrahedral recognition site* in which the substrates are bound in a tetrahedral array of hydrogen bonds. It represents a state of the art illustration of the molecular engineering involved in abiotic receptor chemistry. Since it binds a tetrahedral cation $NH_4^{\oplus}$, a bent neutral molecule H_2O, or a spherical anion $Cl^{\ominus}$ when unprotonated, diprotonated, or tetraprotonated, respectively, the macrotricyclic cryptand **5** behaves like a sort of molecular chameleon responding to pH changes in the medium!

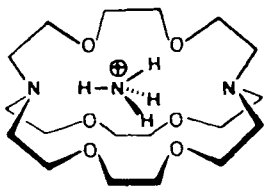

11

The macrobicycle **3** also binds $NH_4^{\oplus}$, forming cryptate **11**. The dynamic properties of **11** compared with **9** reflect the receptor-substrate binding complementarity: whereas $NH_4^{\oplus}$ is firmly held inside the cavity in **9**, it undergoes internal rotation in **11**.[41]

2.5. Recognition of Ammonium Ions and Related Substrates

In view of the important role played by substituted ammonium ions in chemistry and in biology, the development of receptor molecules capable of recognizing such substrates is of special interest. Macrocyclic polyethers bind primary ammonium ions by anchoring the $NH_3^{\oplus}$ group into their circular cavity via three $^{\oplus}N-H\cdots O$ hydrogen bonds as shown in **12**;[12-15,25,42] however, they complex alkali cations such as $K^{\oplus}$ more strongly. Selective binding of $R-NH_3^{\oplus}$ may be achieved by extending the results obtained for $NH_4^{\oplus}$ complexation by **5** and making use of the oxa-aza macrocycles[15,43] developed in the course of the synthesis of cryptands.[29a,b,30] Indeed, the triazamacrocycle [18]-N_3O_3,[*] which forms a complementary array of three $^{\oplus}N-H\cdots N$ bonds, **13**, selects $R-NH_3^{\oplus}$ over $K^{\oplus}$ and is thus a receptor unit for this functional group.[43]

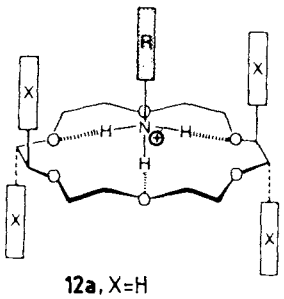

12a, X=H
12b, X=$CO_2^{\ominus}$
12c, X=CONYY'

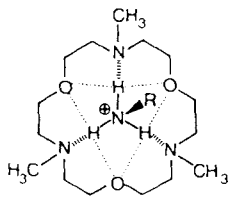

13

A great variety of macrocyclic polyethers have been shown to bind $R-NH_3^{\oplus}$ molecules with structural and chiral selectivity.[12,13,42] Particularly strong binding is shown by the tetracarboxylate **12b**, which conserves the desirable, basic [18]-O_6 ring and adds electrostatic interactions, thus forming the most stable metal-ion and ammonium complexes of any polyether macrocycle.[44] Very marked *central discrimination* is observed in favor of primary ammonium ions compared with more highly substituted ones; it allows preferential binding of biologically active ions such as noradrenaline or norephedrine compared with their *N*-methylated derivatives adrenaline and ephedrine.[44]

Modulation of the complexation features of **12** by varying the side groups X so as to make use of specific interactions (electrostatic, H-bonding, charge transfer, lipophilic) between X and the R group of the centrally bound $R-NH_3^{\oplus}$ substrate, brings about *lateral discrimination* effects. This also represents a general way of modeling interactions present in biological receptor-substrate complexes, such as that occurring between nicotinamide and tryptophane.[45] One may thus attach to **12** amino-acid residues (leading to "parallel peptides"[44] as in **12c**), nucleic acid bases or nucleosides, saccharides, etc.

Binding of metal-amine complexes $[M(NH_3)_n]^{m\oplus}$ to macrocyclic polyethers via $N-H\cdots O$ interactions with the NH_3 groups, leads to a variety of supramolecular species of "supercomplex type" by second-sphere coordination.[46] As with $R-NH_3^{\oplus}$ substrates, binding to aza-oxa or polyaza macrocycles (see **13**) may also be expected. Strong complexation by macrocycles bearing negative charges (such as **12b** or the hexacarboxylate in **14**[47]) should make it possible to induce various processes between centrally bound metal-amine species and lateral groups X in **12** (energy and electron transfer, chemical reaction, etc.).

Receptor sites for secondary and tertiary ammonium groups are also of interest. $R_2NH_2^{\oplus}$ ions bind to the [12]-N_2O_2 macrocycle via two hydrogen bonds.[48] The case of quaternary ammonium ions will be considered below.

[*] The designation gives the ring size in brackets followed by the kind and number of heteroatoms.

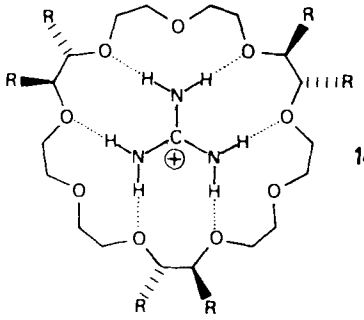

14, R=$CO_2^{\ominus}$

The guanidinium cation binds to [27]-O_9 macrocycles through an array of six H-bonds,[49] yielding a particularly stable complex **14** with a hexacarboxylate receptor, which also binds the imidazolium ion.[49a]

3. Anion Coordination Chemistry and the Recognition of Anionic Substrates

Although anionic species play a very important role in chemistry and in biology, their complexation chemistry went unrecognized as a specific field of research, while the complexation of metal ions and, more recently, cationic molecules was extensively studied. The coordination chemistry of anions may be expected to yield a great variety of novel structures and properties of both chemical and biological significance.[2,6,32] To this end, anion receptor molecules and binding subunits for anionic functional groups have to be devised. Research has been increasingly active along these lines in recent years and anion coordination chemistry is progressively building up.[8,9,50]

Positively charged or neutral electron-deficient groups may serve as interaction sites for anion binding. Ammonium and guanidinium units, which form $^{\oplus}N-H\cdots X^{\ominus}$ bonds, have mainly been used, but neutral polar hydrogen bonds (e.g., with $-NHCO-$ or $-COOH$ functions), electron-deficient centers (boron, tin, etc.), or metal-ion centers in complexes also interact with anions.

Polyammonium macrocycles and macropolycycles have been studied most extensively as anion receptor molecules. They bind a variety of anionic species (inorganic anions, carboxylates, phosphates, etc.) with stabilities and selectivities resulting from both electrostatic and structural effects.

Strong and selective complexes of the spherical halide anions are formed by macrobicyclic and by spherical macrotricyclic polyammonium receptors such as the protonated forms of **5**[32] (see **8**), of bis-tren **15**,[51] and of related compounds.[50,52]

The hexaprotonated form of bis-tren, **15**-6$H^{\oplus}$, complexes various monoatomic and polyatomic anions.[51] The crystal structures of four such anion cryptates (Fig. 1) provide a unique series of anion coordination patterns.[51b] The spherical halide ions are not complementary to the ellipsoidal receptor cavity and distort the structure, $F^{\ominus}$ being bound in a tetrahedral array of $N-H\cdots F^{\ominus}$ bonds and $Cl^{\ominus}$ and $Br^{\ominus}$ having octahedral coordination. The linear triatomic anion $N_3^{\ominus}$ has a shape and size complementary to the cavity of **15**-6$H^{\oplus}$ and is bound inside by a pyramidal array of three H-bonds to each terminal nitrogen, forming the cryptate $[N_3^{\ominus}\subset(\mathbf{15}\text{-}6H^{\oplus})]$ **16**. Thus, **15**-6$H^{\oplus}$ is a molecular receptor recognizing linear triatomic species such as $N_3^{\ominus}$, which is indeed bound much more strongly than other singly charged anions.

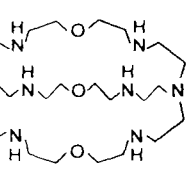

15

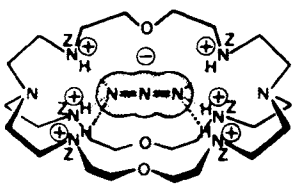

16

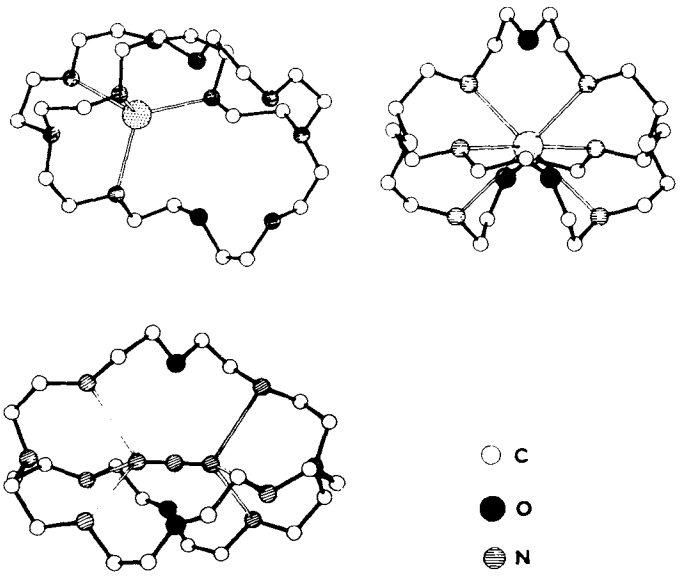

Fig. 1. Crystal structures of the anion cryptates formed by the hexaprotonated receptor molecule **15**-6$H^{\oplus}$ with fluoride (upper left), chloride (upper right), and azide (below) anions [51b].

Carboxylates and *phosphates* bind to polyammonium macrocycles with stabilities and selectivities determined by structure and charge of the two partners.[50,51,53-57] The design of receptor units for these functional groups is of much interest since they serve as anchoring sites for numerous biological substrates. Thus, strong complexes are obtained with macrobicyclic polyammonium pockets in which carboxylate (formate, acetate, oxalate, etc.) and phosphate groups interact with several ammonium sites.[51] The guanidinium group, which serves as a binding site in biological receptors, may form two H-bonds with carboxylate and phosphate functions and has been introduced into acyclic[58] and macrocyclic[59] structures. Binding units mimicking that of vancomycin are being sought.[60]

Complexation of complex anions of transition metals such as the hexacyanides $M(CN)_6^{n\ominus}$ yields second-coordination-sphere complexes, *supercomplexes*,[53a] and affects markedly their electrochemical[61,62] and photochemical[63] properties. Of special interest is the strong binding of adenosine mono-, di-, and triphosphate (AMP, ADP, and

ATP) and related compounds that play a very important biological role.[55-57]

Cascade-type binding[64] of anionic species occurs when a ligand first binds metal ions, which then serve as interaction sites for an anion. Such processes occur for instance in lipophilic cation/anion pairs[65] and with Cu^{II} complexes of bis-tren **15** and of macrocyclic polyamines.[66]

Heteronuclear NMR studies give information about the electronic effects induced by anion complexation as found for chloride cryptates.[67]

Complexation of various molecular anions by other types of macrocyclic ligands have been reported,[50] in particular with cyclophane-type compounds. Two such receptors of defined binding geometries are represented by the protonated forms of the macropolycycles **17**[68] and **18**.[69]

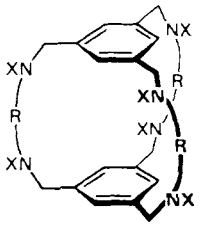

17, X=H, R=$(CH_2)_3$

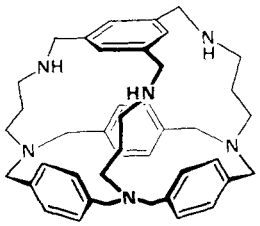

18

Anion coordination chemistry has thus made very significant progress in recent years. The development of other receptor molecules possessing well-defined geometrical and binding features will make it possible to further refine the requirements for anion recognition, so as to yield highly stable and selective anion complexes with characteristic coordination patterns. Theoretical studies may be of much help in the design of anion receptors and in the a priori estimation of binding features, as recently illustrated by the calculation of the relative affinity of **5**-4H$^{\oplus}$ for chloride and bromide ions.[70]

4. Coreceptor Molecules and Multiple Recognition

Once binding units for specific groups have been identified, one may consider combining several of them within the same macropolycyclic architecture. Thus are formed polytopic coreceptor molecules containing several discrete binding subunits which may cooperate for the simultaneous complexation of several substrates or of a multiply bound (polyhapto) polyfunctional species. Suitable modification would yield cocatalysts or cocarriers performing a reaction or a transport on the bound substrate(s). Furthermore, because of their ability to perform multiple recognition and because of the mutual effects of binding site occupation, such coreceptors provide entries into higher forms of molecular behavior such as cooperativity, allostery, and regulation, as well as communication or signal transfer, if a species is released or taken up. Basic ideas and definitions concerning coreceptor molecules have been presented in more detail elsewhere.[7]

The simplest class of coreceptors is that containing two binding subunits, ditopic coreceptors, which may belong to different structural types. Combination of chelating, tripodal, and macrocyclic fragments yields macrocyclic, axial or lateral macrobicyclic, or cylindrical macrotricyclic structures (Fig. 2). Depending on the nature of these units, the resulting coreceptors may bind metal ions, organic molecules, or both.

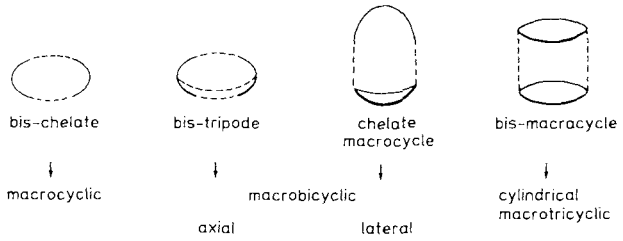

Fig. 2. Combination of chelating, tripodal, and cyclic subunits into ditopic coreceptors of macrocyclic, axial and lateral macrobicyclic, and cylindrical macrotricyclic types.

4.1. Dinuclear and Polynuclear Metal-Ion Cryptates

Coreceptor molecules containing two or more binding subunits for metal ions form dinuclear or polynuclear cryptates in which the arrangement of the metal ions is determined by the macropolycyclic structure. Such complexes may present a multitude of new properties, such as interactions between cations, electrochemical and photochemical processes, and fixation of bridging substrates, which are of interest both for bioinorganic modeling and for multicenter-multielectron reactions and catalysis.

Dinuclear cryptates of ligands belonging to all structural types shown in Figure 2 have been obtained. This vast area will only be illustrated here by a few recent examples (for more details and references see earlier reviews[64,71]).

Axial macrobicyclic ligands give dinuclear cryptates such as the Cu_2^I complex **19** formed by a large hexaimine structure obtained in a one-step multiple condensation reaction; its crystal structure is shown in **20**.[72]

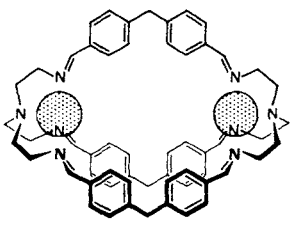

19

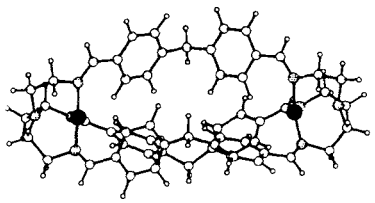

20

Lateral macrobicycles are dissymmetric by construction and make it possible to arrange metal centers of different properties in the same ligand. Thus, complexes of type **21** combine a redox center and a Lewis acid center for activation of a bound substrate.[73]

"*Cluster cryptates*" may be formed by assembling of metal ions and bridging species inside the molecular cavity of polytopic receptors. Thus, in the Cu_3^{II} complex **22** (crystal structure **23**) a bis-μ_3-hydroxo, triscopper(II) group is bound in the cavity of a tritopic macrocycle.[74] Modeling of biological iron-sulfur cluster sites may employ inclusion into appropriate macrocyclic cavities.[75]

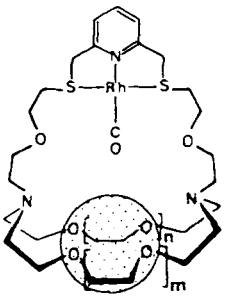

21, m,n=0,1

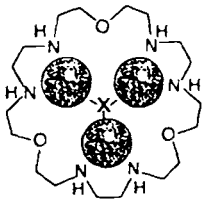

22

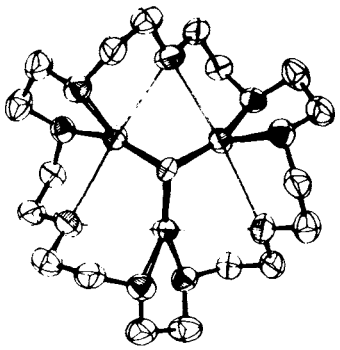

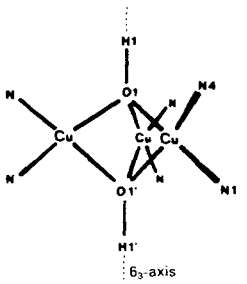

23

This inorganic aspect of supramolecular species represents in itself a field of research in which many novel structures and reactivities await to be discovered.

4.2. Linear Recognition of Molecular Length by Ditopic Coreceptors

Receptor molecules possessing two binding subunits located at the two poles of the structure will complex preferentially substrates bearing two appropriate functional groups at a distance compatible with the separation of the subunits. This distance complementarity amounts to a recognition of molecular length of the substrate by the receptor. Such *linear molecular recognition* of dicationic and dianionic substrates corresponds to the binding modes illustrated by **24** and **25**.

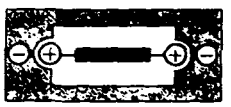

24

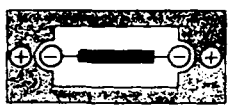

25

Incorporation of macrocyclic subunits that bind $NH_3^{\oplus}$ groups (see above) into cylindrical macrotricyclic[76] and macrotetracyclic[77] structures yields ditopic coreceptors that form molecular cryptates such as **26** with terminal *diammonium cations* $^{\oplus}H_3N-(CH_2)_n-NH_3^{\oplus}$. In the resulting supermolecules the substrate is located in the central molecular cavity and anchored by its two $NH_3^{\oplus}$ groups in the macrocyclic binding sites, as shown by the crystal structure **27** (**26** with R = NA and A = $(CH_2)_5$).[78] Changing the length of the bridges R in **26** modifies the binding selectivity in favor of the substrate of complementary length. NMR relaxation data have also shown that optimal partners present similar molecular motions in the receptor-substrate pair. Thus, complementarity in the supramolecular species expresses itself in both steric *and* dynamic fit.[79]

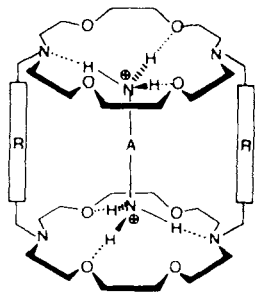

26, R=P,NA,BP,TP

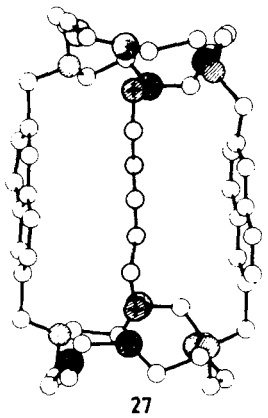

27

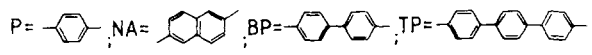

Dianionic substrates, such as the alkyl dicarboxylates $^{\ominus}O_2C-(CH_2)_n-CO_2^{\ominus}$, are bound with length discrimination by ditopic macrocycles such as **28**. These receptors contain two triammonium groups as binding subunits interacting with the terminal carboxylate functions, via a pattern schematically shown in **29**.[80]

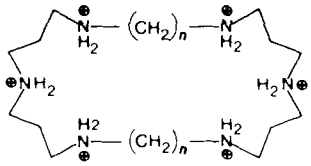

28, n=7,10

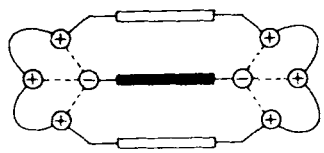

29

Thus, for both the terminal diammonium and dicarboxylate substrates, selective binding by the appropriate receptors describes a linear recognition process based on length complementarity in a ditopic binding mode. Important biological species, such as polyamines, amino-acid and peptide diamines, and dicarboxylates, may also be bound selectively.

Numerous variations in the nature of the binding subunits or of the bridges linking them, are conceivable and may be tailored to specific complexation properties (see, for instance, Refs. [15, 81]). The development of *heterotopic receptors* may allow the binding of ion pairs[82] or zwitterionic species.[83]

Studies on *dynamic coupling*[79,84] between a receptor and a substrate are of much interest. Dynamic features of supermolecules correspond on the intermolecular level to the internal conformational motions present in molecules themselves and define molecular recognition processes by their dynamics in addition to their structural aspects.

4.3. Heterotopic Coreceptors: Speleands, Amphiphilic Receptors

Combination of binding subunits of different nature yields heterotopic receptors that may bind substrates by in-

teracting simultaneously with cationic and anionic neutral sites, making use of electrostatic and van der Waals forces as well as of solvophobic effects.

The natural cyclodextrins were the first receptor molecules whose binding properties towards organic molecules yielded a wealth of results on physical and chemical features of molecular complexation.[21,85]

Numerous types of synthetic macrocyclic receptors that contain various organic groups and polar functions have been developed in recent years. They complex both charged and uncharged organic substrates. Although the results obtained often describe mere binding rather than actual recognition, they have provided a large body of data that make it possible to analyze the basic features of molecular complexation and the properties of structural fragments to be used in receptor design. We describe here mainly some of our own results in this area, referring the reader to specific reviews of the subject.[20,86]

Synergetical operation of electrostatic and hydrophobic effects may occur in *amphiphilic receptors* combining charged polar sites with organic residues, which shield the polar sites from solvation and increase electrostatic forces. Such macropolycyclic structures containing polar binding subunits maintained by apolar shaping components, termed *speleands*, yield molecular cryptates *(speleates)* by substrate binding.[87]

Thus, macrocycle **30**, incorporating four carboxylate groups and two diphenylmethane units,[88] not only forms very stable complexes with primary ammonium ions, but also strongly binds secondary, tertiary, and quaternary ammonium substrates. In particular, it complexes *acetylcholine*, giving information about the type of interactions that may play a role in biological acetylcholine receptors, such as the combination of negative charges with hydrophobic walls. Similar effects operate in other anionic receptors complexing quaternary ammonium cations.[86a,89] Extensive studies have been conducted on the complexation of heterocyclic ammonium ions such as diquat by macrocyclic polyether receptors.[90]

The $CH_3-NH_3^{\oplus}$ cation forms a selective speleate **31** by binding to the [18]-N_3O_3 subunit of a macropolycycle maintained by a cyclotriveratrylene shaping component. The tight intramolecular cavity efficiently excludes larger substrates.[87,91]

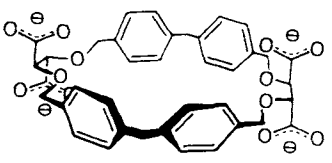

30

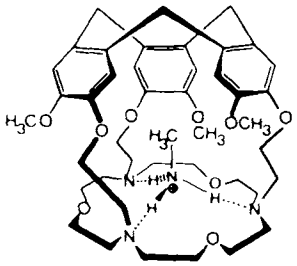

31

Amphiphilic binding also occurs for molecular anionic substrates.[20,86,92] Charged heterocyclic ring systems, such as those derived from the pyridinium group, represent an efficient way to introduce simultaneously electrostatic interactions, hydrophobic effects, structure, and rigidity into a molecular receptor; in addition they may be electroactive and photoactive.[93] Even single planar units such as diazapyrenium dications bind flat organic anions remarkably well in aqueous solution, using electrostatic interactions as well as hydrophobic stacking.[93] A macrocycle containing four pyridinium sites was found to strongly complex organic anions.[94]

Receptors of *cyclointercaland* type, which incorporate intercalating units into a macrocyclic system, are of interest for both the binding of small molecules and their own (selective) interaction with nucleic acids. A *cyclo-bisintercaland* has been found to form an intercalative molecular cryptate **32** in which a nitrobenzene molecule is inserted between the two planar subunits of the receptor.[95] Such receptors are well suited for the recognition of substrates presenting flat shapes and become of special interest if intercalating dyes are incorporated.[96]

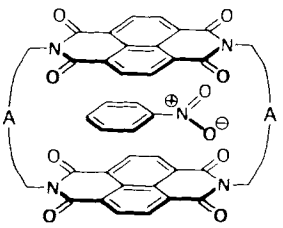

32, A=$(CH_2)_8$

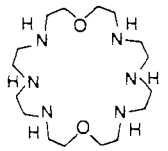

33

Fitting the macrocyclic polyamine **33** with a side chain bearing a 9-aminoacridine group yields a coreceptor that may display both anion binding, via the polyammonium subunit and stacking interaction via the intercalating dye. It interacts with both the triphosphate and the adenine groups of ATP and provides in addition a catalytic site for its hydrolysis (see Section 5.2).[97]

Flat aromatic heterocyclic units bearing lateral acid and amide functional groups function as receptors that perform size and shape recognition of complementary substrates within their molecular cleft.[17b] Receptor units containing heterocyclic groups such as 2,6-diaminopyridine[98a] or a nucleic acid base combined with an intercalator[98b] may lead to recognition of nucleotides via base-pairing.[98c]

The spherically shaped *cryptophanes* allow the study of recognition between neutral receptors and substrates and, in particular, the effect of molecular shape and volume complementarity on selectivity.[99]

4.4. Multiple Recognition in Metalloreceptors

Metalloreceptors are heterotopic coreceptors that are able to bind both metal ions and organic molecules by means of substrate-specific units.

Porphyrin and α,α'-bipyridine (bipy) groups have been introduced as metal-ion binding units in macropolycyclic coreceptors containing also macrocyclic sites for anchoring $NH_3^{\oplus}$ groups.[64,71,100] These receptors form mixed-substrate supermolecules by simultaneously binding metal ions and diammonium cations as shown in **34**. Metalloreceptors, and the supermolecules that they form, thus open

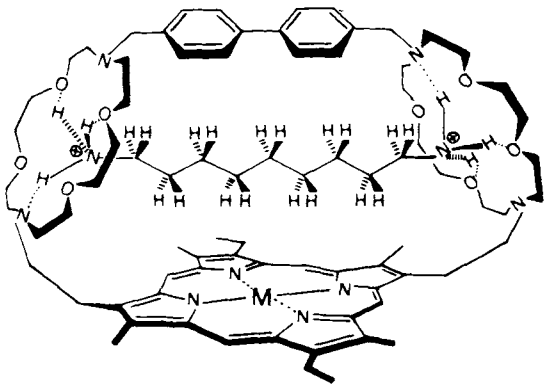

34, M=Zn

up a vast area for the study of interactions and reactions between co-bound organic and inorganic species. In view of the number of metal-ion complexes known and of the various potential molecular substrates, numerous types of metalloreceptors may be imagined which would be of interest as abiotic chemical species or as bioinorganic model systems.[101]

5. Supramolecular Reactivity and Catalysis

Reactivity and catalysis represent major features of the functional properties of supramolecular systems. Molecular receptors bearing appropriate reactive groups in addition to binding sites may complex a substrate (with given stability, selectivity, and kinetic features), react with it (with given rate, selectivity, and turnover), and release the products, thus regenerating the reagent for a new cycle (Fig. 3).

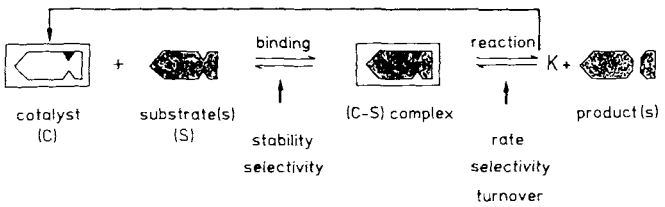

Fig. 3. Schematic representation of the supramolecular catalysis process.

Supramolecular reactivity and catalysis thus involve two main steps: *binding* which selects the substrate and *transformation* of the bound species into products within the supermolecule formed. Both steps take part in the molecular *recognition* of the *productive* substrate and require the correct molecular information in the reactive receptor.[1] Compared to molecular catalysis, a binding step is involved that selects the substrate and precedes the reaction itself.

The design of efficient and selective supramolecular reagents and catalysts may give mechanistic insight into the elementary steps of catalysis, provide new types of chemical reagents, and effect reactions that reveal factors contributing to enzymatic catalysis. This has led to numerous investigations, which have made use mainly of reagents based on functionalized α-cyclodextrin, macrocyclic polyethers, and cyclophanes.[85, 102, 103]

5.1. Catalysis by Reactive Cation Receptor Molecules

Ester cleavage processes have been most frequently investigated in enzyme model studies. Macrocyclic polyethers fitted with side chains bearing thiol groups cleave activated esters with marked rate enhancements and chiral discrimination between optically active substrates.[104–106] The tetra-L-cysteinyl derivative of macrocycle **12c** binds *p*-nitrophenyl (PNP) esters of amino acids and peptides, and reacts with the bound species, releasing *p*-nitrophenol as shown in **35**.[105] The reaction displays (1) substrate selec-

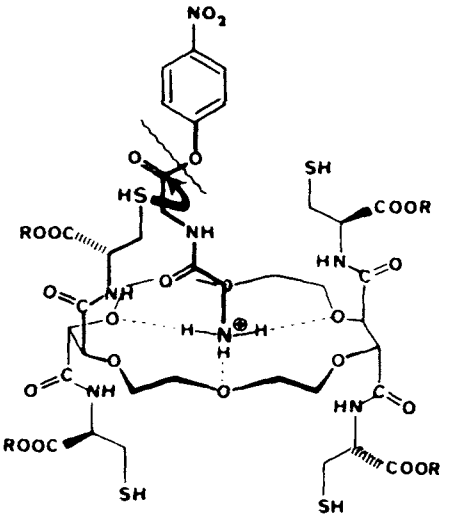

35, R=CH_3

tivity with (2) marked rate enhancements in favor of dipeptide ester substrates, (3) inhibition by complexable metal cations that displace the bound substrate, (4) high chiral recognition between enantiomeric dipeptide esters, and (5) slow but definite catalytic turnover.

Binding of pyridinium substrates to a macrocycle of type **12c** bearing 1,4-dihydropyridyl side chains led to enhanced rates of *hydrogen transfer* from dihydropyridine to pyridinium within the supramolecular species **36** formed. The first-order intracomplex reaction was inhibited and became bimolecular on displacement of the bound substrate by complexable cations.[107]

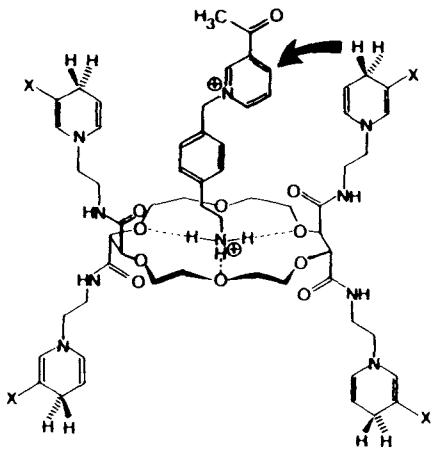

36, X=CONH*n*Bu

Activation and orientation by binding was observed for the hydrolysis of *O*-acetylhydroxylamine. $CH_3COONH_3^{\oplus}$ forms such a stable complex with the macrocyclic tetracarboxylate **12b** that it remains protonated and bound even at neutral pH, despite the low pK_a of the free species (ca. 2.15). As a consequence, its hydrolysis is accelerated and exclusively gives acetate and hydroxylamine, whereas in the presence of $K^{\oplus}$ ions, which displace the substrate, the latter rearranges to acetylhydroxamic acid, $CH_3CONH-OH$ (ca. 50%).[108] Thus, strong binding may be sufficient for markedly accelerating a reaction and affecting its course, a result that also bears on enzyme-catalyzed reactions.

5.2. Catalysis by Reactive Anion Receptor Molecules

The development of anion coordination chemistry and anion receptor molecules has made it possible to perform molecular catalysis on anionic substrates of chemical and biochemical interest, such as adenosine triphosphate (ATP).

ATP hydrolysis was found to be catalyzed by a number of protonated macrocyclic polyamines. In particular, [24]-N_6O_2 **33** strongly binds ATP and markedly accelerates its hydrolysis to ADP and inorganic phosphate over a wide pH range.[109] The reaction presents first-order kinetics and is catalytic with turnover. It proceeds via initial formation of a complex between ATP and protonated **33**, followed by an intracomplex reaction which may involve a combination of acid, electrostatic, and nucleophilic catalysis. Structure **37** represents one possible binding mode of the ATP–**33** complex and indicates how cleavage of the terminal phosphoryl groups might take place. A transient intermediate, identified as phosphoramidate **38**, is formed by

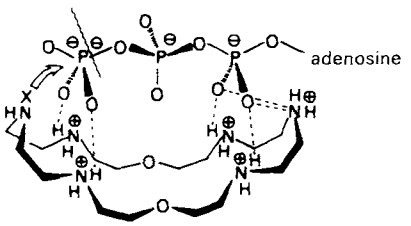

37

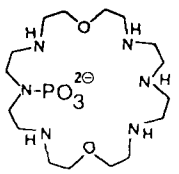

38

phosphorylation of the macrocycle by ATP and is subsequently hydrolyzed. Studies with analogues of ATP indicated that the mechanism was dissociative in character within a preassociative scheme resulting from receptor–substrate binding.[110] In this process, catalyst **33** presents prototypical ATPase activity; i.e., it behaves as a proto-ATPase.

5.3. Cocatalysis: Catalysis of Synthetic Reactions

A further step lies in the design of systems capable of inducing *bond formation* rather than bond cleavage, thus effecting *synthetic* reactions as compared to degradative ones. To this end, the presence of several binding and reactive groups is essential. Such is the case for coreceptor molecules in which subunits may cooperate for substrate binding and transformation.[7] They should be able to perform *cocatalysis* by bringing together substrate(s) and cofactor(s) and mediating reactions between them within the supramolecular structure (Fig. 4).

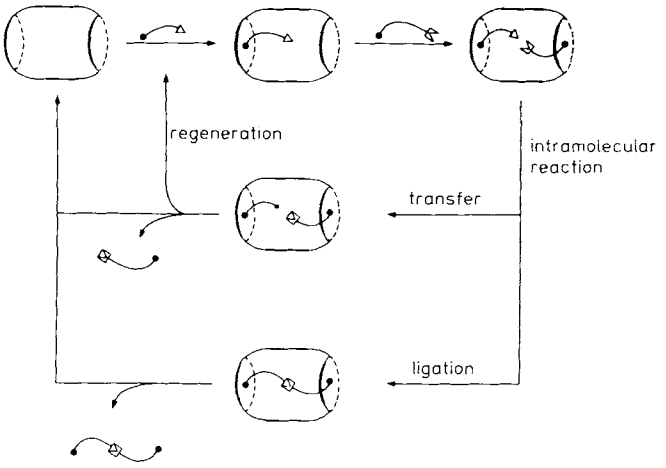

Fig. 4. Schematic illustration of cocatalysis processes: group transfer and ligation reactions occurring within the supramolecular complex formed by the binding of substrates to the two macrocyclic subunits of a macrotricyclic coreceptor molecule.

A process of this type has been realized recently.[111] Indeed, when the same macrocycle **33** used in the studies of ATP hydrolysis was employed as catalyst for the hydrolysis of acetylphosphate ($AcP = CH_3COOPO_3^{2\ominus}$), it was found to mediate the *synthesis of pyrophosphate* from AcP. Substrate consumption was accelerated and catalytic with turnover. The results obtained agree with a catalytic cycle involving the following steps: (1) substrate AcP binding by the protonated molecular catalyst **33**; (2) phosphorylation of **33** within the supramolecular complex, giving the phosphorylated intermediate PN **38**; (3) binding of the substrate $HPO_4^{2\ominus}$ (P); (4) phosphoryl transfer from PN to P with formation of pyrophosphate PP (Fig. 5); (5) release of the product and of the free catalyst for a new cycle.

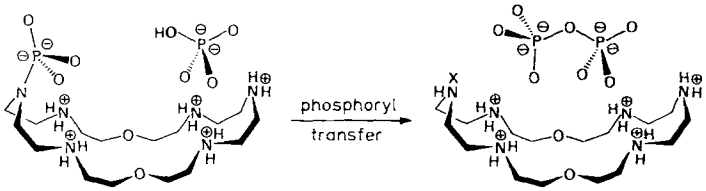

Fig. 5. Cocatalysis: pyrophosphate synthesis by phosphoryl transfer mediated by macrocycle **33** via the phosphorylated intermediate **38**.

The fact that **33** is a ditopic coreceptor containing two diethylenetriamine subunits is of special significance for both PN and PP formation. These subunits may cooperate in binding AcP and activating it for phosphoryl transfer via the ammonium sites, in providing an unprotonated nitrogen site for PN formation, and in mediating phosphoryl transfer from PN to P. Thus **33** would combine electrostatic and nucleophilic catalysis in a defined structural ar-

rangement suitable for PP synthesis via two successive phosphoryl transfers, displaying protokinase-type activity (Fig. 5). This bond-making process extends supramolecular reactivity to cocatalysis, mediating *synthetic reactions* within the supramolecular entities formed by coreceptor molecules. The formation of PP when ATP is hydrolyzed by **33** in the presence of divalent metal ions has also been reported.[112]

Functionalized macrocyclic polyethers were used for peptide bond formation in two successive intracomplex steps[113] and a macrobicyclic cyclophane bearing a thiazolium group was shown to effect supramolecular catalysis of the benzoin condensation of two benzaldehyde molecules.[114]

The systems described in this section possess the properties that define supramolecular reactivity and catalysis: substrate recognition, reaction within the supermolecule, rate acceleration, inhibition by competitively bound species, structural and chiral selectivity, and catalytic turnover. Many other types of processes may be imagined. Thus, supramolecular catalysis of the hydrolysis of unactivated esters and of amides presents a challenge[115] that chemistry has met in natural enzymatic reagents but not yet in abiotic catalysts. Designing modified enzymes by chemical mutation,[116] or by protein engineering,[117] and producing catalytic proteins by antibody induction[118] represent biochemical approaches to artificial catalysts. Of particular interest is the development of supramolecular catalysts performing synthetic reactions that create new bonds rather than cleave them. By virtue of their multiple binding features, coreceptors open the way to the design of cocatalysts for ligation, metallocatalysis, and cofactor reactions, which act on two or more co-bound and spatially oriented substrates.

Supramolecular catalysts are by nature *abiotic* reagents, chemical catalysts that may perform the same *overall* processes as enzymes, without following the detailed pathway by which the enzymes actually realize them. This chemistry may develop reagents effecting highly efficient and selective processes that enzymes do not perform or realizing enzymatic ones under conditions in which enzymes do not operate.

6. Transport Processes and Carrier Design

The organic chemistry of membrane transport processes and carrier molecules has only recently been developed, although the physico-chemical features and the biological importance of transport processes have long been recognized. The design and synthesis of receptor molecules binding selectively organic and inorganic substrates made available a range of compounds which, if made membrane soluble, could become carrier molecules and induce selective transport by rendering membranes permeable to the bound species. Thus, transport represents one of the basic functional features of supramolecular species together with recognition and catalysis.[2, 103, 119, 120]

The chemistry of transport systems comprises three main aspects: to design transport effectors, to devise transport processes, and to investigate their applications in chemistry and in biology. Selective membrane permeability may be induced either by *carrier molecules* or by *transmembrane channels* (Fig. 6).

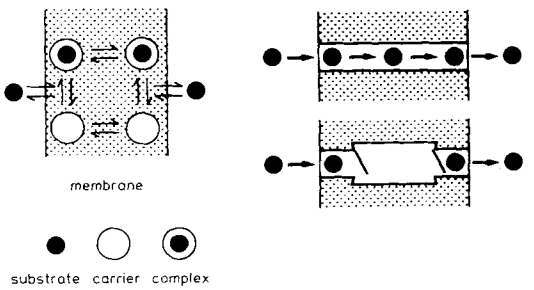

Fig. 6. Left: Transport processes: carrier-mediated. Right: Channel (above), gated channel (below).

6.1. Carrier-mediated Transport

Carrier-mediated transport consists in the transfer of a substrate across a membrane, facilitated by a carrier molecule. The four-step cyclic process (association, dissociation, forward and back-diffusions; Fig. 6) is a *physical catalysis* effecting a translocation of the substrate like chemical catalysis effects a transformation into products. The carrier is the transport catalyst and the active species is the carrier–substrate supermolecule. Transport is a three-phase process, whereas homogeneous chemical and phase-transfer catalyses are single phase and two-phase, respectively.

Carrier design is the major feature of the organic chemistry of membrane transport since the carrier determines the nature of the substrate, the physico-chemical features (rate, selectivity), and the type of process (facilitated diffusion, coupling to gradients and flows of other species, active transport). The carrier must be highly selective, present appropriate exchange rates and lipophilic/hydrophilic balance, and bear functional groups suitable for flow coupling. The transport process depends also on the nature of the membrane, the concentrations in the three phases, and the other species present. More detailed considerations on the internal and external factors that affect transport processes may be found in earlier reports.[1, 103, 120, 121]

Our initial work on the *transport of amino acids*, dipeptides, and acetylcholine through a liquid membrane employed simple lipophilic surfactant-type carriers. It was aimed at the physical organic chemistry of transport processes, exploring various situations of transport coupled to flows of protons, cations, or anions in concentration and pH gradients.[122]

Selective *transport of metal cations*, mainly of alkali cations, has been a major field of investigation, spurred by the numerous cation receptors of natural or synthetic origin that are able to function as cation carriers.[24, 103, 119–121, 123, 124]

Cryptands of type **1**–**3** and derivatives thereof carry alkali cations,[125] even under conditions where natural or synthetic macrocycles are inefficient. The selectivities observed depend on the structure of the ligand, the nature of the cation, and the type of co-transported counteranion. Designed structural changes allow the transformation of a

cation receptor into a cation carrier.[120, 125] The results obtained with cryptands indicated that there was an optimal complex stability and phase-transfer equilibrium for highest transport rates.[125] Combined with data for various other carriers and cations, they gave a bell-shaped dependence of transport rates on extraction equilibrium (see Fig. 3 in Ref. [120]), with low rates for too small or too large (carrier saturation) extraction and highest rates for half-filled carriers.[120, 125] Kinetic analyses allowed the experimental results to be related to the dependence of transport rates and selectivities on carrier properties.[124, 126, 127] Detailed studies of the transport of $K^{\oplus}$ and $Na^{\oplus}$ by lipophilic derivatives of **2** and **3** in vesicles bore on the efficiency, the selectivity, and the mechanism of the processes.[128]

Modifying the nature of the binding sites makes it possible to selectively transport other cations, such as toxic metal ions. Macrocyclic polyethers can carry organic primary ammonium cations, in particular physiologically active ones.[129] The nature of the counterion and the concentrations of species strongly influence rates of transport and may affect its selectivity.[120, 125]

Anion transport may be effected by lipophilic ammonium ions or by metal complexes[120, 130] acting as anion receptors. Progress in anion coordination chemistry should provide a range of anion carriers that will help to develop this area of transport chemistry. The selective transport of carboxylates and phosphates is of great interest. Some results, references, and suggestions have already been given.[120, 131]

Cation–anion cotransport was effected by a chiral macrotricyclic cryptand that carried simultaneously an alkali cation and a mandelate anion (see **39**).[82] Employing together a cation and an anion carrier should give rise to *synergetic transport* with double selection, by facilitating the flow of both components of a salt (see the electron-cation symport below).

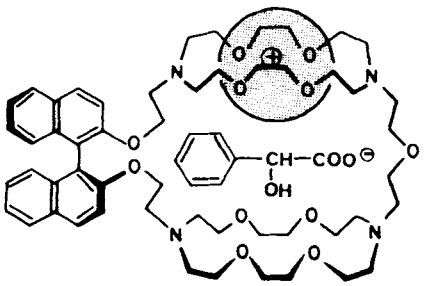

39

Selective transport of amino acids occurs with a macrotricycle containing an internal phosphoric acid group[83b] and with a convergent dicarboxylic acid receptor.[83c] *Neutral* molecules are carried between two organic phases through a water layer by water-soluble receptors containing a lipophilic cavity.[92b, 132]

It is clear that numerous facilitated transport processes may still be set up, especially for anions, salts, or neutral molecules and that the active research in receptor chemistry will make available a variety of carrier molecules. Of special interest are those transport effectors, derived from coreceptors, that allow coupled transport (*cotransport*) to be performed.

6.2. Coupled Transport Processes

A major goal in transport chemistry is to design carriers and processes that involve the coupled flow of two (or more) species either in the same (symport) or in opposite (antiport) direction. Such parallel or antiparallel vectorial processes make it possible to set up pumped systems in which a species is carried in the potential created by physico-chemical gradients of electrons (redox gradient), protons (pH gradient), or other species (concentration gradient). To this end, either two or more individual carriers for different species may be used simultaneously or the appropriate subunits may be introduced into a single species, a *cocarrier*.

6.2.1. Electron-Coupled Transport in a Redox Gradient

Electron–cation symport has been realized in a double carrier process where the coupled, parallel transport of electrons and metal cations was mediated simultaneously by an electron carrier and by a selective cation carrier.[133] The transport of electrons by a nickel complex in a redox gradient was the electron pump for driving the selective transport of $K^{\oplus}$ ions by a macrocyclic polyether (Fig. 7).

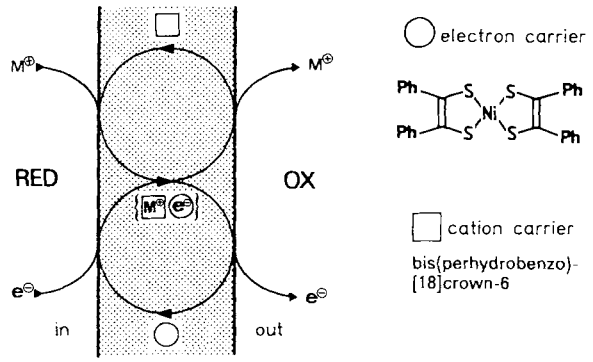

Fig. 7. Electron-cation coupled transport: a redox-driven electron-cation symport consisting of an electron carrier (nickel complex) and a selective cation carrier (macrocyclic polyether). RED, potassium dithionite; OX, $Na_3[Fe(CN_6)]$ [133].

The process has the following features: active $K^{\oplus}$ transport and coupled electron flow; two cooperating carriers acting synergetically; a redox pump; a selection process by the cation carrier; regulation by the cation/carrier pair. This system represents a prototype for the design of other multicarrier coupled transport processes. Electron transport with quinone carriers involves a ($2e^{\ominus}$, $2H^{\oplus}$) symport.[134, 135]

Electron–anion antiports have been realized for instance with carriers such as ferrocene or alkylviologens.[136] The latter have been used extensively in light-driven systems and in studies on solar energy conversion.

6.2.2. Proton-Coupled Transport in a pH Gradient

Carriers bearing negatively charged groups may effect cation antiport across membranes, so that if one cation is a proton, a proton pump may be set up in a pH gradient.

This has been realized for alkali cations with natural or synthetic carboxylate-bearing ionophores.[137]

A case of special interest is that of the transport of divalent ions such as calcium versus monovalent ones. The lipophilic carrier **40**, containing a *single* cation receptor site and *two* ionizable carboxylic acid groups, was found to transport selectively $Ca^{2\oplus}$ in the dicarboxylate form and

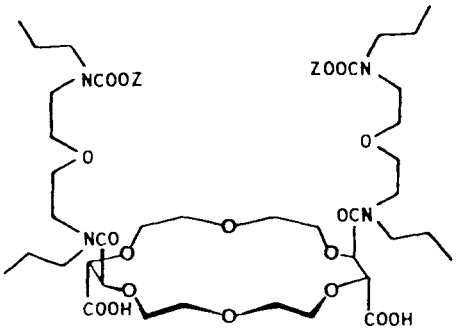

40, $Z = CH_2C_6H_5$

$K^{\oplus}$ when monoionized, thus allowing pH control of the process. This striking change in transport features involves *pH regulation* of $Ca^{2\oplus}/K^{\oplus}$ selectivity in a competitive ($Ca^{2\oplus}$, $K^{\oplus}$) symport coupled to ($Ca^{2\oplus}$, $2H^{\oplus}$) and ($K^{\oplus}$, $H^{\oplus}$) antiport in a pH gradient, which provides a proton pump (Fig. 8).[138]

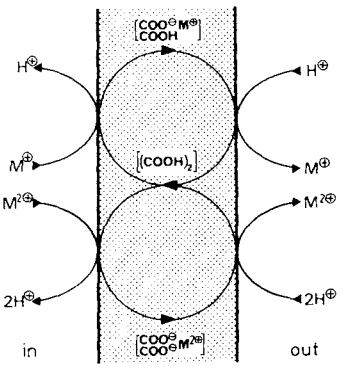

Fig. 8. A competitive divalent/monovalent cation symport coupled to $M^{2\oplus}/2H^{\oplus}$ and $M^{\oplus}/H^{\oplus}$ antiport in a pH gradient by a macrocyclic carrier such as **40**; the state of the carrier is indicated as diprotonated, $[(CO_2H)_2]$, or complexed, $[(CO_2^{\ominus})_2, M^{2\oplus}]$ and $[(CO_2H)(CO_2^{\ominus}), M^{\oplus}]$.

This system demonstrates how carrier design allows transport processes to be endowed with regulation of rates and selectivity, as well as coupling to energy sources, for transport of a species against it own concentration gradient.

6.2.3. *Light-Coupled Transport Processes*

Light-driven transport may be brought about by photogeneration of a species that will induce the process or perturb it.

This has been achieved in a *light-induced electron transport* process involving the proflavine-sensitized photogeneration of reduced methylviologen, $MV^{\oplus}$, which transfers electrons to a quinone-type carrier contained in the membrane.[135] Light-driven (electron, cation) symport occurs when combining this system with the (nickel complex, macrocycle) process described above.[139] The increased lipophilicity of reduced viologens facilitates electron and phase transfer.[140] Such processes are also of interest for solar energy storage systems where electron-permeable membranes separate the reductive and oxidative components. Photocontrol of ion extraction and transport has been realized with macrocyclic ligands that undergo a structural change upon irradiation, resulting in two forms having different ion affinities.[141]

The results obtained on coupled transport processes stress the role of cocarrier systems capable of transporting several substrates with coupling to physical and chemical energy sources.

6.3. Transfer via Transmembrane Channels

Transmembrane channels represent a special type of multi-unit effector allowing the passage of ions or of molecules through membranes by a flow or site-to-site hopping mechanism. They play an important role in biological transport. Natural and synthetic peptide channels (gramicidin A, alamethicin) for cations have been studied.[142, 143]

Artificial *cation channels* would provide fundamental information on the mechanism of cation flow and channel conduction. A solid-state model of cation transfer inside a channel is provided by the crystal structure of the KBr complex of **12c** ($Y = Y' = CH_3$), which contains stacks of macrocycles with cations located alternately inside and above a macrocyclic unit, like a frozen picture of cation propagation through the "channel" defined by the stack.[144]

A polymeric stack of macrocycles has been synthesized[145] and a cyclodextrin-based model of a half-channel has been reported.[146] A derivative of monensin, an acyclic polyether ionophore, forms lithium channels in vesicles,[147] which may be sealed by diammonium salts.[148]

Cylindrical macrotricycles such as **26** (substrate removed) represent the basic unit of a cation channel based on stacks of linked macrocycles; they bind alkali cations,[149] and cation jumping processes between the top and bottom rings have been observed.[150] Theoretical studies give insight into the molecular dynamics[151] of ion transport and the energy profiles[152] in cation channels.

Electron channels, as transmembrane wires, represent the channel-type counterpart to the mobile electron carriers discussed above and will be considered in Section 9.2. *Anion channels* may also be envisaged.

Thus, several types of studies directed towards the development of artificial ion channels and the understanding of ion motion in channels are being carried out. These effectors deserve and will receive increased attention, in view also of their potential role in molecular ionics (see Section 9.2).

A further step in channel design must involve the introduction of (proton-, ion-, redox-, or light-activated) *gates and control elements* for regulating opening and closing, rates, and selectivity. In this respect, one may note that ionizable groups on mobile carriers (as in **40**, see Section 6.2.2) correspond, for these effectors, to the gating mechanisms in channels.

In conclusion, transport studies open ways to numerous developments of this chemically and biologically most important function, such as effector design, analysis of elementary steps and mechanisms, coupling to chemical potentials, energy and signal transduction, models of biological transport processes, construction of vesicular microreactors and artificial cells, with a variety of possible applications, for instance in separation and purification or in batteries and systems for artificial photosynthesis.

By the introduction of polytopic features, which may include selective binding subunits as well as gating components for flow regulation, the design of cocarriers and of artificial molecular channels should add another dimension to the chemistry of the effectors and mechanisms of transport processes.

7. From Endoreceptors to Exoreceptors

The design of receptor molecules has mainly relied on macrocyclic or macropolycyclic architectures (see above) and/or on rigid spacers or templates (see, for instance, Refs. [17b, 26, 76–79, 81b, 83c]) that allow binding sites to be positioned on the walls of molecular cavities or clefts in such a way that they converge towards the bound substrate. The latter is more or less completely surrounded by the receptor, forming an *inclusion* complex. This widely used principle of *convergence* defines a convergent or *endo-supramolecular chemistry* with endoreceptors effecting endo-recognition. Biological analogies are found in the active sites of enzymes where a small substrate binds inside a cavity of a large protein molecule.

The opposite point of view would be to make use of an external *surface* with protuberances and depressions, rather than an internal cavity, as substrate receiving site. This would amount to the passage from a convergent to a *divergent* or *exo-supramolecular chemistry* and from endo- to *exoreceptors*. Receptor–substrate binding then occurs by surface-to-surface interaction, which may be termed *affixion* and symbolized by // or by the mathematical symbol of intersection $\cap$ (if there is notable interpenetration of the surfaces),[153] $[\rho // \sigma]$ and $[\rho \cap \sigma]$, respectively. *Exo-recognition* with strong and selective binding requires a large enough contact area and a sufficient number of interactions as well as geometrical and site (electronic) complementarity between the surfaces of ρ and σ. Such a mode of binding finds biological analogies in protein–protein interactions, for instance at the antibody–antigen interface where the immunological recognition processes occur.[154]

One may note that exo-recognition includes recognition between (rather large) bodies of similar size as well as recognition at interfaces with monolayers, films, membranes, cell walls, etc.

7.1. Metallo-Exoreceptors. Metallonucleates

In order to reinforce the binding strength, one may think of introducing one or more interaction *poles*, for instance, electrical charges, generating strong electrostatic forces. Such could be the case for a metal complex whose central cation would be the electrostatic pole and whose external surface could bear functional groups containing the molecular information required for recognizing the partner. In addition, the metal cation provides a further way of organizing the structure by virtue of its coordination geometry (tetrahedral, square-planar, octahedral, etc.), which leads to a given arrangement of the external interaction sites (Fig. 9).

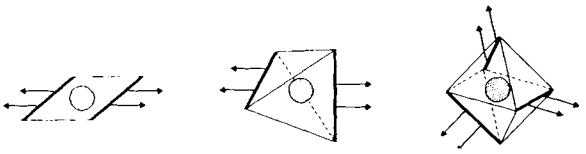

Fig. 9. Schematic representation of the arrangement of external interaction sites (arrows) around a metal ion of given coordination geometry (planar, tetrahedral, octahedral) in mononuclear metallo-exoreceptors.

As a first approach to receptor design along these lines, specific groups, selected for their information content, have been attached to functionalized α,α'-bipyridines, giving ligands of type **41**, which form metal complexes of defined geometry and physico-chemical properties. With nucleosides, species such as the bis-adenosine derivative **42**

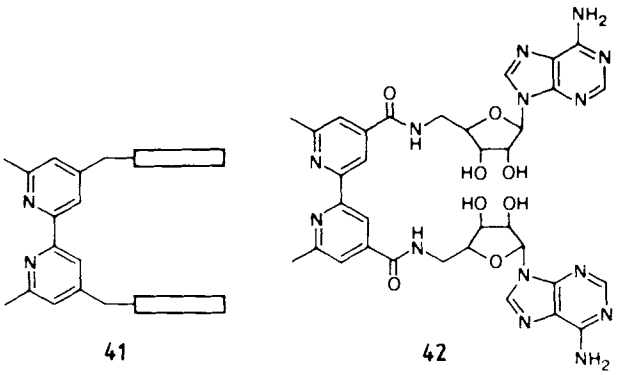

41 **42**

are obtained.[155] The resulting positively charged, *metallonucleate* complexes should interact strongly and selectively with the negatively charged oligonucleotides and nucleic acids, the fixation site depending on the nature and disposition of the external nucleosides. Double-helical metallonucleates[155] may be derived from the helicates described below. Numerous variations may be imagined for the external groups (intercalators, amino acids, oligopeptides, reactive functions) so as to yield metal complexes displaying selective fixation and reactivity (chemical, photochemical) determined by the nature of the attached sites.

7.2. Molecular Morphogenesis

The design of exoreceptors requires means of generating defined external molecular shapes. This may be achieved

in a number of ways, namely by stepwise synthesis of molecular architectures or by assembling on metal templates that impose a given coordination geometry, as noted in the preceding section.

Another approach to such controlled molecular morphogenesis is provided by the generation of globular molecules such as the "starburst dendrimers"[156] and the "arborols,"[157] based on branched structures formed via cascade processes. Starting from a given core, it may be possible to produce a molecule of given size and external shape. On the polymolecular level, this may be related to the generation of shapes and structures in two-dimensional lipid monolayers[158] and in aggregates of amphiphilic molecules[159] (see also Section 8).

8. From Supermolecules to Polymolecular Assemblies

Molecular chemistry is the domain of (more or less) independent *single* molecules. *Supramolecular chemistry* may be divided into two broad, partially overlapping areas: (1) *supermolecules* are well-defined *oligo*molecular species that result from the intermolecular association of a few components (a receptor and its substrate(s)) following a built-in "Aufbau" scheme based on the principles of molecular recognition; (2) *molecular assemblies* are polymolecular systems that result from the spontaneous association of a nondefined number of components into a specific phase having more or less well-defined microscopic organization and macroscopic characteristics depending on its nature (layers, membranes, vesicles, micelles, mesomorphic phases, etc.[160]).

Continuous progress is being made in the design of synthetic molecular assemblies, based on a growing understanding of the relations between the features of the molecular components (structure, sites for intermolecular binding, etc.), the characteristics of the processes which lead to their association and the supramolecular properties of the resulting polymolecular assembly.

Molecular organization, self-assembling and cooperation, construction of multilayer films,[161-164] generation of defined aggregate morphologies,[159] etc. make it possible to build up supramolecular architectures. The polymerization of the molecular subunits has been a major step in increasing control over the structural properties of the polymolecular system.[165,166] Incorporating suitable groups or components may yield functional assemblies capable of performing operations such as energy, electron or ion transfer, information storage, and signal transduction.[160,162,167,168] The combination of receptors, carriers, and catalysts, handling electrons and ions as discussed above, with polymolecular organized assemblies opens the way to the design of what may be termed *molecular* and *supramolecular devices*, and to the elaboration of chemical microreactors and artificial cells.

One may also note that polymolecular assemblies define *surfaces* on which and through which processes occur, a feature that again stresses the interest of designing exoreceptors operating at the interfaces, in addition to endoreceptors embedded in the bulk of the membranes.

9. Molecular and Supramolecular Devices

Molecular devices may be defined as structurally organized and functionally integrated chemical systems built into supramolecular architectures. The development of such devices requires the design of molecular components (effectors) performing a given function and suitable for incorporation into an organized array such as that provided by the different types of polymolecular assemblies (see Section 8). The components may be photo-, electro-, iono-, magneto-, thermo-, mechano-, or chemoactive, depending on whether they handle photons, electrons, or ions, respond to magnetic fields or to heat, undergo changes in mechanical properties, or perform a chemical reaction. A major requirement would be that these components, and the devices that they bring about, perform their function(s) at the *molecular* and *supramolecular* levels as distinct from the bulk material.

Molecular receptors, reagents, catalysts, carriers, and channels are potential effectors that may generate, detect, process, and transfer signals by making use of the three-dimensional information storage and read-out capacity operating in molecular recognition and of the substrate transformation and translocation processes conveyed by reactivity and transport. Coupling and regulation may occur if the effectors contain several subunits that can interact, influence each other, and respond to external stimuli such as light, electricity, heat, and pressure.

The nature of the mediator (substrate) on which molecular devices operate defines fields of molecular photonics, molecular electronics, and molecular ionics. Their development requires the design of effectors that handle these mediators and the examination of their potential use as components of molecular devices. We shall now examine specific features of molecular receptors, carriers, and reagents from this point of view.

9.1. Supramolecular Photochemistry and Molecular Photonics

The formation of supramolecular entities from photoactive and/or electroactive components may be expected to perturb the ground-state and excited-state properties of the individual species, giving rise to novel properties that define a *supramolecular photochemistry* and *electrochemistry*.

Thus, a number of processes may take place within supramolecular systems, modulated by the arrangement of the bound units as determined by the organizing receptor: photoinduced energy migration, charge separation by electron or proton transfer, perturbation of optical transitions and polarizabilities, modification of redox potentials in ground or excited states, photoregulation of binding properties, selective photochemical reactions, etc.

Supramolecular photochemistry, like catalysis, may involve three steps: binding of substrate and receptor, mediating a photochemical process, followed by either restoration of the initial state for a new cycle or by a chemical reaction[169] (Fig. 10). The photophysical and photochemical features of supramolecular entities form a vast area of investigation into processes occurring at the level of intermolecular organization.

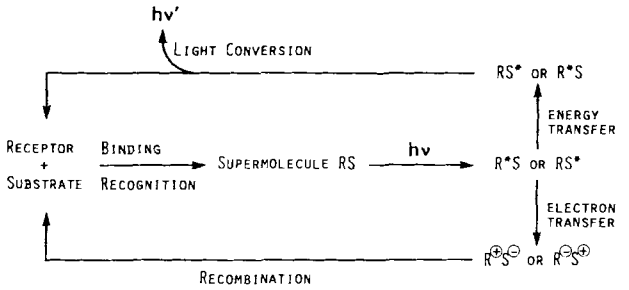

Fig. 10. Representation of the processes involved in supramolecular photochemistry. Generation of R*S, RS*, $R^{\oplus}S^{\ominus}$, or $R^{\ominus}S^{\oplus}$ may be followed by a chemical reaction.

9.1.1. Light Conversion by Energy Transfer

A light conversion molecular device may be realized by an Absorption-Energy-Transfer-Emission (A-ET-E) process in which light absorption by a receptor molecule is followed by intramolecular energy transfer to a bound substrate which then emits. This occurs in the europium(III) and terbium(III) cryptates of the macrobicyclic ligand [bipy·bipy·bipy] **43**.[170] UV light absorbed by the bipy groups is transferred to the lanthanoid cation bound in the molecular cavity, and released in the form of visible lanthanoid emission via an A-ET-E process, as shown in **44**.[171] These Eu^{III} and Tb^{III} complexes display a bright

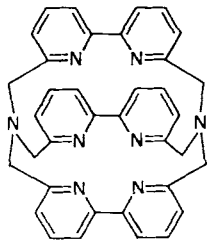

43

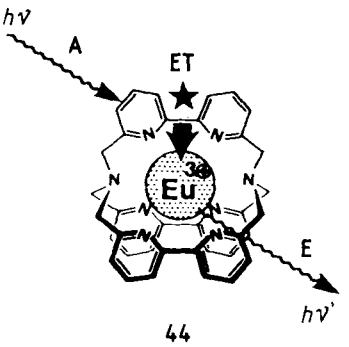

44

luminescence in aqueous solution, whereas the free ions do not emit under the same conditions. Numerous applications may be envisaged for such substances, in particular as luminescent probes for monoclonal antibodies, nucleic acids, and membranes.

Photophysical processes occurring in macrocyclic,[172] cryptate,[173] and molecular[174, 175] complexes have been investigated.

9.1.2. Photoinduced Electron Transfer in Photoactive Coreceptor Molecules

The photogeneration of charge-separated states is of interest both for inducing photocatalytic reactions (e.g., for artificial photosynthesis) and for the transfer of photosignals (e.g., though a membrane). It may be realized in D-PS-A systems in which excitation of a photosensitizer PS, followed by two electron transfers from a donor D to an acceptor A, yields $D^{\oplus}$-PS-$A^{\ominus}$. Numerous systems of this type are being studied in many laboratories from the standpoint of modeling photosynthetic centers.

The D, A units may be metal coordination centers. Thus, binding of silver ions to the lateral macrocycles of coreceptors containing porphyrin groups as photosensitizers introduces electron-acceptor sites, as shown in **45**. This results in quenching of the singlet excited state of the Zn-porphyrin center by an efficient intracomplex electron transfer, leading to charge separation and generating a porphyrinium cation of long half-life.[176]

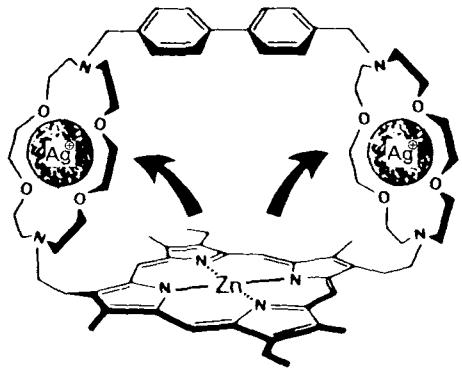

45

Systems performing photoinduced electron transfer processes represent components for *light-to-electron conversion devices*. The light-activated electron transport mentioned above[135] also belongs to this general type.

9.1.3. Photoinduced Reactions in Supramolecular Species

The binding of a substrate to a receptor molecule may affect the photochemical reactivity of either or both species, orienting the course of a reaction or giving rise to novel transformations.

Complexation of coordination compounds may make it possible to control their photochemical behavior via the structure of the supramolecular species formed. Thus, the photoaquation of the $[Co(CN)_6]^{3\ominus}$ anion is markedly affected by binding to polyammonium macrocycles. The results agree with the formation of supramolecular species, in which binding to the receptor hinders some $CN^{\ominus}$ groups from escaping when the Co-CN bonds are temporarily broken following light excitation.[63] It thus appears possible to orient the photosubstitution reactions of transition-metal complexes by using appropriate receptor molecules. Such effects may be general, applying to complex cations as well as to complex anions, and providing an approach to the control of photochemical reactions via formation of defined supramolecular structures.[169, 177, 178]

Structural or conformational changes photoproduced in receptor molecules affect their binding properties, thus causing release or uptake of a species, as occurs in macrocyclic ligands containing light-sensitive groups.[141, 172] Such effects may be used to generate protonic or ionic photosignals in *light-to-ion conversion* devices.

9.1.4. Nonlinear Optical Properties of Supramolecular Species

Substances presenting a large electronic polarizability are likely to yield materials displaying large macroscopic

optical nonlinearities.[179] This is the case for push-pull compounds possessing electron donor and acceptor units. The potential nonlinear optical (NLO) properties of materials based on metal complexes and supramolecular species have been pointed out recently.[179b] The D-PS-A systems investigated for their ability to yield charge-separated states possess such features; they may be metallic or molecular complexes.

Ion-dependent optical changes produced by indicator ligands[180] might lead to cation control of nonlinear optical properties.

Molecular electron-donor-acceptor complexes could present NLO effects since they possess polarized ground states and undergo (partial) intermolecular charge separation on excitation. It is possible to more or less finely tune their polarization, polarizability, extent of charge transfer, absorption bands, etc. by many variations in basic structural types as well as in substituents (see, for instance, Refs. [174, 179c]).

The results discussed above provide illustrations and incentives for further studies of photoeffects brought about by the formation of supramolecular species.

In a broader perspective, such investigations may lead to the development of *photoactive molecular devices*, based on photoinduced energy migration, electron transfer, substrate release, or chemical transformation in supermolecules. Thus would be brought together molecular design, intermolecular bonding, and supramolecular architectures with photophysical, photochemical, and optical properties, building up a kind of *molecular photonics*.

9.2. Molecular Electronic Devices

More and more attention is being given to *molecular electronics* and to the possibility of developing electronic devices that would operate at the molecular level.[3, 181] Molecular rectifiers, transistors, and photodiodes have been envisaged, the latter requiring features such as those of charge-transfer states in organic molecules, in metal complexes, and in D-PS-A systems discussed in Section 9.1.2 (see also references in Ref. [182]).

Among the basic components of electronic circuitry at the molecular level, a unit of fundamental importance is a connector or junction allowing electron flow to take place between different parts of the system, i.e., a *molecular wire*.

An approach to such a unit is represented by the *caroviologens*, vinylogous derivatives of methylviologen that combine the features of the carotenoids and of the viologens.[182] They present features required for a molecular wire: a conjugated polyene chain for electron conduction; terminal electroactive and hydrosoluble pyridinium groups for reversible electron exchange; a length sufficient for spanning typical molecular supporting elements such as a monolayer or bilayer membrane.

Caroviologens have been incorporated into sodium dihexadecyl phosphate vesicles. The data obtained agree with a structural model in which the caroviologens of sufficient length span the bilayer membrane, the pyridinium sites being close to the negatively charged outer and inner surfaces of the vesicles and the polyene chain crossing the lipidic interior of the membrane (Fig. 11). These and other functionalized membranes are being tested in processes in which the caroviologen would function as a continuous, transmembrane electron channel, i.e., a genuine molecular wire. With respect to electron transport by means of redox-active mobile carrier molecules (see Section 6.2.1), the caroviologens represent electron channels, in analogy to cation channels and cation carriers. They portray a first approach to molecular wires, and several modifications concerning the end groups and the chain may be envisaged.[183] For instance, coupling with photoactive groups could yield photoresponsive electron channels, as well as charge separation and signal-transfer devices. Combination with other polymolecular supports, such as polymeric layers or mesomorphic phases, as well as with other components, might make it possible to assemble nanocircuits and more complex molecular electronic systems.

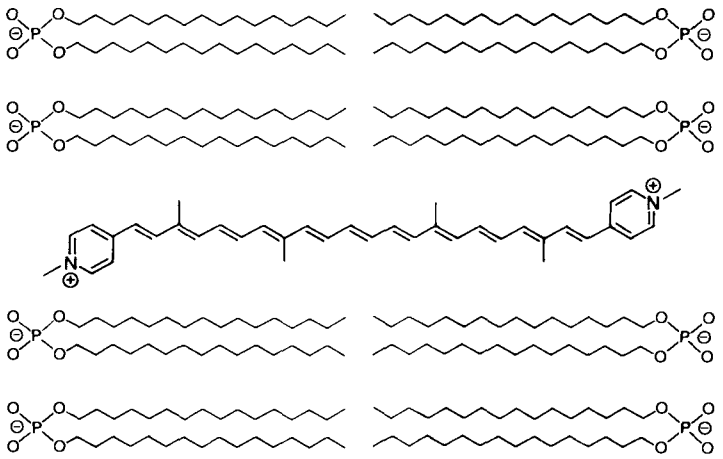

Fig. 11. Transmembrane incorporation of a caroviologen into sodium dihexadecylphosphate vesicles.

Redox modification of an electroactive receptor or carrier molecule leads to changes in binding and transport properties, thus causing release or uptake of the substrate, in a way analogous to the photoeffects discussed above. To this end, redox couples such as disulfide/dithiol[184, 185a] and quinone/hydroquinone[185] have been introduced into receptor molecules and shown to modify their substrate-binding features. Complexation of metal hexacyanides $[M(CN)_6]^{n\ominus}$ by polyammonium macrocycles markedly perturbs their redox properties.[61] These electrochemical features resulting from receptor-substrate association define a *supramolecular electrochemistry*. The mutual effects of redox changes and binding strength in a receptor-substrate pair may make it possible to achieve electrocontrol of complexation and, conversely, to modify redox properties by binding (see also next section).

9.3. Molecular Ionic Devices

The numerous receptor, reagent, and carrier molecules capable of handling inorganic and organic ions are potential components of molecular and supramolecular *ionic devices* that would function via highly selective recognition, reaction, and transport processes with coupling to external factors and regulation. Such components and the devices

that they may build up form the basis of a field of *molecular ionics*, the field of systems operating with ionic species as support for signal and information storage, processing, and transfer. In view of the size and mass of ions, ionic devices may be expected to perform more slowly than electronic devices. However, ions have a very high information content by virtue of their multiple molecular (charge, size, shape, structure) and supramolecular (binding geometry, strength and selectivity) features. Molecular ionics appears to offer a promising field of research which may already draw from a vast amount of knowledge and data on ion-processing by natural and synthetic receptors and carriers.

Selective ion receptors represent basic units for ionic transmitters or detectors; selective ion carriers correspond to ionic transducers. These units may be fitted with triggers and switches sensitive to external physical (light, electricity, heat, pressure) or chemical (other binding species, regulating sites) stimuli for connection and activation.

Binding or transport and triggering may be performed by separate species, each having a specific function, as in multiple carrier transport systems (see Section 6.2).[133] This allows a variety of combinations between photo- or electroactive components and different receptors or carriers. On the other hand, light- and redox-sensitive groups have been incorporated into receptors and carriers and shown to affect binding and transport properties (see Refs. [141, 172, 184, 185] and references therein). Coreceptors and cocarriers provide means for regulation via cofactors, co-bound species that modulate the interaction with the substrate. Thus, a simple ionizable group such as a carboxylic acid function represents a *proton switch* and leads to gated receptors and carriers responding to pH changes, as seen for instance in the regulation of transport selectivity by **40**.[138]

The main problem is the generally insufficient changes brought about in most systems by the switching process. It is worth stressing that proton-triggered yes/no or +/− switches are potentially contained in the ability of polyamine receptors and carriers to bind and transport cations when unprotonated and anions when protonated; also, zwitterions such as amino acids may change from bound to unbound or conversely when they undergo charge inversion as a function of pH. Molecular *protonic devices* thus represent a particularly interesting special case of ionic devices. A proton-conducting channel would be a *proton wire*.

Functional molecular assemblies provide ways of organizing molecular devices and of introducing regulation and cooperative processes which may induce a much steeper response of the system to the stimuli. Vesicles have been fitted with functional units,[168] for instance with a $Li^{\oplus}$ ion channel that may be sealed.[147, 148] Liquid crystals consisting of macrocyclic molecules bearing mesogenic groups, such as **46**, form *tubular mesophases*, composed of stacked rings as in **47**, which may lead to the development of phase-dependent ion-conducting channels.[186, 187] Cooperativity and self-assembly may also be designed directly into the molecular components (see next section).

Biological information and signals are carried by ionic and molecular species ($Na^{\oplus}$, $K^{\oplus}$, $Ca^{2\oplus}$, acetylcholine, cyclic AMP, etc.). Polytopic metalloproteins such as calcium-binding proteins[188] perform complicated tasks of detecting, processing, and transferring ionic signals. These biological functions give confidence and inspiration for the development of molecular ionics.

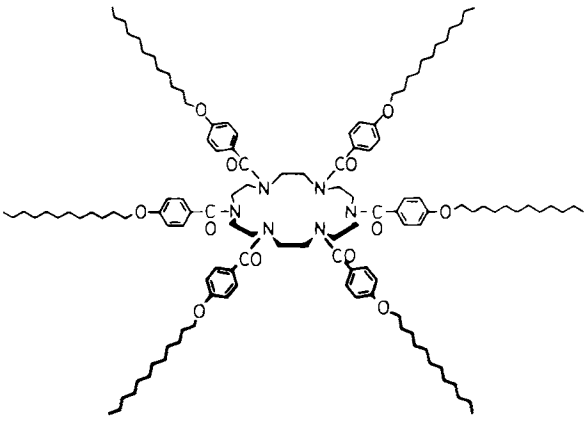

46

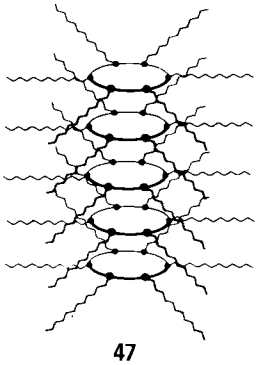

47

One may note that ion receptors, channels, switches, and gates have been considered within a potential European research project on "Ionic Adaptative Computers." Applications such as selective chemical sensors based on molecular recognition are already well advanced.[121]

9.4. Molecular Self-Assembling

Self-assembling and multiple binding with positive cooperativity are processes of spontaneous molecular organization that also allow *amplification molecular devices* to be envisaged. Such phenomena are well documented in biology, but much less so in chemistry. By virtue of their multiple binding subunits, polytopic coreceptors may display self-assembling if substrate binding to one receptor molecule generates binding sites that induce association with another one.

Positive cooperativity in substrate binding is more difficult to set up than negative cooperativity. However, both effects are of interest for regulation processes. Cooperativity is found in the unusual facilitation of the second protonation of **5** by a water effector molecule as in **10**.[40] Allosteric effects on cation binding to macrocyclic polyethers have been studied by inducing conformational changes via a remote site,[17a] and subunit cooperativity occurs in a dimeric porphyrin.[189]

The spontaneous formation of the double helix of nucleic acids represents the self-assembling of a supramole-

cular structure induced by the pattern of intermolecular interactions provided by the complementary nucleic bases. It involves recognition and positive cooperativity in base-pairing.[190]

Such self-assembling has recently been shown to occur in repetitive chain ligands, acyclic coreceptors containing several identical binding sites arranged linearly. Based on earlier work with a "quaterpyridine" ligand, oligo-bipyridine chain ligands incorporating two to five bipy groups were designed. By treatment with Cu^{I} ions they underwent a spontaneous assembling into *double-stranded helicates* containing two ligand molecules and one Cu^{I} ion per bipy site of each ligand, the two receptor strands being wrapped around the metal ions which hold them together. Thus, the tris-bipy ligand **48** forms the trinuclear complex **49**, whose

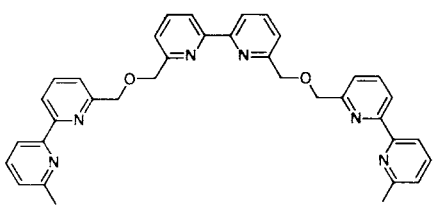

48

49

crystal structure has been determined, confirming that it is indeed an *inorganic double helix*.[191] The results obtained indicate that the process occurs probably with positive cooperativity, binding of a Cu^{I} ion with two ligands facilitating complexation of the next one. Furthermore, it appears that in a mixture of ligands containing different numbers of bipy units, pairing occurs preferentially between the *same* ligands, thus performing *self-self recognition*. This spontaneous formation of an organized structure of intermolecular type opens ways to the design and study of self-assembling systems presenting cooperativity, regulation, and amplification features. Catalytic reactions, gated channels, and phase changes represent other processes that might be used for inducing amplification effects.

Various further developments may be envisaged along organic, inorganic, and biochemical lines. Thus, if substituents are introduced at the *para* positions of the six pyridine units in **48**, treatment with Cu^{I} should form an inorganic double helix bearing twelve outwardly directed functional groups. [155]

Designed self-assembling rests on the elaboration of molecular components that will spontaneously undergo organization into a desired supramolecular architecture. Such control of self-organization at the molecular level is a field of major interest in molecular design and engineering, which may be expected to become a subject of increasing activity.

9.5. Chemionics

Components and molecular devices such as molecular wires, channels, resistors, rectifiers, diodes, and photosensitive elements might be assembled into nanocircuits and combined with organized polymolecular assemblies to yield systems capable ultimately of performing functions of detection, storage, processing, amplification, and transfer of signals and information by means of various mediators (photons, electrons, protons, metal cations, anions, molecules) with coupling and regulation.[3,8,181,182,192]

Molecular photonics, electronics, and ionics represent three areas of this intriguing and rather futuristic field of chemistry which may be termed "*chemionics*"[3,8]—the design and operation of photonic, electronic, and ionic components, devices, circuitry, and systems for signal and information processing at the molecular level. Such perspectives lie, of course, in the distant future,[193] but along the way they could yield numerous spin-offs and they do represent ultimate goals towards which work may already be planned and realized.

10. Conclusion

The present text was aimed at presenting the scope, providing illustration, and exploring perspectives of supramolecular chemistry. Its conceptual framework has been progressively laid down and the very active research on molecular recognition, catalysis, and transport, together with extension to molecular surfaces and polymolecular assemblies, is building up a vast body of knowledge on molecular behavior at the supramolecular level. It is clear that much basic chemistry remains to be done on the design and realization of numerous other systems and processes that await to be imagined. The results obtained may also be analyzed in the view of developing components for molecular devices that would perform highly selective functions of recognition, transformation, transfer, regulation, and communication, and allow signal and information processing. This implies operation via intermolecular interactions and incorporation of the *time* dimension into recognition events. One may note that such functions have analogies with features of expert systems, thus linking processes of artificial intelligence and molecular behavior.

These developments in molecular and supramolecular science and engineering offer exciting perspectives at the frontiers of chemistry with physics and biology. Of course, even with past achievements and present activities, extrapolations and predictions can only be tentative; yet, on such an occasion for the celebration of chemistry, it appears justified to try looking out into the future, for

"He (or she) who sits at the bottom of a well to contemplate the sky, will find it small"
(*Han Yu*, 768-824).

I wish to thank very warmly my collaborators at the Université Louis Pasteur in Strasbourg and at the Collège de France in Paris, whose skill, dedication, and enthusiasm allowed the work described here to be realized. Starting with B. Dietrich and J.-P. Sauvage, they are too numerous to be named here, but they have all contributed to the common goal. I also wish to acknowledge the fruitful collaboration with a number of laboratories in various countries, beginning with the crystal structure determinations of cryptates by Raymond Weiss and his group and extending over various areas of structural and coordination chemistry, electrochemistry,

photochemistry, and biochemistry. Finally, I thank the Université Louis Pasteur, the Collège de France, and the Centre National de la Recherche Scientifique for providing the intellectual environment and the financial support for our work.

Received: January 8, 1988 [A 655 IE]
German version: *Angew. Chem. 100* (1988) 91

[1] J.-M. Lehn, *Struct. Bonding (Berlin) 16* (1973) 1.
[2] J.-M. Lehn, *Pure Appl. Chem. 50* (1978) 871.
[3] J.-M. Lehn, *Leçon Inaugurale*, Collège de France, Paris 1980.
[4] R. Pfeiffer: *Organische Molekülverbindungen*, Enke Verlag, Stuttgart 1927.
[5] K. L. Wolf, H. Frahm, H. Harms, *Z. Phys. Chem. Abt. B 36* (1937) 17; K. L. Wolf, H. Dunken, K. Merkel, *ibid. 46* (1940) 287; K. L. Wolf, R. Wolff, *Angew. Chem. 61* (1949) 191.
[6] J.-M. Lehn, *Acc. Chem. Res. 11* (1978) 49.
[7] J.-M. Lehn in Z. I. Yoshida, N. Ise (Eds.): *Biomimetic Chemistry*, Kodansha, Tokyo/Elsevier, Amsterdam 1983, p. 163.
[8] J.-M. Lehn, *Science 227* (1985) 849.
[9] P. G. Potvin, J.-M. Lehn in R. M. Izatt, J. J. Christensen (Eds.): *Synthesis of Macrocycles: The Design of Selective Complexing Agents (Progress in Macrocyclic Chemistry, Vol. 3)*, Wiley, New York 1987, p. 167.
[10] E. Fischer, *Ber. Dtsch. Chem. Ges. 27* (1894) 2985.
[11] F. Cramer, W. Freist, *Acc. Chem. Res. 20* (1987) 79.
[12] J. F. Stoddart, *Chem. Soc. Rev. 7* (1979) 85; *Annu. Rep. Prog. Chem. Sect. B 1983*, 353.
[13] D. J. Cram, J. M. Cram, *Acc. Chem. Res. 11* (1978) 8.
[14] R. C. Hayward, *Chem. Soc. Rev. 12* (1983) 285.
[15] I. O. Sutherland, *Chem. Soc. Rev. 15* (1986) 63.
[16] G. van Binst (Ed.): *Design and Synthesis of Organic Molecules Based on Molecular Recognition*, Springer, Berlin 1986.
[17] a) J. Rebek, Jr., *Acc. Chem. Res. 17* (1984) 258; b) *Science 235* (1987) 1478.
[18] a) W. Bartmann, K. B. Sharpless (Eds.): *Stereochemistry of Organic and Bioorganic Transformations*, VCH Verlagsgesellschaft 1987; b) P. B. Dervan, R. S. Youngquist, J. P. Sluka in [18a], p. 221; c) W. C. Still in [18a], p. 235.
[19] R. M. Izatt, J. J. Christensen (Eds.): *Progress in Macrocyclic Chemistry, Vol. 1-3*, Wiley, New York 1979, 1981 and 1987.
[20] F. Vögtle (Ed.): *Host Guest Chemistry (Top. Curr. Chem. 98* (1981), *101* (1982)); F. Vögtle, E. Weber (Eds.), *ibid. 121* (1984).
[21] J. L. Atwood, J. E. D. Davies, D. D. MacNicol: *Inclusion Compounds, Vol. 1-3*, Academic Press, London 1984.
[22] G. Wipff, P. Kollman, J.-M. Lehn, *J. Mol. Struct. 93* (1983) 153; G. Ranghino, S. Romano, J.-M. Lehn, G. Wipff, *J. Am. Chem. Soc. 107* (1985) 7873; G. Wipff, P. Kollman, *Nouv. J. Chim. 9* (1985) 457; S. Lifson, M. Levitt (Eds.): *Structure and Dynamics of Macromolecules (Isr. J. Chem. 27* (1986) No. 2).
[23] An idea about the respective role of collection and orientation may be gained from examining the energies calculated for a series of $[Li(NH_3)_n]^{\oplus}$ complexes and of the corresponding $(NH_3)_n$ units in the identical geometry. In the presence of $Li^{\oplus}$ the formation energies of the complexes are obtained at the optimized $Li^{\oplus}\cdots NH_3$ distances. When $Li^{\oplus}$ is removed and the NH_3 molecules are kept at the same position, the energies calculated are for the formation of the coordination shell alone. These energies represent the repulsion between the NH_3 groups; they are a measure of the intersite repulsive energy for bringing together two, three, or four amine binding sites into a polydentate ligand of same coordination geometry. *Results*, $(NH_3)_n$, geometry (repulsive energy [kcal/mol]): $(NH_3)_2$, linear (−2.4), bent (−3.8); $(NH_3)_3$, trigonal (−9.1), pyramidal (−10.8); $(NH_3)_4$, tetrahedral (−20.8). Thus, the total collection energies are appreciably larger than the organization energies represented by the changes from one geometry to another, linear to bent (1.4 kcal/mol) or trigonal to pyramidal (1.7 kcal/mol). Ab initio computations performed with a set of Gaussian-type basis functions, contracted into a double set with polarization; J.-M. Lehn, R. Ventavoli, unpublished results; see also: R. Ventavoli, 3è Cycle Thesis, Université Louis Pasteur, Strasbourg 1972.
[24] a) Yu. A. Ovchinnikov, V. T. Ivanov, A. M. Skrob: *Membrane Active Complexones*, Elsevier, New York 1974; b) B. C. Pressman, *Annu. Rev. Biochem. 45* (1976) 501; c) H. Brockmann, H. Geeren, *Justus Liebigs Ann. Chem. 603* (1957) 217; d) M. M. Shemyakin, N. A. Aldanova, E. I. Vinogradova, M. Yu, Feigina, *Tetrahedron Lett. 1963*, 1921; e) C. Moore, B. C. Pressman, *Biochem. Biophys. Res. Commun. 15* (1964) 562; f) B. C. Pressman, *Proc. Natl. Acad. Sci. USA 53* (1965) 1077; g) J. Beck, H. Gerlach, V. Prelog, W. Voser, *Helv. Chim. Acta 74* (1962) 620; h) Z. Stefanac, W. Simon, *Chimia 20* (1966) 436; *Microchem. J. 12* (1967) 125; i) K. T. Kilbourn, J. D. Dunitz, L. A. R. Pioda, W. Simon, *J. Mol. Biol. 30* (1967) 559; j) P. Mueller, D. O. Rudin, *Biochem. Biophys. Res. Commun. 26* (1967) 398; k) T. E. Andreoli, M. Tieffenberg, D. C. Tosteson, *J. Gen. Biol. 50* (1967) 2527; l) M. M. Shemyakin, Yu. A. Ovchinnikov, V. T. Ivanov, V. K. Antonov, A. M. Skrob, I. I. Mikhaleva, A. V. Evstratov, G. G. Malenkov, *ibid. 29* (1967) 834; m) B. C. Pressman, E. J. Harris, W. S. Jagger, J. H. Johnson, *Proc. Natl. Acad. Sci. USA 58* (1967) 1949.
[25] a) C. J. Pedersen, *J. Am. Chem. Soc. 89* (1967) 7017; b) C. J. Pedersen, H. K. Frensdorff, *Angew. Chem. 84* (1972) 16; *Angew. Chem. Int. Ed. Engl. 11* (1972) 16.
[26] D. J. Cram, *Angew. Chem. 98* (1986) 1041; *Angew. Chem. Int. Ed. Engl. 25* (1986) 1039.
[27] D. Parker, *Adv. Inorg. Chem. Radiochem. 27* (1983) 1; B. Dietrich, *J. Chem. Ed. 62* (1985) 954. For the sepulchrate-type of encapsulated metal ions, see: A. M. Sargeson, *Pure Appl. Chem. 56* (1984) 1603.
[28] a) J.-M. Lehn, J.-P. Sauvage, *J. Am. Chem. Soc. 97* (1975) 6700; b) B. Dietrich, J.-M. Lehn, J.-P. Sauvage, *J. Chem. Soc. Chem. Commun. 1973*, 15.
[29] a) B. Dietrich, J.-M. Lehn, J.-P. Sauvage, *Tetrahedron Lett. 1969*, 2885, 2889; b) B. Dietrich, J.-M. Lehn, J.-P. Sauvage, J. Blanzat, *Tetrahedron 29* (1973) 1629; B. Dietrich, J.-M. Lehn, J.-P. Sauvage, *ibid. 29* (1973) 1647; c) B. Metz, D. Moras, R. Weiss, *J. Chem. Soc. Chem. Commun. 1970*, 217; F. Mathieu, B. Metz, D. Moras, R. Weiss, *J. Am. Chem. Soc. 100* (1978) 4412, and references cited therein.
[30] E. Graf, J.-M. Lehn, *J. Am. Chem. Soc. 97* (1975) 5022; *Helv. Chim. Acta 64* (1981) 1040.
[31] B. Dietrich, J.-M. Lehn, unpublished results.
[32] E. Graf, J.-M. Lehn, *J. Am. Chem. Soc. 98* (1976) 6403.
[33] F. Schmidtchen, G. Müller, *J. Chem. Soc. Chem. Commun. 1984*, 1115.
[34] J. L. Dye, *Angew. Chem. 91* (1979) 613; *Angew. Chem. Int. Ed. Engl. 18* (1979) 587; J. L. Dye, M. G. DeBacker, *Annu. Rev. Phys. Chem. 38* (1987) 271.
[35] J.-M. Lehn, *Pure Appl. Chem. 52* (1980) 2303.
[36] A. I. Popov, J.-M. Lehn in G. A. Melson (Ed.): *Coordination Chemistry of Macrocyclic Compounds*, Plenum Press, New York 1979, p. 537.
[37] I. M. Kolthoff, *Anal. Chem. 51* (1979) 1R.
[38] F. Montanari, D. Landini, F. Rolla, *Top. Curr. Chem. 101* (1982) 203; E. Blasius, K.-P. Janzen, *ibid. 98* (1981) 163.
[39] E. Graf, J.-M. Lehn, J. LeMoigne, *J. Am. Chem. Soc. 104* (1982) 1672.
[40] E. Graf, J.-P. Kintzinger, J.-M. Lehn, unpublished results.
[41] B. Dietrich, J.-P. Kintzinger, J.-M. Lehn, B. Metz, A. Zahidi, *J. Phys. Chem.*, in press.
[42] a) D. J. Cram, K. N. Trueblood, *Top. Curr. Chem. 98* (1981) 43; b) F. De Jong, D. N. Reinhoudt in V. Gold, D. Bethell (Eds.): *Adv. Phys. Org. Chem. 17* (1980) 219.
[43] J.-M. Lehn, P. Vierling, *Tetrahedron Lett. 21* (1980) 1323.
[44] J.-P. Behr, J.-M. Lehn, P. Vierling, *J. Chem. Soc. Chem. Commun. 1976*, 621; *Helv. Chim. Acta 65* (1982) 1853.
[45] J.-P. Behr, J.-M. Lehn, *Helv. Chim. Acta 63* (1980) 2112.
[46] H. M. Colquhoun, J. F. Stoddart, D. J. Williams, *Angew. Chem. 98* (1986) 483; *Angew. Chem. Int. Ed. Engl. 25* (1986) 487.
[47] Stability constants of about 800 and 10^5 L mol^{-1} have been obtained for binding $[Ru(NH_3)_6]^{3\oplus}$ to **12b** and to the hexacarboxylate in **14**, respectively (aqueous solution, pH = 7.3); J.-M. Lehn, P. Vierling, unpublished results.
[48] J. C. Metcalfe, J. F. Stoddart, G. Jones, *J. Am. Chem. Soc. 99* (1977) 8317; J. Krane, O. Aune, *Acta Chem. Scand. B 34* (1980) 397.
[49] a) J.-M. Lehn, P. Vierling, R. C. Hayward, *J. Chem. Soc. Chem. Commun. 1979*, 296; b) see also K. Madan, D. J. Cram, *ibid. 1975*, 427; J. W. H. M. Uiterwijk, S. Harkema, J. Geevers, D. N. Reinhoudt, *ibid. 1982*, 200.
[50] a) F. Vögtle, H. Sieger, W. M. Müller, *Top. Curr. Chem. 98* (1981) 107; b) K. Saigo, *Kagaku to Kogyo (Osaka) 35* (1982) 90; c) J.-L. Pierre, P. Baret, *Bull. Soc. Chim. Fr. II 1983*, 367; d) E. Kimura, *Top. Curr. Chem. 128* (1985) 113; e) F. P. Schmidtchen, *ibid. 132* (1986) 101.
[51] a) J.-M. Lehn, E. Sonveaux, A. K. Willard, *J. Am. Chem. Soc. 100* (1978) 4914; b) B. Dietrich, J. Guilhem, J.-M. Lehn, C. Pascard, E. Sonveaux, *Helv. Chim. Acta 67* (1984) 91; c) for other macrobicyclic receptors see also M. M. Hosseini, *Thèse de Doctorat-ès-Sciences*, Université Louis Pasteur, Strasbourg 1983.
[52] C. H. Park, H. Simmons, *J. Am. Chem. Soc. 90* (1968) 2431.
[53] a) B. Dietrich, M. W. Hosseini, J.-M. Lehn, R. B. Sessions, *J. Am. Chem. Soc. 103* (1981) 1282; b) *Helv. Chim. Acta 68* (1985) 289.
[54] J. Cullinane, R. I. Gelb, T. N. Margulis, L. J. Zompa, *J. Am. Chem. Soc. 104* (1982) 3048; E. Suet, H. Handel, *Tetrahedron Lett. 25* (1984) 645.
[55] M. W. Hosseini, J.-M. Lehn, M. P. Mertes, *Helv. Chim. Acta 66* (1983) 2454.
[56] E. Kimura, M. Kodama, T. Yatsunami, *J. Am. Chem. Soc. 104* (1982) 3182; J. F. Marecek, C. J. Burrows, *Tetrahedron Lett. 27* (1986) 5943.
[57] M. W. Hosseini, J.-M. Lehn, *Helv. Chim. Acta 70* (1987) 1312; see also H. R. Wilson, R. J. P. Williams, *J. Chem. Soc., Faraday Trans. I 83* (1987) 1885.

[58] B. Dietrich, D. L. Fyles, T. M. Fyles, J.-M. Lehn, *Helv. Chim. Acta 62* (1979) 2763.
[59] B. Dietrich, T. M. Fyles, J.-M. Lehn, L. G. Pease, D. L. Fyles, *J. Chem. Soc. Chem. Commun. 1978*, 934.
[60] M. J. Mann, N. Pant, A. D. Hamilton, *J. Chem. Soc. Chem. Commun. 1986*, 158.
[61] F. Peter, M. Gross, M. W. Hosseini, J.-M. Lehn, *J. Electroanal. Chem. 144* (1983) 279.
[62] E. Garcia-Espana, M. Micheloni, P. Paoletti, A. Bianchi, *Inorg. Chim. Acta 102* (1985) L9; A. Bianchi, E. Garcia-Espana, S. Mangani, M. Micheloni, P. Orioli, P. Paoletti, *J. Chem. Soc. Chem. Commun. 1987*, 729.
[63] M. F. Manfrin, L. Moggi, V. Castelvetro, V. Balzani, M. W. Hosseini, J.-M. Lehn, *J. Am. Chem. Soc. 107* (1985) 6888.
[64] J.-M. Lehn, *Pure Appl. Chem. 52* (1980) 2441.
[65] J.-M. Lehn, J. Simon, J. Wagner, *Angew. Chem. 85* (1973) 621, 622; *Angew. Chem. Int. Ed. Engl. 12* (1973) 578, 579.
[66] R. J. Motekaitis, A. E. Martell, B. Dietrich, J.-M. Lehn, *Inorg. Chem. 23* (1984) 1588; R. J. Motekaitis, A. E. Martell, I. Murase, *ibid. 25* (1986) 938; A. Evers, R. D. Hancock, I. Murase, *ibid. 25* (1986) 2160; D. E. Whitmoyer, D. P. Rillema, G. Ferraudi, *J. Chem. Soc. Chem. Commun. 1986*, 677.
[67] J.-P. Kintzinger, J.-M. Lehn, E. Kauffmann, J. L. Dye, A. I. Popov, *J. Am. Chem. Soc. 105* (1983) 7549.
[68] D. Heyer, J.-M. Lehn, *Tetrahedron Lett. 27* (1986) 5869.
[69] T. Fujita, J.-M. Lehn, unpublished work.
[70] T. P. Lybrand, J. A. McCammon, G. Wipff, *Proc. Natl. Acad. Sci. USA 83* (1986) 833.
[71] J.-M. Lehn in K. J. Laidler (Ed.): *IUPAC Frontiers of Chemistry*, Pergamon Press, Oxford 1982, p. 265.
[72] J. Jazwinski, J.-M. Lehn, D. Lilienbaum, R. Ziessel, J. Guilhem, C. Pascard, *J. Chem. Soc. Chem. Commun. 1987*, 1691.
[73] A. Carroy, J.-M. Lehn, *J. Chem. Soc. Chem. Commun. 1986*, 1232.
[74] J. Comarmond, B. Dietrich, J.-M. Lehn, R. Louis, *J. Chem. Soc. Chem. Commun. 1985*, 74.
[75] Y. Okuno, K. Uoto, O. Yonemitsu, T. Tomohiro, *J. Chem. Soc. Chem. Commun. 1987*, 1018; J. R. Holmes, J.-M. Lehn, work in progress.
[76] F. Kotzyba-Hibert, J.-M. Lehn, P. Vierling, *Tetrahedron Lett. 21* (1980) 941.
[77] F. Kotzyba-Hibert, J.-M. Lehn, K. Saigo, *J. Am. Chem. Soc. 103* (1981) 4266.
[78] C. Pascard, C. Riche, M. Cesario, F. Kotzyba-Hibert, J.-M. Lehn, *J. Chem. Soc. Chem. Commun. 1982*, 557.
[79] J.-P. Kintzinger, F. Kotzyba-Hibert, J.-M. Lehn, A. Pagelot, K. Saigo, *J. Chem. Soc. Chem. Commun. 1981*, 833.
[80] M. W. Hosseini, J.-M. Lehn, *J. Am. Chem. Soc. 104* (1982) 3525; *Helv. Chim. Acta 69* (1986) 587.
[81] a) F. P. Schmidtchen, *J. Am. Chem. Soc. 108* (1986) 8249; b) J. Rebek, Jr., D. Nemeth, P. Ballester, F.-T. Lin, *ibid. 109* (1987) 3474.
[82] J.-M. Lehn, J. Simon, A. Moradpour, *Helv. Chim. Acta 61* (1978) 2407.
[83] a) F. P. Schmidtchen, *J. Org. Chem. 51* (1986) 5161; b) J. Simon, *Thèse de Doctorat d'Etat*, Université Louis Pasteur, Strasbourg 1976; see also **28** in [14], p. 305; c) J. Rebek, Jr., B. Askew, O. Nemeth, K. Parris, *J. Am. Chem. Soc. 109* (1987) 2432.
[84] J.-P. Behr, J.-M. Lehn, *J. Am. Chem. Soc. 98* (1976) 1743.
[85] F. Cramer: *Einschlußverbindungen*, Springer, Berlin 1954; M. L. Bender, M. Komiyama: *Cyclodextrin Chemistry*, Springer, Berlin 1978.
[86] a) J. Franke, F. Vögtle, *Top. Curr. Chem. 132* (1986) 137; b) F. Vögtle, W. M. Müller, W. H. Watson, *ibid. 125* (1984) 131; c) for calixarenes, see C. D. Gutsche, *ibid. 123* (1984) 1; *Acc. Chem. Res. 16* (1983) 161; d) for cavitands, see D. J. Cram, *Science 219* (1983) 1177.
[87] J. Canceill, A. Collet, J. Gabard, F. Kotzyba-Hibert, J.-M. Lehn, *Helv. Chim. Acta 65* (1982) 1894.
[88] M. Dhaenens, L. Lacombe, J.-M. Lehn, J.-P. Vigneron, *J. Chem. Soc. Chem. Commun. 1984*, 1097.
[89] H.-J. Schneider, D. Güttes, U. Schneider, *Angew. Chem. 98* (1986) 635; *Angew. Chem. Int. Ed. Engl. 25* (1986) 647.
[90] B. L. Allwood, F. H. Kohnke, J. F. Stoddart, D. J. Williams, *Angew. Chem. 97* (1985) 584; *Angew. Chem. Int. Ed. Engl. 24* (1985) 581.
[91] For dissymmetric cylindrical macrotricyclic coreceptors that bind ammonium ions see: A. D. Hamilton, P. Kazanjian, *Tetrahedron Lett. 26* (1985) 5735; K. Saigo, R.-L. Lin, M. Kubo, A. Youda, M. Hasegawa, *Chem. Lett. 1986*, 519.
[92] For macrocyclic cyclophane-type receptors see also a) K. Odashima, T. Soga, K. Koga, *Tetrahedron Lett. 21* (1980) 5311; b) F. Diederich, K. Dick, *J. Am. Chem. Soc. 106* (1984) 8024, and references cited therein.
[93] A. J. Blacker, J. Jazwinski, J.-M. Lehn, *Helv. Chim. Acta 70* (1987) 1.
[94] I. Bidd, B. Dilworth, J. M. Lehn, unpublished work.
[95] J. Jazwinski, A. J. Blacker, J.-M. Lehn, M. Cesario, J. Guilhem, C. Pascard, *Tetrahedron Lett. 28* (1987) 6057.
[96] J.-M. Lehn, F. Schmidt, J.-P. Vigneron, work in progress.
[97] A. J. Blacker, M. W. Hosseini, J.-M. Lehn, unpublished work.
[98] a) J.-P. Behr, J.-M. Lehn, unpublished work; b) J.-M. Lehn, I. Stibor, work in progress; c) for recent examples see J. Rebek, Jr., B. Askew, P. Ballester, C. Buhr, S. Jones, D. Nemeth, K. Williams, *J. Am. Chem. Soc. 109* (1987) 5033; A. D. Hamilton, D. Van Engen, *ibid. 109* (1987) 5035.
[99] J. Canceill, M. Cesario, A. Collet, C. Riche, C. Pascard, *J. Chem. Soc. Chem. Commun. 1986*, 339; J. Canceill, L. Lacombe, A. Collet, *C. R. Acad. Sci. Ser. 2 Paris 304* (1987) 815.
[100] A. D. Hamilton, J.-M. Lehn, J. L. Sessler, *J. Chem. Soc. Chem. Commun. 1984*, 311; *J. Am. Chem. Soc. 108* (1986) 5158.
[101] For other metalloreceptor-type species see for instance references in [15]; N. M. Richards, I. O. Sutherland, P. Camilleri, J. A. Pape, *Tetrahedron Lett. 26* (1985) 3739; M. C. Gonzalez, A. C. Weedon, *Can. J. Chem. 63* (1985) 602; D. H. Busch, C. Cairns in [9], p. 1; V. Thanabal, V. Krishnan, *J. Am. Chem. Soc. 104* (1982) 3643; G. B. Maiya, V. Krishnan, *Inorg. Chem. 24* (1985) 3253.
[102] a) R. Breslow, *Science 218* (1982) 432 and [21], *Vol. 3*, p. 473; b) R. M. Kellogg, *Top. Curr. Chem. 101* (1982) 111; c) I. Tabushi, K. Yamamura, *ibid. 113* (1983) 145; d) Y. Murakami, *ibid. 115* (1983) 107; e) C. Sirlin, *Bull. Soc. Chim. Fr. II 1984*, 5; f) R. M. Kellogg, *Angew. Chem. 96* (1987) 769; *Angew. Chem. Int. Ed. Engl. 23* (1984) 782; g) V. T. D'Souza, M. Bender, *Acc. Chem. Res. 20* (1987) 146.
[103] J.-M. Lehn, *Pure Appl. Chem. 51* (1979) 979; *Ann. N. Y. Acad. Sci. 471* (1986) 41.
[104] Y. Chao, G. R. Weisman, G. D. Y. Sogah, D. J. Cram, *J. Am. Chem. Soc. 101* (1979) 4948.
[105] J.-M. Lehn, C. Sirlin, *J. Chem. Soc. Chem. Commun. 1978*, 949; *New J. Chem. 11* (1987) 693.
[106] S. Sasaki, K. Koga, *Heterocycles 12* (1979) 1305.
[107] J.-P. Behr, J.-M. Lehn, *J. Chem. Soc. Chem. Commun. 1978*, 143.
[108] J.-M. Lehn, T. Nishiya, *Chem. Lett. 1987*, 215.
[109] M. W. Hosseini, J.-M. Lehn, M. P. Mertes, *Helv. Chim. Acta 66* (1983) 2454; M. W. Hosseini, J.-M. Lehn, L. Maggiora, K. B. Mertes, M. P. Mertes, *J. Am. Chem. Soc. 109* (1987) 537.
[110] G. M. Blackburn, G. R. J. Thatcher, M. W. Hosseini, J.-M. Lehn, *Tetrahedron Lett. 28* (1987) 2779.
[111] M. W. Hosseini, J.-M. Lehn, *J. Chem. Soc. Chem. Commun. 1985*, 1155; *J. Am. Chem. Soc. 109* (1987) 7047.
[112] P. G. Yohannes, M. P. Mertes, K. B. Mertes, *J. Am. Chem. Soc. 107* (1985) 8288.
[113] S. Sasaki, M. Shionoya, K. Koga, *J. Am. Chem. Soc. 107* (1985) 3371.
[114] H.-D. Lutter, F. Diederich, *Angew. Chem. 98* (1986) 1125; *Angew. Chem. Int. Ed. Engl. 25* (1986) 1125.
[115] F. M. Menger, M. Ladika, *J. Am. Chem. Soc. 109* (1987) 3145.
[116] E. T. Kaiser, D. S. Lawrence, *Science (Washington) 226* (1984) 505.
[117] See, for instance A. R. Fersht, J. P. Shi, A. J. Wilkinson, D. M. Blow, P. Carter, M. M. Y. Waye, G. P. Winter, *Angew. Chem. 96* (1984) 455; *Angew. Chem. Int. Ed. Engl. 23* (1984) 467; J. A. Gerlt, *Chem. Rev. 87* (1987) 1079; A. J. Russell, A. R. Fersht, *ibid. 328* (1987) 496.
[118] A. Tramontano, K. D. Janda, R. A. Lerner, *Science (Washington) 234* (1986) 1566; S. J. Pollack, J. W. Jacobs, P. G. Schultz, *ibid. 234* (1986) 1570; R. A. Lerner, A. Tramontano, *Trends Biochem. Sci. 12* (1987) 427.
[119] Selective cation transport was one of the initial objectives of our work on cryptates; see Refs. [29a, 125].
[120] J.-M. Lehn in G. Spach (Ed.): *Physical Chemistry of Transmembrane Ion Motions*, Elsevier, Amsterdam 1983, p. 181.
[121] W. Simon, W. E. Morf, P. C. Meier, *Struct. Bonding (Berlin) 16* (1973) 113; W. E. Morf, D. Amman, R. Bissig, E. Pretsch, W. Simon in [19], *Vol. 1*, p. 1.
[122] J.-P. Behr, J.-M. Lehn, *J. Am. Chem. Soc. 95* (1973) 6108.
[123] B. C. Pressman, *Annu. Rev. Biochem. 45* (1976) 501.
[124] J. D. Lamb, J. J. Christensen in [21], *Vol. 3*, p. 571.
[125] M. Kirch, J.-M. Lehn, *Angew. Chem. 87* (1975) 542; *Angew. Chem. Int. Ed. Engl. 14* (1975) 555; M. Kirch, *Thèse de Doctorat-ès-Sciences*, Université Louis Pasteur, Strasbourg 1980.
[126] J.-P. Behr, M. Kirch, J.-M. Lehn, *J. Am. Chem. Soc. 107* (1985) 241.
[127] T. M. Fyles, *Can. J. Chem. 65* (1987) 884.
[128] M. Castaing, F. Morel, J.-M. Lehn, *J. Membr. Biol. 89* (1986) 251; M. Castaing, J.-M. Lehn, *ibid. 97* (1987) 79.
[129] E. Bacon, L. Jung, J.-M. Lehn, *J. Chem. Res. (S) 1980*, 136.
[130] H. Tsukube, *Angew. Chem. 94* (1982) 312; *Angew. Chem. Int. Ed. Engl. 21* (1982) 304; *Angew. Chem. Suppl. 1982*, 575.
[131] Anion transport with anion cryptands has been observed recently: T. M. Fyles, J.-M. Lehn, unpublished results.
[132] A. Harada, S. Takahashi, *J. Chem. Soc. Chem. Commun. 1987*, 527.
[133] J. J. Grimaldi, J.-M. Lehn, *J. Am. Chem. Soc. 101* (1979) 1333.
[134] S. S. Anderson, I. G. Lyle, R. Paterson, *Nature (London) 259* (1976) 147.
[135] J. J. Grimaldi, S. Boileau, J.-M. Lehn, *Nature (London) 265* (1977) 229.

[136] J. K. Hurst, D. H. P. Thompson, *J. Membr. Sci. 28* (1986), and references cited therein; I. Tabushi, S.-i. Kugimiya, *Tetrahedron Lett. 25* (1984) 3723.
[137] M. Okahara, Y. Nakatsuji, *Top. Curr. Chem. 128* (1985) 37.
[138] A. Hriciga, J.-M. Lehn, *Proc. Natl. Acad. Sci. USA 80* (1983) 6426.
[139] R. Frank, H. Rau, *Z. Naturforsch. A 37* (1982) 1253.
[140] I. Tabushi, S.-i. Kugimiya, *J. Am. Chem. Soc. 107* (1985) 1859.
[141] S. Shinkai, O. Manabe, *Top. Curr. Chem. 121* (1984) 67.
[142] D. W. Urry, *Top. Curr. Chem. 128* (1985) 175.
[143] R. Nagaraj, P. Balaram, *Acc. Chem. Res. 14* (1981) 356; R. O. Fox, Jr., F. M. Richards, *Nature (London) 300* (1982) 325.
[144] J.-P. Behr, J.-M. Lehn, A.-C. Dock, D. Moras, *Nature (London) 295* (1982) 526.
[145] U. F. Kragten, M. F. M. Roks, R. J. M. Nolte, *J. Chem. Soc. Chem. Commun. 1985*, 1275.
[146] I. Tabushi, Y. Kuroda, K. Yokota, *Tetrahedron Lett. 23* (1982) 4601.
[147] J.-H. Fuhrhop, U. Liman, *J. Am. Chem. Soc. 106* (1984) 4643.
[148] J.-H. Fuhrhop, U. Liman, H. H. David, *Angew. Chem. 97* (1985) 3371 *Angew. Chem. Int. Ed. Engl. 24* (1985) 339.
[149] J.-M. Lehn, J. Simon, *Helv. Chim. Acta 60* (1977) 141.
[150] J.-M. Lehn, M. E. Stubbs, *J. Am. Chem. Soc. 96* (1974) 4011.
[151] W. Fischer, J. Brickmann, P. Läuger, *Biophys. Chem. 13* (1981) 105.
[152] C. Etchebest, S. Ranganathan, A. Pullman, *FEBS Letters 173* (1984) 301.
[153] For an earlier use of the intersection sign, see: E. Kauffmann, J. L. Dye, J.-M. Lehn, A. I. Popov, *J. Am. Chem. Soc. 102* (1980) 2274.
[154] A. G. Amit, R. A. Mariuzza, S. E. V. Phillips, R. J. Poljak, *Science (Washington) 233* (1986) 747; H. M. Geysen, J. A. Tainer, S. J. Rodda, T. J. Mason, H. Alexander, E. D. Getzoff, R. A. Lerner, *ibid. 235* (1987) 1184.
[155] M. M. Harding, J.-M. Lehn, unpublished work.
[156] D. A. Tomalia, M. Hall, D. M. Hedstrand, *J. Am. Chem. Soc. 109* (1987) 1601, and references cited therein.
[157] G. R. Newkome, Z.-q. Yao, G. R. Baker, V. K. Gupta, P. S. Russo, M. J. Saunders, *J. Am. Chem. Soc. 108* (1986) 849; G. R. Newkome, G. R. Baker, M. J. Saunders, P. S. Russo, V. K. Gupta, Z.-q. Yao, J. E. Miller, K. Bouillion, *J. Chem. Soc. Chem. Commun. 1986*, 752.
[158] H. M. McConnell, L. K. Tamm, R. M. Weiss, *Proc. Natl. Acad. Sci. USA 81* (1984) 3249; R. M. Weiss, H. M. McConnell, *Nature (London) 310* (1984) 47.
[159] T. Kunitake, Y. Okahata, M. Shimomura, S.-i. Yasunami, K. Takarabe, *J. Am. Chem. Soc. 103* (1981) 5401; N. Nakashima, S. Asakuma, T. Kunitake, *ibid. 107* (1985) 509.
[160] J. H. Fendler: *Membrane Mimetic Chemistry*, Wiley, New York 1982.
[161] H. Kuhn, D. Moebius, *Angew. Chem. 83* (1971) 672; *Angew. Chem. Int. Ed. Engl. 10* (1971) 620.
[162] D. Moebius, *Acc. Chem. Res. 14* (1981) 63; *Ber. Bunsenges. Phys. Chem. 82* (1978) 848; *Z. Phys. Chem. (Munich) 154* (1987) 121.
[163] J. A. Hayward (Ed.): *New technological applications of phospholipid bilayers, thin films and vesicles*, Plenum Press, London 1986.
[164] J. Sagiv in [163]; L. Netzer, J. Sagiv, *J. Am. Chem. Soc. 105* (1983) 674.
[165] H.-H. Hub, B. Hupfer, H. Koch, H. Ringsdorf, *Angew. Chem. 92* (1980) 962; *Angew. Chem. Int. Ed. Engl. 19* (1980) 938; L. Gros, H. Ringsdorf, H. Schupp, *ibid. 93* (1981) 311 and *20* (1981) 305; see also: H. Ringsdorf, B. Schlarb, J. Venzmer, *ibid. 100* (1988) 117 and *27* (1988) 113.
[166] G. Wegner, *Chimia 36* (1982) 63; C. M. Paleos, *Chem. Rev. 14* (1985) 45.
[167] H. Kuhn, *Pure Appl. Chem. 53* (1981) 2105.
[168] a) J.-H. Fuhrhop, J. Mathieu, *Angew. Chem. 96* (1984) 124; *Angew. Chem. Int. Ed. Engl. 23* (1984) 100; b) J.-H. Fuhrhop, D. Fritsch, *Acc. Chem. Res. 19* (1986) 130; c) Y. Okahata, *Acc. Chem. Res. 19* (1986) 57.
[169] a) V. Balzani (Ed.): *Supramolecular Photochemistry*, Reidel, Dordrecht, Netherlands 1987; b) J.-M. Lehn in [169a], p. 29.
[170] J.-C. Rodriguez-Ubis, B. Alpha, D. Plancherel, J.-M. Lehn, *Helv. Chim. Acta 67* (1984) 2264.
[171] B. Alpha, J.-M. Lehn, G. Mathis, *Angew. Chem. 99* (1987) 259; *Angew. Chem. Int. Ed. Engl. 26* (1987) 266; B. Alpha, V. Balzani, J.-M. Lehn, S. Perathoner, N. Sabbatini, *ibid. 99* (1987) 1310 and *26* (1987) 1266; N. Sabbatini, S. Perathoner, V. Balzani, B. Alpha, J.-M. Lehn, in Ref. [169a], p. 187.
[172] a) H. Bouas-Laurent, A. Castellan, J.-P. Desvergne, *Pure Appl. Chem. 52* (1980) 2633; b) H. Bouas-Laurent, A. Castellan, M. Daney, J.-P. Desvergne, G. Guinand, P. Marsau, M.-H. Riffaud, *J. Am. Chem. Soc. 108* (1986) 315.
[173] J. P. Konopelski, F. Kotzyba-Hibert, J.-M. Lehn, J.-P. Desvergne, F. Fagès, A. Castellan, H. Bouas-Laurent, *J. Chem. Soc. Chem. Commun. 1985*, 433.
[174] D. F. Eaton, *Tetrahedron 43* (1987) 1551, and references cited therein.
[175] A. Guarino, *J. Photochem. 35* (1986) 1.
[176] M. Gubelmann, J.-M. Lehn, J. L. Sessler, A. Harriman, *J. Chem. Soc., Chem. Commun.*, in press.
[177] V. Balzani, N. Sabbatini, F. Scandola, *Chem. Rev. 86* (1986) 319.
[178] Photoactive units may photoxidize complexed substrates [93] and effect DNA photocleavage: A. J. Blacker, J. Jazwinski, J.-M. Lehn, F.-X. Wilhelm, *J. Chem. Soc. Chem. Commun. 1986*, 1035.
[179] a) D. S. Chemla, J. Zyss (Eds.): *Non-linear Optical Properties of Organic Molecules and Crystals, Vol. 1*, Academic Press, New York 1987; b) J.-M. Lehn in [179a], p. 215; c) J. F. Nicoud, R. J. Twieg in [179a], p. 221.
[180] M. Takagi, K. Ueno, *Top. Curr. Chem. 121* (1984) 39; H.-G. Löhr, F. Vögtle, *Acc. Chem. Res. 18* (1985) 65; R. Klink, D. Bodart, J.-M. Lehn, B. Helfert, R. Bitsch, *Eur. Pat. Apl. 83100281.1* (14 January 1983), Merck GmbH.
[181] R. C. Haddon, A. A. Lamola, *Proc. Natl. Acad. Sci. USA 82* (1985) 1874; R. W. Munn, *Chem. Br. 1984*, 518; J. Simon, J.-J. André, A. Skoulios, *Nouv. J. Chim. 10* (1986) 295; J. Simon, F. Tournilhac, J.-J. André, *New J. Chem. 11* (1987) 383, and references cited therein; for other related work see, for instance: J. K. Nagle, J. S. Bernstein, R. C. Young, T. J. Meyer, *Inorg. Chem. 20* (1981) 1760; E. T. T. Jones, O. M. Chyan, M. S. Wrighton, *J. Am. Chem. Soc. 109* (1987) 5526.
[182] T. S. Arrhenius, M. Blanchard-Desce, M. Dvolaitzky, J.-M. Lehn, J. Malthête, *Proc. Natl. Acad. Sci. USA 83* (1986) 5355.
[183] Biological effectors may also be sought: I. Tabushi, T. Nishiya, M. Shimomura, T. Kunitake, H. Inokuchi, T. Yagi, *J. Am. Chem. Soc. 106* (1984) 219.
[184] R. Schwyzer, A. Tun-Kyi, M. Caviezel, P. Moser, *Helv. Chim. Acta 53* (1970) 15; *Experientia 26* (1970) 577; see also [1], p. 19.
[185] a) S. Shinkai, *Pure Appl. Chem. 59* (1987) 425; b) D. A. Gustowski, M. Delgado, V. J. Gatto, L. Echegoyen, G. W. Gokel, *J. Am. Chem. Soc. 108* (1986) 7553, and references cited therein.
[186] J.-M. Lehn, J. Malthête, A.-M. Levelut, *J. Chem. Soc. Chem. Commun. 1985*, 1794.
[187] For phthalocyanine derived columnar mesophases see: D. Masurel, C. Sirlin, J. Simon, *New J. Chem. 11* (1987) 455, and references cited therein.
[188] E. Carafoli, J. T. Penniston, *Sci. Am. 253* (1985) No. 11, p. 50; *Spektrum Wiss. 1986*, No. 1, p. 76; T. Hiraoki, H. J. Vogel, *J. Cardiovasc. Pharm. 10 (Suppl. 1)* (1987) S 14.
[189] I. Tabushi, S.-i. Kugimiya, T. Sasaki, *J. Am. Chem. Soc. 107* (1985) 5159, and references cited therein.
[190] D. Pörchske, M. Eigen, *J. Mol. Biol. 62* (1971) 361, and references cited therein.
[191] J.-M. Lehn, A. Rigault, J. Siegel, J. Harrowfield, B. Chevrier, D. Moras, *Proc. Natl. Acad. Sci. USA 84* (1987) 2565; J.-M. Lehn, A. Rigault, unpublished results.
[192] K. E. Drexler, *Proc. Natl. Acad. Sci. USA 78* (1981) 5275; C. Joachim, J.-P. Launay, *Nouv. J. Chim. 8* (1984) 723.
[193] *Opportunities in Chemistry* ("Pimentel-Report"), National Academy Press, Washington, DC, USA, pp. 219f.

ANGEWANDTE CHEMIE

International Edition in English

Volume 27 · Number 1
January 1988
Pages 113–158

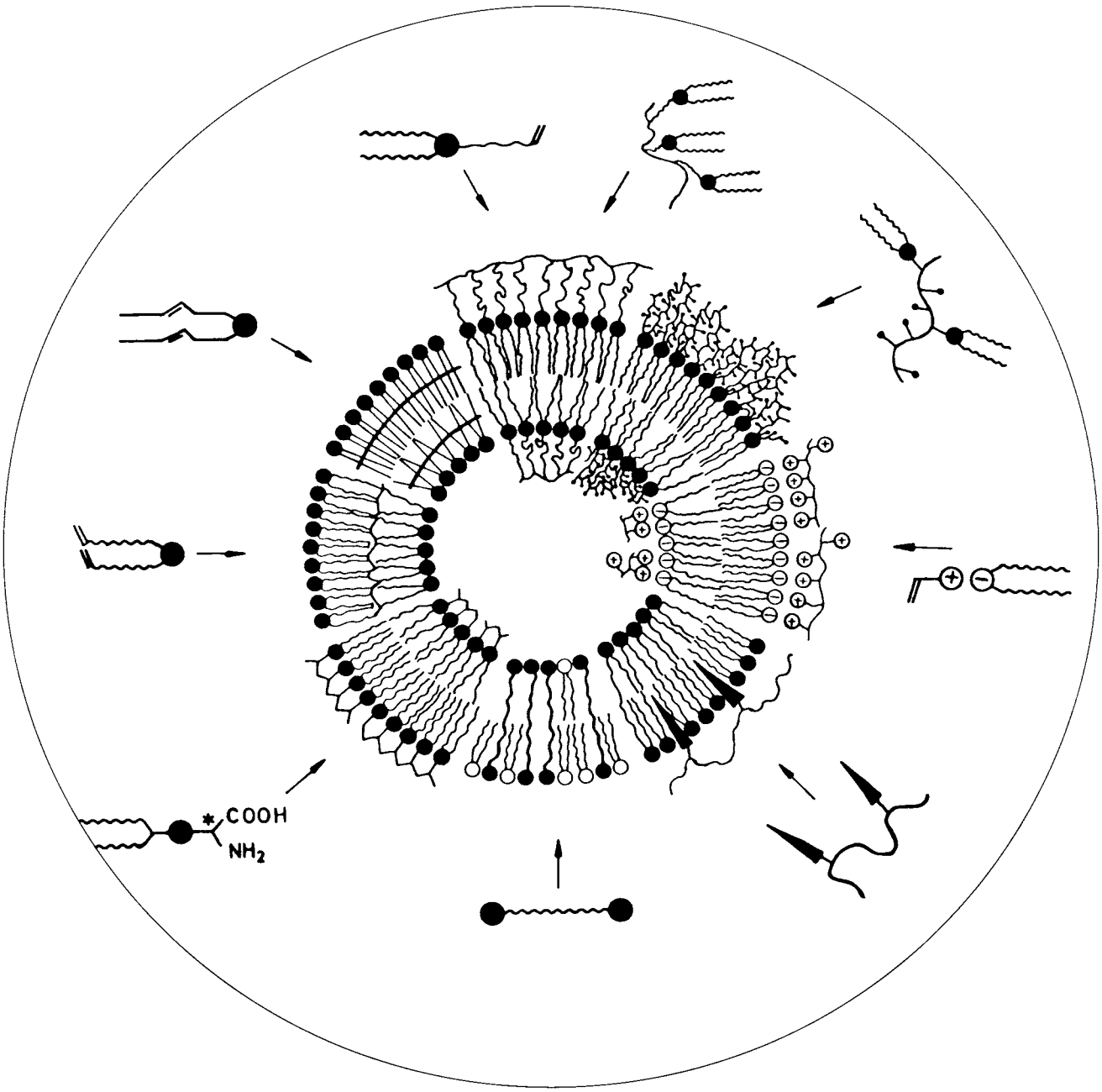

Helmut Ringsdorf, Bernhard Schlarb, and Joachim Venzmer

Molecular Architecture and Function of Polymeric Oriented Systems: Models for the Study of Organization, Surface Recognition, and Dynamics of Biomembranes

© VCH Verlagsgesellschaft mbH, D-6940 Weinheim, 1988

0570-0833/88/0101-0113 $ 02.50/0

Molecular Architecture and Function of Polymeric Oriented Systems: Models for the Study of Organization, Surface Recognition, and Dynamics of Biomembranes**

By Helmut Ringsdorf,* Bernhard Schlarb, and Joachim Venzmer

The Part and the Whole. The principle of self-organization for the creation of functional units is not an invention of modern natural sciences. It was already a basic idea of the ancient philosophies in Asia and Europe: only the mutuality of the parts creates the whole and its ability to function. Translated into the language of chemistry this means: the self-organization of molecules leads to supramolecular systems and is responsible for their functions. Thermotropic and lyotropic liquid crystals are such functional units, formed by self-organization. As highly oriented systems, they exhibit new properties. The importance of lyotropic liquid crystals for the life sciences has been known for a long time. They are a prerequisite for the development of life and the ability of cells to function. In materials science this concept of *function through organization* led to the development of new liquid-crystalline materials. From the point of view of macromolecular chemistry, this review tries to combine these two different fields and especially hopes to stimulate their interaction and joint treatment. To exemplify this, the molecular architecture of polymeric organized systems will be discussed. Polymeric liquid crystals combine the ability to undergo spontaneous self-organization—typical of liquid-crystalline phases—with the polymer-specific property of stabilizing these ordered states. As new materials, polymeric liquid crystals have already been investigated intensively. As model systems for biomembranes as well as for the simulation of biomembrane processes, they so far have been little discussed. The intention of this review article is to show that polymer science is able to contribute to the simulation of cellular processes such as the stabilization of biomembranes, specific surface recognition, or even the "uncorking" of cells. Polymer science, having an old tradition as an interdisciplinary field, can no longer restrict itself to common plastics. Attempts to reach new horizons have already begun. The borderland between liquid crystals and cells will certainly play an important role. Basic requirements to work in this frontier area between organic chemistry, membrane biology, life science, and materials science will be the delight in scientific adventures as well as the courage to go ahead. The most important prerequisite will be the willingness to cooperate with disciplines which so far have not really accepted each other. From this point of view, this review does not aim at giving defined answers. It wants instead to encourage the scientific venture: too often we cling to painfully acquired knowledge, fearing adventures.

To the question of what he was up to at the moment, Mr. K. answered: "I'm hard at work preparing my next error"
Bertolt Brecht[1]

1. Introduction: Polymer Science Today—Ancient Roots, Young Branches?[2]

1.1. Tradition and Innovation in Science

Two decisive aspects in the field of science are tradition and innovation. Tradition is the basis, for it is the cumulation of wisdom in the body of knowledge. To know what a subject is all about and to control it creates self-confidence, thus paving the way for innovations. Innovation is the adventure, since with the challenge comes the risk of calling into question (or even losing) one's own scientific identity, gained through tradition.

Persisting in tradition without innovation, however, soon leads to tiresome routine, to the science of yesterday: the longing for new adventures withers and dies.[3] On the other hand, pure innovation harbors the danger of superficiality. The sum of knowledge is immense and growing! Tradition and solid, successful work are honored and admired. Nevertheless, science can only be justified by a challenge, and demands the willingness to give up long-held classical or traditional views[4] in the attempt to discover new horizons.

1.2. One Example to Introduce the Topic: Order versus Chaos

Only a few years ago, it was still difficult to bring the evolution of life in line with the basic laws of physics. Ac-

[*] Prof. Dr. H. Ringsdorf, Dipl.-Chem. B. Schlarb, Dipl.-Chem. J. Venzmer
Institut für Organische Chemie der Universität
J.-J.-Becher-Weg 18-20, D-6500 Mainz 1 (FRG)
[**] The preceding page shows Figure 24.

cording to the principles of classical thermodynamics, disorder in the world was supposed to increase constantly. All controlled functional processes should therefore end one fine day; all order should dissipate. During the big bang, when the world evolved from chaos, there was no order at all. So how could organized structures, living organisms, develop from this start?[5]

It was a stormy development in the field of nonequilibrium phenomena that helped to resolve this dilemma. During the last few decades, the term self-organization has been synonymous with theories developed in various disciplines that deal with the further development, dynamics, and differentiation of systems. On the borderland between chemistry and biology, these include, in particular, concepts for the development of highly complicated organic molecules and the role they play in the evolution of biological information in a prebiotic world.[6b] Even the somewhat new overlapping discipline of synergetics,[6] with its concepts of ordered, self-organized, and collective behavior, had its share in this process.

The fascinating phenomena of self-organization, which can be observed in physical, chemical, and biological systems (either near to or far from thermodynamical equilibrium), are characterized by great variety and complexity. A large number of molecules organize spontaneously, eventually exhibiting well-organized behavior on the macroscopic scale. The variety of organized states ranges from relatively simple spatial or chronological forms of organization all the way to the complicated interaction between order and function in biological systems. Over the last few years, the phenomenon of self-organization has developed into a subject of interdisciplinary research with overlapping topics.[5,6]

1.3. From Polymeric Liquid Crystals to Functional Biomembrane Models?

Right from its very beginnings, polymer science was a field on the borderland between chemistry and physics, i.e., between two classical disciplines. Thus, scientists in this field had to dare to make innovations. It was no less a man than *Hermann Staudinger* who experienced this. It is highly instructive to observe how at the height of his creativity in the field of organic chemistry, he left his traditional field of work to enter the frontier between chemistry and physics in order to tackle the problems of macromolecular chemistry.[7] In the meantime, macromolecular chemistry, too, has become a classical discipline, a mature science, with all the advantages and handicaps of maturity. Harvest is plentiful, the results are abundant—but one has to ask: where is the future, where are the adventures?

Modern materials science once developed out of the interaction between metallurgy, ceramics, and macromolecular technology, and in the jubilee issue of *Angewandte Chemie* in honor of the 100th anniversary of *Hermann Staudinger*'s birth, the old "Geheimrat" *Hermann Mark* asked the question of what direction polymer science was about to take:[2] Is it going in the direction of life science? Is it possible to reduce polymer science, cell biology, and medicine to a common denominator? So from that point of view, polymer science finds itself not only on the borderland between chemistry and physics, but also between materials science and life science (Fig. 1).

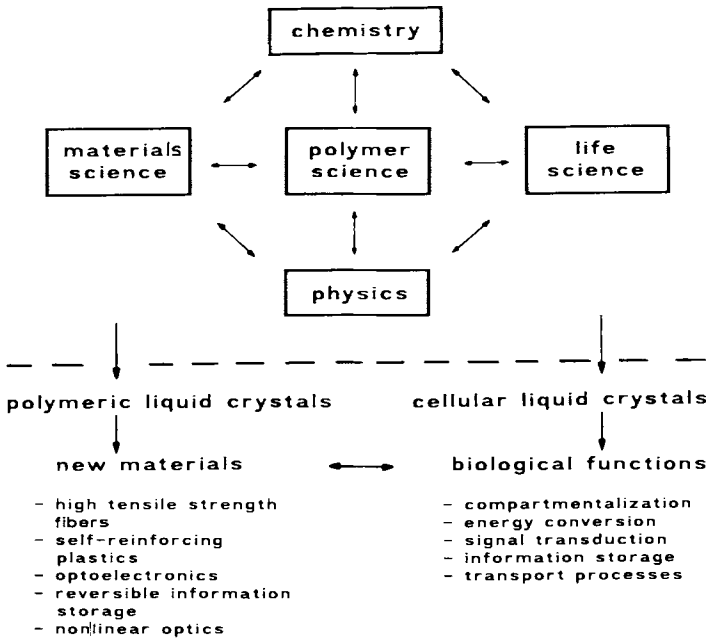

Fig. 1. Polymer science as an interdisciplinary field of science.

Taking self-organization and the molecular architecture of macromolecular systems as examples, this article aims to show that these fields of science can no longer be dealt with separately. In this review, the biological macromolecules of the cell such as polysaccharides or nucleic acids are not discussed as such. Molecular biology today is able to understand the central role which these polymers play in life science. But it has to be pointed out that their functions are based in all cases on the combination of molecular mobility and high order. This is achieved by their incorporation into membranes, by self-organization in solution, or by orientation at cell surfaces. These are combinations of properties which are typical of liquid-crystalline behavior. Thus, liquid crystals are chosen as *one* principal example of self-organizing systems, which are important for materials science as well as for life science (Fig. 1).

It was not by chance that, about 50 years ago, *J. D. Bernal* called the cell itself a natural liquid crystal, based on the knowledge of that time.[8] Liquid crystals really feature a behavior which is considered to be typical of a living cell: they react to a large number of stimulations such as light, sound, mechanical pressure, heat, and electric and magnetic fields as well as to changes in the chemical environment. The significance of cellular liquid crystals has been accepted for quite a long time. The significance of low-molecular-weight and of polymeric liquid crystals is on its way to becoming widely accepted. However, although the basic principles of self-organization are the same for both cellular and technical liquid crystals, only on rare occasions have they been looked at together.[9]

But what about the molecular architecture of the building blocks of self-organizing systems such as synthetic and biological liquid crystals and what about the structure of the resulting highly oriented supramolecular systems?

How does the molecular architecture relate to the functions of these materials? A hint as to possible answers to this problem will be given in an overview in Section 2. The goal is to stimulate interest in the overlapping fields of synthetic and biological liquid crystals in the broadest sense (cf. Fig. 2). In Section 3, thermotropic and lyotropic mesogens will briefly be defined and exemplified. Section 4 will show that scientists today are learning, step by step, what Mother Nature has long since known, namely to stabilize ultrathin, organized membranes and to functionalize them. Sections 5 and 6 will then concentrate on the connection between structure, function, and organization in biomembrane models. Even though the subject is still in its infancy, it is fascinating to observe how chemistry, physics, and membrane biology have to cooperate in order to mimic surface reactions (Section 5) and dynamic processes of biomembranes (Section 6).

Endocytosis and exocytosis, patching and capping—foreign words to chemists? Corkscrews for corked lipo somes?—a funny, maybe even nonscientific question? They originate from biology and are used on the borderland of polymer science between liquid crystals and the cell, an area of research which is only just beginning. The willingness to closely cooperate with adjacent disciplines, which hitherto have often been ignorant of one another,[10] will be a basic requirement to go ahead in this field. From that point of view, this article can neither be a perfect summary nor a presentation of detailed research results. To give definite answers is out of the question. It is simply meant to encourage innovations and scientific ventures: much too often we cling to our own knowledge out of the fear of new adventures.[11]

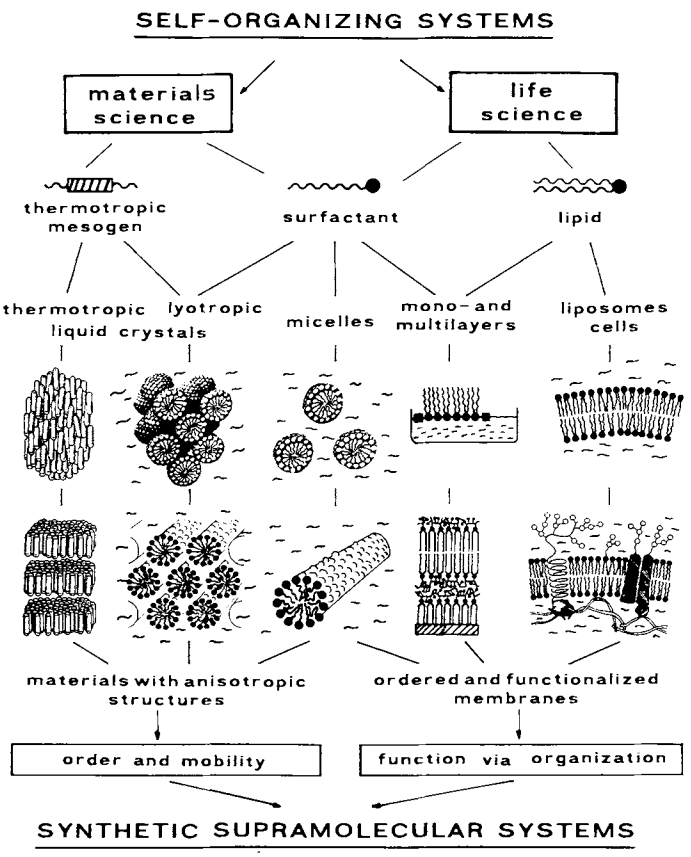

Fig. 2. Self-organization and supramolecular systems [12] in materials science and life science. The supramolecular structures range from simple nematic liquid crystals to complex biomembranes.

2. Self-Organization and Formation of Supramolecular Systems

Order and mobility are two basic principles of Mother Nature. On a molecular level two extreme cases can be found: the perfect order of crystals, in which the molecules exhibit almost no mobility at all, and the disordered state in gases and liquids, which exhibit randomness of highly mobile molecules. Both principles, order and mobility, are combined in liquid-crystalline phases. Although there are many possibilities for self-organization, the molecular basis is almost always simple: form-anisotropic or amphiphilic molecules make up the simplest building blocks. These already suffice—as shown in Figure 2—to construct a broad range of substances able to form supramolecular systems,[12] from thermotropic and lyotropic liquid crystals and the manifold micellar systems up to the highly ordered membranes in liposomes and cells.

In materials science, the significance of liquid crystals and micellar systems has long been known; it is based on exactly that combination of order and mobility in form-anisotropic molecules, leading to anisotropic (i.e., direction-dependent) properties of their materials and solutions.

From the life sciences we know that no life would be possible without the lipids' self-organization into bilayers within the cell membrane. In this case, too, order and mobility are related to the structure of functional units formed by lipids and proteins. In all cases, the functions of such supramolecular systems, formed by aggregation, are based on their organization.

The self-organization and the construction of supramolecular systems is an interdisciplinary area which cannot be understood without the cooperation of different fields of science: chemistry alone does not fulfill that task nor does physics or biology. Over the last few years it has been possible to observe an increase in the number of studies which reveal the connection between synthetic and cellular liquid crystals and in which a mutual understanding opens up new perspectives. Macromolecular chemistry may play an important role in this context. On the one hand, macromolecules can stabilize organized systems without hampering their mobility. On the other hand, it is well known in macromolecular chemistry that creative curiosity for new compounds leads to new properties due to novel structures.

3. Molecular Architecture of Synthetic Self-Organizing Structures—or How to Attract Molecules to Form Supramolecular Systems

3.1. Structure and Properties of Thermotropic Polymeric Liquid Crystals

Numerous organic compounds with a rigid, rodlike molecular geometry (mesogens) do not directly go from the

crystalline into the isotropic state when they melt. Instead, they form intermediate liquid-crystalline phases (Fig. 3),[13] known as mesophases. These mesophases combine the order of the crystal with the mobility of the isotropic liquid. The parallel orientation of the longitudinal molecular axes is common to all mesophases (long-range orientational order). Two major classes can be distinguished: nematic (molecular centers distributed isotropically) and smectic (molecular centers organized in layers) phases. The individual smectic phases are further subdivided[14] into phases with or without tilt of the mesogens in the direction of the normal to the smectic layer. The molecules can either be in a disordered state within the respective layers or show different states of order. On the one hand, the driving forces

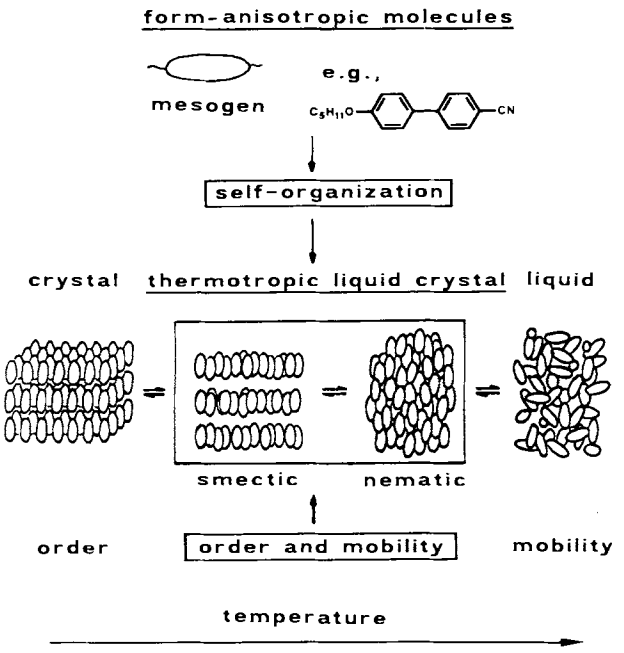

Fig. 3. Structure and phase behavior of thermotropic liquid crystals.

for the formation of mesophases are the anisotropic dispersion interactions[15] caused by the form-anisotropy of the mesogens. On the other hand, there are the steric repulsion forces[16] which are also orientation dependent.

The mesophases of rod-shaped compounds had been known for almost 100 years[17] when, in 1977, the discotic liquid-crystalline phases of disc-shaped molecules were found by *Chandrasekhar* et al.[18]. One can distinguish between a nematic discotic phase and several columnar discotic phases.[19] In the latter, molecular discs form stacks which, in turn, are organized in a two-dimensional lattice (cf. Fig. 5). These investigations reopened the game of molecular design of liquid-crystalline systems. So, additional phases were found: tubular,[20] pyramidic,[21] phasmidic,[22] and sanidic[23] phases. However, it still remains uncertain whether this is only a funny nomenclature or whether these are really new phases.

The development in the field of polymeric liquid crystals[24] started with polymers whose stiff main chain as a whole functions as the mesogen. Such polymers form liquid-crystalline phases either in solution[25] or in the melt.[26] At present, they are used as high-tensile-strength fibers (e.g., Kevlar®) or as thermoplastically processable, self-reinforcing plastics (e.g., Xydar®, Vectra®, Ultrax®).

Parallel to these industrial developments, numerous studies have been carried out in the area of basic research during the last ten years. They have dealt with the incorporation of rod-shaped mesogenic groups, known from low-molecular-weight liquid crystals, into polymers. This incorporation is either carried out by connecting the mesogenic groups via flexible spacers,[27] thus forming semiflexible liquid-crystalline (LC) main-chain polymers[28] (type B, Fig. 4) or, as in the case of the LC side-group polymers, by fixing the mesogens via flexible spacers to the polymer backbone[29] (type A, Fig. 4). Both types of liquid-crystalline polymers were, and still are, intensively investigated. Their structure-property relationships are discussed in numerous monographs[30] and reviews.[31]

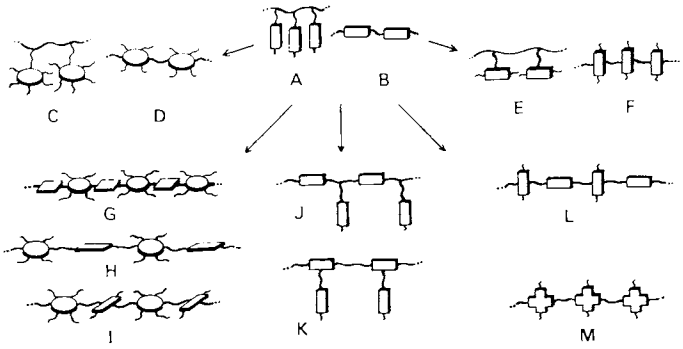

Fig. 4. Molecular architecture of polymeric liquid crystals: A) side-group polymers; B) main-chain polymers; C) discotic side-group polymers [32]; D) discotic main-chain polymers [33]; E) side-group polymers with laterally fixed mesogens [34, 35]; F) main-chain polymers with laterally linked mesogens [35]; G, H, I) combined disc-rod polymers, i.e., combinations of disc- and rod-shaped mesogens [23, 36, 37]; J, K) combined main-chain/side-group polymers [38]; L) polymers with laterally and terminally linked mesogenic groups; M) polymers with cross-shaped mesogenic groups [35].

From these two "classical" types (A and B), variations of the macromolecular architecture of liquid-crystalline polymers have recently been carried out. They are illustrated schematically in Figure 4.

On the one hand, it is possible to realize discotic phases, as observed in the case of low-molecular-weight liquid crystals, by using side-group[32] (type C) and main-chain[33] (type D) polymers. On the other hand, it is, of course, also possible to incorporate rod-shaped mesogens in different ways than in the two classical types A and B: examples are side-group polymers[34,35] (type E) as well as main-chain polymers[35] (type F) with laterally fixed mesogens. These strange-looking architectures do not prevent the formation of liquid-crystalline phases. As far as polymers of type E are concerned, the limited rotation of the mesogenic groups around their longitudinal axes leads to the formation of biaxial nematic phases.[34a-c] These phases have not been observed yet with low-molecular-weight liquid crystals. The third group of structural variations makes use of a well-known principle in polymer chemistry, which is rarely used in the field of liquid-crystalline materials: the com-

binations of different structural elements and different building principles to design one macromolecule. This includes the different combinations of rod- and disc-shaped mesogens[23, 36, 37] (types G, H, and I) and the combination of the structural principles of the two classical types of liquid-crystalline polymers (types A and B) in the combined main-chain/side-group polymers[38] (types J and K). Furthermore, the polymers with cross-shaped mesogens[35] (type M) should be mentioned, as well as the idea of combining laterally and terminally connected mesogenic groups (type L), which has not yet been realized.

Here only two examples are given to illustrate the structure-property relationships of such new polymeric liquid crystals. Figure 5 shows a discotic main-chain polymer[33a, b] of type D. This one features a columnar phase which can be mechanically oriented and frozen below the glass transition temperature. It is noteworthy that this polymer forms a highly ordered D_{ho} phase. Thus, the polymer chains do not disturb the packing of the discs.

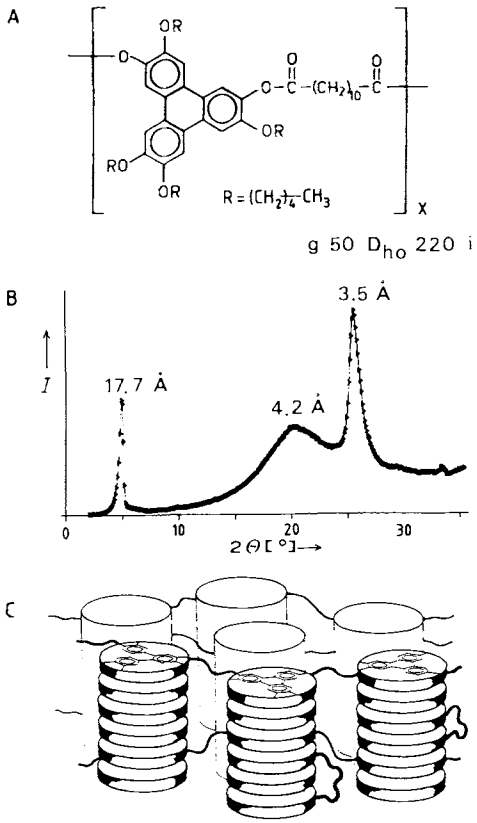

Fig. 5. A) Chemical structure and phase behavior of a discotic main-chain polymer with triphenylene moieties as core of the discogen [33a] (g = *g*lassy; D_{ho} = *d*iscotic *h*exagonal *o*rdered; i = *i*sotropic). B) X-ray scattering diagram (λ = 1.54 Å) of the polymer (I = scattering intensity, θ = scattering angle) [33b]. The scattering maxima are given by the Bragg spacings and can be interpreted in analogy to the values found for low-molecular-weight triphenylene derivatives [19b] as follows: 17.7 Å corresponds to the columnar distance in the hexagonal lattice; 4.2 Å corresponds to the nonoriented liquid-like arrangement of the alkyl chains; 3.5 Å corresponds to the constant distance of the triphenylene cores in the column. C) Structural model for the D_{ho} phase of the discotic main-chain polymer based on results from X-ray measurements of mechanically oriented samples [33b]. The columns are perpendicular to the stretching direction.

In Figure 6, a combined main-chain/side-group liquid-crystalline polyester of type J (A) is compared to one of type K (B). Depending on the point of attachment of the mesogenic side group, either mostly smectic (A) or nematic (B) mesophases are observed.

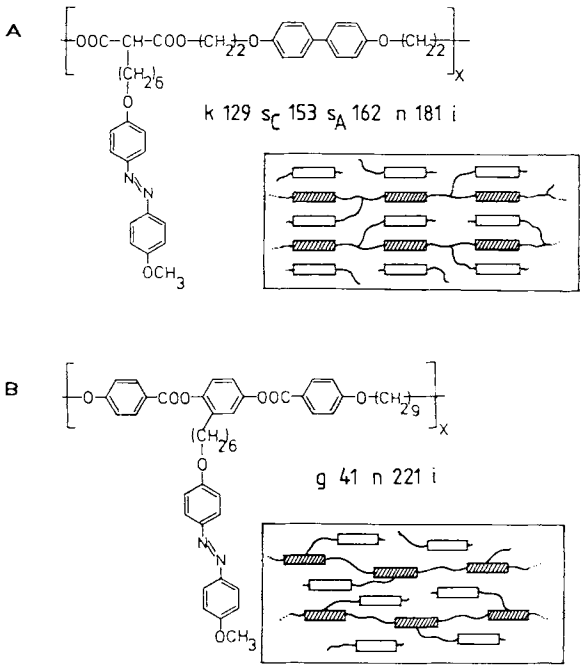

Fig. 6. Chemical structure, phase behavior, and structural models of the mesophase of combined main-chain/side-group liquid-crystal polymers. A) The attachment of the mesogenic groups to the flexible spacer of the polymalonate main chain [38a] favors smectic mesophases (s). B) The attachment of the mesogenic side groups directly to the polyester main-chain mesogens [38b] leads to broad nematic phases (n).

3.2. Structural Variations in Micellar and Lyotropic Liquid-Crystalline Systems

Contrary to thermotropic ones, lyotropic liquid-crystalline systems always consist of at least two components. One of them is a solvent, which plays a crucial role in determining order and mobility. The state of lyotropic liquid crystallinity is not primarily achieved by a change in temperature, but, as shown in Figure 7, by a change in solvent content.[39]

With decreasing solvent content, molecules that are isotropically dispersed at lower concentrations only form aggregates. These aggregates organize into nematic phases or into the more ordered lamellar (comparable to the thermotropic smectic phases), columnar, and cubic mesophases. Nematic phases differ from the isotropic solution by the long-range orientational order of the aggregates only, lamellar and columnar phases additionally by a long-range positional order of the aggregate centers in one or two dimensions; cubic phases merely show a long-range positional order in three dimensions. On further decreasing the solvent content, solvent-free crystals are formed—often via solvent-containing crystals. As typical of amphiphiles, lyotropic mesogens are composed of soluble (solvatophilic) and insoluble (solvatophobic) moieties within one molecule. Fatty acid salts and long-chain alkyl ammonium salts are representatives of this type of structure. In aqueous solution, they aggregate—if their concentration lies above

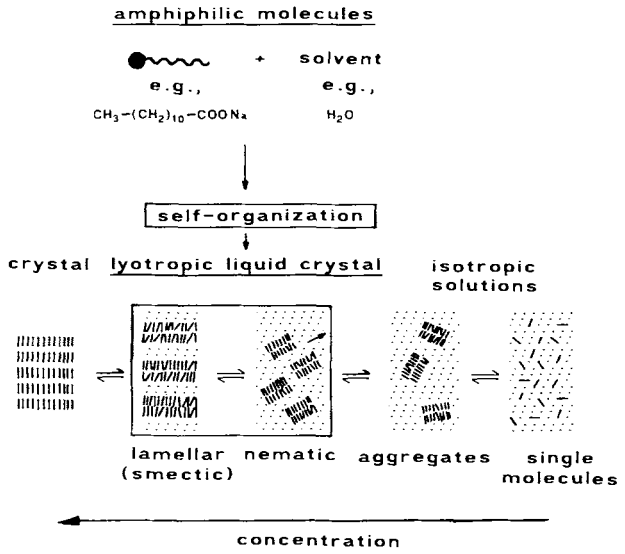

Fig. 7. Structure and phase behavior of lyotropic liquid crystals.

the critical micelle concentration (CMC)—to micelles, which may be spherical, cylindrical, or plate-shaped (Fig. 8).

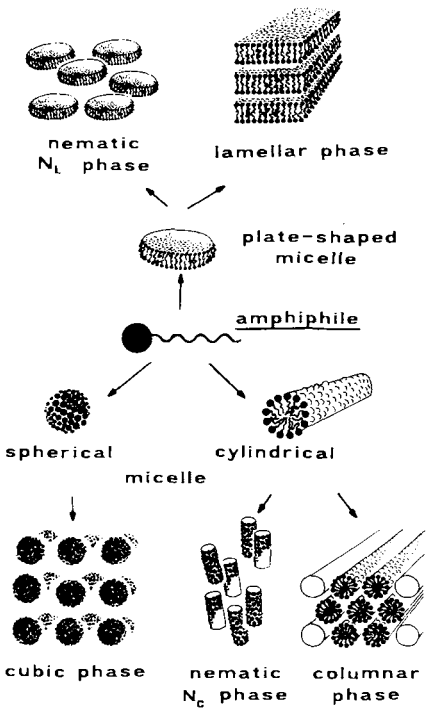

Fig. 8. Aggregation of amphiphiles to form micelles of various shapes and the formation of lyotropic mesophases from these micelles.

For spherical micelles, intermicellar interactions lead to cubic mesophases; for cylindrical micelles, to nematic N_C as well as to columnar mesophases. Plate-shaped micelles can form an additional type of nematic phase (N_L) and further a lamellar mesophase.[40] Thus, the different types of lyotropic mesophases are not directly determined by the structure of the single molecule (mesogen)—as is the case of thermotropic systems—but by the structure of the micelle[41] or the aggregate. The structure of the micelle, however, depends on several factors, such as temperature, concentration, and the structure of the amphiphile itself. The latter refers, in particular, to the hydrophobic-hydrophilic balance between the head group and the alkyl chain as well as to the geometry of the amphiphile.[42] Most of the amphiphiles form micelles of different shapes and thus often several types of lyotropic mesophases.

It is mainly this complexity of the aggregation behavior that has stimulated the syntheses of various types of amphiphilic compounds. So as to get to specific supramolecular systems, one now tries to influence the shape, size, and stability of the aggregates through molecular architecture of low-molecular-weight and polymeric amphiphiles. Two different approaches have been taken so far (Fig. 9).

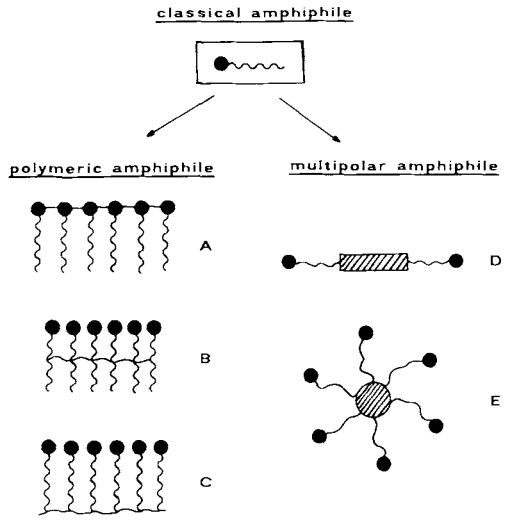

Fig. 9. Molecular architecture of polymeric (A, B, C) and multipolar amphiphiles (D, E).

The first approach starts from polymeric amphiphiles. Although they have long been known, the relationship between their structure and mesophase behavior has hardly been investigated. As depicted in Figure 9, amphiphiles can be synthesized with the polymerizable unit in the head group, in the hydrophobic chain, or attached to its end. Their polymerization leads to polymers of type A, B, or C, with the mobility of the amphiphiles, which are now fixed by the polymer, being extremely different from that of the monomeric compounds. As a consequence, aggregation and mesophase behavior may also change. In view of the few examples known,[43] hardly any changes have been observed as to the type of mesophase—not so as to the concentration and temperature ranges which were largely extended through polymerization. This is demonstrated by the amphiphilic polymer of type C shown in Figure 10.[43a]

Monomer **1** and the respective polymer only form lamellar phases in water. The monomer exhibits lyotropic liquid-crystalline behavior within a concentration range of 65–88 wt%, whereas the polymer exhibits such behavior in the range of 37–100 wt%. The maximum clearing tempera-

ture of the lyotropic mesophase of the monomer is 87 °C, that of the lyotropic mesophase of the polymer, however, 185 °C.

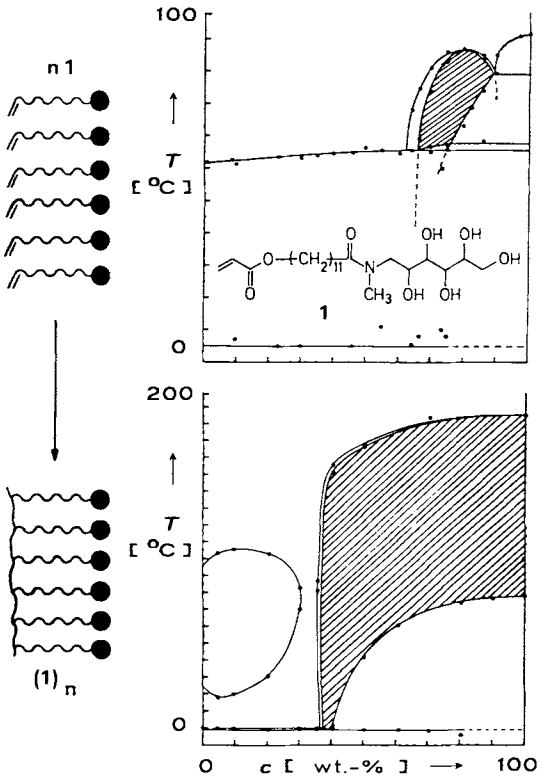

Fig. 10. Extension of the concentration and temperature ranges of the lyotropic mesophases (hatched) of **1** due to polymerization [43a].

The second approach to achieve a specific type of mesophase starts from amphiphiles of novel structure. These new structures combine the molecular design of thermotropic and lyotropic mesogens (see Section 3.3), i.e., the form-anisotropy of thermotropic liquid crystals (rod- and disc-shaped) with the amphiphilic character of lyotropic liquid crystals (see Fig. 9, types D and E). Some examples are shown in Figure 11. If, for instance, the alkyl chains of rod-shaped thermotropic liquid crystals are replaced by hydrophilic chains,[43i,k,44] rod-shaped bipolar amphiphiles result (e.g., **2** and **3**). In water, compound **2** forms only platelike aggregates, which arrange into a lamellar or smectic phase in a concentration range of 53–84 wt% at temperatures between 8.7 °C and 33.5 °C.[43i] As for the rod-shaped amphiphiles **2** and **3**, disc-shaped multipolar amphiphiles (e.g., **4**–**7**) are obtained by introducing hydrophilic chains into discotic molecules such as benzene or triphenylene derivatives. The amidation of the triphenylene-hexayl hexaester **8** with amino alcohols to form hexaamides,[47] e.g., **7** (Fig. 12), provides a simple reaction that involves this transformation of a thermotropic discotic liquid crystal to a lyotropic discotic liquid crystal. In this case, the structural similarity between the thermotropic discotic mesogen and the new lyotropic discotic mesogen is responsible for the same type of mesophase, namely, the columnar one. The lyotropic mesophase is formed by cylindrical aggregates present in the isotropic solution.

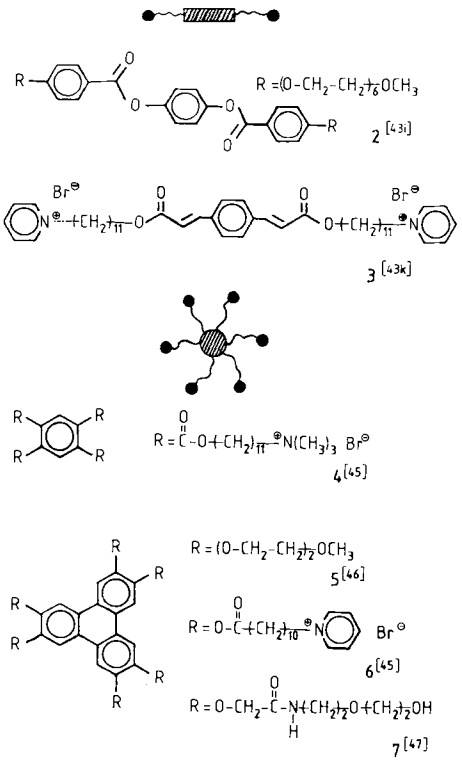

Fig. 11. Examples of multipolar amphiphiles (types D and E from Fig. 9).

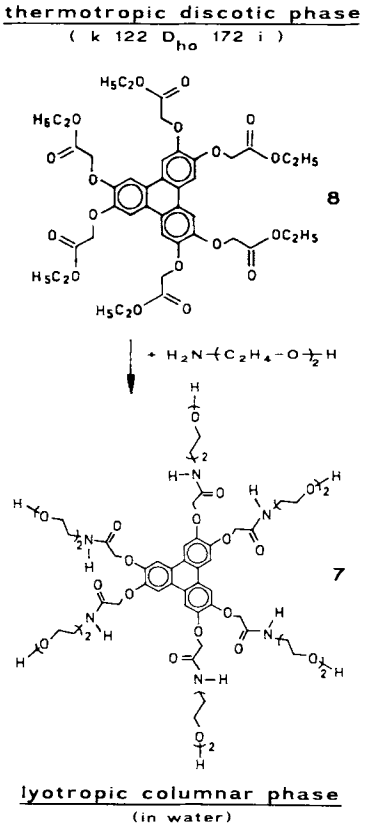

Fig. 12. Transformation of a thermotropic discotic mesogen to a multipolar amphiphile [47] (k = crystalline). Distances between the columns in the thermotropic phase (cf. Fig. 5C) at 140 °C, 19.2 Å; in the aqueous lyotropic phase (cf. Fig. 8) at 20 °C and 60 wt%, 28 Å.

3.3. Amphotropic Systems—All-round Compounds

In lyotropic mesophases, the combination of order and mobility can be achieved by using a solvent. The formation of thermotropic liquid-crystalline phases is based on the temperature-induced mobility of form-anisotropic molecules in the melt.

Amphotropic molecules (Greek: ampho = both, in two ways; trepein = align, direct) are compounds which can be organized according to at least two different principles owing to their structural properties. Figure 13 illustrates this using an example from the field of liquid crystals.

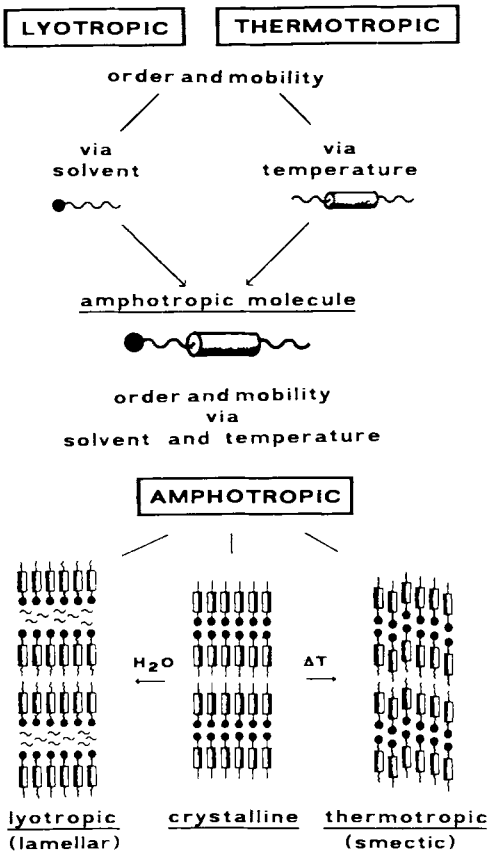

Fig. 13. Schematic representation of an amphotropic system.

Although the term amphotropic liquid crystal has not been used so far, there are many examples of amphotropic behavior:[39b, 43a, 48] some phospholipids,[48a] alkylated monosaccharides,[48b, c] and amphiphilic metal salts[39b, 48d] not only form lyotropic but also thermotropic mesophases. As regards their molecular structure, these molecules are normal amphiphiles. However, they reveal amphotropic behavior.

The range of amphotropic compounds can be considerably increased by the additional incorporation of typical thermotropic liquid-crystal building blocks (rod- or disc-shaped) into amphiphiles. *Kunitake* et al. have investigated a large number of amphiphilic substances which contain rod-shaped mesogens in the hydrophobic chains (e.g., biphenyl, azobenzene, diphenylazomethine moieties).[48e] Apart from various ordered structures in the aqueous phase, thermotropic liquid-crystalline behavior was observed for some of these compounds. Moreover, some polymers also show amphotropic properties.[43a, 48f, g, h] For example, it is possible to organize modified hydroxycellulose derivatives[48f, g] and various polyisocyanates,[48h] not only lyotropically, but also thermotropically.

As for amphotropic molecules, promising perspectives turn up in the field of Langmuir-Blodgett (LB) multilayers.[49, 50] A large number of possible technical applications of these ordered layer systems are nowadays a focal point of discussion. They could be used, for example, as electron beam resists[51] and photoresists,[52] in nonlinear optics (NLO),[53] in the field of reversible information storage,[54] and in the development of bio- and immunosensors.[55, 82]

LB multilayers show—owing to the stepwise transfer mechanism—a well-defined layer structure in the vertical direction. However, within each individual layer, the amphiphiles form two-dimensional lattices with a distinct domain structure (Fig. 14).

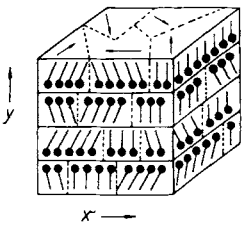

Fig. 14. Structure of LB multilayers: perfectly ordered layers in vertical direction y; irregular domain structure in horizontal direction x.

The crystalline packing of the molecules in the individual layers and the related severe limitation of the molecular mobility have so far not allowed a subsequent, specific manipulation of the molecular order. It has not yet been possible to obtain homogeneous, domain-free (i.e., uniformly oriented) lipid layers. Indeed, it is possible to induce a slight mobility of the molecules and thus a minute change in orientation by heating the multilayers within a certain temperature range. The melting of the layers, however, usually leads to the irreversible collapse of order.[56] On the one hand, amphotropic molecules are amphiphiles, i.e., capable of building up LB multilayers. On the other hand, they are thermotropic liquid crystals owing to the incorporation of mesogenic building blocks. Thus, amphotropic molecules could be used as an approach to introduce mobility within the individual layers, necessary for the subsequent manipulation process. The orientation of the molecules in the individual layers could then, for example, be carried out by means of electric or magnetic fields (Fig. 15).

Mesogen-containing amphiphiles have already been investigated in multilayers.[57] The example discussed here demonstrates that it is indeed possible to introduce thermal mobility in multilayers by using amphotropic molecules. The polymeric malonate **9** contains azobenzene

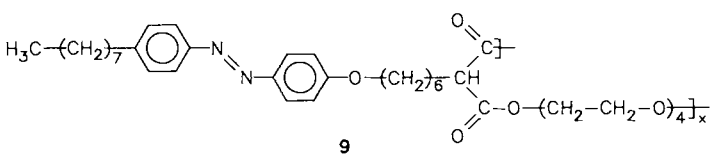

9

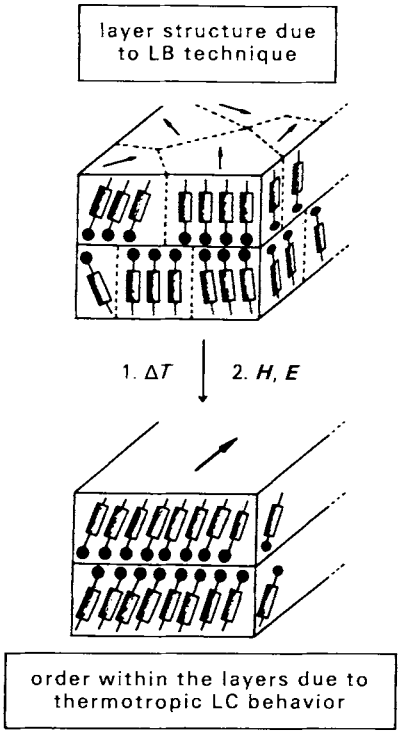

Fig. 15. LB multilayers made from amphotropic molecules: orientation within the layers by electric (*E*) or magnetic (*H*) fields in the mobile LC phase.

moieties as mesogens and an ethylene glycol main chain as the hydrophilic part.[58] In bulk, the polyester **9** is liquid crystalline (g - 275 55i). At the gas/water interface it forms a solid-analogous monolayer, which can be transferred onto solid substrates by means of the LB technique. The organization of the layers has been demonstrated by using small angle X-ray scattering (Fig. 16).

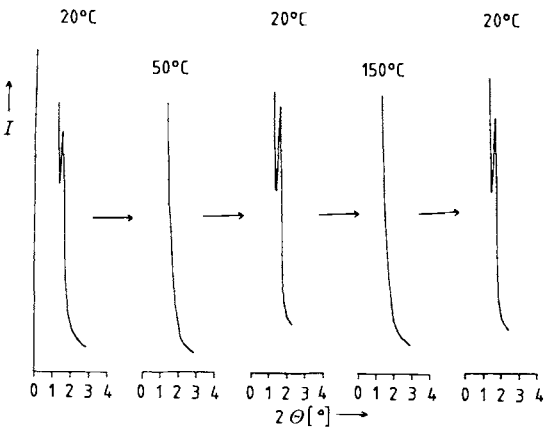

Fig. 16. Temperature-dependent small angle X-ray scattering of 30 layers of the polymer **9** on a polyethylene-therephthalate support: layer structure reappears at 20°C after melting above 50°C.

If the temperature is increased to about 50°C, the scattering reflex in the X-ray diagram disappears. The multilayer melts and the highly ordered structure is lost. It is decisive, however, that the capacity to reorientate is maintained: after cooling to 20°C, the scattering reflex reappears with its original intensity. Even after heating to 150°C, the multilayer structure reassembles at room temperature. The incorporation of mesogenic building blocks into the amphiphilic system and their fixation to the polymer seems to prevent a direct isotropic melting. Although the layer correlation is lost, the parallel alignment of the polymer-fixed mesogenic amphiphiles is maintained (cf. Fig. 13).

The field of molecular engineering of thermotropic and lyotropic liquid crystals is broad. The search for compounds capable of self-organization and formation of specific supramolecular structures will lead to numerous new classes of substances. The first examples have already been described.[48d, 59]

One compound that is capable of self-organization in manifold ways—and thus amphotropic—is the cholesterol derivative **10**. Its different possibilities of orientation are described in Figure 17.[60]

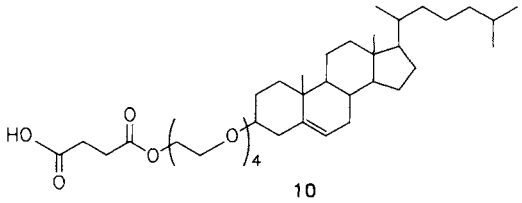

Owing to its form-anisotropy, this compound forms a thermotropic mesophase of the type "bilayer smectic S_A" between −28°C and 113°C (g −28 S_A 113 i). If it is slowly cooled, the substance solidifies at −28°C in the form of an anisotropic glass which does not crystallize even after a long period of annealing.

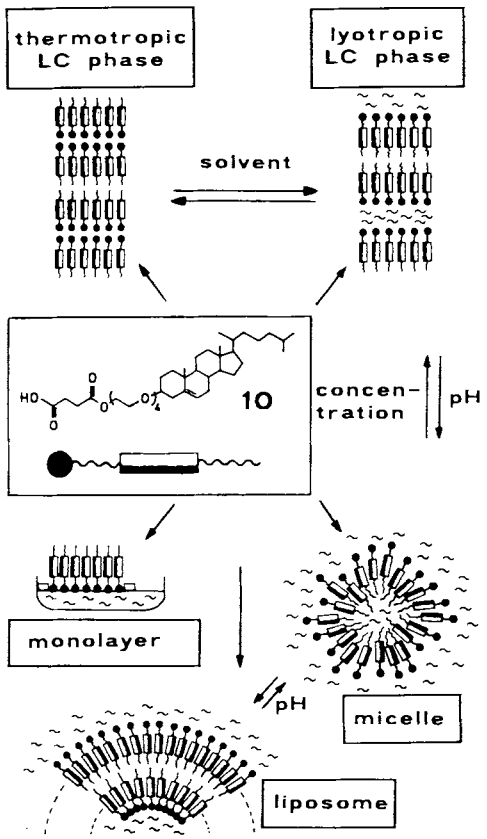

Fig. 17. Example of an amphotropic system: various ways of self-organization of the cholesterol derivative **10** [60].

Since the cholesterol derivative **10** is also an amphiphile, it can form numerous supramolecular structures in aqueous media: lyotropic LC phases, liposomes, micelles, and ordered monolayers. A lyotropic lamellar phase can be obtained by swelling in water or even in absolute diethylene glycol. In both media, spherically closed lipid bilayers (liposomes) develop spontaneously from the lamellar phase after further dilution. The formation of liposomes was demonstrated by means of entrapment of a water-soluble fluorescent marker as well as by phase contrast and electron microscopy. In addition, pH variations lead to the reversible formation of micelles. With a value of 1.6×10^{-3} mol L^{-1} (pH = 9.3), its CMC is in the range of normal surfactants. Drying of the aqueous aggregates leads back to the thermotropic liquid crystal.

As vesicle-forming molecules, ethylene oxide cholesterol derivatives[60,61] possess an atypical structure, since the hydrophobic portion of bilayer-forming lipids usually consists of fatty acid chains. The molecular architecture of these "normal" lipids will be dealt with in greater detail in the next section.

3.4. Lipids as Bilayer-Forming Amphiphiles

Whereas the micelle-forming amphiphiles discussed in Section 3.2 still show a rather high solubility in water (CMC about 10^{-3} mol L^{-1}), it is a lot lower for membrane-forming lipids (CMC about 10^{-8} mol L^{-1}). Lipid molecules, i.e., double-chain amphiphiles, are the basic building blocks of all biological membranes.[62,63] Their self-organization in water is the result of the hydrophobic effect,[64] as is the case with surfactants, and depends also on the relative proportion of hydrophobicity and hydrophilicity of the lipid, as well as on its geometry.[42]

The phase diagram of a mixture of water with a typical lecithin lipid such as dipalmitoylphosphatidylcholine (DPPC) features the lipid bilayer as the basic structure over a very broad temperature and concentration range.[65] Depending on the water content, homogeneous, smectic phases of parallel lipid bilayers (lyotropic phases) and heterogeneous dispersions of multilamellar or single-walled liposomes can be observed. For low water content and high temperature, other lyotropic liquid-crystalline phases exist, such as the hexagonal, the cubic, and the ribbon phase.

In accordance with the importance of lipids for the formation of biomembranes, Nature is equipped with a wide range of possibilities in order to vary the molecular architecture of its membrane-forming amphiphiles (Scheme 1). Most of the natural lipids are zwitterionic (e.g., lecithin **11a** or ethanolamine **11b**) or negatively charged (e.g., phosphatidic acid **11c** or phosphatidylserine **11d**). There are also uncharged lipid structures found in Nature (e.g., glycolipids[66] such as **12a**). Not only the head-group structure but also the hydrophobic region is varied to a large extent. Depending on whether rigid or fluid membranes are needed, either saturated or unsaturated fatty acid chains are incorporated, respectively. Hydrogen bonds between the head groups, as, for example, in the case of sphingolipids (e.g., **12**), lead to an additional stabilization of the membrane.[67]

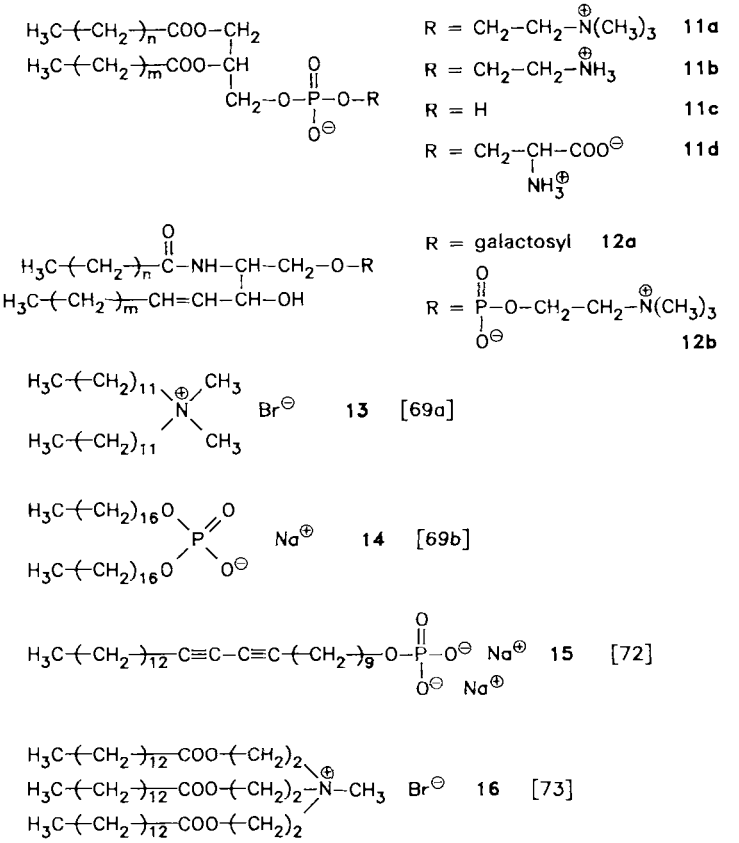

Scheme 1. Examples of natural and synthetic bilayer-forming amphiphiles.

Many of the lipids occurring in Nature have been synthesized.[68] In 1977, *Kunitake* et al. described fully synthetic amphiphiles having simple structures, which, just like natural lipids, are capable of forming bilayer membranes. Typical examples are the quaternary ammonium salts (e.g., **13**) and dialkyl phosphates (e.g., **14**) with two long chains.[69] The idea that even such simple amphiphilic structures can form bilayer membranes soon resulted in a large arsenal of artificial membrane-forming lipids.[70] These also include chiral compounds,[71] as they usually occur in Nature. Apart from the double-chain "classical" lipids discussed so far, synthetic bilayer-forming amphiphiles with only one (e.g., **15**[72]) or three (e.g., **16**[73]) hydrophobic alkyl chains also exist. Furthermore, there are membrane-spanning lipids; some of these bipolar amphiphiles will be presented in Section 4.7.

4. Stabilization and Surface Variation of Model Membranes

4.1. The Architecture of Biomembranes[74,75]

A decisive step in the development of the early forms of life was the self-organization of amphiphiles to form plasma membranes. It is unknown which principles led to the formation of macromolecules from purines, pyrimidines, or amino acids, but their self-replication would not have been possible without the protective shell of the lipid membrane. The cell membrane plays an important role in all essential biological phenomena. These include prob-

lems related to biological transport, energy metabolism, cell division, and macromolecular synthesis. The cell surface, in particular, is of significant importance as regards many aspects of cell biology, immunology, and cell-cell interaction as well as cell differentiation and the transformation of normal cells into malignant ones.

The biomembrane can be divided into three layers that are connected with one another: glycocalix, protein-lipid bilayer, and cytoskeleton (Fig. 18). The middle, protein-containing lipid bilayer is the component which indeed separates the cell into compartments.[76] Furthermore, it functions as an active filter and participates in motion and transport processes.

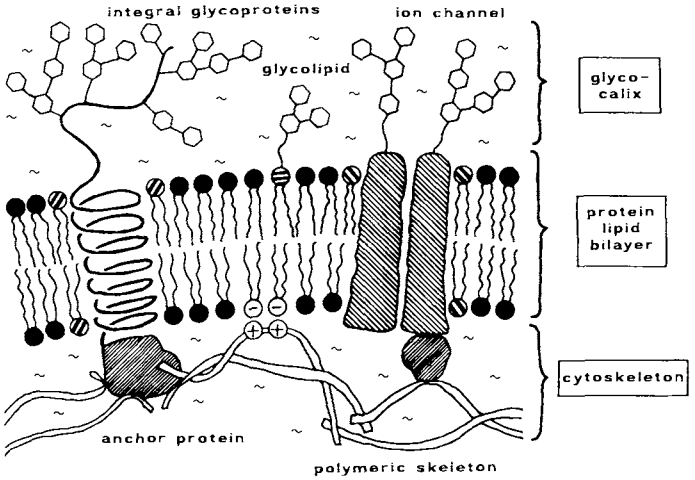

Fig. 18. Schematic representation of a biomembrane. The three layers are the glycocalix, the protein-lipid bilayer, and the cytoskeleton.

Outside, the phospholipid membrane is coated by a carbohydrate-rich layer, the glycocalix. It mainly consists of the oligosaccharide head groups of the glycoproteins and glycolipids, which are usually incorporated into the membrane. The glycocalix determines the surface recognition of cells: the oligosaccharide side chains, for example, are antigenic determinants in reactions of the immune system (see Section 5). In the case of plant cells, the glycocalix usually occurs as a solid, closed cell wall, in which the sugar groups (polysaccharides) additionally act as a skeleton (see Section 4.8.1). In the case of bacteria, the polysaccharide chains are cross-linked by oligopeptide chains. Thus, they form an extremely stable murein coat which represents one single macromolecule.

In animal cells, the stabilization of the cell membrane is mainly achieved by the cytoskeleton, which is linked to the inner side of the central lipid bilayer (see Section 4.8.2). From the point of view of polymer science, the cytoskeleton, in particular, as a polymeric network, represents an ideal basis for simulation experiments: reversible cross-linking, fixing of networks to membranes, dynamical processes in gels—these are all processes the cell constantly carries out in manifold ways.

To get a deeper insight into the structure-function relationships of biomembranes, a large number of bioorganic investigations are necessary. This is therefore an attractive and broad field of activity for synthetic chemists. However, natural membranes show a high complexity. Thus, in order to study the properties of individual membrane components, it is necessary to concentrate, at first, on simple model membranes having a defined chemical composition.

4.2. Model Membranes as Supramolecular Systems

In order to study the structure-property relationships of individual membrane components (lipids or proteins) at a supramolecular level, one has to rely on model membranes. On the one hand, they can provide information about the physical properties of membranes that only consist of lipids (pure or in mixture). On the other hand, in reconstitution experiments, membrane proteins can be incorporated into a physically and chemically defined surrounding. Then, the activity of the individual membrane proteins can be studied. Figure 19 gives a survey of the commonly used model membrane systems.

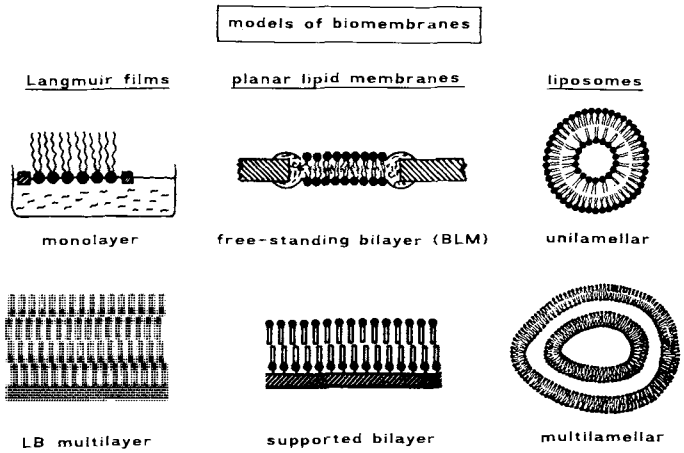

Fig. 19. Commonly used model membranes.

The spreading of a lipid at a gas/water interface leads to the formation of monolayers.[49c, 77] Formally, they represent only one-half of the lipid bilayer of a cell membrane. Thus, the monomolecular films—compared with other model membranes—seem to be the least similar to biomembranes. Nevertheless, investigations of monolayers supply precise information about the molecular packing and orientation of amphiphiles which cannot be gained from other model membranes. With the help of a film balance, monomolecular films can be characterized in the form of surface pressure-area diagrams (isotherms). This is a very sensitive method which responds to the slightest change in the structure of lipids. By means of isotherms, it is possible to gain information not only as to the orientation behavior of amphiphiles, their mobility in membranes, but also as regards the interactions with substances dissolved in the subphase (e.g., proteins; see Sections 5.2 and 5.3). Furthermore, by using a fluorescence microscope, phase-separation processes within the monolayer can be visualized.[78]

Highly ordered, ultrathin Langmuir-Blodgett (LB) films are obtained by transferring monolayers onto solid substrates.[49, 50, 79] As model membranes, multilayers are less

interesting. They seem to be technically more important as functional ultrathin films (see Section 3.3).

Planar lipid bilayers resemble much more the structure of biological membranes. They can be prepared either as free-standing black lipid membranes or as supported planar membranes. Black lipid membranes (BLMs)[80] are lipid bilayers which span a hole in a separating wall between two aqueous compartments. That is why they are ideal to carry out electrical measurements from which conclusions can be drawn as regards membrane capacity, thickness, and resistance. Thus, they are often used to study transport processes (e.g., of ions) through lipid membranes.[81] Supported planar membranes permit the use of measuring methods that cannot be applied to other model membranes.[82] If, for instance, such a planar membrane is fixed on a quartz substrate, one can detect fluorescence probes by means of TIRF spectroscopy (TIRF: total internal reflection fluorescence) only when they are close to the surface of the lipid bilayer. Therefore, such supported membranes are especially suitable for the investigation of surface recognition reactions.[82, 83, 163b]

Liposomes (vesicles)[84] are spherically closed lipid bilayers, which, in analogy to the cell membrane, enclose an aqueous compartment. Vesicles can be prepared by numerous methods,[84h, 85] which lead to the formation of completely different vesicle systems. These differ in diameter (between 20 nm and 100 μm) as well as in the number of bilayers. The sonication of lipid suspensions in water, for example, leads to small unilamellar vesicles (SUV, 20–100 nm). The swelling of lipid films, however, leads to uni- or multilamellar vesicles of the size of a cell. Liposomes are suitable for a large number of biophysical and biochemical investigations: e.g., for the measurement of membrane permeability,[84a] for the reconstitution of active membrane proteins,[86] and for the study of surface recognition reactions[84d, e] or dynamic membrane processes.[155] Furthermore, the possible use of liposomes as drug carriers is also being discussed.[87, 144a]

The five following sections (Sections 4.3 to 4.8) mainly deal with liposomes as model membranes. Apart from their surface variations, strategies for the preparation of polymerized liposomes are also discussed. On the one hand, these attempts should lead to more stable model membranes; on the other hand, they should help to simulate the stabilizing elements of the biomembrane.

4.3. Surface Variation of Model Membranes

In addition to direct variations of the membrane components, chemical surface variations of the cell membrane also play an important role in Nature: the generation of asymmetrical membranes or variations of the glycocalix are important examples. In model membranes, the molecular architecture of lipids can subsequently be varied within the supramolecular structure by means of chemical reactions. Such reactions in ordered systems are of interest because the highly organized lipid matrix represents a medium to control them. Differences in the course of these reactions, compared with the ones in isotropic solution, are caused by the orientation or the local concentration of the molecules involved.[88] Such reactions can be regarded not only as models for the transformation of lipids within biomembranes, but also, more generally, as models of enzymatic catalysis.[89] If vesicles are used as model membranes, a separation into different reaction sites[70e] (entrapped volume, hydrophobic interior of the membrane, membrane surface, aqueous outer volume), i.e., a spatial division of reaction partners, has to be considered. Thus, vesicles have been used, for example, to study artificial photosynthetic processes.[90] Moreover, the formation of spherically closed lipid bilayers by using reactive lipid molecules allows reactions to be carried out with water-soluble agents located only at the outer membrane surface. Thus, vesicle membranes with an asymmetrical distribution of head groups can be prepared.[70c, 90a] In the following examples, some reactions taking place at the surface of ordered membranes are illustrated.

The transformation of a negatively charged membrane surface to a positively charged one, under mild conditions, has been investigated in monolayers.[91] The maleic acid monoamide **17** with a carboxylic acid head group was used as an anionic reactive lipid. Under acidic conditions, the *cis* carboxyl group of **17** catalyzes the intramolecular hydrolysis of the amide bond.[92] In the course of this process, the dioctadecylammonium ion is formed. In order to observe the cleavage process, **17** was spread onto an acidic subphase. The isotherms of the acid, as well as that of the ammonium salt formed by the cleavage of the amide bond, are shown in Figure 20.

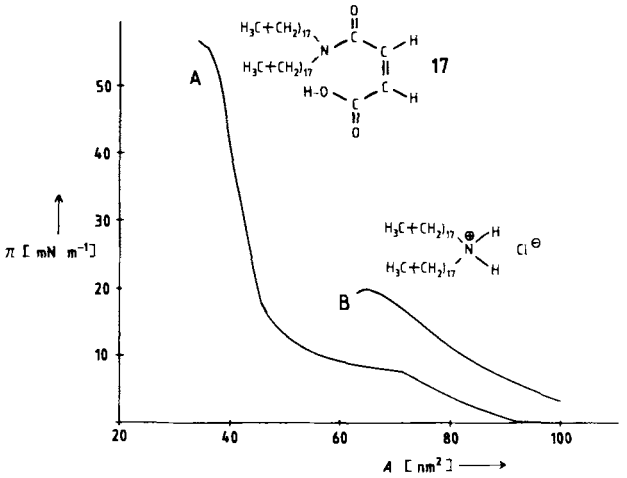

Fig. 20. Variation of the head-group charge in a monolayer [91]. A) Isotherm of the maleic acid amide **17** ($T = 31$ °C, pH of the subphase = 2). B) Isotherm of a monolayer from the amide **17** after head-group cleavage with the formation of the corresonding ammonium salt. The cleavage was achieved by leaving the film for 14 h at 0 mN m^{-1} and 31 °C on the acidic subphase (pH = 2). π = surface pressure, A = area per molecule.

Apart from a liquid-analogous phase, **17** also features a solid-analogous phase (curve A). In contrast, the isotherm of the product, the ammonium salt, shows only a liquid-analogous film (curve B). This behavior is in good agreement with the isotherm of a reference sample of dioctadecylamine. The formation of this amine in the monolayer was also demonstrated by means of thin layer chromatography and by mass spectrometry. The intramolecular

cleavage of the head group of this compound depends on its structure; it does not take place in the case of the analogous succinic acid monoamide of dioctadecylamine.

The variation of membrane properties can also be achieved photochemically;[93,94] some examples are summarized in Figure 21. The alteration of the membrane per-

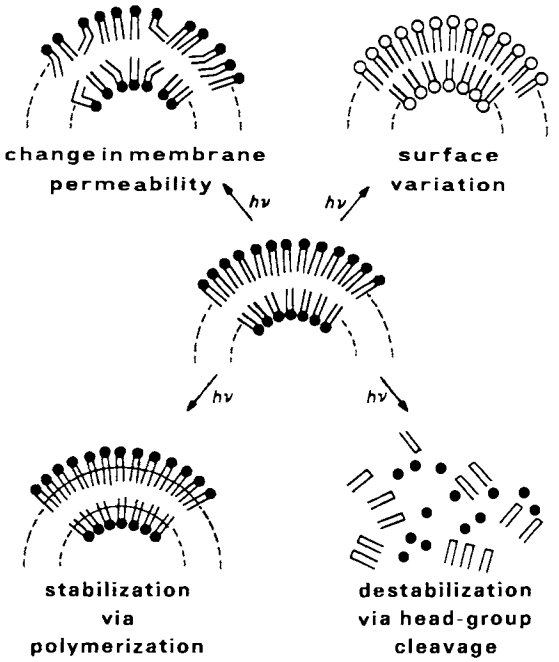

Fig. 21. Possibilities for the photochemical variation of membrane properties.

meability by means of the photochemical *cis-trans* isomerization of amphiphilic dyes has already been described.[94] The stabilization of model membranes via photochemically initiated polymerization reactions will be described in Section 4.5.1.

The photochemical variation and destabilization of the surface of monolayers and liposomes has been investigated by using lipids containing a zwitterionic photoreactive *N*-(1-pyridinio)amidate head group[95] (e.g., **18**).

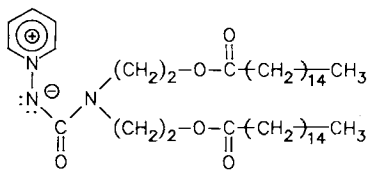

18

Upon UV irradiation, these ylides can undergo ring expansion to give the isomeric 1,2-diazepines, or their head group can be cleaved, thus forming pyridine and an intermediary nitrene.[96] In liposomes composed of **18**, the photoreaction leads to the formation of 1,2-diazepine in high yield (Fig. 22).

Although the hydrophilicity of the diazepine formed in the head group is rather low, the vesicles neither aggregate nor precipitate during the photoreaction. However, these diazepine liposomes are metastable and can therefore be destroyed by mechanical stress such as shearing forces. A

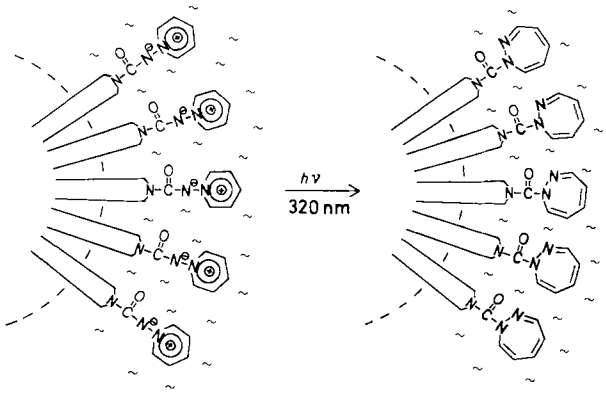

Fig. 22. Photochemical reaction of *N*-(1-pyridinio)amidate head groups forming diazepines in liposomal membranes: reduction of the head-group hydrophilicity [95].

subsequent reformation of vesicles from the isolated photoproduct is not possible. Thus, vesicle membranes composed of molecules that are not able to form such supramolecular systems by themselves can be generated by means of photochemical variation within the supramolecular system.

In a different photoreaction, lipid **19** is destroyed upon photolysis of its quaternary benzylammonium head group.[97] UV irradiation of **19** in monolayers and lipo-

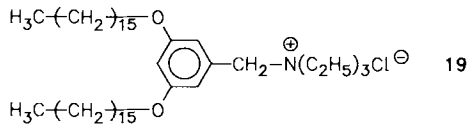

19

somes mainly leads to the formation of the corresponding toluene derivative.[93a] The ordered membranes then collapse and form crystals (Fig. 23).

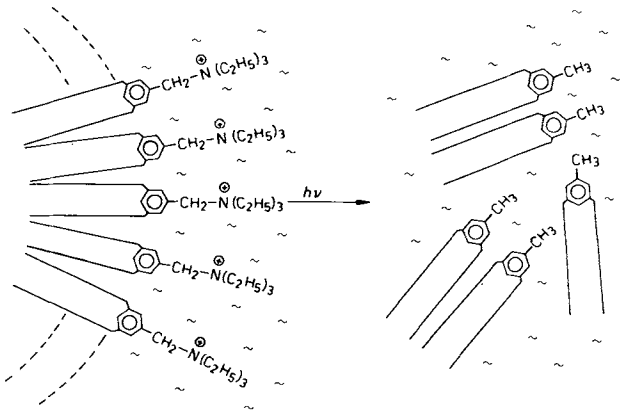

Fig. 23. Photochemical destruction of liposomes made from benzylammonium lipids [93a].

This process has also been studied in giant liposomes by means of phase contrast microscopy.[93a] Upon extended irradiation (about 40 s) the formation of crystallites is observed. A short irradiation (about 2 s), which does not result in a quantitative conversion of the reactive head groups, leads to the detachment of small liposomes from the larger ones. This process will again be dealt with briefly in Section 6.2 (Fig. 61).

4.4. Strategies for the Stabilization of Model Membranes

In the last few years, numerous methods to stabilize model membranes have been developed, mainly by using polymeric systems. A survey of the possible molecular architectures of stabilized liposomes is given in Figure 24.

The polymerization of lipids before or after their orientation in model membranes has been studied most intensively (see Section 4.5). As an alternative, the polycondensation of lipid molecules has also been described (see Section 4.6). Apart from such covalent binding reactions of lipid molecules, other possibilities to stabilize lipid bilayers are based on the noncovalent binding of polymers to the membrane surface (see Section 4.8). One method to achieve stabilization without using polymers involves the incorporation of membrane-spanning lipids into the bilayer (see Section 4.7).

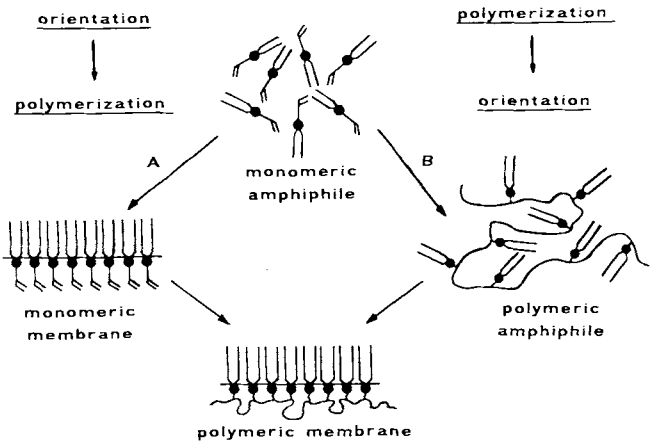

Fig. 25. Strategies for the preparation of polymeric model membranes. A) Orientation of the monomers in model membranes with subsequent polymerization. B) Polymerization of the monomers in isotropic solution and subsequent orientation of the polymeric amphiphiles.

4.5. Ordered Membranes from Monomeric and Prepolymerized Amphiphiles

Two approaches, schematically shown in Figure 25, have been used to prepare ordered polymeric model membranes. On the one hand, polymerizable amphiphiles can be used to build up monomeric model membranes, which can then be converted into polymeric ones (approach A). On the other hand, the use of oligomeric amphiphiles or the incorporation of spacer groups into the polymeric amphiphile to decouple the disordered polymer chain from the ordered membrane allows the formation of membranes from prepolymerized amphiphiles (approach B).[98]

4.5.1. Polymerizable Lipids

The polymerization behavior of amphiphiles with polymerizable units was first studied in monomolecular films.[99] In 1979, the formation of polymerized vesicles by using a lipid containing butadiyne units was mentioned for the first time.[100] In the meantime, many polymerizable groups have been incorporated into various lipid structures (see Scheme 2) to prepare polymerized liposomes.

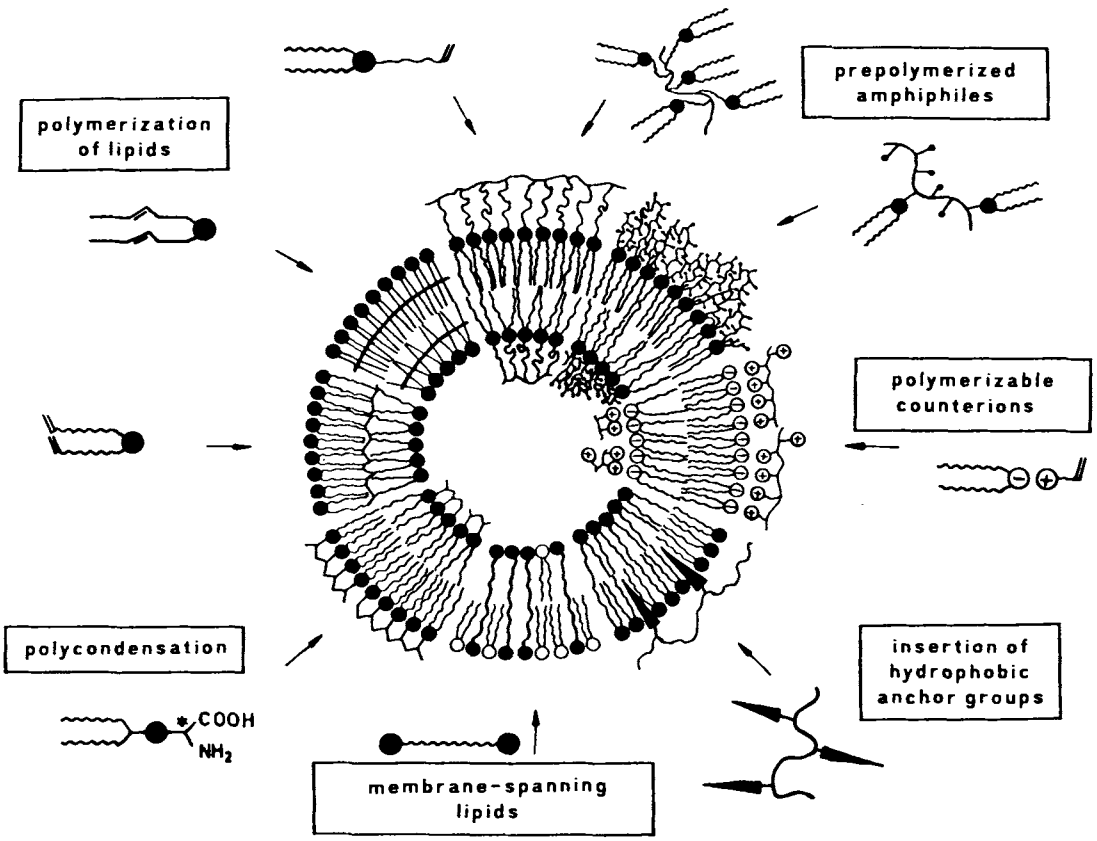

Fig. 24. Strategies for the stabilization of lipid bilayer membranes.

Scheme 3 shows only a few characteristic examples from the large number of polymerizable lipids.

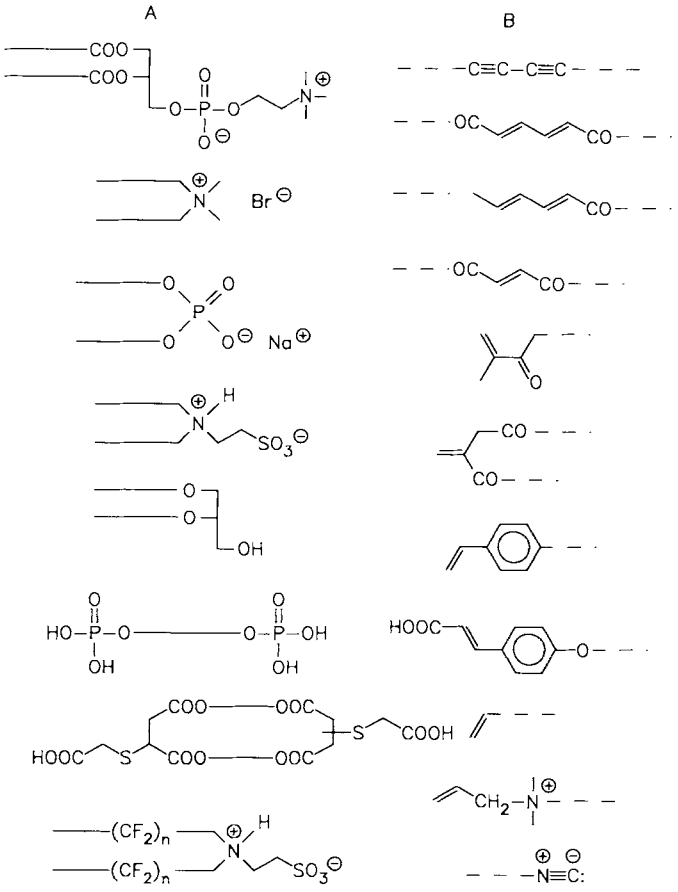

Scheme 2. Building blocks of polymerizable lipids: A) lipid structures; B) polymerizable groups.

The game of structural variations of polymerizable amphiphiles (lipids, surfactants) and their use in monolayers, liposomes, and multilayers have enriched the monomeric and polymeric landscape and given rise to new hopes. These compounds and their perspectives of application will not be discussed further, since quite a few reviews on that topic already exist.[114]

4.5.2. *Model Membranes from Prepolymerized Amphiphiles*

A more recent concept for the preparation of polymeric membranes is based on the use of amphiphiles which have already been polymerized. At first sight, it seems surprising that this approach was taken much later than that via monomers. The problem with prepolymerized amphiphiles is the two-dimensional orientation of a three-dimensional polymer coil: An individual, motile molecule can easily be incorporated into a membrane. For a polymer-fixed molecule, however, its incorporation as a cooperative process is more complicated. Two different pathways can be followed to organize the membrane-forming alkyl chains of a polymer into ordered mono- or bilayers, despite the unordered structure of the polymer chain. On the one hand, polymers with low degrees of polymerization can be used. On the other hand, the incorporation of flexible spacers allows the decoupling of the different motion and organization processes taking place between the alkyl chains and the polymer main chain. Nature commonly uses the spacer concept, especially when functional groups with high mobility have to be kept close together. Already used for pharmacologically active polymers,[115] a similar concept has also been applied to the synthesis of liquid-crystalline polymers.[28,29] As regards polymeric amphiphiles, there exist three different possibilities as to the incorporation of a spacer group (Fig. 26).[116]

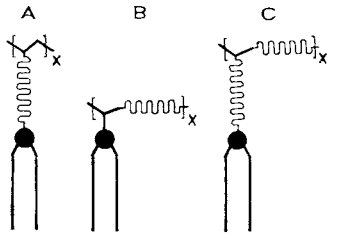

Fig. 26. Three possible ways to introduce hydrophilic spacer groups into polymeric amphiphiles [116a]: A) side-group spacer; B) main-chain spacer; C) main-chain and side-group spacer.

Homopolymers with side-group spacers (A) have been synthesized from lipids containing a hydrophilic spacer group between the membrane-forming amphiphilic part and the polymerizable unit. By means of copolymerization of simple lipids with hydrophilic comonomers, amphiphilic copolymers with main-chain spacers (B) can be prepared. The combination of both spacer types (C) can be realized by the copolymerization of spacer-containing lipids with hydrophilic comonomers.[116] The formation of polymeric model membranes by using such amphiphilic spacer-containing copolymers is illustrated in Figure 27.

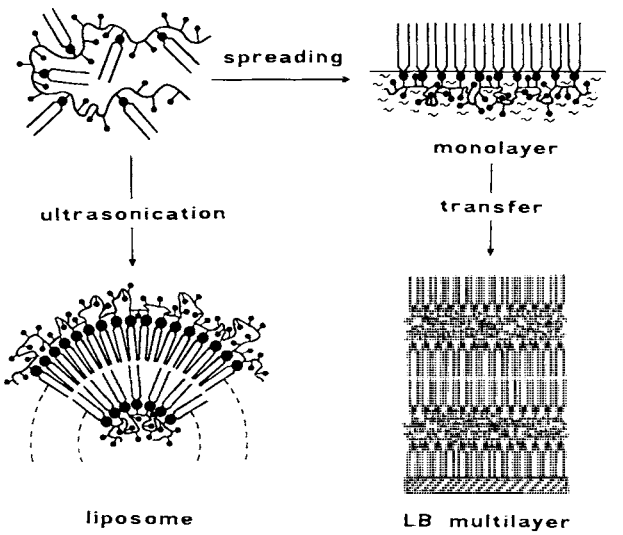

Fig. 27. Preparation of polymeric model membranes from copolymers containing hydrophilic comonomers.

The preparation of vesicles from prepolymerized lipids has so far only been described for homopolymers with

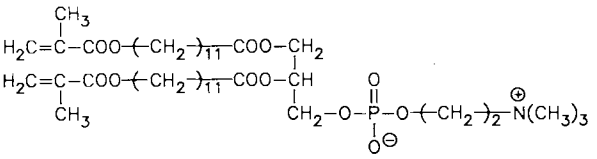

20 [101]

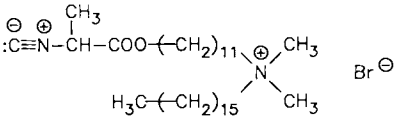

21 [102]

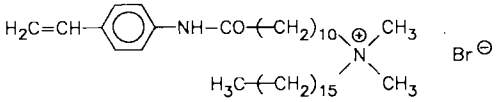

22 [103]

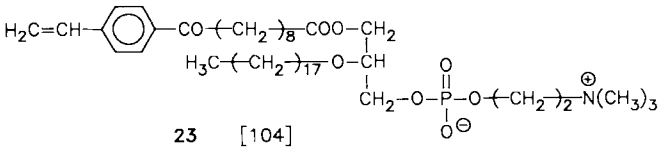

23 [104]

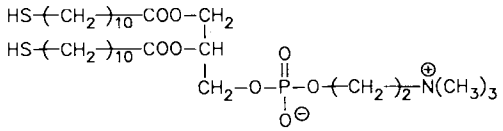

24 [105]

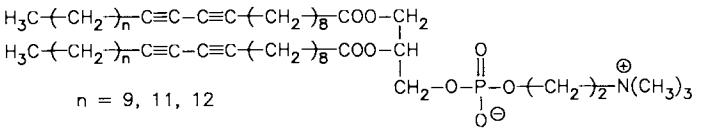

25 [72,106]

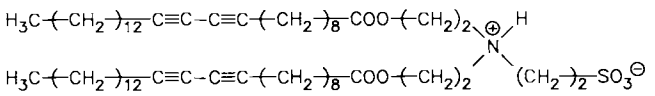

26 [106a,107]

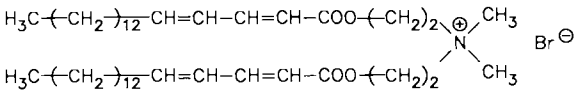

27 [72,108]

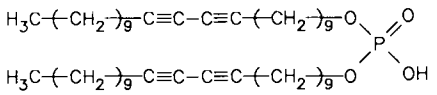

28 [106e, f]

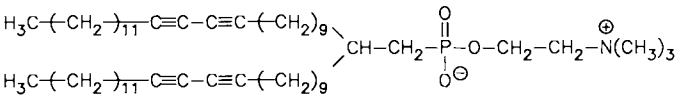

29 [109]

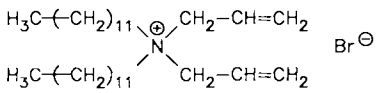

30 [110]

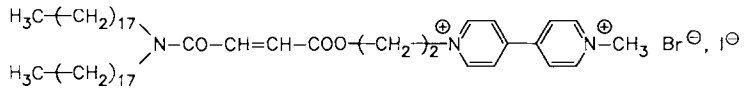

31 [111]

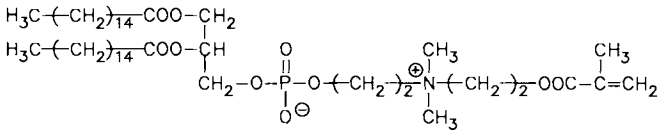

32 [112]

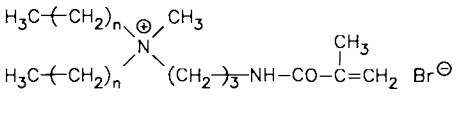

n = 15, 17

33 [113]

Scheme 3. Typical examples of liposome-forming polymerizable lipids.

side-group spacers (type A, Fig. 26).[98] In addition, the self-organization of a polyionene as a vesicle membrane has also been discussed.[98a]

Fendler et al. described the copolymerization of maleic acid derivatives (e.g., **31**) with isotropically dissolved acrylonitrile as comonomer.[90a, 111] This kind of copolymerization also leads to the formation of polymers with main-chain spacers.

It is possible to prepare and investigate highly ordered stable monolayers by spreading the prepolymerized lipids (Fig. 27). They can also be used for the preparation of polymeric LB films via transfer onto solid substrates according to the LB technique.[116–119]

Scheme 4 shows some of the monomers from which amphiphilic homo- and copolymers with main-chain, side-group, or combined spacers have been synthesized. A fur-

ther interesting system consists of alternating copolymers made from maleic anhydride (e.g., with long-chain vinyl ethers or olefins), which have been investigated, in particular, by *Hodge* et al.[119]

A

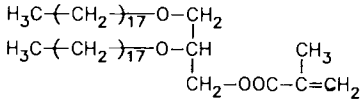

34 [116a]

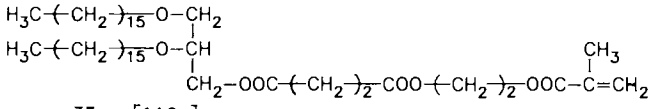

35 [116a]

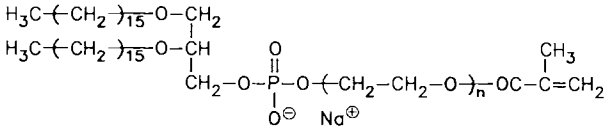

n = 1: **36a** [116a]
n = 4: **36b** [98b]

B

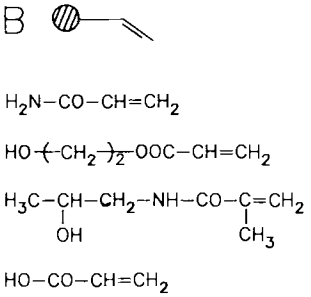

Scheme 4. A) Polymerizable lipids; B) hydrophilic comonomers for the synthesis of spacer-containing amphiphilic copolymers.

The necessity of introducing a decoupling spacer becomes obvious when looking at the isotherms of the monomeric and polymerized spacer-free lipid **34** (Fig. 28). The

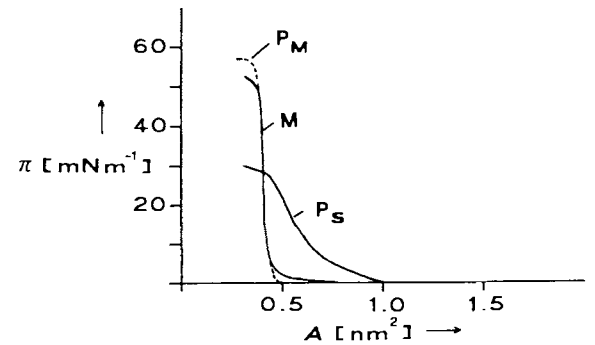

Fig. 28. Comparison of the isotherms of the spacer-free monomeric lipid **34** with its polymers [116a]. M) Monomeric lipid forms a highly ordered monolayer with a solid-analogous phase. P_M) Polymerization in the ordered monolayer leads to a slightly increased stability of the solid-analogous phase. P_S) Upon spreading of the polymer after polymerization in isotropic solution, only a liquid-analogous phase is formed. π = surface pressure, A = area per molecule.

monomeric lipid **34** forms a stable film with solid-analogous packing (curve M). After polymerization in the ordered monolayer, the isotherm exhibits a similar behavior, showing a slightly increased stability of the film (curve P_M). If, however, this spacer-free lipid is polymerized in isotropic solution and then spread, it is no longer capable of forming a highly ordered solid-analogous film (curve P_S). Here, an important role should be played by the molecular weight as well as the tacticity:[118c, 120] The isotherm of a lipid polymerized in isotropic solution should show a similar behavior to that of a monomeric lipid when a small degree of polymerization and a high fraction of syndiotactic units are used.

The isotherms in Figure 29 show that it is possible to maintain mobility and orientability of the alkyl side chains of a copolymer with a main-chain spacer. Whereas the monomeric lipid **35** with a short side-group spacer exhibits a liquid- and a solid-analogous phase (Fig. 29A), the corresponding polymer **37**, prepolymerized in solution, can

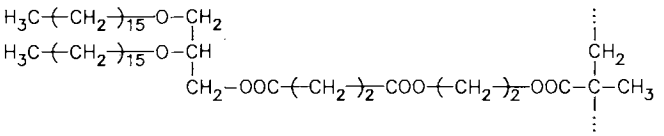

37

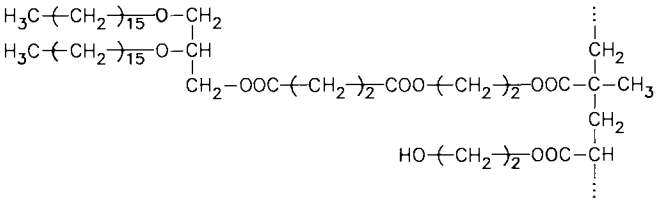

38

only form a solid-analogous phase (Fig. 29B). After the polymerization of the lipid in the head-group region, the mobility of the alkyl chains is extremely hindered. However, it is recovered by incorporating hydrophilic comonomer units. Indeed, the introduction of an equimolar amount of hydroxyethylacrylate as hydrophilic comonomer (**38**) already suffices to give rise to a liquid-analogous phase (Fig. 29C).

In ordered multilayers, the polymerization of amphiphiles[121] usually leads to the formation of defects.[52, 122] An elegant way to avoid defects induced by polymerization is to prepare LB films from prepolymerized amphiphiles. In Figure 30, the example of copolymer **39** illustrates in how far the content of hydrophilic comonomer influences the structure of LB multilayers. By means of small angle X-ray scattering, it has been shown that the spacings between the individual layers increase with increasing comonomer content.[116a] Furthermore, an increased portion of hydroxyethylacrylate allows a higher layer correlation.

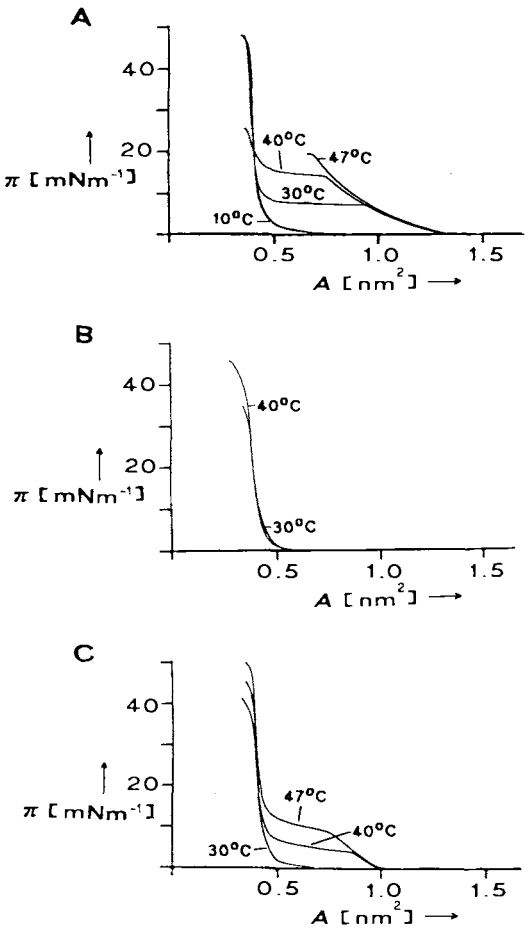

Fig. 29. Isotherms of the monomeric methacrylate **35** and its homo- and copolymers [116a]. A) The monomer **35** with a short side-group spacer forms temperature-dependent liquid- and solid-analogous phases. B) The homopolymeric methacrylate **37** (= $(\mathbf{35})_n$) is only capable of forming solid-analogous phases. C) The statistical 1:1 copolymer **38** from lipid **35** with hydroxyethylacrylate as main-chain spacer forms temperature-dependent liquid- and solid-analogous phases. π = surface pressure, A = area per molecule.

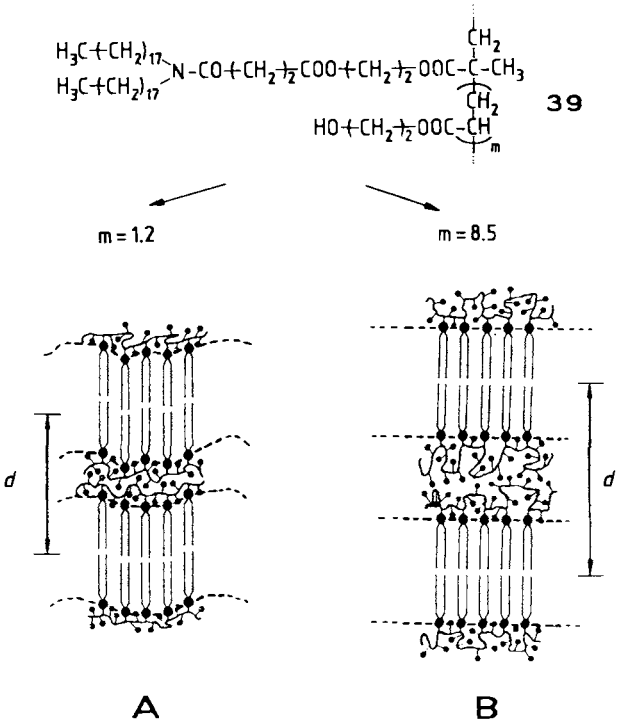

Fig. 30. Multilayers from the amphiphilic copolymer **39**. Schematic representation of the layer thickness d and the layer correlation depending on comonomer contents [116a]. A) Hydroxyethylacrylate content $m = 1.2$ (short hydrophilic main-chain spacer); small distance between layers, poor layer correlation. B) Hydroxyethylacrylate content $m = 8.5$ (long hydrophilic main-chain spacer); larger distance between layers, good layer correlation.

4.6. Polypeptide Liposomes—Bilayers from Polycondensable Lipids

Considering the interest placed in liposomes as drug carrier systems,[87,114a] the idea of building up stabilized but biologically degradable systems looks exciting. The first attempts to prepare biodegradable polymerized liposomes have been described by *Regen* et al. They have used a reversibly polymerizable dimercaptolecithin[105] (cf. lipid **24**, Scheme 3). In this context, polypeptide liposomes seem to be promising.

Up to now, only a few papers exist on polycondensation reactions in ordered systems. The first one was published as early as 1948 by *Katchalsky* et al. It describes the condensation of octadecyl or hexadecyl esters of glycine and alanine in *LB* multilayers.[123] By simply allowing the films to stand, the corresponding polypeptides could be obtained within the films via aminolysis of the esters. In an isotropic solution, no reaction takes place under comparable mild conditions. Thus, the increased reactivity of the amphiphiles in the multilayers is presumably due to their orientation. *Fukuda* et al. later resumed these investigations.[124] Other attempts to achieve a polycondensation in ordered systems are the cross-linking of long-chain urea derivatives with formaldehyde[125] and of glycolipids with epichlorohydrin or divinylsulfone.[126]

The aminolysis of long-chain amino acid esters has also been tried in vesicle membranes. However, the transformation of free amino groups to amide groups leads to a decrease in the hydrophilicity of the lipid head groups to such an extent that the liposomes precipitate.[127] If long-chain Leuchs anhydrides are used for the polycondensation in vesicle membranes, neither educts nor products are capable of forming vesicles. Thus, it is necessary to use mixed membranes with lipids such as the phosphatidylcholine DPPC.[128]

To prepare stable polypeptide liposomes, amino dicarboxylic acid lipids have been introduced by *Neumann* et al.[129] Some examples of polycondensable amino acid and amino dicarboxylic acid lipids are the compounds **40** and **41**–**45**. Liposomes prepared by using the lipids **41**–**45** remain in solution after polycondensation, owing to the additional hydrophilic carboxyl group (Fig. 31).

The lipids **40**–**45** were synthesized by the addition of cysteine or homocysteine to maleic acid derivatives. In water, they form vesicles upon ultrasonication. Furthermore, giant vesicles can be obtained from the glycerine ether derivatives **42**–**45** by means of swelling. The polycondensation of liposomes was achieved by sonicating the lipids **41**–**45** in the presence of a water-soluble carbodiimide at pH = 6.5. The formation of amide bonds, under these conditions, was confirmed by FTIR spectroscopy. Vapor-pressure osmometry reveals that oligopeptides with a mean de-

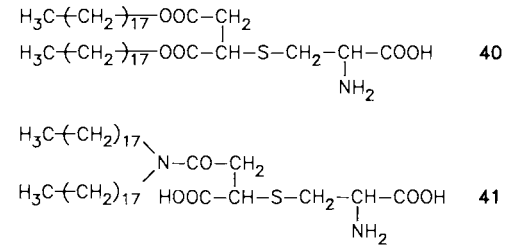

40

41

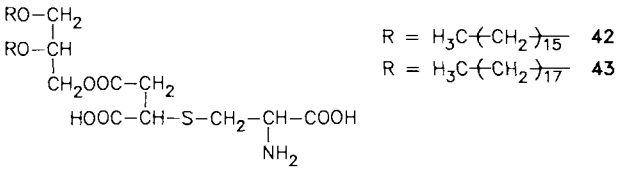

42

43

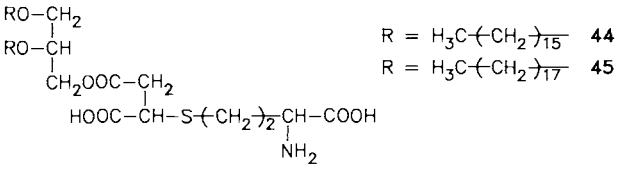

44

45

gree of polymerization of 4 are formed by the polycondensation reaction.

In order to characterize the permeability of the monomeric and oligomeric amino acid vesicles, the release of entrapped markers was measured.[129b] The twofold negatively charged fluorescent dye 6-carboxyfluorescein (6-CF) as well as [^{3}H]glucose were used as markers. The monomeric liposomes feature a remarkably small permeability towards these two markers. By using the relatively bulky, charged 6-CF, for example, less than 0.1% release is measured within 30 h at room temperature. The permeability is remarkably higher after polycondensation; however, it is still rather low: after 30 h, these vesicles lose about 1.5% of 6-CF. The diffusion through the membrane is much faster for the uncharged marker compared with the charged 6-CF. The release behavior of monomeric and polycondensed vesicles from lipid **43** is exemplified in Figure 32.

As a comparison, the release kinetics of distearoylphosphatidylcholine (DSPC) vesicles is also given. This lipid was chosen since, just like the monomeric and condensed amino acid lipids, it is in the gel state at room temperature.

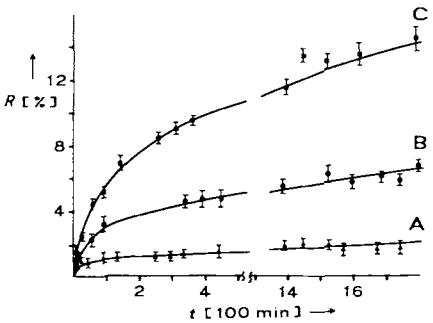

Fig. 32. Release of [^{3}H]glucose from amino acid liposomes (24 °C) [129b]. A) Liposomes made from the monomeric amino acid lipid **43**. B) Peptide liposomes made from the lipid **43**. C) Liposomes made from DSPC.

Figure 32 shows that monomeric amino acid liposomes exhibit a low permeability even when [^{3}H]glucose is used as a marker; their release rate is the lowest found for monomeric vesicles. In this case, too, the permeability is increased by the polycondensation; i.e., the packing density of the lipids is impaired by the oligopeptide formation. Nevertheless, the release rates of polycondensed liposomes are clearly below those of DSPC vesicles.

By means of sonication, isolated oligopeptides can also be used to prepare liposomes, analogously to the use of prepolymerized amphiphiles (see Section 4.5.2). The peptides of the lipids **42**–**45**, together with cholesterol, are even capable of forming giant liposomes.

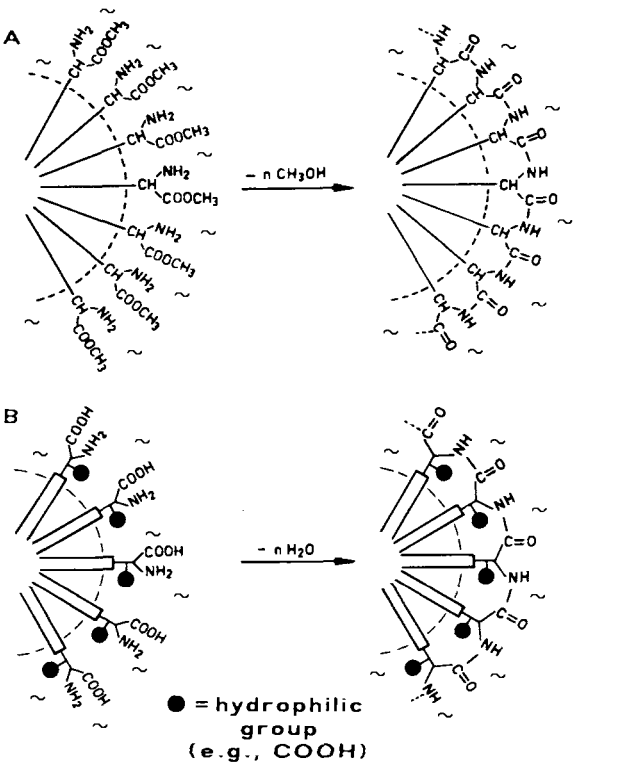

Fig. 31. Formation of peptide liposomes. A) Aminolysis of amino acid esters: reduction of the head-group hydrophilicity leads to the precipitation of liposomes [127]. B) Polycondensation of aminodicarboxylic acids: owing to the additional hydrophilic head group (COOH), such peptide liposomes remain in solution [129].

4.7. Stabilization by Means of Membrane-Spanning, Polymerizable Lipids

In archebacteria Nature offers an interesting example of membranes with high stability. They survive under extreme conditions and are therefore able to fill ecological niches. Thermophilic archebacteria thrive at temperatures up to 110 °C, acidophilic bacteria at pH values around 1, and halophilic ones even in saturated sodium chloride solution. Owing to their adaption to unusual habitats, the membrane components of these microorganisms also exhibit unusual structures.[130] The most important membrane lipid fraction is composed of membrane-spanning bipolar lipids (e.g., **46**). They consist of two isoprenoid diphytanyl (C_{40}) chains which are connected via acid-stable ether linkages to form macrocyclic glycerol tetraethers.

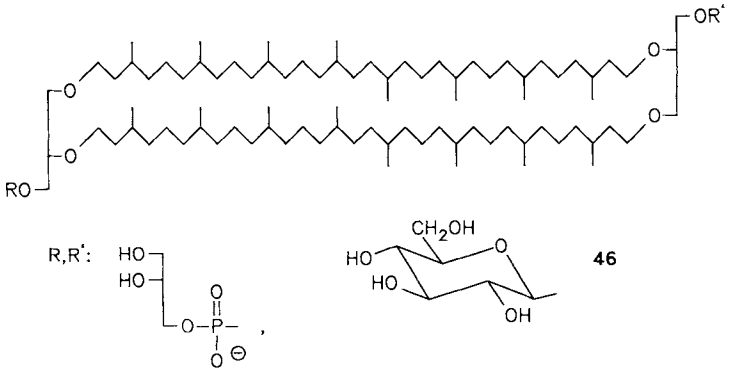

46

An asymmetrical structure of the bacterial membrane can be achieved with macrocycles carrying two different head groups. Commonly occurring polar head groups are phosphatidylglycerol and mono- or oligosaccharides. Some representatives of these archebacteria do not even possess a cell wall. Thus, the cell membrane is the only barrier towards the aggressive external environment.

Synthetic analogues of the membrane-spanning lipids of archebacteria have been prepared (e.g., **47**–**52**).

Okahata and *Kunitake* succeeded in preparing monolayer vesicle membranes by using a single-chain bipolar ammonium salt like **47**.[44] The term "bola amphiphile" was used by *Fuhrhop* et al. to describe numerous vesicle-forming bipolar, double-chain (macrocyclic) lipids (e.g., **48**).[131]

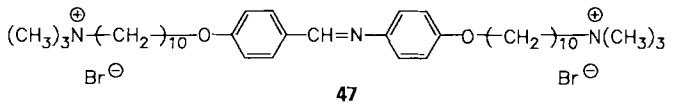

47

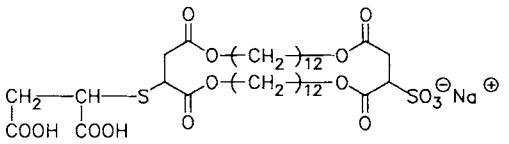

48

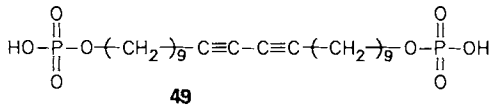

49

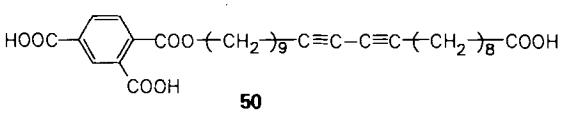

50

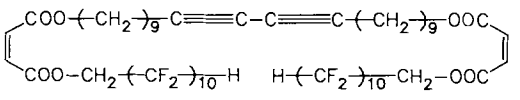

51

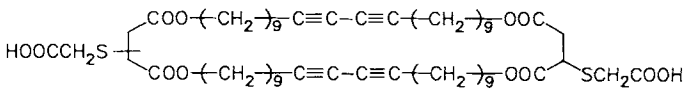

52

Polymerizable bipolar amphiphiles containing butadiyne units, such as **49**–**52**, were introduced by *Bader* et al.[132] In the presence of cholesterol, the single-chain bipolar amphiphile **49** forms vesicle membranes which can be polymerized by UV irradiation at 0 °C.[132a] By using the macrocyclic dicarboxylic acid **52**, small unilamellar vesicles as well as giant liposomes can be obtained. They are in the liquid state and exhibit no phase transition to the solid-analogous state down to a temperature of 4 °C. Since the topochemical polymerization of butadiynes takes place only in the solid-analogous phase,[164] it is not possible to polymerize vesicles of the macrocycle **52**.

Asymmetrical vesicle membranes can be obtained by using the bipolar amphiphiles **48** and **50**, bearing head groups of different size, since the smaller and bigger head groups will preferably point inwards and outwards, respectively, in small liposomes of asymmetrical amphiphiles (Fig. 33). This concept was first used by *Fuhrhop* et al.[131b]

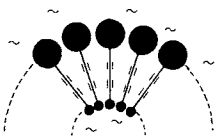

Fig. 33. Asymmetrical membranes of small, unilamellar vesicles made from membrane-spanning butadiyne lipids with head groups of different sizes [132b].

From **50**, vesicles can be prepared by sonication in the presence of 20–30 mol% of an amine (*N*-methylmorpholine, cyclohexylamine). The packing of **50** meets the requirements for a topochemical polymerization. Upon UV irradiation at 0 °C, the clear, colorless vesicle solution of **50** can be polymerized, forming a deep blue solution.[132b] The bulky trimellitic acid head group is located preferentially at the outside of the vesicle. This was proven by NMR experiments using the line-broadening effect of externally added $Mn^{2\oplus}$ ions on the signals of the aromatic protons.

Although liposomes made from a single lipid species are useful in studying basic membrane properties, those made from mixtures of structurally different lipids are a closer match to the complexity of natural systems. One can expect that mixed membranes prepared with membrane-spanning amphiphiles and conventional lipids should show a higher stability, as is schematically pointed out in Section 4.4 (Fig. 24). This stabilizing effect corresponds to that of archebacterial membranes and can also be compared to that of integral proteins. Indeed, electron microscopy reveals that mixed liposomes, made from the membrane-spanning macrocyclic amphiphile **52** and dimyristoylphosphatidylcholine (DMPC) (1:1), have homogeneously mixed membranes.[132b] Differences as to head groups or chain lengths do not result in phase separation (no DMPC domains can be seen by means of their ripple structures; cf. Section 4.8.1, Fig. 39, and Section 6.3.2, Fig.

64). Moreover, the thermal stability of these vesicles is increased by the membrane-spanning component. This has been demonstrated by temperature-dependent measurements of their permeability using 6-CF as an entrapped fluorescent marker.[132b]

4.8. "Liposomes in a Net"—Stabilization of Model Membranes by Polymeric Skeletons

Whereas model membranes can be stabilized by polymerization or polycondensation, i.e., by connecting the lipid molecules covalently, Nature makes use of completely different strategies to stabilize its membranes. Polymeric frames that are attached to the biomembrane provide it with flexibility and stability. Depending on the type of cell, these supporting elements differ considerably. Usually, they are attached to only one side of the membrane. Typical representatives are the cytoskeleton of erythrocytes and the cell walls of plant cells and bacteria.

Can model membranes be stabilized analogously to biomembranes by using polymeric frames?

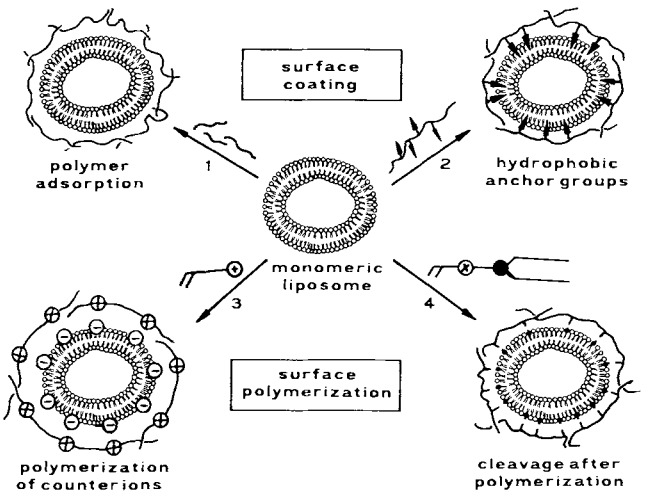

Fig. 34. Possible ways to prepare "liposomes in a net."

The four ways to bind polymers to liposomal membranes, shown in Figure 34, which are also common in Nature, are summarized as follows:

1. Water-soluble polymers can be adsorbed to vesicle membranes by means of hydrophilic or ionic interactions. Examples are the stabilization of lecithin vesicles by the adsorption of carboxymethyl chitin[133] as well as the binding of polylysine to negatively charged vesicle surfaces.[134] *Tirrell* et al. investigated the interaction between synthetic polyelectrolytes and liposomal membranes.[135]
2. Water-soluble polymers can be hydrophobized by modification with fatty acids or cholesterol. By inserting the hydrophobic anchor groups into membranes, these micellar, water-soluble, polymeric amphiphiles can be attached to membrane surfaces. *Sunamoto* et al. made use of this method in order to stabilize liposomes by coating them with hydrophobized polysaccharides.[136] These "artificial cell walls" will be dealt with in greater detail in Section 4.8.1.
3. In order to fix polyelectrolytes to membrane surfaces, charged monomers can be linked to the membrane-forming lipids via ionic forces. The subsequent "matrix polymerization" then proceeds at the membrane surface.[137] The introduction of polymerizable counterions only at the inside of vesicles leads to the formation of polymeric networks attached to the inner membrane surface. Such "artificial cytoskeletons" will be discussed in Section 4.8.2.
4. Liposomes might also be prepared from polymerizable lipids which carry a cleavable spacer (X) between the lipid part and the polymerizable group. The covalent linkage between the liposomal membrane and the enveloping polymer net can be split by the subsequent cleavage of that spacer. Such systems have not been realized yet.

4.8.1. Artificial Cell Walls or Wigs for Liposomes

To simulate the cell wall of plants, water-soluble polymers can be anchored in membranes via hydrophobic residues (Fig. 35). The driving force for the insertion of the anchor groups is the gain in free energy resulting from the transition from a dynamic, micellar system with partially solvent-exposed alkyl chains to a system in which the hydrophobic residues lie in the hydrophobic interior of the membrane.

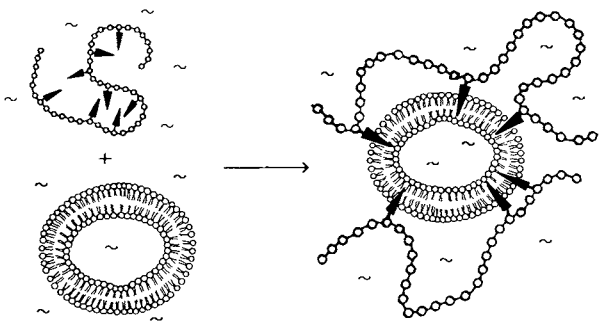

Fig. 35. Schematic drawing of the interaction of a liposomal membrane with a micellar polymer with hydrophobic anchor groups.

Examples of such interactions between polymers and membranes have been known for some time: The adsorption of synthetic polymers with hydrophobic anchor groups to cell membranes, for example, was described as early as 1964.[138] The first experiments with *O*-stearoyl derivatives of the polysaccharide dextran followed soon after.[139] *Wolf* et al. used similar polymers to study the lateral diffusion of polymers incorporated or attached to BLMs and cells.[140] In 1984 *Sunamoto* et al. introduced polysaccharide-coated liposomes as carrier systems for drugs.[136, 141] These are small, uni- or multilamellar vesicles, coated with palmitoyl- or cholesteryl-derivatized polysaccharides (pullulan, amylopectin). These asymmetrically coated liposomes feature a decreased permeability for 6-CF and an increased stability towards enzymatic de-

gradation by phospholipase D. *Kobayashi* et al. described mixed liposomes made from DPPC and synthetic *O*-octadecyl dextran.[142]

The coating of liposomes with polymers is of interest not only as regards the increase in stability, but also as regards surface variation. For example, it was demonstrated that a polysaccharide coating of liposomes leads to an altered distribution in the body.[136, 141, 143] Recently, even fragments of monoclonal antibodies were attached to a polysaccharide in addition to the hydrophobic anchor groups.[144] In vitro, the resulting "immunoliposomes" are bound to specific cells to a higher extent than the corresponding antibody-free liposomes.

Hydrophobized polysaccharides interact also with BLMs. Indeed, *Möllerfeld* et al. observed a dramatic increase in the mechanical stability of BLMs made from glycerol monoleate.[145] All other membrane properties, such as the transport of the lipophilic ion dipicrylamine, however, are influenced only slightly by this method of stabilization.

So far, attempts to simulate an artificial cell wall have only been made as regards the BLM and small vesicle model systems. However, for a direct observation of the insertion process of the anchor groups and its consequent effects on the membrane (e.g., morphological changes in the system), one has to use giant liposomes[146] as model membranes. These are form-flexible and can be observed with a light microscope. For these measurements, a temperature-controlled flow chamber[148] has been constructed, in which giant liposomes (ca. 20 μm in diameter) are prepared directly by swelling a lipid film. By using a syringe, the medium can be exchanged or additional components can be injected (Fig. 36).

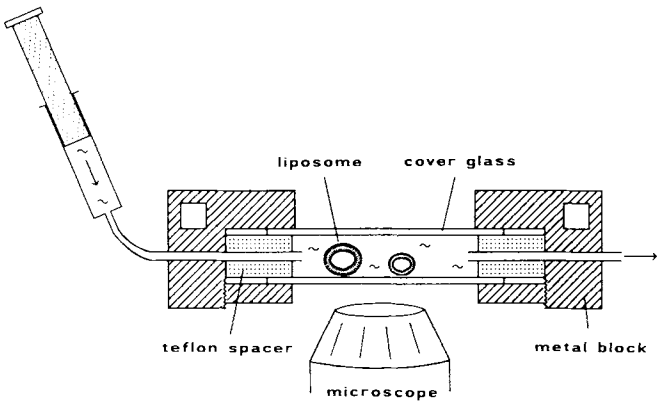

Fig. 36. Construction of the flow chamber for the observation of giant liposomes (schematic cross sectional view). The volume is 200 μL; the metal block is temperature-controlled. With the help of a syringe the medium can be gradually exchanged. Observations are carried out by using an inverse microscope (phase contrast and epifluorescence).

A series of amphiphilic polymers consisting of *O*-palmitoyl derivatives of the natural, linear polysaccharide dextran have been synthesized[60] (Fig. 37).

When a solution of one of those amphiphilic polymers is added to a preparation of giant liposomes, above a critical concentration, a significant morphological change can be observed: tubelike liposomes become constricted. In the course of this process structures resembling strings of pearls develop along the original longitudinal axis of the liposome (Fig. 38). These morphological changes are due to the insertion of the hydrophobic anchor groups into the bilayer. On the one hand, the unmodified dextran, without hydrophobic residues, shows no effect. On the other hand, a clearly membrane-associated fluorescence can be observed when a hydrophobized and fluorescence-labeled dextran is used. The critical concentration, above which these "strings of pearls" are formed, decreases with increasing degree of substitution and increasing molecular weight of the dextran derivative.[147] The formation of structures resembling strings of pearls is shown in Figure 38 together with a schematic representation of the insertion process.

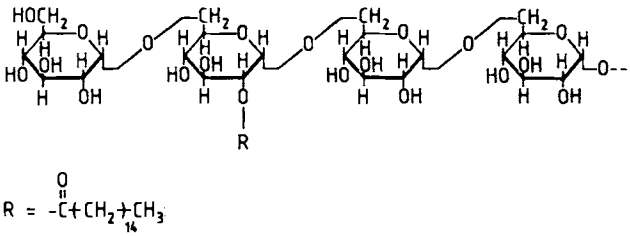

$R = -\overset{O}{\overset{\|}{C}}-CH_2-(CH_2)_{14}-CH_3$

Fig. 37. *O*-Palmitoyldextrans [60] with mean molecular weights ranging from 43000 to 160000 and degrees of substitution between 3 and 6 mol% were used for the studies of giant liposomes described in the text. These dextrans have 15 to 40 anchor groups per polymer chain.

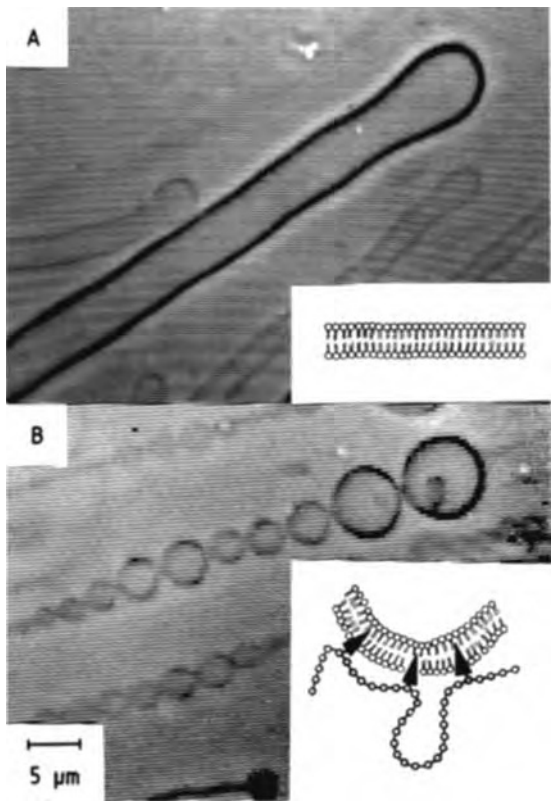

Fig. 38. Morphological change of a tubelike liposome owing to the interaction with a hydrophobized dextran (phase contrast micrograph and schematic explanation) [60, 147]. A) Before injection of the micellar polymer. B) After the injection.

According to these observations, the insertion of the anchor groups only in the outer half of the membrane induces a curvature (see Section 6.2) which leads to the formation of the "string of pearls." This is obviously a case of a polymer effect: Unsubstituted dextrans do not induce this process, whereas it occurs with octyl glucoside only at concentrations which are five orders of magnitude higher. This polymer effect is based on the fact that the locally high concentration of the anchor groups leads to a cooperative insertion into small membrane regions.

A similar kind of constriction process plays an important role in Nature in receptor-mediated endocytosis. In this case, the attachment of the protein clathrin to the inside of the cell membrane leads to the formation of "coated pits" and to the consequent detachment of "coated vesicles." They have an important transport function in the uptake of LDL (low-density lipoproteins).[149] These types of biomembrane processes will be discussed in detail in Section 6.2.

By means of freeze fracture electron microscopy,[150] it is possible to directly demonstrate the insertion of the hydrophobic anchor groups into the outer membrane of DMPC liposomes.[60, 147] By using this method, surface structures of membranes can be observed with a transmission electron microscope. Upon annealing between the pretransition and the main transition, typical ordered structures develop in liposomes from natural lecithins.[151] Owing to their appearance, they are called ripple phases. A liposomal membrane made from pure DMPC exhibits homogeneous ripple spacings of 12 ± 2 nm. Small amounts of impurities in the membrane already lead to a significant disturbance of these ripple structures.[152] Figure 39 explicitly illustrates the insertion of the hydrophobic anchor groups by means of the interaction between a hydrophobized polyvinylpyrrolidone derivative and DMPC liposomes.[60] The outer surface of the liposome shows a disturbed and widened ripple structure. However, the inner membrane surfaces of the multilamellar vesicle, which are made visible by the fracture, exhibit the perfect, original ripple structure of pure DMPC. This demonstrates that the added amphiphilic polymers, as schematically shown in Figure 35, only interact with the outer liposome surface and cannot penetrate through the membrane. A further attempt to insert amphiphilic compounds into liposomal membranes is described in Section 5.4.

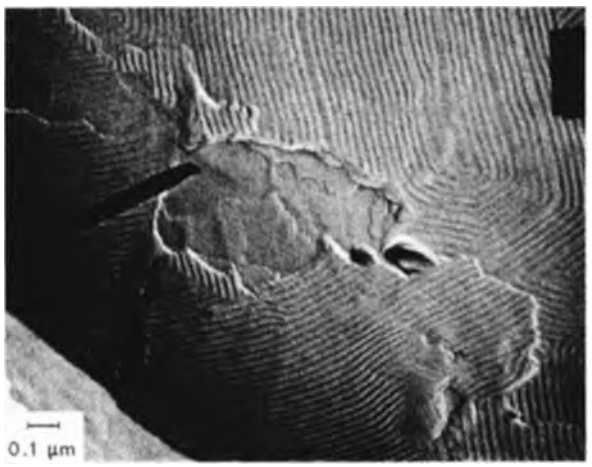

Fig. 39. Freeze fracture electron micrograph [204] of a multilamellar DMPC liposome after the interaction with a hydrophobized polyvinylpyrrolidone derivative; widened and disturbed ripple structure in the outer surface; undisturbed ripple structure of pure DMPC in the inner membrane layers [60].

4.8.2. Cytoskeleton Models or the Stabilization from Inside

In animal cells, the highly structured interior is spanned by a three-dimensional protein network, namely, the cytoskeleton. Among other functions, it serves as a static skeleton of the cell, thus maintaining its shape and stabilizing the plasma membrane. A typical example for the stabilizing function of the cytoskeleton is the spectrin network of erythrocytes.[153] Here, the combination of stability and flexibility is achieved by a two-dimensional protein network which is coupled to the lipid/protein bilayer (cf. Fig. 18). The protein network consists of filamentous spectrin molecules. Tetramers of this protein are cross-linked by another protein, actin. Some of these actin molecules are fixed to the cytoplasmic end of an integral membrane protein (Band III) by an anchor protein, known as ankyrin. A similar coupling of the cytoskeleton probably exists to the membrane-spanning protein glycophorin.[153a] Furthermore, it is assumed that the spectrin molecules are bound to negatively charged lipids in the inner-membrane leaflet by electrostatic forces.[154]

Because of the high complexity of the interaction between plasma membrane and cytoskeleton, it is hardly possible to understand the mechanical and structural properties of erythrocyte membranes without parallel model investigations. A simple model of an erythrocyte membrane was prepared from a mixture of DMPC and the polymerizable lipid **36b**.[154, 155] Here, the polymerizable methacrylate unit is kept in the aqueous phase by the hydrophilic tetraethylene oxide spacer[98b] (see Section 4.5.2).

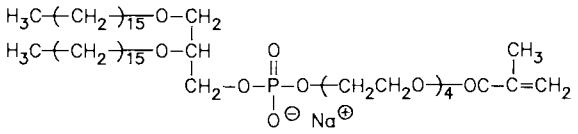

36b

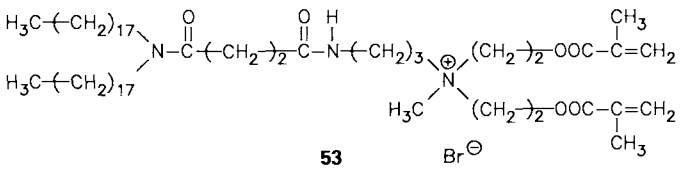

53

The polymerization of such mixed liposomes leads to the formation of linear macromolecules at both membrane surfaces. By using a mixture of **36b** and lipid **53**, which contains two polymerizable units in the head-group region, cross-linked macrolipids are obtained. This leads to the formation of polymeric networks at both bilayer leaflets (Fig. 40).

An even better approach to simulate the cytoskeleton of the cell is a liposome, in which polymeric networks are

only inside the vesicles. It is possible either to attach two-dimensional networks to the inner membrane surface or to fill the interior of vesicles with three-dimensional cross-linked polymeric gels. Such three-dimensional networks,

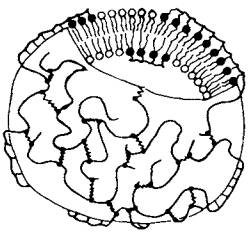

Fig. 40. Schematic drawing of a mixed liposome composed of polymerized lipids which are embedded in the monomeric lipid matrix. Additionally, the polymer chains are connected with one another forming a polymer network [155].

which span the complete interior of liposomes, are readily accessible by the polymerization of liposome-encapsulated hydrophilic monomers. By using this method, cross-linked polyacrylamide gels in the aqueous interior of liposomes have been prepared.[156] After destroying the lipid bilayer by addition of a surfactant, the size of the gel particles, as determined by light scattering and electron microscopy, remains nearly unchanged.

Two-dimensional polymeric networks that are attached only to the inner or the outer surface of the vesicle membrane via electrostatic interactions can be prepared by the exchange of the counterions at the outside of SUVs.[157] This is shown schematically in Figure 41.

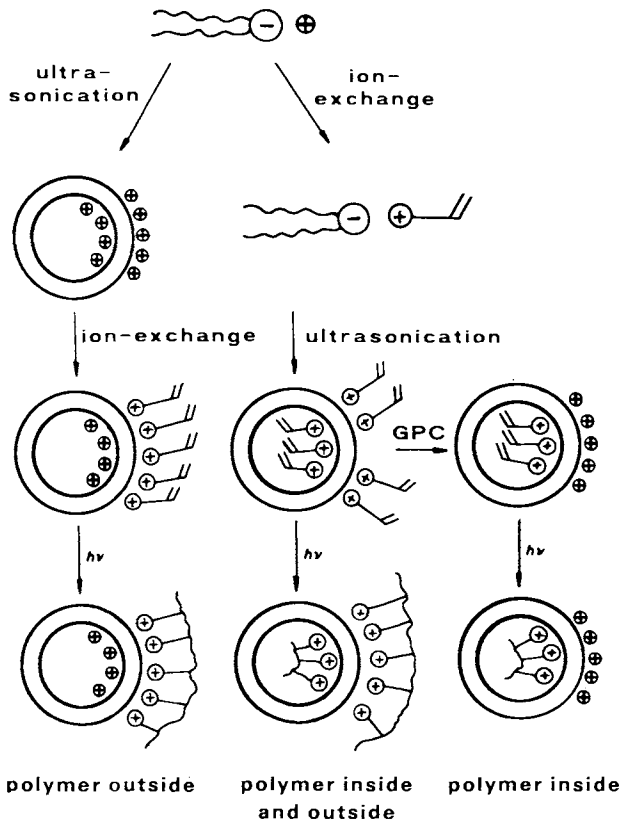

Fig. 41. Preparation of vesicle membranes with asymmetrically or symmetrically bound polyelectrolytes from lipids with polymerizable counterions [157]. GPC = gel permeation chromatography.

To realize this concept, the salts **54**–**57**, prepared from anionic lipids and polymerizable counterions, were used.[157] In the case of **54** and **56**, choline methacrylate is

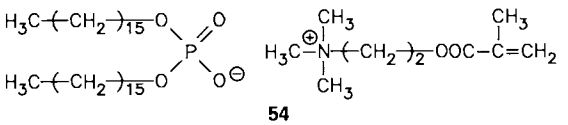

54

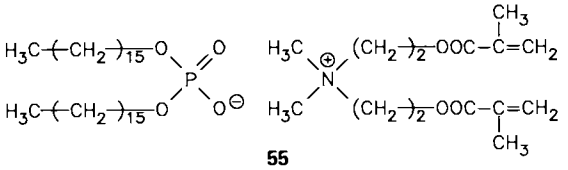

55

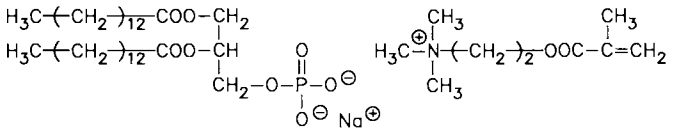

56

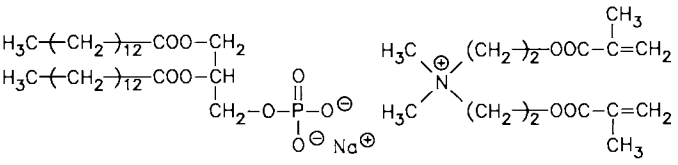

57

bound as a counterion to negatively charged lipids (dihexadecyl phosphate or the anion of dimyristoylphosphatidic acid (DMPA)). This leads to linear polymer chains. Additionally, the salts **55** and **57**, with a counterion bearing two polymerizable groups, were used to prepare polymeric networks. The different routes to prepare vesicles with ionically linked polymers made with these lipids, as shown in Figure 41, are discussed briefly below.

Polymerizable counterions are introduced to the outer surface of unilamellar vesicles by exchanging $Na^{\oplus}$ against alkylammonium ions containing a methacrylate moiety. This process can be monitored by UV spectroscopy. Upon irradiation with UV light, the counterions can be polymerized at the outer membrane surface. In order to create macromolecules at the inner membrane surface, vesicles with polymerizable counterions on both sides of the lipid bilayer have to first be prepared. The polymerizable counterions at the outer membrane surface can then be replaced by $Na^{\oplus}$ by means of gel permeation chromatography (GPC). The polymerization of this vesicle system leads, in the case of lipid **55**, to a highly cross-linked polymeric network which is only attached to the inside of the vesicle membrane.

The phase transition temperature of the lipid bilayers strongly depends on the sort of counterion bound to the vesicle. Here, DMPA vesicles with a symmetrical distribution of the counterions are given as an example. Liposomes made from **56** with polymerizable counterions exhibit a phase transition temperature which is decreased to 31 °C, compared with liposomes made from the corresponding disodium salt (50 °C). By polymerization of the

cations of **56** at both membrane surfaces, the phase transition temperature is increased again.[157] Analogous results were obtained for dihexadecyl phosphate vesicles.[158] Figure 42 shows a model for the strong influence of the monomeric or the polymeric counterions on the phase transition.

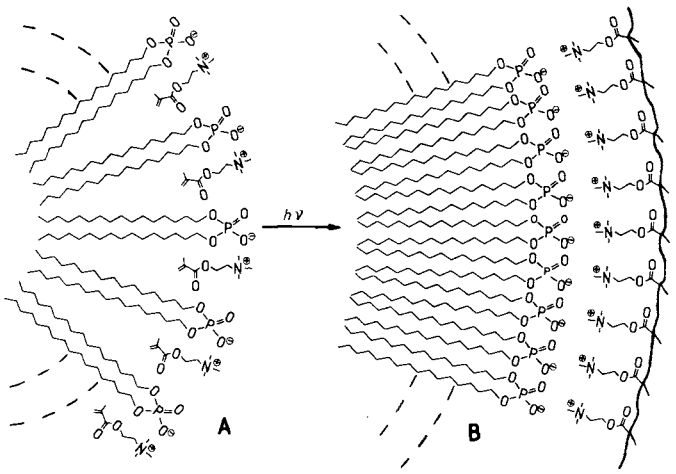

Fig. 42. Schematic drawing of the influence of choline methacrylate counterions on the packing of lipids in the membrane [158]. A) The monomeric counterions are partially inserted in the membrane, thus disturbing the packing of the lipids. B) The polymer is not inserted in the membrane, thus allowing a denser packing of the lipid molecules.

The monomeric choline methacrylate counterion thus leads to a fluidization of the membrane, owing to its partial insertion into the lipid bilayer. Since the phase transition temperature is shifted to higher values after polymerization, it can be assumed that the resulting polymer is no longer embedded in the membrane, thus allowing a denser packing of the lipid molecules. This model is also supported by results from permeability measurements.[158] Furthermore, comparative investigations of the stability of symmetrical vesicles of lipid **54** towards organic solvents were carried out using monomeric and polymeric counterions. Turbidity measurements reveal that the polymeric "liposomes in a net," in contrast with the unpolymerized counterparts, are even stable in 60% methanol.

A further step in simulating the cytoskeleton of erythrocytes is the additional fixation of an ionically fixed polymeric network to the inner membrane surface via covalently bound hydrophobic anchor groups. Such an "artificial cytoskeleton" was built up with vesicles consisting of a mixture of the lipids **53** and **54**[158] (Fig. 43). First, the polymerizable counterions are removed only from the outer vesicle surface. Then, the choline methacrylate counterions, bound to the inner membrane leaflet, are copolymerized with the cross-linking lipid **53** by means of UV irradiation. Thus, a two-dimensional polyelectrolyte network is formed at the inner-membrane surface. In addition to its electrostatic bonds, this network is fixed to the lipid bilayer via covalently linked hydrophobic anchor groups.

Comparative release measurements carried out on monomeric and polymerized vesicles using [^{3}H]glucose revealed that such an "artificial cytoskeleton" does not change the membrane permeability. Thus, it is the lipid bilayer, and not the polymeric skeleton, which indeed acts as the permeability barrier.[158] Hence, these polymerized vesicles formally behave like erythrocytes: the polymer controls their physical stability as well as their shape, whereas the lipid bilayer controls their permeability.

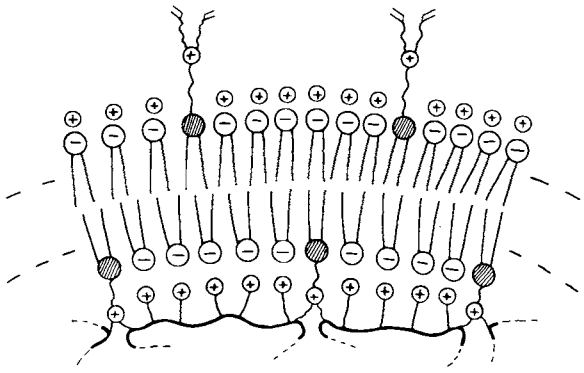

Fig. 43. "Artificial cytoskeleton" at the inner surface of vesicle membranes, prepared according to the following procedure [158]: (1) preparation of liposomes from 90 mol% of **54** (polymerizable counterions) with 10 mol% of **53** as a cross-linker (covalently bound methacrylate groups); (2) removal of the polymerizable counterions from the outer surface of the vesicle membrane via GPC; (3) copolymerization of the ionically or covalently bound methacrylates at the inner surface of the vesicle membrane.

5. The Use of Model Membranes to Study Biological Recognition Processes

The complex molecular processes in biological systems can only proceed along ordered paths if they are selectively controlled. Thus, the development of multicellular organisms can hardly be imagined without the capability of intercellular communication. The decisive step in such an information exchange is the binding of a signal molecule to a specific receptor which is usually bound to the membrane. Analogous recognition reactions are of significant importance for the immune system of vertebrates, too. The various responses of the immune system recognize and eliminate invading organisms as well as toxic substances produced by them. Because immune reactions are destructive, it is essential that they be made only in response to molecules which are foreign to the host. Without this distinction between foreign and autologous molecules, fatal autoimmune reactions would result. Therefore, biologists, biochemists, and biophysicists place great interest in the structure and the function of biological membranes as well as their interaction with signal molecules. In the course of these investigations, simple model membranes have also been used during the last few years.[82,159] In addition, the surface recognition of liposomes by target cells is of decisive importance for specific drug delivery.[87]

What kind of substances play a role in the manifold recognition reactions in Nature? The most important membrane components for surface recognition are those of the glycocalix, the glycoproteins and the glycolipids.[66] In the cell membrane, they are responsible for vital functions and properties such as cell recognition, antigenicity, histocom-

patibility, and lectin affinity. Sections 5.1, 5.3, and 5.4 will deal with the recognition of sugar structures in model membranes by means of lectins and antibodies. Moreover, the most well known and the best-investigated regulated process is the replication and transcription of DNA as well as the translation of RNA.[160] In this case, the recognition reaction is the base-coupling of nucleic acids. Model experiments in which these reactions are applied will be discussed in Section 5.2.

5.1. Reversible Sugar–Lectin Interaction with Polymerized Liposomes

Sugar structures attached to membranes can be recognized by lectins. These proteins, originally only found in plants, possess specific binding sites for certain sugars.[161] A well-studied representative is concanavalin A (Con A) which can bind α-glucopyranosides and α-mannopyranosides. It is a tetrameric protein where each subunit carries one binding site. The saturation of these binding sites with the low-molecular-weight sugars does not lead to aggregation of Con A. If, however, several of those sugar units are components of a supramolecular system such as a cell, agglutination and precipitation occurs after lectin addition. This process is reversible since the addition of a large amount of one of those pyranosides leads to the dissolution of the precipitate, thus reforming the original cell dispersion.[162]

Two principles can be used to carry out such biological recognition reactions with polymerized membrane systems. On the one hand, natural lipids with recognizable structures can be incorporated into polymeric membranes. On the other hand, polymerizable lipids with a recognizable head group can be synthesized.

Several polymerizable glycolipids with different sugar head groups were prepared a few years ago.[163] These carry a butadiyne unit as the polymerizable group in the hydrophobic chain.

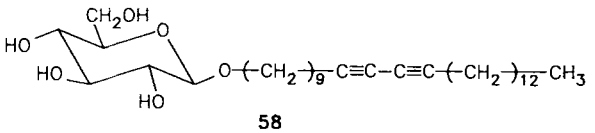

58

The interaction between the glucose derivative **58** and Con A has been investigated in monolayers[163] and liposomes.[114a,b] Liposomes of **58** can be polymerized by UV irradiation, exhibiting a color change from colorless via blue to red, which is typical for butadiyne derivatives.[72,164] The experiment with Con A and sugar-bearing polymerized liposomes is schematically shown in Figure 44.

After adding Con A to a deep red solution of polymerized liposomes prepared from **58**, agglutination occurs within a few seconds: a red precipitate is formed, the supernatant becoming colorless. If, however, α-methylmannopyranoside, which binds much stronger to Con A, is then added, the precipitate is redispersed, thus leading to the original clear red solution of the liposomes. So the result is a competitive replacement of the liposomal-bound sugar groups by the soluble sugar.

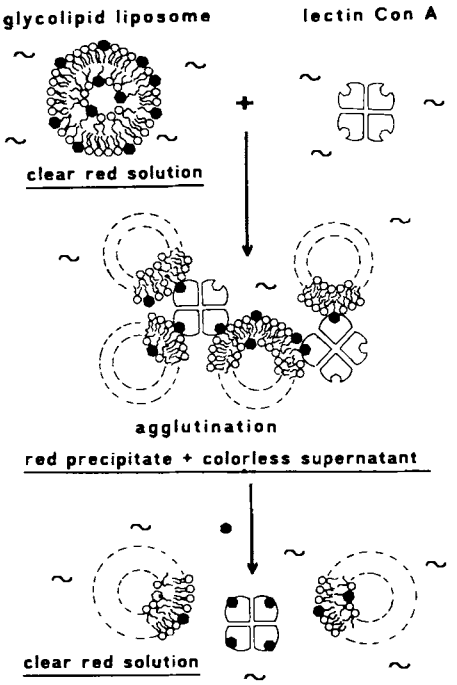

Fig. 44. Schematic representation of the reversible interaction of concanavalin A with polymerized glycolipid liposomes made from **58** [114b]. ● = sugar.

From simple qualitative experiments of this kind, one can proceed to investigations using synthetic and biologically relevant sugar structures[165] or natural glycolipids. Such model investigations gain increasing significance, for example, as regards the simulation of immunological phenomena and their medical application (affinity chemotherapy[166]).

5.2. Nucleolipid–Nucleobase Interaction in Monolayers

Another recognition reaction that occurs in Nature is the base-pairing in DNA. To learn more about the base–base interaction and the relation between structure and function, a large number of polynucleotide analogues have been synthesized.[167] The most common models are linear, uncharged polymers with nucleobases as side groups. With these polymers, specific interactions have been observed.[167,168] In none of these investigations were the nucleobases in an oriented state. In order to use the specific base-pairing in surface recognition reactions, nucleolipid monolayers and their interaction with nucleobases, dissolved in the subphase, were also recently investigated.[169] *Kornberg* et al. used such ordered nucleolipid monolayers to show that certain proteins, such as the B1 subunit of ribonucleotide reductase, are specifically bound in the form of a two-dimensional crystal.[170]

Compounds **59**–**62** are examples of new, uncharged nucleolipids, which form ordered structures like monolayers and liposomes.[169b,171] Despite their consistently big and only weakly hydrophilic head group, these nucleolipids

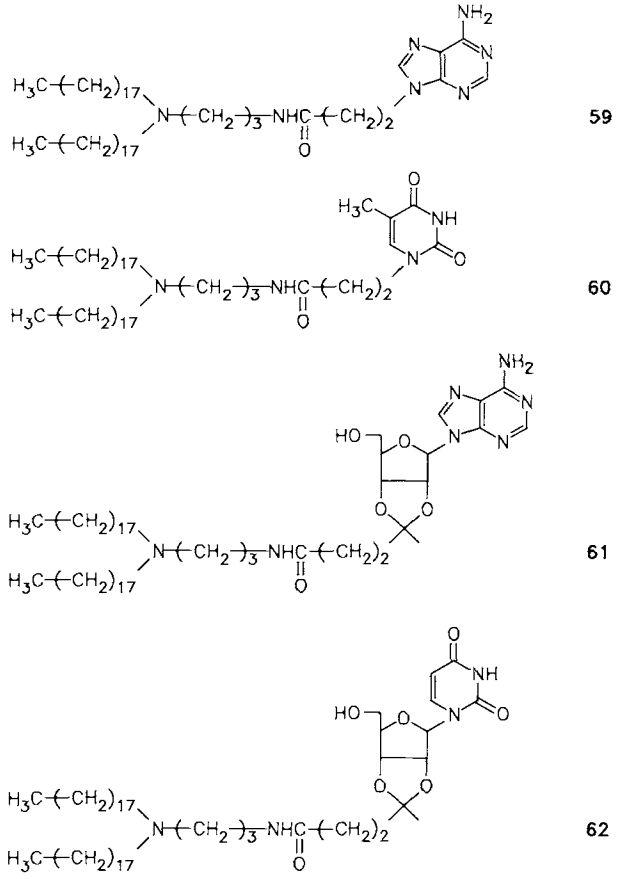

59

60

61

62

form stable, solid-analogous monolayers, with the nucleobase head groups dipping into the subphase. Their isotherms should be affected by the interaction of these nucleolipids with nucleobases as substratum in the aqueous phase. Figure 45 exhibits the surface-pressure behavior of the uridine lipid **62** to exemplify the influence of a monomeric nucleobase dissolved in the subphase.

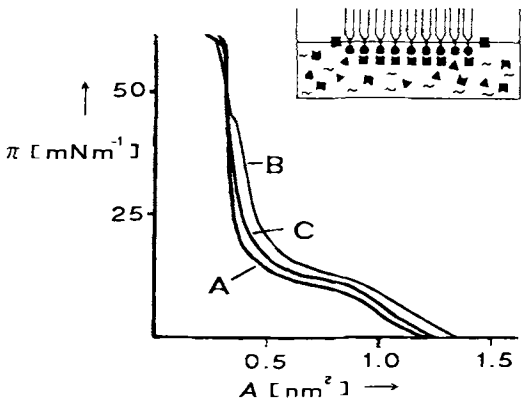

Fig. 45. Isotherms of the uridine lipid **62** on different subphases (20°C) [169b]: A) water; B) 0.01 M adenine (complementary) (■); C) 0.01 M thymine (noncomplementary) (▲). π = surface pressure, A = area per molecule.

The characteristic phase behavior of the nucleolipid **62** (curve A) is basically not changed by the dissolved nucleobases. Liquid-analogous as well as solid-analogous phases are observed, and the molecular area is slightly increased after addition of the bases. The influence of adenine (curve B), which is complementary to the nucleolipid, is slightly stronger than that of thymine (curve C).

The interaction between a nucleolipid monolayer and polymeric nucleotide bases is illustrated by means of the adenosine lipid **61** (Fig. 46). The two polynucleotides re-

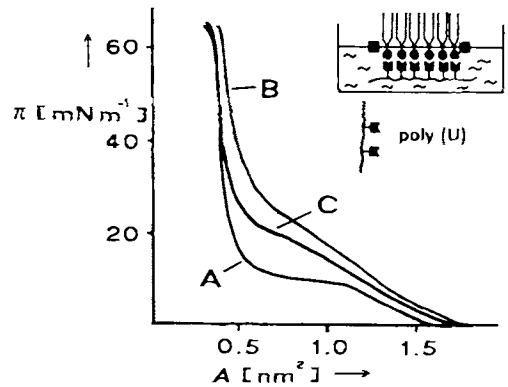

Fig. 46. Isotherms of the adenosine lipid **61** [169b] (subphase: PBS (= phosphate-buffered saline) buffer, pH 7.3, 1.5×10^{-3} M): A) in the absence of a polymeric nucleobase; B) 1.5×10^{-5} mol base L^{-1} poly(U) (complementary); C) 1.5×10^{-5} mol base L^{-1} poly(A) (noncomplementary). π = surface pressure, A = area per molecule.

veal a noticeably different influence on the isotherms of **61** if the surface pressure exceeds 15 mN m^{-1}. As regards the noncomplementary polyadenine nucleotide poly(A), it is already expelled from the head-group region at a surface pressure of 40–50 mN m^{-1}. Thus it loses all influence on the solid-analogous packing of the monolayer (curve C). In contrast, the poly(U) base, which is complementary to the lipid head group, exhibits a considerable interaction with the monolayer (curve B) even at high surface pressures.

In the case of liposomes made with nucleolipids and the phosphatidylcholine DPPC (3 : 1), no clear interaction with monomeric nucleobases can be demonstrated. Nevertheless, a significant interaction between liposomes and polymeric nucleobases was observed. However, the hypochromicity effects (decrease of the extinction coefficient after base-coupling) display no significant difference between specific and nonspecific interaction.[169b] This may be due to the fact that the stronger ionic interaction (see Section 4.8) of the polynucleotides with DPPC is superimposed on the weaker base–base interaction.

5.3. Model Investigations of the Interaction between Bacteria and the Complement System

In humoral immune reactions, the outer membrane of gram-negative bacteria is damaged by the complement system. The resulting hydrophilic pores lead to the death of the bacterium. The complement cascade (C) consists of at least 14 serum proteins which are activated in a specific order.[172] The classical pathway of C-activation is initiated by the adsorption of the first component C1 to the surface of the bacterium. This involves the binding of the C1 subcomponent C1q to the lipid A (**63**) of the outer membrane.[173] This first step of the complement cascade can

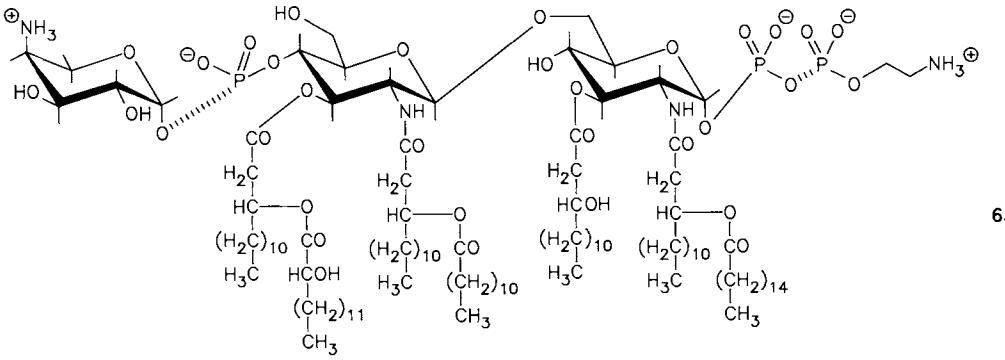

63

also be investigated by using model membrane systems. Indeed, **63**, the lipid anchor of the lipopolysaccharide (LPS), has already been incorporated into model membranes.[174] In cooperation with the group of *Loos*, the interaction between the complement component C1q and **63** was studied in monolayers and liposomes.[175] Lipid A (**63**) consists of seven hydrophobic alkyl chains of different lengths and one hydrophilic head group made up of glucosamine units as well as phosphate and ammonium groups.[176] C1q is built up of six collagen-like triple-stranded helices which are linked together at one end (Fig. 47). The free ends carry globular head groups that function as recognition sites. The C1q molecule has a molecular weight of 410000 and consists of 18 polypeptide chains.[177]

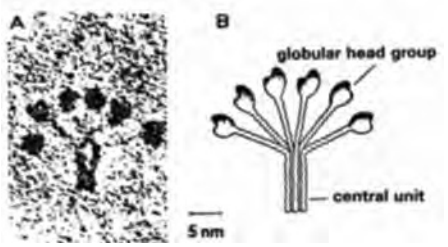

Fig. 47. A) Electron micrograph; B) schematic representation of the complement component C1q [177].

Figure 48 shows the isotherms of the purified oligomer-like **63** at different temperatures. The monolayers exhibit liquid- and solid-analogous phases and have a remarkable stability up to a temperature of 37 °C. The molecular area of about 1.3 nm^2 per molecule in the solid-analogous phase is within the range expected for a lipid with seven alkyl chains.

In order to investigate the interaction between **63** and C1q, the lipid A monolayer was kept under constant pressure while C1q was injected into the subphase. After the injection of C1q, one can clearly see a strong increase in molecular area if the monolayer is kept at a pressure of 2 mN m^{-1}, i.e., in the liquid-analogous state (Fig. 49). If, however, a higher surface pressure (20 mN m^{-1}) is applied, no change in the area per molecule is observed. In the solid-analogous state, the lipid A molecules are evidently so densely packed that the C1q head groups cannot penetrate the monolayer. For a recognition reaction to take place, not only does the specificity of the recognizable

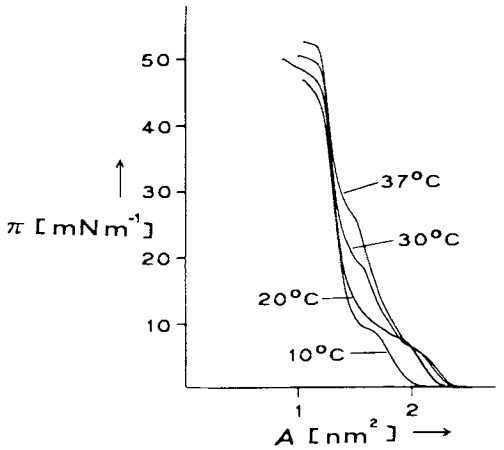

Fig. 48. Isotherms of **63** at 10, 20, 30, 37 °C (subphase: water). π = surface pressure, A = area per molecule.

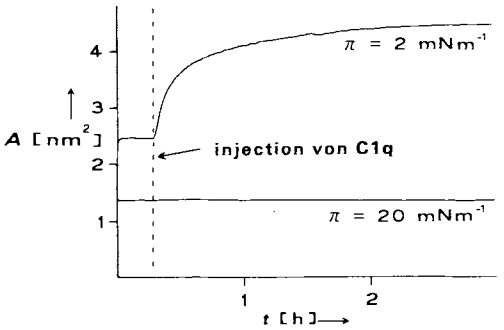

Fig. 49. Interaction of the protein C1q (1 μg mL^{-1}) with lipid A monolayers (20 °C): Injection of C1q (----) into the subphase at a constant pressure of 20 mN m^{-1} (solid-analogous phase) and 2 mN m^{-1} (liquid-analogous phase); strong interaction (expansion of the monolayer) only in the fluid state. A = area per molecule.

groups seem to be important, but also the existence of a liquid-analogous phase, common in biological membranes.[178]

The binding of C1q to lipid A monolayers was confirmed by investigations with a fluorescein-labeled anti-C1q antibody. These experiments were carried out with a film balance which was combined with a fluorescence microscope[180] (Fig. 50). Mixing diagrams of **63** and DPPC exhibit a complete miscibility of both components. However, these experiments do not give evidence as to whether the phase separation, which can be seen in Figure 50 (see also Section 6.1), already occurs owing to the adsorption

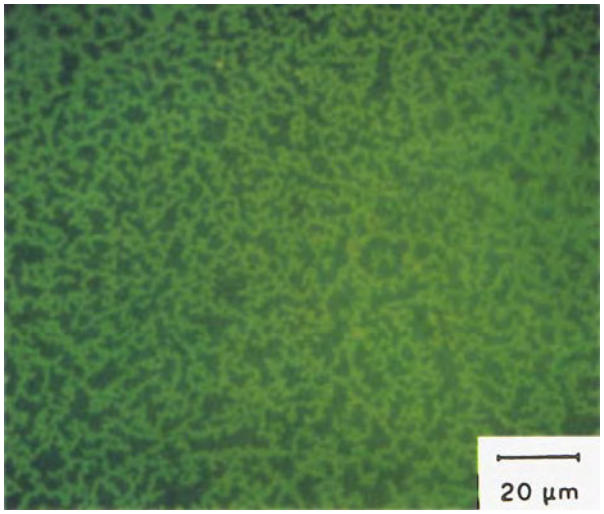

Fig. 50. Epifluorescence micrograph to show the binding of C1q to a monolayer formed from lipid A and DPPC (1:4) (cf. Fig. 51). Injection of a fluorescein-labeled antibody against C1q (anti-C1q FITC IgG [179], FITC = fluorescein isothiocyanate) into the subphase of the monolayer with bound C1q, resulted in the appearance of a fluorescence due to binding of the FITC antibody to the membrane-fixed C1q-lipid A complex.

of C1q to the lipid A monolayer, or if it is caused later by the C1q-antibody interaction.

As is known from other studies, C1q binds to **63** via its globular head-group structures. Therefore, the simplified model shown in Figure 51 can be postulated to explain the monolayer results described above.

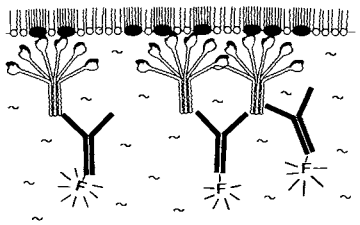

Fig. 51. Schematic representation of the adsorption of C1q to a monolayer formed from lipid A and DPPC and the binding of the fluorescein-labeled antibody. F stands for fluorescein isothiocyanate.

By making use of giant liposomes, it was also possible to demonstrate the interaction between C1q and **63** using FITC-labeled antibodies (for this method see Section 5.4). Here, too, it was found that, after the addition of C1q, only those liposomes containing **63** are made visible in the fluorescence microscope by the antibody.

5.4. Induction of Membrane Processes by Recognition Reactions at the Surface of Vesicles

A further example of a recognition reaction at the membrane surface is the binding of a specific antibody to its corresponding antigen at the membrane. Together with the group of *Bitter-Suermann*,[181] the polysaccharide K1 (**64**) from *E. coli* was used as a model system to investigate such surface reactions.[60]

K1 consists of α-(2-8)-linked sialic acid units[182] which are connected to a lipid residue. It belongs to the group of acidic capsular polysaccharides of the outer bacterial membrane. They are supposed to play a role in the serum and phagocytosis resistance of gram-negative bacteria.[181a] To prove the incorporation of **64** into model membranes, giant liposomes of the phosphatidylcholine DMPC were used. A micellar solution of **64** is injected into the chamber, shown in Figure 36, containing such a liposome preparation (Fig. 52A). After the insertion of the lipid anchors into the liposomal membrane (Fig. 52B, see also Section 4.8.1), the fluorescence-labeled anti-K1 antibody[181b] is added. The recognition between antigen and antibody (Fig. 52C) can be shown by means of fluorescence microscopy:

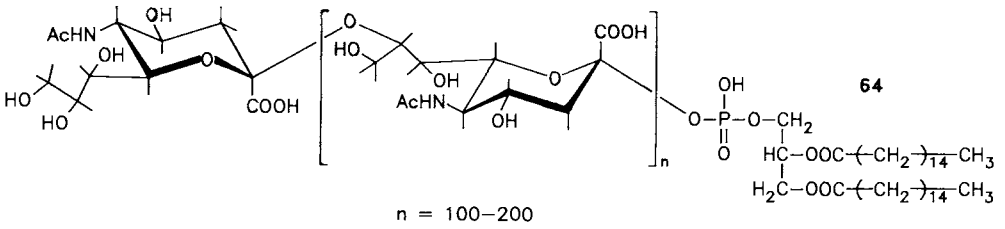

the originally diffuse fluorescence of the dissolved antibody becomes concentrated on the liposome surface.

The comparison of a phase-contrast micrograph (Fig. 53A) with the corresponding epifluorescence one (Fig.

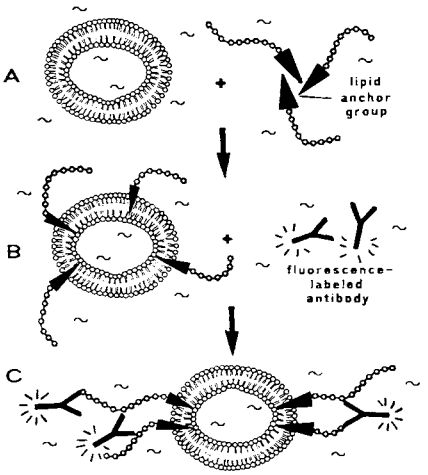

Fig. 52. Schematic representation of the experiment to prove the insertion of the capsular polysaccharide K1 (**64**) into liposomal membranes by using immunofluorescence [60]. A) Addition of a micellar solution of K1 to a liposome preparation. B) Insertion of the lipid anchor groups into the lipid bilayers; addition of the fluorescein-labeled anti-K1 antibody. C) Binding of the antibody and induction of a phase separation due to cross-linking of the K1 molecules (patching).

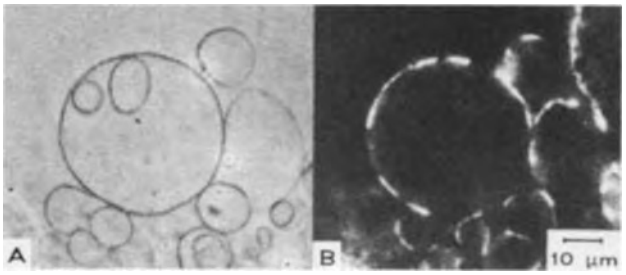

Fig. 53. Proof for the incorporation of **64** into DMPC liposomes [60]. A) Phase-contrast micrograph; B) epifluorescence micrograph of the same liposome (patching according to schematic drawing in Fig. 52C).

53B) clearly shows that the fluorescence of the antibody is associated with the membrane; i.e., **64** is detected at the membrane surface. Furthermore, it becomes evident that the fluorescence, dependent on time and concentration, is no longer distributed homogeneously in the membrane: patching[183] can be observed. It is caused by the reaction between the multivalent antigen, which is capable of lateral diffusion within the membrane, and the bivalent antibody, thus leading to a phase separation. This process might be compared to a precipitation reaction in two dimensions. Therefore, this experiment is not only an example of a recognition reaction between antigen and antibody; the final result, the clustering of one membrane component, also represents a simple membrane process (see Section 6.1).

6. Simulation of the Dynamics of Biomembranes

The dynamics of biomembranes (shape fluctuations, membrane instabilities), which is responsible for motion and transport processes, is fascinating and of great biological importance. It is a challenging task to explain cellular processes by phenomenological physical properties of the plasma membrane.[155a] The plasma membrane with its manifold functions is much more than just a passive permeability barrier which encloses cytosol from the surrounding medium. On the one hand, membrane transport proteins or ion carriers provide for a "local," ordered exchange of substances in both directions. On the other hand, dynamic processes are responsible for the important "bulky" transport through the membrane. Examples of these uptake and release processes of the cell are illustrated in Figure 54.

Cells ingest macromolecules and particles by a process called endocytosis: the substances are progressively enclosed by a small portion of the plasma membrane, which first invaginates and then pinches off to form an intracellular vesicle containing the ingested material.[185] Analogous mechanisms exist for the release of substances from the cell: as regards exocytosis, the intracellular vesicles, containing the substance to be released, fuse with the plasma membrane and open to the extracellular space. In the case of budding, bulges of the membrane to the outside are detached, whereby the substances given off remain enclosed by a lipid bilayer. This process plays a role when, for example, a virus leaves its host cell.

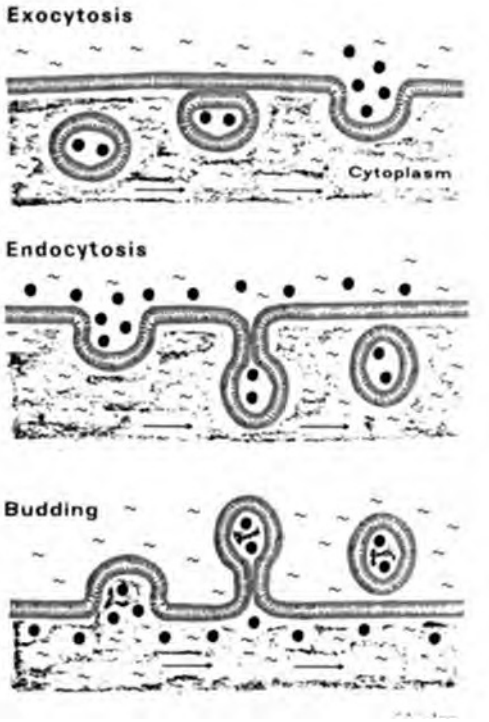

Fig. 54. Schematic drawing of three important transport processes of biological membranes [184]: exocytosis, endocytosis, and budding.

All these events require dynamic processes within the membrane, including the possibility of forming local domains in the membrane (patching and capping). In membrane biology, the mechanism of such dynamic cell processes is habitually described as extremely complex, usually involving proteins and being energy-consuming. Phase-separation phenomena, however, can be triggered off in lipid bilayers depending on counterions or temperature.[186] Simplified model membranes thus help to answer the question of what minimum requirements are necessary in a given system for a certain process to take place at all. The following sections illustrate how dynamic processes can be induced in purely synthetic, polymeric model systems in such a way that they correspond, at least formally, to biomembrane processes.

6.1. Patching and Capping in Polymerized Mixed Liposomes

Patching and capping are simple dynamic processes of the biomembrane caused by lateral diffusion. They are triggered off at the cell surface by antigen–antibody interactions and can be observed directly with a light microscope by using a fluorescence-labeled antibody.[183, 187] This is schematically shown in Figure 55. The fluorescence-labeled antibodies bind to the antigens at the cell surface (Fig. 55A) and a diffuse fluorescence, which is homogeneously distributed over the whole cell membrane, can be observed. Since the antibody molecules are bivalent, they are able to cross-link with the antigens. This soon leads to a phase separation within the membrane and thus to the fluorescent patches (Fig. 55B). An example of such a patching process in a vesicle membrane has already been described in Section 5.4. In the cell, the individual

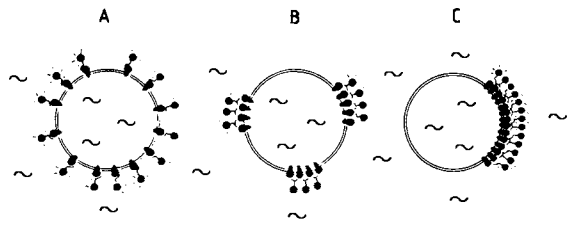

Fig. 55. Schematic drawing of the aggregation of membrane receptors induced by the binding of bifunctional fluorescence-labeled antibodies. A) Diffuse fluorescence of the homogeneously bound antibody. B) Clustering of the receptors forming fluorescent domains (patching). C) Aggregation of the domains forming a single fluorescent area (capping).

domains move, within a few minutes, to one certain area of the membrane, thus forming a cap (Fig. 55C). Whereas patching only requires lateral diffusion, it is assumed that the subsequent aggregation to one single cap is an energy-promoted process.[183, 187]

In mixed membranes of unsaturated and natural lipids, a phase separation can be induced via polymerization. This domain formation resembles the immunologically important processes of patching and capping.[188] Such experiments have been carried out with mixed giant liposomes made from the polymerizable lipid **27** (Scheme 3) and DMPC (1:1). Their membrane dynamics are made visible by the addition of a small amount of a fluorescent lipid. The liposomes composed of the monomeric components reveal complete miscibility of both lipids and the incorporated fluorescent dye, as can be seen by the diffuse fluorescence of the giant liposomes. After photopolymerization of **27** at 40°C (diffuse fluorescence still observable, Fig. 56A) and cooling down of these partially polymerized liposomes below the phase transition of the polymeric lipid, isolated areas of intense fluorescence occur (Fig. 56B).

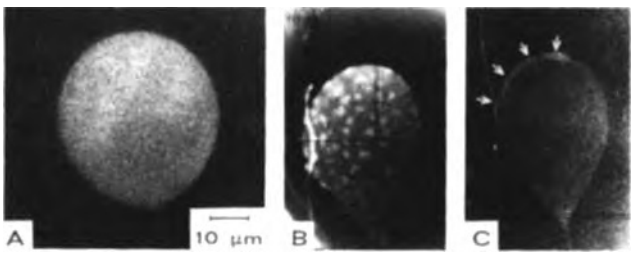

Fig. 56. Simulation of patching and capping in polymerized giant liposomes; epifluorescence micrographs of a giant liposome made from a mixture of the butadiene derivative **27** and DMPC (1:1) (0.1 mol% fluorescent lipid as marker) [188a]. A) Homogeneous fluorescence in the polymerized liposome at 40°C (above the phase transition of the polymer). B) Phase separation forming fluorescent domains in the same liposome immediately after lowering the temperature to 28°C (below the phase transition of the polymer). C) Formation of a single fluorescent cap in the same liposome after a few minutes.

This is caused by the immiscibility between the polymeric lipid, which is in the crystalline state, and the other membrane components, which are still in the fluid state. After a few minutes, the visible patches "flow" together, thus forming one single membrane cap (Fig. 56C). The time scale and appearance of these processes are completely analogous to the patching and capping observed on cell surfaces during their interaction with bivalent antibodies.

These natural biomembrane processes can thus be mimicked with striking similarity using polymeric model systems. The initiating mechanisms are, however, completely different. Nevertheless, such experiments may contribute to the understanding of the biological phenomenon. It is generally assumed that the process of capping is actively driven, thus requiring ATP. However, the results reported here provide the first experimental evidence that such a cap formation can take place passively without energy consumption.

6.2. Morphological Changes of Giant Liposomes

The transport mechanisms of endocytosis and budding involve a local bulge either to the inside or to the outside of the membrane with the subsequent detachment of a small vesicle (cf. Fig. 54). The first step of this two-stage process is a local reversible change in the spontaneous curvature of the membrane. In contrast, the second step, the detachment of the vesicle, is irreversible. Figure 57 schematically illustrates how this process is triggered off in Nature by taking erythrocytes as an example. Here a local change in the spontaneous curvature of the membrane occurs, probably due to a lateral contraction of the cytoskeleton.[154]

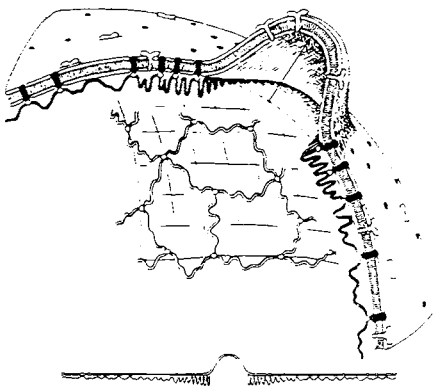

Fig. 57. Proposed pathway of triggering of endocytosis in an erythrocyte; by a local lateral contraction of the cytoskeleton, the removal of the network is expected to lead to a local change in the spontaneous curvature [154].

Protrusions caused by lateral phase separation can also occur in synthetic model systems. Figure 58A shows a giant liposome composed of a mixture of DMPC and the polymerizable spacer lipid **36b** (Scheme 4). Upon UV polymerization under a light microscope, clearly visible protrusions (Fig. 58B) develop out of the initially smooth surface. They continue to grow even after the UV light has been turned off, and their number increases with increasing amount of polymerizable lipid. This leads to the conclusion that a phase separation between the formed polymeric lipid and DMPC takes place, as shown schematically in Figure 58C.

Fairly well known examples of reversible transitions between different cell morphologies are the shape changes of erythrocytes. These can be achieved by different environmental changes such as changes in pH, temperature, and ionic strength or by the addition of drugs.[189] In the last

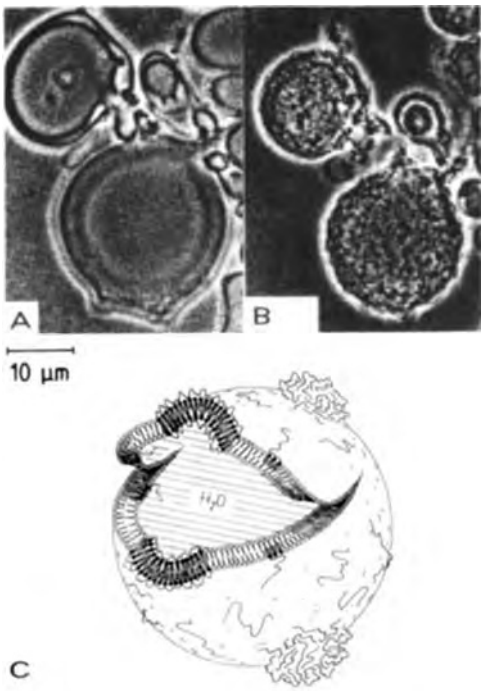

Fig. 58. Polymerization-induced protrusions in a giant liposome made from DMPC and **36b** (1:1) [154]. A) Phase-contrast micrograph of monomeric giant liposomes. B) After UV polymerization (100 s). C) Schematic representation of the microstructure of the bilayer after polymerization; lateral phase separation leads to domains of the polymeric lipid exhibiting a higher spontaneous curvature than the monomeric lipid matrix.

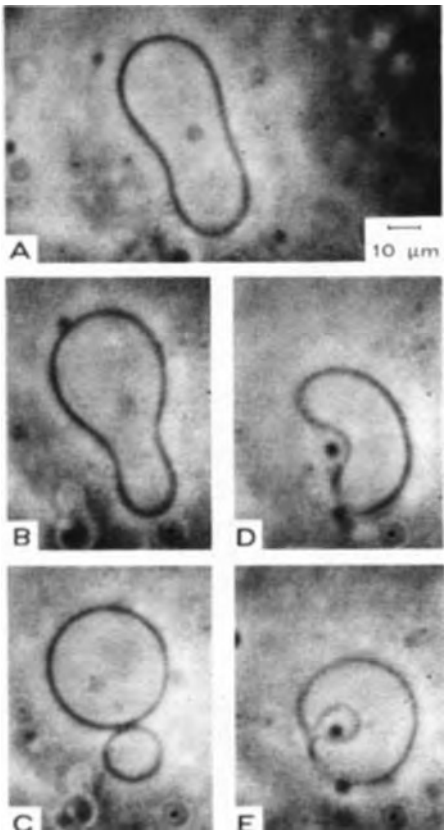

Fig. 59. Phase-contrast micrographs of temperature-induced, reversible morphology changes of a giant liposome made from the ammonium lipid **27** [155b]. A–B–C: Constriction of a discoid liposome at increasing temperature, reminiscent of exocytosis (cf. Fig. 54). A–D–E: Invagination in the same discoid liposome at decreasing temperature, reminiscent of endocytosis (cf. Fig. 54). A) 42°C; B) 42.5°C; C) 43°C; D) 41.5°C; E) 41°C.

few years, a series of theoretical studies have been published in order to explain the stability of the different cell shapes observed.[190] In this context, the model of *Svetina* and *Zeks* must be mentioned in particular.[190d] This model explains the stability of the different cell morphologies without any assumption as to the structure of the cell membrane. It is based on the idea that both leaflets of the lipid bilayer can expand and contract independently of one another. If, however, the changes in area of the two bilayer halves differ, the result is a change in the spontaneous curvature and thus a morphological change of the cell.

This concept has been confirmed by the observation of giant unilamellar liposomes.[155b] Figure 59 shows a series of reversible morphological changes of a giant vesicle made from the ammonium lipid **27**. These processes are temperature dependent and occur near the phase transition temperature (42°C). At a temperature of 42°C, the vesicle has a discoid shape (A). When the temperature is raised to 43°C, the vesicle constricts (C) via a bulge (B) to the outside. If, however, the temperature is lowered to 41°C, the opposite, i.e., a bulge to the inside, can be observed (D, E). Formally, these processes resemble budding and endocytosis and are completely reversible. By using the model of *Svetina* and *Zeks*, they can be explained in terms of a difference in the electric surface potential between the inner and outer membrane halves.[155b]

An additional example of an invagination involving a giant vesicle made from DMPC and the spacer lipid **36b** (4:1) is shown in Figure 60. In this case, however, the process is not triggered off by changing the temperature,

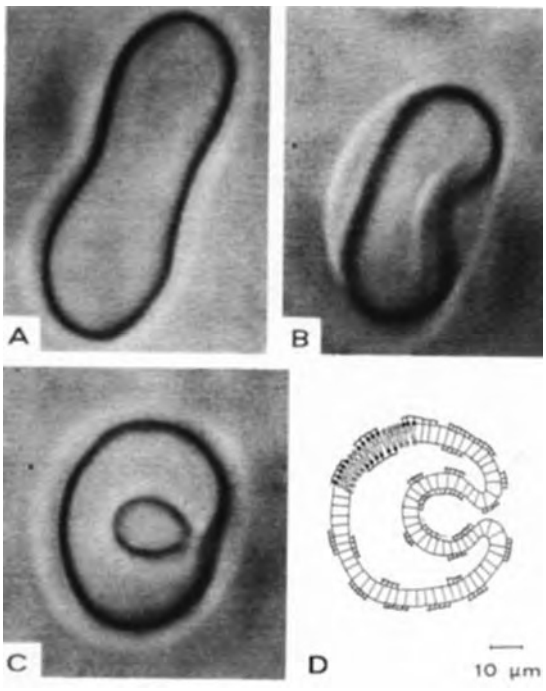

Fig. 60. Endocytosis-like shape change of a giant liposome made from DMPC and **36b** (4:1) caused by UV polymerization [155a]. A) Monomeric liposome at 29°C. B, C) Transformation occurring after 2 min of UV irradiation. D) Possible explanation for the shape transition in terms of a larger reduction of the area per lipid molecule in the outer monolayer compared with the inner leaflet. This might be due to an asymmetric distribution of **36b** which is probably preferentially distributed in the outer leaflet because of its large head group.

but by UV polymerization of one membrane component. This experiment does not lead to the protrusions of phase-separated polymer (cf. Fig. 58), because the portion of the polymerizable lipid is only 20 mol%. The membrane process observed is a bulge of the membrane to the inside, analogous to endocytosis. This can also be explained by the model of *Svetina* and *Zeks*: It can be assumed that the concentration of the spacer lipid **36b** is slightly higher in the outer membrane half than in the inner one, owing to its large head group. The polymerization going hand in hand with a decrease in area per molecule then leads to a reduction in area of the outer leaflet of the membrane, thus causing the invagination.[155a]

The experiments described show that even slight changes in the membrane or its environment may cause the morphological changes which are important for transport processes in biological systems. The second step of these processes, the irreversible detachment of smaller vesicles, however, requires more than only a change in curvature. In Section 4.3, a photoreactive system has already been presented which allows the realization of this process in model membranes. Upon short-term irradiation of interconnected, giant vesicles of the benzylammonium lipid **19**

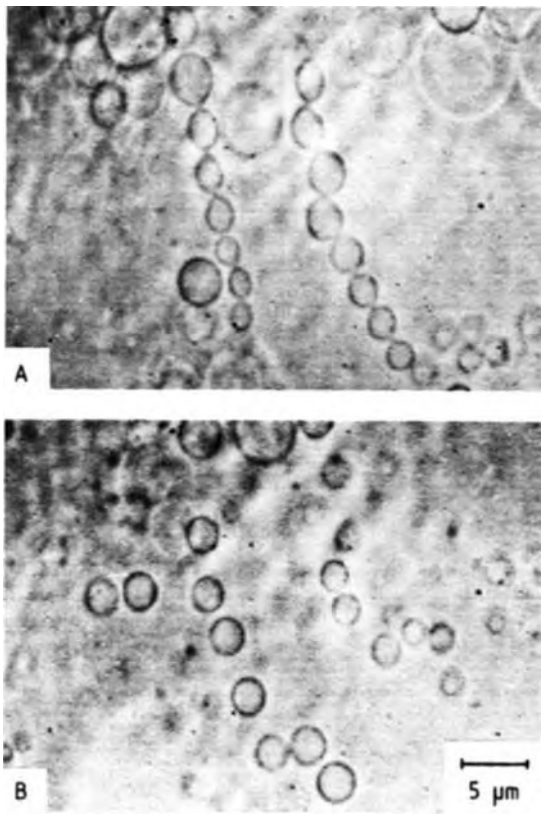

Fig. 61. Photochemically induced separation of interconnected giant liposomes made from the benzylammonium lipid **19** (cf. Fig. 23) [155b, 191]: A) before irradiation; B) after 2 s of UV irradiation.

(Fig. 61A), which resemble strings of pearls, the individual vesicles undergo separation via a photoinduced phase-separation process (Fig. 61B).[155b, 191]

6.3. Selective Opening of Phase-Separated Liposomes

6.3.1. Death of a Tumor Cell—Is Simulation Possible?

The great variety of biomembrane processes and the interaction of molecular and cellular events is reflected in a rather fascinating way in the death of a tumor cell that cannot escape from the immune system (Fig. 62).[192] The scanning electron micrograph shows the attack of an activated macrophage on a tumor cell (Fig. 62A).

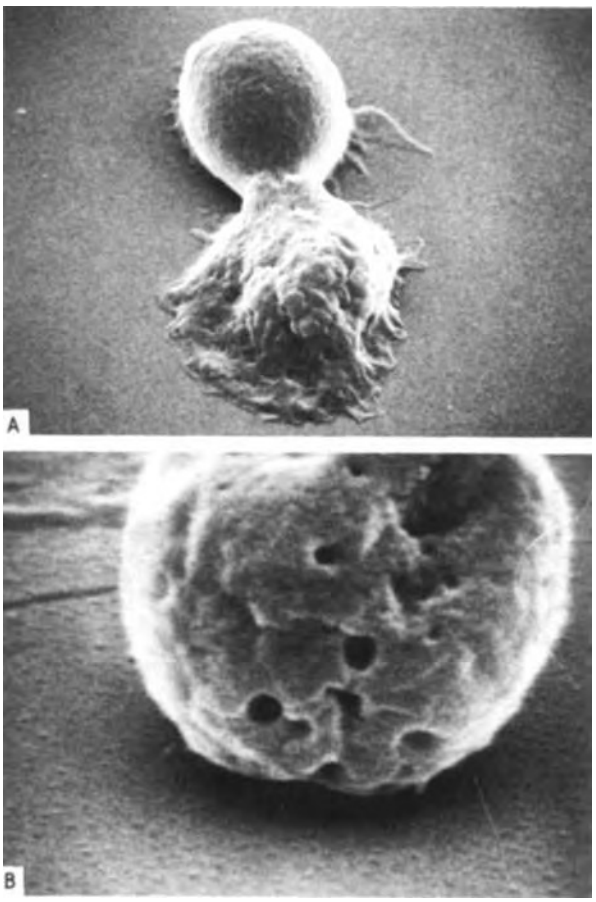

Fig. 62. Scanning electron micrograph of a tumor cell attacked by an activated macrophage [192]. A) Close contact between tumor cell (upper part) and activated macrophage (lower part). B) Holes in the membrane of the tumor cell after the attack.

On a molecular level, via antigen–antibody interaction, the macrophage recognizes the target cell and establishes a close membrane contact. Then, on a cellular level, a patching of the antigen–antibody complexes presumably takes place. In the subsequent membrane processes, which are not yet completely understood, the defense cell is able to drill holes in the originally stable membrane of the tumor cell. As a result, the cytoplasmic interior leaks out, which causes the death of the cell. What remains is a ghost cell (Fig. 62B).

Can this process be simulated? And if so, what is needed to do so? On the one hand, it is surprising that the lipid–protein bilayer does not collapse despite the visible holes. This gives evidence for its stability, the simulation of which has been discussed several times in this article. On

the other hand, the question of how these holes are created comes up. Conceivably, this occurs by means of a local process in the phase-separated membrane. One possibility could be that the macrophage tears open the tumor cell's membrane by means of a local endocytosis process of its own membrane. Another possibility is that the opening process is triggered by the macrophage and is accomplished by the cytoskeleton of the tumor cell. A further possible approach would be the lysis of membrane domains by enzymatic cleavage of the phospholipids, forming water-soluble lysophospholipids. The real course of this process is unknown.

The following sections describe the formal simulation of this process using the simple model of phase-separated polymerized liposomes.

6.3.2. *Formation of Domains in Vesicle Membranes*

Phase-separated liposomes can be used to simulate the hole formation process of the cell. In order to avoid a complete destruction of these liposomes by "uncorking," it is important that they are composed of a polymerized lipid matrix surrounding the labile domains of cleavable or nonpolymerizable lipids (Fig. 63).

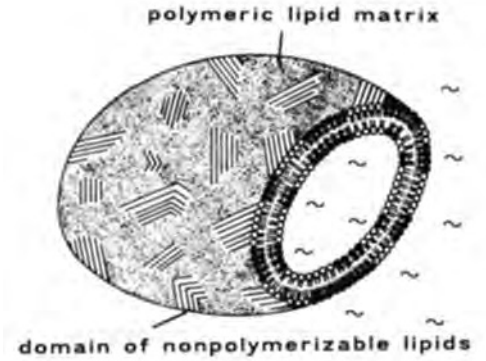

Fig. 63. Schematic drawing of a phase-separated liposome; the polymerized lipids form the stable matrix, surrounding the domains of nonpolymerizable lipids.

The induction of such a phase separation via polymerization has already been described in Section 6.1. Alternatively, the formation of domains can be predetermined by choosing suitable, incompatible lipid mixtures. Examples are mixtures of hydrocarbon and fluorocarbon lipids.[193] Mixed liposomes made from DMPC and the fluorocarbon amine **65** feature two phase transitions, e.g., in differential

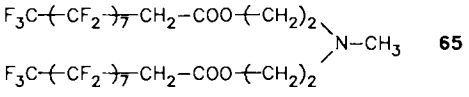

65

scanning calorimetry (DSC) measurements. This observation clearly demonstrates that these two lipids are immiscible since these phase transition temperatures are identical with those of the corresponding pure lipids.[193a] Freeze fracture electron micrographs reveal that, indeed, phase-separated liposomes with domains of the individual lipids are formed from the lipid mixture instead of two different liposome populations. Thus, domain formation in mixed membranes prepared from DMPC and **65** (95:5) can be made directly visible (Fig. 64) by means of the ripple structure typical of lecithin liposomes (see Section 4.8.1).

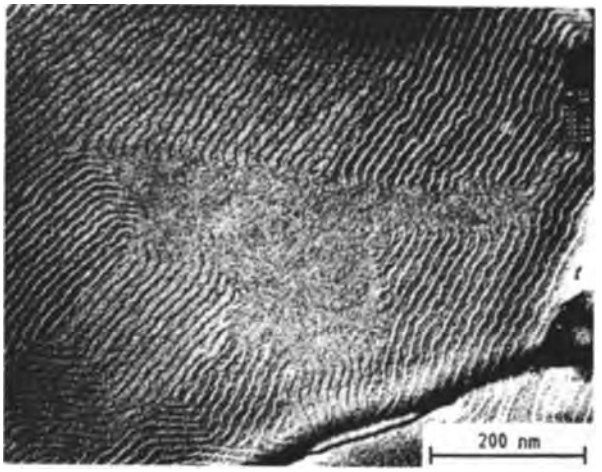

Fig. 64. Freeze fracture electron micrograph of a phase-separated liposomal membrane (95 mol% DMPC and 5 mol% fluorinated lipid **65**). The ripple structure shows the parts of the membrane composed of DMPC, surrounding a domain of the fluorinated lipid (smooth surface) [193a, 204].

To obtain a stable polymeric matrix needed for uncorking experiments of mixed liposomes, the polymerizable lipids **66** and **67** with hydrocarbon and fluorocarbon chains, respectively, have been used.

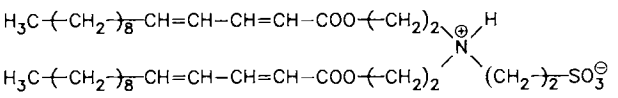

66

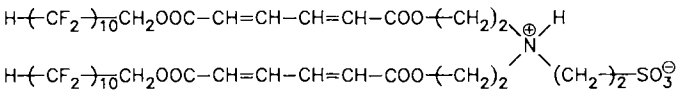

67

Small unilamellar liposomes can be prepared from both lipids by means of sonication. The tightness of the polymeric matrix of vesicles formed by lipid **66** was demonstrated by time-dependent release measurements using eosin as a fluorescent marker. Figure 65 shows a comparison of the eosin release of monomeric and polymeric vesicles

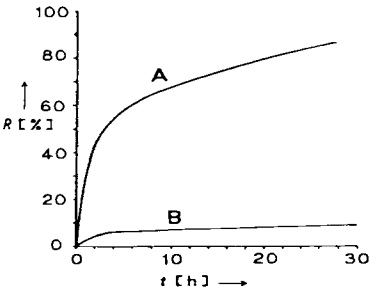

Fig. 65. Release R of eosin from vesicles (SUV) made from **66** [200]: A) monomeric; B) polymerized (5 mol% azobisisobutyronitrile, 60°C, 12 h).

made from the lipid **66**. The monomeric vesicles release half of the dye within 5 h, whereas the polymeric ones have lost only about 10% of their contents after 30 h.

6.3.3. *Corkscrews for Corked Liposomes*[194]

Numerous works proposing various mechanisms to destabilize membranes of liposomes have already been published. These include photochemical[94] as well as temperature-induced[195] increases in permeability or the use of pH-sensitive liposomes.[196] These investigations have exclusively been carried out with liposomes made from nonpolymerizable lipids.

In order to simulate the attack on a tumor cell by a macrophage, as shown in Figure 62, it is important not to destroy the whole liposome by membrane-destabilizing processes. Only labile domains within a stable lipid matrix should be selectively dissolved.[197] Figure 66 shows different processes that result in selective opening of such stabilized, phase-separated liposomes.

The polymeric components of these mixed liposomes form the stabilizing, shape-maintaining matrix. In order to destroy the labile domains, at least two methods are conceivable: dissolving or cleavage of the lipids. On the one hand, it is possible to dissolve the lipids of those domains with surfactants (detergents), thus forming mixed micelles, or by using organic solvents (e.g., acetone or ethanol). On the other hand, lipid cleavage through enzymatic or chemical reactions can be carried out. The enzymatic hydrolysis of phospholipids, forming lysophospholipids, by means of phospholipase A_2 (cf. Fig. 75) is the method Nature uses to synthesize and decompose membranes.[198] Several years ago, *Büschl* et al. already succeeded in transferring these reactions to polymeric model systems.[199]

The simulation of such lipid cleavage reactions by means of chemical processes offers a great number of synthetic ways to locally open the labile lipid domains in polymerized liposomes. Two principles are shown in Figure 66: head-group cleavage of double-chain lipids or chain cleavage of membrane-spanning lipids, each of them forming two surfactant molecules. To realize this concept by chemical reactions, a series of double-chain (**68**, **69**) or membrane-spanning (**70**) lipids with a disulfide group as

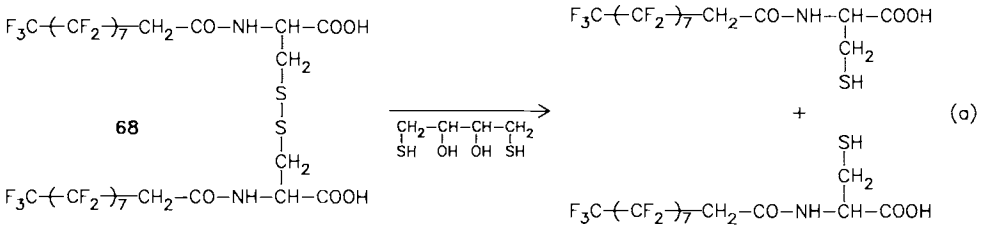

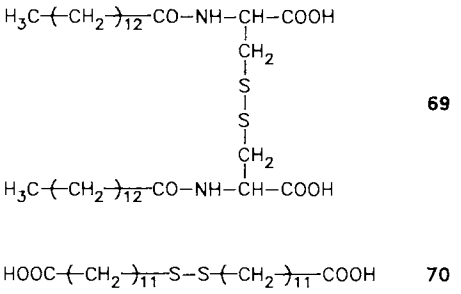

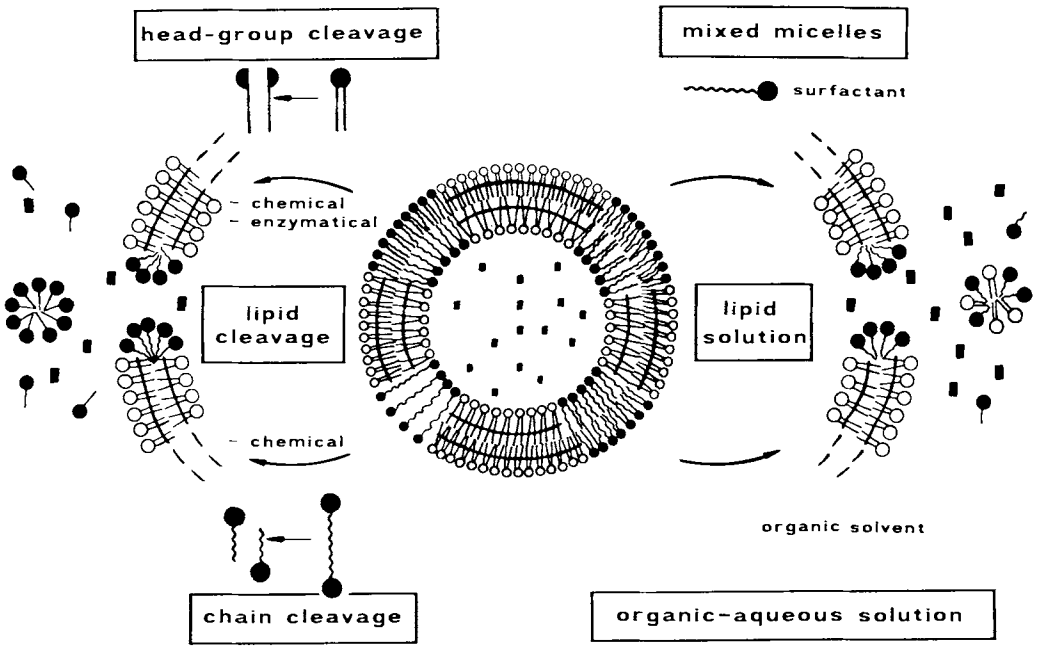

Fig. 66. Methods to uncork phase-separated liposomes composed of a stable polymeric matrix with labile domains.

cleavable unit have been synthesized.[200] The reductive cleavage of the water-insoluble disulfides—for example, with dithiothreitol (DTT)—leads to the formation of the corresponding partially water-soluble, single-chain thiols [Eq. (a)].

The cystine lipids **68** and **69** are capable of forming liposomes by sonication. The membrane-destruction process was followed by fluorescence spectroscopy using liposomes (made from **68**) containing eosin (Fig. 67). The

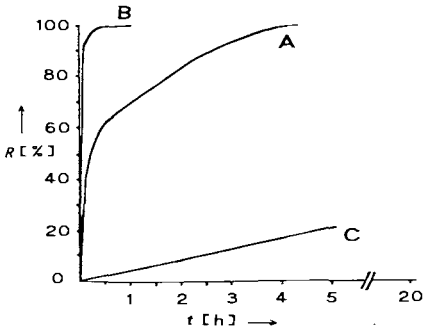

Fig. 67. Release R of eosin from vesicles (SUV) made from the fluorinated cystine derivative **68** at pH = 9 [200]. A) Cleavage of the disulfide bond by using 0.1 M Na_2SO_3. B) Cleavage by using dithiothreitol (DTT) (2 mg mL^{-1}). C) In the absence of a cleaving reagent.

cleavage process of the disulfide bonds within the cystine-lipid liposomes is much faster with DTT compared with sodium sulfite. Thus, DTT was used as a corkscrew[201] for all further opening reactions.

6.3.4. Chemical and Enzymatic Opening of Polymerized Mixed Liposomes

The combination of polymerizable taurine lipids (**66** and **67**) with cork-forming amphiphiles (**68**–**70**) results in stable polymeric liposomes with cleavable "cork" domains, as discussed in Section 6.3.3. Evidence for the opening of the labile domains in mixed liposomes was provided by electron microscopy as well as by the release of entrapped eosin.[202] Figure 68 schematically illustrates the opening process.

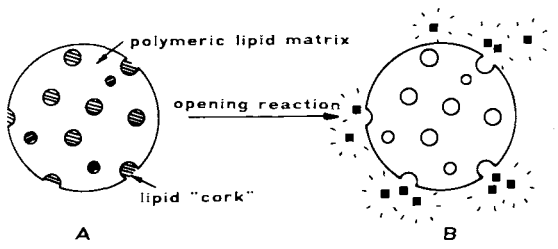

Fig. 68. Proof of the hole formation in polymerized vesicles containing labile domains. A) No fluorescence of the entrapped marker owing to self-quenching. B) Fluorescence of the released and therefore diluted marker after the hole formation in the membrane.

Head-group cleavage of lipids: In order to confirm the effect of phase separation on the release behavior of entrapped markers, liposomes with a homogeneous distribution of the cork component (i.e., not phase-separated) were studied as a comparison. Therefore, mixed liposomes from the polymerizable lipid **66** and the cystine lipid **69** (9 : 1), which form a homogeneous mixture, were used (Fig. 69).

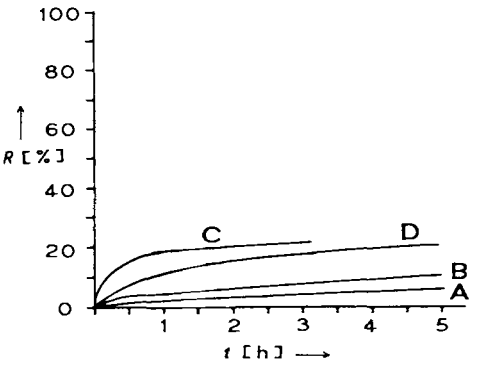

Fig. 69. Release R of eosin from domain-free vesicles (SUV) (90 mol% **66**, 10 mol% **69**, pH = 9) [200]. A) Polymerized vesicles in the absence of a cleaving reagent. B) Monomeric vesicles in the absence of a cleaving reagent. C) Polymerized vesicles after addition of DTT (1 mg mL^{-1}). D) Monomeric vesicles after addition of DTT (1 mg mL^{-1}).

In the absence of DTT as a cleavage reagent for the disulfide group of **69**, the release rates of the monomeric (curve B) and the polymerized liposomes (curve A) differ only very little. After the addition of DTT, the cleavage of the lipids does not lead to the formation of holes, because the cleavable lipids are distributed homogeneously within the membrane. The compatible lysolipids, formed during that process, cannot be pushed out of the membrane. Thus, after a short period of time, the release rates (curves C and D) are comparable to those measured without DTT (curves A and B).

A dramatic change in release behavior occurs if phase-separated liposomes from the same polymerizable lipid **66** and the domain-forming "fluorocarbon cork" **68** (9 : 1) are used (Fig. 70).

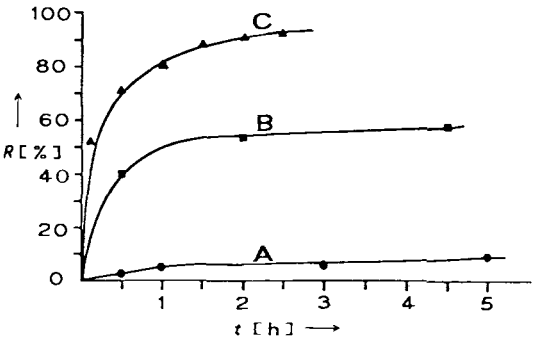

Fig. 70. Release R of eosin from phase-separated, domain-containing vesicles (SUV) (90 mol% **66**, 10 mol% **68**, pH = 9) [200]. A) Polymerized vesicles in the absence of cleaving reagent. B) Monomeric vesicles after addition of DTT (1 mg mL^{-1}). C) Polymerized vesicles after addition of DTT (1 mg mL^{-1}).

In this case, the domains of **68** are rapidly destroyed by DTT during the disulfide cleavage in unpolymerized liposomes. However, owing to the lateral diffusion of the monomeric lipids, the membrane defects are healed rather quickly. After cleavage of the whole cork component (about 1 h), the release rate (curve B) decreases to that

without DTT (curve A). After addition of DTT to the polymerized liposomes, the stiff polymeric matrix is uncorked and eosin is rapidly and almost completely released (curve C).

Is the hole formation in these experiments really similar to that which occurs in a cell (cf. Fig. 62)? It was possible to confirm this using two electron microscopy techniques. Figure 71 shows a scanning electron micrograph of a phase-separated polymeric liposome made from the taurine lipid **66** and the cleavable cystine lipid **68** before and after the destruction of the labile domains. As can be seen,

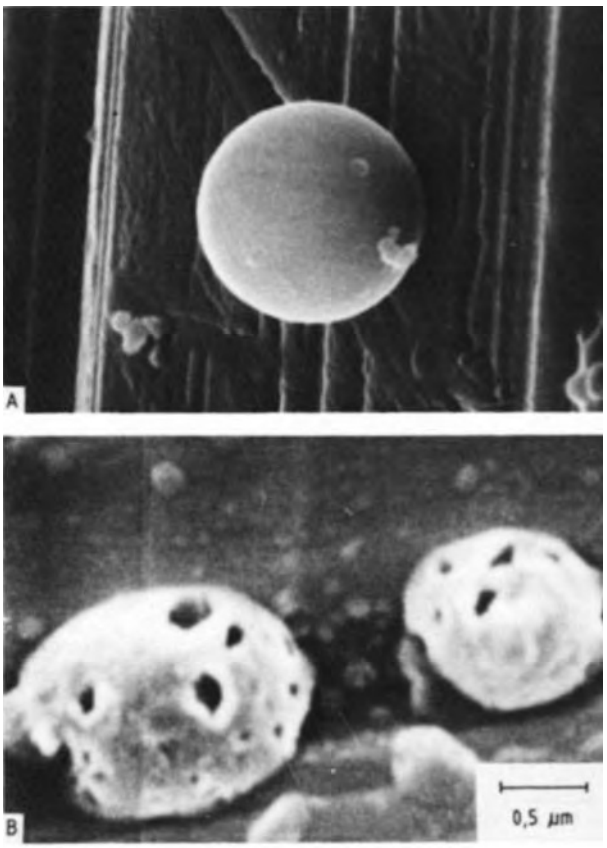

Fig. 71. Scanning electron micrograph of phase-separated, polymerized liposomes (90 mol% **66**, 10 mol% **68**) [200, 203]. A) Liposome before the cleavage reaction. B) Perforated membrane after the cleavage reaction (uncorked liposome!).

the lipid bilayers do not collapse. The function of the cytoskeleton of the cell, i.e., the stabilization of the membrane, is thus fulfilled by the polymeric matrix of the liposomes. The pore formation observed is not an artifact of the preparation technique for the scanning electron micrograph. This was proven by means of freeze fracture electron microscopy (Fig. 72). Figure 72A shows the smooth, unstructured surface of the polymeric mixed liposome before it is uncorked. In Figure 72B the membrane again features clearly visible holes after the cleavage has been carried out. The different diameters of the holes in the uncorked liposomes (Figs. 71B and 72B) are due to varying domain sizes, caused by different annealing times of the mixed liposomes before their polymerization.

Chain cleavage of lipids: All experiments discussed so far have been carried out with the cystine derivative **68** as the lipid cork. An analogous behavior has been observed with

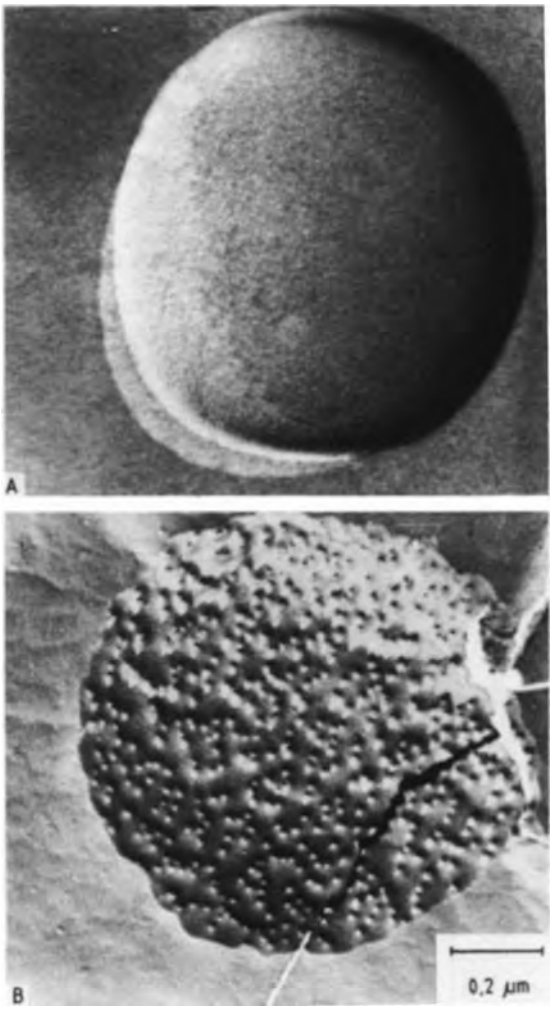

Fig. 72. Freeze fracture electron micrograph of phase-separated, polymerized liposomes [200, 204] (see caption to Fig. 71).

the bipolar disulfide amphiphile **70**. The release of eosin from phase-separated liposomes containing this cleavable lipid and the fluorinated muconic acid derivative **67** is shown in Figure 73.

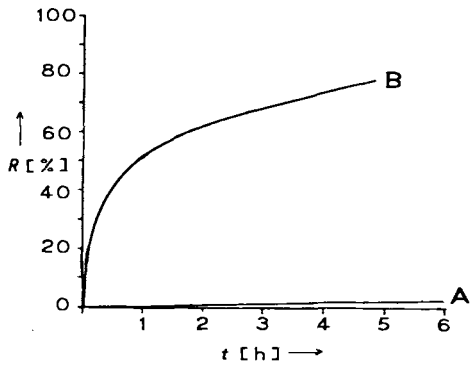

Fig. 73. Release R of eosin from phase-separated, domain-containing vesicles (SUV) (90 mol% muconic acid derivative **67**, 10 mol% disulfide **70**, pH = 9) [200]. A) Polymerized vesicles in the absence of a cleaving reagent. B) Polymerized vesicles after addition of DTT (1 mg mL^{-1}).

Polymerized vesicles with 10 mol% of the supposedly membrane-spanning cork **70** again exhibit only minor eosin release before cleavage (curve A). In this case, also, the

addition of DTT leads to a rapid release of the fluorescent marker, even though the rate is slower than that observed in the cleavage experiments with the cystine lipid **68**. This is quite understandable since the cleavage reagent does not attack the head groups; it first needs to diffuse into the membrane. However, no difference can be seen by electron microscopy between the double-chain and membrane-spanning cleavable lipid systems (Fig. 74).

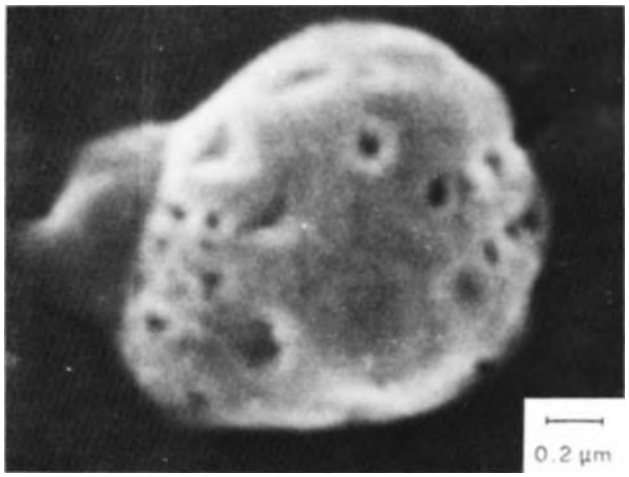

Fig. 74. Scanning electron micrograph of phase-separated, domain-containing liposomes (90 mol% **67**, 10 mol% **70**); hole formation after addition of DTT [200, 203].

Dissolving the cork without cleavage: As already illustrated schematically (Fig. 66), apart from a cleavage reaction, even the simple dissolving of the labile domains out of a polymeric matrix can lead to the formation of pores in a vesicle membrane.[200] This concept is based on the well-known fact that polymerized vesicles exhibit a higher stability towards surfactants or solvents than their monomeric analogues.[72,205]

To carry out an opening reaction by using solvents, mixed membranes made from the cationic polymerizable ammonium lipid **27** with the fluorinated amine **65** (9:1) were prepared. The dissolving of the domains formed by the fluorocarbon lipid after the addition of acetone to the solution of polymerized vesicles (1:1) was demonstrated by scanning electron microscopy. Here, too, holes are formed in the vesicle. In the course of this process, the polymerized lipid matrix again maintains its shape. In the meantime, *Tsuchida* et al. have also reported similar experiments.[206]

Enzymatic uncorking:[207] The opening reactions discussed so far proceed under nonphysiological conditions and with a relatively high concentration of cleavage reagent. The biochemical opening, in contrast, uses phospholipases and allows the process to take place under physiological conditions. Phospholipase A_2 specifically catalyzes the hydrolysis of the ester bond at the C-2 position of L-α-glycerophospholipids (Fig. 75).

This enzymatic reaction can be transferred to model membranes composed of polymerized and natural lipids. This was demonstrated first by using monolayers.[199] To investigate this cleavage reaction in liposomes,[208] mixed

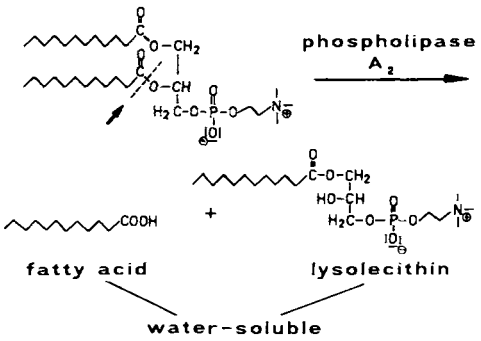

Fig. 75. Enzymatic cleavage of the C-2 ester bond of a lecithin by phospholipase A_2; the products (fatty acid and lysolecithin) are water-soluble surfactants.

membranes of the polymerizable lecithin **71** and DPPC (1:1) were used. Here, DPPC acts as the cork, cleavable by

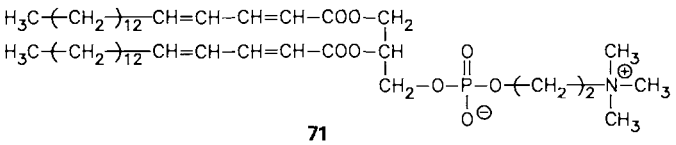

71

enzymes. The liposomes formed from these two lipids do not show domains since they are homogeneously miscible. Polymerization, however, induces a phase separation. It has to be pointed out that the highly specific phospholipase A_2 attacks the ester group of the dienoyl lecithin neither in the monomeric nor in the polymeric form. Indeed, liposomes prepared only from the dienoyl lecithin **71** remain tight and do not release eosin after addition of the enzyme. Thus, the release of 6-CF from mixed liposomes (Fig. 76) is clearly due only to the cleavage of the saturated lecithin (DPPC).

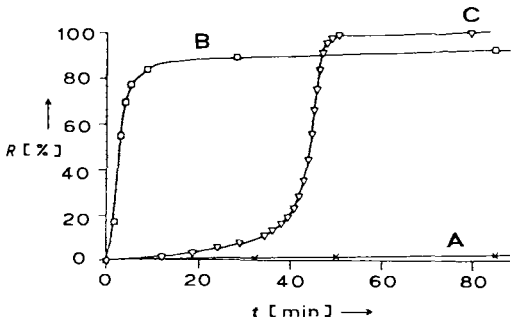

Fig. 76. Release R of 6-CF from monomeric and polymerized mixed vesicles (SUV) (50 mol% **71**, 50 mol% DPPC) [208]. A) Monomeric and polymerized vesicles in the absence of the enzyme. B) Polymerized vesicles after addition of phospholipase A_2 (30 µg mL^{-1}). C) Monomeric vesicles after addition of phospholipase A_2 (30 µg mL^{-1}).

In the absence of the enzyme, the release rate of 6-CF for the monomeric as well as the polymeric liposomes remains below 1% (curve A) during the experiment. After the addition of phospholipase A_2, a dramatic change in the release behavior occurs. The polymerized, phase-separated vesicles very rapidly lose the entrapped marker: already after 10 min, 90% of the vesicle contents are released

(curve B). In contrast, the analogous monomeric system exhibits an "incubation time" of about 40 min. In this case, too, a fast and almost complete release of the marker subsequently takes place within a few minutes (curve C). How can these different release rates be explained?

At first the 6-CF marker is only slowly released from the homogeneously mixed membrane of the monomeric liposomes. This is due to the fact that the lysolipids formed dissolve in the membrane, thus disturbing it only slowly. Since the ratio of cleavable to noncleavable lipid is 1 : 1, the membrane reaches such a high content of lysolipids and fatty acids after a certain incubation time (40 min) that the liposomes spontaneously decay, forming mixed micelles. The difference between the monomeric and the polymerized mixed system can be explained by the polymerization-induced phase separation. Experiments with monolayers of analogous systems also revealed that phospholipase A_2 attacks phase-separated membranes much faster than the corresponding homogeneous mixtures.[199] Due to phase separation, the lysolipid- and fatty-acid-rich domains are rapidly dissolved. However, the formation of a stable polymeric matrix may be impossible in these systems owing to the high contents (50 mol%) of DPPC. Thus, the polymerized liposomal membrane, too, is completely destabilized during the cleavage reaction with the formation of mixed micelles.

These concepts are supported by release measurements with mixed liposomes of the same composition but with different extents of polymerization (conversion).[208] As can be seen in Figure 77, the incubation time for the spontaneous destabilization depends on the amount of polymer in the membrane. Due to the polymerization-induced phase separation, the portion of cleavable lipid within the monomeric areas increases with increasing polymerization. Therefore, the time needed to reach the critical concentration of water-soluble products in the monomeric domains, i.e., the incubation time, depends on the extent of polymerization.

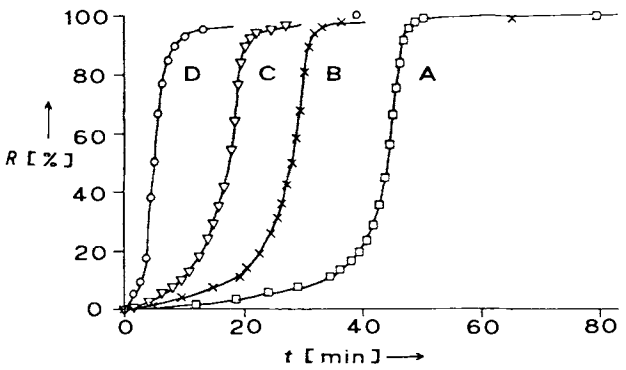

Fig. 77. Enzymatic release of 6-CF from partially polymerized vesicles (SUV) (50 mol% **71**, 50 mol% DPPC, 30 μg mL^{-1} phospholipase A_2) [208]. Dependence of the release kinetics on the extent of polymerization: A) 0%; B) 15%; C) 45%; D) 85%.

Synthetic corkscrews for cells? The experiments discussed so far show that it is indeed possible to formally simulate the biological process of local cell membrane opening by using phase-separated, partially polymerized liposomes. However, one is still miles away from the natural process. Figure 78 leads back to biological processes and does not merely show an additional polymerized liposome before and after it has been uncorked.

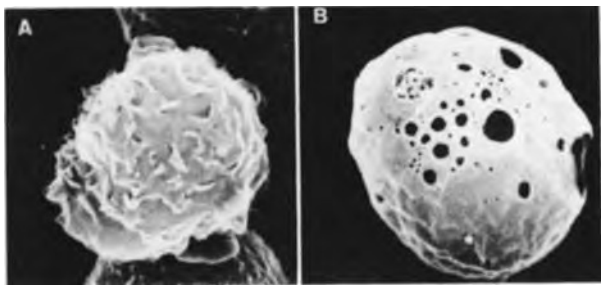

Fig. 78. Scanning electron micrograph of the hole formation in leukemia cells [209e]. A) Untreated leukemia cell. B) Leukemia cell after treatment with *O*-methyllysolecithin.

This scanning electron micrograph shows leukemia cells of a cell culture before (A) and after (B) treatment with special surfactants, namely, methyl ether derivatives of lysophospholipids which are, at present, also considered as anti-tumor agents.[209,68a] The result of the uncorking process of the cell by the synthetic lysolipid can clearly be seen. In whatever form the natural process of uncorking cells by activated macrophages (cf. Fig. 62) may proceed, it can at least be simulated in cells by using surfactants.

7. Outlook or Where to Go?

Many parts of this review are certainly incomplete. This is due partly to a lack of sufficient insight, partly to insufficient data. The reader should therefore not look at this contribution as a crystal-clear definition of facts and problems, but rather as an impulse for possible developments. This review represents an attempt, using the concept of self-organization, to jointly discuss the molecular architecture of supramolecular systems such as liquid crystals, micelles, liposomes, and biomembranes as a problem of mutual interest.[210]

The attempt to review different areas, which have traditionally been separate, is always a risky enterprise. It is impossible without generalizations and one thus, and rightly so, has to accept the eventuality of becoming superficial.[211]

On the other hand, *Georg Christoph Lichtenberg*, already 200 years ago, stated clearly: "He who understands nothing but chemistry doesn't even understand chemistry." Originally discussed in a more philosophical context, it nowadays (in times of rapidly increasing specialization) certainly holds true even for the natural sciences alone. Additionally, one has to accept that, owing to modern methods of measurements and sophisticated computer techniques, it is possible to measure to high precision and to evaluate more and more exactly: to measure and to verify is intensively taught and studied, but, too often, intuitive thinking is neglected.[212] Interdisciplinary research, however, is one way to stimulate intuition. In a refreshingly encouraging contribution, which recently appeared

in this journal, *Roald Hoffmann* describes "How Chemistry and Physics Meet in the Solid State."[211a] He stresses intuition as a strength of chemists. This frontier area of solid-state chemistry and physics can also only be tackled jointly and, like the formation and investigation of functional supramolecular systems, represents a fascinating chapter of modern materials science.

The fascination evoked in human beings by biological processes is old. The fascination of simulating these processes and transferring them into technical dimensions has just begun. The field is open and modern chemistry can offer essential contributions to it. Where to go? At present, materials science certainly can profit more from life science than vice versa. A technical analogue for biological membranes mimicking the specificity of their recognition and translocation processes has not yet been found—despite the countless varieties of synthetic polymer membranes already known. There have been many attempts to mimic the natural prototype and a few examples have been mentioned in this contribution. The breakthroughs are still missing: the knowledge is available, but innovation is a long time coming. Especially with respect to the next generation of technical membranes—switchable, functional, asymmetric, and suitable for specific and selective transport—the chemist should not leave the field of oriented supramolecular systems to the physicist and biologist alone. The physicists tend to like "too simplified" models, while biologists tend to reject all approaches which are not in accord with the "too complicated" prototypes of Mother Nature. Thus organic chemistry and macromolecular chemistry can play the important role of a mediator. One hint that this might work is given in the contribution by *J.-M. Lehn* in this issue.[12d] Molecular recognition processes for organic and inorganic compounds are a first step towards simulating highly specific recognition reactions common in biology.[12c,213] It will also be exciting to see what possibilities will be opened by the synthesis of glycolipids and glycoproteins representing tumor-specific antigens. They might be a bridge between organic chemistry and immunology.[214]

The art of synthesizing exceedingly complex molecules and characterizing them perfectly has reached dizzying heights and opens fascinating opportunities in the area of molecular engineering. But what is it good for? This art certainly will remarkably increase our chemical knowledge—but is this enough? It is not unlikely that, independent of the enormously increasing number of new synthetic compounds, the number of true innovations or innovative compounds has constantly decreased during the last few decades. In his aggressively but optimistically written contribution on "Chemical Needs and Possibilities at the End of the Century,"[215] *C. Frejacques* points out the importance of chemical systems based on self-organization. He stresses that, above and beyond the chemistry of covalent bonds, a chemistry of supramolecular systems is now emerging.

This review on the molecular architecture and function of polymeric oriented systems intends to show that such chemical systems, like their natural prototypes, may lead to functional units which can contribute to the understanding of biological processes and to the development of new materials. Both tradition and innovation are needed for that. On the borderland between the different disciplines of science, adventures are waiting. Neither uncritical optimism nor obstructive pessimism are justified. The excitement and the courage to set out for new frontiers and the willingness for close cooperation are basic prerequisites for this adventure of science. All the knowledge is available, we only have to learn to use it.

We are grateful to the Deutsche Forschungsgemeinschaft, the Bundesministerium für Forschung und Technologie, and the Fonds der Chemischen Industrie for support of our work. And what about thanks to the coworkers? See Ref. [216]!

Received: September 29, 1987 [A 653 IE]
German version: *Angew. Chem. 100* (1988) 117
Translated by *Eva Grunwald* and Dr. *Christian Salesse*, Mainz

[1] B. Brecht: *Geschichten*, Bibliothek Suhrkamp, Frankfurt am Main 1962, p. 167. In this essay and under the heading "Hardship of the best," Mr. K. answers this question. But he certainly was a scientist! Don't you think so?

[2] H. Mark, *Angew. Chem. 93* (1981) 309; *Angew. Chem. Int. Ed. Engl. 20* (1981) 303.

[3] a) *Ronald Searle*, the scalpel-sharp British cartoonist, illustrates that even for the old gold diggers it was an absurd adventure to pan for gold by the light of the silvery neon in the main street of downtown Klondike (see [3b], p. 25):

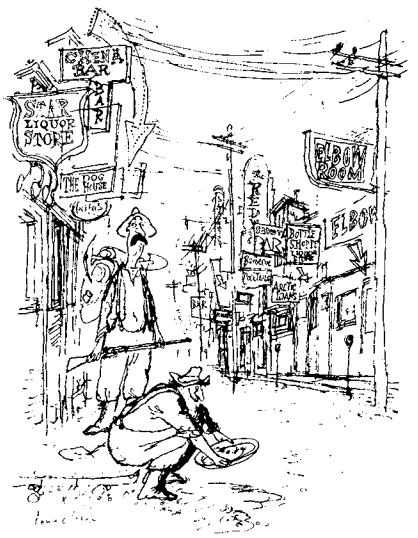

Already in 1788 (!) *Georg Christoph Lichtenberg*, the great and critical philosopher and physicist from Göttingen, was very clear and outspoken in this respect when he characterized one of his colleagues: "... he was still hanging at his university like a wonderful chandelier without a tiny candle lit for years" (G. Ch. Lichtenberg, "*Sudelbücher*"). b) R. Searle: *From Frozen North to Filthy Lucre*, Viking Press, New York 1964.

[4] *Erwin Chargaff*, biochemist and critical essayist, depicts this as follows: "In science today smaller and smaller rooms are furnished more and more luxuriously and completely." (E. Chargaff: *Bemerkungen*, Klett-Cotta, Stuttgart 1981, p. 33).

[5] A. Dress, H. Hendrichs, G. Küppers: *Selbstorganisation - Die Entstehung von Ordnung in Natur und Gesellschaft*, Piper, München 1986.

[6] a) H. Haken: *Erfolgsgeheimnisse der Natur - Synergetik: Die Lehre vom Zusammenwirken*, Deutsche Verlags-Anstalt, Stuttgart 1986; b) B.-O. Küppers (Ed.): *Ordnung aus dem Chaos. Prinzipien der Selbstorganisation und Evolution des Lebens*, Piper, München 1987.

[7] From the standpoint of the history of science, it is most interesting to see how, very often, out of controversies between different disciplines, new research areas develop. The famous and historical controversy in the twenties between the then well-established colloid science (*W. Ostwald*) and the rising macromolecular chemistry (*H. Staudinger*) is an

instructive example for that: weak interactions in the formation of aggregates (colloids) as opposed to covalently linked small molecules (macromolecules). These competitive concepts have long since inevitably fused, as perfectly demonstrated in the supramolecular systems of biological membranes. However, it is also interesting to note that—at least in Germany—colloid science did not recover from this controversy for quite a while. For at least two or three decades colloid chemistry nearly disappeared from German universities. It regained its reputation only via its industrial importance. a) H. Morawetz, *Angew. Chem. 99* (1987) 95; *Angew. Chem. Int. Ed. Engl. 26* (1987) 93; b) *Polymers. The Origins and Growth of a Science*, Wiley, Chichester 1985; c) E. Jostkleigrewe (Ed.): *Makromolekulare Chemie - Das Werk Hermann Staudingers in seiner heutigen Bedeutung*, Schnell und Steiner, München 1987.

[8] a) J. D. Barnal, *Trans. Faraday Soc. 29* (1933) 1022; b) *The Physical Basis of Life*, Routledge and Kegan, London 1951.

[9] a) G. H. Brown, J. J. Wolken: *Liquid Crystals and Biological Structures*, Academic Press, New York 1979; b) D. M. Small, *J. Colloid Interface Sci. 58* (1977) 581; c) D. Chapman in F. D. Saeva (Ed.): *Liquid Crystals: The Fourth State of Matter*, Dekker, New York 1979, p. 305; d) Y. Bouligand in L. Liebert (Ed.): *Liquid Crystals (Solid State Phys. Suppl. 14* (1978) 259).

[10] As far as the often discussed and adjured willingness of scientists to cooperate is concerned, one has to be skeptical. Again one can use the point of view of *Ronald Searle* to describe the situation: People tend to cling to the old ways; a homesteader's cabin is still his castle (see [3b], p. 14 and [4]):

[11] The courage to set out and the willingness to turn around and search for prey from a different perspective are prerequisites for the adventure of science (see [3b], p. 21):

[12] Supermolecules ("Übermolekeln") were already defined by *K. L. Wolf* in 1937 to describe associations of molecules, the function of which was based on their organization: a) K. L. Wolf, F. Frahm, H. Harms, *Z. Phys. Chem. Abt. B 36* (1937) 17; b) K. L. Wolf, R. Wolff, *Angew. Chem. 61* (1949) 191. The conception of "Supramolecular Chemistry" has been realized by *Jean-Marie Lehn* and his group during the last few years: c) J.-M. Lehn, *Science (Washington) 227* (1985) 849; d) *Angew. Chem. 100* (1988) 91; *Angew. Chem. Int. Ed. Engl. 27* (1988) 89. In this contribution the term *supramolecular systems* is not only used for small molecular complexes of single molecules, such as substrate-receptor complexes. It is also applied to large molecular aggregates (high aggregation numbers), the function of which is again based on their organization. The ideal system to exemplify this definition is the biomembrane.

[13] a) H. Kelker, R. Hatz: *Handbook of Liquid Crystals*, Verlag Chemie, Weinheim 1980; b) D. Demus, H. Demus, H. Zaschke: *Flüssige Kristalle in Tabellen, Band 1/Band 2*, VEB Verlag für Grundstoffindustrie, Leipzig 1974/1984.

[14] H. Sackmann, *Prog. Colloid Polym. Sci. 69* (1984) 73.

[15] W. Maier, A. Saupe, *Z. Naturforsch. A 14* (1959) 882; *ibid. 15* (1960) 287.

[16] P. J. Flory, G. Ronca, *Mol. Cryst. Liq. Cryst. 54* (1979) 311.

[17] F. Reinitzer, *Monatsh. Chem. 9* (1888) 421.

[18] S. Chandrasekhar, B. K. Sadashiva, K. A. Suresh, *Pramana 9* (1977) 471; *Chem. Abstr. 88* (1978) 30566y.

[19] a) C. Destrade, P. Foucher, H. Gasparoux, Nguyen Huu Tinh, A.-M. Levelut, J. Malthête, *Mol. Cryst. Liq. Cryst. 106* (1984) 121; A.-M. Levelut, *J. Phys. Lett. 40* (1979) L 81.

[20] J.-M. Lehn, J. Malthête, A.-M. Levelut, *J. Chem. Soc. Chem. Commun. 1985*, 1794.

[21] a) H. Zimmermann, R. Poupko, Z. Luz, J. Billard, *Z. Naturforsch. A 40* (1985) 149; b) J. Malthête, A. Collet, *Nouv. J. Chim. 9* (1985) 151.

[22] a) J. Malthête, A.-M. Levelut, Nguyen Huu Tinh, *J. Phys. Lett. 46* (1985) L 875; b) Nguyen Huu Tinh, C. Destrade, A.-M. Levelut, J. Malthête, *J. Phys. 47* (1986) 553.

[23] a) O. Herrmann-Schönherr, J. H. Wendorff, H. Ringsdorf, P. Tschirner, *Makromol. Chem. Rapid Commun. 7* (1986) 791; b) H. Ringsdorf, P. Tschirner, O. Herrmann-Schönherr, J. H. Wendorff, *Makromol. Chem. 188* (1987) 1431; c) M. Ballauff, G. F. Schmidt, *Makromol. Chem. Rapid Commun. 8* (1987) 93.

[24] a) J. L. White, *J. Appl. Polym. Sci. Appl. Polym. Symp. 41* (1985) 3; b) E. T. Samulski, *Faraday Discuss. Chem. Soc. 79* (1985) 7.

[25] a) C. Robinson, *Trans. Faraday Soc. 52* (1956) 571; b) P. W. Morgan, *Macromolecules 10* (1977) 1381; c) S. L. Kwolek, P. W. Morgan, J. R. Schaefgen, L. W. Gulrich, *ibid. 10* (1977) 1390; d) T. I. Bair, P. W. Morgan, F. L. Killian, *ibid. 10* (1977) 1396; e) M. Panar, L. F. Beste, *ibid. 10* (1977) 1401.

[26] a) W. J. Jackson, H. F. Kuhfuss, *J. Polym. Sci. Polym. Chem. Ed. 14* (1976) 2043; b) W. J. Jackson, *Br. Polym. J. 12* (1980) 154.

[27] P. G. de Gennes, *C. R. Hebd. Seances Acad. Sci. Ser. B 281* (1975) 101.

[28] A. Roviello, A. Sirigu, *J. Polym. Sci. Polym. Lett. Ed. 13* (1975) 455.

[29] a) H. Finkelmann, H. Ringsdorf, J. H. Wendorff, *Makromol. Chem. 179* (1978) 273; b) V. P. Shibaev, N. A. Platé, Ya. S. Freidzon, *J. Polym. Sci. Polym. Chem. Ed. 17* (1979) 1655.

[30] a) A. Ciferri, W. R. Krigbaum, R. B. Meyer (Eds.): *Polymer Liquid Crystals*, Academic Press, New York 1982; b) M. Gordon, N. A. Platé (Eds.): *Liquid Crystal Polymers Vol. I–III (Adv. Polym. Sci. 59/60–61* (1984)); c) A. Blumstein (Ed.): *Polymer Liquid Crystals*, Plenum, New York 1985.

[31] a) A. Blumstein, J. Asrar, R. B. Blumstein in A. C. Griffin, J. F. Johnson (Eds.): *Liquid Crystals and Ordered Fluids, Vol. 4*, Plenum, New York 1984, p. 311; b) H. Finkelmann, *Angew. Chem. 99* (1987) 840; *Angew. Chem. Int. Ed. Engl. 26* (1987) 816; c) S. K. Varshney, *J. Macromol. Sci. Rev. Macromol. Chem. Phys. C 26* (1986) 551.

[32] W. Kreuder, H. Ringsdorf, *Makromol. Chem. Rapid Commun. 4* (1983) 807.

[33] a) W. Kreuder, H. Ringsdorf, P. Tschirner, *Makromol. Chem. Rapid Commun. 6* (1985) 367; b) O. Herrmann-Schönherr, J. H. Wendorff, W. Kreuder, H. Ringsdorf, *ibid. 7* (1986) 97; c) G. Wenz, *ibid. 6* (1985) 577.

[34] a) F. Hessel, H. Finkelmann, *Polym. Bull. 14* (1985) 375; b) *ibid. 15* (1986) 349; c) F. Hessel, R.-P. Herr, H. Finkelmann, *Makromol. Chem. 188* (1987) 1597; d) Q. Zhou, H. Li, X. Feng, *Macromolecules 20* (1987) 233.

[35] S. Berg, V. Krone, H. Ringsdorf, *Makromol. Chem. Rapid Commun. 7* (1986) 381.

[36] W. Kreuder, H. Ringsdorf, O. Herrmann-Schönherr, J. H. Wendorff, *Angew. Chem. 99* (1987) 1300; *Angew. Chem. Int. Ed. Engl. 26* (1987) 1249.

[37] a) M. Ballauff, *Macromolecules 19* (1986) 1366; b) *Makromol. Chem. Rapid Commun. 7* (1986) 407.

[38] a) B. Reck, H. Ringsdorf, *Makromol. Chem. Rapid Commun. 6* (1985) 291; b) *ibid. 7* (1986) 389.

[39] a) G. W. Gray, P. A. Winsor (Eds.): *Liquid Crystals and Plastic Crystals, Vol. I, II*, Ellis Horwood, Chichester 1974; b) G. J. T. Tiddy, *Phys. Rep. 57* (1980) 1; c) B. J. Forrest, L. W. Reeves, *Chem. Rev. 81* (1981) 1.

[40] H. Hoffmann, *Ber. Bunsenges. Phys. Chem. 88* (1984) 1078, and references cited therein.

[41] P. Fromherz, *Ber. Bunsenges. Phys. Chem. 85* (1981) 891.

[42] a) J. N. Israelachvili, S. Marčelja, R. G. Horn, *Q. Rev. Biophys. 13* (1980) 121; b) J. N. Israelachvili in V. Degiorgio, M. Corti (Eds.): *Physics of Amphiphiles: Micelles, Vesicles and Microemulsions*, North-Holland Physics Publishing, Amsterdam 1985, p. 24; c) D. F. Evans, B. W. Ninham, *J. Phys. Chem. 90* (1986) 226.

[43] a) H. Finkelmann, M. A. Schafheutle, *Colloid Polym. Sci. 264* (1986) 786; b) E. Jahns, H. Finkelmann, *ibid. 265* (1987) 304; c) B. Lühmann, H. Finkelmann, G. Rehage, *Angew. Makromol. Chem. 123/124* (1984) 217; d) J. Herz, F. Reiss-Husson, P. Rempp, V. Luzzati, *J. Polym. Sci.*

Part C4 (1964) 1275; e) A. Schmitt, R. Varoqui, A. Skoulios, *C. R. Hebd. Seances Acad. Sci. Ser. C268* (1969) 1469; f) R. Thundathil, J. O. Stoffer, S. E. Friberg, *J. Polym. Sci. Chem. Ed. 18* (1980) 2629; g) R. Keller, *Diplomarbeit*, Universität Mainz 1982; h) S. M. Hamid, D. C. Sherrington, *Polymer 28* (1987) 332; i) H. Finkelmann, M. A. Schafheutle, *17th Arbeitstagung Flüssigkristalle*, Freiburg, April 8–10, 1987, Abstr.; j) B. Lühmann, H. Finkelmann, *Colloid Polym. Sci. 265* (1987) 506; k) M. Wibbing, *Diplomarbeit*, Universität Mainz 1986.

[44] Y. Okahata, T. Kunitake, *J. Am. Chem. Soc. 101* (1979) 5231.

[45] R. Keller-Griffith, H. Ringsdorf, A. Vierengel, *Colloid Polym. Sci. 264* (1986) 924.

[46] N. Boden, R. J. Bushby, L. Ferris, C. Hardy, F. Sixl, *Liq. Cryst. 1* (1986) 109.

[47] a) H. Ringsdorf, R. Wüstefeld, *Int. Conf. Liq. Cryst. Polym., Bordeaux*, July 20–24, 1987, Abstr.; b) R. Wüstefeld, *Diplomarbeit*, Universität Mainz 1986.

[48] a) D. Chapman in [39a], Vol. I, p. 288; b) G. A. Jeffrey, *Acc. Chem. Res. 19* (1986) 168; c) M. A. Marcus, P. L. Finn, *Mol. Cryst. Liq. Cryst. Lett. Sect. 2* (1985) 159; d) D. W. Bruce, D. A. Dunmur, E. Lalinde, P. M. Maitlis, P. Styring, *Nature (London) 323* (1986) 791; e) T. Kunitake, Y. Okahata, M. Shimomura, S. I. Yasunami, K. Takarabe, *J. Am. Chem. Soc. 103* (1981) 5401; f) S. L. Tseng, A. Valente, D. G. Gray, *Macromolecules 14* (1981) 715; g) G. V. Laivins, P. Sixou, D. G. Gray, *J. Polym. Sci. Polym. Phys. Ed. 24* (1986) 2779; h) S. M. Aharoni, *Macromolecules 12* (1979) 94.

[49] a) I. Langmuir, *Trans. Faraday Soc. 15* (1920) 62; b) K. B. Blodgett, *J. Am. Chem. Soc. 57* (1935) 1007; c) G. L. Gaines: *Insoluble Monolayers at Liquid-Gas Interfaces*, Wiley Interscience, New York 1966; d) G. G. Roberts, *Adv. Phys. 34* (1985) 475; e) M. Sugi, *J. Mol. Electron. 1* (1985) 3.

[50] *Thin Solid Films 132–134* (1985); *ibid. 99* (1983); *ibid. 68* (1980).

[51] R. Jones, C. S. Winter, R. H. Tredgold, P. Hodge, A. Hoorfar, *Polymer 28* (1987) 1619.

[52] A. Barraud, *Thin Solid Films 99* (1983) 317.

[53] a) J. Zyss, *J. Mol. Electron. 1* (1985) 25; b) D. Lupo, W. Prass, U. Scheunemann, A. Laschewsky, H. Ringsdorf, I. Ledoux, *J. Opt. Soc. Am. B Opt. Phys.*, in press.

[54] M. Eich, J. H. Wendorff, B. Reck, H. Ringsdorf, *Makromol. Chem. Rapid Commun. 8* (1987) 59.

[55] a) M. G. McNamee, E. L. M. Ochoa, *Neuroscience 7* (1982) 2305; b) T. M. Ginnai, *Ind. Eng. Chem. Prod. Res. Dev. 24* (1985) 188.

[56] a) J. P. Rabe, J. D. Swalen, J. F. Rabolt, *J. Chem. Phys. 86* (1987) 1601; b) D. D. Saperstein, *J. Phys. Chem. 90* (1986) 1408.

[57] a) A. J. Vickers, R. H. Tredgold, P. Hodge, E. Khoshdel, I. Girling, *Thin Solid Films 134* (1985) 43; b) R. Jones, R. H. Tredgold, A. Hoorfar, R. A. Allen, P. Hodge, *ibid. 134* (1985) 57.

[58] A. Schuster, *Diplomarbeit*, Universität Mainz 1986.

[59] a) N. Boden, R. J. Bushby, C. Hardy, *J. Phys. Lett. 46* (1985) L325; b) J.-H. Fuhrhop, D. Fritsch, B. Tesche, H. Schmiady, *J. Am. Chem. Soc. 106* (1984) 1998.

[60] G. Decher, *Dissertation*, Universität Mainz 1986.

[61] a) K. R. Patel, M. P. Li, J. R. Schuh, J. D. Baldeschwieler, *Biochim. Biophys. Acta 814* (1985) 256; b) *ibid. 797* (1984) 20.

[62] M. S. Bretscher, *Spektrum Wiss. 1985*, No. 12, p. 90; *Scientific American 253* (1985) No. 10, p. 86.

[63] a) H. Hauser, *Chimia 39* (1985) 252; b) P. R. Cullis, M. J. Hope, B. de Kruijff, A. J. Verkleij, C. P. S. Tilcock in J. F. Kuo (Ed.): *Phospholipids and Cellular Regulation, Vol. 1*, CRC Press, Boca Raton, FL, USA 1985, p. 1; c) J. N. Hawthorne, G. B. Ansell (Eds.): *Phospholipids (New Compr. Biochem. 4* (1982)).

[64] C. Tanford: *The Hydrophobic Effect*, 2nd ed., Wiley, New York 1980.

[65] a) E. Sackmann, *Ber. Bunsenges. Phys. Chem. 78* (1974) 929; b) *ibid. 82* (1978) 891.

[66] a) H. Wiegandt (Ed.): *Glycolipids (New Compr. Biochem. 10* (1985)); b) J. N. Kanfer, S. Hakomori (Eds.): *Sphingolipid Biochemistry (Handbook of Lipid Research, Vol. III)*, Plenum, New York 1983.

[67] a) I. Pascher, *Biochim. Biophys. Acta 455* (1976) 433; b) W. Curatolo, A. Bali, C. M. Gupta, *J. Pharm. Sci. 74* (1985) 1255; c) T. Kunitake, N. Yamada, N. Fukunaga, *Chem. Lett. 1984*, 1089; d) Y. Murakami, A. Nakano, A. Yoshimatsu, K. Uchitomi, Y. Matsuda, *J. Am. Chem. Soc. 106* (1984) 3613; e) Y. Murakami, J. Kikuchi, T. Takaki, *Bull. Chem. Soc. Jpn. 59* (1986) 3145.

[68] a) H. Eibl, *Angew. Chem. 96* (1984) 247; *Angew. Chem. Int. Ed. Engl. 23* (1984) 257; b) M. Kates in E. D. Korn (Ed.): *Methods in Membrane Biology, Vol. 8*, Plenum, New York 1977, p. 219.

[69] a) T. Kunitake, Y. Okahata, *J. Am. Chem. Soc. 99* (1977) 3860; b) *Bull. Chem. Soc. Jpn. 51* (1978) 1877.

[70] a) T. Kunitake, *J. Macromol. Sci. Chem. A 13* (1979) 587; b) J. H. Fendler: *Membrane Mimetic Chemistry*, Wiley, New York 1982; c) J.-H. Fuhrhop, J. Mathieu, *Angew. Chem. 96* (1984) 124; *Angew. Chem. Int. Ed. Engl. 23* (1984) 100.

[71] a) D. Marr-Leisy, R. Neumann, H. Ringsdorf, *Colloid Polym. Sci. 263* (1985) 791; b) J.-H. Fuhrhop, P. Schnieder, J. Rosenberg, E. Boekema, *J. Am. Chem. Soc. 109* (1987) 3387; c) T. Kunitake, N. Nakashima, M. Shimomura, Y. Okahata, K. Kano, T. Ogawa, *ibid. 102* (1980) 6642.

[72] B. Hupfer, H. Ringsdorf, H. Schupp, *Chem. Phys. Lipids 33* (1983) 355.

[73] T. Kunitake, N. Kimizuka, N. Higashi, N. Nakashima, *J. Am. Chem. Soc. 106* (1984) 1978.

[74] B. Alberts, D. Bray, J. Lewis, M. Raff, K. Roberts, J. D. Watson: *Molecular Biology of the Cell*, Garland, New York 1983; *Molekularbiologie der Zelle*, VCH Verlagsgesellschaft, Weinheim 1986.

[75] a) G. Benga (Ed.): *Structure and Properties of Cell Membranes, Vol. 1–III*, CRC Press, Boca Raton, FL, USA 1985; b) J. B. Finean, R. H. Michell (Eds.): *Membrane Structure (New Compr. Biochem. 1* (1981)); c) D. Chapman (Ed.): *Biological Membranes, Vol. 4*, Academic Press, London 1982; d) *Biomembrane Structure and Function*, Verlag Chemie, Weinheim 1984.

[76] S. J. Singer, G. L. Nicolson, *Science (Washington) 175* (1972) 720.

[77] D. A. Cadenhead in [75a], Vol. III, p. 21.

[78] a) M. Lösche, E. Sackmann, H. Möhwald, *Ber. Bunsenges. Phys. Chem. 87* (1983) 848; b) V. von Tscharner, H. M. McConnell, *Biophys. J. 36* (1981) 409; c) P. Meller, *Dissertation*, Technische Universität München 1985; d) K. Beck in J. Bereiter-Hahn, O. R. Anderson, W.-E. Reif (Eds.): *Cytomechanics*, Springer, Berlin 1987, p. 79.

[79] H. Kuhn, D. Möbius, *Angew. Chem. 83* (1971) 672; *Angew. Chem. Int. Ed. Engl. 10* (1971) 620.

[80] a) P. M. Vassilev, H. Ti Tien in [75a], Vol. III, p. 63; b) H. Ti Tien: *Biomolecular Lipid Membranes, Theory and Practice*, Dekker, New York 1974; c) M. K. Jain: *The Bimolecular Lipid Membrane: A System*, Van Nostrand, New York 1972; d) R. Latorre, O. Alvarez, X. Cecchi, C. Vergara, *Annu. Rev. Biophys. Biophys. Chem. 14* (1985) 79.

[81] P. Läuger, *Angew. Chem. 97* (1985) 939; *Angew. Chem. Int. Ed. Engl. 24* (1985) 905.

[82] H. M. McConnell, T. H. Watts, R. M. Weis, A. A. Brian, *Biochim. Biophys. Acta 864* (1986) 95.

[83] V. Hlady, R. A. van Wagenen, J. D. Andrade in J. D. Andrade (Ed.): *Surface and Interfacial Aspects of Biomedical Polymers, Vol. 2*, Plenum, New York 1985, p. 81.

[84] a) A. D. Bangham, M. W. Hill, N. G. A. Miller in E. D. Korn (Ed.): *Methods in Membrane Biology, Vol. 1*, Plenum, New York 1974, p. 1; b) D. W. Deamer, P. Uster in [75a], Vol. III, p. 103; c) A. D. Bangham (Ed.): *Liposome Letters*, Academic Press, London 1983; d) M. J. Ostro (Ed.): *Liposomes*, Dekker, New York 1983; e) *Liposomes: From Biophysics to Therapeutics*, Dekker, New York 1987; f) G. Gregoriadis, A. C. Allison (Eds.): *Liposomes in Biological Systems*, Wiley, Chichester 1980; g) C. G. Knight (Ed.): *Liposomes: From Physical Structure to Therapeutic Applications*, Elsevier, Amsterdam 1981; h) G. Gregoriadis (Ed.): *Liposome Technology, Vol. I–III*, CRC Press, Boca Raton, FL, USA 1984.

[85] F. Szoka, D. Papahadjopoulos, *Annu. Rev. Biophys. Bioeng. 9* (1980) 467.

[86] Z. I. Cabantchik, A. Darmon in [75a], Vol. III, p. 123.

[87] a) D. A. Tirrell, L. G. Donaruma, A. B. Turek (Eds.): *Macromolecules as Drugs and as Carriers for Biologically Active Materials (Ann. NY Acad. Sci. 446* (1985)); b) T. N. Palmer, H. M. Patel, L. E. Readings (Eds.): *Use of Liposomes in Medicine (Biochem. Soc. Trans. 12* (1984) 331); c) G. Poste, *Biol. Cell 47* (1983) 19; d) see also [84], especially d)–g) and h), Vol. III.

[88] a) N. J. Turro, G. S. Cox, M. A. Paczkowski, *Top. Curr. Chem. 129* (1985) 57; b) V. Ramamurthy, *Tetrahedron 42* (1986) 5753; c) D. G. Whitten, *Angew. Chem. 91* (1979) 472; *Angew. Chem. Int. Ed. Engl. 18* (1979) 440; d) H. Koch, A. Laschewsky, H. Ringsdorf, K. Teng, *Makromol. Chem. 187* (1986) 1843; e) [70b], p. 293.

[89] a) T. Kunitake, S. Shinkai, *Adv. Phys. Org. Chem. 17* (1980) 435; b) [70b], p. 235.

[90] a) P. Tundo, K. Kurihara, D. J. Kippenberger, M. Politi, J. H. Fendler, *Angew. Chem. 94* (1982) 73; *Angew. Chem. Int. Ed. Engl. 21* (1982) 81; b) [70b], p. 492; c) D. H. P. Thompson, W. C. Barrette, J. K. Hurst, *J. Am. Chem. Soc. 109* (1987) 2003; d) Y.-M. Tricot, J. H. Fendler, *ibid. 106* (1984) 2475.

[91] B. Schlarb, *Diplomarbeit*, Universität Mainz 1983.

[92] a) M. L. Bender, *J. Am. Chem. Soc. 79* (1957) 1258; b) W.-C. Shen, H. J.-P. Ryser, *Biochem. Biophys. Res. Commun. 102* (1981) 1048; c) P. J. G. Butler, J. I. Harris, B. S. Hartley, R. Leberman, *Biochem. J. 103* (1967) 78p.

[93] a) M. Haubs, H. Ringsdorf, *Nouv. J. Chim. 11* (1987) 151; b) D. A. Holden, H. Ringsdorf, V. Deblauwe, G. Smets, *J. Phys. Chem. 88* (1984) 716; c) D. A. Holden, H. Ringsdorf, M. Haubs, *J. Am. Chem. Soc. 106* (1984) 4531.

[94] a) D. F. O'Brien, *Photochem. Photobiol. 29* (1979) 679; b) K. Kano, Y. Tanaka, T. Ogawa, M. Shimomura, T. Kunitake, *ibid. 34* (1981) 323; c) C. Pidgeon, C. A. Hunt, *ibid. 37* (1983) 491.

[95] M. Haubs, H. Ringsdorf, *Angew. Chem. 97* (1985) 880; *Angew. Chem. Int. Ed. Engl. 24* (1985) 882.

[96] J. Streith, J.-M. Cassal, *Angew. Chem. 80* (1968) 117; *Angew. Chem. Int. Ed. Engl. 7* (1968) 129.
[97] M. A. Ratcliff, J. K. Kochi, *J. Org. Chem. 36* (1971) 3112.
[98] a) T. Kunitake, N. Nakashima, K. Takarabe, M. Nagai, A. Tsuge, H. Yanagi, *J. Am. Chem. Soc. 103* (1981) 5945; b) R. Elbert, A. Laschewsky, H. Ringsdorf, *ibid. 107* (1985) 4134.
[99] a) G. Gee, *Trans. Faraday Soc. 32* (1936) 187; b) A. Cemel, T. Fort, J. B. Lando, *J. Polym. Sci. Part A-1 10* (1972) 2061; c) R. Ackermann, O. Inacker, H. Ringsdorf, *Kolloid-Z. Z. Polym. 249* (1971) 1118; d) G. Scheibe, H. Schuller, *Z. Elektrochem. 59* (1955) 861.
[100] D. Day, H.-H. Hub, H. Ringsdorf, *Isr. J. Chem. 18* (1979) 325.
[101] S. L. Regen, A. Singh, G. Oehme, M. Singh, *J. Am. Chem. Soc. 104* (1982) 791.
[102] M. F. M. Roks, R. S. Dezentjé, V. E. M. Kaats-Richters, W. Drenth, A. J. Verkleij, R. J. M. Nolte, *Macromolecules 20* (1987) 920.
[103] W. Reed, L. Guterman, P. Tundo, J. H. Fendler, *J. Am. Chem. Soc. 106* (1984) 1897.
[104] a) E. Hasegawa, Y. Matsushita, K. Eshima, N. Nishide, E. Tsuchida, *Makromol. Chem. Rapid Commun. 5* (1984) 779; b) Y. Matsushita, E. Hasegawa, K. Eshima, H. Ohno, E. Tsuchida, *ibid. 8* (1987) 1.
[105] N. K. P. Samuel, M. Singh, K. Yamaguchi, S. L. Regen, *J. Am. Chem. Soc. 107* (1985) 42.
[106] a) H.-H. Hub, B. Hupfer, H. Koch, H. Ringsdorf, *Angew. Chem. 92* (1980) 962; *Angew. Chem. Int. Ed. Engl. 19* (1980) 938; b) B. Hupfer, H. Ringsdorf, *Chem. Phys. Lipids 33* (1983) 263; c) J. Leaver, A. Alonso, A. A. Durrani, D. Chapman, *Biochim. Biophys. Acta 732* (1983) 210; d) D. S. Johnston, S. Sanghera, M. Pons, D. Chapman, *ibid. 602* (1980) 57; e) E. Lopez, D. F. O'Brien, T. H. Whitesides, *ibid. 693* (1982) 437; f) *J. Am. Chem. Soc. 104* (1982) 305.
[107] a) H. Koch, H. Ringsdorf, *Makromol. Chem. 182* (1981) 255; b) N. Wagner, K. Dose, H. Koch, H. Ringsdorf, *FEBS Lett. 132* (1981) 313; c) R. Pabst, H. Ringsdorf, H. Koch, K. Dose, *ibid. 154* (1983) 5.
[108] A. Akimoto, K. Dorn, L. Gros, H. Ringsdorf, H. Schupp, *Angew. Chem. 93* (1981) 108; *Angew. Chem. Int. Ed. Engl. 20* (1981) 90.
[109] B. Ostermayer, O. Albrecht, W. Vogt, *Chem. Phys. Lipids 41* (1986) 265.
[110] D. Babilis, P. Dais, L. H. Margaritis, C. M. Paleos, *J. Polym. Sci. Polym. Chem. Ed. 23* (1985) 1089.
[111] P. Tundo, D. J. Kippenberger, M. J. Politi, P. Klahn, J. H. Fendler, *J. Am. Chem. Soc. 104* (1982) 5352.
[112] A. Kusumi, M. Singh, D. A. Tirrell, G. Oehme, A. Singh, N. K. P. Samuel, J. S. Hyde, S. L. Regen, *J. Am. Chem. Soc. 105* (1983) 2975.
[113] a) K. Dorn, E. V. Patton, R. T. Klingbiel, D. F. O'Brien, H. Ringsdorf, *Makromol. Chem. Rapid Commun. 4* (1983) 513; b) K. Dorn, R. T. Klingbiel, D. P. Specht, P. N. Tyminski, H. Ringsdorf, D. F. O'Brien, *J. Am. Chem. Soc. 106* (1984) 1627; c) R. Ebelhäuser, H. W. Spiess, *Makromol. Chem. Rapid Commun. 5* (1984) 403; d) *Ber. Bunsenges. Phys. Chem. 89* (1985) 1208.
[114] a) L. Gros, H. Ringsdorf, H. Schupp, *Angew. Chem. 93* (1981) 311; *Angew. Chem. Int. Ed. Engl. 20* (1981) 305; b) H. Bader, K. Dorn, B. Hupfer, H. Ringsdorf, *Adv. Polym. Sci. 64* (1985) 1; c) J. H. Fendler, *Science (Washington) 223* (1984) 888; d) J. H. Fendler, P. Tundo, *Acc. Chem. Res. 17* (1984) 3; e) D. F. O'Brien, R. T. Klingbiel, D. P. Specht, P. N. Tyminski, *Ann. NY Acad. Sci. 446* (1985) 282; f) S. L. Regen in [84e], p. 73.
[115] a) H. P. Kim, S. M. Byum, Y. T. Ylom, S. W. Kim, *J. Pharm. Sci. 72* (1983) 225; b) H. Ringsdorf, *J. Polym. Sci. Polym. Symp. 51* (1975) 135; c) J. B. Lloyd, R. Duncan, J. Kopeček, *Biochem. Sci. Trans. 14* (1986) 391.
[116] a) A. Laschewsky, H. Ringsdorf, G. Schmidt, J. Schneider, *J. Am. Chem. Soc. 109* (1987) 788; b) A. Laschewsky, H. Ringsdorf, J. Schneider, *Angew. Makromol. Chem. 145/146* (1986) 1; c) W. Frey, J. Schneider, H. Ringsdorf, E. Sackmann, *Macromolecules 20* (1987) 1312; d) H. Ringsdorf, G. Schmidt, J. Schneider, *Thin Solid Films 152* (1987) 207.
[117] E. Orthmann, G. Wegner, *Angew. Chem. 98* (1986) 1114; *Angew. Chem. Int. Ed. Engl. 25* (1986) 1105.
[118] a) T. Kawaguchi, H. Nakahara, K. Fukuda, *Thin Solid Films 133* (1985) 29; b) S. J. Mumby, J. D. Swalen, J. F. Rabolt, *Macromolecules 19* (1986) 1054; c) G. Duda, A. J. Schouten, T. Arndt, G. Lieser, G. F. Schmidt, C. Bubeck, G. Wegner, *Thin Solid Films*, in press.
[119] a) P. Hodge, E. Khoshdel, R. H. Tredgold, A. J. Vickers, C. S. Winter, *Br. Polym. J. 17* (1985) 368; b) R. H. Tredgold, A. J. Vickers, A. Hoorfar, P. Hodge, E. Khoshdel, *J. Phys. D Appl. Phys. 18* (1985) 1139.
[120] a) N. Beredjick, H. E. Ries, *J. Polym. Sci. 62* (1962) S64; b) D. Naegele, H. Ringsdorf in H. G. Elias (Ed.): *Polymerization of Organized Systems (Midl. Macromol. Monogr. 3* (1977) 79).
[121] a) M. Breton, *J. Macromol. Sci. Rev. Macromol. Chem. C21* (1981) 61; b) B. Tieke, *Adv. Polym. Sci. 71* (1985) 79.
[122] a) D. Naegele, J. B. Lando, H. Ringsdorf, *Macromolecules 10* (1977) 1339; b) O. Albrecht, A. Laschewsky, H. Ringsdorf, *ibid. 17* (1984) 937; c) *J. Membr. Sci. 22* (1985) 187; d) A. Laschewsky, H. Ringsdorf, G. Schmidt, *Thin Solid Films 134* (1985) 153; e) H. Cackovic, H.-P. Schwengers, J. Springer, A. Laschewsky, H. Ringsdorf, *J. Membr. Sci. 26* (1986) 63; f) F. Grunfeld, C. W. Pitt, *Thin Solid Films 99* (1983) 249; g) B. Tieke, G. Lieser, K. Weiss, *ibid. 99* (1983) 95; h) J. P. Rabe, J. F. Rabolt, C. A. Brown, J. D. Swalen, *J. Chem. Phys. 84* (1986) 4096.
[123] A. Baniel, M. Frankel, I. Friedrich, A. Katchalsky, *J. Org. Chem. 13* (1948) 791.
[124] a) K. Fukuda, Y. Shibasaki, H. Nakahara, *J. Macromol. Sci. Chem. A 15* (1981) 999; b) *Thin Solid Films 99* (1983) 87; c) *ibid. 113* (1985) 39.
[125] a) A. Barraud, A. Ruaudel-Teixier, C. Rosilio, *Ann. Chim. 10* (1975) 195; b) C. Rosilio, A. Ruaudel-Teixier, *J. Polym. Sci. Polym. Chem. Ed. 13* (1975) 2459; c) A. Barraud, C. Rosilio, A. Ruaudel-Teixier, *Thin Solid Films 68* (1980) 7.
[126] W. N. Emmerling, B. Pfannemüller, *Colloid Polym. Sci. 261* (1983) 677.
[127] T. Folda, L. Gros, H. Ringsdorf, *Makromol. Chem. Rapid Commun. 3* (1982) 167.
[128] A. Shibata, S. Yamashita, Y. Ito, T. Yamashita, *Biochim. Biophys. Acta 854* (1986) 147.
[129] a) R. Neumann, H. Ringsdorf, *J. Am. Chem. Soc. 108* (1986) 487; b) R. Neumann, H. Ringsdorf, E. V. Patton, D. F. O'Brien, *Biochim. Biophys. Acta 898* (1987) 338.
[130] a) S. C. Kushwaha, M. Kates, G. D. Sprott, I. C. P. Smith, *Science (Washington) 211* (1981) 1163; b) T. A. Langworthy, *Curr. Top. Membr. Transp. 17* (1982) 45.
[131] a) J.-H. Fuhrhop, K. Ellermann, H. H. David, J. Mathieu, *Angew. Chem. 94* (1982) 444; *Angew. Chem. Int. Ed. Engl. 21* (1982) 440; *Angew. Chem. Suppl. 1982*, 980; b) J.-H. Fuhrhop, J. Mathieu, *J. Chem. Soc. Chem. Commun. 1983*, 144; c) J.-H. Fuhrhop, H. H. David, J. Mathieu, U. Limann, H.-J. Winter, E. Boekema, *J. Am. Chem. Soc. 108* (1986) 1785; d) J.-H. Fuhrhop, D. Fritsch, *Acc. Chem. Res. 19* (1986) 130.
[132] a) H. Bader, H. Ringsdorf, *J. Polym. Sci. Polym. Chem. Ed. 20* (1982) 1623; b) *Faraday Discuss. Chem. Soc. 81* (1986) 329.
[133] a) A. Kato, M. Arakawa, T. Kondo, *J. Microencapsulation 1* (1984) 105; b) H. Izawa, M. Arakawa, T. Kondo, *Biochim. Biophys. Acta 855* (1986) 243.
[134] a) W. Hartmann, H.-J. Galla, E. Sackmann, *FEBS Lett. 78* (1977) 169; b) W. Hartmann, H.-J. Galla, *Biochim. Biophys. Acta 509* (1978) 474; c) B. de Kruijff, A. Rietveld, N. Telders, B. Vaandrager, *ibid. 820* (1985) 295; d) D. Carrier, J. Dufourcq, J.-F. Faucon, M. Pézolet, *ibid. 820* (1985) 131; e) D. Carrier, M. Pézolet, *Biochemistry 25* (1986) 4167; f) A. Walter, C. J. Steer, R. Blumenthal, *Biochim. Biophys. Acta 861* (1986) 319; g) A. E. Gad, G. Elyashiv, N. Rosenberg, *ibid. 860* (1986) 314.
[135] a) K. A. Borden, K. M. Eum, K. H. Langley, D. A. Tirrell, *Macromolecules 20* (1987) 454; b) D. A. Tirrell, A. B. Turek, D. A. Wilkinson, T. J. McIntosh, *ibid. 18* (1985) 1512; c) K. Seki, D. A. Tirrell, *ibid. 17* (1984) 1692; d) D. Y. Takigawa, D. A. Tirrell, *Makromol. Chem. Rapid Commun. 6* (1985) 653.
[136] M. Takada, T. Yuzuriha, K. Katayama, K. Iwamoto, J. Sunamoto, *Biochim. Biophys. Acta 802* (1984) 237.
[137] a) K. V. Aliev, H. Ringsdorf, B. Schlarb, K.-H. Leister, *Makromol. Chem. Rapid Commun. 5* (1984) 345; b) S. L. Regen, J.-S. Shin, K. Yamaguchi, *J. Am. Chem. Soc. 106* (1984) 2446; c) S. L. Regen, J.-S. Shin, J. F. Hainfeld, J. S. Wall, *ibid. 106* (1984) 5756; d) H. Fukuda, T. Diem, J. Stefely, F. J. Kezdy, S. L. Regen, *ibid. 108* (1986) 2321; e) J. E. Brady, D. F. Evans, B. Kachar, B. W. Ninham, *ibid. 106* (1984) 4279.
[138] T. Tsumita, M. Ohashi, *J. Exp. Med. 119* (1964) 1017.
[139] U. Hammerling, O. Westphal, *Eur. J. Biochem. 1* (1967) 46.
[140] a) D. E. Wolf, J. Schlessinger, E. L. Elson, W. W. Webb, R. Blumenthal, P. Henkart, *Biochemistry 16* (1977) 3476; b) D. E. Wolf, P. Henkart, W. W. Webb, *ibid. 19* (1980) 3893.
[141] J. Sunamoto, K. Iwamoto, M. Takada, T. Yuzuriha, K. Katayama in E. Chiellini, P. Giusti (Eds.): *Polymers in Medicine*. Plenum, New York 1984, p. 157.
[142] K. Kobayashi, H. Sumitomo, H. Ichikawa, *Macromolecules 19* (1986) 529.
[143] J. Sunamoto, M. Goto, T. Iida, K. Hara, A. Saito, A. Tomonaga in G. Gregoriadis, G. Poste, J. Senior, A. Trouet (Eds.): *Receptor-Mediated Targeting of Drugs*. Plenum, New York 1985, p. 359.
[144] J. Sunamoto, T. Sato, M. Hirota, K. Fukushima, K. Hiratani, K. Hara, *Biochim. Biophys. Acta 898* (1987) 323.
[145] J. Möllerfeld, W. Prass, H. Ringsdorf, H. Hamazaki, J. Sunamoto, *Biochim. Biophys. Acta 857* (1986) 265.
[146] J. P. Reeves, R. M. Dowben, *J. Cell. Physiol. 73* (1968) 49.
[147] E. Kuchinka, *Diplomarbeit*, Universität Mainz 1986.
[148] Analogous construction: K. Fricke, E. Sackmann, *Biochim. Biophys. Acta 803* (1984) 145.
[149] See [74], pp. 307 ff. (338 ff).
[150] R. Krbecek, C. Gebhardt, H. Gruler, E. Sackmann, *Biochim. Biophys. Acta 554* (1979) 1.
[151] a) C. Gebhardt, H. Gruler, E. Sackmann, *Z. Naturforsch. C32* (1977) 581; b) E. J. Luna, H. M. McConnell, *Biochim. Biophys. Acta 466* (1977) 381.

[152] a) E. Sackmann, D. Rüppel, C. Gebhardt, *Springer Ser. Chem. Phys. 11* (1980) 309; b) D. Rüppel, E. Sackmann, *J. Phys. (Les Ulis Fr.) 44* (1983) 1025.
[153] a) J. Darnell, H. Lodish, D. Baltimore: *Molecular Cell Biology*, Scientific American Books, Freeman, New York 1986, p. 592ff; b) K. Weber, M. Osborn, *Spektrum Wiss. 1985*, No. 12, p. 102; *Scientific American 253* (1985) No. 10, p. 92; c) V. T. Marchesi, *J. Membr. Biol. 51* (1979) 101; d) D. Branton, C. M. Cohen, J. Tyler, *Cell 24* (1981) 24; e) C. Koszka, *Chem. Unserer Zeit 20* (1986) 19.
[154] E. Sackmann, P. Eggl, C. Fahn, H. Bader, H. Ringsdorf, M. Schollmeier, *Ber. Bunsenges. Phys. Chem. 89* (1985) 1198.
[155] a) E. Sackmann, H.-P. Duwe, H. Engelhardt, *Faraday Discuss. Chem. Soc. 81* (1986) 281; b) E. Sackmann, H.-P. Duwe, K. Zeman, A. Zilker in E. Clementi, S. Chin (Eds.): *Structure and Dynamics of Nucleic Acids, Proteins, and Membranes*, Plenum, New York 1986, p. 251.
[156] V. P. Torchilin, A. L. Klibanov, N. N. Ivanov, H. Ringsdorf, B. Schlarb, *Makromol. Chem. Rapid Commun. 8* (1987) 457.
[157] a) H. Ringsdorf, B. Schlarb, *Polym. Prepr. (Am. Chem. Soc. Div. Polym. Chem.) 27 (2)* (1986) 195; b) *Makromol. Chem.*, in press.
[158] H. Ringsdorf, B. Schlarb, P. N. Tyminski, D. F. O'Brien, *Macromolecules*, in press.
[159] L. B. Margolis, *Biochim. Biophys. Acta 779* (1984) 161.
[160] Cf. [74], pp. 98ff., 199ff. and 105ff., 217ff.
[161] M. Monsigny, C. Kieda, A.-C. Roche, *Biol. Cell 47* (1983) 95.
[162] R. R. Rando, J. S. Slama, F. W. Bangerter, *Proc. Natl. Acad. Sci. USA 77* (1980) 2510.
[163] a) H. Bader, H. Ringsdorf, J. Skura, *Angew. Chem. 93* (1981) 109; *Angew. Chem. Int. Ed. Engl. 20* (1981) 91; b) H. Bader, R. van Wagenen, J. D. Andrade, H. Ringsdorf, *J. Colloid Interface Sci. 101* (1984) 246.
[164] B. Tieke, G. Lieser, G. Wegner, *J. Polym. Sci. Polym. Chem. Ed. 17* (1979) 1631.
[165] a) R. R. Schmidt, *Angew. Chem. 98* (1986) 213; *Angew. Chem. Int. Ed. Engl. 25* (1986) 212; b) H. Kunz, *ibid. 99* (1987) 297 and *26* (1987) 294.
[166] M. Wilchek, *Makromol. Chem. Suppl. 2* (1979) 207.
[167] K. Takemoto in C. G. Gebelein, C. E. Carraher (Eds.): *Bioactive Polymeric Systems*, Plenum, New York 1985, p. 417.
[168] a) C. G. Overberger, Y. Inaki, *J. Polym. Sci. Polym. Chem. Ed. 17* (1979) 1739; b) J. Pitha, M. Akashi, M. Draminski in P. Goldberg, A. Nakajima (Eds.): *Biomedical Polymers*, Academic Press, New York 1980, p. 271.
[169] a) H. Kitano, H. Ringsdorf, *Bull. Chem. Soc. Jpn. 58* (1985) 2826; b) M. Ahlers, *Diplomarbeit*, Universität Mainz 1985.
[170] a) H. O. Ribi, P. Reichard, R. D. Kornberg, *Biochemistry 26* (1987) 7974; b) see also E. E. Uzgiris, R. D. Kornberg, *Nature (London) 301* (1983) 125.
[171] a) H. Rosemeyer, M. Ahlers, B. Schmidt, F. Seela, *Angew. Chem. 97* (1985) 500; *Angew. Chem. Int. Ed. Engl. 24* (1985) 501; b) synthesis of the head groups: F. Seela, F. Cramer, *Chem. Ber. 108* (1975) 1329.
[172] M. Loos, *Curr. Top. Microbiol. Immunol. 102* (1983) 1.
[173] a) M. Loos, D. Bitter-Suermann, M. P. Dierich, *J. Immunol. 112* (1974) 935; b) F. Clas, M. Loos, *Infect. Immun. 31* (1981) 1138.
[174] a) M. Ivanova, I. Panaiotov, M. Eshkenazy, R. Tekelieva, R. Ivanova, *Colloids Surf. 17* (1986) 159; b) C. R. Alving, S. Shichijo, I. Mattsby-Baltzer in [84h], Vol. II, p. 157; c) B. Banerji, C. R. Alving, *J. Immunol. 126* (1981) 1080.
[175] M. Loos, M. Latsch, M. Ahlers, R. Nagata, H. Ringsdorf, unpublished results.
[176] a) E. T. Rietschel, H. Mayer, H.-W. Wollenweber, U. Zähringer, O. Lüderitz, O. Westphal, H. Brade in J. Y. Homma (Ed): *Bacterial Endotoxin*, Verlag Chemie, Weinheim 1984, p. 16; b) H.-W. Wollenweber, K. W. Broady, O. Lüderitz, E. T. Rietschel, *Eur. J. Biochem. 124* (1982) 191.
[177] a) K. B. M. Reid, R. Porter, *Biochem. J. 155* (1976) 19; b) H. R. Knobel, W. Villiger, H. Isliker, *Eur. J. Immunol. 5* (1975) 78.
[178] Cf. [74], pp. 256ff. (278ff).
[179] F. Stemmer, M. Loos, *J. Immunol. Methods 74* (1984) 9.
[180] P. Meller, H. Ringsdorf, unpublished.
[181] a) K. N. Timmis, G. J. Boulnois, D. Bitter-Suermann, F. C. Cabello, *Curr. Top. Microbiol. Immunol. 118* (1985) 197; b) M. Frosch, I. Görgen, G. J. Boulnois, K. N. Timmis, D. Bitter-Suermann, *Proc. Natl. Acad. Sci. USA 82* (1985) 1194.
[182] E. J. McGuire, S. B. Binkley, *Biochemistry 3* (1964) 247.
[183] Cf. [74], pp. 276ff. (302ff).
[184] Cf. [74], p. 303 (332).
[185] a) D. J. Morré in [75a], Vol. II, p. 181; b) J. Aggeler, Z. Werb, *J. Cell Biol. 94* (1982) 613; c) M. K. Pratten, J. B. Lloyd, G. Hörpel, H. Ringsdorf, *Makromol. Chem. 186* (1985) 725.
[186] a) E. Sackmann in W. Hoppe, W. Lohmann, H. Markl, H. Ziegler (Eds.): *Biophysik*, 2nd ed., Springer, Berlin 1982, p. 439; b) H. Hauser, M. C. Phillips in D. A. Cadenhead, J. F. Danielli (Eds.): *Progress in Surface and Membrane Science*, Academic Press, New York 1979, p. 297.
[187] G. Lenaz, G. P. Castelli in [75a], Vol. I, pp. 93ff., 124.
[188] a) H. Gaub, E. Sackmann, R. Büschl, H. Ringsdorf, *Biophys. J. 45* (1984) 725; b) H. Gaub, R. Büschl, H. Ringsdorf, E. Sackmann, *Chem. Phys. Lipids 37* (1985) 19.
[189] M. Bessis: *Living Blood Cells and their Ultrastructure*, Springer, Berlin 1973.
[190] a) E. A. Evans, *Biophys. J. 14* (1974) 923; b) H. J. Deuling, W. Helfrich, *ibid. 16* (1976) 861; c) M. P. Sheetz, S. J. Singer, *Proc. Natl. Acad. Sci. USA 71* (1974) 4457; d) S. Svetina, B. Zeks, *Biomed. Biochim. Acta 42* (1983) 86.
[191] M. Haubs, *Dissertation*, Universität Mainz 1986.
[192] a) W. E. Fleming (Upjohn Company, USA), private communication; b) see also *Der Spiegel 35* (1981) No. 7, p. 201.
[193] a) R. Elbert, T. Folda, H. Ringsdorf, *J. Am. Chem. Soc. 106* (1984) 7687; b) T. Kunitake, S. Tawaki, N. Nakashima, *Bull. Chem. Soc. Jpn. 56* (1983) 3235.
[194] a) The abundance of methods to open stabilized liposomes selectively can only be surpassed by the number of techniques to uncork a bottle of wine. This also holds true for the manifold concepts used to approach scientific problems and is certainly influenced by the personal and national character of the bon vivants. So, how do the Germans open a bottle of wine? b) Taken from: R. Searle: *Something in the Cellar ... Wonderful World of Wine*, Souvenir Press, London 1986):

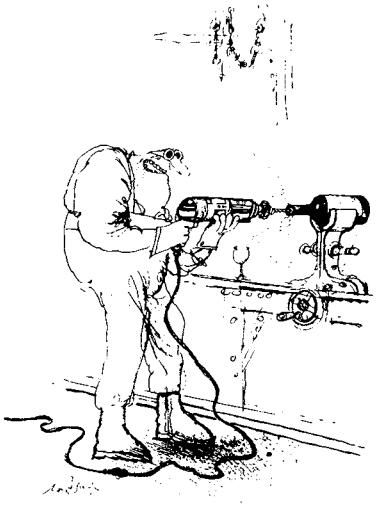

[195] a) J. N. Weinstein, R. L. Magin, M. B. Yatvin, D. S. Zaharko, *Science (Washington) 204* (1979) 188; b) S. M. Sullivan, L. Huang, *Biochim. Biophys. Acta 812* (1985) 116.
[196] a) M. B. Yatvin, W. Kreutz, B. A. Horwitz, M. Shinitzky, *Science (Washington) 210* (1980) 1253; b) R. Nayar, A. J. Schroit, *Biochemistry 24* (1985) 5967; c) D. A. Tirrell, D. Y. Takigawa, K. Seki, *Ann. NY Acad. Sci. 446* (1985) 237; d) B. P. Devlin, D. A. Tirrell, *Macromolecules 19* (1986) 2465; e) O. O. Petrukhina, N. N. Ivanov, M. M. Feldstein, A. E. Vasil'ev, N. A. Plate, V. P. Torchilin, *J. Controlled Release 3* (1986) 137; f) J.-H. Fuhrhop, U. Liman, H. H. David, *Angew. Chem. 97* (1985) 337; *Angew. Chem. Int. Ed. Engl. 24* (1985) 339.
[197] a) R. Büschl, T. Folda, H. Ringsdorf, *Makromol. Chem. Suppl. 6* (1984) 245; b) H. Bader, H. Ringsdorf, B. Schmidt, *Angew. Makromol. Chem. 123/124* (1984) 457.
[198] M. Butler, L. G. Abood, *J. Membrane Biol. 66* (1982) 1.
[199] R. Büschl, B. Hupfer, H. Ringsdorf, *Makromol. Chem. Rapid Commun. 3* (1982) 589.
[200] T. Folda, *Dissertation*, Universität Mainz 1984.
[201] A pretty rapid method to uncork a bottle is the so-called "Sicilian opening" also known in chess and from time to time applied in science too (see [194b]):

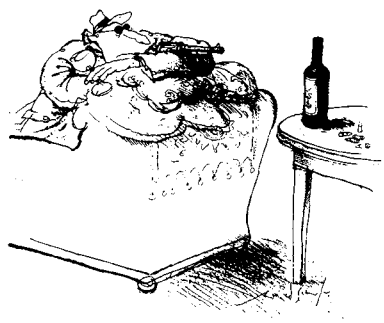

[202] For the use of fluorescent dyes to measure the permeability of liposomal membranes see: a) J. N. Weinstein, S. Yoshikami, P. Henkart, R. Blumenthal, W. A. Hagins, *Science (Washington) 195* (1977) 489; b) J. N. Weinstein, E. Ralston, L. D. Leserman, R. D. Klausner, P. Dragsten, P. Henkart, R. Blumenthal in [84h], Vol. III, p. 183.
[203] The sanning electron micrographs were taken at Case Western Reserve University, Cleveland, Ohio, USA (Prof. *J. B. Lando*).
[204] The freeze fracture electron micrographs were taken by *C. Fahn* at the Physics Department of the Technische Universität München (Prof. *E. Sackmann*).
[205] a) W. F. Reed, L. R. Guterman, *J. Radiat. Curing 1986*, 18; b) R. L. Juliano, M. J. Hsu, S. L. Regen, M. Singh, *Biochim. Biophys. Acta 770* (1984) 109.
[206] H. Ohno, S. Takeoka, E. Tsuchida, *Polym. Bull. 14* (1985) 487.
[207] Enzymatic processes are common in the wine business. To uncork bottles, however, physical methods are usually preferred. As far as elegance is concerned, the Swiss variant can hardly be surpassed (see [194b]):

[208] R. Büschl, *Dissertation*, Universität Mainz 1984.
[209] a) P. G. Munder, M. Modolell, W. Bausert, H. F. Oettgen, O. Westphal, *Prog. Cancer Res. Ther. 16* (1981) 411; b) R. Andreesen, A. Schulz, U. Costabel, P. G. Munder, *Immunobiology 163* (1982) 335; c) M. Modolell, R. Andreesen, W. Pahlke, U. Brugger, P. G. Munder, *Cancer Res. 39* (1979) 4681; d) M. H. Runge, R. Andreesen, A. Pfleiderer, P. G. Munder, *JNCI J. Natl. Cancer Inst. 64* (1980) 1301; e) R. Andreesen, M. Modolell, G. H. F. Oepke, P. G. Munder, *Exp. Hematol. (NY) 11* (1983) 564.
[210] "It is just like someone dragging a stone and claiming: I'm building a Gothic cathedral."
[211] a) R. Hoffmann, *Angew. Chem. 99* (1987) 871; *Angew. Chem. Int. Ed. Engl. 26* (1987) 846; b) *Roald Hoffmann*—certainly one of the last ones to be reproached for superficiality—defines the problem of generalization saying: "Typologies and generalizations often point not so much to reality as to the weakness of the mind that proposes them." This has to be accepted!
[212] *Georg Christoph Lichtenberg* in his *"Aphorisms"*: "The wit is the finder and the intelligence the observer". "It is really necessary to seriously investigate why most inventions have to be made by chance. The main reason might be the fact that people tend to accept the views of their teachers and their environment. It thus might be beneficial to develop instructions how to systematically deviate from rules." *Aphorismen*, Inseltaschenbuch Suhrkamp, Frankfurt am Main, 1979, p. 202 and 204.
[213] a) F. Vögtle, H.-G. Löhr, J. Franke, D. Worsch, *Angew. Chem. 97* (1985) 721; *Angew. Chem. Int. Ed. Engl. 24* (1985) 727; b) F. Vögtle, E. Weber (Eds.): *Host Guest Complex Chemistry I–III, Top. Curr. Chem. 98* (1981), *101* (1982), *121* (1984); c) F. Vögtle, E. Weber (Eds.): *Biomimetic and Bioorganic Chemistry I–III, Top. Curr. Chem. 128* (1985), *132* (1986), *136* (1986); d) D. J. Cram, *Angew. Chem. 98* (1986) 1041; *Angew. Chem. Int. Ed. Engl. 25* (1986) 1039.
[214] See [165] and references cited therein.
[215] C. Frejacques, *Chem. Ind. (London) 1985*, 780.
[216] Thanks to all the coworkers for their diligent and devoted ...!

However, one really should remember that the Chinese already knew 2000 years ago: you learn a lot from your teachers, you learn more from your friends but you learn most from your students. (Picture taken from [3b], p. 101.)

ANGEWANDTE CHEMIE

International Edition in English

Volume 27 · Number 1
January 1988
Pages 159–183

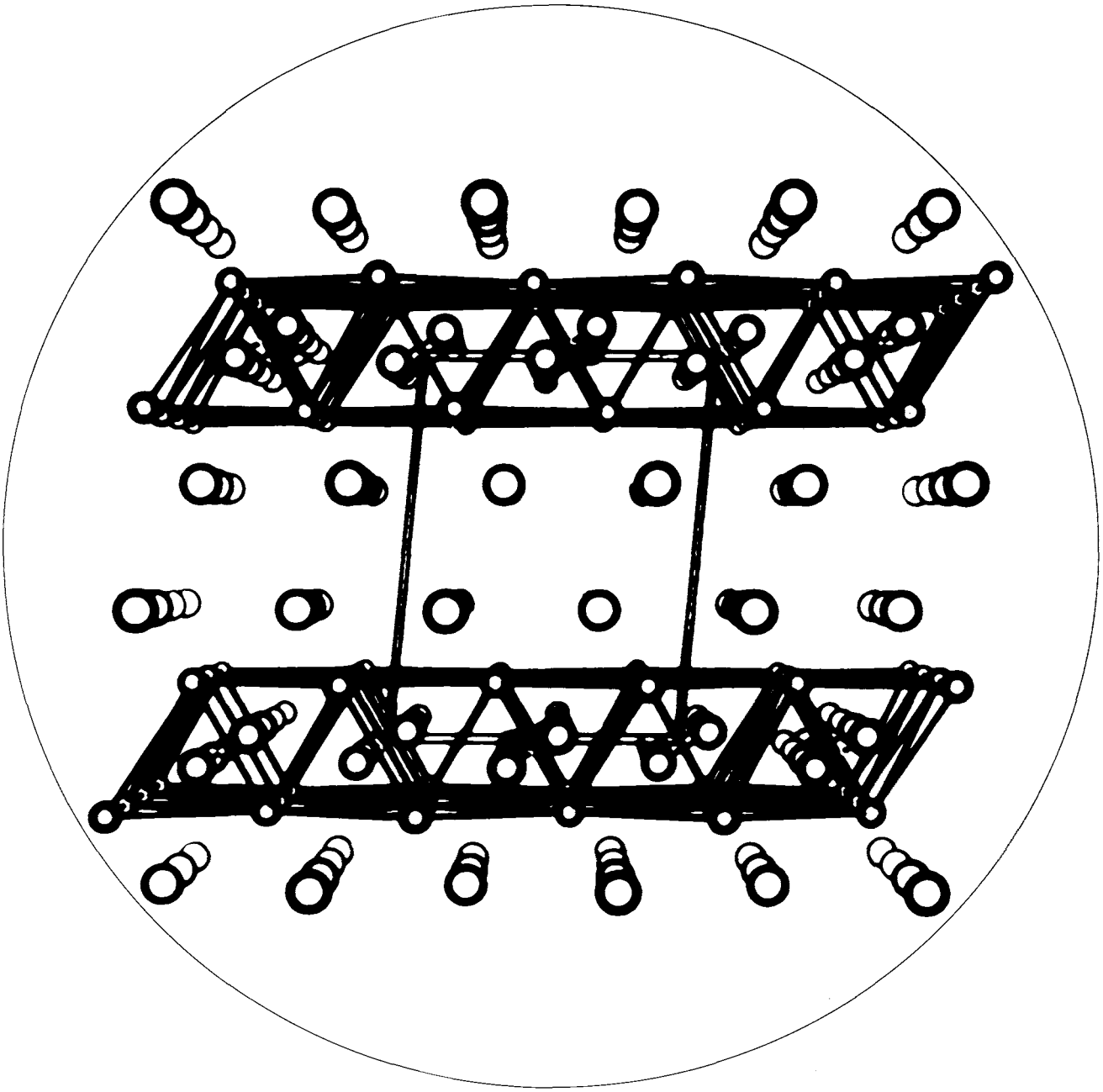

Arndt Simon

Clusters of Valence Electron Poor Metals—Structure, Bonding, and Properties

 © VCH Verlagsgesellschaft mbH, D-6940 Weinheim, 1988 *0570-0833/88/0101-0183 $ 02.50/0*

Clusters of Valence Electron Poor Metals—Structure, Bonding, and Properties**

By Arndt Simon*

Metals in low oxidation states are capable of forming metal–metal bonds. An attempt has been made to classify the numerous phases and structures occurring in such metal-rich systems of valence electron poor metals in some sort of order from a rather general point of view. With this purpose in mind, clusters of these elements, their different types of interconnections, and their condensation via shared metal atoms, which finally leads to extended M–M bonded structures, are described. Interstitial atoms play an important role in stabilizing electron deficient clusters, and can actually lead to the loss of all M–M bonds. Surprising similarities emerge between apparently very different systems as the metal-rich oxides of alkali metals, the oxides, halides, and chalcogenides of d transition metals, and the halides and carbide halides of the lanthanoids.

1. Introduction

It is immediately apparent from the literature that chemists are becoming more conscious of the behavior of solids and of the interrelationships between their structure, bonding, and chemical and physical properties. Superficially analyzed, this is due to the fact that single crystal structural analysis—the development of solid state chemistry without this technique would be unthinkable—has become a routine analytical method in molecular chemistry. With this technique, one is compelled to consider additional atomic interactions present in the "extended" crystalline state that may be absent in the "molecular" state. As illustrated in the following amusing story, such additional interactions might be very special: We succeeded in solving the crystal structure of the unstable compound F_3CCSF_3, which melts at $-123\,^{\circ}C$, and found, contrary to the predicted angle of 180.0°,[2] one of 171.5° at the central carbon atom.[1] Obviously due to the influence of crystal packing forces![3] Later, calculations taking into account electronic correlation effects predicted a much larger deviation from linearity,[4] and now the experimental value was too large. Once again, packing influences? *The solid state is something very special!*

From the above it is not obvious that the last sentence is meant seriously. Naturally, an assembly of 10^{23} atoms in a crystal must have significant consequences with respect to bonding and properties like non-stoichiometry or cooperative phenomena. Besides these real peculiarities, however, there are a number of apparent ones originating from a different development of description in different fields of chemistry. The carbon suboxide C_3O_2 is not puzzling to chemists, because its conventional formulation O=C=C=C=O obeys the accepted and well-known valence rules. The formula Rb_9O_2 is more likely to raise eyebrows. Yet, the principle of bonding in both compounds is the same. Only a part of the valence electrons of C (Rb) is used for heteronuclear C–O (Rb–O) bonds, while the extra electrons are used for homonuclear C–C (Rb–Rb) bonds.

The reverse is also true. Certain bonding features in a molecule are considered most unusual, even though comparable features are quite normal in solid compounds. Thus, the carbon in the stable molecule Li_6C was believed to be hypervalent,[5,6] even though the occurrence of octahedrally coordinated carbon atoms was known to be widespread in transition metal carbides with the rock salt-type structure. The hypervalency is not required in a simple ionic formulation. With $(Li^+)_6C^{4-}(e^-)_2$ the only surprising feature is the surplus of electrons. Yet, even this feature is familiar in the case of interstitial carbides like V_2C. Again, it holds that valence electrons of V (Li) that are not used for heteronuclear V–C (Li–C) bonding are used for homonuclear V–V (Li–Li) bonds, as suggested by the 8 − n rule.[7]

The structures and properties of metal-rich compounds are well suited for illustrating the sometimes different but supplementary views in molecular and solid-state chemistry. The examples already discussed throw light on important facets of the following treatise: Metal-rich compounds contain more metal atoms than the number of free valencies of the nonmetal atoms. The excess of metal-centered valence electrons can lead to bonding, nonbonding, or even antibonding interactions between adjacent metal atoms. As a rule, these interactions are bonding with the valence electron-poor metals under discussion and therefore result in the formation of discrete metal clusters or extended M–M bonded structures.

A surprisingly uniform picture has been developed for the bonding in metal-rich alkali metal oxides, cluster compounds of d-metals, and metal-rich compounds of the lanthanoids, especially the carbide halides, allowing us to relate these seemingly different classes of compounds under one unified theme.

2. Alkali Metal Suboxides—"Cluster Metals"

The alkali metals have been considered rather boring due to their exclusive monovalency. Contrary to this, the

[*] Prof. Dr. A. Simon
Max-Planck-Institut für Festkörperforschung
Heisenbergstrasse 1, D-7000 Stuttgart 80 (FRG)

[**] The preceding page shows Figure 27c of this article.

previously mentioned compounds Li_6C and Rb_9O_2 indicate that metal-metal bonding occurs and results in a fascinating chemistry, even with these elements. The molecule Li_6C, which is stable toward all conceivable decomposition reactions in the gas phase, is by no means unique. Numerous comparable hypermetalated molecules (e.g., Li_3O, Li_4O, Li_5N, Na_3O, Na_4O, and Na_2OH) have been estimated to be stable and have been observed experimentally.[8] The existence of M–M bonds between alkali metal atoms should not be surprising at all, for it has long been known that vapors of these metals contain M_2 molecules. Larger homonuclear clusters are formed by high-energy ion bombardment[9] or expansion of the vapors,[10] although such homonuclear clusters have a rather low stability. If Cs vapor is expanded into an atmosphere of pure He gas, no Cs clusters are observed. The situation changes drastically when small amounts of O_2 (0.01%) are introduced into the He. A large number of homonuclear Cs_n clusters can be detected by mass spectroscopy; they are obviously formed by fractionation during the ionization process (e.g., Cs_n^{2+} with $n > 19$). On increasing the proportion of O_2, hypermetalated species like $[Cs_5O]^+$, $[Cs_7O]^+$, and $[Cs_7O_2]^+$ are formed in high concentrations.[11–13]

These findings can be summarized in the following simple way: Clusters of valence electron-poor metals have a rather low stability. They are stabilized by the insertion of heteroatoms, which leads to strong bond formation to these atoms at the expense of a further weakening of the already weak M–M bonds.

Although metal-rich solids appear to be more complicated, their bonding can be explained in a similar fashion provided one uses a sufficiently simplified description. The formulation of Li_6C as $(Li^+)_6C^{4-}(e^-)_2$ should not be taken as an ideology of chemical bonding, but as providing a simple and easily visualized counting scheme. A more detailed description tells us that in the octahedral molecule, all bonding states are occupied by ten electrons, $(3a_{1g})^2(2t_{1u})^6(4a_{1g})^2$, and that the HOMO $4a_{1g}$ has Li–Li bonding character.[6]

During the transition from the gas phase to the solid state, even the alkali metal clusters that are stabilized by interstitial nonmetal atoms are threatened with decomposition. The metals are entirely miscible with their molten halides, provided the temperature is high enough.[14, 15] The colorful and experimentally difficult cluster chemistry that results[16] is lost with decreasing temperature due to the dominance of the heteroatom bonds. This results in a phase separation and crystallization of the monohalides with their high lattice stabilities.

A small island of stability of alkali metal clusters in the solid state only exits so far in the suboxides of the heavy alkali metals, Rb and Cs,[17] although only at relatively low temperatures (Table 1). Similar compounds of the lighter metals and the higher homologs of O do not exist because of the ease of formation of the normal valence compounds M_2X.

As shown in Figure 1, the Rb and Cs suboxides contain Rb_9O_2 and $Cs_{11}O_3$ clusters, which are composed of two and three face-sharing octahedral M_6O units, respectively. They are the only constituents of the compounds Rb_9O_2 and $Cs_{11}O_3$, but occur together with a stoichiometric amount of Rb and Cs in a variety of thermally unstable phases that have even higher M:O ratios. Most of these compounds have been characterized by single crystal structural analyses. The clusters are largely decomposed in melts that have the composition of the solid phases. The decomposition follows, inter alia, from the fact that the quenching of a melt of composition Rb_7O to $-109\,^\circ C$ yields an amorphous product. Upon annealing at $-103\,^\circ C$ this product deposits crystalline metastable $Rb_{6.33}O$ but no Rb_9O_2 clusters.[25] Crystalline Rb_9O_2 is finally generated along with elemental Rb upon warming to $-90\,^\circ C$. Rb_9O_2 and $Cs_{11}O_3$ clusters do not occur in the gas phase, as has been demonstrated by mass spectroscopic investigation of the partially oxidized metal vapors.[12, 13]

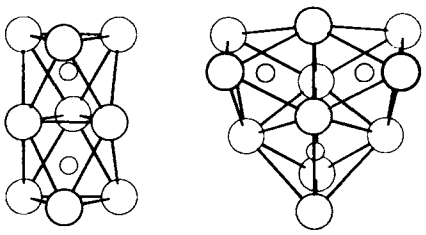

Fig. 1. Characteristic clusters Rb_9O_2 and $Cs_{11}O_3$ in Rb and Cs suboxides, respectively [17] (the large circles represent the metal atoms).

According to *Pauling*'s estimation of the ionicity based on differences in electronegativities, the O–M bonds in the Rb_9O_2 and $Cs_{11}O_3$ clusters are approximately 85% ionic. Therefore, the formulations $(Rb^+)_9(O^{2-})_2(e^-)_5$ and $(Cs^+)_{11}(O^{2-})_3(e^-)_5$ represent a rather realistic description of the bonding in these clusters. Their stability is due to strong O–M bonds, although additional (weaker) M–M bonds are essential for their existence. Model calculations using a simple Born-Mayer potential show that no stable configurations exist for the purely ionic clusters $[(Rb^+)_9(O^{2-})_2]^{5+}$ and $[(Cs^+)_{11}(O^{2-})_3]^{5+}$.[26] Such hypothetical species are unstable and lose cations. For a stable configuration, M–M bonds, i.e., additional electrons in metal centered states, are necessary, which in the electrostatic model are taken into account as a partial shielding of the positive charges. As shown in Figure 2, the energy minimum for the Rb_9O_2 cluster is reached at a global charge of

Table 1. Melting or decomposition temperature T and structural principle of alkali metal suboxides [17, 18].

Compound	T [°C]	Structural principle
Rb_9O_2	40	Rb_9O_2-Cluster
Rb_6O	− 8	$Rb_9O_2Rb_3$; three Rb atoms per Rb_9O_2 cluster
$Rb_{6.33}O$	−93 (metastable)	probably $(Rb_6O)_3Rb$; discrete Rb_6O units
$Cs_{2.78-3.19}O$	< 166	*anti*-TiI_3 type for anticipated composition Cs_3O (to be revised; additional diffuse scattering effects)
$Cs_{11}O_3$	52	$Cs_{11}O_3$ cluster
Cs_4O	ca. 12	$Cs_{11}O_3Cs$; one Cs atom per $Cs_{11}O_3$ cluster
Cs_7O	4	$Cs_{11}O_3Cs_{10}$; ten Cs atoms per $Cs_{11}O_3$ cluster
$Cs_{11}O_3Rb$	—	one Rb atom per $Cs_{11}O_3$ cluster
$Cs_{11}O_3Rb_2$	—	two Rb atoms per $Cs_{11}O_3$ cluster
$Cs_{11}O_3Rb_7$	−22	seven Rb atoms per $Cs_{11}O_3$ cluster

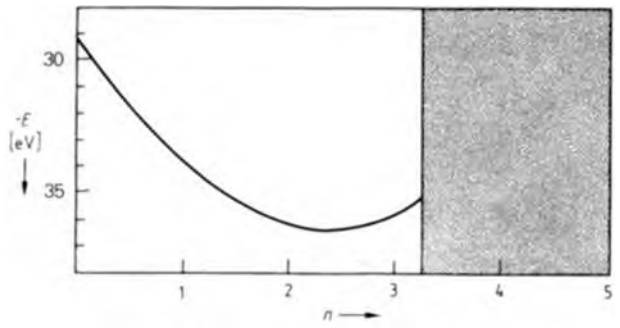

Fig. 2. Calculation of the stable configuration of the cluster $[Rb_9O_2]^{n+}$ assuming two body interactions of the kind $V_{ij}=Z_iZ_j/r_{ij}+A\cdot\exp(-r_{ij}/\rho)$ [26]. For $n>3.2$ no stable arrangement exists. In the shaded range the cluster looses a Rb atom [27].

+2.3. The incomplete shielding of the cationic charges by the additional electrons is probably associated with the anisotropic charge distribution around the Rb^+ ions, which has further interesting consequences discussed later. The vibrational states of the cluster calculated for the equilibrium configuration are in good agreement with the observed Raman spectrum of Rb_9O_2.[26] Therefore, the simple model accounts for both the static and dynamic features of the cluster.

The atomic arrangement in $Cs_{11}O_3$ (Fig. 3) is reminiscent of a molecular crystal structure exhibiting short "intramolecular" Cs-Cs distances (367–431 pm) as a consequence of the strong ionic O-Cs bonds (275–292 pm). Contrary to this, the large "intermolecular" Cs-Cs distances between the clusters, which with only one exception are longer than 500 pm, correspond to the distances in elemental Cs. $Cs_{11}O_3$ and all other alkali metal suboxides have metallic luster[29] and are good metallic conductors.[30] Thus, the electrons in M–M bonding states do not stay localized within the clusters but delocalize throughout the crystal due to the close contacts between the clusters. Accordingly, the characteristic features of the bonding in $Cs_{11}O_3$ can be described in two alternative ways, presented graphically in Figure 3: on the one hand as a "cluster metal", in which the simple ionic cores in the cesium (Cs^+) are replaced by complex ion clusters $[Cs_{11}O_3]^{5+}$ (Fig. 3, top) and, on the other, as a cesium metal that is largely contaminated with oxygen. The localization of negative charges on the O atoms and the regular arrangement of accumulated negative charge in the crystal create a lattice with regions of atomic dimensions that are repulsive to the conduction electrons. The comparison of such a void metal with a "microscopically foamed metal" might be allowed (Fig. 3, bottom).

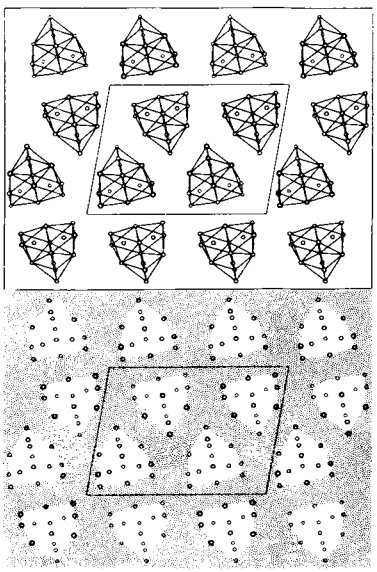

Fig. 3. Projections of the crystal structure of $Cs_{11}O_3$ [28] along [010]. The unit cell is outlined. Top: The $Cs_{11}O_3$ clusters are emphasized by interconnections between the Cs atoms. Bottom: The metallic bonding between the $Cs_{11}O_3$ clusters is emphasized (hatched) leaving repulsive regions for the conduction electrons near the O^{2-} ions (white).

Both model descriptions, the first rather chemical and molecular in character, the second rather physical and related to the quasi-infinite nature of the crystal, allow for a quantitative understanding of the properties of the alkali metal suboxides from very different viewpoints. The cluster metals Rb_9O_2 and $Cs_{11}O_3$ form "intermetallic compounds" with Rb and Cs,[17] e.g. $Rb_9O_2Rb_3$, $Cs_{11}O_3Cs_{10}$, and $Cs_{11}O_3Rb_7$ (Table 1). The molar volumes of these compounds closely correspond to the sum of the molar volumes of Rb_9O_2 and $Cs_{11}O_3$ and the atomic volumes of Rb and Cs, respectively. For example, the molar volumes of $Cs_{11}O_3Cs$ and $Cs_{11}O_3Cs_{10}$ exceed the volume of $Cs_{11}O_3$ by 69.9 and 696.5 $cm^3\ mol^{-1}$ respectively, with the volume of elemental Cs at $-50\,^\circ C$ being 69.4 $cm^3\ mol^{-1}$. Clearly, the Cs in these suboxides forms purely metallic bonds to the $Cs_{11}O_3$ cluster. In Rb-Cs mixed suboxides, under equilibrium conditions, pure $Cs_{11}O_3$ clusters are formed[17,31,32] (for example, $Cs_{11}O_3Cs_{10-x}Rb_x$, $Cs_{11}O_3Rb_{7-x}Cs_x$, and $Cs_{11}O_3Cs_{1-x}Rb_x$). It is only when there is no Cs left for the purely metallic regions between the clusters that the Rb starts to substitute Cs in the cluster itself (e.g., in $Cs_{11-x}Rb_xO_3Rb_7$ and $Cs_{11-x}Rb_xO_3$). There is evidence for the existence of K-Cs mixed suboxides that should, according to what has been said about the Rb-Cs suboxides, have the general composition $Cs_{11}O_3(Cs,K)_n$. Unfortunately, they decompose at $-60\,^\circ C$ with deposition of K_2O and only preliminary X-ray and thermal analysis data have been obtained.

Aside from these chemical aspects of the cluster metal model there emerges a number of physical aspects. Thus, for example, the temperature dependence of the specific heat[33] of $Cs_{11}O_3Cs_{10}$ closely corresponds to the sum of the appropriately scaled values of $Cs_{11}O_3$ and Cs. In particular, the separate contributions to the specific heat of the lattice vibrations of the clusters and the purely metallic regions at low temperatures are of interest. Elemental Cs shows a larger increase in the specific heat in the range $1\le T^2\le 8\,K^2$ than would be expected according to the T^3 law; this is due to the excitation of phonons of the lowest-lying acoustic branch. In the same temperature interval an anomalous increase of c_p is also found for $Cs_{11}O_3Cs_{10}$ which is caused by the excitation of vibrations of the individual isolated Cs atoms (Fig. 4). A similar, although much less pronounced behavior is found in the region $0.1\le T^2\le 1\,K^2$ (Fig. 4, inset). Here one expects excitation of the very soft vibrations of the clusters as a whole, which have more than eleven times the mass of a single Cs atom.

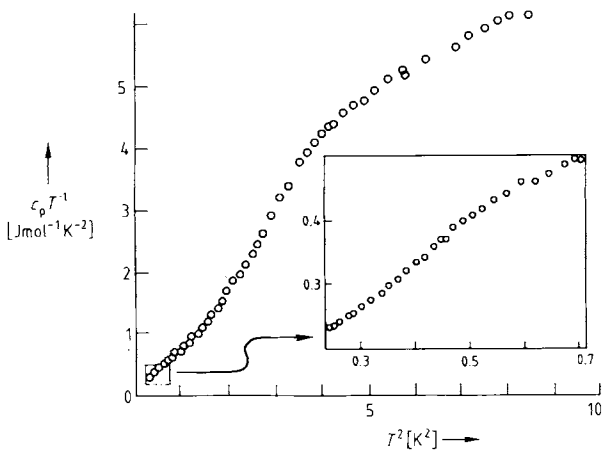

Fig. 4. Specific heat [33] of $Cs_{11}O_3Cs_{10}$ ($\triangleq Cs_7O$) as a function of T, plotted as $c_p/T = f(T^2)$ in the range $0.2 \leq T^2 \leq 9\,K^2$ (inset: $0.24 \leq T^2 \leq 0.72\,K^2$).

An additive behavior of the components in alkali metal suboxides is observed, in particular, in the electronic densities of states. At first glance, the photoelectron (PE) spectrum of $Cs_{11}O_3Cs_{10}$[34] looks like a superposition of the spectra of $Cs_{11}O_3$ and Cs (Fig. 5). All spectra exhibit densities of states at the Fermi level ($E_F = 0$ eV) as one would expect for metallic samples. In the spectrum of $Cs_{11}O_3$ the spin-orbit-split Cs 5p band is shifted by 0.5 eV to smaller binding energies compared to that of Cs, and in the spectrum of $Cs_{11}O_3Cs_{10}$ the photoemission from the 5p band is both characteristic for the $Cs_{11}O_3$ cluster and for pure Cs. The narrow O 2p band provides evidence for the localization of electrons in the O^{2-} ion, and the measured binding energy ($E_B = 2.7$ eV), which is the lowest for all oxides, is consistent with the given description of chemical bonding in terms of O^{2-} ions that are stabilized by a weak Coulomb field of surrounding cations.

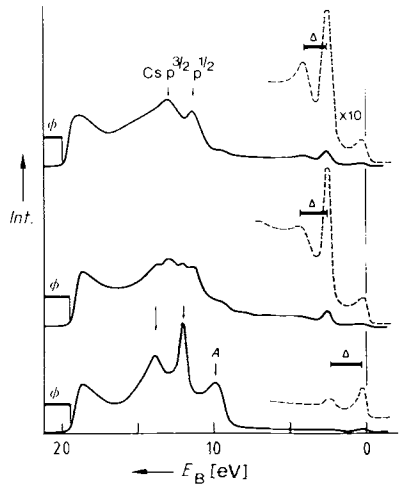

Fig. 5. PE spectra (He(I), $h\nu = 21.2$ eV) of Cs (bottom), $Cs_{11}O_3Cs_{10}$ (middle) and $Cs_{11}O_3$ (top) [34]. The binding energy E_B is referred to the Fermi level $E_F = 0$ eV (ϕ = work function, A = Auger transition $O_{III}VV$, Δ = energy loss structure $\hbar\omega$ (surface plasmon), Int. = intensity.

The measured spectrum of $Cs_{11}O_3Cs_{10}$ could stem from a heterogeneous mixture of Cs and $Cs_{11}O_3$, were it not for features of the spectrum that provide clear evidence of a homogeneous sample. Each sample has a characteristic value for the work function Φ that decreases with increasing O content and shows up as a gap between 21.2 eV (excitation energy) and the threshold of photoemission. The energy loss also changes systematically and leads to satellite structures Δ on the high-E_B side in the spectra due to reduced kinetic energies of the photoemitted electrons. The losses are caused by excitation of surface plasmons, whose energies depend on the number of quasi free electrons. The number of free electrons determined from the measured energy values for $Cs_{11}O_3$ and $Cs_{11}O_3Cs_{10}$ (5 and 14 electrons per formula unit respectively) are in excellent agreement with the simple ionic bond model explained earlier.

The PE spectroscopic investigation not only enables a quantitative proof of this model of the chemical bonding in alkali metal suboxides but also provides information of importance regarding applications and fundamental aspects. Thin composite layers of Cs_2O and Cs on Ag play an important role in the IR-sensitive S1 photocathodes that have now been manufactured for approximately fifty years.[35] The characteristic spectral response of such cathodes can be explained in terms of the presence of alkali metal suboxides ($Cs_{11}O_3$ or "Cs_2O"), which have the necessary electronic properties, namely, a low work function (approximately 1 eV compared to 2 eV for elemental Cs) and low energies of the surface plasmons (1.5 eV), which due to their decay, enhance the photoelectric yield.[36]

The small value for the plasmon energy is simply related to the low carrier concentration and intimately connected with the electron-poor nature of the alkali metals. But what is the origin of the low work function? An interesting explanation is based on the "microscopically foamed metal" model (see Fig. 3, bottom).[37] The conduction electrons in a suboxide crystal find a regular array of accumulated netative charges or "forbidden regions" and reside in narrow regions of atomic scale between the $Cs_{11}O_3$ clusters. As with extremely thin wires, quantization effects are to be expected. In fact, the estimation of such quantum size effects for $Cs_{11}O_3$ predicts a work function that is 0.9 eV lower than that for Cs. Recently, metastable de-excitation spectroscopic (MDS) investigations on cesium suboxide surfaces gave further support for such a quantum size effect.[38,39]

It is a long way from the hypermetalated molecules at the beginning of this Section to the unique electronic properties of alkali metal suboxides. The electron gas and its plasma oscillations call for a quasi-infinitely extended metal. The work function describes a surface property of a solid, and the mentioned quantum size effect is related to the unique bonding in the extended crystal. Yet, the way to molecules is not as far as it might seem. The work function is closely related to the electronegativity of atoms and to the ionization energy of molecules. Much in the same way as the work function of Cs decreases with the addition of oxygen, the ionization energy for a Cs_nO cluster in the gas phase, as a rule, is lower than for the corresponding Cs_n cluster.[11] Does the photoelectron simply experience an additional repulsion by an O^{2-} ion that acts from the interior of an isolated Cs_nO cluster or from a position be-

neath the outermost atomic layer in a suboxide crystal? Does this simple explanation of an experimental observation hold for both the crystal and the isolated molecule?

3. Discrete Clusters—Transition from Insulators to Metals

In alkali metal suboxides an extreme of cluster chemistry involving metals that are especially deficient in valence electrons is realized. The weakness of the M-M bonding in alkali metals is already apparent in the properties of cesium, which is as soft as paraffin, has a low melting point, and is easy to distill. The clusters are stabilized by interstitial atoms, and the metals lack electrons to surround the clusters by nonmetal atoms. On searching for metals with strong M-M bonds one arrives at the transition metals with approximately half-filled d-shells. These have the maximum number of electrons capable of bonding in the elements. Metals like Nb, Ta, Mo, and W are distinguished by high melting points and high values for the heats of atomization. In fact, these metals also exhibit a broad and already frequently described chemistry of metal-rich compounds.[40-59]

It is attractive to extend along the line of thoughts developed so far with a few chosen systems. Particularly suitable as model systems are compounds containing metal clusters with octahedral M_6 units. These units are surrounded by eight nonmetal atoms X above the faces (M_6X_8) or twelve X atoms above the edges (M_6X_{12}), with square coordination geometry of the X atoms at each M atom. The chemical bonding in these clusters has been repeatedly analyzed.[60] The number of M-M bonding states results in a simple way: Each M atom bonds four X atoms via s, p, and d_{xy} orbitals. In the case of the M_6X_8 cluster the remaining four d states mix to yield a fourfold degenerate valence state that bonds along the octahedral edges and leads to twelve 2 electron-2 center (2e-2c) bonds. In the case of the M_6X_{12} cluster the MX_4 planes are rotated through 45° and the corresponding d valence hybrids overlap in the octahedral faces to yield eight 2e-3c bonds.[67] Therefore, ions like $[Mo_6Cl_8]^{4+}$ and $[Nb_6Cl_{12}]^{2+}$ are effectively isoelectronic, for in both cases 20 electron pairs occupy M-X and M-M bonding states.[68]

In addition to the atoms X^i located above the edges and faces of the M_6 octahedra, there are X^a atoms located above the apices of the octahedra (Fig. 6a). In compounds such as $K_4Nb_6Cl_{18}$ ($= K_4Nb_6Cl^i_{12}Cl^a_6$)[69] or $HgMo_6Cl_{14}$ ($= HgMo_6Cl^i_8Cl^a_6$)[70] all coordination sites are occupied without any linkage between the clusters. There is a variety of different ways in which adjacent clusters can be linked, as indicated schematically for the M_6X_8 cluster in Figure 6b. For sake of clarity only bridging between two clusters is shown. Bridges between three discrete clusters are the exception, although they exist, e.g., in $Nb_6Cl_{12}I^{a-a}_{6/3}$.[71] In the condensed cluster systems discussed later, bridges between 3 or even 4 adjacent M_6 units are found.

The electronic balance and the degree of coverage of the M_6 units by X atoms critically determine the physical properties of the compounds. A total coverage always

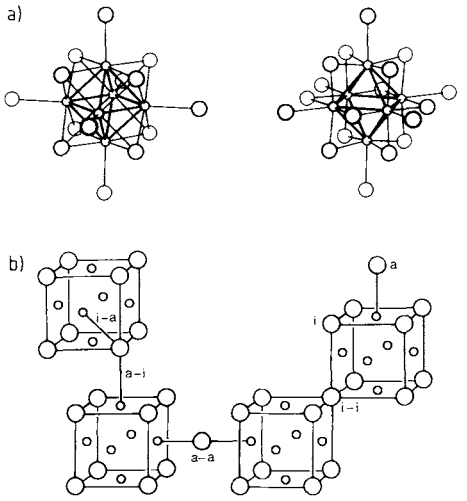

Fig. 6. a) $M_6X^i_8X^a_8$ (left) and $M_6X^i_{12}X^a_6$ clusters (right). b) Different kinds of cluster linkages via X atoms and the symbols used for their description [41]. The cube of X^i atoms is emphasized.

Table 2. Halides, halide chalcogenides and chalcogenides with Mo_6X_8 clusters; structures and properties [55] (cf. Fig. 6); the value of z indicates the number of electrons in M-M bonding states.

Compounds		Structural principle	z/Mo_6	Properties
$A_2Mo_6X_{14}$	A = Li, K, Rb, Cs, Cu; X = Cl $Cs_2Mo_6Cl_8Br_6$	$Mo_6X^i_8X^a_6$	24	insulators
AMo_6X_{14}	A = V–Ni, Zn–Hg, Sn, Pb, Mg–Ba, Eu, Yb; X = Cl	$Mo_6X^i_8X^a_6$	24	insulators
AMo_6X_{13}	A = Na, Ag; X = Cl	$Mo_6X^i_8X^a_{4/2}X^{a-a}_{2/2}$	24	insulators
Mo_6X_{12}	X = Cl, Br, I	$Mo_6X^i_8X^a_{4/2}X^{a-a}_{4/2}$	24	insulators
$Mo_6X_{10}\hat{X}$	X = Cl, Br; $\hat{X}$ = S–Te X = I; $\hat{X}$ = Se, Te	$Mo_6(X_7\hat{X})^i_8X^{a-a}_{6/2}$	24	insulators
$Mo_6X_8\hat{X}_2$	X = Br; $\hat{X}$ = S X = I; $\hat{X}$ = S, Se	$Mo_6(X_5\hat{X})^iX^{i-i}_{2/2}X^{a-a}_{6/2}$	24	insulators
$Mo_6X_6\hat{X}_3$	$Mo_6Br_6S_3$	$Mo_6X^i_4X^{i-i}_{2/2}\hat{X}^{i-a}_{2/2}X^{a-a}_{4/2}\hat{X}^{a-i}_{2/2}$	24	narrow band gap semiconductor (0.02 eV at $T < 100$ K)
$Mo_6X_2\hat{X}_6$	X = Br, I; $\hat{X}$ = S	$Mo_6X^i_2X^{i-a}_{6/2}\hat{X}^{a-i}_{6/2}$	22	metals, superconductors $T_c \approx 14$ K
$Mo_6\hat{X}_8$	$\hat{X}$ = S, Se, Te	$Mo_6\hat{X}^i_2\hat{X}^{i-a}_{6/2}\hat{X}^{a-i}_{6/2}$	20	metals, superconductors
$AMo_6\hat{X}_7$	$Cs_{0.6}Mo_6S_7$	$Mo_6X^{i-i}_{2/2}\hat{X}^{i-a}_{6/2}\hat{X}^{a-i}_{6/2}$	22	metal, superconductors $T_c \approx 8$ K

means insulating or semiconducting behavior even when the important condition for metallic conductivity, namely, partial occupation of the M–M bonding cluster states, is met. An increasing degree of cluster linkage leads to a stepwise closer approach of the M_6 units, especially if the X^i atoms are involved. Following the Herzfeld-Mott criterion,[72–74] the metallic state is finally reached, which we already met with in the bare clusters of the alkali metals. The stepwise transition from insulators to metals is immediately recognizable in the examples of Mo compounds listed in Table 2.

In the case of the valence electron poor metal Nb, the M_6X_8 cluster is found as an exception in iodides,[57–77] but is common in (chalcogenide) halides of Mo[54–58] and (halide) chalcogenides of Re.[55,78,79] There are sufficient d electrons in the halides of Mo to fill all M–M bonding states in the M_6X_8 cluster. When the halogen atoms X are successively replaced by divalent chalcogen atoms $\hat{X}$ the d electron concentration is concomitantly kept high by a stepwise reduction of the $(X,\hat{X})/Mo$ ratio. In the case of valence electron rich Re, a large portion of $\hat{X}$ atoms is needed to avoid the occupation of M–M antibonding states. The decrease in the nonmetal content in the cluster compounds of Re occurs to a lesser extent than in Mo.

The different patterns of interconnection and the increasing degree of interconnection of clusters with decreasing $(X,\hat{X})/M$ ratio are shown schematically for selected compounds in Figure 7. In the chloromolybdates, and also in the ternary molecular compound $Re_6S_4Cl_{10}$ $(= Re_6S_4^iCl_4^iCl_6^a)$,[80] discrete clusters occur. The increasing degree of interconnection via X^a atoms results in one-, two-, and three-dimensional frameworks. The salts AMo_6Cl_{13} and the compound $Re_6Se_5Cl_8$[81] contain cluster chains. The structures of the Mo dihalides[82] and of the isostructural $Re_6S_6Cl_6$[81] are made up of layers, and the complete connection of clusters in all directions according to $M_6X_8^iX_{6/2}^{a-a}$ is reached in the structures of Nb_6I_{11}[75] and the isostructural compounds $Mo_6X_{10}\hat{X}$.[83] $Li_4Re_6S_{11}$[84] is isoelectronic with the latter compounds if a full charge transfer from the Li atoms to the Re_6S_{11} clusters is assumed, which are linked as in Nb_6I_{11}. Besides simple bridges of the X^{a-a} type, polyanionic bridges have been known for a long time, as in W_6Br_{16} $(= W_6Br_8^iBr_4^a(Br_4)_{2/2}^{a-a})$ and in $K_4Re_6S_{12}$ $(= K_4Re_6S_8^iS_{4/2}^{a-a}(S_2)_{6/6}^{a-a})$.[85,86] For Re_2Te_5 $(= Re_6Te_8^i(Te_7)_{6/6}^{a-a})$ a particularly interesting structure has been found.[87,88] The bridges consist of Te_7 units containing a central Te atom with a square planar environment of Te atoms.

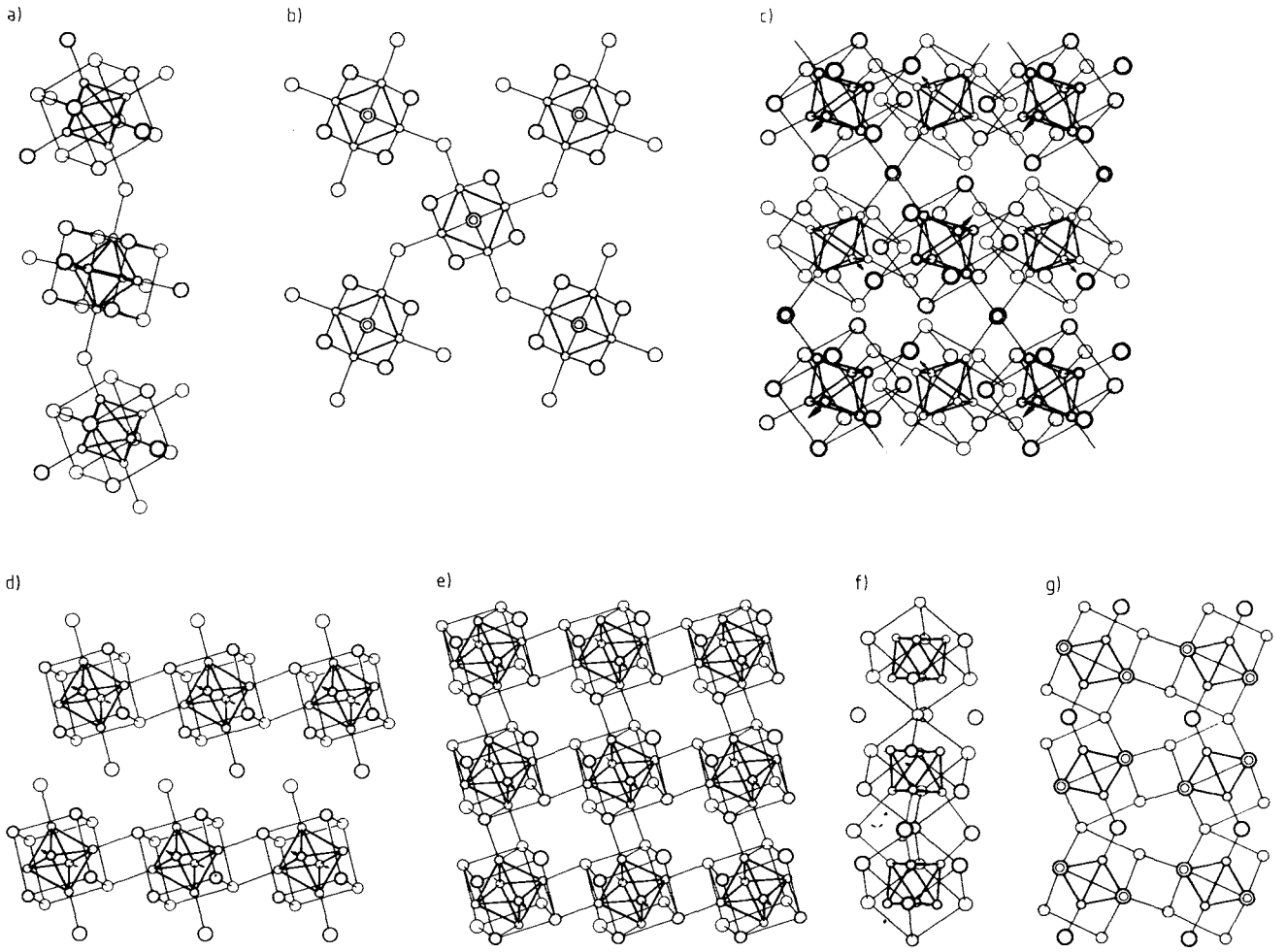

Fig. 7. Increasing connectivity of $M_6(X,\hat{X})_8^i$ clusters in halides, halide-chalcogenides and chalcogenides of the metals Nb, Mo and Re. X^{a-a} links in a) $Re_6Se_5Cl_8$ (chain), b) Mo_6Cl_{12} (layer), c) Nb_6I_{11} (network); X^{i-a} links in (d) $Re_6Se_8Cl_2$ (layer) and e) $Mo_6S_6Br_2$ (network); X^{i-i} $(+X^{i-a})$ links in f) $Mo_6Br_8S_2$ (chain) and g) $Mo_6Br_6S_3$ (layer). M, $\hat{X}$ and X atoms are drawn with increasing size (cf. Table 2 and text).

At low nonmetal contents, $(X,\hat{X})/M \leq 10$, X^{i-a} and X^{i-i} linkage becomes important. In the structure of $Re_6Se_8Cl_2$ ($= Re_6Se_4^{i}Se_4^{i-a}Cl_2^{a}$)[89] the clusters are connected via X^{i-a} bonds to form layers that are surrounded by Cl atoms and are held together via van der Waal forces. Omitting these X^{a}-type Cl atoms results in the $M_6\hat{X}_8$-type structure that consists of $M_6\hat{X}_8$ clusters connected in all directions via X^{i-a} bonds. The X^{i-i}-type interconnection always occurs via opposite atoms of the cluster and leads to linear chains. Such chains, which are van der waals bonded, are found in the structure of the compounds $Mo_6X_8\hat{X}_2$. The connection of these adjacent chains via X^{i-a} contacts results in layers as in the structure of $Mo_6Br_6S_3$. When these layers are linked via X^{i-a} contacts, the Mo-S framework of $Cs_{0.6}Mo_6S_7$ is formed. At this point, a critical limit is reached in the structural chemistry of these cluster compounds. A further reduction of the X/M ratio must lead to a condensation of the M_6 octahedra themselves.

All compounds with 24 electrons in M-M bonding states within the M_6 unit, i.e., with a fully occupied valence band, are insulators or semiconductors, even when close contacts due to interconnections via X^{i} atoms occur. In the case of $Mo_6Br_6S_3$, the energy gap is nearly closed. The gap is 0.037 eV at room temperature. A partial occupation of M-M bonding states does not, of course, result in a metal when the electrons of neighboring clusters are well separated due to X^{a-a} bridges and remain localized on the clusters. The dark green Ta_6Cl_{15} ($= Ta_6Cl_{12}^{i}Cl_{6/2}^{a-a}$)[90] or the brownish-black Nb_6I_{11} ($= Nb_6I_8^{i}I_{6/2}^{a-a}$) are insulators or semiconductors (depending where one draws the line), although only 15 and 19 electrons respectively (instead of 16 and 24) fill M-M bonding states. The description of Nb_6I_{11} as $(Nb^{5+})_6(I^{-})_{11}(e^{-})_{19}$ only serves as a unified counting scheme for electrons. It does not provide a good description of the chemical bonding. A quantitative analysis of bonding, at least within the limits of the one-electron approximation, has been performed.[91] In view of the weak electronic interaction between the clusters, the valence bands are narrow enough to describe the bonding within the MO scheme for the discrete cluster.

In compounds with such discrete units, the d electrons are only delocalized within the cluster. A partial occupation of the M-M bonding states may lead to interesting magnetic properties, which have been investigated in some depth with Nb_6I_{11}.[92-94] At low temperatures all 19 electrons in the M-M bonding states except one are spin paired. The calculated spin density distribution was also verified experimentally with polarized neutrons.[95] In a second order phase transition near 0°C the deformation pattern of the Nb_6I_8 cluster changes slightly. As a result, the states around the HOMO-LUMO gap approach each other, and when their separation becomes smaller than the spin pairing energy, one pair decouples. The phase transformation is accompanied by a change in the magnetic ground state from doublet to quartet (Fig. 8). Such spin crossover transitions should occur frequently in metal cluster compounds, since numerous closely spaced levels with M-M bonding character exist, whose energies are sensitive to small changes in the geometry of the clusters.

The compounds at the end of Table 2 combine a partial occupation of the M-M bonding states with a close approach of the clusters, which leads to broadened valence bands. These compounds are metallic. The strong electronic interactions between neighboring clusters are mainly due to the short distances between Mo and $\hat{X}$ atoms and not due to direct Mo-Mo intercluster bonding.[64] For example, the Mo-Mo distances in the structure of $Mo_6S_6Br_2$ are 272 and 273 pm within and 322.5 pm between Mo_6 octahedra. In contrast, the intracluster Mo-S distances of 240-247.5 pm are only slightly shorter than the inter-cluster Mo-S distances of 248.5 pm.[97]

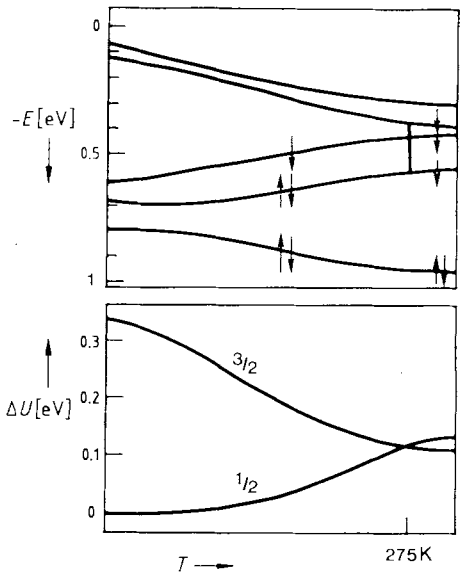

Fig. 8. Top: Changes in the one-electron energies of the highest occupied (HOMO's) and lowest unoccupied (LUMO's) d states in Nb_6I_{11} as a function of temperature (or deformation of the Nb_6 octahedron respectively) [91, 92]. When the separation of the marked states becomes equal to the spin pairing energy at 275 K the energy difference between low-spin ($S = 1/2$) and high-spin state ($S = 3/2$) disappears and a doublet-quartet transition occurs (bottom). ΔU = total energies.

Wide variations for the d electron concentration are found in the Chevrel phases $(M,M')_6(X,\hat{X})_8A_x$. One possibility for changing the electron balance is by substitution of the nonmetal atoms, as seen in the last example. Substitution of the Mo atoms by more electron-rich transition metals is also possible, and the "magic number" of 24 electrons per $(M,M')_6$ unit is reached in the semiconductors $Mo_4Ru_2Se_8$ or $Mo_2Re_4Se_8$.[98] A third possibility for varying the electronic count is the intercalation of metals A that act as electron donors. Metal atoms from the entire Periodic Table can be incorporated between the clusters. The Mo-Mo distances are a sensitive probe for the number of electrons transferred from A into the cluster. At low electron concentrations, the M_6 unit is an elongated trigonal antiprism and becomes increasingly regular as the 24 electron limit is approached.[99, 100]

The chemical and physical properties of Chevrel compounds have been covered in detail in textbooks.[101] The enormous interest in these compounds is due to the fact that Mo_6S_8Pb turned out to be a superconductor ($T_c \approx 14$ K),[102, 103] which, from the very beginning, set a new record to accessible upper critical fields ($H_{c2} \approx 60$ Tesla). Figure 9 compares Mo_6S_8Pb with the technically used superdonductors NbTi and Nb_3Sn. Incidentally, the compound initiating all the interest, Mo_6S_8Pb, already repre-

sented the nearly optimized system. In the meantime cold-drawn multifilament wires have been produced that contain thin Mo_6S_8Pb fibers in a Cu matrix.[104]

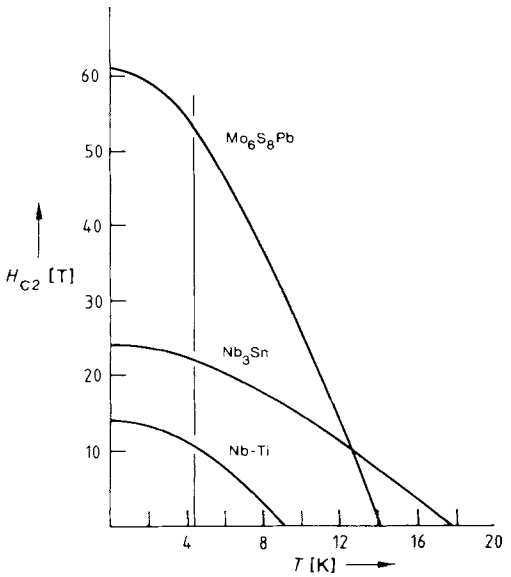

Fig. 9. Comparison of the upper critical fields H_{c2} for Mo_6S_8Pb and the technologically employed superconductors Nb-Ti and Nb_3Sn [105]. The boiling point of He (4.2 K) is marked.

Magnetic fields normally decrease the superconducting transition temperature, no matter whether the field is independent of or created by the flow of current through the wire itself. Hence, the high value of the critical field H_{c2} for Mo_6S_8Pb is of interest for any technical application of this superconductor. Moreover, the investigations carried out on Chevrel compounds have contributed significantly to our understanding of the antagonism between superconductivity and magnetism.

Superconductivity of the element Mo at $T_c < 1$ K could only be demonstrated after the metal had been purified from ppm traces of magnetic impurities, Fe in particular. In the compound Mo_6S_8Pb a contamination by 0.5 atom-% Fe suppresses superconductivity.

In contrast, large magnetic ions like those of the lanthanoids can be introduced between the clusters in a strictly ordered arrangement. The distances to the Mo atoms are large (d(Ln–Mo) > 410 pm), and their influence on the superconductivity of the phases is small. The coexistence of superconductivity and long-range magnetic order could be demonstrated in these systems for the first time.[101] The Ln sublattice (e.g., Ln = Dy, Pr, Gd, Tb) in Mo_6S_8Ln orders antiferromagnetically without affecting the superconductivity. It needs a ferromagnetic ordering of the Ln^{3+} ions, corresponding to a strong external field, to break the Cooper pairs and destroy the superconductivity. Such competition between superconductivity and magnetism is responsible for the remarkable properties of Mo_6S_8Ho, which becomes superconducting upon cooling ($T_c = 1.2$ K) and normal again at the lower temperature of 0.65 K. At this temperature, the ferromagnetic ordering of the Ho^{3+} moments occurs. Still more unusual is the behavior of $Mo_6S_{7.2}Se_{0.8}Sn_{0.25}Eu_{0.75}$ (Fig. 10).[108, 109] At $T < 1$ K the superconductivity is suppressed in a weak field of approximately 1 T, but reoccurs at higher fields. Finally, above 22 T the phase becomes a normal conductor again. This phenomenon is explained in terms of the Eu 4f electrons generating an exchange field in opposition to the external field, which it therefore compensates.

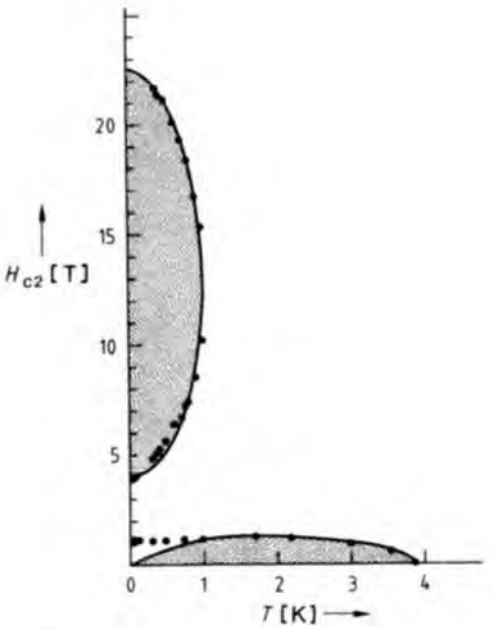

Fig. 10. Field induced superconductivity of $Mo_6S_{7.2}Se_{0.8}Sn_{0.25}Eu_{0.75}$ [108, 109]. The regions with superconductivity are shaded (lines calculated, points measured).

The intriguing physical properties of the Chevrel phases, as well as their comparatively simple crystal structures based on a primitive packing of quasi-molecular $Mo_6\hat{X}_8$ units, prompted a series of theoretical investigations in order to understand the chemical bonding in these phases.[64, 65, 110, 111] They provided evidence of strong electronic interactions between the closely spaced clusters. The transition from the local bonding scheme for the "molecule" $Mo_6\hat{X}_8$ to the band structure for the extended crystal can be illustrated in a most obvious way (Fig. 11). In the discrete regular $Mo_6\hat{X}_8$ cluster the twelve M–M bonding states lying above the M–$\hat{X}$ bonding ones are followed by the antibonding e_g, t_{1u}, a_{2g}, t_{1g}, and t_{2u} states. Their degeneracy is partly removed due to the deformations in the real clusters.

In Figure 11 the molecular orbitals (MO's) are drawn around the HOMO-LUMO gap for the real clusters in Mo_6S_8 and Mo_6S_8Pb. The interactions between the cluster systems in the extended crystal leads to a band-like broadening of all levels. Their dispersion in momentum space is shown for the symmetry direction along the threefold axis of the rhombohedral system. The bands are filled to the Fermi level, E_F.

The special arrangements of the clusters in the $M_6\hat{X}_8$ structure (Fig. 7e) allows each Mo atom to form a donor-acceptor bond with an $\hat{X}$ atom (type $X^{i\text{-}a}$) of an adjacent cluster. The bonding originates from an opening of the HOMO-LUMO gap. The M–M bonding e_g state remains

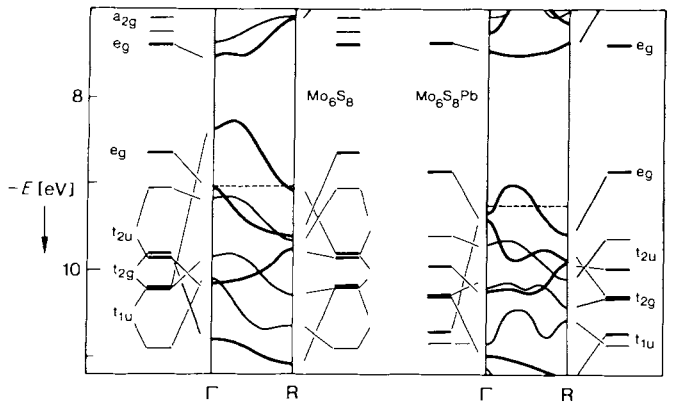

Fig. 11. MOs around the HOMO-LUMO gap for the discrete clusters in Mo_6S_8 and Mo_6S_8Pb together with the band structures for the extended crystals. The band dispersions are shown in the direction of the threefold axis of the rhombohedral system [64]. The Fermi levels are marked by dashed lines.

virtually unchanged in energy as there is hardly any overlap with the p orbitals on the $\hat{X}^{a-i}$ atom (δ bond). According to the result of a population analysis, the Mo-$\hat{X}$ bonds between clusters are essentially as strong as those within the clusters, whereas the *inter*-cluster Mo-Mo bonds have only approximately 10% of the strength of the *intra*-cluster Mo-Mo bonds. This result is fully consistent with the qualitative interpretation of the bonding presented earlier for $Mo_6S_6Br_2$ on the basis of the experimental Mo-Mo and Mo-$\hat{X}$ distances.

The self-consistent band structure calculation performed for the Chevrel phases with 20 to 23 d-electrons in M-M bonds leads to a result that is of significance to an understanding of their superconductivity. Obviously, the band scheme is not rigid but changes drastically with the electron concentration in the cluster. The conduction band, in particular, changes its shape dramatically.[112] These changes can be traced back to the antibonding interactions between e_u and the p orbitals at the $\hat{X}^{a-i}$ atom. These have π character and therefore are sensitive to changes in the intercluster distances. In the case of a filled conduction band (24 electrons) these antibonding interactions between the clusters lead to large Mo-$\hat{X}^{a-i}$ distances. The depletion of the conduction band reduces the repulsive interaction between the clusters, and as a consequence, the intercluster distances decrease and the conduction band near Γ is raised. This change is evident from a comparison of the band structure of Mo_6S_8 (20 electrons) and Mo_6S_8Pb (22 electrons).

In Mo_6S_8Pb the electrons occupy the local minimum at Γ. Vibration of the clusters as a whole changes the Mo-$\hat{X}^{a-i}$ distances and, hence, raises and lowers the conduction band near Γ. These states will fill and deplete periodically with the same rhythm of the vibrations. One might argue that the resulting strong electron–phonon coupling is essential for the superconductivity of these phases. But how is the coupling of the electrons in Cooper pairs effected? Is there a tendency for a pairwise localization of electrons in a cluster state, and do the magnetic properties of the insulating Nb_6I_{11} and the superconductivity in the metallic Mo_6S_8Pb therefore have anything in common?

4. Condensed Clusters, "Polymers" and "Oligomers"

In the previous section it was shown how stepwise lowering of the nonmetal-to-metal ratio in compounds with M_6X_8 and M_6X_{12} clusters leads to an increasing degree of bridging and, thus, to a change from insulators to semiconductors to metals. But, in the most metal-rich systems, i.e. the $Mo_6\hat{X}_8$ Chevrel phases, the relative number of $\hat{X}$ atoms is sufficiently high to occupy all inner positions of the cluster completely and even the X^a positions are all occupied by $\hat{X}$ atoms of adjacent clusters. Intercluster M-M bonding has thus far played only a subordinate role.

Further reduction of the nonmetal-to-metal ratio creates a qualitatively new situation, since not only X atoms but also M atoms now have to be shared between clusters. Such a condensation can occur via corners, edges or faces of the M_6 octahedron. In fact, numerous structures of metal-rich compounds of d metals and p elements can be interpreted in terms of condensed clusters forming the characteristic partial structures. A more comprehensive treatise of the concept has been given elsewhere.[49] In the present review, only some recent results will be summarized to illustrate the structural chemical concept, and in particular, those results will be discussed which shift emphasis from "structure" to "chemistry".

The condensation of M_6X_8 clusters via *trans*-positional corners of the M_6 octahedron is the most simple case, as the monomeric unit is kept complete in this process. The resulting chain has the composition $M_{2/2}M_4X_{8/2} = M_5X_4$. In this case the M atoms as well as the X atoms surrounding the clusters are shared between adjacent clusters. This type of cluster chain was first found in the structure of Ti_5Te_4.[113] There exists quite a number of isostructural compounds with M = V, Nb, Ta, Mo and X = S, Se, Te, As, Sb. The structure is shown as a projection along the tetragonal axis in Figure 12. The complete M_6X_8 clusters in

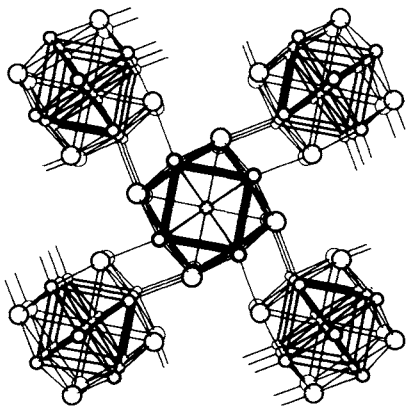

Fig. 12. Central projection of the structure of Ti_5Te_4 [113] along the tetragonal c axis. The Ti atoms (small circles) are connected by strong lines.

the chains are easily recognized. The intercluster contacts (M-X^{a-i}) are the same as those found in the Chevrel phases. Figure 13 shows, in a rather simplified way, how the bonding in the chain is derived from the bonding in the discrete cluster.[67, 114] The ordering of the d states remains,

in principle, the same in the discrete cluster as in the cluster chain structure. The four atoms in the equatorial plane of the M_6 unit are not involved in condensation. Their valence orbitals combine (2e-2c bonding) to form four bonding and four antibonding MO's respectively. In contrast, each apical M atom bonds to the atoms of two adjacent octahedron bases via four degenerate 2e-2c bonds resulting in four bonding, four nonbonding and four antibonding combinations respectively. In spite of some rather strong dispersion of the bands their origin is still recognizable, at least at low energies. Deviations from the very simplified MO scheme are mostly due to severe distortions of the clusters in the chain. The M_6 octahedra are always compressed to some degree such that the M-M distances in the octahedron bases are only slightly shorter than the intercluster distances (322 pm vs. 343 pm in Ti_5Te_4). The M-X distances between chains (d(Ti-Te) = 277 pm) are also of the same length or shorter than in the chains (277, 282, 295 pm).[113]

The M_5X_4 structure type exists with variable occupation of the M-M bonding states; Ti_5Te_4 (12 electrons) and Mo_5As_4 (18 electrons)[115] indicate the wide range of electronic balance. The experimentally established range of electron counts is in agreement with the calculated band structure (Fig. 13), which, at first glance, does not exhibit

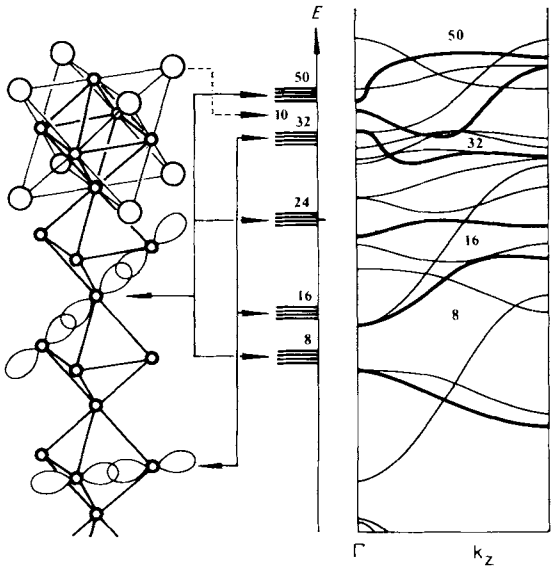

Fig. 13. Development of the band structure of a M_5X_4 chain in the [001] direction by the condensation of M_6X_8 clusters [67, 114]. The 2e-2c bond in the octahedral basis and the 2e-3c bond via the apex atom are indicated. The total number of electrons in the bands is given.

any region of low density of states. One-dimensional band structure calculations for distorted chains as in the real compounds, on the other hand, lead to electronic gaps or regions of low densities of states for the ranges 12 to 13 and 17 to 18 electrons, making the experimental observation of a certain concentration of compounds with these electron counts understandable.[116, 117]

The M_5X_4 chain is a characteristic structural component of a variety of compounds of quite different composition. The beautiful structure of $Nb_{21}S_8$[118] is shown as an example in Figure 14. The structure contains M_5X_4 chains as

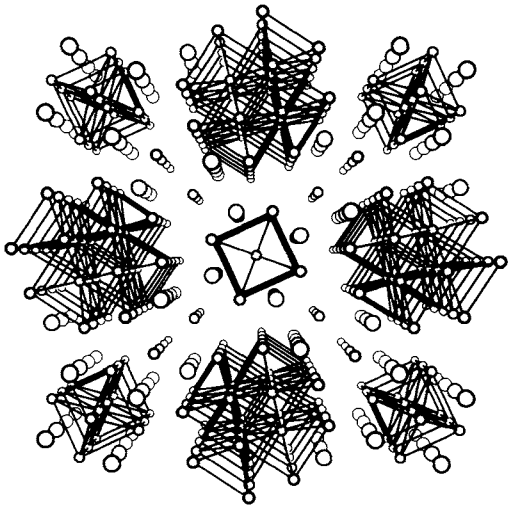

Fig. 14. Central projection of the structures of $Nb_{21}S_8$ [118] along the tetragonal c axis. The substructures derived from the M_6X_8 cluster are emphasized. Lines connect the Nb atoms.

well as parallel linear units formed by condensation of four such chains. In this process of condensation the X atoms of the single chains are largely substituted by M atoms of an adjacent chain. All Nb_6 octahedra are compressed to such a degree that the inner atoms of the unit have a cubic environment very similar to that found in the bcc structure of Nb metal. The structure gives the impression of a eutectic separation which stopped within atomic dimensions and resulted in a suspension of metallic Nb in a sulfide matrix. In fact, it is only a matter of the viewpoint one takes, whether the structures of metal-rich compounds are discussed in terms of condensed monomers or as pieces of the elemental structures cut out from the pure metals.[47] In this sense, the polycyclic arenes could equally be considered as derivatives of benzene and of graphite.

Structures are also known which are built up from M_6X_{12} clusters condensed via apices of the M_6 octahedra. In the low-temperature modification of TiO, chains occur in which the Ti_6 octahedra are condensed via *trans*-positional apices similarly as in M_5X_4 chains.[49] In NbO the clusters are condensed via all apical atoms, thus leading to a rigid three-dimensional framework with extended M-M bonding.[41] Band structure calculations impressively reveal the close relationship between the chemical bonding in the extended arrays of TiO and NbO and the bonding in a discrete M_6O_{12} unit.[119, 120] Consideration of these structures from another standpoint is helpful here: The structures of TiO and NbO almost correspond to the rock-salt type structure except for the fact that 1/6 and 1/4 of the available positions for the M and O atoms, respectively, are unoccupied. The loss of lattice energy caused by the vacancies has to be compensated for by M-M bonding. The proportion of vacancies therefore increases with the number of d electrons for M-M bonding. In the case of d^1 systems (e.g. TiN, NbC ...) the rock-salt structure is stable; the structure of the d^2 system TiO is between the rock-salt type structure and the structure of the d^3 system NbO. The conclusions drawn for metal-rich complexes in the gas phase also hold true here: if only few electrons are available for M-M bonding, then the clusters are stabilized, in

our case in the rock salt structure, by interstitial nonmetal atoms. TiO is an interesting borderline case. All clusters are empty in the structure of the low-temperature modification, but at high temperature a transition to a (statistically disordered) rock salt structure occurs.

When M_6 octahedra are condensed via apices the entire M_6X_8 and M_6X_{12} clusters remain complete and the directions of the valence orbitals are not changed significantly. The situation must change in the case of a condensation via edges or faces of the octahedra. In these systems one X atom is replaced by two or three M atoms respectively, which can only be bonded via drastically reoriented orbitals (rehybridization) compared to the discrete cluster. A correlation of the electronic band structures of extended systems of condensed clusters and the MO pictures of discrete clusters is therefore scarcely possible, and one might ask whether a description of, for example, an octahedra chain in terms of condensed clusters is meaningful. On the other hand, in recent years numerous compounds have been found which contain "polymeric" or even "oligomeric" clusters based on edge- and face-sharing M_6 octahedra. A kind of "macromolecular chemistry" with metal clusters is emerging.

Table 3. Oxomolybdates with chains of edge-sharing Mo_6 octahedra [50, 51, 53, 57]. The number z of metal centered valence electrons was derived from (a) the ionic formula, (b) from the bond-order sums Σs_i(Mo-O) for all Mo atoms [121]. **2** contains an excess of Mo in octahedral voids. Therefore, the value of z derived according to (a) is minimal.

Compounds		Interconnection of the chains	z/Mo$_4$ (a)	(b)
$A_xMo_4O_6$ **1**	A_x = Li–Rb	$Mo_4O_4^iO_2^{i-a}$	13.0	12.8
	A_x = In		13.0	13.1
	$A_x = Ba_{0.62}$		13.2	– [a]
	$A_x = Pb_{0.8}$		13.6	13.3
	$A_x = Sn_{0.9}$		13.8	13.4
$A_{2-x}A'_xMo_4O_7$ **2**	$A_{2-x}A'_x = Sc_{0.75}Zn_{1.25}$	$Mo_4O_4^iO_{2/2}^{i-i}O_2^a$	≥ 14.7	14.5
	$A_{2-x}A'_x = Ti_{0.5}Zn_{1.5}$		≥ 14.5	14.4
	$A_{2-x}A'_x = Sc_{0.5}Fe_{1.5}$		≥ 14.5	14.3
$Mn_{1.5}Mo_8O_{11}$ **3**		$Mo_4O_3^iO^{i-a}O_{1/2}^{i-i}O^{i-a}$	14.5	14.0
$A_xMo_8O_{10}$ **4**	A_x = Li	$Mo_4O_4^{i-a}O_{2/2}^{i-i}$	14.5	14.3
	A_x = Zn		15.0	14.7
$Ca_{5.45}Mo_{18}O_{32}$ **5**		–	14.6	15.6

[a] Not calculated.

Table 3 summarizes the different crystal structures of the known reduced oxomolybdates, all of which contain chains of *trans*-edge-condensed Mo_6 octahedra. The particularly simple structure of $NaMo_4O_6$ is reproduced in Figure 15. It contains parallel chains of Mo_6 octahedra with O atoms located above all free edges (as in the M_6X_{12} cluster). The chains have the composition $Mo_{4/2}Mo_{2/2}O_2O_{8/2}$ (= Mo_4O_6). The Mo and O atoms not involved in the condensation interconnect the chains according to $Mo_4O_4^iO_2^{i-a}$ (as in rutile), and the cations occupy the cubic voids in the channels between the cluster chains. The structure is also formed with a series of other cations. Pb as cation occupies an acentric position in the cube and is coordinated in the typical pyramidal configuration of the "lone pair" Pb^{2+} ion. When the cations are In or Sr, the position of occupancy is approximately in or exactly in the cube faces respectively, and the coordination geometry is square planar. This special coordination, in conjunction with the short interactomic distances (e.g. d(In–In) = 286.3 pm), indicates that M–M bonds not only occur in the anionic part but also in the cationic part of the structure (vide infra).

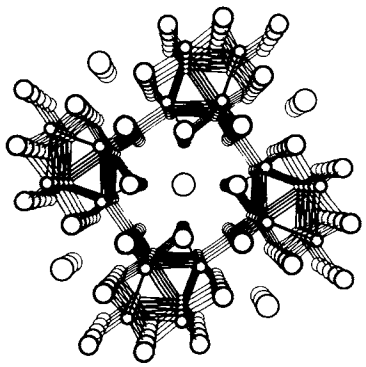

Fig. 15. Central projection of the structure of $NaMo_4O_6$ along the tetragonal c axis [122]. The Mo_6 octahedra are emphasized by strong lines. The Na^+ ions occupy the channels between the cluster chains (e.g. in the center of the drawing).

The structures of the compounds summarized in Table 3 exhibit different patterns of interconnection between the Mo_4O_6 chains. In **1**, **2**, **3**, and **5** the chains are parallel, whereas in **4** they form layers which are stacked crosswise. In **5**, in addition to the Mo_4O_6 chains there are chains of single Mo atoms and ribbons of edge-sharing Mo_4 rhomboids. These ribbons are the only structural element in $NaMo_2O_4$. The bridging O atoms in these oxomolybdates are coordinated by up to four Mo atoms, in contrast to the X atoms which bridge two discrete clusters. Oxygen atoms with trigonal and square planar or SF_4-like coordination geometries are quite common.

There are several independent ways in which the number of electrons in M–M bonding states can be estimated. The formal counting scheme via oxidation states used so far (e.g. $Na^+(Mo^{6+})_4(O^{2-})_6(e^-)_{13}$) leads to very similar results as the detailed analysis of all Mo–O distances with the aid of an empirical bond length-bond strength relationship.[121] According to this analysis 13 to 15 d electrons populate M–M bonding orbitals in the Mo_4 fragment. At high electron counts the sum of M–M bonds as determined from the Mo–Mo distances using *Pauling*'s formula is somewhat low. The logarithmic equation of *Pauling* might be too simplified for an analysis of M–M bonds between heavy transition metal atoms.[123] On the other hand, the too-low bond order sums could indicate that a portion of the d electrons have entered nonbonding or antibonding states, since chain distortions are typically found at high electron counts. For example, in **2** the Mo_6 octahedra are tilted around the common edges, leading to alternating short and long distances between the apical atoms. In **3** and **4** the apical atoms are pairwise associated and the corresponding common edge in the octahedron basis is considerably lengthened. Of course, the cation distribution in the structures as well as the interchain connections might influence these distortions. In any event, the distortions are electronically favored, as indicated from Ex-

tended Hückel (EH) calculations on an undistorted chain compared to a distorted chain as in **2**.[124]

The essential features of the band structures of compounds containing the Mo_4O_6 chains can be worked out from a one-dimensional calculation because the dispersion of the bands is small in the directions orthogonal to the chain. The decomposition of the calculated density of states into bonding and antibonding contributions for the different kinds of Mo-Mo contacts is particularly instructive. The corresponding diagrams are plotted in Figure 16. As one would expect from the crystal structure, the bonds

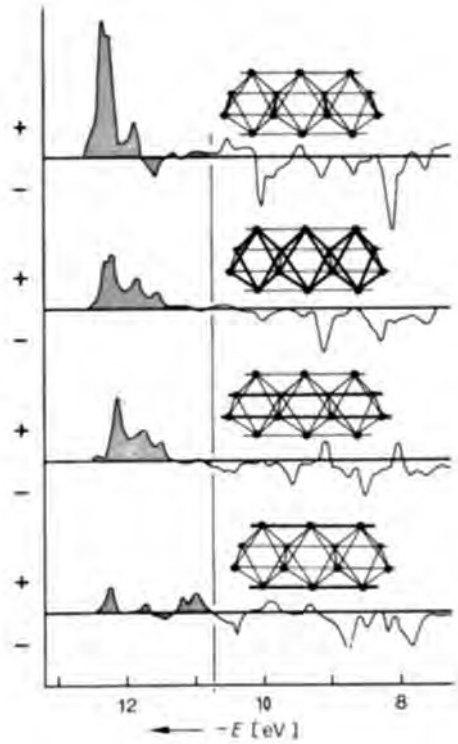

Fig. 16. COOP diagrams (crystal orbital overlap population) [161] indicating bonding (+) and antibonding (−) character of the bands for the different kinds of Mo-Mo contacts in the octahedra chain of $NaMo_4O_6$ [124]. The shaded bands are filled to the Fermi level (vertical line).

along the joined edges are the strongest and the bonds between the apical atoms the weakest. Thirteen electrons per Mo_4 fragment enter the bands without occupying antibonding states. Yet even with 15 electrons the energy balance is still good because the weakening of the bonds along the chain direction is compensated for by a strengthening of the bonds along the joined edges. At high electron counts, however, the formation of one strong bond from two weak bonds between apical atoms of adjacent octahedra leads to a decrease in energy.

The structures of the previously discussed oxomolybdates all contain quasi-infinite chains. Under weakly oxidizing conditions phases of the general composition $In_{1+x}Mo_4O_{6+2x}$ can be prepared which are built up from finite parts of the chain. X-ray crystallographic and high-resolution electron microscopic investigations indicate that many structural variations are possible.[125,126] In the structure of $In_3Mo_{11}O_{17}$, layers of clusters occur which contain five Mo_6 octahedra (Fig. 17a). The structure of $In_{11}Mo_{40}O_{62}$ is made up of alternating layers which contain clusters with four and five Mo_6 octahedra (Fig. 17b). In the electron microscope clusters of six condensed Mo_6 octahedra could also be observed (Fig. 17c), and the occurrence of diffuse and "incommensurate" superstructure reflections in X-ray diagrams of "$InMo_4O_6$" crystals furnished evidence of the existence of even longer clusters. The preparation of homogeneous phases incurs severe problems because they differ only marginally in composition. Thus, a compound which contains only clusters with five Mo_6 octahedra has the composition $In_{1.091}Mo_4O_{6.182}$ ($\triangleq In_3Mo_{11}O_{17}$); a hypothetical phase formed from clusters with six Mo_6 octahedra has the composition $In_{1.077}Mo_4O_{6.154}$. When mixtures of different layers appear as irregular patterns in the crystal a more or less continuous change of composition can occur.

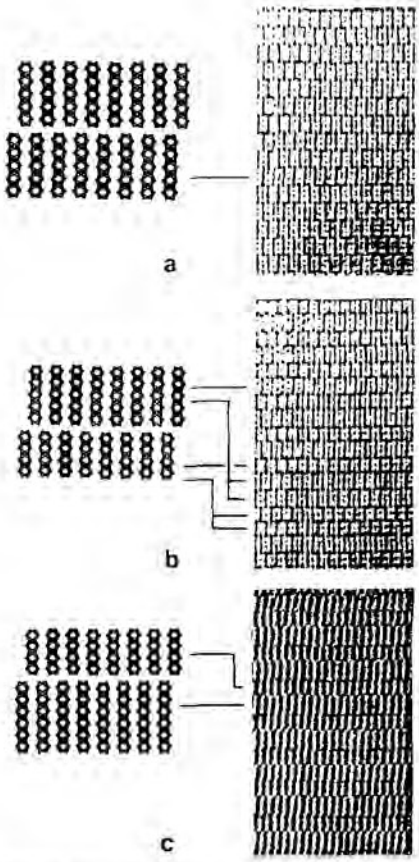

Fig. 17. High-resolution electron microscopic images of a) $In_3Mo_{11}O_{17}$ with uniform layers of $n=5$ clusters, b) $In_{11}Mo_{40}O_{62}$ exhibiting alternating layers of $n=4$ and $n=5$ clusters, respectively, and some faults indicated, and c) a phase (projected in a different direction) with layers of $n=4$, 5 and 6 in an irregular sequence [126]. The units of n edge-condensed octahedra are shown on the left-hand side.

As in the monomeric M_6X_{12} cluster, the oligomeric clusters with n edge-sharing Mo_6 octahedra are surrounded by O atoms above all free edges. The structure of $In_{11}Mo_{40}O_{62}$ therefore contains alternating layers of $Mo_{18}O_{30}$ and $Mo_{22}O_{36}$ clusters which are oriented parallel to each other and are interconnected at top and bottom according to $(Mo_{18}O_{26}O^{i-i}_{4/2})(Mo_{22}O_{32}O^{i-i}_{4/2})$. Bonds of the X^{i-a} type link the clusters within the layers. In the channels between

these clusters are suspended chains of five and six In atoms respectively.

The $Mo_{18}O_{30}$ cluster and the In_5 chain with the nearest O neighbors are shown in Figure 18. Here, we find the interesting situation where M–M bonded polycations and polyanions occur simultaneously in $In_{11}Mo_{40}O_{62}$. The In_5 chain can be formally decomposed into $2\times In^{2+}$ and $3\times In^{+}$ and can thus be described as $(In_5)^{7+}$. The summation of all In–O bond orders leads to the same ionic charge, which also corresponds to the anionic charge derived from all Mo–O distances.

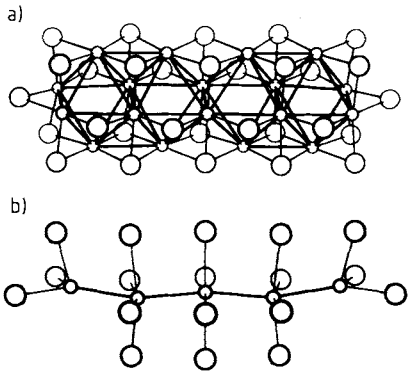

Fig. 18. a) $Mo_{18}O_{30}$ cluster in $In_{11}Mo_{40}O_{62}$ [125]. The coordination of all Mo atoms by O atoms of adjacent clusters O^{a-i} is omitted. b) $(In_5)^{7+}$ cation in $In_{11}Mo_{40}O_{62}$ with the nearest neighbor O atoms. The central In atom has an exactly planar coordination by four O atoms.

Normally, the outer two electrons of the In^+ ion are nonbonding (lone pair). In the structures of these oxomolybdates the rigid matrix of the cluster anions parallel to the In chains (Mo-Mo distances between 276 and 284 pm) forces the In^+ cations into such close proximity that the lone pair configuration is changed into two In–In bonds for each In atom. The bonds manifest themselves in the even closer approach of the atoms within the In chain (d(In–In) $\geq$ 262 pm) than required by the matrix. Thus, hitherto unknown chain-like polycations of In (and possibly other main group metals) can be stabilized by suitable anionic clusters.

The compositions of the cluster layers or, in the case of only one cluster type, the compounds $In_{1+x}Mo_4O_{6+2x}$ follow the general formula $In_{n+1}^{(n+3)+}(Mo_{4n+2}O_{6n+4})^{(n+3)-}$. The number of Mo_6 octahedra in the cluster is designated n. What values may n have?

The oligomeric clusters can be dissembled into Mo_4O_7 (top) and Mo_2O_5 (bottom) fragments, which together constitute a divided Mo_6O_{12} cluster and $n-1$ inserted Mo_4O_6 fragments (from the infinite chain). The fragment orbitals correspond to those in the monomeric cluster and in the polymeric chain. Therefore, 16 electrons (or rather 14[128]) per Mo_6O_{12} fragment and 13 to 15 electrons per Mo_4O_6 fragment can enter metal centered d states in the oligomeric clusters. Within these limits the allowed range of d-electron counts is calculated for different n and compared with the cluster electron counts derived via the anionic charges (Fig. 19). Apparently, only clusters with $n\geq 3$ are favorable in the case of the In compounds. The characteristic distortion of the $Mo_{18}O_{30}$ cluster ($n=4$) with the pairwise short distances between apical atoms, as in the infinite chains of **3** and **4** (cf. Fig. 18a), indicates a high d electron concentration. When the metal is Sn instead of In the d electron concentration is so high that, according to Figure 19, clusters with $n\leq 7$ should not occur. In fact, with Sn only the infinite chain compound has been observed so far and the Sn deficiency in $Sn_{0.9}Mo_4O_6$ can even be taken as evidence that the upper stability limit in Figure 19 should be slightly lower.

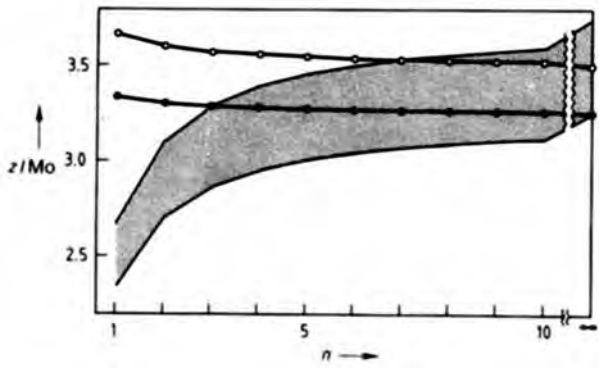

Fig. 19. Stability range for oligomeric clusters of n edge-sharing Mo_6 octahedra in the phases $A_{1+x}Mo_4O_{6+2x}$ (A = Sn (○) and In (●)). The shaded region corresponds to optimal electron concentrations. It was derived by dissembling the oligomer into a Mo_6O_{12} fragment (14–16 electrons) and $n-1$ Mo_4O_6 fragments (13–15 electrons) [127] (cf. text).

It is natural to seek for smaller oligomeric clusters with more electron poor d metals. Indeed, a variety of recently discovered reduced oxo compounds exists in the case of the neighboring element Nb. Nearly all of them have unusually complicated stoichiometries.[131] Their structures frequently contain discrete Nb_6O_{12} clusters, but so far no condensed clusters have been found. In the structure of $SrNb_8O_{14}$ (Fig. 20, bottom) the clusters are aligned in such a way that their close relation between the monomer and the polymeric chain is immediately recognizable (Fig. 20, top).

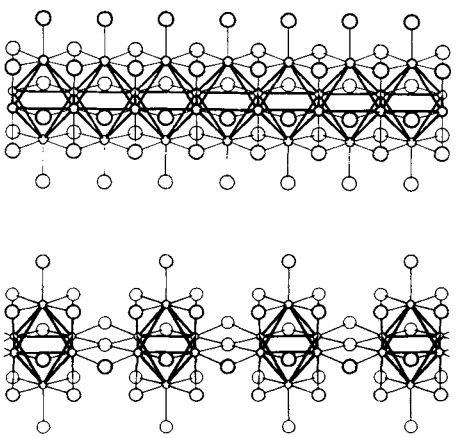

Fig. 20. Comparison of a chain of condensed Mo_6O_{12} clusters in oxomolybdates (top) and the arrangement of discrete Nb_6O_{12} clusters in the structure of $SrNb_8O_{14}$ (bottom) [133].

Table 4. Ternary molybdenum chalcogenides $A_xMo_{3n+3}\hat{X}_{3n+5}$ characterized by single crystal investigations. Those in the first group contain one individual kind of clusters with n face-condensed Mo_6 octahedra; those in the second group contain different kinds of clusters [54, 58]. In the first group the number of electrons per Mo atom, z/Mo, in M–M bonding states as derived from the composition is compared to the optimum range estimated through a fragmentation of the clusters.

n	Compound	Clusters	Charge	z/Mo Experimental	z/Mo Estimated
Clusters of one kind					
1	$A_xMo_6\hat{X}_8$ ($\hat{X}$ = S, Se, Te)	$Mo_6\hat{X}_8$	0 to 4−	4.00–3.33	—
2	$Ag_{2.3}CsMo_9Se_{11}$	Mo_9Se_{11}	3.3−	3.92	4.11–3.67
2	$Ag_{3.4}ClMo_9Se_{11}$	Mo_9Se_{11}	3.4−	3.93	4.11–3.67
2	$Ag_{3.6}Mo_9Se_{11}$	Mo_9Se_{11}	3.6−	3.96	4.11–3.67
3	$Cs_2Mo_{12}Se_{14}$	$Mo_{12}Se_{14}$	2−	3.83	4.17–3.83
5	$Rb_4Mo_{18}Se_{20}$	$Mo_{18}Se_{20}$	4−	4.00	4.22–4.00
7	$Cs_6Mo_{24}Se_{26}$	$Mo_{24}Se_{26}$	6−	4.08	4.25–4.08
9	$Cs_8Mo_{30}Se_{32}$	$Mo_{30}Se_{32}$	8−	4.13	4.27–4.13
∞	$TlMo_3Se_3$	$Mo_{6/2}Se_{6/2}$	1−	4.33	—
Clusters of different kinds					
1	$In_{\sim 1}Mo_{15}Se_{19}$	Mo_6Se_8			
2		Mo_9Se_{11}			
1	$In_2Mo_{15}Se_{19}$	Mo_6Se_8			
2		Mo_9Se_{11}			
1	$Tl_4Mo_{18}S_{22}$	Mo_6S_8			
3		$Mo_{12}S_{14}$			

The chemistry of the last variant of cluster condensation, namely the condensation via faces of the M_6 octahedron is particularly impressive. Figure 21 shows the discrete $Mo_6\hat{X}_8$ cluster and the final product of the condensation of

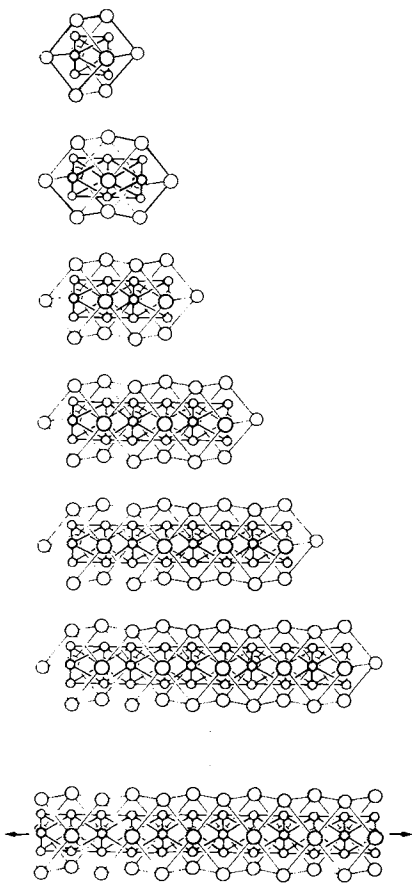

Fig. 21. Monomeric, oligomeric and polymeric clusters $Mo_{3n+3}\hat{X}_{3n+5}$ (Mo small circles) containing Mo_6 octahedra condensed via faces [54, 58]. The compositions of the clusters are $Mo_6\hat{X}_8$, $Mo_9\hat{X}_{11}$, $Mo_{12}\hat{X}_{14}$, $Mo_{18}\hat{X}_{20}$, $Mo_{24}\hat{X}_{26}$, $Mo_{30}\hat{X}_{32}$, and for the polymeric chain $Mo_3\hat{X}_3$.

such clusters via *trans*-faces of the octahedron, the $Mo_3\hat{X}_3$ chain as it occurs in the compounds $AMo_3\hat{X}_3$ with univalent elements such as A = K, Tl, etc. In the last few years, numerous compounds have been synthesized and structurally characterized[54, 58] which contain the intermediate oligomeric clusters of stepwise increasing sizes (Fig. 21). Table 4 lists some compounds which have been characterized by single crystal structure investigations.

The compounds have the general composition $A_xMo_{3n+3}\hat{X}_{3n+5}$ and can contain either one kind of cluster exclusively or different clusters together in an ordered array. The structures containing only one kind of cluster exhibit (with the exception of the Ag compounds) a particularly close relationship with the structure of the first member of the series. All compounds crystallize in the space group $R\bar{3}$ as do the Chevrel phases $A_xMo_6\hat{X}_8$: The $Mo_6\hat{X}_8$ cluster is stretched along its threefold axis, and inserted in the channels between the elongated clusters there are $n-1$ planar $Mo_3\hat{X}_3$ fragments together with the corresponding number of A atoms. This genesis of the oligomeric clusters allows for a suitable fragmentation procedure to estimate the optimal electron counts. All intra- and intercluster contacts of the $Mo_3\hat{X}_4$ fragments (top and bottom) are the same as in the Chevrel phases. Both fragments together can have 20 to 24 d electrons for M–M bonding. The number of electrons in M–M bonding states per $Mo_3\hat{X}_3$ fragment in the infinite chain is 13. Therefore the number of electrons (z) in M–M bonding states of an oligomeric cluster with n condensed Mo_6 octahedra should be within the limits $13n+7 \leq z \leq 13n+11$, where the upper limit corresponds to the closed configuration.[135] This estimate is in agreement with the results of MO calculations for the ions $[Mo_9S_{11}]^{4-}$ and $[Mo_{12}S_{14}]^{6-}$.[65] With $z = 13n+11$ and $n=2$ and 3 we get $z=37$ and $z=50$, respectively. The MO calculation gives 50 electrons in M–M bonding states for $n=3$. In the case where $n=2$ (and all clusters with even n) there is some ambiguity in the electron count due to a non-bonding state in the HOMO-LUMO gap. The cluster contains 38 electrons when this level is occupied and 36 if unoccupied.

All the examples in Table 4 have less d electrons than expected for the closed configuration. There is no ambiguity in the electron counts for the large cluster compounds with alkali metal cations; in each case four electrons are missing for the closed configuration.

Band structure calculations for the quasi infinite $^1_\infty[(Mo_3\hat{X}_3)^-]$ chain[65, 111] yield a band with very strong dispersion for the six equivalent bonds between the $Mo_3\hat{X}_3$ fragments along the chain direction. With an electron count of 13 this band is half-filled, i.e. the compounds $AMo_3\hat{X}_3$ are metals with distinctly one-dimensional character, and the Peierls distortion expected for such a system obviously occurs with the alkali metal compounds. They show a gradual transition to semiconducting behavior with decreasing temperature,[138] while the electronic coupling between the cluster chains through the Tl ions in $TlMo_3Se_3$ is apparently strong enough to suppress the metal-semiconductor transition. The compound stays metallic at low temperatures and becomes superconducting at $T<6$ K.[139]

Chemically, the one-dimensional character of these phases expresses itself in a fascinating reaction: $LiMo_3Se_3$

forms colloidal suspensions in polar solvents such as DMSO. Electron microscopic investigations reveal single $Mo_3\hat{X}_3$ chains in such systems.[140] Numerous topochemical reactions with these cluster compounds proceed without a disassembly of the entire structural framework ("soft chemistry").[141] For example, the In can be extracted from $InMo_3Se_3$ as InCl by reaction with HCl at 420 °C. Electrochemically, the residual Mo_3Se_3 can be intercalated reversibly by up to 4.5 Li.[142] Thus, Mo_3Se_3 is an interesting candidate for a solid state battery. The theoretical energy density of a Li/Mo_3Se_3 cell (referred to the volume) is nearly the same as for the widely used Li/TiS_2 cell.

The topochemical reaction described for $InMo_3Se_3$ can be exploited for the preparation of new binary and ternary molybdenum chalcogenides which are not accessible directly. Starting from $In_2Mo_{15}Se_{19}$ or $In_{\sim 3}Mo_{15}Se_{19}$, prepared directly from the elements, pure $Mo_{15}Se_{19}$ can be obtained by the removal of In.[143, 144] As the arrangement of the clusters is different in the two starting compounds, the $Mo_{15}Se_{19}$ is obtained in two modifications. The empty cluster frameworks can be reloaded by a direct reaction with metals at elevated temperatures or by electrochemical reactions (e.g. with alkali metals, Zn, Cd, Tl, Sn, Pb) and new ternary compounds are formed.

The last mentioned reactions leave the cluster framework unchanged. All attempts to disassemble the framework in a chemically controlled way have so far failed. Is such a disassembly possible and does it lead to a solution chemistry with oligomeric clusters which is offered by the defined bulk solids?

5. Clusters Containing Interstitial Atoms

Clusters with only a few valence electrons for M–M bonding can be stabilized by interstitial atoms with the consequence of a partial substitution of weak M–M bonds by strong bonds with these atoms. This conclusion drawn for clusters of alkali metals at the beginning is also valid for transition metals. The metals of the third and fourth groups form numerous cluster compounds, which are, to a great extent, isostructural with corresponding compounds of the more electron-rich neighboring metals, but differ from them by the additional atoms in the clusters of the M_6 octahedra. The list in Table 5 gives an overview of the broad spectrum of interstitial atoms and structure types known to date.

The occupation of a metal cluster center by a nonmetal atom was first demonstrated in $Nb_6I_{11}H$.[145, 155] At the same time $[Ru_6(CO)_{17}C]$[156] was prepared, and was the first molecular example containing an interstitial C atom in an M_6 octahedron. In the meantime a large variety of related organometallic compounds have been synthesized.[157, 158]

Only $Nb_6I_{11}H$ and $CsNb_6I_{11}H$ contain the M_6X_8 cluster with an interstitial atom. There is no evidence for interstitial atoms being incorporated, for example, in the clusters of the Chevrel phases, despite their electron deficiency ($M_6\hat{X}_8$: 20 electrons in M–M bonding states).

$Nb_6I_{11}H$ and $CsNb_6I_{11}H$ are formed by heating the binary and the ternary compound in H_2 respectively. Hence, the Nb_6I_8 cluster is known with and without an interstitial atom. The hydrogen is lost only in vacuum at such a high temperature that further decomposition of the residue occurs due to the formation of gaseous NbI_4. If this decomposition reaction is suppressed by sealing the sample in an H_2-permeable Nb ampoule, the hydrogenation reaction can be performed reversibly.

Table 5. Halides with interstitial atoms in M_6X_8 and M_6X_{12} clusters and their interconnection patterns together with corresponding structure types based on empty clusters.

"Empty" Cluster	"Filled" Cluster	Interconnection
Nb_6I_{11} [75]	$Nb_6I_{11}H$ [145]	$M_6X_8^iX_{6/2}^a$
$CsNb_6I_{11}$ [76]	$CsNb_6I_{11}H$ [76]	$M_6X_8^iX_{6/2}^a$
—	$Sc_7Cl_{12}Y$ (Y = B, N) [146] $Sc_7I_{12}M'$ (M' = Co, Ni) [147] $M_7I_{12}M'$ (M = Y, Gd; M' = Fe, Co) [147] $Pr_7I_{12}M'$ (M' = Mn, Fe, Co, Ni) [147]	$M_6X_6^iX_{6/2}^iX_{6/2}^a$
—	$Zr_6I_{12}Y$ (Y = B, C) [66, 148] $Zr_6Cl_{12}Be$ [149] $Zr_6I_{12}Mn$ [147]	$M_6X_6^iX_{6/2}^iX_{6/2}^a$
—	$Zr_6X_{13}B$ (X = Cl, Br) [149] $KZr_6Cl_{13}Be$ [149]	$M_6X_{10}^iX_{2/2}^iX_{6/3}^a$
Nb_6Cl_{14} [150]	$Zr_6Cl_{14}Y$ (Y = B, C) [148] $Zr_6X_{14}Fe$ (X = Br, I) [147]	$M_6X_{10}^iX_{2/2}^iX_{2/2}^aX_{4/2}^a$
—	$AZr_6I_{14}C$ (A = K_x–Cs) [66] $AZr_6Cl_{14}B$ (A = Na–Cs) [148, 149] $Cs_xZr_6I_{14}Y$ (Y = Al, Si, Mn, Fe, Co) [147, 148]	$M_6X_{10}^iX_{2/2}^iX_{2/2}^aX_{4/2}^a$
Nb_6F_{15} [151]	$Th_6Br_{15}M'$ (M' = Mn, Fe, Co) [152]	$M_6X_{12}^iX_{6/2}^a$
Ta_6Cl_{15} [90]	$Zr_6Cl_{15}N$ [149]	$M_6X_{12}^iX_{6/2}^a$
$NaNb_6Cl_{15}$ [153]	$Na_xZr_6Cl_{15}Y$ (Y = B, C) [149]	$M_6X_{12}^iX_{6/2}^a$
$CsNb_6Cl_{15}$ [153]	$AZr_6Cl_{15}C$ (A = K–Cs) [154] $KZr_6Cl_{15}N$ [154] $CsZr_6Br_{15}Fe$ [147] $CsRbZr_5Cl_{15}B$ [154]	$M_6X_{12}^iX_{6/2}^a$
—	$K_2Zr_6Cl_{15}B$ [149]	$M_6X_{12}^iX_{6/2}^a$
—	$A_3Zr_6Cl_{15}Be$ (A = K, Rb) [154]	$M_6X_{12}^iX_{6/2}^a$
—	$Na_4Zr_6Cl_{16}Be$ [149]	$M_6X_{12}^iX_{4/2}^aX_2^a$

The magnetic properties of Nb_6I_{11} change drastically with the absorption of H_2. $Nb_6I_{11}H$ is nonmagnetic at low temperature, and above room temperature it exhibits a similar kind of singlet-triplet spin crossover transition as Nb_6I_{11}. Apparently, the H atom adds its electron to the electron deficient cluster system. Yet, the H atom does not play the role of a simple electron donor as is found, e.g., for the Cs atom, which lies between the clusters in $CsNb_6I_{11}$. The large difference in the electronegativities of H and Nb indicates that H is rather hydridic in nature. In fact, the calculated electron density distribution shows cumulated density at the H atom in the cluster.[159]

The solution of this apparent contradiction[91, 114, 160, 162] leads to simple general conclusions on the bonding of interstitial atoms in clusters and the meaning of "counting rules" for this case.

The interaction of the H 1s function with the fully occupied a_{1g} state of the cluster leads to a drastic lowering of the energy of this state; the antibonding combination lies well above the HOMO-LUMO gap. Therefore, the number of bonding cluster states remains unchanged, and only the number of electrons in these states is increased by the electron of the H atom. The stabilization of the cluster is not primarily due to the additional electron (in the nearly nonbonding HOMO), but to the low energy of the originally

M-M bonding a_{1g} state that becomes essentially localized at the H atom. This description of the chemical bonding for the H atom in a cluster is identical with the description of bonding in metal hydrides except for the different terms used. In NiH_x or PdH_x an "impurity band" that has strong H 1s character occurs below the conduction band formed from low-lying d band states. The additional electrons from H fill band holes at the Fermi levels.[163-165]

The transition from Nb to the more electron-deficient neighbor Zr creates a qualitatively new situation. The d electron concentration does not suffice for the formation of the M_6X_8 cluster. The number of electrons is even too low for the formation of the M_6X_{12} type cluster. Other than in the case of Nb_6I_{11}, where the cluster centers can be occupied reversibly by impurity atoms (H), interstitial atoms are a requirement for the formation of the Zr_6X_{12} unit.[166]

The Zr_6X_{12} cluster is able to incorporate a variety of atoms (cf. Table 5), with B, C, and N being the least surprising examples. The previously discussed bonding scheme for interstitial H needs only a minor extension to understand the bonding of these other interstitial atoms.[66, 168, 169] The 2s (a_{1g}) and 2p (t_{1u}) states of the central atom strongly lowers the four clusters states that have the same symmetries. The antibonding combinations are too high in energy to be reached; therefore, the relevant number of orbitals is the same as for the empty cluster. Only the number of electrons in these states is increased by the number of valence electrons of the central atom.[170] The cluster in $Zr_6I_{12}C$ has the same number of available MO's and electrons as the empty cluster in Nb_6Cl_{14}. The essential difference, though, is due to the fact that all 16 electrons in Nb_6Cl_{12} occupy M-M bonding states, whereas in the $Zr_6I_{12}C$ cluster the strong bonds between anionic C and surrounding cationic Zr atoms only allow a few direct M-M bonds.[172] It is true that the formulation $(Zr^{4+})_6(I^-)_{12}C^{4-}(e^-)_8$ ignores the covalency between Zr and C (and I), yet it yields a realistic estimate of the number of electrons involved in M-M bonding. Moreover, it links the Zr compound with simple molecules like $(Li^+)_6C^{4-}(e^-)_2$ (see Section I).

Of particular interest is the recently discovered introduction of transition metal atoms into M_6X_{12} clusters of Zr[147] and Th.[152] Figure 22 shows the cluster occupied by a Fe atom in $Th_6Br_{15}Fe$ ($= Th_6Br^i_{12}FeBr^{a\text{-}a}_{6/2}$).

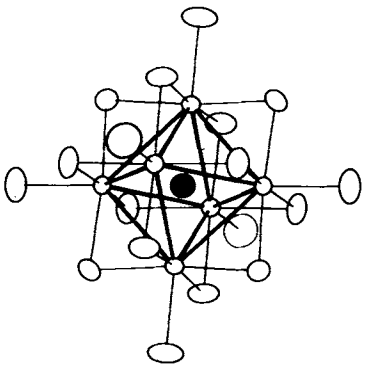

Fig. 22. $Th_6Br^i_{12}FeBr^a_6$ cluster with an interstitial Fe atom in the structure of $Th_6Br_{15}Fe$ [152]. Ellipsoids at the 90% probability level.

The chemical bonding of the 3d metal atom is described via the MO diagram for the $[Zr_6I^i_{12}FeI^a_6]^{4-}$ cluster in Figure 23. With respect to the bonding of interstitial nonmetal atoms, there are two main differences. The polarity of the bonds is smaller and reversed in direction, and the a_{1g} state is primarily Zr-Zr bonding. Furthermore, four additional electrons can be localized at the interstitial d metal atom in degenerate e_g states, which hardly interact with the states of the Zr_6 frame.

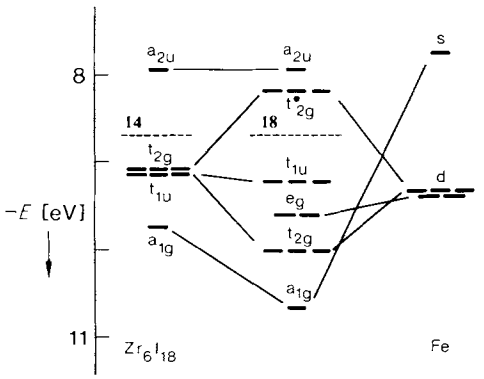

Fig. 23. MO diagram for a regular $Zr_6I^i_{12}I^a_6$ cluster with a central Fe atom [147]. The cluster with the interstitial atom contains 18 electrons up to the Fermi level (dashed line).

What criterion decides whether an element is able to contribute to the stabilization of an electron-deficient cluster as an interstitial atom? Obviously, the M_6 octahedron behaves like a microscopically small piece of metal, and therefore, the question should be, which elements form stable compounds with the bulk metal of the cluster atoms. The answer to this question gives a qualitative explanation for the fact that the electron-deficient Nb_6 unit incorporates H, while the Mo_6 octahedron does not.[173] Zr forms numerous intermetallic compounds with Be, Al, and 3d metals[175, 176] and, obviously, does not lose this ability in the case of only six Zr atoms being joined. *Miedema*'s concept of the stability of intermetallic systems[177, 178] proves helpful in the search for possible interstitial atoms, when this search is limited to atoms of appropriate size to fit into the octahedral site.[179] The comparison of $Cs_{0.3}Zr_6I_{14}Si$ (Si in the Zr octahedron[148]) and $Na(Si,Nb)Nb_{10}O_{19}$ (Si in a O_4 tetrahedron[132]) clearly indicates that the competition of different kinds of bonds (Si-Zr vs. Si-I or Si-Nb vs. Si-O) finally decides about the position of the additional atom, whether in the cluster center or between clusters.

Interstitial atoms frequently occur in discrete clusters. Even more frequently, such interstitial atoms are found in structures that can be described in terms of condensed clusters. As discussed previously, there are compounds that allow the reversible insertion of additional atoms under equilibrium conditions as well as many compounds that are only stable upon inclusion of interstitial atoms.

The Zr halides ZrCl and ZrBr[181] contain characteristic layer units X-Zr-Zr-X composed of single close-packed X and Zr layers. The units can be discussed in terms of edge-condensed Zr_6 octahedra coordinated by X atoms above all free faces (as in the M_6X_8 cluster).

The compounds reversibly absorb H_2.[182] It is remarkable that for a composition ZrX, *two* H atoms are located in each trigonally elongated Zr_6 octahedron.[183, 184] For reasons of electrostatic repulsion the X atoms move above the edges of the octahedra. Hence, the Zr/X arrangement is now related to the M_6X_{12} cluster.

The absorption of H_2 by the halides ZrX can be taken as direct chemical evidence for the deficiency of electrons in M–M bonding states. The hypothetical chalcogenides $Ta\hat{X}$, which are isoelectronic with ZrX, do not exist at all. Yet, the compound Ta_2S_2C, which has a C atom in the center of the Ta_6 octahedron (again the $\hat{X}$ atoms are above the octahedron edges), has been prepared.[186] The compounds "MX" formed with the valence electron poor metals Sc, Y, and Ln exhibit the ZrX type structure and were first thought to be binary compounds.[187–189] Later it was determined that they were stabilized by interstitial H.[52, 146, 190] Gd_2Br_2C, which is isostructural with Ta_2S_2C, has also been prepared.

An important borderline is reached with the last example. No matter what the distribution of valence electrons in Ta_2S_2C looks like, the formulation $(Ta^{5+})_2(S^{2-})_2C^{4-}(e^-)_2$ leaves electrons for M–M bonding. In contrast, all electrons are used up for strong heteroatomic bonds in Gd_2Br_2C $(=(Gd^{3+})_2(Br^-)_2C^{4-})$. The "stabilization of the clusters" by interstitial atoms has led to a decomposition of the cluster, at least if one associates M–M bonds with the term "cluster". Gd_2Br_2C is a normal simple ionic compound, like the isostructural and isoelectronic La_2O_2S.[192] What does the borderline between cluster compounds and simple salts look like?

6. d-Metal Chemistry of the Lanthanoids

All the facets of cluster compounds presented in the preceeding chapters apply to the chemistry of metal-rich halogeno compounds of the lanthanoids. The clusters exist in empty and filled, discrete and condensed forms, and the bonding ranges from M–M bonded species that may be stabilized with additional strong heteropolar bonding to interstitial atoms to species that have only ionic bonding and are simple salts. The latter still have the atomic arrangement in common with cluster compounds, yet have no electrons for M–M bonding. The compounds Gd_2Cl_3 (condensed cluster) and $Gd_7I_{12}C$ (discrete filled cluster) mark the limits of the broad spectrum.[193]

The structure of Gd_2Cl_3[195, 196] contains parallel chains of *trans* edge-sharing Gd_6 octahedra (Fig. 24) which are coordinated by Cl atoms above all free edges (as in the M_6X_8 cluster). The Gd–Gd interatomic distances along the joined edges are shorter than in elemental Gd (337 vs. 357 pm). The octahedron is extremely elongated (390 pm) and the Gd–Gd distances involving the apical atoms are 373 and 378 pm. It is clear from this that the Gd–Gd distances are much longer than in the case of the clusters of the 4d and 5d metals (d(M–M) < 300 pm) previously discussed. The larger cages with lanthanoid clusters have interesting consequences concerning the incorporation of interstitial atoms (vide infra).

The PE spectrum of Gd_2Cl_3[196] immediately affords an insight into the essentials of the chemical bonding com-

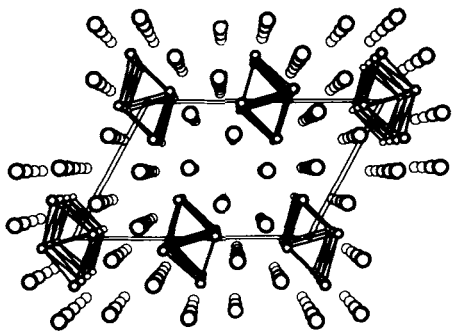

Fig. 24. Central projection of the structure of Gd_2Cl_3 [194, 195] along the monoclinic b axis. The chains of edge-sharing Gd_6 octahedra are emphasized by bold lines.

pared to that of Gd (Fig. 25). The Gd 4f band 10 eV below the Fermi level exhibits no trace of multiplet splitting and therefore corresponds to a $4f^7$ configuration as is typical for the ionic core of Gd^{3+}. The low-lying Cl 3p band gives evidence for strongly polar Gd–Cl bonds. Residual metal valence electrons are present according to the formulation $(Gd^{3+})_2(Cl^-)_3(e^-)_3$. These electrons have d character and fill M–M bonding states. Surprisingly, these electrons are localized in spite of their non-integral number per metal atom (1.5 e^-). Missing density of states at the Fermi level and the band gap of 0.85 eV determined from electrical measurements[197] are clear evidence of the electronic localization in the black compound. This result finds an interpretation from band structure calculations.[198]

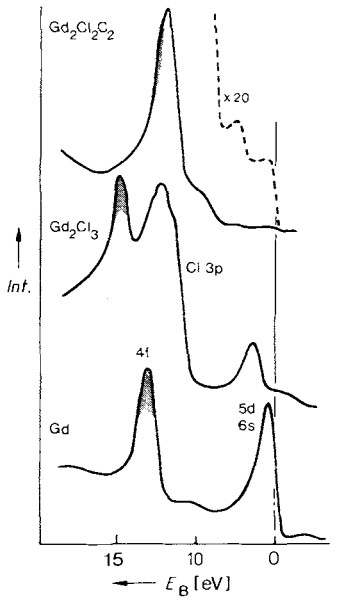

Fig. 25. PE spectra of Gd and Gd_2Cl_3, both taken with He(II) radiation (40.8 eV) [196], and of $Gd_2Cl_2C_2$ (He(I), 21.2 eV) [199]. The narrow 4f band is marked. The structures above the Fermi level ($E_B = 0$) in the spectra of Gd and Gd_2Cl_3 arise from excitations of electrons from the 4f band by the 50.3 eV satellite line.

Few valence electrons are available for M–M bonding in Gd_2Cl_3. The subchloride readily decomposes into Gd and $GdCl_3$; the enthalpy of this reaction, obtained from the

calorimetrically determined enthalpy of formation of Gd_2Cl_3, is 30 ± 15 kJ mol^{-1}.[200] Experiments on the co-crystallization of other lanthanoids in Gd_2Cl_3 indicate that only Tb is incorporated in significant amounts.[201] Obviously, the island of stability of subhalides of the lanthanoids is small.

The "stabilization" of Gd_2Cl_3 with two interstitial N atoms per Gd_6 octahedron is formally achieved in the compound Gd_2Cl_3N.[202] This step is even possible to follow structurally: According to the formulation $(Gd^{3+})_2(Cl^-)_3N^{3-}$ all electrons are removed from M-M bonding states and are now involved in strong Gd-N bonds. Nevertheless, the distances between neighboring Gd atoms are, within a few pm, the same as in Gd_2Cl_3. The mutual repulsion of the N^{3-} ions deforms the Gd_6 octahedron into two edge-sharing Gd_4 tetrahedra, each with a centered N. The Cl^- ions rearrange around the chains of tetrahedra. The Cl and N atoms together form the typical coordination polyhedron of a tricapped trigonal prism around the Gd^{3+} ion.

The band structure calculation and population analysis for Gd_2Cl_3N[198] provide a more quantitative interpretation of the bonding situation with the formulation $(Gd^{2+})_2(Cl^{0.7-})_3N^{1.8-}$ instead of the extreme ionic picture used above. However, it does not change the essential point, namely that the Gd d bands are empty and, therefore, no M-M bonds are possible. The outlined transition from Gd_2Cl_3 to Gd_2Cl_3N, however, is an unconvincingly formal one, for a topochemical reaction of this kind is not possible and the topological similarity of the two structures is more or less accidental. The jump from the black Gd_2Cl_3 to the colorless Gd_2Cl_3N is too large to see in detail what happens when the borderline between cluster systems and simple salts is crossed. The multitude of existing carbide halides of the lanthanoids allows smaller steps.

Table 6. Gd carbide halides. Crystallographically different C-C distances deviate by less than ± 5 pm from the given values. The number of electrons z (per formula unit) in M-M bonding states is derived via the ionic limit on the basis of the experimental C-C distances $((C_2)^{4-}$ and $(C_2)^{6-}$ corresponding to 130 and 145 pm, respectively).

Compound	"Linkage" of the Gd_6-Octahedra	C_n	d(C-C) [pm]	z	Ref.
$Gd_7I_{12}C$	one octahedron	C	—	5	[203]
$Gd_{10}Cl_{18}C_4$	two octahedra	C_2	145	0	[204, 205]
$Gd_{10}Cl_{17}C_4$	two octahedra	C_2	145	1	[205]
$Gd_{10}I_{16}C_4$	two octahedra	C_2	145	2	[206]
Gd_4I_5C	straight chain	C	—	3	[206]
$Gd_{12}X_{17}C_6$ (X = Br, I)	folded chain	C_2	145	1	[207, 208]
$Gd_7I_{10}C_2$	twin chain	C	—	3	[206]
$Gd_6X_7C_2$ (X = Br, I)	twin chain	C	—	3	[209]
Gd_3I_3C	twin chain	C	—	2	[210]
Gd_2Br_2C	planar layer	C	—	0	[191]
$Gd_2X_2C_2$ (X = Cl, Br)	planar layer	C_2	130	0	[191, 210]
Gd_2XC (X = Cl, Br, I)	planar layer	C	—	1	[210]
$Gd_6Cl_5C_{3.0-3.5}$	undulated layer	C	—	1-0	[211]
Gd_3Cl_3C	network	C	—	2	[212]

Table 6 summarizes the carbide halides of Gd that have been structurally characterized. All structures contain octahedral Gd_6 units, which are discrete or condensed via edges and surrounded above all free edges (as in the M_6X_{12} cluster) by halogen atoms. A special feature, when compared to previously treated clusters, is that C_2 units are found in the octahedral voids, in addition to single C atoms. The occurrence of C and C_2 species as well as the observation of different C-C distances in the C_2 species can be used to test the electron counting scheme on a finely graded chemical scale.

$Gd_7I_{12}C$ has the same structure as $Sc_7Cl_{12}N$.[213] It contains $Gd_7I_{12}C$ clusters, whose very low d electron concentration is increased by an extra Gd atom incorporated between the clusters which acts as a three-electron donor.[214] The clusters are additionally stabilized by interstitial C atoms.

The compounds $Gd_{10}Cl_{18}C_4$ (discrete), $Gd_{10}Cl_{17}C_4$ $(= Gd_{10}Cl^i_{16}Cl^{i-i}_{2/2})$ and $Gd_{10}I_{16}C_4$ $(\cong Gd_{10}I^i_{14}I^{i-i}_{4/2})$ contain Gd_6X_{12} dimers condensed via edge sharing. C_2 groups, which are oriented parallel to each other, fill the octahedral voids (Fig. 26). The $Gd_{10}Cl_{18}C_4$ arrangement corresponds to the first step of condensation of M_6 octahedra via edges and closely follows the (empty) oligomeric clusters and chains in the reduced oxomolybdates discussed in Section 4. Even the X^{i-i} type interconnection in $Gd_{10}I_{16}C_4$ is identical to that in $In_{11}Mo_{40}O_{62}$.

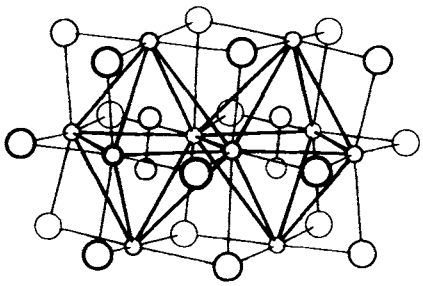

Fig. 26. $Gd_{10}Cl_{18}C_4$ unit in the structures of $Gd_{10}Cl_{18}C_4$, $Gd_{10}Cl_{17}C_4$, and $Gd_{10}I_{16}C_4$ [204-206]. Two Gd_6 octahedra centered by C_2 units are joined via a common edge and surrounded by X atoms above all free edges, as in the M_6X_{12} cluster.

The increasing degree of condensation of (C-containing) Gd_6X_{12} units via common edges of the octahedra is easy to see for the chosen examples in Figure 27. The straight chains of *trans*-edge linked Gd_6C octahedra in the structure of Gd_4I_5C (Fig. 27a) together with their immediate anionic surrounding correspond entirely to the chains in $NaMo_4O_6$. Only the connections between the chains are of a different type. The next step in cluster condensation, which involves the coupling of two parallel M_4X_6 chains with the loss of X atoms above the joined edge, has not yet been realized with empty clusters. With Gd_6C octahedra it is realized, e.g., in the structure of $Gd_6X_7C_2$ (X = Br, I) (Fig. 27b). The crystal contains parallel oriented twin chains formed from edge-sharing Gd_6C octahedra. Extension of this construction principle leads to a hypothetical series of compounds of the general composition $Gd_{2a+2}X_{2a+2}$ for the metal/halogen framework, where a is the number of condensed octahedra chains. Apart from the starting members ($a = 1$, 2), so far only the final members ($n = \infty$) have been realized in the compounds Gd_2Br_2C and $Gd_2X_2C_2$ (X = Cl, Br) (Fig. 27c). These compounds have typical layer structures with van der Waals bonds between

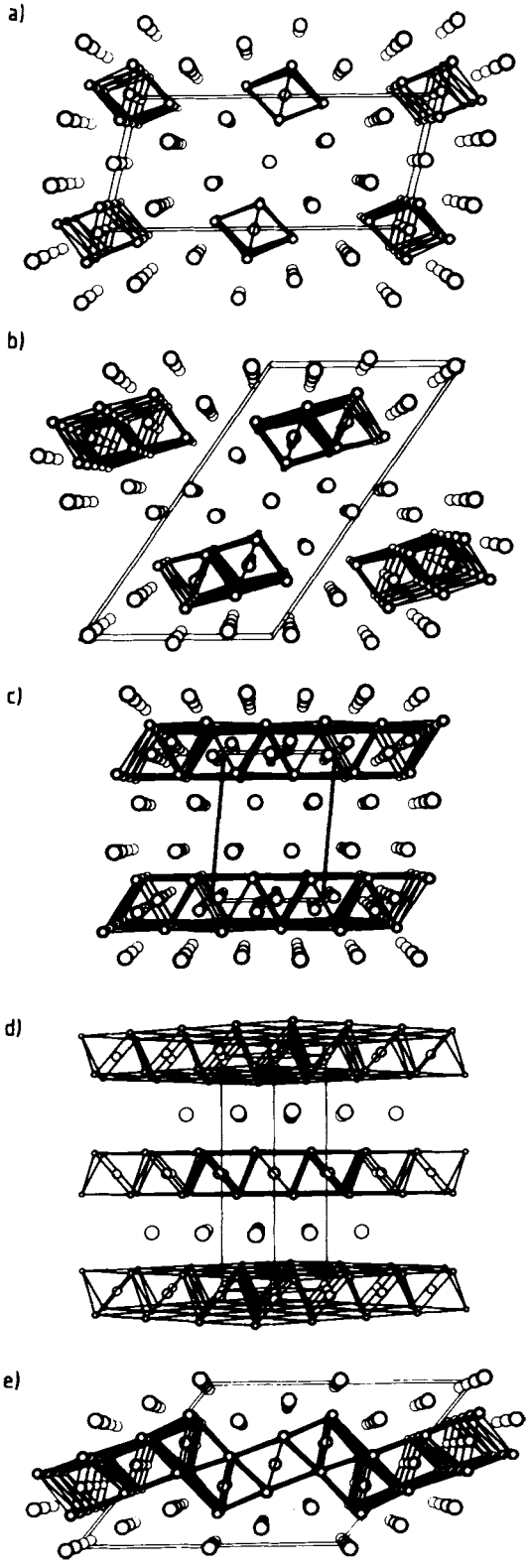

Fig. 27. Central projections along the shortest axes of a) Gd_4I_5C (octahedra chains), b) $Gd_6Br_7C_2$ (twin chains), c) $Gd_2Cl_2C_2$ (planar layers), d) Gd_2IC (planar layers), and e) $Gd_6Cl_5C_3$ (undulated layers). The frameworks of Gd_6 octahedra are outlined with bold lines (cf. Table 6).

adjacent X atom layers. In the structures of the compounds Gd_2XC (X = Cl, Br, I) the layers of octahedra are linked via X^{i-i} bridges (Fig. 27d). Finally, the structure of Gd_3Cl_3C contains a three-dimensional network of edge-sharing Gd_6C octahedra. Numerous other structural variations like the folded chains in $Gd_{12}I_{17}C_6$ or the undulated layers in $Gd_6Cl_5C_{3.0-3.5}$ (Fig. 27e) are possible. Further carbide halide variations have been identified X-ray crystallographically, but have not yet been characterized in any detail.

The way of drawing the structures of the lanthanoid carbide halides in Figure 27 has been chosen so as to relate the structures to those of the reduced d metal compounds discussed in Sections 4 and 5. One should be careful not to be mislead by the drawings, for the lines between the metal atoms might have entirely different meanings. In $NaMo_4O_6$, they indicate M-M bonds, while in the case of $Gd_2Cl_2C_2$, where there are no electrons available for M-M bond formation, they are used only to emphasize the topology of the structure.

The borderline separating cluster compounds and simple salts is well illustrated with Gd_2ClC. The structure is built up of close-packed layers of Gd (abc), Cl (ABC) and C atoms ($\alpha\beta\gamma$) in a cubic sequence $Ac\beta aCb\alpha cBa\gamma b\ldots$ This arrangement bears a similarity to the structure of the silver subfluoride Ag_2F,[215] a structure containing layers of condensed empty Ag_6 octahedra. In the structure of Gd_2ClC, all octahedral voids are occupied by interstitial C atoms, which stabilize the clusters. If one ignores the chemical differences between the anions in Gd_2ClC ($ABC \cong \alpha\beta\gamma$), one has the rock salt structure.

The interstitial C_2 units will commonly have C-C distances of around 145 pm, which corresponds to a shortened single bond, but the C-C distance of 130 pm found in $Gd_2X_2C_2$ (X = Cl, Br) is indicative of a double bond. In the Raman spectra, the C-C stretching vibration was observed at 1158 cm^{-1} for $Gd_{10}Cl_{18}C_4$ and 1175 cm^{-1} for both $Gd_{10}Cl_{17}C_4$ and $Gd_{12}Br_{17}C_6$. In $Gd_2Cl_2C_2$ the stretching vibration was found to be at 1578 cm^{-1}.[216] According to *Siebert*[217] the bond orders, which were derived from the corresponding force constants, are 1.2 and 1.9.

As expected, the hydrolysis[208] of $Gd_{10}Cl_{18}C_4$ with H_2O at room temperature yields a hydrocarbon mixture containing 95 mol-% C_2H_6. The unequivocal assignment of the solvolysis products to a C species in a crystal, similarly as in the case of CaC_2 is rather an exception. It has long been known that when delocalized electrons are present in the solid, the observed gas phase species need not be related to the actual units in the solid. The gases liberated in the hydrolysis of Gd_2ClC under comparable conditions (55% CH_4, 30% H_2, and 15% C_2 hydrocarbons) might still be within the range expected for the decomposition of a "methanide", although side reactions are obvious. These dominate in the case of $Gd_2Cl_2C_2$, where one finds only 15% C_2H_4 besides 45% C_2H_2 and 30% C_2H_6, as well as a certain amount of C_4 hydrocarbons.

Can the different C species in the structures of lanthanoid carbide halides be rationalized in terms of the simple concept of a stabilization of electron deficient clusters by interstitial atoms?

It has been demonstrated with the example of $Nb_6I_{11}H$ that the interstitial atom depletes the M-M bonding states of an electron deficient cluster. This effect is further enhanced in the case of the electropositive lanthanoids because the Fermi level of the metals is high with respect to

the s and p states of carbon. One only needs to check how many electrons are left with the metal atoms after bonding the X atoms. These electrons will be transferred to the empty, π, π^* and σ_p^* states of the neutral C_2 unit. In the case of $Gd_2Cl_2C_2$ ($= (Gd^{3+})_2(Cl^-)_2(C_2)^{4-}$) the framework donates four electrons to the C_2 unit. Effectively two antibonding states are not occupied and the observed short C–C distance corresponds to a double bond. In $Gd_{10}Cl_{18}C_4$ ($\cong (Gd^{3+})_5(Cl^-)_9(C_2)^{6-}$) the highest antibonding state remains unoccupied and a C–C single bond results. Finally, in Gd_2Br_2C ($= (Gd^{3+})_2(Br^-)_2(C^{4-})$ the eight electrons donated from the framework for C_2 occupy all bonding and antibonding states and only single C atoms occur. All the structures listed in Table 6 correspond to this naive counting scheme for electrons on the basis of an ionic limit in the sense of the generalized $8-n$ rule.[7]

The examples chosen to demonstrate the electron counting are special in so far as the available number of electrons from the framework corresponds exactly to the number taken up by the C_2 unit. In the more general case these numbers are different, and the excess electrons then occupy M–M bonding states. Making this balance leads to several obvious conclusions: One or more electrons per C atom in M–M bonding states are only possible when no C_2 units are present. There are also restrictions for the simultaneous presence of different C species in a compound. Thus, despite the structural similarity of Gd_2Br_2C and $Gd_2Br_2C_2$ no mixed crystals between these compounds exist, in which C^{4-} and $(C_2)^{4-}$ would be mutually exchanged. Because of a synproportionation reaction leading to $(C_2)^{6-}$, the simultaneous occurrence of these ions is not to be expected. In contrast, C^{4-} and $(C_2)^{6-}$ (as well as $(C_2)^{4-}$ and $(C_2)^{6-}$) may occur simultaneously in a compound, if the structure allows it. The range of homogenity of $Gd_6Cl_5C_{3.0-3.5}$ is rationalized in terms of a partial substitution of C^{4-} by $(C_2)^{6-}$, which proceeds until all M–M bonding states are depleted.[218]

In the previous discussions, the electron concentration in M–M bonding states was derived by assuming the ions to carry conventional formal charges (e.g., Gd^{3+} or $(C_2)^{6-}$). To avoid any misunderstanding about the relevance of such a procedure, Figure 28 (top) presents the result of a self-consistent calculation for $Gd_{10}Cl_{18}C_4$.[219] The MO's of the weakly interacting (free) C_2 units are lowered in the $Gd_{10}Cl_{18}C_4$ unit to such an extent that the π^* level falls below the Fermi level[220] and becomes occupied. The Gd 4d bands are empty. Of course, there is a significant Gd 5d contribution to the valence bands, especially by back bonding from π^* into the empty d states. But this mixing-in of d states leads to a covalency of the Gd–C and Gd–Cl bonds in the sense of the more realistic bonding description $(Gd^{1.3+})_{10}(Cl^{0.45-})_{18}(C_2^{2.4-})_2$, without any Gd–Gd bonds being present. Only the lowering of the halogen content in the compounds $Gd_{10}Cl_{17}C_4$ and $Gd_{10}I_{16}C_4$ leaves electrons with Gd and leads to the occupation of the narrow band split off from the Gd 5d block. This band has 90% d character (Fig. 28, bottom), and it is clear that it has M–M bonding character in the equitorial plane of the bioctahedron and, in particular, along the joined edge between the two octahedra. The experimentally observed shortening of this edge by 9 pm on going from $Gd_{10}Cl_{18}C_4$ to $Gd_{10}Cl_{17}C_4$ is in agreement with the result of this calculation.

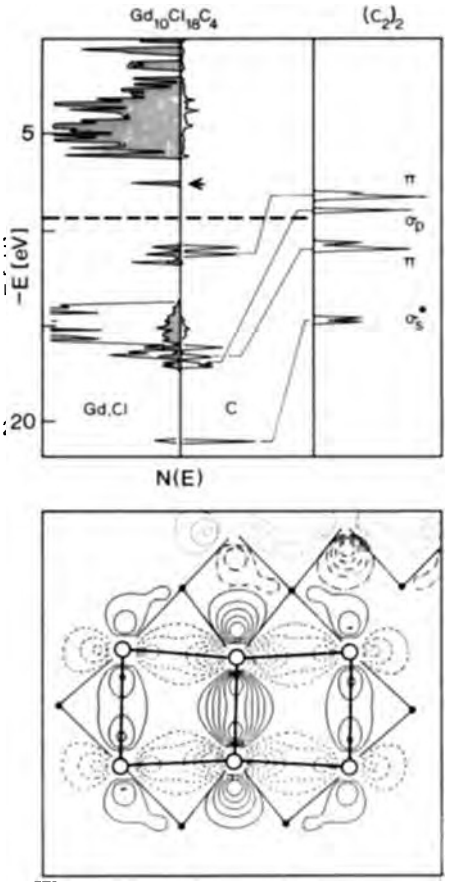

Fig. 28. Top: MO diagram of two free C_2 units arranged as in $Gd_{10}Cl_{18}C_4$ (right) and projected densities of states (Gd contribution shaded) for the unit $Gd_{10}Cl_{18}C_4$ [216, 217]. The Fermi level corresponds to the dashed line. Bottom: Representation of the discrete M–M bonding orbital above the Fermi level marked by an arrow. The orbital is drawn in the plane of the Gd_6 octahedra bases (Gd circles, Cl points). The state is singly occupied in $Gd_{10}Cl_{17}C_4$ and doubly in $Gd_{10}I_{16}C_4$.

The structures scarcely reflect that a borderline between the simple salt $Gd_{10}Cl_{18}C_4$ and the cluster compound $Gd_{10}Cl_{17}C_4$ has been passed through. The "cluster" in $Gd_{10}Cl_{18}C_4$ also results from an fcc type packing of low and highly charged anions (Cl^- and $(C_2)^{6-}$, resp.) in the ratio 9 : 1. Only the favorable octahedral voids around the highly charged anions are filled by the cations. $Gd_{10}Cl_{18}C_4$ is just a defect variant of rock salt.

The discussion shows that a simple ionic model is suitable for counting electrons in M–M bonding states. In the case of the alkali metal suboxides dealt with in Section 2 the estimated numbers were verified by physical measurements, namely by measuring the energy losses caused by these electrons. In the case of lanthanoid carbide halides, the C_n species serve as chemical checks for the correct electron balances. Physical properties, particularly the electric conductivity, are also in agreement with these balances. Metallic behavior is always observed with extended M–M bonded systems (chains, twin chains, layers, and networks) in conjunction with an excess of metal valence electrons. Insulators and semiconductors are found with discrete clusters (cf. Section 3) and in extended structures with close M–M contacts that have no electrons in the M–M bonding bands.

Only $Gd_2Cl_2C_2$ and $Gd_2Br_2C_2$ seem to be exceptions. They form golden crystals with high (two-dimensional) metallic conductivity, although all bands with M–M bonding character should be empty.

The explanation for this apparent disagreement is trivial. The statement about a filling of energy bands does not give any clue to the separation of these bands. Metallic properties might occur "accidentally" if filled valence and empty conduction bands are not separated by an energy gap.

The PE spectrum of $Gd_2Cl_2C_2$ (Fig. 25) exhibits density of states at the Fermi level. The dramatic shift of the Gd 4f band to higher energy might indicate the cause for the non-vanishing density at $E_B = 0$, namely, backbonding from occupied C_2 π^* states (valence band) into empty Gd d states (conduction band). The analysis of bonding in $Gd_2Cl_2C_2$ with the aid of EH calculations[199] verifies this interpretation. The calculated density of states (4f omitted) and the projected densities for Gd 5d (shaded) are plotted in Figure 29 (top). The character of the states at the Fermi

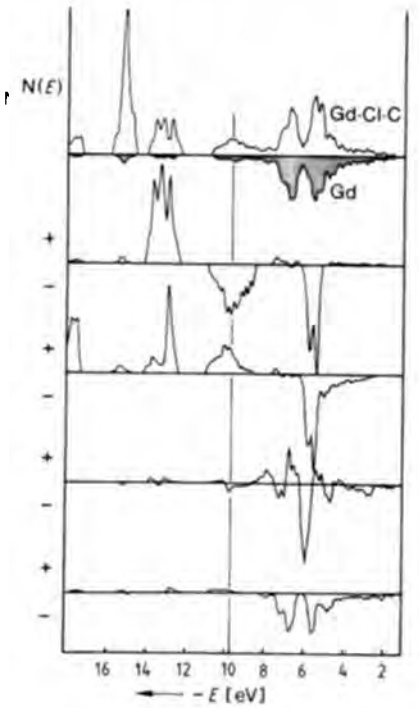

Fig. 29. Results of EH calculations for $Gd_2Cl_2C_2$ [199]. From top to bottom: total density of states and projected part of Gd 5d (shaded); COOP curves for C–C, C–Gd_{axial}, Gd_{basal}–Gd_{basal}, and Gd_{axial}–Gd_{basal} interactions, the latter in the sequence. The Fermi level is marked by the vertical line.

level are obtained from the corresponding COOP diagrams for C–C, Gd–C, and Gd–Gd interactions. As expected, they are C–C antibonding (π^*), but bonding with respect to Gd–C interactions and in particular involve those Gd atoms that are collinear with the C_2 unit. The occupation of these states is a compromise between the loosening of the C–C bonding and formation of π bonds between C and Gd. It is evident from Figure 29 that the comparatively high Gd 5d contribution to the bands at E_F is almost entirely due to the covalent Gd–C bonds and does not lead to M–M bonding. According to the population analysis, the bonding is described as $(Gd^{1.36+})_2(Cl^{0.46-})_2(C^{0.90-})_2$ and there are no electrons for Gd–Gd bonds. It should be possible to introduce weak M–M bonds (accompanied by a change from C–C double to C–C single bonding) by a chemical reduction of $Gd_2Cl_2C_2$. In fact, the compound can be intercalated, e.g., by electrochemical methods, with lithium to yield a limiting composition $Gd_2Cl_2C_2Li_{0.9}$.[208] Unfortunately, the layers become disordered during this reaction and can not be characterized structurally.

The formation and breaking of M–M bonds by means of a chemical reaction can be nicely shown with the hydride halides of the trivalent lanthanoids that are structurally closely related to $Gd_2Cl_2C_2$. Because of the strong absorption of neutrons by Gd, the diffraction studies are carried out with the isostructural Tb compounds.

TbClH has the structure of ZrBr if one considers only the TbCl framework.[189, 190, 221] Tb_6 octahedra are condensed via edges into layers, and these are surrounded by Cl atoms above the octahedral faces (as in the M_6X_8 cluster). The Tb atoms are close packed, and neutron diffraction of the deuterated compounds shows the tetrahedral voids within the Tb twin layers to be occupied by D atoms[222] (cf. Fig. 30). The compound has a range of homogeneity $TbClD_{0.67-1.00}$ due to a partial occupation of the voids.

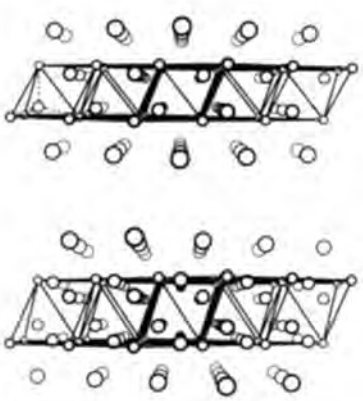

Fig. 30. Top: Characteristic part of the structure of $TbClD_{0.8}$ [223]. The D atoms are located in tetrahedral voids in the twin-layers of Tb atoms which are interconnected. Bottom: Corresponding part of the structure of $TbBrD_2$ [225] with additional occupation of the "octahedral" voids by two D atoms each. These D atoms are almost coplanar with the Tb atoms.

$TbClH_{1-x}$ looks like graphite and is a good (two-dimensional) metallic conductor, as expected from the formulation $Tb^{3+}Cl^-(H^-)_{1-x}(e^-)_{1+x}$. Heating the phase in a H_2 atmosphere topochemically leads to $TbClH_2$. A neutron diffraction study[224] showed that the Tb_6 "octahedra" are considerably elongated and filled by two H(D) atoms each. In addition, all Cl atoms are moved from positions above faces to positions above edges.

The reaction of $TbClH_{1-x}$ with H_2 is accompanied by a dramatic change in the physical properties. $TbClH_2$ forms transparent crystals and is an insulator. In $TbClH_{1-x}$ the excess valence electrons of the metal are delocalized in a band that has M–M bonding character. The reaction with H_2 results in a localization of all electrons in a narrow band that is essentially H 1s in character (the former "impurity band"). When $TbClH_2$ (and the isostructural $GdClH_2$) is heated in vacuo, hydrogen is lost and the M–M

bonds are "switched on" in a synchronized way. The resistivity of such a sample drops by several orders of magnitude with the formation of $TbClH_{1-x}$ (Fig. 31).

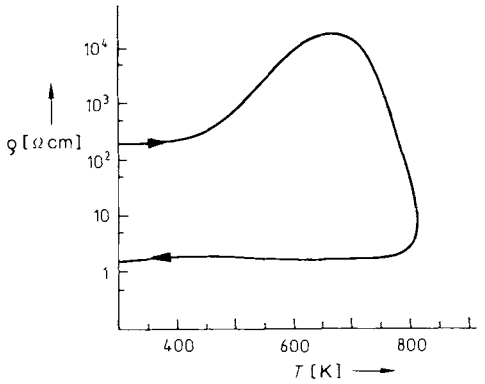

Fig. 31. Change of the electrical resistivity ϱ of a polycrystalline $GdClH_2$ pellet upon heating in vacuo [226]. $GdClH_{1-x}$ is formed, which is metallic.

Naturally, such reactions have been known for a long time. The transition from a metal to a salt is observed with the reaction of alkali metals and hydrogen. The recovery of the metal by the thermal decomposition of the hydride is also a similar reaction. The terbium example was chosen, for it demonstrates how the ideas outlined—starting from molecular clusters, their interconnection and condensation, the role of interstitial atoms, and finally the removal of any metal-metal bonding by these atoms—allow for a rather unified view of a large field. This field comprises molecules and solids, metals, and salts, and one hardly recognizes borderlines but only gradual differences.

This review article contains several, in part still unpublished, results collected by my co-workers, whose enthusiastic cooperation I gratefully acknowledge. Special thanks are due to the Fonds der Chemischen Industrie for generous long-term support of our investigations, and to I. Remón and B. Krauter for their help with the preparation of the text and drawings.

Received: September 3, 1987 [A 652 IE]
German version: *Angew. Chem. 100* (1988) 163

[1] B. Pötter, K. Seppelt, A. Simon, E.-M. Peters, B. Hettich, *J. Am. Chem. Soc. 107* (1985) 980.
[2] J. E. Boggs, *Inorg. Chem. 23* (1984) 3577.
[3] D. A. Dixon, B. E. Smart, *J. Am. Chem. Soc. 108* (1986) 2688.
[4] D. Christen, H.-G. Mack, C. J. Marsden, H. Oberhammer, G. Schatte, K. Seppelt, H. Willner, *J. Am. Chem. Soc. 109* (1987) 4009.
[5] P. von R. Schleyer, E.-U. Würthwein, J. A. Pople, *J. Am. Chem. Soc. 104* (1982) 5839.
[6] P. von R. Schleyer in P.-O. Löwdin, B. Pullman (Eds.): *New Horizons of Quantum Chemistry*, Reidel, Dordrecht, Niederlande 1983, p. 95.
[7] A. Kjekshus, T. Rakke, *Struct. Bonding (Berlin) 19* (1974) 45.
[8] E.-U. Würthwein, P. von R. Schleyer, J. A. Pople, *J. Am. Chem. Soc. 106* (1984) 6973.
[9] S.-S. Lin, *Rev. Sci. Instrum. 44* (1973) 576.
[10] O. F. Hagena, W. Obert, *J. Chem. Phys. 56* (1972) 1793.
[11] T. P. Martin in P. Grosse (Ed.): *Festkörperprobleme XXIV*, Vieweg, Braunschweig 1984, p. 1.
[12] T. P. Martin, *Angew. Chem. 98* (1986) 197; *Angew. Chem. Int. Ed. Engl. 25* (1986) 197.
[13] T. P. Martin, H. Limberger in G. Benedek, T. P. Martin, G. Pacchioni (Eds.): *Elemental and Molecular Clusters*, Springer, Berlin 1987, in press.
[14] M. A. Bredig, J. W. Johnson, W. T. Smith, *J. Am. Chem. Soc. 77* (1955) 307.
[15] M. A. Bredig, H. R. Bronstein, W. T. Smith, *J. Am. Chem. Soc. 77* (1955) 1454.
[16] J. F. Jal, P. Chieux, J. Dupuy, J. P. Dupin, *J. Phys. (Les Ulis, Fr.) 41* (1980) 657.
[17] A. Simon, *Struct. Bonding (Berlin) 36* (1979) 81.
[18] All compounds with the exception of $Rb_{6.33}O$ and $Cs_{2.78-3.19}O$ have been characterized by single crystal structure investigations. The phase relationships [19] were established thermoanalytically and with the aid of a modified Guinier technique [20]. Recent investigations [21, 22] on the Cs/Cs_2O system re-establish the state of the art as it was before our own investigations. Despite the numerous experiments in our laboratory we have no evidence for the recently postulated stable Rb_3O [23,24].
[19] A. Simon, *Z. Anorg. Allg. Chem. 395* (1973) 301.
[20] A. Simon, *J. Appl. Crystallogr. 3* (1970) 11; *4* (1971) 138.
[21] C. F. Knights, B. A. Phillips, *J. Nucl. Mater. 84* (1979) 196.
[22] H. U. Borgstedt in R. W. Ohse (Ed.): *Handbook of Thermodynamic and Transport Properties of Alkali Metals, IUPAC Chem. Data Ser. 30* (1985) 901.
[23] T. Suzuki, S. Masuda, Y. Tanazawa, *J. Nucl. Mater. 127* (1985) 113.
[24] T. Suzuki, S. Masuda, Y. Matsui, Y. Nakanishi, *J. Nucl. Mater. 137* (1986) 250.
[25] H.-J. Deiseroth, A. Simon, *Z. Naturforsch. B 33* (1978) 714.
[26] T. P. Martin, H.-J. Stolz, G. Ebbinghaus, A. Simon, *J. Chem. Phys. 70* (1979) 1096.
[27] The following distances [pm] are derived for the minimum of the total energy ($3 \times$ Rb1, $6 \times$ Rb2, experimental values in brackets): d(Rb1–Rb1) = 384 (394), d(Rb2–Rb2) = 325 (354), d(Rb1–O) = 262 (270), d(Rb2–O) = 279 (280).
[28] A. Simon, E. Westerbeck, *Z. Anorg. Allg. Chem. 428* (1977) 187.
[29] G. Metsch, W. Bauhofer, A. Simon, *Z. Naturforsch. A 40* (1985) 303.
[30] W. Bauhofer, A. Simon, *Z. Anorg. Allg. Chem. 447* (1978) 29.
[31] H.-J. Deiseroth, A. Simon, *Rev. Chim. Miner. 20* (1983) 475.
[32] A. Simon, B. Hettich, unpublished.
[33] E. Gmelin, A. Simon, W. Brämer, R. Villar, *J. Chem. Phys. 76* (1982) 6256.
[34] G. Ebbinghaus, A. Simon, *Chem. Phys. 43* (1980) 117.
[35] A. H. Sommer: *Photoemissive Materials*, Wiley, New York 1968.
[36] G. Ebbinghaus, W. Braun, A. Simon, K. Berresheim, *Phys. Rev. Lett. 37* (1976) 1770.
[37] M. G. Burt, V. Heine, *J. Phys. C 11* (1978) 961.
[38] B. Woratschek, G. Ertl, J. Kuppers, W. Sesselmann, H. Haberland, *Phys. Rev. Lett. 57* (1986) 1484.
[39] B. Woratschek, W. Sesselmann, J. Küppers, G. Ertl, H. Haberland, *J. Chem. Phys. 86* (1987) 2411.
[40] S. Rundquist, *Ark. Kemi 20* (1962) 67.
[41] H. Schäfer, H. G. Schnering, *Angew. Chem. 76* (1964) 833.
[42] K. Schubert: *Kristallstrukturen zweikomponentiger Phasen*, Springer, Berlin 1964.
[43] F. Hulliger, *Struct. Bonding (Berlin) 4* (1968) 83.
[44] H. Nowotny, *Prog. Solid State Chem. 5* (1971) 27.
[45] W. Jeitschko, *MTP Int. Rev. Sci., Inorg. Chem. Ser. 2 5* (1974) 219.
[46] M. J. Taylor: *Metal-to-Metal Bonded States of Main Group Elements*, Academic Press, London 1975.
[47] H. F. Franzen, *Prog. Solid State Chem. 12* (1978) 1.
[48] J. D. Corbett, *Adv. Chem. Ser. (Solid State Chem.) 186* (1980) 329.
[49] A. Simon, *Angew. Chem. 93* (1981) 23; *Angew. Chem. Int. Ed. Engl. 20* (1981) 1.
[50] R. E. McCarley, *Phil. Trans. R. Soc. London A 308* (1982) 141.
[51] R. E. McCarley, *ACS Symp. Ser. 211* (1983) 273.
[52] A. Simon, *J. Solid State Chem. 57* (1985) 2.
[53] R. E. McCarley, K.-H. Lii, P. A. Edwards, L. F. Brough, *J. Solid State Chem. 57* (1985) 17.
[54] R. Chevrel, P. Gougeon, M. Potel, M. Sergent, *J. Solid State Chem. 57* (1985) 25.
[55] C. Perrin, M. Sergent, *J. Less-Common Met. 123* (1986) 117.
[56] E. Parthé, B. Chabot in K. A. Gschneidner, LeRoy Eyring (Eds.): *Handbook of Physics and Chemistry of Rare Earths, Vol. 6*, North Holland, Amsterdam 1984, p. 113.
[57] a) J. Rouxel (Ed.): *Crystal Chemistry and Properties of Materials with Quasi-One-Dimensional Structures*, Reidel, Dordrecht, Netherlands 1986; b) J. D. Corbett, R. E. McCarley in [57a], p. 179.
[58] R. Chevrel, M. Sergent in [57a], p. 315.
[59] A. Simon in A. K. Cheetham, P. Day (Eds.): *Solid State Chemistry, Vol. 2*, Clarendon Press, Oxford 1987, in press.
[60] The M–M bonding states in the M_6X_8 cluster have the symmetries (in order of increasing energy) a_{1g}, t_{1u}, t_{2g}, t_{2u} und e_g. They can accommodate 24 electrons. The corresponding states for the M_6X_{12} cluster are a_{1g}, t_{2g}, t_{1u} and a_{2u}, and they can accommodate 16 electrons [61–66].
[61] F. A. Cotton, R. E. Haas, *Inorg. Chem. 3* (1964) 10.
[62] L. J. Guggenberger, A. W. Sleight, *Inorg. Chem. 8* (1969) 2041.

[63] B. E. Bursten, F. A. Cotton, G. G. Stanley, *Israel J. Chem. 19* (1980) 132.
[64] H. Nohl, O. K. Andersen, *Supercond. d-f-Band Met., Proc. Conf. 4th*, Karlsruhe 1982, p. 161.
[65] T. Hughbanks, R. Hoffmann, *J. Am. Chem. Soc. 105* (1983) 1150.
[66] J. D. Smith, J. D. Corbett, *J. Am. Chem. Soc. 107* (1985) 5704.
[67] O. K. Andersen, unpublished.
[68] S. F. A. Kettle, *Theor. Chim. Acta 3* (1965) 211.
[69] A. Simon, H. G. von Schnering, H. Schäfer, *Z. Anorg. Allg. Chem. 367* (1969) 1.
[70] H. G. von Schnering, *Z. Anorg. Allg. Chem. 385* (1971) 75.
[71] A. Simon, M. Sägebarth, unpublished.
[72] K. F. Herzfeld, *Phys. Rev. 29* (1927) 701.
[73] N. F. Mott, *Proc. Phys. Soc. A 62* (1949) 416.
[74] P. P. Edwards, M. J. Sienko, *Int. Rev. Phys. Chem. 3* (1983) 83.
[75] A. Simon, H. G. von Schnering, H. Schäfer, *Z. Anorg. Allg. Chem. 355* (1967) 295.
[76] H. Imoto, J. D. Corbett, *Inorg. Chem. 19* (1980) 1241.
[77] F. Stollmaier, A. Simon, *Inorg. Chem. 24* (1985) 168.
[78] A. Perrin, C. Perrin, M. Sergent, *J. Less-Common Met.*, in press.
[79] W. Bronger, M. Spangenberg, *J. Less-Common Met. 76* (1980) 73.
[80] L. Leduc, A. Perrin, M. Sergent, F. LeTraon, J. C. Pilet, A. LeTraon, *Mater. Lett. 3* (1985) 209.
[81] L. Leduc, A. Perrin, M. Sergent, *C. R. Acad. Sci. (Paris) Ser. II 296* (1983) 961.
[82] H. Schäfer, H. G. von Schnering, J. Tillack, F. Kuhnen, H. Wöhrle, H. Baumann, *Z. Anorg. Allg. Chem. 353* (1967) 281.
[83] C. Perrin, M. Sergent, F. LeTraon, A. LeTraon, *J. Solid State Chem. 25* (1978) 197.
[84] W. Bronger, H. J. Miessen, P. Müller, R. Neugroschel, *J. Less-Common Met. 105* (1985) 303.
[85] R. Siepmann, H. G. von Schnering, *Z. Anorg. Allg. Chem. 357* (1968) 289.
[86] W. Bronger, H.-J. Miessen, R. Neugroschel, D. Schmitz, M. Spangenberg, *Z. Anorg. Allg. Chem. 525* (1985) 41.
[87] F. Klaiber, W. Petter, F. Hulliger, *J. Solid State Chem. 46* (1983) 112.
[88] V. E. Federov, N. V. Podberezskaya, A. V. Mischenko, G. F. Khudorozko, I. P. Asanov, *Mater. Res. Bull. 21* (1986) 1335.
[89] L. Leduc, A. Perrin, M. Sergent; *Acta Crystallogr. C39* (1983) 1503.
[90] D. Bauer, H. G. von Schnering, *Z. Anorg. Allg. Chem. 361* (1968) 259.
[91] H. Nohl, O. K. Andersen, *Conf. Ser. Inst. Phys. 55* (1980) 61.
[92] J. J. Finley, H. Nohl, E. E. Vogel, H. Imoto, R. E. Camley, V. Zevin, O. K. Andersen, A. Simon, *Phys. Rev. Lett. 46* (1981) 1472.
[93] J. J. Finley, R. E. Camley, E. E. Vogel, V. Zevin, E. Gmelin, *Phys. Rev. B24* (1981) 1023.
[94] H. Imoto, A. Simon, *Inorg. Chem. 21* (1982) 308.
[95] P. J. Brown, K. R. A. Ziebeck, A. Simon, M. Sägebarth, *J. Chem. Soc. Dalton Trans.*, in press.
[96] P. Gütlich, *Struct. Bonding (Berlin) 44* (1981) 83.
[97] C. Perrin, R. Chevrel, M. Sergent, Ø. Fischer, *Mater. Res. Bull. 14* (1979) 1505.
[98] A. Perrin, M. Sergent, Ø. Fischer, *Mater. Res. Bull. 13* (1978) 259.
[99] K. Yvon, *Curr. Top. Mater. Sci. 3* (1979) 53.
[100] J. D. Corbett, *J. Solid State Chem. 39* (1981) 56.
[101] Ø. Fischer, M. B. Maple (Eds.): *Superconductivity in Ternary Compounds; Vol. 1, 2 (Top. Curr. Phys. 32)*, Springer, Berlin 1982.
[102] B. T. Matthias, M. Marezio, E. Corenzwit, A. S. Cooper, H. E. Barz, *Science 175* (1972) 1465.
[103] R. Odermatt, O. Fischer, H. Jones, G. Bongi, *J. Phys. C7* (1974) L 13.
[104] The wires of 1 mm thickness contain 285 superconducting filaments of 10 to 30 μm diameter. A transition temperature $T_c \approx 14$ K and critical current densities of 10^4 A cm^{-2} at 4.2 K/5 T are reached with such wires. dH_{c2}/dT ist 4 T K^{-1} [105]. The recently found high-T_C materials of the $YBa_2Cu_3O_{7-x}$ type ($T_c > 90$ K) [106] presumably allow critical fields $H_{c2} > 250$ T at 4.2 K [107]. Within half a year after the discovery of $YBa_2Cu_3O_{7-x}$ wires could be produced (0.8 mm diameter: inclusion in Ag) which stand critical current densities of 4×10^4 A cm^{-2} (*Nature 327* (1987), 356).
[105] R. Chevrel, H. Hirrien, M. Sergent, *Polyhedron 5* (1986) 87.
[106] M. K. Wu, J. R. Ashburn, C. J. Torug, P. H. Hor, R. L. Meng, L. Gao, Z. J. Huang, Y. Q. Wang, C. W. Chu, *Phys. Rev. Lett. 58* (1987) 908.
[107] J. C. Ousset, M. F. Ravet, M. Maurer, A. Menny, J. P. Ulmet, H. Rakoto, J. M. Broto, S. Askenazy, J. Durand, *Abstr. Eur. Mater. Res. Soc. Meet.*, Strassburg, June 1987, B 20.
[108] N. E. Alekseevskii, M. Glinski, N. M. Dobrovolskii, V. I. Isebro, *JETP Lett. (Engl. Transl.) 23* (1976) 412.
[109] T. Luhmann, D. Dew-Hughes, *J. Appl. Phys. 34* (1979) 409.
[110] O. K. Andersen, W. Klose, H. Nohl, *Phys. Rev. B 17* (1978) 1209.
[111] H. Nohl, W. Klose, O. K. Andersen in [101], p. 166.
[112] This is due to a mixing-in of the (bonding) Mo d like t_{1u} states which are raised in energy by the interaction with low-lying (anti-bonding) X p like t_{1u} states. The conduction band states in Γ therefore are low for X = S and high for X = Te. The result is in contrast to the simple e_g conduction band model [58], which does not lead to any significant change in the conduction band energy as a function of the inter-cluster distances, because the intractions between the clusters are δ type.
[113] F. Grønwold, A. Kjekshus, F. Raaum, *Acta Crystallogr. 14* (1961) 930.
[114] A. Simon, *Ann. Chim. (Paris) 7* (1982) 539.
[115] P. Jensen, A. Kjekshus, *Acta Chem. Scand. 20* (1966) 1309.
[116] V. Kumar, V. Heine, *Inorg. Chem. 23* (1984) 1498.
[117] V. Kumar, V. Heine, *J. Phys. F14* (1984) 365.
[118] H. F. Franzen, T. A. Beineke, B. R. Conrad, *Acta Crystallogr. B24* (1968) 412.
[119] O. K. Andersen, S. Satpathy in A. Dominguez, J. Castaing, R. Marquez (Eds.): *Basic Properties of Binary Oxides*, Serv. Publ. Univ. Sevilla, Sevilla, Spain 1983, p. 21.
[120] J. K. Burdett, T. Hughbanks, *J. Am. Chem. Soc. 106* (1984) 3103.
[121] R. E. McCarley, *Polyhedron 5* (1986) 51.
[122] C. C. Torardi, R. E. McCarley, *J. Am. Chem. Soc. 101* (1979) 3963.
[123] A. Simon, *Angew. Chem. 95* (1983) 94; *Angew. Chem. Int. Ed. Engl. 22* (1983) 95.
[124] T. Hughbanks, R. Hoffmann, *J. Am. Chem. Soc. 105* (1983) 3528.
[125] H. Mattausch, A. Simon, E.-M. Peters, *Inorg. Chem. 25* (1986) 3428.
[126] A. Simon, W. Martin, H. Mattausch, R. Gruehn, *Angew. Chem. 98* (1986) 831; *Angew. Chem. Int. Ed. Engl. 25* (1986) 845.
[127] The width of the stability range is $(15n+1)/(4n+2) \leq z/Mo \leq (13n+1)/(4n+2)$. Lines for In $(13n+7)/(4n+2)$ and Sn $(14n+8)/(4n+2)$ are shown.
[128] As a rule, the Nb_6O_{12} cluster in oxoniobates contains 14 electrons in M-M bonding states, e.g. in $Mg_3Nb_6O_{11}$ $(=(Mg^{2+})_3(Nb^{5+})_6(O^{2-})_{11}(e^-)_{14}$ [129, 130].
[129] B. O. Marinder, *Chem. Scr. 11* (1977) 97.
[130] R. Burnus, J. Köhler, A. Simon, *Z. Naturforsch. B42* (1987) 536.
[131] The structures of $Mg_3Nb_6O_{11}$ and $Mn_3Nb_6O_{11}$ [129, 130] as well as the new compounds $Na(Si,Nb)Nb_{10}O_{19}$ [132], $Na_3Al_2Nb_{34}O_{64}$ [132], $SrNb_8O_{14}$ [133] and $Na(Nb,V)_2Nb_7O_{14}$ [134] contain Nb_6O_{12} clusters besides single Nb atoms and Nb_2 units.
[132] J. Köhler, A. Simon, *Z. Anorg. Allg. Chem.*, in press.
[133] J. Köhler, A. Simon, S. Hibble, A. Cheetham, unpublished.
[134] J. Köhler, A. Simon, unpublished.
[135] According to an earlier formulated rule [136, 137] the closed configuration should correspond to an occupation of the M-M bonding states by 12n + 12 electrons. The rule predicts a non-varying valence electron concentration $z/Mo = 4.0$.
[136] W. Hönle, H. G. von Schnering, A. Lipka, K. Yvon, *J. Less-Common Met. 71* (1980) 135.
[137] K. Yvon in [101], p. 87.
[138] J. M. Tarascon, F. J. DiSalvo, J. V. Waszczak, *Solid State Commun. 52* (1984) 227.
[139] R. Lepetit, P. Monceau, M. Potel, P. Gougeon, M. Sergent, *J. Low Temp. Phys. 56* (1984) 219.
[140] J. M. Tarascon, F. J. DiSalvo, C. H. Chen, P. J. Carroll, M. Walsh, L. Rupp, *J. Solid State Chem. 58* (1985) 290.
[141] M. Potel, P. Gougeon, R. Chevrel, M. Sergent, *Rev. Chim. Miner. 21* (1984) 509.
[142] J. M. Tarascon, *Solid State Ionics 18/19* (1986) 802.
[143] J. M. Tarascon, G. W. Hull, J. V. Waszczak, *Mater. Res. Bull. 20* (1985) 935.
[144] J. M. Tarascon, *Solid State Ionics 18/19* (1986) 768.
[145] A. Simon, *Z. Anorg. Allg. Chem. 355* (1967) 295.
[146] S.-J. Hwu, J. D. Corbett, *J. Solid State Chem. 64* (1986) 331.
[147] T. Hughbanks, G. Rosenthal, J. D. Corbett, *J. Am. Chem. Soc. 108* (1986) 8289.
[148] J. D. Smith, J. D. Corbett, *J. Am. Chem. Soc. 108* (1986) 1927.
[149] R. P. Ziebarth, J. D. Corbett, *J. Am. Chem. Soc. 107* (1985) 4571.
[150] A. Simon, H. G. von Schnering, H. Wöhrle, H. Schäfer, *Z. Anorg. Allg. Chem. 339* (1965) 155.
[151] H. Schäfer, H. G. von Schnering, K.-J. Niehues, H. G. Niedervahrenholz, *J. Less-Common Met. 9* (1965) 95.
[152] A. Simon, F. Böttcher, unpublished.
[153] H. Imoto, M. Sägebarth, A. Simon, unpublished.
[154] R. P. Ziebarth, J. D. Corbett, *J. Am. Chem. Soc. 109* (1987) 4844.
[155] A. Simon, F. Stollmaier, D. Gregson, H. Fuess, *J. Chem. Soc. Dalton Trans. 1987*, 431.
[156] B. F. G. Johnson, R. D. Johnston, J. Lewis, *Chem. Commun. 1967*, 1057.
[157] V. G. Albano, S. Martinengo, *Nachr. Chem. Tech. Lab. 28* (1980) 654.
[158] J. N. Nicholls, *Polyhedron 3* (1984) 1307.
[159] H.-G. Fritsche, F. Dübler, H. Müller, *Z. Anorg. Allg. Chem. 513* (1984) 46.
[160] A. Simon, *Naturwissenschaften 71* (1984) 171.
[161] R. Hoffmann: *Angew. Chem. 99* (1987) 871; *Angew. Chem. Int. Ed. Engl. 26* (1987) 846.
[162] F. Dübler, H. Müller, C. Opitz, *Chem. Phys. Lett. 88* (1982) 467.

[163] D. E. Eastman, J. K. Cashion, A. C. Switendick, *Phys. Rev. Lett. 27* (1971) 35.
[164] O. Jepsen, R. M. Nieminen, J. Madsen, *Solid State Commun. 34* (1980) 375.
[165] A. C. Switendick in G. Alefeld, J. Volkl (Eds.): *Hydrogen in Metals I*, Springer, Berlin 1978.
[166] The phases initially described as pure halides (e.g Zr_6I_{12} or $CsZr_6I_{14}$ [167]) are stabilized by impurity atoms in the clusters, most of which are carbide halides [66].
[167] D. H. Guthrie, J. D. Corbett, *Inorg. Chem. 21* (1982) 3290.
[168] J. W. Lauher, *J. Am. Chem. Soc. 100* (1978) 5305.
[169] S. D. Wijeyesekera, R. Hoffmann, *Organometallics 3* (1984) 949.
[170] The highest lying, nearly nonbonding a_{1u} state can be occupied or not (e.g. in $Zr_6I_{12}C$, $CsZr_6I_{14}C$ or $Zr_6I_{14}C$), much in the same way as with empty clusters (e.g. $[Ta_6Cl_{12}]^{2+}$, $[Ta_6Cl_{12}]^{3+}$ or $[Ta_6Cl_{12}]^{4+}$ [171]. As a rule, $z = 14$ is approached in the case of $Zr_6X_{12}Y$ clusters. Incidently this is the same electron count as for the Nb_6O_{12} cluster in oxoniobates [128].
[171] B. Spreckelmeyer, *Z. Anorg. Allg. Chem. 358* (1968) 148.
[172] The population analysis leads to a charge of 1.8− on the C atom [66].
[173] The vibrational frequency of the H atom in the Nb_6H unit of $Nb_6I_{11}H$ is nearly identical with the frequency of H in the metallic hydride NbH, [174].
[174] A. N. Fitch, S. A. Barrett, B. E. Fender, A. Simon, *J. Chem. Soc. Dalton Trans. 1984*, 501.
[175] M. Hansen: *Constitution of Binary Alloys*, McGraw-Hill, New York 1958.
[176] T. B. Massalski, J. L. Murray, L. H. Bennett, H. Baker: *Binary Alloy Phase Diagrams, Vol. 1, 2*, Am. Soc. Metals, Metals Park, OH, USA 1986.
[177] A. R. Miedema, R. Boom, F. R. de Boer in C. J. M. Rooymans, A. Rabenau (Eds.): *Crystal Structure and Chemical Bonding in Inorganic Chemistry*, North Holland, Amsterdam 1975, p. 163.
[178] A. K. Niessen, F. R. de Boer, R. Boom, P. F. Châtel, W. C. M. Mattens, A. R. Miedema, *CALPHAD: Comput. Coupling Phase Diagrams Thermochem. 7* (1983) 51.
[179] The interstitial K atom in $Zr_6I_{14}K$ [180] cannot be rationalized in terms of these criteria.
[180] J. D. Smith, J. D. Corbett, *J. Am. Chem. Soc. 106* (1984) 4618.
[181] A. W. Struss, J. D. Corbett, *Inorg. Chem. 9* (1970) 1373.
[182] A. W. Struss, J. D. Corbett, *Inorg. Chem. 16* (1977) 360.
[183] S. D. Wijeyesekera, J. D. Corbett, *Solid State Commun. 54* (1985) 657.
[184] A phase $ZrHX_{0.5}$ is known which has the tetrahedral voids between the Zr twin-layers occupied and the same stacking sequence AbcA as the binary halide [185].
[185] S. D. Wijeyesekera, J. D. Corbett, *Inorg. Chem. 25* (1986) 4709.
[186] H. Nowotny, H. Boller, O. Beckmann, *J. Solid State Chem. 2* (1970) 462.
[187] K. R. Poeppelmeier, J. D. Corbett, *Inorg. Chem. 16* (1977) 694.
[188] H. Mattausch, J. B. Hendricks, R. Eger, J. D. Corbett, A. Simon, *Inorg. Chem. 19* (1980) 2128.
[189] H. Mattausch, A. Simon, N. Holzer, R. Eger, *Z. Anorg. Allg. Chem. 466* (1980) 7.
[190] A. Simon, Hj. Mattausch, R. Eger, *Z. Anorg. Allg. Chem.*, in press.
[191] U. Schwanitz-Schüller, A. Simon, *Z. Naturforsch. B 40* (1985) 710.
[192] W. H. Zachariasen, *Acta Crystallogr. 2* (1949) 60.
[193] The isostructural compounds Y_2X_3 [188], Gd_2X_3 [194, 195] (X = Cl, Br) and Tb_2Cl_3 [195] are binary subhalides which can be prepared in large yield and pure state. Those phases with X/M < 1.5 which were prepared only in low yields and characterized via single crystal X-ray investigations and described as binary phases [49] turned out to be stabilized by impurity atoms [52]. They can be prepared in high yields as carbide halides (or hydride halides MXH_n) by purposely adding the contaminants.
[194] D. A. Lokken, J. D. Corbett, *Inorg. Chem. 12* (1973) 556.
[195] A. Simon, N. Holzer, H. Mattausch, *Z. Anorg. Allg. Chem. 456* (1979) 207.
[196] G. Ebbinghaus, A. Simon, A. Griffith, *Z. Naturforsch. A 37* (1982) 564.
[197] W. Bauhofer, A. Simon, *Z. Naturforsch. A 37* (1982) 568.
[198] D. W. Bullett, *Inorg. Chem. 24* (1985) 3319.
[199] G. J. Miller, J. K. Burdett, C. Schwarz, A. Simon, *Inorg. Chem. 25* (1986) 4437.
[200] L. R. Morss, H. Mattausch, R. Kremer, A. Simon, J. D. Corbett, *Inorg. Chim. Acta*, in press.
[201] A. Simon, H. Mattausch, N. B. Mikheev, C. Keller, *J. Naturforsch. B 42* (1987) 666.
[202] U. Schwanitz-Schüller, A. Simon, *Z. Naturforsch. B 40* (1985) 705.
[203] A. Simon, E. Warkentin, K. Berroth, unpublished.
[204] A. Simon, E. Warkentin, R. Masse, *Angew. Chem. 93* (1981) 1071; *Angew. Chem. Int. Ed. Engl. 20* (1981) 1013.
[205] E. Warkentin, R. Masse, A. Simon, *Z. Anorg. Allg. Chem. 491* (1982) 323.
[206] E. Warkentin, A. Simon, unpublished.
[207] A. Simon, E. Warkentin, *Z. Anorg. Allg. Chem. 497* (1983) 79.
[208] C. Schwarz, A. Simon, unpublished.
[209] A. Simon, E. Warkentin, U. Schwanitz-Schüller, C. Schwarz, unpublished.
[210] H. Mattausch, C. Schwarz, A. Simon, unpublished.
[211] A. Simon, C. Schwarz, W. Bauhofer, *J. Less-Common Met.*, in press.
[212] E. Warkentin, A. Simon, *Rev. Chim. Miner. 20* (1983) 488.
[213] J. D. Corbett, K. R. Poeppelmeyer, *J. Solid State Chem. 57* (1985) 43.
[214] Single crystal investigations of $Ln_7I_{12}C$ (Ln = La, Gd, Tb, Er) [203] have met with several problems, which even have rendered an unambiguous characterization impossible: (i) Variable lattice constants indicate a range of homogeneity; (ii) the scattering density in the cluster centers varies largely, perhaps due to the presence of different interstitial atoms (cf. Tab. 5); (iii) with the exception of $Er_7I_{12}C$ the "vibrational" ellipsoids of the single Ln^{3+}-Ionen ions are extremely elongated (as in the case of $Sc_7Cl_{12}N$).
[215] G. Argay, I. Naray-Szabo, *Acta Chim. Acad. Sci. Hung. 49* (1966) 329.
[216] R. Kliche, C. Schwarz, A. Simon, unpublished.
[217] H. Siebert, *Z. Anorg. Allg. Chem. 273* (1953) 170.
[218] 1/6 of the single C atoms (C^{4-}) can be substituted by C_2 units ($(C_2)^{6-}$) due to the electron balance [211] (see Table 6). For electrostatic reasons the undulation of the layers in $Gd_6Cl_5C_3$ allows incorporation of the more highly charged ion.
[219] S. Satpathy, O. K. Andersen, *Inorg. Chem. 24* (1985) 2604.
[220] The lowest and highest states, σ_s and σ_p^* respectively, are omitted from the drawing.
[221] H. Mattausch, W. Schramm, R. Eger, A. Simon, *Z. Anorg. Allg. Chem. 530* (1985) 43.
[222] The investigation was performed on $TbClD_{0.8}$ [223].
[223] H. Mattausch, A. Simon, K. Ziebeck, *J. Less-Common Met. 113* (1985) 149.
[224] The investigation was performed on $TbBrD_2$ [225].
[225] F. Ueno, K. Ziebeck, H. Mattausch, A. Simon, *Rev. Chim. Miner. 21* (1984) 804.
[226] W. Bauhofer, A. Simon, unpublished.

ANGEWANDTE CHEMIE

International Edition in English

Volume 27 · Number 1
January 1988
Pages 185–206

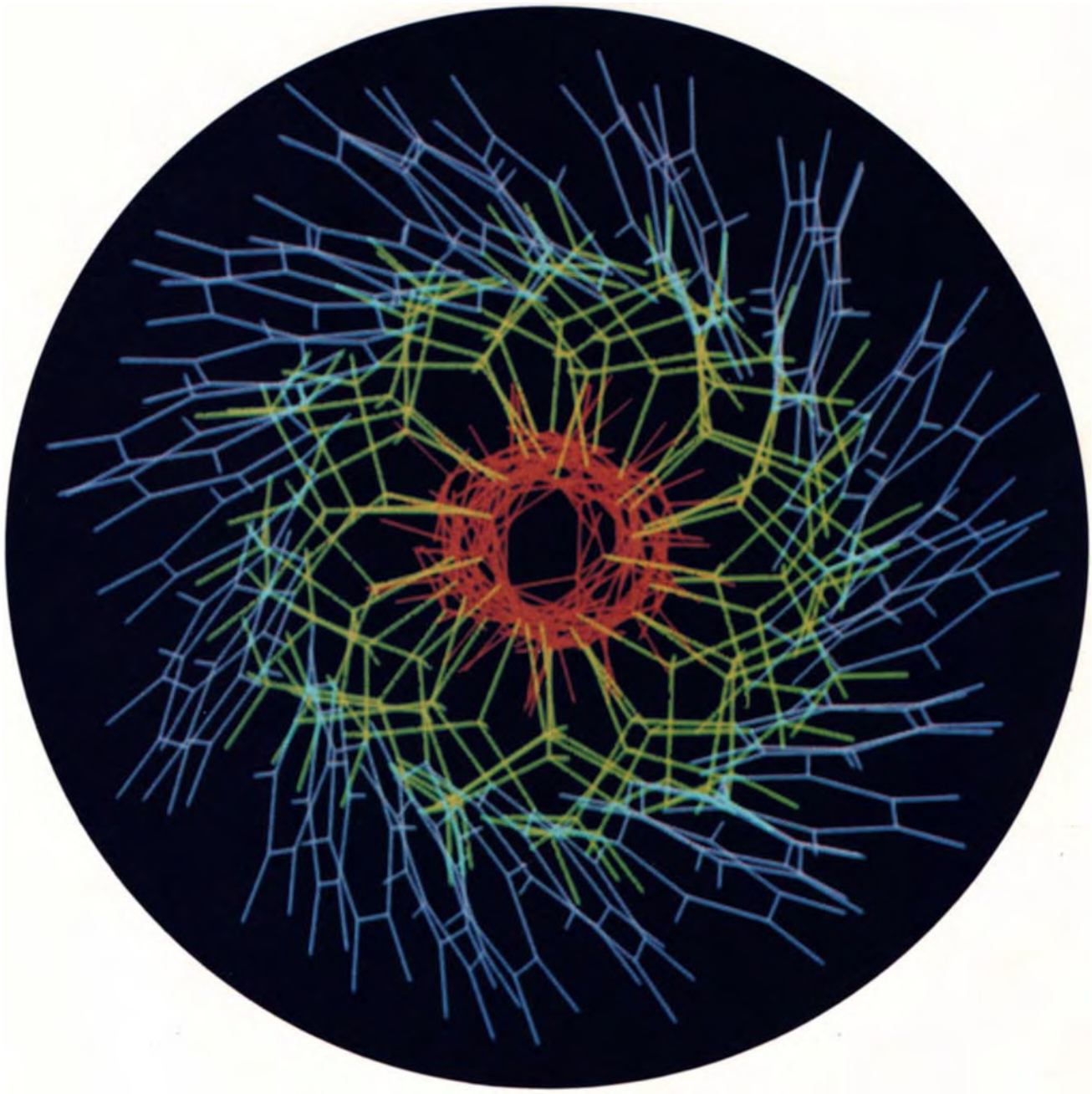

Günther Wilke

Contributions to Organo-Nickel Chemistry

 © VCH Verlagsgesellschaft mbH, D-6940 Weinheim, 1988 *0570-0833/88/0101-0185 $ 02.50/0*

Contributions to Organo-Nickel Chemistry**

By Günther Wilke*

One hundred years of organonickel chemistry have generated a wealth of new knowledge and a history of examples of accidental discoveries which have finally led to industrial applications. The historical development is associated with the names of *Mond*, *Sabatier*, *Reppe* and *Ziegler* and, with the methods and techniques available today, many of the original discoveries and unsolved problems are attracting renewed attention. For example, 70 years were to go by before a synthesis first conceived by *Sabatier* could finally be realized. The path leading from nickel-catalyzed hydrogenation to highly enantioselective homogeneous catalysts is one of the contributions to organonickel chemistry which is described here.

1. Introduction and Historical Development

The scientist in his search for new knowledge is continually confronted with the interaction between planning and chance, the precise experiment and the unexpected results, rational thinking and intuition. This interaction is a favorite topic in science politics, and nickel is one of the few elements whose chemistry provides examples which can be regarded as pioneer achievements in chemical research and hence can provide insight into the way new knowledge evolves. For this reason, a review of the historical development accompanied by appropriate quotations and reminiscences seems a suitable introduction to the topic of this article.

100 years of "Angewandte Chemie" is almost synonymous with 100 years of organonickel chemistry. In 1890 *Mond*, *Langer*, and *Quincke*[1] reported the synthesis of "nickel carbonyl" from metallic nickel and carbon monoxide. *Mond* quickly realized the significance of this discovery and developed a technical process for purifying nickel based upon the formation and decomposition of the carbonyl. 20 years later, in an obituary for *Mond*, *Langer*[2] described the beginnings:

> "The experiments had been proceeding for some time when we discovered nickel carbonyl by accident. We treated nickel, as we had often done before, with carbon monoxide in a combustion tube and led the resulting gases into a Bunsen-burner in order to render them harmless. My assistant, who looked after these experiments, asked me to switch off the apparatus since he had to go home earlier. Some time after I had turned off the burners, I noticed that the flame of the Bunsen-burner into which the liberated gas was being led had a peculiar greenish yellow color which became more intense as the tube cooled. My first thought was that arsenic must be present in the carbon monoxide since it had been prepared from normal sulfuric acid. I therefore heated the glass tube through which the gas was led into the burner in order to obtain an arsenic mirror. The mirror was formed immediately but consisted not of arsenic but of nickel!
>
> My assistant told me later that he had often observed this flame coloration but had considered it of no importance. I mention these circumstances in such detail in order to illustrate how easily an important discovery can be overlooked and upon what insignificant details new industries are often based."

This discovery had consequences which went far beyond the creation of a new industry: a few years later *Sabatier* and *Senderens*[3] were led to attempt the preparation of volatile nickel compounds similar to $Ni(CO)_4$ using gases other than carbon monoxide. More than 40 years later, *Sabatier*[4] lectured on the background and the results before the Academy:

> "What led M. Senderens and I to develop our general direct hydrogenation method in the presence of finely divided metals and in particular of nickel?
>
> The initial objective of our research was quite a different one. A few years earlier, Ludwig Mond had managed to attach carbon monoxide directly to finely divided nickel (which he obtained by reduction of the oxide) and had prepared tetracarbonyl nickel $Ni(CO)_4$ as a well defined, volatile substance. (...)
>
> We hoped that a similar fixation would take place with other unsaturated gaseous molecules such as dinitrogen oxide, nitrogen oxide, nitrogen dioxide, ethylene, acetylene. (...)
>
> With this idea, which we later found to be incorrect, we studied the effect of ethylene upon reduced nickel.
>
> If ethylene is passed into a column of nickel in the cold nothing happens. Not much happens at 100°C, 200°C, 250°C but at 300°C the system becomes incandescent and the gas decomposes, whereby not only carbon and hydrogen are formed but also considerable amounts of *ethane*. This last compound must have been formed by hydrogenation of ethylene as the result of

[*] Prof. Dr. G. Wilke
Max-Planck-Institut für Kohlenforschung
Postbox 011325, D-4330 Mülheim a. d. Ruhr (FRG)

[**] Including unpublished results by *A. Aradi*, *O. Behrens*, *H. Kuhn*, *T. Leven*, *J. Neuffer*, *J. Monkiewicz*, *K. R. Pörschke*, *L. Stehling*, and *K. H. Walter* and unpublished crystal structure determinations by *C. Krüger*, *E. Raabe*, and *Y.-H. Tsay*, and model calculations by *K. Angermund*. The preceding page shows Figure 19 of this article.

some special property of the nickel which caused it to act as a hydrogenation catalyst. This was subsequently confirmed in a direct experiment.

A mixture of equal volumes of hydrogen and ethylene when passed into a column of freshly reduced nickel at slightly elevated temperatures (30° to 40°C is sufficient) is converted into ethane without any by-products being formed. We then extended this hydrogenation behavior of nickel by using acetylene: a mixture of equal volumes of hydrogen and acetylene react *in the cold* with nickel to give exclusively ethylene; two volumes of hydrogen and one volume of acetylene giving one volume of ethylene.

The nickel was completely unchanged and could be used repeatedly."

During a meeting in 1912 which led to the founding of the Kaiser-Wilhelm-Institut für Kohlenforschung, *Emil Fischer* paid tribute to this discovery by *Sabatier* and *Senderens*, for which *Sabatier* had just received the Nobel Prize:[5]

"Gentlemen, a new era has begun for the chemistry of the gases and these have now moved into the constellation of catalysis. Using catalysts, some amazing conversions of hydrogen, oxygen, nitrogen, carbon monoxide can be carried out at temperatures which are many hundreds of degrees lower than that at which these gases normally react. This chapter on catalysis is unlimited and it is here that a systematic investigation promises to bring a rich reward."

75 years later, this program with which *Emil Fischer* sent the Institute on its way has, without doubt, a prophetic note and the original ideas of *Sabatier* were realized in part when we managed to prepare tris(ethylene)nickel **1**,

$[(C_2H_4)_3Ni]$ **1**

which although extremely labile can be isolated in crystalline form.[6] This discovery had been preceded by no less than 20 years of intense activity in the field of nickel chemistry.

In 1948, the 60th anniversary of the founding of this Journal, another milestone in the chemistry of nickel, was reached. *Reppe*, *Schlichting*, *Klager*, and *Toepel*[7] reported the completely unexpected discovery of the "cyclic polymerization of acetylene" to cyclooctatetraene (COT) using nickel catalysts. Well ahead of their time, the authors formulated the mechanism shown in Scheme 1.

Even with hindsight, the accompanying explanation sounds surprisingly modern:

"We assume that a bond is formed consisting of a hypothetical biradical composed of four acetylene molecules, whereby both terminal radical-electrons are accepted into the 3d levels of the nickel."

This description implies what we would now describe as the formation of a metallacycle[*] by oxidative addition and its cleavage by reductive elimination. There has been much speculation concerning the mechanism of the formation of cyclooctatetraene which will not be discussed in detail here, but it is now believed that the cyclotetramerization of acetylene with a nickel catalyst does not take place in an electrocyclic manner as an example of "forbidden to allowed catalysis" but that a number of steps are involved. Recent investigations carried out both in the Mülheim Institute and by BASF in Ludwigshafen led us to suggest a mechanism involving two nickel atoms. A comparison was made using *Reppe*'s original conditions and either nickel acetylacetonate or our bis(cyclooctatetraene)dinickel $[(cot)_2Ni_2]$[10] **2** as catalyst. It turns out that in the presence of **2**, in contrast to nickel acetylacetonate, no incubation period is observed, the formation of cuprene[**] is significantly suppressed and the selectivity increases considerably. **2** is apparently the most effective catalyst known for the synthesis of cyclooctatetraene. The X-ray structural analysis of **2** shows that it is a sandwich complex in which two nickel atoms are held between two, essentially planar, cyclooctatetraene molecules[10c] (cf. Fig. 3 in Section 2). Based on this structure and the structure and chemical properties of a model—the chromium compound **3**,[11] in which a C_8H_8 chain bridges both Cr atoms, reacts further upon warming with conversion of the chain into COT which itself interacts again with both Cr-atoms—we proposed the formulation shown in Scheme 2 for the formation of COT.[11]

$[(\eta^5\text{-}C_5H_5)Cr(C_8H_8)Cr(\eta^5\text{-}C_5H_5)]$ **3**

This proposal is supported by recent experiments[12] which have led to the isolation and characterization of a

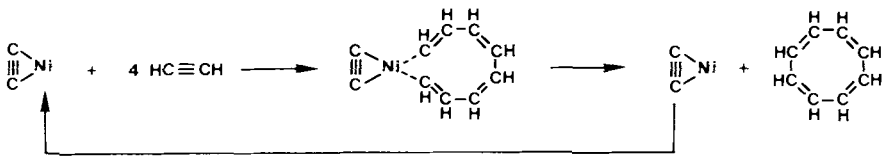

Scheme 1. The reaction mechanism for cyclooctatetraene formation as formulated by *Reppe* et al. [7].

[*] *Reppe* and *Vetter* [8] can be regarded as the fathers of the metallacycles: although they were unaware of the structure of the compound $Fe_2C_{12}H_4D_8$ which they had synthesized, a three dimensional crystal structure analysis by *Hock* and *Mills* [9] revealed the presence of a metallacycle.

[**] Cuprene is polyacetylene.

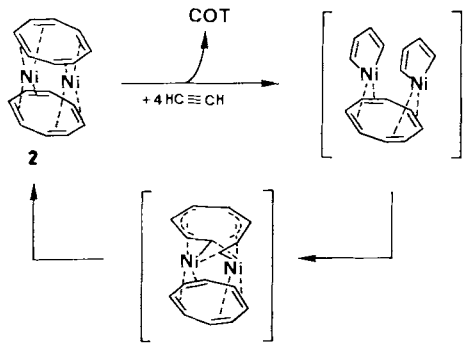

Scheme 2. The $[(cot)_2Ni_2]$-catalyzed cyclotetramerization of acetylene.

nickelacyclopentadiene complex **6** from the reaction of a nickel(0) complex with acetylene (Scheme 3).

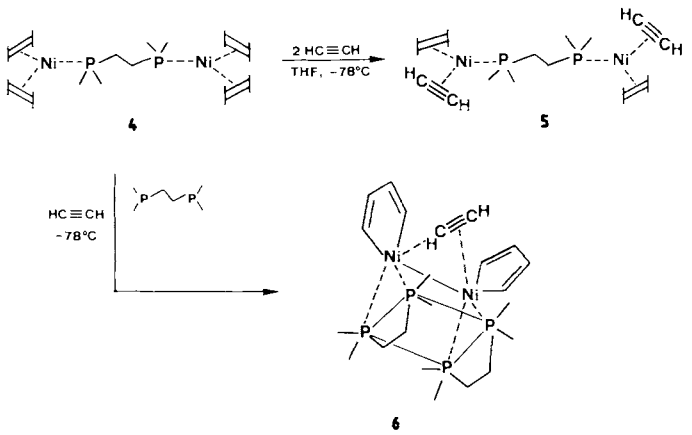

Scheme 3. Formation of the nickelacyclopentadiene **6** from the complex **4** and acetylene by oxidative addition. Isopropyl groups are attached to the phosphorus.

Should the mechanism discussed above turn out to be correct, then we would have the interesting situation in which two metal atoms are involved in a catalytic process in a homogeneous phase and in which the product of the catalysis plays a decisive role as a ligand by holding the two Ni atoms a suitable distance apart. The incubation period mentioned above is probably associated with an initial reduction of the nickel(II) compound introduced as the catalyst.

These remarks on the third phase in the development of organonickel chemistry illustrate that modern developments have given a new actuality to discoveries made 40 years ago.

In 1953, five years after the publication of the most important aspects of the Reppe-chemistry, an initially annoying case of the failure of a routinely successful experiment occurred in the Mülheim Institute. Subsequently, however, the recognition of the reason for the failure was to become the starting point for a revolution in some areas of chemistry. For no apparent reason, the Aufbau reaction of triethylaluminum and ethylene which had been discovered by *Ziegler* and *Gellert*[13] quite unexpectedly failed. Instead of the usual higher aluminum alkyl compounds, *Holzkamp*[14] observed the formation of 1-butene. After a long search it was discovered that traces of nickel catalyzed a termination reaction after each insertion step. We described this development along with our explanation of the phenomenon in detail 15 years ago in an article in Angewandte Chemie under the title "The Nickel Effect."[15] Some recent results will be discussed in Section 4.2. The "nickel effect" was to lead step by step to the discovery of the "Ziegler catalysts."[16] These are associated by every chemist with unique scientific and economic success so that it is hardly an exaggeration to describe the development following the discovery of the "nickel effect" as revolutionary.

The "nickel effect" also marks the beginning of the extensive work on organonickel chemistry which developed in the Institute in Mülheim after 1959. The immediate impulse, however, came from two unrelated directions. In order to use the "nickel effect" for the continuous dimerization of ethylene to butene, it was necessary to develop a stable nickel cocatalyst. This problem was solved by treating nickel acetylacetonate in toluene with Et_2AlOEt in the presence of, for example, phenylacetylene.[14] This recipe was developed in 1954 and the desired cocatalyst was formed as a reddish orange solution. Nothing was known about its structure or even about its composition; all that mattered was that it worked. Five years later in 1959—in the meantime the cyclotrimerization of butadiene to 1,5,9-cyclododecatriene (CDT) using Ziegler catalysts had been discovered[17]—the use of this mixture, i.e. the red-orange solution, acted as the fuse for a new research strategy: the controlled oligomerization of unsaturated compounds.[18] In an attempt to develop a catalyst which would convert butadiene into a cyclic dimer instead of the cyclic trimer, experiments were carried out with various metals including nickel—*Reed*[19] having been able to dimerize butadiene with tetracarbonylnickel derivatives. To our satisfaction, the very first experiments with the "cocatalyst solution" gave 1,5-cyclooctadiene as well as cyclododecatriene. The further development in this direction will be described in Section 4.1.

The second idea led unexpectedly to a novel method for preparing transition-metal complexes. During the nickel-cocatalyzed ethylene dimerization and olefin displacement reaction, double bond isomerization had frequently been observed and we wanted to use this effect to find out which was the thermodynamically more stable isomer of cyclododecatriene. Nickel acetylacetonate was treated with Et_2AlOEt, exactly as before, in the presence of all-*trans*-cyclododecatriene. It was anticipated that the nickel produced during the reaction would cause isomerization. Instead of a precipitate of black elemental nickel, a dark red solution was formed from which an extremely air-sensitive but thermally stable, red, crystalline compound was finally isolated: the first nickel(0)-olefin complex, all-*trans*-cyclododecatrienenickel(0) **7**,[20] had been born and at the same time a general synthesis for complexes of this type had been discovered.[21]

This review of the historical development of organonickel chemistry will be followed by sections devoted to the results of our recent work with nickel complexes, their stoichiometric reactions, and their use as homogeneous catalysts.

2. Nickel(0) Complexes

all-*trans*-Cyclododecatrienenickel(0) **7**, which has been known for over 25 years, was the first nickel(0)–olefin complex and it still attracts attention because of its structure and reactivity. The X-ray structural analysis[22] shows that the three *trans* double bonds adopt a propeller-like arrangement around the nickel atom to give a racemate in which the propeller can have a left-hand or a right-hand screw (see Fig. 1).

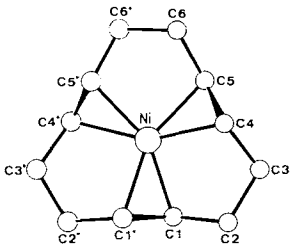

7

Fig. 1. The structure of all-*trans*-1,5,9-cyclododecatrienenickel(0) **7**.

The deep red color of this 16e-complex is remarkable and is presumably associated with the unusual arrangement of the double bonds. According to *R. Hoffmann* et al.,[23] the energetically most stable structure would be one in which the six C atoms of the three double bonds lie in the same plane as the nickel(0). Indeed, **7** reacts in a 1 : 1 ratio with all-*cis*-1,5,9-cyclododecatriene to give the almost colorless all-*cis*-cyclododecatrienenickel(0) **8**[24] in which the *cis*-double bonds have this arrangement. We believe that this is also the reason why the chelating ligand all-*trans*-CDT can be displaced even at low temperatures by ethylene. Similar behavior is observed for norbornene[15] and *trans*-cyclooctene.[25] The resulting tris(olefin)-16e-nickel(0) complexes **1**, **9**, and **10** (cf. Scheme 4) are also colorless, and the X-ray structural analysis of **9** confirms the coplanar geometry.[26]

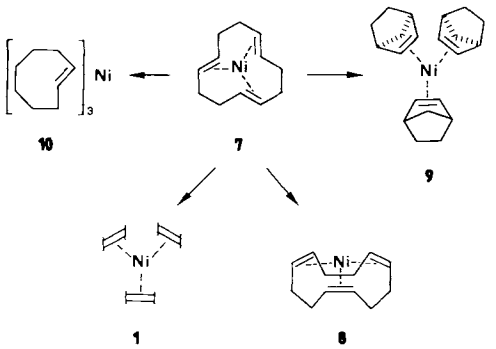

Scheme 4. Tris(olefin)-16e-nickel(0) complexes, **1** and **7**–**10**.

The high reactivity and sensitivity of these 16e-complexes is of course associated with the unoccupied fourth coordination position. **7** readily adds ligands such as CO, CNR, and PR_3 as well as a hydride (see Section 4.2), and the red color disappears. For example, with Me_3P, the yellow colored complex [(Me_3P)Ni(cdt) **11** is formed. The conversion of the 16e-system into an 18e-system is accompanied by a displacement of the nickel atom out of the plane such that an almost tetrahedral coordination results, and this has been confirmed by an X-ray structural analysis of [(menthyldimethylphosphane)Ni(cdt)] **12a** (Fig. 2).[27]

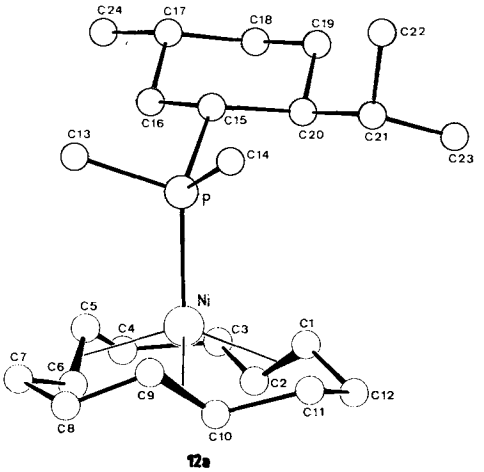

12a

Fig. 2. The structure of the adduct **12a** of menthyldimethylphosphane and [(cdt)Ni] **7**.

The fourth coordination position plays a key role in the separation of the racemate (cf. Scheme 5). We have converted **7** into the diastereomers **12a** and **12b** by a 1 : 1 reaction with menthyldimethylphosphane, separated these by recrystallization, and then displaced the optically active phosphane by reaction with PMe_3 to give the enantiomers **11a** and **11b**. The next step, the removal of the Me_3P to give the enantiomers **7a** and **7b**, created problems, which, however, were solved by treating **11a** and **11b** with the allylnickel complex **13**: at low temperatures the phosphane is transferred to **13** with liberation of **7a** and **7b**. It is also possible to go directly from **12a** and **12b**.[28]

The specific rotation of **7a** is $[\alpha]_D^{-30^\circ} = +104^\circ$. The successful separation shows that a racemization **7a** ⇌ **7b** by a simple rotation of the double bonds is not possible. The

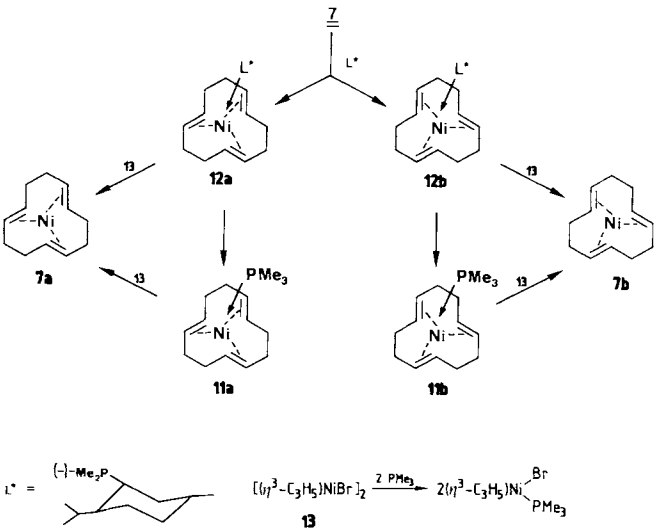

Scheme 5. Separation of the racemates of **7** and the isolation of the enantiomers **7a** and **7b**.

chirality of **7a** and **7b** has a certain similarity with that of the helicenes and they are presumably the simplest optically active transition metal complexes known.

The discovery of bis(cyclooctadiene)nickel(0) **14**[10] occurred almost simultaneously with that of 7and was prepared by a similar reduction of nickelacetylacetonate with Et_2AlOEt in the presence of 1,5-cyclooctadiene. **14** can also be easily prepared from **7** and is now used all over the world either as a stoichiometric reagent or in the preparation of catalysts. It is appropriate to mention here that we have prepared **14** in our pilot plant on a 10-kg scale with no trouble at all. Particularly effective is the reaction of nickel(II) ethoxide,[29] which we prepare by an electrochemical procedure, with Et_3Al in the presence of cyclooctadiene. **14** has now become a readily available product and its synthesis is a standard exercise with which newcomers to the Institute gain experience.

It is appropriate while discussing the olefin-nickel(0) complexes to comment further on bis(cyclooctatetraene)dinickel **2**[10] which we mentioned in Section 1. Because of its low solubility we initially regarded this complex as a polymer ("**2**"), and formulated it as such using the non-planar form of free cyclooctatetraene (Scheme 6).

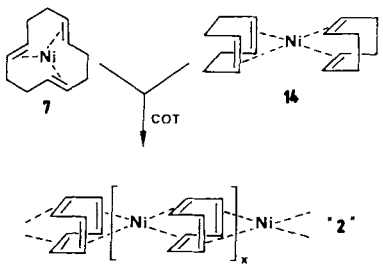

Scheme 6. The initially suggested polymeric structure for **2**.

The black, metallic crystalline compound, which can be prepared in practically quantitative yield either by reduction or by a displacement reaction from **7** or **14**, has been examined by X-ray diffraction (cf. Fig. 3)[10c]: each nickel atom is bonded to two *syn*-η^3-allyl groups and the Ni-Ni distance varies between 2.719(9) and 2.947(1) Å (the nickel positions are disordered) which presumably excludes a strongly bonding Ni-Ni interaction.

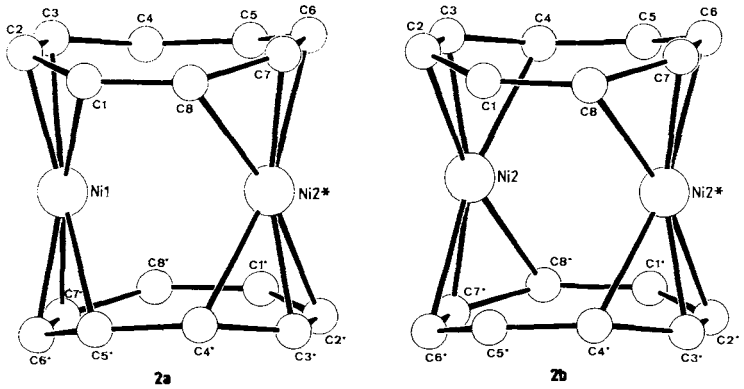

Fig. 3. The two structures of $[(cot)_2Ni_2]$ **2** (the Ni positions are disordered).

3. Stoichiometric Reactions: Oxidative Addition

The "pure" or homoleptic olefin-nickel(0) complexes have considerable synthetic potential. The driving force for these reactions is the oxidation of nickel(0) to nickel(II) and this will be illustrated in the following with a few examples.

Certain catalysts, which will be discussed in Section 4, can be easily prepared by the oxidative addition of an allyl halide to nickel(0)[30] and dimeric η^3-allylnickel halides result. *E. O. Fischer* and *G. Bürger* originally used $Ni(CO)_4$,[31] but the yields were unsatisfactory since the liberated CO can obviously interfere.[30] By using $[(cod)_2Ni]$ **14** we were able to obtain a practically quantitative yield.[30] An example is the synthesis of the rather unusual compound discussed below which later found use in a quite different area.[32]

(+)-(1*R*,5*R*)-η^3-pinenylnickel bromide **16** was prepared from (−)-(1*R*,5*S*)-pinenylbromide **15** (Scheme 7) and used

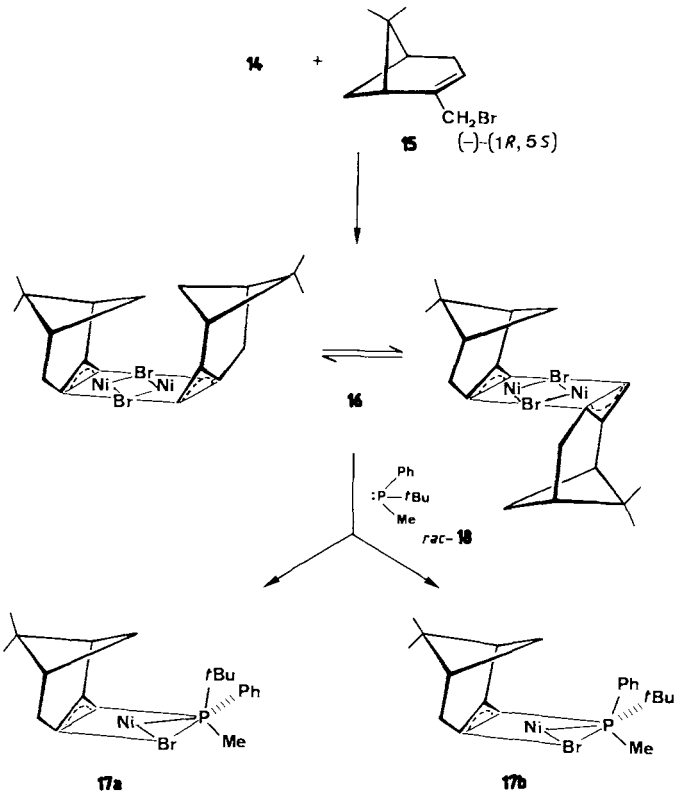

Scheme 7. Reaction of the racemic Horner-phosphane *rac*-**18** with pinenylnickel bromide **16** to give the diastereomers **17a** and **17b**.

to separate Horner-phosphanes into their enantiomers by means of diastereomer formation. For example, **16**, which according to ^{1}H-NMR spectroscopy exists at −20°C in two forms, reacts with racemic *tert*-butyl(methyl)phenylphosphane *rac*-**18** in a 1:1 ratio to give the diastereomers **17a** and **17b**.

17a could be crystallized[32] and was analyzed by X-ray crystallography[33] (cf. Fig. 4). The absolute configuration turns out to be 1*R*,5*R* in the pinenyl part and *S* in the phosphane part.

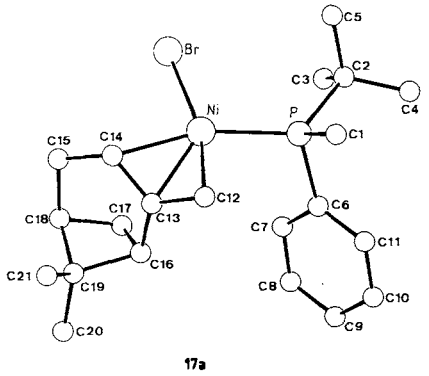

17a

Fig. 4. The structure of the dextrorotatory complex **17a**.

The (−)-(*S*)-*tert*-butyl(methyl)phenylphosphane (−)-(*S*)-**18** can be displaced from **17a** by treatment with Me_3P and has an optical purity of 96.6%, which increases to almost 100% after one further complexation. We have used this separation procedure for a series of Horner-phosphanes of the type $PR^1R^2R^3$, and in each case the optical purity after a single crystallization lies between 60 and 96%. The example discussed above turns out to be the best, but nevertheless the method appears to be general.[32] It should also be mentioned that the preparative complexation of a Horner-phosphane to **16** can also be used analytically to determine its optical purity: the diastereomers can be distinguished in the NMR spectrum and used to measure their relative proportions.[34]

A formal oxidative addition also occurs when $[(cod)_2Ni]$ **14** is treated with butadiene at −10°C. The COD is displaced and three butadiene molecules couple together to give a C_{12}-chain which is bonded to the nickel atom by terminal η^3-allyl groups. By definition the nickel is now regarded as nickel(II). The complex $[(C_{12}H_{18})Ni]$ **19** was the first intermediate to be isolated from a catalytic cyclooligomerization reaction of butadiene.[35] It can be recrystallized from liquid butadiene and melts at +1°C. If **19** is treated with excess butadiene at elevated temperatures, the C_{12}-chain undergoes reductive elimination to give CDT. This is accompanied by the transient formation of nickel(0), which immediately undergoes a renewed oxidative addition with butadiene. Since this sequence continues repeatedly, the result is the catalytic cyclotrimerization of butadiene accompanied by a repeated change in the formal oxidation state of the nickel [$Ni^0 \rightleftharpoons Ni^{II}$].[18]

Detailed NMR-spectroscopic investigations[36] have shown that **19** exists as two stereoisomers which differ only in the arrangement of the internal double bond (Scheme 8).

Many years previous to the elucidation of these structures by NMR spectroscopy, the chemical behavior had convinced us that a C_{12}-chain is formed and that this bonds through η^3-allyl groups.[35a] The successful synthesis of bis(η^3-allyl)nickel **20** was based upon this conclusion.

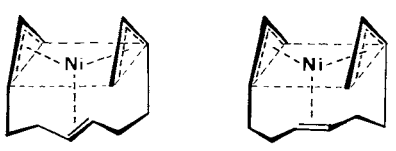

19a **19b**

Scheme 8. The two stereoisomers of η^3,η^3-dodecatrienediylnickel **19**.

$[(\eta^3\text{-}C_3H_5)_2Ni]$ **20**

20, a highly volatile and reactive compound, is the simplest transition metal sandwich compound and is the prototype of the "pure" or homoleptic allyl-transition metal compounds.[37] It is mentioned here because recent structural investigations and independent ab-initio calculations have produced some interesting results and corrected some earlier misconceptions. It is hardly surprising that **20** attracted the attention of theoreticians at an early date and several groups carried out ab-initio calculations. However, it was assumed that the three C atoms and five H atoms of the allyl group lie in one plane. *F. Mark*,[38] without knowing the latest results obtained by *C. Krüger* and *R. Goddard*[38] from low temperature X-ray analysis and neutron diffraction data, found by double-ζ-ab-initio calculations that the displacement of the H atoms out of the plane of the three C atoms produces an energy minimum. The agreement between the calculated and experimental results is remarkable, as is also the stabilization of the molecule by 187 KJ/mol. Figure 5 speaks for itself.

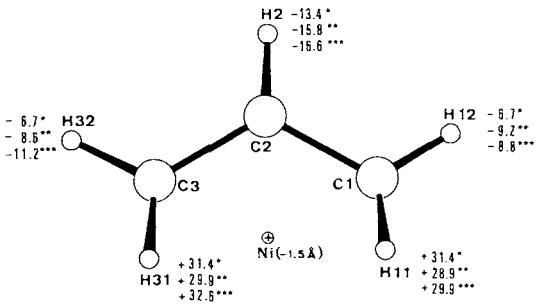

Fig. 5. The displacement of the H atoms out of the plane formed by the three C atoms of an allyl group in bis(η^3-allyl)nickel **20**. The values [°] are taken from an ab initio calculation (*), a neutron diffraction study (**), and a low-temperature X-ray structural analysis (***).

The calculations also suggest that the nickel atom has a net charge of +0.81, which is significantly higher than that calculated for a system having planar allyl groups (+0.65,[39] +0.55, and +0.485[40]).

It is appropriate to mention these results at this point since η^3-allyl systems of this type are frequently observed as intermediates in the transition metal-catalyzed reactions of 1,3-dienes.

The oxidation of nickel(0) by butadiene, which we have mentioned above, takes quite a different course if the reaction is carried out in the presence of aldehydes or ketones.[41] In the simplest case of acetone, butadiene and nickel(0) (in the form of **14**) react to give a nickel dialkoxide **21** in which two equivalents of acetone are coupled with one equivalent each of butadiene and nickel (Scheme 9). Hydrolysis leads to (*E*)-2,7-dimethyl-4-octene-2,7-diol **22**, which can be easily converted by conventional dehydration into (*E*)-2,7-dimethyl-2,4,6-octatriene **23**. This nickel-induced coupling of butadiene with a carbonyl

compound forms the basis of an effective polyene synthesis.

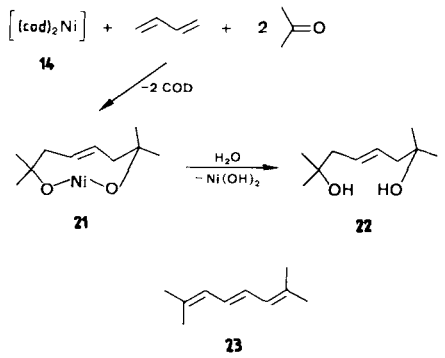

Scheme 9. The nickel-induced synthesis of the diol **22** and the triene **23**.

Analogous reactions have been used to convert benzaldehyde, cinnamaldehyde, phenylpentadienal and vitamin-A-aldehyde into the polyenes **24**–**27** (Scheme 10). Compound **27** can be regarded as a homologue of β-carotene.

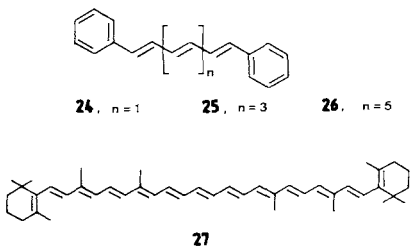

Scheme 10. The polyenes **24**–**27** prepared by reaction of butadiene with benzaldehyde, cinnamaldehyde, phenylpentadienal and vitamin-A-aldehyde, respectively.

Particularly convincing examples of the oxidative addition to nickel(0) have resulted from the investigations of the reactivity of cyclopropabenzene **28** towards Ni(0) (Scheme 11).[42] Steric factors have an obvious influence upon the reaction which can lead to completely different products. The three-membered ring opens in the reaction between **28** and $[(Et_3P)_2Ni(cod)]$ **29**, and the nickelacyclobutabenzene derivative **30** can be isolated.[43]

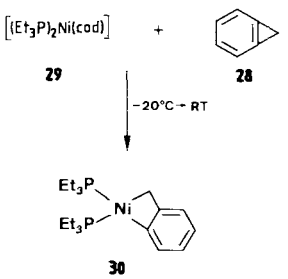

Scheme 11. The synthesis of the nickelacyclobutabenzene derivative **30**.

31, the methyl analogue of **29**, on the other hand, reacts under the same conditions with two equivalents of **28** to give the bismethano-bridged nickelaannulene **32** (Scheme 12).[42] The *anti* arrangement of the bridging methano-

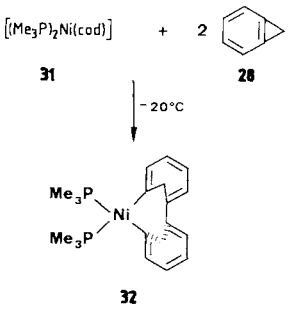

Scheme 12. The synthesis of the nickelaannulene **32**.

group in **32** has been established by NMR spectroscopy and an X-ray structural analysis[44] (Fig. 6).

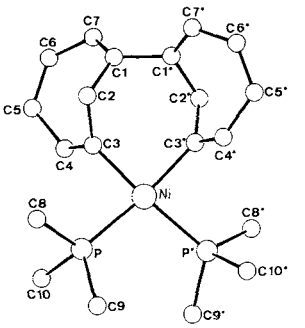

Fig. 6. The structure of the nickelaannulene **32**.

The chemistry of **32** has produced some interesting results (Scheme 13). Carbonylation leads to the ketone **33**, which has been shown by NMR-spectroscopy and an X-ray structural analysis to be a derivative of norcaradiene. Upon conversion into the alcohol **34**, the cycloheptatriene structure of **32** is re-formed.[45]

In addition to the expected product **35**, hydrolysis also produces lesser amounts of the dimer **36** indicating that **32** adopts a transient dimeric form. This tendency to dimerize or even oligomerize is also observed in the reaction with CH_3I: terminally methylated di-, tri- and tetrameric (n = 1-

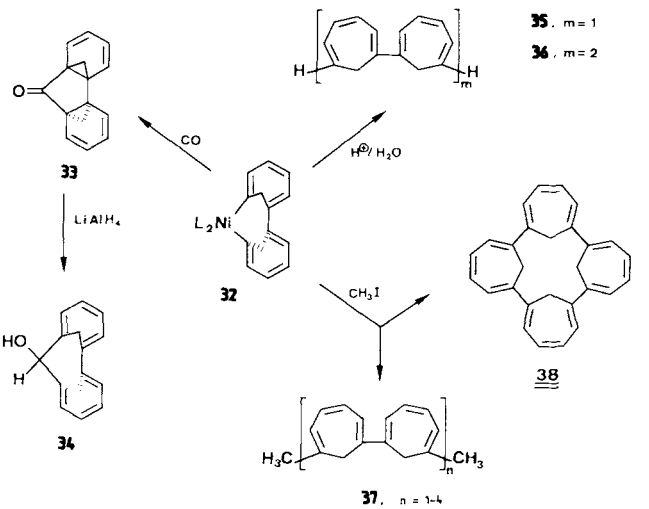

Scheme 13. The reactions of **32**, L = CH_3.

4) units are formed, i.e. the products **37** contain from two to eight coupled cycloheptatriene units.[46] The most spectacular product from this reaction, however, is the tetramethano-bridged [24]annulene **38**, which is formed as a red crystalline solid in ca. 10% yield.

An X-ray structural analysis[47] (Fig. 7) shows that **38** does not have a planar structure, as the formula would suggest, but rather has a cylindrical form.

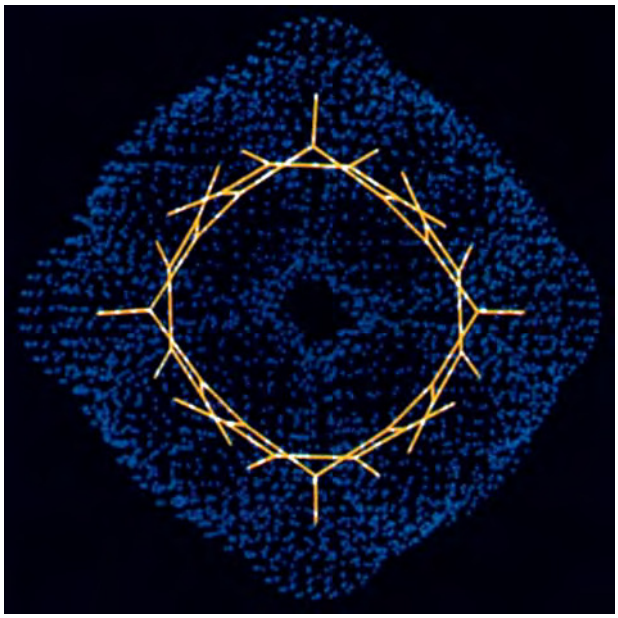

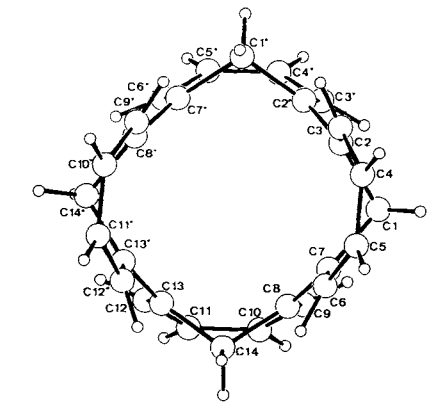

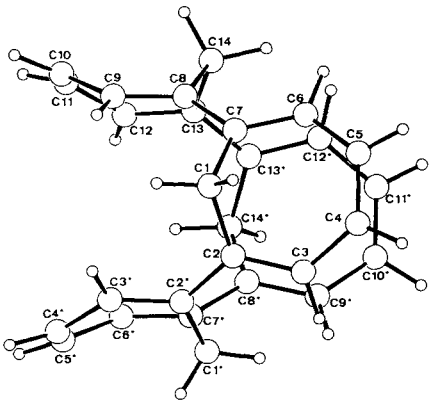

38

Fig. 7. The structure of the bridged [24]annulene **38**. Top: space-filling computer graphic representation. Middle and bottom: two views of the molecule **38**.

It is worth considering for a moment how one would synthesize **38** by conventional means. Without a doubt considerable effort would be involved, underlining the synthetic possibilities which such nickel complexes offer. However, we have not been able to prepare **38** catalytically from **28**, presumably because of a side reaction in which **32** reacts with excess **28** to give what is formally a trimer of **28** but which does not have a trismethano-bridged [18]annulene structure. During the reaction of **28** with **32**, the three-membered ring opens (in a manner similar to that discussed above for **30**) and couples with the annulene fragment of **32**. The product consists of the two isomeric hydrocarbons **39a** and **39b** (Scheme 14).[42]

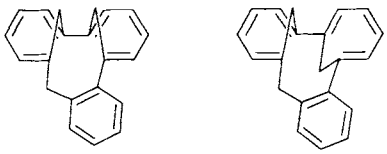

39a **39b**

Scheme 14. The two stereoisomers **39a** and **39b** from the formal cyclotrimerization of **28**.

4. Catalytic Reactions

The stoichiometric reactions discussed above clearly indicate that, with the help of suitable organonickel compounds, organic syntheses can be carried out which would either be impossible or extremely tedious by conventional means. The only drawback is that the nickel is used as a stoichiometric reagent; although under suitable conditions a regeneration should be possible. This disadvantage is avoided if the nickel component acts as a catalyst and in one case, discussed below, over a million cycles have been achieved.

4.1. Cyclooligomerization

We have already mentioned a catalytic cycle which forms the basis of the cyclotrimerization of butadiene as part of the discussion of the oxidative addition of butadiene to nickel(0) or as it has been called "naked nickel".[18] Scheme 15 summarizes a number of catalytic cyclooligomerization reactions in which butadiene is one of the substrates and in which either "naked nickel" or a ligand-nickel system (LNi) are involved.

The "naked nickel", in the form of, for example [(cdt)Ni] **7** or [$(cod)_2$Ni] **14**, loses its ligands under the influence of the butadiene, and the nonisolable intermediate **I** is presumably formed in which η^4- or η^2-systems are complexed to the nickel. Further reaction occurs at low temperature ($-20°$ to $-30°C$) with butadiene to give **II**, which has also not been isolated. In the presence of ligands such as $L' = PPh_3$ or $P(OC_6H_4\text{-}o\text{-}Ph)_3$ or $L'' = P(cyclohexyl)_3$, the intermediates **42** to **44** can be isolated, while in the presence of butadiene, **19** is formed. The structures of these species have been unequivocably established by NMR spectroscopy.[36,48] It is almost certain that **19** as well as **42**–**44** are involved in the catalysis—particularly

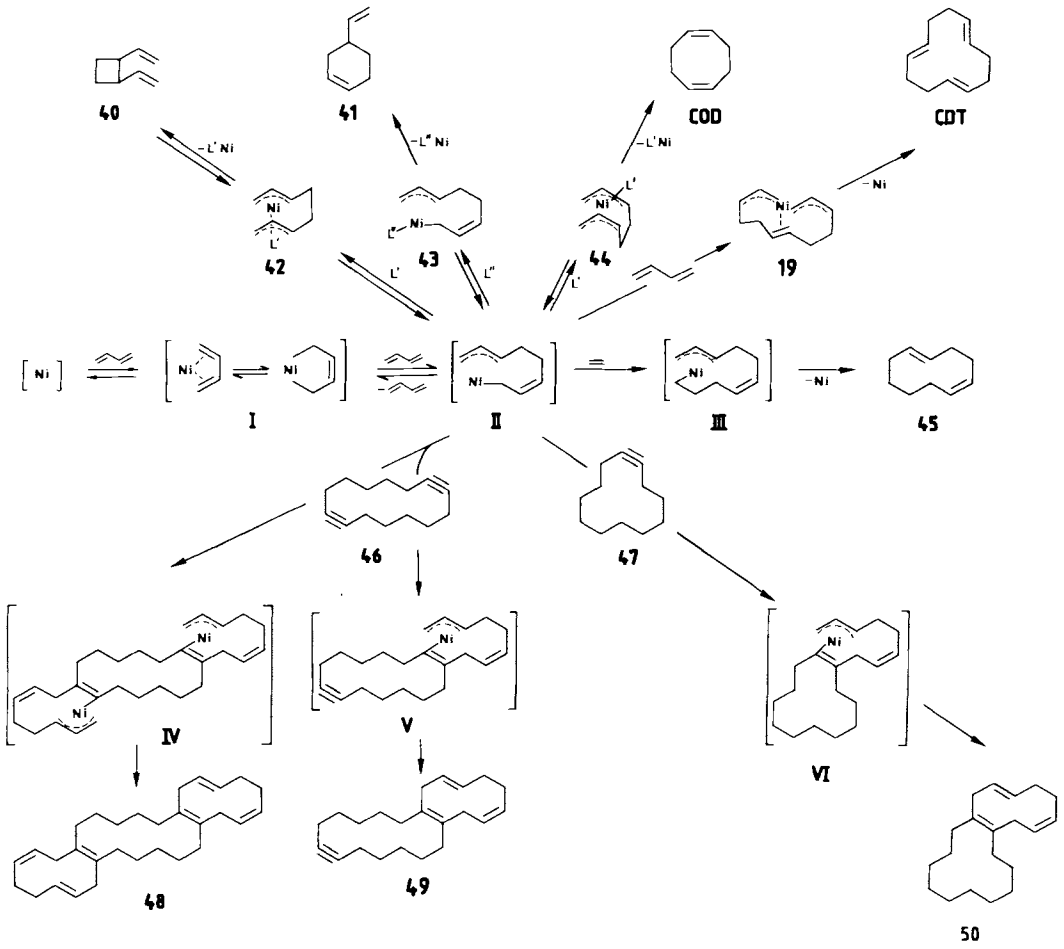

Scheme 15. The nickel-catalyzed cyclooligomerization of butadiene alone or with ethylene or cycloalkynes.

since these compounds take part in stoichiometric reductive elimination reactions to give the cyclic dimers **40**, **41** and COD as well as the cyclic trimer CDT. Related intermediates of the type **III**–**IV** are involved in the catalytic reactions of butadiene with ethylene or alkynes (here the cycloalkynes **46** and **47**) to give the cyclic oligomers **40**, **41**, COD, CDT, **45**, and **48** to **50**.[35b,49] All these products of the catalysis are formed in high yield and in principle the number of catalytic cycles should be unlimited—assuming that it were possible to guarantee the absolute purity of all the reagents involved. We have never met with a substrate specific termination reaction.

It is apparent that the catalytic syntheses leading to **48**–**50**[49c] offer a route to large ring systems. Partial hydrogenation gives bi- or tricyclic systems containing one or two tetrasubstituted double bonds. These can be cleaved by ozone to give di- or tetraketones of the 20-, 22-, and 30-membered rings **51**–**53** (Scheme 16).[49c]

1,5,9-Cyclododecatriene is produced on a large scale in various countries and is the starting material for the preparation of lauryl lactam or dodecanoic acid, which can be converted into polyamides (e.g. Vestamide and Qiana). In addition, a plant for the industrial production of 1,5-cyclooctadiene (COD) is under construction. COD is partially hydrogenated to cyclooctene and this is converted by metathesis into the polymer polyoctenamer—a rubber having interesting technical potential.

Cyclooligomerization with nickel(0) catalysts is by no means limited to dienes. Reactive monoolefins also react and intermediates in the form of nickelacyclopentane derivatives can be isolated. These can have considerable stabil-

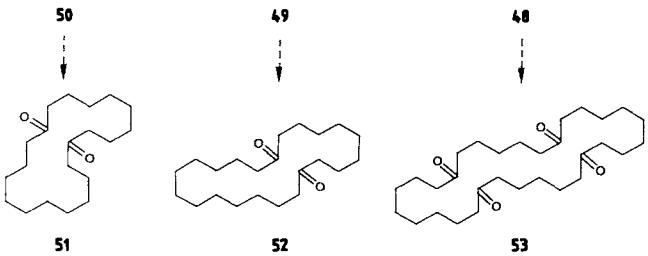

Scheme 16. Macrocyclic ketones **51**–**53** derived from catalytically prepared di- and tricyclic systems.

ity depending upon the nature of the associated ligands. The following example (Scheme 17) illustrates the unusual stability of the Ni–C bond in the presence of suitable ligands: whereas the reaction of nickel acetylacetonate or nickel ethoxide with $AlMe_3$ results in the immediate precipitation of elemental nickel even at $-120\,^{\circ}C$, the unstable $NiMe_2$ can be stabilized by carrying the reaction out in the

presence of, for example, α,α′-bipyridyl, and the thermally stable [(bpy)Ni(CH_3)$_2$] **54** can be isolated and can even be recrystallized from boiling benzene.[50]

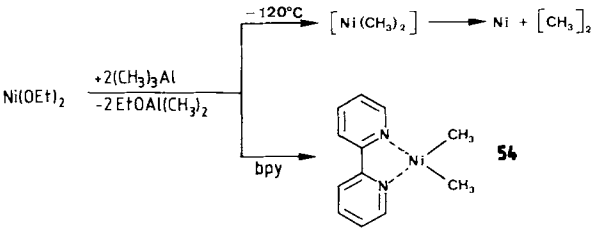

Scheme 17. Example of the ligand-induced stabilization of a Ni-C bond.

In this way it has proved possible to isolate a number of products of oxidative addition reactions involving monoolefins in the form of the nickelacyclopentane derivatives, e.g. **55** and **56**[51] (Scheme 18).

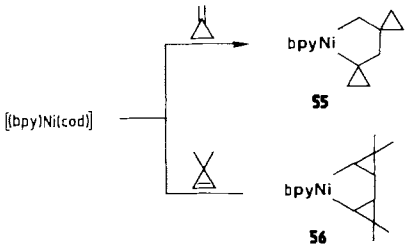

Scheme 18. Formation of the nickelacyclopentanes **55** and **56** from a nickel(0) complex and methylenecyclopropane or 3,3-dimethylcyclopropene.

Nickelacyclopentane species of this type are probably formed during the catalytic cyclodimerization of these monoolefins (Scheme 19).[51]

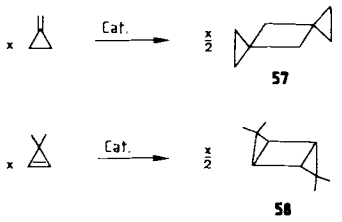

Scheme 19. The catalytic cyclodimerization of methylenecyclopropane and 3,3-dimethylcyclopropene to **57** and **58**. Cat. = catalyst.

As part of another project, an interest existed in the radialenes. These were first prepared by *Iyoda* et al.[52] from dimethylhexatriene and we were able to demonstrate that it is also possible here to isolate a nickelacyclopentane derivative **59** by reaction of the hexatriene with [(bpy)Ni(cod)] (Scheme 20).[53a]

59 takes part in insertion reactions: CO reacts to give the ketone **60** and acetylenedicarboxylic acid ester gives the six-membered ring **61**. Reductive elimination to the [4]-radialene **62** can be induced in the presence of electron withdrawing species such as maleic anhydride (MA).[53a] The stoichiometric reaction can be converted into a catalytic cyclooligomerization in the presence of [(cod)$_2$Ni] (Scheme

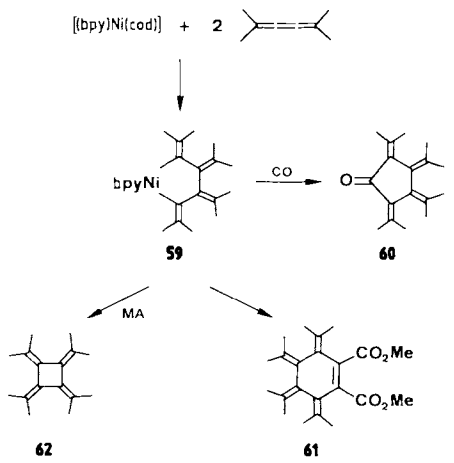

Scheme 20. The formation of the nickelacyclopentane **59** by the oxidative addition of 2,5-dimethyl-2,3,4-hexatriene (MA = maleic anhydride).

21) and, depending upon the conditions, it is possible to obtain either the cyclodimer[53a] or the cyclotrimer.[53b]

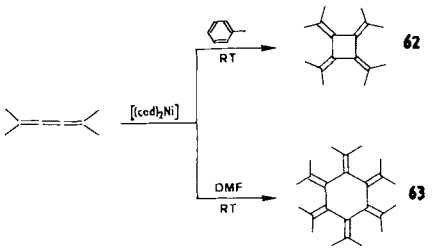

Scheme 21. The catalytic cyclodimerization and cyclotrimerization of 2,5-dimethyl-2,3,4-hexatriene to **62** and **63**, respectively.

The catalytically prepared radialenes **62** and **63** have been investigated by X-ray methods (see Fig. 8). The four-membered ring in **62** is found to be folded, while the six-membered ring in **63** adopts a chair conformation.[54]

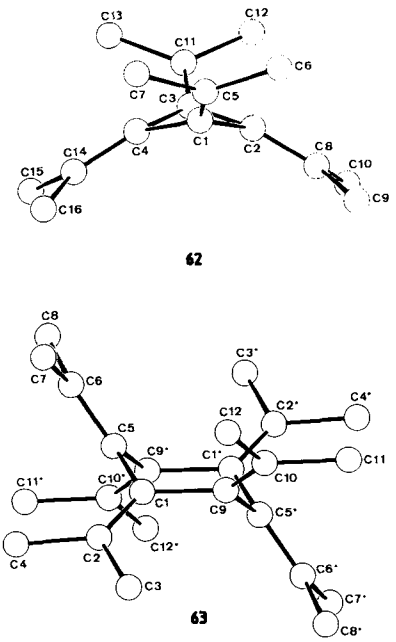

Fig. 8. The structures of the [4]- and [6]-radialenes **62** and **63**.

62 and **63** behave quite differently towards dienophiles (Scheme 22) and whereas **63** does not react with either tetracyanoethylene or *N*-phenyltriazoledione, **62** reacts immediately to give a 1:1 adduct. Steric hindrance apparently prevents the isopropylidene group in **63** from adopting an arrangement suitable for a Diels-Alder reaction. It should also be mentioned that **62** can react in a 1:2 manner with *N*-phenyltriazoledione—the product is not, however, a cyclobutadiene derivative. Whereas the 1:1 addition takes place in a Diels-Alder manner to give **64**, the second molecule of the dienophile reacts in an unusual manner to give **65**,[53b] which has been shown by X-ray analysis to have a betaine-like structure.[54]

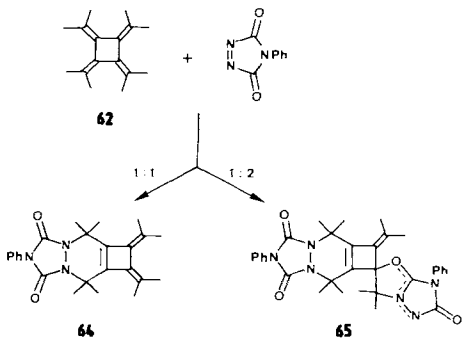

Scheme 22. Formation of a Diels-Alder adduct (**64**) and a betaine-like product (**65**) from **62**.

As far as we are aware, this is the first report of an addition of this type and it enables **64** to avoid adopting a cyclobutadiene-like structure.

4.2. The Interaction between Nickel(0) and Main Group Metal-Alkyls and -Hydrides

In 1973 we summarized for the first time the chemistry associated with the "nickel effect" (see above) and developed a model **66** based upon the assumption that in this catalytic system a key role is played by a complex involving nickel(0), the appropriate olefin and the trialkylaluminum derivative (Scheme 23).[15]

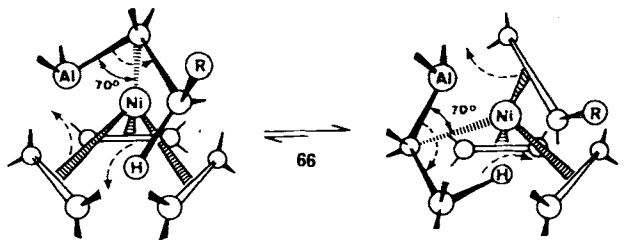

Scheme 23. A model of an intermediate in the "nickel effect".

According to this model, ethylene complexes to nickel(0) in a manner similar to that found in $[(C_2H_4)_3Ni]$ **1**. The R_3Al occupies a further coordination site and forms a three-centered bond through the α-C atom. The transalkylation of the type observed in the "nickel effect" can then occur in an electrocyclic manner.

This proposal acted as a stimulus for efforts to discover systems in which nickel(0) interacts with alkyl derivatives of main group metals. Before discussing the results, it is appropriate to mention an example of this catalytic transalkylation reaction to indicate its usefulness.[55]

$(C_8H_{17})_3Al$, which is used in the synthesis of certain tin compounds, is prepared on a technical scale by heating $(i\text{-}C_4H_9)_3Al$ with 1-octene at ca. 140°C, whereby isobutene is eliminated. However, during this purely thermal transalkylation, small amounts of undesirable higher alkyls are formed as a result of the addition of the Al-C bond to 1-octene.

The catalytic reaction, on the other hand, is carried out as shown in Scheme 24;[55] $[(cod)_2Ni]$ **14**, $(i\text{-}C_4H_9)_3Al$ and 1-octene are mixed in the ratio 5:1000:6000 and kept at −10°C. After 5 hours a quantitative reaction has occurred to give $(n\text{-}C_8H_{17})_3Al$. The catalyst can then be removed in the form of $Ni(CO)_4$ by using gaseous CO. Other α-olefins can be converted in an analogous manner.

$$(i\text{-}C_4H_9)_3Al + 3\,CH_2{=}CH{-}C_6H_{13} \xrightarrow{[(cod)_2Ni]} (n\text{-}C_8H_{17})_3Al + 3\,CH_2{=}C(CH_3)_2$$

Scheme 24. The synthesis of tri-*n*-octylaluminum by nickel-catalyzed transalkylation of triisobutylaluminum.

It is of significance that we have never been able to detect an interaction between, for example, **1** and Et_3Al. If a mixture of **1** and Et_3Al is treated with C_2D_4 below −50°C, then an exchange with the C_2H_4 molecules occurs without the ethyl groups of the Et_3Al being involved, while above −50°C the "nickel effect" causes statistical scrambling of the D atoms of the C_2D_4 over all the ethyl groups and ethylene molecules. The catalytic reaction takes place, however, without it being possible to detect any complex formation[55] by NMR spectroscopy. This is not, however, adequate proof against complex formation, since, particularly in catalysis, minimal concentrations of such intermediates (or complexes) are frequently sufficient to ensure a rapid reaction.

The chemistry of the organoaluminum compounds suggests that hydrides in particular have a marked tendency to form multicentered bonds. For example, the dialkylaluminum hydrides form Al-H-Al bridges which are so stable that they are only partially cleaved by ether (see Scheme 25). It is therefore remarkable that [(cdt)Ni] **7** reacts with diethylaluminum hydride in pentane at −78°C with cleavage of the Al-H-Al bridges to give the 1:1 adduct **67**, which contains a Ni-μ-H-Al bridge.[56] In ether, a 1:1:1 adduct **68** is formed in which the fourth coordination position at the aluminum is occupied by ether.[56] Both **67** and **68** are crystalline solids but are only stable below −60°C. A 1:1 adduct is also formed between **7** and the complex derived from $(CH_3)_2AlH$ and quinuclidine.[57] **69** is also crystalline and in this case the solid is stable up to 20°C. An analogous complex **70**[58] is formed with $LiAlH_4$.

70 is an example in which the Ni atom in **7** interacts with a complex anion through a hydride bridge. Of even greater relevance to the "nickel effect" are complexes such

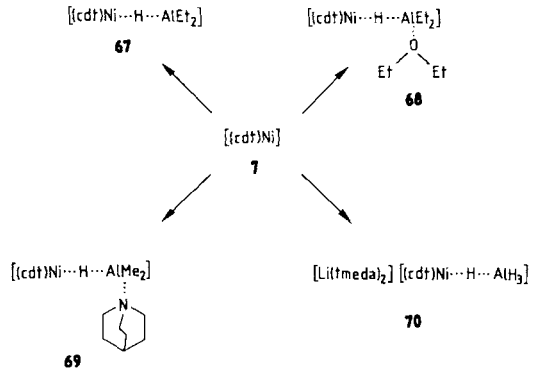

Scheme 25. CDT-Ni complexes **67**–**70** with Ni-μ-H-Al bridges.

as **71** to **73**, which can be prepared from **1** and in which both a C_2H_4 molecule and a hydride are bonded to nickel(0) (Scheme 26).[57]

$$[(C_2H_4)_3Ni] \longrightarrow [Na(tmeda)_2][(C_2H_4)_2Ni\cdots H\cdots AlEt_2]$$
1 **71**

$$[(C_2H_4)_3Ni] \longrightarrow [Na(thf)_6][(C_2H_4)_2Ni\cdots H\cdots AlEt_3]$$
1 **72**

$$[(C_2H_4)_3Ni] \longrightarrow [Na(thf)_6][(C_2H_4)_2Ni\cdots H\cdots Al(i\text{Bu})_3]$$
1 **73**

Scheme 26. Ethylene complexes **71**–**73** with Ni-μ-H-Al bridges.

In these cases the Ni atom is the anion center, while the cation is coordinated with THF or tetramethylethylenediamine (TMEDA). In **66** it is assumed that both olefinic ligands as well as the α-C atom of trialkylaluminum derivative are bonded to nickel(0). If **7** is allowed to react instead with alkyllithium compounds, then (depending upon the nature of the chelating ligand bonded to the lithium) complexes are formed which contain either a Ni-μ-C-Li bridge (**74**) or an alkyl anion (**75**) (Scheme 27).[59]

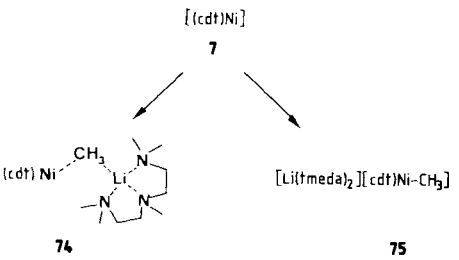

Scheme 27. The CDT-complex **74** with a Ni-μ-C-Li bridge and the ate-complex **75** derived from (CDT)Ni **7**.

The structures of the related complexes **76**–**78** derived from **1** (Scheme 28) have been determined by X-ray diffraction (Fig. 9): **76**[59] and **78**[60a] are characterized by the presence of a Ni-μ-C-Li bridge, while **77**[61] is an ion pair. **76** can be readily converted into **77**.

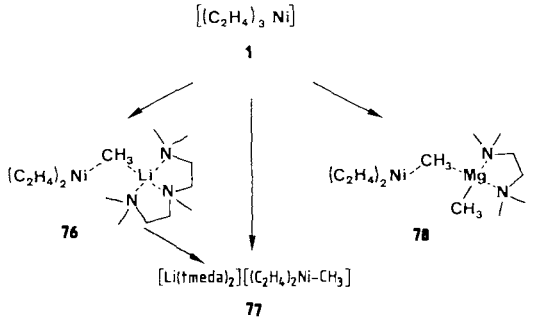

Scheme 28. The ethylene-nickel complexes **76** and **78** with Ni-μ-C-Li bridges and the related ate-complex **77**.

Recent results show that dialkylmagnesium compounds can be coordinated to nickel(0), but in these cases the products frequently react further—the driving force apparently being the formation of a Mg-Ni-hydride.[60b]

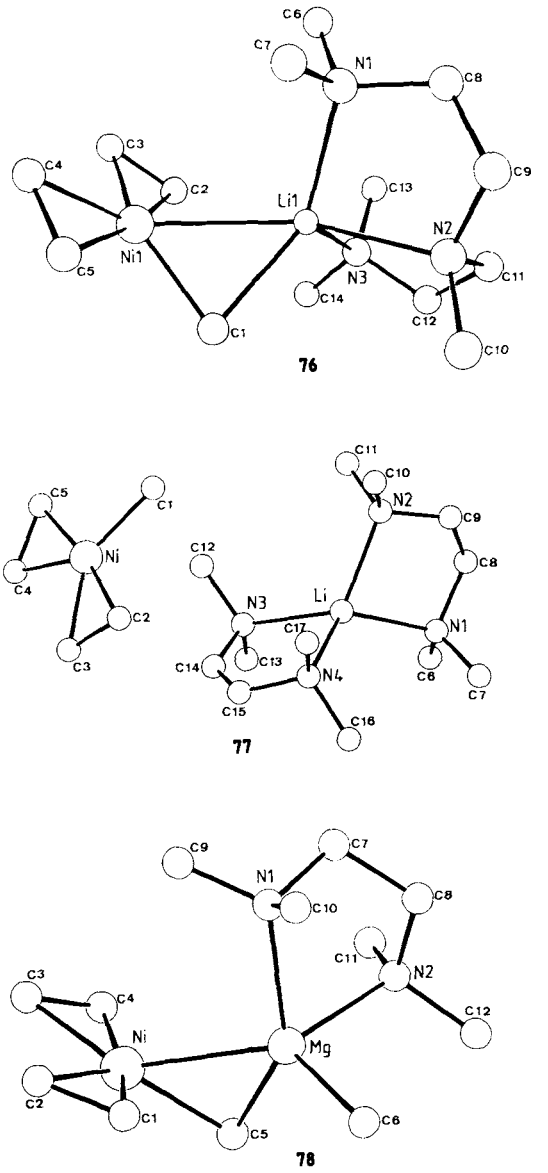

Fig. 9. The structures of the $[(C_2H_4)_2Ni]$ complexes **76** and **77** with MeLi and **78** with Me_2Mg.

These results suggest that the interaction of alkyl derivatives and hydrides of main group metals with nickel(0) is possible as long as the M-C or M-H bonds are sufficiently polar. The polarity of the Al-C bond appears to be so low that at most only low equilibrium concentrations of an adduct are formed.

Finally, the catalytic "nickel effect" can be elegantly demonstrated with the following example (Scheme 29).[62] $[(C_2H_4)_3Ni]$ **1** reacts in the presence of pentamethyldiethylenetriamine (PMDTA) with butyllithium in ether at $-30°C$ to give **79**, in which a Ni-μ-C-Li arrangement is present. **79** reacts with ethylene to give an unstable intermediate **80**, which rearranges to **81** by transalkylation of the butyllithium to give ethyllithium and 1-butene. Displacement of the PMDTA in **81** by tetramethylethylenediamine (TMEDA) furnishes the ion-pair **82**, whose structure is analogous to that of **77**.

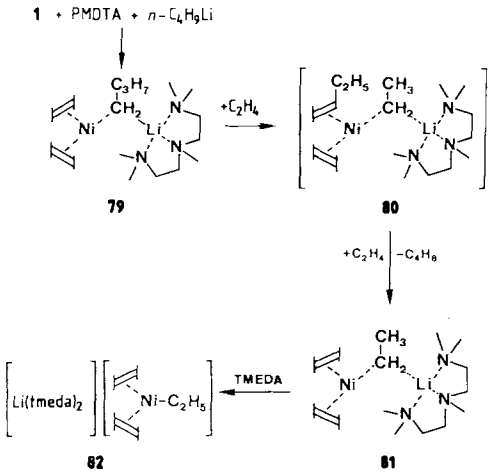

Scheme 29. The transalkylation of butyllithium during the "nickel-effect" (see text).

It is clear that these results do not prove the suggested mechanism for the "nickel effect", but the behavior of these model complexes is good evidence. The use of models of this type to describe catalytic processes as well as the isolation of intermediates could lead to incorrect conclusions, but, nevertheless, they are of assistance in understanding a complex catalytic cycle.

4.3. Asymmetric Catalysis and the Dimerization and Codimerization of Olefins

We described a series of catalysts based upon the η^3-allylnickel halides[30] in an article published in this Journal in 1966. This was followed in 1968 by a review of the use of ligand-modified η^3-allylnickel halide catalysts to control the course of catalytic reactions[63] and was subsequently extended to asymmetric syntheses.[64] The catalysts are prepared in a homogeneous phase by activating the 1:1 adducts of the η^3-allylnickel halide and trialkyl- or triarylphosphanes with Lewis acids such as $EtAlCl_2$. The structure of one such complex has been determined by X-ray methods (Fig. 10).[64c]

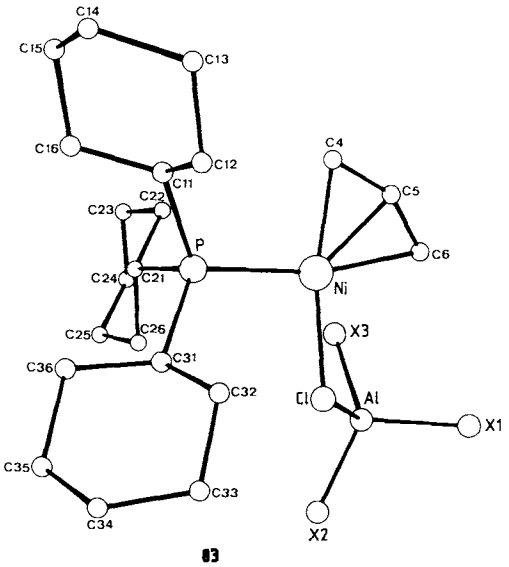

Fig. 10. The structure of a catalyst complex **83**. X1, X2, X3 = Cl or Me.

In polar solvents (CH_2Cl_2 or chlorobenzene) these catalysts dimerize olefins such as propene even at $-70°C$, whereby the structure of the dimers is dependent upon the nature of the phosphane present.[63] Although it was realized at an early date that the catalysts have a quite remarkable activity, it is only recently that we have become aware of how active they are, and experiments carried out in liquid propene and chlorobenzene suggest that they are the most active homogeneous catalysts known.[65]

It is relevant to briefly indicate the mechanism of the formation of one of the dimers of propene (Scheme 30) before discussing the latest results.

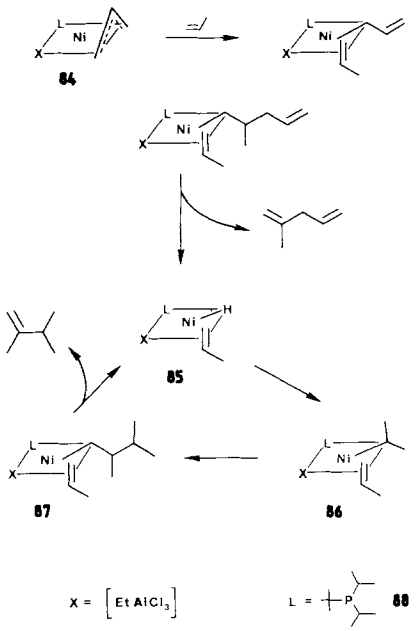

Scheme 30. The catalytic cycle for the dimerization of propene.

The η^3-allyl group in **84** has been shown to react in an initial step with propene to give the catalytically active

species—the nickel hydride **85**—with displacement of a diene. **85** then adds to propene to give the alkylnickel compound **86**, which reacts further by addition of the Ni-C bond to propene to give **87**, from which β-hydrogen transfer leads to displacement of the product (in this case 2,3-dimethyl-1-butene) with regeneration of the hydride **85**.[63]

2,3-Dimethyl-1-butene is formed preferentially in the presence of sterically demanding phosphanes such as *tert*-butyldiisopropylphosphane **88**. The initial addition of the Ni–H bond to propene takes place in a Ni→C2 manner to give an isopropylnickel species, while in the second step the Ni-C bond adds to propene in a Ni→C1 sense, and the subsequent β-H-elimination produces the branched chain dimer with regeneration of the nickel hydride **85**. Sterically less demanding phosphanes favor the formation of hexene and the methylpentenes, and 2,3-dimethyl-1-butene is only a side product.

The latest investigations[66] on the activity of the catalyst were carried out as follows: a solution of liquid propene (300 g), chlorobenzene (90 g) and $EtAlCl_2$ (0.6 g) was cooled to −45 °C and treated with 0.017 g of the complex $[(\eta^3-C_3H_5)NiX(PR_3)]$ **89**, X = Br, $PR_3 = P(iPr)_2tBu$ ($C_3 : Al : Ni \approx 7 \times 10^6 : 5 \times 10^3 : 0.5 \times 10^1$). The catalytic dimerization starts immediately and effective cooling is necessary to maintain the temperature at −45 °C. The catalysis can be stopped at will by adding NH_3. The relevant conversion data are given in Table 1.

Table 1. Catalyic dimerization of propene; for conditions see text. The conversion is calculated for 1 mol of catalyst.

Reaction time	C_3H_6 molecules per Ni atom	Conversion C_3H_6 molecules per Ni atom per s	C_6(metric tons) per mol catalyst
150 s	175000	1170	7.4
2 h	1250000	173	52.2

The activity is highest at the start of the reaction and decreases with increasing conversion: the main problem under these extreme conditions rests in the exclusion of impurities. As mentioned above, the product distribution can be controlled by varying the ligand[63] and we were therefore interested in the relationship between catalyst activity and the nature of the ligand.[66] The ligand was characterized by the ^{31}P-NMR chemical shift of the corresponding complex **89**. The catalytic reaction was stopped after 30 minutes and the catalytic activity (C_3H_6/Ni/s) was calculated from the conversion. It is remarkable, that a practically linear correlation exists between the catalyst activity and the ^{31}P-NMR chemical shift (δ) of the complexed ligand involved.[66]

As can be seen in Figure 11, trimethylphosphane and tri-*tert*-butylphosphane behave anomalously, but for different reasons. In both cases the activity is that of a phosphane-free catalyst. The PMe_3-modified catalyst **89**, X = BrAl$EtCl_2$, disproportionates to give **91**, which is inactive, and the phosphane-free species **90**, which is of only low activity (Scheme 31). The situation is somewhat different in the case of tri-*tert*-butylphosphane: the bulkiness of the ligand

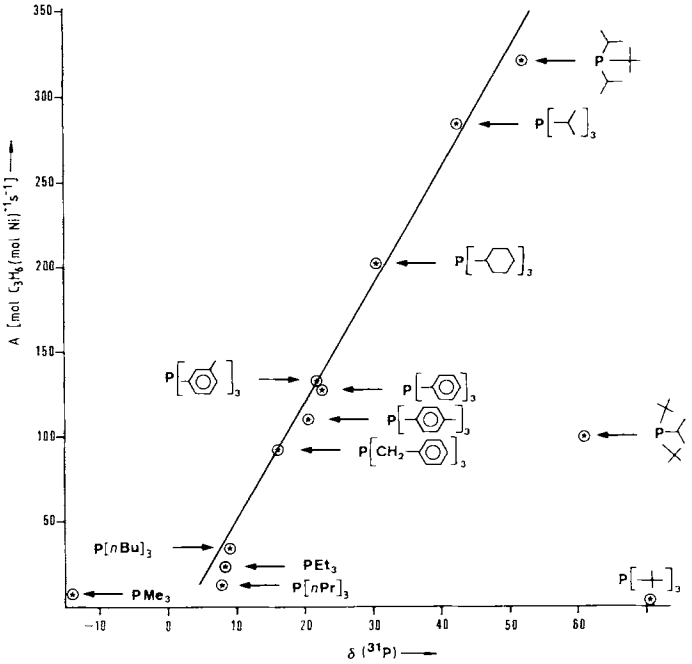

Fig. 11. The dependence of catalyst activity A on the phosphane ligand and the correlation of the activity with the $\delta(^{31}P)$-NMR values of the complexes **89**, X = BrAl$EtCl_2$, at −45 °C.

labilizes the 1 : 1 (Ni : P) adduct in solution above −78 °C, and at the reaction temperature (−45 °C) it dissociates so that the phosphane has no influence upon either the activity or the course of the reaction. The most active catalyst involves diisopropyl-*tert*-butylphosphane and is, moreover, the most selective for 2,3-dimethyl-1-butene formation. Di-*tert*-butylisopropylphosphane **92** is an exception—the corresponding complex is not noticeably dissociated but, nevertheless, the catalyst has a reduced activity. This appears to be the result of a high steric shielding which manifests itself in the formation of 2-methyl-1-pentene as the main product, i.e. the catalytic cycle proceeds through two Ni→C1 additions. In the first step, steric effects cause addition to occur in a Ni→C1-sense (in contrast to that shown in Scheme 30) to give an *n*-propylnickel species. The values in Figure 11 are based upon duplicate experiments and are reproducible.[66]

The physical basis for the essentially linear correlation between the activity and $\delta(^{31}P)$ values is not clear, but Figure 11 does show that the activity of the catalyst increases with increasing bulkiness of the modifying ligand up to a certain point beyond which a sharp decline is observed. Steric interaction within the catalyst influences both the regioselectivity and the reactivity.

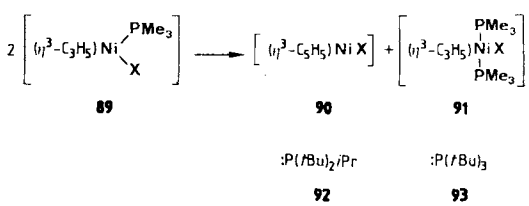

Scheme 31. Disproportionation of the catalyst **89**.

It is remarkable that the most active catalyst has the highest selectivity for the formation of one of the products (in this case 2,3-dimethyl-1-butene). That activity and selectivity run parallel has also been observed in the cyclodimerization of butadiene to 1,5-cyclooctadiene[49] and a further example will be discussed later. It seems to be a general principle of catalysis that activity and selectivity are coupled.

We have already drawn attention in Figure 11 to the sudden jump in the regioselectivity on going from diisopropyl-*tert*-butylphosphane **88** to di-*tert*-butylisopropylphosphane **92**. This jump is the result of steric changes in the ligand caused by the substitution of a single H atom by a CH_3 group. A particularly impressive example of this effect is found in the catalytic conversion of ethylene: a diisopropyl-*tert*-butylphosphane-modified catalyst is highly active for the dimerization of ethylene to 1-butene. If excess tri-*tert*-butylphosphane **93** is used instead, then the product is a high molecular weight, linear polyethylene (Scheme 32).[67]

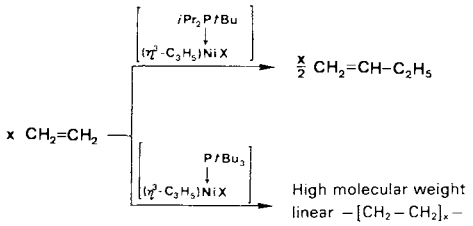

Scheme 32. The dimerization and polymerization of ethylene using a catalyst modified with **88** or **93**.

Here again, the difference in behavior is associated with the apparently small change in the steric situation associated with the substitution of a H atom by a CH_3 group. The β-H-elimination step which would lead to dimerization is apparently suppressed and instead polymerization occurs. This suggests that the more sterically demanding ligand prevents access to the required coordination position at the nickel atom. Although this explanation seems plausible, it remains speculation.

It has not proved possible to isolate the intermediate hydride **85** shown in Scheme 30—presumably it is only present in minimal concentrations in the presence of excess propene. Recent work has led to a model for the addition of a Ni-H (either as a preformed complex or as an intermediate) to an olefin[66] (cf. Scheme 33). The olefins used were di(3-butenyl)methylphosphane **94** and 3-butenyldiphenylphosphane. **94** reacts with nickel(0) (in **7**) to give a complex in which both the P atom and the C=C double bonds are complexed to the nickel atom. Protonic acids such as acetylacetone undergo an oxidative addition with this complex to give a hydride species **95**, which reacts immediately with the complexed olefin. The result is a Ni→C2 addition to give **96**. The complex **96** has been fully characterized and can be regarded as a model for an intermediate in the catalytic cycle—the alkylnickel group in **96** being equivalent to **86** in Scheme 30.

In the presence of 3-butenyldiphenylphosphane **97**, the compound **98** as well as the stable hydride **100** could be converted into the intermediate hydride species **99**, which reacts further to give **101** (Scheme 34).

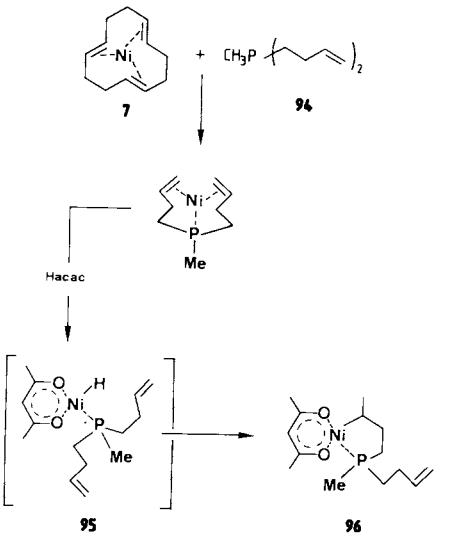

Scheme 33. Di-(3-butenyl)methylphosphane **94** as a hydride trapping reagent.

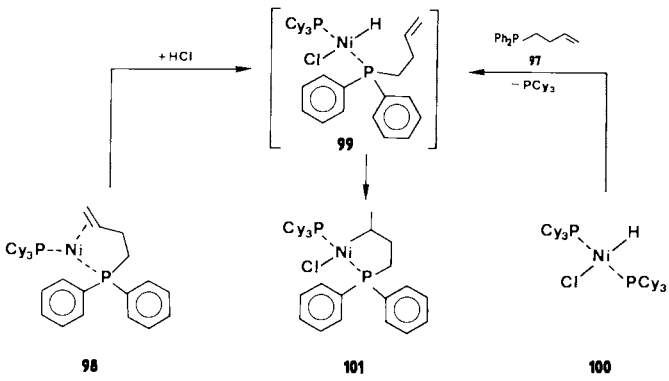

Scheme 34. Trapping of a preformed (**100**) or intermediate hydride **99** with 3-butenyldiphenylphosphane **97**. Cy = cyclohexyl.

Phosphanes of the type **94** and **97** are ideal hydride-trapping reagents.[66] The NMR spectrum of the complex **96** indicates that diastereomers are present.

The use of **94** or **97** to trap a nickel-hydride species can, in principle, be applied to the catalytic reaction but the P-bonded butenyl groups react further with, for example, propene. In other words, the resulting Ni-C bond becomes itself involved in the catalytic cycle. Investigations on this problem are continuing.[66]

Catalysts containing a complex anion of the type $[EtAlCl_3]^{\ominus}$ (see Scheme 30) cannot be used in reactions involving olefins substituted by functional groups such as $-CO_2R$ or $-OR$, since these groups coordinate to the anion and bring about cleavage and deactivation of the catalyst. This can be avoided by using complex anions which resist cleavage. The $BF_4^{\ominus}$ ion has proven particularly effective. The catalyst can be prepared by reacting, for example $[(cod)_2Ni]$ **14**, $[(\eta^3\text{-}(C_3H_5)_2Ni]$ **20** or $[(C_{12}H_{18})Ni]$ **19** with HBF_4 or $[(\eta^3\text{-}C_3H_5)NiBr]_2$ **13** with $AgBF_4$, and here again phosphanes influence the direction of reaction.[68]

The dimerization of methyl acrylate using a variety of catalysts has attracted considerable attention.[69] In all cases relatively high temperatures (80–200 °C) are needed and the turnover numbers achieved are modest.

We have shown[68] that methyl acrylate can be smoothly dimerized at 0 °C using a nickel catalyst containing the $BF_4^{\ominus}$ ion and turnover numbers of 600 are easily achieved. One unusual facet is that, in contrast to the dimerization of propene, effective modification of the catalyst is achieved only in the presence of PMe_3. In this case also disproportionation leads to deactivation of the catalyst (see Scheme 31). The catalytic cycle is similar to that proposed for the dimerization of propene: cycle A is activated ten times more frequently than cycle B (Scheme 35) and as a result the dimers **102** and **103** are formed in a 10 : 1 ratio.

upon optically-pure natural products. As early as 1967 we obtained an optical induction during the codimerization of 2-butene with propene using (−)-tris(*trans*-myrtanyl)phosphane: among others (−)-*trans*-4-methyl-2-hexene was formed with an *ee* of ca. 3%.[64b]

In later work, we used the codimerization of norbornene with ethylene to give 2-*exo*-vinylnorbornane **104** (Scheme 36) as a test for the effectiveness of a particular catalyst in inducing optical activity.[64b]

The codimerization with introduction of a vinyl group is now referred to in the literature as hydrovinylation.[70]

A maximum induction was obtained in the presence of isopropyldimenthylphosphane at −70 °C and an *ee* value of 65% was obtained, i.e. 82.5% of (+)-(1*S*,2*R*,4*R*)-2-vinylnorbornane **104a** is formed. Both the selectivity and the

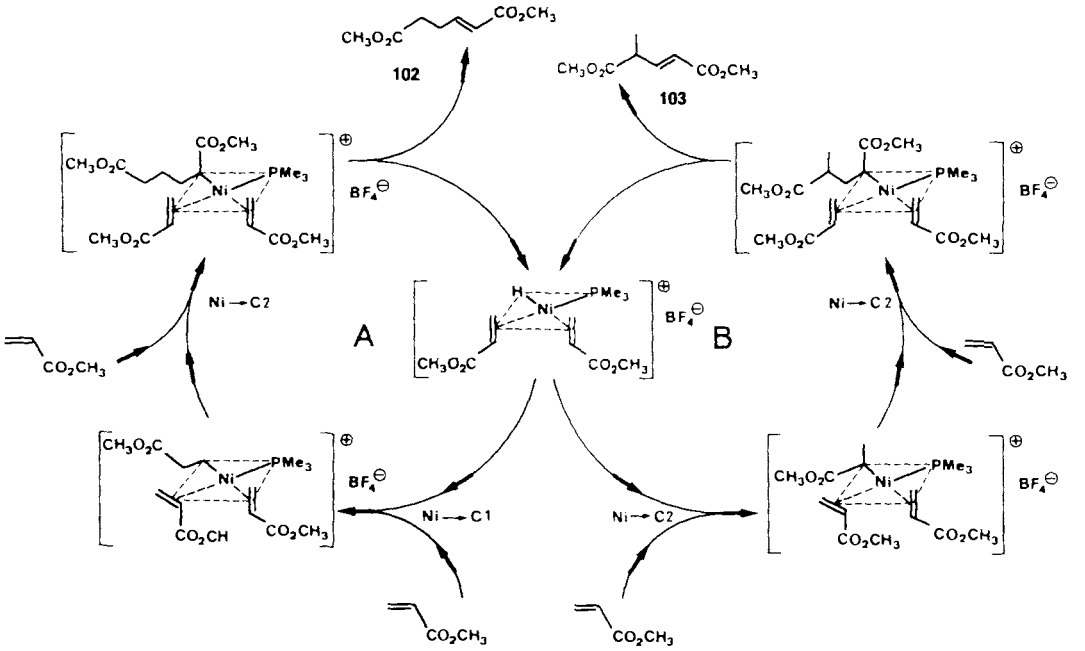

Scheme 35. The catalytic cycle for the dimerization of acrylic ester. **A**, **B** see text.

In contrast to the sequence shown in Scheme 30, the main cycle A involves an initial Ni→C1 addition which is followed by a Ni→C2 addition, whereas in cycle B both steps involve Ni→C2 additions. The absence of a ^{19}F-coupling to the ^{31}P-signal of the complexed PMe_3 in the NMR spectrum indicates that the $BF_4^{\ominus}$ ion is not coordinated to the Ni atom—coupling of this type is observed in non-dissociated model compounds.

Our activities in the field of catalyzed asymmetric synthesis stem from the idea of depositing a typical Ziegler catalyst onto finely ground optically-active quartz and to use the system to dimerize isoprene to optically-active limonene. However, before we could get round to trying this out we started to investigate homogeneous catalysts, since it had been shown that the direction of the dimerization of propene could be controlled by various modifying ligands. Optically-pure Horner-phosphanes are not easy to prepare and so we synthesized a series of phosphanes having optically-active substituents such as menthyl or myrtanyl based

activity of this catalyst were unsatisfactory, so the search for more effective ligands was continued.

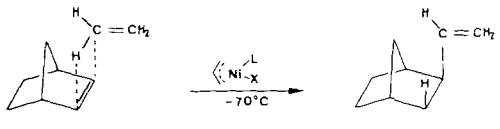

104a

Scheme 36. The hydrovinylation of norbornene with ethylene to give chiral *exo*-2-vinylnorboraane **104a**.

I have already indicated several times in this article the role which an accidental discovery can play and in the case of the further development of the catalyst, chance helped us further. Our attempts to prepare a highly rigid ligand by combining a pinene derivative, an optically active amine and a phosphorus component led to a mixtura mirabilis (^{31}P-NMR) composed of various phosphorus compounds.[71] In spite of our disappointment, a catalytic experiment was carried out with the mixture and at −70 °C

we obtained **104** with an *ee* of ca. 50% and almost 100% selectivity in a reaction whose activity was the highest we had observed.[71]

Our objective was to prepare the ligand **108** according to Scheme 37. (−)-(*R*)-myrtenal (−)-**105** was treated with (+)-(*R*)-1-phenylethylamine to give the azomethine **106**,

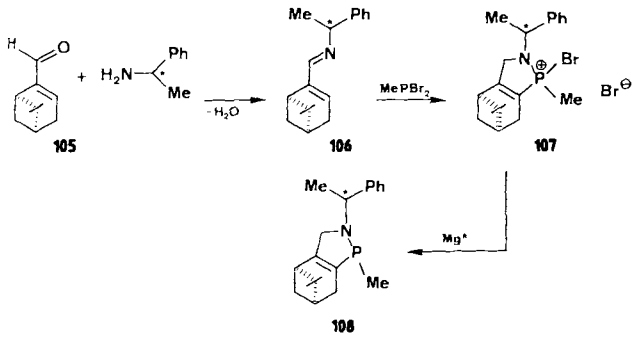

Scheme 37. The synthesis of the ligand **108**.

which underwent a McCormack reaction to give the salt **107**. Dehalogenation of **107** using activated magnesium (prepared by the thermal decomposition of MgH_2) led to the mixture of phosphorus compounds from which we finally isolated the component **109** responsible for the catalytic reaction.[72] **109** was isolated in crystalline form and the X-ray structural analysis (Fig. 12) showed it to be a dimeric form of **108**. The absolute configuration of all twelve chiral centers has been determined.[73]

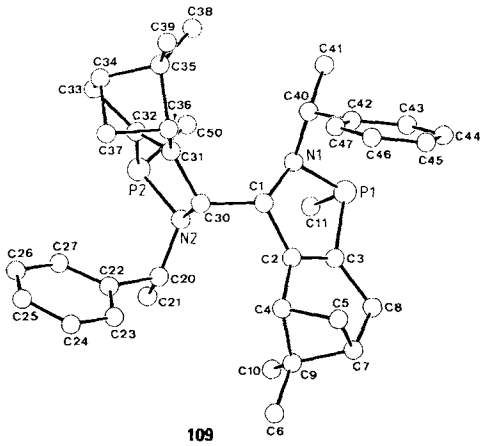

Fig. 12. The structure of the ligand **109** having an *R*-configuration at C20 and C40.

The catalyst modified with **109** produced (−)-**104** in almost quantitative yield with an *ee* of 53% and at a rate of 20000 cycles per Ni atom and hour at −65°C, i.e. the induction is modest but the activity and selectivity are excellent:[72] It should be emphasized that this catalyst does not react with norbornene alone and only very slowly with ethylene. The fast catalytic reaction occurs only when both olefins are present. This behavior is reminiscent of biocatalysts.

The enantiomeric form of **109** was prepared similarly by reaction of (+)-(*S*)-myrtenal (+)-**105** and (−)-(*S*)-1-phenylethylamine and as expected the use of this ligand led to the formation of (+)-**104**.[72]

The next step was the synthesis of the dimer **110** from (−)-(*R*)-myrtenal (−)-**105** and (−)-(*S*)-1-phenylethylamine.[72] **110** also formed crystals suitable for an X-ray structure analysis (Fig. 13).[73]

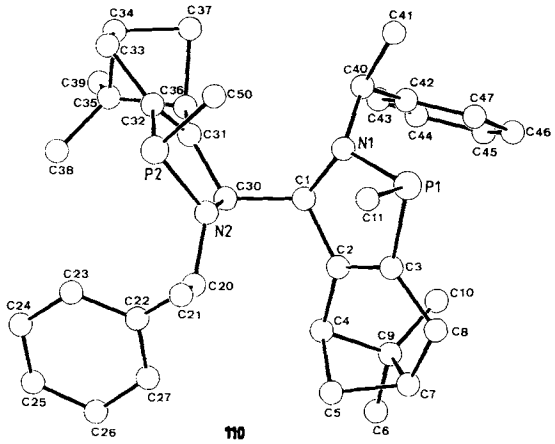

Fig. 13. The structure of ligand **110** having an *S*-configuration at C20 and C40.

The structural differences between **109** and **110** will be discussed later. The results of the catalysis with **110** were a surprise; the activity was only one hundredth of that involving **109**, and (+)-**104** was formed with an *ee* of 40%. What appeared at first glance to be only a slight change in the space-filling properties of the ligand had led to dramatic changes in the catalytic behavior.

This result induced us to try a further variation: the effect of changing the substitution at the amine, which had been unexpectedly high on going from the *R*- to the *S*-configuration, should be completely different in the presence of an isopropyl group. The resulting dimer **111** was also analyzed by X-ray diffraction (Fig. 14)[73] and used in the catalysis. At −60°C we observed ca. 1800 cycles per Ni atom and hour, but the *ee* value dropped to 26% while the yield of **104** decreased to ca. 30% and was accompanied by the formation of (*E*)- and (*Z*)-ethylidenenorbor-

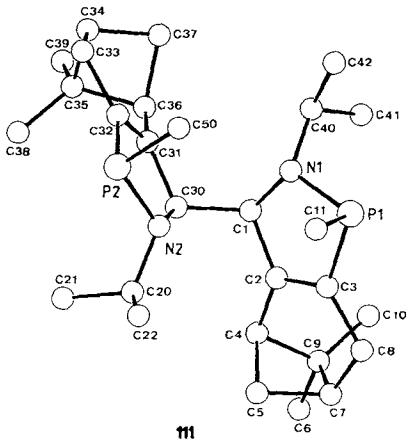

Fig. 14. Structure of the ligand **111** having isopropyl groups at N1 and N2.

nane and a vinylated dimer of norbornene. In other words, the selectivity decreases markedly, while the activity of the catalyst lies between that of systems modified with **109** or **110**.

How can we explain these experimental results? Firstly, it is necessary to compare the crystal structures. Both **109** and **110** consist of two equal parts and therefore the discussion can center initially on one of them. The two structures are similar in that the hetero five-membered rings in **109** and **110** lie in the same plane as C4, C7, and C8, while the substituents at the P and Ni atoms are arranged *trans* to each other. The CH_3 group on the P atom and the second half of the molecule, i.e. the bond C1-C30, adopt a *cis*-arrangement. A basic difference is observed in the arrangement of the substituents at the N atom relative to the $(CH_3)_2C$-bridge of the pinene group: in **109** this group occupies a position *trans* to the plane defined above, while in **110** it adopts a *cis*-position. These steric differences are the result of a difference in the induction from the *R*- and *S*-amine during the syntheses (see Fig. 15).

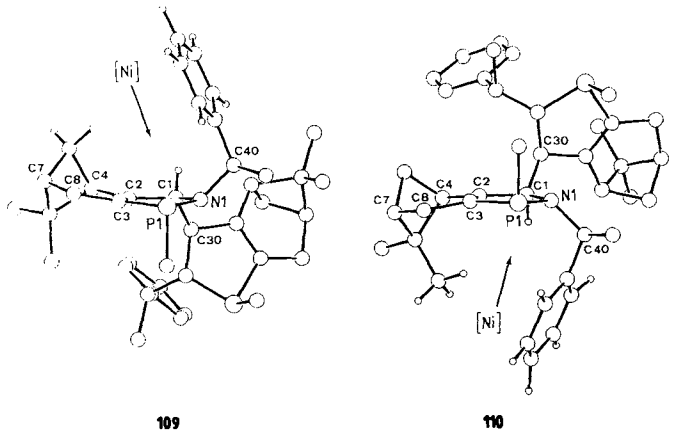

Fig. 15. The structures of the ligands **109** and **110** comparing the arrangement of the substituents in the plane defined by the five-membered heterocyclic ring and C4, C7, C8.

The interamolecular rotations have been studied using a computer simulation based on the X-ray data[74] and from this it can be seen that rotations about C1-C30 and N1-C40 are limited to ca. 50° and ca. 40°, respectively. Further rotation of the two halves of the molecule is hindered by steric effects (as is the case in atropisomers), i.e. several pairs of H atoms approach each other by less than 2 Å. The result is that **109** and **110** are relatively rigid systems.

In the catalysts the lone pairs at the P atoms form a bond to the Ni atom. The picture of the structures of **109** and **110** with incorporation of the van der Waals radii suggest that **109** can form a tunnel which can take up the Ni atom, whereas in **110** the P atom appears to be more protected—perhaps as a result of the *cis* arrangement of the $(CH_3)_2C$-bridge with respect to the substituents on the N atom.

The reduced activity of the catalyst involving **110** is then seen to be a result of the shielding of the active center. The situation resembles that discussed previously for the dimerization of propene in the presence of a catalyst modified by di-*tert*-butylisopropylphosphane **92**.

The computer simulation[74] also shows that in the nickel complex involving the ligand **109**, the 40° rotation about the N1-C40 bond causes the phenyl groups to act as a "windshield wiper" across the catalytically active center, thereby causing the H atom bonded to C43 to enter the sphere of the Ni atom, i.e. the rotation about the C40-C42 bond is also restricted (Fig. 16; for numbering see Fig. 12).

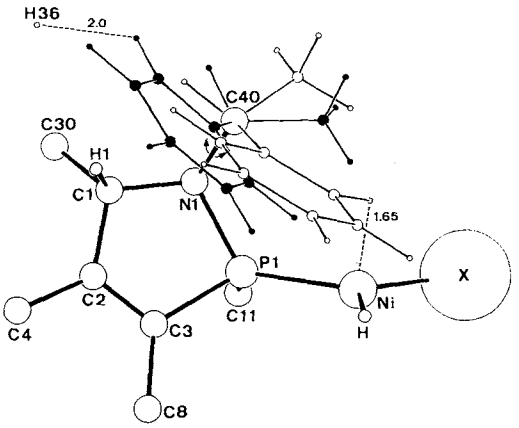

Fig. 16. A schematic representation of the rotation of the N1-C40 bond (ca. 40°). The arrangement of the substituents at N1 upon contact of the phenyl group with H36 of the second half of the molecule (phenyl group depicted by black spheres) or with the Ni atom (phenyl group depicted by white spheres).

Intramolecular, directed collisions of the "windshield wiper" type between the phenyl groups and groups bonded to nickel, in as far as they are not immediately turned into translational energy, might well be expected to lead to a weakening of those bonds which are to be broken in the catalytic cycle and in this way the catalysis would be accelerated. The simulation supported suggestions are only of a preliminary nature and will need further study. We have already mentioned that a certain similarity exists between the phenomenon observed using these catalysts and those typical for biocatalysts. The similarities include the substrate selectivity as well as the sequence within the catalytic cycle. We will return to this topic after discussing a further catalytic reaction.

Recently,[72] we have investigated the hydrovinylation of styrene using a catalyst modified by the ligand **109** and to our surprise a highly selective reaction occurs to give (*R*)-(−)-3-phenyl-1-butene **112** (Scheme 38).

The interest in this hydrovinylation reaction lies both in the high selectivity and in the observation that (−)-**112** is produced at −70°C with an *ee* of 95.2%, i.e. only 2% of the second enantiomer (+)-**112** is formed.

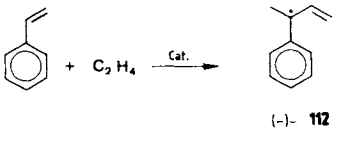

Scheme 38. The catalytic synthesis of (−)-3-phenyl-1-butene (−)-**112**. Cat. = catalyst.

Here again, it is found that the individual components are either inactive or react only slowly with the catalyst, whereas the substrates react together with high activity. The selectivity is presumably the result of the Ni-H bond reacting more rapidly with the activated C=C bond of the styrene than with that of the ethylene. Steric effects then prevent a second styrene molecule from approaching the resulting Ni-C bond and as a result the styrene is neither oligomerized or polymerized. The much smaller ethylene molecule, however, reacts with insertion into the Ni-C bond and this is followed by β-H-elimination and displacement of **112** from the catalyst. Similar effects are observed in the hydrovinylation of norbornene. This explanation accounts for the selectivity but not for the induction.

Some insight into this problem has been obtained from a computer simulation of a complete catalytic cycle.[74] The possible pathways for the approach of a styrene molecule were simulated with incorporation of the X-ray data for **109** as well as the coordination of the H-Ni-X group to the P atom with estimated van der Waals radii for the complex anion X (Fig. 17).

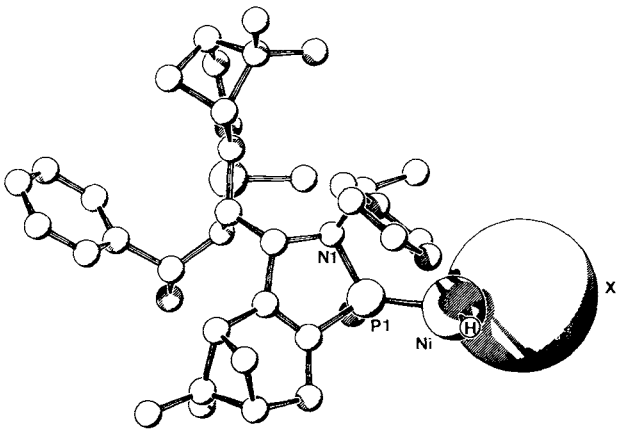

Fig. 17. A model for simulating a catalytic cycle incorporating the estimated spacial volume of the complexed anion $[EtAlCl_3]^{\ominus}$ (symbolized here as X).

These investigations clearly show that the styrene preferentially approaches the Ni atom such that, after coordination and rotation about the complexation axis, Ni→C2 addition gives an alkylnickel species having the configuration needed for the synthesis of (−)-3-phenyl-1-butene, (−)-**112**. The subsequent addition to the ethylene and the final β-H-elimination have no further influence on the configuration of the product. The catalytic cycle has been simulated using an interactive graphics system and recorded as a video film to give an impression of the spacial properties from various perspectives. A simulation of this type does not of course mirror reality; nevertheless such pictorial representations certainly widen the chemist's conceptional horizon.

After this purely academic presentation, it should be mentioned that we have carried out the hydrovinylation of both norbornene and styrene on a 10-kg scale in our pilot plant, since both products—2-*exo*-vinylnorbornane **104** and 3-phenyl-1-butene **112**—are of interest as starting materials for further syntheses and as monomers for homopolymerization or copolymerization. Initial investigations[75] of the homopolymerization of **104** and **112** using certain Ziegler catalysts have produced polymers which decompose only above 400°C. Of particular interest is the polymer derived from (−)-**112** which is produced in an isotactic polymerization and whose orientation is controlled by both the catalyst and the chirality of the monomers (Scheme 39).

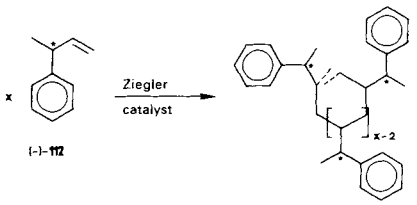

Scheme 39. The isotactic polymerization of (−)-**112**.

The polymer formed is amorphous, or at least only partially crystalline, but has an IR spectrum with remarkably sharp bands in the phenyl region. The ^{1}H-NMR solid-state spectrum is also well resolved, indicating a high regularity within the polymer. A transparent pressling formed by tempering at high temperature and pressure, rotates plane-polarized light and gives sharp Debye-Scherrer reflections, i.e. the tempering causes crystallization. Force field calculations[76] suggest that in polymeric (−)-**112**, helices can be formed which have the same configuration at the asymmetric C-atom but may be left-handed or right-handed. The identity period is made up of ca. eleven monomer units. A polymer chain containing 40 monomer units is shown in Figure 18, while Figure 19 shows a view into the left-handed helix. Both the polymerization and the structure of the polymer are the subject of ongoing investigations.

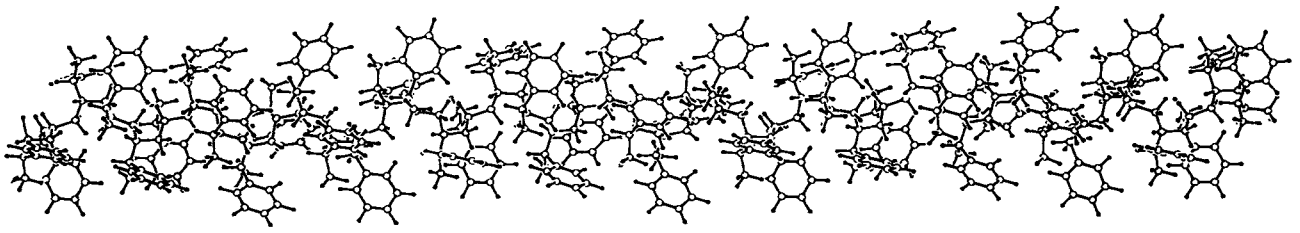

Fig. 18. Model of the polymer chain of poly-(−)-**112** based on force field calculations.

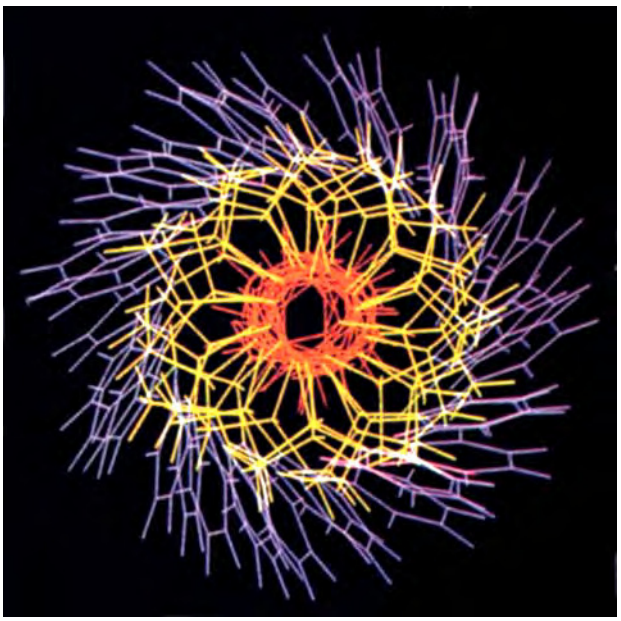

Fig. 19. A view down the helix of the computer simulated model for poly-(−)-**112**.

5. Outlook

The results described in this article indicate that the element nickel, in the form of its organometallic compounds and complexes, is able to induce a wide variety of stoichiometric and, more significantly, catalytic organic syntheses in the homogeneous phase. The highly selective and enantioselective catalytic reaction discussed above suggests some of the possibilities for further developments. In particular the incorporation of unsaturated compounds containing functional groups should open up new areas for further research. The same applies to the development of substrate-specific and enantioselective homogeneous catalysts, whereby the construction of suitable ligands using, inter alia, the principles described in this article, will play an important role—particularly since the structural permutations are practically unlimited. It can be predicted that synthetic catalysts will be developed whose properties and activities will be comparable with those of the biocatalysts. The aim will certainly not be to partially replace these but rather to develop in vitro syntheses which are not possible in vivo.

100 years of organonickel chemistry seems to be just a beginning.

Received: August 19, 1987 [A 648 IE]
German version: *Angew. Chem. 100* (1988) 189

[1] L. Mond, C. Langer, F. Quincke, *J. Chem. Soc. 1890*, 749.
[2] C. Langer, *Ber. Dtsch. Chem. Ges. 43* (1910) 3665.
[3] P. Sabatier, J.-B. Senderens, *C. R. Hebd. Séances Acad. Sci. 124* (1897) 616, 1358.
[4] P. Sabatier, *Bull. Soc. Chim. Fr. 6* (1939) 1261.
[5] E. Fischer, *Stahl Eisen 32* (1912) 1898.
[6] K. Fischer, K. Jonas, G. Wilke, *Angew. Chem. 85* (1973) 620; *Angew. Chem. Int. Ed. Engl. 12* (1973) 565.
[7] W. Reppe, O. Schlichting, K. Klager, T. Toepel, *Justus Liebigs Ann. Chem. 560* (1948) 1.
[8] W. Reppe, H. Vetter, *Justus Liebigs Ann. Chem. 582* (1953) 133.
[9] A. A. Hock, O. S. Mills, *Proc. Chem. Soc. 1958*, 233.
[10] a) G. Wilke, *Angew. Chem. 72* (1960) 581; b) B. Bogdanović, M. Kröner, G. Wilke, *Justus Liebigs Ann. Chem. 699* (1966) 1; c) D. J. Brauer, C. Krüger, *J. Organomet. Chem. 122* (1976) 265.
[11] a) G. Wilke, *Pure Appl. Chem. 60* (1978) 677; b) W. Geibel, G. Wilke, R. Goddard, C. Krüger, R. Mynott, *J. Organomet. Chem. 160* (1978) 139.
[12] K. R. Pörschke, unpublished.
[13] K. Ziegler, *Brennst.-Chem. 33* (1952) 193.
[14] K. Ziegler, H.-G. Gellert, E. Holzkamp, G. Wilke, *Brennst.-Chem. 35* (1954) 321.
[15] K. Fischer, K. Jonas, P. Misbach, R. Stabba, G. Wilke, *Angew. Chem. 85* (1973) 1002; *Angew. Chem. Int. Ed. Engl. 12* (1973) 943.
[16] K. Ziegler, E. Holzkamp, H. Breil, H. Martin, *Angew. Chem. 67* (1955) 426.
[17] G. Wilke, *Angew. Chem. 69* (1957) 397.
[18] G. Wilke, *Angew. Chem. 75* (1963) 10; *Angew. Chem. Int. Ed. Engl. 2* (1963) 105.
[19] H. W. Reed, *J. Chem. Soc. 1954*, 1931.
[20] G. Wilke, *Angew. Chem. 72* (1960) 581.
[21] G.Wilke, E. W. Müller, M. Kröner, P. Heimbach, H. Breil, DBP 1191375 (Prior. 28. 4. 1960).
[22] D. J. Brauer, C. Krüger, *J. Organomet. Chem. 44* (1972) 397.
[23] N. Rösch, R. Hoffmann, *Inorg. Chem. 13* (1974) 2656.
[24] K. Jonas, P. Heimbach, G. Wilke, *Angew. Chem. 80* (1968) 1033; *Angew. Chem. Int. Ed. Engl. 7* (1968) 949.
[25] K. Jonas, *Dissertation*, Universität Bochum 1968.
[26] C. Krüger, Y.-H. Tsay in [15], Fig. 4.
[27] C. Krüger, K. Angermund, crystal structure analysis of **12a**: $C_{24}H_{43}NiP$; $P2_1$, $a=9.277(2)$, $b=8.606(1)$, $c=15.383(3)$ Å, $\beta=106.89(1)°$, RT, $Z=2$, $\rho_{calc}=1.19$ g cm^{-3}, $\mu(Mo_{K\alpha})=9.01$ cm^{-1}, Enraf-Nonius diffractometer; 6399 measured reflections averaged to 5940, 4341 observed ($I\geq 2\sigma(I)$); $R=0.072$, $R_w=0.089$ ($w=1/\sigma^2(F_0)$) for 235 refined parameters [77].
[28] A. Aradi, J. Neuffer, G. Wilke, unpublished.
[29] W. Eisenbach, H. Lehmkuhl, G. Wilke, DBP 2349561 (Austrian Prior. 5. 10. 1972).
[30] G. Wilke, B. Bogdanović, P. Hardt, P. Heimbach, W. Keim, M. Kröner, W. Oberkirch, K. Tanaka, E. Steinrücke, D. Walter, H. Zimmermann, *Angew. Chem. 78* (1966) 157; *Angew. Chem. Int. Ed. Engl. 5* (1966) 151.
[31] a) E. O. Fischer, G. Bürger, *Z. Naturforsch. B 16* (1961) 77; b) *Chem. Ber. 94* (161) 2409; c) G. Bürger, *Dissertation*, Universität München 1962.
[32] a) O. Behrens, G. Wilke, unpublished; b) O. Behrens, *Dissertation*, Universität Bochum 1973.
[33] C. Krüger, *Chem. Ber. 109* (1976) 3574.
[34] R. Mynott, W. J. Richter, G. Wilke, *Z. Naturforsch. B 41* (1986) 85.
[35] a) G. Wilke, M. Kröner, B. Bogdanović, *Angew. Chem. 73* (1961) 755; b) B. Bogdanović, P. Heimbach, M. Kröner, G. Wilke, *Justus Liebigs Ann. Chem. 727* (1969) 143.
[36] B. Henc, P. W. Jolly, R. Salz, G. Wilke, R. Benn, E. G. Hoffmann, R. Mynott, J. Schroth, K. Seevogel, J. C. Sekutowski, C. Krüger, *J. Organomet. Chem. 191* (1980) 425.
[37] G. Wilke, B. Bogdanović, *Angew. Chem. 73* (1961) 756.
[38] R. Goddard, C. Krüger, F. Mark, R. Stansfield, X. Zhang, *Organometallics 3* (1985) 285.
[39] M. M. Rohmer, J. Demuynck, A. Veillard, *Theor. Chim. Acta 36* (1974) 93.
[40] D. Moncrieff, J. H. Hillier, V. R. Saunders, W. von Niessen, *Inorg. Chem. 24* (1985) 4247.
[41] C. De Ortueta Spiegelberg, G. Wilke, only published in part; C. De Ortueta Spiegelberg, *Dissertation*, Universität Bochum 1965.
[42] a) R. Mynott, R. Neidlein, H. Schwager, G. Wilke, *Angew. Chem. 98* (1986) 374; *Angew. Chem. Int. Ed. Engl. 25* (1986) 367; b) H. Schwager, *Dissertation*, Universität Bochum 1986.
[43] R. Neidlein, A. Rufińska, H. Schwager, G. Wilke, *Angew. Chem. 98* (1986) 643; *Angew. Chem. Int. Ed. Engl. 25* (1986) 640.
[44] C. Krüger, Y.-H. Tsay, crystal structure analyses of **32**: $C_{20}H_{30}NiP_2$; $I\bar{4}$, $a=10.440(1)$, $b=10.440(1)$, $c=38.015(3)$ Å, RT, $Z=8$, $\rho_{calc}=1.25$ g cm^{-3}, $\mu(Cu_{K\alpha})=27.82$ cm^{-1}. Enraf-Nonius diffractometer; 8493 measured reflections, averaged to 2202, of which 1332 observed ($I\geq 2\sigma(I)$); $R=0.070$, $R_w=0.088$ ($w=1/\sigma^2(F_0)$) for 210 parameters [77].
[45] H. Schwager, G. Wilke, *Chem. Ber. 120* (1987) 79.
[46] K.-H. Walter, G. Wilke, unpublished.
[47] K. Angermund, C. Krüger, crystal structure analysis of **38**: $C_{28}H_{24}$; *Aba2*, $a=7.987(1)$, $b=16.141(2)$, $c=15.163(2)$ Å, RT, $Z=4$, $\rho_{calc}=1.22$ g cm^{-3}, $\mu(Mo_{K\alpha})=0.64$ cm^{-1}. Enraf-Nonius diffractometer; 2483 measured reflections, averaged to 1734, of which 1125 observed ($I\geq 2\sigma(I)$); $R=0.035$, $R_w=0.032$ ($w=1/\sigma^2(F_0)$) for 174 parameters [77].
[48] R. Brenn, B. Büssemeier, S. Holle, P. W. Jolly, R. Mynott, J. Tkatschenko, G. Wilke, *J. Organomet. Chem. 279* (1985) 63.
[49] a) W. Brenner, P. Heimbach, H.-J. Hey, E.W. Müller, G. Wilke, *Justus Liebigs Ann. Chem. 727* (1969) 161; b) W. Brenner, P. Heimbach, G. Wilke, *ibid. 727* (1969) 183; c) P. Heimbach, W. Brenner, *Angew. Chem. 78* (1966) 983; *Angew. Chem. Int. Ed. Engl. 5* (1966) 961.

[50] G. Wilke, G. Hermann, *Angew. Chem. 78* (1966) 591; *Angew. Chem. Int. Ed. Engl. 5* (1966) 581.

[51] a) P. Binger, M. J. Doyle, R. Benn, *Chem. Ber. 116* (1983) 1; b) P. Binger, M. J. Doyle, *J. Organomet. Chem. 162* (1978) 195.

[52] M. Iyoda, S. Tanaka, M. Nose, M. Oda, *J. Chem. Soc. Chem. Commun. 1983*, 1058.

[53] a) L. Stehling, G. Wilke, *Angew. Chem. 97* (1985) 505; *Angew. Chem. Int. Ed. Engl. 24* (1985) 496; b) L. Stehling, G. Wilke, unpublished.

[54] C. Krüger, crystal structure analysis of **62**: $C_{16}H_{24}$; $P\bar{1}$, $a=9.070(1)$, $b=11.045(2)$, $c=15.030(1)$ Å, $\alpha=97.729(7)$, $\beta=95.023(7)$, $\gamma=96.33(1)°$, RT, $Z=4$, $\rho_{calc}=0.97$ g cm^{-3}, $\mu(Mo_{K\alpha})=0.50$ cm^{-1}. Enraf-Nonius diffractometer; 6666 measured reflections of which 4600 observed ($I\geq 2\sigma(I)$); $R=0.051$, $R_w=0.062$ ($w=1/\sigma^2(F_0)$) for 482 parameters [77]. - **63**: $C_{24}H_{36}$; $P\bar{1}$, $a=9.466(4)$, $b=9.784(5)$, $c=6.990(4)$ Å, $\alpha=103.04(6)$, $\beta=110.14(7)$, $\gamma=109.36(4)$, RT, $Z=1$, $\rho_{calc}=1.03$ g cm^{-3}, $\mu(Mo_{K\alpha})=0.53$ cm^{-1}. Enraf-Nonius diffractometer; 3050 measured reflections of which 2190 observed ($I\geq 2\sigma(I)$); $R=0.047$, $R_w=0.062$ ($w=1/\sigma^2(F_0)$) for 181 parameters [77].

[55] K. Fischer, K. Jonas, A. Mollbach, G. Wilke, *Z. Naturforsch. B 39* (1984) 1011.

[56] K. Fischer, *Dissertation*, Universität Bochum 1973.

[57] W. Kleinmann, *Dissertation*, Universität Bochum 1983.

[58] K. R. Pörschke, G. Wilke, *Chem. Ber.*, in press.

[59] K. R. Pörschke, K. Jonas, G. Wilke, R. Benn, R. Mynott, R. Goddard, C. Krüger, *Chem. Ber. 118* (1985) 275.

[60] a) C. Krüger, K. Angermund, crystal structure analysis of **78**: $C_{12}H_{30}N_2NiMg$; $P2_1/a$, $a=14.308(5)$, $b=8.372(3)$, $c=14.891(6)$ Å, $\beta=114.65(3)°$, RT, $Z=4$, $\rho_{calc}=1.17$ g cm^{-3}, $\mu(Mo_{K\alpha})=12.21$ cm^{-1}. Enraf-Nonius diffractometer; 9174 measured reflections, averaged to 4901, of which 4128 observed ($I\geq 2\sigma(I)$); $R=0.043$, $R_w=0.055$ ($w=1/\sigma^2(F_0)$) for 265 parameters [77]; b) W. Kaschube, *Dissertation*, Universität Bochum 1987.

[61] K. Jonas, K. R. Pörschke, C. Krüger, Y.-H. Tsay, *Angew. Chem. 88* (1976) 682; *Angew. Chem. Int. Ed. Engl. 15* (1976) 622.

[62] K. R. Pörschke, K. Jonas, G. Wilke, *Chem. Ber.*, in press.

[63] B. Bogdanović, G. Wilke, *Brennst.-Chem. 49* (1968) 323.

[64] a) B. Bogdanović, B. Henc, B. Meister, H. Pauling, G. Wilke, *Angew. Chem. 84* (1972) 1070; *Angew. Chem. Int. Ed. Engl. 11* (1972) 1023; b) B. Bogdanović, B. Henc, A. Löser, B. Meister, H. Pauling, G. Wilke, *Angew. Chem. 85* (1973) 1013; *Angew. Chem. Int. Ed. Engl. 12* (1973) 954; c) B. L. Barnett, C. Krüger in [64b], Fig. 3.

[65] B. Bogdanović, B. Spliethoff, G. Wilke, *Angew. Chem. 92* (1980) 633; *Angew. Chem. Int. Ed. Engl. 19* (1980) 622.

[66] T. Leven, *Dissertation*, Universität Bochum 1987.

[67] G. Wilke in M. Tsutsui (Ed.): *Fundamental Research in Homogeneous Catalysis. Vol. 3*, Plenum Press, New York 1979, p. 1–24.

[68] a) K. Sperling, *Dissertation*, Universität Bochum 1983; b) K. Sperling, L. Stehling, F. Wilke, DOS 3336691 (October 8, 1983); c) F. Wilke, *Proc. 5th IUPAC Symp. Org. Synth. 1984*, Blackwell Scientific Publications, Oxford 1985, p. 1.

[69] a) T. Alderson, E. L. Jenner, R. V. Lindsey, Jr., *J. Am. Chem. Soc. 87* (1965) 5638; b) M. G. Barlow, M. J. Bryant, R. N. Hazeldine, A. G. Mackie, *J. Organomet. Chem. 21* (1970) 215; c) H. Pracejus, H. J. Krause, G. Oehme, *Z. Chem. 20* (1980) 24; d) P. Grenouillet, D. Neibecker, I. Tkatschenko, *Abstract 3rd I.S.H.C. Mailand*, p. 186.

[70] G. Wilkinson, F. G. A. Stone, E. W. Abel (Hrsg.): *Comprehensiv Organometallic Chemistry, Vol. 8*, Pergamon Press, Oxford 1982, p. 486.

[71] H. Kuhn, *Dissertation*, Universität Bochum 1983.

[72] J. Monkiewicz, G. Wilke, unpublished.

[73] C. Krüger, E. Raabe, K. Angermund, crystal structure analyses of **109**: $C_{38}H_{50}N_2P_2$; $P2_12_12_1$, $a=11.562(2)$, $b=14.237(2)$, $c=21.511(2)$ Å, RT, $Z=4$, $\rho_{calc}=1.12$ g cm^{-3}, $\mu(Cu_{K\alpha})=13.00$ cm^{-1}. Enraf-Nonius diffractometer; 3817 measured reflections of which 2934 observed ($I\geq 2\sigma(I)$); $R=0.042$, $R_w=0.050$ ($w=1/\sigma^2(F_0)$) for 579 parameters [77]. - **110**: $C_{38}H_{50}N_2P_2$; $P2_12_12_1$, $a=10.970(1)$, $b=13.007(2)$, $c=24.484(2)$ Å, RT, $Z=4$, $\rho_{calc}=1.13$ g cm^{-3}, $\mu(Mo_{K\alpha})=1.47$ cm^{-1}. Enraf-Nonius diffractometer; 7282 measured reflections, averaged to 6988, of which 4624 observed ($I\geq 2\sigma(I)$); $R=0.051$, $R_w=0.054$ ($w=1/\sigma^2(F_0)$) for 380 parameters [77]. - **111**: $C_{28}H_{46}P_2N_2$; $P2_1$, $a=12.658(2)$, $b=8.253(1)$, $c=14.591(1)$ Å, $\beta=108.193(8)°$, RT, $Z=2$, $\rho_{calc}=1.08$ g cm^{-3}, $\mu(Mo_{K\alpha})=1.62$ cm^{-1}. Enraf-Nonius diffractometer; 8452 measured reflections, averaged to 7841, of which 5418 observed ($I\geq 2\sigma(I)$); $R=0.052$, $R_w=0.058$ ($w=1/\sigma^2(F_0)$) for 288 parameters [77].

[74] K. Angermund, unpublished results; the simulation was carried out with an Evans & Sutherland PS390 graphics system and the program MOGLI.

[75] H. Bretinger, F. Fürbach and H. Martin, unpublished results.

[76] K. Angermund, unpublished results; the force field calculations were carried out with the program MM2 (QCPE No. 395).

[77] Further details concerning the crystal structure determinations can be obtained from the Fachinformationszentrum Energie Physic Mathematik, D 7514 Eggenstein-Leopoldshafen GmbH (FRG), on quoting the depositary number CSD-52660, the names of the authors, and the jounal citation.

Registered names, trademarks, etc. used in this journal, even when not marked as such, are not to be considered unprotected by law.

© VCH Verlagsgesellschaft mbH, D-6940 Weinheim, 1988. - Printed in the Federal Republic of Germany by Zechnersche Buchdruckerei, Speyer/Rhein.

All rights reserved (including those of translation into foreign languages). No part of this issue may be be reproduced in any form – by photoprint, microfilm, or any other means – nor transmitted or translated into a machine language without written permission from the publishers. Only single copies of contributions, or parts thereof, may be made for personal use.

Valid for users in the USA: The appearance of the code at the bottom of the first page of an article in this journal (serial) indicates the copyright owner's consent that copies of the article may be made for personal or internal use, or for the personal or internal use of specific clients. This consent is given on the condition, however, that the copier pay the stated per-copy fee through the Copyright Clearance Center, Inc., for copying beyond that permitted by Sections 107 or 108 of the U.S. Copyright Law. This consent does not extend to other kinds of copying, such as copying for general distribution, for advertising or promotional purposes, for creating new collective works, or for resale. For copying from back volumes of this journal see 'Permissions to Photo-Copy: Publisher's Fee List' of the CCC.

Editorial office: Pappelallee 3, D-6940 Weinheim, Federal Republic of Germany, Telephone (06201) 602315, Telex 465516 vchwh d, Telefax (06201) 602328.

Editor: *P. Gölitz*

Associate editors: *D. I. Loewus, A. Stimson.* **Editorial assistant:** *E. Schweikart*

Publishers: VCH Verlagsgesellschaft mbH. (Managing Directors: *Prof. Dr. Helmut Grünewald* and *Hans Dirk Köhler*), Pappelallee 3, D-6940 Weinheim, Federal Republic of Germany. Correspondence concerning advertisements should be addressed to VCH Verlagsgesellschaft mbH. (Advertising Manager *R. J. Roth*), Boschstr. 12, P.O. Box 1260/1280, D-6940 Weinheim, Federal Republic of Germany, Telephone Weinheim (06201) 602-0, Telex 465516 vchwh d, Telefax (06201) 602328.

ANGEWANDTE CHEMIE
International Edition in English
Volume 27 · Number 2
February 1988
Pages 207–308

Pharmaceutical Proteins**

By Dietmar Blohm,* Claus Bollschweiler, and Heinz Hillen

Dedicated to Professor Helmut Dörfel on the occasion of his 60th birthday

There is currently great interest in pharmaceutical proteins, and work in this area, from basic research to drug marketing, is expanding vigorously. The starting points of these developments are genetic engineering and biotechnology, which contribute to the discovery of new proteins and allow them to be produced on a worthwhile scale. Ever since the commercial introduction of insulin in 1923, of thyroid hormone in 1934, of factor VIII in 1948, and of calcitonin in 1970, hormones, serum proteins, and enzymes have been firmly established as therapeutic agents. Immunomodulators and various tissue proteins are in a turbulent phase of development as a new approach to the therapy of tumors. Increasingly, diagnostic aids now take the form of enzymes and monoclonal antibodies, and recently there has even been development of vaccines based on defined single proteins and oligopeptides. Of the more than 200 pharmaceutical proteins which have been investigated to date, more than half are undergoing research and development, about 100 are in clinical trials, and a dozen or so have already been marketed. The most important indications for them are cardiovascular disorders, tumors, autoimmune diseases, and infections. Genetically engineered proteins can be used as active substances, which are chemically and biologically exactly defined, for new drug products and in research to acquire new information on therapeutic use, based on the concept of therapy with endogenous proteins. Very recent developments have shown that proteins, either in their natural form or modified, are becoming of increasing importance for research into active substances.

1. Introduction—Definition of Terms

Active substances from medicinal herbs and other natural sources form, together with the compounds which chemists have been synthesizing for about 100 years, the backbone of drug therapy. Nevertheless, there are still many diseases which cannot be satisfactorily treated with substances derived from either of these sources.

1.1. From the Beginnings to Genetic Engineering

The active substances in many traditional medicines, such as bee-sting ointments, enzyme and snake venom products, and preparations used in "alternative medicine," are proteins, usually in the form of poorly defined mixtures. Table 1 shows some examples of proteins isolated from a wide variety of biological sources and used for

[*] Dr. D. Blohm [+], Dr. C. Bollschweiler, Dr. H. Hillen
BASF Aktiengesellschaft, Main Laboratory
D-6700 Ludwigshafen (FRG)

[+] Present address:
Dana-Faber Cancer Institute, Biochemical Pharmacology
44 Binney Street, Boston, MA 02115 (USA)

[**] Abbreviations: AA, amino acid(s); ch., chain; CHO, glycosylation site with carbohydrate chain; SS, disulfide bridge; MP, membrane protein; Pre, protein containing pre(pro)-sequences; sia, sialylated; Mo, monomer; Di, dimer; Tri, trimer; Tet, tetramer; het., heterogenous.

 © VCH Verlagsgesellschaft mbH, D-6940 Weinheim, 1988 0570-0833/88/0202-0207 $ 02.50/0

Table 1. Active proteins isolated from animals, plants, or microorganisms.

Substance	Origin	Examples of use
Aprotinin	cattle	stopping bleeding, treatment of shock
L-Asparaginase	*E. coli*	leukemia
Collagenase, Nucleases	microorganisms	healing of wounds
Dextranase	penicillium	prophylaxis of caries
Eglin	leeches	emphysema
Hirudin	leeches	prophylaxis of thrombosis
Hyaluronidase	cattle	percutaneous infiltration
Insulin	cattle/hogs	diabetes
Kallikrein	hogs	circulatory disturbances
Lysozyme	chicken eggs	bacterial infections
Thyroid hormones	cattle	metabolic disturbance
Streptokinase	streptococci	thrombolysis
Superoxide dismutase	cattle	rheumatoid arthritis
Toxins	snakes, bees, etc.	circulatory disturbances, rheumatism
Digestive enzymes, e.g., amylase, carboxy peptidase, chymotrypsin, lipase, pepsin, trypsin	cattle/hogs and, in some cases, microorganisms	digestive disturbances, healing of wounds

every type of medicinal therapy—for causal and symptomatic treatment and for prophylaxis.

Up to the late 1970s virtually the only source for endogenous substances needed for replacement therapy—for example, for deficiency of growth hormone or coagulation factor VIII—was the human body. Proteins of this type are listed in Table 2.

Table 2. Active proteins isolated from the human body (for further details, see Sections 3 and 6).

Substance	Origin	Examples of use
α1 protease inhibitor	blood	emphysema
Antithrombin III	blood	anticoagulant
Angiotensinase	placenta	high blood pressure
Factor VII, Factor VIII, Factor IX, Factor X, Fibrinogen, Thrombin	blood	blood coagulation diseases
Immunglobulins	blood	passive immunization
Interferons	blood	virus infection, tumor therapy
Plasmin	blood	thrombolysis
Serum albumin	blood	plasma replacement
Urokinase	urine	thrombolysis
Growth hormone	pituitary	dwarfism

This situation began to change in 1977, when a human hormone was synthesized for the first time using *E. coli* bacteria which had undergone gene manipulation.[90] Table 3 shows that it took less than ten years to progress from the comparatively simple somatostatin molecule to apolipoprotein B, the largest and most complicated pharmaceutical protein which can now be produced with the aid of these new methods.

Table 3. Gene cloning and expression of various complex pharmaceutical proteins (cf. Fig. 1 in Section 2.1).

Protein	AA	Structural pecularities	Successfully cloned	Ref.	Expression
Somatostatin	14	1 SS	1977	[90]	*E. coli*
Insulin	51	α and β chains, 3 SS	1979	[70]	*E. coli*
Growth hormone	191	2 SS	1979	[123]	*E. coli*
Tissue plasminogen activator	527	one- and two-chain forms, 17 SS, 3 CHO	1983	[157]	mammalian cells
Factor VIII	2332	12 SS, 25 CHO	1984	[203]	mammalian cells
Apolipoprotein B	4536	25 SS, 20 CHO	1986	[29]	

The result of these developments in method is that now more than 480 human proteins have had their primary structure elucidated by gene cloning,[183] and most of them are now available in substantial quantities by expression in host cells. This route is particularly important for substances such as interferons, interleukins, and growth factors which are often formed only in nanogram quantities in the body.

1.2. The Concept of Therapy with Endogenous Pharmaceutical Proteins

Based on these developments in molecular biology and as a result of advances in cell biology and protein chemistry, a new concept of therapy with active substances is about to become reality—the concept of therapy with endogenous active proteins.

The idea behind this concept is to supplement the research aimed at finding new active substances, the costs of which are still increasing, by the use of endogenous active proteins. At present, about 15000 chemical compounds, on average, have to be prepared and tested in order to find a new marketable therapeutic agent. In contrast, a protein that carries out the relevant function in the human body already has, by its nature, the desired biological effect. The concept essentially comprises the following three stages:

1. Discovery and preparation by gene manipulation of proteins having therapeutic potential;
2. Examination of their spectra of biological effects in vitro and in vivo;
3. Development of drug products based on these proteins and on a knowledge of their mechanisms of action.

Examples of these proteins are hormones, components in enzyme cascades, immunological mediators, and growth and differentiation factors. They are either used for therapy in the form found in nature or their structures are used as "leads" for the preparation of derivatives with improved properties.

There are no problems in the administration (e.g., in replacement treatment) of endogenous proteins which normally circulate in the blood, such as insulin and other hormones. Problems, which are largely unsolved, derive from the fact that, under physiological conditions, there is very

localized release of many active proteins, and they have short half-lives, which ensure that they have no effects on neighboring tissues or organs.

1.3. Definition

Strictly speaking, pharmaceutical proteins usually have regulatory functions in maintaining biochemical or cellular equilibria in the healthy body, and they may be involved both in pathophysiological events and in the healing process. They can be defined as proteins or polypeptides which, by reason of their natural functions in the human body, are suitable as therapeutic substances, or they are derivatives of these proteins prepared by mutagenesis or proteolysis, hybrid proteins, protein aggregates, or conjugates with other molecules.

In the wider sense, however, pharmaceutical proteins also include polyclonal and monoclonal antibodies and proteins which are derived from viruses, microorganisms, plants, or animals, and are of clinical use either directly or after modification.

It is impossible within the scope of this review to deal comprehensively with all the proteins meeting this definition. Thus, selected examples will be presented, mainly of those pharmaceutical proteins having particular importance for cardiovascular/blood and cancer/immunology indications. However, no mention is made of the various clinical aspects of pharmaceutical proteins because the pharmacology of these large molecules is very specialized—in particular, their kinetics of distribution, their protection from proteases and inhibitors (half-life), their possible antigenicity, and the fact that they cannot be administered orally.

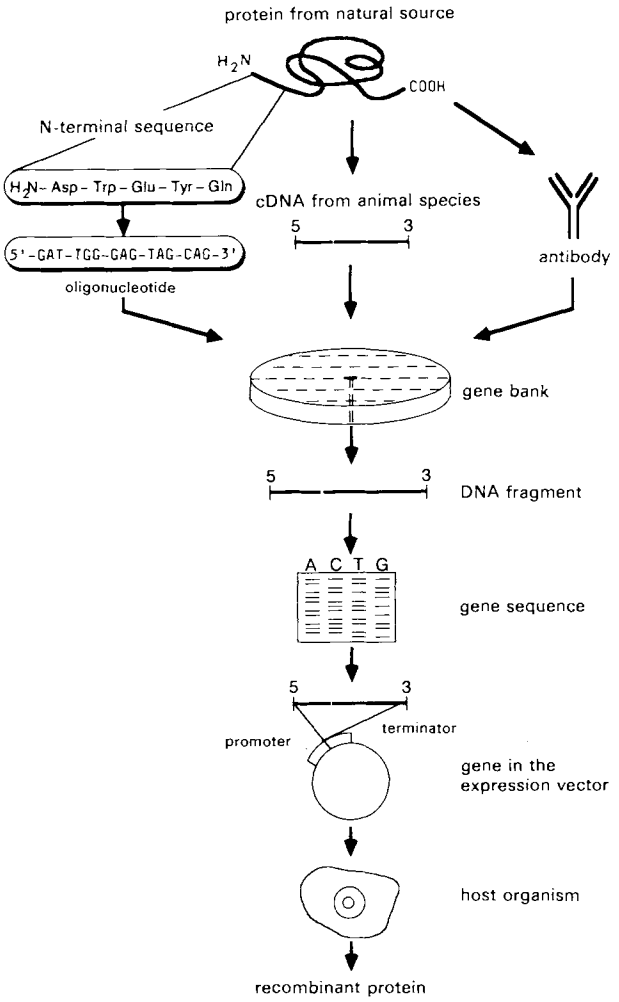

Fig. 1. Schematic summary of the gene-cloning procedure. For explanation see text.

2. Methodological Bases and Developments

The rapid developments in pharmaceutical proteins have been based primarily on the biosynthetic methods for preparation of proteins which have emerged in recent years from genetic engineering and biotechnology.[217]

The story of insulin is a particularly good illustration of these developments: although it was used clinically for the first time in 1922 by *Banting, Best,* and *Collip,* crystallized in 1926 by *Abel,* sequenced in 1955 by *Sanger,* its total synthesis published in 1963 by *Zahn, Katsoyannis,* and others, and its crystal structure elucidated in 1969 by *Crowfoot-Hodgkin*, until 1979 the only way of obtaining it was by extraction from either porcine or bovine pancreas.[70, 111]

2.1. Gene Cloning

The developments in genetic engineering in the 1970s made it possible for the first time to prepare insulin and other proteins by biosynthetic methods (for an introductory review see Ref. [28]). Nowadays, the time taken from the discovery of a protein to its preparation on a production scale has been reduced to a few years (Fig. 1).

This process usually begins with the development of straightforward biological tests for detecting the new protein. These tests are needed in order to make it possible to purify at least microgram quantities of the protein from the biological material. In favorable cases, these quantities are sufficient for the preparation of antibodies and for partial amino acid sequencing of the *N*-terminal end of the protein or fragments isolated after proteolysis. The corresponding genes are isolated from previously prepared gene banks. These are populations of recombinant host cells, usually hundreds of thousands of them, which together contain, randomly distributed, the genetic information of an organism in the form of cloned DNA fragments. Human genes for the proteins, which occur in only very small amounts, are usually isolated from cDNA banks derived from enriched messenger RNA fractions from specifically induced cell cultures or specific tissues. A variety of strategies can be used to discover the genes—for example, the use of radiolabeled DNA hybridization probes in the form of oligonucleotides whose sequence is established from the amino acid sequence and which can easily be obtained using automatic synthesizers. If the DNA fragments can be expressed in the host cells of the gene bank, it is possible to use antibodies to find the gene. The final steps are the sequencing of the DNA segment harboring the gene, and incorporation of the gene into expression vectors of suitable host cells.

The primary structure of a protein, and the information about functional domains and modifications which can be deduced from this, is now usually determined via gene cloning more rapidly than by investigation of the protein itself.

2.2. Gene Expression

Since pharmaceutical proteins are mainly extracellular, the most common modification is the attachment via nitrogen to certain asparagine residues or via oxygen to serine or threonine residues of carbohydrate chains which vary in length and are composed of either mannose and *N*-acetylglucosamine (*N*-glycosylation) or galactose and *N*-acetylgalactosamine (*O*-glycosylation). It has been shown in some cases that the glycosylation is important for transport of the protein out of the cell. In addition, there is sometimes an improvement in the solubility and resistance to proteolysis. With few exceptions, the biological activity of the protein is only slightly altered by glycosylation (but see Ref. [137]).

Proteins produced in *E. coli* bacteria are usually not glycosylated, while some glycosylations are possible in yeasts. However, only mammalian cells are suitable as host cells for the expression of proteins having complex modifications, such as γ-carboxylation of glutamyl residues, and for obtaining the same glycosylation pattern as in the human product.

Whereas genetically manipulated mammalian cell cultures rarely produce more than 50 mg of the relevant protein per liter of culture medium, it is usually possible to produce several grams per liter by use of recombinant bacteria (Fig. 2).

However, foreign proteins synthesized by bacteria are often attacked by their proteases. Proteins of low solubility may occasionally form crystalloid, denatured protein aggregates (inclusion bodies) within the cells.

2.3. Protein Chemistry

Advances in the discovery of new proteins and in retaining their biologically relevant molecular structure during purification are essentially based on developments in methods of protein chemistry. New and efficient separating materials—e.g., for HPLC, FPLC (fast protein liquid chromatography), and affinity chromatography—have considerably improved the isolation of proteins on an analytical and preparative scale. Detailed knowledge of the folding mechanisms and the structural principles assist in assessing the natural state of proteins, and this knowledge has increasingly been obtained by methods of circular dichroism and dynamic fluorescence or 2D NMR spectroscopy.

However, the renaturation of complex proteins with a high cysteine content remains a problem, particularly because of the large number of possible disulfide bridges, which are important in determining the folding of the protein and thus its biological activity.[16]

Modification of pharmaceutical proteins by chemical or genetic means—i.e., the preparation of protein derivatives ("muteins"), hybrid proteins, and protein fragments—is now performed by routine methods using in vitro mutagenesis of the relevant gene or by defined proteolysis.

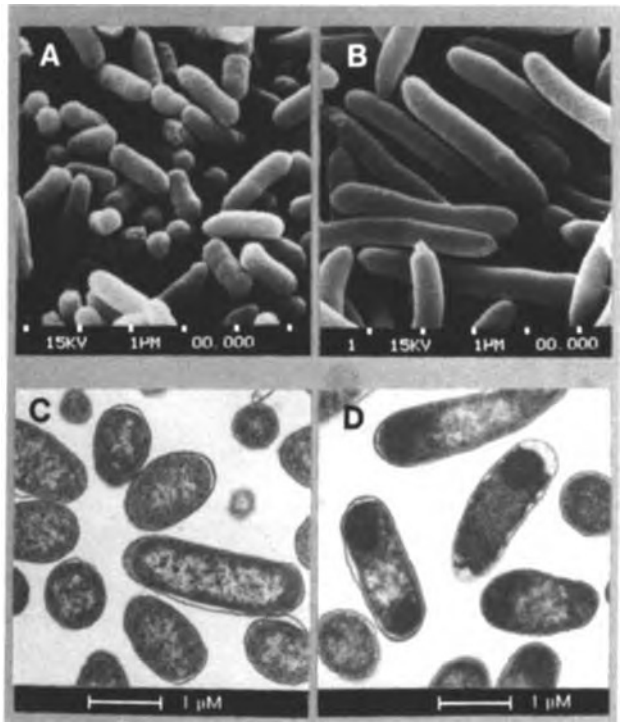

Fig. 2. *E. coli* bacteria before and after genetic manipulation A) Wild-type bacteria under the scanning electron microscope; B) TNF-producing bacteria (TNF = tumor necrosis factor; TNF remains dissolved within the cell); C) ultrathin section of wild-type bacteria; D) IFN-γ-producing bacteria (INF-γ = interferon-γ; IFN-γ forms inclusion bodies within the cell). See text for explanation.

In addition, the complete synthesis of polypeptides on polymeric supports in automatic apparatuses has recently been improved. Polypeptides having a chain length of up to 140 amino acids can be synthesized on a milligram scale in a few days.[31] Although proteins prepared in this way cannot be used as drugs because of impurities arising from side reactions, they can be used to test structural variants, which can then be produced by gene-technological methods.

3. Marketed Products

The great expectations aroused by the new methods in molecular biology were manifested in the USA back in the late 1970s by the setting up of more than 300 "gene companies" aimed at producing new pharmaceutical proteins. Many of these companies now develop their cloned proteins in cooperation with larger pharmaceutical companies, because the costs of developing a drug product are 10 to 50 times those for the research needed to prepare a protein. Examples of successful cooperation are that of Genentech with Eli Lilly for insulin and that of Genentech with Hoffmann-La Roche and of Biogen with Schering-Plough for interferon-α.

The sales of pharmaceutical proteins amounted to less than 1.5 billion US $ in 1985, scarcely 1% of world drug sales,[204] the main uses being for tumor therapy and the regulation of fibrinolysis and coagulation, and for infec-

tions, autoimmune and inflammatory diseases, hormonal disturbances, and vaccines. Market projections[5] predict for cardiovascular and antitumor agents alone a more than tenfold increase in the world sales of proteins in only four years, from about 0.2 billion DM in 1986 to more than 2.3 billion DM in 1990. It is likely that the conventional products on the market, such as animal insulins and the hepatitis B vaccines produced from inactivated viruses, will be gradually replaced by improved recombinant products.

The main advantages of recombinant products are their virtually unlimited availability, the economic aspects and, in particular, the product safety. For example, hepatitis B surface protein produced in yeast contains no viral nucleic acid (i.e., no viable particles) and consequently is far superior to vaccines produced from virions in the matter of safety. The same is true of proteins conventionally isolated from blood fractions, such as serum albumin and factor VIII, where production of them using genetically engineered microorganisms or cell cultures reduces the risk of virus infection (e.g., with hepatitis B or the AIDS virus) far below the level hitherto possible.

It is necessary to choose between classical and genetic engineering alternatives for the most economical process for preparing a pharmaceutical protein. Some of the pharmaceutical proteins now reaching the market are produced not by the recombinant DNA technique but by peptide synthesis, isolation from blood fractions, or by means of conventional cell cultures (Table 4).

In some cases, the requisite genes are not yet available, or the recombinant proteins, such as some interferons, differ slightly in structure or action from the natural forms.[170] In addition, in some cases the conventional processes are still more economical than the new biotechnological methods as is the case with human serum albumin. However, it is now possible in some cases to choose between alternative methods of gene technology.

3.1. Insulin

Insulin is an instructive example of this situation; the world demand is about 2000 kg per annum, with a market value of about 1.3 billion DM.[204] Although human insulin is less immunogenic than bovine or porcine insulin, it cannot replace the latter right away because, for many diabetics, there is no reason to change the product, which keeps diabetes well under control. Human insulin produced from porcine insulin by enzymatic amino acid replacement (i.e., semisynthetically) competes with genetically engineered human insulin, there now being at least two different processes for its production.[135]

The first step in the production of Huminsulin®, which was launched by Eli Lilly in 1982, is the separate preparation of the A and B chains in the form of fusion proteins in *E. coli* (Fig. 3a).

The individual chains are isolated and then joined together to form the active hormone via disulfide bridges produced by successive reductive thiolysis and air oxidation.

An alternative procedure starts from proinsulin, an insulin precursor (Fig. 3b). Proinsulin is likewise produced as a fusion protein in *E. coli* and is converted into human insulin by reaction with cyanogen bromide, oxidative sulfitolysis, and reductive thiolysis to give the correctly folded molecule of proinsulin, followed by treatment with trypsin and carboxypeptidase B (see Table 7).

3.2. Growth Hormone

At present, recombinant growth hormone is being used in the USA to treat several thousands of children suffering from dwarfism, a disorder brought about by a deficient endogenous production of the hormone, which is also called somatotropin. It is possible for growth to be completely normalized by administering the protein during the critical

Table 4. Examples of recently approved protein-based products on the market [a].

Protein	Product name	Company, year approved	Preparation
Calcitonin	Cibacalcin®	Ciba-Geigy, 1986	synthetic
Epidermal growth factor (EGF)	Gentel®	Zambon, 1986	
Factor VIII	Haemate®	Behringwerke (Hoechst), 1982	blood fraction
	Koate-Tropon®	Tropon-Cutter, 1985	blood fraction
Tissue plasminogen activator (tPA)	*Actilyse®*	*Boehringer Ingelheim, 1987*	*rDNA*
Hepatitis B vaccine	Heptavax-B®	Merck & Co., 1982	blood virions,
	Gen-H-B-vax®	Merck & Co., 1986	rDNA
Insulin	Novolin®	Novo, 1982	semisynthetic
	H-Insulin®	Hoechst, 1983	semisynthetic
	Huminsulin®	Eli Lilly, 1983	rDNA
Interferon-α	Berofor®	Boehringer Ingelheim, 1983	cell culture
Interferon-α-2C	Berofor alpha 2®	Boehringer Ingelheim, 1985	rDNA
Interferon-α-2A	Roferon A®	Hoffmann-La Roche, 1986	rDNA
Interferon-α-2B	Intron A®	Schering-Plough, 1986	rDNA
Interferon-α-N1	Wellferon®	Wellcome, 1986	cell culture
Interferon-β	Fiblaferon®	Bioferon/Rentschler, 1983	cell culture
Monoclonal antibodies	Orthoclone OKT 3®	Ortho, 1986	cell culture
Secretin	Sekretolin®	Hoechst, 1982	synthetic
Streptokinase	Streptase®	Behringwerke, 1985	microbial
Somatostatin	Stilamin®	Serono, 1980	synthetic
Growth hormone	Protropin®	Genentech + KabiVitrum, 1985	rDNA
	Humatrop®	Eli Lilly, 1987	rDNA (Met-free)
	Saizen®	Serono, 1987	rDNA (Met-free)

[a] Approvals relate mainly to the Federal Republic of Germany. Further details on the proteins mentioned here are to be found in the following sections and in Tables 6-11.

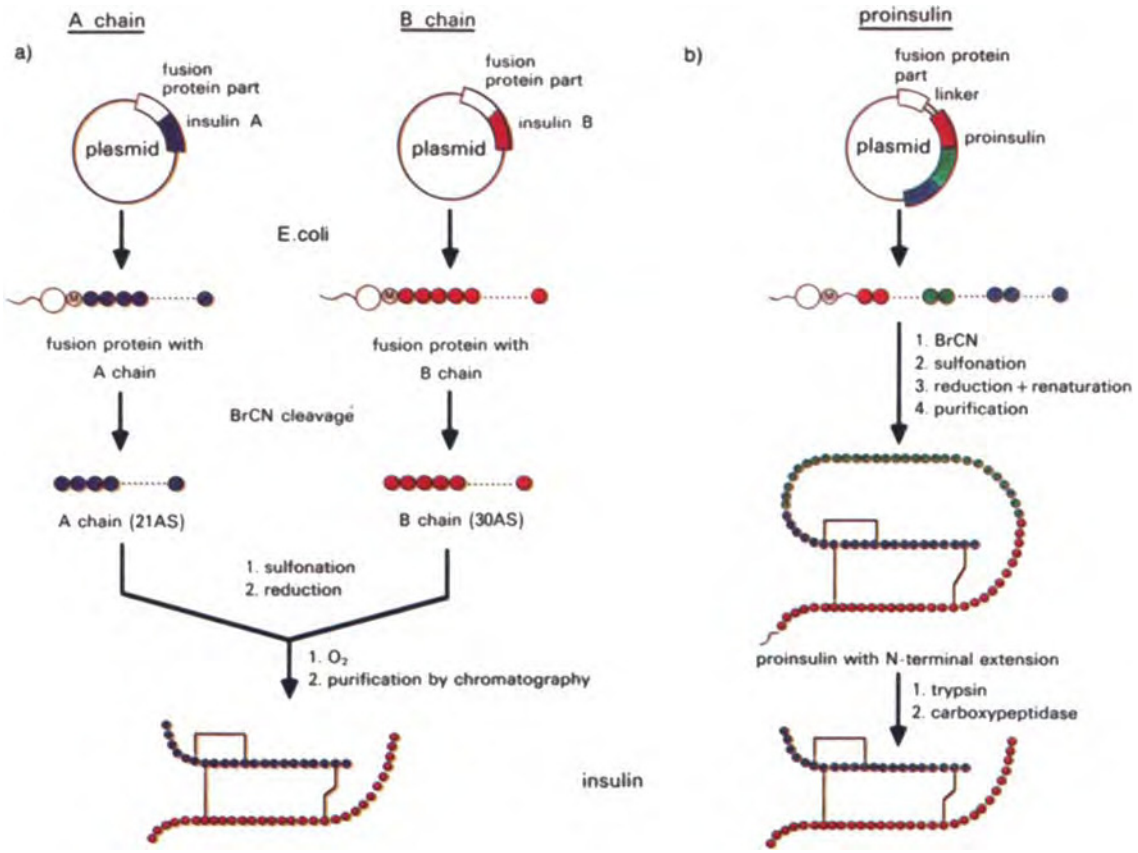

Fig. 3. Diagrammatic representation of the various genetic engineering methods for the production of insulin; see text for explanation.

years of development. Until 1985 the hormone was obtained from human pituitaries at autopsy.

This product was criticized because of the suspicion of viral contamination. Approval in 1985 of Protropin®, a human somatotropin which has an additional methionine residue at the *N*-terminal end and is produced in *E. coli* by Genentech, was rapidly followed by the Eli Lilly growth hormone Humatrop®, which contains no methionine and is thus identical with the endogenous substance.[84]

Other indications for human growth hormone, such as injuries, osteoporosis, and cachexia, are undergoing clinical trials (see Table 7).

3.3. Tissue Plasminogen Activator

Tissue plasminogen activator (tPA) is a serine protease which liberates plasmin from plasminogen and does not act until it has bound to fibrin. In contrast to streptokinase and urokinase, tPA acts on plasminogen only in the presence of fibrin, and thus can dissolve blood clots without long-lasting interference with blood coagulation.[39,210] It is a complex glycoprotein which has 17 disulfide bridges, undergoes post-translational modification, and consists of several domains to which defined functions can be assigned by examination of genetically engineered variants (Fig. 4).

Modifications in the pattern of glycosylation may also result in functional alterations in the tPA molecule. For example, it is possible in this way to increase the half-life of tPA in the blood without loss of biological activity.[113]

Indications for tPA are acute myocardial infarct and other thrombotic obstructions of vessels. With a therapeutic dose of just over 1 mg/kg body weight and 1.5 million myocardial infarcts each year in the USA alone, tPA is expected to be the "big" product giving genetically engineered pharmaceutical proteins their commercial breakthrough. Its sale has recently been approved in the USA, Canada, the Federal Republic of Germany, France, Austria, New Zealand, and the Philippines (see Table 8).

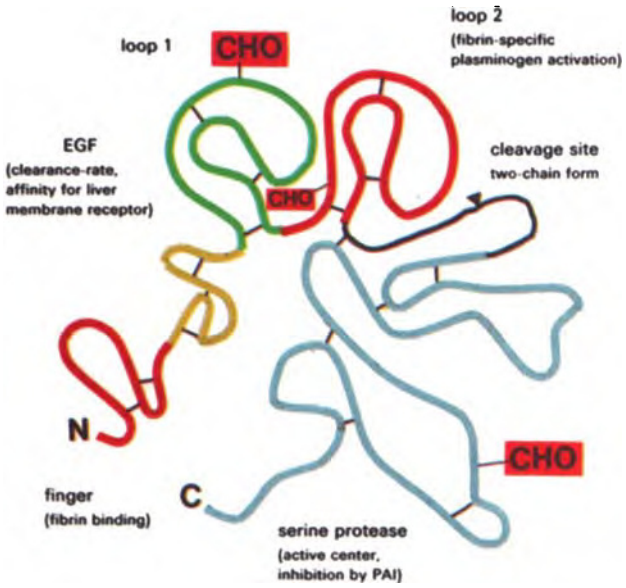

Fig. 4. Structural model of the tissue plasminogen activator (tPA) molecule: assignment of the biological functions to the domains of the protein. PAI = plasminogen activator inhibitor. EGF = epidermal growth factor. As noted at the beginning, CHO represents a carbohydrate chain.

3.4. Interferons

This group of active proteins undergoes local synthesis in picogram quantities only after induction, and it was discovered in 1957 that they have antiviral activity. They have been available in adequate quantities and high purity only since they were cloned in the early 1980s, which marked a breakthrough in gene technology methods. More than 24 natural interferons have been described to date, and these are essentially divided, according to their biological origin, into IFN-α, -β, and -γ as well as "concensus interferons" (see Table 5).

Table 5. Interferons (IFNs).

Name	Origin	Production	Stage of development	Indication
Interferon-α1 to α21	leukocytes	recombinant *E. coli*	launched (IFN-α2)	hairy cell leukemia (Kaposi sarcoma, multiple myeloma)
Interferon-β1 and β2	fibroblasts	cultured fibroblasts	launched (IFN-β1)	herpes zoster, viral encephalitis
Interferon-γ	lymphocytes	recombinant *E. coli*	clin. phase III	arthritis, leukemia
Consensus-IFN	artificial	recombinant *E. coli*	development	tumors

Interferon-β isolated from cell cultures was approved in the Federal Republic of Germany for serious viral diseases and tumors in 1983. The early expectations were great, but they have been only partially fulfilled. However, further preclinical and clinical trials on the recombinant product are in progress; these are particularly aimed, as are those on other interferons, at combinations with other active substances, especially for tumors. The best clinical results to date have been achieved with interferon-α products.[149] The first interferons produced by *E. coli* were launched in 1986 in the USA: Roferon A® of Hoffmann-La Roche and Intron A® of Schering-Plough. They differ by only one amino acid and as yet have been approved in the USA only for the treatment of the rare hairy cell leukemia. This malignant blood disease was previously incurable but about 90% of cases can now be cured by treatment with interferon-α for several months.[6]

The "immune interferon" IFN-γ is being tested for its antitumor action and recent tests have begun for the treatment of arthritis. It has a wide variety of immunological control functions and, in this respect, is more closely related to the interleukins than to the interferons, but it shares the antiviral and cytostatic activity of the latter.[211]

"Consensus" interferons are constructed by gene manipulation in order to combine sequences of the various natural types of interferons (see Table 9).

3.5. Hepatitis B Vaccines

In some countries in South-East Asia and Africa, up to 20% of the population is infected with the highly infectious hepatitis B virus, which causes jaundice and, as a late consequence of chronic infection, liver tumors. The vaccine, which has been available since 1982, is produced from virions isolated from the blood of virus carriers. In contrast, the first vaccine based on a recombinant protein, which has recently been approved for use in humans, contains the pure viral surface antigen.[105] On secretion from the genetically manipulated yeast, it spontaneously forms aggregates which substantially resemble the natural virus shell and are highly immunogenic.[206] Seroconversion rates with the new vaccine range from 80 to 100%, without there being any serious side effects or production of antibodies against yeast proteins[24] (see Table 11).

3.6. OKT3 Monoclonal Antibodies

The therapeutic uses of monoclonal antibodies (MAbs), which are mainly obtained from mouse hybridomas and thus are endogenous proteins only in the wider sense, have essentially three different aims.[102] One is the production of immunotoxins—which are molecular conjugates of MAbs with cytotoxins such as gelonin, ricin, or radionuclides. Based on the principle of drug-targeting, they are intended to attach themselves to, for example, tumor cells and selectively kill them. Immunotoxins of this type are currently undergoing initial clinical trials. The second aim is to use MAbs to act in vivo as normal antibodies. The intention is that they densely occupy the antigen-carrying cells, thus enabling them to be destroyed, particularly by the complement system and antibody-dependent cell-mediated cytotoxicity (ADCC). The third approach aims at blocking specific cell receptors in order to inhibit the biological function of these cells—e.g., T cells which are responsible for transplant rejection.

Orthoclone, OKT3®, was developed by Ortho and was the first MAb marketed for therapeutic purposes. It follows the last of the approaches mentioned, being directed against the T3 receptors of human T cells and having a strong immunosuppressant action. Where there is an acute risk of rejection, especially with kidney transplants, it is superior to conventional steroid therapy.[152] However, since it is a mouse MAb, its antigenicity makes it unsuitable for long-term therapy. It is hoped to eliminate this general disadvantage of the current MAbs by developing human MAbs[34] or producing hybrid antibodies by methods of gene technology (see Table 11).

4. Diagnostic Aids

Whereas endogenous proteins are of most interest as therapeutic agents, the greatest importance of the MAbs is as diagnostic aids, which made up about 5% of world pharmaceutical sales in 1982.[204]

MAbs are increasingly being used as components of in vitro test systems. By the middle of 1983 more than 40 MAbs from 22 different companies had already been approved in the USA as in vitro diagnostic aids. At present, in vivo uses, such as tumor imaging, still tend to be the exception.

Determinations of chorionic gonadotropin, large numbers of which are carried out with the commercially available do-it-yourself pregnancy tests, now mainly make use of MAbs. The conventional polyclonal kits are being re-

placed, especially in the area of immunology, by ELISAs, RIAs, and similar determination methods based on MAbs, because the latter have higher specificity and the MAbs can be reproducibly manufactured in virtually unlimited quantities.[182]

5. Veterinary Products

Proteins are becoming of increasing importance in veterinary medicine too, e.g., as vaccines, therapeutics, growth promoters, and diagnostic aids. The losses from livestock epidemics throughout the world amount to about 160 billion DM annually, and this has prompted intensive work on the development of, in particular, recombinant vaccines, e.g., against foot and mouth disease, which alone is the cause of more than half these losses. Bovine growth hormone is able to increase milk production by 20% or more, and porcine interferons successfully control the economically important shipping fever. In the Federal Republic of Germany alone, more than ten veterinary products based on genetically engineered proteins are already on the market.

6. Research and Development Projects

Pharmaceutical proteins provide a good example of the intermeshing of basic and applied research in molecular biology which has increased over the last ten years. The isolation of a new pharmaceutical protein usually starts with the discovery of a biological effect, for example from the observation that the supernatant from an in vitro culture of a cell line causes interesting biological reactions in another cell culture. The subsequent steps, such as characterization of the "factors," protein purification, preparation of antibodies, use of suitable animal models, and isolation of the gene, are still of the nature of basic research, but do provide a chemically defined protein for the first time. This stage is followed, as a rule, by application for a patent and preparation by gene technological methods. This arouses interest in the protein in the pharmaceutical industry. Although it is difficult to estimate the therapeutic potential of the protein at this stage, the companies have to decide whether they wish to produce it as a potential pharmaceutical protein or not. It is usually only after a company has made a recombinant protein available that further basic research reveals details of its biological function(s) and thus allows assessment of its clinical relevance—both of which are needed to justify the high costs of preclinical and clinical development of the pharmaceutical product.

It has sometimes occurred in the past that proteins have been discovered by different approaches and have appeared to be different biologically active substances and then proved to be similar or identical on comparison of the protein or DNA sequences. Thus, for example, it has slowly emerged that tumor necrosis factor, cachectin, and differentiation inhibiting factor are the same protein.

This is why the following tables include only those proteins which, while still undergoing research and development, are either in the preclinical or clinical stage of development or, at the least, chemically defined at the protein or gene level.

Given the large number of protein names and "factor" designations, synonyms have been given, if at all, only in the form of the usual abbreviations. Molecular families,[55] or polypeptides emerging as divergent by proteolysis,[176] and peptides having fewer than 30 amino acids are, as a rule, represented by only one example which has been well investigated and has important uses. Apart from a few exceptions, which are noted, all the data in the tables relate to human proteins and are merely by way of example—i.e., they only partially reflect the current state of knowledge. Further, more detailed information on the individual pharmaceutical proteins may be found in the recent reviews, to which reference is made.

6.1. Peptide Hormones

Many polypeptide hormones consist of fewer than 30 amino acids, which is the current limit below which biotechnological production processes are hardly economic because smaller peptides can, as a rule, be produced at lower cost by chemical synthesis (Table 6).

Table 6. Processes for the production of peptide hormones of various sizes.

Hormone	AA	Production process		
		chemical synthesis	extraction from tissue	gene technology
Thyrotropin-releasing factor	3	X		
Vasopressin	9	X		
LH-releasing hormone	10	X		
Secretin	27	X		
Glucagon	29	(X)	X	
Calcitonin	32	X	X	
Adrenocorticotropin	39	(X)	X	(X)
Insulin	51		X	X
Parathyroid hormone	84		X	X
Growth hormone	191		(X)	X

Some of the hormones in Tables 6 and 7 are already marketed as pharmaceuticals, and some of them have been for quite a few years. Further developments will be aimed at discovering new structural variants with improved therapeutic properties and less costly production processes.

The distinctions between hormones (Table 7), the cytokines, which are occasionally called tissue hormones (Table 9), and growth and differentiation factors (Table 10) are not sharp. For example, the molecules of the insulin family,[18] colony-stimulating factors, interleukins, and other proteins have properties which are characteristic both of hormones and of growth factors.

Many polypeptides are present in vivo as heterogeneous populations of molecules—e.g., atrial natriuretic peptide (ANF), endorphins, somatomedins, and the fertility hormones. The reasons for this are, occasionally, gene families, such as the insulin/somatomedin family, alternative splicing of the mRNA or differences in aggregation, such as with chorionic gonadotropin (HCG), follicle-stimulating hormone (FSH), luteinizing hormone (LH), and thyroid-stimulating hormone (TSH), proteolytic processing

Table 7. Peptide hormones [a].

Protein (abbreviation)	Rev. ref.	AA	Structural peculiarities	Isolated from	Ref.	Cloned	Ref.	Example of use	Preclinical	Clinical
Adrenocorticotropin (ACTH)	[92]	39	1 ch.	—	via bovine cDNA	1980	[33]	inflammation		
ACTH releasing factor (CRF)	[92]	41	1 ch.	—	via ovine cDNA	1983	[188]	inflammation		
Atrial natriuretic peptide (ANF, ANP)	[179]	28	het., 1 SS	1984 atria	[95]	1984	[150]	hypertension	A11, B18, B19, C10, F2, G8, M6, M7, M12, S3, S6, S11, S14, S20, U2, Y3	C1+W6, S16
Calcitonin	[92]	32	C-term. amide, 1 SS, 1 ch.	1968	[172]	1982	[40]	osteoporosis	C3+S3, E1, E7+U3, M4, M7, S2, S16	R6, T3
Cholecystokinin (CCK)		33	1 ch.	—	via porcine protein	1985	[197]	digestion		
Chorionic gonadotropin (CG, HCG)	[165]	237	α-ch., β-ch., CHO	1975 placenta	[134]	1979 1980	[60] [61]	fertility		S15
Endorphin-β	[176]	31	1 ch., CHO	1977 tumor	[54]	1983	[44]	pain		
Follicle-stimulating hormone (FSH)	[163]	210	α-ch., β-ch., CHO	1975 1976 pituitary	[167] [181]	1981	[62]	infertility	I3+S9	
Growth hormone releasing factor (GHRF)	[120]	44	1 ch.	1982 pancreatic tumor	[173]	1983	[126]	rheumatoid arthritis	A5+M11, B7+K1+S12, C8	K1, S4
Growth hormone, Somatotropin (HGH)	[127]	191	1 ch., 2 SS	1972 1971 pituitary tumor	[15] [146]	1979	[123]	dwarfism wound healing	C7, E5, H3, N1, T5	A1+B12+D7, C3+S9, G1, N8, S4
Inhibin	[118]	335	Di, CHO	—	via porcine cDNA	1986	[125]	contra-ception	B10, G1	
Insulin	[192]	51	2 ch., 3 SS	1960 pancreas	[145]	1979	[70]	diabetes	B6+S12, C7, C8+N8, H3, P5, S11	A6+C1+E4, C2, H3, N9, P2
Insulin-like growth factor-1, somatomedin C (IGF1)	[190]	70	1 ch. (incl. C-peptide), 3 SS	1978 plasma	[171]	1983	[93] [94]	injuries	A4, B7+K1+S15, B12, C8+C10, C15, F2, G1, M5, P1	
						1981	[62]			
Luteinizing hormone (LH)	[163]	204–213	α-ch., β-ch., CHO	1979 pituitary	[99]	1983	[198]	fertility	I3+S9	
Parathyroid hormone (PTH)	[164]	84	1 ch.	1978	[98]	1981	[80]	osteoporosis		T7
					via bovine cDNA					
Prolactin release-inhibiting factor (PIF)		56	1 ch.	—		1986	[2]	fertility		
Relaxin	[192]	60	2 ch., 3 SS	—	via porcine cDNA	1983	[86]	obstetrics	G1	
Renin	[144]	340		—	via mouse cDNA	1983	[89]		C1	
Somatostatin	[18]	14	1 ch., 1 SS	1973	[20]	1977 (synth.) 1982	[90] [187]	gastric bleeding	C2, S9	S18
Thyroid-stimulating hormone (TSH)	[163]	201–209	α-ch., β-ch., CHO	1977 pituitary	[180]	1981 1986	[62] [53]	metabolic disorders		

[a] Rev. ref. = reference to review; for company code see Appendix.

steps, such as with ANF and endorphins, or combinations of these possibilities. The physiological significance of these mixtures of molecules of varying biological activity, in which the spectra of action of the components overlap, for example, is largely unknown.

The molecular size of the hormone-like active proteins means that they tend to be near the limit of suitability for oral administration. Oligopeptides that have five or six, or fewer, amino acids and that are protected from peptidases, which is possible by introduction of modified amino acids, for example, are adsorbed from the digestive tract. In contrast, administration of larger polypeptides is possible only by injection or by use of delivery systems. Besides the subcutaneous insulin pump, which has to be inserted surgically, the nasal spray, and the liposome technique, other approaches now being examined are microencapsulation in biocompatible or metabolizable polymers and transmucosal administration. With respect to methodology, however, pharmaceutical proteins still have a lot to catch up on compared with the current lower-molecular-weight active

substances—at least for agents which have to be administered frequently or over long periods.

6.2. Hemostasis and Blood Proteins

Proteins having therapeutic potential for clotting and fibrinolysis indications can be roughly divided into two groups corresponding to the possibilities of treating pathological changes in hemostasis:

- coagulation-promoting proteins for conditions where there is a deficiency of clotting components or for local improvement of coagulation, or
- fibrinolytic proteins for dissolving blood clots, and anticoagulant proteins for preventing fibrin formation.

The therapeutic effect of the protein is decided by whether it acts as an activator or inhibitor, or even as an activator-inhibitor, for example, plasminogen activator-inhibitor (PAI), in the complex interactions regulating blood clotting and fibrinolysis. The functions of some proteins, such as protein C and protein S, vary widely, depending on the local situation in the blood vessel, some of them taking place on the surfaces of endothelial cells and being connected with reactions in the immune system. There are many borderline cases, so that the active proteins are to be found either in Table 8 under hemostasis, in Table 9 under immunomodulators, or in Table 10 as growth factors. Typical examples are the angiogenesis factors, such as angiogenin and fibroblast growth factors.

Development of pharmaceuticals using active proteins of these types must be based on detailed knowledge of the progress and regulation of the processes, and is thus closely tied to basic research.

In the case of human serum albumin, the annual world demand for which is currently about 100 t, with a market

Table 8. Hemostasis and blood proteins [a].

Protein (abbreviation)	Rev. ref.	AA	Structural peculiarities	Isolated from	Ref.	Cloned	Ref.	Example of use	Preclinical	Clinical
Albumin (HSA)		585	SS	1975 liver	[128]	1981	[114]	plasma expander	C7, D4+G1+M7, G3+G6	
α1-antitrypsin (AAT)	[140]	394	1 ch., 3 CHO	1978 1978 blood	[189] [136]	1981	[108]	anti-coagulant	C8, C13, C14+Z1, D4, G1, S14, T9	
Antithrombin III (AT3)	[130]	432	CHO, 3 SS	1979 liver	[161]	1983 1982	[32] [19]	anti-coagulant	D4, G1	C6, H3
Factor VII	[115]	406	1 ch., CHO	1980	[25]	1986	[77]	blood clotting		N9, Z1
Factor VIII	[115]	2332	1 ch., 25 CHO	1983 liver	[177] via porcine cDNA	1984 1984	[69] [203]	hemophilia A	A1, B7+K1+T2, C18+G1, G5, G6, T9	B1+G2, H3, R6
Factor IX	[43]	416	1 ch., CHO	1975 plasma	[153]	1982 1982	[35] [109]	hemophilia B	B12, G1, G2, R5+T9, Z1	
Factor XIII	[115]	1372	Tet, α-ch., β-ch., CHO	1971 plasma	[185]	1986	[88]	surgical adhesive	H3	
Tissue plasminogen activator (tPA)	[39]	527	17 SS, 1 ch. and 2 ch., 3 CHO	1979 uterus	[168]	1983	[157]	myocardial infarct, embolism	B2+M9, B3, B4+C8, B11+R4, C3+S3, C4, C5+H2+N5+N6+S1+T8, C10, C12, C15+M4, E4, G3, G4, I6+S8, K1+W4, K2, M1, M8, P4, S13+W4, W2, Y1	A10+K5, B1+G2+W5+S15, B2+Y1, B7+F2+S14, B13+G1+K6+M7, D1+I3+K4+T6, D3+S14, G6+Y3, M10
Leuserpin 2 (LS 2)		480	CHO	— via DNA probes of homol. protein		1986	[166]	blood clotting		
Plasminogen activator inhibitor (PAI 1)	[17]	376-379	CHO	1984 lymphosarcoma	[202]	1986	[148]	blood clotting	H3	
Protein C (PC)	[56]	262	2 ch., CHO, SS	1979 plasma	[101]	1984	[64]	anti-coagulant	E4, H3, I3+K4+T6, T2+Z1	
Protein S		635	1 ch., CHO, 2βHA	— via bovine cDNA		1986	[121]	anti-coagulant	I3+K4	
Prourokinase (SCUPA, PUK, KPA)	[17]	411	1 ch., 1 CHO, SS	1982	[219]	1985 1985	[84] [143]	myocardial infarct, thromboses	D3, N5+N6+T5	C13+S2, G1+G7, G6+Y3, M10
Streptokinase [b]	[156]			microbial				myocardial infarct, thromboses	P3	D5
Urokinase (UK)	[156] [37]	366	1 ch. and 2 ch., SS, 1 CHO	1982 urine	[75]	1984	[209]	thromboses, embolism	D3, G6, H1, N2	G1, G7

[a] Rev. ref. = reference to review; for company code see Appendix. [b] APSAC (B3) see text.

value of about 1.3 billion DM,[204] the research and development is concentrated primarily on improving the biological and industrial processes for producing it using recombinant yeasts in order to be able to compete in economic terms with the conventional isolation from human blood.

Streptokinase, which is also now commercially available, is an example of the successful chemical modification of pharmaceutical proteins. The "acylated plasminogen streptokinase activator complex" (APSAC) of Beecham is distinguished from streptokinase by having less affinity for fibrinogen and a longer half-life.

6.3. Immunomodulators (Cytokines)

The immune system is, in association with the healing processes which take place following inflammation, the real source of the "natural healing powers" of the body and thus is central to the therapeutic concept of endogenous proteins. The pharmaceutical proteins that act on immunological functions include, in particular, the interferon and interleukin groups (Table 9) as well as the growth and differentiation factors (Table 10) which, as immunomodulators inter alia, control the maturation, activation, and

Table 9. Immunmodulators (cytokines) [a].

Protein (abbreviation)	Rev. ref.	AA	Structural peculiarities	Isolated from	Ref.	Cloned	Ref.	Example of use	Preclinical	Clinical
Interferon-α (IFN-α)	[160]	166	CHO, het., sia, acid-stable	1979 leucocytes	[178]	1980	[141]	hairy cell leukemia, tumors	A9, B4, B7+S11, B15, B15+G1+G6, C8+S7, C10+K6, D1+G1, I1, N3, T7, S15+W5	A4, C7, C13+I4, E3, E8, G6, H1+M10+O2, K1, V1
Interferon-β (IFN-β1)	[160]	166	CHO, SS, sia	1979 fibroblasts	[199]	1980	[47]	keratitis, hepatitis B	B4, B7+S5, K6, S15, W5	C6+T10, K6, M10, S7
Interferon-γ (IFN-γ, MAF)	[211]	146	CHO, acid-labile	1981 lymphocytes	[212]	1982	[74]	tumors, arthritis	A10+B2, B4, C3+S3, C7, C8+S7, E3, H1+O2, K2, M3, S9+Y2, S14, S15+S16, W5	A4, A8+I4+R7+T8, B1+B7+R1+S11, B13+D1+G1+T4, C10+K6, G1+G6, M2+M12, N4+T1, S5+S16, S12
Interleukin-1 (*IL-1, ETAF, LAF*)	[51]	152	MP	1984 *neutrophils*	[50]	1984	[10]	tumors	C11+D7, D2, I2+S17, I4, M5, O2, R2, S7, S14	
Interleukin-2 (IL-2, TCGF)	[7]	133	sia, het.	1980 T cells	[132]	1983	[200]	tumors	A2+H3+I2+T1, A9, B9, B15, C8, D7, G3+Y3, H3, K6, O2, Q1	A2+H4, A4+J1, B7+S11, C6, C13+T10, F2, G6, H1, H3, I2, I5, L1+T1, O2, R7+S4+T9, T4, V1
Interleukin-3 (IL-3, Multi-CSF, BPA, MCGF)	[184]	133	CHO, het.	—	via gibbon cDNA	1986	[221]	leukemia, other tumors	B7, D6, G2, H3+I2, Z1	
Interleukin-4 (*IL-4*, BSF-1, BCGF-I)		129	CHO	—	via mouse cDNA	1986	[222]	leukemia, infections	D6+S5, E2, O1	
Interleukin-5 (IL-5, TRF, BCGF-II)		112	2 CHO	—	via mouse cDNA	1986	[11]	autoimmune diseases	B9, C13, D6, E2+I2, I4, Q1, S16	
Interleukin-6 (IL-6, BSF2, IFN-β2, BCDF)	[186]	184	1 ch., CHO	1985 T cells	[81]	1986	[82]	leukemia	A2	
Lymphotoxin (LT, TNF-β)	[154, 213]	171	CHO	1984 lymphocytes	[4]	1984	[73]	tumors	F2+G1, K2, S13, U2	
Macrophage inhibitory factor (MIF)	[191]		het.	1981 lymphocytes	[216]	1987	[196]			
Thymopoietin (TPO)	[71]	48		1987 thymus	[9]			infections		H4
Transforming growth factor-α (TGF-α)	[46]	50	1 ch.	1982 tumor cells	[122]	1984	[49]	wound healing	C15, G1	
Transforming growth factor-β (TGF-β)	[97]	112	homo-Di, 2 ch., SS	1983 kidney tumor	[8]	1985	[48]	wound healing, tumors	C15, G1	
Tumor necrosis factor (TNF-α, cachectin, DIF)	[14, 154]	157	1 SS	1985	[3]	1984	[159]	tumors	A10+N7, C6+C8, G6, I4, S7, S9+Y2, Y1	A10, B7+K4+S16, B13+G1, C6, D2+G1, H1+M10+O2, W1
Uromodulin, Tamm-Horsfall protein (UK)		616	CHO, 24 SS, sia	1985 urine	[139]	1987	[158]	inflammations	B7	

[a] Rev. ref. = reference to review; for company code see Appendix.

suppression of the various blood cells. Dysregulation within the immune system not only causes weakening of the body's defenses, resulting in an increased susceptibility to infection and, possibly, tumors too, but may also give rise to hyperreactivity towards autologous tissue, resulting in autoimmune diseases such as rheumatoid arthritis and multiple sclerosis.

Cells of the immune system pass through two phases of growth and differentiation which differ in character. The process of hemopoiesis initially results in bone marrow cells being converted into precursors of lymphocytes, monocytes, and granulocytes, which develop into, for example, T cells and their subpopulations, various macrophages and eosinophilic, neutrophilic, or basophilic granulocytes. Cells persisting after this first phase of growth and differentiation, called resting cells, may be activated in the case of immunological reactions to renewed proliferation and special differentiation steps. Proteins that mainly act in this second phase are listed as immunomodulators in Table 9, and proteins that control the first development phase of the immune cells or exert analogous functions on other cells are listed as growth factors in Table 10. The two groups belong together since different functions may be combined in one molecule, a good example being tumor necrosis factor (TNF). Originally isolated as a protein able to kill tumor cells selectively in vitro and in vivo, TNF has now proved to be a central immunomodulator which may act, inter alia, as a growth factor for fibroblasts, as an activator for neutrophilic granulocytes, and as an inhibitor in the differentiation of bone marrow cells to lymphocytes. The spectra of action of immunomodulators show distinct redundancies even more often than those of hormones (see Table 7). For example, TNF and interleukin-1[151] are now known to have about 30 biological effects which, for the most part, are common to both but differ quantitatively.[116] The same is true of the antiviral and cytostatic effects of interferon-α and -β.

Although they bind to the same receptor molecule on the target cell, they may trigger different cellular reactions. The biological significance of this phenomenon and the possible consequences for the development of drugs are largely unclear. Whether a cell reacts to an immunomodulator molecule or not depends equally on the presence or absence of the immunomodulator and on the presence or absence of the appropriate receptors on the target cells. In some tumor cells, for example, interferon-γ appears to influence the cytotoxic action of TNF by inducing TNF receptors and thus making the initially TNF-resistant cells sensitive. Receptors for some cytokines, such as interleukin-1 and interleukin-2, have already been isolated. Intensive work is being carried out on many others to make it possible to establish, and influence, the structural components of the receptor/ligand interaction. A requirement for structural investigations of this type is the preparation of

Table 10. Growth and differentiation factors [a].

Protein (abbreviation)	Rev. ref.	AA	Structural peculiarites	Isolated from	Ref.	Cloned	Ref.	Example of use	Preclinical	Clinical
Angiogenin (TAF)	[124]	123	1 ch., 3 SS	1985 1985 bowel cancer calls	[59] [194]	1985	[110]	wound healing, tumors	M12	
Endothelial cell growth factor (ECGF-β)		155		—	via bovine ECGF	1986	[94]	wound healing	R6	
Epidermal growth factor, urogastrone (EGF)	[67]	49	MP, 1 ch., 3 SS	1975	[36]	1984 1985	[23] [195]	burns, ulcers	A4, A7, B16, C15, E1, J1+M12, O2, S9, S15, T6, W3, W5	C8, J1, K3
Erythrocyte differentiation factor (EDF)		110	homo-Di, SS	1987 leukemia cells	[57]	1987		tumors	A2	
Erythropoietin (EPO)		167	CHO, sia	1977 urine	[133]	1984	[117]	aplastic anemia	B5, C1, C12, H1, H3+I3+T6, S13, S15+W5	A4+K3+S3+J1, B4+I3, B7, B14+C9+G2
Fibroblast growth factor (bFGF (basic))	[201]	146	het.	1986	[68] via bovine cDNA	1986	[1]	wound healing, tumors	C1+A3, C8, M5, T9	
Granulocyte colony-stimulating factor (G-CSF)	[30]	174–177	CHO	1986 tumor cells	[147]	1986	[142]	leukemia, other tumors	B4+I2, B7, C9, K6	A4+K3, I2
Granulocyte-macrophage colony stimulating factor (GM-CSF, CSF-2)	[129]	127	CHO	1984 T cell 1981	[66] [42]	1985	[218]	anemia, tumors	B7+S15, C9, D6, I3, T4, Z1	A4+K3, G2+S2, I2+H3
Macrophage colony stimulating factor (CSF-1, M-CSF)	[30]	224	CHO, homo-Di	1982 urine	[41]	1985	[96]	leukemia, tumors	B4+I2, B7, C6, G2, O2	
Nerve growth factor (NGF-β)	[72]	118	homo-Di	—	via mouse cDNA	1983	[205]	injuries	F1+G1, G2	
Platelet-derived growth factor (PDGF)	[175]	241	homo-Di, SS	1983 1983 platelets	[215] [52]	1985	[38]	wound healing	A4, C8+J1, C15, Z1	

[a] Rev. ref. = reference to review; for company code see Appendix.

sufficiently large protein crystals for X-ray structural analysis, and these are already available in the case of TNF, for example (Fig. 5).

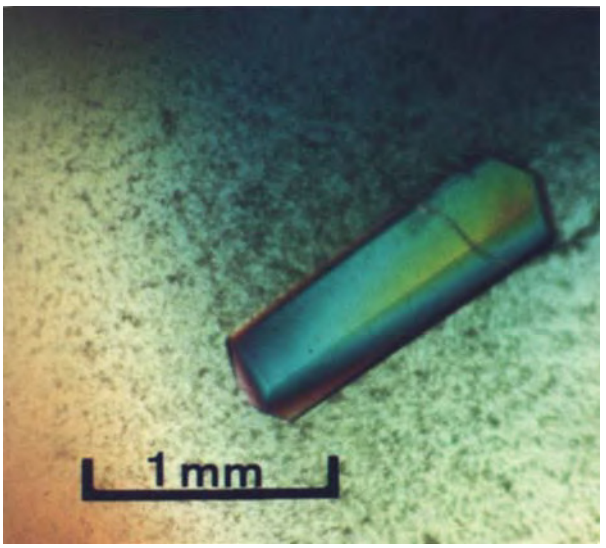

Fig. 5. Crystal of recombinant tumor necrosis factor under the polarizing microscope.

Thus, as understanding of the functioning of humoral and cell-mediated immunity increases, there is an increase in the importance not only of the soluble mediator molecules as "biological response modifiers" (BRM) for therapeutic purposes, but also of their receptors on the cell membrane and similar signal transfer molecules.

6.4. Growth and Differentiation Factors

The group of growth and differentiation factors (Table 10) includes, in particular, the colony-stimulating factors (CSFs) to which interleukin-3 and, in the wider sense, erythropoietin and erythrocyte differentiation factor also belong.[72] They are highly specific triggers of the differentiation steps in hemopoiesis. Although G-CSF activates neutrophilic granulocytes, in addition to the hemopoietic action, and GM-CSF increases the biological activity of macrophages and granulocytes, nevertheless these effects are confined to precursor and fully differentiated cells of the populations which are stimulated to differentiate by CSFs.[30] This specificity is a possible reason why the initial clinical studies, with, for example, erythropoietin on dialysis patients, and G-CSF and GM-CSF on cancer patients following chemotherapy, were so successful and were not complicated by the undesired side effects otherwise found with immunomodulators, such as fever[103] (Fig. 6).

Vastly more complicated is the development of endogenous proteins that are normally not distributed with the blood but formed locally, for example in the neighborhood of inflammations, tumors, or injuries, and display their effects only there, and are then rapidly inactivated. Typical examples are the angiogenesis factors such as angiogenin and fibroblast growth factors. Apart from wound healing, their importance is in tumor therapy, in particular, although not directly but as part of the search for antagonists or inhibitors preventing the vascularization of solid tumors and thus hindering their growth or even inducing necrosis. These proteins show that, on occasion, pharmaceutical proteins are not themselves of clinical interest but they must be available and their mode of functioning must be known in order for them to serve, for example, as test and screening systems for other proteins or low-molecular-weight active substances.

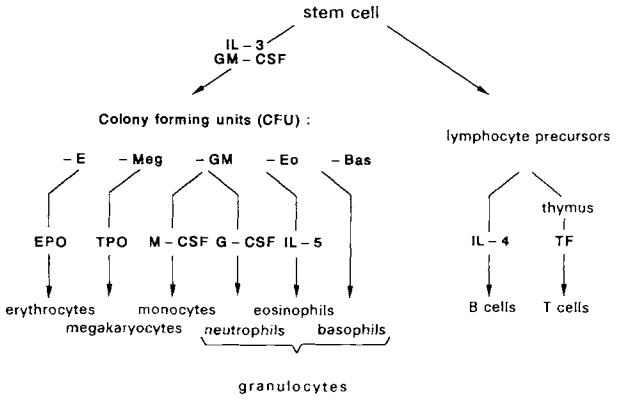

Fig. 6. Diagram showing hemopoiesis with the main sites of action of some growth and differentiation factors. Abbreviations: IL-3, -4, -5, interleukin-3, -4, -5; GM-CSF, granulocyte-macrophage colony-stimulating factor; CFU-E, -Meg, -GM, -Eo, -Bas, precursor cells for erythrocytes, megakaryocytes, granulocytes-macrophages, and eosinophilic and basophilic granulocytes; EPO, erythropoietin; TPO, thymopoietin; M-CSF, macrophage colony-stimulating factor; G-CSF, granulocyte colony-stimulating factor; TF, T-cell maturation factor (for further details see Ref. [30]).

6.5. Other Pharmaceutical Proteins

The hepatitis B surface antigen, which is already marketed as a vaccine, is included in Table 11 as a representative of many other vaccines currently under development. Genetically engineered surface proteins, or parts of these molecules, occasionally also produced by peptide synthesis, also form the basis for the development of vaccines against malaria, leprosy, meningitis, AIDS, influenza, herpes, and other infectious diseases. The first malaria and AIDS vaccines are now sufficiently advanced to have been tested on humans, but they have not proved to be sufficiently antigenic as yet.

Promising approaches to new vaccines based on anti-idiotype antibodies have recently been reported;[208] these "anti-antibodies" are directed against the antibodies previously formed in the body, and consequently have elements of the molecular structure of the original antigen. They can apparently be used in place of the antigen for vaccination.

There are great hopes that superoxide dismutase will be of use for diminishing the risk of reocclusion and necrosis following fibrinolytic treatment of myocardial infarcts, because reperfusion of tissue that has been depleted of oxygen results in the formation of O_2 radicals which are damaging to tissues.

7. Protein Purification

Apart from the few digestive enzymes that can be administered orally, at present injection is the only practica-

Table 11. Other pharmaceutical proteins [a].

Protein (abbreviation)	Rev. ref.	AA	Structural peculiarities	Isolated from	Ref.	Cloned	Ref.	Example of use	Preclinical	Clinical
Apolipoprotein A1 (APO)	[21]	243	1 ch.	1975 1975 plasma	[12] [45]	1982	[22]	arterio-sclerosis	B12, M7	
Fibronectin (FN)	[87]	96	CHO, MP, 2 ch., SS	1970	[138]	1983	[104]	wound healing	D4, S12	
Hepatitis-B surface antigen (HBS, HBsAg)	[131, 207]	226	CHO	1977 virions	[162]	1979	[155]	hepatitis vaccine		A4+J1, B7+G6+W5, C8, G1, R5
Human collagenase inhibitor (HCI, TIMP)		184	CHO	1983 fibro-blasts	[193]	1986	[26]	arthritis	C3, R5	
Hyaluronidase			CHO	1982 serum	[58]			ophthalmolo-gical in-filtrations	B8	
Lipase		135	Pre	microbial		1986	[106]	digestive disturbances	C3	
Lung surfactant protein (LSP, PSP)		248	CHO, sia	1986 sputum	[63]	1986 1987	[63] [91]	emphysema, pulmonary infections	B17, C1	
Lipomodulin, Lipocortin (AIP)	[83]	346	1 CHO	—	via rat sequence	1986	[214]	arthritis, allergies	B7+Y1, U3	
Monoclonal antibody OKT3 (OKT3)	[102]			1979 hybridoma	[107]			transplan-tation		
Muellerian inhibiting substance (MIS)		560	CHO, SS, Di	—	via bovine cDNA	1986	[27]	ovarian tumors	B7+M5	
Neuroleukin (NL)		558		1986 salivary gland	[76]	1986 (mouse)	[76]			
Superoxide dismutase (SOD)	[65]	153	Di, contains Cu and Zn	1972 1980 placenta	[78] [13]	1982	[119]	after-treat-ment of myocar-dial infarct	N3, S19, T7, U1	B12+B15+Y2, C2, C8+G7+P1, E2+E6+R3
Trypsin inhibitor (HPSTI)	[79, 112]	56	3 SS, 1K	1985 pancreas	[100]	1985	[220]	pancreatitis	S20	

[a] Rev. ref. = reference to review; for company codes see Appendix.

ble method of administering pharmaceutical proteins. This is why purification processes must be designed to meet the stringent purity requirements applying to solutions for injection. Figure 7 outlines a typical purification process for a recombinant protein from *E. coli*.

The final purification is an attempt to ensure the purity and homogeneity of the protein, usually by successive chromatography steps based on differing principles of separation, e.g., on charge, molecular weight, hydrophobicity, and other affinity properties. These separation processes are aimed at reducing the contents in the desired product of not only foreign proteins but also protein aggregates, biologically inactive isomers, and species with *N*-terminal methionine. A reliable statement about the homogeneity of a complex protein can be based only, if at all, on a combination of many results from different analytical methods. These include high-precision chemical analyses, quantitative amino acid determinations, *N*- and *C*-terminal sequencing, peptide mapping, gel electrophoreses and isoelectric focusing, in combination with spectroscopic methods and appropriate bioassays. The amounts of impurities, the most important being endotoxin, nucleic acids, and host cell proteins, tolerable per dose of active substance are usually in the picogram range, and thus at the limit of sensitivity of the currently available methods. A demonstration of the absence of viruses may be omitted for proteins produced in *E. coli*, for example, whereas great efforts must be made in this direction where the genetically modified cells used are derived from rodents or, in particular, humans.

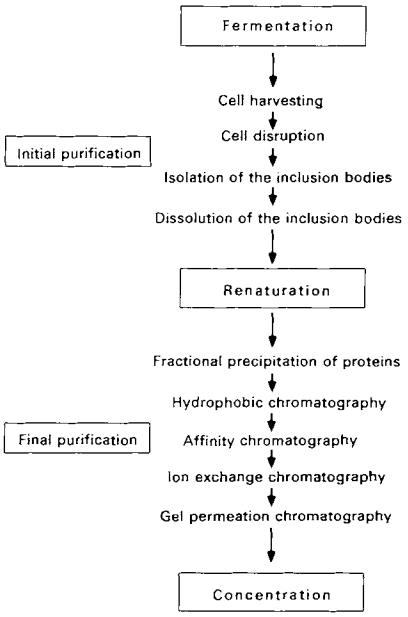

Fig. 7. Diagram of the steps in the purification of a recombinant protein produced in the form of inclusion bodies in *E. coli*.

8. Official Approval

In most countries, a staged scheme is applied to each individual protein by the authorities approving clinical trials on, or the marketing of pharmaceuticals based on, genetically engineered proteins. The requirements for this are accurate data on the purity of the protein together with preclinical investigations of the pharmacokinetics, toxicology, formulation, and biological activity in various animal models. In this connection it has to be remembered that species-specific pharmaceutical proteins in an animal model comprise a heterologous system, so that there are provisos about applying the results to humans. Where the data warrant initial clinical use, the protein is made available to physicians who, in the Federal Republic of Germany, may administer it to patients only after approval by the relevant ethical committee.

The clinical trials are conducted to determine in the first phase the dose required, in the second phase the efficacy, and in the third phase the therapeutic safety. These trials usually take three to five years, and only after this will the authority make a decision, based on the available data, about approval for marketing.

9. Patent Aspects

A plethora of questions about patent law have arisen since the results of research in genetic engineering and biotechnology have reached the level of economic decisions, and conclusive answers to these will emerge only gradually. Whereas, for example, up to 1979 it was absolutely impossible to patent microorganisms in the USA, it is now possible in most countries to protect a very wide variety of cultivated cells. This requires that the microorganism is described in such a way that those skilled in the art are able to reproduce the invention at any time and as often as required. If this is impossible, description may be replaced by deposition of the organism in a type collection accessible to the public.

Patent protection in the area of biotechnology tends at present to be limited, and efforts are being made internationally to extend and facilitate it not only by providing protection for microorganisms and results of molecular biological research (e.g., cell lines, plasmids, monoclonal antibodies), but also by improving the existing protection available for the results of breeding (e.g., for new plant varieties and animal breeds).

The importance of harmonization in the industrial property area rights is evident from the fact that, for example, in the USA and Japan a patent application can still be filed twelve and six months, respectively, after publication of the invention, whereas in the European and German proceedings any publication is immediately "prejudicial to novelty."

It will take some years for many of the questions to be answered in the courts, and only after this will it be possible to assess accurately the value of genetic engineering and biotechnological patents. The basic question of whether, in the case of a known protein which has been produced for the first time by gene manipulation, the product or only the process can be patented has been answered, for the moment, as follows: The High Court in the UK recently annulled a patent of Genentech which claimed, inter alia, comprehensive product protection for tPA, on the grounds that the patent was too broad and the substance and its use were already known.

Besides these general questions, there are many specific problems. For example, the breadth of protection conferred by a product claim for a new protein remains undetermined. Does it include genetically engineered mutants, and is it enough to replace a single amino acid, or even a nucleotide, to circumvent such a patent?

Gene patents that relate not to the protein but to the sequence of a section of human DNA and claim all the proteins, antibodies, diagnostic aids, etc. derived from it[169] have given rise to discussion about whether it is acceptable for property rights on human DNA sequences to be acquired in the course of sequencing the human genome.[174]

10. Prospects

Despite a 65-year history of the use of proteins in therapy, interest in it has perceptively increased only in recent years. The basis for this development is the enormous increase in knowledge in the biomedical disciplines which, in the last two decades, has derived from, in particular, advances in molecular biology (genetic engineering), cell biology, and protein chemistry, as well as new physicochemical measurement techniques and high-tech laboratory equipment, such as automatic analyzers and synthesizers and computers.

It now often takes less than a year for the DNA and amino acid sequences of a new protein of defined biological activity to become available. Comparison of these sequences with the several thousand already known sometimes reveals the functions and biological relationships of at least parts of the structures of these proteins. These parts of the structure, called domains, are often the structural elements responsible for biological action. Important tasks for protein chemists in the future will be to detect them in the folded protein molecule, to isolate them and stabilize their structures, and to modify them for appropriate effects. These aims are a development in the direction of "synthetic biology" and will be successfully achieved only by interdisciplinary cooperation between the molecular and cell biologists and the protein or peptide chemists and specialists in molecular modeling.

At present, most effort is still directed at finding new proteins with pharmaceutical potential. In view of the fact that there are about 30000 human genes and about 200 different tissues, i.e., mutually interacting cell types, and that the proteins suitable as pharmaceuticals are mainly extracellular proteins, each of which, in many cases, has several biological functions, it may be assumed that the number of proteins of potential use for pharmaceuticals will be in the hundreds, although hardly more than one thousand. However, it is hardly likely that the possible combinations and variations of active substances derived from them will be exhausted in the forseeable future. In addition, there is the large repertoire of "natural protein design" which is the

basis for the synthesis of antibodies in cells and which now can be artificially modified in a variety of ways.

However, work in the immediate future will be concentrated more on the clinical application of the active proteins already available, in order to make the breakthrough with new genetically engineered proteins which is now necessary after almost ten years of development in this area of molecular biology.

Thus, drug research and pharmaceutical treatment are at the beginning of an entirely new development which raises hopes of new approaches to indications as important as virus infections, inflammatory rheumatic diseases, arteriosclerosis, autoimmune diseases, and tumors.

We express our thanks to Dr. W. Heckmann for the electron micrographs and to Dr. N. Walker for the picture of the TNF crystal. The valuable assistance with the preparation of the manuscripts by M. Kern and S. Petersen-Werner is gratefully acknowledged.

Received: September 9, 1987 [A 656 IE]
German version: *Angew. Chem. 100* (1988) 213

Appendix: Company Codes

A 1 ABI Biotechnology, Winnipeg, Canada
A 2 Ajinomoto, Tokyo, Japan
A 3 Akzo Pharma, Oss, The Netherlands
A 4 Amgen, Thousand Oaks, USA
A 5 American Cyanamid, Wayne, USA
A 6 American Home Products, New York, USA
A 7 Amersham International, Little Chalfont, UK
A 8 Anheuser-Busch, St. Louis, USA
A 9 Antibioticos (Montedison), Madrid, Spain
A 10 Asahi Chemical, Osaka, Japan
A 11 Abbott, Chicago, USA
B 1 Baxter Travenol, Deerfield, USA
B 2 Beckmann Research Institute, City of Hope, USA
B 3 Beecham, Brentford, UK
B 4 Behringwerke (Hoechst), Marburg, FRG
B 5 Bioassay Systems, Woburn, USA
B 6 Biobras, Brazil
B 7 Biogen, Willemstad, NL Antilles
B 8 Biopharm, Swansea, UK
B 9 Biotech Research, Rockville, USA
B 10 Biotechnology Australia, Sydney, Australia
B 11 Bio-Response, Hayward, USA
B 12 Bio-Technology General, New York, USA
B 13 Boehringer Ingelheim, FRG
B 14 Boehringer Mannheim, FRG
B 15 Bristol-Myers, New York, USA
B 16 British Bio-Technology, Cowley, UK
B 17 Byk Gulden (Altana), Konstanz, FRG
B 18 Bayer, Leverkusen, FRG
B 19 Bio-Mega, Montreal, Canada
C 1 California Biotechnology, Mountain View, USA
C 2 Carlbiotech, Kopenhagen, Denmark
C 3 Celltech, Berkshire, UK
C 4 Centocor, Malvern, USA
C 5 Central Glass, Tokyo, Japan
C 6 Cetus, Emeryville, USA
C 7 Cheil Sugar, Samsung, Korea
C 8 Chiron, Emeryville, USA
C 9 Chugai, Tokyo, Japan
C 10 Ciba-Geigy, Basel, Switzerland
C 11 Cistron Biotechnology, Pine Brook, USA
C 12 Codon, Brisbane, UK
C 13 Collaborative Research, Lexington, USA
C 14 Cooper Development, Palo Alto, USA
C 15 Creative Biomolecules, Hopkinton, USA
D 1 Daichi Seiyaku, Tokyo, Japan
D 2 Dainippon, Tokyo, Japan
D 3 Damon Biotech, Needham Heights, USA
D 4 Delta Biotechnology, Nottingham, UK
D 5 Diversified Tech, Salt Lake City, USA
D 6 DNAX (Schering Plough), Palo Alto, USA
D 7 DuPont, Wilmington, USA
E 1 Earth Chemical, Ako City, Japan
E 2 Eastman Kodak, Rochester, USA
E 3 Egis Pharmaceuticals, Budapest, Hungary
E 4 Eli Lilly, Indianapolis, USA
E 5 Endotronics, Coon Rapids, USA
E 6 Enzon, South Plainfield, USA
E 7 Erbamont, Italy
E 8 Exovir, New York, USA
F 1 Fidia, Abano Terme, Italy
F 2 Fujisawa, Osaka, Japan
G 1 Genentech, San Francisco, USA
G 2 Genetics Institute, Cambridge, USA
G 3 Genex, Gaithersburg, USA
G 4 Genzyme, Boston, USA
G 5 Gist-Brocades, Delft, The Netherlands
G 6 Green Cross, Osaka, Japan
G 7 Grünenthal, Stolberg, FRG
G 8 Glaxo, London, UK
H 1 Hayashibara, Okayama, Japan
H 2 Hodogaya Chemical, Tokyo, Japan
H 3 Hoechst, Frankfurt (Main), FRG
H 4 Hoffmann-La Roche, Basel, Switzerland
I 1 ICI, London, UK
I 2 Immunex, Seattle, USA
I 3 Integrated Genetics, Framingham, USA
I 4 Interferon Sciences (NPDC), New Brunswick, USA
I 5 Interleukin-2 Inc., Alexandria, USA
I 6 Invitron, Redwood City, USA
J 1 Johnson & Johnson, New Brunswick, USA
K 1 KabiVitrum, Stockholm, Sweden
K 2 Kanegafuchi, Osaka, Japan
K 3 Kirin Brewery, Tokyo, Japan
K 4 Knoll (BASF), Ludwigshafen, FRG
K 5 Kowa Spinning, Tokyo, Japan
K 6 Kyowa Hakko, Tokyo, Japan
L 1 Liposome Company, Princeton, USA
M 1 Meiji Milk, Tokyo, Japan
M 2 Meiji Seika Kaisha, Tokyo, Japan
M 3 Meloy Laboratories (Rorer), Springfield, USA
M 4 Menarini, Florenz, Italy
M 5 Merck & Co., Rahway, USA
M 6 Merrell Dow (Dow), Cincinnati, USA
M 7 Mitsubishi Chemical, Tokyo, Japan
M 8 Mitsui, Tokyo, Japan
M 9 Mitsui Toatsu, Tokyo, Japan
M 10 Mochida, Tokyo, Japan
M 11 Molecular Genetics, Minnetonka, USA
M 12 Monsanto, St. Louis, USA
N 1 Nippon Chemical Ind. Co., Tokyo, Japan
N 2 Nippon Chemiphar, Tokyo, Japan
N 3 Nippon Kayaku, Tokyo, Japan
N 4 Nippon Roche (Roche), Tokyo, Japan
N 5 Nippon Soda, Tokyo, Japan
N 6 Nissan Chemical, Tokyo, Japan
N 7 Nihon Seiyaku, Tokyo, Japan
N 8 Nordisk, Gentofte, Denmark
N 9 Novo, Bagsvaerd, Denmark
O 1 Ono Pharmaceutical, Osaka, Japan
O 2 Otsuka, Tokyo, Japan
P 1 Pharmacia (Fortia), Uppsala, Sweden
P 2 Pharmed, Westbury, USA
P 3 Phillips Petroleum, Bartlesville, USA
P 4 Porton International, London, UK
P 5 Procter & Gamble, Cincinnati, USA
Q 1 Quidel, La Jolla, USA
R 1 Rentschler, Laupheim, FRG
R 2 Repligen, Cambridge, USA
R 3 Research Corporation, USA
R 4 Retroperfusion Corporation, USA
R 5 Rhone-Poulenc, Courbevoie, France
R 6 Rorer, Fort Washington, USA
R 7 Roussel-Uclaf, Paris, France
S 1 Sagami Chemical Research Center, Tokyo, Japan
S 2 Sandoz, Basel, Switzerland
S 3 Sankyo, Tokyo, Japan
S 4 Sanofi, Paris, France
S 5 Schering Plough, Madison, USA
S 6 Schwarz, Monheim, FRG
S 7 Sclavo (Eni), Siena, Italy
S 8 Searle (Monsanto), Skokie, USA

S 9 Serono, Randolph, USA
S 10 Seyaku, Japan
S 11 Shionogi, Osaka, Japan
S 12 Sidus, Buenos Aires, Argentina
S 13 Snow Brand, Tokyo, Japan
S 14 SmithKline, Philadelphia, USA
S 15 Sumitomo, Osaka, Japan
S 16 Suntory, Osaka, Japan
S 17 Syntex, Palo Alto, USA
S 18 Schering AG, Berlin, FRG
S 19 Syn-tek, Sweden
S 20 Squibb, New York, USA
T 1 Takeda, Osaka, Japan
T 2 Teijin, Osaka, Japan
T 3 Teikoku Hormone, Tokyo, Japan
T 4 Toray, Tokyo, Japan
T 5 Tosoh Corporation, Japan
T 6 Toyobo, Osaka, Japan
T 7 Toyo Jozo, Tokyo, Japan
T 8 Toyo Soda, Tokyo, Japan
T 9 Transgene, Paris, France
T 10 Triton Biosciences, Alameda, USA
U 1 Ube Industries, Ube City, Japan
U 2 Upjohn, Kalamazoo, USA
U 3 Unigene, Fairfield, USA
V 1 Viragen, Hialech, USA
W 1 Wadley Institute, Dallas, USA
W 2 Wakamoto Pharmaceuticals, Tokyo, Japan
W 3 Wakunaga, Osaka, Japan
W 4 Weizmann Institute (Yeda), Tel Aviv, Israel
W 5 Wellcome, Dartford, UK
W 6 Wyeth Laboratories (Ferm.), Radnor, USA
Y 1 Yamanouchi, Tokyo, Japan
Y 2 Yeda, Tel Aviv, Israel
Y 3 Yoshitomi, Osaka, Japan
Z 1 Zymo-Genetics, Seattle, USA

[1] J. A. Abraham, J. L. Whang, A. Tumolo, A. Mergia, J. Friedman, D. Gospodarowicz, J. C. Fiddes, *EMBO J. 5* (1986) 2523.
[2] J. P. Adelman, A. J. Mason, J. S. Hayflick, P. H. Seeburg, *Proc. Natl. Acad. Sci. USA 83* (1986) 179.
[3] B. B. Aggarwal, W. J. Kohr, P. E. Hass, B. Moffat, S. A. Spencer, W. J. Henzel, T. S. Bringman, G. E. Nedwin, D. V. Goeddel, R. N. Harkins, *J. Biol. Chem. 260* (1985) 2345.
[4] B. B. Aggarwal, B. Moffat, R. N. Harkins, *J. Biol. Chem. 259* (1984) 686.
[5] *Newswatch*, Nov. 1986, p. 5.
[6] *Roche Intern*, Aug. 1987, p. 5.
[7] S. K. Arya, M. G. Sarngadharan, *NATO ASI Ser., Ser. A 120* (1986) 165.
[8] R. K. Assoian, A. Komoriya, C. A. Meyers, D. M. Miller, M. B. Sporn, *J. Biol. Chem. 258* (1983) 7155.
[9] T. Audhya, D. H. Schlesinger, G. Goldstein, *Proc. Natl. Acad. Sci. USA 84* (1987) 3545.
[10] P. E. Auron, A. C. Webb, L. J. Rosenwasser, S. F. Mucci, A. Rich, S. M. Wolff, C. A. Dinarello, *Proc. Natl. Acad. Sci. USA 81* (1984) 7907.
[11] C. Azuma, T. Tanabe, M. Konishi, T. Kinashi, T. Noma, F. Matsuda, Y. Yaoita, K. Takatsu, L. Hammarström, C. I. E. Smith, E. Severinson, T. Honjo, *Nucleic Acids Res. 14* (1986) 9149.
[12] H. N. Baker, A. M. Gotto, Jr., R. L. Jackson, *J. Biol. Chem. 250* (1975) 2725.
[13] D. Barra, F. Martini, J. V. Bannister, M. E. Schinina, G. Rotilio, W. H. Bannister, F. Bossa, *FEBS Lett. 120* (1980) 53.
[14] B. Beutler, A. Cerami, *N. Engl. J. Med. 316* (1987) 379.
[15] T. A. Bewley, J. S. Dixon, C. H. Li, *Int. J. Pept. Protein Res. 4* (1972) 281.
[16] H. Bialy, *Bio/Technol. 5* (1987) 883.
[17] F. Blasi, J.-D. Vassalli, K. Danø, *J. Cell Biol. 104* (1987) 801.
[18] T. L. Blundell, R. E. Humbel, *Nature (London) 287* (1980) 781.
[19] S. C. Bock, K. L. Wion, G. A. Vehar, R. M. Lawn, *Nucleic Acids Res. 10* (1982) 8113.
[20] P. Brazeau, W. Vale, R. Burgus, N. Ling, M. Butcher, J. Rivier, R. Guillemin, *Science 179* (1973) 77.
[21] J. L. Breslow, *Annu. Rev. Biochem. 54* (1985) 699.
[22] J. L. Breslow, D. Ross, J. McPherson, H. Williams, D. Kurnit, A. L. Nussbaum, S. K. Karathanasis, V. I. Zannis, *Proc. Natl. Acad. Sci. USA 79* (1982) 6861.
[23] J. E. Brissenden, A. Ullrich, U. Francke, *Nature (London) 310* (1984) 781.
[24] S. E. Brown, C. Stanley, C. R. Howard, A. J. Zuckerman, M. W. Stewart, *Br. Med. J. 292* (1986) 159.
[25] G. J. Broze, Jr., P. W. Majerus, *J. Biol. Chem. 255* (1980) 1242.
[26] D. F. Carmichael, A. Sommer, R. C. Thompson, D. C. Anderson, C. G. Smith, H. G. Welgus, G. P. Stricklin, *Proc. Natl. Acad. Sci. USA 83* (1986) 2407.
[27] R. L. Cate, R. J. Mattaliano, C. Hession, R. Tizard, N. M. Farber, A. Cheung, E. G. Ninfa, A. Z. Frey, D. J. Gash, E. P. Chow, R. A. Fisher, J. M. Bertonis, G. Torres, B. P. Wallner, K. L. Ramachandran, R. C. Ragin, T. F. Manganaro, D. T. McLaughlin, P. K. Donahoe, *Cell (Cambridge, Mass.) 45* (1986) 685.
[28] W.-M. Catenhusen, H. Neumeister (Eds.): *Chancen und Risiken der Gentechnologie*, Schweitzer Verlag, München 1987; see also H. G. Gassen, *Angew. Chem. 94* (1982) 19; *Angew. Chem. Int. Ed. Engl. 21* (1982) 23; F. Wengenmeyer, *ibid. 95* (1983) 874 and *22* (1983) 842.
[29] C. Cladaras, M. Hadzopoulou-Cladaras, R. T. Nolte, D. Atkinson, V. I. Zannis, *EMBO J. 5* (1986) 3495.
[30] S. C. Clark, R. Kamen, *Science 236* (1987) 1229.
[31] I. Clark-Lewis, R. Aebersold, H. Ziltener, J. W. Schrader, L. E. Hood, S. B. H. Kent, *Science 231* (1986) 134.
[32] T. Chandra, R. Stackhouse, V. J. Kidd, S. L. C. Woo, *Proc. Natl. Acad. Sci. USA 80* (1983) 1845.
[33] A. C. Y. Chang, M. Cochet, S. N. Cohen, *Proc. Natl. Acad. Sci. USA 77* (1980) 4890.
[34] N. Chiorazzi, *Bio/Technol. 4* (1986) 210.
[35] K. H. Choo, K. G. Gould, D. J. G. Rees, G. G. Brownlee, *Nature (London) 299* (1982) 178.
[36] S. Cohen, G. Carpenter, *Proc. Natl. Acad. Sci. ZSA 72* (1975) 1317.
[37] D. Collen, *J. Cell. Biochem. 33* (1987) 77.
[38] T. Collins, D. Ginsburg, J. M. Boss, S. H. Orkin, J. S. Pober, *Nature (London) 316* (1985) 748.
[39] S. J. Crabbe, C. C. Cloninger, *Clin. Pharm. 6* (1987) 373.
[40] R. K. Craig, L. Hall, M. R. Edbrooke, J. Allison, I. MacIntyre, *Nature (London) 295* (1982) 245.
[41] S. K. Das, E. R. Stanley, *J. Biol. Chem. 257* (1982) 13679.
[42] S. K. Das, E. R. Stanley, L. J. Guilbert, L. W. Forman, *Blood 58* (1981) 630.
[43] E. W. Davie, *J. Protein Chem. 5* (1986) 247.
[44] C. R. DeBold, M. E. Schworer, T. B. Connor, R. E. Bird, D. N. Orth, *Science 220* (1983) 721.
[45] T. Delahunty, H. N. Baker, A. M. Gotto, Jr., R. L. Jackson, *J. Biol. Chem. 250* (1975) 2718.
[46] R. Derynck, *J. Cell. Biochem. 32* (1986) 293.
[47] R. Derynck, J. Content, E. DeClerq, G. Volckaert, J. Tavernier, R. Devos, W. Fiers, *Nature (London) 285* (1980) 542.
[48] R. Derynck, J. A. Jarrett, E. Y. Chen, D. H. Eaton, J. R. Bell, R. K. Assoian, A. B. Roberts, M. B. Sporn, D. V. Goeddel, *Nature (London) 316* (1985) 701.
[49] R. Derynck, A. B. Roberts, M. E. Winkler, E. Y. Chen, D. V. Goeddel, *Cell (Cambridge, Mass.) 38* (1984) 287.
[50] C. A. Dinarello, *Rev. Infect. Dis. 6* (1984) 51.
[51] C. A. Dinarello, *UCLA Symp. Mol. Cell. Biol., New Ser. 41* (1987) 335.
[52] R. F. Doolittle, M. W. Hunkapiller, L. E. Hood, S. G. Devare, K. C. Robbins, S. A. Aaronson, H. N. Antoniades, *Science 221* (1983) 275.
[53] N. C. Dracopoli, W. J. Rettig, G. K. Whitfield, G. J. Darlington, B. A. Spengler, J. L. Biedler, L. J. Old, I. A. Kourides, *Proc. Natl. Acad. Sci. USA 83* (1986) 1822.
[54] N. Dragon, N. G. Seidah, M. Lis, R. Routhier, M. Chretien, *Can. J. Biochem. 55* (1977) 666.
[55] T. J. Dull, A. Gray, J. S. Hayflick, A. Ullrich, *Nature (London) 310* (1984) 777.
[56] C. T. Esmon, *Science 235* (1987) 1348.
[57] Y. Eto, T. Tsuji, M. Takezawa, S. Takano, Y. Yokogawa, H. Shibai, *Biochem. Biophys. Res. Commun. 142* (1987) 1095.
[58] M. Fenger, *J. Chromatogr. 240* (1982) 173.
[59] J. W. Fett, D. J. Strydom, R. R. Lobb, E. M. Alderman, J. L. Bethune, J. F. Riordan, B. L. Vallee, *Biochemistry 24* (1985) 5480.
[60] J. C. Fiddes, H. M. Goodman, *Nature (London) 281* (1979) 351.
[61] J. C. Fiddes, H. M. Goodman, *Nature (London) 286* (1980) 684.
[62] J. C. Fiddes, H. M. Goodman, *J. Mol. Appl. Genet. 1* (1981) 3.
[63] J. Floros, R. Steinbrink, K. Jacobs, D. Phelps, R. Kriz, M. Recny, L. Sultzman, S. Jones, H. W. Taeusch, H. A. Frank, E. F. Fritsch, *J. Biol. Chem. 261* (1986) 9029.
[64] D. Foster, E. W. Davie, *Proc. Natl. Acad. Sci. USA 81* (1984) 4766.
[65] A. Gaertner, U. Weser, *Top. Curr. Chem. 132* (1986) 1.
[66] J. C. Gasson, R. H. Weisbart, S. E. Kaufman, S. C. Clark, R. M. Hewick, G. G. Wong, D. W. Golde, *Science 226* (1984) 1339.
[67] G. N. Gill, P. J. Bertics, J. B. Santon, *Mol. Cell. Endocrinol. 51* (1987) 169.
[68] G. Gimenez-Gallego, G. Conn, V. B. Hatcher, K. A. Thomas, *Biochem. Biophys. Res. Commun. 135* (1986) 541.

[69] J. Gitschier, W. I. Wood, T. M. Goralka, K. L. Wion, E. Y. Chen, D. H. Eaton, G. A. Vehar, D. J. Capon, R. M. Lawn, *Nature (London) 312* (1984) 326.
[70] D. V. Goeddel, D. G. Kleid, F. Bolivar, H. L. Heyneker, D. G. Yansura, R. Crea, T. Hirose, A. Kraszewski, K. Itakura, A. D. Riggs, *Proc. Natl. Acad. Sci. USA 76* (1979) 106.
[71] G. Goldstein, *UCLA Symp. Mol. Cell. Biol., New Ser. 41* (1987) 51.
[72] A. S. Goustin, E. B. Leof, G. D. Shipley, H. L. Moses, *Cancer Res. 46* (1986) 1015.
[73] P. W. Gray, B. B. Aggarwal, C. V. Benton, T. S. Bringman, W. J. Henzel, J. A. Jarrett, D. W. Leung, B. Moffat, P. Ng, L. P. Svedersky, M. A. Palladino, G. E. Nedwin, *Nature (London) 312* (1984) 721.
[74] P. W. Gray, D. W. Leung, D. Pennica, E. Yelverton, R. Najarian, C. S. Simonsen, R. Derynck, P. J. Sherwood, D. M. Wallace, S. L. Berger, A. D. Levinson, D. V. Goeddel, *Nature (London) 295* (1982) 503.
[75] W. A. Günzler, G. J. Steffens, F. Ötting, G. Buse, L. Flohé, *Hoppe-Seyler's Z. Physiol. Chem. 363* (1982) 133.
[76] M. E. Gurney, S. P. Heinrich, M. R. Lee, H.-S. Yin, *Science 234* (1986) 566.
[77] F. S. Hagen, C. L. Gray, P. O'Hara, F. J. Grant, G. C. Saari, R. G. Woodbury, C. E. Hart, M. Insley, W. Kisiel, K. Kurachi, E. W. Davie, *Proc. Natl. Acad. Sci. USA 83* (1986) 2412.
[78] J. W. Hartz, H. F. Deutsch, *J. Biol. Chem. 247* (1972) 7043.
[79] H. Heydtmann, J. Travis, *Res. Monogr. Cell Tissue Physiol. 12* (1986) 441.
[80] G. N. Hendy, H. M. Kronenberg, J. T. Potts, Jr., A. Rich, *Proc. Natl. Acad. Sci. USA 78* (1981) 7365.
[81] T. Hirano, T. Taga, N. Nakano, K. Yasukawa, S. Kashiwamura, K. Shimizu, K. Nakajima, K. H. Pyun, T. Kishimoto, *Proc. Natl. Acad. Sci. USA 82* (1985) 5490.
[82] T. Hirano, K. Yasukawa, H. Harada, T. Taga, Y. Watanabe, T. Matsuda, S.-I. Kashiwamura, K. Nakajima, K. Koyama, A. Iwamatsu, S. Tsunasawa, F. Sakiyama, H. Matsui, Y. Takahara, T. Taniguchi, T. Kishimoto, *Nature (London) 324* (1986) 73.
[83] F. Hirata, Y. Notsu, R. Yamada, Y. Ishihara, Y. Wano, I. Kunos, G. Kunos, *Agents Actions 17* (1985) 263.
[84] W. E. Holmes, D. Pennica, M. Blaber, M. W. Rey, W. A. Günzler, G. J. Steffens, H. L. Heyneker, *Bio/Technol. 3* (1985) 923.
[85] H. M. Hsiung, N. G. Mayne, G. W. Becker, *Bio/Technol. 4* (1986) 991.
[86] P. Hudson, J. Haley, M. John, M. Cronk, R. Crawford, J. Haralambidis, G. Tregear, J. Shine, H. Niall, *Nature (London) 301* (1983) 628.
[87] R. O. Hynes, *Spektrum Wiss. 1986*, No. 8, p. 80; *Scientific American 1986*, No. 6, p. 32.
[88] A. Ichinose, L. E. Hendrickson, K. Fujikawa, E. W. Davie, *Biochemistry 25* (1986) 6900.
[89] T. Imai, H. Miyazaki, S. Hirose, H. Hori, T. Hayashi, R. Kageyama, H. Ohkubo, S. Nakanishi, K. Murakami, *Proc. Natl. Acad. Sci. USA 80* (1983) 7405.
[90] K. Itakura, T. Hirose, R. Crea, A. D. Riggs, H. L. Heyneker, F. Bolivar, H. W. Boyer, *Science 198* (1977) 1056.
[91] K. A. Jacobs, D. S. Phelps, R. Steinbrink, J. Fisch, R. Kriz, L. Mitsock, J. P. Dougherty, H. W. Taeusch, J. Floros, *J. Biol. Chem. 262* (1987) 9808.
[92] H.-D. Jakubke, H. Jeschkeit: *Aminosäuren, Peptide, Proteine*, Verlag Chemie, Weinheim 1982; see also H.-D. Jakubke, P. Kuhl, A. Könnecke, *Angew. Chem. 97* (1985) 79; *Angew. Chem. Int. Ed. Engl. 24* (1985) 85.
[93] M. Jansen, F. M. A. van Schaik, A. T. Ricker, B. Bullock, D. E. Woods, K. H. Gabbay, A. L. Nussbaum, J. S. Sussenbach, J. L. Van den Brande, *Nature (London) 306* (1983) 609.
[94] M. Jaye, R. Howk, W. Burgess, G. A. Ricca, I. M. Chiu, M. W. Ravera, S. J. O'Brien, W. S. Modi, T. Maciag, W. N. Drohan, *Science 233* (1986) 541.
[95] K. Kangawa, H. Matsuo, *Biochem. Biophys. Res. Commun. 118* (1984) 131.
[96] E. S. Kawasaki, M. B. Ladner, A. M. Wang, J. Van Arsdell, M. K. Warren, M. Y. Coyne, V. L. Schweickart, M.-T. Lee, K. J. Wilson, A. Boosman, E. R. Stanley, P. Ralph, D. F. Mark, *Science 230* (1985) 291.
[97] J. Keski-Oja, E. B. Leof, R. M. Lyons, R. J. Coffey, Jr., H. L. Moses, *J. Cell. Biochem. 33* (1987) 95.
[98] H. T. Keutmann, M. M. Sauer, G. N. Hendy, J. L. H. O'Riordan, J. T. Potts, Jr., *Biochemistry 17* (1978) 5723.
[99] H. T. Keutmann, R. M. Williams, R. J. Ryan, *Biochem. Biophys. Res. Commun. 90* (1979) 842.
[100] N. Kikuchi, K. Nagata, N. Yoshida, M. Ogawa, *J. Biochem. (Tokyo) 98* (1985) 687.
[101] W. Kisiel, *J. Clin. Invest. 64* (1979) 761.
[102] A. Klausner, *Bio/Technol. 4* (1986) 185.
[103] G. Kolata, *Science 236* (1987) 517.
[104] A. R. Kornblihtt, K. Vibe-Pedersen, F. E. Baralle, *Proc. Natl. Acad. Sci. USA 80* (1983) 3218.
[105] T. Kozlovskaya, P. Pumpen, *Mol. Biol. (Moscow) 20* (1986) 884.
[106] W. Kugimiya, Y. Otani, Y. Hashimoto, Y. Takagi, *Biochem. Biophys. Res. Commun. 141* (1986) 185.
[107] P. C. Kung, G. Goldstein, E. L. Reinherz, S. F. Schlossman, *Science 206* (1979) 347.
[108] K. Kurachi, T. Chandra, S. J. Friezner-Degen, T. T. White, T. L. Marchioro, S. L. C. Woo, E. W. Davie, *Proc. Natl. Acad. Sci. USA 78* (1981) 6826.
[109] K. Kurachi, E. W. Davie, *Proc. Natl. Acad. Sci. USA 79* (1982) 6461.
[110] K. Kurachi, E. W. Davie, D. J. Strydom, J. F. Riordan, B. L. Vallee, *Biochemistry 24* (1985) 5494.
[111] J. Larner in L. S. Goldman, A. Gilman (Eds.): *The Pharmacological Basis of Therapeutics*, 6th ed., Macmillan, New York 1980, p. 1497.
[112] M. Lasowski, Jr., I. Kato, *Annu. Rev. Biochem. 49* (1980) 593.
[113] D. Lau, G. Kuzma, C.-M. Wei, D. J. Livingston, N. Hsiung, *Bio/Technol.* (1987), in press.
[114] R. M. Lawn, J. Adelman, S. C. Bock, A. E. Franke, C. M. Houck, R. C. Najarian, P. H. Seeburg, K. L. Wion, *Nucleic Acids Res. 9* (1981) 6103.
[115] J. Lazerson in J. S. Holcenberg, J. Roberts (Eds.): *Enzymes as Drugs*, Wiley, New York 1981, p. 332.
[116] J. Le, J. Vilcek, *Lab. Invest. 56* (1987) 234.
[117] S. Lee-Huang, *Proc. Natl. Acad. Sci. USA 81* (1984) 2708.
[118] C. H. Li, K. Ramasharma, *Annu. Rev. Pharmacol. Toxicol. 27* (1987) 1.
[119] J. Lieman-Hurwitz, N. Dafni, V. Lavie, Y. Groner, *Proc. Natl. Acad. Sci. USA 79* (1982) 2808.
[120] N. Ling, F. Zeytin, P. Böhlen, F. Esch, P. Brazeau, W. B. Wehrenberg, A. Baird, R. Guillemin, *Annu. Rev. Biochem. 54* (1985) 403.
[121] Å. Lundwall, W. Dackowski, E. Cohen, M. Shaffer, A. Mahr, B. Dahlbäck, J. Stenflo, R. Wydro, *Proc. Natl. Acad. Sci. USA 83* (1986) 6716.
[122] H. Marquardt, G. J. Todaro, *J. Biol. Chem. 257* (1982) 5220.
[123] J. A. Martial, R. A. Hallewell, J. D. Baxter, H. M. Goodman, *Science 205* (1979) 602.
[124] J. L. Marx, *Science 237* (1987) 23.
[125] A. J. Mason, H. D. Niall, P. H. Seeburg, *Biochem. Biophys. Res. Commun. 135* (1986) 957.
[126] K. E. Mayo, W. Vale, J. Rivier, M. G. Rosenfeld, R. M. Evans, *Nature (London) 306* (1983) 86.
[127] S. H. Mellon in S. Raiti, R. A. Tolman (Eds.): *Human Growth Hormon*, Plenum, New York 1986, p. 179.
[128] B. Meloun, L. Moravek, V. Kostka, *FEBS Lett. 58* (1975) 134.
[129] D. Metcalf, *Science 229* (1985) 16.
[130] P. Meusel, K. T. Preissner, U. Delvos, G. Mueller-Berghaus, *Verh. Dtsch. Ges. Inn. Med. 92* (1986) 120.
[131] M. L. Michel, P. Tiollais, *Hepatology (Baltimore) 7*, 1. Suppl. (1987) 61s.
[132] J. W. Mier, R. C. Gallo, *Proc. Natl. Acad. Sci. USA 77* (1980) 6134.
[133] T. Miyake, C. K.-H. Kung, E. Goldwasser, *J. Biol. Chem. 252* (1977) 5558.
[134] F. J. Morgan, S. Birken, R. E. Canfield, *J. Biol. Chem. 250* (1975) 5247.
[135] K. Morihara, T. Oka, H. Tsuzuki, *Nature (London) 280* (1979) 412.
[136] M. Morii, S. Odani, T. Koide, T. Ikenaka, *J. Biochem. (Tokyo) 83* (1978) 269.
[137] P. Moonen, J.-J. Mermod, J. F. Ernst, M. Hirschi, J. F. Deamarter, *Proc. Natl. Acad. Sci. USA 84* (1987) 4428.
[138] M. W. Mosesson, R. A. Umfleet, *J. Biol. Chem. 245* (1970) 5728.
[139] A. V. Muchmore, J. M. Decker, *Science 229* (1985) 479.
[140] S. Müllertz, *Fibrinolysis 4* (1987) 3.
[141] S. Nagata, H. Taira, A. Hall, L. Johnsrud, M. Streuli, J. Ecsödi, W. Boll, K. Cantell, C. Weissmann, *Nature (London) 284* (1980) 316.
[142] S. Nagata, M. Tsuchiya, S. Asano, Y. Kaziro, T. Yamazaki, O. Yamamoto, Y. Hirata, N. Kubota, M. Oheda, H. Nomura, M. Ono, *Nature (London) 319* (1986) 415.
[143] M. Nagai, R. Hiramatsu, T. Kanéda, N. Hayasuke, H. Arimura, M. Nishida, T. Suyama, *Gene 36* (1985) 183.
[144] S. Nakanishi, N. Kitamura, H. Ohkubo, *Bio/Technol. 3* (1983) 1089.
[145] D. S. H. Nicol, L. F. Smith, *Nature (London) 187* (1960) 483.
[146] H. D. Niall, M. L. Hogan, R. Sayer, I. Y. Rosenblum, F. C. Greenwood, *Proc. Natl. Acad. Sci. USA 68* (1971) 866.
[147] H. Nomura, I. Imazeki, M. Oheda, N. Kubota, M. Tamura, M. Ono, Y. Ueyama, S. Asano, *EMBO J. 5* (1986) 871.
[148] T. Ny, M. Sawdey, D. Lawrence, J. L. Millan, D. J. Loskutoff, *Proc. Natl. Acad. Sci. USA 83* (1986) 6776.
[149] H. F. Oettgen, *Arzneim.-Forsch. 37* (1987) 251.
[150] S. Oikawa, M. Imai, A. Ueno, S. Tanaka, T. Noguchi, H. Nakazato, K. Kangawa, A. Fukuda, H. Matsuo, *Nature (London) 309* (1984) 724.
[151] J. J. Oppenheim, E. J. Kovacs, K. Matsushima, S. K. Durum, *Immunol. Today 7* (1986) 45.

[152] Ortho Multicenter Transplant Study Group, *N. Engl. J. Med. 313* (1985) 337.
[153] B. Østerud, R. Flengsrud, *J. Biochem. 145* (1975) 469.
[154] M. A. Palladino, B. S. Finkle, *Trends Pharmacol. Sci. 1986*, 388.
[155] M. Pasek, T. Goto, W. Gilbert, B. Zink, H. Schaller, P. McKay, G. Leadbetter, K. Murray, *Nature (London) 282* (1979) 575.
[156] E. P. Paques, *Haemostasis 16*, 3. Suppl. (1986) 21.
[157] D. Pennica, W. E. Holmes, W. J. Kohr, R. N. Harkins, G. A. Vehar, C. A. Ward, W. F. Bennett, E. Yelverton, P. H. Seeburg, H. L. Heyneker, D. V. Goeddel, D. Collen, *Nature (London) 301* (1983) 214.
[158] D. Pennica, W. J. Kohr, W.-J. Kuang, D. Glaister, B. B. Aggarwal, E. Y. Chen, D. V. Goeddel, *Science 236* (1987) 83.
[159] D. Pennica, G. E. Nedwin, J. S. Hayflick, P. H. Seeburg, R. Derynck, M. A. Palladino, W. J. Kohr, B. B. Aggarwal, D. V. Goeddel, *Nature (London) 312* (1984) 724.
[160] S. Pestka, J. A. Langer, *Annu. Rev. Biochem. 56* (1987) 727.
[161] T. E. Petersen, G. Dudek-Wojciechowska, L. Sottrup-Jensen, S. Magnusson in D. Collen, B. Vilman, M. Verstraete (Eds.): *The Physiology of Inhibitors of Blood Coagulation and Fibrinolysis*, Elsevier, Amsterdam 1979, p. 43.
[162] D. L. Peterson, I. M. Roberts, G. N. Vyas, *Proc. Natl. Acad. Sci. USA 74* (1977) 1530.
[163] J. G. Pierce, T. F. Parsons, *Annu. Rev. Biochem. 50* (1981) 465.
[164] I. T. Potts, H. M. Kronenberg, M. Rosenblatt, *Adv. Protein Chem. 35* (1982) 323.
[165] D. Puett, *BioEssays 4* (1986) 70-
[166] H. Ragg, *Nucleic Acids Res. 14* (1986) 1073.
[167] P. Rathnam, B. B. Saxena, *J. Biol. Chem. 250* (1975) 6735.
[168] D. C. Rijken, G. Wijngaards, M. Zaal-de Jong, J. Welbergen, *Biochim. Biophys. Acta 580* (1979) 140.
[169] G. Riethmüller, T. Meo, E. Weiß, H. Szöts, DOS 3542024 (1987).
[170] E. Rinderknecht, B. H. O'Connor, H. Rodriguez, *J. Biol. Chem. 259* (1984) 6790.
[171] E. Rinderknecht, R. E. Humbel, *J. Biol. Chem. 253* (1978) 2769.
[172] B. Riniker, R. Neher, R. Maier, F. W. Kahnt, P. G. H. Byfield, T. V. Gudmundsson, L. Galante, I. McIntyre, *Helv. Chim. Acta 51* (1968) 1738.
[173] J. Rivier, J. Spiess, M. Thorner, W. Vale, *Nature (London) 300* (1982) 276.
[174] L. Roberts, *Science 237* (1987) 358.
[175] R. Ross, *Annu. Rev. Med. 38* (1987) 71.
[176] J. Rossier, G. Chapouthier, *Umschau 1983*, 153.
[177] F. Rotblat, D. P. O'Brien, S. M. Middleton, E. G. D. Tuddenham, *Thromb. Haemostasis 50* (1983) 108.
[178] M. Rubinstein, S. Rubinstein, P. C. Familletti, R. S. Miller, A. A. Waldman, S. Pestka, *Proc. Natl. Acad. Sci. USA 76* (1979) 640.
[179] G. A. Sagnella, G. A. MacGregor, *Trends Biochem. Sci. 11* (1986) 299.
[180] M. R. Sairam, C. H. Li, *Can. J. Biochem. 55* (1977) 755.
[181] B. B. Saxena, P. Rathnam, *J. Biol. Chem. 251* (1976) 993.
[182] A. Becker, R. Neumeier, *Biol. Unserer Zeit 14* (1984) 72.
[183] J. Schmidtke, D. N. Cooper, *Nucleic Acids Res. 15* (1987) Suppl. r1.
[184] J. W. Schrader, *Annu. Rev. Immunol. 4* (1986) 205.
[185] M. L. Schwartz, S. V. Pizzo, R. L. Hill, P. A. McKee, *J. Biol. Chem. 246* (1971) 5851.
[186] P. B. Sehgal, L. T. May, I. Tamm, J. Vilcek, *Science 235* (1987) 731.
[187] L.-P. Shen, R. L. Pictet, W. J. Rutter, *Proc. Natl. Acad. Sci. USA 79* (1982) 4575.
[188] S. Shibahara, Y. Morimoto, Y. Furutani, M. Notake, H. Takahashi, S. Shimizu, S. Horikawa, S. Numa, *EMBO J. 2* (1983) 775.
[189] D. Shochat, S. Staples, K. Hargrove, J. S. Kozel, S. K. Chan, *J. Biol. Chem. 253* (1978) 5630.
[190] A. Skottner, L. Fryklund, H. A. Hansson, *Acta Paediatr. Scand., Suppl. 325* (1986) 107.
[191] C. Sorg, K. Odink, *Proc. 5th Int. Lymphokine Workshop*, Clearwater Beach 1987.
[192] D. F. Steiner, S. J. Chan, J. M. Welsh, S. C. M. Kwok, *Annu. Rev. Genet. 19* (1985) 463.
[193] G. P. Stricklin, H. G. Welgus, *J. Biol. Chem. 258* (1983) 12252.
[194] D. J. Strydom, J. W. Fett, R. R. Lobb, E. M. Alderman, J. L. Bethune, J. F. Riordan, B. L. Vallee, *Biochemistry 24* (1985) 5486.
[195] T. C. Südhof, D. W. Russell, J. L. Goldstein, M. S. Brown, R. Sanchez-Pescador, G. I. Bell, *Science 228* (1985) 893.
[196] G. Swadlo, J. Brüggen, G. Gerhards, R. Schlegel, C. Sorg, Clin. Exp. Immunol. (1987), in press.
[197] Y. Takahashi, K. Kato, Y. Hayashizaki, T. Wakabayashi, E. Ohtsuka, S. Matsuki, M. Ikehara, K. Matsubara, *Proc. Natl. Acad. Sci. USA 82* (1985) 1931.
[198] K. Talmadge, W. R. Boorstein, J. C. Fiddes, *DNA 2* (1983) 281.
[199] Y. H. Tan, F. Barakat, W. Berthold, H. Smith-Johannsen, C. Tan, *J. Biol. Chem. 254* (1979) 8067.
[200] T. Taniguchi, H. Matsui, T. Fujita, C. Takaoka, N. Kashima, R. Yoshimoto, J. Hamuro, *Nature (London) 302* (1983) 305.
[201] K. A. Thomas, G. Gimenez-Gallego, *Trends Biochem. Sci. 11* (1986) 81.
[202] S. Thorsen, M. Philips, *Biochim. Biophys. Acta 802* (1984) 111.
[203] J. J. Toole, J. L. Knopf, J. M. Wozney, L. A. Sultzman, J. L. Buecker, D. D. Pittman, R. J. Kaufman, E. Brown, C. Shoemaker, E. C. Orr, G. W. Amphlett, W. B. Foster, M. L. Coe, G. J. Knutson, D. N. Fass, R. M. Hewick, *Nature (London) 312* (1984) 342.
[204] E. Truscheit, *Pharm. Ind. 48* (1986) 741.
[205] A. Ullrich, A. Gray, C. Berman, T. J. Dull, *Nature (London) 303* (1983) 821.
[206] P. Valenzuela, A. Medina, W. J. Rutter, G. Ammerer, B. D. Hall, *Nature (London) 298* (1982) 347.
[207] P. Valenzuela, P. Tekamp-Olson, D. Coit, U. Heberlein, G. Kuo, F. R. Masiarz, M. A. Medina-Selby, S. Rosenberg, I. Whitney, A. Burlingame, W. J. Rutter in R. M. Chanock, R. A. Lerner (Eds.): *Modern Approaches to Vaccines*, Cold Spring Harbor Laboratory, Cold Spring Harbor 1984, p. 209.
[208] J. Van Brunt, *Bio/Technol. 5* (1987) 421.
[209] P. Verde, M. P. Stoppelli, P. Galeffi, P. Di Nocera, F. Blasi, *Proc. Natl. Acad. Sci. USA 81* (1984) 4727.
[210] M. Verstraete, D. Collen, *Blood 67* (1986) 1529.
[211] J. Vilcek, P. W. Gray, E. Rinderknecht, C. G. Sevastopoulos, *Lymphokines (N. Y.) 11* (1985) 1.
[212] D. M. Wallace, M. J. M. Hitchcock, S. B. Reber, S. L. Berger, *Biochem. Biophys. Res. Commun. 100* (1981) 865.
[213] D. Wallach, *Interferon (London) 7* (1986) 89.
[214] B. P. Wallner, R. J. Mattaliano, C. Hession, R. L. Cate, R. Tizard, L. K. Sinclair, C. Foeller, E. P. Chow, J. L. Browning, K. L. Ramachandran, R. B. Pepinsky, *Nature (London) 320* (1986) 77.
[215] M. D. Waterfield, G. T. Scrace, N. Whittle, P. Stroobant, A. Johnsson, Å. Wasteson, B. Westermark, C.-H. Heldin, J. S. Huang, T. F. Deuel, *Nature (London) 304* (1983) 35.
[216] W. Y. Weiser, D. K. Greineder, H. G. Remold, J. R. David, *J. Immunol. 126* (1981) 1958.
[217] R. G. Werner, *Arzneim.-Forsch./Drug Res. 36* (1986) 1429.
[218] G. G. Wong, J. S. Witek, P. A. Temple, K. M. Wilkens, A. C. Leary, D. P. Luxenberg, S. S. Jones, E. L. Brown, R. M. Kay, E. C. Orr, C. Shoemaker, D. W. Golde, R. J. Kaufman, R. M. Hewick, E. A. Wang, S. C. Clark, *Science 228* (1985) 810.
[219] T.-C. Wun, L. Ossowski, E. Reich, *J. Biol. Chem. 257* (1982) 7262.
[220] T. Yamamoto, Y. Nakamura, T. Nishide, M. Emi, M. Ogawa, T. Mori, K. Matsubara, *Biochem. Biophys. Res. Commun. 132* (1985) 605.
[221] Y.-C. Yang, A. B. Ciarletta, P. A. Temple, M. P. Chung, S. Kovacic, K. S. Witek-Giannotti, A. C. Leary, R. Kriz, R. E. Donahue, G. G. Wong, S. C. Clark, *Cell (Cambridge, Mass.) 47* (1986) 3.
[222] T. Yokota, T. Otsuka, T. Mosmann, J. Banchereau, T. DeFrance, D. Blanchard, J. E. DeVries, F. Lee, K.-I. Arai, *Proc. Natl. Acad. Sci. USA 83* (1986) 5894.

Zeolites: Catalysts for Organic Syntheses

By Wolfgang Hölderich,* Michael Hesse, and Fritz Näumann

Dedicated to Professor Helmut Dörfel on the occasion of his 60th birthday

Zeolites have proved to be valuable technical catalysts in petrochemistry and in oil processing. The characteristic properties of zeolites, such as acidity, shape-selectivity and thermal stability also enable them to be used for highly selective synthesis in the fields of chemical intermediates and fine chemicals. This interesting area of application has grown continuously in recent years. The present article summarizes the various standard types of reaction involved in organic syntheses which can be catalyzed by zeolites; these include, inter alia, electrophilic and nucleophilic substitution reactions, isomerization of double bonds and carbon skeletons, as well as addition, elimination and hydrogenation reactions.

1. Introduction

1.1. Possible Applications

The industrial use of zeolites as catalysts started at the beginning of the 1960s with the replacement of cracking catalysts based on amorphous aluminosilicates.[1–4] Metal doped Y-zeolites proved successful as bifunctional catalysts in the field of hydrocracking.[4–7] The discovery of ZSM-5,[8] the first representative of the family of pentasil zeolites,[9,10] was a milestone in zeolite chemistry during the 1970s. The use of silicon-rich pentasil zeolites as highly acidic, extremely shape-selective and heat-stable catalysts led to new industrial petrochemical processes:[11,12] selectoforming,[13] olefin oligomerization,[15] dewaxing[4,16,17] and the MTG (methanol to gasoline) process[4,18,21] have established themselves as industrial processes alongside cracking and hydrocracking. They will probably soon be joined by the dehydrocyclization of ethane, propane or LPG (liquified petroleum gas) to arenes[14,19,20] and in the somewhat more distant future by the MTO (methanol to olefins) process.[4,21,22] A common feature in all these processes is a broad spectrum of products. However, the petrochemical industry also uses selective reactions such as the Mobil-Badger process for the alkylation of arenes,[4,23,24] the *para*-directed isomerization of xylenes[4,25] and the disproportionation[25–27] or alkylation of monosubstituted arenes.[28]

The combination of acidity and shape selectivity in the zeolite catalysts is an important factor for organic chemistry. The tendency to utilize this potential for specific, highly selective syntheses in the field of intermediates and fine chemicals has continued steadily in recent years.[29] The numerous modifications of zeolites in respect of the number and strength of acid centers, isomorphous substitution[47] and doping with metals provide an opportunity of employing catalysts that are tailored to suit the reactions desired. In this regard the experience gained in zeolite-catalyzed processes in petrochemistry offers valuable guidance.

[*] Dr. W. Hölderich, Dr. M. Hesse, Dr. F. Näumann
BASF Aktiengesellschaft, Ammoniaklaboratorium
D-6700 Ludwigshafen (FRG)

1.2. Structure and Properties

As originally conceived, zeolites are crystalline aluminosilicates with a highly ordered crystalline structure. Cavities of a definite size are formed in the rigid, three-dimensional network composed of SiO_4- and AlO_4-tetrahedra. The lattice contains cavities of varying diameters, depending on the type of zeolite.[30] A distinction is made between large-, medium- and small-pore zeolites (Fig. 1, Table 1). In the case of large-pore Y-zeolites, for example, a cavity of this type having a diameter of 7.4 Å is formed by twelve

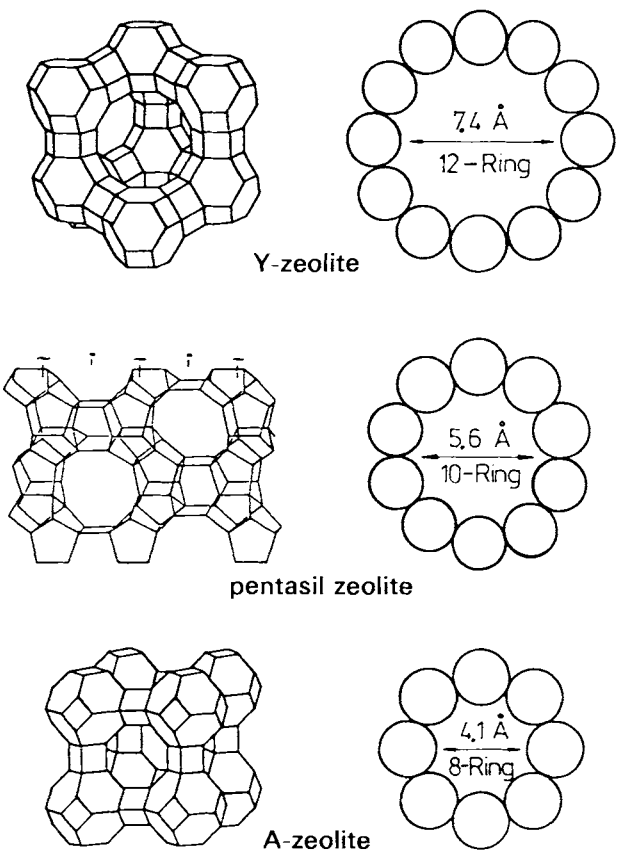

Fig. 1. Zeolite structures (see text).

Table 1. Classification of zeolites according to their pore size.

Small-pore	Ref.	Medium-pore [a]	Ref.	Large-pore	Ref.
A	[31-36]	ZSM-5	[8]	Faujasite	[31-36]
Erionite	[32-34]	ZSM-11	[32-34]	X-/Y-zeolite	[31-36]
Chabazite	[32-34]	ZSM-22	[41-44]	Mordenite	[32-34]
		NU-10	[41-44]	Offretite	[32-34]
		Theta 1	[41-44]	L	[32-34]
		ZSM-23	[42, 45, 46]	Omega	[32-34]
		ZSM-48	[32-34]	ZSM-4	[31-36]
		TS-1	[397]	ZSM-12	[31-36]
		Silicalite	[59]	Z	[102]

[a] All medium-pore zeolites are pentasil zeolites.

SiO_4 tetrahedra.[31-36] In the case of small-pore A-zeolites, eight tetrahedra form a ring of diameter 4.1 Å.[31-36] The medium-pore pentasil zeolites have a 10-ring system with an ellipsoidal tubular diameter of 5.5 Å × 5.6 Å.[8,31-40] The structural assembly of uniform channels (Fig. 2) is an advantageous special feature of the pentasil zeolites.[41-46] In contrast, the other types of zeolites contain larger cavities behind the pore openings.

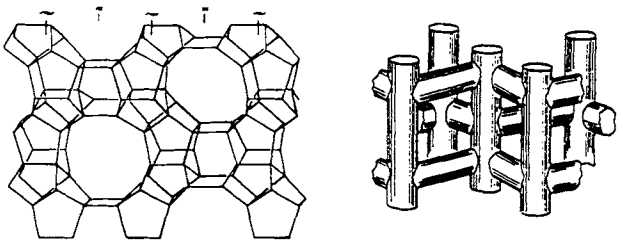

Fig. 2. Pentasil zeolites with emphasized channel system (right).

The central atoms of the tetrahedra in the zeolite lattice can be replaced in an isomorphous manner by a large number of other tri- and tetravalent atoms.[47] For example, B, Fe, Cr, Sb, As, and Ga[51-56] can be incorporated into the zeolite skeleton instead of Al, and, for example, Ge, Ti, Zr, and Hf[51-58] can be incorporated instead of Si. The pure SiO_2-pentasil zeolite (Silicalit®) is also known.[59] Isomorphous substitution results in altered lattice constants and can therefore be monitored by X-ray diffraction. In the case of some elements, such as boron, incorporation can be detected by means of MAS-NMR spectroscopy.[48,49] The nature and the extent of incorporation of the isomorphous replacement affect the catalytic properties, e.g. the acidity of the zeolites. Quantification can be attained by appropriate test reactions.[50]

The use of organic cations[31,60,61] is an important step in the hydrothermal synthesis of silicon-rich types of zeolites, whose characteristic features are high acidity, high resistance to water and acids, and high thermal stability. Amongst the large number of organic components, known as templates, which control the crystallization of new zeolite structures, the organic amines have a dominating position.[e.g. 8,31-46] Syntheses in alcohols,[54,62] ethers,[54,64] dodecylbenzenesulfonate,[65] and water[63] are also known. Further important structure-determining parameters are the Si/Al ratio[66-69] and the condition of the silicate present in the synthesis mixture, which can be described, e.g. in terms of the amount and degree of polymerization of the dissolved silicate anions.[70,71]

Zeolites are inorganic cation exchangers. Their catalytic activity is associated with the presence of acid centers in the intracrystalline surface. In their acid-form, the zeolites can be employed without further treatment as catalysts or as carrier material for active components. The following advantages of zeolite catalysts may be mentioned:

- The acid strength and number of the acid centers (Brønsted and Lewis acid centers) can be adjusted in a controlled manner during synthesis and/or by subsequent ion exchange. The acid centers can also be arranged regularly within the zeolite skeleton.[32-34,72,74-81]
- The shape selectivity means that only molecules smaller than the pore diameter of the zeolite can react with the zeolite catalyst. In addition only such molecules can be formed whose transition state geometry is smaller than the pore diameter (transition state shape selectivity).[32,33,36,82-90]

These advantageous properties make zeolites suitable for wide application in both petrochemical processes and organic syntheses of intermediates and fine chemicals:

- The most important application of zeolites is in reactions catalyzed by proton acids and Lewis acids, where the change from a homogeneous to a heterogeneous procedure brings advantages in respect of easy separation and disposal of the catalyst, avoidance of corrosion etc. In this regard, their shape selectivity has an advantageous effect on the composition of the product, e.g. on the preferred selectivity for the *p*-isomer in isomerization reactions of aromatic compounds (see Section 4).
- As carriers for active components, zeolites make it possible to increase the activity and stability of the catalyst towards steam and high temperature, e.g. by doping with rare earths.[3,72-74] Doping with suitable metals enables hydrogenation (Section 7) and oxidation (Section 8) reactions to be carried out. In all these cases the shape selectivity of the support is an additional factor controlling the reaction. The introduction of the active components can be carried out by ion exchange or by impregnation. In these cases the acid H-form of the zeolite (H-Y-zeolite, H-ZSM-5 etc.) is converted, for example, into the doped form (Ce-Y-zeolite, Pd-ZSM-5 etc.).
- The thermal stability of the zeolites permits them to be used above 150 °C. They are therefore advantageous for reactions in which the thermodynamic equilibrium requires high temperatures. At the same time carrying out the reaction at a high temperature level makes it possible to recover process heat effectively.
- Zeolite catalysts can be regenerated readily with air merely by burning off the coke, which is frequently responsible for their deactivation; after this treatment they generally regain their initial activity.

2. Substitution Reactions with Arenes

2.1. The Alkylation of Arenes

The liquid-phase Friedel-Crafts alkylation of arenes using Lewis-acid catalysts ($AlCl_3$, $FeCl_3$ or BF_3) is carried out on a large industrial scale, e.g. for the preparation of ethylbenzene. The use of such catalysts entails problems of corrosivity, toxicity, work-up and effluent pollution. This makes it desirable to replace homogeneous catalysis for electrophilic substitution reactions by heterogeneous catalysis. Furthermore, the gas phase also offers advantages in the field of process technology, such as utilization of the reaction heat.[4, 91, 92]

The Mobil-Badger process is an outstanding and technically proven example of the alkylation of aromatic compounds;[24, 93, 94] in the USA ethylbenzene has been produced since 1980 in a 500000 t/year plant from ethylene and benzene over phosphorus-doped ZSM-5-zeolite at approx. 400°C. In this case the shape selectivity of the medium-pore pentasil zeolite is a very important factor in the excellent product selectivity (>98% at approx. 20% benzene conversion).

Whereas ethylation ideally takes place in the gas phase, in many alkylation reactions with longer-chain alkenes it is necessary to revert to the liquid phase; as the chain length increases, cracking reactions must be expected in the gas phase. It is then preferable to use the large-pore ZSM-12-, X- and Y-zeolites.[95–98] For example, using H-ZSM-12 at 150–250°C and under pressures of up to 250 bar, isopropyltoluene (32% *p*-, 62% *m*-, and 6% *o*-isomer) or *tert*-butylethylbenzene (90% *p*-isomer and 10% *m*-isomer) are formed at a selectivity of approx. 95% at conversions exceeding 95%.[95] The high proportion of the *p*-isomer in the case of *tert*-butylethylbenzene, in comparison with isopropyltoluene, can be explained by the shape selectivity of H-ZSM-12. The crystallinity of a Y-zeolite is reduced as the result of treatment with ammonium salt, which probably increases its porosity and hence facilitates the diffusion of large molecules; a zeolite of this type produces hexadecyltoluene from toluene and *n*-hexadecene at a selectivity of 98.5% at a conversion of 94.5%,[97] whereas a large-pore, amorphous aluminosilicate only has a selectivity of 65.5% at 94% conversion.[98] The addition of SO_2 to the reaction mixture increases the activity; in the alkylation of benzene with propylene over a Ce-X-zeolite, a 96% conversion and a 96% selectivity are achieved at 120°C, compared with 53% and 90%, respectively, in the absence of SO_2.[96]

The most important selective gas phase alkylation of oligocyclic arenes is the methylation of naphthalene.[106] A 90% selectivity at 20% conversion is achieved at 460°C using H-ZSM-5. The ratio of 2-methylnaphthalene to the other isomer is 0.93 : 1. There is also preferential β-selectivity over Ce-ZSM-5 or Li-ZSM-5; the methylation of 2-methylnaphthalene gives 2,6-dimethylnaphthalene with 78% selectivity at 14% conversion. On Al_2O_3 the β-selectivity is only about half this value. This provides evidence of the shape selectivity of the zeolite.

A very important feature of the pentasil zeolites is their capacity to direct the alkylation of alkylbenzenes selectively into the *para*-position.[28] In most cases pure pentasil zeolites still do not have an adequate *p*-selectivity. However, the thermodynamically favored *m*- and *o*-isomers can be suppressed in favor of the *p*-isomers by modification, e.g. by means of metals or by adding *N*-heterocyclic compounds.[99, 100] In the methylation of toluene, 99% *p*-selectivity at 86% conversion is obtained using Mg-ZSM-5,[101] and 86% *p*-selectivity at 19% conversion is obtained using Ca-P-ZSM-5 or Mg-P-ZSM-5.[102, 103] The part played by doping in increasing *p*-selectivity is discussed comprehensively in several articles.[92, 104, 105]

Alkylation reactions of arenes containing functional groups in accordance with reaction (1) can also be carried out on zeolitic catalysts. A broad spectrum of products, consisting essentially of cresols, xylenols, anisoles and diphenyl ether, is obtained when phenol is methylated using zeolites.[107–110] The formation of the *m*-isomer, which is favored by the acidic zeolite and is difficult to separate, is inhibited by doping the zeolites with alkali or rare earth metals. The expected *p*-selectivity, as is found in the methylation of toluene, is, however, not observed. *p*-Cresol is only formed preferentially at a yield of 22% using K-Y-zeolite at 250°C. In the case of larger molecules, such as amylphenol[111] or octylphenol,[112] the reaction in the liquid phase on large-pore zeolites results preferentially in a high fraction of the *p*-isomer.

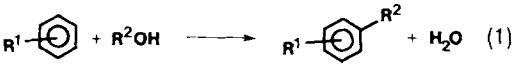

(1)

R^1 = OH, NH_2; R^2 = alkyl

Aniline can be alkylated on faujasite zeolites both in the gas phase[113] and in the liquid phase[114] in the same way as on pentasil zeolites.[115] There is no direct advantage for either of the two types. At an MeOH/aniline molar ratio of 3 : 1 and at 350°C, the selectivity on H-ZSM-5 for toluidines is 20% at 70% conversion, but with Cs-ZSM-5 it is only 3% at 78% conversion, whereas the selectivity of *N*,*N*-dimethylaniline rises from 20% to 59%; alkali-doping increases the *N*-alkylation, whereas acid centers are responsible for *C*-alkylation.

Zeolite-catalyzed nuclear alkylation reactions afford large potential for industrial exploitation in the future as a result of their high selectivity, and the environmentally beneficial as well as energy-saving procedure.

2.2. Side-Chain Alkylation

When alkylbenzenes are alkylated, the reaction at the side chain competes with the reaction at the aromatic nucleus. In the case of alkylating agents of a small molecular size, such as methanol, medium-pore pentasil zeolites lead to selective alkylation of the nucleus, whereas large-pore zeolites, doped with alkali metals or alkaline earth metals[116–125] are employed for side-chain alkylation. The selectivity of side-chain alkylation can also be improved by an additional treatment of the zeolite catalyst with boric acid, borates or phosphates.[126, 127] The reaction of toluene with methanol or formaldehyde to yield styrene and ethylbenzene according to reaction (2) is of industrial interest; an Na-X-zeolite treated with CsOH, H_3BO_3, and LiOH

gives a 49% yield of ethylbenzene and styrene at 430 °C.[116] Doping the catalysts with subgroup elements has also been suggested,[117-119, 126, 127] although no advantage compared with the above modifications can be discerned.

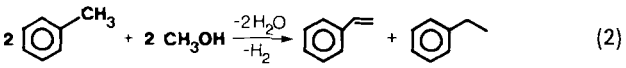

(2)

The side-chain alkylation of picolines with methanol at 400–450 °C using X- and Y-zeolites ion-exchanged with alkali metals (excepting Li) results in ethylpyridine (favored by Cs-Y) and vinylpyridine (favored by Cs-X).[131] It is characteristic that in contrast to the side-chain alkylation of toluene, alkylation also takes place in the nucleus. A 28% yield of ethylpyridine, 7% of vinylpyridine and 2% of lutidine is obtained on Cs-Y-zeolite. The Li-X- or Li-Y-zeolite leads to only nuclear alkylation. If H_2 instead of N_2 is used as the carrier gas, the content of ethylpyridine can be increased at the expense of vinylpyridine (cf. Section 2.3).

It is not yet possible to give a precise explanation of whether the selective side-chain alkylation on X-/Y-zeolites is caused by a particular arrangement of acidic and basic centers[118, 121, 123] or by an alkali metal obtained by reduction[124] or by shielding of the aromatic nucleus as the result of interaction with alkali metal ions in the zeolite cavity.[120] It is difficult to carry out these interesting reactions on an industrial scale, since under the conditions required methanol can react to give, for example, olefins and aromatic compounds. This cannot be completely prevented even by neutralizing the acidity of the zeolites.

2.3. The Alkylation of Heteroarenes

The change from homogeneous catalysis using Lewis acids to heterogeneous catalysis using zeolites can also be recommended for the alkylation of heteroaromatic compounds. For example, thiophene can be alkylated with methanol according to reaction (3) using H-ZSM-5. At 450 °C, the product contains 10% of 2-methylthiophene, 10% of 3-methylthiophene and 9% of dimethylthiophene.[128, 129] The second methylation[130] takes place preferentially in the 5-position with a yield of over 65%. Pyridines can be alkylated in the nucleus using faujasites,[131] the β-position being attacked preferentially on H-Y- or Li-Y-zeolite, and the α-position and γ-positions being attacked preferentially using Y-zeolites doped with alkaline earth metals. At 400 °C on H-Y-zeolite, 3% of α-, 12% of β-, and 3% of γ-picoline are obtained at 32% conversion, whereas on Ba-Y-zeolite 23% of α-, 4% of β-, and 8% of γ-picoline are obtained at 63% conversion (cf. Section 2.2).

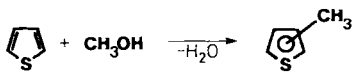

(3)

The zeolite-catalyzed synthesis of alkylated heteroaromatic compounds will become important in the future for environmental reasons, even though the yield and the service life of the catalysts will have to be further improved.

2.4. The Acylation of Arenes

Like alkylation, the acylation of arenes can also be carried out using zeolitic heterogeneous catalysts. Detailed investigations of the acylation of toluene with C_1–C_{20}-carboxylic acids using Ce-Y-zeolite in the liquid phase at 150 °C have been carried out. The yield increases as the chain length of the acylating agent increases. A maximum is achieved at 96% in the case of dodecanoic acid, the *p*-isomer being present to the extent of 93%.[132]

Acylation reactions of arenes using zeolites may gain great industrial importance because of their high selectivity, especially for the production of anthraquinone from benzene and phthalic anhydride. At 350 to 550 °C, Na-X-zeolite loaded with 0.1% of Pt affords a product mixture containing 98% of anthraquinone and 2% of benzophenone.[133–135]

2.5. The Halogenation and Nitration of Arenes

Halogeno- and nitroarenes are prepared industrially in the presence of Lewis or mineral acids at 20–80 °C. A great deal of effort is being directed towards carrying out the halogenation[136–149] and the nitration[150–152] of arenes in the gas and liquid phases using aluminosilicates, especially zeolites, in order to avoid corrosion and disposal problems.

A surprising fact in the chlorination of benzene is that the substitution product chlorobenzene (CB) is obtained on Y-zeolite, whereas on ZSM-5 the addition product hexachlorocyclohexane (HCCH) is formed.[137] At 175 °C, 87% of HCCH and 13% of CB (86% conversion) are obtained on using ZSM-5. In contrast, on Y-zeolite doped with rare earth 3% of HCCH and 97% of CB (100% conversion) are obtained. Although the opposite would be expected on the basis of shape selectivity, evidently H-ZSM-5 induces a free-radical reaction which takes place mainly on the external surface and/or at the pore opening of the zeolite. X-, Y-, and L-zeolites can be employed for the chlorination of anisole,[138] toluene,[139, 140] and halogenotoluenes[141, 142] at 70–100 °C. In these cases, by virtue of the shape selectivity, the *p*/*o* ratio of isomers is higher than with conventional catalysts such as $FeCl_3$. Bromination reactions are carried out analogously.[143] In the chlorination of toluene in the gas phase, a comparison of aluminosilicate, silica gel, faujasite and montmorillonite (a layer silicate) shows that the yield of chlorotoluene achieved using the last-mentioned catalyst is 10% higher than that obtained with faujasite.[144] Since the ratio of isomers is also comparable in the case of these catalysts, the zeolite affords no advantages for the reaction compared with the less expensive layer silicates.

Investigations into the halogenation of halogenobenzenes show that Y-zeolites in which the acidity has been reduced by means of alkali exhibit a higher *p*-selectivity than the H-Y-zeolite in the liquid phase.[142] Dibromobenzene can be prepared by brominating bromobenzene or benzene on Li-faujasite; at 200 °C the conversion is 100% and the *p*-selectivity is 92%.[145] The *p*/*o* ratio is markedly higher in the case of the alkali-doped Y-zeolites than in the case of the conventional catalysts, because of steric factors

which promote the transition state for *p*-selectivity in the zeolite skeleton. Deactivation of the catalyst by HBr can be counteracted by adding $NaHCO_3$ and K-A-zeolite.[148]

Cu-faujasites are suitable for the oxidative chlorination[146,147] and bromination[145] of arenes, whereas Ca-ZSM-5 is suitable for iodination.[149] Iodobenzene is obtained with a selectivity of 97.5% at almost complete conversion.

Arenes, halogenoarenes, and alkoxyarenes are nitrated with NO_2 in the gas phase using zeolite catalysts.[150,151] For example, when chlorobenzene is nitrated on mordenite at 175°C, 10% of *o*-, 0.3% of *m*- and 33% of *p*-nitrochlorobenzene are obtained at a conversion of approx. 43%.[150] Using N_2O_4 as the nitrating agent for benzene, nitrobenzene is formed on H-ZSM-5 with a selectivity of 98% at a conversion of 64%.[151,152]

Irreversible damage is caused to the zeolites by hydrogen halides when arenes are halogenated, so that industrial application, particularly in the gas phase, appears difficult. On the other hand, nitration in the gas phase offers an advantageous alternative to homogeneous catalysis if the conversion can be increased while retaining a high degree of selectivity.

3. Substitution Reactions in Aliphatic Compounds

Nucleophilic substitution—a type of reaction frequently encountered in aliphatic chemistry—has been subjected to many investigations using zeolites, as in the case of electrophilic substitution in aromatic compounds.

3.1. The Formation of Ethers and Esters

Alcohols can be converted into ethers using a large number of zeolitic catalysts. Thus, dimethyl ether can be prepared from methanol at 80% conversion and 100% selectivity on crystalline aluminosilicate at 390°C.[154] In general, ethers are formed analogously from the corresponding alcohols.[155-157] In this case zeolites offer no advantages over montmorillonite.[153] The same applies to the conversion of diols into cyclic ethers; 1,4-butanediol is converted into THF at 100% conversion on Al-doped montmorillonite at 200°C.[157] Ethers containing functional groups are likewise accessible, as shown by the cyclization of 1,2,4-butanetriol to give tetrahydrofuran-3-ol.[158]

The zeolite-catalyzed esterification of acids with alcohols has been described many times.[159-164] For example, acetic acid and alcohols react on wide-pore H-Z-zeolite at 100°C with yields of over 93%.[162] The use of the active centers on the inner surface of the medium-pore pentasil zeolites appears to be limited to small molecules; a kinetic study of the reaction of acetic acid with butanols, catalyzed by ZSM-5, indicates that the activity corresponds only to the acid centers on the surface of the crystallite.[160,161] Transesterification using zeolites, i.e. the formation of a new ester starting from a carboxylate, is described analogously to the synthesis of esters.[165,166] For example, yields of approx. 50% are obtained at 150°C in the preparation of methyl acetate from acetic acid and methyl formate on pentasil zeolites.

In all these reactions, as in the case of homogeneous catalysis, one only achieves an equilibrium distribution, capable of being shifted by the customary methods. Since there is no necessity to change to heterogeneous catalysis for reasons of energy and environmental policy, and since an expensive change in process technology is required, industrial application will only be possible in the case of some etherification reactions in which the zeolites exhibit less coking and hence longer service lives than the conventional catalysts such as Al_2O_3, Al_2O_3/H_3PO_4 etc.

3.2. Thiols from Alcohols and Hydrogen Sulfide

Alcohols ROH react with an excess of H_2S on H-Y-, Na-Y-,[167] and L-zeolite[168] at temperatures below 300°C to give thiols ($\leq$65% yield). At higher temperatures and at a lower H_2S/alcohol ratio dialkyl sulfides are formed in yields of over 50%.[167,169-172] If sulfur is added, it is even possible to prepare dialkyl disulfides, R-S-S-R, in good yields at 310°C.[173] Here too, the chemistry of the thiols is similar to that of the alcohols and the considerations already mentioned apply in this case, the smaller market for thiols being an additional difficulty in the way of changeover, although zeolites afford better yields and service lives than conventional heterogeneous catalysts.

3.3. Amines from Alcohols and Ammonia

The methylamines obtained from methanol and NH_3 are the most important industrial products in this Section. The aim is in most cases to achieve a reaction product having a composition differing from the equilibrium distribution and containing as high a proportion as possible of monomethylamine or dimethylamine (MMA and DMA).[174-180] Thus, it is possible to reduce the proportion of trimethylamine to less than 20% when the reaction is carried out on mordenite at 350°C, but only at conversions of less than 80%.[180-181] DMA, which is particularly in demand, is produced at approx. 60% conversion with a selectivity of up to 70% on using dealuminized mordenites or erionites[182] or zeolite A and Rho.[183,184] It is not yet possible to control the reaction to give only one component, but the composition of the product mixture can be controlled better than in the classical reaction on Al_2O_3.[185,186] The synthesis of higher alkylamines, for example from NH_3 and ethanol, is also possible on H-Y- and RE-Y-zeolite[187] or from NH_3 and butanol on Na-X- and Na-Y-zeolite,[188] but only at low conversions. $EtNH_2$ is formed at 55°C and 18 bar with a selectivity of 85% at 6% conversion. The synthesis of anilines from phenols and NH_3 using ZSM-5 (if necessary doped with Cu) under pressure at 400–500°C is of industrial interest.[189-191] Selectivities to anilines of up to 99% are achieved at over 90% conversion.

Analogously to cyclic ethers, cyclic amines can be prepared from corresponding educts by elimination of H_2O or NH_3. Thus, morpholine is formed from diglycolamines.[192] Azabicyclooctane and diazabicyclooctane, respectively, are formed in accordance with reaction (4) from substi-

tuted piperidines or piperazines in yields of up to 87% using H-ZSM-5 at 400°C.[193]

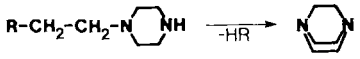

(4)

R = OH, NH_2

Industrial application of the amination of alcohols on zeolitic catalysts, which is being investigated by many research groups, can be expected particularly in the case of the methylamines, if the control of the reaction in favor of MMA or DMA can be improved further.

4. Isomerization Reactions of Arenes

The conversion of substituted arenes into their isomers is of industrial interest and frequently serves as a model reaction for the shape selectivity of the zeolites.[50,87] An important example is the isomerization of xylenes. It is one of the processes already carried out on a large industrial scale using zeolites as catalysts. It forms the subject of numerous publications[84,194-199] and is in operation, e.g., in the UK in a 250000 t/year plant. In this instance the shape selectivity of the zeolites is utilized to increase the proportion of *p*-xylene in C_8-arene fractions.[200-202]

The principle of this reaction is applicable to a number of aromatic intermediates. The reaction generally studied is the equilibration of the *o*-compound to give a mixture of *o*-, *m*- and *p*-isomers. Examples are the isomerization of *o*-toluidine (at 340–430°C on zirconium zeolite to give 51% of *o*-, 37% of *m*- and 12% of *p*-toluidine),[203] of *o*-bromotoluene[208] or of *o*-chlorotoluene (at 250–340°C on zirconium zeolite to give 85% of *o*-, 12% of *m*- and 1.8% of *p*-chlorotoluene).[203,206] ZSM-5 is suitable for the isomerization of 3,4-dichlorotoluene to 2,5-dichlorotoluene at 310°C, and it offers advantages compared with the classical catalyst $AlCl_3$, with which six isomers are formed.[207]

A comparison of the isomerization of tolunitriles and dimethylbenzonitriles shows that, in the case of tolunitrile, the three isomers are distributed in accordance with the thermodynamic equilibrium,[205] whereas in the case of the dimethylbenzonitriles the shape selectivity results in a product distribution such that no 1,2,3-isomers or 1,3,5-isomers are formed. This limitation does not apply to trimethylbenzenes; in this case the 1,2,3-isomer and the 1,3,5-isomer are formed from 1,2,4-trimethylbenzene in a ratio between 1.3 : 1 and 2.7 : 1.[201]

The shape selectivity of the zeolites is particularly pronounced in the isomerization of substituted phenols. 2,4-Dichlorophenol reacts at 400°C on pentasil, mordenite or faujasite zeolites to give a 26% yield of 2,5-dichlorophenol.[204] The 2,5-isomer is not accessible by conventional routes by chlorinating phenol.

Isomerization reactions of heteroaromatic compounds, for example alkylthiophenes or halogenothiophenes, are also catalyzed by zeolites;[211] 2-chlorothiophene can be converted into 3-chlorothiophene according to reaction (5) using Na-ZSM-5 at 250°C, partial dechlorination taking place. The 2-chlorothiophene formed preferentially in the chlorination of thiophene can thus be converted into 3-chlorothiophene. A comprehensive review of the isomerization of halothiophenes has been published recently.[455]

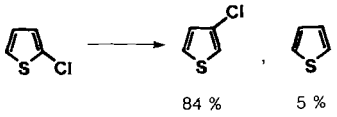

(5)

Polynuclear aromatic compounds can also be isomerized using zeolites. 1-Methylnaphthalene is converted (40%) into 2-methylnaphthalene at a selectivity of 95% using H-Na-Y-zeolite at 270°C in a stream of hydrogen, but there is a loss of activity of ca. 50% in the course of 10 h.[209] 2,6-Dimethylnaphthalene in benzene solution reacts on pentasils at 350°C, with a conversion of 65% to yield a mixture of naphthalene, methylnaphthalene (6.5%) and dimethylnaphthalene isomers (42% of 1,6- and 1,5-DMN and 16% of 1,7- and 1,8-DMN).[210]

In the case of some of these reactions it must be pointed out that only equilibration takes place. Mixtures of products are always obtained in the isomerization reactions. If the isomers can be separated easily, as in the case of 2-chlorothiophene/3-chlorothiophene, it is also possible to obtain compounds which are initially only formed in small amounts. Additionally, isomerization using zeolites instead of Lewis acids offers the customary advantages of a heterogeneous process. In contrast to the isomerization of xylenes, the isomerization of functionalized aromatic compounds still awaits realization on an industrial scale. It may, however, be expected when catalyst service lives are adequate.

5. Isomerization Reactions of Aliphatic Compounds

In isomerization reactions of aliphatic compounds, a distinction must be drawn between rearrangements of the carbon skeletons, in which C–C single bonds are broken and formed, and double bond isomerization reactions, in which the carbon skeleton remains unchanged, but hydrogen atoms are shifted. The shape selectivity of the zeolites is intended to cause the reactions to take the desired path.

5.1. Double Bond Isomerization in Olefins

In the steam cracking of naphtha, after butadiene and isobutene have been removed, a C_4 fraction containing a varying proportion of 2-butene to 1-butene is obtained; this proportion can be increased as desired in an isomerization stage. The reaction can be controlled to give the desired isomer by adjusting the acidity of the catalyst and the temperature. At 175–200°C, using an acid boron pentasil, 88% of the 1-butene is converted into 2-butene in a *trans/cis* ratio of 5 : 3. Na-boron zeolite is suitable for isomerization in the reverse direction; at 450°C *trans*-2-butene is converted in a yield of 60% into 1-butene and *cis*-2-butene in a ratio of 7 : 5.[226-229] Like the isomerization of longer-chain olefins over zeolites, the isomerization of butene is the subject of numerous publications.[212-220,224,225]

If zeolites are used for double bond isomerization in linear olefins containing functional groups, it is also possible for the latter to be attacked. In the isomerization of 2-alkylacroleins into 2-methyl-2-alkenals according to reaction (6) the boron zeolite converts the terminal double bond in the 2-alkylacroleins into an internal double bond in the 2-methyl-2-alkenals, without reduction in selectivity through skeleton isomerization or reactions at the aldehyde group.[230] Ce-boron zeolite is an effective heterogeneous catalyst which, at 300°C, gives an 82% selectivity of tiglaldehyde (reaction (6), $R = CH_3$) at a conversion of 20%;[230] conventional catalysts such as S-poisoned supported Pd catalyst in the presence of H_2[231] exhibit the fundamental disadvantage of considerable formation of hydrogenation products.

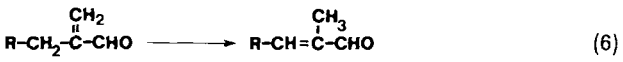

(6)

R = alkyl, aryl, arylalkyl

If the olefin is substituted by an acetoxy group, the pentasil zeolites are not only capable of isomerizing the double bond, but they also produce a rearrangement through a simultaneous shift of the functional group,[233] as in the allyl rearrangement of diacetoxybutenes in accordance with reaction (7). 1,4-Diacetoxybutene is converted into 3,4-diacetoxybutene on boron and aluminum pentasils at 300°C, at a conversion of over 50%. The selectivity is 50–60%. This transformation is reversible; if 3,4-diacetoxybutene is passed over boron zeolite at 200°C, 25% of it reacts to give the 1,4-product with a selectivity of 80%. Hitherto, allyl rearrangements of this type have only been carried out in the liquid phase using SeO_2[234] or Pt or Pd halides in the presence of O_2.[235,236] The use of pentasil zeolites in the gas phase offers an alternative to this, even if the yields achieved in the former case are not always reached.

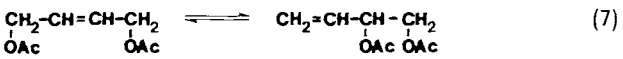

(7)

The aim of selective double bond isomerization is only attained to a limited extent, since, inter alia, mixtures of isomers are formed. The target product can, however, be obtained by removing and recycling the undesired isomers. The double bond isomerization of butenes is of industrial importance for the production of 1-butene for l-LDPE (l-low density polyethylene) and also for the production of isoprene by hydroformylation of 2-butene (cf. Section 6.2), in which zeolites offer an alternative to ion exchange resins. At present it is not possible to estimate the extent to which the isomerization of substituted olefins can be carried out on an industrial scale.

5.2. The Skeletal Rearrangement of Paraffins and Olefins

Skeletal rearrangement reactions play an important part in petrochemical cracking reactions on zeolites, a wide variety of products being obtained. In the chemistry of intermediates, however, a selective rearrangement of the carbon skeleton is the desired objective. Skeletal isomerization reactions of alkanes take place under surprisingly mild conditions over strongly acidic zeolites. A high selectivity can be achieved at a low conversion. Thus, *n*-butane is converted into isobutane at 200°C on H-Y- or La-Y-zeolite at a conversion of 15% and a selectivity of approx. 85%; propane and pentanes are formed as by-products.[215] Alkanes containing only one side chain are formed as the primary products when long-chain alkanes are isomerized using bifunctional catalysts. Thus, *n*-undecane is isomerized on Pt/Ce-Y-zeolite in a stream of hydrogen at 275°C at conversions of up to 40% into a mixture of isoundecanes, without cracking processes manifesting themselves.[221] Reactions of this type can also be used to characterize shape-selective zeolites.[87]

Another reaction of interest is the isomerization of linear olefins into branched olefins, particularly *n*-butenes into isobutene,[214] but double bond isomerization takes place as a side reaction. On Silicalite at 300°C at a conversion of 16% the yield of isobutene is only 11%.

One example, even though not of commercial interest, is the complex rearrangement of tetrahydrodicyclopentadiene into adamantane in accordance with reaction (8). Selectivities of 41%, at 81% conversion, are obtained at 250°C using an La-Y-zeolite containing Pt and Co as promoters in the presence of H_2.[222,223]

(8)

With the exception of the *n*-butene/isobutene isomerization, which, however, only affords low yields, the skeletal isomerizations mentioned have no commercial importance for the chemistry of intermediates.

5.3. Skeletal Rearrangement of Compounds Containing Functional Groups

It is already evident from the allyl rearrangement of diacetoxybutenes (Section 5.2) that the skeleton of hydrocarbons containing carbonyl groups can be isomerized by pentasil zeolites without the carbonyl group being attacked. A further example is the aldehyde-ketone rearrangement according to reaction (9). Pentasils are particularly suitable for this.[240] For example, 2-phenylpropanal is converted into phenylacetone with a selectivity of 97% and a conversion of 63% at 400°C using a boron zeolite. Here too, as in other reactions,[242] iron zeolite exhibits a higher activity than boron zeolite; a selectivity of 98% at a conversion of 95% is found under the same conditions. Only a low selectivity[241] at high conversions is found with aluminum zeolite ZSM-5. In the competition between the phenyl and benzyl and methyl group, the only migration observed is, surprisingly, that of the methyl group. This could be explained by the high shape selectivity of the pentasil zeolites.

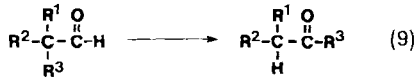

(9)

R^1–R^3 = alkyl, aryl, arylalkyl

The preparation of ketones from aldehydes is a desirable reaction, since the latter are readily accessible via the oxo synthesis. Isomerization reactions of this type using conventional catalysts composed of mixed oxides containing tin, molybdenum, and copper,[237] using cerium on aluminum oxide[238] or using an Al_2O_3 containing 10% of ZnF_2[232] are known. Only a low selectivity at satisfactory conversions is achieved in these reactions, and the best results in respect of selectivity and service life can only be obtained if steam is added. The industrial preparation of asymmetrically substituted ketones is, therefore, carried out as a condensation reaction between different organic acids followed by decarboxylation,[239] the inevitable production of symmetrically substituted ketones and carbon dioxide being a disadvantage. All these drawbacks can be avoided if zeolite catalysts are employed. As a result the potential for industrial application is high.

A reaction in which both hydrogen shifts and a migration of a methyl group take place is the rearrangement of 3,5,5-trimethylcyclohex-2-ene-1,4-dione to give trimethylhydroquinone, which occurs on H-Y-zeolite at 450°C in a stream of H_2 at a conversion of 23% and a selectivity of 50%. A conversion of 33% and a selectivity of 50% are obtained with amorphous aluminosilicates.[243] In this case the conventional catalyst is superior to the zeolite.

5.4. The Pinacolone Rearrangement

The dehydration of 1,2-diols using acid catalysts results in a carbonyl compound; conjugated dienes are only produced in a few cases. This applies regardless of the homogeneous or heterogeneous catalyst used. If the temperatures are raised to 400°C or higher, dienes are obtained, as can be seen from the example of the formation of isoprene from 2-methylbutanal (cf. Section 6.2).

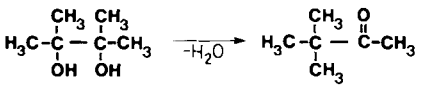

(10)

In the pinacolone rearrangement according to reaction (10) using zeolites of the faujasite and pentasil type,[244] the carbenium ion which is formed as an intermediate is stabilized by the migration of an alkyl group. Yields between 41 and 83% are achieved at 105°C, the best performance being obtained with H-Y-zeolite. 1,2-Diols containing a primary OH group are rearranged, after dehydration, to give aldehydes. For example, phenylglycols, which can contain a wide variety of substituents in the aromatic nucleus, are converted in accordance with reaction (11) into phenyl-

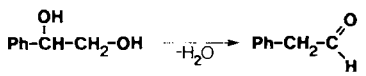

(11)

acetaldehydes on aluminum and boron pentasils at 250–300°C. The selectivity at complete conversion is between 88 and 96%.[250] In this reaction, the zeolites are superior to the amorphous metal-doped or undoped aluminum silicates, by means of which yields between 50 and 86% are attained.[245] Like phenylglycol itself, ethers and esters of the latter can be isomerized in high yields (91–96%).[250] These reactions are only of academic interest and will probably not be used in industry, since the 1,2-diols are usually prepared from the corresponding epoxides, which undergo rearrangement by zeolites to give such aldehydes too (cf. Section 5.6).

5.5. The Wagner–Meerwein Rearrangement

The Wagner–Meerwein or retro-pinacolone rearrangement is very closely related to the pinacolone rearrangement. The reaction of dihydro-5-(hydroxymethyl)-2-furanones on zeolites and phyllosilicates results, according to reaction (12), in 3,4-dihydro-2-pyrones, which are impor-

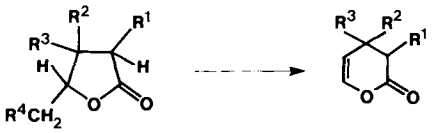

(12)

R^1–R^3 = alkyl; R^4 = OH, alkoxy

tant intermediates, inter alia, for insecticides.[246] It is also known[247] that 2,3-dihydro-1*H*-pyran is obtained in accordance with reaction (13) from 1,2,5-pentanetriol using

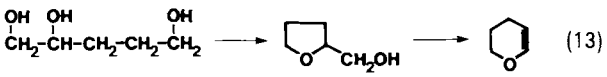

(13)

zeolites directly or via the intermediate stage of tetrahydrofurfuryl alcohol. Using a W-boron zeolite at 350°C, the pentanetriol is completely converted, and the dihydropyran is obtained with a selectivity of approx. 88%. One advantage of the zeolitic catalyst over Al_2O_3 is the fact that the dehydration and the Wagner–Meerwein rearrangement are carried out in a single reaction stage. Furthermore, the yield is markedly higher than the value of 50% achieved with Al_2O_3.[248]

5.6. The Rearrangement of Epoxides

The same considerations as for the pinacolone rearrangement (Section 5.4) apply to the opening of the epoxide ring to give aldehydes using acid, heterogeneous catalysts, such as zeolites, in the liquid or gas phase. The reaction of styrene oxide or alkyl-substituted or alkoxy-substituted styrene oxides using titanium zeolites in acetone or methanol at 30–100°C results in phenylacetaldehydes, according to reaction (14) with selectivities higher than 90%

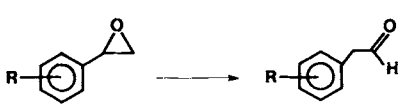

(14)

R = alkyl, aryl, arylalkyl, halogen, haloalkyl, alkoxy, alkylthio

at conversions between 90 and 100%.[249] It is also possible to prepare phenylacetaldehydes containing a very wide variety of substituents on zeolites in the gas phase, without using solvents. Particularly attractive features of the acidic

boron-, iron- and aluminum-pentasils are their high service lives and yields (>90%).[250,251]

The rearrangement of butene-1 oxide by Zn, Cd, and Ag ion-exchanged A-zeolites has also been investigated,[252] but in this case the desired butyraldehyde (55–72%) is also accompanied by a number of by-products, such as methyl ethyl ketone, *cis*- and *trans*-crotyl alcohol and 3-buten-1-ol. For the rearrangement on X-zeolite it is necessary to reduce the number of strongly acidic centers by alkali doping, as shown by the example of propylene oxide, giving acetone and propionaldehyde.[253] The formation of the acetone is catalyzed by the basic centers, while that of the propionaldehyde is catalyzed by the weakly acidic centers. Although zeolites such as faujasite catalyze the rearrangement of cyclic epoxides such as 1-methylcyclopentene oxide[254] into 2-methylcyclopentanone, methylcyclopentenol and methylcyclopentadiene are also formed in this reaction. In the case of cyclododecane oxide,[255] zeolites are inferior to Al_2O_3 catalysts doped with Pd or Rh.

Consideration of the mechanism of epoxide rearrangement over minerals and silica/alumina surfaces[256] shows that the (OH)Si-O-Al grouping acts as the active center. This model is also applicable to zeolites. There are probably opportunities for the industrial use of zeolites for the isomerization of epoxides. This is certainly already one of the established routes for the synthesis of aldehydes, since, in contrast to acid homogeneous catalysts or other acid heterogeneous catalysts, they exhibit higher selectivity, longer service lives and higher conversion rates.

5.7. The Rearrangement of Cyclic Acetals

The isomerization of 1,3-dioxanes to 3-alkoxypropionaldehydes in accordance with reaction (15) was first observed over pumice and silica gels,[257] and acid catalyst properties were considered responsible. It has also been shown, however, that basic catalysts, such as didymium oxide on SiO_2, catalyze this reaction.[258] Use of the zeolites

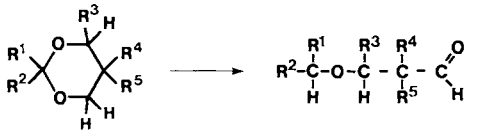

(15)

$R^1 = R^2 = R^4 = R^5 = H$, alkyl, alkenyl, aryl, arylalkyl, alkylaryl, arylalkenyl, alkenylaryl, heterocyclic residue; $R^3 = H$, alkyl

as acid catalysts in this reaction emphasizes once more that they are superior to the conventional catalysts;[259] their shape selectivity has a particularly advantageous effect on the yield of the long-chain neoalkanals. Selectivities of up to 90% or more at a conversion of 50–80% are achieved at 250–400°C.

5.8. The Beckmann Rearrangement

ε-Caprolactam—one of the most important fiber precursors—is mainly prepared by a Beckmann rearrangement of cyclohexanone oxime in which approx. 2.3 t of ammonium sulfate/t of lactam is inevitably formed in the oximation and rearrangement stage. If the reaction were carried out with heterogeneous acidic catalysts, this disadvantage in the rearrangement stage would be eliminated.

The Beckmann rearrangement on H-Y-zeolite was investigated as long ago as the 1960s, when the main problems were found to be the inadequate selectivity and service life of the catalyst.[260] Selectivities of not more than 80%, at an initial quantitative conversion, are achieved in benzene solution at 350°C on H-ZSM-5 with an Si/Al ratio > 1400 : 1, but even these catalysts lose 50% of their activity in the course of 12 h.[261] By-products of the reaction are hexanenitrile and cyclohexanone unsaturated derivatives thereof. The effect of the degree of replacement (H/alkali) on the service life and selectivity of alkali-doped Y-zeolites shows that the rearrangement only takes place on centers having strong Brønsted acidity, whereas nitriles are formed mainly at the alkali metal ions.[262] The rate of nitrile formation decreases in the series Li > Na > K > Cs.[263]

The service life can be improved by selectively covering the outer surface of a boron pentasil zeolite with Na ions.[264] It must, however, be pointed out that the Beckmann rearrangement of cyclohexanone oxime by means of zeolites, and similarly with other supported catalysts and ion exchangers,[265–267] does not at present, for reasons of service life and selectivity problems, constitute an alternative to the homogeneous process now practiced (96% yield).

6. Addition and Elimination Reactions

The acid-catalyzed addition reaction between olefins and polar or polarizable compounds such as acids, alcohols, water or halogens is an important fundamental reaction. Here the use of zeolites offers marked advantages; by virtue of their acidity, the zeolites accelerate the primary stage of the reaction—the formation of a carbenium ion—and it is possible to inhibit olefin polymerization which would reduce the selectivity. The reverse reaction, elimination, takes place particularly advantageously on zeolites.

6.1. Hydration and Dehydration

Alcohols are prepared by the acid-catalyzed hydration of olefins. Catalysis with H_2SO_4 requires the additional stage of hydrolyzing the resulting sulfuric acid ester, and acid heterogeneous catalysts, such as WO_3, SiO_2/Al_2O_3 or cation exchangers, often exhibit an excessively low activity. When zeolites are used it is also necessary to accept low conversions in order to achieve high selectivities. The reaction of C_2 to C_4 olefins with water on H-ZSM-5,[268,269] H-mordenite or H-Y-zeolite,[271] and on offretite, ferrierite and erionite[272] as well as on pillared clays[273] has been described. The conversions at 100–200°C and up to 200 bar are in all cases less than 20%. Special pentasils doped with Cr and rare earths are used,[274,275] but are susceptible to rapid deactivation through coking. The reaction only appears to be of commercial interest in the case of a few cyclic alcohols, where the yields using pentasil zeolites exceed 20%.[270,276–279]

More attention is attracted to the dehydration of alcohols to olefins, which takes place in markedly better yields than the addition reaction. 100% conversion and a selectivity of over 95% are achieved using H-ZSM-5.[269,280-282] Improved selectivities are obtained in this reaction by a high Si/Al ratio in the zeolite and the addition of water, and also by the replacement of the skeletal aluminum by iron.[281] The dehydration of cyclohexanol is suggested[283] as a model reaction for the determination of zeolite activities. In addition to alkyl alcohols,[284-289] aromatic compounds are also converted, e.g. phenylethanol into styrene (95% yield at 220°C).[290] At the present time, the dehydration properties of the pentasil zeolites have found clear recognition in the MTG (methanol to gasoline) and MTO (methanol to olefin) processes, which are of industrial and scientific interest. Further industrial processes can be expected because of their wide field of application, high yields and long catalyst service lives.

6.2. The Dehydration of Aldehydes

The aldehyde-ketone rearrangement of zeolites (Section 5.3) reaches its limit in the case of aldehydes containing not only α- and β-, but also γ-hydrogen atoms. In aldehydes of this type the kinetically favored dehydration to 1,3-dienes according to reaction (16) occurs in preference to migration of the alkyl group. Enolization takes place before migration, particularly at high temperatures. The reason is probably that the enol can react further irreversibly to give the diene via the allyl isomers by 1,4-elimination of water.

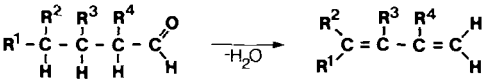

(16)

R^1-R^4 = alkyl

The preparation of dienes from aldehydes by simple dehydration is desirable, since the aldehydes are readily accessible via the oxo synthesis. Examples of catalysts used in this reaction are acids, such as phosphoric acid[291] or boron phosphates.[292-294] Steam dilution, in particular, is a disadvantage in this process. These drawbacks can be avoided if dehydration is carried out by pentasil zeolites.[295] Isoprene is obtained with a selectivity of up 95%, at 51% conversion, from 2-methylbutanal on boron zeolites at 400°C. Aluminozeolites are less suitable for this aldehyde dehydration reaction, since formation of arenes also occurs in this case. The preparation of isoprene by this process could be of commercial interest for the rubber industry and tire manufacturers.

6.3. The Addition and Elimination of Alcohols

In contrast to hydration, the direct addition of alcohols to olefins for the preparation, in particular, of mixed, substituted ethers can be carried out in good yields. This reaction is of commercial interest in regard to the production of the octane booster MTBE (methyl *tert*-butyl ether) from isobutene and methanol. Most of the papers which have appeared are therefore concerned with this synthesis.[296-299] Yields of 86% of MTBE are achieved using boron zeolite AMS-1B at approx. 100°C and 30 bar,[296] while conversions of approx. 35% with selectivities of >95% are attained using H-ZSM-5, NU-2, NU-4, and NU-10.[297,298] Higher temperatures cannot be used for this reaction owing to the formation of symmetrically substituted ethers (cf. Section 9.1). Industrially, MTBE is still produced on acid ion exchangers, since compared with these the zeolites are still inferior.

The preparation of olefins from methanol via dimethyl ether as an intermediate[4,11,20] and the rearrangement of cyclic acetals (cf. Section 5.7) demonstrate the capability of zeolites to cleave C–O bonds selectively. This fact is also utilized for the preparation of enol ethers from acetals according to reaction (17).[300,301] Yields of up to 80% or more

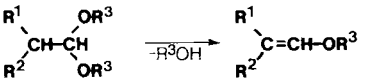

(17)

$R^1 = R^2 = H$, alkyl, aryl; R^3 = alkyl

can be achieved in this reaction within a temperature range from 270 to 340°C, if the acidity of the zeolite is suppressed or eliminated by means of alkali doping. Vinyl ethers are of considerable industrial importance both for special homopolymers and copolymers and as intermediates for organic syntheses such as the Diels-Alder reaction. They are produced industrially by the Reppe process from acetylene and an alcohol in the liquid phase. An alternative method of synthesis would be desirable at plants where acetylene is not available. The industrial use of zeolites is promising in this regard, since they are superior to the conventional catalysts (phosphates, sulfates or carbonates on a carrier).

6.4. The Addition and Elimination of Acids

The addition of acids (in most cases acetic acid) to olefins in accordance with reaction (18) is described in several patents.[302-304] However, conversions of only 30% are achieved with H-ZSM-5 and H-ZSM-12 at 150-200°C and 25 bar. In addition, mixtures of isomers are formed if asymmetrical olefins are used. Thus, 1-olefins afford the 2-carboxylates with a selectivity of 80%.[304] The use of

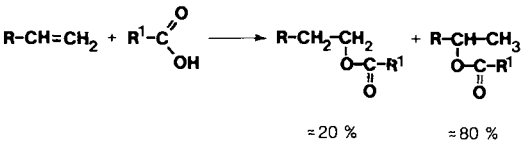

(18)

layer silicates in which replacement has been carried out with trivalent ions offers better results than zeolites. Yields of up to 90%, based on olefins, have been obtained.[305,306]

Dehydrohalogenation is of industrial interest, particularly in regard to the manufacture of vinyl chloride from dichloroethane; in most cases it is carried out by a thermal reaction at 500-600°C. Dehydrohalogenation in the pres-

ence of ZSM-5 or Silicalite, however, can be performed at lower temperatures.[307] At 335°C, 1,2-dichloroethane and 1,1,2-trichloroethane are converted into chloroethylene at 100% conversion and into dichloroethylene at 50% conversion, respectively. Ethylene is a by-product. Analogous reactions on offretite/erionite and Linde L[308] are described, as is also the reaction of 1,2-dichloroethane on La-H-FZ-33 leading to vinyl chloride (conversion 35%, selectivity 61%).[309] However, it appears to be difficult to carry out a process of this type on an industrial scale due to the destruction of the zeolite skeleton by HCl (cf. Section 2.5).

6.5. The Addition of S-Compounds

The acid-catalyzed reaction of olefins with H_2S furnishes thiols and thioethers.[310–312] Non-doped X- and Y-zeolites catalyze the conversion of branched olefins into tertiary thiols in high yields,[313,314] but only give moderate yields in the case of linear olefins.[312] Recourse is made in this case to RE-Y- and Cd-X-zeolites, which give conversions of >99% and selectivities >90%.[310,311] The reactions are carried out at 100–250°C and under elevated pressure (up to 250 bar). Compared with conventional acidic catalysts, zeolites give better yields and service lives.

6.6. The Addition of N-Compounds

The addition of NH_3 or amines to olefins using X- and Y-zeolites is known,[315–316] but suffers from the disadvantage of rapid deactivation. On the other hand, RE-Y-zeolites[317,318] and alumino-, ferro- and borozeolites of the pentasil type[319] afford commercially acceptable yields and service lives. Thus, in the reaction of isobutene with NH_3 at 250–300°C and a pressure of over 100 bar, a conversion into *tert*-butylamine of approx. 8–15% is achieved, with a selectivity of over 98%. The latter has hitherto been obtained by a multistage industrial process using the Ritter reaction from isobutene and hydrogen cyanide, the resulting formamide being saponified. The advantages of using zeolites are evident in this case. Compared with *tert*-butylamine, lower yields are obtained in the production of other amines such as ethylamine or isopropylamine (gradation from primary to secondary to tertiary carbenium ion). In these cases direct addition cannot compete with the conventional methods of preparation.

6.7. Carbonylation and Decarbonylation Reactions

The carbonylation of methanol on Rh- and Ir-doped X-, Y-zeolites[320–325] and H-ZSM-5[326] has been described. Conversions to AcOMe and AcOH of less than 2%, with the formation of large amounts of Me_2O, are obtained when H-ZSM-5 is used at 200–300°C and 10 bar. Co-doped pentasil zeolites, however, enable the reaction to acetic acid (9%) and methyl acetate (45%) to be carried out in acceptable yields,[327] without the addition of iodine, whereby troublesome corrosion problems are avoided. Here too, however, the addition of iodide improves the yields of acetic acid. The preparation of derivatives of the 2-hydroxy acids in yields of up to 40% from aldehydes by means of CO and an alcohol or an acid on various zeolites has been described.[328,329] It is also known that noble metal catalysts decarbonylate branched and unbranched aldehydes.[330,331] In the presence of zeolitic catalysts almost only the unbranched aldehydes contained in the mixture of aldehydes react to yield olefins; using *n*-/iso-butyraldehyde mixtures, conversions of *n*-butyraldehyde of 39–56% are achieved at selectivities of 44–73%. The reason for this behavior is the shape selectivity of the zeolites.

At the present stage of development, the synthesis of acetic acid using zeolites cannot compete with the Monsanto process, in spite of the elimination of environmental problems (iodine-free process), and, at the yields indicated, there is no industrial application for the decarbonylation of aldehydes.

6.8. Addition Reactions to Epoxides

Under mild conditions, 25–100°C, the addition reaction between water and ethylene oxide or cyclohexene oxide on H-ZSM-5 gives the corresponding diols in yields of over 90%. In this case the catalyst service life is commercially acceptable.[332,333] The catalyzed reaction of epoxides with NH_3 or amines gives ethanolamines; ethylene oxide reacts with NH_3 on A-zeolite at 110°C to give an 82% conversion into ethanolamine with a selectivity of 80%.[334] The results with faujasite zeolites and acid ion exchangers are within the same range.[335] Various asymmetric ethanolamines can be obtained analogously.[336] The cost benefit of changing the processes to zeolites is questionable, since the conventional processes operate at very high yields.

7. Reactions with Hydrogen

Hydrocracking[4–7] is one of the large-scale petrochemical processes in which zeolites are used as catalysts. Bifunctional (the hydrogenation property being achieved by deposited metals and the acidity by the zeolitic support), shape selective hydrogenation catalysts of this type are also employed for selective organic syntheses.

7.1. Hydrogenation and Dehydrogenation Reactions

Cyclopentene in a mixture with 4-methylcyclohexene can be hydrogenated selectively to cyclopentane by Rh-X or Rh-ZSM-11. A kinetic study shows that cyclopentene reacts 47 times as fast as 4-methylcyclohexene on Rh-ZSM-11.[337] 1-Hexene in the presence of 4,4-di-methyl-1-hexene is also hydrogenated to hexane on Pt/Cs-, Pd/Cs- or Ni/Cs-ZSM-5 or β-zeolite; because of the shape selectivity of Pd/Cs-ZSM-5, the conversion of 4,4-dimethyl-1-hexene is less than 1% at a 90% conversion of 1-hexene.[338] Ethylene employed for the manufacture of polyethylene must only contain small amounts of acetylene, Pd-Al_2O_3 being used in industry to hydrogenate the acetylene. High standards are thus set for suppressing the hydrogenation and oligomerization of ethylene. Although the activity of Pd-zeolites is somewhat less than that of the conventional

catalysts, comparable selectivities are obtained, especially with Pd-ZSM-5.[339,340]

Aromatic compounds can be hydrogenated partly or completely using zeolite catalysts. The hydrogenation of benzene is virtually the only source of cyclohexane, which is used as feedstock for ε-caprolactam. This hydrogenation is nowadays mainly carried out using nickel homogeneous catalysts. Comparisons of activity have been carried out between zeolites and non-zeolitic catalysts for the hydrogenation of aromatic compounds.[341-345] Using zeolites doped with noble metals, the catalytic activity is found to decrease in the series Pt > Rh > Ru > Ir; this is different from the activity sequence found on SiO_2-supported catalysts (Rh > Ru > Pt > Ir).[343] The partial hydrogenation of benzene to give cyclohexene on Ru-zeolites at 100–200 °C and at a H_2 pressure of 10–100 bar is described.[346] It is not apparent from this patent, however, whether the conversion and selectivity measure up to the values achieved using amorphous supports (Ru/SiO_2; 175 °C, 50 bar H_2; 56% selectivity of cyclohexene at 57% conversion).

The complete hydrogenations of furfuryl alcohol, acetone, 4-methylcyclohexanone and phenylmethyl alcohol using 5% of Ru-doped LZy52-zeolite in methanol according to reaction (19) are described.[347] At 45–55 °C, yields of up to 100% are achieved.

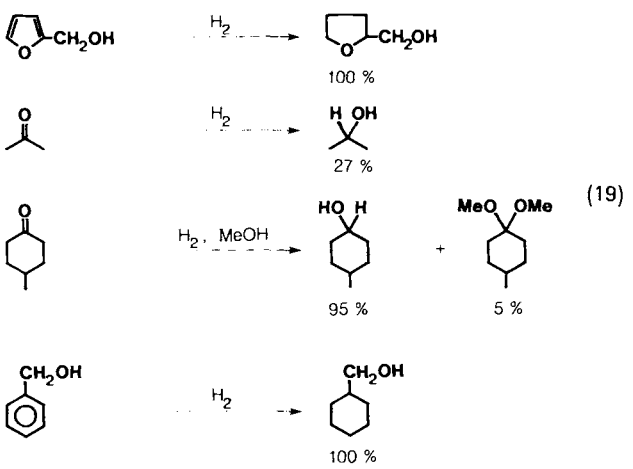

(19)

C_2 to C_5 alkanes can be dehydrogenated to give monoolefins on metal-doped zeolites in the presence or absence of O_2.[348-357] Propane, for example, is dehydrogenated to propylene under non-oxidizing conditions using Pt/Mg-ZSM-5 or Pt/Mn-ZSM-5; at 550 °C a conversion of 23% and a selectivity to propylene of 87% are obtained.[349] Gatheta-1-zeolite is also used for dehydrogenating C_2 to C_5-alkanes; at 600 °C the conversion of butane is 50%, but the selectivity to butenes is only 34%, the total selectivity to olefins is 63% and the remainder is composed of crack products and skeletal isomerization products.[358] A zeolite containing V, Sn, P, and alkali metals is suitable for the oxidative dehydrogenation of C_4 to C_8 monoolefins to give conjugated dienes, for example the dehydrogenation of 1-butene to 1,3-butadiene; at 400 °C a conversion of 61% and a selectivity of 91% are found.[354]

Vinylcyclohexene, which is accessible by cyclodimerization of butadiene (cf. Section 10), can be dehydrogenated oxidatively to give ethylbenzene at 210 °C, e.g. at a conversion of 99% and a selectivity of 99% using Pd-3A-zeolite. The dehydrogenation of ethylbenzene to styrene can be carried out on Na-doped, small- and large-pore zeolites in a stream of O_2.[359] The dehydrogenation of (+)-limonene to *p*-cymene also takes place at a high selectivity at 200 °C on a Pd/Ce-boron pentasil zeolite (conversion 100%, selectivity 84%); in the course of the reaction the double bonds reorient to form an aromatic system.[365] Boron pentasil zeolites[361,362] or gallium pentasil zeolites[363] doped with noble metals are employed for the bifunctionally catalyzed dehydroisomerization of *n*-butane to isobutene at 500–700 °C. Mixtures of *n*-butenes, isobutene, butadiene and isobutane are obtained. Using a Pt-boron zeolite, the maximum proportion of isobutene is approx. 27% at a conversion of 85%.[364]

Although hydrogenation with zeolite catalysts does not as yet take place with very high yields in all cases (for example the hydrogenation of benzene), it must be expected in general that hydrogenation catalysts based on shape selective carriers, such as zeolites, will become of increasing importance for the synthesis of intermediates and fine chemicals. Since dehydrogenation reactions on zeolites often produce a wide spectrum of products, industrial use of these reactions will probably be limited.

7.2. Dehydrocyclization

With the aim of obtaining more valuable products from the raw materials natural gas and petroleum, cyclization reactions of lower alkanes and olefins to aromatic hydrocarbons are being investigated. The conversion of methane to arenes is not possible for thermodynamic reasons, and, under oxidizing conditions (O_2, N_2O), the total oxidation to CO_2 always predominates.[366-369] The dehydrocyclization of ethane, on the other hand, takes place under non-oxidizing conditions at 570–620 °C on Zn/Cu-ZSM-5 or Ga-ZSM-5 at a conversion of 35% and a selectivity of 60%, the proportion of benzene in the mixture of arenes being approx. 65%.[369-371] The aromatization of propane occurs with higher yields; a conversion of 83% and a selectivity of 60% are achieved at 550 °C.[372,373] Even higher yields of arenes can be obtained if olefins are used; propylene gives 81% of aromatic products using Ga-ZSM-5, the main constituents being toluene and xylene.[374] If the raw material situation changes and the demand for arenes increases, these reactions could become commercially interesting and open up new sources of arenes.

7.3. Hydroformylation

The investigation of immobilized carbonyl-transition metal compounds for hydroformylation reactions is attracting considerable interest.[375] The classical hydroformylation of olefins on carbonylcobalt or -rhodium compounds gives mixtures of *n*-aldehydes and isoaldehydes. One aim in using hydroformylation catalysts supported on zeolites is to exploit the shape selectivity in order to shift the *n/iso*-aldehyde ratio in favor of linear isomers.[376-380] When ethylene is reacted (200 °C, 100 bar, $C_2H_4/CO/$

$H_2 = 1.5:2.1:2.5$) using a Ru-Z-zeolite, almost complete conversion is observed with the formation of approx. 12% of propionaldehyde, 36% of *n*-propanol and 12% of 2-methylbutyraldehyde; part of the Ru is removed in the form of the carbonyl complex and the spent catalyst contains ruthenium carbonyl compounds which cannot be extracted. In a further hydroformylation cycle the removal of ruthenium virtually ceases.[376] Hydroformylation over Rh-zeolites under atmospheric pressure[381-389] gives, at minimal conversion rates, *n*/iso-aldehyde ratios that do not exceed the values achieved with homogeneous catalysts.

The principal problems in hydroformylation using zeolites are the occurrence of acid-catalyzed side-reactions (oligomerization or aldol condensation) and removal of the active transition metal component. Application on an industrial scale therefore appears impossible for the present.

8. Oxidation Reactions

In oxidation reactions—as also in hydrogenation and dehydrogenation reactions—zeolites assume the function of the support material for active components and influence the product spectrum by virtue of their shape selectivity.

8.1. Oxidation Reactions with Oxygen

The oxidation of lower olefins to carbonyl compounds according to reaction (20) can be carried out in the gas phase on Pd/Cu-Y-zeolites. It is essential to add water in order to ensure high selectivity and long catalyst service life. The rate of oxidation falls off as the chain length increases, as is known from the homogeneously catalyzed reaction using Pd and Cu salts.[390,391] In the oxidative acetoxylation of propylene to give allyl acetate, Pd/Cu-erionite (approx. 90% selectivity) and Pd/Cu-mordenite (approx. 70% selectivity) are superior to Pd/Cu-faujasite (approx. 40% selectivity). However, the activity and selectivity of conversion in this reaction depend on the alkali metal ion present in the zeolite before replacement by Pd and Cu.[392,393]

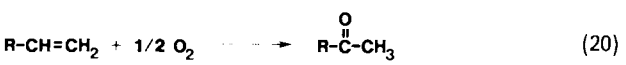

$$R\text{-}CH{=}CH_2 + 1/2\ O_2 \longrightarrow R\text{-}\overset{\overset{O}{\|}}{C}\text{-}CH_3 \qquad (20)$$

The selective partial oxidation of C_4 to C_{10}-hydrocarbons to maleic anhydride offers a commercially interesting alternative to the conventional process by the oxidation of benzene, 2-butene or crotonaldehyde. Maleic anhydride is obtained with a selectivity of 80% at a conversion of 17% from *n*-butane at 525°C using zeolites doped with V, P or alternatively Zn.[395]

Monochlorinated, saturated hydrocarbons can be oxyhalogenated to dihalogenated compounds over Cu-pentasil zeolite at 225–325°C;[394] chloroethane gives a 60% conversion, and the composition of the reaction mixture is 43% by volume of 1,2-dichloroethane, 40% by volume of chloroethane and 16% by volume of ethylene. As a result of the shape selectivity, more highly halogenated ethanes are not observed. The reaction can also be carried out at lower temperatures than the process using conventional catalysts, thereby avoiding the formation of vinyl chloride and separation problems associated therewith. The irreversible damage caused to the zeolite by HCl, however, makes industrial application doubtful.

A comprehensive review article on oxidation reactions, including oxidative dehydrogenation reactions over zeolites, has recently appeared.[396]

8.2. Oxidation Reactions with Peroxides

The discovery of the titanium zeolite TS-1 has enabled remarkable progress to be made in oxidation reactions with H_2O_2 in recent years.[397,398] Liquid phase epoxidation (in methanol or acetone) of olefins and diolefins[399,402] with H_2O_2 takes place over TS-1 between 0 and 80°C with selectivities of 75–96% (relative to the olefin), the conversion of H_2O_2 being in most cases complete. The principal by-product formed is a glycol monomethyl ether (in methanol) or a glycol ketal (in acetone). A great advantage of TS-1 compared with the conventional oxidation catalysts, such as OsO_4 and V_2O_5,[400] is that it is possible to use dilute aqueous peroxide solution in practically stoichiometric proportions. This reaction is of particular interest for the preparation of propylene oxide, at a selectivity of 98%, at 15°C in methanol. The side-reaction leading to glycol monomethyl ether can also be made the main reaction if the process is carried out above 100°C [reaction (21), $R = CH_3$].[401]

$$R\text{-}CH{=}CH\text{-}R^1 + H_2O_2 + CH_3OH \longrightarrow R\text{-}\underset{OH}{CH}\text{-}\underset{OCH_3}{CH}\text{-}R^1 + H_2O \qquad (21)$$

$R = R^1 = H$, alkyl, aryl, alkylaryl, cycloalkyl, alkylcycloalkyl

The direct hydroxylation of aromatic hydrocarbons by means of H_2O_2 is also possible using TS-1;[403] phenol in acetone solution gives hydroquinone at a selectivity of 92% relative to phenol or 80% relative to H_2O_2, at an H_2O_2 conversion of 100%. This process is already being carried out on an industrial scale in Italy. Further examples of its use are the hydroxylation of toluene, ethylbenzene, anisole and cresol. The tendency for the *p*-isomer to be formed preferentially and the minimization of undesired side reactions leading to multinuclear arenes are indications of the shape selectivity of the titanium zeolite. The hydroxylation of phenol can also be carried out in the presence of the aluminozeolites H-ZSM-5 or H-ZSM-11, doped with coinage metals or Fe, Co, and Ni or their homologs, with a selectivity to hydroquinone of 99%.[404]

The extension of the principle of this reaction to primary and secondary alcohols opens up new routes for the preparation of aldehydes and ketones.[405] For example, benzyl alcohol is oxidized to benzaldehyde and cyclohexanol to cyclohexanone by means of H_2O_2 in yields of approx. 90% (relative to H_2O_2) on TS-1 at 70–90°C. Reference should also be made in this connection to the conversion of hydroperoxides. Over Co-4Å-zeolite, cyclohexyl hydroperoxide is converted at 30–160°C into cyclohexanol and cyclo-

hexanone with a selectivity of over 95% at 100% conversion.[406] In contrast, Co on graphite gives a selectivity of only 82% at a peroxide conversion of 94%. The decomposition of cumene hydroperoxide to give phenol (96% selectivity) and acetone can be carried out over a mixed alumino/borozeolite at 40–60°C.[407]

These examples justify the prediction that in the future zeolites, in particular the titanium zeolites, will find widespread application in oxidation reactions. As an alternative to the chlorohydrin route, a heterogeneously catalyzed propylene oxide process using TS-1 is both commercially attractive and environmentally unproblematic.

9. Condensation Reactions

Condensation reactions are catalyzed by acids or bases. This is a suitable field for the use of zeolites, since their acidity can be easily controlled or they can be doped with bases, with the retention of their shape selectivity. In this way it is possible to adjust their catalytic properties in order to suit the desired reaction.

9.1. Aldol Condensations

The base-catalyzed or acid-catalyzed aldol condensation is a classical dehydration reaction undergone by carbonyl compounds. Over acid aluminum zeolites, acetone is converted into mesityl oxide, isobutene, phorones, mesitylene and alkylphenols.[408–412] It has been shown in a detailed investigation[411] that ZSM-5 containing iron oxide as an impurity converts acetone selectively into 2,4-dimethylphenol. The preparation of α,β-unsaturated aldehydes from formaldehyde and aldehydes in accordance with reaction (22) takes place with high selectivity using the boron zeolite H-AMS-1B.[413] For example, a 1:1 molar mixture of propanal and formaldehyde is converted at 300°C into methacrolein at a selectivity of 98% and a propanal conversion of 58%. Citronellal can react with isopropanol according to reaction (23) in a Meerwein–Ponndorf–Verley reduction at 150°C on alkali-containing X-zeolites to give isopulegol or citronellol, depending on the metal used for doping.[414]

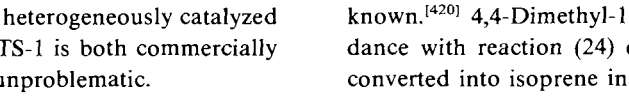

(22)

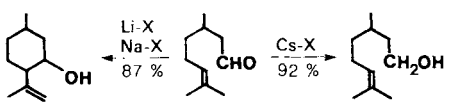

(23)

There have been many investigations of aldol condensations under hydrogenating conditions. Thus butyraldehyde is converted into 2-ethylhexanal and 2-ethylhexanol (80% conversion, >70% selectivity) on Pd/Pt–X-zeolites in the presence of H_2 and at 100–200°C.[415–417] In this case dehydration and hydrogenation take place in a single reaction step. Ketones also give hydrogenated saturated compounds in the presence of H_2;[418,419] acetone reacts with H_2 at 180°C on Pd-ZSM-5 yielding methyl isobutyl ketone with a selectivity of 98% but with a selectivity of only approx. 30% on Pd–Y,[418] the conversion in both cases being 30%. Kinetic studies[419] indicate that the condensation reaction of acetone over zeolites takes place via an intermediate attached to the surface, whereas in the case of higher ketones intermolecular dehydration predominates without the zeolite having an appreciable effect.

The reaction of olefins with formaldehyde, for example for the synthesis of isoprene from isobutene, is well known.[420] 4,4-Dimethyl-1,3-dioxane is formed in accordance with reaction (24) over large-pore zeolites, and is converted into isoprene in the second stage.[42,422] In contrast to this, the reaction according to reaction (24) on

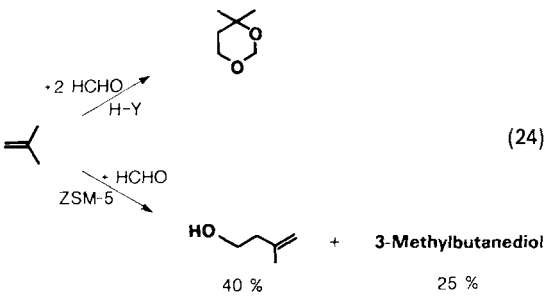

(24)

ZSM-5 or ZSM-11 (70°C, 10 bar) gives 3-methyl-3-buten-1-ol (40%) and a mixture of 3-methylbutanediols (25%) at a conversion of 50%.[423] These findings reflect the shape selectivity of the zeolites. The reaction of methyl acetate or acetic anhydride with formaldehyde over ZSM-5, giving methyl acrylate (50% yield) and acrylic acid (9% yield), offers a possible alternative to the existing method of manufacture on a large industrial scale.[424] In view of their industrial importance, further work is being carried out on both processes, since the yields are still not satisfactory at the present time.

9.2. Synthesis of Aromatic N-Heterocyclic Compounds

Classical processes for the condensation of small molecules to form N-heterocyclic compounds are markedly superior to reactions using zeolites, particularly in the case of compounds with complicated substituents.[425–428] Acetaldehyde reacts with NH_3 on H-ZSM-5 and Cd-H-ZSM-5[425] and Cd-Y[426] at 300–400°C to form picolines in yields of 20% to 60%, in a relatively unspecific manner. Acetaldehyde, formaldehyde and NH_3 give an 83% yield of a mixture of pyridine and β-picoline (molar ratio 2:1) at 450°C on zeolites.[427]

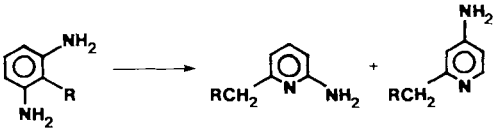

(25)

The synthesis of picolines by rearrangement of aminated arenes constitutes an interesting alternative to the reactions mentioned above. Thus, aniline can be converted into β-picoline by means of NH_3 at 500°C and elevated pressure on H-ZSM-5 (selectivity 52%, conversion 13%).[429] 1,3-

Diaminoarenes afford a mixture of 2-aminopyridines and 4-aminopyridines according to reaction (25) on ZSM-5 at 350–400 °C (selectivity 98%, conversion 40%, R = H, CH_3).[430] These compounds have hitherto only been accessible in good yields by reaction of sodamide with pyridines.

9.3. The Synthesis of Isocyanates and Nitriles

Aromatic isocyanates can be prepared from (nitromethyl)arenes,[434] and nitriles can be prepared from amides (ZSM-5, 400 °C, 85% yield) or from formaldehyde/alcohols in the presence of amines.[435,436] The preparation of aliphatic dinitriles, such as adiponitrile, from dicarboxylic acids and ammonia is carried out in the gas phase on a large industrial scale in fluidized- and fixed-bed processes. Using conventional catalysts,[431,432] the selectivity in reaction (26) is reduced as a result of cyclization to cyclopenta-

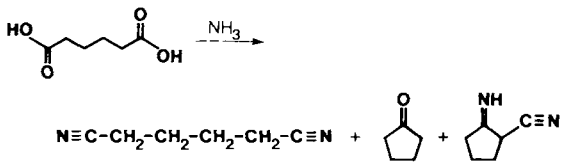

(26)

none and 2-iminocyclopentanecarbonitrile. Side reactions of this type are suppressed if, for example, a boron zeolite doped with 5.6% by weight of Na and 7.6% by weight of P is employed.[433] As shown by comparison with a catalyst based on SiO_2, the content of cyclic compounds is reduced from 6.7% to 1.4%, as a result of which the selectivity for adiponitrile is increased from 83% to 94%. The transition state shape-selectivity of the zeolite, which does not permit the cyclization reaction, is evidently responsible for this. This example shows once more the synergism of dehydration properties and shape selectivity exercised by the pentasil zeolites. The profitability of this process is increased markedly by the zeolites.

9.4. O/N Replacement in Cyclic Compounds

As is known from other acid heterogeneous catalysts, the reaction of lactones and cyclic ethers with ammonia also gives lactams or cyclic imines using zeolite catalysts.[437–441] Tetrahydrofuran is converted into pyrrolidine on H-L-zeolite with a selectivity of 91% at 350 °C or on H-Y-zeolite with a selectivity of only 82%. H-L-zeolite is not very suitable for the preparation of piperidine from tetrahydropyran.[437] Only after it has been dealuminized does this zeolite improve the catalytic activity and selectivity for the O/N exchange in the ring;[439] at 460 °C the H-L-zeolite (Si/Al = 3.2) gives a 24% conversion and a piperidine selectivity of 58%, whereas the dealuminized catalyst (Si/Al = 6.0) gives a 25% conversion and an 80% piperidine selectivity. Butyrolactone is converted into 2-pyrrolidone with a selectivity of 80–90% on Cu-Y-zeolite at 230–260 °C.[440,441] The zeolites offer an interesting alternative to conventional acid, non-shape-selective catalysts for the replacement of O by N in heterocyclic compounds.

10. Oligomerization Reactions

The only oligomerization reactions to be described here are those leading to open-chain and cyclic aliphatic hydrocarbons (cf. also Section 7.3). In general, mixtures of dimers, trimers and tetramers are formed from olefins using zeolites. The deposition of higher oligomers can, however, result in coking and deactivation of the catalyst. Isobutene can be dimerized to give trimethylpentene isomers in accordance with reaction (27) with a selectivity of up to 88% on Bi- or Pb-pentasil zeolites at 100–150 °C; migration of methyl groups also takes place.[443] Ni-ZSM-5 or Ni/Zn-ZSM-5 or ZSM-11 are suitable for the oligomerization of C_2- to C_{20}-olefins; in the case of propylene a selectivity to the dimer of 71% is achieved at almost quantitative conversion at approx. 60 °C.[442,445] C_3-olefins and C_4-olefins can be tetramerized in a two-stage process on Ni-H-ZSM-5 at 120–230 °C with a selectivity of over 60%.[444]

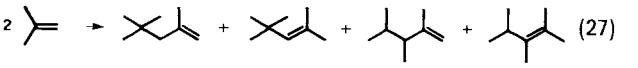

(27)

The selective oligomerization of lower olefins to give terminal C_8- to C_{12}-monoolefins is of interest. Hydroformylation of these monoolefins to aldehydes or alcohols yields intermediates which are used in the synthesis of surfactants and lubricants. Oligomerization reactions of this type[15] are already carried out on an industrial scale.

11. Summary and Prospects

The present exposition is intended to demonstrate the numerous possibilities in which zeolitic catalysts can be employed. It also illustrates the opportunities afforded by these shape selective acid catalysts, and emphasizes the future importance of such catalyst systems. Numerous economically interesting organic reactions, which were hitherto not feasible because of low activity, selectivity and/or service life of the catalyst, can now be commercially exploited using zeolites. It has now become easier to change from homogeneously catalyzed processes to heterogeneous catalysis if environmental and process engineering problems occur in the separation, work-up or possible recycling of the homogeneous catalyst. Existing processes can be improved merely by replacing the conventional heterogeneous catalyst.

Furthermore, publications are beginning to appear in the literature which indicate the importance of zeolite catalysts in stereochemistry[446,447] and as carriers for enzymes and microorganisms in biotechnology.[448] This opens up a wide range of new applications.

The new developments in the fields of phosphates having a zeolite structure,[449–452] artificially expanded clay minerals (so-called pillared clays)[453] and modified carbon molecular sieves[124] as well as certain crystalline cyanometalates[454] offer the possibility of combining the catalytic properties of these materials with a shape selective behavior. Solid-state chemistry will consequently provide materials which can give a new impetus to shape selective catalysis. This will enable us to proceed further along the road

leading to enzyme catalysis, the most subtle form of shape selectivity.

In our constant endeavor to look over Nature's shoulder and to learn from her, the future will certainly bring us surprises, but also insights into a deeper understanding of shape-selective catalysis. Even if we shall never quite attain the perfection of our teacher, new horizons will nevertheless open up.

The authors are grateful to Dr. H. Lermer of BASF for his helpful assistance in screening the literature and discussions leading to the preparation of Section 2.

Received: August 19, 1987 [A 654 IE]
German version: *Angew. Chem. 100* (1988) 232

[1] P. B. Weisz, V. J. Frilette, R. W. Maatman, E. B. Mower, *J. Catal. 1* (1962) 307.
[2] C. J. Plank, E. J. Rosinski, M. P. Howthorne, *Ind. Eng. Chem. Prod. Res. Dev. 3* (1964) 165.
[3] B. P. Venuto, E. T. Habib, Jr.: *Chemical Industries, Vol. 1*, Marcel Dekker, New York 1979.
[4] W. Hölderich, E. Gallei, *Chem.-Ing.-Tech. 56* (1984) 908.
[5] A. P. Bolton, *ACS Monogr. 171* (1976) 714.
[6] E. Gallei, *Chem.-Ing.-Tech. 52* (1980) 99.
[7] K. Hedden, J. Weitkamp, *Chem.-Ing.-Tech. 55* (1983) 907.
[8] R. J. Argauer, G. R. Landolt, *US-Pat. 3702886* (April 14, 1967), Mobil Oil Corp.
[9] T. E. Whyte, Jr., R. A. Dalls, *Catal. Rev.-Sci. Eng. 24* (1982) 567.
[10] G. T. Kokotailo, W. M. Meier, *Spec. Publ. Chem. Soc. 33* (1980) 133.
[11] P. B. Weisz, *Pure Appl. Chem. 52* (1980) 2091.
[12] N. Y. Chen, W. E. Garwood, *Catal. Rev.-Sci. Eng. 28* (1986) 185.
[13] N. Y. Chen, J. Maziuk, A. B. Schwartz, P. B. Weisz, *Oil Gas J. 66* (1968) 154.
[14] N. Y. Chen, *US-Pat. 3729409* (November 4, 1971), Mobil Oil Corp.
[15] W. E. Garwood, *ACS Symp. Ser. 218* (1983) 383.
[16] K. W. Smith, W. C. Starr, N. Y. Chen, *Oil Gas J. 78* (1980) 75.
[17] N. Y. Chen, R. L. Gorring, H. R. Ireland, T. R. Stein, *Oil Gas J. 75* (1977) 165.
[18] S. C. Meisel, J. P. McCullough, C. J. Lechthaler, P. B. Weisz, *CHEMTECH 6* (1976) 86.
[19] A. W. Chester, F. Yung, *US-Pat. 4350835* (September 21, 1982), Mobil Oil Corp.
[20] W. J. Ball, D. G. Stewart, *US-Pat. 4376104* (August 6, 1980), BP Co. Ltd.
[21] W. O. Haag in D. H. Olson, A. Bisio (Eds.): *Proceedings of the 6th International Zeolite Conference*, Reno, NV (USA) 1983, Butterworth, Guildford 1984, p. 466.
[22] W. Hölderich, H. Eichhorn, R. Lehnert, L. Marosi, W. D. Mross, R. Reinke, W. Ruppel, H. Schlimper in [21], p. 545.
[23] F. G. Dwyer, P. J. Lewis, F. M. Schneider, *Chem. Eng. (N.Y.) 83* (1976) 90.
[24] F. G. Dwyer: "Catalysis of Organic Reactions" in W. R. Moser (Ed.): *Chemical Industries, Vol. 5*, Marcel Dekker, New York 1981, p. 39.
[25] W. O. Haag, F. G. Dwyer, *Am. Inst. Chem. Eng., 8th Meeting*, Boston, MA (USA) 1979.
[26] J. Weitkamp, S. Ernst, P. A. Jacobs, H. G. Karge, *Erdöl-Kohle-Erdgas-Petrochem. 39* (1986) 13.
[27] W. W. Keading, C. Chu, L. B. Young, S. A. Butter, *J. Catal. 69* (1981) 392.
[28] D. G. Parker, *Appl. Cat. 9* (1984) 53.
[29] a) W. Hölderich in Y. Murakami, A. Iijima, J. W. Ward (Eds.): *Proceedings of the 7th International Zeolite Conference, Tokyo 1986*, Kodansha-Elsevier, Tokyo 1986, p. 827; b) *Pure Appl. Chem. 58* (1986) 1383.
[30] R. Gramlich, W. M. Meier, *J. Solid State Chem. 44* (1982) 41.
[31] L. Puppe, *Chem. Unserer Zeit 4* (1986) 117.
[32] D. W. Breck: *Zeolite Molecular Sieves*, Wiley, New York 1974.
[33] R. M. Barrer: *Zeolites and Clay Minerals as Sorbents and Molecular Sieves*, Academic Press, London 1978.
[34] J. A. Rabo, *ACS Monogr. 171* (1976) 332.
[35] F. Schwochow, L. Puppe, *Angew. Chem. 87* (1975) 659; *Angew. Chem. Int. Ed. Engl. 14* (1975) 620.
[36] E. G. Derouane: *Diffusional Limitations and Shape Selective Catalysis in Zeolites*, Academic Press, New York 1982, p. 101.
[37] G. T. Kokotailo, W. M. Meier, *Spec. Publ. Chem. Soc. 33* (1980) 133.
[38] Z. Gabelica, E. G. Derouane, N. Blom, *Appl. Catal. 5* (1983) 109, 227.
[39] E. M. Flanigen, *Adv. Chem. Ser. 121* (1973) 119.
[40] S. B. Kulkarni, V. P. Shiralkar, A. N. Kotasthane, R. B. Borade, P. Ratnasamy, *Zeolites 2* (1982) 313.
[41] G. T. Kokotailo, J. L. Schlenker, F. G. Dwyer, E. W. Valyocsik, *Zeolites 5* (1985) 349.
[42] L. M. Parker, D. M. Bibb, *Zeolites 3* (1983) 8.
[43] A. Araya, B. M. Lowe, *Zeolites 4* (1984) 280.
[44] S. A. I. Barri, G. W. Smith, D. White, D. Young, *Nature (London) 312* (1984) 533.
[45] A. C. Rohrmann, Jr., R. B. La Pierre, J. L. Schlenker, J. D. Wood, E. W. Valyocsik, M. K. Rubin, J. B. Higgins, W. I. Rohrbaugh, *Zeolites 5* (1985) 352.
[46] P. A. Wright, J. M. Thomas, G. R. Millward, S. Ramdas, S. A. I. Barri, *J. Chem. Soc. Chem. Commun. 1985*, 1117.
[47] M. Thielen, M. Geelen, P. A. Jacobs, *Proc. ZEOCAT Symp.*, Siofok (Hungary) 1985, *Acta Phys. Chem. (Szeged) 1985*, p. 1.
[48] Z. Gabelica, J. B. Nagy, P. Bodart, G. Debras, *Chem. Lett. 1984*, 1059.
[49] S. Hayashi, K. Suzuki, S. Shin, K. Hayamizu, O. Yamamoto, *Bull. Chem. Soc. Jpn. 58* (1985) 52.
[50] J. A. Martens, M. Thielen, P. A. Jacobs, J. Weitkamp, *Zeolites 4* (1984) 98.
[51] H. W. Kouwenhoven, W. H. J. Stork, L. Schapert, DOS 2755770 (December 16, 1976), Shell Int. Res. Maatschappij B. V.
[52] M. R. Klotz, DOS 2746790 (April 20, 1978), Standard Oil Corp.
[53] L. Marosi, J. Stabenow, M. Schwarzmann, DBP 2830787, DBP 2830830 (both January 31, 1980), BASF AG.
[54] W. Hölderich, W. D. Mross, M. Schwarzmann, Eur. Pat. 77946 (May 4, 1983), Eur. Pat. 91508 (October 19, 1983), BASF AG.
[55] M. Taramasso, G. Perego, B. Notari in L. V. C. Rees (Ed.): *Proceedings of the 5th International Zeolite Conference, Naples 1980*, Heyden and Sons, London 1980, p. 40.
[56] E. E. Davies, A. J. Kolombos, DBP 2755901 (July 6, 1978), BP Co. Ltd.
[57] H. Baltes, H. Litterer, E. Leupold, F. Wunder, DBP 3217323, DBP 3217324 (both November 10, 1983), DBP 3141283 (April 28, 1983), Hoechst AG.
[58] M. Taramasso, G. Perego, B. Notari, Belg. Pat. 886812 (June 22, 1981), Snamprogetti.
[59] E. M. Flanigen, J. H. Bennett, R. W. Grose, J. P. Cohen, R. L. Patton, R. M. Kirchner, J. V. Smith, *Nature (London) 271* (1978) 512.
[60] E. Moretti, S. Contessa, M. Padovan, *Chim. Ind. (Milan) 67* (1985) 21.
[61] B. M. Lok, T. R. Cannan, C. A. Messina, *Zeolites 3* (1983) 282.
[62] J. L. Casci, B. M. Lowe, T. V. Whittam, Eur. Pat. 42225 (December 23, 1981), ICI Ltd.
[63] R. W. Grose, E. M. Flanigen, US-Pat. 4257885 (March 24, 1981), Union Carbide Corp.
[64] W. Hölderich, L. Marosi, W. D. Mross, M. Schwarzmann, Eur. Pat. 51741 (May 19, 1982), BASF AG.
[65] H. Hagiwara, Y. Kiyozumi, M. Kurita, T. Sato, H. Shimada, K. Suzuki, S. Shin, A. Nishijima, N. Todo, *Chem. Lett. 1981*, 1653.
[66] L. D. Rollmann, E. W. Valyoscik, Eur. Pat. 15132 (September 3, 1980), Mobil Oil Corp.
[67] L. D. Rollmann, E. W. Valyoscik, DBP 2817576 (November 2, 1978), Mobil Oil Corp.
[68] L. Marosi, J. Stabenow, M. Schwarzmann, Eur. Pat. 7098 (January 23, 1981), Eur. Pat. 46504 (March 3, 1982), DBP 2830787 (January 31, 1980), BASF AG.
[69] L. D. Rollmann, E. W. Valyocsik, US-Pat. 4108881 (August 22, 1978), Mobil Oil Corp.
[70] E. G. Derouane, S. Detremmerie, Z. Gabelica, N. Blom, *Appl. Catal. 1* (1981) 201.
[71] Z. Gabelica, E. G. Derouane, *ACS Symp. Ser. 248* (1984) 229.
[72] P. A. Jacobs: *Carboniogenic Activity of Zeolites*, Elsevier, Amsterdam 1977.
[73] J. N. Miale, N. Y. Chen, P. B. Weisz, *J. Catal. 5* (1966) 278.
[74] J. S. Magee, J. J. Blazek, *ACS Monogr. 171* (1976) 615.
[75] R. A. Morrison, DBP 2848849 (May 22, 1980), Mobil Oil Corp.
[76] S. T. Butter, W. W. Keading, US-Pat. 3906054 (September 16, 1975), Mobil Oil Corp.
[77] V. S. Nayak, V. R. Choudhary, *J. Catal. 81* (1983) 26.

[78] H. Nakamoto, H. Takahasi, *Zeolites 2* (1982) 67.
[79] J. S. Sherry, *Adv. Chem. Ser. 101* (1971) 350.
[80] D. Barthomeuf, *ACS Symp. Ser. 40* (1977) 453.
[81] L. Marosi, J. Stabenow, M. Schwarzmann, DBP 3006471 (August 27, 1981), BASF.
[82] P. B. Weisz, V. J. Frilette, *J. Phys. Chem. 64* (1960) 382.
[83] P. B. Weisz, *Catal. Proc. Int. Congr. 7th, 1980, Part A*, 3.
[84] W. O. Haag, R. Lago, P. B. Weisz, *Faraday Discus. Chem. Soc. 72* (1981) 317.
[85] S. M. Csicsery, *ACS Monogr. 171* (1976) 680; *Am. Chem. Soc. Div. Fuel Chem. 28* (1983) 116; *Chem. Br. 5* (1985) 473.
[86] E. G. Derouane, *Stud. Surf. Sci. Catal. 5* (1980) 5.
[87] J. Weitkamp, S. Ernst, H. Dauns, E. Gallei, *Chem.-Ing.-Tech. 58* (1986) 623.
[88] E. G. Derouane, *J. Catal. 100* (1986) 541.
[89] I. E. Maxwell, *J. Inclusion Phenom. 4* (1986) 1.
[90] N. Y. Chen, W. E. Garwood, *Catal. Rev.-Sci. Eng. 28* (1986) 185.
[91] J. Weitkamp, *Acta Phys. Chem. 31* (1985) 271.
[92] W. W. Keading, G. C. Barile, M. M. Wu, *Catal. Rev.-Sci. Eng. 26* (1984) 597.
[93] P. E. Keown, C. C. Meyers, R. G. Wetherold, US-Pat. 3751504 (August 7, 1973), Mobil Oil Corp.
[94] P. J. Lewis, F. G. Dwyer, *Oil Gas J. 75* (1977) 55.
[95] G. T. Burress, Eur. Pat. 12514 (June 25, 1980), Mobil Oil Corp.
[96] R. Q. Kluttz, L. H. Slaugh, US-Pat. 4395372 (July 26, 1983), Shell Oil Co.
[97] H. A. Bouncer, I. A. Cody, Eur. Pat. 160144 (November 6, 1985), Exxon Comp.
[98] H. A. Bouncer, Eur. Pat. 160145 (November 6, 1985), Exxon Comp.
[99] L. D. Rollmann, Eur. Pat. 39205 (November 4, 1981), Mobil Oil Corp.
[100] X. Qinhua, J. Zhu, *Acta Phys. Chem. 31* (1985) 181.
[101] J. P. McWilliams, US-Pat. 4447666 (May 8, 1984), Mobil Oil Corp.
[102] C. C. Chu, US-Pat. 4420418 (December 13, 1983), Mobil Oil Corp.
[103] N. P. Forbus, W. W. Keading, Eur. Pat. 89787 (September 28, 1983), Mobil Oil Corp.
[104] W. W. Keading, L. B. Young, C. C. Chu, *J. Catal. 89* (1984) 267.
[105] K. H. Chandavar, S. G. Hedge, S. B. Kulkarni, P. Ratnasamy, G. Chitlangia, A. Singh, A. V. Deo, in [21], p. 325.
[106] K. Eichler, E. Leupold, DBP 3334084 (April 28, 1985), Hoechst AG.
[107] P. D. Chantal, S. Kaliaguine, J. L. Grandmaison, *Appl. Catal. 18* (1985) 133; *Stud. Surf. Sci. Catal. 19* 1194) 93.
[108] S. Namba, T. Yashima, Y. Itaba, N. Hara, *Stud. Surf. Sci. Catal. 5* (1980) 105.
[109] S. Balsama, P. Beltrame, P. L. Beltrame, P. Carniti, L. Forni, G. Zuretti, *Appl. Catal. 13* (1984) 161.
[110] T. G. Dakuchaeva, S. A. Kozhevnikov, D. A. Sibarov, V. F. Timofeer, *Neftekhimiya 1985*, 57.
[111] H. Miki, T. Shivahata, Y. Iwase, Jap. Pat. 60181042 (September 24, 1985), Mitsui Petrochem. Ind.
[112] L. B. Young, Eur. Pat. 29333 (May 27, 1981), Mobil Oil Corp.
[113] G. O. Chivadze, L. Z. Chkheidze, *Izv. Akad. Nauk Gruz. SSR, Ser. Khim. 10* (1984) 232.
[114] M. N. Magerramov, A. G. Lyutfaliev, R. A. Khalilova, I. Sh. Dadasheva, *Azerb. Khim. Zh. 1985*, 25.
[115] P. Y. Chen, M. C. Chen, H. Y. Chu, N. S. Chang, T. K. Chuang, *Stud. Surf. Sci. Catal. 28* (1986) 739.
[116] K. Eichler, E. Leupold, DBP 3330790 (March 14, 1985), DBP 3316929 (November 15, 1984), Hoechst AG.
[117] Jap. Pat. 58020233 (February 5, 1983), Jap. Pat. 58189039 (November 4, 1983), Jap. Pat. 60097922 (May 31, 1985), Mitsubishi Chem. Ind.
[118] T. Yashima, K. Sato, T. Hayasaka, N. Hara, *J. Catal. 26* (1972) 303.
[119] Jap. Pat. 57068144 (April 26, 1982), Jap. Pat. 8281419 (May 21, 1982), Ube Ind.
[120] M. L. Unland, G. E. Barker in [24], p. 51.
[121] H. Itoh, A. Miyamoto, Y. Murakami, *J. Catal. 64* (1980) 284.
[122] J. Engelhardt, J. Szanyi, B. Jover, *Actas Simp. Iberoam. Catal. 9th, 2*, (1984) 1435.
[123] H. Itoh, T. Hattori, K. Suzuki, Y. Murakami, *J. Catal. 79* (1983) 21.
[124] J. M. Garces, G. E. Vrieland, S. I. Bates, F. M. Scheidt, *Stud. Surf. Sci. Catal. 20* (1985) 67.
[125] C. Lacroix, A. Deluzarche, A. Kiennemann, A. Boyer, *Zeolites 4* (1984) 109; *J. Chim. Phys. Phys.-Chim. Biol. 81* (1984) 413, 481, 486.
[126] H. C. Liu, Eur. Pat. 123536 (October 31, 1984), Exxon Comp.
[127] H. C. Liu, R. J. Spohn, US-Pat. 4483936 (November 20, 1984), Exxon Comp.
[128] K. Eichler, E. Leupold, Eur. Pat. 175969 (March 20, 1986), Hoechst AG.
[129] V. Solinas, R. Monaci, G. Longu, L. Forni, *Acta Phys. Chem. 31* (1985) 291.
[130] V. B. Abramovich, M. F. Pankratova, R. M. Masagutov, Russ. Pat. 278708 (August 21, 1970).
[131] H. Kashiwagi, Y. Fujiki, S. Enomoto, *Chem. Pharm. Bull. 30* (1982) 404, 2575; *Nippon Kagaku Kaishi 4* (1980) 551.
[132] B. Chiche, A. Finiels, C. Gauthier, P. Geneste, J. Graille, D. Pioch, *J. Org. Chem. 51* (1986) 2128.
[133] Jap. Pat. 56142233 (November 6, 1981), Mitsui Toatsu Chem. Inc.
[134] G. Leston, DBP 2616583 (October 28, 1976), Koppers Co., Inc.
[135] G. Friedhofen, O. Immel, H. H. Schwarz, DBP 2633458 (January 26, 1978), Bayer AG.
[136] Jap. Pat. 57077631 (May 15, 1982), Kureha Chem. Ind. KK.
[137] T. Huizinga, J. J. F. Scholten, T. M. Wortel, H. van Bekkum, *Tetrahedron Lett. 21* (1980) 3809.
[138] Jap. Pat. 6048943 (March 16, 1985), Ihara Chem. Ind.
[139] Y. Higuchi, T. Suzuki, Eur. Pat. 112722 (July4, 1984), Ihara Chem. Ind.
[140] K. Sekizawa, T. Hironaka, Y. Tsutsumi, Eur. Pat. 171265 (February 12, 1986), Toyo Soda Mfg.
[141] Y. Higuchi, T. Suzuki, Eur. Pat. 118851 (September 19, 1984), Eur. Pat. 154236 (September 11, 1985), Ihara Chem. Ind.
[142] T. Miyake, K. Sekizawa, T. Hironaka, M. Nakano, S. Fujii, Y. Tsutsumi, *Stud. Surf. Sci. Catal. 28* (1986) 747.
[143] T. Suzuki, C. Komatsu, Jap. Pat. 6153234 (March 17, 1986), Ihara Chem. Ind.
[144] J. M. Bakke, J. Liaskar, G. B. Lorentzen, *J. Prakt. Chem. 324* (1983) 488.
[145] S. Kai, Jap. Pat. 60224644, Jap. Pat. 60224645 (November 9, 1985), Asahi Chem. Ind.
[146] Y. Sasaki, M. Fushida, N. Hatto, Jap. Pat. 74010658 (March 12, 1974), Hodogaya Co.
[147] M. Vadekar, DBP 1915393 (December 4, 1969), Esso AG.
[148] T. M. Mortel, D. Oudijn, C. J. Vleugel, D. P. Roelofsen, H. van Bekkum, *J. Catal. 60* (1979) 110.
[149] G. Papavatto, M. Saetti, Eur. Pat. 181790 (May 21, 1986), Montedipe S.p.A.
[150] J. Schumacher, K. Wang, Eur. Pat. 53031 (June 2, 1982), Eur. Pat. 78247 (May 4, 1983), US-Pat. 4107220 (August 15, 1978), Monsanto.
[151] Jap. Pat. 59216851 (1984), Japan Synthetic Rubber.
[152] Jap. Pat. 58157748 (1983), Sumitomo Chem. Co.
[153] T. Kometoku, T. Nozawa, Jap. Pat. 60215642 (October 28, 1985), Shoma Deuko.
[154] J. Topp-Jorgensen, Eur. Pat. 148626 (July 17, 1985), Haldor Topsoe.
[155] L. D. Brake, Eur. Pat. 99676 (February 1, 1984), DuPont de Nemours Comp.
[156] S. W. Kaiser, Eur. Pat. 115071 (August 8, 1984), Union Carbide Corp.
[157] D. Kotkar, P. K. Ghosh, *J. Chem. Soc. Chem. Commun. 1986*, 650.
[158] H. Müller, D. Voges, DBP 3308931 (March 12, 1983), BASF AG.
[159] E. Santacesaria, D. Gelosa, P. Danise, S. Carra, *J. Catal. 80* (1983) 427.
[160] S. Namba, Y. Wakushima, T. Shimizu, H. Mosumoto, T. Yashima, Stud. Surf. Sci. Catal. 20 (1985) 205.
[161] R. Gregory, D. J. Westlake, Eur. Pat. 45618 (March 26, 1986), BP Comp.
[162] Zh. Yurni, H. Lijun, C. Shuxing, *Shiyou Huagong 15* (1986) 411.
[163] Zh. Huaibin, Zh. Baozhen, L. Hexuan, *Shiyou Huagong 15* (1986) 476.
[164] E. Santacesaria, G. Carra, F. Silva, *J. Catal. 85* (1984) 519.
[165] H. Eckhardt, K. Halbritter, W. Hölderich, W. D. Mross, DBP 3506632 (February 26, 1985), BASF AG.
[166] L. A. Hamilton, US-Pat. 3328439 (June 27, 1967), Mobil Oil Corp.
[167] M. Ziolek, J. Bresinska, *Zeolites 5* (1985) 245.
[168] R. B. Hager, US-Pat. 4313006 (January 26, 1982) and Eur. Pat. 82500 (June 19, 1983), Pennwalt Corp.
[169] B. Buchholz, E. J. Dzierza, Eur. Pat. 38540 (October 28, 1981), Pennwalt Corp.
[170] T. F. Doumani, US-Pat. 2816146 (December 10, 1957), Union Oil Co.

[171] K. Eichler, E. Leupold, Eur. Pat. 175969 (April 2, 1986), Hoechst AG.

[172] M. Ziolek, J. Bresinska, H. G. Karge in [47], p. 551.

[173] R. S. Custer, P. G. Haines, Eur. Pat. 171092 (October 17, 1985), Pennwalt Corp.

[174] F. J. Weigert, Eur. Pat. 25693 (March 3, 1981) and Eur. Pat. 26071 (April 1, 1981), DuPont de Nemours Comp.

[175] L. D. Brake, Eur. Pat. 62428 (October 13, 1982), DuPont de Nemours Comp.

[176] G. E. Heinsohn, Eur. Pat. 64380 (November 10, 1982), DuPont de Nemours Comp.

[177] A. J. Tompsett, Eur. Pat. 76034 (April 6, 1983), ICI PLC.

[178] M. Deeba, R. N. Cochran, Eur. Pat. 85408 (August 10, 1983), Air Prod. Chem. Inc.

[179] A. J. Tompsett, A. Stewart, Eur. Pat. 107457 (May 2, 1984) and Eur. Pat. 118193 (September 12, 1984), ICI PLC.

[180] Y. Ashina, T. Fujita, M. Fukatsu, J. Yagi, Eur. Pat. 125616 (November 21, 1984), Jap. Pat. 57169444 (October 19, 1982), Jap. Pat. 59227841 (June 8, 1983), Jap. Pat. 60045550 (August 22, 1983) and Neth. Pat. 8201523 (April 10, 1981), Nitto Chem. Ind.

[181] Jap. Pat. 5849340 (March 23, 1983), Toyo Soda Co.

[182] Y. Ashina, T. Fujita, M. Fukatsu, J. Yagi, Eur. Pat. 130407 (January 9, 1985), Nitto Chem. Ind.

[183] L. Abrams, T. E. Gier, R. D. Shannon, G. C. Sonnichson, Eur. Pat. 183423 (June 4, 1983), DuPont de Nemours Comp.

[184] M. Deeba, W. J. Ambs, R. N. Cochran, US-Pat. 4434300 (February 28, 1984), Air Prod. Chem. Inc.

[185] G. Schmitz, *J. Chim. Phys. Phys.-Chim. Biol. 77* (1980) 393.

[186] I. Machida, A. Yatsutake, H. Fujitsu, *J. Catal. 82* (1983) 313.

[187] M. Deeba, Eur. Pat. 180983 (November 6, 1985), Air Prod. Chem. Inc.

[188] A. I. Maksimov, K. H. Minachev, I. V. Mishin, I. I. Levitskii, *Dokl. Akad. Nauk SSSR 280* (1985) 1154.

[189] C. D. Chang, W. H. Lang, US-Pat. 4434299 (November 12, 1982) and Eur. Pat. 062542 (October 13, 1982), Mobil Oil Corp.

[190] K. K. Pitale, M. G. Warawdekar, R. A. Rajadhyasaka, *Advances in Catalysis, Science and Technology*, Wiley Eastern Ltd., New York 1985, p. 263.

[191] K. K. Pitale, R. A. Rajadhyasaka, *Curr. Sci. 54* (1985) 447.

[192] V. Eskinazi, J. E. Wells, US-Pat. 4446320 (December 20, 1982), Air Prod. Chem. Inc.

[193] R. A. Budnik, M. R. Sandner, Eur. Pat. 158319 (October 16, 1985), Union Carbide Corp.

[194] L. B. Young, S. A. Butter, W. W. Kaeding, *J. Catal. 76* (1982) 418.

[195] J. Nunan, J. Cronin, J. Cunningham, *J. Catal. 87* (1984) 77.

[196] R. A. Morrison, US-Pat. 3856872 (December 14, 1974), Mobil Oil Corp.

[197] W. W. Kaeding, L. B. Young, US-Pat. 4034053 (June 5, 1977), Mobil Oil Corp.

[198] F. A. Smith, A. B. Schwartz, L. L. Breckenridge, Eur. Pat. 0000432 (February 15, 1979), Mobil Oil Corp.

[199] *Chem. Age* (London) (May 15, 1981), p. 19.

[200] D. Seddon, *J. Catal. 98* (1986) 1.

[201] P. Cartraud, A. Cointot, M. Dufour, N. S. Gnet, G. Joly, J. Tejada, *Appl. Catal. 21* (1986) 85.

[202] D. H. Olson, R. B. Calvert, E. W. Valyocsik, Eur. Pat. 102716 (March 14, 1984), Mobil Oil Corp.

[203] K. Eichler, E. Leupold, H. J. Arpe, H. Baltes, DBP 3420707 and DBP 3420706 (December 5, 1985), Hoechst AG.

[204] H. Baltes, E. Leupold, DBP 3345808 (June 27, 1985), Hoechst AG.

[205] F. J. Weigert, *J. Org. Chem. 51* (1986) 2653.

[206] H. J. Arpe, H. Litterer, N. Mayer, Eur. Pat. 72008 (February 16, 1983), Hoechst AG.

[207] Jap. Pat. 6042340 (March 6, 1985), Toray Ind.

[208] G. A. Olah, M. W. Meyer, *J. Org. Chem. 27* (1962) 3464.

[209] V. Solinas, R. Monaci, B. Marongiu, L. Forni, *Appl. Catal. 9* (1984) 109.

[210] T. Maki, T. Masuyama, Y. Asahi, US-Pat. 4556751 (December 3, 1985), Mitsubishi Chem.

[211] K. Eichler, E. Leupold, DBP 3433813 (March 20, 1986), DBP 3419555 (November 28, 1985) and Eur. Pat. 166182 (January 2, 1986), Hoechst AG.

[212] A. V. Timofeev, L. Ya. Romanchenko, *Khim Prom-st. (Moscow) 1986*, 146.

[213] J. A. Martens, P. J. Grobet, W. J. Vermeiren, R. H. Jacobs in [29a], p. 935.

[214] G. E. M. J. DeClippeleir, R. M. Cahen, G. L. G. Debras, DBP 3512057 (October 3, 1985), Labofina S.A.

[215] M. Stoecker, P. Hemmersbach, J. H. Raeder, J. K. Grepstad, *Appl. Catal. 25* (1986) 223.

[216] M. M. Ermilova, Z. V. Gryaznova, *Russ. J. Phys. Chem (Engl. Transl.) 44* (1970) 985, 987.

[217] K. Otsuka, A. Morikawa, *J. Catal. 46* (1977); *56* (1979) 88.

[218] K. Otsuka, N. Kazuo, A. Morikawa, *J. Chem. Soc. Faraday Trans. 76* (1980) 1196.

[219] T. Nishizawa, H. Hattori, T. Uenatsu, T. Shiba in J. W. Hightower (Ed.): *Proc. 4th Int. Congr. Catal. Moscow*, Rice University Printing and Reproduction Department, Houston, TX 1969, p. 994.

[220] V. Y. Volf, M. N. Zhavoronkov, A. Z. Dorojochinski, *Izv. Vyssh. Uchebn. Zaved. Khim. Khim. Tekhol. 28* (1985) 21.

[221] J. Weitkamp, W. Gerhard, P. A. Jacobs in [47], p. 261.

[222] K. Honna, M. Sugimoto, N. Shimizu, K. Kurisaki, *Chem. Lett. 1986*, 315.

[223] H. Iida, K. Honna, Jap. Pat. 60246333 (December 6, 1985), Idemitsu Kosan Co.

[224] J. D. N. Irving, H. F. Leach, D. A. Whan, M. S. Spencer, *J. Chem. Res. Synop. 1983*, 66, 108.

[225] R. M. Dessau, *J. Catal. 80* (1984) 520.

[226] W. Hölderich, A. Lindner, W. D. Mross, M. Schwarzmann, K. Volkamer, U. Wagner, Eur. Pat. 129899 (January 2, 1985), BASF AG.

[227] A. Lindner, U. Wagner, K. Volkamer, W. Hölderich, W. Hochstein, W. Immel, Eur. Pat. 129000 (January 2, 1985), BASF AG.

[228] W. Hölderich, A. Lindner, W. D. Mross, M. Strohmeyer, DBP 3427979 (January 30, 1986), BASF AG.

[229] D. L. Sikkenga, US-Pat. 4503282 (March 5, 1985), Standard Oil Co.

[230] R. Fischer, W. Hölderich, W. D. Mross, H. M. Weitz, Eur. Pat. 0167021 (January 8, 1986), BASF AG.

[231] P. Fitton, H. Moffet, DBP 2621224 (December 16, 1976), Hoffmann-La Roche.

[232] V. Alexandrov, V. Smirnov, S. Kryukov, *Neftekhimiya 25* (1985) 645.

[233] W. Hölderich, R. Fischer, W. D. Mross, H. M. Weitz, Eur. Pat. 0132737 (February 13, 1985), BASF AG.

[234] G. B. Fozzard, J. R. Norell, US-Pat. 4182901 (January 8, 1980), Phillips Petrol.

[235] S. Mabuchi, H. Kisaki, US-Pat. 3830833 (January 13, 1972), Toyo Soda Co.

[236] Y. Yoshinori, S. Hironobu, Br. Pat. 2051805 (December 18, 1980), Japan Synthetic Rubber Co.

[237] L. J. Velenyi, A. S. Krupa, US-Pat. 4329506 (May 11, 1982), Standard Oil Co.

[238] J. W. Reynolds, H. S. Young, US-Pat. 3466334 (June 14, 1968), Eastmann Kodak Co.

[239] H. Fröhlich, M. Schneider, W. Himmele, M. Strohmeyer, G. Sandrock, K. Baer, DBP 2758113 (July 5, 1979), BASF AG.

[240] W. Hölderich, F. Merger, W. D. Mross, R. Fischer, Eur. Pat. 0162387 (November 27, 1985), BASF AG.

[241] H. C. Linstid, G. S. Koermer, US-Pat. 4537995 (August 27, 1985), Celanese Co.

[242] K. G. Ione, L. A. Vostrikova, A. V. Petrova, V. M. Mastikin, *Catal., Proc. Int. Congr. 8th*, Berlin 1984, *Vol. 4*, p. 519.

[243] M. Baudoin, R. Perrony, DBP 2646172 (April 28, 1977), Rhône Poulenc Ind.

[244] Q. Wang, Z. Chen, *Kexue Tongbao 29* (1984) 1130.

[245] Jap. Pat. 74025654 (July 2, 1974), Mitsubishi Petrochem. Co.

[246] H. G. Schmidt, Eur. Pat. 75680 (November 20, 1986), Dynamit Nobel AG.

[247] W. Hölderich, R. Fischer, W. Mesch, DOS 3636430 (February 5, 1986), BASF AG.

[248] J. Colange, G. Descotes, B. Girond-Abel, J. C. Martin, *C. R. Hebd. Séances Acad. Sci. Ser. 258* (1964) 2096.

[249] C. Neri, F. Buonomo, Eur. Pat. 100117 (July 13, 1983), Enichem Anic S.p.A.

[250] W. Hölderich, N. Götz, L. Hupfer, R. Kropp, H. Theobald, B. Wolf, DOS 3546372 (July 2, 1987), BASF AG.

[251] M. Orisaku, K. Sano, Jap. Pat. 61112040 (May 30, 1986), Mitsubishi Gas Chem.

[252] K. Aomura, M. Nitta, S. Matsumoto, *Kogakubu Kenkyu Hokoku (Hokkaido Daigaku) 67* (1973) 171.

[253] S. Fujii, S. Mori, *Rikogaku Kenkyusho Hokoku, Waseda Daigaku 67* (1974) 26.

[254] M. R. Musaev, E. S. Guseinova, F. M. Mamedov, *Azerb. Khim. Zh. 5* (1976) 21.
[255] F. A. Chernyshkova, D. V. Mushenko, *Neftekhimiya 16* (1976) 250.
[256] E. Ruiz-Hitzky, B. Casal, *J. Catal. 92* (1985) 291.
[257] C. S. Rondestvedt, G. J. Mantell, *J. Am. Chem. Soc. 82* (1960) 6419; *84* (1962) 3307.
[258] H. J. Arpe, DOS 2922698 (December 11, 1980), Hoechst AG.
[259] W. Hölderich, F. Merger, R. Fischer, Eur. Pat. 199210 (October 29, 1986), BASF AG.
[260] P. S. Landis, P. B. Venuto, *J. Catal. 6* (1966) 245.
[261] M. Sato, N. Ishii, K. Hirose, S. Nakamura in [29a], p. 755.
[262] A. Aucejo, M. Burguet, A. Corma, V. Fornes, *Appl. Catal. 22* (1986) 187.
[263] J. Ward, *J. Catal. 13* (1969) 321.
[264] P. M. G. Frenken, Eur. Pat. 86543 (May 7, 1986), Stamicarbon B. V.
[265] H. Fuchs, O. A. Brand-Grosskinsky, R. Schmitz, DBP 2837793 (March 13, 1980), BASF AG.
[266] O. Immel, B. U. Kaiser, W. Litz, H. H. Schwarz, K. Starke, DBP 2641408 (March 16, 1978), Bayer AG.
[267] A. DeRooij, J. Elmendorp, W. J. Wassen, DBP 2223643 (December 30, 1972), Stamicarbon N.V.
[268] C. D. Chang, N. J. Morgan, US-Pat. 4214107 (July 22, 1980), Mobil Oil Corp.
[269] L. B. Young, US-Pat. 4461729, US-Pat. 4461730 (both July 24, 1984), Mobil Oil Corp.
[270] Jap. Pat. 57070828 (May 1, 1982), Maruzen Oil.
[271] Y. Okumura, S. Kamiyama, H. Furukawa, K. Kaneko, Eur. Pat. 130697 (May 31, 1983), Eur. Pat. 127486 (May 31. 1984), Toa Nenryo.
[272] T. Sakamoto, DBP 3337301 (April 19, 1984), Toyo Soda Mfg.
[273] R. Gregory, D. J. Westlake, Eur. Pat. 45618 (February 10, 1982), BP Co. Ltd.
[274] C. Gueguen, F. Figueras, F. Fajula, Fr. Pat. 2545480 (November 9, 1984), Elf Co.
[275] L. N. Tolkacheva, L. A. Novikova, I. D. Miheikin, L. M. Kuster, K. M. Minachev, *Neftekhimiya 25* (1985) 610.
[276] M. Tojo, Y. Fukuoka, Eur. Pat. 162475 (May 24, 1985), Asahi Chem. Ind.
[277] O. Mitsui, Y. Fukuoka, O. Kurashiki, DBP 3441072 (May 23, 1985), Asahi Chem. Ind.
[278] O. Mitsui, Y. Fukuoka, Fr. Pat. 2554440 (May 10, 1985), Asahi Chem. Ind.
[279] Jap. Pat. 60104029 (June 8, 1985), Asahi Chem. Ind.
[280] J. Jacobs, P. A. Jacobs, J. Uytterhoeven, Eur. Pat. 175399 (August 13, 1985).
[281] R. M. Cursetji, A. N. Singh, A. V. Deo: *Advances in Catal.* 1985, p. 345.
[282] P. Lurang, J. Delin, L. Hexuan, *Shiyou Huagong 15* (1986) 155.
[283] H. G. Karge, H. Koesters, Y. Wada in [21], S. 308.
[284] Union Carbide Corp., *Res. Discl. 264* (1986) 222.
[285] A. Molnar, I. Bucsi, M. Bartok, *Acta Phys. Chem. 31* (1985) 571.
[286] P. L. Yue, O. Olaofe, *Chem. Eng. Res. Des. 62* (1984) 81.
[287] M. R. Musaev, B. A. Dadashev, K. G. Mirzoeva, *Azerb. Khim. Zh. 1983*, 30.
[288] L. N. Malashevich, A. V. Pismennaya, *Neftekhimiya 24* (1984) 664.
[289] E. Paukstis, K. Jiratova, R. V. Soltanev, *Collect. Czech. Chem. Commun. 50* (1985) 643.
[290] Y. Aoki, Jap. Pat. 61072727 (April 14, 1986), Nippon Sheet Class Co.
[291] H. Fischer, G. Schnuchel, DBP 2163396 (June 28, 1973), Erdölchemie GmbH.
[292] D. Forster, G. E. Barker, Eur. Pat. 80449 (July 3, 1985), Monsanto Comp.
[293] A. Vavere, US-Pat. 4547614 (October 15, 1985), Monsanto Comp.
[294] W. L. Hsu, N. A. Maly, B. A. Matrana, L. G. Wideman, US-Pat. 4524233 (June 18, 1985), Goodyear Tire and Rubber.
[295] W. Hölderich, F. Merger, W. D. Mross, G. Fouquet, Eur. Pat. 0162385 (November 27, 1985), BASF AG.
[296] M. R. Klotz, US-Pat. 4584415 (April 22, 1986), Amoco.
[297] P. Chu, G. H. Kuehl, US-Pat. 4605787 (August 12, 1986), Mobil Oil Corp.
[298] J. A. Daniels, A. Stewart, Eur. Pat. 55045 (December 19, 1986), ICI Ltd.
[299] V. Macho, M. Kavala, M. Matas, C. Hybl, Czech. Pat. 189071 (December 15, 1981), Ustav pre Petrochemin.
[300] J. A. Bogod, V. R. Gurevich, L. E. Mezklumyan, *Khim. Promst. (Moscow) 9, 1972*, 657; Russ. Pat.-Anm. 232967 (August 1969).
[301] D. Arntz, M. Baacke in [29a], Poster 2 D-13.
[302] L. B. Young, US-Pat. 4365084 (December 21, 1982), US-Pat. 4447642 (May 8, 1984), Mobil Oil Corp.
[303] Jap. Pat. 56092833 (December 27, 1979), Mitsubishi Gas Chem. Ind.
[304] S. Haruhito, DBP 3149979 (July 22, 1982), Idemitsu Kosan Co., Ltd.
[305] R. Gregory, D. J. Westlake, J. J. Harry, Eur. Pat. 45618 (March 26, 1986), BP Co.
[306] J. A. Ballantine, M. Davies, R. M. O'Neil, I. Patel, J. H. Purnell, M. Rayanakorn, K. J. Williams, *J. Mol. Catal. 26* (1984) 57.
[307] R. W. Diesen, US-Pat. 4384159 (May 17, 1983), Dow Chemical Co.
[308] K. Sekizawa, S. Fujii, Y. Tsutumi, Jap. Pat. 60252433 (May 29, 1984), Toyo Soda.
[309] A. J. Magistro, Eur. Pat. 162457 (November 27, 1985), Goodrich, B. F., Co.
[310] H. E. Fried, Eur. Pat. 122654 (October 24, 1984), Shell Int. Research.
[311] D. Kallo, G. Onyestyak, J. Papp in [21], p. 444.
[312] G. Onyestyak, D. Kallo, J. Papp, J. E. Detrekoy, Hung. Pat. 29972 (February 28, 1984).
[313] G. T. Kerr, P. S. Landis, US-Pat. 3312751 (April 4, 1967), Mobil Oil Corp.
[314] B. Buchholz, US-Pat. 4102931 (July 25, 1978), Pennwalt Corp.
[315] J. Peterson, H. S. Fales, US-Pat. 4307250 (April 8, 1981), Eur. Pat. 39918 (February 29, 1984), Air Prod. Chem. Inc.
[316] M. E. Deeba, W. J. Ambs, Eur. Pat. 77016 (June 19, 1985), Air Prod. Chem. Inc.
[317] J. Peterson, H. S. Fales, US-Pat. 4375002 (February 22, 1983), Air Prod. Chem. Inc.
[318] W. J. Ambs, M. E. Deeba, J. F. White, Eur. Pat. 101921 (April 16, 1986), Air Prod. Chem. Inc.
[319] V. Taglieber, W. Hölderich, R. Kummer, W. D. Mross, G. Saladin, DBP 3326579 (January 31, 1985), DBP 3327000 (February 7, 1985), BASF AG.
[320] S. L. Andersson, M. Scurrell, *J. Mol. Catal. 18* (1983) 375.
[321] R. Gelin, F. Lefebvre, B. Elleuch, C. Naccache, Y. Ben Taarit, *ACS Symp. Ser. 218* (1983) 455.
[322] D. R. Denley, R. H. Raymond, S. C. Tang, *J. Catal. 87* (1984) 414; *Springer Ser. Chem. Phys. 27* (1983) 325.
[323] S. L. Andersson, M. Scurrell, *Zeolites 3* (1983) 261.
[324] M. Scurrell, S. K. Johnsen, H. Svendsen, *Heterog. Katal. 5th 1983, Pt. 2*, 39.
[325] F. Kaoru, S. Tsutomu, O. Kohji, T. Hiro, *Chem. Lett. 12* (1984) 2047.
[326] D. Feitler, US-Pat. 4612387 (September 16, 1986), Air Prod. Chem. Inc.
[327] W. Hölderich, G. Fouquet, W. Harder, F. Cäsar, DOS 3606169 (February 26, 1986), BASF AG.
[328] T. Suzuki, I. Nakana, Jap. Pat. 59161328 (September 12, 1984), Mitsubishi Gas Chem.
[329] T. Suzuki, S. Hashimoto, M. Orisaku, I. Nakana, Eur. Pat. 114567 (August 1, 1984), Mitsubishi Gas Chem. Co.
[330] I. Tsuji, K. Ohno, *J. Am. Chem. Soc. 90* (1968) 94.
[331] F. A. Pesa, M. W. Blaskie, I. R. Fox, US-Pat. 4517400 (May 14. 1985).
[332] C. D. Chang, S. P. Hellringe, US-Pat. 4620044 (October 16, 1985), Mobil Oil Corp.
[333] C. A. Hamilton, US-Pat. 3328467 (June 27, 1967), Mobil Oil Corp.
[334] F. L. Johnson, US-Pat. 4438281 (March 20, 1984), Texaco.
[335] L. Vamling, L. Cider, *Ind. Eng. Chem. Prod. Res. Dev. 25* (1986) 424.
[336] M. Onaka, M. Kamai, Y. Izumi, *Chem. Lett. 1985*, 779.
[337] D. R. Corbin, W. C. Seidel, L. Abrams, N. Herron, G. D. Stucky, C. A. Tolman, *Inorg. Chem. 24* (1985) 1800.
[338] Jap. Pat. 59156437 (September 5, 1984), Mobil Oil Corp.
[339] W. Kranich, A. Weiss, Z. Schay, L. Guzy, *Appl. Catal. 13* (1985) 257.
[340] R. Denkewicz, A. Weiss, W. Kranich, *J. Wash. Acad. Sci. 74* (1984) 19.
[341] L. Tebassi, A. Sayari, A. Ghorbel, M. Dufaux, C. Naccache, *J. Mol. Catal. 25* (1984) 397.
[342] A. A. Galinskii, V. S. Gutyrya, *Neftеperearab. Neftekhim. (Kiev) 25* (1983) 22.
[343] M. Goldwasser, C. Naccache, *Actas Simp. Iberoam. Catal. 9th 2* (1984) 1398.
[344] G. DelAngel, B. Coq, R. Dutartre, F. Fajula, F. Figueras, C. Leclercq, *Stud. Surf. Sci. Catal. 17* (1983) 301.
[345] M. Dufaux, P. Gelin, C. Naccache, *Stud. Surf. Sci. Catal. 5* (1980) 261.
[346] Jap. Pat. 59186929 (October 23, 1984), Asahi Chem. Ind.

[347] P. D. Seemuth, US-Pat. 4459419 (July 10, 1984), Ethyl Corp.
[348] R. Ottana, A. Parmaliana, C. Zipelli, N. Giordano, *Ann. Chim. (Rome) 73* (1983) 403.
[349] N. P. Forbus, US-Pat. 4547618 (October 15, 1985), Mobil Oil Corp.
[350] N. M. Page, Eur. Pat. 186399 (July 2, 1986), Mobil Oil Corp.
[351] S. A. I. Barri, D. Dave, D. Young, Eur. Pat. 150107 (July 31, 1985), BP Co. Ltd.
[352] K. M. Minachev, V. V. Kharlamov, J. B. Tagiev, Z. G. Zul'fugarov, *Zeolites 4* (1983) 270.
[353] J. P. Lucien, Eur. Pat. 98622 (March 5, 1986), Shell.
[354] P. R. Robinson, E. L. Moorehead, US-Pat. 4564603 (January 14, 1986), Union Oil Co.
[355] R. Cid, P. Ryes, G. Pecchi, *J. Chem. Res. Synop. 1986*, 64.
[356] S. D. Mekhtiev, Kh. M. Alimardanov, M. R. Musaev, M. M. Damirov, Russ. Pat. 1074853 (February 23, 1984), Inst. Petrochem. Process; *Otkrytiya Isobret. 1984*, 85.
[357] M. R. Musaev, Kh. M. Alimardanov, G. T. Makhmudova, Russ. Pat. 1133253 (January 7, 1985); *Otkrytiya Isobret. 1985*, 93.
[358] L. S. Marchenko, D. Z. Levin, V. A. Plakhotnik, E. S. Mortikov, *Izv. Akad. Nauk SSSR Ser. Khim. 1986*, 94.
[359] Kh. M. Minachev, D. B. Tagiev, Z. G. Zul'fugarov, V. V. Kharlamov, *Geterog. Katal. 4* (1979) 505.
[360] J. L. Cihonski, US-Pat. 4429175 (January 31, 1984), El Paso Products Co.
[361] D. L. Sikkenga, T. N. Nevitt, N. F. Jerome, US-Pat. 4433190 (February 21, 1984), Standard Oil Co.
[362] D. L. Sikkenga, US-Pat. 4435311 (March 6, 1984), Standard Oil Co.
[363] A. J. Kolombos, C. D. Telford, D. Young, Eur. Pat. 42252 (October 5, 1983), BP Co.
[364] N. A. Kutz in B. L. Shapiro (Ed.): *Heterogeneous Catalysis, Proceedings of the Second Symposium College Station*, Texas A & M University Press, College Station 1984, p. 121.
[365] W. Hölderich, R. Fischer, W. D. Mross, F. F. Pape, DBP 3513570 (October 16, 1986), BASF AG.
[366] J. R. Anderson, P. Tsai, *Appl. Catal. 19* (1985) 141.
[367] S. Shepelev, K. Ione, *React. Kinet. Catal. Lett. 23*, (1983) 129, 323.
[368] D. Young, Eur. Pat. 0093543 (February 26, 1986), BP Co. Ltd.
[369] C. Pochen, US-Pat. 4120910 (October 17, 1978), Mobil Oil Corp.
[370] N. Y. Chen, T. Y. Yan, *Ind. Eng. Chem. Process Des. Dev. 25* (1986) 151.
[371] A. W. Chester, Y. F. Chu, US-Pat. 4350835 (September 21, 1982), Mobil Oil Corp.
[372] W. J. Ball, D. G. Stewart, US-Pat. 4354049 (October 12, 1982), BP Co. Ltd.
[373] T. Inui, Y. Makino, F. Okazumi, A. Miyamoto, *J. Chem. Soc. Chem. Commun. 1986*, 571.
[374] G. Sirokman, Y. Sendoda, Y. Ono, *Zeolites 6* (1986) 299.
[375] D. C. Bailey, S. H. Langer, *Chem. Rev. 81* (1981) 109.
[376] P. F. Jackson, F. G. Brian, J. Lewis, R. Ganzerla, M. Lenarda, M. Graziani, *J. Organomet. Chem. 190* (1980) C1.
[377] E. Mantovani, N. Palladino, A. Zanobi, *J. Mol. Catal. 3* (1978) 285; DBP 2804307 (August 3, 1978), Snamprogetti SPA.
[378] R. J. Davis, J. A. Rossin, M. E. Davis, *J. Catal. 98* (1986) 477.
[379] M. E. Davis, P. M. Butler, J. A. Rossin, B. E. Hanson, *J. Mol. Catal. 31* (1985) 385.
[380] L. H. Simons, D. C. Alexander, US-Pat. 4435517 (March 6, 1984), Texaco Inc.
[381] N. Takahashi, S. Hasegawa, N. Hanada, M. Kobyashi, *Chem. Lett. 1983*, 945.
[382] H. Arai, H. Tominaga, *J. Catal. 75* (1982) 188.
[383] N. Takahashi, M. Kobayashi, *J. Catal. 85* (1984) 89.
[384] N. Takahashi, H. Matsuo, M. Kobayashi, *J. Chem. Soc. Faraday Trans. 1 80* (1984) 629.
[385] P. Centola, G. Terzaghi, R. DelRosso, I. Pasquon, *Chim. Ind. (Milan) 54* (1972) 775.
[386] E. Rode, M. Davis, B. Hanson, *J. Chem. Soc. Chem. Commun. 1985*, 1477.
[387] B. E. Hanson, M. E. Davis, D. Taylor, E. Rode, *Inorg. Chem. 23* (1984) 52.
[388] M. E. Davis, E. Rode, D. Taylor, B. E. Hanson, *J. Catal. 86* (1984) 67.
[389] E. J. Rode, M. E. Davis, B. E. Hanson, *J. Catal. 96* (1985) 563; *J. Chem. Soc. Chem. Commun. 1985*, 716.
[390] H. Arai, T. Yamashiro, T. Kubo, H. Tominaga, *Bull. J. Pet. Inst. 18* (1976) 39.
[391] Kh. M. Minachev, N. Y. Usachev, A. P. Rodin, V. P. Kalinin, Y. I. Isakov, *Neftekhimiya 19* (1979) 751; *Izv. Akad. Nauk SSSR Ser. Khim. 1981*, 267, 724; *1982*, 132.
[392] Kh. M. Minachev, O. M. Nefedov, V. V. Kharlamov, S. Y. Panov, S. F. Politanskii, *Izv. Akad. Nauk SSSR Ser. Khim. 1981*, 1490.
[393] Kh. M. Minachev, V. V. Kharlamov in [47], p. 497.
[394] R. W. Diesen, Eur. Pat. 106356 (April 25, 1984), Dow Chemical Comp.
[395] E. L. Moorehead, US-Pat. 4604371 (August 5, 1986), Union Oil Comp.
[396] D. B. Tagiev, Kh. M. Minachev, *Russ. Chem. Rev. (Engl. Transl.) 50* (1981) 1009.
[397] M. Taramasso, G. Perego, B. Notari, US-Pat. 4410501 (August 18, 1983), Snamprogetti S.p.A.
[398] G. Perego, G. Bellussi, C. Corno, M. Taramasso, F. Buonomo, A. Esposito in [29a], p. 129.
[399] C. Neri, B. Anfossi, A. Esposito, F. Buonomo, Eur. Pat. 100119 (February 8, 1984), Anic S.p.A.
[400] R. A. Sheldon, *J. Mol. Catal. 7* (1980) 107.
[401] C. Neri, F. Buonomo, B. Anfossi, Eur. Pat. 100118 (February 8, 1984), Anic S.p.A.
[402] C. Neri, F. Buonomo, Eur. Pat. 102097 (March 7, 1984), Anic S.p.A.
[403] A. Esposito, M. Taramasso, C. Neri, F. Buonomo, Br. Pat. 2116974 (October 5, 1985), Anic S.p.A.
[404] C. D. Chang, S. D. Hellring, US-Pat. 4578521 (March 25, 1986), Mobil Oil Corp.
[405] A. Eposito, C. Neri, F. Buonomo, US-Pat. 4480135 (October 30, 1984), Anic S.p.A.
[406] J. Hartig, A. Stoessel, G. Hermann, L. Marosi, DOS 3222144 (December 15, 1983), BASF AG.
[407] U. Romano, M. G. Clerici, G. Bellussi, F. Buonomo, Eur. Pat. 203632 (December 3, 1986), Enichem Sintesi S.p.A.
[408] M. A. Tobias, US-Pat. 3728408 (April 17, 1973), Mobil Oil Corp.
[409] C. J. Plank, E. J. Rosinski, G. T. Kerr, US-Pat. 4011278 (March 8, 1977), Mobil Oil Corp.
[410] J. Novakva, L. Kubelkova, P. Jiru, S. Beran, K. Nevodova in [47], p. 561.
[411] Y. Servotte, J. Jacobs, P. A. Jacobs in [47], p. 609.
[412] C. D. Chang, W. H. Lang, W. K. Bell in [24], p. 73.
[413] G. P. Hagen, US-Pat. 4433174 (February 21, 1984), Standard Oil Co.
[414] J. Shabtai, R. Lazar, E. Biron, *J. Mol. Catal. 27* (1984) 35.
[415] Y. Isakov, N. Y. Usachev, T. Isakova, K. Minashev, *Izv. Akad. Nauk SSSR Ser. Khim. 1985*, 1965.
[416] Y. Isakov, N. Y. Usachev, T. Isakova, K. Minachev, *Izv. Akad. Nauk SSSR Ser. Khim. 1986*, 299.
[417] Y. Isakov, K. Minachev, T. Isakova, *Dokl. Akad. Nauk SSSR 1985*, 284.
[418] T. J. Huang, W. O. Haag, US-Pat. 4339606 (July 13, 1982), Eur. Pat. 112821 (July 16, 1986), Mobil Oil Corp.
[419] G. I. Golodets, N. V. Pavlenko, L. F. Korzhova, K. M. Vaisberg, Y. I. Churkin, *Kinet. Katal. 25* (1984) 1015.
[420] K. Weissermel, H.-J. Arpe: *Industrielle Organische Chemie*, Verlag Chemie, Weinheim 1978, p. 108.
[421] D. G. Jones, US-Pat. 3414588 (December 3, 1968), Mobil Oil Corp.
[422] K. Okumura, M. Sasamoto, K. Tanaka, Jap. Pat. 60226834 (November 12, 1985), Jap. Pat. 60252432 (May 28, 1984), Jap. Pat. 60224642 (April 23, 1984), Nippon Zeon.
[423] C. Chang, W. Lang, N. Morgan, Eur. Pat. 13600 (July 23, 1980), Mobil Oil Corp.
[424] M. T. Barlow, D. G. Stewart, Eur. Pat. 122782 (October 24, 1984), BP Co. Ltd.
[425] C. D. Chang, W. H. Lang, US-Pat. 4220783 (May 9, 1979), Mobil Oil Corp.
[426] S. K. Roy, N. S. Rawat, P. N. Mukherjee, *Natl. Symp. Catal. 7th, 1985*, 121.
[427] D. Feitler, W. Schimming, H. Wetstein, Eur. Pat. 131887 (January 23, 1985), Nepera.
[428] Nederlandse Org. voon Zuiver Wetenschappelijk Onderzoek, Neth. Pat. 8202884 (February 16, 1984).
[429] C. D. Chang, P. D. Perkins, Eur. Pat. 82613 (June 29, 1983), US-Pat. 4388461 (June 14, 1983), Mobil Oil Corp.
[430] H. LeBlanc, L. Puppe, K. Wedemeyer, DBP 3332687 (March 28, 1985), Bayer AG.
[431] K. Baer, M. Decker, J. Schmidt, G. Leibner, H. Sperber, US-Pat. 3324165 (June 6, 1967), BASF AG.

[432] F. Foley, F. C. Mawer, DBP 2056295 (May 27, 1971), ICI Ltd.
[433] W. Hölderich, H. Lendle, P. Magnussen, H. Leitner, J. H. Manegold, W. Leitenberger, Eur. Pat. 196554 (October 8, 1986), BASF AG.
[434] B. Milligan, R. K. Pinschmidt, US-Pat. 4341898 (July 27, 1982), Air Prod. Chem.
[435] A. V. Rao, M. N. Rao, K. Garyali, P. Kumar, *Chem. Ind. (London) 1984*, 270.
[436] C. D. Chang, W. H. Lang, R. B. Lapierre, US-Pat. 4231955 (November 4, 1980), Mobil Oil Corp.
[437] Y. Ono, K. Hatada, K. Fujita, A. Halgeri, T. Keii, *J. Catal. 41* (1976) 322.
[438] K. Fujita, K. Hatada, Y. Ono, T. Keii, *J. Catal. 35* (1974) 325.
[439] Y. Ono, A. Halgeri, M. Kaneko, K. Hatada, *ACS Symp. Ser. 40* (1977) 596.
[440] K. Hatada, M. Shimada, K. Fujita, Y. Ono, T. Keii, *Chem. Lett. 1974*, 439.
[441] K. Hatada, M. Shimada, Y. Ono, T. Keii, *J. Catal. 37* (1975) 166.
[442] D. Mravec, J. Balko, J. Ilavsky, *Chem. Prum. 36* (1986) 82.
[443] W. Hölderich, H. Hoffmann, H. Lermer, Eur. Pat. 2242220 (June 3, 1987), BASF AG.
[444] S. J. Miller, US-Pat. 4608450 (August 26, 1986), Chevron Res. Co.
[445] S. J. Miller, US-Pat. 4542251 (September 17, 1985), Chevron Res. Co.
[446] P. J. Garegg, S. Koepper, P. Ossowski, J. Thiem, *J. Carbohydr. Chem. 5* (1986) 59.
[447] R. M. Dessau, US-Pat. 4554262 (November 19, 1985), Mobil Oil Corp.
[448] H. Tiltscher, K. Dialer, W. Jaeger, DBP 3421049 (December 12, 1985).
[449] S. T. Wilson, B. M. Lok, C. A. Messina, E. M. Flanigen in [21], p. 97.
[450] E. M. Flanigen, B. M. Lok, R. L. Patton, S. T. Wilson in [29a], p. 103.
[451] *Chem. Eng. News 63* (1985) No. 1, p. 47.
[452] *Chem. Eng. News 63* (1985) No. 1, p. 15.
[453] T. J. Pinnavaia, *Science 220* (1983) 365.
[454] G. Boxhoorn, J. Moolhuysen, J. G. F. Coolegem, R. A. van Santen, *J. Chem. Soc. Chem. Commun. 1985*, 1305.
[455] U. Dettmeier, K. Eichler, K. Kühlein, E. J. Leupold, H. Litterer, *Angew. Chem. 99* (1987) 470; *Angew. Chem. Int. Ed. Engl. 26* (1987) 468.

Structure Elucidation and Artificial Intelligence

By Wolfgang Bremser*

Dedicated to Professor Helmut Dörfel on the occasion of his 60th birthday

The difference between the older and the more recent computer systems amounts, in the final analysis, to the difference between an insect and a human being. The insect comes "fully programmed" into the world—programmed by instincts which it follows without using any thought processes. On the other hand, the human being must first learn the correct behavior—however, such learning can develop an impetus all its own: becoming, indeed, proceeding from his own decision and his awareness, the human being can change his former action programs. The creation of a computer system of the x-th generation will actually far more resemble educating a child than the traditional programming of a computer.

Stanisław Lem[1]

1. Elucidation of Structure in Organic Chemistry

There is no need for any discussion concerning the increasing importance of structure elucidation in organic chemistry. During the past years, increasing emphasis has been placed not only on the classical analysis of constitution, but also on the investigation of configuration and conformation, these activities reaching their peak in the accurate imaging of entire protein structures by means of X-ray structural analysis or NMR spectroscopy. Even natural and synthetic mixtures are identified as a matter of routine, be it after previous separation, by time-dependent observation of chemical reactions or, in the case of high polymers, by sequence analysis. Finally, by measuring the isotope ratios, it is possible to retrace the history of the origin of a substance in synthetic or biological reactions with a relatively high degree of accuracy.

By means of electronics and computer control, the level of performance of modern analytic equipment has reached such an advanced stage that an abundance of accurate and highly specific data—which awaits detailed evaluation—is being generated, to a large extent fully automatically. Indeed, in our spectroscopy laboratory approximately 40 MBytes of data are handed over, each day, to our colleagues in charge of interpretation, and there await processing; this is a colossal task, which can be performed only with the aid of electronic data processing.

On the other hand, the need for detailed information about our chemical substances is also increasing daily. In the present-day political environment, with its requirements imposed by the legislature and the demands of environmental protection, as well as the high quality standard which, in the situation of fierce industrial competition, offers the only chance of survival, analytical procedures are challenged afresh every day. Moreover, an improvement of the properties of a substance is possible only by means of an accurate knowledge of the substance, and the controlled synthesis of an active substance only by means of a knowledge of the mechanism of action. It is frequently possible, by means of improved analytical data, to avoid unnecessary effort in the synthesis and testing of compounds which are unwanted, because they are inactive.

Only by the consistent application of modern computer technology in the recording and interpretation of spectroscopic data can these constantly increasing demands be met. The present article cannot and will not deal with every aspect of the problem. On the contrary the intention is to present a brief excursion into the facilities and problems of automation from the viewpoint of a modern spectroscopy laboratory, and, above all, to survey the tools which permit an "intelligent" evaluation of the raw data. In this connection, it should be borne in mind that the person commissioning a spectroscopic analysis is, in most cases, not interested in the spectrum per se, but has a direct interest in the structural information. If it proves to be possible to translate the spectroscopic parameters directly into topologies and the associated structural pictures (topograms), then a further decisive step towards the improvement of the level of performance of analytical methods has been taken.

2. Automated Recording of Spectra

Components for the fully automatic control of the recording of NMR, IR and MS spectra are nowadays included in the basic equipment of the majority of spectrometers which are commercially available. Accordingly, the experiments are designed, the measurement parameters are optimized, the desired number of runs is summed, and the data processed and printed out in standardized form on the screen or printer. The entire procedure is set up by the user in a flexible programming language and executed by the computer. In this way, it is also possible for series of experiments, such as 2D correlations, reaction kinetics,[2]

[*] Dr. W. Bremser
Molekülspektroskopie, ZHV/S
Hauptlaboratorium der BASF Aktiengesellschaft
D-6700 Ludwigshafen (FRG)

 © VCH Verlagsgesellschaft mbH, D-6940 Weinheim, 1988 0570-0833/88/0202-0247 $ 02.50/0

Fig. 1. An interior view of a modern spectroscopy laboratory with a high-field nuclear resonance spectrometer including an automatic sample changer in the foreground and a robot system for the automatic preparation of the substance samples in the background. A human being is intentionally employed at the intermediate monitoring stage; he inspects the solution and places it, after grading, into the changer.

daughter scans, etc., to be performed without supervision (Fig. 1).

Automatic switching-over between chemical ionization (CI) and electron impact (EI) excitation in mass spectrometry is mentioned as example of a more recent development. The CI experiment is necessary in order to determine the molecular mass and thus the overall formula with precision. This information is an important prerequisite, especially for fully automatic interpretation (see Section 10). In contrast, EI spectra supply the characteristic fragmentation of the molecule and thus the fingerprint of the structure, which is required for the library search. Switching-over between the two types of ionization during the measurement is achieved by the ACE (*A*lternate *C*hemical Ionization/*E*lectron Impact) technique. Although, in the standard method, a medium-sized aperture is used as a compromise between the small CI and the large EI slit, and the spectra produced are mixed spectra—which are not suitable for comparisons of identity—in the modification[3] developed in collaboration with an equipment manufacturer switching-over between optimal apertures takes place pneumatically. As illustrated in Figure 2, in the EI spectrum no CI components are present any longer and even in the course of a GC/MS coupling or a fractionated evaporation CI and EI spectra can be measured "simultaneously".

2.1. Automatic Sample Changers

An automatic changing of the prepared substance sample is required for a fully automatic measurement of different compounds. Automatic changers for small sample tubes (Fig. 1) in nuclear magnetic resonance and for KBr pellets in IR are nowadays included among the accessories supplied with most commercial systems, although care should be taken not to underestimate the complexity of the task with the numerous safety monitoring devices which are required. If separation techniques are carried out in advance in IR or MS, an autosampler is available, which, with its cleaning and drying cycle, can also be used for the

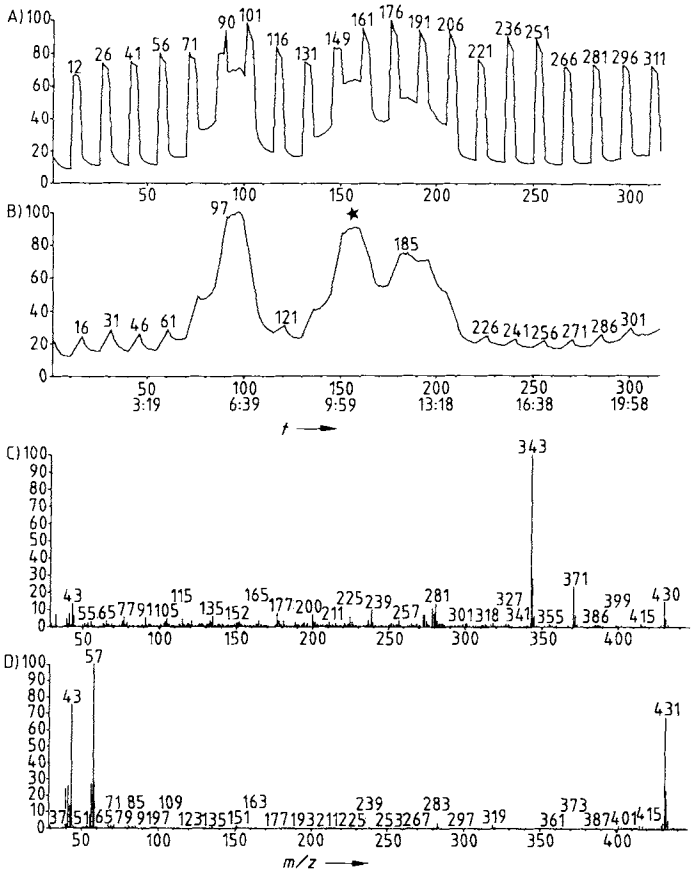

Fig. 2. Direct evaporation of a solid-sample mixture, with monitoring of the total ion current, using automatic switching-over between EI and CI. A, B) Reconstructed total ion current as a function of time. The maxima at constant intervals are due to the reactant gas ions during the CI setting. The progress of the evaporation is best reproduced by the trace B, which is derived from the ion current under EI conditions. C) EI spectra and D) CI spectra of the component which is associated with the second maximum of the evaporation profile (*). The molecular mass of 430 derived from the EI spectrum is confirmed by $(M+H)^{\oplus}$ in the CI spectrum. The EI spectrum is essentially free of impurities due to the preceding CI experiment.

filling of cells in IR.[3] In mass spectrometry, the development of automatic solid-substance charging valves (cf. AUDEVAP[4]) is in progress. Films of liquid samples on KBr windows can also be made and then inserted into the spectrometer by robots (see Fig. 3). By tireless employment, day and night and at the weekend, the automatic changers permit a large throughput of samples and an efficient utilization of the expensive spectrometers. Thus, in nuclear magnetic resonance experiments it is possible to process more than 200 samples per machine per day, and, in mass spectrometric measurements, more than 24 GC/MS couplings with an average of ten components. The information output of these systems can be processed only by resort to computer systems for the documentation and interpretation of the measured results.

2.2. Automatic Preparation of Samples

The aforementioned technical facilities for the automatic execution of the sequences of, in some cases, complicated experiments have not only relieved the burden on laboratory personnel and increased the throughput of sam-

ples but also have improved the quality of the analyses. The only significant manual work remaining is the preparation of the substance samples, especially in IR and NMR spectroscopy. And even here, it is possible to obtain a robot system, which, as a result of the flexibility of its movements and operations, can react rapidly to the required decisions associated with problems specific to certain substances.

Figure 1 shows, in the background, a robot system for the preparation of solutions for NMR spectroscopy (for details see Ref. [3]). The system can handle solid and liquid substance samples alike, from the opening of the sample vessel to the closing of the small measurement tube. Up to 100 substances can be handled in one run, which corresponds to a typical daily throughput of one employee.

In IR spectroscopy, use is made not only of an automatic system for the preparation of KBr pellets[3, 5] but also of a robot for the application of films on KBr windows (Fig. 3). The following steps are executed:

- A KBr disk is taken from the dispenser.
- The sample vessel is screwed on and the sample is pipetted onto the KBr disk, using the injection hand.
- A second KBr disk is taken from the dispenser and pressed onto the first one; the two KBr disks are then placed together with the sample film in a holder and pressed firmly together.
- The holder moves into the measurement beam of the spectrometer, and the start signal for the measurement is passed to the spectrometer. Meanwhile, the sample vessel is again screwed up and put back into position.
- After completion of the measurement, the holder travels upwards again and the measured sample is filed away. The procedure can now recommence from the start.

With this technique, it is possible for 90% of all liquid samples to be prepared and measured fully automatically;

Fig. 3. Laboratory robot (Zymark) for the preparation of films on KBr windows. A small sample tube is just being placed ready for the preparation. Left: spectrometer computer. Right: optical bench where the robot delivers the prepared KBr window.

the time required for the preparation of the robot is approximately half an hour.

By means of the robot it has thus become possible to circumvent the time-consuming filling, cleaning and drying of the standard cells and also to provide the necessary technical prerequisites for the routine recording of liquid substance samples in IR spectroscopy. In this way, the use of autosamplers with a rinsing/drying cycle[3] has been supplemented in a significant manner.

3. The Flow of Information in the Laboratory

Figure 4 shows the flow of information in an IR laboratory. The substance sample is sent by the chemist, together with a statement of the desired experiments, to the appropriate laboratory. In the case of solid state samples, the

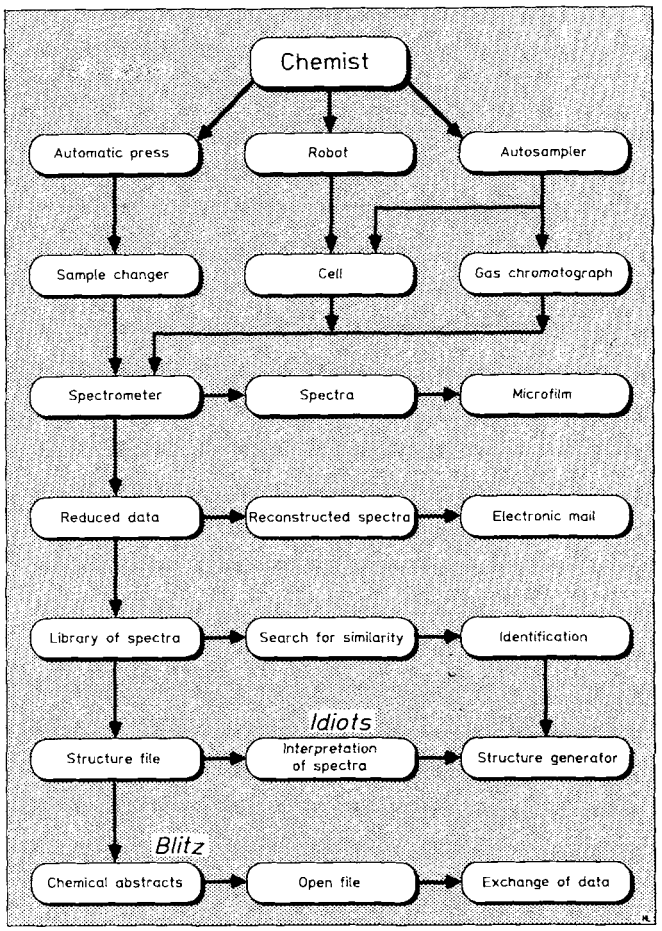

Fig. 4. The flow of information in an IR spectroscopy laboratory. A comparison of the structures present in the structure file with those of Chemical Abstracts by means of the *Blitz* system permits a decision to be made as to whether the compounds have already been published and the data sets can be cleared for exchange with partners in the development of knowledge-based expert systems.

compound is mixed with KBr, formed into pellets in an automatic press and deposited in the sample-changer wheel of the spectrometer. Liquid samples are either applied to KBr windows by the robot (see Section 2.2) or filled into a cell by means of an autosampler or introduced into the gas cell (light pipe) via a short GC column. The

automatic FT-IR spectrometer records the measurement data and plots a spectrum, which, after microfilming, is transmitted in the original to the person commissioning the investigation.

In the spectrometer computer, the data are reduced to band position, band intensity and band width, and are filed in a library of spectra. Using this condensed information, it is possible at any time to reconstruct a spectrum whose form of appearance does not differ from the original, within the limits of reproducibility. In future, the spectra will be fed directly to the chemists via LAN (=Local Area Network).

For the final evaluation, a comparison is made between the measured IR spectra and all reference data stored to date. This permits a rapid and reliable identification of unknown products. In most cases, the desired reference spectra are not present, since the substance to be analyzed is a novel type of product.

Accordingly, it is necessary to conduct a computer-assisted interpretation of the spectra,[6] whose variants will be explained in the following. The structure file is used to carry out a transformation of the spectral parameters into structure parameters and, by means of the structure generator, novel types of topological structures are proposed. These are also documented and sent to the person requesting the investigation, thus completing the analytical cycle.

4. Estimation of Chemical Shifts

As has already been stated, the spectral information $\{\nu\}$ should be capable of being directly converted into the structure information {S} desired by the person commissioning the investigation. On the other hand, the function $\{S\}=f\{\nu\}$ is just as unknown and complex as its inverse $\{\nu\}=f\{S\}$, where ν describes the entirety of the spectral parameters δ (chemical shift), J (coupling) and τ (relaxation time) and their interactions.

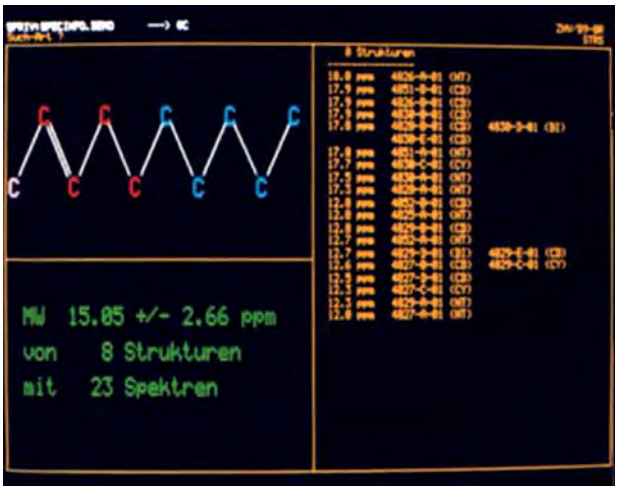

Fig. 5. Result of the search for partial structures including a methyl group at an isolated double bond. The focus is situated on the carbon shown in purple, and the range of the HOSE code with four spheres is marked in red. An evaluation of the chemical shifts derived from 23 spectra of eight structures gives a mean value of 15.05 for δ with a standard deviation of 2.66 ppm. The reference compounds listed on the right-hand side are shown, for some cases, in Figure 6.

Most appropriately, this correlation is also to be implemented in NMR spectroscopy, where, since the incremental rules of *Shoolery* et al.[7] and *Grant* et al.,[8] the relation $\delta=f(S)$ has been applied to a structural element S including the spherically surrounding α, β, γ, and δ substituents. This concept forms the basis of the HOSE code[9] with its hierarchically ordered spherical presentation (*H*ierarchically *O*rdered *S*pherical Description of *E*nvironment) of the environment. In searching for all reference data for a characteristic node in the description of the topological structure (methyl group at double bond in Fig. 5), after the desired structure has been built up the number of the node is entered, the partial structure code is computed and the corresponding entries in the index are printed out. Figure 5 shows the individual values together with the short codes for the solvent, as well as the mean value, the standard deviation and the number of reference compounds on which this estimate of the ^{13}C chemical shift is based. It emerges that the standard deviation is relatively large and the individual values can be grouped about two maxima at $\delta=12.5$ and 17.8. Inspection of the associated structures (Fig. 6) reveals that the well-known steric interactions are responsible for this: cisoid methyl groups absorb at $\delta\approx 12$ ppm and transoid ones at $\delta\approx 18$ ppm.

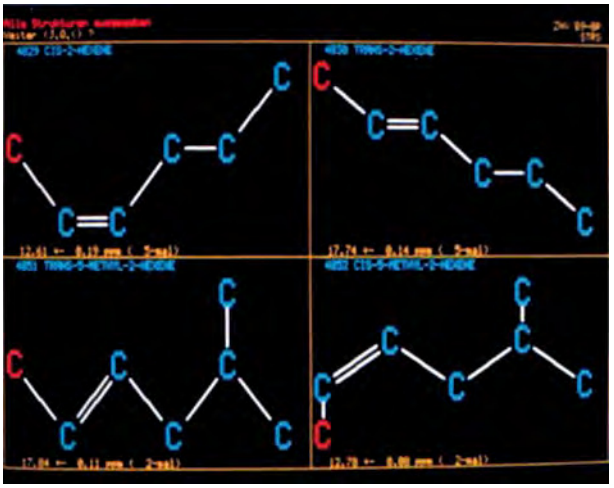

Fig. 6. Display of the first four reference compounds, indication of the atoms whose chemical shifts are sought and listing of the assigned chemical shifts. Where several spectra are recorded, mean values are indicated.

Three findings emerge from this simple example:

- Stereochemical interactions have a great effect on the physical appearance of the spectrum; the topological structure coding should therefore also include the stereochemistry (at least the configuration at double bonds). In quite general terms, it must be stated that a structure coding—if it is to serve not only for the simple objective of documentation and retrieval, but also for the explanation and modelling of physical properties—must specify the interactions in the molecule with the greatest possible accuracy.
- A pictorial recording of the interactions by means of marked structural images is in accord with the chemist's line of thinking. An expert system should not really re-

place an expert, but should serve the expert as a competent "interlocutor". Any aids necessary for making a decision about a structure should be prepared on a user-friendly basis and should provide an incentive for "browsing" through stored chemical structures, correlated with spectroscopic information for creative thought.

— If a partial structure ↔ chemical shift correlation is possible, the total spectrum can also be predicted as the sum of the partial data. However, in all cases a test of the whole set of data for multiple maxima should be carried out,[10] and double entries should be specified in the data expression. In most cases, an experienced spectroscopist can immediately decide which effect was left unaccounted for in the coding of the data; if not, browsing through the detailed data is recommended.

5. Recording of Spin–Spin Interactions

In addition to tracking down the individual items of information, the spectroscopist is also interested in the interaction between the individual parts of molecules, so as to be able to put together the components of the puzzle without ambiguity. In this connection, the spin-spin coupling is of particular importance. Figure 7 shows the search for the magnitude of a coupling between a ^{19}F atom on C4 and the carbon atom C5 of quinoline.

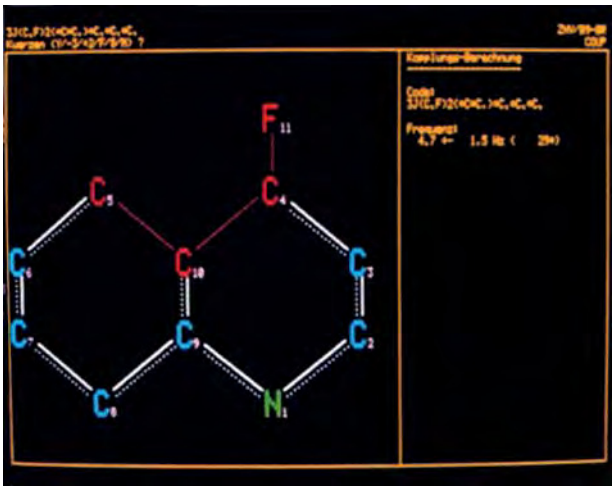

Fig. 7. Estimation of the coupling between C5 and a fluorine substituent on C4 in quinoline.

The computer supplies, as the mean value of five reference spectra, a coupling $^3J_{C,F}=4.7$ Hz with an expected range of ± 1.5 Hz. In a similar way to the above described method for estimating chemical shifts by using HOSE codes, a hierarchically ordered coupling code HOCC was developed, which describes the distance and nature of the interacting nuclei (in this case, 3J(C,F)). This is followed by the number of π electrons (in this instance two) and a precise characterization of the coupling path together with the bonds lying between the element and symbols (here *C*C.). Finally, the environment of the individual nuclei is determined in accordance with the HOSE code. The desired information can be found very quickly as

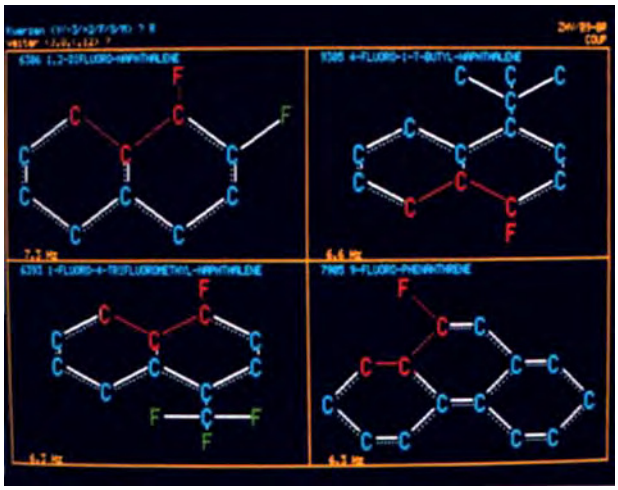

Fig. 8. Display of the first four reference compounds for the coupling searched for in Figure 7. The influence of the differing substituents is reflected in the characteristic variations of the measured coupling parameters.

an index entry under the resulting coupling code 3J(C,F)2(*C*C.)*C,*C,*C. However, if such a coupling is not described in the reference file, the search can be generalized by stepwise abbreviation, until a corresponding structure is present in the file. In this case, an inspection of the individual structures as illustrated in Figure 8 is recommended, in order to derive the best value for the specific problem. A similar example is given in Reference [3] for 4-fluoro-*N*,*N*,3-trimethylaniline.

An interaction of a specified order of magnitude is frequently observed in a spectrum. In this instance, an inspection of the reference structures proposed by the computer is likewise recommended. Thus, the coupling of 19.9 Hz measured in a ^{13}C-NMR spectrum may result from an interaction between C and F, P or D, via one or two bonds, saturated or unsaturated. Further browsing would reveal a variety of possibilities to which the expert has certainly not always given consideration and which (with the exception of $J_{C,D}$ on account of the differing pattern of splitting) cannot always be ruled out (Fig. 9).

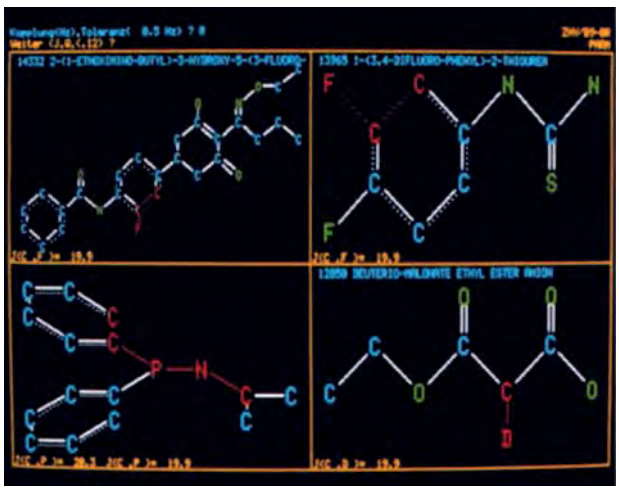

Fig. 9. Search for a coupling of 19.9 Hz, observed in a ^{13}C-NMR spectrum, with any nuclei (apart from hydrogen). The coupling path marked in the case of the first four reference compounds shows differing possibilities of interaction, which can, if desired, be restricted to specific nuclei.

6. Computation of the Spectra

As shown in Sections 4 and 5, chemical shifts and coupling constants for defined structural elements can be estimated on the basis of a reference file. If this is done for all nuclei in the molecule, a computed spectrum for an overall structure is obtained (Fig. 10).

The individual data are characterized by the standard deviation and the number of entries or a statement referring to how many spheres the abbreviation process was implemented in the course of the interpolation (INT*2), and can, at any time, be retraced to the original data in accordance with the above indicated process. Double entries (e.g. in the case of C15) result from double maxima of the total entity, which reflects steric or electronic interactions, or alternatively erroneous data.

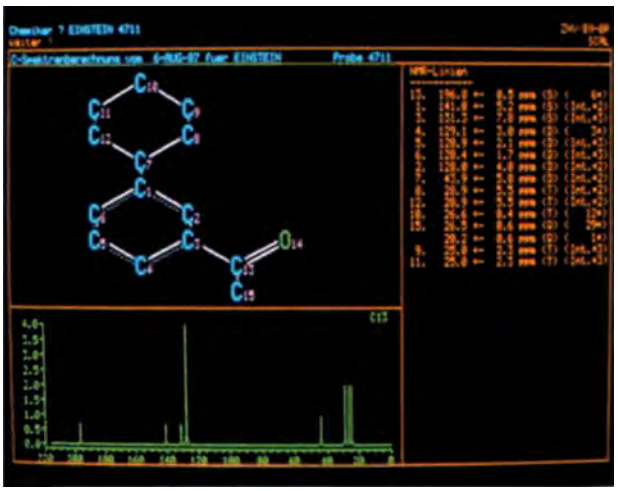

Fig. 10. Estimation of the ^{13}C-NMR spectrum of 3-cyclohexylacetophenone. The diagram shows not only the reconstructed spectrum, but also, listed on the right-hand side, the individual data which permit a good survey of the reliability of the computation. The standard format includes all essential information for subsequent documentation, and is sent to the person requesting the investigation together with the experimental results.

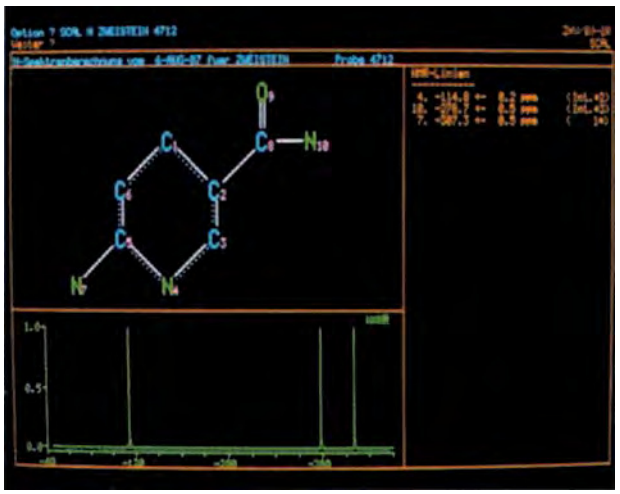

Fig. 11. Estimation of the ^{15}N-NMR spectrum of 6-aminonicotinamide on the basis of a reference file containing 1000 ^{15}N-NMR spectra [11].

This method can be applied to all nuclei, as illustrated in Figure 11 for ^{15}N, provided that the necessary structure-oriented spectral file[11] is available. In our laboratory, the data sets for ^{13}C, ^{31}P, ^{15}N, and ^{19}F are available, but in the case of ^{1}H there is as yet no assignment of the resonance frequencies, and in this instance the computation of a spectrum is possible only with difficulty in accordance with the above principle on account of the strong influence of solvation, stereochemistry and the splitting of the coupling.

On the other hand, infrared spectroscopy is not a form of atomic spectroscopy, but genuine molecular spectroscopy. In this case as well, the simulation of spectra is possible, by comparison with similar reference structures and a corresponding modification of the associated spectra. A typical result, as represented in Figure 12 for anthranilic acid hydrazide, is very promising, particularly if one compares the spectrum with the experimental spectra in the catalogs.[12]

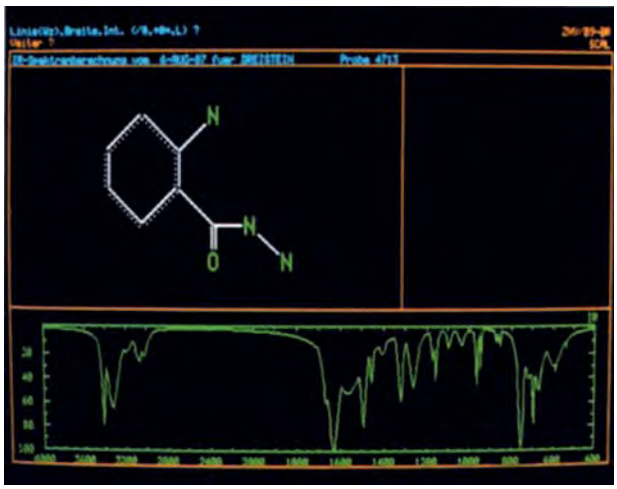

Fig. 12. Estimation of the IR spectrum of anthranilic acid hydrazide as KBr pellet.

In the simulation of mass spectra, statements are made concerning the probable sites of ionization, in the first instance on the basis of observations concerning ionization potentials. For each radical cation obtained in this manner, fragmentation and rearrangement sequences are then set up; in this procedure, each stage and each intermediate state is assessed in accordance with the physical parameters computed according to the above indicated methods.[13]

Figure 13 shows preliminary results for 3-hydroxytetrahydrofuran. The two free electron pairs on the oxygen atom come under consideration as ionization sites, whereby the radical cations **A** and **B** are obtained. The mass spectra simulated in accordance with the fragmentation mechanisms which differ for these two species are shown at the top; the superposition of the two processes gives spectrum C, which shows a very good level of agreement with the experimental data in the lower spectrum (spectrum D).

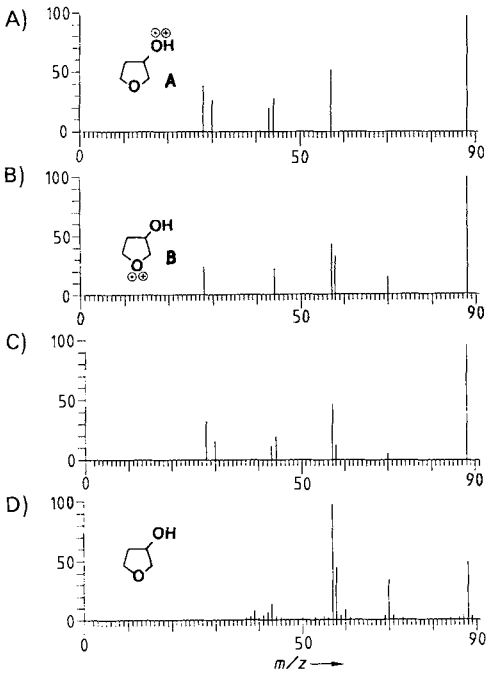

Fig. 13. Simulation of the fragmentation properties of 3-hydroxytetrahydrofuran. The two possible radical cations **A** and **B** give the partial spectra A and B, the simple combination of which yields the computed mass spectrum C. Apart from the masses at m/z 28 and 30, which were not included in the experiment (spectrum D), the physical appearance of the spectra is reproduced quite well.

7. Search for Spectra

The search for similar reference compounds can be carried out by computer in a variety of ways.[14] The method which is simplest and frequently very effective for carrying out a search for spectral patterns is the line search with reference to numbers of correlations. In the present case, a search was carried out for the features of a quartet at $\delta = 14.0$, a triplet at $\delta = 60.5$ and a singlet at $\delta = 173.1$ in a ^{13}C-NMR spectrum, using a spectral window of 0.5 ppm. The three most similar reference spectra are shown in Figure 14, with the required line positions indicated in red.

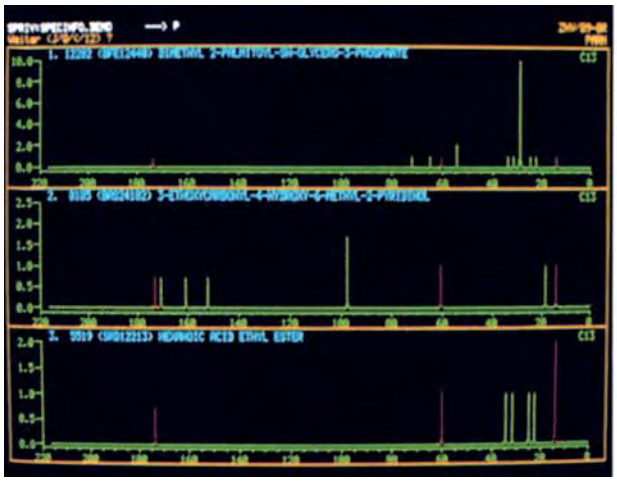

Fig. 14. The three most similar reference spectra, placed in order of increasing sum of the deviations of the chemical shifts. The signal combination required is entered in red, and the associated structures are shown in Figure 15.

More information is again provided by the associated structures (Fig. 15), which reveal that an ethyl ester could be involved. A survey of the situation is facilitated by the fact that, as a result of the assignment of the chemical shifts to the nodes of the topological matrix, the atoms with corresponding resonance frequencies can be made identifiable. In spite of this, the picture is confusing, because structures with purely random similarities at differing positions of the molecule also obscure the interrelationships. An effective suppression of this structural noise is possible by means of the partial structure analysis, as indicated in Section 8.

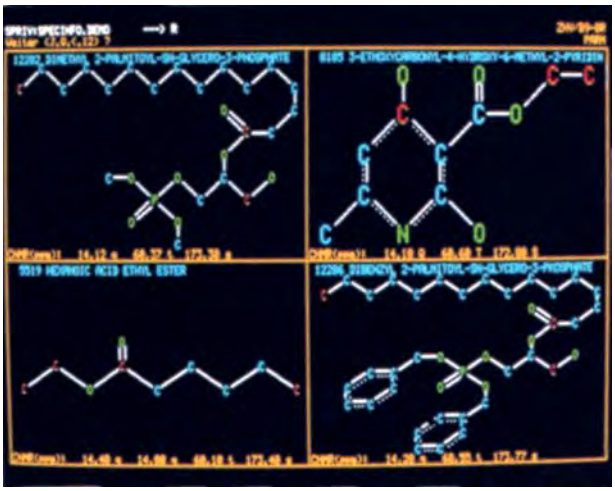

Fig. 15. The structures of the four most similar reference spectra (cf. Fig. 14) with a listing of the corresponding chemical shifts, and marking of the appropriate carbon atoms (in red).

The situation is even more difficult in IR and MS spectroscopy, where the association of spectral properties with defined structural components is possible only with difficulty. The search for IR spectra with band positions at 3305, 1255, 747, and 564 cm^{-1} (tolerance $\pm 5\ cm^{-1}$) furnishes the three most similar reference spectra shown in Figure 16. A comparison of the corresponding structures

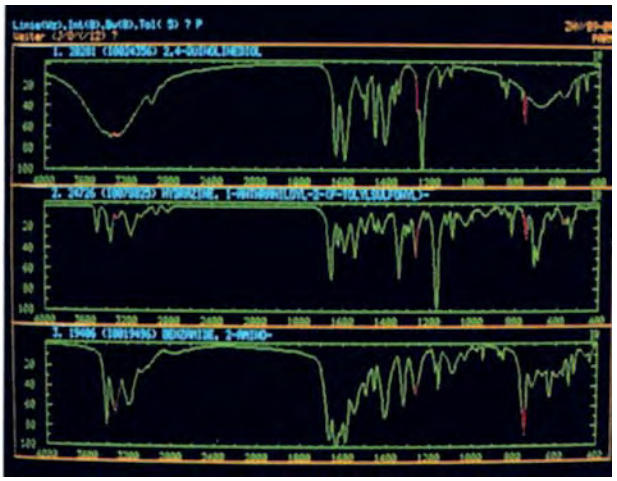

Fig. 16. The three most similar IR reference spectra, placed in order of increasing deviation of the band positions. The combination of four wave numbers which was sought is marked in red, and the associated structures are shown in Figure 17.

without marking of the common structural components is confusing (Fig. 17). In this instance, further help can be provided only by a computer analysis of the corresponding partial structures.

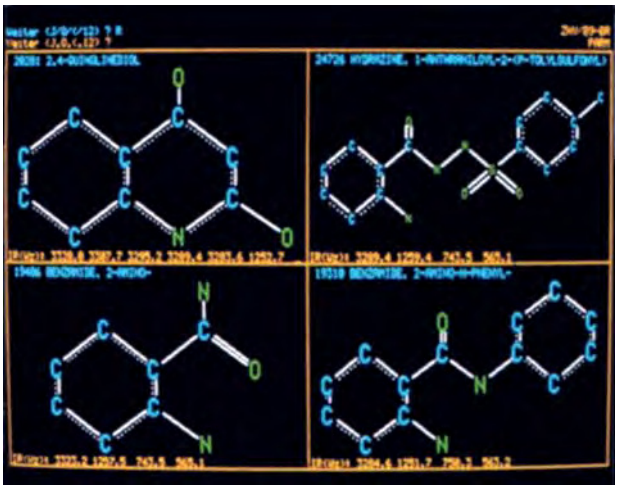

Fig. 17. The structures of the four most similar reference spectra (cf. Fig. 16) with a listing of the corresponding band positions.

8. Substructural Analysis

In substructural analysis, the structures which are found are broken down into their smallest components and are characterized in relation to their environment by means of the HOSE code (one to four spheres, according to choice). Accordingly, a topological matrix including 15 nodes would be converted into 15 HOSE codes and a specified number of HORD codes (*H*ierarchically *O*rdered *R*ing *De*scription) for the ring system. These data are generated for the desired number of structures (typically 20), combined and displayed in the form of a histogram (Fig. 18). Thereby, the information given in green (third column of figures) describes the statistical probability of finding the predetermined substructure in a total of 20 structures in the file. If the partial structure is observed more frequently (second column of figures), then the red coding exceeds the trivial standard frequency (green). This is the relevant information which defines the probability with which a specified partial structure should be present in the unknown compound, on the basis of the spectral similarities.

Fig. 18. Substructural analysis of the results of a search for ^{13}C-NMR reference spectra with the same spectral pattern (Fig. 14). The occurrence of the substructures set forth on the left-hand side is represented in the form of a histogram; in this case, the green information characterizes the standard frequency in the ^{13}C-NMR file, and the red symbols characterize the nodes going beyond that information in the data set. The first column of figures is the quotient of occurrence and standard frequency, which are then listed as individual values (second and third columns respectively).

Although far from being difficult, it is not necessary to understand the coding of the partial structures in order to use this method. The computer can indicate the substructures corresponding to the spectral patterns,[15] and can use the information in order to emphasize the conforming partial structures in the proposed structures (Figs. 15, 17) in color (Figs. 19, 20). The centers marked in red occur in 70%, and the centers marked in purple only in 35% of the best 20 reference structures. The presentation (Fig. 19) has now changed, and the structural interrelationships are more

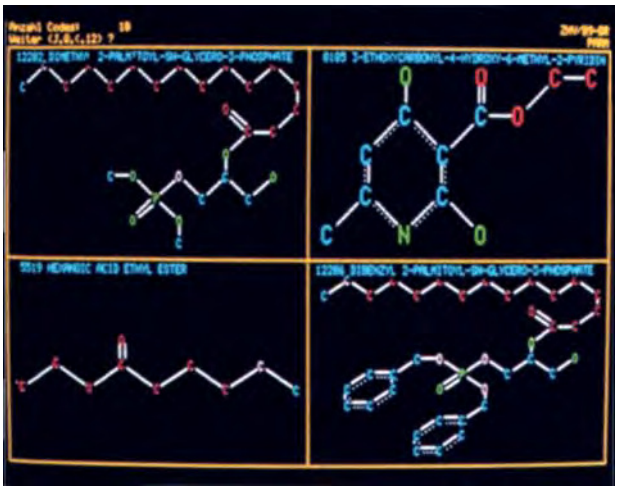

Fig. 19. Characterization of the most probable substructures on the basis of a partial structural analysis (Fig. 18, cf. Fig. 15). The most frequent nodes are marked in red, as are the bonds of the dominant ring systems. Less frequent, but significant structural components are shown in purple. The threshold magnitude for this presentation can readily be optimized in interactive dialog, in order to render the common structural elements visible.

Fig. 20. Marking of the most probable partial structures for the IR band search of Figure 16.

clearly emphasized. In the IR reference structures in particular (Fig. 20), it is now possible to discern very rapidly the common features and thus the probable structural components. There is certainly no need to add that the computer also "understands" the information which it can display, and can use that information in more extensive algorithms.

By means of the substructural analysis, it is therefore possible to convert spectral information into structural information, regardless of whether chemical shifts, band positions, masses, neutral losses,[15] couplings, splitting patterns, etc. are involved. The structural information obtained is unitary, normalized and computer-oriented. This has several advantages: it is possible to combine the results of various experiments and methods with one another. In "multidimensional spectroscopy",[15] each method contributes to the total result only with the statistically relevant, i.e. cogent findings. The structural noise is effectively suppressed. In the final proposed structure it is possible, by marking the particular methods concerned, to demonstrate which technique has confirmed which partial structural information.[15]

It is found thereby that ^{13}C-NMR spectroscopy and mass spectrometry are the most important for the elucidation of constitution, because they principally define the molecular skeleton, which the chemist usually regards as the principal characteristic of the structure. IR and ^{1}H-NMR spectroscopy, with their information about substituents and configuration, contribute to a refinement of the picture.

Following the concept of overlapping partial structures,[16] the partial structure codes may readily be combined into topological structures. Thereby, the feeding-in of additional information is permitted, and a combinatorial explosion during structure generation is restrained (see Section 9).

9. Intelligent Evaluation of Spectra

The expression "Artificial Intelligence" is defined in different ways by different authors. "Intelligence" is derived from the Latin intelligentia = concept, insight, understanding. "According to general understanding, intelligence is the superior capability (or a group of capabilities), which expresses itself in the grasping and creation of distinct and abstract relationships, and thus enables new types of situations to be coped with by problem-solving activity."[17] In this sense, the tools which we have considered so far are certainly "intel-ligent" and must simply be combined in order to solve new types of problems.

"Intelligent" systems normally possess a regulating mechanism (inference engine) and a knowledge base.[18] Let us now consider the previously discussed hypotheses from this point of view (Table 1). The library search requires a collection of reference spectra and operates on the basic principle that a relationship exists between spectrum and structure. Similar spectra should characterize similar structures, this being a simplified assumption which is not valid in all cases.

The similarity search is to a greater extent optimized with respect to the search for similar rather than identical compounds. As a matter of necessity, more degrees of freedom for deviations must be tolerated. Accordingly, in the sequential procedure *all* properties of the spectrum with respect to position, intensity, form and probability of their occurrence are compared.

Table 1. Various strategies for the elucidation of structure of differing intelligence and abstraction with the associated system of rules and knowledge base.

Method	Rule	Knowledge
Library search	Spectrum ↔ structure	Library of spectra
Similarity search	Spectrum ↔ structure	Library of spectra Tolerance
Interpretation	Partial spectrum ↔ partial structure	Rules of interpretation
Spectrum calculation	Shift ↔ chemical environment	$\delta = f(S)$
Structure elucidation	Shift ↔ chemical environment Chemical structures Spectroscopy	$S = f(\delta)$

This is implemented in an excellent way with the aid of assessment matrices (according to *Clerc* et al.[19]), but requires upstream relatively crude presearch algorithms (pre-

```
------------------------------------------------------------
   I N T E R P R E T A T I O N   O F   S P E C T R A
------------------------------------------------------------
                  WITH 1500 TRANSCRIPTS

STANDARD ASSESSMENT ? (J/N)
=J

RESULT:    17 FITTINGS TRANSCRIPTS     (1423 VR-HITS)

   QUALITY    CNMR    HNMR  IR  T-NR.    NAME

 1.  1.933  1.997  0.968       103  ETHYL ESTER (-)
 2.  0.946  1.183  0.800      1112  CHLORO-METHYL (=)
 3.  0.946  1.183  0.800      1112  CHLORO-METHYL (=)
 4.  0.916  1.308  0.701       104  ETHYL ESTER (*)
 5.  0.449  0.915  0.491         9  METHYL (*), TWO ORTHO-SUBST.
 6.  0.339  0.782  0.434      1393  3-HYDROXY-BUTANOIC ACID ESTER
 7.  0.278  0.775  0.359      1042  2-HYDROXY-ACETIC ACID ESTER
 8.  0.268  1.049  0.256      1306  AMINOMETHYL (*)
 9.  0.191  0.806  0.237      1398  1,2-ETHYLENEDIAMINE-N1,N2-DIYL (*,*)
10.  0.103  1.039  0.100      1197  2-HYDROXY-ETHYL-AMIDE

FITTING TRANSCRIPT COMBINATION

      QUALITY    T-NR.        NAME

       1.997      103     ETHYL ESTER (-)
       1.183     1112     CHLORO-METHYL (=)
       1.183     1112     CHLORO-METHYL (=)


REMAINING LINES  171.2   S   1
                 122.4   S   1
                  84.3   S   1
                  63.9   D   1
                  39.1   S   1
                  24.4   Q   1
                  23.3   Q   1

TRANSCRIPT STRUCTURES ?
=J

 103. TRANSCRIPT            1112. TRANSCRIPT

          C       &                    C
        . .     .                    . .
      .     . .                    .     .
     C       O                   CL       &
```

Fig. 21. Example of the combined interpretation of ^{1}H- and ^{13}C-NMR spectra. The possible basic structural components which were proposed on the basis of the first run may not, in this case, be unified into a consistent data set, because, apart from the ethoxy group, the partial structures which are present in the molecule have not yet been coded in the form of a rule.

liminary search and intermediate search[14]), in order to be able to undertake a search using large files containing over 50000 spectra within a reasonable time. This approach thus operates with spectroscopic expert knowledge, which defines, on the basis of experience, whether and what deviations can be tolerated. Thus, for example, the spectroscopist knows that in the ^{1}H-NMR spectra, in the event of a change of the solvent, triplets can be converted into doublets of doublets and acid protons are particularly strongly displaced. In similarity assessments, the computer should also apply this knowledge.

In the course of interpretation, subspectra are correlated with substructures. The knowledge base employed is a library of interpretation rules,[20] which define, for example, that the signals for an ethoxy group (in ethyl esters) occur in the ^{13}C-NMR spectrum at $\delta = 60.4 \pm 0.5$ (triplet) and $\delta = 14.2 \pm 0.5$ (quartet). Whenever this spectral pattern is observed, there is a high probability that an ethoxy group is present in the unknown structure, especially if further conditions, such as ^{1}H-NMR resonances at $\delta = 4.1 \pm 0.2$ (quartet, intensity 2) and 1.2 ± 0.2 (triplet, intensity 3) are fulfilled. By way of example, Figure 21 (see preceding page) shows the search for 4,6,6-trichloro-7,7,7-trifluoro-3,3-dimethylheptanoic acid ethyl ester as a fictitious unknown substance. The list of the proposed structural elements contains essential fragments of the structure sought, placed in order of decreasing probability. In a second run, the list is again processed sequentially and examined for consistency, i.e. each ^{13}C-NMR resonance may be documented only once in the correlation. In contrast to the cited instructional examples,[20] in the case of this unusual structure it is very difficult to compose the unknown from the results. The method has three essential disadvantages:

- The partial structures are predefined in the file, and only these substructures can be found by the computer. In view of the variety of feasible structural elements, the number of the presently used 1500 rules is certainly too small, but will, in practice, never become large enough. The method of substructural analysis described in Section 8 is certainly the more flexible and more promising.
- The rules were coded to a large extent manually, with reliance upon the reference spectra. This laborious process has to be periodically repeated, in order to reflect the latest state of knowledge (= the library of spectra). Rules[21] derived purely by fully automatic means from a structure-oriented library of spectra will exist in the future. This is especially true in the case of IR spectroscopy and mass spectrometry, where the relationships between partial structures and partial spectra are very complex and can be made visible only by statistical processing of the spectral material (cf. program package IDIOTS[21]).
- The probable structural fragments must be brought together by hand. As a rule, this task is time-consuming and should therefore be transferred to a computer (see Section 10). On the other hand, the expression "substructure" does not have a precise definition, and the translation of the topological fragments, which in some cases are large, in some cases small and in some cases imprecise, into the language of the structure generator presents difficulties.

While the computer interpretation yields essentially structural concepts within the meaning of "brain storming", the estimation of spectra in NMR spectroscopy is a relatively precise method. We are now at the highest level of abstraction, and, as a rule, correlate chemical shifts with chemical environments. The knowledge base, which is an index file storing the mean resonance frequencies for all chemical environments which are present, is generated entirely automatically from the spectral file, and in all cases reflects the latest state of knowledge. The application of this has already been described (Figs. 10 and 11).

The reverse process, i.e. the elucidation of structure, is the dream of the chemist and has been accomplished only in some areas. The knowledge base required in this instance is the inverted information, where, for each chemical shift, all associated chemical environments are stored. Finally, such a strategy should also take into account the basic rules of structural chemistry and spectroscopy, principally for the purpose of permitting an effective combination of the multidimensional information.

10. Fully Automatic Structure Elucidation

The essential basic components and the flow of information of a system for automatic elucidation of structures are presented with reference to the example of the program package ACCESS[16] (= *A*utomatic *C*omputer *C*orrelation and *E*valuation of *S*pectra based on *S*ubstructures) (Figs. 22 and 23). The spectral parameters (chemical shift, multiplicity, intensity, coupling) of an unknown compound are analyzed and compared with the substructure file $S = f(\delta)$. The overall formula, which can readily be obtained (especially when the number of C atoms is known) from high-resolution mass spectra, serves to eliminate substructure codes on the basis of the elemental composition. Thus, for example, there is no need to consider any $SiCH_3$

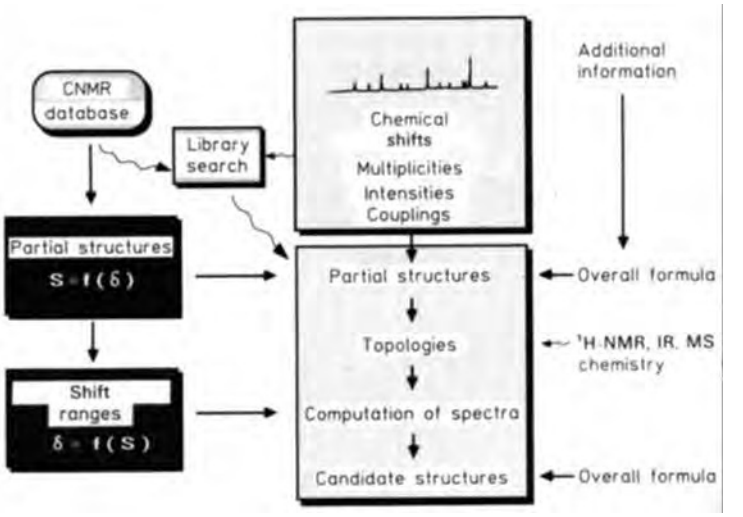

Fig. 22. Flow of information in the automatic interpretation of spectra using ACCESS.

```
-------------------------------------------------
 E L U C I D A T I O N   O F   S T R U C T U R E
-------------------------------------------------

(1) OVERALL FORMULA
=C11 H16 CL3 F3 O2

THERE IS/ARE 1 DOUBLE BONDS OR RINGS

SEARCH FOR 1 SPHERE CODE
SEARCH FOR 2 SPHERE CODES

(2) CONSIDERATION OF THE RESULTS OF OTHER SEARCHES?
=S
-------------------------------------------------
   S E A R C H   F O R   S A H O   S P E C T R A
-------------------------------------------------

WITH 77486 SPECTRA

RESULT:  1 SPECTRUM

11 HOSE CODES WITH LINE POSITION ARE STORED

(3) AT HOW HIGH A LEVEL IS EACH ONE OF THESE CODES TO BE ASSESSED ?
(RETURN=1.00)
=0.8

FILE WITH 239235 EXPECTED RANGES OF 84335 SPECTRA

(4) NUMBER OF THE START LINE ? (RETURN = AUTOMATIC)
=

PROCESSING BEGINS WITH THE 2ND LINE (122.4 PPM)

ONLY THE BEST 8 CODES OF EACH LINE ARE PROCESSED

USING THESE INPUT DATA, NO STRUCTURE WAS FOUND. PERHAPS YOU SHOULD
INCREASE THE NUMBER OF PROCESSED CODES OR THE ADDITIONAL WIDTHS OR
REDUCE THE MINIMUM ASSESSEMENT.  HOWEVER, IT IS ALSO POSSIBLE THAT
AN UNUSUAL STRUCTURE IS INVOLVED AND NO FITTING PARTIAL STRUCTURES
ARE PRESENT IN THE FILE.

BEST APROXIMATION:

                F CL
                . .
              F.2..3.6
                . .
                F CL

THE NUMBER OF CODES TO BE PROCESSED PER LINE WAS SET AT 16. AND
THE MINIMUM ASSESSMENT AT 1.00

PROCESSING BEGINS WITH THE 2ND LINE (122.4 PPM)

ONLY THE BEST 16 CODES OF EACH LINE ARE PROCESSED.

 1ST PROPOSED SOLUTION:  OVERALL FORMULA C11 H16 CL3 F3 O2

                CL   CL       O
                  . .         =
               F   3          1.0.5.11
                . . .       .
                 2   6      7
                ..    .     .
               F F     4..8
                       .   ..
                     CL   10 9
```

```
COMPARISON WITH ESTIMATED CNMR SPECTRUM              EXP.        DEV.

C 1  (S)  171.0 PPM  #  0.1 PPM   (    4 X )      171.2 PPM    0.2 PPM
C 2  (S)  122.4 PPM  #  0.  PPM   (    1 X )      122.4 PPM    0.  PPM
C 3  (S)   84.3 PPM  #  0.  PPM   (    1 X )       84.3 PPM    0.  PPM
C 4  (D)   64.0 PPM  #  0.  PPM   (    1 X )       63.9 PPM    0.1 PPM
C 5  (T)   60.4 PPM  #  0.3 PPM   ( 386 X )       60.4 PPM    0.  PPM
C 6  (T)   43.9 PPM  #  0.8 PPM   (    3 X )       44.9 PPM    1.0 PPM
C 7  (T)   43.5 PPM  #  0.  PPM   (    1 X )       43.5 PPM    0.  PPM
C 8  (S)   38.9 PPM  #  0.2 PPM   (    3 X )       39.1 PPM    0.2 PPM
C 9  (Q)   23.9 PPM  #  0.5 PPM   (    6 X )       24.4 PPM    0.5 PPM
C10  is symmetrical to C9                           23.3 PPM    0.6 PPM
C11  (Q)   14.2 PPM  #  0.1 PPM   (2000 X )       14.3 PPM    0.1 PPM

SYMMETRY DEVIATION: 1.1 PPM (THIS WAS ADDED TO THE STANDARD DEVIATION)

THIS PROPOSAL HAS A STANDARD DEVIATION OF 1.59 PPM

  2ND PROPOSED SOLUTION:  OVERALL FORMULA C11 H16 CL3 F3 O2

                                        0
                                        =
                              F F       1
                               ..      . .
                                2   CL      0   11
                              . . .       .
                              F   3         5
                                . .       .
                               CL   6     7
                                    .     .
                                     4..8
                                    .   ..
                                  CL   10 9

COMPARISON WITH ESTIMATED CNMR SPECTRUM              EXP.        DEV.

C 1  (S)  170.6 PPM  #  0.5 PPM   ( 136 X  )      171.2 PPM    0.6 PPM
C 2  (S)  122.4 PPM  #  0.  PPM   (   1 X  )      122.4 PPM    0.  PPM
C 3  (S)   84.3 PPM  #  0.  PPM   (   1 X  )       84.3 PPM    0.  PPM
C 4  (D)   69.5 PPM  #  1.6 PPM   ( INTERP.)       63.9 PPM    5.6 PPM
C 5  (T)   63.6 PPM  #  1.0 PPM   ( INTERP.)       60.4 PPM    3.2 PPM
C 6  (T)   43.5 PPM  #  0.  PPM   (   1 X  )       44.9 PPM    1.4 PPM
C 7  (T)   40.1 PPM  #  5.1 PPM   ( INTERP.)       43.5 PPM    3.4 PPM
C 8  (S)   36.5 PPM  #  1.4 PPM   ( INTERP.)       39.1 PPM    2.6 PPM
C 9  (Q)   28.5 PPM  #  2.4 PPM   ( INTERP.)       24.4 PPM    4.1 PPM
C10  is symmetrical to C9                           23.3 PPM    5.2 PPM
C11  (Q)   20.7 PPM  #  0.2 PPM   ( 822 X  )       14.3 PPM    6.4 PPM

SYMMETRY DEVIATION: 1.1 PPM ( THIS WAS ADDED TO THE STANDARD DEVIATION)

THIS PROPOSAL HAS A STANDARD DEVIATION OF 4.69 PPM
THIS PROPOSAL WAS DISCARDED.

   -->    1 K CYCLE WAS EXECUTED (14.59 S CPU)

   AND FURTHER?
   =

   -->    2 K CYCLES WERE EXECUTED (25.74 S CPU)

(5) AND FURTHER?
=

      SE      SEQN. #    IDENT. OVERALL FORMULA
    1.59        1            C11 H16 CL3 F3 O2
    4.69        2            C11 H16 CL3 F3 O2              (DISCARDED)
```

Fig. 23. Example of an automatic structure elucidation (① through ⑤) using ACCESS. The version of the program currently available cannot yet discern that, because of the interaction with the adjacent chlorine, C_9/C_{10} should exhibit different chemical shifts. A feature worthy of note is the rapid convergence of the program in only 25 s CPU.

groups, if, according to the mass spectrum or elemental analysis, no silicon is present. Alternatively, aromatic groups can be ruled out, if only three double bonds/rings are permitted on the basis of the number of hydrogen atoms.

All topologies which are at all feasible are now constructed from the partial structures which have been collected and ranked in order of their probability. With increasing molecular size and/or number of hetero atoms and double bonds, there is a combinatorial explosion, so that the hierarchical tree must be pruned at an early stage, in order to facilitate convergence. The best way for this to happen is by means of the inclusion of additional measurement results, for example by substructural analysis of the library search results in IR or MS.[15] In addition, a knowledge of the chemical reaction and the reaction partners can play an important role. In a similar way to the procedure in synthesis planning with the computer, the chemist can observe the progress of the program and take assisting action, if "nonsensical" proposals appear. Since, from the point of view of the computer, there are no nonsensical proposals, great care is required here in order to prevent wishful thinking from falsifying the information provided by the unbiased "interlocutor." However, if there is a lack of information, then the computer should be able to take account of this knowledge of the human partner.

Furthermore, it becomes evident that additional controlled experiments increase the probability of individual substructures and give these pre-eminence over the structural noise. By this means, the convergence is accelerated, and the result becomes clearer. Accordingly, it is a good idea to carry out, in advance, a library search with subsequent substructural analysis using the same data. The library search sees the spectral features in combination, and can therefore deliver more specific structural information.

The spectra of all structures proposed by the computer are computed with the aid of the shift-range file and compared with the experimental data. This generates a list—ranked in order of probability—of candidate structures, which is examined once again for conformity with the overall formula. Structures exhibiting a large deviation between computation and experiment are discarded. A

detailed inspection of the most probable structures frequently shows that further measurement data are necessary in order to achieve final clarification.

Figure 23 illustrates the progress of an automatic structure elucidation (using ACCESS) regarding the example of 4,6,6-trichloro-7,7,7-trifluoro-3,3-dimethylheptanoic acid ethyl ester. When the overall molecular formula ① has been entered, the computer determines the number of double bonds or rings. If desired, the results of other search procedures can be incorporated ②, and in this case a library search was carried out with reference to the Hash code (SAHO = *S*pectral *A*ppearance in *H*ierarchical *O*rder[14,22]) and the partial structures found were assigned a probability of 0.8 ③.

At this point, the actual search begins in an index file of the ^{13}C-NMR shift ranges for 240000 partial structures, generated from 84000 data sets of ^{13}C-NMR spectra with topological structures. The starting line position for the assembly of the structural components determined, with the aid of the structure generator, is selected by the computer itself ④. The line at $\delta = 122.4$ with the large coupling to F is clearly the most characteristic. In a first rapid run with only eight substructure codes per line, only part of the molecule is built up; some basic structural components important for a convergence are still absent. This coarse testing procedure is comparable with the "lightning chess setting" with commercial chess computers, where a superficial assessment permits a rapid overview of the complexity of the problem.

The computer switches over automatically to detailed processing of the problem with 16 substructures in each instance and a minimum probability of 1.0. Now two proposed structures follow, the second of which was discarded, on account of the great deviation (4.7 ppm) between computation and experiment. After 2 K cycles, i.e. 2000 unsuccessful attempts to synthesize a new structure, the computer went through all possibilities and interrupted its evaluation with a compilation of the result ⑤. The structure sought was correctly predicted; the alternative can readily be ruled out, on account of the resonance of C11.

11. Structural Similarity

The question of the similarity of chemical structures cannot be answered in general terms, since it is dependent upon the content of the query. Thus, the materials chemist, the pharmacist and the spectroscopist, for example, classify entirely different molecules as similar. Even the spectroscopists who are frequently specialists in one method view structural differences in relation to the distinguishing capability of their technique, and will accordingly weight similarities differently. However, a measure of structural similarity/dissimilarity as a function of the method is important, in order to select the correct experiment when additional information is required, and to take the necessary decision between alternative structures.

The basic molecular components which are most important and in most cases unchanged in syntheses are the ring systems. Ring searches[22] and the inclusion of the HORD (*H*ierarchically *O*rdered *R*ing *D*escription) ring code in the partial structural analysis[16] are necessary strategies. In the case of condensed ring systems, the CAS ring index is available, which, in modified form, is employed as a search criterion.[22] However, an analysis of the given structure from the standpoint of its characteristic fundamental components is promising. These are predefined in a library as short codes[24] and can be assessed on a basis specific to the method concerned.

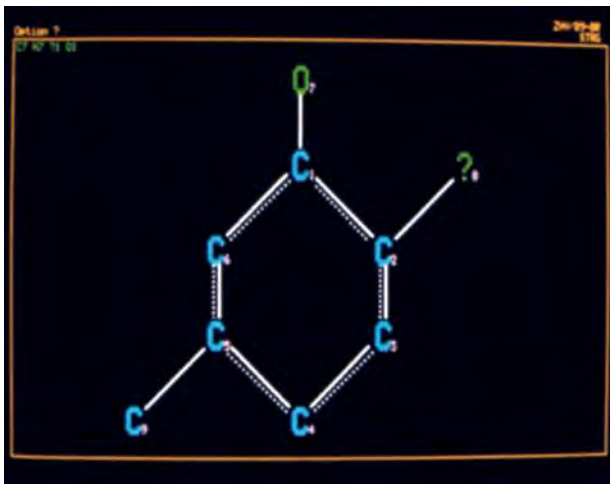

Fig. 24. Query in respect of a search for similar structures with an open substituent.

Fig. 25. Short codes [24] of a search criterion for the query in Figure 24. This control list can be edited by the experienced user prior to the search, i.e. it can be supplemented or abbreviated. Entries marked in red are already included in preceding, more specific short codes, and are therefore not taken into account in the search.

Figures 24 and 25 illustrate the procedure. The target structure 3-methylphenol with an unknown substituent in position 5 is entered and subjected to a fragment analysis

(at the present time, 240 fragments are employed). Figure 25 shows the required fundamental molecular components and their occurrence in the structure database.

The entries marked in red are redundant, because they are already included in the preceding data set, and are not searched. The resulting similar structures are shown in Figure 26. Since, at the present time, the procedure has been optimized for IR spectroscopy, all these compounds exhibit similar IR spectra, in spite of the dramatic differences in composition and constitution.

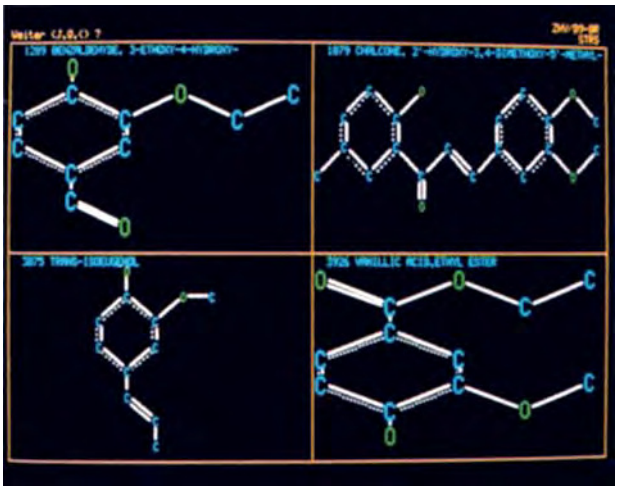

Fig. 26. Four structures which satisfy the query in Figure 24 and the automatically generated short codes in Figure 25.

12. Outlook

In spite of the difficulties which intelligent systems had in the past and still have in the interpretation of spectra, there is justification for the hope that, after the recording of spectra, they will also revolutionize the evaluation of spectra. Accordingly, in conclusion, the outlook for future development should be permitted; this might, indeed, become reality in the course of the next 5 years.

Figure 27 shows the flow of information in a spectroscopy laboratory of the future. The computers at the chemists desks are connected via LAN to the spectroscopy laboratory; the chemists send their requested analysis, including a proposed structure, direct to the Information Management System of the laboratory. Depending upon the set task and capacity, the appropriate system is selected and the sample required for the experiment is requested. After the measurement, the spectrometer checks whether the results are in accord with the structure. If so, the person requesting the investigation receives confirmation and, if desired, the spectrum as well, which he can copy into his electronic laboratory journal. If the quality standards are complied with, the data set is completed and included in the databank as knowledge base.

If discrepancies are observed between experiment and computation, the central information system SPECINFO[25] makes proposals of alternative structures, which are sent to the chemist for examination and possibly confirmed by measurements which are automatically set up. In this case, it is recommended that experiments should be carried out on the same spectrometer, since then there is no need for the sample to be transported (see Section 2). Only if the system still fails to converge must the human expert intervene and tackle the problem in partnership with the not very "creative," but extremely "hard-working" and "well-read" computer.

As has already been mentioned, a proportion of this great knowledge and experience should be transferred to a special program, which is present in the spectrometer and can directly take intelligent decisions.

The knowledge base is of decisive importance to the level of performance of the entire system. It should at the same time be broadly based and optimized for the specific problems of the working group, i.e. it should combine commercially available databanks and the organization's own measured data.

A brief overview of the commercially available reference data is given in Reference [20]. An important factor from the point of view of small laboratory units is the facility of access to ^{13}C-NMR, IR,[26] and MS databanks[27] and the corresponding expert systems via telecommunication, even though joint application with company internal information and specialist chemistry is not possible. A good compromise is frequently offered by the dedicated systems which are installed on minicomputers and which, in some cases, are supplied by instrument manufacturers directly as components of the analysis systems and, in some cases, can also be used on desk-top computers of the IBM PC type.[28] The level of performance of the programs and data files is, however, a very variable factor.[29]

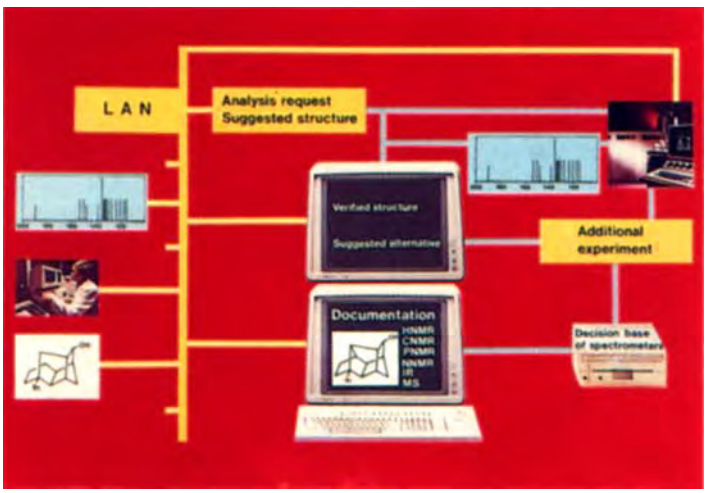

Fig. 27. Flow of information in a spectroscopy laboratory of the nineties. The individual components are essentially already available, and simply need to be combined into an operational system.

In future, increasing emphasis must be placed on the quality of these data, since erroneous data file entries lead to incorrect predictions. As *Lem* mentioned in the introduction, intelligent systems have a tendency to become independent. We shall certainly continue to experience

many, hopefully pleasant surprises while working with computers (Fig. 28).

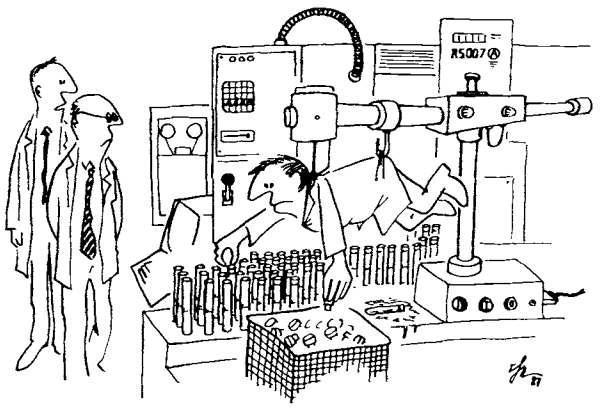

Fig. 28. "We were able to remove some initial difficulties this way."

Such an ambitious project can be pursued only in close cooperation with committed colleagues, who all made a decisive contribution to the present-day level of performance of the entire system: M. Beckmann, W. Fachinger, Prof. Dr. J. Gasteiger, A. Hardt, C. Heistermann, C. Köhler, Dr. R. Neudert, Dr. M. Passlack, R. Rupprecht, C. Schäfer, H. Wagner, and F. Wolf. We wish to express our gratitude to the research management of BASF, Prof. Dr. H. Dörfel, Dr. U. Schenck, and Dr. H. W. Schmidt, for their continuous support, and to the Bundesministerium für Forschung und Technologie and the Fachinformationszentrum Energie, Physik, Mathematik GmbH (FRG) for their financial support over many years.

Received: August 27, 1987 [A 657 IE]
German version: *Angew. Chem. 100* (1988) 252

[1] S. Lem, *Also sprach Golem (Thus Spoke Golem)*, Insel-Verlag, Frankfurt 1984.
[2] R. Neudert, E. Ströfer, W. Bremser, *Magn. Reson. Chem. 24* (1986) 1089.
[3] W. Bremser, R. Neudert, *Eur. Spectrosc. News 75* (1987) 10.
[4] Finnigan MAT, Bremen, AUDEVAP Application Note (1982).
[5] Maschinenfabrik Herzog GmbH, Osnabrück; M. Passlack, *Bruker Rep. 1* (1986) 11.
[6] M. E. Munk, M. Forkas, A. H. Lipkis, B. D. Christie, *Mikrochim. Acta 1986 II*, 199; K. Funatsu, C. A. Del Carpio, S. Sasaki, *Comput. Enhanced Spectrosc. 3* (1986) 133.
[7] J. N. Shoolery, L. F. Johnson, W. A. Anderson, *J. Mol. Spectrosc. 5* (1960) 110.
[8] D. M. Grant, E. G. Paul, *J. Am. Chem. Soc. 86* (1964) 2948.
[9] W. Bremser, *Anal. Chim. Acta 103* (1978) 355.
[10] W. Bremser, B. Franke, H. Wagner: *Chemical Shift Ranges in Carbon-13 NMR Spectroscopy*, Verlag Chemie, Weinheim 1982.
[11] R. Neudert, G. Goizet, W. Bremser, M. Martin, unpublished.
[12] Stadtler Grating Spectra No. 11671, Sadtler Research Laboratories, Philadelphia, PA, USA (1968).
[13] J. Gasteiger, *Nachr. Chem. Tech. Lab. 34* (1986) 228; J. Gasteiger, M. G. Hutchings, B. Christoph, L. Gaun, C. Hiller, P. Löw, M. Marsili, H. Saller, K. Yuki, *Top. Curr. Chem. 137* (1987) 19.
[14] W. Bremser, H. Wagner, B. Franke, *Org. Magn. Reson. 15* (1981) 178; W. Bremser, *Fresnius Z. Anal. Chem. 286* (1977) 1.
[15] R. Neudert, W. Bremser, H. Wagner, *Org. Mass Spectrom. 22* (1987) 321.
[16] W. Bremser, W. Fachinger, *Magn. Reson. Chem. 23* (1985) 1056.
[17] *Meyers Neues Lexikon, Band 4*, Bibliographisches Institut, Mannheim 1979, p. 164.
[18] J. W. Frazer, *Microchim. Acta 1986 II*, 163.
[19] J. T. Clerc, F. Erni, *Top. Current Chem. 39* (1973) 91.
[20] W. Bremser, *Nachr. Chem. Tech. Lab. 31* (1983) 456.
[21] M. Passlack, W. Bremser in J. Zupan (Ed.): *Computer-Supported Spectroscopic Databases*, Ellis Horwood, Chichester 1986.
[22] W. Bremser, L. Ernst, W. Fachinger, R. Gerhards, A. Hardt, P. M. E. Lewis, *Carbon-13 NMR Spectral Data*, 4th Edit., VCH Verlagsgesellschaft, Weinheim 1987.
[23] *Ring Systems Handbook*, Chemical Abstracts Service, Columbus, OH, USA 1984.
[24] M. Passlack, W. Bremser, M. Beckmann, H. Wagner: *Infrared Spectral Data*, VCH Verlagsgesellschaft, Weinheim 1986.
[25] W. Bremser, W. Fachinger, H. Wagner, SPECINFO—*Multidimensionales Expertensystem zur Strukturaufklärung (Multidimensional Expert System for the Elucidation of Structure)*, unpublished.
[26] Databank INKADATA, Fachinformationszentrum für Energie, Physik, Mathematik GmbH, D-7514 Eggenstein-Leopoldshafen 2 (FRG).
[27] Databank MASSLIB, Fachinformationszentrum Chemie, D-1000 Berlin.
[28] B. Wittig, M. Zeitler, W. Schmidt, W. Bremser, W. Fachinger: *Data Documentation 11*, Wissenschaftliche Software, VCH Verlagsgesellschaft, Weinheim 1987.
[29] J. T. Clerc, E. Pretsch, M. Zürcher, *Mikrochim. Acta 1986 II*, 217.

When submitting manuscripts, authors of articles intended for publication as "Communications" are requested to read the "Notice to Authors" reproduced in the January issue of the journal following the list of contents; upon request, a copy can be obtained from the editorial office.

$[\{Hg_3Co(C_4H_6NO)_6\}(NO_3)_2]_n$: A Macrobicyclic Bimetallic Chain Polymer Incorporating Deprotonated 2-Pyrrolidone Bridges**

By *David M. L. Goodgame,* David J. Williams,** and *Richard E. P. Winpenny*

Recently we have reported the discovery and structural characterization of complex **1**,[1] an exciting new bimetallic cationic polymer comprising contiguous 32-membered macrocycles containing Hg and Cu atoms linked by 2-pyrrolidone anions, $C_4H_6NO^{\ominus}$, and with either $NO_3^{\ominus}$ or $ClO_4^{\ominus}$ as counterions. In **1** the geometry about the Cu atom can formally be described as a severely tetragonally distorted octahedron, the $ClO_4^{\ominus}$ or $NO_3^{\ominus}$ ions being only weakly coordinated in the axial positions. We thus considered it important to investigate the influence of replacing Cu by a metal ion preferring a more rigorously octahedral geometry, e.g., Mn, Fe, Co, or Ni. To this end we have prepared an analogous Co^{II} complex, **2**,[2] though its stoichiometry differs notably from that of the Cu^{II} complex **1**. As **2** was readily obtained as good single crystals, an X-ray analysis has been carried out[3] to establish the structure of this complex and the implications of the different stoichiometry.

$[\{Hg_2Cu(C_4H_6NO)_4\}X_2]_n$ **1**, $X = NO_3^{\ominus}, ClO_4^{\ominus}$
$[\{Hg_3Co(C_4H_6NO)_6\}(NO_3)_2]_n$ **2**

The analysis has revealed the structure of **2** to be dramatically different to the contiguous 32-membered macrocyclic structure of the Cu complex **1**. Here we have a macrobicyclic chain polymer (Fig. 1). Each link of the chain is comprised of two interlocking 16-membered rings, each containing two Co, two Hg, four C, four N, and four O atoms. Alternatively, each link may be visualized as a 16-membered macrocycle with an additional $Hg(C_4H_6NO)_2$ central strut connecting adjacent Co atoms. The structure is highly symmetric, with both the Co and Hg atoms that form the central backbone lying on crystallographic centers of symmetry.

There are two nonequivalent Hg environments. One-third of the Hg atoms lie on the backbone and are centrally disposed with respect to adjacent pairs of Hg and Co atoms.[4] The remainder lie on the exterior of the chain and loosely bind the $NO_3^{\ominus}$ counterions.[5] This interaction is reflected in a noticeable bending of the associated N-Hg-N unit (175.1(2)°; cf. 180° for the central N-Hg-N units).[6]

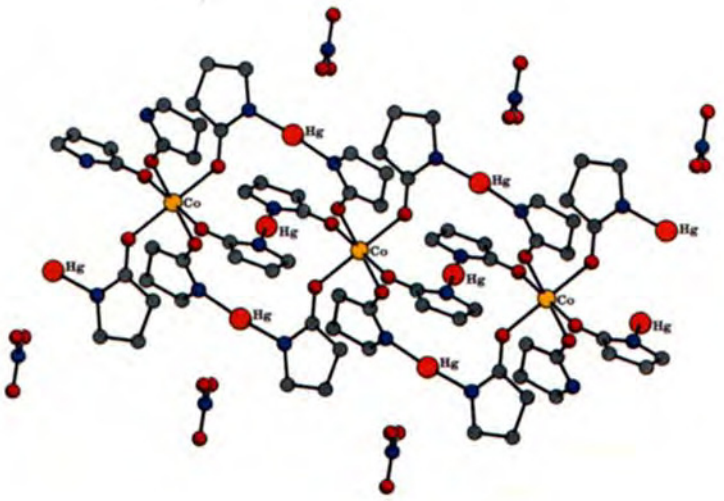

Fig. 1. Part of the contiguous macrobicyclic chain polymer formed by **2** in the crystal.

The polymer chains are not cross-linked; they are parallel[7] and lie along the crystallographic *a* direction. The $NO_3^{\ominus}$ ions are similarly aligned, occupying columns between the polymeric cations.

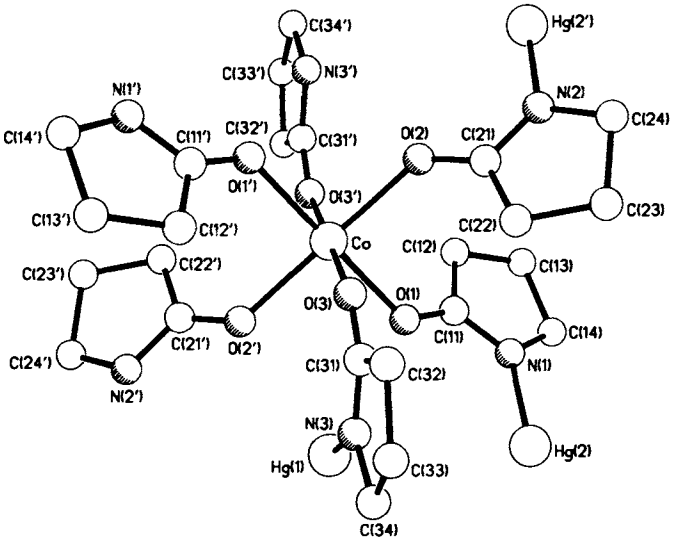

Fig. 2. The structure of **2** in the crystal. Selected bond distances and angles: Co-O(1) 2.122(5), Co-O(2) 2.120(5), Co-O(3) 2.052(7) Å; O(1)-Co-O(2) 89.8(2), O(1)-Co-O(3) 87.0(2), O(2)-Co-O(3) 94.4(2)°. O(3) is the oxygen of the 2-pyrrolidone unit that forms the central strut in the polymer chain (see Fig. 1).

As expected, the Co coordination geometry closely approaches a regular octahedron (Fig. 2). There are, however, some significant small deviations associated with Co-O bonds to the ligands that form the central strut of the chain. These result in a small axial compression as well as a slight angular distortion. This has no noticeable effect, however, on the electronic spectrum of the complex, which

[*] Dr. D. M. L. Goodgame, Dr. D. J. Williams, R. E. P. Winpenny
Chemistry Department, Imperial College of Science and Technology
London SW7 2AY (UK)

[**] This work was supported by the Science and Engineering Research Council.

is unexceptional.[8] Previously[1] we considered the possible application of the polymeric complex **1** in anion exchange. Here the exclusion of nitrate from the coordination sphere of the Co leads to the anion being even more loosely bound. Also its confinement to channel-like domains in the crystal offers the potential for diffusion. Experiments to investigate this possibility are being undertaken.

Received: August 21, 1987;
supplemented: October 13, 1987 [Z 2406 IE]
German version: *Angew. Chem. 100* (1988) 266

[1] D. M. L. Goodgame, D. J. Williams, R. E. P. Winpenny, *Angew. Chem. 99* (1987) 1053; *Angew. Chem. Int. Ed. Engl. 26* (1987) 1044.

[2] *Experimental Procedure:* $Hg(C_4H_6NO)_2$ was made by dissolving $Hg(OAc)_2$ (2 mmol) and 2-pyrrolidone (4 mmol) in a minimum volume of methanol and reprecipitating with diethyl ether. The precipitate was then dissolved with hydrated $Co(NO_3)_2$ (1 mmol) in methanol (25 mL) and the pink solution allowed to evaporate at room temperature. Small pink, air-stable crystals for X-ray analysis formed after 3 d, yield 70%, m.p. = 170–174 °C (dec.). The compound gave a satisfactory elemental analysis. The compound was soluble in water but insoluble in dimethylformamide, alcohols, and other common organic solvents. X-ray powder diffraction photographs show the Cd^{II} homologue to be isostructural, but the Ni^{II} compound is not. To date, crystals of the latter of suitable quality for X-ray structure analysis have not been obtained.

[3] **2**: Triclinic, $a = 7.476(2)$, $b = 11.040(3)$, $c = 11.383(3)$ Å, $\alpha = 64.39(2)$, $\beta = 77.45(2)$, $\gamma = 81.95(2)°$, $V = 825$ Å^3, $P\bar{1}$, $Z = 1$, $\mu(Cu_{K\alpha}) = 310$ cm^{-1}, $\rho_{calcd} = 2.59$ g cm^{-3}. Nicolet R3m diffractometer, ω-scan, graphite-monochromated $Cu_{K\alpha}$ radiation. The structure was solved by the heavy-atom method, corrected for absorption, and refined anisotropically to give $R = 0.032$ ($R_w = 0.034$) for 2061 independent observed reflections [$\theta \leq 58°$, $|F_o| > 3\sigma(|F_o|)$]. Further details of the crystal structure investigation can be obtained from the Director of the Cambridge Crystallographic Data Centre, Lensfield Road, Cambridge, CB2 1EW (England), by quoting the full literature citation.

[4] The central chain Co···Hg distances are 3.74 Å and the "interior" to "exterior" Hg···Hg contact distances are 3.62 Å.

[5] The approach distances of the $NO_3^{\ominus}$ oxygen atoms to the "exterior" Hg atoms in **2** are very similar to those of the $NO_3^{\ominus}$ and $ClO_4^{\ominus}$ oxygen atoms to the Hg atoms in the Cu^{II} complex **1**, with Hg(2)···O(5) = 2.855 and Hg(2)···O(4) = 2.733 Å. Interestingly, whereas all three O atoms of the $NO_3^{\ominus}$ ion in the Cu^{II} complex are involved in interactions to Hg, here only two interact.

[6] Hg(1)-N(3) = 2.041(9), Hg(2)-N(1) = 2.041(8), and Hg(2)-N(2) = 2.010(9) Å.

[7] The closest inter-polymer contact is 3.23 Å between O(6) (the nitrate oxygen not bound to Hg(2)) in one chain and C(23), a pyrrolidone carbon, in the next.

[8] Electronic spectrum of **2** by reflectance technique (Beckmann DK2 spectrometer): $\lambda = 7580$, 14000, 18520 cm^{-1}. The magnetic moment (5.1, Gouy method) and infrared spectrum of the complex are unexceptional. NMR spectrum of **2** recorded in D_2O (JEOL FX90 spectrometer) shows breakdown of the complex giving $Hg(C_4H_6NO)_2$ and $[Co(H_2O)_6]^{2\oplus}$. Interestingly, the Cu^{II} complex **1** did not dissolve in D_2O.

B_6H_{14}, a Dimeric B_3H_7?**

By *Bernd Brellochs* and *Herbert Binder**

The higher boranes B_4H_{10}, B_5H_9, B_5H_{11}, and $B_{10}H_{14}$ are usually prepared by pyrolysis of B_2H_6.[1] During the course of these complex reactions, the highly reactive, unstable molecules BH_3, B_3H_7, B_4H_8, and B_3H_9 are formed; with the exception of the latter species, however, they have only been identified so far by mass spectroscopy.[2] We found that the oxidation of $B_3H_8^{\ominus}$[3] with I_2 in inert solvents below −40 °C is a simple way to prepare "B_3H_7" in situ [Eqs. (a) and (b)]. The counterions are $NEt_4^{\oplus}$ or $PPh_4^{\oplus}$. B_3H_7 **1** may be described by the valence structures shown in Scheme 1.

$$B_3H_8^{\ominus} + I_2 \longrightarrow B_3H_7 + HI + I^{\ominus} \quad (a)$$

$$B_3H_8^{\ominus} + HI \longrightarrow B_3H_7 + H_2 + I^{\ominus} \quad (b)$$

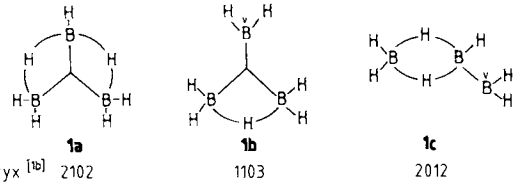

Scheme 1. Valence electron structures for B_3H_7 **1**. s = number of hydrogen bonds; t = number of closed two-electron three-center bonds; y = number of B-B bonds; x = additional H atoms on boron; v = free orbital.

Calculations have shown[4] that **1a** is 4.4 and 7.4 kcal mol^{-1} more stable than **1b** and **1c**, respectively; accordingly, a fluxional process is expected between **1a** and **1b**. The ^{11}B-NMR spectrum (28.88 MHz) of a solution of "B_3H_7" in CH_2Cl_2 consists of two broad, separated signals at $\delta = -10.7$ and -30.4 (intensity ratio 2:1, half-widths 180 and 172 Hz, respectively, the region of tetracoordinated boron atoms). In the $^{11}B\{^1H\}$-NMR spectrum, the half-widths of the two signals are reduced to 68 and 80 Hz, respectively. This indicates ^{11}B-^1H coupling. The ^1H-NMR spectrum (400 MHz) of "B_3H_7" in CD_2Cl_2 at −50 °C exhibits only one broad unresolved signal at $\delta = 1.38$, overall half-width 130 Hz. In the case of monomeric B_3H_7, the dynamics of the H atoms should result in the three B atoms being magnetically equivalent, in analogy to those in $B_3H_8^{\ominus}$;[5,6] thus, only one signal should be observed in the ^{11}B-NMR spectrum. The small difference in energy between **1a** and **1b**, as well as the electron sextet in **1b**, suggests that "B_3H_7" is stabilized through hydrogen bonds as B_6H_{14} **2**. The analogy to the dimerization of BH_3 to B_2H_6 is readily apparent. B_6H_{14} is formally a member of the series of *hypho*-boranes B_nH_{n+8}, whose structures may be described in terms of *Wade*'s rules with (2n + 8) skeleton electrons.[7] The examples of this class of compounds so far known are B_8H_{16}, $B_{10}H_{18}$,[8] $B_{14}H_{22}$, and $B_{15}H_{23}$;[9] the latter two examples are probably "*conjuncto*-boranes."

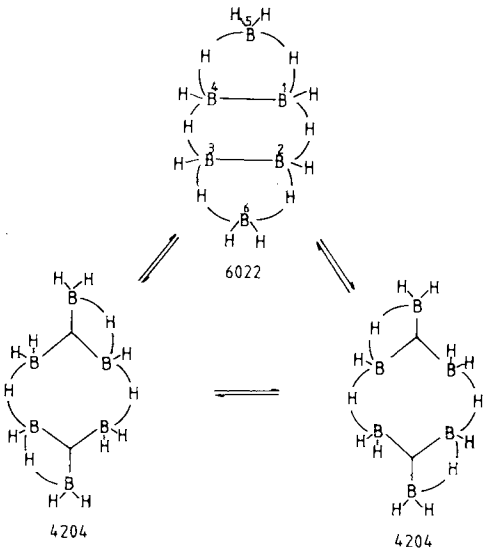

Scheme 2. Valence structures for B_6H_{14} **2**. The "styx" values are given once again for each structure (see caption to Scheme 1).

[*] Prof. Dr. H. Binder, Dr. B. Brellochs
Institut für Anorganische Chemie der Universität
Pfaffenwaldring 55, D-7000 Stuttgart 80 (FRG)

[**] This work was supported by the Deutsche Forschungsgemeinschaft and the Fonds der Chemischen Industrie. We thank Bayer AG for the donation of chemicals.

Scheme 2 shows the probable valence structures of **2**, which would also explain the 2:1 ratio of intensities found in the ^{11}B-NMR spectrum: $B^1B^2B^3B^4 \neq B^5B^6$.

Two further observations support this interpretation. (1) The ^{11}B-NMR spectrum is independent of the solvent employed; this rules out an interaction between B_3H_7 and the solvent. (2) Since $NEt_4^{\oplus}I^{\ominus}$ precipitates in the synthesis carried out according to (a) and (b), $B_3H_7I^{\ominus}$ can also be ruled out as a product. Determination of the molecular weight by means of vapor-pressure depression, however, is not useful owing to partially dissolved $NEt_4^{\oplus}I^{\ominus}$.

Another route to **2** is via $Cl^{\ominus}$ abstraction from $B_3H_7Cl^{\ominus}$[10] with $AlCl_3$ at -45 °C in CH_2Cl_2 [Eq. (c)]. Com-

$$NEt_4^{\oplus}B_3H_7Cl^{\ominus} + AlCl_3 \longrightarrow 1/2\ \mathbf{2} + NEt_4^{\oplus}AlCl_4^{\ominus} \qquad (c)$$

pound **2** cannot be isolated from the reaction solution, however, since it decomposes upon removal of the solvent or above -40 °C to give B_4H_{10} and B_5H_9 along with H_2 [Eq. (d)]. The low stability of **2** might be due to the relatively large number of hydrogen bonds.

$$3/2\ \mathbf{2} \longrightarrow B_4H_{10} + B_5H_9 + H_2 \qquad (d)$$

Compound **2** reacts with a series of Lewis bases at -78 °C to give the B_3H_7 adducts **3**[11] [Eq. (e)]. L–BH_3 adducts are not observed. Compound **2** reacts with some carboxylic and thiocarboxylic acids at -45 °C within a few minutes to give exclusively the bicyclic compound **4** [Eq. (f)]. (For R = Ph, it was possible to characterize **4** by an X-ray structure analysis.[12]) $NEt_4^{\oplus}BH_4^{\ominus}$ reacts with **2** to form the starting compound $NEt_4^{\oplus}B_3H_8^{\ominus}$ [Eq. (g)].

$$\mathbf{2} + 2\,L \longrightarrow 2\,L\text{–}B_3H_7\ \mathbf{3} \qquad (e)$$

L = NH_3, NMe_3, PPh_3, THF, CH_3CN

$$1/2\ \mathbf{2} + RCOOH\ (CH_3COSH) \longrightarrow \mathbf{4} + H_2 \qquad (f)$$

R = H, CH_3, C_2H_5, Ph

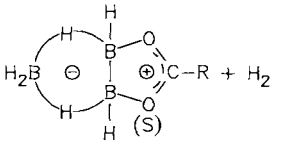

$$\mathbf{2} + 2\,BH_4^{\ominus} \longrightarrow 2\,B_3H_8^{\ominus} + B_2H_6 \qquad (g)$$

Examples (e)–(g) show that **2** presumably contains the original B_3H_7 fragments and that the linking hydrogen bonds are the reactive positions. Of particular interest is the fact that B_3H_7 can be viewed as an isoelectronic system to the allyl cation $C_3H_5^{\oplus}$ and, like this, can therefore function as a ligand in metal complexes.[13]

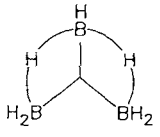

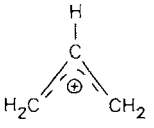

Experimental Procedure

a) $NEt_4(B_3H_8)$ (204 mg, 1.2 mmol) was added to a suspension of I_2 (152 mg, 0.6 mmol) in 2 mL of CH_2Cl_2 ($CHCl_3$, $C_2H_4Cl_2$, $MeNO_2$, $nPrNO_2$, or toluene) at -40 to -50 °C [14]. H_2 evolved and NEt_4I precipitated. After 1 h, only **2** was observed in the solution by ^{11}B-NMR spectroscopy. With $PPh_3(B_3H_8)$, soluble PPh_4I was formed, but **2** as well, as shown by the ^{11}B-NMR spectrum.

b) $NEt_4(B_3H_7Cl)$ (682 mg, 4 mmol) was added to a suspension of $AlCl_3$ (534 mg, 4 mmol) in CH_2Cl_2 (10 mL) at ca. -45 °C. After 6 h, only signals of **2** were still observable in the ^{11}B-NMR spectrum.

Received: September 11, 1987 [Z 2427 IE]
German version: *Angew. Chem. 100* (1987) 270

CAS Registry numbers:
1, 12429-70-8; **3** (L = NH_3), 57808-44-3; **3** (L = NMe_3), 57818-48-7; **3** (L = PPh_3), 64506-31-6; **3** (L = THF), 52842-96-3; **3** (L = CH_3CN), 59796-67-7; **4** (R = H), 112373-60-1; **4** (R = CH_3), 112373-64-5; **4** (R = C_2H_5), 112373-61-2; **4** (R = Ph), 112373-62-3; **4** (CH_3COSH deriv.), 112373-63-4; $NEt_4^{\oplus}B_3H_8^{\ominus}$, 12555-74-7; $PPh_4^{\oplus}B_3H_8^{\ominus}$, 12572-64-4; I_2, 7553-56-2; HI, 10034-85-2; $NEt_4^{\oplus}B_3H_7Cl$, 112373-59-8; $AlCl_3$, 7446-70-0; B_4H_{10}, 18283-93-7; B_5H_9, 19624-22-7; HCOOH, 64-18-6; CH_3COOH, 64-19-7; CH_3CH_2COOH, 79-09-4; PhCOOH, 65-85-0; CH_3COSH, 507-09-5; $NEt_4^{\oplus}BH_4^{\ominus}$, 17083-85-1.

[1] a) A. E. Stock: *Hydrides of Boron and Silicon*, Cornell University Press, Ithaca, NY, USA 1933; b) W. N. Lipscomb: *Boron Hydrides*, Benjamin, New York 1966, p. 154; c) M. F. Hawthorn in E. L. Muetterties: *The Chemistry of Boron and Its Compounds*, Wiley, New York 1967, p. 223.
[2] a) R. T. Paine, G. Sodeck, F. E. Stafford, *Inorg. Chem. 11* (1972) 2593; b) G. W. Mappes, T. P. Fehlner, *J. Am. Chem. Soc. 92* (1970) 1562; c) O. Herstad, G. A. Pressley, Jr., F. E. Stafford, *J. Phys. Chem. 74* (1970) 874; d) R. E. Hollins, F. E. Stafford, *Inorg. Chem. 9* (1970) 877; e) A. B. Baylis, G. A. Pressley, Jr., F. E. Stafford, *J. Am. Chem. Soc. 88* (1966) 2428; A. B. Baylis, G. A. Pressley, Jr., M. E. Gordon, F. E. Stafford, *ibid. 88* (1966) 929.
[3] *Gmelin Handbuch der Anorganischen Chemie, Erg. Werk zur 8. Aufl. Band 53, Teil 18*, Springer, Berlin 1978.
[4] M. L. McKee, W. N. Lipscomb, *Inorg. Chem. 21* (1982) 2846.
[5] a) W. C. Phillips, H. C. Miller, E. L. Muetterties, *J. Am. Chem. Soc. 81* (1959) 4496; b) D. Marynick, T. Onak, *J. Chem. Soc. A 1970*, 1160; c) H. Beall, C. H. Bushweller, W. J. Dewkett, M. Grace, *J. Am. Chem. Soc. 92* (1970) 3484; d) R. T. Paine, E. Fukushima, S. B. W. Roeder, *Chem. Phys. Lett. 32* (1976) 566.
[6] W. N. Lipscomb, *J. Inorg. Nucl. Chem. 11* (1959) 1.
[7] K. Wade, *Chem. Br. 11* (1975) 177.
[8] J. Dobson, R. Maruca, R. Schaeffer, *Inorg. Chem. 9* (1970) 2161.
[9] J. Rathke, R. Schaeffer, *Inorg. Chem. 13* (1974) 3008.
[10] G. B. Jacobsen, J. H. Morris, *Inorg. Chim. Acta 59* (1982) 207.
[11] S. G. Shore in E. L. Muetterties: *Boron Hydride Chemistry*, Academic Press, New York 1975.
[12] H. Binder, *VI. Int. Meet. Boron Chem.* (Bechyně bei Tábor, CSSR, June 22–26, 1987); these results will be reported elsewhere.
[13] C. E. Housecroft, T. P. Fehlner, *Inorg. Chem. 21* (1982) 1739.
[14] K. Wolfer, *Dissertation*, Universität Stuttgart 1985.

A New Type of Unsaturated *triangulo* Transition-Metal Cluster and Homogeneous Catalyst

By *Hans-Jürgen Haupt,* Peter Balsaa,* and *Ulrich Flörke*

The synthesis of $[Re_3(CO)_6(\mu_3\text{-}H)_2\{\mu\text{-}P(C_6H_5)_2\}_3]$ **2**, which has 44 cluster valence electrons (CVE), closes the gap between transition-metal clusters with 48 and 46 CVE, on the one hand, and those with 42 CVE, on the other (Fig. 1). Numerous examples of clusters with 48 CVE (three covalent M–M bonds) are known (e.g., $[M_3(CO)_{12}]$, M = Fe, Ru, Os). Those with 46 CVE (one double and two single bonds) are exemplified by at least $(NEt_4)[Re_3(CO)_9(\mu\text{-}H)_4(L)]$, L = $P(C_6H_5)_3$, C_5H_5N,[1] and $[Co_3(\mu_5\text{-}C_5Me_5)_3(\mu_3\text{-}$

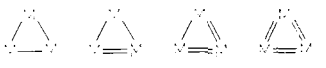

Fig. 1. Cluster valence electrons (CVE) in trinuclear transition-metal clusters fulfilling the 18-valence-electron rule for transition-metal atoms M.

[*] Prof. Dr. H.-J. Haupt, Dr. P. Balsaa, Dr. U. Flörke
Anorganische Chemie der Universität-Gesamthochschule
Warburger Strasse 100, D-4790 Paderborn (FRG)

$CO)_2]$.[2] An example of those with 42 CVE (three double bonds) is provided by the Re_3X_9 structural unit (X = Cl, Br, I).[3]

However, cluster **2** is not only of theoretical interest for understanding the bonding in clusters with metal-metal multiple bonds,[4] but is also of interest as a potential hydrogenation reagent. Of particular interest would be its possible suitability as a homogeneous catalyst.[5]

Cluster **2** may be prepared from the dirhenium starting clusters $[Re_2(CO)_8(PPh_3)_2]$, $[Re_2(CO)_8(\mu\text{-}H)(\mu\text{-}PPh_2)]$,[6] and $[Re_2(CO)_8(\mu\text{-}PPh_2)_2]$. To this end, the two phosphido-bridged starting clusters must be subjected to thermolysis, while, for the nonbridged starting cluster, hydrogenolysis at 210 °C proved successful [Eqs. (a)-(c)]. The two products

$$[Re_2(CO)_8(PPh_3)_2] + H_2 \rightleftharpoons 2[HRe(CO)_4PPh_3] \quad (a)$$

$$3[HRe(CO)_4PPh_3] \xrightarrow{-3CO} 3\,PhH + [Re_3(CO)_9(\mu\text{-}PPh_2)_3] \quad (b)$$

1, 48 CVE

$$[Re_3(CO)_9(\mu\text{-}PPh_2)_3] + H_2 \xrightarrow{-3CO} [Re_3(CO)_6(\mu_3\text{-}H)_2(\mu\text{-}PPh_2)_3] \quad (c)$$

2, 44 CVE

1 and **2** were identified by means of single-crystal X-ray structure analysis,[7,8] while the existence of the μ_3-hydrido bridge in **2** was shown by ^{1}H-NMR spectroscopy.

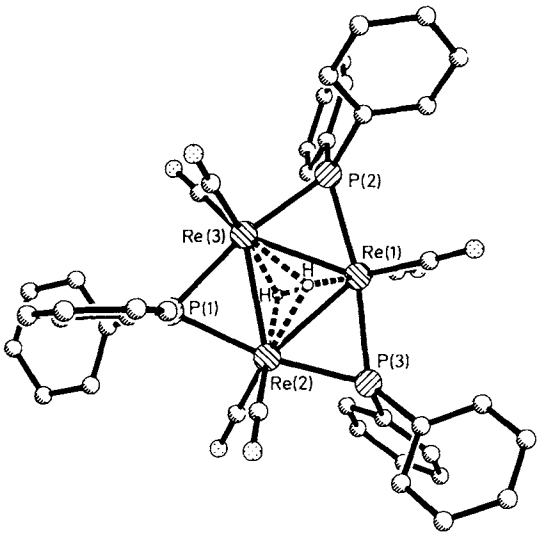

Fig. 2. Molecular structure of **2**.

Cluster **2** (Fig. 2) exhibits three comparable Re-Re bonds with multiple-bond character. This indicates that the four π electrons in the rhenium three-membered ring are not localized as shown in Figure 1. The double-bond character of the Re-Re bonds in **2** is clearly revealed by comparison of the Re-Re bond lengths of Re clusters having different CVE (Table 1) (compare also the values for Re-Re double bonds in Ref. [9]). The consequences of the short Re-Re bonds include a reduction in the Re-(μ-P)-Re bond angle by 3(1)° and a reduction in the Re-(μ-P) bond lengths. An alternative description of **2** as a system with two π electrons (analogous to the cyclopropenyl cation), which would correspond to a formulation as $[Re_3(CO)_6(\mu\text{-}PPh)_2)_3]^{2\oplus}\,2\,H^{\ominus}$, is considered less likely on the basis of the ^{1}H-NMR data, the estimated Re-H bond lengths,[8] and the behavior of **2** as a nonelectrolyte in dichloromethane.

Table 1. Selected bond lengths [pm].

Compound	CVE	d(Re-Re)	d(Re-(μ-Y))	Ref.
1	48	291.4(4) [a]	2.422(20) [b]	[7]
2	44	273.0(1)	2.369(6) [b]	[8]
$[Re_3(CO)_9(PPh_3)(\mu\text{-}H)_4]^{\ominus}$	46	279.7(1) [c]	2.481(2) [d]	[1]
		319.3(1)		
		323.4(1)	1.84 [a, e]	

[a] Mean value; [b] Y = P; [c] d(Re=Re); [d] d(Re−PPh$_3$); e) Y = H.

Phosphido bridging, such as that observed in **2**, has recently been used quite often in order to hold metals together stably.[4,10] Preliminary experiments to determine the homogeneous-catalysis properties of **2** (hydrogenation of cyclohexene in tetrahydrofuran) gave TON values [cycles h^{-1}] of 63 (20 °C) and 285 (60 °C).[11] Analysis of the activation energies of hydrogenations with these and other soluble hydridorhenium complexes will establish the prerequisites for the determination and evaluation of the catalytic activity of different types of hydrido complexes.

Experimental Procedure

Hydrogenolysis: A solution of $[Re_2(CO)_8(PPh_3)_2]$ (0.5 g, 0.45 mmol) in dry xylene (9 mL) was placed in a steel autoclave; hydrogen was then admitted at room temperature until a pressure of 2×10^5 Pa was obtained. The reaction was complete after 4 d at 210 °C. The products were separated by means of thick layer chromatography (eluant $CHCl_3$/*n*-hexane 3 : 2). **1** (0.02 g, 5%) was isolated from the red fraction and **2** (0.1 g, 26%; dec. >250 °C) from the orange-red fraction. Analytical data for **2**: $M^{\oplus}$(^{187}Re) = 1268 (150 °C vaporization temperature; 70eV-EI-MS; IR ($\tilde{\nu}_{CO}$, KBr): 1974 (s), 1938 (s) cm^{-1}; NMR ($CDCl_3$): ^{31}P{^{1}H} (standard H_3PO_4): δ = 198.2 (s, μ-P); ^{1}H: δ = 7.45 (m, 30 H, Ph), −18.20 (q, 2 H, μ_3-H), J(PH) = 7.3 Hz. Analytical data for **1**: ^{31}P{^{1}H}-NMR ($CDCl_3$): δ = 56.53 (s, μ-PPh_2), in agreement with literature value [7].

Thermolyses: $[Re_2(CO)_8(\mu\text{-}H)(\mu\text{-}PPh_2)]$ (0.08 g, 0.1 mmol) [6] in xylene (3 mL) was heated in a sealed glass tube (inner volume ca. 10 mL) for 1 d at 230 °C. The solvent was then removed under oil-pump vacuum, the remaining yellow-brown solid was dissolved in 2 mL of chloroform, and crystallization was achieved by means of the vapor-pressure equalization method ($CHCl_3$/*n*-pentane): 0.02 g (25%) of orange crystals of **2** and 0.04 g (50%) of a white crystalline mixture consisting of the starting material and $[Re_2(CO)_8(\mu\text{-}PPh_2)_2]$, which were identified by comparison of their ^{31}P-NMR data with those of authentic reference compounds. Similar treatment of $[Re_2(CO)_8(\mu\text{-}PPh_2)_2]$ (0.26 g, 0.27 mmol) also afforded **2**.

Received: June 26, 1987;
revised: September 15, 1987 [Z 2312 IE]
German version: *Angew. Chem. 100* (1988) 280

CAS Registry numbers:
1, 18757-73-8; **2**, 112373-66-7; $Re_2(CO)_8(PPh_3)_2$, 14172-94-2; cyclohexene, 110-83-8.

[1] T. Beringhelli, G. D'alfonso, M. Freni, G. Ciani, A. Sironi, H. Molinari, *J. Chem. Soc. Dalton Trans. 1986*, 2691.
[2] L. F. Dahl, A. D. Rae, R. L. Bedard, *J. Am. Chem. Soc. 108* (1986) 5924.
[3] F. A. Cotton, G. Wilkinson: *Advanced Inorganic Chemistry*, Wiley, New York 1980, p. 1097.
[4] W. A. Herrmann, *Angew. Chem. 98* (1986) 57; *Angew. Chem. Int. Ed. Engl. 25* (1986) 56.
[5] P. E. Garrou, *Chem. Rev. 85* (1985) 171.
[6] H.-J. Haupt, P. Balsaa, U. Flörke, *Z. Anorg. Allg. Chem. 548* (1987) 151.
[7] H.-J. Haupt, P. Balsaa, U. Flörke, *Inorg. Chem. 27* (1988), in press.
[8] H.-J. Haupt, U. Flörke, P. Balsaa, *Acta Crystallogr. Sect. C 43* (1987), in press.
[9] W. A. Herrmann, R. Serrano, A. Schäfer, U. Küsthardt, M. L. Ziegler, E. Guggolz, *J. Organomet. Chem. 272* (1984) 55.
[10] G. Huttner, K. Knoll, *Angew. Chem. 99* (1987) 765; *Angew. Chem. Int. Ed. Engl. 26* (1987) 743.
[11] The homogeneously catalyzed hydrogenations were carried out in a steel autoclave (200 mL) under the following standard conditions: 1.0 MPa H_2 pressure, 20 mL cyclohexene in dry tetrahydrofuran (1 mol L^{-1}); $[Re_3(CO)_6(\mu_3\text{-}H)_2(\mu_2\text{-}PPh_2)_3]$ (5×10^{-3} g; 1.95×10^{-4} mol L^{-1}).

Tris(2,2'-bipyridyl-5-sulfonic acid)rhodium(III), an Improved Redox Catalyst for the Light-Induced and the Electrochemically Initiated Enzymatic Reduction of Carbonyl Compounds**

By *Marlene Franke* and *Eberhard Steckhan**

Many enzyme-catalyzed reductions require reduced nicotinamide cofactors such as NADH or NADPH as reducing equivalents. Nicotinamide cofactors also play an important role in photosynthesis for the transfer and storage of reducing equivalents. In order to use such reactions in biotechnological processes or for the transformation and storage of solar energy, it is necessary to develop simple and effective chemical, and especially photochemical, methods for the regeneration of the cofactors and, wherever possible, to couple these in situ with an NAD(P)H-dependent enzyme reaction. Enzyme-catalyzed regeneration is the most frequently used procedure.[1] Such a process, although often well-developed technologically,[2] is not optimal, because it is usually necessary to work with two enzymes, two substrates, and two products. The most advantageous procedure, which is also employed technologically, makes use of formate dehydrogenase with formate as donor; CO_2 is thereby formed as a gaseous, noninterfering product.[2] However, it is still of principal importance to develop alternative methods that do not operate with a second enzyme system. Electrochemical and photochemical procedures are possible techniques. The difficulty in solving the problem of nonenzymatic NADH regeneration consists in finding systems that are able to transfer two electrons simultaneously or a hydride ion to $NAD^{\oplus}$. One-electron transfer, however, results in formation of the NAD radical, which undergoes dimerization to form enzyme-inactive $(NAD)_2$. As a consequence, electrochemical regeneration can only be carried out by an indirect process.[3] Several research groups have shown that the indirect electrochemical regeneration of NADH can also be performed using electrochemically generated one-electron transfer agents. However, in these cases, an additional enzyme system is once again necessary.[4–6] This must be capable of accepting two electrons stepwise from the most commonly used viologen radical cations and of then transferring these electrons as a pair to $NAD^{\oplus}$. More promising seems to be the attempt to use intact microorganisms for the electromicrobial reduction.[6,7] Also for the especially interesting photochemical in situ regeneration of NAD(P)H, only one-electron transfer agents have been so far used as electron relays, which, for the above reasons, require the introduction of an additional enzyme such as ferredoxin reductase or lipoamide dehydrogenase.[8] The sensitizers used in these cases were $[Ru(bpy)_3]^{2\oplus}$ or zinc(II) *meso*-tetramethylpyridiniumporphyrin, the donors, $(NH_4)_3EDTA$ (EDTA = ethylenediaminetetraacetate) or 2-mercaptoethanol.

We showed earlier that it is possible to dispense with the use of an additional enzyme or microorganisms in the indirect electrochemical and photochemical regeneration, if electrochemically or photochemically generated and regenerated two-electron or hydride transfer agents are employed. Tris(2,2'-bipyridyl)rhodium(III), $[Rh(bpy)_3]^{3\oplus}$,[9] originally used as a redox catalyst or electron relay, however, exhibited several disadvantages. For instance, the relatively negative potential of the rhodium complex (−0.92 V vs. SCE) results in the formation of small amounts of $(NAD)_2$ by direct reduction of $NAD^{\oplus}$ at the cathode. Furthermore, the passivation of the electrode surfaces by a sparingly soluble intermediary rhodium complex occurred. We were able to solve these problems by using bipyridyl-5-sulfonic acid as ligand L. The sulfonic acid moiety in $[Rh(L_3)]^{3\oplus}$ makes the complex and its intermediates more soluble and shifts the reduction potential by almost 200 mV to more positive values ($E_p = -0.73$ V vs. Ag/AgCl). It is thereby possible to completely suppress the NAD dimerization upon electrochemical reduction of this complex in the presence of $NAD^{\oplus}$. Further improvements were achieved by adding tetraethylene glycol and by working at relatively high substrate concentrations. We carried out the electrolysis of a system that contained 0.332 mmol of the complex $[Rh(L_3)]^{3\oplus}$, 0.15 mmol of $NAD^{\oplus}$, 10.7 mg of horse liver alcohol dehydrogenase (HLADH) (16 units based on the system ethanol/acetaldehyde), 25.6 mmol of cyclohexanone, and 3 mL of tetraethylene glycol in 80 mL of Tris-H_2SO_4 buffer at pH 7.4 (Fig. 1). At a potential of −0.73 V vs. Ag/AgCl, we were able to obtain 15.2 mmol of cyclohexanol after 33 days. This corresponds to 101 cycles based on $NAD^{\oplus}$ and 46 cycles based on the rhodium complex. In this reaction, an intermediary hydrido rhodium complex is evidently involved as a hydride ion transfer agent.

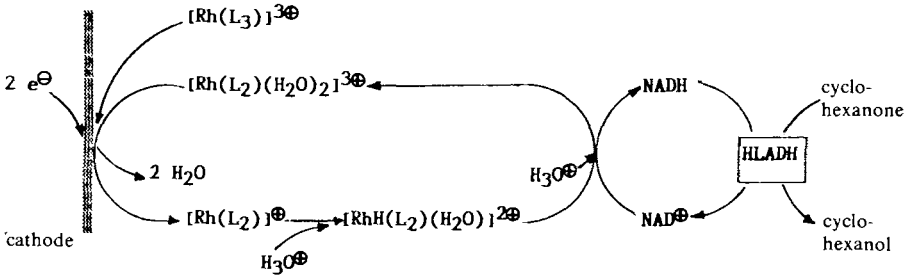

Fig. 1. Reaction scheme for the electrochemically initiated enzymatic reduction of cyclohexanone catalyzed by horse liver alcohol dehydrogenase and with tris(2,2'-bipyridyl-5-sulfonic acid)rhodium(III) $[Rh(L_3)]^{3\oplus}$ as redox catalyst.

After an induction period of several days, the rate of conversion remains constant for 20 days at approximately 0.73 mmol of cyclohexanone per day, corresponding to 4.9 cycles/day based on $NAD^{\oplus}$ and 2.2 cycles based on the redox catalyst.

Similarly, NADH can be regenerated in situ photochemically, if $[Ru(bpy)_3]^{2\oplus}$ is used as a sensitizer and 2,2,2-nitrilotriethanol (triethanolamine, TEOA) as a donor. Contrary to our former apprehension, the oxidative degradation products of TEOA do not disturb the reaction. In this way it was possible to reduce carbonyl compounds under HLADH catalysis in the presence of a catalytic amount of coenzyme in a continuous fashion (Fig. 2).

[*] Prof. Dr. E. Steckhan, Dipl.-Chem. M. Franke
Institut für Organische Chemie und Biochemie der Universität
Gerhard-Domagk-Strasse 1, D-5300 Bonn (FRG)

[**] This work was supported by the Minister für Wissenschaft und Forschung des Landes Nordrhein-Westfalen and by the Fonds der Chemischen Industrie.

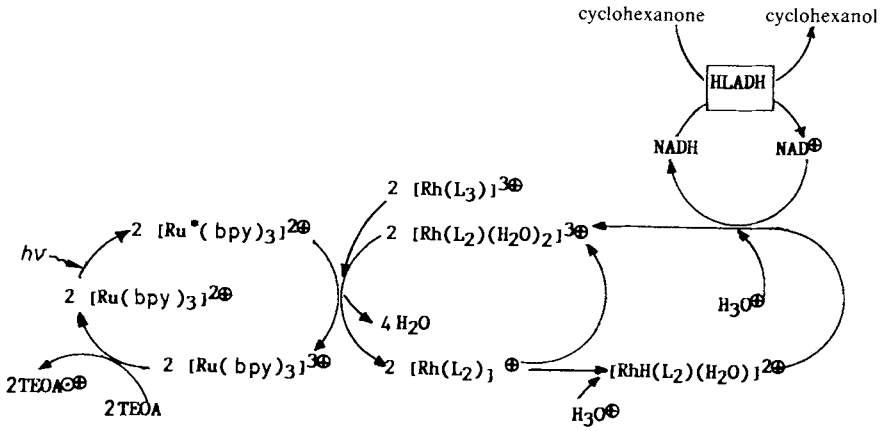

Fig. 2. Reaction scheme for the light-induced enzymatic reduction of cyclohexanone with $[Rh(L_3)]^{3\oplus}$ as electron relay.

Blank experiments with or without irradiation, in the absence of one of the components mentioned above, however, were negative. The photochemically initiated enzyme reaction (Table 1), with 11 or 12 cycles per day based on $[Rh(L_3)]^{3\oplus}$, is faster than the indirect electrochemical coenzyme regeneration by a factor of 5.

Table 1. Results of the light-induced enzymatic reduction of cyclohexanone using tris(2,2'-bipyridyl-5-sulfonic acid)rhodium(III) as electron relay [a].

No.	t [h]	Cyclohexanone [mmol]	$[Ru(bpy)_3]^{2\oplus}$ [mmol]	$[Rh(L_3)]^{3\oplus}$ [mmol]	$NAD^{\oplus}$ [mmol]	Product cyclohexanol [mmol]	Cycles based on NADH	Cycles based on $[Rh(L_3)]^{3\oplus}$
1	24	5.1	0.003	0.0114	0.022	0.128	6.0	11
2	24	5.1	0.0026	0.0167	0.032	0.204	6.3	12
	36	5.1	0.0026	0.0167	0.032	0.320	10.0	19

[a] In 50 mL of TEOA(0.42 M)/Tris-H_2SO_4 buffer at pH 7.4; irradiation with a 250-W slide projector, only $\lambda \geq 395$ nm used; 8.8 mg (15 units, No. 1) and 3.6 mg (6 units, No. 2) HLADH were used.

The time dependence of the photolysis is shown in Figure 3. After 36 h, the linear increase in the amount of cyclohexanol formed is still observed. This demonstrates that the activity of the system is fully maintained up to this length of time.

Since it was known that $[Ru(bpy)_3]^{3\oplus}$ oxidizes oxalate,[10] experiments were carried out with ammonium oxalate or formate in place of nitrilotriethanol as the effective donor to trap this Ru^{III} complex. In this case, CO_2 would be formed as an inert oxidation product. UV spectroscopic measurements showed, however, that the photochemically initiated Rh^{I} generation was too slow in these cases.

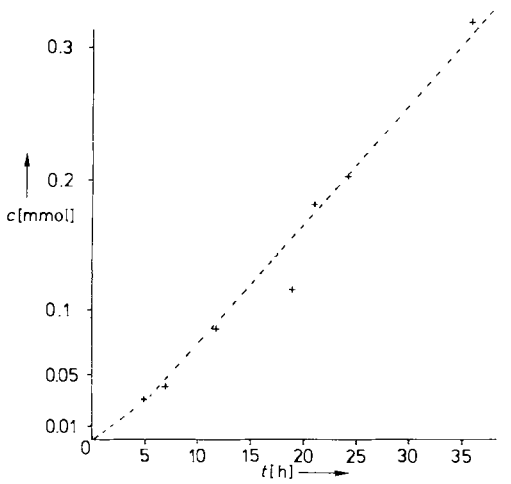

Fig. 3. Time dependence of the light-induced enzymatic reduction of cyclohexanone with $[Rh(L_3)]^{3\oplus}$ as electron relay (reaction conditions given in Table 1, No. 2). c = amount of cyclohexanol formed.

The rhodium complexes employed by us differ from other complexes in that, in their reduced form, they do not directly reduce carbonyl compounds. Thus, the stereospecificity of the enzyme can be fully exploited. In order to test this under the conditions of the photolysis, we used racemic 2-methylthiacyclohexan-4-one **1** in place of cyclohexanone. Starting from 0.003 mmol of $[Ru(bpy)_3]^{2\oplus}$, 0.174 mmol of $[Rh(L)_3]^{3\oplus}$, 0.21 mmol of $NAD^{\oplus}$, 17 units of HLADH, and 3.34 mmol of **1** in 50 mL of TEOA (0.42 M)/Tris-H_2SO_4 buffer at pH 7.4, it was possible to isolate 1.34 mmol (40% conversion) of the two diastereomeric alcohols **2** after 24 hours. This corresponds to 6.4 regenerative cycles based on the coenzyme and 7.7 cycles based on the rhodium complex. Flash chromatography (eluant *n*-hexane/ether = 3 : 7, subsequently 5 : 5) afforded initially 0.61 mmol of the (2*R*,4*S*) alcohol followed by 0.19 mmol of the (2*S*,4*S*) alcohol with specific optical rotations $[\alpha]_D$ of $+12°$ and $+3.8°$, respectively; this corresponds to an optical purity of $p = 0.81$ for the *trans* alcohol and 0.95 for the *cis* alcohol (Scheme 1). Within the limits of experimental accuracy, these results are identical with those obtained by the enzyme-catalyzed regeneration of the coenzyme.[11]

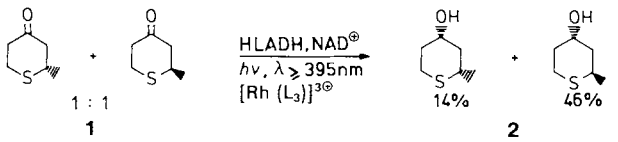

Scheme 1. Yields based on conversion (40%).

Thus, it has been shown that, for the photochemical regeneration of NADH in the presence of horse liver alcohol dehydrogenase described here, the stereospecificity of the enzyme is maintained and a direct reduction of the carbonyl compound by the reduced rhodium complex, which would circumvent the enzyme system, can be ruled out.

On the basis of these results, it should be possible to develop complexes as electron relays or redox catalysts that make possible an appreciably faster conversion.

Received: August 3, 1987;
revised: October 2, 1987 [Z 2386 IE]
German version: *Angew. Chem. 100* (1988) 295

[1] J. B. Jones, J. F. Beck in J. B. Jones, C. J. Sih, D. Perlman (Eds.): *Applications of Biochemical Systems in Organic Chemistry, Part 1*, Wiley-Interscience, New York 1976, pp. 370–376; J. B. Jones in R. Porter, S. Clark (Eds.): *Enzymes in Organic Synthesis*, Pitman, London 1985, p. 3; G. M. Whitesides, *ibid.*, p. 76.
[2] C. Wandrey, R. Wichmann, A. F. Bückmann, M. R. Kula, *Umschau 84* (1984) 88; C. Wandrey, R. Wichmann, W. Berke, M. Morr, M. R. Kula in: *Eur. Congr. Biotechnol. (Third), Vol. 1*, Verlag Chemie, Weinheim 1984, p. 239; C. Wandrey, R. Wichmann in A. I. Laskin (Ed.): *Enzymes and Immobilized Cells in Biotechnology*, Benjamin/Cummings, Menlo Park, CA, USA 1985, p. 177; M. R. Kula, C. Wandrey, *Methods Enzymol. 136* (1986).
[3] E. Steckhan, *Angew. Chem. 98* (1986) 681; *Angew. Chem. Int. Ed. Engl. 25* (1986) 683; *Top. Curr. Chem. 142* (1987) 1.
[4] M. Ito, T. Kuwana, *J. Electroanal. Chem. 32* (1971) 415.
[5] R. DiCosimo, C.-H. Wong, L. Daniels, G. M. Whitesides, *J. Org. Chem. 46* (1981) 4622.
[6] H. Simon, H. Günther, J. Bader, W. Tischer, *Angew. Chem. 93* (1981) 897; *Angew. Chem. Int. Ed. Engl. 20* (1981) 861; H. Simon, H. Günther, J. Bader, S. Neumann in R. Porter, S. Clark (Eds.): *Enzymes in Organic Synthesis*, Pitman, London 1985, p. 97; H. Simon, J. Bader, H. Günther, S. Neumann, I. Thanos, *Angew. Chem. 97* (1985) 541; *Angew. Chem. Int. Ed. Engl. 24* (1985) 539.
[7] H. Skopan, H. Günther, H. Simon, *Angew. Chem. 99* (1987) 139; *Angew. Chem. Int. Ed. Engl. 26* (1987) 128.
[8] D. Mandler, I. Willner, *J. Am. Chem. Soc. 106* (1984) 5352; *J. Chem. Soc. Perkin Trans. 2 1986*, 805.
[9] R. Wienkamp, E. Steckhan, *Angew. Chem. 94* (1982) 786; *Angew. Chem. Int. Ed. Engl. 21* (1982) 782; *Angew. Chem. Suppl. 1982*, 1739; *ibid. 95* (1983) 508 and *22* (1983) 497.
[10] I. Rubinstein, A. J. Bard, *J. Am. Chem. Soc. 103* (1981) 5007.
[11] J. Davies, J. B. Jones, *J. Am. Chem. Soc. 101* (1979) 5405.

The Copper Salt of 2-Iodo-5-methyl-*N,N'*-dicyanoquinonediimine—a Radical Anion Salt Exhibiting Metallic Conductivity down to Low Temperatures**

By *Peter Erk, Siegfried Hünig,* Jost Ulrich von Schütz, Hans-Peter Werner,* and *Hans Christoph Wolf*

Dedicated to Professor Helmut Dörfel on the occasion of his 60th birthday

Organic metals whose electrical conductivity continuously increases down to very low temperatures are of particular interest, since special properties, e.g., superconductivity, are then expected. Superconductivity has so far been found for several salts containing organic radical cations.[1] We recently described the salt **1a**, the first radical-anion-containing compound whose single-crystal conductivity increases to ca. 500000 S cm^{-1} at 0.45 K.[2] It is derived from the new class of *N,N'*-dicyanoquinonediimine (DCNQI) acceptors,[3] whose 2,5-disubstituted derivatives preferentially form radical anion salts that are close-packed in segregated stacks having the stoichiometry $(DCNQI)_2M$.[4]

We have now investigated whether these special properties are exhibited by other 2,5-disubstituted DCNQI salts.

1. Radical anion salts of type **1**,[5] with X = Me, Cl, Br, and M = Cu[6] (except for **1a**), Ag, and alkali metals,[7] exhibit a nearly constant conductivity of $\sigma = 700$–1000 S cm^{-1} (Cu salts) and $\sigma = 100$–300 S cm^{-1} (Ag and alkali-metal salts) between 300 and 100 K. Below a phase transition (Peierls distortion) these salts undergo a transition to a semiconducting state. In addition to their high electrical conductivity, they all exhibit very similar magnetic properties.[8] Similar conductivities have meanwhile been reported for the salts **1**, X = Me, M = Cu (= **1a**), Ag, Li, Na, K, and **1**, X = Cl, M = Cu (= **1c**), Li, NH_4.[9]

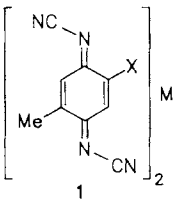

1

1a, X = Me, M = Cu
1b, X = I, M = Cu
1c, X = Cl, M = Cu

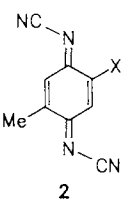

2

2a, X = Me
2b, X = I

2. In contrast, the derivative **1b** surprisingly exhibits a continuous increase in conductivity down to the lowest temperatures measured (1.2 K) (Fig. 1).

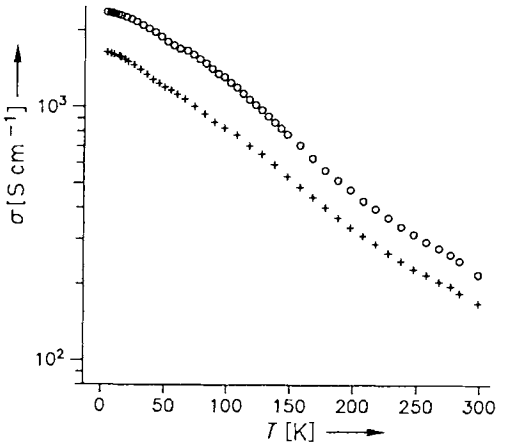

Fig. 1. Temperature dependence of the electrical conductivity of single crystals of the radical anion salt **1b**. O, + see text.

The salt **1b** was synthesized analogously to **1a**.[2] Combination of solutions of **2b**[10] and CuI in acetonitrile results in the precipitation of **1b** in the form of microcrystalline needles exhibiting a powder conductivity[11] of 0.2 S cm^{-1}.

Large single crystals of **1b** can be grown by electrolysis of **2b** and copper(II) bromide in acetonitrile (cf. Ref. [2]). A new method, which makes numerous DCNQI copper salts readily available, affords single crystals of **1b** by dipping a bright copper wire into a solution of **2b** and copper(II) bromide in acetonitrile.[12]

The single crystals of **1b** obtained in this way, which are up to 2 cm long, are indistinguishable in crystal habitus from those of **1a**. The X-ray powder diagram revealed that **1b** is isomorphous with the copper salts of the series **1**, $X = CH_3$ (= **1a**), Cl, Br,[13] so far synthesized and crystallizes in the tetragonal space group $I4_1$ (or $I4_1/a$) with the lattice constants $a = 21.687$ (± 0.003) and $c = 3.867$ (± 0.003).[14] This finding is surprising, since iodine (van der Waals radius 215 pm) is significantly larger than the other substituents of this series (CH_3 200, Br 195, Cl 180 pm).[15] In the crystal of **1a**, four molecules of **2a** are coordinated to each copper atom, and the separations of

[*] Prof. Dr. S. Hünig, Dipl.-Chem. P. Erk
Institut für Organische Chemie der Universität
Am Hubland, D-8700 Würzburg (FRG)
Dr. J. U. von Schütz, Dipl.-Phys. H.-P. Werner,
H. C. Wolf (physical measurements)
Physikalisches Institut der Universität (Teil 3)
Pfaffenwaldring 57, D-7000 Stuttgart 80 (FRG)

[**] This work was supported by the Stiftung Volkswagenwerk, the Fonds der Chemischen Industrie, and BASF AG, Ludwigshafen.

the methyl groups (392 pm) are already less than the sum of the van der Waals radii. In the case of the iodine-substituted derivative **1b**, the van der Waals radii of the substituents also overlap.

According to Figure 1, the slope of the conductivity curve between 300 and ca. 150 K is $\sigma(T) \approx T^{-\alpha}$ ($\alpha \approx 2$); at low temperatures, the slope becomes smaller. No convergence of the conductivity is evident. The different absolute values for the two series of measurements (○, +) are due to errors in the determination of the sample dimensions.

An electron spin resonance experiment revealed no ESR signal, either in the X band (9.6 GHz) or in the Q band (35 GHz). This is in accord with the finding for **1a**; in that case, the absence of an ESR signal is explained by the extreme line broadening due to spin-orbit coupling and points to multidimensionality owing to mixed valence states of copper.[2,6-9]

In the case of **1c**, a discontinuous contraction of the lattice in the stacking direction was demonstrated for a phase transition at 210 K. The size of the substituents appears to inhibit such a contraction for **1a** without significantly perturbing the overlap of the π systems. The methyl substituents show a similar effect in the superconducting radical cation salts of tetramethyltetraselenafulvalene.[16]

We presume that the "large" van der Waals radius of the iodine substituents in **1b** causes high strain in the crystal and suppresses a Peierls distortion. At the same time, the size of iodine is responsible for a poor overlap of the π systems and thus the lower absolute conductivity at 300 K. This effect may also be ascribed, however, to a low transverse conductivity through the CN-Cu-NC bridges, since, in this case, defects in the anion stack, have a stronger effect.

The small increase in conductivity in the low-temperature region indicates that the electron-phonon interaction might be significantly increased.[17] Thus, **1b** is a potential candidate for superconductivity at even lower temperatures, if necessary under pressure. Less likely is the possibility of Cooper pair formation in the case of **1a**, which would be required for superconductivity. Its stronger increase in conductivity at low temperatures is an indication of weak electron-phonon coupling.

Received: October 2, 1987 [Z 2454 IE]
German version: *Angew. Chem. 100* (1988) 286

[1] a) D. Jerome, A. Mazaud, M. Ribault, K. Bechgaard, *J. Phys. Lett. (Orsay, Fr.) 41* (1980) 41; b) E. B. Yagubshii, I. F. Shchegolev, V. N. Laukhin, P. A. Konovich, M. V. Kartsounik, A. V. Zvarykinau, L. I. Buravov, *Zh. Eksp. Teor. Fiz. Pis'ma Red. 39* (1984) 12; J. M. Williams, T. J. Enge, H. H. Wang, M. A. Beno, P. T. Copps, K. D. Carlson, G. W. Wabtree, *Inorg. Chem. 23* (1984) 2558; E. Amberger, H. Fuchs, K. Polborn, *Angew. Chem. 97* (1985) 968; *Angew. Chem. Int. Ed. Engl. 24* (1985) 968; F. Creuzet, D. Jerome, D. Schweitzer, H.-J. Keller, *Europhys. Lett. 1* (1986) 461.

[2] A. Aumüller, P. Erk, G. Klebe, S. Hünig, J. U. von Schütz, H.-P. Werner, *Angew. Chem. 98* (1986) 759; *Angew. Chem. Int. Ed. Engl. 25* (1986) 740.

[3] A. Aumüller, S. Hünig, *Angew. Chem. 96* (1984) 437; *Angew. Chem. Int. Ed. Engl. 23* (1984) 447; *Liebigs Ann. Chem. 1986*, 142, 165.

[4] Unpublished experiments with *P. Erk* and Dr. *G. Klebe*.

[5] Patent protection for these salts: see, inter alia, S. Hünig, A. Aumüller, P. Erk, German patent application 3522232 (June 21, 1985), BASF AG; S. Hünig, A. Aumüller, P. Erk, German patent application P3718365 (June 2, 1987), BASF AG.

[6] **1**, X = Cl, M = Cu (= **1c**), Ag: J. U. von Schütz, H. P. Werner, H. C. Wolf, A. Aumüller, P. Erk, S. Hünig in B. Maraviglia (Ed.): *Magn. Reson. Relat. Phenom. Proc. Congr. Ampere 23th* (1986) 158.

[7] **1**, X = Me, M = Cu (= **1a**), Ag, Li: J. U. von Schütz, M. Bair, H. P. Werner, H. C. Wolf, A. Aumüller, P. Erk, S. Hünig in P. Delhaes, M. Drillon (Eds.): NATO Advanced Research Workshop Amorca, May 3, 1987; *NATO ASI Series Vol. Organic and Inorganic Low Dimensional Crystalline Materials*, Plenum, New York 1987.

[8] J. U. von Schütz, H.-P. Werner, H. C. Wolf, A. Aumüller, P. Erk, S. Hünig, *Mater. Sci. 13* (1987) 255.

[9] R. Kato, H. Kobayashi, T. Mori, H. Inokuchi, *Chem. Lett. 1987*, 1579; A. Kobayashi, R. Kato, H. Kobayashi, T. Mori, H. Inokuchi, *Solid State Commun. 64* (1987) 45.

[10] P. Erk, S. Hünig, H. Meixner, J.-U. von Schütz, J. P. Werner, *Liebigs Ann. Chem. 1987*, 997.

[11] Method of measurement, cf. [10].

[12] P. Erk, S. Hünig, H. Meixner, J. U. von Schütz, H. P. Werner, H. C. Wolf, *Liebigs Ann. Chem. 1988*, in press.

[13] A. Aumüller, P. Erk, S. Hünig, J. U. von Schütz, H. P. Werner, H. C. Wolf, manuscript in preparation.

[14] We thank Prof. Dr. *E. Tillmanns* for the powder diagrams.

[15] *CRC Handbook of Chemistry and Physics 1984*, 64th ed. Chemical Rubber Co., Cleveland, OH 1983-1984, p. D-191.

[16] K. Bechgaard, K. Carneiro, M. Olsen, F. B. Rasmussen, C. S. Jacobsen, *Phys. Rev. Lett. 46* (1980) 852.

[17] A. Nowack, M. Weger, D. Schweitzer, H. J. Keller, *Solid State Commun. 60* (1986) 199.

A New Route to *trans*-Substituted γ-Lactones**

By *Thomas Kunz* and *Hans-Ulrich Reissig**

Dedicated to Professor Klaus Hafner on the occasion of his 60th birthday

The addition of nucleophiles to chiral carbonyl compounds (Cram/anti-Cram selectivity) is one of the best-studied reactions in organic chemistry. New reagents, which unequivocally attack with or without chelate control, have recently given these investigations new impetus.[1] Carbonyl compounds with functional groups in the α or β position—mostly protected hydroxyl groups—have been investigated intensively. This is not true for γ-functionalized compounds.[2] We report here on the chemo- and diastereoselective additions of organometallic reagents to the formyl group of the readily accessible chiral methyl γ-oxocarboxylates **1**,[3] which, after ring closure, afford γ-lactones with a high excess of the *trans* isomer.[4]

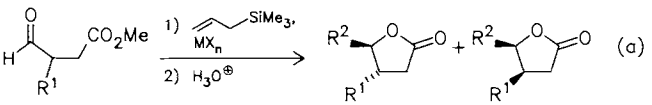

	R^2 = allyl	
1a, R^1 = Me	**2a**	**3a**
1b, R^1 = *i*Pr	**2b**	**3b**
1c, R^1 = Ph	**2c**	**3c**

In the reaction of allyltrimethylsilane with **1a** in the presence of Lewis acids,[5] the largest diastereoselectivity is observed with the bidentate titanium tetrachloride as acid (*trans* : *cis* = 63 : 37). $TiCl_4$ is also the most selective promoter in the case of **1b** and **1c** (*trans* : *cis* > 90 : 10) [Eq. (a), Table 1).

The ratio **2a** : **3a** is independent of whether one or two equivalents of $TiCl_4$ are used.[6] We interpret this as evidence for the formation of the seven-membered ring che-

[*] Prof. Dr. H.-U. Reissig, Dipl.-Chem. T. Kunz
Institut für Organische Chemie der
Technischen Hochschule
Petersenstrasse 22, D-6100 Darmstadt (FRG)

[**] This work was supported by the Fonds der Chemischen Industrie and by the Karl-Winnacker-Stiftung (Hoechst AG).

Table 1. Reaction of the aldehydes **1** with allyltrimethylsilane in the presence of Lewis acids MX_n (complexation at ca. 20°C, addition of the nucleophile at −78°C, warm-up to room temperature, treatment with acid).

1	MX_n	Yield [%]	2 : 3 [a, b]
a	$1BF_3 \cdot OEt_2$	62	52 : 48
a	$2BF_3 \cdot OEt_2$	65	59 : 41
a	$1SnCl_4$	92	58 : 42
a	$1HfCl_4$	80	59 : 41
a	$1ZrCl_4$	78	62 : 38
a	$1TiCl_4$	99	63 : 37
a	$2TiCl_4$	93	65 : 35
b	$1BF_3 \cdot OEt_2$	45	75 : 25
b	$1ZrCl_4$	63	87 : 13
b	$1TiCl_4$	69	92 : 8
c	$1BF_3 \cdot OEt_2$	75	70 : 30
c	$1ZrCl_4$	68	85 : 15
c	$1TiCl_4$	63	93 : 7

[a] Isomer ratio and assignment by high-field ^{1}H-NMR spectroscopy (cf. Refs. [4] and [12]). [b] Product distribution after kugelrohr distillation (purity ca. 90–97%); chromatography afforded samples giving satisfactory elemental analyses.

late **8**, which involves *both* carbonyl groups of **1** and *one* molecule of $TiCl_4$.[7] The formation of this chelate ring is also supported by the spectroscopic data—in particular, the significant downfield shift of the signals of both carbonyl C atoms in the ^{13}C-NMR spectrum of **1a** · $TiCl_4$.[8] The attacking nucleophile approaches **8** preferentially from the sterically less shielded face (*trans* to R^1), leading to formation of the *trans*-substituted lactone **2**. The flexibility of the seven-membered ring results in only moderate diastereoselectivity for R^1 = Me, whereas the larger substituents R^1 = *i*Pr and Ph (**1b**, **1c**) almost completely prevent *cis* attack on **8**.

With $MeTiCl_3 \cdot (OEt_2)_2$ instead of allyltrimethylsilane/$TiCl_4$ as reagent, the corresponding lactones **4** and **5** are obtained in essentially the same *trans/cis* ratio ([Eq. (b),

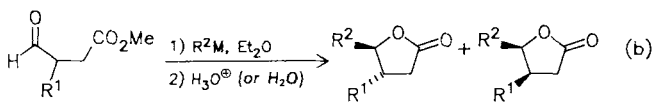

(b)

1a–c R^2 = Me **4** **5**

R^2 = *n*Bu **6** **7**

Table 2)]. This points once again to a chelate-controlled reaction at the formyl group. Better stereoselectivity is achieved with $MeTi(OiPr)_3$ and, in particular, with Me_2CuLi. In the case of these reagents, addition probably occurs without initial complexation.[9] The transfer of a butyl group is also possible, most efficiently by using the corresponding cuprate. Starting from **1a–c**, practically only the *trans*-substituted lactones **6a–c** are obtained!

Table 2. Reactions of the aldehydes **1** with other organometallic reagents R^2M.

1	R^2M	Yield [%]	4 : 5 [a, b] or 6 : 7
a	$MeTiCl_3$	59	68 : 32
a	$MeTi(OiPr)_3$	60 [c]	79 : 21
a	Me_2CuLi	34	95 : 5
b	$MeTiCl_3$	74	92 : 8
c	$MeTiCl_3$	79	93 : 7
c	Me_2CuLi	53	97 : 3
a	*n*BuMgBr	39	60 : 40
a	$nBu_2Cu(CN)Li_2$	47	75 : 25
a	nBu_2CuLi	50	>95 : 5
b	nBu_2CuLi	82	>95 : 5
c	nBu_2CuLi	65	>97 : 3

[a], [b] See Table 1. [c] Purity <90%.

The stereoselectivity of the additions to aldehydes **1** can be interpreted in terms of the Felkin-Anh model[10] with the reactive conformation **9**, provided that $R^1 > CH_2CO_2Me > H$ is valid for the size of the substituents.[11] However, conformation **9** might also be fixed by chelation (cf. **8**) for reagents that exhibit less Lewis acidity.

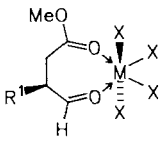

8

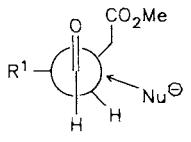

9

Such *trans*-substituted γ-lactones are of importance as intermediates in synthesis and are also found as natural products (e.g., whisky lactone **6a**[12]). Since some of the aldehydes **1** are available in optically active form,[13] the concept described here may also be employed to prepare nonracemic *trans*-substituted γ-lactones.

Received: July 31, 1987;
revised: October 19, 1987 [Z 2383 IE]
German version: *Angew. Chem. 100* (1988) 297

[1] Review: M. T. Reetz, *Angew. Chem. 96* (1984) 542; *Angew. Chem. Int. Ed. Engl. 23* (1984) 556; *Organotitanium Reagents in Organic Synthesis*, Springer, Berlin 1986.

[2] a) G. Maier, M. Schneider, T. Sayrac, *Chem. Ber. 111* (1978) 3412; b) T. Fukuyama, B. Vranesic, D. P. Negri, Y. Kishi, *Tetrahedron Lett. 1978*, 2741; c) M. T. Reetz, R. Steinbach, J. Westermann, R. Urz, B. Wenderoth, R. Peter, *Angew. Chem. 94* (1982) 133; *Angew. Chem. Int. Ed. Engl. 21* (1982) 135; *Angew. Chem. Suppl. 1982*, 257; d) M. T. Reetz, K. Kesseler, S. Schmidtberger, B. Wenderoth, R. Steinbach, *ibid. 95* (1983) 1007 and *22* (1983) 989 and *1983*, 1511; e) G. Maier, C. Roth, R. K. Schmitt, *Chem. Ber. 118* (1985) 704; f) I. Fleming, H. Kühne, K. Takai, *J. Chem. Soc. Perkin Trans. 1 1986*, 725; g) R. Bloch, L. Gilbert, *Tetrahedron Lett. 28* (1987) 423; h) R. Frenette, M. Kakushima, R. Zamboni, R. N. Young, T. R. Verhoeven, *J. Org. Chem. 52* (1987) 304.

[3] Compounds **1a–c** were synthesized similarly to published examples: E. Kunkel, I. Reichelt, H.-U. Reissig, *Liebigs Ann. Chem. 1984*, 512, 802. The sensitive aldehydes should only be prepared immediately prior to use.

[4] Recent syntheses of *trans*-substituted γ-lactones: a) D. Hoppe, A. Brönneke, *Tetrahedron Lett. 24* (1983) 1687; b) H. Frauenrath, T. Philips, *Liebigs Ann. Chem. 1985*, 1951; c) J.-M. Fang, B.-C. Hong, L.-F. Liao, *J. Org. Chem. 52* (1987) 855.

[5] A. Hosomi, H. Sakurai, *Tetrahedron Lett. 1976*, 1295.

[6] The small but significant change in the diastereoselectivity on going from one to two equivalents of $BF_3 \cdot OEt_2$ indicates the involvement of a doubly complexed species: cf. M. T. Reetz, K. Kesseler, *J. Chem. Soc. Chem. Commun. 1984*, 1079.

[7] Five- and six-membered ring chelates have meanwhile unequivocally been identified by spectroscopy: M. T. Reetz, M. Hüllmann, T. Seitz, *Angew. Chem. 99* (1987) 478; *Angew. Chem. Int. Ed. Engl. 26* (1987) 477, and references cited therein; G. E. Keck, S. Castellino, M. R. Wiley, *J. Org. Chem. 51* (1986) 5478; S. V. Frye, E. L. Eliel, R. Cloux, *J. Am. Chem. Soc. 109* (1987) 1862; b) crystal structure analysis of a seven-membered ring chelate: T. Poll, J. O. Metter, G. Helmchen, *Angew. Chem. 97* (1985) 117; *Angew. Chem. Int. Ed. Engl. 24* (1985) 116; a seven-membered ring chelate analogous to **8** is suggested in Ref. [2h] and has been proposed to be involved in a 1,4 addition to an enone [D. Mobilio, B. De Lange, *Tetrahedron Lett. 28* (1987) 1483].

[8] ^{1}H-NMR ($CDCl_3$) for **1a**: δ = 9.70 (s, 1H; 4-H), 3.69 (s, 3H; CO_2Me), ABM part of an $ABMX_3$ system (2.38, 2.74, 2.86, 3H, 3-H, 2-H), 1.20 (d, 3H, 3-Me); ^{1}H-NMR ($CDCl_3$) for **1a** + $BF_3 \cdot OEt_2$: δ = 9.70 (br. s, 1H; 4-H), 3.75 (s, 3H; CO_2Me), 3.1–2.2 (m, 3H; 3-H, 2-H), 1.40 (d, 3H; 3-Me) + signals for OEt_2; ^{1}H-NMR (CD_2Cl_2) for **1a** + $TiCl_4$: δ = 9.82 (s, 1H; 4-H), 4.14 (s, 3H; CO_2Me), 3.7–3.5, 3.4–3.0 (2m, 1H and 2H; 3-H, 2-H), 1.48 (d, 3H; 3-Me). ^{13}C-NMR ($CDCl_3$) for **1a**: δ = 202.6 (d; C-4),

172.1 (s; C-1), 51.5 (q; OMe), 42.5 (d; C-3), 34.6 (t; C-2), 13.3 (q; 3-Me); ^{13}C-NMR (CD_2Cl_2) for **1a** + $TiCl_3$: δ = 215.0 (d; C-4), 180.9 (s; C-1), 58.4 (q; OMe), 43.3 (d; C-3), 35.9 (t; C-2), 14.1 (q; 3-Me). IR ($CDCl_3$) for **1a** + $TiCl_4$: $\tilde{\nu}$(CO) = 1658 cm^{-1}.

[9] For (presumably) chelate-controlled addition of cuprates to chiral aldehydes, see: W. Clark Still, J. A. Schneider, *Tetrahedron Lett. 21* (1980) 1035; see also Y. Yamamoto, K. Maruyama, *J. Am. Chem. Soc. 107* (1985) 6411.

[10] a) M. Cherest, H. Felkin, N. Prudent, *Tetrahedron Lett. 1968*, 2199; N. T. Anh, *Top. Curr. Chem. 88* (1980) 145; b) a recent theoretical study supporting the Felkin-Anh model: Y.-D. Wu, K. N. Houk, *J. Am. Chem. Soc. 109* (1987) 908; c) recent experimental work: E. P. Lodge, C. H. Heathcock, *ibid. 109* (1987) 3353.

[11] Since R^1 = Me is expected to be sterically less demanding than the CH_2CO_2Me group, the latter possibly exerts a dominating electronic effect as well.

[12] For synthesis of **6a** see Ref. [4] as well as C. Günther, A. Mosandl, *Liebigs Ann. Chem. 1986*, 2112, and references cited therein.

[13] a) **1a** is accessible with 93% *ee* if an optically active auxiliary reagent is used in equimolar amounts: A. Bernardi, S. Cardani, G. Poli, C. Scolastico, *J. Org. Chem. 51* (1986) 5041; b) **1a–c** have been synthesized with up to 50% *ee* by means of asymmetric catalysis: T. Kunz, H.-U. Reissig, unpublished.

How High is the Activation Barrier to Helix Inversion of 1,4,5,8-Tetrasubstituted Phenanthrenes?**

By *Albrecht Mannschreck,* Erich Gmahl, Thomas Burgemeister, Fritz Kastner,* and *Volker Sinnwell*

In 1947, the synthesis of (4,5,8-trimethyl-1-phenanthryl)acetic acid **1** and the enrichment of its (+) enantiomer were reported.[2] This kind of enantiomerism was termed isomerism of the 4,5-phenanthrene type[2] and must be considered the starting point of helicene chemistry.[3] This isomerism, described by equilibrium (a), contributed substantially to our knowledge of what is presently called molecular helicity.[4] The above enrichment of an enantiomer has been frequently cited, its significance being shown by its appearance in several textbooks.[5]

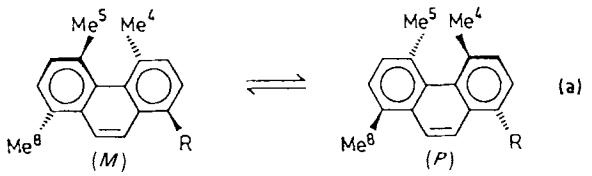

1, R = CH_2CO_2H; **2**, R = CH_2OH; **3**, R = CH(Me)OH; **4**, R = CH(CMe_3)OH

Although no information regarding the rate of racemization of (+)-**1** was given, a few optical rotations between $+0.11 \pm 0.02$ and 0.00°, measured in $CHCl_3$ with respect to time, were mentioned.[2] Since no other data on the enantiomerization of 1,4,5,8-tetrasubstituted phenanthrenes have been available until now, the above optical rotations have been used by several groups[6–10] to estimate the half-life $t_{0.5}$ at room temperature and/or $\Delta G^{\neq}$ for the inversion.

[*] Prof. Dr. A. Mannschreck, Dipl.-Chem. E. Gmahl, Dr. T. Burgemeister, F. Kastner
Institut für Organische Chemie der Universität
Universitätsstrasse 31, D-8400 Regensburg (FRG)
Dr. V. Sinnwell
Institut für Organische Chemie und Biochemie der Universität
Martin-Luther-King-Platz 6, D-2000 Hamburg (FRG)

[**] Helical Phenanthrenes, Part 2. Support of this work by the Fonds der Chemischen Industrie is acknowledged. We thank Drs. *W. Fischer* and *H. Scherübl* for helpful discussions and *N. Pustet* for experimental assistance. — Part 1: [1].

The values obtained differ slightly[6–10] but are in agreement concerning the orders of magnitude ($t_{0.5} \approx 4$ h, $\Delta G^{\neq} \approx 99$ kJ mol^{-1}). These values are similar to the ones obtained for 4,5-dimethyl-9,10-dihydrophenanthrene (2.8 h, 98.4 kJ mol^{-1}, 24.8 °C, benzene).[6, 11] This result was unexpected[6] because under analogous conditions another phenanthrene derivative had shown a considerably *lower* activation barrier than the comparable 9,10-dihydrophenanthrene.[12] The $\Delta G^{\neq}$ values of 4,5-bis(acetoxymethyl)phenanthrene (75.7 kJ mol^{-1}, 24.8 °C)[7] and 4,5-dimethylphenanthrene (67 kJ mol^{-1}, 25 °C)[10] are also considerably *lower* than the value of ca. 99 kJ mol^{-1} obtained for **1**. It has been pointed out by several groups[7, 8, 10] that these differences remain to be explained. Toward the solution of these discrepancies, we report here the determination of the activation barrier to helix inversion (*M*) ⇌ (*P*) of phenanthrenes **1–4**.

Our preparation of **1** is directed toward cyclodehydrogenation as the last step (Scheme 1). This reaction was unknown at the time of the reported 20-step synthesis.[2] The primary alcohol **2** and the secondary alcohols **3** and **4** were also prepared (Scheme 1) because their $\Delta G^{\neq}$ values should be similar to that of **1**. Contrary to (*MP*)-**1** and (*MP*)-**2**, four stereoisomers of **3** and of **4** are possible ((*MP*)(*RS*)-**3** and (*MP*)(*RS*)-**4**).

The mass spectra of **1–4** were in agreement with the constitutions. The ^{1}H-NMR assignments of all aliphatic (Table 1) and aromatic protons of **1**, **2**, and **4** were obtained by nuclear Overhauser difference spectra. The HPLC peaks for the enantiomers of **1** and **2**, obtained on an optically active sorbent at −40 °C, coalesced to a single averaged peak during HPLC at +15 °C (Table 1), owing to enantiomerization.[13, 14] The melting point given in the literature (142.8–143.6 °C, corr.)[2] is close to that of our acid **1** (137.5–138.5 °C, corr.). Its UV absorption in $CHCl_3$ resembles the spectrum depicted earlier[2] (solvent not specified). The $\Delta G^{\neq}$ values for helix inversion (Table 2) were obtained by dynamic ^{1}H-NMR spectroscopy and/or thermal racemization. For the latter measurements the flow during HPLC on an optically active sorbent was stopped

Table 1. ^{1}H-NMR and HPLC data for the phenanthrenes **1–4**.

	δ(^{1}H) [a]				k [c]	$\bar{k}$ [c]
	Aryl-CH_3 [b]	Aryl-CH_2	Aryl-CH	⩾CCH_3		
	2.52 (5)				0.7 (−)	
1	2.55 (4)	4.08 (s) [d]	—	—	1.1 (+)	0.7
	2.68 (8)					
	2.53 (5)	5.07 [e]			0.6 (−)	
2	2.56 (4)	5.16 [e]	—	—	1.2 (+)	0.5
	2.70 (8)					
	2.52 (5)		5.65 [f]	1.65 [f]		
3	2.55 (4)	—	5.67 [f]	1.71 [f]	—	—
	2.70 (8)					
	2.53 (5)		5.32 [h]	0.93 [i]		
4	[g] (4)	—	5.41 [i]	1.06 [h]	—	—
	2.69 (8)					

[a] 250 MHz; 24 °C; $Cl_2CDCDCl_2$. [b] Position of CH_3 group (4, 5, or 8) is given in parentheses. [c] HPLC capacity factors $k = (v - v_0)/v_0$ at −40 °C for each enantiomer (retention volumes v) and averaged capacity factor $\bar{k} = (\bar{v} - v_0)/v_0$ at 15 °C for both enantiomers (retention volume $\bar{v}$) after coalescence [13, 14] of their peaks. v_0 = retention volume of water that is not retained [15]. Sorbent: (+)-poly(tritylmethacrylate) [15] coated on silica. Eluent: CH_3OH. Dual detection by photometry (350 nm) and polarimetry (365 nm). At 15 °C no polarimetric detections were obtained. [d] In C_5D_5N (400 MHz; 22 °C): δ(^{1}H) = 4.38 and 4.41, ^2J(AB) = 15.4 Hz. [e] ^2J(AB) = 12.3 Hz. [f] ^3J = 6.5 Hz. Diastereomeric ratio for **3** = 1 : 1. [g] δ = 2.54 and 2.56 for the diastereomers of **4** (ratio 2.2 : 1). [h] Minor diastereomer of **4**. [i] Main diastereomer of **4**.

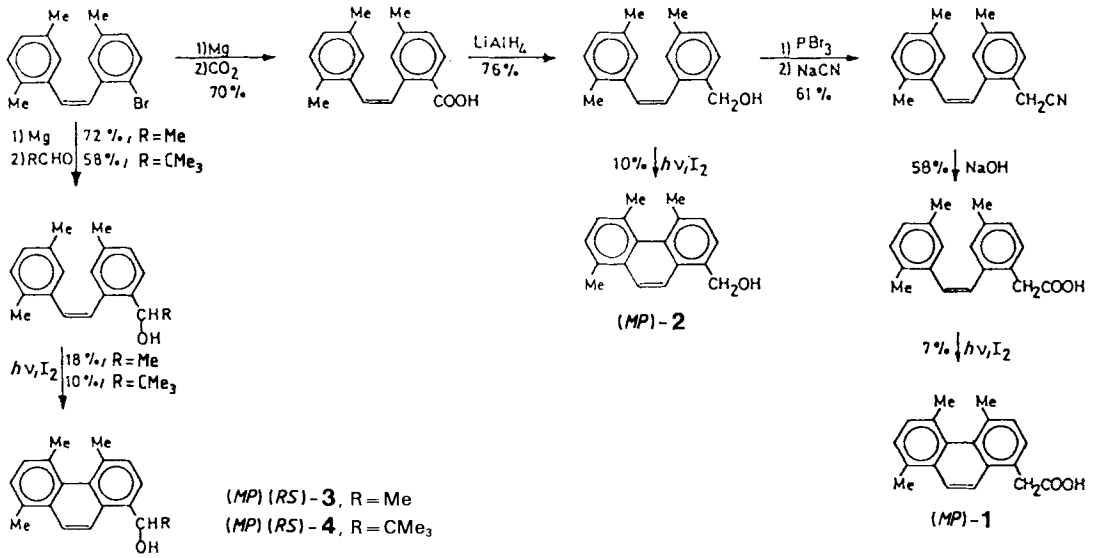

Scheme 1. Synthesis of the 1,4,5,8-tetrasubstituted phenanthrenes **1**–**4**. In most cases, the substituted stilbenes were (*E*)/(*Z*) mixtures.

when the cell of the polarimetric detector contained one enriched enantiomer. Subsequently, the cell was thermostated to a temperature suitable for on-line racemization.[14, 17, 18]

Since the known entropies of activation are not far from zero,[7, 10] it is permissible in most cases to compare $\Delta G^{\neq}$ values determined at different temperatures. The $\Delta G^{\neq}$ value of our acid **1** (78 kJ mol^{-1}, Table 2) corresponds to a half-life of enantiomerization of only 3 s at 24.8 °C and is incompatible with the above estimated values of ca. 99 kJ mol^{-1} and ca. 4 h. At the same time, our result clarifies all reported discrepancies.[6–8, 10] We have not yet been able to attempt a crystallization of the diastereomeric salts[2] of our acid **1**, since the amount available was low owing to the low yields of the cyclodehydrogenation (Scheme 1).

Our $\Delta G^{\neq}$ value for **1** is confirmed by the results for its analogues **2**–**4**. A comparison of **1** and 4,5-dimethylphenanthrene **5** or **2** and **5** shows a decrease of $\Delta G^{\neq}$ by about 10 kJ mol^{-1} (Table 2) when the 1- and 8-substituents are removed. A similar decrease of $\Delta G^{\neq}$ is found when going from 1,3,4,5,6,8-hexamethylphenanthrene **6** to 3,4,5,6-tetramethylphenanthrene **7**. These observations indicate that the interaction of the 1- and 8-substituents with the 10- and 9-hydrogens contributes significantly to the helicity of 1,4,5,8-tetrasubstituted phenanthrenes.

Table 2. $\Delta G^{\neq}$ for the helix inversion described by (a).

	$\Delta G^{\neq}$ [kJ mol^{-1}]	T [°C]	Solvent	Method
1	78.3 ± 0.7	−11	CH_3OH	[a]
	77.9 ± 0.4	78	C_5D_5N	[b]
2	78.0 ± 0.6	−10	CH_3OH	[a]
	79.4 ± 0.4	96	$Cl_2CDCDCl_2$	[c]
3	80 ± 1	90	$Cl_2CDCDCl_2$	[d]
4	84 ± 1 (I) 81 ± 1 (II)	108	$Cl_2CDCDCl_2$	[d]
5	67 ± 6 [10]	25	n-C_6H_{14}	[e]
6	105.1 ± 0.4 [16]	49	$CHCl_3$	[f]
7	95.8 ± 0.2 [1]	30	$CHCl_3$	[f]

[a] On-line racemization, monitored by polarimetry, after enrichment of one enantiomer in solution by HPLC on silica coated with (+)-poly(tritylmethacrylate) [15]; cf. text and [14, 17, 18]. [b] Coalescence (400 MHz) of the ^{1}H-NMR CH_2 absorption. $^2J(AB) = 15.4$ Hz, $\delta_A - \delta_B = 0.016$ ppm extrapolated to 78 °C; cf. Table 1. [c] Coalescence (250 MHz) of the ^{1}H-NMR CH_2 absorption upon decoupling from the OH proton at $\delta = 1.83$ (broadened). $^2J(AB) = 12.3$ Hz, $\delta_A - \delta_B = 0.065$ ppm extrapolated to 96 °C; cf. Table 1. [d] Coalescence (250 MHz) of two ^{1}H-NMR singlets, originating from the methyl groups bonded to sp^3 C atoms of the diastereomers I and II; cf. Ref. [19]. The spectrum of **4** exhibits two singlets for these methyl groups; the spectrum of **3** consists of two singlets when decoupled from the methine absorption. $|\delta_I - \delta_{II}| = 0.045$ (**3**) and 0.121 ppm (**4**), extrapolated to the coalescence temperatures. The equilibrium constants [I] : [II] = 1 : 1 (**3**) and 2.2 : 1 (**4**) did not depend appreciably upon temperatures; cf. Table 1. [e] Off-line racemization, monitored by circular dichroism, after HPLC enrichment of one enantiomer in solution; cf. Ref. [10]. [f] Off-line racemization, monitored by polarimetry, after preparative enrichment of one enantiomer; cf. Ref. [1].

Received: August 10, 1987 [Z 2394 IE]
German version: *Angew. Chem. 100* (1987) 299

[1] H. Scherübl, U. Fritzsche, A. Mannschreck, *Chem. Ber. 117* (1984) 336.
[2] M. S. Newman, A. S. Hussey, *J. Am. Chem. Soc. 69* (1947) 978, 3023.
[3] M. S. Newman, D. Lednicer, *J. Am. Chem. Soc. 78* (1956) 4765; W. H. Laarhoven, W. J. C. Prinsen, *Top. Curr. Chem. 125* (1984) 63.
[4] Cf. G. Krow, *Top. Stereochem. 5* (1970) 31.
[5] See, e.g., E. L. Eliel: *Stereochemistry of Carbon Compounds*, McGraw-Hill, New York 1962, p. 176; H. A. Staab, *Einführung in die theoretische organische Chemie*, 4th ed., Verlag Chemie, Weinheim 1966, p. 555; W. J. le Noble, *Highlights of Organic Chemistry*, Dekker, New York 1974, p. 154; H. Kagan, *La stéréochimie organique*, Presses Universitaires, Paris 1975, p. 142; S. Hauptmann, *Organische Chemie*, H. Deutsch, Frankfurt/M. 1985, p. 100.
[6] K. Mislow, H. B. Hopps, *J. Am. Chem. Soc. 84* (1962) 3018.
[7] R. Munday, I. O. Sutherland, *J. Chem. Soc. B 1968*, 80.
[8] R. E. Carter, P. Berntsson, *Acta Chem. Scand. 22* (1968) 1047.
[9] W. H. Laarhoven, W. H. M. Peters, A. H. A. Tinnemans, *Tetrahedron 34* (1978) 769.
[10] R. N. Armstrong, H. L. Ammon, J. N. Darnow, *J. Am. Chem. Soc. 109* (1987) 2077.
[11] Cf. O. Yamamoto, H. Nakanishi, *Tetrahedron 29* (1973) 781.
[12] D. M. Hall, E. E. Turner, *J. Chem. Soc. 1955*, 1242.
[13] A. Eiglsperger, F. Kastner, A. Mannschreck, *J. Mol. Struct. 126* (1985) 421.
[14] A. Mannschreck, D. Andert, A. Eiglsperger, E. Gmahl, H. Buchner, *Chromatographia 23* (1988), in press.
[15] Y. Okamoto, K. Hatada, *J. Liq. Chromatogr. 9* (1986) 369.
[16] A. Mannschreck, E. Hartmann, H. Buchner, D. Andert, *Tetrahedron Lett. 28* (1987) 3479.
[17] M. Mintas, Z. Orhanović, K. Jakopčić, H. Koller, G. Stühler, A. Mannschreck, *Tetrahedron 41* (1985) 229.
[18] Cf. C. Roussel, A. Djafri, *Nouveau J. Chim. 10* (1986) 399.
[19] A. Jaeschke, H. Münsch, H. G. Schmid, H. Friebolin, A. Mannschreck, *J. Mol. Spectrosc. 31* (1969) 14.

Reactivity of Tri-*tert*-butylazete**

By *Uwe Josef Vogelbacher, Martin Ledermann, Thomas Schach, Gisbert Michels, Udo Hees,* and *Manfred Regitz**

So far, only spectroscopic properties have been reported for the recently synthesized tri-*tert*-butylazete **1**, the first kinetically stabilized azacyclobutadiene.[1] We have investigated several aspects of its reactivity and report here the oxidation and hydrolytic behavior as well as the addition potential of this electronically genuine antiarene.[2]

Triplet oxygen adds exclusively to the CC double bond of **1** in *n*-butane at −78 °C to give the dioxetane **2** (95%). Both in the crystalline state and in the same solvent (25 °C, half-time ≈ 4 h), the bicyclic ring opens as expected to give the dicarbonyl compound **3** (40%).

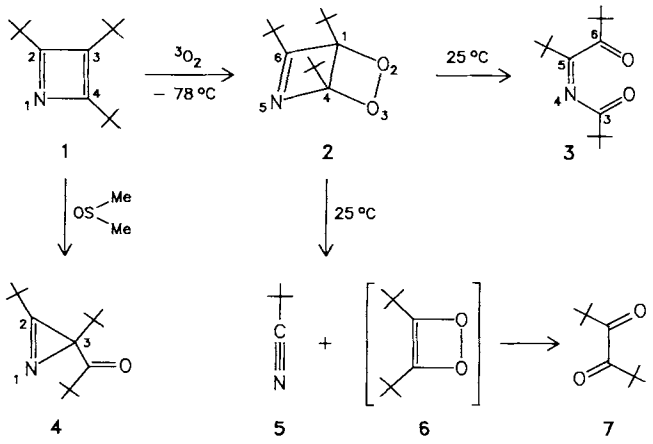

However, the cycloreversion of **2** to give the nitrile **5** and the dioxete **6** dominates over this ring opening; **6** undergoes immediate isomerization to give the α-diketone **7**. Both final products were distilled under high vacuum and identified by comparison of their ^{1}H-NMR spectra with those of authentic compounds. Surprisingly, smooth oxidation of **1** by dimethyl sulfoxide occurred at 25 °C with ring contraction to give the azirine **4**.[3] We became aware of this reaction when a sample of the azete underwent change during NMR measurements in the same solvent.[4]

Upon hydrolysis of **1** with water-saturated tetrahydrofuran (25 °C, catalytic amount of hydrochloric acid), the azomethine bond is smoothly cleaved; the β-iminoketone **8** (68%) is formed. Reaction with concentrated hydrogen bromide in the same solvent results in transformation of **8** to the iminium bromide **9** (36%), which, in turn, undergoes dehydrobromination with sodium carbonate to give **8**.

Protic nucleophiles such as methanol, dimethyl malonate, and acetic acid exclusively undergo 1,4-addition at N-1 and C-4 of **1** (25 °C, *n*-pentane or chloroform) to give the 1,2-dihydroazetes **10a–c** (81–100%);[5] the reaction is presumably initiated by *N*-protonation. In chloroform, **10c** undergoes acetic acid–catalyzed rearrangement to give the

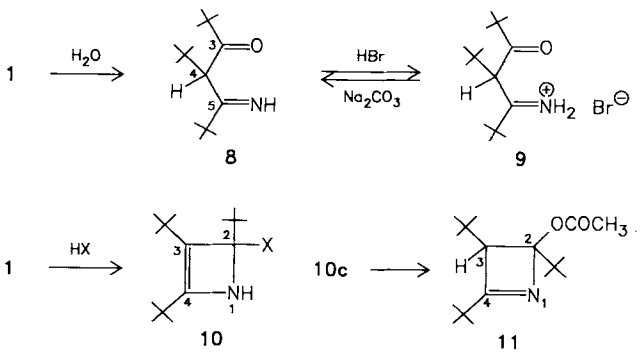

10a: X = OMe; b: X = $CH(CO_2Me)_2$; c: X = O_2CCH_3

evidently thermodynamically more stable 2,3-dihydroazete **11**. It may be assumed that the *t*Bu groups in the 2- and 3-position are in the *trans* arrangement.

Both the 1,3-diene and the olefin character of **1** are reflected in its reactions with cyclopentadiene (25 °C, *n*-pentane). The reaction occurs exclusively at two *t*Bu-substituted carbon atoms and affords a 4:1 mixture of **12** and **13**, which may be separated by medium-pressure chromatography on silica gel (petroleum ether/ether, 4:1).

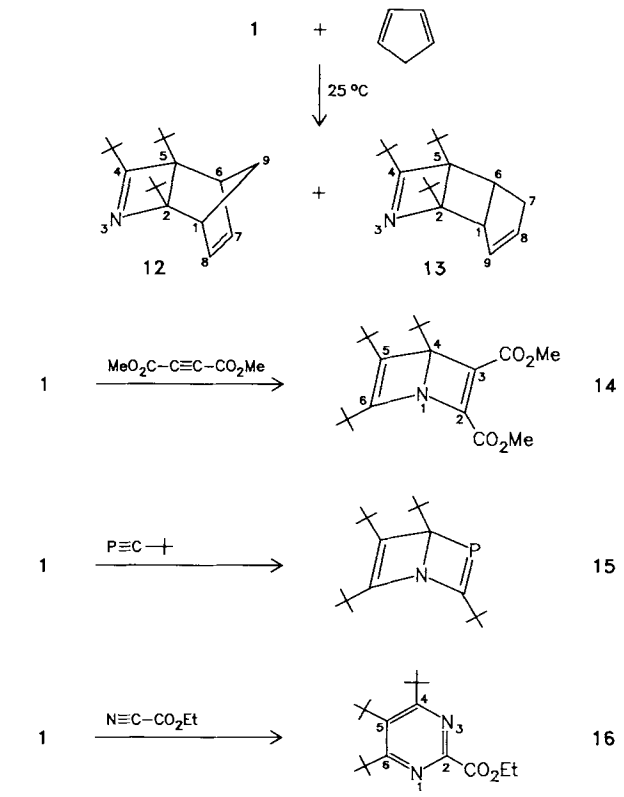

The two tricyclic compounds exhibit fundamental differences in their ^{1}H-NMR spectra in that the framework-bonded protons of **12** form an AA'MM'XX' spin system whereas those of **13** form an ABMNXY spin system (Table 1).[6]

In contrast to the reaction of **1** with cyclopentadiene, the Diels–Alder reaction with dimethyl acetylenedicarboxylate (pentane, 25 °C) takes place exclusively at a nitrogen and a neighboring carbon atom; it affords the 1-Dewarpyridine **14** (93%).[7] (2,2-Dimethylpropylidyne)phosphane,[8] a compound containing a PC triple bond, reacts

[*] Prof. Dr. M. Regitz, Dr. U. J. Vogelbacher, Dipl.-Chem. M. Ledermann, Dipl.-Chem. T. Schach, Dr. G. Michels, Dipl.-Chem. U. Hees
Fachbereich Chemie der Universität
Erwin-Schrödinger-Strasse, D-6750 Kaiserslautern (FRG)

[**] Syntheses with Cyclobutadienes, Part 21. This work was supported by the Deutsche Forschungsgemeinschaft and the Fonds der Chemischen Industrie. — Part 20: G. Michels, R. Mynott, M. Regitz, *Chem. Ber. 120* (1987), in press.

analogously with **1** to give the 1-Dewar-1,3-azaphosphinine **15** (92%). The orientation of the phosphaalkyne is established unequivocally by ^{13}C-NMR comparison of **15** with the known 2-Dewar-phosphinines.[9] Compounds containing electron-deficient CN triple bonds such as ethyl cyanoformate ("ethoxycarbonylnitrile") also add readily to **1** (dichloromethane, 25°C): Instead of a bicyclic product like **14** or **15**, the reaction affords the pyrimidine **16** (83%), formed by subsequent electrocyclic ring opening.

Depending on the size of the substituents, either the CC or the CN double bond of **1** is attacked in 1,3-dipolar cycloadditions with diazo compounds: diazomethane (ether) affords regiospecifically the dihydropyrazole **17** (81%),[10] and 1-diazo-1-phenylethane the *endo/exo* isomeric dihydrotriazoles **18** (57%, ratio 2:3);[11] in the *endo* phenyl derivative, the signal for the 7-*t*Bu group ($\delta = 0.53$) is shifted markedly to high field owing to an anisotropy effect.

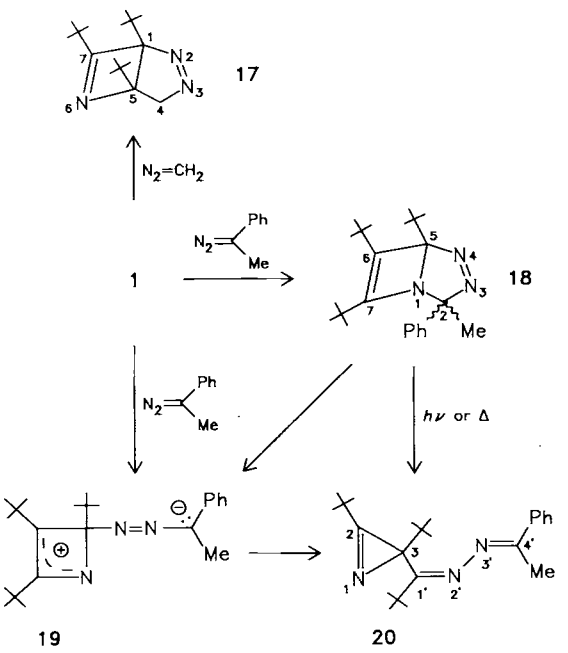

In addition to the cycloadducts **18**, the azirine **20** (43%) is formed; it is also formed upon irradiation (Philips HPK 125 W) of *endo*- and *exo*-**18** in chloroform or upon warming to 80°C (neat). A crystal structure analysis has been carried out for **20**[12] which indirectly established the constitution of **18** as well. Intermediate **19** is assumed to be involved both in the azirine formation occurring in the cycloaddition and in the isomerization.

Correct elemental analyses were obtained for all the reaction products. Of particular importance for establishing the reaction centers of **1** is the presence or absence of the C=C or C=N increment, respectively, above all in the ^{13}C-NMR spectra (Table 1).

Tri-*tert*-butylcyclobutadienecarboxylic esters (**1**, C-CO_2R instead of N) are of primary interest in comparing the reactivity of **1** with other antiarenes. These esters undergo 1,4 addition and cycloaddition mainly at neighboring carbon atoms bearing ester and *t*Bu substituents.[13] The azete **1** shows corresponding behavior only toward protic nucleophiles (→ **10**). Cycloadditions take place at C-2/C-3 (→ **2**, **12**, **13**, **17**) until steric hindrance is so large that a reaction is forced to take place at N-1/C-2 (or C-4) (→ **14**, **15**, **16**, **18**).

Table 1. Some physical data for the compounds **2**–**4**, **8**, **10a**–**c**, **11**, **12**–**18**, and **20** [a].

2: colorless crystals [b]; IR (CCl_4): $\tilde{\nu} = 1570$ cm^{-1} (C=N); ^{13}C-NMR (CD_2Cl_2, −55°C): $\delta = 109.7$, 113.2 (C-1/C-4), 200.8 (C-6)

3: colorless crystals, m.p. = 52°C; IR: $\tilde{\nu} = 1675$ cm^{-1} (br., C=O/C=N); ^{13}C-NMR: $\delta = 174.9$ (C-5), 190.7 (C-3), 214.5 (C-6)

4: colorless liquid, b.p. = 60°C/0.1 mbar; IR (film): $\tilde{\nu} = 1750$ (C=N), 1690 cm^{-1} (C=O); ^{13}C-NMR: $\delta = 33.7$ (C-3), 44.1 [$(H_3C)_3CCO$], 178.3 (C-2), 214.1 (CO)

8: colorless crystals, m.p. = 67°C; IR: $\tilde{\nu} = 3270$ (NH), 1690 (C=O), 1610 cm^{-1} (C=N); ^{13}C-NMR: $\delta = 55.4$ (d, $^1J_{H,C} = 131$ Hz, C-4), 185.3 (C-5), 215.0 (C-3)

10a: colorless oil, b.p. = 60°C/5 × 10^{-2} mbar; IR (film): $\tilde{\nu} = 1620$ cm^{-1} (C=C); ^{1}H-NMR: $\delta = 1.07$, 1.19, 1.22 (3s, 9H, *t*Bu), 2.7 (s, 1H, NH), 3.28 (s, 3H, OMe); ^{13}C-NMR: $\delta = 98.9$ (C-2), 125.6 (C-3), 156.0 (C-4)

10b: colorless crystals, m.p. = 61°C; IR: $\tilde{\nu} = 3310$ (NH), 1760, 1730 cm^{-1} (C=O); ^{13}C-NMR: $\delta = 51.8$, 52.2 (q, $^1J_{C,H} = 150$ Hz, OCH_3), 55.0 (d, $^1J_{C,H} = 134$ Hz, CH-malonate), 75.2 (C-2), 130.9 (C-3), 159.8 (C-4), 167.6, 168.8 (CO)

10c: viscous oil (not distilled); IR: $\tilde{\nu} = 1750$ cm^{-1} (CO); ^{13}C-NMR: $\delta = 22.8$ (q, $^1J_{C,H} = 127$ Hz, $COCH_3$), 97.7 (C-2), 128.2 (C-3), 154.4 (C-4), 169.5 (CO)

11: colorless crystals, m.p. = 48°C; IR: $\tilde{\nu} = 1760$ (C=O), 1590 cm^{-1} (C=N); ^{13}C-NMR: $\delta = 22.4$ (q, $^1J_{C,H} = 127$ Hz, $COCH_3$), 62.2 (d, $^1J_{C,H} = 131$ Hz, C-3), 101.3 (C-2), 200.4 (C-4)

12: colorless oil, b.p. = 100°C/0.01 mbar; IR (film): $\tilde{\nu} = 1590$ cm^{-1} (C=N); ^{1}H-NMR: $\delta = 1.14$, 1.20, 1.25 (3s, 9H, *t*Bu), 1.6–1.7 (m, 1H, H-9$_{endo}$), 1.9–2.0 (m, 1H, H-9$_{exo}$), 2.7–2.8 (m, 2H, H-1/H-6), 6.1–6.2 (m, 2H, H-7/H-8); ^{13}C-NMR: $\delta = 47.3$, 49.0 (C-1/C-6), 57.0 (C-9), 82.0 (C-5), 86.6 (C-2), 138.6, 139.1 (C-7/C-8), 197.6 (C-4)

13: colorless oil, b.p. = 80°C/0.01 mbar; IR (film): $\tilde{\nu} = 1585$ cm^{-1} (C=N); ^{1}H-NMR: $\delta = 1.02$, 1.08, 1.16 (3s, 9H, *t*Bu), 2.1–2.4 (m, 2H, H-7), 2.9–3.1, 3.2–3.4 (m, 1H, H-1/H-6), 5.4–5.8 (m, 2H, H-8/H-9); ^{13}C-NMR: $\delta = 32.9$, 35.9 (C-1/C-6), 47.80 (C-7), 74.5, 80.4 (C-2/C-5), 131.1, 136.4 (C-8/C-9), 197.2 (C-4)

14: colorless crystals, m.p. = 83°C; IR: $\tilde{\nu} = 1710$ cm^{-1} (CO); ^{13}C-NMR: $\delta = 85.5$ (C-4), 132.5, 138.9 (C-2/C-3), 160.7, 163.1 (C-5/C-6)

15: colorless crystals, m.p. = 76°C; ^{13}C-NMR: $\delta = 82.6$ (d, $^1J_{P,C} = 19.5$ Hz, C-4), 139.5 (C-5), 161.10 (d, $^3J_{P,C} = 19.6$ Hz, C-6), 242.8 (d, $^1J_{P,C} = 38.3$ Hz, C-2); ^{31}P-NMR ($CDCl_3$): $\delta = 202.2$

16: colorless crystals, m.p. = 52°C; ^{13}C-NMR: $\delta = 139.6$ (C-5), 146.1 (C-2), 174.8 (C-4/C-6)

17: colorless oil, b.p. = 75°C/0.01 mbar; IR (film): $\tilde{\nu} = 1597$, 1559 cm^{-1} (C=N/N=N); ^{1}H-NMR: $\delta = 1.10$ (s, 9H, *t*Bu), 1.25 (s, 18H, *t*Bu), 4.38, 4.49 (AB system, $^2J_{H,H} = 19.4$ Hz, CH_2); ^{13}C-NMR: $\delta = 77.5$ (C-4), 79.1 (C-5), 115.0 (C-1), 199.7 (C-7)

18 (*exo*-phenyl derivative): pale yellow crystals, m.p. = 139°C; ^{1}H-NMR: $\delta = 0.98$, 1.20, 1.23 (3s, 9H, *t*Bu); ^{13}C-NMR: $\delta = 101.7$ (C-2), 128.7 (C-5), 152.2 (C-6), 160.8 (C-7)

18 (*endo*-phenyl derivative): pale yellow crystals, m.p. = 129°C; ^{1}H-NMR: $\delta = 0.53$, 1.25, 1.33 (3s, 9H, *t*Bu); ^{13}C-NMR: $\delta = 100.7$ (C-2), 151.7 (C-6), 161.3 (C-7), C-5 lies in the aromatic carbon region

20: pale yellow crystals, m.p. = 140°C; IR: $\tilde{\nu} = 1600$ (C=N azine), 1730 cm^{-1} (C=N azirine); ^{13}C-NMR: $\delta = 49.7$ (C-3), 161.6/173.6 (C-1′/C-4′), 180.0 (C-2)

[a] IR spectra in KBr, ^{1}H- and ^{13}C-NMR spectra in $CDCl_3$ [TMS (int.)], unless noted otherwise. The b.p. data are based on kugelrohr distillation. [b] M.p. not determined owing to danger of explosion.

Received: August 31, 1987 [Z 2419 IE]
German version: *Angew. Chem. 100* (1988) 304

[1] U. J. Vogelbacher, M. Regitz, R. Mynott, *Angew. Chem. 98* (1986) 835; *Angew. Chem. Int. Ed. Engl. 25* (1986) 842.
[2] For the reactivity of thermodynamically stabilized 2-phenylbenzazetes see B. M. Adger, C. W. Rees, R. C. Storr, *J. Chem. Soc. Perkin Trans. 1 1975*, 45.
[3] The three-membered ring exhibits ^{13}C resonances similar to those of **20**, whose structure was established by X-ray analysis. In addition, the pivaloyl group is revealed by the typical downfield signal, which is also observed for **8** (Table 1).
[4] From the research of S. Haber, Universität Kaiserslautern 1987.
[5] Acetyl chloride reacts similarly with **1** (25°C, pentane) to give **10** (H_3CCO instead of H, X = Cl); 65%, colorless crystals, m.p. = 65°C.

[6] The *endo* arrangement of **12** cannot be derived definitively from the NMR data, but it is presumably favored owing to secondary orbital interactions in the transition state.
[7] Little is known on compounds having this type of structure. Summary: Y. Kobayashi, I. Kumadaki, *Top. Curr. Chem. 123* (1984) 103.
[8] G. Becker, G. Gresser, W. Uhl, *Z. Naturforsch. B36* (1981) 16. Optimized procedure: W. Rösch, M. Hees, M. Regitz, *Chem. Ber. 120* (1987) 1645.
[9] J. Fink, W. Rösch, U. J. Vogelbacher, M. Regitz, *Angew. Chem. 98* (1986) 265; *Angew. Chem. Int. Ed. Engl. 25* (1986) 280.
[10] The establishment of the dipolar orientation was achieved by comparison of the ^{13}C-NMR data with those of the corresponding adduct of diazomethane to *tert*-butyl tri-*tert*-butylcyclobutadienecarboxylate: U. J. Vogelbacher, P. Eisenbarth, M. Regitz, *Angew. Chem. 96* (1984) 691; *Angew. Chem. Int. Ed. Engl. 23* (1984) 708. Diazoethane and Diazo(phenyl)methane react similarly.
[11] Comparable cycloadditions with 1-diazo-2,2-dimethylpropane and diazo(diphenyl)methane.
[12] Selected bond lengths [Å] and angles [°]: N1-C3 1.554(5), N1-C2 1.249(5), C2-C3 1.470(5), C1′-N2′ 1.272(4), N2′-N3′ 1.402(4), N3′-C4 1.281(4); C3-N1-C2 62.2(3), N1-C3-C2 48.7(2), N1-C2-C3 69.2(3), C3-C1′-N2′ 122.4(3), C1′-N2′-N3′ 115.7(3), N2′-N3′-C4′ 114.5(3), C1′-N2′-N3′-C4′ 139.8.
[13] See the preceding articles in this series as well as S. Masamune, N. Nakamura, M. Suda, H. Ona, *J. Am. Chem. Soc. 95* (1973) 8481.

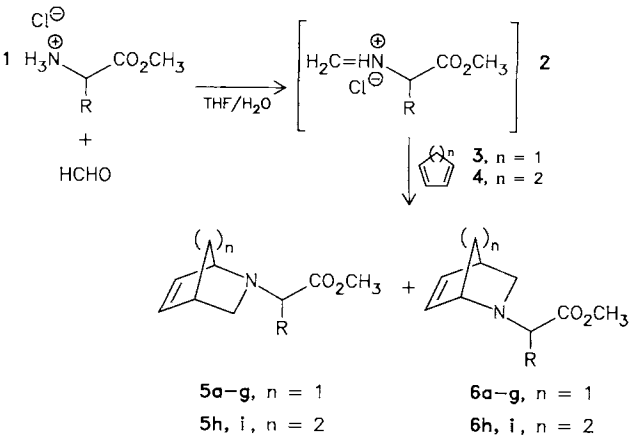

Scheme 1. For the hydrochlorides used see Table 1.

Amino Acid Methyl Esters as Chiral Auxiliaries in Aza-Diels–Alder Reactions in Aqueous Solution**

By *Herbert Waldman**

Diels–Alder reactions make it possible to synthesize carbo- and heterocycles in a regio- and diastereoselective fashion and are therefore employed in the synthesis of natural products, for example in the de novo synthesis of carbohydrates and alkaloids.[1] To achieve higher diastereoselectivities, asymmetric Diels–Alder reactions are often carried out at low temperature (−78 °C) under Lewis acid catalysis. Of particular interest for syntheses, however, are processes that take place at higher temperatures with satisfactory stereoselectivities and allow large quantities of the products to be prepared. Uncatalyzed homo- and hetero-Diels–Alder reactions involving nonactivated dienophiles can be accelerated by carrying them out in aqueous medium.[2] *Grieco* et al. have studied aza-Diels–Alder reactions in aqueous medium with iminium ions prepared in situ from ammonium salts and aldehydes. They have shown that these reactions are diastereoselective when (*S*)-1-phenylethylamine hydrochloride is used as the ammonium salt.[3] We report here on the use of (*R*)- and (*S*)-amino acid methyl ester hydrochlorides **1**, which are readily accessible in large amounts, as chiral auxiliaries in analogous aza-Diels–Alder reactions.[4]

Amino acid methyl ester hydrochlorides **1** react with cyclopentadiene **3** and cyclohexadiene **4** in the presence of formaldehyde in THF/water at 0 °C to form the diastereomeric bicyclic aza compounds **5** and **6** (Scheme 1) in very good yields. The iminium ion **2** is assumed to be the reactive intermediate. Depending on the steric demands of the amino acid side chain, good stereoselectivities are achieved even at this reaction temperature, which is high for diastereoselective reactions (Table 1, **5a/6a–5i/6i**). The ratios of the diastereomers were determined from the 400-MHz ^{1}H-NMR spectra of the crude products.

Table 1. Yields and diastereomeric ratios in the aza-Diels–Alder reactions using (*R*)- or (*S*)-amino acid methyl ester hydrochlorides as chiral auxiliaries.

Amino acid in **1**	Diene	Compd	*T* [°C]	Diastereomeric ratio **5**:**6** or **8**:**9**	Yield [%]
(*S*)-Ile	**3**	**5a/6a**	0	93 : 7	57
(*S*)-Val	**3**	**5b/6b**	0	86 : 14	74
(*S*)-Ser	**3**	**5c/6c**	0	87 : 13	63
(*S*)-Phg	**3**	**5d/6d**	0	78 : 22	97
(*R*)-Val	**3**	**5e/6e**	0	17 : 83	69
(*R*)-Ser	**3**	**5f/6f**	0	12 : 88	66
(*R*)-Phg	**3**	**5g/6g**	0	20 : 80	90
(*S*)-Ile	**4**	**5h/6h**	25	80 : 20	35
(*R*)-Ser	**4**	**5i/6i**	25	27 : 73	40
(*R*)-Phg	**7a**	**8a/9a**	0	37 : 63	22
(*S*)-Ile	**7b**	**8b/9b**	0	71 : 29	45
(*S*)-Phg	**7b**	**8c/9c**	0	66 : 34	63
(*R*)-Ser	**7c**	**8d**=**9d**	25	—	50

The reaction of isoleucine (*S*)-Ile with **3** afforded the best stereoisomeric ratio (**5a** : **6a** = 93 : 7), which is significantly better than that obtained for (*S*)-1-phenylethylamine (80 : 20).[3] In the case of the less reactive cyclohexadiene **4**, the diastereomers (**5h/6h**) are even formed at 25 °C in a ratio of 80 : 20. The main isomers formed in these reactions, which can readily be carried out on a 30-g scale, can be obtained easily in pure form, e.g., by flash chromatography. If the (*S*)-amino acid methyl esters are used as auxiliary groups, the (1*R*,4*S*)-2-azabicycloheptenes or -octenes **5** are preferentially formed. Amino acid esters of (*R*)-configuration give preferentially the (1*S*,4*R*) isomers **6**. The configurations of these cycloadducts were established by means of NOE difference spectra.[5]

The hetero-Diels–Alder reactions can also be carried out with open-chain 1,3-dienes **7** (Scheme 2, Table 1, **8a/9a–8d**). Although the diastereoselectivities in these cases are only moderate, the substituted didehydropiperidines **8** and **9** are easy to separate by chromatography. As has already been observed for the simpler amines, the reactions with isoprene **7c** and *trans*-2-methyl-1,3-pentadiene **7b** afford only one regioisomer in each case and the reaction with *trans,trans*-2,4-hexadiene **7a** results in the formation of only one pair of diastereomers.[3]

[*] Dr. H. Waldmann
Institut für Organische Chemie der Universität
Johann-Joachim-Becher-Weg 18–20, D-6500 Mainz (FRG)

[**] This work was supported by Degussa AG and by the Fonds der Chemischen Industrie (Liebig-Stipendium). I wish to thank Prof. Dr. *Kunz*, Mainz, for his generous support.

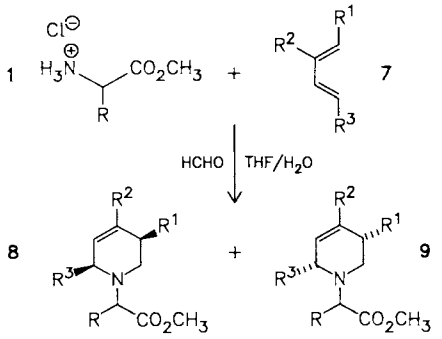

Scheme 2. **7a**, $R^1=R^3=CH_3$, $R^2=H$; **7b**, $R^1=H$, $R^2=R^3=CH_3$; **7c**, $R^1=R^3=H$, $R^2=CH_3$.

The underlying nitrogen heterocycles can be obtained in a number of ways from the cycloadducts. The benzylamine moiety in the phenylglycine derivatives (**5d/6d**, **5g/6g**, **8a/9a**, **8c/9c**) can be removed quantitatively by hydrogenolysis following selective hydrogenation of the olefinic double bond. Thus, for example, (−)-2-azabicyclo[2.2.1]octane hydrochloride **10** can be obtained in enantiomerically pure form.[6] Similarly, **8a/9a** and **8c/9c** can be converted into the corresponding piperidines.

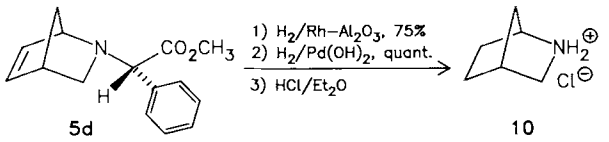

In the case of the serine derivatives, the amino acid side chain can be removed, for example, by conversion to the enamine by means of the Mitsunobu reaction followed by its hydrolytic cleavage. For instance, the didehydropiperidinium hydrochloride **12** is obtained, albeit in achiral form, from **8d** via **11**. The double bond in the ring (allylic to N) is not attacked.

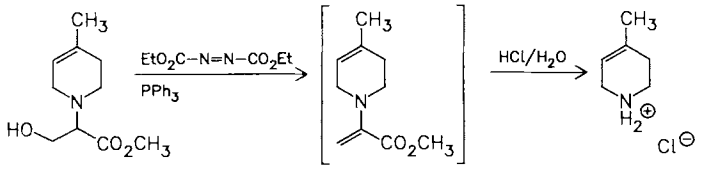

Experimental Procedure

A mixture made up of **1** (0.15 mol), **3**, **4**, or **7** (0.3 mol), water (55 mL), THF (6.5 mL), and a 35% solution of formaldehyde (19 mL, 0.22 mol formaldehyde) was stirred at the temperatures listed in Table 1 for 72 h. The reaction mixture was then diluted with 100 mL of water and extracted with ether, the pH value was adjusted to 12, and the resulting mixture was extracted three times with ether. After drying of the organic phases and evaporation of the solvent, the products were purified by distillation under high vacuum or by flash chromatography. They were characterized by ^{1}H- and ^{13}C-NMR spectroscopy as well as by elemental analysis.

Received: September 21, 1987 [Z 2435 IE]
German version: *Angew. Chem. 100* (1987) 307

[1] For recent reviews see: R. R. Schmidt, *Acc. Chem. Res. 19* (1986) 250; S. Danishefsky, *Angew. Chem. 99* (1987) 15; *Angew. Chem. Int. Ed. Engl. 26* (1987) 15; G. Helmchen, P. Karge, J. Weetmann in R. Scheffold (Ed.): *Modern Synthetic Methods, Vol. 4*, Springer, Berlin 1986, p. 261; W. Oppolzer, *Angew. Chem. 96* (1984) 840; *Angew. Chem. Int. Ed. Engl. 23* (1984) 876; S. M. Weinreb, R. R. Staib, *Tetrahedron 38* (1982) 3087.

[2] R. Breslow, D. Rideout, *J. Am. Chem. Soc. 102* (1980) 7816.

[3] S. Larsen, P. Grieco, *J. Am. Chem. Soc. 107* (1985) 1768.

[4] For the use of amino acid derivatives in asymmetric synthesis, see K. Drauz, A. Kleemann, J. Martens, *Angew. Chem. 94* (1982) 590; *Angew. Chem. Int. Ed. Engl. 21* (1982) 584.

[5] Characteristic NOE effects are observed between the amino acid β-protons and H1 as well as between the amino acid α-proton and H1 and $H3_{ax}$: H. Waldmann, unpublished.

[6] $[\alpha]_D^{25}=-19.1$ ($c=1$, CH_3OH). The compound has already been described in racemic form: J. R. Malpass, N. J. Tweddle, *J. Chem. Soc. Perkin Trans. 1 1977*, 874. The ^{1}H-NMR spectrum of **10** agrees with the reported spectrum.

Heterogeneous, Bimetallic Metathesis Catalysts by Reaction of Fischer-type Carbene Complexes with Reduced Phillips Catalyst**

By *Karin Weiss,* Wilfried Guthmann,* and *Sergio Maisuls*

Tungsten carbene complexes of the Fischer type are frequently used as model catalysts for stoichiometric metathesis reactions.[1-3] However, for catalytic metathesis reactions cocatalysts must be added to increase the activity, or the reaction temperatures should be in the range where the carbene complexes decompose. Since 1964, when *Banks* and *Bailey* discovered the metathesis of linear olefins,[4] heterogeneous metathesis catalysts have repeatedly proved to be more reactive and have been chosen for industrial processes.

We therefore tested inorganic supports such as silica or alumina as cocatalysts for Fischer-type carbene complexes, but carbene complexes were fixed only in small concentrations to alumina suspended in pentane. The metathesis activity (tested with 1-octene in hexane at 69 °C), moreover, was low. For this reason, we looked for modified inorganic supports as carriers for the carbene complexes.

Reduced Phillips catalyst, surface chromium(II) on silica,[5] abbreviated SiO_2/Cr^{II}, is thought to be the catalytically active species involved in ethylene polymerization according to the Phillips process. It contains isolated chromium atoms which are anchored through O–Si bridges and have free coordination sites for the complexation of ligands. Not only ethylene but also higher 1-olefins such as 1-octene give polymerization in high yields with SiO_2/Cr^{II} as catalyst.[6] We have now used this polymerization catalyst as an inorganic support for Cr, Mo, and W Fischer-type carbene complexes[7] (Scheme 1). Reaction of the Cr and W carbene complexes with SiO_2/Cr^{II} in pentane resulted in the evolution of an amount of CO corresponding to the cleavage of one CO ligand per coordinated Cr and W complex and more per Mo complex.

In each case, the carbene complex was used in excess (1.5 mmol per mmol Cr). The unreacted carbene complex was subsequently extracted with pentane and its amount in the eluate determined. The new bimetallic catalysts were thereby found to have a Cr:M molar ratio of 1:1.1 (M = Cr, W) and 1:1.5 (M = Mo). Thus, the Cr and W carbene complexes reacted in nearly equimolar amounts with the chromium atom of reduced Phillips catalyst. In the case of Mo, on the other hand, subsequent reactions, possibly involving cluster formation, occurred.

In principle, these bimetallic catalysts can react with alkenes in two ways:

[*] Dr. K. Weiss, W. Guthmann, S. Maisuls
Laboratorium für Anorganische Chemie der Universität
Postfach 101251, D-8580 Bayreuth (FRG)

[**] Investigations of Polymerization and Metathesis Reactions, Part 11.—Part 10: K. Weiss, K. Hoffmann, *Z. Naturforsch. B42* (1987) 769.

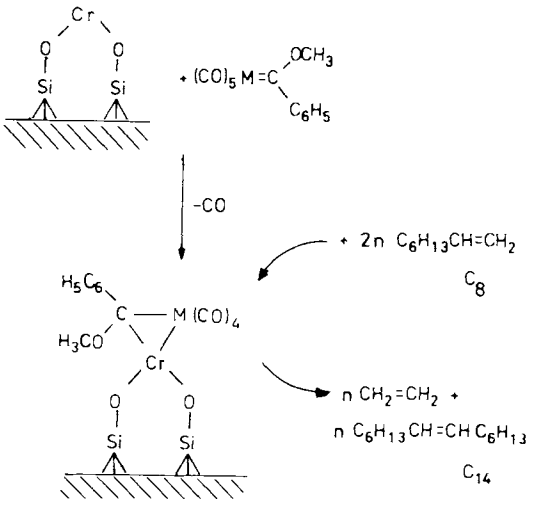

Scheme 1. Bimetallic catalysts from reduced Phillips catalyst and carbene complexes. M = Cr, Mo, W, and 1-octene metathesis with M = Mo, W.

1. Polymerization at the carrier-bound Si–O–Cr centers.
2. Metathesis at the bound Cr, Mo, or W carbene complex fragments.

The reactivity toward 1-octene was tested in each case with a suspension of the bimetallic catalyst in refluxing hexane and the metathesis products were analyzed by gas chromatography.[8] To test for poly-1-octene, the metathesis products were distilled under high vacuum at 100 °C and the residue was investigated by IR spectroscopy. The starting carbene complexes $[(CO)_5M{=}C(OCH_3)(C_6H_5)]$, M = Cr, Mo, W, under the same conditions, in hexane solution, exhibited neither polymerization nor metathesis activity. Furthermore, no polymerization or metathesis activity toward 1-octene was observed when silica, which, except for Cr doping, had been subjected to all steps in the synthesis of SiO_2/Cr^{II}, was used as carrier for the carbene complexes (only trace amounts of the starting carbene complex were adsorbed). Polymerization or metathesis activity was not observed for the bimetallic catalyst $SiO_2/Cr/Cr$ (prepared from SiO_2/Cr^{II} and $[(CO)_5Cr{=}C(OCH_3)(C_6H_5)]$) either. We therefore conclude that the polymerization activity of the SiO_2/Cr^{II} centers is lost by reaction with the Cr carbene complex. Metathesis activity of the Cr carbene complex bound to the SiO_2/Cr^{II} centers was not expected, since Cr carbene complexes yield no catalytic metathesis reactions with unsubstituted alkenes.

Metathesis:

$$2\,C_6H_{13}CH{=}CH_2 \rightleftharpoons CH_2{=}CH_2 + \underbrace{C_6H_{13}CH{=}CHC_6H_{13}}_{C_{14}}$$

Isomerization + metathesis:

$$C_6H_{13}CH{=}CH_2 \rightleftharpoons C_5H_{11}CH{=}CH{-}CH_3$$

$$2\,C_6H_{13}CH{=}CH_2 + 2\,C_5H_{11}CH{=}CH{-}CH_3 \rightleftharpoons$$

$$\underbrace{C_6H_{13}CH{=}CHC_5H_{11}}_{C_{13}} + CH_2{=}CHCH_3$$

$$+\ \underbrace{C_6H_{13}CH{=}CHCH_3}_{C_9} + C_5H_{11}CH{=}CH_2$$

Scheme 2. Products of the metathesis of 1-octene on $SiO_2/Cr/M$ catalysts.

In contrast, $SiO_2/Cr/Mo$ and $SiO_2/Cr/W$ exhibited high metathesis activity (see Fig. 1). The amount of side products C_n (primarily C_9 and C_{13}, formed by isomerization followed by metathesis, Scheme 2) at the start of the reaction is significantly less with $SiO_2/Cr/W$ than with $SiO_2/Cr/Mo$. Possibly, these side reactions are favored by cluster formation with excess $[(CO)_5Mo{=}C(OCH_3)(C_6H_5)]$. When the concentration of 1-octene becomes less, the amount of side products of type C_n, due to isomerization and subsequent metathesis, generally increases.

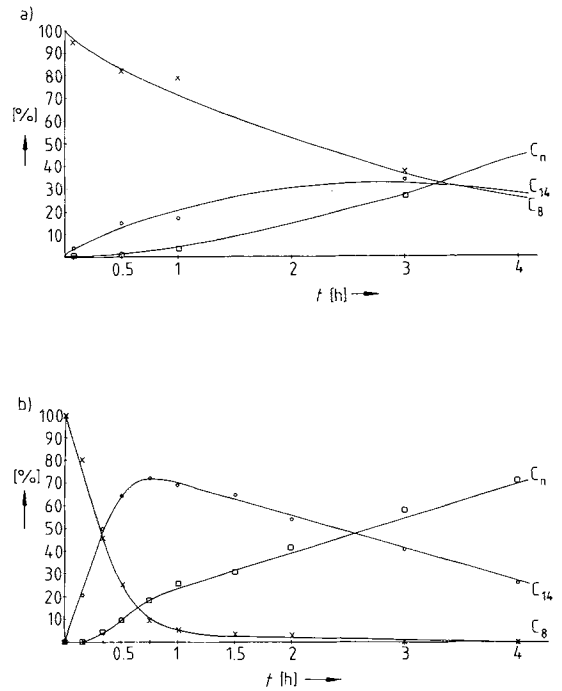

Fig. 1. Turnover/time diagrams for the metathesis of 1-octene with $SiO_2/Cr/M$ (69 °C, hexane). a) M = Mo; b) M = W.

Poly-1-octenes are not formed with any of the bimetallic catalysts. This indicates that, by reaction with the carbene complexes, the originally polymerization-active SiO_2/Cr^{II} loses fully its polymerization activity. On the other hand, the Mo and W centers in the bimetallic catalysts exhibit high metathesis activity, due to the activation by the "co-catalyst" SiO_2/Cr^{II}. In order to make statements about the exact structures of these bimetallic catalysts, numerous further investigations are still required. The first FT IR investigations in diffuse reflectance from $SiO_2/Cr/W$ revealed CO absorptions of terminal CO ligands at $\tilde{\nu} = 2137$, 2094, 2075, and 2062 cm^{-1}. These absorptions might be due to a $W(CO)_4$ fragment having a positive central atom (e.g., carbyne complexes such as $[Cl(CO)_4W{\equiv}CC_6H_5]$: $\tilde{\nu}(CO) = 2123$ and 2038 cm^{-1}). Carbonyl complexes of SiO_2/Cr^{II}, on the other hand, have the most intense CO absorptions in the region around 2185 cm^{-1}.[9]

A proposed structure for $SiO_2/Cr/W$ provides a possible explanation for the especially high activity of this catalyst (Scheme 3). After having failed to prepare so far a metathesis-active bimetallic catalyst by reaction of $W(CO)_6$ with SiO_2/Cr^{II}, we believe that the carbene complex is also bound to SiO_2/Cr through the carbene ligand. The carbene complex fragment would thereby become a platform for

alkenes, the O-Cr-O fragment serving as "activating spacer" to the silica surface.

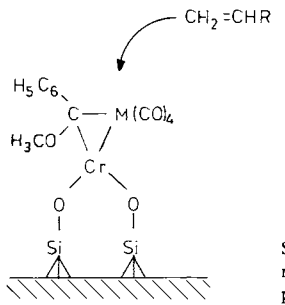

Scheme 3. Structural proposal for the bimetallic catalyst $SiO_2/Cr/W$, which explains its high activity.

Received: September 16, 1987;
revised: November 5, 1987 [Z 2429 IE]
German version: *Angew. Chem. 100* (1988) 268

[1] K. J. Ivin: *Olefin-Metathesis*, Academic Press, London 1983.
[2] V. Dragutan, A. T. Balaban, M. Dimonie: *Olefin Metathesis and Ring-opening Polymerisation of Cyclo-Olefins*, Wiley, New York 1985.
[3] K. Weiss in U. Schubert, H. Fischer, P. Hofmann, K. Weiss, K. H. Dötz, F. R. Kreissl (Eds.): *Transition Metal Carbene Complexes*, Verlag Chemie, Weinheim 1983, p. 237.
[4] R. L. Banks, G. C. Bailey, *Ind. Eng. Chem. Prod. Res. Develop. 3* (1964) 170.
[5] H. L. Krauss, B. Rebensdorf, U. Westphal, *Z. Anorg. Allg. Chem. 414* (1975) 97; A. Clark, I. N. Finch, B. H. Ashe, *Proc. 3rd Int. Congr. Catal.* (1964), p. 1001.
[6] K. Weiss, H. L. Krauss, *J. Cat. 88* (1984) 424.
[7] *Preparation of the bimetallic catalysts:* A suspension of ca. 20 g of SiO_2/Cr^{II} (Cr^{II} = 0.78%, ΣCr = 1.13%, Cr oxidation number = 2.3, activated at 800°C, reduced with CO at 350°C, see Ref. [5]) was treated at 0°C with a 1.5-fold molar excess (based on ΣCr) of $[(CO)_5M{=}C(OCH_3)(C_6H_5)]$, M = Cr, Mo, W, in pentane. The color of SiO_2/Cr^{II} turned from bright green to brown and gas evolution occurred. The unreacted carbene complex was subsequently extracted with pentane.
[8] *Reaction of the bimetallic catalysts with 1-octene:* 5 g of $SiO_2/Cr/M$, M = Cr, Mo, W, (corresponding to 1 mmol of Cr and 1 mmol of $Cr_{carbene}$, 1.5 mmol of $Mo_{carbene}$, or 1 mmol of $W_{carbene}$) was suspended in 60 mL of hexane, treated with 5 mL (32 mmol) of 1-octene, and heated under reflux (69°C). The decrease in the amount of 1-octene and the increase in the amount of the metathesis products was followed by gas chromatography. The catalytic turnovers were not optimized.
[9] R. Höpfl, *Dissertation*, Universität Bayreuth 1981.

New Complex Cations of Aluminum(III) and Gallium(III)**

By *Alan H. Cowley,* Carl J. Carrano, Rolf L. Geerts, Richard A. Jones,** and *Christine M. Nunn*

Recently, $[MX_4]^{\ominus}$ salts of cations of the genre $[(\eta^6\text{-arene})_2M]^{\oplus}$ (M = Ga^{I}, In^{I}; X = Cl, Br) have been isolated and structurally characterized.[1] Interestingly, it has not yet been possible to synthesize cyclopentadienyl-substituted cations of the group 13 elements of the type $[(\eta^5\text{-}C_5R_5)_2M]^{\oplus}$ (M = Al^{III}, Ga^{III}, In^{III}; R = H, Me).[2] Recognizing the formal analogy between cyclopentadienyl and tris(pyrazolyl)borato ligands,[3] we were prompted to attempt the preparation of the corresponding $[HB(pz^*)_3]$-substituted cations ($[HB(pz^*)_3]^{\ominus}$ = tris(3,5-dimethyl-1-pyrazolyl)hydridoborate anion). In passing we note that the use of (pyrazolyl)borato ligands in main-group chemistry is relatively unexplored.

Treatment of $GaCl_3$ with an equimolar quantity of $K[HB(pz^*)_3]$ in THF resulted in formation of the salt **1**.

$[\{HB(pz^*)_3\}_2Ga][GaCl_4]$ **1**

The ^{71}Ga-NMR spectrum of **1** (THF, 91.54 MHz, 25°C) exhibited two sharp singlets of equal intensity at $\delta = 2.8$ ($w_{1/2} = 60$ Hz) and $\delta = 239.2$ ($w_{1/2} = 60$ Hz). The latter peak corresponds to the $[GaCl_4]^{\ominus}$ anion,[1a,4] leading to the conclusion that the former peak is due to the cation $[\{HB(pz^*)_3\}_2Ga]^{\oplus}$. This was confirmed by a single-crystal X-ray diffraction study.[5] The solid-state of **1** comprises discrete $[\{HB(pz^*)_3\}_2Ga]^{\oplus}$ and $[GaCl_4]^{\ominus}$ ions with no short interionic contacts. Within experimental error, all Ga-N bond lengths of the cation are identical and the GaN_6 geometry is close to regular octahedral (Fig. 1). The N11-N21-N31 and N41-N51-N61 planes are therefore parallel.

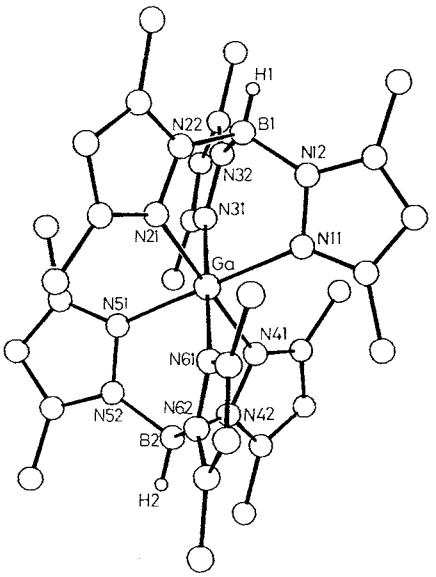

Fig. 1. Structure of **1** in the crystal. Selected bond lengths [Å]: Ga-N11 2.070(7), Ga-N21 2.066(6), Ga-N31 2.057(7), Ga-N41 2.060(6), Ga-N51 2.066(7), Ga-N61 2.064(7).

If the view is taken that the hydridotris(pyrazolyl)borate and cyclopentadienyl ligands are chemically similar, then $[\{HB(pz^*)_3\}_2Ga]^{\oplus}$ corresponds to the unknown "gallocene" cations, $[(\eta^5\text{-}C_5R_5)_2Ga]^{\oplus}$ (R = H, Me). The $[(arene)_2Ga]^{\oplus}$ cations have been shown to possess bent-sandwich structures;[1i] however, since the $[(\eta^5\text{-}C_5R_5)_2Ga]^{\oplus}$ cations feature two less electrons on the central atom, they are expected to adopt a parallel ring sandwich structure as observed for **1**.

The reaction of $K[HB(pz^*)_3]$ with $AlCl_3$ in CH_2Cl_2 proceeded similarly and afforded **2**. Unfortunately, the crys-

$[\{HB(pz^*)_3\}_2Al][AlCl_4]$ **2**

tals of **2** were not suitable for X-ray diffraction study; however, the presence of $[AlCl_4]^{\ominus}$ in solution was evident from the ^{27}Al-NMR spectrum (CH_2Cl_2, 78.21 MHz, 25°C) which exhibited a sharp singlet at $\delta = 98.5$ ($w_{1/2} = 6$ Hz).[6]

[*] Prof. Dr. A. H. Cowley, Prof. Dr. R. A. Jones,
Dr. R. L. Geerts, Dr. C. M. Nunn
Department of Chemistry, The University of Texas at Austin
Austin, TX 78712 (USA)
Prof. Dr. C. J. Carrano
Department of Chemistry, The University of Vermont
Burlington, VT 05405 (USA)

[**] This work was supported by the National Science Foundation, The Robert A. Welch Foundation, and the Texas Advanced Technology Research Program.

A second sharp singlet of equal intensity at $\delta = 6.2$ ($w_{1/2} = 12$ Hz) is attributed to the cation $[\{HB(pz^*)_3\}_2Al]^{\oplus}$.

Interestingly, the reaction of $K[HB(pz^*)_3]$ with $InCl_3$ took a different course and afforded the covalent dichloride **3**. An X-ray crystal structure determination of

$[HB(pz^*)_3]InCl_2$ **3**

$\mathbf{3} \cdot CH_3CN$[5] revealed that each indium atom is bonded to two chlorines and four nitrogens (Fig. 2). Three of the nitrogens are associated with the pyrazolylborato ligand, the fourth being from a coordination CH_3CN molecule. The binding of the $(CH_3CN)InCl_2$ moiety to the pyrazolylborate face is not symmetrical as indicated by the fact that the In–N21 distance is somewhat shorter than the other two $In-N_{pyrazolyl}$ distances.

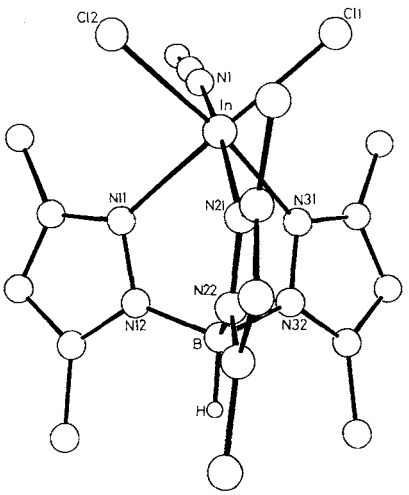

Fig. 2. Structure of **3** in the crystal. Selected bond lengths [Å]: In-Cl1 2.428(2), In-Cl2 2.429(2), In-N1 2.379(7), In-N11 2.268(4), In-N21 2.233(6), In-N31 2.249(5).

Experimental

All operations were performed under dry, oxygen-free conditions.

1: A THF (150 mL) solution of $K[HB(pz^*)_3]$ [3] (1.91 g, 5.7 mmol) was added dropwise to a THF (150 mL) solution of $GaCl_3$ (1.0 g, 5.7 mmol) at room temperature. After stirring the reaction mixture for 18 h, the solvent was removed in vacuo. The resulting solid residue was extracted with CH_2Cl_2 (2×100 mL) and filtered. Recrystallization from CH_3CN afforded colorless **1** in >80% yields. ^{1}H-NMR (90 MHz, CD_3CN, 25 °C) $\delta = 1.13$ (s, 18 H, aryl-CH_3), 2.50 (s, 18 H, aryl-CH_3), 5.90 (s, 6 H, aryl-H).

2 was prepared in the same manner as **1** except that CH_2Cl_2 was employed as the reaction solvent. Recrystallization from CH_3CN afforded colorless, microcrystalline **2** in virtually quantitative yield. ^{1}H-NMR (300.15 MHz, $CDCl_3$, 25 °C) $\delta = 1.07$ (s, 18 H, aryl-CH_3), 2.56 (s, 18 H, aryl-CH_3), 5.88 (s, 6 H, aryl-H).

3 was prepared in the same fashion as **1**. Recrystallization from CH_3CN afforded colorless, crystalline **3** in essentially quantitative yield. ^{1}H-NMR (300.15 MHz, C_6D_6, 25 °C) $\delta = 0.58$ (s, CH_3CN), 2.03 (s, 9 H, aryl-CH_3), 2.80 (s, 9 H, aryl-CH_3), 5.45 (s, 3 H, aryl-H).

Received: September 7, 1987 [Z 2425 IE]
German version: *Angew. Chem. 100* (1988) 306

CAS Registry numbers:
1, 112439-51-7; **2**, 112439-53-9; **3**, 112439-54-0; $\mathbf{3} \cdot CH_3CN$, 112439-55-1; $K[HB(pz^*)_3]$, 17567-17-8; $GaCl_3$, 13450-90-3; $AlCl_3$, 7446-70-0; $InCl_3$, 10025-82-8.

[1] a) H. Schmidbaur, U. Thewalt, T. Zafiropoulos, *Organometallics 2* (1983) 1150; b) *Chem. Ber. 117* (1984) 3381; c) J. Ebenhöch, G. Müller, S. Riede, H. Schmidbaur, *Angew. Chem. 96* (1984) 367; *Angew. Chem. Int. Ed. Engl. 23* (1984) 386; d) *ibid. Angew. Chem. 97* (1985) 893; *Angew. Chem. Int. Ed. Engl. 24* (1985) 893. For somewhat related chemistry of C_5H_5- and Me_5C_5-substituted In^I and Tl^I compounds, see, e.g., H. Werner, H. Otto, H. J. Kraus, *J. Organomet. Chem. 315* (1986) C57; O. T. Beachley, M. R. Churchill, J. C. Fettinger, J. C. Pazik, L. Victoriano, *J. Am. Chem. Soc. 108* (1986) 4666, and references therein.

[2] A. H. Cowley, R. L. Geerts, unpublished results.

[3] S. Trofimenko, *Prog. Inorg. Chem. 34* (1986) 115.

[4] B. R. McGarvey, M. J. Taylor, D. G. Tuck, *Inorg. Chem. 20* (1981) 2010.

[5] **1**: monoclinic, space group $P2_1/c$ (No. 14), $Z = 4$; $a = 10.796(6)$, $b = 27.272(2)$, $c = 14.825(2)$ Å, $\beta = 97.27(2)°$, $V = 4330$ Å^3; $\rho_{calcd} = 1.406$ g cm^{-3}, $3° < 2\theta < 55°$ ($Mo_{K\alpha}$ $\lambda = 0.71069$ Å, $\mu = 15.28$ cm^{-1}, 9879 unique reflections collected, of which 3846 ($I > 3.\sigma(I)$) were used to solve (direct methods) and refine (full matrix, least squares) the structure of **1**. $R = 0.0558$, $R_w = 0.0649$. **3**: triclinic, space group $P\bar{1}$ (No. 2), $Z = 2$; $a = 8.125(2)$, $b = 13.848(2)$, $c = 14.574(2)$ Å, $\alpha = 72.34(1)$, $\beta = 74.76(2)$, $\gamma = 70.24(2)°$, $V = 1447$ Å^3, $\rho_{calcd} = 1.295$ g cm^{-3}, $3 < 2\theta < 48°$ ($Mo_{K\alpha}$ $\lambda = 0.71069$ Å), $\mu = 10.07$ cm^{-1}; 4520 unique reflections, of which 3457 ($I > 3.\sigma(I)$) were used to solve (Patterson) and refine (full matrix, least squares) the structure of **3**. $R = 0.0386$, $R_w = 0.0492$. Further details of these crystal structure investigations can be obtained from the Fachinformationszentrum Energie Physik Mathematik GmbH, D-7514 Eggenstein-Leopoldshafen 2 (FRG), by quoting the depository number CSD-52717, the names of the authors, and the journal citation.

[6] J. W. Akitt, *Annu. Rep. NMR Spectrosc. 5* (1972) 465.

Asymmetric Induction in the [2,3] Wittig Rearrangement by Chiral Substituents in the Allyl Moiety**

By *Reinhard Brückner** and *Henning Priepke*

Recently, the Wittig rearrangement of allyloxy carbanions (**1** → **2**) has attracted renewed interest in terms of developing novel methodologies for stereoselective C–C bond formation.[1] The relative configuration of the newly formed stereogenic centers ("stereocenters") is influenced by the configuration of the double bond in the allyl ether **1** and by the R^5 moiety; the absolute configuration of the newly formed stereocenters has been controlled so far by a stereocenter at C-3 of the educt or by a chiral substituent R^5.[1,2] Here we describe two examples of high asymmetric induction by a stereocenter in the R^1 moiety.

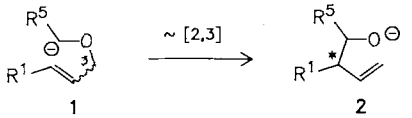

1 **2**

In the first example, the allyl ether **3**, containing a double bond with *trans* configuration, was rearranged upon lithiation (Scheme 1).[3] Due to the influence of the chiral dioxolane ring, the new stereocenter was formed with a diastereoselectivity of 86%. The configuration of this stereocenter in the major product **4** was determined by ^{1}H-NMR spectroscopy[4] after transformation to the lactone **6**. Upon irradiation of the CH_2OH resonance of **6**, we observed a nuclear Overhauser effect (NOE) of 6% for the $CH{=}CH_2$ signal, which indicates a *cis* arrangement of the vinyl and hydroxymethyl groups. In the isomeric *trans* lactone, a corresponding NOE was not observed.[5]

The second example of the novel asymmetric induction was found when we deprotonated the allyl ether **7**,[6] containing a double bond with *cis* configuration. The Wittig rearrangement of the lithium enolate of **7** gave a 40% yield of only one homoallylic alcohol, **8**,[7] along with <2% of the other three possible stereoisomers (Scheme 2). The

[*] Dr. R. Brückner, H. Priepke
Fachbereich Chemie der Universität
Hans-Meerwein-Strasse, D-3550 Marburg (FRG)

[**] This work was supported in part by the Deutsche Forschungsgemeinschaft (Project Br 881/2-1). *R. B.* thanks the Fonds der Chemischen Industrie for a Liebig-Stipendium.

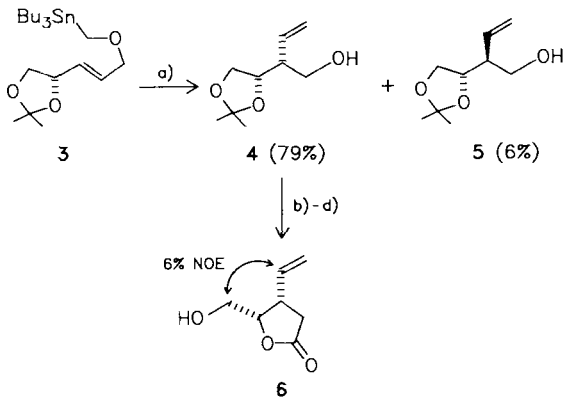

Scheme 1. a) 0.2 M in THF; +2 equiv. 1.5 M *n*BuLi in hexane, −78°C, 1 h. b) nBu$_3$P, Ph_2S_2, CH_2Cl_2, room temp., 4 h; 84%. c) LiNaphth/THF, then $ClCO_2Me$, both −78°C, 30 min; 29%. d) Ref. [5]; 49%.

configuration of the stereocenters of **8** was determined after conversion to the diol **9**. Glycol cleavage and reduction lead to compound **4** mentioned above; hence, C-3 has the (*S*) configuration in **9** and **8**. The configuration of C-2 of **8** was obtained after transformation of the diol **9** into the bisacetonide **10**; this compound is optically inactive and displays only *one* set of signals for the *two* dioxolane rings in both the ^{1}H- and ^{13}C-NMR spectra. This means that **10** contains a symmetry plane, which, in turn, proves the (*R*) configuration of C-2 in **8**.

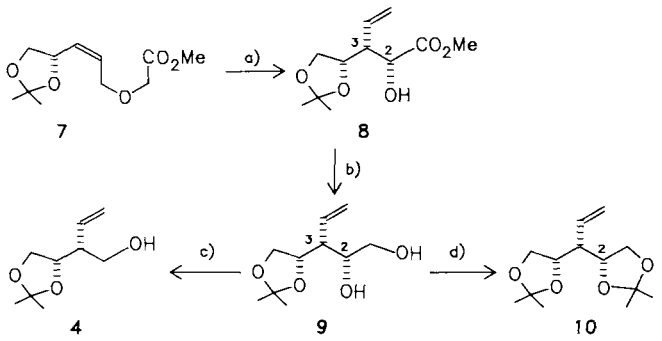

Scheme 2. a) 0.2 M in THF to 1.25 equiv. 0.2 M lithiumdiisopropylamide, −78°C, 30 min; then 5.5 equiv. tetramethylethylenediamine, −40°C, 3 h; 40%. b) $LiAlH_4$/THF; 92%. c) 1. $NaIO_4$/aq. MeOH, 2. $NaBH_4$/EtOH; 58%. d) $Me_2C(OMe)_2$, acetone, *p*-TsOH; 76%.

We observed the same 1,2-asymmetric induction in both Wittig rearrangements, in **3**→**4** as well as in **7**→**8**. The vinyl group of the preferred rearrangement product is *syn* to the C-O bond at the stereocenter originally present. This finding becomes plausible by examining the reaction path with the lowest-energy transition state in the frontier orbital model. For this purpose, the Wittig rearrangement is regarded as an S_N2' nucleophilic attack on an allylic ether. The crucial orbital interaction occurs between the $HOMO_{anion\ moiety}$ and the $LUMO_{allyl\ ether\ moiety}$, whereby the latter approximately can be taken as the $\pi^*_{C=C}$ orbital. The energy of the $\pi^*_{C=C}$ orbital is lowered through overlap with the adjacent allylic σ* orbitals,[8] such as are present in the dioxolane ring of **3** and **7**. The lower in energy the $\pi^*_{C=C}$ orbital thereby becomes, the better is the HOMO/LUMO interaction in the transition state and the faster is the [2,3]-sigmatropic rearrangement. Since a σ^*_{C-O} orbital is lower in energy than a σ^*_{C-C} orbital, the former lowers the $\pi^*_{C=C}$ energy more than the latter. Consequently, in the preferred transition state **11** of the Wittig rearrangement, the C-O bond of the allyl substituent is perpendicular to the plane of the double bond; of the remaining allylic substituents, the larger is found "outside" for steric reasons.

We therefore propose that **12** and **13** are transition states for the Wittig rearrangements **3**→**4** and **7**→**8**, respectively. Here, the bulky heterocycle prefers the "outside" position and the H atom the "inside" position.[9]

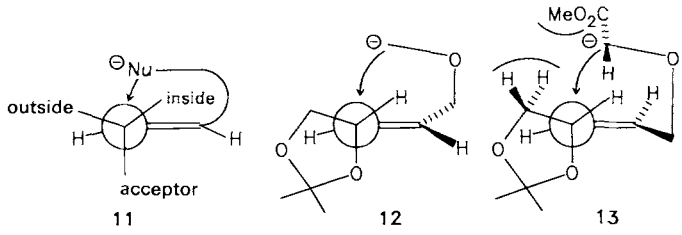

Cha et al. investigated the Claisen-Ireland rearrangements related to the Wittig rearrangements described here, but they found lower asymmetric inductions by the chiral dioxolanes.[10] A possible explanation is that, in the rearrangement of the neutral ketene acetal, less charge has to be stabilized in the transition state by the σ^*_{C-O} orbital than in the rearrangement of the carbanions.

Thus, the reactions **3**→**4** and **7**→**8** represent a novel stereocontrol in the Wittig rearrangement, which can be interpreted by a Felkin-Anh-type transition state **11**. Compounds **4** and **8** are needed for the synthesis of amphotericin B.

Received: July 15, 1987;
Final version: November 26, 1987 [Z 2357 IE]
German version: *Angew. Chem. 100* (1988) 285

[1] Review: T. Nakai, K. Mikami, *Chem. Rev. 86* (1986) 885.
[2] a) M. Uchikawa, T. Hanamoto, T. Katsuki, M. Yamaguchi, *Tetrahedron Lett. 27* (1986) 4577; b) M. Uchikawa, T. Katsuki, M. Yamaguchi, *ibid. 27* (1986) 4581.
[3] Method: W. C. Still, A. Mitra, *J. Am. Chem. Soc. 100* (1978) 1927. The stannyl ether **3** ($[\alpha]_D^{20}$ (c = 1.63, $CDCl_3$) + 11.2) was prepared in 60% yield from (4′*S*)-*trans*-3-(2,2-dimethyl-1,3-dioxolan-4-yl)prop-2-en-1-ol ($[\alpha]_D^{20}$ (c = 6.37, CH_2Cl_2) + 23.7; Ref. [5]: $[\alpha]_D$ (c = 0.21, $CHCl_3$) + 26.7; N. Minami, S. S. Ko, Y. Kishi, *J. Am. Chem. Soc. 104* (1982) 1109: $[\alpha]_D$ (c = 3.63, $CHCl_3$) + 33.9) by treatment with KH/Bu_3SnCH_2I.
[4] **4**: $[\alpha]_D^{22}$ (c = 1.26, $CDCl_3$) + 13.9. 300-MHz ^{1}H-NMR ($CDCl_3$): δ = 1.30 and 1.36 (2s; 2′-$(CH_3)_2$), 1.89 (dd, J = 7.0, J = 5.0; OH), 2.39 (mc; 2-H), 3.59-3.70 (m; 1-H_2 and 5′-H^3), 3.97 (dd, J_{gem} = 8.2, $J_{5'\text{-}H^2,4'}$ = 6.4; 5′-H^2), 4.22 (ddd, $J_{4',5'\text{-}H^3} = J_{4',5'\text{-}H^2}$ = 6.9, $J_{4',2}$ = 4.6; 4′-H), 5.15 (ddd, J_{trans} = 17.3, J_{gem} = 1.7, $J_{4,2}$ = 0.8; *Z*-4-H), 5.22 (dd, J_{cis} = 10.4, J_{gem} = 1.7; *E*-4-H), 5.75 (ddd, J_{trans} = 17.3, J_{cis} = 10.4, $J_{3,2}$ = 8.7; 3-H).
[5] The *cis* lactone **6** and its *trans* isomer have been described: T. Suzuki, E. Sato, S. Kamada, H. Tada, K. Unno, T. Kametani, *J. Chem. Soc. Perkin Trans. 1 1986*, 387; T. Kametani, T. Suzuki, M. Nishimura, E. Sato, K. Unno, *Heterocycles 19* (1982) 205. The configurational proof given by the authors is not convincing in our opinion.
[6] The ester **7** ($[\alpha]_D^{20}$ (c = 4.02, CH_2Cl_2) + 1.2) was obtained in 89% yield from (4′*S*)-*cis*-3-(2,2-dimethyl-1,3-dioxolan-4-yl)prop-2-en-1-ol ($[\alpha]_D^{20}$ (c = 2.42, CH_2Cl_2) + 13.5; Ref. [5]: $[\alpha]_D$ (c = 0.34, $CHCl_3$) + 17.1; N. Minami, S. S. Ko, Y. Kishi, *J. Am. Chem. Soc. 104* (1982) 1109: $[\alpha]_D$ (c = 4.52, $CHCl_3$) + 14.0) by the sequence 1. dimsyl-Na; $ClCH_2CO_2Na$, 2. CH_2N_2.
[7] **8**: $[\alpha]_D^{20}$ (c = 5.36, CH_2Cl_2) −25.7. 300-MHz ^{1}H-NMR ($CDCl_3$): δ = 1.37 and 1.42 (2s; 2′-$(CH_3)_2$), 2.65 (ddd, $J_{3,4}$ = 9.4, J' = 6.2, J'' = 2.6; 3-H), 3.12 (d, J = 4.6; OH), 3.78 (s; OCH_3), 3.85 (dd, J_{gem} = 8.1, $J_{5'\text{-}H^1,4'}$ = 7.1; 5′-H^1), 4.10 (dd, J_{gem} = 8.2, $J_{5'\text{-}H^2,4'}$ = 6.2; 5′-H^2), 4.33-4.39 (m; 2-H, 4′-H), 5.15 (ddd, J_{trans} = 17.2, J_{gem} = 1.7, $J_{5,3}$ = 0.7; *Z*-5-H), 5.25 (dd, J_{cis} = 10.4, J_{gem} = 1.8; *E*-5-H), 5.87 (ddd, J_{trans} = 17.2, J_{cis} = 10.3, $J_{4,3}$ = 9.5; 4-H).
[8] K. N. Houk, M. N. Paddon-Row, N. G. Rondan, Y.-D. Wu, F. K. Brown, D. C. Spellmeyer, J. T. Metz, Y. Li, R. L. Loncharich, *Science 231* (1986) 1108.

 © VCH Verlagsgesellschaft mbH, D-6940 Weinheim, 1988 0570-0833/88/0202-0279 $ 02.50/0

[9] The configuration of C-2 of **8** arises because in the transition state **13** the ester function gives way to the bulky dioxolane ring and therefore occupies *exclusively* the *exo* position (cf., however, Ref. [1]).—If the dioxolane ring in **13** is replaced by the smaller methyl group, i.e., in the transition state of the Wittig rearrangement of the (cis-crotyloxy)acetic ester anion, the ester function is no longer forced completely into the *exo* position. Accordingly, the hydroxy ester resulting in *this* case, contrary, to **8**, shows only a 2:1 preference for the *syn* arrangement of the hydroxyl group and the vinyl group [2b].

[10] J. K. Cha, S. C. Lewis, *Tetrahedron Lett. 25* (1984) 5263.

On the Pentaphosphacyclopentadienide Ion, $P_5^{\ominus}$**

By *Marianne Baudler,* Stilianos Akpapoglou, Dimitrios Ouzounis, Fritz Wasgestian, Bernd Meinigke, Herbert Budzikiewicz,** and *Helmut Münster*

Dedicated to Professor Emanuel Vogel on the occasion of his 60th birthday

We recently reported on the formation of the pentaphosphacyclopentadienide ion **1** upon cleavage of white phosphorus with sodium in diethylene glycol dimethyl ether (diglyme) or with lithium dihydrogen phosphide in tetrahydrofuran (THF); in addition, other polyphosphides (in particular, $M_2^IP_{16}$, $M_3^IP_{21}$, and $M_3^IP_{19}$) were formed.[1] Compound **1** was identified by a low-field singlet in the ^{31}P-NMR spectrum ($\delta = +470.2$) and a singlet in both the ^{23}Na- and ^{7}Li-NMR spectra as well as by the Na:P ratio of 1:5 determined analytically for solutions of NaP_5. We report here further findings that have been made in the meantime concerning the formation, characterization, stability, and reactivity of **1**.

1

Preparation of a pure NaP_5 solution: The lithium salt was the first alkali-metal pentaphosphacyclopentadienide that could be obtained pure in solution.[1] In the case of the sodium compound, the other polyphosphides formed could not be separated by crystallization from diglyme. As observed by chance,[2] the formation tendency of NaP_5 in THF is significantly increased by the presence of [18]crown-6, which simultaneously favors the precipitation of other polyphosphides, so that a pure NaP_5/[18]crown-6/THF solution can be obtained;[3] NaP_5 is formed in 12% yield.

Properties and stability: The NaP_5 solutions prepared in this way are golden orange, extremely sensitive to oxidation, and stable for 7–10 days in concentrations of 10^{-2} M at room temperature. These solutions are considerably more stable than the solutions of coronand-free LiP_5 in THF.[1] Upon further concentration, NaP_5 undergoes rearrangement, in particular with formation of Na_2P_{16} and Na_3P_{21}. The addition of dimethylformamide effects stabilization, whereas hydrocarbons or active charcoal cause immediate decomposition.

Characterization. The composition and structure of **1** were corroborated by extensive spectroscopic characterization of the NaP_5/[18]crown-6/THF solutions. The ^{31}P-NMR singlet appears at somewhat higher field ($\delta = +467.2$) than in diglyme, corresponding to the larger polarity of the solvent mixture used.

The first determination of the ion mass of **1** in solution[4] was achieved by means of negative-ion FAB mass spectrometry. The use of method a) (cf. Ref. [5]) revealed, in addition to ions of the solvent mixture, a species of mass *m/z* 155 ($P_5^{\ominus}$) when the solution was warmed. This peak disappeared upon further warming, while *m/z* 62 ($P_2^{\ominus}$) increased in intensity. After averaging of the separate spectra obtained in the temperature region where *m/z* 155 appears and subtraction of the spectrum of the solvent mixture recorded under the same conditions, the difference spectrum exhibits (in addition to weak peaks corresponding to ions of the series $[(CH_2)_xO_y \pm H]^{\ominus}$, due to incomplete subtraction) only the phosphorus-containing species $P_5^{\ominus}$, $P_2^{\ominus}$, and $P_2O^{\ominus}$ (*m/z* 78, oxidation upon admission of the sample). The use of method b) (cf. Ref. [5]) resulted in the immediate transient appearance of the $P_5^{\ominus}$ ion with high intensity in addition to the matrix ions.

In the IR and Raman spectrum of the NaP_5 solution, an intense band at 815 cm^{-1} (IR) and a medium-intense polarized band at 463 cm^{-1} (Raman) are observed (in addition to the bands of the solvent mixture). These bands can be assigned to the vibrational modes E_1' and A_1', respectively, of a planar, five-atom ring of symmetry D_{5h} ($\overline{10}2m$).

The UV spectrum[6] (Fig. 1) exhibits two π–π^* bands of medium intensity at 260 and 320 nm as well as an n–π^* transition at 370 nm. When freshly prepared, dilute solutions ($c < 10^{-4}$ M) are employed, the 260-nm band shows a vibrational fine structure with maxima at 271, 266, 258, 252, 246, and 241 nm. The low intensity of the longest-wavelength vibronic maximum (271 nm) is an indication for a symmetry-forbidden transition corresponding to $^1A_1' \rightarrow {}^1E_2'$ of a 6π-electron system of the cyclopentadienide type.[7] Overall, the shape of the UV spectrum confirms the aromatic character of **1**.

Reactivity: The chemistry of **1** is characterized by analogies to and differences from that of the $C_5H_5^{\ominus}$ ion. For instance, **1** reacts with alkyl halides to form, mainly, P_7R_3

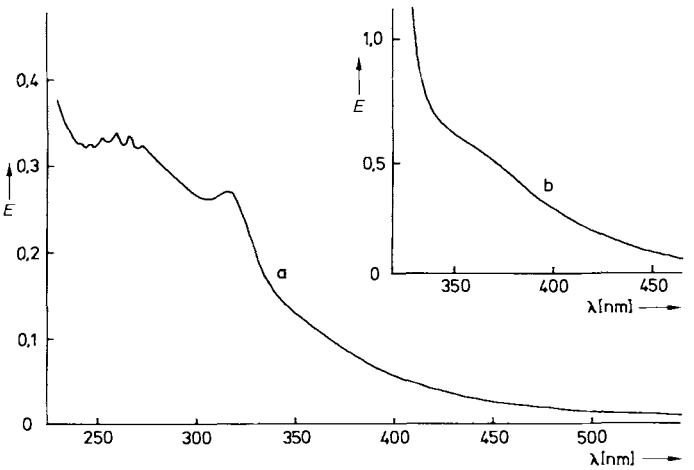

Fig. 1. Electronic spectrum of NaP_5/[18]crown-6/THF solutions; concentration of NaP_5 ca. 3×10^{-5} M (a) and 10^{-4} M (b).

[*] Prof. Dr. M. Baudler, S. Akpapoglou, D. Ouzounis, Prof. Dr. F. Wasgestian, B. Meinigke
Institut für Anorganische Chemie der Universität
Greinstrasse 6, D-5000 Köln 41 (FRG)
Prof. Dr. H. Budzikiewicz, H. Münster
Institut für Organische Chemie der Universität
Greinstrasse 4, D-5000 Köln 41 (FRG)

[**] Contributions to the Chemistry of Phosphorus, Part 185. This work was supported by the Deutsche Forschungsgemeinschaft and the Fonds der Chemischen Industrie.—Part 184: M. Baudler, J. Simon, *Chem. Ber.*, in press.

and P_9R_3. The nonaromatic primary product **2** is apparently so unstable that it spontaneously rearranges to give the thermodynamically favored alkylpolyphosphanes. No evidence for dimers of **2** was found.

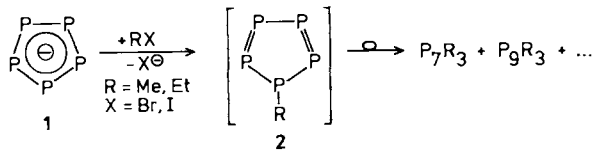

1 2

$$LiP_5 + LiC_5Me_5 + FeCl_2 \xrightarrow[-2\,LiCl]{THF} [(\eta^5\text{-}P_5)Fe(\eta^5\text{-}C_5Me_5)]$$

3

Compound **1** reacts with compounds of the transition metals Fe, Ni, Rh, Mn, Cr, or Mo to form dark brown to black solids, whose insolubility and relative nonvolatility make their characterization difficult. However, black "FeP_{10}," formed immediately upon reaction with $FeCl_2$ in THF at room temperature exhibits—like **1**—an IR band at 815 cm^{-1}, which is evidence for an intact aromatic P_5 ring as structural element, since it is definitely not caused by free **1**. That a "decaphosphaferrocene" might indeed be present was further supported by direct one-pot synthesis of the mixed sandwich complex **3** (in addition to "FeP_{10}" and $[(C_5Me_5)_2Fe]$) from LiP_5, LiC_5Me_5, and $FeCl_2$;[8] **3** is identical with the compound recently obtained by *Scherer* et al.[9] by cothermolysis of $[(\eta^5\text{-}C_5Me_5)Fe(CO)_2]_2$ and P_4.

Received: October 1, 1987 [Z 2452 IE]
German version: *Angew. Chem. 100* (1988) 288

[1] M. Baudler, D. Düster, D. Ouzounis, *Z. Anorg. Allg. Chem. 544* (1987) 87; see also M. Baudler, *Phosphorus Sulfur 30* (1987) 345; *Angew. Chem. 99* (1987) 429; *Angew. Chem. Int. Ed. Engl. 26* (1987) 419.

[2] M. Baudler, D. Düster, unpublished work.

[3] *NaP_5 solution:* Freshly distilled white phosphorus (1.27 g, 0.041 g atom) in a mixture of THF (160 mL) and [18]crown-6 (5.04 g, 0.019 mol) was allowed to react under inert gas at reflux temperature with powdered sodium (0.44 g, 0.019 g atom) with stirring for 3.5 h. After standing for 24 h at room temperature, the reaction solution was separated from the sparingly soluble P-rich polyphosphides by siphoning off over a frit. Concentration to half of the original volume under oil-pump vacuum (bath temperature 55 °C, cold trap −78 °C) and renewed crystallization at −30 °C followed by filtration in the cold gave a pure, ca. 10^{-2} M NaP_5/[18]crown-6/THF solution. Additional NaP_5 can be extracted from the precipitate with boiling THF. Overall yield (by comparison of the intensity of the ^{31}P-NMR singlet with the signal of a Ph_4PCl solution of known concentration) 0.18 g (12%, based on phosphorus).

[4] The appearance of **1** in the negative ion mass spectrum of red phosphorus at 325 °C has been reported by J. T. Snodgrass, J. V. Coe, C. B. Freidhoff, K. M. McHugh, K. H. Bowen, *Chem. Phys. Lett. 122* (1985) 352.

[5] Mass spectrometer MAT-731 (acceleration voltage 8 kV, post-acceleration 7.5 kV) equipped with an 11 NF FAB ion source (Ion Tech Ltd., Teddington; 10^{-5} torr Xe, 7 kV, Cu target). The sample was admitted either by a) application of a NaP_5/[18]crown-6/THF solution, concentrated to 1/6 of its volume, onto a liquid-nitrogen-cooled target followed by slow warming in the ion source accompanied by continuous recording of the spectra or b) by mixing the concentrated solution with dibenzyl ketone as matrix at 25 °C.

[6] Cary 2300. The concentrations of the stock solutions (ca. 10^{-2} M) were estimated from the intensity of the ^{31}P-NMR singlet [3].

[7] B. O. Wagner, H. F. Ebel, *Tetrahedron 26* (1970) 5155.

[8] **3**: Anhydrous $FeCl_2$ (60 mg, 0.47 mmol) in refluxing THF (20 mL) was stirred under inert gas until all material had gone into solution. The solution was treated at the same temperature over 10 min with a suspension of LiC_5Me_5 (67 mg, 0.47 mmol) and LiP_5 (19 mg, 0.12 mmol) [1] in 30 mL of THF. After 1 h of stirring, the solvent was completely removed under reduced pressure at room temperature. The residue was extracted three times with 30 mL of boiling dichloromethane with stirring (20 min each time). Removal of the solvent from the combined extracts and recrystallization from *n*-pentane gave 11 mg (27%) of pure **3** (^{31}P-NMR, MS).

[9] O. J. Scherer, T. Brück, *Angew. Chem. 99* (1987) 59; *Angew. Chem. Int. Ed. Engl. 26* (1987) 59.

Synthesis and Optical Properties of Terminally Substituted Conjugated Polyenes**

By *Franz Effenberger,* Hubert Schlosser, Peter Bäuerle, Stefan Maier, Helmut Port,* and *Hans Christoph Wolf**

Dedicated to Professor Helmut Dörfel on the occasion of his 60th birthday

The mechanisms of energy transport in molecular systems have been the subject of numerous studies in recent years.[1] Aside from investigations on the elucidation of processes involved in biological systems, e.g., in photosynthesis,[2] increasing attention has been directed to the synthesis of compounds which are suitable for the transport and storage of information on a molecular basis.[3]

Herein we report on the synthesis of conjugated polyenes of various lengths with terminal substituents whose spectroscopic properties differ from those of the polyene chains. The selective optical excitation of these model compounds and the possibility of an intramolecular energy transport are discussed on the basis of absorption, emission, and excitation spectra.

Starting from the polyene dialdehydes **1** and **7** we have synthesized, via Wittig reactions, numerous conjugated polyenes bearing the following terminal groups: 9-anthryl (A), 1-naphthyl (N) and 5,10,15,20-tetraphenylporphyrin-2-yl (TPP) as well as *p*-nitrophenyl, *p*-dimethylaminophenyl, ferrocenyl, alkoxycarbonyl, carboxy, and methyl. In the present communication, however, only those compounds shown in Schemes 1 and 2 (see overleaf) and 4,8,13,17-tetramethyl-2,4,6,8,10,12,14,16,18-eicosanonaene (TMEN) used as reference compound will be discussed.[4]

Upon Wittig reaction and purification of the products by column chromatography, the dialdehydes **1** and **7** with all-*E*-configuration initially yield *E*/*Z* isomeric mixtures in which the all-*E*-isomers dominate. The all-*E*-isomers can be enriched by recrystallization: for example, the compounds **2**-A and **3**-A,N are enriched to the extent of 100%, **3**-A,A and **3**-N,N to 99%, **3**-A,TPP to 95% and **6** to 70% in the all-*E*-form. The isomeric ratios were determined by HPLC and the respective isomers assigned by ^{1}H-NMR and UV/VIS spectroscopy.

Figure 1a shows the absorption spectra of anthracene, 5,10,15,20-tetraphenylporphyrin and TMEN, while Figure 1b shows, as selected examples, those of the polyenes **3**-A,TPP, **6** and **9**-A,A (concentrations between 10^{-6} and 10^{-4} mol L^{-1}, CH_2Cl_2, $T = 295$ K). The shapes of the spectra are concentration-independent. The anthrylpolyenes **2**-A, **8**-A, and **10**-A all show an absorption maximum at 256 nm independent of the chain length, which is not observed in the case of **1**, **7**, and TMEN, and which corresponds to the ^1B_b state[5] of anthracene. As expected, in the case of the bilaterally anthryl-substituted polyenes **3**-A,A, **9**-A,A, and **11**-A,A, the extinction coefficients of the absorption at 256 nm are doubled. In the absorption spectra of the mixed-substituted compounds **3**-A,N, **9**-A,N, and **11**-A,N a further band aside from that at 256 nm appears at 220 nm; this corresponds to the excitation of the ^1B_b

[*] Prof. Dr. F. Effenberger, Dipl.-Chem. H Schlosser, Dr. P. Bäuerle
Institut für Organische Chemie der Universität
Pfaffenwaldring 55, D-7000 Stuttgart 80 (FRG)
Prof. Dr. H. C. Wolf, Dipl.-Phys. S. Maier, Dr. H. Port
3. Physikalisches Institut der Universität
Pfaffenwaldring 57, D-7000 Stuttgart 80 (FRG)

[**] This work was supported by the Deutsche Forschungsgemeinschaft, the Fonds der Chemischen Industrie, and BASF AG (supply of polyenedialdehydes). We thank *H. Strobel* for valuable assistance.

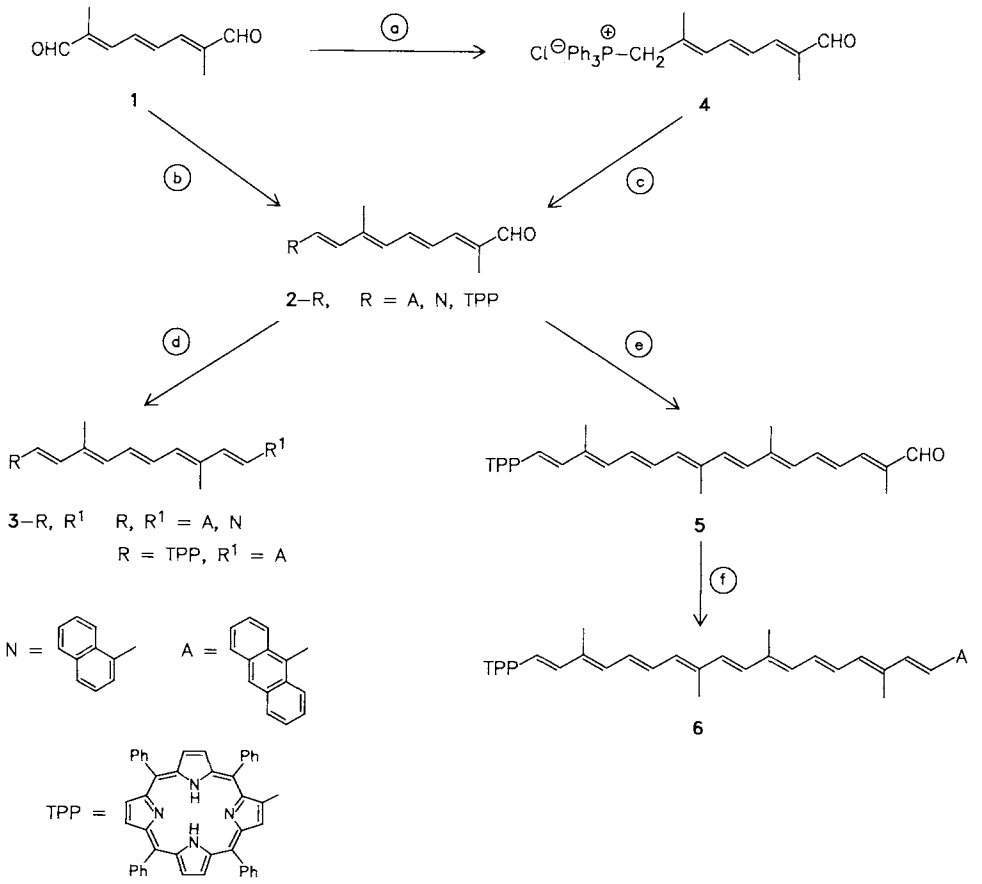

Scheme 1. ⓐ 1) $NaBH_4$, 2) HCl, 3) PPh_3, according to [10]. ⓑ **2**-A: A–CH_2–$\overset{\oplus}{P}Ph_3Br^{\ominus}$, *n*BuLi, Et_2O/1 h/RT; dropwise addition to **1**, CH_2Cl_2/2 h/RT; 1 h stirring; chromatography on SiO_2/CH_2Cl_2; recrystallization from toluene/CH_3OH; 60%, 100% all-*E*.—**2**-N: analogous to **2**-A with N–CH_2–$\overset{\oplus}{P}Ph_3Cl^{\ominus}$; recrystallization from hexane; 21%; 97% all-*E*. ⓒ **2**-TPP: **4**, $HC(OCH_3)_3$, TsOH, CH_3OH/2 h/RT; pyridine; $NaOCH_3/CH_3OH$; TPP–CHO, CH_2Cl_2 added; 17 h/RT; chromatography on SiO_2/CH_2Cl_2; recrystallization from CH_2Cl_2/hexane; 59%, 98% all-*E*. ⓓ **3**-A,A: A–CH_2–$\overset{\oplus}{P}Ph_3Br^{\ominus}$, *n*BuLi, Et_2O/1 h/RT; **1**, CH_2Cl_2 added; 4 h/RT; chromatography on SiO_2/CH_2Cl_2; recrystallization from toluene; 40%; 99% all-*E*.—**3**-N,N: by-product of **2**-N; recrystallization from toluene/CH_3OH; 13%; 99% all-*E*.—**3**-A,N: analogous to **3**-A,A with N–CH_2–$\overset{\oplus}{P}Ph_3Cl^{\ominus}$ and **2**-A; 2 h/RT; recrystallization from toluene/CH_3OH; 72%; 100% all-*E*.—**3**-TPP,A: analogous to **3**-A,A with **2**-TPP; 5 h/RT; recrystallization from CH_2Cl_2/CH_3OH; 26%, 95% all-*E*. ⓔ **5**: analogous to **2**-TPP with **2**-TPP; 49%; 99% all-*E*. ⓕ **6**: analogous to **3**-A,A with **5**; 22 h/RT; recrystallization from CH_2Cl_2/CH_3OH; 18%; 70% all-*E*.

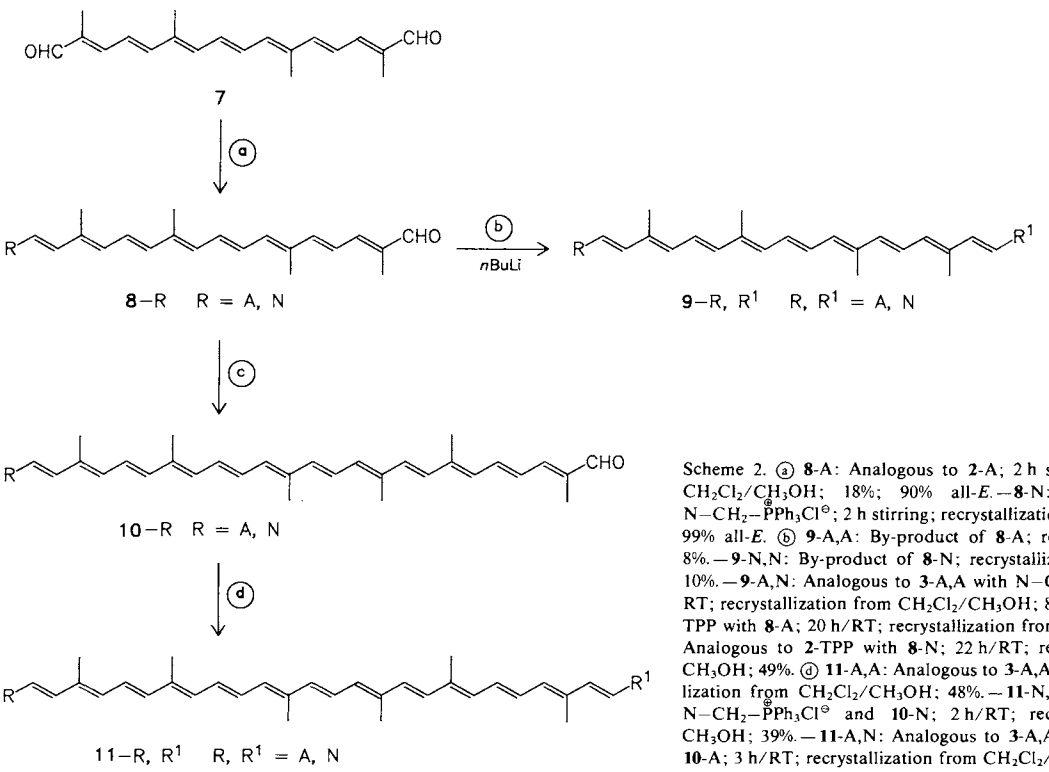

Scheme 2. ⓐ **8**-A: Analogous to **2**-A; 2 h stirring; recrystallization from CH_2Cl_2/CH_3OH; 18%; 90% all-*E*.—**8**-N: Analogous to **2**-A with N–CH_2–$\overset{\oplus}{P}Ph_3Cl^{\ominus}$; 2 h stirring; recrystallization from CH_2Cl_2/hexane; 18%; 99% all-*E*. ⓑ **9**-A,A: By-product of **8**-A; recrystallization from CH_2Cl_2; 8%.—**9**-N,N: By-product of **8**-N; recrystallization from CH_2Cl_2/CH_3OH; 10%.—**9**-A,N: Analogous to **3**-A,A with N–CH_2–$\overset{\oplus}{P}Ph_3Cl^{\ominus}$ and **8**-A; 15 h/RT; recrystallization from CH_2Cl_2/CH_3OH; 88%. ⓒ **10**-A: Analogous to **2**-TPP with **8**-A; 20 h/RT; recrystallization from CH_2Cl_2/Et_2O; 45%.—**10**-N: Analogous to **2**-TPP with **8**-N; 22 h/RT; recrystallization from CH_2Cl_2/CH_3OH; 49%. ⓓ **11**-A,A: Analogous to **3**-A,A with **10**-A; 2 h/RT; recrystallization from CH_2Cl_2/CH_3OH; 48%.—**11**-N,N: Analogous to **3**-A,A with N–CH_2–$\overset{\oplus}{P}Ph_3Cl^{\ominus}$ and **10**-N; 2 h/RT; recrystallization from CH_2Cl_2/CH_3OH; 39%.—**11**-A,N: Analogous to **3**-A,A with N–CH_2–$\overset{\oplus}{P}Ph_3Cl^{\ominus}$ and **10**-A; 3 h/RT; recrystallization from CH_2Cl_2/MeOH; 58%.

state[5] of naphthalene. The intensity ratios of the anthryl and naphthyl bands (2 : 1) of these polyenes approximately correspond to those of the free arenes anthracene and naphthalene. The spectra of **3**-A,TPP and **6** show the typical anthryl band at 256 nm, in addition to the Q bands (500–650 nm) as well as the intense Soret band (425 nm)[6] of the TPP group. The TPP bands are more or less largely superimposed by the polyene absorptions.

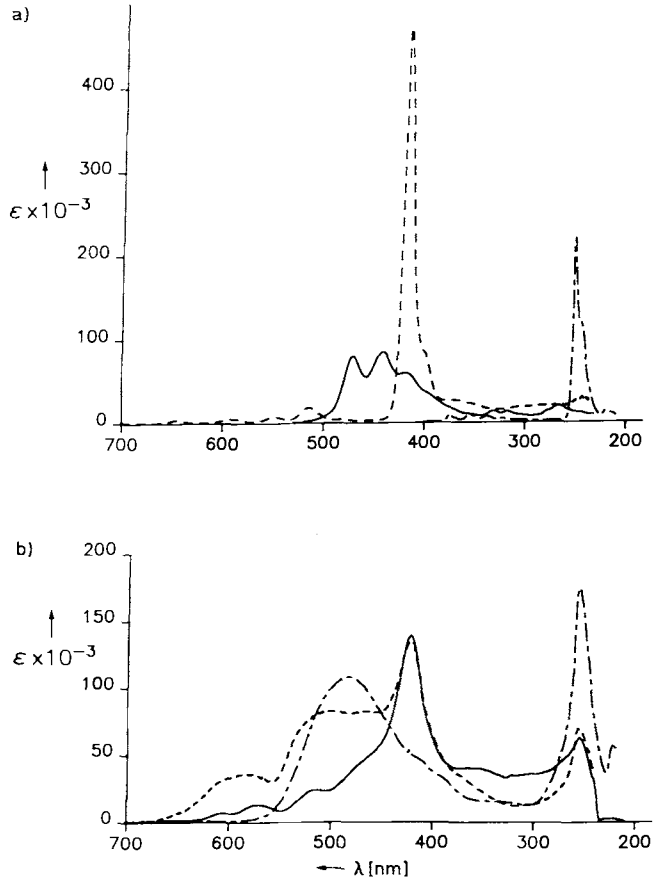

Fig. 1. Absorption spectra (CH_2Cl_2, T=295 K) of a) TMEN (——), anthracene (—·—·—), and 5,10,15,20-tetraphenylporphyrin (— — —), and of b) **3**-A,TPP (——), **6** (— — —), and **9**-A,A (—·—·—).

Evaluation of the absorption spectra accordingly reveals the not fully expected but important finding, especially as regards an application in the sense alluded to in the introduction, that a localized excitation of terminal groups is possible in the conjugated π-systems mentioned here.

In order to check whether an energy transport from an electronically excited terminal group via the conjugated polyene to another terminal group is possible we chose the compounds **3**-A,TPP and **6**, in which the absorption and emission bands of the relevant molecular moieties are adequately separated. Figures 2a and 2b show the corrected emission spectra[7] of anthracene and tetraphenylporphyrin and of **3**-A,TPP, respectively (*n*-hexane, T=180 K, excitation at 257 nm). Compared to the emission spectrum of the anthracene-tetraphenylporphyrin mixture, the emission spectrum of **3**-A,TPP shows a decrease in the anthryl emission with concomitant increase in the tetraphenylporphyrinyl emission.

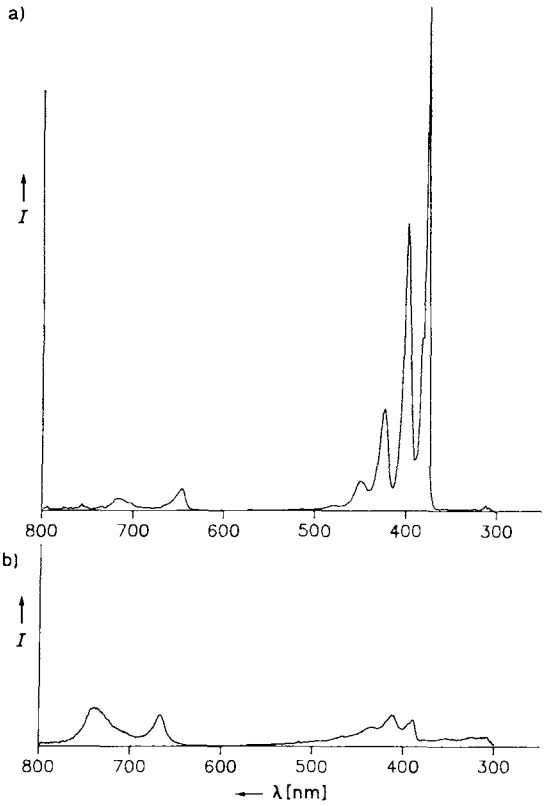

Fig. 2. Emission spectra (*n*-hexane, T=180 K, excitation at 257 nm) of a) anthracene/5,10,15,20-tetraphenylporphyrin (1/1), concentration 10^{-6} mol L^{-1} (the spectrum corresponds to a superposition of the individual spectra) and of b) **3**-A,TPP, concentration 2×10^{-5} mol L^{-1} (the origin of the weak emission between 300 and 380 nm is still unknown).

From the corrected excitation spectra of the compounds **3**-A,TPP and **6** shown in Figure 3 it clearly follows that, depending upon the excitation wavelength, the emission intensity of the TPP terminal group at 665 nm shows a

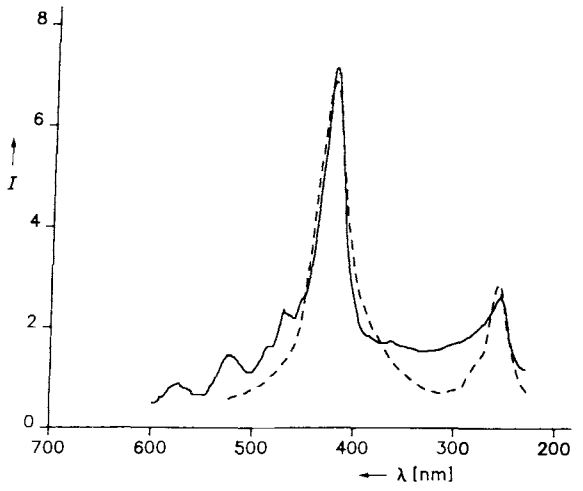

Fig. 3. Excitation spectra at T=295 K. Detection at 665 nm. **3**-A,TPP (——) and **6** (— — —).

maximum upon excitation with 256 nm, corresponding to the absorption band of the anthryl substituent. A TPP emission is not observed upon excitation in the range of

the polyene absorption of the compound **6** (at ca. 500 nm).

The time resolved measurements of the emission (picosecond laser pulse excitation, single-photon counting detection) gave no significant changes of the time constants for the growth and decay behavior of the coupled systems **3**-A,TPP and **6** compared to anthracene and tetraphenylporphyrin. The time constants for the growth are in all cases <25 ps, while those for the decay lie between 3.6 and 5.5 ns.

All the emission and excitation spectroscopic findings are consistent with an intramolecular energy transport from the excited anthryl group via the polyene chain to the TPP substituent, which then emits in competition with the anthryl group. Other known energy transfer mechanisms such as reabsorption,[8] Förster mechanism[9] or light-induced electron transfer[1] are not involved. The independence of the emission spectra on the concentration and the short growth times of the TPP emission rule out reabsorption and an intermolecular energy transfer by Förster mechanism. In the case of an intramolecular energy transfer by long distance interactions as described by *Förster* a shortening of the anthryl emission decay time should be observed, as also in the case of an electron transfer from the anthryl- to the TPP-substituent.

For an explanation of the observed energy transport we must therefore assume that the energy absorbed in the anthryl substituent leads only to partial relaxation into the anthryl S_1 state, which then emits. Occupation of an energy state delocalized over the molecule competes with this; after relaxation into the first excited singlet state of the TPP group the corresponding emission finally takes place.

Received: November 2, 1987;
revised: November 30, 1987 [Z 2491 IE]
German version: *Angew. Chem. 100* (1988) 274

Formation of Cycloheptatriene/Norcaradiene Systems in the Decomposition of Diaryldiazomethanes in Benzene**

By *Klaus Hannemann**

Whereas numerous carbenes are known to react with benzene to form cycloheptatriene/norcaradiene systems,[1] to our knowledge this reaction has hitherto not been observed with diphenylcarbene. Benzophenone azine **3a** and small amounts of tetraphenylethane **4a** and tetraphenylethene **5a** were mainly obtained as products of the thermal and photochemical decomposition of diphenyldiazomethane **1a** (Scheme 1).[2] We have now been able to observe addition of the corresponding carbenes **2** to benzene in the thermal decomposition of diphenyldiazomethane **1a** and its *ortho*-methyl derivative **1b** and to isolate the previously unknown cycloheptatriene/norcaradiene systems **6/7** in substantial yields.[3,4]

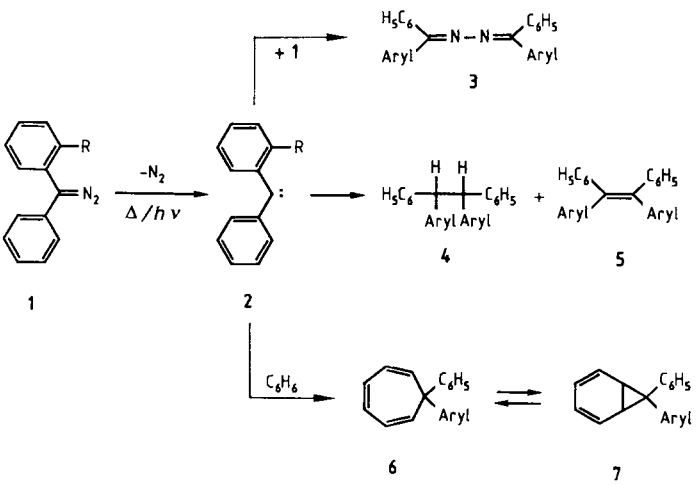

Scheme 1. Aryl = C_6H_4R; **a**, R = H; **b**, R = CH_3.

When the diazomethanes **1** are decomposed in boiling benzene the product composition strongly depends on the concentration of the starting material. At high concentrations of **1** the reaction of the carbene **2** with its precursor **1** dominates.[2] At greater dilution, reactions of **2** with the solvent and with traces of impurities such as water and oxygen predominate.

In the thermolysis of **1b** in boiling benzene (on a preparative scale, high dilution, complete absence of moisture and oxygen) an addition product of **2b** and benzene could be isolated in 31% yield.[5] Diphenylcarbene **2a** is less reactive: under the same conditions, only 8% of the addition products **6a/7a** were obtained. The same compounds are also formed on photolysis, but the yields are lower.[6]

The NMR spectra of the compounds are consistent with a cycloheptatriene/norcaradiene equilibrium.[7] The chemical shifts of the 1,6 H and C atoms of pure cyclohepta-

[1] a) H. Kuhn in W. Hoppe, W. Lohmann, H. Markl, H. Ziegler (Eds.): *Biophysik*, Springer, Berlin 1982, p. 289; b) J. R. Miller, L. T. Calcaterra, G. L. Closs, *J. Am. Chem. Soc. 106* (1984) 3047; c) H. Heitele, M. E. Michel-Beyerle, *ibid. 107* (1985) 8286; d) A. Leitner, M. E. Lippisch, S. Draxler, M. Riegler, F. R. Aussenegg, *Thin Solid Films 132* (1985) 55; e) J. A. Schmidt, A. Siemiarczuk, A. C. Weedon, J. R. Bolton, *J. Am. Chem. Soc. 107* (1985) 6112; f) D. Gust, T. A. Moore, P. A. Lidell, G. A. Nemeth, L. R. Makings, A. L. Moore, D. Barret, P. J. Pessiki, R. V. Bensasson, M. Rougée, C. Chachaty, F. C. De Schryver, M. Van der Auweraer, A. R. Holzwarth, J. S. Connolly, *ibid. 109* (1987) 846; g) D. N. Beratan, *ibid. 108* (1986) 4321.

[2] a) M. Calvin, *Acc. Chem. Res. 11* (1978) 369; b) H. B. Gray, *Chem. Soc. Rev. 15* (1986) 17; c) H. Kuhn, *Phys. Rev. A 34* (1986) 3409; d) A. D. Joran, B. A. Leland, P. M. Felker, A. H. Zewail, J. J. Hopfield, P. B. Dervan, *Nature (London) 327* (1987) 508.

[3] a) R. W. Munn, *Chem. Br. 20* (1984) 518; b) T. S. Arrhenius, M. Blanchard-Desce, M. Dvolaitzky, J. M. Lehn, J. Malthete, *Proc. Natl. Acad. Sci. USA 83* (1986) 5355; c) J. M. Lehn, *Angew. Chem. 100* (1988) 91; *Angew. Chem. Int. Ed. Engl. 27* (1988) 89.

[4] All the new compounds **2**, **3**, **5**, **6** and **8**–**11** gave correct analyses and/or correct values in the high resolution mass spectrum. The IR and ^{1}H-NMR spectroscopic data are in agreement with the given structures.

[5] E. Clar: *Polycyclic Hydrocarbons*, Academic Press, New York 1964.

[6] J. R. Platt in A. Hollaender (Ed.): *Radiation Biology, Vol. III*, McGraw-Hill, New York 1956, p. 96.

[7] The experimental results are independent of the sample volume and concentration ($2\times10^{-5}>c>2\times10^{-6}$ mol L^{-1}) upon 90° detection (range of optical density (OD): $0.84>OD_{max}>0.028$). The samples were degassed in five freeze-thaw cycles.

[8] F. Dörr in W. Hoppe, W. Lohmann, H. Markl, H. Ziegler (Eds.): *Biophysik*. Springer, Berlin 1982, p. 275.

[9] T. Förster, *Z. Naturforsch. A 4* (1949) 321.

[10] a) G. Pattenden, J. E. Way, B. C. L. Weedon, *J. Chem. Soc. C 1970*, 235; b) K. Bernhard, F. Kienzle, H. Mayer, R. K. Mueller, *Helv. Chim. Acta 63* (1980) 1473.

[*] Dr. K. Hannemann
Institut für Physikalische Chemie der Universität
Klingelbergstrasse 80, CH-4046 Basel (Switzerland)

[**] The author thanks the Fonds der Chemischen Industrie for a Liebig fellowship, Professor *J. Wirz* for his generous support of this work, and Professor *H. Fritz* (Ciba-Geigy) for the 400-MHz NMR spectrum. This work was financed by the Schweizerischen Nationalfonds zur Förderung der Wissenschaftlichen Forschung (Project No. 2.034-086) and the CIBA-Stiftung.

trienes lie at $\delta = 5.2$–5.3 and 120–130, respectively, whereas typical norcaradienes absorb at $\delta = 2.8$–3.5 and 35–45, respectively (Table 1). The resonances of equilibrium systems lie between these values, and from their position the position of the cycloheptatriene/norcaradiene equilibrium can be estimated.[8] The addition compound of **2a** and benzene shows shifts of $\delta = 4.54$ and 96.20 for the 1,6 H and C atoms, from which it can be estimated that ca. 35% of the norcaradiene form **7a** is present in the equilibrium at room temperature. In contrast, the resonances at $\delta = 2.87$ and 42.27 for the 1,6 H and C atoms, respectively, of the addition product of **2b** and benzene show that this is present entirely as the norcaradiene **7b**. Hence, the *ortho*-methyl group influences the position of the cycloheptatriene/norcaradiene equilibrium considerably.

Table 1. NMR data of some cycloheptatrienes (CHT) and norcaradienes (NCD).

Substitution pattern	Isomer	^{1}H-NMR [a] 1,6-H	2,5-H	3,4-H	^{13}C-NMR [a] 1,6-C	7-C
7-*tert*-Butyl [b] [8b]	CHT	5.21	6.09	6.57	126.0	50.6
7-Phenyl [b]	CHT	5.31	6.14	6.63		
7-Spirofluorenylidene [c]	CHT/NCD	4.74	6.16			
7,7-Diphenyl (**6a**) [d]	CHT/NCD	4.54	6.36	6.02	96.20	43.76
7-Phenyl-7-*o*-tolyl (**7b**) [d]	NCD	2.87	6.25	5.71	42.27	26.06
7,7-Dicyano [e]	NCD	3.47	6.2–6.8			
1,6-(1,3-Propanediyl) [8b]	NCD				38.6	20.2

[a] Chemical shift δ relative to TMS. [b] H. Günther, M. Görlitz, H.-H. Hinrichs, *Tetrahedron 24* (1968) 5665. [c] H. Dürr, H. Kober, *Angew. Chem. 83* (1971) 362; *Angew. Chem. Int. Ed. Engl. 10* (1971) 342. [d] ^{1}H-NMR in [D$_6$]acetone, ^{13}C-NMR in $CDCl_3$. [e] C. Ganter, J. D. Roberts, *J. Am. Chem. Soc. 88* (1966) 741.

Studies on the influence of substituents on the cycloheptatriene/norcaradiene equilibrium showed that the norcaradiene form can be stabilized by π-acceptors in position 7,[9] by incorporation of the norcaradiene in ring systems,[8b, 10] and by steric effects.[11] Electronic effects are unlikely to be responsible for the shift in the equilibrium **6** ⇌ **7** on going from **6a/7a** to **6b/7b**, since a *para*-methyl group in similar systems shows no comparable effect[9f] and the methyl group shows a +I effect (negative Hammett constant) instead of a −I effect stabilizing the norcaradiene system. The strong influence of the *ortho*-methyl group on the cycloheptatriene-norcaradiene equilibrium is therefore probably due to steric interactions and thus represents a considerable "*ortho*" effect.

The addition of diarylcarbenes to benzene opens up the possibility of systematic studies on the influences of aryl substituents on the cycloheptatriene/norcaradiene equilibrium.

Experimental

A solution of **1** in benzene was added dropwise over a period of 24 h to 250 mL of boiling anhydrous benzene under N_2; the mixture was then heated under reflux for a further 24 h. After removal of the benzene, the crude product was separated by column chromatography (silica gel, gradient elution with hexane containing 0.5–3% ethyl acetate).

a) Products of the reaction with **1a** (1.40 g, 7.21 mmol) in benzene (150 mL): 4 mg (0.7%) of biphenyl, 140 mg (8%) of **6a/7a**, 102 mg of a mixture of **4a**, **5a** and two further unidentified compounds, 78 mg (6%) of benzophenone, 770 mg (59%) of **3a**.

b) Products of the reaction with **1b** (500 mg, 2.40 mmol) in benzene (50 mL): traces of biphenyl, 55 mg (13%) of phenylcyclobutabenzene, 210 mg (34%) of **7b**, 20 mg (4%) of **4b**, 27 mg (6%), of 2-methylbenzophenone, 95 mg (20%) of **3b**.

Received: September 4, 1987 [Z 2421 IE]
German version: *Angew. Chem. 100* (1988) 273

CAS Registry numbers:
1a, 883-40-9; **1b**, 52506-26-0; **3a**, 983-79-9; **3b**, 71104-26-2; **4a**, 632-50-8; **4b**, 37834-54-1; **5a**, 632-51-9; **6a**, 112423-70-8; **7a**, 112423-71-9; **7b**, 112423-72-0; 2-methylbenzophenone, 131-58-8; phenylcyclobutabenzene, 55190-64-2.

[1] a) W. Kirmse: *Carbene Chemistry*, 2nd Edit., Academic Press, New York 1971; b) M. Jones, Jr., R. A. Moss (Eds.): *Carbenes*, Wiley, New York 1973.

[2] a) H. Staudinger, E. Anthes, F. Pfenninger, *Chem. Ber. 49* (1916) 1928; b) W. E. Parham, W. R. Hasek, *J. Am. Chem. Soc. 76* (1954) 935; c) W. Kirmse, L. Horner, H. Hoffmann, *Justus Liebigs Ann. Chem. 614* (1958) 19; d) D. R. Dalton, S. A. Liebman, *Tetrahedron 25* (1969) 3321; e) L. Benati, P. C. Montevecchi, P. Spagnolo, *J. Chem. Soc. Perkin Trans. 2 1981*, 1437.

[3] A tricarbonylchromium complex of **6a** has already been described: G. Simonneaux, G. Jaouen, R. Dabard, *Tetrahedron 36* (1980) 893. **6a** and other substituted cycloheptatrienes are also accessible via addition of diazomethanes to benzvalene after denitrogenation of the adduct and subsequent catalyzed rearrangement. We thank Prof. *M. Christl* for informing us of these unpublished results.

[4] Reviews: a) G. Maier, *Angew. Chem. 79* (1967) 446; *Angew. Chem. Int. Ed. Engl. 6* (1967) 402; b) D. Wendisch in *Houben-Weyl-Müller: Methoden der organischen Chemie, Vol. IV/3*, 4th Edit., Thieme, Stuttgart 1972, p. 509; c) H. Kessler, *ibid., Vol. V/1d*, p. 301.

[5] Aside from other products, 12% of phenylcyclobutabenzene could be isolated, which is formed by intramolecular H-abstraction and subsequent ring closure. At room temperature, cyclobutabenzene is formed in traces only; upon pyrolysis (325°C), however, it is formed in more than 50% yield. This is consistent with findings on comparable systems: H. E. Zimmermann, D. H. Paskovich, *J. Am. Chem. Soc. 86* (1964) 2149.

[6] The efficiency of the photochemical addition of carbene to benzene is temperature-dependent: photolysis of **1b** at 50°C furnished 13% of **6b/7b**, that at room temperature 10% of **6b/7b**.

[7] 7-(2-Methylphenyl)-7-phenylbicyclo[4.1.0]hepta-2,4-diene **7b**: colorless needles, m.p. 70–71°C (MeOH), b.p. 100–110°C/0.05 torr (Kugelrohr), ^{1}H-NMR ($CDCl_3$, 400 MHz): $\delta = 2.22$ (s, 3H; Me), 2.87 (m, $J_{1,2} = 5.7$, $J_{1,6} = 8$ Hz, 2H; 1,6-H), 5.71 (m, $J_{2,3} = 9.6$, $J_{2,4} = 0.7$, $J_{3,4} = 6.2$ Hz, 2H; 3,4-H), 6.25 (m, $J_{2,5} = 0.8$ Hz, 2H; 2,5-H), 6.86 (m, 2H; aryl-H), 7.00–7.22 (m, 7H; aryl-H).—^{13}C-NMR ($CDCl_3$): $\delta = 19.95$ (q), 26.06 (s), 42.27 (d), 123.71 (d), 124.49 (d), 124.75 (d), 125.21 (d), 126.31 (d), 126.77 (d), 128.07 (d), 130.70 (d), 134.21 (d), 135.67 (s), 139.02 (s), 146.03 (s).—MS (70 eV): *m/z* 258 (79%, $M^{\oplus}$), 243 (70%), 181 (33%), 179 (30%), 178 (22%), 167 (35%), 166 (43%), 165 (100%), 152 (16%).—7,7-Diphenylcycloheptatriene **6a**: colorless needles, m.p. 104–105°C (MeOH), ^{1}H-NMR ([D$_6$]acetone, 90 MHz): $\delta = 4.54$ (m, 2H; 1,6-H), 6.02 (m, 2H; 3,4-H), 6.36 (m, 2H; 2,5-H), 7.05–7.24 (m, 10H; aryl-H).—^{13}C-NMR ($CDCl_3$): $\delta = 43.76$ (s), 96.20 (d), 125.44 (d), 125.92 (d), 127.58 (2d), 128.94 (d), 145.71 (s).—MS (70 eV): *m/z* 244 (30%, $M^{\oplus}$), 243 (12%), 167 (44%), 166 (36%), 165 (100%), 152 (12%), 115 (12%), 51 (10%).

[8] For examples see a) M. Görlitz, H. Günther, *Tetrahedron 25* (1969) 4467; b) H. Günther, T. Keller, *Chem. Ber. 103* (1970) 3231; c) G. E. Hall, J. D. Roberts, *J. Am. Chem. Soc. 93* (1971) 2203; d) K. Takeuchi, H. Fujimoto, K. Okamoto, *Tetrahedron Lett. 22* (1981) 4981.

[9] H. Günther, *Tetrahedron Lett. 1970*, 5173; b) R. Hoffmann, *ibid. 1970*, 2907; c) H. Günther, W. Peters, R. Wehner, *Chem. Ber. 106* (1973) 3683; d) W. Betz, J. Daub, *Chem. Ber. 107* (1974) 2095; e) G. Maas, M. Regitz, *Chem. Ber. 109* (1976) 2039; f) K. Takeuchi, H. Fujimoto, T. Kitagawa, H. Fujii, K. Okamoto, *J. Chem. Soc. Perkin Trans. 2 1984*, 461.

[10] H. Günther, H.-H. Hinrichs, *Justus Liebigs Ann. Chem. 706* (1967) 1.

[11] a) H. Tsuruta, S. Mori, T. Mukai, *Chem. Lett. 1974*, 1127; b) K. Takahashi, K. Takase, H. Toda, *ibid. 1981*, 979; c) K. Takeuchi, T. Kitagawa, A. Ueda, Y. Senzaki, K. Okamoto, *Tetrahedron 41* (1985) 5455, and references cited therein.

C_5 Building Blocks for Terpene Syntheses: γ-Acetoxylation of (*E*)-2-Methyl-2-butenals

By *Rolf H. Fischer,* Heinz Krapf,* and *Joachim Paust*

Dedicated to Professor Helmut Dörfel on the occasion of his 60th birthday

The (*E*)-2-methyl-2-butenals **1** and **2** containing acetoxy groups are important C_5 building blocks for the synthesis of terpenes by means of the Wittig reaction. Thus, (*E*)-3-

[*] Dr. R. H. Fischer, Dr. H. Krapf, Ammoniaklaboratorium
Dr. J. Paust, Hauptlaboratorium
BASF Aktiengesellschaft, D-6700 Ludwigshafen (FRG)

 © VCH Verlagsgesellschaft mbH, D-6940 Weinheim, 1988 0570-0833/88/0202-0285 $ 02.50/0

formyl-2-butenyl acetate **1** is of industrial importance for the production of vitamin A.[1] In unilaterally protected dialdehydes, such as (*E*)-3-formyl-2-butenylidene diacetate **2**, first the free, then—after hydrolysis of the protecting group—the capped aldehyde can each be allowed to react with a different ylide.[2]

1: R^1=OAc, R^2=H
2: R^1, R^2=OAc

3

1 can either be prepared from C_1- to C_3-starting compounds such as acetylene and acetone or acetylene, formaldehyde and carbon monoxide,[1] or by functionalization of the C_5 skeleton already present in isoprene.[3] For the synthesis of **2**, only the oxidation of 3-methyl-2-butenylidene diacetate ("4,4-diacetoxy-2-methyl-2-butene") with selenium dioxide has previously been described.[2a]

An attractive starting compound for the preparation of **1** and **2** is (*E*)-2-methyl-2-butenal (tiglaldehyde) **3**, which contains all the structural elements of **1** excepting the acetoxy group and, e.g., is readily accessible from isoprene epoxide[3a] or 2-methyl-2-butenylene diacetate ("1,4-diacetoxy-2-methyl-2-butene").[4]

Attempts to convert **3** into **1** in one step by acetoxylation have thus far met with little success.[5] On the other hand, if **3** is first converted into 2-methyl-1,3-butadienyl acetate **4** with isopropenyl acetate,[6] then a method already described for the 1,4-bisacetoxylation of butadiene can be used successfully for the synthesis of **1**.[7]

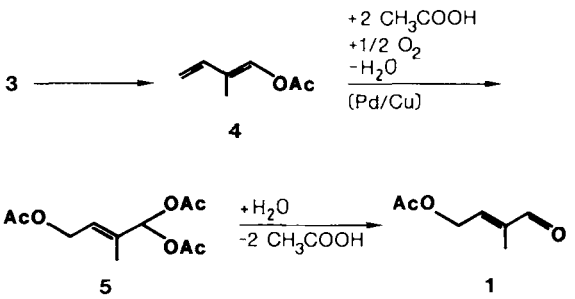

After reaction of **4** with glacial acetic acid and oxygen at 95°C in the presence of a suspension of supported Pd/Cu catalyst (5% Pd, 9% Cu on activated carbon)[8] we isolated **1** in 28% yield and (*E*)+(*Z*)-2-methyl-2-butene-1,1,4-triyl triacetate **5** in 37% yield. For the preparation of pure **1**, the reaction products, after removal of catalyst by filtration, were worked-up by hydrolysis. Although **5** is present as an (*E*)/(*Z*)-mixture (53% *E*, 47% *Z*), **1** can be isolated (yield 66%), after hydrolysis of **5**, with an (*E*)-content of 98%.

Using the same principle, other α,β-unsaturated aldehydes instead of **3**, such as 2-butenal, 3-methyl-2-butenal, and 3-formylallyl acetate ("4-acetoxy-2-butenal"), can be acetoxylated via dienyl acetates to tri- and tetraacetoxylated 2-butenes.

For the conversion of **1** into **2** via 2-methyl-1,3-butadienylene diacetate **6**[9] we could not use the 1,4-bisacetoxylation method: namely, the (*E*)/(*Z*)-mixture of the 1,1,4,4-tetraacetates obtained by acetoxylation of **6** could not be hydrolyzed to **2** with sufficient regioselectivity.

On the other hand, it was possible to oxidize **6** to **2** with anhydrous peracetic acid[10] at 100°C in glacial acetic acid as solvent (yield ca. 50%).[11] The (*E*)-fraction of **2** amounted to 69% and could be increased to 83% by addition of strongly acidic ion-exchangers.[12]

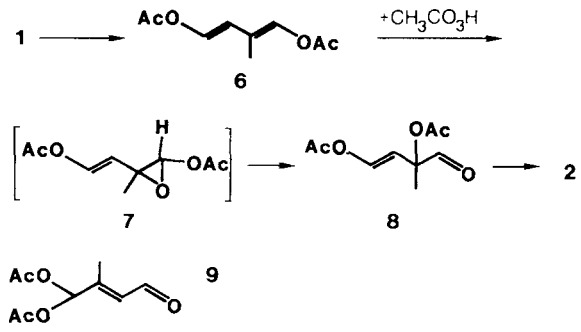

In the reaction of **6** with peracetic acid the methyl-substituted double bond should be epoxidized with high regioselectivity, as in the case of isoprene.[3a] The epoxide **7** formed thereby is presumably converted into **2** via the aldehyde **8** (allyl rearrangement). Consistent with this explanation is the fact that, after epoxidation of **6** with *m*-chloroperbenzoic acid in chloroform, a mixture of **8** and its (*Z*)-isomer together with **2** could be isolated and identified by ^{1}H-NMR spectroscopy.[13] The ester **9**, isomeric with **2**, was isolated as by-product (yield 2%). The (*E*)-form shown here is consistent with the ^{1}H-NMR spectrum.

Interesting secondary products are accessible from **2**: Thus, on heating with acetic acid in the presence of *p*-toluenesulfonic acid, **2** is converted into 3-methyl-2(5*H*)-furanone **10**.[14] Upon acetalization with trimethyl orthoformate the C_5 building block (*E*)-4,4-dimethoxy-3-methyl-2-butenal is formed in the form of its acylal **11**.[15]

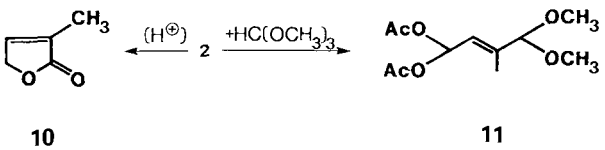

10 **11**

Experimental

1+5: 63 g (0.5 mol) of **4** was added dropwise within 4 h at −95°C to a stirred suspension of 25 g of Pd/Cu catalyst (5% Pd, 9% Cu on activated carbon) [8a] in 600 g of glacial acetic acid in a three-necked flask fitted with a gassing stirrer; at the same time 12 L of O_2 were passed into the solution. A further 3 L of O_2 were then passed into the solution within 1 h at 95°C and stirring continued for 15 min with simultaneous passage of N_2. After cooling, the catalyst was removed by suction. According to combined GC/MS the reaction product (663 g) contained **1** and **5** together with small amounts of **3** and 1-formyl-1-methylallyl acetate ("2-acetoxy-2-methyl-3-butenal"). After fractional distillation, 20.4 g of **1**, b.p. 92–95°C/16 mbar ((*E*)/(*Z*) ratio according to GC 98:2) (28% based on **4**) and 44.9 g of **5**, b.p. 118–124°C/0.8 mbar, n_D^{20} = 1.4492 ((*E*)/(*Z*) ratio according to ^{1}H-NMR ca. 1:1) (37% based on **4**) were isolated.—^{1}H-NMR (250 MHz, $CDCl_3$, TMS int.): (*E*)-**5**: δ = 1.78 (s, CH_3, 3 H), 2.03–2.12 ($COCH_3$, 9 H), 4.66 (d, OCH_2, *J* = 6.6 Hz, 2 H), 5.86 (t, =CH−, 6.6 Hz, 1 H), 7.05 (s, −OCHO−, 1 H). (*Z*)-**5**: δ = 1.84 (s, CH_3, 3 H), 2.03–2.12 ($COCH_3$, 9 H), 4.79 (d, OCH_2, *J* = 7.0 Hz, 2 H), 5.61 (t, =CH−, *J* = 7.0 Hz, 1 H), 7.48 (s, −OCHO−, 1 H).

1: The reaction product, after removal of catalyst by filtration and addition of 29 g (1.6 mol) of H_2O, was heated under reflux for 4 h. After work-up by distillation, 48.1 g of **1** (66% based on **4**) ((*E*)/(*Z*) ratio 98:2) was obtained.

2: A suspension of 10 g of acidic ion-exchanger (®Amberlite IR-120, H-form; previously washed anhydrously with glacial acetic acid) in a solution of **6**

(184 g, 1 mol) (60% (*E,E*), 18% (*Z,E*), 17% (*E,Z*), and 5% (*Z,Z*)) and 500 g of glacial acetic acid was treated at 100±2°C within 1 h with a solution of 806 g (1.2 mol) of 11.3% anhydrous peracetic acid [10] in glacial acetic acid and then stirred a further 10 min at the same temperature. After removal of ion-exchanger from the peroxide-free solution by filtration, removal of the acetic acid (rotary evaporator, 45°C/215 mbar), and distillation (Vigreux column), 141 g of crude **2**, b.p. 86–102°C/0.9 mbar was obtained (GC analysis: 80% **2** + (*Z*)-isomer, 2% **8**, 3% (*Z*)-isomer of **8** and 6% **9**; the percentage amounts are based on peak areas in the gas chromatogram). Fractional distillation (1 m rotary band column) furnished 117 g of **2**, b.p. 79–81°C/0.1 mbar (GC purity: 97%, (*E*)/(*Z*) ratio according to ^{1}H-NMR (ratio of aldehyde protons) 83:17) (47% based on **6**) and 4 g of **9**, b.p. 87–88°C/0.15 mbar (GC purity 86%) (2% based on **6**). **2** and **9** gave correct elemental analyses.—Under the same conditions, but without ion-exchanger, 125 g of **2** ((*E*)/(*Z*)-ratio 69:31) (43% based on **6**) was obtained after fractional distillation.—^{1}H-NMR (250 MHz, $CDCl_3$, TMS int.). **2**: δ=1.90 (d, CH_3, J=1.5 Hz, 3H), 2.15 (s, $COCH_3$, 6H), 6.40 (q, d, =CH–, J=1.5 Hz, 7.7 Hz, 1H), 7.60 (d, –OCHO–, J=7.7 Hz, 1H), 9.50 (s, –CHO, 1H).—(*Z*)-form of **2**: δ=1.87 (d, CH_3, J=ca. 1.6 Hz, 3H), 2.15 (s, $COCH_3$, 6H), ca. 6.40 (q, d, =CH–, J=ca. 2 Hz, ca. 8 Hz, 1H), 7.98 (d, –OCHO–, J=8.6 Hz, 1H), 10.30 (s, –CHO, 1H).—**9**: δ=2.14 (s, $COCH_3$, 6H), 2.22 (d, CH_3, J=2 Hz, 3H), 6.19 (q, d, –CH=, J=2 Hz, 7 Hz, 1H), 7.15 (s, –OCHO–, 1H), 10.08 (d, –CHO, J=7 Hz, 1H).

Received: October 7, 1987;
revised: December 18, 1987 [Z 2468/2469 IE]
German version: *Angew. Chem. 100* (1988) 301

CAS Registry numbers:
1, 26586-02-7; (*E*)-**2**, 56269-66-0; (*Z*)-**2**, 101513-14-8; **3**, 497-03-0; **4**, 72808-94-7; (*E*)-**5**, 72808-95-8; (*Z*)-**5**, 72808-96-9; (*E,E*)-**6**, 52884-86-3; (*Z,E*)-**6**, 59491-15-5; (*E,Z*)-**6**, 59491-14-4; (*Z,Z*)-**6**, 55378-59-1; (*E*)-**8**, 88543-51-5; (*Z*)-**8**, 88543-52-6; **9**, 112549-36-7; **10**, 22122-36-7; **11**, 112549-37-8; Isoprenyl acetate, 108-22-5; 1-formyl-1-methylallyl acetate, 88031-98-5; 4-hydroxy-2-methyl-2-butenylidene diacetate, 88032-00-2.

[1] H. Pommer, A. Nürrenbach, *Pure Appl. Chem. 43* (1975) 527.
[2] a) J. Paust, W. Reif, H. Schumacher, *Liebigs Ann. Chem. 1976*, 2194; b) K. Schmieder, J. Paust, R. Fischer, H.-M. Weitz, Eur. Pat. 112502 (1983), BASF AG; *Chem. Abstr. 101* (1984) 171563.
[3] a) G. Eletti-Bianchi, F. Centini, L. Re, *J. Org. Chem. 41* (1976) 1648; b) J. H. Babler, M. J. Coghlan, M. Feng, F. Fries, *ibid. 44* (1979) 1716, and references cited therein.
[4] R. Fischer, H.-M. Weitz, Eur. Pat. 4622 (1978), BASF AG; *Chem. Abstr. 92* (1980) 75861.
[5] The conversion of **3** into (*E*)-4-chloro-2-methyl-2-butenal (yield 55%), which can be acetoxylated to **1** with alkali-metal acetates, was already known. However, stoichiometric amounts of alkali-metal chloride are thereby formed (K. H. Dietl, J. R. Normark, D. A. Payne, J. G. Thweatt, D. A. Young, *Tetrahedron Lett. 1973*, 1719).
[6] H. J. Hagemeyer, D. C. Hull, *Ind. Eng. Chem. 41* (1949) 2920. Analogously to 2-ethylacrolein, **3** could be converted with isopropenyl acetate into **4** (yield 79%).
[7] Butadiene reacts with acetic acid and oxygen in the presence of doped, supported Pd catalysts to give (*E*)/(*Z*)-2-butenylene diacetate ("1,4-diacetoxy-2-butene"); a) T. Onoda, J. Haji, DOS 2217452 (1971), Mitsubishi Chem. Ind.; *Chem. Abstr. 78* (1973) 57786; b) K. Takehira, H. Mimoun, J. S. De Roch, *J. Catal. 58* (1979) 155. This reaction is the key step of a 1,4-butanediol synthesis that has been realized on an industrial scale (Y. Tanabe, *Hydrocarbon Process. 60* (1981) 187).
[8] Preparation of the Pd/Cu catalysts: a) H.-M. Weitz, J. Hartig, L. Marosi, DOS 2820519 (1978), BASF AG; *Chem. Abstr. 92* (1980) 110551.—Pd/Te [7a] and Pd/Cu/Te catalysts [8b] can also be used instead of the Pd/Cu catalysts; b) H. M. Weitz, R. Fischer, R. Schnabel, DOS 2943407 (1979), BASF AG; *Chem. Abstr. 95* (1981) 61536).
[9] a) J. F. Keana, P. E. Eckler, *J. Org. Chem. 41* (1976) 2625; b) H.-M. Weitz, R. Fischer, J. Paust, Eur. Pat. 110309 (1982), BASF AG; *Chem. Abstr. 101* (1984) 170716.
[10] R. Criegee in Houben-Weyl: *Methoden der Organischen Chemie, Vol. VIII*, 4th Edit., Thieme, Stuttgart 1952, p. 41.
[11] The epoxidation of **4**, on the other hand, proceeds less selectively under the conditions given for **2** in the experimental section. Not only the expected **1** is isolated (22%) but also 1-formyl-1-methylallyl acetate ("2-acetoxy-2-methyl-3-butenal") (23%) and a mixture of 4-hydroxy-2-methyl-2-butenylidene diacetate ("1,1-diacetoxy-4-hydroxy-2-methyl-2-butene") and **5**.
[12] Larger amounts of ion-exchanger in the epoxidation, or heating of (*Z*)-isomer containing **2** in the presence of this exchanger increase the (*E*)-fraction—albeit with losses in yield—to ca. 95%.
[13] H.-M. Weitz, R. Fischer, J. Paust, Eur. Pat. 89586 (1983), BASF AG; *Chem. Abstr. 100* (1984) 51088.
[14] R. Fischer, H.-M. Weitz, DOS 3210705 (1982), BASF AG; *Chem. Abstr. 100* (1984) 34399.
[15] B. Schulz, R. Fischer, DOS 3622601 (1986), BASF AG.

Synthesis and Structure of an Azastibacubane**

By *Walter Neubert, Hans Pritzkow,* and *Hans P. Latscha**

Antimony(v)-nitrogen compounds are formed only when the basicity of the nitrogen is reduced by electron-attracting groups or by mesomeric effects. Furthermore, the nitrogen-containing reaction partner must be relatively insensitive towards oxidation.[1–3] Amines, for example, react with antimony pentachloride to give, inter alia, mixed valence compounds;[4] single valence products can only be obtained if trimethylsilyl-substituted amines are used.

On allowing antimony pentachloride to react with methylbis(trimethylsilyl)amine [Eq. (a)] we obtained pale yellow crystals of **1** in good yield.

$$4\,SbCl_5 + 4((CH_3)_3Si)_2(CH_3)N \longrightarrow (CH_3NSbCl_3)_4 + 8\,(CH_3)_3SiCl \quad \text{(a)}$$

1

1 is the first compound whose cubane-like structure is entirely made up of nitrogen and antimony atoms (Fig. 1).[5] The molecule has a fourfold rotary inversion axis; the Sb–N distances are comparable with those in Sb_2N_2 four-membered rings.[2,6]

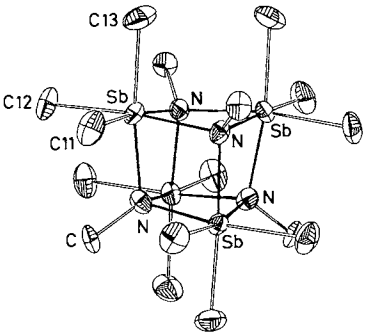

Fig. 1. Molecular structure of **1**. Important bond lengths [Å] and angles [°]: Sb–Cl 2.320–2.337(3), Sb–N 2.151–2.189(10), N–C 1.504(13); Sb–N–Sb 99.6–100.8(4), N–Sb–N 78.2–79.1(3).

Experimental

Separate solutions of equimolar amounts of $SbCl_5$ and of $((CH_3)_3Si)_2(CH_3)N$ in CH_2Cl_2 were prepared. Both were made as dilute as possible. The $SbCl_5$ solution was added dropwise and slowly at room temperature to the stirred silylamine solution. After addition was complete the mixture was heated for about 1 h under reflux. Finally, the solvent together with trimethylchlorosilane was removed from the mixture by distillation. The residue was then extracted with CH_2Cl_2. On evaporation of the extract to dryness, yellow crystals of **1** were obtained. They are soluble in aromatic and chlorinated hydrocarbons, and were purified by chromatography on silica gel (eluent cyclohexane/dichloromethane 3/1); m.p. 180°C (decomp.) yield ca. 55%.—IR spectrum (KBr pellet): $\tilde{\nu}$ [cm^{-1}]=3500–3400 (w, KBr), 3250 (w, NH), 2930 (w, ν(CH)), 2860 (w, ν(CH), 1440 (s, δ(CH)), 1410 (m, δ(CH)), 970 (s, ν(N–CH)), 780 (m), 635 (w), 530 (s, ν_{as}(SbN)), 395 (m, ν($SbCl_2$)), 330 (m, ν(SbCl), ν_s(SbN_2)).—^{1}H-NMR spectrum ($CDCl_3$, TMS as standard): δ=3.65. ^{13}C-NMR spectrum ($CDCl_3$): δ=35.9.—MS: *m/z* 984 ($M^{\oplus}$ – HCl).—Correct elemental analysis (C,H,N,Cl,Sb).

Received: August 6, 1987;
revised: October 7, 1987 [Z 2391 IE]
German version: *Angew. Chem. 100* (1988) 298

[*] Prof. Dr. H. P. Latscha, Dipl.-Chem. W. Neubert, Dr. H. Pritzkow
Anorganisch-chemisches Institut der Universität
Im Neuenheimer Feld 270, D-6900 Heidelberg (FRG)

[**] This work was supported by the Fonds der Chemischen Industrie.

CAS Registry numbers:
1, 112373-65-6; $SbCl_5$, 7647-18-9; $((CH_3)_3Si)_2(CH_3)N$, 920-68-3.

[1] a) B. Milewsky, W. Dietrich, H. P. Latscha, *Chem. Ztg. 103* (1979) 401; b) U. Müller, *Z. Anorg. Allg. Chem. 422* (1976) 134; c) O. Morschheuser, H. P. Latscha, *ibid. 525* (1985) 29, see also references [1] and [2] cited therein; d) N. Wiberg, K. H. Schmid, *Chem. Ber. 100* (1967) 741.

[2] G. Rajca, W. Schwarz, J. Weidlein, *Z. Naturforsch. B39* (1984) 1219.

[3] H. D. Hausen, W. Schwarz, G. Rajca, J. Weidlein, *Z. Naturforsch. B41* (1986) 1223.

[4] a) G. Birke, H. P. Latscha, H. Pritzkow, *Z. Naturforsch. B31* (1976) 1285; b) W. Dietrich, H. Eisinger, H. P. Latscha, J. Pebler, K. Schmid, *ibid. 34* (1979) 1454; c) H. Eisinger, H. P. Latscha, *ibid. 34* (1979) 1059.

[5] **1**: space group $P\bar{4}2_1c$, $a=b=10.044(1)$, $c=12.472(2)$ Å, $V=1258$ Å^3, $Z=2$, $R=0.033$ for 595 independent reflections (Siemens-Stoe AED, ω-scan, $Mo_{K\alpha}$ radiation). Further details of the crystal structure investigation, are available on request from the Fachinformationszentrum Energie, Physik, Mathematik GmbH, D-7514 Eggenstein-Leopoldshafen 2 (FRG), on quoting the depository number CSD-52713, the names of the authors, and the journal citation.

[6] U. Müller, *Z. Anorg. Allg. Chem. 388* (1972) 207.

A Conjugated Bis(tetrathiafulvalene) System with Tetrathia-*s*-indacene Structure**

By *Peter Wolf, Herbert Naarmann,* and *Klaus Müllen**

Dedicated to Professor Helmut Dörfel on the occasion of his 60th birthday

The anisotropy of the charge transport in stacked charge-transfer (CT) complexes of the tetrathiafulvalene (TTF) series[1,2] leads, below a critical temperature, to reorganizations of the crystal lattice and thus to the breakdown of "metallic" states.[3,4] The distortions in the crystal lattice can be prevented if the electron transfer between neighboring donor stacks is facilitated and the dimensionality of the conduction process thus increased. Typical examples are CT complexes of bis(ethylenedithio)tetrafulvalene, in which the increase in dimensionality results from the special, unpredictable crystal structure.[5] Another more rarely investigated strategy consists in enabling the delocalization of electrons via neighboring donor stacks by covalent bonds. Following this concept we developed donor systems of larger molecules which contain conjugatively coupled TTF units.

We describe here the dibenzo-"bis"-TFF **1c** containing a benzene unit as "conjugative bridge". The tetrathia-*s*-indacenedithione system **2** appeared to be a suitable candidate as precursor, but the parent compound **2a** (R = H) is unsuitable due to its insolubility in organic solvents.[6] The advantage of **2** is that groups which improve the solubility can be readily incorporated. As starting material for the synthesis of soluble derivatives of **1** we chose the dihydroxy compound **2b**,[7] which we (cf. Ref. [8]) etherified with 3,5-di-*tert*-butylbenzyl bromide to give **2c** (acetone, K_2CO_3, 62%; m.p. 237 °C).[9] Possible disadvantageous effects of the bulky benzyl residue on the distance of neighboring donor units within TTF stacks were put up with in favor of the easy accessibility and improved solubility of the compounds **1**.

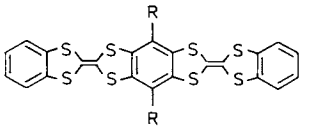

1c

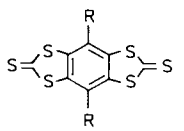

2a–c

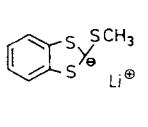

3·Li$^{\oplus}$

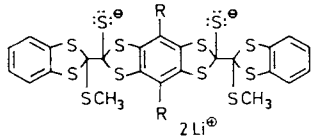

4c·2 Li$^{\oplus}$

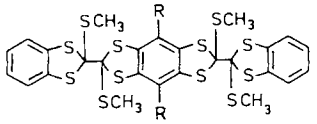

5c

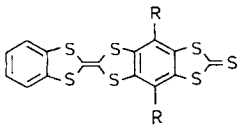

6c

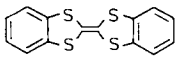

7

a, R = H; **b**, R = OH; **c**, R = 3,5-Di-*tert*-butylbenzyloxy

The method of choice for the coupling of the readily soluble dithione **2c** to bis-TFF systems proved to be that described by *Lindsay* et al.[10,11] and previously used only for the synthesis of unsymmetrical benzotetrathiafulvalenes. A solution of the trithioorthoformate anion **3** in tetrahydrofuran (THF) was treated (argon, −78 °C) dropwise with a THF-solution of **2c** (molar ratio 2 : 1), and the dithiolate ion **4c** that was formed initially was converted by addition of methyl iodide into the bis(hexathioorthooxalate) **5c** (colorless microcrystals, m.p. 119 °C; yield 66% after chromatography on silica gel [petroleum ether/chloroform 2 : 1] and recrystallization). An attempted reaction of the anion **3** with the unsubstituted analogue **2a** yielded only unchanged **2a** and methylated **3**.

Heating of a tetrachloroethane solution of **5c** resulted in extrusion of dimethyl disulfide and formation of the desired compound (orange needles, m.p. 242 °C [decomp.]; yield 45% after chromatography on silica gel [petroleum ether/chloroform 1 : 1] and recrystallization), which is readily soluble in organic solvents. Characteristic in the NMR spectra of **1c** are the resonances of the aromatic protons ($\delta_H = 7.10$–7.30 [8 H] and 7.30–7.48 [6 H]) due to an AA'BB' and an AB_2 system, and the resonances of the fulvalenic carbon atoms ($\delta_C = 110.7$ and 112.2).

Reaction of **2c** with only one equivalent of the anion **3** and work-up as previously described affords the monothione **6c**, which is a useful starting material for further coupling reactions.

The electrochemical oxidation of **1c** leads, according to cyclovoltammetry (dichloromethane, tetraethylammonium perchlorate, Ag/AgCl reference electrode), to reversible electron transfers at +0.70 and +1.00 V. These potentials largely correspond to those of the model system dibenzo-

[*] Prof. Dr. K. Müllen, Dipl.-Chem. P. Wolf
Institut für Organische Chemie der Universität
J.-J.-Becher-Weg 18–20, D-6500 Mainz 1
Dr. H. Naarmann
BASF Aktiengesellschaft, Kunststofflabor
D-6700 Ludwigshafen (FRG)

[**] This work was supported by the Bundesminister für Forschung und Technologie.

TFF 7, which under our conditions lie at +0.66 and +1.08 V.[12] In the ESR spectrum of the oxidatively generated radical cation $\mathbf{1c}^{\odot\oplus}$ (aluminum chloride, dichloromethane, hyperfine couplings of ^1H not resolved) the couplings of ^{32}S obtained from the satellites are of the same magnitude as those in the radical cation $7^{\odot\oplus}$.[13] Apparently the spin density in $\mathbf{1c}^{\odot\oplus}$ remains localized in a TTF unit.

Reaction of **1c** with dichlorodicyano-*p*-benzoquinone (DDQ) and with iodine, bromine and chlorine leads to the formation of CT complexes, but not, however, the attempted reaction with tetracyanoquinodimethane. In the case of the deep-green DDQ complex the composition determined by elemental analysis is 1:2, i.e. each TFF subunit binds one acceptor molecule. The IR spectrum of the complex shows a very broad, intense absorption band, which stretches from the NIR region to a wavelength of ca. 2000 cm^{-1}. This band is typical for mixed valence CT complexes with separate donor and acceptor stacks; it is generally attributed to an electron transition between neighboring donor molecules within a stack.[14]

The IR spectrum of the iodine complex of **1c** is similar, only the broad absorption band is shifted to shorter wavelengths. The composition determined by elemental analysis is, in this case, 1:1.52, i.e. 76% of the fulvenic centers are present in the oxidized state. The powder conductivity of the DDQ complex of **1c** is $10^{-8}\ \Omega^{-1}\ cm^{-1}$. This possibly reflects a greater TTF layer separation caused by the bulky substituents.

Further possibilities of the synthesis described here are the construction of higher molecular TTF systems and the variation of the substituents R, which also includes the generation of water-soluble substances.

Received: September 9, 1987 [Z 2426 IE]
German version: *Angew. Chem. 100* (1988) 290

CAS Registry numbers:
1c, 112549-49-2; **1c**·xI_2, 112549-51-6; **1c**·xBr_2, 112549-52-7; **1c**·xCl_2, 112549-53-8; **1c**·2DDQ, 112549-54-9; **2b**, 65211-71-4; **2c**, 112549-46-9; **3**, 90703-69-8; **4c**, 112549-47-0; **5c**, 112549-48-1; **6c**, 112549-50-5; 3,5-di-*tert*-butylbenzylbromide, 62938-08-3.

[1] M. Narita, C. U. Pittman, *Synthesis 1976*, 489.
[2] A. Krief, *Tetrahedron 42* (1986) 1209.
[3] W. E. Hatfield (Ed.): *Molecular Metals*, Plenum Press, New York 1979.
[4] L. Alcácer (Ed.): *The Chemistry and Physics of Low Dimensional Solids*, Reidel, Dordrecht, Holland 1980.
[5] E. Amberger, H. Fuchs, K. Polborn, *Angew. Chem. 98* (1986) 751; *Angew. Chem. Int. Ed. Engl. 25* (1986) 729.
[6] P. Wolf, K. Müllen, M. Przybylski, *Chimia 40* (1986) 200.
[7] N. G. Demetriadis, S. J. Huang, E. T. Samulski, *Tetrahedron Lett. 28* (1977) 2223.
[8] J. Heinze, J. Mortensen, K. Müllen, R. Schenk, *J. Chem. Soc. Chem. Commun. 1987*, 107.
[9] All the new compounds gave correct elemental analyses. **1c**: ^1H-NMR (CD_2Cl_2, 200 MHz): $\delta = 1.38$ (s, 36H, *t*Bu), 5.02 (s, 4H, OCH_2), 7.10–7.30 (AA'BB', 8H), 7.30–7.48 (AB_2, 6H); ^{13}C-NMR ($CDCl_3$, 50 MHz): $\delta = 31.6$, 35.0, 75.2, 110.7, 112.2, 121.9, 122.8, 123.3, 126.0, 129.6, 134.8, 136.6, 142.0, 151.2 [recorded in the presence of Co(acac)$_2$ as relaxation accelerator]; FD-MS ($CHCl_3$): *m/z* 968.5 [$(M-H)^{\odot\oplus}$, 100%].—**2c**: ^1H-NMR ($CDCl_3$, 200 MHz): $\delta = 1.32$ (s, 36H, *t*Bu), 5.02 (s, 4H, OCH_2), 7.13 (d, 4H), 7.44 (t, 2H); ^{13}C-NMR ($CDCl_3$, 50 MHz): $\delta = 31.4$, 34.9, 76.7, 123.5, 123.6, 133.6, 134.6, 139.2, 151.7, 209.7.—**5c**: ^1H-NMR ($CDCl_3$, 200 MHz): $\delta = 1.38$ (s, 36H, *t*Bu), 2.50 (s, 6H, SCH_3), 2.56 (s, 6H, SCH_3), 4.62 (s, 4H, OCH_2), 6.98–7.42 (m, 14H, AA'BB' and AB_2); ^{13}C-NMR ($CDCl_3$, 50 MHz): $\delta = 18.0$, 18.2, 31.5, 34.9, 74.1, 95.1, 96.6, 120.3, 122.4, 123.2, 125.2, 129.8, 135.1, 138.2, 140.5, 150.8; FD-MS ($CHCl_3$): *m/z* 1061.8 ($M^{\odot\oplus} - CH_3SSCH_3$, 17%), 967.5 ($M^{\odot\oplus} - 2 \times CH_3SSCH_3$, 100%).—**6c**: ^1H-NMR ($CDCl_3$, 90 MHz): $\delta = 1.33$ (s, 36H, *t*Bu), 5.00 (s, 4H, OCH_2), 7.15–7.44 (m, 10H, AA'BB' and AB_2); ^{13}C-NMR ($CDCl_3$, 50 MHz): $\delta = 31.5$, 34.9, 75.8, 109.0, 114.1, 121.9, 123.2, 123.5, 126.1, 131.8, 133.3, 134.2, 136.4, 140.5, 151.4, 210.7.
[10] C. A. Brown, R. D. Miller, C. M. Lindsay, K. Smith, *Tetrahedron Lett. 25* (1984) 991.
[11] C. M. Lindsay, K. Smith, C. A. Brown, K. Betterton-Cruz, *Tetrahedron Lett. 25* (1984) 995.
[12] a) P. Wolf, H. Naarmann, K. Müllen, unpublished results; b) S. Hünig, G. Kiesslich, H. Quast, D. Scheutzow, *Liebigs Ann. Chem. 1973*, 310.
[13] L. Cavara, F. Gerson, D. O. Cowan, K. Lerstrup, *Helv. Chim. Acta 69* (1986) 141.
[14] S. Matsuzaki, T. Moriyama, M. Onomichi, K. Toyoda, *Bull. Chem. Soc. Jpn. 56* (1983) 369.

Photochemical Reaction of $[(CO)_4Co(SiEt_3)]$ with Ethylene: Implications for Cobaltcarbonyl-Catalyzed Hydrosilation of Alkenes**

By *Friedrich Seitz* and *Mark S. Wrighton**

Dedicated to Prof. Dr. Helmut Dörfel on the occasion of his 60th birthday

The commonly proposed Chalk-Harrod mechanism (Scheme 1)[1–3] for transition metal catalyzed hydrosilation of alkenes involves as the key steps the insertion of an alkene into a M–H bond [step (3)] and the reductive elimination of an alkyl and a silyl ligand to form an alkylsilane [step (5)]. Whereas the insertion of alkenes into M–H bonds is well documented,[4] the reductive elimination of an alkylsilane has only been reported for $[(CO)_4Fe(alkyl)(SiR_3)]$,[5] and this is a slow reaction at 298 K. More importantly, the mechanism in Scheme 1 cannot explain the formation of alkenylsilanes, which are frequently observed as by-products of hydrosilation reactions.[6–9]

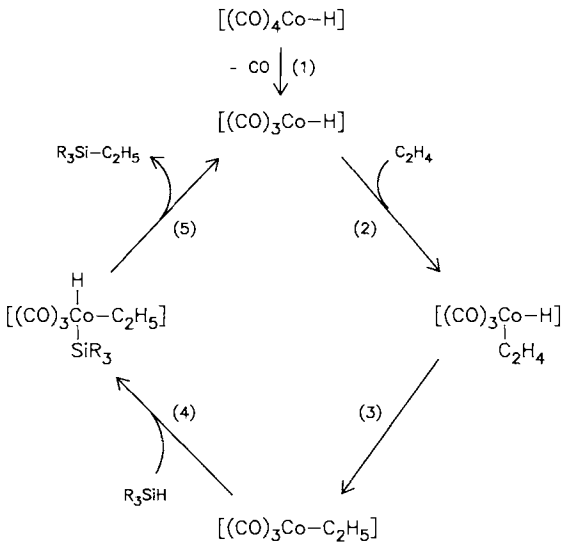

Scheme 1. Chalk-Harrod mechanism of the catalytic hydrosilation by insertion of C_2H_4 into a M–H bond, with $[(CO)_4Co-H]$ as model example [1–3].

An alternative mechanism (Scheme 2) has been suggested for the photocatalyzed hydrosilation of alkenes using $Fe(CO)_5$,[6] $M_3(CO)_{12}$ (M = Fe, Ru, Os)[7] or $[(CO)_4Co-SiR_3]$[8] as catalysts. The key steps of this mechanism are

[*] Prof. Dr. M. S. Wrighton
Department of Chemistry, Massachusetts Institute of Technology
Cambridge, Massachusetts 02139 (USA)
Dr. F. Seitz
BASF AG, Kunststofflaboratorium
D-6700 Ludwigshafen (FRG)

[**] This work was supported by the Deutsche Forschungsgemeinschaft, the Office of Naval Research (USA), and the National Science Foundation.

the insertion of an alkene into a M–Si bond [step (3)] and the reductive elimination of an alkyl and a hydrido ligand [step (5)]. Evidence for all steps required by this mechanism has been obtained for $[(\eta^5\text{-}C_5Me_5)(CO)_2Fe\text{-}SiR_3]$.[10] We have now extended these investigations to the complex $[(CO)_4Co\text{-}SiR_3]$, which is known to be an efficient hydrosilation catalyst under irradiation.[8]

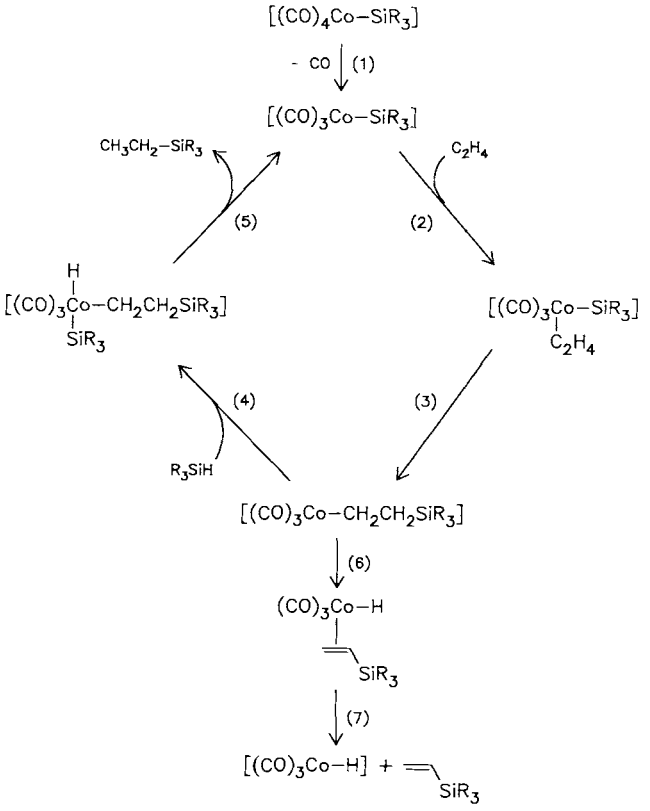

Scheme 2. Newly proposed mechanism for the catalytic hydrosilation by insertion of C_2H_4 into a Co–Si bond (R = Et).

It has been shown[11] that near-UV photolysis of $[(CO)_4Co\text{-}SiEt_3]$ at 77 K in a methylcyclohexane (MCH) matrix yields the 16-electron complex $[(CO)_3Co\text{-}SiEt_3]$ and CO as the only species detectable by FTIR.[12] The same coordinatively unsaturated complex is obtained at 77 K, when the matrix contains ethylene. However, in this case warm-up of the matrix leads to disappearance of bands attributed to $[(CO)_3Co\text{-}SiEt_3]$ and formation of new bands at 1968 (sh) and 1961 cm^{-1}. These bands are also observed upon near-UV irradiation of a solution of $[(CO)_4Co\text{-}SiEt_3]$ and ethylene in MCH at 210 K. We attribute the bands at 1968 and 1961 cm^{-1} to $[(CO)_3(C_2H_4)Co\text{-}SiEt_3]$, formed by addition of ethylene to photogenerated $[(CO)_3Co\text{-}SiEt_3]$. Coordination of ethylene is also evidenced by ^{1}H-NMR spectroscopy.[13]

According to Scheme 2 the next step in the catalytic cycle is insertion of the coordinated alkene into the Co–Si bond [step (3)]. To investigate this reaction a solution of $[(CO)_3(C_2H_4)Co\text{-}SiEt_3]$ was slowly warmed to 298 K and monitored by FTIR. Upon warming, a reaction is observed which under the experimental conditions has a half-life of about 2 minutes at 265 K. The unexpected reaction product is the acyl complex $[(CO)_4Co\text{-}C(O)C_2H_5]$, established spectroscopically by comparison with independently synthesized material.[14] We assume that insertion into the Co–Si bond [step (3)] does indeed take place, but, since no R_3SiH necessary for step (4) is present, β-H transfer takes place instead [step (6)]. The complex obtained is expected to undergo loss of vinyl(triethyl)silane [step (7)]. Free vinyl(triethyl)silane can be detected in the reaction mixture by gas chromatography by comparison with an authentic sample. We have thus demonstrated formation of an alkenylsilane. This result is consistent with the finding that photolysis of $[(CO)_4Co\text{-}SiEt_3]$ in the presence of 1-pentene yields triethyl(pentenyl)silane[8] and the photolysis of $[(\eta^5\text{-}C_5Me_5)(CO)_2Fe\text{-}SiMe_3]$ in the presence of ethylene yields trimethyl(vinyl)silane.[10] Since we have used a large excess of ethylene the 16-electron metal complex formed in step (7) undergoes addition of ethylene, followed by insertion into the Co–H bond and addition of two molecules of CO to form $[(CO)_4Co\text{-}C(O)C_2H_5]$ [reactions (a–c)]. Consistent

$$[(CO)_3Co\text{–}H] + C_2H_4 \longrightarrow [(CO)_3Co(C_2H_4)\text{–}H] \quad \text{(a)}$$

$$[(CO)_3Co(C_2H_4)\text{–}H] \longrightarrow [(CO)_3Co\text{–}CH_2CH_3] \quad \text{(b)}$$

$$[(CO)_3Co\text{–}CH_2CH_3] + 2\,CO \longrightarrow [(CO)_4Co\text{–}C(O)CH_2CH_3] \quad \text{(c)}$$

with consumption of two molecules of CO for one metal complex, the formation of $[(CO)_4Co\text{-}C(O)C_2H_5]$ stops, once 40% of photogenerated $[(CO)_3(C_2H_4)Co\text{-}SiEt_3]$, i.e. 80% of CO, reacts. The rate-determining step in this reaction sequence appears to be the ethylene insertion into the Co–Si bond, since none of the intermediates could be observed. Insertion of ethylene into the Co–Si bond [step (3)] is the first example of insertion of an unactivated alkene into the M–Si bond of a catalytically active complex. In the presence of R_3SiH, step (7) in Scheme 2 is presumably followed by reaction of $[(CO)_3Co\text{-}H]$ with R_3SiH to regenerate $[(CO)_3Co\text{-}SiR_3]$ and H_2.

We have so far demonstrated steps (1)–(3) and (6) and (7) of Scheme 2. To obtain evidence for steps (4) and (5), we turned to $[(CO)_4Co\text{-}Me]$ as model compound for the alkyl complex $[(CO)_4Co\text{-}CH_2CH_2SiR_3]$. Due to the lability of cobalt alkyl complexes, the reactions could not be spectroscopically monitored. We therefore allowed $[(CO)_4Co\text{-}Me]$ to react with Me_3SiH and analyzed the products by ^{1}H-NMR.[15] We assume thermal CO loss occurs from $[(CO)_4Co\text{-}Me]$ giving $[(CO)_3Co\text{-}Me]$, corresponding to the intermediate $[(CO)_3Co\text{-}CH_2CH_2SiR_3]$ in Scheme 2, but also to $[(CO)_3Co\text{-}C_2H_5]$ in Scheme 1. In both cases, as well as with our model complex, the next step is oxidative addition of the silane [reaction (d)].

$$[(CO)_3Co\text{–}Me] + Me_3SiH \longrightarrow (CO)_3Co(H)(SiMe_3)\text{–}Me \quad \text{(d)}$$

In Scheme 2 this is followed by elimination of the alkyl and the hydrido ligand to yield, in the case of our model compound, CH_4 and $[(CO)_3Co\text{-}SiMe_3]$ [reaction (e)]. In

$$(CO)_3Co(H)(SiMe_3)\text{–}Me \longrightarrow CH_4 + (CO)_3Co\text{–}SiMe_3 \quad \text{(e)}$$

contrast, from Scheme 1 we would expect elimination of the silyl and the alkyl ligand to yield $SiMe_4$ and $[(CO)_3Co-H]$ [reaction (f)]. We find CH_4, not $SiMe_4$ by ^{1}H-NMR

$$(CO)_3Co(H)(SiMe_3)-Me \longrightarrow SiMe_4 + (CO)_3Co-H \qquad (f)$$

($\delta = 0.18$) and $[(CO)_4Co-SiMe_3]$ by FTIR. We cannot completely rule out the possibility that some $SiMe_4$ is also formed, but formation of CH_4 is certainly the predominant reaction.

We have thus found evidence for all steps postulated in Scheme 2. Formation of CH_4, not $SiMe_4$, in the reaction of $[(CO)_4Co-Me]$ with Me_3SiH is clearly inconsistent with the Chalk-Harrod mechanism, Scheme 1. We therefore propose the mechanism depicted in Scheme 2 for hydrosilation catalysis, at least with carbonylcobalt complexes. This new mechanism involves as key step the insertion of an olefin into a Co-Si bond.

Received: September 23, 1987 [Z 2439 IE]
German version: *Angew. Chem. 100* (1988) 281

[1] J. F. Harrod, A. J. Chalk in I. Wender, P. Pino (Ed.): *Organic Syntheses via Metal Carbonyls, Vol. 2*, Wiley, New York 1977, p. 673.
[2] J. L. Speier, *Adv. Organomet. Chem. 17* (1979) 407.
[3] a) A. J. Chalk, J. F. Harrod, *J. Am. Chem. Soc. 87* (1965) 16; b) J. F. Harrod, A. J. Chalk, *ibid. 87* (1965) 1133.
[4] a) G. W. Parshall: *Homogeneous Catalysis*, Wiley, New York 1980, p. 29; b) N. M. Doherty, J. E. Bercaw, *J. Am. Chem. Soc. 107* (1985) 2670; c) D. C. Roe, *J. Am. Chem. Soc. 105* (1983) 7770.
[5] a) A. J. Blakeney, J. A. Gladysz, *Inorg. Chim. Acta 53* (1980) L25; b) K. C. Brinkman, A. J. Blakeney, W. Krone-Schmidt, J. A. Gladysz, *Organometallics 3* (1984) 1325.
[6] M. A. Schroeder, M. S. Wrighton, *J. Organomet. Chem. 128* (1977) 345.
[7] R. G. Austin, R. S. Paonessa, P. J. Giordano, M. S. Wrighton, *Adv. Chem. Ser. 168* (1978) 189.
[8] C. L. Reichel, M. S. Wrighton, *Inorg. Chem. 19* (1980) 3858.
[9] a) A. Millan, M. J. Fernandez, P. Bentz, P. M. Maitlis, *J. Mol. Catal. 26* (1984) 89; b) A. J. Cornish, M. F. Lappert, *J. Organomet. Chem. 271* (1984) 153; c) A. Onopchenko, E. T. Sabourin, D. L. Beach, *J. Org. Chem. 49* (1984) 3389; d) A. Onopchenko, E. T. Sabourin, D. L. Beach, *ibid. 48* (1983) 5101; e) Y. Seki, K. Takeshita, K. Kawamoto, S. Murai, N. Sonoda, *Angew. Chem. 92* (1980) 974; *Angew. Chem. Int. Ed. Engl. 19* (1980) 928; f) A. N. Nesmeyanov, R. K. Freidlina, E. C. Chukovskaya, R. G. Petrova, A. B. Belyavsky, *Tetrahedron 17* (1962) 61; g) B. Marciniec, J. Gulinski, *J. Organomet. Chem. 253* (1983) 349.
[10] C. L. Randolph, M. S. Wrighton, *J. Am. Chem. Soc. 108* (1986) 3366.
[11] F. R. Anderson, M. S. Wrighton, *J. Am. Chem. Soc. 106* (1984) 995.
[12] IR spectroscopic data (CO stretching region) for relevant complexes [cm^{-1}]: $[(CO)_4Co-SiEt_3]$: 2089 m, 2026, 1995 s; $[(CO)_3Co-SiEt_3]$: 1957 s, 1953 s; $[(CO)_3(C_2H_4)Co-SiEt_3]$: 1968 sh, 1961 s; $[(CO)_4Co-C(O)CH_2CH_3]$: 2105 m, 2045 m, 2023 s, 2002 s.
[13] When a solution of $[(CO)_4Co-SiEt_3]$ in ethylene containing [D$_8$]toluene is irradiated, signals at $\delta = 1.15$ (m) for Et_3Si and 3.00 (s) for coordinated ethylene are observed. For the resonance of coordinated ethylene cf. Y.-M. Wuu, J. G. Bentsen, C. G. Brinkley, M. S. Wrighton, *Inorg. Chem. 26* (1987) 530.
[14] Under 1 atm of CO at 0°C, 210 mg (0.3 mmol) of $[(Ph_3P)_2N][Co(CO)_4]$ in 2 mL of THF was added to 200 mg (1.1 mmol) of $[Et_3O][BF_4]$. After stirring the solution for 15 min, the solvent was removed in vacuo. The residue was redissolved in 1 mL of methylcyclohexane. $[(Ph_3P)_2N][BF_4]$ and excess $[Et_3O][BF_4]$ was removed via filtration and the solution was used without further purification. Only signals due to $[(CO)_4Co-C(O)CH_2CH_3]$ were observed in the FTIR spectrum; cf. L. Marko, G. Bor, G. Almasy, P. Szabo, *Brennst. Chem. 44* (1963) 184.
[15] At 0°C 45 mg (0.3 mmol) of MeI was added to a solution of 70 mg (0.4 mmol) of $Na[Co(CO)_4]$ in 1 mL [D$_8$]THF. After 2 min the resulting $[(CO)_4Co-Me]$ was allowed to react with 100 mg (1.3 mmol) of Me_3SiH. The solution was stirred for 20 min at 0°C and then warmed up. Immediately after the solution reached room temperature, a ^{1}H-NMR spectrum was recorded: $\delta = 0.18$ for methane. Formation of $[(CO)_4Co-C(O)CH_3]$ accompanies formation of $[(CO)_4Co-Me]$ in the synthesis (see [14]) and the thermolysis of the $[(CO)_4Co-Me]/[(CO)_4Co-C(O)CH_3]$ mixture in the presence of Me_3SiH gives CH_3CHO in addition to CH_4 (cf. also R. W. Wegman, *Organometallics 5* (1986) 707, which shows formation of CH_3CHO from reaction of $[(CO)_3(PPh_3)Co-C(O)CH_3]$ with Et_3SiH or Ph_3SiH).

CD Spectroelectrochemistry, a Method for the Characterization of Chiral Electron Transfer Reagents and Chiral Reaction Intermediates**

By *Jörg Daub,* Josef Salbeck,* and *Irmgard Aurbach*

The combination stereochemistry/electron transfer (ET) has so far never been dealt with in monographs on stereochemistry even though a close relationship exists between both fields.[1,2] Only a slight stereoselectivity has thus far been observed in ET reactions carried out in homogeneous solution. This holds true for diastereoselective reactions and in particular for enantioselective reactions.[3]

We now show that chiral ET reagents can be investigated by the use of chiroptic methods (here measurement of the circular dichroism) in spectroelectrochemical measurements.[4] For this purpose a thin-layer cell developed for spectrochemical investigations, which consisted of an optically transparent working electrode (OTTLE = optically transparent thin-layer electrode, indium oxide doped with tin oxide, coated on glass), a platinum disk as counter electrode and an Ag/AgCl reference electrode,[5] was mounted in the beam of a CD and UV/VIS spectrometer. By means of this instrumental coupling of potentiostatic intermediate generation and electron spectroscopic (UV/VIS) and chiroptic (CD) detection, both electrochemical as well as structural properties of chiral intermediates can be determined. Thus, a method is available which provides access to important information about the properties of chiral electron transfer compounds and about their use for enantioselective redox reactions.[6] Herein we shall outline the application of the method to the study of the axially chiral bisanthraquinone **1**.

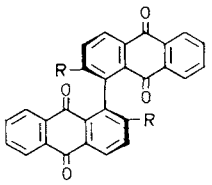

(*R*)-**1** - (*R*)-**5**

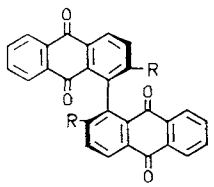

(*S*)-**1** - (*S*)-**5**

1, R = CO_2CH_3; **2**, R = CH_3; **3**, R = $CHBr_2$; **4**, R = CHO; **5**, R = CO_2H

The enantiomeric forms of **1** are readily accessible on a preparative scale: starting from *rac*-2,2'-dimethyl-1,1'-bianthraquinone **2**, the dicarboxylic acid *rac*-**5** was prepared via *rac*-**3** and *rac*-**4**;[7] this was then separated into the two enantiomers (*R*)-(−)-**5** and (*S*)-(+)-**5**.[8] Subsequent reaction with diazomethane furnished the optically active esters (*R*)-(−)-**1** and (*S*)-(+)-**1** respectively, in good yields.[9] The optical purity of both enantiomers was determined ^{1}H-NMR spectroscopically (250 MHz): in the presence of (−)-9-(1-hydroxy-2,2,2-trifluoroethyl)anthracene as chiral auxiliary reagent the ^{1}H-NMR spectra of the enantiomers each show only the signals of one diastereomeric associate. The absolute configurations of (*R*)-(−)-**1** and (*S*)-(+)-**1** were derived from the known configurations of (*R*)-(−)-**2**, (*S*)-(+)-**2** and (*R*)-(−)-**5**, (*S*)-(+)-**5**.[10]

[*] Prof. Dr. J. Daub, Dipl.-Chem. J. Salbeck, Dipl.-Chem. I. Aurbach
Institut für Organische Chemie der *Universität*
Universitätsstrasse 31, D-8400 Regensburg (FRG)

[**] This work was supported by the Stiftung Volkswagenwerk and the Deutsche Forschungsgemeinschaft. We thank Prof. *H. Brunner* for placing the CD spectrometer (circular dichrograph J-40A, Jasco) at our disposal and Frau *D. Andert* for instructions on the use of the apparatus.

For the electrochemical and spectroscopic measurements, **1** was dissolved in acetonitrile. Bu_4NPF_6 served as supporting electrolyte; the substrate concentration was 5.4×10^{-3} mol L^{-1}.

$$\mathbf{1} \overset{E^1}{\rightleftharpoons} \mathbf{1}^{\odot\ominus} \overset{E^2}{\rightleftharpoons} \mathbf{1}^{2(\odot\ominus)} \overset{E^3}{\rightleftharpoons} \mathbf{1}^{(\odot\ominus)2\ominus} \overset{E^4}{\rightleftharpoons} \mathbf{1}^{4\ominus} \qquad \text{(a)}$$

The cyclovoltammograms of (*S*)- and (*R*)-**1** show the reversible reaction cycle (a) with the following half-wave potentials: $E^1 = 1190$ mV; $E^2 = -1360$ mV, $E^3 \approx E^4 = -1780$ mV (Fig. 1). In the electronic spectra obtained by UV/VIS

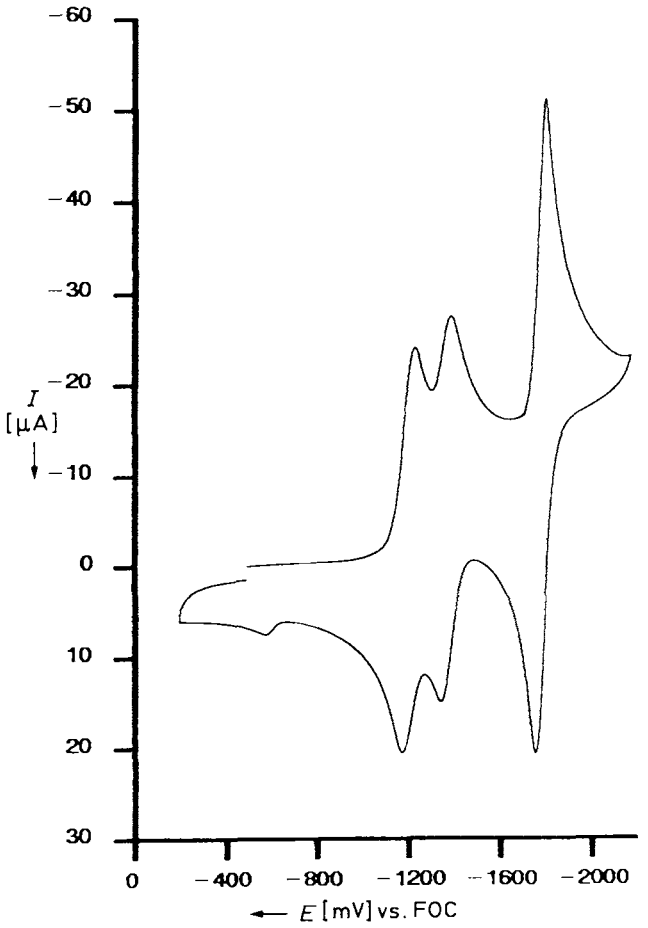

Fig. 1. Cyclovoltammogram of (*S*)-(+)-**1** in CH_3CN, $c = 5.4 \times 10^{-3}$ mol L^{-1}, scan 200 mV s^{-1}; FOC = ferrocene.

spectroelectrochemical inspection of **1** the formation of the monoanion $\mathbf{1}^{\odot\ominus}$ is recognizable only by one isosbestic point at $\lambda_{max} = 360$ nm. $\mathbf{1}^{\odot\ominus}$ is thereby formed at a stationary potential of -1275 mV. The dianion $\mathbf{1}^{2(\odot\ominus)}$ (absorptions at 403 and 614 nm, Fig. 2b) is formed at a stationary potential of -1600 mV. At a potential of -2200 mV the tetraanion $\mathbf{1}^{4\ominus}$ is then formed. Its absorption spectrum shows an intense band at $\lambda_{max} = 490$ nm with a shoulder extending to 800 nm.

The dianion $\mathbf{1}^{2(\odot\ominus)}$ is a bisradical anion (Scheme 1), as is clearly shown by comparison of its electronic spectrum (Fig. 2b) with that of 9,10-anthraquinone **6** obtained by UV/VIS spectroelectrochemistry (Fig. 3). The most intense

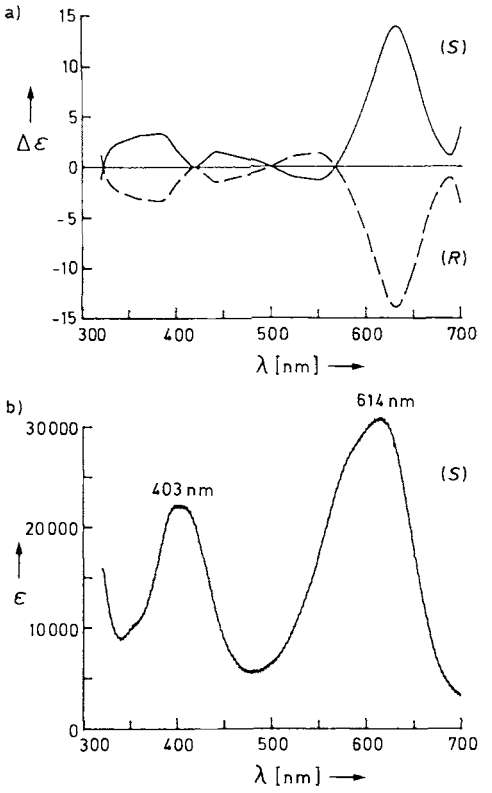

Fig. 2. Spectroelectrochemistry of (*R*)-(−)-**1** and (*S*)-(+)-**1**. a) CD spectra of the enantiomeric bisradical anions $\mathbf{1}^{2(\odot\ominus)}$. b) Electronic spectrum of (*S*)-(+)-$\mathbf{1}^{2(\odot\ominus)}$.

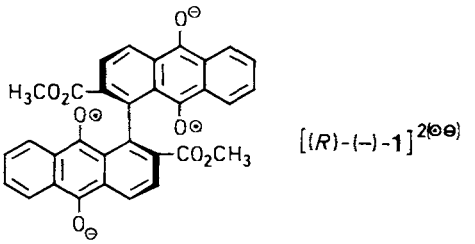

Scheme 1. $\mathbf{1}^{2(\odot\ominus)}$ as bisradical anion.

absorptions of the radical anion $\mathbf{6}^{\odot\ominus}$ appear at $\lambda_{max} = 390$, 410, and 540 nm. The dianion $\mathbf{6}^{2\ominus}$ has its most intense band at $\lambda_{max} = 480$ nm and a weaker absorption at 645 nm.

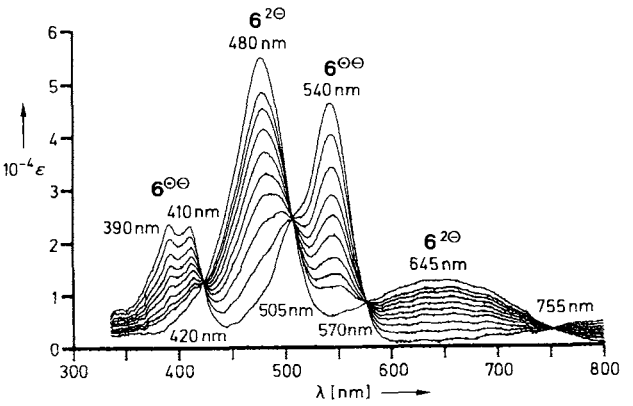

Fig. 3. UV/VIS spectroelectrochemistry of **6**. Potential range 0 to −2300 mV.

The CD spectra of electrochemically generated ions of (*R*)-(−)-**1** and (*S*)-(+)-**1** were recorded over the potential range 0 to −2200 mV. Figure 2a shows the CD spectra of both enantiomeric forms of $\mathbf{1}^{2(\odot\ominus)}$, which were generated at a stationary potential of $=-1600$ mV.[11] (*S*)-$\mathbf{1}^{2(\odot\ominus)}$ shows a positive $\Delta\varepsilon$ for the longest wavelength absorption; in the case of (*R*)-$\mathbf{1}^{2(\odot\ominus)}$ the corresponding band has a negative $\Delta\varepsilon$ value of equal intensity. The tetraanion (*S*)-(+)-$\mathbf{1}^{4\ominus}$ generated at a potential of −2200 mV has a positive $\Delta\varepsilon$ value for the intense band at $\lambda_{max}=490$ nm. A further band with positive $\Delta\varepsilon$ is observed at 630 nm.

The reaction cycle between bianthraquinone **1** and bisradical anion $\mathbf{1}^{2(\odot\ominus)}$ is electrochemically reversible over several measuring cycles. Racemization could not be observed. On the other hand, during the electrochemical formation of the tetraanion $\mathbf{1}^{4\ominus}$ with Bu_4NPF_6 as supporting electrolyte, a chemical secondary reaction can already be observed after the first cycle.[12]

Received: August 17, 1987;
revised: October 12, 1987 [Z 2402 IE]
German version: *Angew. Chem. 100* (1988) 278

[1] J. D. Morrison (Ed.): *Asymmetric Synthesis, Vol. 1-5,* Academic Press, New York 1983-1985.
[2] a) J. Deisenhofer, O. Epp, K. Miki, R. Huber, H. Michel, *J. Mol. Biol. 180* (1984) 385; b) R. J. Cave, P. Siders, R. A. Marcus, *J. Chem. Phys. 90* (1986) 1436.
[3] For studies on this theme see: a) B. Grossman, R. G. Wilkins, *J. Am. Chem. Soc. 89* (1967) 4230; b) N. A. P. Kane-Maguire, R. M. Tollison, D. E. Richardson, *Inorg. Chem. 15* (1976) 499; c) M. Hatano, T. Nozawa, S. Ikeda, T. Yamamoto, *Makromol. Chem. 141* (1979) 11; d) G. B. Porter, R. H. Sparks, *J. Chem. Soc. Chem. Commun. 1979,* 1094; e) D. A. Geselowitz, H. Taube, *J. Am. Chem. Soc. 102* (1980) 4525; f) Y. Kaizu, T. Mori, H. Kobayashi, *J. Phys. Chem. 89* (1985) 332; g) B. Pispisa, A. Palleschi, M. Bateri, S. Nardini, *J. Phys. Chem. 89* (1985) 1767; h) P. Osvath, A. G. Lappin, *Inorg. Chem. 26* (1987) 195.
[4] In the redox titrations of soluble ferredoxin, isolated from spinach leaves, CD spectroscopy was employed as method of analytical detection: F. M. Hawkridge, B. Ke, *Anal. Biochem. 78* (1977) 76.
[5] a) J. Bindl, P. Seitz, U. Seitz, E. Salbeck, J. Salbeck, J. Daub, *Chem. Ber. 120* (1987) 1747; b) all potentials referred to ferrocene (FOC); c) for a review of UV/VIS spectroelectrochemistry see: T. Kuwana, W. R. Heineman, *Acc. Chem. Res. 9* (1976) 241.
[6] J. Bindl, G. Pilidis, J. Daub, *Angew. Chem. 96* (1984) 294; *Angew. Chem. Int. Ed. Engl. 23* (1984) 314; J. Daub, L. Jakob, J. Salbeck, Y. Okamoto, *Chimia 39* (1985) 393.
[7] F. Bell, D. H. Waring, *J. Chem. Soc. 1949,* 1579.
[8] F. Bell, W. H. D. Morgan, *J. Chem. Soc. 1950,* 1963; cf. also R. Kuhn, O. Albrecht, *Justus Liebigs Ann. Chem. 464* (1928) 91.
[9] Physical data of *rac*-**1**, (*R*)-(−)-**1** and (*S*)-(+)-**1**. *rac*-**1**: m.p. 259-260 °C; IR (KBr): $\tilde{\nu}=3080$, 2970, 1740, 1680, 1595, 1575, 1320, 1270, 1230, 1150, 1005, 955, 725 cm^{-1}; (*R*)-(−)-**1**: $[\alpha]_D^{20}=-132$ ($c=0.25$, CH_3CN), m.p. 198 °C; (*S*)-(+)-**1**: $[\alpha]_D^{20}=+124$ ($c=0.37$, CH_3CN), m.p. 200 °C.
[10] S. Yamada, H. Akimoto, *Tetrahedron Lett. 1968,* 3967; H. Akimoto, S. Yamada, *Tetrahedron 27* (1971) 5999.
[11] The CD spectra of the two enantiomers were fitted to the same zero line.
[12] In order to observe reversibility up to formation of the tetraanion, Me_4NBF_4 must be used as supporting electrolyte.

$[TiSCl_4]^{2\ominus}$ and $[Ti_3O(S_2)_3Cl_6]^{2\ominus}$, a Multinuclear Complex with a Structure Typical for Clusters

By *Ulrich Müller** and *Volker Krug*

For molybdenum, a series of cluster compounds of the composition $[Mo_3(\mu_3\text{-}S)(\mu\text{-}S_2)_3X_6]^{2\ominus}$ with molybdenum in the oxidation state +IV (X = Cl, CN, S etc.) are known.[1-5] Such compounds contain metal-metal bonds, as is evident from, inter alia, the Mo-Mo distances of between 272 and 278 pm. In the case of titanium, however, far fewer cluster compounds are known. Examples are $[Cp_5Ti_5(\mu_3\text{-}S)_6]$ with bridging sulfur atoms[6] and $[Cp_6Ti_6(\mu_3\text{-}O)_8]$ with bridging oxygen atoms;[7] in these compounds the titanium has an oxidation number between +III and +IV and the Ti-Ti distances are on average 317 and 289 pm, respectively. The Ti-Ti distances in $[(MeC_5H_4)_4Ti_4S_8O_2]$ are of the same order of magnitude;[8] this compound has been described as a cluster, although according to *Cotton*'s definition[9] it should not be regarded as a cluster, since the titanium has oxidation number +IV and therefore no metal-metal bonds should be present. We report here on a further Ti^{IV} compound with a structure typical for clusters.

In the reaction of titanium tetrachloride with bis(trimethylsilyl) sulfide [Eq. (a)] a black precipitate is formed which mainly consists of $TiSCl_2$. When the precipitate is treated with a solution of tetraphenylphosphonium chloride or tetraethylammonium chloride in dichloromethane the greater part turns green or orange in color respectively; the tetrachlorothiotitanate ion **1** is formed.

$$\begin{array}{l} TiCl_4 + S(SiMe_3)_2 \longrightarrow TiSCl_2 + 2\,ClSiMe_3 \\ \qquad\qquad\qquad\qquad\quad \downarrow +2Cl^{\ominus} \\ \qquad\qquad\qquad\qquad\quad [TiSCl_4]^{2\ominus}\ \mathbf{1} \end{array} \qquad (a)$$

At the same time a small amount of the precipitate dissolves, resulting in a red solution. After addition of CCl_4, red $(PPh_4)_2[Ti_3(\mu_3\text{-}O)(\mu\text{-}S_2)_3Cl_6]$ **2a** or $(NEt_4)_2[Ti_3(\mu_3\text{-}O)(\mu\text{-}S_2)_3Cl_6]$ **2b**, respectively, crystallizes from the solution. The oxygen in the anion **2** presumably comes from the inert gas (anhydrous N_2 containing small amounts of O_2). This assumption is supported by the finding that the yield of **2** is considerably greater on repeating the experiment in an atmosphere of pure oxygen [Eq. (b)].

$$\begin{array}{l} 3\,TiCl_4 + 6\,S(SiMe_3)_2 + 3/2\,O_2 \longrightarrow \\ \qquad\qquad [Ti_3O(S_2)_3Cl_4] + 8\,ClSiMe_3 + 2\,O(SiMe_3)_2 \\ \qquad\qquad\quad \downarrow +2Cl^{\ominus} \\ \qquad\qquad [Ti_3O(S_2)_3Cl_6]^{2\ominus}\ \mathbf{2} \end{array} \qquad (b)$$

$(PPh_4)_2[TiSCl_4]$ **1a** and $(NEt_4)_2[TiSCl_4]$ **1b** can be recrystallized from warm acetonitrile. Crystalline **1a** is green, crystalline **1b** orange. **1b** crystallizes tetragonally with the $[TiSCl_4]^{2\ominus}$ ions on fourfold axes of rotation.[10] The ions have a square-pyramidal structure with a short TiS bond (211 pm) (Fig. 1). This can be interpreted in terms of a Ti-S double bond, consistent with the IR spectrum ($\nu(TiS)=530$ cm^{-1}).

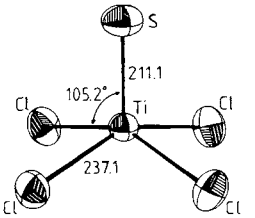

Fig. 1. Structure of the $[TiSCl_4]^{2\ominus}$ ion in the crystal of **1b**, with ellipsoids of thermal vibration (50% probability level at 22 °C). Bond lengths in pm, standard deviations: 0.2 pm.

When recrystallized from acetonitrile, **2a** contains one mol. equivalent of CH_3CN. Its structure analysis[11] reveals

[*] Prof. Dr. U. Müller, Dipl.-Chem. V. Krug
Fachbereich Chemie der Universität
Hans-Meerwein-Strasse, D-3550 Marburg (FRG)

the same type of structure (Fig. 2) for the anion **2** as mentioned above for the case of the molybdenum compounds. The oxygen atom bridges all three titanium atoms and each pair of Ti atoms is linked via a side-on coordinated disulfide unit. The Ti-Ti distances of 314 to 318 pm are markedly greater than the Mo-Mo distances in the molybdenum clusters—as to be expected for a Ti^{IV} compound,

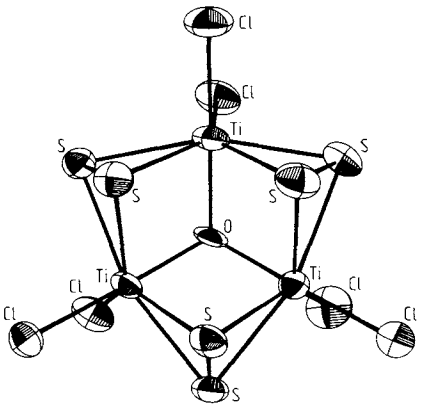

Fig. 2. Structure of the $[Ti_3O(S_2)_6Cl_6]^{2\ominus}$ ion in the crystal of **2a** · CH_3CN. Important bond lengths [pm]: Ti-Cl 231.3 to 235.7(5) (mean 232.3), Ti-S (in the plane of the Ti atoms) 250.9 to 252.4(5) (mean 252.3), remaining Ti-S 245.8 to 248.7(5) (mean 247.0), Ti-O 190 to 193(1) (mean 191.6), S-S 203.3 to 205.0(5) (mean 204.0), Ti···Ti 314.0 to 317.9 (mean 316.3); mean bond angles [°]: Ti-O-Ti 111.3(5), Cl-Ti-Cl 93.9(2), O-Ti-Cl 96.1(4) and 170.0(4).

owing to the absence of metal-metal bonds. On the other hand, however, these distances are not longer than those in the titanium clusters with Ti oxidation numbers between +III and +IV.[6,7] In the perthiotitanate Tl_2TiS_4, in which there are chains of edge-sharing octahedra, the Ti-Ti distances are 349 pm,[12] whereas in the triangular Ti_3 groups of Ti_7Cl_{16}, Ti-Ti distances of 295 pm have been found.

Received: August 24, 1987 [Z 2411 IE]
German version: *Angew. Chem. 100* (1988) 277

[1] A. Müller, R. Jostes, F. A. Cotton, *Angew. Chem. 92* (1980) 921; *Angew. Chem. Int. Ed. Engl. 19* (1980) 875.
[2] F. A. Cotton, R. Llusar, D. O. Marler, W. Schwotzer, *Inorg. Chim. Acta 102* (1985) L25.
[3] B. Meyer, H. Wunderlich, *Z. Naturforsch. B37* (1982) 1437.
[4] J. Huang, M. Shang, J. Huang, H. Zhueng, S. Lu, J. Lu, *Jiegou Huaxue 1* (1982) 1; *Chem. Abstr. 99* (1983) 186292; S. Lu, Y. Lin, J. Huang, J. Lu, J. Huang, *Jiegou Huaxue 3* (1984) 147; *Chem. Abstr. 103* (1984) 62905.
[5] P. Klingelhöfer, U. Müller, C. Friebel, J. Pebler, *Z. Anorg. Allg. Chem. 543* (1986) 22.
[6] F. Bottomley, G. O. Egharevba, P. S. White, *J. Am. Chem. Soc. 107* (1985) 4353.
[7] J. C. Huffman, J. G. Stone, W. C. Krusell, K. G. Caulton, *J. Am. Chem. Soc. 99* (1977) 5829.
[8] G. A. Zank, C. A. Jones, T. B. Rauchfuss, A. L. Rheingold, *Inorg. Chem. 25* (1986) 1886.
[9] F. A. Cotton, *Q. Rev. Chem. Soc. 20* (1968) 389.
[10] a) X-ray structure analysis of **1b** with 966 observed reflections, $R = 0.053$. $a = 923.9(3)$, $c = 1406.7(2)$ pm, space group $P4/n$, $Z = 2$. b) Further details of the structure analyses are available on request from the Fachinformationszentrum Energie, Physik, Mathematik GmbH, D-7514 Eggenstein-Leopoldshafen 2 (FRG), on quoting the depository number CSD-52824, the names of the authors, and the journal citation.
[11] X-ray structure analysis of **2a** · CH_3CN with 3035 reflections, $R = 0.070$. $a = 1138.8(3)$, $b = 1268.8(4)$, $c = 2166.4(6)$ pm, $\alpha = 101.26(3)$, $\beta = 97.2(2)$, $\gamma = 109.24(2)°$, space group $P\bar{1}$, $Z = 2$ [10b].
[12] K. O. Klepp, *Z. Naturforsch. B40* (1985) 229.
[13] B. Krebs, G. Henkel, *Z. Anorg. Allg. Chem. 474* (1981) 149.

The Structures of 1*H*-Cyclopropabenzene and Its 1,1-Bis(triisopropylsilyl) Derivative

By *Richard Neidlein,* Detlev Christen, Volker Poignée, Roland Boese,* Dieter Bläser, Alfred Gieren,* Catalina Ruiz-Pérez,* and *Thomas Hübner*

Dedicated to Professor Helmut Dörfel on the occasion of his 60th birthday

1*H*-Cyclopropabenzene **1a**,[1a] which has recently found increasing interest because of its reactivity and regioselectivity,[2] has also been the subject of intensive spectroscopic[1c,3] and theoretical[4] studies. X-ray structure analyses, however, have thus far only been carried out on the derivatives **1b** and **1c**.[4e,5] We have now prepared the parent compound **1a** (from 3-bromocyclohexene **2**) and the derivative **1d**, 1,1-disubstituted with the very bulky triisopropylsilyl residue,[2c,1d] and have carried out single-crystal X-ray structure analyses on both compounds[6] (**1a** at 120 K, **1d** at room temperature).

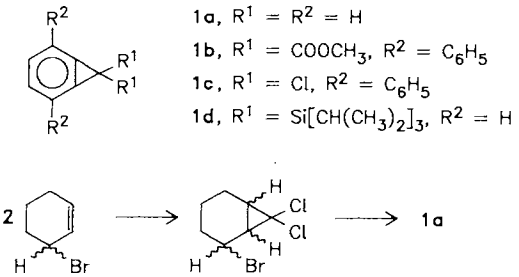

Figure 1 shows the structures of **1a** and **1d**; the bond lengths and bond angles for the 1*H*-cyclopropabenzene skeleton of **1a** and **1d** are listed together for comparison in Table 1. A significant difference (0.043 Å) appears only in the C-C bond lengths in the cyclopropene ring (C6-C7). As a result the bond angles in the cyclopropene ring differ slightly. The remaining differences in bond lengths and bond angles are not significant on taking into account the standard deviations. Both in **1a** as well as in **1d** the 1*H*-cyclopropabenzene moiety deviates from a strictly planar conformation, albeit with a different reduction in symmetry. In the case of **1a** the *mm*2 symmetry is reduced to *m*; the six-membered ring and the three-membered ring are tilted at an angle of 2.4° to each other. In **1d** there is a reduction in symmetry from *mm*2 to 2. This is induced by the bulky triisopropylsilyl groups, which, for steric reasons, are so arranged that they are interconverted into each other, not via a mirror plane but via a twofold molecular symmetry axis (Fig. 1). This symmetry continues in the 1*H*-cyclopropabenzene skeleton. The maximum deviation from an *mm*2 symmetry here, however, corresponds to a torsion angle of only 1.9°. A slight non-planarity of the 1*H*-cyclopropabenzene moiety has also been observed in the case of **1b**.[4e]

[*] Prof. Dr. R. Neidlein, Dr. D. Christen, Dr. V. Poignée
Pharmazeutisch-Chemisches Institut der Universität
Im Neuenheimer Feld 364, D-6900 Heidelberg (FRG)
Dr. R. Boese, Dipl.-Ing. D. Bläser
Institut für Anorganische Chemie der Universität - Gesamthochschule
Universitätsstr. 5-7, D-4300 Essen 1 (FRG)
Prof. Dr. A. Gieren, Dr. C. Ruiz-Pérez, Dr. T. Hübner
Institut für Anorganische und Analytische Chemie der Universität
Innrain 52a, A-6020 Innsbruck (Austria)

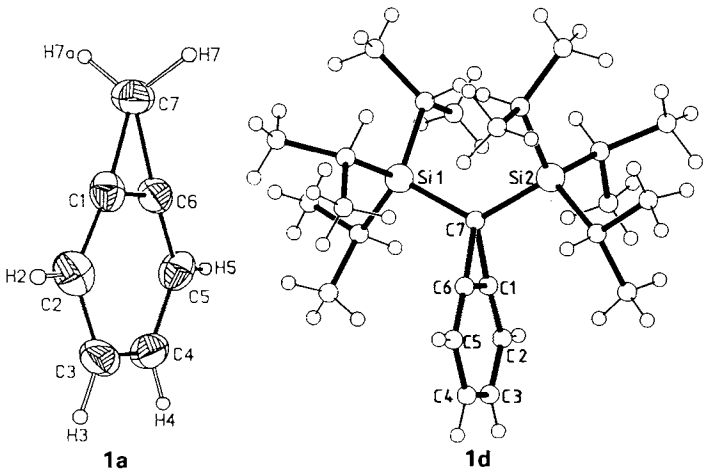

Fig. 1. Molecular structures of 1*H*-cyclopropabenzene **1a** and its derivative **1d**.

The structure of the benzene ring in **1a** and **1d** is, in principle, comparable with that in **1b** and **1c**, i.e. the angles in the benzene ring are deformed in the same manner by the annelation of the three-membered ring, and, in all cases, the C-C bond lengths give no indication of bond localization but rather of an aromatic delocalization. The C1-C6 bond is equally short in all the compounds **1**: **a**, 1.334(4); **b**, 1.333 (max. 8);[4e] **c**, 1.35(2);[5] **d**, 1.336(3) Å. The mean length of the five longer bonds in the benzene ring is also the same in **1a** (1.378) and **1d** (1.381 Å), and is 0.04 Å greater than the length of a C=C double bond. The C1-C6 bond in **1a** and **1d** is also lengthened to a similar extent compared to the C=C bond in cyclopropene.[7,8] Thus, the aromatic π-electron delocalization in the benzene ring is retained.

Table 1. Bond lengths [Å] and angles [°] averaged by the molecular symmetry of **1a** and **1d**.

	Bond lengths			Bond angles	
	1a	**1d**		**1a**	**1d**
C1-C6	1.334(4)	1.336(3)	C3-C4-C5	122.4(2)	122.4(2)
C3-C4	1.390(5)	1.379(6)	C4-C5-C6	113.2(2)	112.9(2)
C4-C5	1.387(4)	1.401(4)	C1-C6-C5	124.5(2)	124.6(1)
C5-C6	1.363(3)	1.361(2)	C1-C6-C7	63.6(1)	64.3(1)
C6-C7	1.498(3)	1.541(1)	C5-C6-C7	171.7(2)	171.0(1)
C4-H4	0.93(3)	0.90(2)	C1-C7-C6	52.8(2)	51.4(1)
C5-H5	0.94(3)	0.92(2)	C3-C4-H4	121(2)	116(1)
			C5-C4-H4	117(2)	121(1)
			C4-C5-H5	122(2)	124(1)
			C6-C5-H5	125(2)	123(1)

A comparison of **1a** and **1d** shows that the C-C bond lengths in the cyclopropene ring are strongly dependent on the substituents at the sp^3-hybridized carbon atom. That this is due to a steric effect is immediately evident upon comparison with the structure of **1b**. In **1d**, whose triisopropylsilyl groups are bulkier than the carboxy groups in **1b**, the C-C bonds are lengthened by 0.04 Å compared to those in **1a** but by only 0.02 Å compared to those in **1b**.

The C-C bonds in the cyclopropene ring of **1a** are ca. 0.02 Å shorter than those in cyclopropene,[7,8] obviously as a result of the widening of the C5-C6-C7 angle to almost 180° caused by the annelation. An X-X map of deformation energy shows a marked bonding electron density maximum for each C-C bond which is shifted from the center of the bond outwards in the case of **1a**, as would be expected for bent bonds.

Received: April 21, 1987;
revised: July 2, 1987 [Z 2211 IE]
German version: *Angew. Chem. 99* (1987) 292
Publication delayed at authors' request

CAS Registry numbers:
1a, 4646-69-9; **1d**, 109874-78-4.

[1] a) W. E. Billups, A. J. Blakeney, W. Y. Chow, *Org. Synth. 55* (1976) 12; b) E. Vogel, S. Korte, W. Grimme, H. Günther, *Angew. Chem. 80* (1968) 279; *Angew. Chem. Int. Ed. Engl. 7* (1968) 289; c) M. A. Cooper, S. L. Manatt, *J. Am. Chem. Soc. 92* (1970) 1605; d) V. Poignée, *Dissertation*, Universität Heidelberg 1986.

[2] a) R. Neidlein, A. Rufińska, H. Schwager, G. Wilke, *Angew. Chem. 98* (1986) 643; *Angew. Chem. Int. Ed. Engl. 25* (1986) 640; b) R. Mynott, R. Neidlein, H. Schwager, G. Wilke, *Angew. Chem. 98* (1986) 374; *Angew. Chem. Int. Ed. Engl. 25* (1986) 367; c) R. Neidlein, D. Christen, *Helv. Chim. Acta 69* (1986) 1623; d) H. Schwager, C. Krüger, R. Neidlein, G. Wilke, *Angew. Chem. 99* (1987) 72; *Angew. Chem. Int. Ed. Engl. 26* (1987) 65; e) B. Halton, C. J. Randall, P. J. Stang, *J. Am. Chem. Soc. 106* (1984) 6109.

[3] a) F. Brogli, E. Giovannini, E. Heilbronner, R. Schurter, *Chem. Ber. 106* (1973) 961; b) J. B. Pawliczek, H. Günther, *J. Am. Chem. Soc. 93* (1971) 2050.

[4] a) B. Halton, *Ind. Eng. Chem. Prod. Res. Dev. 19* (1980) 349; b) Y. Apeloig, D. Arad, *J. Am. Chem. Soc. 108* (1986) 3241; c) W. E. Billups, W. Y. Chow, K. M. Leavell, E. S. Lewis, J. L. Margarve, R. L. Sax, J. J. Shieh, P. G. Werness, J. L. Wood, *J. Am. Chem. Soc. 95* (1973) 7878; d) B. Halton, *Chem. Rev. 73* (1973) 113; e) E. Carstensen-Oeser, B. Müller, H. Dürr, *Angew. Chem. 84* (1972) 434; *Angew. Chem. Int. Ed. Engl. 11* (1972) 440.

[5] B. Halton, T. J. McLennan, W. T. Robinson, *Acta Crystallogr. Sect. B 32* (1976) 1889.

[6] X-ray structure analysis of **1a** at 120 K, crystal growth at 193 K by a computer-controlled miniature-zone melting technique [9]. (*R. B.* and *D. B.*): orthorhombic, $P2_12_12_1$, $a = 5.772(3)$, $b = 7.505(5)$, $c = 11.565(7)$ Å, $V = 501.0$ Å^3, $Z = 4$, $\rho_{calc} = 1.167$ g cm^{-3}; 768 observed, independent reflections; $2\theta_{max} = 70°$, $F_0 \geq 4.5\sigma(F)$; Nicolet R3, $Mo_{K\alpha}$, graphite monochromator, ω-scan; structure solution, refinement and graphic representation with SHELXTL, $R = 0.058$, $R_w = 0.051$. Room temperature analysis of **1d** (*A. G., C. R-P., T. H.*): monoclinic, $P2_1/n$, $a = 15.799(3)$, $b = 9.297(2)$, $c = 17.738(5)$ Å, $\beta = 90.20(2)°$, $V = 2605.3$ Å^3, $Z = 4$, $\rho_{obs} = 1.025$ g cm^{-3}, $\rho_{calc} = 1.027$ g cm^{-3}; 4496 observed, independent reflections; $1.5° < \theta < 28.0°$, $I > 2\sigma(I)$; CAD4, $Mo_{K\alpha}$, graphite monochromator, $\omega/2\theta$-scan; direct methods, E-Fourier and successive Fourier syntheses, Si, C atoms with anisotropic, H atoms with isotropic temperature factors, $R = 0.047$, $R_w = 0.049$. Further details of the crystal structure investigations of **1a** and **1d** are available on request from the Fachinformationszentrum Energie, Physik, Mathematik GmbH, D-7514 Eggenstein-Leopoldshafen 2 (FRG), on quoting the depository numbers CSD-52860 for **1a** and CSD-52409 for **1d**, the names of the authors, and the journal citation.

[7] J. D. Dunitz, H. G. Feldman, V. Schomaker, *J. Chem. Phys. 20* (1952) 1708.

[8] P. H. Kasai, R. J. Myers, D. F. Eggers, K. B. Wiberg, *J. Chem. Phys. 30* (1959) 512.

[9] D. Brodalla, D. Mootz, R. Boese, W. Osswald, *J. Appl. Crystallogr. 18* (1985) 316.

Nitrogen Fixation by Borabenzene**

By *Günther Maier,* Hans Peter Reisenauer, Jochem Henkelmann,* and *Christine Kliche*

Dedicated to Professor Helmut Dörfel on the occasion of his 60th birthday

Free borabenzene **3** (borinine[1]) is still unknown. The nearest related species so far reported is the betaine **4**, which was recently prepared by us[2] from the boracyclo-

[*] Prof. Dr. G. Maier, Dr. H. P. Reisenauer, Dr. J. Henkelmann, C. Kliche
Institut für Organische Chemie der Universität
Heinrich-Buff-Ring 58, D-6300 Giessen (FRG)

[**] Hetero π-Systems, Part 15. This work was supported by the Deutsche Forschungsgemeinschaft and the Fonds der Chemischen Industrie.—Part 14: [5].

hexadiene **1** and pyridine using the method described by *Paetzold*.[3] It is questionable whether borabenzene occurs as an intermediate in this reaction. Presumably pyridine is first bound to the boron atom in **1** and then elimination of the ether **2** follows in a secondary reaction.

In continuation of our investigations[4] of the borabenzene[3] and boraethene problem[5] we have studied the flash-thermolytic fragmentation of **1** (770 °C; condensation of the products on a 10 K cold window), not only with argon[3,4] but also with nitrogen as carrier gas.

On changing over from argon to nitrogen, a remarkable effect was observed. When the flash thermolysis of **1** was carried out in a stream of argon only the ether **2** could be detected on the matrix support,[2,4] whereas when it was carried out in a stream of nitrogen an additional set of IR bands was recorded, the most intense of which was observed at 2197.6 cm^{-1} (Table 1). In the UV spectrum of the condensate, absorptions appear at 235, 240, and 361 nm.

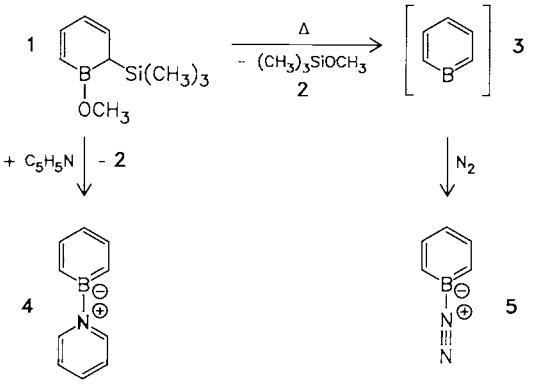

The long wavelength band shows a vibrational fine structure with maxima at 315, 337, and 361 nm. We ascribe these spectroscopic data to the adduct **5** of nitrogen and borabenzene **3**. The main argument for this is the intense IR band at 2197.6 cm^{-1}. It shifts by 73.3 cm^{-1} to 2143.3 cm^{-1} when $^{15}N_2$ is used as carrier gas,[6] and can therefore be assigned to the N≡N stretching vibration (Table 1). The assignment of the other IR absorptions listed in Table 1 to **5** follows from their synchronous decrease with the disappearance of the diazonium band upon irradiation of the matrix with 366-nm light. As to whether free borabenzene **3** is formed during this decomposition reaction cannot be ascertained on the basis of the experimental findings thus far available.

Table 1. IR data (10 K, N_2 matrices) of [$^{14}N_2$]-**5** and [$^{15}N_2$]-**5**.

[$^{14}N_2$]-**5**		[$^{15}N_2$]-**5**	
$\tilde{\nu}$ [cm^{-1}]	Int. (rel.)	$\tilde{\nu}$ [cm^{-1}]	Int. (rel.)
3048.0	(0.03)	3049.0	(0.03)
2197.6	(1.00)	2124.3	(1.00)
1529.3	(0.04)	1529.3	(0.03)
963.3	(0.08)	960.9	(0.08)
944.5	(0.13)	941.1	(0.37)
939.7	(0.11)	—	—
918.0	(0.09)	917.0	(0.09)
712.6	(0.22)	712.1	(0.28)
492.7	(0.04)	—	—

According to theoretical calculations[7] borabenzene **3** is characterized by a very low-lying σ*-MO, mainly localized on the boron atom. The resulting pronounced acceptor property is responsible for the trapping of nitrogen. From MNDO calculations[8] it follows that the nitrogen adduct **5** has an energy minimum, and that the trapping of nitrogen by borabenzene **3** is exothermic (reaction enthalpy $\Delta H = -25.2$ kcal/mol). The values for the reaction of **3** with pyridine ($\Delta H = -39.6$ kcal/mol) and with carbon monoxide[9] ($\Delta H = -73.6$ kcal/mol) are much more favorable.

The nitrogen fixation by borabenzene **3** is reminiscent of the N_α,N_β-rearrangement of diazonium salts,[10] in which the phenyl cation (isoelectronic with **3**) formed by dediazonation is capable of trapping nitrogen in the same way. The observations outlined above indicate that borabenzene **3** is formed—as hoped—in the pyrolysis of **1**. In an argon stream it does not survive the thermolysis, since owing to its extreme Lewis acidity, it is absorbed on the surface of the pyrolysis tube, where it decomposes. With nitrogen as carrier gas, borabenzene **3** can give the stable adduct **5** in competition with the wall reaction, and in this way, can be flushed through the hot tube.

Received: September 24, 1987 [Z 2442 IE]
German version: *Angew. Chem. 100* (1988) 303

CAS Registry numbers:
1, 96911-15-8; **3**, 31029-61-5; **5**, 112375-15-2.

[1] Nomenclature: *Pure Appl. Chem. 55* (1983) 409.
[2] J. Henkelmann, *Dissertation*, Universität Giessen 1985.
[3] R. Boese, N. Finke, J. Henkelmann, G. Maier, P. Paetzold, H. P. Reisenauer, G. Schmid, *Chem. Ber. 118* (1985) 1644.
[4] Review: G. Maier, *Pure Appl. Chem. 58* (1986) 95.
[5] G. Maier, J. Henkelmann, H. P. Reisenauer, *Angew. Chem. 97* (1985) 1061; *Angew. Chem. Int. Ed. Engl. 24* (1985) 1065.
[6] In the benzenediazonium ion ($^{14}N\equiv{}^{14}N$: 2302.1 cm^{-1}; $^{15}N\equiv{}^{15}N$: 2227.5 cm^{-1}) the corresponding $^{14}N/^{15}N$ isotopic shift of the N≡N stretching vibration is 74.6 cm^{-1}: L. S. Gray, Jr., V. A. Fassel, R. N. Kniseley, *Spectrochim. Acta 16* (1960) 514.
[7] a) G. Raabe, E. Heyne, W. Schleker, J. Fleischhauer, *Z. Naturforsch. A 39* (1984) 678; b) G. Raabe, W. Schleker, E. Heyne, J. Fleischhauer, *ibid. 42* (1987) 352.
[8] QCPE Program No. 506.—The likewise calculated IR spectra give—assuming the calculated frequencies lie about 10% too high—a value of 79.5 cm^{-1} for the mentioned $^{14}N/^{15}N$ isotopic shift of **5**.
[9] Preliminary experiments show that the adduct of CO and **3** can be matrix-isolated on using an argon/CO mixture as carrier gas.
[10] a) E. S. Lewis, R. E. Holliday, *J. Am. Chem. Soc. 91* (1969) 426; b) I. Szele, H. Zollinger, *ibid. 100* (1978) 2811; Y. Hashida, R. G. M. Landells, G. E. Lewis, I. Szele, H. Zollinger, *ibid. 100* (1978) 2816; see also: D. M. A. Grieve, G. E. Lewis, M. D. Ravenscroft, P. Skabral, T. Sonoda, I. Szele, H. Zollinger, *Helv. Chim. Acta 68* (1985) 1427.

The Central Propellane Bond as Polymerizable CC Single Bond: Poly(tricyclo[4.2.0.0^{2,7}]octane-1,7-diyl) — a "Poly([1.1.1]propellane)"**

By *Arnulf-Dieter Schlüter**

Small ring propellanes[1] are characterized by a special bonding geometry ("inverted tetrahedra"[2]) at the bridgehead C-atoms. They exhibit high ring strain concentrated over a few bonds,[3] an unusual electron distribution in the central σ bond,[4] and considerable reactivity.[5,6] Acceptor-

[*] Dr. A.-D. Schlüter
Max-Planck-Institut für Polymerforschung
Postfach 3148, D-6500 Mainz (FRG)

[**] I thank Prof. Dr. *G. Wegner*, Mainz, and Prof. Dr. *W. J. Feast*, Durham (UK), for their interest in and support of this work. I also wish to thank Frau Dr. *C. Böffel* for recording the solid-state NMR spectra and Herrn *K. Opitz* for help with some of the experiments.

substituted cyclopropanes and bicyclobutanes polymerize with ring-opening (cleavage of a CC single bond).[7] This poses the question whether small-ring propellanes can also undergo polymerization with ring-opening. Such a polymerization should lead, assuming exclusive cleavage of the central σ-bond, to a novel type polymer with a rigid rod-like structure.[8] Polymerization of [n.1.1]propellanes (n > 1) has occasionally been observed,[9] but neither the directed synthesis nor the structure of a "polypropellane" has thus far been described.[10] We report here on the first anionically-induced polymerization of [1.1.1]propellane **1**[11] leading to formation of the polymers **2**, whose structure could be established by solid-state ^{13}C-NMR spectroscopy.

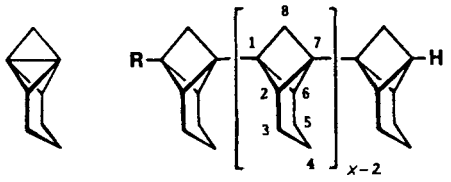

1 **2a**, R = *t*Bu
2b, R = Ph

Reaction of monomer **1**, which is readily accessible in gram amounts, with 0.15 equivalents of *tert*-butyllithium in a small amount of hexane at 20°C led to exothermic formation of a white precipitate, to which we assign the structure **3a**. After 30 min, the mixture was treated with ethanol and filtered through a frit; the remaining precipitate was then carefully washed with hot water and hot chloroform to remove inorganic and oligomeric components. Finally, the white, powdery polymer **2a** was dried to constant weight at 10^{-6} torr and 100°C (mass balance: 50% polymeric, 46% oligomeric material). The polymer **2b** could be obtained analogously in 35% yield by reaction of **1** with phenyllithium.

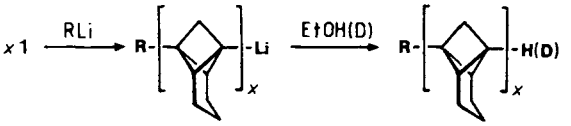

3 **2**

a, R = *t*Bu ; b, R = Ph

The CP-MAS-^{13}C-NMR spectra[12] of **2b** (Fig. 1) and **2a** show as expected five well-resolved signals in the region $\delta = 20$–60; these could be assigned by special pulse techniques which enable differentiation of C atoms according to the number of H atoms bonded to them. The assignment given in Figure 1 is consistent with the ^{13}C-NMR data of **2a**, x = 1.[11] The *t*Bu and Ph terminal groups in **2a** and **2b**, respectively, give rise to very low intensity signals at $\delta \approx 30$ and 128.[13] The spectrum of **2a** shows no signals for olefinic C-atoms or signals that could be assigned to bicyclobutanes. Hence, the signal of **2b** at $\delta \approx 128$ must indeed originate from the Ph terminal group, and, what is more important, only the central bond of the propellane **1** must have been opened in the polymerization step.

By exploiting the decreasing solubility of the oligomer in THF with increasing degree of polymerization (P_n) a fraction of **2a** could be isolated whose P_n value (average number) was, according to ^{1}H-NMR integration, ca. 11. The

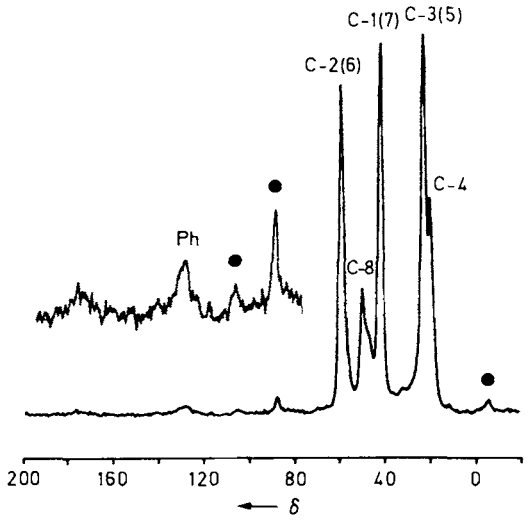

Fig. 1. CP-MAS-^{13}C-NMR spectrum (75 MHz) [12] of polymer **2b** with amplified downfield portion. The spinning side bands are indicated by black dots; the broad signal at $\delta \approx 180$ could not be assigned.

signals at $\delta = 2.29$ for 2-H and 6-H of one of the terminal repeat units are not superposed by the broad signals of the oligomeric mixture,[14] and thus enable a comparison with the intensity of the likewise unmasked *t*Bu signal. The ^{1}H- and ^{13}C-NMR spectra[14] are consistent with the given oligomeric structure, and thus further confirm the postulated polymeric structure.

A remarkable finding is that, at a P_n value of ca. 11, these rigid rods can still be readily dissolved in chloroform.[15] The rotation of the individual repeat units about the rods' axis and the folding back of the trimethylene bridges might play an important role regarding this finding. The P_n value of 11 found for the oligomer is a lower threshold value for the P_n value of the polymer **2**. We obtained direct information about the P_n value by quantitative determination of the lithium content in **3**. Atomic absorption spectroscopy gave a lithium content of 0.38% (±0.1%), which corresponds to a minimum value of P_n[16] of 17. This finding and the low intensity of the signals of the *t*Bu and Ph terminal groups, respectively, in the solid-state NMR spectra of **2a** and **2b** suggest P_n values of over 20.

The ring-opening polymerization of the propellane **1** presumably proceeds according to an anionic mechanism. This is indicated in the work-up of the lithiated species **3a** with EtOD, in which monomeric and dimeric compounds **2a**, x = 1, and **2a**, x = 2, are formed, each of which are deuteriated to more than 96% in position 7—that is, at the bridgeheads formerly bearing lithium. Furthermore, it follows from the ^{1}H-NMR spectra of all oligomers that there are two different terminal groups, likewise an indication of the postulated mechanism.

Received: August 5, 1987 [Z 2387 IE]
German version: *Angew. Chem. 100* (1988) 283

CAS Registry numbers:
1, 98577-41-4; **1** (homopolymer), 112347-61-2; **1** (SRU), 112347-62-3; *t*BuLi, 594-19-4; PhLi, 591-51-5.

[1] D. Ginsburg: *Propellanes*, Verlag Chemie, Weinheim 1975.
[2] K. B. Wiberg, J. E. Hiatt, *Tetrahedron Lett. 1968*, 5855; K. B. Wiberg, G. B. Ellison, J. J. Wendolowski, *J. Am. Chem. Soc. 98* (1976) 1212.
[3] K. B. Wiberg, *Angew. Chem. 98* (1986) 312; *Angew. Chem. Int. Ed. Engl. 25* (1986) 312.

[4] D. Feller, E. R. Davidson, *J. Am. Chem. Soc. 109* (1987) 4133, and references cited therein.
[5] K. B. Wiberg, *Acc. Chem. Res. 17* (1984) 379.
[6] K. B. Wiberg, S. T. Waddell, K. Leidig, *Tetrahedron Lett. 27* (1986) 1553; K. J. Morf, G. Szeimies, *ibid. 27* (1986) 5363.
[7] H. K. Hall, Jr., L. G. Snow in K. J. Ivin, T. Saegusa (Eds.): *Ring-Opening Polymerization, Vol. 1*, Elsevier, London 1984.
[8] For polyamides and polyesters whose rigidity is due to mesomeric effects see, e.g.: J.-I. Jin, S. Autoun, C. Ober, R. W. Lenz, *Br. Polym. J. 12* (1980) 132, and references cited therein.
[9] W. B. Scott, R. E. Pincock, *J. Am. Chem. Soc. 95* (1973) 2040; P. G. Gassman, G. S. Proehl, *ibid. 102* (1980) 6882; K. B. Wiberg, F. H. Walker, W. E. Pratt, J. Michl, *ibid. 105* (1983) 3638.
[10] I thank Dr. *W. Marx*, Max-Planck-Institut für Festkörperforschung, Stuttgart, for a CAS online search.
[11] For the first efficient synthesis of a [1.1.1]propellane see: K. Semmler, G. Szeimies, J. Belzner, *J. Am. Chem. Soc. 107* (1985) 6410.
[12] Spin frequency 3.516 kHz; cross-polarization time 3 ms; in KBr; room temperature; standard: TMS external.
[13] The intensity of the signal at $\delta = 128$ representing five C atoms is only 5% of that of the C-2/C-6 signal.
[14] **2a**, $x \approx 11$: ^{1}H-NMR ($CDCl_3$, 50°C): $\delta = 0.84$ (s; CH_3), 1.15 (s; H(terminal(t)-8), 1.27 (H-8), 1.35 (s; H(t)-8), 1.43 (H-4), 1.59 (H-3(5), H(t)-3(5)), 2.16 (H-2(6)), 2.29 (poorly resolved t; H(t)-2(6)); ^{13}C-NMR ($CDCl_3$, 50°C): $\delta = 17.92$ (t; C-4), 22.56 (t; C-3, C-5), 27.76 (q; CH_3), 41.12 (s; C-1, C-7), 47.30 (t; C-8), 57.75 (d; C-2, C-6).
[15] For comparison, the solubility of quinquiphenyl, which also has a rigid structure, is already less than 0.1 g/L: W. Kern, M. Seibel, H. O. Wirth, *Makromol. Chem. 29* (1959) 165.
[16] We presume that a part of the initiator forms mixed aggregates with the lithiated species **3**. Moreover, the initiator may contain small amounts of the hydrolysis product lithium hydroxide. Both effects lead to an underestimation of the true P_n of **2**.
[17] Especially indicative are the H-8 signals: small, sharp singlets at $\delta = 1.15$ and 1.35, respectively, for both terminals.

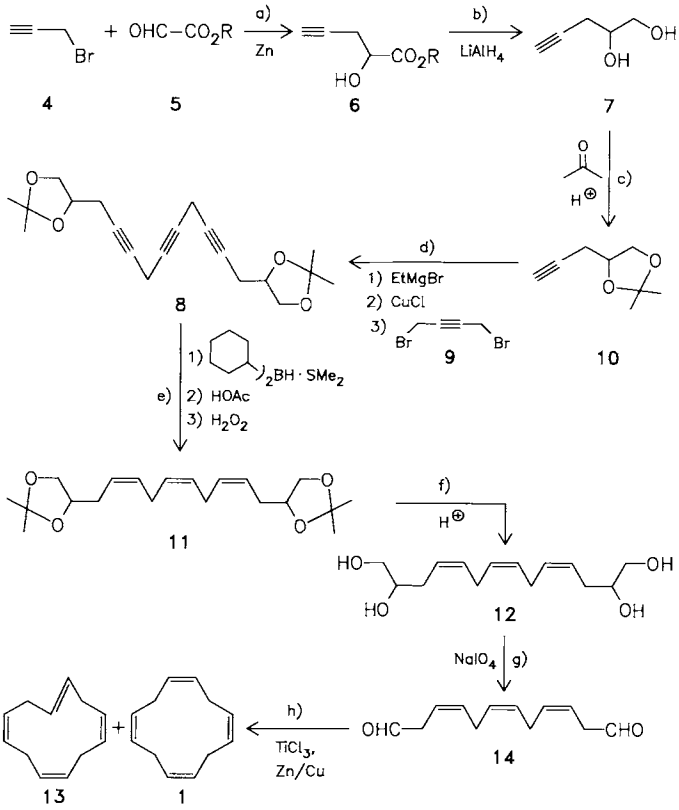

Synthesis of all-*cis*-1,4,7,10-Cyclododecatetraene**

By *Martin Brudermüller* and *Hans Musso**

Dedicated to Professor Emanuel Vogel on the occasion of his 60th birthday

Reflecting on the known ability of cyclic olefins to form π-complexes such as, e.g., bis(cyclooctadiene)nickel,[1] with transition metals it seemed worthwhile trying to synthesize the title compound **1**. Depending on the conformation of the olefin and molar ratio of the reactants there are numerous possibilities for complex formation (see, e.g. **2**). Intra- and intermolecular cycloadditions of **1** are of interest; e.g. tetraasterane **3** could be formed in a double intramolecular [2+2] cycloaddition.

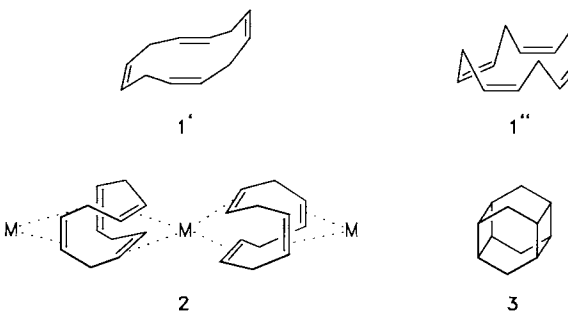

[*] Prof. Dr. H. Musso, Dr. M. Brudermüller
Institut für Organische Chemie der Universität
Richard-Willstätter-Allee, D-7500 Karlsruhe (FRG)

[**] This work was supported by the Deutsche Forschungsgemeinschaft and the Fonds der Chemischen Industrie. We thank *A. Kuiper, P. Lang, I. Mayer, I. Süss*, and *U. Tanger* for numerous spectra and analytical data.

Scheme 1. a), b), c) Ref. [9], 30% yield of **10**.—d) 7.0 g (50 mmol) of **10** was added slowly under N_2 to a solution of ethylmagnesium bromide (55 mol) in THF (70 mL) such that the temperature did not exceed 40°C; the mixture was heated at 60°C for 45 min, allowed to cool to room temperature, and treated firstly with 150 mg of CuCl, then, after 20 min, with 4.76 (22.5 mmol) of **9** within 20 min. Finally, the mixture was heated under reflux for 16 h. After hydrolysis with NH_4Cl/KCN solution, extraction, and chromatography on SiO_2 with CH_2Cl_2 and $CHCl_3$, 6.60 g (89%) of a light-brown oil was obtained whose spectra were consistent with the constitution **8**.[17] Compound **8**, which turns black after a few hours, was immediately reduced. ^{1}H-NMR: $\delta = 1.36$ (s, 6H; CH_3), 1.44 (s, 6H; CH_3), 2.33-2.60 (m, 4H; CH_2—C≡), 3.14 (t, 4H; =CCH_2C≡), 3.75 (dd, 2H; CH_2O *trans*), 4.10 (dd, 2H; CH_2O *cis*), 4.22 (m, 2H; CHO).—e) A solution of dicyclohexylborane-dimethyl sulfide (3.2 g, 41 mmol) in THF (50 mL) was treated at 0°C with 6.9 g (82 mmol) of cyclohexene and the mixture stirred for 2 h; a solution of **8** (3.3 g, 10 mmol) in THF (10 mL) was then added dropwise at 0°C. The mixture was allowed to warm to 20°C within 2 h, stirred for a further 2 h, and treated dropwise with 16 mL of ethyl acetate. After a further 15 hours' stirring, addition of 60 mL of 5 M NaOH and 16 mL of 30% H_2O_2, work-up, and chromatography on SiO_2 with ethyl acetate and $CHCl_3$, **11** was obtained in 72% yield as a yellowish oil. ^{1}H-NMR: $\delta = 1.35$ (s, 6H; CH_3), 1.43 (s, 6H; CH_3), 2.25-2.51 (m, 4H; CH_2C=), 2.83 (t, 4H; =CCH_2C=), 3.56 (dd, 2H; CH_2O *trans*), 4.03 (dd, 2H; CH_2O *cis*), 4.12 (m, 2H; CHO), 5.34-5.57 (m, 6H; CH=).—f) After 15 hours' stirring with 3% H_2SO_4 at room temperature, extraction with ether, and chromatography with CH_2Cl_2, 1.4 g (74%) of **12** was obtained as an almost colorless oil. ^{1}H-NMR: $\delta = 2.50$ (m, 4H; CH_2C=), 2.90 (t, 4H; =CCH_2C=), 3.51 (dd, 2H; CH_2O), 3.63 (dd, 2H; CH_2O), 3.78 (m, 2H; CHO), 5.57 (m, 6H; CH=).—g) A solution of **12** (1.9 g, 7.4 mmol) in H_2O (20 mL) was treated portionwise at 0°C with a solution of $NaIO_4$ (3.2 g, 15 mmol) in H_2O (15 mL). After 1.5 h the mixture was extracted with ether and the extract dried over $MgSO_4$ and evaporated to dryness; 1.16 g (82%) **14**, IR: $\tilde{\nu} = 1720$ cm^{-1}; ^{1}H-NMR: $\delta = 9.67$ (t, 2H; CHO), 5.64 (m, 4H; C=CH), 5.38 (t, 2H; =C*H*–CH_2), 3.03 and 2.82 (m, each 4H; CH_2).—h) A mixture of $TiCl_3$ (10.3 g) and Zn/Cu couple (10.0 g) in 200 mL of DME was boiled for 1 h and then a solution of **14** (1.5 mmol) in DME (200 mL) was added dropwise over a period of 8 h. After a further 15 hours' heating under reflux and further dropwise addition of **14** under the same conditions, the final mixture was heated to boiling for 12 h, allowed to cool, and filtered over Florosil. The filtrate was evaporated down to a few mL and the residue extracted with *n*-pentane. After evaporation of the extract to 3 mL, half of the residue was separated chromatographically on a QF1 column at 95°C (injection block 200°C): **1** (retention time 69 min), 4 mg (2%), colorless liquid which solidified in the cold trap; **2** (retention time 64 min), 10 mg (4%), colorless liquid.

All-*cis*-1,4,7-cyclononatriene has a crown conformation,[2] and its photoelectron spectrum reveals a weak through-space interaction between the three double bonds (6π-electron system),[3] which according to *Winstein* can be regarded as an indication of homoaromaticity.[4] In the case of **1**, as 8π-electron system and homolog of cyclooctatetraene, the crown conformation **1''** should be unstable, and an interaction between the double bonds is highly unlikely.

Following a number of unsuccessful attempts to synthesize **1**, including even the use of the Wittig reaction,[5] we have now found that the McMurry reaction[6] is suitable for this purpose (Scheme 1).[7]

Reaction of propargyl bromide **4** and the glyoxylic acid ester **5**, $R=C_2H_5$,[8] in the presence of zinc furnishes the 2-hydroxy-4-pentynoate **6**,[9] which is reduced to the pentynediol **7**. After protection of the hydroxy groups with acetone, the acetal **10**[9] is coupled via the Grignard compound to both ends of the 1,4-dibromobutyne **9**[10] to give the triyne **8**. Hydrogenation of **8** with Lindlar catalyst does not afford the pure all-*cis*-triene **11**. This could be achieved, however, with the dicyclohexylborane-dimethyl sulfide complex;[11] the product was chromatographically >94% isomerically pure, and the ^{1}H-NMR spectra showed a *cis* configuration for all three double bonds. The protecting groups were removed hydrolytically with dilute sulfuric acid, and the tetraol **12** was cleaved with sodium periodate in water. The sensitive dialdehyde **14** could be obtained as crude product in 82% yield and sufficiently pure for cyclization. **14** was immediately added slowly and dropwise as a 7.5×10^{-3} molar dimethyloxyethane (DME) solution to a large excess of the McMurry reagent prepared from titanium trichloride and zinc/copper couple. Two cyclic tetraolefins $C_{12}H_{16}$ were formed which could be isolated analytically pure on a preparative scale by gas chromatography as colorless liquids; 4% of **13** from the front fraction and 2% of **1** from the end fraction. Both compounds show molecular ion peaks at *m/z* 160 and afford cyclododecane upon catalytic hydrogenation.

The isomer formed in lower yield and with somewhat longer retention time must be the all-*cis*-isomer **1**, since it shows a symmetric quintet for the olefin protons at $\delta=5.41$ and a triplet for the CH_2 groups at $\delta=2.98$ in the ^{1}H-NMR spectrum. Since the spectrum does not alter down to -110°C we assume that a very flexible conformer predominates in the equilibrium in which the H atoms of the CH_2 groups can very rapidly occupy homotopic sites. The fine splitting of the signals is remarkably similar to that which is observed for 1,4,7-cyclononatriene at 80°C.[2]

The other $C_{12}H_{16}$ isomer, one and a half to four times more of which is formed than 1, depending on the amounts of starting material used, is regarded as the *trans-cis*[3]-isomer **13**, since its ^{1}H-NMR spectrum shows two signals for olefin protons, a multiplet of $\delta=5.40$–5.62 corresponsing to 6 H, and a sharp q at $\delta=5.37$ for 2 H. The signal for the CH_2 groups at $\delta=2.80$–2.87 is also broadened in two regions in the ratio 1 : 1. The McMurry reaction[6] often furnishes the more stable *trans*-olefin. For example, from dodecanedial we obtained pure *trans*-cyclododecene in 76% yield.

Received: September 28, 1987 [Z 2446 IE]
German version: *Angew. Chem. 100* (1988) 267

CAS Registry numbers:
1, 112681-65-9; **4**, 106-96-7; **5**, 924-44-7; **6**, 89898-34-0; **7**, 89364-28-3; **8**, 112681-61-5; **9**, 2219-66-1; **10**, 90199-16-9; **11**, 112681-62-6; **12**, 112681-63-7; **13**, 112790-14-4; **14**, 112681-64-8.

[1] G. Wilke, *Angew. Chem. 72* (1960) 581; *75* (1963) 10; *Angew. Chem. Int. Ed. Engl. 2* (1963) 105.
[2] K. G. Untch, R. J. Kurland, *J. Am. Chem. Soc. 85* (1963) 346; W. R. Roth, W. P. Bang, P. Göbel, R. L. Sass, R. B. Turner, A. P. Yü, *ibid. 86* (1964) 3178.
[3] P. Bischof, R. Gleiter, E. Heilbronner, *Helv. Chim. Acta 53* (1970) 1425.
[4] S. Winstein, *J. Am. Chem. Soc. 81* (1959) 6524; *Q. Rev. Chem. Soc. 23* (1969) 141; P. Radlick, S. Winstein, *J. Am. Chem. Soc. 85* (1963) 344.
[5] H. Hopf, H. Musso, unpublished results from 1970; P. Fielder, *Dissertation*, Universität Karlsruhe 1980.
[6] J. E. McMurry, M. P. Fleming, K. L. Kees, L. P. Krepski, *J. Org. Chem. 43* (1978) 3255.
[7] M. Brudermüller, *Dissertation*, Universität Karlsruhe 1987.
[8] M. E. Jung, K. Shishido, L. H. Davis, *J. Org. Chem. 47* (1982) 892.
[9] F. Bohlmann, P. Herbst, H. Gleinig, *Chem. Chem. 94* (1961) 948.
[10] A. W. Johnson, *J. Chem. Soc. 1946*, 1011.
[11] J. G. Millar, E. W. Underhill, *Can. J. Chem. 64* (1986) 2427.

1,3-Dihydro-1,3-diborafulvene Derivatives**

By *Volker Schäfer, Hans Pritzkow,* and *Walter Siebert**

Dedicated to Professor Helmut Dörfel on the occasion of his 60th birthday

1,4-Diboracyclohexadienes **1** are stabilized by π-donor substituents (e.g. $R^1=F$, OMe) at the boron atoms, whereas when $R^1=$alkyl, rearrangement to *nido*-carbaboranes **2** takes place.[1] *Herberich* et al. recently described two further isomers, 2,6-diborabicyclo[3.1.0]hex-3-ene **3** ($R^1=NiPr_2$)[2a] and 1,2-dibora-3,5-cyclohexadiene **4** ($R^1=NMe_2$) as ligands in Ru- and Rh-complexes.[2b]

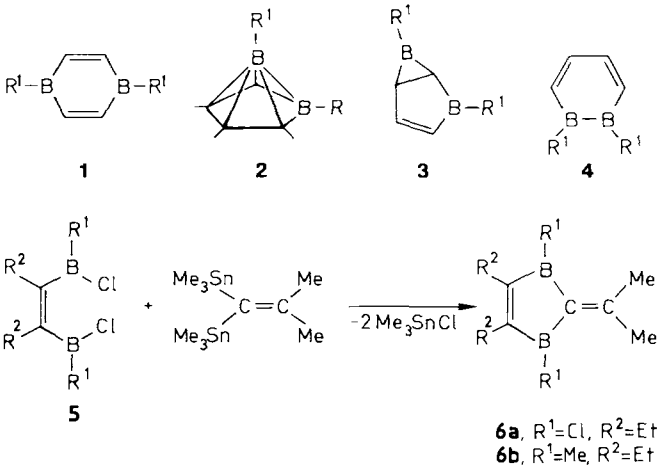

6a, $R^1=Cl$, $R^2=Et$
6b, $R^1=Me$, $R^2=Et$

Herein we report on derivatives of the novel $C_4B_2R_6$ isomer 1,3-dihydro-1,3-diborafulvene **6** which are obtained in good yields by reaction of (*Z*)-bis(dichloroboryl)alkenes **5**, $R^1=Cl$, with 1,1-bis(trimethylstannyl)-2-methyl-1-propene.[3] Substitution of the chlorine atoms in the pale yellow **6a** with Al_2Me_6 leads to the yellowish-orange derivative **6b**. The ^{13}C-NMR spectra of **6a**, **b** at 25°C contain sharp signals at $\delta=172.3$ and $\delta=154.6$, respectively, for the exocyclic olefinic C-atom. Broad signals are observed at $\delta=176$ and 179, respectively, which we assign to the C

[*] Prof. Dr. W. Siebert, V. Schäfer, Dr. H. Pritzkow
Anorganisch-chemisches Institut der Universität
Im Neuenheimer Feld 270, D-6900 Heidelberg (FRG)

[**] This work was supported by the Deutsche Forschungsgemeinschaft, the Fonds der Chemischen Industrie, and BASF AG.

atoms of the ring double bonds. The signal for C2 is not observable at 25 °C because of the quadrupole effect of the two boron atoms. In the case of **6b** the signal for C2 ($\delta = 151.8$) is first observed on cooling to −45 °C; **6a** already crystallizes out at this temperature.

Prolonged heating of the air-sensitive derivative **6b** under nitrogen at 120 °C leads to rearrangement to a carbaborane whose constitution has still not been clarified.[4] As a Lewis acidic dihydrodiborafulvene, **6b** has good donor and acceptor properties for the formation of mononuclear and dinuclear complexes.[5] Typical examples are the tetracarbonylmetal complexes **7a** and **7b** formed on reaction of **6b** with $Cr(CO)_6$ and $Mo(CO)_6$, respectively. Their constitution follows from the spectroscopic data and an X-ray structure analysis of **7b**.[6]

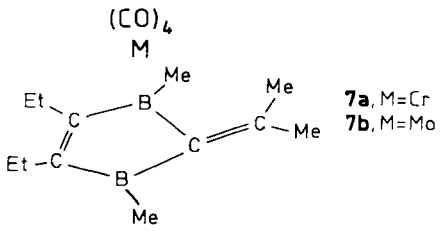

7a, M=Cr
7b, M=Mo

Complexation of **6b** at the $M(CO)_4$ fragment results in an upfield shift of the NMR signals for the ring atoms, while the signal for C6 remains virtually unaffected (cf. [(fulvene)$Cr(CO)_3$] complexes[7a]). The donor groups coordinate the molybdenum atom in a distorted octahedral geometry with the ligands C18–O4 and C15–O1 and the double bonds C2–C6 and C4–C5 (midpoint) in one plane (Fig. 1). Prerequisite for a favorable interaction of the molybdenum atom with the π-electrons of the C2–C6 double bond

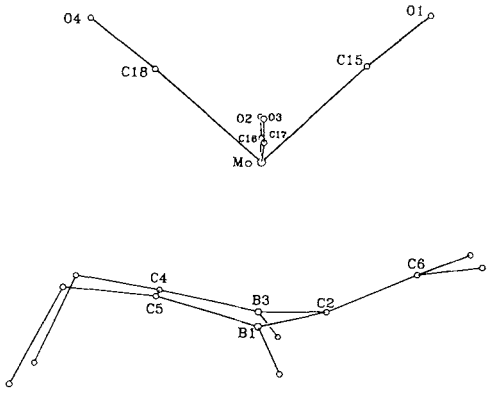

Fig. 1. Schematic representation of the crystal structure of **7b** [6]. Bond lengths [Å] and angles [°, esd 0.2°]: Mo-C2 2.324(1), Mo-C4(C5) 2.461, 2.469(2), Mo-B1(B3) 2.563, 2.546(2), Mo-C6 2.714(2), C2-C6 1.387(3), C2-C1(B3) 1.580, 1.574(3), C4-C5 1.407(3), B1(B3)-C5(C4) 1.558, 1.558(3), Mo-C15(C18) 1.994, 1.983(2), Mo-C16(C17) 2.041, 2.033(2), distances to the midpoints of the C=C bonds: Mo-(C4,C5) 2.362, Mo-(C2,C6) 2.430; C4C5B1B3/B1B3C2 20, B1B3C2/C2C6 14, C18MoC15 96.7, C16MoC17 162.7, B1C2B3 104.7, C2B3C4 105.0, B3C4C5 110.8, C4C5B1 110.2, C5B1C2 105.1; C6C2B1 125.7, C6C2B3 125.6.

is the bending at C2 (14°) and along B1B3 (20°). The distance Mo-C6 (2.71 Å) is longer than in analogous fulvene(η^6-arene)molybdenum complexes (2.37, 2.31 Å),[7b] since the donor centers (midpoint of the double bonds) are further apart because of the longer B–C bonds and the different disposition of the double bonds.

Experimental

6a: A solution of **5** (1.97 g, 8 mmol) in toluene (10 mL) was added dropwise to a solution of 1,1-bis(trimethylstannyl)-2-methyl-1-propene (3.06 g, 8 mmol) [3] in toluene (50 mL) at −10 °C. The mixture was then stirred for 2 h at 20 °C. Finally, the solvent was removed in a vacuum and **6a** (1.4 g, 77%) isolated by distillation at 55 °C/10^{-3} torr.—^{1}H-NMR (C_6D_6): $\delta = 0.96$ (t, 6H, $^3J(HH) = 7.6$ Hz), 2.15 (s, 6H), 2.28 (q, 4H); ^{11}B-NMR (C_6D_6): $\delta = 62.6$; ^{13}C-NMR ([D_8]toluene): $\delta = 14.1$ (CH_3CH_2), 21.8 (CH_2), 26.6 (CH_3C), 172.3 (C_{exo}), 176 (C4/C5, br.); EI-MS: *m/z* 228 ($M^{\oplus}$, 100%).

6b: A solution of trimethylaluminum (0.5 g, 3.5 mmol) in pentane (10 mL) was added dropwise with stirring to a solution of **6a** (0.79 g, 3.5 mmol) in pentane (10 mL) at −60 °C. The mixture was warmed to 20 °C, filtered, and the solvent removed from the filtrate in a vacuum. **6b** (0.54 g, 82%) was then recovered by distillation at 35 °C/10^{-3} torr.—^{1}H-NMR (C_6D_6): $\delta = 0.98$ (t, 6H, $^3J(HH) = 7.6$ Hz), 1.08 (s, 6H; B-CH_3), 1.99 (s, 6H), 2.34 (q, 4H); ^{11}B-NMR (C_6D_6): $\delta = 68.6$; ^{13}C-NMR ([D_8]toluene, −45 °C): $\delta = 7.4$ (B-CH_3), 14.7 (CH_3CH_2), 22.2 (CH_2CH_3), 26.4 (CCH_3), 151.8 (C2), 154.6 (C6), 179.3 (C4/5), Assignments by means of 2D-NMR measurements (^{1}H-,^{13}C-correlated) at 25 °C); EI-MS: *m/z* 188 ($M^{\oplus}$, 2.6%); 108 ($M^{\oplus} - C_5H_9B$, 53.1%).

7a: A solution of $Cr(CO)_6$ (0.26 g, 1.18 mmol) and **6b** (0.22 g, 1.17 mmol) in toluene (20 mL) was heated under reflux for 4 h. After removal of the solvent the red residue was dissolved in petroleum ether and the resulting solution chromatographed on an Al_2O_3 column (5% H_2O): 0.35 g of red **7a** (85%, m.p. 63 °C, from hexane, −35 °C). Yellow **7b** (69%, m.p. 75 °C, from hexane, −35 °C) was obtained analogously.—Spectroscopic data for **7a**: ^{11}B-NMR (C_6D_6): $\delta = 34.0$; ^{1}H-NMR (C_6D_6): $\delta = 0.91$ (s, 6H, B-CH_3), 1.05 (t, 6H, $^3J(HH) = 7.7$ Hz), 1.52 (s, 6H), 1.87 (m, 2H), 2.20 (m, 2H); ^{13}C-NMR (C_6D_6): $\delta = 3.3$ (br., B-CH_3), 15.5 (CH_3CH_2), 22.5 (CH_2CH_3), 28.1 (CCH_3), 140 (br., C4,5), 157.2 (C6), 218.0 (CO), 219.2 (2CO), 228.0 (CO). MS-EI: *m/z* 352 ($M^{\oplus}$, 3.2%), 324 ($M^{\oplus} - CO$, 4%), 296 ($M^{\oplus} - 2CO$, 3.4%), 268 ($M^{\oplus} - 3CO$, 25.3%), 240 ($M^{\oplus} - 4CO$, 81.7%). IR (ν(CO), pentane): 2026.0, 1960.0, 1936.5, 1907.5 cm^{-1}). **7b**: ^{11}B-NMR (C_6D_6): $\delta = 37.2$; ^{1}H-NMR (C_6D_6): $\delta = 0.98$ (s, 6H, B-CH_3), 1.08 (t, 6H, $^3J(HH) = 7.7$ Hz), 1.65 (s, 6H), 2.13 (m, 2H), 2.22 (m, 2H); ^{13}C-NMR (C_6D_6): $\delta = 1.35$ (br., B-CH_3), 16.1 (CH_3CH_2), 22.6 (CH_2CH_3), 28.3 (CCH_3), 138.5 (br., C4,5), 150.3 (C6), 211.1 (CO), 211.4 (2CO), 217.3 (CO); MS-EI: *m/z* 396 ($M^{\oplus}$, 34.1%), 368 ($M^{\oplus} - CO$, 54.1%), 340 ($M^{\oplus} - 2CO$, 100%), 312 ($M^{\oplus} - 3CO$, 56.5%), 284 ($M^{\oplus} - 4CO$, 11.8%). IR (ν(CO), pentane): 2029.0, 1964.0, 1920.5, 1909.5 cm^{-1}.

Received: August 26, 1987 [Z 2418 IE]
German version: *Angew. Chem. 100* (1988) 271

CAS Registry numbers:
5 (R^1=Cl, R^2=Et), 112375-16-3; **6a**, 112375-17-4; **6b**, 112375-18-5; **7a**, 112375-19-6; **7b**, 112375-20-9; $(Me_3Sn)_2C=C(CH_3)_2$, 103670-41-3; $Cr(CO)_6$, 13007-92-6; $Mo(CO)_6$, 13939-06-5.

[1] G. E. Herberich in G. Wilkinson, F. G. A. Stone, E. W. Abel (Eds.): *Comprehensive Organometallic Chemistry, Vol. 1*, Pergamon Press, Oxford 1982, p. 399 ff.
[2] a) G. E. Herberich, H. Ohst, H. Mayer, *Angew. Chem. 96* (1984) 975; *Angew. Chem. Int. Ed. Engl. 23* (1984) 969; b) G. E. Herberich, B. Hessner, M. Hostalek, *ibid. 98* (1986) 637 and *25* (1986) 637.
[3] T. N. Mitchell, W. Reimann, *Organometallics 5* (1986) 1991.
[4] ^{11}B-NMR (C_6D_6): $\delta = 16.6$, −45.4 (in the ratio 1:1). This points to a *nido*-carbaborane derivative **2**; cf. H. O. Berger, H. Nöth, B. Wrackmeyer, *Chem. Ber. 112* (1979) 2884.
[5] V. Schäfer, W. Siebert, unpublished.
[6] **7b**: space group $P2_12_12_1$, $a = 10.911(1)$, $b = 11.299(1)$, $c = 15.383(1)$ Å, $V = 1896.5$ Å^3, $Z = 4$, $R = 0.027$ for 3039 observed reflections (two-circle diffractometer, $Mo_{K\alpha}$ radiation, ω-scan; Mo,O,B,C anisotropic, H isotropic, CH_3 as rigid group). Further details of the crystal structure investigation are available on request from the Fachinformationszentrum Energie, Physik, Mathematik GmbH, D-7514 Eggenstein-Leopoldshafen 2 (FRG), on quoting the depository number CSD-52712, the names of the authors, and the journal citation.
[7] a) B. Lubke, F. Edelmann, U. Behrens, *Chem. Ber. 116* (1983) 11, and references cited therein; b) M. L. H. Green, A. Izquierdo, J. J. Martin-Polo, V. S. B. Mtetwa, K. Prout, *J. Chem. Soc. Chem. Commun. 1983*, 538.

A New Route to Nitrile Oxides via α-Nitrosodiazo Derivatives**

By *Ghislaine Sicard, Antoine Baceiredo, Guy Crocco,* and *Guy Bertrand**

It has been known since 1889 that 1,2-bisdiazo derivatives spontaneously decompose to the corresponding alkynes—thus indicating that 1,2-biscarbenes are acetylenic in nature.[1] Recently, we have extended this concept to λ^3-phosphanes which are directly bound to a diazomethyl[2] or an azido group[3] and have been able to synthesize new heteroelement multiply bonded systems.

$$-\underset{\underset{N_2}{\|}}{C}-\underset{\underset{N_2}{\|}}{C}- \xrightarrow[-\,2\,N_2]{} -\ddot{C}-\ddot{C}- \longleftrightarrow -C\equiv C-$$

$$\gtrdot\ddot{P}-\underset{\underset{N_2}{\|}}{E} \xrightarrow[-\,N_2]{} \gtrdot\ddot{P}-\ddot{E} \longleftrightarrow \gtrdot P\equiv E \qquad E = CR, N$$

Nitrile oxides[4] can be formally considered as "nitrene oxides" α to a carbene carbon atom:[5]

$$-\ddot{C}-\ddot{N} \longrightarrow O \longleftrightarrow -C\equiv N \longrightarrow O$$

Therefore, α-nitrosodiazo derivatives are potential precursors of these species. We have already shown that the carbon-silicon bond of trimethylsilyldiazo derivatives easily reacts with activated halogen compounds.[2b] Since no phosphorus-substituted nitrile oxide was known, we first chose to study the reaction of nitrosyl chloride with the [diazo(trimethylsilyl)methyl]phosphonic acid derivative **1**.[6-8]

$$R_2P(=S)-\underset{\underset{N_2}{\|}}{C}-SiMe_3 \xrightarrow[-\,Me_3SiCl\ -\,78\,^\circ C]{+\ ClN=O} \left[R_2P(=S)-\underset{\underset{N_2}{\|}}{C}-\ddot{N}=O\right] \xrightarrow[-\,N_2]{} R_2P(=S)-C\equiv N\rightarrow O$$

1 **2** **3**

R = iPr_2N

The α-nitroso derivative **2** was not stable enough to be characterized, even at −78 °C; in contrast, the λ^5-phosphorus-substituted nitrile oxide **3**[8] was obtained in 90% isolated yield as white crystals (m.p. 60 °C, decomp.). Characteristic nitrile oxide reactivity was observed for derivative **3**. With triphenylphosphane, the nitrile **4**[8] was obtained in nearly quantitative yield, while irradiation ($\lambda = 254$ nm) gave rise to the isomeric isocyanate **5** in 71% yield.[8]

$$R_2P(=S)-C\equiv N \xleftarrow[-\,Ph_3PO]{+\,Ph_3P} \mathbf{3} \xrightarrow{h\nu} R_2P(=S)-N=C=O$$

4 **5**

R = iPr_2N

[*] Dr. G. Bertrand, G. Sicard, Dr. A. Baceiredo, Dr. G. Crocco
Laboratoire des Organométalliques, U.A. 477,
Université Paul Sabatier
118, route de Narbonne, F-31062 Toulouse Cedex (France)

[**] We thank Dr. *I. Tkatchenko,* Dr. *Y. Dartiguenave,* and Dr. *M. Dartiguenave* (Laboratoire de Chimie de Coordination du CNRS, Toulouse) for providing us with laboratory facilities following the destruction, on March 25, 1987, of the Chemistry building of the Université Paul Sabatier.

Since α-nitroso-α-phosphino carbenes such as **8a** can be considered either as nitroso λ^5-phosphaacetylenes **8b** (formulated as zwitterion) or as λ^3-phosphinonitrile oxides **8c**, it was of interest synthesizing the diazo(nitroso) precursor **7** (analogously to **2**[7]), starting from the [diazo(trimethylsilyl)methyl]phosphane **6**.[2a] In fact, **7** appeared to be unstable as well as **8**, which spontaneously rearranged, via a 1-3 oxygen shift,[2b] to the corresponding nitrile of the phosphane oxide **9**,[8] in 75% isolated yield. A small

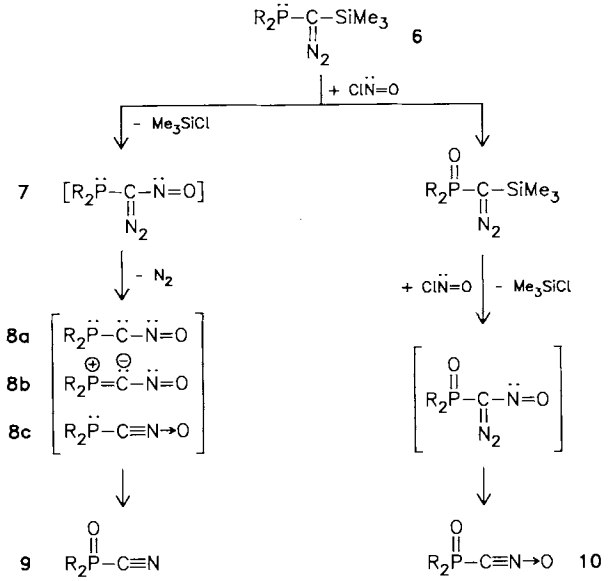

R = iPr_2N

amount (15% yield) of the corresponding nitrile oxide **10**[8] was also obtained, presumably resulting from oxidation of the starting material **6** followed by a subsequent reaction with a second molecule of nitrosyl chloride.

Note that in all the methods described so far for the synthesis of nitrile oxides, organic systems already containing the C-N-O sequence have been used as starting material. That the conversion of organic compounds possessing a CN single, double or triple bond into nitrile oxides or even that the introduction of an NO group into organic compounds is possible has hitherto never been clearly indicated.

Received: September 21, 1987 [Z 2433 IE]
German version: *Angew. Chem. 100* (1988) 289

CAS Registry numbers:
1, 112550-05-7; **3**, 112575-03-8; **4**, 112550-06-8; **5**, 112550-07-9; **6**, 97135-48-3; **9**, 112550-08-0; **10**, 112550-09-1; ClN=O, 2696-92-6; Ph_3P, 603-35-0.

[1] T. Curtius, *Ber. Dtsch. Chem. Ges. 22* (1889) 2161.
[2] a) A. Baceiredo, G. Bertrand, G. Sicard, *J. Am. Chem. Soc. 107* (1985) 4781; b) A. Baceiredo, A. Igau, G. Bertrand, M. J. Menu, Y. Dartiguenave, J. J. Bonnet, *ibid. 108* (1986) 7868; c) A. Baceiredo, G. Bertrand, *Phosphorus Sulfur 26* (1986) 57; d) G. Bertrand, A. Baceiredo, G. Sicard, M. Granier, *ibid. 30* (1987) 353.
[3] a) G. Sicard, A. Baceiredo, G. Bertrand, J. P. Majoral, *Angew. Chem. 23* (1984) 450; *Angew. Chem. Int. Ed. Engl. 23* (1984) 459; b) A. Baceiredo, G. Bertrand, J. P. Majoral, G. Sicard, J. Jaud, J. Galy, *J. Am. Chem. Soc. 106* (1984) 6088; c) A. Baceiredo, G. Bertrand, J. P. Majoral, F. El Anba, G. Manuel, *ibid. 107* (1985) 3948; d) J. P. Majoral, G. Bertrand, A. Baceiredo, E. Ocando, *Phosphorus Sulfur 27* (1986) 75; e) J. Boske, E. Niecke,

E. Ocando, J. P. Majoral, G. Bertrand, *Inorg. Chem. 25* (1986) 2695; f) G. Bertrand, J. P. Majoral, A. Baceiredo, *Acc. Chem. Res. 19* (1986) 17.

[4] For reviews see for example: a) A. Quilico, *Chim. Ind. (Milan) 53* (1971) 157; b) C. Grundmann, P. Grunanger: *The Nitrile Oxides*, Springer, Berlin 1971; c) J. Andree, *Chem. Listy 67* (1973) 1138; d) H. Stamm, *Method. Chim. 6* (1975) 329.

[5] R. Huisgen, *Angew. Chem. 75* (1963) 604; *Angew. Chem. Int. Ed. Engl. 2* (1963) 565.

[6] Synthesis of **1**: A toluene solution of **6** [2a] (344 mg) and sulfur (64 mg) was stirred at room temperature for 1 h. After removal of the solvent, **1** (357 mg, 95% yield) was purified by column chromatography.

[7] Through a solution of **1** (200 mg) in toluene was bubbled, at −78°C, an excess of nitrosyl chloride. After warming to room temperature and removal of the solvent, **3** was purified by column chromatography (hexane/ether 90/10, $R_F = 0.8$).

[8] **1**: yellow oil; R_F(hexane/ether 90/10) 0.8; ^{31}P-NMR (C_6D_6): $\delta = +65$; ^{1}H-NMR (C_6D_6): $\delta = 0.55$ (s, 9H, CH_3Si), 1.4 (d, J(H,H) = 7 Hz, 12H, CH_3), 1.5 (d, J(H,H) = 7 Hz, 12H, CH_3), 3.8 (sept d, J(H,H) = 7 Hz, J(P,H) = 16 Hz, 4H, CH); IR (KBr): $\tilde{\nu} = 2050$ (CN_2) cm^{-1}; MS: m/z 376 ($M^{\oplus}$).—**3**: ^{31}P-NMR (C_6D_6): $\delta = +27$; ^{1}H-NMR ($CDCl_3$): $\delta = 1.3$ (d, J(H,H) = 7 Hz, 12H, CH_3), 1.4 (d, J(H,H) = 7 Hz, 12H, CH_3), 3.7 (sept d, J(H,H) = 7 Hz, J(P,H) = 14 Hz, 4H, CH); ^{13}C-NMR ($CDCl_3$): $\delta = 22.17$, 22.82 (s, CH_3), 46.87 (d, J(P,C) = 5.3 Hz, CH), CNO carbon was not observable (cf. [9]); IR (KBr): $\tilde{\nu} = 2610$, 2210, 1310 (CNO) cm^{-1}; MS: m/z 305 ($M^{\ominus}$), 263 ($M^{\oplus} - CNO$).—**4**: m.p. 115°C; R_F(pentane/ether 95/5) 0.4; ^{31}P-NMR ($CDCl_3$): $\delta = +23$; ^{1}H-NMR ($CDCl_3$): $\delta = 1.1$ (d, J(H,H) = 7 Hz, 12H, CH_3), 1.3 (d, J(H,H) = 7 Hz, 12H, CH_3), 3.5 (sept d, J(H,H) = 7 Hz, J(P,H) = 20 Hz, 4H, CH); IR (KBr): $\tilde{\nu} = 2180$ (CN) cm^{-1}; MS: m/z 289 ($M^{\oplus}$).—**5**: ^{31}P-NMR ($CDCl_3$): $\delta = +49$; ^{1}H-NMR ($CDCl_3$): $\delta = 1.2$ (d, J(H,H) = 7 Hz, 12H, CH_3), 1.4 (d, J(H,H) = 7 Hz, 12H, CH_3), 3.5 (sept d, J(H,H) = 7 Hz, J(P,H) = 14 Hz, 4H, CH); IR ($CDCl_3$): $\tilde{\nu} = 2250$ (NCO) cm^{-1}.—**9**: m.p. 68°C; R_F(ether) 0.5; ^{31}P-NMR ($CDCl_3$): $\delta = -10$; ^{1}H-NMR (C_6D_6): $\delta = 1.4$ (d, J(H,H) = 7 Hz, 12H, CH_3), 1.6 (d, J(H,H) = 7 Hz, 12H, CH_3), 3.7 (sept d, J(H,H) = 7 Hz, J(P,H) = 14 Hz, 4H, CH); IR (KBr): $\tilde{\nu} = 2190$ (CN), 1245 (PO) cm^{-1}; MS: m/z 273 ($M^{\ominus}$).—**10**: yellow oil; ^{31}P-NMR (C_6D_6): $\delta = -7$; ^{1}H-NMR (C_6D_6): $\delta = 1.3$ (d, J(H,H) = 7 Hz, 12H, CH_3), 1.4 (d, J(H,H) = 7 Hz, 12H, CH_3), 3.4 (sept d, J(H,H) = 7 Hz, J(P,H) = 18 Hz, 4H, CH); IR (C_6D_6): $\tilde{\nu} = 2220$, 1330 (CNO), 1250 (PO) cm^{-1}; MS: m/z 289 ($M^{\ominus}$).

[9] M. Christl, J. P. Warren, B. L. Hawkins, J. D. Roberts, *J. Am. Chem. Soc. 95* (1973) 4392.

$[Os(\eta^2\text{-}PHS)(CO)_2(PPh_3)_2]$, a Stable η^2-Thioxophosphane(H−P=S)-Metal Complex**

By *D. Scott Bohle, Clifton E. F. Rickard,* and *Warren R. Roper**

A variety of reactive, small molecules such as CF_2,[1] Se_2,[2] $S_2Me^{\oplus}$,[3] PH(OMe)Ph,[4] and PC(O)CF_3[5] form stable complexes with the 16-electron fragment $[Os(CO)_2(PPh_3)_2]$. As part of our attempts to stabilize a terminal phosphanediyl (phosphinidene) complex $[L_nM{=}PR]$[5] utilizing this metal fragment we have prepared a mononuclear example of complexed η^2-thioxophosphane, H−P=S, that is, the sulfide of a terminal phosphinidene complex. This unusual ligand is the parent molecule of the class of compounds R−P=S, examples of which are found in the two binuclear complexes, $[(OC)_4Mn(\eta^2\text{-}\mu^2\text{-}PMeS)Mn(CO)_5]$,[6] and $[(C_5H_5)_2Mo_2(CO)_3(\mu\text{-}CO)(\eta^2,\mu^2\text{-}PRS)]$ ($R = C_6H_4OCH_3$).[7] Free thioxophosphanes are very reactive and their existence has been demonstrated only by matrix isolation vibrational spectroscopy[8] and by trapping experiments with dienes and alcohols.[9] Thioxophosphanes are also of interest as an extension of the emerging chemistry of R′P=A (A = CR_2, NR, and PR). Herein we report the preparation of the osmium complexes **2a** and **2b**, and the crystal structure and reactions of **2a**.

$[Os(\eta^2\text{-}PHX)(CO)_2(PPh_3)_2]$ **2a**, X = S; **2b**, X = Se

Addition of one equivalent of trifluoromethanesulfonic acid to the phosphane sulfide (or selenide) complexes **1a**, **b** (Scheme 1) followed immediately by addition of an excess of the base DBU (1,8-diazabicyclo[5.4.0]undec-7-ene), results in good yields of the η^2-thioxo- and η^2-selenoxophosphane complexes **2a** and **b**, respectively.

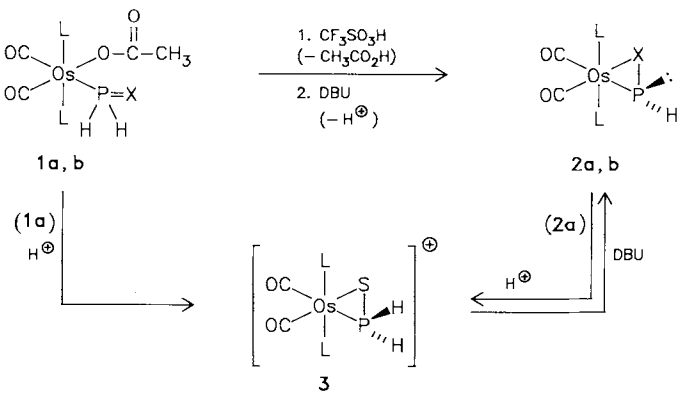

Scheme 1. Synthesis of **2a**, **b**. L = PPh_3; **a**, X = S; **b**, X = Se.

While attempts to isolate the cationic H_2PS complex **3** have failed, both ^{1}H- and ^{31}P-NMR spectra (Table 1) indicate that **3** is the initial product when either **1a** or **2a** is treated with strong acids. At room temperature, solutions of **3** quickly decompose. Spectroscopic data for **2a** ($\tilde{\nu}$(PH) = 2196 cm^{-1} and $^1J_{HP} = 117.5$ Hz) suggest a weakened phosphorus-hydrogen bond. However **2a**,**b** are prepared in the presence of excess base and there is no evidence for the deprotonation of **2a**,**b** under these conditions. Only very low yields (< 7%) of **2a** result when **1a** is treated directly with base.

Table 1. Selected NMR and IR spectroscopic data of **1**–**3** and **5**–**7** [a].

1a: ^{1}H: $\delta = 1.44$ (s; O_2CCH_3), 5.82 (dt, $^1J_{HP} = 374.8$, $^3J_{HP} = 7.9$; H_2PS); ^{31}P{^{1}H}: $\delta = -3.48$ (d, $^2J_{PP} = 27.7$; PPh_3), −56.29 (t, $^2J_{PP} = 27.7$; H_2PS); IR: 2050, 1969

1b: IR: 2056, 1980

2a: ^{1}H: $\delta = 0.82$ (dt, $^1J_{HP} = 117.5$, $^3J_{HP} = 6.6$, HPS); ^{31}P{^{1}H}: $\delta = 12.5$ (dd, $^2J_{PP} = 285.9$, $^2J_{PP} = 6.5$; PPh_3), 1.6 (dd, $^2J_{PP} = 285.9$, $^2J_{PP} = 13.9$; PPh_3), −140.4 (dd, $^2J_{PP} = 13.9$, $^2J_{PP} = 6.5$; HPS); IR: 1989, 1922

2b: ^{1}H: $\delta = 0.83$ (dt, $^1J_{HP} = 118.5$, $^3J_{HP} = 7.8$; HPSe); ^{31}P{^{1}H}: $\delta = 10.7$ (d, $^2J_{PP} = 282.4$; PPh_3), 0.1 (dd, $^2J_{PP} = 282.4$, $^2J_{PP} = 16.6$; PPh_3), −137.6 (dd, $^2J_{PP} = 16.6$, $^2J_{PP} = 5.1$; HPSe); ^{77}Se{^{1}H}: $\delta = -472$ (ddd, $^1J_{PSe} = 280$, $^2J_{PSe} = 9.5$, $^2J_{PSe} = 4.4$; HPSe); IR: 1987, 1924

3: ^{1}H: $\delta = 5.01$ (dt, $^1H_{HP} = 444.7$, $^3J_{HP} = 8.7$; H_2PS); ^{31}P{^{1}H}: $\delta = -3.66$ (d, $^2J_{PP} = 21.1$; PPh_3), −64.63 (t, $^2J_{PP} = 21.1$; H_2PS)

5: IR: 2050, 1978, 1957 (cs), 1924 (cs)

6: IR: 2022, 1940

7a: IR: 2057, 2000

7b: IR: 2056, 1998

[a] NMR spectra: Bruker-AM400 spectrometer, $CDCl_3$, 21°C; δ values referred to TMS (^{1}H), 85% H_3PO_4 (^{31}P) or Me_2Se (^{77}Se); coupling constants J in Hz. IR spectra of Nujol mulls between KBr pellets. $\tilde{\nu}$ (CO stretching vibration) in cm^{-1}; cs = crystal splitting band.

[*] Prof. Dr. W. R. Roper, D. S. Bohle, Dr. C. E. F. Rickard
Department of Chemistry, The University of Auckland
Private Bag, Auckland (New Zealand)

[**] We thank Dr. *Jan Coddington* for assistance in obtaining NMR data; Johnson Matthey for the loan of OsO_4; and the New Zealand Universities Grants Committee for grants towards the purchase of instrumental facilities and the award of a Postgraduate Scholarship to *D. S. B.*

Both NMR spectroscopy and the reactions of **2a** suggest that there is a lone pair of electrons on the phosphorus in the HPS and HPSe ligands. The $^{31}P\{^1H\}$-NMR spectrum of **2a** indicates that there are two strongly coupled ($^2J_{PP}=285.9$ Hz), inequivalent, *trans*-triphenylphosphane ligands (Table 1). The X-ray diffraction study of **2a** (Fig. 1)[10] reveals that the phosphorus and sulfur atoms are almost coplanar with the metal and the two carbon monoxide ligands. Therefore, the inequivalence of the triphenylphosphane ligands arises from there being a lone pair on one side of this plane and a hydrogen atom on the other side. Because of the inability to distinguish phosphorus and sulfur crystallographically little can be inferred from the specific geometry of **2a** except that the phosphorus–sulfur bond length, 209.0(5) pm, is significantly longer than the average value for the thiophosphoryl phosphorus–sulfur double bond, 193 pm; in fact it is at the long end of the range (203–209 pm) associated with phosphorus–sulfur single bonds.[11] Weakened phosphorus–selenium bonding in **2b** is also implied by both the ^{31}P- and ^{77}Se-NMR spectra which show that the one bond phosphorus–selenium coupling ($^1J_{PSe}=280$ Hz) is about half of that found in **1b** ($^1J_{PSe}=531$ Hz).

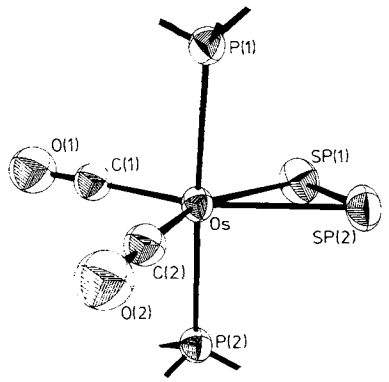

Fig. 1. Crystal structure of **2a** [10]. Because phosphorus and sulfur were not distinguished these atoms are represented by SP(1) and SP(2). Bond lengths [pm]: Os-P(1) 240.3(3), Os-P(2) 239.4(3), Os-SP(1) 245.7(3), Os-SP(2) 244.3(3), SP(1)-SP(2) 209.0(5). Bond angles [°]: SP(1)-Os-SP(2) 50.5(1), Os-SP(1)-SP(2) 64.4(1), Os-SP(2)-SP(1) 65.1(1). The phenyl rings of the triphenylphosphane ligands have been omitted for clarity.

These structural and spectroscopic results suggest that the bonding in **2a,b** may be similar to that in the complexes $[Os(CO)_2(PPh_3)_2L]$, L = alkene and alkyne. Interaction of the empty π^* orbital of HPS with filled metal orbitals of the appropriate symmetry would be expected to weaken the phosphorus–sulfur bond, as observed. There is no evidence of a *monohapto* HPS interaction as depicted in **4**, although this is the geometry present in the related $R_2N-\ddot{P}=O$ complex $[(OC)_5Cr\{P(O)NR_2\}]$, R = *i*Pr.[12] Both geometries are found in phosphaalkene[13] and diphosphene[14] transition metal complexes.

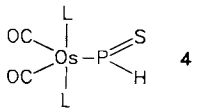

4

Electrophiles readily add to the phosphorus in **2a** (Scheme 2). Stable adducts result when **1a** is treated with methyl trifluoromethanesulfonate, to give **5**, and with $[NBu_4][AuI_2]$, to give **6**. In the presence of alcohol, however, reaction with acid results in phosphorus–sulfur bond cleavage and the product, a cationic mercaptoalkylphosphinite complex, **7a,b**, is formed from overall ROH and $H^{\oplus}$ addition. This reaction is reversible and addition of base (DBU) to **7a,b** leads to abstraction of $H^{\oplus}$, loss of ROH, and return of **2a** in high yield. The HPSe complex **2b** behaves similarly when treated with acidic alcohol but the resulting product is stable only in the presence of acid. In the presence of D_2O, NMR experiments indicate that the SH protons exchange more rapidly than the $ROPH_2$ protons.

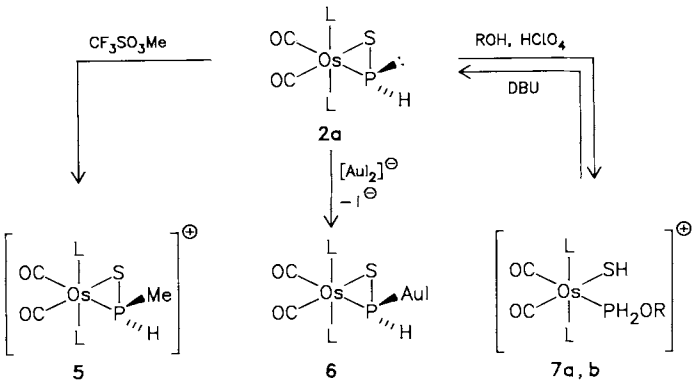

Scheme 2. Reactions of **2a**. L = PPh_3; **7a**, R = Me; **7b**, R = Et.

At low temperatures the cationic complex **5** is deprotonated rapidly with DBU to give $[Os(\eta^2\text{-}PMeS)(CO)_2(PPh_3)_2]$.[15]

Experimental

2a: **1a** (0.5 g, 0.59 mmol) in 10 mL of anhydrous THF is treated with CF_3SO_3H (0.59 mmol, 0.084 g, 0.049 mL), and to this colorless solution excess DBU (1.7 mmol, 0.25 g, 0.25 L) is immediately added. The bright yellow color of **2a** is produced instantly. The THF is removed and dichloromethane/ethanol is used to recrystallize **2a** in 63% yield (0.31 g, m.p. 188 °C). **2b** is prepared analogously (in 70% yield) from **1b**. The starting materials **1a**, **b** are prepared in three steps from $[OsCl(PH_3)(CO)(NCCH_3)(PPh_3)_2]ClO_4$ (**A**) [5, 16]: **A** (0.7 g, 0.73 mmol) and CH_3CO_2Na (1.4 g, 17.1 mmol) are heated at reflux for 20 min in 20 mL of methanol, cooled, and the product $[Os(PH_2)(\eta^2\text{-}O_2CCH_3)(CO)(PPh_3)_2]$ (**B**) (0.56 g, 0.67 mmol, 92% yield, m.p. 171 °C) is isolated by filtration and washing with water, methanol and ethanol. **B** (0.1 g) is carbonylated (dichloromethane, 300 kPa CO, 20 min, 25 °C) and the product $[Os(PH_2)(\eta^1\text{-}O_2CCH_3)(CO)_2(PPh_3)_2]$ (**C**) is recrystallized from dichloromethane/ethanol to give 0.1 g (95% yield) of white solid, m.p. 177 °C. **1a** is prepared from **C** (0.28 g, 0.32 mmol) by treating it with sulfur (1.1 equivalents, 0.35 mmol, 0.011 g) in 20 mL of benzene for 5 h. The benzene is removed in vacuo and dichloromethane/ethanol used to recrystallize **1a** (0.28 g, 98% yield, m.p. 153 °C). **1b** is prepared analogously from **C** and selenium. All isolated compounds have given satisfactory elemental analyses.

Received: September 30, 1987 [Z 2449 IE]
German version: *Angew. Chem. 100* (1988) 308

[1] W. R. Roper, *J. Organomet. Chem. 300* (1986) 167.
[2] D. H. Farrar, K. R. Grundy, N. C. Payne, W. R. Roper, A. Walker, *J. Am. Chem. Soc. 101* (1979) 6577.
[3] G. R. Clark, D. R. Russell, W. R. Roper, A. Walker, *J. Organomet. Chem. 136* (1977) C1.
[4] D. S. Bohle, T. C. Jones, C. E. F. Rickard, W. R. Roper, *J. Chem. Soc. Chem. Commun. 1984*, 865.
[5] D. S. Bohle, C. E. F. Rickard, W. R. Roper, *J. Chem. Soc. Chem. Commun. 1985*, 1594.
[6] E. Lindner, K. Auch, W. Hiller, R. Fawzi, *Angew. Chem. 96* (1984) 287; *Angew. Chem. Int. Ed. Engl. 23* (1984) 320.
[7] H. Alper, F. W. B. Einstein, J. F. Petrignani, A. C. Willis, *Organometallics 2* (1983) 1422.

[8] H. Schnöckel, M. Lakenbrink, *Z. Anorg. Allg. Chem. 507* (1983) 70; M. Binnewies, *ibid.* (1983) 66.
[9] L. D. Quin, J. Szewczyk, *J. Chem. Soc. Chem. Commun. 1986*, 844; S. Nakayama, M. Yoshifuji, R. Okazaki, N. Inamoto, *Chem. Commun. 1971*, 1186; R. Hussong, H. Heydt, M. Regitz, *Phosphorus Sulfur 25* (1985) 201.
[10] **2a**: Crystal suitable for X-ray diffraction grown from dichloromethane/ethanol under nitrogen. Triclinic $P\bar{1}$, $a=1052.4(4)$, $b=1801.0(3)$, $c=1038.9(5)$ pm, $\alpha=103.26(3)$, $\beta=115.63(3)$, $\gamma=76.11(2)°$, $V=1.70562\times10^6$ pm^3, $Z=2$; $\lambda(Mo_{K\alpha})=71.069$ pm; $R=0.0398$, $R_w=0.0409$ for 3455 unique reflections [$2<2\theta<46°$, $I>3\sigma(I)$], measured on a CAD4 diffractometer and solved using SHELX76. Further details of the crystal structure investigation are available on request from the Director of the Cambridge Crystallographic Data Centre, University Chemical Laboratory, Lensfield Road, Cambridge CB2 1EW (UK).
[11] D. E. C. Corbridge: *The Structural Chemistry of Phosphorus*, Elsevier, Amsterdam 1974, p. 218-228.
[12] E. Niecke, M. Engelmann, H. Zorn, B. Krebs, G. Henkel, *Angew. Chem. 92* (1980) 739; *Angew. Chem. Int. Ed. Engl. 19* (1980) 710.
[13] J. G. Kraaijkamp, G. van Koten, T. A. van der Knaap, F. Bickelhaupt, *Organometallics 5* (1986) 2014.
[14] K. M. Flynn, H. Hope, B. D. Murray, M. M. Olmstead, P. P. Power, *J. Am. Chem. Soc. 105* (1983) 7750; E. Cannillo, A. Coda, K. Prout, J. C. Daran, *Acta Crystallogr. Sect. B33* (1977) 2608.
[15] D. S. Bohle, W. R. Roper, unpublished.
[16] D. S. Bohle, W. R. Roper, *Organometallics 5* (1986) 1607.

tinue, albeit in a weaker form, in the case of 1,2-dihydrocyclobutabenzene **2a**[2] and more markedly so in the case of 1,2,4,5-tetrahydrodicyclobuta(*a,d*)benzene **3**.[3,4]

So far X-ray structure analyses have been reported only for derivatives of **2a** (**2b**–**2d**),[5] while in the case of **3** only one structure determination (from the year 1969)[6] exists, whose standard deviations do not permit an interpretation of the bond lengths in the benzene ring.

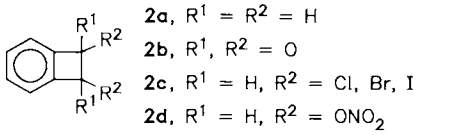

2a, $R^1 = R^2 = H$
2b, $R^1, R^2 = O$
2c, $R^1 = H$, R^2 = Cl, Br, I
2d, $R^1 = H$, $R^2 = ONO_2$

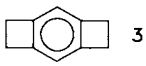

3

The substituents in **2b**–**2d** give rise to reductions in symmetry and electron shifts that are not observed in the parent compound (cf. also the situation in **1**[11]). We have therefore carried out an X-ray structure analysis of **2a** (m.p. ca. −75 °C) at −170 °C and calculated the X–X deformation electron density; single crystals prepared by a

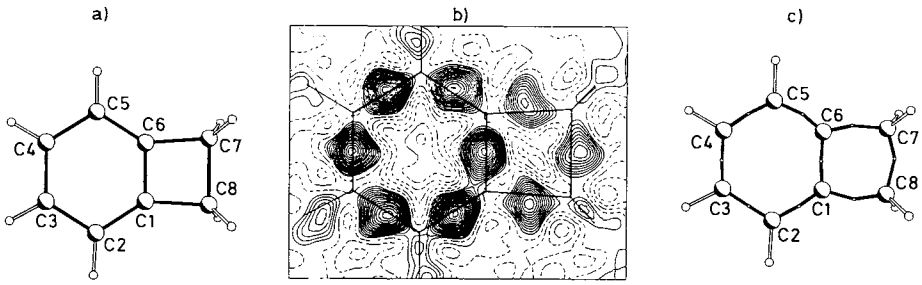

Fig. 1. a) **2a** with atomic labeling and important distances [Å] and angles [°] (standard deviations 0.001 Å and 0.1° resp.) averaged for *mm*2 symmetry (corrected values according to *Schomaker* and *Trueblood* [13] in brackets): C3-C4 1.399 (1.402), C4-C5 1.400 (1.402), C5-C6 1.385 (1.387), C6-C1 1.391 (1.395), C6-C7 1.518 (1.520), C7-C8 1.576 (1.580); C3-C4-C5 121.7, C4-C5-C6 116.0, C5-C6-C1 122.3, C5-C6-C7 144.2, C1-C6-C7 93.5, C6-C7-C8 86.5. b) X-X-deformation electron densities of **2a** in the plane of the molecule. Contour interval 0.025 eÅ^3, negative electron densities dashed, intervals 0.05 eÅ^3. c) Bond lengths [Å] and angles [°] of **2a**, calculated in each case linearly via the maximum of the deformation electron densities (estimated standard deviations about 1 in the last decimal place): C3-C4 1.40, C4-C5 1.41, C5-C6 1.40, C6-C1 1.41, C6-C7 1.56, C7-C8 1.65; C3-C4-C5 127, C4-C5-C6 124, C5-C6-C1 123, C1-C6-C7 106, C6-C7-C8 112.

Structures and Deformation Electron Densities of 1,2-Dihydrocyclobutabenzene and 1,2,4,5-Tetrahydrodicyclobuta[*a,d*]benzene**

By *Roland Boese** and *Dieter Bläser*

X-ray crystallographic analysis of cyclopropabenzene **1** reveals no bond localization in the sense of the Kekulé resonance structures **A** or **B**, but rather a reduction in symmetry with retention of the aromatic π-electron delocalization in the benzene nucleus (**C**).[1] This trend should con-

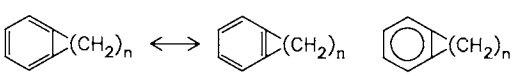

A B C

n = 1 : 1
n = 2 : **2a**

previously described method[7] were used for the analysis.[8] A redetermination of the structure at −170 °C and calculation of the X–X deformation electron density were also carried out for **3**.[9] The results are presented in Figures 1a (**2a**) and 2a (**3**).

The molecules of **2a** and **3** in the solid state are, within the limits of error, planar. **2a** has *mm*2 symmetry, while **3** has *mmm* symmetry; the resulting symmetry element *i* is identical with the crystallographic inversion center in $P\bar{1}$.

Unlike in **1**, in **2a** and **3** there is no significant shortening of the annelated bond, and an alternation of the bonds is also not observed. In **2a** the bonds in the benzene ring adjacent to the annelated bond (C1-C2, C5-C6) are shortened (1.385 Å). Both types of σ-bonds in the cyclobutene ring in **2a** and in **3** are of equal length (1.518 Å and 1.576 Å in **2a**, 1.521 Å and 1.575 Å in **3**) and are comparable with those in 1-cyclobutene-1,2-dicarboxylic acid (1.50 Å and 1.56 Å).[10] This is consistent with the concept of bent bonds; the respective shifts of the bonding electron density maxima are clearly recognizable in Figures 1b and 2b. The angular deformation of the benzene ring in **3** is almost as large as that in **1** (C3′-C1-C2 112.1° in **3**, C1-C2-C3 113.2° in **1**), but smaller in both cases than that in

[*] Dr. R. Boese, Dipl.-Ing. D. Bläser
Institut für Anorganische Chemie der Universität - Gesamthochschule Universitätsstrasse 5-7, D-4300 Essen 1 (FRG)

[**] We thank Herrn Prof. Dr. *W. Roth*, Universität Bochum, for generously supplying the substances.

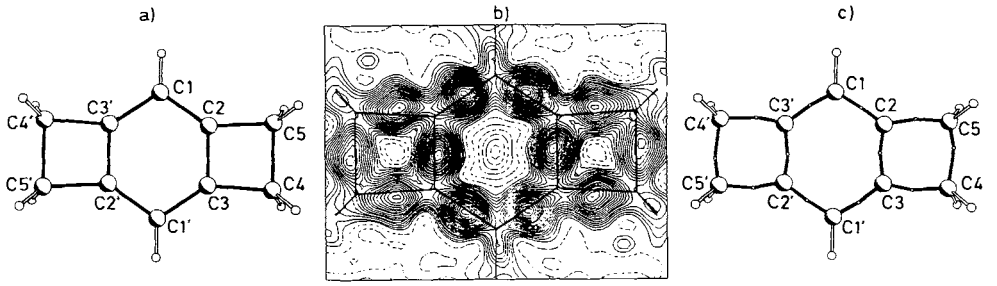

Fig. 2. a) **3**, distances and angles averaged for *mmm* symmetry, other data as for Fig. 1a: C1-C2 1.394 (1.396), C2-C3 1.399 (1.402), C2-C5 1.521 (1.522), C5-C4 1.575 (1.579); C3'-C1-C2 112.1, C1-C2-C3 124.0, C1-C2-C5 142.7, C3-C2-C5 93.4, C2-C5-C4 86.6. b) X-X deformation electron densities of **3**, other data as for Fig. 1b. c) Bond lengths and angles of **3**, other data as for Fig. 1c: C1-C2 1.40, C2-C3 1.41, C2-C5 1.53, C5-C4 1.60; C3'-C1-C2 119, C1-C2-C3 120, C3-C2-C5 107, C2-C5-C4 102.

2a (C1-C2-C3 116.0°). If, on the other hand, the angles are calculated with the assumption of bent bonds, i.e. bonds which do not correspond to the nucleus-nucleus bond axes but to lines joining the maxima of the deformation densities (Figs. 1c and 2c), angles result which compare far better with those expected for sp^2 and sp^3 hybridized C-atoms.

From Figures 1b and 2b it is clear that the ring strain of the cyclobutene ring is transferred to the annelated bond, whose bonding electron density shifts to the center of the benzene ring. This causes an outward shift of the electron densities in the neighboring bonds. As a result the C-C-C angles at C2 and C5 of **2** become smaller. Due to double annelation, the ring strain in **3** is much greater, and leads to even smaller angles (at C1 and C1'). Attempts to annelate two cyclopropene rings to a benzene ring in order to increase the ring strain still further have hitherto failed.[11] So far only the annelation of a cyclopropene ring and a cyclobutene ring to a benzene ring has been achieved.[12] Determination of the structure of this species is presently under way.

Received: April 21, 1987;
revised: July 8, 1987 [Z 2212 IE]
German version: *Angew. Chem. 100* (1988) 293
Publication delayed at authors' request

CAS Registry numbers:
2a, 694-87-1; **3**, 1610-51-1.

[1] R. Neidlein, D. Christen, V. Poignée, R. Boese, D. Bläser, A. Gieren, C. Ruiz-Pérez, T. Hübner, *Angew. Chem. 100* (1988) 292; *Angew. Chem. Int. Ed. Engl. 27* (1988) 294.

[2] M. P. Cava, D. R. Napier, *J. Am. Chem. Soc. 80* (1958) 2225.

[3] M. P. Cava, A. A. Deana, K. Muth, *J. Am. Chem. Soc. 82* (1960) 2524.

[4] a) Y. Apeloig, D. Arad, *J. Am. Chem. Soc. 108* (1986) 3241; b) F. Brogli, E. Giovannini, E. Heilbronner, R. Schurter, *Chem. Ber. 106* (1973) 961; c) B. Halton, *Ind. Eng. Chem. Prod. Res. Dev. 19* (1980) 349; d) M. A. Cooper, S. L. Manatt, *J. Am. Chem. Soc. 92* (1970) 1605.

[5] a) F. H. Allen, J. Trotter, *J. Chem. Soc. B 1970*, 916; b) G. L. Hardgrove, L. K. Templeton, D. H. Templeton, *J. Phys. Chem. 72* (1968) 668; c) F. H. Allen, J. Trotter, *J. Chem. Soc. B 1970*, 1551.

[6] J. Lawrence, S. G. G. MacDonalds, *Acta Crystallogr. 35* (1969) 978.

[7] D. Brodalla, D. Mootz, R. Boese, W. Osswald, *J. Appl. Crystallogr. 18* (1985) 316.

[8] a) X-ray structure analysis of **2a**: $a=6.369(2)$, $b=7.359(2)$, $c=7.382(2)$ Å, $\alpha=85.41(2)$, $\beta=66.72(2)$, $\gamma=66.12(2)°$, $V=289.41(14)$ Å^3; -170 ± 0.4vC, triclinic, space group $P\bar{1}$, $Z=2$, $\rho_{calc}=1.175$ g cm^{-3}, $Mo_{K\alpha}$ radiation, $\mu=0.62$ cm^{-1}, $2\theta_{max}=90°$, 4765 independent intensities 3884 observed ($F_0 \geq 4\sigma(F)$), solution of structure by direct methods, structure refinement (C atoms anisotropic, H atoms isotropic) with SHELXTL, extinction and cylinder correction, 105 parameters, $R=0.038$, $R_w=0.042$, $w^{-1}=\sigma(F_0)^2+9.3\times10^{-4}\,F_0^2$. High angle refinement: according to $w=1-\exp(5(\sin\theta/\lambda)^2)$, H-atom parameters fixed from previous refinement. 74 parameters, $R=0.039$, $R_w=0.042$; b) further details of the crystal structure analysis are available on request from the Fachinformationszentrum Energie, Physik, Mathematik GmbH, D-7514 Eggenstein-Leopoldshafen 2 (FRG), on quoting the depository number CSD-52571, the names of the authors, and the journal citation.

[9] X-ray structure analysis of **3** [8b]: $a=5.421$, $b=5.515(1)$, $c=6.197(1)$ Å, $\alpha=106.60(1)$, $\beta=98.05(1)$, $\gamma=94.68(1)°$, $V=174.35(3)$ Å^3; -170 ± 0.4 °C, triclinic space group $P\bar{1}$, $Z=1$, $\rho_{calc}=1.240$ g cm^{-3}, $\mu=0.65$ cm^{-1}, $2\theta_{max}=90°$, 2743 independent intensities, 2421 observed ($F_0 \geq 4\sigma(F_0)$), 66 parameters, $R=0.037$, $R_w=0.039$, $w^{-1}=\sigma(F_0)+8.2\times10^{-4}\,F_0^2$. High angle refinement: 46 parameters, $R=0.038$, $R_w=0.038$; for further details see [8].

[10] D. Belluš, H.-C. Mez, G. Rihs, *J. Chem. Soc. Perkin Trans. 2 1974*, 884.

[11] a) M. G. Bauwell, B. Halton, *Austr. J. Chem. 32* (1979) 849, 2689; b) E. Vogel, W. Püttmann, W. Duchatsch, T. Schieb, H. Schmickler, J. Lex, *Angew. Chem. 98* (1986) 727; *Angew. Chem. Int. Ed. Engl. 25* (1986) 720; c) U. H. Brinker, H. Wüster, G. Maas, *Angew. Chem. 99* (1987) 585; *Angew. Chem. Int. Ed. Engl. 26* (1987) 577.

[12] a) D. Davalin, P. J. Garatt, *J. Am. Chem. Soc. 87* (1975) 6883; b) D. Davalin, P. J. Garatt, M. M. Mansuri, *ibid. 100* (1978) 980; c) C. J. Saward, K. P. C. Vollhardt, *Tetrahedron Lett. 1975*, 4539.

[13] V. Schomaker, K. N. Trueblood, *Acta Crystallogr. Sect. B 24* (1968) 63.

Protein Chemistry in Vogue

The last few years have seen advances in molecular biology which break new ground. Since in most cases the end product of a piece of research in molecular biology is a protein, there has also been a new upsurge of interest in protein chemistry. The importance of collaboration between molecular biologists and protein chemists can be seen by considering an example. Thus, the protein chemist begins by determining a part of the sequence, starting at the terminal NH_2 group, for a very small quantity of an unknown protein. Next the molecular biologist, using an oligodeoxynucleotide which corresponds to the sequenced portion, isolates the gene or the cDNA of the unknown protein and expresses this in a foreign organism. The recombinant protein which is thereby obtained in a sufficient quantity can now be characterized by the protein chemist (physico-chemical properties, perhaps a sequence analysis to confirm the cDNA sequence, determining the positions of any post-translational modifications such as disulfide bridging, glycosylation, or proteolytic scissions, determining secondary and tertiary structure, and identifying biological activity). The combined efforts may culminate in selective mutagenesis of the protein being studied ("protein engineering"). The techniques of protein chemistry needed in order to attain these and other objectives are described in detail in

Practical Protein Chemistry—a Handbook. Edited by *A. Darbre*. Wiley, Chichester 1986. xix, 620 pp., bound, $ 91.55.—ISBN 0-471-90673-5

The book includes chapters on affinity chromatography, disulfide bonds, fragmentation of proteins, separation of peptide and protein mixtures, X-ray crystallography, predicting likely secondary and tertiary structures, a section on analysis of glycoproteins, and, occupying a central position, several contributions on manual and automatic methods of sequence analysis. The most important methods used in protein chemistry are here summarized in a single volume by prominent experts, the only exceptions being peptide synthesis and the chemical modification of proteins, which have already been covered in detail elsewhere.

The term "protein engineering" is relatively new, but the field to which it mainly refers has been in existence since the beginnings of sequence analysis and peptide synthesis, being previously described less succinctly as "the study of protein structure and function". Protein engineering in its broadest sense means modifying the properties of proteins, e.g. their stability, specificity towards particular substrates, or enzymic activity. One must also include in this the developing field of designing new polypeptides which do not occur naturally. The current popularity of protein engineering arises from the possibility of being able, through site-directed mutagenesis, to effect any desired amino-acid exchange at any desired position on a protein chain. It is therefore not surprising that we now have the first monographs dealing with this field. The book to be discussed here is

Protein Engineering. Edited by *M. Inouye* and *R. Sarma*. Academic Press, New York 1986. xiii, 424 pp., bound, $ 49.95.—ISBN 0-12-372485-6

The work is divided into four sections. The first (Structure and Design) includes articles on the importance of data banks of protein sequences, the construction of models of biologically active polypeptides, the molecular analysis of thermophilic proteins, the total chemical synthesis of a gene for bovine rhodopsin, "surface simulation synthesis", and a particularly important chapter on the analysis of homologous tertiary structures. The second section (Mutant Analysis) deals with mutants of individual proteins; examples are the hemagglutinin of the influenza virus, bacterio-opsin, staphylococcal nuclease, and the lysozyme of the T4 bacteriophage. In the third section (Complex Systems), the protein engineering of antibody molecules deserves particular attention. The antigen binding sites of the variable regions of light and heavy chains suggest the possibility of manipulations which could lead to completely new proteins; experiments along these lines are still at an early stage. The fourth section (Applications) includes chapters on enzymic reactions in non-aqueous media, on directed transport of toxins by using monoclonal antibodies, on the production of new antibiotics, on genetic transformation of plants, and on the application of genetic engineering to bioinsecticides.

The individual contributions have undoubtedly been written by authors competent in their fields, but it must be said that the editors of the book have shown some lack of care, especially in the fourth section, in what has been included under the heading of protein engineering which is not identical with genetic engineering and biotechnology; some of the chapters are at best only marginally related to the book's title. Conversely, some topics which ought to have been covered in an introduction to this field and an account of its main features are not included, e.g. the prediction of likely protein structures and their experimental determination, the design of new proteins, and a good summary of the methods of site-directed mutagenesis (all of which are covered in another book on protein engineering, edited by *Oxender* and *Fox*). Also, some of the contributions in this monograph are not very up-to-date; a glaring example is a chapter with 50 references, of which 42 are to papers published in the 1960's and 1970's and only eight relate to the 1980's. Despite these shortcomings, the book can be recommended for the predominantly high quality of the contributions. However, newcomers to the field should begin with a better structured work than this.

Bernd Gutte [NB 860/861 IE]
Biochemisches Institut
der Universität Zürich (Switzerland)

Aromaticity. By *P. J. Garratt*. Wiley-Interscience, New York 1986. xi, 318 pp., bound, $ 65.00.—ISBN 0-471-80703-6

The many-faceted concept of aromaticity has had a profound effect on progress in organic chemistry from its beginnings up to the present day, involving an interplay of experiment and theory. This monograph, intended for use as a student textbook, attempts to convey something of that continuing process. The arrangement of the present work follows that of the text published by the same author 15 years ago, under the same title. After a short historical introduction, the first of the eleven chapters continues by defining the problem of aromaticity, then gives a very con-

cise introduction to the HMO and VB methods, as exemplified in the prototype molecule benzene. By way of providing a key to all that follows, Chapter 2 then gives a detailed account of the physical, chemical and theoretical differences between anti-aromatic, aromatic and non-aromatic systems, based on the example of the classical triad cyclobutadiene-benzene-cyclooctatetraene. The following chapter, which is newly introduced material, first briefly describes the chemistry of simple arenes, taking as examples the different substitution mechanisms as well as thermal and photochemical addition reactions; this is followed by a discussion of the synthesis, chemistry and properties of the valence isomers of benzene, dehydroarenes, and arenes whose structures are distorted by bridging, by sterically hindered substitutions, or by annelation of small rings. The following chapters deal with all the main classes of compounds that are connected with the concept of aromaticity: annulenes, monocyclic aromatic and anti-aromatic ions, annulenones, fulvenes and related systems. Further chapters are devoted to heterocyclic compounds—subdivided into π-excessive compounds of the pyrrole type, π-deficient compounds of the pyridine type and heterocyclic compounds with two or more heteroatoms—and polycyclic benzenoid and non-benzenoid arenes. The penultimate chapter discusses homo-aromatic and topologically related compounds such as bicycloaromatic and longicyclic ions with non-coplanar π-electron systems. The final chapter is concerned with the aromatic transition states in pericyclic reactions, and gives a concluding summary of aromaticity criteria. An adequate index is provided (14 double column pages) with cross-references, giving quick access to particular topics, though it fails to include some of the key phrases that are used frequently in the text, e.g. delocalization energy.

New passages of greater or less detail, which one only notices on close comparison with the earlier book, have been interlaced into all the chapters. These take particular account of the progress made during the past one and a half decades. The wide scope of subjects covered in the book is supported by a wealth of factual material, in particular by a large amount of magnetic, kinetic, spectroscopic and structural data. One especially welcomes the ^{13}C- and ^{1}H-NMR data, explicitly given for many molecules to establish the diatropic, paratropic or atropic character of the compounds under discussion. The persistent use of the Frost-Musulin formalism, and of *Dewar*'s PMO method for estimating delocalization energies, has to be considered as instructionally very successful. It affords the reader an easy approach, free of more severe mathematical hurdles, to these quantities, which are fundamental to an understanding of aromaticity. Reference is also made to more recent theoretical approaches to this topic. In keeping with the textbook character of the work, the references which are given at the end of each chapter are nearly all to review articles, arranged according to topics (extending up to 1986 in many cases). Sometimes, though, the lack of references to original papers is a disadvantage.

In the chapter on homo-aromaticity, insufficient account is taken of recent new knowledge, especially concerning neutral compounds. Particularly noticeable is the absence of quantitative data which are now available on aromatic stabilization or destabilization. There is no mention of anti-homo-aromaticity. The treatment of aromatic transition states, which is very relevant in the context of this book, deserved to be covered in more detail in view of its importance, which is not confined to mechanistic organic chemistry alone. Here too, it would have been desirable to include data on the order of magnitude of the energy advantage conferred by reaction routes involving aromatic transition states, compared with alternative reaction channels.

The book is written in a very readable style, and is richly illustrated by figures and clearly presented reaction schemes. Some typographical errors need to be corrected in a later edition. With regard to errors of content, only two will be mentioned here. The conversion of hexatriene to 1,3-cyclohexadiene is not a Cope rearrangement but an electrocyclic reaction. The homo-aromatic ions involved in solvolysis with retention (p. 292) are reaction intermediates, not transition states.

Despite the shortcomings mentioned here, this monograph certainly offers to advanced students, and to chemists who wish to refresh their knowledge of the whole topic of aromaticity, the quickest, most complete, and most up-to-date means of access to the subject that is now available. The book will undoubtedly be a valuable addition to every chemistry library, especially since it can also be useful as a work of reference.

Dieter Hasselmann [NB 855 IE]
Fakultät für Chemie
der Universität Bochum (FRG)

The Practice of Enantiomer Separation by Capillary Gas Chromatography. By *W. A. König*. Hüthig, Heidelberg 1987. xii, 104 pp., bound, DM 48.00.—ISBN 3-7785-1324-3

The separation and quantitative analysis of enantiomers is still a difficult problem even today. One method which has been developed and perfected in recent years for this purpose is capillary gas chromatography. This little book by *König* gives a complete and easily understood account of the present state of knowledge on this topic.

It begins with a general section dealing with the principle of the technique, with the preparation of chiral coating materials for columns and that of the columns themselves, and—so far as this is known—the mechanisms whereby such columns effect separation of enantiomers. As the compounds to be separated are usually strongly polar, it is necessary in nearly all cases to prepare a derivative of the sample. The following chapters of the book describe methods for derivatization and the difficulties encountered, illustrated by many actual examples. Detailed experimental conditions for preparing the derivatives are appended to each chapter. Further sections follow in which other chromatographic techniques for separating and determining enantiomers are discussed, such as by forming metal complexes and preparing diastereomeric derivatives to achieve separation of enantiomers. The book thus provides a good survey of the different techniques for enantiomeric separation, enabling the reader to choose the best method for the problem in hand.

In this description of enantiomer separation by gas chromatography, *König* has provided a valuable aid to the experimentalist. The book's outstanding characteristics are the clear and helpful discussion of the various methods, with their advantages and disadvantages, and the relationship to practical examples, the whole book being a pleasure to read. Everyone who is at some time involved in the separation and determination of chiral substances will find this book valuable.

Gerhard Spiteller [NB 841 IE]
Laboratorium für Organische Chemie I
der Universität Bayreuth (FRG)

The Manipulation of Air-Sensitive Compounds. 2nd Edition. By *D. F. Shriver* and *M. A. Drezdzon*. Wiley, Chichester 1986. x, 326 pp., bound, $ 62.95.—ISBN 0-471-86773-X

This book, the fully updated second edition of a classic work, deals with all the currently used techniques for handling air-sensitive substances, including gases. The book is both a practical work of reference and a laboratory handbook for use in many fields of organic, inorganic, physical and analytical chemistry, and in biochemistry, materials science and solid state physics. It can be recommended not only for experts who have a considerable experimental background, but also for students and for practising scientists who are unfamiliar with these techniques.

The book is arranged in two parts: Part 1 (Chapters 1–4) describes inert gas techniques, and Part 2 (Chapters 5–10) describes vacuum work.

Chapter 1 is concerned with those inert gas techniques which can be used directly at the bench without elaborate apparatus, i.e. work under argon using manifolds, syringes, Schlenk tubes, and fritted funnels, and with flushing of apparatus and the supplying and handling of gases, etc. Chapter 2 describes glove box and glove bag techniques: providing and maintaining the inert gas atmosphere, gas locks for introducing and withdrawing samples, work using microscopes, etc. Chapter 3 deals with the purification of inert gases, including the use of chemical drying agents, freezing, adsorption, oxygen removal, and the design of gas purifying systems. Chapter 4 contains information on purifying solvents and reagents. Systems for distillation under inert gas and for storing solvents of high purity are described, as are purification methods for specific cases. Chapter 5 is devoted to classical high vacuum techniques as used particularly in preparative inorganic chemistry. The authors discuss various aspects of the design of high vacuum systems suitable for handling volatile compounds without loss of material. Out-gassing, trap-to-trap distillation (using a partial condenser), measurement of gas quantities, various types of baths for cold traps, and even a Töpler pump, are described. The sixth chapter describes the principles of construction of different types of vacuum pumps, including vacuum seals, cold traps, etc., and compares performance data. Pressure measurements and leak-finding are discussed in detail in Chapter 7, and Chapter 8 deals with ground joints, taps and valves. High vacuum systems and techniques for special purposes are treated in Chapter 9; these include tensimeters, measurement of vapor pressures, determinations of molecular weights and melting points, sample preparation methods for different spectroscopic techniques (IR, NMR etc.), filtration, storage of gases, use of break seals, and high vacuum handling of purified alkali metals. Chapter 10 is concerned with systems of metallic construction for work at higher pressures, for handling reactive fluorine compounds, or for applications requiring extreme vacuum tightness. The book concludes with six appendices which deal in turn with safety, glass-blowing techniques, plastics, metals, calculations of vapor pressures (using various empirical equations, approximations and tables), and lastly conversion factors (for pressures, flow rates, mercury data).

Since the book has been written by American authors, equipment which is commercially available from European manufacturers has in some cases not been mentioned; some examples to which this applies are dosing funnels for powdery substances, dosing funnels and fritted funnels with temperature control jackets, and sublimation apparatus suitable for air-sensitive substances (all available from Normag, Hofheim am Taunus, FRG). Considered as a whole, the book is certainly worth the price, and no laboratory in which techniques of this sort are used should be without it.

Thomas Laube [NB 852 IE]
Laboratorium für Organische Chemie
der Eidgenössischen Technischen
Hochschule Zürich (Switzerland)

Registered names, trademarks, etc. used in this journal, even when not marked as such, are not to be considered unprotected by law.

© VCH Verlagsgesellschaft mbH, D-6940 Weinheim, 1988. - Printed in the Federal Republic of Germany by Zechnersche Buchdruckerei, Speyer/Rhein.

All rights reserved (including those of translation into foreign languages). No part of this issue may be be reproduced in any form – by photoprint, microfilm, or any other means – nor transmitted or translated into a machine language without written permission from the publishers. Only single copies of contributions, or parts thereof, may be made for personal use.

Valid for users in the USA: The appearance of the code at the bottom of the first page of an article in this journal (serial) indicates the copyright owner's consent that copies of the article may be made for personal or internal use, or for the personal or internal use of specific clients. This consent is given on the condition, however, that the copier pay the stated per-copy fee through the Copyright Clearance Center, Inc., for copying beyond that permitted by Sections 107 or 108 of the U.S. Copyright Law. This consent does not extend to other kinds of copying, such as copying for general distribution, for advertising or promotional purposes, for creating new collective works, or for resale. For copying from back volumes of this journal see 'Permissions to Photo-Copy: Publisher's Fee List' of the CCC.

Editorial office: Pappelallee 3, D-6940 Weinheim, Federal Republic of Germany, Telephone (06201) 602315, Telex 465516 vchwh d, Telefax (06201) 602328.

Editor: *P. Gölitz.*

Associate editors: *D. I. Loewus, A. Stimson.* **Editorial assistant:** *E. Schweikart*

Publishers: VCH Verlagsgesellschaft mbH. (Managing Directors: *Prof. Dr. Helmut Grünewald* and *Hans Dirk Köhler*), Pappelallee 3, D-6940 Weinheim, Federal Republic of Germany. Correspondence concerning advertisements should be addressed to VCH Verlagsgesellschaft mbH. (Advertising Manager *R. J. Roth*), Boschstr. 12. P.O. Box 1260/1280, D-6940 Weinheim, Federal Republic of Germany, Telephone Weinheim (06201) 602-0, Telex 465516 vchwh d, Telefax (06201) 602328.

ANGEWANDTE CHEMIE
International Edition in English
Volume 27 · Number 3
March 1988
Pages 309–446

Tetrahedrane and Cyclobutadiene

By Günther Maier

Tetra-*tert*-butyltetrahedrane—a useless molecule? In the first part of this progress report an attempt is made to answer this provoking question in order that the reader can evaluate why it is worthwhile to track such an esoteric molecule. An account of the unusual properties of tetra-*tert*-butyltetrahedrane, the only tetrahedrane unequivocally identified so far, and the most highly strained saturated hydrocarbon of all, is followed by a summary of attempts to synthesize the parent compound. The emphasis in these two sections is on our own research achievements. Since any discussion of the tetrahedranes must necessarily include the corresponding cyclobutadienes, it was found appropriate to organize the article at the same time as a final account of the cyclobutadiene problem. *Masamune*[8c] characterized his excellent report in 1980 in the journal Tetrahedron as a *comma* in the history of cyclobutadiene. Meanwhile, the significant questions have been answered. The time is now ripe to replace the comma by a *full stop*.

1. Introduction

Why does the tetrahedrane molecule fascinate the organic chemist? Is it the aesthetic appeal of the topology of the tetrahedron or the hope that the unusual bonding properties of this molecule could lead to otherwise inaccessible knowledge of general importance, or is it indeed the synthetic challenge of the highly reactive—if at all capable of existence[1]—tetrahedrane, together with the sporting ambition to reach the goal first?

Let us start with the first mentioned aspect. If symmetrical objects are considered beautiful, harmonic, and inwardly balanced, this is no modern trend. Behind lies a long tradition, reaching back into antiquity. *Plato* assigned four of the five regular polyhedra described by him to what he called the elements of matter, of which the world was assumed to be composed, namely the tetrahedron to fire, the cube to earth, the octahedron to air, and the icosahedron to water. No terrestrial room was left for the fifth, the pentagonal dodecahedron (nothing material is envisaged for the "ether" (Fig. 1)). This object should serve to

Fig. 1. The Platonic solids: tetrahedron, cube, pentagonal dodecahedron (upper row); octahedron, icosahedron (lower row).—Reproduced by kind permission of the publisher from: L. Pauling, R. Hayward: *The Architecture of Molecules*, W. Freeman, San Francisco 1964.

[*] Prof. Dr. G. Maier
Institut für Organische Chemie der Universität
Heinrich-Buff-Ring 58, D-6300 Giessen (FRG)

 © VCH Verlagsgesellschaft mbH, D-6940 Weinheim, 1988 0570-0833/88/0303-0309 $ 02.50/0

organize the universe into a beautiful whole.[2] It is easy to bridge the gap to the present day.[3] Replacing the corners of the regular polyhedra by methine groups in which three of the bonds go to neighboring ring carbon atoms and the fourth to a hydrogen atom[4] leads in the case of the first three structures of Figure 1 to the so-called "Platonic hydrocarbons", tetrahedrane, cubane, and dodecahedrane. It is now understandable why the synthetic chemist, whose daily routine surely also consists of an artistic component, finds it attractive to create these "beautiful" molecules in the laboratory. Previous efforts in this area are documented by two milestones: *Eaton* et al.[5] constructed cubane over 20 year ago. The synthesis of dodecahedrane by *Paquette* et al.[6] is much more recent.

The equating of the tetrahedron with the element fire has a chemical parallel. According to theory, tetrahedrane (**1**) is the most highly strained (fiery) of the formally saturated hydrocarbons. Therefore, it is also the most likely to satisfy the second criterion, namely to show properties that are not otherwise experimentally accessible. Any such chemical "extravagances" of tetrahedrane could by far exceed the importance of its mere synthesis. It is the purpose of this article to demonstrate whether or not the tetra-*tert*-butyl derivative (**2**) can fulfill the above-mentioned expectations.

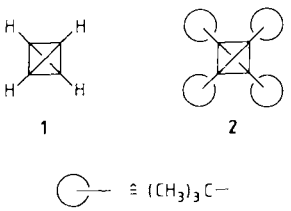

As for the sporting ambition,[7] a piece of evidence is given here. How else could it be understood why we, in spite of discouraging predictions by the theoreticians as well as many previous unsuccessful attempts, are still engaged in finding a route to the unsubstituted tetrahedrane?

The chemistry of tetra-*tert*-butyltetrahedrane is closely associated with that of the corresponding valence isomeric cyclobutadiene. Although the present article focuses on our own work, it also includes important results from other groups, and it can be seen at the same time as a progress report on the subject tetrahedrane/cyclobutadiene.[8]

2. Tetra-*tert*-butyltetrahedrane

If only a minimal lifetime is expected of the unsubstituted tetrahedrane (**1**), it is appropriate to replace the hydrogen atoms by *tert*-butyl groups. Examples of this trick of attaining kinetic stabilization through steric hindrance of attack of external reaction partners are legion. Apart from the intermolecular effect of mutual shielding, the voluminous substituents in tetra-*tert*-butyltetrahedrane (**2**) play a second role of decisive importance for the stability. The intramolecular repulsion of the four *tert*-butyl groups is at a minimum when their mutual distance is at a maximum. This condition is fulfilled by the T_d symmetry of the tetrahedron. Any other imaginable arrangement causes the substituents to be closer to each other. The breaking of a tetrahedrane bond in **2** must equally lead to strong steric strain. In other words: the favored spherical arrangement of the four peripheral groups in **2** forces the tetrahedral geometry on the molecule. The two *tert*-butyl groups which would recede from each other on stretching a ring bond are forced back again by the other two. This "corset effect" must stabilize **2** relative to **1**. If, however, only one of the substituents in **2** is replaced by a smaller group, the situation must change drastically. Since, in general, alkyl groups lower the thermal stability of a CC bond, all tetrahedranes less highly substituted than **2** should undergo ring opening more easily than the parent molecule itself. In this context it is logical that phenyl-[9] and methyl-substituted[10] tetrahedrane derivatives remain undetectable even under matrix conditions.

2.1. Preparation

The concept for the synthesis of tetrahedrane **2** is based on our experience gained during the photochemical formation of tri-*tert*-butylcyclobutadiene (**6**) from the cyclopentadienone **4**.[8b, 11, 12] The anhydride **3** ought to be an ideal precursor for **6**. However, the photochemical cleavage at room temperature gives exclusively the two cyclopentadienones **4** and **5**.[13] In contrast to the positional isomer **5**, **4** is photolabile at 77 K and gives the desired cyclobutadiene **6**.[11] Meanwhile, the mysterious origin of the strange

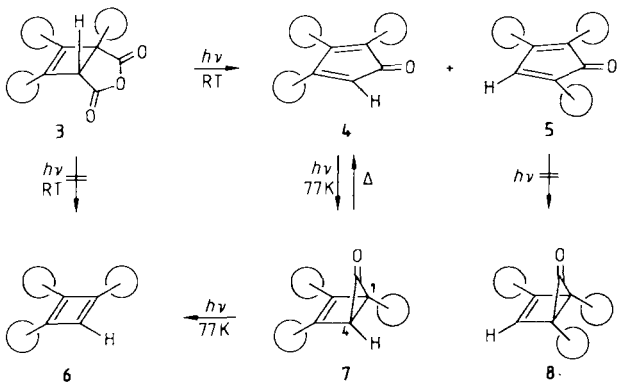

temperature-dependence of the photochemical behavior of **4** has been solved:[14] irradiation of **4** at 10 K gives the housenone **7**, which subsequently is transformed into **6** via CO elimination. The thermal ring-opening of **7** to **4** already takes place at −80 °C.[15] Therefore, at room temperature the stationary concentration of **7** is so low that no formation of **6** is observable. The fact that the cyclopentadienone **5** does not undergo any photofragmentation at any temperature (room temperature, organic matrix at 77 K, or argon matrix at 10 K[16]) demonstrates the importance of the mutual orientation of the *tert*-butyl groups. Apparently, the corresponding housenone **8** is so strained

that it is either not formed by photochemical excitation, or rapidly undergoes ring opening to **5** even at 10 K. This view is supported by theoretical studies.[17] MNDO calculations give a C1–C4 distance of 1.587 Å for **7**. The corresponding bond in **8** must be longer (1.647 Å) and hence weaker.

From the above observations it may be inferred that introduction of a fourth *tert*-butyl group in **4** or **5** should drastically influence the ability to undergo photoisomerization. This expectation finally led to the successful synthesis of the tetrahedrane **2**:[18] the photochemical behavior of tetra-*tert*-butylcyclopentadienone **9** is entirely different from that of **4**. Excitation of the dienone **9** isolated in argon with 254-nm light results in exclusive criss-cross addition to give the tricyclopentanone **10** as observed by IR spectroscopy. Continued irradiation leads to carbon monoxide elimination. At the same time, the typical band of ketene **11** appears. This ketene is likewise photolabile and eliminates CO, albeit very slowly. Irradiation in an organic matrix at 77 K permits isolation of the hydrocarbons formed.

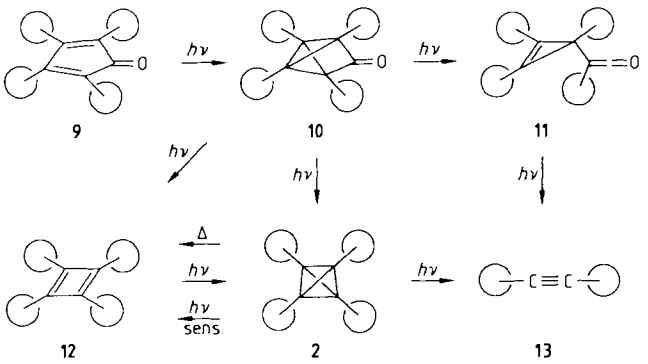

Apart from di-*tert*-butylacetylene (**13**), which is the only end product of the room temperature irradiation, *Pfriem*[18] isolated the tetrahedrane **2** as stable, colorless crystals. On heating to 135 °C, **2** is transformed into the corresponding cyclobutadiene **12**. This valence isomerization is photochemically reversible. It may be assumed, therefore, that the bicyclobutanediyl diradical primarily formed on irradiation of **10** is converted into the cyclobutadiene **12** by cleavage of the backbone bond; the cyclobutadiene then furnishes the tetrahedrane derivative **2** under the conditions of irradiation.

2 is the only isolated and unequivocally identified tetrahedrane so far.[19] The route to **2** should also be applicable to other highly strained systems. Unfortunately, however, this is not so. An examination of the differently substituted cyclopentadienones **14**–**24**[20] showed that **14**–**19** are totally unchanged by irradiation ($\lambda = 254$ nm) in argon at 10 K. Only **20**, **21**, and **22** undergo photoisomerization to the related tricyclopentanones of type **10** to an increasing extent.[20b] At least **22** undergoes the criss-cross addition about as easily as the reference substance **9**. However, no tetrahedrane derivative is detectable on subsequent CO elimination. Although the extremely bulky adamantyl residue favors tricyclopentanone formation, it may already be too large to permit the planarization of the cyclobutadiene ring necessary for decarbonylation. Apparently, it is only in the tetra-*tert*-butyl series, which also includes **23** and **24**, that everything fits nicely together.

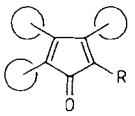

14–24

Cpd.	R	Cpd.	R
14	phenyl	**20**	ethyl
15	pentafluorophenyl	**21**	isopropyl
16	*o*-tolyl	**22**	1-adamantyl
17	benzyl	**23**	$C(CD_3)_3$
18	1-phenylethyl	**24**	$^{13}C(CH_3)_3$
19	trimethylsilyl		

The very different photochemical behavior of the cyclopentadienones **4**, **5**, and **9** still requires an explanation. The X-ray structure analyses carried out by *Boese* provide an indication (Fig. 2).[21]

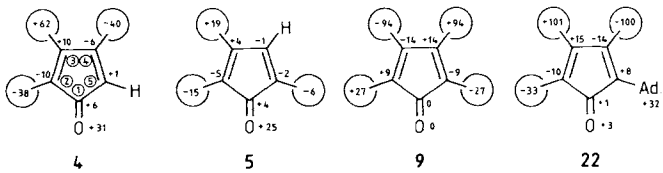

Fig. 2. Deformations [pm] of the cyclopentadienones **4**, **5**, **9**, and **22** relative to a "best" plane through the rings, determined by X-ray crystallography. +: above; −: below the plane.—The distance to the "best" plane refers, in the case of the adamantyl moiety (Ad), to C1.

The structures demonstrate that the direction of the photochemically induced reaction is already given by the distortion of the rings in the ground state. The deviations are relatively small in the case of **5**. Therefore, no photoreaction takes place. In ketone **4**, the four *tert*-butyl groups and therefore also the neighboring ring C-atoms are in a staggered arrangement. Here, less energy is required in order to achieve photoisomerization. From the structure, one could expect a criss-cross reaction. Nevertheless, when a housenone is formed, this is because it is preferred over the tricyclopentanone on the grounds of ring strain. According to MNDO calculations,[22] the enthalpy of formation of **26** is 26.8 kcal mol^{-1} higher than that of **25**. The

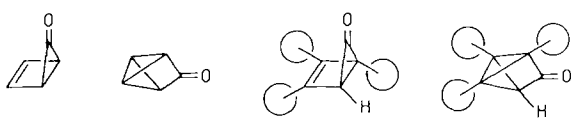

introduction of three *tert*-butyl groups reduces this energy difference between **27** and **7** to 4.8 kcal mol^{-1}. It is therefore no wonder that the tricycle **27** is known; however, the

compound is completely photostable.[23] Following the trend, the tricyclopentanone **10** could already be more stable than the corresponding housenone in the tetra-*tert*-butyl series. Furthermore, the structure of **9** (Fig. 2) implies that photoexcitation should lead to the tricycle (corset effect, see above). Since the deviations are larger still in the adamantyl derivative **22**, the same reaction should be observed here, in agreement with experiment.

2.2. Structure and Spectroscopic Properties

In view of the erroneous announcements of successful syntheses of compounds with tetrahedrane structure, we endeavored to gather as many data as possible and thus prove the structure of **2** unambiguously. The first indication was given by the ^{13}C-NMR spectrum [in $CDCl_3$; three signals at $\delta = 9.27$ (ring-C), 27.16 ($C(CH_3)_3$), and 31.78 (CH_3)]. The observation that the quaternary C atoms of the *tert*-butyl groups appeared at higher field than the primary ones was a first indication of the peculiarity of **2**. The bond between the *tert*-butyl groups and the neighboring C atoms must possess a high degree of s character (as in di-*tert*-butylacetylene, **13**). The high field position of the signal for the ring carbon atoms is even more revealing. It is in exact agreement with expectations.[24] Naturally, the ^{1}H-NMR spectrum of **2** features only a single signal (even in a nematic phase[25]) at $\delta = 1.18$ ($CDCl_3$). The mass spectrum (field desorption) gives the correct molecular mass (*m/z* 276.1). The PE-spectroscopic examination by *Heilbronner* et al.[26] played an important role in the structural analysis of **2** and **12**. As required, the lowest energy band of **2** (centered at $I \approx 7.9$ eV) is a doublet due to Jahn-Teller splitting. Cyclobutadiene **12** shows a singlet at $I = 6.35$ eV.

In addition to the spectroscopic properties already reported,[25] two investigations of isotopically labeled derivatives of **2** should be mentioned. *Saunders*, for example, queried whether in the case of **2** perhaps a dynamic system of rapidly equilibrating singlet diradicals exists rather than a static molecule. Tetrahedrane derivative **2** possessing one perdeuterated *tert*-butyl group is obtainable from the cyclopentadienone **23**[20b] and the isotopic perturbation observable by ^{13}C-NMR spectroscopy was studied in this regard.[27] However, no effect over and above an "intrinsic shift" was detectable. Accordingly, **2** possesses a rigid, fixed structure. Another important point concerns the electron distribution in **2**. ^{13}C–^{13}C coupling constants can give information on this. The couplings are observable by labeling one of the *tert*-butyl groups in **2** with ^{13}C at the quaternary center. The required substance can be obtained from the dienone **24**.[20b,28] The analysis of the ^{13}C-NMR spectrum carried out by *Lüttke* et al.[29] allows the following conclusions to be drawn: the axes of the endocyclic hybrid orbitals ($sp^{5.20}$ hybrids) are bent outward by 28.4° with respect to the lines connecting the nuclei (record value for banana bonds). The bond connecting the tetrahedral corner with the *tert*-butyl group has a high degree of s character ($sp^{1.04}$ hybridization; closely related to *tert*-butylacetylene). These bond properties are in good agreement with predictions.[30–32]

The remaining spectroscopic information[25] has become less significant as a consequence of a recent X-ray structure analysis of **2**. After many unsuccessful attempts with the room-temperature modification of **2** (plastic, i.e. soft and easily deformed crystals), *Irngartinger* et al.[33] succeeded in growing a more highly ordered modification at low temperature. Recent, impressive results by *Irngartinger* et al.[34] show that this low-temperature form of **2** is "stabilized" by entrapped gases (N_2, Ar). This has allowed the solution of the structural problem. The result shown in Figure 3[33] should remove any remaining doubt about the

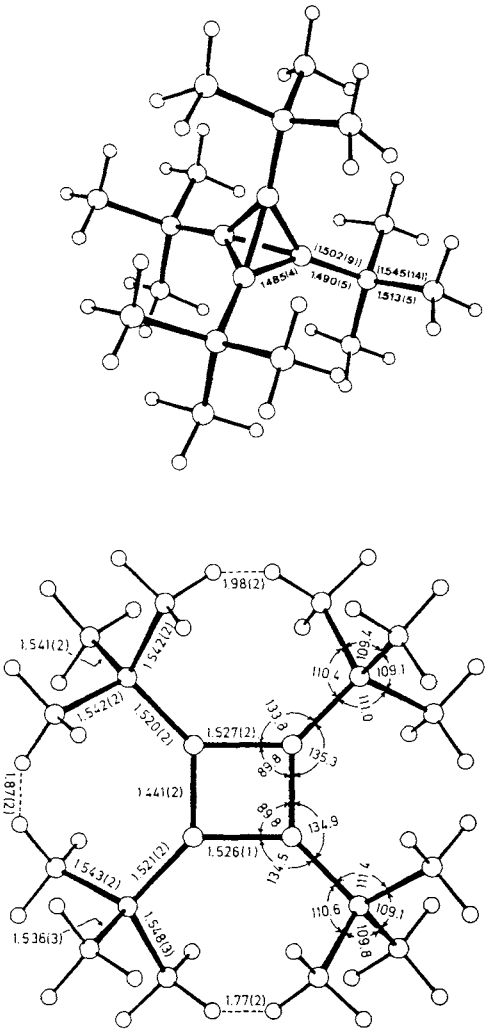

Fig. 3. Crystal structure of **2** [33] with averaged bond lengths ([Å]; deviations in parentheses; corrected values in square brackets); crystal structure of **12** at −150°C with bond lengths [Å] and angles [°].

correctness of structure **2**. The bond lengths in the tetrahedron are relatively short (average 1.485 Å;[33] 1.497 Å[34]) in comparison with normal CC single bonds (1.54 Å) as a consequence of the bending of the bonds. The deformation densities determined for the Ar-clathrate of **2** demonstrate a bending of the ring bonds by 26°.[34] The agreement with the value mentioned above (28.4°) is remarkable. Incidentally, the quantum chemically calculated bond lengths vary between 1.470 and 1.520 Å.[30,32,35,36,37] Of these, the distance originally computed by *Schulman* and *Venanzi*[30] us-

ing an ab initio method comes closest to reality. The appearance of relatively large vibrational ellipsoids of the methyl carbons could indicate that enantiomeric molecules of chiral T symmetry are disorderly arranged about the mirror plane in the crystal. *Mislow* et al.[38] has predicted such deviation from the maximal T_d symmetry to the lower T symmetry on the basis of force field calculations for the free molecule **2**. MNDO calculations have confirmed this.[36]

In this context, it is worth mentioning the curious history of the structural analysis of tetra-*tert*-butylcyclobutadiene (**12**). At room temperature, slight but nevertheless significant alternation is found (1.482 and 1.464 Å) for the ring bonds. The quaternary C atoms of the *tert*-butyl groups deviate from the ring plane by 0.37 Å above or below in an alternating fashion. Also, the four-membered ring itself is not planar but folded with a dihedral angle of 170°.[39] Whereas in other stable cyclobutadienes prepared by *Krebs*[40] and *Masamune*[41] (**65a**, **65b**, **66a**; see Section 2.5) the single bond is stretched, thereby causing a clear alternation (up to 0.26 Å),[42,43] the double bond in **12** is elongated, and therefore the difference in the bond lengths reduced. It has been argued that the stretching of the double bonds (caused by the amassing of four *tert*-butyl groups) should lead to a shortening of the single bonds and hence a nearly square structure.[44] Doubt[45] about this X-ray structure of **12** with "almost equal bond lengths in the four-membered ring" motivated *Irngartinger* to repeat the structure analysis at −150 °C.[46a] Under these conditions, the constitution given in Figure 3 results. The folding of the four-membered ring remains, also at −150 °C. However, the bond alternation is now found to be noticeably larger (0.086 Å). The strange "temperature-dependence of the structure" can be explained by disordering phenomena. The experimentally determined bonding electron density distribution in **12**[46a,b] shows bent bonds in the four-membered ring. The single bond having a lower electron density is more bent than the double bond. A part of the above-mentioned disorder is possibly still present even at −150 °C. A detailed analysis of the anisotropic displacement parameter of ring carbon atoms of **12** shows that the measured data can be reconciled with an averaging, in the sense of a superposition of two rectangular rings rotated through 90°, with the bond alternations found for the other cyclobutadienes mentioned above.[46c]

2.3. Physical Properties

Tetra-*tert*-butyltetrahedrane forms colorless crystals, stable in air and melting at 135 °C with red coloration; i.e. at this temperature **2** is transformed into the valence isomeric cyclobutadiene **12**. This high thermal stability appeared to make a tetrahedrane structure very unlikely. On the other hand, the high melting point is an expression of the high symmetry of **2**. A model based on the van der Waals radii leads to a sphere whose surface is covered with hydrogen atoms (Fig. 4). The volatility is correspondingly high: **2** sublimes very easily in a water aspirator vacuum at room temperature.

Fig. 4. Space-filling model (SCHAKAL [47]) of tetra-*tert*-butyltetrahedrane **2**. The carbon atoms of the ring skeleton are shown in red.

Of course, the ring strain of **2**, which must be an absolute record, is of most interest. There is no other molecule that could surpass tetrahedrane in terms of the strain theory postulated by *Baeyer*[48] just over 100 years ago. Theoretical calculations are in agreement with this, although at first strongly scattered expectation values between 97 and 150 kcal/mol were mentioned.[30,48-50] Using the *Franklin* increments as a reference point,[30] a comparison with the most recently calculated heat of formation of tetrahedrane[36,37,51-55] yields expected strain energies of 136 (MNDO[36]), 134 (ab initio[37]), 126 [MINDO/3[52]), and 132–134 kcal/mol (ab initio).[53-55]

What does the experiment tell? The enthalpy of combustion of **2** determined by *Månsson*[56] ($\Delta H_c^\circ = -3099.8 \pm 1.8$ kcal mol^{-1}) leads to an enthalpy of formation in the condensed phase of $\Delta H_f^\circ(c) = -10.9 \pm 1.9$ kcal mol^{-1}. The enthalpy of sublimation measured by *Rüchardt* et al.[57] ($\Delta H_{sub} = 17.1 \pm 0.8$ kcal mol^{-1}) gives an enthalpy of formation of **2** in the gas phase of $\Delta H_f^\circ(g) = +6.2 \pm 2.1$ kcal mol^{-1}. *Schleyer*'s increments[58] give a calculated enthalpy of formation for the strain free molecule $\Delta H_f^\circ(g) = -123.0$ kcal mol^{-1}. Thus, the strain enthalpy of **2** is calculated as $\Delta H_s = 129.2 \pm 2.1$ kcal/mol (541 kJ mol^{-1}). Since the *tert*-butyl groups contribute very little to the strain of **2**,[59] each ring bond in the tetrahedrane skeleton of **2** can be assigned a strain enthalpy of 21.5 kcal/mol. This is the highest value ever found.[60,61]

Because of the high strain energy, tetrahedrane **1** possesses a higher enthalpy of formation than cyclobutadiene (**29**). All theoretical calculations agree in this. Table 1 gives information on the enthalpy differences thus determined. According to force field calculations by *Mislow*,[64] the substitution by four *tert*-butyl groups in the system **2/12** causes a strong preference for the tetrahedrane form (by 43.8 kcal mol^{-1}). MNDO calculations[36] give the same result (preference by 39.2 kcal mol^{-1}; without *tert*-butyl groups $\Delta\Delta H^\circ = 45.9$ kcal mol^{-1}, i.e. **2** is only 6.7 kcal mol^{-1} higher in energy than **12**). Therefore, the driving force for the conversion **2** → **12** should be significantly weaker than for the unsubstituted parent compounds. If it was previously claimed that tetrahedrane (**1**) would isomerize to cyclobutadiene (**29**) without activation on the grounds of the thermodynamics,[49] recent calculations per-

mit somewhat more optimism. Perhaps one may expect a certain kinetic stability of **1** after all, firstly because both the synchronous ring-opening **1** → **29** and the cleavage of **1**

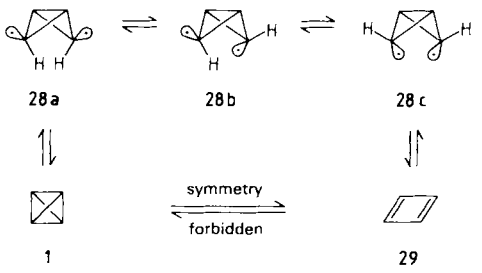

Table 1. Calculated enthalpy differences $\Delta\Delta H°$ between tetrahedrane **1** and cyclobutadiene **29**.

Ref.	[48]	[62]	[35]	[36]	[37]	[52]	[54]	[55]	[63]
Year	1967	1969	1975	1979	1980	1981	1985	1985	1987
$\Delta\Delta H°$ [kcal mol^{-1}]	84	70	27	46	26	32	23	29	29

to two acetylene molecules are symmetry forbidden processes, and secondly because a noticeable barrier must be expected also for a multistep reaction via bicyclobutanediyl diradicals **28**.[37] According to *Gleiter* et al.[65] this is due to a HOMO-LUMO crossover on the way from **28a** to **28c**. The activation enthalpy $\Delta H^{\neq}$ calculated for this process spans from 10 to 50 kcal mol^{-1}.[30,36,37,49,52] Some prominent values are: 11 (MINDO/3[52]), 15 (MNDO),[36] 18 (ab initio[30]), and 30 kcal mol^{-1} (ab initio[37]). In this connection *Kollmar*[37] points out that the actual bond cleavage **1** → **28a** only requires 10 kcal mol^{-1}, and this diradical could possibly play a role as a reactive intermediate in bimolecular reactions.

How does the fourfold substitution with *tert*-butyl groups influence the activation barrier? An activation enthalpy of 20 kcal mol^{-1} has been predicted for the process **2** → **12**.[36] The successful isolation of **2** again allows a comparison between theory and experiment for the first time. It is possible to monitor the kinetics of isomerization of the tetrahedrane **2** to cyclobutadiene **12**. The activation parameters thus derived are $\Delta G^{\neq} = 28.6 \pm 2.9$ kcal/mol, $\Delta H^{\neq} = 25.5 \pm 2.3$ kcal mol^{-1}, and $\Delta S^{\neq} = -10.3 \pm 5.8$ cal mol^{-1} K^{-1}.[25] If it is true that the activation enthalpy for the unsubstituted tetrahedrane (**1**) is about 5 kcal mol^{-1} lower,[36] then a value of about 20 kcal mol^{-1} would be expected. Given this barrier, the lifetime of **1** at −40 °C would be about 10 s.[49] From this point of view the matrix isolation of **1** does not appear hopeless.

As described in more detail in the next section, the most important chemical property of **2** is its ease of oxidation.[66] This is to be expected from the exceptionally low ionization potential of **2**[26] and is confirmed by results from chemical ionization.[67] These show that **2** is not protonated by the plasma ion, but oxidized. It was now enticing to attempt the deliberate oxidation of **2**. Several aspects were of interest: a) is the same radical cation **30** formed from both **2** and **12**? b) how high is the barrier for a possible isomerization of the radical cation **31** to **30**? c) is **30** a π or a σ radical? d) what is the structure of the cyclobutadiene radical cation? *Bock* et al.[66] succeeded in finding answers to all these questions. **2** and **12** afford the

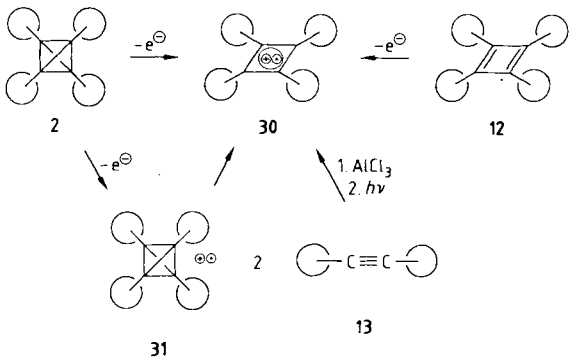

same radical cation **30** on one-electron oxidation with aluminum chloride in dichloromethane at −70 °C. The radical cation **31** initially formed from **2** spontaneously isomerizes to **30**. As indicated by calculations, no activation barrier is expected for the conversion of **31** into **30** (**31** is a C_4 cluster with the "wrong" number of electrons). Thus, the radical cation of **2** behaves completely differently from the neutral precursor (see above). The ESR spectrum of **30** features 36 equivalent, coupled protons and four equivalent ring C atoms. The coupling constants argue for a π radical. Moreover, the values measured [$a(H_\gamma) = 0.28$ G; $a(^{13}C_\alpha) = 10.0$ G] can be taken as indications of a roof-like bending. This interpretation is supported by subsequently published work. *Hogeveen* et al.[68] have prepared the radical cation of tetramethylcyclobutadiene by treatment of 2-butyne with aluminum chloride followed by irradiation of the σ complex so formed. This method can be applied to other acetylenes.[68,69] According to *Davies* et al.[69] it is even possible to generate the radical cation **30** in sufficient quantity for ESR spectroscopic detection, starting from di-*tert*-butylacetylene (**13**). These studies also reveal that the cyclobutadiene radical cations are to be regarded as planar π radicals. The folding in the case of **30** is an exception, although it is in agreement with the structure of the electroneutral cyclobutadiene **12**. Furthermore, the bending becomes still more noticeable in the radical cation bearing four 1-adamantyl groups.[70,71]

One problem remains: inspired by the preparation of **30**, *Borden* et al.[72] carried out an ab initio calculation of the cyclobutadiene radical cation **32**. As expected, **32** is subject to Jahn-Teller distortion. The rectangular geometry **33** represents the minimum (the same is true of the radical cation of tetramethylcyclobutadiene[66,73]). The two valence isomers **33** and **33'** can be transformed into each

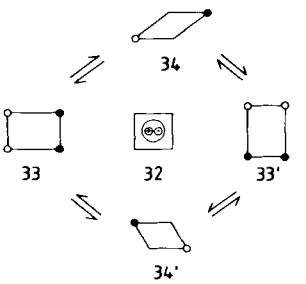

other via the 6 kcal mol^{-1} higher energy rhombohedral forms **34** and **34'**. In this regard the situation differs from that of cyclobutadiene itself, in which the transition state for valence isomerization is described by a square geometry (see below). Accordingly, one may very well conclude that the experimental ESR spectrum of **30**[66] is the result of exchange between two folded structures with alternating bond lengths, occurring rapidly on the ESR time-scale.

The picture is rounded off by experiments on electrochemical oxidation of **2** and **12** by *Fox* and *Hünig* et al.[74] The oxidation potentials determined by cyclic voltammetry are exceptionally low and again constitute record values for saturated and unsaturated hydrocarbons, respectively. At $E_{pa} = 0.50 \pm 0.10$ V the tetrahedrane **2** gives a radical cation **31**, which is transformed into **30** in an unmeasurably fast reaction.[66,75] **30**, in turn, is reversibly formed from cyclobutadiene **12** at $E_{1/2} = 0.15 \pm 0.10$ V. Knowing these data, we examined[76] whether **2** might be convertible into cyclobutadiene **12** in a photochemically induced electron transfer reaction.[77] In fact, **2** isomerizes smoothly and quantitatively to the cyclobutadiene **12** on irradiation in tetrahydrofuran in the presence of catalytic amounts of 9,10-dicyanoanthracene, and even in the absence of the acceptor by irradiation in benzene solution. Thus, the equilibrium **2** ⇌ **12** can be entirely displaced in one or the other direction depending on the conditions of irradiation (see Section 2.1); this is not an everyday occurrence.

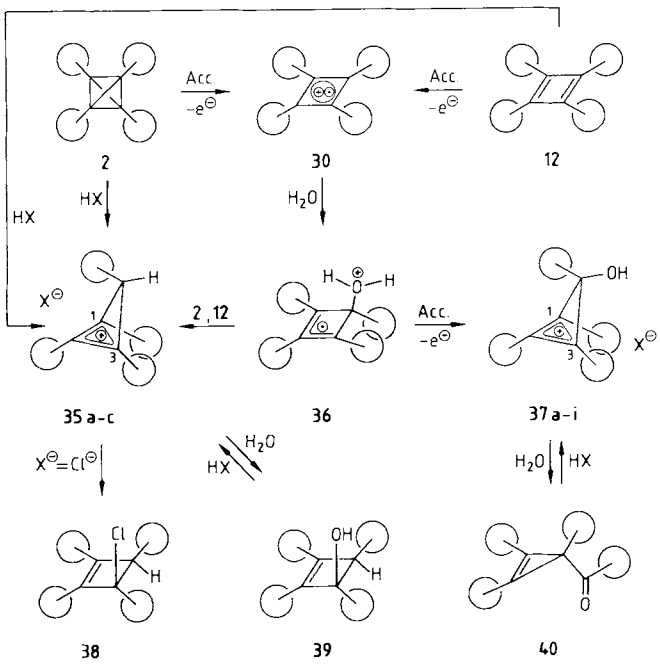

35/37	X	35/37	X	35/37	X
a	Cl	d	I_3	g	SbF_6
b	Br	e	F_3CCOO	h	ClO_4
c	I	f	BF_4	i	NO_3

2.4. Chemical Properties

In contrast to the valence isomeric cyclobutadiene **12**, tetra-*tert*-butyltetrahedrane (**2**) is insensitive to air and humidity under ordinary conditions. It is now known that only two reaction channels are open to **2**, viz. protonation and oxidation.[76,78-80] A proton can just fit in between the *tert*-butyl groups. Apart from this, all reactions start with an oxidation step, and the chemistry of **2** is characterized by the primary formation of the radical cation **30**.

The high degree of p character of the ring bonds in **2** must result in high reactivity toward electrophiles. It has even been predicted[81] that the tetrahedrane **2** should still be protonated at pH = 16.2, i.e. in molten sodium hydroxide. Nevertheless, **2** is completely inert to aqueous hydrochloric acid. The relatively large $H_9O_4^{\oplus}$ ions[82] cannot penetrate the shield of *tert*-butyl groups (Fig. 4). Therefore, protonation of **2** is possible only with anhydrous hydrogen chloride. The same reaction is much faster for the cyclobutadiene **12**, which smoothly reacts with water to give the cyclobutenol **39**.[39] This proceeds via the homocyclopropenylium chloride **35a** which in non-polar solvents and in substance captures a chloride ion, forming an adduct **38** with covalently bonded chlorine. This type of nucleophilic attack is not possible in the case of the bromide and iodide ions. Hydrogen bromide leads only to the formation of the salt **35b**; there is no indication any more of a covalent form. The other salts **35c-g** are likewise obtained either by treatment of **2** with the corresponding acid, or by exchange of the chloride ion in **35a** or the OH group in cyclobutenol **39**. The alcohol **39** is formed again by hydrolysis of these salts.

A first indication of how to "activate" the unreactive tetrahedrane derivative **2** was obtained in the attempt to catalyze the valence isomerization **2** → **12** which requires heating to 135 °C in the absence of a catalyst. The use of $Ag^{\oplus}$ ions as a catalyst[83] did not result in the expected reaction; instead **2** was oxidized. The nature of the isolable end-product, cyclobutenol **39** or ketone **40**, depends on the reaction conditions. It has taken some effort to unravel the ensuing intricacies.[84] Silver tetrafluoroborate, silver hexafluoroantimonate, and silver perchlorate cause oxidation of **2** and **12** to the radical cation **30** (both valence isomers **2** and **12** were always employed in parallel in these experiments).

Steric shielding by the four *tert*-butyl groups hinders the immediate conversion of **30**. In this regard **30** is an ideal molecule for the study of the chemical properties of radical cations.[85] It is also understandable why **2** is an ideal precursor for **30**: ordinary reactants cannot approach the ring skeleton of **2** sufficiently. This is less serious in the oxidation. The electron can overcome a distance of up to 15 Å[86] in SET (single electron transfer) reactions. If no other suitable reagent is available, **30** reacts with traces of water, which in spite of much effort cannot be entirely removed, giving the adduct **36**. The latter can be transformed into the HO-salts **37f-h** in a second oxidation step. In fact, two equivalents of $Ag^{\oplus}$ ions are consumed as long as the hydrocarbon is added slowly to an excess of the oxidant. However, the intermediate **36** can also transfer a proton to **2** or **12**. This latter reaction occurs on inverse addition. Here, the radical cation **36** acts as an acid toward **2** or **12** still present.[87] In this manner the salts **35f-h** are formed. Hydrolysis of the hydroxy salts **37** leads to ketone

40. Also this reaction is reversible; reaction with trifluoroacetic or nitric acid results in regeneration of the salts **37e** and **37i**, respectively. This means that **40** is much more basic than ordinary ketones. In this connection, it is worth mentioning that nitric acid oxidizes the tetrahedrane **2** faster than it protonates, i.e. **37i** is formed exclusively, and not **35i**. On prolonged standing in concentrated nitric acid subsequent cleavage of **37i** gives tri-*tert*-butylcyclopropenylium nitrate and pivalic acid.

Also halogenations of **2** may be looked upon as redox reactions. The first step is again oxidation to the radical cation **30**. The subsequent course is determined by the nature of the halogen. Xenon difluoride, (dichloroiodo)-benzene (or chlorine), and pyridinium perbromide (or bromine) react with **2** to give dihalocyclobutenes **42** via **30** → **41**. The stability of the dihalocyclobutenes decreases strongly from the difluoro to the dichloro and dibromo-compound. The ketone **40** is again the hydrolysis product of the compounds of type **42**. The rate of this reaction followed by ease of ionization **42** → **41** and the subsequent addition of water to give the intermediate **43**. If traces of water are not entirely excluded, the hydroxy salts **37a–c**

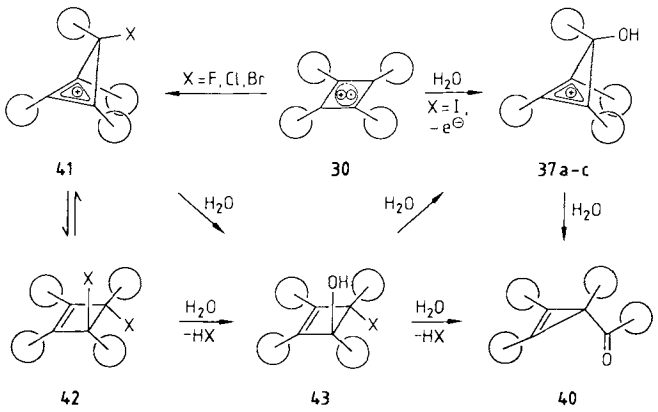

are formed as well in competition to **41** during halogenation. The iodide ion is too large for an addition to **30**, and hence with iodine the hydroxy salt **37c** or the ketone **40** is obtained exclusively.

The above-mentioned properties engendered the hope that examples of Diels–Alder type reactions with radical ion pair intermediates could be found for **2** or **12**. Although the two reactions described below do not constitute a proof, they provide strong indication of such a course of reaction.[88] Both **2** and **12** give rise to the 1:2 adduct **46** with tetracyanoethylene (TCNE). This substance is a rarity with regard to structure and reactivity.[89] It may be assumed that the radical ion pair **30** · **44** is formed in the first step. Due to steric hindrance, the radical anion **44** attacks **30** with the nitrogen atom as the "spear head". The end product **46** is formed via **45** after addition of a second TCNE molecule. The "normal" Diels Alder adduct **49** can be formed analogously from **2** and **12** and dicyanoacetylene via the radical ion pair **30** · **47** and the zwitterion **48**.[90,91]

What is the evidence for the intermediate appearance of the radical ion pair **30** · **47**? It is simply the fact that while

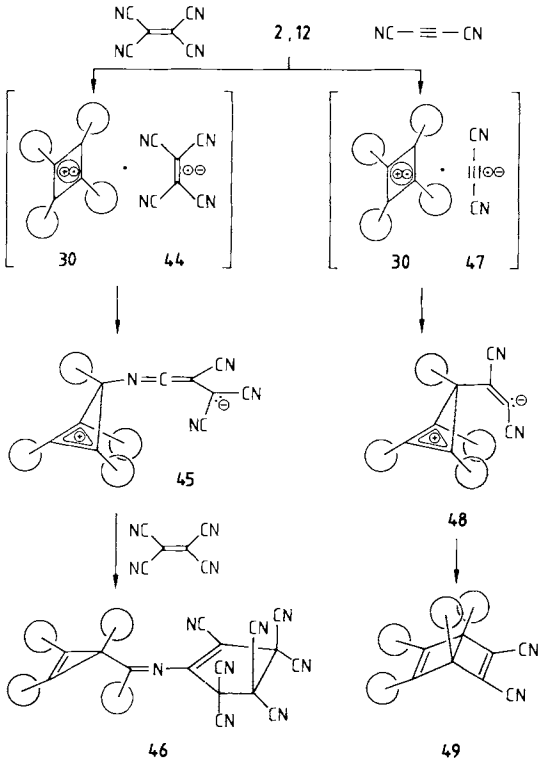

cyclobutadiene **12** gives the Diels–Alder adduct **50** with acetylene dicarboxylic ester, tetrahedrane **2** remains unchanged under the same conditions. If, however, dicyanoacetylene is used, both **2** and **12** give the adduct **49**. The explanation is obvious: the oxidation potential of dicyanoacetylene, but not that of acetylene dicarboxylic acid esters, suffices in order to generate the radical cation **30** from **2** (and **12**).

The adduct **50** also has no shortage of surprising properties.[92] The genetic connections between the valence isomers **50**, **51**, and **52** are shown in the scheme. The crucial point is the thermal isomerization of the arene **51** to the thermodynamically more stable Dewar-benzene **52**. This

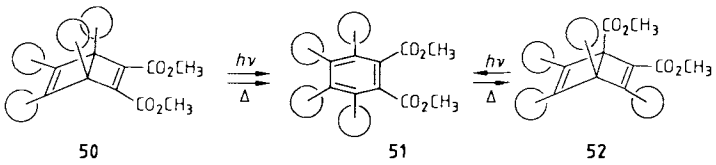

reversal of stabilities relative to the habitual situation once again documents the drastic influence exerted by four directly neighboring *tert*-butyl groups.[93,94]

Autoxidation is a subject where the importance of the tetrahedrane **2** for cognition in apparently very remote areas becomes particularly clear. **2** and cyclobutadiene **12** behave entirely differently in the presence of oxygen. Furthermore, the product formation is also very sensitive to the reaction conditions: tetra-*tert*-butyltetrahedrane **2** is completely stable in air. The corresponding cyclobutadiene **12** reacts smoothly with oxygen to give the dioxetane **54**. This picture changes completely in the presence of an acceptor. Addition of 0.1–0.3 equivalents of silver

ions or iodine to an O_2-saturated solution of **2** results in the formation of at least four products, of which the oxete **55** is the major component. At least the spectra support this unusual structure. The last doubt has not yet been removed, however, for in contrast to known oxetes,[95,96] **55** is stable up to 200°C. Perhaps the accumulation of four sterically demanding groups is once again responsible.[97] The other products are the diketones **56** and **57**, which incidentally are photochemically interconvertible, and the cyclopropenyl ketone **40**. The latter is formed also when **2** is allowed to stand for several days in oxygen-saturated chloroform, and by oxidation of cyclobutadiene **12** in the presence of 0.1–0.5 equivalents of the acceptor. The use of an excess of oxygen in diiodomethane, or the addition of a trace of iodine in chloroform or carbon tetrachloride results in the exclusive formation of the cyclic peroxide **53**. This is the only product from **2** in which only one bond has been broken.

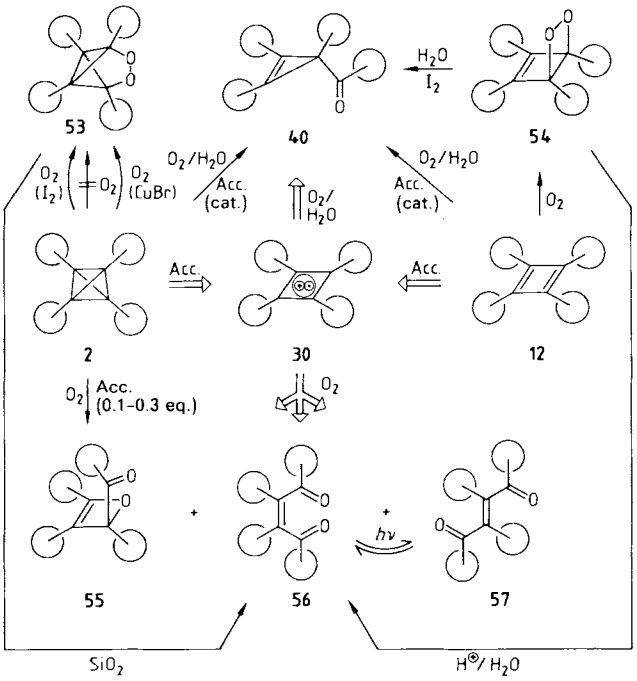

Two reactions in which the oxidation state remains unchanged should also be mentioned: chromatography of the peroxide **53** on silica gel gives rise to the diketone **56**.[80] The latter is also obtained by acid treatment of the dioxetane **54**.[97] Apparently, mineral acid catalyzes ring opening of **56** and not elimination of hydrogen peroxide to give the cyclopropenyl ketone **40**. Strangely, this is the only product when the dioxetane **54** is treated with water in the presence of iodine.

Apart from **53**, all the products of the reaction of **2** with oxygen are likely formed via the radical cation **30**. It is difficult to provide an overall picture of the branching observed in the autoxidation of **2** and **12**. Nevertheless, it will be attempted: the normal potential of oxygen [$E_{1/2}(O_2/O_2^{2\ominus}) = -0.57$,[98a] -0.8,[99] -0.83,[100] -0.94 V[98b]] is too low to oxidize **2** ($E_{pa} = 0.5$ V, see above). In order to make **2** reactive enough, a sufficiently strong acceptor is needed ($Ag^{\oplus}$ ions, iodine, TCNE, and similar acceptors). The crucial intermediate **30** is formed via **31**. At this stage oxygen is consumed, and the two radical cations **60** and **61** are formed. Ring opening of **61** leads to the open-chain intermediates **63** and **64**.[101] These are in equilibrium with **62**. All three species, **62**–**64**, can be reduced by tetra-*tert*-butyltetrahedrane **2** to **55**, **56**, and **57**. Compound **30** is regenerated in this process. Such a reaction chain can explain the rapid oxidation of **2**.

The formation of ketone **40** is more difficult to interpret. As described above, **40** can be formed from **30** by addition of water and repeated oxidation. However, another route via the oxygen adduct **60** (or **61**) is also open. In the presence of water, the adduct can give the intermediate **59** (the reverse reaction, i.e. first addition of water to **30** and then reaction of the intermediate **36** with oxygen is also possible). Reduction of **59** (by the iodide ions resulting from the oxidation of **2** with iodine, or by either **2** or **12** within the reaction chain) leads to the hydroperoxide corresponding to compound **59**. Elimination of hydrogen peroxide then gives the cyclopropenyl ketone **40**. If this purely speculative mechanism is correct, it implies that an unusual process has been discovered as follows:

$$H_2O^* + O_2 + \text{substrate} \xrightarrow{I_2} H_2O_2 + \text{substrate}\cdot O^*$$

The substrate molecule is transformed into an oxidation product carrying only *one* more oxygen atom; this takes place under catalysis by iodine, which is at first consumed but reappears at the end of the reaction. The asterisk denotes that the added oxygen atom originates in the water, not in the actual oxidant (O_2).

Finally, the question of how the peroxide **53** is formed from **2** is still unanswered. Several interpretations are possible: oxygen, present in excess, captures the radical cation **31** postulated as the primary product; this requires that in contrast to the outcome of the calculations (see above) **31** possesses a finite lifetime. Reduction of the peroxide radical cation **58** could then give **53**.

Another possibility is that a charge transfer complex between **2** and iodine is formed initially; in the presence of excess oxygen the peroxide **53** would result at once.

Or perhaps the attacking oxygen is activated rather than **2**. This phenomenon is not altogether unknown.[102] This would imply that some iodine–oxygen complex is the attacking agent. This type of oxygen activation with iodine has not to our knowledge been reported in the literature.[103] There are, however, accounts of a corresponding function of transition metal–oxygen complexes.[104] Accordingly, we also treated **2** with copper(I) bromide in acetonitrile and oxygen.[105] Indeed, peroxide **53** is the exclusive product of this reaction.[76] Since **2** is inert toward copper bromide alone (the normal potential of copper(I) is strongly reduced under these conditions[105]), oxygen activation cannot be dismissed as the mechanism of the reaction **2** → **53**.

The system presented above also offers the specific possibility to elucidate the autoxidation of cyclobutadienes.[106] Presumably, dioxetane **54** is not formed via the radical cation **30** (this leads, as mentioned above, to other products), but is more likely the result of the diradicaloid

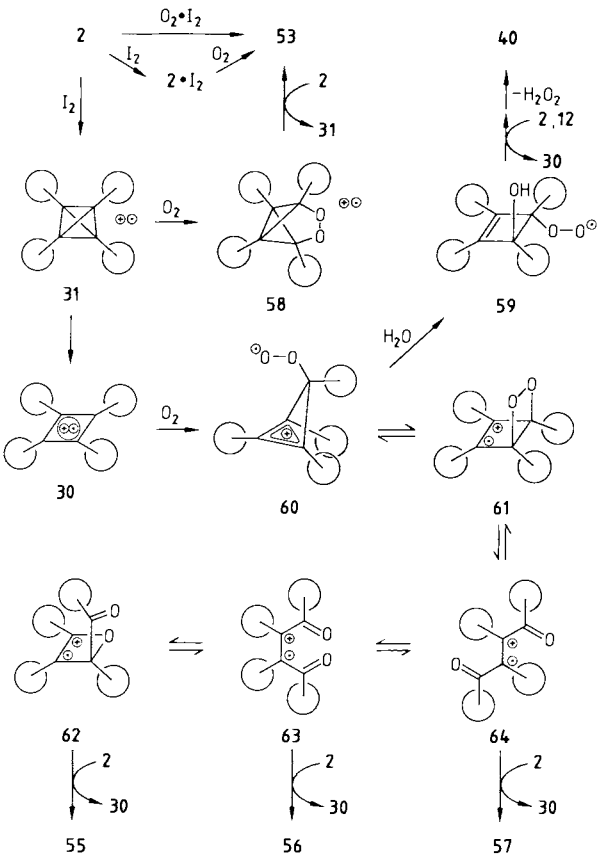

character of **12**.[107] The relevance of the results for the discussion of SET oxidations in general[108] (excitation by irradiation or addition of an oxidizing agent, trapping of the radical cation by the radical anion $O_2^{\odot\ominus}$ of triplet oxygen, possible chain reaction with radical cation catalysis) is obvious.

2.5. Guide to New Fields

The tetrahedrane **2** and the cyclobutadiene **12** are end members of a chain starting with the still very reactive tri-*tert*-butylcyclobutadiene **6** whose principal reaction channels have been clarified.[8b, 11, 12, 107, 109] Other members of

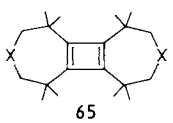

65

a, X = S ; b, X = CH_2

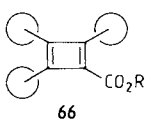

66

a, R = CH_3 ; b, R = $C(CH_3)_3$

the chain include *Krebs*' stable cyclobutadienes **65a** and **65b**,[40, 43, 106, 110] *Masamune*'s ester **66a**[8c, 12] and the *tert*-butyl ester **66b** recently widely employed by *Regitz* et al.[111]

To what extent can occupying oneself with **2** still generate new questions? A few examples will illustrate this. The bottleneck in the study of **2** is still its poor accessibility. An alternative was sought in the reaction of lithiated *tert*-butyldiazomethane with the cyclopropenylium salt **68**. We have found no mention of the synthetic use of anions of alkyl-substituted diazomethanes in the literature. It is all

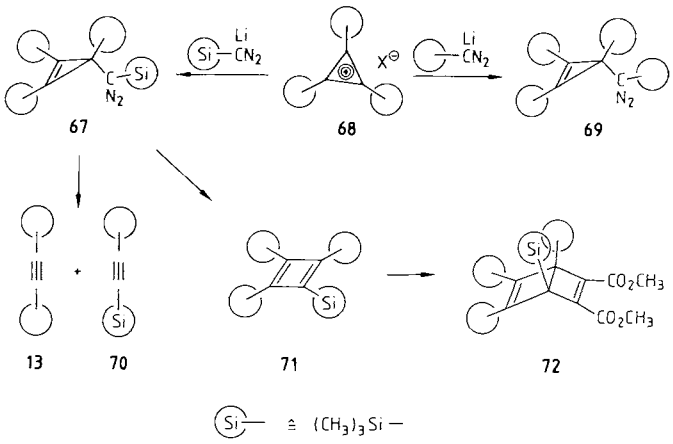

the more surprising, therefore, that the reaction **68** → **69** can be accomplished. The diazo compound **69** is surprisingly stable thermally [20a] and melts at 120 °C. Future experiments[112] will show whether a route to **12** and hence **2** can be found from **69**. The known[113] lithium salt of (trimethylsilyl)diazomethane reacts with **68** to give the silylated cyclopropenyldiazomethane **67**. Pyrolysis or irradiation of the latter results in fragmentation to **13** and **70**. Catalysis with copper(I) chloride and trapping with acetylenedicarboxylic acid ester allows isolation of the adduct **72**,[114] a proof for the presence of the new cyclobutadiene **71** — which itself is a potential candidate for tri-*tert*-butyl(trimethylsilyl)tetrahedrane[112] — in the crude product.

In this context, the specific utilization of trimethylsilyl residues has singled out a new synthetic concept. These substituents have the advantage to be larger still than the *tert*-butyl groups. Furthermore, they are easily eliminated and thereby permit access to the unsubstituted parent compounds (see next section). Thirdly, our own experience demonstrates that in the presence of trimethylsilyl groups polycyclic compounds are preferentially formed.[115–119] Finally, the kinetic stabilization by TMS-substituents is particularly large. However, there are disadvantages too.

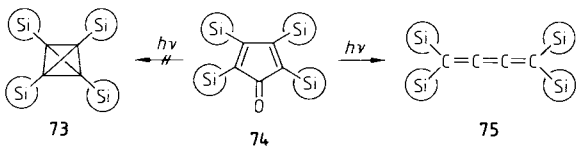

Due to the long C–Si bond, the corset effect in **73** should be weaker than that in **2**. Furthermore, silyl groups tend to rearrange. This is the reason why **74** furnishes the butatriene **75** rather than the tetrahedrane **73**.[120]

The occupation with the chemistry of **2** has also opened our eyes to some aspects of carbenium ion chemistry. Redox reactions of **2** permit the isolation of crystalline cyclobutenylium salts of the types **35** and **37** for the first time, as well as the X-ray determination of their crystal and molecular structures (Fig. 5).[84] This is of importance in connection with *Winstein*'s[121] postulate that these ions should have homoaromatic character. Numerous investigations of this point have been carried out — but all in solution.[122] The structural data now available for **35d** and **37g**[84]

(folded rings; relatively short C1-C3 distances) justify the description of these compounds as homocyclopropenylium salts in spite of the scepticism of theoreticians.[123]

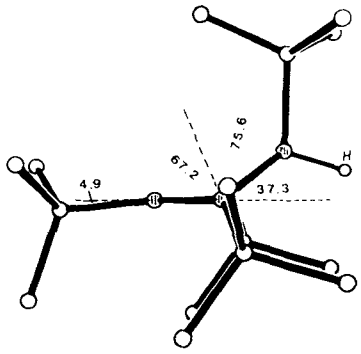

35d

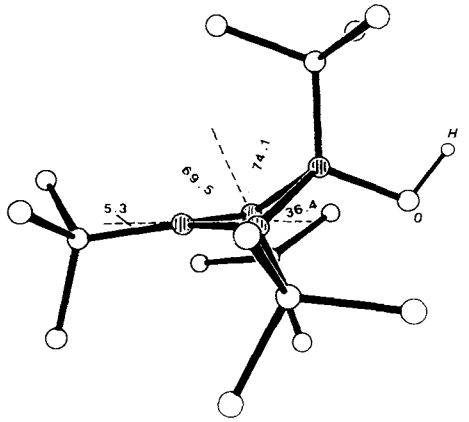

37g

Fig. 5. Crystal structure (folding angle [°]) of the cyclobutenylium ions of **35d** (C1-C3 = 1.806 Å) and of **37g** (C1-C3 = 1.833 Å). C1 and C3 are the atoms at the site of folding.

The ion **37** offers a further surprise. Its NMR spectrum is temperature-dependent as a result of a carousel rearrangement **37** ⇌ **76** ⇌ **37'**.[124]

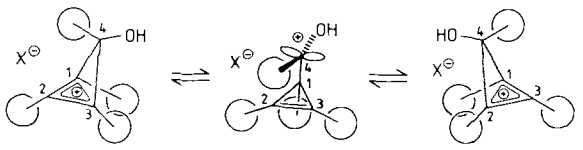

37 **76** **37'**

It is of particular interest that, in contrast to the predictions of the Woodward-Hoffmann rules, this reaction proceeds with inversion at the migrating C-atom, i.e. the bisected transition state **76** is preferred—as predicted.[125]

Incidentally, if the *tert*-butyl group at C1 is missing in cation **76**, the cyclopropenylmethylium system becomes an energy minimum relative to the corresponding homocyclopropenylium system; accordingly, direct observation is possible.[126] The interplay between cyclobutenylium and cyclopropenylmethylium system culminates in the dynamic behavior of the cation **77**.[127] The latter is obtainable from the diazo compound **67** via an unconventional

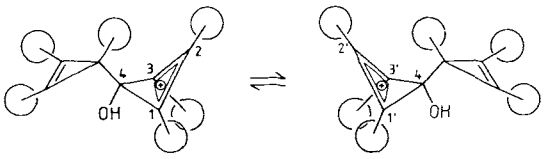

77 **77'**

route. Compound **77** can undergo a tandem walk rearrangement, i.e. a consecutive migration of C4 around the segment C1/C2/C3 accompanied by a mutual exchange of ring moieties in the sense **77** ⇌ **77'**. As a consequence, the carbon atom carrying the hydroxyl group migrates around six equivalent ring positions.

The study of the system **2/12** has also caused a small renaissance concerning our previous model molecule **6**. The consideration that *Saunder*'s isotope perturbation method, which proves a static structure for tetrahedrane, should reveal a dynamic equilibrium [D_9]-**6** ⇌ [D_9]-**6'** in the case of deuterated tri-*tert*-butylcyclobutadiene was confirmed in the first attempt.[128] The splitting found in the

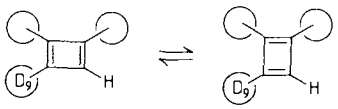

[D_9]-**6** [D_9]-**6'**

^{13}C-NMR spectrum is the first direct spectroscopic proof for the postulate that cyclobutadiene is not a resonance-stabilized molecule but consists instead of a valence tautomeric equilibrium between two rectangular singlet ground state structures (a kinetic proof due to *Carpenter*[129] will be described in Section 4.1).

Another peculiarity of **6** concerns the stereochemistry of its dimerization. In contrast to previous belief,[8b] the dimer does not have the structure **78** expected from a reaction of the Diels-Alder type, but is in reality the *anti*-tricyclic compound **79**.[130] The transition **6** → **79** must be a two-step process. The first step may be either a nucleophilic addition of singlet **6** to another molecule of singlet **6** (with **80** as an intermediate), or a reaction between one molecule of singlet **6** with a thermally populated triplet **6** (with **81** as

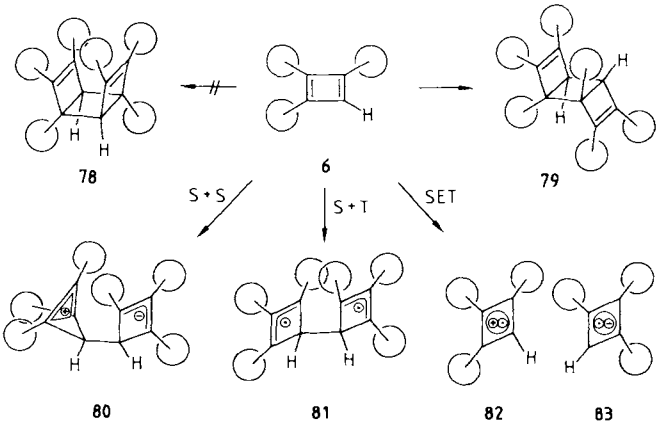

78 **6** **79**

80 **81** **82** **83**

an intermediate). Thermal activation of a singlet ground state to the excited triplet state has been reported for antiaromatic dianions.[131] Admittedly, a singlet-triplet gap of at least 12 (adiabatic triplet energy) or 29 kcal mol^{-1} (vertical energy) has been measured for **65b** by *Wirz* and *Krebs* et al.[110a] However, it cannot be excluded that the energy difference is significantly smaller in the case of **6** (e.g. due to less alternation, as in **12**). There is a third and bolder hypothesis, namely that electron transfer in a triplet excimer complex ^{3}(**6***,**6**) could generate a radical ion pair **82**·**83** and thence the dimer **79**. We know of no example of such a thermally induced "disproportionation",[132a] but it could perhaps be the result of the small HOMO-LUMO distance in **6** caused by the pseudo-Jahn–Teller distortion.

However, a chain reaction catalyzed by the radical cation **82**[85d, 132b]—as the "effectiveness" of the dimerization would suggest—cannot be ruled out either. In some way or other traces of the radical cation **82** are formed by external

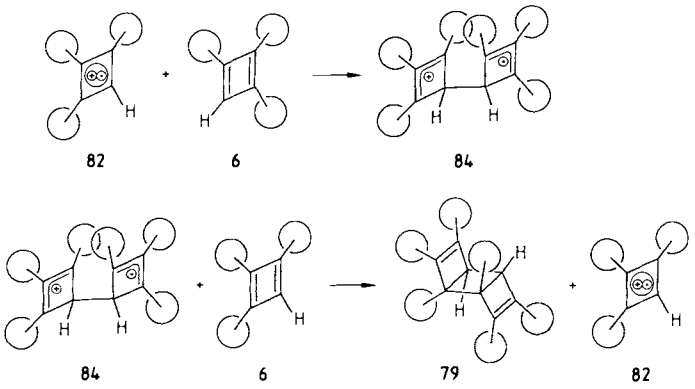

effects. This reacts with a further molecule of **6**—probably via a π-complex between the two species[132c]—to give the coupling product **84**, which undergoes a redox process with **6** again, leading to renewed liberation of a radical cation **82**.

In this context it is important to realize that, in contrast to previous experience with other cyclobutadienes,[8] **6** and **12**[133, 134] as well as *Masamune*'s ester **66a**[135] give poorly resolved ESR signals in the region expected for monoradicals. It is, unfortunately, very difficult to give an assignment of the observed signals to a particular species.

3. Unsubstituted Tetrahedrane

The risks associated with a search for the unsubstituted parent compound are obvious.[1] As briefly discussed in Section 2, the corset principle no longer applies when there are less than four substituents on the tetrahedrane skeleton. Indeed, bond breaking becomes easier than in the unsubstituted tetrahedrane if only one substituent is removed. Thus, if one hopes to synthesize less sterically demanding tetrahedranes, there is only one consequence: to dare the attempt at the wholly unsubstituted parent molecule **1**. In view of the energetic situation mentioned above, a matrix isolation appears possible. The question is whether a usable way to **1** exists. If one accepts the theoretical predictions slavishly, one need not even commence

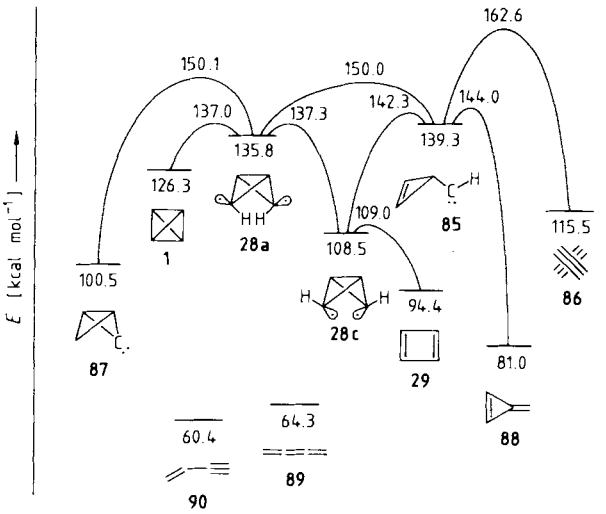

Scheme 1. Calculated [52] enthalpies of formation of the most important C_4H_4 minima and the energies of the connecting transition states.

such a project. A section of the C_4H_4 energy hypersurface is given in Scheme 1 for clarity. The calculated[52] enthalpies of formation of the C_4H_4 minima **1**, **28a**, **28c**, and **29**, and **85**–**90** as well as the barrier heights connecting them demonstrate that there is only one reasonable route to **1**, namely the one from diradical **28a**. However, isomerization to diradical **28c** can compete, having the same activation barrier. It is more difficult still to obtain **28a** in the first place. Regardless of the starting point, there are always more favorable escape routes. The only consolation in this awkward situation is the fact that the calculations only indicate the general trend, and the absolute numerical values are less meaningful. Moreover, the picture should be valid for thermally induced transitions. Electronically excited species generated by photochemical fragmentation of suitable precursors could react quite differently. In this hope, and guided by the "trimethylsilyl trick" as a method for the preparation of reactive unsubstituted tetrahedrane precursors, we have attempted to defy the difficulties.

3.1. Experiments on the Preparation of Tetrahedrane

Tetrahedrane (**1**) might be formed by ring closure of **28** or by intramolecular carbene addition of **85**. As further routes the two carbenes **87** and **91** are of particular interest. Both precursors have been approached experimentally, and were claimed on the basis of labeling experiments[136–138] to dissociate into two molecules of acetylene via tetrahedrane (**1**). The precursor **87** was reportedly formed by addition of atomic carbon[136] or C_2O[136, 137] to cyclopropene, in the latter case followed by CO elimination. Dicarbene **91** or cyclopropenylcarbene **85** are considered as the

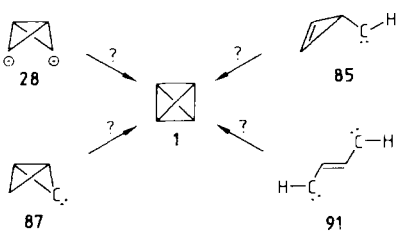

products of pyrolysis of the lithium salt **96** of the bistosylhydrazone of fumaric dialdehyde.[138]

We have endeavored to generate all the tetrahedrane precursors **28**, **85**, **87**, and **91** selectively in order to trap the expected tetrahedrane in a matrix at 10 K. It is possible to isolate the anhydride **92**[115, 139] and the ketone **26**[116, 140] by desilylation of the corresponding trimethylsilyl derivatives and then subject them to photofragmentation in a noble gas matrix at 10 K. Neither these conditions nor flash pyrolysis with matrix isolation permit the IR-spectroscopic detection of tetrahedrane (**1**) (tricyclopentanone **26** gives cyclobutadiene and cyclopentadienone **142** as well as methylenecyclobutenone **119** under these conditions).[135] If the target molecule **1** were present in the matrix, at least the strongest (calc.: 895[54] and 940[30] cm^{-1}, resp.) of the three theoretically possible IR bands ought to be recognizable. The diradical **28** might also be formed from the *Corey* lactone **93**.[141] However, **93** is photostable under matrix conditions. Flash pyrolysis does not give **1** but cyclobutadiene (**29**).[142, 143]

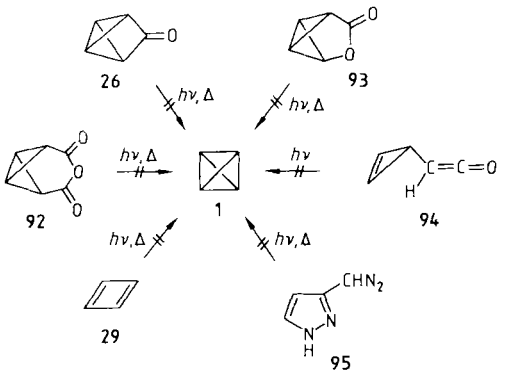

The question of the properties of dicarbene **91** remains open. In our hands, repetition of the procedure by *Rodewald* and *Lee*[138] did not show the reported result. According to our results[117] vacuum pyrolysis of the lithium salt **96** does not give any acetylene. Rather, the only spectroscopically identifiable product is 3-pyrazolyldiazomethane (**95**). An independent structure proof for **95** is given by the fact that the same substance results from the oxidation of the hydrazone **98** with MnO_2,[144] and also by vacuum pyrolysis of the bishydrazones **97a**, **b**.[145] These hydrazones, prepared by the method of *Eschenmoser*[146] have the advantage over **96** that they are obtained in analytically pure form, free of solvent, and are cleaved to the desired carbenes[147] in the same manner as the still missing cyclopropenyldiazomethane.[148]

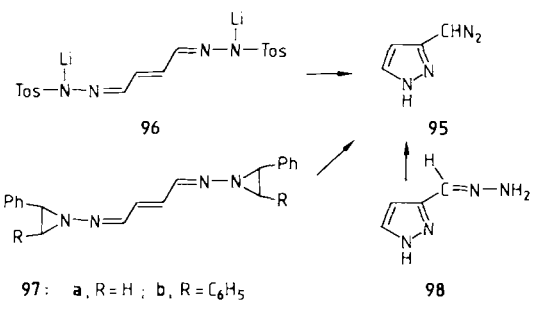

It may be concluded, therefore, that the pyrazolyldiazomethane **95** was an intermediate also in the experiments of *Rodewald* and *Lee*.[138] In these circumstances it is surprising that **95**, in contrast to the literature statement for the pyrolysis of the salt **96**, does not give any acetylene or vinylacetylene. Nevertheless, **95** is a good source of C_4H_4 species. Matrix irradiation[144] results in a complicated picture. The two thermodynamically most stable isomers (cf. Scheme 1), namely butatriene (**89**) and vinylacetylene (**90**), can be discerned in the products together with methylenecyclopropene (**88**) and acetylene (**86**).

A further procedure reported in the literature[149] and involving dehydrogenation of the bishydrazone **99** to the bisdiazo compound **100** likewise could not be reproduced by us. We[145] believe, however, to have prepared **100** as a violet substance, which is only isolable at −196 °C, starting from the urea derivative **101**. Preliminary matrix-irradiations of **100** in argon at 10 K have unfortunately yielded only acetylene.

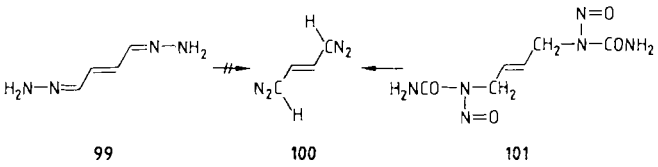

The third potential tetrahedrane precursor, viz. bicyclobutylidene (**87**), has not been mentioned so far. The enthalpy of formation of this candidate is relatively low. A problem could be that in **87** a concerted ring opening to vinylacetylene (**90**)[150a] takes precedence over the formal insertion giving tetrahedrane (**1**). There are hurdles in the practical execution too; the common procedure for carbene generation (Bamford–Stevens reaction) is prohibited for this species since the bicyclobutane ring system does not readily tolerate an sp^2-hybridized C-atom.[150b] Studies using cyclopropenylidene (**103**) as a model give an indication of the procedure to follow. This carbene was recently prepared for the first time in collaboration with *R. W. Hoffmann* by flash pyrolysis of the polycyclic **102** with subsequent matrix isolation.[151] The bisperoxy ester **104** also serves as a precursor.[152, 153] This access is not only new in principle, but also synthetically simpler.

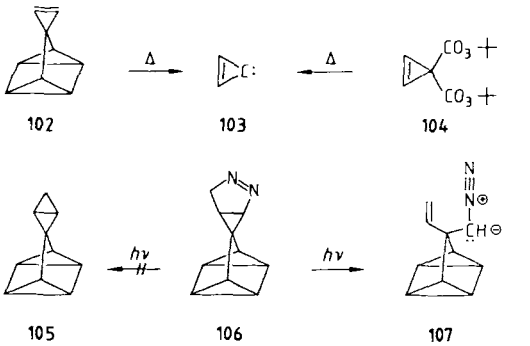

Applying the reaction **102** → **103** to the bicyclobutylidene problem it seems logical to utilize the dihydropyrazole **106**, obtainable from **102**,[144] in the preparation of

87. However, matrix irradiation of **106** does not give the desired starting material for **87**, namely **105**, but instead the diazo compound **107**.[154] Surprisingly, the latter is unchanged by further matrix irradiation although this is in agreement with analogous observations for diazomethane itself.[155] The preparation and flash pyrolysis of the diester of bicyclobutane-2,2-bis(peroxycarboxylic acid) is a logical extension of this work[152] (cf. **104**). Access to the diester **110**[119] has in the meantime been considerably improved.[152] When heated in the presence of copper(I) bromide, **108** is converted quantitatively into **109**. The subsequent desilylation with tetra-*n*-butylammonium fluo-

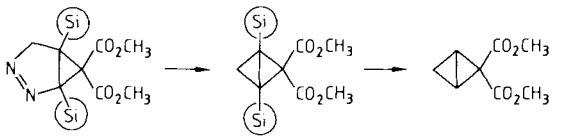

108 109 110

ride can be accomplished only in dioxane (but with 60–70% yield). The last step has thus far failed in that the free dicarboxylic acid—in contrast to the dianion—is not able to exist.

Summarizing: an unquestionable proof of the existence of tetrahedrane (**1**) is still wanting. The diradical **28** preferentially undergoes ring opening to cyclobutadiene (see Section 4.1). Not unexpectedly, cyclopropenylcarbene **85** avoids carbene addition to give **1**;[156] instead, ring expansion to cyclobutadiene (**29**) and ring opening to vinylacetylene (**90**) (see Section 3.2), or fragmention to two molecules of acetylene[143] occur. Presumably, the dicarbene **91** is not formed at all by decomposition of compounds of the type **96**. This is not surprising since this species should not be a minimum on the C_4H_4 energy hypersurface.[52] With regard to bicyclobutylidene (**87**) the experimental material is still too meager for a clear verdict. The catalog of negative results is easily extended: in contrast to the photoisomerization **12** → **2**, matrix irradiation of cyclobutadiene (**29**) does not furnish tetrahedrane (**1**), but mainly acetylene and a little vinylacetylene.[135, 157] This fragmentation of **29** to two molecules of acetylene is also seen in the gas-phase pyrolysis of cyclobutadiene.[135, 142] In view of these disappointing results[158, 159] it would seem reasonable to turn the synthetic efforts toward more promising goals. But the cards have not been completely outbidden yet, and there is one small consolation: at least it is known how tetrahedrane *cannot* be made.

3.2. Other C_4H_4 Isomers

Of the C_4H_4 isomers mentioned in Scheme 1, butatriene (**89**) and vinylacetylene (**90**) have been known for a long time. Both occupy energy sinks and there are many routes to these thermodynamically favored species. The three remaining bond-saturated hydrocarbons **1**, **29**, and **88** are much more interesting. If tetrahedrane itself still needs a lot of pressing, at least the efforts can be turned into success regarding cyclobutadiene (**29**) and methylenecyclopropene (**88**).

The experiment shows that almost all of the above-mentioned tetrahedrane precursors lead to cyclobutadiene (**29**) on either flash pyrolysis or matrix irradiation. The cyclopropenylketene **94** is generated either by low-temperature irradiation of diazoketone **111** in a matrix[143] or by pyrolysis of the formal adduct between **111** and hexafluoro-*o*-xylene with condensation of the fragments (**94** and hexafluoro-*o*-xylene) on the cold window.[144] The diiodides **112**[160] and **113**[161] are additional thermal precursors.[143] These results are of importance for several reasons: firstly, the existing range[8] of cyclobutadiene precursors is significantly extended; secondly, the pyrolyses demonstrate that cyclobutadiene is sufficiently long-lived in the gas phase to

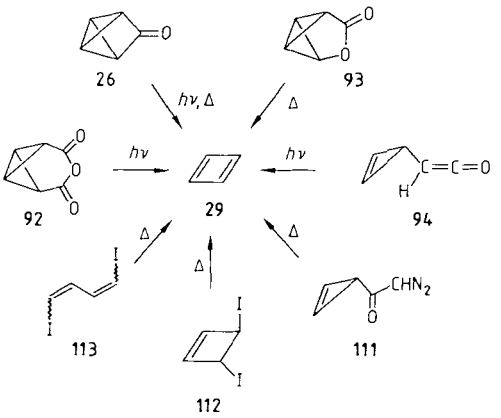

survive the distance to the cold finger.[162] Thus, the unequivocal determination of the PE spectrum of cyclobutadiene starting from **93** was achieved recently.[163] Thirdly, the case of the diiodide **113** has shown that it is even possible to thermally close open-chain starting materials to a cyclobutadiene ring![142, 143]

Two further examples of abortive attempts to synthesize tetrahedrane (**1**) must be cited because they were to start from "optimal" precursors. The polycycle **114** prepared by *Christl* et al.[164a] evades fragmentation in the matrix irradiation (Ar, 10 K) by an intramolecular [2+2]-photoaddition of the two double bonds (the same is true for derivatives of **114** substituted in the six-membered ring). The azo compound **115**[164b] affords only the dimer of cyclobutadiene and pyridazine after irradiation in an organic glass

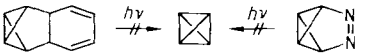

114 1 115

at 77 K and thawing (irradiations in an argon matrix have not yet been attempted). As we have found earlier,[135] no **115** or even **1** can be detected in the matrix irradiation of pyridazine — formally the "most elegant" route to tetrahedrane. Only an isomerization to pyrazine is observed.

Also the preparation of methylenecyclopropene (**88**) has been a long time coming. This substance was obtained only recently by *Billups* et al.[165a] and *Staley* et al.[165b] by treatment of **116** or **117** with potassium *tert*-butoxide. The

same compound, **88**, is also obtained by gas-phase pyrolysis of the sulfoxide **118**[166] or the diazoketone **111** with condensation of the products at 10 K.[142,143] It should be noted that a band at 904 cm^{-1} previously assigned to **88**[165a] is absent when using **111** and **118** as precursors.

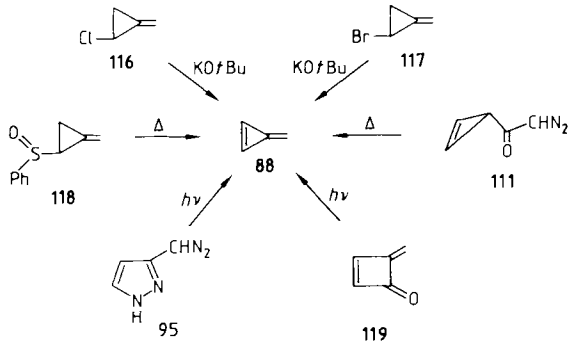

This absorption is also absent in the calculated IR spectrum.[167] Meanwhile it has become clear that the said band is not due to **88**,[168] and this is a further proof of the quality of state-of-the-art calculations of positions and intensities of IR absorptions for molecules of a reasonable size.[169] While the reaction **111**→**88** is strange enough (insertion of the carbene center in the bridgehead C–H bond followed by CO elimination), it is even more surprising that matrix irradiation of **95** likewise leads to methylenecyclopropene.[144] As the IR spectrum of **88** is now known, it is easily confirmed that also the irradiation of methylenecyclobutenone **119** gives **88** as previously reported by *Chapman*.[158] Long-time irradiation of **88** finally leads to vinylacetylene.

4. Completion of the Picture

As a supplement to the two previous reviews of the cyclobutadiene problem,[8b,8c] recent work that has not already been mentioned will be briefly outlined here. It will emerge that large segments of the cyclobutadiene theme can now be regarded as "closed".

4.1. Unsubstituted Cyclobutadiene

There exists a whole range of further cyclobutadiene precursors apart from the ones mentioned in Section 3.2. The tricarbonyliron complex **120** of *Pettit*[170] is still unbeaten from the point of view of preparative chemistry. Several compounds have played an important role in the spectroscopic identification of cyclobutadiene (**29**): photo-α-pyrone **121** (*Chapman* et al.,[171] *Krantz* et al.[172]), Dewar-pyridine **122** (*Chapman* et al.[171a]), the ether **123** (*Masamune* et al.[173]), the anhydride **124** (*Maier* et al.[157,174a]), the heterocycle **125** (*Maier* et al.[174a]), adducts of the type **126** (*Maier* et al.[157]), and the polycyclic **127** (*Maier* et al.[174b]). The azo-compound **128** (*Masamune* et al.[175a]) motivated *Carpenter* et al. to investigate the automerization of cyclobutadiene.[129] It is amazing that the related azoxide[175b] furnishes no cyclobutadiene upon pyrolysis, and only traces thereof in the matrix pyrolysis.[135] The photo-

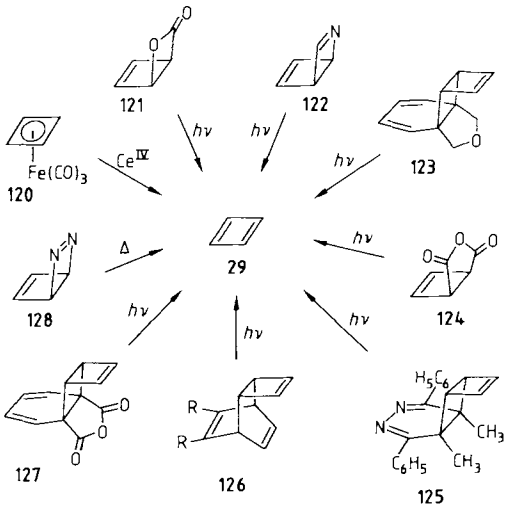

chemical cleavage of the anhydride **124** is the most convenient method for matrix isolation of cyclobutadiene, whereas it is obtained in the purest form from tricyclopentanone **26**.

The first argon matrix isolation of cyclobutadiene in 1973 by *Chapman* et al.[171] and *Krantz* et al.[172b] is now a classical experiment. However, the correct interpretation of the experimental IR results has been going on till today. A square structure was originally claimed [D_{4h} geometry allows four, and the rectangular D_{2h} seven fundamental vibrations], but this became questionable as we[157] and *Masamune* et al.[173b] demonstrated that one of the postulated cyclobutadiene bands was due to an absorption of carbon dioxide imbedded in a matrix cavity together with **29**. Subsequent isotope labeling experiments have confirmed this assumption.[172c] Such association (**129**) is reminiscent of neighboring phenomena previously postulated by us in

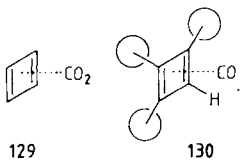

terms of formula **130**.[14] The square geometry of **29** was definitively ruled out when *Masamune* et al.[173c] found four bands below 2000 cm^{-1}, i.e. one more than allowed for D_{4h} symmetry. Calculations[169,176,177] support the now accepted D_{2h} symmetry.

The two lines at the highest frequency (>3000 cm^{-1}) are expectedly due to the C–H stretching vibrations. They were not recorded by *Masamune*. However, bands are observable in this region (3105, 3073 cm^{-1}) on irradiation of tricyclopentanone **26** in argon.[135] The difference spectrum (Fig. 6, see over) shows the IR spectrum of cyclobutadiene (**29**) in the upper half, and in the lower half that of its photolysis products (much acetylene (**86**) and traces of vinylacetylene (**90**)). Provided that the bands at 3105 and 3073 cm^{-1} are due to the two expected fundamental vibrations, at least six of the seven bands expected for D_{2h} symmetry are discernible in the spectrum of **29** (a seventh band at 1028 cm^{-1} is too weak for an unambiguous assignment; it would, however, correspond to the required sev-

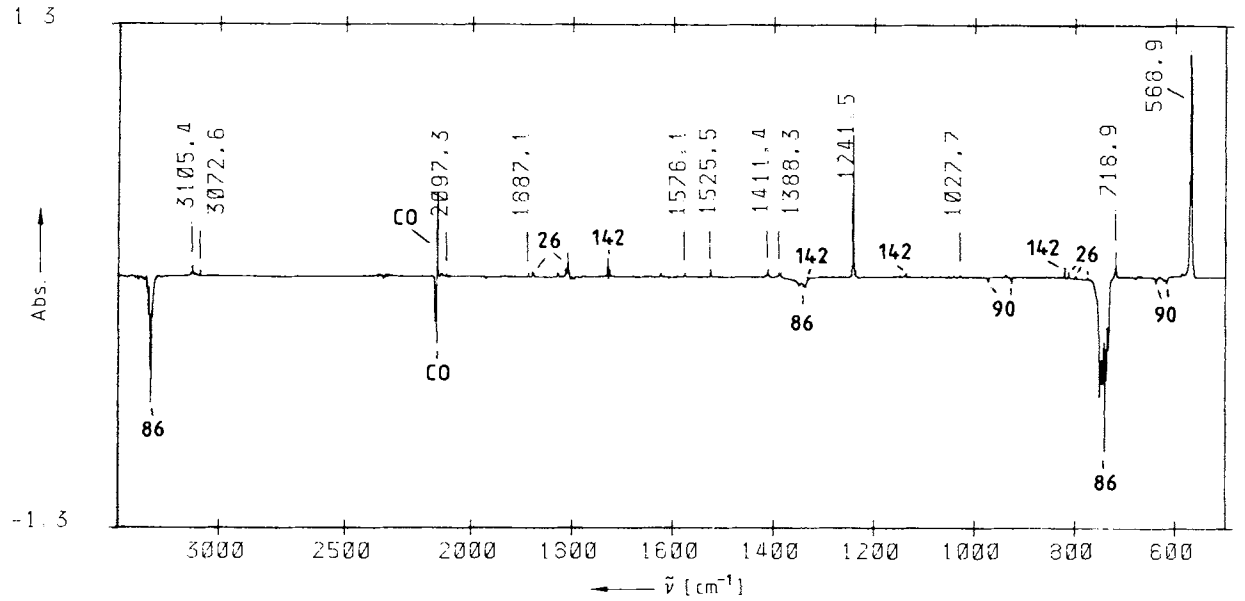

Fig. 6. IR subtraction spectra (Ar matrix, 12 K; irradiated **26** minus irradiated **29**) of cyclobutadiene (**29**) (upper part; 3.5 h irradiation of **26**, $\lambda = 254$ nm) and its photoproducts (lower part, after 3 h additional irradiation of **29** at $\lambda = 250$–420 nm).

enth absorption band at 1081 cm^{-1} (Table 2). Very weak additional absorptions at 2098, 1887, 1576, 1411, 1388, and 1386 cm^{-1} are presumably combination bands).

Table 2 demonstrates the good agreement between the measured spectrum and that calculated by *Hess* and *Schaad*[177c] for a rectangular geometry (Fig. 7).

Table 2. Comparison of experimental [135] and calculated [177c] IR spectrum of D_{2h}-cyclobutadiene [cm^{-1}] (E, relative intensity).

Assignment		Calculated		Experimental	
B_{1u}	ν(CH)	3299	(14.4)	3105	(4.2)
B_{2u}	ν(CH)	3279	(6.8)	3073	(1.7)
B_{1u}	ν(C=C)	1619	(1.0)	1526	(1.2)
B_{2u}	$\delta i.p.$(CH)	1293	(24.4)	1242	(25.1)
B_{1u}	$\delta i.p.$(CH)	1081	(0.6)	1028	(0.6)
B_{2u}	δ(Ring)	750	(4.4)	719	(5.7)
B_{3u}	$\delta o.o.p.$(CH)	560	(100)	569	(100)

The last flaw has also been eliminated in the meanwhile: according to the IR spectrum, *Chapman*[171b] had obtained but a single cyclobutadiene from two positionally isomeric deuterated photo-α-pyrones; the two valence isomers [D_2]-**29** and [D_2]-**29′** would have been expected for a rectangular structure. Hence it was concluded that cyclobutadiene was square. However, a comparison with the spectra calculated by *Hess*, *Schaad* et al.[169,177,178] demonstrates that here, too, an equilibrium mixture of the rectangular 1,2-D_2 and 1,4-D_2 isomers was actually present. The fact that both species were formed each time could be due to photoequilibration already in the precursors.[172d] At any rate, *Chapman* had the two valence isomeric rectangular forms of the cyclobutadiene present in his experiment already in 1973 without noticing it.

The UV spectrum of cyclobutadiene is more problematic. The handicap here is the low extinction of the expected band. We have tried several times but without success to ascertain the validity of the maximum at ca. 300 nm ($\varepsilon \leq 100$) postulated by *Masamune* et al.[173] and previously by ourselves.[174a] The band is not unequivocally documented.[157] Perhaps the inconsistencies are due to the fact that this extremely weak band is seen only in the difference spectrum,[173a] and not in the direct measurement.[135,157]

The weak band in question (300 nm; 4.13 eV) would be in good agreement with theory, which requires a forbidden transition between 338 nm (3.67 eV) and 358 nm (3.46 eV) as the longest-wavelength UV absorption band of the rectangular singlet cyclobutadiene.[179] Evidence for a relatively long-wavelength absorption of **29** is also given by the fact that cyclobutadiene is cleaved into two molecules of acetylene much faster using low energy light (Hg high-pressure lamp; range $\lambda = 250$–420 nm) than with short wavelength irradiation (Hg low-pressure lamp; $\lambda = 254$ nm; see caption to Fig. 6). Further support is given by a comparison of the UV spectra of cyclobutadienes and the "isoelectronic" cyclopentadienones: in analogy to other substituted cyclopentadienones,[180] the tetra-*tert*-butyl derivative **9** absorbs at a very long wavelength (420 nm; $\varepsilon = 186$).[18c] The corresponding cyclobutadiene **12** absorbs at 425 nm ($\varepsilon = 38$),[18c] again in agreement with other cyclobutadiene derivatives.[8c] Due to the easily polarizable π system in both classes of compounds, a hypsochromic shift is expected for the unsubstituted parent systems. In accordance with this, cyclopentadienone features a maximum at 360 nm.[181] Accordingly, a similar value is expected for cyclobutadiene (**29**).

If cyclobutadiene forms matrix "complexes" such as **129** and **130** already with CO_2 and CO,[182] particularly drastic effects must be brought about by partners that can engender a stabilizing electronic interaction. In fact, phthalic anhydride gives a yellow charge transfer complex **131** with an absorption maximum at 375 nm ($\varepsilon \approx 500$) due to interaction with **29** in either organic or argon matrices.[174b]

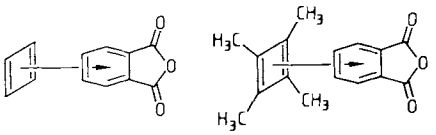

131 132

The donor-acceptor influence is even more distinct in the tetramethylcyclobutadiene complex **132**, which absorbs at 495 nm in an organic matrix,[183] and at 525 nm in argon.[184] Hence, the donor property of cyclobutadiene can be exploited in the spectroscopic identification. For example, the appearance of the complex **132** in the photocleavage of a precursor expected to yield tetramethyltetrahedrane[10d, 184] quickly destroyed that hope.

As already mentioned in Section 3.2, the photoelectron spectrum of **29** was recently recorded by *Schweig* et al.[163] The lowest vertical ionization potential is 8.24 eV, in ideal agreement with the previous indirectly determined value of 8.29 eV[185] as well as the ionization energies of substituted cyclobutadienes.[26, 186] Because the observed band is relatively sharp, whereas a square radical **32** should show first order Jahn-Teller splitting, the authors consider the appearance of the PE spectrum an independent proof for the rectangular geometry of the cyclobutadiene ring.

Thus, all information speaks for a rectangular singlet ground state of cyclobutadiene **29**. The following structural data, used in the calculation of the IR spectrum,[177c] should be rather close to reality.

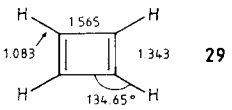

29

Fig. 7. Bond lengths [Å] and angles [°] in cyclobutadiene **29** [177c].

Difficulties with the theoretical treatment of cyclobutadiene[8c] have also been removed in the meanwhile. The outcome is decidedly dependent on whether or not configuration interaction is taken into account. When it is, the singlet turns out to be favored over the triplet species, even in the case of square geometry.[187] The preference of the rectangular vis-a-vis the square arrangement of singlet cyclobutadiene is due to mixing of energetically close states (pseudo Jahn-Teller or second order Jahn-Teller effect).[8c, 188] The quintessence is: a square geometry is a minimum for triplet cyclobutadiene, but it is a transition state for the interconversion of two degenerate and rectangular singlet ground states on the singlet energy hypersurface (Fig. 8).

According to the most recent calculations, the barrier height for automerization is about 10 kcal mol^{-1} (MINDO/3: 8.1;[189] ab initio: 8.3,[190] 9.0,[179c] 9.0,[191] 13.4[188]). A similar value is also given for the difference between SS and ST cyclobutadiene (8.6,[188] 11.0,[191] 14.1[190] kcal mol^{-1}). Incidentally, a rhombohedral transition state for the RS,RS equilibration is less favorable[8c, 190, 191] than the square. Likewise, folding of RS-cyclobutadiene does not cause any gain in energy.[192, 193] Accordingly, the non-planar structure of the cyclobutadiene **12** is caused by steric repulsion between the *tert*-butyl groups. The further effect

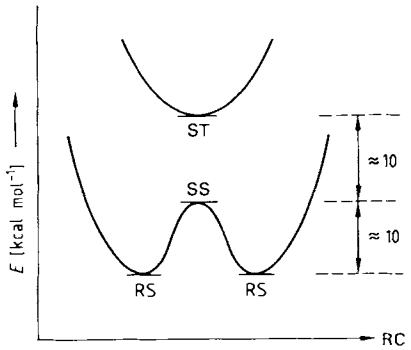

Fig. 8. Reaction diagram for interconversion of two rectangular cyclobutadienes. RS = rectangular singlet; SS = square singlet; ST = square triplet molecule.

of the four sterically demanding groups, viz. the increased similarity of the bond lengths,[39, 44, 46] was discussed in Section 2.2. However, the accumulation of four voluminous substituents not only favors the tetrahedrane **2** relative to **12**, it also favors SS-**12** relative to RS-**12**. According to force field calculations by *Mislow* et al.,[64, 187] this effect is approximately equal to the RS, SS difference in unsubstituted cyclobutadiene. Therefore, it would be completely understandable if the parent compound **29** (Fig. 7) were to show a stronger alternation than the tetra-*tert*-butyl derivative **12** (Fig. 3). A further consequence is that the rate of valence isomerization and the size of the HOMO-LUMO gap will be smaller in **12** than in cyclobutadiene itself.

The high reactivity of cyclobutadiene (**29**) is often associated with its "antiaromaticity". It is difficult enough to clearly define the concept of "aromaticity",[194] and this is even more true of the determination of "antiaromaticity".[8c, 193, 195] Yet, the heuristic value of this notation cannot be denied, regardless which point of reference is used (cf. the different definitions by *Hückel*, *Dewar*, *Hess*, and *Schaad*, or *Hadden*, *Herndon*, *Trinajstic*, *Aihara*, *Randić*, and others[8b, c, 196]). The division of the "excess energy" of cyclobutadiene into two entities, namely strain energy and electronic destabilization[197, 198] is also informative. The former accounts for about 40%, the latter for 60% (e.g. the heat of formation of cyclobutadiene (Scheme 1) is composed of a strain energy of 24, and an "antiaromaticity" of 35 kcal mol^{-1}[198]). While the starting material already has a high energy content, the ready dimerization of **29** to give the *syn*-tricyclic compound (**78** without *tert*-butyl groups) is facilitated by virtue of the orbital symmetry-allowed [4+2]-cycloaddition. The preference for the *syn*-transition state is due to a secondary orbital interaction.[88a]

Thus, we have a feeling for the nature of the peculiarities of the cyclobutadiene system. The molecule has by no means lost its fascination for the theoreticians, however.[199]

The discussion of the unsubstituted cyclobutadiene will be terminated with the work of *Carpenter* et al.,[129] who in elegant kinetic studies determined the activation parameters for the valence isomerization [D_2]-**29** ⇄ [D_2]-**29**′. The cyclobutadiene is generated by thermal [4+2]-cycloreversion from 1,4-dideuterio-2,3-diazobicyclo[2.2.0]hexa-2,5-diene ([D_2]-**128**) and trapped with 3-cyanoacrylic ester in a Diels-Alder reaction. The concentration- and temperature-

dependence of the products lead to an activation enthalpy for the valence isomerization [D$_2$]-**29** $\rightleftarrows$ [D$_2$]-**29**′ between 1.6 and 10 kcal mol^{-1} (the "classical" barrier for the RS$\rightleftarrows$SS$\rightleftarrows$RS process is 8.1–13.4 kcal mol^{-1}; see above]. Furthermore, the activation entropy so obtained is strongly negative (-17 to -32 cal mol^{-1} K^{-1}). On the basis of

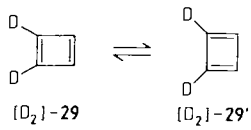

these parameters, *Carpenter*[129c] postulates that the automerization of cyclobutadiene is dominated by tunneling of the CH units. This process is believed to account for 97% of the total rate below 0°C. The demonstration of such a heavy-atom tunneling is of general importance. Scepticism about the ability of the large methine units in cyclobutadiene to tunnel has been largely removed,[189,200] if not completely so,[201] by theoretical calculations. It cannot be ruled out that tunneling of carbon atoms may play a role in other bond migrations such as in cyclooctatetraene[129c] and the unsubstituted norbornyl cation.[202]

4.2. Cyclobutadiene Dications and Dianions

In contrast to the electroneutral cyclobutadiene (**29**) (and the radical cation **32** and radical anion **134**), its dication **133** and dianion **135** should be "aromatic" according to the Hückel rule. Yet, elaborate calculations indicate that

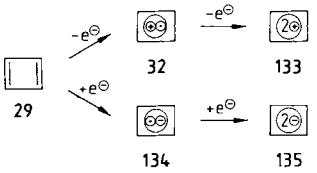

both **133**[197c,203,204] and **135**[203b,204,205] should be regarded as non-aromatic because of destabilizing 1,3-interactions. In other words, the stabilization due to cyclic delocalization is not sufficient in these doubly charged systems. Accordingly, the Hückel-type D_{4h} geometry is not to be expected. Calculations by *Schleyer* et al.[203a] indicate that the dication is folded (**133**′, D_{2d} symmetry); for the dianion a

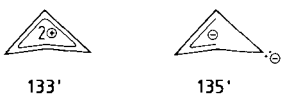

square geometry is predicted by ab initio calculations,[204,205] but an additional vibrational analysis demonstrated that the minimum is occupied by the C_s conformation **135**′,[204] which is composed of an allyl anion and a localized negative charge.

For these reasons it is understandable why the unsubstituted dication **133** has not so far been detected. The hope to generate a stable dication **136** from the hydroxy salt **37** in magic acid was not fulfilled. Presumably, **136** is formed as an intermediate but rearranges immediately to the ring-expanded dication **137**.[76] It is reasonable that a series of Wagner–Meerwein rearrangements takes preference over a cleavage into two acetylene fragments—another potential stabilizing reaction for cyclobutadiene dications.[206]

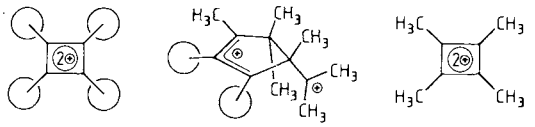

In contrast, the tetrakis(dimethylamino) derivative is a stable substance.[207b] But even alkyl groups suffice, in principle, to delocalize the positive charge. Thus, *Olah* et al.[207a] succeeded in the unambiguous identification of tetramethylcyclobutadiene dication (**138**). Folding is expected for this species too.[203a] Unfortunately, the NMR spectra allow no decision on this question. Therefore, information about the exact structure of cyclobutadiene dication is still lacking. The isolable tetrakis(dimethylamino) derivative is not a good reference substance since its charges are essentially delocalized in the substituents.[207b]

An alkyl group does not help in the case of cyclobutadiene dianions.[208] Therefore, the dianion **135** and its alkyl derivatives are unknown. In agreement with this, the cyclovoltammetric investigation[74] of tetra-*tert*-butylcyclobutadiene (**12**) gave no indication of either the dication **136** or the dianion **139**, which is also not accessible by deprotonation of the corresponding monoanion.[109b]

However, *Garratt* et al.[209] successfully used ester groups to delocalize the negative charge so extensively that the dianion **140** was stable at room temperature.

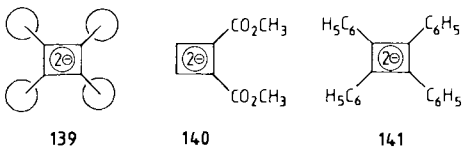

According to the authors, only 40% of the negative charge in **140** remains in the four-membered ring. pK_a measurements indicate that the dianion does not experience any "aromatic" stabilization. The same applies to the tetraphenylcyclobutadienediide **141** synthesized by *Boche* et al.[210] Again, the charge resides predominantly (64%) on the phenyl groups. This is true also for the dication.[207a] The destabilizing electron repulsion in the dianion compensates for any energy gain expected for a closed (4n + 2) π-electron system.

4.3. Cyclopentadienone

The relationship between cyclobutadiene and cyclopentadienone was pointed out in the previous review.[8b] Meanwhile, the secrets of this ring system have also been explored.[133,180,181] The unsubstituted cyclopentadienone (**142**) can be prepared from a multitude of precursors (**26**,

92, **111**, **119**, **120**, **124**, **143**–**150**). The molecule is stable in an argon matrix and behaves in the ground state like its derivatives as a normal α,β-unsaturated ketone (PE, NMR,

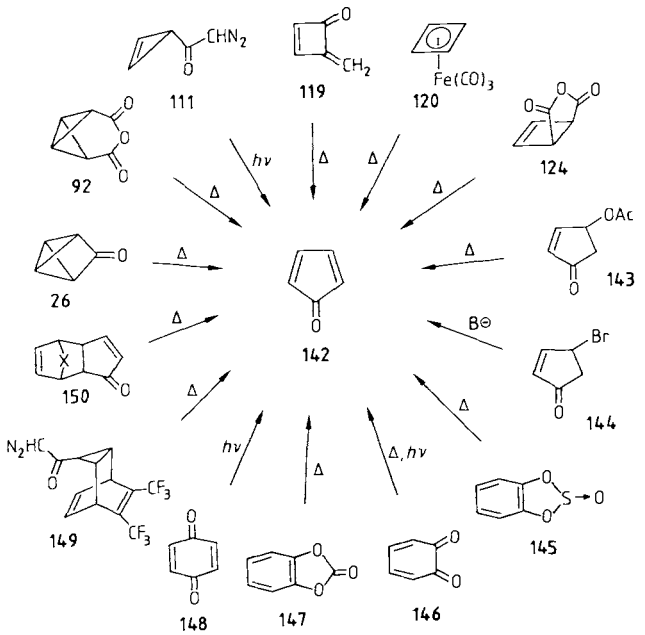

IR spectra; dipole moment; bond alternation). The resonance structures with a cyclopentadienyl cation, or a "wrongly" polarized C=O double bond hardly contribute. The unusual properties gleaned from the UV-spectra, redox behavior, and Diels–Alder reactivity are due to a strongly delocalized and hence low-lying LUMO.[211]

5. Outlook

A proof for the existence of the unsubstituted tetrahedrane (**1**) and the synthesis of modified derivatives of tetra-*tert*-butyltetrahedrane **2** are still challenges.

Heterocyclobutadienes and tetrahedranes will experience increasing importance in the future. There is a whole range of possibilities between the $(HC)_4$ cluster **1** and the tetrahedral structure of white phosphorus.[212] The preparation of tri-*tert*-butylazacyclobutadiene (**151**) by *Regitz* et al.[213] is a first success. Monosila-[214a] and tetrasila-deriva-

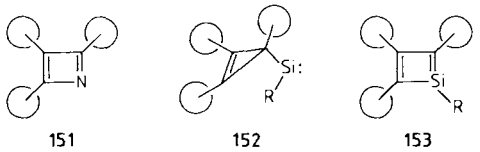

151 152 153

tives[214b,c] are further exciting targets. In this connection a rewarding object of study is silylene (silanediyl) **152**.[215] Every possible stabilization reaction is interesting, whether it is the ring-expansion to the silacyclobutadiene **153**, the ring-closure to the corresponding silatetrahedrane, or the cleavage with formation of a silaacetylene.[216]

Likewise, it is not difficult to predict future activities regarding the unsubstituted C_4H_4 systems. *Dewar* et al.[52] located no less than 19, and *Hehre* and *Pople*[35] ten minima on the singlet C_4H_4 hypersurface (Scheme 1 only represents a small selection). Only four (**29**, **88**, **89**, **90**) are known today. The race for new exotic molecules will not be slow in coming, or to put it better, is already underway: upon photochemical elimination of CO from vinylpropadienone[152] one presumably obtains butadienylidene **154**, a "suppressed" C_4H_4 isomer in the global treatment.[52] The direct detection of **154** is very difficult since it immediately transforms into vinylacetylene **90** under the conditions employed. There is already some information about cyclobutenylidene (**155**). *Shevlin* et al.[217] attempted to prepare this species by reaction of cyclobutenone with atomic carbon but isolated only vinylacetylene (**90**). This was probably formed by ring cleavage of **155**. According to MINDO/3 calculations, the cleavage is faster than both ring contraction to methylenecyclopropene (**88**) and CH-insertion to give cyclobutadiene (**29**). It may be, however, that **155** is only a transition state for the ring inversion in bicyclo[1.1.0]but-1-ene (**156**). According to *Dewar* et al.,[52] the latter is one of the lowest energy minima of the 19 calculated. Thus, the matrix isolation of **156** is a logical experiment. The same is true for bicyclo[1.1.0]but-1(3)-ene (**157**) and cyclobutyne (**158**).

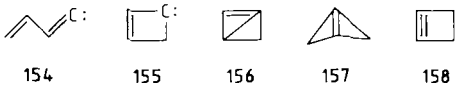

154 155 156 157 158

Bicyclobutene **157** is expected to have a folded structure. Its IR-spectrum has been calculated.[63] Impressive experiments by *Szeimies* et al.[218a] have already demonstrated the existence of bridged derivatives of **157**. Unfortunately, no bicyclobutenes are formed in the absence of the bridge. Only butatrienes or vinylacetylenes are detectable in such cases.[218b] The theoretical IR-spectrum of cyclobutyne (**158**) is also available.[219] The likelihood of isolating **158** is somewhat remote, however. The compound is higher in energy than tetrahedrane.[63] Perhaps it is not a minimum on the energy hypersurface at all.[52]

Two final examples will illustrate that there are always practical or theoretical facets worth investigating. It is synthetically attractive to have good access to the polyfunctional cyclobutadiene **159**, the intermediacy of which has been demonstrated previously by *Scharf* et al.[220] The treatment of 1,2-dibromocyclobutane-1,2,3,4-tetracarboxylic acid ester with potassium *tert*-butoxide at −78 °C gave the anion **160**, which on warming to room temperature gave very good yields of products (e.g. Diels–Alder adducts) formally derived from **159**.[221] On the theoretical side, one may ask how a square structure may be forced upon a cyclobutadiene. The simplest possible and hitherto "forgotten" circulene **161** could be such a molecule.[222,223] According to the method proposed by *Hess* and *Schaad*[197]

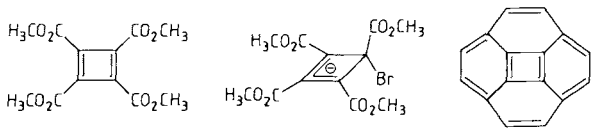

159 160 161

calculations give a molecule with D_{4h} symmetry and a resonance energy per electron (REPE) of 0.028 β.[135] Perhaps the synthesis[224] of **161** will be successful in spite of the considerable angular strain expected for this molecule.

6. Conclusion

Our present knowledge about cyclobutadiene (**29**) allows this chapter to be terminated. It is now secured textbook material.

Nobody knows whether the unsubstituted tetrahedrane (**1**) can ever be synthesized. It is easy, however, to answer the question posed in the preamble: the excitement caused by an unusual molecule such as the tetrahedrane **2** does not end with its mere synthesis. The real importance lies in the new fundamental knowledge obtainable from working with such rarities.

The study of tetra-*tert*-butyltetrahedrane has a) sharpened our feeling for the subtle influence of sterically demanding groups (favoring of otherwise impracticable synthetic routes; reversal of thermodynamic stabilities), b) led to broadly applicable concepts (corset principle, silyl-trick, formation of radical ion pairs), c) opened up access to several unknown or at least difficultly accessible classes of substances, d) allowed the isolation of crystalline derivatives of highly reactive systems, e) caused X-ray investigations with surprising results (extremely bent bonds, dependency of alternation on degree of substitution, gas inclusion compounds, structural indicators of "homoaromatic" character), f) allowed detailed insight into the behavior of radical cations, and g) made the discovery of new reaction mechanisms possible (in addition reactions, autoxidation, and cationic rearrangements). The molecules **2** and **12** have delivered non-stop record values of physical data (NMR, ionization potentials, redox potentials etc.).

Having successfully prepared the highly strained tetrahedrane **2**, any shyness toward other sterically loaded molecules disappears.[225,226] The synthetic building blocks designed for **1** and **2** (geminal diperoxy esters, lithiated diazoalkanes, etc.) may also become important in other areas of research. Finally, the work with tetrahedrane required extensive use of matrix isolation techniques in combination with photolytic and flash thermolytic fragmentations. The skills thus acquired encouraged us to transfer the methodology to many other fields, ranging from unsaturated silicon[227] and boron[228] compounds to radicals,[229] carbenes,[153] new isomers of polyhalomethanes,[230] and interstellar molecules.[231] These simple molecules open another aspect: they are small enough to allow "reliable" predictions to be made with modern computational methods and thus offer an ideal opportunity to test the quality of theoretical calculations by experimentation.[135,151,153] In brief, an originally very specific and for many outsiders "irrelevant" quest has led to many fields previously totally unknown to us and far from the primary goal. Hence, it pays off to "seek the adventure, without which science as well as life would be insipid" (*R. Criegee*).[232]

The results reported from our own research group are due to the efforts of a series of risk-taking and motivated coworkers. Their names are given in the appropriate references. I am indebted to them, as also to the Fonds der Chemischen Industrie and the Deutsche Forschungsgemeinschaft for financial support.

Received: February 2, 1987;
revised: January 4, 1988 [A 659 IE]
German version: *Angew. Chem. 100* (1988) 317
Translated by Dr. *Edeline Wentrup-Byrne*, Brisbane (Australia)

[1] Review covering the tetrahedrane problem: N. S. Zefirov, A. S. Koz'min, A. V. Abramenkov, *Russ. Chem. Rev. (Engl. Transl.) 47* (1978) 163. This review also mentions the alleged preparation of tetrahedrane.

[2] Platon: *Timaios*.

[3] W. Grahn, *Chem. Unserer Zeit 15* (1981) 52.

[4] H. P. Schultz, *J. Org. Chem. 30* (1965) 1361.

[5] a) P. E. Eaton, T. W. Cole, Jr., *J. Am. Chem. Soc. 86* (1964) 962, 3157; b) summary: P. E. Eaton, *Tetrahedron 35* (1979) 2189.

[6] a) R. J. Ternansky, D. W. Balogh, L. A. Paquette, *J. Am. Chem. Soc. 104* (1982) 4503; b) L. A. Paquette, R. J. Ternansky, D. W. Balogh, G. Kentgen, *ibid. 105* (1983) 5446; c) summary: L. A. Paquette, *Top. Curr. Chem. 119* (1984) 1; d) Pagodane route to dodecahedrane according to *Prinzbach*: W.-D. Fessner, B. A. R. C. Murty, J. Wörth, D. Hunkler, H. Fritz, H. Prinzbach, W. D. Roth, P. von R. Schleyer, A. B. McEwen, W. F. Maier, *Angew. Chem. 99* (1987) 484; *Angew. Chem. Int. Ed. Engl. 26* (1987) 452.

[7] If the synthesis of dodecahedrane has been compared with the first ascent of Mount Everest, the air is not thinner in the case of tetrahedrane, more so in terms of the high energy content than the number of synthetic steps.

[8] a) Earlier summaries: M. R. Cava, M. J. Mitchell: *Cyclobutadiene and Related Compounds*, Academic Press, New York 1967; b) G. Maier, *Angew. Chem. 86* (1974) 491; *Angew. Chem. Int. Ed. Engl. 13* (1974) 425; c) T. Bally, S. Masamune, *Tetrahedron 36* (1980) 343; d) D. Lloyd: *Non-benzenoid Conjugated Carbocyclic Compounds*, Elsevier, Amsterdam 1984, p. 197-244. – Note: cyclobutadiene complexes and annelated systems are not discussed in the present paper.

[9] E. H. White, R. E. K. Winter, R. Graeve, U. Zirngibl, E. W. Friend, H. Maskill, U. Mende, G. Kreiling, H. P. Reisenauer, G. Maier, *Chem. Ber. 114* (1981) 3906.

[10] a) G. Maier, H. P. Reisenauer, H.-A. Freitag, *Tetrahedron Lett. 1978*, 121; b) G. Maier, H. P. Reisenauer, *Chem. Ber. 114* (1981) 3916; c) G. Maier, M. Schneider, G. Kreiling, W. Mayer, *ibid. 114* (1981) 3922; d) G. Maier, W. Mayer, H.-A. Freitag, H. P. Reisenauer, R. Askani, *ibid. 114* (1981) 3935; e) G. Maier, H. P. Reisenauer, *ibid. 114* (1981) 3956.

[11] G. Maier, A. Alzérreca, *Angew. Chem. 85* (1973) 1056; *Angew. Chem. Int. Ed. Engl. 12* (1973) 1015.

[12] **6** was obtained independently and simultaneously by *Masamune* et al. using another route: S. Masamune, N. Nakamura, M. Suda, H. Ona, *J. Am. Chem. Soc. 95* (1973) 8481.

[13] G. Maier, F. Bosslet, *Tetrahedron Lett. 1972*, 1025.

[14] G. Maier, U. Schäfer, W. Sauer, H. Hartan, R. Matusch, J. F. M. Oth, *Tetrahedron Lett. 1978*, 1837.

[15] W. Sauer, *Dissertation*, Universität Marburg 1977.

[16] H.-G. Hartan, *Dissertation*, Universität Marburg 1976.

[17] A. Schweig, W. Thiel, *J. Comput. Chem. 1* (1980) 129.

[18] a) G. Maier, S. Pfriem, *Angew. Chem. 90* (1978) 551; *Angew. Chem. Int. Ed. Engl. 17* (1978) 519; b) G. Maier, S. Pfriem, U. Schäfer, R. Matusch, *ibid. 90* (1978) 552 and *17* (1978) 520; c) G. Maier, S. Pfriem, U. Schäfer, K.-D. Malsch, R. Matusch, *Chem. Ber. 114* (1981) 3965.

[19] a) Almost simultaneously with the synthesis of **2** the preparation of an alleged tetralithiotetrahedrane was reported: G. Rauscher, T. Clark, D. Poppinger, P. von R. Schleyer, *Angew. Chem. 90* (1978) 306; *Angew. Chem. Int. Ed. Engl. 17* (1978) 276. A structural proof is still lacking (lithium atoms are presumed to be arranged above the planes of the carbon tetrahedron). Review of unusual structures of lithium compounds: P. von R. Schleyer, *Pure Appl. Chem. 56* (1984) 151. b) More recently it has been questioned whether the assumed structure represents an energy minimum at all: J. P. Ritchie, *J. Am. Chem. Soc. 105* (1983) 2083; R. L. Disch, J. M. Schulmann, J. P. Ritchie, *ibid. 106* (1984) 6246. c) More elaborate calculations (K. Raghavachari, P. von R. Schleyer) confirm the T_d symmetry of Li_4C_4 (see footnote [12] in H. G. von Schnering, M. Schwarz, R. Nesper, *Angew. Chem. 98* (1986) 558; *Angew. Chem. Int. Ed. Engl. 25* (1986) 566). d) Tetralithiotetrahedrane has been reported to give tetramethyltetrahedrane with methyl iodide: N. S. Zefirov, V. N. Kirin, N. M. Yur'eva, A. S. Koz'min, N. S. Kulikov, Y. N. Luzikov, *Tetrahedron Lett. 1979*, 1925. This is incorrect (N. S. Zefirov, private communication).

[20] a) G. Maier, K. A. Reuter, L. Franz, H. P. Reisenauer, *Tetrahedron Lett. 26* (1985) 1845; b) L. H. Franz, *Dissertation*, Universität Giessen 1982.

[21] R. Boese, unpublished. We are indebted to Dr. *Boese*, Universität Essen, for these structural investigations.

[22] W. Thiel, unpublished. We thank Prof. *Thiel*, Universität Wuppertal, for these data (private communication).

[23] Cf. [8c], footnote 58. In [8c], Scheme 10, the arrow should start from **22a** instead of **22b**.

[24] A chemical shift of $\delta = -15.9$ is calculated for tetrahedrane **1**: M. Schindler, W. Kutzelnigg, *J. Am. Chem. Soc. 105* (1983) 1360; application of a low-field shift of 25 ppm due to the *tert*-butyl groups gives a value of $\delta \approx 9$ for **2**. For the calculation of shielding tensors, see also J. C. Facelli, A. M. Orendt, M. S. Solum, G. Depke, D. M. Grant, J. Michl, *ibid. 108* (1986) 4268.

[25] Summary of the spectroscopic properties of **2**: G. Maier, S. Pfriem, K.-D. Malsch, H.-O. Kalinowski, K. Dehnicke, *Chem. Ber. 114* (1981) 3988.

[26] E. Heilbronner, T.-B. Jones, A. Krebs, G. Maier, K.-D. Malsch, J. Pocklington, A. Schmelzer, *J. Am. Chem. Soc. 102* (1980) 564.

[27] M. Saunders, G. E. Walter, unpublished; G. E. Walter, *Dissertation*, Yale University 1983.

[28] T. Loerzer, *Dissertation*, Universität Göttingen 1983.

[29] T. Loerzer, R. Machinek, W. Lüttke, L. H. Franz, K.-D. Malsch, G. Maier, *Angew. Chem. 95* (1983) 914; *Angew. Chem. Int. Ed. Engl. 22* (1983) 878.

[30] J. M. Schulman, T. J. Venanzi, *J. Am. Chem. Soc. 96* (1974) 4739.

[31] The NMR coupling constants for **1** given in [30] should be $^1J_{CC} = 14.5$, $^1J_{CH} = 273$ Hz, according to another calculation (Coupled Hartree-Fock Perturbation Theory; J. M. Schulman, private communication, 1978).

[32] K. Kovačevič, Z. B. Maksič, *J. Org. Chem. 39* (1974) 539.

[33] H. Irngartinger, A. Goldmann, R. Jahn, M. Nixdorf, H. Rodewald, G. Maier, K.-D. Malsch, R. Emrich, *Angew. Chem. 96* (1984) 967; *Angew. Chem. Int. Ed. Engl. 23* (1984) 993.

[34] H. Irngartinger, R. Jahn, G. Maier, R. Emrich, *Angew. Chem. 99* (1987) 356; *Angew. Chem. Int. Ed. Engl. 26* (1987) 356.

[35] W. J. Hehre, J. A. Pople, *J. Am. Chem. Soc. 97* (1975) 6941.

[36] A. Schweig, W. Thiel, *J. Am. Chem. Soc. 101* (1979) 4742.

[37] H. Kollmar, *J. Am. Chem. Soc. 102* (1980) 2617.

[38] W. D. Hounshell, K. Mislow, *Tetrahedron Lett. 1979*, 1205.

[39] H. Irngartinger, N. Riegler, K.-D. Malsch, K.-A. Schneider, G. Maier, *Angew. Chem. 92* (1980) 214; *Angew. Chem. Int. Ed. Engl. 19* (1980) 211.

[40] H. Kimling, A. Krebs, *Angew. Chem. 84* (1972) 952; *Angew. Chem. Int. Ed. Engl. 11* (1972) 932; A. Krebs, H. Kimling, R. Kemper, *Liebigs Ann. Chem. 1978*, 431; see also [43].

[41] L. T. J. Delbaere, M. N. G. James, N. Nakamura, S. Masamune, *J. Am. Chem. Soc. 97* (1975) 1973.

[42] H. Irngartinger, H. Rodewald, *Angew. Chem. 86* (1974) 783; *Angew. Chem. Int. Ed. Engl. 13* (1974) 740; see also [39].

[43] H. Irngartinger, M. Nixdorf, N. H. Riegler, A. Krebs, G. Maier, K.-D. Malsch, K. A. Schneider, *Chem. Ber.*, in press.

[44] W. T. Borden, E. R. Davidson, *J. Am. Chem. Soc. 102* (1980) 7958.

[45] O. Ermer, E. Heilbronner, *Angew. Chem. 95* (1983) 414; *Angew. Chem. Int. Ed. Engl. 22* (1983) 402.

[46] a) H. Irngartinger, M. Nixdorf, *Angew. Chem. 95* (1983) 415; *Angew. Chem. Int. Ed. Engl. 22* (1983) 403; b) *Chem. Ber.*, in press; c) J. D. Dunitz, C. Krüger, H. Irngartinger, M. F. Maverick, Y. Wang, M. Nixdorf, *Angew. Chem. 100* (1988) 415; *Angew. Chem. Int. Ed. Engl. 27* (1988) 387.

[47] Drawing program SCHAKAL: E. Keller, *Chem. Unserer Zeit 14* (1980) 56; *20* (1986) 178; we thank Dr. *Keller* for providing us with Figure 4.

[48] a) A. Baeyer, *Ber. Dtsch. Chem. Ges. 18* (1885) 2269; summaries: b) R. Huisgen, *Angew. Chem. 98* (1986) 297; *Angew. Chem. Int. Ed. Engl. 25* (1986) 297; c) K. B. Wiberg, *ibid. 98* (1986) 312 and *25* (1986) 312; see also: d) A. Greenberg, J. F. Liebman: *Strained Organic Molecules*, Academic Press, New York 1978.

[49] a) N. C. Baird, M. J. S. Dewar, *J. Am. Chem. Soc. 89* (1967) 3966; b) N. C. Baird, *Tetrahedron 26* (1970) 2185.

[50] I. J. Miller, *Tetrahedron 25* (1969) 1349.

[51] A. B. Bolotin, V. A. Bolotin, J. Sulskus, S. S. Yarovoi, *Zh. Strukt. Khim. 25* (1984) 161; *Chem. Abstr. 101* (1984) 170253f.

[52] J. Kollmar, F. Carrion, M. J. S. Dewar, R. C. Bingham, *J. Am. Chem. Soc. 103* (1981) 5292.

[53] a) K. B. Wiberg, *J. Comput. Chem. 5* (1984) 197; b) K. B. Wiberg, R. F. W. Bader, C. D. H. Lau, *J. Am. Chem. Soc. 109* (1987) 985, 1001.

[54] B. A. Hess, Jr., L. J. Schaad, *J. Am. Chem. Soc. 107* (1985) 865.

[55] R. L. Disch, J. M. Schulman, M. L. Sabio, *J. Am. Chem. Soc. 107* (1985) 1904.

[56] M. Månsson, unpublished. - We thank Dr. *Månsson*, Universität Lund (Sweden), for carrying out the calorimetric measurements.

[57] C. Rüchardt, H.-D. Beckhaus, B. Dogan unpublished. We also thank the group in Freiburg for the determination of the heat of sublimation.

[58] P. von R. Schleyer, J. E. Williams, K. R. Blanchard, *J. Am. Chem. Soc. 92* (1970) 2377.

[59] According to force field calculations the strain energy of **2** is only 33 kJ mol^{-1} (7.9 kcal mol^{-1}) higher than that of **1** (C. Rüchardt, H.-D. Beckhaus, private communication).

[60] The strain is also greater than in [1.1.1]propellane, in which it is 14 kcal mol^{-1} per ring bond [48c, 61].

[61] M. D. Newton, J. M. Schulman, *J. Am. Chem. Soc. 94* (1972) 773.

[62] R. J. Buenker, S. D. Peyerimhoff, *J. Am. Chem. Soc. 91* (1969) 4342.

[63] B. A. Hess, Jr., W. D. Allen, D. Michalska, L. J. Schaad, H. F. Schaefer III, *J. Am. Chem. Soc. 109* (1987) 1615; see also: B. A. Hess, Jr., D. Michalska, L. J. Schaad, *ibid. 109* (1987) 7546.

[64] a) K. Mislow, W. D. Hounshell, private communication, March 1978; b) cited in [187].

[65] M. C. Böhm, R. Gleiter, *Tetrahedron Lett. 1978*, 1179.

[66] a) H. Bock, B. Roth, G. Maier, *Angew. Chem. 92* (1980) 213; *Angew. Chem. Int. Ed. Engl. 19* (1980) 209; b) *Chem. Ber. 117* (1984) 172.

[67] Experiments by H. Schwarz, Technische Universität Berlin; already cited in [25]. We thank Prof. *Schwarz* for these measurements.

[68] a) Q. B. Broxterman, H. Hogeveen, P. M. Kok, *Tetrahedron Lett. 22* (1981) 173; b) Q. B. Broxterman, H. Hogeveen, *ibid. 24* (1983) 639.

[69] a) J. L. Courtneidge, A. G. Davies, J. Lusztyk, *J. Chem. Soc. Chem. Commun. 1983*, 893; b) J. L. Courtneidge, A. G. Davies, J. E. Parkin, *ibid. 1983*, 1262; c) J. L. Courtneidge, A. G. Davies, E. Lusztyk, J. Lusztyk, *J. Chem. Soc. Perkin Trans. 2 1984*, 155; d) J. L. Courtneidge, A. G. Davies, *Acc. Chem. Res. 20* (1987) 90.

[70] Q. B. Broxterman, H. Hogeveen, R. F. Kingma, *Tetrahedron Lett. 25* (1984) 2043.

[71] M. Chan, J. L. Courtneidge, A. G. Davies, J. C. Evans, A. G. Neville, C. C. Rowlands, *Tetrahedron Lett. 26* (1985) 4121.

[72] W. T. Borden, E. R. Davidson, D. Feller, *J. Am. Chem. Soc. 103* (1981) 5725.

[73] M. Shiotani, K. Ohta, Y. Nagata, J. Sohma, *J. Am. Chem. Soc. 107* (1985) 2562.

[74] M. A. Fox, K. A. Campbell, S. Hünig, H. Berneth, G. Maier, K.-A. Schneider, K.-D. Malsch, *J. Org. Chem. 47* (1982) 3408.

[75] The calculated barrier is also practically zero for the radical cations of the unsubstituted tetrahedrane **1** and cyclobutadiene **29** [74].

[76] R. Emrich, *Dissertation*, Universität Giessen 1986.

[77] Summaries: a) G. J. Kavarnos, N. J. Turro, *Chem. Rev. 86* (1986) 401; b) M. A. Fox, *Adv. Photochem. 13* (1986) 237; cf. also c) P. G. Gassman, B. A. Hay, *J. Am. Chem. Soc. 108* (1986) 4227; d) J. Mattay, *Angew. Chem. 99* (1987) 849; *Angew. Chem. Int. Ed. Engl. 26* (1987) 825.

[78] The experimental and largely unpublished details of the chemistry of **2** and **12** are given in the dissertations of *K.-D. Malsch* [79], *K. A. Schneider* [80] and *R. Emrich* [76].

[79] K.-D. Malsch, *Dissertation*, Universität Giessen 1982.

[80] K.-A. Schneider, *Dissertation*, Universität Giessen 1982.

[81] I. J. Miller, *Aust. J. Chem. 24* (1971) 2013.

[82] Holleman-Wiberg: *Lehrbuch der Anorganischen Chemie*, de Gruyter, Berlin 1985, p. 246.

[83] Reviews on $Ag^{\oplus}$-catalysis: a) L. A. Paquette, *Synthesis 1975*, 347; b) K. C. Bishop III, *Chem. Rev. 76* (1976) 461.

[84] G. Maier, R. Emrich, K.-D. Malsch, K.-A. Schneider, M. Nixdorf, H. Irngartinger, *Chem. Ber. 118* (1985) 2798.

[85] Reviews on the generation and reactions of radicalions: a) L. Eberson, *Adv. Phys. Org. Chem. 18* (1982) 79; b) O. Hammerich, V. D. Parker, *ibid. 20* (1984) 55; c) A. Pross, *Acc. Chem. Res. 18* (1985) 212; d) L. Eberson: *Electron Transfer Reactions in Organic Chemistry*, Springer, Berlin 1987.

[86] a) J. R. Miller, J. A. Peeples, M. J. Schmitt, G. L. Closs, *J. Am. Chem. Soc. 104* (1982) 6488; b) L. T. Calcaterra, G. L. Closs, J. R. Miller, *ibid. 105* (1983) 670.

[87] Acid strengths of radical cations: F. G. Bordwell, M. J. Bausch, *J. Am. Chem. Soc. 108* (1986) 2473.

[88] This extreme case of a Diels-Alder reaction has barely been discussed previously, also not in: a) J. Sauer, R. Sustmann, *Angew. Chem. 92* (1980) 773; *Angew. Chem. Int. Ed. Engl. 19* (1980) 779. b) Meanwhile *R. Sustmann* et al. have reported convincing evidence for a radical ion pair intermediate in another system: M. Dern, H.-G. Korth, G. Kopp, R. Sustmann, *ibid. 97* (1985) 324 and *24* (1985) 337.

[89] G. Maier, K.-A. Schneider, K.-D. Malsch, H. Irngartinger, A. Lenz, *Angew. Chem. 94* (1982) 446; *Angew. Chem. Int. Ed. Engl. 21* (1982) 437; *Angew. Chem. Suppl. 1982*, 1072.

[90] Similar zwitterions have been discussed in the context of addition of tetracyanoethylene to olefins: a) R. Huisgen, J. P. Ortega, *Tetrahedron Lett. 1978*, 3975. Relevant summaries: b) R. Gompper, *Angew. Chem. 81* (1969) 348; *Angew. Chem. Int. Ed. Engl. 8* (1969) 312; c) R. Huisgen, *Acc. Chem. Res. 10* (1977) 117.

[91] A detailed discussion of SET activation of Diels-Alder reactions between tetracyanoethylene and anthracene has appeared meanwhile: S. Fukuzumi, J. K. Kochi, *Tetrahedron 38* (1982) 1035.

[92] G. Maier, K.-A. Schneider, *Angew. Chem. 92* (1980) 1056; *Angew. Chem. Int. Ed. Engl. 19* (1980) 1022.

[93] 2,3,4,5-Tetra-*tert*-butylbiphenyl shows the same phenomenon (A. Krebs, private communication); cf. also: A. Krebs, E. Franken, S. Müller, *Tetrahedron Lett. 22* (1981) 1675.

[94] a) The Dewar-benzene analogue of hexakis(pentafluorethyl)benzene becomes energetically favored above 278 °C for entropic reasons: E. D. Clifton, W. T. Flowers, R. N. Haszeldine, *J. Chem. Soc. Chem. Commun. 1969*, 1216; A.-M. Dabbagh, W. T. Flowers, R. N. Haszeldine, P. J. Robinson, *ibid. 1975*, 323. b) For a thermal valence isomerization between the dianions of a napthalene and a hemi-Dewar naphthalene see: I. B. Goldberg, H. R. Crowe, R. W. Franck, *J. Am. Chem. Soc. 98* (1976) 7641.

[95] a) L. E. Friedrich, G. B. Schuster, *J. Am. Chem. Soc. 93* (1971) 4602; b) L. E. Friedrich, J. D. Bower, *ibid. 95* (1973) 6869; c) Y. Kobayashi, Y. Hanzawa, W. Miyashita, T. Kashiwagi, T. Nakano, I. Kumadaki, *ibid. 101* (1979) 6445.

[96] P. C. Martino, P. B. Shevlin, *J. Am. Chem. Soc. 102* (1980) 5429.

[97] The problem is the subject of further investigation: H. Rang, *Diplomarbeit*, Universität Giessen 1986.

[98] a) J. Eriksen, C. S. Foote, T. L. Parker, *J. Am. Chem. Soc. 99* (1977) 6455; b) J. Eriksen, C. S. Foote, *ibid. 102* (1980) 6083.

[99] K. Okada, K. Hisamitsu, Y. Takahashi, T. Hanaoka, T. Miyashi, T. Mukai, *Tetrahedron Lett. 25* (1984) 5311.

[100] H. Bock, D. Jaculi, *Angew. Chem. 96* (1984) 298; *Angew. Chem. Int. Ed. Engl. 23* (1984) 305.

[101] Ring opening of radical cations is often very easy; see [85b].

[102] G. Henrici-Olivé, S. Olivé, *Angew. Chem. 86* (1974) 1; *Angew. Chem. Int. Ed. Engl. 13* (1974) 29.

[103] See, however: a) $Cl_2 \cdot O_2$: G. Porter, I. J. Wright, *Discuss. Faraday Soc. 14* (1953) 23; b) $ICl \cdot O_2$: M. Hawkins, L. Andrews, A. J. Downs, D. J. Drury, *J. Am. Chem. Soc. 106* (1984) 3076.

[104] Reviews: a) S. Fallab, *Angew. Chem. 79* (1967) 500; *Angew. Chem. Int. Ed. Engl. 6* (1967) 496; b) L. Vaska, *Acc. Chem. Res. 9* (1976) 175; c) A. B. P. Lever, H. B. Gray, *ibid. 11* (1978) 348; d) D. Cremer in S. Patai (Ed.): *The Chemistry of Functional Groups, Peroxides*, Wiley, London 1983, p. 1-84.

[105] R. D. Gray, *J. Am. Chem. Soc. 91* (1969) 56.

[106] A. Krebs, H. Schmalstieg, O. Jarchow, K.-H. Klaska, *Tetrahedron Lett. 21* (1980) 3171.

[107] G. Maier, W. Sauer, *Angew. Chem. 89* (1977) 49; *Angew. Chem. Int. Ed. Engl. 16* (1977) 51.

[108] Recent papers with literature "reviews": a) Y. Kabe, T. Takata, K. Ueno, W. Ando, *J. Am. Chem. Soc. 106* (1984) 8174; b) L. E. Manring, M. K. Kramer, C. S. Foote, *Tetrahedron Lett. 25* (1984) 2523; c) K. Gollnick, A. Schnatterer, *ibid. 25* (1984) 185; d) R. Curci, L. Lopez, L. Troisi, S. M. K. Rashid, A. P. Schaap, *Tetrahedron Lett. 28* (1987) 5319; e) S. F. Nelsen, *Acc. Chem. Res. 20* (1987) 269.

[109] a) G. Maier, W. Sauer, *Angew. Chem. 87* (1975) 675; *Angew. Chem. Int. Ed. Engl. 14* (1975) 648; b) G. Maier, F. Köhler, *ibid. 91* (1979) 327 and *18* (1979) 308.

[110] a) J. Wirz, A. Krebs, H. Schmalstieg, H. Angliker, *Angew. Chem. 93* (1981) 192; *Angew. Chem. Int. Ed. Engl. 20* (1981) 192; b) J. Pocklington, *Dissertation*, Universität Hamburg 1979.

[111] Part 1: P. Eisenbarth, M. Regitz, *Chem. Ber. 115* (1982) 3796; Part 19: J. Fink, H. Gümbel, P. Eisenbarth, M. Regitz, *Chem. Ber. 120* (1987) 1027, and references cited therein.

[112] D. Born, Giessen, unpublished.

[113] U. Schöllkopf, H.-U. Scholz, *Synthesis 1976*, 271.

[114] I. Bauer, *Dissertation*, Universität Giessen 1986.

[115] H. W. Lage, *Dissertation*, Universität Giessen 1982.

[116] M. Hoppe, *Dissertation*, Universität Giessen 1984.

[117] B. Wolf, *Dissertation*, Universität Giessen 1985.

[118] D. Volz, *Dissertation*, Universität Giessen 1987.

[119] G. Maier, B. Wolf, *Synthesis 1985*, 871.

[120] G. Maier, H. W. Lage, H. P. Reisenauer, *Angew. Chem. 93* (1981) 1010; *Angew. Chem. Int. Ed. Engl. 20* (1981) 976.

[121] Reviews: a) S. Winstein, *Q. Rev. Chem. Soc. 23* (1969) 141; b) P. Warner, *Top. Nonbenzenoid Aromat. Chem. 2* (1977) 283; c) L. A. Paquette, *Angew. Chem. 90* (1978) 114; *Angew. Chem. Int. Ed. Engl. 17* (1978) 106.

[122] a) G. A. Olah, J. S. Staral, G. Liang, *J. Am. Chem. Soc. 96* (1974) 6233; G. A. Olah, J. S. Staral, R. J. Spear, G. Liang, *ibid. 97* (1975) 5489; however, see also: W. J. Hehre, A. J. P. Devaquet, *ibid. 98* (1976) 4370; b) A. E. Lodder, H. M. Buck, L. J. Oosterhoff, *Recl. Trav. Chim. Pays-Bas 89* (1970) 1229; c) G. A. Olah, R. J. Spear, *J. Am. Chem. Soc. 97* (1975) 1845.

[123] More recent theoretical studies: a) R. C. Haddon, K. Raghavachari, *J. Am. Chem. Soc. 105* (1983) 118; b) D. Cremer, E. Kraka, T. S. Slee, R. F. W. Bader, C. D. H. Lau, T. T. Nguyen-Dang, P. J. MacDougall, *ibid. 105* (1983) 5069; R. F. W. Bader, T. S. Slee, D. Cremer, E. Kraka, *ibid. 105* (1983) 5061; c) D. Cremer, J. Gauss, P. von R. Schleyer, P. H. M. Budzelaar, *Angew. Chem. 96* (1984) 370; *Angew. Chem. Int. Ed. Engl. 23* (1984) 370.

[124] G. Maier, R. Emrich, H.-O. Kalinowski, *Angew. Chem. 97* (1985) 427; *Angew. Chem. Int. Ed. Engl. 24* (1985) 429.

[125] a) ab initio: W. J. Hehre, A. J. P. Devaquet, *J. Am. Chem. Soc. 98* (1976) 4370; *96* (1974) 3644; b) MINDO/2: K. Morio, S. Masamune, *Chem. Lett. 1974*, 1251.

[126] G. Maier, K. Euler, R. Emrich, *Tetrahedron Lett. 27* (1986) 3607.

[127] G. Maier, I. Bauer, D. Born, H.-O. Kalinowski, *Angew. Chem. 98* (1986) 1132; *Angew. Chem. Int. Ed. Engl. 25* (1986) 1093.

[128] G. Maier, H.-O. Kalinowski, K. Euler, *Angew. Chem. 94* (1982) 706; *Angew. Chem. Int. Ed. Engl. 21* (1982) 693. It should be remembered that the equilibrium **6** ⇌ **6'** cannot be frozen out in the ^{13}C-NMR even at −185 °C, indicating an activation barrier of probably less than 2.5 kcal mol^{-1} [14]. Perhaps this low value may be due to some contribution from tunneling [129].

[129] a) D. W. Whitman, B. K. Carpenter, *J. Am. Chem. Soc. 102* (1980) 4272; b) *104* (1982) 6473; c) B. K. Carpenter, *ibid. 105* (1983) 1700.

[130] G. Maier, K. Euler, H. Irngartinger, M. Nixdorf, *Chem. Ber. 118* (1985) 409.

[131] a) A. Minsky, A. Y. Meyer, M. Rabinovitz, *Angew. Chem. 95* (1983) 45; *Angew. Chem. Int. Ed. Engl. 22* (1983) 45; b) A. Minsky, A. Y. Meyer, R. Poupko, M. Rabinovitz, *J. Am. Chem. Soc. 105* (1983) 2164.

[132] a) However, a radical ion pair $C_6F_6^{\oplus\cdot}C_6F_6^{\cdot\ominus}$ has been postulated to explain the photophysical behavior of hexafluorobenzene: J. L. G. Suijker, C. A. G. O. Varma, *Chem. Phys. Lett. 97* (1983) 513; b) N. L. Bauld, D. J. Bellville, B. Harirchian, K. T. Lorenz, R. A. Pabon, Jr., D. W. Reynolds, D. D. Wirth, H.-S. Chiou, B. K. Marsh, *Acc. Chem. Res. 20* (1987) 371; c) W. Lau, J. K. Kochi, *J. Org. Chem. 51* (1986) 1801.

[133] H.-O. Kalinowski, L. H. Franz, G. Maier, *Org. Magn. Reson. 17* (1981) 6.

[134] G. Maier, *Pure Appl. Chem. 58* (1986) 95.

[135] G. Maier, H. P. Reisenauer, unpublished.

[136] R. F. Peterson, R. T. K. Baker, R. L. Wolfgang, *Tetrahedron Lett. 1969*, 4749.

[137] P. B. Shevlin, A. P. Wolf, *J. Am. Chem. Soc. 92* (1970) 406, 5291.

[138] L. B. Rodewald, H.-K. Lee, *J. Am. Chem. Soc. 95* (1973) 623, 3084.

[139] H. W. Lage, H. P. Reisenauer, G. Maier, *Tetrahedron Lett. 23* (1982) 3893.

[140] a) G. Maier, M. Hoppe, H. P. Reisenauer, *Angew. Chem. 95* (1983) 1009; *Angew. Chem. Int. Ed. Engl. 22* (1983) 990; b) the PE spectrum of tricyclopentanone **26** was measured by Prof. *Gleiter* (unpublished). The first three bands appear at 9.7 ($4b_1$, HOMO, oxygen lone pair), 10.4 ($7a_1$) und 11.0 eV ($1a_2$); for the dimethyl derivative see: R. Gleiter, R. Haider, P. Bischof, N. S. Zefirov, A. M. Boganov, *J. Org. Chem. 49* (1984) 375.

[141] E. J. Corey, W. H. Pirkle, *Tetrahedron Lett. 1967*, 5255.

[142] K. Lanz, *Dissertation*, Universität Giessen 1985.

[143] G. Maier, M. Hoppe, K. Lanz, H. P. Reisenauer, *Tetrahedron Lett. 25* (1984) 5645.

[144] U. Köhler, *Dissertation*, Universität Giessen 1986.

[145] J. Gebhardt, *Diplomarbeit*, Universität Giessen 1985.

[146] a) D. Felix, J. Schreiber, K. Piers, U. Horn, A. Eschenmoser, *Helv. Chim. Acta 51* (1968) 1461; b) D. Felix, C. Wintner, A. Eschenmoser, *Org. Synth. 55* (1976) 52, and references cited therein.

[147] Irradiation of **97a** or **97b** in solution gives the corresponding aziridinyl imine of cyclopropenecarbaldehyde [145], also obtainable from the analogous bistrimethylsilylated hydrazones of this aldehyde by desilylation (A. Rubo, Diplomarbeit, Giessen 1986). Attempts to obtain the unsubstituted cyclopropenyldiazomethane [148] via this route are underway.

[148] G. Maier, M. Hoppe, H. P. Reisenauer, C. Krüger, *Angew. Chem. 94* (1982) 445; *Angew. Chem. Int. Ed. Engl. 21* (1982) 437; *Angew. Chem. Suppl. 1982*, 1061.

[149] H. Lee, *Daehan Hwahak Hwoejee (J. Korean Chem. Soc.) 13* (1969) 333.

[150] a) S.-W. Chiu, W.-K. Li, *Croat. Chem. Acta 54* (1981) 183; b) For experiments in this direction (bicyclobutanone) see: O. L. Chapman, *Pure Appl. Chem. 51* (1979) 331.

[151] H. P. Reisenauer, G. Maier, A. Riemann, R. W. Hoffmann, *Angew. Chem. 96* (1984) 596; *Angew. Chem. Int. Ed. Engl. 23* (1984) 641.

[152] W. Schwab, *Dissertation*, Universität Giessen 1987.

[153] G. Maier, H. P. Reisenauer, W. Schwab, P. Čársky, B. A. Hess, Jr., L. J. Schaad, *J. Am. Chem. Soc. 109* (1987) 5183.

[154] H. Teles, Giessen, unpublished.

[155] G. Maier, H. P. Reisenauer, *Angew. Chem. 98* (1986) 829; *Angew. Chem. Int. Ed. Engl. 25* (1986) 819.

[156] O. Sinanoğlu, C. Trindle, *Middle East Tech. Univ. J. Pure Appl. Sci. 7* (1974) 265.

[157] G. Maier, H.-G. Hartan, T. Sayrac, *Angew. Chem. 88* (1976) 252; *Angew. Chem. Int. Ed. Engl. 15* (1976) 226.

[158] See also: O. L. Chapman, *Pure Appl. Chem. 40* (1974) 511.

[159] Summary also in [134].

[160] H. Hoberg, C. Fröhlich, *Synthesis 1981*, 830.

[161] Mixture of isomers, obtained by heating **112** to 120°C [142].

[162] For direct evidence for the existence of free cyclobutadiene in the gas phase see: a) E. Hedaya, R. D. Miller, D. W. McNeil, P. F. D'Angelo, P. Schissel, *J. Am. Chem. Soc. 91* (1969) 1875; b) E. Hedaya, I. S. Krull, R. D. Miller, M. E. Kent, P. F. D'Angelo, P. Schissel, *ibid. 91* (1969) 6880, and references cited therein.

[163] J. Kreile, N. Münzel, A. Schweig, H. Specht, *Chem. Phys. Lett. 124* (1986) 140.

[164] a) M. Christl, S. Freund, *Chem. Ber. 118* (1985) 979; b) D. A. Kaisaki, D. A. Dougherty, *Tetrahedron Lett. 28* (1987) 5263.

[165] a) W. E. Billups, L.-J. Lin, E. W. Casserly, *J. Am. Chem. Soc. 106* (1984) 3698; b) S. W. Staley, T. D. Norden, *ibid. 106* (1984) 3699.

[166] A. Weber, N. Neuenschwander, *Angew. Chem. 93* (1981) 788; *Angew. Chem. Int. Ed. Engl. 20* (1981) 774; see also: J. Krebs, D. Guggisberg, U. Stämpfli, M. Neuenschwander, *Helv. Chim. Acta 69* (1986) 835.

[167] a) B. A. Hess, Jr., D. Michalska, L. J. Schaad, *J. Am. Chem. Soc. 107* (1985) 1449; b) D. Michalska, B. A. Hess, Jr., *Int. J. Quantum Chem. 29* (1986) 2217.

[168] Cited in [167a].

[169] a) B. A. Hess, Jr., L. J. Schaad, P. Čársky, *Pure Appl. Chem. 55* (1983) 253; b) B. A. Hess, Jr., L. J. Schaad, P. Čársky, *Pure Appl. Chem. 55* (1983) 253; b) B. A. Hess, Jr., L. J. Schaad, P. Čársky, R. Zahradnik, *Chem. Rev. 86* (1986) 709.

[170] G. F. Emerson, L. Watts, R. Pettit, *J. Am. Chem. Soc. 87* (1965) 131.

[171] a) O. L. Chapman, C. L. McIntosh, J. Pacansky, *J. Am. Chem. Soc. 95* (1973) 614; b) O. L. Chapman, D. De La Cruz, R. Roth, J. Pacansky, *ibid. 95* (1973) 1337.

[172] a) C. Y. Lin, A. Krantz, *J. Chem. Soc. Chem. Commun. 1972*, 1111; b) A. Krantz, C. Y. Lin, M. D. Newton, *J. Am. Chem. Soc. 95* (1973) 2744; c) R. G. S. Pong, B. S. Huang, J. Laureni, A. Krantz, *ibid. 99* (1974) 4153; d) B. S. Huang, R. G. S. Pong, J. Laureni, A. Krantz, *ibid. 99* (1977) 4154.

[173] a) S. Masamune, M. Suda, H. Ona, L. M. Leichter, *J. Chem. Soc. Chem. Commun. 1972*, 1268; b) S. Masamune, Y. Sugihara, K. Morio, J. E. Bertie, *Can. J. Chem. 54* (1976) 2679; c) S. Masamune, F. A. Souto-Bachiller, T. Machiguchi, J. E. Bertie, *J. Am. Chem. Soc. 100* (1978) 4889.

[174] a) G. Maier, B. Hoppe, *Tetrahedron Lett. 1973*, 861; b) G. Maier, H. P. Reisenauer, *ibid. 1976*, 3591.

[175] a) S. Masamune, N. Nakamura, J. Spadaro, *J. Am. Chem. Soc. 97* (1975) 918; b) W. R. Roth, M. Dogan, C. Beck, unpublished.

[176] H. Kollmar, V. Staemmier, *J. Am. Chem. Soc. 100* (1978) 4304.

[177] a) L. J. Schaad, B. A. Hess, C. S. Ewig, *J. Am. Chem. Soc. 101* (1979) 2281; b) B. A. Hess, Jr., P. Čársky, L. J. Schaad, *ibid. 105* (1983) 695; c) B. A. Hess, Jr., L. J. Schaad, private communication; basis set: MP2/6-31G* (Gaussian 82, Version K).

[178] L. J. Schaad, B. A. Hess, Jr., C. S. Ewig, *J. Org. Chem. 47* (1982) 2904.

[179] a) R. C. Haddon, G. R. J. Williams, *J. Am. Chem. Soc. 97* (1975) 6582; b) M. D. Newton in H. F. Schaefer III (Ed.): *Modern Theoretical Chemistry. Vol. IV*, Plenum Press, New York 1977, p. 264ff; c) F. Fratev, V. Monev, R. Janoschek, *Tetrahedron 38* (1982) 2929.

[180] M. A. Fox, K. Campbell, G. Maier, L. H. Franz, *J. Org. Chem. 48* (1983) 1762.

[181] G. Maier, L. H. Franz, H.-G. Hartan, K. Lanz, H. P. Reisenauer, *Chem. Ber. 118* (1985) 3196.

[182] For calculations on the interaction of cyclobutadiene with partner molecules, see: a) K. B. Lipkowitz, R. Larter, *Tetrahedron Lett. 1978*, 33; b) K. B. Lipkowitz, *J. Am. Chem. Soc. 100* (1978) 7535; c) A. Schweig, W. Thiel, *Tetrahedron Lett. 1978*, 1841; d) S. Fraga, *ibid. 22* (1981) 3343; see also e) Q. B. Broxterman, H. Hogeveen, R. F. Kingma, F. van Bolhuis, *J. Am. Chem. Soc. 107* (1985) 5722.

[183] G. Maier, W. Mayer, C. Haacke, R. Askani, *Angew. Chem. 85* (1973) 1051; *Angew. Chem. Int. Ed. Engl. 12* (1973) 1016.

[184] G. Maier, H. P. Reisenauer, H.-A. Freitag, *Tetrahedron Lett. 1978*, 121.

[185] S. D. Worley, T. R. Webb, D. H. Gibson, T.-S. Ong, *J. Organomet. Chem. 168* (1979) C 16.

[186] a) G. Lauer, C. Müller, K.-W. Schulte, A. Schweig, A. Krebs, *Angew. Chem. 86* (1974) 597; *Angew. Chem. Int. Ed. Engl. 13* (1974) 544; b) G. Lauer, C. Müller, K.-W. Schulte, A. Schweig, G. Maier, A. Alzérreca, *ibid. 87* (1975) 194 and *14* (1975) 172.

[187] W. T. Borden, E. R. Davidson, *Acc. Chem. Res. 14* (1981) 69.

[188] H. Kollmar, V. Staemmler, *J. Am. Chem. Soc. 99* (1977) 3583.

[189] M. J. S. Dewar, K. M. Merz, J. J. P. Stewart, *J. Am. Chem. Soc. 106* (1984) 4040.

[190] W. T. Borden, E. R. Davidson, P. Hart, *J. Am. Chem. Soc. 100* (1978) 388.

[191] J. A. Jafri, M. D. Newton, *J. Am. Chem. Soc. 100* (1978) 5012.

[192] L. J. Schaad, B. A. Hess, Jr., private communication.

[193] A. F. Voter, W. A. Goddard, III, *J. Am. Chem. Soc. 108* (1986) 2830.

[194] a) G. Binsch, *Naturwissenschaften 60* (1973) 369; b) G. Maier, *Chem. Unserer Zeit 9* (1975) 131.

[195] N. L. Bauld, T. L. Welsher, J. Cessac, R. L. Holloway, *J. Am. Chem. Soc. 100* (1978) 6920.

[196] See summary in [197].

[197] a) B. A. Hess, Jr., L. J. Schaad, *J. Am. Chem. Soc. 105* (1983) 7500; b) L. J. Schaad, B. A. Hess, Jr., *Pure Appl. Chem. 54* (1982) 1097; c) B. A. Hess, Jr., L. A. Schaad, *ibid. 52* (1980) 1471.

[198] M. J. S. Dewar, K. M. Merz, Jr., *J. Am. Chem. Soc. 107* (1985) 6175.

[199] Further papers concerning the Hückel rule: a) J. J. Aihara, *J. Am. Chem. Soc. 98* (1976) 2750; b) S. Inagaki, Y. Hirabayashi, *ibid. 99* (1977) 7418; c) S. Kuwajima, *ibid. 106* (1984) 6496; d) D. J. Klein, N. Trinajstić, *ibid. 106* (1984) 8050; e) J. K. Burdett, S. Lee, W. C. Sha, *Nouv. J. Chim. 9* (1985) 757; f) C. Zhising, H. Siqun, *Theor. Chim. Acta 67* (1985) 409.

[200] M.-J. Huang, M. Wolfsberg, *J. Am. Chem. Soc. 106* (1984) 4039.

[201] J. Michl, note in a book review, *Angew. Chem. 97* (1985) 1005. Note added in proof (February 24, 1988): Quite recently the static ^{13}C-NMR dipolar spectrum and polarized IR spectrum of vicinally ^{13}C-labeled cyclobutadiene (**29**) have been recorded. If the barrier for the automerization is ≈ 10 kcal mol^{-1} (Fig. 8), the interconversion in an argon matrix must be due to tunneling at a rate of at least 10^3 s^{-1} (*J. Michl*, private communication).

[202] The experimental findings reported by *Yannoni* et al. make a tunneling effect appear questionable: a) C. S. Yannoni, V. Macho, P. C. Myhre, *J. Am. Chem. Soc. 104* (1982) 907, 7380; b) P. C. Myhre, K. L. McLaren, C. S. Yannoni, *ibid. 107* (1985) 5294. c) According to *Dewar* et al. this effect does not play a role in the case of the 1,2-dimethyl-2-norbornyl cation [202b] but does in the case of the parent compound [202a]: M. J. S. Dewar, K. A. Merz, Jr., *ibid. 108* (1986) 5634.

[203] a) K. Krogh-Jespersen, P. von R. Schleyer, J. A. Pople, D. Cremer, *J. Am. Chem. Soc. 100* (1978) 4301; b) T. Clark, D. Wilhelm, P. von R. Schleyer, *Tetrahedron Lett. 23* (1982) 3547.

[204] B. A. Hess, Jr., C. S. Ewig, L. J. Schaad, *J. Org. Chem. 50* (1985) 5869.

[205] A. Skancke, I. Agranat, *Nouv. J. Chim. 9* (1985) 577.

[206] L. Radom, H. F. Schaefer III, *J. Am. Chem. Soc. 99* (1977) 7522.

[207] a) G. K. Surya Prakash, T. N. Rawdah, G. A. Olah, *Angew. Chem. 95* (1983) 356; *Angew. Chem. Int. Ed. Engl. 22* (1983) 390, and references cited therein; b) A. Bouvy, Z. Janousek, H. G. Viehe, *Synthesis 1983*, 718.

[208] K. Müllen, *Chem. Rev. 84* (1984) 603.

[209] P. J. Garratt, R. Zahler, *J. Am. Chem. Soc. 100* (1978) 7753.

[210] G. Boche, H. Etzrodt, M. Marsch, W. Thiel, *Angew. Chem. 94* (1982) 141; *Angew. Chem. Int. Ed. Engl. 21* (1982) 133; G. Boche, H. Etzrodt, *Tetrahedron Lett. 24* (1983) 5477. Dianion of 1,2-diphenylcyclobutabenzene: G. Boche, H. Etzrodt, M. Marsch, W. Thiel, *Angew. Chem. 94* (1982) 141; *Angew. Chem. Int. Ed. Engl. 21* (1982) 132; G. Boche, H. Etzrodt, W. Massa, G. Baum, *ibid. 97* (1985) 858 and *24* (1985) 863.

[211] See references in [181].

[212] H. G. von Schnering, *Angew. Chem. 93* (1981) 44; *Angew. Chem. Int. Ed. Engl. 20* (1981) 33.

[213] U.-J. Vogelbacher, M. Regitz, R. Mynott, *Angew. Chem. 98* (1986) 835; *Angew. Chem. Int. Ed. Engl. 24* (1986) 842.

[214] a) Calculation: M. S. Gordon, *J. Chem. Soc. Chem. Commun. 1980*, 1131; b) calculation: D. A. Clabo, Jr., H. F. Schaefer III, *J. Am. Chem.*

Soc. 108 (1986) 4344; c) attempts to prepare tetra-*tert*-butyltetrasilacyclobutadiene/tetrahedrane: U. Wessolek, unpublished.
[215] P. Lingelbach, Giessen, unpublished.
[216] From a very recently published work it emerges that this aspect is also being studied from another point of view: M. J. Fink, D. B. Puranik, *Organometallics 6* (1987) 1809.
[217] a) S. F. Dyer, S. Kammula, P. B. Shevlin, *J. Am. Chem. Soc. 99* (1977) 8104; b) tetraphenyl derivative: H. Nickels, H. Dürr, F. Toda, *Chem. Ber. 119* (1986) 2249.
[218] a) K.-D. Baumgart, H. Harnisch, U. Szeimies-Seebach, G. Szeimies, *Chem. Ber. 118* (1985) 2883, and references cited therein; b) A. Düker, G. Szeimies, *Tetrahedron Lett. 26* (1985) 3555, and references cited therein.
[219] a) G. Fitzgerald, P. Saxe, H. F. Schaefer III, *J. Am. Chem. Soc. 105* (1983) 690; b) H. F. Schaefer III, Y. Yamaguchi, *J. Mol. Struct. 135* (1986) 369.
[220] H. D. Scharf, K. R. Stahlke, *Angew. Chem. 82* (1970) 835; *Angew. Chem. Int. Ed. Engl. 9* (1970) 810.
[221] R. Wilmes, *Dissertation*, Universität Giessen 1987.
[222] Preparative studies: a) W. E. Barth, R. G. Lawton, *J. Am. Chem. Soc. 93* (1971) 1730; b) K. Yamamoto, T. Harada, M. Nakazaki, *ibid. 105* (1983) 7171.
[223] Calculations: a) M. Randić, N. Trinajstić, *J. Am. Chem. Soc. 106* (1984) 4428; b) J. Aihara, *ibid. 107* (1985) 298; c) I. Agranat, B. A. Hess, Jr., L. J. Schaad, *Pure Appl. Chem. 52* (1980) 1399.
[224] M. Scholtissek, Giessen, unpublished.
[225] Attempted synthesis of tetra-*tert*-butylethene: H.-O. Kalinowski, E. Röcker, G. Maier, *Org. Magn. Reson. 21* (1983) 64.
[226] Experiments toward hexa-*tert*-butylbenzene: G. Maier, I. Bauer, U. Huber-Patz, R. Jahn, D. Kallfass, H. Rodewald, H. Irngartinger, *Chem. Ber. 119* (1986) 1111.
[227] a) Silaethene: G. Maier, G. Mihm, H. P. Reisenauer, *Chem. Ber. 117* (1984) 2351; b) Silabenzene: G. Maier, G. Mihm, R. O. W. Baumgärtner, H. P. Reisenauer, *ibid. 117* (1984) 2337.
[228] a) Boraethenes: G. Maier, J. Henkelmann, H. P. Reisenauer, *Angew. Chem. 97* (1985) 1061; *Angew. Chem. Int. Ed. Engl. 24* (1985) 1065; b) Pyridine-borabenzene: R. Boese, N. Finke, J. Henkelmann, G. Maier, P. Paetzold, H. P. Reisenauer, G. Schmid, *Chem. Ber. 118* (1985) 1644; c) Nitrogen fixation by borabenzene: G. Maier, H. P. Reisenauer, J. Henkelmann, C. Kliche, *Angew. Chem. 100* (1988) 303; *Angew. Chem. Int. Ed. Engl. 27* (1988) 295.
[229] G. Maier, H. P. Reisenauer, B. Rohde, K. Dehnicke, *Chem. Ber. 116* (1983) 732.
[230] G. Maier, H. P. Reisenauer, *Angew. Chem. 98* (1986) 829; *Angew. Chem. Int. Ed. Engl. 25* (1986) 819.
[231] a) Cyclopropenylidene **103** has recently been detected in interstellar space: P. Thaddeus, J. M. Vrtilek, C. A. Gottlieb, *Astrophys. J. 299* (1985) L63; b) simply substituted nitrile oxides as further potential candidates: G. Maier, J. H. Teles, *Angew. Chem. 99* (1987) 152; *Angew. Chem. Int. Ed. Engl. 26* (1987) 155; c) the list includes a new oxide of carbon (C_5O_2) [135] and the isofulminic acid [154]; unpublished.
[232] See also G. Maier: "*Rudolf Criegee*", Chem. Ber. 110 (1977) XXVII.

Enzymic Baeyer–Villiger Oxidations by Flavin-Dependent Monooxygenases

By Christopher T. Walsh* and Y.-C. Jack Chen

There has recently been a revival of interest in microbial biochemistry. Part of this resurgence is due to the increased presence of man-made organic compounds in the biosphere and the resultant interest in microorganisms which can degrade these xenobiotic molecules. Also, advances in genetic engineering have raised the possibility of utilizing the chemical machinery of bacteria for commercial profit and social benefit. The Baeyer–Villiger reaction is a useful transformation in organic synthesis which provides chemists with a gentle means of converting ketones into esters or lactones. The reaction, however, suffers from the problems of low yield and the need, in some cases, to utilize harsh conditions. There exist bacteria, capable of growth on aliphatic molecules, that contain enzymes which can catalyze Baeyer–Villiger reactions. These enzymes, known as monooxygenases, are involved in the breakdown of acyclic and alicyclic ketones to provide simpler carbon units for further catabolism. The gamut of reactions catalyzed by some of these enzymes is remarkable. This diversity, plus their availability in pure form in quantity by genetic engineering raises the possibility that these biocatalysts can be useful as reagents in organic synthesis.

1. Introduction

The oxidation of ketones to esters and lactones by the Baeyer–Villiger reaction is a reliable and highly useful transformation in synthetic chemistry and is typically effected by a peroxide or peracid reagent.[1–3] In general, the Baeyer–Villiger reaction is conducted with peracids, and the reaction with simple peroxides proceeds in low yields or not at all because the readily formed, and often isolable, tetrahedral peroxy adducts of ketones with H_2O_2[4] or alkyl hydroperoxides are resistant to the alkyl migration step needed to generate the ester or lactone.[5–11] Some rate data are collected in Table 1.

With these few facts on the chemical Baeyer–Villiger process as backdrop, this review turns to biological Baeyer–Villiger transformations as its focus and summarizes the current knowledge on the enzymes and the cofactors and cosubstrates required for the biological counterpart.

Table 1. Rate of Baeyer–Villiger oxidations of three substrates by peroxides and peracids.

Reagent	Cyclohexanone	Cyclohexyl methyl ketone	Acetophenone
*t*BuOOH	slow	slow	slow
H_2O_2	slow	slow	slow
$C_6H_5CO_3H$	$96\text{–}158 \times 10^{-5}$ $M^{-1}\,s^{-1}$ ($CHCl_3$, 25 °C)	$11.7\text{–}14.1 \times 10^{-5}$ $M^{-1}\,s^{-1}$ ($CHCl_3$, 15 °C)	1.5×10^{-5} $M^{-1}\,s^{-1}$ ($CHCl_3$, 28 °C)
CF_3CO_3H	6.1×10^{-2} $M^{-1}\,s^{-1}$	5.7×10^{-3} $M^{-1}\,s^{-1}$ [a]	1.7×10^{-3} $M^{-1}\,s^{-1}$

[a] For isopropyl methyl ketone.

Collected in Table 2 are seven examples of transformations which appear by stoichiometry, and, in some cases, by detailed mechanistic analysis, to be enzyme-catalyzed Baeyer–Villiger reactions. The first five transformations, (a)–(e), camphor to the "1,2-campholide,"[12] 2-tridecanone to undecyl acetate,[13] progesterone to testosterone acetate,[14] cyclohexanone to ε-caprolactone,[15] and tetradecanal to tetradecanoate,[16] are all catalyzed by bacterial enzymes that have been purified to homogeneity and characterized as pure biocatalysts. As will be detailed in the next section, all five enzymes require O_2 as the cosubstrate for oxidation, contain or utilize a riboflavin-based coenzyme, and contain no transition metals. Reaction (e) is catalyzed by luminescent bacteria, and a coproduct of the oxidation of an aldehyde to an acid is a photon of blue-green light.[16] Many luminescent fish give off light by this mechanism from colonies of photobacteria harbored in specialized light organs.

The last two transformations, (f) and (g), occur in the metabolism of the hepatotoxic, carcinogenic aflatoxin mold metabolites. One involves oxygenative ring expansion of the cyclopentanone moiety to a six-membered ring lactone in the conversion of aflatoxin B to G_1. The other transformation, occurring in earlier stages of aflatoxin biogenesis, is proposed for conversion of averufin to versiconal acetate.[17] No further biochemical information is available on these latter transformations. There are dozens of other natural products and biogenetic routes to accumulating secondary plant metabolites where biological Baeyer–Villiger reactions have been postulated or are likely.

Given the observations that molecular oxygen is cosubstrate and flavin coenzymes are cofactors in the five

[*] Prof. C. T. Walsh [+], Dr. Y.-C. J. Chen
Departments of Chemistry and Biology
Massachusetts Institute of Technology
Cambridge, MA 02139 (USA)

[+] Present address:
Departments of Biological Chemistry and Molecular Pharmacology,
Harvard Medical Schoool,
Boston, MA 02115 (USA)

Table 2. Biological transformations effected by enzymes catalyzing Baeyer-Villiger oxidations.

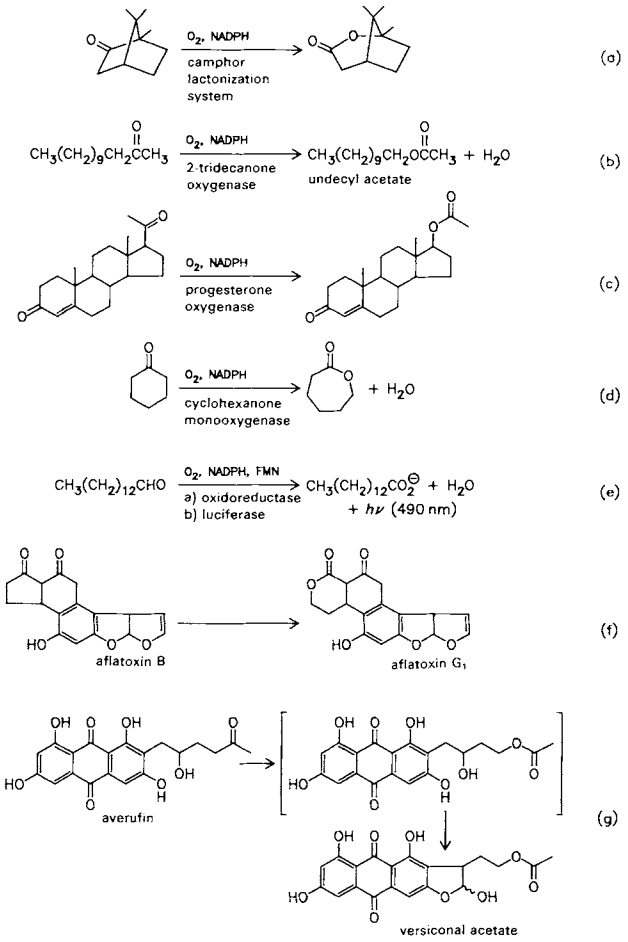

Baeyer-Villiger enzymes so far purified, we briefly analyze oxygenase enzymes and their cofactor requirements in the next section.

2. Oxygenase Categories

Enzymes that reductively activate oxygen for insertion into some cosubstrate can be broadly classified as dioxygenases or monooxygenases based on whether two or only one of the oxygen atoms from O_2 is incorporated into a cosubstrate as it is transformed into product[18] (Fig. 1). Dioxygenases usually contain tightly associated iron, in heme or non-heme environments, and are exemplified by the enzymes involved in 1,4-dioxygenations in prostaglandin and leukotriene biogenesis, in aromatic ring functionalizations by microbes such as the conversion of benzene to its *cis*-1,2-dihydroxy derivative, and in oxygenative aromatic fissions of phenols and catechols in aromatic ring biodegradations. Monooxygenases, of which the Baeyer-Villiger oxygenases are a subset, show a wider range of cofactor content, and also convert one atom of O_2 into H_2O as a coproduct of the oxygenation process. To convert O_2

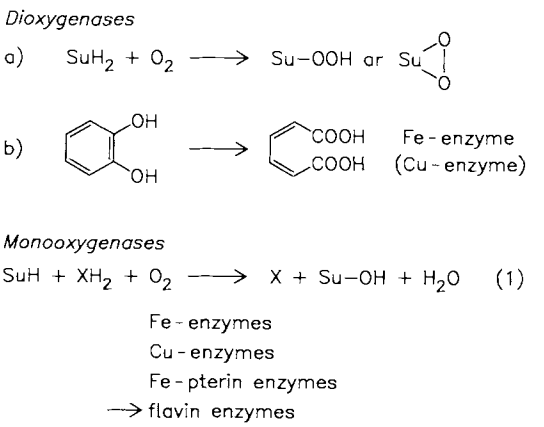

Fig. 1. The two classes of oxygenases and the reactions they catalyze. Dioxygenases require metal cofactors whereas monooxygenases utilize either metal or organic cofactors.

into an activated oxygen transfer reagent, monooxygenases generally use a two-electron reductant and either a redox-active transition metal (Fe, Cu) or a conjugated organic cofactor (pterin or flavin coenzyme) to facilitate passage of electrons one at a time to O_2 via an oxo-metal or oxygenated cofactor intermediate. The general stoichiometry is given by Equation 1 in Figure 1.

The four types of monooxygenases, based on the redox cofactor, are exemplified in Table 3. A typical flavoprotein monooxygenase is represented by the bacterial *p*-hydroxybenzoate hydroxylase, which produces the catecholic product by *ortho* hydroxylation of an activated aryl ring.[19] The second type using a conjugated organic cofactor is phenylalanine hydroxylase, the first enzyme in adrenergic neurotransmitter biosynthesis, which carries out a much more difficult functionalization of the unactivated phenylalanine ring, regiospecifically, to yield tyrosine. Whereas the reductant for the flavoenzyme(s) is the readily available dihydronicotinamide NADPH, the phenylalanine hydroxylase uses tetrahydrobiopterin and generates as initial product the bridgehead hydroxy pterin that is enzymically dehydrated to H_2O and the quinoid tautomer of dihydrobiopterin. Phenylalanine hydroxylase also requires one equivalent of iron in its active site to be catalytically active and it is likely that the oxygenating species may be a high-valent oxo-iron reagent in the enzyme's active site.[20] The third type of monooxygenase, a copper enzyme, is dopamine β-hydroxylase, which functions further along the same catecholamine biosynthetic pathway to convert dopamine into noradrenaline by benzylic hydroxylation.[21] Here the reductant, XH_2, is vitamin C in a biologically well-documented role for ascorbic acid. The fourth example is an iron enzyme, here a heme protein of the cytochrome P_{450} family, acting to convert camphor into the 5-*exo* alcohol at the start of the bacterial catabolic pathway for this bicyclic substrate, a regio- and stereoselective hydroxylation of an unactivated carbon site.[22]

Because the Baeyer-Villiger enzymes (Table 2) are flavoprotein monooxygenases, we focus on the catalytic capacity of this vitamin B_2-based class further. In Figure 2 are shown the coenzymically active forms of riboflavin, the 5'-monophosphate, FMN (active with luciferase), and the 5'-

Table 3. The four different classes of monooxygenases. All monooxygenases catalyze reduction of molecular oxygen to water with concomitant oxidation of a substrate molecule. The differences stem from the cofactors which are required to effect these reactions.

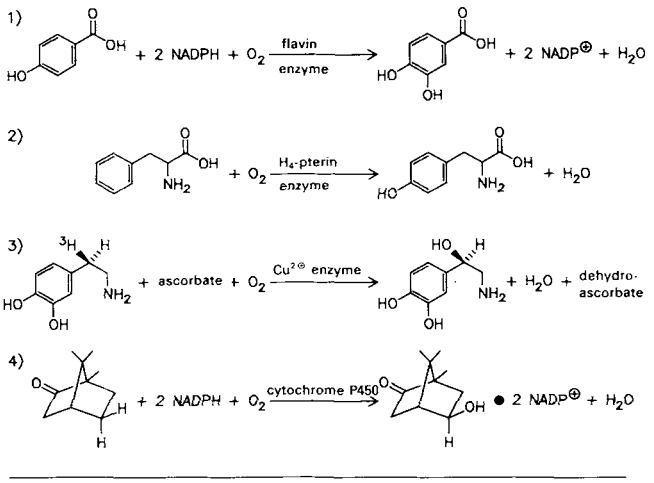

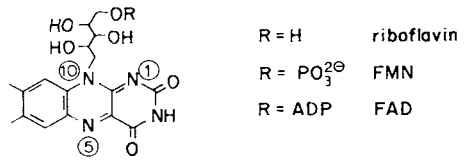

Fig. 2. Riboflavin (vitamin B_2) and coenzyme forms which are active as enzyme cofactors.

ADP ester, FAD (the predominant coenzyme form in the flavin-linked monooxygenases where it stays tightly bound to the enzyme active site through multiple catalytic turnovers). The tricyclic isoalloxazine ring system is the key locus for redox catalysis and the role of the exogenous reductant NADPH is to deliver hydride ion and reduce bound FAD to $FADH_2$, the 1,5-dihydro regioisomer.

Because $FADH_2$ (and $FMNH_2$) has a central dihydropyrazine ring, it is readily reoxidized by both one-electron (to the semiquinone radical) and two-electron routes and so can function as a two-electron/one-electron redox switch in biochemistry (Fig. 3).[22] The kinetic and thermodynamic accessibility of the semiquinone radical is the structural feature enabling rapid reaction of $FADH_2$ with O_2 to yield, by one-electron transfer, $O_2^{\ominus\ominus}$ (superoxide anion radical) and $FADH^{\ominus}$. Rapid radical recombination yields a bridgehead 4a-hydroperoxyflavin, first characterized with bacterial luciferase where its accumulation as an intermediate was detected by cryoenzymologic investigation.[23] The hydroperoxyflavin can break down intramolecularly to yield reoxidized flavin and H_2O_2 or it can undergo O–O bond fission at the active site of a specific flavoenzyme to monooxygenate, intermolecularly, a cosubstrate bound in its proximity and yield the 4a-hydroxyflavin as initial coproduct; intramolecular loss of H_2O from this pseudobase then regenerates FAD for a subsequent catalytic cycle (Fig. 4).

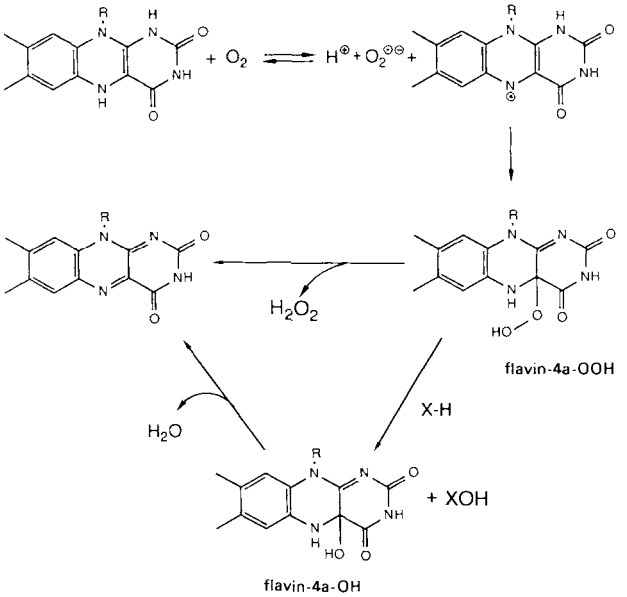

Fig. 4. Proposed reaction of reduced flavins with oxygen. The flavin hydroperoxide intermediate can either fragment to oxidized flavin and H_2O_2 or can oxygenate a cosubstrate with concomitant generation of a 4a-hydroxyflavin which then breaks down to oxidized flavin and water.

The types of substrates that undergo monooxygenation by flavoenzymes can be divided into three categories: (1) phenols are transformed into catechols; (2) heteroatom-containing compounds into the corresponding oxides; (3) ketones or aldehydes into esters or acids. This last category is our focus.

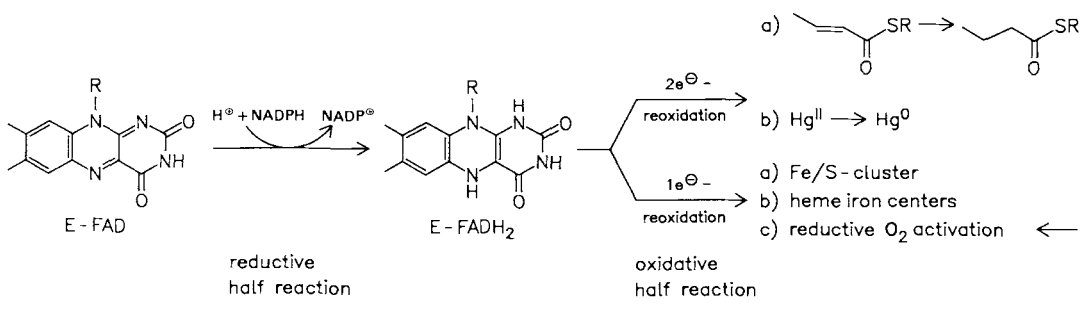

Fig. 3. The redox versatility of the flavin cofactor arises from its ability to perform both one- and two-electron transfers. E = enzyme.

3. Baeyer-Villiger Flavoprotein Monooxygenases

Although we shall focus on cyclohexanone monooxygenase as the example of the Baeyer-Villiger enzyme subjected to closest mechanistic scrutiny, we note first some contextual features of the other flavoenzymes of Table 2. *Pseudomonas* can grow on camphor as a sole carbon source, and its strategy for disconnection of the bicycloheptane skeleton to return its carbons to metabolically useful building blocks is remorselessly monooxygenative in attack. As shown in Figure 5, camphor can undergo a

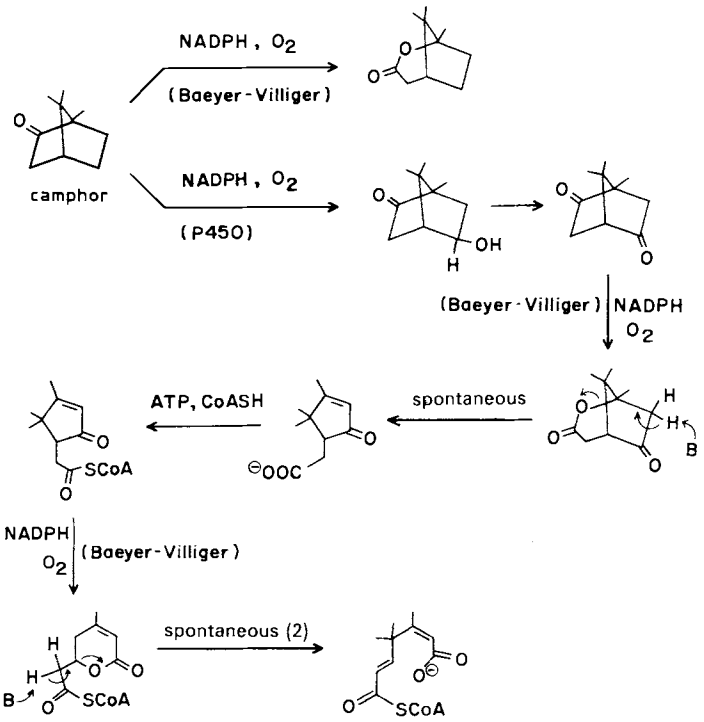

Fig. 5. The oxygenative pathway for camphor dissimilation. Initial hydroxylation by a cytochrome P_{450} monooxygenase activates the bicyclic system for subsequent fragmentation of each ring via successive Baeyer-Villiger oxidations.

Baeyer-Villiger enzymic oxygenation directly, but the major metabolic flux is by initial 5-*exo*-alcohol formation by the P_{450} camphor hydroxylase (entry 4, Table 3), oxidation of the alcohol to yield the diketone, and then Baeyer-Villiger oxidation with insertion of oxygen, as anticipated, between the carbonyl C atom and the bridgehead.[12,24,25] The resultant lactone is unstable in mild base and fragments to the monocyclic conjugated cyclopentenone with a pendant acid grouping. The acid is thioesterified with coenzyme A and then yet another Baeyer-Villiger-type flavoprotein oxygenase is brought to bear to convert the last ring by oxygenative fragmentation into acyclic metabolites. Note the key role of multiple Baeyer-Villiger enzymes in the skeletal disconnection strategy.

The 2-tridecanone oxygenase from *Pseudomonas cepacia* turns out to be a highly nonselective oxygen-insertion enzyme. It will take C_7 to C_{14} methyl ketones and convert them into the corresponding alkyl acetates. Further, it will take any other ketone isomer of tridecanone and insert oxygen into either side as exemplified (Fig. 6) by the conversion of 6-tridecanone to heptyl hexanoate and pentyl octanoate.[13] This enzyme has also been reported to act on cyclopentanone and cyclohexanone. The pure FAD-containing steroid oxygenase from *Cylindrocarpon radicicola*[26] will not only convert progesterone into testosterone acetate but also androstenedione into testolactone, with a broad specificity suggested for other 17- and 20-ketosteroids.

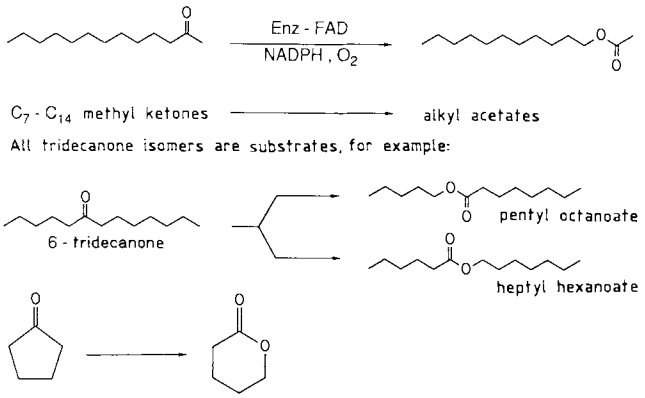

Fig. 6. Alkyl methyl ketone catabolism by *Pseudomonas cepacia* tridecanone oxygenase. Note the ability of this enzyme to insert oxygen into either side of the carbonyl moiety. This oxygenase is a dimeric flavoprotein (2 × 55 kDa); it constitutes 3% of the soluble protein in the cell. $k_{cat} = 100\ min^{-1}$.

Luciferase, in structural terms, is the best characterized of this class of flavoenzymes and has been available in homogeneous form from several photobacteria for about 20 years.[27] This enzyme is an $\alpha\beta$ dimer. However, the enzyme differs from the other flavoenzymes in that it binds FMN only weakly and requires a separate feeder enzyme to reduce free FMN to $FMNH_2$. The $FMNH_2$ then diffuses to luciferase's active site. With purified luciferase enzyme, O_2, $FMNH_2$, and tetradecanal, only a single turnover ensues (due to competing nonenzymic autoxidation of $FMNH_2$), so steady-state kinetic determinations have been difficult. The main focus in luciferase study has been on the emission of blue-green light ($\lambda_{max} = 490$ nm, quantum yield = 0.1) generated as coproduct of luciferase action. Possibly, the FMN-4a-OOH reacts with aldehyde to yield the tetrahedral adduct which then could decompose with C-H cleavage in a Baeyer-Villiger mode[28] and yield product acid and FMN-4a-OH. This route does not obviously explain light emission. *Hastings* and colleagues have suggested that the excited state of FMN-4a-OH is the initial species which can emit light directly or transfer energy to an accessory chromophore. To produce the excited FMN-4a-OH, they proposed that luciferase fragments the O-O bond via intramolecular electron transfer to yield carboxylic acid and diradical. Then "charge annihilation results in the formation of the excited state of the hydroxy flavin"[29] (Fig. 7). This type of mechanism has also been proposed by *Ghisla* and coworkers.[30,31] In model studies with N_5-ethyl-4a-hydroperoxyflavin and aldehydes, a low-quantum-yield chemiluminescence has been reported.[32]

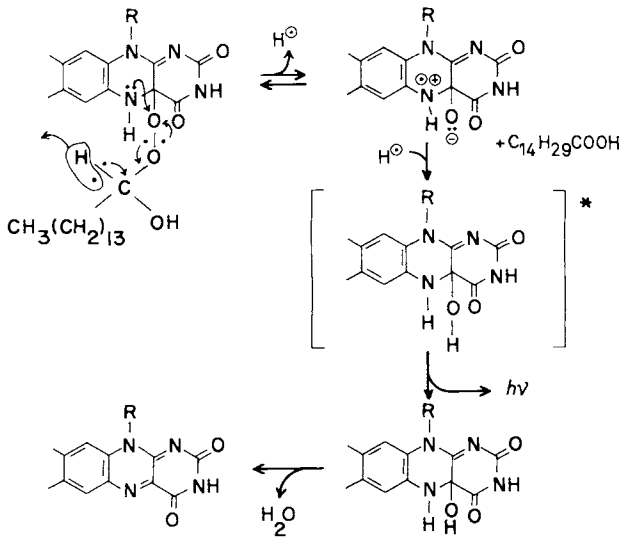

Fig. 7. A possible catalytic cycle for the bacterial luciferase reaction.

The enzyme cyclohexanone monooxygenase has been detected in soil bacteria—*Nocardia, Pseudomonas, Acinetobacteria*—that can grow on cyclohexanol as sole carbon source.[33] The key step in cyclic ketone carbon assimilation is the Baeyer-Villiger ring expansion to the seven-membered ring lactone. Subsequent enzymic hydrolysis leads to the hydroxy acid which can be processed to standard C_2 and C_4 metabolites (Fig. 8).

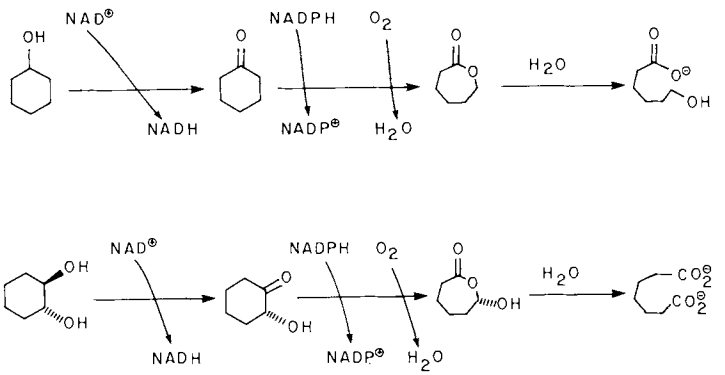

Fig. 8. Metabolic path of cyclohexanol and *trans*-1,2-cyclohexanediol catabolism in *Acinetobacteria*. Cyclohexanone monooxygenase catalyzes the second step in this pathway.

4. Properties of Cyclohexanone Monooxygenase

The enzyme was initially purified from *Acinetobacteria* and *Nocardia* by *Trudgill* et al.[15] and found to be a yellow FAD-containing enzyme of about 60000 daltons. The enzyme is active as a monomer and contains one tightly but noncovalently bound FAD per monomer. The *Acinetobacter* gene has recently been cloned and expressed in *E. coli* and the DNA sequence determined, leading to the first primary sequence of a Baeyer-Villiger enzyme.[53] Analysis of the first 50 residues at the NH_2-terminus reveals a homology to the FAD-binding domain of other flavoenzymes such as glutathione reductase, whose X-ray structure is known, where the glycine clusters represent part of an FAD nucleotide binding domain in the enzyme (Fig. 9).

Fig. 9. Sequence alignment of the FAD-binding region of cyclohexanone monooxygenase (A) and glutathione reductase from human liver (B) and *E. coli* (C). All three sites are located near the NH_2-terminus and display strong homology across species.

The optical spectrum of the enzyme is displayed in Figure 10, showing the characteristic two absorption maxima of FAD in the 375- and 450-nm region.

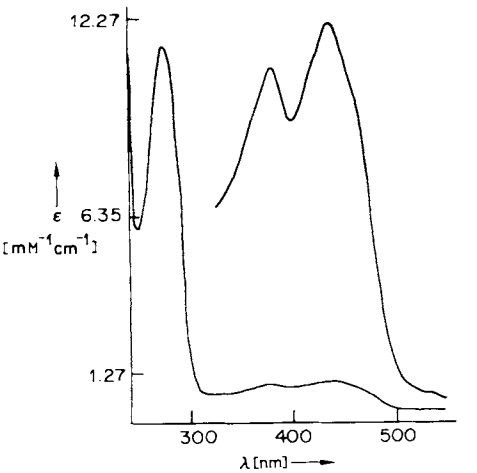

Fig. 10. UV/VIS spectrum of pure cyclohexanone monooxygenase. $\varepsilon_{450} = 11.3\ mM^{-1}\ cm^{-1}$.

Trudgill et al. established that the enzyme would process C_4 to C_8 cyclic ketones (Fig. 11)[15,33] and we have also seen cyclononanone-dependent O_2 and NADPH consumption by the pure enzyme. In fact, the enzyme shows even broader specificity, working on some acyclic ketones and aryl ketones such as acetophenone.[34] The enzyme also oxygenates camphor and fenchone and even, slowly, pregnelone.[35] On initial isolation, there is good coupling of NADPH oxidation to ketone oxygenation with only 0.3% of O_2 being reduced and appearing as H_2O_2, presumably by intramolecular breakdown of the FAD-4a-OOH in the enzyme's active site.[36] As the pure enzyme ages and perhaps denatures a bit in its active site integrity, the uncoupled oxidase rate may rise to 2-3% of the flux.

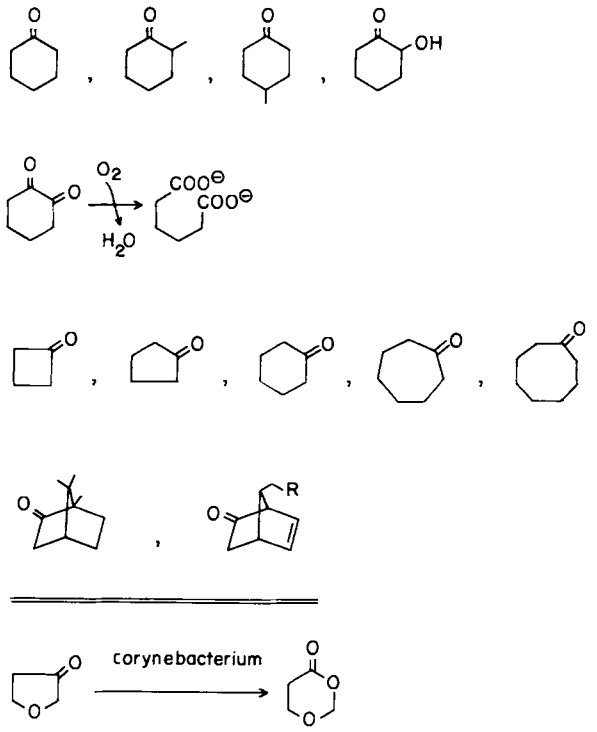

Fig. 11. Cyclic ketone substrate range for cyclohexanone monooxygenase.

4.1. A Baeyer–Villiger Biocatalyst

The migratory aptitude of the enzymic oxygen insertion process has been probed with two types of substrates. First, 2-methylcyclohexanone gives oxygen insertion only between the carbonyl group and the substituted carbon center.[37] Also, phenylacetone is converted into benzyl acetate, reflecting exclusive benzyl migration[34] in accord with the nonenzymic reaction of phenylacetone with trifluoroperacetic acid (Fig. 12). Enzymic processing of the aldehydic substrate phenylacetaldehyde results in both hydrogen and benzyl migration (2:1 hydrogen:benzyl) to yield 65% phenylacetic acid, 12% benzyl formate, and 23% benzyl alcohol. An inverted preference (7:1 to 2:1 benzyl:hydrogen) is seen with various peracids nonenzymically.[38] Aliphatic aldehydes, e.g., butyraldehyde (Fig. 12), yield only carboxylic acids with either cyclohexanone monooxygenase[34] or peroxide reagents.[7] In aldehyde oxidations by this enzyme, in contrast to luciferase, no light emission was detected. The molecular bases for these distinctions are unknown.

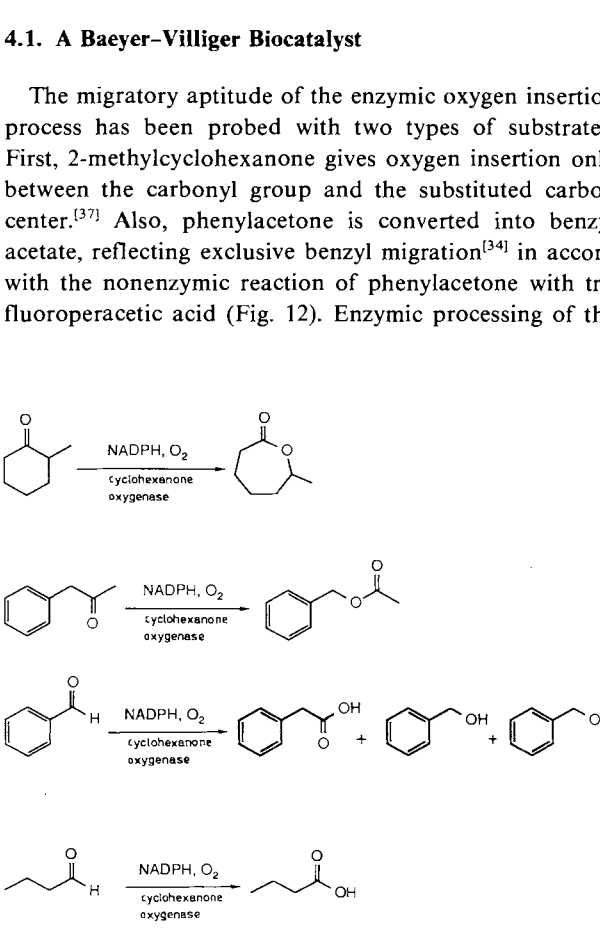

Fig. 12. Migratory aptitude of cyclohexanone monooxygenase-mediated oxygen insertion parallels that of chemical reagents such as trifluoroperacetic acid. Some inverted preferences are observed, possibly as a result of the steric constraints of the active site.

The nonenzymic Baeyer–Villiger reaction proceeds with retention of configuration at the migrating carbon center[39] (Fig. 13a). This aspect of mechanism has been probed with cyclohexanone monooxygenase using (2*R*)-[D_1]cyclohexanone; retention of stereochemical configuration in the monodeuterolactone product was confirmed by NMR spectroscopy.[37] To rule against an enolization, epoxidation, rearrangement route (Fig. 13b), 2,2,6,6-tetradeuteriocyclohexanone was incubated with enzyme and the retention of all deuteriums in the lactone product confirmed by GC/MS analysis. These data, taken in aggregate, strongly support a Baeyer–Villiger mechanism involving formation of a tetrahedral adduct at the cyclohexanone carbonyl in the active site.

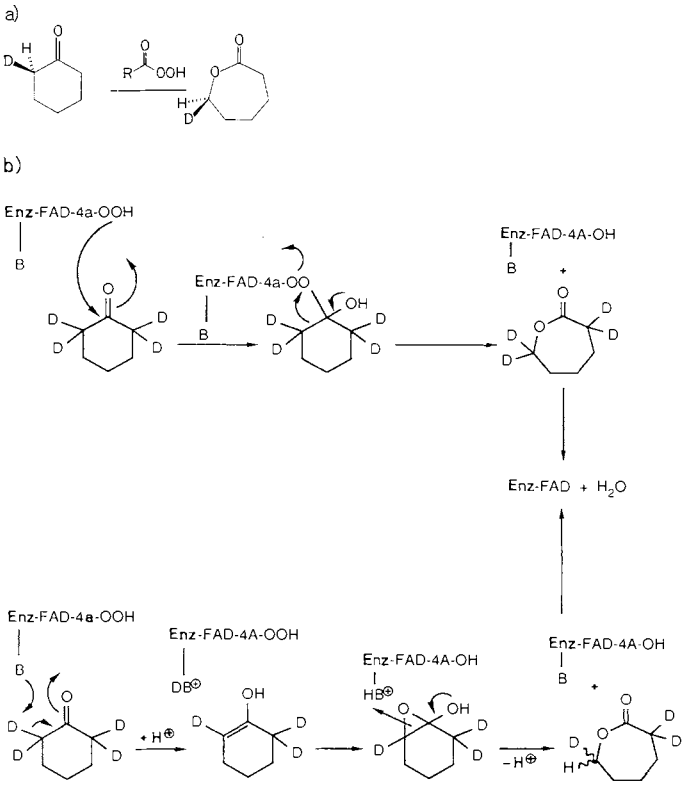

Fig. 13. a) Migration of the carbon center in the enzymic reaction proceeds with retention of stereochemical configuration in accord with the chemical Baeyer–Villiger process. b) Oxygen insertion is suggested to proceed by way of formation of a tetrahedral intermediate which breaks down to products (above). Studies with 2,2,6,6-[D_4]cyclohexanone argue against the enol epoxidation route (below).

To determine whether nascent H_2O_2 generated by two-electron reduction of O_2 might be the oxidant, we determined that incubation with $NADP^{\oplus}$, H_2O_2, cyclohexanone, and enzyme did not yield any lactone product.[40] This negative result coupled with pre-steady-state spectrophotometric kinetic studies supports the idea of an enzyme-bound FAD-4a-OOH intermediate.[41] A corresponding FMN-4a-OOH species is chemically and kinetically competent in luciferase catalysis.[23]

Thus, the mechanism shown in Figure 14 has been proposed as a minimal mechanism for cyclohexanone monooxygenase.[40] NADPH binds to and reduces the enzyme-bound FAD (E-FAD) with a very fast rate (>50000 min^{-1}). The $FADH_2$ likewise reoxidizes with O_2 much more rapidly than catalytic turnover to produce the FAD-4a-OOH. The flavin hydroperoxide can form the hydroperoxy anion (pH optimum of enzyme = 9.0) and act as nucleophile at the ketone (or aldehyde) carbonyl. The tetrahedral adduct then decomposes in the forward direction by typical Baeyer–Villiger migration of one of the carbon–carbon bonds (or the carbon–hydrogen bond for aldehydes) with fragmentation of the weak O–O bond to yield ester (or acid) and flavin-4a-OH, which returns to FAD by internal loss of H_2O.

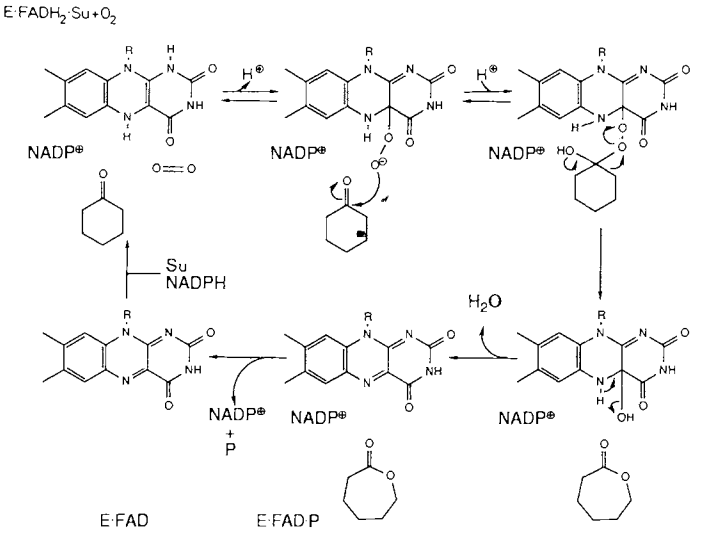

Fig. 14. Mechanistic proposal for oxygen insertion by cyclohexanone monooxygenase. Oxidation of the reduced flavin generates E-FAD-4a-OOH which serves as the oxygen donor. Elimination of water regenerates oxidized flavin for the next catalytic cycle.

One can write more elaborate variants of this mechanism in which the flavin-4a-OOH is not the actual oxygen transfer agent but rather a progenitor of a more activated species such as a flavin oxaziridine, a cyclic 4a,10a-peroxide, a flavin perepoxide, or a ring-opened flavin carbonyl oxide, to name a few (Fig. 15). However, no discrete evidence for such species has been obtained and, by Occam's razor, one stays with the peroxyflavin until proven otherwise. There is the issue of whether the flavin bridgehead hydroperoxide is a sufficiently reactive peroxide reagent. Model data from *Bruice* et al. exist at least for *N*- and *S*-oxygenation, albeit not for Baeyer–Villiger reactions.[41] For *N*- or *S*-oxygenations, the N_5-alkylflavin-4a-hydroperoxide is almost 200000 times more reactive than *tert*-butyl hydroperoxide. *Bruice* et al. have conducted structure–activity studies on these flavin hydroperoxides and find they are well-behaved in an activated peroxide–peracid series[41] where the oxygen-transfer potential of various ROOH species, including flavin-4a-OOH, is correlated with the pK_a of the leaving group alcohol.

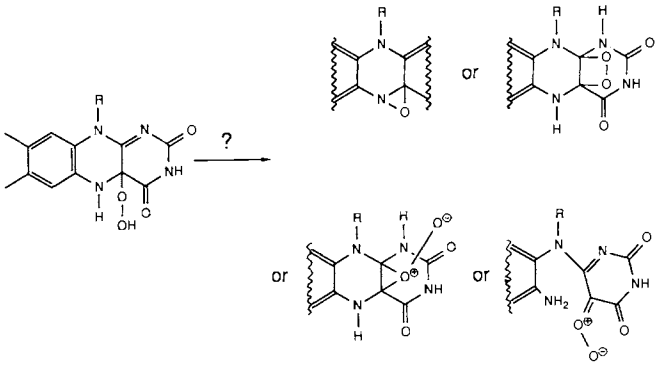

Fig. 15. Other possible flavin oxygen transfer agents derived from FAD-4a-OOH. No evidence yet exists to support these species.

4.2. Heteroatom Oxygenation by Cyclohexanone Monooxygenase

Given the reactivity of flavin-4a-OOH in model *S*- and *N*-oxygenations, one can inquire whether the flavoenzyme oxygenases capable of Baeyer–Villiger catalysis can also oxygenate such heteroatoms. Further, one expects an activated alkyl hydroperoxide equivalent to show ambident reactivity in oxygen transfer, both as initiating nucleophile at ketone carbonyls and for electrophilic transfer to nucleophilic substrates. Indeed, cyclohexanone monooxygenase will oxygenate trimethyl phosphite to trimethyl phosphate, and will also oxidize iodide ion, a classic reagent for titrimetric determination of peroxides.[42]

The enzyme is also active with sulfide substrates, processing thiacyclohexane with 88% the V_{max} of cyclohexanone ($K_m = 24$ μM).[40] If enough product sulfoxide builds up, it can be oxidized on to the sulfone. The K_m for the sulfoxide ($K_m = 170$ μM) is eightfold higher than for thiacyclohexane, and the V_{max} is 60% that of cyclohexanone (Fig. 16a).[34] This qualitatively parallels peracid oxidation of sulfides to sulfoxides with one equivalent of oxidizing reagent and to sulfones with two equivalents.[1,43] As a probe for stereoselectivity of sulfoxidation, ethyl *p*-tolyl sulfide was incubated with the enzyme and found to give 82% *S*-sulfoxide, suggesting only a 4:1 kinetic preference in enantiomeric sulfide recognition (Fig. 16b).[44] No further studies of sulfur stereochemical analysis have been reported with this oxygenase.

Initial studies to evaluate the preference of cyclohexanone monooxygenase for sulfide oxidation versus Baeyer–Villiger oxygenation utilized isomers of thiacyclohexanone. The enzyme converted 3- and 4-thiacyclohexanone exclusively into the lactone products with no detectable

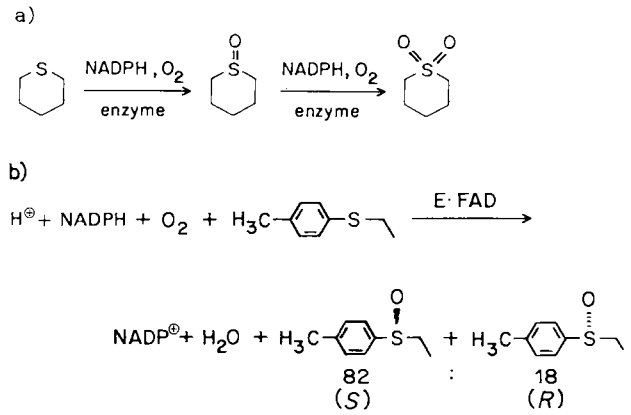

Fig. 16. a) Oxidation of sulfides to sulfones proceeds in two steps by way of the isolable sulfoxide. b) Cyclohexanone monooxygenase-mediated sulfur oxidation appears to be enantioselective as evidenced by a ca. 4 : 1 preference for generation of the (*S*)-sulfoxide.

sulfoxidation.[36] This may reflect preferential recognition of the carbonyl group in initial binding near the flavin peroxide species (Fig. 17).

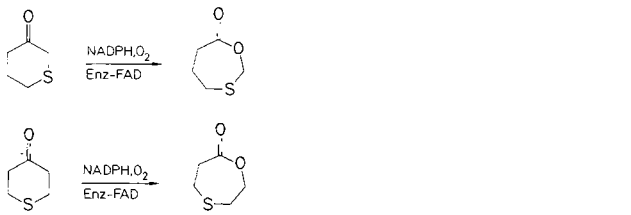

Fig. 17. Enzymic oxidation of thiacyclohexanones is regioselective with a preference for insertion of oxygen adjacent to the carbonyl.

Studies with allyl phenyl sulfide indicated smooth conversion to the sulfoxide by cyclohexanone monooxygenase with no inactivation from potential 2,3-sigmatropic rearrangement of the product allyl sulfoxide (Fig. 18a).[34] The

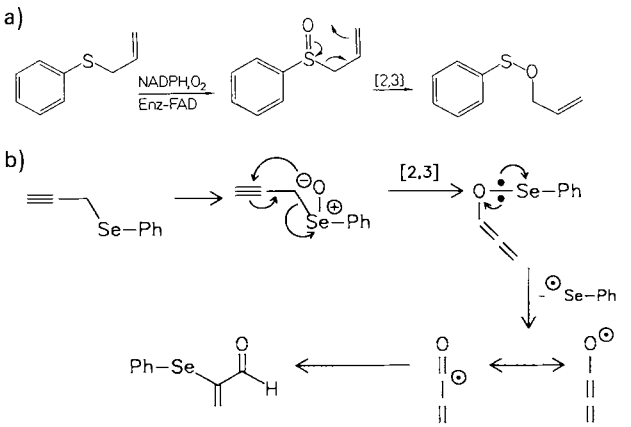

Fig. 18. a) Oxidation of allyl phenyl sulfide to the sulfoxide did not cause enzymic inactivation (from potential 2,3-sigmatropic rearrangement to an electrophilic species). b) Enzymic oxidation of phenyl propargyl selenide [45] yielded the same products of 2,3-sigmatropic rearrangement as those generated by chemical oxidation of the selenide [46].

corresponding selenide was readily oxygenated, again without detectable loss of enzyme activity. When the corresponding phenyl propargyl selenide was enzymically processed (Fig. 18b), the sole product detected was α-phenylselenoacrolein,[45] a product likely to have arisen from enzymic selenoxidation, followed by 2,3-sigmatropic rearrangement to an allenyl selenenic ester, then fragmentation and recombination to the accumulating product. This route is precedented by treatment of the same selenide with ozone in dry organic solvents.[46]

At this point, cyclohexanone monooxygenase has shown versatility in delivery of electrophilic oxygen to a variety of electron-rich heteroatom-containing substrates. To test further for nucleophilic oxygen-transfer initiation beyond the Baeyer–Villiger reaction, we analyzed for oxygen transfer to boron, specifically boronic acid substrates.[34] Both alkylboronic and arylboronic acids are smoothly converted into the corresponding alcohols (Fig. 19) via the intermediate borate esters as hydrolytically labile initial enzyme products. For example, *n*-octylboronic acid is converted into *n*-octanol and boric acid with a K_m lower than that for cyclohexanone (2.5 μM versus 6 μM) and a higher k_{cat} (580 min^{-1} versus 400 min^{-1}), making it the most efficient substrate yet detected for this oxygenase ($k_{cat}/K_m = 3.8 \times 10^6\ M^{-1}\ s^{-1}$).

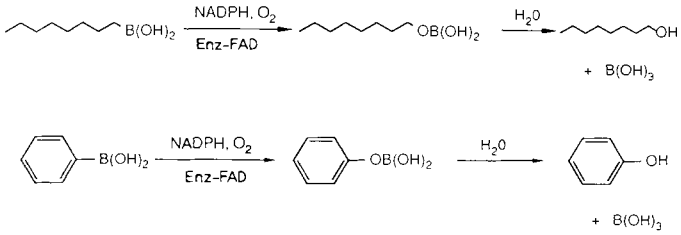

Fig. 19. Cyclohexanone monooxygenase catalyzed the first example of an enzymic boron oxidation, converting boronic acids into the corresponding alcohols.

This was the first example of any enzymic boron oxygenation and seemed likely to proceed by analogy to the Baeyer–Villiger process with attack by a flavin hydroperoxy anion on boron and then decomposition of the adduct with R group migration and O–O bond fission (Fig. 20). The reaction is so facile nonenzymically with peracids that oxygen insertion into carbon–boron bonds is used both synthetically and in organoboron quantitative analy-

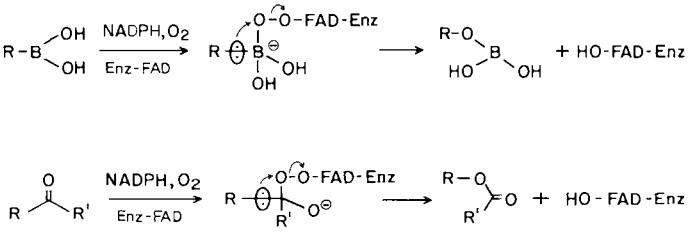

Fig. 20. Mechanistic proposal for oxidation of boronic acids by cyclohexanone monooxygenase via a tetrahedral peroxyboron adduct and alkyl or aryl group migration (top) in analogy to the Baeyer–Villiger process (bottom).

sis.[12,47] It seems that boronic acid substrates may be useful probes for *nucleophilic oxygen equivalents*.[34]

If boronic acid enzymic oxygenation proceeds by a boron equivalent to a Baeyer–Villiger process, then the R group migrating from boron to oxygen should retain stereochemical configuration. This prediction has been validated with (*S,S*)-2-methylcyclohexylboronic acid. Enzymic oxidation yielded the (*S,S*)-2-methylcyclohexanol with quantitative retention of configuration at the migrating cyclohexyl group[48] (Fig. 21). This finding parallels the results obtained for oxidation of dimethyl (*S,S*)-2-methylcyclohexylboronate with H_2O_2 in alkaline medium.[48b]

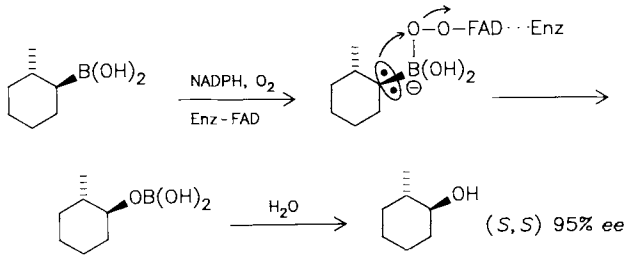

Fig. 21. The enzymic conversion of boronic acids to the borate esters proceeds with retention of stereochemical configuration at the migrating center. Incubation of (*S,S*)-2-methylcyclohexylboronic acid yields the corresponding (*S,S*)-2-methylcyclohexanol.

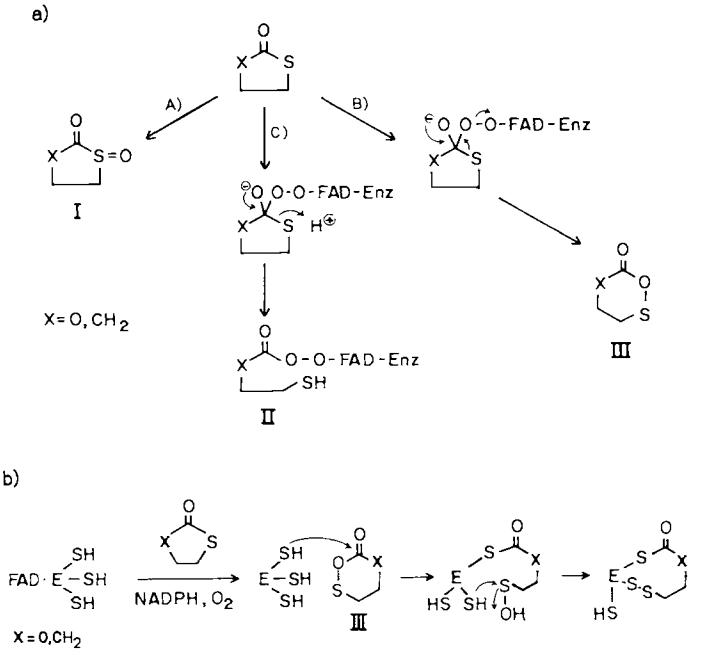

Fig. 22. a) Possible routes for enzymic inactivation by thiolactone substrates. Three pathways involving oxidation of the substrate to extremely reactive electrophilic species, **I**–**III**. b) Acylation of **III** unmasks a second electrophilic site for a cross-linking step, leading to an enzyme disulfide thioester adduct.

4.3. Enzymic Inactivation by Thiolactones and Thiocarbonates

In contrast to the 3-thia- and 4-thiacyclohexanones, cyclohexanone monooxygenase processes 2-thiacyclohexanone and in the process inactivates itself.[36] This thiacyclohexanone isomer is of course a thiolactone which itself could be a reactive acylating agent, but the inactivation of cyclohexanone monooxygenase requires NADPH and O_2 and is clearly mechanism-based. The processing of thiolactones to products is in kinetic competition with enzymic suicidal inactivation. γ-Thiobutyrolactone undergoes 33 turnovers per inactivation event while ethylenethiocarbonate yields 110 turnovers per killing event.[36] With [^{35}S]-γ-thiobutyrolactone, inactivation results in stoichiometric incorporation of one radiolabel per enzyme molecule, but the covalent adduct structure has not yet been determined. Nonetheless, one can propose three alternatives: (1) oxygen transfer to sulfur to yield an acyl sulfoxide, **I**, a known active acylating species, (2) a Baeyer–Villiger-type oxygen insertion to a mixed sulfenic carboxylic anhydride, **III**, or (3) decomposition of the tetrahedral adduct to a perester species, **II** (Fig. 22a). All routes involve generation of an activated acylating species and then uncovering of an electrophilic sulfenic acid group capable of a second cross-linking reaction with a protein residue (e.g., to form a disulfide) (Fig. 22b). This route may have some generality beyond cyclohexanone monooxygenase since thiocarbamate herbicides are known to require enzymic oxygenation in the plants by oxygenases, probably of the cytochrome P_{450} type, to yield acyl sulfoxides, isolable at low temperatures, as active herbicidal acylating agents.[49–50] There is also the possibility that some of the toxicity of the antihypertensive and diuretic agent spironolactone is due to tissue-specific (adrenal and kidney) enzymic *S*-oxygenation (Fig. 23).[51]

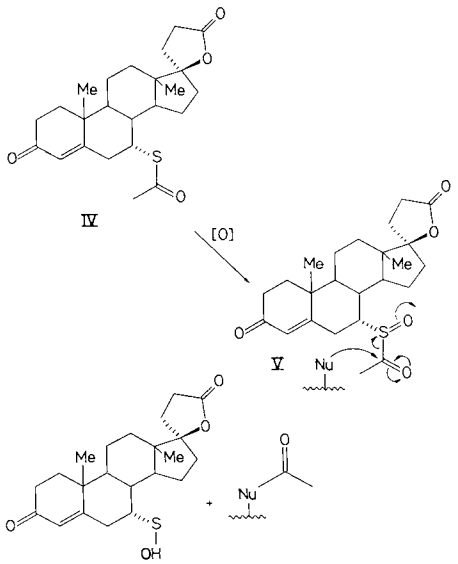

Fig. 23. Possible mode of action for the drug spironolactone **IV**. Enzyme-mediated *S*-oxygenation generates an acyl sulfoxide **V** which captures a free nucleophile to yield an acetylated molecule and an electrophilic sulfenic acid moiety.

5. Concluding Remarks

As a well-studied flavoprotein monooxygenase apparently designed as a Baeyer–Villiger catalyst to degrade cycloalkanones in bacterial metabolism,[33] cyclohexanone

monooxygenase has shown remarkable versatility as an oxygenation reagent. This enzyme has an activated FAD-4a-OOH, bound tightly in its active site, to deliver either a formal "nucleophilic" or "electrophilic" oxygen equivalent, depending on the electron-poor or electron-rich nature of the bound cosubstrate. A representative list of cyclohexanone monooxygenase substrates with K_{cat} values ranging from 50 min^{-1} to ca. 700 min^{-1} is presented in Table 4. It might seem that the enzyme can oxygenate almost any substrate that can diffuse into the active site. However, as Table 5 shows, there are some exceptions, among them 1,3-cyclohexanedione, 2-cyclohexenone, 4-phenylcyclohexanone, 2-butanone, triphenylphosphane, and such ketones as carvone, pulegone, and menthone.

The regiochemistry of Baeyer–Villiger migration has only been examined in a few cases but appears as predicted chemically. Retention of configuration of the migrating group occurs, in the two cases examined, for 2-methylcyclohexanone and for 2-cyclohexylboronic acid oxygenation. We have observed no preference in lactonization of 4-methylcyclohexanone as determined by NMR analysis after derivatization (Y.-C. J. Chen, P. Lodi, C. Walsh, unpublished results);[52] both D- and L-camphor are substrates. There is an apparent 2:1 kinetic preference for (*R*)-2- over (*S*)-2-methylcyclohexanone reacting with the enzyme.[39]

Table 4. Substrate range of cyclohexanone monooxygenase from *Acinetobacteria*.

	K_m [μM]	k_{cat} [min^{-1}]
	6	400
	16	455
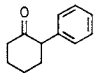	-	86
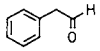	350	68
	25	159
	29	521
	21	491
	10	692
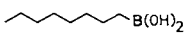	2.5	660
	24	396
	30	373
$P(OEt)_3$	360	228
NaI	2500	196
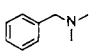		50

Table 5. Scope of oxygenations catalyzed by cyclohexanone monooxygenase. The enzyme appears to be sensitive to large functionalities on the substrate molecule.

Substrates	Not substrates
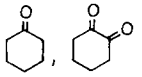	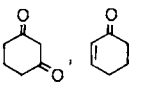
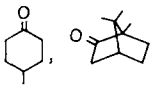	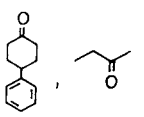
$P(OMe)_3$	PPh_3
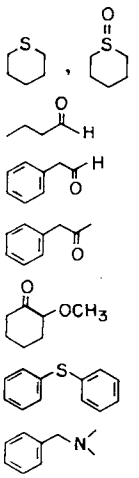	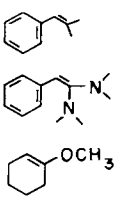

Repeated efforts to epoxidize olefinic double bonds such as that of dimethyl styrene and enols such as the methyl enol ether of cyclohexanone or an enamine, 2-phenylvinylidenebis(dimethylamine), have all failed with this enzyme (J. Latham, Y.-C. J. Chen, C. Walsh, unpublished results) and we raise the question whether the intrinsic reactivity of the enzyme-bound FAD-4a-OOH (or a reactive species derived therefrom) is sufficient for olefin epoxidations. Thus, in Table 6, we list the scope of oxygenations known to be carried out by flavin-based or iron-based monooxygenases. Below the dashed line, and well-exemplified by cyclohexanone monooxygenase, is the province of flavin-linked oxygenases. Above the line are the epoxidations of isolated double bonds and of aromatic double bonds (where the initial dihydroaromatic arene oxides rearrange unimolecularly to phenols) and the hydroxylation at unactivated sp^3 carbon centers (e.g., in camphor). To date, these constitute the exclusive province of oxo-iron enzyme reagents (and also a few oxo-copper enzymes). While flavin-dependent monooxygenases may yet be shown to epoxidize olefins, it may be that epoxidations and alkane hydroxylations require the oxo-iron enzyme biological "oxygen-guns" to be wheeled up.

Lastly, all examples yet characterized of Baeyer–Villiger enzymes are flavoproteins and it is likely one can antici-

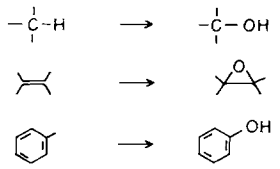

Flavin-dependent monooxygenases

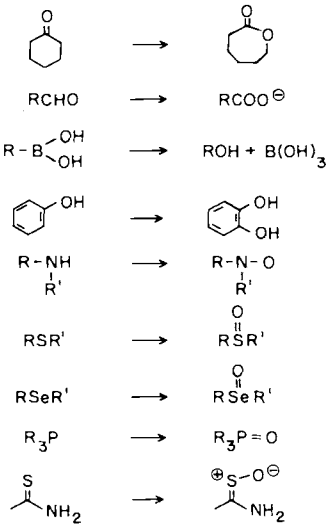

pate them to be the biological reagents for many other biological Baeyer–Villiger transformations occurring in more complex natural product structures.

Received: April 22, 1987;
revised: August 31, 1987 [A 660 IE]
German version: *Angew. Chem. 100* (1988) 342

[1] J. B. Lee, B. C. Uff, *Q. Rev. 21* (1967) 429.
[2] C. Rugero, J. C. Edwards in D. Swern (Ed.): *Organic Peroxides*, Wiley-Interscience, New York 1970, p. 199.
[3] H. Mimoun, *Angew. Chem. 94* (1982) 750; *Angew. Chem. Int. Ed. Engl. 21* (1982) 734.
[4] H. A. Milas, S. A. Harris, P. C. Panagiotakos, *J. Am. Chem. Soc. 61* (1939) 2430.
[5] D. H. R. Barton, W. D. Ollis, J. F. Stoddart (Eds.): *Comprehensive Organic Chemistry*. Pergamon Press, Oxford 1979, p. 920.
[6] R. Criegee, W. Schnorrenberg, J. Becke, *Justus Liebigs Ann. Chem. 565* (1949) 7.
[7] R. Hiatt in D. Swern (Ed.): *Organic Peroxides*, Wiley-Interscience, New York 1971, p. 1.
[8] C. M. Hassall, *Org. React. 9* (1957) 73.
[12] H. E. Conrad, R. Dubus, M. J. Namvedt, I. C. Gunsales, *J. Biol. Chem. 240* (1965) 495.
[13] L. N. Britton, A. J. Markavetz, *J. Biol. Chem. 252* (1977) 8561.
[14] M. A. Rahum, C. J. Sih, *J. Biol. Chem. 241* (1966) 3615.
[15] N. A. Donoghue, D. B. Norris, P. W. Trudgill, *Eur. J. Biochem. 63* (1976) 175.
[16] K. H. Nealson, J. W. Hastings, *Microbiol. Rev. 43* (1979) 496.
[17] C. A. Townsend, S. B. Christiansen, S. G. Davis, *J. Am. Chem. Soc. 104* (1982) 6154.
[18] C. Walsh: *Enzymatic Reaction Mechanisms*, Freeman, San Francisco 1979, p. 501.
[19] B. Entsch, D. P. Ballou, V. Massey, *J. Biol. Chem. 251* (1976) 2550.
[20] T. A. Dix, S. J. Benkovic, *Biochemistry 24* (1985) 5839.
[21] R. C. Rosenberg, W. Lovenberg in M. Youdim, W. Lovenberg, D. F. Sharman, J. R. Lagnado (Eds.): *Essays in Neurochemistry and Neuropharmacology*. Wiley, New York 1980, p. 163.
[22] C. Walsh, *Acc. Chem. Res. 13* (1980) 148.
[23] S. Ghisla, J. W. Hastings, V. Favaudon, J. M. Lhoste, *Proc. Natl. Acad. Sci. USA 75* (1978) 5860.
[24] C. A. Yu, J. C. Gunsalus, *J. Biol. Chem. 244* (1969) 6149.
[25] H. J. Ougham, D. G. Taylor, P. W. Trudgill, *J. Bacteriol. 153* (1983) 140.
[26] E. Itagake, M. Katagiri in R. Bray (Ed.): *Flavins and Flavoproteins*. de Gruyter, Berlin 1984, p. 639.
[27] D. H. Cohn, R. C. Ogden, J. N. Abelson, T. O. Baldwin, K. H. Nealson, M. I. Simon, A. J. Mileham, *Proc. Natl. Acad. Sci. USA 80* (1983) 120.
[28] J. W. Hastings, K. H. Nealson, *Annu. Rev. Microbiol. 31* (1977) 549.
[29] J. W. Hastings, C. J. Potrikus, S. C. Gupta, M. Kurfurst, J. C. Makemson, *Adv. Microbial Physiol. 26* (1985) 236.
[30] S. Ghisla, P. Macheroux, J. Eckstein in D. McCormick, D. Edmondson (Eds.): *Flavins and Flavoproteins*. de Gruyter, Berlin 1987, in press.
[31] P. Macheroux, S. Ghisla, *Nachr. Chem. Tech. Lab. 33* (1985) 785.
[32] T. C. Bruice in V. Massey, C. Williams (Eds.): *Flavins and Flavoproteins*, Elsevier/North Holland, New York 1982, p. 265.
[33] P. W. Trudgill in D. T. Gibson (Ed.): *Microbial Degradation of Organic Compounds*, Marcel Dekker, New York 1984, p. 131.
[34] B. P. Branchaud, C. Walsh, *J. Am. Chem. Soc. 107* (1985) 2153.
[35] O. Abril, *Ph. D. Thesis*, Massachusetts Institute of Technology, Cambridge, MA, USA 1983.
[36] J. A. Latham, C. Walsh, *J. Am. Chem. Soc. 109* (1987) 3421.
[37] J. Schwab, W. B. Li, L. P. Thomas, *J. Am. Chem. Soc. 105* (1983) 4800.
[38] M. J. Rayer, M. Beugelmas-Verrier, *C. R. Acad. Sci. Ser. C272* (1971) 1818.
[39] J. Schwab, *J. Am. Chem. Soc. 103* (1981) 1976.
[40] C. C. Ryerson, D. P. Ballou, C. Walsh, *Biochemistry 21* (1982) 2644.
[41] T. C. Bruice, J. B. Noar, S. S. Ball, U. V. Venkataram, *J. Am. Chem. Soc. 105* (1983) 2452.
[42] S. Siggia: *Quantitative Organic Analysis Via Functional Groups*, Wiley-Interscience, New York 1979, p. 325.
[43] B. Plesnicar in W. Trahanovsky (Ed.): *Oxidation in Organic Chemistry*, Academic Press, New York 1978, p. 211.
[44] D. Light, D. Waxman, C. Walsh, *Biochemistry 21* (1982) 2490.
[45] J. A. Latham, B. P. Branchaud, Y.-C. J. Chen, C. Walsh, *J. Chem. Soc. Chem. Commun. 1986*, 528.
[46] H. J. Reich, K. E. Yelm, S. Wallowitz, *J. Am. Chem. Soc. 105* (1983) 2503.
[47] R. D. Strahm, M. F. Hawthorne, *Anal. Chem. 32* (1960) 530.
[48] a) J. A. Latham, C. Walsh, *J. Chem. Soc. Chem. Commun. 1986*, 527; b) H. C. Brown, B. Singaram, *J. Am. Chem. Soc. 106* (1984) 1797.
[49] M. M. Lay, J. P. Hubbell, J. E. Casida, *Science 189* (1975) 287.
[50] Y. S. Chen, J. E. Casida, *J. Agric. Food Chem. 27* (1979) 1601.
[51] R. H. Menard, T. M. Guenther, H. Kon, J. R. Gillette, *J. Biol. Chem. 254* (1979) 1726.
[52] I. J. Jakovac, B. J. Jones, *J. Org. Chem. 44* (1979) 2165.
[53] Y.-C. J. Chen, O. Peoples, C. Walsh, *J. Bacteriol.*, in press.

Oxo-Bridged Polyiron Centers in Biology and Chemistry**

By Stephen J. Lippard*

The functions of iron in biology are often associated with heme or iron-sulfur proteins. But dioxygen transport, reduction of ribo- to deoxyribonucleotides, acid phosphatase activity, oxidation of methane to methanol, and iron storage are among the growing list of biological phenomena known or believed to be associated with a newly emerging class of proteins having oxo-bridged di- or polyiron aggregates at their metallic cores. The recognition of these iron-oxo proteins as a separate class has stimulated efforts on the part of inorganic chemists to prepare and characterize model compounds that replicate the physical properties and functions of the polymetallic protein cores. As a consequence, a variety of new oxo-bridged di-, tri-, tetra-, hexa-, octa-, and undecairon aggregates has been synthesized. These novel molecules promise not only to provide insight into the detailed characteristics of the metal centers in iron-oxo proteins, but also to serve as a focal point for preparing new materials, including oxidation catalysts and corrosion inhibitors, for the evolution of new theories to describe their physical properties, for developing new strategies for the treatment of iron-related disease, and for building links between the chemistry of the biosphere and the geosphere.

1. Introduction

Of all the transition elements, none is more prevalent in the sea or the earth's crust than iron.[1] In aqueous solution, the chemistry of iron is dominated by ferrous ($Fe^{2\oplus}$) and ferric ($Fe^{3\oplus}$) species, and its complexes are well known to undergo facile acid-base and electron transfer reactions.[2] Iron is therefore ideally suited for its many roles in biology, which include the transport and storage of dioxygen (O_2) and the catalysis of numerous reactions that utilize O_2.[1] In much of its biological chemistry, iron is chelated by a porphyrin ligand. In this form, it transports and stores O_2, in hemoglobin (Hb) and myoglobin (Mb), respectively, and catalyzes the oxidation of organic substrates, in cytochrome P-450, for example.[3] Another common source of Fe in biology are the iron-sulfur proteins, which function as electron transfer catalysts and participate in nitrogen fixation.[4] A third major class of iron-binding proteins contains neither cofactors nor sulfur clusters and includes transferrin and catechol dioxygenases.[5] The present discussion focuses on proteins in this third category that have two or more iron atoms known or thought to be linked by one or more oxygen atoms as bridging oxo, hydroxo, or alkoxo ligands. Although some of these proteins, such as ferritin and hemerythrin, have been known and studied for several decades, others have been subjects of interest only recently, as similarities among the structural and physical properties of their polyiron centers have begun to emerge.

Table 1 lists proteins currently known to contain an oxo-bridged binuclear or, in the case of ferritin, polynuclear iron center, together with their functions.[6-13] Although the properties of several of these proteins are discussed in greater detail below, some general observations are relevant in the present context. Hemerythrin (Hr), ribonucleotide reductase (RR), and methane monooxygenase (MMO) may all be comprised of the same or closely related (μ-oxo)bis(μ-carboxylato)diiron cores (Fig. 1). Their functions differ distinctly, however, Hr being a reversible oxygen carrier, whereas MMO and RR catalyze the oxidation of methane and reduction of ribonucleotides, respectively. Thus, the local protein environment may alter the properties of similar bimetallic centers to evoke the desired bio-

Table 1. Polyiron-oxo proteins: their abbreviations and biological functions.

Protein	Biological function	Occurrence	M_r	Ref.
Hemerythrin (Hr)	Oxygen transport	Marine invertebrates	108000[a]	[6]
Ribonucleotide reductase (RR)	Reduction of ribo- to deoxyribonucleotides	Animals, viruses, bacteriophages, prokaryotes	200000-300000[b]	[7, 8]
Purple acid phosphatases (PAP), uteroferrin	Unknown	Mammals, plants	35000-110000	[9]
Methane monooxygenase (MMO)	Methane oxidation	Methanotrophic bacteria	272000[c]	[10-12]
Ferritin (Ft) hemosiderin	Iron storage	Most life forms	450000	[13]

[a] Refers to the octamer. Dimers, trimers, and tetramers also exist. The molecular weight of monomeric myohemerythrin is 13900. [b] Comprised of two identical 80-90-kD and two identical 35-55-kD subunits, the former of which bind iron. In bacterial forms, these are designated B1 and B2, respectively. [c] Comprised of non-heme iron component A ($M_r = 210000$), 20-kD component B, and iron-sulfur flavoprotein component C ($M_r = 42000$). Component A has three subunits ($M_r = 54000$, 42000, 17000) present in stoichiometry $\alpha_2\beta_2\gamma_2$.

[*] Prof. S. J. Lippard
Department of Chemistry, Massachusetts Institute of Technology
Cambridge, MA 02139 (USA)

[**] In this article, "oxo-bridged" is usually taken to mean a bridging oxygen atom derived from an oxo ligand, but also refers generically to species with bridging $OH^{\ominus}$ or $OR^{\ominus}$ ligands.

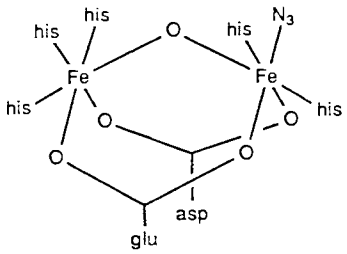

Fig. 1. Binuclear unit found in azidomet- and azidometmyohemerythrin. Similar (μ-oxo)bis(μ-carboxylato)diiron cores may occur in RR and MMO.

logical response. This phenomenon has interesting parallels in the biochemistry of other iron and copper metalloproteins.[1,14] The diiron center in Hr, like the dicopper center in hemocyanin and the iron porphyrin centers in Hb and Mb, binds O_2 reversibly, while the putative $[Fe_2O(O_2CR)_2]$ and $[Fe_2(OH)(O_2CR)_2]$ cores in RR and MMO, like the respective dicopper and iron porphyrin cores in tyrosinase and cytochrome P-450, for example, catalyze reactions involving oxygen-atom transfer steps. Uncovering the principles used by Nature to tune these centers to perform such diverse functions is a major incentive for investigating their chemistry.

			pK_a
$Fe^{3\oplus} + H_2O$	⟶	$Fe(OH)^{2\oplus} + H^{\oplus}$	2.2
$2Fe^{3\oplus} + 2H_2O$	⟶	$Fe_2(OH)_2^{4\oplus} + 2H^{\oplus}$	2.9
$Fe(OH)^{2\oplus} + H_2O$	⟶	$Fe(OH)_2^{\oplus} + H^{\oplus}$	3.5
$Fe(OH)_2^{\oplus} + H_2O$	⟶	$Fe(OH)_3 + H^{\oplus}$	6
$Fe(OH)_3 + H_2O$	⟶	$Fe(OH)_4^{\ominus} + H^{\oplus}$	10

Fig. 2. Hydrolysis reactions of iron(III) at 25°C, $\mu = 0$. Data were taken from Ref. [15].

Figure 2 reveals the tendency for iron(III) to hydrolyze in the physiological pH range 6–8, forming the familiar brown precipitate known as rust.[15] As a consequence, there were few well-characterized classes of soluble, oxo-bridged polyiron complexes prior to the work that is the major focus of this article. Among the better known discrete oxo-bridged polyiron complexes are the basic iron carboxylates first prepared early in this century.[16] The magnetic behavior of these trinuclear iron(III) oxo complexes (Fig. 3a) has been the subject of extensive investigations.[17–21] These compounds have recently formed the basis for a new class of alkane oxidation catalysts,[22] and many derivatives[23] and mixed-valence analogues[24] are now known. Another important species has been (μ-oxo)diiron(III) (Fig. 3b), recognized as a thermodynamically very stable entity in the hydrolytic coordination chemistry of iron.[2] Numerous complexes containing the linear $[Fe_2O]^{4\oplus}$ core have been characterized.[25,26] The molecular geometries of species depicted in Figures 1 and 3 differ significantly, however, and except for a structurally poorly characterized mineral known as ferrihydrite,[27,28] postulated as a model for the polyiron oxo core in the iron-storage protein ferritin (Ft),[29] accurate model compounds for oxo-bridged polyiron centers in biology did not exist prior to 1984.

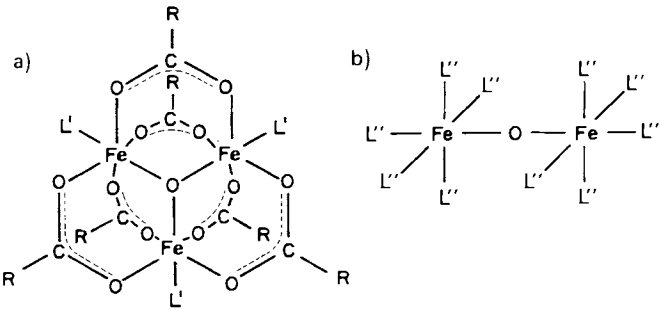

Fig. 3. Two common oxo-bridged polyiron species: a) the basic iron carboxylate structure; b) the (μ-oxo)diiron(III) structure. $L' = H_2O$, pyridine, etc.; e.g., $R = CH_3$.

In the following discussion, we first describe what is known about various members that constitute the class of iron-oxo proteins and, more importantly, what remains to be learned. Relevant iron chemistry is then described, building from simple binuclear hemerythrin model complexes to Fe_3, Fe_4, Fe_6, Fe_8, and Fe_{11} aggregates of higher nuclearity. In comparing the physical and chemical properties of well-defined inorganic complexes with those of the protein cores, we hope to learn, ultimately, "how Nature has managed to fashion a bioinorganic chemistry of rust."[30]

2. Proteins Containing Oxo-Bridged Polyiron Centers

2.1. Hemerythrin

Hemerythrins (Hr's) are the oxygen transport proteins of marine invertebrates including members of the Sipunculida, Priapulida, and Brachiopoda phyla.[6,31,32] Single- and multi-subunit forms are known and referred to as myoHr and Hr, respectively. X-ray crystal structure studies of the functionally inactive, oxidized (met) forms of myoHr and Hr have been determined, in which the dioxygen binding site is either occupied by $N_3^{\ominus}$ or vacant.[33,34] The structure of the diiron(III) center in azidometmyoHr is shown in Figure 4. The two iron atoms are bridged by an oxygen atom and two bidentate carboxylate groups from glutamate and aspartate amino acid residues. The $[Fe_2O(O_2CR)_2]^{2\oplus}$ core is further anchored to the protein by the imidazole side chains of five histidine residues, three of which occupy an octahedral face of one iron atom and two of which coordinate to the other iron atom. The sixth octahedral site on the second iron atom is filled by the azide nitrogen atom. This structure is consistent with magnetic and spectroscopic data on met forms of the protein, indicating two strongly antiferromagnetically coupled ($J \approx -134$ cm^{-1}), high-spin Fe^{III} atoms.[35]

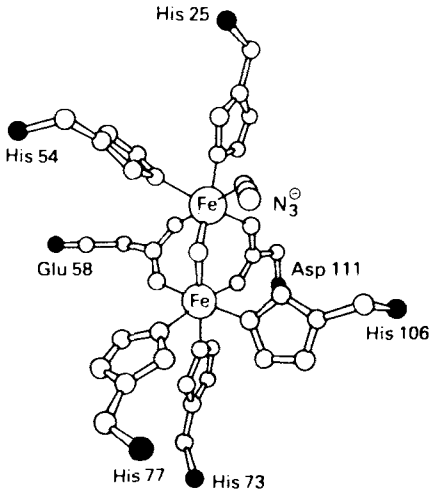

Fig. 4. Structure of the diiron center in azidometmyohemerythrin from *T. zostericola* [34] (reproduced by permission from Ref. [34]).

Magnetic susceptibility, Mössbauer, MCD (magnetic circular dichroism), EXAFS, ^{1}H-NMR, and low-resolution (3.9 Å) X-ray data on deoxy Hr suggest the presence of a $[Fe_2(OH)(O_2CR)_2]^{\oplus}$ core with one five-coordinate (Fe_A) and one six-coordinate (Fe_B) high-spin Fe^{II} center and weak antiferromagnetic coupling ($J \approx -15$ cm^{-1}).[36-40] Similar studies, including resonance Raman spectroscopic experiments, indicate that oxy Hr is best formulated as a hydroperoxy derivative of the (μ-oxo)bis(μ-carboxylato)diiron(III) core, with the hydroperoxide ligand filling the sixth coordination site of Fe_A.[4] Thus, the reversible dioxygen binding reaction of Hr may be viewed as oxidative addition and reductive elimination of O_2 to the diiron center (Fig. 5). Since dioxygen binding to *P. gouldii* Hr is pH-independent, internal proton transfer from the bridging hydroxide ligand in deoxy Hr to the hydroperoxide group in oxy Hr is postulated (Fig. 5).[41] Moreover, resonance Raman studies of oxy Hr, including ^{18}O and ^{2}H isotope substitution experiments, suggest that the proton on the hydroperoxide ligand is hydrogen bonded to the μ-oxo group. This hydrogen bond may be a key component that facilitates the kinetics of the oxygen binding reactions (see Section 3.5).

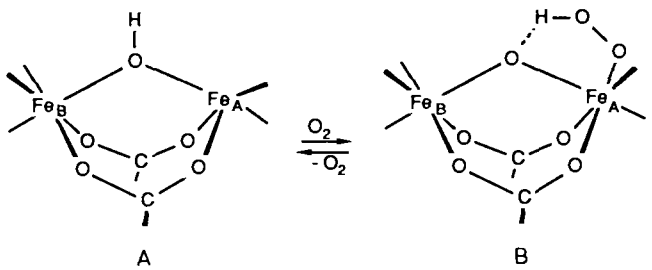

Fig. 5. Proposed model for reversible oxygen binding to hemerythrin [41]. **A** = deoxy Hr, **B** = oxy Hr.

Although the main features of the functional center in Hr are reasonably well understood, the protein continues to be a focus for physical and chemical studies because it is the prototype for other oxo-bridged diiron proteins about which much less is known. One point of interest is the existence of various redox states of Hr, for in addition to deoxy [Fe^{II},Fe^{II}], oxy [Fe^{III},Fe^{III}], and functionally inactive met [Fe^{III},Fe^{III}] Hr, several mixed-valence semimet [Fe^{II},Fe^{III}] forms are known (Fig. 6).[6] Numerous kinetic studies of electron transfer to, from, and among these forms have been reported.[6,42,43] Recent ^{1}H-NMR probes of the binuclear core have correlated chemical shifts with the extent of antiferromagnetic exchange between iron atoms in the different forms and, in particular, estimated J for semimet Hr to be ca. -20 cm^{-1}.[39] Derivatives have been prepared in which the bridging oxide atom in Hr has been replaced by sulfide or selenide, the semimet versions of which have been characterized.[44-46] The iron atoms of azidosemimet Hr have a trapped [Fe^{II},Fe^{III}] valence state on the NMR time scale (ca. 10^{-4} s) and the sulfide-bridged form of semimet Hr has the same trapped valence on the Mössbauer time scale (10^{-7} s).[39]

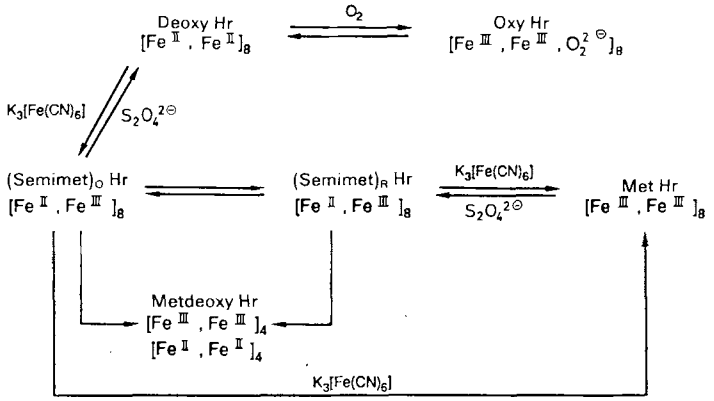

Fig. 6. Redox states of hemerythrin and their interconversion (after Ref. [6]).

The met form of Hr, very little of which is found in freshly isolated sipuncular worm erythrocytes, is unable to function in the oxygen-binding reaction (Fig. 5) unless first reduced to deoxy Hr. Recently, a cytochrome b_5 in *P. gouldii* erythrocytes was discovered, which appears to be one component of a potential system for reduction of met Hr in vivo.[47]

2.2. Ribonucleotide Reductase

Ribonucleotide reductases (RR's) catalyze the conversion of ribonucleotides to deoxyribonucleotides (Fig. 7), the first committed step in DNA biosynthesis. There are at least two major classes of this enzyme, a bacterial and cyanobacterial form that is dependent upon coenzyme B_{12}, and a form containing iron that occurs in bacteria including *Escherichia coli*, in mammals including man, and in herpes simplex and Epstein Barr viruses.[7,8,48] Although the detailed mechanism by which these enzymes catalyze reduction of the 2′ hydroxyl group of ribose is unknown, they are both believed to function by radical reactions in which $H^{\odot}$ is abstracted from the 3′ carbon atom of the sugar ring.[48,49] Adenosylcobalamin cofactors are well

known to promote such free radical reactions through homolytic cleavage of the Co-C bond.[50] The iron-containing RR enzymes have, in addition to a binuclear iron center with properties similar to the $[Fe_2O(O_2CR)_2]^{2\oplus}$ core in Hr,

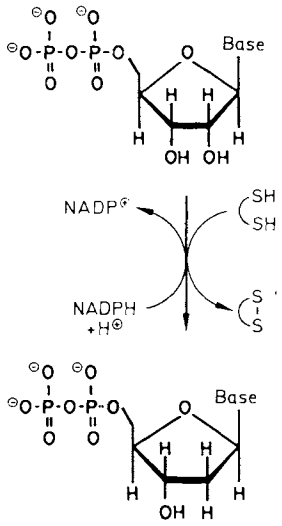

Fig. 7. Reaction catalyzed by RR.

a stable deprotonated tyrosine radical that has been implicated in the catalytic mechanism.[51] The protein is made up of two subunits, designated in the bacterial enzymes as B1 and B2. The B1 subunit ($M_r \approx 170000$) is comprised of two nearly identical protein chains, α and α′, binds substrates and allosteric effectors, and contains mercapto groups required for reducing the substrate. The B2 subunit ($M_r \approx 87000$) is made up of two identical chains, β, either one of which may contain the free radical tyrosine residue (Tyr 122)[52] and which together bind the binuclear iron unit.

Although X-ray crystallographic structural information is not yet available to define the diiron center in RR (the B2 dimer has been crystallized[53]), resonance Raman,[54] magnetic and UV/VIS spectroscopic data,[55] and Mössbauer results[56] all support an oxo-bridged diiron(III) formulation. This assignment is especially convincing, given the similarity of these properties to those of azidomet Hr and met Hr[33,34] and model complexes,[57,58] discussed in Section 3.3, having the $[Fe_2O(O_2CR)_2]^{2\oplus}$ core (Table 2).

Recent EXAFS studies of the B2 subunit obtained from a heat-inducible overproducing *E. coli* strain[59] have yielded the metrical parameters given in Table 2. Similar results were obtained in an independent study.[60] Since the shell due to the five Fe-O/Fe-N bonds around each iron other than the Fe-$O_{\mu\text{-oxo}}$ bond is 0.07 Å shorter for B2 RR than for azidomet Hr or the model compound $[Fe_2O(O_2CCH_3)_2(HBpz_3)_2]$, **2b** (see Section 3.3), one or more of the terminal nitrogen atoms in these latter two species is postulated to be replaced by hydroxide, phenolate, or carboxylate in RR. Paramagnetically shifted ^{1}H-NMR resonances observed for the B2 subunit of *E. coli* RR have been assigned to histidine ligands.[62] Taken together, these results have been interpreted in terms of the structural model shown in Figure 8.[61] Resonance Raman work on B2 RR and its ^{18}O-substituted derivative supports the presence of terminal hydroxide ligands and an Fe-O-Fe angle of 138°.[61]

Table 2. Properties of the $[Fe_2O(O_2CR)_2]^{2\oplus}$ cores of hemerythrin (Hr), ribonucleotide reductase (RR), and a model complex.
a) Structural features [34, 57, 59].

	AzidometmyoHr	RR	$[Fe_2O(O_2CCH_3)_2(HBpz_3)_2]$ **2b**
d(Fe-$O_{\mu\text{-oxo}}$) [Å]	1.80, 1.77	1.78	1.784
Fe-O-Fe angle [°]	132	127	123.6
d(Fe···Fe) [Å]	3.26	3.2	3.146

b) Mössbauer and magnetic features [32, 35, 56, 57]

	Met Hr	RR	**2b**
Isomer shift [mm s^{-1}]	0.46	0.53, 0.44	0.52
Quadrupole splitting [mm s^{-1}]	1.57	1.66, 2.45	1.60
J [cm^{-1}]	−134	−108	−121

c) Vibrational spectroscopic features [32, 41, 57, 61].

	Azidomet Hr	RR	**2b**
$\tilde{\nu}$ (ν_s) [cm^{-1}]	507	492	528
$\tilde{\nu}$ (ν_{as}) [cm^{-1}]	770	756	751

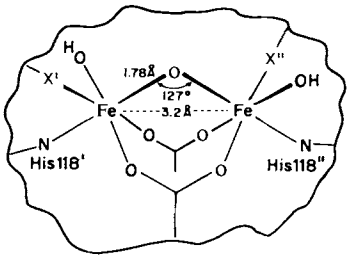

Fig. 8. Postulated structure [61] for the diiron center of RR, based on information provided in Refs. [57-62]. N represents a histidine nitrogen atom, OH, a hydroxide anion, and X, an unassigned ligand. Ligands from different subunits are designated by superscripts (′ and ″) (after Ref. [61]).

Very little is known about the role of the oxo-bridged diiron(III) center in the function of RR. Removal of iron by prolonged dialysis against chelating agents inactivates the enzyme and destroys the ESR signal of the tyrosine free radical. Both the enzymatic activity and the ESR signal can be restored upon addition of iron(II) in the presence of O_2.[49] It has been suggested that nucleotide phosphate groups might bind the binuclear $[Fe_2O]^{4\oplus}$ core, by analogy to the chemistry of model compounds,[63] but no experiments bearing on this point have been carried out. Establishing the role of iron in the catalytic function of RR is clearly an important objective. Further discussion of the inhibition of the enzyme by chelators, redox agents, or hydroxyurea, the role of such agents in chemotherapy, and other details about the formation of the tyrosine radical is available.[48,49,61]

2.3. Methane Monooxygenase

Methanotrophic bacteria, which utilize methane as their sole carbon and energy source, oxidize methane to methanol, formaldehyde, formate, and eventually carbon dioxide.[10] The initial oxidation to methanol has been shown for *Methylococcus capsulatus* (Bath) to be catalyzed by a

multicomponent methane monooxygenase (MMO). Component A of this enzyme system is comprised of three subunits, α, β, and γ, having molecular weights of 54000, 42000, and 17000, respectively, with the native protein having the stoichiometry $\alpha_2\beta_2\gamma_2$.[12] The active site of the enzyme appears to consist of a binuclear iron center capable of accessing the redox states [Fe^{II},Fe^{II}], [Fe^{II},Fe^{III}], and [Fe^{III},Fe^{III}] with midpoint potentials of -25 mV and $+350$ mV, respectively.[64] ESR studies[64] of the mixed-valence state revealed a signal showing principal g values of $g_z = 1.78$, $g_y = 1.88$, $g_x = 1.95$, values similar to those reported for semimet Hr. The ESR study also revealed a broad free radical signal at $g = 2.011$ with some partly resolved hyperfine structure. Very recent iron EXAFS data on semimet component A reveal an Fe–Fe distance of 3.41 Å and no short Fe–$O_{\mu\text{-oxo}}$ bond.[65] These results suggest that a binuclear iron core functions to promote the oxidation of methane to methanol in MMO, although considerably more work is required to establish its structure and role in the catalytic mechanism.

That Nature may have chosen a binuclear iron center to catalyze both the reduction of the hydroxyl group in ribonucleotides (RR) and oxidation of alkanes to alcohols (MMO) may be no coincidence. The latter reaction, the oxidation of saturated hydrocarbons, is of considerable industrial interest.[22]

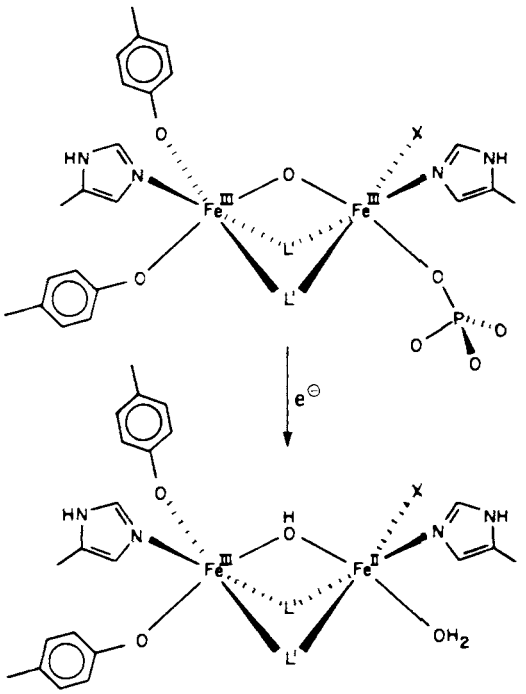

Fig. 9. Proposed structures for the oxidized, purple (top) and reduced, pink (bottom) forms of purple acid phosphatases (after Ref. [67]). L' and X are unidentified.

2.4. Purple Acid Phosphatases (Uteroferrin)

These enzymes have been isolated from a variety of microbial, plant, and animal sources. They occur in a purple ($\lambda_{max} = 550$–575 nm), catalytically inactive diiron(III) form and an enzymatically active, mixed-valence pink ($\lambda_{max} = 505$–515 nm) diiron(II,III) form.[9] Although the true biological function of the purple acid phosphatases is unknown, they catalyze the dephosphorylation of phosphoproteins and nucleotides and are assayed by their ability to hydrolyze *p*-nitrophenyl phosphate to *p*-nitrophenol and inorganic phosphate. The magnetic and ESR properties of the mixed-valence form of the enzymes obtained from beef spleen and porcine uterine fluid (uteroferrin) resemble those of semimet Hr. As a consequence, it has been suggested that the $[Fe_2O]^{3\oplus}$ core might be present in these enzymes.[66,67] From resonance Raman and ^{1}H-NMR spectroscopy, it is known that tyrosine ligands are coordinated to the binuclear iron center[67,68] at the ferric site in the mixed-valence form.[69] A tightly bound phosphate group has also been found for purple acid phosphatase (PAP), but there is presently some controversy over whether or not addition of phosphate to the reduced form is accompanied by rapid oxidation.[66,70] Recent X-ray absorption studies of this enzyme reveal an Fe···Fe distance of 3.00 Å, consistent with a bridged binuclear iron center, Fe–$O_{tyrosine}$ linkages of 1.8–1.9 Å, which prohibit positive identification of Fe–$O_{\mu\text{-oxo}}$ linkages, and an Fe···P distance of 3.06 Å assigned to a monodentate phosphate ligand.[71] From this information, the structures shown in Figure 9 have been proposed for the binuclear iron center in PAP.[67] Further work is required, however, to verify this assignment.

2.5. Ferritin

Ferritin (Ft) is a protein found in bacteria, plants, and animals. Its functions are to store iron, which it does in the form of a polyiron oxo aggregate, and to detoxify and recycle iron.[13,72,73] A related iron-storage protein is hemosiderin,[74] isolated as insoluble granules believed to arise from ferritin breakdown. Less is known about hemosiderin than Ft. Much of our knowledge about the latter is based on the X-ray crystal structure of horse spleen apoferritin, which consists of 24 subunits arranged in a hollow shell of crystallographically imposed 432 symmetry (Fig. 10). The resulting molecule of apoFt is roughly spherical with an inner diameter of 80 Å; it can store up to 4500 iron atoms. Eight hydrophilic and six hydrophobic channels are located respectively along molecular threefold and fourfold symmetry axes. The funnel-shaped hydrophilic channels, 3–4 Å wide at the protein interior and broadening outward towards the protein surface, are lined with three aspartate and three glutamate residues. Suggestions that these channels are the entry and departure routes for iron have been supported by probes with various paramagnetic metal ions.[75,76] Peptide-specific antibodies have recently been used to demonstrate that iron probably enters the core via the threefold channels and is released via the fourfold channels.[77] Details of the loading and unloading of iron from the Ft core in vivo are unknown, however, and it is even uncertain whether Fe^{II}, Fe^{III} or some combination of the two is a kinetically competent species for this process.[78]

Although crystallographic information about ferritin is available, less is known about how the iron atoms are arranged inside the hollow protein core. Five characteristic

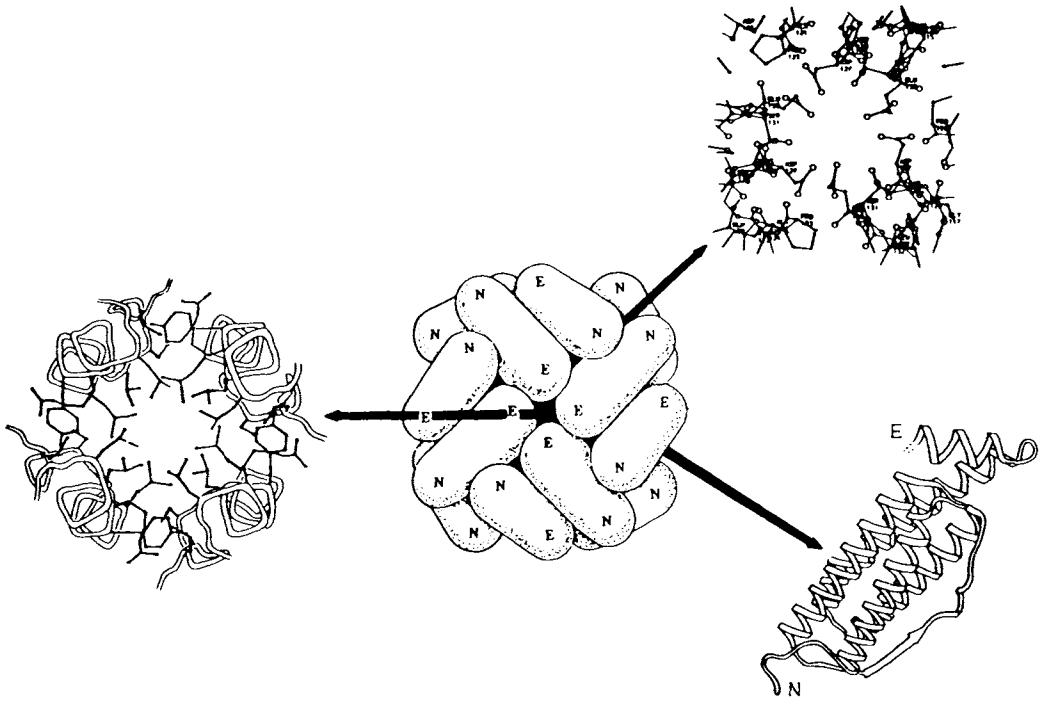

Fig. 10. Structural features of apoFt. In the center is shown the gross quaternary structure of the protein and more details on the fourfold channels (left-hand side), threefold channels (upper right), and the subunits (lower right) are also illustrated (reproduced by permission from Ref. [75]).

electron or X-ray powder diffraction rings have been observed which resemble those of the mineral ferrihydrite.[28,29] Ferrihydrite has the composition $5\,Fe_2O_3 \cdot 9\,H_2O$, but details of its structure are obscure.[27] From spectroscopic data,[79,80] it seems clear that iron in ferritin is present as polymeric (Fe-Fe distance ≈ 3.5 Å), octahedrally coordinated Fe^{III}, with oxygen donor atoms contributed by one or more of the ligands $O^{2\ominus}$, $OH^{\ominus}$, H_2O, and possibly inorganic phosphate (P_i). Variable amounts of phosphate have been found to be associated with the iron core in Ft, and early workers postulated the formula $[\{FeO(OH)\}_8\{FeO(H_2PO_4)\}]$.[81] In human thalassemic ferritin, the Fe/P_i ratio is 21.0 : 1 and, as this ratio increases, the core exhibits more crystallinity.[82] Bacterial ferritin has significantly higher amounts of inorganic phosphate, the Fe/P_i ratio being measured at 1.71 : 1.[82] Estimates of the crystallite sizes of ferritin cores range from 40 to 80 Å.[29] The variability in size, shape, and composition of the iron(III) oxo-hydroxo-phosphato species that constitute the ferritin core is perhaps not surprising in view of the function of the protein. Rapid access to and egress from the hollow core[83] might be better facilitated by a sponge-like structure comprised of small aggregates of iron atoms than by an extended three-dimensional crystalline matrix.

2.6. Other Polyiron Oxo Centers in Biology

Magnetotactic bacteria are aquatic microorganisms that orient and swim along magnetic field lines.[84] They contain crystals of magnetite, Fe_3O_4, with typical dimensions of 400 to 1200 Å, the magnetic moment of which is large enough to facilitate their orientation in the earth's magnetic field.[85] They tend to migrate downward towards the North or South Pole, depending upon the hemisphere in which they are found, ostensibly to avoid oxygen-rich surface waters. In the organism *Aquaspirillum magnetotacticum*, the iron comprises more than 2% of the total dry weight of the cell. Wrapped in a membrane, the Fe_3O_4 particles are called magnetosomes. Mössbauer spectroscopic studies revealed the presence of octahedral high-spin Fe^{II} and both tetrahedral and octahedral Fe^{III}, consistent with the inverse spinel structure of magnetite.

The presence of magnetite in magnetotactic bacteria and the less well defined ferrihydrite in biological organisms provides examples of what has been termed the biomineralization[86] of iron oxides.[87] Another illustration of this phenomenon is the deposition of the iron(III) mineral goethite, α-FeO(OH), in the teeth of marine mollusks known as limpets.[88] Magnetite also occurs in the radula teeth of chitons, in homing pigeons,[89] and in honey bees,[90] where it may also serve as a homing mechanism.[89] The diversity of structures and functions of oxo-bridged polyiron centers in biology is fascinating, and its attraction to the bioinorganic chemical community is understandable.

3. Oxo-Bridged Diiron(III) Cores

3.1. The Hydrolytic Chemistry of Iron(III)

The hydrolysis of iron(III) salts in dilute aqueous solutions has been extensively studied.[15,26,91] Equilibrium constants corresponding to the formation of some of the

known species are given in Figure 2. As the pH is raised from very acidic to conditions near neutrality, binuclear and then species of higher nuclearity form within milliseconds. At low pH, the major binuclear complex is $[(H_2O)_4Fe(OH)_2Fe(OH_2)_4]^{4\oplus}$, which contains the di(μ-hydroxo)diiron(III) core. In 0.2 M NaCl, needle-shaped polynuclears form, which laser light-scattering methods have shown to be rotational ellipsoids that achieve a polynuclearity of 21000 and 400–500 Å lengths within several days at 25 °C.[92] As the pH is raised into the neutral region, $Fe(OH)_3$ or $FeO(OH)\cdot H_2O$ precipitates. It is therefore clear that hydrated ferric ion is an unrealistic source of Fe^{III} at physiological pH in biological systems, and that either hydrated ferrous ion or a complexed form of Fe^{III}, such as found in microbial iron transport compounds called siderophores,[93] will be required.

3.2. Early Studies of the (μ-Oxo)diiron(III) Center

In the presence of chelating agents, discrete oxo-bridged polyiron complexes can be crystallized and structurally characterized. An early example was [(hedta)FeOFe(hedta)]$^{2\ominus}$, where hedta = (*N*-hydroxyethyl)ethylenediaminetriacetate, in which the two ferric centers are connected by an oxo bridge (Fe-O-Fe angle = 165.0°).[94] Numerous binuclear oxo-bridged iron(III) complexes were soon available, and their electronic structures and magnetic exchange interactions were thoroughly investigated.[26] Close scrutiny of the properties of these (μ-oxo)diiron(III) complexes revealed, however, that despite their ready synthesis by reaction (a), their physical properties did not match in

$$2[L'Fe(OH_2)]^{3\ominus} + 2OH^{\ominus} \longrightarrow [L'FeOFeL']^{4\oplus} + 3H_2O \qquad (a)$$

detail those of the diiron(III) center in the oxidized forms of hemerythrin. A critical ingredient was missing, namely, the two additional bridging carboxylate ligands.

3.3. Accurate Models for the Hemerythrin Core

Significant progress was made in the synthesis of models for azidomet Hr in 1983 by two groups working independently.[57,58] As shown in reactions (b) and (c), the (μ-oxo)bis(μ-carboxylato)diiron(III) core readily assembles from mononuclear ferric salts in the presence of water, an alkyl carboxylate salt, and a facially coordinating tridentate nitrogen donor ligand, hydrotris(1-pyrazolyl)borate ($HBpz_3^{\ominus}$) or 1,4,7-triazacyclononane (tacn) (Fig. 11). The benzoate-bridged analogue **2d**, which could not be synthesized by reaction (b), was subsequently obtained by using $(Et_4N)_2[Fe_2OCl_6]$, according to reaction (d).[57] This synthesis and several others discussed below (cf. reactions (k) and (l) in Section 5.1) have been greatly facilitated by the use of $(Et_4N)_2[Fe_2OCl_6]$, containing the "preformed" (μ-oxo)diiron(III) synthon.[95] The $[Fe_2O(O_2CR)_2]^{2\oplus}$ unit appears to be exceptionally stable, however, and can be assembled even by using basic iron acetate as the source of metal.[96] Structurally related $[M_2O(O_2CR)_2]^{n\oplus}$ centers have recently been reported for $M = Ti^{IV}$,[97] V^{III},[98] Mn^{III},[99,100] and Os^{IV}.[101]

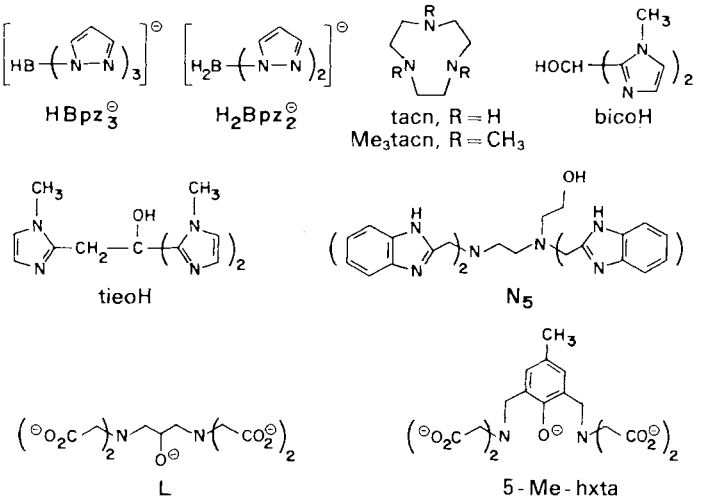

Fig. 11. Structures and abbreviations of ligands used to coordinate polyiron oxo complexes.

$$Fe(ClO_4)_3\cdot 10H_2O + 2NaO_2CR \xrightarrow{H_2O} \xrightarrow[10\,h]{K(HBpz_3)} \text{red precipitate}$$

After fractional crystallization from CH_3CN:

$[Fe(HBpz_3)_2](ClO_4)$ + $[Fe_2O(O_2CR)_2(HBpz_3)_2]$ (b)
1·$ClO_4^{\ominus}$, red crystals **2**, green-brown crystals,
2a–c, R = H, CH_3, C_2H_5; R ≠ Ph

$$FeCl_3\cdot 6H_2O \xrightarrow[EtOH]{tacn} [FeCl_3(tacn)] \xrightarrow[NaI]{NH_4OAc} [Fe_2O(O_2CCH_3)_2(tacn)_2]I_2 \qquad (c)$$

yellow precipitate

3·$2I^{\ominus}$, brown crystals

$$(Et_4N)_2[Fe_2OCl_6] \xrightarrow[CH_3CN]{2\,NaO_2CPh} \xrightarrow{2\,K(HBpz_3)} \text{olive-green solution} \xrightarrow{H_2O} \text{green precipitate} \qquad (d)$$

After recrystallization from acetone:

$[Fe_2O(O_2CPh)_2(HBpz_3)_2]$
2d, green microcrystals

The simple binuclear iron(III) complexes are excellent models for the azidomet Hr core, as demonstrated by comparing their physical properties with those of the protein.[57,58,102] Single-crystal X-ray diffraction studies of complexes **2** and **3** revealed geometries (Fig. 12) nearly congruent with those of the azidomet forms of Hr and myoHr (Fig. 4). A significant feature of these structures is the short Fe-$O_{\mu\text{-oxo}}$ bond (ca. 1.78 Å) compared with the Fe-O distances of ca. 2.05 Å to the bridging carboxylate ligands. As a consequence, the Fe-N bond *trans* to the Fe-$O_{\mu\text{-oxo}}$ bond is lengthened (2.20 Å, compared to 2.15 Å for the *cis* Fe-N bonds), and the quadrupole splitting parameter in the Mössbauer spectrum is 1.6 mm s^{-1}. Moreover, the short Fe-$O_{\mu\text{-oxo}}$ bridge bond mediates substantial antiferromagnetic spin exchange between the two high-spin ferric centers, with coupling constants J in the range -115 to -135 cm^{-1} for the protein and model compounds. The residual paramagnetism of the complex at ambient temper-

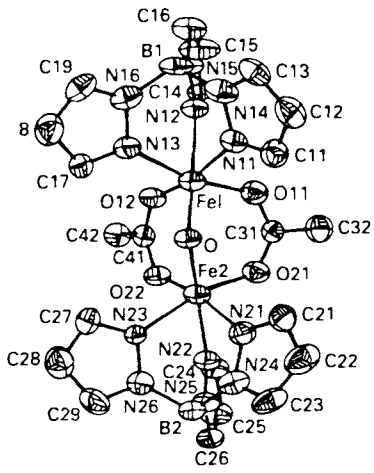

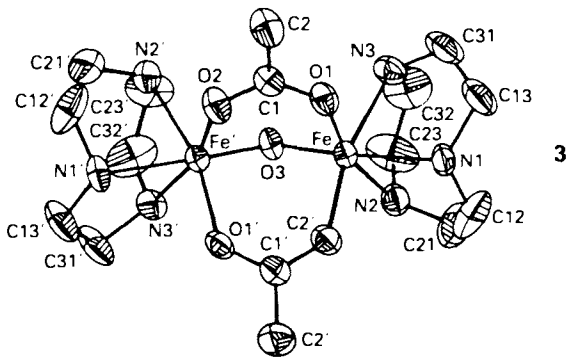

Fig. 12. Crystal structure of two model compounds, **2b** and **3**, for the active center of met Hr (cf. Fig. 4) (reproduced by permission from Ref. [30]).

ature, $\mu_{eff}/Fe \approx 1.71\,\mu_B$, gives rise to broad, characteristic ^{1}H-NMR resonances that are isotropically shifted. A resonance at $\delta = 10.5$ ppm in **2b**, assigned to the acetate methyl protons, has a counterpart in the ^{1}H-NMR spectrum of azidomet Hr which could, by analogy, be identified as broad, unresolved aspartate β-CH_2 and glutamate γ-CH_2 proton resonances.[39] Resonance Raman and IR spectroscopic studies of **2** and a derivative, in which ^{18}O had been exchanged into the bridging position, identified symmetric (ν_s) and asymmetric (ν_{as}) stretching vibrations of the $[Fe_2O]^{4\oplus}$ core at 528 and 751 cm^{-1}, respectively.[57, 103] These values are similar to those of azidomet Hr, 507 and 770 cm^{-1} (Table 2). A rich pattern of overtones has been observed upon excitation of the model complex with 4067-Å laser light.[103] Although the optical spectra (UV/VIS, near IR) of the models and proteins are in good agreement and some tentative assignments have been made,[57] the electronic spectroscopic analysis of the $[Fe_2O(O_2CR)_2]^{2\oplus}$ chromophore is not yet completely satisfactory.

An excellent model for the reduced, deoxy form of hemerythrin has been prepared according to reaction (e).[104, 105] The success of this synthesis is due at least in

$$Fe(ClO_4)_2 \cdot 6H_2O + 2\,Me_3tacn \xrightarrow[Ar]{CH_3OH} \xrightarrow[Ar]{2\,NaO_2CCH_3} [Fe_2(OH)(O_2CCH_3)_2(Me_3tacn)_2](ClO_4) \cdot H_2O \quad (e)$$

4·$ClO_4^{\ominus}$·H_2O

part to the fact that the ligand Me_3tacn (Fig. 11) is too sterically encumbered to form a mononuclear bis(chelate) iron(II) complex. The structure of **4** is similar to that of **3** (cf. Fig. 12), except that the Fe-O bond length to the bridging oxygen atom has increased to 1.99 Å, owing largely to protonation and, secondarily, to the lower charge at the metal center. Consequently, the *trans* Fe-N bond is no longer lengthened and the spin exchange coupling constant is diminished to $J = -13$ cm^{-1}.[105] This value is in good agreement with that estimated by MCD and ESR ($-13 > J > -38$ cm^{-1})[40] and by ^{1}H-NMR ($J = -15 \pm 2$ cm^{-1})[39] studies of deoxy Hr. Additional changes in the Mössbauer and electronic spectra of the reduced diiron(II), compared to the oxidized diiron(III), model compound parallel those observed in going from azidomet Hr to deoxy Hr.

Although semimet, mixed-valence diiron(II,III) forms of hemerythrin are known, it has not yet been possible to isolate and fully characterize the (μ-oxo)bis(μ-acetato)diiron(II,III) core in a model compound. Such a mixed-valence species, $[Fe_2O(O_2CCH_3)_2(Me_3tacn)_2]^{\oplus}$, has been generated electrochemically in dilute solution, however, as revealed by ESR spectroscopy.[105] Reaction (f) illustrates

$$[Fe_2(OH)(O_2CCH_3)_2(Me_3tacn)_2]^{\oplus} \xrightleftharpoons[Et_3N]{-0.29\ V} Fe^{II}Fe^{III}\ \text{species} \quad (f)$$

4

$$\xrightleftharpoons{-0.37\ V} [Fe_2O(O_2CCH_3)_2(Me_3tacn)_2]^{2\oplus}$$

5

that the $Fe^{II}Fe^{III}$ center can be obtained both from diiron(II,II) and diiron(III,III) precursors, **4** and **5**, respectively, but the redox potentials (vs. SCE) reveal that the mixed-valence species is unstable with respect to disproportionation. This behavior parallels that of the Hr proteins, the semimet forms of which also disproportionate. A small amount of triethylamine was added in reaction (f) to simplify the cyclic voltammetric waves by converting hydroxo- into oxo-bridged mixed-valence diiron(I,III) species. In the absence of added base, two closely spaced cathodic peaks appear following the oxidation of **4**. These peaks were assigned to reduction of $Fe^{II}Fe^{III}$ oxo- and hydroxo-bridged species. Controlled-potential electrolysis of **5** produced a reasonably stable species after addition of one electron. ESR studies at 9.6 K of the product revealed features at $g < 2.0$ that integrated to 65% of the value expected for one unpaired spin. The synthesis and X-ray crystal structure determination of an isolated mixed-valence model complex containing the $[Fe_2O(O_2CR)_2]^{\oplus}$ or $[Fe_2(OH)(O_2CR)_2]^{2\oplus}$ core remains an important, if formidable, objective. Two mixed-valence, phenoxo-bridged diiron(II,III) complexes have been characterized.[106, 107]

3.4. Relevance of Models to Ribonucleotide Reductase

A detailed comparison of the Mössbauer spectral parameters, magnetic spin exchange coupling constants, UV/VIS spectroscopic properties, Fe-O-Fe symmetric stretching frequency, and EXAFS spectra of ribonucleotide re-

ductase subunit B2 and the complexes **2** (Table 2) reveals many similarities, strongly suggesting that the (μ-oxo)bis(μ-carboxylato)diiron(III) core occurs in the enzyme. The presence of the bridging carboxylate groups was questioned at an early stage since, unlike Hr, which is known to have an $[Fe_2O(O_2CR)_2]^{2\oplus}$ core structure, RR readily exchanges ^{18}O into the bridging position upon equilibration with $H_2{}^{18}O$.[54] Studies with the model compounds **2** revealed ^{18}O exchange to occur at a rate comparable to that of RR, however.[57] This result is thus consistent with the triply bridged $[Fe_2O(O_2CR)_2]^{2\oplus}$ core model for RR and suggests that the failure of Hr to exchange ^{18}O into its bridging site may be due to the inaccessibility to water of the bimetallic center in that protein. A definitive structural characterization of the B2 subunit of RR to high resolution by X-ray diffraction methods is awaited with interest.

3.5. Chemistry of Diiron Centers: Possible Functional Significance

Thus far, we have compared only the physical and geometric properties of molecules containing the $[Fe_2O(O_2CR)_2]^{n\oplus}$ or $[Fe_2(OH)(O_2CR)_2]^{m\oplus}$ core with those of the proteins. In order for model chemistry to have functional significance, the reaction chemistry of the metalloprotein cores must be reproduced. In the case of hemerythrin models, this requirement includes reversible redox (electron transfer) chemistry and, most importantly, reversible binding of O_2. Additional reactions of the oxo-bridged diiron cores of biological relevance would be catalysis of the reduction of diols to monoalcohols, oxidation of hydrocarbons, and phosphate ester hydrolysis. Ligand substitution and exchange reactions are also of interest, for they help to define the parameters that control substrate molecule access to oxo-bridged diiron centers in proteins.

As previously illustrated by reaction (f), the model complexes **4** and **5** can be interconverted electrochemically. Cyclic voltammetric studies of **2b**, however, revealed decomposition to the mononuclear Fe^{II} complex $[Fe(HBpz_3)_2]$ **6**.[57] Consequently, a desirable design feature for achieving reversible electron transfer involving the $[Fe_2O(O_2CR)_2]^{2\oplus}$ core is to use ligands that either cannot form $Fe^{II}L_2$ complexes, such as the sterically bulky Me_3tacn molecule, or have a framework that ties together the triply bridged binuclear iron center, rendering it kinetically inaccessible to redox-activated decomposition. Two published attempts to achieve the latter objective have not been successful.[96, 108]

The (μ-oxo)bis(μ-carboxylato)diiron(III) core can be reversibly protonated, as shown in reaction (g), which was

$$\underset{\textbf{2b}}{[Fe_2O(O_2CCH_3)_2(HBpz_3)_2]} \xrightarrow[Et_3N]{HBF_4} \underset{\textbf{7}}{[Fe_2(OH)(O_2CCH_3)_2(HBpz_3)_2]^{\oplus}} \quad (g)$$

carried out in CH_2Cl_2/Et_2O solutions.[109] Table 3 compares the structural, magnetic, and spectroscopic properties of the diiron(III) cores in these oxo- and hydroxo-bridged complexes.[57, 109, 110] Protonation of the bridging oxygen atom results in elongation of the two Fe-O bridge bonds by ca. 0.17 Å. The corresponding reduction in Fe-O bridge bond order eliminates the structural *trans* influence on the pyrazole ring nitrogen atom *trans* to the bridging oxygen atom, and substantially diminishes the antiferromagnetic exchange interaction. The latter leads to larger isotropic shifts in the ^{1}H-NMR spectrum, while the former, which produces a much more symmetric electric field gradient at the iron atoms, markedly reduces the quadrupole splitting parameter in the Mössbauer spectrum. All of these differences serve to validate the assignment of the binuclear centers in oxidized forms of met Hr and RR as μ-oxo, rather than μ-hydroxo, carboxylate-bridged diiron(III) units.

Table 3. Comparison of structural, magnetic, and spectroscopic properties of μ-oxo and μ-hydroxo diiron(III) complexes [57, 109, 110].

Property	**2b**	**7**
d (Fe–μ-O) [Å]	1.780(2), 1.788(2)	1.952(4), 1.960(4)
Fe-O-Fe angle [°]	123.6(1)	123.1(2)
$\bar{d}$ (Fe-N, *cis* to μ-O) [Å]	2.15	2.10
$\bar{d}$ (Fe-N, *trans* to μ-O) [Å]	2.19	2.11
d (Fe···Fe) [Å]	3.146(1)	3.439(1)
$\bar{d}$ (Fe–O_{OAc}) [Å]	2.043	1.999
J [cm^{-1}]	−121	−17
Isomer shift [mm s^{-1}]	0.52	0.47
Quadrupole splitting [mm s^{-1}]	1.60	0.37
δ(^{1}H)	3.0 (BH), 10.5 (CH_3), 12.3	−13.6 (BH), 28.0, 37.1, 61.0, 68.7 (CH_3)
Electronic spectrum: λ [nm] (ε_{Fe})	262 (3375), 339 (4635), 358, (sh, 457 (505)), 492 (460), 528 (sh), 695 (70), 995 (3.5)	375 (4750), 700 (2.1), 1115 (0.9)

It is instructive to compare the geometric features of four bridged binuclear iron complexes containing $[Fe_2O(O_2CR)_2]^{2\oplus}$, $[Fe_2(OH)(O_2CR)_2]^{3\oplus}$, or $[Fe_2(OH)(O_2CR)_2]^{\oplus}$ centers (Table 4). Protonation of the (μ-oxo)diiron(III) unit (**2b**→**7**) lengthens the bridge bonds by ca. 0.17 Å, but reduction of $[Fe_2(OH)(O_2CR)_2]^{3\oplus}$ to $[Fe_2(OH)(O_2CR)_2]^{\oplus}$ increases the bridge bond lengths by only an additional few hundredths of an angstrom (cf. **7** and **4**). Let us now consider the reversible binding of O_2 by the hemerythrin core, as represented in Figure 5. Formation of a hydrogen bond in oxy Hr between the proton on the hydroperoxy ligand and the μ-oxo oxygen atom will tend to increase the Fe-O bridge bond length from its 1.8 Å value in metazido Hr towards the ca. 1.95 Å value expected for the deoxy form of the protein. In the absence of

Table 4. Comparison of Fe-$O_{\mu\text{-oxo}}$ bond lengths (average) [Å] and Fe-$O_{\mu\text{-oxo}}$-Fe angles [°] for hemerythrin model compounds [a].

Compound	d (Fe–μ-O)	Fe-μ-O-Fe-angle
2b	1.784(4)	123.6(1)
5	1.800(3)	113.2(2)
7	1.956(4)	123.1(2)
4	1.987(8)	119.7(1)

[a] Data from Refs. [57, 105, 109].

models containing the $[N_3FeO(O_2CR)_2FeN_2(O_2H)]^{\oplus}$ moiety, the Fe-O bridge bond lengths in such an internally hydrogen-bonded complex are unknown. Nevertheless, the existing models suggest such hydrogen bonding would minimize the Franck-Condon reorganizational barrier to electron transfer involved in shortening the Fe-O bridge bond during oxidative addition of the bimetallic center from diiron(II) in deoxy Hr to diiron(III) in oxy Hr (Fig. 5).

Protonation of the μ-oxo group in **2** also facilitates exchange of the bridging ligands.[63] As shown in reactions (h)-(j), the bridging carboxylate ligands exchange with perdeuterioacetic and with diphenyl phosphoric acid. Reactions (h) and (i) were readily followed by

$$\mathbf{2b} + CD_3CO_2D(\text{excess}) \xrightarrow{CD_2Cl_2} [Fe_2O(O_2CCD_3)_2(HBpz_3)_2] \quad (h)$$

$$7 + CD_3CO_2D(\text{excess}) \xrightarrow{CD_3CN} [Fe_2(OD)(O_2CCD_3)_2(HBpz_3)_2]^{\oplus} \quad (i)$$

$$\mathbf{2b} + 2(PhO)_2PO_2H \xrightarrow{CH_2Cl_2} [Fe_2O\{O_2P(OPh)_2\}_2(HBpz_3)_2] + 2CH_3CO_2H \quad (j)$$

8

^{1}H-NMR spectroscopy. Protonation of a bridging ligand, probably the μ-oxo group, is necessary for exchange to occur, since $[Fe_2(OH)(O_2CCH_3)_2(HBpz_3)_2]^{\oplus}$ **7** exchanges its bridging acetates with $(Et_4N)(O_2CCH_3)$, whereas $[Fe_2O(O_2CCH_3)_2(HBpz_3)_2]$ **2b** does not.[110] Protonation might also facilitate ^{18}O exchange into the bridging position, but information on this point is not yet available.

The diphenyl phosphate-bridged product of reaction (j), **8**, has been isolated and structurally characterized (Fig. 13).[63] The slightly larger bite distance of the bridging $(PhO)_2PO_2^{\ominus}$ ligands in this complex (2.576(7) Å, compared to 2.236(3) Å for the bridging acetate groups in **2b**[57]) leads to longer $Fe-O_{\mu\text{-oxo}}$ and Fe···Fe distances. As a consequence, the antiferromagnetic exchange interaction constant is less negative in **8** ($J = -98\ cm^{-1}$). The sensitivity of the J values to even minor changes in the geometry of the $[Fe_2O]^{4\oplus}$ core is of interest in interpreting the magnetic properties of Hr, RR, and related proteins. Exchange reactions of the $[Fe_2O(O_2CR)_2]^{2\oplus}$ core that lead to new phosphate ester- and carboxylate-bridged complexes are potentially useful as models for naturally occurring iron-phosphate interactions in biology.

Attempts to synthesize asymmetric diiron complexes of the kind $[L^3FeO(O_2CR)_2FeL^2]$, where L^3 is a tridentate and L^2 a bidentate nitrogen donor ligand, as functional models for Hr, RR, or MMO have led to tetranuclear compounds containing the $[Fe_4O_2]^{8\oplus}$ core. This chemistry is further discussed in Section 5.2. An unsymmetrical (μ-oxo)diiron(III) complex $[N_5Fe-O-FeCl_3]^{\oplus}$, where N_5 = 2-{*N*-(2-benzimidazolylmethyl)-*N'*-{2-[bis(2-benzimidazolylmethyl)-amino]ethyl}amino}ethanol (Fig. 11), has been prepared and structurally characterized.[111] Quasi-reversible cyclic voltammetric formation of the mixed-valence diiron(II,III) form was mentioned. Several other binuclear mixed-valence iron(II,III) complexes with a variety of ligands have recently been reported,[106,107,112] but their relevance to uteroferrin and semimet Hr is uncertain. Also of interest is the discovery that phenoxo-bridged diiron(III) complexes can serve as catalysts for catechol oxidation[113] and olefin epoxidation.[114] Detailed mechanisms and the relevance of this chemistry to MMO or RR remain to be established.

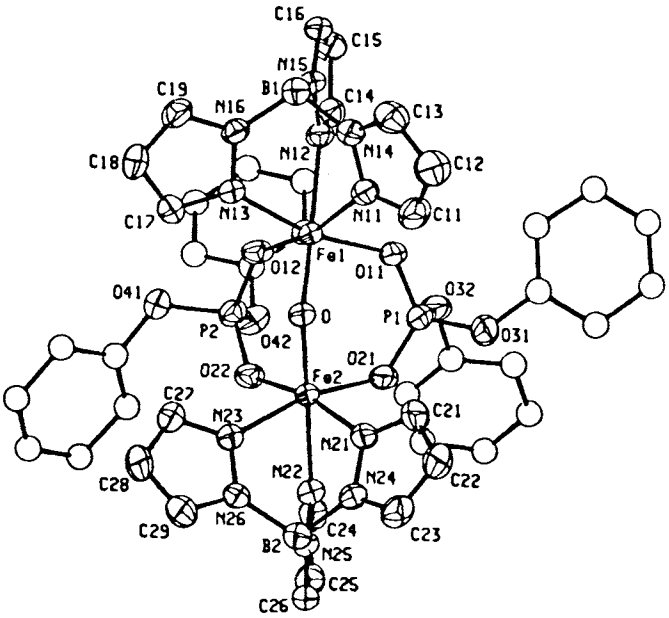

Fig. 13. Structure of **8** (reproduced by permission from Ref. [63]).

4. Oxo-Bridged Triiron(III) Systems

4.1. Basic Iron Acetates; An Equilateral Triangle of Iron Atoms[115]

Solutions of ferric ions in the presence of carboxylate salts have been known for over a century to form stable (μ_3-oxo)hexakis(μ-carboxylato)triiron(III) complexes, referred to as basic iron acetates.[16] As depicted in Figure 3, the structures of these complexes consist of an equilateral triangle of iron atoms with a triply bridging oxygen atom at its center, two bidentate bridging carboxylate ligands along each edge of the triangle, and one centripetally directed terminal ligand (L') completing the octahedral coordination sphere of each metal atom. A variety of mixed-valence, especially $Fe_2^{III}Fe^{II}$, species as well as heterometallic and sulfate-bridged analogues are also known.[23,24] In several cases, the bridging carboxylate group is part of an amino acid.[116,117] The magnetic properties of $[Fe_3O(O_2CR)_6L'_3]^{\oplus}$ complexes were extensively investigated long before their structures were known.[18,19] The three high-spin d^5 iron(III) atoms are antiferromagnetically coupled, giving rise to a total ground-state spin of $S_T = 1/2$ which determines their magnetic properties at 4.2 K. The spin exchange coupling constants J fall in the range -20 to $-40\ cm^{-1}$.[115] The magnitudes of these coupling constants are substantially smaller than observed for the binuclear $[Fe_2O]^{4\oplus}$ complexes, but larger than for

$[Fe_2(OH)(O_2CCH_3)_2(HBpz_3)_2]^{\oplus}$ **7**. The proton thus appears to be more effective at withdrawing electron density from Fe-$O_{\mu\text{-oxo}}$ bonds than a third iron(III) atom. Antiferromagnetic exchange interactions between iron(III) atoms linked both by a bridging oxygen atom and by other bridging ligands are qualitatively correlated with the Fe-$O_{\mu\text{-oxo}}$ distances,[118] although a theoretical model for this behavior remains to be developed. Vibrational spectroscopic studies of $[Fe_3O(O_2CCH_3)_6(py)_3]^{\oplus}$ and its ^{18}O and [D_5]pyridine isotopically substituted derivatives have identified in-plane ν_{as} and out-of-plane δ_s IR bands characteristic of the $[Fe_3O]^{7\oplus}$ core.[119]

Apart from structural, magnetic, and spectroscopic correlations, there has been considerable interest in mixed-valence derivatives of the basic iron acetates.[24,115] In particular, $[Fe_2^{III}Fe^{II}O(O_2CCH_3)_6L'_3]$ complexes, where L' = H_2O, pyridine, or a substituted pyridine, exhibit temperature-dependent internal electron transfer rates in the solid state. These intramolecular electron transfer reactions can be substantially influenced by dynamic disorder phenomena of the ligands L', counterions, and/or solvate molecules in the crystal lattice.[24]

4.2. An Isosceles Triangle of Iron Atoms

Although the mixed-valence forms of the basic iron acetates show distortions from an equilateral towards an isosceles triangle of iron atoms, especially at low temperatures,[120] a much more dramatic deformation of this kind was recently discovered for the $[Fe_3O]^{7\oplus}$ core in $[Fe_3O(tieo)_2(O_2CPh)_2Cl_3]\cdot 2C_6H_6$, where tieoH is 1,1,2-tris(*N*-methyl-2-imidazolyl)ethanol (Fig. 11).[121] The structure of the complex (Fig. 14) is characterized by two short Fe-$O_{\mu\text{-oxo}}$ bridge bonds of 1.865(7) Å and one long one (2.067(6) Å), while the Fe-$O_{\mu\text{-oxo}}$-Fe bond angles are also very asymmetric. Their values are 159.1(3)° for Fe1-O3-Fe2 and 100.3(3)° and 100.5(3)° for Fe1-O3-Fe3 and Fe2-O3-Fe3, respectively. Magnetization and magnetic Mössbauer studies revealed the ground state of this unusual molecule to be $S_T = 5/2$, in contrast to the value of $S_T = 1/2$ for the symmetrically bridged $[Fe_3O]^{7\oplus}$ cores described in Section 4.1. Fits of the temperature-dependent magnetic susceptibility data to a theoretical expression for isotropic spin exchange in a trinuclear Fe^{III} cluster of C_{2v} symmetry gave coupling constants $J_{12} = -55(1)\ cm^{-1}$ and $J_{13} = J_{23} = -8.0(4)\ cm^{-1}$, where the subscripts refer to the iron atom labels given in Figure 14. These J values fit the correlation of spin exchange coupling constant with Fe-O bond distance[118] and readily explain the $S_T = 5/2$ ground state of the cluster. At 4.2 K, iron atoms Fe1 and Fe2 are magnetically coupled to form a diamagnetic (S = 0) pair, leaving the magnetically isolated third, high-spin Fe3 center to account for the ground-state spin. As the temperature is raised, the magnetic moment of the trinuclear system actually decreases, due to the fact that the first excited magnetic state has $S_T = 3/2$, reaching a minimum at 60 K, before increasing towards the maximum theoretical value expected for $S_T = 15/2$.

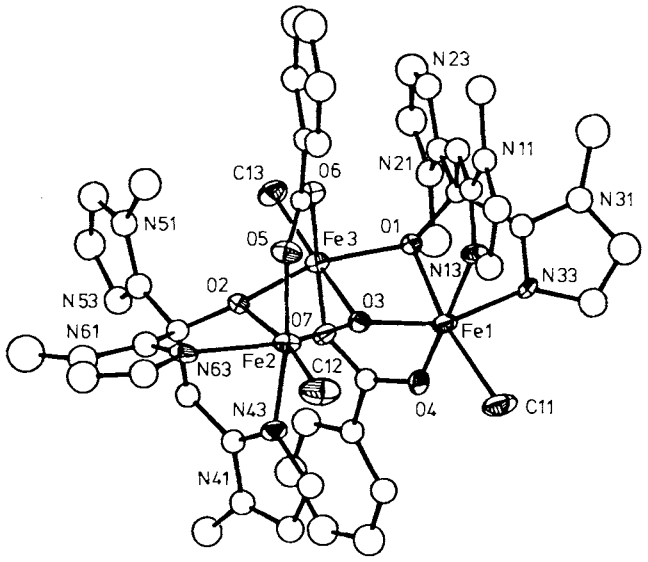

Fig. 14. Structure of $[Fe_3O(tieo)_2(O_2CPh)_2Cl_3]$ (reproduced by permission from Ref. [121]).

This example illustrates the importance of measuring the magnetic properties of polynuclear iron oxo centers over as wide a temperature range as possible, and of fitting the data to the proper theoretical model. Moreover, the unusual asymmetric $[Fe_3O]^{7\oplus}$ core, a topological isomer of the symmetric structure found in the basic iron acetates and their analogues, results from complexation by the new polyimidazole ligand, tieoH.

5. Oxo-Bridged Tetrairon(III) Complexes

5.1. Tetranuclear $[Fe_4O_2]^{8\oplus}$ Cores by Formal Dimerization of $[Fe_2O]^{4\oplus}$ Units

In order to explore chemistry of (μ-oxo)bis(μ-carboxylato)diiron(III) centers relevant to their functions in biology, it is desirable to have one or more terminal coordination sites available for ligand substitution. Attempts to achieve this goal by using KH_2Bpz_2 (Fig. 11) in place of $KHBpz_3$ in reaction (b) led instead to the novel tetranuclear complex **9** [reaction (k), R = Me, Ph], the structure of which is

$$2(Et_4N)_2[Fe_2OCl_6] + 7\,NaO_2CR + 2\,KH_2Bpz_2 \xrightarrow{MeCN} (Et_4N)[Fe_4O_2(O_2CR)_7(H_2Bpz_2)_2] + 7\,NaCl + 2\,KCl + 3\,Et_4NCl \quad \text{(k)}$$

$Et_4N \cdot$ **9**

shown in Figure 15 for R = Ph.[122] A manganese(III) analogue with seven bridging carboxylate ligands and bipyridine instead of dihydrobis(pyrazolyl)borate, $[Mn_4O_2(O_2CR)_7(bpy)_2]^{\oplus}$, has also been synthesized, attesting to the stability of the $[M_4O_2(O_2CR)_7L'_2]$ stoichiometry.[123]

A very similar $[Fe_4O_2]^{8\oplus}$ core was also obtained when bis(*N*-methyl-2-imidazolyl)methanol (bicoH, Fig. 11) was used in a parallel attempt to prepare functional models for oxo-bridged diiron(III) protein cores [reaction (l) and Fig. 16].[124] Although there are additional bridging ligands in **10**, complexes **9** and **10** have the same core structure, depicted in Scheme 1, where the curved lines represent car-

$$2(Et_4N)_2[Fe_2OCl_6] + 4\,NaO_2CPh + 4\,bicoH \xrightarrow[-2\,Et_3NHCl]{MeCN/Et_3N} [Fe_4O_2(bicoH)_2(bico)_2(O_2CPh)_4]Cl_2 + 4\,NaCl + 4\,Et_4NCl \quad (1)$$

10 · 2 Cl

boxylate ligands. This structure further illustrates the propensity of the μ-oxo ligand in the $[Fe_2O(O_2CR)_2]^{2\oplus}$ core to become triply bridging by coordination to a third iron(III) center. These reactions, to form tri- or tetranuclear aggregates, are formally depicted in Scheme 2.

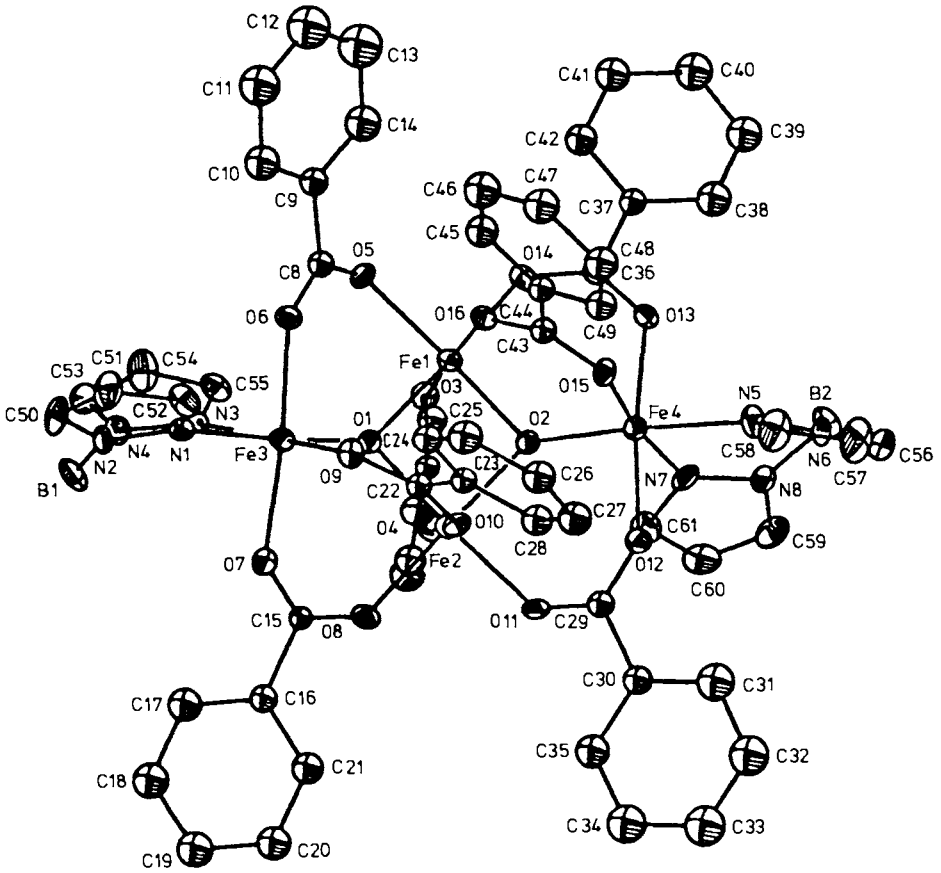

Fig. 15. Structure of **9**, R = Ph [122].

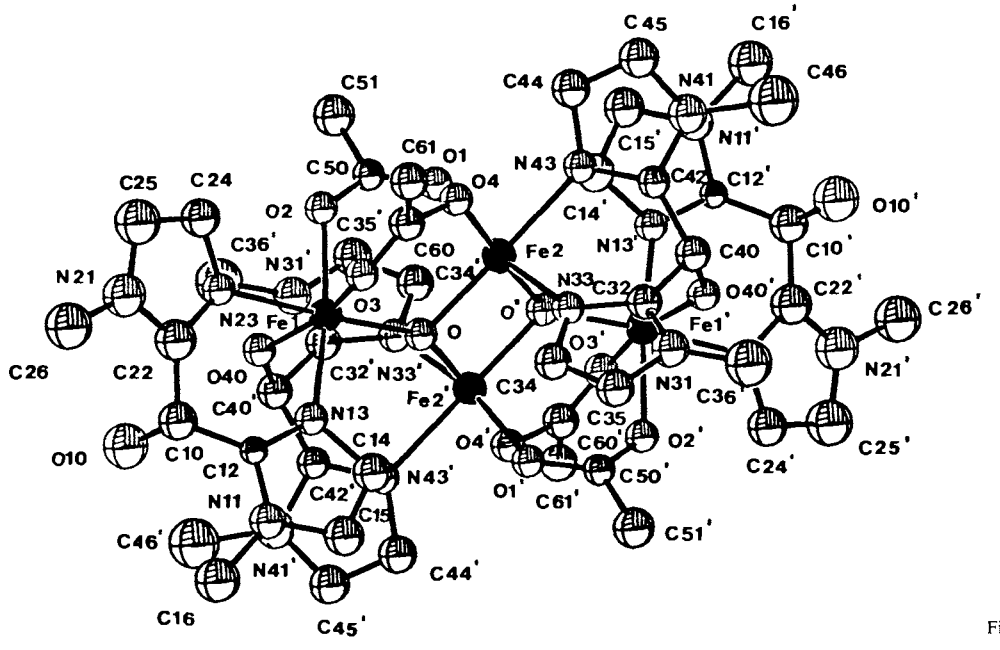

Fig. 16. Structure of **10** [124].

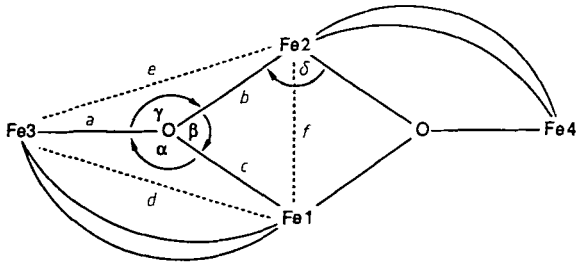

Scheme 1. Structure of the $[Fe_4O_2]^{8\oplus}$ core of **9** and **10**.

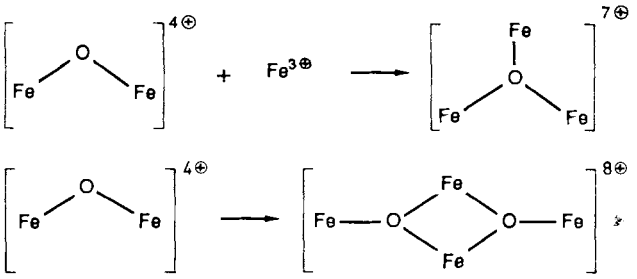

Scheme 2.

A related tetranuclear compound, **11**·$2H_2O$, has been synthesized by slow evaporation in air of solutions containing the trinuclear mixed-valence iron complex $[Fe_3O(O_2CCF_3)_6(H_2O)_3]\cdot 3.5H_2O$.[125] The structure of **11** is

$[Fe_4O_2(O_2CCF_3)_8(H_2O)_6]$ **11**

illustrated in Figure 17 and, schematically, in Scheme 3. Magnetic susceptibility and Mössbauer spectroscopic studies of all three of these novel $[Fe_4O_2]^{8\oplus}$-containing complexes reveal a diamagnetic (S = 0) ground state,[122, 124, 126] consistent with antiferromagnetic coupling

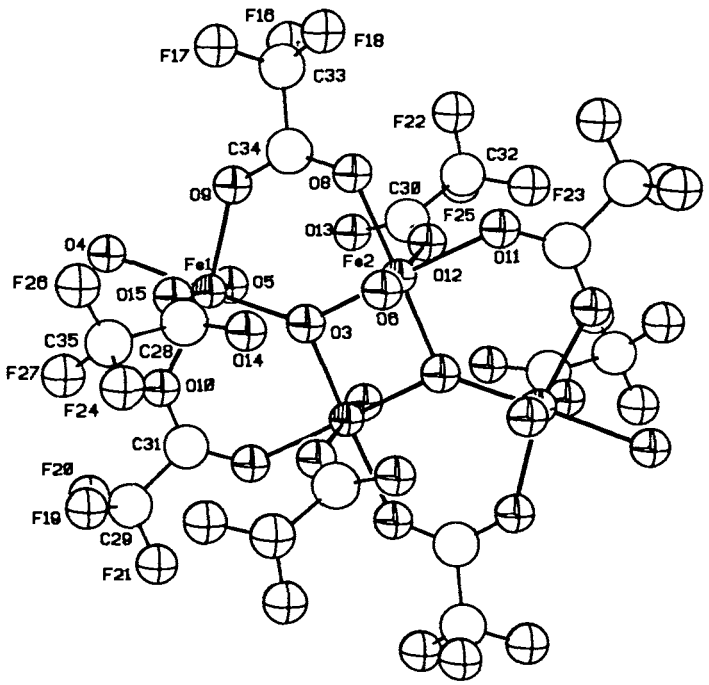

Fig. 17. Structure of **11** (drawn from the coordinates in Ref. [125]).

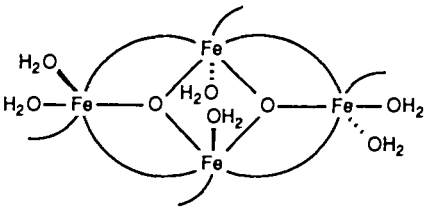

Scheme 3. Schematic structure of **11**.

through the μ_3-oxo bridges. Geometric comparisons of the $[Fe_4O_2]^{8\oplus}$ cores in **10**,[125] **11**,[126] and the mineral amarantite, $[Fe_4O_2(SO_4)_4]$,[127] reveal the central $[Fe_2O_2]$ unit ("kernel") to be a structural invariant,[124] with parameters *b*, *c*, *f*, β, and δ (see Scheme 1) being in the respective ranges 1.96–1.97 Å, 1.93–1.94 Å, 2.90–2.93 Å, 95.7–96.8°, and 82.9–83.7°. The geometry of the $[Fe_4O_2]^{8\oplus}$ core in **9**, R = Ph,[122] is similar, with small but significant differences arising from its nonplanarity.

5.2. Other Tetranuclear Iron(III) Oxo Aggregates

Two other complexes of this class have been recently synthesized, in which the iron-oxo core geometries differ from those of the $[Fe_4O_2]^{8\oplus}$-containing molecules **9**–**11**. Addition of NaOH to an aqueous solution of $Fe(NO_3)_3$ and the protonated ligand 5-Me-hxta (Fig. 11) gives rise first to a red binuclear complex, $[Fe_2(5\text{-Me-hxta})(OH)(H_2O)_2]$, and eventually to the orange tetranuclear compound (pyrrH)$_4$·**12**·$2CH_3OH$, where

$[Fe_4O_2(OH)_2(5\text{-Me-hxta})_2]^{4\ominus}$ **12**

pyrrH is the pyrrolidinium cation, $C_4H_{10}N^{\oplus}$.[128] As shown in Figure 18, the complex is comprised of a tetrahedral array of iron atoms bridged on its six edges by oxygen atoms, two from oxo ligands, two from hydroxo ligands, and two from the 5-Me-hxta phenolate groups. The resulting $[Fe_4O_6]$ core has the adamantane structure (Scheme 4). The

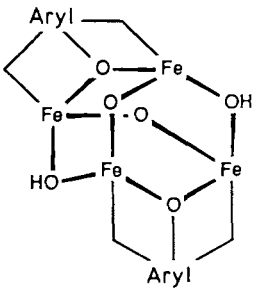

Scheme 4. Adamantane structure of the $[Fe_4C_6]$ core of **12**.

$Fe-O_{\mu\text{-oxo}}$ bonds are short (1.791(3) Å) and the Fe–O–Fe bond angle is 151.23(19)°. Magnetic susceptibility studies reveal a singlet (S = 0) ground state.[129]

Another, topologically distinctive, tetranuclear iron oxo complex is $Na_6[Fe_4O_2(CO_3)_2L_2]$, where L is the pentaanionic form of 1,3-diamino-2-hydroxypropane-*N*,*N*,*N'*,*N'*-tetraacetic acid (Fig. 11).[130] The structure of this aggregate is illustrated in Figure 19. Iron centers Fe(1) and Fe(2′) are linked by μ-oxo bridges (Fe–O distances,

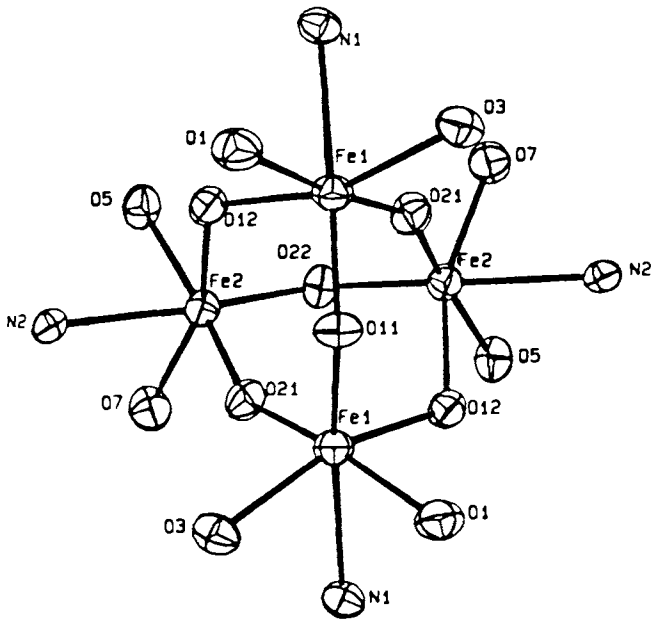

Fig. 18. Structure of the $[Fe_4O_x]$ core of **12** (reproduced by permission from Ref. [128]). The oxo and hydroxo groups are labeled O21 and O11/O22, respectively.

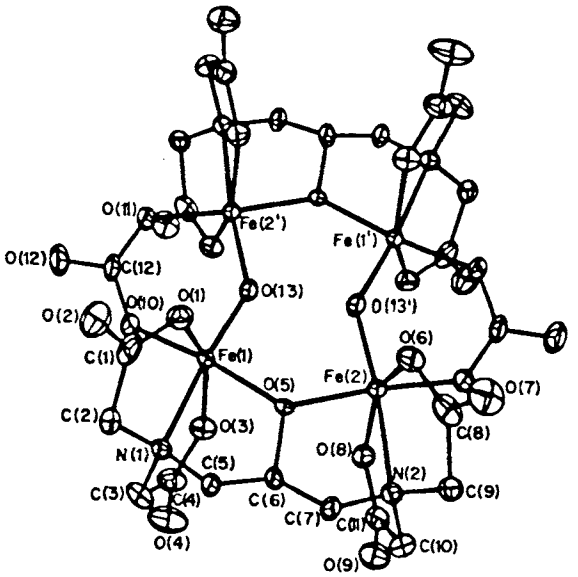

Fig. 19. Structure of $[Fe_4O_2(CO_3)_2L_2]^{6\ominus}$ (reproduced by permission from Ref. [130]).

1.828(4) and 1.830(4) Å; Fe-O-Fe angle, 136.4(3)°) and carbonate bridges, previously unknown in iron(III) chemistry. The $Fe\text{-}O_{\mu\text{-oxo}}$ bridge bonds are among the longest of their kind, and a very short intramolecular nonbonded oxygen-oxygen contact of 2.408(9) Å occurs between O(13) and O(13'). Both of these results are suggestive of H-bonding between O(13) and O(13'), although the evidence seems to favor the bridges being purely oxo, rather than a mixture of oxo and hydroxo.[130] The temperature dependence of the magnetic susceptibility of this complex reveals a superexchange pathway through the oxo bridges, characterized by an antiferromagnetic exchange coupling constant J of $-63.4\ cm^{-1}$. The two alkoxide bridges mediate a weaker antiferromagnetic exchange interaction having $J = -11.2\ cm^{-1}$. The former value is nicely consistent with the correlation[118] between $Fe\text{-}O_{\mu\text{-oxo}}$ bond distances and the magnitude of J for multiply bridged diiron(III) complexes. The $[Fe_4O_2(CO_3)_2L_2]^{6\ominus}$ ion is the only structurally characterized tetrairon oxo aggregate studied thus far for which J values have been determined.

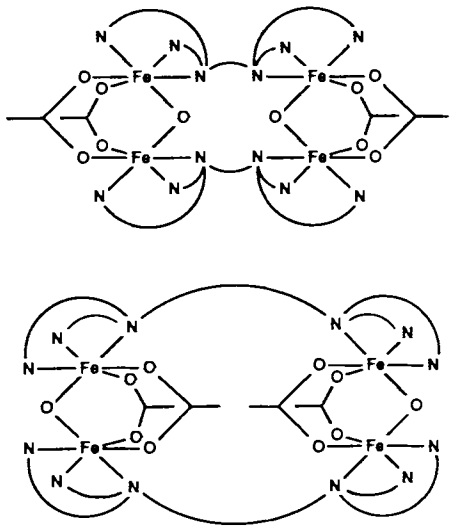

Scheme 5. Schematic structure of $[Fe_2O(O_2CCH_3)_2L'_2]^{2\oplus}_2$.

Two tetranuclear complexes of general formula $[Fe_2O(O_2CCH_3)_2L'_2]^{4\oplus}_2$, where L' is a hexadentate *N,N'*-tetrapicolinyl(xylylene)diamine or -(alkylene)diamine ligand, have been structurally characterized (Scheme 5).[96,131] Both of these molecules arose from unsuccessful attempts to link the two halves of a binuclear complex containing the (μ-oxo)bis(μ-carboxylato)diiron(III) core. Tetranuclear iron halo/methoxo and methoxo/alkanoato complexes have been postulated, but not structurally defined.[132-134]

6. Higher Nuclearity Iron(III) Oxo Complexes

6.1. Hexairon(III) Species

Although there is good evidence for the existence of the cyclic hexanuclear complex $[Fe_6(OH)_{12}](OH)_6$ (Scheme 6) in solution,[91,92] the only hexairon(III) oxo/hydroxo com-

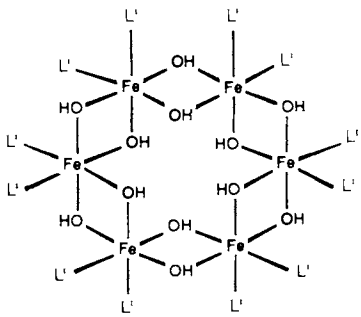

Scheme 6. Proposed structure of the complex $[Fe_6(OH)_{12}]^{6\oplus}$ in solution.

plex to be crystallographically characterized is $[Fe_6O_2(OH)_2(O_2CR)_{12}]$, where R is *tert*-butyl.[135] As shown in Scheme 7, two (μ-hydroxo)bis(μ-pivalato)diiron(III)

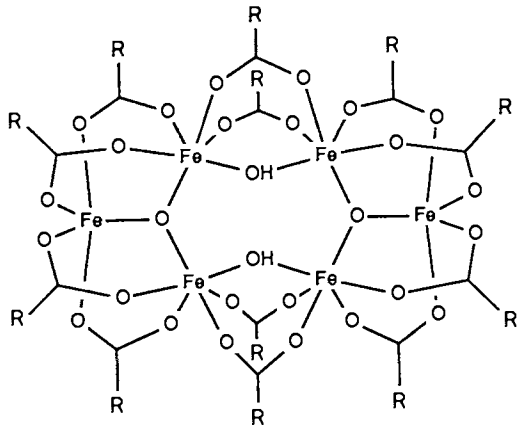

Scheme 7. Structure of $[Fe_6O_2(OH)_2(O_2CR)_{12}]$, R = *tert*-butyl.

units are linked to two trigonal-bipyramidally coordinated iron(III) centers by a triply bridging μ-oxo and two bridging pivalate ligands. This fascinating molecule was first detected in gas-phase mass spectroscopic studies of $[Fe_3O(O_2CR)_6(H_2O)_3]RCO_2 \cdot 2RCO_2H$ and subsequently generated from the latter, basic iron acetate type molecule by thermolysis in tetradecane at 200–220 °C for 15–20 min. The $Fe\text{-}O_{\mu\text{-oxo}}$ and $Fe\text{-}OH_{\mu\text{-hydroxo}}$ bond lengths are 1.946(6) Å and 1.962(9) Å, respectively, for the six-coordinate iron atoms; the equatorial Fe–O bond distance to the pentacoordinate iron atom is 1.848(5) Å.

6.2. An Octairon(III) Aggregate

Hydrolysis of $[Fe(tacn)Cl_3]$ at pH 9 in the presence of bromide ion over a 24-h period leads to brown crystals of the octairon(III) complex $[Fe_8O_2(OH)_{12}(tacn)_6]Br_8 \cdot 9H_2O$, where tacn is defined in Figure 11.[136] The structure of the cation is shown in Figure 20. At the center of the octairon(III) aggregate is an $[Fe_4O_2]^{8\oplus}$ core with geometric properties remarkably similar to those in the tetranuclear iron complexes described in Section 5.1.[124] Apart from its structure, there is little additional information available about this interesting cluster. The compound is reported to obey the Curie–Weiss law between 103 and 193 K with $\mu_{eff} = 3.72\mu_B$ and $\theta = 59.9$ K, but the ground state is unknown.[136]

6.3. Undecairon(III) Oxo-Hydroxo Complex

The largest discrete oxo-bridged polyiron compound known thus far is $[Fe_{11}O_6(OH)_6(O_2CPh)_{15}]$ **13**, synthesized by hydrolytic polymerization in nonaqueous solvents of simple mononuclear $[FeCl_4]^{\ominus}$ and binuclear $[Fe_2OCl_6]^{2\ominus}$ salts.[137] At least four different crystalline forms of this novel undecairon(III) aggregate exist,[129, 137–139] two of which, **13** · 6THF and **13** · (H_2O) · 8CH_3CN, have been described in detail.[138] The eleven iron atoms are arranged at the corners of a pentacapped twisted trigonal prism having a twist angle, α, of 17.4° (Fig. 21). Six triply bridging pla-

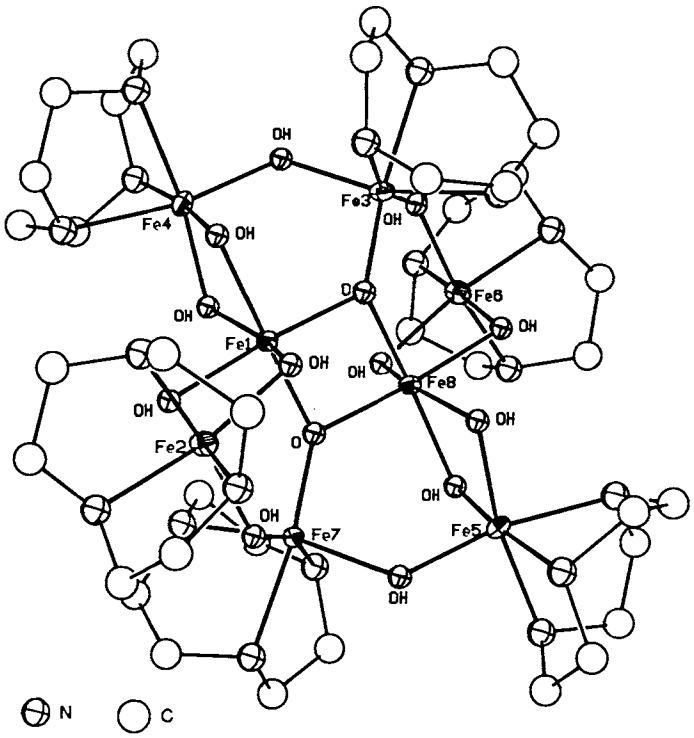

Fig. 20. Structure of $[Fe_8O_2(OH)_{12}(tacn)_6]^{8\ominus}$ (drawn from deposited coordinates, see Ref. [136]).

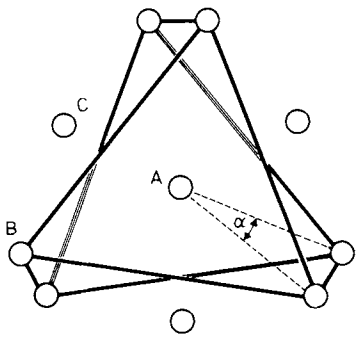

Fig. 21. Arrangement of iron atoms in **13**, showing the three types of iron atoms and twist angle α. The view is down the C_3 axis, which obscures one of the type-A iron atoms. For more discussion, see Ref. [138] (reproduced by permission from Ref. [138]).

nar μ-oxo and six triply bridging pyramidal μ-hydroxo ligands link the iron atoms together, while 30 oxygen atoms of bidentate bridging benzoate ligands fill the remaining, distorted octahedral coordination positions at each iron atom (Fig. 22). Hydrogen bonding of the hydroxyl group protons to THF, H_2O, or CH_3CN acceptor atoms of solvent in the lattice occurs in all structures (Fig. 23). The benzoate groups provide a hydrophobic sheath about the aggregate through which these hydrogen-bonding interactions can occur, and also serve further to knit together the structure.

Magnetic and Mössbauer studies of **13** reveal a ground state spin of $S_T = 1/2$ per aggregate and internal antiferro-

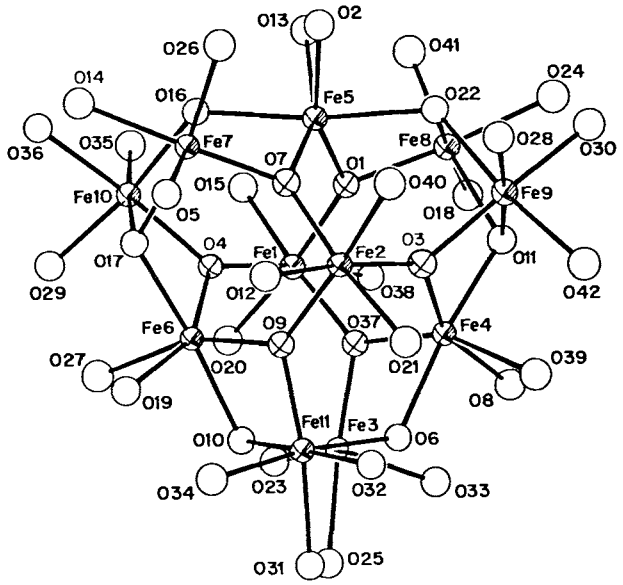

Fig. 22. Structure of **13**, omitting only the benzoate group carbon atoms (reproduced by permission from Ref. [138]).

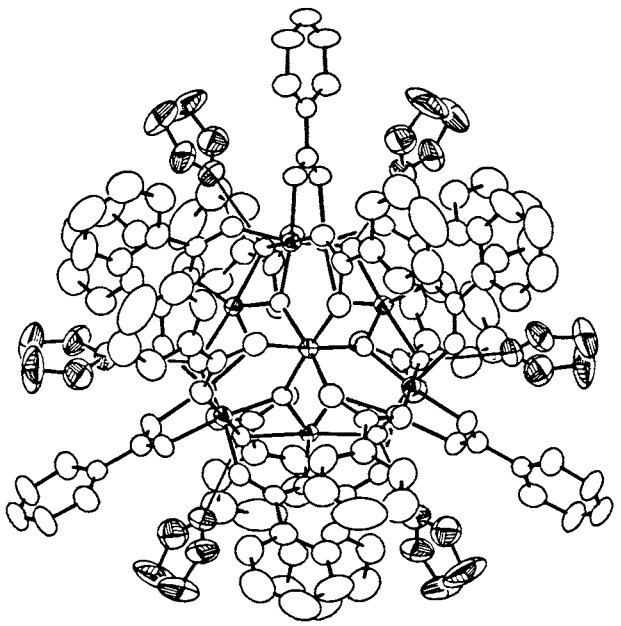

Fig. 23. Full structure of **13**·6THF. The THF solvent molecules, drawn using shaded ellipsoids, are hydrogen-bonded to the six hydroxyl groups (reproduced by permission from Ref. [138]).

magnetic spin exchange among the eleven bridged high-spin ferric centers.[138] A quasi-reversible reduction at $E_{1/2} = -0.31$ V vs. SCE has been observed by cyclic voltammetry and tentatively assigned to the formation of the $[Fe_{11}O_6(OH)_6(O_2CPh)_{15}]^{\ominus}$ anion. At more negative potentials, additional electrons may be added to the aggregate, but the waves are irreversible, possibly due to fragmentation of the undecairon unit. The mode of formation and ligands employed in the synthesis of **13** make it an attractive model for the polyiron core in ferritin, and detailed comparisons of the magnetic, spectroscopic, and structural properties of the two systems are available.[138]

6.4. Analogies to the Ferritin Core

The stability of **13** has led to speculations that in ferritin cores the iron atoms may be stored as discrete Fe_{11} units in which the bridging carboxylate groups are replaced by phosphate, oxo, or hydroxo ions.[138] A total of 409 ± 3 such Fe_{11} units have been shown to be sufficient to fill the entire core. Other synthetic iron polymers, including one of approximate composition $[Fe_4O_3(OH)_4(NO_3)_2] \cdot 1.5\,H_2O$[140,141] and a large ($\geq 250$) polynuclear iron cluster formed from a 4:1 ratio of Fe^{III} and ATP,[142] have been suggested as models for the polyiron core in ferritin. The synthesis, structural characterization, physical properties, redox behavior, and reactions, especially the stepwise release and addition of mononuclear or small polynuclear iron units, of these and related higher-order polyiron aggregates will continue to be of interest and importance in helping to define the true chemical nature of ferritin cores.

7. Conclusion

Attempts to model polynuclear iron oxo centers in biology have produced a fascinating array of novel aggregates scarcely imagined only a few years ago. Parallel work in manganese chemistry, some of it similarly motivated, has also resulted in a variety of di-, tri-, tetra-, nona-, and dodecanuclear oxo-bridged complexes.[99,100,115,123,143–145] These complexes have undoubtedly sharpened our insights into the structural and physical properties of polyiron oxo centers in biology. While such synthetic achievements can be admired for their intrinsic beauty, they are limited in their ability to elucidate chemical details underlying the biological functions of these units. Attention must now turn to systems with reaction chemistry that mimics that of the natural systems, including binuclear iron oxo centers that bind O_2 reversibly, oxygenate hydrocarbon substrates, reduce geminal diols, or hydrolyze phosphate esters. What features of the metal coordination chemistry of (μ-oxo)bis(μ-carboxylato)diiron(III) units, for example, dictate whether reversible oxygen binding or oxygen activation will occur? How much of this distinction arises from fine tuning of the electronic and steric properties of the bimetallic center and how much requires the protein chains? A precisely analogous question applies to binuclear copper centers that bind or activate O_2 in different proteins.[146]

Progress in studying the bioinorganic chemistry of rust is likely to have an impact in several related disciplines. New strategies for the synthesis of ceramic materials, catalysts for alkane oxidation, and corrosion inhibitors should arise from fundamental knowledge about the chemistry of polyiron oxo complexes. In the search for molecular systems that hydroxylate hydrocarbons, attention is already beginning to shift towards non-heme iron compounds, some of which are certain to be polynuclear. Applications to medicine may derive from a better understanding of the coordination chemistry of iron in aqueous media and of the principles that govern the loading and unloading of iron from ferritin cores. It will be interesting to follow these developing areas in the next several years.

Studies performed in the author's laboratory were supported by grant GM-32134 from the National Institute of General Medical Sciences, which is gratefully acknowledged. I also wish to thank my talented former MIT coworkers William H. Armstrong (currently at the University of California at Berkeley), Sergiu M. Gorun (Exxon), Alan Spool (IBM, San Jose), and Ian M. Williams (Oxford), as well as current MIT students and postdoctoral associates Robert H. Beer, James G. Bentsen, Judithann R. Hartman, R. Lynn Rardin, Mary E. Roth, and Petra N. Turowski for their hard work and stimulating ideas. Several excellent collaborators also contributed greatly to our progress, specifically Richard B. Frankel and Georgia Papaefthymiou of the Francis Bitter National Magnet Laboratory at MIT, Chuck Dismukes (Princeton), Britt Hedman and Keith Hodgson (Stanford), JoAnne Stubbe (Wisconsin, now at MIT), and Karl Wieghardt (Bochum). Dave Hendrickson, Don Kurtz, and Larry Que kindly sent preprints of their work prior to publication. Finally, I appreciate the assistance of Kazi Ahmed and Petra N. Turowski in preparing some figures and drawings for this article.

Received: August 31, 1987 [A 658 IE]
German version: *Angew. Chem. 100* (1988) 353

[1] E.-i. Ochiai: *Bioinorganic Chemistry - An Introduction*, Allyn and Bacon, Boston 1977.
[2] F. A. Cotton, G. Wilkinson: *Advanced Inorganic Chemistry*, 4th ed., Wiley, New York 1980, p. 752–766; *Anorganische Chemie*, 4th ed., Verlag Chemie, Weinheim 1982, p. 765–782.
[3] Review articles: D. Dolphin (Ed.): *Porphyrins 1978–1979*, Academic Press, New York.
[4] Review articles: W. Lovenberg (Ed.): *Iron-Sulfur Proteins 1973–1977*, Academic Press, New York.
[5] E. C. Theil, G. L. Eichhorn, L. G. Marzilli (Eds.): *Adv. Inorg. Biochem. 5* (1983).
[6] P. C. Wilkins, R. G. Wilkins, *Coord. Chem. Rev. 7* (1987) 195.
[7] M. Lammers, H. Follmann, *Struct. Bonding (Berlin) 54* (1983) 27.
[8] B.-M. Sjöberg, A. Gräslund, *Adv. Inorg. Biochem. 5* (1983) 87.
[9] B. C. Antanaitis, P. Aisen, *Adv. Inorg. Biochem. 5* (1983) 111.
[10] H. Dalton, *Adv. Appl. Microbiol. 26* (1980) 71.
[11] J. Lund, M. P. Woodland, H. Dalton, *Eur. J. Biochem. 147* (1985) 297.
[12] M. P. Woodland, H. Dalton, *J. Biol. Chem. 259* (1984) 53.
[13] E. C. Theil, *Annu. Rev. Biochem. 56* (1987) 289.
[14] See, for example, H. A. O. Hill in H. B. Dunford, D. Dolphin, K. N. Raymond, L. Sieker (Eds.): *The Biological Chemistry of Iron*, Reidel, Dordrecht, Holland, 1981, p. 12; E.-i. Ochiai, *J. Chem. Educ. 63* (1986) 942.
[15] C. M. Flynn, Jr., *Chem. Rev. 84* (1984) 31.
[16] R. Weinland: *Einführung in die Chemie der Komplex-Verbindungen*, Verlag von Ferdinand Enke, Stuttgart 1919, p. 345ff, and references cited therein.
[17] L. A. Welo, *Philos. Mag. [7] 6* (1928) 481.
[18] K. J. Kambe, *J. Phys. Soc. Jpn. 5* (1960) 48.
[19] J. Yvon, J. Horowitz, A. Abragam, *Rev. Mod. Phys. 25* (1953) 165.
[20] A. Earnshaw, B. N. Figgis, J. Lewis, *J. Chem. Soc. A 1966*, 1656.
[21] M. Takano, *J. Phys. Soc. Jpn. 33* (1972) 1312.
[22] D. H. R. Barton, M. J. Gasteiger, W. B. Motherwell, Fr. Pat.-Anm. 2543542 (1983).
[23] For leading references: B. P. Straughan, O. M. Lam, *Inorg. Chim. Acta 98* (1985) 7; J. A. Thich, B. H. Toby, D. A. Powers, J. A. Potenza, H. J. Schugar, *Inorg. Chem. 20* (1981) 3314.
[24] S. E. Woehler, R. J. Wittebort, S. M. Oh, T. Kambara, D. N. Hendrickson, D. Inniss, C. E. Strouse, *J. Am. Chem. Soc. 109* (1987) 1063, and references cited therein.
[25] H. J. Schugar, G. R. Rossman, C. G. Barraclough, H. B. Gray, *J. Am. Chem. Soc. 94* (1972) 2683.
[26] K. S. Murray, *Coord. Chem. Rev. 12* (1974) 1.
[27] F. V. Chukrov, B. B. Zvyagin, A. I. Gorschkov, L. P. Yermilova, V. V. Balashova, *Izv. Akad. Nauk SSSR Ser. Geol. 1973*, 23; *Int. Geol. Rev. 16* (1974) 1131.
[28] K. M. Towe, W. F. Bradley, *J. Colloid. Interface Sci. 24* (1967) 384.
[29] P. M. Harrison, F. A. Fischbach, T. G. Hoy, G. H. Haggis, *Nature (London) 216* (1967) 1188.
[30] S. J. Lippard, *Chem. Br. 22* (1986) 222.
[31] I. M. Klotz, D. M. Kurtz, Jr., *Acc. Chem. Res. 17* (1984) 16.
[32] D. M. Kurtz, Jr., D. F. Shriver, I. M. Klotz, *Coord. Chem. Rev. 24* (1977) 145, and references cited therein.
[33] R. E. Stenkamp, L. C. Sieker, L. H. Jensen, *J. Am. Chem. Soc. 106* (1984) 618.
[34] S. Sheriff, W. A. Hendrickson, J. L. Smith, *Life Chem. Rep. Suppl. Ser. 1* (1983) 305; *J. Mol. Biol. 197* (1987) 273.
[35] J. W. Dawson, H. B. Gray, H. E. Hoenig, G. R. Rossman, J. M. Schredder, R. H. Wang, *Biochemistry 11* (1972) 461.
[36] R. E. Stenkamp, L. C. Sieker, L. H. Jensen, J. D. McCallum, J. Sanders-Loehr, *Proc. Natl. Acad. Sci. USA 82* (1985) 713.
[37] W. T. Elam, E. A. Stern, J. D. McCallum, J. Sanders-Loehr, *J. Am. Chem. Soc. 105* (1983) 1919.
[38] J. M. Nocek, D. M. Kurtz, Jr., J. T. Sage, P. G. Debrunner, M. J. Maroney, L. Que, Jr., *J. Am. Chem. Soc. 107* (1985) 3382.
[39] M. J. Maroney, D. M. Kurtz, Jr., J. M. Nocek, L. L. Pearce, L. Que, Jr., *J. Am. Chem. Soc. 108* (1986) 6871.
[40] R. C. Reem, E. I. Solomon, *J. Am. Chem. Soc. 109* (1987) 1216.
[41] A. K. Shiemke, T. M. Loehr, J. Sanders-Loehr, *J. Am. Chem. Soc. 108* (1986) 2437, and references cited therein.
[42] L. L. Pearce, D. M. Kurtz, Jr., Y.-M. Xia, P. G. Debrunner, *J. Am. Chem. Soc. 109* (1987) 7286.
[43] See, for example, G. D. Armstrong, A. G. Sykes, *Inorg. Chem. 25* (1986) 3725.
[44] D. M. Kurtz, Jr., J. T. Sage, M. Hendrich, P. G. Debrunner, G. S. Lukat, *J. Biol. Chem. 258* (1983) 2115.
[45] G. S. Lukat, D. M. Kurtz, Jr., A. K. Shiemke, T. M. Loehr, J. Sanders-Loehr, *Biochemistry 23* (1984) 6416.
[46] G. S. Lukat, D. M. Kurtz, Jr., *Biochemistry 24* (1985) 3464.
[47] R. E. Utecht, D. M. Kurtz, Jr., *Inorg. Chem. 24* (1985) 4458. A similar role is performed by sipuncular NADH diaphorase: C. Maxwell, *Comp. Biochem. Physiol. 58B* (1977) 331.
[48] G. W. Ashley, J. Stubbe, *Pharmacol. Ther. 30* (1987) 301.
[49] P. Reichard, A. Ehrenberg, *Science (Washington) 221* (1983) 514, and references cited therein.
[50] P. J. Toscano, L. G. Marzilli, *Prog. Inorg. Chem. 31* (1984) 105, and references cited therein.
[51] A. Gräslund, M. Sahlin, B.-M. Sjöberg, *EHP Environ. Health Perspect. 64* (1985) 139.
[52] A. Larsson, B.-M. Sjöberg, *EMBO J. 5* (1986) 2037.
[53] T. Joelson, U. Uhlin, H. Eklund, B.-M. Sjöberg, S. Hahne, M. Karlsson, *J. Biol. Chem. 259* (1984) 9076.
[54] B.-M. Sjöberg, T. M. Loehr, J. Sanders-Loehr, *Biochemistry 21* (1982) 96.
[55] L. Petersson, A. Gräslund, A. Ehrenberg, B.-M. Sjöberg, P. Reichard, *J. Biol. Chem. 255* (1980) 6706.
[56] C. L. Atkin, L. Thelander, P. Reichard, G. Lang, *J. Biol. Chem. 248* (1973) 7464.
[57] W. H. Armstrong, S. J. Lippard, *J. Am. Chem. Soc. 105* (1983) 4837; W. H. Armstrong, A. Spool, G. C. Papaefthymiou, R. B. Frankel, S. J. Lippard, *ibid. 106* (1984) 3653.
[58] K. Wieghardt, K. Pohl, W. Gebert, *Angew. Chem. 95* (1983) 739; *Angew. Chem. Int. Ed. Engl. 22* (1983) 727.
[59] R. C. Scarrow, M. J. Maroney, S. M. Palmer, L. Que, Jr., A. L. Roe, S. P. Salowe, J. Stubbe, *J. Am. Chem. Soc. 109* (1987) 7857.
[60] G. Bunker, L. Petersson, B.-M. Sjöberg, M. Sahlin, M. Chance, B. Chance, A. Ehrenberg, *Biochemistry 26* (1987) 4708.
[61] B.-M. Sjöberg, J. Sanders-Loehr, T. M. Loehr, *Biochemistry 26* (1987) 4242.
[62] M. Sahlin, A. Ehrenberg, A. Gräslund, B.-M. Sjöberg, *J. Biol. Chem. 261* (1986) 2778.
[63] W. H. Armstrong, S. J. Lippard, *J. Am. Chem. Soc. 107* (1985) 3730.
[64] M. P. Woodland, D. S. Patil, R. Cammack, H. Dalton, *Biochim. Biophys. Acta 873* (1986) 237.
[65] A. Ericson, B. Hedman, K. O. Hodgson, J. Green, H. Dalton, J. G. Bentsen, R. Beer, S. J. Lippard, *J. Am. Chem. Soc.*, in press.
[66] J. W. Pyrz, J. T. Sage, P. G. Debrunner, L. Que, Jr., *J. Biol. Chem. 261* (1986) 11015, and references cited therein.
[67] B. A. Averill, J. C. Davis, S. Burman, T. Zirino, J. Sanders-Loehr, T. M. Loehr, J. T. Sage, P. G. Debrunner, *J. Am. Chem. Soc. 109* (1987) 3760, and references cited therein.
[68] B. C. Antanaitis, T. Strekos, P. Aisen, *J. Biol. Chem. 257* (1982) 3766.
[69] R. B. Lauffer, B. C. Antanaitis, P. Aisen, L. Que, Jr., *J. Biol. Chem. 258* (1983) 14212.
[70] K. Doi, R. Gupta, P. Aisen, *J. Biol. Chem. 262* (1987) 6982.
[71] S. M. Kauzlarich, B. K. Teo, T. Zirino, S. Burman, J. C. Davis, B. A. Averill, *Inorg. Chem. 25* (1986) 2781.
[72] G. C. Ford, P. M. Harrison, D. W. Rice, J. M. A. Smith, A. Treffry, J. L. White, J. Yariv, *Philos. Trans. R. Soc. London Ser. B304* (1984) 551.
[73] R. R. Crichton, *Angew. Chem. 85* (1973) 53; *Angew. Chem. Int. Ed. Engl. 12* (1973) 57.
[74] G. J. Kontoghiorghes, S. Chambers, A. V. Hoffbrand, *Biochem. J. 241* (1987) 87, and references cited therein.

[75] P. M. Harrison, A. Treffry, T. H. Lilley, *J. Inorg. Biochem. 27* (1986) 287, and references cited therein.
[76] J. G. Wardeska, B. Viglione, N. D. Chasteen, *J. Biol. Chem. 261* (1986) 6677.
[77] A. Treffry, P. M. Harrison, *Proc. Eighth Int. Conf. Proteins of Iron Transp. Storage*, Montreal 1987, p. 8.
[78] N. D. Chasteen, B. C. Antanaitis, P. Aisen, *J. Biol. Chem. 260* (1985) 2926.
[79] J. Webb, H. B. Gray, *Biochim. Biophys. Acta 351* (1974) 224.
[80] C.-Y. Yang, A. Meagher, B. H. Huynh, D. E. Sayers, E. C. Theil, *Biochemistry 26* (1987) 497.
[81] L. Michaelis, C. D. Coryell, S. Granick, *J. Biol. Chem. 148* (1943) 463.
[82] S. Mann, J. V. Bannister, R. J. P. Williams, *J. Mol. Biol. 188* (1986) 225.
[83] T. Jones, R. Spencer, C. Walsh, *Biochemistry 17* (1978) 4011.
[84] R. P. Blakemore, *Annu. Rev. Microbiol. 36* (1982) 217.
[85] R. B. Frankel, G. C. Papaefthymiou, R. P. Blakemore, W. O'Brien, *Biochim. Biophys. Acta 763* (1983) 147, and references cited therein.
[86] H. A. Lowenstam, *Science (Washington) 211* (1981) 1126.
[87] S. Mann, *Chem. Br. 1987*, 137, and references cited therein.
[88] J. Webb, S. Mann, J. V. Bannister, R. J. P. Williams, *Inorg. Chim. Acta 124* (1986) 37.
[89] C. Walcott, J. L. Gould, J. L. Kirschvink, *Science (Washington) 205* (1979) 1027.
[90] J. L. Gould, J. L. Kirschvink, K. S. Deffeyes, *Science (Washington) 202* (1978) 1026.
[91] W. Schneider, *Comments Inorg. Chem. 3* (1984) 205.
[92] B. Schwyn, *Dissertation*, Eidgenössische Technische Hochschule Zürich, No. 7404.
[93] K. N. Raymond, T. P. Tufano in H. B. Dunford, D. Dolphin, K. N. Raymond, L. Sieker (Eds.): *The Biological Chemistry of Iron*, Reidel, Dordrecht, Holland 1981, p. 85.
[94] S. J. Lippard, H. J. Schugar, C. Walling, *Inorg. Chem. 6* (1967) 1825.
[95] W. H. Armstrong, S. J. Lippard, *Inorg. Chem. 24* (1985) 981.
[96] H. Toftlund, K. S. Murray, P. R. Zwack, L. F. Taylor, O. P. Anderson, *J. Chem. Soc. Chem. Commun. 1986*, 191.
[97] N. W. Alcock, P. N. Bartlett, D. Gordon, T. F. Illson, M. G. H. Wallbridge, *J. Chem. Soc. Chem. Commun. 1986*, 614.
[98] K. Wieghardt, M. Köppen, B. Nuber, J. Weiss, *J. Chem. Soc. Chem. Commun. 1986*, 1530.
[99] K. Wieghardt, U. Bossek, D. Ventur, J. Weiss, *J. Chem. Soc. Chem. Commun. 1985*, 347.
[100] J. E. Sheats, R. S. Czernuszewicz, G. C. Dismukes, A. L. Rheingold, V. Petrouleas, J. Stubbe, W. H. Armstrong, R. H. Beer, S. J. Lippard, *J. Am. Chem. Soc. 109* (1987) 1435.
[101] J. E. Armstrong, W. R. Robinson, R. A. Walton, *Inorg. Chem. 22* (1983) 1301.
[102] A. Spool, I. D. Williams, S. J. Lippard, *Inorg. Chem. 24* (1985) 2156.
[103] R. S. Czernuszewicz, J. E. Sheats, T. G. Spiro, *Inorg. Chem. 26* (1987) 2063.
[104] P. Chaudhuri, K. Wieghardt, B. Nuber, J. Weiss, *Angew. Chem. 97* (1985) 774; *Angew. Chem. Int. Ed. Engl. 24* (1985) 778.
[105] J. R. Hartman, R. L. Rardin, P. Chaudhuri, K. Pohl, K. Wieghardt, B. Nuber, J. Weiss, G. C. Papaefthymiou, R. B. Frankel, S. J. Lippard, *J. Am. Chem. Soc. 109* (1987) 7387.
[106] M. Suzuki, A. Uehara, K. Endo, *Inorg. Chim. Acta 123* (1986) L9.
[107] A. S. Borovik, B. P. Murch, Jr., V. Papaefthymiou, E. Münck, *J. Am. Chem. Soc. 109* (1987) 7190.
[108] K. Wieghardt, I. Tolksdorf, W. Herrmann, *Inorg. Chem. 24* (1985) 1230.
[109] W. H. Armstrong, S. J. Lippard, *J. Am. Chem. Soc. 106* (1984) 4632.
[110] W. H. Armstrong, S. J. Lippard, unpublished results.
[111] P. Gomez-Romero, G. C. DeFotis, G. B. Jameson, *J. Am. Chem. Soc. 108* (1986) 851.
[112] F. Arena, C. Floriani, A. Chiesi-Villa, C. Guastini, *J. Chem. Soc. Chem. Commun. 1986*, 1369.
[113] U. Russo, M. Vidali, B. Zarli, R. Purrello, G. Maccarrone, *Inorg. Chim. Acta 120* (1986) L11.
[114] B. P. Murch, F. C. Bradley, L. Que, Jr., *J. Am. Chem. Soc. 108* (1986) 5027.
[115] Comprehensive reviews: R. D. Cannon, R. P. White, *Prog. Inorg. Chem. 36* (1988), in press.
[116] E. M. Holt, S. L. Holt, N. W. Alcock, *Cryst. Struct. Commun. 11* (1982) 505, and references cited therein.
[117] R. D. Cannon, L. Montri, D. B. Brown, K. M. Marshall, C. M. Elliott, *J. Am. Chem. Soc. 106* (1984) 2591.
[118] S. M. Gorun, S. J. Lippard, *Recl. J. R. Neth. Chem. Soc. 106* (1987) 417.
[119] L. Montri, R. D. Cannon, *Spectrochim. Acta Part A41* (1985) 643.
[120] S. M. Oh, D. N. Hendrickson, K. L. Hassett, R. E. Davis, *J. Am. Chem. Soc. 107* (1985) 8009.
[121] S. M. Gorun, G. C. Papaefthymiou, R. B. Frankel, S. J. Lippard, *J. Am. Chem. Soc. 109* (1987) 4244.
[122] W. H. Armstrong, M. E. Roth, S. J. Lippard, *J. Am. Chem. Soc. 109* (1987) 6318.
[123] J. B. Vincent, C. Christmas, J. C. Huffman, G. Christou, H.-R. Chang, D. N. Hendrickson, *J. Chem. Soc. Chem. Commun. 1987*, 236.
[124] S. M. Gorun, S. J. Lippard, *Inorg. Chem. 27* (1988) 149.
[125] V. I. Ponomarev, L. O. Atovmyan, S. A. Bobkova, K. I. Turté, *Dokl. Akad. Nauk SSSR 274* (1984) 368.
[126] R. A. Stukan, V. I. Ponomarev, V. P. Nifontov, K. I. Turté, L. O. Atovmyan, *Zh. Strukt. Khim. 26* (1985) 197.
[127] P. Susse, *Z. Kristallogr. 127* (1968) 261.
[128] B. P. Murch, F. C. Bradley, P. D. Boyle, V. Papaefthymiou, L. Que, Jr., *J. Am. Chem. Soc. 109* (1987) 7993.
[129] R. L. Rardin, S. J. Lippard, unpublished results.
[130] D. L. Jameson, C.-L. Xie, D. N. Hendrickson, J. A. Potenza, H. J. Schugar, *J. Am. Chem. Soc. 109* (1987) 740.
[131] J. R. Hartman, S. J. Lippard, unpublished results.
[132] G. A. Kakos, G. Winter, *Austr. J. Chem. 22* (1969) 97.
[133] E. Kokot, G. M. Mockler, G. L. Sefton, *Austr. J. Chem. 26* (1973) 2105.
[134] J. Cattesick, P. Thornton, *J. Chem. Soc. Dalton Trans. 1977*, 1420.
[135] N. V. Gerbeleyeu, A. S. Batsanov, G. A. Timko, Yu. T. Struchkov, K. M. Indrichan, G. A. Popovich, *Dokl. Akad. Nauk SSSR 293* (1986) 364.
[136] K. Wieghardt, K. Pohl, I. Jibril, G. Huttner, *Angew. Chem. 96* (1984) 66; *Angew. Chem. Int. Ed. Engl. 23* (1984) 77.
[137] S. M. Gorun, S. J. Lippard, *Nature (London) 319* (1986) 666.
[138] S. M. Gorun, G. C. Papaefthymiou, R. B. Frankel, S. J. Lippard, *J. Am. Chem. Soc. 109* (1987) 3337.
[139] M. E. Roth, C. Pulla Rao, S. J. Lippard, unpublished results.
[140] T. G. Spiro, S. E. Allerton, J. Denner, A. Terzis, R. Bils, P. Saltman, *J. Am. Chem. Soc. 88* (1966) 2221.
[141] G. W. Brady, C. R. Kurkjian, E. F. Lyden, M. B. Robin, P. Saltman, T. G. Spiro, A. Terzis, *Biochemistry 7* (1968) 2185.
[142] A. N. Mansour, C. Thompson, E. C. Theil, N. D. Chasteen, D. E. Sayers, *J. Biol. Chem. 260* (1985) 7975.
[143] T. Lis, *Acta Crystallogr. Sect. B36* (1980) 2042.
[144] K. Wieghardt, U. Bossek, L. Zsolnai, G. Huttner, G. Blondin, J.-J. Girerd, F. Babonneau, *J. Chem. Soc. Chem. Commun. 1987*, 651.
[145] C. Christmas, J. B. Vincent, H.-R. Chang, J. C. Huffman, G. Christou, D. N. Hendrickson, *J. Am. Chem. Soc. 110* (1988) 823.
[146] K. D. Karlin, J. Zubieta (Eds.): *Biological & Inorganic Copper Chemistry*, Adenine Press, Guilderland, NY, USA, 1983.

Complexation of Neutral Molecules by Cyclophane Hosts

By François Diederich*

In memoriam Iwao Tabushi

Since the discovery of the crown ethers by *Pedersen* twenty years ago, the chemistry of synthetic hosts for the selective complexation of organic and inorganic guests has seen an extraordinarily rapid development. This article discusses in particular the contributions provided by synthetic cyclophanes as hosts to the understanding of molecular complexation of neutral organic guest molecules in aqueous and organic solvents. In aqueous solution, cyclophanes form stoichiometric complexes with neutral aromatic guests which can approach enzyme-substrate complexes in their stability. Efficient molecular complexation is also observed in organic environments. Here, as a result of large solvation effects, the strength of complexation is strongly dependent on the nature of the organic solvent. Electron donor–acceptor interactions can contribute significantly to the stability of complexes formed between cyclophane hosts and aromatic guests. Force-field calculations together with computer graphics are powerful tools in the design of water-soluble, optically active hosts for chiral recognition of complexed racemic guests. Simple and selective functionalization of the cyclophane framework leads to stable, bioorganic catalysts. Like enzymes, these catalysts bind their substrates in a rapid equilibrium prior to the reaction steps. As a perspective, some fascinating research objectives in the field of molecular recognition and catalysis which can be targeted with designed cyclophane hosts are shown.

1. Introduction

The first descriptions of clathrate formation, the inclusion of organic and inorganic guests in the interstices of the crystal lattices of hosts such as hydroquinone, urea, and cholic acids, date back to the middle of the nineteenth century.[1–4] In contrast, the first evidence for the inclusion of a guest within the intramolecular cavity of a host was first reported in 1938. At that time, *Freudenberg* and *Meyer-Delius* proposed that the formation of an adduct between iodine and cyclodextrins was a result of a cavity formed by the cyclodextrin ring.[5] During his habilitation with *Freudenberg* at the end of the forties and at the beginning of the fifties, *Cramer* pioneered the research area which is now known as host-guest chemistry[6] or molecular recognition. At that time, he undertook the first systematic studies on the cavity inclusion complexation between cyclodextrins and organic guests in aqueous solution and in the solid state.[7] *Cramer* et al. also explored for the first time the acceleration and the stereoselectivity of reactions as a result of substrate binding in the cyclodextrin cavity.[8] This early work of *Cramer* et al. was well ahead of its time and it subsequently initiated numerous successful studies of natural and modified cyclodextrins as receptor and enzyme models. Without doubt, the development of fully synthetic hosts, especially of the water-soluble cyclophanes, has been stimulated by the past and the on-going creative research with cyclodextrins in the laboratories of *Bender*,[9] *Breslow*,[10] *Tabushi*[11], and others.[12–17]

Despite the successful studies of *Cramer* at the beginning of the fifties on molecular complexation and catalysis by the *natural* cyclodextrins, the progression to synthetic hosts for organic and inorganic guests did not occur until fifteen years later. Only *Stetter* and *Roos*[18] in 1955 published a paper in this direction. The long interval between the first studies on cyclodextrins and the development of synthetic hosts can certainly be explained in terms of insufficient understanding of the intermolecular interactions that hold together complexes formed by enzymes, biological receptors, and the natural cyclodextrins. The fundamental discovery of the *synthetic* crown ethers by *Pedersen* in 1967[19] was needed to trigger the development of efficient synthetic hosts. *Pedersen*'s discovery demonstrated that molecular complexation is not limited to natural systems but can also occur effectively with fully synthetic receptors. The scope of this article does not allow for a discussion of the wide variety of molecular hosts that have been prepared since 1967 for the selective complexation of anionic, cationic, and hydrogen-bonding neutral guests. The reader is referred to numerous monographs[20–29] and to some of the reviews that have appeared.[30–48] However, the inspiring work of *Lehn* et al.[49] and *Cram* et al.[6, 50] should be specifically mentioned here. These researchers quickly recognized the implications of *Pedersen*'s discovery. With their stimulating and innovative contributions to supramolecular complexation, chiral recognition and catalysis, they have established the constituency of the field of synthetic host-guest chemistry. With great joy the author of this article may now add to this introduction that *Pedersen*, *Cram*, and *Lehn* were awarded the 1987 Nobel Prize in Chemistry for their future-oriented work.

The above mentioned work of *Stetter* and *Roos*,[18] reported in 1955, has to be seen as the first approach towards

[*] Prof. Dr. F. Diederich
Department of Chemistry and Biochemistry
University of California at Los Angeles
Los Angeles, CA 90024 (USA)

 © VCH Verlagsgesellschaft mbH, D-6940 Weinheim, 1988 0570-0833/88/0303-0362 $ 02.50/0

the synthesis of systems with binding sites for apolar molecules. They recognized the potential of cyclophanes for inclusion complexation and prepared the macrocycles **1–3** derived from benzidine. In their paper, they described the formation of stable crystalline 1:1 complexes with benzene and dioxane when the macrocycles **2** and **3** were recrystallized from these solvents. Until 1982, these complexes were thought to be of the cavity inclusion type. At that time, *Hilgenfeld* and *Saenger*[51] showed by X-ray crystallography that the largest macrocycle **3** and benzene do not form an intramolecular cavity inclusion complex but rather a clathrate in which benzene is accomodated between host molecules in the crystal lattice.

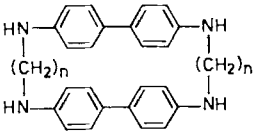

1, n = 2
2, n = 3
3, n = 4

In the seventies, the research groups of *Tabushi*,[11b,52] *Murakami*,[53] and *Koga*[54] in Japan and of *Whitlock*[55] in the United States started developing water-soluble, cyclophane-type macrocycles and analyzed their ability to act as hosts in aqueous solution. Among theses studies, the work of *Koga* et al. is considered a milestone contribution. In 1980, they reported the first stoichiometric inclusion of an apolar guest in the cavity of a synthetic cyclophane-host both in aqueous solution as well as in the solid state.[54a] By ^{1}H-NMR spectroscopy, they demonstrated the formation of a 1:1 complex ($K_a = 2.8 \times 10^3$ L mol^{-1}) between host **4** and 2,7-naphthalenediol in dilute hydrochloric acid at pH < 2. From acidic aqueous solution, they crystallized a 1:1 complex of **4** and durene and characterized it unambiguously by X-ray crystallography as a cavity inclusion complex. By variation of the bridges between the diphenylmethane units as well as of the aromatic spacers, *Koga* et al. subsequently prepared other tetraazaparacyclophanes and studied the complexation of aromatic guests, especially of those bearing anionic residues, in aqueous solution.[54b–e]

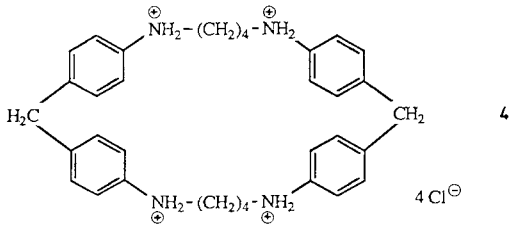

4

2. Concept for the Design of Water-Soluble Cyclophane Hosts with Pronounced Hydrophobic Cavity Binding Sites

Our original interest in the development of water-soluble hosts stems from a desire to study in detail the hydrophobic effect, i.e. the specific driving force for the association of apolar binding partners in aqueous solution.[56–65] All theories of the hydrophobic effect agree that this driving force for complexation originates from the specific interactions between the water molecules; these cohesive forces are larger than the forces between the water molecules and apolar solutes. In modern biochemistry texts, the hydrophobic effect is mainly attributed to a specific, highly positive entropic contribution.[66] As an example, water-molecules around the apolar surfaces at an enzyme active site and around an apolar guest arrange to form a highly structured hydrogen-bonding network. Upon complexation, these structured surface water molecules are released into the bulk solution, which results in a positive entropy change. Despite many experimental and theoretical studies, it is still unclear as to what extent the entropy change due to desolvation in an aqueous solution is more positive than the corresponding entropy change in an organic solvent.[65c]

A favorable (negative) enthalpic contribution to the complexation process in aqueous solution is explained by the lower polarizability of the OH-residues of water as compared to CH_2-units.[63,66a] Since the polarizability, in addition to the interatomic distance, predominantly defines the attractive potential of the London dispersion interactions, these interactions are stronger between associated hydrocarbons than between hydrocarbon solutes and water molecules. A negative heat capacity change (ΔC_p^0) is often measured upon association or complexation of apolar binding partners in aqueous solution and is considered another criterion for the hydrophobic effect.[62,67] The negative heat capacity change of the aqueous system can be explained by the high thermal lability of the layer of water molecules which are arranged in a structured way around the free binding partners and which are released into the bulk upon complexation. A large negative heat capacity change was measured for the complexation between 1-adamantanecarboxylic acid and cyclodextrins in aqueous solution.[68a]

A multitude of binding interactions are effective in complex biological systems and consequently the hydrophobic effect, isolated from other driving forces for complexation, is difficult to study. We therefore planned to undertake such a study using geometrically well-defined water-soluble cyclophane hosts. The host components described by *Koga* et al.[54] were not ideal for such studies since the hydrophobic character of their binding sites is perturbed by ionic, strongly hydrated ammonium centers in the periphery of the macrocyclic cavity. For the construction of water-soluble hosts with apolar cavity binding sites shaped by hydrocarbon residues, we proposed to locate water-solubility-providing ionic groups remote from the cavity.[69,70] To achieve this goal, quaternary ammonium centers providing water-solubility at neutral pH could either be introduced by bicyclic, propellane or spiro-type arrangements (Fig. 1).

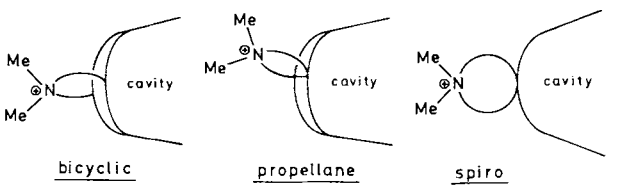

Fig. 1. Possible arrangements which locate water-solubility providing quaternary ammonium nitrogens remote from the cavity. Ammonium centers as shown here effect solubility of the host molecule at pH 7 in water.

We chose spiro piperidinium rings, since **5**–**7** provide building blocks which combine the spiro system with the diphenylmethane unit in a desired spatial arrangement. The building blocks **5**–**7**, introduced in our macrocycles, e.g. **11**–**18**,[71] can be readily prepared in one step in 90% yield from the corresponding phenol and *N*-acetylpiperidine. In other cyclophane hosts, e.g. **19**, we have introduced carboxylate residues to provide water-solubility. The specific fixation at the central carbon atom of the diphenylmethane spacer orients the carboxylate residues away from the binding site.[55e,72,73] The building blocks **8**–**10**, needed to prepare hosts such as **19**, can also be obtained in one step in very good yield starting with the corresponding phenol and diethyl acetonedicarboxylate.[74]

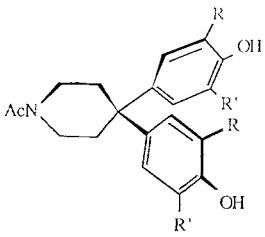

5, R = R' = H
6, R = CH_3, R' = H
7, R = R' = CH_3

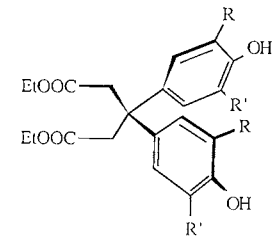

8, R = R' = H
9, R = CH_3, R' = H
10, R = R' = CH_3

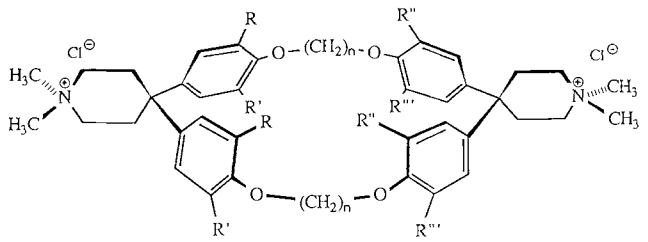

	R–R'''	n		R	R'	R''	R'''	n
11,	H	2	**15**,	CH_3	H	H	H	4
12,	H	3	**16**,	CH_3	CH_3	H	H	4
13,	H	4	**17**,	CH_3	CH_3	CH_3	H	4
14,	H	5	**18**,	CH_3	CH_3	CH_3	CH_3	4

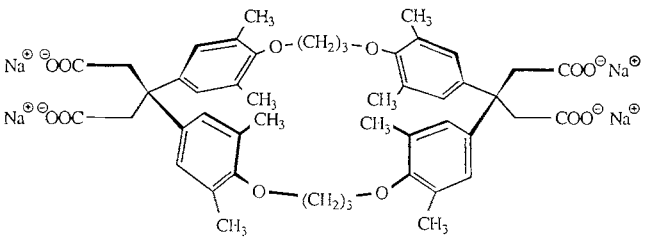

19

Other research groups have introduced bicyclic aromatic units, e.g. derivatives of *Tröger*'s base[75,76] or 9,10-bridged 9,10-dihydroanthracenes[77] into macrocyclic hosts. These units are spacers similar to **5**–**10** in their ability to shape cavity binding sites and direct water-solubility-providing groups outwards. Water-soluble hosts with propellane units have also been prepared.[78] In the latter systems, however, the ionic groups are aligned in the cavity periphery.

The diphenylmethane units of our macromonocyclic hosts are bridged by α,ω-dioxaalkane chains. Variation of the chain length leads to cavity binding sites of variable size (**11**–**14**).[69,71] The X-ray structure analyses and the computer modeling studies described below show that the lone pairs of the four ether oxygens in the cavity periphery are directed outwards. This enhances the hydrophobic character of the binding site. In the series **15**–**18**, two, four, six, and eight methyl groups are attached to the host. As a result, the cavity becomes successively deeper and more hydrophobic.[71]

To increase the molecular-dispersed water-solubility (see Section 4.1), we attached spiro piperidinium groups to the bridging chains in host **20** to locate two additional ionic centers away from the cavity binding site.[79,80] The two spiro units also help to enforce the binding site by limiting the number of conformations of the aliphatic bridges in the sense of a "*gem*-dimethyl effect". For a tighter encapsulation of the complexed guests, we prepared the macrobicyclic hosts **21** and **22** which are soluble in weakly acidic aqueous solution. These compounds are designed according to the cryptand-concept of *Lehn*[49a] and possess three diphenylmethane units bridged by chains stemming from two "cryptand" nitrogen atoms.[81,82]

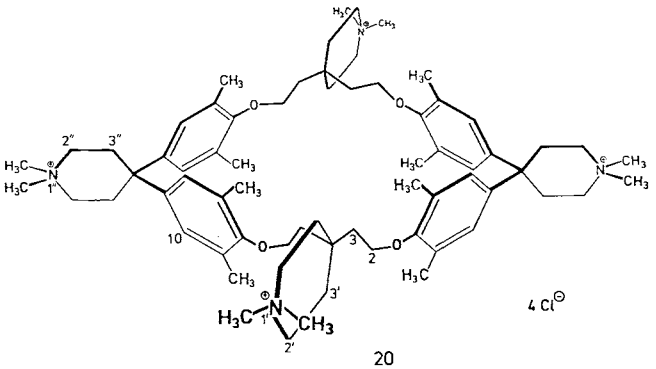

20

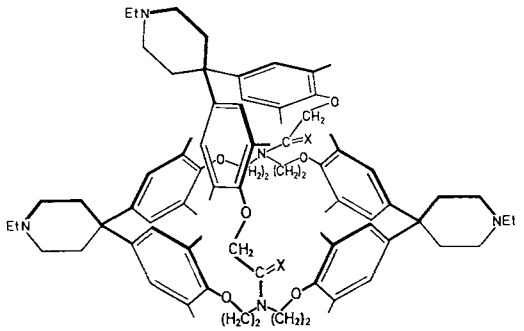

21, X = O
22, X = 2H

3. Crystal Structures of the Host Molecules

In the entire field of host-guest chemistry, two principles have been found to be of special importance for the successful design of strongly binding host molecules: (i) the principle of stereoelectronic complementarity between host and guest and (ii) the principle of preorganization of a binding site prior to complexation. The former essentially represents a modern formulation of the lock-and-key principle of *Emil Fischer*.[83] The latter principle has been defined by *Cram* et al.[50d] in a series of systematic and elegant studies. It states that the preorganization of a host prior to complexation is an essential factor controlling the association strength. If a host binding site is not completely organized, a reorganization must occur upon complexation of the guest. This reorganization can cost part of the free binding energy. In the most unfavorable case, the energy needed to reorganize the binding site is larger than the free complexation energy and no binding will occur. *Cram* et al. also showed that the guest selectivity increases with increasing preorganization of a binding site.[50d]

A comparison of the X-ray crystal structures of hosts and their complexes is often used to determine the degree of preorganization of a binding site.[50d,84,85] Solid state structures, of course, are only of limited value for making predictions about the conformations of hosts and complexes in solution. When **13a**, the bis(*N*-methylpiperidine) precursor of bisquaternary host **13**, was recrystallized from aromatic solvents, crystalline complexes suitable for an X-ray analysis were obtained (Fig. 2).[86,87] In the 1:1 host-guest complex obtained from toluene, the disordered toluene molecules are located in the interstitial spaces of the crystal lattice (Fig. 2A). From wet benzene, we obtained a crystalline 1:2:1 (host/benzene/water) complex. One of the two benzene rings is perfectly enclosed within the intramolecular cavity of the host (Fig. 2B). The second benzene ring and the water molecule are located in the interstitial spaces of the crystal lattice. A third crystalline 1:1 host-guest complex of **13a** was obtained from *p*-xylene. In

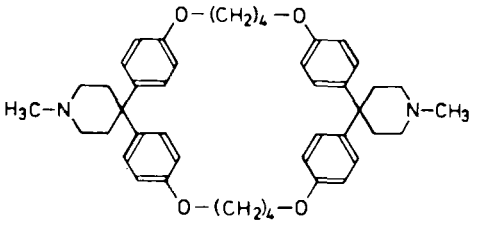

13a

this complex, which is not shown, the host molecules stack along a crystal axis. The guest molecules are enclosed in a sandwich-type array between host molecules in the stacks.[86] The methyl groups of the guest extend into the intramolecular cavities of the two surrounding host molecules.

The inclusion of benzene,[18,88-90] toluene,[91,92a,b] *p*-xylene,[93] durene,[54a] naphthalene,[54e] anisole,[92c] and *p*-nitrophenol[85] was demonstrated by X-ray analysis for crystalline complexes of a variety of cyclophane hosts with

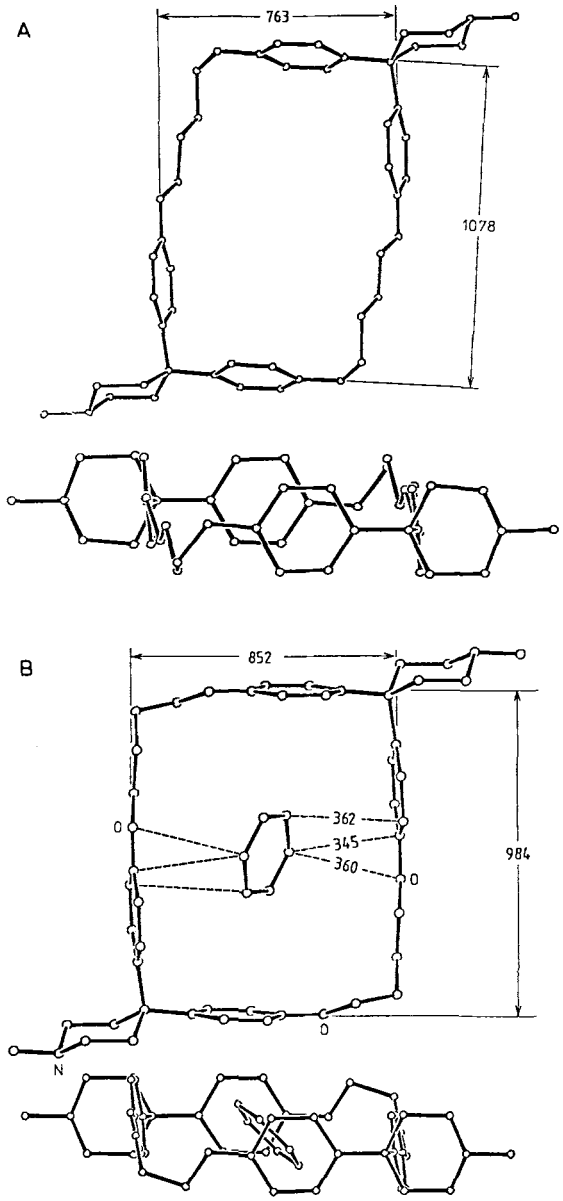

Fig. 2. View onto the least square plane of the host and view parallel to the least square plane of the host: A) in the **13a** · toluene (1:1) complex (only the host is shown and not the toluene molecules which are located in a disordered way in the crystal lattice); B) in the **13a** · benzene (1:2) monohydrate (only the host and the benzene ring in the intramolecular cavity are shown; an additional benzene ring and a water molecule are located in the crystal lattice).

apolar cavities, e.g. the calix[4]arenes.[91,92] In analogy to our results, the guests in these complexes are found both in the intramolecular cavity of the host[54a,e,85,88,91,92a] as well as in the crystal lattice.[18,89,90,92b,c,93] A crystal lattice inclusion of the guest is often observed even if the binding site of the host is sufficiently large and preorganized for intramolecular cavity inclusion. The large cyclophane hosts often crystallize with large interstitial spaces in the crystal lattice. If such interstices have geometric complementarity for the guests, the guests can encounter a large number of tight van der Waals contacts and crystal lattice inclusion can become very favorable. The formation of crystalline complexes between cyclophane hosts with apolar cavities and neutral molecules is not limited to aromatic guests. The inclusion of chloroform,[94-96] dichloromethane,[96,97]

1,2-dichloroethane,[85] carbon disulfide,[98] and acetonitrile[99] in the intramolecular cavities of cyclophane hosts, and of acetone[100] and 1,4-dioxane[93,101] in the crystal lattice between host molecules has been observed.

In the three crystalline complexes of **13a** with benzene, toluene, and *p*-xylene, the host adopts the face-to-face conformation.[52c] The four benzene rings are oriented more or less perpendicular to the mean molecular plane. The three crystal structures only differ in the sequence of the three antiperiplanar and the two synclinical torsion angles in the C_{aryl}-O-$(CH_2)_4$-O-C_{aryl}-bridges. Depending on the position of the two synclinal torsional angles, the cavity adopts a more rectangular (Fig. 2A) or a more square (Fig. 2B) shape. The structure of the host in the toluene clathrate (Fig. 2A) resembles the structure of the host in the benzene complex (Fig. 2B) and in the *p*-xylene complex which is not shown.[86] Hence, we conclude that, in the solid state, the hosts shaped by two diphenylmethane units possess highly preorganized binding sites.

4. Complexation in Aqueous Solution

4.1. Aggregation Behavior of the Host Molecules in Aqueous Solution

A serious problem in previous studies of the complexation between apolar hosts and guests in aqueous solution involved the potential self-aggregation of the host and/or guest molecules leading to the formation of aggregates of higher molecular weight.[53b,102,103] The same hydrophobic interactions that act as a driving force for stoichiometric host-guest complexation can also lead to the segregated association of host and/or guest molecules and to the formation of mixed aggregates with poorly defined orientation of host and guest, similar to micellar systems. The formation of stoichiometric complexes should therefore be studied in a concentration range in which the complexation equilibrium is not perturbed by additional equilibria leading to aggregation. Hence, the aggregation behavior of both host and guest should be known. We suggest that a study of stoichiometric complexation with a new host, designed to provide significant thermodynamic and kinetic data, should always begin with the investigation of the aggregation behavior of the host component.

We found that the critical aggregation concentration (CAC) of cyclophane hosts, below which stoichiometric complexation is studied, can be determined in an easy way by ^{1}H-NMR spectroscopy.[69-71] This method has been applied to measure the critical micelle concentration (CMC) of micellar systems.[104-106] As an example, Figure 3 shows the chemical shifts of the protons of **20** plotted as a function of the concentration of this host in aqueous solution. In the curves, a well-defined discontinuity is observed at approximately the same concentration. This concentration can be considered as the ^{1}H-NMR CAC of this compound. Below this value, the host is present in a molecular-dispersed form and the chemical shifts are independent of concentration. Above the CAC, the chemical shifts become dependent on concentration, since the anisotropic regions of the aromatic rings influence the signal positions of the

Table 1. Critical aggregation concentrations (CAC's) of the hosts determined by ^{1}H-NMR spectroscopy and maximum water-solubilities (T = 303 K).

Host	CAC [mol L^{-1}]	Maximum water-solubility [mol L^{-1}]
11 [a]	2.5×10^{-3}	$\approx 2\times10^{-2}$
12 [a]	2.5×10^{-3}	$\approx 1\times10^{-1}$
13 [a]	1.6×10^{-4}	$\approx 1\times10^{-1}$
18 [a]	$\leq 2\times10^{-5}$	$\approx 6\times10^{-2}$
19 [b]	1.5×10^{-3}	$\approx 1\times10^{-2}$
20 [a]	7.5×10^{-3}	$\approx 1\times10^{-1}$
21 [c]	1.0×10^{-3}	$\approx 1\times10^{-2}$
22 [c]	5.0×10^{-3}	$\approx 1\times10^{-1}$

[a] D_2O. [b] 0.05 M K_2CO_3. [c] 0.5 M KD_2PO_4.

aggregating hosts. In addition, a strong line-broadening, increasing at higher concentrations, of the signals is observed for some but not for all hosts above the CAC. A good agreement was observed between the ^{1}H-NMR CAC of the host **13** and the CAC value determined by monitoring the light scattering at a 90° angle.[71] Table 1 includes the CAC values for some of our host systems.[70-72,82] The table clearly shows the large reduction in aggregation tendency which occurs upon introduction of the two additional spiro piperidinium units in host **20**. The CAC of **20** (7.5×10^{-3} mol L^{-1}) is more than two magnitudes higher than the CAC of the comparable host **18** with only two ionic centers ($\leq 2\times10^{-5}$ mol L^{-1}). Below the very low CAC of **18**, the application of ^{1}H-NMR spectroscopy to host-guest complexation analysis was not possible.

Figure 3 shows that the aggregation-induced shifts of the host signals above the CAC are quite significant.[71] These shifts can be of the same magnitude as the shifts resulting from the formation of a stoichiometric molecular complex. Therefore, it is not possible to decide whether shifts of the host resonances observed in solutions of host and guest above the CAC result from molecular complexation or from aggregation. Future investigations have to clarify

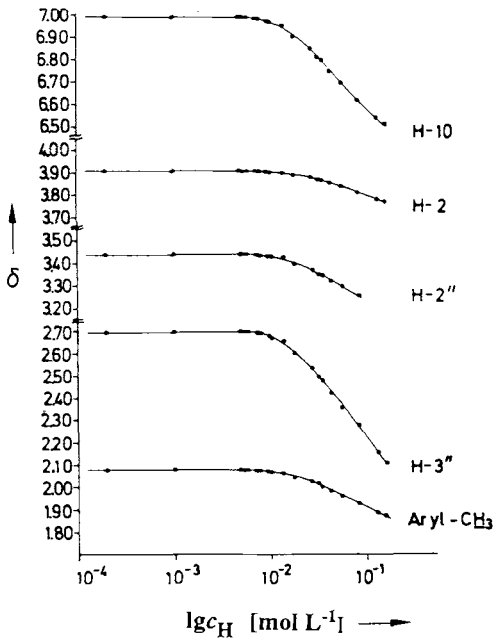

Fig. 3. Chemical shifts (δ values) of the protons of **20** as a function of the concentration (c_H) of **20** in D_2O [360 MHz, 303 K, ext. standard: sodium 2,2,3,3-tetradeuterio-3-(trimethylsilyl)propionate (TSP)].

how aggregation equilibria interfere with the equilibrium of stoichiometric, geometrically well defined molecular complexation. Studies must also address how the guest alters the aggregation behavior of the host. We have obtained preliminary evidence that the aggregation tendency of complexes can be considerably reduced if complexed guest components possess ionic groups extending out of the cavity.[107] These preliminary observations must be supported by additional quantitative studies.

In all binding studies described below, aqueous solutions with host concentrations below the CAC have been used.

4.2. Evidence for the Formation of Inclusion Complexes in Solution and Determination of the Association Constant K_a of Host-Guest Complexes

A large variety of analytical methods has been employed to provide conclusive evidence for inclusion complex formation by cyclodextrins in aqueous solution.[9, 12a, 13] To provide such evidence in studies with cyclophane hosts, ^{1}H-NMR spectroscopy is by far the method of choice.[33, 108–111] This method allows the thermodynamics and the kinetics of complexation equilibria to be analyzed quantitatively.[33, 82, 111–116] In addition, extensive information can be obtained about the structures of the cyclophane complexes as shown in Section 4.3.[117] Since the inclusion of a guest in the intramolecular cavity of a cyclophane can be demonstrated in the most convincing way by ^{1}H-NMR spectroscopy, this method should be applied in the first place to the analysis of the complexation behavior of a new cyclophane host in solution.

A versatile methodology has been developed for the determination of the stability constants of molecular charge-transfer complexes[118–122] and of cyclodextrin inclusion complexes.[9, 12, 13, 123] These methods have also been used for the quantitative analysis of the stability of synthetic host-guest complexes. For a comprehensive discussion of the methods available for measuring binding constants of molecular complexes, the reader is referred to a new excellent monograph by *Connors*.[124] The application of computers to the evaluation of experimental binding data and to the determination of complex stability constants has also been recently reviewed in a monograph.[125] Included are print-outs of computer programs which can be applied directly or, after modifications, to a given problem.

For the quantitative determination of the thermodynamic stability of the inclusion complexes formed by our hosts in aqueous and organic solutions, we have relied on various methodologies. For all host-guest interactions discussed in this review, we could demonstrate the exclusive formation of complexes with 1 : 1 host-guest stoichiometry in the concentration ranges used in the binding studies. In many cases, the association constant K_a (L mol^{-1}) of a given host-guest complex was determined by several independent methods,[70, 82] and we always found good agreement between such values. The following methods were employed:

1. *Solid-Liquid and Liquid-Liquid Extractions.* These procedures are indispensable for the preparation of aqueous solutions of complexes formed by guests that are extremely insoluble in water, e.g. perylene, pyrene, fluoranthene, naphthalene, or durene. For the preparation of aqueous solutions of complexes by solid-liquid extraction, an excess of finely powdered solid guest was extracted at constant temperature with an aqueous solution of the hosts **20** or **21**[70, 77, 82, 126] by vigorous stirring and shaking or ultrasonic radiation until establishment of the extraction equilibrium; the excess of solid guest was then removed by centrifugation and filtration. The complex stability constants K_a from solid-liquid extraction procedures were in good agreement with those obtained by other procedures. For accurate K_a values, it is important that residual microcrystals of the solid guest are completely removed by centrifugation and filtration from the aqueous complex solution obtained by the extraction. For the solutions of the complexes formed by perylene, pyrene, or fluoranthene, the absence of microcrystals could be elegantly demonstrated by the complete absence of the excimer fluorescence which is characteristic of the crystalline materials.[127]

Liquid-liquid extraction procedures are often the methods of choice to prepare organic solutions of polyethercation complexes and to determine the thermodynamic constants of the association, distribution, and extraction equilibria [Eq. (1)–(4)] which define the efficiency of the extraction.[128, 129] For the preparation of aqueous solutions of arenes that are extremely insoluble in water, we extracted at constant temperature solutions of the guests in *n*-hexane with aqueous solutions of the hosts **20** or **21**.[70, 82] Using Equations (1)–(4), the association constant K_a, the distribution constant K_d, and the extraction constant K_e could be determined in a very reproducible way.

$$[\text{host}_{H_2O}] + [\text{guest}_{H_2O}] \overset{K_a}{\rightleftharpoons} [\text{host-guest complex}_{H_2O}] \quad (1)$$

$$[\text{guest}_{\text{hexane}}] \overset{K_d}{\rightleftharpoons} [\text{guest}_{H_2O}] \quad (2)$$

$$[\text{guest}_{\text{hexane}}] + [\text{host}_{H_2O}] \overset{K_e}{\rightleftharpoons} [\text{host-guest complex}_{H_2O}] \quad (3)$$

$$K_e\,[\text{L mol}^{-1}] = K_a K_d \quad (4)$$

2. *Determination of the Stoichiometry and Stability of the Complexes by ^{1}H-NMR Titration and Optical Titration.* In these titrations at constant guest concentration, the change of a guest property X is monitored as a function of increasing host concentration.[70, 71, 82] The property X can be the chemical shift of a guest proton or the intensity of an electronic absorption or fluorescence band of the guest. The titration curves are obtained by plotting the change of the guest property (ΔX) as a function of increasing host concentration. From these curves, the stoichiometry of the complexes and the K_a values are obtained using the following methods of analysis.

a) If a 1 : 1 complex is formed exclusively, the titration curves are described by a quadratic equation[124] with the change of the guest property ΔX_{sat} at saturation binding and the association constant K_a as the two unknowns. In some fluorescence and ^{1}H-NMR titrations, especially with host **20**, saturation binding could be reached[70, 82] and ΔX_{sat} could therefore be directly determined. In these experiments, K_a was the only unknown quantity and could be easily and directly evaluated from the titration curve.

b) If saturation binding was not observed, the association constant K_a as well as ΔX_{sat} could be determined from the straight lines in the double reciprocal plots obtained by evaluation of the titration data according to *Benesi* and *Hildebrand*.[130] To evaluate titration data according to *Benesi* and *Hildebrand* or by using the related semi-reciprocal treatments described by *Scott*[131] or *Scatchard*,[132] the concentration of free host must be considerably larger than the concentration of the host-guest complex over the entire titration range.[133-135] This boundary condition can be best obeyed by choosing over the entire titration range a total host concentration $[host]_0$ which is much larger (≥ 10 times) than the total guest concentration $[guest]_0$.[135]

c) Over the past two years, we have switched to a computer-assisted, non-linear curve-fitting evaluation of those titrations in which saturation binding was not reached.[136] Figure 4 shows the experimental data points of a ^{1}H-NMR titration to determine the association constant of the **18** · 2,6-naphthalenedicarbonitrile complex in [D$_4$]methanol and the non-linear least square curve fit to calculate the saturation shift $\Delta\delta_{sat}$ of the guest proton 1-H and the association constant K_a. The non-linear curve fitting has a

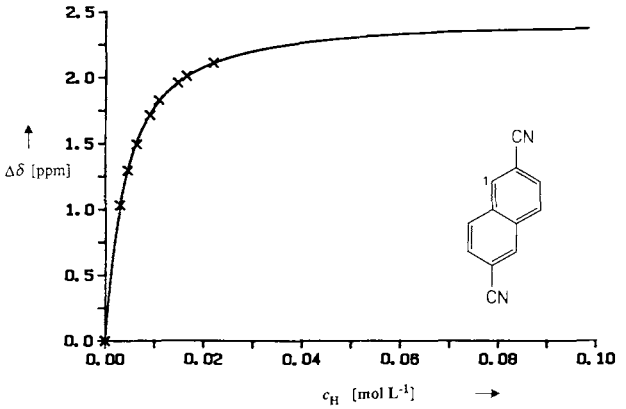

Fig. 4. Determination of the association constant (K_a) of the **18** · 2,6-naphthalenedicarbonitrile complex in [D$_4$]methanol (T=303 K) by computer-assisted non-linear curve fitting of the experimental data [x] of a ^{1}H-NMR titration (500 MHz, CH_3OD as internal standard, $[host]=2\times10^{-3}$–2×10^{-2} mol L^{-1}; $[guest]=5\times10^{-3}$ mol L^{-1}). The complexation-induced shifts $\Delta\delta$ observed for the guest proton 1-H are plotted against the host concentration c_H.

major advantage over the treatment of *Benesi* and *Hildebrand*, since no boundary condition with respect to the ratio of the concentrations of the two binding partners must be obeyed during the titration. Hence, this evaluation is of much broader applicability and, in view of the increasing use of computers, will presumably displace in the future the evaluations according to *Benesi* and *Hildebrand*, and to *Scott*, or *Scatchard*.[76,77,137-139a]

3. *Competitive Inhibition of the Complexation of a Fluorescing Guest by a Non-Fluorescing Inhibitor.* This method was applied in binding studies with the host **20**, when the complex stability constants could not be determined from extraction procedures or from the titration methods described above.[70] In a fluorescence titration with the boundary condition $[inhibitor]_0 \gg [host]_0 \gg [guest]_0$, the host concentration is continuously increased at constant inhibitor and guest concentration. Evaluation of the change in fluorescence intensity in a procedure analogous to the *Benesi* and *Hildebrand* treatment afforded the unknown association constant K_i of the inhibitor complex.[140] It is essential for the accuracy of this method that the association constant of the complex of the fluorescing guest, whose binding is competitively inhibited, can be determined exactly. As fluorescing guests in our studies, we used 6-(4-methylphenyl)amino-2-naphthalenesulfonate (TNS) **23** and 8-phenylamino-1-naphthalenesulfonate (ANS) **24**. These compounds form highly stable 1 : 1 complexes with the host **20** in aqueous solution and their stability constants could be very accurately determined from direct evaluations of the fluorescence titration curves.[70]

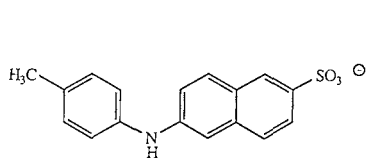

23

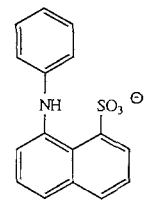

24

The two fluorescence probes TNS (**23**) and ANS (**24**) have been preferentially employed in the analysis of the complexation behavior of cyclophane hosts with apolar binding sites in aqueous solution.[52c,53d,54b,55c,69-71,78,123,141-147] In these studies, valuable information on the micropolarity of the binding sites is obtained from the fluorescence intensity as well as from the position of the emission maximum.[148-150]

4. *^{1}H-NMR Spectroscopic Estimation of the Association Constant of a Host-Guest Complex in a Series of Solvents.*[82] The degree of complexation and subsequently the stability constant in a given solvent is calculated from the complexation shifts $\Delta\delta_{obs}$ of host and guest protons observed in this solvent and the complexation shifts at saturation binding ($\Delta\delta_{sat}$) observed in another solvent. This method allowed the rapid determination of the complexing properties of host **22** in a larger series of solvents without resorting to the more exact but significantly more time-consuming NMR titrations.[82] Comparisons showed that the K_a-values calculated in this manner are in good agreement with the values determined from complete titrations. Significant binding constants are only obtained by this rapid method if, as demonstrated for the complexes of **22**, the geometry of the given host-guest complex is very similar in the two solvents. Only then can one expect similar complexation shifts at saturation binding ($\Delta\delta_{sat}$) in both solvents. This, however, is the prerequisite for using the $\Delta\delta_{sat}$ value from one solvent to determine the degree of complexation and the complex stability constant in a second one.

4.3. Stability and Structure of Complexes Formed by Polycyclic Aromatic Hydrocarbons in Aqueous Solution

With the host molecule **20**, by using solid-liquid and liquid-liquid extraction procedures, we were able to prepare for the first time a series of 1 : 1 complexes of polycyclic

aromatic hydrocarbons of variable size in aqueous solution.[70, 79] The amount of extremely insoluble hydrocarbon that can be solubilized in water is dramatically increased by host-guest complexation. As an example, the maximum solubility of pyrene in water is only 8×10^{-7} mol L^{-1}. With a 5.5×10^{-3} M aqueous solution of **20** in solid-liquid extractions, however, a complex solution can be prepared containing a total pyrene concentration of 2.8×10^{-3} mol L^{-1}. The association constants of the 1 : 1 complexes of arenes, determined from the two extraction procedures, are listed in Table 2.

Table 2. Association constants (K_a) and free enthalpies of complexation ($-\Delta G$)[a] for the 1 : 1 complexes of the hosts **20** and **21** with aromatic hydrocarbons in aqueous solution (T = 293-295 K).

Guest	K_a [L mol^{-1}]	$-\Delta G$ [kcal mol^{-1}]
a) Complexes of host **20** *in water:*		
Perylene	1.6×10^7	9.6
Fluoranthene	1.8×10^6	8.4
Pyrene	1.8×10^6	8.4
Biphenyl	2.2×10^4	5.8
Azulene	2.1×10^4	5.8
Naphthalene	1.2×10^4	5.5
Durene	1.9×10^3	4.4
b) Complexes of host **21** *in 0.5 M* KH_2PO_4, *pH* = 4.7:		
Pyrene	3.1×10^6	8.7
Naphthalene	1.6×10^4	5.6

[a] Free enthalpies are also known as Gibbs free energies of systems at constant T,p.

Table 2 shows that host **20** can form complexes with apolar guests in aqueous solution which are comparable in stability to enzyme-substrate complexes. The most stable complex is formed with perylene, the guest with the highest complementarity to the binding site and with the largest surface for hydrophobic and van der Waals interactions. The geometric complementarity between **20** and smaller arenes is less favorable and, expectedly, the complex stability decreases. Perylene binds better than pyrene and fluoranthene and a strong decrease in complex stability is observed with the smaller guests biphenyl, azulene, and naphthalene.[151] Durene is similar in size and shape to naphthalene and azulene. However, the association constant of the durene complex is about one magnitude smaller than those of the naphthalene and azulene complexes. This demonstrates the importance of van der Waals interactions for the stability of the complexes. These interactions are more effective in the complexes of the more polarizable guests naphthalene and azulene than in the durene complex. Hydrophobic interactions, however, represent the single most important driving force for complexation, as shown by the solvent dependency of the binding strength. Strong complexation is only observed in aqueous solution. In methanol, the free binding enthalpy of the **20** · pyrene complex ($K_a \approx 75$ L mol^{-1}) is 5.9 kcal mol^{-1} smaller than in water and, in dimethyl sulfoxide, almost no complexation at all is observed. In concentration ranges below 10^{-2} mol L^{-1}, we could not detect any molecular complexation of arenes in water by comparison compounds lacking the macrocyclic binding site.

The comparison of the two hosts **21** and **22** in weakly acidic aqueous solution underscores in an impressive way the importance of locating ionic groups remote from the binding site if strong hydrophobic complexation is to occur. In host **21**, only the three piperidine nitrogen atoms directed outwards are protonated. Hence, this macrocycle is a very good host for neutral arenes (Table 2). In addition to the three piperidine nitrogens, host **22** possesses two tertiary cryptand nitrogen atoms in the periphery of the cavity which are also protonated and favorably solvated. Hence, the hydrophobic character of the binding site is reduced and the complexation of arenes is much weaker. By solid-liquid extraction, the association constant of the **22** · pyrene complex in 0.5 M KH_2PO_4 was estimated as $K_a \approx 10^4$ L mol^{-1}. The complexation of pyrene in 0.5 M KH_2PO_4 by host **22** is therefore about 3.5 kcal mol^{-1} less favorable than the complexation of this guest by host **21** (Table 2).

Similar stability constants were measured for the arene complexes of the hosts **20** and **21** (Table 2).[82] The **21** · pyrene complex is only slightly more stable than the pyrene complex of **20**, and naphthalene even forms complexes of very similar stability with the two ligands. This high similarity in the complexing properties of two geometrically very different hosts was quite surprising at first. We had expected a considerably better binding by the more spherical host **21** as consequence of a much better encapsulation of the enclosed guest. The small difference in complexing ability between hosts **20** and **21** in aqueous solution indicates that the macromonocyclic host **20** already envelops and encapsulates efficiently arenes of complementary size. In addition, favorable solvation of the two amide groups in the periphery of the binding site of **21** interferes with hydrophobic complexation.

Detailed information about the spatial relationship between the two binding partners in the complexes of hosts **20**-**22** could be obtained by ^{1}H-NMR spectroscopy.[82, 111] In the complexes, the diatropic ring currents of both host and guest mutually influence the positions of their proton resonances and selective complexation shifts are observed. The extent of these complexation shifts depends on the distance and orientation of the two binding partners in the complex. Extensive ^{1}H-NMR studies showed that all aromatic guests prefer a location in a specific plane in the cavity of the host **20**.[111] This plane, which we have named the arene-guest plane of **20**, passes through the two spiro carbon atoms of the two diphenylmethane units and perpendicular to the mean molecular plane of the host. An incorporation of an aromatic guest in this plane is easily recognized in the ^{1}H-NMR spectrum by a characteristic pattern of upfield and downfield shifts of the host signals as well as by specific upfield shifts of the guest signals. Table 3 shows the complexation-induced shifts of the host and guest resonances in an aqueous solution of the **20** · pyrene complex. These characteristic signal shifts support the preferred orientation of pyrene in the arene-guest plane of **20** shown in Figure 5A. As depicted schematically in Figure 5A, the piperidinium rings attached to the aliphatic bridges approach and further envelop the enclosed guest. This

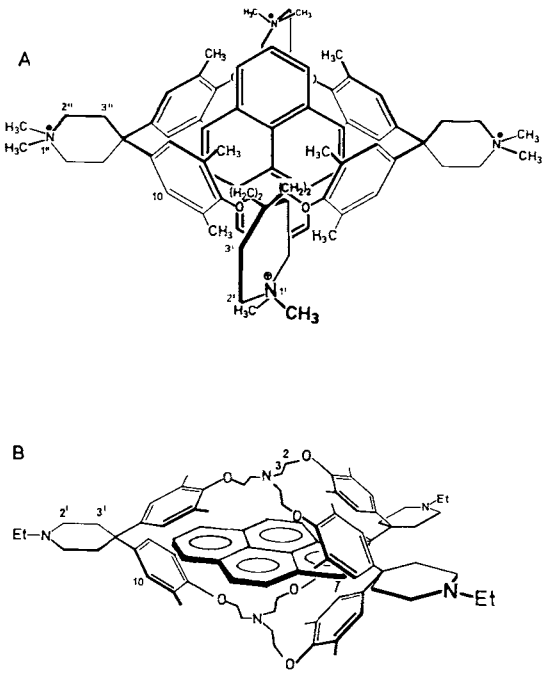

Fig. 5. Schematic drawing of the geometry of the complex which, according to ^{1}H-NMR, is highly favored for A) the **20** · pyrene complex in aqueous solution (the piperidinium rings of the bridges can also be oriented to the same cavity side), and for B) the **22** · pyrene complex in methanol (for the **21** · pyrene complex in aqueous solution, a very similar geometry is supported by ^{1}H-NMR spectroscopy).

leads to additional favorable shielding of the complexed apolar guest from the solvent.

In the complexes of **21** and **22** in aqueous as well as in organic solutions, the arene guests are exclusively located in the plane of the cavity passing through the three spiro centers of the host (Fig. 5B). Table 3 includes the complexation-induced shifts of the host and guest resonances for methanol solutions of the **22** · pyrene complex. These signal shifts clearly support the inclusion complex geometry shown in Figure 5B.

Table 3. Complexation-induced shifts ($\Delta\delta$ values, + = upfield shift) of host and guest proton resonances in the 360-MHz ^{1}H-NMR spectra of solutions of the **20** · pyrene complex in D_2O and of the **22** · pyrene complex in [D_4]methanol (see Fig. 5).

*a) **20** · pyrene complex in D_2O* [a]:

Host **20**	$\Delta\delta$ [ppm]	Pyrene	$\Delta\delta$ [ppm]
2-H	+0.81	1-H	+1.02
2′-H	+0.49	2-H	+0.44
2″-H	−0.07	4-H	+1.25
3-H	+0.52		
3′-H	+0.77	N(1′)-CH_3	+0.20
3″-H	−0.16	N(1″)-CH_3	−0.02
10-H	−0.31		
ArylCH_3	−0.02		

*b) **22** · pyrene complex in [D_4]methanol* [b]:

Host **22**	$\Delta\delta$ [ppm]	Pyrene	$\Delta\delta$ [ppm]
2-H	+2.14	1-H	+1.79
2′-H	−0.16	2-H	+1.21
3-H	+0.85	4-H	+1.98
3′-H	−0.43		
10-H	−0.60	N−CH_2−CH_3	−0.04
Aryl-CH_3	+0.08	N−CH_2−CH_3	−0.04

[a] This complex solution, obtained by solid-liquid extraction, contains [**20**] = 5.5×10^{-3} mol L^{-1} and [pyrene] = 2.8×10^{-3} mol L^{-1}. 2 H and 3 H, see formula **20** in Section 2. [b] Pyrene signals in a solution with [**22**] = 2.0×10^{-2} mol L^{-1} and [pyrene] = 2.0×10^{-3} mol L^{-1} and host signals in a solution with [pyrene] = 2.0×10^{-2} mol L^{-1} and [**22**] = 2.0×10^{-3} mol L^{-1}.

The ^{1}H-NMR studies have provided preliminary information on the kinetics of complex formation between our hosts and arenes in aqueous solution.[152] On the ^{1}H-NMR time scale (360 MHz), the dissociation of the **20** · pyrene and the **20** · fluoranthene complexes is slow at 273 K, while the dissociation of the **21** · pyrene complex is slow at 303 K. For the dissociation of the **20** · pyrene complex, the first order decomplexation rate constant was determined at the coalescence temperature as $k_{-1} = 495\ s^{-1}$ ($T = 273$ K). With an association constant $K_a = k_1/k_{-1}$ of 1.8×10^6 L mol^{-1} ($T = 293$ K), the second order complexation rate constant can be estimated as approximately $k_1 \approx 9 \times 10^8$ s^{-1} L mol^{-1}. Hence, the formation of the highly stable complexes of pyrene and fluoranthene in aqueous solution is not much slower than diffusion controlled. This fast complexation rate is not unexpected in view of the easy steric accessibility of the binding sites of our hosts. In addition, the desolvation of apolar binding sites and of the apolar arenes during the complexation step apparently requires only a small activation energy. The dissociation of the complexes formed by the smaller and weaker binding arenes, e.g. naphthalene and azulene, is fast on the NMR time scale.

Different kinetics are observed if the aromatic guests possess polar neutral substituents capable of forming strong hydrogen bonds to the solvent (−$CONH_2$, −NH_2, −COOH, −OH). In the ^{1}H-NMR spectra of aqueous or methanolic solutions of complexes formed between the hosts **18** or **20** and 2,6-disubstituted naphthalenes as guests with these substituents, extreme signal broadening is observed at room temperature.[152] This broadening indicates decomplexation rates on the ^{1}H-NMR time scale. From the association constants measured in aqueous solution ($K_a = 10^4$ L mol^{-1}) and in methanol in particular ($K_a \approx 30$–350 L mol^{-1}), which are considerably smaller than in the case of the **20** · pyrene complex in water, it follows that the complexation steps must be significantly slower than diffusion controlled for the dissociation of the complexes to be observed on the NMR time scale. We explain the slower complexation step by the higher activation energy needed to desolvate the polar, hydrogen-bonding substituent upon penetration of the guest into the cavity binding site. The application of faster relaxation methods, e.g. ultrasonic relaxation, for studying the kinetics of the complexation of cyclophane hosts and organic molecules seems very desirable.[42a, 153] From such studies, interesting information on the energies needed to desolvate neutral polar substituents could be obtained.

In the meantime, other efficient hosts for the complexation of larger arenes in aqueous solutions have been described. *Dougherty* et al.[77] reported on the inclusion of anthracene as well as of pyrene ($K_a = 2 \times 10^6$ L mol^{-1}) by the macrocyclic ligand **25**. *Vögtle* et al.[126] obtained in a very short synthetic sequence the macrobicyclic host **26** which is soluble in dilute hydrochloric acid. Following the extraction procedures described above, solutions of complexes with large arenes, including benzo[*g,h,i*]perylene,

benzo[*a*]pyrene and triphenylene, could be prepared. The host **26** forms a very stable complex with phenanthrene but binds anthracene only weakly. This binding selectivity could be exploited for the separation of phenanthrene from anthracene by solid-liquid extraction. Furthermore, it was possible through complex formation with host **26** to separate partially hydrogenated arenes from the parent arenes, e.g. hexahydropyrene from pyrene and dodecahydrotriphenylene from triphenylene. In liquid-liquid extractions, only the strongly binding arenes are transferred from a *n*-hexane phase into the aqueous solution, whereas the poorly binding partially hydrogenated compounds are not extracted.

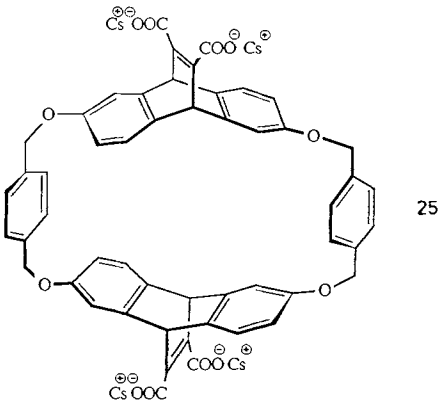

25

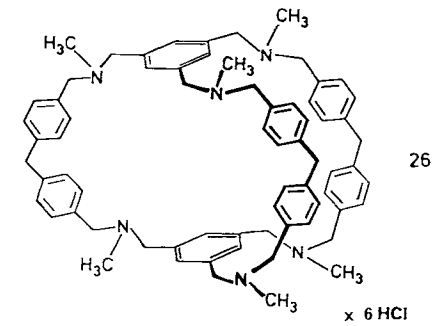

26 x 6 HCl

4.4. Acceleration of the Transport of Arenes through Aqueous Solutions

With the host **20**, we observed for the first time the molecular carrier-mediated acceleration of the transport of lipophilic arenes through an aqueous phase along a concentration gradient.[70, 154] Such a transport represents the inverted form of the molecular transport of cations through lipophilic membranes mediated by natural or synthetic ionophores.[155–159] The U-type cell shown in Figure 6 was used in our transport experiments. We measured the relative rate of transport of arenes from one hexane phase into a second hexane phase through an aqueous phase in the presence of and absence of host **20** in the aqueous phase. When the aqueous phase contained the host, the transport, especially of the larger arenes, was considerably accelerated. Competitive inhibition experiments demonstrated that the acceleration is a consequence of host-guest complexation in the aqueous phase. High guest selectivity in the transport acceleration was observed. Table 4 shows

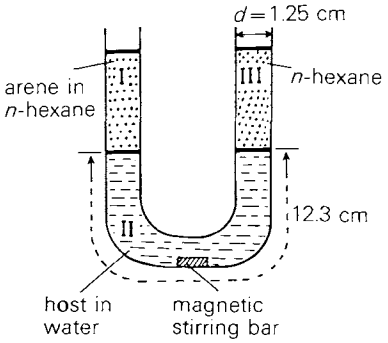

Fig. 6. U-type cell for studying the transport of arenes through an aqueous phase mediated by **20** as molecular carrier. The transport data of Table 4 were obtained with this cell.

that the highest acceleration is measured for the arenes with the lowest distribution constant K_d [Eq. (2)] and the highest association constant K_a of the complex formed with **20** in the aqueous phase.

Table 4. Acceleration of the transport of arenes through a 5×10^{-4} M solution of **20** as aqueous phase II against the transport through pure water ($T = 293$–295 K). The experiments were run in the U-type cell shown in Fig. 6. The initial concentration of the arenes in the *n*-hexane phase I was 10^{-2} mol L^{-1}. The association and distribution constants included in the table were obtained by liquid-liquid extractions.

Arene	Acceleration factor	K_a[L mol^{-1}]	K_d
Pyrene	430	1.8×10^6	8.3×10^{-6}
Fluoranthene	395	1.8×10^6	1.1×10^{-5}
Naphthalene	3.7	1.2×10^4	3.8×10^{-4}
Azulene	3.6	2.1×10^4	6.0×10^{-4}
Durene	1.8	1.9×10^3	3.8×10^{-5}

The molecular carrier-mediated transport of lipophilic molecules through aqueous solutions has also been studied by other research groups.[126, 160, 161] *Vögtle* et al.[126] described the separation of naphthalene from phenanthrene in transport experiments using U-type cells and the macrobicycle **26** as molecular carrier. Only phenanthrene forms a very stable carrier complex and, hence, only the transport of this arene is accelerated.

The molecular understanding of the carrier-mediated transport through aqueous solutions is still poorly developed. In particular, the relationship between the rate of transport and the stability constant of the carrier-complex needs to be determined. For the cation transport through lipophilic membranes, *Kirch* and *Lehn*[162, 163] as well as *Izatt*, *Christensen* et al.[159] have shown that the rate of transport initially increases with the cation-carrier complex stability to reach a plateau at K_a-values around 10^4–10^5 L mol^{-1}. Finally, at still higher K_a-values, the transport rate starts to decrease. It would be interesting to explore within a series of hosts, whether a similar dependency exists between the rates of transport in aqueous solution and the association constants of the arene-carrier complexes.

The transport monitored in our U-type cell is a "passive transport" along a concentration gradient. After approximately 10–15% of the total quantity of arene initially present in the source phase has been transported into the receiving phase, back transport becomes significant. The occurrence of back transport limits the utilization of the high

transport selectivity for efficient material separations. To take advantage of the high transport selectivity[70, 126] and to obtain higher separation yields, the transport has to occur in one defined direction. For the transport and separation of cations through lipophilic membranes, a variety of carrier-ligands which allow for "active transport" in one defined direction have been described.[43b, 164] As a characteristic feature, the complexing properties of these ligands can be rapidly and reversibly altered. The driving force for the unidirectional "active transport" can be provided by the electron flow in a redox process,[163, 165] by the light energy in a photochemical process,[43b, 164, 166] or by the proton flux in a pH-gradient.[164]

The complexing properties of the flavin-host **40** can be controlled by a redox process (Section 7). This system represents the first stage in the development of carriers for the separation of neutral molecules by "active transport" through aqueous solutions.[74]

4.5. Structure and Stability of Complexes of the Host 20 with Naphthalene Derivatives in Aqueous Solution

To explore the influence of guest substituents on the stability and structure of complexes in aqueous solution, we carried out extensive studies on the binding between the host **20** and a variety of naphthalene derivatives.[70]

Table 5. K_a and $-\Delta G$ of the 1 : 1 complexes of the host **20** und naphthalene derivatives in aqueous solution ($T = 293$ K). For comparison: naphthalene: $K_a = 1.2 \times 10^4$ L mol^{-1}; $-\Delta G = 5.5$ kcal mol^{-1} ($T = 293$–295 K); see Table 2.

Guest	K_a [L mol^{-1}]	$-\Delta G$ [kcal mol^{-1}]
a) Naphthalene derivatives with neutral substituents:		
1,5-Dimethylnaphthalene	3.3×10^4	6.0
2,6-Dimethylnaphthalene	2.6×10^4	5.9
2,7-Naphthalenediol	1.9×10^4	5.7
1,3-Naphthalenediol	9.8×10^3	5.4
1,5-Bis(dimethylamino)naphthalene [a]	9.7×10^3	5.4
1-(Dimethylamino)naphthalene	9.3×10^3	5.3
b) Naphthalene derivatives with ionic substituents:		
TNS **23**	5.0×10^6	9.0
ANS **24**	3.2×10^6	8.7
2,6-Naphthalenedisulfonate	$> 10^6$	> 8.0
1,5-Naphthalenedisulfonate	4.4×10^5	7.6
2-Naphthalenesulfonate	4.0×10^5	7.5
1-Naphthalenesulfonate	3.5×10^5	7.4
5-Dimethylamino-1-naphthalenesulfonate	1.4×10^5	6.9
1-(Trimethylammonium)naphthalene-fluorosulfonate	1.7×10^3	4.3
1,5-Bis(dimethylammonium)naphthalenebis(deuterium chloride) [b]	$\approx < 10$	$\approx < 1.3$

[a] 1.5×10^{-2} M K_2CO_3, pH ≈ 11. [b] D_2O/DCl/KCl; pD = 1.2, ionic strength $I = 0.27$ mol L^{-1}.

Table 5a shows that naphthalene itself and derivatives with non-ionic substituents form complexes of similar stability ($K_a \approx 10^4$ L mol^{-1}, $\Delta G \approx -5.4$ kcal mol^{-1}). Our initial study included only naphthalene derivatives with donor substituents; such guests have unfavorable electronic complementarity to the electron-rich host **20**. At that time, the importance of electron donor-acceptor interactions in molecular complexes of our hosts had not yet been recognized. More recent studies (Section 5.2)[136] have demonstrated that a higher stability can be expected for complexes of **20** and naphthalene derivatives with acceptor substituents ($-CN$, $-NO_2$) than for the complexes of the non-ionic derivatives included in Table 5a.

^{1}H-NMR studies[111] have shown that substituents of the complexed guests extend out of the cavity into the aqueous solution; this occurs both for steric reasons and for reasons of favorable solvation of polar and ionic groups. The spectra indicated that, depending on the position of the substituents, the guests, especially the disubstituted naphthalenes, take a highly preferred orientation in the arene-guest plane of the cavity of **20** (Fig. 7). Naphthalene itself does not seem to prefer a specific orientation; Figure 7 shows its equatorial inclusion. Both 1,3- and 2,3-naphthalenediol prefer an axial, 2,6- and 2,7-disubstituted derivatives a pseudo-axial, and 1,5-disubstituted naphthalenes a pseudo-equatorial position in the arene-guest plane. These structural assignments are based on characteristic upfield shift patterns of the guest resonances in the ^{1}H-NMR spectra. It is apparent from Figure 7 that protons 1,4,5,8-H of an axially enclosed guest should encounter a specifically large upfield complexation shift. Similarly, a large upfield shift can be expected for the resonances of 4,8-H in a preferred pseudo-axial inclusion and for the resonances of 3,7-H in a preferred pseudo-equatorial inclusion. Experimentally, these complexation shifts are observed in the NMR spectra. The preferred pseudo-axial inclusion of disubstituted naphthalenes could be further supported by docking experiments in computer modeling studies. For the complexes formed by **4** or other tetraaza[n.1.n.1]paracyclophanes and naphthalene derivatives, *Koga* et al. had derived similar structures to those shown in Figure 7 from ^{1}H-NMR experiments.[54e, 110] They also proposed the nomenclature which we use to describe the different orientations of the guests in the cavity.

Additional ion-pairing can lead to extraordinary binding selectivity in a series of guests which fit well into the binding site (Table 5b). The host **20** forms complexes with naphthalene mono- and disulfonates that are considerably more stable than those of the neutral naphthalene derivatives in Table 5a. Thus, for example, host **20** forms the most stable complexes known with the anionic fluorescence probes ANS and TNS.[54b, 70, 144d, e] In the complexes of the naphthalenesulfonates, both apolar interactions in the cavity and ion-pairing interactions at the cavity periphery are operative. Efficient ion-pairing results from the electrostatic attraction between the anionic residues of the guests and the quaternary nitrogen atoms of the piperidinium rings attached to the aliphatic bridges of the host. This is shown in Figure 8 for the **20** · 2,6-naphthalenedisulfonate complex, a highly structured complex according to ^{1}H-NMR analysis. The importance of ionic interactions is demonstrated in an impressive way by the weaker binding of 1-(trimethylammonium)naphthalene fluorosulfonate and especially by the almost complete absence of complexation of 1,5-bis(dimethylammonium)naphthalene dihydrochloride (Table 5b).[80] This strongly reduced complexation is explained by the electrostatic repulsion between the cationic centers of both binding partners. Table 5b shows, that favorable versus unfavorable ionic interactions in

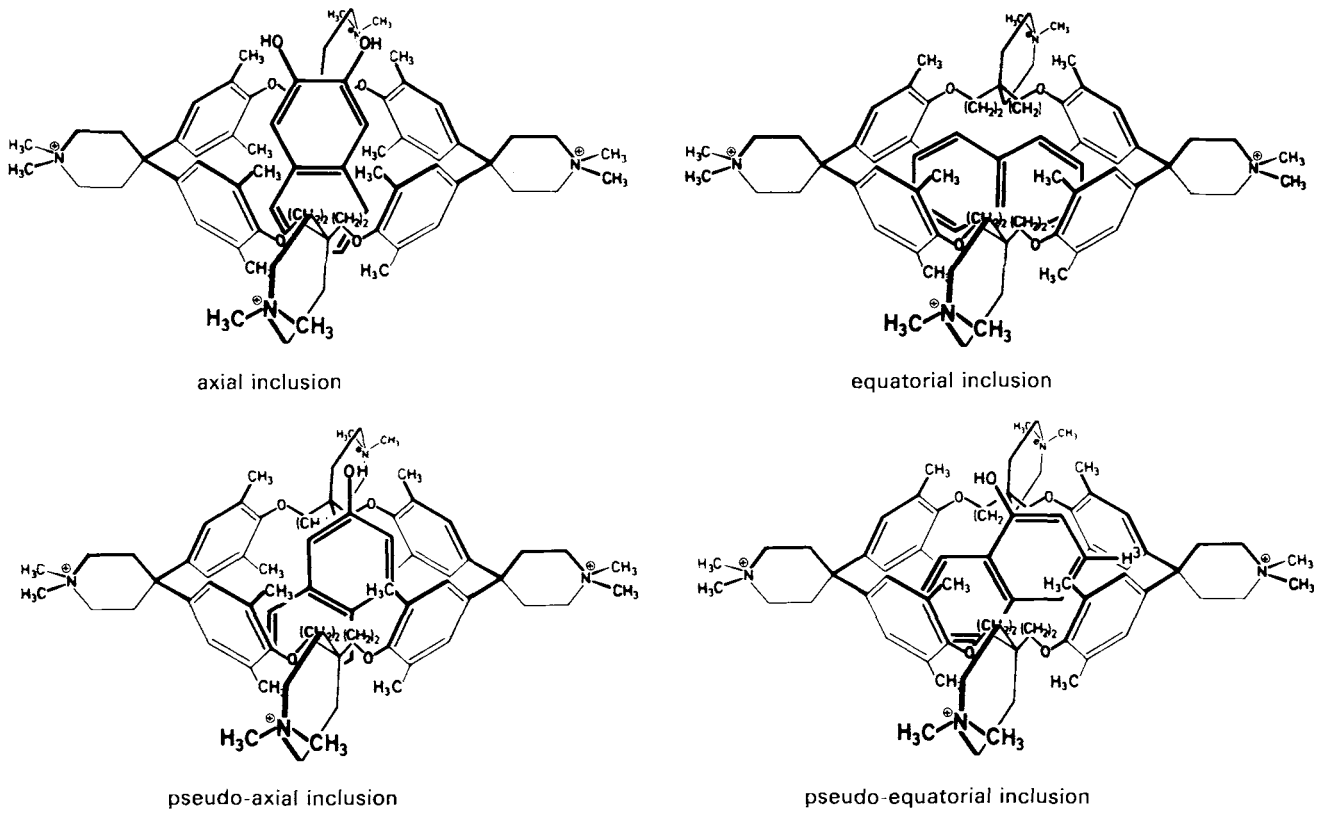

Fig. 7. Different possible positions of naphthalene and of substituted naphthalene derivatives in the cavity of **20**. The position of the spiro piperidinium rings fixed in the aliphatic chains of **20** is arbitrarily chosen. The inclusion of the following guests is shown: 2,3-naphthalenediol (axial), naphthalene (equatorial), 2,6-naphthalenediol (pseudo-axial), 1,5-naphthalenediol (pseudo-equatorial).

complexes of **20** with substrates of similar geometry [2,6-naphthalenedisulfonate and 1,5-bis(dimethylammonium)-naphthalene dihydrochloride] can lead to differences in the free enthalpy of complexation (ΔG) of more than 6.5 kcal mol^{-1}! Hence, multiple interactions in the complexes of cyclophanes lead to excellent, enzyme-like selectivity in the binding of a variety of guests which all fit well in the binding site. The efficient complexation of *p*-toluenesulfonate (Table 6) in the cavity of **20**, which is too spacious for a good fit of benzene guests, represents another example of hydrophobic interactions combined with ion-pairing acting as the driving force for complexation. This combination of binding modes is also at the origin of the strong complexation between the cationic hosts described by *Koga* et al., e.g. **4**, and arenesulfonates.[54b, 167]

Table 6. K_a and $-\Delta G$ of the 1:1 complexes of the hosts **20** and **12** with benzene derivatives and alicyclic compounds in aqueous solution ($T = 293$ K).

Host	Guest	K_a [L mol^{-1}]	$-\Delta G$ [kcal mol^{-1}]
a) Benzene derivatives:			
20	*p*-Toluenesulfonate	7.6×10^3	5.2
	Durene	1.9×10^3	4.4
12	TNS (**24**) [a]	1.5×10^3	4.3
	p-Benzenedicarbonitrile	1.5×10^3	4.3
	p-Dinitrobenzene	1.3×10^3	4.2
	p-Nitrotoluene	6.2×10^2	3.7
	Ethyl anthranilate	2.0×10^2	3.1
	p-Dimethoxybenzene	78	2.5
	p-Xylene	< 10	< 1.3
b) Alicyclic guests:			
20	Cyclohexyl acetate	7.4×10^2	3.8
	trans-1,4-Cyclohexanedimethanol	5.0×10^2	3.6
	1-Adamantanol	1.6×10^2	2.9

[a] Only the toluidine residue fits into the cavity.

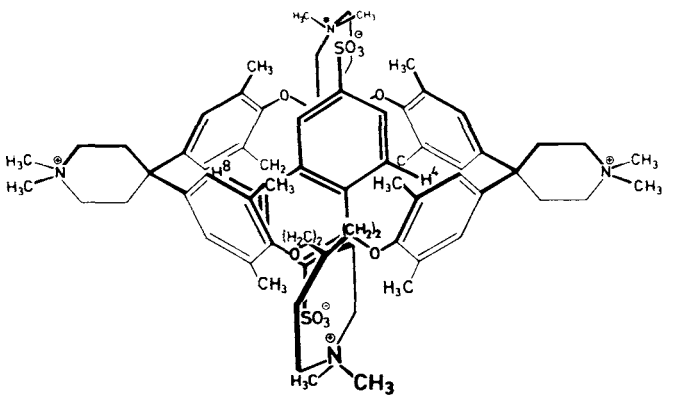

Fig. 8. Schematic drawing of the geometry of the **20** · 2,6-naphthalenedisulfonate complex, which, according to the ^{1}H-NMR spectrum is highly favored in aqueous solution. Observed complexation shifts of the guest resonances in an aqueous solution with [host] = [guest] = 4×10^{-3} mol L^{-1}: $\Delta\delta$ [in ppm] = 1.36 (1-H), 0.94 (3-H), and 3.09 (4-H).

Dissociation of the highly stable **20** · 2,6-naphthalenedisulfonate complex is slow on the ^{1}H-NMR time scale at room temperature. This is also observed for the less stable complexes formed in methanol between host **18** and 2,6-disubstituted naphthalene derivatives with ionic substituents ($-SO_3^{\ominus}$, $-COO^{\ominus}$, $-SMe_2^{\oplus}$, $-NR_3^{\oplus}$). This again indi-

cates that the complexation rate is much slower than diffusion controlled. The slow complexation rates can be easily explained by the energetically unfavorable desolvation of one of the two ionic substituents required for the penetration of the guest into the cavity.

4.6. Complexation of Benzene Derivatives in Aqueous Solution

With the spherands, *Cram* et al. have designed the most efficient systems for the strong complexation of inorganic cations. CPK (*C*orey-*P*auling-*K*oltun) molecular models of the spherand complexes indicate an extremely tight encapsulation of these ions.[50d, 168, 169] In the design of hosts with specificity for benzene or naphthalene derivatives, however, we found that efficient complexation did not occur if CPK model examinations predicted the formation of such a tight complex. The modeling suggested the formation of a very stable complex between benzene derivatives and host **11** with the $(CH_2)_2$-bridges and between axially enclosed naphthalene guests and host **12** with the $(CH_2)_3$-bridges. In both cases, we did not observe any significant inclusion complexation.[71] Inclusion complexation only occurs with hosts that are larger: benzene derivatives form stable complexes with **12** and naphthalene derivatives take axial positions in the cavity of host **13** with the $(CH_2)_4$-bridges.

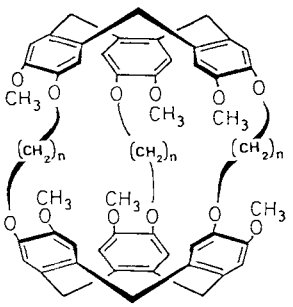

27a, n = 2
27b, n = 3

A similar discrepancy between CPK molecular model predictions and experimentally observed binding was also reported by *Collet* et al. who studied the binding of halogenated methanes by the bis(cyclotriveratrylenyl) hosts **27a,b** in 1,1,2,2-tetrachloroethane.[170] The host **27a** was designed to specifically bind chloroform; experimentally, however, the complexation of the smaller guest dichloromethane was preferred. Similarly, host **27b** was designed for carbon tetrachloride, but the complex formed with chloroform was two magnitudes more stable. We conclude from studies in *Collet*'s and in our laboratories that a host designed to complex a neutral organic molecule must incorporate a larger cavity than that suggested by CPK model examinations.[71]

The cavity of the host **12** with three methylene units in each bridge possesses optimum complementarity for benzene derivatives.[71] By ^{1}H-NMR spectroscopy, we observed the axial inclusion of more than ten *p*-disubstituted benzene derivatives in aqueous solution. This study revealed that the guest components with the most pronounced hydrophobic character, e.g. *p*-xylene, do not form the most stable complexes with **12** in aqueous solution. The complex stability is highest, as shown in Table 6, when host and guest possess optimum electronic complementarity in terms of electron donor-acceptor interactions (Section 5.2).[171]

A better complexation of benzene derivatives[144c] can be expected when the aromatic rings of a host similar to **12** are substituted with eight methyl groups in *ortho* positions to the ether oxygen atoms. An incremental increase in binding ability was observed upon stepwise introduction of two, four, six, and eight methyl groups in hosts **15**–**18**.[71] The methyl groups deepen the cavity and increase the hydrophobic character of the binding site. In addition, force-field calculations and computer graphics show[172, 173] that the methyl groups favorably influence the torsional angles in the dioxaalkane chains and enforce conformations of the host having a preorganized binding site.

The ^{1}H-NMR spectra recorded on solutions of complexes formed between **12** and benzene derivatives show only weak complexation shifts of the host resonances. There appears to be no preferred orientation of benzene in the cavity of **12**. Figure 9A includes a space-filling computer graphics representation of the complex formed between *p*-benzodicarbonitrile and the bis(*N*-methylpiperidine) precursor of **12**. The graphics suggest that π-π-interactions ("stacking interactions") between the almost cofacially oriented aromatic rings of host and guest as well as aryl-H_{guest}-aryl$_{host}$ interactions can contribute significantly to the stability of the complex. Similar stabilizing interactions are also apparent from the crystal structure of the **13a** · benzene complex shown in Figure 2B. The complex formed between the bis(*N*-methylpiperidine) precursor of

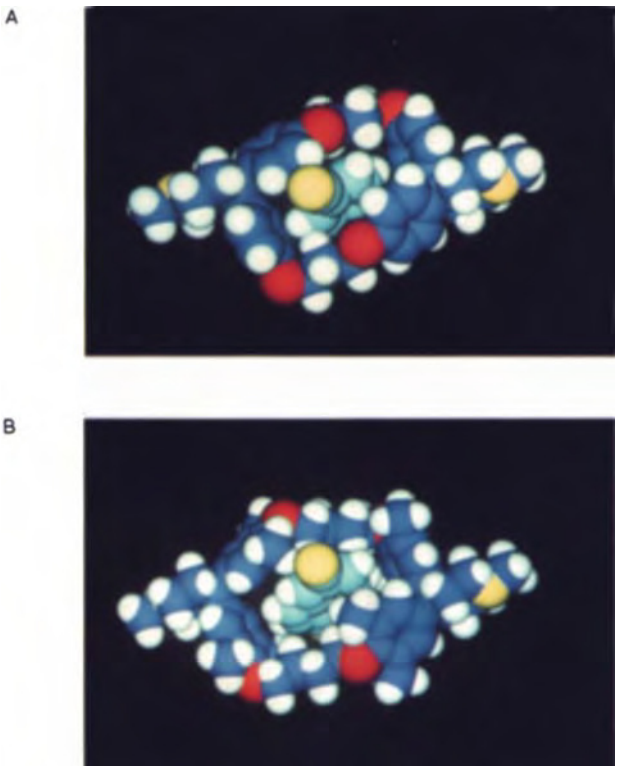

Fig. 9. Optimized space-filling structures generated on a Silicon Graphics IRIS 3130 workstation by the Hydra color graphics software A) for the complex formed between the bis(*N*-methylpiperidine) precursor of **12** and *p*-benzenedicarbonitrile and B) for the complex formed between the bis(*N*-methylpiperidine) precursor of **18** and 2,6-naphthalenedicarbonitrile.

18 and 2,6-naphthalene dicarbonitrile is reproduced in Figure 9B. The color graphics of Figure 9 were generated by docking the guests into low energy conformations of the host that have been calculated by using a modified MM2 force-field.[173-175] The docking procedure involves the minimization of van der Waals energy during complex formation.[174]

Wilcox et al. recently described the formation of stable complexes between host **28** and benzene derivatives in acidic aqueous solution.[144c] The binding site of **28** is shaped by a diphenylmethane unit and a derivative of *Tröger*'s base.[76]

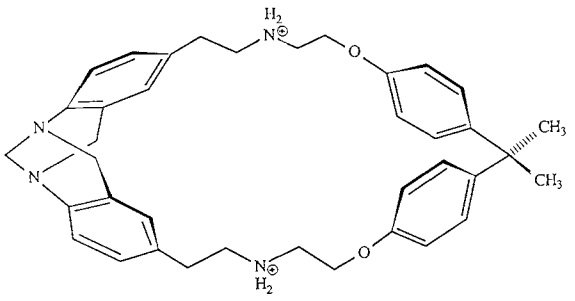

28

4.7. The Complexation of Neutral Non-Aromatic Molecules in Aqueous Solutions

The host **20** is also capable of complexing alicyclic derivatives[176] in aqueous solution (Table 6).[80] Since the cavity of **20** is quite narrow between the aliphatic chains, only flat alicyclic compounds possess complementary size to the binding site. Hence, **20** forms more stable complexes with cyclohexane than with the more spherical adamantane derivatives.

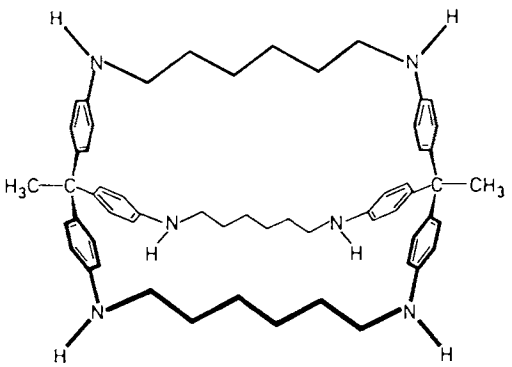

29a

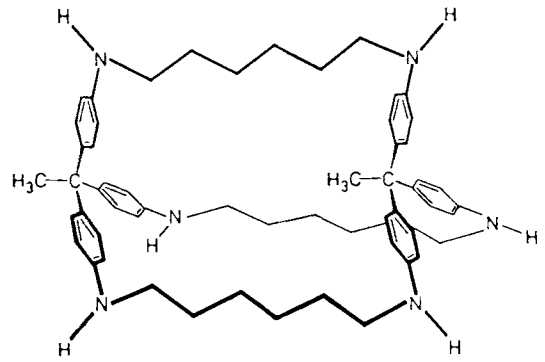

29b

Water-soluble hosts with larger binding sites for the inclusion of adamantane derivatives and of steroids have been reported by *Vögtle* et al.,[144a] by *Koga* et al.,[54d] and by *Dougherty* et al.[77b] The interesting hosts **29a** and **29b**, which show very different complexation ability have been prepared by *Vögtle* et al.[144a] With its two triphenylethane methyl groups turned outwards, host **29a** possesses a spacious cavity and incorporates adamantane as well as derivatives with neutral substituents in acidic aqueous solution. In host **29b**, one of the two triphenylethane methyl groups is turned into the cavity, which drastically reduces the space available to a guest. Hence, **29b** does not complex molecules as large as adamantane. With $K_a = 1.2 \times 10^5$ L mol^{-1}, host **25** forms a very stable complex with 1-adamantyltrimethylammonium iodide. It would be of interest to determine the contribution of ion-pairing interactions to this strong binding.[77b]

By condensation of four acetaldehyde and four resorcinol molecules, *Schneider* et al.[177,178] prepared a host which, in basic aqueous solution, is soluble as a tetraanion and which shows a high binding affinity for quaternary ammonium ions.[139] Thus, for example, choline and the tetraanionic macrocycle form a 1:1 complex with a free enthalpy of formation of $\Delta G = -6.4$ kcal mol^{-1}. *Lehn* et al. have also reported a host for the specific complexation of quaternary aliphatic ammonium ions in aqueous solution.[179] The binding site of this host is shaped by two diphenylmethane units bridged by two tartrate residues. Complexation of neutral molecules was not described for these anionic host systems; ion-pairing rather than apolar interactions can be assumed as the major binding force in the complexes. Apolar host-guest interactions represent a major driving force for the inclusion complexation between cucurbituril (**30**) and aliphatic or aromatic primary

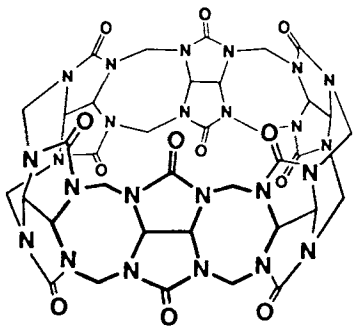

30

and secondary ammonium salts in aqueous formic acid.[114,180] In systematic binding studies, *Mock* et al. determined stability constants of $K_a = 10^3$–10^7 L mol^{-1} for the complexes of these ionic guests. In addition, they obtained ^{1}H-NMR spectroscopic evidence for the inclusion of cyclopentane, tetrahydrofuran (THF), and tetrahydrothiophene in the cavity of **30**. The binding of these neutral guests is, however, weaker than the binding of the ammonium compounds. The complexes of the latter guests are stabilized by ionic hydrogen bonding between the guest ammonium hydrogens and the host urea carbonyls in addition to the hydrophobic interactions.

Busch et al.[181] described relaxation time measurements and ^{13}C-NMR titrations to demonstrate the interactions in

aqueous solutions between aliphatic alcohols or phenols and the molecular cavities of transition metal complexes. Interesting ternary complexes are formed when the organic guests, e.g. *n*-butanol, are incorporated in the molecular cavity binding sites of these macrocyclic cobalt(II) and iron(II) complexes and when, in addition, oxygen binds reversibly to the transition metal ion.

By replacing the six methoxy groups in **27a** by OCH_2COOH residues, *Collet* et al.[182] prepared a water-soluble cyclophane host. The stability of the complexes formed by this host and dichloromethane or chloroform in aqueous solution is much higher than the stability of the complexes of host **27a** with these guests in 1,1,2,2-tetrachloroethane. The driving force for chloroform complexation by the modified host in water is $\Delta G = -5.3$ kcal mol^{-1} ($T = 300$ K); in the organic solvent the **27a** · chloroform complex is stabilized by only $\Delta G = -3.3$ kcal mol^{-1}.

Despite isolated progress, our understanding of the principles of molecular recognition of aliphatic guests by synthetic ligands and by cyclodextrins[68] in aqueous solution still leaves much to be desired compared to our understanding of the principles of molecular recognition of aromatic molecules.

5. Complexation of Neutral Molecules by Cyclophane Hosts in Organic Solution

When we extended our studies with cyclophanes to non-aqueous solutions,[81,82] few examples of the molecular complexation of neutral molecules by macrocycles in organic solvents had been reported. In 1974, *Cram* et al.[183] described the formation of a crystalline complex between [18]crown-6 and acetonitrile. In the following years, the structures of many solid-state complexes of crown ethers with neutral small molecules possessing C–H, N–H, and O–H acidic functionalities were determined by X-ray crystallography.[184,185] However, first thermodynamic studies of the interactions between crown ethers and these neutral polar compounds in solution were only described in recent years.[138,186] An article in 1975 by *Siegel* and *Breslow*[187] first reported on the complexation of neutral, apolar molecules in organic solvents. In this paper, the authors described the inclusion complexation of arenes, e.g. toluene and anisole, as well as of ferrocence by cyclodextrins in dimethyl sulfoxide (Me_2SO) and in dimethylformamide (DMF). Other studies with cyclodextrins in organic solvents[188,189] include the interesting observation of complexation of nitrophenols and indoles by a peralkylated cyclodextrin in heptane by *Menger* et al.[190] Furthermore, it was observed that cyclophane hosts form complexes in organic solvents with carbon disulfide or methylacetylene[98a] and dichloromethane.[97c]

5.1. Complexation of Polycyclic Arenes

For our complexation studies in non-aqueous environments, we chose the neutral host molecules **21** and **22**, since these macrobicycles are readily soluble in almost the entire range of organic solvents. We investigated the complexation of the arenes perylene, pyrene, fluoranthene, naphthalene, and durene and were initially surprised by the magnitude of complexation observed in many organic solvents, specially for the larger guests. The ^{1}H-NMR spectra showed that all arene guests are encapsulated in the cavities of **21** and **22** as shown schematically for pyrene in Figure 5B. The geometry of a given complex, e.g. of the **22** · pyrene complex, is very similar in all solvents. Following the methodology described in Section 4.2, we determined the stability constants of the 1 : 1 complexes over a wide solvent polarity range.

To our surprise, host **22** with its two tertiary cryptand nitrogen atoms is a much better binder in organic solvents than host **21** with the two amide groups in the periphery of the cavity. The association constants of the perylene complexes formed by hosts **21**, **22**, and **31** in methanol ($T = 303$ K) are listed in Table 7. The free enthalpy of formation (ΔG) of the **22** · perylene complex is -7.0 kcal mol^{-1}, whereas the complexation of perylene by **21** is less favorable by 3.2 kcal mol^{-1} and thus similar only in strength to the complexation of this guest by the macromonocyclic host **31**. CPK model examinations do not support an explanation based on geometrical factors for the large difference in binding ability between the two spherical hosts **21** and **22**. We explain this difference, which is observed in all solvents, by complexation-induced unfavorable changes in the solvation of the two amide groups in the periphery of the cavity of **21**. We have accumulated additional experimental evidence both in aqueous and organic solutions of the impact of complexation-induced changes in the solvation of functional groups, especially of amide groups, on the binding strength.[192] If the energetically favorable solvation of a polar functional group of one of the binding partners is reduced in the complex compared to the free component and if no new binding interactions in the complex compensate for this loss in solvation energy, a considerably lower complexation strength will be observed.

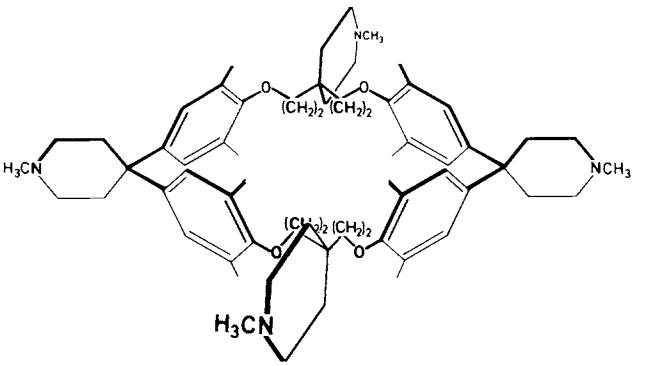

31

Table 7. K_a and $-\Delta G$ of the 1 : 1 complexes of the hosts **21**, **22** and **31** with perylene in methanol ($T = 303$ K).

Host	K_a [L mol^{-1}]	$-\Delta G$ [kcal mol^{-1}]
22	1.1×10^5	7.0
21	5.6×10^2	3.8
31	8.4×10^2	4.0

Similar to aqueous solutions, the complementarity between host and guest in organic solvents is crucial in determining the strength of complexation. The sequence of the stability of the arene complexes shown in Table 8 for methanol is also observed in all other solvents. The same sequence was observed for the complexes of host **20** in aqueous solution (Table 2). The driving force for complexation in organic solvents is predominantly enthalpic in nature. For the **22** · perylene complex in ethanol, the enthalpic and the entropic contributions to ΔG were determined as $\Delta H = -10.7$ kcal mol^{-1} and $\Delta S_{303\,K} = -13.4$ cal mol^{-1} K^{-1}.

Table 8. K_a and $-\Delta G$ for the 1:1 complexes formed between the host **22** and arenes in methanol ($T = 303$ K).

Guest	K_a [L mol^{-1}]	$-\Delta G$ [kcal mol^{-1}]
Perylene	1.1×10^5	7.0
Fluoranthene	7.2×10^4	6.7
Pyrene	4.4×10^4	6.4
Naphthalene	1.2×10^2	2.9
Durene	27	2.0

Complexation of arenes occurs in a large variety of solvents. In each case, however, the binding is considerably weaker than in aqueous solution. An impressive dependency of the complexation strength on the nature of the solvent was observed. This dependency is shown in Table 9 for the **22** · pyrene complex. The driving force for complexation decreases from $\Delta G = -6.4$ kcal mol^{-1} in methanol to $\Delta G = -1.3$ kcal mol^{-1} in carbon disulfide. The strongest binding is observed in alcohols. Weaker but still considerable complexation occurs in dipolar-aprotic solvents, e.g. acetone, Me_2SO, DMF, and THF. The binding is weakest in chloroform, benzene, and carbon disulfide. Nevertheless, it is remarkable that arenes such as perylene, pyrene, and fluoranthene can be complexed in an aromatic solvent like benzene. For all complexes of hosts **21**, **22**, and **31** and the guests of Table 8, the same solvent dependency of the complexation strength as shown in Table 9 for the **22** · pyrene complex was observed.

Table 9. K_a and $-\Delta G$ of the **22** · pyrene complex in various organic solvents ($T = 303$ K).

Solvent	K_a [L mol^{-1}]	$-\Delta G$ [kcal mol^{-1}]
Methanol	4.4×10^4	6.4
Ethanol	2.5×10^4	6.1
Acetone	1.2×10^3	4.3
Dimethyl sulfoxide	6.9×10^2	3.9
Dimethylformamide	1.2×10^2	2.9
Tetrahydrofuran	84	2.7
Chloroform	43	2.3
Benzene	12	1.5
Carbon disulfide	9	1.3

According to the ^{1}H-NMR spectrum the geometry of the **22** · pyrene complex is very similar in all solvents (Fig. 5B). The large decrease in binding strength upon changing the solvent from methanol to carbon disulfide therefore cannot result from differences in attractive van der Waals interactions between host and guest in the complexes formed in these solvents. Rather, solvation phenomena must be responsible for the observed differences in complexation strength. In agreement with this hypothesis, the solvent-dependent free enthalpies of formation of the **22** · pyrene complex shown in Table 9 can be nicely correlated with empirical solvent parameters, e.g. with the Dimroth-Reichardt parameter E_T as shown in Figure 10.[193]

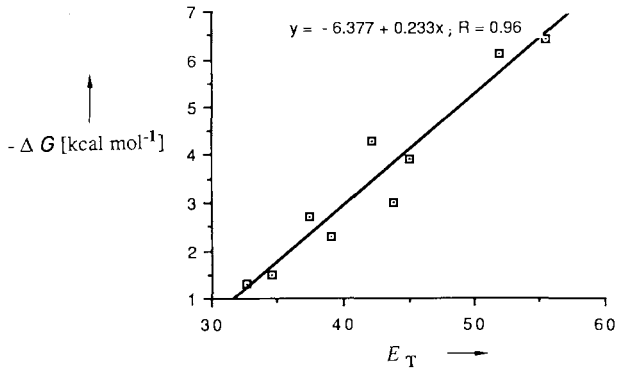

Fig. 10. Free enthalpies of complexation $-\Delta G$ (kcal mol^{-1}) of the **22** · pyrene complex in various organic solvents (see Table 9) plotted against the empirical solvent polarity parameters E_T [193] of these solvents.

For an explanation on a molecular basis of the observed differences in complexation strength, several parameters like the cohesive interactions of the solvent and the solvation of host, guest, and host-guest complex have to be considered. Differences in the external solvation of the complex as compared to the free host should not be of great importance since the encapsulated guest has no solvation-sensitive functional groups that extend out of the binding site. The observed sequence (Table 9) cannot be explained by the loss of heat of solvation upon desolvation of the guest during the inclusion process. There exists no significant correlation between heats of solvation[194] measured for benzene in the various solvents and the ΔG values of Table 9.

A larger part of the observed gradual change in binding strength could result from differences in the desolvation entropy gained upon inclusion of the solvated guest into the highly preorganized, solvated cavity of the host. In protic organic solvents, a favorable solvation-desolvation process similar to the hydrophobic effect in water could assist complexation, although such an effect will certainly be weaker here.

The weakest binding is observed in chloroform, benzene, and carbon disulfide. These solvents can compete with the guest for the binding site. As solvent molecules, these compounds are present in very large excess and, hence, their affinity for the cavity does not need to be very strong. Experimental evidence for favorable interactions between these molecules and the binding site of **22** are available. The affinity of carbon disulfide for apolar binding sites had been observed independently by *Cram* et al.[98a] Specific aromatic solvent induced shifts (ASIS)[55a,b] in the ^{1}H-NMR spectra of **22** in benzene indicate interactions of the benzene molecules with the cavity.[82] A chloro-

form molecule enclosed in the cavity can form a N···H-CCl_3 hydrogen bond to the cryptand nitrogen atoms of **22**.

The extent to which a solvent molecule can act as an efficient competitor of the guest for the cavity binding site is largely determined by the cohesive interactions in the solvent. These forces determine the energy needed to disrupt the interactions of a solvent molecule with the surrounding solvent molecules in the bulk and to transfer it for solvation into the host cavity. The molar heat of vaporization, ΔH_{vap} [kcal mol^{-1}] or, alternatively, the internal pressure, can be considered as a measure for the cohesive interactions in a given solvent.[195] We found a significant correlation, analogous to the one shown in Figure 10, between the ΔG values of the **22** · pyrene and the **22** · perylene complexes and the molar heats of vaporization ΔH_{vap} of the solvents. The decrease in free binding energy upon changing from protic solvents to dipolar aprotic solvents and to benzene and carbon disulfide is parallel to the decrease of the cohesive forces, expressed by the molar heats of vaporization. At smaller ΔH_{vap} values, it becomes increasingly favorable to transfer a solvent molecule for solvation from the bulk into the cavity. In this sequence, therefore, a solvent molecule becomes a more and more efficient competitor of the substrate for the host cavity.

Our studies clearly show that predictions of the stability of host-guest complexes based on computer-modeling can only be successful if specific solvation free energies are taken into account.

As mentioned in Section 4.6, *Collet* et al.[97,170] studied the complexation in organic solvents between hosts such as **27a** or **27b** and halogenated methanes. Recently, they described the molecular complexation of isobutane in 1,1,2,2-tetrachloroethane, and this represents the first report of alkane binding in an organic solvent.[191] Despite *Collet*'s and our work, the complexation of neutral molecules at apolar binding sites in organic solvents still remains relatively unexplored. Progress in this area is of special interest in the development of bioorganic, enzyme-like catalysts that complex their substrates prior to the actual reaction steps. Although enzymes are water-soluble and take their substrates mostly from aqueous environment, the catalytic processes occur in non-aqueous media at their active sites. Evidence is accumulating of the importance of desolvation for the large rate enhancements in enzymatic reactions. These reactions occur at active sites, dipolar-aprotic in nature, rather than in aqueous environment where solvation processes often lead to much higher reaction transition states.[196-198] The complete shielding from the solvent of the reactive sites of bioorganic, enzyme-like catalysts that are active in water could require the construction of very complex molecules. An easier alternative could well be the design and synthesis of hosts that bind and catalyze in dipolar-aprotic solvents.

Rebek et al.[40b,199] have described the stoichiometric complexation of heterocyclic arenes, e.g. pyrazine, phenoxaline, phenazine, pyridine, purine, and 9-ethyladenine[199b] by non-macrocyclic, cleft-type receptors. These complexes are held together mainly by hydrogen-bonding interactions. Hydrogen-bonding can also lead to selective complexation by cyclophane hosts as was shown by *Whitlock* et al.[85,200] In 1,2-dichloroethane solution and in the solid state, they observed the preferred inclusion of *p*-nitrophenol ($K_a = 3 \times 10^3$ L mol^{-1}) as well as of *p*-hydroxybenzonitrile ($K_a = 1.1 \times 10^3$ L mol^{-1}) in the completely preorganized cavity of **32**. At the desolvated binding site, a firm hydrogen bond forms between the pyridine nitrogen of the host and the phenolic hydroxyl group of the guest. *Whitlock* et al. found that geometrically comparable guests without a hydrogen-bond donor center did not undergo complexation with **32**. Interestingly, a large binding selectivity is also observed among guests which possess both geometric complementarity and a hydrogen-bond donor center. This selectivity is explained by the need for a special favorable relationship between the pK_a values of host and guest.

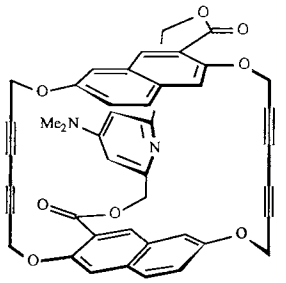

32

5.2. Electron Donor-Acceptor Interactions in Host-Guest Complexes

Over the past decades, the important role of electron donor-acceptor (EDA) interactions[201-205] for selective molecular complexation in biological systems[206-207] and also in synthetic host-guest complexes[50c,208,209] has been recognized. These interactions are also of key importance in chromatographic optical resolution processes on chiral phases and especially on Pirkle phases.[210] Major components of the interaction in EDA complexes are defined as electrostatic interaction, polarization interaction, and charge-transfer interaction as well as dispersion energy.[201,202] To explore the contribution of these interactions to the stability of the complexes formed by our cyclophane hosts, we studied the binding between host **18** and a series of 2,6-disubstituted naphthalene derivatives, e.g. **33a-i**, in methanol (Table 10).[136] These guests adopt a pseudo-axial position in the cavity of **18**, which allows for efficient π-π-interactions in the complexes. This can be seen in Figure 9B which shows in a space-filling computer graphics representation the energetically favorable location of 2,6-naphthalenedicarbonitrile (**33i**) in the cavity of the bis(*N*-methylpiperidine) precursor of **18** (Fig. 9B).

Our complexation studies revealed that the electron-deficient guests **33g-i** with two acceptor substituents form more stable complexes than the electron-rich guests **33a-c**, while the complexes of guests having one donor and one acceptor substituent (**33d-f**) demonstrate an intermediate stability (Table 10). The differences in free enthalpy, ΔG, determined from ^{1}H-NMR titrations (Fig. 4),[136] are as large as 1.48 kcal mol^{-1} at 303 K and result from a major contribution of intermolecular EDA interac-

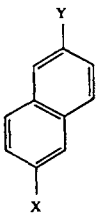

33a-i

Table 10. K_a and $-\Delta G$ for the 1:1 complexes formed between the host **18** and the naphthalene derivatives **33a-i** in [D_4]methanol ($T = 303$ K).

Guest	X	Y	K_a [L mol^{-1}]	$-\Delta G$ [kcal mol^{-1}]
a) Donor-donor guests:				
33a	OH	OH	24	1.91
33b	NH_2	NH_2	33	2.11
33c	OCH_3	OCH_3	47	2.32
b) Donor-acceptor guests:				
33d	NH_2	NO_2	102	2.78
33e	OCH_3	NO_2	109	2.82
33f	OCH_3	CN	117	2.87
c) Acceptor-acceptor guests:				
33g	$COOCH_3$	$COOCH_3$	188	3.15
33h	NO_2	NO_2	213	3.23
33i	CN	CN	277	3.39

tions in the complexes. With its four trialkylsubstituted anisole units, compound **18** can be considered as a donor host. As expected for EDA interactions, the most stable complexes are formed with the acceptor guests **33g-i**. The importance of attractive interactions in the complexes of the acceptor guests is reflected in the enthalpic and entropic contributions to the free enthalpy of complexation ΔG. For the **18-33i** complex in methanol, these contributions were determined as $\Delta H = -7.6$ kcal mol^{-1} and $\Delta S_{303\,K} = -14.1$ cal mol^{-1} K^{-1}.

In the meanwhile, our studies have shown that EDA interactions are of general importance in the complexes of our hosts with aromatic guests. This extra stabilization of complexes formed between donor hosts like **11-20** and acceptor guests has been observed in a large variety of solvents, e.g. in water, methanol, Me_2SO, and cyclohexane,[211] and results mainly from electrostatic and polarization interactions. Even the complexes with very good acceptor guests, e.g. *p*-benzoquinone, *p*-benzodicarbonitrile, *p*-dinitrobenzene, do not give a charge transfer band in the electronic absorption spectra,[204] since the ionization potential of the trialkylsubstituted anisole units of our hosts presumably is too high.

6. Chiral Recognition in Diastereomeric Host-Guest Complexes in Aqueous Solution

With increased understanding of molecular complexation in aqueous solution, we next addressed the development of optically active hosts for chiral recognition in water-soluble diastereomeric complexes. Free or polymer bound macrocycles with asymmetric binding sites could have great potential for the resolution of racemic guests in chromatographic, transport, or extraction processes. Asymmetric synthesis and catalysis in supramolecular complexes represents another fascinating perspective of this research.

The first reports on the synthesis of chiral macrocyclic polyethers by *Wudl* and *Gaeta*[212] and *Cram* et al.[213] appeared about fifteen years ago. Since then, a large variety of optically active macrocyclic polyethers have been prepared for the resolution of racemic cationic guests through complexation in organic solutions.[30,31,33a,47b,214,215] Chiral recognition of non-cationic racemic guests in diastereomeric complexes of macrocyclic hosts has until recently almost exclusively been limited to free or polymer-bound cyclodextrins.[9a,216,217] Only a few reports have appeared in recent years describing the formation of diastereomeric complexes between fully synthetic, optically active ligands and non-cationic guests in aqueous and organic solutions.[218-220] *Koga* et al. replaced the alkyl bridges in the host **4** by bridges derived from L-tartaric acid [$-CH_2-CH(OCH_3)-CH(OCH_3)-CH_2-$] and observed the formation of diastereomeric complexes in acidic aqueous solution with racemic guests like mandelic acid and atrolactic acid.[218] *Collet* et al. described the formation of diastereomeric inclusion complexes in chloroform between an optically active host resembling compound **27a** and (*R,S*)-bromofluoroiodomethane.[219]

In our first approach to the development of chiral hosts, we chose the biphenyl-macrocycle **35** as the target molecule.[221] This host, in optically active form, was designed to differentiate via complexation between the enantiomers of aromatic α-amino acids and arylpropionic acids, e.g. naproxen (**36**), an inhibitor of the enzyme cyclooxygenase responsible for prostaglandin biosynthesis. Differences in apolar interactions and ion-pairing as well as in steric interactions were expected to lead to the formation of diastereomeric complexes of different stability. Binding studies with **34** in acidic aqueous solution, however, clearly revealed that this biphenyl macrocycle did not act as a host. Contrary to expections based on CPK model examinations, compound **34** does not possess an efficient binding site for aromatic guests. Force-field calculations in combination with computer graphics provided an explanation for this absence of binding. According to the calculations, the biphenyl unit in **34** is not a suitable spacer group. With an O···O distance of 8.91 Å (in free form), the diphenylmethane unit incorporated in **34** and in our other hosts, e.g. **11-18**, favorably shapes and widens binding sites for arenes and flat cycloalkanes. At an O···O distance of only 4.10 Å (in free form), the biphenyl unit of **34** does not sufficiently widen the macrocyclic cavity binding site. In ad-

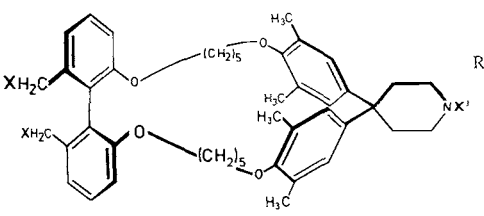

34, X = NMe_2, X' = Me
35, X = $NMe_3^{\oplus}Cl^{\ominus}$, X' = $Me_2^{\oplus}Cl^{\ominus}$

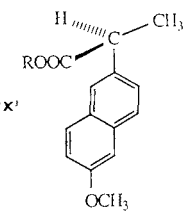

36, R = H
37, R = CH_3

dition, the computer graphics of the MM2 optimized[175] structure of **34** revealed that this macrocycle prefers an extensively twisted helical geometry. This helical twist further reduces the size of a possible binding site and was not expected from CPK model examinations.[172] The helical conformation seems to be imposed on the macrocycle by the tendency of the bridging alkane chains, which connect two spacers of very different O···O distances, to maximize the number of antiperiplanar torsional angles.

Force-field calculations indicated that the critical O···O distance in the 4-phenyl-1,2,3,4-tetrahydroisoquinoline derivative **38** would be considerably larger than in the biphenyl unit of **34**, and that **38** would consequently be a more favorable chiral spacer.[172] Starting from (−)-**38**, we prepared the optically active host (+)-**39**[222,223] and found its binding properties consistent with the force-field predictions. In water/methanol (60:40), (+)-**39** preferentially binds 2,6-disubstituted naphthalenes which take a pseudo-axial position in the cavity. By ^{1}H-NMR spectroscopy, we could clearly demonstrate the formation of diastereomeric complexes between (+)-**39** and (*R,S*) naproxen (**36**) or its methyl ester (*R,S*)-**37**. In the host conformation which is the most preorganized for complexation, but not however the most energetically favorable, the O···O distance at the chiral spacer is 7.58 Å.[172]

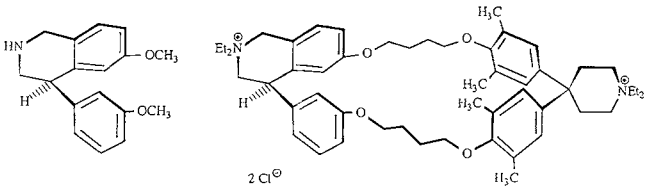

(−)-38 (+)-39

Besides providing clear evidence for the formation of diastereomeric complexes by host **39** in aqueous solution, our research efforts in the area of chiral recognition so far have shown ways to a more rational design of host systems.[55c,172] The ability of aromatic building blocks, especially of those with several energetically favorable conformations, to act as spacers in macrocyclic hosts can be tested prior to synthesis by force-field calculations. According to these calculations, a correct O···O distance in the aromatic spacers is crucial for the complexation properties of our macrocycles. For design purposes, diphenylmethane units like **5**–**7** with their favorable cavity opening O···O distance can be taken as a reference for new spacer building blocks suitable for the construction of binding sites for flat alicyclic and aromatic guests.[54c,224] We predict, that efficient hosts for these guests are formed when an achiral or chiral aromatic spacer unit with an O···O distance of ≥6.5 Å and a diphenylmethane unit like **5**–**10** are bridged by suitably sized aliphatic chains.

The computer modeling not only provided aesthetic visualizations of our macrocycles (e.g. in Fig. 9), it also advanced our knowledge on the principles of molecular recognition.[172] The experimentally observed binding properties of our macrocycles could be reproduced in the docking experiments. Further support could be provided for complex geometries, e.g. for the preferred pseudo-axial inclusion of 2,5-disubstituted naphthalenes (Fig. 9B), which had been previously deduced experimentally from extensive ^{1}H-NMR binding studies. The influence of the aliphatic bridge conformations on the spatial structure of our macrocycles has been recognized more clearly through the modeling studies. Affordable computers and sophisticated graphics programs are available to chemists, and it is safe to predict that computer assisted design will play a very important role in the future development of synthetic chiral and achiral receptors and catalysts.

7. Cyclophane Hosts as Enzyme Mimics: From Complexation to Catalysis

Soon after his first fundamental studies on molecular complexation by cyclodextrins, *Cramer* investigated the enzyme-like catalytic properties of these systems.[7,8] Following this, a large variety of stimulating and innovative studies on the catalytic properties of the cyclodextrins have been conducted by *Cramer* himself[8c] and by research workers in the laboratories of *Bender*,[9] *Breslow*,[10] and *Tabushi*.[11] These together with the pioneering work in the seventies in the laboratories of *Cram*,[50] *Lehn*,[49] *Murakami*,[53] and *Kellogg*[39] on catalysis in synthetic supramolecular complexes have generated a fascination for the rational development of efficient bioorganic catalysts. Since then, an increasing number of chemists became interested in this important new area of research. The scope of this article does not allow discussion of the original work of these researchers. It should, however, be noted that cyclophanes with binding sites for neutral molecules[11b,43,52c,53,144a,176,218b,225–228] have been designed and studied in an increasing number as bioorganic catalysts.[35,45a,103b,180c,229–237] The remaining part of this article will provide a short account of our first studies in the field of molecular catalysis.[74,238,239]

Current research objectives in our laboratories address the activation of coenzymes by the specific microenvironment of an apolar active site as well as the influence of coenzymes on the strength of substrate binding.[74] For these studies, we prepare water-soluble macrocycles with coenzyme models attached in a defined way to the periphery of the preorganized binding sites.[10,11e] A considerable influence of the coenzyme on the strength of substrate binding can be expected especially for flavoenzymes. The flavin coenzymes FMN (flavin mononucleotide) or FAD (flavin adenine dinucleotide) are known to be tightly bound or, in some cases, even covalently attached to the active sites of flavoenzymes.[240] To explore how the large isoalloxazine unit of these coenzymes affects the complexation ability of a molecular binding site, we prepared the flavin host **40a** with an isoalloxazine unit as cavity wall. In aqueous alkaline borate buffer (pH = 10) under argon, the flavin host **40a** could be readily and quantitatively reduced to the trianionic host **40b** with a dihydroisoalloxazine unit as the cavity wall. Upon introduction of oxygen into the solution of **40b**, the oxidized flavin host **40a** is regenerated quantitatively. The redox cycles **40a** ⇌ **40b** can be repeated numerous times without affecting the molecular structure of the host.

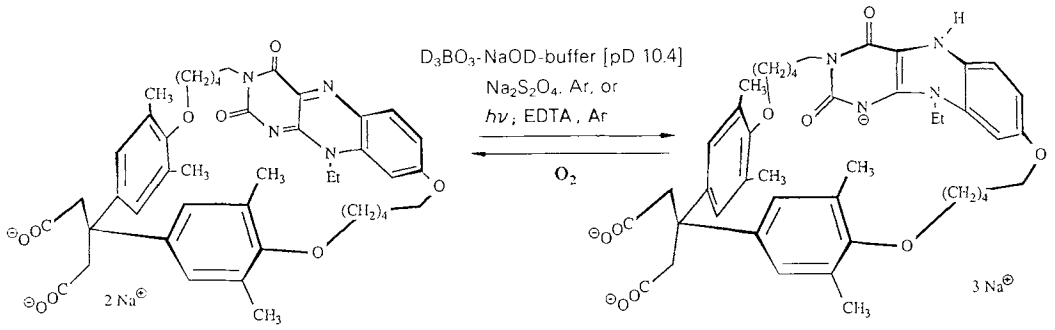

40a 40b

The geometry of the binding site of the host systems **40a/b** is highly dependent on the redox state of the flavin unit. The oxidized isoalloxazine unit in **40a** is planar while the $2e^{\ominus}$-reduced dihydroisoalloxazine unit in **40b** is butterfly shaped as shown in the formula. Values of 30° have been observed in X-ray crystal structures for the angle about the two nitrogens N-5 and N-10 of the central ring in the dihydroisoalloxazine unit.[240] The different geometry of the tricyclic system in the two redox states influences the binding properties of the macrocycles. Both **40a** and **40b** form complexes in aqueous solution with 2,6-disubstituted naphthalene derivatives ($K_a \approx 100$–500 L mol^{-1}). In the cavity of **40a**, the guests assume a near cofacial orientation to the isoalloxazine unit. In the cavity of **40b**, the guests take a similar position as in the complexes of the bis(diphenylmethane) hosts, e.g. **18**. Differences in the stability of the complexes of **40a** and **40b** can result from differences in the charge and geometry of the binding sites as well as from electron donor-acceptor interactions. EDA interactions are responsible for the strongly redox-dependent complexation of acceptor-acceptor substituted guests. Compounds like 2,6-naphthalenedicarbonitrile or 2,6-dinitronaphthalene only undergo complexation with the reduced host **40b** and not with the oxidized host **40a**. We explain this different complexing behavior by favorable electronic complementarity between the electron-rich host **40b** and the acceptor guests only. Electrostatic repulsion between the electron-accepting isoalloxazine unit of the oxidized host **40a** and these guests leads to a complete absence of binding. In addition to further quantitative binding studies involving biological substrates, we now focus on the catalysis of redox processes in the supramolecular complexes formed by the flavin host systems **40a/b**.[241,242]

A major advantage for the development of bioorganic catalysts is the easy and selective functionalization of our tetraoxa[n.1.n.1]paracyclophanes, especially at the aromatic rings.[238,239,243] We prepared the thiazolium derivative **41** in order to explore the influence of an apolar macrocyclic cavity binding site on the activity of thiazolium ions in the benzoin condensation.[244,245] In this macrobicyclic system, a thiazolium ring is attached in a favorable position to the binding site which provides space for the two benzaldehyde molecules to react to give benzoin. The entropically favorable proximity and orientation of the substrate and the coenzyme model were expected to effect catalysis.[66a]

The macrobicycle **41** represents a very complete model system for thiamine pyrophosphate-dependent ligases. In protic solvents, where complexation of benzaldehyde takes place, **41** is a better turnover catalyst ($k_{cat} = 1.1$ min^{-1} in

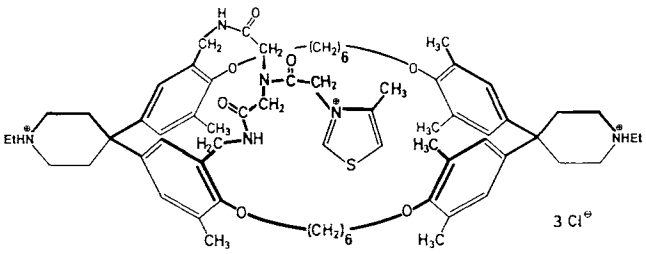

41

methanol, [Et_3N] = 160 mmol L^{-1}, [$Et_4N^{\oplus}Cl^{\ominus}$] = 100 mmol L^{-1}, $T = 35$°C) for the benzoin condensation than non-macrocyclic thiazolium derivatives. The observed saturation kinetics, describing a sigmoid curve, could be best evaluated by assuming the formation of a 1:2 Michaelis–Menten complex. In methanol, the equilibrium of the benzoin condensation is far on the benzoin side, and in reactions catalyzed by **41**, benzoin could be isolated in 93% yield. In Me_2SO, the equilibrium is far less on the side of benzoin, and by starting from pure benzoin, benzaldehyde could be isolated. In aqueous buffers, we could demonstrate a specific activation of the thiazolium ring by the binding site of **41** which is of lower polarity than the surrounding solution.[238,244] We observed a strong influence of the cavity of **41** on the H/D exchange,[246,247] which is considerably faster at C-2 of the thiazolium ring of **41** than at C-2 of thiazolium derivatives without a macrocyclic binding site. We explain this H/D exchange rate enhancement by a micropolarity effect of the cavity of **41** on the (kinetic) acidity of the proton 2-H of the thiazolium ring. Therefore, one of the catalytic advantages of **41** relative to non-macrocyclic thiazolium derivatives could be the formation of a larger amount of reactive ylide at a given pH.

Like many other researchers [8–11,49,50f,53,103b,226,228c,229–231,234–237] we also focus on the development of synthetic hydrolases.[239] At the active sites of proteases[66a], e.g. the well studied serine proteases, the thiol proteases, or the aspartyl proteases, highly efficient catalytic mechanisms are generated through a specific array of functional groups. The isolated forms of these functionalities demonstrate lit-

tle or no catalytic activity. Only by their cooperative action at the specific active site do catalytic mechanisms such as transition state binding and stabilization, acid-base catalysis, nucleophilic and electrophilic catalysis become effective.[66a, 248] It is not surprising that the possibility of generating such catalytic mechanisms in designed supramolecular complexes is a fascinating objective for many research groups.

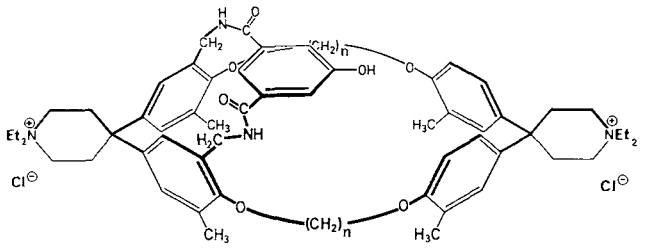

42, n = 4
43, n = 6

On the way to synthetic hydrolases, we have prepared the macrobicycles **42** and **43**.[239] These systems possess phenolic hydroxyl groups as nucleophiles that are active at near physiological pH. The nucleophiles are positioned in a well defined way atop the macrocyclic binding sites. By comparing the esterase activity of **42** and **43**, we have obtained a fine example for the concept of *productive versus non-productive binding*, a mechanism believed to generate substrate specificity in enzymatic catalysis.[249] Both macrocycles form complexes of similar stability with naphthalene guests in aqueous solution. With 4-nitro-1-naphthylacetate as a substrate, we observed a large difference in the transacylation rates. In aqueous phosphate buffer at pH 8.0 ($T = 20°C$; [host] $= 5.0 \times 10^{-4}$ mol L^{-1}; [4-nitro-1-naphthylacetate] $= 2.0 \times 10^{-5}$ mol L^{-1}) the acylation of **42** by the naphthyl ester is only 14 times ($k_{obs} = 2.43 \times 10^{-4}$ s^{-1}) faster than the hydrolysis in pure buffer. Under these conditions, the acylation of **43** by the complexed ester is 178 times faster ($k_{obs} = 3.21 \times 10^{-3}$ s^{-1}) than the hydrolysis in pure buffer. For the acyl transfer in the presence of **43**, saturation kinetics is observed, whereas the reaction in the presence of **42** strictly follows second order kinetics. Only host **43** forms a productive complex with a favorable proximity between the phenolic hydroxyl group and the substrate carbonyl group. The smaller host **42** also forms a stable complex with the naphthyl ester. In this complex, however, the phenol ring completely blocks one side of the cavity. The ester residue of the guest extends in a non-productive manner out of the cavity on the side opposite to the nucleophile and undergoes an intermolecular reaction with the phenol group of another host molecule.

The phenolic OH group in **43** is not only a good nucleophile in the transacylation step but, with its estimated pK_a of ≈ 8.4, also represents a favorable leaving group in the deacylation step as indicated by a weak but significant catalytic turnover.[239, 250] With [**43**] $= 1.0 \times 10^{-5}$ mol L^{-1} and [4-nitro-1-naphthylacetate] $= 1.0 \times 10^{-4}$ mol L^{-1} under the above mentioned conditions, the covalently catalyzed ester hydrolysis is accelerated by a factor of 1.3 compared to the hydrolysis in pure buffer. Under these conditions, only $\approx 15\%$ of the total amount of host is complexed. Having discovered the optimum size of the binding site and the favorable role of the phenolic nucleophile in covalently catalyzed ester hydrolysis, we will now continue the further development of the host system **43** to a synthetic hydrolase to give high catalytic turnover in aqueous solution.[239a]

8. Perspectives

One of the more fascinating and gratifying aspects of research in the field of molecular complexation and catalysis is the multidisciplinary approach to generate interesting research objectives and to subsequently target them in experiments. Inspiration is provided by studying problems of interest and importance in biological sciences. Open fundamental questions are recognized which can be better answered with the methods of more exact, molecular-based chemical science. In addition, the intensive occupation with the extraordinary properties of biological systems such as enzymes and receptors stimulates a strong desire to generate similar properties in designed systems. The application of computer modeling to the design of molecular receptors and catalysts is becoming increasingly important. A large variety of state of the art synthetic, analytical, and physical-organic techniques are applied during the experimental research phase. This multidisciplinary approach breaks new frontiers in organic chemistry. In addition, it guarantees a future-oriented and flexibility-mediating education of chemists. This is of special importance at a time where many chemists enter professional careers where barriers between organic chemistry, biochemistry, and biotechnology can no longer be defined.

In this article, interesting open questions have been discussed which need to be answered for a better understanding of the principles of molecular recognition and catalysis. Some additional research objectives, to be targeted with cyclophane hosts, are added at the end of this article. Studies of complexation at binding sites of pronounced apolar character will contribute to a clearer definition, on a molecular basis, of the hydrophobic effect. The discovery of efficient complexation of neutral apolar molecules in a variety of organic solvents has made it possible to determine specific effects of the solvent in comparative binding studies in organic and aqueous solutions.

Efficient synthetic receptors are currently not available for many important classes of compounds, e.g. for sugars and, despite isolated progress, for neutral aliphatic and heteroaliphatic guests. Also, the preparation of hosts with spacious binding sites for large biological molecules, e.g. for double stranded DNA, can be expected in the near future.

Host systems with two or more neighboring binding sites in a well-defined spatial orientation should be subject to increasing research efforts. Multiple interactions in the complexes of these hosts allow for very high guest selectivity.[45b, 49e, 54f] It is unknown how the complexing ability of one binding site is influenced by a second, adjacent binding site and its solvation pattern. An improved understanding of multiple interactions in molecular complexes will

benefit the rational development of optically active hosts which discriminate effectively between racemic guests. The immobilization of optically active cyclophane hosts with apolar binding sites could lead to novel chiral phases of hydrophobic character.

The interaction between binding sites located at larger but still well-defined distances in molecular hosts deserves increasing attention for several reasons. These di- or polytopic host systems will mimic and contribute to the understanding of cooperative and allosteric effects in biological systems.[40a] Such systems will allow one to explore how the information of complexation can be selectively transferred from one binding site to a second binding site over larger distances in a molecule. Novel molecular sensors could be obtained by the conversion of binding information into an electrical signal. In materials science research, there is a need for novel crystalline host systems which, by specific orientation of complexed dipolar guests, could generate non-linear optical properties.[16]

In environmental science and technology, host-guest systems could be useful to sequester extremely toxic compounds from soils and waters even if these compounds are present in high dilution only. Polymer-bound cyclophane hosts could be very effective in removing carcinogenic polycyclic aromatic hydrocarbons and substituted dibenzofurans and dibenzodioxins from aqueous solution.

Research in the field of bioorganic catalysis will lead to compounds with specific advantages such as superior stability and broad applicability compared to organometallic catalysts, to enzymes and their mutants,[66a] or to other catalysts derived from biological materials, e.g. catalytic antibodies[251] and semi-synthetic enzymes.[252] These synthetic catalysts could recognize a large variety of substrates and accelerate many reactions for which no biological catalysts are available. The most worthwile objective of the current research efforts on the way to such catalysts is to learn how to generate the efficient principles and mechanisms of enzymatic catalysis in synthetic organic systems. The successful development of bioorganic catalysts could well represent an ultimate test for the depth of our understanding of enzymatic catalysis. The author of this article is convinced that we possess a true understanding of enzymatic catalytic mechanisms only if we are able to reproduce them with the same or even at enhanced efficiency in synthetic systems. In this sense, the development of bioorganic catalysts will help to define, from a chemical viewpoint, the degree of molecular understanding of enzymatic catalysis that has been achieved.

I warmly thank my coworkers who, by their skills, their engagement and their enthusiasm, contributed to the development of cyclophane molecules as efficient receptors and catalysts. I would like to express on this occasion my special thanks to Mr. Klaus Dick, now at BASF Ludwigshafen, who has made major experimental contributions to all the results obtained during my Habilitation time in Heidelberg. I warmly thank my coworkers Dr. Eileen Seward and Stephen B. Ferguson for assisting in the English translation of the original German manuscript. The work performed at the Department of Organic Chemistry at the Max-Planck-Institute for medical research in Heidelberg was generously supported by the Max-Planck-Society through funding provided by Prof. Dr. H. A. Staab and by the Deutsche Forschungsgemeinschaft. The work performed at the University of California at Los Angeles and the writing of this article was supported in a generous way by the Office of Naval Research and the National Science Foundation. We also thank BASF and Merck Sharp & Dohme for additional support of our work.

Received: September 2, 1987 [A 661 IE]
German version: *Angew. Chem. 100* (1988) 372

[1] F. Wöhler, *Ann. Chem. Pharm. 69* (1849) 294.
[2] A. Clemm, *Ann. Chem. Pharm. 110* (1859) 345.
[3] F. Mylius, *Ber. Dtsch. Chem. Ges. 19* (1886) 999.
[4] R. Anschütz, *Ber. Dtsch. Chem. Ges. 25* (1892) 3512.
[5] K. Freudenberg, M. Meyer-Delius, *Ber. Dtsch. Chem. Ges. 71* (1938) 1596.
[6] D. J. Cram, J. M. Cram, *Science (Washington, DC) 183* (1974) 803.
[7] F. Cramer: *Einschlussverbindungen*, Springer, Berlin 1954.
[8] a) F. Cramer, *Chem. Ber. 86* (1953) 1576; b) F. Cramer, W. Dietsche, *ibid. 92* (1959) 1739; c) F. Cramer, *Angew. Chem. 73* (1961) 49.
[9] a) M. L. Bender, M. Komiyama: *Cyclodextrin Chemistry*, Springer, Berlin 1978; b) V. T. D'Souza, M. L. Bender, *Acc. Chem. Res. 20* (1987) 146.
[10] a) R. Breslow, *Science (Washington, DC) 218* (1982) 532; b) *Adv. Enzymol. Relat. Areas Mol. Biol. 58* (1986) 1.
[11] a) I. Tabushi, *Acc. Chem. Res. 15* (1982) 66; b) I. Tabushi, Y. Kuroda, *Adv. Catal. 32* (1983) 417; c) I. Tabushi, *Pure Appl. Chem. 58* (1986) 1529; d) I. Tabushi, T. Mizutani, *Tetrahedron 43* (1987) 1439; e) I. Tabushi, M. Kodera, *J. Am. Chem. Soc. 109* (1987) 4734.
[12] a) W. Saenger, *Angew. Chem. 92* (1980) 343; *Angew. Chem. Int. Ed. Engl. 19* (1980) 344; b) W. Saenger in J. L. Atwood, J. E. D. Davies, D. D. MacNicol (Eds.): *Inclusion Compounds, Vol. 2*, Academic Press, London 1984, p. 231.
[13] R. J. Bergeron in J. L. Atwood, J. E. D. Davies, D. D. MacNicol (Eds.): *Inclusion Compounds, Vol. 3*, Academic Press, London 1984, p. 391.
[14] J. Szejtli (Ed.): *Cyclodextrins*, Reidel, Dordrecht 1982.
[15] A. P. Croft, R. A. Bartsch, *Tetrahedron 39* (1983) 1417.
[16] D. F. Eaton, *Tetrahedron 43* (1987) 1551.
[17] A. Ueno, F. Moriwaki, T. Osa, F. Hamada, K. Murai, *Tetrahedron 43* (1987) 1571.
[18] H. Stetter, E.-E. Roos, *Chem. Ber. 88* (1955) 1390.
[19] a) C. J. Pedersen, *J. Am. Chem. Soc. 89* (1967) 2495; b) *ibid. 89* (1967) 7017; c) C. J. Pedersen, H. K. Frensdorff, *Angew. Chem. 84* (1972) 16; *Angew. Chem. Int. Ed. Engl. 16* (1972) 16.
[20] R. M. Izatt, J. J. Christensen (Eds.): *Synthetic Multidentate Macrocyclic Compounds*, Academic Press, New York 1978.
[21] R. M. Izatt, J. J. Christensen (Eds.): *Progress in Macrocyclic Chemistry, Vol. 1-3*, Wiley-Interscience, New York 1979, 1981, 1987.
[22] G. A. Melson (Ed.): *Coordination Chemistry of Macrocyclic Compounds*, Plenum Press, New York 1979.
[23] F. Vögtle, E. Weber (Eds.): *Host Guest Complex Chemistry, Parts I-III (Top. Curr. Chem. 98, 101, 121)*, Springer, Berlin 1981, 1982, 1984.
[24] M. Hiraoka (Ed.): *Crown Compounds*, Elsevier, Amsterdam 1982.
[25] G. W. Gokel, S. H. Korzeniowski (Eds.): *Macrocyclic Polyether Syntheses*, Springer, Berlin 1982.
[26] J. L. Atwood, J. E. D. Davies, D. D. MacNicol (Eds.): *Inclusion Compounds, Vol. 1-3*, Academic Press, London 1984.
[27] F. Vögtle, E. Weber (Eds.): *Host Guest Complex Chemistry, Macrocycles (Synthesis, Structures, Applications)*, Springer, Berlin 1985.
[28] F. Vögtle, E. Weber (Eds.): *Bioorganic and Biomimetic Chemistry, Parts I-III (Top. Curr. Chem. 128, 132, 136)*, Springer, Berlin 1985, 1986, 1986.
[29] E. Weber (Ed.): *Molecular Inclusion and Molecular Recognition - Clathrates, Vol. 1 (Top. Curr. Chem. 140)*, Springer, Berlin 1987.
[30] V. Prelog, *Pure Appl. Chem. 50* (1978) 893.
[31] F. DeJong, D. N. Reinhoudt, *Adv. Phys. Org. Chem. 17* (1980) 279.
[32] a) R. C. Hayward, *Chem. Soc. Rev. 12* (1983) 285; b) C. Sirlin, *Bull. Soc. Chim. Fr. II 1984*, 5.
[33] a) J. O. Sutherland in P. M. Keehn, S. M. Rosenfeld (Eds.): *Cyclophanes, Vol. 2*, Academic Press, New York 1983, p. 679; b) I. O. Sutherland, *Chem. Soc. Rev. 15* (1986) 63.
[34] V. K. Majestic, G. R. Newkome, *Top. Curr. Chem. 106* (1982) 79.
[35] N. J. Turro, *Pure Appl. Chem. 58* (1986) 1219.
[36] F. Diederich, *Nachr. Chem. Tech. Lab. 32* (1984) 787.
[37] K. N. Raymond, G. Müller, B. F. Matzanke, *Top. Curr. Chem. 123* (1984) 49.
[38] C. D. Gutsche, *Top. Curr. Chem. 123* (1984) 1.
[39] a) R. M. Kellogg, *Angew. Chem. 96* (1984) 769; *Angew. Chem. Int. Ed. Engl. 23* (1984) 782; b) R. M. Kellogg in [27], p. 283.

[40] a) J. Rebek, Jr., *Acc. Chem. Res. 17* (1984) 258; b) J. Rebek, Jr., *Science (Washington, DC) 235* (1987) 1478.
[41] a) F. Franke, F. Vögtle, *Top. Curr. Chem. 132* (1986) 135; b) F. Vögtle, H.-G. Löhr, J. Franke, D. Worsch, *Angew. Chem. 97* (1985) 721; *Angew. Chem. Int. Ed. Engl. 24* (1985) 727.
[42] a) R. M. Izatt, J. S. Bradshaw, S. A. Nielsen, J. D. Lamb, J. Christensen, D. Sen, *Chem. Rev. 85* (1985) 271; b) R. M. Izatt, G. C. Lindh, R. L. Bruening, J. S. Bradshaw, J. D. Lamb, J. J. Christensen, *Pure Appl. Chem. 58* (1986) 1453.
[43] a) S. Shinkai, *Pure Appl. Chem. 58* (1986) 1523; b) S. Shinkai, *ibid.* 425.
[44] a) H. M. Colquhoun, J. F. Stoddart, D. J. Williams, *New Scientist*, May 1, 1986, p. 44; b) H. M. Colquhoun, J. F. Stoddart, D. J. Williams, *Angew. Chem. 98* (1986) 483; *Angew. Chem. Int. Ed. Engl. 25* (1986) 487.
[45] a) F. P. Schmidtchen, *Top. Curr. Chem. 132* (1986) 101; b) *J. Am. Chem. Soc. 108* (1986) 8249.
[46] C. O. Dietrich-Buchecker, J. P. Sauvage, *Chem. Rev. 87* (1987) 671.
[47] a) A. Shanzer, J. Libman, F. Frolow, *Acc. Chem. Res. 16* (1983) 60; b) J. Jurczak, M. Pietrazkiewicz, *Top. Curr. Chem. 130* (1986) 183; c) S. Quici, P. L. Anelli, H. Molinari, T. Beringhelli, *Pure Appl. Chem. 58* (1986) 1503.
[48] E. Kimura, *Top. Curr. Chem. 128* (1985) 113.
[49] a) J.-M. Lehn, *Struct. Bonding (Berlin) 16* (1973) 1; b) *Pure Appl. Chem. 50* (1978) 871; c) *Acc. Chem. Res. 11* (1978) 49; d) *Science (Washington, DC) 227* (1985) 849; e) A. Hamilton, J.-M. Lehn, J. L. Sessler, *J. Am. Chem. Soc. 108* (1986) 5158; f) M. W. Hosseini, J.-M. Lehn, L. Maggiora, K. B. Mertes, M. P. Mertes, *ibid. 109* (1987) 537; g) J.-M. Lehn, *Angew. Chem. 100* (1988) 91; *Angew. Chem. Int. Ed. Engl. 27* (1988) 89.
[50] a) D. J. Cram, J. M. Cram, *Acc. Chem. Res. 11* (1978) 8; b) D. J. Cram, K. N. Trueblood, *Top. Curr. Chem. 98* (1981) 43; c) D. J. Cram, *Science (Washington, DC) 219* (1983) 1177; d) *Angew. Chem. 98* (1986) 1041; *Angew. Chem. Int. Ed. Engl. 25* (1986) 1039; e) D. J. Cram in J. B. Jones, C. J. Sih, D. Perlman (Eds.): *Applications of Biochemical Systems in Organic Chemistry;* A. Weissberger (Ed.): *Techniques in Chemistry, Vol. 10, Part II*, Wiley, New York 1976, p. 815; f) D. J. Cram, P. Y. Lam, S. P. Ho, *J. Am. Chem. Soc. 108* (1986) 839.
[51] R. Hilgenfeld, W. Saenger, *Angew. Chem. 94* (1982) 788; *Angew. Chem. Int. Ed. Engl. 21* (1982) 781; *Angew. Chem. Suppl. 1982*, 1690.
[52] a) I. Tabushi, H. Yamada, K. Matsushita, Z. Yoshida, H. Kuroda, R. Oda, *Tetrahedron 28* (1972) 3381; b) I. Tabushi, Y. Kuroda, Y. Kimura, *Tetrahedron Lett. 1976*, 3327; c) I. Tabushi, K. Yamamura, *Top. Curr. Chem. 113* (1983) 145; d) I. Tabushi, K. Yamamura, H. Nonoguchi, K. Hirotsu, T. Higuchi, *J. Inclusion Phenom. 2* (1984) 85.
[53] a) Y. Murakami, J. Sunamoto, K. Kano, *Bull. Chem. Soc. Jpn. 47* (1974) 1238; b) Y. Murakami, *Top. Curr. Chem. 115* (1983) 107; c) *J. Inclusion Phenom. 2* (1984) 35; d) Y. Murakami, J. Kikuchi, T. Hirayama, *Chem. Lett. 1987*, 161.
[54] a) K. Odashima, A. Itai, Y. Iitaka, K. Koga, *J. Am. Chem. Soc. 102* (1980) 2504; b) T. Soga, K. Odashima, K. Koga, *Tetrahedron Lett. 21* (1980) 4351; c) K. Odashima, A. Itai, Y. Iitaka, K. Koga, *J. Org. Chem. 50* (1985) 4478; d) H. Kawakami, O. Yoshino, K. Odashima, K. Koga, *Chem. Pharm. Bull. 33* (1985) 5610; e) K. Odashima, K. Koga in P. M. Keehn, S. M. Rosenfeld (Eds.): *Cyclophanes, Vol. 2*, Academic Press, New York 1983, p. 629; f) C.-F. Lai, K. Odashima, K. Koga, *Tetrahedron Lett. 26* (1985) 5179.
[55] a) E. T. Jarvi, H. W. Whitlock, Jr., *J. Am. Chem. Soc. 102* (1980) 657; b) B. J. Whitlock, E. T. Jarvi, H. W. Whitlock, *J. Org. Chem. 46* (1981) 1832; c) S. P. Adams, H. W. Whitlock, *J. Am. Chem. Soc. 104* (1982) 1602; d) E. T. Jarvi, H. W. Whitlock, *ibid. 104* (1982) 7196; e) S. P. Miller, H. W. Whitlock, Jr., *ibid. 106* (1984) 1492.
[56] H. S. Frank, M. W. Evans, *J. Chem. Phys. 13* (1945) 507.
[57] W. Kauzmann, *Adv. Protein Chem. 14* (1959) 1.
[58] I. M. Klotz, *Science (Washington, DC) 128* (1958) 815.
[59] a) G. Nemethy, H. A. Scheraga, *J. Chem. Phys. 48* (1962) 3382, 3401; b) H. A. Scheraga, *Acc. Chem. Res. 12* (1979) 7.
[60] W. P. Jencks: *Catalysis in Chemistry and Enzymology*, McGraw-Hill, New York 1969, Chap. 8, p. 393.
[61] M. H. Klapper, *Prog. Bioorg. Chem. 2* (1973) 55.
[62] C. Tanford: *The Hydrophobic Effect: Formation of Micelles and Biological Membranes*, 2nd Edit., Wiley, New York 1980.
[63] M. H. Abraham, *J. Am. Chem. Soc. 101* (1979) 5477; *104* (1982) 2085.
[64] A. Ben-Naim, *Hydrophobic Interactions*, 2nd Edit., Plenum, New York 1983.
[65] For examples of critical discussions of the nature of hydrophobic interactions see: a) R. D. Cramer, III, *J. Am. Chem. Soc. 99* (1977) 5408; b) M. S. Ramadan, D. F. Evans, R. Lumry, *J. Phys. Chem. 87* (1983) 4538; c) F. A. Greco, *ibid. 88* (1984) 3132.
[66] a) A. Fersht: *Enzyme Structure and Mechanism*, 2nd Edit., Freeman, New York 1985; b) L. Stryer: *Biochemistry*, 2nd Edit., Freeman, San Francisco 1981.
[67] J. M. Sturtevant, *Proc. Natl. Acad. Sci. USA 74* (1977) 2236.
[68] a) J. C. Harrison, M. R. Eftink, *Biopolymers 21* (1982) 1153; b) W. C. Cromwell, K. Byström, M. R. Eftink, *J. Phys. Chem. 89* (1985) 326.
[69] F. Diederich, K. Dick, *Tetrahedron Lett. 23* (1982) 3167.
[70] F. Diederich, K. Dick, *J. Am. Chem. Soc. 106* (1984) 8024.
[71] F. Diederich, K. Dick, D. Griebel, *Chem. Ber. 118* (1985) 3588.
[72] E. Seward, P. Inocencio-Szweda, F. Diederich, unpublished.
[73] K. Odashima, K. Koga, *Heterocycles 15* (1981) 1151.
[74] E. Seward, F. Diederich, *Tetrahedron Lett. 28* (1987) 5111.
[75] M. Fukae, T. Inazu, *J. Inclusion Phenom. 2* (1984) 223.
[76] C. S. Wilcox, M. D. Cowart, *Tetrahedron Lett. 27* (1986) 5563.
[77] a) M. A. Petti, T. J. Shepodd, D. A. Dougherty, *Tetrahedron Lett. 27* (1986) 807; b) T. J. Shepodd, M. A. Petti, D. A. Dougherty, *J. Am. Chem. Soc. 108* (1986) 6085.
[78] Y. Tobe, H. Fujita, I. Wakaki, K. Terashima, K. Kobiro, K. Kakiuchi, Y. Odaira, *J. Chem. Soc. Perkin Trans. 1 1984*, 2681.
[79] F. Diederich, K. Dick, *Angew. Chem. 95* (1983) 730; *Angew. Chem. Int. Ed. Engl. 22* (1983) 715; *Angew. Chem. Suppl. 1983*, 957.
[80] F. Diederich, K. Dick, *Chem. Ber. 118* (1985) 3817.
[81] F. Diederich, K. Dick, *Angew. Chem. 96* (1984) 789; *Angew. Chem. Int. Ed. Engl. 23* (1984) 810.
[82] F. Diederich, K. Dick, D. Griebel, *J. Am. Chem. Soc. 108* (1986) 2273.
[83] E. Fischer, *Ber. Dtsch. Chem. Ges. 27* (1894) 2985.
[84] a) B. L. Allwood, F. H. Kohnke, J. F. Stoddart, D. J. Williams, *Angew. Chem. 97* (1985) 584; *Angew. Chem. Int. Ed. Engl. 24* (1985) 581; b) B. L. Allwood, H. Shahriari-Zavareh, J. F. Stoddart, D. J. Williams, *J. Chem. Soc. Chem. Commun. 1987*, 1058; c) B. L. Allwood, N. Spencer, H. Shahriari-Zavareh, J. F. Stoddart, D. J. Williams, *ibid. 1987*, 1061.
[85] R. E. Sheridan, H. W. Whitlock, Jr., *J. Am. Chem. Soc. 108* (1986) 7120.
[86] C. Krieger, F. Diederich, *Chem. Ber. 118* (1985) 3620.
[87] C. Krieger, F. Diederich, unpublished.
[88] D. O'Krongly, S. R. Denmeade, M. Y. Chiang, R. Breslow, *J. Am. Chem. Soc. 107* (1985) 5544.
[89] a) K. Saigo, M. Kubo, R.-J. Lin, A. Youda, M. Hasegawa, *Tetrahedron Lett. 26* (1985) 1325; b) K. Saigo, R.-J. Lin, M. Kubo, A. Youda, M. Hasegawa, *J. Am. Chem. Soc. 108* (1986) 1996.
[90] T. Takemura, K. Kozawa, T. Uchida, N. Mori, *Chem. Lett. 1984*, 1839.
[91] S. G. Bott, A. W. Coleman, J. L. Atwood, *J. Am. Chem. Soc. 108* (1986) 1709.
[92] a) G. D. Andreetti, R. Ungaro, A. Pochini, *J. Chem. Soc. Chem. Commun. 1979*, 1005; b) G. D. Andreetti, A. Pochini, R. Ungaro, *J. Chem. Soc. Perkin Trans. 2 1983*, 1773; c) R. Ungaro, A. Pochini, G. D. Andreetti, P. Domiano, *ibid. 1985*, 197.
[93] F. Vögtle, W. M. Müller, H. Puff, E. Friedrichs, *Chem. Ber. 116* (1983) 2344.
[94] F. Vögtle, H. Puff, E. Friedrichs, W. M. Müller, *J. Chem. Soc. Chem. Commun. 1982*, 1398.
[95] J. Jazwinski, J.-M. Lehn, R. Méric, J.-P. Vigneron, M. Cesario, J. Guilhem, C. Pascard, *Tetrahedron Lett. 28* (1987) 3489.
[96] I. Tabushi, K. Yamamura, H. Nonoguchi, K. Hirotsu, T. Higuchi, *J. Am. Chem. Soc. 106* (1984) 2621.
[97] a) J. Canceill, M. Cesario, A. Collet, J. Guilhem, C. Riche, C. Pascard, *J. Chem. Soc. Chem. Commun. 1986*, 339; b) J. Canceill, M. Cesario, A. Collet, J. Guilhem, C. Pascard, *ibid. 1985*, 361; c) J. Canceill, L. Lacombe, A. Collet, *C. R. Acad. Sci. Sec. II 298* (1984) 39.
[98] a) D. J. Cram, K. D. Stewart, I. Goldberg, K. N. Trueblood, *J. Am. Chem. Soc. 107* (1985) 2574; b) I. Goldberg, *J. Inclusion Phenom. 4* (1986) 191.
[99] M. A. McKervey, E. M. Seward, G. Ferguson, B. L. Ruhl, *J. Org. Chem. 51* (1986) 3581.
[100] R. Ungaro, A. Pochini, G. D. Andreetti, V. Sangermano, *J. Chem. Soc. Perkin Trans. 2 1984*, 1979.
[101] S. J. Abbott, A. G. M. Barrett, C. R. A. Godfrey, S. B. Kalindjian, G. W. Simpson, D. J. Williams, *J. Chem. Soc. Chem. Commun. 1982*, 796.
[102] Y. Murakami, Y. Aoyama, M. Kida, *J. Chem. Soc. Perkin Trans. 2 1977*, 1947.
[103] a) J. P. Guthrie, *J. Chem. Soc. Chem. Commun. 1972*, 897; b) J. P. Guthrie, J. Cossar, B. A. Dawson, *Can. J. Chem. 64* (1986) 2456.
[104] J. H. Fendler: *Membrane Mimetic Chemistry*, Wiley, New York 1982.
[105] B. Lindman, H. Wennerström, *Top. Curr. Chem. 87* (1980) 1.
[106] E. J. Fendler, V. G. Constien, J. H. Fendler, *J. Phys. Chem. 79* (1975) 917.
[107] G. Schürmann, F. Diederich, unpublished.
[108] F. Kotzyba-Hibert, J.-M. Lehn, K. Saigo, *J. Am. Chem. Soc. 103* (1981) 4266.
[109] M. R. Johnson, I. O. Sutherland, R. F. Newton, *J. Chem. Soc. Chem. Commun. 1979*, 309.
[110] K. Odashima, A. Itai, Y. Iitaka, Y. Arata, K. Koga, *Tetrahedron Lett. 21* (1980) 4347.

[111] F. Diederich, D. Griebel, *J. Am. Chem. Soc. 106* (1984) 8037.
[112] J. H. Prestegard, S. I. Chan, *J. Am. Chem. Soc. 92* (1970) 4440.
[113] F. H. Kohnke, J. F. Stoddart, *J. Chem. Soc. Chem. Commun. 1985*, 314.
[114] W. L. Mock, N.-Y. Shih, *J. Org. Chem. 51* (1986) 4440.
[115] T. Anthonsen, D. J. Cram, *J. Chem. Soc. Chem. Commun. 1983*, 1414.
[116] J.-P. Kintzinger, F. Kotzyba-Hibert, J.-M. Lehn, A. Pagelot, K. Saigo, *J. Chem. Soc. Chem. Commun. 1981*, 833.
[117] E. P. Kyba, J. M. Timko, L. J. Kaplan, F. deJong, G. W. Gokel, D. J. Cram, *J. Am. Chem. Soc. 100* (1978) 4555.
[118] G. Briegleb: *Elektronen-Donator-Acceptor-Komplexe*, Springer, Berlin 1961.
[119] K. J. Andrews, R. M. Keefer: *Molecular Complexes in Organic Chemistry*, Holden-Day, San Francisco 1964.
[120] R. S. Mulliken, W. B. Person: *Molecular Complexes*, Wiley-Interscience, New York 1969.
[121] R. Foster: *Organic Charge-Transfer Complexes*, Academic Press, London 1969.
[122] R. Foster, C. A. Fyfe, *Prog. Nucl. Magn. Reson. Spectrosc. 4* (1969) 1.
[123] F. Cramer, W. Saenger, H.-C. Spatz, *J. Am. Chem. Soc. 89* (1967) 14.
[124] K. A. Connors: *Binding Constants, The Measurement of Molecular Complex Stability*, Wiley, New York 1987.
[125] D. J. Leggett (Ed.): *Computational Methods for the Determination of Formation Constants*, Plenum, New York 1985.
[126] F. Vögtle, W. M. Müller, U. Werner, H.-W. Losensky, *Angew. Chem. 99* (1987) 930; *Angew. Chem. Int. Ed. Engl. 26* (1987) 901.
[127] D. Schweitzer, K. H. Hausser, R. G. H. Kirrstetter, H. A. Staab, *Z. Naturforsch. A 31* (1976) 1189.
[128] H. K. Frensdorff, *J. Am. Chem. Soc. 93* (1971) 4684.
[129] K. E. König, G. M. Lein, P. Stuckler, T. Kaneda, D. J. Cram, *J. Am. Chem. Soc. 101* (1979) 3553.
[130] H. A. Benesi, J. H. Hildebrand, *J. Am. Chem. Soc. 71* (1949) 2703.
[131] R. L. Scott, *Recl. Trav. Chim. Pays-Bas 75* (1956) 787.
[132] G. Scatchard, *Ann. N. Y. Acad. Sci. 51* (1949) 660.
[133] W. B. Person, *J. Am. Chem. Soc. 87* (1965) 167.
[134] D. A. Deranleau, *J. Am. Chem. Soc. 91* (1969) 4050.
[135] R. J. Bergeron, W. P. Roberts, *Anal. Biochem. 90* (1978) 844.
[136] S. B. Ferguson, F. Diederich, *Angew. Chem. 98* (1986) 1127; *Angew. Chem. Int. Ed. Engl. 25* (1986) 1127.
[137] H. J. Schneider, K. Philippi, J. Pöhlmann, *Angew. Chem. 96* (1984) 907; *Angew. Chem. Int. Ed. Engl. 23* (1984) 908.
[138] a) J. A. A. de Boer, D. N. Reinhoudt, S. Harkema, G. J. van Hummel, F. de Jong, *J. Am. Chem. Soc. 104* (1982) 4073; b) C. J. van Staveren, V. M. L. J. Aarts, P. D. J. Grootenhuis, J. van Eerden, S. Harkema, D. N. Reinhoudt, *ibid. 108* (1986) 5271.
[139] a) C. D. Gutsche, M. Iqbal, I. Alam, *J. Am. Chem. Soc. 109* (1987) 4314; b) L. J. Bauer, C. D. Gutsche, *ibid. 107* (1985) 6063.
[140] K. Mochida, A. Kagita, Y. Matsui, Y. Date, *Bull. Chem. Soc. Jpn. 46* (1973) 3703.
[141] J.-M. Lehn, J. Simon, J. Wagner, *Angew. Chem. 85* (1973) 622; *Angew. Chem. Int. Ed. Engl. 12* (1973) 579.
[142] I. Tabushi, H. Sasaki, Y. Kuroda, *J. Am. Chem. Soc. 98* (1976) 5727.
[143] Y. Murakami, Y. Aoyama, M. Kida, A. Nakano, *Bull. Chem. Soc. Jpn. 50* (1977) 3365.
[144] a) J. Franke, F. Vögtle, *Angew. Chem. 97* (1985) 224; *Angew. Chem. Int. Ed. Engl. 24* (1985) 219; b) F. Vögtle, T. Merz, H. Wirtz, *ibid. 97* (1985) 226 bzw. *24* (1985) 221; c) T. Merz, H. Wirtz, F. Vögtle, *ibid. 98* (1986) 549 and *25* (1986) 567; d) J. Franke, T. Merz, H.-W. Losensky, W. M. Müller, U. Werner, F. Vögtle, *J. Inclusion Phenom. 3* (1985) 471; e) U. Werner, W. M. Müller, H.-W. Losensky, T. Merz, F. Vögtle, *ibid. 4* (1986) 379.
[145] H.-J. Schneider, J. Pöhlmann, *Bioorg. Chem. 15* (1987) 183.
[146] H. L. Larkins, A. D. Hamilton, *Tetrahedron Lett. 27* (1986) 2721.
[147] G. Lepropre, J. Fastrez, *J. Inclusion Phenom. 5* (1987) 157.
[148] D. Turner, L. Brand, *Biochemistry 7* (1968) 3381.
[149] G. M. Edelman, W. O. McClure, *Acc. Chem. Res. 1* (1968) 65.
[150] L. Stryer, *Science (Washington, DC) 162* (1968) 526.
[151] F. M. Menger, M. Takeshita, J. F. Chow, *J. Am. Chem. Soc. 103* (1981) 5938.
[152] D. Griebel, S. B. Ferguson, F. Diederich, unpublished.
[153] G. W. Liesegang, E. M. Eyring in [20], p. 245.
[154] A. Xenakis, C. Tondre, *J. Phys. Chem. 87* (1983) 4737.
[155] G. R. Painter, B. C. Pressman, *Top. Curr. Chem. 101* (1982) 83.
[156] S. Lindenbaum, J. H. Rytting, L. A. Sternson, *Prog. Macrocyclic Chem. 1* (1979) 219.
[157] Y. A. Ovchinnikov, V. T. Ivanov, A. M. Shkrob: *Membrane Active Complexones*, Elsevier, Amsterdam 1974.
[158] W. E. Morf, D. Ammann, R. Bissig, E. Pretsch, W. Simon, *Prog. Macrocyclic Chem. 1* (1979) 1.
[159] a) J. D. Lamb, R. M. Izatt, J. J. Christensen, *Prog. Macrocyclic Chem. 2* (1981) 41; b) D. W. McBride, Jr., R. M. Izatt, J. D. Lamb, J. J. Christensen in [26], Vol. 3, p. 571.
[160] W. H. Mandeville, G. M. Whitesides, *J. Org. Chem. 51* (1986) 3257.
[161] A. Harada, S. Takahashi, *J. Chem. Soc. Chem. Commun. 1987*, 527.
[162] a) M. Kirch, J.-M. Lehn, *Angew. Chem. 87* (1975) 542; *Angew. Chem. Int. Ed. Engl. 14* (1975) 555; b) J.-M. Lehn, *Pure Appl. Chem. 51* (1979) 979.
[163] P. G. Potvin, J.-M. Lehn, *Prog. Macrocyclic Chem. 3* (1987) 167.
[164] M. Okahara, *Top. Curr. Chem. 128* (1986) 37.
[165] L. Echeverria, M. Delgado, V. J. Gatto, G. W. Gokel, L. Echegoyen, *J. Am. Chem. Soc. 108* (1986) 6825.
[166] J. D. Winkler, K. Deshayes, *J. Am. Chem. Soc. 109* (1987) 2190.
[167] K. Odashima, T. Soga, K. Koga, *Tetrahedron Lett. 22* (1981) 5311.
[168] D. J. Cram, T. Kaneda, R. C. Helgeson, S. B. Brown, C. B. Knobler, E. Maverick, K. N. Trueblood, *J. Am. Chem. Soc. 107* (1985) 3645.
[169] W. L. Koltun, *Biopolymers 3* (1965) 665.
[170] J. Canceill, L. Lacombe, A. Collet, *J. Am. Chem. Soc. 108* (1986) 4230.
[171] E. Seward, S. B. Ferguson, F. Diederich, unpublished.
[172] R. Dharanipragada, S. B. Ferguson, F. Diederich, *J. Am. Chem. Soc.*, in press.
[173] S. B. Ferguson, F. Diederich, unpublished.
[174] The computer-modeling program HYDRA 1.1 of Polygen Corporation, 200 Fifth Ave, Waltham, MA 02254 (USA) was used on a Silicon Graphics IRIS 3130 workstation.
[175] U. Burkert, N. L. Allinger: *Molecular Mechanics*, American Chemical Society, Washington, DC 1982. The program used has been modified by *D. Spellmeyer*, University of California at Los Angeles, to enable calculations on compounds with up to 200 atoms. The Beckhaus-parameters [H.-D. Beckhaus, *Chem. Ber. 116* (1983) 86] for alkyl-substituted aromatic rings were incorporated in the program.
[176] F. Vögtle, W. M. Müller, *Angew. Chem. 96* (1984) 711; *Angew. Chem. Int. Ed. Engl. 23* (1984) 712.
[177] H.-J. Schneider, D. Güttes, U. Schneider, *Angew. Chem. 98* (1986) 635; *Angew. Chem. Int. Ed. Engl. 25* (1986) 647.
[178] A. G. S. Högberg, *J. Org. Chem. 45* (1980) 4498.
[179] M. Dhaenens, L. Lacombe, J.-M. Lehn, J.-P. Vigneron, *J. Chem. Soc. Chem. Commun. 1984*, 1097.
[180] a) W. A. Freeman, W. L. Mock, N.-Y. Shih, *J. Am. Chem. Soc. 103* (1981) 7367; b) W. L. Mock, N.-Y. Shih, *J. Org. Chem. 48* (1983) 3618; c) W. L. Mock, T. A. Irra, J. P. Wepsiec, T. L. Manimaran, *ibid. 48* (1983) 3619.
[181] a) D. H. Busch, C. Cairns, *Prog. Macrocyclic Chem. 3* (1987) 1; b) T. J. Meade, K. J. Takeuchi, D. H. Busch, *J. Am. Chem. Soc. 109* (1987) 725.
[182] J. Canceill, L. Lacombe, A. Collet, *J. Chem. Soc. Chem. Commun. 1987*, 219.
[183] G. W. Gokel, D. J. Cram, C. L. Liotta, H. P. Harris, F. L. Cook, *J. Org. Chem. 39* (1974) 2445.
[184] a) F. Vögtle, H. Sieger, W. M. Müller in [27], p. 321; b) F. Vögtle, W. M. Müller, W. H. Watson, *Top. Curr. Chem. 125* (1984) 131.
[185] R. Kaufmann, A. Knöchel, J. Kopf, J. Oehler, G. Rudolph, *Chem. Ber. 110* (1977) 2249.
[186] P. A. Mosier-Boss, A. I. Popov, *J. Am. Chem. Soc. 107* (1985) 6168.
[187] B. Siegel, R. Breslow, *J. Am. Chem. Soc. 97* (1975) 6869.
[188] A. Harada, S. Takahashi, *Chem. Lett. 1984*, 2089.
[189] Y. Nakai, K. Yamamoto, K. Terada, H. Horibe, *Chem. Pharm. Bull. 30* (1982) 1796.
[190] F. M. Menger, M. A. Dulany, *Tetrahedron Lett. 26* (1985) 267.
[191] J. Canceill, L. Lacombe, A. Collet, *C. R. Acad. Sci. Sec. II 304* (1987) 815.
[192] S. B. Ferguson, F. Diederich, unpublished.
[193] C. Reichardt, *Angew. Chem. 77* (1965) 30; *Angew. Chem. Int. Ed. Engl. 4* (1965) 29.
[194] E. Washburn (Ed.): *International Critical Tables of Numerical Data, Physics, Chemistry and Technology, Vol. 5*, McGraw-Hill, New York 1929.
[195] a) F. Diederich, unpublished; I thank *J. Tucker*, University of California at Los Angeles, for valuable discussions to these issues; b) I. Tabushi, Y. Kiyosuke, T. Sugimoto, K. Yamamura, *J. Am. Chem. Soc. 100* (1978) 916.
[196] A. Warshel, *Proc. Natl. Acad. Sci. USA 75* (1978) 5250.
[197] J. D. Madura, W. L. Jorgensen, *J. Am. Chem. Soc. 108* (1986) 2517.
[198] M. J. S. Dewar, D. M. Storch, *Proc. Natl. Acad. Sci. USA 82* (1985) 2225.
[199] a) J. Rebek, Jr., B. Askew, M. Killoran, D. Nemeth, F.-T. Lin, *J. Am. Chem. Soc. 109* (1987) 2426; b) J. Rebek, B. Askew, P. Ballester, C. Buhr, S. Jones, D. Nemeth, K. Williams, *ibid. 109* (1987) 5033.
[200] A. D. Hamilton, D. Van Engen, *J. Am. Chem. Soc. 109* (1987) 5035.
[201] P. A. Kollman in H. F. Schaefer III (Ed.): *Applications of Electronic Structure Theory*, Plenum, New York 1977.
[202] K. Morokuma, *Acc. Chem. Res. 10* (1977) 294.
[203] M. W. Hanna, J. L. Lippert in R. Foster (Ed.): *Molecular Complexes, Vol. 1*, Elek Science, London 1973, p. 1.

[204] H. A. Staab, C. P. Herz, C. Krieger, M. Rentea, *Chem. Ber. 116* (1983) 3813, and references cited therein.
[205] C. J. Bender, *Chem. Soc. Rev. 15* (1986) 475.
[206] B. Pullman, A. Pullman: *Quantum Biochemistry*, Wiley-Interscience, New York 1963.
[207] See [121], Chap. 12, p. 335.
[208] a) H. M. Colquhoun, E. P. Goodings, J. M. Maud, J. F. Stoddart, J. B. Wolstenholme, D. J. Williams, *J. Chem. Soc. Perkin Trans. 2 1985*, 607; b) H. M. Colquhoun, S. M. Doughty, J. F. Stoddart, A. M. Z. Slawin, D. J. Williams, *ibid. 1986*, 253.
[209] J. Rebek, Jr., D. Nemeth, *J. Am. Chem. Soc. 107* (1985) 6738.
[210] W. H. Pirkle, T. C. Pochapsky, *J. Am. Chem. Soc. 108* (1986) 5627, 352; *109* (1987) 5975.
[211] Y. Rubin, F. Diederich, unpublished.
[212] F. Wudl, F. Gaeta, *J. Chem. Soc. Chem. Commun. 1972*, 107.
[213] E. P. Kyba, M. G. Siegel, L. R. Sousa, G. D. Y. Sogah, D. J. Cram, *J. Am. Chem. Soc. 95* (1973) 2691.
[214] S. T. Jolley, J. S. Bradshaw, R. M. Izatt, *J. Heterocycl. Chem. 19* (1982) 3.
[215] J. F. Stoddart, *Prog. Macrocyclic Chem. 2* (1981) 173.
[216] D. Sybilska, E. Smolková-Keulemansová in [26], Vol. 3, p. 173.
[217] D. W. Armstrong, T. J. Ward, A. Czech, B. P. Czech, R. A. Bartsch, *J. Org. Chem. 50* (1985) 5556.
[218] a) I. Takahashi, K. Odashima, K. Koga, *Tetrahedron Lett. 25* (1984) 973; b) *Chem. Pharm. Bull. 33* (1985) 3571.
[219] J. Canceill, L. Lacombe, A. Collet, *J. Am. Chem. Soc. 107* (1985) 6993.
[220] J. Rebek, Jr., B. Askew, P. Ballester, M. Doa, *J. Am. Chem. Soc. 109* (1987) 4119.
[221] Y. Rubin, K. Dick, F. Diederich, T. M. Georgiadis, *J. Org. Chem. 51* (1986) 3270.
[222] R. Dharanipragada, F. Diederich, *Tetrahedron Lett. 28* (1987) 2443.
[223] No correlation exists between the arbitrarily chosen absolute configuration at the chiral centers of compounds shown by perspective drawings and the experimentally determined sign of optical rotation.
[224] J. C. Barnes, J. D. Paton, J. R. Damewood, Jr., K. Mislow, *J. Org. Chem. 46* (1981) 4975.
[225] J. Winkler, E. Coutouli-Argyropoulou, R. Leppkes, R. Breslow, *J. Am. Chem. Soc. 105* (1983) 7198.
[226] J. Tabushi, Y. Kimura, K. Yamamura, *J. Am. Chem. Soc. 103* (1981) 6486.
[227] Y. Murakami, Y. Hisaeda, J. Kikuchi, T. Ohno, M. Suzuki, Y. Matsuda, *Chem. Lett. 1986*, 727.
[228] a) H. J. Schneider, R. Busch, *Angew. Chem. 96* (1984) 910; *Angew. Chem. Int. Ed. Engl. 23* (1984) 911; b) H. J. Schneider, N. K. Sangwan, *J. Chem. Soc. Chem. Commun. 1986*, 1787; c) H.-J. Schneider, A. Junker, *Chem. Ber. 119* (1986) 2815.
[229] R. Hershfield, M. L. Bender, *J. Am. Chem. Soc. 94* (1972) 1376.
[230] F. M. Menger, M. Ladika, *J. Am. Chem. Soc. 109* (1987) 3145.
[231] a) T. Matsui, K. Koga, *Tetrahedron Lett. 1978*, 1115; b) S. Sasaki, M. Kawasaki, K. Koga, *Chem. Pharm. Bull. 33* (1985) 4247.
[232] S. Sasaki, M. Shionoya, K. Koga, *J. Am. Chem. Soc. 107* (1985) 3371.
[233] M. Komiyama, I. Sugiura, H. Hirai, *J. Mol. Catal. 36* (1986) 271.
[234] T. Ikeda, R. Kojin, C. Yoon, H. Ikeda, M. Iijima, F. Toda, *J. Inclusion Phenom. 5* (1987) 93.
[235] H. Dugas, C. Penney: *Bioorganic Chemistry*, Springer, New York 1981.
[236] J. H. Fendler, E. J. Fendler: *Catalysis in Micellar and Macromolecular Systems*, Academic Press, New York 1975.
[237] For micellar catalysis see a) C. A. Bunton, L. S. Romsted in S. Patai (Ed.): *The Chemistry of Functional Groups, Suppl. B: The Chemistry of Acid Derivatives, Part II*, Wiley, New York 1979, p. 945; b) T. Kunitake, S. Shinkai, *Adv. Phys. Org. Chem. 17* (1981) 435; c) F. M. Menger, L. G. Whitesell, *J. Am. Chem. Soc. 107* (1985) 707; d) F. M. Menger, R. A. Persichetti, *J. Org. Chem. 52* (1987) 3451; e) R. A. Moss, K. W. Alwis, J. S. Shin, *J. Am. Chem. Soc. 106* (1984) 2651; f) R. A. Moss, S. Bhattacharya, P. Scrimin, S. Swarup, *ibid. 109* (1987) 5740.
[238] a) H.-D. Lutter, F. Diederich, *Angew. Chem. 96* (1986) 1125; *Angew. Chem. Int. Ed. Engl. 25* (1986) 1125; b) F. Diederich, L. Jiminez, H.-D. Lutter, unpublished.
[239] a) G. Schürmann, F. Diederich, *Tetrahedron Lett. 27* (1986) 4249; b) F. Diederich, G. Schürmann, I. Chao, *J. Org. Chem.*, in press.
[240] C. Walsh: *Enzymatic Reaction Mechanisms*, Freeman, San Francisco 1979.
[241] C. Walsh, *Acc. Chem. Res. 13* (1980) 148.
[242] T. C. Bruice, *Acc. Chem. Res. 13* (1980) 256.
[243] S. B. Ferguson, L. Jimenez, I. Chao, F. Diederich, unpublished.
[244] J. Crosby, R. Stone, G. E. Lienhard, *J. Am. Chem. Soc. 92* (1970) 2891.
[245] D. Hilvert, R. Breslow, *Bioorg. Chem. 12* (1984) 206.
[246] R. Breslow, *J. Am. Chem. Soc. 80* (1958) 3719.
[247] P. Haake, L. P. Bausher, W. B. Miller, *J. Am. Chem. Soc. 91* (1969) 1113.
[248] F. Diederich, *Chem. Unserer Zeit 17* (1983) 105.
[249] See [66a], Chap. 12, p. 311.
[250] D. Jaeger, D. Bolikal, *J. Org. Chem. 51* (1986) 1352.
[251] a) S. Pollack, J. Jacobs, P. G. Schultz, *Science (Washington, DC) 234* (1986) 1570; b) A. Tramontano, K. Janda, R. Lerner, *ibid. 234* (1986) 1566.
[252] a) K. D. Stewart, C. Radziejewski, E. T. Kaiser, *J. Am. Chem. Soc. 108* (1986) 3480; b) T. Nakatsuka, T. Sasaki, E. T. Kaiser, *ibid. 108* (1987) 3808.

When submitting manuscripts, authors of articles intended for publication as "Communications" are requested to read the "Notice to Authors" reproduced in the January issue of the journal following the list of contents; upon request, a copy can be obtained from the editorial office.

Equilibrium Structure, Stabilized Transition State, or Disorder in the Crystal? Studies of the Antiaromatic Systems Tetra-*tert*-butyl-*s*-indacene and Tetra-*tert*-butylcyclobutadiene by Low-Temperature Crystal Structure Analysis**

By *Jack D. Dunitz,* Carl Krüger, Hermann Irngartinger, Emily F. Maverick, Yu Wang,* and *Matthias Nixdorf*

The crystal structure of 1,3,5,7-tetra-*tert*-butyl-*s*-indacene **1** as determined at room temperature[1] shows effective D_{2h} symmetry of the carbon skeleton. Similarly, the

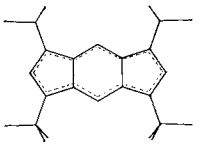

1

presence of only four ^{13}C-NMR signals that show no perceptible line broadening down to -130 °C for the twelve C atoms of the perimeter is consistent either with a very low energy barrier between the valence isomers or with a completely delocalized twelve-electron π system. According to calculations[1] (MINDO/3 method), the energy barrier is only about 8 kJ mol^{-1} for the tetrasubstituted molecule **1**, although it is considerably larger for the parent hydrocarbon.[2]

We now report results of a new, more accurate low-temperature (100 K) X-ray analysis of **1**, which substantiate and extend these indications.[3,4] Although the (crystallographic) molecular site symmetry is only C_i ($\bar{1}$), the molecular geometry (Fig. 1) shows no significant deviations from D_{2h} symmetry.

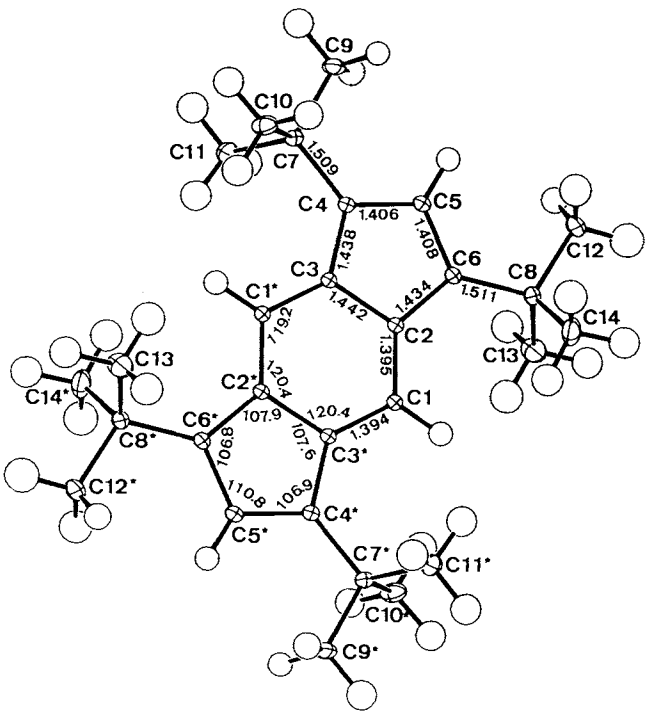

Fig. 1. ORTEP [27] drawing of **1** at 100 K; parameters from the HO refinement [3]. Bond lengths [10^2 pm] and angles [°] are indicated. Ellipsoids are scaled to enclose 50% probability.

Moreover, as described below, a detailed analysis of the anisotropic displacement parameters U^{ij} (ADPs)[5] of the carbon atoms gives no evidence for disorder between two sets of atomic positions for the skeletal atoms. We conclude that either the equilibrium structure of **1** has D_{2h} symmetry with a localized π system or we are observing not the ground-state molecular structure in the crystal but rather the transition state for the valence isomerization, which may be stabilized by crystal packing forces. The example of biphenyl, planar in its crystal structure, nonplanar as a free molecule, can serve as a precedent.[7]

Analysis of the ADPs with *Trueblood*'s THMA program[8] leads to the following indications:

(1) Calculation of mean-square displacement amplitudes (MSDAs)[9] along all interatomic vectors shows that the molecule does not behave as a rigid body in the crystal. The MSDAs between nonbonded pairs of atoms—and indeed the ellipsoids in Figure 1—reveal appreciable motions of the *tert*-butyl groups relative to the indacene skeleton. On the other hand, the rigid-bond criterion[10] is satisfied reasonably well, especially for the indacene skeleton, for which $\langle\Delta(\mathrm{MSDA})^2\rangle^{1/2} = 7$ pm^2.

(2) The translational (***T***) and librational (***L***) analysis,[11] including allowance for internal libration of the *tert*-butyl groups about the exocyclic bonds C4–C7 and C6–C8, leads to mean-square libration amplitudes, $\langle\phi^2\rangle$, of 9 and 20 (°)^2, respectively,[12] considerably larger than the eigenvalues of the **L** tensor (4.9, 0.9, 0.4 (°)^2, with the major eigenvalue approximately along the long axis of the molecule).[13]

[*] Prof. Dr. J. D. Dunitz
Laboratory of Organic Chemistry,
Swiss Federal Institute of Technology
Universitätstrasse 16, CH-8092 Zürich (Switzerland)
Prof. Dr. C. Krüger
Max-Planck-Institut für Kohlenforschung
Kaiser-Wilhelm-Platz 1, D-4330 Mülheim a. d. Ruhr (FRG)
Prof. Dr. H. Irngartinger, Dr. M. Nixdorf
Organisch-chemisches Institut der Universität
Im Neuenheimer Feld 270, D-6900 Heidelberg 1 (FRG)
Prof. Dr. E. F. Maverick
Los Angeles City College
Los Angeles, CA 90029 (USA)
Prof. Dr. Y. Wang
Department of Chemistry, National Taiwan University
Roosevelt Road, Section 4, Taipei (Taiwan)

[**] This work was supported by the Swiss National Science Foundation, the Deutsche Forschungsgemeinschaft, and the Fonds der Chemischen Industrie. We thank *K. H. Claus* (MPI Mülheim) für experimental assistance.

(3) Although the above model leads to reasonable agreement between observed and calculated U tensors ($\langle(\Delta U^{ij})^2\rangle^{1/2} = 15$ pm^2), the residual discrepancies show systematic features. In the direction perpendicular to the ring plane, U_{obsd} is significantly larger than U_{calcd} for the ring atoms C2, C3, and especially C5 ($\Delta U^{33} = 51$ pm^2); for C7 and C8, the reverse is true. Thus the model tends to ascribe too much motion to the quaternary C atoms C7 and C8, and too little to the ring atoms that are not attached to *tert*-butyl groups. This suggests that the ring atoms (especially C5) are moving in a direction perpendicular to the plane. Allowance for out-of-plane bending or buckling of the ring skeleton, as inferred in a variable-temperature study of naphthalene,[15] would reduce these discrepancies. Within the molecular plane there are no significant differences between U_{obsd} and U_{calcd} components for the ring atoms, whereas in an averaged structure involving superposition of two valence isomers with localized single and double bonds, we would expect $U_{obsd} > U_{calcd}$ to allow for the effect of disorder.[16] If the observed structure were such a superposition, the two sets of atomic positions could not differ from the averaged positions by more than about 3 pm.

The observed structure, if it is indeed the transition state for interconversion of the free molecules, may be stabilized relative to the structures with localized bonds by better packing of the *tert*-butyl groups. Model calculations suggest that the packing energy would be reduced by about 4 kJ mol^{-1} per *tert*-butyl group for the small in-plane displacements of these groups that would be associated with the reorganization of the indacene skeleton.

In contrast, a comparable analysis of the ADPs from a low-temperature study of tetra-*tert*-butylcyclobutadiene **2**[17] shows that in this crystal at 123 K there is still residual

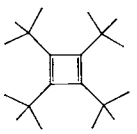

2

disorder of the atoms of the central four-membered ring, corresponding to the coexistence of both valence isomers (although not in equal amounts).

The room-temperature X-ray analysis of **2** led to a structure in which the sides of the slightly nonplanar four-membered ring were almost equal (146.4 and 148.3 pm).[18] This result was in conflict with those obtained for other cyclobutadiene derivatives where much larger differences (14–26 pm) between the ring bonds were observed.[19] On the basis of quantum-mechanical model calculations, *Borden* and *Davidson*[20] suggested that the bulky *tert*-butyl groups could exert a considerable "quadratization effect," but this was countered by *Ermer* and *Heilbronner*,[21] who argued from photoelectron spectroscopic evidence and force-field calculations that **2** must have a rectangular structure with appreciably different ring bond lengths. They proposed that the nearly square arrangement of the ring atoms found in the room-temperature analysis did not correspond to the actual molecular structure but rather to averaged atomic positions resulting from disorder among two rectangular structures. Indeed, ring bond lengths found in the subsequent low-temperature crystal structure analysis at 123 K were different (144.1 and 152.7 pm),[17] but the question of whether residual disorder was still present at this temperature was left open. From a detailed analysis of the anisotropic displacement parameters U^{ij}[5] of the carbon atoms in the 123 K structure, we now conclude that residual disorder is indeed still present at this temperature. The results are compatible with an averaged superposition of two mutually perpendicular rectangular rings with sides approximately 160 and 134 pm,[22] and with one orientation several times more probable than the other.

ADPs from the 123 K structure determination were analyzed, as for the indacene derivative **1**, with THMA.[8] Standard deviations of U tensor components are of the order of 5 pm^2. Casual inspection of the probability ellipsoids (Fig. 2) shows that those of the methyl group carbon atoms are systematically larger than those of the other atoms. Calculation of MSDAs[9] along interatomic vectors shows that in contrast to the indacene derivative **1** the rigid-bond criterion[10] is not obeyed for **2**. For example, for the C1–C6 bond Δ(MSDA) is 19 pm^2. This in itself is an indication of possible disorder. However, MSDA differences between nonbonded pairs of atoms are much larger (up to 100 pm^2) and indicate appreciable motions of the *tert*-butyl groups relative to the inner ring.[24]

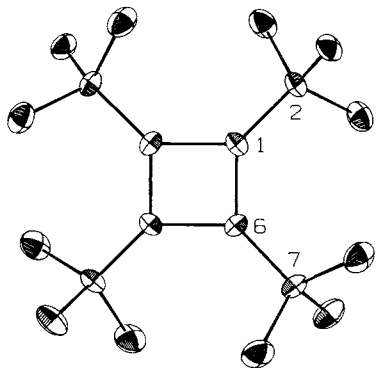

Fig. 2. ORTEP [26] drawing of **2** at 123 K. Ellipsoids are scaled to enclose 50% probability. Hydrogen atoms are omitted for clarity.

The T, L, and screw tensor (S) analysis, including internal libration of the two independent *tert*-butyl groups about the C1–C2 and C6–C7 bonds, leads to mean-square libration amplitudes $\langle\phi^2\rangle$ of 14 and 23 (°)^2 for the two internal motions, respectively.[12] These are several times larger than the eigenvalues of the L tensor (4.4, 2.4, 2.2 (°)^2, with the lowest value along the crystallographic twofold rotation axis; the molecule has effective D_2 symmetry but only one of the symmetry elements is imposed by the space group).[25]

The residual discrepancies between observed and calculated U tensors show systematic features. One of these is the striking excess of 51 and 31 pm^2 of the observed over the calculated tangential components of C1 and C6 (Table 1). This feature cannot be attributed to underestimation of the overall molecular libration (this would affect the outer atoms rather than the inner ones), but it is qualitatively in

Table 1. Calculated and observed mean-square displacement amplitudes [pm^2] for the ring atoms C1 and C6 in **2** along the tangential, radial, and ring-normal directions.

	Observed	Calculated
C1	221, 126, 170	170, 166, 154
C6	210, 126, 164	179, 157, 145

accord with the disorder model proposed by *Ermer* and *Heilbronner* (see Fig. 1 in Ref. [21]). In the crystal it is not necessary that the two perpendicular orientations of the rectangular ring have a common center (indeed, the above-mentioned Δ(MSDA) of 19 pm^2 between C1 and C6 suggests that they do not). However, if we wish to make a rough estimate of the proportions of major and minor orientation present, it simplifies the argument somewhat if we assume this condition to be satisfied and use the averaged tangential MSDA excess of 41 pm^2.

For equal occupancy of the two perpendicular orientations of a rectangular ring with sides of 134 and 160 pm[22] and a common center, we expect an excess MSDA of 84 pm^2 in the tangential direction (in agreement with *Ermer* and *Heilbronner*'s estimate of 80 pm^2[21]). For other occupancy factors p, the excess is then $336\,p(1-p)$ and hence $p \approx 0.86$ for the observed excess MSDA of 41 pm^2 at 123 K.[26]

These examples, 1,3,5,7-tetra-*tert*-butyl-*s*-indacene with indications of delocalization consistent with a stabilized transition state between two valence isomers, and tetra-*tert*-butylcyclobutadiene with evidence for disorder among the two isomers, show how ADPs derived from high-quality diffraction data can provide information about the nature and extent of mean displacements of atoms from their equilibrium positions and hence allow differentiation among alternative models compatible with these positions.

Received: July 7, 1987;
revised: December 28, 1987 [Z 2332/2333 IE]
German version: *Angew. Chem. 100* (1988) 415

CAS Registry numbers:
1, 101998-70-3; **2**, 66809-05-0.

[1] K. Hafner, B. Stowasser, H. P. Krimmer, S. Fischer, M. C. Boehm, H. J. Lindner, *Angew. Chem. 98* (1986) 646; *Angew. Chem. Int. Ed. Engl. 25* (1986) 630.

[2] For HMO arguments showing that **1** should have a more delocalized π system than the unsubstituted *s*-indacene, see also E. Heilbronner, Z.-z. Yang, *Angew. Chem. 99* (1987) 369; *Angew. Chem. Int. Ed. Engl. 26* (1987) 360.

[3] Crystal structure of **1**: monoclinic, space group $P2_1/n$, $Z=2$, $a=970.0(3)$, $b=1174.6(3)$, $c=1085.8(2)$ pm, $\beta=107.67°$, $T=100$ K, $\rho_{calcd}=1.06$ g cm^{-3}, $Mo_{K\alpha}$ radiation ($\lambda=71.069$ pm), $\mu=0.52$ cm^{-1} (no absorption correction applied), 22565 measured reflections, reduced to 5636 independent reflections ($R_{av}=0.022$), 4383 observed ($I>2\sigma(I)$), 207 parameters refined, $R=0.043$, $R_w=0.039$, $R_{HO}=0.030$ ($\sin\theta/\lambda>0.0065$ pm^{-1}). Measured reflections: $\pm h\ \pm k\ l$ $0<\theta<42°$, $\psi=0°$; $\pm h\ \pm k\ l$ $0<\theta<42°$, $\psi=15°$; $\pm h\ \pm k\ l$ $0<\theta<16°$, $\psi=-45/45°$. Normal data set 45 kV/32 mA; attenuated reflection set 50 kV/8 mA, 40 kV/8 mA. Further details of the crystal structure investigation may be obtained on request from the Fachinformationszentrum Energie Physik Mathematik, D-7514 Eggenstein-Leopoldshafen 2 (FRG), by quoting the number CSD-52900, the names of the authors, and the complete citation of the article.

[4] We thank Prof. *K. Hafner* for supplying samples and Prof. *H. J. Lindner* for sending the room-temperature crystal data and other information.

[5] U^{ij} are the components of the symmetric second-order tensor $\boldsymbol{U}$ which defines the matrix of second moments of the probability distribution function for each atom. They are obtained along with positional coordinates of the atoms by least-squares analysis of the experimental structure amplitudes from X-ray or neutron diffraction. The interpretation of ADPs is discussed in some detail in a recent review [6].

[6] J. D. Dunitz, V. Schomaker, K. N. Trueblood, *J. Phys. Chem.* (1988), in press.

[7] W. R. Busing, *Acta Crystallogr. Sect. A 39* (1983) 340.

[8] K. N. Trueblood, *Acta Crystallogr. Sect. A 34* (1978) 950. Several versions of this program are in circulation, the latest being THMA 11.

[9] The mean-square displacement amplitude in the direction of a unit vector $\boldsymbol{n}$ is given by $\boldsymbol{n}^T\boldsymbol{U}\boldsymbol{n}$, where the components of $\boldsymbol{n}$ are referred to unit-length reciprocal basis vectors.

[10] F. L. Hirshfeld, *Acta Crystallogr. Sect. A 32* (1976) 239.

[11] For the analysis of **1** described here, the screw tensor $\boldsymbol{S}$ vanishes because of the molecular site symmetry. In the $\boldsymbol{T}$, $\boldsymbol{L}$ analysis we used the parameters from refinement of the full data set, but results obtained with parameters from the HO refinement [3] are practically the same.

[12] As discussed by *V. Schomaker* and *K. N. Trueblood, Acta Crystallogr. Sect. A 40* Suppl. (1984) C-339 (see also [6]), these values correspond strictly not to $\langle\phi^2\rangle$ but to $\langle\phi^2\rangle+\langle\phi\lambda^{II}\rangle$, where $\langle\phi\lambda^{II}\rangle$ is the parallel component of the overall molecular libration. However, since the overall libration is here small compared with the internal libration, their quadratic average must also be small.

[13] Values of mean-square libration amplitudes $\langle\phi^2\rangle$ were also estimated by numerical integration of

$$\int \phi^2 \exp(-V(\phi)/RT)\,d\phi \Big/ \int \exp(-V(\phi)/RT)\,d\phi$$

where $V(\phi)$ was obtained from calculated potential energy curves [14] for step-by-step rotation of the *tert*-butyl groups about the appropriate axes without relaxation of the surrounding crystal structure. The calculated values of $\langle\phi^2\rangle$ are about 50% too small, but larger for C6-C8 than for C4-C7, as found in the ADP analysis.

[14] U. Shumueli, P. A. Kroon, *Acta Crystallogr. Sect. A 30* (1974) 768.

[15] C. P. Brock, J. D. Dunitz, *Acta Crystallogr. Sect. B 38* (1982) 2218.

[16] The U components arising from this kind of disorder would not be completely absorbed in a model involving additional librational motion.

[17] H. Irngartinger, M. Nixdorf, *Angew. Chem. 95* (1983) 415; *Angew. Chem. Int. Ed. Engl. 22* (1983) 403.

[18] H. Irngartinger, N. Riegler, K.-D. Malsch, K.-A. Schneider, G. Maier, *Angew. Chem. 92* (1980) 214; *Angew. Chem. Int. Ed. Engl. 19* (1980) 211.

[19] a) H. Irngartinger, H. Rodewald, *Angew. Chem. 86* (1974) 783; Angew. Chem. Int. Ed. Engl. 13 (1974) 740; b) L. R. J. Delbaere, M. N. G. James, N. Nakamura, S. Masamune, *J. Am. Chem. Soc. 97* (1975) 1973.

[20] W. T. Borden, E. R. Davidson, *J. Am. Chem. Soc. 102* (1980) 7958.

[21] O. Ermer, E. Heilbronner, *Angew. Chem. 95* (1983) 414; *Angew. Chem. Int. Ed. Engl. 22* (1983) 402.

[22] These bond lengths are chosen to agree with values found in other cyclobutadiene derivatives [18, 19a, 23].

[23] H. Irngartinger, M. Nixdorf, N. H. Riegler, A. Krebs, H. Kimling, J. Pocklington, G. Maier, K.-D. Malsch, K.-A. Schneider, *Chem. Ber.*, in press.

[24] R. E. Rosenfield, K. N. Trueblood, J. D. Dunitz, *Acta Crystallogr. Sect. A 34* (1978) 828.

[25] Calculations [13] reproduce the difference in internal motion between these groups but the values of $\langle\phi^2\rangle$ are too small. However, since the intramolecular overcrowding among the *tert*-butyl groups is so severe, allowance for correlated motion will certainly need to be included in a more realistic model.

[26] From the observed bond lengths of 144.1 and 152.7 pm we would estimate $p \approx 0.7$, assuming the same rectangular ring. For a more thorough discussion of the disorder on Δ(MSDA) values see K. Chandrasekhar, H. B. Bürgi, *Acta Crystallogr. Sect. B 40* (1984) 387.)

[27] C. K. Johnson: ORTEP-II: A FORTRAN Thermal-Ellipsoid Plot Program for Crystal Structure Illustrations (report ORNL-5138), Oak Ridge National Laboratory, Oak Ridge, TN, USA 1976.

Reaction of 1,3-Azaphosphinines with 2-*tert*-Butyl-1-phosphaethyne: 9-Aza-2,4,6-triphosphatetracyclo-[5.3.0.0^{2,4}.0^{3,6}]deca-8,10(1)-diene

By *Gottfried Märkl,* Stefan Dietl, Manfred L. Ziegler,* and *Bernd Nuber*

Recently, we reported the synthesis of 1,3-azaphosphinines **1** from 3-azapyrylium salts by O/P exchange with $(Me_3Si)_3P$.[1]

In contrast to phosphinines, which only undergo Diels-Alder reactions with highly reactive alkyne dienophiles (e.g., hexafluorobutyne) under drastic reaction conditions to give 1-phosphabarrelenes,[2] 1,3-azaphosphinines **1** react with all alkynes so far investigated even under mild condi-

[*] Prof. Dr. G. Märkl, S. Dietl
Institut für Organische Chemie der Universität
Universitätsstrasse 31, D-8400 Regensburg (FRG)
Prof. Dr. M. L. Ziegler, Dr. B. Nuber
Anorganisch-chemisches Institut der Universität
Im Neuenheimer Feld 270, D-6900 Heidelberg (FRG)

tions to give the [4+2] cycloadducts **2**. The initially formed heterobarrelenes **2** eliminate (substituted) benzonitrile, undergoing cycloreversion with aromatization to give the corresponding substituted phosphinines.[3]

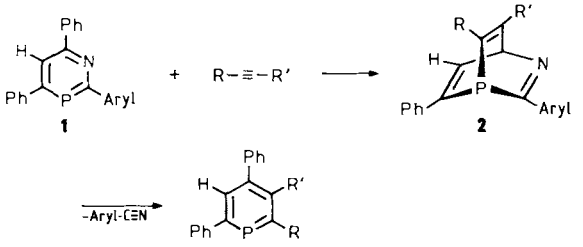

As heteroalkyne, 2-*tert*-butyl-1-phosphaethyne **3**[4] reacts with the 2,4,6-triaryl-substituted 1,3-azaphosphinines **1** at about 100°C in toluene (reaction bomb)—as investigated so far—completely different. The mass spectrum and elementary analysis show that **1** and **3** react in a molar ratio of 1:2 without elimination of (substituted) benzonitrile. Thus, a secondary product of the possibly expected 1,3-diphosphinine **4** is not present.

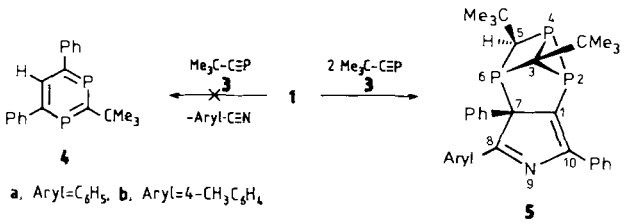

The crystal structure analysis (Fig. 1) shows that the tetracyclic triphosphane **5a** is formed from **1a**. It contains a 3*H*-pyrrole, a 1,3-diphosphacyclopentane, a 1,3-diphosphacyclobutane, and a diphosphacyclopropane system[5] (numbering of **5** according to IUPAC nomenclature).

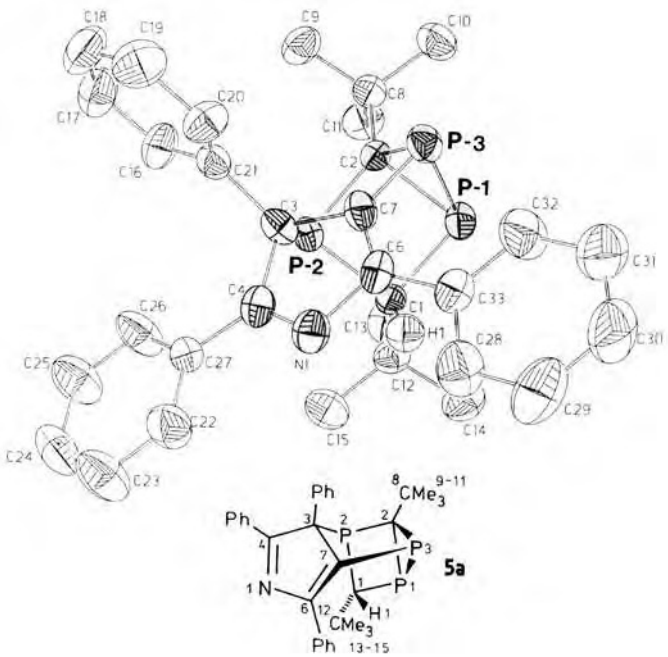

Fig. 1. Molecular structure of **5a** (arbitrary numbering) [5].

Thus, the six-membered 1,3-azaphosphinine system of **1** undergoes rearrangement and ring contraction to give a 3*H*-pyrrole system containing phosphorus in the *exo* position. The positions of the phenyl moieties and the nitrogen show that P-2 is derived from **1**.

The formation of **5** presumably begins with a cycloaddition of **3** at the 3,5 position of **1** to give the heterosemibullvalene **6**. This cycloaddition to give **6** may be initiated by a nucleophilic attack of the sp ethyne carbon atom in **3** on the $\lambda^3\sigma^2$ phosphorus of **1**; there exists a purely formal analogy to the cycloaddition of alkenes to benzene to give tetrahydrosemibullvalenes, which presumably occurs via the photochemically excited singlet state $^1B_{2u}$ ("prefulvene").[6]

Under the reaction conditions, **6** rearranges to give the secondary phosphane **7** having a dihydropentalene structure. The cycloaddition of the second molecule **3** begins with an ene reaction with the vinylphosphane structural element in **7** leading to the formation of **8**.[7] An intramolecular [2+2] cycloaddition of the two phosphaalkene units in **8** affords the 1,3-diphosphabutane and the diphosphapropane ring in **5**. It has not been possible so far to isolate intermediates, even by changing the stoichiometry or the reaction conditions.

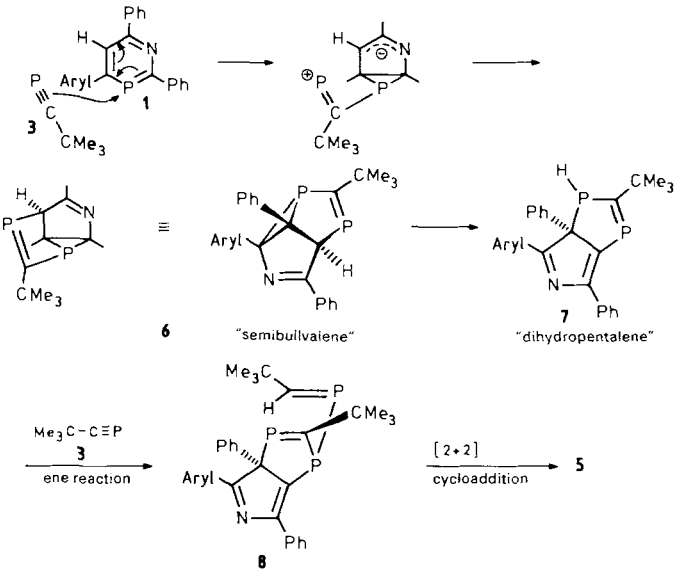

The exceptional stability of **5** is indicated by the mass spectra,[8] in which, apart from the molecular-ion peaks, only a few low-intensity fragment peaks are observed.

In the ^{1}H-NMR spectra of **5a** and **5b**,[8] the signal for H-1 is observed at $\delta = -0.76$ owing to strong shielding; the assignment of the signals for the *t*Bu groups was accomplished by means of NOE difference spectra. The assignment of the $^{31}P\{^1H\}$-NMR signal of P-1 ($\delta = -158.8$, d ($J_{P\text{-}1/P\text{-}3} = 176.0$ Hz)) and of P-3 ($\delta = -56.8$, d) is based on observations made for other diphosphacyclopropanes.[7] The downfield shift of P-2 ($\delta = +77.4$ (s)) lies far beyond the values observed for tertiary phosphanes, but is in agreement with more recent observations made for phosphanes of similar structure; however, an interpretation is not yet possible.[9]

Experimental Procedure

1a (0.81 g, 2.5 mmol) and **3** (0.55 g, 5.5 mmol) in dry toluene (4 mL) were allowed to react in a reaction bomb at 145°C for 48 h. After removal of the solvent, the reaction products were chromatographed on silica 60 (dried by heating under vacuum): **5a** was eluted with benzene/petroleum ether (1:1).

Recrystallization from $CHCl_3$/EtOH afforded yellow needles, m.p. = 214–215°C. Yield: 15%. **5b** was synthesized analogously, m.p. = 192–196°C. Yield: 10%. In addition to **5** and a small amount of azaphosphinine **1**, only amorphous, nondefinable products were obtained.

Received: August 6, 1987 [Z 2392 IE]
German version: *Angew. Chem. 100* (1988) 426

[1] G. Märkl, G. Dorfmeister, *Tetrahedron Lett. 28* (1987) 1093.
[2] G. Märkl, F. Lieb, *Angew. Chem. 80* (1968) 702; *Angew. Chem. Int. Ed. Engl. 7* (1968) 733; G. Märkl, F. Lieb, C. Martin, *Tetrahedron Lett. 1971*, 1215.
[3] T. Riedl, *Diplomarbeit*, Universität Regensburg 1987; see also [1].
[4] G. Becker, G. Gresser, W. Uhl, *Z. Naturforsch. B 36* (1981) 16.
[5] Crystal data of **5a**: crystal system, monoclinic, space group $C_{2h}^5 P2_1/C$, $a = 9.555(6)$, $b = 9.569(5)$, $c = 30.80(2)$ Å, $\beta = 95.64(5)°$, $V = 2802.5$ Å^3, $Z = 4$, $\rho_{calcd} = 1.25$ g cm^{-3}, $F_{000} = 1112$, $\mu(Mo_{K\alpha}) = 2.28$ cm^{-1}. In the range h 0/12, k 0/12, l −40/40; $3° < 2\theta < 55°$, 2473 measured reflections, (ω-scans; $J > 2\sigma(J)$) 2160 unique reflections (R_{merge} 0.032), Lp and absorption correction (empirical, 5 reflections ($4.3° \leq 2\theta \leq 35.8°$)), ψ scans, transmission factors: min. 0.84, max. 1.0, $Mo_{K\alpha}$ ($\lambda = 0.71069$ Å), graphite monochromator, AED II Siemens-Stoe. The structure was solved by direct methods (SHELXTL program), residual electron density: max. 0.30, min. −0.30 e/Å^3; $R = 0.057$, $R_w = 0.047$; Goof 1.71, shift/esd: −0.1 (max), 0.02 (mean); LS-parameter 310.—Origin of H-1: differential Fourier analysis.—Selected bond lengths [Å] and angles [°]: P1-P3 2.238(2), P1-C1 1.892(5), P1-C2 1.903(5), P2-C1 1.885(5), P2-C2 1.860(5), P2-C3 1.916(5), P3-C2 1.860(5), P3-C7 1.806(6), C3-C4 1.519(8), C3-C7 1.522(7), C4-N1 1.313(7), C6-N1 1.430(7), C6-C7 1.341(7); C1-P1-P3 98.4(2), C2-P1-P3 52.6(2), C2-P1-C1 85.6(2), C2-P2-C1 87.1(2), C3-P2-C1 98.4(2), C3-P2-C2 96.4(2), C2-P3-P1 54.4(2), C7-P3-P1 100.1(2), C7-P3-C2 96.4(2), P2-C1-P1 93.2(2), P2-C2-P1 93.7(2), P3-C2-P1 73.0(2), P3-C2-P2 109.1(3), C4-C3-P2 113.9(4), C7-C3-P2 102.1(4), C7-C3-C4 99.7(4), N1-C4-C3 112.5(5), C6-N1-C4 107.3(4), C7-C6-N1 112.0(4), C3-C7-P3 117.2(4), C6-C7-P3 131.6(4), C6-C7-C3 108.2(5). Further details of the crystal structure investigation may be obtained from the Fachinformationszentrum Energie, Physik, Mathematik GmbH, D-7514 Eggenstein-Leopoldshafen 2 (FRG), on quoting the depository number CSD-52613, the names of the authors, and the journal citation.
[6] See, for example, D. Bryce-Smith, H. C. Longuet-Higgins, *Chem. Commun. 1966*, 593; D. Bryce-Smith, *Pure Appl. Chem. 16* (1968) 47.
[7] The ene reactions of phosphaalkynes **3** with cyclic phosphaalkenes were recently described by E. P. O. Fuchs, W. Rösch, M. Regitz, *Angew. Chem. 99* (1987) 1058; *Angew. Chem. Int. Ed. Engl. 26* (1987) 1011. The diphosphacyclopropane derivatives described there exhibit $\delta(^{31}P)$ values of −165 to −210 ($J(P/P) = 150$–158 Hz).
[8] **5a**: MS (70 eV): $M^{\oplus\ominus}$, m/z 525 (100%), $[M - C_4H_8]^{\oplus\ominus}$, 469 (11%); ^{1}H-NMR (250 MHz, $CDCl_3$): H-1: $\delta = -0.76$ (d, $J = 2.0$ Hz), tBu(CH): 1.03 (s), tBu(C): 0.71 (s), aromat. H: 7.15–7.60 (m, 11H), 7.94–7.98 (m, 2H), 8.34–8.47 (m, 2H); UV (acetonitrile): $\lambda_{max} = 360$ nm ($\varepsilon = 4700$).—**5b**: MS (70 eV): $m^{\oplus\ominus}$, m/z 539 (100%), $[M - {}^{\ominus}CH_3]^{\oplus}$, 524 (1%), $[M - C_4H_8]^{\oplus\ominus}$, 483 (4%), $[M - {}^{\ominus}C_4H_9]^{\oplus}$, 482 (4%), $M^{2\oplus}$, 269.5 (2%); ^{1}H-NMR (250 MHz, $CDCl_3$): H-1: $\delta = -0.76$ (d, $J = 2.0$ Hz), tBu(CH): 1.02 (s), tBu(C): 0.71 (s), CH_3: 2.32 (s), aromat. H: 7.11–7.24 (m, 4H), 7.42–7.61 (m, 6H), 7.85–7.89 (m, 2H), 8.42–8.46 (m, 2H); UV (acetonitrile): $\lambda_{max} = 371$ nm ($\varepsilon = 6600$).
[9] L. D. Quin, K. C. Caster, J. C. Kisalus, K. A. Mesch, *J. Am. Chem. Soc. 106* (1984) 7021; L. D. Quin, F. C. Bernhardt, *Magn. Reson. Chem. 23* (1985) 929; G. Märkl, H. J. Beckh, K. K. Mayer, M. L. Ziegler, T. Zahn, *Angew. Chem. 99* (1987) 255; *Angew. Chem. Int. Ed. Engl. 26* (1987) 236; G. Märkl, E. Eckl, U. Jakobs, M. L. Ziegler, B. Nuber, *Tetrahedron Lett. 28* (1987) 2119.

The Fluoronium Ions $H_2F^{\oplus}$ and $H_3F_2^{\oplus}$: Characterization by Crystal Structure Analysis**

By *Dietrich Mootz** and *Klemens Bartmann*

In relation to their existence, structure, and hydrogen bonding in the solid state, mostly in hydrates of strong acids, oxonium ions, such as $H_3O^{\oplus}$ and $H_5O_2^{\oplus}$, but also species containing more water, have been thoroughly investigated by crystal structure analysis.[1] A corresponding characterization of fluoronium ions, in particular $H_2F^{\ominus}$ and $H_3F_2^{\oplus}$, has so far been completely missing. It has now been accomplished for the first time, viz. for crystalline compounds in the system hydrogen fluoride–antimony pentafluoride.

According to an IR-spectroscopic study, this system as the strongest known liquid superacid[2] contains the $H_3F_2^{\oplus}$ ion as the predominant cationic species for concentrations up to 40 mol% SbF_5, whereas at higher concentrations the $H_2F^{\oplus}$ ion is observed.[3] Concerning the formation of solid phases in this system, two investigations yield largely contradictory results.[4] In initial examinations of our own, we managed to grow single crystals of two phases at temperatures between −20 and −30°C, containing 40 and 50 mol% SbF_5 (molecular formulae $3HF \cdot 2SbF_5$ and $HF \cdot SbF_5$, respectively), and characterize them by X-ray structure analysis as the fluoronium salts **1** and **2**.[5]

$H_3F_2^{\oplus}Sb_2F_{11}^{\ominus}$ **1** $H_2F^{\oplus}Sb_2F_{11}^{\ominus}$ **2**

The $H_3F_2^{\oplus}$ ion of **1** (Fig. 1) is located on a symmetry center of the space group and thus has *trans* conformation. With an F···F distance of 2.30(1) Å its inner hydrogen bond is only slightly weaker than the strongest known hydrogen bonds (F···F down to 2.26 Å) in a series of hydrogen difluorides[6] and poly(hydrogen fluorides).[7] By longer hydrogen bonds of 2.41(1) Å the cations are linked with the anions in infinite chains. The dioctahedral $Sb_2F_{11}^{\ominus}$ ion is also centrosymmetric and thus its central fluorine bridge linear.

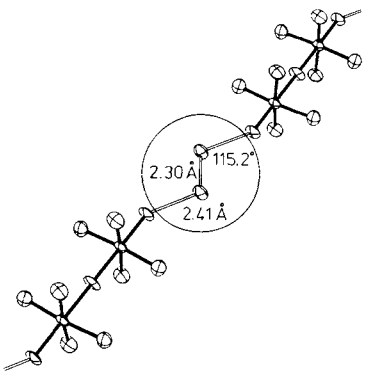

Fig. 1. Detail of the crystal structure of **1**. The fluoronium ion $H_3F_2^{\oplus}$ with its hydrogen bonds is shown in the circle (without the hydrogen atoms, which were not localized in the structure analysis). Thermal ellipsoids at the 50% probability level.

In the structure of **2** the ions occupy general positions. With much longer and less gradated F···F distances to the anions (six distances between 2.64 and 2.78 Å) the $H_2F^{\oplus}$ ion exhibits orientational disorder. The bridging angle of the anion amounts to 144.2(3)°.

Received: September 4, 1987 [Z 2424 IE]
German version: *Angew. Chem. 100* (1988) 424

CAS Registry numbers:
$H_2F^{\oplus}$, 12206-67-6; $H_3F_2^{\oplus}$, 112481-61-8;
$H_3F_2^{\oplus}Sb_2F_{11}^{\ominus}$, 112482-63-0; $H_2F^{\oplus}Sb_2F_{11}^{\ominus}$, 112482-64-1.

[*] Prof. Dr. D. Mootz, Dipl.-Chem. K. Bartmann
Institut für Anorganische Chemie und Strukturchemie der Universität Universitätsstrasse 1, D-4000 Düsseldorf 1 (FRG)

[**] Fluorides and Fluoro Acids, Part 19. This work was supported by the Fonds der Chemischen Industrie and by the Deutsche Forschungsgemeinschaft. Part 18: D. Boenigk, D. Mootz, *J. Am. Chem. Soc.*, in press.

[1] a) C. I. Ratcliffe, D. E. Irish in F. Franks (Ed.): *Water Science Reviews, An Annual Journal, Vol. 2*, Cambridge University Press, Cambridge 1986. b) I. Taesler, *Acta Univ. Upsal. Abstr. Uppsala Diss. Fac. Sci. 591* (1981) 1; c) J.-O. Lundgren, I. Olovson in P. Schuster, G. Zundel, C. Sandorfy (Eds.): *The Hydrogen Bond, Vol. II*, North-Holland, Amsterdam 1976, p. 471.

[2] G. A. Olah, G. K. S. Prakash, J. Sommer: *Superacids*, Wiley-Interscience, New York 1985, p. 48.
[3] B. Bonnet, G. Mascherpa, *Inorg. Chem. 19* (1980) 785.
[4] a) B. Bonnet, C. Belin, J. Potier, G. Mascherpa, *C. R. Hebd. Séances Acad. Sci. Ser. C 281* (1975) 1011; b) V. K. Ezhov, *Russ. J. Inorg. Chem. 17* (1972) 345.
[5] Crystal growth and structure determination: miniature zone-melting with focused heat radiation (D. Brodalla, D. Mootz, R. Boese, W. Osswald, *J. Appl. Crystallogr. 18* (1985) 316) in sealed capillaries made of Teflon PFA; Syntex $P2_1$ diffractometer equipped with a low-temperature device: $Mo_{K\alpha}$ radiation, graphite monochromator, ω scan. **1** at -20°C: space group $P\bar{1}$, $Z=1$; $a=5.268(4)$, $b=6.653(4)$, $c=7.479(5)$ Å, $\alpha=115.90(5)$, $\beta=93.65(6)$, $\gamma=94.93(6)$°; $2\theta_{max}=65$°; 1465 unique observed reflections, $R=0.049$, no improvement upon refinement in $P1$. **2** at -155°C: $P2_12_12_1$, $Z=4$; $a=7.241(4)$, $b=9.704(3)$, $c=12.956(3)$ Å; $2\theta_{max}=70$°, 2159 unique observed reflections, $R=0.047$. Owing to the strongly scattering Sb atoms, the H atoms, which are presumed to be partially disordered in the two structures, could not be definitely localized. Further details of the crystal structure determinations may be obtained from the Fachinformationszentrum Energie, Physik, Mathematik GmbH, D-7514 Eggenstein-Leopoldshafen 2 (FRG), on quoting the depository number CSD-52728, the names of the authors, and the journal citation.
[6] J. Emsley, *Chem. Soc. Rev. 9* (1980) 91.
[7] a) D. Mootz, D. Boenigk, *Z. Anorg. Allg. Chem. 544* (1987) 159; b) *J. Am. Chem. Soc. 108* (1986) 6634.

The Crystal Structure of Hypofluorous Acid: Chain Formation by O–H···O Hydrogen Bonds**

By *Wolfgang Poll, Gottfried Pawelke, Dietrich Mootz,** and *Evan H. Appelman*

Hypofluorous acid, HOF, can be isolated only at very low temperature as an intermediate of the well-known reaction of fluorine with water to hydrogen fluoride and oxygen.[1] So far, it is the only hypohalogenous acid obtained pure in condensed phase. Initial IR- and Raman-spectroscopic examinations of the solid-state structure of HOF[2] led to the assumption that the molecules are linked in planar zigzag chains by O–H···F hydrogen bonds. However, according to a recent interpretation of the data, supported by the results of theoretical calculations, O–H···O type hydrogen bonds are more probable.[3] We have now carried out a single-crystal X-ray structure analysis which confirms the linking of the molecules by O–H···O hydrogen bonds to form infinite angular chains.

Due to the ready and often explosive decomposition of the substance even at low temperatures, the handling of samples was quite difficult. A tube made of Teflon-PFA, with its middle section drawn to a capillary ca. 60 cm long, was attached to a vacuum system at both ends, evacuated, and then dipped into liquid nitrogen. An amount of roughly one drop of the compound, prepared by means of a circulation method,[4] was condensed from a cold trap (-78 °C) into one of the narrowing ends of the tube. From there it was sucked as a liquid into a part of the capillary suitable for the X-ray measurements and at last resolidified. After sealing the capillary at both ends of the solid, it had a length of ca. 3 cm and was fixed mechanically in a Lindemann glass capillary which was then mounted on a four-circle diffractometer (Syntex $P2_1$) equipped with a low-temperature device.

The sample was again liquefied, apart from a tiny residue, and this nucleus was used to grow a single crystal by slowly lowering the temperature (6 K/h) from a starting point at -130 °C. After further cooling to -160 °C, the dimensions and symmetry of the lattice were determined and the reflection intensities of one hemisphere in the range of $3° \leq 2\theta \leq 70°$ were measured (ω scan). The determination and refinement of the structure were carried out with the common methods using the program SHELXTL (Nicolet) on an ECLIPSE S/140 (Data General) computer.[5]

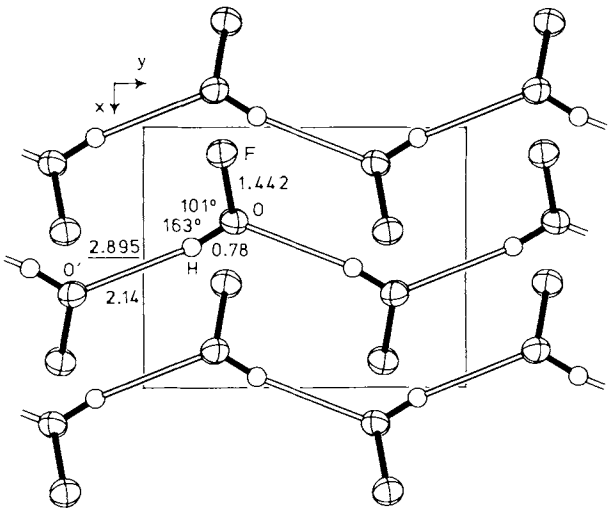

Fig. 1. Structure of HOF in the crystal with interatomic distances [Å] and angles [°] (O···O' distance of the hydrogen bond underlined). The standard deviations are 0.001 Å for the distances O-F and O···O', 0.02 Å for O-H and H···O, and 1° for the angles. The atom O' is generated from the atom O by the operation of a 2_1 screw axis parallel to the *b* axis (symmetry operation $1-x, -1/2+y, 1/2-z$). The chains appearing to be contiguous in the drawing are displaced in the *z* direction by half a lattice constant *c*. The thermal ellipsoids are drawn at the 50% probability level.

The geometry of the molecule obtained (Fig. 1) is in good agreement with that in the gaseous state;[6] only the O-H bond shows the usual systematic shortening, due to the X-ray method, as compared to the distance between the nuclei in question. The rather small bond angle may result from intramolecular Coulomb attraction of opposite charges of the hydrogen and the fluorine atom. Presumably in this connection the clearly dominating proton acceptor of the *intermolecular* hydrogen bonding is the oxygen atom. By almost linear O–H···O hydrogen bonds the molecules are linked to form angular chains (Fig. 1). The chains have the direction [010]; their polarity alternates along [100].

Received: September 16, 1987 [Z 2430 IE]
German version: *Angew. Chem. 100* (1988) 425

CAS Registry number:
HOF, 14034-79-8.

[*] Prof. Dr. D. Mootz, Dr. W. Poll
Institut für Anorganische Chemie und Strukturchemie der Universität
Universitätsstrasse 1, D-4000 Düsseldorf 1 (FRG)
Dr. G. Pawelke
Anorganische Chemie, FB 9, Universität - Gesamthochschule
Postfach 100127, D-5600 Wuppertal 1 (FRG)
Dr. E. H. Appelman
Chemistry Division, Argonne National Laboratory
9700 South Cass Avenue, Argonne, IL 60439 (USA)

[**] Fluorides and Fluoro Acids, Part 20. This work was supported by a NATO Research Grant, by the Fonds der Chemischen Industrie, and by the Office of Basic Energy Sciences, Division of Chemical Sciences, U. S. Department of Energy (*E. H. A.*). Part 19: D. Mootz, K. Bartmann, *Angew. Chem. 100* (1988) 424; *Angew. Chem. Int. Ed. Engl. 27* (1988) 391.

[1] E. H. Appelman, R. C. Thompson, *J. Am. Chem. Soc. 106* (1984) 4167.
[2] E. H. Appelman, W. W. Wilson, H. Kim, *Spectrochim. Acta A 37* (1981) 385; H. Kim, E. H. Appelman, *J. Chem. Phys. 76* (1982) 1664.

[3] K. O. Christe, *J. Fluorine Chem. 35* (1987) 621.
[4] E. H. Appelman, A. W. Jache, *J. Am. Chem. Soc. 109* (1987) 1754.
[5] Crystallographic data: $a=4.075(1)$, $b=5.040(1)$, $c=5.939(2)$ Å; $P2_12_12_1$; $Z=4$; 329 observed unique reflections; $R=0.027$. Coordinates (atom, x, y, z): F, 0.10128(9), 0.24300(9), 0.34039(9); O, 0.36012(12), 0.28006(11), 0.17792(11); H, 0.460(3), 0.149(4), 0.194(2). Further details of the crystal structure investigation may be obtained from the Fachinformationszentrum Energie, Physik, Mathematik GmbH, D-7514 Eggenstein-Leopoldshafen 2 (FRG), on quoting the depository number CSD-52727, the names of the authors, and the journal citation.
[6] H. Kim, E. F. Pearson, E. H. Appelman, *J. Chem. Phys. 56* (1972) 1; E. F. Pearson, H. Kim, *ibid. 57* (1972) 4230.

Cyclodextrins Increase Surface Tension and Critical Micelle Concentrations of Detergent Solutions

By *Wolfram Saenger** and *Anke Müller-Fahrnow*

The amphiphilic detergent molecules have a characteristic tendency to self-aggregate in aqueous solution such that their hydrophobic parts are removed from and their hydrophilic parts are exposed to the solvent. At low concentrations, the detergents form a variety of low-molecular-weight aggregates in solution, and monolayers are formed at the surface of the solvent which reduces the surface tension. Above the "critical micelle concentration" (*cmc*), micelles coexist in solution. It should in principle be possible to destroy the surface monolayers and the micelles, and to change the properties of the detergent solutions, by transferring the amphiphilic molecules to bulk solvent, i.e., by making them better soluble.

Based on this assumption, we have added cyclodextrins to detergent solutions, because these cyclically closed oligosaccharides with six, seven, or eight α-D-glucoses per macrocycle (α-, β-, γ-cyclodextrins) are able to form inclusion complexes[1,2] and have been used to enhance the solubility of organic molecules in water.[3,4]

The central cavity of the cyclodextrins is of hydrophobic character and has a diameter of 5 Å (α), 6–7 Å (β), and 7–8 Å (γ),[1,2] which is ideally suited to accommodate the hydrophobic, aliphatic part of the chosen detergent molecules with a diameter of about 5 Å (*n*-dodecylmaltoside (*n*-DM), *N*,*N*-dimethyl-*N*-lauryl-*N*-amine oxide (LDAO), decanoyl-*N*-methylglucamide (MEGA-10), β-octylglucoside (β-OG), Triton X-100). Moreover, the rims of the cyclodextrins are lined with OH groups, which should be able to form hydrogen bonds with the hydrophilic parts of the enclosed amphiphilic molecules and thus add to the stability of the formed complexes.

Experiments were carried out by the ring removal method with an interfacial tensiometer based on the concept of *Lecomte du Noüy*. The detergent solution (20 mL) was contained in a quartz beaker thermostated at 20 °C, in which a platinum ring was immersed. The ring was attached to a balance and by lowering the beaker, the surface tension (σ) could directly be measured in mN m^{-1} when the surface film broke. As calibration, pure water was used ($\sigma \approx 72$ mN m^{-1}).

Solutions of the detergents used were prepared with concentrations about 10 times the literature *cmc* values, and then diluted in series to afford solutions with concentration ratios of 1 : 1/2 : 1/4 : 1/8, etc. The surface tensions of these solutions were first measured and then a 10-, 100-, or 300-μL aliquot of a 10^{-1} M α-cyclodextrin solution was added to each of the 20-mL solutions and the surface tension again measured. The obtained values were plotted versus the logarithms of the detergent concentrations to derive the *cmc* (see the results for *n*-DM in Fig. 1a). For *n*-DM, we have also added β- and γ-cyclodextrin (Fig. 1b, c) and the permethylated tri-*O*-methyl-β-cyclodextrin (Fig. 2) to study the dependence of surface tension and *cmc* of the detergent solutions on ring size and hydrophilic character of the cyclodextrin.

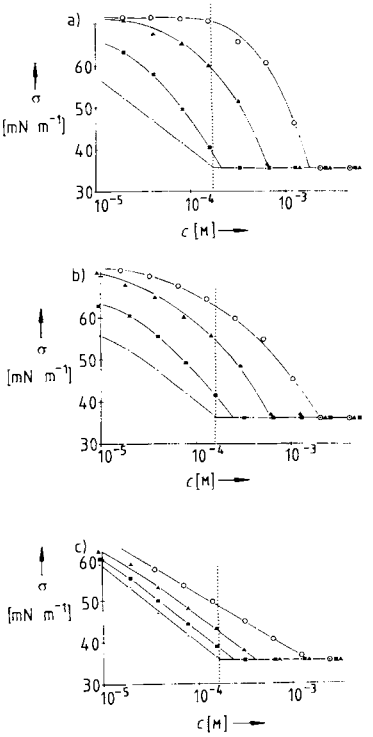

Fig. 1. Dependence of surface tension σ on the concentration c of the detergent *n*-DM without (•) and with added cyclodextrin. a) ■ 10^{-4} M, ▲ 6×10^{-4} M, ○ 21×10^{-4} M α-cyclodextrin. b) ■ 10^{-4} M, ▲ 5.7×10^{-4} M, ○ 17.4×10^{-4} M β-cyclodextrin. c) ■ 6×10^{-4} M, ▲ 20×10^{-4} M, ○ 66.3×10^{-4} M γ-cyclodextrin. The concentration at the vertical dotted line corresponds to the *cmc* of *n*-DM in water.

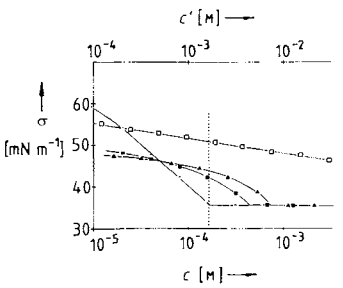

Fig. 2. Dependence of surface tension σ on the concentration c of the detergent *n*-DM without (•) cyclodextrin and in the presence of 5.66×10^{-4} M (■) and 17.44×10^{-4} M (▲) tri-*O*-methyl-β-cyclodextrin. Additional measurements were carried out without detergent (□) and with varying concentration c of tri-*O*-methyl-β-cyclodextrin (top abscissa). The dotted line corresponds to the *cmc* of *n*-DM in water.

[*] Prof. Dr. W. Saenger, Dipl. Biochem. A. Müller-Fahrnow
Institut für Kristallographie
Takustrasse 6, D-1000 Berlin 33

[**] We are grateful to *Barbara Saenger* for carrying out the measurements, and to the Institut für Physikalische Chemie, Freie Universität Berlin, for providing the Interfacial Tensiometer. This work was supported in part by the Deutsche Forschungsgemeinschaft (Sonderforschungsbereich 312, Teilprojekt D1) and by the Fonds der Chemischen Industrie.

For all the investigated detergents, the addition of α-cyclodextrin shifts the *cmc* to higher concentrations by up to one order of magnitude, depending on the detergent. A similar effect is observed with the surface tension, as indicated by the dotted line in Figure 1 and by the data in Table 1. For *n*-DM and LDAO, the addition of 2.1×10^{-3} and 6.5×10^{-3} M α-cyclodextrin, respectively, shifts the surface tension from that measured at the *cmc* (ca. 36 mN m^{-1}) to that of pure water.

The change of surface tension induced by 6.5×10^{-3} M α-cyclodextrin at *cmc* condition is medium for MEGA-10 (56 mN m^{-1}) but only modest for the other detergents used, Triton X-100 and β-OG (see Table 1).

Table 1. Dependence of *cmc* and surface tension of detergents on the concentration of added α-, β-, and γ-cyclodextrin (α-CD, β-CD, γ-CD).

Detergent and added cyclodextrin	*cmc* (M) (Literature values in parentheses)	σ at *cmc* of pure detergent [mN m^{-1}]
n-DM	1.7×10^{-4}	35.8
	(1.6×10^{-4})	
10^{-4} M α-CD	2×10^{-4}	38.5
6×10^{-4} M α-CD	6.2×10^{-4}	58.5
21×10^{-4} M α-CD	18×10^{-4}	70.2
10^{-4} M β-CD	2.4×10^{-4}	41.2
5.7×10^{-4} M β-CD	6×10^{-4}	54.5
17.4×10^{-4} M β-CD	2×10^{-3}	63.0
6×10^{-4} M γ-CD	2.3×10^{-4}	39.0
20×10^{-4} M γ-CD	4×10^{-4}	43.5
66.3×10^{-4} M γ-CD	1.4×10^{-3}	49.2
LDAO	2.35×10^{-3}	36.0
	(2.1×10^{-3})	
5×10^{-4} M α-CD	3.2×10^{-4}	41.5
20×10^{-4} M α-CD	6.4×10^{-4}	59.8
65×10^{-4} M α-CD	12.5×10^{-4}	72.0
MEGA-10	2.6×10^{-2}	33.6
	(3×10^{-2})	
5×10^{-4} M α-CD	2.8×10^{-2}	34.0
20×10^{-4} M α-CD	3.2×10^{-2}	38.0
65×10^{-4} M α-CD	4.6×10^{-2}	56.0
β-OG	23×10^{-3}	32.5
	(24.5×10^{-3})	
5×10^{-4} M α-CD	$23 \times \times 10^{-3}$	32.5
20×10^{-4} M α-CD	28×10^{-3}	34
65×10^{-4} M α-CD	32×10^{-3}	37
Triton X-100	1.75×10^{-4}	32.5
	(2×10^{-4})	
5.3×10^{-3} M α-CD	3.6×10^{-4}	38.2
17.1×10^{-3} M α-CD	5.8×10^{-4}	43.7

For the larger analogues β- and γ-cyclodextrin and for the permethylated β-cyclodextrin, a systematic study was only performed with *n*-DM. The effects are smaller with β-cyclodextrin and even more reduced with γ-cyclodextrin (Table 1). As to the permethylated β-cyclodextrin, it gives rise to a large increase in *cmc*, which is, however, smaller compared to unmethylated β-cyclodextrin (cf. Figs. 1b and 2). The change in surface tension is much less with permethylated β-cyclodextrin and, in the range of measurement, does not exceed 50 mN m^{-1}. At a detergent concentration of 5×10^{-4} M the data points describing surface tension in the presence of the permethylated β-cyclodextrin even cross that found for pure detergent, suggesting that permethylated β-cyclodextrin itself reduces the surface tension. In order to test this finding, the surface tension of aqueous solutions of permethylated β-cyclodextrin was measured (see Fig. 2). It is in fact surface active, but the concentration dependence is low.

The effects of the cyclodextrins on the surface tension and on the *cmc* of the different detergents studied here can be explained with the formation of inclusion complexes. This interpretation is suggested by the complex-forming ability of the cyclodextrins for *n*-DM which decreases in the series α- > β- > γ-cyclodextrin, probably because the fit of the aliphatic part of the detergent is tightest with α-cyclodextrin with a cavity diameter of ca. 5 Å. We have tried to determine the equilibrium constants assuming a simple 1 : 1 complex formation. Since we did not obtain a consistent value from the measured data, we have to infer that the complex formation between the detergents and the cyclodextrins is of a more complicated nature.

The detergent molecules become more water soluble by inclusion complexation, and are transported from the micelles or from the surface of the solution into bulk aqueous solvent. This obviously interferes with the aggregation of the detergent molecules into micelles, thereby shifting the *cmc* to higher concentration, and, as is indicated by the large rise in surface tension, it also removes the amphiphilic molecules from the surface monolayer.

The addition of cyclodextrins to detergent solutions can be used to advantage in all cases where micelles have to be destroyed or where the surface tension should be increased, e.g., in order to avoid foaming. The detergents chosen in this study were taken from our work with membrane proteins, but we expect that the effects also apply to other detergents as long as they are able to form inclusion complexes with the cyclodextrins.

Received: August 13, 1987 [Z 2399 IE]
German version: *Angew. Chem. 100* (1988) 429

[1] J. Szejtli: *Cyclodextrins and their Inclusion Complexes*, Akadémiai Kiadó, Budapest 1982.
[2] W. Saenger, *Angew. Chem. 92* (1980) 343; *Angew. Chem. Int. Ed. Engl. 19* (1980) 344.
[3] J. L. Lach, W. A. Pauli, *J. Pharm. Sci. 55* (1966) 32.
[4] K. H. Frömming, I. Weyermann, *Arch. Pharm. (Weinheim) 305* (1972) 290.

Methylrhenium Oxides: Synthesis from R_2O_7 and Catalytic Activity in Olefin Metathesis**

By *Wolfgang A. Herrmann,* Josef G. Kuchler, Josef K. Felixberger, Eberhardt Herdtweck,* and *Werner Wagner*

The system Re_2O_7/Al_2O_3 is an effective heterogeneous catalyst for carrying out olefin metatheses under mild conditions. Its activity can be further increased by the addition of alkyltin compounds SnR_4, and tin-containing cocatalysts are essential for the metathesis of *functionalized* olefins (e.g., unsaturated carboxylic esters and nitriles), which is of special industrial importance.[1] Since the first synthesis of hexamethylrhenium(VI) and several alkylrhenium oxides was reported by *Wilkinson* et al., the general accessibility of alkyl complexes of rhenium is no longer in question.[2] However, there has been little subsequent investiga-

[*] Prof. Dr. W. A. Herrmann, Dipl.-Chem. J. G. Kuchler, Dipl.-Chem. J. K. Felixberger, Dr. E. Herdtweck, Dipl.-Chem. W. Wagner
Anorganisch-chemisches Institut der Technischen Universität München
Lichtenbergstrasse 4, D-8046 Garching (FRG)

[**] Multiple Bonds between Main-Group Elements and Transition Metals, Part 50.—Part 49: W. A. Herrmann, R. A. Fischer, E. Herdtweck, *J. Organomet. Chem. 329* (1987) C 1.

tion of this class of substances and, therefore, virtually nothing is known about the chemistry of rhenium-containing metathesis catalysts.[1f] We have now found that simple methylation of dirhenium heptoxide provides a straightforward, extremely useful approach to these catalysts.

The components of the catalyst, dirhenium heptoxide and tetramethyltin, react rapidly and quantitatively in refluxing THF (Scheme 1) to give the mononuclear com-

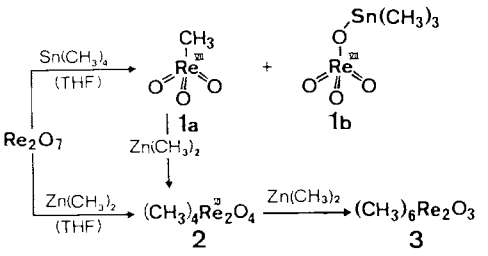

Scheme 1.

pounds trioxomethylrhenium(VII) **1a** and trioxo(trimethylstannoxy)rhenium(VII) **1b** (Scheme 1). The organorhenium oxide **1a**, which is stable toward air and moisture, can—like its CD_3 derivative **1a'**—be isolated from the crude product by vacuum sublimation (50–70 °C/10^{-2} torr) and is obtained as colorless, strongly refractive needles (Table 1). By way of contrast, the perrhenium ester **1b** can be extracted with THF from the residue remaining after sublimation. The (redox-neutral) monomethylation stage is not surpassed even if an excess of tetramethyltin is used. Re_2O_7 also reacts with other alkyltin compounds. If their alkyl groups contain β hydrogen atoms, however, low-valent rhenium oxides are formed with alkane/alkene liberation (e.g., C_4H_{10}/*cis*- and *trans*-C_4H_8 in the case of tetra(*n*-butyl)tin); an analogous reaction had been observed in the reaction of $Sn(n\text{-}C_4H_9)_4$ with $[(\eta^5\text{-}C_5H_5)ReCl_4]$.[3] The corresponding alkylsilanes, e.g., $Si(CH_3)_4$, do not react with dirhenium heptoxide under comparable conditions.

Until now, **1a** has only been accessible by oxidation of paramagnetic $[(CH_3)_4ReO]$ with O_2, a long and laborious route, which was not always reproducible;[4a] owing to the poor accessibility of **1a**, nothing was known about its chemistry, in contrast to the case for the structurally analogous π-complex $[(\eta^5\text{-}C_5Me_5)ReO_3]$.[5] The perrhenium ester **1b**[4b] is also now available for the first time by a clearly defined route and in an analytically pure form.

The methylrhenium oxide **1a** effects the metathesis of acyclic olefins in the presence of $AlCl_3$ even at room temperature; an example is the conversion of 2-pentene to 2-butene and 3-hexene (*cis/trans* mixture). In addition, the system **1a**/$Sn(CH_3)_4$/$AlCl_3$ is also able to catalyze the ring-opening polymerization of cycloolefins to polyalkenamers having elastomeric properties. Likewise, the π-complex $[(\eta^5\text{-}C_5Me_5)ReO_3]$ and its derivatives catalyze metathetic ring opening, for instance by virtue of the systems

$[(\eta^5\text{-}C_5Me_5)ReOCl_2]/Sn(CH_3)_4/AlCl_3$,
$[(\eta^5\text{-}C_5Me_5)ReX_4]/Sn(CH_3)_4/AlCl_3$ (X = Cl, Br), and
$[(\eta^5\text{-}C_5Me_5)Re(CH_3)X_3]/Sn(CH_3)_4/AlCl_3$ (X = Cl, Br).

It is to be noted that both a Lewis acid (AlX_3) and a cocatalyst (SnR_4) are required to achieve metathesis.

Complex **1a** is further methylated only upon treatment with dimethylzinc (Scheme 1). In the temperature region −78 to 30 °C and for short reaction times, reduction and dimerization lead to the new, likewise sublimable, lemon-yellow methylrhenium oxide **2**. A single-crystal X-ray structure analysis[6] establishes the binuclear structure of this Re^{VI} compound, which, owing to a metal–metal single bond (259.3(< 1) pm) is spin-paired and therefore diamagnetic. In addition, the four methyl groups are *cis* with respect to the Re_2O_2 core structure, which is puckered along the Re–Re bond (Fig. 1); the same geometry was found for the complex $[R_4Re_2O_4]$ ($R = CH_2C(CH_3)_2C_6H_5$) obtained by a different, albeit poorly defined route.[7] Solid-state thermolysis of **2** ($T = 200$ °C) affords 90% methane and higher hydrocarbons up to C_4 (GC/MS analysis). In contrast, heating of **1a** even at 200 °C results in only trace amounts of methane and ethane, indicating the thermal robustness of the Re^{VII} title compound.

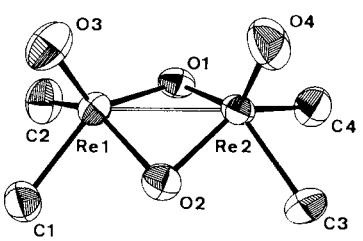

Fig. 1. Molecular structure of **2** (ORTEP, hydrogen atoms omitted, thermal ellipsoids at the 50% probability level). Selected bond lengths [pm] and angles [°]: Re1-Re2 259.3(< 1), Re1-C1 210.8(6), Re1-C2 210.2(6), Re2-C3 213.9(6), Re2-C4 210.3(7), Re1-O1 193.4(4), Re1-O2 197.5(4), Re1-O3 165.2(4), Re2-O1 193.0(4), Re2-O2 193.2(4), Re2-O4 165.9(5); Re1-O1-Re2 84.3(1), Re1-O2-Re2 83.1(2), between the planes Re1/O2/Re2 and Re1/O1/Re2 139.0. Further details of the crystal structure investigation may be obtained from the Fachinformationszentrum Energie, Physik, Mathematik GmbH, D-7514 Eggenstein-Leopoldshafen 2 (FRG), on quoting the depository number CSD-52591, the names of the authors, and the journal citation.

The binuclear complex **2** also catalyzes the metathetic ring-opening polymerization of cyclopentene in the presence of $Sn(CH_3)_4/AlCl_3$. This particular compound represents the so far missing member of the series

$(CH_3)_6Re$ $(CH_3)_4ReO$ $[(CH_3)_2ReO_2]_2$ $[ReO_3]_\infty$,
A **B** **C** = 2 **D**

Table 1. Data for the rhenium oxides **1**, **2**, and **3** [a].

1a: colorless, air-stable needles or cubes, m.p. = 106 °C.—IR (cm^{-1}, KBr): $\tilde{\nu}$ = 2984 (m), 2899 (m, ν(CH)), 953 (vs, br), 1002 (s, shoulder, ν(Re=O)).—^{1}H-NMR: δ(CH_3) = 2.61 (s).—^{13}C-NMR: δ(CH_3) = 19.03 [^1J(C,H) = 138 Hz].—EI-MS: *m/z* 250 ($M^\oplus$).—^{17}O-NMR: δ(O) = 824.

1a': From Re_2O_7 and $Sn(CD_3)_4$; properties similar to **1a**.—IR (cm^{-1}): $\tilde{\nu}$ = 2238 (m), 2100 (m, ν(CD)), ν(ReO) cf. **1a**.—EI-MS: *m/z* 253 ($M^\oplus$)

1b: colorless, air-stable powder, m.p. = 213 °C (dec.).—IR (cm^{-1}, KBr): $\tilde{\nu}$ = 946 (vs), 909 (vs, ν(ReO)).—^{1}H-NMR ([D$_8$]THF): δ(CH_3) = 0.69 (s, $^2J(^1H,^{117}Sn)$ = 64.0, $^2J(^1H,^{119}Sn)$ = 66.9, ^1J(H,C) = 132.0 Hz).—^{13}C-NMR ([D$_8$]THF): δ(CH_3) = −0.86 ($^1J(^{13}C,^{117}Sn)$ = 459.3, $^1J(^{13}C,^{119}Sn)$ = 480.7 Hz).—^{119}Sn-NMR ([D$_8$]THF, standard $SnMe_4$): δ(Sn) = 91.8.—EI-MS: *m/z* 399 ([*M* − CH_3]$^\oplus$, base peak; weak molecular-ion peak *m/z* 414 at 12 eV).—^{17}O-NMR: δ(O) = 564.

2: yellow, air-stable needles, m.p. = 120 °C.—IR (cm^{-1}, KBr): $\tilde{\nu}$ = 1017/1007 (vs, ν(Re=O)).—^{1}H-NMR: δ(CH_3) = 2.81 (s).—^{13}C-NMR: δ(CH_3) = 30.36.—EI-MS: *m/z* 498 ($M^\oplus$), 249 (base peak, 1/2 $M^\oplus$)

3: red, air-stable needles, m.p. = 88 °C.—IR (cm^{-1}, KBr): $\tilde{\nu}$ = 1005 (vs, ν(Re=O)), 850 (m, ν(ReORe).—^{1}H-NMR: δ(CH_3) = 2.45, 2.52 (2 s; rel. int. 2:1).—^{13}C-NMR: δ(CH_3) = 30.70, 40.46 (^1J(H,C) = 131 Hz).—EI-MS (12 eV): *m/z* 512 ($M^\oplus$), 248 ([$ReMe_3O$]$^\oplus$)

[a] Correct C, H, O, and Re analyses were obtained. Unless noted otherwise: NMR spectra recorded at 28 °C in $CDCl_3$, JEOL JNM GX-270 and JNM GX-400 (the NMR spectra do not change upon lowering the temperature (−80 °C)); mass spectra at 70 eV, T_Q = 30–70 °C, Finnigan MAT 311-A.

in which the degree of aggregation increases as a result of decreasing ligand/metal ratio (CN 5 or 6). With the exception of **2**, the Re^{VI} complexes of the series $R_{6-2n}ReO_n$ are either paramagnetic (**A** and **B**) or metallic conducting (**D**; perovskite-type structure).

Excess dimethylzinc effects even further methylation of **2** within 1 h at 30–60 °C (Scheme 1). The oxo ligand of **2** is thereby replaced by two methyl groups with retention of the binuclear structure and the bright red compound **3** is obtained (Table 1). This compound, which was obtainable earlier only via the siloxy derivative $[(Me_3SiO)ReO_3]$ in a two-step reaction,[8] is diamagnetic despite the d^1 configuration ("spin superexchange" in the linear ReORe framework). According to Scheme 1, **3** is now obtained quantita-

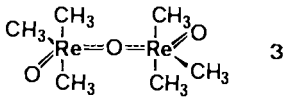

3

tively directly from dirhenium heptoxide and dimethylzinc in a molar ratio of 1:3 (in refluxing THF). Complex **3** catalyzes ring-opening polymerization (cyclopentene), even when the catalyst $Sn(CH_3)_4$ necessary in the case of **1a** and **2** is absent. Solid-state thermolysis of **3** at 200 °C gives mainly methane and isobutylene along with small amounts of other C_2–C_4 hydrocarbons.

Although the methylrhenium oxides **1a** and **3** are not new compounds, the reactions of Re_2O_7 with alkyltin and alkylzinc reagents described here offer a selective and high-yield route to these compounds. Important for future studies of catalysis is the observation that *one* methyl group in the rhenium-containing catalytic component is not necessary for the catalytic activity but is also not sufficient: **1b** also catalyzes olefin metathesis in the presence of $Sn(CH_3)_4/AlCl_3$, while **3** no longer needs the cocatalyst $Sn(CH_3)_4$ which provides the additional methyl groups.

On the basis of the findings presented here, there can no longer be any doubt that complexes **1a** and **1b** are the actual catalytic precursors in the system $Re_2O_7/Sn(CH_3)_4$. At present $AlCl_3$ is thought to be required for the generation of the catalyst because it opens up additional coordination sites for consecutive alkylations by the alkyltin cocatalysts.[1a–e, 9] We are currently investigating this question in terms of a preparative approach.

Received: August 13, 1987;
revised version: October 9, 1987 [Z 2417 IE]
German version: *Angew. Chem. 100* (1988) 420

[1] a) Recent monographs on olefin metathesis: V. Dragutan, A. T. Balaban, M. Dimonie: *Olefin Metathesis and Ring-Opening Polymerization of Cyclo-Olefins*, Wiley, New York 1985; K. J. Ivin: *Olefin Metathesis*, Academic Press, London 1983; b) industrial applications of olefin metathesis: R. Streck, *Chem. Ztg. 99* (1975) 397; c) recent work: R. H. A. Bosma, G. C. N. van den Aardweg, J. C. Mol, *J. Organomet. Chem. 255* (1983) 159; d) X. Xiaoding, J. C. Mol, *J. Chem. Soc. Chem. Commun. 1985*, 631 (metathesis of unsaturated carboxylic esters); e) G. C. N. van den Aardweg, R. H. A. Bosma, J. C. Mol, *ibid. 1983*, 262 (metathesis of unsaturated nitriles with $C \geq 5$); f) *not a single* well-defined organometallic complex has been obtained so far from catalytically active WCl_6/SnR_4 and $Re_2O_7/SnR_4/Al_2O_3$ systems; cf. the contributions to the *VIth International Symposium on Olefin Metathesis* (August 26–30, 1985, Hamburg) in *J. Mol. Catal. 36* (1986).

[2] K. Mertis, J. F. Gibson, G. Wilkinson, *J. Chem. Soc. Chem. Commun. 1974*, 93; J. F. Gibson, K. Mertis, G. Wilkinson, *J. Chem. Soc. Dalton Trans. 1975*, 1093; K. Mertis, D. H. Williamson, G. Wilkinson, *ibid. 1975*, 607; K. Mertis, G. Wilkinson, *ibid. 1976*, 1488.

[3] W. A. Herrmann, J. K. Felixberger, E. Herdtweck, A. Schäfer, J. Okuda, *Angew. Chem. 99* (1987) 466; *Angew. Chem. Int. Ed. Engl. 26* (1987) 466.

[4] a) Four-week reaction time: cf. I. R. Beattie, P. J. Jones, *Inorg. Chem. 18* (1979) 2318; b) H. Schmidbaur, D. Koth, *Chem. Ztg. 100* (1976) 290.

[5] Reviews: a) W. A. Herrmann, *J. Organomet. Chem. 300* (1986) 111; b) W. A. Herrmann, J. Okuda, *J. Mol. Catal. 41* (1987) 109; c) W. A. Herrmann, E. Herdtweck, M. Flöel, J. Kulpe, U. Küsthardt, J. Okuda, *Polyhedron 6* (1987) 1165.

[6] Yellow needles grown by vacuum sublimation, $0.70 \times 0.15 \times 0.05$ mm; monoclinic, *Pn* (Int. Table No. 7); $a = 608.6(1)$, $b = 856.4(1)$, $c = 923.4(2)$ pm, $\beta = 95.08(2)°$; $V = 479 \times 10^6$ pm^3; $Z = 2$; $F(000) = 436$; $\rho_{calcd} = 3.440$ g cm^{-3}; $\lambda = 71.073$ pm ($Mo_{K\alpha}$ radiation); systematic absences $h0l$ $(h+l = 2n+1)$; $T = 23 \pm 1$ °C; Enraf-Nonius CAD-4; range of measurement: $2.0° \leq \theta \leq 30.0°$; ω scan; scan width: $(0.75 + 0.35 \cdot \mathrm{tg}\theta)° \pm 25\%$ before and after each reflection for determination of background; t_{max}: 90 s; 2927 measured reflections, 2668 unique reflections with $I > \sigma(I)$; $R = \Sigma \| F_0 | - | F_c \| / \Sigma | F_0 | = 0.033$; $R_w = [\Sigma w(|F_0| - |F_c|)^2 / \Sigma w |F_0|^2]^{1/2} = 0.044$ with $w = 1/\sigma^2(F_0)$, $GOF = [\Sigma w(|F_0| - |F_c|)^2/(NO - NV)]^{1/2} = 7.004$. Structure solved by Patterson methods; numerical absorption correction, $\mu = 255.5$ cm^{-1}; correction for extinction, $\varepsilon = 0.3425 \times 10^{-6}$. The positions of the hydrogen atoms were calculated for an ideal geometry (d(C–H) = 95 pm) and used with collective isotropic temperature factors in the calculation of structural factors, but not refined. Anomalous dispersion was taken into consideration. Shift/error < 0.00 in the final refinement cycle; residual electron density, $+3.99\, e_0 \cdot$ Å^{-3} at 68 pm next to the heavy atom rhenium. Upon refinement of the enantiomorphic presentation, the R values did not change significantly.

[7] J. M. Huggins, D. R. Whitt, L. Lebioda, *J. Organomet. Chem. 312* (1986) C 15.

[8] P. Stavropoulos, P. G. Edwards, G. Wilkinson, M. Motevalli, K. M. Abdul Malik, M. B. Hursthouse, *J. Chem. Soc. Dalton Trans. 1985*, 2167.

[9] Cf., for example, J. Kress, A. Aguero, J. A. Osborn, *J. Mol. Catal. 36* (1986) 1.

$[Cp_2Co][Bi\{Co(CO)_4\}_4]$: A Paramagnetic, Ten-Electron, Tetrahedral Complex of Bismuth**

By *J. Scott Leigh* and *Kenton H. Whitmire**

It is well established that the incorporation of main-group heteroatoms into transition-metal clusters has a pronounced effect on cluster reactivity. Studies of mixed main-group/transition-metal clusters have led to the stabilization of intriguing metal-cluster geometries.[1] The extremely large element bismuth has shown surprising structural versatility in its compounds. For example, structures with EM_3 frameworks (E = main-group atom, M = transition metal) of the first-row transition metals have been isolated in which the Bi atom is surrounded by an open framework, as in $[BiCo_3(CO)_{12}]$,[2] $[BiMn_3(CO)_{15}]$,[3a] and $[BiFe_3(CO)_6Cp_3]$.[3b] Other open structures for mixed clusters in which a main-group atom is tetrahedrally surrounded by four ML_n units have been proposed for In and Tl,[4] as well as Sn and Pb,[5] and confirmed for $[Et_4N]_3[BiFe_4(CO)_{16}]$.[6] It was thought at one time that the large size of the Bi atom would prevent the formation of transition-metal–transition-metal bonds in these compounds, yet closed EM_3 structures for Bi have also been isolated, as in $[BiCo_3(CO)_9]$,[7] $[Bi_2Fe_3(CO)_9]$,[8] and $[BiFe_3(CO)_3Cp_3]$.[3b] More complicated structures with more than one Bi atom have been reported for $[Et_4N]_2[Bi_2Fe_4(CO)_{13}]$ and $[Et_4N][Bi_2Fe_2Co(CO)_{10}]$,[9] $[Et_4N]_2[Bi_4Fe_4(CO)_{13}]$,[10] and $[Bi_2W_3(CO)_{15}]$.[11] The latter three complexes are believed to have some degree of Bi–Bi bonding. Here we present the isolation and characterization of $[Cp_2Co][Bi\{Co(CO)_4\}_4]$, **1** ($Cp = C_5H_5$), a paramagnetic, ten-electron, tetrahedral complex of bismuth.

[*] Dr. K. H. Whitmire, J. S. Leigh
Department of Chemistry, Rice University
P.O. Box 1892, Houston, TX 77251 (USA)

[**] This work was supported by the National Science Foundation (CHE-8421217) and the Alexander von Humboldt Foundation. Note added in proof: Another synthesis of the anion $[Bi\{Co(CO)_4\}_4]^{\ominus}$ was recently reported: S. Martinengo, G. Ciani, *J. Chem. Soc. Chem. Commun. 1987*, 1589.

Complex **1**[12] is synthesized by treating $[BiCo_3(CO)_{12}]$ with $[Cp_2Co][Co(CO)_4]$ generated in situ [Eq. (a)]. Isolated

$$[Cp_2Co][Co(CO)_4] + [BiCo_3(CO)_{12}] \rightleftharpoons \underset{\mathbf{1}}{[Cp_2Co][BiCo_4(CO)_{16}]} \quad (a)$$

yields of up to 86% have been obtained. Complex **1** is also formed from the direct reaction of $[BiCo_3(CO)_{12}]$ with $[Cp_2Co]$ in CH_2Cl_2. This process probably proceeds via the intermediate formation of $[Cp_2Co][Co(CO)_4]$, generated from the degradation of $[BiCo_3(CO)_{12}]$ by $[Cp_2Co]$. The $[Cp_2Co][Co(CO)_4]$ may then react with another $[BiCo_3(CO)_{12}]$ to form **1**.

X-ray quality reddish-brown crystals of **1**[13,14] were obtained from a concentrated CH_2Cl_2 solution cooled at $-20\,^{\circ}C$ for several days. The crystal structure of **1** (Fig. 1)

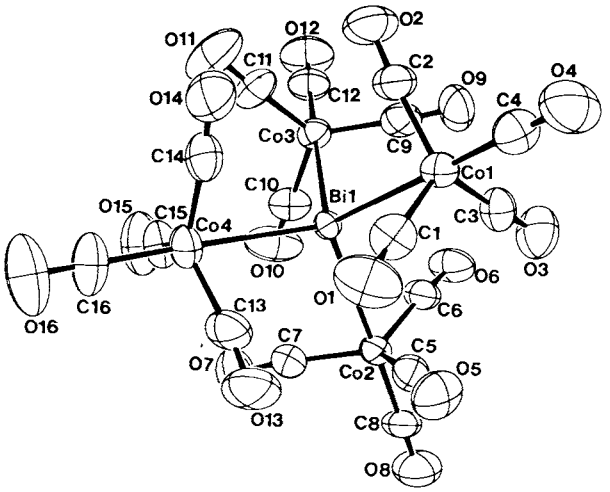

Fig. 1. ORTEP diagram of the $[Bi\{Co(CO)_4\}_4]^-$ anion showing 50% thermal probability ellipsoids and atom labeling. Important bond distances [Å] and angles [°]: Bi1-Co1 2.939(2), Bi1-Co2 2.898(2), Bi1-Co3 2.912(3), Bi1-Co4 2.876(2), Co-C(average) 1.79, C-O(average) 1.14; Co4-Bi1-Co2 109.76(6), Co4-Bi1-Co3 110.31(7), Co4-Bi1-Co1 108.74(7), Co2-Bi1-Co3 108.31(7), Co2-Bi1-Co1 108.96(6), Co3-Bi1-Co1 110.73(6).

consists of ordered $[Cp_2Co]^{\oplus}$ cations and $[BiCo_4(CO)_{16}]^{\ominus}$ anions in a 1:1 ratio. The Cp rings of the cation are staggered as in most standard $[Cp_2Co]^{\oplus}$ salts such as $[Cp_2Co][ClO_4]$[15] and $[CoCp(C_5H_4CO_2H)][PF_6]$.[16] The molecular structure of the anion, which approaches T_d point group symmetry, consists of a bismuth atom that is tetrahedrally surrounded by four $[Co(CO)_4]^{\ominus}$ units. The Bi–Co bonds are extremely long, ranging from 2.876 to 2.939 Å (average 2.906 Å). For comparison, the average Bi–Co bond distance in $[BiCo_3(CO)_{12}]$ is 2.766 Å,[2] and the Bi–Co distance in $[BiCo_3(CO)_9]$ is 2.613 Å.[7] The Co–Bi–Co bond angles range from 108.31 to 110.73° (average 109.47°).

The unusual feature of $[Cp_2Co][Bi\{Co(CO)_4\}_4]$ **1** that separates it from other open, tetrahedral $[E\{ML_4\}_4]$ complexes such as $[ECo_4(CO)_{16}]^{\ominus}$ (E = In, Tl),[4] $[ECo_4(CO)_{16}]$ (E = Sn, Pb),[5] and $[Et_4N][BiFe_4(CO)_{16}]$[6] is the electron count. The bismuth is a 10-electron center, having two electrons more than required to meet the EAN rule. Similar "hypervalency" has been observed in $[CpMoFe(CO)_5\{Te_2Br\}]$ and $[CpMoFe(CO)_5\{Te_2\text{-}(S_2CNEt_2)\}]$.[17] The two extra electrons, which are apparently stereochemically inactive, are unpaired, making **1** paramagnetic ($\mu_{eff} = 3.40\,\mu_B$ at room temperature).[18] Thus, the extremely long Bi–Co bonds may result from the extra electron density in the metal framework.

Experimental Procedure

1: Under nitrogen atmosphere, $[Co_2(CO)_8]$ (0.059 g, 0.17 mmol) and $[Cp_2Co]$ (0.066 g, 0.35 mmol) were mixed in a Schlenk flask with a magnetic stir bar. CH_2Cl_2 (30 mL) was added via syringe, and the solution was stirred a little over 1 h. The solution was then filtered onto solid $[BiCo_3(CO)_{12}]$ (0.250 g, 0.346 mmol), and the resulting solution was stirred a little over 1 h. The solution was filtered, and the solvent was removed under vacuum. The solid, **1**, was isolated in 86% yield (0.324 g, 0.299 mmol). The product is formed quite cleanly in this reaction if nearly exact stoichiometric amounts of reactants are used. Slight stoichiometric variations in the reactants cause the formation of small amounts of neutral byproducts, which can be removed easily by washing the solid with toluene.

Received: September 21, 1987;
supplemented: November 30, 1987 [Z 2436 IE]
German version: *Angew. Chem. 100* (1988) 399

CAS Registry numbers:
1, 112839-88-0; $Co_2(CO)_8$, 10210-68-1; Cp_2Co, 1277-43-6; $BiCo_3(CO)_{12}$, 43164-49-4.

[1] a) W. A. Herrmann, *Angew. Chem. 98* (1986) 57; *Angew. Chem. Int. Ed. Engl. 25* (1986) 58; b) W. A. Herrmann, J. Rohrmann, M. L. Ziegler, T. Zahn, *J. Organomet. Chem. 295* (1985) 175; c) G. Huttner, U. Weber, B. Sigwarth, O. Scheidsteger, H. Lang, L. Zsolnai, *ibid. 282* (1985) 331; d) H. Lang, G. Huttner, B. Sigwarth, I. Jibril, L. Zsolnai, O. Orama, *ibid. 304* (1986) 137; e) G. Schmid, *Angew. Chem. 90* (1978) 417; *Angew. Chem. Int. Ed. Engl. 17* (1978) 392; f) A. Vizi-Orosz, G. Pályi, L. Markó, R. Boese, G. Schmid, *J. Organomet. Chem. 288* (1985) 179; g) P. Gusbeth, H. Vahrenkamp, *Chem. Ber. 118* (1985) 1746; h) T. Jaeger, S. Aime, H. Vahrenkamp, *Organometallics 5* (1986) 245; i) R. D. Adams, J. E. Babin, M. Tasi, *Inorg. Chem. 26* (1987) 2807; j) R. D. Adams, J. E. Babin, *ibid. 25* (1986) 3418; k) T. D. Weatherill, T. B. Rauchfuss, R. A. Scott, *ibid. 25* (1986) 1466; l) D. A. Lesch, T. B. Rauchfuss, *ibid. 22* (1983) 1854; m) C. F. Campana, L. F. Dahl, *J. Organomet. Chem. 127* (1977) 209; n) L. D. Lower, L. F. Dahl, *J. Am. Chem. Soc. 98* (1976) 5046; o) A. L. Rheingold, P. J. Sullivan, *Organometallics 3* (1984) 1417; p) A. P. Rheingold, M. J. Foley, P. J. Sullivan, *J. Am. Chem. Soc. 104* (1982) 4727.

[2] G. Etzrodt, R. Boese, G. Schmid, *Chem. Ber. 112* (1979) 2574.

[3] J. M. Wallis, G. Müller, H. Schmidbaur, *Inorg. Chem. 26* (1987) 458; b) *J. Organomet. Chem. 325* (1987) 159.

[4] W. R. Robinson, D. P. Schussler, *J. Organomet. Chem. 30* (1971) C5.

[5] G. Schmid, G. Etzrodt, *J. Organomet. Chem. 131* (1977) 477.

[6] M. R. Churchill, J. C. Fettinger, K. H. Whitmire, C. B. Lagrone, *J. Organomet. Chem. 303* (1986) 99.

[7] K. H. Whitmire, J. S. Leigh, M. Gross, *J. Chem. Soc. Chem. Commun. 1987*, 926.

[8] M. R. Churchill, J. C. Fettinger, K. H. Whitmire, *J. Organomet. Chem. 284* (1985) 13.

[9] K. H. Whitmire, K. S. Raghuveer, M. R. Churchill, J. C. Fettinger, R. F. See, *J. Am. Chem. Soc. 108* (1986) 2778.

[10] K. H. Whitmire, M. R. Churchill, J. C. Fettinger, *J. Am. Chem. Soc. 107* (1985) 1056.

[11] G. Huttner, U. Weber, L. Zsolnai, L. Zsolnai, *Z. Naturforsch. B37* (1982) 707.

[12] IR of **1** (crystals in CH_2Cl_2): $\tilde{\nu}(CO) = 2066$ (m), 2028 (vs), 1969 (s), 1890 (w corresponds to the presence of $[Co(CO)_4]^{\ominus}$) cm^{-1}. The IR pattern, neglecting the band due to small amounts of $[Co(CO)_4]^{\ominus}$, which probably results from a slight equilibrium as indicated in Eq. (a), agrees with local C_{3v} symmetry at Co and is similar to other $[XCo(CO)_4]$ compounds such as $[HCo(CO)_4]$ and $[MeCo(CO)_4]$ [19]. Solubility of **1**: insoluble in hexane, toluene; partially soluble in diethyl ether; soluble in dichloromethane, methanol, acetone, acetonitrile, tetrahydrofuran. Correct Bi, Co elemental analysis.

[13] X-ray data: Triclinic; $P\bar{1}$; $a = 11.300(6)$, $b = 11.320(6)$, $c = 16.077(6)$ Å; $\alpha = 106.16(4)$, $\beta = 95.08(4)$, $\gamma = 117.58(4)^{\circ}$; $V = 1693(2)$ Å^3; $Z = 2$; diffractometer, Rigaku AFC5S; radiation, $Mo_{K\alpha}$; data collection temperature, 23 °C; 5293 observed reflections with $I > 3.00\,\sigma(I)$; 436 variables; $R = 0.046$, $R_w = 0.054$; GOF, 1.30; solved and refined using a combination of SHELX-86 and the TEXSAN structure solution package. Further details of the crystal structure investigation are available on request from the Fachinformationszentrum Energie, Physik, Mathematik GmbH, D-7514 Eggenstein-Leopoldshafen 2 (FRG), on quoting the depository number CSD-52815, the names of the authors, and the journal citation.

[14] Professor *George M. Sheldrick*, Göttingen, and Dr. *Nigel Walker*, BASF AG, Ludwigshafen are thanked for their helpful suggestions concerning the X-ray crystal structure analysis.

[15] E. Frasson, G. Bombieri, C. Panattoni, *Acta Crystallogr. 16* (1963) A68.
[16] P. E. Riley, R. E. Davis, *J. Organomet. Chem. 152* (1978) 209.
[17] L. E. Bogan, Jr., T. B. Rauchfuss, A. L. Rheingold, *Inorg. Chem. 24* (1985) 3720.
[18] *D. W. Lee*, Houston, is thanked for his help in performing the magnetic moment measurements on **1**.
[19] G. Bor, *Inorg. Chim. Acta 1* (1967) 81.

3,3,6,6-Tetramethylcyclohexyne**

By *Wolfram Sander* and *Orville L. Chapman**

Thermolysis and photolysis of cyclopropenones provide attractive routes to strained acetylenes.[1] We now describe 3,3,6,6-tetramethylcyclohexyne **1**, prepared from 2,2,5,5-tetramethylbicyclo[4.1.0]hept-1(6)-en-7-one **2**. *Suda* and *Masamune* showed **2** to be stable at 100°C in CH_2Cl_2 for 5 h.[2] In our hands, irradiation ($\lambda > 208$ nm) of **2** matrix-isolated in argon gave only a small amount of carbon monoxide.[3] Compound **2** thus shows remarkable thermal and photochemical stability for a cyclopropenone, and more vigorous methods were required.

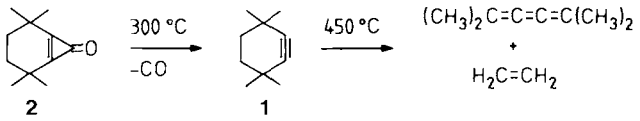

Thermolysis of **2**[4] at 600°C (10^{-6} torr) and trapping the product in argon at 12 K gives carbon monoxide, ethylene, and tetramethylbutatriene[5] as the only products. The products were identified by comparison of the IR spectra with those of authentic samples.[6] Tetramethylbutatriene was further characterized by ^{1}H-NMR spectroscopy[7] after warming the matrix and isolation. At temperatures of 300–450°C a new product was trapped in addition to tetramethylbutatriene. This product is 3,3,6,6-tetramethylcyclohexyne **1** [IR (Ar, 12 K): $\tilde{\nu}$ = 2977 (s), 2939 (m), 1470 (w), 1455 (m), 1365 (m), 1305 (w), 1256 (m), 1215 (m), 894 (w), 838 (w), 815 (w), 798 (w), 700 (w), 563 (w), 445 (s), 405 (m) cm^{-1}] (see Fig. 1). The optimum yield of **1** is obtained at 370°C (10^{-6} torr) with argon trapping at 12 K.

Thermolysis (370°C) of **2** at slightly higher pressure followed by trapping at 12 K in argon gives **1** with a small amount of dimer **3**, ethylene, and tetramethylbutatriene (Fig. 2, top). When the matrix is warmed above 40 K, the argon vaporizes. Continued deposition at 45 K gives only dimer **3** and small amounts of ethylene and tetramethylbutatriene (Fig. 2, bottom). At the higher temperature (45 K) in the absence of argon, 3,3,6,6-tetramethylcyclohexyne **1** dimerizes to **3**. Thermolysis of **2** at 370°C (0.02 torr) and warming the product to room temperature gave dimer **3**, tetramethylbutatriene, and one minor, unidentified product. An authentic sample of dimer **3** was prepared from **4**.[8]

[*] Prof. Dr. O. L. Chapman
Department of Chemistry and Biochemistry, University of California
Los Angeles, CA 90024 (USA)
Dr. W. Sander
Organisch-chemisches Institut der Universität
Im Neuenheimer Feld 270, D-6900 Heidelberg (FRG)

[**] This research was supported by the National Science Foundation (grant CHE-11196) and the IBM Corporation. The Humboldt Foundation provided a fellowship for *W. Sander*.

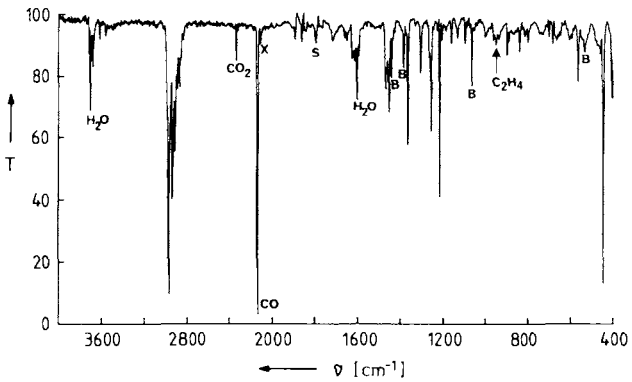

Fig. 1. IR spectrum of 3,3,6,6-tetramethylcyclohexyne **1** produced by pyrolysis of **2** at 350°C and trapping the products in argon at 12 K. The bands of the remaining cyclopropenone **2** were subtracted. S = cyclopropenone **2**, B = tetramethylbutatriene (T = transmission).

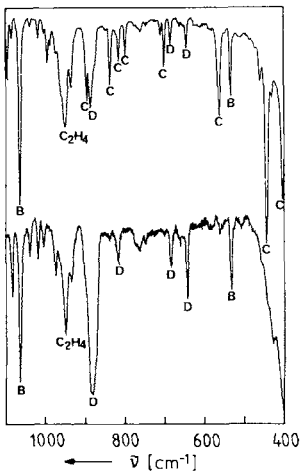

Fig. 2. Top: IR spectrum of 3,3,6,6-tetramethylcyclohexyne **1** from pyrolysis at 370°C with argon trapping at 12 K. Bottom: IR spectrum from same thermolysis with window at 45 K. B = tetramethylbutatriene, C = **1**, D = dimer **3**.

Irradiation ($\lambda > 208$ nm) of **1** generated by thermolysis of **2** and trapping in argon gave no tetramethylbutatriene but did give small amounts of **2**. This observation suggested that **1** photochemically adds carbon monoxide giving **2**.[9] If the photostationary state in the system favored **2**, the reason for failure in the photodecarbonylation of **2**

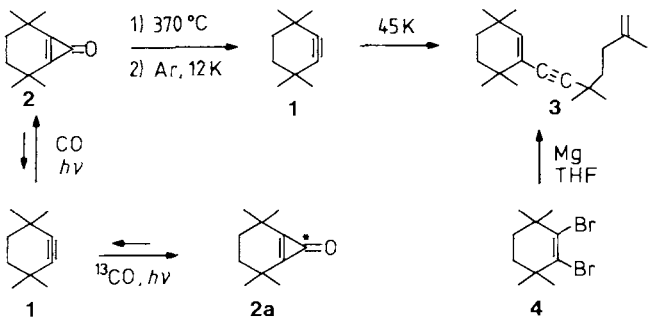

would be clear. Irradiation of **2** matrix-isolated in argon containing ^{13}C-carbon monoxide (95 atom% ^{13}C; 1.5% CO in Ar) gave ^{13}C-labeled **2a**. A similar experiment using thermally generated **1** in an argon matrix containing ^{13}C-carbon monoxide (95 atom% ^{13}C; 1.5% CO in Ar) gave **2a** on irradiation. The shifts in the IR bands in the spectrum of **2a** relative to **2** (Table 1) are in excellent agreement with the corresponding shifts in diphenylcyclopropenone.[10]

Table 1. IR bands of **2** and **2a** matrix-isolated in argon at 12 K.

$\tilde{\nu}$ [cm^{-1}]		$\Delta\tilde{\nu}$ [cm^{-1}]
2	**2a**	
1890 s	1856 s	34
1858 vs	1825 vs	33
1789 s	1775 s	14
1629 s	1619 s	10

The only disappointment in the IR spectrum of **1** (Fig. 1) is the absence of an identifiable triple-bond stretch. It is probably either hidden under the carbon monoxide bands (2139, 2149 cm^{-1}) or is very weak compared to other bands in **1** and thus not observed.[11] The other IR bands of **1** are due to vibrations very similar to those of the hydrocarbon portion of **2**. The most striking shifts are those of the bands at 684 and 643 cm^{-1} in **2** to 445 and 405 cm^{-1} in **1**.

Received: September 22, 1987 [Z 2437 IE]
German version: *Angew. Chem. 100* (1988) 402

CAS Registry numbers:
1, 37494-11-4; **2**, 54283-14-6; **2a**, 112897-94-6; **3**, 59129-90-7; **4**, 37490-74-7; ^{13}CO, 1641-69-6; $H_2C{=}CH_2$, 74-85-1; $(CH_3)_2C{=}C{=}C{=}C(CH_3)_2$, 2431-31-4.

[1] O. L. Chapman, J. Gano, P. R. West, M. Regitz, G. Maas, *J. Am. Chem. Soc. 103* (1981) 7033.
[2] M. Suda, S. Masamune, *J. Chem. Soc. Chem. Commun. 1974*, 504.
[3] The photodecarbonylation of **2** in Ar at 15 K was described by *Krebs* et al. Our results clearly show that the spectrum, tentatively assigned to **1** by these authors, has to be reassigned to an unknown photoproduct: A. Krebs, W. Cholcha, M. Müller, T. Eicher, H. Pielartzik, H. Schnöckel, *Tetrahedron Lett. 25* (1984) 5027.
[4] **2**: IR (Ar, 12 K): 2976 (s), 2941 (m), 2879 (w), 1890 (s), 1858 (vs), 1842 (m), 1789 (s), 1629 (s), 1463 (w), 1456 (w), 1367 (m), 1205 (m), 1159 (m), 758 (w), 684 (m), 643 (w) cm^{-1}.
[5] The thermal decomposition of cyclohexyne to give ethylene and butatriene was observed recently: a) J. Tseng, M. L. McKee, P. B. Shevlin, *J. Am. Chem. Soc. 109* (1987) 5474; b) A. Runge, W. Sander, unpublished results.
[6] Tetramethylbutatriene: IR (Ar, 12 K): $\tilde{\nu}$=2998 (s), 2936 (s), 2914 (vs), 2894 (m), 2873 (m), 2857 (m), 2714 (w), 1664 (w), 1452 (s), 1375 (m), 1365 (s), 1205 (w), 1064 (s), 815 (w), 534 (m), 433 (m) cm^{-1}. For a discussion of the IR spectrum (gas-phase) see: A. Rogstadt, *Spectrochim. Acta A 36* (1980) 131.
[7] L. Skattebøl, *Tetrahedron Lett. 1965*, 2175.
[8] a) D. E. Applequist, P. A. Gebauer, D. E. Gwynn, K. H. O'Connor, *J. Am. Chem. Soc. 94* (1972) 4272; b) C. N. Bush, D. E. Applequist, *J. Org. Chem. 42* (1977) 1076.
[9] Photochemical addition of carbon monoxide to 1,2-dehydronaphthalene has been observed, unpublished observation of F. Diederich and O. L. Chapman.
[10] Y. Takehira, F. Toda, *Bull. Chem. Soc. Japan 51* (1978) 2441.
[11] Recently, the triple-bond stretching frequency for unsubstituted cyclohexyne was calculated to be 2003 cm^{-1}: S. Olivella, M. A. Pericàs, A. Riera, A. Solé, *J. Org. Chem. 52* (1987) 4160. The intensities of the bands were not calculated and therefore the comparison with the experimental values is difficult. The IR spectrum of **1** shows no IR band in the range 1900–2100 cm^{-1} (Fig. 1).

Novel Boron–Phosphorus Cages with $C_4B_4P_4$ and $C_2B_4P_4$ Frameworks**

By *Matthias Driess, Hans Pritzkow,* and *Walter Siebert**

In contrast to aminoboranes, phosphinoboranes exist mainly as cyclic dimers or trimers.[1,2] However, if electronic stabilization is achieved by amino substituents on the boron atom or if kinetic stabilization is achieved by bulky substituents on the boron and phosphorus atoms, then the corresponding phosphinoboranes are monomeric.[2b,3] Derivatives of the heterocycles 2,5-dihydro-1*H*-1,2,5-phosphadiborol **1**[4] and 1,2,3,6-tetrahydro-1,2,3,6-diphosphadiborin **2**[5] with amino substituents on boron are also monomeric. We have now synthesized a derivative of **2** that is dimeric.

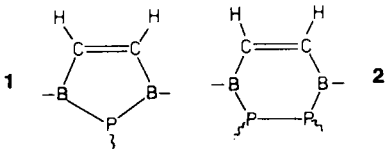

Reaction of **3** with 1,2-di-*tert*-butyl-1,2-bis(trimethylsilyl)diphosphane **4** results in elimination of Me_3SiCl and formation of a dimeric product, which is not the cubane-like compound **5** but, surprisingly, the colorless, constitutionally isomeric compound **6**, having the cuneane cage as a structural element. Thus, its structure is analogous to that of S_4N_4 or Hittorf phosphorus. Compound **6** is stable toward oxygen and moisture up to ca. 100°C. In contrast to compounds of types **1** and **2**, compound **6** does not react with sulfur or selenium in refluxing toluene.

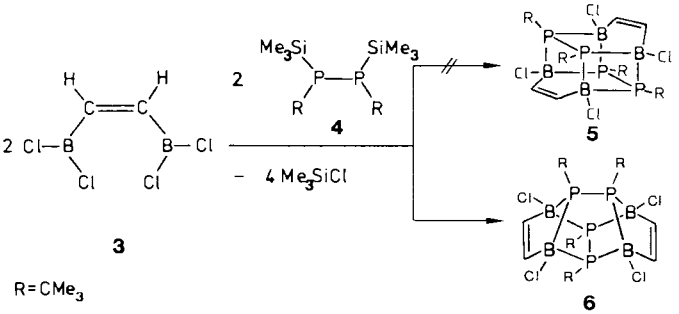

The $^1H\{^{31}P\}$-NMR spectrum of **6** exhibits two singlets for the *tert*-butyl protons and the $^{31}P\{^1H\}$-NMR spectrum exhibits two triplets at 220 K, which are broadened owing to ^{11}B–^{31}P coupling. The ^{11}B-NMR signal at $\delta = 4.2$ ($b_{1/2} = 170$ Hz) is in a region characteristic for tetracoordinated boron. These findings are not in agreement with structure **5** but rather with structure **6**. This conclusion is further corroborated by the result of X-ray structure analyses (Fig. 1),[6] according to which **6** is present in two modifications, one of which contains two independent molecules in the unit cell. The structures of the molecules, however, are not significantly different.

The formation of **6** within twelve hours (at 300 K) can be followed by ^1H-, ^{11}B-, and ^{31}P-NMR spectroscopy. The elimination of Me_3SiCl was thereby shown to proceed in two steps via an intermediate that has not yet been characterized. The intermediate, in turn, gives **6** quantitatively (^1H-NMR spectroscopy).

In order to determine what effect the kind of hydrocarbon bridge has on the cage formation, we incorporated the methylene group in place of the ethenylene group. The reaction of $CH_2(BCl_2)_2$ **7** with **4** does not result in formation of compound **8**, which is analogous to **6**, but rather in formation of the colorless, constitutionally isomeric compound **9**, which is moderately soluble in CH_2Cl_2 and

[*] Prof. Dr. W. Siebert, M. Driess, Dr. H. Pritzkow
Anorganisch-chemisches Institut der Universität
Im Neuenheimer Feld 270, D-6900 Heidelberg (FRG)

[**] This work was supported by the Deutsche Forschungsgemeinschaft, the Fonds der Chemischen Industrie, and BASF AG.

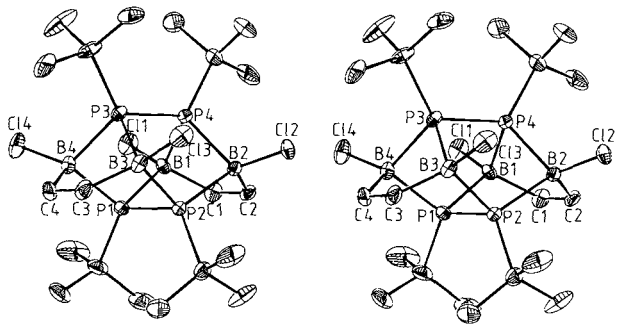

Fig. 1. Stereodrawing of the molecular structure of **6**. Important bond lengths [Å] and angles [°] (standard deviations for modification I: 0.003–0.015 Å, 0.2–0.8°; for modification II: 0.002–0.009 Å, 0.1–0.5°; averages for three molecules): P1-P2 2.273, P3-P4 2.254, P1(2)-B 2.02, P3(4)-B 2.000, B-C 1.573, C-C 1.330; B-P1(2)-B 110.3, B-P3(4)-B 86.7, P1(2)-P2(1)-B 96.7, P3(4)-P4(3)-B 104.9, P1(2)-B-C 110.2, P3(4)-B-C 100.8, P-B-P 95.0, C-C-B 116.7.

CH_3CN and whose stability toward oxygen and moisture is similar to that of **6**.

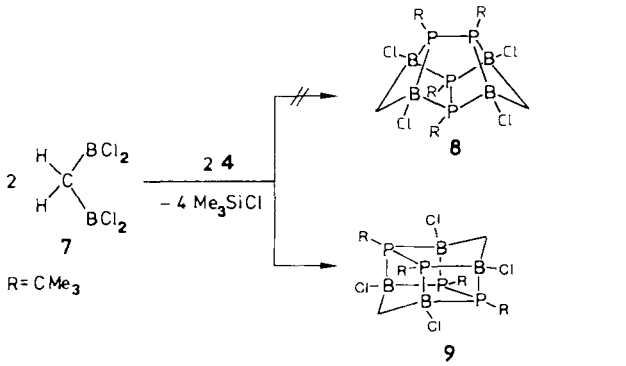

The $^1H\{^{31}P\}$- and $^{31}P\{^1H\}$-NMR spectra[7] of **9** indicate a highly symmetric arrangement of atoms in the molecule, which is confirmed by the results of an X-ray structure analysis (Fig. 2).[8] Compound **9** contains two CB_2P_2 five-membered rings joined by donor-acceptor bonds, whereas **8** displays two less favorable CB_2P four-membered rings.

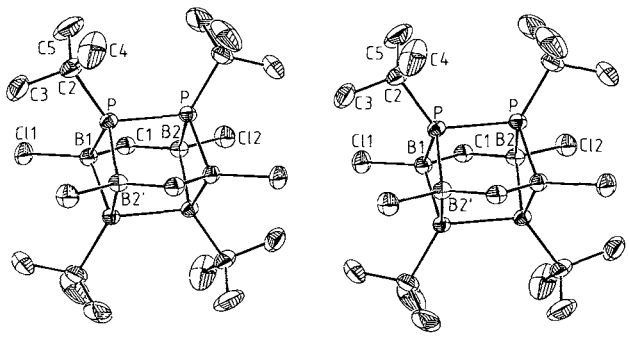

Fig. 2. Stereodrawing of the molecular structure of **9**. Important bond lengths [Å] and angles [°]: P-P 2.242(1), P-B 2.041, 2.036(2), B-C 1.584, 1.587(4); P-P-B 95.0(1), B1-P-B2' 93.9(1), C1-B-P 110.3, 110.0(1), B1-C1-B2 110.3(2).

Experimental Procedure

6 (2,3,8,9-tetra-*tert*-butyl-1,4,7,10-tetrachloro-2,3,8,9-tetraphosphonia-1,4,7,10-tetraboratapentacyclo[6.4.0.0^{2,10}.0^{3,7}.0^{4,9}]dodeca-5,11-diene): **3** (3.4 g, 17.8 mmol) was dissolved in CH_2Cl_2 (200 mL) at −20°C. **4** (5.73 g, 17.8 mmol) in CH_2Cl_2 (100 mL) was then added to this vigorously stirred solution. The clear orange-yellow solution was then allowed to warm to room temperature and stirred for an additional 12 h. After removal of all readily volatile components under vacuum, an orange powder remained, which was recrystallized from toluene (−30°C). Yield: 2.95 g (56%) **6**, m.p. = 308°C (dec.), correct C,H,P elemental analysis.—$^1H\{^{31}P\}$-NMR (300 MHz, CD_2Cl_2, 300 K): δ = 1.49 (s, 18H), 1.61 (s, 18H), 6.23 (br. s, 4H); $^{31}P\{^1H\}$-NMR (80.0 MHz, CD_2Cl_2, 220 K): δ = 19.92 (t, 2P, ^2J(PP) = 87.5 Hz), 14.70 (t, 2P); ^{13}C-NMR (50.3 MHz, CD_2Cl_2, 300 K): δ = 32.82 (m, 6C; CH_3), 33.38 (m, 6C; CCH_3), 43.18 (m, 2C; CCH_3), 43.26 (m, 2C; CCH_3), 145.08 (br. s, 4C; CB); MS (CI, CH_4): *m/z* 588 (4%, $M^{\oplus}$), 531 (6%, $[M-t\mathrm{Bu}]^{\oplus}$), 474 (4%, $[M-2t\mathrm{Bu}]^{\oplus}$), 57 (100%, $t\mathrm{Bu}^{\oplus}$).

9 (2,3,7,8-tetra-*tert*-butyl-1,4,6,9-tetrachloro-2,3,7,8-tetraphosphonia-1,4,6,9-tetraboratapentacyclo[5.3.0.0^{2,6}.0^{3,9}.0^{4,8}]decane): **4** (5.49 g, 17 mmol) in CH_2Cl_2 (100 mL) was added slowly at −40°C to **7** (3.03 g, 17 mmol) in CH_2Cl_2 (300 mL). After warming to room temperature, the clear orange reaction solution was concentrated to ca. 80 mL and allowed to stand for 24 h, resulting in the crystallization of **9**, which was further purified by washing with warm CCl_4. Yield: 2.02 g (42%) **9**, m.p. = 218°C (dec.). Correct C,H,P elemental analysis.—$^1H\{^{31}P\}$-NMR (300 MHz, $CDCl_3$, 300 K): δ = 1.78 (s, 36H), 1.45 (br. s, 4H); $^{31}P\{^1H\}$-NMR (121.5 MHz, $CDCl_3$, 210 K): δ = 2.03 (br. s); ^{11}B-NMR (29.8 MHz, $CDCl_3$, 300 K): δ = 8.6 (s, $b_{1/2}$ = 130 Hz); $^{13}C\{^1H\}$-NMR (50.3 MHz, $CDCl_3$, 300 K): δ = 33.45 (m, 12C; CCH_3), 43.41 (m, 4C, CCH_3), a signal for CB was not observed; MS (EI, 70 eV): *m/z* 564 (3%, $M^{\oplus}$), 507 (23%, $[M-t\mathrm{Bu}]^{\oplus}$), 451 (24%, $[M-t\mathrm{Bu}-C_4H_8]^{\oplus}$), 282 (4%, $[M/2]^{\oplus}$), 57 (100%, $t\mathrm{Bu}^{\oplus}$).

Received: October 5, 1987 [Z 2458 IE]
German version: *Angew. Chem. 100* (1988) 410

CAS Registry numbers:
3, 18447-36-4; **4**, 55793-25-4; **6**, 112969-18-3; **7**, 40710-68-7; **9**, 112969-19-4.

[1] J. R. Wasson, *Boron-Phosphorus Compounds* in: *Gmelin, Handbuch der Anorganischen Chemie, Borverbindungen Band 19/3*, p. 93.
[2] a) G. Fritz, E. Sattler, *Z. Anorg. Allg. Chem. 413* (1975) 193; b) R. Köster, *Diorganophosphinoborane* in: *Houben-Weyl-Müller, Borverbindungen, Band 13/3b*, p. 386.
[3] H. Nöth, W. Schrägle, *Z. Naturforsch. B 16* (1961) 473.
[4] M. Driess, H. Pritzkow, W. Siebert, *Angew. Chem. 99* (1987) 789; *Angew. Chem. Int. Ed. Engl. 26* (1987) 781.
[5] M. Driess, H. Pritzkow, W. Siebert, unpublished results.
[6] **6** crystallizes in two modifications. I: space group $P2_1ab$, a = 12.703(3), b = 14.894(7), c = 16.263(4) Å; V = 3077 Å^3, Z = 4. Refinement with 2475 reflections ($I \geq \sigma(I)$, two-circle diffractometer, $Mo_{K\alpha}$ radiation, ω scan), R = 0.058 (Cl, P, C, B anisotropic, methyl groups as rigid groups) [9].—II: space group $P2_1/c$, a = 10.236(4), b = 18.107(7), c = 33.239(11) Å, β = 98.66(3)°; V = 6090 Å^3, Z = 8. Refinement with 5411 reflections ($I = 2\sigma(I)$, four-circle diffractometer, $Mo_{K\alpha}$ radiation, ω scan), R = 0.042 (Cl, P, C, B anisotropic, methyl groups as rigid groups) [9].
[7] We thank Mr. *Domnick*, Universität Karlsruhe, for the spectra.
[8] **9**: space group $C2/m$, a = 13.564(4), b = 11.657(3), c = 9.910(3) Å, β = 113.84(3)°; V = 1433 Å^3, Z = 2. Refinement with 1584 reflections ($I \geq 2\sigma(I)$, four-circle diffractometer, $Mo_{K\alpha}$ radiation, ω scan), R = 0.034 (Cl, P, C, B anisotropic, methyl groups in part as rigid groups) [9].
[9] Further details of the crystal structure investigations may be obtained from the Fachinformationszentrum Energie, Physik, Mathematik GmbH, D-7514 Eggenstein-Leopoldshafen 2 (FRG), on quoting the depository number CSD-52758, the names of the authors, and the journal citation.

Synthesis and Properties of N^{α}-Di-*tert*-Butoxycarbonyl and N^{α}-Benzyloxycarbonyl *tert*-Butoxycarbonyl Amino Acids**

By *Kerstin Gunnarsson, Leif Grehn,* and *Ulf Ragnarsson**

Benzyloxycarbonyl[1] (Z) and *tert*-butoxycarbonyl[2,3] (Boc) amino acids are derivatives of fundamental importance in modern peptide synthesis.[4] The two groups

[*] Dr. U. Ragnarsson, K. Gunnarsson, B. Sc., Dr. L. Grehn
Institute of Biochemistry, University of Uppsala, BMC
Box 576, S-751 23 Uppsala (Sweden)

[**] This work was supported by grants from the Swedish Natural Science Research Council and the National Swedish Board for Technical Development and by a research scholarship (to *K. G.*) from the Sven and Lilly Lawski Foundation.

complement each other for protection purposes since both of them can be selectively removed under rather mild conditions.

We recently demonstrated that *N*-Boc_2 derivatives of simple model compounds could be prepared and that they were surprisingly stable.[5,6] Also mixed *N*-Boc(Z) derivatives were made.[6,7] This led us to try the synthesis of Boc_2-(**1**) and Boc(Z)-amino acids (**2**).

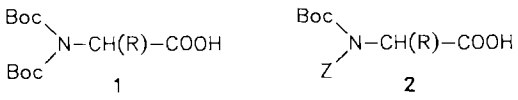

For the synthesis of compounds **1** three methods are used. In the first one (method A), a Boc-amino acid is converted into its benzyl ester,[8] which is then exhaustively *tert*-butoxycarbonylated[5] with Boc_2O and dimethylaminopyridine to give the Boc_2-amino acid benzyl ester. In the case of glycine, the corresponding derivative can be prepared from benzyl α-bromoacetate by a Gabriel reaction with di-*tert*-butyl iminodicarboxylate $HNBoc_2$.[9] The benzyl ester is then cleaved by catalytic hydrogenolysis over Pd/C or catalytic transfer hydrogenolysis to give the Boc_2-amino acid **1**.

If the Boc-amino acid contains a benzyl protecting group in its side chain, method A cannot be applied. Therefore, an alternative method, not requiring catalytic hydrogenolysis, was sought. First, we tried the base-labile 9-fluorenylmethyl esters[10] (method B). This approach also offered a possibility for the synthesis of mixed Boc(Z)-amino acids **2** and was applied to compounds **2a** and **2b**. However, although this procedure worked reasonably well for Boc- and Z-glycine and Z-alanine, in the case of Boc-Ser(Bzl) and Boc-Tyr(Bzl) difficulties were encountered already in the *tert*-butoxycarbonylation step, whereas for Boc(Z)-Phe the ester could not be subsequently cleaved with piperidine. From these experiments it was concluded that the 9-fluorenylmethyl esters were not the ideal solution to our problem, mainly due to their size and concomitant steric hindrance.

With the shortcomings of method B in mind, we directed our attention instead toward small protecting groups for the carboxyl function and we decided to try allyl esters[11] (method C). Their *tert*-butoxycarbonylation seemed much easier to accomplish and also their subsequent specific cleavage with tris(triphenylphosphane)rhodium(I) chloride at 70°C presented no particular problems. This procedure was tried in three cases, **1e**, **1f**, and **2a**, all with good results.

All Boc_2- and Boc(Z)-amino acids made so far are stable for several months at room temperature. The Boc_2 derivatives are resistant to moderately strong bases like piperidine, which was used for the final cleavage of the carboxyl protecting group in method B. With respect to their other properties, it can be mentioned that these *N*-protected amino acids form salts with dicyclohexylamine and active esters with *p*-nitrophenol and hydroxysuccinimide.

The new derivatives have been employed in the synthesis of a few dipeptides related to Leu-enkephalin: Boc_2-Gly-Phe-OBzl [via the *p*-nitrophenyl ester, 88% yield, m.p. = 74–75°C; $[\alpha]_D^{25}$ −1.2 (*c* = 1, DMF)], Boc_2-Gly-Phe-ONb [Nb = *p*-nitrobenzyl, via the *p*-nitrophenyl ester, 90% yield, m.p. = 165–166°C; $[\alpha]_D^{25}$ −9.7 (*c* = 1, DMF)], Boc_2-Phe-Leu-OBzl [via the *p*-nitrophenyl ester, 92% crude yield, 59% yield after chromatography, m.p. = 61.5–62°C; $[\alpha]_D^{25}$ −53.8 (*c* = 1, DMF); also made with dicyclohexylcarbodiimide (DCC) in 99% crude yield], Boc(Z)-Gly-Phe-ONb [with DCC, 88% yield, m.p. = 139–140°C; $[\alpha]_D^{25}$ −9.4 (*c* = 1, DMF)]. All peptides were chromatographically and spectroscopically pure and gave on amino acid analysis, after hydrolysis, the expected amino acid ratios.

Table 1. Yields and physical data of the new Boc_2- and Boc(Z)-amino acids **1** and **2**, respectively.

Compd [a]	R	Method [b]	Yield [%] [c]	M.p. [°C]	$[\alpha]_D^{25}$ [c = 1] [d]	^{1}H-NMR ($CDCl_3$, rel. TMS, δ values)
1a	H	A	93	113.5–114	—	4.39 (s, 2H), 1.50 (s, 18H)
		B	70			
1b	CH_3	A	85	141–141.5	−39.0 (DMF)	5.03 (q, 1H), 1.51 (s + d, 21H)
1c	i-C_4H_9	A	83	119–121	−37.3 (HOAc)	7.7 (br. s, 1H), 4.99 (dd, 1H), 1.84 (m, 1H), 1.45–1.6 (s + overlapping signal, 20H), 0.93 (d, 6H)
1d	CH_2Ph	A	92	136.5–137.5	−116.6 (DMF)	7.22 (overlapped s, 5H), 5.24 (dd, 1H), 3.0–3.5 (m, 2H), 1.39 (s, 18H)
1e	CH_2OBzl	C	75	105–106	−61.2 (DMF)	7.31 (s, 5H), 5.32 (dd, 2H), 4.55 (q, 1H), 3.8–4.2 (m, 2H), 1.47 (s, 18H)
1f	CH_2CH_2-COOBzl	C	67	82.5–84	−31.7 (MeOH)	7.73 (br. s, 1H), 7.34 (s, 5H), 5.12 (s, 2H), 5.03 (dd, 1H), 2.1–2.7 (m, 4H), 1.48 (s, 18H)
2a	H	B	64	97.5–98	—	7.35 (s, 5H), 5.25 (s, 2H), 4.46 (s, 2H), 1.46 (s, 9H)
		C	77	97–98		
2b	CH_3	B	45	88.5–89	−35.3 (DMF)	7.36 (s, 5H), 5.25 (s, 2H), 5.08 (q, 1H), 1.52 (d, 3H), 1.45 (s, 9H)

[a] All compounds are new and gave satisfactory elemental analysis (C, H, N). [b] A, catalytic hydrogenolysis of the corresponding benzyl ester over Pd/C; B, hydrolysis of the 9-fluorenylmethyl ester with piperidine; C, hydrolysis of the allyl ester with tris(triphenylphosphane)rhodium(I) chloride at 70°C. [c] Yields refer to crude, chromatographically and spectroscopically pure products. [d] DMF = dimethylformamide.

Received: October 6, 1987 [Z 2465 IE]
German version: *Angew. Chem. 100* (1988) 411

[1] M. Bergmann, L. Zervas, *Ber. Dtsch. Chem. Ges. 65* (1932) 1192.
[2] F. C. McKay, N. F. Albertson, *J. Am. Chem. Soc. 79* (1957) 4686.
[3] G. W. Anderson, A. C. McGregor, *J. Am. Chem. Soc. 79* (1957) 6180.
[4] Review: E. Wünsch in *Houben-Weyl-Müller: Methoden der Organischen Chemie, Band 15/1*, Thieme, Stuttgart 1974, pp. 47–69, 117–132.
[5] L. Grehn, U. Ragnarsson, *Angew. Chem. 97* (1985) 519; *Angew. Chem. Int. Ed. Engl. 24* (1985) 510.
[6] L. Grehn, K. Gunnarsson, U. Ragnarsson, *Acta Chem. Scand. Ser. B40* (1986) 745.
[7] M. L. S. Almeida, L. Grehn, U. Ragnarsson, *J. Chem. Soc. Chem. Commun. 1987*, 1250.
[8] S.-S. Wang, B. F. Gisin, D. P. Winter, R. Makofske, I. D. Kulesha, C. Tzougraki, J. Meienhofer, *J. Org. Chem. 42* (1977) 1286.
[9] L. Grehn, U. Ragnarsson, *Synthesis 1987*, 275.
[10] a) M. A. Bednarek, M. Bodanszky, *Int. J. Pept. Protein Res. 21* (1983) 196; b) H. Kessler, R. Siegmeier, *Tetrahedron Lett. 24* (1983) 281.
[11] a) H. Waldmann, H. Kunz, *Liebigs Ann. Chem. 1983*, 1712; b) H. Kunz, *Angew. Chem. 99* (1987) 297; *Angew. Chem. Int. Ed. Engl. 26* (1987) 294, and references cited therein.

 © VCH Verlagsgesellschaft mbH, D-6940 Weinheim, 1988 0570-0833/88/0303-0401 $ 02.50/0

Tetranuclear Complexes as Intermediates in Transannular Oxidative-Addition Reactions. Structure of the First Tetrairidium Linear Cluster**

By *Miguel A. Ciriano, Santiago Sebastián, Luis A. Oro,* Antonio Tiripicchio, Marisa Tiripicchio Camellini,* and *Fernando J. Lahoz*

One of the emerging patterns of reactivity of bridged binuclear complexes significantly different from those of the mononuclear counterparts is the transannular oxidative-addition reaction discovered by *Schmidbaur* et al.[1a] [Eq. (a)]. This reaction[1b] results in a formal one-electron

$$X-Y + \overset{\frown}{M\quad M} \longrightarrow X-\overset{\frown}{M-M}-Y \qquad (a)$$

oxidation of each metal center and in creation of a metal-metal bond. Although a free-radical mechanism has been suggested for this type of reaction, e.g., the addition of iodine to the complexes $[\{Ir(\mu\text{-}StBu)(CO)(PR_3)\}_2]$,[2a] mechanistic studies are scarce,[2b] intermediates have not been isolated, and the role of the second metal center is not fully understood.

On the other hand, there is an increasing interest in binuclear complexes that are bridged through both hard and soft donor atoms. Our activity in this area began in 1984 when it was found that the binuclear complexes $[\{M(\mu\text{-}X)L_2\}_2]$ (X = 2-pyridinethiolate (C_5H_4NS) or benzothiazole-2-thiolate ($C_7H_4NS_2$); L_2 = diolefin or $(CO)_2$) may lead to: (1) the construction of homo- or hetero-trinuclear aggregates in which the metal atoms are in close proximity;[3] (2) the stabilization of otherwise reactive species such as the binuclear iodomethyldiiridium complex $[Ir_2(\mu\text{-}C_5H_4NS)_2(CH_2I)I(CO)_4]$.[4] Herein we describe the isolation and characterization of the unique linear Ir_4 cluster $[Ir_4(\mu\text{-}C_7H_4NS_2)_4(I)_2(CO)_8]$ **3** as intermediate in a transannular oxidative-addition reaction (see Scheme 1).

The red-orange binuclear complex $[\{Ir(\mu\text{-}C_7H_4NS_2)(cod)\}_2]$ **1** (cod = 1,5-cyclooctadiene) can be prepared in excellent yield as described for the analogous rhodium compound.[3b] Complex **1** is fluxional but its ^1H- and $^{13}C\{^1H\}$-NMR spectra[5] in the slow-exchange region are in accordance with the presence of a single species in solution, either the head-to-head (C_s) or the head-to-tail (C_2) isomer depicted in Scheme 1. Carbon monoxide immediately replaces the diolefin in **1** to yield a deep purple solution of the highly air-sensitive compound $[\{Ir(\mu\text{-}C_7H_4NS_2)(CO)_2\}_2]$ **2**.[6] Isomerization arising from the relative disposition of the bridging ligands occurs during this reaction and results in an equilibrium mixture of the head-to-tail and the head-to-head *cis*-tetracarbonyl isomers of **2** in 1:3 ratio in $[D_6]$benzene at 20°C. Iodine reacts with **2**, in dichloromethane upon exposure to sunlight, affording the red-orange transannular oxidative-addition product

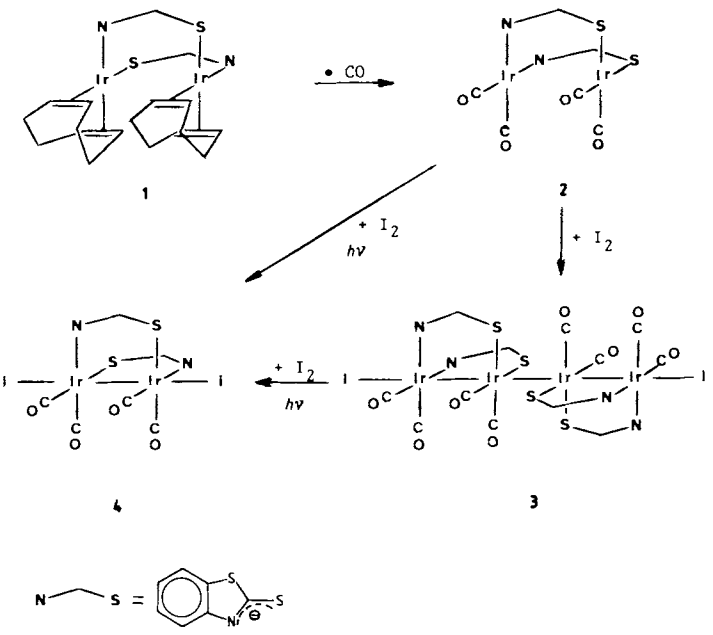

Scheme 1.

$[\{Ir(\mu\text{-}C_7H_4NS_2)I(CO)_2\}_2]$ **4**. If the reaction is carried out in toluene, the tetranuclear cluster **3** crystallizes out rapidly as a dichroic golden-brown solid in 85% yield. Further reaction of **3** with iodine in dichloromethane rapidly gives complex **4**; in toluene, in which **3** is slightly soluble, this step requires intense irradiation with visible light.

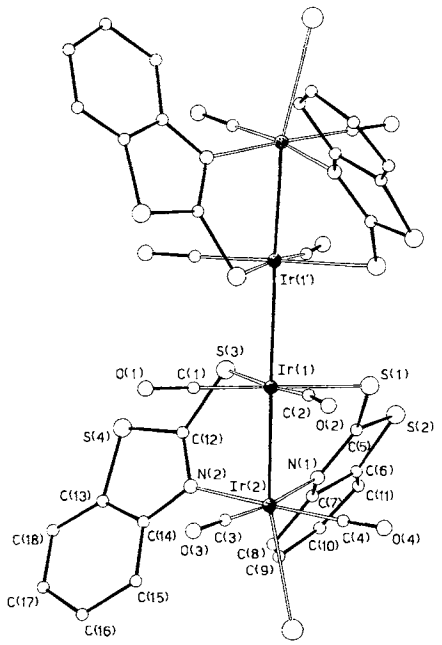

Fig. 1. View of the structure of $[Ir_4(\mu\text{-}C_7H_4NS_2)_4I_2(CO)_8]$ **3**. Selected bond lengths [Å] and angles [°]: Ir(1)-Ir(1') 2.828(2), Ir(1)-Ir(2) 2.731(2), Ir(2)-I 2.892(3), Ir(1)-S(1) 2.408(6), Ir(1)-S(3) 2.382(7), Ir(2)-N(1) 2.09(2), Ir(2)-N(2) 2.11(2); Ir(1)-Ir(2)-I 168.5(1), Ir(2)-Ir(1)-Ir(1') 170.2(1). The primed atoms are related to the nonprimed ones by a twofold axis.

The structures of complexes **3** (as toluene solvate) and **4**, determined by single-crystal X-ray diffraction studies, are depicted in Figures 1 and 2, respectively.[7] Complex **3**

[*] Prof. Dr. L. A. Oro, Dr. M. A. Ciriano, Dr. F. J. Lahoz, Dipl.-Chem. S. Sebastián
Departamento de Química Inorgánica,
Instituto de Ciencia de Materiales de Aragon
Universidad de Zaragoza—C.S.I.C.
E-50009 Zaragoza (Spain)
Prof. Dr. A. Tiripicchio, Prof. Dr. M. Tiripicchio Camellini
Istituto di Chimica Generale ed Inorganica, Universitá di Parma
Centro di Studio per la Strutturistica Diffrattometrica del CNR
Viale delle Science, I-43100 Parma (Italy)

[**] This work was supported by C.A.I.C.Y.T. (Spain) and by the joint program C.S.I.C.-C.N.R.

shows a novel linear arrangement of the four metal atoms and can be considered to be made up of two binuclear halves related by a crystallographic twofold axis. Each half is formed by two iridium atoms separated by a distance of 2.731(2) Å, corresponding to a metal-metal bond, bridged by two benzothiazole-2-thiolate ligands through the N atom and the S atom exterior to the heterocycle, and bonded to two terminal carbonyl groups. The outer iridium atom, Ir(2), completes its octahedral coordination with a iodine atom, whereas the inner one, Ir(1), forms a nonbridged metal-metal bond, of 2.828(2) Å, with its symmetry-related atom. The almost linear chain of three metal-metal bonds makes **3** "EPR-silent." Noteworthy is the head-to-head coordination of the four ligands, which are bonded to the inner iridium atoms through the sulfur atoms and to the outer iridium atoms through the nitrogen atoms. As far as we know, a similar linear M_4 disposition has only been reported for $[Rh_4(1,3\text{-diisocyanopropane})_8Cl]^{5\oplus}$[8a] and in a small number of platinum-blue analogues.[8b]

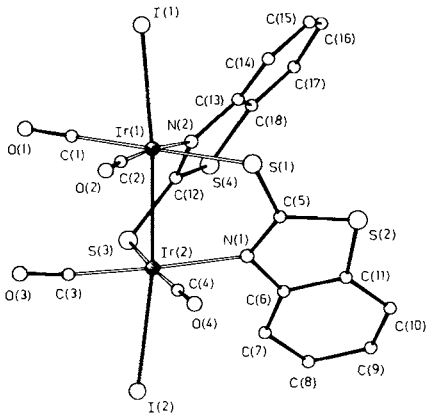

Fig. 2. View of the structure of $[\{Ir(\mu\text{-}C_7H_4NS_2)I(CO)_2\}_2]$ **4**. Selected bond lengths [Å] and angles [°]: Ir(1)-Ir(2) 2.676(2), Ir(1)-I(1) 2.797(2), Ir(2)-I(2) 2.788(2), Ir(1)-S(1) 2.386(5), Ir(2)-S(3) 2.395(6), Ir(1)-N(2) 2.10(2), Ir(2)-N(1) 2.13(1); Ir(2)-Ir(1)-I(1) 175.1(1), Ir(1)-Ir(2)-I(2) 173.5(1).

The final product of the oxidative addition, **4**, is a dimeric molecule with two iridium atoms separated by a typical metal-metal bond distance of 2.676(2) Å and bridged by two benzothiazole-2-thiolate ligands, which are coordinated in a head-to-tail manner. Both iridium atoms show analogous octahedral environments, each being additionally bonded to two carbonyls and to an iodine. All the features of this structure are reminiscent of those of the complex $[Ir_2(\mu\text{-}C_5H_4NS)_2(CH_2I)I(CO)_4]$ with the analogous N-C-S 2-pyridinethiolate ligand.[4]

The structure of **3** suggests that iodine attacks one of the metal centers in **2** to give presumably the radical complex $[Ir_2(\mu\text{-}C_7H_4NS_2)_2I(CO)_4]^{\odot}$ having a metal-metal bond,[9] which dimerizes rapidly. In this way, the second metal center, which is involved in the formation of the tetranuclear intermediate complex, can also provide "anchimeric assistance"[10] in cleaving the added molecule (in this case, I_2). The addition of iodine to the nonbridged metal-metal bond in **3** corresponds to the visible-light-assisted reaction. The change in the relative disposition of the bridging ligands on going from **3** to **4** is probably associated with their mobility since both compounds exhibit a fluxional behavior.

In conclusion, we have presented factual evidence of the so far unsuspected feature that tetranuclear complexes can be involved in oxidative-additions to binuclear complexes.

Received: October 7, 1987 [Z 2467 IE]
German version: *Angew. Chem. 100* (1988) 406

[1] a) H. Schmidbaur, R. Franke, *Inorg. Chim. Acta 13* (1975) 85; b) for leading references see: A. L. Balch, C. T. Hunt, C. L. Lee, M. M. Olmstead, J. P. Farr, *J. Am. Chem. Soc. 103* (1981) 3764; R. Poilblanc, *Inorg. Chim. Acta 62* (1982) 75; J. L. Atwood, K. A. Beveridge, G. W. Bushnell, K. R. Dixon, D. T. Eadie, S. R. Stobart, M. J. Zaworotko, *Inorg. Chem. 23* (1984) 4050; J. D. Basil, H. H. Murray, J. P. Fackler, Jr., J. Tocher, A. M. Mazany, B. Trzcinska-Bancrost, H. Knachel, D. Dufis, T. J. Delord, D. O. Marler, *J. Am. Chem. Soc. 107* (1985) 6908; J. D. Scott, R. J. Puddephatt, *Organometallics 5* (1986) 2522.

[2] a) P. Kalck, J. J. Bonnet, *Organometallics 1* (1982) 1211; b) R. J. Puddephatt, J. D. Scott, *ibid. 4* (1985) 1221; J. V. Caspar, H. B. Gray, *J. Am. Chem. Soc. 106* (1984) 3029.

[3] a) L. A. Oro, M. A. Ciriano, F. Viguri, A. Tiripicchio, M. Tiripicchio Camellini, F. J. Lahoz, *Proc. XII. Int. Conf. Organomet. Chem.*, Wien 1985, p. 410; *Nouv. J. Chim. 10* (1986) 75; b) M. A. Ciriano, L. A. Oro, J. J. Pérez-Torrente, A. Tiripicchio, M. Tiripicchio Camellini, *J. Chem. Soc. Chem. Commun. 1986*, 1737.

[4] M. A. Ciriano, F. Viguri, L. A. Oro, A. Tiripicchio, M. Tiripicchio Camellini, *Angew. Chem. 99* (1987) 452; *Angew. Chem. Int. Ed. Engl. 26* (1987) 444.

[5] ^{1}H-NMR (200 MHz, $CDCl_3$, −20°C): δ=8.56 (d, 2H; H-4), 7.38 (t, 2H), 7.25-7.08 (overlapping m, 4H), 4.6 (br. s, 2H; cod), 4.1 (br. s, 4H; cod), 3.4 (br. s, 2H; cod), 2.6-2.1 (br., 8H; cod), 1.8-1.3 (br., 8H; cod).—^{13}C{^{1}H}-NMR (50 MHz, $CDCl_3$, −50°C): δ=178.2 (2C; C=S), 150.8, 134.5 (4C; C-3a, C-7a), 125.9, 124.3, 120.4, 119.9 (8C; C4, C5, C6, C7), 66.1, 65.4, 63.9, 62.6 (8C; =CH cod), 32.2-31.1 (16C; CH_2 cod). The carbon atoms of the heterocyclic ligand are numbered according to the IUPAC rules starting from the heterocyclic sulfur.

[6] We have not been able to isolate **2** analytically pure in the solid state. Nevertheless, **2** shows the same pattern of $\tilde{\nu}$(CO) bands and comparable NMR data as the related compounds *cis* head-to-tail $[\{Rh(\mu\text{-}C_5H_4NS)(CO)_2\}_2]$ and *cis* head-to-head $[\{Rh(\mu\text{-}C_5H_4NO)(CO)_2\}_2]$ (C_5H_4NO = "2-pyridonate"), whose structures have been determined by X-ray methods, and *cis*-$[\{Rh(\mu\text{-}C_7H_4NS_2)(CO)_2\}_2]$ (unpublished results). Spectroscopic data: IR (toluene): $\tilde{\nu}$(CO)=2080 (s), 2045 (m), 2005 (s), 1990 (w, sh) cm^{-1}. Major species: 200-MHz ^{1}H-NMR (C_6D_6): δ=8.54 (dd of d, 2H; H4), 7.03 (dd of d, 2H; H5), 6.75 (dd of d, 2H; H6), 6.53 (dd of d, 2H, H7); 50-MHz ^{13}C{^{1}H}-NMR (C_6D_6): δ=182.7 (2C, C=S), 172.6, 172.1 (4C; CO), 151.3, 133.0 (4C; C3a, C7a), 126.1, 125.4, 120.6, 120.1 (8C; C4, C5, C6, C7). Minor species: 200-MHz ^{1}H-NMR (C_6D_6): δ=8.05 (d, 2H; H4), 6.88 (dd of d, 2H), 6.72 (dd of d, 2H), 6.57 (dd of d, 2H, H7); 50-MHz ^{13}C{^{1}H}-NMR (C_6D_6): δ=187.6 (2C; C=S), 173.6, 171.6 (4C, CO), 151.0, 133.4 (4C; C3a, C7a), 126.3, 125.1, 121.3, 118.9 (8C; C4, C5, C6, C7).

[7] Siemens AED diffractometer ($Cu_{K\alpha}$): **3** (toluene solvate): orthorhombic, *Pccn*, Z=4, a=12.563(4), b=20.122(8), c=23.363(7) Å; V=5906(3) Å^3; $3<\theta<70°$, 5913 unique reflections, 2510 observed with $I>2\sigma(I)$, R=0.0629, R_w=0.0892. Philips PW-1100 diffractometer ($Mo_{K\alpha}$): **4**: triclinic, $P\bar{1}$, Z=2, a=17.800(5), b=9.607(3), c=8.036(2) Å, α=113.31(1), β=92.23(2), γ=78.32(1)°; V=1234.6(6) Å^3, $3<\theta<24°$, 3855 unique reflections, 2107 observed with $I>3\sigma(I)$, R=0.0416, R_w=0.0479. Further details of the crystal structure analyses may be obtained from the Cambridge Crystallographic Data Centre, University Chemical Laboratory, Lensfield Road, Cambridge CB2 1EW, UK, on quoting the names of the authors and the journal citation.

[8] a) K. R. Mann, M. J. DiPierro, T. P. Gill, *J. Am. Chem. Soc. 102* (1980) 3965; b) K. Matsumoto, H. Takahashi, K. Fuwa, *ibid. 106* (1984) 2049; *Inorg. Chem. 22* (1983) 4086.

[9] The structure and bonding of the related paramagnetic cationic complex $[\{Rh(\mu\text{-}RNNNR)(CO)(PPh_3)\}_2][PF_6]$ (R=*p*-tolyl) (N. G. Connelly, C. J. Finn, M. J. Freeman, A. Orpen, J. Stirling, *J. Chem. Soc. Chem. Commun. 1984*, 1025) and the preparation and ESR spectra of the cationic radicals $[M(\mu\text{-}3,5\text{-}Me_2pz)(cod)]_2^{\oplus}$ (M=Rh, Ir; pz=pyrazolate) (D. O. K. Fjeldsted, S. R. Stobart, *J. Chem. Soc. Chem. Commun. 1985*, 908) have been described recently.

[10] S. S. M. Ling, N. C. Payne, R. J. Puddephatt, *Organometallics 4* (1985) 1546.

A Tetramethylene-1,4-distannacyclohexane from 3,4-Dilithio-2,5-dimethyl-2,4-hexadiene and Dichlorodimethylstannane: the First Dimetalla[6]radialene**

By *Adalbert Maercker,* Franz Brauers, Walter Brieden, Michael Jung,* and *Heinz Dieter Lutz*

2,3-Dilithio-1,3-butadiene derivatives are readily accessible by addition of lithium to the central double bond of aliphatic butatriene derivatives **1**[1,2] and are therefore of value for the synthesis of heterocyclic radialene derivatives. The formation of three-membered ring products **3** or six-membered ring products **4** is expected. So far, only one example of each of the compounds **3** and **4** (X = S, R = CH_3) is known; the yields of the multistep syntheses, however, are unsatisfactory.[3]

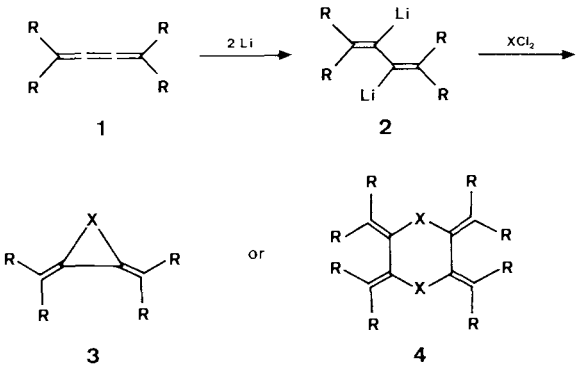

The reaction of 3,4-dilithio-2,5-dimethyl-2,4-hexadiene **2a**[1,2] with dichlorodimethylstannane in diethyl ether at 0°C does not result in formation of the three-membered ring compound **3** (X = $Sn(CH_3)_2$, R = CH_3), but rather of the formal dimer, the six-membered ring compound 1,1,4,4-tetramethyl-2,3,5,6-tetra-2-propylidene-1,4-distannacyclohexane **4a** (yield 45%, not optimized, the remainder being presumably polymer), a colorless, crystalline, air-stable substance.

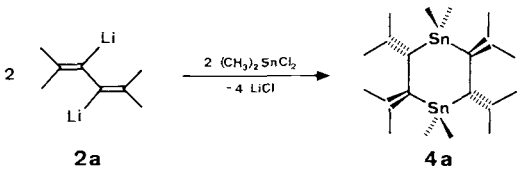

The six-membered ring structure is indicated by the long-range SnH and SnC couplings in the ^{1}H- and ^{13}C-NMR spectrum, respectively, and by the mass spectrum (Table 1). Thus, the signals of the allyl protons of **4a** at $\delta = 1.59$ and 1.75, for example, exhibit not only a $^4J_{SnH}$ coupling to *one* tin atom but also an additional $^5J_{SnH}$ coupling to a second tin atom. The different SnC couplings to the two tin atoms make it possible to assign unequivocally the ^{13}C-NMR signals of the olefinic C atoms. Differences in the magnitudes of the coupling constants to the nuclei ^{117}Sn and ^{119}Sn are only observed for the Sn-bonded C atoms and for the protons of the Sn-bonded methyl groups.

Table 1. ^{1}H- and ^{13}C-NMR data and MS data for **4a**; J values in Hz for ^{119}Sn in each case.

^{1}H-NMR (80 MHz, $CDCl_3$): $\delta = 0.25$ (s, 12H, $2 \times Sn(CH_3)_2$, $^2J(SnH) = 52.2$), 1.59 (s, 12H, $4 \times CH_3$, $^4J(SnH) = 12.3$, $^5J(SnH) = 7.6$), 1.75 (s, 12H, $4 \times CH_3$, $^4J(SnH) = 16.7$, $^5J(SnH) = 10.6$)

^{13}C-NMR (20.1 MHz, $CDCl_3$): $\delta = -5.63$ ($Sn(CH_3)_2$, $^1J(SnC) = 302.7$), 21.03 (CH_3, $^3J(SnC) = 53.7$), 26.24 (CH_3, $^3J(SnC) = 45.2$), 135.71 (CMe_2, $^2J(SnC) = 28.1$, $^3J(SnC) = 41.5$), 142.25 (SnC, $^1J(SnC) = 468.8$, $^2J(SnC) = 28.1$)

MS: m/z 514 ($M^{\oplus}$, 14%), 499 ($M^{\oplus}$ – Me, 12%), 297 (66%), 135 (100%)

The Sn-bonded methyl groups gave rise to only a single, temperature-independent signal in the ^{1}H-NMR spectrum (even at −90°C) and in the ^{13}C-NMR spectrum. This is evidence in disfavor of a rigid chair conformation. On the other hand, a rapid ring inversion is not expected, since the bulky isopropylidene groups—as revealed by examination of models—can only move past one another with difficulty. In order to clarify unequivocally the conformation of **4a**, an X-ray structure analysis[4] was carried out; it shows that **4a** exists in a twist conformation (Fig. 1).

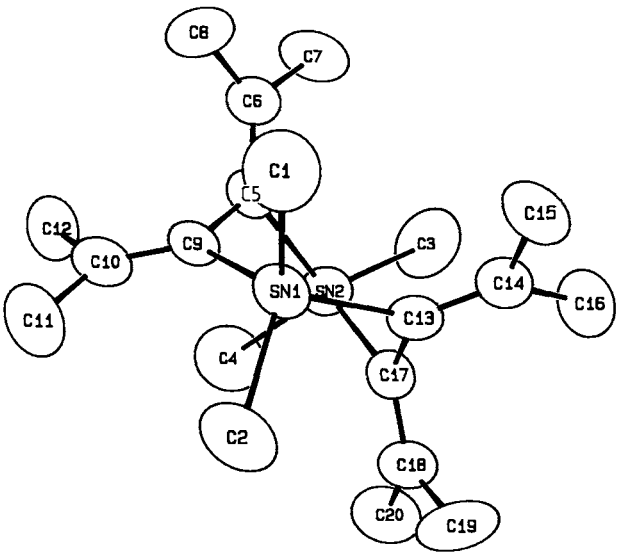

Fig. 1. Molecular structure of **4a** (thermal ellipsoids at the 50% probability level). Important distances [Å] and angles [°]: Sn1-C1 2.155(10), Sn1-C2 2.178(10), Sn2-C3 2.152(10), Sn2-C4 2.182(11), Sn1-C9 2.128(9), Sn1-C13 2.154(8), Sn2-C5 2.129(8), Sn2-C17 2.144(10), C13-C17 1.522(10), C5-C9 1.517(10), C5-C6 1.348(13), C9-C10 1.344(13), C13-C14 1.334(12), C17-C18 1.337(13); C1-Sn1-C2 110.3(4), C3-Sn2-C4 110.0(4), C9-Sn1-C13 101.6(3), C5-Sn2-C17 102.1(3), Sn2-C5-C9 109.0(5), C6-C5-C9 121.8(7), Sn2-C5-C6 129.1(5), Sn1-C9-C10 127.4(6), C5-C9-C10 121.4(8), Sn1-C9-C5 111.1(6), Sn1-C13-C17 109.1(6), Sn1-C13-C14 128.6(5), C14-C13-C17 122.0(7), Sn2-C17-C13 110.4(6), Sn2-C17-C18 127.1(6), C13-C17-C18 122.5(8), dihedral angle C6-C5-C9-C10 84.4(8), C14-C13-C17-C18 83.1(8).

In addition to molecules having the conformation shown, molecules having the enantiomeric conformation exist in the crystal. Attempts to separate the enantiomers

[*] Prof. Dr. A. Maercker, Dipl.-Chem. F. Brauers, Dipl.-Chem. W. Brieden
Institut für Organische Chemie der Universität
Adolf-Reichwein-Strasse, D-5900 Siegen (FRG)
Prof. Dr. H. D. Lutz [+], Dr. M. Jung [+]
Institut für Anorganische Chemie der Universität
Adolf-Reichwein-Strasse, D-5900 Siegen (FRG)

[+] X-ray structure analysis.

[**] Polylithium Organic Compounds, Part 8. This work was supported by the Fonds der Chemischen Industrie and the Stiftung Volkswagenwerk.—Part 7: A. Maercker, B. Grebe, *J. Organomet. Chem. 334* (1987) C21.

of **4a** by HPLC on chiral stationary phases have been unsuccessful so far,[5] indicating that the stationary phases were not suitable or that the barrier to inversion of **4a** is too low.

Noteworthy in the structure of **4a** are, on the one hand, the large dihedral angles within the two butadiene units—the angles C6-C5-C9-C10 and C14-C13-C17-C18 (Fig. 1) are 84 and 83°, respectively—and, on the other, the torsion angle of 48° between the two $C_{CH_3}SnC_{CH_3}$ planes; both indicate that the six-membered ring is strained. The central bonds of the butadiene units, which are not conjugated, have lengths of 1.522(10) (C13-C17) and 1.517(10) Å (C5-C9).

In contrast to the analogous disulfur compound **4** (X = S, R = CH_3),[3] **4a** does not undergo [4+2] cycloaddition with 4-phenyl-1,2,4-triazole-3,5-dione. Presumably, the coplanar arrangement of the isopropylidene groups is rendered even more difficult by the Sn methyl groups.

Experimental Procedure

4a: A 1.0 molar solution of **2a** (55 mL) in diethyl ether (450 mL) was added over 2 h to a stirred solution of dichlorodimethylstannane (11.0 g, 0.05 mol; Merck) in diethyl ether (50 mL) at 0°C. After aqueous workup, the residue was distilled (135–145°C/0.01 torr). After addition of *n*-hexane, **4a** crystallized at −25°C. It was then recrystallized from *n*-hexane. Yield according to GC: 45% (standard: *trans*-stilbene); yield of pure product, 2.3 g (18%); m.p. = 195–196°C; correct C,H analysis.

Received: October 19, 1987 [Z 2479 IE]
German version: *Angew. Chem. 100* (1988) 413

CAS Registry numbers:
2a, 96445-43-1; **4a**, 112897-93-5; $(CH_3)_2SnCl_2$, 753-73-1.

[1] A. Maercker, R. Dujardin, *Angew. Chem. 97* (1985) 612; *Angew. Chem. Int. Ed. Engl. 24* (1985) 571.

[2] A. Maercker, R. Dujardin, F. Brauers, *Organomet. Synth. 4* (1988), in press.

[3] W. Ando, Y. Hanyu, T. Takata, K. Ueno, *Tetrahedron Lett. 26* (1985) 3019.

[4] **4a**: crystal dimensions 0.5 mm × 0.5 mm × 0.2 mm, space group $P2_1/c$, $a = 19.824(3)$, $b = 15.219(3)$, $c = 17.196(9)$ Å, $\beta = 114.13(2)°$, $V = 4734.7$ Å^3, $Z = 8$, $\rho_{calcd} = 1.44$ g cm^{-3}, $\rho_{obs} = 1.43$ g cm^{-3}, $Mo_{K\alpha}$, measurement temperature 20°C, maximum angle $\theta_{max} = 30°$, 5098 measured reflections, 3905 observed ($I > 3\sigma(I)$), 398 parameters, $R = 0.047$. Further details of the crystal structure investigation are available on request from the Fachinformationszentrum Energie, Physik, Mathematik GmbH, D-7514 Eggenstein-Leopoldshafen 2 (FRG), on quoting the depository number CSD-52748, the names of the authors, and the journal citation.

[5] Columns: Bakerbond Chiral (DNBPG-Covalent) HPLC columns (J. T. Baker Research Products, Phillipsburg, NJ, USA), EC 250/8/4 Cel-Ac-40XF (Macherey-Nagel GmbH + Co. KG, Düren, FRG).

[(η⁵-C_5Me_4Et)Rh(μ,η²-P_2)]$_2$Rh(η⁵-C_5Me_4Et)], a Sandwich Complex with a P_4 Rectangle**

By *Otto J. Scherer,* Magdalena Swarowsky,* and *Gotthelf Wolmershäuser*

Triple-decker sandwich complexes containing a *cyclo*-P_x middle deck are known for *cyclo*-P_3,[1] *cyclo*-P_5,[2] and *cyclo*-P_6.[3] The question of what form planar P_4 (square **A**, rectangles **B** and **C**) would be stabilized in such complexes remains to be answered.[4a]

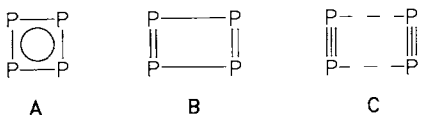

A partial answer is provided by the structural elucidation of the binuclear sandwich complex **2b**, which we obtained from **1b** and white phosphorus (P_4).

$$2[LRh(CO)_2] \xrightarrow[8\ h,\ 150°C]{P_4,\ xylene} [LRh(P_4)RhL]$$

1 **2**

a, L = (η⁵-C_5Me_5); **b**, L = (η⁵-C_5Me_4Et)

Complexes **2a,b** form orange crystals, which may be handled in the air and which are moderately soluble in *n*-pentane and readily soluble in dichloromethane and toluene. The ^{1}H- and ^{31}P{^{1}H}-NMR data[5] of **2a,b** show hardly any differences. Noteworthy in both cases is the small ^1J(RhP) coupling of ca. 27 Hz; values of this order of magnitude are also found for **3**[6] and **4a,b**, which contain 1,3-diphosphacyclobutadiene as ligand.[7] In the mass spectrum[5] of **2a,b**, the most intense peak is due to the molecular ion; P_4 and P_2 appear as P_x fragments.

[(η³-P_3)Rh{$MeC(CH_2PPh_2)_3$}] **3**[6]

[{η⁴-(*t*BuCP)$_2$}Rh(η⁵-C_5R_5)] **4a**, R = H; **4b**, R = Me[7]

The X-ray structure analysis[8] shows that the two five-membered rings and the P_4 structural unit of **2b** are planar and parallel to one another (Fig. 1). Whereas the P1–P2

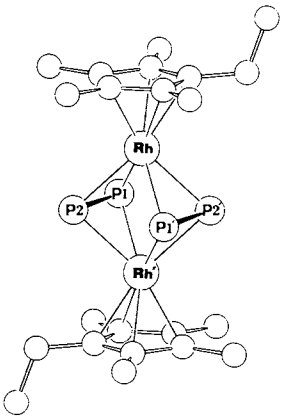

Fig. 1. Molecular structure of **2b**. Selected bond lengths [Å] and angles [°]: Rh···Rh' 3.324(1), Rh-P1 2.418(1), Rh-P2 2.413(1), Rh-P1' 2.416(1), Rh-P2' 2.418(1), Rh-C 2.198(4)–2.220(4), P1-P2 2.052(2), P1···P2' 2.845(2), $C_{(r)}$-$C_{(r)}$ 1.414(6)–1.438(6), $C_{(r)}$-$C_{(t)}$ 1.493(7)–1.513(6), Rh-$L_{(centr.)}$ 1.851, Rh-$P_{4(centr.)}$ 1.662; P1-P2-P1' 90.0(1), P2-P1-P2' 90.0(1), Rh-P1-Rh' 86.9(1), Rh-P2-Rh' 86.9(1), P1-Rh-P2 50.3(1), P1-P2-Rh 65.0(1), P2-P1-Rh 64.8(1). — (r) = ring, (t) = terminal, L = η⁵-C_5Me_4Et.

distance (2.052(2) Å) of the shorter side of the P_4 rectangle lies in the range expected for μ,η²-P_2 units,[4] the length of its long side (P1···P2' 2.845(2) Å) is nearly identical with that of the "short" P···P side (2.849(5) Å) of the P_4 trapezoid of **5**;[9] this value lies just in the range found for the "long" P–P distances (2.4–2.8 Å) of metal phosphides.[10] The RhP_4Rh framework of **2** may be regarded as the molecular pendant to the three-dimensionally linked NbP_4Nb fragment of the NbPS solid-state structure.[11] Whereas **2b**

[*] Prof. Dr. O. J. Scherer, Dipl.-Chem. M. Swarowsky, Dr. G. Wolmershäuser [+]
Fachbereich Chemie der Universität
Erwin-Schrödinger-Strasse, D-6750 Kaiserslautern (FRG)

[+] X-ray structure analysis.

[**] This work was supported by the Fonds der Chemischen Industrie.

should be regarded as a binuclear sandwich complex having two four-electron donor μ,η^2-P_2 ligands (i.e., 18 valence electrons (VE) per Rh atom), the bonding in the Co analogue **6** is more complicated. The X-ray structure analysis reveals two independent molecules per unit cell,[12] each of whose Co-Co distances is ca. 3.1 Å. In this case, the P_4

cis-$[(\eta^5\text{-}C_5Me_5)(CO)MoP_2\{Cr(CO)_5\}]_2$ **5**[9]

$[(\eta^5\text{-}C_5Me_4Et)Co(P_4)Co(\eta^5\text{-}C_5Me_4Et)]$ **6**[12]

$[Rh_2Cl_2\{(\eta^5\text{-}C_5H_5)Rh\{\eta^4\text{-}(t\text{BuCP})_2\}\}_4]$ **7**[14]

bridging ligand forms a "long" (similar to that of **2b**) and a "short" (32-VE triple-decker with *cyclo*-P_4?) rectangle, whose average P-P values correspond almost exactly to the distance of 2.38 Å in the cubic (metallic) modification[13] of black phosphorus ($\bar{d}$(P-P) = 2.45 Å for **2b**). The Rh-Rh' distance of **2b** (3.324(1) Å) is significantly longer than d(M-M) for triple-decker complexes (2.63–2.73 Å) containing a *cyclo*-$P_{5(6)}$ middle deck and exhibiting metal-metal interaction;[2,3] the average Rh-P value for **2b** (2.416 Å) is larger than that observed for 7 (2.335 Å).[14]

Experimental Procedure

2a,b: **1a** (650 mg, 2.2 mmol) [15a] [**1b** (600 mg, 1.95 mmol) [15b]] and P_4 (547 mg, 4.4 mmol) [483 mg, 3.9 mmol) were stirred in refluxing xylene (ca. 30 mL) for 8 h. The reaction solution (containing small amounts of insoluble components) was concentrated to 10 mL under oil-pump vacuum, treated with 3 g of Al_2O_3 (basic, activity II), and then dried under oil-pump vacuum to afford a freely flowing solid. Upon chromatography (column: 25 × 2.5 cm), excess P_4 was eluted as a yellow forerun with pentane. Elution with pentane/toluene (1 : 1) then afforded **2a,b** as a yellow-orange fraction. After removal of the solvent under oil-pump vacuum, **2a,b** were obtained as spectroscopically pure, orange powders. Recrystallization from pentane (ca. −18 °C) afforded **2a** as needle-shaped and **2b** as cube-shaped, orange crystals. Yield **2a**: 207 mg (31%) [**2b**: 190 mg (31%)].

Received: November 4, 1987 [Z 2492 IE]
German version: *Angew. Chem. 100* (1988) 423

CAS Registry numbers:
1a, 32627-01-3; **1b**, 113035-21-5; **2a**, 113035-19-1; **2b**, 113035-20-4.

[1] Review: M. Di Vaira, L. Sacconi, *Angew. Chem. 94* (1982) 338; *Angew. Chem. Int. Ed. Engl. 21* (1982) 330.
[2] O. J. Scherer, J. Schwalb, G. Wolmershäuser, W. Kaim, R. Gross, *Angew. Chem. 98* (1986) 349; *Angew. Chem. Int. Ed. Engl. 25* (1986) 363.
[3] O. J. Scherer, H. Sitzmann, G. Wolmershäuser, *Angew. Chem. 97* (1985) 358; *Angew. Chem. Int. Ed. Engl. 24* (1985) 351; O. J. Scherer, J. Schwalb, H. Swarowsky, G. Wolmershäuser, W. Kaim, R. Gross, *Chem. Ber.*, in press.
[4] a) O. J. Scherer, *Comments Inorg. Chem. 6* (1987) 1; b) M. Di Vaira, P. Stoppioni, M. Peruzzini, *Polyhedron 6* (1987) 351.
[5] ^{1}H-NMR (200 MHz, C_6D_6, TMS int.): **2a**: δ = 1.71 (sext., ^3J(RhH) = ^4J(PH) = 0.55 Hz); **2b**: δ = 1.70 (s, 24H), 2.27 (q, 4H), 0.79 (t, 6H). ^{31}P{^{1}H}-NMR (80.82 MHz, [D_8]toluene, 85% H_3PO_4 ext.): **2a**: δ = −37.5 (t, ^1J(RhP) = 27.4 Hz); **2b**: δ = −40.4 (t, ^1J(RhP) = 27.0 Hz). EI-MS: **2a** (70 eV): *m/z* 600 ($M^{\oplus}$, 100%), $P_4^{\oplus}$ (8.3), $P_2^{\oplus}$ (4.2), and other peaks; **2b** (18 eV): *m/z* 628 ($M^{\oplus}$, 100%), $P_4^{\oplus}$ (15.4), $P_2^{\oplus}$ (14.7), and other peaks.
[6] M. Di Vaira, L. Sacconi, P. Stoppioni, *J. Organomet. Chem. 250* (1983) 183.
[7] P. B. Hitchcock, M. Jamil Maah, J. F. Nixon, *J. Chem. Soc. Chem. Commun. 1986*, 737; see also: P. Binger, R. Milczarek, R. Mynott, M. Regitz, W. Rösch, *Angew. Chem. 98* (1986) 645; *Angew. Chem. Int. Ed. Engl. 25* (1986) 644.
[8] **2b**: monoclinic, $P2_1/n$, a = 7.9175(9), b = 8.2345(6), c = 19.4581(15) Å, β = 96.47(1)°, Z = 2, V = 1260.5(2) Å^3, ρ_{calcd} = 1.655 g cm^{-3}. 1693 of 2074 unique reflections observed ($Mo_{K\alpha}$, $F_o^2 \geq 2.0\sigma(F_o^2)$, $2\theta \leq 50°$). 180 refined parameters, R = 0.027, R_w = 0.032. Further details of the crystal structure investigation may be obtained from the Fachinformationszentrum Energie, Physik, Mathematik GmbH, D-7514 Eggenstein-Leopoldshafen 2 (FRG), on quoting the depository number CSD-52788, the names of the authors, and the journal citation.
[9] O. J. Scherer, H. Sitzmann, G. Wolmershäuser, *J. Organomet. Chem. 309* (1986) 77.
[10] D. E. C. Corbridge: *The Structural Chemistry of Phosphorus*, Elsevier, New York 1974.
[11] Detailed theoretical investigations: D. A. Keszler, R. Hoffmann, *J. Am. Chem. Soc. 109* (1987) 118 and references cited therein concerning related solid-state structures (cf. also [10] for MP and MP_2 structures).
[12] O. J. Scherer, M. Swarowsky, G. Wolmershäuser, unpublished results; see also O. J. Scherer, *Nachr. Chem. Tech. Lab. 35* (1987) 1140.
[13] J. C. Jamieson, *Science 139* (1963) 1291.
[14] P. B. Hitchcock, M. Jamil Maah, J. F. Nixon, C. Woodward, *J. Chem. Soc. Chem. Commun. 1987*, 844.
[15] a) J. W. Kang, P. M. Maitlis, *J. Organomet. Chem. 26* (1971) 393; b) O. J. Scherer, M. Swarowsky, unpublished results.

Tetraoxaporphyrin Dication**

By *Emanuel Vogel,* Wilhelm Haas, Bernd Knipp, Johann Lex,* and *Hans Schmickler*

Sondheimer's [18]annulene **1**,[1] the classic example of a simple benzene homologue that conforms to the Hückel rule, exhibits a striking dichotomy with respect to aromatic character: although the molecule fulfills the physical criteria for aromaticity, it displays a high reactivity similar to that of polyenes owing to its conformational flexibility. Comparison of the chemical behavior of **1** with that of bridged annulenes, such as 1,6-methano[10]annulene,[2] clearly highlights the fact that the rigidity of the ring skeleton is an essential prerequisite for the stability of a [4n + 2]annulene with n > 1.

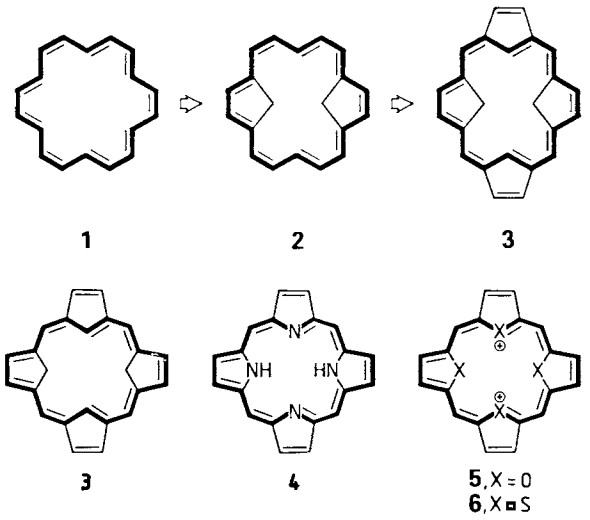

Among the numerous possible ways of making the [18]annulene **1** rigid while maintaining planarity,[3] the incorporation, according to **2** and **3**, of two CH_2 and two CH=CH groups as inner and outer bridges, respectively, is a representative case. The resulting bridged [18]annulene **3**, which has not been reported so far, commands great scientific interest since it constitutes the hydrocarbon parent structure of the *porphyrins* (**4**: porphyrin[4]) — *the*

[*] Prof. Dr. E. Vogel, Dr. W. Haas, B. Knipp, Dr. J. Lex, Dr. H. Schmickler
Institut für Organische Chemie der Universität
Greinstrasse 4, D-5000 Köln 41 (FRG)
[**] Presented in a plenary lecture at the Autumn Meeting of the Royal Society of Chemistry, Nottingham (England), September 22–24, 1987.

bridged annulenes of nature. Like **3**, the no less intriguing oxygen and sulfur analogues of the porphyrins,[5,6] tetraoxaporphyrin and tetrathiaporphyrin, **5** and **6**, respectively, still await synthesis. In terms of 18π-electron systems, **5** and **6** are dications[7] describable by resonance structures with oxonium oxygen and sulfonium sulfur atoms, respectively (see structural formula), as well as by those with a dicationic C_{20} perimeter. Similar to square-planar metalloporphyrins, **5** most likely exhibits D_{4h} symmetry, whereas, in the case of **6**, the possibility must be considered that the molecule deviates from planarity owing to the large sulfur atoms. Despite the fact that porphyrins are now commonly regarded as NH-bridged diaza[18]annulenes, quite a number of questions remain unanswered regarding the π-electron structure of these chemically and biologically extremely important tetrapyrrolic macrocycles.[8] The prospect of arriving at a deeper understanding of the bonding in porphyrins by means of **3**, **5**, and **6** makes these three new ring systems attractive synthetic goals.

We report here on a route to the tetraoxaporphyrin dication **5** as its perchlorate **5a**. A possible synthetic approach to **5** suggesting itself is the two-electron oxidation of the oxygen-bridged [20]annulene **7**, which is likewise unknown. Since **5** is certain to exhibit considerable resonance stabilization, the readiness with which the annulene **7** undergoes electron transfer might be so pronounced that it could be regarded as a "pseudometal."[9] Such reasoning about **5**/**7** also provided the motivation for the synthesis of the tetraoxaporphycene dication **10** (as the perchlorate), which was realized in a parallel investigation.[10]

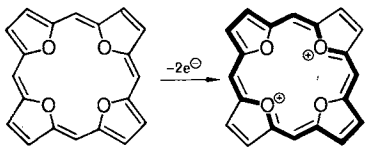

7 **5**

Synthetic approach

Compound **7**[11] should, in principle, be easy to synthesize by a MacDonald condensation[9, 12] of 5,5′-methylenedi-2-furaldehyde **8**[13] with 2,2′-difurylmethane **9**. Unlike the case in porphyrin syntheses, this condensation would not be followed by a dehydrogenation step. Reaction of **8** (1.02 g, 5 mmol) with **9** (0.74 g, 5 mmol) in dichloromethane (100 mL) in the presence of 40 mL of trifluoroacetic acid (2 h, room temperature) was not encouraging, however, since it resulted in the formation of a reaction mixture showing no spectroscopic evidence of **7**. A closer inspection of the literature on porphyrins made us speculate that **7** might be present in latent form and thus led us to oxidize the mixture (after removal of solvent) by direct addition of 30 mL of 65% nitric acid (48 h, room temperature) — as in the preparation of the tetraoxaporphycene dication **10**.[10] This unconventional experiment was indeed successful. A reddish-brown solution formed from which, upon slow addition of 10 mL of 70% perchloric acid, the desired tetraoxaporphyrin dication **5** separated as the perchlorate **5a** in the form of violet crystals (needles) [dec. above 310°C; yield 206 mg (8%)].

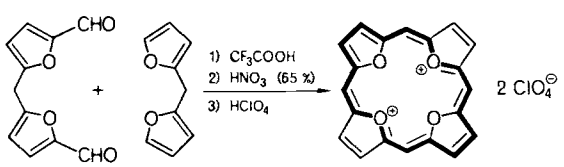

8 **9** **5a**

Compound **5a** is virtually insoluble in common organic solvents. In water, it undergoes decomposition in a surface reaction. Thus, strong mineral acids, preferably concentrated sulfuric acid (good solubility) are the primary solvents of choice.[14] The spectroscopic structural proof of **5a** was very easy owing to the high symmetry of the compound as well as to the fact that the tetraoxaporphycene dication **10** provided an ideal reference substance.[10]

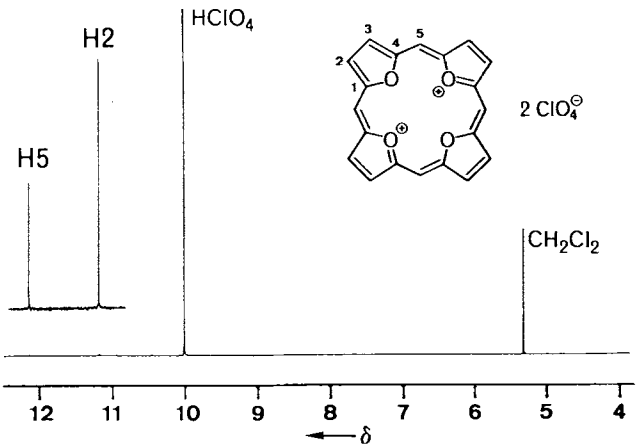

Fig. 1. ^{1}H NMR spectrum of **5a** (300 MHz, 68% $DClO_4$, CH_2Cl_2 int.).

The ^{1}H NMR spectrum (Table 1 and Fig. 1) shows only two signals ($\delta = 12.13$ and 11.17) in the region expected for an aromatic dication **5** describable by resonance structures involving oxonium oxygen atoms,[10, 15] while the ^{13}C NMR spectrum complements these results in displaying three signals, one for a quaternary and two for proton-bearing sp^2-hybridized carbon atoms. If any further argument were needed to demonstrate the close structural relationship between porphyrin and porphycene systems,[10, 16] it is provided by the striking agreement in the ^{1}H and ^{13}C NMR parameters between **5a** and **10**.

Table 1. ^{1}H NMR (300 MHz) and ^{13}C NMR data (75.5 MHz) of **5a** and **10** (68% $DClO_4$, CH_2Cl_2 int.). Chemical shifts δ_H and δ_C and coupling constants J [Hz].

	H2	H3	H5	C1	C2	C3	C4	C5
		$^3J(^1H\text{-}^1H)$				$^1J(^{13}C\text{-}^1H)$		
5a	11.17		12.13	157.03	139.61			104.87
	$J(2,3)=4.71$ [a]			—	188 [a]			168 [a]
10	10.93	11.46	11.30 [b]	159.25	140.52	135.91	148.12	118.84 [b]
	$J(2,3)=4.87$			—	188	189	—	166
	$J(9,10)=11.6$							

[a] The coupling constants were taken from the spectrum of **5a** in 68% DNO_3 (better solubility of **5a**); [b] δ_H of H9, δ_C of C9 (for numbering of **10** see [10]).

The UV/VIS spectrum of **5a** [in 96% H_2SO_4: $\lambda_{max} = 298$ nm ($\varepsilon = 7500$), 325 (7100), 341 (16700) sh, 351 (51000), 359 (79000), 370 (1020000), 470 (430) sh, 486 (1330) sh, 494 (1580) sh, 499 (1910), 524 (18600), 529 (14600) sh, 543 (3400) sh, 569 (1600)] has — like that of **10** — the shape characteristic of porphyrin spectra: a strong B band (Soret

band) in the near ultraviolet and weak Q bands in the visible region.[8b] As revealed in Figure 2, the change from **10**

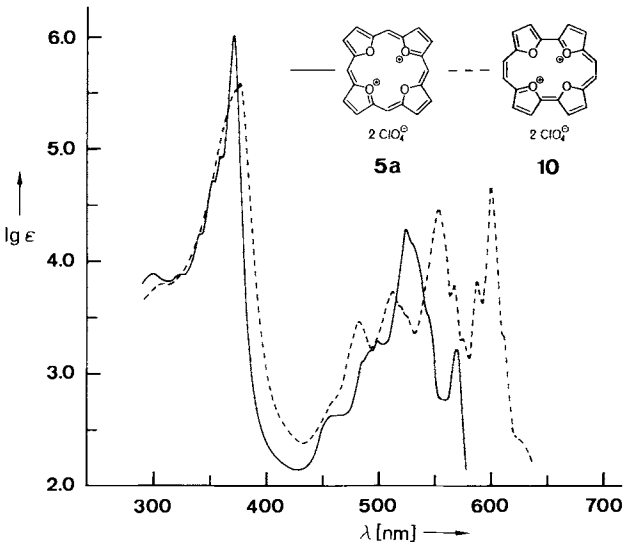

Fig. 2. UV/VIS spectra of **5a** (96% H_2SO_4) and **10** (70% $HClO_4$).

to **5a** is reflected in the spectrum primarily by a reduction in the splitting of both types of bands, especially the Q bands. It seems reasonable to interpret these differences in terms of a transformation from a D_{2h}- to a D_{4h}-type of spectrum (in analogy to porphyrin versus metalloporphyrin spectra).[17]

The IR spectrum of **5a** exhibits relatively few bands,[18] which is in agreement with the assumption that, in analogy to square-planar-coordinated metalloporphyrins,[19] **5** possesses D_{4h} symmetry (for **5**, this symmetry leads to the expectation of seventeen IR-active in-plane and five IR-active out-of-plane normal mode vibrations).

An insight into the molecular structure of **5a** is provided by an X-ray structure analysis[20] (Fig. 3). The dication **5** is very nearly planar (maximum deviation of the C and O atoms from the mean plane, ±0.03 Å; maximum torsional angle, 2.6°) and has virtually the postulated D_{4h} symmetry. The molecular shape of **5** (Fig. 3, top) is largely in agreement with that of porphyrin **4**,[21] but the replacement of nitrogen by oxygen atoms results in the C_α–C_β bond lengths in the heterocyclic five-membered rings being strikingly short [1.442 versus 1.406 Å (average values)], the C_β–C_β bond lengths remaining roughly constant. In parallel herewith, the internal bond angles at the *meso*-methine carbon atoms are expanded by ca. 3.7° [from 127.1 to 130.8° (average values)]. Interestingly, these structural changes, which amount to a contraction of the C_{20} molecular perimeter, do not have an effect on the dimensions of the inner cavity: The O···O distances (O···O′, 2.869 Å; O···O‴, 2.900 Å) are the same within the limits of error as the N···N distances in porphyrin (between 2.879 and 2.901 Å).[22] As shown in the side view of the molecule (Fig. 3, bottom), the dicationic tetraoxaporphyrin, in accordance with the stoichiometry, is associated with two perchlorate ions, which are situated above and below the ring framework.

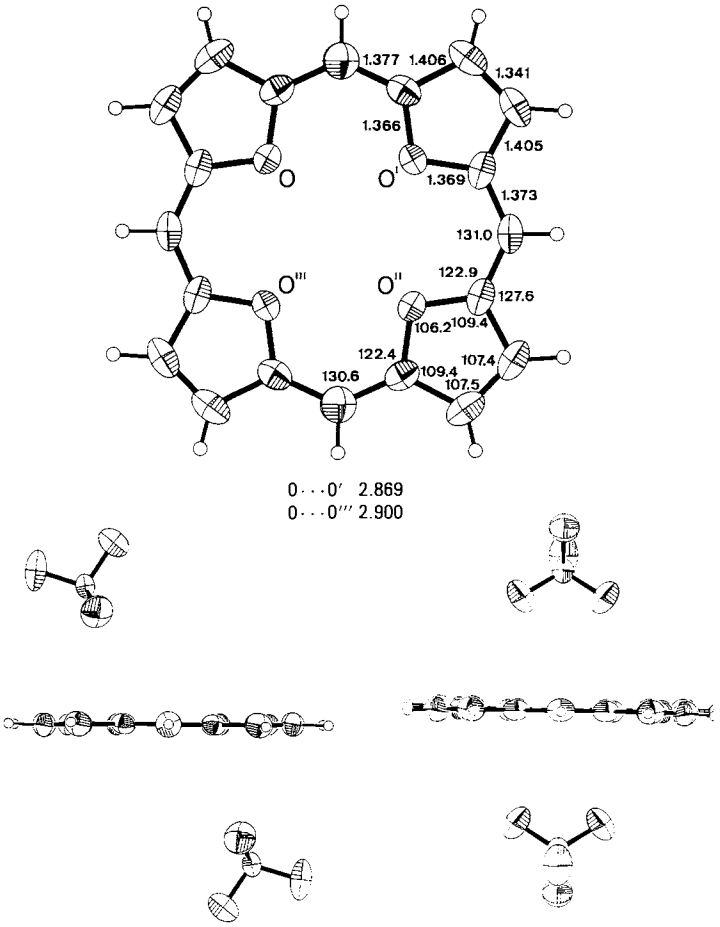

Fig. 3. Molecular structure of **5a**. Top: Viewed from above (tetraoxaporphyrin dication). Bottom: Two side views (rotated by 90°) of an isolated unit consisting of a tetraoxaporphyrin dication and two perchlorate ions. Selected bond lengths, nonbonded contacts [Å], and bond angles [°]; standard deviations ca. 0.003 Å and 0.2°. The thermal ellipsoids are drawn at the 40% probability level.

In view of the long history of porphyrin chemistry, it is amazing that the conceptually very simple tetraoxaporphyrin dication **5** remained unknown for so long. The synthesis of this compound occupies a position of central importance in our research, since it establishes a bridge between annulene and porphyrin chemistry, a connection we have sought since the first NH-bridged [4n+2]annulene, i.e., 1,6-imino[10]annulene,[23] was made in this laboratory more than two decades ago.

Received: September 22, 1987 [Z 2438 IE]
Publication delayed at authors' request
German version: *Angew. Chem. 100* (1988) 445

[1] F. Sondheimer, I. C. Calder, J. A. Elix, Y. Gaoni, P. J. Garratt, K. Grohmann, G. di Maio, J. Mayer, M. V. Sargent, R. Wolovsky in: *Aromaticity. Special Publication No. 21*, Chemical Society, London 1967, p. 75; K. Stöckel, F. Sondheimer, *Org. Synth. 54* (1974) 1; P. J. Garratt: *Aromaticity*, Wiley, New York 1986.

[2] E. Vogel in: *Aromaticity. Special Publication No. 21*, Chemical Society, London 1967, p. 113; E. Vogel, W. Klug, A. Breuer, *Org. Synth. 54* (1974) 11.

[3] G. M. Badger, J. A. Elix, G. E. Lewis, *Aust. J. Chem. 19* (1966) 1221; T. Otsubo, R. Gray, V. Boekelheide, *J. Am. Chem. Soc. 100* (1978) 2449; H. Ogawa, N. Sadakari, T. Imoto, I. Miyamoto, H. Kato, Y. Taniguchi, *Angew. Chem. 95* (1983) 412; *Angew. Chem. Int. Ed. Engl. 22* (1983) 417;

Angew. Chem. Suppl. 1983, 471. Kekulene [F. Diederich, H. A. Staab, *Angew. Chem. 90* (1978) 383; *Angew. Chem. Int. Ed. Engl. 17* (1978) 372] can be regarded formally as a conformationally rigid [18]annulene.

[4] According to the new IUPAC nomenclature for tetrapyrroles [*Pure Appl. Chem. 59* (1987) 779] the porphyrin parent compound is no longer called porphin but instead porphyrin.

[5] Mono- and dioxaporphyrins are known through the elegant work of *A. W. Johnson* on structural variants of porphyrins: A. W. Johnson in K. M. Smith (Ed.): *Porphyrins and Metalloporphyrins*, Elsevier, Amsterdam 1975, p. 729. 21,22-Dioxa- and 21,23-dioxaporphyrins (alkyl-substituted) exhibit an unexpectedly high basicity and have not yet been obtained as such; they are isolated as the stable hydrobromides [6a].

[6] There have been several reports on mono- and dithiaporphyrins and on diselenaporphyrins: a) M. J. Broadhurst, R. Grigg, A. W. Johnson, *J. Chem. Soc. C 1971*, 3681; b) A. Ulman, J. Manassen, *J. Am. Chem. Soc. 97* (1975) 6540; c) A. Ulman, J. Manassen, F. Frolow, D. Rabinovich, *ibid. 101* (1979) 7055; d) R. L. Hill, M. Gouterman, A. Ulman, *Inorg. Chem. 21* (1982) 1450; e) L. Latos-Grażyński, J. Lisowski, M. M. Olmstead, A. L. Balch, *J. Am. Chem. Soc. 109* (1987) 4428; f) for an attempted synthesis of tetrathiaporphyrins, see M. Ahmed, O. Meth-Cohn, *J. Chem. Soc. C 1971*, 2104.

[7] Strictly speaking, **5** and **6** correspond to diprotonated porphyrin.

[8] a) J. Michl, *J. Am. Chem. Soc. 100* (1978) 6801 (in this work, the tetraoxaporphyrin dication **5** was discussed for the first time); b) M. Gouterman in D. Dolphin (Ed.): *The Porphyrins, Vol. III*, Academic Press, New York 1978, p. 1; c) I. Gutman, *Croat. Chem. Acta 58* (1985) 359.

[9] The nitrogen analogue of **7**, the likewise unknown isophlorin **11**, probably possesses such a high tendency to undergo two-electron oxidation (formation of diprotonated porphyrin **12**) that there is little likelihood of its being isolated; see the discussion of *R. B. Woodward* in connection with the synthesis of chlorophyll [*Angew. Chem. 72* (1960) 651].

[10] E. Vogel, M. Sicken, P. Röhrig, H. Schmickler, J. Lex, O. Ermer, *Angew. Chem. 100* (1988) 450; *Angew. Chem. Int. Ed. Engl. 27* (1988) 411.

[11] The [20]annulene **7** is probably prone to polymerize owing to the presence of two *o*-quinonoid furan units; for pertinent references see: H. E. Winberg, F. S. Fawcett, W. E. Mochel, C. W. Theobald, *J. Am. Chem. Soc. 82* (1960) 1428; W. S. Trahanovsky, M.-G. Park, *J. Org. Chem. 39* (1974) 1448.

[12] G. P. Arsenault, E. Bullock, S. F. MacDonald, *J. Am. Chem. Soc. 82* (1960) 4384; J. A. S. Cavaleiro, A. M. d'A. Rocha Gonsalves, G. W. Kenner, K. M. Smith, *J. Chem. Soc. Perkin Trans. 1 1974*, 1771.

[13] P. S. Clezy, V. Diakiw, *Aust. J. Chem. 24* (1971) 2665; P. S. Clezy, C. Parnis, *ibid. 25* (1972) 2055.

[14] Attempts to prepare salts having more favorable solubility properties are underway.

[15] The signals of the vinylic protons of diprotonated dioxaporphyrins are found in the same resonance region ($\delta = 10$–12) [6a].

[16] E. Vogel, M. Köcher, H. Schmickler, J. Lex, *Angew. Chem. 98* (1986) 262; *Angew. Chem. Int. Ed. Engl. 25* (1986) 257.

[17] A detailed analysis of the absorption spectra will be carried out in collaboration with *G. Hohlneicher* (Universität Köln) and *J. Michl* (University of Texas at Austin).

[18] IR spectrum (Nujol) of **5a**: $\tilde{\nu} = 3129, 3112, 3062, 1569, 1495, 1446, 1365, 1221, 1149, 1096$ ($ClO_4^{\ominus}$), 1049 ($ClO_4^{\ominus}$), $972, 959, 936, 900, 845, 819, 798, 696, 685, 623$ ($ClO_4^{\ominus}$) cm^{-1}.

[19] H. Ogoshi, Y. Saito, K. Nakamoto, *J. Chem. Phys. 57* (1972) 4194.

[20] $C_{20}H_{12}Cl_2O_{12}$, dec. above 310°C, crystals from $HNO_3/HClO_4$; monoclinic, space group $C2/m$, $Z = 2$; $a = 14.330(3)$, $b = 12.237(3)$, $c = 5.887(1)$ Å, $\beta = 100.97(2)°$; $\rho_{calcd} = 1.688$ g cm^{-3}; intensities measured on a four-circle diffractometer [room temperature, $\lambda_{Mo} = 0.71069$ Å, $\theta_{Mo}(max) = 27°$], refinement (C, Cl, O anisotropic, H isotropic) using 937 reflections with $F_0 > 4\sigma(F_0)$; $R = 0.043$, $R_w = 0.049$. Further details of the crystal structure investigation may be obtained from the Fachinformationszentrum Energie, Physik, Mathematik GmbH, D-7514 Eggenstein-Leopoldshafen 2 (FRG), on quoting the depository number CSD-52872, the names of the authors, and the journal citation.

[21] B. M. L. Chen, A. Tulinsky, *J. Am. Chem. Soc. 94* (1972) 4144.

[22] On going from **4** to **5**, the structural parameters of the heterocyclic five-membered rings are influenced in the same way as on going from porphycene to the tetraoxaporphycene dication.

[23] E. Vogel, W. Pretzer, W. A. Böll, *Tetrahedron Lett. 1965*, 3613.

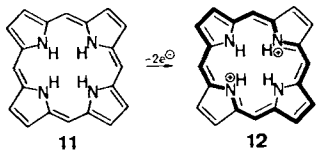

11 **12**

Tetraoxaporphyrinogen (Tetraoxaquaterene): Oxidation to the Tetraoxaporphyrin Dication

By *Wilhelm Haas, Bernd Knipp, Martin Sicken, Johann Lex,* and *Emanuel Vogel**

The porphyrinogens, colorless tetrapyrrolic macrocycles having the structure type **2**, play a central role in porphyrin chemistry, since they are the primary cyclic intermediates in the biosynthesis of hemins and chlorophylls[1] as well as in important laboratory syntheses of porphyrins.[2] The most pertinent chemical feature of these hexahydroporphyrins is the ease with which they undergo oxidation (even in the solid state) to the corresponding porphyrins upon exposure to oxygen or upon treatment with other oxidants. In order to isolate porphyrinogens, therefore, anaerobic conditions are usually required.

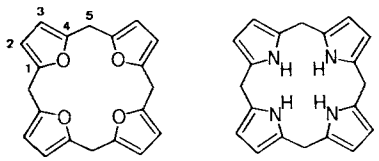

1 **2**

After we synthesized the tetraoxaporphyrin dication **4** as its perchlorate **4a**,[3] the question was raised whether tetraoxaporphyrinogen **1**—in analogy to the biologically significant porphyrinogen-porphyrin transformation—would be oxidizable to **4**. Surprisingly, the parent compound **1** was unknown,[4] although an extensive literature exists regarding the synthesis of tetraoxaporphyrinogens —the so-called tetraoxaquaterenes[5]—by cyclocondensation of furan with ketones and aldehydes.[6] Whereas the route to tetraoxaporphyrin dications is blocked by the geminal substituents in the case of tetraoxaporphyrinogens prepared from ketones, those made from aldehydes, such as 5,10,15,20-tetramethyltetraoxaporphyrinogen,[6c, g] constitute potential precursors of dications of the present kind. We have now succeeded in obtaining **1** and in extending the porphyrinogen-porphyrin transformation to the "tetraoxa series."

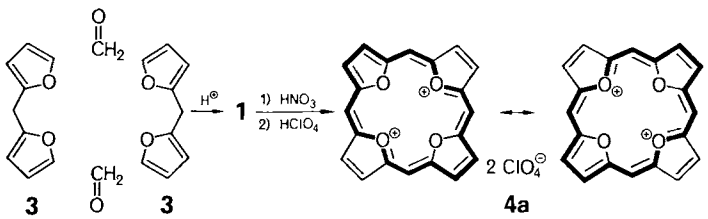

3 **3** **4a**

The acid-catalyzed condensation of furan with formaldehyde[7] affords a complex mixture of products, consisting mainly of polymers, which did not encourage us to search for tetraoxaporphyrinogen **1** that might possibly have been formed. The conjecture that it might be easier to detect **1** if the condensation component furan were replaced by the conceivable intermediate 2,2′-difurylme-

[*] Prof. Dr. E. Vogel, Dr. W. Haas, B. Knipp, M. Sicken, Dr. J. Lex
Institut für Organische Chemie der Universität
Greinstrasse 4, D-5000 Köln 41 (FRG)

thane **3** turned out to be correct. When **3** was allowed to react in methanol/water in the presence of lithium perchlorate and perchloric acid with a 30% aqueous solution of formaldehyde (room temperature, 3 d),[8] the desired **1** could be isolated in small amounts by conventional chromatographic workup of the reaction products on silica gel with toluene as eluent.[9] After sublimation and crystallization from ethanol,[10] **1** was obtained as colorless needles (m.p. = 158–159 °C, yield 0.5–1%).

The ^{1}H NMR spectrum (300 MHz, $CDCl_3$) of **1** exhibits two singlets at $\delta = 5.95$ (H2, $^3J_{2,3} = 2.87$ Hz) and 3.83 (H5), while the ^{13}C NMR spectrum (75.5 MHz, $CDCl_3$), in parallel herewith, shows three resonances at $\delta = 150.91$ (C1), 106.63 (C2, $^1J_{CH} = 172.8$ Hz), and 27.47 (C5, $^1J_{CH} = 128.5$ Hz). The presence of the tetraoxa compound, rather than of an oligomer, is indicated by the base peak at m/z 320 ($M^{\oplus}$) in the mass spectrum (EI, 75 eV). The UV spectrum [in cyclohexane: $\lambda_{max} = 222$ nm ($\varepsilon = 34\,400$)] is in fair agreement with that of 2,5-dimethylfuran[11] with respect to the position of the maximum, but displays an extinction coefficient that is more than four times higher. In the IR spectrum (KBr), strong to medium-strong bands are found at $\tilde{\nu} = 3104$, 2914, 1557, 1217, 1016, 955, 790, 770, and 758 cm^{-1}.

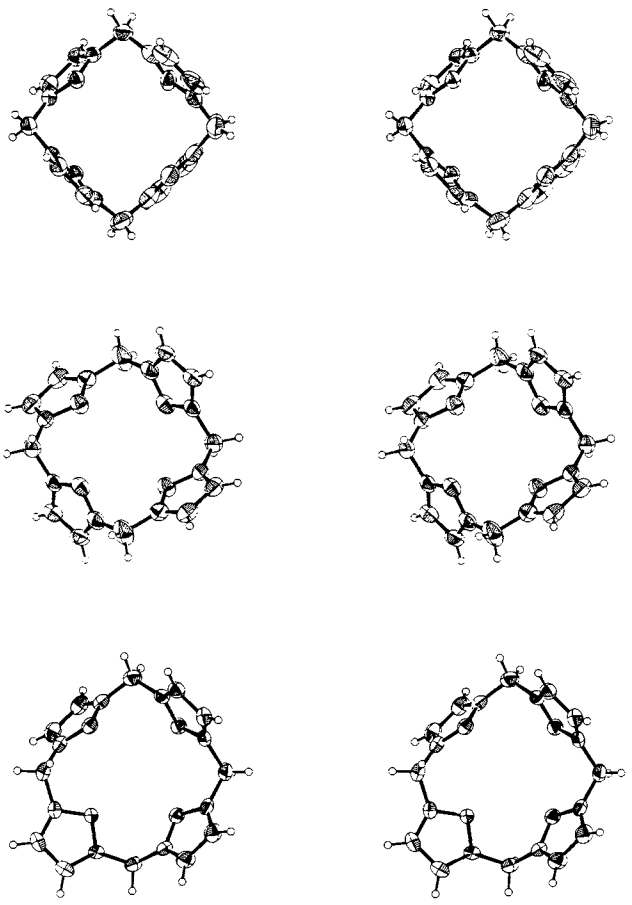

Fig. 1. Top: Stereoprojection of the molecular structure of **1** in the monoclinic crystal modification. Middle and bottom: Stereoprojections of the two independent molecules of **1** in the triclinic crystal modification. The thermal ellipsoids are drawn at the 40% probability level.

According to the X-ray structure analysis (Fig. 1), **1** crystallizes from ethanol in two modifications (form A, monoclinic;[12] form B, triclinic[13]). In form A, **1** exists in only one conformation, whereas two conformations are present in form B, both of which differ significantly from that in form A. The molecules in form A have approximately D_{2d} symmetry (Fig. 1, top). In the case of the two molecular structures in form B, two related conformations are involved (Fig. 1, middle and bottom), one of which (Fig. 1, middle) is characterized by a center of symmetry.[4] In all three conformations, the bond lengths and bond angles are normal.

In contrast to porphyrinogens, tetraoxaporphyrinogen **1** is stable toward oxygen, but it can be converted into **4** by employing nitric acid, the oxidizing agent used advantageously in the original synthesis of the tetraoxaporphyrin dication **4**.[3] Upon treatment of **1** at 0 °C with 65% nitric acid, a reddish-brown solution forms after a short time. Slow addition of perchloric acid to this solution results in the crystallization of the perchlorate **4a** (violet needles, yield 10%). The **4a** thus obtained is identical (^{1}H NMR, UV/VIS, and IR) with an authentic sample.[3]

The attempt to oxidize the known 5,10,15,20-tetramethyltetraoxaporphyrinogen[6c, g] with nitric acid to give the 5,10,15,20-tetramethyl derivative of **4** led, unexpectedly, to complete degradation of the molecule. If, on the other hand, the compound is treated with bromine in dichloromethane and the bromination product, after removal of the solvent, is dissolved in perchloric acid, the perchlorate of the 5,10,15,20-tetramethyltetraoxaporphyrin dication precipitates on standing. A more detailed investigation of this product is currently in progress.[14]

Received: November 26, 1987 [Z 2512 IE]
German version: *Angew. Chem. 100* (1988) 448

CAS Registry numbers:
1, 281-97-0; **3**, 1197-40-6; **4a**, 113086-62-7; formaldehyde, 50-00-0; 5,10,15,20-tetramethylporphyrinogen, 61093-51-4; perchlorate of 5,10,15,20-tetramethyltetraoxaporphyrin dication, 113087-04-0.

[1] A. R. Battersby, E. McDonald in K. M. Smith (Ed.): *Porphyrins and Metalloporphyrins*, Elsevier, Amsterdam 1975, p. 61; D. Mauzerall in D. Dolphin (Ed.): *The Porphyrins, Vol. II*, Academic Press, New York 1978, p. 91; B. Franck, G. Bringmann, C. Wegner, U. Spiegel, *Liebigs Ann. Chem. 1980*, 263.

[2] P. Rothemund, A. R. Menotti, *J. Am. Chem. Soc. 63* (1941) 267; G. P. Arsenault, E. Bullock, S. F. MacDonald, *J. Am. Chem. Soc. 82* (1960) 4384; R. B. Woodward, *Angew. Chem. 72* (1960) 651; D. Dolphin, *J. Heterocycl. Chem. 7* (1970) 275; K. M. Smith in A. R. Katritzky, C. W. Rees (Eds.): *Comprehensive Heterocyclic Chemistry. Vol. 4*, Pergamon Press, Oxford 1984, p. 377.

[3] E. Vogel, W. Haas, B. Knipp, J. Lex, H. Schmickler, *Angew. Chem. 100* (1988) 445; *Angew. Chem. Int. Ed. Engl. 27* (1988) 406; for the synthesis of the tetraoxaporphycene dication analogous to **4**, as the perchlorate, see E. Vogel, M. Sicken, P. Röhrig, H. Schmickler, J. Lex, O. Ermer, *ibid. 100* (1988) 450 and *27* (1988) 411.

[4] The only investigation of **1** so far reported is a semiempirical SCF-MO calculation on the structure and conformation of the molecule carried out using the MNDO method [A. F. Cuthbertson, C. Glidewell, *J. Mol. Struct. (Theochem.) 94* (1983) 407]. According to this study, the molecule has overall S_4 symmetry; the four oxygen atoms, however, display local D_{4h} symmetry.

[5] Systematic name for **1**: 21,22,23,24-tetraoxapentacyclo-[16.2.1.1^{3,6}.1^{8,11}.1^{13,16}]tetracosa-3,5,8,10,13,15,18,20-octaene. For the origin of the name tetraoxaquaterene, see the first reference in [6a].

[6] a) R. G. Ackman, W. H. Brown, G. F. Wright, *J. Org. Chem. 20* (1955) 1147; R. E. Beals, W. H. Brown, *ibid. 21* (1956) 447; W. H. Brown, W. N. French, *Can. J. Chem. 36* (1958) 537; W. H. Brown, B. J. Hutchinson, *ibid. 56* (1978) 617; b) M. Chastrette, F. Chastrette, J. Sabadie, *Org. Synth. 57* (1977) 74; c) Y. Kobuke, K. Hanji, K. Horiguchi, M. Asada, Y. Nakayama, J. Furukawa, *J. Am. Chem. Soc. 98* (1976) 7414; d) G. R. Newkome, J. D. Sauer, J. M. Roper, D. C. Hager, *Chem. Rev. 77* (1977) 513; e) K. W. Field, A. D. Glover, J. S. Moroz, D. J. Collander, K. E. Kolb, *J. Chem. Educ. 56* (1979) 269; f) P. D. Williams, E. LeGoff, *J. Org. Chem. 46* (1981) 4143; g) A. G. S. Högberg, M. Weber, *Acta Chem. Scand. B 37* (1983) 55; h) A. D. Baker, G. H. Armen, S. Funaro, *J. Chem. Soc. Dalton Trans. 1983*, 2519; i) M. de Sousa Healy, A. J. Rest, *J. Chem. Soc. Perkin Trans. 1 1985*, 973.

[7] W. H. Brown, H. Sawatsky, *Can. J. Chem. 34* (1956) 1147. 2,2'-Difurylmethane (yield 1.7%) was obtained as the only defined product in the reaction of furan and formaldehyde.
[8] The relative amounts of 2,2'-difurylmethane, formaldehyde, lithium perchlorate, and perchloric acid are the same as those reported by *Högberg* and *Weber* [6g] for the condensation of 1,1-di(2-furyl)ethane with acetaldehyde.
[9] In order to detect **1**, the HNO_3 oxidation to **4** proved useful: If the TLC plate was sprayed with concentrated HNO_3, **1** could be localized on the basis of the characteristic red fluorescence (upon excitation with light of 366-nm wavelength) of the dication **4**.
[10] The (preliminary) low yield of **1** serves to illustrate the importance of the *gem*-dialkyl effect involved in the tetraoxaquaterene syntheses with ketones as carbonyl components [N. L. Allinger, V. Zalkow, *J. Org. Chem. 25* (1960) 701]. The yield of **1** did not improve appreciably when **3** was condensed with the diol 5,5'-methylenedifurfuryl alcohol instead of with formaldehyde.
[11] H. Nozaki, T. Koyama, T. Mori, *Tetrahedron 25* (1969) 5357.
[12] $C_{20}H_{16}O_4$, crystals from ethanol; monoclinic, space group $P2_1/n$, $Z=4$; $a=9.971(1)$, $b=16.625(4)$, $c=11.214(2)$ Å, $\beta=113.90(2)°$; $\rho_{calcd}=1.252$ g cm^{-3}; intensities measured on a four-circle diffractometer [room temperature, $\lambda_{Mo}=0.71069$ Å, $\theta_{Mo}(max)=27°$]; refinement (C, O anisotropic, H isotropic) using 1100 reflections with $F_0>4\sigma(F_0)$; $R=0.044$, $R_w=0.046$ [15].
[13] $C_{20}H_{16}O_4$, crystals from ethanol; triclinic, space group $P\bar{1}$, $Z=3$; $a=10.009(2)$, $b=10.477(2)$, $c=12.399(3)$ Å, $\alpha=84.27(2)$, $\beta=88.19(2)$, $\gamma=66.09(2)°$; $\rho_{calcd}=1.349$ g cm^{-3}; same conditions of measurement as for the monoclinic modification but with $\theta_{Mo}(max)=30°$; refinement (C, O anisotropic, H isotropic) using 4564 reflections with $F_0>4\sigma(F_0)$; $R=0.043$, $R_w=0.049$ [15].
[14] The X-ray structure analysis of the 5,10,15,20-tetramethyltetraoxaporphyrin dication (as the perchlorate) remains to be carried out, but the NMR spectra (68% $DClO_4$, CH_2Cl_2 int.) already show unequivocally that the dication is present: ^{1}H NMR (300 MHz): $\delta=10.91$ (s, H2, $^3J_{2,3}=5.71$ Hz), 4.97 (s, CH_3); ^{13}C NMR (75.5 MHz): $\delta=157.55$ (C1), 136.23 (C2, $^1J_{CH}=187.4$ Hz), 116.09 (C5), 21.23 (CH_3, $^1J_{CH}=132.4$ Hz); unpublished results with P. Walgenbach.
[15] Further details of the crystal structure investigations may be obtained from the Fachinformationszentrum Energie, Physik, Mathematik GmbH, D-7514 Eggenstein-Leopoldshafen 2 (FRG), on quoting the depository number CSD-52873, the names of the authors, and the journal citation.

Tetraoxaporphycene Dication

By *Emanuel Vogel,* Martin Sicken, Peter Röhrig, Hans Schmickler, Johann Lex,* and *Otto Ermer*

The conception and synthesis of the tetraoxaporphyrin dication[1] demonstrate the significance of [18]annulene, possessing D_{6h} symmetry,[2] as the underlying structure of important macrocyclic rings, in particular the porphyrins, which can be regarded as bridged [18]annulenes. Bridging of the hypothetical [18]annulene **1**, which exhibits C_{2h} symmetry and which presumably does not exist owing to conformational strain, should also lead to interesting ring systems. Surprisingly, however, such systems, although closely related structurally to the porphyrins, have not been investigated until very recently.

If, in analogy to the pattern described for the higher-symmetry [18]annulene,[1] two inner CH_2 and two outer CH=CH bridges are incorporated into **1**, the rigid [18]annulene **3** is obtained (via the still relatively flexible **2**). Compound **3**, which is expected to have a rectangular molecular framework, is the hydrocarbon parent structure of the recently synthesized porphycene **4**,[3] a planar and aromatic, tetrapyrrolic macrocycle resembling porphyrin in many ways. The H···H repulsions in the center of **3** need not necessarily result in a nonplanar ring framework; hence this hydrocarbon, although considerably strained, might also exhibit aromaticity. The oxygen analogue of **4**, the tetraoxaporphycene dication **5**, can be predicted with great confidence to exist as an 18π Hückel arene having D_{2h} symmetry. Obviously, not only the resonance structures with oxonium oxygen atoms shown here but also resonance structures having a dicationic C_{20} perimeter should contribute to the stabilization of **5**. A prognosis concerning the π-electron structure of the tetrathiaporphycene dication **6** is more problematical, since it is not certain whether the spatial demands of the sulfur atoms would still permit a planar conformation of the molecule.[4]

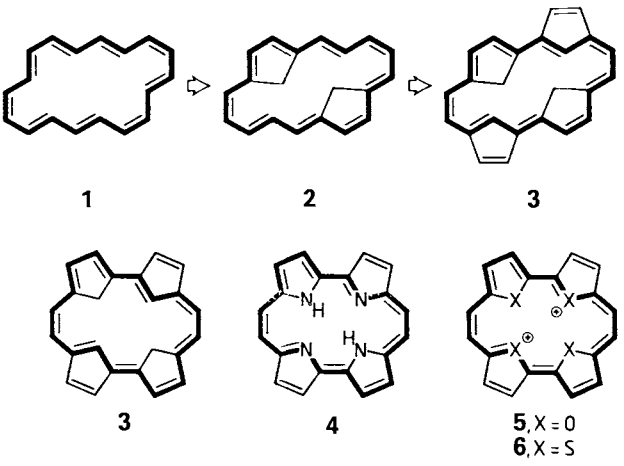

Having already prepared porphycene **4**, we have now succeeded in synthesizing the tetraoxaporphycene dication **5** as the perchlorate **5a** and the hydrogen dinitrate **5b** and have confirmed the porphyrinoid nature of the compound. As the method of choice for the synthesis of the dication **5**, the two-electron oxidation of the oxygen-bridged [20]annulene **8** corresponding to **5** suggested itself. Ready oxidizability of the [4n]annulene **8** appeared guaranteed in view of the observation that the nitrogen analogue of **8**, 22,24-dihydroporphycene, underwent dehydrogenation to **4** even under the reducing conditions of its formation.[3a]

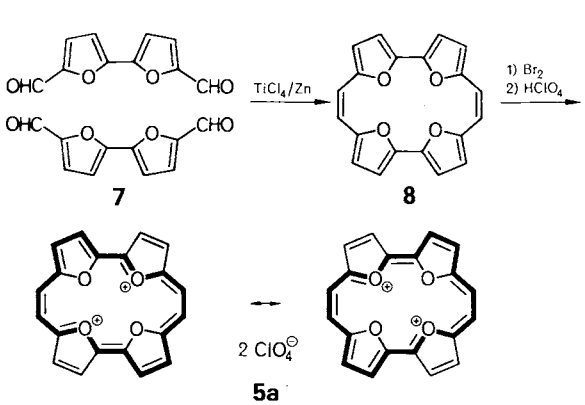

The required [20]annulene **8** is formed as the main low-molecular-weight product[5] when 5,5'-bi-2,2'-furaldehyde[6] **7** is subjected to reductive coupling using low-valent titanium[7] according to the procedure reported for 5,5'-bi-2,2'-pyrrolecarbaldehyde.[3a] In contrast to 22,24-dihydroporphycene, **8** is a relatively stable [4n]annulene,

[*] Prof. Dr. E. Vogel, M. Sicken, P. Röhrig, Dr. H. Schmickler, Dr. J. Lex, Prof. Dr. O. Ermer
Institut für Organische Chemie der Universität
Greinstrasse 4, D-5000 Köln 41 (FRG)

whose isolation requires no special protective measures [violet leaflets (from ether/hexane), m.p. = 270–271 °C; yield 16%].

The ^{1}H NMR spectrum of **8** (Table 1 and Fig. 1, top), which, as expected, consists of an AB system and a singlet, reveals a pronounced paramagnetic ring current; the ^{1}H resonances (center of gravity $\bar{\delta}_H = 4.68$) appear at relatively high field, similar to those of the corresponding vinylic protons in simple[8] and bridged[9] macrocyclic [4n]annulenes, especially in 1,6:9,14-dimethano[16]annulene ($\bar{\delta}_H = 4.96$).[9c-e] The assumption that **8** is present in the form of the thermodynamically more stable double-bond isomer having four furan units is supported by the magnitudes of the vicinal coupling constants.

An X-ray structure analysis[10] (Fig. 2a) reveals **8** as a crystallographically centrosymmetric molecule having a slightly puckered ring framework [maximum deviation of the C and O atoms from the mean plane, ±0.13 Å (C_β of the furan rings); maximum torsional angle, 8.2° (C7-C8-C9-C10)]. This slight nonplanarity may be due to O···O repulsions or to packing effects. The olefinic character of **8** is clearly evident from the alternation of the CC bond lengths, which is most pronounced in the ring segment C8-C9-C10-C11. Further noteworthy structural features of **8** are the nearly square configuration of the four oxygen atoms (O1···O2, 2.778 Å; O1···O2′, 2.729 Å) and the large increase in the CCC bond angles in the inner 16-membered ring to 134.6°.

The base peak in the mass spectrum is due to the doubly positively charged molecular ion. This finding provides further support for the expectation that the dication **5** is sufficiently stabilized as an 18 π arene to allow it to be isolated in the chemical two-electron oxidation of the [20]annulene **8**. Indeed, the transformation of **8** to **5** was achieved under conditions reminiscent of those involved in the formation of the tropylium ion from tropilidene.[11] When **8** is treated in dichloromethane with one equivalent of bromine, an apparently saltlike amorphous product separates spontaneously, which dissolves in 70% perchloric acid to give a reddish-violet solution (weak red fluorescence). Slow addition of water to this solution results in the formation of microcrystalline tetraoxaporphycene dication **5** as the perchlorate **5a** (95% crude product); recrystallization from 50% perchloric acid affords **5a** as violet needles [dec. above 300 °C; yield 90%].[12]

Table 1. ^{1}H NMR (300 MHz) and ^{13}C NMR data (75.5 MHz) of **8** (C_6D_6) and **5a** (68% $DClO_4$, CH_2Cl_2 int.). Chemical shifts δ_H and δ_C and coupling constants J [Hz].

	H2	H3	H9	C1	C2	C3	C4	C9
	$^3J(^1H,^1H)$			$^1J(^{13}C,^1H)$				
8	4.90	4.94	4.19	155.58	116.36	109.33	149.42	113.98
	$J(2,3) = 3.45$	$J(9,10) = 13.6$	—	175	176	—	157	
5a	10.93	11.46	11.30	159.25	140.52	135.91	148.12	118.84
	$J(2,3) = 4.87$	$J(9,10) = 11.6$	—	188	189	—	166	

The presence of the aromatic tetraoxaporphycene dication in the perchlorate **5a** is shown very convincingly in the ^{1}H NMR spectrum (Table 1 and Fig. 1, bottom) by the fact that the oxidation of **8** to the dication causes the center of gravity $\bar{\delta}_H$ of the ^{1}H chemical shift (with reversal of the relative positions of the signals of H2 and H9) to be moved downfield by no less than 6.6 ppm. The position of the ^{1}H resonances of the dication is in accordance with expectation, if dioxaporphyrins, which exist in diprotonated form,[13] are taken as reference compounds. That **5a**, in contrast to **8**, is delocalized is revealed not only by the chemical shifts, but also by a partial equalization of the vicinal coupling constants. In the ^{13}C NMR spectrum of **5a**, like in that of **8**, five resonance signals are observed.

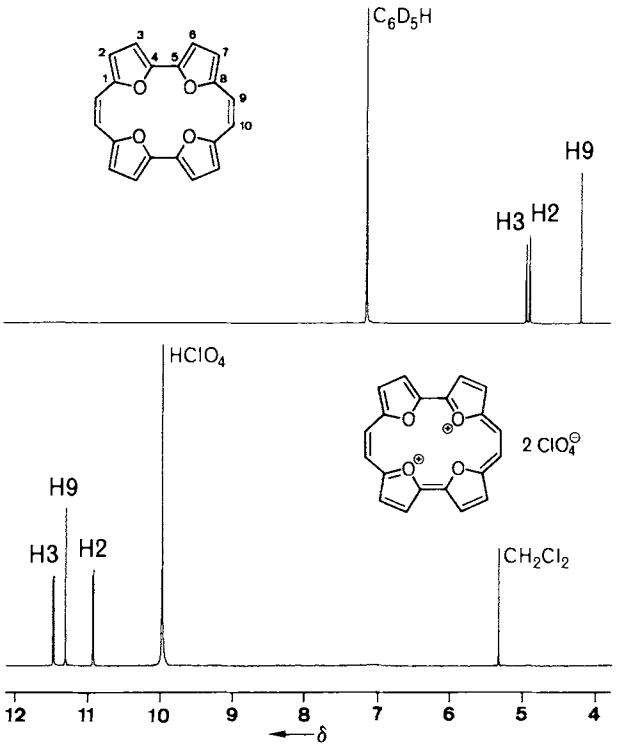

Fig. 1. ^{1}H NMR spectra of **8** (300 MHz, C_6D_6) and **5a** (300 MHz, 68% $DClO_4$, CH_2Cl_2 int.).

Significantly, on conversion of **8** into **5a** the center of gravity $\bar{\delta}_C$ of the ^{13}C chemical shifts migrates downfield by only 12 ppm ($\Delta\bar{\delta}_C$), while, according to the correlation between chemical shift and charge density (160 ppm/π electron) that holds for numerous (4n + 2)π-electron systems, a value of $\Delta\bar{\delta}_C = 16$ ppm[14] would have been expected for a system in which two positive charges are distributed over twenty C atoms. From the difference between the measured and estimated $\Delta\bar{\delta}_C$ values it is apparent that the oxygen atoms also bear charge. It seems justified, therefore, to describe **5** primarily by resonance structures in which the 18 π conjugation pathway includes two oxonium oxygen atoms as shown in the formula.

The UV/VIS spectrum of **5a** is similar to that of porphycene,[3a,e] apart from the larger number of bands in the long-wavelength region.

Although the X-ray analysis of **5a** supported the molecular structure derived from the spectra, a complete structure determination was prevented by partial disorder effects (two orientations of **5** mutually rotated in the molecular plane). Guided by the notion that a planar anion should allow better intermolecular contacts than the more spherical perchlorate ion, and thus should reduce the propensity toward disorder in the crystal, the prepara-

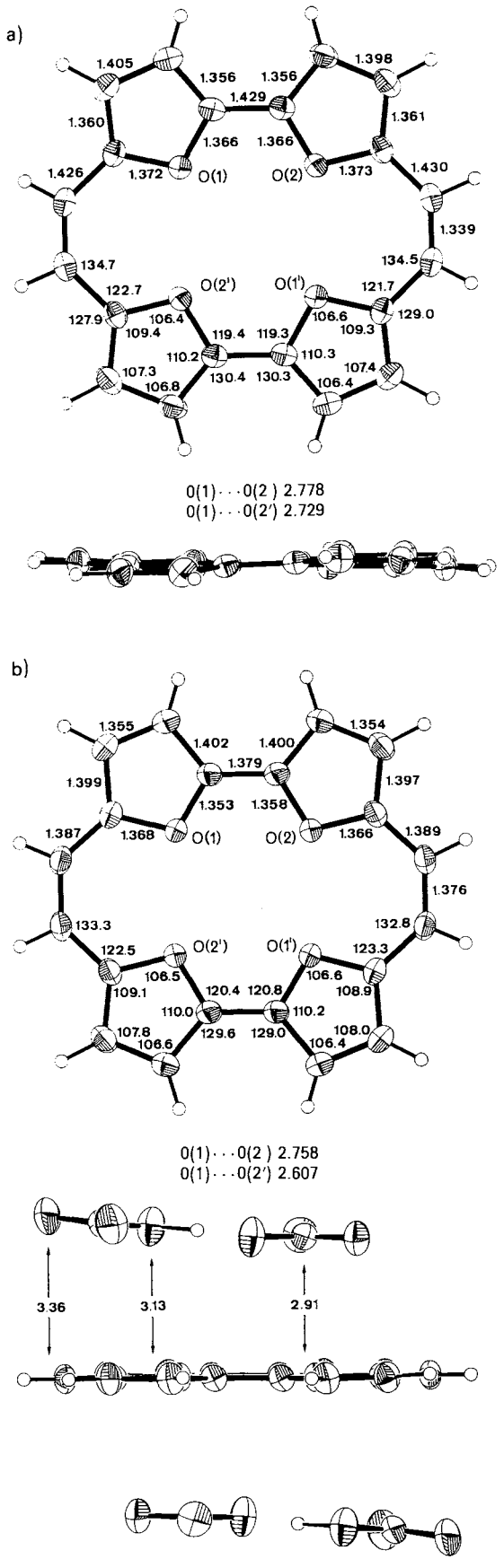

Fig. 2. a) Structure of **8**. Top: View perpendicular to the molecular plane. Bottom: Side view. b) Structure of **5b**. Top: View of dication. Bottom: Side view of a "sandwich" consisting of one tetraoxaporphycene dication and two hydrogen dinitrate ions situated above and below the dication. Selected bond lengths, nonbonded contacts [Å], and bond angles [°]; standard deviations ca. 0.002 Å and 0.1°. The thermal ellipsoids are shown at the 40% probability level.

tion of the nitrate of **5** was attempted. Whereas **8** did not give a well-defined crystalline product with silver nitrate (various media), upon treatment with 65% nitric acid (!) at room temperature it immediately afforded a salt, which, surprisingly, differed from the expected nitrate by containing two additional equivalents of HNO_3 (yield almost quantitative). Violet rhombs (dec. above 270°C upon rapid heating) were grown by slow crystallization from concentrated nitric acid. In fact, these crystals did not suffer from crystallographic disorder perturbations and turned out to consist of the hydrogen dinitrate **5b** $[(C_{20}H_{12}O_4)^{2\oplus}2(NO_3\cdot HNO_3)^{\ominus}]$[15] of the tetraoxaporphycene dication **5** (**5b** tends to decompose, presumably by loss of HNO_3).

The X-ray structure of **5b**[16] (Fig. 2b) confirms that, in contrast to its annulene precursor **8**, the dication features a "porphyrinoid ring system." The following structural changes on going from **8** to **5b** are evident (Fig. 2): (1) *Planarity:* While **8** is slightly puckered, the dication **5** is practically planar (maximum deviation of the C and O atoms from the mean plane, ±0.02 Å; maximum torsional angle, 1.4°). (2) *Bond lengths:* Bond alternation is no longer present in the ring segment C8-C9-C10-C11, whereas the length relation C_β-$C_\beta > C_\alpha$-C_β is reversed, similar to what is observed in porphyrins and porphycenes. (3) *Configuration of the four heteroatoms:* The almost square O_4 core in **8** adopts a more rectangular shape in the dication (O1···O2, 2.758 Å; O1···O2′, 2.607 Å), presumably due in part to attractive $O^{\ominus}\cdots O$ 1,6 interactions (similar to the N-H···N hydrogen bonds in porphycene). As expected, the decrease in the O1···O2′ separation is accompanied by a CCC angle contraction in the inner 16-membered ring (by about 2°).

Table 2. Selected physical data for **8** and **5a, b**.

1,4:5,8:11,14:15,18-tetraoxido[20]annulene **8**: for ^1H and ^{13}C NMR data see Table 1; MS (70 eV): m/z 316 ($M^{\oplus}$, 30%), 158 ($M^{2\oplus}$, 100); IR (KBr): $\tilde{\nu}$ = 3132, 2977, 1899, 1673, 1632, 1619, 1530, 1439, 1403, 1393, 1348, 1206, 1030, 971, 958, 953, 848, 781, 773, 756, 751, 627 cm^{-1}; UV/VIS (benzene): λ_{max} = 303 nm (ε = 107000), 307 (106000), 317 (159000), 354 (5600) sh, 380 (3900) sh, 400 (1550) sh, 517 (640)

5a: for ^1H and ^{13}C NMR data see Table 1; IR (Nujol): $\tilde{\nu}$ = 3103, 3054, 3040, 3010, 1582, 1523, 1511, 1438, 1402, 1259, 1194, 1090 ($ClO_4^{\ominus}$), 1050 ($ClO_4^{\ominus}$), 959, 934, 913, 861, 818, 654, 624 ($ClO_4^{\ominus}$) cm^{-1}; UV/VIS (70% $HClO_4$): λ_{max} = 307 nm (ε = 6500), 372 (340000) sh, 376 (383000), 457 (550) sh, 482 (2900), 512 (5300), 523 (3400) sh, 552 (27900), 567 (6100), 575 (2050), 587 (6550), 599 (45300), 610 (2200) sh, 623 (280) sh

5b: ^1H NMR (300 MHz, 68% DNO_3, CH_2Cl_2 int.): δ = 11.65 (d, H3), 11.47 (s, H9), 11.08 (d, H2); ^{13}C NMR (75.5 MHz, 68% DNO_3, CH_2Cl_2 int.): δ = 158.58, 147.44, 139.49, 134.92, 117.85; IR (Nujol): $\tilde{\nu}$ = 3111, 3088, 3062, 3049, 1579, 1518, 1437, 1357 ($NO_3\cdot HNO_3^{\ominus}$), 1303, 1294, 1201, 934, 910, 864 cm^{-1}. UV/VIS (65% HNO_3): The λ_{max} values are in agreement with those of **5a**, whereas the ε values exhibit a slight scatter, presumably owing to loss of HNO_3 from **5b**.

The structure of the hydrogen dinitrate ion serving as counterion in **5b** is noteworthy; it consists of two nearly coplanar nitrate groups connected by a short asymmetric hydrogen bond (O···O, 2.490 Å).[15] The two hydrogen dinitrate ions are arranged layerlike above and below the dication, the layer separation being slightly different for $NO_3^{\ominus}$ and HNO_3 (Fig. 2b, bottom). In the crystal, these "sandwich-type" triple layers are stacked in a laterally displaced pattern.

Received: August 18, 1987 [Z 2416 IE]
Publication delayed at authors' request
German version: *Angew. Chem.* *100* (1988) 450

[1] E. Vogel, W. Haas, B. Knipp, J. Lex, H. Schmickler, *Angew. Chem. 100* (1988) 445; *Angew. Chem. Int. Ed. Engl. 27* (1988) 406.

[2] F. Sondheimer, *Pure Appl. Chem. 7* (1963) 363; H. Baumann, J. F. M. Oth, *Helv. Chim. Acta 65* (1982) 1885; J. Bregman, F. L. Hirshfeld, D. Rabinovich, G. M. J. Schmidt, *Acta Crystallogr. 19* (1965) 227; F. L. Hirshfeld, D. Rabinovich, *ibid. 19* (1965) 235.

[3] a) E. Vogel, M. Köcher, H. Schmickler, J. Lex, *Angew. Chem. 98* (1986) 262; *Angew. Chem. Int. Ed. Engl. 25* (1986) 257; b) E. Vogel, M. Balci, K. Pramod, P. Koch, J. Lex, O. Ermer, *ibid. 99* (1987) 909 and *26* (1987) 928; c) E. Vogel, M. Köcher, M. Balci, I. Teichler, J. Lex, H. Schmickler, O. Ermer, *ibid. 99* (1987) 912 and *26* (1987) 931; d) B. Wehrle, H.-H. Limbach, M. Köcher, O. Ermer, E. Vogel, *ibid. 99* (1987) 914 and *26* (1987) 934; e) P. F. Aramendia, R. W. Redmond, S. Nonell, W. Schuster, S. E. Braslavsky, K. Schaffner, E. Vogel, *Photochem. Photobiol. 44* (1986) 555; f) H. Ofir, A. Regev, H. Levanon, E. Vogel, M. Köcher, M. Balci, *J. Phys. Chem. 91* (1987) 2686.

[4] Compare the loss of peripheral cyclic delocalization on going from 1,4:7,10:13,16-trioxido[18]annulene to the corresponding trithia compound: G. M. Badger, J. A. Elix, G. E. Lewis, *Aust. J. Chem. 18* (1965) 70; *ibid. 19* (1966) 1221.

[5] In addition to tetraoxido[20]annulene **8**, small amounts of higher macrocyclic products can be isolated, but only hexaoxido[30]annulene has been identified so far.

[6] R. Grigg, J. A. Knight, M. V. Sargent, *J. Chem. Soc. C 1966*, 976.

[7] T. Mukaiyama, T. Sato, J. Hanna, *Chem. Lett. 1973*, 1041; J. E. McMurry, M. P. Fleming, *J. Am. Chem. Soc. 96* (1974) 4708; J. E. McMurry, *Acc. Chem. Res. 16* (1983) 405; D. Lenoir, *Synthesis 1977*, 553.

[8] G. Schröder, J. F. M. Oth, *Tetrahedron Lett. 1966*, 4083; B. W. Metcalf, F. Sondheimer, *J. Am. Chem. Soc. 93* (1971) 6675; I. C. Calder, F. Sondheimer, *Chem. Commun. 1966*, 904.

[9] a) H. Ogawa, M. Kubo, I. Tabushi, *Tetrahedron Lett. 1973*, 361; b) J. A. Elix, *Aust. J. Chem. 22* (1969) 1951; c) D. Tanner, O. Wennerström, E. Vogel, *Tetrahedron Lett. 23* (1982) 1221; d) E. Vogel, U. Kürschner, H. Schmickler, J. Lex, O. Wennerström, D. Tanner, U. Norinder, C. Krüger, *ibid. 26* (1985) 3087; e) see also E. Vogel, B. Neumann, W. Klug, H. Schmickler, J. Lex, *Angew. Chem. 97* (1985) 1044; *Angew. Chem. Int. Ed. Engl. 24* (1985) 1046.

[10] $C_{20}H_{12}O_4$, m.p. = 270–271 °C, crystals from ether/hexane; monoclinic, space group $P2_1/c$, $Z=2$; $a=9.926(2)$, $b=4.855(1)$, $c=15.507(3)$ Å, $\beta=106.17(2)°$; $\rho_{calcd}=1.464$ g cm^{-3}; intensities measured on a four-circle diffractometer [room temperature, $\lambda_{Mo}=0.71069$ Å, $\theta_{Mo}(max)=27°$]; refinement (C, O anisotropic, H isotropic) using 1369 reflections with $F_0>4\sigma(F_0)$; $R=0.045$, $R_w=0.048$ [17].

[11] W. von E. Doering, L. H. Knox, *J. Am. Chem. Soc. 76* (1954) 3203.

[12] **5** is unstable in nonacidic aqueous medium, since, as oxonium ion, it is subject to rapid nucleophilic attack by the solvent. The possibility of making **5** resistant to water by the introduction of alkyl substituents is being investigated. Cf. the stabilization of the pyrylium ion by 2,4,6-trialkyl substitution: G. P. Ellis in A. R. Katritzky, C. W. Rees (Eds.): *Comprehensive Heterocyclic Chemistry, Vol. 3*, Pergamon Press, Oxford 1984, p. 652.

[13] M. J. Broadhurst, R. Grigg, A. W. Johnson, *J. Chem. Soc. C 1971*, 3681; A. W. Johnson in K. M. Smith (Ed.): *Porphyrins and Metalloporphyrins*, Elsevier, Amsterdam 1975, p. 729. We will describe elsewhere dioxaporphycenes (as salts), which are obtainable from the corresponding bridged [20]annulenes by two-electron oxidation.

[14] H.-O. Kalinowski, S. Berger, S. Braun: *^{13}C-NMR-Spektroskopie*, Thieme, Stuttgart 1984, p. 88; see also B. Eliasson, U. Edlund, K. Müllen, *J. Chem. Soc. Perkin Trans. 2* 1986, 937.

[15] The hydrogen dinitrate ion takes on two distinctly different configurations in the crystal. The configuration observed for **5b**, containing coplanar nitrate groups linked by a short hydrogen bond, has precedence in the structure of tetraphenylarsonium hydrogen dinitrate (B. D. Faithful, S. C. Wallwork, *Chem. Commun. 1967*, 1211), but this appears to be an exception. In most cases, a configuration is present in which four oxygen atoms of two nitrate groups form a distorted tetrahedron around the bridging hydrogen atom: J. Roziere, M.-T. Roziere-Bories, J. M. Williams, *Inorg. Chem. 15* (1976) 2490, and other examples listed there.

[16] $C_{20}H_{14}N_4O_{16}$, dec. above 270 °C, crystals from 65% HNO_3; triclinic, space group $P\bar{1}$, $Z=1$; $a=8.097(2)$, $b=8.707(2)$, $c=9.365(2)$ Å, $\alpha=73.18(2)$, $\beta=89.81(2)$, $\gamma=66.32(2)°$; $\rho_{calcd}=1.638$ g cm^{-3}; conditions of measurement as for **8**, refinement (C, N, O anisotropic, H isotropic) using 1889 reflections with $F_0>4\sigma(F_0)$; $R=0.032$, $R_w=0.044$ [17].

[17] Further details of the crystal structure investigations may be obtained from the Fachinformationszentrum Energie, Physik, Mathematik GmbH, D-7514 Eggenstein-Leopoldshafen 2 (FRG), on quoting the depository number CSD-52871, the names of the authors, and the journal citation.

Electron–Electron/Spin–Spin Long-Range Interaction as Studied in the Diradical Dication [Di{bis(dimethylphosphino-η^6-benzene)chromium(I)}-nickel(0)]$^{++}$ **

By *Christoph Elschenbroich,* Gottfried Heikenfeld, Martin Wünsch, Werner Massa,* and *Gerhard Baum*

Facile change in the oxidation state and favorable ESR properties make the $(\eta^6\text{-arene})_2M(d^5)$[2] unit a suitable probe for the study of mixed valence and intermediate valence states as well as of electron–electron/spin–spin interaction. After considering the cases of rigid parallel orientation (e.g., **1**[3]) and conformationally flexible orientation (e.g., **2**[4]), we focused our attention on oligonuclear sandwich compounds with orthogonally arranged moieties. A tetrahedrally coordinated Ni atom lends itself well as a spacer for the two orthogonal halves of the molecule.

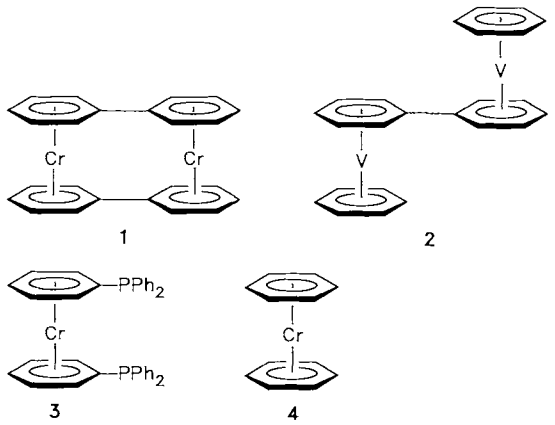

In continuation of earlier work (**3**[5]), we have now synthesized the "organometallic diphos ligand" bis(dimethylphosphino-η^6-benzene)chromium **6** and allowed it to react with bis(1,5-cyclooctadiene)nickel to obtain the title compound **7** (Scheme 1).

The air-sensitive dimethylphosphino derivatives **5** and **6** are also labile towards hydrolysis; they are rapidly dephosphinylated in THF/5% H_2O, especially at the complex cation stage. The C–P bond in the bis(chelate) complex **7** as well as in the $Ni(CO)_2$ adduct **8**, synthesized for comparison, is more inert. Figure 1 shows the molecular structure of **7**.[7] Physical data are collected in Table 1.

The structural features of both the NiL_4 and $(\eta^6\text{-arene})_2Cr$ units are largely retained upon formation of **7**. The methyl groups of the PMe_2 bridges assume axial and equatorial positions with respect to the plane of the arene; overall, the "ligands" **6** coordinate to Ni to produce the *meso* form. The axes of the two sandwich moieties lie mutually perpendicular and the distance between their central atoms is 8.49 Å. The eclipsed arrangement of the benzene rings and the C–P–Ni bond angle, however, result in the three central atoms Cr, Ni, and Cr being non-colinear. In solution, **7** is conformationally flexible; only one ^{1}H-

[*] Prof. Dr. C. Elschenbroich, Dr. G. Heikenfeld, Dipl.-Chem. M. Wünsch, Priv.-Doz. Dr. W. Massa, G. Baum
Fachbereich Chemie der Universität
Hans-Meerwein-Strasse, D-3550 Marburg (FRG)

[**] Metal π Complexes of Benzene Derivatives, Part 31. This work was supported by the Deutsche Forschungsgemeinschaft and the Fonds der Chemischen Industrie. — Part 30: [1].

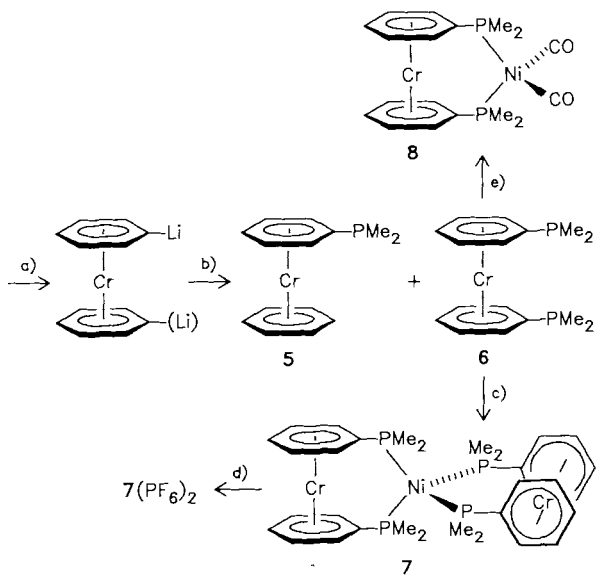

Scheme 1. a) *n*BuLi, TMEDA, cyclohexane, 80°C, 1 h; b) Me_2PPMe_2 in cyclohexane, 0°C, 1 h, then 20°C, 24 h; chromatography on silylated silica: **5** golden yellow flakes (38%), **6** brown needles (40%) from petroleum ether; c) (1,5-cyclooctadiene)$_2$Ni, toluene, 20°C, 2d: **7** brown crystals (13%) from toluene/petroleum ether; d) two-phase system toluene, KPF_6/H_2O (O_2-free), and 4-pyridinecarbaldehyde [6], 0°C, 10 min, precipitation: $7(PF_6)_2$ brown powder (quantitative); e) $Ni(CO)_4$, toluene, 20°C, 3d; chromatography on Al_2O_3 (active, neutral): **8** brownish yellow needles (42%) from toluene/petroleum ether.

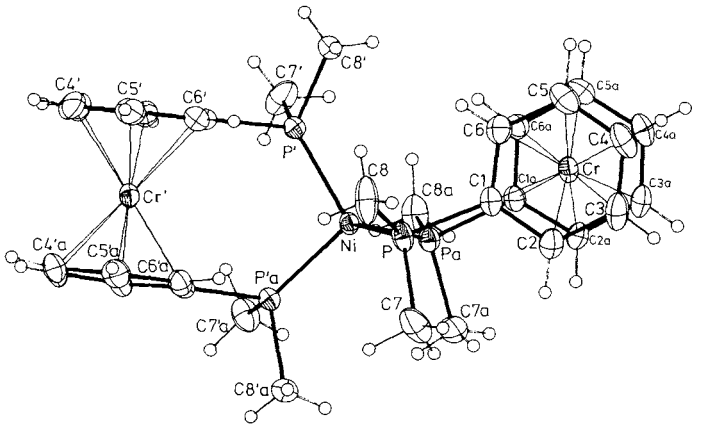

Fig. 1. Molecular structure of **7** (ORTEP). The thermal ellipsoids are drawn at the 30% probability level. Atoms that are symmetrically equivalent with respect to the C_2 axis are indicated by primes. Important interatomic distances [Å] and angles [°]: Ni-P 2.146(1), Ni-P_a 2.151(1), P-C_{methyl} (mean) 1.839, P-C1 1.845(5), P_a-Cl_a 1.844(4), Cr-C (mean) 2.144, Cr-ring center (Z) (mean) 1.617, Cr-Ni 4.319; Cr-Cr' 8.490; Cr-Ni-Cr' 150.4, P-Ni-P_a 103.0(1), P-Ni-P' 116.9(1), P_a-Ni-P'_a 107.5(1), P_a-Ni-P' 113.2(1), Ni-P-C1 118.9(2) Ni-P_a-$C1_a$ 119.2(2), Z-Cr-Z_a 177.6(4), angle between the sandwich axes 84.5.

Table 1. Physical data for the new compounds **5**-**8**. ^{1}H-NMR, 400 MHz; ^{13}C-NMR, 100.6 MHz; MS (electron-impact ionization), 70 eV; ESR, X band.

5: m.p. = 69–71°C; MS: *m/z* 268 (23.9, $5^{\oplus}$), 190 (79.7, $LCr^{\oplus}$), 175 (7.2, $H_3CPC_6H_5Cr^{\oplus}$), 138 (20.5, $L^{\oplus}$), 123 (18.6, $C_6H_5PCH_3^{\oplus}$), 78 (25.6, $C_6H_6^{\oplus}$), 77 (9.1, $C_6H_5^{\oplus}$), 52 (100, $^{52}Cr^{\oplus}$), L = $C_6H_5P(CH_3)_2$; ^{1}H-NMR (C_6D_6): δ = 1.06 (d, H_{Me}, ^1J(H, P) = 3.6 Hz), 4.12 (m, H_p), 4.16 (m, H_m, $H_{\eta\text{-}Bz}$), 4.42 (m, H_o); ^{13}C-NMR (C_6D_6): δ = 15.3 (C_{Me}, ^1J(C, P) = 14.4 Hz, ^1J(C, H) = 128 Hz), 74.3 (C_p, J(C, P) < 2 Hz, ^1J(C, H) = 162 Hz), 75.3 (C_m, J(C, P) ≈ 4 Hz, ^1J(C, H) = 167 Hz), 77.1 (C_o, J(C, P) = 19.1 Hz, ^1J(C, H) = 166 Hz), 86.2 (C_{ipso}, J(C, P) = 13.4 Hz), 75.9 ($C_{\eta\text{-}Bz}$, ^1J(C, H) = 167 Hz); ^{31}P{^{1}H}-NMR (C_6D_6): δ = −42.2; ESR ($5^{\odot\oplus}$, THF, +25 and −140°C): $\langle g\rangle$ = 1.9863, a(11 ^{1}H) = 3.29 G, a(^{31}P) ≦ 0.55 G, a(^{53}Cr) = 17.5 G, $g_\perp$ = 1.9764, $g_\parallel$ = 2.0057, $A_\parallel$(^{1}H) = 3.75 G, $A_\perp$(^{1}H) = 2.96 G, $A_\perp$(^{53}Cr) = 24.6 G; cyclic voltammetry (DME, TBAP 0.1 M, 20°C versus SCE): $E_{1/2}(5/5^{\odot\oplus})$ = −0.62 V, reversible.

6: m.p. = 65–67°C, MS: *m/z* 328 (32.0, $6^{\oplus}$), 190 (100, $6^{\oplus}$−L), 175 (7.1, $H_3CPC_6H_5Cr^{\oplus}$), 138 (24.2, $L^{\oplus}$), 123 (16.0, $C_6H_5PCH_3^{\oplus}$), 78 (19.6, $C_6H_6^{\oplus}$), 52 (96.0, $^{52}Cr^{\oplus}$), L = $C_6H_5P(CH_3)_2$; ^{1}H-NMR (C_6D_6): δ = 1.13 (d, H_{Me}, J(H, P) = 3.5 Hz), 4.30 (m, $H_{m,p}$), 4.51 (m, H_o); ^{13}C-NMR (C_6D_6): δ = 15.3 (C_{Me}, J(C, P) = 14.1 Hz, ^1J(C, H) ≈ 127.8 Hz), 75.7 (C_p, J(C, P) < 2 Hz, ^1J(C, H) = 168.8 Hz), 76.6 (C_m, J(C, P) = 6.4 Hz, ^1J(C, H) = 166.5 Hz), 78.1 (C_o, J(C, P) = 19.3 Hz, ^1J(C, H) = 169.4 Hz), 87.7 (C_{ipso}, J(C, P) = 17.7 Hz); ^{31}P{^{1}H}-NMR (C_6D_6): δ = −42.6; ESR ($6^{\odot\oplus}$, THF, 25 and −140°C): $\langle g\rangle$ = 1.9865, a(10 ^{1}H) = 3.23 G, a(2 ^{31}P) ≦ 0.55 G, a(^{53}Cr) = 17.7 G, $g_\perp$ = 1.9780, $g_\parallel$ = 2.0027, $A_\perp$(^{1}H) = 3.35 G, $A_\parallel$(^{1}H) = 3.00 G; cyclic voltammetry: $E_{1/2}(6/6^{\oplus})$ = −0.57 V, reversible at 20°C.

7: m.p. = 140°C (dec.); MS: *m/z* 714 (16.5, $7^{\oplus}$), 386 (2.6, (**6**)Ni$^{\oplus}$), 328 (27.3, $6^{\oplus}$), 190 (63.9, **6**−$L^{\oplus}$), 138 (100.0, $L^{\oplus}$), 123 (91.4, $C_6H_5PCH_3^{\oplus}$), 121 (69.7, $C_7H_6P^{\oplus}$), 91 (44.5, $C_7H_7^{\oplus}$), 58 (2.1, $^{58}Ni^{\oplus}$), 52 (62.3, $^{52}Cr^{\oplus}$), L = $C_6H_5P(CH_3)_2$; ^{1}H-NMR ([D$_8$]toluene: δ = 1.48 [s, H_{Me}], 4.17 (t, H_p, $J(H_p, H_m)$ ≈ 5.1 Hz), 4.22 (t, H_m, $J(H_m, H_p) \approx J(H_m, H_o)$ = 5.1 Hz), 4.80 (m, H_o); ^{13}C-NMR ([D$_8$]toluene): δ = 23.9 (C_{Me}, ^1J(C, H) = 127 Hz, ^{13}C{^{1}H}: "quint," line separation 8 Hz [13]), 74.5 (C_p, ^1J(C, H) = 166 Hz), 75.4 (C_m, ^1J(C, H) = 169 Hz), 78.7 (C_o, ^1J(C, H) = 164 Hz, ^{13}C{^{1}H}: "quint," line separation 3.5 Hz [13]), 98.9 (C_{ipso}, ^{13}C{^{1}H}: "quint," line separation 10 Hz [13]); ^{31}P{^{1}H}-NMR (C_6D_6): δ = −11.1; ESR and cyclic voltammetry, see text.

8: m.p. = 140°C (dec.), FDMS: *m/z* 442 (*M* = 443.02); ^{1}H-NMR (C_6D_6): δ = 1.32 (d, H_{Me}, J(H, P) = 4.4 Hz), 4.14 (m, $H_{m,p}$), 4.29 (m, H_o); ^{13}C-NMR (C_6D_6): δ = 19.7 (C_{Me}, ^1J(C, H) = 130 Hz); ^{13}C{^{1}H}-NMR: m, 6 lines, overall width 42 Hz), 74.7 (C_p, ^1J(C, H) = 169 Hz; ^{13}C{^{1}H}-NMR: s), 77.2 (C_m, ^1J(C, H) = 168 Hz; ^{13}C{^{1}H}-NMR: "t," line separation 3 Hz), 79.7 (C_o, ^1J(C, H) = 165 Hz; ^{13}C{^{1}H}-NMR: m, 5 lines, overall width 40 Hz), 85.9 (C_{ipso}, ^{13}C{^{1}H}-NMR: m, 6 lines, overall width 47 Hz), 202 (CO, ^2J(P, C) = 5 Hz); ^{31}P{^{1}H}-NMR (C_6D_6): δ = −3.9; ESR ($8^{\odot\ominus}$, CH_3OH, +25°C): $\langle g\rangle$ = 1.9872, a(10 ^{1}H) = 3.25 G, a(^{53}Cr) = 18.2 G, $8^{\odot\ominus}$ (CH_3OH, −140°C): $g_\parallel$ = 2.0019, $g_\perp$ = 1.9794; cyclic voltammetry: $E_{1/2}(8/8^{\odot\ominus})$ = −0.54 V, reversible, (20°C, DME, TBAP, 0.1 M, versus SCE).

and $v > 100$ mVs^{-1}. Comparison of the peak currents for samples of known concentration of **7** using **6** as standard indicates that $E^1_{1/2}$ is associated with the transfer of two electrons. Thus, the following assignment accrues (in DME, $(n\text{Bu})_4NClO_4$ (TBAP), at a glassy carbon electrode versus the saturated calomel electrode (SCE), v = 100 mVs^{-1}):

$$7 \equiv [(\mathbf{6})_2Ni] \xrightleftharpoons{-2e^{\ominus}} [(\mathbf{6}^{\odot\oplus})_2Ni]^{2\oplus} \xrightleftharpoons{-e^{\ominus}} [(\mathbf{6}^{\odot\oplus})_2Ni]^{3\oplus} \xrightarrow{-e^{\ominus}} [(\mathbf{6}^{\odot\oplus})_2Ni]^{4\oplus}$$

+20°C:	$E^1_{1/2} = -0.70$ V	$E^2_{1/2} = -0.52$ V	$E^3_{pa} = -0.12$ V (irrev.)
−25°C:	$E^1_{1/2} = -0.73$ V	$E^2_{1/2} = -0.55$ V	$E^3_{1/2} = -0.16$ V (rev.)

NMR signal is observed for the methyl groups in the range $-80°C < T < +40°C$.

The redox behavior of **7** was investigated by cyclic volt-ammetry (Fig. 2c). It is characterized by three electron-transfer steps, the first and second of which ($E^1_{1/2} = -0.70$ V, $E^2_{1/2} = -0.52$ V) are reversible in dimethoxyethane (DME) at room temperature. The third step ($E^3_{1/2} = -0.16$ V) becomes reversible only at $T < -25°C$

The potentials $E^2_{1/2}$ and $E^3_{1/2}$ are similar to those of the mononuclear complex bis(diphenylphosphinoethane)nickel;[8] $E^1_{1/2}$ is shifted cathodically in comparison to the value observed for the free ligand **6** ($E_{1/2} = -0.57$ V, reversible at 25°C). The shape of the signal and the peak current of the first wave indicate that no electrochemically measurable interaction exists between the two redox centers of the sandwich moieties; that is, electron transfer at

 © VCH Verlagsgesellschaft mbH, D-6940 Weinheim, 1988 0570-0833/88/0303-0415 $ 02.50/0

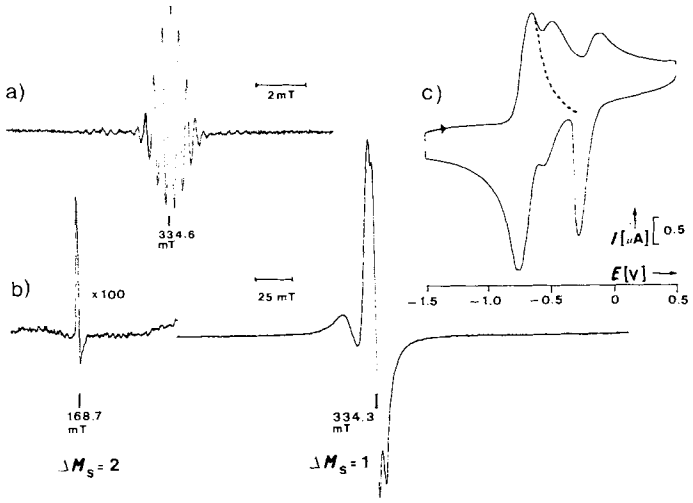

Fig. 2. a) ESR spectrum (2nd derivative) of $7(PF_6)_2$ in dimethylformamide (DMF)/chloroform (1:1), $T=25°C$. b) ESR spectrum of $7(PF_6)_2$ in glassy solution, DMF/$CHCl_3$ (1:1), $T=-160°C$; * not identified. c) Cyclic voltammogram of 7 in DME/TBAP (0.1 M), 20°C, at the glassy carbon electrode versus SCE, $v=50\ mVs^{-1}$.

the two centers occurs independently and in a purely statistical fashion.[9]

The first redox step $7 \rightarrow 7^{2\oplus}$ can also be realized on a preparative scale if the dication, once formed, is precipitated from solution as the hexafluorophosphate, thus preventing further attack by the oxidizing agent (see Scheme 1); O_2 or—preferentially—4-pyridinecarbaldehyde are suitable as oxidants.[6] From the ESR spectra of $7(PF_6)_2$ in fluid solution, hyperfine coupling constants $a(10\ ^1H_{arene})$ and $a(1\ ^{53}Cr)$ can be derived. The multiplicity and the magnitude of these hyperfine splittings, which largely correspond to those of the monoradical cation $8^{\odot\oplus}$, indicate that, for the diradical dication $7^{\ddagger\ddagger}$, the exchange interaction J is much smaller than the hyperfine interactions $a(^1H)$ and $a(^{53}Cr)$. Thus, in fluid solution, the ESR line width for $7^{\ddagger\ddagger}$ is only slightly increased compared with $8^{\odot\ominus}$. This behavior is in accord with the presence of two singly occupied, orthogonal, $Cr(3d_{z^2})$ orbitals centered at a distance of 8.49 Å. A sensitive means of detecting long-range electron-electron/spin-spin interaction is provided by the classical dipole-dipole coupling, which is manifested most clearly in the appearance of a "half-field signal" ($\Delta M_s=2$) in glassy solutions[10] (Fig. 2b). In accordance with the large separation of the two unpaired electrons in $7^{\ddagger\ddagger}$, the intensity of the half-field signal is only ca. 10^{-4} that of the main-field signal.[11] From the latter may be derived—and confirmed by spectral simulation[12]—the zero-field splitting parameters $D=2.7\times10^{-3}\ cm^{-1}$, $E=0.67\times10^{-3}\ cm^{-1}$, which, according to the equation $r=(0.650\ g^2/D)^{1/3}$ [Å],[10b] in turn, give an average interspin distance r and thus a Cr···Cr distance of 9.91 Å. In order to account for the only moderate agreement of this value with the results of the X-ray structure analysis, we are attempting to replace Ni in 7 by other bridging metal atoms.

Received: August 25, 1987;
revised: November 11, 1987 [Z 2414 IE]
German version: *Angew. Chem. 100* (1988) 397

CAS Registry numbers:
4, 1271-54-1; **5**, 113008-25-6; **6**, 113008-26-7; **7**, 112988-51-9; $7\cdot(PF_6)_2$, 113034-67-6; **8**, 112988-52-0; $Ni(CO)_4$, 13463-39-3; Ni (cod)$_2$, 1295-35-8.

[1] C. Elschenbroich, J. Schneider, M. Wünsch, J.-L. Pierre, P. Baret, P. Chautemps, *Chem. Ber. 121* (1988) 177.
[2] C. Elschenbroich, R. Möckel, U. Zenneck, D. W. Clack, *Ber. Bunsenges. Phys. Chem. 83* (1979) 1008.
[3] C. Elschenbroich, J. Heck, *J. Am. Chem. Soc. 101* (1979) 6773.
[4] C. Elschenbroich, J. Heck, *Angew. Chem. 93* (1981) 278; *Angew. Chem. Int. Ed. Engl. 20* (1981) 267.
[5] C. Elschenbroich, F. Stohler, *Angew. Chem. 87* (1975) 198; *Angew. Chem. Int. Ed. Engl. 14* (1975) 174.
[6] 4-Pyridinecarbaldehyde has proved to be a mild, homogeneous one-electron oxidant for the generation of organometallic radical cations which contributes no signal of its own to the ESR spectrum.
[7] $C_{32}H_{44}P_4Cr_2Ni$, space group $P2_12_12_1$, $Z=2$, $a=15.185(6)$, $b=9.562(5)$, $c=11.260(7)$ Å; 2765 unique reflections with $F_0>3\sigma$; four-circle diffractometer (CAD4, Enraf-Nonius), $Mo_{K\alpha}$ radiation, 295 K; no absorption correction ($\mu=13.6\ cm^{-1}$), H atoms refined with istropic temperature factors. 265 parameters, $R_w=0.036$ (weighting $w=1/\sigma^2(F_0)$). Further details of the crystal structure investigation may be obtained from the Fachinformationszentrum Energie, Physik, Mathematik GmbH, D-7514 Eggenstein-Leopoldshafen 2 (FRG), on quoting the depository number CSD-52822, the names of the authors, and the journal citation.
[8] a) M. Martelli, G. Pilloni, G. Zotti, S. Daolio, *Inorg. Chim. Acta 11* (1974) 155; b) G. Gontempelli, F. Magno, G. Schiavon, B. Corain, *Inorg. Chem. 20* (1981) 2579.
[9] a) F. Ammar, J. M. Savéant, *J. Electroanal. Chem. 47* (1973) 215; b) J. B. Flanagan, S. Margel, A. J. Bard, F. C. Anson, *J. Am. Chem. Soc. 100* (1978) 4248; c) A. J. Bard, L. Faulkner: *Electrochemical Methods*, Wiley New York 1980, p. 232.
[10] a) S. P. McGlynn, T. Azumi, M. Kinoshita: *Molecular Spectroscopy of the Triplet State*, Prentice Hall, Englewood Cliffs 1969; b) N. D. Chasteen, R. L. Belford, *Inorg. Chem. 9* (1970) 169.
[11] S. S. Eaton, G. R. Eaton, *J. Am. Chem. Soc. 104* (1982) 5002; S. S. Eaton, K. M. More, B. M. Sawant, G. R. Eaton, *ibid. 105* (1983) 650.
[12] Simulation program POWDER, C. Daul, B. Mohos, C. W. Schläpfer, Universität Fribourg, Switzerland.
[13] C atoms bonded to P in metal complexes containing *cis* phosphane ligands can give rise to five-line multiplets in the ^{13}C-NMR spectrum if $^2J(P,P')$ is small. (D. A. Redfield, L. W. Cary, J. H. Nelson, *Inorg. Chem. 14* (1975) 50).

The First Diphosphaallyl System Coordinated to Two Metal Centers**

By *Rolf Appel,* Winfried Schuhn,* and *Martin Nieger*

The complexation of transition-metal complex fragments to compounds in which phosphorus is involved in multiple bonding has been intensively investigated in recent years. Both terminal (η^1) coordination, as found for phosphanes, and side-on (η^2) coordination, as found for alkenes and alkynes, have been observed. Combination of both types of bonding has also been described.[1] The two modes of coordination of phosphaallyl compounds (η^3 and η^1) have so far only been realized with the 1-phosphaallyl system.[2]

We have now obtained the first diphosphaallyl complex in which, in addition to the η^3 coordination of the tricarbonyliron fragment via the lone pairs of the two phosphorus atoms, a further metal atom is bonded. Reaction of the sodium [(diphosphaallyl)ferrate] **1**[3] with nickelocene **2** in THF at room temperature results in cleavage of cyclopentadienylsodium and formation of a black-brown solution of **3**. Chromatographic workup of this solution afforded black crystals of **3**.

Elemental analysis, IR and NMR spectroscopic data (Table 1), and the mass spectrum are in agreement with the structure given. Particularly characteristic is the singlet for the two phosphorus atoms in the ^{31}P-NMR spectrum at high field.

[*] Prof. Dr. R. Appel, W. Schuhn, M. Nieger
Anorganisch-chemisches Institut der Universität
Gerhard-Domagk-Strasse 1, D-5300 Bonn 1 (FRG)

[**] Low-Coordinate Phosphorus Compounds, Part 63.—Part 62: R. Appel, J. Kochta, V. Winkhaus, *Chem. Ber.*, in press.

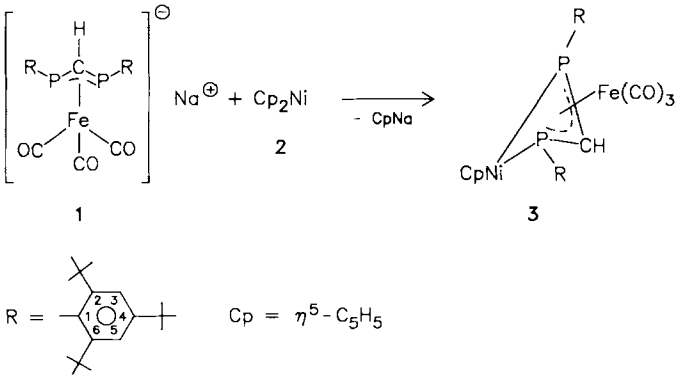

Table 1. Selected NMR and IR spectroscopic data for **3**.

^{31}P-NMR (32.2 MHz, H_3PO_4 ext., C_6D_6): $\delta = -125.8$ (s)

^{1}H-NMR (90 MHz, TMS int., C_6D_6): $\delta = 1.20$ (s, 18 H; 2× *p*-*t*Bu), 1.55 (s, 18 H; 2× *o*-*t*Bu), 1.95 (s, 18 H; 2× *o*-*t*Bu), 5.05 (s, 5 H; C_5H_5), 6.22 (s, 1 H; CH), 7.31 (s, 2 H; 3/5-H), 7.34 (s, 2 H; 3/5-H)

^{13}C{^{1}H}-NMR (50.288 Mhz, CD_2Cl_2): $\delta = 30.66$ (s, *p*-CCH_3), 33.59 (s, *o*-CCH_3), 34.89 (s, *o*-CCH_3), 34.43 (s, *p*-CCH_3), 39.81 (s, *o*-CCH_3), 40.39 (s, *o*-CCH_3), 63.27 (t, $J(CP) = 12.8$ Hz; CH), 91.45 (s; Cp), 122.97 (s, C3/5), 123.32 (t, C3/5), 125.38 (br. s, C1), 150.66 (s, C4), 154.87 (s, C2/6), 159.07 (t, C2/6), 195.0 (br., CO)

IR (KBr): $\tilde{\nu}$(CO) = 1930, 1945, 2010 cm^{-1}

According to an X-ray structure determination (Fig. 1),[4] the C^1 atoms of the aryl moieties and the PCHP framework form a plane, which is typical for phosphaallyl systems.[5] The η^3 coordination to the iron atom is confirmed by the short distance to the allyl C atom (202.5 pm). The lengths of the coordinative bonds to the nickel atom (220 pm) correspond to those in other (phosphane)nickel complexes.[6]

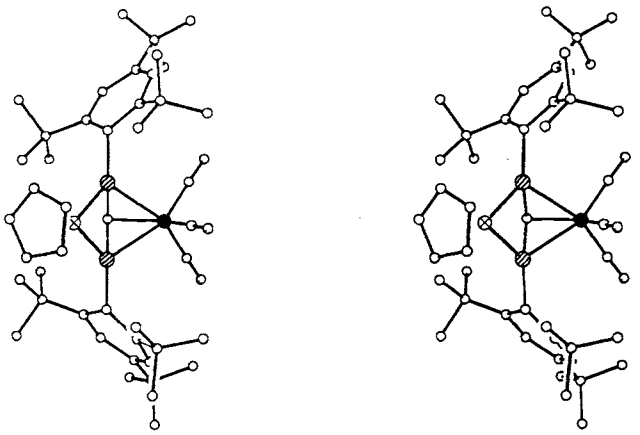

Fig. 1. Stereoprojection of the molecular structure of **3**: ● Fe, ⊗ Ni, ◎ P. Important distances [pm] and angles [°] (standard deviations in parentheses): Fe-P 231.0(2)/230.7(2), Fe-C(allyl) 202.5(7), P-C(allyl) 176.0(7)/176.8(7), Ni-P 219.4(2)/220.1(2); PCP 91.1(3), PFeP 66.1(1), PNiP 69.9(1); dihedral angle PCP/PNiP 35.1.

Experimental Procedure

A solution of **2** (0.40 g, 2.1 mmol) in THF (50 mL) was added to a solution of **1** (1.46 g, 2 mmol) in THF (50 mL) at room temperature over 15 min. The reaction mixture was allowed to stir for 6 h, then concentrated under vacuum and extracted with 150 mL of pentane. After separation of the precipitate, the filtrate was purified by column chromatography on Al_2O_3 (activity I, neutral, eluent toluene). Recrystallization from toluene/pentane (1:1) afforded 1.24 g (75%) of **3**; m.p. = 232 °C.

Received: October 13, 1987 [Z 2473 IE]
German version: *Angew. Chem. 100* (1988) 437

CAS Registry numbers:
1, 112987-72-1; **2**, 1271-28-9; **3**, 112987-80-1.

[1] a) O. J. Scherer, *Angew. Chem. 97* (1985) 905; *Angew. Chem. Int. Ed. Engl. 24* (1985) 924; b) S. Holand, C. Charrier, F. Mathey, J. Fischer, A. Mitschler, *J. Am. Chem. Soc. 106* (1984) 826; c) R. Appel, C, Casser, F. Knoch, *J. Organomet. Chem. 293* (1985) 213; d) N. Hoa Tran Huy, J. Fischer, F. Mathey, *J. Am. Chem. Soc. 109* (1987) 3475.

[2] a) F. Mercier, J. Fischer, F. Mathey, *Angew. Chem. 98* (1986) 347; *Angew. Chem. Int. Ed. Engl. 25* (1986) 357; b) J. F. Nixon, *Xth Int. Conf. Phosphorus Chem.* (Bonn, 1986), lecture B-48.

[3] R. Appel, W. Schuhn, *J. Organomet. Chem. 329* (1987) 179.

[4] **3**: black crystals from toluene, crystal dimensions 0.15 × 0.2 × 0.4 mm^3. Monoclinic, space group $P2_1/n$, $a = 949.9(5)$, $b = 2650.8(23)$, $c = 1816.1(9)$ pm, $\beta = 90.68(4)°$, $V = 4.573$ nm^3, $Z = 4$, $\rho_{calcd} = 1.20$ g cm^{-3}; $\mu = 0.83$ mm^{-1} ($Mo_{K\alpha}$); 6631 measured, 5957 unique reflections ($2\theta_{max} = 45°$), 3710 reflections with $|F| > 4\sigma(F)$ used in the structure solution (direct methods) and refinement (469 parameters), non-hydrogen atoms anisotropic, H atoms (localized by difference electron density determination) refined with a riding model (allyl H atom freely refined, $R = 0.063$ ($R_w = 0.055$, $w^{-1} = \sigma^2(F) + 0.0002F^2$). Further details of the crystal structure investigation are available on request from the Fachinformationszentrum Energie, Physik, Mathematik GmbH, D-7514 Eggenstein-Leopoldshafen 2 (FRG), by quoting the depository number CSD-52777, the names of the authors, and the journal citation.

[5] a) R. Appel, W. Schuhn, F. Knoch, *Angew. Chem. 97* (1985) 421; *Angew. Chem. Int. Ed. Engl. 24* (1985) 420; b) cf. [2]; c) R. Appel, W. Schuhn, F. Knoch, *J. Organomet. Chem. 319* (1987) 345.

[6] P. W. Jolly, G. Wilke: *The Organic Chemistry of Nickel, Vol. 1*, Academic Press, New York 1974.

Weak Intramolecular Bonding Relationships: The Conformation-Determining Attractive Interaction between Gold(I) Centers**

By *Hubert Schmidbaur,* Wilhelm Graf*, and *Gerhard Müller*

Structural analyses[1, 2] and spectroscopic studies[3, 4] on mono- and polynuclear gold(I) compounds have provided a wealth of indirect evidence of an attractive interaction between the d^{10}-configurated gold atoms. This weak bonding relationship occurs perpendicular to the principle axis of the linearly two coordinated structural moieties and leads either to catenated or layered aggregation of the molecules via Au···Au contacts, some less than 3.0 Å in length, or to the intramolecular pairing of the gold atoms with similar equilibrium distances. The 5d^{10}–5d^{10} interaction concerned stems from a mixing of the 6s^2 states,[5] whose energy gap is reduced by relativistic effects.[6, 7] In the case of the neighboring element mercury these effects are already less pronounced, so the phenomenon rarely occurs.[8]

We have searched for convincing evidence for these interactions and for a possibility of measuring their strengths quantitatively. From the numerous structural data available[1] there emerged astonishingly many striking indications of such interactions,[9] yet proof thereof is so far still lacking, even after specially planned tests.[10] A new series of experiments have now furnished the positive results reported here.

[*] Prof. Dr. H. Schmidbaur, Dipl.-Chem. W. Graf, Dr. G. Müller [+]
Anorganisch-chemisches Institut der Technischen Universität München
Lichtenbergstrasse 4, D-8046 Garching (FRG)

[+] X-ray structure analysis.

[**] This work was supported by the Deutsche Forschungsgemeinschaft (Leibniz program), by the Fonds der Chemischen Industrie, and by Hoechst AG and Degussa AG. We thank Prof. Dr. *F. E. Wagner*, Physik-Department der Technischen Universität München, for the ^{197}Au-Mössbauer spectrum, and Herr *J. Riede* for supplying the crystallographic data sets.

Both in solution and in the crystalline state the doubly phosphino-substituted ylide **1** has the conformation given in the formula **1a** with *syn*- and *anti*-orientation, respectively, of the lone pairs.[11] A P-C rotation with establishment of the *syn/syn* conformation **1b** requires an activation energy of 11 kcalmol^{-1}. It was to be expected that after double complexation of **1** with AuCl—assuming sufficiently strong attraction of the gold atoms — the relative stability of these conformations should change in favor of the symmetrical form. Surprisingly, however, the unsymmetrical conformation is retained, both in the 1:1 adduct **2** as well as in the 1:2 adduct **3**.[10] Apparently the ground state conformation of **3** is still too strongly favored due to

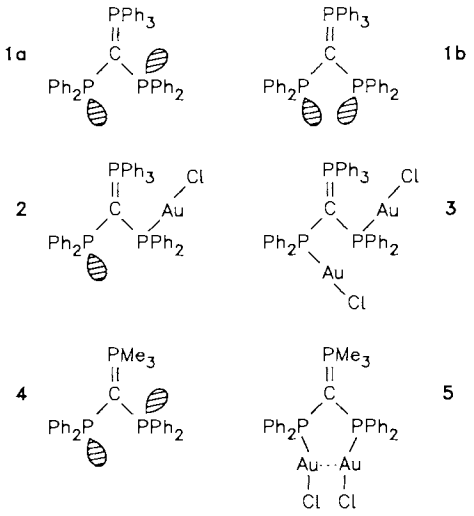

the steric hindrance of the seven phenyl groups. Therefore, in order to make the Au···Au attraction recognizable, the steric hindrance had to be reduced. We first showed that the threefold methyl-substituted ylide **4** has the same *syn/anti* conformation as **1a**[12] (Fig. 1). Compound **4** was synthesized by methods, which, in principle, are known.[13-15] The ^{31}P-NMR spectroscopically determined activation energy of the P-C rotation, with $\Delta G^{\neq} = 9.5$ kcal mol^{-1}, is only slightly less than that of **1**.

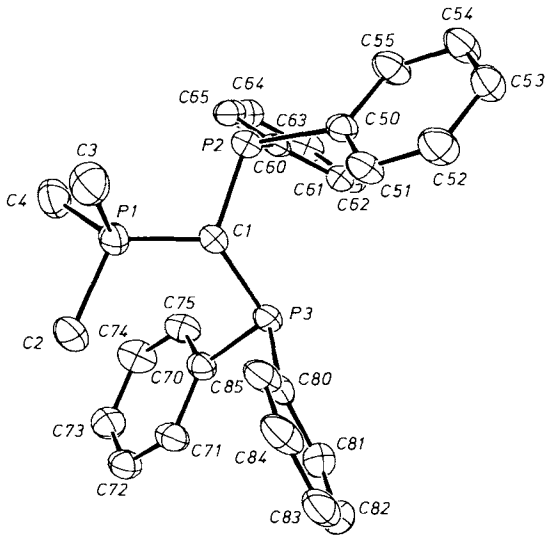

Fig. 1. Crystal structure of **4** (ORTEP, vibrational ellipsoids at the 50% probability level, H atoms omitted). Important bond lengths [Å] and angles [°]: P1-C1 1.725(2), P2-C1 1.792(2), P3-C1 1.777(3); P1-C1-P2 109.8(1), P1-C1-P3 126.4(1), P2-C1-P3 121.6(1).

Reaction of **4** with two equivalents of [(CO)AuCl] readily leads via elimination of CO to the 2:1 complex **5** in high yields. The ^{1}H-, ^{13}C-, and ^{31}P-NMR spectra of **5** already showed that the two Ph_2PAuCl moieties in this molecule are equivalent in solution at low temperatures.[16] The X-ray crystallographic structure analysis[12] and the ^{197}Au-Mössbauer spectra subsequently also proved that the molecule has the hoped for *syn/syn* conformation (Fig. 2) in

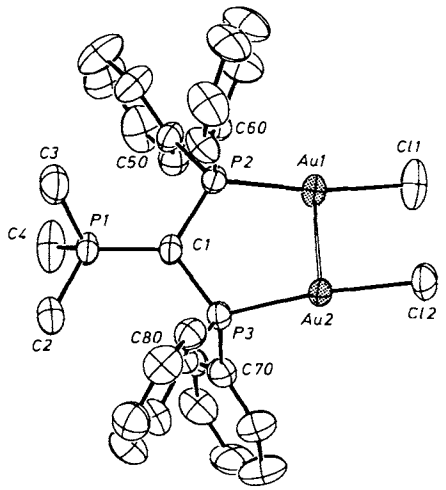

Fig. 2. Crystal structure of **5** (ORTEP, vibrational ellipsoids at the 50% probability level, H atoms omitted). Important bond lengths [Å] and angles [°]: P1-C1 1.742(6), P2-C1 1.772(6), P3-C1 1.777(6), P2-Au1 2.246(2), P3-Au2 2.247(2), Au1-Au2 3.000(1), Au1-Cl1 2.290(2), Au2-Cl2 2.290(2); P1-C1-P2 120.1(3), P1-C1-P3 125.2(4), P2-C1-P3 114.6(3), P2-Au1-Cl1 170.3(1), P3-Au2-Cl2 172.9(1).

the crystalline state, in which the two gold atoms are at a distance of only just over 3.000(1)Å from each other. With this interaction taken into account, the structure corresponds to a twist configurated five-membered ring. One of the two Ph_2P moieties rotates about the P-C bond during the transition from **4** to **5** such that the two gold centers are brought into contact. The mutual attraction of the metal atoms is also manifested in the marked decrease in the angle of the P-Au-Cl axes. Thus, through the reduction of the mutual hindrance of the organic groups on going from **1** to **4**, the Au···Au interaction can effectively function as a conformation-determining force. It should be pointed out that the P-C bond lengths in the free ylide **4** remain practically unchanged during complex formation. In contrast, the changes in the P-C-P angle very nicely reflects the repulsive interactions between organic groups and lone pairs in **4**, while the Au···Au attraction in **5** is manifested by virtue of a distinctly smaller P2-C1-P3 angle. That is, the attachment of the gold atoms to the phosphorus atoms does not lead to profound geometrical changes in the ligand with which the conformational change could be explained. The same agreement of bond distances was also observed in the case of **1a** and **3**,[10] in which no change in conformation occurs.

Interestingly, the ^{31}P-NMR spectrum of **5** is also temperature-dependent. The equivalence of the two PPh_2 groups is maintained over a wide temperature range, but the $J(P^{V}P^{III})$ coupling constant decreases with decreasing temperature. Below -35 °C (in CD_2Cl_2 as solvent) even a broadening of the P^{III} signal and disappearance of its multiplicity takes place. We attribute the decrease in the coupling constant to the different proportions of the possible

conformers according to the dihedral dependence of the spin-spin interaction. The signal-broadening may be due to a further hindering of P-C rotations. A similar situation is observed in the case of **3**.

From the above-mentioned energy barrier it can be estimated that the energy of the Au···Au interaction lies in the order of 7–8 kcal mol^{-1}. It is thus comparable with hydrogen bonding, wherein its conformation-determining influence finds a good parallel.

Experimental

$Me_3P{=}CH{-}PPh_2$: A solution of $Me_3P{=}CH_2$ [17] (4.15 g, 46 mmol) in toluene (50 ml) was treated at 0°C with a solution of Ph_2PCl (5.08 g, 4.23 mmol) in a little toluene. After 16 hours' stirring at 20°C the mixture was filtered and the filter-cake washed with toluene. Concentration of the combined filtrates by evaporation and careful addition of a layer of pentane led to crystallization of the desired product: yield 5.25 g (83%), m.p. 88–89°C; ^{31}P-NMR ([D$_8$]toluene, 25°C): $\delta = 4.4$, -21.3 (AX, $^2J(PP) = 163.3$ Hz).

4: A solution of $Me_3P{=}CH{-}PPh_2$ (820 mg, 2.99 mmol) in toluene (25 mL) was treated at 0°C with a solution of Ph_2PCl (330 mg, 1.49 mmol) in a small amount of the same solvent. Yield after analogous work-up as above: 590 mg (86%); m.p. 152–153°C; ^{31}P-NMR ([D$_8$]toluene, -80°C): $\delta = 16.6$ (dd, $^2J(PP) = 187.7$, 30.4 Hz), -1.9 (dd, $^2J(PP) = 187.7$, 10.5 Hz), -8.2 (dd, $^2J(PP) = 30.4$, 10.5 Hz); +50°C: $\delta = 14.1$ (t), 2.7 (d, $^2J(PP) = 77.1$ Hz); ^{1}H-NMR (C_6D_6, 25°C): $\delta = 0.90$ (d, $J(PH) = 11.4$ Hz, Me), 7.02–7.69 (m, Ph); ^{13}C-NMR ([D$_8$] toluene): $\delta = 17.2$ (dt, $J(PC) = 57.7$, 5.3 Hz, Me), 126.7, 127.9, 133.0 and 144.1 (Ph).

5: A solution of **4** (120 mg, 0.26 mmol) in toluene (25 mL) was treated with a solution of [(CO)AuCl] (136 mg, 0.52 mmol) in a small amount of toluene. Evolution of CO was observed. After 16 hours' stirring at 20°C any small amounts of pale violet precipitate of colloidal gold that separated out were removed by filtration, washed with toluene and the combined filtrates treated with nitrobenzene/pentane. The desired compound **5** crystallized out: yield 200 mg, (74%), m.p. 200–202°C (decomp), soluble in CH_3CN, CH_2Cl_2, nitrobenzene. ^{31}P-NMR (CD_2Cl_2, 0°C): $\delta = 20.9$(d), 6.9 (t, $J(PP) = 17.9$ Hz); -30°C: $\delta = 23.3$ (d), 6.8 (t, $J(PP) = 15.6$ Hz); -60°C: $\delta = 26$ (br.), 6.6 (t, $J(PP) = 12.1$ Hz); ^{13}C-NMR ($C_6D_5NO_2$, 25°C): $\delta = 18.1$ (d, $J(PC) = 58.7$ Hz, Me); ^{1}H-NMR (CD_2Cl_2, 25°C): $\delta = 1.50$ (d, $J(PH)$ 12.2 Hz, Me), 7.42–7.78 (m, Ph); ^{197}Au-Mössbauer spectrum (4 K): $I.S. = 2.6935$, $Q.S. = 6.9274$ mm s^{-1}.

Received: November 30, 1987 [Z 2518 IE]
German version: *Angew. Chem. 100* (1988) 439

CAS Registry numbers:
4, 113109-84-5; **5**·$C_6H_5NO_2$, 113109-82-3; [(CO)AuCl], 50960-82-2; $Me_3P{=}CHPPh_2$, 113109-83-4; $Me_3P{=}CH_2$, 14580-91-7; Ph_2PCl, 1079-66-9.

[1] P. G. Jones, *Gold Bull. 14* (1981) 102, 159; *16* (1983) 114; *19* (1986) 46.
[2] H. Schmidbaur, T. Pollok, R. Herr, F. E. Wagner, R. Bau, J. Riede, G. Müller, *Organometallics 5* (1986) 566; H. Schmidbaur, A. Wohlleben, U. Schubert, G. Huttner, *Chem. Ber. 110* (1977) 2751.
[3] W. Ludwig, W. Meyer, *Helv. Chim. Acta 65* (1983) 934; W. Bensch, M. Prelati, W. Ludwig, *J. Chem. Soc. Chem. Commun. 1986*, 1762.
[4] H. Schmidbaur, C. Hartmann, F. E. Wagner, *Hyperfine Interact.*, in press.
[5] Y. Jiang, S. Alvarez, R. Hoffmann, *Inorg. Chem. 24* (1985) 749; P. K. Mehrotra, R. Hoffmann, *ibid. 17* (1978) 2187.
[6] P. Pyykkö, J. P. Desclaux, *Acc. Chem. Es. 12* (1979) 276; K. S. Pitzer, *ibid. 12* (1979) 271.
[7] T. Ziegler, J. G. Snijders, E. J. Baerends, *J. Chem. Phys. 74* (1981) 1271.
[8] J. Bravo, J. S. Casas, Y. P. Mascarenhas, A. Sanchez, C. de O. P. Santos, J. Soedo, *J. Chem. Soc. Chem. Commun. 1986*, 1100.
[9] H. Schmidbaur, G. Reber, A. Schier, J. Riede, G. Müller, *Inorg. Chim. Acta*, in press.
[10] H. Schmidbaur, W. Graf, G. Reber, G. Müller, *Helv. Chim. Acta 69* (1986) 1748.
[11] H. Schmidbaur, U. Deschler, B. Milewski-Mahrla, *Chem. Ber. 116* (1983) 1393.
[12] Crystal structure data **4**: $C_{28}H_{29}P_3$, $M_r = 458.47$, monoclinic, space group $P2_1/c$, $a = 10.464(1)$, $b = 20.422(2)$, $c = 12.788(1)$ Å, $\beta = 113.16(1)$°, $V = 2512.5$ Å^3, $\rho_{calc} = 1.212$ g cm^{-3}, $Z = 4$, 3943 independent reflections, 3108 with $F_o \geq 4.0\sigma(F_o)$ ($+h$, $+k$, $\pm l$, $(\sin\theta/\lambda)_{max} = 0.572$, $Mo_{K\alpha}$ radiation, $\lambda = 0.71069$ Å, $T = -35$°C, Syntex $P2_1$). Solution by direct methods (SHELXS-86), $R(R_w) = 0.059$ (0.043), $w = 1/\sigma^2(F_o)$ for 289 refined parameters and all reflections (anisotropic, Me rigid groups, SHELX-76), $\Delta\rho_{fin}(max/min) = 0.33/-0.31$ e/Å^3. — **5**·1 nitrobenzene: $C_{28}H_{29}Au_2Cl_2P_3 \cdot C_6H_5NO_2$, $M_r = 1046.42$, triclinic, $P\bar{1}$, $a = 10.796(1)$, $b = 12.486(1)$, $c = 15.168(1)$ Å, $\alpha = 67.96(1)$, $\beta = 75.21(1)$, $\gamma = 75.12(1)$°, $V = 1802.6$ Å^3, $\rho_{calc} = 1.928$ g cm^{-3}, $Z = 2$, $\mu(Mo_{K\alpha}) = 84.2$ cm^{-1}. 7816 reflections, 5754 "observed" ($+h$, $\pm k$, $\pm l$, $(\sin\theta/\lambda)_{max} = 0.638$, $T = 23$°C, Enraf-Nonius CAD4). Patterson methods, $R(R_w) = 0.066$ (0.033) for 340 refined parameters and all reflections (anisotropic, Me and nitrobenzene as rigid groups). $\Delta\rho_{fin}(max/min) = 1.86/-1.67$ e/Å^3 on disordered nitrobenzene. — Further details of the crystal structure investigations are available on request from the Fachinformationszentrum Energie, Physik, Mathematik GmbH, D-7514 Eggenstein-Leopoldshafen 2 (FRG), on quoting the depository number CSD 52765/52766, the names of the authors, and the journal citation.
[13] H. Schmidbaur, W. Tronich, *Chem. Ber. 101* (1968) 3345.
[14] K. Issleib, R. Lindner, *Justus Liebigs Ann. Chem. 699* (1966) 40; K. Issleib, H.-P. Abicht, *J. Prakt. Chem. 312* (1976) 721.
[15] H. Schmidbaur, A. Wohlleben-Hammer, *Chem. Ber. 112* (1979) 510; M. S. Hussain, H. Schmidbaur, *Z. Naturforsch. B 31* (1976) 721.
[16] Cf. experimental procedures.
[17] H. Schmidbaur, *Inorg. Synth. 18* (1978) 136.

Polyauriomethane Compounds**

By *Hubert Schmidbaur,* Franz Scherbaum, Brigitte Huber,* and *Gerhard Müller*

Polynuclear gold compounds are of great current interest, since, on the one hand, their structures and properties provide a fruitful framework on which to discuss the concepts of intermetallic interactions[1] and, on the other, they should open up improved routes to the thermal, chemical or photochemical deposition of metallic gold, e.g. in electronics and electron microscopy.

Not only gold clusters, in which the metal atoms are directly bonded to each other,[2] but also organogold compounds in which several metal atoms are bonded via a common carbon atom are of special importance. The close proximity of the gold atoms in such compounds should not only lead to clearly recognizable Au···Au bonding relationships but should also facilitate metal nucleation, which is important for the controlled deposition of gold. (The concomitant formation of a gold carbide is not to be expected.) The number of known polyaurioalkanes has increased significantly in recent years,[4–6] yet all attempts to prepare compounds in which more than two gold atoms are fixed to one carbon atom have thus far failed.[6, 7] In contrast, polymercuriomethanes including even tetramercuriomethanes have been relatively well documented.[8]

We were able to show already in 1976 that carbodiphosphoranes are suitable precursors for diauriomethane compounds, since the phosphonium centers facilitate polyauration.[4] In continuation of these studies we have now succeeded in synthesizing numerous further examples of this series of compounds. Not only hexamethylcarbodiphosphorane **1a** but also the dimethyltetraphenyl- and methylpentaphenyl-homologues proved to be exceptionally good donors for gold(I) centers. In contrast to **1a**, these phenylated double ylides only form 1:1 complexes with [MeAuPPh$_3$], namely **3a** and **3b**, respectively; but reaction of **1b** with [BrAuPPh$_3$] once again furnishes a cationic 1:2 complex (**4**).

[*] Prof. Dr. H. Schmidbaur, Dipl.-Chem. F. Scherbaum, Dipl.-Chem. B. Huber [+], Dr. G. Müller [+]
Anorganisch-chemisches Institut der Technischen Universität München
Lichtenbergstrasse 4, D-8046 Garching (FRG)

[+] X-ray structure analysis.

[**] This work was supported by the Deutsche Forschungsgemeinschaft (Leibniz-Program), the Fonds der Chemischen Industrie, Hoechst AG, and Degussa AG, We thank Prof. Dr. *F. E. Wagner*, Physik-Department der Technischen Universität München, for recording the ^{197}Au-Mössbauer spectrum and *J. Riede* for supplying the crystallographic data sets.

$Me_3P{=}C{=}PMe_3 + 2[MeAuPPh_3] \longrightarrow 2\,PPh_3 + [(Me_3P)_2C(AuMe)_2]$
1a **2**

$MePh_2P{=}C{=}PPh_2Me + [MeAuPPh_3] \longrightarrow PPh_3 + [(MePh_2P)_2CAuMe]$
1b **3a**

$MePh_2P{=}C{=}PPh_2Me + 2[BrAuPPh_3] \longrightarrow [\{(MePh_2P)_2C(AuPPh_3)_2\}Br_2]$
1b **4**

$MePh_2P{=}C{=}PPh_3 + [MeAuPPh_3] \longrightarrow PPh_3 + [MePh_2P(Ph_3P)CAuMe]$
1c **3b**

Attempts to synthesize non-ylidic diauriomethanes, on the other hand, have so far met without success. Neither reaction of boryl-substituted alkanes nor the treatment of halogenoalkylated gold complexes of the type $[ClCH_2AuPPh_3]$ with CsAu in the presence of PPh_3 led to satisfactory results.[9]

The desilylation of suitable silylphosphonium salts and their corresponding ylides,[10] however, proved to be favorable methods even for the synthesis of higher auriated products. For example, even a triply auriated cation such as **7** could be obtained by silyl cleavage with cesium fluoride in acetonitrile.[11]

Reaction of trimethylphosphonio(trimethylsilylmethanide) **5**[10] with $[ClAuPPh_3]$ affords, in quantitative yield, the adduct **6**, which corresponds to the homologue already mentioned previously.[12] Treatment of this precursor with CsF in the presence of further $[ClAuPPh_3]$, or the direct reaction of **5** with at least two equivalents of $[ClAuPPh_3]$, lead via several similar but not isolated intermediate stages to the [trimethyl(triauriomethyl)phosphonium] chloride **7**.

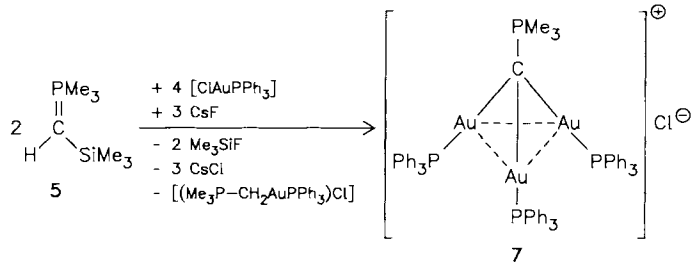

$[\{Me_3P{-}CH(SiMe_3)AuPPh_3\}\,Cl]$ **6**

The colorless salt **7** is stable towards air, light and water, and can be crystallized from aqueous acetonitrile as a, likewise, colorless and very stable hemihydrate **7a**. ^1H-, ^{13}C- and ^{31}P-NMR data for the solutions are consistent with the structural equivalence of the three Ph_3PAu moieties and the onium character of the Me_3P group on the common central C-atom. The ^{197}Au-Mössbauer spectrum, with a single, completely symmetrical quadrupole doublet of equal intensity also indicates, within the limits of accuracy, a comparable position of the gold centers in the crystal (Fig. 1). The FD-mass spectrum shows the mass of the cation at *m/z* 1465.

The X-ray structure analysis[13] confirms the proposed structure. The unit cell contains two crystallographically independent formula units, which merely differ in conformational details. The three gold atoms are about equidistant from the common carbon atom. Pairwise they form

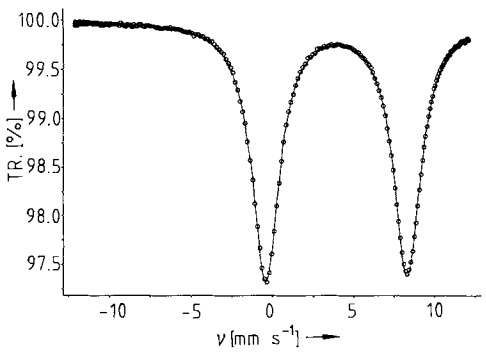

Fig. 1. ^{197}Au-Mössbauer spectrum of the triauriomethane compound **7** (at 4 K). TR = relative transmission, ν = relative rate.

angles with the ylidic C atom which are significantly less than the tetrahedral angle of 109° (Fig. 2); hence the P1–C1–Au angles are greater than 109°. The C1–Au–P axes deviate only slightly from linearity. The P1–C1 distance, with a mean value of 1.72 Å, compares very well with the values found for other metalated phosphonium salts and ylide complexes.[14] The P–Au and Au–C distances are also as would be expected. The chloride ion and the water of crystallization have no discrete contacts to the cations.

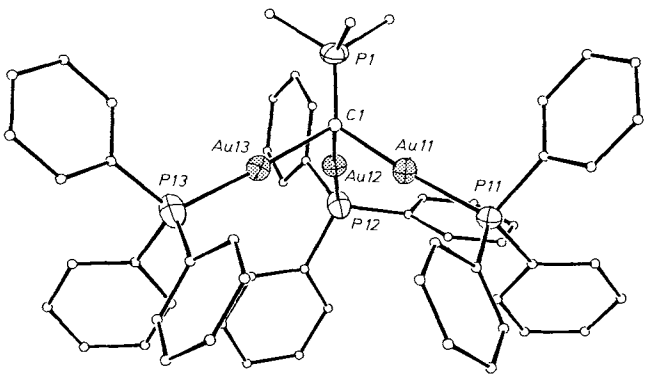

Fig. 2. Structure of one of the two crystallographically independent cations of **7a** ($7 \cdot \frac{1}{2}H_2O$; ORTEP, vibrational ellipsoids at the 50% probability level, C atoms with arbitrary radii). Important bond lengths [Å] and angles [°] for both cations: Au11–Au12 3.117(2)/3.138(2), Au11–Au13 3.233(2)/3.140(2), Au12–Au13 3.266(2)/3.166(2), Au11–C1 1.96(4)/1.95(3), Au12–C1 2.21(3)/2.05(3), Au13–C1 2.13(4)/2.04(4), Au11–P11 2.27(1)/2.29(1), Au12–P12 2.30(1)/2.27(1), Au13–P13 2.28(1)/2.29(1), P1–C1 1.62(4)/1.83(3); Au11–C1–Au12 96(1)/103(1), Au11–C1–Au13 104(2)/104(2), Au12–C1–Au13 97(1)/102(2), P1–C1–Au11 124(2)/116(2), P1–C1–Au12 115(2)/114(2), P1–C1–Au13 115(2)/117(2), C1–Au11–P11 173(1)/178(1), C1–Au12–P12 176(1)/176(1), C1–Au13–P13 175(1)/171(1).

The structure is in the first place remarkable in that all other previously known triaurioelement cations $[X(AuL)_3]^{\oplus}$ with X=O, S, Se oligomerize in such a way via Au···Au contacts that one Au_2-pair is bound other than the remaining third gold atom.[15] Particularly significant, however, is the clearly recognizable approach of the gold atoms in **7** to within an average 3.18 Å, which, despite the repulsion to be expected between the large PPh_3 ligands and the equidirectional formal charge on the metal atoms, leads to the above-mentioned narrowing of the Au–C1–Au angle. It confirms anew the concept of structure- and conformation-determining d^{10}-d^{10} interactions in the heavy late d-block elements.

Experimental

3b: A solution of [MeAuPPh$_3$] (0.92 g, 1.94 mmol) in diethyl ether (10 mL) was treated at −78 °C with a solution of **1c** (1.01 g, 2.10 mmol) in 35 mL of the same solvent and the stirred mixture allowed to warm within 2 h to room temperature. A yellow precipitate separated out, yield 1.15 g (86%), which decomposed on warming. ^{1}H-NMR (CD_2Cl_2, 25 °C): $\delta = -0.1$ (s, MeAu), 1.83 (d, J(PH) = 11.8 Hz, MeP), 7.1–8.1 (m, Ph); ^{31}P{^{1}H}-NMR (CD_2Cl_2, 25 °C): $\delta = 7.5$ and 9.7 (per d, J(PP) = 51.9); ^{13}C-NMR (CD_2Cl_2, 25 °C): $\delta = -3.65$ (s, MeAu), 21.5 (d, J(PC) = 74.2, MeP), two sets of resonances for PPh_2 and PPh_3.

4: A suspension of [BrAuPPh$_3$] (1.93 g, 3.6 mmol) in THF (40 mL) was treated at −78 °C with a solution of **1b** (0.74 g, 1.8 mmol) in 20 mL of THF. The stirred mixture was allowed to warm to room temperature within 3 h and treated with 50 mL of pentane; after filtration, the precipitate was dried under vacuum. Yield 2.6 g (98%), m.p. 180–182 °C (decomp.). ^{1}H-NMR (CD_3OD, 25 °C): $\delta = 2.60$ ($A_3XX'A'_3$, N = 12.6, Me), 7.1–8.6 (m, Ph), ^{31}P{^{1}H}-NMR (CD_3OD, 25 °C): $\delta = 21.19$ and 34.26 (s).

6: The colorless product obtained from equimolar amounts of **5** and [ClAuPPh$_3$] in THF was characterized by the following spectroscopic data: ^{1}H-NMR ($CDCl_3$, 25 °C): $\delta = 0.23$ (s, $SiMe_3$), 1.18 (dd, J(PH) = 18.8 and 8.8 Hz, CHP), 1.84 (d, J(PH) = 12.9, PMe_3), 7.3–7.6 (m, PPh_3); ^{31}P{^{1}H}-NMR ($CDCl_3$, 25 °C): $\delta = 26.68$ (d) and 41.93 (d, per J(PP) = 15.26 Hz); ^{29}Si-NMR ($CDCl_3$, −30 °C): $\delta = 1.72$ (dd, J(PSi) = 5.63 and 3.19); ^{13}C-NMR ($CDCl_3$, 25 °C): $\delta = 3.87$ (dd, J(PC) = 4.42 and 0.96, $SiMe_3$), 16.88 (dd, J(PC) = 57.22 and 1.96 Hz, PMe_3), 23.02 (dd, J(PC) = 68.23 and 36.44, CHP), 129.56 (J = 11.2), 132.09 (J = 2.45) and 133.82 (J = 13.7) for C2 to C4 in PPh_3 (C1 masked).

7/7a: A solution of [ClAuPPh$_3$] (1.16 g, 2.34 mmol) in THF (65 mL) was treated with a solution of **5** (0.19 g, 1.17 mmol) in 15 mL of THF and the mixture allowed to stand for 3.5 h at room temperature. The solvent was then removed and the residue treated with a solution of CsF (0.5 g, 3.3 mmol) in acetonitrile (70 mL); the mixture was then stirred for 23 h at 60–65 °C. After filtration under vacuum, the filtrate was evaporated to dryness and the residue extracted several times with benzene. On evaporation of the combined extracts to dryness a colorless product, **7**, precipitated which after washing with pentane could be crystallized from a mixture of acetonitrile and diethyl ether; yield 0.65 g (54%) **7a**, m.p. 190–192 °C. ^{1}H-NMR (CD_3CN, 25 °C): $\delta = 1.65$ (d, ^2J(PH) = 12.5 Hz, Me), 7.2–7.5 (m, Ph); ^{31}P{H}-NMR (CD_3CN, 25 °C): $\delta = 27.23$ (s, PMe_3), 37.95 (s, PPh_3); ^{13}C-NMR (CD_3CN, 25 °C): $\delta = 25.82$ (d, ^1J(PC) = 58.2 Hz, Me), 132.43 (d, J = 49.39), 134.88 (d, J = 14.18), 130.12 (d, J = 10.76), 132.34 (s) for C1 to C4 of C_6H_5; ^{197}Au-Mössbauer spectrum (4 K): $I.S.$ = 3.926(1) mm s^{-1}; $Q.S.$ = 8.705(2) mm s^{-1}.

Received: November 30, 1987 [Z 2519 IE]
German version: *Angew. Chem. 100* (1988) 441

[1] P. G. Jones, *Gold Bull. 14* (1981) 102, 159; *16* (1983) 114; *19* (1986) 46.
[2] K. P. Hall, D. M. P. Mingos, *Prog. Inorg. Chem. 32* (1984) 237; C. Malatesta, *Gold Bull. 8* (1975) 48; G. Schmid, R. Pfeil, R. Boese, F. Bandermann, S. Meyer, G. H. M. Calis, J. W. A. van der Velden, *Chem. Ber. 11* (1981) 3634.
[3] H. Schmidbaur: *"Organogold Compounds"* in *Gmelin Handbuch der Anorganischen Chemie*, Springer Berlin 1980.
[4] H. Schmidbaur, O. Gasser, *Angew. Chem. 88* (1976) 542; *Angew. Chem. Int. Ed. Engl. 15* (1976) 501.
[5] P. Jandik, U. Schubert, H. Schmidbaur, *Angew. Chem. 94* (1982) 74; *Angew. Chem. Int. Ed. Engl. 21* (1982) 73; *Angew. Chem. Suppl. 1982*, 1; H. Schmidbaur, C. Hartmann, *Angew. Chem. 98* (1986) 573; *Angew. Chem. Int. Ed. Engl. 25* (1986) 575; H. Schmidbaur, C. Hartmann, J. Riede, B. Huber, G. Müller, *Organometallics 5* (1986) 1652; H. H. Murray, A. M. Mazany, J. P. Fackler, Jr., *ibid. 4* (1985) 154, and references cited therein; J. Vicente, M. C. Chicote, J. A. Cayuelas, J. Fernandez-Baeza, P. G. Jones, G. M. Sheldrick, P. Espinet, *J. Chem. Soc. Dalton Trans. 1985*, 1163, and references cited therein; E. G. Perevalova, K. I. Grandberg, T. V. Baukova, V. P. Dyadchenko, Yu. L. Slovokhotov, Yu. T. Struchkov, *Koord. Khim. 8* (1982) 1337.
[6] In contrast, a tetraaurioammonium cation is already known: Yu. L. Slovokhotov, Yu. T. Struchkov, *J. Organomet. Chem. 277* (1984) 143.
[7] W. Kress, *Diplomarbeit* 1978, *Dissertation* 1983, Universität Erlangen-Nürnberg.
[8] D. K. Breitinger, W. Kress, *J. Organomet. Chem. 256* (1983) 217; D. K. Breitinger, W. Kress, R. Sendelbeck, *ibid. 243* (1983) 245; D. K. Breitinger, K. Geibel, W. Kress, R. Sendelbeck, *ibid. 191* (1980) 7.
[9] F. Scherbaum, *Diplomarbeit*, Technische Universität München 1986.
[10] H. Schmidbaur, W. Tronich, *Chem. Ber. 101* (1968) 595, 3545; *100* (1967) 1932.
[11] E. Vedejs, F. G. West, *Chem. Rev. 86* (1986) 941; E. Vedejs, G. R. Martinez, *J. Am. Chem. Soc. 101* (1979) 6452.
[12] H. Schmidbaur, R. Franke, *Chem. Ber. 108* (1975) 1321; H. Schmidbaur, W. Richter, W. Wolf, F. H. Köhler, *ibid. 108* (1975) 2649.
[13] Crystal structure data of **7a** (7·½H$_2$O): monoclinic, space group $P2_1/n$, a = 21.277(3), b = 20.338(3), c = 27.154(4) Å, β = 106.82(1)°, V = 11247.7 Å^3, Z = 8, ρ_{calc} = 1.784 g cm^{-3}, μ(Mo$_{K\alpha}$) = 79.8 cm^{-1}, Syntex $P2_1$ diffractometer, Mo$_{K\alpha}$ radiation, λ = 0.71069 Å, T = −40 °C, 11230 independent reflections, 9008 "observed" with $F_0 \geq 2.0\sigma(F_0)$. Solution by Patterson methods (SHELXS-86), $R(R_w)$ = 0.110 (0.083), $w = 1/\sigma^2(F_0)$ for 387 refined parameters (Au, P anisotropic, Cl, O, C isotropic, phenyl rings as rigid groups, SHELX-76). $\Delta\rho_{fin}$(max/min) = +3.3/−2.1 e/Å^3. The high R values and the large standard deviations arise from the poor quality of the crystals of **7a**. Further details of the crystal structure investigation are available on request from the Fachinformationszentrum Energie, Physik, Mathematik GmbH, D-7514 Eggenstein-Leopoldshafen 2 (FRG), on quoting the depository number CSD-52881, the names of the authors, and the journal citation.
[14] H. Schmidbaur, *Angew. Chem. 95* (1983) 980; *Angew. Chem. Int. Ed. Engl. 22* (1983) 907.
[15] E. I. Smyslova, E. G. Perevalova, V. P. Dyadchenko, K. I. Grandberg, Yu. L. Slovokhotov, Yu. T. Struchkov, *J. Organomet. Chem. 215* (1981) 269; A. N. Nesmeyanov, E. G. Perevalova, Yu. T. Struchkov, M. Yu. Antipin, K. I. Grandberg, V. P. Dyadchenko, *ibid. 201* (1980) 343; P. G. Jones, G. M. Sheldrick, E. Hädicke, *Acta Crystallogr. B36* (1980) 2777; H. Schmidbaur, R. Franke, J. Eberelin, *Chem.-Ztg. 99* (1975) 91; E. W. Abel, C. R. Jenkins, *J. Organomet. Chem. 14* (1968) 285; C. Kowala, J. M. Swan, *Aust. J. Chem. 19* (1966) 547.

Structure of Molecular PNO, Matrix Isolation and ab initio Calculations**

By *Reinhart Ahlrichs, Stephan Schunck,* and *Hansgeorg Schnöckel**

Dedicated to Professor Harald Schäfer on the occasion of his 75th birthday

We have already reported the synthesis and characterization of numerous molecules that are of theoretical interest regarding their bonding, e.g. SiO_2,[1] $SiOCl_2$,[2] and PO_2Cl[3] [Eq. (a)-(c)].

$$SiO + O \longrightarrow O{=}Si{=}O \quad (a)$$

$$SiO + Cl_2 \longrightarrow O{=}SiCl_2 \quad (b)$$

$$O{=}PCl + O \longrightarrow O_2P{-}Cl \quad (c)$$

PO_2Cl belongs to a type of compounds that has recently attracted increasing interest.[4] We now wanted to clarify whether P^V can also occur in compounds with coordination number two. By reaction of PN[5] and O_3 under matrix conditions it should be possible to prepare $N{\equiv}P^{\oplus}{-}O^{\ominus}$,[6] which is analogous to N_2O and isoelectronic with SiO_2. Figure 1 shows sections of the IR spectra which were recorded after cocondensation of PN and O_3[3] with an excess of Ar, and after subsequent photolysis.[7,8] After the photolysis, a series of low intensity absorptions is observed, together with a medium-strength band at 1755 cm^{-1} (1727 cm^{-1}).[9] This is not to be assigned to a PN vibration (e.g. in NPO),[10] but to an NO vibration. Numerous experiments carried out under different reaction conditions showed that only the band at 865 cm^{-1} (844 cm^{-1})[9] is changed simultaneously with that at 1755 cm^{-1}. On the basis of frequency calculations (GF method[13]) these

[*] Prof. Dr. H. Schnöckel, Dr. S. Schunck
Anorganisch-chemisches Institut der Universität
Wilhelm-Klemm-Strasse 8, D-4400 Münster (FRG)
Professor Dr. R. Ahlrichs
Institut für Physikalische Chemie und Elektrochemie der Universität
Kaiserstrasse 12, D-7500 Karlsruhe (FRG)

[**] This work was supported by the Deutsche Forschungsgemeinschaft and the Fonds der Chemischen Industrie.

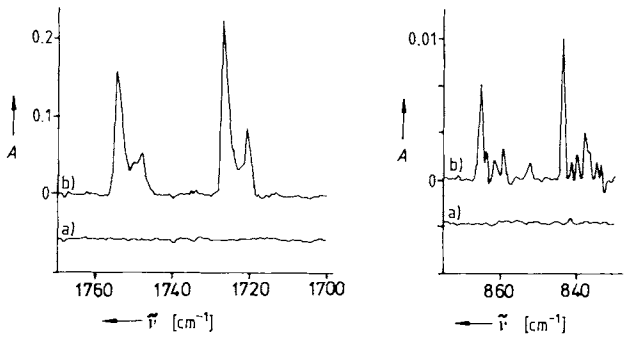

Fig. 1. Sections of the IR spectra of PN + $^{16}O_2/^{18}O_2$ (1:1) in an Ar matrix; a) before and b) after the photolysis (310 nm, 20 min). A = absorption.

Table 1. Measured and calculated frequencies of the PN and NO vibrations of PNO as wave numbers $\tilde{\nu}$ [cm^{-1}].

	$\tilde{\nu}$(PN) measured	$\tilde{\nu}$(NO) measured	$\tilde{\nu}$(PN) [12] calculated [11]	$\tilde{\nu}$(NO) calculated [11]
PN^{16}O	865.2	1754.7	865.2	1754.7
PN^{18}O	843.5	1727.2	842.5	1727.1

bands can only be assigned to a molecule P≡N$^{\oplus}$–O$^{\ominus}$ (Table 1). The force constants determined by these calculations are consistent with expectation (Scheme 1).

	P≡N$^{\oplus}$–O$^{\ominus}$		P≡N	N≡N$^{\oplus}$–O$^{\ominus}$		N≡N
f(XY)	7.95	11.5	9.9[11]	17.7	11.4[13]	22.4[11]
f(XY/YZ)	0.8			1.2		

Scheme 1. Stretching force constants f(X/Y) and interaction force constants f(XY/YZ) [mdyn Å^{-1}].

In connection with these experimental investigations we have carried out ab initio SCF calculations for some molecules XYZ (X,Y = P,N; Z = O,S).[14] Here also, the isomer PNO proved to be more stable than NPO (ΔE = 28 kJ mol^{-1}). The same trend is observed for the isomeric pair PNS/NPS. The most important results of these calculations are collected in Table 2. In addition, CI calculations by the CPF method using extended basis sets were carried out for the molecules PNO and NPO.[15] Once again PNO proved to be more stable than NPO (ΔE = 22 kJ mol^{-1}). Thus, all the quantum chemical calculations confirm the experimental result: in its highest oxidation state P avoids twofold coordination. The calculated structural data (bond lengths, charge and SEN,[16] Table 2) confirm the data obtained from force constants: in PNO the PN bond is weaker than in PN;[18] the NO bond is comparable to that in N_2O.

Summarizing, it can be said that the structure of PNO contradicts "chemical intuition," according to which the most electropositive atom should assume the central position in a triatomic molecule (e.g. O=N–F, N≡S–F),[19] since the molecule acquires an additional ionic stabilization in this way (cf. the charges q obtained from the population analysis in Table 2 for PNO and NPO).

Comprehensive quantum chemical calculations, on the other hand, are consistent with the experimental findings.[20] Apparently the absence of a possibility for ionic stabilization in PNO is overcompensated by other effects, e.g. the formation of an NO bond which is stronger than the PO bond in NPO.[21]

Received: September 24, 1987 [Z 2440 IE]
German version: *Angew. Chem. 100* (1988) 418

CAS Registry numbers:
^{18}O, 14797-71-8; Ar, 7440-37-1; P≡N$^{\oplus}$–O$^{\ominus}$, 113110-84-2.

[1] The oxygen atoms were generated in a microwave discharge: H. Schnöckel, *Angew. Chem. 90* (1978) 638; *Angew. Chem. Int. Ed. Engl. 17* (1978) 616.
[2] H. Schnöckel, *Z. Anorg. Allg. Chem. 460* (1980) 37.
[3] R. Ahlrichs, C. Ehrhardt, M. Lakenbrink, S. Schunck, *H. Schnöckel, J. Am. Chem. Soc. 108* (1986) 3596; the oxygen atoms were generated by photolysis of O_3.
[4] H. Germa, J. Navech, *Phosphorus Sulfur 26* (1986) 327; E. Nieke, W. Flick, *Angew. Chem. 86* (1974) 128; *Angew. Chem. Int. Ed. Engl. 13* (1974) 134; T. A. Van der Knaap, F. Bickelhaupt, *Phosphorus Sulfur 18* (1983) 47; E. Niecke, R. Rüger, M. Lysek, W. W. Schöller, *ibid. 18* (1983) 35; R. Appel, J. Peters, A. Westerhaus, *Angew. Chem. 94* (1982) 76; *Angew. Chem. Int. Ed. Engl. 21* (1982) 80; R. Appel, E. Gaitzsch, F. Knoch, *ibid. 97* (1985) 574 and *24* (1985) 589.
[5] R. M. Atkins, P. L. Timms, *Spectrochim. Acta Part A 33* (1977) 853; *Inorg. Nucl. Chem. Lett. 14* (1978) 113.
[6] This formulation is the same as the usual description for $NO_2^{\oplus}$ (N≡N$^{\oplus}$–O$^{\ominus}$) and was therefore chosen. The results described in this communication, however, show that the true bonding relationships are not reproduced with this formula or with the formula $^{\ominus}$P=N$^{\oplus}$=O.
[7] An isotopomeric mixture of O_3, formed from a 1:1 mixture of $^{16}O_2$ and $^{18}O_2$ in a high-frequency discharge, was used. For the photolysis of O_3 the mixture was irradiated with a high pressure Hg lamp for 20 min using a 310 nm filter (interfering thermal radiation was excluded by means of an H_2O filter).
[8] The spectra were recorded with an FT-IR spectrometer (Bruker IFS 113v).
[9] The frequency quoted in brackets refers to the isotopomer with ^{18}O.
[10] In the PN molecule $\tilde{\nu}_e$ = 1337 cm^{-1}. As model calculations show, in NPO the frequency should be shifted up to maximally 1500 cm^{-1} by coupling with the PO vibration.
[11] H. J. Becher: *Fortschr. Chem. Forsch. 10* (1968) 155. The constants of the diatomic molecules PN and NO were taken as basic for the anharmonicity correction: K. P. Huber, G. Herzberg: *Molecular Spectra and Molecular Structure. Vol. IV*, Van Nostrand Reinhold, New York 1979.

Table 2. Results of ab initio SCF calculations [a] and population analysis [6].

Molecule XYZ [c]	d(XY) [pm]	d(YZ) [pm]	E [a.u.]	SEN(XY)	SEN(YZ)	q(X)	q(Y)	q(Z)
PNO	149.16	116.71	−469.942633	2.31	1.69	−0.06	0.46	−0.40
NPO	146.14	144.76	−469.932036	2.43	1.61	−0.63	1.30	−0.67
PNS	148.44	158.86	−792.594898	2.41	1.44	0.17	0.00	−0.17
NPS	146.13	189.15	−792.567277	2.48	1.53	−0.58	0.98	−0.40
NNO				2.50	1.55	−0.26	0.74	−0.48 [d]
PN				2.86		0.30	−0.30	[e]
NN				2.94 [b, f]				

[a] [14]; the following basis sets were used: P(11,7,1) [6,4,1], η(d) = 0.4; N(9,5) [5,3,1], η(d) = 0.8; O(9,5,1) [5,3,1], η(d) = 1.0. [b] [16] [c] The sequence in which the elements are described reflects the structure of the molecules. [d] [17]. [e] Calculated energy −395.121777 a.u.; d(PN) (calc.) = 146.2 pm; d(PN) (exp.) = 149 pm. [f] d(NN) = 109 pm.

[12] The calculated isotopic shift for the PN vibration is about 4% greater than the measured shift. We attribute this to an interaction between the fundamental of the stretching vibration and the overtone of the unobserved deformation vibration (Fermi resonance). Since the deformation vibration should absorb at 450 cm^{-1}, on the basis of a comparison of the corresponding frequencies of COS, CO_2 and N_2O (cf. [21]), an interaction of its overtone with the PN stretching vibration is conceivable. Such an effect is frequently observed (see, e.g., Refs. [2, 21]). For the PN vibration this would lead to an experimentally determined isotopic shift smaller than the calculated one. This is observed.

[13] H. Siebert: *Anwendungen der Schwingungsspektroskopie in der Anorganischen Chemie*, Springer, Berlin 1966; E. B. Wilson, J. C. Decius, P. C. Cross: *Molecular Vibrations*, McGraw-Hill, New York 1955.

[14] The "Karlsruhe version" of the Columbus program systems was used: R. Ahlrichs, H. J. Böhm, C. Ehrhardt, P. Scharf, H. Schiffer, H. Lischka, M. Schindler, *J. Comput. Chem. 6* (1985) 200.

[15] R. Ahlrichs, P. Scharf, C. Ehrhardt, *J. Chem. Phys. 82* (1985) 890; with a larger basis set [P(11,7,2,1) [6,4,2,1], N, O (9,5,2,1) [5,3,2,1] and η(d,d,f) 0.7, 0.23, 0.5 (P); 1.78, 0.49, 1.085 (N); 2.47, 0.68, 1.5 (O)] the results listed in Table 3 were obtained. From these results the following frequencies were calculated for the XY and YZ vibrations: NPO 1604/1150 cm^{-1}; PNO 1922/945 cm^{-1}. The frequencies ca. 10% higher than the experimental values are consistent with expectation. They likewise confirm the greater stability of the isomer PNO.

Table 3. Results of CI calculations for NPO and PNO.

XYZ	d(XY) [pm]	d(YZ) [pm]	E(CPF) [a.u.]	f(XY) [mdyn Å^{-1}]	f(YZ) [mdyn Å^{-1}]	f(XY/YZ) [mdyn Å^{-1}]
NPO	149.8	147.3	−470.565219	12.1	11.1	0.2
PNO	152.3	119.4	−470.573433	10.4	13.7	1.2

[16] Here, the electronic structure is elucidated by a population analysis on the basis of occupation numbers: SEN (shared electron number) and charge on the relevant atom (q). For further detailed literature see, e.g., ref. [3]; for an introduction to this problem see R. Ahlrichs, C. Ehrhardt, *Chem. Unserer Zeit 19* (1985) 12. The SEN is regarded as a reliable measure of the strength of a covalent bond. To demonstrate this some typical values are: strong σ-bonds (CC, CH) 1.4; double bonds (CC) 2.2; triple bonds (CC, NN) ca. 3; lower SEN values are found for polar (NaF 0.3) and weak bonds (F_2 0.6).

[17] The experimentally determined structure is based on the calculations for N_2O: d(NN) = 112.6, d(NO) = 118.6 pm: A. E. Douglas, C. K. Moller, *J. Chem. Phys. 22* (1954) 275.

[18] a) The energy calculated for PN at the SCF level is −395.121777 a.u.; d(PN)(calc.) = 146.2, d(PN)(exp.) = 149 pm; b) the following PN distances are obtained for NPF_2 and $NPCl_2$ at the SCF level (singlet state, C_{2v} symmetry): in NPF_2 146.2, in $NPCl_2$ 147.6 pm: H. Plitt, S. Schunk, H. Schnöckel, unpublished.

[19] See, e.g., R. Ahlrichs, R. Becherer, M. Binnewies, H. Borrmann, M. Lakenbrink, S. Schunck, H. Schnöckel, *J. Am. Chem. Soc. 108* (1986) 7905.

[20] On critical assessment of the methods of calculation available today, calculations which afforded comparable energies for PNO and NPO would also support our experimental findings.

[21] Similar unusual bonding situations are present in SNO, which could be prepared in an Ar matrix. M. Hawkins, A. J. Downs, *J. Phys. Chem. 88* (1984) 3042.

Evidence for a Folded Conformation of Methotrexate in Solution

By *Peter Faupel* and *Volker Buss**

Methotrexate (MTX) is a powerful antimetabolite: by complexing with dihydrofolate reductase (DHFR), it inhibits the reduction of dihydrofolate to tetrahydrofolate, an essential step in the biosynthesis of nucleotide bases. While the binding of this widely used chemotherapeutic agent to DHFR of *E. coli* has been investigated in detail using high resolution X-ray data,[1] the crystal structure of MTX itself was determined only recently:[2] the molecule is twisted through an angle of almost 90° at the CH_2 group between the rings.

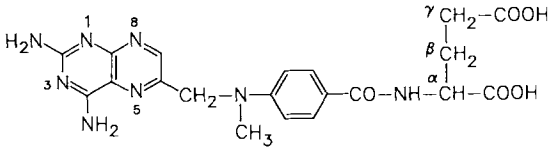

MTX

The question as to what the conformation in solution might be has not yet been settled. We now present evidence, from low-temperature UV and CD spectroscopic studies in nonpolar solvents, to show that under these conditions the molecule adopts a folded conformation stabilized by intramolecular hydrogen-bonding.

The UV-spectrum of MTX in THF/CH_2Cl_2 (10:1) exhibits a pronounced temperature-dependence (Fig. 1, left): on cooling to −130°C, the main absorption band at 290 nm is red-shifted by about 13 nm while the bands at 265 and 380 nm disappear, making place for two new bands at 253 and 350 nm, respectively. These changes strikingly resemble the spectral changes observed for MTX in aqueous medium with decreasing pH-values, the low-temperature spectrum in THF/CH_2Cl_2 corresponding to the acidic form in water (Fig. 1, right).[3] There are several isosbestic points in the spectra, and we note a distinct hypochromic effect in going from −40 to −60°C.

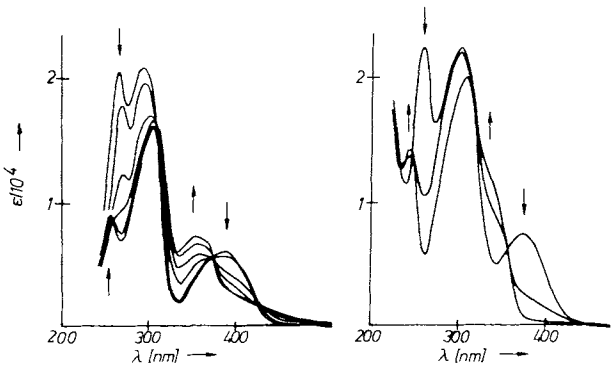

Fig. 1. Left: Temperature dependence of UV-spectra of MTX in THF/CH_2Cl_2 (10:1), $c = 7.7 \times 10^{-5}$ mol L^{-1}. Curves shown correspond to measurements at +10, −40, −60, −80, −110, and −130°C, respectively. Arrows indicate spectral changes with decreasing temperature; they are at 254, 265, 350, and 383 nm. Right: pH-dependence of UV-spectrum of MTX in water. Curves shown correspond to pH-values of, respectively, 1 and 5.6 ($c = 8.0 \times 10^{-5}$ mol L^{-1}) and > 10 ($c = 5.0 \times 10^{-5}$ mol L^{-1}). Arrows indicate spectral changes with increasing acidity; they are at 244, 259, 335, and 373 nm.

The CD-spectra obtained under identical conditions reflect the spectral changes observed in the UV (Fig. 2, left). At room temperature, there are three broad unstructured bands of low intensities at 260, 290, and 350 nm. The low-temperature spectra show three intense bands developing, with alternating signs and maxima at 280, 307, and 345 nm.

Within the limits set by the solubility of MTX and experimental accuracy, these spectra are independent of concentration (Fig. 2, right). This suggests that the CD absorptions are not caused by intermolecular interactions such as dimerization or stacking processes, but result from a pre-

[*] Prof. Dr. V. Buss, Dipl.-Chem. P. Faupel
Fachgebiet Theoretische Chemie der Universität
Lotharplatz 1, D-4100 Duisburg (FRG)

ferred molecular conformation evolving at low temperature.

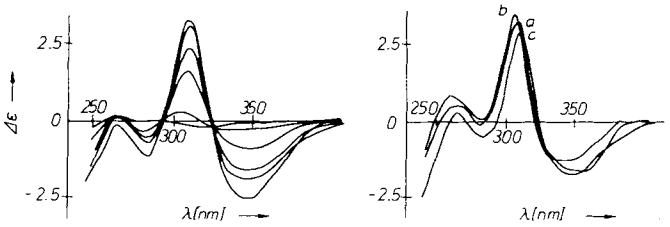

Fig. 2. CD-spectra of MTX in THF/CH_2Cl_2 (10:1), corrected for volume contraction. Left: Temperature dependence. Curves shown correspond to measurements at +10, −40, −60, −80, −100, and −115°C, $c = 8.0 \times 10^{-5}$ mol L^{-1}. Right: Concentration dependence; $c = 10 \times 10^{-5}$ (a), 8×10^{-5} (b), and 4.5×10^{-5} mol/L (c), $T = -120$°C.

Both the UV and CD data can be interpreted by assuming a folded MTX conformation characterized by close contact of the pteridine and benzene chromophores (Fig. 3). Evidence for electronic interaction between these two groups has led to the proposal of a similarly folded conformation of folic acid in water at high dilution.[4]

The folded MTX conformation is held together by a hydrogen-bond most probably involving the γ-carboxyl group of the glutamic acid and N1 of the pteridine moiety. Protonation of this site has been suggested[5] to account for the observed spectral shifts of 2,4-diaminopteridine in acid medium. In agreement with these observations, we calculate[6] for the protonated form a 30-nm blue-shift of the 380-nm absorption and a 20-nm red-shift of the 265-nm band. This latter band presumably appears in the low-temperature spectra as a shoulder of the strong 300-nm absorption, which is essentially an excitation of the *p*-aminobenzoic acid chromophore. Also, according to STO-3G calculations[7] N1 is favored relative to the other ring nitrogens with respect to protonation, though steric constraints could easily overcome any differences in basicity.

In addition to any chirality originating from non-planar conformations, MTX has a constitutional source of chirality in the asymmetric α-carbon atom of the glutamic acid moiety which obviously can differentiate between otherwise enantiomeric conformations. The reason why the absolute conformation depicted in Figure 3 should be preferred over the (distinguishable) inverted form is easily seen: with the hydrogen atom of the asymmetric center pointing towards the observer, the α-carboxyl group points down towards the C2-amino group, in perfect orientation to make a second hydrogen bond.

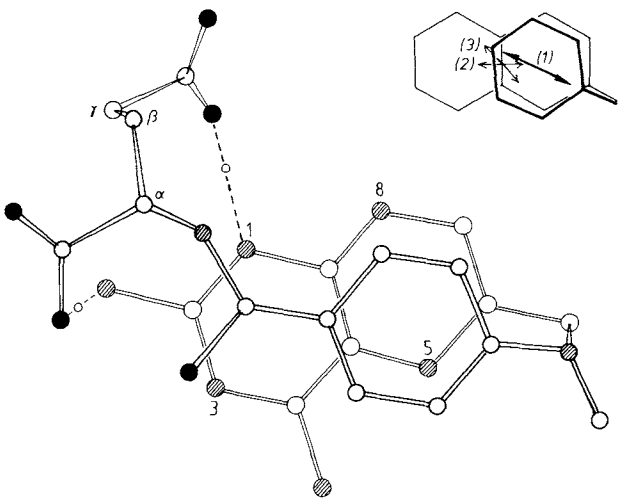

Fig. 3. Proposed structure of folded MTX conformation in solution. Open circles represent carbon atoms, hatched circles nitrogen atoms and black circles oxygen atoms. Small figure, top right: transition moments of the two chromophoric systems as obtained from CNDO/S calculations.

The signs of the three prominent CD bands can be rationalized on the basis of the proposed structure (Fig. 3, top right). According to our calculations, the direction of the 300-nm band transition moment (1) lies inside the acute angle formed by the transitions at 330 nm (2) and 280 nm (3). This results in positive rotational strengths for both the lower and higher energy absorptions from the interaction with the 300-nm band, while for the latter, negative rotational strengths are to be expected, in agreement with the experimental CD spectrum.—Quantitative calculations are in progress to test the viability of the proposed structure.

Received: October 14, 1987 [Z 2477 IE]
German version: *Angew. Chem. 100* (1988) 422

[1] J. T. Bolin, D. J. Filman, D. A. Matthews, R. C. Hamlin, J. Kraut, *J. Biol. Chem. 257* (1982) 13650.
[2] T. W. Hambley, H.-K. Chan, I. Gonda, *J. Am. Chem. Soc. 108* (1986) 2103; P. A. Sutton, V. Cody, G. D. Smith, *ibid. 108* (1986) 4155.
[3] The pH-dependence of the UV-spectra of MTX as well as of folic acid have been documented before: M. Poe, *J. Biol. Chem. 248* (1973) 7025; however, only the former shows the peculiar changes at low temperature in the UV.
[4] C. Thiery, *Eur. J. Biochem. 37* (1973) 100.
[5] G. Konrad, W. Pfleiderer, *Chem. Ber. 103* (1970) 722.
[6] Reported values are based on CNDO/S calculations employing standard parameters. Also, the transition moments in Fig. 3 are taken from these calculations.
[7] J. E. Gready, *J. Comput. Chem. 6* (1985) 377.

Preparation of 2,3,4-Tris(η^5-cyclopentadienyl)-1,5-diphenyl-1-phospha-2,3,4-tricobaltapentaborane(5); Phenyl Group Migration from Phosphorus to Boron**

By *Jiang Feilong, Thomas P. Fehlner,** and *Arnold L. Rheingold**

Only a few metal-rich metallaboranes (M/B > 1, direct metal boron interactions) are known[1]. We have shown that the reaction of [CpCoLL'] with $BH_3 \cdot THF$ is a source of metal-rich cobaltaboranes[2]. For low $BH_3 \cdot THF$/[CpCoLL'] ratios and $L = L' = PPh_3$, PPh_x (x = 1,2) fragments are incorporated into the clusters[3]. We have now demonstrated that C_6H_6 is a product of the preparative reaction and is formed, presumably, by the reaction of phenyl groups with hydrides[4, 5]. Here we report the formation of a metal-rich phosphacobaltaborane **1** which contains a BPh fragment in which the phenyl group on boron is also derived from the PPh_3 ligand of $[CpCo(PPh_3)_2]$. Hence, in addition to being eliminated as C_6H_6, the Ph group on PPh_3 can migrate from phosphorus to boron[6]. This behavior constitutes another manifesta-

[*] Prof. T. P. Fehlner, J. Feilong
Department of Chemistry, University of Notre Dame
Notre Dame, IN 46556 (USA)
Dr. A. L. Rheingold
Department of Chemistry, University of Delaware
Newark, DE 19716 (USA)
[**] This work was supported by the National Science Foundation under Grant CHE 8498251 and the Petroleum Research Fund, administered by the American Chemical Society.

tion of the "metallic" character of boron when found in a cluster environment.[7]

$[Cp_3CoPBPh_3]\cdot 0.5\,C_6H_6$ **1**

The new compound **1** was characterized by an X-ray structure analysis (Fig. 1)[8]. The structure exhibits a metal-

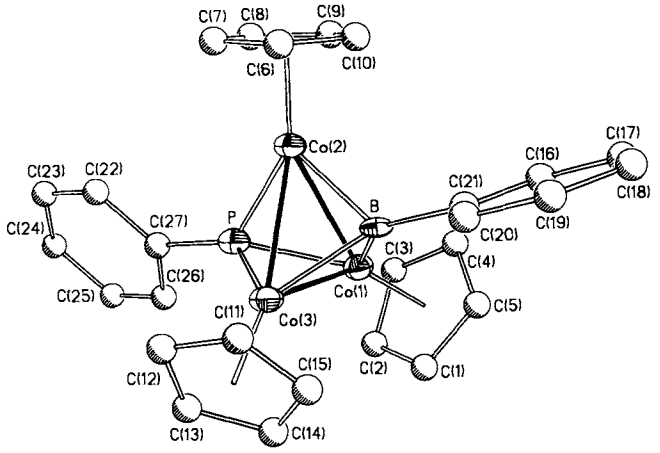

Fig. 1. The molecular structure of **1**. The solvent molecule and hydrogen atoms have been omitted for clarity. Important bond distances [Å] and angles [0]: Co(1)-Co(2) 2.553(1), Co(1)-Co(3) 2.473(2), Co(2)-Co(3) 2.561(1), P-Co(1) 2.089(8), P-Co(2) 2.082(2), P-Co(3) 2.100(2), B-Co(1) 2.065(8), B-Co(2) 2.018(8), B-Co(3) 2.031(9); Co(1)-Co(2)-Co(3) 57.81(7), Co(2)-Co(3)-Co(1) 60.87(7), Co(3)-Co(1)-Co(2) 61.21(8).

metal bonded, equilateral triangular array of Co atoms each bound to a η^5-C_5H_5 ligand and capped on one side by a μ_3-PPh fragment and on the other by a μ_3-BPh fragment. The metal-metal and metal-main group element distances lie within the ranges typical for clusters. However, note that the average CoB distance is only 0.05 Å shorter than the average CoP distance despite the fact that the difference in covalent radii is 0.24 Å. The three Co atoms, the P atom and the B atom of **1** form a trigonal bipyramidal cluster core which is isoelectronic with the cluster found in **2**[9], analogous to the cluster in **3**[10] and isolobal with the *closo* carbaborane **4**[11]. Comparison of the cobalt com-

$[Cp_3Co_3C_2R_2]$ **2** $[Cp_3Rh_3C_2R_2]$ **3** $C_2B_3H_5$ **4**

pounds **1** and **2** reveals a dependence of the structural parameters on the main group element. The average Co-Co distance in **1** is 0.15 Å longer than that in **2** and the difference in the average Co-B distance in **1** and the Co-C distance in **2** is larger than expected (0.13 Å). Thus, even though identical in terms of electron counting rules[12], these structural differences suggest significant differences in the bonding, perhaps associated with the fact that **1** has a polar character relative to **2** (i.e. BR, CR, and PR function as 2-, 3-, and 4-electron donors, respectively, in the cluster).

The NMR spectra of **1** in solution are consistent with the solid state structure[13]. Although main group elements capping transition metal triangles are very well known in general, there are only two well characterized examples involving boron without B-H-M bridge interactions[14]. Of particular note is the downfield chemical shift of the μ_3-boron atom in the ^{11}B-NMR spectrum. Extreme downfield shifts appear to be characteristic of BR fragments directly bound (no B-H-M bridges) to three or more transition metals.

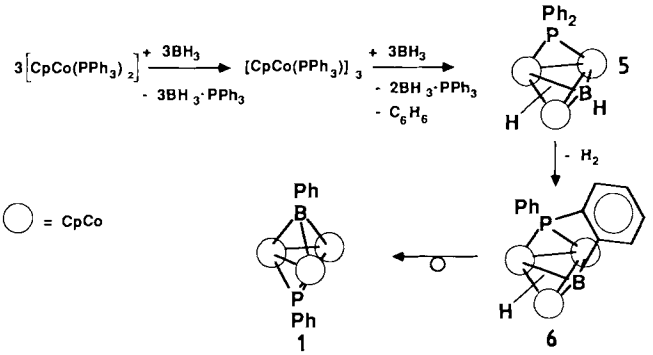

Based on literature precedents, a reasonable mechanism for the production of **1** can be postulated. The trimerization of $[CpCo(CO)_2]$ is known[15]; in our system, $[CpCo(PPh_3))]_3$ is a likely intermediate in the formation of trinuclear clusters. Loss of PPh_3 (as $BH_3\cdot PPh_3$) and C_6H_6 from the Co_3 species and boronation lead to the critical intermediate **5**[16], which eliminates H_2 and yields a dehydrobenzene intermediate **6**[17] by orthocycloboronation. **6** affords directly the observed product. Orthocycloboronation is well documented[18]. But this is the first example of the complete transfer of a phenyl substituent from phosphorus to boron. We have no evidence for this mechanism but it serves to show that a chemically reasonable route to the unusual and unexpected product **1** exists.

Experimental Procedure

A solution of 2.8 mmol of $[CpCo(PPh_3)_2]$ in 20mL of toluene was treated with 5.5 mL (5.5 mmol) of 1 M BH_3·THF at −78°C. After warming to 25°C, the mixture was stirred for 24 h. According to the ^{11}B-NMR spectrum the major boron-containing product (besides $BH_3\cdot PPh_3$) is **1**. After concentration of the solution and partial precipitation of $BH_3\cdot PPh_3$, chromatography on silica gel (hexane/toluene) yielded a dark brown band ($R_f = 0.3$, hexane/toluene 1:1) which produced brown crystals in 7% yield (based on cobalt). The compound decomposes slowly in solution but is reasonably stable in the solid state. Mass spectrum: M^+ 568 (parent ion envelope for $C_{27}H_{25}BPCo_3$), *m/z* 567:568:569:570 = 0.15:0.63:0.19:0.03(obsd); 0.147: 0.639: 0.187: 0.027(calcd).

Received: September 25, 1987 [Z 2445 IE]
German version: *Angew. Chem. 100* (1988) 400

CAS Registry numbers:
1, 112897-50-4; **1**·0.5 C_6H_6, 112897-51-5; $[CpCo(PPh_3)_2]$, 32993-07-0.

[1] N. N. Greenwood, *Chem. Soc. Rev. 13* (1984) 353; R. N. Grimes, *Acc. Chem. Res. 16* (1983) 22; J. D. Kennedy, *Prog. Inorg. Chem. 32* (1984) 519; *34* (1986) 211; C. E. Housecroft, T. P. Fehlner, *Adv. Organomet. Chem. 21* (1982); C. E. Housecroft, *Polyhedron 6* (1987) 1935.

[2] J. Feilong, T. P. Fehlner, A. L. Rheingold, *J. Am. Chem. Soc. 109* (1987) 1860.

[3] J. Feilong, T. P. Fehlner, A. L. Rheingold, *J. Chem. Soc. Chem. Commun. 1987*, 1395.

[4] Demonstrated by infrared and ^{1}H-NMR spectroscopic examination of the less volatile fraction of the reaction mixture.

[5] The elimination of phenyl groups as benzene is well documented in the reactions of substituted transition metal clusters; cf. R. D. Adams, I. T. Horvath, *Prog. Inorg. Chem. 33* (1985) 127.

[6] This transfer can be either intra- or intermolecular, although the former appears more likely.

[7] R. D. Barreto, T. P. Fehlner, L.-Y. Hsu, D.-Y. Jan, S. G. Shore, *Inorg. Chem. 25* (1986) 3572.

[8] Crystallographic data for $C_{27}H_{25}BCo_3P\cdot 0.5\,C_6H_6$ (**1**) (293 K): $a = 11.166$ (3) Å, $b = 13.807(4)$ Å, $c = 17.435(7)$ Å, $\beta = 101.69(3)^0$, $V = 2632.4(16)$ Å^3, $Z = 4$, space group $P2_1/n$, $\rho_{(calcd)} = 1.433$ g cm^{-3}. Of 3420 reflections col-

lected ($4° \le 2\theta \le 44°$; limited by weak diffraction), 3138 were unique, and 2238 were observed ($F_0 = 4\sigma(F_0)$). For each molecule of **1**, the lattice contains a half-molecule of benzene. $R(F) = 0.0539$, $R(wf) = 0.0652$ for 292 variables. Further details of the crystal structure determination are obtainable from the director of the Cambridge Crystallographic Data Centre, Lensfield Road, Cambridge CB2 1EW (UK), on quoting the names of the authors and the journal citation.

[9] J. R. Fritch, K. P. C. Vollhardt, M. R. Thompson, V. W. Day, *J. Am. Chem. Soc. 101* (1979) 2768; H. Yamazaki, Y. Wakatsuki, K. Aoki, *Chem. Lett. 1979*, 1041; R. B. A. Pardy, G. W. Smith, M. E. Vickers, *J. Organomet. Chem. 252* (1983) 341.

[10] A. D. Clauss, J. R. Shapley, C. N. Wilker, R. Hoffmann, *Organometallics 3* (1984) 619. A. Vazquez deMiguel, K. Isobe, P. M. Bailey, N. J. Meanwell, P. M. Maitlis, *ibid. 1* (1982) 1604.

[11] I. Shapiro, C. E. Good, R. E. Williams, *J. Am. Chem. Soc. 84* (1962) 3837.

[12] K. Wade, *Adv. Inorg. Chem. Radiochem. 18* (1976) 1; D. M. P. Mingos, *Acc. Chem. Res. 17* (1984) 311.

[13] NMR: ^{11}B (toluene, 25°C): $\delta = 143.7$ (s, $b_{1/2}$ 360 Hz); ^1H (C_6D_6, 25°C): $\delta = 8.6$–7.3 (m, Ph), 4.45 (s, Cp); ^{31}P (C_6D_6, 25°C): $\delta = 122.5$ (s).

[14] J. R. Pipal, R. N. Grimes, *Inorg. Chem. 16* (1977) 3255; S. G. Shore, D.-Y. Jan, L.-Y. Hsu, H.-L. Hsu, *J. Am. Chem. Soc. 105* (1983) 5923.

[15] K. P. C. Vollhardt, J. E. Bercaw, R. G. Bergman, *J. Organomet. Chem. 97* (1975) 283.

[16] Analogous to $[(\mu\text{-H})Fe_3(CO)_9(\mu\text{-CO})HBH]$: J. C. Vites, C. E. Housecroft, G. B. Jacobsen, T. P. Fehlner, *Organometallics 3* (1984) 3.

[17] Dehydrobenzene ligands derived from phenyl groups of PPh_3 are known. C. W. Bradford, R. S. Nyholm, G. J. Gainsford, J. M. Guss, P. R. Ireland, R. Mason, *J. Chem. Soc. Chem. Commun. 1972*, 87. G. J. Gainsford, J. M. Guss, P. R. Ireland, R. Mason, C. W. Bradford, R. S. Nyholm, *J. Organometal. Chem. 40* (1972) C70.

[18] The work of *Greenwood* et al. provides several examples of the orthocycloboronation in "boron rich" metallaboranes. See for example: J. Bould, J. E. Cook, N. N. Greenwood, J. D. Kennedy, W. S. McDonald, *J. Chem. Soc. Chem. Commun. 1983*, 949.

Reduction with Yeast Cells, the Key Step of an Efficient Synthesis of (3*S*, 4*S*)-4-Amino-3-hydroxypentanoic Acids**

By *Peter Raddatz, Hans-Eckart Radunz,* Günter Schneider,* and *Harry Schwartz**

Pepstatin,[1] a pentapeptide first isolated by *H. Umezawa,* contains the unusual γ-amino acid statine ((3*S*, 4*S*)-4-amino-3-hydroxy-6-methylheptanoic acid). Statine and its analogues are central building blocks for many highly active, specific aspartyl protease inhibitors, including even renin inhibitors,[2] which are of interest as hypotensive drugs. Kinetic studies have shown that the hydroxy group in statines must be *S*-configurated, but the carbon chain at C-4 can be chemically modified.[3]

The current importance of such drugs warranted the search for a synthetic strategy enabling a flexible, diastereoselective synthesis of statine from readily accessible starting materials. At best, the methods of synthesis published so far[4] only partly fulfill these requirements, if at all.

In principle, in the case of the statine synthesis presented here any α-amino acid can be used as starting compound. This is allowed to react with a malonic acid building block, and the resulting γ-amino-β-ketoester can be diastereoselectively reduced to the β-hydroxy derivative with certain yeasts. The strategy will be described here for the synthesis of (3*S*, 4*S*)-*N*-Boc-4-amino-3-hydroxy-5-cyclohexylpentanoic acid methyl ester **5** (Scheme 1).

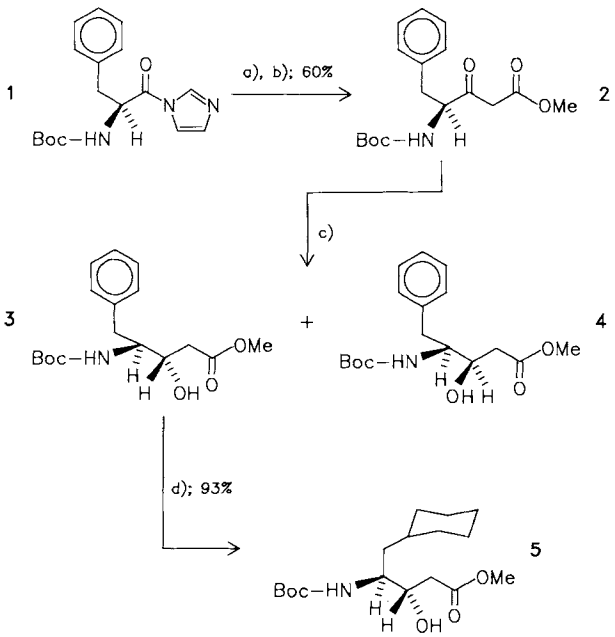

Scheme 1. Synthesis of **5**. a) $HO_2C-CH_2-CO_2Me$, *i*PrMgBr; b) 15% HCl; c) reduction with yeast; d) Rh/Al_2O_3. Boc = *tert*-butoxycarbonyl. For physical and spectroscopic data of **2**–**5** see Table 1.

The crucial step is the stereoselective reduction of **2**, which is formed from *N*-Boc-L-phenylalanine-imidazolide **1** and the magnesium enolate of the malonic acid monomethyl ester,[4b] to the alcohol **3** with *S* configuration at C-3. The catalytic hydrogenation of **2** with Raney nickel affords a 1:1 mixture of the diastereomeric alcohols **3** and **4**. Neither of the diastereomers is preferentially formed, even with complex, sterically bulky hydrides. In order to alter the conditions in favor of one of the diastereomers, reduction of the β-ketoester with bakers' yeast was attempted.[5] The attempts with commercially available yeast (*Saccharomyces cerevisiae*) merely resulted in incomplete reaction (30–50%), but nevertheless the desired 3*S*, 4*S*-diastereomer **3** was formed (*de* = 60%).

Table 1. Selected physical and spectroscopic data of the compounds **2**–**5** [a]. $[\alpha]_D^{20}$ values with $c = 0.68$ to 1.26 g/100 mL methanol. 500-MHz ^1H-NMR spectra ([D$_6$]DMSO, coupling constants *J* in Hz).

2: m.p. 91°C (petroleum ether/methyl *tert*-butyl ether): $[\alpha]_D^{20} = -64.8°$; ^1H-NMR: $\delta = 1.35$ (s, 9 H; $C(CH_3)_3$), 2.73 (dd, $J = 10.2$, 14, 1 H; CH_2Ph), 3.06 (dd, $J = 4.6$, 14, 1 H; CH_2Ph), 3.26 (br. s, 2 H; CH_2CO), 3.65 (s, 3 H; OCH_3), 4.25 (m, 1 H; CHN), 6.85 (br. m, 1 H, NH), 7.25 (m, 5 H; C_6H_5)

3: m.p. 99°C (diisopropyl ether); $[\alpha]_D^{20} = -35.4°$; ^1H-NMR: $\delta = 1.32$ (s, 9 H; $C(CH_3)_3$), 2.30 (dd, $J = 9.2$, 15, 1 H; CH_2CO), 2.5 (dd, $J = 4$, 15, 1 H; CH_2CO), 2.60 (dd, $J = 9.5$, 13, 1 H; CH_2Ph), 2.84 (dd, $J = 5.3$, 13, 1 H; CH_2Ph), 3.55 (s, 3 H; OCH_3), 3.68 (m, 1 H; CHN), 3.9 (m, 1 H; C*H*OH), 4.9 (br. d, $J = 7$, 1 H; OH), 6.48 (br. d, $J = 7.5$, 1 H; NH), 7.23 (m, 5 H; C_6H_5)

4: m.p. 139°C (methyl *tert*-butyl ether); $[\alpha]_D^{20} = -17.1°$; ^1H-NMR: $\delta = 1.25$ (s, 9 H; $C(CH_3)_3$), 2.30 (dd, $J = 9.3$, 15, 1 H; CH_2CO), 2.55 (m, 2 H; CH_2CO, CH_2Ph), 3.05 (dd, $J = 3.5$, 14, 1 H; CH_2Ph), 3.52 (m, 1 H; CHN), 3.6 (s, 3 H; OCH_3), 3.80 (m, 1 H; C*H*OH), 5.07 (br. d, $J = 7$, 1 H; OH), 6.61 (br. d, $J = 8$, 1 H; NH), 7.22 (m, 5 H; C_6H_5)

5: m.p. 69°C (petroleum ether); $[\alpha]_D^{20} = -36.5°$; ^1H-NMR: $\delta = 0.7$–1.3 (m, 8 H), 1.42 (s, 9 H; $C(CH_3)_3$), 1.5–1.85 (m, 5 H), 2.25 (dd, $J = 9.2$, 15, 1 H; CH_2CO), 2.45 (dd, $J = 4$, 15, 1 H; CH_2CO), 3.55 (m, 1 H; CHN), 3.60 (s, 3 H; OCH_3), 3.85 (m, 1 H; C*H*OH), 4.75 (br. d, $J = 7$, 1 H; OH), 6.25 (d, $J = 7.5$, 1 H; NH)

[a] All the compounds gave correct elemental analyses.

[*] Dr. H.-E. Radunz, Dr. P. Raddatz, G. Schneider
E. Merck
Leitung Pharmazeutische Chemie
Frankfurter Strasse 250, D-6100 Darmstadt (FRG)
Dr. H. Schwartz
E. Merck
Zentrale Forschung und Entwicklung Chemie
Frankfurter Strasse 250, D-6100 Darmstadt (FRG)

[**] We thank Dr. *M. Heinrich* for caryying out the fermentation and Herr *O. Kaser* for valuable assistance with the experiments.

Since baker's yeast behaves differently depending on its origin and strain we tried to improve the stereoselectivity by using pure cultures of selected yeast strains of the genera *Kloeckera*, *Hansenula*, *Candida*, and *Torulopsis*.[6] Only five of 74 yeast strains tested reduced the β-ketoester **2** completely. Four strains, including *Hansenula anomala*, formed the 3*S*, 4*S*-diastereomer **3** with *de* = 92%, whereas predominantly the 3*R*, 4*S*-diastereomer **4** was formed (90% *de*) by the yeast *Candida boidinii*. Further optimization attempts with resting cells of the yeast *Hansenula anomala* during fermentation of glucose revealed that reduction of the β-ketoester **2** proceeds almost quantitatively if the glucose concentration is 10%, the yeast concentration 1%, and the substrate concentration 0.1%; this holds true for sample volumes of 100 mL to 1000 L. Irrespective of whether intact cells, cells immobilized in polyacrylamide gel[7] or cell-free crude extracts of the strain *Hansenula anomala* were used, **2** was reduced almost completely (90–95% conversion) on a laboratory scale (100 mg to 1 g). The procedure optimized for small amounts was then extended to larger substrate amounts (50 g to 1000 g). On using 50 g of **2**, 96% was reduced after 48 hours' incubation; the ratio of the alcohols **3** and **4** was 23:1. After work-up and recrystallization from diisopropyl ether we obtained 35 g of **3** with 98% *de*. Subsequent recrystallization from cyclohexane increased the diastereomeric excess to >99%.

Experimental

For the production of cell masses, yeasts of the genus *Hansenula* were incubated under sterile conditions in 100-L fermenters with continuous aeration at 28 °C in a medium consisting of 2% glucose, 0.3% malt extract, 0.3% yeast extract and 0.5% peptone from casein. After reaching the stationary growth phase the cells were separated from the medium and washed with cold 0.9% NaCl solution. The reduction was carried out in a 100-L fermenter at 28 °C. 500 g of yeast (wet weight) was suspended in 50 L of a 10% glucose solution. After commencement of fermentation, a solution of 50 g of β-ketoester **2** in 500 mL of ethanol was added and the mixture incubated for 48 h with continuous stirring (200 rpm) and gentle aeration.

For the extraction, the yeast suspension was treated twice with dichloromethane (a total of 35 L) and stirred for one hour. The separated organic phase was filtered over diatomaceous earth and the filtrate dried over Na_2SO_4. After removal of solvent the residue was recrystallized from 500 mL of diisopropyl ether.

The enantiomeric purity was determined HPL chromatographically and NMR spectroscopically via the MTPA amides[8] of **3** (MTPA = α-methoxy-α-trifluoromethylphenylacetic acid) and gave >98% *ee*. Subsequent hydrogenation of the benzene ring of **3** with Rh on Al_2O_3 in methanol afforded **5** in 93% yield.[9]

Received: September 28, 1987 [Z 2447 IE]
German version: *Angew. Chem. 100* (1988) 414

[1] H. Umezawa, T. Aoyagi, H. Morishima, M. Matzusaki, H. Hamada, T. Takeuchi, *J. Antibiot. 23* (1970) 259.
[2] a) D. H. Rich, *J. Med. Chem. 28* (1985) 263; b) S. Thaisrivongs, D. T. Pats, W. M. Kati, S. R. Turner, L. M. Thomasco, *J. Med. Chem. 28* (1985) 1553; c) T. L. Blundell, B. L. Sibanda, A. Hemmings, S. F. Foundling, I. J. Tickle, L. H. Pearl, S. P. Wood, A. S. V. Burgen, G. C. K. Roberts, M. S. Tute (Eds.): *Molecular Graphics and Drug Design*, Elsevier, Amsterdam, New York 1986, p. 323.
[3] D. H. Rich, E. T. O. Sun, *J. Med. Chem. 23* (1980) 27.
[4] a) D. H. Rich, E. T. Sun, A. S. Boparai, *J. Org. Chem. 43* (1978) 3624; b) R. Steulmann, H. Klostermeyer, *Justus Liebigs Ann. Chem. 1975*, 2245; c) M. W. Holladay, F. G. Salituro, D. H. Rich, *J. Med. Chem. 30* (1987) 374; d) S. Danishefsky, S. Kobayashi, J. F. Kerwin, Jr., *J. Org. Chem. 47* (1982) 1981; e) P. W. K. Woo, *Tetrahedron Lett. 26* (1985) 2973; f) M. N. Dufour, P. Jouin, A. Pantaloui, B. Castro, *J. Chem. Soc. Perkin Trans. 1 1985*, 1985; g) H. Kogen, T. Nishi, *J. Chem. Soc. Chem. Comm. 1987*, 311.
[5] a) H.-U. Reissig, *Nachr. Chem. Tech. Lab. 34* (1986) 782; b) C. J. Sih, C.-S. Chen, *Angew. Chem. 96* (1984) 556; *Angew. Chem. Int. Ed. Engl. 23* (1984) 570; c) D. Seebach, M. A. Sutter, R. H. Weber, M. F. Züger, *Org. Synth. 63* (1985) 1; d) D. W. Brooks, M. Wilson, M. Webb, *J. Org. Chem. 52* (1987) 2244; e) D. W. Brooks, R. P. Kellog, C. S. Cooper, *ibid. 52* (1987) 192; f) M. Hirama, T. Nakamine, Sho Ito, *Tetrahedron Lett. 27* (1986) 5281; g) M. Soukup, B. Wipf, E. Hochuli, H. G. W. Leuenberger, *Helv. Chim. Acta 70* (1987) 232.
[6] a) Y. Takaishi, Y.-L. Yang, D. DiTullio, C. J. Sih, *Tetrahedron Lett. 23* (1982) 5489; b) R. N. Patel, C. T. Hou, A. I. Laskin, P. Derelanko, A. Felix, *Eur. J. Biochem. 101* (1979) 401; c) D. Buisson, R. Azerad, *Tetrahedron Lett. 27* (1986) 2631.
[7] I. Chibata, T. Tosa, T. Sato, *Appl. Microbiol. 27* (1974) 878.
[8] J. A. Dale, D. L. Dull, H. S. Mosher, *J. Org. Chem. 34* (1969) 2543.
[9] J. Boger, L. S. Payne, D. S. Perlow, N. S. Lohr, M. Poe, E. H. Blaine, E. H. Ulm, T. W. Schorn, B. I. LaMont, D. F. Veber, *J. Med. Chem. 28* (1985) 1779.

Formation of Dioxirane from Carbonyl Oxide**

By *Dieter Cremer,* Thomas Schmidt, Jürgen Gauss,* and *T. P. Radhakrishnan*

Dedicated to Professor Emanuel Vogel on the occasion of his 60th birthday

Dioxirane **1** is an effective oxygen carrier for regio- and stereoselective epoxidations.[1] Spectroscopic investigations have provided evidence that **1** can be formed by thermal or photochemical isomerization of carbonyl oxide **2**, e.g. in the ozonolysis[2, 3] or the oxidation of carbenes.[4] According to ab initio calculations, the activation energy for the isomerization in the gas phase is 22.8 kcal mol^{-1}.[5] The transition state **3** (Fig. 1) of this reaction resembles **2** more closely than it does **1**, as is clear from the calculated geometries, in particular the large distance between C and the terminal O atom in **3** (Fig. 1).

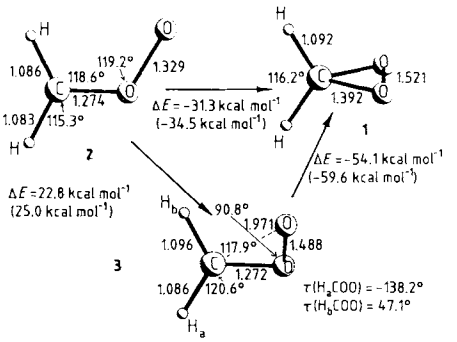

Fig. 1. Isomerization of carbonyl oxide **1** to dioxirane **2**. MP4(SDQ)/6-31G* energies and geometries for **1**, **2**, and **3**; distances in Å. The values in brackets are MP2/6-31G* results [5].

Further, the calculations show that the isomerization is not initiated by rotation about the CO bond but by pyramidalization at the central O atom. Negative charge is shifted from the C atom to the neighboring O atom, resulting in a weakening of the OO bonding due to enhanced charge repulsion (Fig. 1). The CO double-bond character, however, is essentially retained, since back-bonding between the orbital of a lone pair on the O atom and the depopulated 2pπ orbital on the C atom is possible (see **3a**).[6]

[*] Prof. Dr. D. Cremer, Dr. T. Schmidt, Dipl.-Chem. J. Gauss
Institut für Organische Chemie der Universität
Greinstrasse 4, D-5000 Köln 41 (FRG)
Dr. T. P. Radhakrishnan
Department of Chemistry, University of Texas
El Paso (USA)

[**] This work was supported by the Deutsche Forschungsgemeinschaft and the Fonds der Chemischen Industrie.

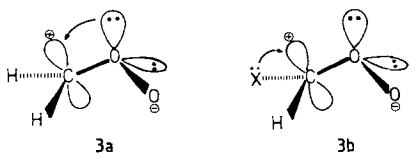

3a 3b

Accordingly, a substituent X with π-donor properties should stabilize the transition state (see **3b**), while π-acceptors should have a slight or noticeable destabilizing influence. These predictions are confirmed in the case of the monofluorocarbonyl oxides **4a** and **4b** (Fig. 2), whose isomerization to monofluorodioxirane **6** via **5a** and **5b** requires activation energies of 8 and 17 kcal mol^{-1}, respectively, according to ab initio calculations.[7] On the basis of these findings the formation of epoxides observed in the ozonolysis of fluoroalkenes[8] can be explained in terms of an enhanced formation of fluorodioxiranes, which epoxidize unchanged alkene.

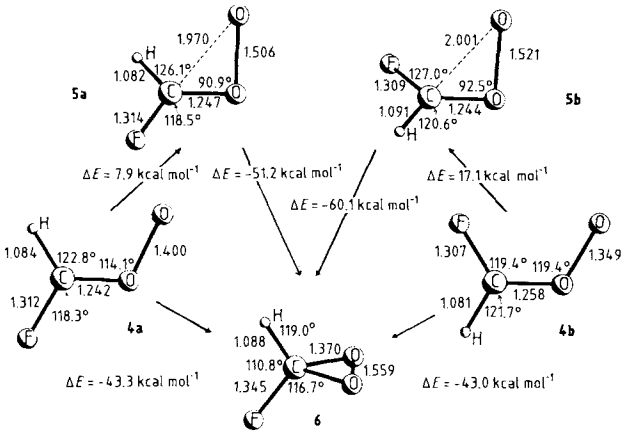

Fig. 2. Isomerization of monofluorocarbonyl oxide **4** to monofluorodioxirane **6**. MP2/6-31G* energies and geometries for **4**, **5**, and **6**; distances in Å. The dihedral angles τ(FCOO) and τ(HCOO) calculated for **5a** are −143.0 and 42.2°; for **5b** they are 53.6 and −137.3°, respectively.

Although **1** is 31.3 kcal mol^{-1} more stable than **2**, it cannot be detected under normal conditions.[2] Ring strain and the repulsion of lone pairs lead to a weak OO bond (R(OO) = 1.521 Å, Fig. 1), which is readily cleaved, either homolytically or, in the presence of Lewis acids, heterolytically.

The strain energy (SE) of **1** is estimated by ab initio calculations for the homodesmotic reaction (a) to be 24.7 kcal mol^{-1}.[9]

$$\mathbf{1} + H_2O_2 + 2CH_3OH \longrightarrow 2CH_3OOH + HOCH_2OH \qquad (a)$$

For the comproportionation of **1** and cyclopropane **7** leading to **8** [Eq. (b)], a reaction energy ΔE of −38.2 kcal

$$\mathbf{1} + \mathbf{7} \longrightarrow 2\,\mathbf{8} \qquad (b)$$

mol^{-1} is calculated.[9] If one assumes that ΔE(b) is determined by the difference in the SE values of the three-membered rings (SE(**1**) = 24.7, SE(**7**) = 27.5,[10] SE(**8**) = 26.9 kcal mol^{-1}[10]) and the bond energies (BE) of C–C (80 kcal mol^{-1}), C–O (78 kcal mol^{-1}[11]), and O–O bonds, then BE(O–O) is estimated at 36 kcal mol^{-1}, a value which is close to the calculated dissociation energy of 31 kcal mol^{-1}.[12] In the isomerization, **2** is formed with an excess energy of 54 kcal mol^{-1}, which, if not reduced by collision deactivation, leads to cleavage of the O–O bond and subsequent decomposition of the molecule.

A thermodynamic stabilization of **1** is achieved by geminal methyl groups. It can be estimated via the reaction energy ΔE(c) to be 21 kcal mol^{-1}.[13] Geminal methyl groups

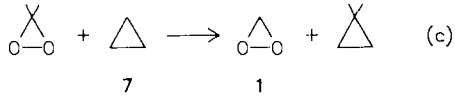

7 1 (c)

also increase the kinetic stability of **1**; they fix the CCC bond angle at a value of 117° by steric interaction and thereby render difficult a rehybridization at the C atom during cleavage of the OO bond. This explains the relatively high stability of dimethyldioxirane, which was recently prepared by oxidation of acetone with $KHSO_5$.[14]

Fluorine as substituent also increases the thermodynamic stability of **1**, but at the same time it reduces its kinetic stability, as manifested in the relatively large O–O distance (1.56 Å) and the reduction in the exocyclic angle to 110.8°. Intermediary fluorodioxiranes are therefore probably stronger epoxidizing agents than dialkyl dioxiranes.

Received: October 5, 1987 [Z 2457 IE]
German version: *Angew. Chem. 100* (1988) 431

CAS Registry numbers:
1, 157-26-6; **2**, 78894-19-6; **4a**, 112897-49-1; **6**, 76694-11-6; dimethyldioxirane, 74087-85-7; dioxirane, 157-26-6.

[1] G. Cicala, R. Curci, M. Fiorentino, O. Laricchiuta, *J. Org. Chem. 47* (1982) 2670; R. Jeyaraman, R. W. Murray, *J. Am. Chem. Soc. 106* (1984) 2462; see also H. Mimoun, *Angew. Chem. 94* (1982) 750; *Angew. Chem. Int. Ed. Engl. 21* (1982) 734.

[2] F. J. Lovas, R. D. Suenram, *Chem. Phys. Lett. 51* (1977) 453; R. D. Suenram, F. J. Lovas, *J. Am. Chem. Soc. 100* (1978) 5117.

[3] D. Cremer, *J. Am. Chem. Soc. 103* (1981) 3619, 3627.

[4] I. R. Dunkin, G. A. Bell, *J. Chem. Soc. Chem. Commun. 1983*, 1213; O. Chapman, T. C. Hess, *J. Am. Chem. Soc. 106* (1984) 1842; G. A. Ganzer, R. S. Sheridan, M. T. H. Liu, *ibid. 108* (1986) 1517; W. Sander, *Angew. Chem. 98* (1986) 255; *Angew. Chem. Int. Ed. Engl. 25* (1986) 254.

[5] 4th order Møller-Plesset calculations with the 6-31G* basis set (MP4(SDQ)/6-31G*) gave the following energies: −189.12016 (**1**), −189.07021(**2**), −189.03391 Hartree (**3**). The MP4 geometries were calculated using analytical gradients. J. Gauss, D. Cremer, *Chem. Phys. Lett. 138* (1987) 131.—For 2nd order Møller-Plesset calculations with the 6-31G* basis set (MP2/6-31G*) see D. Cremer, *J. Am. Chem. Soc. 101* (1979) 7199. Since MP2 calculations in the case of **2** favor diradical structures with a balanced π system, there results an isomerization barrier of 2.2 kcal mol^{-1} higher than with the more reliable MP4 calculations. This can be taken into account on correcting the MP2 calculations.

[6] The same holds true for the rotation about the CO bond of alkoxycarbenium ions: D. Cremer, J. Gauss, R. F. Childs, C. Blackburn, *J. Am. Chem. Soc. 107* (1985) 2435.

[7] MP2/6-31G* calculations gave the following energies: −288.07412 (**4a**), −288.07462 (**4b**), −288.05798 (**5a**), −288.04385 (**5b**), −288.14818 Hartree (**6**). The estimated MP4 correction[5] for the activation energy is −2.2 kcal mol^{-1}.

[8] J. W. Agopovich, C. W. Gillies, *J. Am. Chem. Soc. 104* (1982) 813; *ibid. 105* (1983) 5047.

[9] MP2/6-31G*-energies: −151.13492 (H_2O_2), −115.35329 (CH_3OH), −190.29560 (CH_3OOH), −190.39760 ($HOCH_2OH$), −117.46275 (**7**), −153.31569 Hartree (**8**).

[10] S. W. Benson: *Thermochemical Kinetics*, Wiley, New York 1976, Table A2, p. 271-310.

[11] BE at 0 K without zero point vibrational energies. At room temperature BE values are 83 and 81 kcal mol^{-1}, respectively. D. Cremer, E. Kraka in J. F. Liebman, A. Greenberg (Eds.): *Molecular Structure and Energetics, Vol. 6*. VCH Publishers, Deerfield Beach, FL, USA, in press; D. Cremer, J. Gauss, *J. Am. Chem. Soc. 108* (1986) 7467.

[12] L. B. Harding, W. A. Goddard, *J. Am. Chem. Soc. 100* (1978) 7180.

[13] MP2/6-31G*-result: D. Cremer, M. Schindler, *Chem. Phys. Lett. 133* (1987) 293; W. Adam, Y.-Y. Chan, D. Cremer, J. Gauss, D. Scheutzow, M. Schindler, *J. Org. Chem. 52* (1987) 2800.

[14] R. W. Murray, R. Jeyaraman, *J. Org. Chem. 50* (1985) 2847.

Facile Reduction of 1,2-Dioxetanes by Thiols as Potential Protective Measure against Photochemical Damage of Cellular DNA**

By *Waldemar Adam,* Bernd Epe, Dietmar Schiffmann, Franklin Vargas,* und *Dieter Wild*

In recent biological studies[1] it was demonstrated that 1,2-dioxetanes are genotoxic. Since these strained four-membered ring cyclic peroxides are known to be efficient chemical sources of n,π*-excited triplet carbonyl products,[2] we postulated that the observed DNA damage was of photochemical origin. However, in view of the quite moderate photo-genotoxicity displayed by the dioxetanes studied, we suspected that these labile peroxides were efficiently detoxified in the cell through chemical action. For example, the living cell guards itself against "oxidative stress"[3] by engaging glutathione, a tripeptide which deactivates reactive oxygen species including peroxides by reduction, itself being oxidized to its disulfide. We now report on the quantitative reduction of dioxetanes to the corresponding vicinal diols by glutathione [Eq. (a)], a reaction which also takes place with other thiols. The results are listed in Table 1.

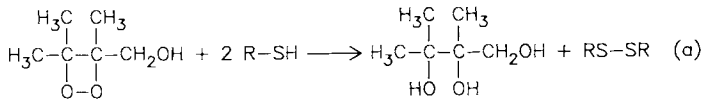

1 2 (a)

Table 1. Reaction of **1** with thiols.

No.	Thiol [a] R-SH	Solvent	Reaction conditions T [°C]	t [h]	Product balance [%]	Product yields [mol] [b, c] Disulfide	**2**	Ketone [d]
1.	L-Glutathione	H_2O	5	0.16	97	0.97	0.96	–
2.	L-Cysteine	H_2O	20	0.16	95	0.98	0.92	–
3.	L-Penicillamine	H_2O	20	0.16	93	0.96	0.90	–
4.	*threo*-1,4-Dimercapto-2,3-butanediol	MeOH	10	1	99	0.99	0.99	–
5.	1,3-Propanedithiol	MeOh	−40	24	97	0.98	0.93	0.03
6.	Thiobenzyl alcohol	MeOH	−50	72	89	0.78	0.82	0.18
7.	Mercaptoacetic Acid	MeOH	−40	72	78	0.56	0.56	0.44
8.	Methyl Mercaptoacetate	MeOH	−40	72	80	0.59	0.58	0.42
9.	Thiophenol	MeOH	−100	22	50	0.49	0.49	0.51

[a] Stoichiometry 2:1 except entries 4 and 5, for which it was 1:1. [b] 100% conversion; normalized to 1.00 mol; ±2% error limits. [c] Determined ^{1}H-NMR spectroscopically and/or isolated. [d] Acetone and hydroxyacetone formed in equal amounts.

On mixing aqueous solutions of the hydroxydioxetane **1** with glutathione at 5°C in a 1:2 stoichiometry, a fast reaction (100% conversion in 10 min, monitored by ^{1}H-NMR) ensued, leading essentially quantitatively to the glutathione dimer [m.p. 178–180°C (decomp.)[4], m.p.$_{obs.}$ 178–182°C (decomp.)] and the triol **2**. Both products were isolated and identified by comparison with authentic materials. Similar results were obtained for cysteine, penicillamine, and *threo*-1,4-dimercapto-2,3-butanediol (Entries 2–4 in Table 1), except that in the latter case the cyclic disulfide 1,2-dithiane was isolated and small amounts (ca. 3%) of the dioxetane cleavage products (acetone and hydroxyacetone) were detected by ^{1}H-NMR. Such cleavage products gain greater importance for the simple thiols (Entries 6–9, Table 1), although the reactions were conducted at subambient temperatures, at which thermal decomposition of the dioxetane is negligible. For example, with thiophenol (Entry 9 in Table 1) the extent of dioxetane cleavage was as much as 50%, even at −100°C, thus seriously competing with reduction to the triol **2**. Similar results were obtained for tetramethyl-1,2-dioxetane, undergoing quantitative reduction by glutathione to pinacol, but appreciable cleavage into acetone with thiophenol.

That glutathione is an efficient reagent for the reduction of peroxides is well established,[3] but that the labile dioxetanes can be so cleanly transformed into vicinal diols is somewhat astonishing, since in the few reported studies with divalent sulfur compounds, oxygen transfer prevails. Thus, the dioxetane is converted into an epoxide and/or a ketone, while the sulfide is oxidized to the sulfoxide.[5] Furthermore, dialkyl sulfoxylates $S(OR)_2$ are transformed via intermediary tetraalkylorthosulfites $S(OR)_4$ into dialkyl sulfites.[6] These oxygen transfer reactions have been mechanistically interpreted in terms of either a nucleophilic attack by the sulfide[5] on the peroxide linkage or a biphilic insertion by the dialkylsulfoxylate.[6] Consequently, we likewise expected oxygenated products rather than disulfides in the reaction with thiols. Indeed, when only equimolar amounts of glutathione and dioxetane **1** were used, the glutathione was converted quantitatively in a fast reaction into its dimer, and in a subsequent slow reaction (hours) the disulfide was oxidized to its *S*-monoxide, as anticipated for an oxygen transfer reaction. With L-methionine (in H_2O, 20°C, 20 min, 1:1 stoichiometry), **1** was quantitatively converted into the epoxide 2,3-dimethyl-2,3-epoxy-1-butanol, while the methionine itself was converted into the sulfoxide. In the case of dimethyl sulfide (in $CHCl_3$, −5°C, 3 h, 1:1 stoichiometry) oxygen transfer was the major reaction (ca. 85%), affording 60% sulfoxide and 12% sulfone as sulfide derived products, and 44% 2,3-dimethyl-2,3-epoxy-1-butanol and 41% of the rearranged, ketone 1-hydroxy-3,3-dimethyl-2-butanone as dioxetane derived products. Dioxetane cleavage into equal amounts of acetone and hydroxyacetone was observed as secondary reaction (ca. 15%). A control experiment showed that in a much slower reaction dimethyl sulfoxide was oxidized by dioxetane **1** to its sulfone. Clearly, the sulfides behave differently than the thiols in their reaction with dioxetanes.

[*] Prof. Dr. W. Adam, Dipl.-Chem. F. Vargas
Institut für Organische Chemie der Universität
Am Hubland, D-8700 Würzburg (FRG)
Dr. B. Epe, Dr. D. Schiffmann, Dr. D. Wild
Institut für Toxikologie und Pharmakologie der Universität
Versbacher Str. 9, D-8700 Würzburg (FRG)

[**] This work was supported by the Deutsche Forschungsgemeinschaft (Sonderforschungsbereich No. 172), the Fritz-Thyssen Stiftung, and the Fonds der Chemischen Industrie. *F. Vargas* thanks the DAAD for a doctoral fellowship.

In this context it was of interest to explore whether other cyclic peroxides, e.g. dimethylmalonyl peroxide **3**, would exhibit such differentiated chemical behavior towards thiols and sulfides. The results of the reactions of **3** with glutathione (GSH) and with dimethyl sulfide are shown in Scheme 1. The former gave quantitatively glutathione dimer (GSSG) and malonic acid, a reduction process identical to that of GSH with **1**. With dimethyl sulfide, on the other hand, the major reaction (ca. 62%) was oxygen transfer leading to malonic anhydride[7] and dimethyl sulfoxide.

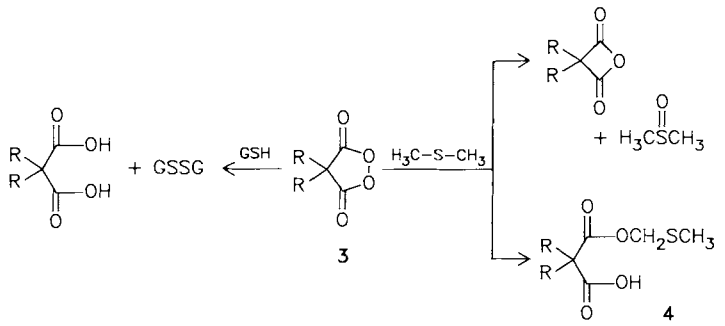

Scheme 1. R=CH_3

A mechanistically most revealing minor process (ca. 38%) gave rise to the insertion product **4**. The latter is indicative of electron transfer chemistry, as observed in the cytochrome P-450-catalyzed dealkylation of sulfides via α-hydroxylation of the intermediary sulfur-centered radical cation.[8] The fortunate happenstance of the present case, the first example of this type of electron transfer for a peroxide-sulfide reaction, is that the acetal moiety ($RO-CH_2-SR$) survives work-up. Preliminary experiments indicate that such an insertion product as structure **4** is formed also with dioxetane **1**, when allowed to react with thioanisole.

That product **4** is of free radical origin is immediately clear from preliminary CIDNP experiments, in that ^{1}H-NMR monitoring of the malonyl peroxide-sulfide reaction in $CDCl_3$ at $-30°C$ exhibited enhanced polarization of the methylene hydrogens of the acetal linkage. Moreover, it is of interest to mention that preliminary results with trimethylsilyl phenyl sulfide show that it behaves like a thiol in that reduction of the malonyl peroxide **3** takes place affording phenyl disulfide. The analogous reduction by trimethylsilyl phenyl sulfide obtains also for the dioxetane **1**.

In view of these findings, we propose that the reaction of dioxetanes with divalent sulfur compounds (thiols and sulfides) are induced by electron transfer, as outlined in Scheme 2. With the help of such electron transfer, one can rationalize in a unified manner all three reaction types observed for thiols and sulfides, i.e. reduction for thiols (X=H, route A), oxygen transfer for sulfides (X=R″, route B), and catalyzed cleavage for both (X=H, R″, route C).

Electron transfer involving dioxetanes constitutes the basis of the CIEEL mechanism[9] and also their dark catalytic decomposition by amines[10] is interpreted to proceed via radical ion pairs. In view of the relatively low oxidation potentials of divalent sulfur compounds,[11] such electron transfer with peroxide oxidants is likely. Although radical cations of sulfides[8] and thiols[12] are well documented, the novel feature in the present report is that such reactive intermediates can be generated in redox reactions with peroxides. Work is in progress employing polycyclic aromatic sulfur compounds as one-electron donors, whose radical cation chemistry is well established, e.g. chloropromazine.[13] Preliminary results with phenothiazine afford indeed its radical cation on treatment[14] with dioxetane **1** or malonyl peroxide **3**. Significant and relevant for our purposes is that it evidently also takes place on treatment of dioxetanes with thiols such as glutathione. That hydrogen abstraction from the thiol may be involved, generating thiyl radicals directly rather than via electron transfer (Scheme 2), seems to be unlikely, as substantiated by the finding that trimethylsilyl derivatives of thiols also reduce dioxetanes affording disulfides. We concede that mechanisms other than electron transfer (Scheme 2) can be proposed to rationalize the present observations and that

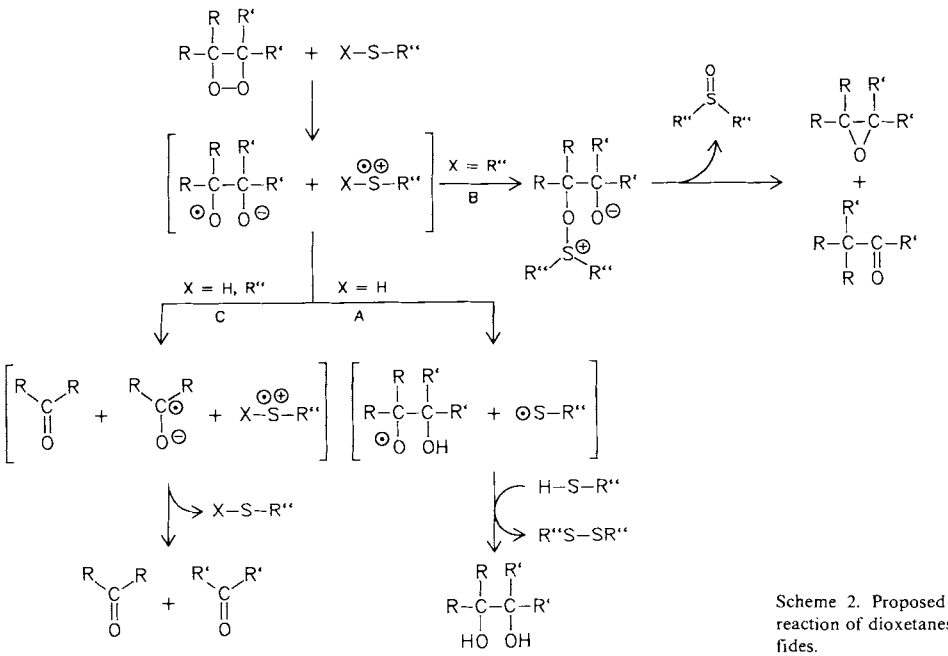

Scheme 2. Proposed mechanism for the reaction of dioxetanes with thiols and sulfides.

more work will be necessary to substantiate the novel redox process postulated here.

Irrespective of this mechanistic query, the fact that glutathione and other biological thiols such as cysteine and penicillamine (Table 1) quantitatively reduce dioxetanes to their vicinal diols provides an effective means for the detoxification of such genotoxic agents in the cell. Indeed, in this context it is important to mention that preliminary studies have revealed that addition of glutathione diminishes the mutagenic activity of dioxetane **1** in the Ames test. Furthermore, buthionine sulfoximine (an inhibitor of glutathione synthesis) increases the cytotoxicity of dioxetane **1** in studies with HL60 (promyelocytic leukemia) cells and SHE (Syrian hamster embryo) cells. Future studies plan using glutathione deficient bacterial strains and cell lines to enhance the photogenotoxity of 1,2-dioxetanes.

Received: October 23, 1987 [Z 2487 IE]
German version: *Angew. Chem. 100* (1988) 443

[1] a) W. Adam, A. Beinhauer, B. Epe, R. Fuchs, A. Griesbeck, H. Hauer, P. Mützel, L. Nassi, D. Schiffmann, D. Wild in T. Friedberg, F. Oesch (Eds.): *Primary Changes and Control Factors in Carcinogenesis*, Deutscher Fachschriften-Verlag, Wiesbaden 1986, pp. 64–67; b) J. W. Lown, R. R. Koganty, K. R. Kopecky, *Photobiochem. Photobiophys. 12* (1986) 295; c) L. Nassi, B. Epe, D. Schiffmann, W. Adam, A. Beinhauer, A. Griesbeck, *Carcinogenesis (London) 8* (1987) 947; d) L. Nassi, D. Schiffmann, A. Favre, W. Adam, R. Fuchs, *Mutat. Res.*, in press.
[2] W. Adam, G. Cilento, *Angew. Chem. 95* (1983) 525; *Angew. Chem. Int. Ed. Engl. 22* (1983) 529.
[3] H. Sies, *Angew. Chem. 98* (1986) 1061; *Angew. Chem. Int. Ed. Engl. 25* (1986) 1058.
[4] C. Berse, R. Boucher, L. Piché, *Can. J. Chem. 37* (1959) 1733.
[5] H. H. Wasserman, E. Saito, *J. Am. Chem. Soc. 97* (1975) 905.
[6] B. S. Campbell, D. B. Denney, D. Z. Denney, L. S. Shih, *J. Am. Chem. Soc. 97* (1975) 3850.
[7] a) C. L. Perrin, T. Arrhenius, *J. Am. Chem. Soc. 100* (1978) 5249; b) W. Adam, J. W. Diehl, *J. Chem. Soc. Chem. Commun.* (1972) 797.
[8] Y. Watanabe, T. Numata, T. Iyanagi, S. Oae, *Bull. Chem. Soc. Jpn. 54* (1981) 1163.
[9] G. B. Schuster, *Acc. Chem. Res. 12* (1979) 366.
[10] T. Wilson, D. Chia-Sen in M. J. Cormier, D. M. Hercules, J. Lee (Eds.): *Chemiluminescence and Bioluminescence*. Plenum, New York 1973, pp. 265–283.
[11] H. Lindley, *Biochem. J. 82* (1962) 418.
[12] a) R. L. Petersen, D. J. Nelsen, M. C. R. Symons, *J. Chem Soc. Perkin Trans 2 1978*, 225; b) V. T. D'Souza, R. Nanjudiah, J. Baeza, H. H. Szmant, *J. Org. Chem. 52* (1987) 1729.
[13] G. R. Buettner, A. G. Motten, R. D. Hall, C. F. Chignell, *Photochem. Photobiol. 44* (1986) 5.
[14] C. Bodea, I. Silberg, *Adv. Heterocycl. Chem. 9* (1968) 321.

The Reagent Diphenyldiselane/Iodine: No Phenylselenenyl Iodide but a Charge Transfer Complex with Cyclic Moieties**

By *Silvia Kubiniok, Wolf-Walther du Mont,* Siegfried Pohl,** and *Wolfgang Saak*

The elements sulfur and selenium do not react with elemental iodine to give stable molecular compounds containing chalcogen–iodine bonds. Only recently has it been possible to demonstrate, in special cases, that—by cleavage of selenium–selenium bonds with iodine—uncharged molecules with covalent selenium–iodine bonds can be generated and even isolated.[1] Thus, bis(2,4,6-tri-*tert*-butylphenyl)diselane **1a** and apparently also bis(2,4,6-trimethylphenyl)diselane **1b** give dismutation equilibria with iodine:[1] in solution the aryl(iodine) selenides **2a** and **2b**, respectively, as well as the starting diselanes **1a** and **1b** can be detected by ^{1}H- and ^{77}Se-NMR spectroscopy;[2] crystalline iodine(2,4,6-tri-*tert*-butylphenyl) selenide **2a** consists of monomeric molecules with selenium–iodine single bonding.[1]

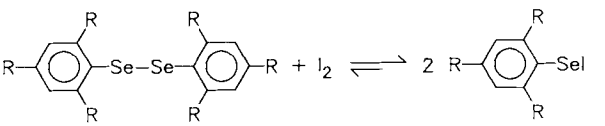

1a, R = t-C_4H_9
1b, R = CH_3

2a, R = t-C_4H_9
2b, R = CH_3

The reagent diphenyldiselane **1c**/iodine,[3] which *Toshimitsu*, *Uemura*, and *Okano* recommend for specific CC coupling reactions, has been available commercially under the name "phenyl selenenyl iodide"[4] [alternative to iodine(phenyl) selenide] for some time. Indeed chemical reactions with the "Toshimitsu reagent" suggest the formation of a reactive species C_6H_5SeI **2c**;[5] thus, e.g., it was possible to carry out the iodoselenation of 1-hexyne with diphenyldiselane **1c**/iodine in the same way as with the product of the reaction of phenylselenenyl chloride with iodotrimethylsilane.[6]

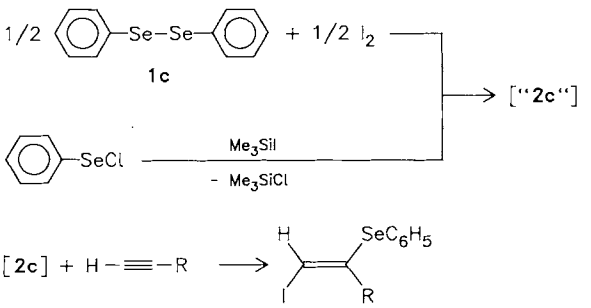

^{13}C- and ^{77}Se-NMR spectra of the solution obtained upon reaction of **1c** with iodine, however, provided no reliable indication of the formation of molecular species **2c**.[7] On addition of half an equivalent of iodine to **1c** in chloroform, changes in the NMR shifts were observed but no separate signals could be resolved for the reaction product. When diselane **1c** is treated with an excess of iodine further shift changes occur compared to the ^{13}C-NMR values[6] quoted earlier for the Toshimitsu reagent.[7] These findings leave it undecided whether a dismutation equilibrium between **1c**/iodine and **2c** exists in solution which is rapidly established on the NMR time scale, or whether a (kinetically labile) charge transfer adduct is formed from the diselane **1c** with iodine.

The product of the reaction of **1c** with iodine can be prepared just as easily as the aryl(iodine) selenide **2a**. Mixing of the reactants in petroleum ether 40/60 and crystallization at −14 °C afford reddish-black shiny crystals, which after brief drying have the correct analytical composition.[8] If the product is left for a prolonged time (2–4 h) under reduced pressure, it gradually loses some iodine; this might explain why the compound was previously obtained only "almost pure" or "98%".[4–6]

[*] Prof. Dr. W.-W. du Mont, Prof. Dr. S. Pohl,
Dipl.-Chem. S. Kubiniok, Dipl.-Chem. W. Saak
Fachbereich Chemie der Universität
Carl-von-Ossietzky-Strasse 9-11, D-2900 Oldenburg (FRG)

[**] Properties of Chalcogen–Chalcogen Bonds, Part 9. This work was supported by the Deutsche Forschungsgemeinschaft and the Fonds der Chemischen Industrie.—Part 8: [1].

An X-ray structure analysis[9] of the compound obtained in crystalline form from petroleum ether revealed without doubt that *no* iodine(phenyl) selenide **2c** is present in the solid state but rather the diphenyldiselane–iodine charge transfer complex **3c** (Fig. 1). Two diphenyldiselane molecules are coupled with two I_2 molecules in such a way that a slightly puckered eight-membered ring containing two Se_2-groups and two I_2-groups is formed. Since the angles in this ring are alternately approximately 90° and 180°, almost a square geometry results. The Se–Se bonds (234.7 pm) and I–I bonds (277.5 pm)[9] are longer than those in **1c** (229 pm)[10] or elemental iodine (271.5 pm).[11] Diphenyldiselane coordinates a diiodine molecule, with one selenium atom acting as donor toward an iodine atom. In addition there are interactions between the other selenium atom and an iodine atom of the adjacent R_2Se_2–I_2 moiety; in this case the selenium atom plays the role of the acceptor. The mutual selenium/iodine donor/acceptor relationships can be analyzed on the basis of the characteristic coordination geometries of hypervalent (10-Se-3) acceptor selenium atoms (linear I-Se-Se arrangement) and (10-I-2) acceptor iodine atoms (linear Se-I-I moiety):[9] The donor atoms are located at the corners of the "square", the atoms with acceptor character at the midpoints of the edges (Fig. 1). Selenium–iodine contacts in **3c**, which result from Se(donor)–I(acceptor) interaction (299.2 pm), are about 50 pm longer than the Se–I single bond in the aryl(iodine) selenide **2a** (252.9 pm).[1, 12] The other selenium–iodine contacts in **3c**, which can be explained in terms of an I(donor)–Se(acceptor) interaction, already exceed the lengths of Se–I single bonds by about 100 pm. These internuclear distances are in the range of "secondary bonding"; they are comparable, e.g., with intermolecular contacts in the chain structure of the thermochromic tetramethyldistibane.[13] Contacts of this kind also exist in the solid between iodine molecules (350 pm) and between the chains of grey selenium (344 pm); the structure of **3c** is a remarkable heteronuclear variant thereof.[11] Iodine–iodine contacts (412.7 pm) between the corner iodine atoms (I2, I2a) lead to chain-like repeat linking of the square moieties in the crystal.

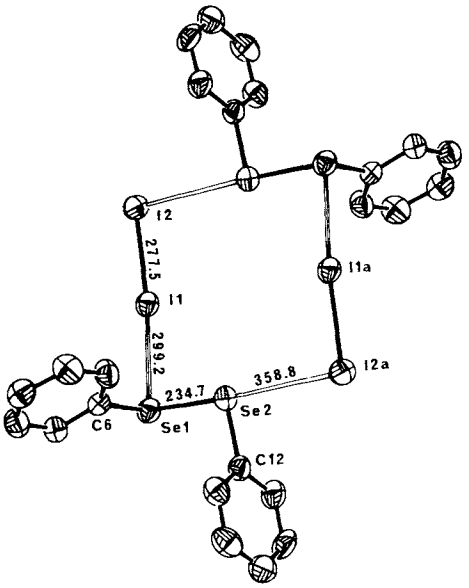

Fig. 1. Dimeric centrosymmetric moiety of $Ph_2Se_2 \cdot I_2$ **3c** in the crystal, without H atoms; vibration ellipsoids at the 50% probability level. Important bond lengths [pm] and angles [°] not quoted in the figure: Se1-C6 194.4(7), Se2-C12 192.8(6); Se2-Se1-I1 90.2(1), Se2-Se1-C6 104.3(2), I1-Se1-C6 94.7(2), Se1-Se2-I2a 176.5(1), Se1-Se2-C12 98.4(2), I2a-Se2-C12 84.0(2), Se1-I1-I2 174.2(1), I1a-I2a-Se2 88.4(1).

3c is labile in solution (NMR), and an association/dissociation equilibrium is established between the reactants **1c**/iodine (UV: weak absorption at 524 nm) and the charge transfer adduct **3c**. The well known chemical reactions with the reagent "C_6H_5SeI"[3,5,6] and the occurrence of the molecular peak of **2c** (C_6H_5SeI, m/z 284 with ^{80}Se) in the mass spectrum of **3c** suggest that scrambling reactions will take place between **1c**/iodine, **2c** and **3c**, which are favored by small differences in energy and low activation energies.

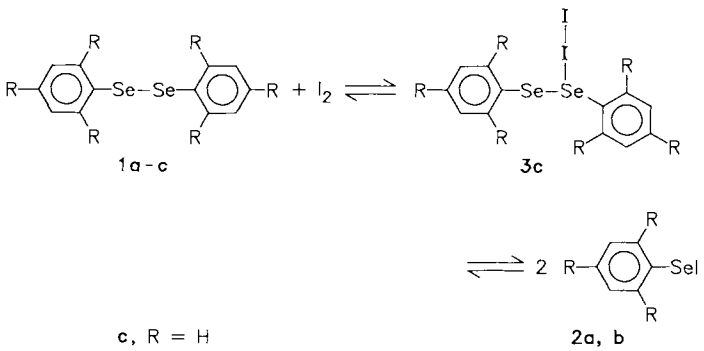

The formation of the cyclic diselane-diiodine charge transfer adduct **3c** with weakening of Se–Se and I–I bonds (compared to the educts **1c** and I_2) is already the primary step of a 2+2 dismutation of Se–Se bonds with I–I bonds. Sterically demanding substituents on selenium disfavor the tendency of formation of charge transfer complexes with iodine.[14] In the case of the diselanes **1a**, **b** the steric hindrance of the reactants favors the tendency to undergo dismutation with formation of molecules having covalent Se–I bonding (**2a**, **b**); the first example, **2a**, was recently confirmed by an X-ray structure analysis.[1] The ability of compounds **3** to exist alongside **2**, **1** and I_2 also provides an improved explanation of the catalytic action of iodine on the crystallization of elemental selenium.[15]

Received: October 8, 1987 [Z 2470 IE]
German version: *Angew. Chem. 100* (1988) 434

CAS Registry number:
3c, 59411-08-4.

[1] a) W.-W. du Mont, S. Kubiniok, K. Peters, H.-G. von Schnering, *Angew. Chem. 99* (1987) 820; b) *Angew. Chem. Int. Ed. Engl. 26* (1987) 780.

[2] ^{1}H-NMR: **1a**, **2a**, see [1]; **1b**/**2b** (300 MHz, in C_6D_6): **1b**: δ = 2.02 (6H), 2.32 (12H), 6.66 (4H); **2b**: δ = 1.96 (3H), 2.45 (6H), 6.59 (2H). ^{77}Se-NMR (57.24 MHz, Me_2Se/C_6D_6 standard): **1a**/**2a** (in C_6D_6): **1a**: δ = 515.6; **2a**: δ = 517.6 (the ^{77}Se-NMR data quoted in [1a] are incorrect); **1b**/**2b** (in C_6D_6): **1b**: δ = 369; **2b**: δ = 400. Correct analytical data were obtained for **2b**.

[3] A. Toshimitsu, S. Uemura, M. Okano, *J. Chem. Soc. Chem. Commun. 1982*, 87.

[4] Aldrich-Katalog 1986/87, Best. Nr. 30.259-7.

[5] A. Toshimitsu, K. Terao, S. Uemura, *J. Org. Chem. 51* (1986) 1724.

[6] S. Tomoda, Y. Takeuchi, Y. Nomura, *Synthesis 1985*, 212.

[7] ^{13}C-NMR (75.47 MHz, 20°C, in $CDCl_3$): **1c**: δ = 127.7 (C-4), 129.2 (C-3,5), 131.5 (C-2,6); **1c** + I_2 (1:0.5): δ = 128.2, 129.2, 132.4; **1c** + I_2 (1:1): δ = 128.8, 129.3, 133.1; **1c** + I_2 (1:2): δ = 129.2, 129.4, 133.6. Measurement at −30°C showed no coalescence phenomena.

[8] Procedure for **3c**: A solution of **1c** (1.0 g, 3.2 mmol) in petroleum ether 40/60 (200 mL) was treated at room temperature with iodine (0.81 g, 3.2 mmol). After three hours' stirring the solution was cooled to −14°C for the crystallization. Filtration and brief drying under reduced pressure afforded 1.72 g (95%) of **3c** as reddish-black shiny crystals. **3c** is

readily soluble in benzene and toluene, but only moderately soluble in aliphatic solvents. M.p. = 58 °C. ^{1}H-NMR: $\delta = 6.8$–8.0 (m); ^{77}Se-NMR (57.24 MHz, Me_2Se/C_6D_6 standard), in C_6D_6: $\delta = 477.7$, in CH_3CN/C_6D_6 (3 : 1): $\delta = 470.4$, in $CDCl_3$: $\delta = 485.3$; shifts concentration-dependent. MS (70 eV, DIR, 55 °C): *m/z* [%] 314 (4, $Ph_2Se_2^{\oplus}$), 284 (10, $PhSeI^{\oplus}$), 254 (100, $I_2^{\oplus}$), 234 (2, $Ph_2Se^{\oplus}$), 157 (14, $PhSe^{\oplus}$), 127 (36, $I^{\oplus}$), 77 (13, $C_6H_5^{\oplus}$).

[9] **3c** crystallizes triclinically, space group $P\bar{1}$, $a = 975.6(4)$, $b = 991.0(4)$, $c = 1009.6(4)$ pm, $\alpha = 116.04(2)$, $\beta = 91.77(2)$, $\gamma = 115.26(2)°$, $V = 764.04 \times 10^6$ pm^3, $Z = 2$, based on the formula $Ph_2Se_2 \cdot I_2$; 2227 symmetry-dependent reflections, 1875 observed ($I > 2\sigma(I)$); $R_w = 0.0296$ (measurement: Siemens-Stoe AED 2; solution SHELX 76). Further details of the crystal structure investigation are available on request from the Fachinformationszentrum Energie, Physik, Mathematik GmbH, D-7514 Eggenstein-Leopoldshafen 2 (FRG), on quoting the depository number CSD-52950, the names of the authors, and the journal citation.

[10] R. E. Marsh, *Acta Crystallogr. 5* (1952) 458.

[11] H. Krebs, *Angew. Chem. 70* (1958) 615; F. van Bolhuis, P. P. Koster, T. Michelsen, *Acta Crystallogr. 23* (1967) 90.

[12] G. Y. Chao, J. D. McCullough, *Acta Crystallogr. 14* (1961) 940; H. Hope, J. D. McCullough, *ibid. 17* (1964) 712; H. D. Maddox, J. D. McCullough, *Inorg. Chem. 5* (1966) 522.

[13] A. J. Ashe III, E. G. Ludwig, J. Oleksyszyn, J. C. Huffmann, *Organometallics 3* (1984) 337; O. Mundt, M. Riffel, G. Becker, A. Simon, *Z. Naturforsch. B 39* (1984) 317.

[14] P. Laur, *5th Int. Symposium on the Chemistry of Selenium and Tellurium*, Oak Ridge, TN (USA) 1987; Abstract 10.

[15] H. Krebs, *Angew. Chem. 65* (1953) 293.

Enantioselective Synthesis of (*R*)-*N*-Boc-1-amino-2-arylcyclopropene-1-carboxylic Acid Methyl Ester**

By *Ulrich Schöllkopf,* Bernd Hupfeld, Stephan Küper, Ernst Egert,** and *Michael Dyrbusch*

Dedicated to Professor Emanuel Vogel on the occasion of his 60th birthday

β,γ-Unsaturated amino acids of the β-methylenephenylalanine type **1**[1] are of special interest as suicide-inhibitors[2] for pyridoxal phosphate-dependent enzymes. 1-Amino-2-aryl-cyclopropene-1-carboxylic acids (Type **7**)[3]—

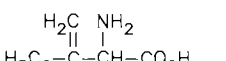

1

structural variants of **1**—should be particularly effective inhibitors because of their extremely strained and thus highly reactive double bond. Since—as usual[4]—only one enantiomer may be biologically active, each enantiomer should be investigated separately. We describe here an enantioselective synthesis of *N*-Boc-1-amino-2-phenyl-, -(4-methylphenyl)-, and -(4-chlorophenyl)cyclopropene-1-carboxylic acid methyl esters **7a**, **b** and **c** utilizing the bislactim ether carbene **3**. The amino acid esters **7** are obtained in almost enantiomerically pure form (*ee* > 95%): with **3** the (*R*)-enantiomers and with *ent*-**3** the (*S*)-enantiomers.

The synthesis starts from **2**, the bislactim ether of cyclo(L-Val-Gly).[5] This is converted via the 2-lithium compound and the 2-diazo compound into the bislactim ether carbene **3**,[6] which is trapped with the arylethyne **4**. Within analytical accuracy only one diastereomer is formed, namely (*R*)-**5**. The configuration was confirmed by an X-ray structure analysis of **5a** (Fig. 1).[7]

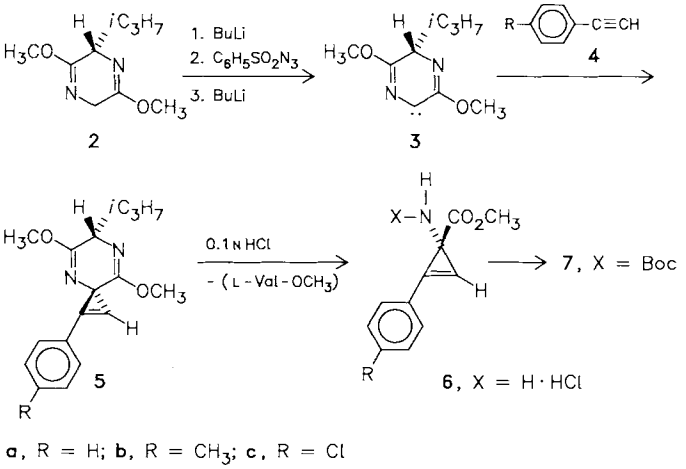

a, R = H; **b**, R = CH_3; **c**, R = Cl

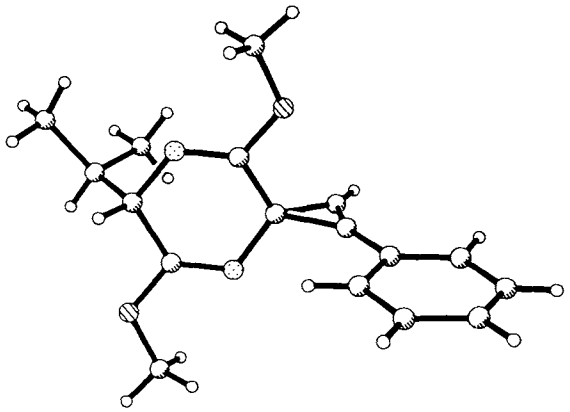

Fig. 1. Structure of the carbene adduct **5a** in the crystal [7]; ⊙ = N, ⊚ = O. Noteworthy is that the phenyl ring and the cyclopropene double bond are completely coplanar, thus indicating an effective conjugation of the two π-systems.

Hydrolysis of the carbene adducts **5** to **6**, the hydrochlorides of the amino acid esters, was achieved with two equivalents of 0.1 N HCl at room temperature. The salts **6** were transformed into the *N*-Boc derivatives **7**. After separation from Boc-L-Val-OMe these were reconverted into the compounds **6** by treatment with 0.5 N HCl in methanol (6 h, 60 °C).

Experimental

5: A solution of **2** (0.55 g, 3.0 mmol) in THF (7 mL) was treated dropwise at −78 °C with a solution of *n*BuLi (3.0 mmol) in hexane. After 15 min stirring, the resulting mixture was added via a Teflon tube (cooled with dry-ice) to a solution of 0.53 g (3.0 mmol) of benzenesulfonyl azide in 7 mL of THF. Stirring was continued for 2.5 h at −78 °C and then *n*-BuLi (3.0 mmol) was added to the mixture at such a rate that the temperature did not rise above −70 °C. After 10 min the mixture was added dropwise within 15 min through a Teflon tube (cooled with dry-ice) to 30 mL of **4**, which was warmed to 50–60 °C. After 30 min vigorous stirring, the mixture was allowed to cool to room temperature, treated with 150 mL of Et_2O, and washed with 3 × 30 mL of a 10% NaCl solution. The organic phase was dried over magnesium sulfate and the solvent removed in vacuo. Excess **4** was distilled off at 30–40 °C/0.01 torr and the residue chromatographed on silica gel (Kieselgel 60, 500 × 15 mm^2 column, petroleum ether/ether 15/1). — **5a**: 0.43 g (50%), m.p. 112–113 °C; **5b**: 0.45 g (50%), m.p. 70–71 °C; **5c**: 0.62 g (65%), m.p. 103–104 °C. Diastereomeric ratio > 49 : 1 [8].

[*] Prof. Dr. U. Schöllkopf, Dipl.-Chem. B. Hupfeld, Dipl.-Chem. S. Küper
Institut für Organische Chemie der Universität
Tammannstrasse 2, D-3400 Göttingen (FRG)
Dr. E. Egert, M. Dyrbusch
Institut für Anorganische Chemie der Universität
Tammannstrasse 4, D-3400 Göttingen (FRG)

[**] Asymmetric Syntheses via Heterocyclic Intermediates, Part 37.—Part 36: U. Schöllkopf, J. Schröder, *Liebigs Ann. Chem. 1988*, 87.

7: A solution of **5** (2.0 mmol) in MeCN (15 mL) was treated with 40 mL of 0.1 N HCl and the resulting mixture stirred for 2 days. The solution was extracted twice with Et_2O and the extracts discarded. The aqueous phase was evaporated to dryness under vacuum and the amino acid ester hydrochlorides subsequently suspended in 25 mL of CH_2Cl_2. The suspension was treated at 0 °C with 1.1 g (5.0 mmol) of Boc_2O and 1.5 g (15.0 mmol) of Et_3N and, after 4 h, the mixture was poured into 20 mL of water, the phases separated, and the organic phase rewashed with 2 × 10 mL of water and dried over magnesium sulfate. The solvent was removed in vacuo and the residue chromatographed on silica gel (Kieselgel 60, 300 × 10 mm² column, ether/petroleum ether 1/1). — **7a**: 0.34 g (58%), m.p. 133–134 °C, $[\alpha]_D^{20} = +53.4$, $R_f = 0.304$; **7b**: 0.36 g (59%), m.p. 103–104 °C, $[\alpha]_D^{20} = +51.4$, $R_f = 0.294$; **7c**: 0.39 g (60%), m.p. 90–91 °C, $[\alpha]_D^{20} = 51.0$, $R_f = 0.275$; recrystallized from ether/pentane 1/2; optical rotation: $c = 1$ in CCl_4. All the compounds described gave correct elemental analyses.

Received: October 12, 1987 [Z 2475 IE]
German version: *Angew. Chem. 100* (1988) 438

[1] R. V. J. Chari, J. Wemple, *Tetrahedron Lett. 1979*, 111.
[2] a) R. R. Rando, *Acc. Chem. Res. 8* (1975) 281; b) R. H. Abeles, A. L. Maycock, *ibid. 9* (1976) 313; c) R. H. Abeles, *Pure Appl. Chem. 53* (1981) 149; d) C. Walsh, *Tetrahedron 38* (1982) 871.
[3] For the synthesis of the achiral 1-amino-2,3-diphenylcyclopropene-1-carboxylic acid methyl ester via the 1-methoxycarbonyl-2,3-diphenylcyclopropenylium ion, see I. N. Domnin, E. F. Zhuravleva, M. I. Komendantov, A. I. Ritari, *Zh. Org. Khim. 13* (1977) 1789.
[4] E. J. Ariens, W. Soudijn, W. M. Timmermann: *Stereochemistry and Biological Activity of Drugs*, Blackwell, Oxford 1983.
[5] U. Schöllkopf, U. Groth, C. Deng, *Angew. Chem. 93* (1981) 791; *Angew. Chem. Int. Ed. Engl. 20* (1981) 798; **2** and *ent*-**2** are commercially available: Merck-Schuchardt, D-6100 Darmstadt, *MS-Info 85-14*.
[6] U. Schöllkopf, M. Hauptreif, J. Dippel, *Angew. Chem. 98* (1986) 187; *Angew. Chem. Int. Ed. Engl. 25* (1986) 192.
[7] **5a**: space group $P2_12_12_1$, $a = 861.4(1)$, $b = 1209.1(1)$, $c = 1577.2(1)$ pm, $V = 1.643$ nm³, $Z = 4$, $\mu = 0.07$ mm⁻¹ ($Mo_{K\alpha}$); crystal dimensions: $0.3 \times 0.3 \times 0.5$ mm³; 2367 measured intensities, $2\theta_{max} = 50°$, 1537 symmetry-independent reflections with $|F| > 3\sigma(F)$ used for the structure solution (direct methods) and refinement; C, N and O atoms refined anisotropically, H atoms located by difference electron density determination and refined with a riding model, $R = 0.062$ ($R_w = 0.052$, $w^{-1} = \sigma^2(F) + 0.0003F^2$). Further details of the crystal structure investigation are available on request from the Fachinformationszentrum Energie, Physik, Mathematik GmbH, D-7514 Eggenstein-Leopoldshafen 2 (FRG), on quoting the depository number CSD-52781, the names of the authors, and the journal citation.
[8] In each case only one set of signals could be recognized in the ^{13}C-NMR spectrum (200 MHz).

Bis([1,2,5]thiadiazolo)[3,4-*b*;3′,4′-*e*]pyrazine, a Novel 14π-Electron Heterocycle with High Electron Affinity

By *Yoshiro Yamashita,* Kenichi Saito, Takanori Suzuki, Chizuko Kabuto, Toshio Mukai,* and *Tsutomu Miyashi*

Cyclic thiazyl compounds have recently attracted considerable attention because of the interesting redox properties of the sulfur-nitrogen linkage.[1] We have already shown that the thiadiazole rings in 2,2′-(benzo[1,2-*c*;4,5-*c*′]-bis[1,2,5]thiadiazole-4,4,8,8-tetrayl)dimalononitrile, **1**, a new type of electron acceptor,[2] play an important role in decreasing Coulomb repulsion by delocalization of negative charge[3] and in forming two-dimensional networks by intermolecular interactions between the heteroatoms.[4] In this connection, bis([1,2,5]thiadiazolo)[3,4-*b*;3′,4′-*e*]pyrazine, **2**, is an interesting hypervalent sulfur-nitrogen heterocycle for which resonance structures such as **2a–c** come into consideration. We have succeeded in preparing **2** and found that it is a strong electron acceptor, in spite of its being a 14π-electron heterocycle.

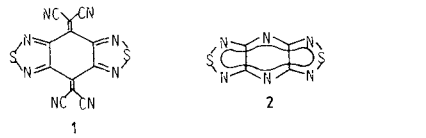
1

2

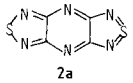
2a

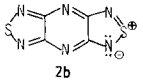
2b

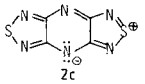
2c

5,6-Diamino[1,2,5]thiadiazolo[3,4-*b*]pyrazine **3a** was prepared by reaction of the dichloro compound **3b**[5] with potassium phthalimide followed by hydrolysis with hydrazine hydrate (yield 63%). Reaction of **3a** with thionyl chloride in the presence of pyridine in dichloromethane afforded, after sublimation, stable red crystals of **2** in 66% yield.[6]

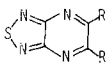
3a, R=NH₂
3b, R=Cl

The half-wave reduction potentials ($E_1 = +0.10$, $E_2 = -0.82$ V vs. SCE) were measured by cyclic voltammetry.[7] The first reduction potential is more positive than that of **1** (−0.02 V),[2] i.e. **2** is a stronger electron acceptor than **1**, even though it does not contain any electron-withdrawing substituents. Moreover, the log K_{sem} value (15.86) is larger than that for **1** (8.10),[8] indicating that the radical anion of **2** is thermodynamically more stable than that of **1**. The high electron affinity of **2** can possibly be attributed to the generation of a new aromatic sextet in one thiadiazole ring by one-electron reduction to give the radical anion **4**. This assumption is supported by the fact that the reduction potential of **5**[9] ($E_1 = \doteq -0.46$ V vs. SCE) is less negative than that of the dichloro compound **3b** ($E_1 = -0.56$ V vs. SCE).

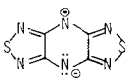
4

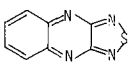
5

The single crystal required for an X-ray structure analysis[10] was obtained by sublimation.[11] Figure 1 shows two views of the crystal structure. In the crystal there exist two different kinds of **2** (abbreviated as BTPY-1 and BTPY-2); the molecular structures, however, are almost identical.[12] Figure 2 shows the molecular structure of BTPY-1, the center of which is related with the unit cell (Fig. 1a). The molecule is planar. The S–N bond lengths lie between those of an S–N single bond (1.73 Å)[13] and an S–N double bond in sulfur diimide (1.53 Å).[14] The C–N bonds and C–C bonds also have intermediate π-bond orders,[15, 16] although significant differences in the C–N bond lengths of the thiadiazole rings and a little bond alternation are observed. The calculated π-bond orders show a delocalization of the π-electrons.

From Figure 1 it is clear that the molecules form a three-dimensional network via S–N contacts. The BTPY-2 molecules are linked by strong S–N contacts between the thiadiazole rings (3.19 Å) to give a ribbon-like structure. The

[*] Dr. Y. Yamashita, K. Saito, T. Suzuki, Dr. C. Kabuto, Prof. Dr. T. Mukai, Prof. Dr. T. Miyashi
Department of Chemistry, Faculty of Science, Tohoku University, Aramaki, Sendai 980 (Japan)

ribbons are, in turn, bridged by BTPY-1 molecules, the S atoms of BTPY-1 and the N atoms of the pyrazine ring of BTPY-2 forming the contacts (3.11 Å). In addition, the BTPY-1 molecules form their own ribbons, although here the S-N contact distances are somewhat larger (3.30 Å) (Fig. 1a). The BTPY-2 ribbons interact with each other via

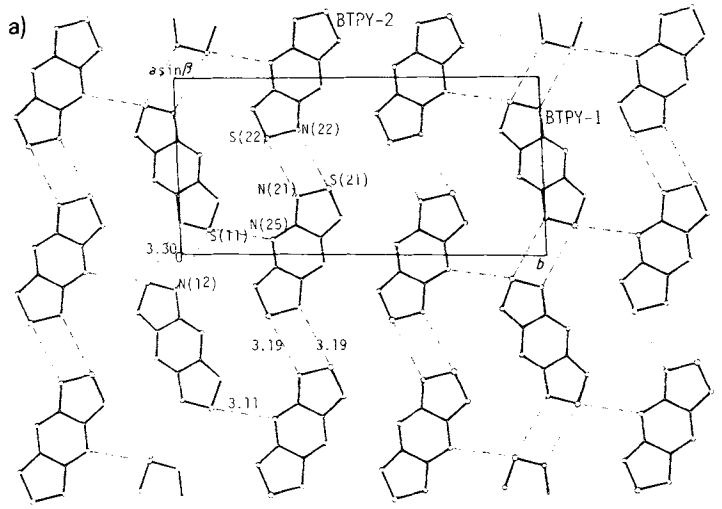

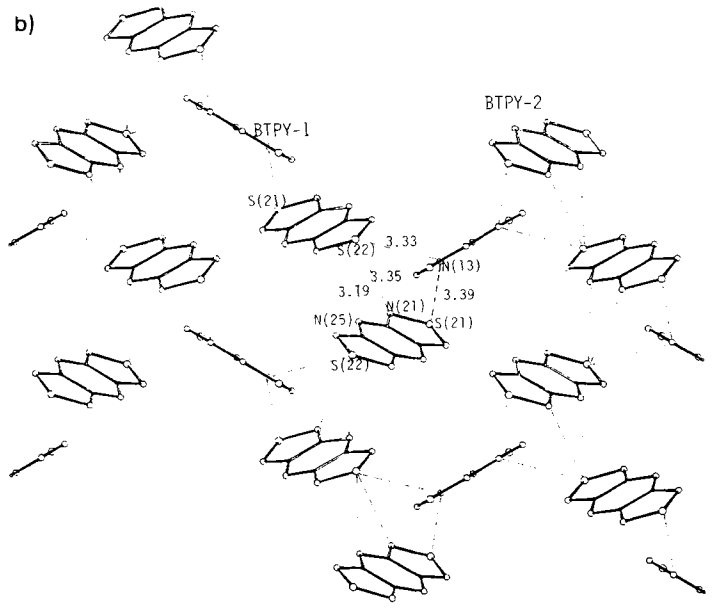

Fig. 1. Two views of the network structure of **2** in the crystal. Broken lines = S-N interactions. a) View of ribbon networks (*c* projection). S(11)-N(12) 3.30 Å, S(11)-N(25) 3.11 Å, S(21)-N(22) 3.19 Å, S(22)-N(21) 3.19 Å. b) Side view of the networks. S(21)-N(13) 3.39 Å, S(22)-N(13) 3.33 Å, S(22)-N(25) 3.19 Å, S(22)-N(21) 3.35 Å.

S-N contacts between the upper and lower sides along the [101] direction (Fig. 1b) but not in the *ab* plane including the ribbons. Such interactions lead to a dense packing in the crystal and thus to the calculated high density. The ribbon formation seems to be related to the bond alternation (Fig. 2), since the S-N contacts are via the longer S-N bonds (Fig. 1a). The observed participation of the N atoms of the pyrazine ring in the formation of a ribbon-like structure suggests that the resonance structure **2c** contributes considerably to the overall atructure of **2**.

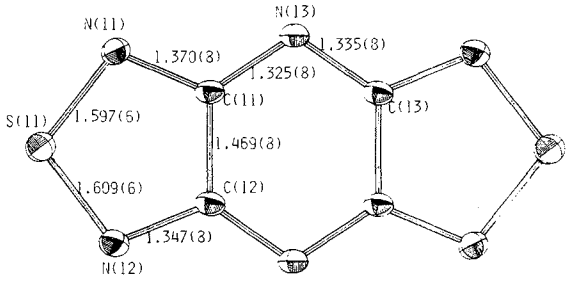

Fig. 2. Molecular structure of BTPY-1, with bond lengths [Å] (ORTEP).

On the basis of the results presented here, **2** should be suitable for the preparation of highly conductive compounds with multidimensionality. Studies on its charge transfer complexes with electron donors and its radical-ion salts are in progress.

Received: November 13, 1987 [Z 2499 IE]
German version: *Angew. Chem. 100* (1988) 428

CAS Registry numbers:
2a, 113055-86-0; **3a**, 113055-18-0; **3b**, 55387-77-4.

[1] P. J. Hayers, R. T. Oakley, A. W. Cordes, W. T. Pennigton, *J. Am. Chem. Soc. 107* (1985) 1346; R. T. Boeré, C. L. French, R. T. Oakley, A. W. Cordes, J. A. Privett, S. L. Craig, J. B. Graham, *ibid. 107* (1985) 7710; E. Dormann, M. J. Nowak, K. A. Williams, R. O. Angus, Jr, F. Wudl, *ibid. 109* (1987) 2594.

[2] Y. Yamashita, T. Suzuki, T. Mukai, G. Saito, *J. Chem. Soc. Chem. Commun. 1985*, 1044.

[3] Y. Yamashita, T. Suzuki, T. Mukai, *J. Chem. Soc. Chem. Commun. 1987*, 1184.

[4] C. Kabuto, T. Suzuki, Y. Yamashita, T. Mukai, *Chem. Lett. 1986*, 1433; T. Suzuki, C. Kabuto, Y. Yamashita, T. Mukai, *Bull. Chem. Soc. Jpn. 60* (1987) 2111.

[5] Y. C. Tong, *J. Heterocyclic Chem. 12* (1975) 451.

[6] M.p. 323-329°C (decomp); UV (CH_2Cl_2): λ (log ε) = 365 (sh, 4.46), 372 (4.52), 421 nm (sh, 3.40).

[7] Measured at a Pt electrode in acetonitrile with 0.1 M Et_4NClO_4 as a supporting electrolyte; scan rate 100 mV s^{-1}.

[8] Calculated as log $K_{sem} = (E_1 - E_2)/0.058$.

[9] A. P. Komin, M. Carmack, *J. Heterocyclic Chem. 13* (1976) 13.

[10] Crystal data for **2**: monoclinic, space group $P2_1/n$, $a = 8.461(1)$, $b = 17.316(2)$, $c = 6.847(1)$ Å, $\beta = 102.76(2)$, $V = 978.06(2)$ Å^3, $Z = 6$, $\rho_{calcd} = 2.00$ g/cm^3. Rigaku AFC-5R, $Mo_{K\alpha}$ radiation, graphite monochromator; 3009 reflections for $2\theta_{max} = 60°$; solution of structure by direct methods; refinement by block-diagonal least-squares method to $R = 0.063$ for 2483 reflections with $|F_0| > 3\sigma|F_0|$. Further details of the crystal structure investigation are available on request from the Director of the Cambridge Crystallographic Data Centre, University Chemical Laboratory, Lensfield Road, Cambridge CB2 1EW (UK) on quoting the names of the authors and the full literature citation.

[11] The sublimation was carried out using an apparatus with a temperature gradient ($T_{max} = 250$°C) under a pressure of 1 torr.

[12] The differences in the bond lengths and angles of BTPY-1 and BTPY-2 are within the standard deviations.

[13] A. Gieren, B. Dederer, H. W. Roesky, N. Amin, O. Petersen, *Z. Anorg.Allg. Chem. 440* (1978) 119.

[14] V. Luzzati, *Acta Crystallogr. 4* (1951) 193.

[15] The π-bond orders calculated from the bond lengths according to established equations [16] are 0.44, 0.57, 0.65, and 0.71 for the C-N bonds, and 0.24 vor the C-C bond.

[16] G. Häfelinger, *Chem. Ber. 103* (1970) 2902.

2,4,6-$Ph_3C_6H_2M$ (M = Cu, Ag), Monomeric Cu^I- and Ag^I-Complexes with Coordination Number 1**

By *Regine Lingnau* and *Joachim Strähle**

Only few alkyl- and aryl-complexes of Ag^I and Au^I are known. *Floriani* et al.[1] synthesized tetrameric mesitylgold(I) in which the aryl moiety functions as bridging ligand between two metal centers and thereby has a coordination number 2 (multicenter bonding). In the case of univalent copper even some polymeric or oligomeric complexes $(RCu)_n$ have been obtained[1,2] in which aryl moieties function as bridging ligands. An interesting aspect of the complexes $(RM)_n$ is that the univalent metals form very short metal-metal bonds, despite their d^{10}-electron configuration. We report here on a novel complex, in which for the first time 2,4,6-$Ph_3C_6H_2$ ("2,4,6-triphenylphenyl"[***]) is bound as ligand to Cu^I and Ag^I. The bulkiness of the ligand precludes formation of a bridge, so monomeric complexes 2,4,6-$Ph_3C_6H_2M$ (M = Cu: 1; M = Ag: 2) in which the metal atom has coordination number 1 are formed.

For the synthesis of **1** and **2**, 2,4,6-$Ph_3C_6H_2MgBr$ is allowed to react with CuCl and AgCl, respectively, at −80 °C in THF. Colorless, air-stable crystals are formed which are readily soluble in organic solvents such as THF, acetone, or toluene. The compounds were characterized by elemental analyses, ^{1}H-NMR spectra, and crystal structure analyses. The ^{1}H-NMR spectra of **1** and **2** are almost identical and differ only slightly from the spectrum of the starting compound 2,4,6-$Ph_3C_6H_2Br$. No signals which would suggest the presence of a metal-bonded hydride could be observed.

Crystals of **1** and **2** were isolated from a concentrated $CHCl_3$ solution by careful addition of a layer of ethanol. **1** and **2** crystallize isotypically in the space group $P2_1/c$.[3] Figure 1 shows a unit cell of the crystal structures of **1** and **2**. The complexes are monomeric, and no further ligands are attached in the *trans* position to the aryl ligand. The nearest non-bonding neighbors of the metal atom are the atoms C21 and C61 of the phenyl substituents in the 2- and 6-positions, respectively, with distances of 3.185 Å and 3.158 Å as well as the atoms C21 to C26 of a neighboring complex at a distance of 3.613–3.962 Å and the respective H atoms H22 to H26 at distances of 3.96–4.64 Å. The Cu–C11 and Ag–C11 bond distances (1.890(6) and 1.902(5) Å, resp.) are very short because of the low coordination number. The values commonly observed for such covalent single bonds lie in the ranges 1.97–2.16 Å and 2.04–2.17 Å, respectively.[2c]

The unusual coordination number of 1 gave reason for investigating the reactivity of the complexes. So far such studies have mainly been carried out on **1** as example. Sterically demanding Lewis bases such as the solvent THF or pyridine and *tert*-butyl isocyanide are not coordinated. Small molecules such as CO and NO, on the other hand, are bonded. NO reacts with **1** in THF to give the adduct $[Ph_3C_6H_2Cu(NO)]$ **3**. Pale yellow crystals can be crystallized from the solution. The NO ligand gives rise to a characteristic NO stretching vibration at 1740 cm^{-1} in the IR spectrum. Reaction of **1** with CO in THF leads to formation of the adduct $[Ph_3C_6H_2Cu(CO)]$ **4**, which, however, decomposes with separation of elemental copper upon slow removal of solvent by passage of CO. The IR spectrum of the solution of **4** shows the $\nu_{(CO)}$ band at 1965 cm^{-1}.

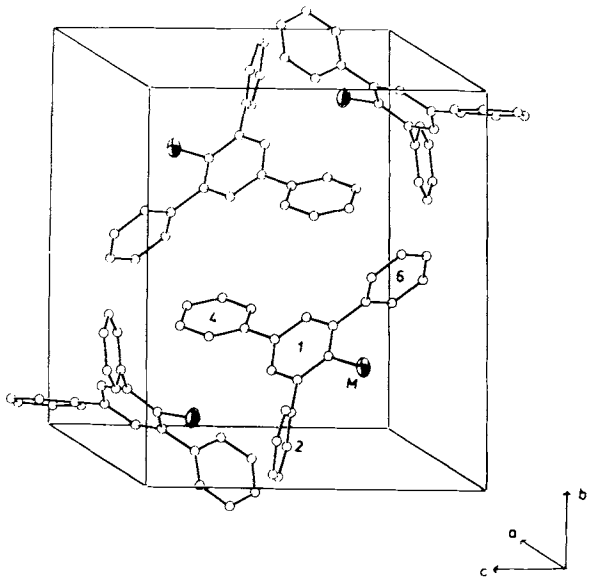

Fig. 1. Unit cell of the isotypic compounds **1** and **2** in the crystal (M = Cu and Ag, resp.). Important bond lengths [Å] and angles [°] of **1** [values for **2** in brackets]: M–C11 = 1.890(6) [1.902(5)], M–C21 = 3.185(5) [3.171(6)], M–C61 = 3.158(5) [3.214(5)]; interplanar angles: 2–1: 61.66 [61.1], 6–1: 73.73 [74.0], 4–1: 31.78 [32.4].

Experimental

1/2: The Grignard solution was treated with CuCl and AgCl respectively (2 equiv. in each case) at −80 °C in the complete absence of air and moisture.[4] The resulting white suspension was stirred for 24 h at −80 °C, slowly warmed to −10 °C, and then stirred for a further 12 h. After removal of insoluble material by filtration and evaporation of the filtrate to dryness the pale yellow crude product was dissolved in a little chloroform for crystal growing by addition of ethanol. After a few days at room temperature, colorless, transparent platelet-like crystals of **1** and **2**, respectively, were isolated (yields: 65%).

Received: December 1, 1987 [Z 2520 IE]
German version: *Angew. Chem. 100* (1988) 409

CAS Registry numbers:
1, 113088-35-8; **2**, 113088-36-1; **3**, 113088-37-2; **4**, 113088-38-3; 2,4,6-$Ph_3C_6H_2MgBr$, 36719-77-4; CuCl, 7758-89-6; AgCl, 7783-90-6; NO, 10102-43-9; CO, 630-08-0.

[*] Prof. Dr. J. Strähle, Dipl.-Chem. R. Lingnau
Institut für Anorganische Chemie der Universität
Auf der Morgenstelle 18, D-7400 Tübingen 1 (FRG)

[**] This work was supported by the Deutsche Forschungsgemeinschaft and the Fonds der Chemischen Industrie.

[***] According to the IUPAC rules the ligand should be named 5′-phenyl-*m*-terphenyl-2′-yl (Rule A54-3).

[1] S. Gambarotta, C. Floriani, A. Chiesi-Villa, C. Guastini, *J. Chem. Soc. Chem. Commun. 1983*, 1087, 1156, 1304.

[2] a) G. van Koten, J. G. Noltes in G. Wilkinson, F. G. A. Stone, E. W. Abel (Eds.): *Comprehensive Organometallic Chemistry*, Pergamon Press, Oxford 1982, *Vol. II*, Chap. 14, p. 709; b) R. J. Puddephatt, *ibid. Vol. II*, Chap. 15, p. 766; c) *ibid. Vol. II*, Chap. 14, p. 725 ff.

[3] Monoclinic, space group $P2_1/c$, $Z = 4$, $Mo_{K\alpha}$ radiation (graphite monochromator). **1**: $a = 10.657(4)$, $b = 15.083(9)$, $c = 12.526(9)$ Å, $\beta = 113.61(4)°$, $V = 1844.4$ Å^3, $\rho_{calcd} = 1.329$ g cm^3. **2**: $a = 10.636(2)$, $b = 15.105(4)$, $c = 12.534(4)$ Å, $\beta = 113.55(2)°$, $V = 1845.9$ Å^3, $\rho_{calcd} = 1.487$ g cm^{-3}. 1946 (1710) independent observed reflections with $I > 3\sigma(I)$ ($3° \le \theta \le 24°$ [$3° \le \theta \le 25°$]). The structures were solved by Patterson synthesis and refined anisotropically. All H atoms for **1** were located by difference Fourier methods and taken into account in the structure factor calculation in the refinement. In the case of **2**, the positions of all H atoms were calculated. $R = 0.041$, $R_w = 0.044$ [$R = 0.082$, $R_w = 0.107$]. Further details of the crystal structure investigation are available on request from the Fachinformationszentrum Energie, Physik, Mathematik GmbH, D-7514 Eggenstein-Leopoldshafen 2 (FRG), on quoting the depository number CSD-52835, the names of the authors, and the journal citation.

[4] W. Rundel, *Chem. Ber. 101* (1968) 2956.

$[M(CO)_4\{CH_3C(CH_2PMe_2)_3\}]$, M = Ti, Zr, Hf, Complexes of Zerovalent Titanium, Zirconium, and Hafnium. First Structural Characterization of a Zr^0-Carbonyl Complex**

By *David W. Blackburn, Kai Ming Chi, Scott R. Frerichs, Mary L. Tinkham*, and *John E. Ellis**

So far, only three carbonylzirconium(0) complexes have been described: $[Zr(C_5H_5)(CO)_4]^{\ominus}$,[1] $[Zr(C_5Me_5)(CO)_4]^{\ominus}$[2] and the thermally unstable [Zr(butadiene)$_2$(dmpe)(CO)], dmpe = 1,2-bis(dimethylphosphino)ethane.[3] We have now found that the tripodal ligand, 1,1,1-tris(dimethylphosphinomethyl)ethane (trmpe), is unusually effective in stabilizing the unknown $Zr(CO)_7$ as well as the titanium and hafnium analogues and now present the first structural characterization of a Zr^0-carbonyl, $[Zr(CO)_4(trmpe)]$. The hafnium compound $[Hf(CO)_4(trmpe)]$ is of particular interest in that it is the first zerovalent hafnium species to have been prepared without the use of a metal atom vapor reactor. Only four Hf^0compounds have thus far been reported: $[Hf(C_6H_5R)_2(PMe_3)]$, R = H, CH_3,[4] $[Hf(1,3,5\text{-}tBu_3C_6H_3)_2]$ and its carbonyl adduct.[5] All were prepared with atomic hafnium.

The procedure [Eq. (1)] used for the synthesis of the complexes $[M(CO)_4(trmpe)]$, M = Ti **1**, M = Zr **2**, M = Hf **3**, is similar to that employed in the synthesis of the aforementioned $[Zr(C_5Me_5)(CO)_4]^{\ominus}$ (THF = tetrahydrofuran, DME = 1,2-dimethoxyethane, trmpe = $CH_3C(CH_2PMe_2)_3$, $C_{10}H_8$ = naphthalene).

$$MCl_4 \cdot 2THF + trmpe + 4KC_{10}H_8 + 4CO \xrightarrow[-60\text{ to }-70\,^{\circ}C]{THF\text{ or }DME} [M(CO)_4(trmpe)] + 4KCl + 4C_{10}H_8 + 2THF \quad (a)$$

1, M = Ti
2, M = Zr
3, M = Hf

Compounds **1**–**3** were isolated as air sensitive and thermally stable (20 °C) orange-red (**1**), deep violet (**2**), and red violet (**3**) microcrystalline materials of satisfactory purity.[6] Some spectroscopic data for these materials are shown in Table 1 and indicate that all three substances are likely to have the same basic molecular geometry. Also, comparison of the IR spectra in the ν(CO) region of **2** and $[Zr(C_5H_5)(CO)_4]^{\ominus}$ (1923 (m), 1781 cm^{-1} (s))[1] reveals strong similarities but indicates that $C_5H_5^{\ominus}$ is a somewhat better donor ligand than trmpe in these systems. Additional support for the composition of **1** was obtained from the proton-decoupled ^{13}C- and ^{31}P-NMR spectra of 99% ^{13}CO-enriched $[Ti(^{13}CO)_4(trmpe)]$. These temperature-independent spectra (down to −90 °C) show the expected splitting patterns for a fluxional seven coordinate molecule in which four equivalent carbonyls are coupled to three equivalent phosphane units.[7] Exceptionally zirconium-free $HfCl_4$[8] was used in the synthesis of compound **3** to minimize its contamination by **2**. Spectral data shown in Table 1 for these two materials are sufficiently different to leave no doubt that **3** is a genuine Hf^0-carbonyl complex.

Table 1. Selected spectroscopic properties of **1**–**3**.

Compound	M	IR [a] $\tilde{\nu}$(CO) [cm^{-1}]	$^{13}C\{^1H\}$-NMR [b] δ(CO)	$^{31}P\{^1H\}$-NMR [c] $\delta(^{31}P)$
1	Ti	1931 m, 1833 sh, 1810 s	278.9 quartet	−10.6 s
2	Zr	1938 m, 1820 s	284.4 br s	−25.1 s
3	Hf	1934 m, 1814 s	282.1 br s	−29.2 s

[a] Solvent: THF for **1**, DME for **2** and **3**. [b] 85.5 MHz, 23 °C, $[D_8]$THF, $J(^{13}C\text{-}^{31}P) = 9$ Hz for **1**. [c] 121.5 MHz, 23 °C, $[D_8]$THF; uncoordinated trmpe gives a ^{31}P-NMR signal at $\delta = -61$.

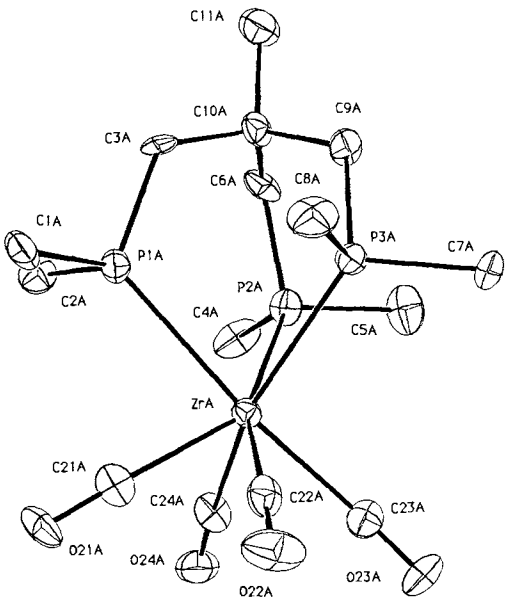

Fig. 1. ORTEP drawing of an independent molecule A of $[Zr(CO)_4(trmpe)]$ **2**. Thermal ellipsoids are drawn with 50% probability boundaries. Important interatomic distances [Å] and angles [°]: ZrA–P1A = 2.755(3); ZrA–P2A = 2.760(3); ZrA–P3A = 2.762(3); ZrA–C21A = 2.133(11), ZrA–C22A = 2.168(12); ZrA–C23A = 2.221(12); ZrA–C24A = 2.155(11); C21A–O21A = 1.182(13); C22A–O22A = 1.150(15); C23A–O23A = 1.120(14); C24A–O24A = 1.171(14); C–P (mean) = 1.83(2); C–C (mean) = 1.55(2); P1A–ZrA–P2A = 74.35(9); P1A–ZrA–P3A = 75.28(9); P2A–ZrA–P3A = 75.87(9); C21A–ZrA–C22A = 67.5(4); C21A–ZrA–C23A = 109.0(5); C21A–ZrA–C24A = 71.5(4); C22A–ZrA–C23A = 68.5(4); C22A–ZrA–C24A = 106.2(4); C23A–ZrA–C24A = 71.0(5); ZrA–C–O (mean) = 176(1).

The X-ray structural characterization of the complex $[Zr(CO)_4(trmpe)]$, **2**, revealed a unit cell containing two independent molecules of very similar structure.[9] One of these is shown in Figure 1 along with selected interatomic distances and angles. The structure may be described as a 4:3 piano stool structure,[10] and resembles that observed for $[Ti(C_5H_5)(CO)_4]^{\ominus}$,[1] where the cyclopentadienyl group is best considered a tridentate ligand. None of the interatomic distances are unusual; all are close to values obtained previously for zirconium carbonyls and phosphines. For example, in the independent molecules A and B, the respective mean Zr–C, C–O, and Zr–P distances are 2.17(4) and 2.17(3), 1.16(3) and 1.17(2), and 2.759(4) and 2.733(11), respectively. These values are similar to corresponding distances observed for $[Cp_2Zr(CO)_2]$ (mean value for Zr–C = 2.187(4) Å)[11] and $[\{(iPr_2PCH_2SiMe_2)_2N\}ZrCl_3]$ (mean

[*] Prof. Dr. J. E. Ellis, D. W. Blackburn, K. M. Chi, S. R. Frerichs, Dr. M. L. Tinkham
Chemistry Department, University of Minnesota
Minneapolis, MN 55455 (USA)

[**] Highly Reduced Organometallics, Part 24. This work was supported by the U. S. National Science Foundation and the Petroleum Research Fund administered by the American Chemical Society. *D. W. B.* thanks the NSF for a predoctoral fellowship (1986–1989).—Part 23: K. M. Chi, S. R. Frerichs, S. B. Philson, J. E. Ellis, *J. Am. Chem. Soc. 101* (1988) 303.—Note added in proof (February 17, 1988): A related complex, $[Ti(CO)_4\{tBuSi(CH_2PMe_2)_3\}]$, was reported after submission of this communication: T. G. Gardner, G. S. Girolami, *Organometallics 6* (1987) 2551.

value for Zr–P = 2.78(1) Å).[12] Somewhat shorter Zr–C and Zr–P distances have been found in $[Zr(C_5Me_5)_2(CO)_2]$ (mean value for Zr–C = 2.145(9) Å)[13] and $[Zr(C_5H_5)(PMe_3)(cyclohexyne)]$ (Zr–P = 2.689(3) Å).[14]

Since the tripodal ligand "trmpe" is readily obtained from Me_4P_2[15] and $[Zr(CO)_4(trmpe)]$ is thermally robust and available in reasonable yields (40–45%) from $ZrCl_4 \cdot 2THF$,[16] this new Zr^0-carbonyl compound and its Ti^0- and Hf^0-analogues should prove to be useful precursors for the investigation of zerovalent group 4 carbonyl metal compounds.

Experimental Procedure

$[Zr(CO)_4(trmpe)]$ **2**: 1.8 g (7.1 mmol) of trmpe was added to a cold (−30°C) solution of 2.69 g (7.14 mmol) of $ZrCl_4 \cdot 2THF$ in 100 mL of DME. A white precipitate of unknown composition formed immediately. The resulting slurry was stirred at ambient temperature for 0.5 h, cooled to −60°C, and then transferred by cannula to a mechanically stirred solution/slurry of 4.88 g (29.3 mmol) of $KC_{10}H_8$ and 3.75 g (29.3 mmol) of $C_{10}H_8$ in 150 mL DME under argon at −65°C. After 20 min, the solution had assumed a beautiful deep purple color and stirring was stopped. Argon was removed by evacuation, purified carbon monoxide was added to slightly above atmospheric pressure and stirring was resumed for 16 h at −65°C. After this time, the now deep red solution was warmed to −10°C over a 5 h period and filtered through Celite. Following removal of solvent under reduced pressure and thorough washing with pentane (2 × 200 mL; 2 × 50 mL) to remove naphthalene, 1.45 g (3.19 mmol, 45% yield) of microcrystalline dark violet **2** (decomp. at 150–153°C) was obtained which provided satisfactory analyses (C, H) without further purification. Crystals for the X-ray study were grown from pentane/CH_2Cl_2 over a six day period at −30°C. Similar syntheses starting from the corresponding $MCl_4 \cdot 2THF$ adducts provided $[Ti(CO)_4(trmpe)]$ **1** (decomp. at 163–166°C) and $[Hf(CO)_4(trmpe)]$ **3** (decomp. above 165°C, slow darkening) in 56 and about 2% yields, respectively, as thermally stable (20°C) materials which provided satisfactory elemental analyses (C, H). The yield of the hafnium compound **3** could be considerably improved (ca. 20%) by performing the low-temperature carbonylation step at about 5 atmospheres pressure of CO.

Received: December 8, 1987 [Z 2531 IE]
German version: *Angew. Chem. 100* (1988) 408

CAS Registry numbers:
1, 111379-11-4; **2**, 113035-22-6; **3**, 113035-23-7; trmpe, 77609-83-7; $TiCl_4 \cdot 2THF$, 31011-57-1; $ZrCl_4 \cdot 2THF$, 21959-01-3; $HfCl_4 \cdot 2THF$, 21959-05-7; $KC_{10}H_8$, 4216-48-2.

[1] B. A. Kelsey, J. E. Ellis, *J. Am. Chem. Soc. 108* (1986) 1344.
[2] B. A. Kelsey, J. E. Ellis, *J. Chem. Soc. Chem. Commun. 1986*, 331.
[3] R. P. Beatty, S. Datta, S. S. Wreford, *Inorg. Chem. 18* (1979) 3139.
[4] F. G. N. Cloke, M. L. H. Green, *J. Chem. Soc. Dalton Trans. 1981*, 1938.
[5] F. G. N. Cloke, M. F. Lappert, G. A. Lawless, A. C. Swain, *J. Chem. Soc. Chem. Commun. 1987*, 1667.
[6] Somewhat darker hues have been noted for the corresponding dicarbonyl(dicyclopentadienyl)metal complexes $[(C_5H_5)_2M(CO)_2]$—the Ti-complex is maroon red, the Zr-complex is black, and the Hf-complex is purple—but the color changes on proceeding from Ti to Hf for these compounds are qualitatively similar to those observed for compounds **1**–**3**. See D. J. Sikora, K. J. Moriarty, M. D. Rausch, *Inorg. Syn. 24* (1986) 147.
[7] Selected data, IR (THF, $\tilde{\nu}(^{13}CO)$ [cm^{-1}]): 1886 m, 1768 s; $^{13}C\{^1H\}$ NMR (85.5 MHz, 23°C, [D$_8$]THF): $\delta = 278.9$ (q, $J(^{13}C\text{-}^{31}P) = 9$ Hz, CO). $^{31}P\{^1H\}$ NMR (121.5 MHz, 23°C, [D$_8$]THF): $\delta = -10.7$ (quint., $J = 9$ Hz coordinated trmpe).
[8] Anhydrous $HfCl_4$ containing about 40 ppm Zr by spectrographic analysis was obtained from a commercial source (Cerac Inc., Milwaukee, WI, USA).
[9] **2** is orthorhombic, space group *Pbca* (No. 61), $a = 14.890(31)$, $b = 19.216(15)$, $c = 29.530(16)$, $V = 8449(29)$ Å^3, $Z = 16$; $\rho_{calcd} = 1.432$ g cm^{-3}; $\lambda(Mo_{K\alpha}) = 0.71073$ Å, $\mu(Mo_{K\alpha}) = 7.48$ cm^{-1}; crystal dimensions $0.05 \times 0.10 \times 0.50$ mm^3. The intensities of 3960 reflections were measured at −86°C ($0 < \theta < 24°$) on an Enraf-Nonius CAD4 diffractometer using $Mo_{K\alpha}$ radiation. The structure was solved by the heavy atom method and refined anisotropically (full-matrix least squares). For 3170 unique observed reflections [$I \geq 2.0\sigma(I)$], $R = 0.054$ and $R_w = 0.070$. Further details of the crystal structure analysis are available on request from the Director of the Cambridge Crystallographic Data Centre, University Chemical Laboratory, Lensfield Road, Cambridge CB2 1EW (England) on quoting the full journal citation.
[10] E. L. Muetterties, C. M. Wright, *Q. Rev. Chem. Soc. 21* (1967) 109.
[11] J. L. Atwood, R. D. Rogers, W. F. Hunter, C. Floriani, G. Fachinetti, A. Chiesi-Villa, *Inorg. Chem. 19* (1980) 3812.
[12] M. D. Fryzuk, A. Carter, A. Westerhaus, *Inorg. Chem. 24* (1985) 642.
[13] D. J. Sikora, M. D. Rausch, R. D. Rogers, J. L. Atwood, *J. Am. Chem. Soc. 103* (1981) 1265.
[14] S. L. Buchwald, R. T. Lum, J. C. Dewan, *J. Am. Chem. Soc. 108* (1986) 7441.
[15] G. M. Whitesides, C. P. Casey, C. Krieger, *J. Am. Chem. Soc. 93* (1971) 1379.
[16] L. E. Manzer, J. Deaton, P. Sharp, R. R. Schrock, *Inorg. Syn. 21* (1982) 136.

Template Synthesis of Macrocyclic Multiphosphane Ligands with Functional Groups**

By *David J. Brauer, Thomas Lebbe,* and *Othmar Stelzer**

Multidentate macrocyclic phosphane ligands—crown phosphanes—exhibit an unusual bonding behavior towards transition metals, which is determined by the sequence of the donor atoms.[1] Moreover, by suitable choice of substituents at the P atoms, such behavior can be controlled. These ligands, however, which are as potentially important as the known synthetic macrocyclic donor systems, have hitherto proven to be difficult to synthesize.

By exploiting the template effect[2] of Ni^{II} we have now been able to prepare a 14-membered crown phosphane with the donor sequence $P-C_2-P-C_2-P-C_3-P-C_3$ in almost quantitative yield by cyclization of a tertiary disecondary triphosphane **2** with a divinylphosphane **1**. In order to suppress formation of polymers in the reaction of **1** and **2**—which is favored even on using the dilution principle—the terminal PRH groups of **2** have to be fixed by coordination to a transition metal in a position which favors the cyclization reaction with **1** with formation of the macrocyclic ring system **3**.

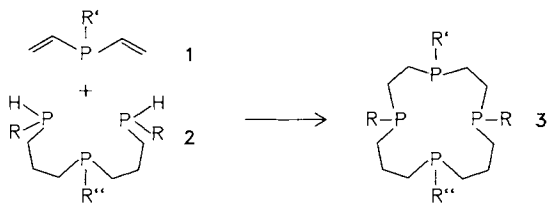

The construction of a suitable template (**5**) for the ring closure reaction was possible starting from the Ni^{II}-complex $[NiBr_2(L)]$ **4** of the tertiary disecondary triphosphane $MeHP-(CH_2)_3-PPh-(CH_2)_3-PMeH$ (L) by extrusion of an anionic halide ligand $Br^{\ominus}$ with $Et_2N-P(CH=CH_2)_2$.[3] Complexes of the type $[MX_2(L)]$ (M = Ni, Pd; X = Cl, Br) are readily accessible from the phosphane ligand L and the M^{II}-halides ($NiBr_2 \cdot 3H_2O$, K_2PdCl_4, $PdCl_2$).[4]

The intermediary formation of the template complex **5** fixes the reaction partners in close proximity. Subsequent rapid addition of the two vinyl groups of the unsaturated phosphane ligand in **5** to the terminal PMeH moieties af-

[*] Prof. Dr. O. Stelzer, Prof. Dr. D. J. Brauer, Dipl-Chem. T. Lebbe
Fachbereich 9,
Anorganische Chemie der Universität-Gesamthochschule
Gaussstrasse 20, D-5600 Wuppertal 1 (FRG)

[**] Reactions of Coordinated Ligands, Part 17. This work was supported by the Deutsche Forschungsgemeinschaft and the Fonds der Chemischen Industrie. — Part 16: G. Hasselkuss, S. Heitkamp, O. Stelzer, *Z. Anorg. Allg. Chem. 534* (1986) 50.

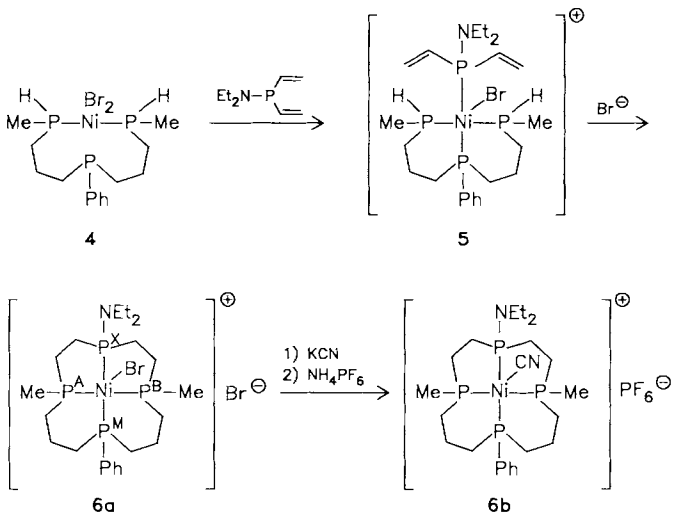

fords **6a**, the complex of a 14-membered crown-phosphane with a functional group (NEt_2), as a mixture of four diastereomers, as shown by analysis of the $^{31}P\{^1H\}$-NMR spectrum of the crude product (Table 1). The phosphorus atoms of the diastereomers I–IV represent spin systems of the type A_2MX or ABMX (A, B = PMe, M = PPh, X = $PNEt_2$). A further isomer is formed in very small amounts. The isomer III ($^{31}P\{^1H\}$-NMR spin system A_2MX) can be precipitated and recovered in pure form from the CH_2Cl_2 solution of the crude product by addition of ether.

Table 1. $^{31}P\{^1H\}$-NMR data of the complexes **6a** and **6b** (δ(P) values relative to 85% H_3PO_4 ext.; labeling of the P-atoms as in formula **6a**).

Stereo-isomer	δ P^A	P^B	P^M	P^X	^2J(PP) [Hz] AX	BX	MX	AB	AM	BM
6a I	44.8		−3.0	148.4	45.0		223		72	
II	34.9		5.4	176.6	36.0		189		64	
III	38.4		−14.2	169.1	38		216		77	
IV	19.8	24.4	7.4	173.7	35	44	256	200	77	77
6b I	55.5		−21.0	164.2	39		140		63	
II	36.9		9,7	175.5	29		172		58	
III	49.8		−21.1	155.1	35		154		76	
IV	13.2	36.7	−24.1	180.0	−19	−34	223	113	−62	68

Treatment of **6a** in aqueous solution with an equimolar amount of KCN furnishes the monocyano cation **6b**, which can be precipitated as hexafluorophosphate with NH_4PF_6. The isomer IV ($^{31}P\{^1H\}$-NMR spin system ABMX) can be obtained in pure form by recrystallization from ethanol. According to an X-ray structure analysis this isomer of **6b**[5] contains a 14-membered ring system with the donor sequences P-C_2-P and P-C_3-P, which is folded along the P(2)-Ni-P(4) edge (Fig. 1). Ni is coordinated in a distorted trigonal-pyramidal fashion, with P(2) (=*P*NEt_2) and P(4) (=*P*Ph) in the axial positions. The $CN^\ominus$ ligand, P(1), and P(3) (= 2 × *P*Me) occupy the equatorial positions. Owing to steric interaction with the NEt_2 group on P(2), the $CN^\ominus$ ligand is not symmetrically arranged between P(1) and P(3). The P(3)–Ni–C(23) angle of 102.1(2)° is markedly smaller than the P(1)–Ni–C(23) angle (140.6(2)°); this is also constistent with the large Ni–P(3) distance (2.235(1) Å).

The $PNEt_2$ moiety in **6a** permits a variety of modifications of the macrocyclic ligand system. Thus, in **6a** (used as a mixture of the isomers II and III) the NEt_2 group

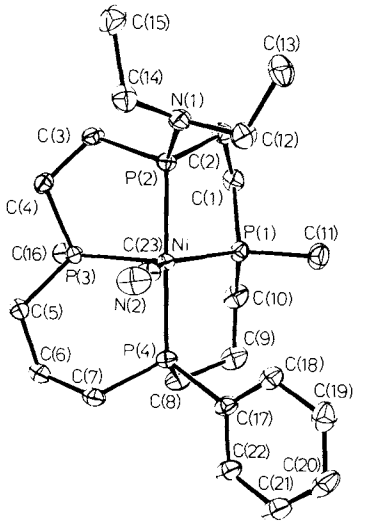

Fig. 1. Perspective view of the structure of the cation of **6b** in the crystal, without H atoms. Selected bond lengths [Å] and angles [°]: Ni-P(1) 2.173(2), Ni-P(2) 2.178(1), Ni-P(3) 2.235(1), Ni-P(4) 2.177(2), Ni-C(23) 1.910(5); P(2)-Ni-P(4) 178.87(6), P(1)-Ni-P(3) 117.17(6), P(1)-Ni-C(23) 140.6(2), P(3)-Ni-C(23) 102.1(2).

can be replaced by $Cl^\ominus$ by reaction with HCl, whereas with H_2S the NEt_2 group and the $Br^\ominus$ ligand are replaced by $HS^\ominus$. The macrocyclic phosphane ligand cannot be removed from **6a** with aqueous KCN in excess, even at elevated temperatures (80–100°C). By reaction with 10% H_2O_2, however, it is possible to convert **6a** via oxidative hydrolytic cleavage of the P–N bond into a phosphane oxide complex of the composition $Et_2NH_2[(C_{18}H_{31}P_4O_5)NiBr_2]\cdot 2H_2O$, from which the nickel can be extracted with ammonium sulfide or diacetyl dioxime.

Experimental

6a: [Bromo(4-diethylamino-1,7-dimethyl-11-phenyl-1,4,7,11-tetraphosphacyclotetradecane)nickel(II) bromide]: Solutions of $Et_2N-P(CH=CH_2)_2$ (3.53 g, 22.5 mmol) and **4** (11.36 g, 22.5 mmol) in CH_2Cl_2 (in each case 250 mL) were added dropwise at the same rate within 3h to 300 mL of CH_2Cl_2. The volume of the deep-red reaction mixture was reduced under vacuum (20°C, 0.2 mbar) to 20 mL and subsequently treated with 500 mL of ether. The brownish-yellow precipitate was filtered off and dried under vacuum (20°C, 0.02 mbar). Yield: 14.5 g (98%) of **6a** (correct elemental analyses).

Received: September 4, 1987 [Z 2423 IE]
German version: *Angew. Chem. 100* (1988) 432

CAS Registry numbers:
1, 63034-50-4; **2**, 79345-74-7; **4**, 79351-76-1; **6a**, 112896-24-9; **6b** (isomer 1), 112896-26-1; **6b** (isomer 2), 112965-95-4; $Et_2NH_2[(C_{18}H_{31}P_4O_5)NiBr_2]$, 112925-46-9.

[1] R. Bartsch, S. Hietkamp, H. Peters, O. Stelzer, *Inorg. Chem. 23* (1984) 3304; D. J. Brauer, F. Gol, S. Hietkamp, H. Peters, H. Sommer, O. Stelzer, W. S. Sheldrick, *Chem. Ber. 119* (1986) 349; L. Horner, P. Walach, H. Kunz, *Phosphorus Sulfur 5* (1978) 171; M. A. Fox, K. A. Campbell, E. P. Kyba, *Inorg. Chem. 20* (1981) 4163.
[2] G. A. Melson in G. A. Melson (Ed.): *Coordination Chemistry of Macrocyclic Compounds*, Plenum, New York 1979, p. 1ff.
[3] K. Issleib, H. Becker, *Z. Anorg. Allg. Chem. 428* (1977) 282.
[4] M. Baacke, S. Hietkamp, S. Morton, O. Stelzer, *Chem. Ber. 114* (1981) 2568.
[5] Crystallographic data of **6b**: space group $P2_1/c$, $a = 12.342(2)$, $b = 14.076(2)$, $c = 19.928(2)$ Å, $\beta = 104.92(2)°$, $Z = 4$, $\rho_{calc} = 1.428$ g cm^{-3}, Siemens AED1 diffractometer, Zr-filtered $Mo_{K\alpha}$ radiation, 5864 independent reflections, $R = 0.052$, $R_w = 0.065$ for 3975 reflections with $|F_o| \geq 4\sigma(F_o)$ and 356 parameters. Further details of the crystal structure investigation are available on request from the Fachinformationszentrum Energie, Physik, Mathematik GmbH, D-7514 Eggenstein-Leopoldshafen 2 (FRG), on quoting the depository number CSD-52841, the names of the authors, and the journal citation.

Oriented Domains and Twins in the "Tetragonal" Superconductor $LaBa_2Cu_3O_{6.7}$

By *M. Hervieu,* B. Domengès, J. Provost, F. Deslandes, B. Raveau, B. Chevalier,* and *J. Etourneau*

A recent investigation of the system La-Ba-Cu-O allowed the oxide $LaBa_2Cu_3O_{6.7}$ to be isolated as superconductor with a critical temperature close to 70 K.[1] A preliminary X-ray diffraction study[2] has shown that the structure of this oxide is different from that of the superconductor $YBa_2Cu_3O_7$,[3–9] although closely related to it. Like $YBa_2Cu_3O_7$, $LaBa_2Cu_3O_{6.7}$ can be described as an ordered oxygen-deficient perovskite. Its structure differs from that of $YBa_2Cu_3O_7$ (Fig. 1) by its tetragonal symmetry

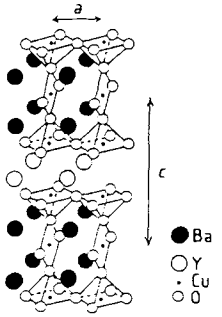

Fig. 1. Idealized representation of the structure of $YBa_2Cu_3O_7$.

involving at least a different ordering of the oxygen vacancies in the structure. Our recent high resolution electron microscopy studies[10, 13] showed that the orthorhombic superconductor $YBa_2Cu_3O_{7-x}$ is characterized by numerous twins and domains, closely related to the orthorhombic symmetry and to the orthorhombic-tetragonal phase transition. It was suggested that such domains could be correlated with the superconducting properties of this oxide. A different behavior should be expected for $LaBa_2Cu_3O_{6.7}$, owing to its tetragonal character. We report here on the results of a preliminary electron diffraction study of this oxide.

$LaBa_2Cu_3O_{6.7}$ was synthesized from $BaCO_3$, La_2O_3 and CuO as previously described.[1, 2] The sample is superconductive with midpoint resistive transition corresponding to $T_c = 70$ K. According to an X-ray structure analysis, the cell is tetragonal with $a = 3.895$ Å and $c = 11.727$ Å. The oxygen content was determined by microthermogravimetry (Setaram TAG24). The electron diffraction study was carried out with a Jeol 120 CX electron microscope fitted with a side entry eucentric goniometer ($\pm 60°$).

Most of the crystals show one or several boundaries which separate the crystals into very large domains (Fig. 2a). Most often, these domains are large enough to be characterized by selected area electron diffraction and medium resolution images, thus allowing the direction of the layer stacking ($\vec{c}$) to be displayed. The existence of two domains whose $\vec{c}$ axis are perpendicular are very often observed in the electron diffraction patterns (Fig. 2b). The weaker reflections are due to multiple diffraction phenom-

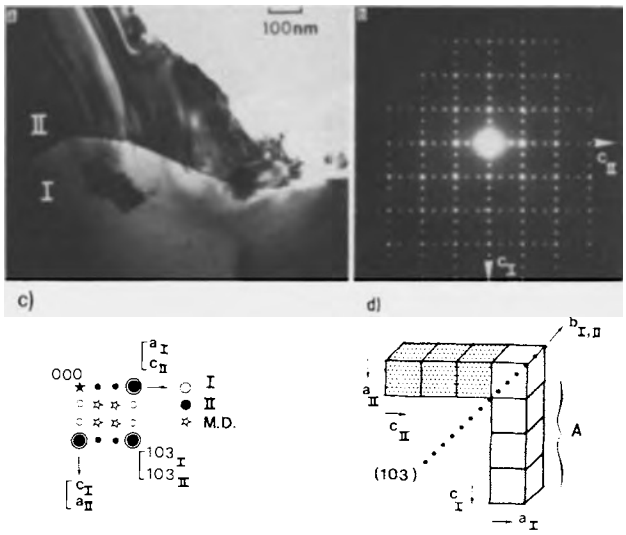

Fig. 2. a) Low-resolution electron micrographs of a crystal of $LaBa_2Cu_3O_{6.7}$; oriented domains are clearly visible. b) Electron diffraction pattern. c) Schematic representation of the electron diffraction patterns. M.D. = multiple diffraction. d) Relative orientations of the unit cells. A = Schematic cell built up from three perovskite units.

ena (Fig. 2c). Also, the [103]* direction deduced from the electron diffraction pattern is common to both domains. However, the corresponding low resolution image (Fig. 2a) shows that the boundary between the two domains does not correspond to a well-defined plane but wanders in the bulk. This type of oriented domains is labeled [103] owing to the role played by this family of planes (Fig. 2d). The same feature is illustrated in Figure 3, where a and b are the electron diffraction patterns of the domains I and II:

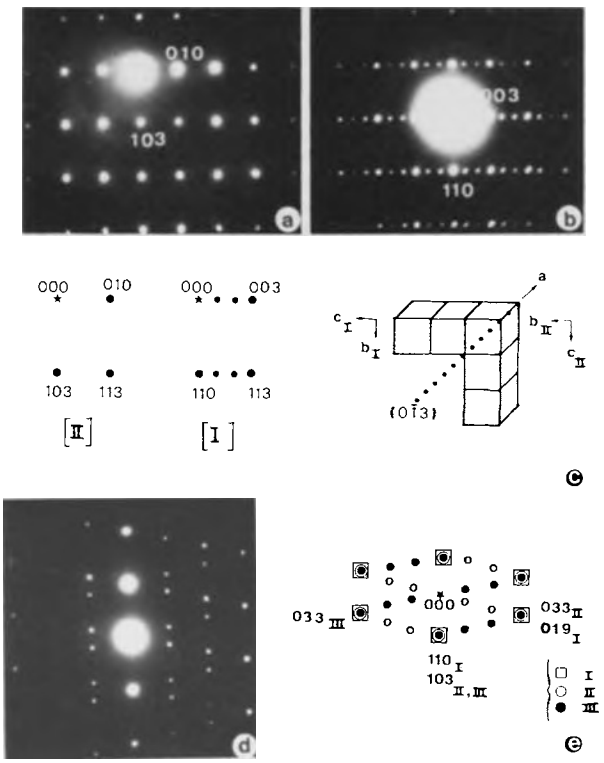

Fig. 3. a) and b) Electron diffraction patterns of domains II and I, respectively. c) Schematic drawings of the patterns (left) and the relative orientations of the unit cells (right). d) Intermediate electron diffraction pattern and e) schematic drawing.

[*] Prof. M. Hervieu, Dr. B. Domengès, Dr. J. Provost, Dr. F. Deslandes, Prof. B. Raveau
Laboratoire de Cristallographie et Sciences des Matériaux, ISMRA, Université de Caen, Campus 2, boulevard du Maréchal Juin, F-14032 Caen Cedex (France)
Dr. B. Chevalier, Prof. J. Etourneau
Laboratoire de Chimie du Solide du CNRS, Université de Bordeaux I
351 cours de la Libération, F-33400 Talence (France)

 © VCH Verlagsgesellschaft mbH, D-6940 Weinheim, 1988 0570-0833/88/0303-0440 $ 02.50/0

$[1\bar{1}0]_I$ and $[30\bar{1}]_{II}$. The schematic representation (Fig. 3c) shows the equivalent roles played by $[(110)_I$ and $(103)_{II}]$ and $[(003)_I$ and $(010)_{II}]$; in this case, the plane $(0\bar{1}3)$ is common to both domains I and II. However, from the reconstruction of the reciprocal space, it appears that the phenomenon is more complex. Indeed, the intermediate electron diffraction pattern (Fig. 3d) and its schematic representation (Fig. 3e) show that three domains (I, II and III) coexist in the bulk, and it is clear that domains II and III share the (103) plane.

The relative orientations of the unit cells and common planes between the domains are drawn schematically in Figure 4b; the corresponding low resolution image (Fig. 4a) shows the three domains and their overlapping. For the

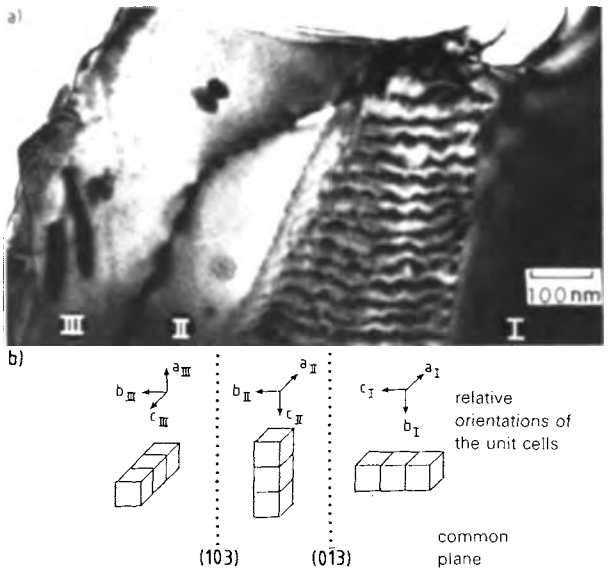

Fig. 4. a) Low-resolution electron micrograph of the crystal and b) relative orientation of the three unit cells.

particular orientation of the crystal providing the electron diffraction patterns in Figures 3a (i.e. $[30\bar{1}]_{II}$) and 3b (i.e. $[1\bar{1}0]_I$), the pattern corresponding to domain III is superimposed by the patterns of the other two domains. Such oriented domains can easily form, owing to the particular values of the parameter ratios $a/b(=1)$ and $c/3a$ (very close to 1). They correspond to the formation of a superstructure along the three perpendicular axes of the cubic perovskite subcell. This behavior is different from that observed for the superconductor $YBa_2Cu_3O_{7-x}$, for which the parameter ratios deviate significantly from 1.[3-9] However, such phenomena are often observed, especially in the oxygen-deficient perovskite[14-19] where they generally appear as localized domains.

A second group of domains has been encountered in a rather large number of crystals, which suggests that the corresponding crystals are, in fact, pseudo-tetragonal. These domains differ from those mentioned above in that they are distinctly smaller (a few 100 Å) and can thus be described as microdomains. Two types of behavior are observed: the microdomains are either stable or disappear upon slight heating by the electron beam. A large number of these domains are obviously microtwins, related to a distortion of the crystal cells; it is important to note that the amplitude of these distortions is variable and besides crystals exhibiting diffraction patterns with clearly visible splitting of the reflections (Fig. 5a) some show electron diffraction patterns and dark field images corresponding to very slight distortion of the unit cells (Fig. 5b, c). Some crystals are characterized by a more complex splitting of the reflections (Fig. 6a) in the electron diffraction patterns;

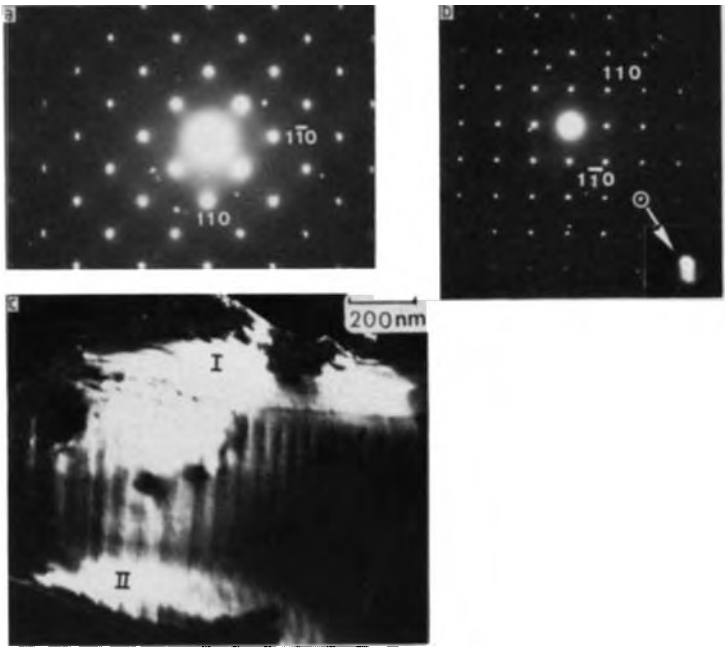

Fig. 5. a) Splitting of the reflections in the [001] pattern. b) Electron diffraction pattern along [001] and enlargement of the (220) reflection (bottom, right) of a slightly distorted crystal. c) Corresponding dark field image (domain I is not twinned).

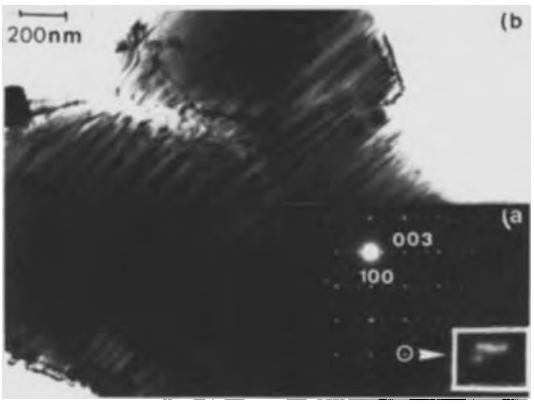

Fig. 6. a) Complex splitting of the reflections of a [010] pattern; the (303) reflection is enlarged. b) Low-resolution image.

the low resolution image (Fig. 6b) shows the corresponding microdomains and the slight misorientations observed between the different areas of the crystals; these "domains" vary upon slight heating by the electron beam. The nature of such domains is not quite clear; even if they remind one of the characteristic features of the superconductor $YBa_2Cu_3O_{7-x}$, it must be pointed out that they behave differently and that numerous distorted perovskites exhibit this type of twinning domains. Such distortions may indeed arise from local variations of the oxygen distribution (especially in the oxygen-deficient $BaO_{(1)}$ plane[2]) which

 © VCH Verlagsgesellschaft mbH, D-6940 Weinheim, 1988 0570-0833/88/0303-0441 $ 02.50/0

can lead to oriented domains and/or antiphase boundaries. High resolution electron microscopic investigations will help us elucidate these features.

Finally, numerous crystals exhibit both phenomena simultaneously (Fig. 5c); microtwins can then appear in only one of the crystal domains (domain II). Moreover, the microtwins are not observed anymore for the non-superconducting tetragonal phase $LaBa_2Cu_3O_{7-x}$, obtained from a different thermal treatment (quenched sample). This is to be compared with the absence of twinning domains for the tetragonal non-superconducting phase $YBa_2Cu_3O_{6.5}$[12, 20–23].

The preliminary electron microscopy investigations of the superconductor $LaBa_2Cu_3O_{6.7}$ thus show that this oxide is characterized, like $YBa_2Cu_3O_{7-x}$, by the presence of numerous domains, in spite of its apparent tetragonal symmetry deduced from X-ray observation. Indeed, it appears that two sorts of crystals exist in the bulk of the superconducting oxide $LaBa_2Cu_3O_{6.7}$: rigorous tetragonal crystals and distorted, presumably orthorhombic crystals which exhibit microtwins. This deviation from tetragonal symmetry observed for many crystals which could not be observed by X-ray powder diffraction is most informative: both phenomena—structural distortion and superconductivity—could be closely related.

Received: October 5, 1987 [Z 2461 IE]
German version: *Angew. Chem. 100* (1988) 403

CAS Registry number:
$LaBa_2Cu_3O_{6.7}$, 111592-75-7.

[1] C. Michel, F. Deslandes, J. Provost, P. Lejay, R. Tournier, M. Hervieu, B. Raveau, *C.R. Acad. Sci. Ser. 2, 304* (1987) 1169.
[2] M. Hervieu, N. Nguyen, C. Michel, F. Deslandes, B. Raveau, *C. R. Acad. Sci. Ser. 2, 305* (1987) 1244.
[3] C. Michel, F. Deslandes, J. Provost, P. Lejay, R. Tournier, M. Hervieu, B. Raveau, *C. R. Acad. Sci. Ser. 2 304* (1987) 1059.
[4] R. J. Cava, B. Battlog, R. B. Vandover, D. W. Murphy, S. Sunshine, T. Siegrist, J. P. Remeika, E. A. Reitman, S. Zahurak, G. P. Espinosa, *Phys. Rev. 58* (1987) 1676.
[5] Y. Lepage, W. R. McKinnon, J. M. Tarascon, L. H. Greene, G. W. Hull, D. M. Hwang, *Phys. Rev. B 35* (1987) 7245.
[6] T. Siegrist, S. Sunshine, D. W. Murphy, R. V. Cava and S. M. Zahurak, *Appl. Phys. Soc.* March Meeting in New York (1987).
[7] J. J. Capponi, C. Chaillout, A. W. Hewat, P. Lejay, M. Mareizio, N. Nguyen, B. Raveau, J. L. Soubeyroux, J. L. Tholence, R. Tournier, *Europhys. Lett. 12* (1987) 1301.
[8] L. Soderlhom, *2nd Int. Conf. Chem. Tech. Lanthanides and Actinides*, Lisbon, April 8, 1987.
[9] B. Raveau, *2nd Int. Conf. Chem. Tech. Lanthanides and Actinides*, Lisbon, April 8, 1987.
[10] M. Hervieu, B. Domengès, C. Michel, G. Heger, J. Provost, B. Raveau, *Phys. Rev. B 36* (1987) 3920.
[11] G. Roth, D. Ewert, G. Heger, M. Hervieu, C. Michel, B. Raveau, F. D'Yvoire, A. Revcolevschi, *Z. Phys. B 69* (1987) 21.
[12] G. Roth, B. Renker, G. Heger, M. Hervieu, B. Domengès, B. Raveau, *Z. Phys. B 69* (1987) 53.
[13] M. Hervieu, B. Domengès, C. Michel, J. Provost, B. Raveau, *J. Solid State Chem. 71* (1987), in press.
[14] A. Reller, J. M. Thomas, D. A. Jefferson, M. K. Uppal, *Proc. R. Soc. A 394* (1984) 223.
[15] T. J. White, R. L. Segall, J. C. Barry, J. L. Hutchison, *Acta Crystallogr. B 41* (1985) 93.
[16] V. Caignaert, *Thesis*, Caen 1986.
[17] V. Caignaert, M. Hervieu, N. Nguyen, B. Raveau, *J. Solid State Chem. 62* (1986) 281.
[18] V. Caignaert, M. Hervieu, B. Raveau, *Mater. Res. Bull. 21* (1986) 1147.
[19] V. Caignaert, M. Hervieu, J. M. Greneche, B. Raveau, *Chem. Scri.*, in press.
[20] G. van Tendeloo, HW. Zandvergen, S. Amelynckx, *Solid State Commun.*, in press.
[21] H. W. Zandbergen, G. van Tendeloo, T. O. Kabe, S. Amelinckx, *Phys. Status Solidi A*, in press.
[22] B. Raveau, C. Michel, M. Hervieu in: *Chemistry of High-Temperature Superconductors (ACS Symp. Ser. 351* (1987)), p. 122.
[23] B. Domengès, M. Hervieu, V. Caignaert, B. Raveau, J. L. Tholence, R. Tournier, J. Microsc. Spectrosc. Electron., in press.

Synthesis, Structure and Bonding of $[Cl_2Sn\{Rh(PMe_3)_3Cl\}_2]\cdot THF$, an Unusual Sn^{II}-Rh^{I} Adduct**

By *Dominic M. T. Chan** and *Todd B. Marder**

It has long been known that Group 8 transition metal complexes react with tin(II) halides to produce effective catalysts for hydrogenation, hydroformylation and isomerization.[1, 2] Although there has been intense interest in these systems, the exact nature of the active catalysts still remains uncertain. It is therefore of interest to examine possible geometries and bonding modes available to Sn^{II} adducts of group 8 metals.

Two recent studies of the reaction of $SnCl_2$ with *trans*-$[M(PR_3)_2(CO)Cl]$ complexes ($M=Ir$[3] and $M=Rh$[4]) in which unusual 1:1 (Ir:Sn) and 2:2 (Rh:Sn) adducts were obtained respectively and a study[5] of Ir^{I}_2–Pb^{II}- and I^{I}_2–Tl^{I}-adducts prompt us to report the syntheses and structural characterization of the first Lewis acid-base adducts involving one $SnCl_2$ and *two* L_3MCl units ($M=Rh$, Ir; $L=PMe_3$). In contrast to the previously reported Rh_2- and Ir_2-complexes[4, 5] in which the two Rh or Ir centers are constrained by a pair of bridging phosphane ligands, the adducts reported herein do not arise from any such constraints. We also discuss the bonding interactions between formal Sn^{II} and Rh^{I}, Ir^{II} centers in light of the observed structure of the Rh_2Sn adduct.

$SnCl_2$ reacts readily and cleanly with 2 equivalents of $[Rh(PMe_3)_3Cl]$, **1a**, at room temperature in THF to produce an intense purple solution. Evaporation of solvent results in an 89% yield of the diamagnetic complex $[Cl_2Sn\{Rh(PMe_3)_3Cl\}_2]$, **2a**,[6] as crystals which appear red by transmitted light and green by reflected light. Similarly, reaction of $SnCl_2$ with 2 equivalents of [Ir(cyclooctene)-$(PMe_3)_3Cl$][7], **1b**, gives a blue solution from which a 97% yield of $[Cl_2Sn\{Ir(PMe_3)_3Cl\}_2]$, **2b**,[6] was obtained [Eq. (a)].

$$2\,L_nMCl + SnCl_2 \longrightarrow [Cl_2Sn\{M(PMe_3)_3Cl\}_2] \qquad (a)$$

1a, $M=Rh$, $L_n=(PMe_3)_3$ **2a**, $M=Rh$
1b, $M=Ir$, $L_n=(C_8H_{14})(PMe_3)_3$ **2b**, $M=Ir$

A single-crystal X-ray diffraction study of the Sn–Rh adduct[8] confirms our structural assignment for **2a** (Fig. 1). The Rh_2SnCl_2 moiety adopts a highly distorted geometry, neither tetrahedral nor trigonal bipyramidal at tin, with essentially no interaction between the two rhodium atoms (d(Rh-Rh) = 5.1 Å). The P_3RhCl units are slightly pyramidalized with the Rh atom located 0.33 Å above the least square plane defined by the chlorine and phosphorus atoms.[9]

No adduct formation was observed between $SnCl_2$ and other complexes such as $[Rh(PPh_3)_3Cl]$[10] and

[*] Prof. T. B. Marder [+], Dr. D. M. T. Chan [++]
Central Research and Development Department
E. I. Du Pont de Nemours and Company, Experimental Station
Wilmington, DE 19898 (USA)

[+] New address:
The Guelph-Waterloo Centre for Graduate Work in Chemistry
Waterloo Campus, Department of Chemistry
University of Waterloo
Waterloo, Ontario N2L 3G1 (Canada)

[++] New address: Imaging Systems Department Research and Development Division E. I. DuPont de Nemours and Company, Experimental Station Wilmington, DE 19898 (USA)

[**] We gratefully acknowledge the technical assistance of *J. Feaster, B. West, M. A. Cushing, Jr.* and Molecular Structure Corporation. We also thank Dr. *D. L. Thorn* for many helpful suggestions concerning the bonding.

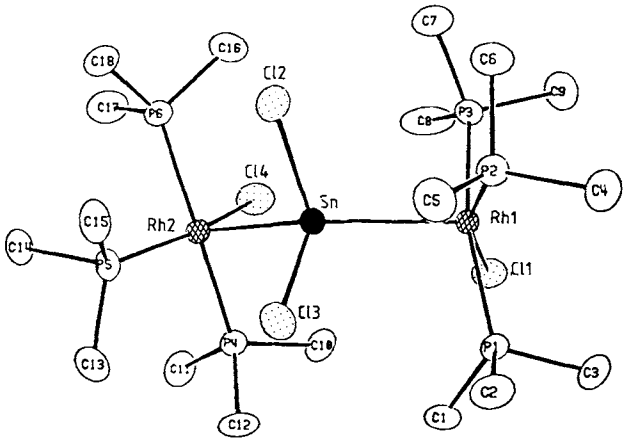

Fig. 1. Perspective drawing of the structure of $[Cl_2Sn\{Rh(PMe_3)_3Cl\}_2]$ in the crystal of **2a**. THF (thermal ellipsoids at the 30% probability level). The THF molecule and hydrogen atoms have been omitted for clarity. Selected distances [Å], Sn–Rh(1) = 2.712(1), Sn–Rh(2) = 2.721(1), Rh(1)–Cl(1) = 2.417(2), Rh(2)–Cl(4) = 2.420(2), Sn–Cl(2) = 2.557(2), Sn–Cl(3) = 2.543(2), and angles [°], Rh(1)–Sn–Rh(2) = 142.52(3), Cl(2)–Sn–Cl(3) = 92.28(9), P(1)–Rh(1)–Sn = 100.81(6), Cl(1)–Rh(1)–P(2) = 159.04(9).

$[Ir(PEt_3)_3Cl]$.[7] Reaction of Sn^{II}-halides with a ligated d^8 metal halide often result in the insertion of Sn^{II} into the metal-halide bond to produce a trihalogentin complex[4, 10] [Eq. (b)]. Formation of simple Rh_2–Sn and Ir_2–Sn adducts is apparently unique to the trimethylphosphane ligand system.[11] Thus, both high electron density and lack of steric hindrance around the metal center are essential for successful complexation.

$$L_nMX + SnX_2 \longrightarrow [L_nM{-}SnX_3] \qquad (b)$$
$M = Rh^{I}, Ir^{I}, Pt^{II}$; X = Cl, Br

The bonding between Rh and Sn in **2a** requires some comment. A valence bond approach yields two extreme models for the Rh–Sn interactions. Thus, the Rh^0 units each possess filled dz^2 orbitals capable of σ-donation to an empty p orbital on Sn^{II}. This would result in Sn having ten valence electrons; a TBP structure involving a linear Rh–Sn–Rh arrangement and an equatorial lone pair on Sn might be expected. However, the Cl–Sn–Cl and Rh–Sn–Rh angles (92.28° and 142.6° respectively) combined with the pyramidization at Rh are not consistent with this simple model. The other extreme would involve sp^3 hybridization at Sn producing two orbitals with a total of two electrons which could be used to form an electron deficient 2e,3c bonding arrangement with the symmetry adapted linear combinations of the two vacant Rh $5p_z$ orbitals. This would lead to a tetrahedral geometry at Sn with an Rh–Sn–Rh angle near 109°. Clearly, neither model suffices to explain the novel structure for **2a**. The bonding picture is most likely intermediate between the two extremes, i.e. some degree of participation of both filled Th $4d_{z^2}$ and empty Rh $5p_z$ orbitals. Preliminary results of molecular orbital calculations combined with a careful examination of the structural models outlined above suggest that the extreme cases may be precluded by severe steric interactions. The extreme oxygen sensitivity of **2a**, **b** indicates their electron-rich nature (i.e. high-lying HOMO) and the absorption spectra[6] indicate a low-lying allowed electronic transition. Further synthetic studies and molecular orbital calculations (extended Hückel and SCF-Xα) are underway to elucidate the bonding, spectra and reactivity of the novel complexes.

Received: October 9, 1987 [Z 2471 IE]
German version: *Angew. Chem. 100* (1988) 436

CAS Registry numbers:
1a, 36103-64-7; **1b**, 59390-28-2; **2a**·THF, 112988-71-3; **2b**, 112988-72-4; Rh, 7440-16-6; Sn, 7440-31-5; Ir, 7439-88-5.

[1] K. A. Ostoja Starzewski, P. S. Pregosin in E. C. Alyea, D. W. Meek (Eds.): *Catalytic Aspects of Metal Phosphine Complexes*, American Chemical Society, Washington 1982, p. 23, and references cited therein; G. K. Anderson, H. C. Clark, J. A. Davies, *Inorg. Chem. 22* (1983) 427, 434; G. K. Anderson, C. Billard, H. C. Clark, J. A. Davies, C. S. Wong, *ibid. 22* (1983) 439

[2] H. Moriyama, T. Aoki, S. Shinoda, Y. Saito, *J. Chem. Soc. Perkin Trans. 2 1982*, 369; A. V. Romanenko, V. L. Kuznetsov, A. P. Shepelin, V. I. Zaikovskii, P. A. Zhdan, L. M. Plyasova, Y. Z. Yermakov, *React. Kinet. Catal. Lett. 21* (1982) 55; H. Singer, J. D. Umpleby, *Tetrahedron 28* (19/82) 5769; J. Kasper, R. Spogliarich, M. Graziani, *J. Organomet. Chem. 231* (1982) 71.

[3] M. Kretschmer, P. S. Pregosin, *Inorg. Chim. Acta 61* (1982) 247.

[4] A. L. Balch, H. Hope, F. E. Wood, *J. Am. Chem. Soc. 107* (1985) 6936.

[5] A. L. Balch, J. K. Nagle, M. M. Olmstead, P. E. Reedy, Jr., *J. Am. Chem. Soc. 109* (1987) 4123.

[6] **2a**: ^1H NMR (360 MHz, [D$_8$] toluene): δ = 3.55 (m, 4 H, THF), 1.56 (bt, J_{PH} = 4 Hz, 36 H, PMe_3), 1.45 (m, 4 H, THF), 1.41 (bd, J_{PH} = 9 Hz, 18 H, PMe_3). ^{13}C NMR (100 MHz, [D$_8$] THF): δ = 22.50 (d, J_{PC} = 30 Hz), 19.00 (t, J_{PC} = 15 Hz). ^{119}Sn NMR (149 MHz, THF): δ = 473.3 (bs, width at half height = 450 Hz). ^{31}P NMR (121.7 MHz, [D$_8$] toluene): δ = 4 75 (d of t, J_{RhP} = 165 Hz, J_{PP} = 36 Hz, 1 P). −9.53 (d of d, J_{RhP} = 116 Hz, J_{PP} = 36 Hz, 2 P) m.p. 160–200 °C (decomp). UV/VIS: λ_{max}(THF) = 550.7 nm (ε = 83,500). **2b**: ^1H NMR (360 MHz, [D$_8$] toluene): δ = 3.55 (m, 4 H, THF), 1.67 (bt, J_{PH} = 3.5 Hz, 36 H), 1.61 (bd, J_{PH} = 9.5 Hz, 18 H), 1.45 (m, 4 H, THF). ^{13}C NMR (100 MHz, [D$_8$] THF): δ = 23.60 (d, J_{PC} = 39 Hz), 19.12 (t, J_{PC} = 17.5 Hz). ^{31}P NMR (121.7 MHz, [D$_8$] toluene): δ = 27.73 (d, J_{PP} = 24 Hz, 2 P), −44.41 (t, J_{PP} = 24 Hz, 1 P). m.p. 160 °C (decomp). UV/VIS: λ_{max}(THF) = 581 nm (ε = 16,000).

[7] T. Herskovitz, unpublished results.

[8] **2a**·THF: $C_{22}H_{62}Cl_4OP_6Rh_2Sn$; 994.89: needle-like crystals were obtained by slow evaporation from benzene; monoclinic; C_2^5-P_{2_1} (No. 7); a = 10.296(5), b = 15.628(7), c = 12.960(3) Å; β = 98.41(3)°; V = 2063(3) Å^3; Z = 2; $\rho_{(calcd)}$ = 1.60 g cm^{-3}. Enraf Nonius CAD 4 diffractometer; $Mo_{K\alpha}$ radiation (λ = 0.71073 Å), graphite monochromator; 23 ± 1°; $2 \leq 2\theta \leq 50°$; 3609 reflections; no absorption correction was made, μ = 18.7 cm^{-1}; solution and refinement (PDP-11/60 based TEXRAY System): The structure was solved by direct methods which yielded the positions of the three heavy atoms. The remaining atoms were located in succeeding difference Fourier syntheses. Hydrogens were included in calculated positions (assuming idealized geometry with C–H = 0.95 Å, B_H = 6.0) and were not refined. Full least squares refinement, 324 variables, 3177 observations [$|F_0|^2 > 3\sigma(F_0^2)$], R = 0.027, R_w = 0.034; Fourier residuals 0.55 e$^{\ominus}$ Å^{-3}. Crystallographic analysis performed by Molecular Structure Corporation, College Station, TX (USA).—Further details of the crystal structure investigation are available on request from the Fachinformationszentrum Energie, Physik, Mathematik GmbH, D-7514 Eggenstein-Leopoldshafen 2 (FRG) on quoting the depository number CSD-52816, the names of the authors, and the journal citation.

[9] For the synthesis and X-ray structure of **1a**, see: R. A. Jones, F. M. Real, G. Wilkinson, A. M. R. Galas, M. B. Hursthouse, K. M. A. Malik, *J. Chem. Soc. Dalton Trans. 1980*, 511.

[10] J. F. Young, R. D. Gillard, G. Wilkinson, *J. Chem. Soc. 1964*, 5176; D. P. Krut'ko, A. B. Permin, V. S. Petrosyan: Abstracts of Papers, *4th Int. Symp. Homogeneous Catalysis*, Leningrad, USSR, September 1984; PI-63.

[11] Our complex *may* be considered to be related to the reported $[SnX_2(NMe_3)_2]$ system (C. C. Hsu, R. A. Geanangel, *Inorg. Chem. 16* (1977) 2529.

Organoselenium and Organotellurium Chemistry in an Up-Current

Organic compounds containing selenium and tellurium have been known since the middle of last century, but because they have been found to be mostly evil-smelling and toxic, and often obtainable in pure form only with difficulty, they have been relegated to the small print of the textbooks. Only during the last two decades have organoselenium compounds, like modern organometallic transition metal reagents, established themselves as important tools in organic synthesis. Modern organoselenium chemistry began around 1973/1974, at the same time as the publication of two basic monographs by *Klayman* and *Günther* (Wiley, 1973) and *Zingaro* and *Cooper* (Van Nostrand Reinhold, 1974), and also of the standard work on organotellurium chemistry by *Irgolic* (Gordon and Breach, 1974). The volumes reviewed here, namely

Selenium Reagents and Intermediates in Organic Synthesis. By *C. Paulmier*. Pergamon Press, Oxford 1986. xiii, 463 pp., paperback, $ 30.00.—ISBN 0-08-032485-1

The Chemistry of Organic Selenium and Tellurium Compounds, Vol. 1. Edited by *S. Patai* and *Z. Rappoport*. Wiley, Chichester 1986. xiv, 939 pp., bound, £ 150.00.—ISBN 0-471-90425-2

Organoselenium Chemistry. Edited by *D. Liotta*. Wiley, Chichester 1987. ix, 422 pp., bound, $ 62.25.—ISBN 0-471-88867-2

are evidence of the much increased interest in organoselenium and organotellurium reagents that has arisen during the past 15 years. The main reason for this is summarized by *Sir Derek Barton* in his preface to *Paulmier*'s book: although organoselenium reagents are in general more costly and more toxic than the corresponding sulfur compounds, they react under much milder conditions. For example, selenolate ions are better nucleophiles, and can be more easily introduced by substitution reactions; selenenyl chlorides are easier to handle and react more effectively with enolates. Mild reaction conditions are especially important in reactions of unsaturated molecules with various functional groups, e.g. in natural products chemistry. Some organoselenium reagents also fulfil the needs which arise nowadays with regard to chemo-, regio- and stereoselectivity.

The decrease in bonding strength in the series S—Se—Te leads to reduced stability in certain selenium and tellurium compounds, e.g. those with small rings, or molecules with C=Se or C=Te bonds. However, it is exactly this behavior which is often useful in organic synthesis, as shown, for example, by the ease of the RSe/Li exchange in selenoacetals, or in epoxide ring opening followed by spontaneous loss of selenium or tellurium.

The book by *Paulmier* is aimed at preparative organic chemists. The book, written in a fluent style, begins with a short outline describing classes of compounds, commercially available selenium reagents, and the *inorganic selenium reagents* of greatest importance for organic chemists. The preparation and reactions of organoselenium functional groups are described in Chapters II to VI. I especially like the treatment of their reactive properties, e.g. the sections on *syn* elimination (p. 132 onwards), and on the 2,3-sigmatropic rearrangements of allylic selenium oxides (p. 143 onwards). Equally useful are the systematically organized chapters on addition reactions (VII), addition reactions with cyclization (VIII), oxidation reactions (XII), and reduction reactions (XIII), the latter including special reactions using elemental selenium, alkali metal selenolates and COSe. The chemistry of selenium substituted carbocations is outlined briefly, and Chapter IX is devoted to carbanions; the main features of selenocarbonyl chemistry are also clearly presented.

As the title of the book indicates, *Paulmier* is mainly concerned with synthetic aspects, and limits the discussions about structure, bonding and spectroscopic data to what is essential. This leads to a pleasingly concise treatment, which after covering the serious business of the book still leaves room for a more relaxed chapter (XIV) on special structures, natural products and biologically active compounds. In this chapter *Paulmier* also describes examples of syntheses to illustrate the methodology of organoselenium chemistry.

Literature references, which are mainly to work published in the period 1974–1984, are included with each chapter, and there are useful author and key word indexes. Although the book has been prepared by photoreproduction of the original typescript, the text (supported by clear structural formula diagrams and reaction schemes) is easy to read—it is well worth buying!

Volume 1 of the two-volume work "The Chemistry of Organic Selenium and Tellurium Compounds", edited by *Patai* and *Rappoport*, is not in competition with *Paulmier*'s book, as it is totally different in concept. Following the general pattern of this series "The Chemistry of Functional Groups", the 18 chapters by recognized experts deal with the topics in greater depth. This has resulted in a comprehensive compilation of material in which some of the individual chapters are monographs in themselves. Following the guidelines laid down by the editors, most of the authors have concentrated on the latest developments rather than aiming at completeness. However, two particularly comprehensive articles are the one of nearly 100 pages on structural chemistry by *I. Hargittai* and *B. Rozsondai*, which may serve as a Se/Te sequel to *Hargittai*'s book on the structures of volatile sulfur compounds, and that of more than 170 pages on complexes with Se and Te ligands, by *H. J. Gysling*, which is superbly compiled, and is a mine of information for inorganic chemists. Other highlights are contributions on NMR and ESR spectroscopy, mass spectrometry, analysis, heterocycles, and directing and activating effects. The articles on functional groups with Se and Te in various oxidation states (*N. Sonada* and *A. Ogawa*) and on derivatives of Se and Te with valencies of four or more (*J. Bergmann, L. Engman*, and *J. Sidén*) include synthetic applications, but the complete treatment of synthetic methods and applications is not due to appear until the publication of Volume 2[*]. The two volumes together will certainly constitute an indispensable, but unfortunately

[*] Volume 2 appeared late in 1987:
The Chemistry of Organic Selenium and Tellurium Compounds. Vol. 2. Edited by *S. Patai*. Wiley, Chichester 1987. xiv, 864 pp., bound, £ 140.00.—ISBN 0-471-91020-1

very expensive, handbook on organoselenium and organotellurium chemistry. It is to be welcomed, since this subject has not been covered in "Comprehensive Organometallic Chemistry". It is an advantage to have selenium and tellurium chemistry treated together, with frequent comparisons of structure and reactivity in the S—Se—Te series. This helps the reader to understand the basic trends and relationships in Main Group VI, and contributes to the systematization of our knowledge.

Liotta's "Organoselenium Chemistry", which is likewise published by Wiley, consists of nine review articles, dealing with the electrophilic, nucleophilic and free radical reactions of organoselenium compounds, their oxidation reactions, and the chemistry of selenium-containing carbanions and organic conductors. These specialized aspects of selenium chemistry are very well described (e.g. in the article by *H. J. Reich* on selenoacetals, carbanions and sigmatropic rearrangements). However, the book as a whole is by no means an alternative to Volume I of the *Patai* series, especially as the excellent contributions by *T. G. Back* on electrophilic and free radical reactions, and by *F. S. Guziec* on selenocarbonyls, in the book edited by *Liotta*, are to be followed by articles from the same authors in Volume 2 of *Patai/Rappoport*[*].

Wolf-Walther du Mont [NB 857 IE]
Fachbereich Chemie
der Universität Oldenburg (FRG)

Tin in Organic Synthesis. By *M. Pereyre, J.-P. Quintard,* and *A. Rahm.* Butterworths, London 1986. 342 pp., bound, £ 50.00.—ISBN 0-408-01435-0

This book, containing 17 chapters, is divided into four parts: Part I is an introduction, containing two chapters. Part II concerns the reduction of various functional groups with tin hydrides, each of five chapters treating a different functional group. Part III covers the synthetic applications, including chapters on the cleavage of tin-carbon bonds by various reagents, transmetallation reactions (primarily for the synthesis of organolithium reagents) and the coupling reactions of organotin reagents in the formation of carbon-carbon bonds. Part IV covers syntheses involving tin-heteroatom bonds in seven chapters. The references are collected at the end of each part (rather than at the end of each chapter). There is an excellent compilation of references on organotin chemistry. Unfortunately the references cover only through 1984 (with a few 1985 references) so there is a two year gap between writing and publication at a time when the field was undergoing an explosive development. A few noteworthy books and references on the synthesis of tin compounds have not been listed in the references for Part I. With these exceptions, the references are quite inclusive.

All areas of tin reagents in organic synthesis have good coverage, with the possible exception of the synthesis of certain organostannanes in Part I. For example, the reaction of tin amides with monosubstituted acetylenes to yield tin acetylides and the mild, palladium catalyzed reaction of hexaalkylditins with vinyl and aryl halides to yield vinyl- and arylstannanes are omitted. Perhaps too much coverage was given to desulfurization reactions of xanthates with tin hydrides and on the benzylation, acylation and alkylation of sugars. The discussion of radical cyclization reactions in Chapter 3 could have been made more coherent and presented more clearly by utilizing the framework of Baldwin's rules.

In most of the book the chemistry is easy to follow. In some chapters, however, the material is not as logically organized as it could be, and this leads to a somewhat disjointed presentation. In some places the equations are not adequately explained and consequently are not readily understood. In many cases, results from the literature are given without comment or a critical evaluation of the results; occasionally the equation for an unusual reaction is presented without comment or speculation as to the mechanism. To include this kind of commentary, however, is a formidable task, so it is understandable that the authors chose not to do so. In other chapters, the chemistry becomes repetitive such that it possibly would have been better to include tables rather than going through example after example, each with an equation and verbal explanation.

There are relatively few mistakes and inconsistencies, most of which will be apparent to organic chemists.

Overall, I highly recommend this book both for those involved in organotin chemistry and in general organic chemistry. It not only serves as an excellent text for introducing organotin chemistry, but also is an excellent reference source. It is the only book of its kind available.

John K. Stille [NB 856 IE]
Department of Chemistry
Colorado State University
Fort Collins, CO 80523 (USA)

Fine Chemicals for the Electronics Industry. By *P. Bamfield.* The Royal Society of Chemistry, London 1986. v, 247 pp., bound, £ 27.50.—ISBN 0-85186-636-0

This book contains 14 papers presented at a specialist symposium in April 1986, and provides a good insight into the manufacture of chemicals for high-technology applications. Although each of the papers relates to a specialist topic, the combined effect provides an excellent and nearly up-to-date picture of this fascinating branch of materials science. In addition to the more conventional materials such as luminescent substances, the topics covered include newer ones such as optical fibers, ceramics and semiconductors, including materials used in solar energy conversion. It is pleasing that the materials discussed include not only inorganic, but also organometallic and organic substances. The interaction between manufacturing technology and the requirements to be met for different applications (including those concerning purity) comes out very clearly. It would have been helpful to have a little more information under the topic "Sampling and Analysis", including the techniques and their limitations, e.g. limits of detection. The chemistry involved in the applications is explained more effectively than the chemical manufacturing processes, owing to the more informative diagrams provided in the former case.

Nearly every contribution illustrates the complexity of the materials problems nowadays encountered in the area of advanced technology. In almost every case one is concerned with high value products which are used only in relatively small quantities. Some discussion of the international competitive situation, and of the availability of raw materials, would have been useful, but would have gone beyond the scope of the report.

A clear impression emerges that much of this high-technology business still relies to a very large extent on providing tailormade systems designed on an empirical basis for specific applications. Many such areas are still at a development stage, and one cannot yet predict the final out-

come. How quickly the state of knowledge can change in these areas is strikingly illustrated by the topic "Superconducting Materials", where already now, only a year and a half after the symposium, a new era has begun. It is also clearly evident that here, more than in most other areas of knowledge, there is a close interaction between materials science research, development and production, which calls for much interdisciplinary work. Just as the papers from this symposium deal with levels of purity which were inconceivable 20 years ago, so one might envisage that the next 20 years will see the development of a materials scene altered beyond recognition from that of today.

Ulrich Wiese [NB 870 IE]
Wacker-Chemitronic GmbH,
Burghausen (FRG)

Organosilicon Chemistry. By *S. Pawlenko*. W. de Gruyter, Berlin 1986. xi, 186 pp., bound, DM 180.00.—ISBN 3-11-010329-X

According to the preface the aim of this monograph is to give an account of the organic chemistry of silicon for industrial and academic chemists. A brief glance through the list of contents reveals straight away that the book is not much concerned with the uses of organosilicon compounds for organic synthesis, as one might have assumed from its title. Instead there is a strong emphasis on systems containing a silicon-heteroatom bond, with the remaining silicon valences being usually occupied by alkyl or aryl groups, which, of course, can therefore be regarded as organic compounds. Nevertheless, the majority of the reactions described belong more to inorganic than to organic chemistry, even though organic chemists will find them of interest and may occasionally use them.

The first short chapter (12 pages) introduces the reader to the bonding properties of silicon. However, the discussion of the Si-C bond does not include the simple but useful rules as formulated by *Fleming*, which make it easier to understand the chemistry of organosilicon compounds. The industrial production of the basic chemicals concerned is touched upon only briefly, in Chapter 2. The main part of the book (Chapter 3, approx. 90 pages) deals with the preparation and properties of more specialized organosilicon compounds. A considerable amount of information is collected here on compounds of silicon with nearly all the other elements of the Periodic Table. It is, of course, very useful to have a review of the most important results in this field, but it is questionable whether boiling points (with pressures given both in Pa and in mm Hg), melting points, and in some cases details of the preparative procedure, should also be included in a comparatively slim book such as this.

Chapter 4 is devoted to the uses of organosilicon compounds in industry, organic synthesis, and medicine. The synthetic uses of silicon-containing precursors are dealt with in about 15 pages, with in addition a few of the most important reactions being described in the previous chapter. This compression of the topic made it especially important to choose representative examples carefully, so as to illustrate the principles, but such a choice has regrettably not been achieved. The activation (and deblocking) of organosilicon compounds by flouride ions receives practically no attention. The particular affinity of silicon towards fluorine is not mentioned, and in equation 4.29 the essential tetrabutylammonium fluoride is omitted. Again, the discussion of Lewis acid induced reactions fails to point out the general principles involved. The author classifies silyl enol ethers as *protected* carbonyl compounds, despite the importance of their activation for selective reactions with electrophilic reagents, which is in fact described in some of the examples. It is astonishing that none of *Mukaiyama*'s work is cited, and that other pioneers in this field (*Reetz, Fleming, Magnus, Paquette* ...) are ignored or barely mentioned. The index entry Peterson olefination does not appear at all.

The final chapter on analytical methods is again very informative, but on the whole the impression remains that it is scarcely possible in about 150 pages to effectively cover such a large field as organosilicon chemistry has now become. Anyone whose main need is for information on applications to organic synthesis will not get his money's worth from this book. For that purpose there are better and less expensive alternatives (the price of about DM 1.— per page is at a level seldom reached by other publishers).

Hans-Ulrich Reißig [NB 837 IE]
Institut für Organische Chemie und Biochemie
der Technischen Hochschule Darmstadt (FRG)

Registered names, trademarks, etc. used in this journal, even when not marked as such, are not to be considered unprotected by law.

© VCH Verlagsgesellschaft mbH, D-6940 Weinheim, 1988. - Printed in the Federal Republic of Germany by Zechnersche Buchdruckerei, Speyer/Rhein.

All rights reserved (including those of translation into foreign languages). No part of this issue may be be reproduced in any form - by photoprint, microfilm, or any other means - nor transmitted or translated into a machine language without written permission from the publishers. Only single copies of contributions, or parts thereof, may be made for personal use.

Valid for users in the USA: The appearance of the code at the bottom of the first page of an article in this journal (serial) indicates the copyright owner's consent that copies of the article may be made for personal or internal use, or for the personal or internal use of specific clients. This consent is given on the condition, however, that the copier pay the stated per-copy fee through the Copyright Clearance Center, Inc., for copying beyond that permitted by Sections 107 or 108 of the U.S. Copyright Law. This consent does not extend to other kinds of copying, such as copying for general distribution, for advertising or promotional purposes, for creating new collective works, or for resale. For copying from back volumes of this journal see 'Permissions to Photo-Copy: Publisher's Fee List' of the CCC.

Editorial office: Pappelallee 3, D-6940 Weinheim, Federal Republic of Germany, Telephone (06201) 602315, Telex 465516 vchwh d, Telefax (06201) 602328.

Editor: *P. Gölitz.*

Associate editors: *D. J. Loewus, A. Stimson.* **Editorial assistant:** *E. Schweikart*

Publishers: VCH Verlagsgesellschaft mbH. (Managing Directors: *Prof. Dr. Helmut Grünewald* and *Hans Dirk Köhler*), Pappelallee 3, D-6940 Weinheim, Federal Republic of Germany. Correspondence concerning advertisements should be addressed to VCH Verlagsgesellschaft mbH. (Advertising Manager *R. J. Roth*), Boschstr. 12, P.O. Box 1260/1280, D-6940 Weinheim, Federal Republic of Germany, Telephone Weinheim (06201) 602-0, Telex 465516 vchwh d, Telefax (06201) 602328.

ANGEWANDTE CHEMIE

International Edition in English

Volume 27 · Number 4
April 1988
Pages 447–592

Multiphoton-Ionization-Mass Spectrometry (MUPI-MS)**

New Analytical Methods (34)

By Jürgen Grotemeyer* and Edward W. Schlag

Mass spectrometry is one of the most important analytical tools in chemistry, biology, medicine and related areas. During the past 30 years, methods have been developed, both for the qualitative as well as the quantitative analysis of a wide variety of substances. The introduction of lasers into chemistry has also profited mass spectrometry, since its nonlinear properties and its tunability open up fundamentally new frontiers. Multiphoton ionization mass spectrometry combines UV-spectroscopy and mass spectrometry, thus providing a two-dimensional method that enables substance-specific and even state-specific analyses. This progress report presents the fundamentals and possibilities of MUPI mass spectrometry and discusses investigations on amino acids, peptides, chlorophylls and sugars. For each substance, multiphoton ionization can be tuned in such a way that only the molecular ion is formed. An increase of laser intensity induces substance-specific fragmentations of the molecule, thus contributing to a quick and easy identification of the substance.

1. Introduction

Analytical tasks, i.e., the identification of a substance and the elucidation of its structure, have always been the chief concern of mass spectrometry. On the one hand, a compound can be identified via its molecular ion, which leads to the exact determination of the molecular weight and thus to the elemental composition and the empirical formula of the molecule, while on the other, a fragmentation of the molecule giving a specific fragmentation pattern is also important for identification and structure elucidation.[1]

Informative mass spectra are only to be expected, however, if the four principal technical prerequisites of mass spectrometry are met with:

- The substance under investigation must either be evaporated as an intact neutral molecule and ionized later or must be vaporized and ionized in one step.
- Evaporation and ionization should be soft enough to ensure that the signal of the molecular ion is detectable with adequate intensity. However, the signals of substance-specific fragmentation should also be observable.
- The ions produced must be separated according to mass with the highest possible accuracy.
- Finally, these ions must be detected without any discrimination due to their absolute mass.

[*] Dr. J. Grotemeyer, Prof. Dr. E. W. Schlag
Institut für Physikalische und Theoretische Chemie der
Technischen Universität München
Lichtenbergstrasse 4, D-8046 Garching (FRG)

[**] A number of abbreviations exist for photon ionization. All terms like MPI, REMPI, R2PI or REMPI/F describe a two-photon excitation leading to ionization. For *multiphoton ionization* we prefer to use the generic term MUPI, because, as described in this paper, three-, four- or multiphoton ionizations via resonant intermediate states as well as nonresonant absorptions can lead to ionization.

 © VCH Verlagsgesellschaft mbH, D-6940 Weinheim, 1988 0570-0833/88/0104-00447 $ 02.50/0

During the past decade, several techniques have been developed that can fulfill these demands, at least in part, and the mass range for routine investigations has been increased from some 100 Da to some 1000 Da. The driving force thereby has been the ever increasing need to analyze larger molecules, especially in biochemical investigations.

In this progress report it will be demonstrated that the use of a laser light source for "optical ionization" is a new, generally useful ionization method in mass spectrometry. Coupling mass spectrometry with the tunable laser ionization results in a two-dimensional analytical method that gives absorption spectroscopic as well as mass spectrometric data. This technique is somewhat equivalent to other well known two-dimensional methods such as the coupling of mass spectrometry with gas chromatography (GC/MS),[2] with liquid chromatography (LC/MS),[3] or even with mass spectrometry itself (MS/MS).[4]

2. Fundamentals

The methods that have been developed in the last few years for investigating involatile and large molecules[*] by mass spectrometric techniques are often only applicable to special problems. Of general use are the so-called *particle impact* methods that utilize atomic particles to desorb ions from a matrix into the gas phase: secondary ion mass spectrometry (SIMS),[5] fast atom bombardment (FAB),[6] ^{252}Cf-plasma desorption (^{252}Cf-PD),[7] and laser desorption (LD).[8] In addition, direct chemical ionization (DCI)[9] and field desorption (FD)[10] are employed for the investigation of large molecules.

Although these methods differ widely in their technical details they have one principal feature in common: The desorption and the ionization are coupled directly.[11] A steering of the ionization process, and thus of the degree of fragmentation, is therefore impossible. In general, the molecular ion is not detectable, but several adduct ions are found which stem from the addition of protons and/or alkali cations to the molecule. Often, there is also an ionization of the matrix molecules, which leads to a considerable amount of non-substance-specific ions and thereby to further complications in the interpretation of the mass spectrum. To achieve a tunable ionization, the evaporation and ionization must be carried out stepwise.

In a MUPI experiment the substance is first vaporized by some method (see Section 2.2), then the molecules are ionized in the gas phase with laser light and finally mass analyzed. Such a two-step process aims at much higher ion yields and is more flexible than one-step direct ionization.

2.1. Multiphoton Ionization

A molecule that undergoes multiphoton ionization becomes a radical cation. Radical cations also result from all conventional impact ionization methods such as electron impact ionization (EI), ionization via charge exchange (CE), and one-photon ionization (PI).[*] Hence, MUPI must be compared with these methods.

Tunable multiphoton ionization was first used by *Boesl* et al.[12] and *Zandee* et al.[13] in 1978, and since then has been discussed in several reviews.[14–17]

In the conventional ionization methods, an energy that is higher than the ionization energy is supplied to the molecule in *one* step, so that fragmentations occur as well as ionization, whereas in MUPI the energy of a single photon is lower than the ionization energy (Fig. 1). The wavelength of the photon is tuned to the energy difference between the ground state and an excited state of the neutral molecule. For ionization, a multiple absorption of photons in the molecule has to take place to accumulate the necessary energy.

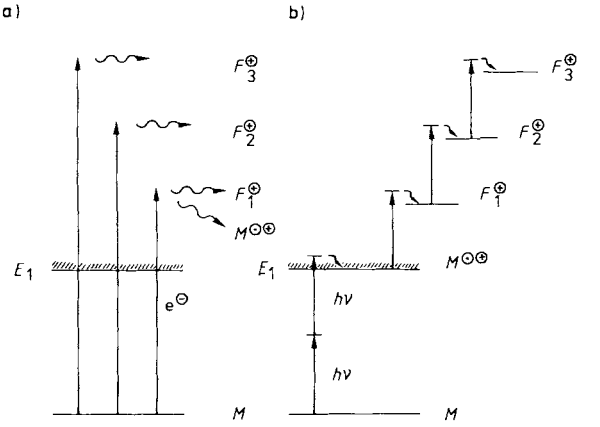

Fig. 1. The difference between a) electron impact ionization (EI) and b) multiphoton ionization (MUPI). E_1 = first ionization energy, $F_1^{\oplus}$, $F_2^{\oplus}$, $F_3^{\oplus}$ = fragmentation ions. Other than in EI, in MUPI the molecular ions are formed with a narrow energy distribution and little excess energy.

In general, the absorption of photons into a molecule is a process of low efficiency. If, however, the wavelength of the absorbed photons just corresponds to the energy difference between the molecular ground state and an excited molecular state, the efficiency of the absorption process is increased by several orders of magnitude (resonance enhancement),[18,19] particularly if the wavelength of the photon corresponds to a maximum in the electronic spectrum of the molecule.

In the most simple case, the absorption of two UV-photons leads to ionization of the molecule. But a three- or four-photon ionization is also possible (2b, c).[20,22] A multiphoton ionization with photons of different wavelength (Fig. 2d) can also be realized. Figure 2e shows the special case of a nonresonant two-photon ionization. This process needs much higher laser intensities than the resonance-enhanced excitation.

MUPI succeeds in state selective formation of molecular ions. As demonstrated by several molecules,[22] MUPI leads to molecular ions that populate a well defined vibrational level, predominantly the vibrational ground state.

[*] The classification of the molecules discussed in this report into small (<300 Da), middle sized (300–1000 Da), and large (>1000 Da) molecules is arbitrary.

[*] In general, SI-, FAB-, CI-, ^{252}PD- and LD-mass spectrometry produce adduct ions containing the molecule and a proton and/or an alkali cation.

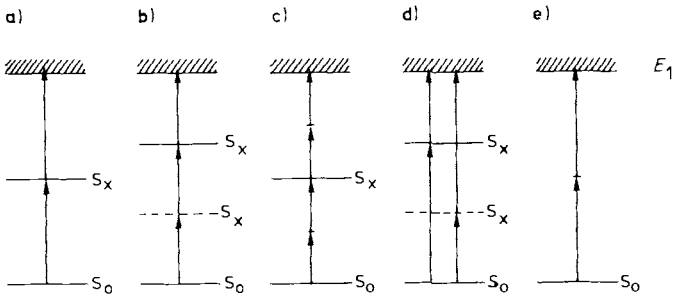

Fig. 2. Some features of multiphoton ionization (MUPI). S_x indicates "allowed" intermediate state, mostly the S_1 state. But the usage of higher states is also possible. a) "Normal" resonant two-photon ionization. b) Resonant three-photon ionization via two intermediate states. c) Four-photon ionization via one intermediate state. d) Resonant two-photon ionization with photons of different wavelength. e) Nonresonant two-photon ionization.

The excess of energy supplied in the ionization step is removed as kinetic energy by the electron leaving the molecule, so the molecular ions have equal or only slightly different energies (Fig. 1). In contrast, in the case of EI the excess energy remains in the ions; this leads to a wide energy distribution, reflecting the energy distribution of the impact electrons. With increasing laser intensity, absorption of photons by the molecular ions induces fragmentation reactions. Several mechanisms have been put forward[23-27] to explain these fragmentations. Generally accepted is the "ladder switching model", which is supported by experimental findings[28] and theoretical studies.[29] As shown in Figure 1, the neutral molecule absorbs two photons on its "absorption ladder" and is ionized. Here the internal energy is only slightly higher than the ionization energy. The molecular ion then absorbs one or several photons, thereby starting the first fragmentation reaction. The system then switches from the molecular absorption ladder to a fragment ion, which can absorb further photons on *its* absorption ladder, inducing further fragmentation reactions. This absorption-fragmentation mechanism may occur several times during typical laser pulses of 6-10 ns and, with sufficient laser densities, result in a total breakdown of the molecule into the atomic particles.

Because of the narrow energy distribution in the molecular ions in MUPI experiments, the absorption-fragmentation mechanism leads to an increased amount of metastable ions.[30, 75, 87] This aspect is of importance in energetic and dynamic investigations of elementary reactions in the gas phase (see Section 3).

2.1.1. *Soft Ionization*

The absorption yield is clearly dependent on the intensity of the laser light. By keeping the intensity low, e.g. 10^6 W/cm^2, the absorption of photons can be limited to form exclusively molecular ions. In Figure 3a, this is demonstrated with the example of *p*-xylene. Since an absorption of photons by the molecular ions is almost impossible at this low laser light intensity, no fragmentation takes place. This possibility of inducing fragmentations in a controlled way is unique in mass spectrometry. Even for large molecules the ionization can be tuned to form only molecular ions.

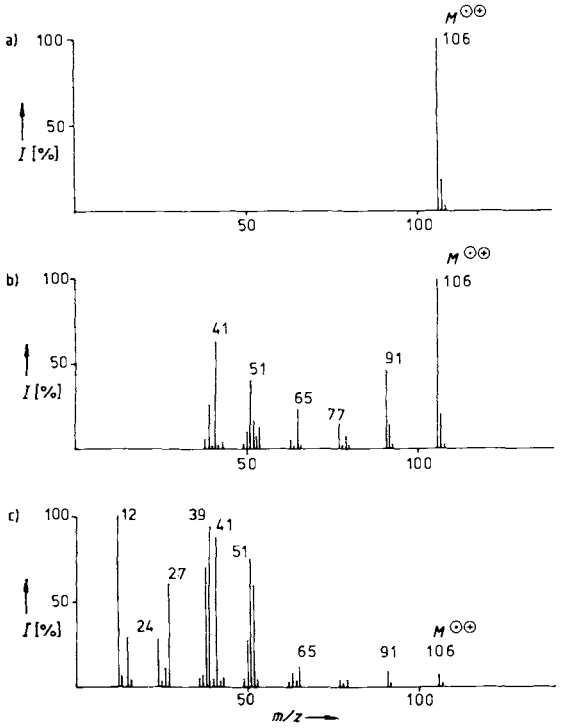

Fig. 3. MUPI-mass spectra of *p*-xylene. a) Soft ionization without fragmentation of the molecular ion, laser intensity about 10^6 W cm^{-2}. b) Partially hard ionization of *p*-xylene with little fragmentation, laser intensity about 10^7 W cm^{-2}. c) Very hard ionization with strong fragmentation, laser intensity about 10^9 W cm^{-2}. I = relative intensity. Excitation wavelength $\lambda = 272$ nm.

2.1.2. *Hard Ionization*

Increasing the laser intensity leads to an additional absorption of photons by the molecular ion, which then undergoes the energetically and kinetically most favored fragmentation. Such a moderate ionization/fragmentation is referred to as "partially hard ionization". For the mass spectrum in Figure 3b, the density of the photons was adjusted to a level that allowed observation of both the signals of the molecular ion as well as of those of the products of the first fragmentation, e.g. m/z 91.

Tuning to higher laser light intensities induces further fragmentations, and, depending on the photon density, the system can switch fragmentation ladders until a decomposition of the molecule into its atomic particles occurs. Figure 3c demonstrates this. Here the fragmentation has advanced to the formation of atomic carbon. This means that the *p*-xylene molecular ion must have absorbed about nine photons of wavelength 272 nm. No other mass spectrometric ionization method can accumulate such a high energy in a molecule. The advantages from the analytical viewpoint, of this possibility of controlling the amount of fragmentation by tuning the laser light intensity are demonstrated in Section 3.

2.1.3. *Wavelength Selectivity*

In multiphoton ionization, not only the intensity but also the wavelength of the light can be varied. The absorption maximum of a molecule and thus the position of the

resonant intermediate state are intrinsic properties of the molecule and therefore substance specific. This is of great importance for the investigation of mixtures, since the component that has an intermediate state in resonance with the wavelength used is preferably ionized; therefore it is possible to detect traces in a mixture with increased sensitivity. Thus, in blood serum, for example, several metals and organometallic compounds can be measured quantitatively in concentrations of about 1 ng per 1 mL serum.[31] Thereby, both the electronic spectrum, measured for one substance-specific mass, as well as the mass spectrum of the substance, measured at a fixed wavelength, can serve for the identification of the components. This method of analysis has been used very successfully,[32-37] both on mixtures of several substances as well as mixtures of structural isomers.[38]

One example of a selective excitation from a mixture is shown in Figure 4.[39] Here a sample of *p*-xylene with natural isotopic composition ($^{12}C_8H_{10}/^{13}C^{12}C_7H_{10}$: 100/8.8%) was investigated. Recording a mass selected optical absorption spectrum of *p*-xylene (*m/z* 106) and the ^{13}C-isotopomer (*m/z* 107) yields absorption lines of the resonant intermediate state shown on the left-hand side of Figure 4. It can be seen that the positions of the absorption maxima of the two molecules differ slightly.

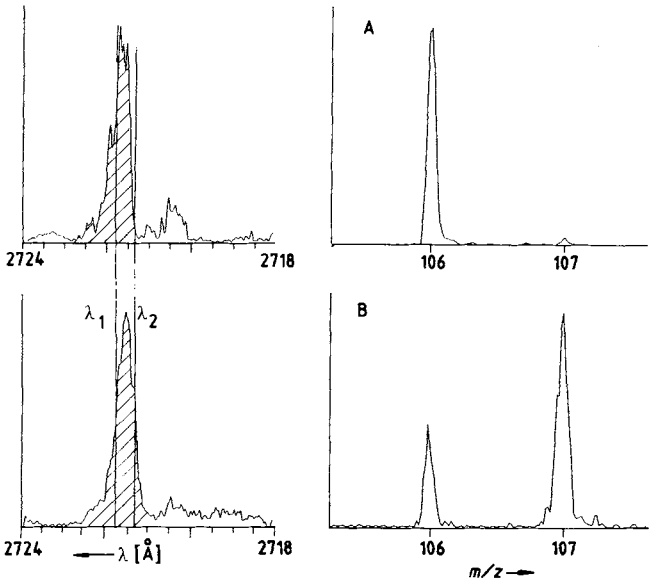

Fig. 4. Left-hand side: mass selective absorption spectrum of *p*-xylene; top: spectrum of the species *m/z* 106; bottom: spectrum of the species *m/z* 107. Normally, the intensity ratio in the mass spectrum of *p*-xylene is *m/z* 106 : *m/z* 107 = 100 : 8.8. As the mass spectra show (right), this ratio is drastically influenced (100 : 0.5 in A; 50 : 100 in B) by the choice of the excitation energy for the MUPI-experiment (λ_1 for A, λ_2 for B).

By choosing the appropriate wavelength from these absorption spectra, the signal of the mono-^{13}C-xylene molecular ion in the mass spectrum can be either amplified or suppressed (Fig. 4, right).

The improvement of the mass spectrum of a substance present in only trace amounts in a mixture is a possibility which only multiphoton ionization can offer.

2.2. Vaporization of Molecules

The gas-phase UV/VIS absorption spectra of polyatomic molecules at room temperature normally show broad and unstructured bands, since a large number of vibrational and rotational states are populated. To investigate molecules with MUPI-mass spectrometry, their thermal excitation should be as low as possible, so that the broad absorption bands become sharp peaks and a selective excitation is possible. Cooling can be achieved by isentropic expansion of a jet of noble gas into the vacuum. Small amounts of the sample under investigation, which must have a sufficiently high vapor pressure, are mixed into the gaseous stream.[40-42]

In typical "seeded supersonic beam expansion" experiments, a gaseous mixture of argon and the sample is allowed to lead from a reservoir through a nozzle of diameter 100–500 μm. The temperature obtainable thereby is about 2 K for the translational degrees of freedom, and 20 K and 50 K respectively for the rotational and vibrational degrees of freedom.[39] This method of injection resembles that of a GC/MS coupling. The reservoir can easily be replaced by a gas chromatograph or a HPLC instrument. Several authors have described a GC/MS coupling under the conditions of supersonic beam expansion and multiphoton ionization.[43-46] *Johnston* et al. have recently reported the coupling of liquid chromatography with MUPI-mass spectrometry.[47] But these methods, using MUPI, are still in the development stage.

Chromatography with supercritical gases, which has found increasing interest during the past few years, is especially suitable for use with MUPI, since highly pressurized gases are used as solvents. In the expansion step, the separation of these gases from the sample is very easy and no clustering with the sample molecules occurs, a problem that is often encountered in liquid chromatography experiments. Up to now, only molecules smaller than 250 Da have been investigated with this method.[50,51]

In an other approach, the thermospray method[52,53] was modified by *Levy* et al.[54] to vaporize involatile samples such as tryptophan as neutral molecules.

All these injection methods are well suited for the separation of mixtures and the evaporation of small, thermally stable molecules, but they cannot be used for the investigation of large, thermally labile molecules. The methods developed for such compounds aim to evaporate and ionize the molecules in one step. But in these methods more neutral molecules are desorbed than there are ions produced. Thus, investigations by *Cotter* et al.[55] have shown that in laser desorption with an IR-laser, the yield of neutral molecules is much larger than the ion yield, as has also been found to be the case by *Budzikiewicz* et al.[56] and *Campana* et al.[57] for the FAB-method. Typical values for the ratio of neutral molecules to ions is about $10^4 : 1$ in laser desorption experiments.[55] Theoretical studies have been undertaken in an attempt to clarify the processes of desorption,[11,58] but many details still remain unexplained.

To make use of the large ratio of neutral molecules to ions we have utilized since 1983 a tandem arrangement of *l*aser *e*vaporation of *i*ntact neutral *m*olecules (LEIM) into a supersonic beam followed by multiphoton ionization.[59,60]

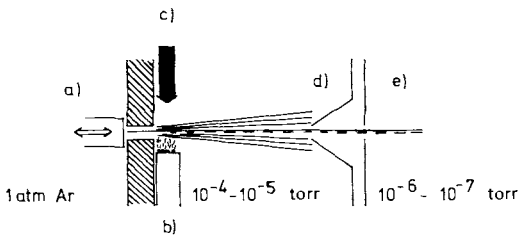

Fig. 5. Typical experimental set-up for the laser desorption into a supersonic beam. a) Pulsed valve with nozzle; b) probe tip mounted in the vacuum in front of the nozzle; c) beam of laser light (produced by a CO_2-IR-laser); d) skimmer; e) ion source.

In a typical LEIM-MUPI experiment (Fig. 5) the sample is dissolved in a suitable solvent, the solution placed on a probe tip, and the solvent evaporated. The probe tip is thus coated with hundreds to thousands of layers of molecules, and is now mounted in the vacuum close to the nozzle for the supersonic beam. The molecules are then desorbed from the surface by IR-photons into the expanding supersonic beam. As described above, the desorbed particles are cooled in their internal degrees of freedom and at the same time transported into the ion source. The pulsed system of this experiment consists of a pulsed valve for the production of the supersonic beam and a small CO_2-laser for the desorption of the neutral molecules.

2.3. Mass Spectrometric Detection

In principle, the ions produced by pulsed MUPI can be analyzed with any type of mass spectrometer. However, instruments that were developed for a continuous cyclic scanning of the mass range, such as magnetic sector instruments, are much less suitable for coupling with MUPI than quadrupole instruments, ICR-spectrometers,[*] and time-of-flight mass spectrometers.

2.3.1. *Quadrupole and ICR-Mass Spectrometry*

In the first studies[12,61,62] concerning the mass spectrometric investigation of ions produced by MUPI, quadrupole instruments were used for the mass separation. Quadrupole instruments are often chosen in GC/MS coupling, because they are easy to handle and have a rapid scanning cycle. However, due to their limited mass range, about 2000 Dalton, and their low mass resolving power,[**] their suitability for coupling with MUPI is somewhat limited. Also the ion transmission of quadrupole fields is not very high.

The coupling of ICR-mass spectrometry with MUPI has also been described.[63-65] It offers the advantage of high mass resolution,[66] but up to now the mass range is still limited to about 4000 Dalton. For technical reasons, the production of ions should be very low in ICR-experiments.[67] But MUPI produces, even with low laser intensities, considerable ion yields, so that the coupling of this ionization method with an ICR-instrument is still complicated. There might be some possibilities in the future, when ICR-mass spectrometry can be operated with high mass resolving power and *simultaneous* recording of the complete mass spectrum.

2.3.2. *Time-of-Flight Mass Spectrometry*

The mass spectrometric method that really takes advantage of the pulsed nature of ion production by MUPI, is the technique of *time-of-flight* (TOF) mass spectrometry.[68] TOF mass spectrometers are simple instruments with extremely high transmission. As opposed to all other mass spectrometers, in these systems a complete mass spectrum is recorded with every laser pulse. The fundamental parts of a TOF mass spectrometer are the ion source, the drift region (flight tube), and the detecting system. On coupling with an EI-ion source, a mass resolving power of only 200-400 could be achieved because of the broad kinetic energy distribution of the ions generated. This low resolution is the reason for TOF mass spectrometers having seldom been used, despite being known for more than 40 years.

Because of the development of pulsed ion sources like SIMS[69] or plasma desorption[70] (but also because of MUPI[39]), the interest in TOF mass spectrometers has grown during the last few years. By using a two-step acceleration field (*Wiley-McLaren*[71]) and multiphoton ionization, a mass resolving power of 400 was reached in a linear TOF mass spectrometer for the *simultaneous* detection of all masses.[72]

Several attempts[72] to increase the mass resolution in TOF instruments have been made, but with limited success. The most promising attempt was made by *Mamyrin* et al.[74] using an electrostatic field that reflects the ion beam at the end of the drift section. This reflecting field not only lengthens the flight distance, but is also able to compensate for most of the differences in the kinetic energy of ions of one nominal mass and thereby the differences in the flight time (Fig. 6). In our experiment, the ions produced by MUPI are accelerated by a constant field of about 800 V and then drift through a length of 80 cm. At the end of this field-free drift region, the mass separated ion packets are slowed down by a short deceleration field and reflected with only low energy in the following reflec-

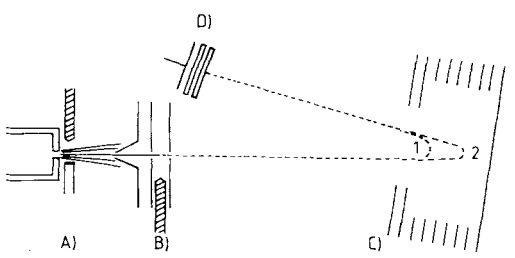

Fig. 6. Schematic representation of the time-of-flight mass spectrometer. 1) Flight path of ions with low kinetic energy; 2) flight path of ions with the same mass but higher kinetic energy. A) Evaporation chamber; B) beam of ionizing laser light; C) reflecting field; D) detector.

[*] ICR = Ion Cyclotron Resonance.

[**] Mass resolving power means the ability to distinguish between two neighboring masses. The signals of two masses are resolved when they are separated by a "valley"; two definitions are usual in mass spectrometry, "10% valley" and "50% valley". In this report the "50% valley" definition is always used. For example a mass resolving power of 1000 separates the masses 500.00 and 500.50.

tor field. After leaving the reflector and deceleration field, the ions fly through the drift region in the opposite direction till they impinge on the detector.

Ions with higher kinetic energy penetrate deeper into the reflector field and therefore have a somewhat longer flight path than ions with lower kinetic energy. As a consequence the differences in the flight time of ions of the same mass are compensated, simultaneously, for all masses. In 1982, *Boesl* et al.[75] succeeded in combining the multiphoton ion source with a reflection time-of-flight (RETOF) mass spectrometer. In these first experiments, a mass resolving power of 3800 could already be reached. *Lubman* et al.[76] and *El-Sayed* et al.[77] have also reported a coupling of MUPI with a reflection TOF instrument, but with different experimental results.

By optimizing the parameters, considerably higher mass resolutions are possible. In particular, it could be shown that the grids used in a classical RETOF-mass spectrometer to define the electrostatical fields lead to a dispersion of the ions and thereby affect the transmission and the mass resolving power. In contrast a gridless ion mirror allows a clean reflection of the ion beam and is autofocussing. *Boesl* et al. succeeded in increasing the mass resolving power to more than 10000[39,78-80] by incorporating a supersonic beam to cool the neutral molecules in their translational degrees of freedom, shortening the laser pulse from 5–8 ns down to 1.5 ns, and lowering the laser intensity. Even further enhancement seems to be possible. Theoretical values of 100000 up to 1000000 have been discussed for the mass resolving power in a RETOF-mass spectrometer.[80]

In the mean time, the reflecting electrostatical field method has also been used in combination with other ionization techniques (SIMS; 1985[81] and ^{252}Cf-PD; 1987[82]).

The advantages of time-of-flight mass spectrometers compared to other mass spectrometers are manifold: first, this technique offers an almost unlimited mass range; with every laser pulse a complete mass spectrum is detected. A registration of up to 100 mass spectra per second is possible; this number is limited only by the capacity of the computer. Today, the mass resolving power and transmission of RETOF instruments are already better than in the case of quadrupole or small magnetic sector instruments.[83] Moreover, time-of-flight mass spectrometry has one physical feature that is unique in comparison to other techniques: the mass resolving power increases with increasing mass. The detection of metastable ions[75] (especially important for MS/MS investigations) is also possible because of the incorporation of the reflecting field.

The location of the evaporation is confined to only a few μm, which is especially important for the investigation of surfaces. The time window of the sampling is limited by the laser pulse to a few ns. Due to the high repetition rate 10–100 spectra can be measured for a signal lasting one second, e.g. from a gas chromatograph.

3. Mass Spectra

MUPI-mass spectrometry was for a long time only used for kinetic investigations of the fragmentation processes of small molecules in the gas phase.[84] It is well suited for this purpose, not only because of the very sharply defined energy for the ionization and fragmentation of molecules, but also because reactions of metastable ions can be investigated.

Since 1983, however, MUPI has found increasing application as a general method of mass spectrometry for the investigation of organic and biochemical samples. A number of examples of such investigations will be outlined in the following sections.

3.1. Small Molecules

Small arenes, such as benzene,[85] alkylbenzenes,[86-88] halogen-substituted aromatic compounds,[89] aromatic amines,[90,91] phenol[92] and aromatic aldehydes,[93] as well as organometallic compounds and several di- and triatomic compounds have been investigated in detail with the help of MUPI. In the main, these experiments were aimed at elucidating the physical processes of ionization by multiphoton excitation or details of certain fragmentation reactions. Interesting reviews of such investigations are to be found in articles by *El-Sayed*[16] and *Neusser*.[84] All the measured samples were volatile and their introduction into the ion source was simple. In this report, we shall concern ourselves with some mass spectra of small, biochemically interesting substances that are either thermally labile or involatile. Amino acids, with their variety of polar, hydrophilic, and hydrophobic residues, are good models in this respect.

The EI mass spectra of free amino acids have been well documented.[94-97] In most cases, the signal for the molecular ion is either small or not detectable at all. Figure 7

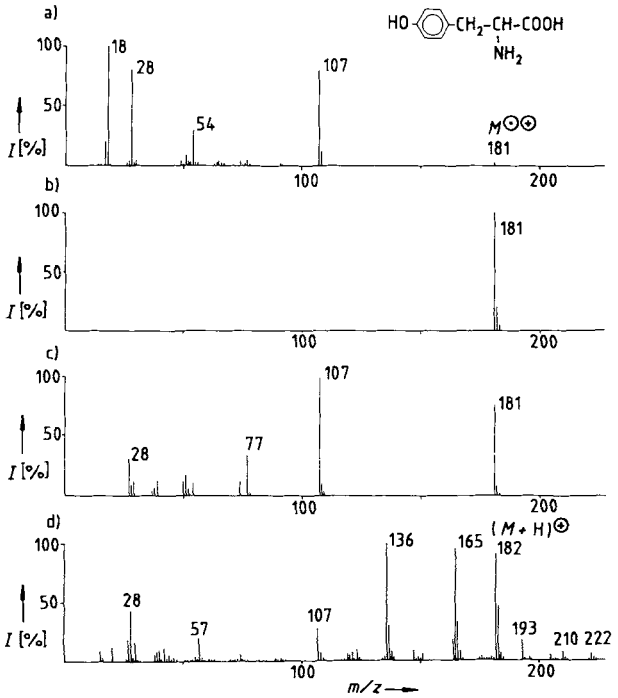

Fig. 7. Comparison of mass spectra of L-tyrosine. a) EI-mass spectrum; note the intensity of the molecular ion signal at m/z 181. b) Soft MUPI-mass spectrum; exclusively the molecular ion is formed. c) Mass spectrum after partially hard MUPI; ionization wavelength $\lambda = 272$ nm. d) CI-(methane)-mass spectrum, corrected for the methane background.

shows two MUPI mass spectra of the amino acid L-tyrosine obtained after laser evaporation, and, for comparison, an EI spectrum and a CI spectrum. The advantages of MUPI are obvious. In the spectrum obtained after soft MUPI (Fig. 7b), the molecular ion signal is the base peak, whereas in the EI spectrum (Fig. 7a), the relative intensity of this signal is only 5%. After background correction, the CI mass spectrum (Fig. 7d) affords the signal of the H-adduct molecular ion with relatively high intensity, but the identification of this ion is clearly complicated by the appearance of the signals of larger adduct ions. Increasing the intensity of the laser light (partially hard ionization) gives rise to the spectrum shown in Figure 7c. Despite pronounced fragmentation, the molecular ion signal is still remarkably intense. It has been shown[98] from the mass spectra of the amino acids that the fragmentation pathways remain virtually unchanged upon tuning the ionization wavelength by up to 40 nm, but the relative intensities of these fragmentations might change drastically. This behavior can be attributed to the different absorption cross sections of the fragmentations. Extreme changes in the relative intensities are observed, for example, in the case of tryptophan.[99]

In the case of aromatic amino acids, the wavelength used for the ionization normally corresponds to an absorption in the aromatic ring system. But the amino acid arginine has no chromophoric group absorbing above 250 nm. Therefore, in this case only a nonresonant absorption can occur (see also Section 2.1). Arginine is known to be particularly thermolabile and neither an EI-spectrum nor a CI-mass spectrum has been published up to now. Field desorption methods give a mass spectrum, but only the protonated molecular ion is detectable.[100] In the MUPI mass spectrum (Fig. 8), the signal of the molecular ion of arginine has been measured for the first time. This ion is of special interest, because arginine is extremely polar and is one of the strongest organic acids.

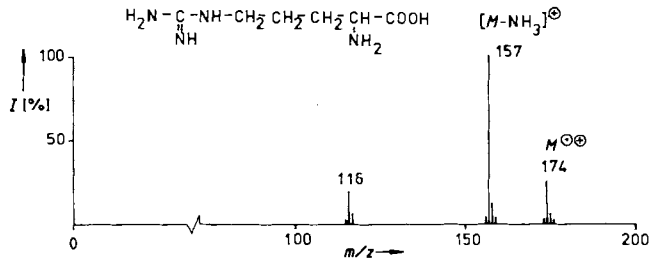

Fig. 8. Mass spectrum of L-arginine after nonresonant MUPI. Ionization wavelength $\lambda = 250$ nm.

Of the amino acid derivatives the phenylhydantoins[101] have already been investigated by MUPI-spectrometry.[98, 102] It was possible to detect less than subfemtogram amounts of these compounds in the gas phase.[102] Some phenylhydantoins, however, proved to be impossible to detect by way of the molecular ion. In contrast, we were able to show[98] that, by optimal tuning of the wavelength, the ionization can be achieved softly enough to obtain exclusively molecular ions.

Lubman et al.[103] also reported that the molecular ion was not always detectable in the investigation of dipeptides containing aromatic amino acids. As example, we shall discuss here phenylalanyl-tyrosine (Fig. 9). According to *Lubman* et al.,[103] the mass spectrum shows only a

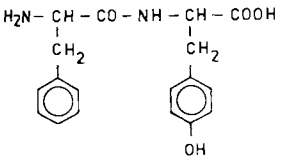

Fig. 9. The dipeptide phenylalanyl-tyrosine.

signal stemming from the loss of an hydroxy radical from the molecule. This fragmentation seems to be an artifact of the special experimental setup of the evaporation and ionization and can easily be avoided. Figure 10 shows the mass spectra of this compound obtained by soft and by partially hard MUPI under various experimental conditions.[104, 105] In the soft ionization spectrum, only the signal of the molecular ion is detected. With increasing laser light intensity, a number of fragmentations occur. The important fragments have *m/z* 236 and *m/z* 208. They correspond to the formation of an acylium ion (*m/z* 236) on rupture of the peptide bond and a further loss of CO from this ion (*m/z* 208). The cleavage of the peptide bond was found to be the favored fragmentation in more than 50 investigated dipeptides.[104–106]

Figure 11 shows a mass spectrum of saccharose that was obtained by nonresonant multiphoton ionization. Saccharose is a classical example for compounds that do not give molecular ions upon electron impact ionization. There

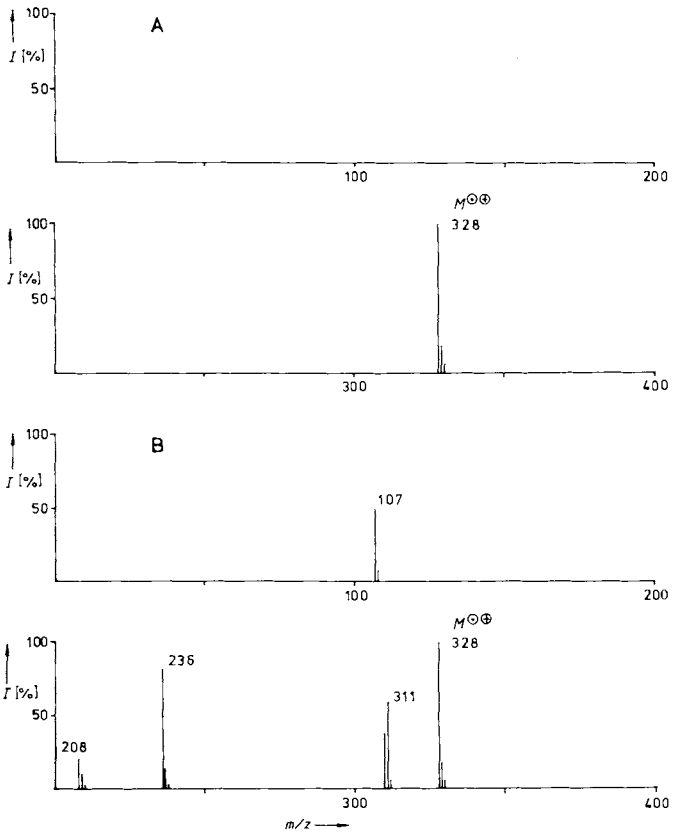

Fig. 10. Comparison of the mass spectra of phenylalanyl-tyrosine obtained by soft (A) and the partially hard (B) MUPI. Ionization wavelength $\lambda = 272$ nm. The signal in B at *m/z* 209 stems from the formation of the X[1] fragment (see Fig. 13).

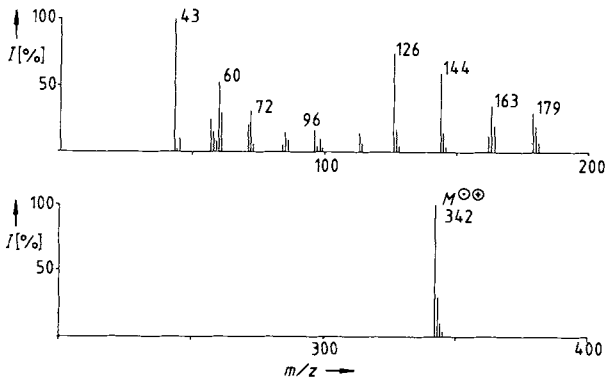

Fig. 11. Mass spectrum of saccharose after partially hard, nonresonant MUPI. Ionization wavelength $\lambda = 252$ nm. The signal at m/z 43 stems from an acylium ion.

have been controversial discussions in the literature[107] on whether molecular ions of sugars actually exist under EI or FD conditions. On the other hand, under MUPI conditions the molecular ion of saccharose is clearly detectable.[108]

The fragmentation reactions of saccharose (Fig. 12) are well known from pyrolysis-FI mass spectra.[109] The main fragmentation is the rupture of the glycosidic bond followed by the successive lost of water molecules.

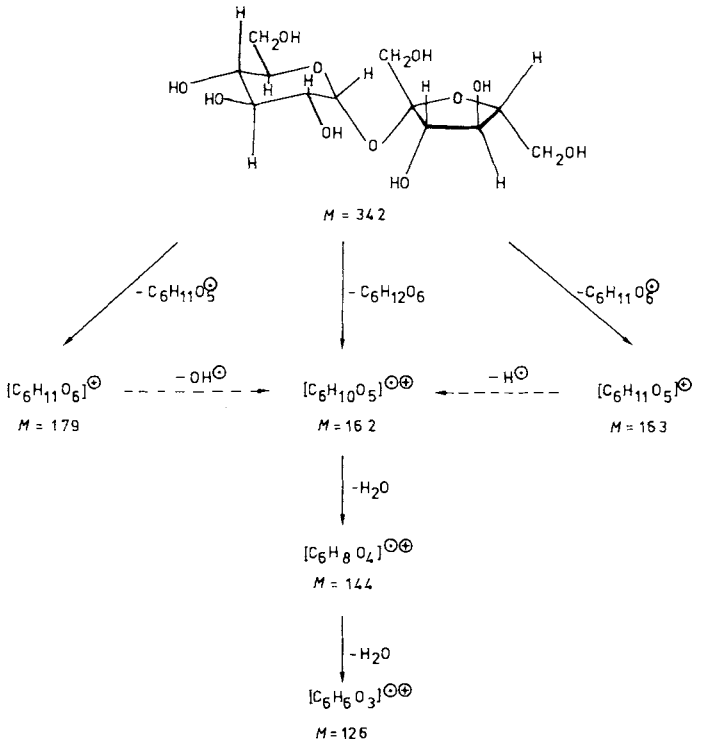

Fig. 12. Fragmentation scheme of saccharose. Some of the decomposition paths have been confirmed by the occurrence of metastable ions.

Further biochemically important small molecules whose MUPI-mass spectra have been obtained include steroids,[104, 107, 110] catecholamines,[111] neuroleptic drugs and vitamins,[112, 113] and purine bases.[114]

3.2. Middle Sized Molecules

The MUPI-mass spectra of several protected tripeptides have also been recorded[115] and compared with EI-spectra.[116] In the mass spectra obtained under partially hard ionization conditions the rupture of the peptide bond is again dominating. Complete series of the A and B fragments are detected (Fig. 13). The nomenclature of the

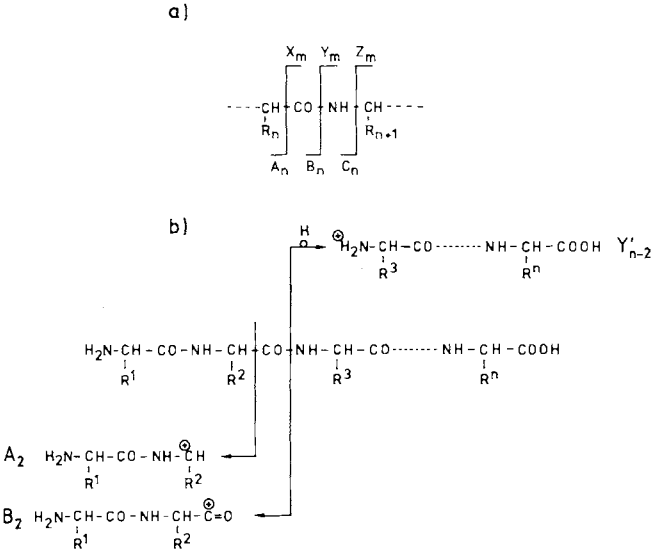

Fig. 13. a) Principal fragmentations of a peptide backbone and the nomenclature of the fragments (*Roepstorff* et al. [117]). The products of proton migrations are labeled, e.g., as A'_n, A''_n, or A'''_n indicating the number of protons isomerized prior to the fragmentation. b) Main fragmentations of peptides that have been observed in MUPI-mass spectra.

acylium ions (B) and the acyliminium ions (A) follows the concept of *Roepstorff* and *Fohlman*.[117] Besides the A and B fragments containing the *N*-terminal end of the peptide chain, also fragments of the Y′-series (Fig. 13) are detectable. These fragment ions contain the *C*-terminal end of the peptide.

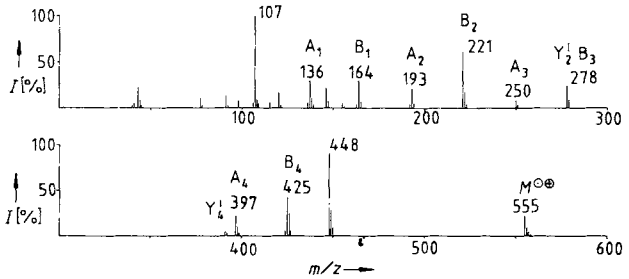

Fig. 14. Mass spectrum of Leu-enkephalin after partially hard MUPI. Ionization wavelength $\lambda = 272$ nm.

Figure 14 shows the mass spectrum of leucine-enkephalin, an unprotected pentapeptide,[118] after partially hard multiphoton ionization; the molecular ion is clearly recognizable. Other intense signals are those of the fragment ions originating from rupture of the peptide chain (Fig. 15). Signals indicating fragmentations in the side chains are only of minor intensity, as is characteristic for MUPI. Once again, besides the complete series of A and B frag-

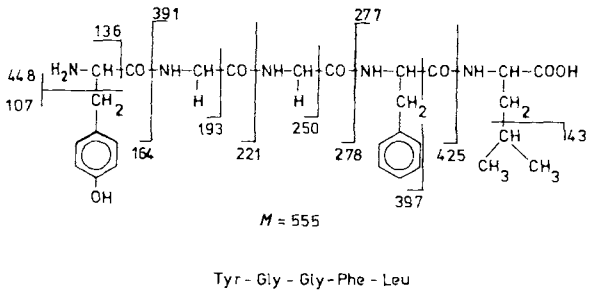

Fig. 15. Structure and fragmentations of Leu-enkephalin.

ments, the signals of some Y′ ions (Fig. 13) are also observed. It should be mentioned here that these complementary fragments are necessary in order to unequivocally prove the sequence of a peptide.

Various smaller peptides, such as pentagastrin,[119] the "sleep inducing peptide" (SLP)[106] and others,[120] have been successfully analyzed by MUPI-mass spectrometry. The favored fragmentation reaction in all cases is the cleavage of the peptide bond.

The spectra of other classes of compounds, for example of erythromycin, have also been recorded.[106] The molecular ions are always formed with high efficiency, and substance-specific ions can be detected without any protection of the molecule prior to the measurements. MUPI enabled the first successful mass spectrometric detection of porphyrins[121] and natural chlorophylls[122] without protecting groups. Natural chlorophyll and its derivatives could be detected in a biological sample containing about 30 different substances, including, inter alia, lipids and glycosides. Figure 16 shows the EI- and MUPI-mass spectra of this sample. It can clearly be seen that the wavelength selectivity of MUPI (Section 2.3.1) enables a separation of the

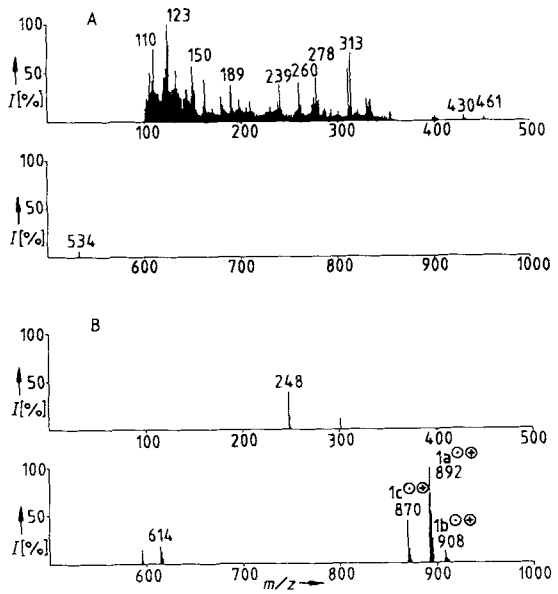

Fig. 16. Comparison of the EI- (A) and MUPI- (B) mass spectra of a biological sample from *Spirulina geitlerie*. In the EI-spectrum, ions of masses below *m/z* 100 are not shown. The ionization wavelength was $\lambda = 281$ nm in the MUPI-mass spectrum. Identifiable are the following molecular ions: *m/z* 870 = pheophytin a; *m/z* 892 = chlorophyll a; *m/z* 908 = 10-hydroxychlorophyll a.

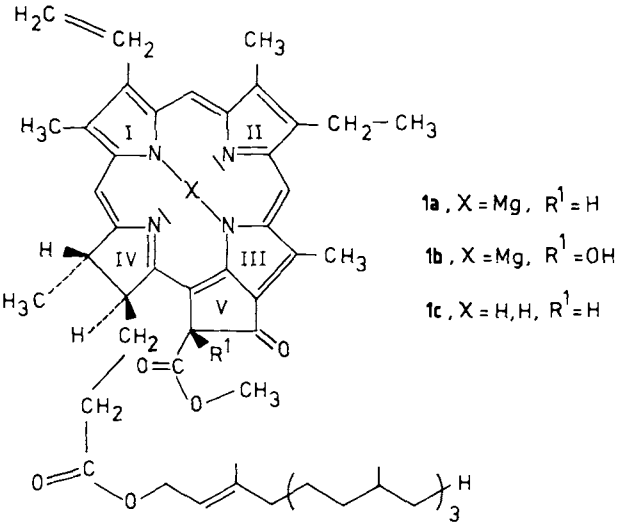

Fig. 17. Structures of the chlorophylls **1a-c** detected mass spectrometrically in a sample of *Spirulina geitlerie*.

substances, and three different chlorophyll derivatives (Fig. 17) can easily be identified. These are pheophytin a (**1c**) at mass *m/z* 870, 10-hydroxychlorophyll a (**1b**) at mass *m/z* 908, and chlorophyll a (**1a**) at mass *m/z* 892.

3.3. Large Molecules

Very informative mass spectra can also be obtained by MUPI combined with LEIM in the mass range above 1000 Da, which hitherto was reserved to SIMS, the FAB method, or plasma desorption. Thus, it could be shown that a soft ionization and controlled fragmentation of the unprotected decapeptide angiotensin I (Fig. 18) is possible by multiphoton excitation.[123] Figure 19 shows the mass spectrum of this compound obtained after partially hard ionization. Fragmentations close to the peptide bonds lead to intense signals; the complete series of A and B fragments are clearly recognizable, and once again the important signals of the Y′ ions containing the C-terminus are also detected. As was found in the smaller peptide chains, fragmentations in the amino acid side chains are only of minor importance.

Figure 21 enables a comparison of the results of peptide investigations with the FAB-MS/MS-method[4, 124] using collisional activation and MUPI-mass spectrometry. The FAB-MS/MS experiment on substance P (Fig. 20) was carried out with a triple sector instrument (*Biemann* et al.[125]). The protonated molecule was mass separated from the fragment ions in the first stage and then fragmentations were induced by collisional activation. By this method predominantly sequence ions of the A series are formed. The signals of the ions of the B series are only of minor intensity. Ions containing the C-terminus are not detectable. In addition, a large number of signals are observed that cannot be definitely assigned (Fig. 21a).

In contrast, the MUPI-mass spectrum (Fig. 21b) of this compound shows signals for all ions of the A series and B series with good intensities. Signals stemming from side-chain fragmentations are of minor significance. As in all of

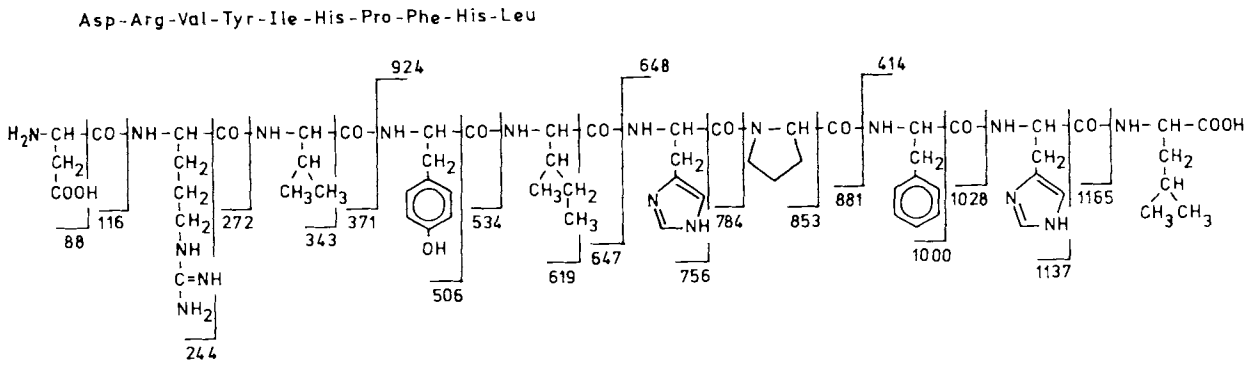

Fig. 18. Structure and fragmentations of angiotensin I (M = 1295).

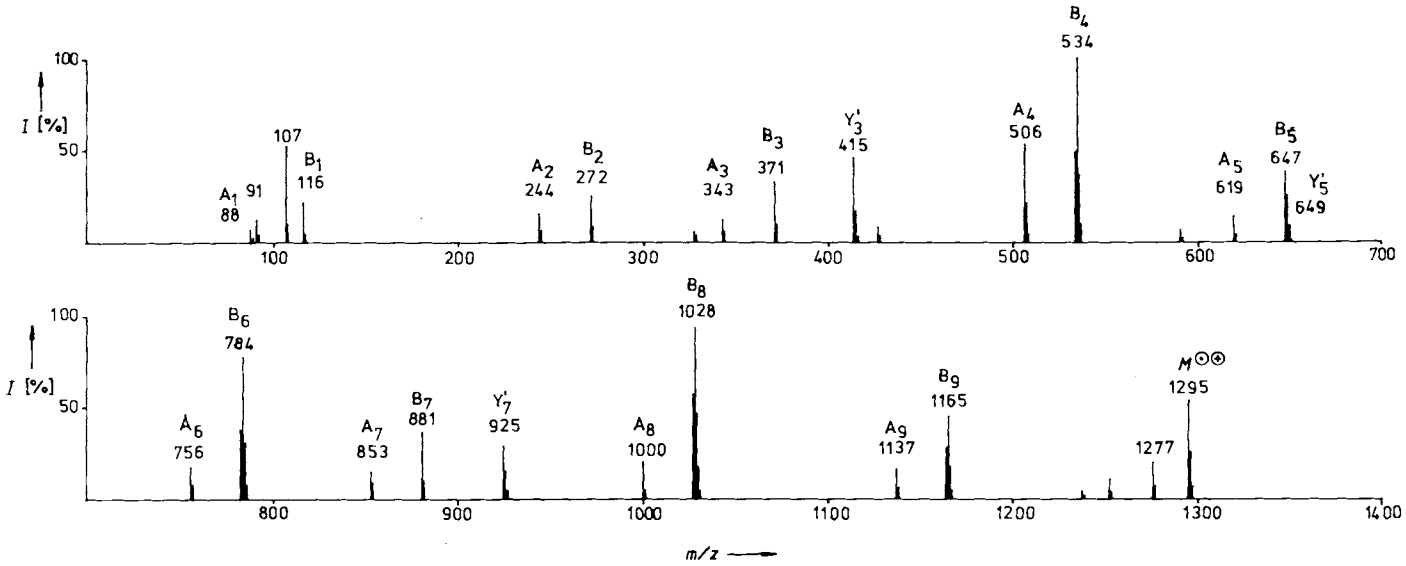

Fig. 19. Mass spectrum of angiotensin I after partially hard MUPI. Ionization wavelength $\lambda = 272$ nm.

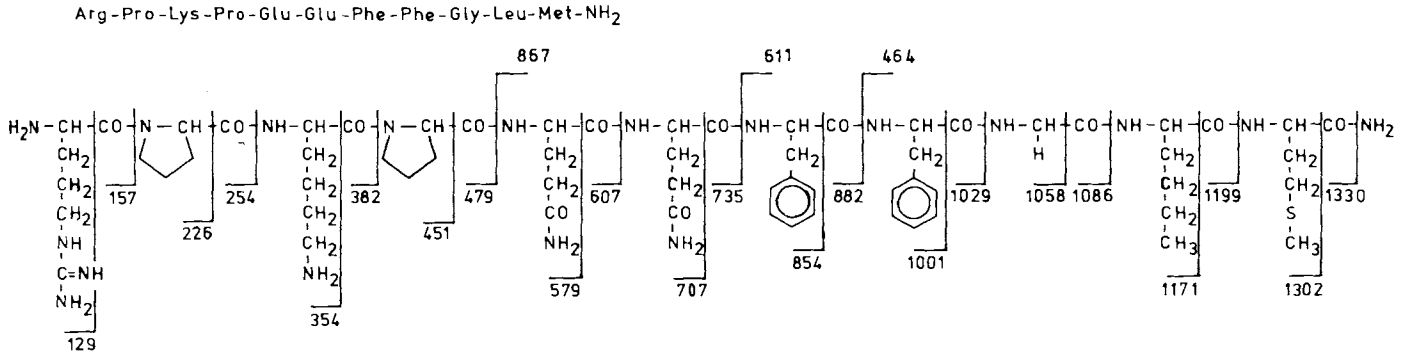

Fig. 20. Structure and fragmentations of substance P.

the above described MUPI-mass spectra of peptides, signals for fragments of the Y′ series are also detectable; hence, the peptide sequence can be unambiguously deduced from the spectrum.

Thus, both methods enable the sequencing of peptides in the gas phase, but the FAB-MS/MS experiment is much more expensive than the investigation by LEIM-MUPI-mass spectrometry.

In Figure 22, a FAB-mass spectrum and a MUPI-mass spectrum of an unknown sample are compared. The aim of the experiment was to investigate whether the compound shown in Figure 23, which should have been formed in a chemical reaction,[126] was present in the sample. MUPI leads to an intense signal corresponding to the molecular ion of the compound, while FAB produces only the signals of the fragmentation products. Thus, together with other

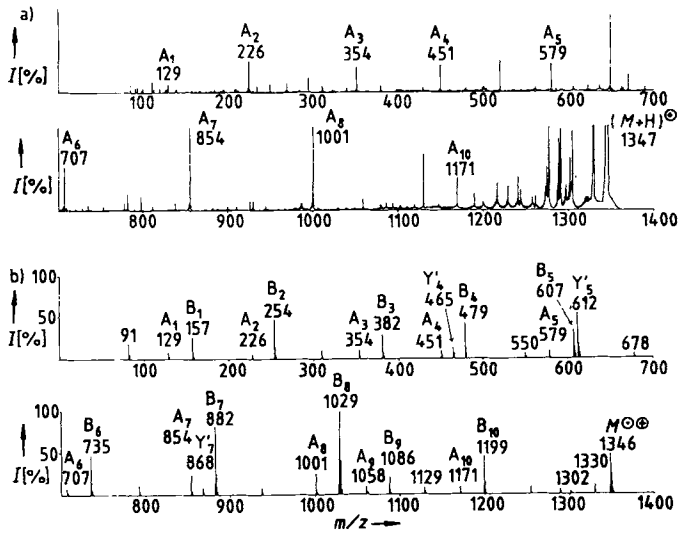

Fig. 21. Comparison of the mass spectra of substance P (a) from a FAB-MS/MS experiment and b) after MUPI.

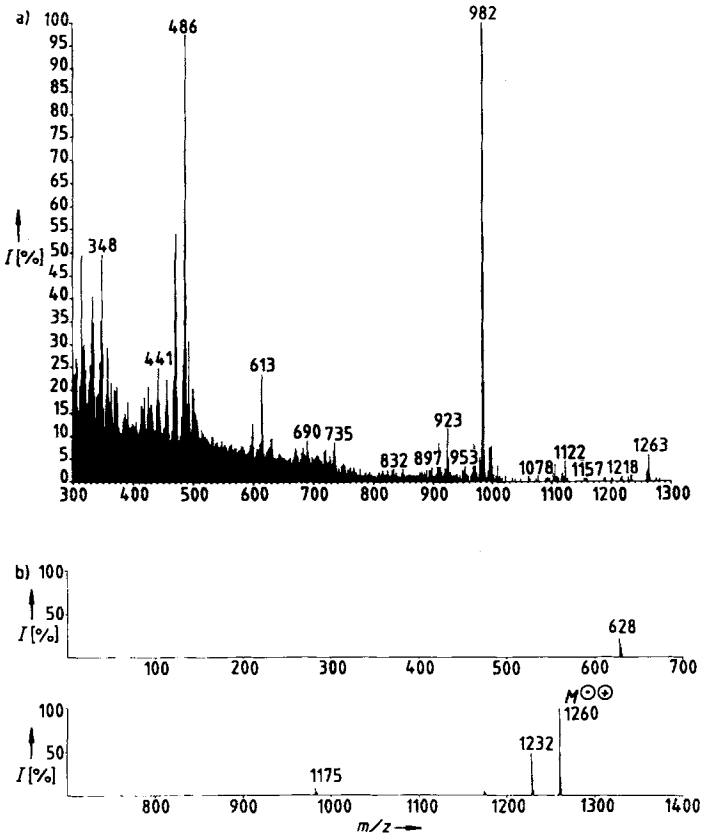

Fig. 22. Comparison of the FAB-mass spectrum (a) and the MUPI-mass spectrum (b) of the product shown in Figure 23.

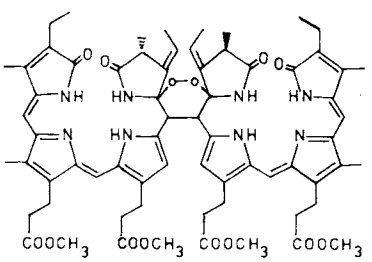

Fig. 23. Postulated structure of a compound in the sample used for the mass spectra in Figure 22.

analytical methods, MUPI-MS was able to give evidence for the existence of the compound.

As a final example of the potential of MUPI-mass spectrometry in the investigation of large molecules, Figure 24 displays the soft ionization spectrum of bovine insulin.[127]

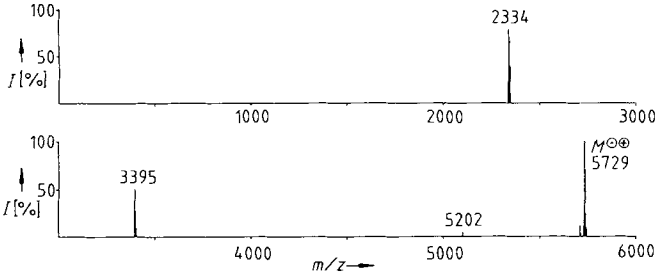

Fig. 24. MUPI-mass spectrum of bovine insulin. Ionization wavelength $\lambda = 272$ nm.

The most intense signal after multiphoton ionization is that of the molecular ion at *m/z* 5729, which is far less noticeable in the mass spectra recorded under FAB or PD-conditions. It should be mentioned again that, unlike in other methods, no background correction is necessary in the case of the MUPI-mass spectra. Figure 25 shows the experimental and calculated patterns of the isotopic distribution for the signal groups of the molecular ion and of the A and B chains.

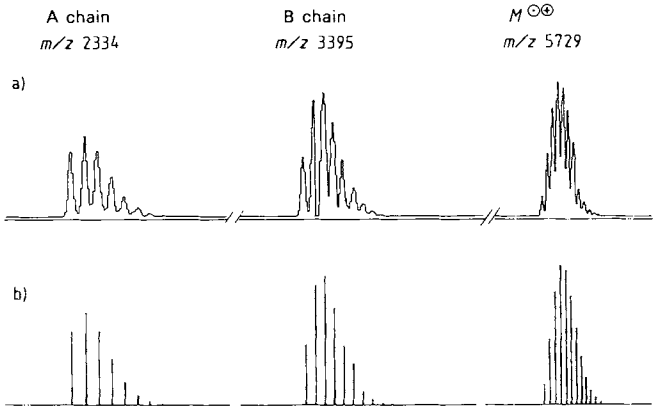

Fig. 25. Comparison of the experimental intensity ratios (a) for the molecular ion of bovine insulin and the fragment signals for the A and the B chains with the isotopic pattern (b) calculated from the elemental composition.

The superimposability of these two patterns for the signal group of the molecular ion proves that the insulin is desorbed into the gas phase as intact molecule without any addition of protons or alkali cations and is then ionized. The main fragmentations can easily be identified on the basis of the signal for the A chain at *m/z* 2334 and the signal for the B chain at *m/z* 3395. These results demonstrate that very large molecules can also be analyzed by MUPI-MS. In the meantime, numerous interesting molecules, like gramicidin and others[105] have also been investigated by this technique.

4. Conclusion and Outlook

The present review has outlined some of the advantages that are gained by combining the laser evaporation of intact neutral molecules with multiphoton ionization and mass spectrometry.

The MUPI-mass spectra of organic and biochemical compounds differ in some particular characteristics from the spectra obtained by other mass spectrometric methods. MUPI-mass spectra always show an intense signal for the molecular ion, thus allowing an easy identification. Since the occurrence of fragmentations can be controlled by appropriately tuning the excitation energy, MUPI-mass spectroscopy enables very detailed analyses.

Investigation of the possibilities opened up by this tunability, not only for mass spectrometric but also absorption spectroscopic analysis, has just begun.

One important aspect of the method described here is that it can be used for nonvolatile and labile compounds; this is possible because of the spatial and temporal separation of the evaporation step from the ionization step. Thus, the intrinsic difficulties caused by simultaneous vaporization and ionization in other mass spectrometric techniques can be avoided. This has a positive effect on the signal to noise ratio, so that, in contrast to other mass spectrometric methods, no background correction is necessary in MUPI-MS.

The very high sensitivity of multiphoton ionization is a further advantage of MUPI-mass spectrometry. Femtogram and subfemtogram amounts of substances can easily be detected by MUPI-MS, thus opening up new applications in trace analysis.

The generation of ions by the influence of light is still more expensive than their production by conventional methods,[128] but the advantages of this excitation method are evident. On the other hand, analysis of the ions in a time-of-flight instrument is very simple, and the overall costs are comparable with those for other types of mass spectrometers.

The range of potential applications of MUPI with respect to the identification of biological material is virtually limitless. The intrinsic features of MUPI, such as soft ionization and the ionization efficiency as a function of the wavelength, the different classes of compounds that can be ionized, and the absolute size of molecules that can be examined, all point to areas of future research and exploitation.

For the investigation of molecules with masses between 20000 and 50000 Da, the main limitation is detection: all commercially available systems have an upper mass limit in this range. Solutions to this problem have been discussed in the literature,[129] but further developments have to be made. Although MUPI-mass spectrometry is still a relatively young method, its future course of development is already forseeable. Parallel with improvements in mass resolving power and higher sensitivity MUPI-mass spectrometry will find increasing importance, in particular, for the elucidation of the structure of biomolecules of higher masses, but also for surface studies and material analyses. Furthermore, the ability of the system to rapidly and selectively (by wavelength changes) mass analyze a sample makes it well suited for the monitoring of technological processes, with the additional dimension of time-selected sampling.

The technique of producing ions with light is still in a state of rapid development, but it is already clear that it will find increasing application during the next few years, not only in mass spectrometric analysis, but also in the quality control of pharmaceutical products and in trace analysis, as well as in resolving diverse clinical and pharmacological problems.

The authors thank the "Deutsche Forschungsgemeinschaft", the "Fonds der Chemischen Industrie" and the "Bundesministerium für Forschung und Technologie" for financial support of this work and Dr. U. Boesl and K. Walter for their cooperation in the development of multiphoton ionization and the set-up of the time-of-flight mass spectrometer.

Received: July 27, 1987 [A 664 IE]
German version: *Angew. Chem. 100* (1988) 461
Translated by Dr. *B. Grotemeyer* and Dr. *R. C. Beavis*, Garching (FRG)

[1] F. W. McLafferty: *Interpretation of Mass Spectra*, University Science Books, Mill Valley, CA, USA 1980.
[2] G. M. Message: *Practical Aspects of Gas Chromatography Mass Spectrometry*, Wiley-Interscience, New York 1984.
[3] C. G. Edmonds, J. A. McCloskey, V. A. Edwards, *Biomed. Mass Spectrom. 10* (1983) 237.
[4] F. W. McLafferty (Ed.): *Tandem Mass Spectrometry*, Wiley-Interscience, New York 1983.
[5] A. Benninghoven, W. Sichtermann, *Anal. Chem. 50* (1978) 1180.
[6] M. Barber, R. S. Bordoli, G. J. Elliot, R. D. Sedgewick, A. N. Tyler, *Anal. Chem. 54* (1982) 645A.
[7] B. Sundqvist, R. D. Macfarlane, *Mass. Spectrom. Rev. 4* (1985) 421.
[8] a) P. G. Kistemaker, G. J. Q. van der Peyl, J. Haverkamp in H. R. Morris (Ed.): *Soft Ionization Biological Mass Spectrometry*, Heyden, London 1981, p. 120; b) M. A. Posthumus, P. G. Kistemaker, H. L. C. Meuzelaar, *Anal. Chem. 50* (1978) 985.
[9] M. A. Baldwin, F. W. McLafferty, *Org. Mass Spectrom. 7* (1973) 1353.
[10] H. D. Beckey, *Field Ionization Mass Spectrometry*, Pergamon Press, Oxford 1971.
[11] I. S. T. Tsong, S. H. Lin, B. V. King in C. J. McNeal (Ed.): *Mass Spectrometry in the Analysis of Large Molecules*, Wiley, Chichester 1986, p. 67.
[12] U. Boesl, H. J. Neusser, E. W. Schlag, *Z. Naturforsch. A 33* (1978) 1546.
[13] L. Zandee, R. B. Bernstein, D. A. Lichtin, *J. Chem. Phys. 69* (1978) 3274.
[14] E. W. Schlag, H. J. Neusser, *Acc. Chem. Res. 16* (1983) 335.
[15] H. Kühlewind, U. Boesl, H. J. Neusser, E. W. Schlag, *Nachr. Chem. Tech. Lab. 32* (1984) 205.
[16] D. A. Gobeli, J. J. Yang, M. A. El-Sayed, *Chem. Rev. 85* (1985) 529.
[17] V. S. Letokhov (Ed.): *Laser Photoionization Spectroscopy*, Academic Press, New York 1987.
[18] G. Petty, C. Tai, F. W. Dalby, *Phys. Rev. Lett. 34* (1975) 1207.
[19] P. M. Johnson, C. E. Otis, *Annu. Rev. Phys. Chem. 32* (1981) 139.
[20] H. Zacharias, H. Rottke, K. H. Welge, *Appl. Phys. 24* (1981) 24.
[21] J. C. Miller, *Anal. Chem. 58* (1986) 1702.
[22] Review: K. Kimura, *Adv. Chem. Phys. 60* (1985) 161, and references cited therein.
[23] D. H. Parker, R. B. Bernstein, *J. Phys. Chem. 86* (1982) 60.
[24] H. Kühlewind, H. J. Neusser, E. W. Schlag, *J. Phys. Chem. 89* (1985) 5600.
[25] J. Silberstein, N. Ohmici, R. D. Levine, *J. Phys. Chem. 89* (1985) 5606.
[26] F. Rebentrost, K. L. Kompa, A. Ben-Shaul, *Chem. Phys. Lett. 77* (1981) 394.
[27] F. Rebentrost, A. Ben-Shaul, *J. Chem. Phys. 74* (1981) 3255.
[28] a) U. Boesl, H. J. Neusser, E. W. Schlag, *J. Chem. Phys. 72* (1980) 4327; b) *Chem. Phys. Lett. 87* (1982) 1.
[29] W. Dietz, U. Boesl, H. J. Neusser, E. W. Schlag, S. H. Lin, *Chem. Phys. 66* (1982) 105.
[30] a) R. G. Cooks, J. H. Beynon, R. M. Caprioli, G. R. Lester: *Metastable Ions*, Elsevier, Amsterdam 1973; b) H. Kühlewind, H. J. Neusser, E. W. Schlag, *Laser Chem. 3* (1983) 3; c) *J. Chem. Phys. 82* (1985) 5452.
[31] a) L. J. Moore, J. E. Hurst, E. H. Taylor, D. W. Beekman, M. T. Spaar, *Int. Phys. Conf. Ser. 84* (1986) 239; b) D. E. Pratt, J. Eagles, R. Self, *Mass Spectrom. 9* (1987) 407, and references cited therein.

[32] U. Boesl, H. J. Neusser, E. W. Schlag, *J. Am. Chem. Soc. 103* (1981) 5058.
[33] S. Leutwyler, U. Even, *Chem. Phys. Lett. 81* (1981) 578.
[34] D. A. Lichtin, S. Datta-Ghosh, K. R. Newton, R. B. Bernstein, *Chem. Phys. Lett. 75* (1980) 214.
[35] R. Trembreull, D. M. Lubman, *Anal. Chem. 54* (1984) 1962.
[36] R. Trembreull, C. H. Sin, P. Li, H. M. Pang, D. M. Lubman, *Anal. Chem. 57* (1985) 1186.
[37] D. M. Lubman, *Anal. Chem. 59* (1987) 31A, and references cited therein.
[38] D. M. Lubman, R. Trembreull, C. H. Sin, *Anal. Chem. 57* (1985) 1084.
[39] U. Boesl, J. Grotemeyer, K. Walter, E. W. Schlag, *Anal. Instrum. (NY) 16* (1987) 151.
[40] R. E. Smalley, L. Wharton, D. H. Levy, *Acc. Chem. Res. 10* (1977) 139, and references cited therein.
[41] J. B. Anderson, R. P. Andres, J. B. Fenn, *Adv. Chem. Phys. 10* (1966) 275.
[42] J. M. Hayes, G. J. Small, *Anal. Chem. 55* (1983) 565 A.
[43] C. M. Klimcak, J. E. Wessel, *Anal. Chem. 52* (1980) 1233.
[44] R. B. Opsal, *Thesis*, Indiana University, Bloomington (USA) 1985.
[45] S. W. Stiller, M. V. Johnston, *Anal. Chem. 59* (1987) 567.
[46] G. Rhodes, R. B. Opsal, J. T. Meek, J. P. Reilly, *Anal. Chem. 55* (1983) 280.
[47] G. R. Kinsel, K. R. Segar, M. V. Johnston, *Proc. 35th Annu. Conf. Mass Spectrom. Allied Top.* (Denver, CO, USA 1987), p. 405.
[48] E. Klesper, A. H. Corvin, D. A. Turner, *J. Org. Chem. 27* (1962) 700.
[49] C. M. White, R. K. Houck, *HRC CC J. High Resolut. Chromatogr. Chromatogr. Commun. 9* (1986) 3.
[50] C. H. Sin, H. M. Pang, D. M. Lubman, *Anal. Chem. 58* (1986) 490.
[51] H. M. Pang, C. H. Sin, D. M. Lubman, *Anal. Chem. 58* (1986) 1581.
[52] C. R. Blakley, M. L. Vestal, *Anal. Chem. 55* (1983) 750.
[53] M. L. Vestal, G. J. Fergusson, *Anal. Chem. 57* (1985) 2373.
[54] T. R. Rizzo, Y. D. Park, D. H. Levy, *J. Am. Chem. Soc. 107* (1985) 277.
[55] a) R. B. van Bremen, M. Snow, R. J. Cotter, *Int. J. Mass Spectrom. Ion Phys. 49* (1983) 35; b) R. J. Cotter, *Anal. Chim. Acta 195* (1987) 45.
[56] E. Schröder, H. Münster, H. Budzikiewicz, *Org. Mass Spectrom. 21* (1986) 707.
[57] R. B. Freas, M. M. Ross, J. E. Campana, *J. Am. Chem. Soc. 107* (1985) 6195.
[58] a) R. N. Zare, R. D. Levine, *Chem. Phys. Lett. 136* (1987) 593; b) R. R. Lucchese in C. J. McNeal (Ed.): *Mass Spectrometry in the Analysis of large Molecules*. Wiley, Chichester 1986, p. 151, and references cited therein.
[59] W. E. Henke, H. von Weyssenhoff, H. L. Selzle, E. W. Schlag, *Verh. Dtsch. Phys. Ges. 3* (1983) 139.
[60] H. von Weyssenhoff, H. L. Selzle, E. W. Schlag, *Z. Naturforsch. A 40* (1985) 674.
[61] L. Zandee, R. B. Bernstein, *J. Chem. Phys. 70* (1979) 1359, 2574.
[62] G. J. Fisanick, T. S. Eichelberger, B. A. Heath, M. B. Robin, *J. Chem. Phys. 72* (1980) 5571.
[63] M. P. Irion, W. D. Bowers, R. L. Hunter, F. S. Rowland, R. T. McIver, Jr., *Chem. Phys. Lett. 93* (1982) 375.
[64] T. J. Carlin, B. S. Freiser, *Anal. Chem. 55* (1983) 955.
[65] T. M. Sack, D. A. McCrery, M. L. Gross, *Anal. Chem. 57* (1985) 1291.
[66] Reported was a mass resolving power of 10^8 at mass 40: H. Bamberg, K. P. Wancek, *Proc. 35th Annu. Conf. Mass Spectrom. Allied Top.* (Denver, CO, USA 1987), p. 1116.
[67] K. P. Wancek, *Int. J. Mass Spectrom. Ion Processes 60* (1984) 11.
[68] a) W. E. Stephens, *Bull. Am. Phys. Soc. 21* (1946) 22; b) A. E. Cameron, D. F. Eggers, Jr., *Rev. Sci. Instrum. 19* (1948) 605; c) M. M. Wolff, W. E. Stephens, *ibid. 24* (1953) 616; d) H. S. Katzenstein, S. S. Freidland, *ibid. 26* (1955) 324.
[69] A. Benninghoven, *Z. Phys. 230* (1970) 403.
[70] D. F. Torgerson, R. P. Skowronski, R. D. Macfarlane, *Biochem. Biophys. Res. Commun. 60* (1974) 616.
[71] W. C. Wiley, I. M. McLaren, *Rev. Sci. Instrum. 26* (1955) 1150.
[72] R. B. Opsal, K. G. Owens, J. P. Reilly, *Anal. Chem. 57* (1985) 1984.
[73] a) W. R. Poschenrieder, *Int. J. Mass Spectrom. Ion Phys. 9* (1972) 357; b) M. L. Muga, *Anal. Instrum. (NY) 16* (1987) 31.
[74] B. A. Mamyrin, V. I. Karataev, D. K. Shmikk, V. A. Zagulin, *Sov. Phys. JETP (Engl. Transl.) 37* (1973) 45.
[75] U. Boesl, H. J. Neusser, R. Weinkauf, E. W. Schlag, *J. Phys. Chem. 86* (1982) 4857.
[76] D. M. Lubman, W. E. Bell, M. N. Kronick, *Anal. Chem. 55* (1983) 1437.
[77] T. L. Tai, M. A. El-Sayed, *Chem. Phys. Lett. 130* (1986) 224.
[78] K. Walter, U. Boesl, E. W. Schlag, *Int. J. Mass Spectrom. Ion Processes 71* (1986) 309.
[79] R. Frey, G. Weiss, R. Kaminski, E. W. Schlag, *Z. Naturforsch. A 40* (1985) 1349.
[80] M. Yang, J. P. Reilly, *Anal. Instrum. (NY) 16* (1987) 133.
[81] E. Niehuis, T. Heller, H. Feld, A. Benninghoven in A. Benninghoven (Ed.): *Ion Formation from Organic Solids IFOS III*, Springer, Berlin 1986, p. 192.
[82] a) R. D. Macfarlane, *Proc. 35th Annu. Conf. Mass Spectrom. Allied Top.* (Denver, CO, USA 1987), p. 1146; b) P. W. Geno, R. D. Macfarlane, *Int. J. Mass Spectrom. Ion Processes 77* (1987) 75.
[83] C. Brunnée, *Int. J. Mass Spectrom. Ion Processes 76* (1987) 125.
[84] See also H. J. Neusser, *Int. J. Mass Spectrom. Ion Processes 79* (1987) 141.
[85] H. Kühlewind, H. J. Neusser, E. W. Schlag, *Int. J. Mass Spectrom. Ion Phys. 51* (1983) 255.
[86] D. W. Squire, M. P. Barbalas, R. B. Bernstein, *J. Phys. Chem. 87* (1983) 1701.
[87] K. R. Newton, R. B. Bernstein, *J. Phys. Chem. 87* (1983) 2246.
[88] J. Grotemeyer, U. Boesl, K. Walter, E. W. Schlag, *Adv. Mass Spectrom. 10 B* (1986) 945.
[89] B. D. Kopiltz, J. M. McVey, *J. Chem. Phys. 80* (1984) 2271.
[90] J. H. Catanzarite, Y. Haas, H. Reisler, C. Wittig, *J. Chem. Phys. 78* (1983) 5506.
[91] D. A. Lichtin, D. W. Squire, M. A. Winnik, R. B. Bernstein, *J. Am. Chem. Soc. 105* (1983) 2109.
[92] R. S. Pandolfi, D. A. Gobeli, J. Lurie, M. A. El-Sayed, *Laser Chem. 3* (1983) 29.
[93] J. J. Young, D. A. Gobeli, R. S. Pandolfi, M. A. El-Sayed, *J. Phys. Chem. 87* (1983) 2255.
[94] S. R. Heller, G. W. A. Milne (Ed.): *EPA/NINH - Mass Spectral Data Base*, NSRDS, Department of Commerce, MA, USA 1978.
[95] W. Vetter in G. R. Waller, O. C. Dermer (Ed.): *Biochemical Applications of Mass Spectrometry, First Suppl. Vol.*, Wiley-Interscience, New York 1980, p. 439 ff.
[96] K. Biemann, J. A. McCloskey, *J. Am. Chem. Soc. 84* (1962) 3192.
[97] G. Junk, H. Svec, *J. Am. Chem. Soc. 85* (1963) 839.
[98] J. Grotemeyer, U. Boesl, K. Walter, E. W. Schlag, *Int. J. Mass Spectrom. Ion Processes 78* (1987) 68.
[99] T. R. Rizzo, Y. D. Park, L. Petenau, D. H. Levy, *J. Chem. Phys. 83* (1985) 4819.
[100] H. U. Winkler, H. D. Beckey, *Org. Mass Spectrom. 6* (1972) 655.
[101] P. Edman, *Acta Chem. Scand. 4* (1950) 283.
[102] F. Engelke, J. H. Hahn, W. Henke, R. N. Zare, *Anal. Chem. 57* (1987) 909.
[103] R. Trembreull, D. M. Lubman, *Anal. Chem. 59* (1987) 1003.
[104] J. Grotemeyer, K. Walter, U. Boesl, E. W. Schlag, *Proc. 35th Annu. Conf. Mass Spectrom. Allied Top.* (Denver, CO, USA 1987), p. 191.
[105] J. Grotemeyer, J. Lindner, K. Walter, E. W. Schlag, *Z. Naturforsch.*, in press.
[106] J. Grotemeyer, E. W. Schlag, unpublished results.
[107] a) H. J. Veith, F. W. Röllgen, *Org. Mass Spectrom. 20* (1985) 689; b) D. E. C. Rogers, P. J. Derrick, *ibid. 19* (1984) 490; c) P. J. Derrick, N. Tang-Trong, D. E. C. Rogers, *ibid. 20* (1985) 690.
[108] J. Grotemeyer, E. W. Schlag, *NATO-ASI Symp. Ser.*, in press.
[109] H. R. Schulten, W. Görtz, *Anal. Chem. 50* (1978) 428.
[110] J. H. Hahn, R. Zenobi, R. N. Zare, *J. Am. Chem. Soc. 109* (1987) 2843.
[111] R. Trembreull, D. M. Lubman, *Appl. Spectrosc. 41* (1987) 431.
[112] R. Trembreull, D. M. Lubman, *Anal. Chem. 59* (1987) 1082.
[113] K. Fujiwara, E. Voigtman, J. D. Winefordner, *Spectrosc. Lett. 17* (1984) 9.
[114] R. Trembreull, D. M. Lubman, *Anal. Chem. 58* (1986) 1299.
[115] J. Grotemeyer, U. Boesl, K. Walter, E. W. Schlag, *Org. Mass Spectrom. 21* (1986) 645.
[116] H. W. Ronge, H. F. Grützmacher, *Anal. Chem. Symp. Ser. 7* (1981) 255.
[117] P. Roepstorff, J. Fohlman, *Biomed. Mass Spectrom. 11* (1984) 601.
[118] J. Grotemeyer, E. W. Schlag in A. Benninghoven (Ed.): *Ion Formation from Organic Solids IV*, Springer, Berlin, in press.
[119] R. Frey, G. Weiss, H. Kaminski, U. Boesl, J. Grotemeyer, K. Walter, E. W. Schlag, *Proc. 35th Annu. Conf. Mass Spectrom. Allied Top.* (Denver, CO, USA 1987), p. 538.
[120] J. Grotemeyer, E. W. Schlag, *Org. Mass Spectrom.*, in press.
[121] U. Boesl, J. Grotemeyer, K. Walter, E. W. Schlag, *Adv. Mass Spectrom. 10 B* (1986) 985.
[122] J. Grotemeyer, U. Boesl, K. Walter, E. W. Schlag, *J. Am. Chem. Soc. 108* (1986) 4233.
[123] J. Grotemeyer, U. Boesl, K. Walter, E. W. Schlag, *Org. Mass Spectrom. 21* (1986) 595.
[124] a) K. Biemann, S. A. Martin, *Mass Spectrom. Rev. 6* (1987) 1; b) B. N. Green, R. S. Bordoli in S. J. Gaskell (Ed.): *Mass Spectrometry in Biomedical Research*, Wiley, Chichester 1986, p. 235; c) M. M. Sheil, P. J. Derrick, *ibid.*, p. 251.
[125] H. A. Scoble, S. A. Martin, K. Biemann, *Biochem. J. 245* (1987) 621.
[126] Kindly supplied by S. Schneider and E. Braslawski, Max-Planck-Institut für Strahlenchemie, Mülheim.
[127] J. Grotemeyer, E. W. Schlag, *Org. Mass Spectrom. 22* (1987) 758.
[128] See also K. Kleinermanns, J. Wolfrum, *Angew. Chem. 99* (1987) 38; *Angew. Chem. Int. Ed. Engl. 26* (1987) 38.
[129] H. Jungclas, H. Danigel, L. Schmidt, *Int. J. Mass Spectrom. Ion Phys. 52* (1983) 223.

Pheromones in Nanogram Quantities: Structure Determination by Combined Microchemical and Gas Chromatographic Methods

New Analytical Methods (35)

By Athula B. Attygalle and E. David Morgan*

What can a chemist do with a few nanograms of valuable organic substance, pure or impure? The answer may be, a great deal. Its components may be quantified, separated, isolated, degraded, derivatized, extracted by solvent partition, as well as the more obvious recording of their mass spectra. Provided a substance is not contaminated by large quantities of solvent, manipulations are possible without much loss or dilution. Necessity is the mother of invention. The examples given in this review show what can be accomplished today in nanochemistry and should act as a stimulus to direct the scientist to discover other applications appropriate to his needs and his circumstances. The examples are largely taken from the field of insect chemistry, but their general applicability is emphasized. This review illustrates how gas chromatography and reaction gas chromatography, alone or combined with mass spectrometry are potent tools in the hands of the chemist to deduce the unique structure of volatile organic substances available only in nanogram quantities.

1. Introduction

From the birth of their subject, organic chemists have devoted a great deal of skill and ingenuity to the determination of the structure of organic molecules. The advances in spectroscopic methods of the past quarter century have made the use of classical methods of degradation and derivatization almost redundant. As a result of this spectroscopic revolution, the elucidation of the structure of natural products has become almost routine. Nuclear magnetic resonance (NMR) spectroscopy, makes the greatest contribution to the assignment of structure to most new natural products. But the chemist probing the secrets of nature often finds substances of interest in quantities far too small for study by NMR spectroscopy. For example, for the pheromone chemist it is difficult to obtain sufficient pure substance for an NMR spectrum. With the exception of mass spectrometry, the other spectral methods usually require microgram to milligram samples of pure substances to obtain useful spectra (Table 1). There are examples of NMR spectra taken on samples as small as 1 to 2 μg,[1,2] but for complex substances it is customary to have about 1 mg.

Fourier transform infrared (FT-IR) spectroscopy is reaching towards the nanogram level when linked to gas chromatography, but the amount of structural information IR spectroscopy can provide is limited.

For the identification of nanogram quantities of natural products a chromatographic separation must precede or accompany spectroscopy. The spectral technique above all others for nanochemistry is mass spectroscopy; and the marriage of gas chromatography and mass spectrometry (GC-MS) is a powerful method of separation, detection and analysis. Although mass spectrometry can provide structural information and may sometimes completely define a compound, usually it does not give enough information for a unique structure of a new natural product. The pheromone chemist, for example, is faced with the choice of the labor and expense of collecting large numbers of insects in order to use NMR spectrometry (perhaps a thousand times that required for a mass spectrum) or to devise some other means of obtaining structural information from the small amount available.

The chemist who sees gas chromatography (GC) only as a high resolution separation and quantitation technique fails to see its potential as a source of structural information. In the simplest way, use of the specific detectors for the elements nitrogen, phosphorus and sulfur (Table 1) can indicate presence of these elements. Noting the retention of the substance on polar and nonpolar stationary phases can indicate the molecular mass and some information about the polarity of a substance. With degradative reactions or by conversion of the compound into a derivative, GC begins to yield more information, and when these are combined with MS, the structural information is increased considerably.

The degradative or derivatizing reaction may be carried out in a separate step, but is more conveniently combined with gas chromatography, either by reaction in the injector, or in a pre-column or a post-column reactor. Such a combined method is called reaction gas chromatography.

2. Solid Injection Techniques

2.1. Disadvantages of Solvents

Generally a mixture is dispersed in a solvent for chromatography, but solvents are a curse to the nanochemist.

[*] Dr. E. D. Morgan, Reader in Chemistry
Chemistry Department, University of Keele
Staffordshire ST5 5BG (England)
Dr. A. B. Attygalle
Alexander-von-Humboldt Stiftung Fellow, Institut für
Organische Chemie der Universität Erlangen-Nürnberg
Henkestrasse 42, D-8520 Erlangen (FRG)

 © VCH Verlagsgesellschaft mbH, D-6940 Weinheim, 1988 0570-0833/88/0404-0460 $ 02.50/0

Table 1. Practical limits of detection of gas chromatographic and spectroscopic detectors [a].

Detector	Abbreviation	Selectivity	Detectable quantity Minimum	Customary	Remarks:
Gas chromatographic [3]					
Flame ionization	FID	non-selective to all organic compounds, however highly oxidized compounds such as HCHO, CS_2 show very low responses	100 pg for alkanes	10 ng	destructive
Electron capture	ECD	selective; responds to electron adsorbing compounds e.g. halogens, nitro compounds, conjugated carbonyls	0.1 pg for lindane	100 pg	non-destructive
Thermal conductivity	TCD	non-selective	100 ng	1 μg	non-destructive
Nitrogen-phosphorus	NPD	highly selective; detection of carbon can be varied	1 pg	1 ng	destructive
Flame photometric	FPD	selective for sulfur and phosphorus	100 pg	10 ng	destructive
Spectroscopic					
Nuclear magnetic Resonance	^{1}H-NMR	selective: protons only	75 μg [b] 1 μg [c]	1 mg	non-destructive
	^{13}C-NMR	selective; ^{13}C only	500 μg [d]	5 mg [e]	non-destructive
Infrared	IR	selective	1 ng [f]	1 mg	non-destructive
Ultraviolet	UV	highly selective for the chromophores present	highly variable depending on the substance		non-destructive
Mass spectrometry	MS	non-selective in general	200 pg	5–500 ng	destructive

[a] This table serves only as a rough comparative guide, the absolute values will depend on the particular substance examined, conditions and the make and model of a particular instrument. [b] Vitamin B_{12} (5.5×10^{-8} mol); accumulation time 10 min. [c] Cortisone-21-acetate; accumulation time 13.9 h. [d] Cholesterol (1.3×10^{-6} mol); accumulation time 10 h. [e] Cholesterol (1.3×10^{-5} mol); accumulation time 10 min. [f] Using Fourier Transform IR spectroscopy.

An injection of 99.9% purity solvent onto a capillary GC system at high sensitivity demonstrates the impurity of such solvents. Moreover, plasticizers, stabilizers and antioxidants are picked up from contact with plastic and rubber with the greatest ease. Very volatile components may be lost in the solvent peak, this can be especially serious when looking for small fragment molecules from a degradation reaction. The solvent chosen may be selective for certain compounds of the mixture, so the composition from these gas chromatograms may not represent the true composition, and, occasionally, the solvent may react with and alter the components. Hence, for sensitive work, solvents are best avoided.

2.2. Solvent-free Techniques

A number of solventless injection techniques have been described, the earliest in 1958.[4] Each method appears to have its own merits depending upon the conditions and type of sample analyzed. Generally they have been used with packed columns, but there is no fundamental difficulty in adapting a solventless injector to capillary columns.

Bridges and *Guinn*, studying bark beetle pheromones, placed a whole beetle in the injection port of a GC, using a wire basket.[5a] A similar method has been used to introduce beetle defensive secretions into the injection port, using a cold plunger with a tiny groove to hold the sample.[5b] In another case, the sample was placed in the open end of a capillary pushed through a hole in the injection septum. However this is reported to give irreproducible retention times.[5c]

Solid injection techniques have been used to study plant tissues containing essential oils.[5d,e] In the study of sex pheromones of Lepidoptera, *Weatherston* and *MacLean* have used a commercially available solid sampler (Perkin–Elmer MS-41) with packed columns.[5f] The insect material was sealed in an aluminum or gold capsule, heated in the injection port and the capsule pierced with a needle. *Descoin*'s group in France have used this method extensively in the study of female lepidopteran pheromones,[6] on packed columns. Although a modification of this system has been used with capillary columns,[7] no applications of its use for natural products have been reported.

Another solvent-less injection technique is the precolumn designed by *Ställberg-Stenhagen*.[8a] Volatile substances from insect or plant material are trapped in a precolumn filled with an adsorbant such as Tenax-GC. The precolumn is then connected to a capillary column and rapidly heated to desorb the collected volatiles.[8b,c]

2.3. A Solid Sampler for Natural Products

A solid injection technique has been in use in our laboratory for insect studies since 1970.[9] Its most obvious advantages are simplicity of operation, reduced chance of contamination, and no dilution. The whole sample available can be placed on the column with minimum manipulations. Even the most volatile substances, such as methanol or acetaldehyde can be recognized and quantified. Most important, the GC instrument can be operated at maximum sensitivity, and accurate quantifications can be made of even minor components without fear of selectivity in extraction.

The sample is sealed inside a glass capillary, and placed in the heated injector for a few minutes to allow the sample to volatilize, or for a biological sample to heat through (Fig. 1). The tube is then crushed with a plunger and the volatile material is swept directly onto the column by the carrier gas.[9,10]

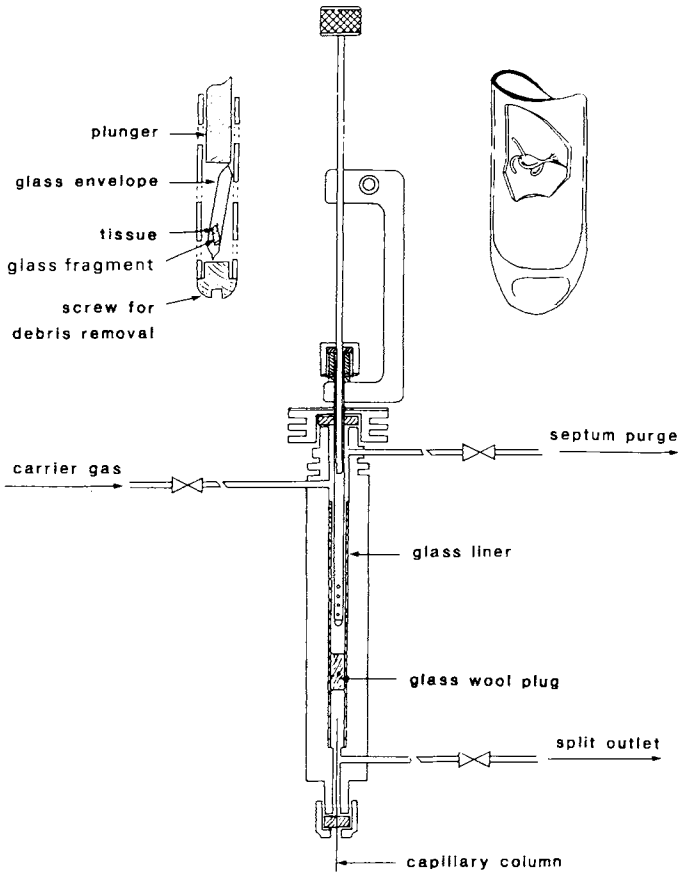

Fig. 1. The solid sample injector, for introducing samples into a gas chromatography column without the intervention of solvent. Illustrated as used with a capillary column. The arrangement is simpler for packed columns. The tip of the device (top left) and the biological tissue on a fragment of glass (top right) are shown enlarged.

2.3.1. *Use with Capillary Columns*

The system is adaptable to capillary columns, when mounted inside the glass insert of a splitless injection system. It is adapted to the Carlo Erba Fractovap splitless injector simply by drilling a larger hole in the metal cap that holds the injection septum. The narrow glass liners used in the injection ports of many other capillary instruments can be replaced by a 4 mm internal diameter glass tube.

The split vent is closed before the sample is crushed, then reopened about 30 seconds later. The oven temperature is initially low for a few min, then rapidly increased at the start of the program. The volatile substances are vaporized in the injector, condensed in the column and are then selectively vaporized with the increasing oven temperature. This yields a better focussing and narrower peaks. With very volatile components, it may be necessary to actively cool the first region of the column.

2.3.2. *Use in Sampling Biological Tissues*

Glandular reservoirs, such as the Dufour gland or poison vesicle of ants, are prepared for chromatography by dissecting under water, then the tissue is attached to a small fragment of glass, excess water is removed by touching with a fragment of paper tissue or filter paper, and the fragment of glass dropped into the glass capillary and the capillary sealed.[9, 11a, b] When a biological tissue is heated inside its sealed capillary and the capillary crushed, the cells are completely disrupted by the steam produced from the cellular fluid. Complete release of volatile material is thereby ensured. If it is necessary to show that the substances examined come from the glandular sac and not from droplets in the tissue, the gland can be pierced by a fine glass capillary of diameter smaller than the gland, the contents removed by capillarity and the fine glass capillary itself is sealed in a larger one and submitted to GC.[12]

Some aphids secrete alarm pheromones from a pair of tubular structures (cornicles) on the posterior abdomen, when disturbed. The cornicle droplets can be collected in capillaries in a similar manner, sealed in larger capillaries and chromatographed. Whole insects that are sufficiently small or pieces of tissue can be examined in this way. A gas chromatogram of the mandibular gland substances from the head of a *Myrmica* ant is shown in Figure 2.

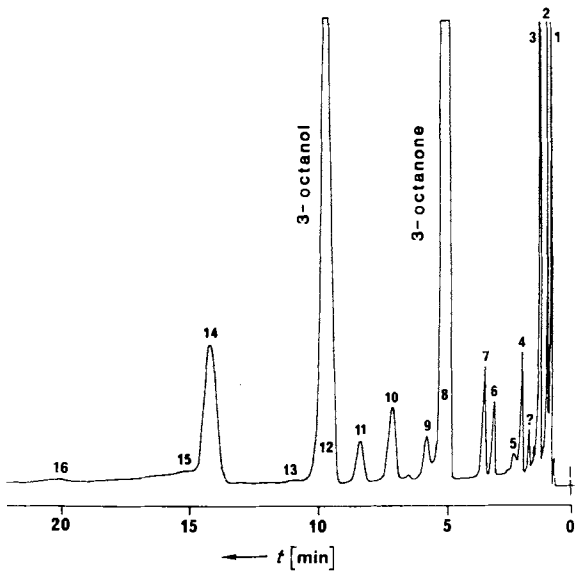

Fig. 2. Gas chromatogram of the mandibular gland contents of one worker of the ant *Myrmica albuferensis*, using the solid sampling technique with a packed column (2.75 m × 4 mm of 10% PEG 20M on Chromosorb W at 130°C). 1, ethanol; 2, acetone; 3, 2-methylpropanal; 4, 3-hexanone; 5, 3-pentanol; 6, 3-heptanone; 7, 3-hexanol; 8, 3-octanone; 9, 3-heptanol; 10, 6-methyl-3-octanone; 11, 3-nonanone; 12, 3-octanol; 13, 6-methyl-3-octanol; 14, 3-decanone; 15, 3-nonanol; 16, 3-undecanone.

The solid sampling method has been used extensively at Keele for the study of glandular substances of ants, generally with packed columns,[13] though with some early applications of capillary columns.[14] The advantages of capillary columns in this work was illustrated when re-examining the Dufour gland substances of the ant *Lasius niger*. Over 50 components were recognized with a capillary column[15a] where only 15 had been identified previously.[15b] A capillary chromatogram from a Dufour gland of *Lasius fuliginosus* is illustrated in Figure 3.

The solid sampling method with capillary columns has been used in analyzing intact sex pheromone glands excised from a number of female moths.[16] These pheromones are located in a small glandular area of the abdom-

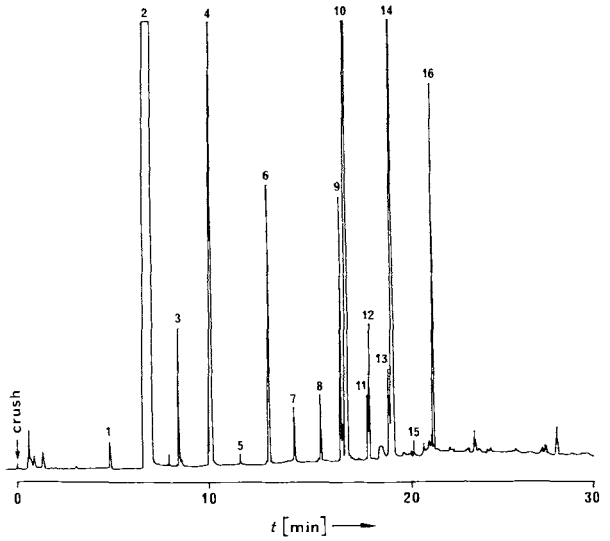

Fig. 3. Gas chromatogram of the Dufour gland contents of one worker of the ant *Lasius fuliginosus*, using the solid sampling technique with a capillary column. 1, decane; 2, undecane; 3, dodecane; 4, tridecane; 5, tetradecane; 6, pentadecane; 7, 2-tridecanone; 8, 2-tetradecanone; 10, 2-pentadecanone; 11, heptadecane; 12, 2-hexadecanone; 14, 2-heptadecanone; 15, 2-octadecanone; 16, 2-nonadecanone; 9 and 13 are two unidentified carbonyl compounds.

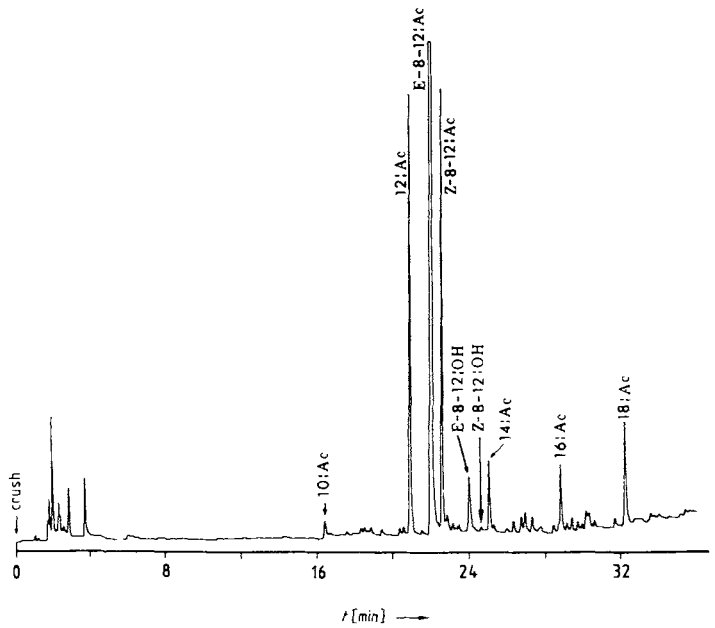

Fig. 4. A gas chromatogram obtained from a sex pheromone gland of an adult female *Cryptophlebia leucotreta*, by solid sampling on a 25 m × 0.22 mm fused silica capillary column, coated with SP-2340. The oven temperature was held at 60 °C for 2 min and programmed to 195 °C at 4 °C/min. 10:Ac, decyl acetate; 12:Ac, dodecyl acetate; 14:Ac, tetradecyl acetate; 16:Ac, hexadecyl acetate; 18:Ac, octadecyl acetate; E-8-12:Ac, (*E*)-8-dodecenyl acetate; Z-8-12:Ac, (*Z*)-8-dodecenyl acetate; E-8-12:OH, (*E*)-8-dodecenol; Z-8-12:OH, (*Z*)-8-dodecen-1-ol.

inal tip, and the females secrete the pheromone only in the period when they are "calling" the males. Hence, the sample must be prepared during this calling period. Figure 4 shows a gas chromatogram obtained from an individual female of the false codling moth *Cryptophlebia leucotreta*.[16c] The technique has been useful in biosynthetic studies, in determining the fate of a precursor after local application.[17]

3. Trapping and Rechromatography

The homogeneity of a peak suspected of being an unresolved mixture of substances can be checked by rechromatographing on a stationary phase of different polarity. But if the mixture is complex, new heterogeneous peaks may occur in the second chromatogram. The solution is to rechromatograph only one peak or a narrow region of the chromatogram. This principle, called multidimensional gas chromatography (MDGC), was first conceived by *Deans*,[18] but did not receive much attention until the appearance of capillary columns.[19] A commercial instrument (Siemens, Sichromat-2) is available with two ovens linked together. Any peak resolved on a nonpolar packed column in the first oven can be switched to a second column, preferably a capillary, for further resolution in the second oven.[20,21] Many other systems of column switching have been devised. MDGC should be useful in determining the optical isomeric composition of chiral pheromones. Columns coated with chiral chromatographic phases[22] have been used for such analyses. These chiral phases are very delicate, hence crude mixtures must be prepurified before chromatography. The use of a chiral column as the second column in MDFG simplifies the manipulation.[23] However, a two-oven chromatograph may be beyond the means or needs of most chromatographers. The same result can be achieved in a simple way by trapping a peak and rechromatographing it on a different phase.

3.1. Effluent Splitting

Trapping of individual peaks may also be required for biological testing, or pure material may be required to accumulate for an NMR or UV spectrum. Structural information may be obtained by chemical reaction on the trapped substance before or during rechromatography. With the nondestructive thermal conductivity detector, the whole of the sample can be collected after the detector, but the low sensitivity of the detector rules it out for many purposes. With the flame ionization detector (FID) a number of effluent splitters have been described, by which a small proportion of the carrier gas reaches the detector and most of it is diverted to a cooled receiver. All-glass splitters are preferred to the early metal ones,[24,25] to avoid catalytic transformations on the hot metal surface. An all-glass splitter for packed columns,[26] simple to make and operate, has been used in our laboratory for a number of years with success (Fig. 5).

No make-up gas is necessary with flow rates normally employed with packed columns (30 to 60 mL min^{-1}). The low flow rates used in capillary columns (0.5 to 2 mL min^{-1}) require a make-up gas if the effluent is split to collect peaks. A few elaborate systems have been described for preparative capillary gas chromatography[27] but a very simple system, such as that of *Williams* and *Vinson*[28] is all that is required.

3.2. Peak Trapping

Many systems of collection and design of traps have been described for gas chromatography.[29] For the collec-

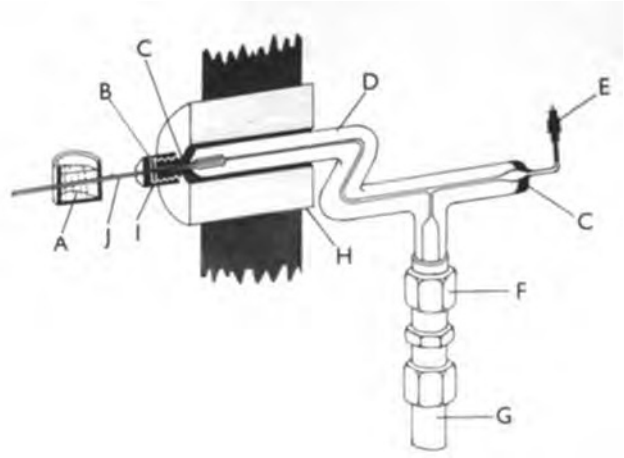

Fig. 5. The effluent splitter for packed columns with trapping capillary attached. A, liquid nitrogen coolant; B, silicone rubber septum; C, glass-to-metal seal; D, glass capillary; E, connection to detector with restrictor wire; F, Swagelok union; G, chromatography column; H, outlet heater; I, hexagonal nut; J, glass capillary.

tion of larger samples (up to μg) we have used steel capillary tubing bent into a U-shape. The U-tube is cooled in liquid nitrogen.[24] Some users prefer glass tubes because of their relative chemical inertness, or to place some column packing, quartz wool or cotton inside the capillary collector or to coat its inside walls. However, others have quoted up to 90% recovery can be achieved with empty glass capillaries, under optimum conditions,[25] and our experience bears this out. It is better to avoid coolant baths using a solvent, because of the chance of contamination, and to use either crushed dry ice[30,31] or liquid nitrogen.[32]

The factors governing trapping efficiency are not well understood, but boiling point, polarity and molecular shape of the compound as well as dimensions of the trapping capillary and gas flow rate all play a part. The temperature of the trap and temperature gradient[25] before the trap seem to affect efficiency. *Klimes* et al.[33] have studied the influence of some of these parameters upon trapping efficiency.

For trapping nanograms of pure compounds from either packed or capillary columns, we have found that a simple arrangement of a glass capillary pushed through two holes in a plastic cap from a specimen tube is convenient and efficient.[32] The internal diameter of the tubes seems critical. Aerosol formation can occur in larger-diameter tubes. One end of the capillary is pushed through a pin-hole in a silicone rubber disc held in the screw or female Luer fitting which fits the splitter of Figure 5. An example of myristic acid trapped in such a capillary is shown in Figure 6. The sharp temperature boundary on the inlet side is clearly seen.

3.3. Rechromatography without Solvent; Melting Point Determination

The glass trapping capillary can be sealed at both ends in a flame and used directly for rechromatography on a different phase or stored until needed. Figure 7 shows the results of a trapping and rechromatography experiment. A synthetic mixture of tetradecane and pentadecane was chromatographed. In a second run the pentadecane was trapped out. Only 5% of the sample went to the detector. The material collected in the glass capillary was sealed and directly rechromatographed; in this way, trapping efficiencies up to 85% have been obtained.[32]

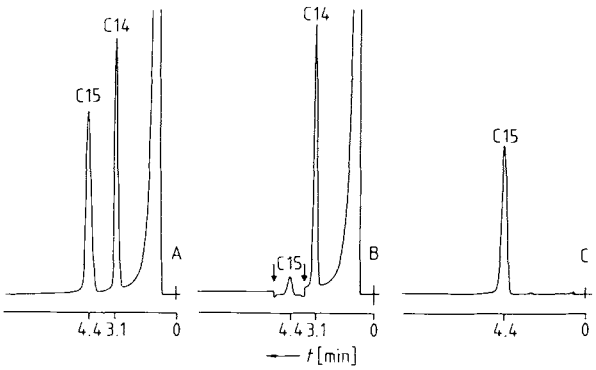

Fig. 7. Efficiency of trapping. A) Tetradecane and pentadecane (250 ng each) in 0.5 μL of hexane chromatographed on a 1.5 m × 4 mm column of 5% SE-30 at 145°C. B) The same amount injected, trapping the effluent between the times indicated by the arrows. C) The total trapped sample is reinjected by the solid injection technique.

When a Dufour gland of the ant *Myrmica rubra* was chromatographed on a polar stationary phase, two components of the secretion, heptadecadiene and (*Z,E*)-α-farnesene eluted together. This peak could be resolved into its components by trapping and rechromatographing on a non-polar SE-30 silicone phase.[32]

Many of the natural products subjected to gas chromatography are liquids at room temperature, but some, including some insect pheromones are solids. The melting points of solids, trapped from the vapor in glass capillaries, such as the myristic acid shown in Figure 6, can be determined with great accuracy using a hot stage microscope.[34] The amount required is chiefly limited by the magnifying power of the microscope. This method can also be used to examine chirality, if both enantiomers are available. Coinjection of each enantiomer in turn with the unknown, trapping the eluate and determining the melting points will reveal which is the racemate by its altered melting point.

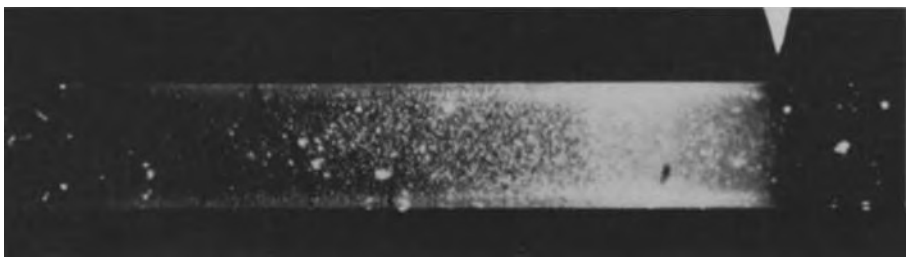

Fig. 6. A few micrograms of myristic acid were trapped in a glass capillary as shown in Fig. 7, from a 1 m × 4 mm 15% FFAP column. Gas flow from the right. The arrow marks the boundary of the cooled zone, and the deposition of crystalline myristic acid.

3.4. Rechromatography with Solvent

The substance trapped in the glass capillaries does not have to be rechromatographed with the solid sampler. If more convenient, 1 μL of a suitable solvent can be injected from a syringe with a fine needle, just inside the capillary end (Fig. 8). The only requirement is that the needle diam-

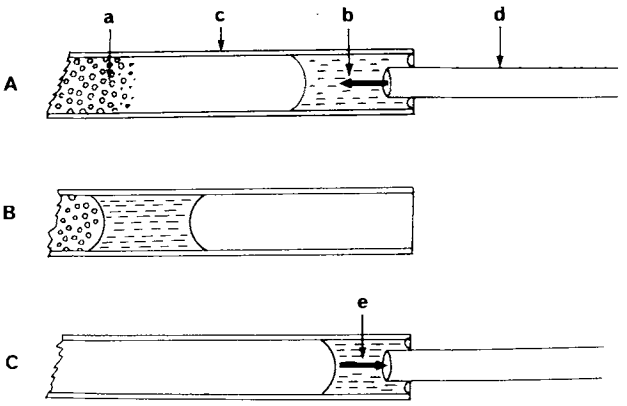

Fig. 8. Reaction in a glass capillary. A) The reagent solution b (1 μL), is added to the trapped material a, in a trapping capillary c, by inserting the tip of a fine syringe needle d (75 mm × 0.17 mm o.d.), just inside the glass capillary. B) The reagent solution is mixed with the trapped material by tilting the capillary. C, the reaction mixture e is tipped back to the end of the capillary and withdrawn with the syringe.

eter should fit easily inside the capillary. By tipping the capillary the column of solvent can be made to mix with the trapped material. The needle is reinserted and the solution is removed. Because of the fine needle used, the material must be rechromatographed through a septumless injector. Efficiencies of recovery of 80–90% have been experienced in our work.[34]

4. Location of Double Bond Positions

The location of the position of double bonds can be an important part of natural product structure determination. Electron impact mass spectrometry is not very helpful unless the spectra of the compound and all its double bond isomers are available. Frequently an indirect method has to be found when dealing with biologically important compounds[35] available only in nanogram quantities.

Even chemical ionization (CI) mass spectrometry with the usual reagent gases such as methane may not help, but methyl vinyl ether and a few other unsaturated gases have been successfully employed as the reagent gas to locate the double bond in mono-unsaturated compounds.[36] The alkene and methyl vinyl ether produce a pair of four-centered addition complexes **1**, **2**, which in turn fragment to produce two characteristic ions **3**, **4** (Scheme 1). The *m/z* values of the ions **3** and **4** can locate the position of the double bond. A mixture of methyl vinyl ether, nitrogen and carbon disulfide as reagent gas are said to give simpler spectra with identifiable molecular ions and characteristic ions to locate the double bond.[36b] However, others[37] report the method is not specific to alkene functions, since adduct ions are also observed with saturated compounds. Similar difficulties with methyl vinyl ether CI spectra have been observed by *Budzikiewicz* and *Busker*.[38] They found that the double bond could be located with isobutane as reagent gas in most cases, in difficult cases they recommend nitric oxide or methylamine. Isobutane CI-spectra have been used[39] for locating conjugated dienes in a range of compounds, including aldehydes, alcohols, formates, acetates, and hydrocarbons.

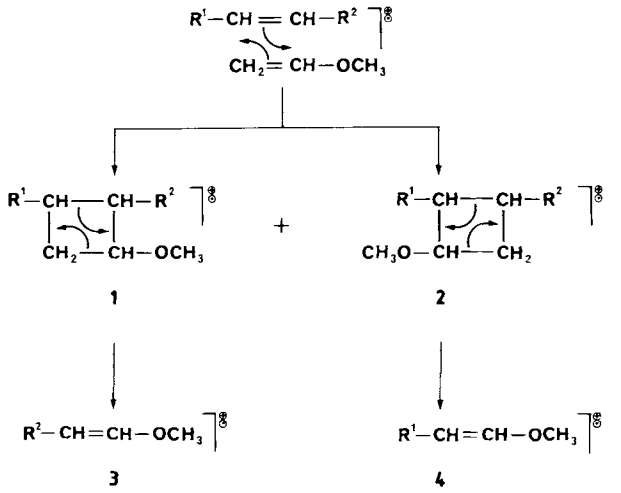

Scheme 1.

It is possible to locate the double bond of mono-unsaturated acetates and alcohols from the relative intensities of some ions of the electron impact spectrum, in spite of the ease of isomerization. *Horiike* et al.[40] first described this empirical approach to double bonds in tetradecenyl acetates. Two other groups have verified and refined the method for C_{12}, C_{14}, and C_{16} linear mono-unsaturated acetates.[41,42] The mass spectra of certain alkatrienes also show fragments characteristic of the double-bond positions.[43] To use this method, all the pure synthetic double-bond isomers are required, to compare with the unknown. Their synthesis alone can be tedious and if they are available, the same results can be achieved by comparing retention times of standards and unknown.

This does not exhaust the mass spectrometric methods that have been proposed, if advanced equipment is available. Negative ion MS/MS has been used to locate double bonds in unsaturated fatty acids. The acids are ionized by fast atom bombardment (FAB) and then collisional activated decomposition (CAD) spectra of the $[M-H]^{\ominus}$ ions are observed.[44]

Generally, the chemist has to resort to derivatization methods, as summarized in Scheme 2, to find the position of double bonds. In all these methods, the compound is converted into a derivative which in GC–MS gives characteristic cleavage ions at the point of attachment of the derivative groups.[45–57] Alternatively, the compound is cleaved at the double bond into smaller fragments that can be identified by GC retention times and possibly mass spectra.[58a–d]

All of these methods tax the skill and ingenuity of the chemist when dealing with nanogram samples.

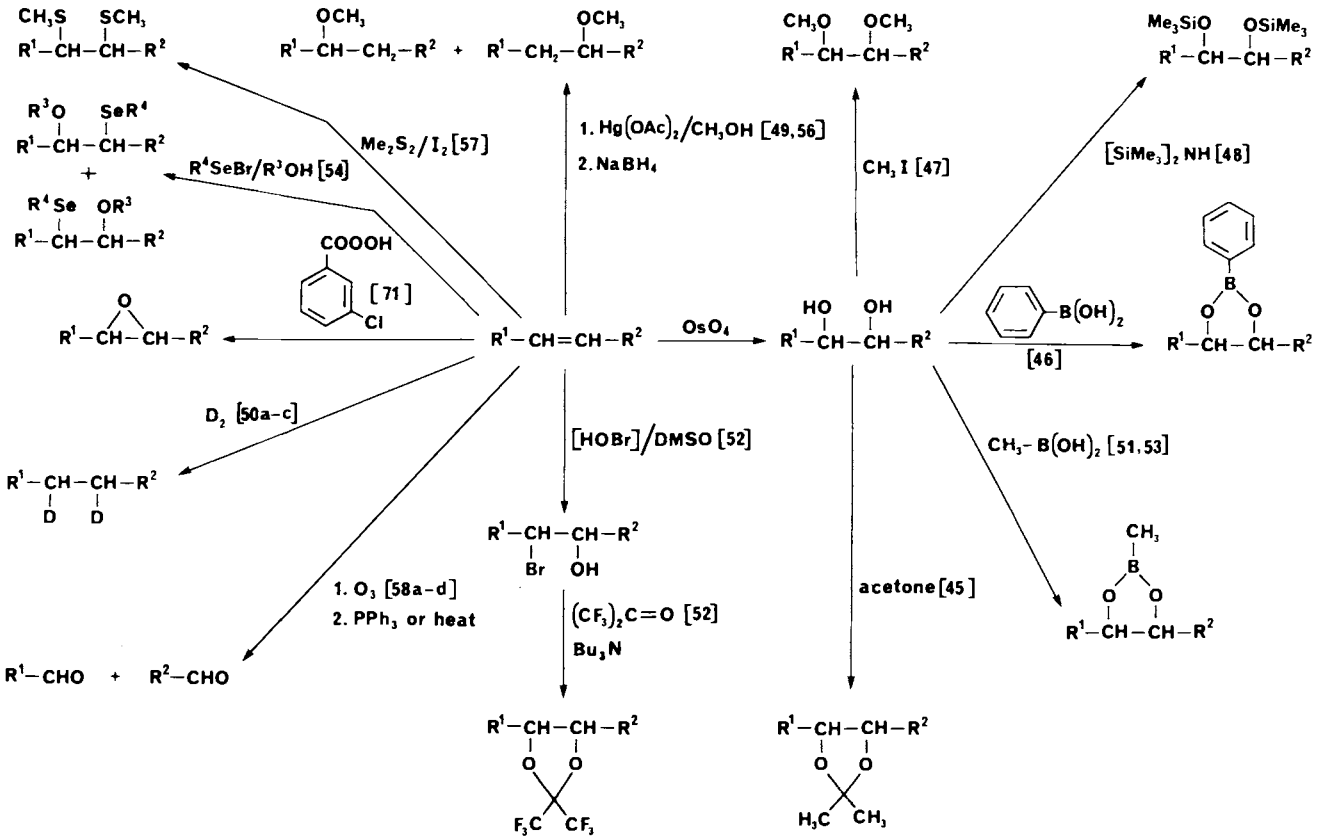

Scheme 2.

5. Nanogram Reactions with Trapped Compounds

Valuable information can be obtained concerning the carbon skeleton or the functional groups of a molecule by performing derivatization or degradation reactions, before, during or after gas chromatography. When the reaction and chromatography are combined, by use of a pre- or post-column reactor, the technique is referred to as reaction gas chromatography.[59,60] Such a technique is particularly useful where only nanograms of sample are available, because of the convenience of handling; however, because of its ease of use and simplicity, the procedure is gaining popularity even when sample size is not a limitation. Some substances must be derivatized to impart better gas chromatographic characteristics to the molecule. Sometimes a crude reaction mixture can be directly injected into the GC. In other cases, the product must be first extracted into an organic solvent.

5.1. Reactions without a Solvent Extraction Step

5.1.1. Ozonolysis

Ozonolysis is a particularly simple and useful technique for the location of carbon-carbon double bonds and has been known for some time.[58a,b] However, its development as a microchemical technique owes much to the work of *Beroza* et al.[58c,d] A relatively inexpensive ozone microgenerator can be assembled from commercially available components, similarly to that described by *Beroza* and *Bierl*,[61] (Fig. 9). The sample is taken up in 5 μL of solvent and, after passage of ozone, is ready for gas chromatography by splitless injection. The customary addition of triphenylphosphane to reduce the ozonides is not essential,[30,32,62] since they are readily cleaved in the GC injection port to carbonyl compounds. Moreover, excess Ph_3P would be only slowly eluted from the column and thus interfere with subsequent analyses.

The main drawback of ozonolysis in a solvent is the difficulty of identifying the small molecular fragments formed because their GC signals are obscured by the solvent peak. *Beroza* and *Bierl*[58c,d] therefore suggested CS_2 as the most suitable solvent for molecules larger than pentanal. More recently, pentyl acetate and hexadecane[58e] have been proposed for molecules smaller than pentanal. The difficulty of solvent peak interference in detecting small molecules is best avoided by "dry" ozonolysis without a solvent.[16d,30-32]

In this technique the alkene is trapped in a glass capillary and ozonized oxygen is passed through a fused silica capillary onto the trapped alkene (Fig. 9). This can be sealed in a larger capillary and kept in the GC injector for three minutes before crushing the tube and releasing onto the column the carbonyl products formed by pyrolytic cleavage of the ozonides. Figure 10 shows the use of the technique in the ozonolysis of a mixture of heptadecane and (*Z*)-8-heptadecene. After ozonolysis, the (*Z*)-8-heptadecene peak disappears completely, octanal and nonanal

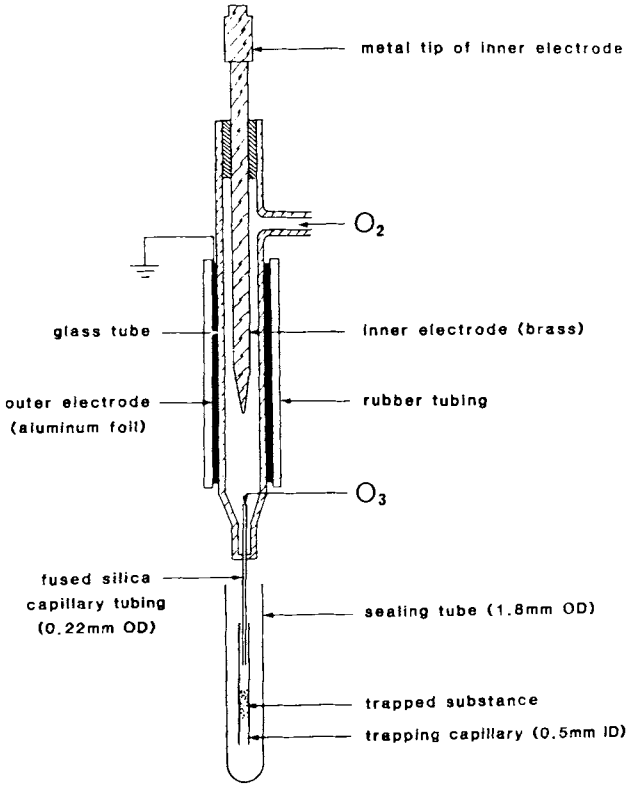

Fig. 9. Microgenerator for ozone. The ozonized air is fed directly to the trapped material through a short length of fused silica capillary tubing.

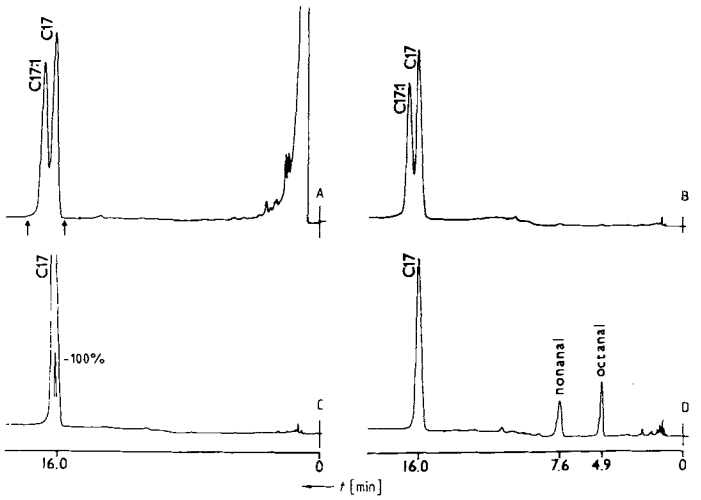

Fig. 10. Trapping, reaction and reinjection. A) Heptadecane and 8-heptadecene (350 ng of each) in 0.5 μL hexane chromatographed on a 10% PEGA column. B) The portion between the arrows in A was trapped and reinjected. C) The trapped portion was reinjected and hydrogenated on-column. D) The trapped portion was ozonized and reinjected. C17:1, (*Z*)-8-heptadecene.

peaks appear, and heptadecane remains unaffected. This method was applied to the pentadecene isolated from the Dufour glands of the ant *Tetramorium caespitum*.[63] The mixture of pentadecane and pentadecene (total of 30 ng) from three Dufour glands was trapped and ozonolyzed. The production of hexanal, heptanal, octanal and nonanal indicated that the pentadecene peak was a mixture of 6- and 7-pentadecene.

This method of "dry" ozonolysis is particularly useful for the determination of the carbon skeleton between the end of the chain and the first double bond. It has been used in the structure elucidation of farnesene **5** and its homologues **6** and **7** from the Dufour glands of *Myrmica* ants.[64] Microozonolysis demonstrated the presence of an

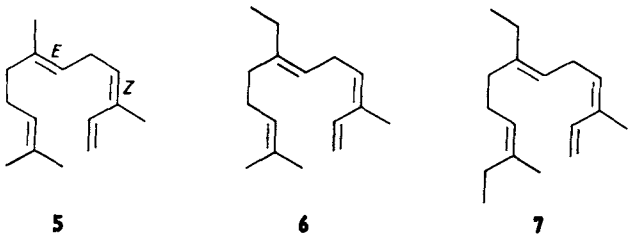

5 **6** **7**

isopropylidene group in farnesene **5** and homofarnesene **6**, through the production of acetone. The formation of butanone confirmed the presence of a 1-methylpropylidene group in bishomofarnesene **7**. About 50 ng of alkene is sufficient for an analysis. The products are introduced into the chromatograph as ozonides, rather than the more volatile carbonyl compounds, and losses are minimal. The use of ozonolysis to cleave alkynes and alkynoic esters has appeared recently.[65]

The detection of formaldehyde, arising from a terminal double bond, or small dialdehydes from the molecular fragment between two double bonds, presents difficulties. These compounds are not detected by FID. Several methods have been recommended for the detection of formaldehyde. In one, it is treated with 1,3-cyclohexanedione to produce the pyran derivative **8**, which is suitable for GC

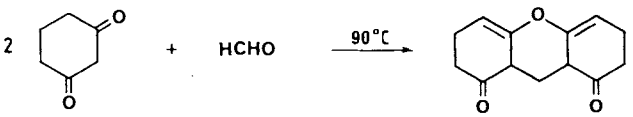

8

detection.[66] Other recommended methods are the formation of pentafluorophenylhydrazones,[67a] *O*-benzyloximes,[67b] *O*-(*p*-nitrobenzyl)oximes,[67b] and *O*-pentafluorobenzyloximes,[67c] all of which are detectable by GC.

We have found two useful methods for determining nanogram quantities of formaldehyde and other low molecular mass carbonyl compounds. In the first, reaction with *O*-benzylhydroxylamine in a Keele microreactor (cf. Section 5.2) gives quantitative yields of benzyloximes, suitable for GC in the usual way.[68] In the second, the carbonyl compounds are reduced with $NaBH_4$ and the corresponding alcohols analyzed on a Porapak column.[69]

Polyfunctional carbonyl compounds have also been converted into derivatives suitable for gas chromatography. 1,2-Dicarbonyl compounds, as are formed, e.g., in the ozonolysis of conjugated double bonds, can be converted into quinoxalines **9** by reaction with *o*-phenylenediam-

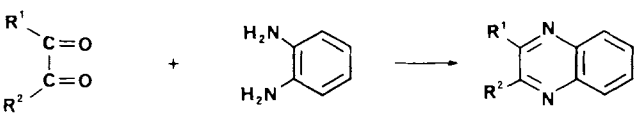

9

ine.[66] Samples as small as 50 ng have been handled by this method.[30] Hydrazine hydrate can convert 1,3- and 1,4-dicarbonyl compounds into pyrazoles **10** and dihydropyridazines **11**, respectively.[66]

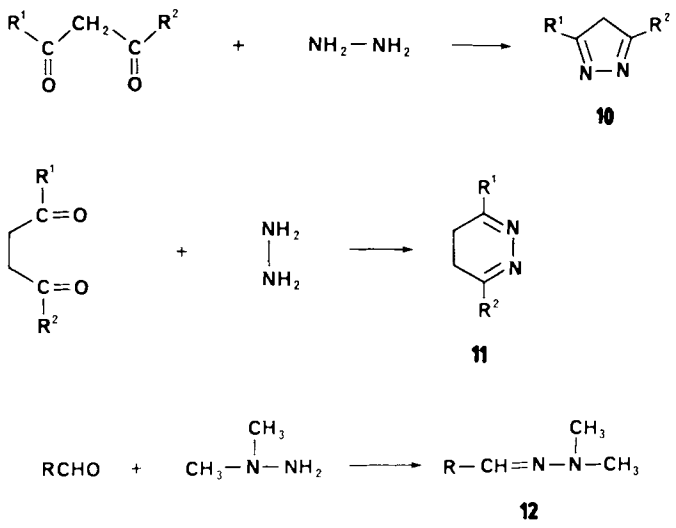

All these derivatives are also suitable for GC-MS analysis. Both quinoxalines and pyrazoles generally give the molecular ion as base peak, while dihydropyridazines give a large [M − 2] peak due to aromatization. Aldehydes as ozonolysis products or unsaturated aldehydes found in many pheromone mixtures tend to give featureless mass spectra. Both aldehydes and ketones can be converted into dimethylhydrazones **12**, which give suitable mass spectra with intense molecular ions (ca. 20–30% relative intensity).[70]

5.1.2. Epoxidation

The epoxides derived from alkenes and other unsaturated compounds can be prepared by reaction with *m*-chloroperbenzoic acid (MCPBA) (Scheme 2).[71] In the case of simple epoxides, electron impact (EI)-MS, and for more epoxides, chemical ionization (CI)-MS, can locate the position of the oxirane ring,[72] thus establishing position of the double bond in the parent compound. When more than one double bond is present in the molecule, epoxidation can still be used successfully.[1,72d] The reaction can be stopped at the monoepoxide stage and CI mass spectra of the two monoepoxides can indicate the positions of unsaturation in the parent compound.

This reaction is particularly useful in determining the (*E*)/(*Z*) ratios of geometrical isomeric mixtures. For many insect pheromones the characteristic (*E*)/(*Z*) ratio gives the maximum biological activity. Capillary columns coated with polar phases such as SP-2340 can yield base line separations of (*E*)- and (*Z*)-isomers of underivatized monoenes.[73a,b] However, the same result can also be achieved on nonpolar capillary columns or packed columns by converting the alkenes into the corresponding epoxides.

Nanogram quantities of alkenes trapped in glass capillaries can be epoxidized while keeping the total reaction volume to 1 μL. For example, a mixture of heptadecane and (*E*)- and (*Z*)-8-heptadecene was trapped and epoxidized by adding MCPBA in hexane, in a manner similar to that described in Section 3.4 (Fig. 11).[34] After the reaction, the 8-heptadecene peak in the chromatogram was completely replaced by the two corresponding epoxide signals, while the heptadecane peak remained unaffected. When the 8-heptadecene from the Dufour gland of the ant *Myrmica rubra* was epoxidized, only a single peak, co-chromatographing with the synthetic (*Z*)-8,9-epoxyheptadecane was obtained (Fig. 11c).

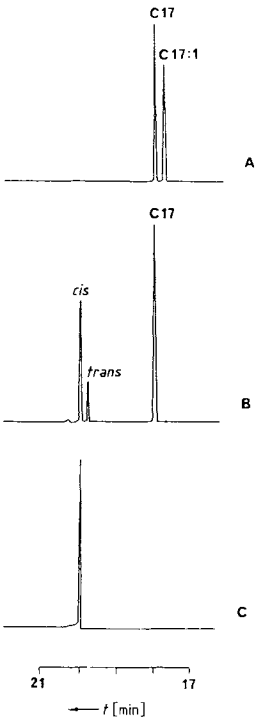

Fig. 11. Separation of (*E*)- and (*Z*)-8-heptadecenes by epoxidation. A) Mixture of heptadecane and heptadecene was chromatographed on an OV-1 capillary column. B) Both peaks from A were trapped in a single fraction, the mixture epoxidized with *m*-chloroperbenzoic acid and reinjected. C) (*Z*)-8-Heptadecene from the Dufour gland of *Myrmica rubra*, trapped, epoxidized and reinjected in the same way.

The epoxides can be converted into a number of secondary derivatives which possess better GC-MS characteristics (Scheme 3). *Minnikin*[77] has critically reviewed these methods. *N,N*-dimethylamino-alcohol derivatives[37] are particularly useful for CI-MS procedures.

5.1.3. Cleavage of Epoxides

Since epoxy groups are encountered in many natural products, e.g. the juvenile hormones **13** and some insect pheromones, microtechniques for locating the epoxide position are very important. Direct mass spectrometry usually

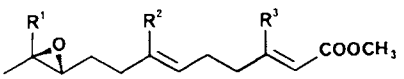

13 a, $R^1 = R^2 = R^3 = Et$ JHO
b, $R^1 = R^2 = Et$; $R^3 = Me$ JH I
c, $R^1 = Et$; $R^2 = R^3 = Me$ JH II
d, $R^1 = R^2 = R^3 = Me$ JH III

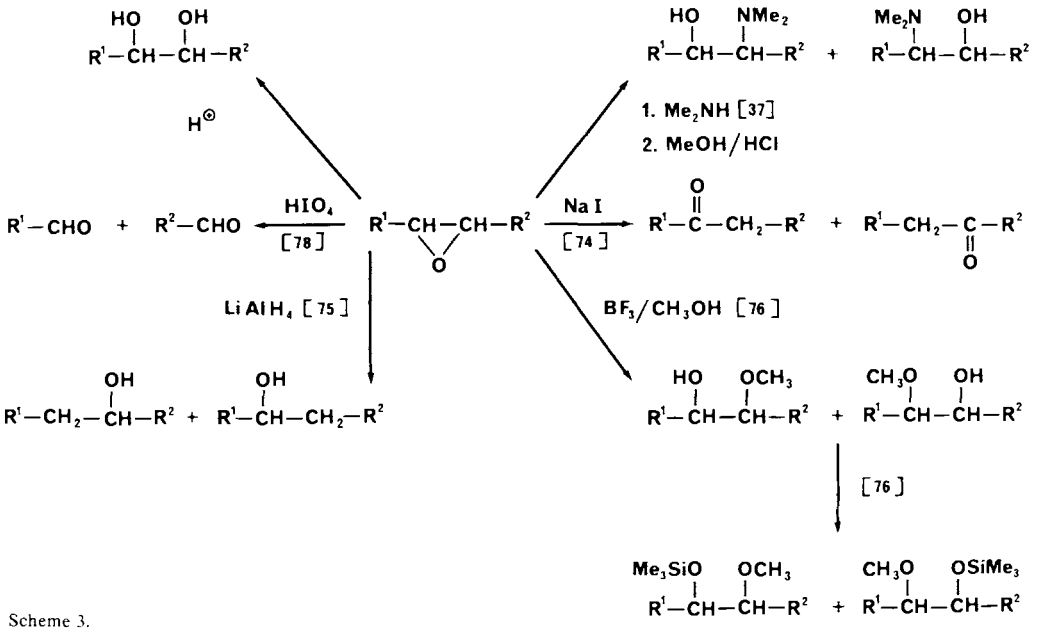

Scheme 3.

signals the presence of the epoxide. For confirmation, the epoxides can be converted into chemically or mass spectrometrically more easily recognizable entities (Scheme 3).

The epoxides can be cleaved with periodic acid to the corresponding carbonyl compounds, which can then be gas-chromatographed.[78] The geometrical configuration of the disubstituted epoxides can be examined by measuring the reaction time. The *trans*-epoxides are cleaved much more slowly than the *cis*-isomers.[78] Epoxide cleavage by reaction gas chromatography can be achieved simply by heating an epoxide collected in a glass capillary, with solid periodic acid in a sealed tube in the injection port of a gas chromatograph.[32] However, it is more convenient to have periodic acid in a precolumn.[79]

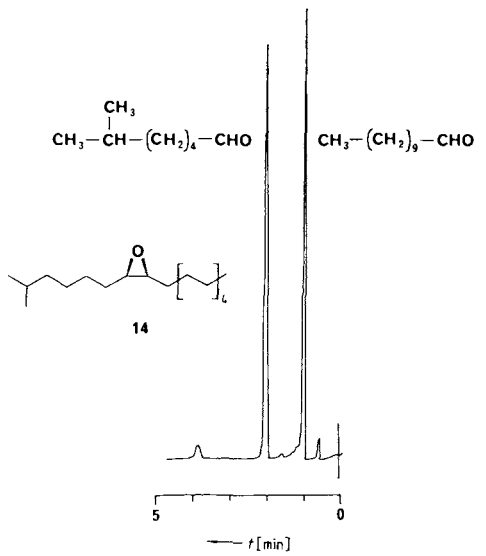

Fig. 12. Epoxide cleavage on a periodic acid precolumn. Disparlure (200 ng) was sealed in a glass capillary and introduced into the gas chromatograph by the solid sampling technique at 180°C. It passed through a periodic acid precolumn and then through a column of 10% PEG 20M.

Figure 12 illustrates the cleavage of the pheromone disparlure **14** by a periodic acid precolumn. Disparlure was trapped in a glass capillary and injected by the solid injection technique. The precolumn cleaved disparlure to 6-methylheptanal and undecanal. A periodic acid precolumn connected to the top of a Porapak Q column is useful for the study of low-mass epoxides. For example, 1,2-epoxypropane and 2,3-dimethyl-2,3-epoxybutane yield acetaldehyde and acetone respectively, whereas 2,3-epoxy-2-methylbutane is cleaved to both acetaldehyde and to acetone. Similarly, juvenile hormones I and II, (**13b**, **13c**) yield butanone as one product, thus indicating that the oxirane ring contains an ethyl group and a methyl group attached to the same carbon atom. In contrast, the juvenile hormone III (**13d**) furnishes acetone. Accordingly, in this case two methyl groups are attached to the same carbon of the epoxide ring.[79] The cleavage of epoxides is quantitative and only a few nanograms of sample are required for a determination.

5.1.4. Hydrogenation

The characterization of alkenes can be facilitated by hydrogenation to saturated analogues which often provide easily interpretable mass spectra. This is particularly useful for determining the carbon skeleton of an unsaturated terpenoid, and combined with mass spectrometry can help determine the number of rings and double bonds in the molecule. Reaction gas chromatographic hydrogenation of unsaturated compounds necessitates employment of a precolumn[32, 80a, b] or a postcolumn[80c] catalyst and hydrogen as the carrier gas. Reduction takes place almost instantaneously. Compounds with up to four C=C groups have been reduced completely using a precolumn catalyst of only a few cm in length.[64] The mass spectra can be obtained in the same step as the reduction when hydrogen is used as the carrier gas. Otherwise the hydrogenated substances can be trapped and re-introduced by the solid-sam-

pling technique. The method is applicable to a few nanograms of unsaturated substance or can be used on a micropreparative scale. The reduction of (*Z*)-8-heptadecene (Fig. 10c) shows that the reaction can be quantitative.

A system of hydrogenation with capillary columns has been described for double-oven chromatography. It has been examined in detail for checking the suitability of the catalysts for the reduction of aromatic hydrocarbons and compounds containing polar functional groups.[81]

An alternative procedure is to trap the alkenes in a glass tube containing the catalyst,[30,31] fill the tube with hydrogen, seal, and heat in the injection port for a few minutes before crushing the tube and chromatographing the products.

5.1.5. *Hydrogenolysis*

The simplest derivative that can be prepared for the characterization of an organic compound is its parent alkane or cycloalkane. Complete hydrogenolysis to this parent, frequently called carbon skeleton chromatography, saturates multiple bonds and replaces functional groups containing halogen, oxygen, sulfur and nitrogen by hydrogen. The resulting products, usually the parent alkane or sometimes the next lower homologue or a mixture of the two can then be identified. The compound is allowed to react with hydrogen in a precolumn containing Pd or Pt catalysts at temperatures much higher than those normally used for hydrogenation.[82a-d] *Brownlee* and *Silverstein* have modified this procedure for use directly with trapped material without the intervention of a solvent.[25] When brevicomin **15**, a sex attractant of the Western pine beetle *Dendroctonus brevicomis*, was subjected to hydrogenolysis, they obtained *n*-nonane. A simpler, alternative procedure has been described by *Bierl-Leonhardt* and *DeVilbiss*.[83a] They heated neat or trapped substances, sealed in a tube, with platinum and $LiAlH_4$. The products were then taken up in hexane or hexadecane, depending upon the molecular mass of the expected products, and examined by GC or GC-MS.[83] $LiAlH_4$ apparently serves as a hydrogen source, since similar reaction with Pt alone yielded unsaturated products.

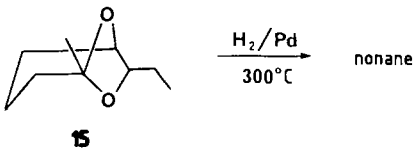

15

A method of structure determination for cyclic sulfur compounds has been devised which involves hydrodesulfurization in a microreactor connected between gas chromatograph and mass spectrometer.[84] Using both hydrogen and deuterium gas, structural information and ring size can be deduced.

5.1.6. *Reduction with $NaBH_4$*

The identification of aldehydes and ketones has been aided by their reduction to the corresponding alcohols with $NaBH_4$, followed by GC and GC-MS analysis.[85] The identification of aldehydes is particularly difficult because of their tendency to oxidize and because they give rather featureless mass spectra. Reduction products larger than hexanol have been identified by reduction with an ethanolic or aqueous solution of $NaBH_4$ in the barrel of a syringe.[86] Surprisingly, it is possible to carry out the reduction with solid $NaHB_4$ in a sealed glass tube, without hydrolysis or additional moisture, at least for a range of carbonyl compounds thus far tested.[14,32,87] An application of this procedure is illustrated in Figure 13. The mandibular gland of *Myrmia* ants contains a mixture of 3-alkanols and 3-alkanones (Figs. 2 and 13A). 3-Octanone, and the minor component 3-heptanol, which elutes as a shoulder on the 3-octanone peak, were trapped in a glass tube, and rechromatographed with finely powdered solid $NaBH_4$. The 3-octanone was quantitatively reduced to 3-octanol and the unchanged 3-heptanol became clearly visible (Fig.

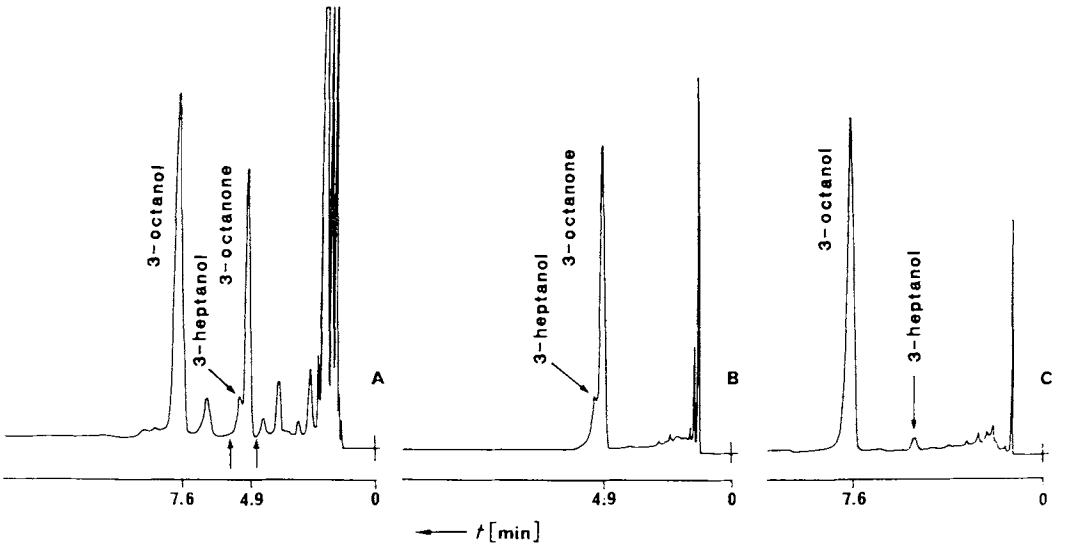

Fig. 13. Reduction of carbonyl compounds. A) The total contents of the mandibular glands of one *Myrmica ruginodis* worker chromatographed on a 10% PEGA column at 125 °C. B) The effluent between the arrows in (A) was trapped and reinjected; C) the effluent was trapped, treated with $NaBH_4$ and injected.

13C). Most probably the reduction takes place between the carbonyl vapors and solid $NaBH_4$ in the injection port.

Alternatively, the reduction can be carried out with $NaBH_4$ in a solvent (not water or ethanol) suitable for on-column injection, such as tetrahydrofuran (THF) or dimethoxyethane, although the solubility of $NaBH_4$ in THF is poor. In one application, saturated $NaBH_4$ in THF was injected into 3-octanone trapped in a glass capillary. The reduction was over 90% complete in 10 minutes[60] (cf. Section 3.4).

A method has been described which is the reverse of this carbonyl reduction. Using a pre-column of activated copper dust at 300–325 °C, primary and secondary alcohols can be dehydrogenated to the corresponding aldehydes and ketones prior to mass spectrometric investigation.[88] This enables a distinction to be made between primary, secondary and tertiary alcohols and dialkyl ethers.

5.1.7. Bromination

A method to differentiate between the peaks of saturated and unsaturated substances in a GC profile is extremely valuable to the microchemist. Bromination shifts all the peaks of the unsaturated compounds, leaving those of the saturated intact. The reaction is instantaneous and the brominated products elute much more slowly than the original alkanes, so that the bromo adducts with more than ten carbon atoms are rarely observed in the chromatogram. Bromination is a stereospecific *trans* addition. Hence the reaction can be used to monitor the geometry of low molecular weight alkenes.[89] Usually the adduct from the *trans*-alkene elutes before that of the corresponding *cis*-isomer. The use of an extremely dilute solution of bromine in a solvent such as hexane or carbon disulfide is recommended. Nanogram amounts of material trapped in glass capillaries can be brominated by the method described in Section 3.4. Figure 14 shows an example of the technique applied to a mixture of heptadecane, 8-heptadecene, nonadecane, and 9-nonadecene.[34] Microscale bromination of glandular components can be achieved by adding 1 μL of bromine solution onto a dissected gland, which can then be chromatographed by a solid injection technique.

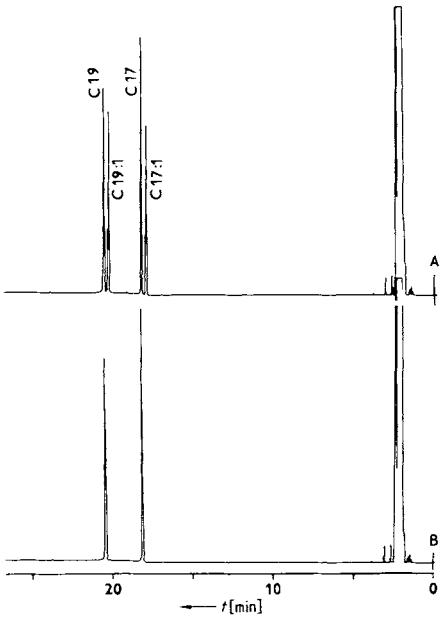

Fig. 14. Bromination of alkenes. A) A mixture of heptadecane, (*Z*)- and (*E*)-8-heptadecene, nonadecane and (*Z*)- and (*E*)-9-nonadecenes (100 ng each) were trapped in a glass capillary and reinjected. B) The same mixture treated with bromine before reinjection. Chromatographed on an OV-1 capillary column programmed from 40 to 300 °C at 10 °C/min.

5.1.8. Esterification with Diazomethane

The lower members of aliphatic monocarboxylic acids are sufficiently volatile to be separated directly by GC. However, adsorption of acids onto the chromatographic support often leads to tailing of the peaks. Esterification is frequently used to convert relatively nonvolatile and polar carboxylic acids into less polar methyl esters with better GC characteristics. The wide variety of techniques available for the esterification of fatty acids has been reviewed.[90a, b] Fatty acids can be trapped from the GC effluent in glass capillaries, and conveniently esterified using CH_2N_2 in THF.[34] The reaction mixture can be rechromatographed as described in Section 3.4. *Huwyler* et al. used a comparable method to esterify low-molecular weight fatty acids and identified the fatty acid components of the trail pheromone of the ant *Lasius fuliginosus*.[91] There is one example reported of a procedure in which octanoic acid was injected into the chromatograph shortly before an ethereal solution of CH_2N_2.[92] Other reaction GC methods available for the esterification of fatty acids have been reviewed by *Harris*.[93]

5.1.9. Acetylation of Alcohols

Acetylation is a useful reaction to check the identification of alcohols and then to distinguish between a primary and a secondary alcohols. Furthermore, if the substance has biological activity, a loss of activity upon acetylation and its return upon saponification may indicate that the active substance is an alcohol.

Primary and secondary alcohols can be acetylated on a microscale by a method similar to that described by *Huwyler*.[94] For primary alcohols trapped in a glass capillary, THF containing acetic anhydride and pyridine can be added, and the mixture examined by GC by on-column injection. Although the reaction is slow for secondary alcohols, it is quantitative. The same procedure can also be used for acetylating phenols, and the number of phenolic groups present can be estimated from the shift in retention time. The method is applicable to samples of a few nanograms.

5.1.10. Dehydration

Dehydration of alcohols to alkenes by reaction GC has been known for some time. Under favorably mild conditions, alcohols can be dehydrated in such a way that the new double bond is formed and remains at the original position of attachment of the hydroxy group. A number of dehydrating agents such as alumina,[87] $KHSO_4$,[87]

H_3PO_4,[95] and hexamethylphosphoric triamide[87] have been employed.

Drawert et al.[59,95] used a precolumn reactor containing phosphoric acid. *Stanley*[87] conducted the dehydration of trapped alcohols in sealed glass capillaries. Recently, *Kobold* et al. and *Bestmann* et al.[96] have used a few milligrams of Al_2O_3 in the insert liner of the injection block for the dehydration of terpene alcohols. *Stanley*[87] found that basic alumina gives fewer rearrangement products than acidic alumina: for example, 1-heptene was the major product of dehydration of 1-heptanol, whereas acidic alumina yielded all five isomeric heptenes.

5.1.11. Subtraction Techniques

Information about functional groups present in a compound can be obtained by the subtraction-loop technique. An appropriate reagent deposited on a solid support, placed before or after the analytical column forms nonvolatile products and thereby abstracts the reacted compounds from a mixture.[82d]

Subtraction techniques for packed columns have been known for some time and many reviews of the subject are available.[97] Only recent advances in this area will be mentioned here. Benzidine has been used to remove carbonyl compounds; however, it is a potent carcinogen and its use is now forbidden. Non-mutagenic 3,3',5,5'-tetramethylbenzidine may be used instead.

Alieshoev et al.[98] have described a reagent for the subtraction of unsaturated aliphatic hydrocarbons. The compound, a styrene-divinylbenzene copolymer with *N,N*-

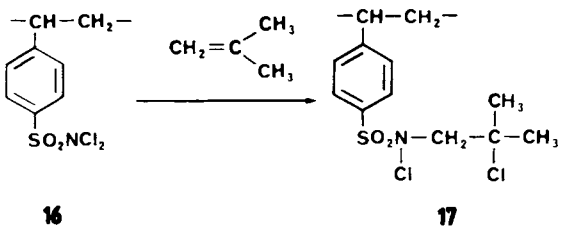

16 **17**

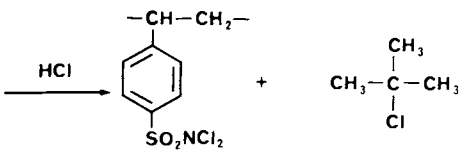

16

dichlorosulfonamide groups (**16**), removes alkenes and alkynes quantitatively, whereas alkanes and aromatic compounds remain unattacked. Furthermore, the used polymer (**17**) can be converted back into the active form **16** by a current of hydrogen chloride. *Kalo*[99] has described the use of subtraction techniques with capillary gas chromatography, where the subtracting agent is deposited on the wall of a glass capillary column.

5.1.12. Other Methods

There are many other reactions which could swell the armory of nanoscale chemistry. Alcohols have been oxidized in sealed glass capillaries[87] to carbonyl compounds by potassium dichromate crystals. A periodic acid precolumn can also convert alcohols into carbonyl compounds, although the yields are poor.[32] A number of microreactions can be performed by leaving the reactants in the syringe barrel for a few minutes[85,86] before chromatography.

In many cases, compounds containing active hydrogen (e.g. **18**) display better gas chromatographic characteristics when silylated (**19**). Moreover, the mass spectra of silyl

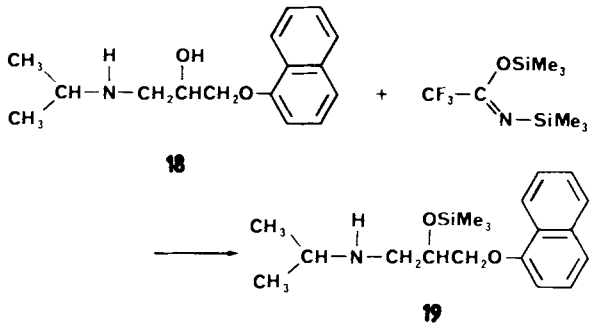

18 **19**

ethers can yield more structural information, e.g. the position of the OH group in a secondary alcohol can often be located in this way.[58e] Many of the large number of silylating techniques available[100] may be adapted for use on a microscale.

Non-esterified, low molecular weight fatty acids have been trapped into tubes containing Ag_2O to give the silver salts **20**. After introducing either methyl iodide or benzyl chloride[101] to the trapped material, it can be rechromatographed in the form of the ester using a solid-injection technique.

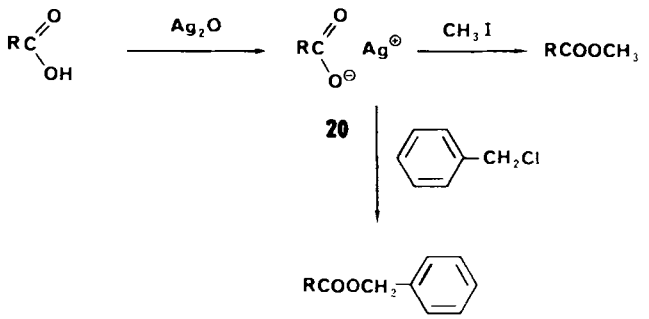

20

A number of other microchemical derivatization methods are available[102] that might be adapted for use on a nanogram scale. It is evident from the examples given that a large number of chemical reactions long practiced on a macroscale are adaptable, with a little ingenuity, to very small quantities.

5.2. Reactions Requiring a Solvent Extraction

Many of the reactions of macroscale organic chemistry require considerable work-up to isolate the product: a compound may have to be released from a salt, excess reagent destroyed, or the product separated from an aqueous mixture of spent reagents. It may not be possible to adapt such reactions directly to the microscale and inject the crude reaction mixture into a gas chromatograph. The reagents and spent products may be corrosive or destructive to the stationary phase or interfere with the analysis. A review by *Poole* and *Schuette*[103] discusses the methods available for sample preparation before capillary GC, including extraction and concentration, and summarizes the problems associated therewith.

Separating funnel partitions require mL quantities of solvent while only a few μL are sufficient for chromatography. Either the small and valuable sample is going to be in very dilute solution, or the solvent must be removed, concentrating impurities in the residue and possibly losing valuable volatile components.

A recent method described by *Cais* and *Shimoni*[104] shows recoveries of more than 80% from extractions, but requires at least 2 mL of extracting solvent. Much lower solvent volumes, have been used by *Grob* et al.[105] for the extraction of organic substances from water samples. *Murray*[106] has improved this method to give better recoveries. A simple but efficient extraction method using a glass syringe has been described by *van Rensburg* and *Hassett*.[107] The sample is extracted in the syringe barrel, which is then turned upside down and the solvent is withdrawn from the tip by gently pushing the plunger.

None of the above methods and devices are suitable for derivatization before extraction, especially when the reaction requires heating. Therefore, we developed a technique that allows derivatization and extraction in the same container with the minimum of manipulation and transfers. The device, which we call the *Keele microreactor*[108] (Figs. 15 and 16), is available commercially.

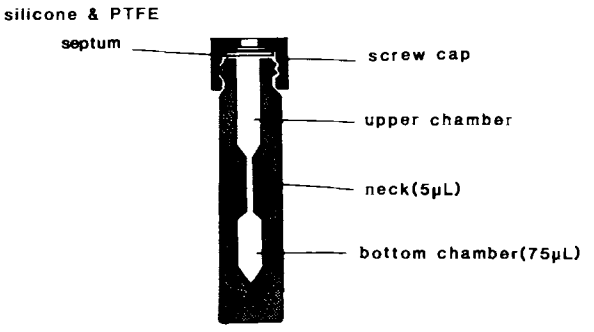

Fig. 15. A sectional view of the Keele microreactor. The microreactor is available from Wheaton Scientific, Millville, NJ 08332 (USA) and their distributors world-wide.

The Keele microreactor has essentially three features; a bottom chamber, a narrow capillary neck, and an upper chamber. When using the microreactor for reaction or extraction, the required liquid layer is drawn into the narrow capillary neck, from which it can be efficiently and almost completely removed for analysis. One of the main advantages of this procedure is that the substances can be extracted with solvents either lighter or heavier than water. The microreactor can be sealed with a teflon liner and screw cap and heated up to 200°C in an oven without any loss of material.

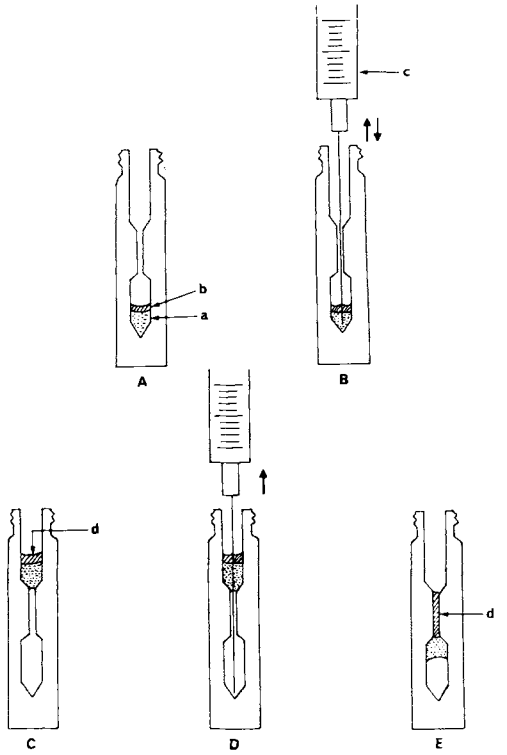

Fig. 16. Use of the Keele microreactor. A) After reaction in the lower chamber, an extraction solvent b is added to the reaction mixture a. B) The two phases are mixed by pumping through a syringe (100 μL). C) The two phases are placed in the upper chamber to separate. D) The spent reagents are drawn into the lower chamber by withdrawing air by a syringe. E) The product in solution is left in the middle chamber d, from which it can be withdrawn efficiently by a microliter syringe.

In a typical extraction procedure the aqueous solution (about 50 μL) is mixed with a solvent such as hexane (10 μL) by pumping the mixture in and out of a glass syringe (Fig. 16B). This process ensures the breakage of the liquid mass into tiny droplets causing an intimate mixing of the two phases. The liquid mixture is allowed to settle in the upper chamber. The surface tension of the liquid in the narrow neck and air in the bottom chamber prevents the liquids running into the lower chamber. A fine syringe needle (0.17 mm OD) is inserted into the lower chamber and air is withdrawn until the desired organic liquid layer enters the neck region (Fig. 16D). Then the organic layer can be withdrawn efficiently for GC or HPLC analysis. Typical recoveries were 40–65% for a single extraction step and nearly 90% for three consecutive extractions.[108]

Some derivatization reactions requiring extraction demonstrate the usefulness of the reactor. Further examples can be devised to suit the chromatographer's problem.

5.2.1. *Pentafluorobenzylation of Carboxylic acids*

Pentafluorobenzyl bromide is a useful reagent for the derivatization of phenols, mercaptans, sulfonamides and carboxylic acids[109] prior to a GC analysis. In a typical derivatization, the acid and pentafluorobenzyl bromide **21**

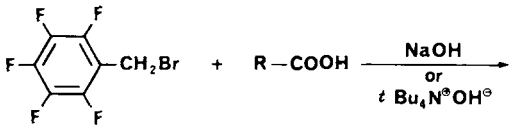

21

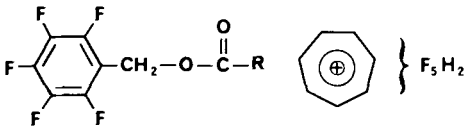

22 **23**

are placed in the bottom chamber of the microreactor. A strong base such as aqueous tetra-*tert*-butylammonium hydroxide is added to remove hydrogen bromide. The reactants are drawn up and down into a glass syringe several times to ensure thorough mixing. The reaction mixture is placed back in the bottom chamber, the vial is closed and shaken. After the reaction is complete 20 µL of water and 10 µL of hexane are added and the organic layer is removed for GC examination.[108] The reaction is fast and quantitative. The derivatives **22** can be identified easily by GC–MS, due to the presence of the pentafluorotropylium cation **23**. Only a few nanograms are required for flame ionization detection. The sensitivity can be increased to picogram level when an electron capture detector (ECD) is used.

5.2.2. *Methoxymercuration–Demercuration of Alkenes*

Methoxymercuration-demercuration has gained popularity as a method for locating the position of double bonds in alkyl chains. *Abley* et al.[49] first described the application of GC–MS to these methoxy derivatives (Scheme 4). The reaction produces two adducts, **24** and **25**, for a single mono-unsaturated compound. The two methoxy derivatives **26** and **27** usually co-elute in GC. The fragmentation of the derivatives in the mass spectrometer results in preferential cleavage on either side of the methoxy group to yield four intense and characteristic fragment ions **28**–**31**. From the masses of these ions, the original double bond position can be deduced.

Many applications of this technique have been reported.[56, 110] The methoxy derivatives **26** and **27** produced must be partitioned between water and ether or hexane before the non-aqueous layer is examined by GC. Such extraction usually requires 50 µL or more of the nonaqueous solvent to allow convenient withdrawal of the upper layer. By the use of the Keele microreactor, 200 ng of alkene samples were conveniently derivatized and the methoxy derivatives could be extracted into 5 µL of hexane.[108]

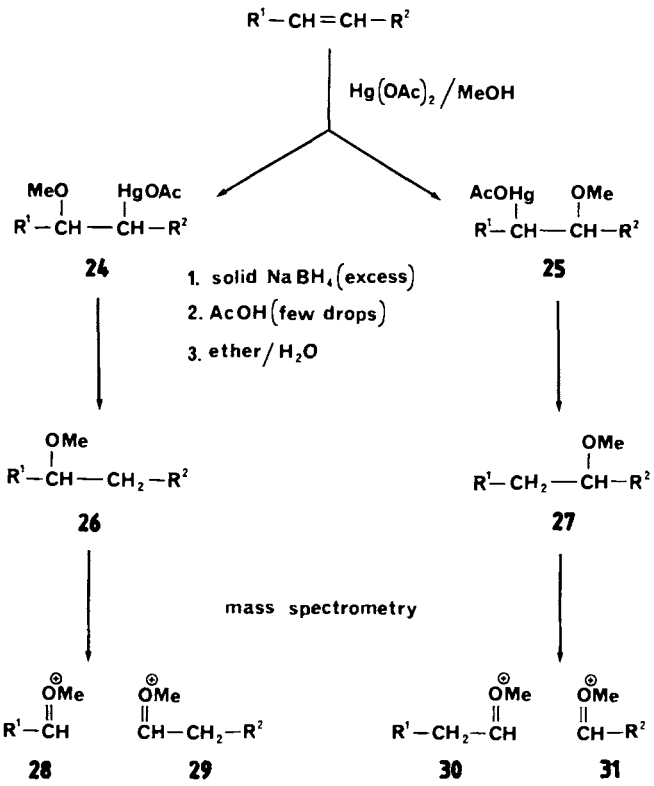

Scheme 4.

5.2.3. *Methylthiolation of Alkenes*

The addition of dimethyl disulfide (DMDS) to monounsaturated alkenes,[57] acetates,[111a] fatty acid esters, aldehydes and alcohols[111b,c] is a more recent method used to locate double bond positions. The addition is stereospecific for both (*E*)- and (*Z*)-isomers yielding a single adduct in each case. The adducts cleave in the mass spectrometer preferentially across the carbon–carbon bond between the CH_3S substituents, leading to two major fragment ions **32** and **33** (Scheme 5). These give intense peaks, one of them usually the base peak, which can be employed to locate the double bond in the parent molecule.

In the procedures described by *Buser* et al.[111a] and *Dunkelblum* et al.[111b] the adducts are finally extracted into 200 µL of hexane and concentrated before chromatographic examination. By employing the Keele microreactor the sensitivity of the method is improved manyfold.[108]

Methylthiolation has a number of advantages over the more widely used methoxymercuration-demercuration method.[63] In the latter the reaction mixture is heterogeneous and is difficult to handle once mercury has been displaced. The reaction is not quantitative, the yields being typically between 55 and 70%. In contrast, methylthiolation is a homogenous reaction, all the components are miscible, much smaller quantities of the unsaturated compound can be used, and the reaction is near quantitative. In methoxymercuration-demercuration a mixed mass spectrum is obtained of the two derivatives (Scheme 4) and each monounsaturated compound gives four characteristic peaks. Methylthiolation leads to only one product with two intense ions (Scheme 5), which are generally more in-

tense than those of methoxy derivatives. Further, the methoxy derivatives rarely show a molecular ion, so identification is less certain. While the underivatized alkenyl acetates, alcohols and aldehydes rarely show molecular ions, the DMDS derivatives examined have always shown a prominent molecular ion. The DMDS adducts of alkenyl acetates and methyl esters of fatty acids show significant fragment ions arising from a loss of acetic acid or methanol respectively from the ion **33**.[111a,b] Similarly, the spectra of unsaturated alcohols and aldehydes show a weak loss of water from the ion **33**.[111c] These ions help to establish the functionality of the compound when a mixture is being examined.

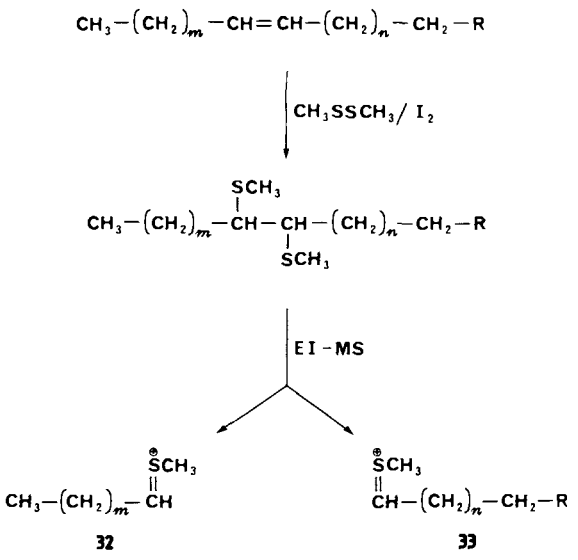

Scheme 5.

Finally, the methoxy-derivative method does not distinguish between (*E*)- and (*Z*)-isomers, whereas the methylthioether method proceeds with stereospecific *trans* addition. The (*E*)- and (*Z*)-isomers yield *erythro*- and *threo*-isomers respectively, which may give almost identical mass spectra, but they are resolved by capillary GC, with the *threo*-isomer usually eluting first. Hence the geometry of an unknown compound can be determined by comparing the retention time with those from a standard (*E*)- and (*Z*)-mixture.

Although methylthiolation has been frequently used only with monoenes, recent results[112] show that it is applicable to dienes also. However, the mass spectra of diene derivatives are not so simple as those of monoenes. Methylthiolation is certainly the preferred method for locating mono-unsaturation.

5.2.4. Esterification of Carboxylic Acids with Boron Trifluoride–Methanol

Esterification with BF_3-methanol is a convenient method for preparing methyl esters of carboxylic acids.[113] However, the crude reaction mixture cannot be injected onto the gas chromatograph because BF_3 is destructive to many stationary phases. The esters must be solvent extracted before injection and sensitivity of the method is substantially increased using the Keele microreactor.[108]

McDaniel and *Howard* have recently reported[70] that 1,1-dimethylhydrazine can also form methyl esters from fatty acids. The reaction is almost quantitative when the acid and 1,1-dimethylhydrazine are heated in a sealed microreactor. The mechanism of the reaction is unknown. The products are partitioned between hexane and dilute sulfuric acid.

6. Liquid Chromatography–Gas Chromatography

In the analysis of crude samples a liquid chromatographic fractionation (LC) is often performed before GC.

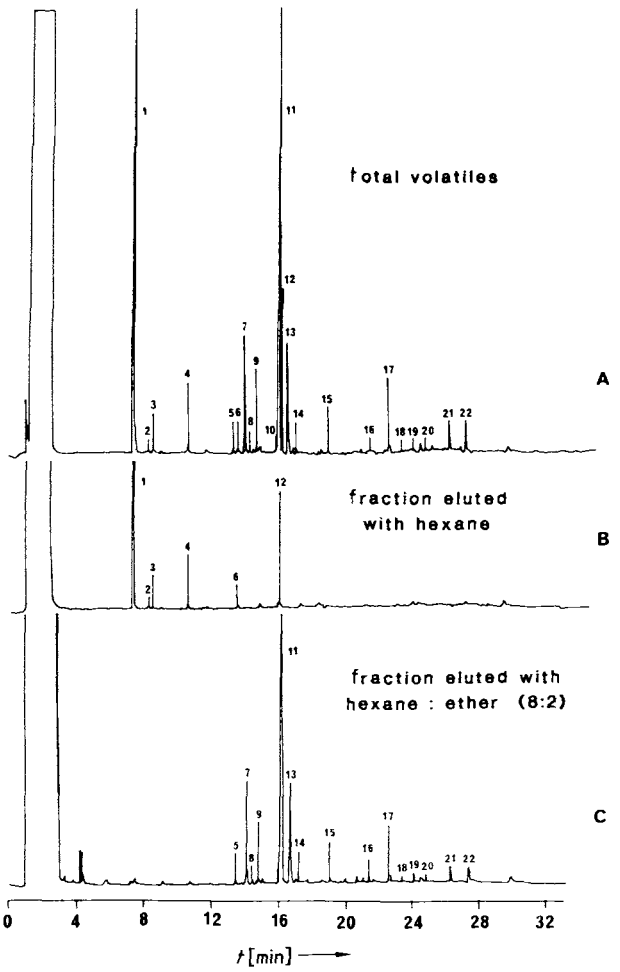

Fig. 17. Use of a microcolumn with gas chromatography to separate classes of compounds. A) An extract of Dufour gland substances of the ant *Lasius niger* in hexane was chromatographed on an OV-17 capillary column, at 60°C for 2 min then programmed at 10°C/min to 270°C. Splitless injection with the split vent kept closed for 30 s. B) A chromatogram of the hexane fraction eluted from a microcolumn directly onto the GC. All peaks are hydrocarbons. C) A chromatogram of the hexane–ether (8:2) eluent from the micro-column directly into the GC. All the peaks (except 9) are due to esters. 1, undecane; 2, 5-methylundecane; 3, 3-methylundecane; 4, tridecane; 5, decyl acetate; 6, pentadecane; 7, 5-methyldecyl acetate; 8, 3-methyldecyl acetate; 9, undecyl acetate + dodecanol; 10, dodecenyl acetate; 11, dodecyl acetate; 12, heptadecane; 13, a branched tridecyl acetate; 14, dodecyl propionate; 15, farnesyl acetate; 16, heptadecyl propionate; 17, octadecyl acetate; 18, octadecyl propionate; 19, dodecyl decanoate; 20, decyl tridecanoate; 21, dodecyl dodecanoate; 22, dodecyl tridecanoate.

However, this procedure is time consuming and wasteful if only a small amount of sample is available. *Sandra*[114] recently described an elegant method for accomplishing liquid chromatographic fractionation before GC in a simple but efficient way. An on-column syringe is used with a polyimide cartridge holding milligram amounts of silica gel or similar materials.

A "microcolumn" of fine silica gel can be made in a similar way in the barrel of a 100 μL syringe[115] and similar devices are now available commercially. An application of the technique for the analysis of a Dufour gland of the ant *Lasius niger* is illustrated in Figure 17. The gland contains over 50 compounds with several functionalities (Fig. 17A).[15a] An individual gland was placed on top of the microcolumn and eluted first with hexane directly into the gas chromatograph via a splitless injector. Only the hydrocarbon peaks were present in the chromatograms obtained from the first two hexane fractions (Fig. 17B). The third hexane fraction contained only the major hydrocarbons, whereas the fourth fraction showed no significant peaks. The microcolumn was then eluted with mixtures of hexane and ether. In the second hexane/ether fraction only the ester peaks were present (Fig. 17C). A subsequent elution of the microcolumn with pure ether gave the alcohols.

The LC-GC method has great potential in the microanalysis of organic functionalities. For example *Bestmann* et al.[115] employed this method for the identification of the sex pheromone of the moth *Cnepasia longana*. Dilute samples can be concentrated before elution into the GC column. When combined with subtraction reactions, this can produce further information about functionality. Further, crude reaction mixtures can be purified before the desired products are eluted into the gas chromatograph.

7. Summary and Outlook

The research worker or analyst may be surprised by what can be done with nanogram samples of organic materials, pure or impure. Provided one does not contaminate them with large quantities of solvents, they may be taken through many manipulations. It is not always necessary to rely on an existing library of mass spectra to deduce the structure of a new substance available only in minute quantities. Conventional chemical training can be called into play, along with a little ingenuity and skill to carry out reactions, degrade or derivatize the substance, even when accompanied by many others, to learn something of its carbon skeleton or its functional groups. Equally minute amounts of substance can be separated from mixtures for further testing. Though the authors' experience has been largely drawn from insect chemistry, the applications are clearly much wider. Examples may be found in forensic science, archaeology, environmental monitoring, pharmacology and drug metabolism.

8. Addendum[*]

Since preparing this manuscript, two reviews have been published on derivatization techniques applicable to microcromethods.[116a,b] Traps coated with a very thick film of stationary phase have been used for recovering material after capillary gas chromatography.[117] A reaction gas chromatographic method for the conversion of water into acetylene has been reported,[118] which could be useful for the determination of water in biological samples. GC-FTIR shows promise of being widely applied in the determination of the geometric configuration of double bonds in pheromones.[119a,b] Water vapor has been used as the carrier gas for the separation of geometric isomers by gas chromatography on a support impregnated with silver nitrate.[120]

Two comprehensive reviews on the location of double bonds in carbon chains have been published.[119a,121] The mass spectra of cycloadducts **35** formed by the addition of 4-phenyl-1,2,4-triazole-3,5-dione **34** to conjugated dienes

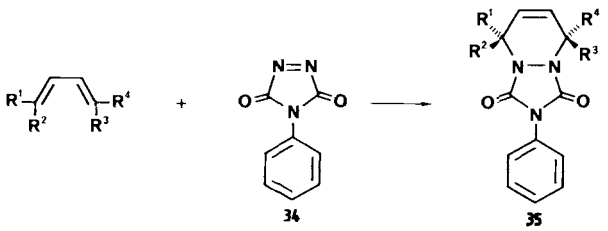

34 **35**

display characteristic ions, diagnostic of the diene position in the chain.[122] The addition of tetracyanoethylene can be used similarly.[123] The methylthiolation procedure for locating double bonds (cf. Section 5.3.2) has been extended to many diene compounds.[124] Recent advances in chemical-ionization mass spectrometry, using reagents such as Fe^{+}[125] and NO,[126] show potential for use in double-bond location, although the principles governing the reactions remain unclear.[127] Further examples of the use of tandem mass spectrometry for double-bond location have been published.[128a,b]

A convenient procedure for determining dialdehydes produced by the ozonolysis of polyenes has been described.[129] The aldehyde groups are converted into 1,3-dioxanes by reducing the ozonides in the presence of 1,3-propanedithiol.

A. B. A. thanks the British Council and the Nuffield Foundation for financial assistance, the Alexander-von-Humboldt Foundation for support, and Professor Dr. H. J. Bestmann for kind hospitality during the preparation of this manuscript. E. D. M. thanks the Royal Society for a grant for equipment, K. T. Alston for help in devising equipment and T. Bolam for many of the illustrations. We thank Dr. O. Vostrowsky for critically reading this manuscript.

Received: June 23, 1987 [A 663 IE]
German version: *Angew. Chem. 100* (1988) 475

[1] J. H. Tumlinson, R. R. Heath, *J. Chem. Ecol. 2* (1976) 87.
[2] R. R. Heath, J. H. Tumlinson in H. E. Hummel, T. A. Miller (Eds.): *Techniques in Pheromone Research*, Springer, Berlin 1984, p. 288.
[3] D. J. David: *Gas Chromatographic Detectors*, Wiley, New York 1974.
[4] R. L. Bowman, A. Karmen, *Nature (London) 182* (1958) 1233.
[5] a) J. R. Bridges, F. H. Guinn, *Z. Angew. Entomol. 89* (1980) 54; b) K. Dettner, G. Schwinger, P. Wunderle, *J. Chem. Ecol. 11* (1985) 859; c) B. V. Burger, Z. Munro, M. Röth, H. S. C. Spies, V. Truter, H. Geertsma, A. Habich, *ibid. 11* (1985) 1093; d) U. M. Senanayake, R. A. Edwards,

[*] Received: January 13, 1988.

T. H. Lee, *J. Chromatogr. 116* (1976) 468; e) D. R. Roberts, *J. Gas Chromatogr. 6* (1968) 126; f) J. Weatherston, W. MacLean, *Can. Entomol. 106* (1974) 281.

[6] a) C. Descoins, M. Gallois, *Ann. Zool. Ecol. Anim. 11* (1979) 521; b) B. Frerot, E. Priesner, N. Gallois, *Z. Naturforsch. C34* (1979) 1248; c) B. Frerot, M. Gallois, M. Lettere, J. Einhorn, D. Michelot, C. Descoins, *J. Chem. Ecol. 8* (1982) 663.

[7] H. V. Buser, H. M. Widmer, *J. High Resolut. Chromatogr. Chromatogr. Commun. 2* (1979) 177.

[8] a) S. Ställberg-Stenhagen, *Chem. Scr. 2* (1972) 97; b) G. Bergström, J. Löfqvist, *J. Insect Physiol. 19* (1973) 877; c) G. Bergström, M. Applegren, A.-K. Borg-Karlson, I. Groth, S. Strömberg, S. Strömberg, *Chem. Scr. 16* (1980) 173.

[9] E. D. Morgan, L. J. Wadhams, *J. Chromatogr. Sci. 10* (1972) 528.

[10] N. W. Davies, J. L. Madden, *J. Chem. Ecol. 11* (1985) 1115.

[11] a) A. B. Attygalle, R. P. Evershed, E. D. Morgan, M. C. Cammaerts, *Insect. Biochem. 13* (1983) 507; b) A. B. Attygalle, E. D. Morgan, *J. Chem. Ecol. 10* (1984) 1453.

[12] E. D. Morgan, R. C. Tyler, *J. Chromatogr. 134* (1977) 174.

[13] a) A. B. Attygalle, M. C. Cammaerts, E. D. Morgan, *J. Insect Physiol. 29* (1983) 27; b) R. P. Evershed, E. D. Morgan, M. C. Cammaerts, *Naturwissenschaften 67* (1981) 374; c) E. D. Morgan, L. J. Wadhams, *J. Insect. Physiol. 18* (1972) 1125.

[14] E. D. Morgan, R. P. Evershed, R. C. Tyler, *J. Chromatogr. 186* (1979) 605.

[15] a) A. B. Attygalle, O. Vostrowsky, H. J. Bestmann, E. D. Morgan, *Insect Biochem. 17* (1987) 219; b) G. Bergström, J. Löfqvist, *J. Insect. Physiol. 16* (1970) 2353.

[16] a) A. B. Attygalle, M. Herrig, O. Vostrowsky, H. J. Bestmann, *J. Chem. Ecol. 13* (1987) 1299; b) A. B. Attygalle, W. Cai-Hong, J. Schwarz, O. Vostrowsky, I. Hasenfuss, H. J. Bestmann, *ibid.*, in press; c) A. B. Attygalle, J. Schwarz, O. Vostrowsky, H. J. Bestmann, *Z. Naturforsch. C41* (1986) 1077; d) H. J. Bestmann, A. B. Attygalle, T. Brosche, J. Erler, H. Platz, J. Schwarz, O. Vostrowsky, W. Cai-Hong, K. E. Kaissling, C. Te-Ming, *ibid. C42* (1987) 631.

[17] H. J. Bestmann, M. Herrig, A. B. Attygalle, *Experientia 43* (1987) 1033.

[18] D. R. Deans, *Chromatographia 1* (1968) 18.

[19] a) T. H. Maugh II, *Science 227* (1985) 1570; b) W. Bertsch, *J. High Resolut. Chromatogr. Chromatogr. Commun. 1* (1978) 85; c) R. J. Miller, S. D. Stearns, R. R. Freeman, *ibid. 2* (1979) 55.

[20] W. Blass, K. Riegner, H. Hulpke, *J. Chromatogr. 172* (1979) 67.

[21] G. Schomburg, H. Husmann, F. Weeke, *J. Chromatogr. 112* (1975) 205.

[22] a) V. Schurig, U. Leyrer, U. Kohule, *Naturwissenschaften 72* (1985) 211; b) V. Schurig, R. Weber, G. J. Nicholson, A. C. Oehlschlager, H. Pierce, A. M. Pierce, J. H. Borden, L. C. Ryker, *ibid. 70* (1983) 92; c) V. Schurig, R. Weber, D. Klimetzek, U. Kohule, K. Mori, *ibid. 69* (1982) 602; d) H. J. Bestmann, A. B. Attygalle, J. Glasbrenner, R. Riemer, O. Vostrowsky, *Angew. Chem. 99* (1987) 784; *Angew. Chem. Int. Ed. Engl. 26* (1987) 784.

[23] G. Schomburg, H. Husmann, E. Hubinger, W. A. König, *J. High Resolut. Chromatogr. Chromatogr. Commun. 7* (1984) 404.

[24] R. K. Odland, E. Glock, N. L. Bodenhamer, *J. Chromatogr. Sci. 7* (1969) 187.

[25] R. G. Brownlee, R. M. Silverstein, *Anal. Chem. 40* (1968) 2077.

[26] R. Baker, J. W. S. Bradshaw, D. A. Evans, M. D. Higgs, L. J. Wadhams, *J. Chromatogr. Sci. 14* (1976) 425.

[27] J. Roeraade, C. R. Enzell, *J. High Resolut. Chromatogr. Chromatogr. Commun. 2* (1979) 123.

[28] H. J. Williams, S. B. Vinson, *J. Chem. Ecol. 6* (1980) 973.

[29] C. F. Poole, S. A. Schuette: *Contemporary Practice of Chromatography*, Elsevier, Amsterdam 1984, p. 403.

[30] D. A. Cronin, J. Gilbert, *J. Chromatogr. 87* (1973) 387.

[31] G. Stanley, B. H. Kennet, *J. Chromatogr. 75* (1973) 304.

[32] A. B. Attygalle, E. D. Morgan, *Anal. Chem. 55* (1983) 1379.

[33] I. Klimes, W. Stünzi, D. Lamparsky, *J. Chromatogr. 136* (1977) 23.

[34] A. B. Attygalle, E. D. Morgan, *J. Chromatogr. 290* (1984) 321.

[35] Y. Tamaki in E. D. Morgan, N. B. Mandava (Eds.): *Handbook of Natural Pesticides: Insects, Vol. 3: Pheromones*, CRC Press, Boca Raton, FL (USA), in press.

[36] a) A. J. Ferrer-Correia, K. R. Jennings, D. K. Sen Sharma, *Adv. Mass Spectrom. 7* (1978) 287; b) R. Chai, A. G. Harrison, *Anal. Chem. 53* (1981) 34.

[37] M. Cervilla, G. Puzo, *Anal. Chem. 55* (1983) 2100.

[38] H. Budzikiewicz, E. Busker, *Tetrahedron 36* (1980) 255.

[39] a) R. E. Doolittle, J. H. Tumlinson, A. Proveaux, *Anal. Chem. 57* (1985) 1625; b) J. Einhorn, H. Virelizier, A. L. Gemal, J. C. Tabet, *Tetrahedron Lett. 26* (1985) 1445.

[40] a) M. Horiike, M. Miyata, C. Hirano, *Biomed. Mass Spectrom. 8* (1981) 41; b) M. Horiike, C. Hirano, *Agric. Biol. Chem. 46* (1982) 2667; c) *Biomed. Mass Spectrom. 11* (1984) 145.

[41] B. A. Leonhardt, E. D. DeVilbiss, J. A. Klun, *Org. Mass Spectrom. 18* (1983) 9.

[42] B. S. Lanne, M. Appelgren, G. Bergström, C. Löfstedt, *Anal. Chem. 57* (1985) 1621.

[43] O. Vostrowsky, K. Michaelis, H. J. Bestmann, *Liebigs Ann. Chem. 1982*, 1001.

[44] a) K. B. Tomer, C. W. Crow, M. L. Gross, *J. Am. Chem. Soc. 105* (1983) 5487; b) N. J. Jensen, K. B. Tomer, M. L. Gross, *Anal. Chem. 57* (1985) 2018.

[45] J. A. McCloskey, M. J. McClelland, *J. Am. Chem. Soc. 87* (1965) 5090.

[46] C. J. W. Brooks, J. Watson, *Chem. Commun. 1967*, 952.

[64] W. G. Niehaus, R. Ryhage, *Tetrahedron Lett. 1967*, 5021.

[48] P. Capella, C. M. Zorzut, *Anal. Chem. 40* (1968) 1458.

[49] P. Abley, F. J. McQuillan, D. E. Minnikin, K. Kusamran, K. Maskens, N. Polgar, *Chem. Commun. 1970*, 348.

[50] a) K. K. Sun, H. W. Hayes, R. T. Holman, *Org. Mass Spectrom. 3* (1970) 1035; b) E. Selke, C. R. Schofield, C. D. Evans, H. J. Dutton, *J. Am. Oil Chem. Soc. 38* (1981) 614; c) V. G. Zaikin, A. I. Mikaya, *J. Chromatogr. 301* (1984) 77.

[51] C. J. W. Brooks, I. Maclean, *J. Chromatogr. Sci. 9* (1971) 18.

[52] B. M. Johnson, J. W. Tylor, *Anal. Chem. 44* (1972) 1438.

[53] V. Dommes, F. Wirtz-Peitz, W. H. Kunau, *J. Chromatogr. Sci. 14* (1976) 360.

[54] G. W. Francis, T. Tande, *J. Chromatogr. 150* (1978) 139.

[55] G. Janssen, G. Parmentier, *Biomed. Mass Spectrom. 5* (1978) 439.

[56] G. J. Blomquist, R. W. Howard, C. A. McDavid, S. Remaley, L. A. Dwyer, D. R. Nelson, *J. Chem. Ecol. 6* (1980) 257.

[57] G. W. Francis, K. Veland, *J. Chromatogr. 219* (1981) 379.

[58] a) V. L. Davison, H. J. Dutton, *Anal. Chem. 38* (1966) 1302; b) E. C. Nickell, O. S. Privett, *Lipids 1* (1966) 166; c) M. Beroza, B. A. Bierl, *Anal. Chem. 38* (1966) 1976; d) *ibid. 39* (1967) 1131; e) B. A. Bierl-Leonhardt, D. S. Moreno, M. Schwarz, H. S. Forster, J. R. Plimmer, E. D. DeVilbiss, *Life Sci. 27* (1980) 399.

[59] F. Drawert, R. Felenhauer, G. Kupfer, *Angew. Chem. 72* (1960) 555.

[60] B. Leonhardt, *Anal. Chem. 57* (1985) 1240A.

[61] M. Beroza, B. A. Bierl, *Mikrochim. Acta 1969*, 720.

[62] E. R. White, B. M. Sutton, J. E. Blank, E. Moeckel, J. E. Zarembo, *Anal. Chem. 44* (1972) 1582.

[63] J. P. J. Billen, R. P. Evershed, A. B. Attygalle, E. D. Morgan, D. G. Ollett, *J. Chem. Ecol. 12* (1986) 669.

[64] A. B. Attygalle, E. D. Morgan, *J. Chem. Soc. Perkin Trans. 1 1982*, 949.

[65] L. S. Silbert, T. A. Foglia, *Anal. Chem. 57* (1985) 1404.

[66] B. P. Moore, W. V. Brown, *J. Chromatogr. 60* (1971) 157.

[67] a) K. Kobayashi, M. Tanaka, S. Kawai, T. Ohno, *J. Chromatogr. 176* (1979) 118; b) D. F. Margin, *ibid. 202* (1980) 255; c) K. Kobayashi, M. Tanaka, S. Kawai, *ibid. 187* (1980) 413.

[68] D. G. Ollett, A. B. Attygalle, E. D. Morgan, *J. Chromatogr. 367* (1986) 207.

[69] D. G. Ollett, E. D. Morgan, *Microchem. J. 35* (1987) 296.

[70] C. A. McDaniel, R. W. Howard, *J. Chem. Ecol. 11* (1985) 303.

[71] N. N. Schwartz, J. H. Blumbergs, *J. Org. Chem. 29* (1964) 1976.

[72] a) R. T. Aplin, L. Coles, *Chem. Commun. 1967*, 858; b) F. D. Gunstone, F. R. Jacobsberg, *Chem. Phys. Lipids 9* (1972) 26; c) B. A. Bierl-Leonhardt, E. D. DeVilbiss, J. R. Plimmer, *J. Chromatogr. Sci. 18* (1980) 264; d) L. R. Hogge, E. W. Underhill, J. W. Wong, *ibid. 23* (1985) 171; e) J. H. Tumlinson, R. R. Heath, R. E. Doolittle, *Anal. Chem. 46* (1974) 1309.

[73] a) R. R. Heath, G. E. Burnsed, J. H. Tomlinson, R. E. Doolittle, *J. Chromatogr. 189* (1980) 199; b) L. R. Hogge, D. J. H. Olson, *J. Chromatogr. Sci. 21* (1983) 524.

[74] G. W. Kenner, E. Stenhagen, *Acta Chem. Scand. 18* (1964) 1551.

[75] T. J. Walton, P. E. Kolattukudy, *Biochemistry 11* (1972) 1885.

[76] R. Kleiman, G. F. Spencer, *J. Am. Oil Chem. Soc. 50* (1973) 31.

[77] D. E. Minnikin, *Chem. Phys. Lipids 21* (1978) 313.

[78] B. A. Bierl, M. Beroza, M. A. Aldridge, *Anal. Chem. 43* (1971) 636.

[79] A. B. Attygalle, E. D. Morgan, *Anal. Chem. 65* (1984) 1530.

[80] a) T. L. Mounts, H. J. Dutton, *Anal. Chem. 37* (1965) 641; b) M. Beroza, R. Sarmiento, *ibid. 38* (1966) 1042; c) A. L. Chaffee, I. Liepa, *ibid. 57* (1985) 2429.

[81] G. Schomburg, E. Hübinger, H. Husmann, F. Weeke, *Chromatographia 16* (1982) 228.

[82] a) M. Beroza, R. Sarmiento, *Anal. Chem. 35* (1963) 1353; b) *ibid. 36* (1964) 1744; c) R. E. Kepner, H. Maarse, *J. Chromatogr. 66* (1972) 229; d) B. A. Bierl, M. Beroza, W. T. Ashton, *Mikrochim. Acta 1969*, 637.

[83] a) B. A. Bierl-Leonhardt, E. D. DeVilbiss, *Anal. Chem. 53* (1981) 936; b) B. A. Bierl-Leonhardt, D. S. Moreno, M. Schwarz, J. Fargerlund, J. R. Plimmer, *Tetrahedron Lett. 22* (1981) 389; c) B. A. Leonhardt, J. N. Neal, J. A. Klun, M. Schwarz, J. R. Plimmer, *Science 219* (1983) 314.

[84] A. I. Mikaya, E. A. Trusova, V. G. Zaikin, N. P. Volinsky, E. N. Karaulova, G. D. Gal'pern, *Org. Mass Spectrom. 19* (1984) 428.
[85] J. E. Hoff, E. F. Feit, *Anal. Chem. 36* (1964) 1002.
[86] K. M. Fredricks, R. Taylor, *Anal. Chem. 38* (1966) 1961.
[87] G. Stanley, *J. Chromatogr. 178* (1979) 487.
[88] A. J. Mikaya, V. I. Smetanin, V. G. Zaikin, A. V. Antonova, N. S. Prostakov, *Org. Mass Spectrom. 18* (1983) 99.
[89] M. J. Burk, R. H. Crabtree, D. V. McGrath, *Anal. Chem. 58* (1986) 977.
[90] a) A. Darbre in K. Blau, G. S. King (Eds.): *Handbook for Derivatives for Chromatography*, Heyden, London 1977, p. 39; b) T. S. Ma, A. S. Ladas: *Organic Functional Group Analysis by Gas Chromatography*, Academic Press, London 1976.
[91] S. Huwyler, K. Grob, M. Viscontini, *J. Insect Physiol. 21* (1975) 299.
[92] D. B. de Oliveira, W. E. Harris, *Anal. Lett. 6* (1973) 1107.
[93] W. E. Harris, *J. Chromatogr. Sci. 13* (1975) 514.
[94] S. Huwyler, *Experientia 28* (1972) 718.
[95] F. Drawert, K.-H. Reuther, *Chem. Ber. 93* (1960) 3066.
[96] a) U. Kobold, O. Vostrowsky, H. J. Bestmann in E. J. Brunke (Eds.): *Progress in Essential Oil Research*, de Gruyter, Berlin 1986, p. 565; b) H. J. Bestmann, U. Kobold, O. Vostrowsky, *Liebigs Ann. Chem. 1986*, 234.
[97] R. Ikan: *Chromatography in Organic Microanalysis*, Academic Press, New York 1982.
[98] V. R. Alieshoev, V. G. Berezkin, E. N. Viktorova, J. Hradil, J. Stamberg, *J. Chromatogr. 246* (1982) 141.
[99] P. Kalo, *J. Chromatogr. 205* (1981) 39.
[100] C. F. Poole, A. Zlatkis, *J. Chromatogr. Sci. 17* (1979) 114.
[101] a) C. B. Johnson, E. Wong, *J. Chromatogr. 109* (1975) 403; b) C. B. Johnson, *Anal. Biochem. 71* (1976) 594.
[102] K. Blau, G. S. King: *Handbook of Derivatives for Chromatography*, Heyden, London 1977.
[103] C. F. Poole, S. A. Schuette, *J. High Resolut. Chromatogr. Chromatogr. Commun. 6* (1983) 526.
[104] M. Cais, M. Shimoni, *Ann. Clin. Biochem. 18* (1981) 317.
[105] K. Grob, K. Grob Jr., G. Grob, *J. Chromatogr. 106* (1975) 299.
[106] D. A. J. Murray, *J. Chromatogr. 177* (1979) 135.
[107] J. F. J. van Rensburg, A. J. Hassett, *J. High Resolut. Chromatogr. Chromatogr. Commun. 5* (1982) 574.
[108] A. B. Attygalle, E. D. Morgan, *Anal. Chem. 58* (1986) 3054.
[109] M. Ma, H. E. Hummel, W. E. Burkholder, *J. Chem. Ecol. 6* (1980) 597.
[110] a) O. Vostrowsky, K. Michaelis, *Z. Naturforsch. B36* (1981) 402; b) O. Vostrowsky, K. Michaelis, H. J. Bestmann, *Liebigs Ann. Chem. 1981*, 1721; c) R. Baker, J. W. S. Bradshaw, W. Speed, *Experientia 38* (1982) 233.
[111] a) H. Buser, H. Arn, P. Guerin, S. Rauscher, *Anal. Chem. 55* (1983) 818; b) E. Dunkelblum, S. H. Tan, P. J. Silk, *J. Chem. Ecol. 11* (1985) 265; c) B. A. Leonhardt, E. D. DeVilbiss, *J. Chromatogr. 322* (1985) 484.
[112] C. Tonini, G. Cassani, P. Massardo, G. Guglielmetti, P. L. Castellari, *J. Chem. Ecol. 12* (1986) 1545.
[113] L. D. Metcalfe, A. A. Schmitz, *Anal. Chem. 33* (1961) 363.
[114] P. Sandra, *J. High Resolut. Chromatogr. Chromatogr. Commun. 6* (1983) 690.
[115] H. J. Bestmann, A. B. Attygalle, H. Platz, O. Vostrowsky, *Z. Naturforsch. C40* (1985) 667.
[116] a) C. F. Poole, S. K. Poole, *J. Chromatogr. Sci. 25* (1987) 434; b) K. Imai, *Adv. Chromatogr. 27* (1987) 215.
[117] S. Blomberg, J. Roeraade, *J. Chromatogr. 394* (1987) 443.
[118] R. Boos, T. Prey, A. Bergert, *J. Chromatogr. 328* (1985) 233.
[119] a) L. R. Hogge, J. G. Millar, *Adv. Chromatogr. 27* (1987) 299; b) R. Yamaoka, M. Tokoro, K. Hayashiya, *J. Chromatogr. 399* (1987) 259.
[120] E. N. Viktorova, V. G. Berezkin, V. S. Gavrichev, *J. Chromatogr. 398* (1987) 317.
[121] B. Schmitz, R. A. Klein, *Chem. Phys. Lipids 39* (1986) 285, 299.
[122] D. C. Young, P. Vouros, B. Decosta, M. F. Holick, *Anal. Chem. 59* (1987) 1954.
[123] A. B. Attygalle, H. J. Bestmann, unpublished.
[124] M. Vincenti, G. Guglielmetti, G. Cassani, C. Tonini, *Anal. Chem. 59* (1987) 694.
[125] D. A. Peake, S.-K. Huang, M. L. Gross, *Anal. Chem. 59* (1987) 1557.
[126] C. Malosse, J. Einhorn, *Org. Mass Spectrom. 21* (1986) 1639.
[127] H. Budzikiewicz, B. Schneider, E. Busker, W. Boland, W. Francke, *Org. Mass Spectrom. 22* (1987) 458.
[128] a) G. Takeuchi, M. Weiss, A. G. Harrison, *Anal. Chem. 59* (1987) 918; b) J. Adams, M. L. Gross, *ibid. 59* (1987) 1576.
[129] G. Lakshminarayana, D. G. Cornwell, *Lipids 21* (1986) 175.

One or Several Pioneers? The Discovery of Noble-Gas Compounds

By Pierre Laszlo* and Gary J. Schrobilgen*

For the general public, science history and restaurant menus share a labeling style. Like Melba peach, Soubise sauce, or tournedos Rossini, many a scientific discovery is credited to a single thinker or tinkerer. Such ultrasimplification rubs into oblivion other important contributors or codiscoverers. The discovery of noble-gas compounds conforms to such a stereotyped and mythic view: according to the standard account, *Neil S. Bartlett*, then at the University of British Columbia, made it a quarter of a century ago on March 23, 1962. We do not attempt here a full and definitive history; it would be premature and we do not have the space. Rather, we shall document the concept and the earlier attempts at synthesis—they antedated *Bartlett*'s success by three decades. The motivation for this note may be summarized in the following questions: (1) What sort of insight and input were those of *Linus Pauling*? (2) What were the likely causes for failure of the attempt by *Yost* and *Kaye* to synthesize noble-gas fluorides in the 1930s? (3) Were there other researchers who envisioned a noble-gas reactivity?

1. The Very Early Story

As always, there are scraps of a prehistory. After the discovery of argon in 1894 by *William Ramsay* and *Lord Rayleigh (J. W. Strutt)*,[1] *Ramsay* provided *Moissan* with about 100 mL of the gas so that he could react it with fluorine, which *Moissan* had isolated in 1886. *Moissan* attempted the reaction of the two gases at room temperature or under the action of an induction spark, but without success.[2] In the same year as *Moissan*'s report, *Marcelin Berthelot* announced that he had combined helium with benzene and with carbon disulfide using a silent electric discharge.[3] *R. J. Strutt* had already drawn attention to the intriguing occlusion of helium in beryl, in the absence of any radioactive source.[4] He repeated *Berthelot*'s experiments and was unable to reproduce his results.[5]

The next episode is epistolary rather than experimental. In 1902, *Giuseppe Oddo*, then a professor in Cagliari, wrote to *Sir William Ramsay* to suggest that, due to the general increase in valence down a row of the periodic table, krypton ought to show a certain tendency toward chemical combination, while xenon ought to have yet a more pronounced such tendency. *Ramsay* agreed that krypton and xenon ought to be more reactive than their lighter relatives. But he could not share the enthusiasm of his Italian correspondent, pointing out that it would be extremely difficult to isolate enough of these two gases to run the experiments. There the matter rested till *Oddo*, reading in 1932 a report of the preparation by *Antropoff* and his co-workers of krypton chloride, decided to publish his correspondence with *Sir William Ramsay* of 30 years back.[6] One should note also the report by *Boomer* of formation of a stable WHe_3 compound under intense electric discharge from a tungsten filament in low-pressure helium.[7] This brings us to the *Antropoff* 1932 "preparation" and to its antecedents.

2. The Early Story

The *Antropoff* part of the story is endearing. He strikes us as an opinionated visionary who knew that he was on the right track. *A. von Antropoff*, then in Karlsruhe, published a paper in the April 17, 1924 issue of *Zeitschrift für angewandte Chemie*.[8] *Antropoff* was building, in part, on the semitheoretical paper of the physicist *Kossel* who predicted, on the basis of ionization potentials, that it should be feasible to form compounds between the heavier noble gases and the most electronegative element. *Kossel* predicted the existence of a xenon fluoride and a krypton fluoride.[9] *Antropoff*'s article discusses the position of the noble gases in the periodic table. In an extremely lucid and well-argued manner, *Antropoff* suggests placing the rare gases in group VIIIb of the periodic system (with the present controversy about the best numbering of the rows in the periodic table, we need no reminder of the importance of such considerations). Accordingly, *Antropoff* pointed out, rare gases will thus be potentially reactive. Such a positioning will give them a maximum valence of eight, and, in *Antropoff*'s words, "one should not forget that as the valence number increases from one group to the next, the intensity of the valence forces decreases." His key sentence is: "*Die Stellung in der Gruppe VIIIb lässt aber die Möglichkeit der Bildung von Verbindungen mit negativen Elementen offen*" (placement in group VIIIb leaves them the possibility to form bonds with negative elements).[8]

This proposal did not go unnoticed. *H. Danneel* published soon afterwards a reply[10] with the all-too-usual

[*] Prof. P. Laszlo
Institut de Chimie Organique, Université de Liège
Sart-Tilman par B-4000 Liège (Belgium)
and
Laboratoire de chimie fine, biomimétique et aux interfaces,
Ecole Polytechnique, F-91128 Palaiseau (France)
Prof. G. J. Schrobilgen
Department of Chemistry, McMaster University
Hamilton, Ontario L8S 4M1 (Canada)

 © VCH Verlagsgesellschaft mbH, D-6940 Weinheim, 1988 0570-0833/88/0404-0479 $ 02.50/0

plea to leave things as they were till more conclusive evidence could be lined up. *Antropoff* jumped back to his desk and penned another article[11] in support of his idea, drawing upon evidence provided by *Danneel* himself and by *Paneth*.[12]

Not only did *Antropoff* stick to his guns, a number of years later he did experiments to form halogen compounds of the noble gases. Taken together with his conceptual considerations,[8,11] they make him a true pioneer in the discovery of noble-gas compounds. *Antropoff* and his coworkers attempted to react krypton with both chlorine and bromine under an intense electric discharge. Not only did reaction take place, as indicated by the drop in gas pressure resulting from combination; they could also isolate a solid, dark red substance.[13] With *Antropoff*'s permission, *Otto Ruff* and *Walter Menzel* in Breslau also conducted similar experiments, with argon-fluorine and krypton-fluorine mixtures, but without success.[15] *Antropoff* was undaunted by their failure, and pointed out that their reaction conditions differed enough from his to explain such lack of success.[14] However, he must have felt the inward challenge. In any case, he decided to reinvestigate his own work. Thus, he had to report in 1933 (he was now at Bonn) that the dark red compound formed in his apparatus was an already known compound of NO and HCl.[16]

This retraction article[16] makes for interesting reading. The authors point out that they still cannot account for certain losses in krypton pressure. Maybe they were still hopeful, and *Antropoff* was still sticking to his guns. One wonders whether he was wont to predict to his associates and students the confirmation of his ideas and the future preparation of noble-gas compounds; it would have been in character for him to do so.

3. *Linus Pauling* Steps In

In 1933, *Linus Pauling* published an article in the *Journal of the American Chemical Society*[17] which dealt ostensibly with the formula of antimonic acid. *Pauling* pointed out that the molecules of oxo acids can be seen as consisting of a central cation surrounded by as many oxygens as will fit around it. Simple consideration of ionic radii is then sufficient to predict reliably coordination numbers: for instance, "the coordination number three is indicated for B, C and N, whose acids should have the formulas H_3BO_3, H_2CO_3 and HNO_3 in agreement with observation."[17] Such simple arguments led *Pauling* to predict oxygen coordination numbers of four and six for krypton and xenon, respectively. He thus conjectured the formula H_4XeO_6 for xenic acid, and predicted quite naturally that it "should form salts such as Ag_4XeO_6 and AgH_3XeO_6."[17] At the end of his paper, *Pauling* moved on to consider fluorides. The same sphere-packing considerations gave him a series of structures in agreement with observation, and led him to the "predicted formulas KrF_6 and XeF_6, with XeF_8 as an unstable compound which might be capable of existence."[17]

Several of these predicted species were actually prepared in the early sixties at Argonne National Laboratory. *Pauling* told us that his conjectures on antimonic acid and noble-gas compounds (perxenic acid and its salts) were really largely directed by reasoning from analogy with other then-known hypervalent species such as $Te(OH)_6$ or $IO(OH)_6$. As for antimonic acid, *Pauling* gave its formula as $HSb(OH)_6$, but, as an ironical footnote to this work, he pointed out in a short note a few months later that, unknown to him, this formula had already been published by *Louis Hammett* a few years before.[18]

4. A Near-Miss, the *Yost* and *Kaye* Experiments

The next and arguably the most fascinating episode took place at Caltech (California Institute of Technology) in 1932 and 1933, with *Linus Pauling* as a most interested onlooker. The senior protagonist was Professor *Don M. L. Yost* (1893–1977), an extremely intent scientist who brought extreme honesty to his work. When *Albert L. Kaye*, who had obtained his B. S. and M. S. engineering degrees at MIT (Massachusetts Institute of Technology), entered the graduate school at Caltech in the fall of 1932, *Yost* recruited him. *Yost* had a very attractive personality, which drew *Kaye* to his work. *Yost* gave *Kaye* the project of forming noble-gas compounds. This was in line with *Yost*'s philosophy that everything could be proved with experiments. He also told *Kaye* of *Antropoff*'s work in 1924 and gave him the initial task of researching all the published attempts at reacting the noble gases.[19] He told *Kaye* to think also of alternative routes to their combination with other elements. *Kaye* must have struck *Yost* as an outstanding choice for such work, because of his earlier training as an electrochemist. *Walter Schumb* had been *Kaye*'s freshman chemistry teacher at MIT and *Schumb* had a strong interest in halogen chemistry. Thus the decision was taken to make an attempt at reacting the noble gases.

Some of the conditions were highly favorable. As *Yost* later wrote,[20] "there were no redundant administrators, safety officers, or editors to bother us or to suggest delicious sins that we might be tempted to commit." Other conditions were less desirable.

In those days the labs at Caltech were small. *Kaye* was eager to get going. He needed good ventilation for handling fluorine. *Yost* answered this request by suggesting that the experiments be run in his office, which doubled as a small laboratory, in the basement of the Gates Chemical Laboratory. The ventilation was inadequate. *Yost* and *Kaye* arranged for a fume hood to be installed. When this was done, in the late fall of 1932, work could start. *Yost* and *Kaye* were very optimistic. They were the brunt of some gentle kidding in the department, and were often told that "they were out to rape xenon."

But first the would-be rapists had to build their own fluorine generator, using the electrolysis of molten HF-KF. They had a cryogenic purification train for fluorine, which caused various difficulties. They blew their own glass[20] [sic; vide infra]. The actual vessel for containing the electric discharge (they used cast-off Ford induction coils as the high-potential source[20]) was machined from a solid bar of copper. *Kaye* himself designed the copper discharge vessel and window.

He now describes it as follows:

> The copper reaction vessel was machined from [an] approximately 4" round bar of solid copper about 12" long. This was bored eccentrically in from both ends and the bores thus met at the center of the bar length which was then enlarged at the center and for a short length toward either end. The enlarged center cavity was provided with a copper stop-cock to drain off any liquid which might accumulate in this area and provided with two holes at the top to accommodate the electrodes. The ends of the vessel were sealed with fitting copper caps with holes for the gas inlet tubes. The only reason the foregoing is clear in my mind is that I remember it taking me quite a while to sell the chemistry department's machine shop foreman on the idea of machining such a maverick contraption to which he contributed a minimum of enthusiasm toward tackling!

Figure 1 shows a (reduced) sketch of the apparatus, which Dr. *A. L. Kaye* drew from memory for this article.

As they were uncertain about the state of aggregation of the product(s), *Yost* and *Kaye* had made provision for observation if the material was solid or liquid. They had a drain on the vessel to allow for the former. *Kaye* had the machine shop make a copper sphere to insert in the copper reactor and to be rolled by gravity to ensure mixing of the xenon and fluorine gases. *Kaye* remembers that they had trouble getting the discharge apparatus leak-tight and had the most trouble with copper-to-glass seals, which they eventually solved by applying some cements. *Kaye* recalls that his relationship with *Yost* was, in his words, like the journeyman and apprentice. Unknown to *Kaye*, the xenon was supplied through *Pauling*; it came from Professor *Fredrick J. Allen* at Purdue. *Linus Pauling* wrote him on September 13, 1932: "I should like to do some work (with Professor Yost) in an attempt to prepare certain compounds of xenon suggested by theoretical arguments. No doubt your xenon is precious; if, however, you could lend us 10 cc. or so ... we would try to return it to you either as such or in some compound (I hope) and we would be properly grateful." The original letter is shown in Figure 2, top left. *Fred Allen* complied with this request and sent a sample (200 mL at less than one-half atmosphere pressure). *Linus Pauling* acknowledged receipt and wrote to *Fred Allen* on October 12, 1932: "We are going to try to make XeF_8 or XeF_6 at once. Some of the excitement is removed by the appearance since I wrote you of a note by von Antropoff et al.[13] in Die Naturw. saying that they have a chloride + bromide of Kr" (the original letter is shown in Fig. 2, rop right).

While *Kaye* was already involved in this project, he was asked to present one of the regular departmental seminars about it. Professor *Arthur A. Noyes* was then chairman. Every Thursday, the chemistry department ran a seminar, usually given by one of the graduate students. *Kaye* presented his seminar in the fall (November) of 1932. *Pauling* attended the seminar. From his remarks, he made it clear that he was already very familiar with *Kaye*'s subject. *Kaye* has a vivid recollection of one particular incident. He *(Kaye)* had prepared what he termed "a pony," i.e., a crib sheet as a guide, on which he had set *Antropoff*'s early predictions. However, in his enthusiasm to portray the experimental aspects, he failed to mention these predictions in his presentation. It was *Linus Pauling* who, in the discussion afterwards, told *Kaye* that he had left out a very important piece of work and brought up *Antropoff*'s 1924 contribution, displaying considerable familiarity with it. More generally, *Kaye* was very much impressed by *Pauling*'s "profound knowledge of the subject." Before he presented his seminar, *Kaye* had no inkling that *Pauling* also had been thinking about the possibility of noble-gas compounds. Obviously, *Yost* must have known of *Pauling*'s in-

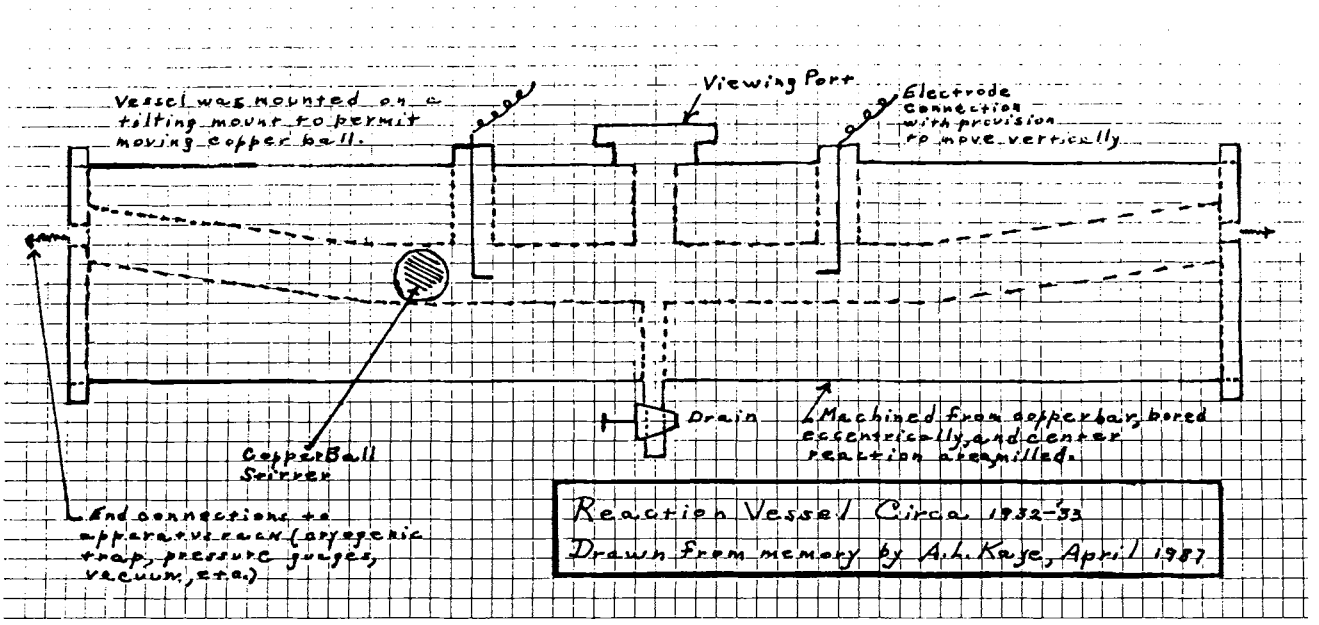

Fig. 1. The copper electrical discharge vessel used by *Yost* and *Kaye* for the reaction of xenon with fluorine (see text).

CALIFORNIA INSTITUTE OF TECHNOLOGY
PASADENA

GATES CHEMICAL LABORATORY

September 13, 1932

Dear Fred:

I should like to do some work (with Professor Yost) in an attempt to prepare certain compounds of xenon suggested by theoretical arguments. No doubt your xenon is precious; if, however, you could lend us 10 cc. or so (of not necessarily pure stuff), we would try to return it to you either as such or in some compound (I hope), and we would be properly grateful. If this is asking too much, or if you can't lend it, could you give us advice as to where we might possibly obtain some?

We were pleased to get your letter & pictures some time ago, and hope our card also arrived. Next Christmas we'll need a larger card, with room for Linda, now 13 weeks old.

We hope you are getting along well.

Sincerely,
Linus Pauling

CALIFORNIA INSTITUTE OF TECHNOLOGY
PASADENA

October 12, 1932.

Dear Fred:

Thanks immensely for the xenon, which arrived safely. We are going to try to make XeF_8 or XeF_6 at once. Some of the excitement is removed by the appearance since I wrote you of a note by von Antropoff et al. in Die Naturw. saying that they have a chloride & bromide of Kr.

I'll let you know if we have any luck.

Yours sincerely,
Linus

This was later retracted but it got an AP front page item in Lafayette Journal Courier

CALIFORNIA INSTITUTE OF TECHNOLOGY
PASADENA

GATES CHEMICAL LABORATORY

Nov. 16, 1933

Dear Fred:

The 70 mm of xenon was the pressure in mm of mercury, the volume of the system being 300 or 400 cc. Hence there was plenty of xenon present. Yost should have mentioned the volume. We still have the xenon, but Yost would like to make another try at preparing a compound, (unless you want the xenon returned soon). I still think XF_6 should be stable.

I wish to offer my congratulations and best wishes on the impending event. We are still satisfied with three little roughnecks.

My work is going on as usual. We are doing a good bit of electron diffraction work. If you prepare any new or unusual compounds, I hope you will remember that we are on the lookout for substances to study with x-rays or electrons.

I hope to be able to stops at Purdue sometime. At present I have no plans for a trip East, except possibly to the Nat. Acad. next April.

Sincerely,
Linus Pauling

CALIFORNIA INSTITUTE OF TECHNOLOGY
PASADENA

1201 - E. California St

July 12, 1933

Dr. F. J. Allen,
Chemistry Department,
Purdue University,
Lafayette, Ind.

Dear Fred:

At last I can send you some information regarding the xenon experiments, which Dr. Yost has been carrying on, inasmuch as he is thoroughly experienced in the chemistry of the halogens. He found that he could not prepare a compound of xenon with either chlorine or fluorine by any of the means that he tried, and he has now given up the investigation. He and his student, Kaye, have sent a note on the experiments to the Journal of the American Chemical Society, in which they thank you for providing the xenon. I am sorry that the experiments have turned out in this way since I felt confident that xenon would combine with fluorine, at any rate. Yost obtained some rod crystals, which he at one time thought contained xenon, but which he later decided were the pink form of hydrogen chloride.

My wife and I have just visited Oregon, where we saw Prof Fulton, Gilbert, and a lot of other people. We had such a good time that we are thinking of spending our vacation there next year.

With best wishes to you and Mrs. Allen, I am

Very sincerely yours,
Linus Pauling

LP:M

P.S. I want to thank you very much for providing the xenon. If there is anything that I can do for you, let me know and I shall try to do it.

Fig. 2. Four letters (reduced facsimiles) of *Linus Pauling* which he wrote to *Fred J. Allen* in connection with attempts to synthesize noble-gas compounds. The handwriting at the bottom of the letter at the top right is due to *F. J. Allen*. In the letter at the bottom right, the line "Gates Chemical Laboratory" at the top is not shown owing to lack of space.

terest and they probably discussed the matter a number of times, which led to the request of a xenon sample from *Fred Allen* at Purdue. This happened, in all likelihood, a few weeks before *Kaye* gave his seminar.

Kaye doesn't recall how they measured the potential. The *actual* value was probably of the order of one kV. *Yost* and *Kaye* repeated the electric discharge experiments 20 times for a week. They failed. *Yost* told *Kaye* that although their experiment had failed, he was going to report their efforts anyway in a letter to the *Journal of the American Chemical Society* to show that they had at least tried. *Linus Pauling* wrote to *Fred Allen*, at Purdue, on July 12, 1933 (the *Yost* and *Kaye* communication to the editor of *J. Am. Chem. Soc.*[21] was received on July 7), as follows:

> At last I can send you some information regarding the xenon experiments, which Dr. Yost has been carrying on, inasmuch as he is thoroughly experienced in the chemistry of the halogens. He found that he could not prepare a compound of xenon with either chlorine or fluorine by any of the means that he tried, and he has now given up the investigation. ... I am sorry that the experiments have turned out in this way since I felt confident that xenon would combine with fluorine, at any rate. Yost obtained some red crystals, which he at one time thought contained xenon, but which he later decided were the pink form of hydrogen chloride.

The original letter is shown in Figure 2, bottom right. The xenon sample was not returned immediately to Professor *Allen*.

The communication to the *Journal of the American Chemical Society*[21] noted that "the side tube was appreciably attacked after some time, and this might be due to the action of a reactive xenon fluoride ... It cannot be said that definitive evidence for compound formation was found. It does not follow, of course, that xenon fluoride is incapable of existing." *Yost* still felt that he had a chance of making such a compound. As *Linus Pauling* wrote to *Fred Allen* on November 16, 1933, "the 70 mm of xenon[21] was the *pressure* in mm of mercury, the volume of the system being 300 or 400 cc. Hence there was plenty of xenon present. Yost should have mentioned the volume. We still have the xenon, but Yost would like to make another try at preparing a compound (unless you want the xenon returned soon). I still think X(e)F_6 should be stable." The original letter is shown in Figure 2, bottom left. Ultimately, the xenon sample was returned to *Fred Allen*. One of us *(G. S.)* was shown it by Professor *Derek Davenport* when he visited Purdue in 1978. According to *Davenport*, the sample was analyzed several years ago by mass spectrometry, showing that *Yost* and *Kaye* had recovered a pure sample of xenon from their apparently failed experiments.

From hindsight, given the success of later attempts using similar reaction conditions, it is tempting to speculate about the most plausible reasons for the failure of the *Yost* and *Kaye* experiments. But first, did they drop the matter there? *Kaye* says now that their failure was as much his as it was *Yost*'s. He remembers them discussing another possible approach, trying various types of radiant energy, or even catalysis. This shows that they were not quitters. However, *Kaye* had decided in the meanwhile to return to MIT to complete his engineering studies. He does not know why *Yost* dropped the matter after his departure. Maybe he simply could not find someone with comparable skills to *Kaye*'s, and/or he lost faith.

5. Reasons for this Non-Happening?

The high initial pressure used in *Yost* and *Kaye*'s experiments (600 torr of fluorine and 30 torr of xenon) apparently precluded the use of lower potentials (a *nominal* potential of 30 kV was reported[21]) making it impossible to achieve a "silent discharge." The ensuing arcing with its accompanying high temperature may have prevented formation of xenon difluoride, particularly in the absence of a "cold finger" for product condensation.

There is also the possibility that the F_2/Xe ratio (20 : 1) used by *Yost* and *Kaye* ought to have led to XeF_6 formation. Once discharge had been initiated in such high-pressure mixtures, the potential would have plummeted, perhaps to a few kV. At these lower potentials, it is now known that xenon fluorides are formed. *Yost* and *Kaye* mention[21] the etching of a side arm used for condensing xenon and fluorine into the "all-quartz"[21] discharge apparatus. This side arm would have probably been the coolest region of the apparatus while a discharge was under way. This would afford the only cold point where a fluoride of relatively low volatility (such as XeF_6) might condense. In so doing, XeF_6 would slowly react with the quartz surface to form the more volatile $XeOF_4$. In such a scenario, the latter oxyfluoride could have reacted further with the quartz apparatus, producing a uniform and virtually imperceptible etch over its entire surface. Decomposition of thin deposits of the resulting thermally unstable XeO_2F_2—if it did not react further with the quartz surface—and XeO_3 presumably would also remain undetected by *Yost* and *Kaye*'s visual inspection.

It is also conceivable that $XeOF_4$ could be fluorinated under electric discharge to give XeF_6, O_2, and/or OF_2. Even a substantial buildup of oxygen difluoride, pale yellow as a liquid, would have been easily masked by the more intense yellow-green color of gaseous fluorine.

In any case, based on the experience in the field of one of us *(G. S.)*, it is probable that a compound was made, that it consisted mostly of xenon hexafluoride, that it reacted with the quartz surface as it formed, leaving only its telltale etch in the cooler (near-ambient) region of the reactor.

This reactor consisted of a quartz-and-copper apparatus. The communication in the *Journal of the American Chemical Society*[21] mentions an all-quartz apparatus but *Pauling* and *Kaye* both recall the use of metal. Borosilicate glass was rare at the time in North America; it was almost exclusive to the French. (Although borosilicate glass was developed in Germany prior to World War I by Schott, its patent was turned over to France as part of Germany's war reparations payment.) This is probably why quartz was used in the *Yost* and *Kaye* apparatus, and it speaks highly of the technical skill within *Yost*'s laboratory. *Pauling* re-

calls that the entire apparatus was metallic, *except* for the cold finger region projecting away from the discharge vessel and associated connections and storage bulbs. He maintains that the discharge region was made of metal (nickel?, copper?), and hence a product if it formed could have been missed because of the opacity.

What were the consequences of the failure of the *Yost* and *Kaye* attempt? As *Yost* wrote:[20] "Mr. Kaye and I will have to rest content with the fringe virtue of having said in print that we hadn't proved by our experiments that a xenon fluoride was incapable of existing." What about *Linus Pauling*, who had been instrumental in getting this experiment launched and who must have been very much interested in its outcome, given his prediction of the existence of several xenon fluorides?

6. *Pauling*'s Change of Heart in the Aftermath of the *Yost* and *Kaye* Experiments

It looks as if *Linus Pauling* back-tracked somewhat. "The Nature of the Chemical Bond"[22] makes no reference to noble-gas compound formation in the second (1940) or third (1960) edition. Nor could we find such a reference in other Pauling books: the second (1953) edition of "General Chemistry,"[23] "College Chemistry"[24] (1952), and "The Chemical Bond"[25] (1967). It appears that the 1933 paper in the *Journal of the American Chemical Society*[17] is the only place where his predictions appear. Interestingly, *Pauling* published an almost-retraction, when he wrote in his 1961 article on general anesthesia:[26] "Xenon is completely unreactive chemically. It has no ability whatever to form ordinary chemical compounds, involving covalent or ionic bonds. The only property it has is that of taking part in the formation of clathrate crystals."

Another indication is provided by the appearance of the periodic table in *Pauling*'s books: as *Antropoff* noted,[8] the position and the labeling of the noble gases had a direct connection with belief or disbelief in their potential reactivity. *Pauling* used a periodic table in all of the above book titles in which the noble gases were alloted to Group 0—even in his 1970 edition of "General Chemistry," long after noble-gas reactivity was discovered. This table also repeats the noble-gas column, placing it to the left of the alkali metals and to the right of the halogens (see Fig. 3). As *Pauling* told us, he prefers his version, based on a very early table (*Moseley*'s), because it makes no break between metals and nonmetals. In that same volume *Pauling* includes a section on his 1933 predictions[17] and a discussion of noble-gas compounds known at the time. In his pre-1962 general chemistry book, *Pauling* describes the noble gases as inert. For example, in the 1952 edition of "College Chemistry"[24a] he stated that these elements are "completely unreactive chemically; they do not form any chemical compounds" and "the failure of these inert elements to form chemical compounds is similarly due to the great stability of their electronic structures." Pauling, however, did make an ex post facto citation of his 1933 predictions in his 1964 edition of "College Chemistry,"[24b] two years after the discovery of noble-gas reactivity: "The possibility of synthesizing fluorides and oxygen compounds of xenon (XeF_6, XeF_8, KrF_6, H_4XeO_6, and others) was predicted long ago from structural arguments [Linus Pauling, *J. Am. Chem. Soc.* 55, 1895 (1933)]. An early effort to make xenon fluoride was unsuccessful [D. M. Yost and A. L. Kaye, *ibid.* 55, 3890 (1933)]."

As to why *Pauling* may not have pursued the matter further, he thinks it was because of his emerging interests in biological molecules in the early 1930s. Back in 1924, in a letter of October 25 when he was trying to fill *Fred Allen* in on the available research areas, were he to come to Caltech, *Pauling* wrote: "The only graduate work in chemistry is in physical, inorganic, and biochemistry. The last is in-

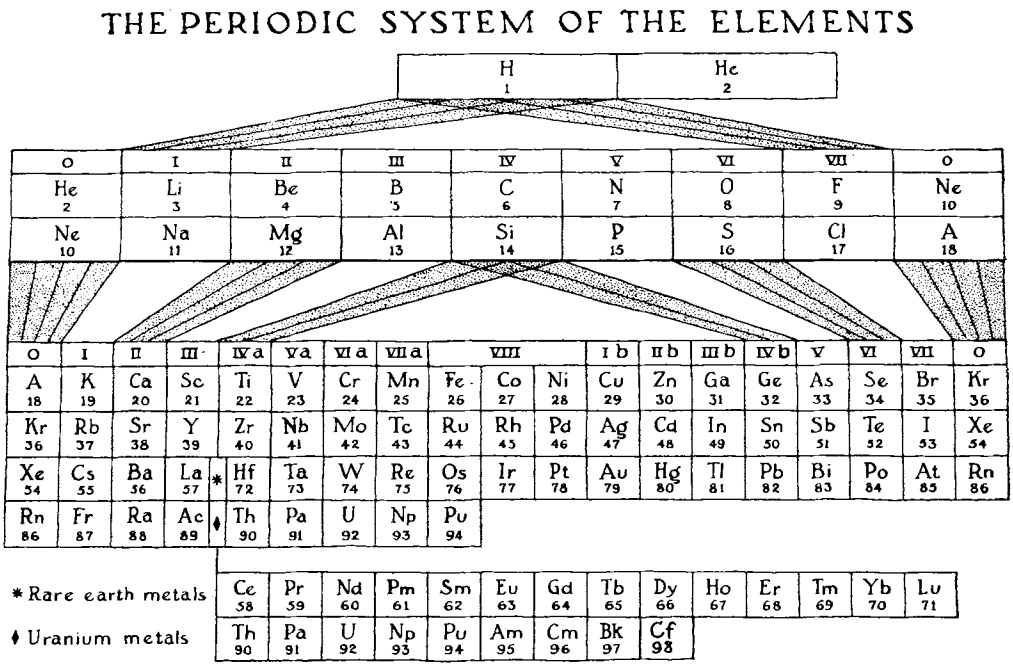

Fig. 3. The periodic table as used by *Pauling* in "General Chemistry" (1970) (cf. [23]).

teresting, but I wouldn't want to do it."[27] His present (1986) feelings are largely the same, he says; he still doesn't care much for biochemistry.

In any case, *Pauling*'s change of attitude about the lack of reactivity of the noble gases and his deep influence may explain the dead calm of the field from 1933 on.[19,28] That year was the turning-point; it saw the retraction of *Antropoff* et al.,[16] the *Pauling* predictions,[17] and the report of the failure of the *Yost* and *Kaye* experiments.[21]

7. Other Attempts

Grimm and *Herzfeld* based on a Born–Haber cycle an estimate of an enthalpy of formation of 246 kcal mol^{-1} for Ne^+Cl^- in 1923.[29] *Booth* and *Willson* carried out in the early 1930s experimental work contemporary with the *Pauling* predictions and the *Yost* and *Kaye* experiment. Their 1935 publication[30] has a footnote to the effect that, on the editor's advice, they withheld publication of a preliminary note submitted on July 17, 1932. *Booth* and *Willson* based their investigation on a sound and well-argued analogy: since boron trifluoride can accept electrons from a full octet in complexes such as dimethyl ether–boron trifluoride, it should be feasible to form likewise compounds between BF_3 and the noble gases. They did a thermal analysis of argon–boron trifluoride mixtures and concluded that formation of $Ar \cdot BF_3$, $Ar \cdot 2BF_3$, $Ar \cdot 3BF_3$, $Ar \cdot 6BF_3$, $Ar \cdot 8BF_3$, and $Ar \cdot 16BF_3$ could occur in the temperature range -127 to -133 °C.[30] *Wiberg* and *Karbe* showed these observations to be in error.[31]

In 1951, *George C. Pimentel* gave a nice MO description of bonding in the trihalides.[32] Overlap of the three atomic p orbitals leads to a bonding, a nonbonding, and an antibonding MO. Two electrons go into the bonding MO, and the other two into the nonbonding MO. This results in two one-electron bonds. *Pimentel* had the foresight to point out that a similar description would be applicable to molecules formed by rare gases with the halogens. He believed that both *Boomer*[7] and *Antropoff*[13] had earlier obtained such compounds. Obviously, he did not know of *Antropoff*'s retraction of 1933.[16] He cited only the *Antropoff, Weil,* and *Frauenhof* 1932 "success."[13] Neither did he refer to *Yost* and *Kaye*.[21] And he predicted confidently[32] formation of rare-gas compounds from mixtures of "helium–iodine, argon–chlorine, krypton–chlorine, and krypton–bromine."

8. The Story: The Multiple Discovery

The rest is history and is well-documented.[19,28] Hence, we shall content ourselves with a brief reminder of the main protagonists, adding only a few footnotes here and there.

Rudolf Hoppe joined the inorganic chemistry group of Professor *W. Klemm* at Münster in 1949. He proposed to his mentor preparation of XeF_4 by direct fluorination of xenon.[33] In 1951, determination of the heat of formation of IF_5 by *A. A. Woolf* served this visionary of noble-gas reactivity to extrapolate it to estimates for the bond energies in XeF_4 and XeF_2 of at least 20–40 kcal mol^{-1}. He provided an estimate by extrapolation for the boiling point of xenon tetrafluoride as 90 °C (1949), revised to 120 °C (1960–1961). *Hoppe* brought to a Gordon Conference in 1961 slides showing this boiling point together with values of the heats of formation predicted for xenon difluoride and xenon tetrafluoride. He showed these to Professor *R. D. Peacock* (now at Leicester University), who felt strongly that it was inadvisable to release such limited information. In August 1961, he decided (against the objections of *Klemm*) to attempt the synthesis. In 1962, the *Hoppe* group in Münster succeeded in preparing xenon difluoride by submitting a mixture of xenon and fluorine (1 : 2) to electric discharges in a sealed quartz vessel (cf. Fig. 4).[34] They missed beating *Bartlett* to the published discovery by just a few weeks. This is a little ironic as the compound made, XeF_2, was well and correctly characterized by *Hoppe*'s group.[33,35] *Bartlett*'s compound is still not definitively characterized after 25 years. Figure 5 shows the first XeF_2 single crystals obtained by *Hoppe* et al.

The other irony was *Hoppe*'s success using a very similar method to that which *Yost* and *Kaye* could not bring to work, which is another reason to believe that *Yost* and *Kaye* may have unknowingly prepared some amount of a xenon fluoride (see Section 4).

At Argonne, the late *Herbert H. Hyman* produced the fine organizational climate that permitted people like *Claassen, Malm, Selig, Chernick,* and others to accomplish so much in such a very short span. They had no prior knowledge of *Hoppe*'s ideas and work, nor of *Pauling*'s predictions.

The context was a wish, on the part of some, to disprove *Bartlett*'s experiment. (The reader is referred here to the cover of the May 1964 issue of *Scientific American*, with a dramatic illustration of the original *Bartlett* experiment as carried out in the hands of the Argonne group. The reaction vessel, containing red-brown PtF_6 vapor, was shown on the left. The same reaction vessel was shown again on the right, this time containing yellow $XePtF_6$ that had partially solidified from the red-brown vapor.) The first time the Argonne group heard of *Bartlett*'s work was when his paper was first published.[36] The general attitude in the Argonne group was lukewarm.

John Malm could bring a lot of expertise to such a test of the *Bartlett* result.[36] Together with *Bernard Weinstock* (died 1984), he had been heavily involved in the Manhattan Project, preparing uranium hexafluoride for isotopic separation. *Malm* and *Weinstock* used to study the periodic table with the view to prepare other hexafluorides (those of platinum, rhodium, and ruthenium). It never occurred to them to try xenon. This group could easily duplicate or refute *Bartlett*'s findings; they had been working with platinum hexafluoride (*Bartlett*'s oxidant) over the past five or six years.

The next day, *Malm* had a glass apparatus made, similar to that described by *Bartlett*,[36] got hold of some xenon (the most difficult part of the experiment), and within two days had repeated *Bartlett*'s experiment. Still, *Malm* was concerned about a possible impurity in xenon such as oxygen, which *Bartlett* had previously shown to be oxidized at ambient temperature by PtF_6 to yield $O_2^+PtF_6^-$. *Malm* neglected to hydrolyze the product. This would also have told him that xenon, not dioxygen, had combined by the

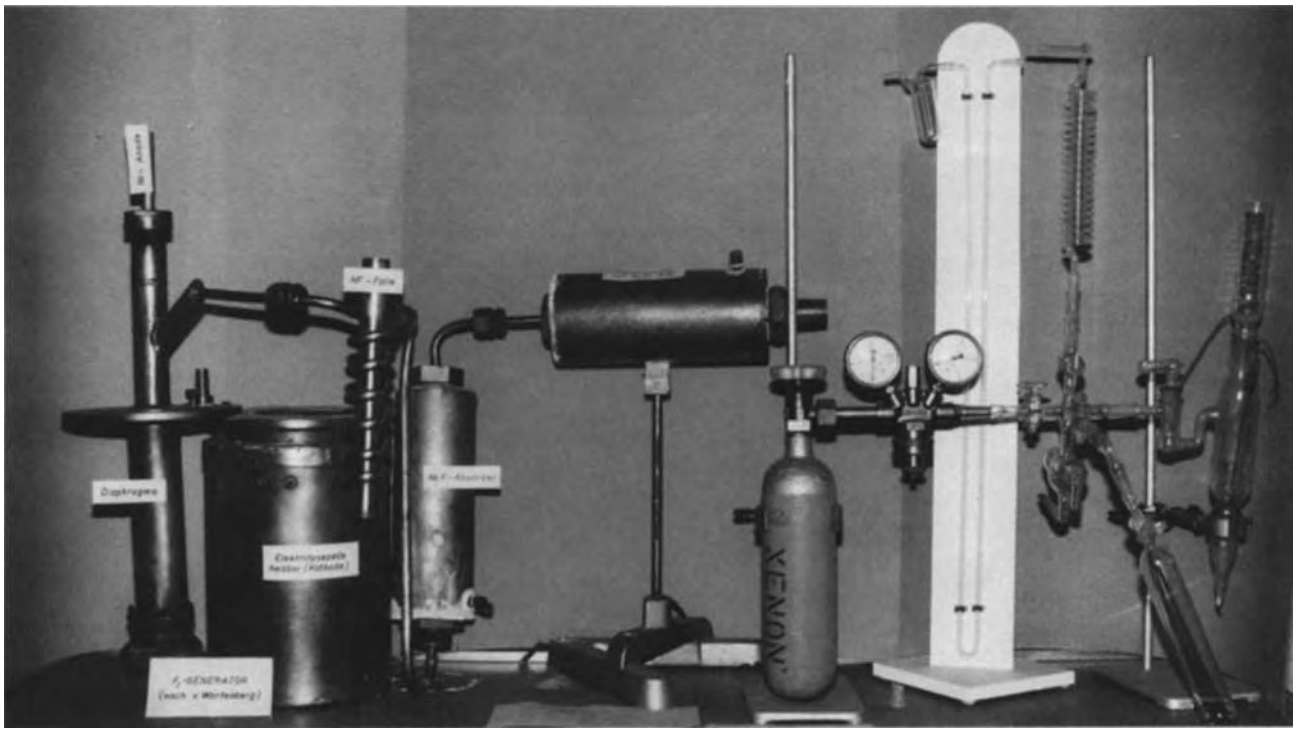

Fig. 4. Apparatus used by *Hoppe* et al. in 1962 to synthesize XeF_2 (cf. [34]). The apparatus is partly disassembled.

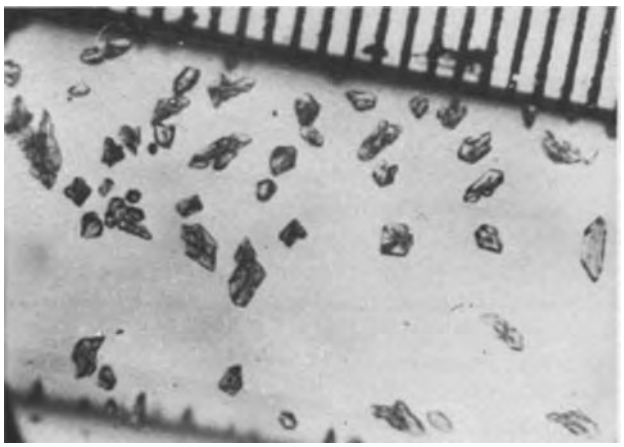

Fig. 5. XeF_2 single crystals (enlarged) prepared by *Hoppe* et al.

liquid-nitrogen-condensible xenon gas released. In the next week he and *Cedric Chernick* ran through all the metal hexafluorides they had on hand, but only platinum hexafluoride worked. They did not have ruthenium hexafluoride on hand at that time, which they later found would also oxidize xenon.

It was then that *Howard Claassen*, a physicist, suggested reacting directly fluorine with xenon to produce a xenon fluoride. This was proposed over coffee and was greeted with skepticism: in *John Malm*'s words, "as a physicist he didn't know any better." The xenon–fluorine reaction was tried by *Claassen* and *Malm*. This was easy since all the high-pressure gear, including a nickel reaction canister were available among *Malm* and *Weinstock*'s paraphernalia. They reacted xenon and fluorine at 400 °C, selecting accidentally the conditions which would give them 97% xenon tetrafluoride. The resulting compound had a very low vapor pressure. Because *Claassen* was a vibrational spectroscopist, his first reaction was to get it into an IR gas cell as quickly as possible. *Howard* knew immediately from the IR spectrum that the molecule was square planar, the only example of a volatile square-planar molecule.

At about this time, *Henry Selig* arrived. He and *Malm* took over the synthetic aspects in *Malm* and *Weinstock*'s laboratory. One of *John Malm*'s tasks was to obtain an analysis of the product. They could obtain the stoichiometry directly from the weights when they employed a small light-weight nickel reaction vessel. He tried hydrolysis. He could titrate fluorine and collect xenon, with a Toepler pump presumably. However, there was always a xenon deficit, later to be shown to arise from disproportionation to the water soluble xenate(VI) and xenon gas. He accomplished the analysis by hydrogen reduction and then titrated the liberated HF as well.

Only two weeks from the first evidence for xenon tetrafluoride, the *Journal of the American Chemical Society* had published their work in a September 1962 issue.[37] The Argonne group only became aware of *Pauling*'s early predictions on perxenate and other noble-gas species after their paper had been published.[17]

Linus Pauling reacted to the Argonne discovery of XeF_4 in a cryptic dictated reply, dated October 24, 1962, to a letter of Professor *F. J. Allen* on the subject: "I must say that I don't understand how Yost could have failed to have discovered xenon tetrafluoride—just bad luck, I guess."

Now, to *Bartlett*'s familiar story. He was the first to knowingly make a compound of a rare gas, beating the Münster and the Argonne groups to it by a few months.

23rd March 1962.

The Preparation of Xenon Hexafluoroplatinate (V) 9.p.m.

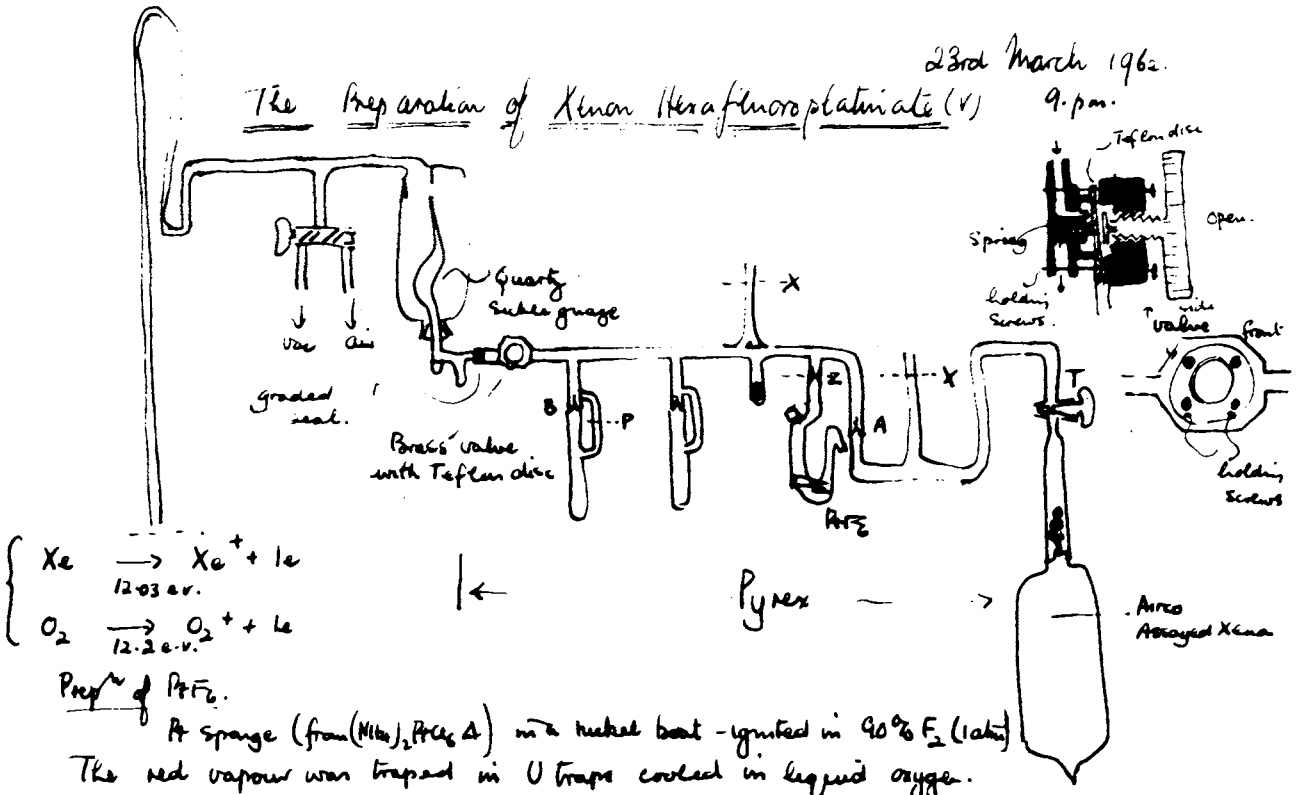

Prep^{n} of PtF_6.

Pt sponge (from $(NH_4)_2PtCl_6$ Δ) in a nickel boat - ignited in 90% F_2 (1 atm). The red vapour was trapped in U traps cooled in liquid oxygen. When the spontaneous platinum ignition stopped the preparation was terminated to reduce contamination by SiF_4 to a minimum.

Measurement of PtF_6

The sample of PtF_6 contained in its original trap (cooled at -183) was connected to a Pyrex - Silica system as shown. The entire system was evacuated and flamed then sealed under vacuum at X. The PtF_6 was transferred to the well of the Pirani gauge (cooled in liq O_2) and the brass valve closed. As the PtF_6 warmed up the pressure developed was balanced by admitting air to the surrounding chamber. A manometer recorded the pressure of the outer chamber. The vapour was deep red (only subdued lighting was used during the experiment to reduce photolysis).

Pressure of PtF_6 taken — 45 mm.
Pressure of Xe taken — 95 "
Residual pressure 40 mm.

The PtF_6 was condensed in the break seal bottle B which was subsequently sealed at P.

Meanwhile the Xenon system - isolated by the breakseal A had been evacuated under vacuum with the tap T open. This system was sealed at X, T closed and the break-seal on the Xenon bottle broken.

Measurement of Xenon.

A was broken and the brass valve opened. Tap T was cautiously opened and the pressure developed balanced by admitting air to the outer Pirani gauge chamber. T was closed when the pressure developed matched that of the PtF_6. The brass valve was closed and the tap T closed. The Xenon between T and the brass valve was pumped out via λ, the system again flamed

Fig. 6. A page from *Bartlett*'s laboratory notebook dated March 23, 1962 (slightly reduced facsimile).

We draw upon *Bartlett*'s recollections, as given to *C. B. Hunt*:[38]

> The crucial step occurred in late February, 1962 ... By chance, as I was flicking through (a textbook), the familiar plot of first ionisation energies of the elements caught my eye. In an instant the old thought, of the possibility of oxidising the noble gases, returned. A quick check confirmed my immediate suspicion that the heavier gases should be oxidisable by PtF_6 ... xenon looked good since its ionisation energy, 1170 $kJ \cdot mol^{-1}$, was marginally less than that of oxygen (1176 $kJ \cdot mol^{-1}$).

Thus, we come full circle to the pioneering insight of *Kossel* 46 years earlier.[9] *Bartlett* was also driven on by another consideration: just about this time he and his graduate student *D. H. Lohmann* had already observed the direct oxidation of oxygen gas by PtF_6 vapor at ambient temperature and they were about to publish these observations (they appeared in the March 1962 issue of the *Proceedings of the Chemical Society*[39]).

Bartlett made himself an apparatus in which he could introduce the deep red-brown PtF_6 vapor and xenon gas, separated by a break-seal. On March 23, 1962, everything was set up. *Bartlett* recalls that "I wasn't ready to break the glass capillary separating the xenon and PtF_6 until about 6.45 p.m. My students had left for supper (they never admitted to scepticism) and I was alone when the capillary was broken. Of course, I was overjoyed when there was an immediate interaction of the gases." Figure 6 shows a page from *Bartlett*'s laboratory notebook, written almost immediately after the successful experiment. On May 14, 1962, he mailed in his communication to the *Proceedings of the Chemical Society*.[36] This achievement is breathtaking and spectacular: single-handedly, *Bartlett* had made a crucial breakthrough, he had revived a whole *problématique*, and opened up a whole avenue of investigation.

9. Concluding Remarks: Rambling Thoughts on Some of the Underlying Patterns

We shall start with the most popular, and arguably least important aspect of the story: the myth of chemical inertness of the rare gases. What this story shows is that it was not in full force till relatively recently, when, for instance, *Neil Bartlett* feared ridicule from his colleagues in the department and from his students.[38] During the whole period 1895–1933, this myth was *not* all-powerful, as the numerous attempts at making compounds of the noble gases show.[19,28] Only after *Yost* and *Kaye*'s failure and the attendant loss of faith by *Linus Pauling* did this myth ascend into a dogma. No doubt, *Pauling*'s influence and his becoming interested in more biological quests had a lot to do with this. In other terms, the octet rule was not seen as a deterrent to the existence of noble-gas compounds till the mid-1930s. It is true that "The Atom and the Molecule" paper by *G. N. Lewis*, with the octet theory, dates back to 1916 and that *Irving Langmuir* published his concept of the atom as made of concentric electronic shells in 1919. However, the *Kossel* paper,[9] coincidentally published also in 1916, and arguing from the same standpoint of a stable configuration of eight electrons, could make the prediction of xenon and krypton fluorides. The 1930s saw the protracted and generalized acceptance by chemists of modern electronic theories of the atom as the basis for the periodic table. After 1933, when *Linus Pauling* himself started to assert the inertness of the noble gases, the octet rule became entrenched. His authority may have made it easier for the octet rule to rigidify into a stultifying dogma. We do not adjudge here between theory and experiment. Theory had the leading role in the earlier *Kossel–Antropoff* part of the story. Theory may have led experiment in the *Yost* and *Kaye* episode. Theory—or rather the watered-down version of theory that percolates into teaching—had the inverse role, it paralyzed experimentation during the whole period 1933–1962.

A tightly coupled reason for the protracted discovery—it *could* have been made at the turn of the century with existing technology and from the supply of xenon that could have been provided; it *should* have been made by *Yost* and *Kaye*, who were particularly unlucky (see below)—is the overwhelming importance of iconic representations: the presentation of the periodic table with the noble gases in the "zero" column. *Antropoff*'s lasting contribution was to explode the myth of chemical inertness and to propose that noble gases be assigned to the VIIIb column.[11]

Yost and *Kaye* also attempted photochemical generation. Their bad luck was that they tried a xenon–chlorine mixture, which did not react. Had they tried a xenon–fluorine mixture in a similar apparatus under their mercury arc lamp, they would have seen xenon difluoride crystals appear in a matter of hours if not sooner (they ran the xenon–chlorine mixture for 12 h). A number of experiments by the *Strengs*[40] show that the photochemical addition of fluorine to xenon readily takes place *Holloway*[41] has shown that XeF_2 can even be produced in a Pyrex glass bulb under the natural sunlight in Aberdeen, Scotland! Figure 7 shows a glass bulb containing photochemically prepared XeF_2.

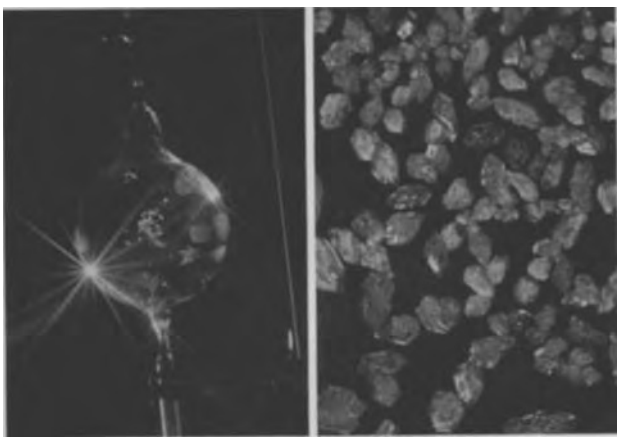

Fig. 7. Left: Glass bulb containing XeF_2 crystals formed by UV irradiation of a 1:1 mixture of Xe and F_2 at McMaster University (*G. S.*). Right: XeF_2 crystals (enlargement).

Alan F. Clifford and a student, *G. R. Zeilenga*, started to investigate the reactions of xenon and fluorine in 1961. Their conditions were similar to those of *Yost* and *Kaye*. They actually obtained white solids and also determined that they contained xenon! The finding was not finalized in time—there may have been a student problem—and it did not receive, like *Hoppe*, priority recognition. After the appearance of *Bartlett*'s work, they assigned the formula Xe_2SiF_6 to their product.[42]

Another interesting story is that of the Oak Ridge fused salt nuclear reactor. *Kirsilis*, *Blankenship*, and *Grimes* had studied molten fluoride fuels. The neutron irradiation was sufficient to cause fission of substantial fractions of the $^{235}UF_4$ present. They noticed that the gas above these melts, if it contained the expected amount of krypton as a fission product, had no xenon! *DeForest Smith*, who was then at Oak Ridge, read the first publication on xenon fluorides to come from Argonne: he remarked that the earlier observation at Oak Ridge, several years before *Bartlett*'s discovery, had been made by engineers rather than by scientists. It was only after they saw the Argonne publication on xenon tetrafluoride that they ascribed the observed absence of xenon above the solidified melts to xenon fluoride formation.[43]

Lastly, there are reasons for the multiple discovery at British Columbia, Münster, and Argonne (in that published order). One is the coming of age of inorganic chemistry, as signaled by *Nyholm*'s 1956 inaugural lecture for his chair at University College, London, entitled "The Renaissance of Inorganic Chemistry"[44] and by the appearance of *Cotton* and *Wilkinson*'s book[45] in the same year, 1962, coincidentally. Another reason was the big progress which World War II, especially the Manhattan Project (Argonne), had led to in the handling of fluorine, and the experience it gave in the chemical properties of hexafluorides.

Yet another factor was the mushrooming of new physical methods, both diffraction and spectroscopic, that became available in many laboratories in the early 1960s. This is apparent in perusal of the Proceedings of the first symposium on noble-gas compounds held at Argonne National Laboratory in 1963;[46] the 58 separate contributions representing the work of 105 researchers published in book form in 1963 are heavily laced with applications of physical methods to structure determinations in the new field of noble-gas chemistry.

The non-discovery of noble-gas compounds in the 1930s can be conjectured to have stifled research on topics such as what we now term hypervalent molecules, van der Waals molecules, strong oxidants, etc. Instead of a fertile area, a desert followed. *Bartlett*'s, *Hoppe*'s too, immense merit was to make it flower again.

We are very deeply indebted to Dr. Albert L. Kaye and John Malm and to Professors Neil Bartlett, Derek Davenport, Rudolf Hoppe, and Linus Pauling for their help. They have shared with us letters and laboratory notes from their archives, giving us permission to quote from them. Yet more importantly, they have entrusted us with their recollections in the course of several interviews, conducted on the phone or in person.

Received: December 29, 1986;
supplemented: March 6, 1987 [A 665 IE]
German version: *Angew. Chem. 100* (1988) 495

[1] P. Laszlo, *Nouv. J. Chim. 6* (1982) 119 (original report: Lord Rayleigh, W. Ramsay, *Phil. Trans. R. Soc. London Ser. A 186* (1) (1895) 187).
[2] H. Moissan, *Bull. Soc. Chim. Fr. 13* (1895) 976.
[3] M. Berthelot, *Ann. Chim. Phys. 11* (1897) 15; *C. R. Hebd. Séances Acad. Sci. 120* (1895) 581, 662, 1386; *124* (1897) 113.
[4] R. J. Strutt, *Proc. R. Soc. London A 80* (1908) 56, 572.
[5] R. J. Strutt, *Proc. R. Soc. London A 87* (1913) 381.
[6] G. Oddo, *Gazz. Chim. Ital. 63* (1933) 380.
[7] E. H. Boomer, *Proc. R. Soc. London A 109* (1925) 198.
[8] A. von Antropoff, *Z. Angew. Chem. 37* (1924) 217.
[9] W. Kossel, *Ann. Phys. (Leipzig) Serie 4 49* (1916) 229.
[10] H. Danneel, *Z. Angew. Chem. 37* (1924) 290.
[11] A. von Antropoff, *Z. Angew. Chem. 37* (1924) 695.
[12] F. Paneth, *Z. Angew. Chem. 37* (1924) 421.
[13] A. von Antropoff, K. Weil, H. Frauenhof, *Naturwissenschaften 20* (1932) 688.
[14] O. Ruff, W. Menzel, *Z. Anorg. Allg. Chem. 213* (1933) 206.
[15] A. von Antropoff, *Z. Anorg. Allg. Chem. 213* (1933) 208.
[16] A. von Antropoff, H. Frauenhof, K. H. Krüger, *Naturwissenschaften 21* (1933) 315.
[17] L. Pauling, *J. Am. Chem. Soc. 55* (1933) 1895.
[18] L. Pauling, *J. Am. Chem. Soc. 55* (1933) 3052.
[19] Besides those already mentioned [2, 3, 7, 12–16] there were many others: see C. L. Chernick, *J. Chem. Educ. 41* (1964) 185.
[20] D. M. Yost in H. H. Hyman (Ed.): *Noble-Gas Compounds*, University of Chicago Press, Chicago 1963, pp. 21, 22.
[21] D. M. Yost, A. L. Kaye, *J. Am. Chem. Soc. 55* (1933) 3891.
[22] L. Pauling: *The Nature of the Chemical Bond, and the Structure of Molecules and of Crystals*, Cornell University Press, Ithaca 1939; 2nd ed. 1940; 3rd. ed. 1960.
[23] L. Pauling: *General Chemistry*, W. H. Freeman, San Francisco 1947; 2nd ed. 1953.
[24] a) L. Pauling: *College Chemistry*, W. H. Freeman, San Francisco 1950; 2nd ed. 1952; b) 3rd ed. 1964.
[25] L. Pauling: *The Chemical Bond*, Cornell University Press, Ithaca 1967.
[26] L. Pauling, *Science 134* (1961) 15.
[27] D. A. Davenport, *J. Chem. Ed. 57* (1980) 35; see also P. Laszlo: *Molecular Correlates of Biological Concepts*, Elsevier, Amsterdam 1986.
[28] J. H. Holloway: *Noble-Gas Chemistry*, Methuen, London 1968, chap. 1.
[29] H. G. Grimm, K. F. Herzfeld, *Z. Phys. 19* (1923) 141.
[30] H. S. Booth, K. S. Willson, *J. Am. Chem. Soc. 57* (1935) 2273.
[31] E. Wiberg, K. Karbe, *Z. Anorg. Chem. 256* (1948) 307.
[32] G. C. Pimentel, *J. Chem. Phys. 19* (1951) 446.
[33] R. Hoppe, H. Mattauch, K. M. Rödder, W. Dähne in H. H. Hyman (Ed.): *Noble-Gas Compounds*, University of Chicago Press, Chicago 1963, p. 98.
[34] R. Hoppe, W. Dähne, H. Mattauch, K. Rödder, *Angew. Chem. 74* (1962) 903; *Angew. Chem. Int. Ed. Engl. 1* (1962) 599.
[35] R. Hoppe, *Angew. Chem. 76* (1964) 455; *Angew. Chem. Int. Ed. Engl. 3* (1964) 538; see also W. Klemm, *Nachr. Chem. Tech. Lab. 30* (1982) 963.
[36] N. Bartlett, *Proc. Chem. Soc. 1962*, 218.
[37] H. H. Claassen, H. Selig, J. G. Malm, *J. Am. Chem. Soc. 84* (1962) 3593.
[38] C. B. Hunt, *Educ. Chem. 20* (1983) 177.
[39] N. Bartlett, D. H. Lohmann, *Proc. Chem. Soc. 1962*, 115.
[40] L. V. Streng, A. G. Streng, *Inorg. Chem. 4* (1965) 1370.
[41] J. H. Holloway, *Chem. Commun. 1966*, 22; *J. Chem. Educ. 43* (1966) 202.
[42] A. F. Clifford, G. R. Zeilenga, *Science 143* (1964) 1431.
[43] W. R. Grimes in M. T. Simnad, L. R. Zumwalt (Eds.): *Materials and Fuels for High-Temperature Nuclear Energy Applications*, MIT Press, Cambridge, MA 1962, p. 117–122.
[44] R. S. Nyholm: *The Renaissance of Inorganic Chemistry*, H. K. Lewis, London 1956.
[45] F. A. Cotton, G. Wilkinson: *Advanced Inorganic Chemistry*, Interscience, New York 1962.
[46] H. H. Hyman (Ed.): Noble-Gas Compounds, University of Chicago Press, Chicago 1963.

Two-Dimensional NMR Spectroscopy: Background and Overview of the Experiments

New Analytical Methods (36)

By Horst Kessler,* Matthias Gehrke, and Christian Griesinger

An exact knowledge of the structure, dynamics, and reactions of molecules provides the key to understand their functions and properties. NMR spectroscopy has developed, through the introduction of two-dimensional methods, into the most important method for the investigation of these questions in solution. A great variety of different techniques is available. However, for their successful application not only the appropriate equipment is required, but also the right choice of experiments and optimum measurement parameters, as well as a careful evaluation of the spectra. This contribution describes the necessary background for modern NMR spectroscopy. With the aid of the so-called product operator formalism it is possible to understand pulsed Fourier transform NMR spectroscopy both qualitatively and quantitatively. Very few, readily understandable assumptions are sufficient for confident application of these methods. This article attempts to introduce in a simple manner this formalism as well as phase cycles necessary for the understanding of pulse sequences, and to train the reader through the discussion of several 2D NMR techniques. An overview of the most important techniques is given in the second part of this article.

1. Introduction

NMR spectroscopy has undergone a revolution with the introduction of 2D techniques.[1-3] Although several reviews on this subject have been published,[2,4-23] we find it useful to provide a readily understandable introduction to and application of the product operator formalism (with Cartesian basis operators).[24-27] In this way the experiments can be understood both qualitatively and quantitatively, without recourse to the somewhat more cumbersome quantum mechanical treatment (keyword: spin density matrix). The product operator formalism makes it possible to describe the behavior of weakly coupled spin systems (i.e., systems in which the difference in chemical shifts of two nuclei is large relative to the J coupling between them) under the influence of pulse sequences by the application of a few simple rules. Thus even nonexperts may follow and apply the experiments.

Along with the description of product operators, some understanding of phase cycles in 2D NMR experiments is also necessary. Phase cycles suppress undesired signals in a multipulse experiment. This concept, as well as the associated "coherence order"[28-32] will be introduced and discussed in Section 2.2.3. Suffice it to mention, at this point, that by following the "coherence-transfer pathways" a simple and powerful tool is provided for the development of phase cycles. The reader will soon recognize that with the product operator formalism and coherence-transfer pathways a theory is now available which in terms of clarity, simplicity, and accuracy by far exceeds the widely used, yet quite cumbersome and insufficient, vector description.

Another reason for writing this article is the experience which has accumulated in applications of the various experiments and which has led to a realization of the advantages and disadvantages of each technique. Thus, for instance, J-resolved[2,33-35] and spin echo correlated spectroscopy,[36-38] which once played a major role in 2D NMR spectroscopy, are now employed only in a few special cases. We can of course only describe a selection of the different 2D NMR techniques. Some 500 pulse sequences for high-resolution NMR spectroscopy have been published. Only a small fraction of those found their way to general recognition and application, and the entire field is still in flux. Thus a whole new series of better experiments is now available, which *quantitatively* measure such parameters as NOE values and vicinal coupling constants, necessary for the determination of structure and dynamics. In addition, the NMR spectroscopy of insensitive nuclei has become more and more accessible, even in large molecules, through the application of inverse techniques.[39-54]

We have tried to write in such a way that the required prior knowledge of the reader be minimal. Therefore the text has been divided into two levels: for a first reading it should be sufficient to cover the normal print. For further discussion and insight the small-print sections should be followed.

2. Background

Nuclear magnetic resonance deals with the interaction between the magnetic moments of atomic nuclei and magnetic fields. The magnetic moment of the nucleus is associated with the nuclear spin S. Only those nuclei for which $S \neq 0$ have a magnetic moment. The high-resolution NMR spectroscopy described in this review is used predomi-

[*] Prof. Dr. H. Kessler, Dipl.-Chem. M. Gehrke
Institut für Organische Chemie der Universität
Niederurseler Hang, D-6000 Frankfurt 50 (FRG)
Dr. C. Griesinger
Laboratorium für Physikalische Chemie der
Eidgenössischen Technischen Hochschule, ETH-Zentrum
Universitätstrasse 22, CH-8092 Zürich (Switzerland)

nantly to investigate nuclei with spin 1/2, which have no quadrupole moment and hence give rise to sharp spectral lines. The nuclei of greatest interest for organic chemistry and biochemistry, H, C, N, and P, all have isotopes with spin 1/2, though for C and N the natural abundance of these isotopes is very small. The proton, the most abundant nucleus in organic compounds, has (with the exception of tritium) the largest nuclear magnetic moment and hence is the simplest nucleus for investigation. However, the NMR spectroscopy of the more "exotic" nuclei, which are of greater significance in organometallic and inorganic chemistry, has also become increasingly important.

2.1. One-Dimensional NMR Spectroscopy

The method now generally used for recording 1D NMR spectra is the Fourier technique introduced by *Ernst* and *Anderson*.[55–57] Since the principles of this technique also underlie 2D NMR spectroscopy, we shall begin with its description.

Nuclei with spin 1/2 are aligned either in a parallel or an antiparallel orientation with respect to the applied $\boldsymbol{B}_0$ field. Only these two states exist, which are marked α and β, respectively. The parallel α state[*] is lower in energy than the antiparallel β state. Therefore, the population of the α state is greater than that of the β state (Boltzmann distribution), and a macroscopic magnetization along the $\boldsymbol{B}_0$ field ("longitudinal magnetization") exists due to this population difference. The macroscopic magnetization can be expressed in terms of the Bloch equations.[58] According to usual convention, the so-called rotating-frame coordinate system is used. The coordinate system rotates about the z axis, which is aligned with the $\boldsymbol{B}_0$ field, at the "carrier frequency" ω_0 of the radio frequency pulse.

Pulses are short-term high-frequency oscillating magnetic fields of the form $\boldsymbol{B}_1 \cos\omega_0 t$. Because the magnetization precesses about $\boldsymbol{B}_0$ during the pulse, a very complicated motion results. A simplified description is achieved in a coordinate system rotating at $\omega_0 = \gamma \boldsymbol{B}_0$ such that the magnetization appears to rotate about $\boldsymbol{B}_1$ alone.

The linearly polarized $\boldsymbol{B}_1$ field (e.g., only the x component) may be divided into two circularly polarized fields [Eq. (1)]. The two vectors rotate at equal frequencies but in opposite directions. In the rotating frame $(\boldsymbol{e}'_x, \boldsymbol{e}'_y)$ one obtains Equation (2).

$$\boldsymbol{B}_1(t) = \boldsymbol{B}_1^\circ \cos\omega_0 t \boldsymbol{e}_x = \tfrac{1}{2}\boldsymbol{B}_1^\circ(\cos\omega_0 t \boldsymbol{e}_x + \sin\omega_0 t \boldsymbol{e}_y) + \tfrac{1}{2}\boldsymbol{B}_1^\circ(\cos\omega_0 t \boldsymbol{e}_x - \sin\omega_0 t \boldsymbol{e}_y) \quad (1)$$

$$\boldsymbol{B}'_1(t) = \tfrac{1}{2}\boldsymbol{B}_1^\circ \boldsymbol{e}'_x + \tfrac{1}{2}\boldsymbol{B}_1^\circ(\cos 2\omega_0 t \boldsymbol{e}'_x - \sin 2\omega_0 t \boldsymbol{e}'_y) \quad (2)$$

The component in (2) rotating at twice the Larmor frequency does not meet the resonance condition and can therefore be neglected. Only the time-independent (!) component $\tfrac{1}{2}\boldsymbol{B}_1^\circ \boldsymbol{e}'_x$ is considered. Thus, the Bloch equation contains only time-independent fields and is readily solved. The static fields ($\boldsymbol{B}_0$ and $\boldsymbol{B}'_1$) cause rotations of the magnetization about the corresponding axes (x or z', respectively). The magnetization rotates by a certain angle, the so-called flip angle, depending on the duration of the $\boldsymbol{B}_1$ field (the pulse length). Therefore pulses are often characterized by their flip angle, rather than by their field strength and duration.

Pulses may be described as rotations by a certain angle (flip angle) about a certain axis in the x,y plane (phase). For example, application of a short radio frequency pulse generally labeled β_y will rotate the magnetization about the y axis by an angle β from the z axis [Eq. (3) and Fig. 1].[*]

$$M_z \xrightarrow{\beta_y} M_z \cos\beta + M_x \sin\beta \quad (3)$$

Equation (3) means that the M_z magnetization[**] transforms under the influence of a β_y pulse in part ($\sin\beta$) into M_x magnetization, the other part ($\cos\beta$) remaining along the z axis.

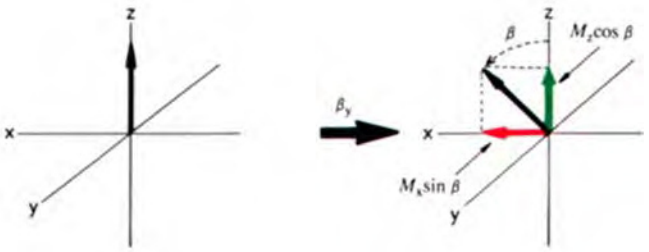

Fig. 1. The effect of an on-resonance radio frequency pulse in the y direction in the rotating frame and a flip angle β on longitudinal magnetization. We have rotated the coordinate system by 90° from the usual representation (x in front) for easier understanding.

After application of the pulse, the transverse magnetization M_x begins to precess about the z axis at a precession frequency $\omega = \gamma \boldsymbol{B}_{\text{eff}}$. The chemical shifts of the different nuclei are represented by $\boldsymbol{B}_{\text{eff}}$. Nuclei of the same isotope (e.g., protons) have equal γ and nearly the same $\boldsymbol{B}_{\text{eff}}$, so that their precession frequencies fall within a narrow range. For protons this frequency varies, depending on individual chemical shifts, within ca. $10^{-5}\,\omega_0$, or 10 ppm. In the rotating-frame the observer (i.e., detector) also rotates about the z axis at the carrier frequency ω_0. The detector "sees" now only difference frequencies $\omega - \omega_0$. Henceforth we shall term these difference frequencies *precession frequencies* or *chemical shifts*, Ω (Fig. 2). In the rotating frame we thus obtain Equation (4).

$$M_x \xrightarrow{\Omega t} M_x \cos\Omega t + M_y \sin\Omega t \quad (4)$$

The precession frequency Ω is the deviation of the Larmor frequency from the carrier frequency ω_0, which is reg-

[*] The assignment α and β for parallel and antiparallel, respectively, follows the notation in Ref. [3], and will be used here throughout. Sometimes the opposite assignment can be found in the literature.

[*] The direction of rotation of the magnetization under the influence of pulses follows Ref. [3], and is in accordance with the mathematical sense of rotation. Frequently, the opposite definition is found in the literature (in our example this would correspond to a rotation to $-x$).

[**] M_x, M_y, and M_z mean unit magnetizations given by the initial polarization along the corresponding axes.

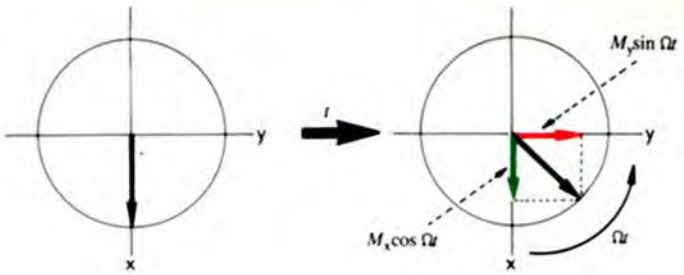

Fig. 2. Evolution of the chemical shift Ω during time t. A view onto the x,y plane in the rotating frame is shown.

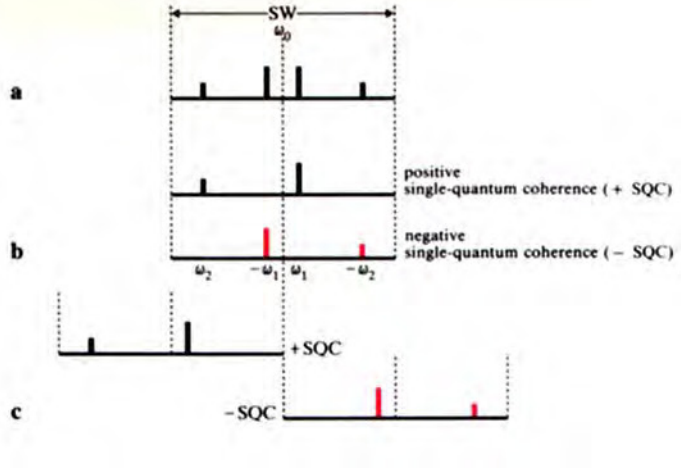

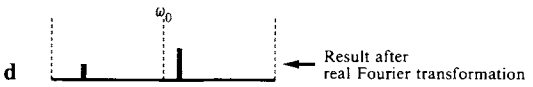

Fig. 3. Principle of the Redfield technique. A single-channel detection spectrum, obtained after complex Fourier transformation (a) contains signals at both positive and negative frequencies, which are shown separately in (b). This corresponds to positive and negative single-quantum coherences. The two spectral parts no longer overlap (c) when the receiver rotates at frequency SW/2 in the rotating frame. After folding about $\omega_t = 0$, , i.e., real Fourier transformation, a spectrum is obtained (d) which contains only the positive frequencies.

istered as a signal by the detector aligned, for example, with the x axis in the rotating frame. Thus a signal $S(t)$ oscillating at frequency Ω is obtained, the so-called *free induction decay* (FID). A Fourier transformation will convert this signal into a spectrum with a single signal ("peak") at frequency Ω (see also Fig. 4).

Fourier transformation is a mathematical procedure by which frequencies, which are detected in an oscillating function of time, are transformed into signals at the corresponding positions on a frequency scale.

The function $\cos\Omega t$ in Equation (4) contains the frequency $\omega = +\Omega$ as well as to $\omega = -\Omega$, and hence a distinction between these frequencies is impossible. It is however desirable to know the sign of a given frequency, for only then can the carrier frequency be placed in the center of the spectral range. Quadrature detection,[59,60] by which both x and y magnetizations in the rotating frame are detected, allows the sign discrimination of the detected frequency. A signal $\cos\Omega t$ is constructed in the x channel (K_x) from the x magnetization M_x in (4), and a signal $\sin\Omega t$ in the y channel (K_y) from the y magnetization M_y. When the two signals are combined, $K_x + iK_y$, the complex expression $e^{i\Omega t}$ is obtained, which after complex Fourier transformation produces a single line at frequency $+\Omega$ (and indeed not also at $-\Omega$). The disadvantage of this procedure is that it requires simultaneous collection of two signals.

A trick introduced by *Redfield* et al.[61,62] is utilized in some instruments, whereby, starting with the (+x) direction, signal detection is alternated among the (+x), (+y), (−x), and (−y) directions (Fig. 3). Hence the receiver rotates in the rotating frame with an additional frequency Ω_R. The recorded signal is then $\cos(\Omega + \Omega_R)t$. Ω_R is set to one-half the spectral width (SW/2) (Fig. 3b). After a complex Fourier transformation, a spectrum is obtained in which signals with positive and negative frequencies no longer overlap (Fig. 3c). Finally, the spectrum may be "folded" about $\Omega = 0$ (Fig. 3d), or, equally well, a real Fourier transformation may be performed.

We now wish to describe the same experiment in terms of the product operator formalism.[24] In contrast to the vector formalism discussed above, in which the macroscopic magnetization rotates under the influence of pulses and/or precesses under the influence of chemical shift, the entire state of the spins or spin system (only the observable magnetization) is described by means of the density matrix. The observable quantities must then be "read out" of the spin state. The following short discussion of the quantum mechanical formalism should be fully sufficient for the understanding of 2D NMR experiments (for detailed discussions of the physical background see Refs. [63–67]).

The ground state of the system in thermal equilibrium is described by a polarization along the z axis, I_z. This state is associated with a magnetization M_z. Under the influence of pulses from the y direction (henceforth termed in short "y pulses") I_z, as well as I_x and I_y, transform according to (5)–(7) (see also Fig. 1).

$$I_x \xrightarrow{\beta I_y} I_x \cos\beta - I_z \sin\beta \tag{5}$$

$$I_y \xrightarrow{\beta I_y} I_y \tag{6}$$

$$I_z \xrightarrow{\beta I_y} I_z \cos\beta + I_x \sin\beta \tag{7}$$

The Cartesian operators[*] (I_x, I_y, I_z) transform like magnetizations when a rotation is performed. The properties of a state I_x, I_y, or I_z can be read off directly in such simple product operators which consist of only *one* operator. I_x is associated with an x magnetization, I_y with a y magnetization, and I_z with a z magnetization.

We have yet to explain the notations used in Equations[**] (5) to (7), as well as in other expressions throughout the paper. The starting state of the spin system is on the left-hand side of the equation. On the right is the end

[*] We use throughout this article the symbols I (or S) for the operator as well as for the expectation value, and not the symbol $\hat{I}$ (or $\hat{S}$) for the operator.

[**] Strictly speaking one should use the term "transformations." However, in this article we use the term "equation" not in its strict mathematical definition.

state after the "propagation," i.e., the evolution under the influence of a particular operator responsible for a specific interaction (e.g., for pulses, chemical shift, coupling). The terms above the arrows are the parts of the Hamiltonian operator (which describes the interactions of the spins with external fields and with each other) under which the system evolves. Thus,

(a) $\beta I_{x,y}$ or in general βI_φ represents a pulse with a flip angle β about an axis in the x,y plane, which forms an angle φ with the x axis,
(b) $\Omega I_z t$ represents the evolution of chemical shift Ω of nucleus I during time t, and
(c) $2\pi J I_{1z} I_{2z} t$ stands for the evolution of coupling J between nuclei I^1 and I^2 during time t.

Equations (8)–(10) apply to the evolution of chemical shifts (see also Fig. 2). The operators behave here again like the magnetizations. For a single particle of spin 1/2 the description is equivalent to that of the vector formalism.

$$I_x \xrightarrow{\Omega t I_z} I_x \cos \Omega t + I_y \sin \Omega t \tag{8}$$

$$I_y \xrightarrow{\Omega t I_z} I_y \cos \Omega t - I_x \sin \Omega t \tag{9}$$

$$I_z \xrightarrow{\Omega t I_z} I_z \tag{10}$$

The detection of x magnetization means that the signal is built up (in Eq. (9), for instance) by the coefficient $-\sin\Omega t$ of I_x. Fourier transformation yields a single line at $\pm\Omega$. Quadrature detection, which is now available on all spectrometers, allows the selection of only one frequency, $+\Omega$ or $-\Omega$.

Quadrature detection means, as we have seen earlier, the addition of the measured x components of the magnetization to i times the corresponding y components ($K_x + i K_y$). This yields the complex signal $e^{i\Omega t}$. This corresponds to the detection of I^- according to the conventions and transformations (11)–(13).

$$I^+ = I_x + iI_y \tag{11}$$

$$I^- = I_x - iI_y \tag{12}$$

$$I_x \cos \Omega t + I_y \sin \Omega t = \tfrac{1}{2}(I^+ e^{-i\Omega t} + I^- e^{i\Omega t}) \tag{13}$$

Figure 4 summarizes again the principles of 1D NMR spectroscopy for a one-spin system. Application of a high-frequency pulse to the z magnetization (spin state I_z), initially at its Boltzmann equilibrium, produces transverse magnetization (state I_x). This state, the so-called *coherence* evolves, i.e., develops during the detection period t. This variation of the intensity with time can be observed by the detection of an induced signal in the receiver coil (I_x, I_y are associated with transverse magnetization). Thus, coherences produced by product operators are displayed in the spectrum at their characteristic frequencies.

The following discussion should serve to clarify the concept of coherence. In contrast to populations (occupation of states in the energy level scheme) the coherences describe transitions among different energy levels. These transitions are characterized by a change Δm_z in the quantum number m_z. This change, Δm_z, is the coherence order p, which is essential for describing phase cycles (see Section 2.2.3). Although in general many of the possible coherences occur under the influence of pulses in a pulse sequence, only a few are associated with observable magnetizations, namely those for which $\Delta m_z = \pm 1$ (the selection rule for NMR spectroscopy). Of these so-called single-quantum coherences only a few are detectable under weak coupling conditions, those in which the state of exactly one spin is changed, i.e., product operators with only *one* transverse operator.

Finally, a technical remark: The induced signal in 1D NMR experiments is not registered in a continuous manner. The signal picked up by the receiver coil is sampled in discrete time intervals Δt ("horizontal" time digitization) and then digitized "vertically" by an analog-to-digital converter. An FID is obtained consisting of N points, where $N \cdot \Delta t$ yields the acquisition time. The horizontal digitization is possible according to the sampling theorem [68–73]

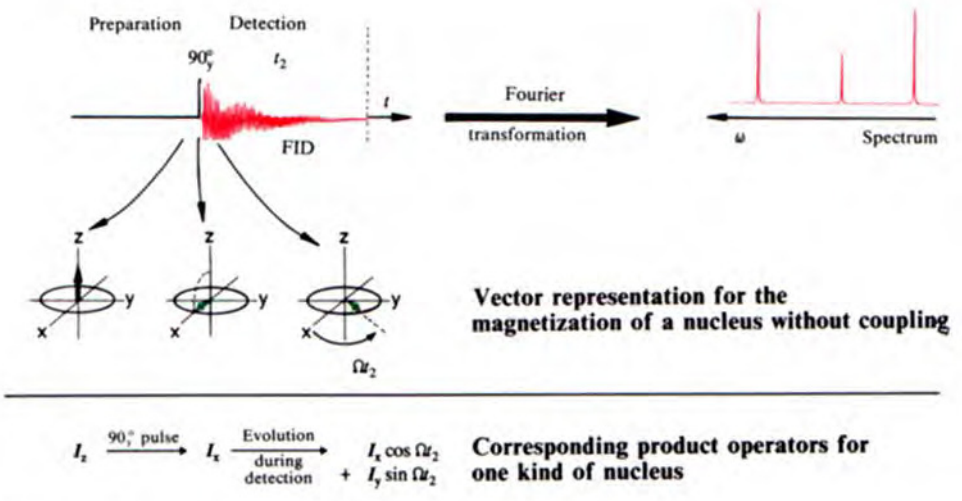

Fig. 4. Principle of 1D NMR spectroscopy. Evolution of magnetization is shown in the vector description and by product operators.

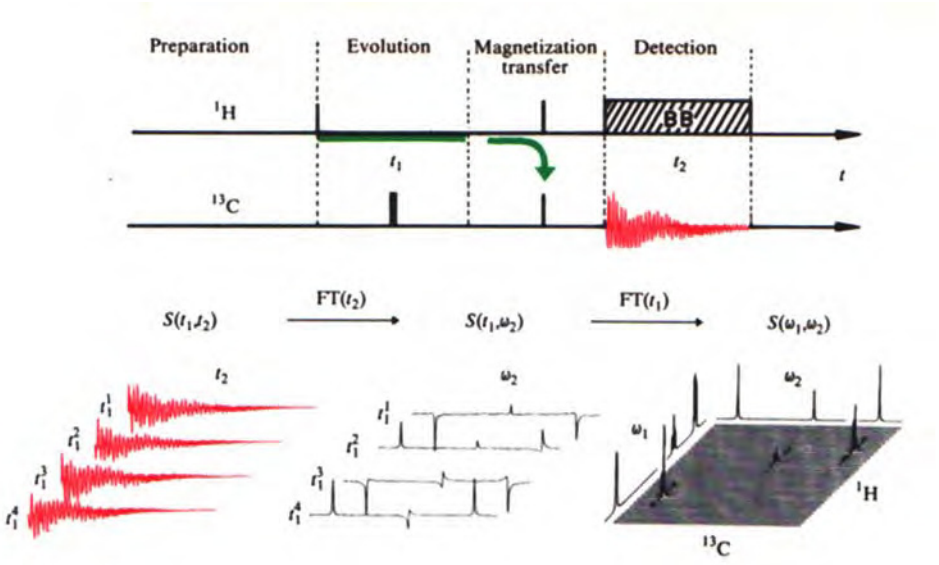

Fig. 5. Principle of 2D NMR spectroscopy, exemplified by H,C-COSY. Note the intensity variation of the carbon signals after the first Fourier transformation (lower center), which reflects the evolution of proton magnetization during t_1.

since the spectral width, i.e., the range of possible frequencies, is limited due to the nature of the sample and to analog filtering. Discrete sampling is essential for 2D NMR spectroscopy, since it enables the definition of a second time scale in digital form (see Section 2.2).

2.2. Two-Dimensional NMR Spectroscopy

The pulse sequence of a 2D NMR experiment may be divided in general into the following blocks:[2]

preparation-evolution(t_1)-mixing-detection(t_2).

The detection period corresponds exactly to the one for 1D NMR spectroscopy (Section 2.1). The time t_2 provides, after Fourier transformation, the ω_2 frequency axis of a 2D NMR spectrum. The trick of 2D NMR spectroscopy is that a second time variable, the evolution time t_1, is introduced. The evolution time t_1 is made stepwise longer, i.e., incremented, in analogy to the detection time t_2. For each t_1 increment a separate FID is detected in t_2. Thus a signal is obtained which is a function of two time variables, t_1 and t_2: $S(t_1,t_2)$. A series of ω_2 spectra is then obtained upon Fourier transformation of each of the FIDs. They differ from one another in the intensities and/or phases of the individual signals, according to the different t_1 increments. A second Fourier transformation over t_1, "perpendicular" to the ω_2 dimension, results in a spectrum as a function of two frequencies (ω_2 horizontal, ω_1 vertical).

The principles of 2D NMR spectroscopy are demonstrated in Figure 5 with an example of proton-carbon chemical shift correlation (H,C-COSY). First, a transverse proton magnetization (coherence) is generated, which is subsequently transferred to carbon during the mixing period by means of ^{1}H and ^{13}C 90° pulses. The exact mechanism of this transfer will be discussed in Section 2.2.1. Finally, the carbon magnetization is detected.

Let us consider this experiment again in greater detail using the pulse sequence of Figure 5 with product operators.[*] After the preparation, which in this case consists of a 90°_y pulse, transverse magnetization I_x (single-quantum coherence) is generated from the equilibrium magnetization. During the evolution time t_1, I_x evolves with its characteristic frequency [Eq. (14)]. Through the mixing sequence consisting of 90° pulses in ^{1}H and ^{13}C, the proton coherence is transferred to ^{13}C coherence (i.e., I_x transforms into S_x). The I_y term is not considered further, since, as we shall see in Section 2.2.1, it is not relevant for this experiment. The mechanism of the coherence transfer is likewise not discussed further at this point. S_x evolves during t_2 with its characteristic frequency [Eq. (15)]. The state of the spin system after a time t_2 is given by Equation (16).

$$I_x \xrightarrow{\Omega_I t_1 I_z} I_x \cos \Omega_I t_1 + I_y \sin \Omega_I t_1 \tag{14}$$

$$S_x \xrightarrow{\Omega_S t_2 S_z} S_x \cos \Omega_S t_2 + S_y \sin \Omega_S t_2 \tag{15}$$

$$\cos \Omega_I t_1 \, (S_x \cos \Omega_S t_2 + S_y \sin \Omega_S t_2) \tag{16}$$

Thus the coefficients of the S operator describing the time evolution in t_1 and t_2 contain not only its own characteristic frequencies Ω_S, but also the I-spin frequency Ω_I. This is sometimes referred to as "labeling." S_{xy} is labeled during t_1 with the I frequency. Quadrature detection converts the operator combination of Equation (16) into a complex signal [Eq. (17)]. Fourier transformation along t_1 and t_2 results in the frequencies, namely, $\pm\Omega_I$ in ω_1 and Ω_S in ω_2. A spectrum like the one shown schematically in Figure 6 is obtained. A line in position (Ω_I, Ω_S) in the 2D NMR spectrum will appear when the signal is modulated in t_1 by the frequency Ω_I and in t_2 by the frequency Ω_S.

$$\cos \Omega_I t_1 \, e^{i\Omega_S t_2} \tag{17}$$

The 2D NMR spectrum is thus a representation of the transfer processes of coherences, whereby peaks arise at the characteristic frequencies of the interconnected coherences. The intensity of the signals is determined by the ef-

[*] Originally I and S were identified with "insensitive" and "sensitive," respectively. Nevertheless we use here I for the proton, although it is magnetically the more sensitive nucleus, and S for the heterospin, to correspond to conventional use.

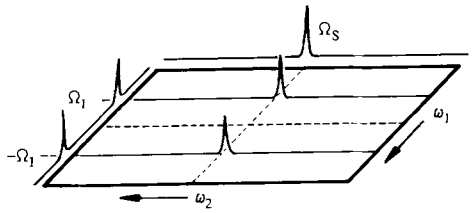

Fig. 6. Schematic cross signals of I and S nuclei in a hypothetical 2D NMR spectrum. The spectra on the margins represent projections along the axes. In ω_2 the Redfield technique (see Fig. 3) was used.

ficiency of the mixing process. The transferability of coherences depends, on the one hand, on the properties of the spin system: on structural, dynamic, and chemical molecular properties which reflect the behavior of the magnetically active nuclei. On the other hand, it is determined by the mixing sequence of the particular 2D NMR experiment. The multitude of 2D NMR experiments relates directly to these various transfer processes.

In high-resolution NMR spectroscopy there are essentially two spin-spin interactions which can be used to effect coherence transfer: one is the through-bond scalar spin-spin coupling (J coupling), well known in 1D NMR spectroscopy since it gives rise to the observed multiplet splitting. It is effective only between spins which are separated by few bonds in the molecule. Therefore it is particularly useful for the elucidation of connectivities, i.e., bonds, between atoms, and serves for the investigation of the *constitution* of organic compounds, as well as for spectral assignments. The magnitude of the scalar coupling is a sensitive measure of the torsion angle about single and double bonds, and hence provides important information about spatial structure *(conformation)*.[74-76]

The other interaction is the *dipolar* coupling of two spins, which operates through space. It is responsible for the dominating mechanism of relaxation in solution,[77-79] but is only indirectly apparent in the 1D NMR spectrum as line broadening. Dipolar coupling generates also the mutual relaxation between spatially neighboring nuclei, the so-called cross relaxation. The intramolecular cross relaxation gives rise to the nuclear Overhauser enhancement (NOE) effect, i.e., to a variation in the intensity of a signal as a result of a disturbance in the populations of another nucleus.[77-82] The NOE effect depends on the distance between the cross-relaxing nuclei, and hence allows the determination of intramolecular interatomic distances.[83-88] NOE values therefore provide the most important parameter for the determination of three-dimensional structures. The quantitative measurement of distances for larger molecules became only practicable[94-101] through 2D NMR spectroscopy.[89-93] NOE effects and J couplings are complementary to each other in their structural information content.

A third mechanism for coherence transfer is provided by exchange processes, such as chemical reactions.[102,103] In contrast to the other processes mentioned above, this coherence transfer does not involve multispin systems. The fact that a nucleus may have different chemical shifts when it is in molecule A or B is sufficient to observe so-called exchange spectra. This was applied very early in kinetic studies.[102-115] The introduction of 2D exchange NMR spectroscopy[89,116,117,371] brought advantages not only for the measurement of rate constants of reactions at equilibrium (such as in vivo reactions), but also for the determination of rates and mechanisms of site exchanges in fluxional molecules.

2.2.1. Scalar Coupling

Scalar coupling underlies most of the 2D NMR experiments. It also leads to the failure of the vector description of NMR experiments. Because of the fundamental role of scalar coupling in 2D NMR spectroscopy we shall discuss it first.

Scalar Coupling in the Product Operator Formalism

Scalar coupling is the interaction between two spins, which occurs predominantly through bonds (indirect coupling) and only occasionally "through space."[118] It leads to splitting of the resonances in the NMR spectrum (multiplet structure). In terms of the product operator formalism, spin-spin coupling between two nuclei 1 and 2 may be described according to (18)-(21). The resulting expressions

$$I_{1x} \xrightarrow{\pi J_{12} t\, 2I_{1z}I_{2z}} I_{1x}\cos \pi J_{12}t + 2I_{1y}I_{2z}\sin \pi J_{12}t \tag{18}$$

$$I_{1y} \xrightarrow{\pi J_{12} t\, 2I_{1z}I_{2z}} I_{1y}\cos \pi J_{12}t - 2I_{1x}I_{2z}\sin \pi J_{12}t \tag{19}$$

$$2I_{1x}I_{2z} \xrightarrow{\pi J_{12} t\, 2I_{1z}I_{2z}} 2I_{1x}I_{2z}\cos \pi J_{12}t + I_{1y}\sin \pi J_{12}t \tag{20}$$

$$2I_{1y}I_{2z} \xrightarrow{\pi J_{12} t\, 2I_{1z}I_{2z}} 2I_{1y}I_{2z}\cos \pi J_{12}t - I_{1x}\sin \pi J_{12}t \tag{21}$$

are quite similar to those obtained for the evolution of chemical shifts. However, here for the first time products of two operators are obtained, to which this formalism owes its name. We turn back for a moment to the vector description in order to clarify the above equations. Coupling between spin 1 and spin 2 is shown in the vector picture as two vectors for spin 1, precessing at different angular velocities corresponding to either the α state or the β state of spin 2 (Fig. 7). The x magnetization of spin 1 is

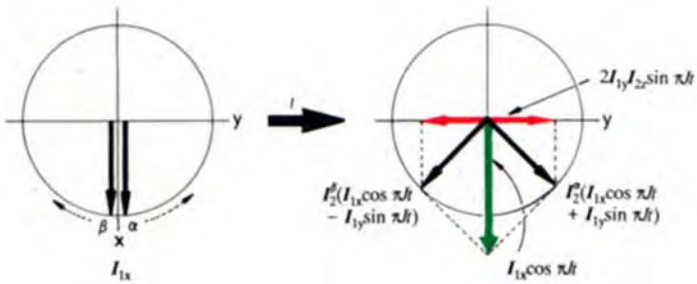

Fig. 7. Evolution of scalar coupling during time t, starting from x magnetization. The resulting anti-phase magnetization is shown in red, the remaining in-phase magnetization in green.

apparently modulated by $\cos \pi Jt$, as is also shown in the first part of Equation (18). In addition there is a magnetization along the y axis (red), which is described by $I_{1y}(I_2^\alpha - I_2^\beta)$ (the y magnetization of spin 1 points to +y for

spin 2 in the α state, and to $-y$ for spin 2 in the β state). This y magnetization is not observable; thus, in the macroscopic sense, it is not really a magnetization, since the positive and negative components cancel exactly. The difference in populations of the α and β levels ($I^{\alpha}-I^{\beta}$) is given by $2I_z$. Hence, $I_{1y}(I_2^{\alpha}-I_2^{\beta})$ is identical with $2I_{1y}I_{2z}$, which is obviously modulated by $\sin \pi Jt$ [cf. Eq. (18)].

In contrast to the evolution under chemical shift and/or pulses, the evolution of coupling "creates" or "annihilates" operators: $I_{1x} \rightarrow 2I_{1y}I_{2z}$ and $2I_{1x}I_{2z} \rightarrow I_{1y}$. Annihilation of operators occurs since a squared operator always equals the unit operator (in this case, $I_zI_z = 1/4$). Only coupling and not chemical shift can "bring other nuclei into the scene." This is the salient point for coherence transfer,[*] since polarization can only be transferred when a second spin is involved in the product operator.

Before we can proceed to use the product operator formalism, we need a number of rules which regulate operator transformations:

(a) A product operator evolves under the effect of chemical shift or pulses such that each operator in the product is transformed separately [Eq. (22)–(24)]. I_z does not evolve under chemical shift [see Eq. (10)].

$$2I_{1x}I_{2z} \xrightarrow{90^{\circ}_{y}} -2I_{1z}I_{2x} \tag{22}$$

$$2I_{1x}I_{2z} \xrightarrow{\Omega_1 tI_{1z}+\Omega_2 tI_{2z}} 2I_{1x}I_{2z}\cos\Omega_1 t + 2I_{1y}I_{2z}\sin\Omega_1 t \tag{23}$$

$$2I_{1x}I_{2y} \xrightarrow{\Omega_1 tI_{1z}+\Omega_2 tI_{2z}} 2(I_{1x}\cos\Omega_1 t + I_{1y}\sin\Omega_1 t)(I_{2y}\cos\Omega_2 t - I_{2x}\sin\Omega_2 t) \tag{24}$$

One must be careful when dealing with scalar coupling, since in this case also pairs of product operators of the mutually coupled nuclei must be treated together. For example, $2I_{1x}I_{2z}$ evolves under a 1,3 coupling according to (25)

$$2I_{1x}I_{2z} \xrightarrow{\pi J_{13}t\,2I_{1z}I_{3z}} 2I_{1x}I_{2z}\cos\pi J_{13}t + 4I_{1y}I_{2z}I_{3z}\sin\pi J_{13}t \tag{25}$$

(i.e., only the transverse operator I_{1x} evolves [cf. Eq. (18)]). Under 1,2 coupling, however, $2I_{1x}I_{2z}$ evolves according to Equation (26).

$$2I_{1x}I_{2z} \xrightarrow{\pi J_{12}t\,2I_{1z}I_{2z}} 2I_{1x}I_{2z}\cos\pi J_{12}t + I_{1y}\sin\pi J_{12}t \tag{26}$$

It is also important to note that product operators of two transverse operators [Eq. (27) and (28)], as well as product operators of two longitudinal operators, do not develop mutual coupling [Eq. (29)].

$$2I_{1x}I_{2x} \xrightarrow{\pi J_{12}t\,2I_{1z}I_{2z}} 2I_{1x}I_{2x} \quad \text{(two transverse operators)} \tag{27}$$

$$2I_{1x}I_{2y} \xrightarrow{\pi J_{12}t\,2I_{1z}I_{2z}} 2I_{1x}I_{2y} \quad \text{(two transverse operators)} \tag{28}$$

$$2I_{1z}I_{2z} \xrightarrow{\pi J_{12}t\,2I_{1z}I_{2z}} 2I_{1z}I_{2z} \quad \text{(two longitudinal operators)} \tag{29}$$

However, $2I_{1x}I_{2y}$ develops coupling to a *third* spin (I_{3z}) [Eq. (30)]. In this equation we have already made use of rule (b).

$$2I_{1x}I_{2y} \xrightarrow{\pi J_{13}t\,2I_{1z}I_{3z}} 2I_{1x}I_{2y}\cos\pi J_{13}t + 4I_{1y}I_{2y}I_{3z}\sin\pi J_{13}t \xrightarrow{\pi J_{23}t\,2I_{2z}I_{3z}}$$
$$2I_{1x}I_{2y}\cos\pi J_{13}t\cos\pi J_{23}t + 4I_{1y}I_{2y}I_{3z}\sin\pi J_{13}t\cos\pi J_{23}t \tag{30}$$
$$-4I_{1x}I_{2x}I_{3z}\cos\pi J_{13}t\sin\pi J_{23}t - 2I_{1y}I_{2x}\sin\pi J_{13}t\sin\pi J_{23}t$$

(b) Couplings and chemical shifts operate simultaneously; in the absence of strong coupling, however, the evolution under these interactions may formally be considered sequential. This is due to the commutation of the operators of chemical shift and weak coupling. This does *not* apply to pulses. Therefore pulses limit the periods of free precession.

The product operators only "come to life" when one realizes to which signals in the spectrum they give rise. The following is valid for weak coupling:

(a) Only product operators with *one* transverse operator (I_x or I_y) are observable. All other products cannot be observed.

(b) Product operators with one transverse operator (I_x, I_y) and any number of longitudinal operators (I_z) evolve into "observable" operators as long as the "transverse" spin is scalar-coupled to all the "longitudinal" ones.

(c) All other product operators are not observable, and do not evolve into observable operators.

We turn now to discuss product operators in a three-spin system, in which nucleus 1 is coupled to two other nuclei, 2 and 3 (Fig. 8). I_{1x} generates the well-known dou-

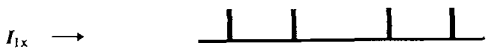

Fig. 8. Schematic in-phase double doublet (line spectrum).

ble doublet at chemical shift Ω_1. This results from Equation (31). We make use of the fact that only I_{1x} and I_{1y} are

$$I_{1x} \longrightarrow I_{1x}\cos\Omega_1 t\cos\pi J_{12}t\cos\pi J_{13}t + I_{1y}\sin\Omega_1 t\cos\pi J_{12}t\cos\pi J_{13}t + \ldots \tag{31}$$

observable, and neglect all other 6 unobservable terms. Before we can show how a spectrum is constructed from this time function we need to add a few comments on phases and Fourier transforms: The absolute phase of a signal cannot be defined in a significant manner. While the phase can change owing to the electronics, it may be corrected by

[*] Most often the expression "polarization transfer" is used instead of "coherence transfer." However, we think the latter is more precise.

the experimenter as desired through zero-order phase correction. However, the definition of relative phases, which remain invariant with respect to phase correction, is significant. The following rule may be formulated: the relative phase equals 90° multiplied by the number of sine factors counted in the coefficients of the x magnetizations. We can, for example, adjust the absolute phase such that an I_x term with only cosine factors as coefficients will be in absorption. The following will then hold for the phases of the other terms (see Fig. 9):

0, 4, ... sine factors: absorption
1, 5, ... sine factor: dispersion
2, 6, ... sine factors: negative absorption
3, 7, ... sine factors: negative dispersion

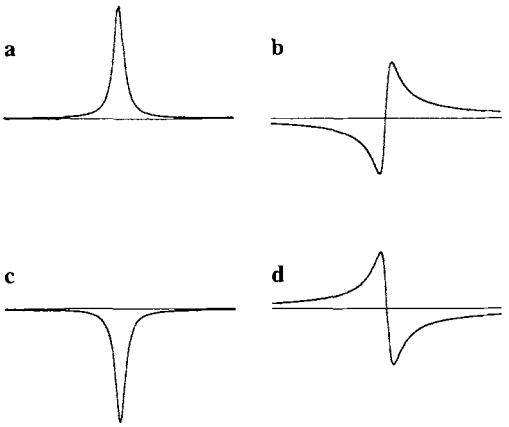

Fig. 9. Line shapes in NMR spectra: a) absorption signal, b) dispersion signal, c) negative absorption signal (emission), d) negative dispersion signal.

The modulation of the time signal by coupling occurs exclusively through amplitude factors of the form $\cos \pi Jt$ and $\sin \pi Jt$. Its Fourier transform is shown in Figure 10.

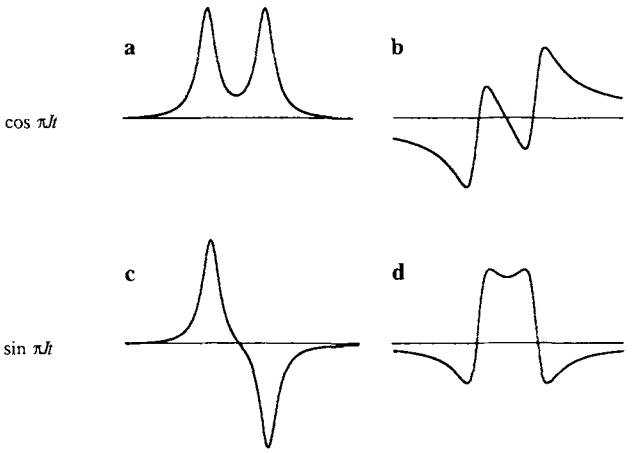

Fig. 10. Signal shapes for a doublet with in-phase structure (a and b), and antiphase structure (c and d). The spectra on the left (a, c) are in absorption, those on the right (b, d) in dispersion.

A starting point for the construction of a signal from a product of functions [see, for instance, Eq. (30)] is the folding principle: The Fourier transform of a product of functions can be constructed from the Fourier transforms of the individual functions by convolution. In our case, the product consists of the trigonometric functions, the Fourier transforms of which are well known. The preceding discussion, applied to the terms in Equation (31), leads to the signals shown in Figure 11.

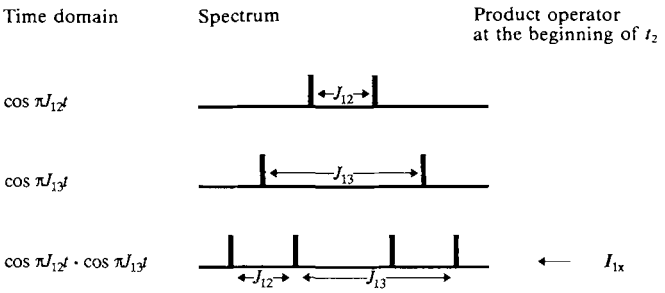

Fig. 11. Construction of an in-phase multiplet from the two in-phase doublets corresponding to J_{12} and J_{13} through convolution.

Antiphase operators behave as follows: $2I_{1x}I_{2z}$ is not directly detectable [rule (a)]; however, it develops observable magnetization according to Equation (32). If the J_{12} coupling equals 0, no observable magnetization evolves [rule (b)], as can also be seen directly in (32).

$$2I_{1z}I_{2z} \xrightarrow{\pi J_{12}t\ 2I_{1z}I_{2z}} I_{1y} \sin \pi J_{12}t \xrightarrow{\pi J_{13}t\ 2I_{1z}I_{3z}} I_{1y} \sin \pi J_{12}t \cos \pi J_{13}t \xrightarrow{\Omega t I_{1z}} I_{1y} \cos \Omega_1 t \sin \pi J_{12}t \cos \pi J_{13}t - I_{1x} \sin \Omega_1 t \sin \pi J_{12}t \cos \pi J_{13}t \quad (32)$$

We apply again the convolution principle and obtain the result shown in Figure 12. An in-phase doublet is obtained

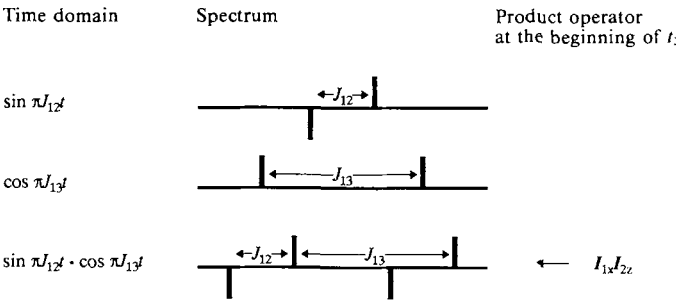

Fig. 12. Construction of a double doublet with antiphase structure with respect to J_{12} and in-phase structure with respect to J_{13}.

for J_{13} (cosine) and an antiphase doublet for J_{12} (sine). The x component contains two sine factors, so that finally a negative absorption signal is obtained, in-phase with respect to J_{13} and antiphase with respect to J_{12}. The spectra for the remaining product operators are likewise obtained using the same "recipe."

At this point we need no longer denote the time domain signal. According to the recipe stating that *every z operator generates an antiphase doublet and the others generate in-*

phase doublets, we can construct the missing spectra, which are shown in Figure 13.

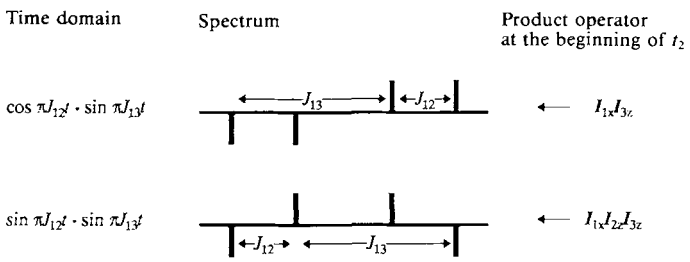

Fig. 13. Double doublets with different antiphase structures: upper part, antiphase with respect to J_{13}. Lower part, with respect to both J_{12} and J_{13}.

There are rules also for the phases of signals (absorption, dispersion): All the terms with an I_x operator (e.g., I_{1x}, $2I_{1x}I_{2z}$, $4I_{1x}I_{2z}I_{3z}$, etc.) are in absorption (an even number of sine factors). It is readily seen that product operators with an I_y operator are in dispersion. Absorption and dispersion can be exchanged by means of a phase correction. In a 2D NMR signal there is an independent phase for each of the frequency dimensions ω_1, ω_2. The phases can hence be either equal or different in both dimensions.

The following is a discussion of the H,H-COSY experiment[1,2] (pulse sequence PI) in greater detail. It has only two pulses and hence is one of the simplest 2D NMR pulse sequences.[*]

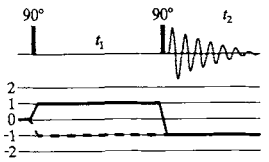

(PI)

Historically 2D COSY was the first 2D NMR experiment,[1] and it remains the most important one. It relates to the earlier mentioned coherence transfer. We have seen that coupling is associated with antiphase terms such as $2I_{1x}I_{2z}$, which can lead to observable magnetization. When a 90°_y pulse is applied to an operator $2I_{1x}I_{2z}$ the latter transforms into $-2I_{1z}I_{2x}$ [cf. also Eq. (22)]. That means that spin 1, which was transverse before the pulse, becomes longitudinal, and the longitudinal spin 2 becomes transverse. Thus the coherence of spin 1 ($2I_{1x}I_{2z}$ evolves with the chemical shift of nucleus 1) has been transferred into the coherence of spin 2. The COSY experiment is based on this coherence transfer.

Let us examine again a three-spin system with spins 1, 2, and 3. The first 90°_y pulse generates from the equilibrium magnetization a transverse magnetization $I_{1x}+I_{2x}+I_{3x}$. In the following discussions we shall not evaluate all the terms, but shall instead ignore the irrelevant ones, which do not lead to signals in the spectrum.

Only terms I_{1x}, I_{2x}, or I_{3x} are detected at the end of the detection period t_2. Let us focus on the I_{2x} term, since the transfer $I_{1x} \rightarrow I_{2x}$ gives rise to a cross signal at Ω_1 in ω_1 (vertical axis) and Ω_2 in ω_2 (horizontal axis). We noted earlier that only coupling can introduce an additional spin into the product operator. The evolution (33) must hence take

$$I_{1x} \longrightarrow 2I_{1x}I_{2z} \tag{33}$$

place during t_1. Only this product operator is converted by a 90°_y pulse completely into $-2I_{1z}I_{2x}$. The transfer diagram for the 1,2 cross signal in the COSY experiment is thus given by Equation 34. There is no other way to transfer magnetization from spin 1 to spin 2 in this pulse sequence. Exactly one z operator, which will subsequently transform into a transverse operator during t_2, is required before the mixing. Spin 1 must be present during t_1 with an x operator I_{1x}. More than one z operator in the product operator would transform into several transverse operators, which are undetectable. The coefficients of these operators are obtained as follows. During t_1, I_{1x} evolves under chemical shift and coupling as in (35). All the couplings to nuclei that are not responsible for the transfer enter as cosine factors. Here only one such coupling, to nucleus 3, was considered. The polarization transfer takes place through the 90°_y pulse, resulting in (36). This evolves into observable magnetization according to Equations (18) and (20). The overall amplitude of the signal, the so-called transfer function, is given by (37).

$$I_{1z} \xrightarrow{90^\circ_y} I_{1x} \xrightarrow{t_1} -2I_{1x}I_{2z} \xrightarrow{90^\circ_y} 2I_{1z}I_{2x} \xrightarrow{t_2} I_{2x} \tag{34}$$

$$-2I_{1x}I_{2z} \sin \Omega_1 t_1 \sin \pi J_{12} t_1 \cos \pi J_{13} t_1 \tag{35}$$

$$2I_{1z}I_{2x} \sin \Omega_1 t_1 \sin \pi J_{12} t_1 \cos \pi J_{13} t_1 \tag{36}$$

$$\sin \Omega_1 t_1 \sin \pi J_{12} t_1 \cos \pi J_{13} t_1 \sin \Omega_2 t_2 \sin \pi J_{12} t_2 \cos \pi J_{23} t_2 \tag{37}$$

Construction of 2D Multiplets

We have discussed the construction scheme for 1D NMR spectra from their time-domain signals, and now apply it to the construction of a 2D NMR spectrum. From the multiplets shown in Figure 14 in ω_1 and ω_2 the 2D NMR spectrum is constructed by placing peaks at the intersection points of the lines. The intensity is obtained from the product of the intensities of the crossing lines. The phases in ω_1 and ω_2 are identical with those of the corresponding "1D NMR spectra" discussed above.

So far we have only dealt with a single cross peak, that for spins 1 and 2. The others are obtained similarly, e.g.,

[*] The "staffs" given under the actual pulse sequences show the corresponding coherence-transfer pathway. They will be explained separately later in the text.

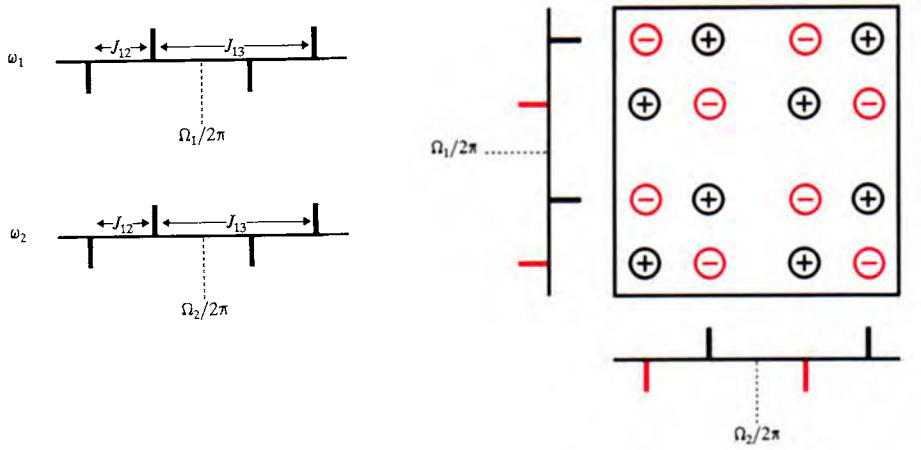

Fig. 14. Construction of a 2D multiplet from the corresponding 1D NMR spectra. The signals in the 2D NMR spectrum (right) arise at the crossing points of the 1D NMR spectra (left). Their intensities result from the product of the intensities of the 1D NMR spectra.

that between 2 and 3 by starting with I_{2x} after the 90° pulse and detecting I_{3x}.

We now summarize again the formation of cross signals. During t_1, coherences evolve under the chemical shift of spin 1; during t_2, under the chemical shift of spin 2. For a coherence transfer with a 90°_y pulse a term $2I_{1x}I_{2z}$ is required, which is converted into $-2I_{1z}I_{2x}$; i.e., antiphase magnetization exists before and after the coherence transfer, caused by the J_{12} coupling. The J_{12} coupling is referred to as *active coupling*. Couplings to other nuclei such as spin 3 appear in-phase and are termed *passive*. They do not participate in the transfer.

Diagonal signals (e.g., $\omega_1=\omega_2=\Omega_1$) are also formed in a COSY spectrum. For a 1,1 diagonal signal the product operator must have *one* transverse operator for spin 1 before the mixing, or else no chemical shift for that spin would evolve during t_1. Likewise the operator for spin 1 must remain transverse after the mixing, in order to appear as a signal at Ω_1 in ω_2. No terms with more than one I_z operator can exist before the mixing pulse, for they would transform into transverse operators by the 90° pulse, and thus generate unobservable terms with more than one transverse operator at the beginning of t_2. The transfer diagram for diagonal signals is given by (38) and the corresponding transfer amplitude by (39).

$$I_{1z} \xrightarrow{90^\circ_y} I_{1x} \xrightarrow{t_1} I_{1y} \xrightarrow{90^\circ_y} I_{1y} \xrightarrow{t_2} I_{1x} \tag{38}$$

$$\sin \Omega_1 t_1 \cos \pi J_{12} t_1 \cos \pi J_{13} t_1 \sin \Omega_1 t_2 \cos \pi J_{12} t_2 \cos \pi J_{13} t_2 \tag{39}$$

The analysis of the multiplet structure reveals dispersive (a single sine factor for both time dimensions) in-phase signals (cosine factors for the couplings) in both frequency dimensions. The diagonal signals in the COSY spectrum are dispersive in both dimensions (double dispersive), while the cross signals are absorptive in both dimensions (double absorptive). Absorption and dispersion can, of course, be exchanged also in 2D NMR spectra by a separate phase correction in each dimension. The diagonal signal is in-phase with respect to all couplings, since they appear as cosines.

So far we have analyzed only the useful transfers (cross and diagonal signals). The undesired signals were simply ignored. In the COSY experiment, so-called *axial peaks* occur as artifacts. They arise when an I_z term at the end of t_1 is converted by the 90° pulse into a transverse operator I_x observable in t_2. Since it is not modulated in t_1 it gives rise to a signal at $\Omega_1=0$ (axial peak). The spectroscopist has, nevertheless, a powerful tool to suppress artifacts: *phase cycling*. Before we elaborate further on this, we wish to describe the second important process for magnetization transfer between two spins, the dipolar coupling.

2.2.2. Dipolar Coupling

The dipolar coupling plays an entirely different role in high-resolution NMR spectroscopy compared to the scalar coupling. In 1D NMR spectroscopy it operates only as a relaxation phenomenon and gives rise to line broadening (T_2), and of course T_1 processes are responsible for the establishment of the Boltzmann state after a certain time. Scalar coupling, on the other hand, leads to oscillations of the FID and splitting of lines in the spectrum. As explained above, J coupling generates during evolution periods operators which cause coherence transfer under the influence of pulses. Thus the scalar coupling generates a state which can then (even without the effect of coupling during the mixing) be converted by pulses into the desired final state [Eq. (40)].

$$I_x \xrightarrow{J(t_1)} 2I_yS_z \xrightarrow{\text{Mixing}} 2I_zS_y \xrightarrow{J(t_2)} S_x \tag{40}$$

The situation is different for mixing through dipolar coupling. There the dipolar coupling must be effective during the mixing period, while it need not be effective in the evolution or detection times [Eq. (41)].

$$I_x \xrightarrow{t_1} I_z \xrightarrow{\text{NOE}} S_z \xrightarrow{t_2} S_x \tag{41}$$

Dipolar Relaxation

Dipolar coupling is the interaction of the magnetic moments of two spins through space.[65,77,78,119] The magnetic field B_D, which is generated by spin 2 at the site of spin 1, is orientation dependent [Eq. (42), where r_{12} is the

internuclear distance and Θ_{12} the angle between the interatomic vector and the B_0 field].

$$B_D^1 = \gamma_2(3\cos^2\Theta_{12} - 1)\, r_{12}^{-3} \tag{42}$$

The rapid reorientation of molecules in solution produces alternating magnetic fields at the sites of the nuclei (Fig. 15). These lead to exchange of spin polarization (z magnetization) and cause relaxation of a spin system, which deviates from the Boltzmann distribution, back to its equilibrium state.

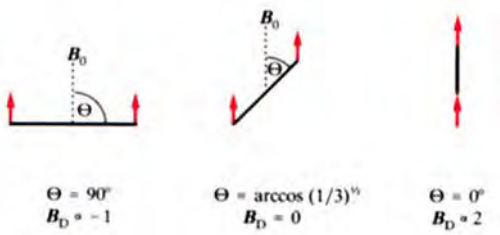

Fig. 15. Dipole-dipole interaction between two spins in the field B_0, and its dependence on the orientation angle Θ. The field reaches a maximum at $\Theta=0$, a minimum at $\Theta=90°$, and vanishes at the magic angle $\Theta=\arccos(1/3)^{1/2}$.

Because of the dipolar coupling, the two spins do not relax independently, but influence each other; i.e., each deviation of a spin state from equilibrium is transferred to the other spin state, which therefore also deviates from equilibrium. This effect is termed nuclear Overhauser enhancement (NOE). Figure 16 depicts the situation for two dipolar coupled spins, I and S:

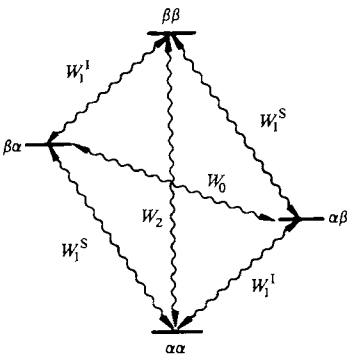

Fig. 16. Relaxation in a two-spin system. Zero-, single-, and double-quantum transitions are labeled W_0, W_1, and W_2, respectively.

Equations (43)–(45)[77] express the transition probabilities W ("rates") under isotropic reorientation of the interatomic vector.

$$W_1^I = \frac{3}{20} \cdot \frac{\gamma_I^2\gamma_S^2\hbar^2}{r^6} \cdot \frac{\tau_c}{1+\omega_I^2\tau_c^2} \tag{43}$$

$$W_0 = \frac{1}{10} \cdot \frac{\gamma_I^2\gamma_S^2\hbar^2}{r^6} \cdot \frac{\tau_c}{1+(\omega_I-\omega_S)^2\tau_c^2} \tag{44}$$

$$W_2 = \frac{3}{5} \cdot \frac{\gamma_I^2\gamma_S^2\hbar^2}{r^6} \cdot \frac{\tau_c}{1+(\omega_I+\omega_S)^2\tau_c^2} \tag{45}$$

To get a feeling for these transition probabilities, we now examine the relaxation generated by polarization of spin I (I_z). Only deviations from the Boltzmann equili-

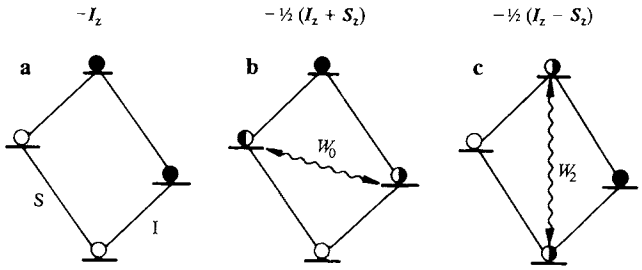

Fig. 17. Population changes due to dipolar relaxation. Note that only deviations from the Boltzmann distribution are shown schematically. a) Initial state I_z, b) after relaxation under the influence of W_0 alone, c) after relaxation under W_2 alone.

brium are shown in Figure 17. Hence, the state shown in Figure 17a corresponds to the Boltzmann equilibrium of spin S and saturation of spin I, resulting in a difference magnetization $-I_z$. We recognize that W_1^S does not affect and W_1^I equalizes the population difference for the I transition, and thus leads to a decay of $-I_z$ (relaxation). Since this applies equally to both I transitions, there is no change in the population difference for the S spin. If W_0 alone is effective, however, the populations of the two middle levels equalize, and the population distribution shown schematically in Figure 17b is obtained, corresponding to a change in population of the S spin at the same time. Thus W_0 relaxation converts an I_z operator in part into S_z, and hence enables magnetization transfer through dipolar coupling. The overall polarization remains unchanged in this process. If W_2 alone operates, the upper and lower levels equalize, resulting in the situation shown in Figure 17c. Magnetization is transferred again from spin I to spin S, however this time with a change in sign, since now the lower levels of S become more densely populated than the higher ones. Evidently the overall polarization is not preserved by this process.

The effectiveness of the relaxation processes W_0 and W_2 is determined by the rate of the molecular reorientation. When the molecular rotation in the external field is slow (corresponding to a long "correlation time," $\tau_c > \omega_0^{-1}$), cross-relaxation occurs mainly through the low-frequency transitions W_0 ($\triangleq \omega_I - \omega_S$) [see Eq. (44)]. Conversely, the relaxation through W_2 ($\triangleq \omega_I + \omega_S$) is only possible when the molecular reorientation is fast [Eq. (45)], corresponding to a short correlation time τ_c. Depending on whether W_0 or W_2 dominates, the cross-relaxation rate $W_2 - W_0$ may be either negative or positive and hence also the NOE effect. For $W_2 - W_0$, the cross relaxation rate vanishes. Conventionally, the positive cross-relaxation rate and the enhanced intensity of the S-spin signal correspond to a positive NOE; conversely, a negative rate and a decreased S-signal intensity correspond to a negative NOE.[78]

Just as COSY is for the coherence transfer, so is the NOESY experiment the fundamental and most important pulse sequence for the incoherent magnetization transfer. We have seen that the transfer of magnetization via NOE is achieved by creating a nonequilibrium situation and then waiting (pulse sequence P2).[89]

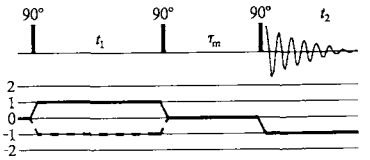

(P2)

The relevant product operators result from the following ideas: at the beginning and the end of τ_m, z magnetization is required. It is converted into transverse magnetization (detectable coherence), and is also generated from transverse magnetization. Hence the transformation (46) results. The transfer amplitude is given by (47), where $\prod_i \cos \pi J_{Ii} t_1$ is the product[*] of all $\cos \pi J_{Ii} t_1$ factors and J_{Ii} are the scalar couplings between spin I and other spins i; $\prod_i \cos \pi J_{Si} t_2$ is the equivalent expression for spin S.

$$I_z \xrightarrow{90°_x} -I_y \xrightarrow{t_1} -I_y \xrightarrow{90°_x} -I_z \xrightarrow{\text{NOE}} -S_z \xrightarrow{90°_x} S_y \xrightarrow{t_2} -S_x \quad (46)$$

$$\cos \Omega_I t_1 \prod_i \cos \pi J_{Ii} t_1 \sin \Omega_S t_2 \prod_i \cos \pi J_{Si} t_2 \quad (47)$$

As far as the relative signs of the diagonal and cross signals in the NOESY spectrum are concerned, when the NOE is positive ($W_2 - W_0 > 0$), I_z evolves into $-S_z$; i.e., the signs of the diagonal and cross signals are opposite. If the NOE is negative ($W_2 - W_0 < 0$), however, I_z evolves into S_z, and the signs of the diagonal and cross signals are the same.

The NOESY signal is in-phase with respect to all the couplings (only cosine factors), and can be corrected to pure absorption. We shall later discuss in greater detail the analysis of NOESY spectra and a few of its variants.

We now come to discuss phase cycles, which are an important means for the elimination of artifact (i.e., unwanted) signals from spectra. For example, it is evident from the NOESY sequence that also the transfer (48) be-

$$I_z \xrightarrow{90°_x} -I_y \xrightarrow{t_1} 2I_yS_z \xrightarrow{90°_x} -2I_zS_y \xrightarrow{\tau_m} S_x \xrightarrow{90°_x} S_x \xrightarrow{t_2} S_x \quad (48)$$

tween two coupled spins is possible. It leads to an undesired signal due to scalar coupling, which overlaps with the NOE signal. Phase cycling allows the suppression of such undesired signals.

2.2.3. Coherence Orders and Phase Cycles

In a phase cycle a pulse sequence is repeated, whereby the phases of the single pulses (transmitter) and the receiver phase are varied systematically ("cycled"), while all other parameters (delays, flip angles, etc.) remain constant. All the FIDs obtained in this way for one t_1 increment are added up. Phase cycles serve to select a desired transfer and simultaneously to suppress undesired magnetizations. They are only useful when the phase dependencies of the desired and undesired transfer processes are different.

A simple example follows. Cross signals arise in the COSY experiment due to the transfer (49). Nothing in the

$$2I_{1x}I_{2z} \xrightarrow{90°_y} -2I_{1z}I_{2x} \quad (49)$$

product operator changes upon rotation of the phase of the 90° mixing pulse by 180° [see (50)].

$$2I_{1x}I_{2z} \xrightarrow{90°_{\bar{y}}} -2I_{1z}I_{2x} \quad (50)$$

Common artifacts in almost all 2D NMR experiments are the so-called axial peaks, which arise from transfer of longitudinal magnetization by the mixing sequence into detectable transverse magnetization. This magnetization is not modulated during t_1, and hence resonates at $\omega_1 = 0$ (the term axial results from "on the $\omega_1 = 0$ axis"). Under $90°_y$ and $90°_{\pm y}$ pulses the axial signals transform according to (51) and (52). Thus, in contrast to the desired cross signals,

$$I_{1z} \xrightarrow{90°_y} I_{1x} \quad (51)$$

$$I_{1z} \xrightarrow{90°_{\bar{y}}} -I_{1x} \quad (52)$$

the axial signals are dependent on the phase of the second pulse in the COSY experiment.

Therefore, the axial signals can be suppressed and the desired signals preserved by adding up the two experiments: $90°_y$-t_1-$90°_y$-t_2 and $90°_y$-t_1-$90°_{\pm y}$-t_2. The axial signals are canceled, while the desired signals add up. We turn now to describe a systematic way which will lead to a recipe for the construction of phase cycles.

Coherence Order[29,30]

As we have seen, pulse phases are related to rotation about the z axis. Hence, let us consider now the behavior of the various operators under such rotation [Eq. (53)-(55), note the analogy with Eq. (8)-(10) with $\varphi = \Omega t$]. It is appar-

$$I_x \xrightarrow{\varphi_z} I_x \cos \varphi + I_y \sin \varphi \quad (53)$$

$$I_y \xrightarrow{\varphi_z} I_y \cos \varphi - I_x \sin \varphi \quad (54)$$

$$I_z \xrightarrow{\varphi_z} I_z \quad (55)$$

ent that the operators I_x and I_y do not transform independently under rotation about the z axis, but rather as a mixture; i.e., a pure I_x operator transforms into a mixture of I_x and I_y. The Cartesian basis is, for reasons beyond the scope of this article, rather unsuitable for describing phase cycles. However, there exists another basis in which operators do transform independently. It is the basis of the one-element operators[120-125] [Eq. (56) and (57)].

[*] Here and later in the text the index i (or j) in the product $\prod_i$ denotes the spins in the system which do not appear in the equation.

$$I^+ = I_x + iI_y \xrightarrow{\varphi_z} I^+ e^{+i\varphi} \quad (56)$$

$$I^- = I_x - iI_y \xrightarrow{\varphi_z} I^- e^{+i\varphi} \quad (57)$$

According to the rules for product operators (successive application of the transformations to each operator), we obtain, for instance, Equation (58) for $I_1^+ I_2^-$. Thus the operator remains invariant under rotation about the z axis. For $I_1^+ I_2^+$, on the other hand, we obtain Equation (59).

$$I_1^+ I_2^- \xrightarrow{\varphi_z} I_1^+ e^{-i\varphi} I_2^- e^{+i\varphi} = I_1^+ I_2^-, \quad (58)$$

$$I_1^+ I_2^+ \xrightarrow{\varphi_z} I_1^+ e^{-i\varphi} I_2^+ e^{-i\varphi} = I_1^+ I_2^+ e^{-2i\varphi} \quad (59)$$

We always find phase factors $e^{-ip\varphi}$ with the rotation about the z axis. p is the so-called *coherence order*. It is the number of I^+ operators minus the number of I^- operators in a product operator. Thus, for $I_1^+ I_2^-$, it follows that $p = 0$ and this coherence is called zero-quantum coherence, while $I_1^+ I_2^+$ is a double-quantum coherence ($p = +2$). $I_1^- I_2^-$ is likewise a double-quantum coherence ($p = -2$). Populations as well as operators that have only longitudinal operators behave like zero-quantum coherences. The significance of coherence order for the classification of coherences results from the fact that it is preserved during periods of free precession.

I^+ is the "raising" operator and I^- the "lowering" operator. "Raising" and "lowering" refer to changes in the quantum number m_z and not the energy. They describe processes in which a single quantum is either emitted ($\beta \rightarrow \alpha$ through I^+) or absorbed ($\alpha \rightarrow \beta$ through I^-), respectively. The number of absorbed quanta equals the number of I^- minus the number of I^+ in the product operator (Fig. 18).

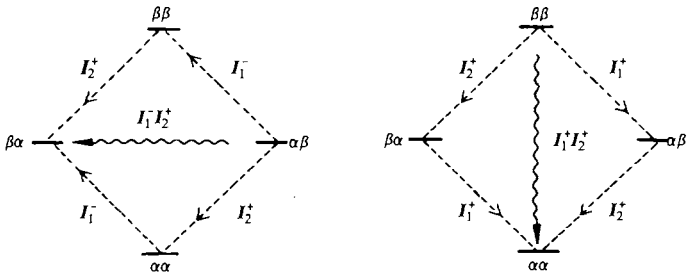

Fig. 18. A graphic representation of zero-quantum coherence (ZQC, left) and double-quantum coherence (DQC, right) in a two-spin energy level scheme. Only one of the two possible transitions is shown in each case, i.e., only absorption in the case of DQC. For further explanation see text.

The symmetry of the spin Hamiltonian for rotations about the z axis (axial symmetry), which is valid during free evolution, forms the basis for classification of coherences by coherence orders. A symmetry corresponds always to a conservation rule,[126] in this case the conservation of coherence order during pulse-free periods. The symmetry breaks down under the influence of pulses; i.e., pulses induce coherence order jumps.

The Cartesian product operators are always associated with a set of coherence orders. Thus I_{1x} and I_{1y} represent sums of positive and negative single-quantum coherences [Eq. (60) and (61), cf. the definitions for I^+ and I^- in Eq. (56) and (57)]. $2I_{1x}I_{2z}$ contains the same coherence orders [Eq. (62)].

$$I_{1x} = \tfrac{1}{2}(I_1^+ + I_1^-) \quad (60)$$

$$I_{1y} = -\tfrac{1}{2}i(I_1^+ - I_1^-) \quad (61)$$

$$2I_{1x}I_{2z} = (I_1^+ + I_1^-)I_{2z} \quad (62)$$

Finally we arrive at the following result: the number of transverse operators determines the highest ($p = +n$) and lowest ($p = -n$) coherence order present in a product operator. All the values from $p = -n$ to $p = +n$ in increments of 2 are valid coherence orders [see (63)–(65)].

$$2I_{1x}I_{2z} \quad : +1, -1 \quad (63)$$

$$4I_{1x}I_{2x}I_{3x} \quad : +3, +1, -1, -3 \quad (64)$$

$$4I_{1y}I_{2x}I_{3z} \quad : +2, 0, -2 \quad (65)$$

We can now see which coherence orders are present at any moment by following the product operators during a 2D NMR experiment. This is commonly represented in a pictorial form (Fig. 19), where lines are drawn (similar to those in musical notation) to indicate the coherence orders during given periods.[30] The straight horizontal lines represent the conservation of coherence orders during periods of free evolution. Figure 19 represents, for example, a positive single-quantum coherence during t_1 and a negative single-quantum coherence during t_2.

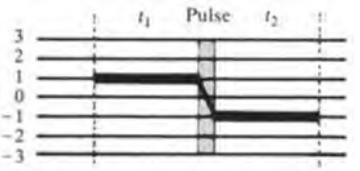

Fig. 19. Representation of various coherence orders in a "staff." In contrast to free evolution, pulses do not conserve the coherence order.

Selection of Coherence Order Jumps

Phase cycles select jumps in the coherence orders. These jumps are generated by pulses. A β_y pulse transforms, for instance, z magnetization into a mixture of x and z magnetizations (Fig. 20). The transfer amplitudes for the various coherence-order jumps are not represented in this diagram.

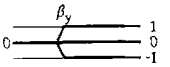

Fig. 20. Coherence orders resulting from longitudinal magnetization after a β pulse.

In general, pulses excite all the coherence orders between p = −n and p = +n, where n is the number of terms in the product operator [Eq. (66)]. This multitude of coher-

$$I_{1x}I_{2y}I_{3z} \xrightarrow{\beta_x} I_{1x}(I_{2y}\cos\beta + I_{2z}\sin\beta)(I_{3z}\cos\beta - I_{3y}\sin\beta) \quad (66)$$

ence-transfer processes (Fig. 21a) can be disentangled with phase cycling. Phase cycles act like masks, in that they only let certain coherence order jumps happen at a certain position. Such a mask may, for instance, act in the form shown schematically in Figure 21b. The form of the mask is determined by two parameters: the selectivity N of the phase cycle and the coherence order jump Δp. There is, however, not just one coherence order jump for a given phase cycle, but an infinite number incremented by N. The selectivity is the interval between successive "holes" in the mask (in the present example N = 3). A phase cycle allows all the coherence order jumps Δp ± k N (where k = 0, 1, 2, ...).

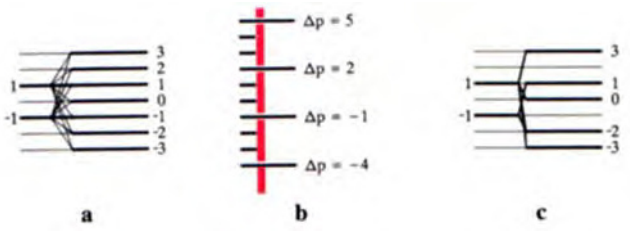

Fig. 21. a) Coherence orders of a three-spin system generated by a pulse from a single-quantum coherence (±SQC). Schematic representation of the phase cycle mask (b), by which certain coherence order jumps (c) can be selected. The mask selects all of the jumps of Δp ± k N (k = 0, 1, 2, ...), where the selectivity N in this example is 3 and Δp is −1. Thus, from ±SQC all of the generated coherence orders can pass the mask which correspond to a jump Δp of −4, −1, 2, or 5 (c).

If we now place this mask over the excitation scheme of Figure 21a, the number of possible coherence-transfer pathways is reduced dramatically (Fig. 21c). Only 5 of the 14 possible ways were selected.

Setting Up Phase Cycles

The selectivity N of a phase cycle for a pulse ($\phi^{(k)} = k\Delta\phi + \phi^{(0)}$ with k = 0, 1 ...) is related to the phase increment $\Delta\varphi$: $\Delta\varphi = 2\pi/N$. It follows that for the mask in Figure 21 with N = 3 the phase increment is $120° = 2\pi/3$. Δp determines the receiver phase φ_{det}: if the pulse phase is increased by $\Delta\varphi$, the receiver phase must also be increased by $-\Delta p \cdot \Delta\varphi$, hereby $-(-1)\cdot 120° = 120°$. It relates to the periodicity of the trigonometric functions that any selected Δp can be chosen. In this way the desired coherence pathway is followed exactly by the receiver. Other unwanted pathways are turned off. Finally, the general formula (67) is obtained for the calculation of phase cycles. Δp_i is the coherence-order jump which should be selected by the i-th pulse.

$$\varphi_{det} = -\sum_i \Delta p_i \cdot \Delta\varphi_i \quad (67)$$

Thus the mask shown in Figure 21 would be realized through the following phase cycle:

k	0	1	2		0	1	2
Pulse	0	120	240	or	3	123	243
Receiver	0	120	240		238	358	118

Only the phase *increments* are of importance. The reference phase $\phi^{(0)}$, to which the phase increments are added, is not determined. The reference phase does not play a role in the selection of coherence-transfer pathways; it is, nevertheless, often significant for the effectiveness by which the selected coherence transfers take place (e.g., even/odd selection of multiple-quantum coherence through 90°-τ-180°-τ-90°).

Before we go into the detailed arrangement of phase cycles, we wish to point out the following two essential facts:

(1) The detector conventionally selects negative single-quantum coherences [cf. the detection of I^-, Eq. (11)–(13)].

(2) The first pulse can only create a single-quantum coherence (positive and negative) from the thermal equilibrium state (p = 0).

Let us proceed one step further and consider now several three-pulse experiments (Table 1) with the pulse sequence (P3). We shall elaborate later on the individual

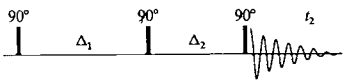

(P3)

Table 1. Various 2D NMR experiments with three 90° pulses [a].

Experiment	Δ_1	Δ_2	Comment	Section
COSY with MQF [b]	t_1	Δ	Δ is very small	3.1
Relayed COSY	t_1	Δ	Refocusing by a 180° pulse during the mixing time is advantageous	3.1.6
NOESY	t_1	τ	Transfer of dipolar coupling during τ	2.2.2
MQ spectroscopy	Δ	t_1	Refocusing in the middle of Δ by a 180° pulse is advantageous	3.1.8

[a] Because there is no generally accepted preference for the meaning of delays Δ and τ, we use in this article mainly Δ if the delay evolves coupling, and τ if other processes such as relaxation or exchange are of importance. [b] Multiple-quantum filter.

techniques. They differ essentially in the function of the second 90° pulse: In the Relayed COSY experiment it creates coherence transfer via single-quantum antiphase magnetization ($2I_{kx}I_{lz} \rightarrow 2I_{kz}I_{lx}$); in the NOESY experiment it generates longitudinal z magnetization ($I_x \rightarrow I_z$); while in DQF-COSY as well as in MQ experiments it produces multiple-quantum coherence ($2I_{kx}I_{lz} \rightarrow 2I_{kx}I_{ly}$). The desired effect is determined by the direction of the second 90° pulse relative to the first one in the selection of antiphase magnetization [see (68)].

$$2I_{kx}I_{ly} \xleftarrow{90°_x} 2I_{kx}I_{lz} \xrightarrow{90°_y} 2I_{kz}I_{lx} \quad (68)$$

The desired coherence order (in the example given above, zero-, single-, or multiple-quantum coherence), and hence the determination of the correct phases, can be achieved by considering the *coherence-transfer pathway*. The derivation of the phase cycle for an H,H-COSY experiment with double-quantum filtering (DQF-COSY) is shown below.

Double-quantum coherence should be selected by the second 90° pulse. The desired changes in coherence orders are presented in the coherence-transfer pathway in Figure 22, left.

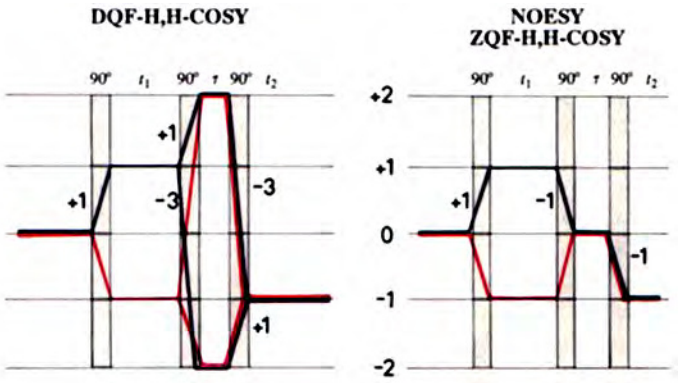

Fig. 22. Coherence-transfer pathways for a phase-sensitive DQF-COSY (left) and a NOESY experiment (right).

On the right-hand side of Figure 22 is shown, for comparison, the here unwanted pathway which would lead to a NOESY experiment (selection of longitudinal magnetization, which in the phase cycles behaves like a zero-quantum coherence). This pathway is successfully suppressed by phase cycling. Sequences with the same coherence-transfer pathway as in NOESY, but with mixing pulses smaller than 90°, are known as z-COSY (Section 3.1.4) and zz spectroscopy (Section 3.4.2).[127-130]

In the DQF-COSY example discussed above the Δp for the first pulse is $+1$ or -1, for the second pulse either $+1/-3$ or $+3/-1$, and in the third pulse $+1$ or -3. The complete phase cycle for an experiment with L pulses consists of $N_1 \times N_2 \times \cdots \times N_L$ variations, where each pulse i is varied independently of other pulses by $2\pi/N_i$ steps. We have seen that in addition to the desired pathways with Δp_i also pathways having $\Delta p_i + k N_i$ are selected. The greater N_i, the more selective is the phase cycle. However, with the increase of N_i also the number of necessary accumulations for each t_1 increment increases. Thus N_i is kept as small as possible; i.e., one must decide whether the undesired transfer pathways which pass the phase cycle really matter. Often this decision is made unnecessary by the availability of only a 90°-phase shifter; hence only $N_i = 2,4$ are available options. If we take $N_i = 4$ in our example, we obtain $4^3 = 64$ variations.

When phase-sensitive spectra are recorded (see Section 2.2.4) it must be noted that during t_1 both the positive and the negative coherence orders (in this case, $p = +1$ and $p = -1$) are necessary. Only in this way can a Fourier transformation over t_1 lead to signals of pure phase (i.e., either absorption or dispersion). It follows that the relative phase shifts of both pulses that limit the t_1 period (in this case, with phases φ_1 and φ_2) can only be 0 or π. Thus the number of variations in a phase-sensitive spectrum is reduced by one-half ($=32$ for our case).

At first the phase of the first pulse (φ_1) is shifted in steps of 90°. The phase variation (φ_2) of the second pulse follows from the rules for phase-sensitive detection. The phase φ_3 for the third pulse is kept constant at first. The receiver phase is calculated in accord with Equation (67). Thus the phases for the first four scans are obtained. The phase variation for the second pulse follows under consideration of the rule for phase-sensitive detection, so that all four directions are included. After these eight scans the phase of the third pulse can be varied. These variations are shown explicitly, whereby the shorthand notation is used ($0 = 0°$, $1 = 90°$, $2 = 180°$, and $3 = 270°$). The entire phase cycle for the above-mentioned spectrum is thus obtained as follows:

φ_1: 0 1 2 3 0 1 2 3 0 1 2 3 0 | 1 | 2 3 0 1 2 3 0 1 2 3 0 1 2 3 0 1 2 3
φ_2: 0 1 0 1 2 3 2 3 0 1 0 1 2 3 | 3 | 2 3 0 1 0 1 2 3 2 3 0 1 0 1 2 3 2 3
φ_3: 0 0 0 0 0 0 0 0 1 1 1 1 1 1 | 1 | 1 1 2 2 2 2 2 2 2 2 3 3 3 3 3 3 3 3
φ_{det}: 0 2 2 0 2 0 0 2 3 1 1 3 1 3 | 3 | 3 1 2 0 0 2 0 2 2 0 1 3 3 1 3 1 1 3

The determination of the receiver phase φ_{det} is demonstrated for the fourteenth scan, which is framed in the above scheme [Eq. (69)].

$$\varphi_{det} = -\{(+1)\cdot 1 + (+1)\cdot 3 + (-3)\cdot 1\} = -1 \qquad (69)$$

This result corresponds to a receiver phase shift of 3, due to the fourfold periodicity of phase shifting ($-1 \triangleq -90° = +270° \triangleq 3$). The alternative way through $p = -1$ during t_1 can similarly be formulated.

Thus a phase-sensitive DQF-COSY experiment requires a 32-scan phase cycle. This could lead to excessively long measuring times in cases where the desired resolution calls for many t_1 increments, or where sample concentrations are high enough to permit fewer scans. A reduction of the phase cycle can be obtained as follows:

(a) Out of the 32 phase constellations introduced above, 24 can be constructed from 8 basic phases, when at the same time all phases are rotated by 90°. This rotation of the phases by 90° serves to compensate for imperfect receiver phase shifts. The eight basic phases are obtained by leaving out the variation of the third pulse. This yields the first eight experiments shown in the scheme above.

(b) Additional reduction is obtained when one realizes that axial peaks, which are formed from z magnetization at the end of t_1, cannot be transformed by the second pulse into double quanta. The double-quantum filter thus suppresses also axial peaks. Therefore the explicit suppression of axial peaks with the second pulse may be left out. The remaining four phases are:

φ_1:	0	1	2	3
φ_2:	0	1	2	3
φ_3:	0	0	0	0
φ_{det}:	0	2	0	2

Experience shows, however, that pulse and phase imperfections are best averaged out when large phase cycles are used. In order to cancel out differences in receiver channels it is useful to apply the CYCLOPS sequence[131] in both 1D and 2D NMR spectroscopy; i.e. all the phases are shifted by 90° increments.

2.2.4. *Phase-Sensitive 2D NMR Spectra*

The expression "phase-sensitive" reception of 2D NMR spectra is somewhat unfortunate, since, in fact, every ac-

quisition is phase sensitive. It is the different method of processing of the data which leads to either phase-sensitive spectra or spectra which are displayed in absolute value mode. Phase-sensitive processing is done in those cases where some or all of the signals in a 2D NMR spectrum can be corrected to pure phases. The sign information thus obtained and the smaller line width relative to the absolute value mode are the main reasons for doing so.

We do not wish to elaborate extensively on the background for phase-sensitive 2D NMR spectroscopy. For a detailed discussion we recommend the article by *J. Keeler* and *D. Neuhaus*.[132] Suffice it to say that phase-sensitive spectra require an amplitude modulation of the signal in t_1. Practically all of the most often used experiments, like COSY, NOESY, Relayed, TOCSY, ROESY, and heteronuclear shift correlation, generate amplitude-modulated signals.

There are two methods for obtaining phase-sensitive spectra. The method of *States, Haberkorn,* and *Ruben*[133, 134] generates two data sets for each t_1 value. In one set the signal in t_1 is cosine-modulated, in the other sine-modulated (in analogy with the synchronous two-channel detection in t_2). If each data set is subjected separately to a complex Fourier transformation, the two spectra shown schematically on the left-hand side of Figure 23 are obtained. The addition of the two spectra results in the desired spectrum (Fig. 23, right).

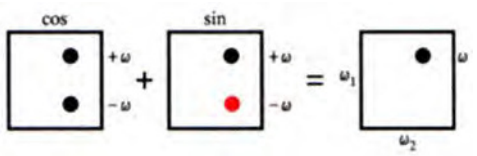

Fig. 23. The result of quadrature detection in t_1 according to *States, Haberkorn,* and *Ruben*. Signals modulated by $\cos\Omega t_1$ are accumulated separately from those modulated by $\sin\Omega t_1$ for each t_1 value, and then, again separately, complex Fourier transformed and added up.

The other method uses a real Fourier transformation and applies in t_1 the same Redfield method already described for quadrature detection in t_2. Detection is done at twice the rate (the t_1 increment is divided by two) and with a 90° phase shift after each t_1 increment. This phase shift in t_1 is a pulse phase, which leads to the name of the method: *T*ime *P*roportional *P*hase *I*ncrementation (TPPI).[135, 136]

The two methods are equivalent. They both require twice as many data points as needed for a non-phase-sensitive spectrum of the same resolution (and equal measuring time).

3. Survey of 2D NMR Techniques

The most important 2D NMR techniques in current use are listed in Tables 2–5. Groups are arranged according to the type of correlated nuclei (homo- or heteronuclear) and according to the type of correlation.[*]

In previous chapters we have explained the underlying principles required in order to understand the currently used techniques. In the following discussion of pulse sequences we shall encounter further methods which, like phase cycles, are designed to discriminate between coherences on the basis of their different properties, in order to either select or suppress them: multiple-quantum filter, z-filter, editing techniques, low-pass *J*-filter, X-filter, and BIRD pulses.

The time t_1, which in contrast to t_2 is not a "real" time, can also be manipulated. Thus particular interactions can be influenced or scaled during t_1. These include, among others, ω_1 decoupling, BIRD pulses during t_1, and selective decoupling.

Manipulation of the t_2 time is relatively difficult. The most common one is heteronuclear decoupling, which is applied in practically all heteronuclear experiments. The associated pulse sequences (see Section 3.2.10) are highly developed and have reached astounding efficiency.

We shall explain these methods in the discussion of pulse sequences and try to show their common features. First we shall describe the most important experiments associated with homonuclear coherence transfer.

3.1. Homonuclear Experiments

3.1.1. H,H-COSY and Variants

The cross signals in a COSY experiment are caused, as we have seen in Section 2.2.1, by two-operator terms like $2I_{1x}I_{2z}$ (with a y-mixing pulse). The cross signals are antiphase with respect to the active J_{12} coupling and in-phase with respect to all other couplings. The diagonal signals are formed from a transfer of the type $I_{1y} \rightarrow I_{1y}$. They are in-phase dispersion signals in both dimensions. Cross signals near the diagonal are often severely distorted and difficult to observe due to the dispersive extensions from the diagonal signals.

This problem can be solved with the application of multiple-quantum filters (pulse sequence (P3), delays as shown in Table 1, coherence-transfer pathways in Fig. 22):[138–141] the product operator responsible for the diagonal signals before the mixing pulse contains a single operator (I_y). In contrast, the one responsible for the cross signals contains two operators ($2I_{1x}I_{2z}$). Double-quantum coherence cannot be generated from a single operator by the mixing pulse; it can, however, be generated from a two-operator term. Thus a $90_x°$ pulse is applied to cause a double-quantum excitation of the two-spin operator term mentioned above, according to Equation (70) [cf. Eq. (60) and (61)].

$$2I_{1x}I_{2z} \xrightarrow{90°_x} -2I_{1x}I_{2y} = -\tfrac{1}{2}\,i(I_1^+I_2^+ - I_1^-I_2^-) - \tfrac{1}{2}\,i(I_1^-I_2^+ - I_1^+I_2^-) \qquad (70)$$

The first term on the right-hand side represents positive and negative double-quantum coherence and the second term zero-quantum coherence. The double-quantum coherence is selected by phase cycling as described in Section 2.3.3 and finally converted back, by a $90_y°$ pulse, into single-quantum magnetization. This leads to filtration of

[*] The explanations of the acronyms used in the text for pulse sequences are given in the Appendix.

Table 2. Homonuclear 2D NMR techniques through mixing by means of coherence transfers.

Symbol	Name	Application	Comment (A: advantage; D: disadvantage)	Reference	Pulse sequence
H–(–)$_n$H	H,H-COSY	Homonuclear shift correlation	Most important technique	[2, 137]	(P1)
	a) normal	Identification of spin systems, signal assignment	Fast routine technique		
	b) with delay	Detection of small couplings	D: No pure phases	[137]	
	c) DQF-COSY	Identification of spin systems, determination of J values	Best standard technique A: Low-intensity diagonal signals	[138–141]	
	d) "Constant time" COSY	Decoupling in t_1	D: Artifacts in case of strong coupling, no pure phases, strong dispersive contributions on the diagonal	[137, 142]	(P7)
	e) β-COSY	Relative sign of J	Alternatives: f, g, h	[2, 137, 143]	
	f) E.COSY	Accurate measurement of J	A: High resolution, good suppression of dispersion signals on the diagonal	[144–146]	
	g) P.E.COSY	Accurate measurement of J	A: Simpler method than E.COSY D: Not as accurate as E.COSY	[147]	
	h) z-COSY	E.COSY-like spectra	A: Absorptive diagonal D: Simultaneous formation of NOE cross signals especially for macromolecules	[130, 148, 149]	(P38)
	i) zz-COSY	Solvent-signal suppression, Determination of J	A: Absorptive diagonal	[127–129]	(P37)
	j) JR-COSY	Solvent-signal suppression	D: No quadrature detection in ω_1	[150]	
	k) X-Filter COSY	Simplification of proton spectra, spectroscopy of very large molecules	Only protons bound to a heteroatom give rise to cross signals	[151, 152]	(P32), (P33)
	l) X-Half-filter COSY	Same applications as k)	A: More flexible than k) since the filter operates only in one frequency domain	[153]	(P34), (P35)
	MQ spectroscopy	a) With emphasis on direct coupling - different representation (in case of overlapping signals in the COSY spectrum)	D: J dependence of excitation efficiency, no pure phases	[154–158]	
		- For measurements in water	A: Cross peaks to resonances under the water signal	[374]	
		b) With emphasis on remote coupling	Information similar to relayed spectrum	[159]	
	TOCSY (HOHAHA)	For macromolecules since cross peaks appear also in case of broad lines (in-phase multiplets)	Transfer across the total spin system possible. This may cause assignment problems	[160–163]	
X–X	INADEQUATE	C connectivity	D: Very insensitive, requires ^{13}C–^{13}C pairs	[50, 164–167]	(P11)
	INEPT-INADEQUATE	C connectivity	Slightly better sensitivity, alternative in some cases: C-relayed H,C-COSY (see Table 5)	[168]	
	Inverse variants			[169]	

the single-spin operator terms (dispersive diagonal signals) introduced above [Eq. (71)].

$$-\tfrac{1}{2}(I_1^+I_2^+ - I_1^-I_2^-) = \tfrac{1}{2}(2I_{1x}I_{2y} + 2I_{1y}I_{2x}) \xrightarrow{90°_y} -\tfrac{1}{2}(2I_{1z}I_{2y} + 2I_{1y}I_{2z}) \quad (71)$$

We thus obtain, through double-quantum coherences, among others the desired transfer from spin 1 to spin 2 [Eq. (72)].

$$2I_{1x}I_{2z} \longrightarrow \tfrac{1}{2}(2I_{1x}I_{2y}) \quad (72)$$

The transfer $2I_{1x}I_{2z} \rightarrow \tfrac{1}{2}(2I_{1y}I_{2z})$, which is effected at the same time, leads to the diagonal peaks in the DQF-COSY experiment. They are now antiphase and absorptive as desired (like the cross peaks). We realize also that, through the factor 0.5, the transfer is now only half as efficient as in a conventional COSY.

The concept of multiple-quantum filtration can also be formulated in a general form: a coherence of the type $I_{1y}I_{2z}\cdots I_{nz}$ can give rise maximally to an n-quantum coherence. An m-quantum filter with $m>n$ would hence suppress such a product operator. Certain spin topologies may then be selected: A spin I^1, which is coupled to $n-1$ other nuclei ($J_{1i}\neq 0$ for $i=2, 3, \ldots, n$), evolves, e.g., after $90°_x$-t_1, product operators with a maximum of n operators. This means that all the peaks that originate from I^1 are suppressed in a spectrum with an m-quantum filter ($m>n$).[138]

The cross signals in an n-quantum-filtered (nQF)-COSY are obtained through the transfer (73). For the generation of the relevant coherence before mixing, I^1 must be coupled to $n-1$ spins; for the

Table 3. Heteronuclear 2D NMR techniques through mixing by means of coherence transfers.

Symbol	Name	Application	Comment (A: advantage; D: disadvantage)	Reference	Pulse sequence
H–X	H,X-COSY (HETCOR)	Heteronuclear shift correlation		[170, 171]	(P14)
	a) normal	Routine method at present		[170–173]	
	b) DEPT-COSY	Permits editing	A: Phase-sensitive representation	[174–177]	(P15), (P16)
	c) H,X-COSY with ω_1 decoupling			[178–180]	(P25)
	d) Modified DEPT-COSY		No advantage over b)	[181]	
	e) COLOC for $^1J_{CH}$	Short measuring time		[182]	
	f) Modified COLOC for $^1J_{CH}$	Short measuring time	A: Not as strongly J dependent as e)	[181]	
	X,H-COSY (inverse heteronuclear correlation)	For small substance quantities, most sensitive method	D: Requires special spectrometer hardware	[39–54, 183, 184]	(P27)
H–$(H)_n$–X	Hetero-TOCSY	Transfer from proton magnetization via TOCSY followed by INEPT transfer	D: Intensity loss through distribution of polarization over many protons	[185, 186]	
H–$(-)_n$X	H,X-COSY for long-range coupling		COLOC should be preferred	[187, 188]	
	COLOC	Assignment of quaternary C, indirect detection of C connectivity, recognition of proton spin systems, qualitative evaluation of $^nJ_{CH}$		[189–193]	(P12)
	modified COLOC (XCORFE)	For discrimination of $^2J_{CH}$ and $^3J_{CH}$ couplings to proton-bearing carbons		[194]	
	"*Freeman* experiment"	Determination of $^nJ_{CH}$	D: Lack of resolution and intensity	[195]	
	X,H correlation through long-range coupling		A: Very sensitive	[50, 54, 196]	
	Hetero E.COSY, β-COSY	Exact determination of $^nJ_{CH}$	D: Relatively insensitive	[143, 197]	

Table 4. 2D NMR techniques with mixing through NOE and/or exchange.

Symbol	Name	Application	Comment (A: advantage; D: disadvantage)	Reference	Pulse sequence
H···H	Homonuclear nuclear Overhauser and exchange spectroscopy				
	NOESY	Distance information, three-dimensional structure of molecules, exchange spectroscopy	Besides COSY most important technique	[17, 89]	(P2)
	zz-NOESY	Solvent-peak suppression, separation of chemical exchange and NOE.		[127, 128]	(P36)
	ROESY (CAMELSPIN)	Separation of chemical exchange and NOE in medium-sized molecules without NOE effects	Suppression of J cross peaks necessary	[198–202]	(P39)
H···X	Heteronuclear nuclear Overhauser and exchange spectroscopy				
	H,X-NOESY, HOESY		D: Low sensitivity	[203–207, 368]	(P20)

$$I_{1x} \longrightarrow 2^{n-1}I_{1x}I_{2z}I_{3z}\ldots I_{nz} \xrightarrow{90^\circ_x} 2^{n-1}I_{1x}I_{2y}I_{3y}\ldots I_{ny} \xrightarrow{nQF} I_{1y}I_{2z}I_{3y}\ldots I_{ny}$$
$$\xrightarrow{90^\circ_x} I_{1x}I_{2x}I_{3z}\ldots I_{nz} \longrightarrow 2^{1-n}I_{2x} \qquad (73)$$

conversion of the resulting coherence into observable magnetization, I^2 must be coupled to the same spins ($J_{i2} \neq 0$ for $i = 1, 3, 4, \ldots, n$).[138]

Cross signals are generated between two coupled spins in an n-quantum-filtered COSY spectrum when they have in common additional $n-2$ coupled nuclei. The multiplet structure of this cross signal shows in both dimensions $n-1$ couplings in antiphase. Multiple-quantum filters with $n > 2$ are not very common. This is due to the reduction of intensity by the factor 2^{n-1}. Another reason is the fact that the higher the order of the multiple-quantum filter the fewer moieties in a molecule "pass it," so that one gets information only on some parts of the structure. Triple-quantum-filtered COSY spectra are used in the analysis of proteins when, for instance, the identification of glycine units is sought; these units are the only amino acids which give rise to cross signals in the TQF-COSY spectrum between the NH protons and both of the α protons.[259]

The net intensity obtained upon integration of the diagonal peak in a multiple-quantum-filtered COSY spectrum ($I_{1x} \rightarrow I_{1x}$, $I_{1y} \rightarrow I_{1y}$) is zero. Thus the problem of the intense diagonal peaks is solved through double-quantum filtration; no dispersion signals are obtained. This is, however, achieved at the cost of a cross-peak intensity reduced by a factor of one-half. The advantage of the strongly reduced diagonal peaks has nevertheless made the DQF-COSY experiment the most widely used technique. An example is shown in Figure 24.[260]

Table 5. Additional 2D NMR methods.

Symbol	Name	Application	Comment (A: advantage; D: disadvantage)	Reference	Pulse sequence
Methods with more than one mixing step					
a) Two consecutive *J* mixings					
H–H–H	H-Relayed H,H-COSY (RCT spectroscopy) or H-Relayed H,H-DQF-COSY	Assignment in crowded spectral regions	A: Stepwise elucidation of connectivities D: Less sensitive than TOCSY For special problems 1D variants [210] are applicable	[208, 209] [211, 212]	(P8)
H–H–X	H-Relayed H,X-COSY	In overcrowded ^{1}H-NMR signals	Mostly well replaceable by COLOC	[213–218]	(P17), (P18)
	Inverse variants			[53, 219]	(P28)
H–X–H	X-Relayed H,H-COSY			[220, 221]	(P29)
H–X–X	X-Relayed H,X-COSY	C connectivity in H-C-C fragments	Also used in a 1D variant A: Relatively insensitive, but more sensitive than INADEQUATE	[222–225]	(P19)
X–H–H	H-Relayed X,H-COSY		D: Useful only for heteronuclei with large γ (e.g. ^{31}P, ^{19}F)	[226, 227]	
b) Mixing through scalar and dipolar coupling					
H–H···H H···H–H	Relayed NOESY	In crowded regions, peptide sequential assignment	D: Useful only when large NOE effects are observed		
	a) normal			[228]	
	b) with DQF	For spectral assignment near the diagonal		[229]	(P40)
	c) with antisymmetrization			[230, 231]	
H–(H)$_n$···H	TORO TOCSY-NOESY	Peptide sequencing	A: No need for α-proton resolution	[232] [233]	(P41)
H···H–(H)$_n$	ROTO			[232]	
H···H–X	Hetero-relayed NOESY		D: Low sensitivity	[234, 368]	
Separation of chemical shift and coupling					
J_H,δ_H	Homonuclear 2D *J* spectroscopy	Determination of *J* and δ	Replaced by DISCO and E.COSY	[5, 235–240]	(P4)
J_{HC},δ_C	Heteronuclear 2D *J* spectroscopy	Determination of multiplicity, determination of *J* Determination of $^nJ_{CH}$	Generally replaceable by DEPT	[241–246] [247, 248]	
	Heteronuclear 2D *J* spectroscopy with selective H pulse	Determination of $^nJ_{CH}$	D: separated H signal required, for coupling to each H one 2D NMR experiment necessary	[249]	
One-dimensional equivalents of 2D NMR experiments					
		Excitation with Gaussian pulses	Traces from 2D NMR spectra obtained A: Time and disc-space saving in case of few well-aimed questions	[210, 250]	
2D NMR spectroscopy with selective excitation					
			Possible with all pulse sequences A: Sometimes sensitivity gained vs. 2D NMR methods with nonselective pulses	[251, 373]	
3D NMR experiments					
	3D J,δ			[252]	
	COSY-COSY			[253–255]	
	NOESY-COSY, and other combinations				
Various					
	CIDNP-COSY	Connection of photochemical excitation with 2D NMR spectroscopy	Part of the molecule must be photochemically active (e.g. arenes)	[256]	
	CIDNP-NOESY			[257]	
	COCONOSY	Simultaneous COSY and NOESY experiment	D: Low resolution in the COSY spectrum	[258]	

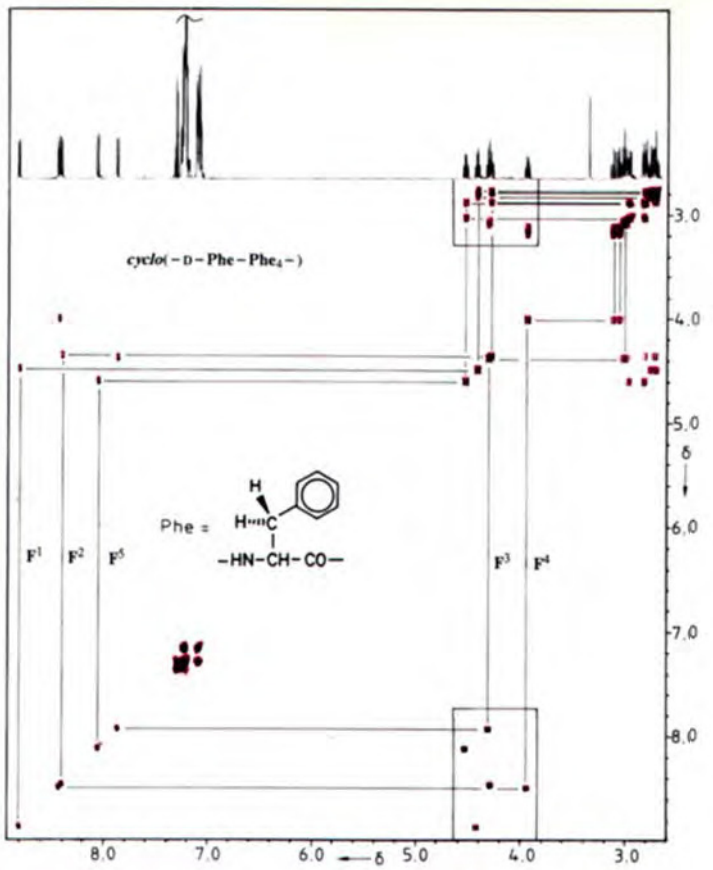

Fig. 24. DQF-H,H-COSY NMR spectrum of *cyclo*(-D-Phe-Phe$_4$-) in [D$_6$]DMSO, 500 MHz. The connectivities within the phenylalanines (F^1 to F^5) are indicated with lines. The signals in the boxes are expanded in Figure 25. The assignment of the amino acids to the peptide sequence does not follow from such a spectrum.

The multiplet structure in COSY spectra contains valuable information about coupling constants. The fine structure of the cross signals in Figure 24 is readily apparent from the enlarged section of the spectrum shown in Figure 25.

The coupling constants over three bonds depend on dihedral angles according to the Karplus relationship.[74,75] The magnitude of the coupling constants is thus related to the spatial structure of the corresponding molecule.

In 1D NMR spectra of complex systems the coupling constants can no longer be read out directly. Therefore 2D NMR methods suitable for the analysis of not-too-strongly coupled systems (see Section 3.1.2) were developed.

3.1.2. 2D *J* Spectroscopy

The first 2D NMR experiment suggested for the analysis of spin systems was the 2D *J*-resolved spectrum.[5] The pulse sequence (P4) for this experiment is the only one, in addition to that in the COSY experiment, with only two pulses and is hence likewise easy to analyze.

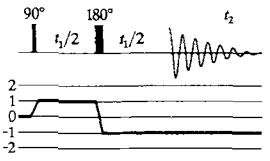

(P4)

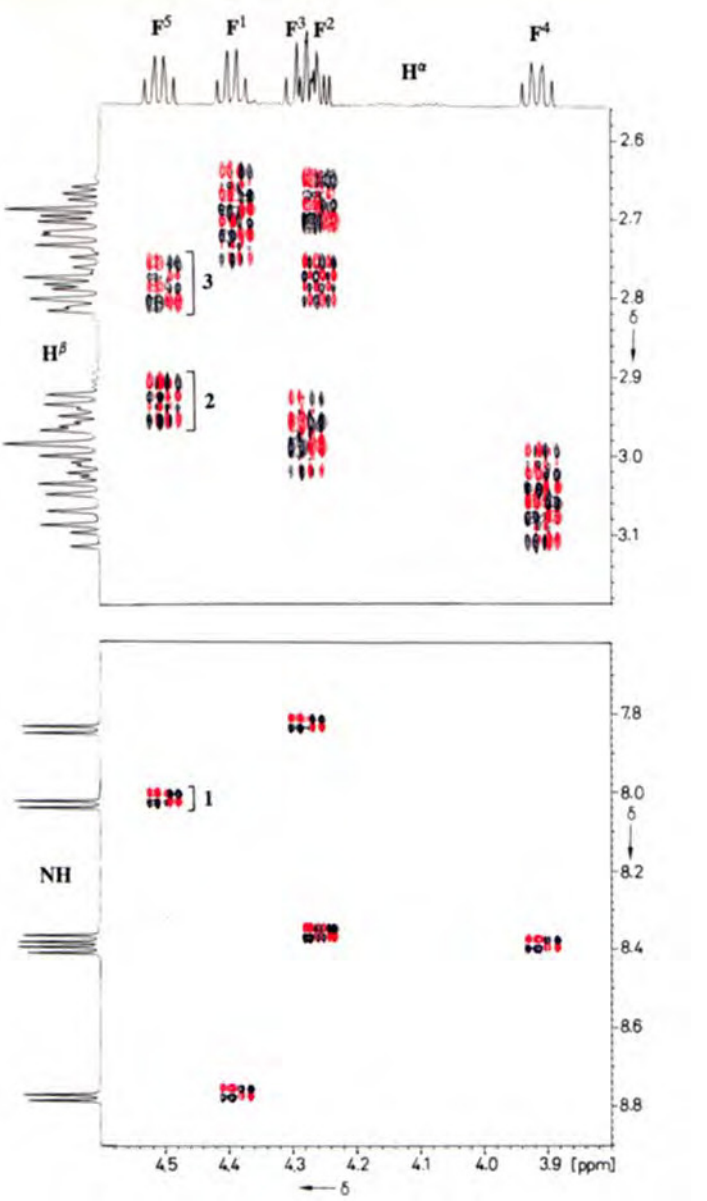

Fig. 25. Expansions from the spectrum in Figure 24: the NH-H$_\alpha$ region (bottom) and H$_\alpha$-H$_\beta$ region (top). The signals labeled 1, 2, and 3 were used for the DISCO procedure (see Fig. 28).

The Effect of 180° Pulses

180° pulses are often used to improve pulse sequences. They have different effects on chemical shift and coupling, and can therefore be utilized to manipulate interactions. We show now that the evolution of coupling is not affected by a 180° pulse [Eq. (74) and (75)]. The *relative* signs of the

$$I_{1x}\cos\pi Jt + 2I_{1y}I_{2z}\sin\pi Jt \xrightarrow{180°_{x,y}} \pm(I_{1x}\cos\pi Jt + 2I_{1y}I_{2z}\sin\pi Jt) \quad (74)$$

$$I_{1y}\cos\pi Jt - 2I_{1x}I_{2z}\sin\pi Jt \xrightarrow{180°_{x,y}} \mp(I_{1y}\cos\pi Jt - 2I_{1x}I_{2z}\sin\pi Jt) \quad (75)$$

two operators remain unchanged; i.e., the evolution of coupling, apart from a possible overall exchange of sign, remains unaffected by the 180° pulse. The chemical shift,

in contrast, reacts differently [Eq. (76)]. The right-hand term in Equation (76) is identical with (77). After the 180° pulse the system is, with respect to chemical shift, in a state

$$I_x \cos \Omega t + I_y \sin \Omega t \xrightarrow{180°_{x,y}} \pm (I_x \cos \Omega t - I_y \sin \Omega t) \quad (76)$$

$$\pm (I_x \cos \Omega(-t) + I_y \sin \Omega(-t)) \quad (77)$$

as if it had evolved in the first period t backward (t has to be replaced by $-t$, time reversal). In other words, further evolution after the 180° pulse will lead after a second period t to the starting situation, i.e., to refocusing of the chemical shift [Eq. (78)].

$$I_x \xrightarrow{t} I_x \cos \Omega t + I_y \sin \Omega t \xrightarrow{180°_x} I_x \cos \Omega t - I_y \sin \Omega t \xrightarrow{t} I_x \quad (78)$$

Thus chemical shift evolves in the 2D J sequence only during t_2, while coupling evolves during both t_1 and t_2. The resulting signal amplitude for spin 1 is given by (79), where

$$\prod_i \cos \pi J_{1i}(t_1 + t_2) \cos \Omega_1 t_2 = \prod_i \cos (\pi J_{1i} t_1 + \pi J_{1i} t_2) \cos \Omega_1 t_2 \quad (79)$$

$\prod_i \cos \pi J_{1i}$ is the product over all couplings of spin 1. Complex Fourier transformation of this expression and absolute value representation yield the multiplets shown schematically in Figure 26a. Projection of such 2D multiplets on the ω_1 or ω_2 axis affords directly the coupling constants. After tilting according to $\omega_1' = \omega_1$, $\omega_2' = \omega_2 - \omega_1$,[34] the spectrum shown in Figure 26b is obtained, in which now ω_2 represents only chemical shifts, and ω_1 only coupling constants. 2D J-resolved NMR spectra are phase-modulated in t_1 ($\pi J_{11} t_1$ is a phase) and hence cannot be corrected to pure phase. The mixed phases lead to false line positions and make the determination of coupling constants unreliable. Furthermore, the resolution achieved through the reduction of multiplets to singlets along ω_2 in tilted 2D J NMR spectra is often insufficient in complex spin systems,[261,262] and artifacts may appear in the presence of strong coupling.

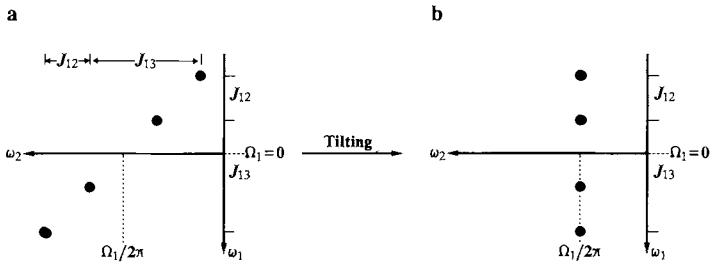

Fig. 26. a) Schematic peak in a homonuclear 2D J-resolved NMR spectrum of a three-spin system; b) separation of chemical shifts (projection on the ω_2 axis) and coupling constants (projection on the ω_1 axis) after tilting.

3.1.3. *Determination of Coupling Constants from COSY Spectra*

Direct Extraction of Coupling Constants from COSY

For very simple multiplets, coupling constants can be measured directly from 2D NMR spectra.[136] However, this is not possible for complex spin systems.

DISCO[263–265]

The disadvantages of 2D J-resolved spectroscopy mentioned in Section 3.1.2 (impure phases, insufficient resolution) are not found in DQF-COSY. The cross signals in DQF-COSY show a rather well resolved multiplet structure, with the active couplings antiphase and all the others in-phase. Consider a three-spin system, in which $J_{13} = 0$. We focus on the two cross signals, the 1,2 and the 2,3 signals. The multiplet structure for the 1,2 cross signal in ω_2 is described by (80) and for the 2,3 cross signal by (81). Summation of the two signals yields a signal in the time domain described by (82); i.e., the active coupling in this "hybrid trace" is $J_{12} + J_{23}$. The number of lines in this signal has been reduced by one-half. Through the reduction in the number of lines, multiplet structures become easier to analyze. The active coupling appears in DISCO spectra as the sum of two couplings and is hence effectively increased, so that cancellation of lines from antiphase signals is less likely (Fig. 27).

$$\sin \pi J_{12} t_2 \cos \pi J_{23} t_2 \prod_i \cos \pi J_{2i} t_2 \quad (80)$$

$$\sin \pi J_{23} t_2 \cos \pi J_{12} t_2 \prod_i \cos \pi J_{2i} t_2 \quad (81)$$

$$\sin \pi (J_{12} + J_{23}) t_2 \prod_i \cos \pi J_{2i} t_2 \quad (82)$$

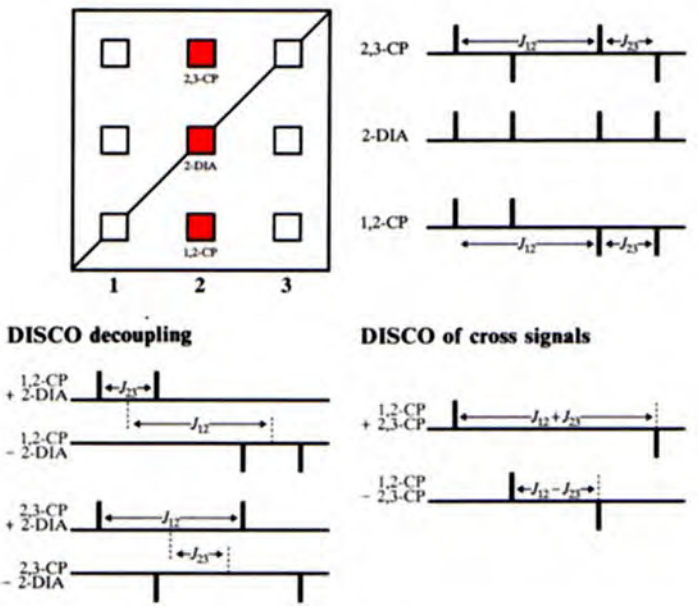

Fig. 27. DISCO with the cross signals of spin 2 of a three-spin system. Note that the diagonal signal is 90° phase-shifted (dispersive). In order to use this signal (2-DIA) for "DISCO-decoupling," the COSY spectrum for the diagonal signals must be calculated with an additional 90° phase correction in both dimensions. Upper left: schematic COSY spectrum. Upper right: cross-sections of 1,2 and 2,3 cross signals (1,2-CP, 2,3-CP) and the diagonal signal (2-DIA) for spin 2 in ω_2. Lower left: DISCO decoupling through addition and subtraction of cross signal and diagonal signal. Lower right: DISCO through addition and subtraction of the cross signals.

If the diagonal signals in a COSY spectrum are free, the DISCO procedure can be applied to these diagonal signals in combination with the corresponding cross signals with equal chemical shifts in ω_2. Since the cross signals are in-phase, Equation (83) is obtained, i.e., a multiplet without

$$\cos \pi J_{12}t_2 \cos \pi J_{23}t_2 \prod_i \cos \pi J_{2i}t_2 \pm i \sin \pi J_{12}t_2 \cos \pi J_{23}t_2 \prod_i \cos \pi J_{2i}t_2$$
$$= e^{\pm i\pi J_{12}t_2} \cos \pi J_{23}t_2 \prod_i \cos \pi J_{2i}t_2 \quad (83)$$

the active coupling (decoupled multiplet), in a position shifted by either $+\pi J_{12}$ or $-\pi J_{12}$. Comparison of the two spectra obtained by addition or subtraction yields the active coupling constant.

A practical example is shown in Figure 28, with a DISCO evaluation of the cross signals due to the α protons of the amino acid Phe[5] in the spectrum of the cyclic pentapeptide from Figure 25.

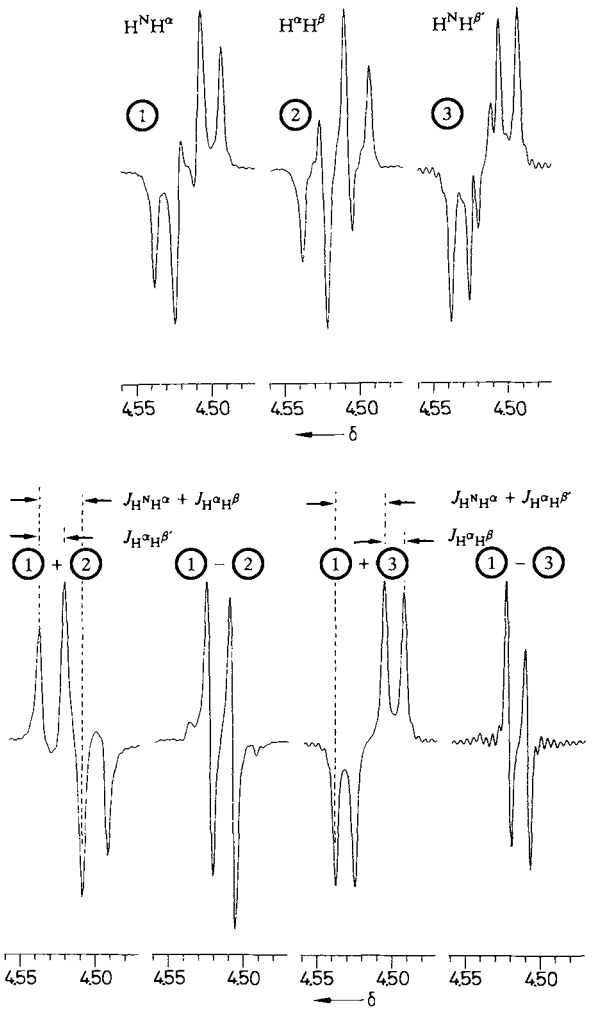

Fig. 28. DISCO spectra from the spectrum of Figure 25. The signals labeled there with 1, 2, and 3 were used. Pseudo 1D spectra (top), obtained by coaddition of the traces, were added up or subtracted (bottom). The simplification of multiplets is clearly evident, particularly after addition, in that the signals are well resolved.

To improve the signal-to-noise ratio, coaddition[*] is performed over the entire cross signal, and the resulting pseudo 1D NMR spectra are summed together.[265] The digital resolution can be improved by a reverse Fourier transformation, zero filling (to 64 K, for example) followed by retransformation. The true scaling factor for the combination of two spectra is unknown and poses some difficulty in the DISCO evaluation. It must be determined from the result of the combination. This makes the application of DISCO in complex or strongly coupled spin systems difficult.

3.1.4. E. COSY

A second procedure (E. COSY[144-146]) simplifies the cross-signal pattern, as shown schematically in Figure 29.

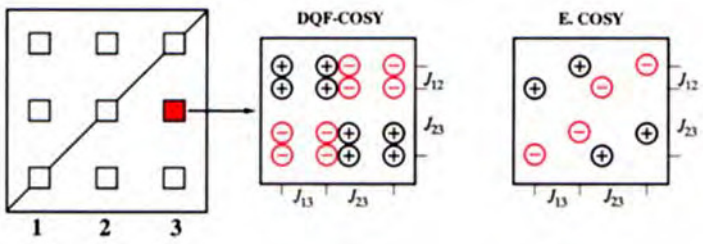

Fig. 29. Multiplet fine structure of a cross signal in a DQF-COSY spectrum (center) and in an E. COSY spectrum (right).

In order to understand this technique we turn back to the multiple-quantum-filtered COSY spectra. We saw that in the DQF-COSY spectrum only two-operator terms contributed. This determines the multiplet structure in COSY and DQF-COSY spectra. Higher-quantum filters (e.g., a triple-quantum filter, TQF) can be used instead of the double-quantum filter. The pulse sequence remains the same (P3, COSY with MQF); only the phase cycle changes. In the TQF-COSY experiment the phases ϕ_1 and ϕ_2 go through the values 0°, 60°, 120°, 180°, 240°, 300°, and during t_2 alternating signals are added and subtracted. The multiplet structure is shown schematically in Figure 30. The cross signals are generated only by the transfer $I_{1x}I_{2z}I_{3z} \rightarrow I_{1z}I_{2x}I_{3z}$. A factor 4 in intensity is lost in such a spectrum, relative to the unfiltered COSY spectrum (a factor 2 in the DQF-COSY spectrum). The multiplet structure is antiphase in both dimensions: with respect to J_{12} and J_{13} in ω_1 and with respect to J_{12} and J_{23} in ω_2.

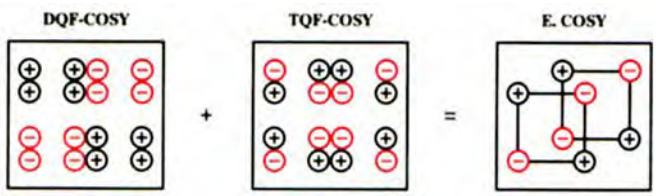

Fig. 30. Fine structure of an E. COSY cross signal from a DQF-COSY and a TQF-COSY spectrum. The E. COSY spectrum is obtained, theoretically, from weighted addition of these two spectra. When additional passive couplings render the spectrum more complex, correspondingly more multiple-quantum spectra must be added.

[*] Coaddition is a special way of addition where each trace is multiplied with the sign of a reference point in that trace in order to avoid cancellation when summing up over antiphase multiplets.

Examination of the multiplet structure in DQF- and TQF-COSY spectra reveals that summation of the two (see Fig. 30) greatly simplifies the multiplet pattern.

A general treatment for more than three spins can be found in the original literature.[144-146] An example of the extraction of coupling constants from an E. COSY spectrum is shown in Figure 31.

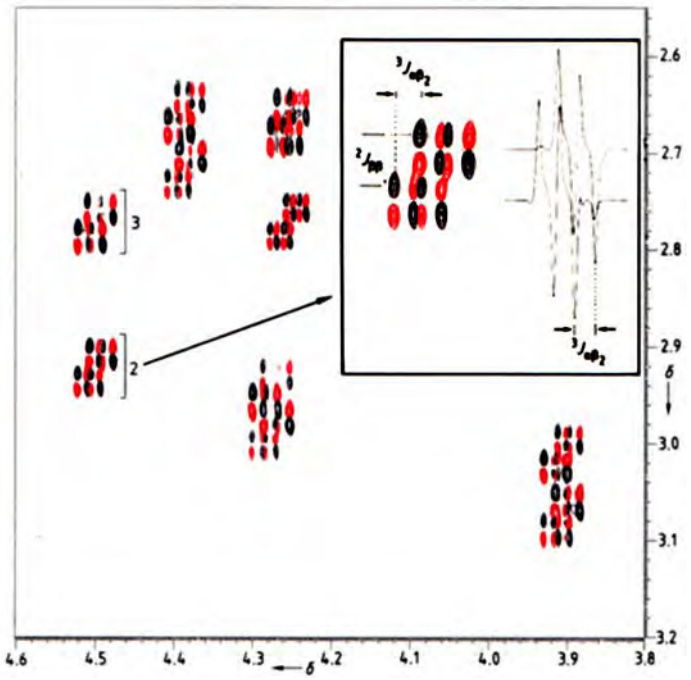

Fig. 31. E. COSY spectrum of *cyclo*(-D-Phe-Phe$_4$-) in [D$_6$]DMSO, the same region as in Figure 25. The expansion of signal 2 is shown in the upper right along with the associated co-added traces. The passive coupling constant $^3J_{\alpha\beta_2}$ can be measured very accurately from the distance between two peaks.

The appearance of a cross signal in an E. COSY spectrum resembles that in a COSY spectrum, in which a mixing pulse with a small flip angle is used (β-COSY).[137] However, there are large dispersive parts in the diagonal peaks, which make the interpretation of cross signals near the diagonal very difficult. This disadvantage is overcome by a technique introduced in Ref. [45] and called later P. E. COSY.[141, 144, 145, 147] Another possibility is the introduction of a z-filter[266] ("z-COSY").[148] However, both methods fail to quantitatively suppress nonconnected transfers. For the last method cross relaxation during the z-filter delay may occur in large molecules.

z-Filter

The z-filter is an additional method to select certain coherences (or in this case populations) which cannot be separated by phase cycles. We saw the multiple-quantum filter as a "high-pass filter" for the number of operators in a product operator, in so far as all the products with fewer operators than the multiple-quantum order were suppressed. In contrast, the z-filter (P5) selects populations and suppresses coherences.

(P5)

With the phase cycle of the β pulses zero-quantum coherences and populations are selected. The zero-quantum coherences are then suppressed by variation of τ_m, which is based on the fact that they are modulated with the difference of the chemical shifts of the two involved spins. Populations, on the other hand, are invariant under variation of τ_m (disregarding relaxation). Therefore, if τ_m is varied and the resulting spectra added, the zero-quantum coherences average out, and ideally only the populations are left.

The z-filter can be used, for instance, to select pure in-phase magnetization just before the detection (P6). Of all

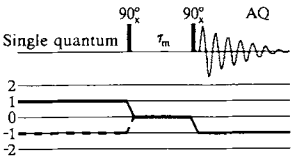

(P6)

the detectable single-quantum coherences only I_y is transformed by the first 90$_x^\circ$ pulse into a population and then regenerated by the second pulse. All the antiphase terms are suppressed, in the ideal case.

This principle is used in the 1D z-filtered COSY technique, where the antiphase terms are refocused after the COSY transfer and undesired contributions with other phases are suppressed by the z-filter. A pure in-phase multiplet for spin 2, which is coupled to spin 1, is obtained through excitation of the latter. This multiplet can then be further simplified through the DISCO procedure.[210]

The z-filter function is more complicated in the z-COSY experiment, for here the z-filter is flanked by pulses with small flip angles. Essentially, transformation (84) should be selected. This then provides substantially simplified cross signals of the E. COSY type.

$$I_{1y}I_{2z}I_{3z}...I_{nz} \xrightarrow{\beta_x} I_{1z}I_{2z}I_{3z}...I_{nz} \xrightarrow{\beta_x} I_{1y}I_{2y}I_{3z}...I_{nz} \qquad (84)$$

3.1.5. *Additional COSY Variants*

Two older COSY variants are described in this section, which were introduced only for signal assignment, i.e., for qualitative NMR spectroscopy. They have lost some of their significance, but are discussed here since they clarify some important principles.

Delay COSY

The signals in a COSY spectrum are antiphase with respect to the active coupling in both frequency domains (see Section 3.1.1). Taking into account the line width, this multiplet structure is not optimal because broad lines in antiphase are likely to cancel partially. Another point is that the resolution determined by t_1^{max} is often not sufficient to resolve small couplings. However, if a delay is introduced before and after the 90° pulse[137] (if necessary, with 180° pulses in the middle of the delays to refocus chemical shifts and compensate for field inhomogeneities: SUPERCOSY[267-269]), in-phase portions are also obtained [Eq. (85)], which do not cancel, irrespective of the ratio of

$$\sin \pi J(t_1+\Delta_1) \sin \pi J(t_2+\Delta_2) = (\sin \pi J t_1 \cos \pi J\Delta_1 + \cos \pi J t_1 \sin \pi J\Delta_1)$$
$$(\sin \pi J t_2 \cos \pi J\Delta_2 + \cos \pi J t_2 \sin \pi J\Delta_2) \qquad (85)$$
$$= \sin \pi J\Delta_1 \sin \pi J\Delta_2 \cos \pi J t_1 \cos \pi J t_2 + ...$$

line width to coupling constant. This type of spectrum[270] therefore produces cross signals with mixed phases, which is the reason why it is now seldom used. In contrast, refocusing and defocusing are widely applied in heteronuclear NMR spectroscopy.

ω_1-Decoupled COSY

ω_1-Decoupling can be achieved almost universally through "constant time" variants of pulse sequences. ω_1-Decoupling causes complete disappearance of the multiplet structure in ω_1, which means a gain in resolution.[137,271] The simplest sequence of this type is the ω_1-decoupled COSY[137] (P7), in which chemical shift evolution is generated by a "wandering" 180° pulse.

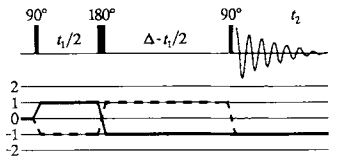

(P7)

In the 2D *J* NMR experiment (Section 3.1.2) 180° pulses do not affect the evolution of coupling, but they reverse the evolution of chemical shifts. As a result the homonuclear coupling in the pulse sequence (P7) evolves during the entire delay Δ between the 90° pulses, whereas chemical shift evolves during $-t_1/2+(\Delta-t_1/2)=\Delta-t_1$. The transfer amplitude for a 1,2 cross signal between two nuclei in constant time COSY is given by (86). The multiplet

$$\sin \pi J_{12}\Delta \prod_i \cos \pi J^{\mathrm{R}}_{1i}\Delta \cos \Omega_1(\Delta-t_1) \sin \pi J_{12}t_2 \prod_i \cos \pi J^{\mathrm{R}}_{2i}t_2 \cos \Omega_2 t_2 \quad (86)$$

structure in ω_1 is lost completely, since the signal is modulated in t_1 only by the chemical shift ($\cos\Omega_1(\Delta-t_1)$). However, the size of the coupling constant enters through the intensity of the cross signal (transfer amplitude). ω_1-Decoupled spectra can, with some difficulty, be corrected to pure phase.

3.1.6. Relayed Spectroscopy

There is only one coherence transfer step in the COSY experiment. Hence magnetization is transferred from one nucleus to another one which is coupled to it: $2I_{1x}I_{2z} \rightarrow 2I_{1z}I_{2x}$. Relayed spectroscopy introduces one or more additional steps of this type. The Relayed COSY pulse sequence is (P8).[208,209]

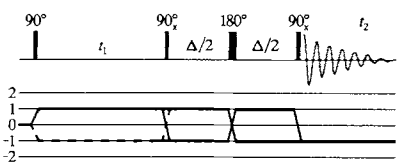

(P8)

We consider again only those terms which are relevant for a relayed signal. Coherence transfer is accomplished by 90° pulses; therefore only two-operator terms are of interest [Eq. (87)]. After preparation (90° pulse) and labeling

$$I_{1z} \xrightarrow{90°_y} I_{1x} \xrightarrow{t_1} 2I_{1y}I_{2z} \xrightarrow{90°_x} -2I_{1z}I_{2y} \xrightarrow{\Delta/2-180°-\Delta/2} 2I_{2y}I_{3z} \xrightarrow{90°_x} 2I_{2z}I_{3y} \xrightarrow{t_2} I_{3x} \quad (87)$$

(evolution of chemical shifts and coupling during t_1) ($2I_{1y}I_{2z}$) the first mixing pulse follows. Antiphase magnetization of spin 2 is obtained ($-2I_{1z}I_{2y}$), labeled with the chemical shift of spin 1. In the following period $\Delta/2$-180°-$\Delta/2$ only coupling evolves, since chemical shifts are refocused. The J_{12} coupling refocuses ($-2I_{1z}I_{2y} \rightarrow I_{2x}$) and antiphase magnetization with respect to spin 3 evolves ($I_{2x} \rightarrow 2I_{2y}I_{3z}$). Spin 3 becomes transverse through the second mixing pulse ($-2I_{2z}I_{3y}$), and, after refocusing of the coupling to spin 2 during t_2, magnetization of spin 3 can be detected. Since the coherence-transfer pathways in Relayed COSY correspond to those in COSY, relayed *as well as* direct COSY signals can always be found in the spectrum. Phase-sensitive processing is possible like in COSY. However, only the phases of the relayed peaks are pure, whereas those of the COSY-type peaks are mixed and depend on Δ. The relayed peaks have no simple multiplet structure when more than one intermediate spin contributes to a cross peak. The transfer amplitude is given by (88).

$$\sin \pi J_{12}t_1 \prod_i \cos \pi J^{\mathrm{R}}_{1i}t_1 \sin \pi J_{12}\Delta \sin \pi J_{23}\Delta \prod_i \cos \pi J^{\mathrm{R}}_{2i}\Delta \sin \pi J_{23}t_2 \prod_i \cos \pi J^{\mathrm{R}}_{3i}t_2 \quad (88)$$

The delay Δ must be optimized with respect to the magnitude of the coupling constants. It must be short enough with respect to the largest coupling, such that $\cos \pi J\Delta \not\approx 0$, for otherwise this passive coupling leads to disappearance of the relayed signals. Long delays should also be avoided in order to keep intensity losses due to relaxation at a minimum.

Relayed spectroscopy enables transfer of magnetization from spin 1 through a relay spin to a third spin not directly coupled with spin 1. This procedure is very useful for spectral assignments. If, for example, in an AMX and a BNY spin system the spins M and N overlap, but spins A and B as well as X and Y do not, assignment of A to X and B to Y can be made with the aid of this technique. An example is shown in Figure 32.

Experiments with several relayed-transfer steps were successfully applied in the spectral assignment of peptides[272] and in the analysis of sugars.[273] When the coupling constants are known the transfer amplitudes can be optimized by the right choice of the delays.[209] Relayed cross signals are often formed through more than one transfer. If there is more than one possible relay spin, the relayed signals consist of the sum of different multiplet structures. This problem of overlapping multiplet patterns in relayed spectra can be solved with the 1D-relayed sequence through selective transfer of magnetization.[210] Such a 1D relayed spectrum is shown in Figure 33.

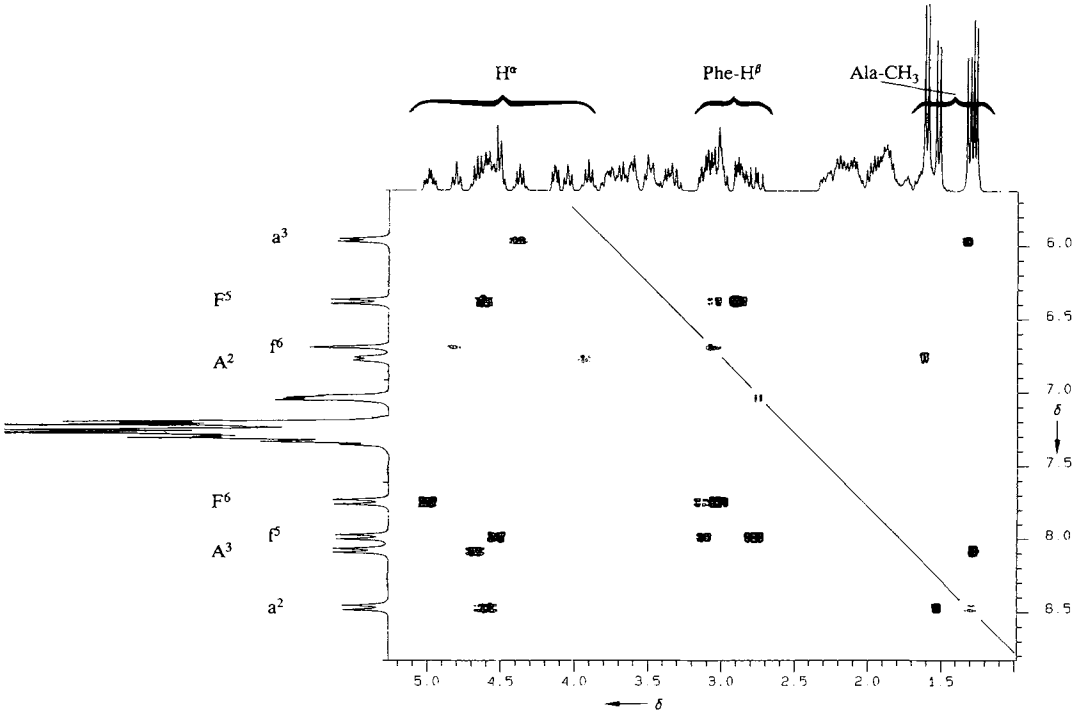

Fig. 32. H-Relayed H,H-COSY of *cyclo*(-Pro^1-Ala^2-Ala^3-D-Pro^4-Phe^5-Phe^6-) in $CDCl_3$ (270 MHz). The NH region in ω_1 is shown and the corresponding cross signals with α and β protons (ω_2). Note that two conformations exist in slow exchange in this solvent (two signal sets labeled with upper- and lower-case letters). The alanine (A and a) and phenylalanine (F, f) spin systems are readily identified through the relayed peaks to the β protons in the right part of the spectrum. This type of spectrum does not lead to assignment of the signals to the peptide sequence. Signals on the counterdiagonal are due to instrument-specific artifacts.

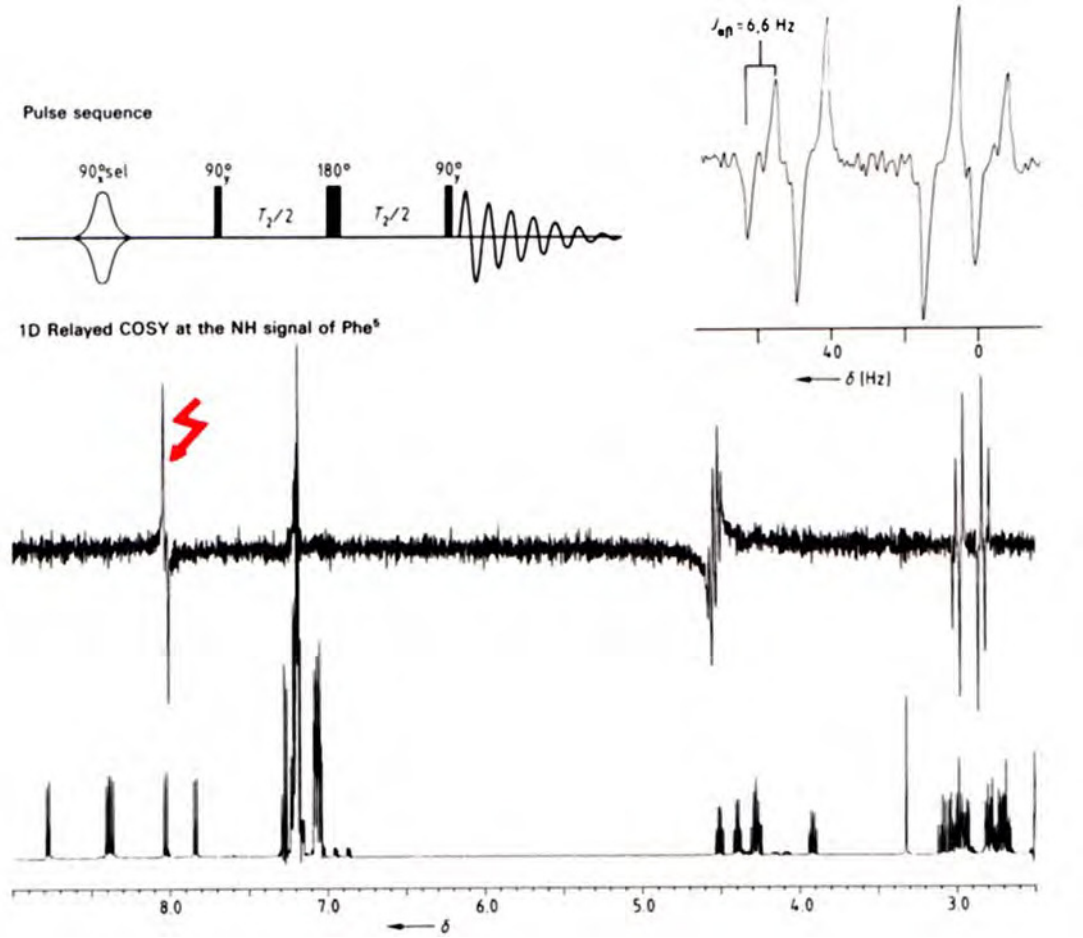

Fig. 33. 1D Relayed spectrum of *cyclo*(-D-Phe-Phe$_4$-). The NH signal of Phe^5 was selectively irradiated. With the right choice of the first delay the corresponding α signal appears dispersive in-phase, while the relayed signals show the multiplet of both β protons in absorptive antiphase. As the expanded region in the upper right corner shows, coupling constants can easily be determined from this multiplet.

3.1.7. TOCSY

A fundamentally different method for the transfer of coupling information is utilized in the TOCSY experiment.[160] In contrast to the COSY experiment, in-phase signals are obtained, i.e., the following transfer takes place: $I_{1x} \rightarrow I_{2x}$ (similar to the NOESY experiment). Mixing is achieved while a spin-lock field is applied, and ideally the effect of chemical shift is completely removed. All the spins are temporarily equivalent (AMX becomes AA'A''). The spin-lock sequences are termed according to *Chandrakumar* et al. as isotropic mixing (no effective field) or as Hartmann-Hahn mixing (with effective field: HOHAHA experiment).[161] Theoretical investigations are described in several publications.[193, 274–280]

The isotropic Hamiltonian includes only the scalar coupling, which is insensitive towards rotation (isotropic). If, however, a residual field remains which is equal for all the chemical shifts, the isotropy of the Hamiltonian is lost and only axial symmetry remains. This condition is termed in analogy to solid-state NMR experiments "Hartmann-Hahn Match." The spins remain strongly coupled, which is essential for the transfer.

Isotropic mixing leads to spectra with mixed phases (phase modulation), whereas in the Hartmann-Hahn mixing pure phases are obtained.[160, 281] The multiplets, even when generated over different mixing times, give rise to combinations of different mirror-symmetric multiplet patterns.[197] Ideally cross signals are formed between all the nuclei in a spin system.

Several pulse sequences have been proposed for the mixing in the TOCSY experiment. The most successful is MLEV-17,[283–285] introduced by *Bax* et al.,[282] which is also used with heteronuclear decoupling (see Section 3.2.10). A further technical realization is found in Ref. [365], theory in Refs. [366, 367].

TOCSY is particularly useful in the analysis of peptides in which the line widths are of the order of couplings, in which case COSY becomes insensitive due to the antiphase structure of the cross signals. The number of nuclei to which magnetization is distributed is controlled through the duration of the spin-lock periods. Short mixing times produce cross signals practically only between directly coupled nuclei, whereas longer mixing times give rise also to relayed and multiple-relayed peaks.

3.1.8. Multiple-Quantum Spectroscopy

We saw in the discussion of the multiple-quantum-filtered COSY technique (Section 3.1.1) that single-quantum coherences were mutually connected through intermediate multiple-quantum coherences. In multiple-quantum spectra,[157, 158, 286–291] however, multiple-quantum coherences are correlated with single-quantum coherences.

Despite the fact that multiple-quantum coherences are not detectable, they can be observed with the aid of 2D NMR spectroscopy. The pulse sequence for an n-quantum

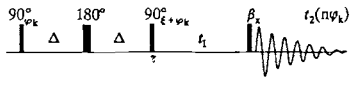

(P9)

spectrum is (P9), where $\xi = (n \bmod 2)90°$ and $\phi_k = k(\pi/n)$ with $k = 0, 1, \ldots, 2n-1$.

We first treat multiple-quantum spectra with two-spin systems. Indeed, double-quantum spectroscopy is used mainly for the correlation of ^{13}C nuclei (INADEQUATE[164]). Due to the small natural abundance of this nucleus (ca. 1%) only signals from two-spin systems are detected.

Double-quantum coherence evolves under chemical shift according to (89) and (90), i.e., the sums of the frequencies evolve. In contrast, J_{12} coupling between the spins participating in the double-quantum coherence does not evolve.

$$2(I_{1x}I_{2y} + I_{1y}I_{2x}) \xrightarrow{(\Omega_1 I_{1z} + \Omega_2 I_{2z})t} 2(I_{1x}I_{2y} + I_{1y}I_{2x})\cos(\Omega_1+\Omega_2)t + 2(I_{1y}I_{2y} - I_{1x}I_{2x})\sin(\Omega_1+\Omega_2)t \quad (89)$$

$$2(I_{1y}I_{2y} - I_{1x}I_{2x}) \xrightarrow{(\Omega_1 I_{1z} + \Omega_2 I_{2z})t} 2(I_{1y}I_{2y} - I_{1x}I_{2x})\cos(\Omega_1+\Omega_2)t - 2(I_{1x}I_{2y} + I_{1y}I_{2x})\sin(\Omega_1+\Omega_2)t \quad (90)$$

The INADEQUATE sequence is (P10), whereby the phase φ changes through 0°, 90°, 180°, and 270°. The first "sandwich" ($90°_{\varphi}$-Δ-180°-Δ-$90°_{\varphi}$) generates double-quantum coherences. For $\varphi = 90°$, for example, (91) is obtained:

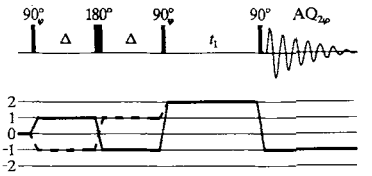

(P10)

$$I_{1x} + I_{2x} \xrightarrow{2\Delta} 2I_{1y}I_{2z} + 2I_{1z}I_{2y} \xrightarrow{90°_x} 2I_{1y}I_{2x} + 2I_{1x}I_{2y} \quad (91)$$

Zero- and single-quantum coherences are suppressed by the appropriate phase cycles. With the correctly tuned delays only molecules with two adjacent ^{13}C nuclei give rise to signals in INADEQUATE spectra.

Chemical shift of the double-quantum coherence, which, as shown in Equation (89), corresponds to the sum of the frequences of the single-quantum coherences of the two spins, evolves during t_1. The 90° pulse that follows converts the double-quantum coherence into antiphase single-quantum coherence, which is evenly distributed between both spins [Eq. (92)]. The resulting spectrum is shown schematically in Figure 34.

$$2(I_{1x}I_{2y} + I_{1y}I_{2x}) \xrightarrow{90°_x} 2(I_{1x}I_{2z} + I_{1z}I_{2x}) \quad (92)$$

There is no multiplet structure in ω_1. Each pair of cross signals at equal ω_1 frequency represents a C-C connectivity. There is hence a direct correlation between constitution

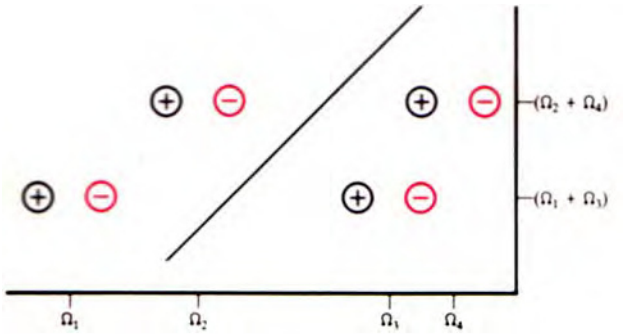

Fig. 34. A schematic INADEQUATE spectrum for an isolated two-spin system, as it appears for "dilute" nuclei. Pairs of antiphase doublets are obtained, symmetrical with respect to the skew diagonal at $\omega_1 = 2\omega_2$.

and spectrum. For a detailed discussion see *J. Buddrus* and *H. Bauer*.[292] The INADEQUATE technique offers maximum sensitivity for the correlation of nuclei of low natural abundance. However, indirect excitation and detection of the heteronuclei by protons as discussed later as "inverse spectroscopy" (Section 3.2.11) leads to an additional increase of intensity.

INADEQUATE spectra with pure phases, as well as quadrature detection in ω_1, are achieved by 45° phase incrementation. Other variants achieve quadrature detection in ω_1 without such phase incrementation, using pulse angles other than 90°. Details of the method can be found in the above-mentioned review[292] or in the original literature.

Double-quantum spectra of larger spin systems (e.g., protons) are substantially more complicated.[157] First we note the coupling to other nuclei. We find (93) and (94). Thus the sum of the coupling constants of the active spins with the passive spins evolves.

$$2(I_{1x}I_{2y} + I_{1y}I_{2x}) \xrightarrow{(\pi J_{13}\, 2I_{1z}I_{3z} + \pi J_{23}\, 2I_{2z}I_{3z})t} 2(I_{1x}I_{2y} + I_{1y}I_{2x})\cos \pi(J_{12}+J_{23})t - 4(I_{1x}I_{2x} + I_{1y}I_{2y})I_{3z} \sin \pi(J_{12}+J_{23})t \quad (93)$$

$$2(I_{1x}I_{2x} + I_{1y}I_{2y}) \xrightarrow{(\pi J_{13}\, 2I_{1z}I_{3z} + \pi J_{23}\, 2I_{2z}I_{3z})t} 2(I_{1x}I_{2x} + I_{1y}I_{2y})\cos \pi(J_{12}+J_{23})t - 4(I_{1x}I_{2y} + I_{1y}I_{2x})I_{3z} \sin \pi(J_{12}+J_{23})t \quad (94)$$

Direct connectivities are found in the double-quantum spectrum according to (95), which leads to the cross-signal pair in ω_1 at the sum of the chemical shifts $(\Omega_1+\Omega_2,\Omega_1)$ and $(\Omega_1+\Omega_2,\Omega_2)$, symmetrical about the diagonal $\omega_1 = 2\omega_2$.

$$2I_{1x}I_{2z} \xrightarrow{90^\circ_x} 2I_{1x}I_{2y} \xrightarrow{t_1} 2I_{1x}I_{2y} + 2I_{1y}I_{2x} \xrightarrow{90^\circ_x} 2I_{1x}I_{2z} + 2I_{1z}I_{2x} \quad (95)$$

In linear spin systems of the type I^1-I^2-I^3 additional "remote" peaks are found according to Equation (96). They appear in ω_2 at the frequency of spin 2, but in ω_1 at the sum of the frequencies for spin 1 and 3 $(\Omega_1+\Omega_3,\Omega_2)$. In contrast to the direct signals, they have no symmetry reflection about the diagonal; they contain, however, the relayed information.

$$4I_{1z}I_{2y}I_{3z} \xrightarrow{90^\circ_x} 4I_{1y}I_{2z}I_{3y} \xrightarrow{t_1} 4I_{1y}I_{2z}I_{3y} \xrightarrow{90^\circ_x} 4I_{1z}I_{2y}I_{3z} \quad (96)$$

For three spins which are all mutually coupled, both types of signals, "direct" as well as "remote" peaks, are found in the spectrum. These signals have mixed phases. For example, the cross peak with the coordinates $(\Omega_1+\Omega_2,\Omega_1)$ arises from (97). This direct signal is in absorption in both frequency dimensions and in-phase with respect to the J_{13} and J_{23} coupling in ω_1. Another pathway is (98). The resulting cross peak is dispersive in ω_1, absorptive in ω_2, and antiphase with respect to both couplings in ω_1. Both transfers give rise to a cross peak at $(\Omega_1+\Omega_2,\Omega_1)$.

$$2I_{1x}I_{2z} \xrightarrow{90^\circ_x} 2I_{1x}I_{2y} \xrightarrow{t_1} 2I_{1x}I_{2y} \xrightarrow{90^\circ_x} 2I_{1x}I_{2z} \quad (97)$$

$$4I_{1z}I_{2z}I_{3y} \xrightarrow{90^\circ_x} 4I_{1y}I_{2y}I_{3z} \xrightarrow{t_1} 2I_{1x}I_{2y} \xrightarrow{90^\circ_x} 2I_{1x}I_{2z} \quad (98)$$

Similarly, for the "remote" peak at coordinates $(\Omega_2+\Omega_3,\Omega_1)$ one obtains (99). The resulting signal is in absorption in both dimensions and in-phase with respect to both couplings in ω_1. Still another transfer route is conceivable [Eq. (100)]. Now dispersion is found in ω_1, absorption in ω_2, and antiphase with respect to both couplings. Again, the cross peak is a mixture of multiplets with different phases and fine structure.

$$4I_{1y}I_{2z}I_{3z} \xrightarrow{90^\circ_x} 4I_{1z}I_{2y}I_{3y} \xrightarrow{t_1} 4I_{1z}I_{2y}I_{3y} \xrightarrow{90^\circ_x} 4I_{1y}I_{2z}I_{3z} \quad (99)$$

$$2I_{2x}I_{3z} \xrightarrow{90^\circ_x} 2I_{2x}I_{3y} \xrightarrow{t_1} 4I_{1z}I_{2y}I_{3y} \xrightarrow{90^\circ_x} 4I_{1y}I_{2z}I_{3z} \quad (100)$$

Because of the different mapping of connectivities in the spectrum, double-quantum spectroscopy is sometimes used to simplify assignments in complex spectra. The use of multiple-quantum spectroscopy is however not widespread, mainly because of the complex multiplet structures of the cross peaks, the dependence of the cross signal intensities upon the length of the delays in the preparation sandwich, the need for phase increments smaller than 90°, and the inconveniency in connection with the evaluation of the ω_1 chemical shift. The use of a z-filter offers some improvement with respect to the phases of the cross peaks.[293]

3.2. Heteronuclear Experiments

Almost all the heteronuclear 1D and 2D NMR techniques are also associated with coherence transfer. Optimal sensitivity of the measurement of heteroatoms is of particular importance, for they practically all (except tritium) have smaller gyromagnetic ratios γ than the proton, and their natural abundance is often very small.

We first comment on the sensitivity of heteronuclear NMR experiments in general. The "global" sensitivity factor of any NMR experiment is $\gamma^{5/2} B_0^{3/2}$. It contains a factor γ, which stems from the polarization at thermal equilibrium. For experiments which start with heteronuclear excitation, the polarization at thermal equilibrium is given by $\gamma_X S_z$, where S stands for the heteronuclear magnetization.

If, however, the experiment starts with proton magnetization, then the corresponding polarization is $\gamma_H I_z$ (I for proton magnetization). Thus the gain in sensitivity in experiments that start with proton rather than heteronuclear magnetization is γ_H/γ_X. The remaining factor $\gamma^{3/2}$ in the global sensitivity is due to detection; when multiplied by the gyromagnetic ratio of the excited nucleus it is proportional to the signal-to-noise ratio (S/N). In conventional heteronuclear experiments the heteronucleus is detected and the factor is $\gamma_X^{3/2}$. In "inverse" spectroscopy protons are detected, and the factor is $\gamma_H^{3/2}$. Thus an additional gain in sensitivity of $\gamma_H^{3/2}/\gamma_X^{3/2}$ is obtained in indirectly detected versus conventionally detected spectra[46] (see Section 3.2.1).

Practically all the homonuclear experiments discussed so far have heteronuclear analogues. A proton pulse of angle β in the homonuclear experiment is analogous to simultaneous pulses of angle β on *both* protons and heteronuclei in the heteronuclear experiment. It follows that every homonuclear 2D NMR experiment can readily be transferred to a heteronuclear system. However, often these direct transfers do not represent the optimum in terms of sensitivity. A nonselective pulse in homonuclear experiments operates equally (neglecting off-resonance effects) on all the nuclei. In contrast, in heteronuclear experiments the two different nuclei can be operated on separately. This leads in certain cases to an enormous gain in sensitivity.

The heteronuclear analogue of the homonuclear COSY experiment (90°(^{1}H)-t_1-90°(^{1}H,^{13}C)-t_2) would only yield, for an HC fragment, one-fourth of the intensity obtained by the conventional H,C shift correlation technique.

A second property of heteronuclear systems, which is significant for the arrangement of pulse sequences, is the large difference in magnitude between direct couplings over one bond, $^1J_{HX}$, and what is termed in heterosystems "long-range coupling" over n bonds ($n \geq 2$), $^nJ_{HX}$. Therefore, to a first approximation, H_nX units can be treated as isolated systems. In addition, the variation in $^1J_{HX}$ is limited, in favorable cases, within a narrow range (the $^1J_{HP}$ coupling is an exception).

3.2.1. The Role of 180° Pulses

Let us first treat the role of 180° pulses in heteronuclear pulse sequences. The effect of a 180°$_I$ pulse on the evolution of chemical shift of spin I after time t (the chemical shift of the heterospin S is obviously unaffected) is shown in (101). Thus a time reversal of period t before the 180° pulse takes place [cf. Eq. (76) and (77)].

$$I_x \cos \Omega t + I_y \sin \Omega t \xrightarrow{180°_{x,y}} \pm (I_x \cos \Omega(-t) + I_y \sin \Omega(-t)) \quad (101)$$

The homonuclear I coupling remains, as we saw earlier, unaffected. The same is true also for homonuclear S coupling. The heteronuclear coupling, however, behaves differently [Eq. (102)]. The corresponding expression for the 180° (S) pulse is (103). Thus, in contrast to homonuclear coupling, after time t and a 180° pulse on one of the heteronuclear species the heteronuclear coupling has evolved backwards, just like chemical shift. It can hence be refocused by a sequence Δ-180°(I)-Δ or Δ-180°(S)-Δ.

$$I_x \cos \pi Jt + 2I_yS_z \sin \pi Jt \xrightarrow{180°_{x,y}(I)} \pm (I_x \cos \pi Jt + 2I_yS_z \sin \pi Jt) = \pm (I_x \cos \pi J(-t) + 2I_yS_z \sin \pi J(-t)) \quad (102)$$

$$S_x \cos \pi Jt + 2S_yI_z \sin \pi Jt \xrightarrow{180°_{x,y}(S)} \pm (S_x \cos \pi Jt + 2S_yI_z \sin \pi Jt) = \pm (S_x \cos \pi J(-t) + 2S_yI_z \sin \pi J(-t)) \quad (103)$$

Two simultaneous 180° pulses on both spins have the same effect as one 180° pulse in a homonuclear system: refocusing of chemical shift, no effect on homo- or heteronuclear coupling.

A final comment: The rules for phase cycling can readily be transferred to heterosystems. It is recommended to use two "staffs" in heteronuclear systems, since the different nuclei are separately excited by pulses.

There are essentially two 1D NMR techniques which perform heteronuclear coherence transfer: INEPT and DEPT.

3.2.2. INEPT

Coherence Transfer in Heteronuclear Spin Systems through $^1J_{CH}$ Couplings

The pulse sequence for INEPT[294] is (P11). It corresponds to COSY: a 90° excitation pulse and a 90° pulse on each of the two nuclei for the coherence transfer. The 180° pulses serve merely for the refocusing of the chemical shift evolution.

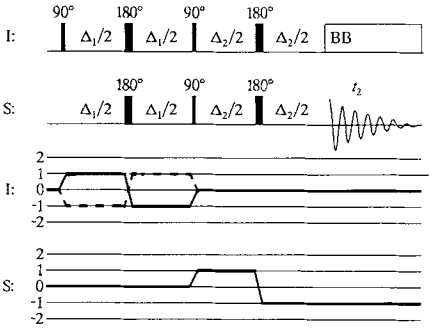

(P11)

We now analyze the INEPT experiment in terms of the product operator formalism. The starting magnetization at thermal equilibrium is $\gamma_I I_z + \gamma_S S_z$. The 90°$_y$ I pulse generates transverse I-spin magnetization: $\gamma_I I_x$. The S-spin magnetization remains longitudinal and can be suppressed by phase cycling (x, −x for the first pulse). During the following period $\Delta_1/2$-180°(I,S)-$\Delta_1/2$, heteronuclear coupling $^1J_{IS}$ as well as homonuclear coupling $^nJ_{II}$ evolve, while chemical shifts for both nuclei are refocused. If the direct heteronuclear coupling $^1J_{IS}$ is large relative to the heteronuclear long-range coupling $^nJ_{IS}$ and the homonuclear coupling J_{II}, one obtains Equation (104). As usual only the antiphase term is effective in the polarization transfer [Eq.

(105)]. The phase of the second 90° pulse must be shifted by 90° relative to the first one.

$$I_x \longrightarrow I_x \cos \pi^1 J_{IS}\Delta_1 + 2I_yS_z \sin \pi^1 J_{IS}\Delta_1 \quad (104)$$

$$2I_yS_z \xrightarrow{90°_x(I,S)} -2I_zS_y \quad (105)$$

The sequence that follows $\Delta_2/2$-180°(I,S)-$\Delta_2/2$ results in refocusing of the heteronuclear coupling into detectable in-phase magnetization of spin S [Eq. (106)].

$$-2I_zS_y \longrightarrow -2I_yS_z \cos \pi J_{IS}\Delta_2 + S_x \sin \pi J_{IS}\Delta_2 \quad (106)$$

The broadband decoupling at the beginning of the acquisition time destroys all the I-spin magnetization. This means that all the product operators that contain I-spin operators are destroyed, and hence can be left out.

The delays Δ_1 and Δ_2 can be set to $\Delta_1 = \Delta_2 = (2J)^{-1}$ so that all the transfer factors equal 1 ($\sin \pi J\Delta = 1$, $\cos \pi J\Delta = 0$); the full factor γ_I/γ_S is gained in sensitivity relative to a broadband decoupled spectrum (without NOE), because of the initial excitation of the I spin. A factor 4 is obtained for $^1H/^{13}C$, and a factor 10 for $^1H/^{15}N$.

When several I nuclei are bound to one S nucleus, care must be taken that the passive I spins contribute a $\cos \pi J\Delta_2$ term during the delay Δ_2. Hence we find for an SI_n group (only relevant operators are observed) Equation (107).

$$n\gamma_I I_z \xrightarrow{90°_x(I)} -n\gamma_I I_y \xrightarrow{\Delta_1} n\gamma_I 2I_xS_z \sin \pi^1 J_{IS}\Delta_1 \xrightarrow{90°(I,S)}$$
$$n\gamma_I 2I_zS_y \sin \pi^1 J_{IS}\Delta_1 \xrightarrow{\Delta_2} -n\gamma_I S_x \sin \pi^1 J_{IS}\Delta_1 \sin \pi^1 J_{IS}\Delta_2 \cos^{n-1} \pi^1 J_{IS}\Delta_2 \quad (107)$$

This transfer function is the key to editing methods, which enable sorting of signals according to the number of I nuclei connected to S. We note the analogy to multiple-quantum filters. Here, however, we are no longer dealing with a high-pass filter, but with a band-pass filter, which selects product operators with *exactly* n operators. With $\pi^1 J_{IS}\Delta_2 = \Theta$ and neglecting the factor $\gamma_I \sin \pi^1 J_{IS}\Delta_1$, which is anyhow always the same, we obtain the factor $n \sin \Theta \cos^{n-1} \Theta$ for the signal intensity.

The cosine factor is negative for $\Theta > 90°$. It follows that $\cos^{n-1} \Theta$ responds to the multiplicity of the S nucleus, i.e., to the number of I nuclei connected to S. Negative signals are obtained for even n, and positive ones for odd n. A selection according to multiplicity is achieved through the combination of spectra with different Θ values. This is done by adding three successive experiments with different Θ values (for the sake of simplicity we use here degrees rather than radians):

$$\Theta_1 = +\Theta;\ \Theta_2 = 90°;\ \Theta_3 = 180° - \Theta$$

If $\Theta = 345°$ is chosen, the coefficients shown in Table 6 are obtained. From the Table we see that the spectrum for SI_3 groups is obtained according to (108), while for SI groups

Table 6. Relative signal intensities for the INEPT experiment as a function of $\Theta = \pi J_{HC}\Delta_2$.

	n	Θ 45°	Θ 90°	Θ 135°
CH	1	$1/\sqrt{2}$	1	$1/\sqrt{2}$
CH_2	2	1	0	−1
CH_3	3	$3/(2\sqrt{2})$	0	$3/(2\sqrt{2})$

it is spectrum(90°). The spectrum for SI_2 groups is always obtained by subtraction of the spectrum for Θ_1 from the one for Θ_3.

$$\text{spectrum}(45°) + \text{spectrum}(135°) - \text{spectrum}(90°) \cdot \sqrt{2} \quad (108)$$

It should further be noted that the quality of the editing by INEPT depends on the assumption of equal coupling constants. A 10% variation in coupling constants changes the angles $\Theta = 45°$, 90°, and 135° to ca. $\Theta \approx 40°$, 80°, and 120°, respectively. The corresponding signal intensities are shown in Table 7. Clearly, the signal suppression under these conditions is no longer complete.

Table 7. Relative signal intensities with editing using the INEPT sequence assuming a 10% deviation of the coupling from the ideal value.

	Intensity of CH	CH_2	CH_3
CH subspectrum	0.99	0.3	0.07
CH_2 subspectrum	−0.2	1.88	0.43
CH_3 subspectrum	0.1	−0.34	1.72

Transfer through Long-Range Couplings

Magnetization can obviously also be transferred in the INEPT experiment from the I spin to the S spin through long-range couplings $^nJ_{IS}$.[188] The delays must be changed for this purpose. In contrast with transfer through direct couplings, homonuclear I,I couplings must also be taken into account, for they are in general of the same order of magnitude as the heteronuclear long-range couplings.

The amplitude for a transfer from I_k to S_i in the INEPT experiment is given by (109). The optimal setting of the delays depends on the actual coupling constants. When these are known approximately, the delays can be optimized, whereby due to relaxation short delays should be preferred.

$$\sin \pi J_{I_kS_i}\Delta_1 \prod_i \cos \pi J_{I_kI_i}\Delta_1 \sin \pi J_{I_kS_i}\Delta_2 \prod_i \cos \pi J_{I_iS_i}\Delta_2 \quad (109)$$

The excitation pathway is not evident from the INEPT experiment; i.e., it is not known from which I spin the measured magnetization was transferred to the S spin. If, however, clarification of this pathway is desired for the elucidation of connectivities, either a selective INEPT or a 2D NMR experiment must be performed.

Selective INEPT

In this method all the I pulses are replaced by selective pulses on I_k.[295,296] In this way all the passive I spins relate to the S spin as well as to the I_k spin as heterospins. The transfer amplitude is thus simplified to (110); i.e., the in-

$$\sin \pi J_{I_kS_i}\Delta_1 \sin \pi J_{I_kS_i}\Delta_2 \quad (110)$$

tensity in this spectrum is substantially higher than in INEPT with nonselective, "hard" pulses. In addition, due to the choice of a particular proton signal for the selective excitation, the transfer pathway is unequivocal. A prerequisite is, of course, a sufficiently resolved proton spectrum.

3.2.3. 2D Variants of INEPT: COLOC

The second possibility to separate the transfer pathways is the constant time 2D variant of INEPT, the COLOC experiment.[189] In the constant time 2D NMR experiment the total evolution time is constant. Evolution of chemical shift is achieved by a 180° pulse, which is shifted within the delay (see Section 3.1.5). In the heteronuclear experiment, after the initial INEPT excitation, two 180° pulses are simultaneously shifted, one for protons and the other for the heteronucleus. Hence the COLOC pulse sequence (P12) is obtained.

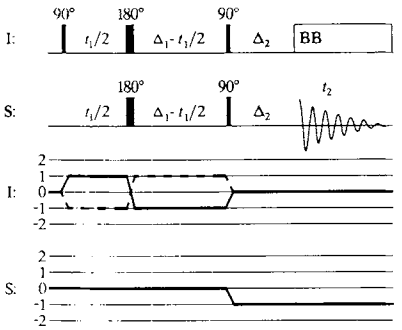

(P12)

There is a direct analogy with the ω_1-decoupled homonuclear COSY experiment (Section 3.1.5): here, too, the cross signals in ω_1 are decoupled (no homonuclear I coupling). The transfer amplitude is, except for the term for chemical shift evolution, the same as for the INEPT experiment. All the signals appear in one spectrum, which makes up for the lower intensity relative to the selective INEPT experiment. However, the selective INEPT experiment is more sensitive if one is only interested in a few correlations, ignoring the greater effort in setting up the experiment.

3.2.4. DEPT

We saw in Section 3.2.2 that the quality of spectral editing in INEPT depends strongly on variations in the coupling constants. The DEPT sequence[297–299] (P13) does not suffer from this disadvantage.

Let us analyze the sequence for an SI_n group. Since the two 180° pulses serve only for the refocusing of chemical

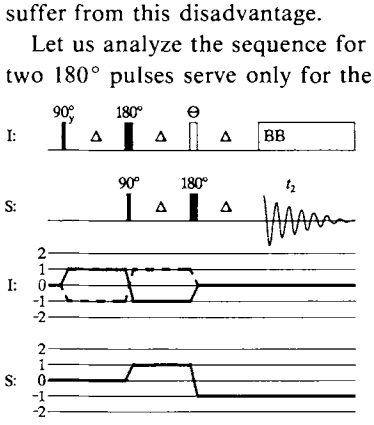

(P13)

shift, we will ignore them in the following discussion, as well as the evolution of chemical shift. The delay should be $\Delta=(2\,{}^1J_{IS})^{-1}$. Equation (111) is obtained. The cosine

$$n\gamma_I I_z \xrightarrow{90°_y(I)} n\gamma_I I_x \xrightarrow{\Delta} n\gamma_I 2I_y S_z \xrightarrow{90°_y(S)} n\gamma_I 2I_y S_x \xrightarrow{\Delta}$$
$$n\gamma_I 2^n I_y S_{x,y}(I_z)^{n-1} \xrightarrow{\Theta_x} 2^n S_{x,y}(I_z)^n n\gamma_I \sin\Theta\cos^{n-1}\Theta \xrightarrow{\Delta} S_x n\gamma_I \sin\Theta\cos^{n-1}\Theta \quad (111)$$

term results from the coupling of protons that do not participate in the generation of heteronuclear antiphase terms $2I_yS_z$, which is effective in the second half of the pulse sequence in transverse $S_{x,y}$ coherence. The transfer function is, like in the INEPT experiment, $\sin\Theta\cos^{n-1}\Theta$; however, here Θ is a tuneable pulse angle, *independent* of J.

So far we have not discussed the J dependence in the transfer amplitude. J was set equal to $(2\Delta)^{-1}$. We repeat the analysis and focus now on terms which originate from SI_n groups, but appear in the edited spectrum as an SI_m group. Such a "cross talk" is possible in an n-spin system when a product operator $S_yI_y(I_z)^{m-1}$ appears before the Θ pulse. It follows immediately that $n \geq m$. This operator behaves in the editing process like an SI_m group. It is built up as shown in (112). When we again assume the values 45°, 90°, and 180°[300] for Θ and a 10% deviation of the coupling constants from the ideal ${}^1J_{IS}=(2\Delta)^{-1}$ is considered, we obtain the

$$n\gamma_I I_z \xrightarrow{90°_y(I)} n\gamma_I I_x \xrightarrow{\Delta} n\gamma_I 2I_y S_z \sin\pi J\Delta \xrightarrow{90°_y(S)} n\gamma_I 2I_y S_x \sin\pi J\Delta$$
$$\xrightarrow{\Delta} n\,\gamma_I\binom{m-1}{n-1}(\sin\pi J\Delta)^m(\cos\pi J\Delta)^{n-m}\,2^m I_y S_x(I_z)^{m-1}$$
$$\xrightarrow{\Theta(I)} n\,\gamma_I\binom{m-1}{n-1}(\sin\pi J\Delta)^m(\cos\pi J\Delta)^{n-m}\,2^m S_x(I_z)^m \sin\Theta\cos^{m-1}\Theta \quad (112)$$
$$\xrightarrow{\Delta} n\,\gamma_I\binom{m-1}{n-1}(\sin\pi J\Delta)^{2m}(\cos\pi J\Delta)^{2(n-m)} S_x \sin\Theta\cos^{m-1}\Theta$$

editing results summarized in Table 8. This result is significantly better in comparison with the INEPT experiment (see Table 7). Further improvement is achieved through DEPT-GL.[301]

Table 8. Relative signal intensities with editing using the DEPT sequence assuming a 10% deviation of the coupling from the ideal value.

	Intensity of		
	CH	CH_2	CH_3
CH subspectrum	1.0	0.02	0.002
CH_2 subspectrum	0.0	1.9	0.14
CH_3 subspectrum	0.0	0.0	2.89

3.2.5. Heteronuclear Shift Correlation

Both INEPT and DEPT serve as the one-dimensional precursor of heteronuclear shift correlation via ${}^1J_{IS}$ coupling. A 2D NMR experiment is formed by the introduction of a variable evolution period (t_1) after the 90° preparation pulse. Decoupling of the heteronuclear coupling in ω_1 is achieved by a 180° pulse on the heteronuclei in the middle of t_1. The spectra that are obtained show no heteronuclear coupling in ω_1. Starting from the INEPT sequence we obtain the pulse sequence for the H,X-COSY experiment[162, 172, 1737][*] (P14), and starting from the DEPT

[*] We use here the term COSY (*C*orrelated *S*pectroscop*y*) also for heteronuclear experiments. Often this term is used only for homonuclear experiments. For H,X-COSY one often finds other expressions in use, such as HETCOR or simply shift correlation.

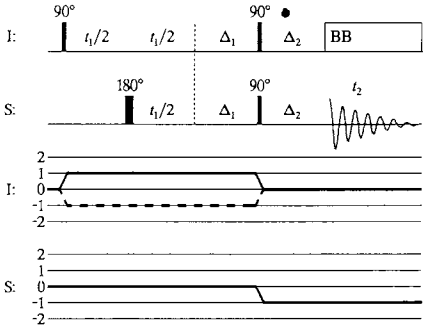

(P14)

sequence that for the DEPT-COSY experiment is obtained,[174-177] (P15) and (P16). The same spectrum is obtained from pulse sequences (P15) and (P16), although (P16) has one pulse less. The evolution of proton chemical shifts takes place in (P15) before the generation of transverse heteronuclear magnetization; in (P16) the two blocks are exchanged.

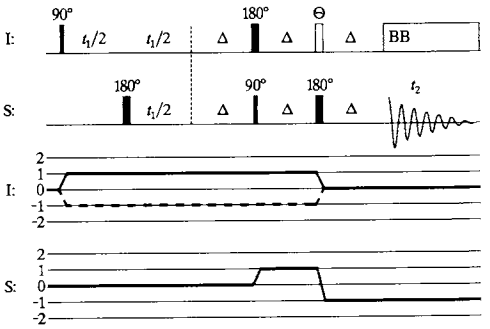

(P15)

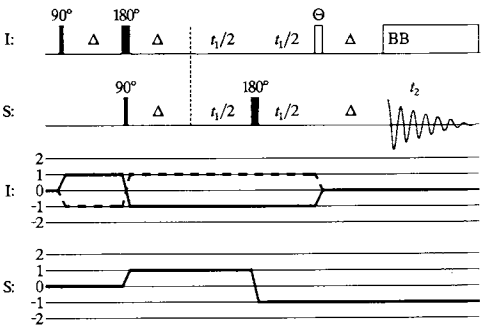

(P16)

The DEPT-COSY sequence is fully refocused; i.e., for $t_1 = t_2 = 0$ no chemical shift evolves. This is an advantage for the phase correction, since only small frequency-dependent phase correction values are obtained. Spectrum editing is equally possible as in the 1D variant.[302] In contrast, the INEPT sequence is less suitable for pure phase 2D spectra, since for $t_1 = t_2 = 0$ proton chemical shift evolves in Δ_1 as well as heteronuclear chemical shift in Δ_2. This introduces a large first-order phase correction in ω_1 and ω_2.[171, 172]

The COLOC sequence and its variant with a BIRD pulse (see Section 3.2.8) can also be used for heteronuclear shift correlation via one bond,[180] if the requirement for resolution in t_1 (protons) is sufficiently small. We only see an advantage in the constant time variants of INEPT and DEPT transfers if the $^1J_{IS}$ dependence of the transfer amplitude is eliminated through the application of a pair of time-shifted "wandering" 180° pulses.[181]

3.2.6. *Heteronuclear Relayed Experiments*

H-Relayed H,X-COSY

Other heteronuclear experiments can be designed through combinations of pulse sequences. Thus by inserting an additional H,H polarization transfer in the H,X-COSY sequence we arrive at the H-Relayed H,X-COSY sequence[213, 214] (P17). After evolution with heterodecou-

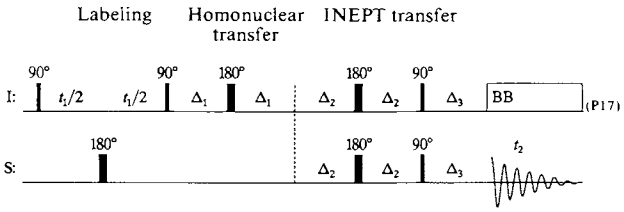

(P17)

pling, polarization is transferred from spin I^1 to other I spins coupled to I^1. The evolution of I-spin chemical shift is refocused in this relay transfer by the first 180° (I) pulse. It is advantageous to refocus the I-spin chemical shift also in the INEPT transfer which follows.[216, 217] The two 180° I-refocusing pulses can be replaced by a single 180° pulse in the middle of the delays ($2\Delta_1$ and $2\Delta_2$), without changing the net effect. Since any addition of pulses to a sequence is a further possible source of artifacts, sequences with fewer pulses are generally preferred. Thus the sequence (P18) is obtained for the heteronuclear H-Relayed H,X-COSY experiment, with $\Delta = \Delta_1 + \Delta_2$.[215, 216] An example of an H-Relayed H,X-COSY is shown in Figure 35b.

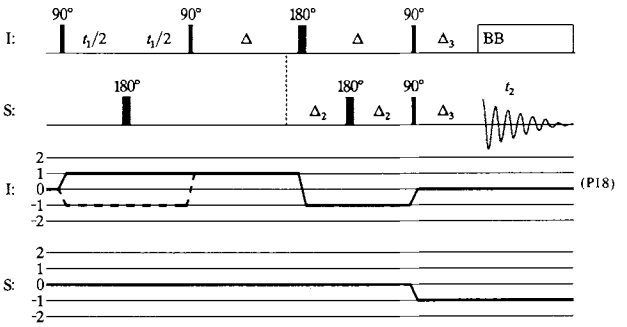

(P18)

We find that in comparison with the H,C-COSY spectrum (Fig. 35a) additional signals, so-called relayed peaks, appear, which are marked by arrows. They are formed by H^1-H^2-C^2 fragments and hence provide indirect information on carbon connectivity.[215] For example, all proton signals and carbon signals of the tetrabenzylglucose ring were assigned as shown in Figure 35. However, the signals due to direct H^2,C^2 coupling are also seen in the spectrum. This is due to the fact that relayed transfer uses single-quantum coherence, like the magnetization remaining on H^1, and thus selection through phase cycling is impossible (see homonuclear relayed experiment). If necessary, the H,X-COSY parts can be filtered with a low-pass *J*-filter, taking advantage of the different magnitudes of the coupling constants (e.g., $^1J_{HC}$ and $^nJ_{HC}$) (see Section 3.2.8).

X-Relayed H,X-COSY

A further variant of the heteronuclear relayed spectroscopy is the X-Relayed H,X-COSY experiment.[222, 223] The pulse sequence is (P19). This experiment, like the INADE-

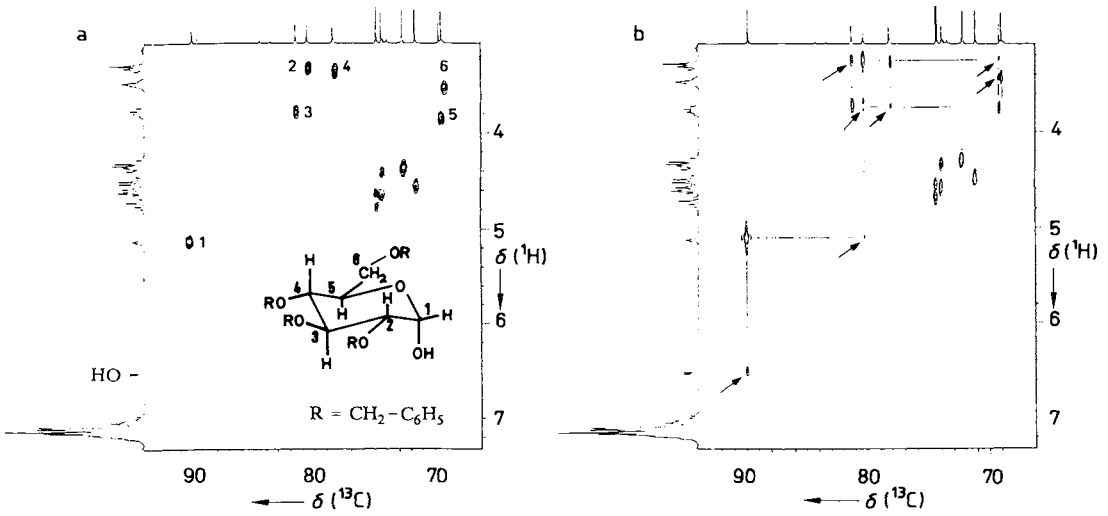

Fig. 35. a) H,C-COSY and b) H-Relayed H,C-COSY of tetrabenzylglucose in [D$_6$]DMSO. The CH cross-signal assignment of the sugar is given in (a). It follows directly from the relayed spectrum (b) without additional assumptions, when the proton signal intensities are consulted (signal 6 is due to two protons attached to one carbon and can hence serve as a starting point for the sequential assignment).

QUATE experiment, serves to resolve connections in which quaternary carbons participate. It also enables extraction of $^1J_{CC}$ coupling constants.

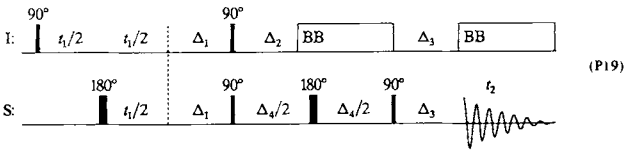

(P19)

3.2.7. Heteronuclear NOESY

The heteronuclear NOESY experiment (P20)[203–207,368] is almost a direct conversion from the homonuclear experiment (P2). Heteronuclear NOEs are often too small to produce useful signals in spectra of larger molecules.

3.2.8. Filters and Their Applications

The low-pass J-filter[303] and BIRD pulses[304] serve to modify the heteronuclear pulse sequences discussed so far. In cases of large differences between $^1J_{IS}$ and $^nJ_{IS}$ and extreme dilution of the S spin, it is possible to selectively manipulate those I spins which have a $^1J_{IS}$ coupling with an S spin. In the isotopomer (**A**) in Figure 36 it is possible to discriminate H^1 and H^2 from H^3, since the first two have a $^1J_{CH}$ coupling, whereas H^3 does not. The opposite is true for the isotopomer **B**.

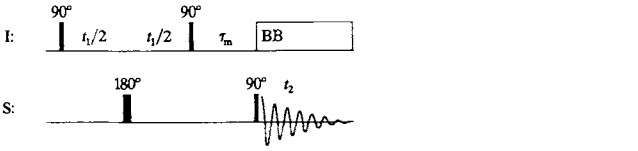

(P20)

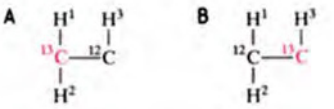

Fig. 36. Different isotopomers of a CH_2CH fragment. The different signals in a ^{13}C-NMR spectrum arise from different isotopomers of the compound investigated.

BIRD

Let us consider the "pulse sandwich"[304] (P21) with $\Delta=(2\,^1J_{IS})^{-1}$. This $BIRD_x$ pulse is essentially a 360° pulse

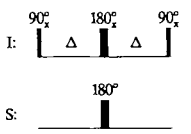

(P21)

for I spins which are not directly connected to an S spin (due to the short delays, long-range and homonuclear couplings can be neglected to a good approximation). For an I spin which is connected to an S spin through $^1J_{IS}$, however, we obtain (for $\Delta=(2J)^{-1}$) Equations (113) and (114). Thus the $BIRD_x$ pulse acts as a 180°_y pulse for I spins which are coupled with S, while for I spins which are not coupled with S it acts as a 0° pulse.

$$I_x \xrightarrow{90^\circ_x} I_x \xrightarrow{\Delta} 2I_yS_z \xrightarrow{180^\circ_x(I,S)} 2I_yS_z \xrightarrow{\Delta} -I_x \xrightarrow{90^\circ_x} -I_x \quad (113)$$

$$I_y \xrightarrow{90^\circ_x} I_z \xrightarrow{\Delta} I_z \xrightarrow{180^\circ_x(I,S)} -I_z \xrightarrow{\Delta} -I_z \xrightarrow{90^\circ_x} I_y \quad (114)$$

If the phase of the 180° pulse is changed to y ($BIRD_y$, P22), the effect of the BIRD sequence is reversed. Now I

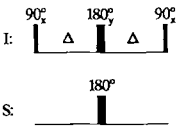

(P22)

spins with $^1J_{IS}$ remain unaffected, and those without $^1J_{IS}$ undergo inversion. (P23) is yet another representation of $BIRD_y$ and (P24) of $BIRD_x$. Applications of BIRD pulses

are presented in the following sections, dealing with proton-carbon correlations.

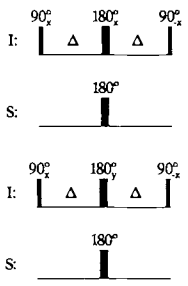

(P23)

(P24)

ω_1-Decoupled Shift Correlation

In H,C shift correlation the spectra of different isotopomers overlap to yield the final spectrum. A line in the ^{13}C-NMR spectrum means that only that carbon in the molecule is a ^{13}C isotope. Only those protons which are directly bound to the ^{13}C atom can be called "carbon bearing," in our way of speech; all the others are not.

ω_1-Decoupling in shift correlation[178] (P25) is achieved by a selective inversion of the passive protons after $t_1/2$, while the active protons are left unaffected.[178-180] This is done with the BIRD$_y$ sandwich. The necessary 180°(S) pulse gives with the 180°(S) decoupling pulse a 360° pulse, and hence can be left out. Homonuclear coupling between geminal protons is not refocused, since geminal protons are always both carbon-bearing. The same concept can be applied in the DEPT-COSY experiment.[305]

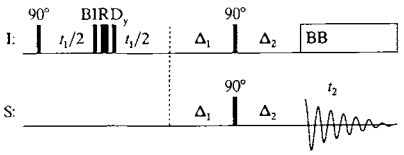

(P25)

COLOC with Protonated Carbons

During the refocusing period Δ_2 in the COLOC experiment also the rapidly oscillating $^1J_{CH}$ couplings evolve with the amplitude $\cos\pi\,^1J_{CH}\Delta_2$. Even a small scatter in $^1J_{CH}$ will therefore have a strong effect on the transfer amplitude. The problem can be solved with a BIRD$_x$ pulse,[195] which inverts protons bound to ^{13}C. In this way the $^1J_{CH}$ couplings are selectively refocused in Δ_2,[194, 195, 306-308] while the long-range couplings remain unaffected.

The BIRD$_y$ pulse in t_1 of the COLOC experiment serves also to discriminate between $^2J_{CH}$ and $^3J_{CH}$ couplings in long-range correlations to proton-bearing ^{13}C nuclei (XCORFE[194]). The pair of wandering 180° pulses in the COLOC sequence is replaced by a BIRD$_y$ pulse. The latter has no effect on protons directly bound to ^{13}C (H^1 in the fragment ^{13}CH^1-^{12}CH^2-^{12}CH^3), as opposed to the other protons. Now protons H^2, which are coupled to H^1 and inverted by the BIRD$_y$ pulse, evolve $^3J_{H^1H^2}$ coupling. If this coupling is large enough, then splitting of the CH^2 cross signal is observed (doublet for ^{13}CH-^{12}CH^2, double doublet for ^{13}CH$_2$-^{12}CH^2, etc.). However, protons that are coupled to that carbon through $^3J_{CH}$ (e.g., in the fragment H^{12}C-^{12}C-^{13}CH$_n^1$) transmit to the corresponding proton H^1 only a negligibly small $^4J_{HH}$ coupling, which does not lead to measurable splitting.[194] In this way the coupling via two bonds can be discriminated from that via three bonds.

Low-Pass J-Filter

It is sometimes desirable, in correlation experiments involving long-range couplings as well as in relayed spectroscopy, to suppress direct I,S correlations, for they generally lead to strong cross signals and thus may interfere with weaker signals. $^1J_{IS}$ cross signals can be suppressed with the low-pass *J*-filter[303] (P26). For $\Delta=(2\,^1J_{IS})^{-1}$, pro-

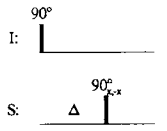

(P26)

tons directly bound to ^{13}C appear after the 90° S pulse as I_xS_y or as $-I_xS_y$, depending on the pulse phase. Thus the magnetization of the I spin directly bound to the S spin is totally destroyed through addition. However, the magnetization of I spins that are coupled to S spins with long-range couplings is only slightly attenuated, by the factor $\cos^n\pi J_{IS}\Delta$.

Low-pass *J*-filters are easy to install in ^{1}H,^{13}C correlation experiments, since the $^1J_{CH}$ and $^nJ_{CH}$ coupling constants lie within narrow ranges. Details about the optimization of these filters can be found in Ref. [303]. They are used in heteronuclear relayed[303] and in COLOC spectroscopy.[197]

3.2.9. Composite Pulses

So far we have worked only with ideal pulses; for example, a 90° pulse should be exactly 90° for all of the nuclei of one type, should have no phase distortions, and should be of zero length. In real pulses there are complications due to off-resonance effects and B_1 inhomogeneity. Off-resonance effects arise because the chemical shift is not "turned off" during the pulse. As a result the magnetization rotates about a tilted field and by a greater angle than the nominal pulse angle. Inhomogeneities in B_1 arise from imperfect coils, which do not generate a constant field within a given volume, and outside this volume generate no field at all.

Composite pulses serve to remove these imperfections. The literature is quite extensive.[333] Yet, with the exception of decoupling and TOCSY sequences, composite pulses have rarely been used. We therefore limit the discussion to a few examples.

180° Pulse

The most common pulse is 90°_x-180°_y-90°_x.[309-327] It achieves an inversion of z magnetization over a large chemical-shift range, and is moderately sensitive to B_1 inhomogeneities. It is applied, for instance, in T_1 measurements of ^{13}C resonances and in shift correlations in the middle of t_1.

90° Pulse

The 90° pulse is substantially self-compensating against offset effects. Similar compensation against B_1 inhomogeneities is achieved through the sequence 90°_x-90°_y.[309,310] Note that this pulse is exactly one-half of the composite inversion pulse.

One must be careful in the construction of pulse sequences with composite pulses, since straightforward substitution of simple pulses by composite pulses does not lead to the goal. The reason is that these pulses introduce additional phases. An example of the construction of a pulse sequence with composite pulses can be found in Ref. [320]. Composite pulses with essentially no phase distortions, as well as pulses that compensate for both offset effects and B_1 inhomogeneities, are discussed in Refs. [312, 323, 326].

3.2.10. Heteronuclear Decoupling

Most of the heteronuclear experiments work with heteronuclear broadband decoupling during detection. The removal of the heteronuclear coupling leads to an increase in intensity, since the multiplet structure due to heteronuclear coupling collapses. The difficulty in broadband heteronuclear decoupling arises from the sometimes huge chemical shift range of the decoupled nucleus. Thus at 300 MHz, for instance, the proton shift range is ca. 3 kHz, whereas for ^{13}C it is 15 kHz and for ^{19}F approximately 60 kHz. On the other hand, the decoupler cannot operate at excessively high power levels because of heating of the sample. The main goal here is to find decoupling sequences which are, as much as possible, offset independent.

This goal is, to state it in a simple way, to keep the decoupled spin rotating in such a way that its α and β states are equally populated. The exchange between α and β states must be faster than the spin-spin interaction, since the multiplet structure (e.g., of a ^{13}C multiplet) depends on the fact that the α and β states of the coupled nucleus are well defined.

The first method introduced for heteronuclear broadband decoupling through stochastic modulation of the decoupler field[328] yielded good results. The decoupled spins are stochastically led around the unit sphere such that all of the orientations of the magnetization are equally probable.

Soon better methods were developed, utilizing composite-pulse decoupling sequences. The first of these sequences, MLEV with 16 composite pulses, uses the composite 180° pulse $(90^\circ_x\text{-}180^\circ_y\text{-}90^\circ_x)$[309,315] to achieve an inversion of the spins to be decoupled with as little as possible offset dependence. A sophisticated expansion[283,284] leads to compensation for imperfections of ever higher order. The band width of MLEV-16 is about $\pm\gamma B_2$, which is the strength of the decoupler field.

Another method, which is now generally used for decoupling of ^{13}C-NMR spectra, is WALTZ-16. Here, in contrast to the MLEV sequences, 90° pulses are permuted. The basic inversion pulse is $90^\circ_x\text{-}180^\circ_x\text{-}270^\circ_x$. WALTZ, like MLEV, has an offset range of $\pm\gamma B_2$. However, the scaling of the coupling is by far better. Precision measurements showed ^{13}C-NMR line broadening of only ca. 10 mHz.[329-321]. WALTZ is also significantly less sensitive to phase errors than MLEV.[333]

The GARP sequence[332] is particularly suitable for very large spectral ranges. It decouples over a range of $\pm 2.5\gamma B_2$, and can hence be applied, for example, for ^{13}C decoupling in proton-detected C,H experiments.

Ref. [333] provides a very good review of decoupling sequences.

3.2.11. Inverse Spectroscopy

All of the heteronuclear spectroscopic methods discussed so far involve the excitation of proton magnetization and the observation of heteronuclear magnetization. When one estimates the sensitivity of a given pulse sequence, there is a factor $\gamma_H(\gamma_X)^{3/2}$ in addition to the specific transfer function of the sequence. Inverse spectroscopy starts likewise with proton magnetization, but also detects proton magnetization, whereby $(\gamma_H)^{5/2}$ is obtained for the sequence-independent sensitivity factor. The factor is thus eight times greater in proton-detected C,H correlation than in conventional spectroscopy. It is, of course, even greater for heteronuclei with smaller γ, e.g., ^{15}N. This substantial gain in sensitivity makes inverse spectroscopy (sometimes called reverse spectroscopy) very attractive. In samples with small natural abundance, however, the suppression of proton signals from molecules without NMR-active heteroatoms is problematic. Thus for ^{13}C the suppression must be 1 to 200, and in ^{15}N 1 to 600. This places a severe stability requirement on the NMR spectrometer, which, when not met, leads to strong t_1 noise (see Appendix). We shall later show methods to suppress t_1 noise by the modification of the NMR experiment. Often, however, the problem can be solved by enrichment of the NMR-active heteronucleus.

Table 9 compares the relative sensitivities of the various detection methods. The first column gives the general signal-to-noise ratio (S/N), the second shows the resulting amplification factor. The last two columns show, for ^{13}C and ^{15}N measurements, respectively, the theoretical gain in intensity for inverse detection.

The most frequently used sequence (P27) is also the simplest one.

Table 9. Comparison of sensitivities of the various heteronuclear NMR experiments as a function of different excitations and detections.

Experiment	S/N	Amplification factor	^{13}C	^{15}N
a) Direct observation	$\gamma_X(\gamma_X)^{3/2}$		1.0	1.0
b) INEPT	$\gamma_H(\gamma_X)^{3/2}$			
compared with a)		(γ_H/γ_X)	4.0	9.9
c) Inverse INEPT	$\gamma_X(\gamma_H)^{3/2}$			
compared with a)		$(\gamma_H/\gamma_X)^{3/2}$	7.9	31.0
compared with b)		$(\gamma_H/\gamma_X)^{1/2}$	2.0	3.1
d) Inverse shift correlation	$\gamma_H(\gamma_H)^{3/2}$			
compared with a)		$(\gamma_H/\gamma_X)^{5/2}$	31.6	306.0
compared with b)		$(\gamma_H/\gamma_X)^{3/2}$	7.9	31.0

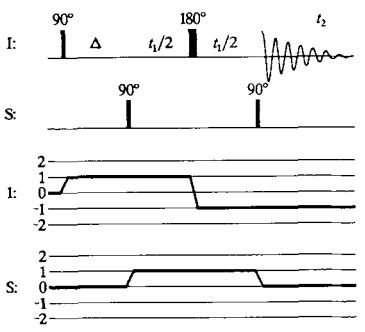

(P27)

We examine only the relevant operators for an $I_k S_i$ cross signal: the transverse proton magnetization following the first 90° pulse evolves homonuclear coupling during $(\Delta + t_1 + t_2$; chemical shift, however, is evolved only during $\Delta + t_2$. The proton network leads therefore to the transfer amplitude (115). This includes all the passive protons. So far the heteronuclear coupling was disregarded, although it is responsible for the cross peak. The active heteronuclear I_h, S_i coupling (J_{ih}) evolves during Δ and contributes a factor $\sin \pi J_{ih} \Delta$ to the transfer amplitude. During t_1 the 180° (I) pulse prevents evolution of heteronuclear coupling. Finally, during t_2 the J_{ih} coupling is refocused and contributes a factor $\sin \pi J_{ih} \Delta t_2$. Combination with Equation (116) leads to the final transfer amplitude (117). The multiplet pattern is like that in a 2D J spectrum

$$\prod_i \cos\{\pi J_{I_k I_i}(t_1 + \Delta + t_2)\} \cos\{\Omega_{I_k}(\Delta + t_2)\} \tag{115}$$

$$\begin{aligned} &I_{kz} \xrightarrow{90°_y} I_{kx} \xrightarrow{\Delta} 2I_{ky}S_{iz} \xrightarrow{90°_y(S)} 2I_{ky}S_{ix} \xrightarrow{t_1} 2I_{ky}S_{ix}\cos\Omega_{S_i}t_1 \\ &\xrightarrow{90°_y(S)} -2I_{ky}S_{iz}\cos\Omega_{S_i}t_1 \xrightarrow{t_2} +I_{kx}\cos\Omega_{S_i}t_1 \sin \pi J_{I_kS_i}t_2 \end{aligned} \tag{116}$$

$$\prod_i \cos\{\pi J_{I_k I_i}(t_1 + \Delta + t_2)\} \cos\Omega_{S_i}t_1 \cos\{\Omega_{I_k}(\Delta + t_2)\} \sin \pi J_{I_kS_i}t_2 \tag{117}$$

(phase-modulated in t_1). It is therefore impossible to obtain pure phases. In the ideal case, in which all of the coupling constants are sufficiently different from each other and greater than the line width, the pattern shown in Figure 37, left, is obtained for a CH^1-CH^2H^3 spin system. Figure 37, right, shows the corresponding pattern which would be obtained in a conventional spectrum.

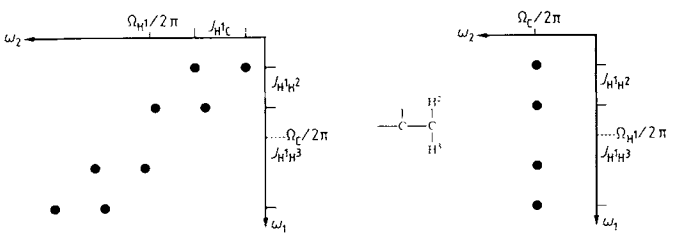

Fig. 37. Schematic representation of the multiplet splitting in the H^1-^{13}C cross signal of a CH^1-CH^2H^3 fragment in an inverse spectrum (left) compared with that in a conventional H,C-COSY spectrum (right).

A factor 4 in sensitivity is gained in the inverse C,H shift correlation; the factor 8 is not gained because the spectrum splits into twice as many lines, as can be seen in Figure 37 (eight lines instead of the four obtained in the usual H,C shift correlation). A factor 16 is obtained for the measuring time, since the sensitivity corresponds to the square root of the measuring time. Such factors in pulse sequences must always be taken into account when an exact comparison of sensitivities is attempted. Thus in the above example only the ^{13}C multiplicity of the protons (in this case 2) is of interest for the comparison of inverse/conventional shift correlation spectroscopy.

A further gain in sensitivity can be reached through the insertion of a refocusing delay after the second 90° S pulse, followed by heterospin decoupling. In this way the $^1J_{IS}$ coupling in ω_2 is removed and, in addition, a factor of 2 in sensitivity is gained. Thus the inverse heteronuclear shift correlation with a refocusing delay should be eight times more sensitive than the conventional shift correlation. This makes even proteins accessible to heteronuclear measurements.[53]

Presaturation of Protons Not Bound to NMR-Active Heteronuclei

A BIRD pulse, which we described earlier in connection with conventional heteronuclear spectroscopy, finds an important use in inverse spectroscopy for reasons mentioned above. By installing a $BIRD_y$ pulse it is possible to eliminate the protons which are not bound to an NMR-active heteroatom. The $BIRD_y$ pulse inverts these protons, and after a delay period of $T_1^H \cdot \ln 2$ the signal due to these protons is minimal (passes through zero). If now the sequence for the inverse shift correlation is started, only coherences due to the protons bound to active heteronuclei are generated. Undesired signals are hence suppressed more effectively.[51] This procedure is only applicable for correlations through direct coupling.

Inverse Correlation through Long-Range Couplings

An increase of the delay Δ enables inverse correlations through heteronuclear long-range couplings. Obviously the common variants, like the low-pass J-filter, can be applied here as well.[196] Long-range couplings contain not only valuable information about constitution, but also about the molecular conformation.[334] Quantitative extraction of heteronuclear long-range coupling constants is possible for the first time with good sensitivity through the use of inverse spectroscopy.[335]

Inverse Relayed Spectroscopy

Relayed spectroscopy has also been successfully carried out in the inverse mode.[53] The suppression of signals due to protons that are not carbon-bearing happens as follows: after the excitation sequence $90°_y(I)$-$\Delta_1/2$-$180°(I,S)$-$\Delta_1/2$ the resulting antiphase magnetization $2I_xS_z$ is transformed by a $90°_y(I)$ pulse into longitudinal two-spin order $(-2I_zS_z)$. The remaining transverse proton magnetization is then destroyed by a homospoil pulse (HS, see Appendix), which results in extensive suppression of signals from protons which are not heteroatom-bearing. The overall pulse sequence is then (P28).

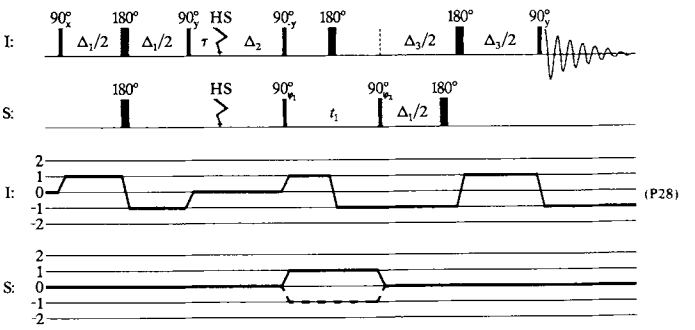

After a recovery period Δ_2 the sequence described in Equation (116) begins: the 90° pulses on both nuclei give rise to heteronuclear double-quantum coherence $(-2I_{1x}S_x)$, which is then labeled during t_1 with the chemical shift of the heteronucleus. This is transformed by the

90°(S) pulse into antiphase magnetization ($2I_{1x}S_z$), which is refocused during Δ_1 to I_{1y}. During $t_1+\Delta_3+\Delta_1$ antiphase magnetization to another proton can evolve ($2I_{1x}I_{2z}$), whereby the last 90°_y(I) pulse generates a coherence transfer to the I^2 spin. With this pulse sequence a successful ^{13}C-NMR spectral assignment of a small protein was achieved.[53] This pulse sequence can be improved if the 90_{-y}(I) pulse is not set directly after Δ_2 but, instead, before the begin of the Δ_3 delay. Then the modulation of the signals by homonuclear coupling in t_1 disappears.

3.3. Homonuclear Correlations through Heterospins

The NMR experiments described in the following sections do not involve proton and heteroatom correlations, but correlations between protons which are, either singly or together, coupled to a heterospin. The experiments that fall in this category are essentially the X-Relayed H,H-COSY, as well as sequences like COSY, NOESY, and TOCSY combined with X-filter or X-half-filter.

3.3.1. X-Relayed H,H-COSY

The oldest of these experiments is the X-Relayed H,H-COSY[220,221] (P29). It correlates protons in a fragment H-X-H. The magnetization is stepwise transferred from H to X and back to H. I-spin magnetization that evolved during t_1 is transferred to S magnetization by the two 90° pulses. The second I spin is activated through the heteronuclear coupling and finally the S magnetization is transferred to the I spin. Consequently the sequence detects a linear H-X-H coupling network. Application of this technique to ^{31}P-NMR spectra has been described in the literature.[220,221]

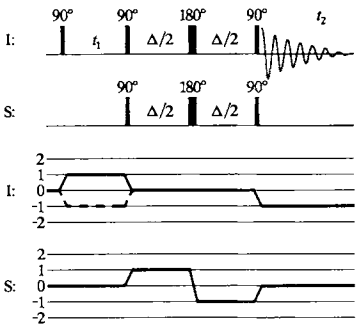

(P29)

3.3.2. X-Filter and X-Half-Filter

Recently, the so-called X-filter and X-half-filter[151-153,336] (P30) have been introduced. They are building blocks which can be incorporated into any homonuclear pulse sequence. The purpose of the filter is to test at a given point in a pulse sequence whether or not a heterospin is involved in the product operator, and depending on the result either to suppress or to select cross signals. Note the similarity with the low-pass *J*-filter. Coherences with an S_z operator remain unchanged under 90°_x-90°_{-x}, but change sign under 90°_x-90°_x. Coherences without an S_z operator remain totally unaffected. Subtraction of two such sequences suppresses all of the coherences which do not contain S_z.

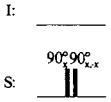

(P30)

The sequence (P31) is a generalized form. Product operators with nS_z operators are influenced as shown in (118).

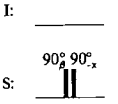

(P31)

$$S_z^n \longrightarrow S_z^n \cos^n\beta \; + \text{ transverse terms} \qquad (118)$$

The spectra can be edited to produce subspectra which result from any desired number of S_z operators. Depending on the pulse phase β one obtains for different n values the different coefficients shown in Table 10, by which the corresponding transfer functions must be multiplied.

Table 10. Coefficients for different numbers n of S_z operators as a function of the phase β in the X-filter.

n	$\beta=0$	60	120	180
0	1	−8	8	1
1	1	−4	−4	1
2	1	−1	−1	1
3	1	−2	2	−1

In the following section we shall examine a series of useful sequences, in which the X-filter has been installed.

X-Filter COSY

In the sequence (P32) only protons that are coupled to a common heterospin should give rise to cross signals. The necessary coupling network is $\overset{\frown}{I^1\text{-}S\text{-}I^2}$. The X-filter is thus applied together with the mixing pulse. Heteronuclear antiphase terms evolve and refocus, respectively, during the evolution and detection periods. The transfer is similar to that of a conventional COSY experiment, except that heteronuclear coupling must be taken into account [Eq. (119)]. A 90°_x-90°_x (S) pulse during the mixing pulse inverts all the terms which contain an S_z operator.

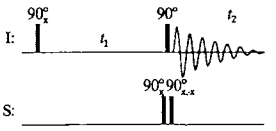

(P32)

$$I_{1z} \xrightarrow{90^\circ_x} I_{1y} \xrightarrow{t_1} -2I_{1x}I_{2x} - 4I_{1x}I_{2z}S_z \xrightarrow{90^\circ_y} 2I_{1x}I_{2x} + 4I_{1z}I_{2z}S_z \qquad (119)$$

If the subspectra for 90°_x-90°_x or for 90°_x-90°_{-x} are added, cross signals resulting from operators without heterospin are formed (i.e., the cross signals are in-phase with respect to the heteronuclear coupling). If, however, the subspectra are subtracted, only cross signals due to I spins that are coupled to a common S spin are obtained, since the terms without an S_z operator are eliminated. The heteronuclear coupling appears in antiphase. The spectrum is substantially simplified compared with the conventional spectrum, since now only a part of the total number of cross signals appears.

The X-filter can obviously be applied not only with a 90° mixing pulse, but with more complicated mixing sequences (MQF-COSY, E.COSY). The heteronuclear coupling is then present as antiphase splitting in the spectrum.

The pulse sequence (P33) selects the same type of coupling network. Here a fixed delay $\Delta=(2^1J_{IS})^{-1}$ serves to build up heteronuclear antiphase terms.[152] These are selected, such that at the beginning of t_1 only coherences of

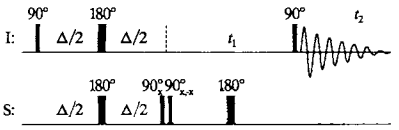

(P33)

S-bound I spins are present. Due to the 180° pulse in the middle of t_1, no heteronuclear coupling evolves, so that coherence of the type $2I_{1x}I_{2z}S_z$ is transformed by the 90° proton mixing pulse into $2I_{1z}I_{2x}S_z$. This coherence refocuses during t_2. The structural requirement is therefore again an $\overset{\frown}{I^1\text{-}S\text{-}I^2}$ system, with $J_{12}\neq 0$. The advantage of this realization of the X-filter is that during t_1 no multiplet structure develops due to the heteronuclear coupling, which would lead to a decrease in the signal-to-noise ratio.

X-Half-Filter COSY

If in the sequence (P33)[153,336] the 180° refocusing pulse in the middle of t_1 is left out, the heteronuclear antiphase magnetization can already refocus in t_1. This enables also spin systems of type $S\text{-}I^1\text{-}I^2$ to pass, and the X-half-filter is

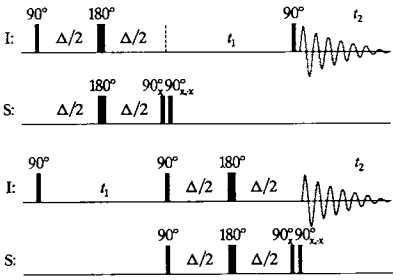

(P34)

(P35)

obtained. The sequence for the (ω_1)-half-filter COSY is thus (P34). This filter can also be introduced at the beginning of t_2 instead of at the beginning of t_1, whereby the (ω_2)-half-filter COSY (P35) is obtained. The simultaneous 90° (S) pulse and 90° (I) mixing pulse serve to select, at the beginning of t_2, only product operators which do not contain heterospin components.

The X-filter and X-half-filter techniques find more and more use, mainly with very large proteins,[337] in which the resolution in conventional 2D NMR spectra is no longer sufficient. The better resolved heterospin resonances are used, or else the NMR-active isotope of the heteronucleus is selectively enriched, so that subspectra of the conventional spectrum are obtained, corresponding to certain subunits of the protein near the isotopic labels. We may expect further success in this area in the future, with the development of ever simpler genetic-engineering methods for the preparation of selectively enriched proteins.

3.4. Experiments Utilizing the Dipolar Coupling

3.4.1. NOESY

Dipolar relaxation and the NOESY experiment have already been discussed briefly. We return to them now in greater detail.

Quantitative Evaluation of NOE Information

Cross signals in a NOESY spectrum rely on the cross relaxation of longitudinal magnetization during the mixing period. The intensity of the signals (the integral) contains valuable information about internuclear distances.[338-344] The exact analysis shows that the cross relaxation rate σ, which determines the efficiency of the NOE transfer, is given (for an isolated two-spin system IS) by Equation (120). Thus the distance information (r) is built into the cross relaxation rate.

$$\sigma = W_2 - W_0 = \frac{\gamma_I^2\gamma_S^2\hbar^2\tau_c}{10r^6}\left(\frac{6}{1+(\omega_I+\omega_S)^2\tau_c^2}-\frac{1}{1+(\omega_I-\omega_S)^2\tau_c^2}\right) \qquad (120)$$

In order to determine the cross relaxation rate from the NOESY spectrum, one either studies the slope of the buildup of the NOE rates for $\tau_m=0$, the so-called "initial buildup rate" (by measuring NOE spectra for various mixing times), or one makes use of the linear approximation. In the second case it is assumed that during the selected mixing time τ_m the system is still linear, i.e., the intensity of the cross signals depends only on the cross relaxation rate. Recently attempts have been made to extract NOE values from a *single* spectrum without the initial rate approximation. These approaches consider multistep transfers, or even solve the entire relaxation matrix.[345-346]

With the aid of one known distance r_{kl} in a molecule (e.g., two protons in a CH_2 group) and the corresponding cross signal rate σ_{kl}, an unknown distance r_{mn} can be calculated from a measured rate σ_{mn} (where I_{kl} and I_{mn} are the intensities of the corresponding cross signals) [Eq. (121)], whereby it is assumed that the correlation times for

$$\sqrt[6]{\frac{I_{kl}}{I_{mn}}} = \frac{r_{mn}}{r_{kl}} \qquad (121)$$

reorientation, τ_c, for the various distance vectors are equal. This can be verified experimentally through ^{13}C relaxation times or steady-state values of the heteronuclear NOEs. A different way is the simultaneous evaluation of NOESY and ROESY, which permits the determination of τ_c and σ.[370]

Artifacts

The phase cycling in a NOESY experiment is set such that during the mixing time τ_m nonzero quantum coherences are filtered out. Zero-quantum coherences are not affected and thus are present in the NOESY spectrum just like the desired NOE cross signals. Let us examine their

$$I_xS_z \xrightarrow{90°_x} \tfrac{1}{2}(I_xS_y+I_yS_x) \xrightarrow{\tau_m} \tfrac{1}{2}(I_xS_y+I_yS_x)\cos(\Omega_I-\Omega_S)\tau_m \xrightarrow{90°_x} \tfrac{1}{2}(I_xS_z+I_zS_x)\cos(\Omega_I-\Omega_S)\tau_m \qquad (122)$$

fine structure as represented by the product operator description [Eq. (122)]. Zero-quantum coherences precess in τ_m and finally lead to dispersion signals with double antiphase structure in the spectrum. Although their integral is zero, they can nevertheless interfere with the integration of cross signals.

Suppression is most successful when a 180° pulse is applied in the mixing period. This pulse is shifted within the constant mixing

time. τ_m thus becomes $\{\Delta/2\text{-}180°\text{-}(\tau_m\text{-}\Delta/2)\}$. The pulse refocuses zero-quantum coherences, so that they evolve with $\cos(\Omega_I-\Omega_S)(\tau_m-\Delta)$. Random[347] or also systematic[93] variation of Δ suppresses the zero-quantum coherences, because the argument of the cosine assumes positive or negative values, depending on Δ, and thus the terms average out. Since in this experiment the mixing time remains constant, no additional t_1 noise is introduced, in contrast with the random variation of τ_m.

Another possibility is to shift the zero-quantum coherence or to split it. If τ_m is incremented synchronously with the evolution time by κt_1, then the zero-quantum coherences give a signal which is modulated by $\cos(\Omega_I-\Omega_S)\kappa t_1$. These signals are placed at $\Omega_I \pm (\Omega_I-\Omega_S)\kappa$ in ω_1, rather than at Ω_I, and are thus shifted out of the region of interest through this procedure.[348]

3.4.2. *Longitudinal Multiple-Spin Orders*

Through the use of 90° mixing pulses in the NOESY experiment, exclusively z magnetization is generated. Operators with more than one z operator cannot be formed from transverse magnetization by 90° pulses. The situation is different when pulses with small flip angles are used. In this case also $2I_{1z}I_{2z}$ operators can be generated from $2I_{1x}I_{2z}$ by a y pulse. This so-called longitudinal multiple-spin order is the cornerstone for several pulse sequences.

zz Spectroscopy

Longitudinal two-spin order can be used to distinguish between certain exchange and cross relaxation signals, as well as between inter- and intramolecular NOEs.[127, 128] Through phase cycling only those cross signals are selected which correspond to the conversion of the operator $2I_{1z}I_{2z}$ to $2I_{3z}I_{4z}$. The spins I^3 and I^4 must likewise be coupled with scalar coupling, like, for instance, for cross signals generated by chemical exchange.

The selection of zz operators (product operators with an even number of z operators) can be achieved by the application of a 180° pulse in every second scan. The resulting signals are added together. Operators with an odd number of z operators are inverted, whereas zz operators are not.

Another possibility for the selection of zz operators is the use of a particular phase cycle with the pulse sequence (P36). Here β equals $45°+n90°$ and the receiver phase is 2β.

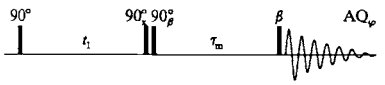

(P36)

zz-COSY

The pulse sequence is the same as in zz spectroscopy. However, in zz-COSY one is only interested in the "COSY"-type cross signals which are formed in zz spectroscopy; hence τ_m is set correspondingly short. zz Operators are selected as above. The transfer efficiency is $\frac{1}{4}\sin^2 2\beta$; i.e., $\beta=45°$ corresponds to the maximum intensity, which is, however, only one-quarter of that of a conventional COSY experiment. The sequence is nevertheless useful, for it offers an effective method for suppression of water signals.[129] By applying a homospoil pulse the undesired transverse magnetization of water is destroyed. The remaining longitudinal magnetization is suppressed, since it cannot evolve into longitudinal multiple-spin order. The pulse sequence is (P37).

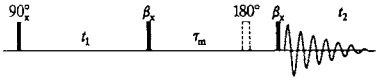

(P37)

z-COSY

We mentioned this sequence earlier (Section 3.1.4) in connection with the E. COSY technique. By using β pulses as flanking pulses for a z-filter one obtains cross signals with E. COSY-like multiplet structure. If the z-filter (P38) is made long enough to permit cross relaxation, it is possible, in ideal cases of coupled spin systems, to separately observe the W_0, W_1, and W_2 rates between two spins.[130]

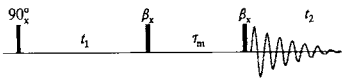

(P38)

3.4.3. *ROESY*

We mentioned earlier (Section 2.2.2) that unfavorable correlation times may lead to $W_2-W_1=0$, and hence to a situation in which there is no cross relaxation. The solution for these cases is provided by the CAMELSPIN experiment,[198] introduced by *Bothner-By* et al., which we shall term ROESY after a suggestion by *Bax*.[199] The mixing in the ROESY experiment (P39) is done in a spin-lock period.

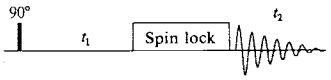

(P39)

NOESY relates to the mutual cross relaxation of z magnetization. In ROESY, transverse components cross-relax, which are prevented by the spin-lock field from precessing about the z axis. For magnetization which is locked along the x axis, for instance, one finds the relaxation rates (123)–(125) for a two-spin system.[77, 198, 202] In contrast to

$$W_1 = \frac{3}{40}\frac{\gamma_I^2\gamma_S^2\hbar^2\tau_c}{r^6}\left(\frac{1}{1+\omega^2\tau_c^2}+\frac{1}{1+4\omega^2\tau_c^2}\right) \quad (123)$$

$$W_0 = \frac{3}{40}\frac{\gamma_I^2\gamma_S^2\hbar^2\tau_c}{r^6}\left(\frac{1}{3}+\frac{1}{1+4\omega^2\tau_c^2}\right) \quad (124)$$

$$W_2 = \frac{3}{40}\frac{\gamma_I^2\gamma_S^2\hbar^2\tau_c}{r^6}\left(3+\frac{4}{1+\omega^2\tau_c^2}+\frac{1}{1+4\omega^2\tau_c^2}\right) \quad (125)$$

$$W_2 - W_0 = \frac{\gamma_I^2\gamma_S^2\hbar^2\tau_c}{10\,r^6}\left(2+\frac{3}{1+\omega^2\tau_c^2}\right) \quad (126)$$

NOE, the ROE is always positive (negative cross signals with respect to the diagonals). This is shown in Figure 38, which gives a graphic representation of the maximum NOE and ROE as a function of the correlation time τ_c in a two-spin system.

In addition, the ROE build-up rates are always (except for $\tau_c=0$) greater than the NOE rates, as shown in Figure 39. However, the time for which the linear approximation is valid is also shorter than in NOESY.

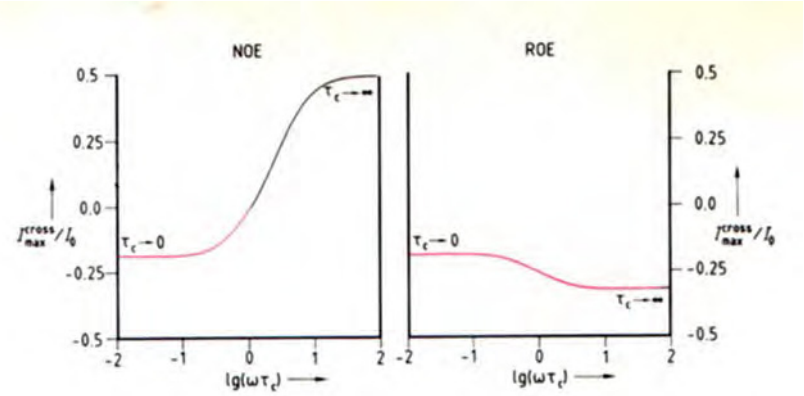

Fig. 38. Maximum intensity I_{max}^{cross} of a cross signal in 2D NOESY and 2D ROESY spectra for a two-spin system, normalized for I_0, the intensity of a diagonal signal with a mixing time $\tau_m = 0$. In the NOESY spectrum the intensity of the cross signal at $\tau_c \to 0$ is ca. 20% of that of a diagonal signal, it vanishes at $\omega_0 \tau_c = 1$, and reaches 50% of the diagonal signal intensity for $\tau_c \to \infty$. In the ROESY spectrum, in contrast, the maximum intensity is about 20% for $\tau_c \to 0$, and ca. 34% for $\tau_c \to \infty$.

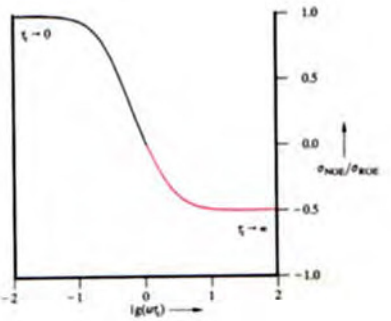

Fig. 39. The relation of the cross relaxation rates σ in a 2D NOESY and a 2D ROESY spectrum. For $\tau_c \to 0$ the rates are equal. Otherwise σ_{ROE} is always greater than σ_{NOE}.

The quantitative evaluation of ROESY spectra[349] is similar to that of NOESY spectra. When the correlation times are near the value $\tau_c \approx (5/4)^{1/2}/\omega_0$, the intensities of NOESY signals are small and can therefore be determined only inaccurately. In addition, cross-peak intensities are very sensitive to different individual correlation times within the same molecule. This can easily lead to errors in the interpretation of molecular distances. In the ROESY experiment, in comparison, this effect is less significant, due to the smaller τ_c dependence of the intensity of the cross signals. The lock field must be weak in order to avoid contributions to the spectrum from transfer through scalar coupling. These contributions are stronger near the diagonal and near the counterdiagonal. A reasonable recommended value is a lock field of the order of one-half of the spectral width [Eq. (127)]. For a quantitative evaluation

$$\gamma B_1 \approx \frac{SW}{2} \qquad (127)$$

one must take into account the ROE dependence on the distance of the resonance from the lock frequency (offset effect).[202]

The spin lock can equally well be generated by a CW irradiation with low power or by a series of pulses $(\beta\tau)_n$. β should be set as small as possible[201] and τ is calculated from Equation (128), where β is given in radians and τ_β is the β pulse length in seconds.

$$\frac{2\pi\beta}{(\tau+\tau_\beta)} = \gamma B_1 \qquad (128)$$

In an improved version with higher sensitivity, 90° pulses are applied before and after the spin-lock period.[202]

3.4.4. *Relayed NOESY*

The combination of NOESY and relayed-pulse sequences is of some significance.[228] Like in the other relayed experiments, one often achieves through the relayed transfer an unequivocal assignment of NOE cross signals in overcrowded spectral regions. The introduction of a double-quantum filter (P40) after the relayed transfer can be useful in order to filter out the (now dispersive) diagonal signals.[229]

(P40)

A second possibility with slightly different spectra is offered by the antisymmetrized pulse sequence.[230,231] The pulse sequence shown above is identical with the NOESY sequence up to the third 90° pulse, which precedes the relayed transfer period. It thus generates in ω_1 absorptive in-phase signals, modulated by the chemical shift of the first spin. After t_1, however, the magnetization is transferred through dipolar coupling to a second spin (NOE transfer), and then transferred again through scalar coupling to a third spin (relayed transfer). Antiphase magnetization of the third spin is thus detected in t_2. Therefore the signal in ω_2 is antiphase. It should be further noted that the spectrum is also asymmetric with respect to the position of the cross signals.[231]

The combination of TOCSY and ROESY (P41) has become particularly useful for medium-sized molecules. It is easily achieved through variation of the mixing se-

(P41)

quence[232] (e.g., 30 ms TOCSY with MLEV-17, followed by 170 ms of a series of pulses with small flip angles). The short TOCSY transfer provides COSY-type in-phase correlations (the transfer goes preferentially via one coupling), which can be used directly for the ROE transfer. The asymmetry of the spectrum directly provides, for example in the NH region of peptides, both the sequence and its direction even when the α-proton region is not resolved. For larger molecules the TOCSY-NOESY combination can be applied.[233]

3.5. Exchange Spectroscopy

A different possibility for the transfer of magnetization from one spin to another is offered by chemical exchange. Two isomers or topomers[102, 103, 350] must exchange moderately rapidly in a chemical equilibrium. Depending on the rate of exchange, either separate sets of signals (slow exchange) or one set of average signals (fast exchange) may be observed in the NMR spectrum. The variation in line shapes in the intermediate region serves to determine the exchange kinetics.[107, 108, 111, 113, 114, 351] In the slow exchange range polarization can be transferred from one site to the other (e.g., saturation transfer[352]). The NOESY and ROESY sequences[353, 354] can be used to determine such exchange processes. The advantage of the 2D NMR technique is straightforward: mutual assignments can be compared,[355, 371] exchange mechanisms are immediately visible,[356–358] and quantitative evaluations are possible.[359, 360] Cross signals due to chemical exchange, as well as those due to negative NOE effects (large molecules, viscous solvent, low temperature, high field), have the same sign as the diagonal signals in spectra with pure phases. In NOESY spectra of small molecules in low-viscosity solvents (positive NOE effects), and in *all* ROESY spectra, exchange signals[361–362] as well as NOEs[201, 363] over several nuclei are readily distinguished from direct NOE cross signals due to the different signs.

An example is shown in Figure 40. This proline-containing cyclic hexapeptide exchanges between two conformations, in which the proline amide bond is either in the *trans* or *cis* configuration. The exchanging NH signals of the two conformations are correlated by positive (black) cross signals (with respect to positive diagonals), while the negative (red) signals represent NOE in the rotating frame (ROE).

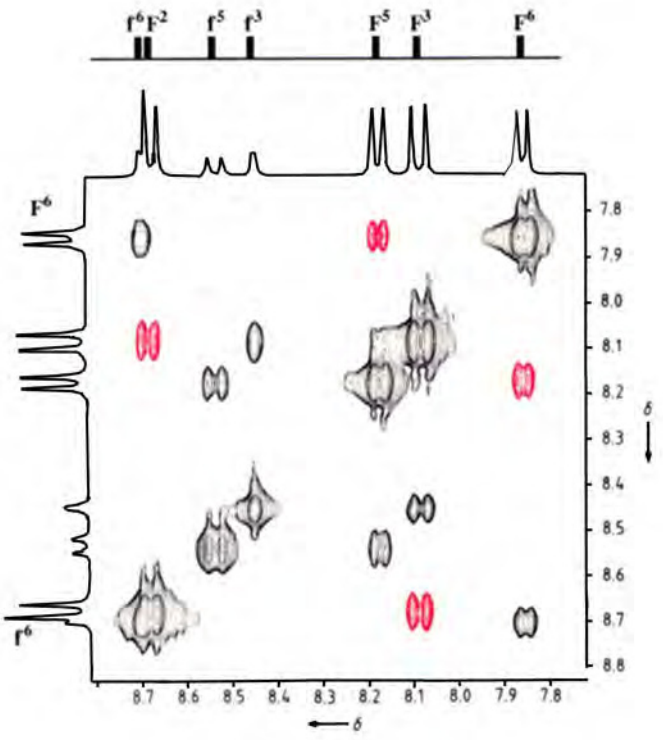

Fig. 40. Section from a 300-MHz ROESY spectrum of *cyclo*(-D-Pro^1-Phe^2-Phe^3-Pro^4-Phe^5-Phe^6-) in [D_6]DMSO, 320 K, β pulse angle 24°, mixing time 200 ms. The molecule is present in two conformations. The exchange between them is evident from the positive cross signals (black). NOE effects between NH signals give rise to negative (red) cross signals (F^2–F^3 and F^5–F^6). Phenylalanine = F, f (the major isomer is labeled with capital letters).

3.6. Further 2D NMR Experiments

A number of additional 2D NMR experiments are obtained by combinations of the techniques discussed above. Variants of these can be created by the introduction of filters,[364] pulse sandwiches, various decoupling schemes, and similar means, and are frequently found in the literature. Conversions of homonuclear techniques into heteronuclear experiments have also been realized (e.g., hetero-TOCSY[185, 186]). Furthermore, photochemical excitation has also been successfully associated with nuclear magnetic resonance (photo-CIDNP).[256, 257]

Recently, a series of 1D variants of 2D NMR techniques have been introduced[210] through the use of semiselective pulses with programmed line shapes, which, for simple problems, open novel aspects. The introduction of semiselective pulses into 2D[251, 335, 372] and 3D NMR spectra[253–255] opens yet another branch for methodological research. A more detailed description of these newest developments would, however, range beyond the scope of this article.

4. Conclusion

In this article we have laid the theoretical foundations for the most important 2D NMR experiments. Thus we now have at our disposal the tool which should enable useful application of these techniques, even though not all of the possible variants could be fully treated. The goal of this article has been to review today's most widely used techniques and to provide experimentalists with the necessary understanding of the theory, so that they can be in a position to:

- select the right experiment for their problem,
- select and set the optimal delays and phase cycles which are most suitable for their particular problem, and
- recognize artifacts in the spectrum and possibly avoid or minimize them.

Thanks to many discussions with various colleagues and the co-workers of our group the manuscript has been considerably improved. However, we especially acknowledge Prof. Dr. D. Kost, Beer Sheva, Israel, for his stimulating discussions and his contributions during the translation into English. Some of the figures were kindly provided from our coworkers U. Anders (Fig. 32), Dr. H. Kogler (Fig. 35), K. Wagner (Fig. 40), and M. Will (Figs. 24, 25, 31, 33). Financial support for the scientific results of our laboratory was provided by the Deutsche Forschungsgemeinschaft and the Fonds der Chemischen Industrie. C. G. thanks Prof. Dr. R. R. Ernst, Zürich, for support.

Received: May 12, 1987;
revised: January 19, 1988 [A 662 IE]
German version: *Angew. Chem. 100* (1988) 507

Appendix 1

Important concepts and abbreviations used in the text:

ω_1	The first frequency domain in a 2D NMR spectrum, obtained by Fourier transformation in t_1
ω_2	Second frequency domain
1D	One dimensional
2D	Two dimensional
Acquisition, AQ	Reception of the NMR signal; in 2D NMR experiments it takes place during the time t_2
Antiphase	Multiplet structure with opposite phases; the multiplet lines change signs
$\boldsymbol{B}_0$	Static magnetic field, oriented along the z axis according to convention
$\boldsymbol{B}_1$	Generally an additional transverse magnetic field, used for instance for pulses
$\boldsymbol{B}_2$	Another magnetic field, used for decoupling sequences, spin lock, etc.
"Band-pass filter"	Filter for the selection of a specified coherence order p
BB	Broadband decoupling of a spin type. Used in heteronuclear experiments to destroy the magnetization of one of the spin types, and generally employed during acquisition time. Nowadays commonly achieved through highly developed composite pulse sequences
$\boldsymbol{B}_{\text{eff}}$	Effective magnetic field, caused by the electronic environment around the nucleus (chemical shift). Often also: the residual field in the rotating frame, generated in cases of incomplete decoupling
Carrier frequency	ω_0, Transmitter frequency of the high-frequency pulses
Chemical shift	The difference in precession frequencies between a nucleus and the carrier frequency. It is often referred to a standard and divided by the carrier frequency (in ppm)
Coherence	Corresponds to a transition between two eigenstates and is an extension of the expression "transverse magnetization," which relates only to allowed transitions. From a quantum mechanical point of view a coherence corresponds to an off-diagonal element in the spin density matrix
Coherence order p	The difference in magnetic quantum numbers Δm_z of two energy levels which participate in the same coherence (e.g., zero-quantum coherence, single-quantum coherence)
Coherence transfer	Transfer of coherence from one nucleus type to another
Coherence-transfer pathway	Progress of a coherence order in a pulse sequence
Composite pulse	A pulse composed of a number of pulses. It is employed in order to compensate for phase errors, $\boldsymbol{B}_1$ field inhomogeneities or offset effects
Constant time	In constant-time variants of NMR experiments, the total duration of each t_1 experiment is constant, since t_1 is limited by pulses within a fixed delay
Convolution	A mathematical operation $F*G=\int_{-\infty}^{+\infty} F(x-y)G(y)\,dy$ Its significance for NMR spectroscopy results from the following relation: $F*G=\mathcal{F}(f\cdot g)$, whereby $\mathcal{F}(f)$ is the Fourier transform of f. That is, the Fourier transform of a product of two functions equals the convolution of the Fourier transforms of the functions
Correlation time	The correlation time τ_c is the mean time required for a rotation of a molecule. It is responsible for relaxation
Cross relaxation	Describes the mutual relaxation (inter- or intramolecular) of magnetically active nuclei, for instance through dipolar relaxation
Density matrix	Describes the state of a quantum mechanical object
Dipolar coupling	A through-space interaction between two spins. It is orientation dependent, and averages out in solution due to rapid reorientation of the molecule. Responsible for relaxation and NOE
DQF	Double-quantum filter
Editing	By setting a few parameters in a pulse sequence (e.g., pulses, delays), a set of subspectra is obtained, which deliver different information, for instance about multiplicities of signals (like subspectra for ^{13}CH, $^{13}CH_2$, and $^{13}CH_3$)
FID	*F*ree *I*nduction *D*ecay of the NMR signal
Flip angle	The angle by which the magnetization vector is rotated
Folding	Used in connection with Fourier transformation. Folding about $\omega_1=0$ means $S_f(\omega_1,\omega_2)=S(\omega_1,\omega_2)+S(-\omega_1,\omega_2)$

Fourier transformation	A mathematical method which determines the frequencies contained in a time-dependent function. The Fourier transform $F(\omega)$ in a complex Fourier transformation is given by $F(\omega) = \int_{-\infty}^{+\infty} e^{-i\omega t} f(t)\,dt$ and in a real Fourier transformation by $F(\omega) = \int_{-\infty}^{+\infty} f(t)\cos(\omega t + \varphi)\,dt$
"High-pass filter"	Filter for the selection of coherence orders $\geq p$
Homospoil pulse, HS	A pulse which generates short-time field inhomogeneities. Serves to eliminate undesired coherences (transverse magnetizations)
In-phase	Multiplet structure with equal phase, multiplet lines do not change signs
Inverse techniques	Heteronuclear experiments which detect the heteronucleus indirectly through proton magnetization. Also called "reversed techniques"
Longitudinal magnetization	Magnetization along the $\boldsymbol{B}_0$ field, i.e., along the z axis
Long-range coupling	Scalar coupling over several bonds
"Low-pass filter"	Filter for the selection of coherence orders $\leq p$
Multiplicity	The splitting of NMR signals by scalar coupling into doublets, triplets, etc.; in ^{13}C-NMR spectra it is also used synonymously to describe the large splitting through direct coupling in order to distinguish quaternary ^{13}C nuclei, CH, CH_2, and CH_3 groups
NOE	*N*uclear *O*verhauser *E*nhancement. An intensity change of an NMR signal induced by another nucleus in a nonequilibrium state. It is caused by dipolar coupling
Peak	Signal in an NMR spectrum; also used for a part of a multiplet
Phase cycle	Pulse sequences used for NMR spectra are mostly combinations of sequences which differ from one another only in the phases of the individual pulses. Systematic variation of the phases constitutes the phase cycle which suppresses unwanted coherences and artifacts
Polarization	It is based on the population difference of energy levels. A polarization must not always be connected with magnetization
Polarization transfer	Transfer of polarization from one nucleus type to another: it is often used synonymously with coherence transfer, even if coherences are transferred
Precession frequency	Larmor frequency ω of the nucleas precessing about the z axis. In the rotating frame it describes only the difference frequency Ω_i from an individual Larmor frequency of the nuclei $\omega_i = \gamma \boldsymbol{B}_{eff}$ and the carrier frequency $\omega_0 = \gamma \boldsymbol{B}_0$
Product operator	Set of orthogonal operators which can be connected to each other by a product
Product operator formalism	Formalism to describe NMR experiments (see extensive explanation in the text)
Pulse	Application of an additional high-frequency magnetic field with a carrier frequency ω_0 for a short time interval
Pulse sequence	Carefully designed series of radio frequency pulses and times of free evolution (delays) with subsequent detection of the produced transverse magnetization
Quadrature detection	A procedure for the detection of NMR signals which allows discrimination of signs of frequencies (in contrast: one-channel detection)
ROE	*R*otating frame N*OE*. NOE caused by relaxation in the rotating frame $T_{1\rho}$
Rotating frame	Frame rotating at frequency ω_0; simplifies the description of pulses and periods of free precession
Scan	A single running of an NMR experiment
Scalar coupling	Mutual interaction between two spins, which is transmitted through chemical bonds. Also called *J* coupling. It is scalar, i.e., independent of the orientation, and yields the multiplet splittings of the NMR signals
t_1	Evolution time. Incremented time in a 2D NMR experiment. Yields after Fourier transformation the first frequency domain
t_2	Detection time, generates after Fourier transformation the second frequency domain
t_1 noise	Noise which appears in 2D NMR spectra parallel to the ω_1 axis, and is particularly visible where there are intense signals in the spectrum. It is mostly due to technical factors associated with the instrument such as random variations of phases, pulses, temperature, $\boldsymbol{B}_0$ inhomogeneity
Thermal equilibrium	A state in which the energy levels are populated according to the Boltzmann distribution: $p(E_i) = e^{-E_i/kT} / \sum_i e^{-E_i/kT}$
Tilting	Transformation of a spectrum by $\omega_1' = \omega$, $\omega_2' = \omega_2 + k \cdot \omega_1$
TQF	Triple-quantum filter

Transverse magnetization	Magnetization in the x,y plane
Transverse operator	Designates I_x or I_y
Weak coupling	J coupling constant for the coupling between two spins is small compared with the difference of their chemical shifts; it causes first-order spectra
Zero-filling	Addition of zeros to the FID in order to improve the digital resolution

Appendix 2

Explanation of acronyms used in the text:

BIRD	*Bi*linear *R*otation *D*ecoupling
CAMELSPIN	*C*ross-Relaxation *A*ppropriate for *M*inimolecules *E*mulated by *L*ocked *Spin*s
CIDNP	*C*hemically *I*nduced *D*ynamic *N*uclear *P*olarization
COCONOSY	*Co*mbined *Co*rrelated and *N*uclear *O*verhauser Enhancement *S*pectroscop*y*
COLOC	*Co*rrelation via *Lo*ng-range *Co*uplings
COSY	*Co*rrelated *S*pectroscop*y*
DEPT	*D*istortionless *E*nhancement by *P*olarization *T*ransfer
DEPT-GL	DEPT-*G*rand *L*uxe
DISCO	*Di*fferences and *S*ums in *COSY* spectra
E. COSY	*E*xclusive COSY
GARP	*G*lobally Optimized *A*lternating Phase *R*ectangular *P*ulse
HETCOR	*Het*eronuclear *Cor*relation
HOESY	*H*eteronuclear 2D N*OE S*pectroscopy
HOHAHA	*Ho*monuclear *Ha*rtmann-*Ha*hn experiment
INADEQUATE	*I*ncredible *N*atural *A*bundance *D*ouble *Qu*antum *T*ransfer *E*xperiment
INEPT	*I*nsensitive *N*uclei *E*nhanced by *P*olarization *T*ransfer
MLEV	*M*alcom *Lev*itt
NOESY	*N*uclear *O*verhauser *E*nhancement and Exchange *S*pectroscop*y*
P. E. COSY	*P*rimitive *E*. COSY
RCT	*R*elayed *C*oherence *T*ransfer
ROESY	*R*otating Frame Nuclear *O*verhauser *E*ffect *S*pectroscop*y*
ROTO	*RO*ESY-*TO*CSY
TOCSY	*To*tal *C*orrelation *S*pectroscop*y*
TORO	*TO*CSY-*RO*ESY
WALTZ	*W*ideband *A*lternating Phase *L*ow-Power *T*echnique for *Z*ero Residue Splitting
XCORFE	*X*-Nucleus *Cor*relation with *F*ixed *E*volution Time

[1] J. Jeener, *Ampere Summer School*, Basko Polje, Yugoslavia 1971.
[2] W. P. Aue, E. Bartholdi, R. R. Ernst, *J. Chem. Phys. 64* (1976) 2229–2246.
[3] R. R. Ernst, G. Bodenhausen, A. Wokaun: *Principles of Nuclear Magnetic Resonance in One and Two Dimensions*, Clarendon, Oxford 1987.
[4] R. R. Ernst, *Chimia 29* (1975) 179–183.
[5] W. P. Aue, J. Karhan, R. R. Ernst, *J. Chem. Phys. 64* (1976) 4226–4227.
[6] R. Freeman, G. A. Morris, *Bull. Magn. Reson. 1* (1979) 5–26.
[7] D. Terpstra, *Top. Carbon-13 NMR Spectrosc. 3* (1979) 62–78.
[8] R. Freeman, *Proc. R. Soc. London A 373* (1980) 149.
[9] A. Bax: *Two-Dimensional NMR in Liquids*, Delft University Press, Delft 1982.
[10] G. A. Morris in A. G. Marshall (Ed.): *Fourier, Hadamard, and Hilbert Transformations in Chemistry*, Plenum, New York 1982, p. 271–307.
[11] A. Bax, *Bull. Magn. Reson. 7* (1985) 167–183.
[12] R. Benn, H. Günther, *Angew. Chem. 95* (1983) 381–411; *Angew. Chem. Int. Ed. Engl. 22* (1983) 350–380.
[13] A. Bax, *Top. Carbon-13 NMR Spectrosc. 4* (1984) 199–240.
[14] H. Kessler, W. Bermel, A. Müller, K.-H. Pook in V. Hruby (Ed.): *The Peptides, Vol. 7*, Academic Press, Orlando, FL, USA 1985, p. 437–473.
[15] K. Nagayama, *Methods Stereochem. Anal. 6* (1986) 155–178.
[16] H. Kessler, W. Bermel, *Methods Stereochem. Anal. 6* (1986) 179–205.
[17] K. Wüthrich: *NMR of Proteins and Nucleic Acids*, Wiley, New York 1986.
[18] G. A. Morris, *Magn. Reson. Chem. 24* (1986) 371–403.
[19] A. Bax, L. Lerner, *Science (Washington) 232* (1986) 960–967.
[20] A. E. Derome: *Modern NMR Techniques for Chemistry Research*, Pergamon, Oxford 1987.
[21] R. M. Carlson, W. R. Croasmun (Eds.): *Methods Stereochem. Anal. 9* (1987).
[22] N. Chandrakumar, S. Subramanian: *Modern Techniques in High Resolution FT-NMR*, Springer, New York 1987.
[23] J. K. M. Sanders, B. K. Hunter: *Modern NMR Spectroscopy*, University Press, Oxford 1987.
[24] O. W. Sørensen, G. W. Eich, M. H. Levitt, G. Bodenhausen, R. R. Ernst, *Prog. Nucl. Magn. Reson. Spectrosc. 16* (1983) 163–192.
[25] F. J. M. van de Ven, C. W. Hilbers, *J. Magn. Reson. 54* (1983) 512–520.
[26] K. J. Packer, P. E. Wright, *Mol. Phys. 50* (1983) 797–813.
[27] L. R. Brown, J. Bremer, *J. Magn. Reson. 68* (1986) 217–231.
[28] A. Wokaun, R. R. Ernst, *Chem. Phys. Lett. 52* (1977) 407–412.
[29] A. D. Bain, *J. Magn. Reson. 56* (1984) 418–427.
[30] G. Bodenhausen, H. Kogler, R. R. Ernst, *J. Magn. Reson. 58* (1984) 370–388.
[31] D. Piveteau, M.-A. Delsuc, J.-Y. Lallemand, *J. Magn. Reson. 63* (1985) 255–270.
[32] T. T. Nakashima, R. E. D. Mellung, *J. Magn. Reson. 70* (1986) 187–203.
[33] K. Nagayama, K. Wüthrich, P. Bachmann, R. R. Ernst, *Biochem. Biophys. Res. Commun. 78* (1977) 99–105.
[34] K. Nagayama, P. Bachmann, K. Wüthrich, R. R. Ernst, *J. Magn. Reson. 31* (1978) 133–148.
[35] G. Bodenhausen, *J. Magn. Reson. 39* (1980) 175–179.
[36] L. Müller, A. Kumar, R. R. Ernst, *J. Magn. Reson. 25* (1977) 383–390.
[37] K. Nagayama, A. Kumar, K. Wüthrich, R. R. Ernst, *J. Magn. Reson. 40* (1980) 321–334.

[38] A. Kumar, R. V. Hosur, K. Chandrasekhar, N. Murali, *J. Magn. Reson. 63* (1985) 107-114.
[39] A. A. Maudsley, R. R. Ernst, *Chem. Phys. Lett. 50* (1977) 368-372.
[40] L. Müller, *J. Am. Chem. Soc. 101* (1979) 4481-4484.
[41] D. A. Vidusek, M. F. Roberts, G. Bodenhausen, *J. Am. Chem. Soc. 104* (1982) 5452-5456.
[42] M. R. Bendall, D. T. Pegg, D. M. Dodrell, *J. Magn. Reson. 52* (1983) 81-117.
[43] A. Bax, R. H. Griffey, B. L. Hawkins, *J. Am. Chem. Soc. 105* (1983) 7188-7190.
[44] D. G. Davis, W. C. Agosta, D. Cowburn, *J. Am. Chem. Soc. 105* (1983) 6189-6190.
[45] A. Bax, R. H. Griffey, B. L. Hawkins, *J. Magn. Reson. 55* (1983) 301-315.
[46] D. H. Live, D. G. Davis, W. C. Agosta, D. Cowburn, *J. Am. Chem. Soc. 106* (1984) 6104-6105.
[47] D. H. Live, I. M. Armitage, D. C. Delgarno, D. Cowburn, *J. Am. Chem. Soc. 107* (1985) 1775-1777.
[48] M. Frey, G. Wagner, M. Vasak, O. W. Sørensen, D. Neuhaus, E. Wörgötter, J. H. R. Kägi, R. R. Ernst, K. Wüthrich, *J. Am. Chem. Soc. 107* (1985) 6847-6851.
[49] J. D. Otvos, H. R. Engeseth, S. Wehrli, *J. Magn. Reson. 61* (1985) 579-584.
[50] A. Bax, M. F. Summers, *J. Am. Chem. Soc. 108* (1986) 2093-2094.
[51] R. A. Byrd, M. F. Summers, G. Zon, C. Spellmeyer Fouts, L. G. Marzilli, *J. Am. Chem. Soc. 108* (1986) 504-505.
[52] A. Bax, S. Subramanian, *J. Magn. Reson. 67* (1986) 565-569.
[53] D. Brühwiler, G. Wagner, *J. Magn. Reson. 69* (1986) 546-551.
[54] W. Bermel, C. Griesinger, H. Kessler, K. Wagner, *Magn. Reson. Chem. 25* (1987) 325-326.
[55] R. R. Ernst, W. A. Anderson, *Rev. Sci. Instrum. 37* (1966) 93-102.
[56] R. R. Ernst, *Adv. Magn. Reson. 2* (1966) 1-135.
[57] T. C. Farrar, E. D. Becker: *Pulse and Fourier Transform NMR*, Academic Press, New York 1971.
[58] F. Bloch, *Phys. Rev. 70* (1946) 460-474.
[59] E. O. Stejskal, J. Schaefer, *J. Magn. Reson. 13* (1974) 249-251.
[60] E. O. Stejskal, J. Schaefer, *J. Magn. Reson. 14* (1974) 160-169.
[61] G. Bodenhausen, R. Freeman, G. A. Morris, R. Niedermeyer, D. L. Turner, *J. Magn. Reson. 25* (1977) 559-562.
[62] A. G. Redfield, S. D. Kunz, *J. Magn. Reson. 19* (1975) 250-254.
[63] U. Fano, *Rev. Mod. Phys. 29* (1957) 74-93.
[64] M. Weißbluth: *Atoms and Molecules*, Academic Press, New York 1978.
[65] C. P. Slichter: *Principles of Magnetic Resonance, 2nd ed.*, Springer, Berlin 1978.
[66] A. Böhm: *Quantum Mechanics*, Springer, New York 1979.
[67] K. Blum: *Density Matrix Theory and Applications*, Plenum, New York 1981.
[68] S. Goldman: *Information Theory*, Practice Hall, Englewood Cliffs, NJ, USA 1953.
[69] B. M. Brown: *The Mathematical Theory of Linear Systems*, Science Paperbacks, Chapman and Hall, London 1965.
[70] R. M. Bracewell: *The Fourier Transform and its Applications*, McGraw-Hill, New York 1965.
[71] D. C. Champeney: *Fourier Transforms and their Physical Applications*, Academic Press, New York 1973.
[72] D. Ziessow: *On Line Rechner in der Chemie, Grundlagen und Anwendungen in der Fourierspektroskopie*, de Gruyter, Berlin 1973.
[73] J. W. Cooper, *Top. Carbon-13 NMR Spectrosc. 2* (1976) 391-431.
[74] M. Karplus, *J. Chem. Phys. 30* (1959) 11-15.
[75] M. Karplus, *J. Am. Chem. Soc. 85* (1963) 2870-2871.
[76] V. F. Bystrov, *Prog. Nucl. Magn. Reson. Spectrosc. 10* (1976) 41-81; V. F. Bystrov, A. S. Arseniev, Yu. D. Gavrilov, *J. Magn. Reson. 30* (1978) 151-184.
[77] I. Solomon, *Phys. Rev. 99* (1955) 559-565.
[78] J. H. Noggle, R. E. Schirmer: *The Nuclear Overhauser Effect, Chemical Applications*, Academic Press, New York 1971.
[79] A. Abragam: *The Principles of Nuclear Magnetism*, Clarendon, Oxford 1978.
[80] R. Kaiser, *J. Chem. Phys. 42* (1965) 1838-1839.
[81] I. D. Campbell, R. Freemann, *J. Magn. Reson. 11* (1973) 143-162.
[82] A. A. Bothner-By in R. G. Shulman (Ed.): *Magnetic Resonance Studies in Biology*, Academic Press, New York 1979, p. 177.
[83] I. O. Campbell, C. M. Dobson, R. J. P. Williamson, *J. Chem. Soc. Chem. Commun. 1974*, 888-889.
[84] W. E. Hull, B. D. Sykes, *J. Chem. Phys. 63* (1975) 867-880.
[85] A. Kalk, H. J. C. Berendsen, *J. Magn. Reson. 24* (1976) 343-366.
[86] S. L. Gordon, K. Wüthrich, *J. Am. Chem. Soc. 100* (1978) 7094-7096.
[87] R. Richarz, K. Wüthrich, *J. Magn. Reson. 30* (1978) 147-150.
[88] G. Wagner, K. Wüthrich, *J. Magn. Reson. 33* (1979) 675-680.
[89] J. Jeener, B. H. Meier, P. Bachmann, R. R. Ernst, *J. Chem. Phys. 71* (1979) 4546-4553.
[90] A. Kumar, G. Wagner, R. R. Ernst, K. Wüthrich, *Biochem. Biophys. Res. Commun. 96* (1980) 1156-1163.
[91] A. Kumar, R. R. Ernst, K. Wüthrich, *Biochem. Biophys. Res. Commun. 95* (1980) 1-6.
[92] G. Wagner, K. Wüthrich, *J. Mol. Biol. 155* (1982) 347-366.
[93] M. Rance, G. Bodenhausen, G. Wagner, K. Wüthrich, R. R. Ernst, *J. Magn. Reson. 62* (1985) 497-510.
[94] P. Balaram, A. A. Bothner-By, J. Dadok, *J. Am. Chem. Soc. 94* (1972) 4015-4017; A. A. Bothner-By, J. H. Noggle, *J. Am. Chem. Soc. 101* (1979) 5152-5155.
[95] H. Kessler, W. Bermel, A. Friedrich, G. Krack, W. E. Hull, *J. Am. Chem. Soc. 104* (1982) 6297-6304.
[96] F. M. Poulsen, J. C. Hoch, C. M. Dobson, *Biochemistry 19* (1980) 2597-2607.
[97] S. Macura, R. R. Ernst, *Mol. Phys. 41* (1980) 95-117.
[98] A. Kumar, G. Wagner, R. R. Ernst, K. Wüthrich, *J. Am. Chem. Soc. 103* (1981) 3654-3658.
[99] C. M. Dobson, E. T. Olejniczak, F. M. Poulsen, R. G. Ratcliffe, *J. Magn. Reson. 48* (1982) 97-110.
[100] E. R. P. Zuiderweg, R. Kaptein, K. Wüthrich, *Proc. Natl. Acad. Sci. USA 80* (1983) 5837-5841.
[101] M. Weiss, D. Petzl, R. Sauer, M. Karplus, *Proc. Natl. Acad. Sci. USA 81* (1984) 130-134.
[102] H. J. Gutowski, D. M. McCall, C. P. Slichter, *J. Chem. Phys. 21* (1953) 279-292.
[103] H. J. Gutowski, A. Saika, *J. Chem. Phys. 21* (1953) 1688-1694.
[104] J. A. Pople, W. G. Schneider, H. J. Bernstein: *High Resolution NMR*, McGraw-Hill, New York 1959.
[105] A. Loewenstein, T. M. Connor, *Ber. Bunsenges. Phys. Chem. 67* (1963) 280-295.
[106] J. Delpuech, *Bull. Soc. Chim. Fr. 1964*, 2697.
[107] H. Kessler, *Angew. Chem. 82* (1970) 237-253; *Angew. Chem. Int. Ed. Engl. 9* (1970) 219-235.
[108] L. M. Jackman, F. A. Cotton: *Dynamic Nuclear Magnetic Resonance Spectroscopy*, Academic Press, New York 1975.
[109] A. Steigel, *NMR Basic Princ. Prog. 15* (1978) 1-53.
[110] H. W. Spiess, *NMR Basic Princ. Prog. 15* (1978) 55-214.
[111] G. Binsch, H. Kessler, *Angew. Chem. 92* (1980) 445-463; *Angew. Chem. Int. Ed. Engl. 19* (1980) 411-428.
[112] M. L. Martin, *G. J. Martin, J. Delpuech: Practical NMR Spectroscopy*, Heyden, London 1980.
[113] J. I. Kaplan, G. Fraenkel: *NMR of Chemically Exchanging Systems*, Academic Press, New York 1980.
[114] J. Sandström: *Dynamic NMR Spectroscopy*, Academic Press, London 1982.
[115] M. Oki, *Methods Stereochem. Anal. 4* (1985).
[116] B. H. Meier, R. R. Ernst, *J. Am. Chem. Soc. 101* (1979) 6441-6442.
[117] Y. Huang, S. Macura, R. R. Ernst, *J. Am. Chem. Soc. 103* (1981) 5327-5333.
[118] J. Hilton, L. H. Sutcliffe, *Prog. Nucl. Magn. Reson. Spectrosc. 10* (1975) 27-39.
[119] C. P. Poole, H. A. Farach: *Relaxation in Magnetic Resonance, Dielectric and Mössbauer Applications*, Academic Press, New York 1971.
[120] A. Wokaun, R. R. Ernst, *J. Chem. Phys. 67* (1977) 1752-1758.
[121] S. Vega, *J. Chem. Phys. 68* (1978) 5518-5527.
[122] D. P. Weitekamp, J. R. Garbow, A. Pines, *J. Chem. Phys. 77* (1982) 2870-2883.
[123] D. P. Weitekamp, *Adv. Magn. Reson. 11* (1983) 111-274.
[124] V. Blechta, J. Schraml, *J. Magn. Reson. 69* (1986) 293-301.
[125] M. H. Levitt in W. S. Brey (Ed.): *Two-Dimensional NMR and Related Techniques*, Academic Press, New York, in press.
[126] E. Noether, *Nachr. Ges. Wiss., Göttingen Math. Phys. Kl. 1918*, 235.
[127] G. Bodenhausen, G. Wagner, M. Rance, O. W. Sørensen, K. Wüthrich, R. R. Ernst, *J. Magn. Reson. 59* (1984) 542-550.
[128] G. Wagner, G. Bodenhausen, N. Müller, M. Rance, O. W. Sørensen, R. R. Ernst, K. Wüthrich, *J. Am. Chem. Soc. 107* (1985) 6440-6446.
[129] E. R. P. Zuiderweg, *J. Magn. Reson. 71* (1987) 283-293.
[130] H. Oschkinat, A. Pastore, G. Bodenhausen, *J. Am. Chem. Soc. 109* (1987) 4110-4111.
[131] D. I. Hoult, R. E. Richards, *Proc. R. Soc. London A 344* (1975) 311-340.
[132] J. Keeler, D. Neuhaus, *J. Magn. Reson. 63* (1985) 454-472.
[133] P. Bachmann, W. P. Aue, L. Müller, R. R. Ernst, *J. Magn. Reson. 28* (1977) 29-39.
[134] D. J. States, R. A. Haberkorn, D. J. Ruben, *J. Magn. Reson. 48* (1982) 286-292.
[135] G. Drobny, A. Pines, S. Sinton, D. P. Weitekamp, D. Wemmer, *Faraday Symp. Chem. Soc. 13* (1979) 49-55.
[136] D. Marion, K. Wüthrich, *Biochem. Biophys. Res. Commun. 113* (1983) 967-974.
[137] A. Bax, R. Freeman, *J. Magn. Reson. 44* (1981) 542-561.

[138] U. Piantini, O. W. Sørensen, R. R. Ernst, *J. Am. Chem. Soc. 104* (1982) 6800-6801.
[139] A. J. Shaka, R. Freeman, *J. Magn. Reson. 51* (1983) 169-173.
[140] M. Rance, O. W. Sørensen, G. Bodenhausen, G. Wagner, R. R. Ernst, K. Wüthrich, *Biochem. Biophys. Res. Commun. 117* (1983) 458-479.
[141] N. Müller, R. R. Ernst, K. Wüthrich, *J. Am. Chem. Soc. 108* (1986) 6482-6492.
[142] M. Rance, G. Wagner, O. W. Sørensen, K. Wüthrich, R. R. Ernst, *Biochem. Biophys. Res. Commun. 121* (1984) 1021-1026.
[143] A. Bax, R. Freeman, *J. Magn. Reson. 45* (1981) 177-181.
[144] C. Griesinger, O. W. Sørensen, R. R. Ernst, *J. Am. Chem. Soc. 107* (1985) 6394-6396.
[145] C. Griesinger, O. W. Sørensen, R. R. Ernst, *J. Chem. Phys. 64* (1986) 6837-6825.
[146] C. Griesinger, O. W. Sørensen, R. R. Ernst, *J. Magn. Reson., 75* (1987) 474-492.
[147] L. Müller, *J. Magn. Reson. 72* (1987) 191-197.
[148] H. Oschkinat, A. Pastore, P. Pfändler, G. Bodenhausen, *J. Magn. Reson. 69* (1986) 559-566.
[149] P. Pfändler, G. Bodenhausen, *J. Magn. Reson. 72* (1987) 475-492.
[150] E. Guittet, M.-A. Delsuc, J.-Y. Lallemand, *J. Am. Chem. Soc. 106* (1984) 4278-4279.
[151] E. Wörgötter, G. Wagner, K. Wüthrich, *J. Am. Chem. Soc. 108* (1986) 6162-6167.
[152] R. H. Griffey, A. G. Redfield, *Q. Rev. Biophys. 19* (1987) 51-82.
[153] G. Otting, H. Senn, G. Wagner, K. Wüthrich, *J. Magn. Reson. 70* (1986) 500-505.
[154] A. Wokaun, R. R. Ernst, *Mol. Phys. 36* (1978) 317-341.
[155] G. Bodenhausen, R. L. Vold, R. R. Vold, *J. Magn. Reson. 37* (1980) 93-106.
[156] G. Bodenhausen, *Prog. Nucl. Magn. Reson. Spectrosc. 14* (1981) 137-173.
[157] L. Braunschweiler, G. Bodenhausen, R. R. Ernst, *Mol. Phys. 48* (1983) 535-569.
[158] T. H. Mareci, R. Freeman, *J. Magn. Reson. 51* (1983) 531-535.
[159] H. Kessler, H. R. Loosli, H. Oschkinat, *Helv. Chim. Acta 68* (1985) 661-681.
[160] L. Braunschweiler, R. R. Ernst, *J. Magn. Reson. 53* (1983) 521-528.
[161] D. G. Davis, A. Bax, *J. Am. Chem. Soc. 107* (1985) 2821-2823.
[162] M. W. Edwards, A. Bax, *J. Am. Chem. Soc. 108* (1986) 918-923.
[163] D. Piveteau, M.-A. Delsuc, E. Guittet, J.-Y. Lallemand, *J. Magn. Reson. 71* (1987) 347-348.
[164] A. Bax, R. Freeman, S. P. Kempsell, *J. Am. Chem. Soc. 102* (1980) 4849-4851.
[165] A. Bax, S. P. Kempsell, R. Freeman, *J. Magn. Reson. 41* (1980) 349-353.
[166] A. Bax, R. Freeman, T. A. Frenkiel, M. H. Levitt, *J. Magn. Reson. 43* (1981) 478-483.
[167] R. Freeman, T. Frenkiel, *J. Am. Chem. Soc. 104* (1982) 5545-5547.
[168] O. W. Sørensen, R. Freeman, T. A. Frenkiel, T. H. Mareci, R. Schuck, *J. Magn. Reson. 46* (1982) 180-184.
[169] P. J. Keller, K. E. Vogele, *J. Magn. Reson. 68* (1986) 389-392.
[170] G. Bodenhausen, R. Freeman, *J. Magn. Reson. 28* (1977) 471-476.
[171] R. Freeman, G. A. Morris, *J. Chem. Soc. Chem. Commun. 1978*, 684-686.
[172] G. Bodenhausen, R. Freeman, *J. Am. Chem. Soc. 100* (1978) 320-321.
[173] A. Bax, S. K. Sarkar, *J. Magn. Reson. 60* (1984) 170-176.
[174] M. H. Levitt, O. W. Sørensen, R. R. Ernst, *Chem. Phys. Lett. 94* (1983) 540-544.
[175] M. R. Bendall, D. T. Pegg, *J. Magn. Reson. 53* (1983) 144-148.
[176] D. T. Pegg, M. R. Bendall, *J. Magn. Reson. 55* (1983) 114-127.
[177] T. T. Nakashima, B. K. John, R. E. D. McClung, *J. Magn. Reson. 59* (1984) 124-131.
[178] A. Bax, *J. Magn. Reson. 53* (1983) 517-520.
[179] V. Rutar, *J. Magn. Reson. 58* (1984) 306-310.
[180] J. A. Wilde, P. H. Bolton, *J. Magn. Reson. 59* (1984) 343-346.
[181] H. Kessler, C. Griesinger, G. Zimmermann, *Magn. Reson. Chem. 25* (1987) 579-583.
[182] W. F. Reynolds, D. W. Hughes, M. Perpick-Dumont, R. G. Enriquez, *J. Magn. Reson. 64* (1985) 304-311.
[183] V. Sklenář, A. Bax, *J. Magn. Reson. 71* (1987) 379-383.
[184] G. Ortiz-Polo, R. Krishnamoorthi, D. H. Live, J. L. Markley, D. G. Davis, D. Cowburn, *J. Magn. Reson. 68* (1986) 303-310.
[185] H. Kessler, W. Bermel, C. Griesinger, *6. Diskussionstag. Fachgruppe Magn. Resonanzspektrosk.* (Berlin, September 25-28, 1985).
[186] A. Bax, D. G. Davis, S. K. Sarkar, *J. Magn. Reson. 63* (1985) 230-234.
[187] K. Hallenga, G. van Binst, *Bull. Magn. Reson. 2* (1980) 343.
[188] C. Wynants, K. Hallenga, G. van Binst, A. Michel, J. Zanen, *J. Magn. Reson. 57* (1984) 93-98.
[189] H. Kessler, C. Griesinger, J. Zarbock, H. R. Loosli, *J. Magn. Reson. 57* (1984) 331-336.
[190] H. Kessler, C. Griesinger, J. Lautz, *Angew. Chem. 96* (1984) 434-435; *Angew. Chem. Int. Ed. Engl. 23* (1984) 444-445.
[191] H. Kessler, W. Bermel, C. Griesinger, *J. Am. Chem. Soc. 107* (1985) 1083-1084.
[192] H. Kessler, W. Bermel, C. Griesinger, C. Kolar, *Angew. Chem. 98* (1986) 352-353; *Angew. Chem. Int. Ed. Engl. 25* (1986) 342-344.
[193] H. Kessler, C. Griesinger, K. Wagner, *J. Am. Chem. Soc. 109* (1987) 6927-6933.
[194] W. F. Reynolds, D. W. Hughes, M. Perpick-Dumont, R. G. Enriquez, *J. Magn. Reson. 63* (1985) 413-417.
[195] C. Bauer, R. Freeman, S. Wimperis, *J. Magn. Reson. 58* (1984) 526-532.
[196] M. F. Summers, L. G. Marzilli, A. Bax, *J. Am. Chem. Soc. 108* (1986) 4285-4294.
[197] C. Griesinger, *Dissertation*, Universität Frankfurt 1986.
[198] A. A. Bothner-By, R. L. Stephens, J. Lee, C. D. Warren, R. W. Jeanloz, *J. Am. Chem. Soc. 106* (1984) 811-813.
[199] A. Bax, D. G. Davis, *J. Magn. Reson. 63* (1985) 207-213.
[200] D. Neuhaus, J. Keeler, *J. Magn. Reson. 68* (1986) 568-574.
[201] H. Kessler, C. Griesinger, R. Kerssebaum, K. Wagner, R. R. Ernst, *J. Am. Chem. Soc. 109* (1987) 607-609.
[202] C. Griesinger, R. R. Ernst, *J. Magn. Reson., 75* (1987) 261-271.
[203] P. L. Rinaldi, *J. Am. Chem. Soc. 105* (1983) 5167-5168.
[204] C. Yu, G. C. Levy, *J. Am. Chem. Soc. 106* (1984) 6533-6537.
[205] K. E. Kövér, G. Batta, *J. Am. Chem. Soc. 107* (1985) 5829-5830.
[206] K. E. Kövér, G. Batta, *J. Magn. Reson. 69* (1986) 519-522.
[207] K. E. Kövér, G. Batta, Z. Mádi, *J. Magn. Reson. 69* (1986) 538-541.
[208] G. Eich, G. Bodenhausen, R. R. Ernst, *J. Am. Chem. Soc. 104* (1982) 3731-3732.
[209] A. Bax, G. Drobny, *J. Magn. Reson. 61* (1985) 306-320.
[210] H. Kessler, H. Oschkinat, C. Griesinger, W. Bermel, *J. Magn. Reson. 70* (1986) 106-133.
[211] S. Macura, N. G. Kumar, L. R. Brown, *Magn. Reson. Relat. Phenom. Proc. Congr. AMPERE 22nd 1984*, 496.
[212] P. L. Weber, L. Müller, *J. Magn. Reson. 73* (1987) 184-190.
[213] P. H. Bolton, G. Bodenhausen, *Chem. Phys. Lett. 89* (1982) 139-144.
[214] P. H. Bolton, *J. Magn. Reson. 48* (1982) 336-340.
[215] H. Kessler, M. Bernd, H. Kogler, J. Zarbock, O. W. Sørensen, G. Bodenhausen, R. R. Ernst, *J. Am. Chem. Soc. 105* (1983) 6944-6952.
[216] A. Bax, *J. Magn. Reson. 53* (1983) 149-153.
[217] P. H. Bolton, *J. Magn. Reson. 54* (1983) 333-337.
[218] S. K. Sarkar, A. Bax, *J. Magn. Reson. 63* (1985) 512-523.
[219] P. H. Bolton, *J. Magn. Reson. 62* (1985) 143-146.
[220] M.-A. Delsuc, E. Guittet, N. Trotin, J.-Y. Lallemand, *J. Magn. Reson. 56* (1984) 163-166.
[221] D. Neuhaus, G. Wider, G. Wüthrich, K. Wagner, *J. Magn. Reson. 57* (1984) 164-168.
[222] H. Kessler, W. Bermel, C. Griesinger, *J. Magn. Reson. 62* (1985) 573-579.
[223] H. Kessler, W. Bermel, C. Griesinger, P. Hertl, E. Streich, A. Rieker, *J. Org. Chem. 51* (1986) 596-601.
[224] K. S. Lee, G. A. Morris, *J. Magn. Reson. 70* (1986) 332-335.
[225] K. S. Lee, G. A. Morris, *Magn. Reson. Chem. 25* (1987) 176-178.
[226] L. D. Field, B. A. Messerle, *J. Magn. Reson. 62* (1985) 453-460.
[227] L. D. Field, B. A. Messerle, *J. Magn. Reson. 66* (1986) 483-490.
[228] G. Wagner, *J. Magn. Reson. 57* (1984) 497-505.
[229] H. Kessler, S. Steuernagel, D. Gillessen, T. Kamiyama, *Helv. Chim. Acta 70* (1987) 726-741.
[230] O. W. Sørensen, C. Griesinger, R. R. Ernst, *Chem. Phys. Lett. 135* (1987) 313-318.
[231] C. Griesinger, C. Gemperle, O. W. Sørensen, R. R. Ernst, *Mol. Phys.*, in press.
[232] G. Kessler, G. Gemmecker, B. Haase, *J. Magn. Reson.* (1988), in press.
[233] G. Kessler, G. Gemmecker, S. Steuernagel, *Angew. Chem. 100* (1988) 600-603; *Angew. Chem. Int. Ed. Engl. 27* (1988) 564-566.
[234] J. L. Dimicoli, A. Volk, J. Mispelter, *J. Magn. Reson. 63* (1985) 605-611.
[235] S. Macura, L. R. Brown, *J. Magn. Reson. 53* (1983) 529-535.
[236] K. Nagayama, K. Wüthrich, P. Bachmann, R. R. Ernst, *Naturwissenschaften 64* (1977) 581-583.
[237] G. Bodenhausen, R. Freeman, D. L. Turner, *J. Magn. Reson. 27* (1977) 511-514.
[238] J. D. Mersh, J. K. M. Sanders, *J. Magn. Reson. 50* (1982) 171-174.
[239] H. Kessler, H. Oschkinat, O. W. Sørensen, H. Kogler, R. R. Ernst, *J. Magn. Reson. 55* (1983) 329-333.
[240] A. J. Shaka, J. Keeler, R. Freeman, *J. Magn. Reson. 56* (1984) 294-313.
[241] L. Müller, A. Kumar, R. R. Ernst, *J. Chem. Phys. 63* (1975) 5490-5491.
[242] G. Bodenhausen, R. Freeman, R. Turner, *J. Chem. Phys. 65* (1976) 839-840.

[243] G. Bodenhausen, R. Freeman, G. A. Morris, *J. Magn. Reson. 26* (1977) 373–378.
[244] G. Bodenhausen, R. Freeman, G. A. Morris, D. L. Turner, *J. Magn. Reson. 28* (1977) 17–28.
[245] M. H. Levitt, G. Bodenhausen, R. R. Ernst, *J. Magn. Reson. 53* (1983) 443–461.
[246] J.-S. Wang, T. C. Wong, *J. Magn. Reson. 61* (1985) 59–66.
[247] A. Bax, *J. Magn. Reson. 52* (1983) 339–344.
[248] V. Rutar, *J. Am. Chem. Soc. 105* (1983) 4095–4096.
[249] A. Bax, R. Freeman, *J. Am. Chem. Soc. 104* (1982) 1099–1100.
[250] C. Bauer, R. Freeman, T. A. Frenkiel, J. Keeler, A. J. Shaka, *J. Magn. Reson. 58* (1984) 442–457.
[251] R. Brüschweiler, J. C. Madsen, C. Griesinger, O. W. Sørensen, R. R. Ernst, *J. Magn. Reson. 73* (1987) 380–385.
[252] G. W. Vuister, R. Boelens, *J. Magn. Reson. 73* (1987) 328–333.
[253] C. Griesinger, O. W. Sørensen, R. R. Ernst, *J. Magn. Reson. 73* (1987) 574–579.
[254] C. Griesinger, O. W. Sørensen, R. R. Ernst, *J. Am. Chem. Soc. 109* (1987) 7227–7228.
[255] H. Oschkinat, C. Griesinger, P. J. Kraulis, O. W. Sørensen, R. R. Ernst, A. M. Gronenborn, G. M. Clore, *Nature 332* (1988) 374.
[256] R. Boelens, A. Podoplelov, R. Kaptein, *J. Magn. Reson. 69* (1986) 116–123.
[257] R. M. Scheek, S. Strob, R. Boelens, K. Dijkstra, R. Kaptein, *J. Am. Chem. Soc. 107* (1985) 705–706.
[258] A. G. Haasnoot, F. J. M. van de Ven, C. W. Hilbers, *J. Magn. Reson. 56* (1984) 343–349.
[259] J. Boyd, C. M. Dobson, C. Redfield, *FEBS Lett. 186* (1985) 35–40.
[260] H. Kessler, M. Will, unpublished results.
[261] G. Wider, R. Baumann, K. Nagayama, R. R. Ernst, K. Wüthrich, *J. Magn. Reson. 42* (1981) 73–87.
[262] K. Nagayama, K. Wüthrich, *Eur. J. Biochem. 114* (1981) 365–374.
[263] H. Oschkinat, R. Freeman, *J. Magn. Reson. 60* (1984) 164–169.
[264] H. Kessler, A. Müller, H. Oschkinat, *Magn. Reson. Chem. 23* (1985) 844–852.
[265] H. Kessler, H. Oschkinat, *Angew. Chem. 97* (1985) 689–690; *Angew. Chem. Int. Ed. Engl. 24* (1985) 690–692.
[266] O. W. Sørensen, R. R. Ernst, M. Rance, *J. Magn. Reson. 56* (1984) 527–534.
[267] A. Kumar, R. V. Hosur, K. Chandrasekhar, *J. Magn. Reson. 60* (1984) 143–148.
[268] R. V. Hosur, K. V. R. Chary, A. Kumar, G. Govil, *J. Magn. Reson. 62* (1985) 123–127.
[269] S. Mayor, R. V. Hosur, *Magn. Reson. Chem. 23* (1985) 470–473.
[270] R. V. Hosur, M. R. Kumar, A. Sheth, *J. Magn. Reson. 65* (1985) 375–381.
[271] M. Rance, G. Wagner, O. W. Sørensen, K. Wüthrich, R. R. Ernst, *J. Magn. Reson. 59* (1984) 250–261.
[272] G. Wagner, *J. Magn. Reson. 55* (1983) 151–156.
[273] W. E. Hull, Heidelberg, personal communication.
[274] N. Chandrakumar, S. Subramanian, *J. Magn. Reson. 62* (1985) 346–349.
[275] N. Chandrakumar, *J. Magn. Reson. 60* (1984) 28–36.
[276] N. Chandrakumar, *J. Magn. Reson. 63* (1985) 174–178.
[277] N. Chandrakumar, *J. Magn. Reson. 63* (1985) 202–206.
[278] N. Chandrakumar, G. V. Visalakshi, D. Ramaswamy, S. Subramanian, *J. Magn. Reson. 67* (1986) 307–318.
[279] N. Chandrakumar, *J. Magn. Reson. 67* (1986) 457–465.
[280] N. Chandrakumar, *J. Magn. Reson. 71* (1987) 322–324.
[281] S. Sankaran, A. Bax, *J. Magn. Reson. 71* (1987) 325–330.
[282] A. Bax, D. G. Davis, *J. Magn. Reson. 65* (1985) 355–360.
[283] M. H. Levitt, R. Freeman, *J. Magn. Reson. 43* (1981) 502–507.
[284] M. H. Levitt, R. Freeman, T. A. Frenkiel, *J. Magn. Reson. 47* (1982) 328–330.
[285] M. H. Levitt, R. Freeman, T. A. Frenkiel, *Adv. Magn. Reson. 11* (1983) 48–110.
[286] A. Bax, R. Freeman, T. A. Frenkiel, *J. Am. Chem. Soc. 103* (1981) 2102–2104.
[287] T. H. Mareci, R. Freeman, *J. Magn. Reson. 48* (1982) 158–163.
[288] M. A. Thomas, A. Kumar, *J. Magn. Reson. 54* (1983) 319–323.
[289] J. Boyd, C. M. Dobson, C. Redfield, *J. Magn. Reson. 55* (1983) 170–176.
[290] G. Wagner, E. R. P. Zuiderweg, *Biochem. Biophys. Res. Commun. 113* (1983) 854–860.
[291] M. Rance, O. W. Sørensen, W. Leupin, H. Kogler, K. Wüthrich, R. R. Ernst, *J. Magn. Reson. 61* (1985) 67–80.
[292] J. Buddrus, H. Bauer, *Angew. Chem. 99* (1987) 642–659; *Angew. Chem. Int. Ed. Engl. 26* (1987) 625–642.
[293] M. Novic, H. Oschkinat, P. Pfändler, G. Bodenhausen, *J. Magn. Reson. 73* (1987) 493–511.
[294] G. A. Morris, R. Freeman, *J. Am. Chem. Soc. 101* (1979) 760–762.
[295] A. Bax, *J. Magn. Reson. 57* (1984) 314–318.
[296] A. Bax, C.-H. Niu, D. Live, *J. Am. Chem. Soc. 106* (1984) 1150–1151.
[297] M. R. Bendall, D. M. Doddrell, D. T. Pegg, *J. Am. Chem. Soc. 103* (1981) 4603–4605.
[298] D. T. Pegg, D. M. Doddrell, M. R. Bendall, *J. Chem. Phys. 77* (1982) 2745–2752.
[299] D. M. Doddrell, D. T. Pegg, M. R. Bendall, *J. Magn. Reson. 48* (1982) 323–327.
[300] H. Bildsøe, S. Dønstrup, H. J. Jakobsen, *J. Magn. Reson. 53* (1983) 154–162.
[301] O. W. Sørensen, S. Dønstrup, H. Bildsøe, H. J. Jakobsen, *J. Magn. Reson. 55* (1983) 347–354.
[302] D. L. Turner, *J. Magn. Reson. 70* (1986) 465–471.
[303] H. Kogler, O. W. Sørensen, G. Bodenhausen, R. R. Ernst, *J. Magn. Reson. 55* (1983) 157–163.
[304] J. R. Garbow, D. P. Weitekamp, A. Pines, *Chem. Phys. Lett. 93* (1982) 504–509.
[305] V. Rutar, *Chem. Phys. Lett. 106* (1984) 258–261.
[306] A. S. Zektzer, M. J. Quast, G. S. Linz, G. E. Martin, *Magn. Reson. Chem. 24* (1986) 1083–1088.
[307] A. S. Zektzer, B. K. John, R. N. Castle, G. E. Martin, *J. Magn. Reson. 72* (1987) 556–561.
[308] A. S. Zektzer, B. K. John, G. E. Martin, *Magn. Reson. Chem. 25* (1987) 752–756.
[309] M. H. Levitt, R. Freeman, *J. Magn. Reson. 33* (1979) 473–476.
[310] R. Freeman, S. P. Kempsell, M. H. Levitt, *J. Magn. Reson. 38* (1980) 453–479.
[311] M. H. Levitt, R. Freeman, *J. Magn. Reson. 43* (1981) 65–80.
[312] R. Tycko, E. Schneider, A. Pines, *J. Chem. Phys. 81* (1984) 680–688.
[313] M. H. Levitt, *J. Magn. Reson. 48* (1982) 234–264.
[314] J. S. Waugh, *J. Magn. Reson. 49* (1982) 517–521.
[315] M. H. Levitt, *J. Magn. Reson. 50* (1982) 95–110.
[316] M. H. Levitt, R. Freeman, *Adv. Magn. Reson. 11* (1983) 47–110.
[317] A. J. Shaka, J. Keeler, R. Freeman, *J. Magn. Reson. 53* (1983) 313–340.
[318] M. H. Levitt, R. R. Ernst, *J. Magn. Reson. 55* (1983) 247–254.
[319] A. J. Shaka, R. Freeman, *J. Magn. Reson. 55* (1983) 487–493.
[320] M. H. Levitt, R. R. Ernst, *Mol. Phys. 50* (1983) 1109–1124.
[321] W. Warren, A. H. Zewail, *J. Chem. Phys. 78* (1983) 2279–2297.
[322] W. Warren, A. H. Zewail, *J. Chem. Phys. 78* (1983) 3583–3592.
[323] R. Tycko, *Phys. Rev. Lett. 51* (1983) 775–777.
[324] M. H. Levitt, D. Suter, R. R. Ernst, *J. Chem. Phys. 80* (1984) 3064–3068.
[325] A. J. Shaka, R. Freeman, *J. Magn. Reson. 59* (1984) 169–176.
[326] R. Tycko, H. M. Cho, E. Schneider, A. Pines, *J. Magn. Reson. 61* (1985) 90–101.
[327] C. Counsell, M. H. Levitt, R. R. Ernst, *J. Magn. Reson. 63* (1985) 133–141.
[328] R. R. Ernst, *J. Chem. Phys. 45* (1966) 3845.
[329] A. Allerhand, R. E. Addleman, D. Osman, *J. Am. Chem. Soc. 107* (1985) 5809–5810.
[330] A. Allerhand, M. Dohrenwend, *J. Am. Chem. Soc. 107* (1985) 6684–6688.
[331] A. Allerhand, R. E. Addleman, D. Osman, M. Dohrenwend, *J. Magn. Reson. 65* (1985) 361–363.
[332] A. J. Shaka, P. B. Barker, R. Freeman, *J. Magn. Reson. 64* (1985) 547–552.
[333] A. J. Shaka, J. Keeler, *Prog. Nucl. Magn. Reson. Spectrosc. 19* (1986) 47–129.
[334] J. L. Marshall, *Methods Stereochem. Anal. 2* (1983).
[335] W. Bermel, K. Wagner, C. Griesinger, *J. Magn. Reson*, in press.
[336] H. Senn, G. Otting, K. Wüthrich, *J. Am. Chem. Soc. 109* (1987) 1090–1092.
[337] A. Volk, J. Mispelter, J. L. Dimicoli, unpublished.
[338] J. W. Keepers, T. L. James, *J. Am. Chem. Soc. 104* (1982) 929–939.
[339] J. W. Keepers, T. L. James, *J. Magn. Reson. 57* (1984) 404–426.
[340] G. B. Young, T. L. James, *J. Am. Chem. Soc. 106* (1984) 7986–7988.
[341] G. M. Clore, A. M. Gronenborn, *J. Magn. Reson. 61* (1985) 158–164.
[342] A. M. Gronenborn, G. M. Clore, *Prog. Nucl. Magn. Reson. Spectrosc. 17* (1985) 1–32.
[343] W. Massefski, Jr., P. H. Bolton, *J. Magn. Reson. 65* (1985) 526–530.
[344] E. Suzuki, N. Pattabiraman, G. Zon, T. H. James, *Biochemistry 25* (1986) 6854–6865.
[345] P. A. Mirau: *Quantitative Interpretation of a Single 2D NOE Spectrum*, Poster, presented at the 28th ENC, (Asilomar, USA, April 5-9, 1987).
[346] T. L. James, B. A. Borgias, A. M. Bianucci, N. Jamin, N. Pattabiraman, E. Suzuki, N. Zhou, G. Zon in J. W. Jarozewski, K. Schaumburg, H. Kofod (Eds.): *NMR Spectroscopy and Drug Design Development*, Munksgard, Copenhagen 1987.
[347] S. Macura, Y. Huang, D. Suter, R. R. Ernst, *J. Magn. Reson. 43* (1981) 259–281.

[348] S. Macura, K. Wüthrich, R. R. Ernst, *J. Magn. Reson. 46* (1982) 269–282.
[349] H. Kessler, J. W. Bats, C. Griesinger, M. Will, K. Wagner, *J. Am. Chem. Soc., 110* (1988) 1033–1049.
[350] G. Binsch, E. L. Eliel, H. Kessler, *Angew. Chem. 83* (1971) 618–619; *Angew. Chem. Int. Ed. Engl. 10* (1971) 570–572.
[351] J. I. Kaplan, G. Fraenkel: *Dynamic Nuclear Resonance Spectroscopy*, Academic Press, New York 1980.
[352] R. A. Hoffman, S. Forsén, *Prog. Nucl. Magn. Reson. Spectrosc. 1* (1966) 15–204.
[353] H. Bleich, J. Wilde, *J. Magn. Reson. 56* (1984) 149–150.
[354] R. Willem, *Prog. Nucl. Magn. Reson. Spectrosc. 20* (1987) 1–94.
[355] H. Kessler, R. Schuck, R. Siegmeier, *J. Am. Chem. Soc. 104* (1982) 4486–4487.
[356] Y. Huang, G. Bodenhausen, R. R. Ernst, *J. Am. Chem. Soc. 103* (1981) 6988–6989.
[357] G. Bodenhausen, R. R. Ernst, *J. Magn. Reson. 45* (1981) 367–373.
[358] G. Bodenhausen, R. R. Ernst, *J. Am. Chem. Soc. 104* (1982) 1304–1309.
[359] E. R. Johnston, M. J. Dellwo, J. Hendrix, *J. Magn. Reson. 66* (1986) 399–409.
[360] E. W. Abel, T. P. J. Coston, K. G. Orrell, V. Sik, D. Stephenson, *J. Magn. Reson. 70* (1986) 34–53.
[361] M. D. Christopher, L. Lian, C. Redfield, K. D. Topping, *J. Magn. Reson. 69* (1986) 201–209.
[362] D. G. Davis, A. Bax, *J. Magn. Reson. 64* (1985) 533–535.
[363] A. Bax, V. Sklenar, M. F. Summers, *J. Magn. Reson. 70* (1986) 327–331.
[364] P. H. Bolton, *J. Magn. Reson. 67* (1986) 391–395.
[365] M. Rance, *J. Magn. Reson. 74* (1987) 557–564.
[366] R. Bazzo, I. O. Campbell, *J. Magn. Reson. 6* (1988) 358–361; R. Bazzo, I. Boyd, *J. Magn. Reson. 75* (1987) 452–466.
[367] J. S. Waugh, *J. Magn. Reson. 68* (1986) 189–192.
[368] K. E. Kövér, G. Batta, *Progr. NMR Spectrosc. 19* (1987) 223–266.
[369] W. Bermel, Bruker, Karlsruhe, personal communication.
[370] D. G. Davies, *J. Am. Chem. Soc. 109* (1987) 3471–3472.
[371] R. Willem, *Progr. NMR Spectrosc. 20* (1988) 1–94.
[372] H. Kessler, U. Anders, G. Gemmecker, *J. Magn. Reson.*, in press.
[373] J. Cavanagh, J. P. Walter, J. Keeler, *J. Magn. Reson. 74* (1987) 386–393.
[374] G. Otting, K. Wüthrich *J. Magn. Reson. 66* (1986) 359–363.

The Cyclopropyl Group in Studies of Enzyme Mechanism and Inhibition

By Colin J. Suckling*

The cyclopropyl group—particularly in compounds such as cyclopropylmethanol, phenylcyclopropylamine, and cyclopropanone hydrate—has proved to be very useful in the study of enzyme reactions. Whether the cyclopropane ring is opened to form a radical or remains intact can provide much information about reactions occurring at the active site.

1. Introduction

One of the most significant developments in the field of bioorganic chemistry in the last ten years has been the symbiosis of studies of the mechanisms of action of enzymes and the design of specific enzyme inhibitors.[1,2] Increasing pressures for specific drugs have encouraged rational approaches to drug design based upon mechanistic arguments and one of the most attractive of these approaches is the design of enzyme-activated inhibitors. Highly specific action at the site of the target enzyme is in principle assured if one can design a drug that is inactive until it encounters the target enzyme, which activates it, thus causing inhibition. One route to designing such biologically active compounds lies in selecting a small, inert functional group that can be modified into a reactive species either by undergoing a transformation itself or through the effect of an altered neighboring group. For example, haloethenyl substituents have been introduced into phenylethylamines to generate inhibitors of amine oxidases and some compounds have great promise as drugs for the treatment of Parkinson's disease.[2a] Similarly, halomethyl groups can lead to potent and selective enzyme inhibitors with potential as antibacterial agents.[2b] This review concerns a further group with this potential, the cyclopropyl group. The intrinsic chemistry of cyclopropane-containing compounds has been of great general interest for many years, but it is only relatively recently that the bioorganic chemistry of cyclopropanes has been extensively explored. The following discussion surveys firstly the scope of cyclopropanes and related small rings in natural product and enzyme chemistry followed by the chemical properties of cyclopropanes relevant to inhibition and mechanistic studies. The third part of the review deals with the interactions of enzymes and cyclopropanes.

1.1. Cyclopropanes in Natural Products

The inherent strain in the cyclopropane ring has not prevented the widespread occurrence of cyclopropane-containing natural products. In many cases, such rings are stable entities and are substructures of molecules at the ends of biosynthetic pathways. For example, many fatty acids, terpenes, and steroids are alkyl cyclopropanes. An especially significant example is pyrethrin **1**, which is the basis of an important series of insecticides.[3] There are equally significant examples, however, in which the reactivity of the cyclopropane is essential for a particular biosynthetic transformation. The conversion of farnesyl pyrophosphate into squalene via presqualene can be understood in terms of a rearrangement reaction of a cyclopropylalkyl cation.[4] A number of cyclopropyl amino acids are known and several have toxic properties;[5] the toxicity of such compounds can often be related to enzyme inhibition (see Section 4). In contrast, 1-aminocyclopropanecarboxylic acid is well known to be the biosynthetic precursor of ethylene, a hormone involved in the ripening of fruit, and has been

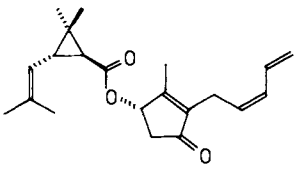

1

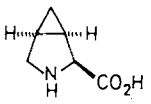

2

isolated from many organisms. The stereochemical details of many of its biosynthetic transformations have been elucidated[6] and there is evidence to implicate the ring opening of cyclopropylammonium radical cations in the biosynthesis.[7a] An ingenious application of the ring opening of cyclopropylalkyl radicals has been shown by *Pirrung* et al. to lead to inhibition of ethylene biosynthesis (see Section 4).[7b] The bicyclic amino acid methanoproline **2** is an inhibitor of proline biosynthesis in plants and can promote sterility in pollen, a feature which has application in the maintenance of true breeding strains of F1 hybrids.[8]

1.2. Unreactive Cyclopropanes

There are several cases of nonnatural cyclopropane-containing compounds in which the small ring is inert but provides a convenient molecular framework to ensure a good match of the compound to its receptor. For example, in

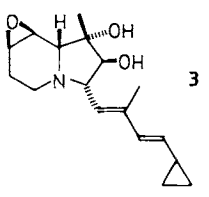

3

[*] Prof. C. J. Suckling
Department of Pure and Applied Chemistry
University of Strathclyde
295, Cathedral Street, Glasgow G1 1XL (UK)

 © VCH Verlagsgesellschaft mbH, D-6940 Weinheim, 1988 0570-0833/88/0404-0537 $ 02.50/0

pyrethroids there is no evidence to suggest that a chemical reaction of the cyclopropane ring is important in insecticidal activity.[3] Fatty alcohol esters of cyclopropanecarboxylic acid have shown to be miticidal agents,[9] again without apparent reactivity in the ring. The active feature of the antibiotic cyclizidine **3** is thought to reside in the indolizidine ring system and not the cyclopropane.[10] *O'Leary* et al. found that 1-hydroxycyclopropanecarboxylic acid phosphate is a reversible inhibitor of enzymes that act upon pyruvate enol phosphate.[11] Presumably in this case, the inhibitor presents the enzymes with a very close geometric match when compared with the substrate. The importance of small groups such as cyclopropanes in providing conformational control of molecules can also be illustrated by its use in investigations of the conformational requirements of the highly flexible neurotransmitter GABA (γ-aminobutyric acid).[12] Such studies are obviously relevant to the design of selective drugs and many compounds containing cyclopropanes have been shown to have biological activity. In some cases, the small ring appears to serve the function of providing favorable binding interactions as a small, rigid alkyl group[13–15] and this may also be the case for a number of compounds with reported central nervous system (CNS) activity.[16] These compounds contain cyclopropyl pyridines and cyclopropyl ketones, structures which would be expected to have reactivity at enzyme sites (see Section 5). The same can be said about several other drugs[17,18] including antimineralocorticoids[19] and antiandrogens.[20]

Cyclopropane-containing compounds with potent biological activities continue to appear. For example, **4** is an inotropic agent that is a competitive inhibitor of cAMP phosphodiesterase.[133]

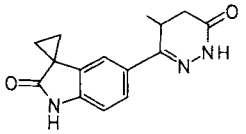

4

1.3. Cyclopropanes and Other Small Rings

The context in which cyclopropane reactivity can be best discussed in terms of biological activity is completed by comparison with small heterocycles. In these compounds, the ring strain is supplemented by the polarization of bonds caused by the heteroatom, leading in many cases to extremely high reactivity and toxicity. For example, aziridines are formed in reactions of β-haloamines, which are components of many drugs (the so-called nitrogen mustards) used in cancer chemotherapy.[21] The naturally occurring antitumor drug mitomycin **5** contains an aziridine

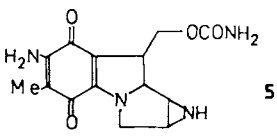

5

that has been implicated in its cytotoxicity.[22] Aziridine-containing amino acids are also known but no enzyme-inhibiting activity of their peptides has been described.[23] Similarly, thiiranes ("epithio derivatives") have high biological activities, exhibited originally in mustard gas[24] and more recently suggested to be responsible for the mutagenicity of 1,2-dihaloethanes through conjugation with glutathione.[25] Epoxides, too, can be used in cancer chemotherapy and they are commonly encountered in enzyme inhibitors.[26,27] Biological activity is not exclusive to three-membered heterocycles. β-Propiolactone was once regarded as a disinfectant but its mutagenicity has limited its use. The most extensively researched area of biologically active small heterocycles, of course, is that of the β-lactam antibiotics. Although it was once thought that the strain in the ring was an important contributor to biological activity, it is now generally accepted that the ability of a β-lactam to acylate its target enzyme is principally a function of the properties of the leaving amino group;[28] in other words, electron-withdrawing groups in the five-membered ring promote activity. Interestingly, a few β-lactams containing cyclopropyl substituents have been reported (e.g., **6** and **7**), but no biological activity attributable to the cyclopropane ring has been described.[29] A number of attempts have been made to prepare antibacterial compounds similar to β-lactams but containing cyclobutanones as the reactive group.[30] The comparison with cyclopropanones is interesting (see Sections 2.2 and 4). However, only in one case (**8**) in which analogues of thienamycin were prepared has antibacterial activity been reported.[30e]

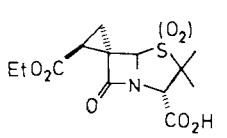

6

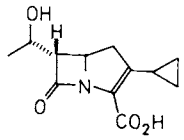

7

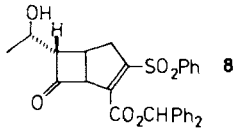

8

2. The Chemical Reactivity of Cyclopropanes

2.1. The Cyclopropane Ring

The acute angles of the three-membered ring in cyclopropanes are obvious sources of ring strain and, in addition, all of the carbon–hydrogen bonds are eclipsed. Together, these factors contribute to a strain energy of 117.6 kJ mol^{-1}.[31,32] The thermodynamic driving force for ring opening is thus great and many of the common reactions of cyclopropanes are addition reactions that parallel those of alkenes: for example, addition of halogen to yield 1,3-dihalides and catalytic hydrogenation to afford alkanes.[32] In common with most vinyl and aryl C–H bonds, the C–H bonds of cyclopropane are strong, which accounts for the lack of radical reactions occurring through hydrogen abstraction pathways. In parallel with reactions of electrophiles, radical reactions tend to lead to net addition to the cyclopropane ring.

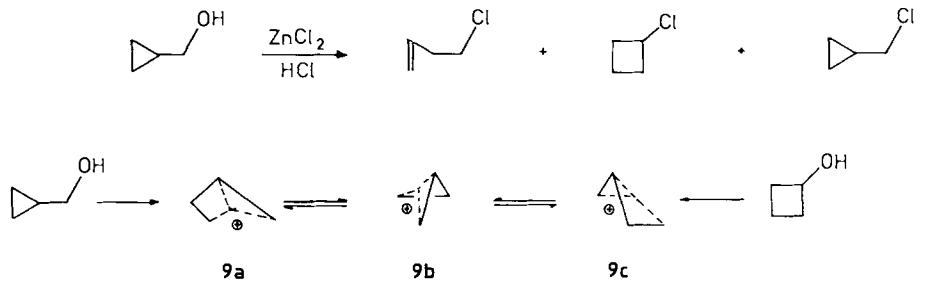

Fig. 1. Cationic rearrangements of cyclopropylmethyl derivatives via cations **9a–c**.

The description of cyclopropanes as homo-alkenes parallels that of epoxides as homo-carbonyl groups and has led to many descriptions of the bonding in cyclopropane. For example, the valence bond treatment generates a bonding picture that includes so-called bent or banana bonds which, because of the nature of the overlap of the component orbitals, have some π character.[33] Alternatively in a description due to *Walsh*,[34] the π character arises from the overlap of centrally pointing p orbitals.

2.2. Cyclopropanones

As will be discussed in Sections 4 and 5.1, cyclopropanones and their imino derivatives have figured greatly in studies of enzyme inhibition. The basic chemical reactivity that accounts for this is the high stability of cyclopropanone hydrate compared with most other ketone hydrates.[35] It has been argued that the cyclopropanone ring is even more strained internally than the cyclopropane ring itself because the preferred bond angle of the carbonyl group (120°) is further away from the enforced bond angle (≈60°) than the tetrahedral bond angle (109°28′).[36] However, a mobile equilibrium between the hydrate and the ketone does exist because ligand exchange occurs readily; this reaction is thought to be the basis for the inhibition of dehydrogenases and some oxidases by cyclopropanones and their equivalents.

2.3. Cyclopropanes Activated by an Electron-Withdrawing Substituent

Into this class of cyclopropane derivatives, two systems can be placed, namely, cyclopropyl aldehydes, ketones, and esters and their relatives, and cyclopropylmethyl halides or cyclopropylmethanols and their esters. The characteristic reaction of this class of compound is nucleophilic attack on the cyclopropane ring leading to ring opening. For cyclopropylcarbonyl derivatives, the stability of the ring to addition by protonic acids is enhanced, a fact that considerably facilitates the synthesis of complex molecules containing cyclopropanes.

The biosynthesis of squalene from presqualene has been reationalized on the basis of the reactivity of a cyclopropylmethyl ester[4] and, in particular, its propensity to rearrange. The prototype rearrangement has been known for many years[37] as the "cyclopropylcarbinyl" rearrangement (Fig. 1). The solvolysis of cyclopropylmethyl halides and toluenesulfonates has been shown to lead to a mixture of products in which the ring is retained, broken, or enlarged, depending upon the reactants and reaction conditions.[38] When experiments with isotopic labels were carried out,[39] it was shown that the connectivity of the labeled carbon atoms was altered even in the products that retained the three-membered ring. Clearly, the intermediate cation has a great many reaction paths of similar energy open to it. Perhaps the best indication of its structure came from experiments in superacid media by *Olah* et al.[40] He interpreted ^{13}C-NMR spectra of the cation in terms of an equilibrium between three species, **9a–c** (Fig. 1), and the same equilibrium was reached with either cyclopropylmethanol or cyclobutanol as the starting material. The point of relevance with regard to squalene biosynthesis is that such reactions allow an apical carbon of the ring to bond to the carbon of the substituent that bears the leaving group. In both this biosynthetic reaction and in transformations of carbocyclic systems, it is believed that the methylene group of the cyclopropane to which the new bond is formed undergoes inversion of configuration.[41] A feature of potential significance of the structure of such rearranging cations with regard to enzyme inhibition is the great opportunity that they give for attack by a nucleophile at the enzyme's active site. Despite this potential, no inhibition reactions have so far been reported to occur through such a mechanism. This is possibly because such solvolysis reactions are relatively slow, with rate constants typically on the order of $10^{-3}\,s^{-1}$ at 30–40°C.[42] Nevertheless, the cyclopropane ring has a strong electron-donating effect that is manifested not only in solvolysis reactions but also in electrophilic aromatic substitution.[32]

Some of the reactions mentioned above (e.g., **10**→**11**) lead to ring-opened products and, in several cases, there is good stereochemical control of the alkene generated. *Julia* et al.[43a] were the first to report such a reaction (Fig. 2) and their work was extended by *Johnson* et al.[43b] The stereochemical course of these reactions has been rationalized by considering the conformation of the cyclopropane ring with respect to the leaving group as illustrated in **12a** and **12b**. The stereoelectronic requirement is for overlap of a cyclopropane bond with the bond to the leaving group. Conformation **12a** minimizes torsional interactions and leads to the observed products with *E* configuration. There is a parallel between these reactions and the inhibition of some dehydrogenases to be described later (see Sections 6.1 and 6.2).

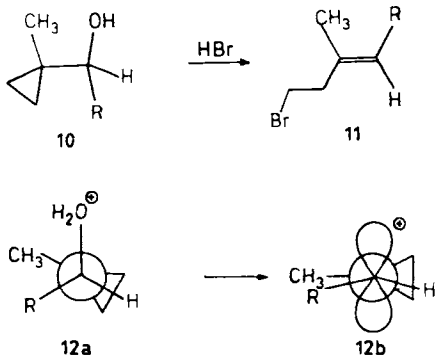

Fig. 2. Formation of alkene **11** from cyclopropylmethanols **10** via cations **12a** and **12b**.

Cyclopropylcarbonyl compounds can be considered as close analogues of the above cationic systems in which the polarized carbonyl group provides the partial positive charge. In many reactions with nucleophiles, addition to a single carbonyl substituent group takes place without cleavage of the small ring. Thus cyclopropyl methyl ketones can be reduced to secondary alcohols with $NaBH_4$ in methanol and esters of cyclopropanecarboxylic acid react with $LiAlH_4$ to yield the corresponding primary alcohols.[44] However, if the carbonyl group's polarization is enhanced by coordination with a Lewis acid, ring opening can take place (e.g., **13** → **14** in Fig. 3); this reaction is a useful synthetic route to homoallylic halides.[45] As will be seen in Section 6, coordination of cyclopropylcarbonyl groups to metal ions is important in the inhibition of metalloenzymes. Under severe conditions, nucleophilic ring

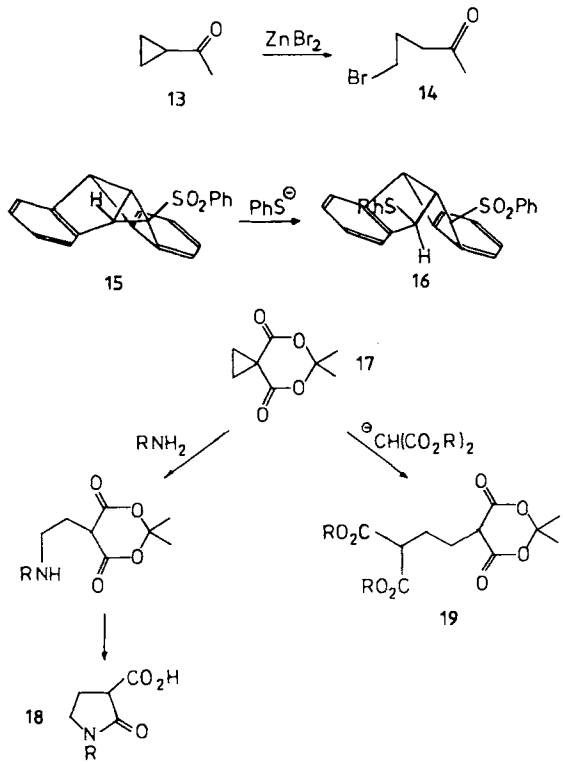

Fig. 3. Nucleophilic substitution with ring opening at cyclopropanes **13**, **15**, and **17** bearing electron-withdrawing substituents.

opening of substituted cyclopropanes is possible without acid catalysis either by a metal ion or a proton. In a particularly interesting example, *Cristol* et al.[46] showed that inversion of configuration occurred when thiophenolate attacked the cyclopropane of the fused ring system (**15** → **16**, Fig. 3). Where the stereochemical course has been determined, nucleophilic ring-opening reactions of activated cyclopropanes have been shown to occur with inversion of configuration at the attacked carbon.

The presence of two electron-withdrawing groups renders the ring susceptible to nucleophilic cleavage without special activation. For example, quite weak nucleophiles can add to the spirocyclic cyclopropane **17**, giving the products **18** and **19** (Fig. 3); the presence of the ester substituents in **18** and **19** opens up further reaction paths that can be useful in synthesis. The ease of this reaction is enhanced by the restricted conformation of the cyclopropane ring which places the scissile C–C bond in a favorable orientation with regard to the electron-accepting carbonyl group.[47] Enzyme inhibitors containing doubly activated cyclopropane rings may therefore be unselective.

2.4. Cyclopropylalkyl Radicals

The cyclopropylmethyl radical (**20**) has held a distinguished place in the chemistry of cyclopropanes and in their bioorganic chemistry since *Ingold* et al. reported that the rate of its ring opening to form the homoallyl radical **21** was $10^8\ s^{-1}$ at 25 °C.[48] It was quickly realized that this

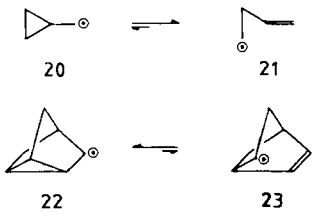

fast reaction could have a useful role in detecting the intermediacy of radicals. There have been many applications of the same general reaction in attempts to elucidate the mechanisms of enzyme-catalyzed reactions and to generate inhibitors. *Ingold* et al. also reported that the ring-opening rate of alkylcyclopropylaminyl radicals, which is very relevant to many inhibition reactions, was too fast to measure by kinetic ESR spectroscopy and was independent of the alkyl substituent.[49a] Very recently, the ring opening of cyclopropylamine radical cation has been shown to proceed via a γ-iminium radical cation[49b] in a manner agreeing with many mechanisms proposed for enzyme inhibition.

The success or otherwise of the enzymic experiments employing cyclopropanes, however, depends critically upon a good understanding of the chemistry of this ring-opening reaction. Several factors must be considered. Firstly, it has been demonstrated that the reaction is an equilibrium;[50] for a monocyclic compound, the equilibrium constant has been determined to be 10^{-5} at 25 °C in favor of the ring-opened radical (cf. **21**). But the position of this equilibrium is decisively influenced by the carbon skeleton into which the cyclopropane is built. The nortri-

cyclyl radical **22** having a cyclopropane ring, for example, is stable at room temperature.[51] Secondly, few enzyme substrates or inhibitors are simple cycloalkanes and so the effect of substituents on the rate of ring-opening reactions must be considered. That cyclopropylalkoxyl radicals readily undergo ring opening has been known for nearly twenty years through the work of *Dauben* et al.[52] who showed that the 3-oxo steroid derivatives **24** and **25** un-

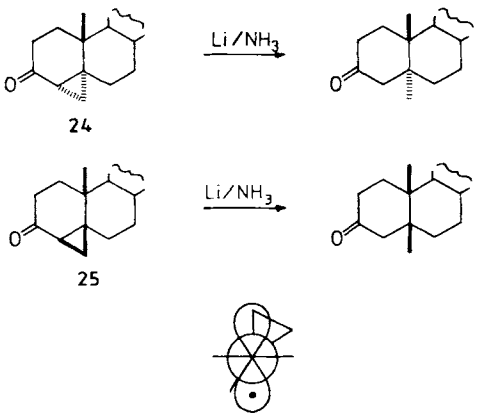

derwent cyclopropane ring opening on treatment with lithium in ammonia. The reaction is quite general[53] and, interestingly, drew attention to a stereoelectronic requirement for ring opening. *Dauben*'s results showed that the cyclopropane C–C bond that better overlaps with the singly occupied orbital of the radical will be broken.[52] None of these results, however, provided a measure of the rate of ring opening of cyclopropylalkoxyl radicals.

Since knowledge of such rates was of critical importance in our work, we have taken some trouble to obtain relevant values (Table 1).[44,54] Using ESR spectroscopic techniques principally with silyl ethers as substrates, we found that the rate of ring opening of a simple cyclopropylalkyl radical was reduced by about a factor of 10 by oxygen substitution. In contrast, the inclusion of alkyl groups, which presumably increase the strain in the cyclopropane ring, accelerates ring opening by a similar factor. A most remarkable result was obtained with disubstituted radicals in which a donor alkoxy group is paired with an acceptor carbonyl or cyano group. In neither case was it possible to observe the ring-opened radical under accessible conditions. The result has been interpreted in terms of the so-called capto-dative stabilization of radicals[55] and is one of the most extreme examples known. Together, all of these observations show that for the ring opening to be rapid and useful as a mechanistic probe for the intermediacy of radicals, several criteria must be satisfied: (1) there must be no substantial stabilization of the radical site itself by delocalization, (2) there must be a conformation available in which a C–C bond of the ring overlaps with the singly occupied orbital, and (3) the structure of the compound must not be so compressed that ring closure is entropically favored. How these factors work out in enzyme-catalyzed reactions will be seen in Section 6.

Table 1. Stability of substituted cyclopropylmethyl radicals and/or alkenyl radicals assessed by variable-temperature ESR spectroscopy.

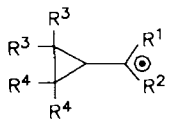

R^1	R^2	R^3	R^4	k [s^{-1}]
H	H	H	H	2.2×10^8
Me	$OSiMe_3$	H	H	2.4×10^7
H	$OSiMe_3$	Me	H	only ring-opened radical observed down to −153 °C
H	$OSiMe_3$	Me	Me	only ring-opened radical observed down to −173 °C
H	CO_2Me	H	H	ring opening not detected up to 7 °C
$OSiMe_3$	CO_2Me	H	H	ring opening not detected up to 110 °C
$OSiMe_3$	CN	H	H	ring opening not detected up to 110 °C

The rates of ring opening of substituted cyclopropylalkyl radicals were studied by photochemical generation of radicals at low temperature.[44,45,54] The temperature dependence of the rate of ring opening in the range 30–89 °C has now been examined using the thermal decomposition of diazo compounds to produce cyclopropylmethyl radicals. It was found that the activation parameters in this temperature range differed significantly from those determined for the range from −120 to −145 °C.[134]

2.5. Cyclopropylalkyl Anions and Their Relatives

Although the π-bonding characteristics of cyclopropanes would suggest that they should stabilize adjacent carbanions, experiments have shown that cyclopropanes are very poor acceptors. Rates of exchange of hydrogen for deuterium in benzyl-substituted cyclopropanes indicate very little stabilization of the anion by the cyclopropyl group[56] in agreement with studies of gas-phase acidities.[57] Nevertheless, cyclopropyl anions have an extensive synthetic chemistry.[58] Interestingly, the cyclopropoxide anion has been found to undergo slow ring opening[59] and the rate of reaction is increased substantially if the carbanion resulting from ring cleavage is delocalized. It can thus be seen that cyclopropylmethyl anions, cations, and radicals can all undergo ring opening, the radical being distinctly the fastest.

3. The Enzyme Chemistry of Cyclopropane and Unactivated Alkylcyclopropanes

Although the majority of cyclopropane derivatives studied in enzyme chemistry contain potentially reactive substituents, some simple alkyl cyclopropanes have been used to characterize the reactivity of oxidizing enzymes. The first example of such experiments using a purified enzyme preparation was reported by *Golding, Dalton* et al.[60] who showed that the monooxygenase enzyme from *Methylococcus capsulatus* was capable of oxidizing cyclopropane to cyclopropanol and methylcyclopropane to cyclopropylmethanol. Interestingly, but-3-en-1-ol, a product of oxidation with ring opening of a cyclopropylmethyl radical, was not observed. Together with other observations, this result suggested to the authors that the oxidase from *M. capsulatus*

functioned through a metal-bound oxygen species that is capable of insertion into a C–H bond and that no radical or cationic intermediates were involved.

Simple cyclopropane derivatives are sometimes cleaved by enzymes. Cyclopropane itself has been oxidized to propanal by *Mycobacterium spp.*[61] Haloperoxidase treats cyclopropane as a typical alkene and adds to afford 3-bromopropanol;[61,62] the orientation of similar reactions using alkenes as substrates suggests that a cationic intermediate is involved in this case. Haloperoxidase is a heme-containing enzyme that is thought to operate through a mechanism different from that of cytochrome P-450. For the latter, model reactions have been very helpful in providing clues as to the reaction mechanism[63] and cyclopropanes have been used as substrates. *Groves* et al.[64] found that bicyclo[4.1.0]heptane was oxidized by manganese(III) tetraphenylporphyrin in the presence of iodosylbenzene to a mixture of products of which 32% were homoallylic alcohols or halides resulting from ring opening. A larger proportion of the products (42%) retained the cyclopropane ring. The results were consistent with a radical mechanism which has become known as the "oxygen rebound" mechanism and has served as a framework for mechanistic discussions relating to cytochromes P-450 (Fig. 4).[63] The proportion of ring-opened products observed in a reaction using an alkylcyclopropane as a mechanistic probe will clearly depend upon the relative rates of ring opening and capture of the intermediate radical. In *Grove*'s case[64] the two rates are comparable.

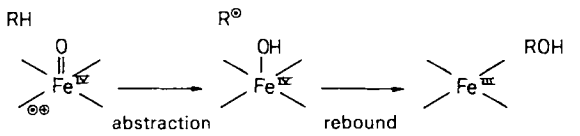

Fig. 4. Hydroxylation of alkanes by cytochromes P450—the oxygen rebound mechanism.

Although many enzymic experiments have been rationalized with the aid of the oxygen rebound mechanism (see Section 5), especially with regard to the intermediacy of radicals, unactivated cyclopropanes as substrates do not provide evidence for the intermediacy of radicals as might be expected from the model reactions. As part of our studies of steroid metabolism,[65] we submitted 5α,6α-methanocholest-3β-ol **26** to oxidation by a purified preparation of cholesterol 7α-hydroxylase. The cyclopropyl steroid **26** proved to be a competitive substrate with respect to cholesterol and was oxidized to the corresponding 7-hydroxy derivative **27** without any evidence of ring opening. We showed that there was no chemical impediment to ring opening of a 7-radical by reducing the 7-oxo-5α,6α-methano steroid **28** with lithium in ether/liquid ammonia following *Dauben* et al.;[52] the product was the ring-opened diol **29**. It seems improbable that cholesterol 7α-hydroxylase, which is otherwise a typical cytochrome P-450 enzyme, should function by a totally different oxidation mechanism from its relatives. However, it is known that the enzyme is especially selective with regard to its substrate; even the loss of one side-chain methyl group causes an appreciable loss of reactivity towards oxidation.[66] If the enzyme is capable of binding the substrate tightly, a radical mechanism can still be accommodated if the oxygen rebound step is faster than the ring-opening step, but an alternative mechanism cannot be ruled out on the basis of this experiment. The cytochrome P-450 responsible for the side-chain cleavage of cholesterol during steroid hormone biosynthesis has also been shown to oxidize a cyclopropane-containing analogue of the substrate without cleaving the three-membered ring.[67] Recently, *Ortiz de Montellano* et al. have provided a rounded background to these results, showing that whereas methylcyclopropane does not undergo ring opening on oxidation by cytochrome P-450, the strained bicyclo[2.1.0]pentane undergoes partial ring opening. These results imply that the radical pair in the rebound mechanism collapses at a rate greater than $10^9\ s^{-1}$.

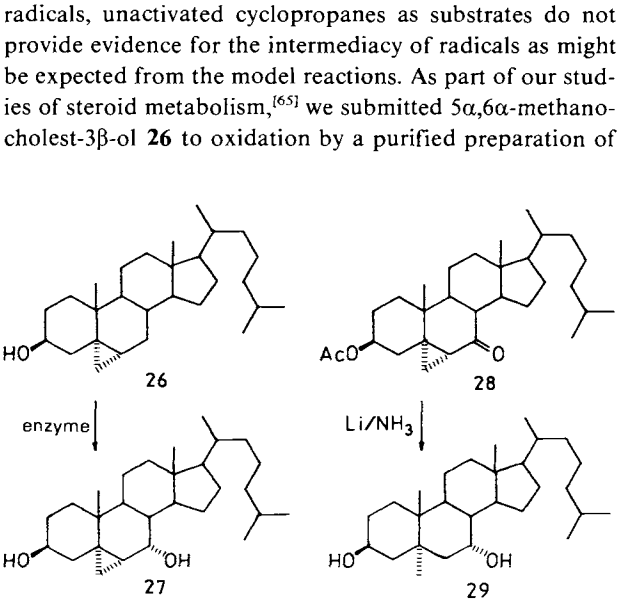

4. Enzyme Inhibition by Amino Acids Containing Cyclopropyl Groups and by Cyclopropanone Derivatives

Two of the first cyclopropane-containing enzyme inhibitors to be described were toxic amino acid derivatives, namely, coprine **30**[69] and hypoglycine A **31** (Fig. 5).[70] Although coprine is clearly a cyclopropanone adduct of glutamine, it is not immediately obvious what biological activity hypoglycine has. *Abeles*[71a] has suggested that deamination and decarboxylation takes place to yield a vinylogous cyclopropanone system as its thiol ester **32**; this compound is suggested to be a substrate of a general acyl-CoA-dependent dehydrogenase which is inactivated by nucleophilic addition. In contrast, *Ghisla*[71b,c] believes that deamination and decarboxylation leads to **33**, the saturated analogue of **32**; the readily formed carbanion from this molecule then adds to the flavin cofactor in a manner similar to alkynes that inhibit lactate oxidase.[72] The inhibition of glutaryl-CoA dehydrogenase has been reported to occur with methylenecyclopropaneacetic acid and its coenzyme A ester,[73] but the detailed mechanism has not been established for either case.

Methylenecyclopropanecarboxylate CoA ester has recently been synthesized and shown to inhibit a general acyl-CoA dehydrogenase from pig kidney.[135]

Coprine, a product of *Coprinus atramentarius*, the common ink cap mushroom, provided the stimulus for the development of a number of enzyme inhibitors. It was

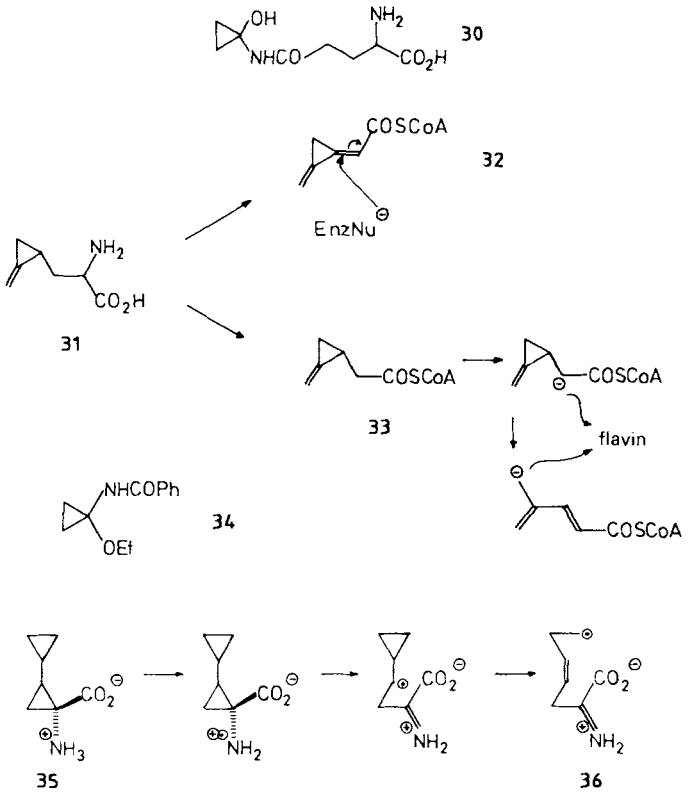

Fig. 5. Enzyme inhibition by cyclopropane-containing amino acids. $EnzNu^{\ominus}$ stands for a nucleophilic group of the enzyme.

shown[74] that coprine is a proinhibitor for aldehyde dehydrogenase, and its ability to inhibit the liver enzyme suggested a use in the treatment of alcoholism. However, neither coprine itself, **30**, nor simple synthetic analogues such as **34**[74] proved suitable for clinical use because of their toxicity. During his studies on ethylene biosynthesis, *Pirrung* et al.[7] reasoned that the cyclopropyl-substituted 1-aminocyclopropanecarboxylic acid **35** should be an inhibitor of the enzyme through the ring-opening reaction **35** → **36**. It was possible to demonstrate time-dependent inhibition of ethylene formation in mungbean hypocotyl segments and substrate protection was observed. The bicyclopropane derivative **35** is an unusual example of a mechanism-based inhibitor of plant enzymes and emphasizes the importance of ring opening of cyclopropylaminium radical cations in ethylene biosynthesis.

The possibility of using cyclopropanones more widely was pursued by many groups. *Abeles* et al. firstly demonstrated that cyclopropanone hydrate was an inhibitor of yeast aldehyde dehydrogenase apparently through addition of a thiol to replace one of the hydroxyl groups.[75] At about the same time, *Singer* et al.[76] and *Silverman* et al.[77] independently described studies of the inhibition of mitochondrial monoamine oxidases (flavoenzymes) by cyclopropylamines. Both groups initially interpreted their results in terms of cyclopropanone chemistry.

trans-2-Phenylcyclopropylamine (tranylcypromine) **37** was the first cyclopropyl enzyme inhibitor to be studied and the first to be shown to follow time-dependent kinetics.[78] *Singer*'s later study showed that inhibition occurred without irreversibly altering the flavin chromophore.[76] He

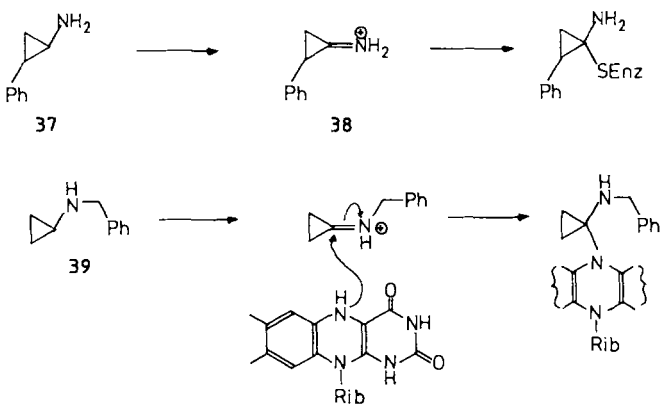

Fig. 6. Proposed mechanisms for the inhibition of monoamine oxidase by cyclopropylamines via cyclopropanone equivalents.

therefore suggested that addition of an enzymic thiol group to the cyclopropyliminium ion **38**, which is the primary oxidation product, again led to inhibition (Fig. 6); this hypothesis was supported by the fact that 2-phenylcyclopropanone had an equivalent inhibitory effect. *Silverman* et al.[77] studied *N*-alkylcyclopropylamines, for example *N*-benzylcyclopropylamine **39**, which were also inhibitors. They found, however, that the flavin chromophore was altered during inhibition and postulated that N-5 of the flavin might also be a suitable nucleophile to add to **38** (Fig. 6). The possibility that electron transfer reactions and multiple pathways might be involved was raised later[79] (see Section 5).

The small cyclopropane ring is attractive for inclusion into many enzyme substrates in order to transform them into inhibitors (see Section 1). *Abeles* et al. have shown that the strategy is successful for hydroxymethylglutaryl-CoA reductase.[80] They synthesized two diastereoisomers of cyclomevalonic acid **40** and showed it to be an inhibitor. It is

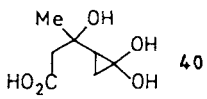

worth noting in passing that addition of nucleophiles to carbonyl groups to form adducts has been successful with electrophilic aldehydes,[81] as well as with trifluoromethyl ketones and peptides.[82, 138]

Further amino acid derivatives of cyclopropanes with biological activity have been described. Although GABA-transaminase was inhibited irreversibly by aminofluoropentenoic acid, the cyclopropane amino acid **41** was a noncompetitive inhibitor. It was suggested that the geometrical structure of this compound made binding at the active site unfavorable.[136]

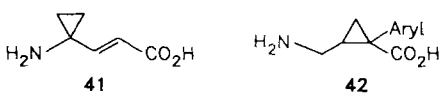

A new series of potential antidepressants, **42**, has been described.[137] Interestingly, these compounds appear to have a different pharmacological profile from tricyclic antidepressants and tranylcypromine **37**; they can also be viewed as GABA analogues.

5. Inhibitors Based Upon Heteroatom-Substituted Cyclopropanes and Their Ring-Opened Derivatives

5.1. Hemoproteins and Monoamine Oxidases

The early experiments with cyclopropylamines seem to have neglected the possibility that radical reactions might lead to inhibition through ring opening prior to radical capture. The first indications that such a mechanism might be reasonable came from studies of the inhibition of cytochromes P-450 by cyclopropylamines. Using *N*-benzylcyclopropylamine **39**, *Hanzlik* et al.[83] showed that cytochrome P-450 from rat liver microsomes was irreversibly inhibited. This result could be accounted for by an addition mechanism (see Section 4), but when it was found that *N*-benzyl-1-methylcyclopropylamine **43** was also an irreversible inhibitor, the possibility of an alternative mechanism became strong, because this inhibitor clearly cannot form a cyclopropanone equivalent. The radical cation **44** was implicated and two modes of reaction were postulated (Fig. 7); firstly, the ring-opening reaction of a cyclopropylalkyl radical equivalent leading to **45**; secondly, ring expansion to an azetidinium radical cation **46**. Chemical analogies existed for each type of reaction[35,84] but the latter was preferred because of the observed tight binding of labeled inhibitors to microsomal protein.

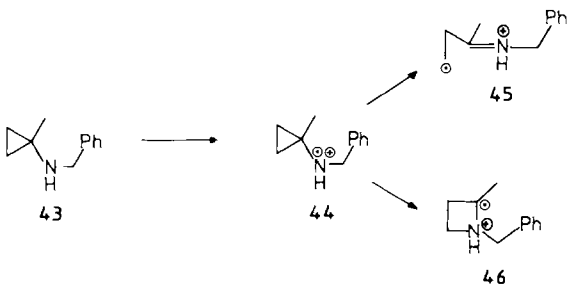

Fig. 7. Formation of radicals in the inhibition of monoamine oxidase by *N*-benzyl-1-methylcyclopropylamine **43**.

Concurrently with this report, *MacDonald, Guengerich* et al.[85] described a further alternative whereby a ring-opened radical such as **45** attacks the porphyrin ring, causing enzyme inactivation. Both *N*-benzylcyclopropylamine **39** and its 1-methyl analogue **43** were studied and it was clearly demonstrated that both benzphetamine and aminopyrine *N*-deethylase activities were inhibited by these compounds, although some activity was recoverable on dialysis.

Naturally, these results have relevance to the mechanism of inhibition of monoamine oxidase[79] and *Silverman* et al. undertook further investigations. When the radical mechanism is applied to 2-phenylcyclopropylamine **37** as an inhibitor, ring opening of the cyclopropane would lead to a benzylic radical, **47** (Fig. 8). By isolation of derivatives of hydrolysis products from the inhibited enzyme it was shown that monoamine oxidase is inhibited not by a cyclopropanone equivalent, but by a cinnamaldehyde equivalent, **49**.[86] Interestingly, further evidence in support of a radical mechanism for monoamine oxidase has been found from experiments with 1-amino-1-phenylcyclobutane.[87]

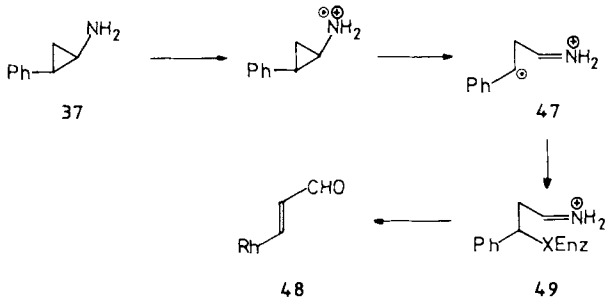

Fig. 8. Possible course of inhibition of monoamine oxidase by 2-phenylcyclopropylamine **37**. Cinnamaldehyde **48** has been detected.

To establish which fragments of cyclopropyl inhibitors were attached to monoamine oxidase, *Silverman* et al. studied labeled *N*-benzyl-1-methylcyclopropylamine **43** and found that only the methyl and cyclopropyl carbon atoms remained attached.[88] The results were interpreted in terms of the mechanism which postulates that a flavin radical couples with the ring-opened radical **45**;[49] hydrolysis of the imine would then liberate benzylamine and leave the inhibitor attached to the flavin as a 3-oxobutyl substituent. In a similar way, the behavior of 1-phenylcyclopropylamine has been rationalized through the observation of phenyl ketones and iminium salts as products.[89] The importance of the cyclopropane in this reaction was shown by the fact that dimethylbenzylamine fails to inactivate the enzyme. The most recent addition to understanding of these reactions has come from the identification of a cysteine residue that forms a transient intermediate with 1-phenylcyclopropylamine during inhibition of mitochondrial monoamine oxidase.[90]

When electron transfer reactions were first considered to be responsible for inhibition of monoamine oxidase, it was felt that related cyclopropanols would not react in this way because of the greater difficulty of removal of an electron from oxygen compared with nitrogen.[83] However, it appears that such reactions can occur if the enzyme possesses a sufficiently powerful oxidizing agent. For example, *Wiseman* et al.[91] found that horse radish peroxidase, a hemoprotein, was inhibited by cyclopropane hydrate **50**. The

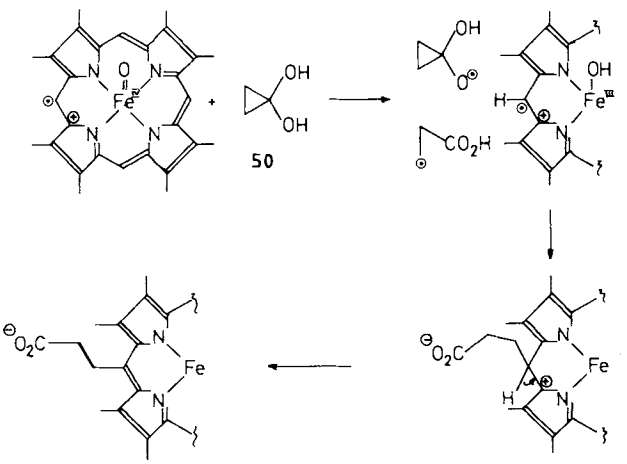

Fig. 9. Mechanism proposed to account for the inhibition of horse radish peroxidase by cyclopropanone hydrate **50**.

visible spectra of the inhibited enzyme were interpreted in terms of alkylation of the porphyrin ring (Fig. 9) in a manner related to the inhibition of cytochrome P-450.

5.2. Methanol Oxidizing Enzymes

Recently there has been a great deal of interest in a newly discovered coenzyme that is responsible for the oxidation of methanol.[92] This cofactor is a pyrroloquinoline quinone (PQQ, **51**) and has also been called methoxatin.[93]

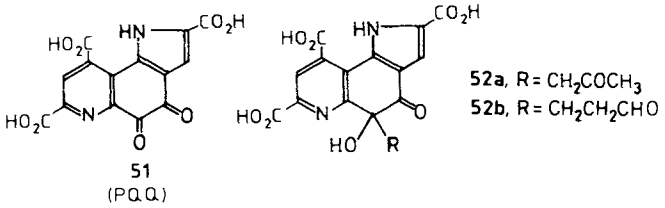

During the course of isolation and structure determination of PQQ, an acetone adduct, **52**, was formed and this compound has influenced thoughts on the mechanism of oxidation of alcohols by PQQ-dependent enzymes.[94,95] The detailed mechanism of action of PQQ is not yet established. Experiments from *Duine*'s laboratory are strongly indicative of a radical pathway, at least for some substrates,[95] although different views have been expressed.[96] Isolated methanol dehydrogenase appears to contain PQQ in a semiquinone form that undergoes one-electron oxidation to the quinone form, which appears to be catalytically active. One of the complications in elucidating the mechanism of action of methanol oxidation is that there are several types of enzyme, some monomeric and some dimeric. One part of the mechanistic problem relates to clarifying the enzymological relationships between the enzymes and the other part relates to the chemical mechanism of oxidation.

Abeles et al.[96] found that cyclopropanol inactivates the enzyme from *M. methanica* in the presence of phenazine methyl sulfate without a measurable primary deuterium or tritium isotope effect.[96b] A base-labile adduct of PQQ and the inhibitor was isolated and assigned the structure **52b**. However, there was no suggestion as to how **52b** might arise except through the radical semiquinone form of the cofactor. *Duine* et al. also have found that cyclopropanol is an inhibitor of dimeric methanol dehydrogenase and also of a monomeric enzyme from *Pseudomonas* BB1[97a] but that cyclopropylmethanol, cyclobutanol, and cyclohexanol are all substrates. In his experiments, enzymes containing PQQ in the semiquinone form were not inactivated. Further it was found that PQQ-dependent dehydrogenases that are capable of oxidizing secondary alcohols (the *Pseudomonas* enzyme) are inhibited by cyclopropanone hydrate **50** and cyclopropanone ethyl hemiketal. The modified PQQs from cyclopropanol and the cyclopropanone derivatives were found to be different, suggesting that a mechanism involving oxidation of cyclopropanol to cyclopropanone is not operative. The structure of the adduct has now been characterized as **52b**[97b] and, with this result in mind, the inhibition of the enzymes was rationalized (Fig. 10) through one-electron oxidation of the alcohol to

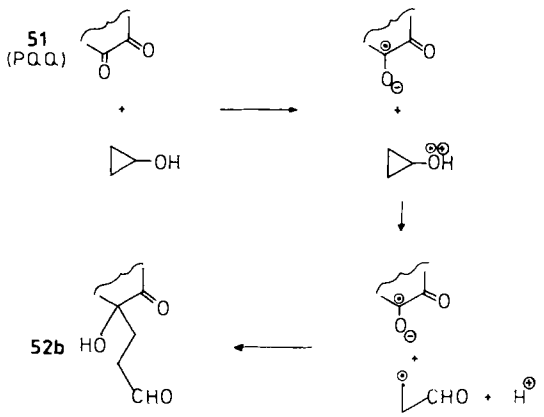

Fig. 10. Suggested mechanism of inhibition of *Pseudomonas* PQQ-dependent methanol dehydrogenase by cyclopropanol.

afford a PQQ radical anion and a cyclopropyloxonium radical. Rapid ring opening of the oxonium radical and combination with the PQQ radical then leads to a molecule with a structure identical to that proposed by *Abeles*, **52b**.

A further class of methanol oxidizing enzyme is known, namely, a flavoprotein oxidase which has also been studied by *Abeles* et al. using cyclopropanol as a probe.[98] The enzyme is inhibited by cyclopropanol through the formation of an *N*-5 flavin adduct as has commonly been suggested. Two possible mechanisms were considered, one in which a cyclopropoxy radical undergoes ring opening before combining with the flavin and the other in which the cyclopropoxide ion undergoes ring opening prior to adding to the oxidized flavin. In view of the very slow rate of the latter ring opening (see Section 2.5),[59] *Abeles* favored the radical mechanism. He also found that cyclopropylmethanol was a substrate for the enzyme and not an inhibitor. This result is consistent with a radical mechanism in which electron transfer from the oxygen atom occurs; the product of this oxidation has a methylene group between the cyclopropane ring and the oxygen radical and would therefore not be expected to undergo rapid ring opening. In contrast, a mechanism involving abstraction of a hydrogen atom from the methylene group might conceivably yield a ring-opened product if the radical formed had a sufficiently long lifetime. Such arguments were raised by *Abeles* in commenting upon our results concerning nicotinamide-dependent dehydrogenases which will be discussed in the following section. He is right to point out, as had been realized earlier, that the lack of ring opening of a cyclopropylalkyl radical is not conclusive evidence against radical intermediates. Indeed, our experience with cytochromes P-450 confirms this.[65,67,68] However we have taken some trouble to establish the limits to which conclusions concerning the intermediacy of radicals can be drawn in the case of nicotinamide-dependent alcohol dehydrogenase[44,45] and these arguments will now be reviewed.

6. Cyclopropylmethanols and Their Derivatives

We have studied the enzyme chemistry of cyclopropylmethanols, and their alkylated and oxidized derivatives

both as inhibitors of enzymes and as mechanistic probes for the intermediacy of radicals in enzyme-catalyzed reactions involving NAD$^{\oplus}$/NADH. It has proved possible to dissect both functions and both will be discussed.

6.1. The Mechanism of Hydrogen Transfer by Nicotinamide Coenzymes

The possibility that hydrogen transfer reactions by nicotinamide coenzymes might involve radical intermediates was strongly raised in 1971 by *Hamilton*[99a] and a great deal of work was stimulated chiefly using model compounds.[99b] We felt, however, that it was important to obtain the best possible information about the reaction occurring at an enzyme's active site. The way to approach this challenge was through the rapid ring opening of cyclopropylalkyl radicals. Since the rates of hydrogen transfer by horse liver alcohol dehydrogenase had been shown to be between 30 and 100 s^{-1},[100] it was possible that a radical intermediate formed during the redox reaction would have ample time to open and hence the products of the reaction would reveal the intermediacy or otherwise of radicals. Our first experiments used horse liver alcohol dehydrogenase with bicyclo[4.1.0]heptane-7-methanol **53** and the corresponding aldehyde.[101] Under preparative conditions with recycling of NAD$^{\oplus}$ or NADH as appropriate, we isolated products and starting material with intact cyclopropane rings. These experiments thus provided no evidence for radical intermediates.

We then extended the investigation to lactate dehydrogenase using cyclopropaneglycolic and cyclopropaneglyoxylic acids. Just as with alcohol dehydrogenase, no ring-opened products were detected in either oxidative or reductive reactions. To correlate these results with those of model studies in which radical intermediates had been postulated,[102] we examined the reduction of methyl cyclopropaneglyoxylate with *N*-benzyl-1,4-dihydronicotinamide in the presence of $Mg^{2\oplus}$ ions. Once again, no ring opening was detected.[103] A parallel study was carried out by *Pandit* et al.[104] who found that *N*-cyclopropylmethylenephenylamines were reduced by Hantzsch ester (dimethyl 1,4-dihydro-2,6-dimethylpyridine-3,5-dicarboxylate) without ring opening. All of the results from these experiments fail to support radical intermediates but it is important to ensure that the stringent conditions for applicability of the cyclopropylalkyl radical as a mechanistic probe mentioned in the introduction have been fulfilled.

At its simplest, it must be shown that radical reagents acting at the site of the redox reaction afford ring-opened products. This condition was satisfied for both cyclopropaneglyoxylate ester[103] and the above-mentioned Schiff base[104] by treatment with tin hydride reagents and an initiator. The important conclusion from these simple experiments is that radical intermediates in the traditional model reactions are most improbable since there are no conformational constraints upon the probe molecules that might militate against ring opening. Similar results were obtained with the bicyclic substrates (cf. **53**)[101] in agreement with previous work.[105] However, in order to evaluate the enzyme-catalyzed reactions, more precise information was needed to establish the effect of substitution upon the rate of ring opening of cyclopropylalkyl radicals (cf. Table 1 in Section 2.4). Thus the introduction of a single oxygen substituent caused a decrease in the rate of ring opening by only a factor of 10 and hence for alcohol dehydrogenase, the mechanistic probe passed this test.[44,45,101] In contrast, the rate of ring opening of cyclopropylalkyl radicals doubly substituted with a donor and an acceptor group was not measurable by ESR spectroscopy under accessible conditions. In this case, therefore, the lack of ring opening in the reactions catalyzed by lactate dehydrogenase is inconclusive. The model reactions are nevertheless indicative of the essential chemical character of the system.[103]

Table 2. Kinetic parameters for the interaction of substituted cyclopropylmethanol and its derivatives with horse liver alcohol dehydrogenase. K_m = Michaelis constant for substrate behavior, k_{ox} = rate constant for oxidation, k_{in} = rate constant for inhibition.

		K_m [$M \times 10^5$]	k_{ox} [s^{-1}]	k_{in} [$s^{-1} \times 10^3$]	$\frac{k_{ox}}{k_{in}}$
53	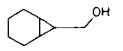	1.92	1.70	13.5	126
54	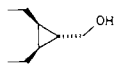	6.38	4.72	5.13	920
55	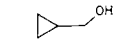	6.89	4.24	4.33	980
56	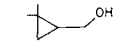	6.3	5.64	1.33	4240
57	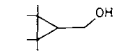	15.9	19.2	0.4	48000

Included in this series of experiments were di- and tetraalkyl cyclopropylmethanols (Table 2) and the rate of ring opening of radicals derived from silyl ethers of these compounds was too rapid to measure by the ESR technique used.[54] This information provided an excellent opportunity to reinforce the conclusions from the first experiments by carrying out preparative reactions with alcohol dehydrogenase. Not only are the methyl-substituted probes intrinsically more reactive with respect to ring opening of the derived radicals, but the alkyl substitution severely reduces their effectiveness as enzyme inhibitors by hindering nucleophilic attack at the cyclopropane ring (see below); experiments with these probes thus concentrate upon the hydrogen-transfer event. As before, no ring-opened products were detectable.[54] It remained then to check that the enzyme presented no impediments to ring opening such as the prevention of attainment of the conformation required for ring opening of a radical intermediate[52,53] or coercion to remain in a ring-closed form. The force of the latter factor is emphasized by the equilibrium position of the nortricyclyl radical **22**[51] which makes its use as a probe for radical intermediates inappropriate.[68,106] The importance of these factors for alcohol dehydrogenase was assessed with the aid of computer graphics techniques.[107] Using a model of the active site of alcohol dehydrogenase constructed from the X-ray crystallographic study of the 4-bromobenzyl alcohol complex,[108] we were able to show that for tetramethylcyclopropaneme-

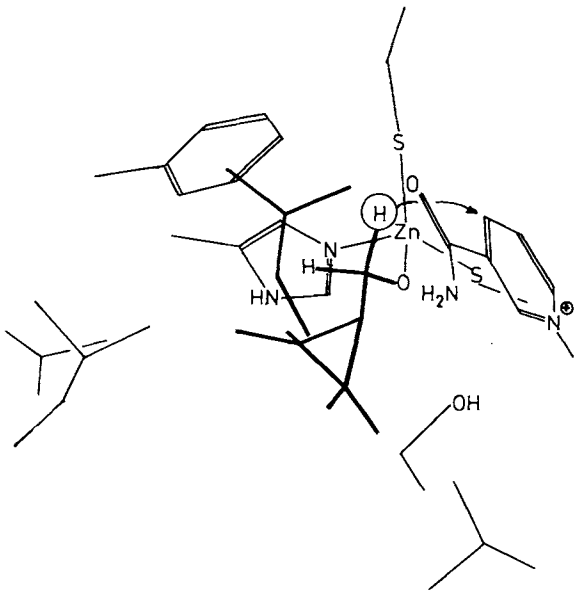

Fig. 11. Active site complex of horse liver alcohol dehydrogenase and tetramethylcyclopropylmethanol in the conformation required for H-transfer and ring opening (deduced from molecular graphics). The probe molecule is shown in bold lines.

thanol **57**, the required conformation for ring opening was accessible (Fig. 11) and that no severe pressure against ring opening existed. These results thus define the limits of confidence within which an interpretation of the lack of ring opening of cyclopropylalkyl substrates can be made. For alcohol dehydrogenase, all of the criteria required of a cyclopropyl probe have been satisfied. Although arguments have been presented for transient intermediates in the oxidation of alcohols by alcohol dehydrogenase and $NAD^{\oplus}$,[109] there is no evidence to support radical intermediates in reactions of simple alkyl aldehydes and ketones with $NAD^{\oplus}$/NADH and alcohol dehydrogenase. It has been argued from other experiments that in any case, single electron transfer mechanisms would only be expected for dihydropyridines reacting with obligate one-electron oxidants such as iron(III) and its complexes.[110]

6.2. Enzyme Inhibition by Alkylcyclopropylmethanol Derivatives

When our work on the inhibition of dehydrogenases began, activation of latent inhibitors by oxidation had not been described. We[111] and others[112] showed that unsaturated alcohols such as but-3-yn-1-ol and 3-ethylthioprop-2-en-1-ol inhibited horse liver alcohol dehydrogenase in a time-dependent manner. However, in the latter case,[111] inhibition proved to be reversible, malondialdehyde and ethanethiol being detected as reaction products. The probable origin of these products was a reverse Michael reaction in which the inhibited enzyme was reactivated; in order to avoid this net hydrolysis, the cyclopropanes were introduced. In this case, reversal of inhibition by ring closure would be improbable. The first series of compounds to be examined was based upon bicyclo[4.1.0]heptane-7-methanol **53**, the compound used initially to probe the mechanism of hydrogen transfer. All the alcohols studied proved to be inhibitors (Table 2), the bicyclic primary alcohols being the most effective, causing inhibition approximately once every 100 catalytic events.

Just as the di- and tetramethylcyclopropylmethanols, **56** and **57** respectively, gave further information on the question of the mechanism of hydrogen transfer, so they also assisted in clarifying the course of the inhibition reactions. A priori there are two sites in the cyclopropylmethanol inhibitors that are capable of reacting with nucleophiles, namely, the carbon bearing the oxygen atom and the remote apices of the cyclopropane ring. If inhibition by the alcohols occurred by nucleophilic attack at the cyclopropane ring, it would be expected that substitution at this site by methyl groups would decrease the rate of inhibition. Tetramethylcyclopropylmethanol **57**, which has the same number of carbon atoms as the prototype inhibitor **53**, was found to bind to the enzyme with comparable affinity.[54] However, it was a poorer inhibitor by 380-fold (Table 2), the dimethyl analogue **56** also being a poorer inhibitor than **53**. Both experiments suggest strongly that the methyl groups interfere with inhibition and implicate the apices of the cyclopropane ring as the target for the enzyme's nucleophile.

From the data in Table 2 and the known affinities of typical substrates for horse liver alcohol dehydrogenase, with the aid of computer graphics it is possible to suggest what the nucleophile responsible for inhibition might be.[107, 108] The inhibitors can bind in two possible orientations at the active site but only in one (Fig. 12) can the *pro-R* hydrogen, the one usually removed by this enzyme,

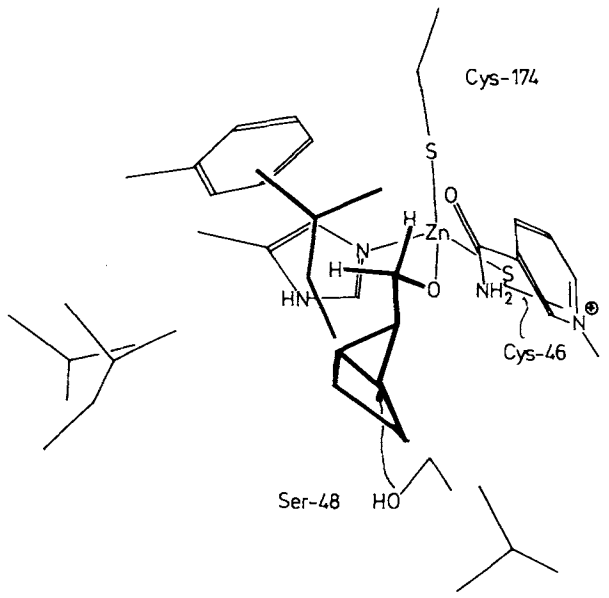

Fig. 12. Mechanism of inhibition of horse liver alcohol dehydrogenase by cyclopropylmethanols as suggested by molecular graphics. The inhibitor is shown in bold lines.

be transferred to $NAD^{\oplus}$ at the same time placing a nucleophile within bonding distance of the apex of the cyclopropane ring. That nucleophile is the hydroxyl group of Ser-48. A comparable situation was found to obtain for lactate dehydrogenase; in this case, the likely nucleophile is the hydroxyl group of threonine-246. Both results are consis-

tent with the stereochemical course of nucleophilic ring opening of cyclopropanes (see Section 2) and with predictions of frontier orbital theory.[107]

6.3. Inhibition of Chemotherapeutically Significant Enzymes by Cyclopropane Derivatives

The examples of alcohol and lactate dehydrogenases show that the cyclopropane derivatives can be effective inhibitors at active sites that involve either metal ions as Lewis acids or proton-transferring groups. It was therefore of interest to extend the concept to other enzymes that possessed similar possibilities for activation, especially enzymes that have relevance in chemotherapy. A most interesting case is dihydrofolate reductase (DHFR), the mechanism of which has been discussed in detail on the basis of both X-ray crystallography[113] and NMR studies.[114] It has been established that diaminopyrimidine inhibitors are protonated by an aspartic acid at the active site of DHFR and this residue has also been implicated in protonating N-5 of the dihydrofolate at some stage in the catalytic mechanism. Bearing in mind the success with lactate dehydrogenase, we wondered whether such protonation could activate a cyclopropane-containing analogue of either diaminopyrimidines or dihydrofolate to generate a reactive inhibitor (Fig. 13). Accordingly we synthesized the pteridine **59** and the pyrimidine **60**.[115] Assay of the inhibition properties of the two compounds showed that the pyrimidine **60** was a competitive inhibitor only, whereas the pteridine **59** behaved as a classic time-dependent irreversible inhibitor. The reason for the difference is being sought in synthetic and modeling studies.

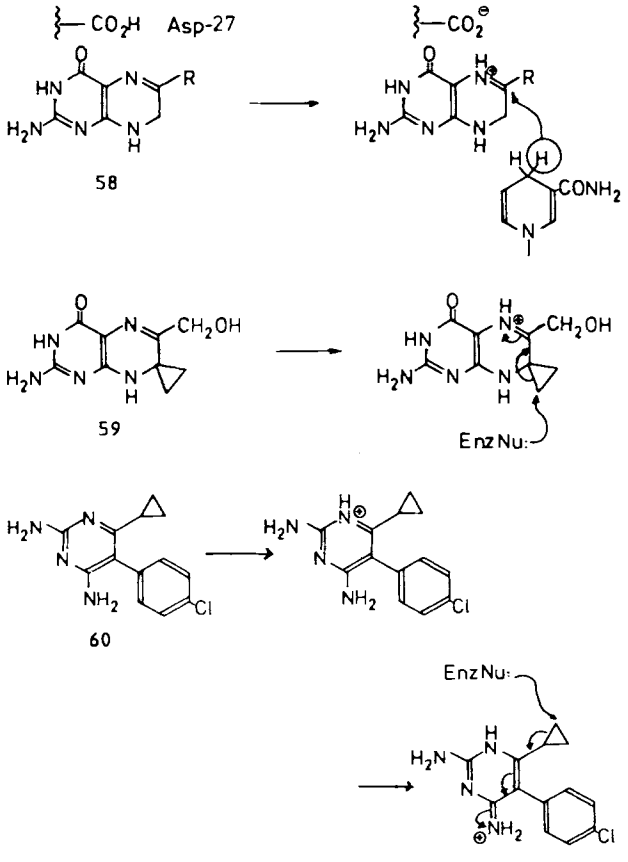

Fig. 13. Mechanism-based design of inhibitors of dihydrofolate reductase.

A further enzyme of interest as a prototype for chemotherapeutic agents is carboxypeptidase A; many important endopeptidases such as angiotensin-converting enzyme are related to carboxypeptidase A.[116] These enzymes are metalloenzymes containing a zinc cation that functions as a Lewis acid at the active site. It was therefore interesting to see whether a cyclopropyl amino acid could be activated in the same way as a cyclopropyl alcohol in alcohol dehydrogenase. We therefore prepared a series of peptides and acyl amino acids based upon 1-aminocyclopropanecarboxylic acid and also using cyclopropanecarbonyl as a simple acyl group. Both types of compounds have been reported as components of peptide inhibitors of enzymes,[117,118] but no evidence for a time-dependent reaction has been presented. We found that the phenylalanyl peptide **61** was a modest inhibitor of carboxypeptidase A and also a poor substrate. In contrast, the prolyl analogue **62** was purely a time-dependent inhibitor with no substrate properties.[119] We have suggested that the close juxtaposition of the proline and cyclopropane rings effectively blocks nucleophilic attack on the scissile carbonyl group.[117,119]

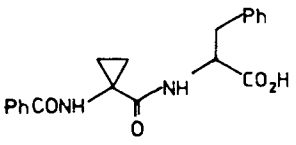

61

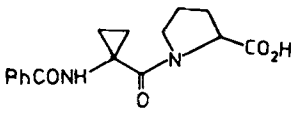

62

The potential of cyclopropane-containing peptides and peptide analogues as inhibitors of peptidases has recently been extended by the demonstration that *N*-cyclopropylamides and the corresponding secondary alcohols are inhibitors of carboxypeptidase A. Further, evidence has been obtained to show that serine and cysteine peptidases can be inhibited by cyclopropane-containing peptides.[139]

The last enzyme that we have so far been able to inhibit by this type of cyclopropane is dihydroorotate dehydrogenase. This enzyme is a key enzyme in the biosynthesis of pyrimidines[120] and after the serendipitous discovery of some hydantoin inhibitors of this enzyme,[121] we found that the spirocyclic compound 5,5-ethylenebarbituric acid was a time-dependent irreversible inhibitor. We have no information regarding the mechanism of this reaction. It is noteworthy, however, that the enzyme is a flavoprotein, and that the inhibitor is intrinsically reactive since it contains a cyclopropane ring substituted by two carbonyl groups. Direct nucleophilic attack or radical pathways are all possible.[122]

7. Aryl- and Benzylcyclopropanes and Hydroxylating Enzymes

Our initial interest in cytochrome P-450 and cyclopropane-containing substrates was to investigate the mechanism of aromatic hydroxylation. We found, however, that reaction took place at the three-membered ring rather than

on the aromatic ring. The first substrate to be examined was cyclopropylbenzene;[123] this compound was competitive for ethoxycoumarin in the enzyme from rabbit liver.[124] Unlike alkenes, which are often inhibitors of cytochrome P-450, no time-dependent inhibition was observed and the surprising major product of the reaction was benzoic acid. We initially interpreted this product as arising from the addition of radicals formed by homolysis of a peroxy intermediate at the active site. The possibility of a peracid or its equivalent was considered,[68] but in view of the recent X-ray analysis of the structure of cytochrome P-450cam, such an intermediate is less likely.[125] However, the essential feature of the mechanism leading to benzoic acid is that a diol would be formed at the active site; such an intermediate can arise via homolytic mechanisms, with or without single electron transfer, or via heterolytic mechanisms. The subsequent oxidative cleavage to benzoic acid was envisaged as occurring in a manner similar to the 19-demethylation of steroids[126] and would afford acetaldehyde as the coproduct. This labile molecule was not detected. However, using 1,2-diphenylcyclopropane as substrate, we were able to characterize benzoic acid and phenylacetaldehyde as products of enzymatic oxidation, a result that supports the general outline of the mechanism proposed for the formation of benzoic acid (Fig. 14). Further research into the chemistry of this intriguing oxidation and its potential biological applications is in progress.

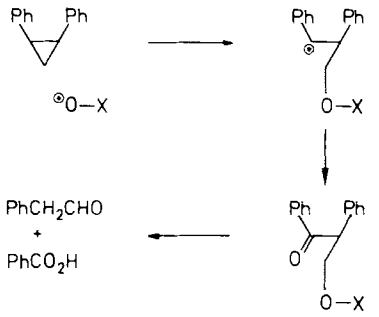

Fig. 14. A possible pathway for the oxidative cleavage of diphenylcyclopropane by cytochrome P-450. $^{\odot}$OX represents an enzyme-bound radical.

The lack of inhibition of cytochrome P-450 by aryl cyclopropanes does not imply that hydroxylating enzymes cannot be inhibited by substituted cyclopropanes. *Fitzpatrick, Villafranca* et al.[127] have shown that dopamine β-hydroxylase, a copper-containing enzyme, is inhibited by alkenes, alkynes, and cyclopropane-containing substrate analogues. The presumed mechanism of action is shown in Figure 15; once again, inhibition was attributed to ring opening of the cyclopropylalkyl radical. Unlike the inhibition of monoamine oxidase by ring-opening reactions, no ring-opened byproducts were detectable in this reaction.

8. Cyclopropanes as Probes of the Mechanism of Coenzyme B_{12}-Mediated Rearrangements

The mechanism by which coenzyme B_{12} directs an intriguing group of molecular rearrangements has been a topic of continuous interest in bioorganic chemistry for

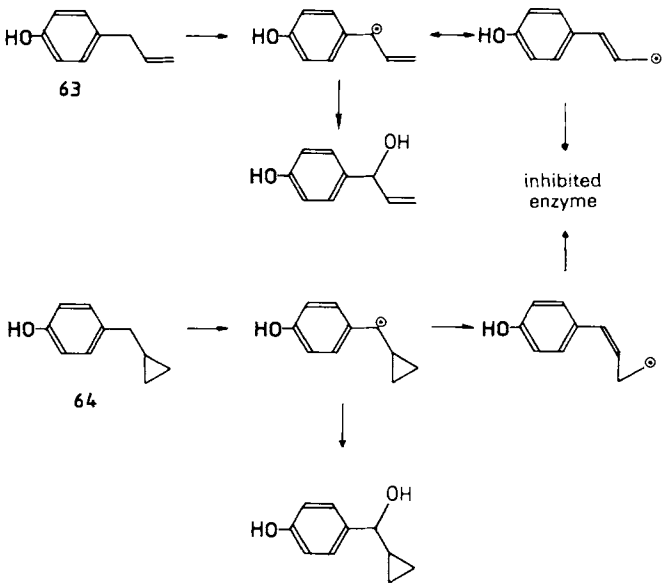

Fig. 15. Inhibition of dopamine β-hydroxylase by alkenyl- and cyclopropyl-substituted phenols as exemplified by *p*-allyl- and *p*-cyclopropylmethylphenol, **63** and **64**, respectively.

more than 20 years.[128] In the early studies, interest was heightened because of the lack of chemical precedent for the 1,2 shifts of both hydrogen and a heavy atom that occur in these reactions (Fig. 16A). The lability of the cobalt–carbon bond of the coenzyme was clearly an important factor; it was known, for example, that homolytic cleavage to give a cobalt(II) complex and an organic radical was possible and such dissociation had been observed in enzyme–substrate complexes. The connection between radical chemistry and the mechanism of action of B_{12} was strengthened when it was found that the reaction of hy-

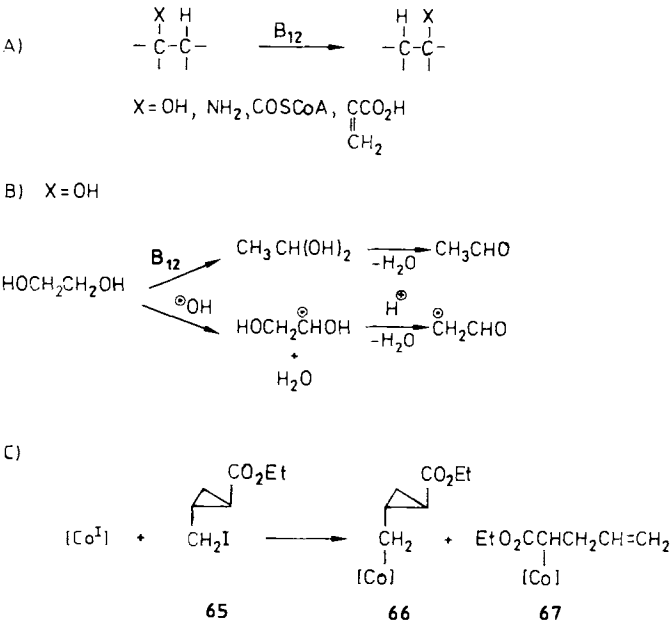

Fig. 16. A) Type of rearrangement catalyzed by coenzyme B_{12}. B) Coenzyme B_{12}-catalyzed rearrangement of ethylene glycol (top) in the presence of $^{\odot}$OH radicals (bottom). C) Model reactions (see text); [Co] stands for bis(dimethylglyoximato)pyridine cobalt.

droxyl radicals with ethylene glycol led to the formation of acetaldehyde radicals (Fig. 16B).[129] There were thus several possible mechanisms for consideration for the rearrangement process once a substrate radical had been formed. Two mechanisms involved electron transfer, but the chief contenders were a radical rearrangement or a mechanism involving a new organocobalt bond formed by combination of the substrate-derived radical with the cobalt; π complexes were also considered. The closest approach to a resolution of this problem has come through studies by *Golding* et al.[130] of model systems that relate to rearrangements in which carbon atoms undergo migration.

Cyclopropane chemistry can be used to study the rearrangement catalyzed by α-methyleneglutarate mutase and *Golding* et al.,[130] using the model compounds **65** and **66** (Fig. 16C), set out to investigate whether the cobalt remained attached to the organic substrate during rearrangement (2-methyleneglutarate→2-methyl-3-methylenesuccinate) or whether a radical free from cobalt was involved. The appropriate probe for a model reaction is a cyclopropyl cobaloxime such as **66**: this was prepared from the corresponding iodide **65** and cobaloxime(I) with partial ring opening to **67**, indicative of a radical substitution pathway. The more hindered *cis* isomer of **66** led exclusively to the ring-opened product **67**, a result that is in keeping with our experience in the ring opening of substituted cyclopropylalkyl radicals.[44] Both isomers of the iodide **65** underwent ring opening upon radiolysis at 77 K thus confirming the sensitivity of the chosen probe to the formation of a radical. In contrast to this reaction, the cyclopropane-substituted cobaloxime **66** did not undergo rearrangement and ring opening. This important result indicates that the cobalt-carbon bond must break for rearrangement to occur and hence that the cobalt is not a direct partner in the rearrangement process. It has, in *Golding*'s words,[130] a "spectator" and not a "conductor" role. The model result thus suggests that in the enzyme-catalyzed reaction, an alkyl cobalamin would be too stable to undergo rearrangement and assigns a role to the deoxyadenosine formed in the reaction, namely to prevent recombination of the rearranging organic substrate radical to afford a stable organocobalt species. In the case of α-methyleneglutarate mutase, it was inferred that the rearrangement takes place via a cyclopropylalkyl radical.[130]

9. Conclusions

The value of the cyclopropyl group in many fields of chemistry is its versatile reactivity. Nowhere is this more true than in the field of enzyme chemistry as the above examples have shown. The interpretations of the likely courses of enzyme-mediated reactions are based upon sound chemical precedent but in many cases, lack of structural information concerning the enzymes makes the interpretations more tentative than one would like. Further examples of the use of cyclopropanes as mechanistic probes in enzyme chemistry nevertheless continue to appear, most recently in a study of the bacterial degradation of phosphonate esters related to nerve gases.[131] The use of cyclopropanol as a tool in the exploration of bacterial alcohol oxidation has been advocated by *Duine* et al.[132] In this application, advantage is taken of the ability of this compound to inhibit only PQQ-dependent enzymes and not NAD-dependent dehydrogenases.

There is a natural scientific progression from basic mechanistic enzymology through metabolic probes to the invention of new drugs. For cyclopropanes, the first two stages have been investigated. It is to be hoped that the third stage will follow. However, the future development of the use of cyclopropanes as mechanistic probes or in inhibitors would benefit from more detailed studies of the intimate interactions of these versatile compounds with the enzymes themselves.

Received: December 19, 1986;
supplemented: January 20, 1988 [A 666 IE]
German version: *Angew. Chem. 100* (1988) 555

[1] a) C. Walsh, *Annu. Rev. Biochem. 47* (1978) 881; b) *ibid. 53* (1984) 493; c) R. H. Abeles, A. L. Maycock, *Acc. Chem. Res. 9* (1976) 313; d) R. R. Rando, *Science* (Washington, D.C.) *185* (1974) 320.
[2] a) M. G. Palfreyman, I. A. McDonald, P. Bey, C. Danzin, M. Zreika, G. A. Lyles, J. R. Fozard, *Biochem. Soc. Trans. 14* (1986) 410; b) C. Walsh, R. Badet, E. Daub, N. Esaki, N. Galakatos in K. W. Lambert (Ed.): *Medicinal Chemistry, Vol. 3*, Royal Society of Chemistry, London 1986, p. 193.
[3] See N. F. James (Ed.): *Recent Advances in the Chemistry of Insect Control*, Royal Society of Chemistry, London 1985, pp. 26, 73, 133.
[4] H. C. Rilling, C. D. Porter, W. W. Epstein, B. Larsen, *J. Am. Chem. Soc. 93* (1971) 1783.
[5] a) Y. Fujimoto, F. Irreverre, J. M. Karle, I. L. Karle, B. Witkop, *J. Am. Chem. Soc. 93* (1971) 3471; b). L. Fowden, C. M. MacGibbon, F. A. Mellon, R. C. Sheppard, *Phytochemistry 11* (1972) 1105; c) L. Fowden, A. Smith, D. S. Millington, R. C. Sheppard, *ibid. 8* (1969) 437; d) A. Ichihara, K. Shiraishi, S. Sakamura, *Tetrahedron Lett. 1977*, 269; e) T. Wakajima, H. Nakamoto, T. Shiba, *ibid. 25* (1984) 4411; f) T. Wakajima, Y. Oda, H. Fujita, T. Shiba, *ibid. 27* (1986) 2143.
[6] a) D. O. Adams, S. F. Young, *Proc. Natl. Acad. Sci. USA 76* (1979) 170; b) K. Lursen, K. Naumann, R. Schroder, *Z. Pflanzenphysiol. 92s* (1979) 285; c) R. M. Adlington, J. E. Baldwin, B. J. Rawlings, *J. Chem. Soc. Chem. Commun. 1983*, 290; d) R. K. Hull, S. R. Prakash, R. Wiesendanger, W. Angst, B. Martinoni, D. Arigoni, H.-W. Liu, C. Walsh, *J. Am. Chem. Soc. 106* (1984) 795; e) G. D. Peiser, T.-T. Wang, N. E. Hoffman, S. F. Young, H.-W. Liu, C. Walsh, *Proc. Natl. Acad. Sci. USA 81* (1984) 3059; f) J. E. Baldwin, R. M. Adlington, G. A. Lajoie, B. J. Rawlings, *J. Chem. Soc. Chem. Commun. 1985*, 1496; g) H.-W. Liu, R. Auchus, C. Walsh, *J. Am. Chem. Soc. 106* (1984) 5335.
[7] a) M. C. Pirrung, *J. Am. Chem. Soc. 105* (1983) 7207; b) M. C. Pirrung, G. M. McGeehan, *Angew. Chem. 97* (1985) 1074; *Angew. Chem. Int. Ed. Engl. 24* (1985) 1044.
[8] See *Chem. Br. 22* (1986) 395.
[9] a) G. B. Stahl, G. F. Ludvik, S. G. Nasser, C. A. Henrick, W. E. Willy, *J. Econ. Entomol. 68* (1975) 91; b) C. A. Henrick, W. E. Willy, G. B. Stahl, G. F. Ludvik, *J. Agric. Food Chem. 24* (1976) 1023.
[10] A. A. Freer, D. Gardner, D. Grentbanks, J. P. Poyer, G. A. Sim, *J. Chem. Soc. Chem. Commun. 1982*, 1160.
[11] M. H. O'Leary, W. J. de Gooyer, T. M. Dougherty, V. Anderson, *Biochem. Biophys. Res. Commun. 100* (1981) 1320.
[12] P. D. Kennewell, S. S. Matharu, J. B. Taylor, R. Westwood, P. G. Sammes, *J. Chem. Soc. Perkin Trans. 1 1982*, 2553, 2563.
[13] a) R. Dahlbom, J. L. G. Nilsson (Eds.): *Medicinal Chemistry, Vol. 1*, Swedish Pharmaceutical Press, Stockholm 1985; b) P. B. M. W. M. Timmermans in [13a], p. 69; c) B. G. Main in [13a], p. 41.
[14] P. Bonnaud, M. Briley, H. Cousse, J. P. Couzinier, P. Lenoble in [13a], p. 119.
[15] J. Lewis in [13a], p. 123.
[16] a) A. P. Gray, H. Kraus, Belg. Pat. 649 145 (1964), Neisler; *Chem. Abstr. 64* (1966) 8151; b) A. P. Gray, H. Kraus, Br. Pat. 1038729 (1966), Neisler; *Chem. Abstr. 65* (1966) 15344.
[17] J. L. Van Gelder, A. H. M. Raeymaekers, L. F. C. Roevers, DBP 2029637 (1971), US-Pat. 3657267 (1972), Janssen; *Merck Index 1983*, No. 2705.
[18] J. M. Teulon, DBP 2446317 (1975), US-Pat. 4005103 (1977), Hexachemie; *Merck Index 1983*, No. 7279.
[19] K. Nickisch, D. Bittler, J. Casals-Stenzel, H. Laurent, R. Nickolson, Y. Nishino, K. Petzold, R. Wiechert, *J. Med. Chem. 28* (1985) 546.

[20] R. Cunningham, D. J. Tindall, A. R. Means, *Steroids 33* (1979) 261.
[21] A. C. Sartorelli, E. Lazo, J. R. Bertino (Eds.): *Molecular Actions and Targets for Cancer Chemotherapeutic Agents*, Bristol Myers Cancer Symposium Series, Academic Press, New York 1981.
[22] R. W. Franck, *Fortschr. Chem. Org. Naturst. 38* (1979) 1.
[23] K. Okawa, K. Nakajima, *Biopolymers 20* (1981) 1811.
[24] D. E. Hathaway: *Molecular Aspects of Toxicology*, Royal Society of Chemistry, London 1984, p. 204.
[25] D. Reichert, *Angew. Chem. 93* (1981) 135; *Angew. Chem. Int. Ed. Engl. 20* (1981) 135.
[26] I. A. Rose, E. L. O'Connell, K. J. Schray, *J. Biol. Chem. 248* (1973) 2214.
[27] a) S. Bantia, C. L. Bevins, R. M. Pollack, *Biochemistry 24* (1985) 2606; b) R. M. Pollack, R. H. Kayser, C. L. Bevins, *Biochem. Biophys. Res. Commun. 91* (1979) 783; c) T. M. Penning, *Biochem. J. 226* (1985) 469.
[28] a) M. I. Page, P. Proctor, *J. Am. Chem. Soc. 106* (1984) 3820; b) P. Proctor, N. P. Gensmantel, M. I. Page, *J. Chem. Soc. Perkin Trans. 2 1982*, 1185.
[29] a) S. R. Lammert, S. Kukolja, *J. Am. Chem. Soc. 97* (1975) 5583; b) R. J. Stoodley, N. S. Watson, *J. Chem. Soc. Perkin Trans. 1 1974*, 1632; c) D. O. Spry, *Tetrahedron Lett. 1973*, 2413; d) T. Kamiya, T. Teraji, M. Hashimoto, O. Nakaguchi, T. Oku, *J. Am. Chem. Soc. 97* (1975) 5020; e) J. E. Arrowsmith, C. W. Greengrass, M. J. Newmann, *Tetrahedron 39* (1983) 2469; f) D. H. Shih, J. A. Fayter, B. G. Christensen, *Tetrahedron Lett. 25* (1984) 1639.
[30] a) E. M. Gordon, J. Pluscac, M. A. Ondetti, *Tetrahedron Lett. 22* (1981) 1871; b) O. Meth-Cohn, A. J. Reason, S. M. Roberts, *J. Chem. Soc. Chem. Commun. 1982*, 90; c) G. Lowe, S. Swain, *ibid. 1983*, 1279; d) G. Lange, M. E. Savard, T. Viswanatha, D. I. Dmitrienko, *Tetrahedron Lett. 26* (1985) 1791; e) A. J. Cocuzza, G. A. Boswell, *ibid. 26* (1985) 5363.
[31] J. F. Liebman, A. Greenberg, *Chem. Rev. 76* (1976) 311.
[32] A. de Meijere, *Angew. Chem. 91* (1979) 867; *Angew. Chem. Int. Ed. Engl. 18* (1979) 809.
[33] C. A. Coulson, W. E. Moffitt, *J. Chem. Phys. 15* (1947) 151.
[34] A. D. Walsh, *Trans. Faraday Soc. 45* (1949) 179.
[35] R. Jornitsma, H. Steinberg, T. J. de Boer, *Recl. Trav. Chim. Pays-Bas 100* (1981) 184, 194.
[36] N. J. Turro, W. B. Hammond, *J. Am. Chem. Soc. 89* (1967) 1028.
[37] N. J. Demjanov, *Ber. Dtsch. Chem. Ges. 40* (1907) 4961.
[38] J. D. Roberts, R. H. Mazur, *J. Am. Chem. Soc. 73* (1951) 2509.
[39] R. H. Mazur, W. N. White, D. A. Semenov, C. C. Lee, M. S. Silver, J. D. Roberts, *J. Am. Chem. Soc. 81* (1959) 4390.
[40] G. A. Olah, C. L. Jerrell, D. P. Kelly, R. D. Porter, *J. Am. Chem. Soc. 94* (1972) 146.
[41] R. Battaglia, *Dissertation No. 4521*, ETH Zürich, 1970.
[42] K. B. Wiberg, A. J. Ashe, *Tetrahedron Lett. 1965*, 1153.
[43] a) M. Julia, S. Julia, R. Guegan, *Bull. Soc. Chim. Fr. 1960*, 1072; b) S. F. Brady, M. I. Ilton, W. S. Johnson, *J. Am. Chem. Soc. 90* (1968) 2882.
[44] D. Laurie, E. Lucas, D. C. Nonhebel, C. J. Suckling, J. C. Walton, *Tetrahedron 42* (1986) 1035.
[45] J. P. McCormick, D. L. Barton, *J. Chem. Soc. Chem. Commun. 1975*, 303.
[46] S. J. Cristol, B. B. Jarvis, *J. Am. Chem. Soc. 89* (1967) 5885.
[47] a) S. Danishevsky, *Acc. Chem. Res. 12* (1979) 66; b) R. V. Stevens, *Pure Appl. Chem. 51* (1979) 1317.
[48] B. Maillard, D. Forrest, K. U. Ingold, *J. Am. Chem. Soc. 98* (1976) 7024.
[49] a) Y. Maeda, K. U. Ingold, *J. Am. Chem. Soc. 102* (1980) 328; b) X.-Z. Quin, F. Williams, *ibid. 109* (1987) 595.
[50] A. Effio, D. Griller, K. U. Ingold, A. L. J. Beckwith, *J. Am. Chem. Soc. 102* (1980) 1734.
[51] P. C. Wong, D. Griller, *J. Org. Chem. 46* (1981) 2327.
[52] a) W. G. Dauben, L. Schutte, R. E. Wolf, E. J. Deviny, *J. Org. Chem. 34* (1969) 2512; b) W. G. Dauben, R. E. Wolf, *ibid. 35* (1970) 374.
[53] a) A. J. Bellamy, E. A. Campbell, I. R. Hall, *J. Chem. Soc. Perkin Trans. 1 1974*, 1347; b) P. S. Mariano, E. Bey, *J. Org. Chem. 45* (1980) 1765.
[54] D. C. Nonhebel, C. J. Suckling, J. C. Walton, *Tetrahedron Lett. 23* (1982) 4477.
[55] H. G. Viehe, R. Merényi, L. Stella, Z. Janousek, *Angew. Chem. 91* (1972) 982; *Angew. Chem. Int. Ed. Engl. 18* (1979) 917.
[56] M. J. Perkins, P. Ward, *J. Chem. Soc. Perkin Trans. 1 1974*, 667.
[57] A. Streitwieser, Jr., cited as a personal communication in [32].
[58] J. Fuhrhop, G. Penzlin: *Organic Synthesis*, Verlag Chemie, Weinheim 1983, pp. 170, 62–67, 270–271.
[59] A. Thibblin, W. P. Jencks, *J. Am. Chem. Soc. 101* (1979) 4963.
[60] H. Dalton, B. T. Golding, B. W. Waters, R. Higgins, J. A. Taylor, *J. Chem. Soc. Chem. Commun. 1981*, 482.
[61] J. J. Perry, *CRC Crit. Rev. Microbiol. 7* (1977) 3878.
[62] J. Geigert, S. L. Neidleman, D. J. Dalietos, *J. Biol. Chem. 258* (1983) 2273.
[63] a) F. P. Guengerich, T. L. MacDonald, *Acc. Chem. Res. 17* (1984) 9; b) R. I. Murray, M. T. Fisher, P. G. Debrunner, S. G. Sligar, *Top. Mol. Struct. Biol. 6* (1985) 157.
[64] J. T. Groves, W. J. Kruper, Jr., R. C. Haushalter, *J. Am. Chem. Soc. 102* (1980) 6375.
[65] a) L. Brown, W. J. S. Lyall, C. J. Suckling, K. E. Suckling, *J. Chem. Soc. Perkin Trans. 1 1987*, 595; b) J. D. Houghton, S. E. Beddows, K. E. Suckling, L. Brown, C. J. Suckling, *Tetrahedron Lett. 27* (1986) 4655.
[66] G. S. Boyd, M. J. G. Brown, N. G. Hattesley, M. E. Lawson, K. E. Suckling, *Adv. Bile Acid Res. Bile Acid Meet. 3rd 1974 3* (1975) 45.
[67] R. M. Hayte, R. B. Hochberg, *J. Biol. Chem. 254* (1979) 2278.
[68] P. R. Ortiz de Montellano, R. A. Stearns, *J. Am. Chem. Soc. 109* (1987) 3415.
[69] O. Ottmar, P. Lindberg, *Acta Pharmacol. Toxicol. 40* (1977) 476.
[70] a) C. H. Hassall, K. Reyle, *Biochem. J. 60* (1955) 334; b) K. Tanaka, E. M. Miller, K. J. Isselbacher, *Proc. Natl. Acad. Sci. USA 68* (1971) 20; C. D. Billington, H. S. A. Sherratt, *Methods Enzymol. 72* (1981) 610.
[71] a) R. H. Abeles in N. Seiler, M. J. Jung, J. Koch-Weser (Eds.): *Enzyme Activated Irreversible Inhibitors*, Elsevier-North Holland Biomedical Press, Amsterdam 1978, p. 1; b) U. Brodbeck (Ed.): *Enzyme Inhibitors*, Verlag Chemie, Weinheim 1980; c) S. Ghisla, A. Wenz, C. Thorpe in [71b], p. 43.
[72] A. Schonbrunn, R. H. Abeles, C. T. Walsh, S. Ghisla, H. Ogata, V. Massey, *Biochemistry 15* (1976) 1798.
[73] a) R. H. Jackson, T. P. Singer, *J. Biol. Chem. 258* (1983) 1857; b) D. B. Hyman, K. Tanaka, *J. Clin. Invest. 73* (1984) 778.
[74] B. Wickberg in [13a], *Vol. 2*, p. 217.
[75] J. S. Wiseman, G. Tayrien, R. H. Abeles, *Biochemistry 19* (1980) 4222.
[76] C. Paech, J. L. Salach, T. P. Singer, *J. Biol. Chem. 255* (1980) 2700.
[77] R. B. Silverman, S. J. Hoffman, *J. Am. Chem. Soc. 102* (1980) 884.
[78] A. R. Mass, M. J. Nimmo, *Nature (London) 184* (1959) 547; E. A. Zeller, S. Sarker, *J. Biol. Chem. 237* (1962) 2333.
[79] R. B. Silverman, S. J. Hoffman, W. B. Catus II, *J. Am. Chem. Soc. 102* (1980) 7126.
[80] P. Dowd, C. Kaufman, R. H. Abeles, *J. Am. Chem. Soc. 106* (1984) 2703.
[81] a) D. O. Shah, K. Lai, D. G. Gorenstein, *J. Am. Chem. Soc. 106* (1984) 4272; b) M. P. Gamscik, J. P. G. Malthouse, W. U. Primrose, N. E. Mackenzie, A. S. F. Boyd, R. A. Russell, A. I. Scott, *ibid. 105* (1983) 6324.
[82] M. H. Gelb, J. P. Svaren, R. H. Abeles, *Biochemistry 24* (1985) 1813; B. Imperiali, R. H. Abeles, *ibid. 25* (1986) 3760.
[83] R. P. Hanzlik, R. H. Tullman, *J. Am. Chem. Soc. 104* (1982) 2048.
[84] a) H. H. Wasserman, H. W. Adickes, O. E. de Ochoa, *J. Am. Chem. Soc. 93* (1971) 5586; b) S. E. Schaafsma, E. J. Molenaar, H. Steinberg, T. J. De Boier, *Recl. Trav. Chim. Pays-Bas 86* (1967) 1301.
[85] T. L. Macdonald, K. Zirvi, L. T. Burka, P. Peyman, F. P. Guengerich, *J. Am. Chem. Soc. 104* (1982) 2050.
[86] R. B. Silverman, *J. Biol. Chem. 258* (1983) 14766.
[87] R. B. Silverman, P. A. Zieske, *Biochemistry 25* (1986) 341.
[88] R. B. Silverman, R. B. Yamasaki, *Biochemistry 23* (1984) 1822.
[89] R. B. Silverman, P. A. Zieske, *Biochemistry 24* (1985) 2128.
[90] R. B. Silverman, P. A. Zieske, *Biochem. Biophys. Res. Commun. 135* (1986) 154.
[91] J. S. Wiseman, J. S. Nichols, M. Kolpak, *J. Biol. Chem. 257* (1982) 6328.
[92] J. A. Duine, J. Frank Jzn., *Trends Biochem. Sci. (Pers. Ed.) 6* (1981) 278.
[93] S. A. Salisbury, H. S. Forrest, W. B. Cruse, O. Kennard, *Nature (London) 280* (1979) 843.
[94] R. H. Dekker, J. A. Duine, J. Frank Jzn., P. E. J. Verwiel, J. Westerling, *Eur. J. Biochem. 125* (1982) 69.
[95] R. De Beer, J. A. Duine, J. Frank Jzn., J. Westerling, *Eur. J. Biochem. 130* (1983) 105.
[96] a) T. Mincey, J. A. Bell, A. S. Mildvan, R. H. Abeles, *Biochemistry 20* (1981) 7502; b) C. Parkes, R. H. Abeles, *ibid. 23* (1984) 6355.
[97] a) M. Dijkstra, J. Frank Jzn., J. A. Jongenjan, J. A. Duine, *Eur. J. Biochem. 140* (1984) 369; b) D. J. Duine, personal communication.
[98] B. Sherry, R. H. Abeles, *Biochemistry 24* (1985) 2594.
[99] a) G. A. Hamilton, *Prog. Bioorg. Chem. 1* (1971) 113; b) M. F. Powell, T. C. Bruice, *J. Am. Chem. Soc. 104* (1982) 5834; *105* (1983) 1014.
[100] a) B. V. Plapp, R. L. Brooks, J. D. Shore, *J. Biol. Chem. 248* (1973) 3470; b) R. L. Brooks, R. H. Gutfreund, *ibid. 247* (1972) 2382; c) R. L. Brooks, J. D. Shore, *Biochemistry 10* (1971) 3855; d) K. Bush, V. J. Shiner, H. R. Mahler, *ibid. 12* (1973) 4802.
[101] I. MacInnes, D. C. Nonhebel, S. T. Orzulik, C. J. Suckling, *J. Chem. Soc. Perkin Trans. 1 1983*, 2776.
[102] S. Yasui, A. Ohno, *Bioorg. Chem. 14* (1986) 70; A. Ohno, H. Yamamoto, S. Oka, *J. Am. Chem. Soc. 103* (1981) 2041.
[103] D. C. Nonhebel, S. T. Orszulik, C. J. Suckling, *J. Chem. Soc. Chem. Commun. 1982*, 1146.
[104] a) J. C. G. van Niel, U. K. Pandit, *J. Chem. Soc. Chem. Commun. 1983*, 149; b) L. H. P. Meijer, J. C. G. van Niel, U. K. Pandit, *Tetrahedron 40* (1984) 5185.

[105] A. G. Davies, B. Muggleton, J.-Y. Godet, M. Pereyre, J.-C. Pommier, *J. Chem. Soc. Perkin Trans. 2 1976*, 1719.
[106] S. K. Chung, S. U. Park, *J. Org. Chem. 47* (1982) 3197.
[107] R. J. Breckenridge, C. J. Suckling, *Tetrahedron 42* (1986) 1035.
[108] E. Horjales, C. I. Branden, *J. Biol. Chem. 260* (1985) 15445.
[109] a) J. Torreilles, M.-C. Guerin, *Biochim. Biophys. Acta 869* (1986) 265; b) C. I. Branden, H. Eklund, *Experientia 36* (1980) 40.
[110] J. W. Verhoeven, W. van Gerresheim, F. M. Martens, S. M. van der Kerk, *Tetrahedron 42* (1986) 975.
[111] I. MacInnes, D. Schorstein, C. J. Suckling, R. Wrigglesworth, *J. Chem. Soc. Perkin Trans. 1 1983*, 2771.
[112] T. A. Alston, L. Mela, H. J. Bright, *Arch. Biochem. Biophys. 197* (1979) 516.
[113] a) D. A. Mathews, R. A. Alden, S. T. Freer, N. Xuong, J. Kraut, *J. Biol. Chem. 254* (1979) 4144; b) J. T. Bolin, D. J. Filman, D. A. Mathews, R. C. Hamlin, *ibid. 257* (1982) 13650; c) D. J. Filman, J. T. Bolin, D. A. Mathews, J. Kraut, *ibid. 257* (1982) 13663.
[114] a) G. C. K. Roberts in J. Blair (Ed.): *Chemistry and Biology of Pteridines*, de Gruyter, Berlin 1983, p. 197; b) H. T. A. Cheng, M. S. Searle, J. Feeney, B. Birdsall, G. C. K. Roberts, I. Kompis, S. J. Hammond, *Biochemistry 25* (1986) 1925.
[115] J. Haddow, C. J. Suckling, H. C. S. Wood, *J. Chem. Soc. Chem. Commun. 1987*, 480.
[116] a) M. A. Ondetti, D. W. Cushman, *Annu. Rev. Biochem. 51* (1982) 283; b) T. Hofmann, *Top. Mol. Struct. Biol. 7* (1985) 1.
[117] R. H. Andreatta, J. Rahuel, M. Wesp, P. Duker in [71b], p. 261.
[118] H. Umezawa, T. Takeuchi, T. Aoyagi, S. Ishii, T. Saino, T. Soweno, Fr. Pat. Appl. 2490632 (1982) Nippon Kayaku; *Chem. Abstr. 97* (1982) P145287m.
[119] A. Bell, S. Ner, C. J. Suckling, R. Wrigglesworth, *J. Chem. Soc. Chem. Commun. 1987*, 480.
[120] T. W. Kensler, D. A. Cooney, *Adv. Pharmacol. Chemother. 18* (1981) 273.
[121] I. G. Buntain, C. J. Suckling, H. C. S. Wood, *J. Chem. Soc. Chem. Commun. 1985*, 242.
[122] I. G. Buntain, J. C. Courtney, C. J. Suckling, H. C. S. Wood, unpublished results.
[123] K. E. Suckling, C. G. Smellie, I. E. Ibrahim, D. C. Nonhebel, C. J. Suckling, *FEBS Lett. 145* (1982) 179.
[124] C. J. Suckling, D. C. Nonhebel, L. Brown, K. E. Suckling, S. Seilman, C. R. Wolf, *Biochem. J. 232* (1985) 199.
[125] T. L. Poulos, B. C. Finzel, I. C. Gunsalus, G. C. Wagner, J. Kraut, *J. Biol. Chem. 260* (1985) 16122.
[126] D. E. Stevenson, J. N. Wright, M. Akhtar, *J. Chem. Soc. Chem. Commun. 1985*, 1078.
[127] a) P. F. Fitzpatrick, D. R. Flory, Jr., J. J. Villafranca, *Biochemistry 24* (1985) 2108; b) P. F. Fitzpatrick, J. J. Villafranca, *J. Am. Chem. Soc. 107* (1985) 5022.
[128] R. G. Finke, D. A. Schiraldi, B. J. Mayer, *Coord. Chem. Rev. 54* (1984) 1.
[129] B. C. Gilbert, J. P. Larkin, R. O. C. Norman, *J. Chem. Soc. Perkin Trans. 2 1972*, 794.
[130] R. M. Dixon, B. T. Golding, S. Mwesigye-Kibende, D. N. Ramakrishna Rao, *Phil. Trans. R. Soc. London Ser. B 311* (1985) 531.
[131] M. L. Cordeiro, D. L. Pompliaro, J. W. Frost, *J. Am. Chem. Soc. 108* (1986) 332.
[132] A. Groenveld, M. Dykstra, J. A. Duine, *FEMS Microbiol. Lett. 25* (1984) 311.
[133] D. W. Robertson, J. H. Krushinski, G. D. Pollock, H. Wilson, R. F. Kauffman, J. S. Hayes, *J. Med. Chem. 30* (1987) 824.
[134] L. Mathew, J. Warkentin, *J. Am. Chem. Soc. 108* (1986) 7981.
[135] J. E. Baldwin, D. W. Parker, *J. Org. Chem. 52* (1987) 1475.
[136] R. B. Silverman, B. J. Invergo, J. Mathew, *J. Med. Chem. 29* (1986) 1841.
[137] B. Bonnaud, H. Cousse, G. Mouzin, M. Briley, A. Stenger, F. Fauran, J.-P. Couzinier, *J. Med. Chem. 30* (1987) 318.
[138] D. A. Trainor, *Trends Pharm. Sci. 18* (1987) 303.
[139] C. J. Suckling in P. J. Leeming (Ed.): *Medicinal Chemistry, Vol. 4*, RSC/SCI Medicinal Chemistry Symposium, Royal Society of Chemistry, London 1988, in press.

When submitting manuscripts, authors of articles intended for publication as "Communications" are requested to read the "Notice to Authors" reproduced in the January issue of the journal following the list of contents; upon request, a copy can be obtained from the editorial office.

First Case of Interannular, Possibly Electronically Transmitted, Asymmetric Induction in an Organometallic Compound**

By *Roland Boese, Dieter Bläser, Ronald L. Halterman,* and *K. Peter C. Vollhardt**

The topic of enantio- and diastereoface control in organic reactions is one of intense current interest.[1] Electronic effects have been invoked in those cases in which steric considerations were insufficient or inappropriate to explain the observed results.[1,2] Although theoretical and experimental analyses have led to the postulation of a variety of phenomena and rules to rationalize both steric and electronic influences,[3] a clear differentiation between these effects has been difficult, in particular because of the lack of systems in which the approaching *reagent and the reacting center* are distant from the chiral auxiliary. Among the more intriguing organometallic examples are $[(\eta^5\text{-}C_5H_5)Re(NO)\{P(C_6H_5)_3\}(C{\equiv}CR)]$[4] and $[(\eta^5\text{-}C_5H_5)Mo(NO)(CO)(allyl)]^{\oplus}$,[5] both of which undergo seemingly remote stereoselective electro- and nucleophilic addition, respectively, controlled by the metal-based stereocenter.[6] We report here the first case of interannular transfer of asymmetry (possibly electronic in nature) in an organometallic system and an unprecedented example of carbon–carbon bond formation to a π-bound ligand in which diastereoselectivity is induced by a chiral unit whose asymmetry originates by complexation of a heterodisubstituted cyclopentadienyl ring to a metal that is thus rendered stereogenic.[7]

Acylation of methylcyclopentadienylsodium produced a nearly equimolar mixture of the salts **1** and **2**[8] which were converted into the dicarbonylcobalt complexes **3** and **4** (17.2%)[8] by treatment with tetracarbonyl(iodo)cobalt.[9] The mixture of **3** and **4** (0.03 M in THF) was photolyzed (450-W Hanovia Hg-vapor lamp, −20°C, 10 h)[10] in the presence of trimethylsilylethyne to give the chiral cyclopentadienone complexes **5** and **6** (73% separated on silica).[8] The chirality in these compounds is due to the presence of the unsymmetrically substituted ligand, from now on referred to as the "bottom" ring. The substitution pattern of the bottom ring in **6** was ascertained using the FUCOUP NMR technique.[11,12] In both isomers the diastereotopic hydrogens attached to the top ring have quite different chemical shifts,[8] boding well for potential differences in reactivity at these two sites.

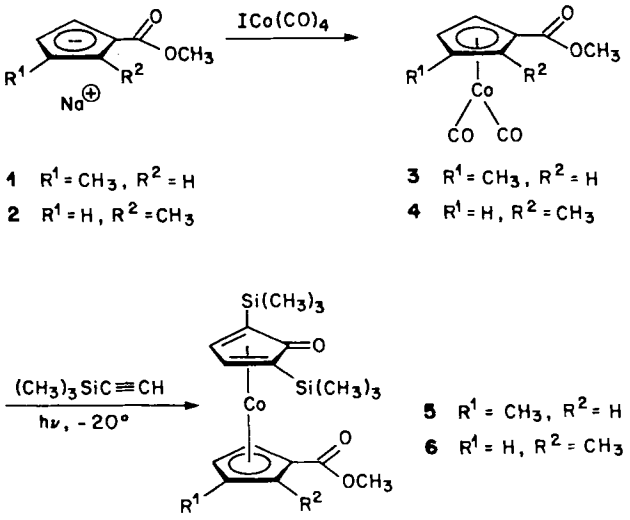

To probe for the origin of this finding and to corroborate the structural assignments, an X-ray structural analysis of **5** was executed (Fig. 1).[13]

There are two rotamers **5a** and **5b** with respect to the orientation of the ester group in the unit cell. Interestingly, while rotamer **5a** contains the relevant carbons C3 and C4

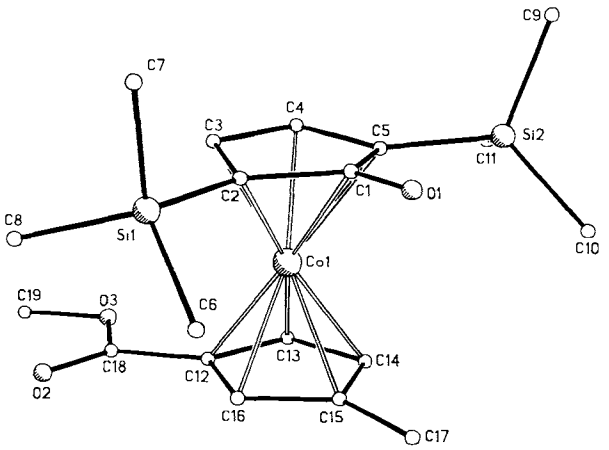

Fig. 1. Crystal structure of **5**. Important bond lengths and nonbonding distances [Å]: **5a**: Co1-C1 2.212(6), Co1-C2 2.057(6), Co1-C3 2.004(7), Co1-C4 2.010(7), Co1-C5 2.069(6), Si1-C2 1.875(6), Si2-C5 1.876(6), C1-O1 1.272(8), C1-C2 1.459(9), C1-C5 1.451(8), C2-C3 1.419(9), C3-C4 1.419(9), C4-C5 1.424(9), C1-C15 3.375, O1-C17 3.452, C2-C16 3.261, C3-C12 3.357, C4-C13 3.375, C5-C14 3.295, C6-O2 5.184, C6-C12 4.943, C6-C16 3.837, C8-O2 3.505, C8-C18 4.133, C8-O2 3.505; **5b**: Co2-C21 2.237(6), Co2-C22 2.059(6), Co2-C23 2.000(7), Co2-C24 2.005(6), Co2-C25 2.066(6), Si4-C22 1.864(6), Si3-C25 1.886(6), C21-O21 1.266(8), C21-C22 1.470(8), C21-C25 1.461(9), C22-C23 1.436(9), C23-C24 1.409(9), C24-C25 1.406(9), C21-C35 3.441, O21-C37 3.518, C22-C36 3.269, C23-C32 3.368, C24-C33 3.380, C25-C34 3.289, C26-O21 3.437, C28-O23 3.511, C28-C39 3.956, C28-C38 4.220.

[*] Prof. Dr. K. P. C. Vollhardt, Dr. R. L. Halterman
Department of Chemistry, University of California,
and the Materials and Chemical Sciences Division,
Lawrence Berkeley Laboratory
Berkeley, CA 94720 (USA)
Dr. R. Boese, Dipl.-Ing. D. Bläser
Institut für Anorganische Chemie der
Universität-Gesamthochschule
Universitätsstrasse 5-7, Postfach 103764, D-4300 Essen 1 (FRG)

[**] This work was supported by the National Institutes of Health (GM 22479). *R. L. H.* was the recipient of a University of California Regents' Fellowship (1982–1984). *K. P. C. V.* was a Miller Research Professor in Residence (1985–1986).

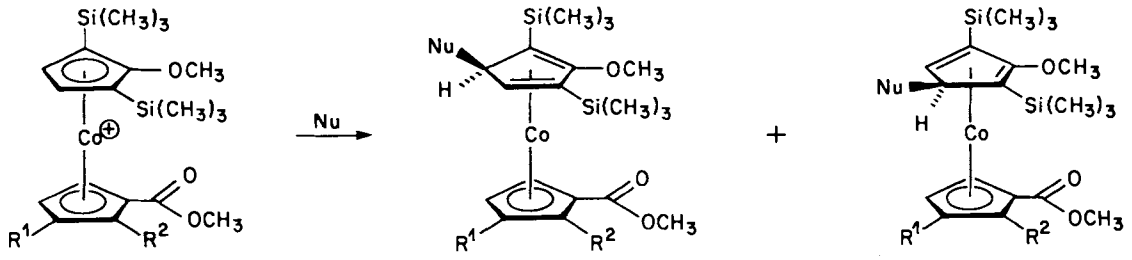

7 $R^1 = CH_3$, $R^2 = H$
8 $R^1 = H$, $R^2 = CH_3$

9a-c $R^1 = CH_3$, $R^2 = H$
10a-c $R^1 = H$, $R^2 = CH_3$

in an (within the error limits) equal environment, **5b** does not, although the differences are subtle. However, it can be seen clearly that the substituents on the bottom ring induce measurable structural changes in its top counterpart compared to [η^4-2,5-bis(trimethylsilyl)cyclopentadienone](η^5-cyclopentadienyl)cobalt,[14] including coplanarity of the respective ring carbons and the enforcement of an eclipsed configuration, *despite the absence of recognizable steric interactions*.[15]

Methylation of **5** or **6** with dimethyl sulfate yielded the (not isolated) cobaltocenium salts **7** and **8**, the substrates required to test for the feasibility of diastereoselective attack. Nucleophilic addition to such structures is known to take place *exo* with respect to the metal, thus clearly avoiding any steric interference by the other ligand.[16,17] Nevertheless, when **7** was exposed to nucleophiles **11**–**13** (chosen to maximize top ring addition),[16] modest but *pronounced and reproducible diastereoselectivity in the formation of* **9**[8] *was observed* (Table 1). The yields of addition (including 20% to the bottom ring) were high, thus ruling out any complications associated with potentially (if unlikely) differing stabilities of the products. The similarity of the ^{1}H-NMR spectral data for the respective sets of isomers suggests that preferential reaction occurred at the same diastereotopic carbon in each instance. The addition to **8** (→**10**) not only gave more bottom ring addition (60%), but also negligible stereoselectivity. To detect any possible involvement of solvent in these transformations, **7** was treated with **11** in THF/hexamethylphosphoramide without any change in the product distribution. Similarly, no change in selectivity was observed over the temperature range −78°C to 20°C.

Table 1. Diastereoselectivities in the additions of nucleophiles **11**–**13** to **7** and **8** [a].

Nucleophile	Stereoselectivity [b] (yield [%] [c])	
	9	**10**
$(CH_3)_3SiC{\equiv}CLi$ **11**	70 : 30 (73.0)	54 : 46 (87.4)
n-$C_6H_{13}C{\equiv}CLi$ **12**	67 : 33 (91.3)	52 : 48 (94.6)
$C_2H_5OC{\equiv}CLi$ **13**	75 : 25 (90.7)	50 : 50 (90.6)

[a] The stereoselectivities were measured by ^{1}H-NMR integration of several characteristic peaks [e.g., those for the cyclopentadienyl and $(CH_3)_3Si$ groups]. [b] Ratio of major to minor isomer. [c] Total yield for the reaction, including bottom ring addition.

It is difficult to find a clear rationale for the observed selectivities. A possible explanation is the operation of a hitherto unobserved interannular electronic transmission of asymmetry. Inter-ring electronic effects in ordinary metallocenes are known and may be related in origin to our observations.[18] Although we cannot completely rule out a subtle steric differentiation between the two transition-state structures when formulated in the form of an extreme conformation that places the methyl ester hydrogens in closest proximity to the reacting top ring carbons, such an effect appears unlikely to be important in view of the fact that the product emerges bearing the resulting complexed cyclopentadiene ring in an envelope configuration in which the sp^3 carbon is *even further* removed from the bottom ring, the potentially interfering hydrogen being located in a pseudo-equatorial position.[17] Regardless of the mechanism by which this preference for nucleophilic attack on **7** and **8** comes about, the present work demonstrates for the first time the feasibility of chiral differentiation in such systems, a phenomenon that, when optimized and properly understood, may be of utility in synthesis.

Experimental Procedure

9a: To a solution of **5** (0.029 g, 0.07 mmol) in diethyl ether (0.5 mL) at room temperature under nitrogen was added dimethyl sulfate (0.030 g, 0.24 mmol) via syringe. This red solution was stirred 40 h until it became clear pale yellow. The solvent was removed by a stream of nitrogen, leaving a yellow oil of the cobaltocenium salt **7**. THF (5 mL) was added and the solution was cooled to −78°C. A solution of **11** in THF, prepared by adding methyllithium (1.0 mL, 1.4 M in diethyl ether/hexane, 1.4 mmol) to trimethylsilylethyne (0.147 g, 1.5 mmol) in THF (5 mL) at −78°C and warming to 0°C over 20 min, was introduced dropwise at −78°C. The reaction mixture turned immediately dark red. After stirring for 1 h at −78°C, water (1 mL) was added and the mixture allowed to warm to room temperature. The deep red solution was extracted with diethyl ether (3 × 5 mL), the combined organic portions were washed with water (1 × 1 mL) and dried over $MgSO_4$, and the volatiles were removed by rotary evaporation. Filtration of the resulting red oil through alumina (2 g, activity 3) with diethyl ether and subsequent reverse-phase HPLC (two 10-mm × 25-cm ODS columns, CH_3CN, 2.8 mL min^{-1}, solvent front 10 min) provided a fraction after 35 min of **9a** [8].

Received: October 12, 1987;
revised: January 15, 1988 [Z 2472 IE]
German version: *Angew. Chem. 100* (1988) 592

[1] M. Nogradi: *Stereoselective Synthesis*, VCH Verlagsgesellschaft, Weinheim 1986; J. W. ApSimon, T. L. Collier, *Tetrahedron 42* (1986) 5157; L. A. Paquette in J. D. Morrison (Ed.): *Asymmetric Synthesis, Vol. 3*, Academic Press, New York 1984, p. 455; H. B. Kagan, *ibid., Vol. 5*, 1984, p. 1; K. E. Koenig, *ibid., Vol. 5*, 1984, p. 71; W. Oppolzer, *Angew. Chem. 96* (1984) 840; *Angew. Chem. Int. Ed. Engl. 23* (1984) 876; H. B. Kagan in G. Wilkinson, F. G. A. Stone, E. W. Abel (Eds.): *Comprehensive Organometallic Chemistry, Vol. 8*, Pergamon Press, New York 1982, p. 463; B. Bosnich, M. D. Fryzuk, *Top. Stereochem. 12* (1981) 119; J. W. ApSimon, R. P. Seguin, *Tetrahedron 35* (1979) 2797; D. Valentine, Jr., J. W. Scott, *Synthesis 1978*, 329.

[2] See, for example, a) N. S. Crossley, A. C. Darby, H. B. Henbest, J. J. McCullough, B. Nicholls, M. F. Stewart, *Tetrahedron Lett. 1961*, 398; b) M. G. Combe, H. B. Henbest, *ibid. 1961*, 404; c) G. Bellucci, F. Marioni, A. Marsili, *Tetrahedron 28* (1972) 3393; d) J. Klein, *ibid. 30* (1974) 3349; e) E. C. Ashby, J. R. Boone, *J. Org. Chem. 41* (1976) 2890; f) M. Chérest,

H. Felkin, P. Tacheau, J. Jacques, D. Varech, *J. Chem. Soc. Chem. Commun. 1977*, 372; g) A. Vasella, *Helv. Chim. Acta 60* (1977) 426, 1273; h) D. Horton, T. Machinami, *J. Chem. Soc. Chem. Commun. 1981*, 88; i) D. Liotta, M. Saindane, C. Barnum, *J. Am. Chem. Soc. 103* (1981) 3224; j) R. W. Franck, T. V. John, K. Olejniczak, J. F. Blount, *ibid. 104* (1982) 1106; k) R. L. Funk, W. E. Zeller, *J. Org. Chem. 47* (1982) 180; l) L. A. Paquette, K. E. Green, R. Gleiter, W. Schäfer, J. C. Gallucci, *J. Am. Chem. Soc. 106* (1984) 8232; m) L. A. Paquette, K. S. Learn, *ibid. 108* (1986) 7873; n) L. A. Paquette, P. F. T. Schirch, S. J. Hathaway, L.-Y. Hsu, J. C. Gallucci, *Organometallics 5* (1986) 490; o) L. A. Paquette, S. J. Hathaway, P. F. T. Schirch, J. C. Gallucci, *ibid. 5* (1986) 500.

[3] See a) N. T. Anh, O. Eisenstein, J.-M. Lefour, M. E. Trân Huu Dău, *J. Am. Chem. Soc. 95* (1973) 6146; b) S. Inagaki, K. Fukui, *Chem. Lett. 1974*, 509; c) N. T. Anh, O. Eisenstein, *Nouv. J. Chem. 1* (1977) 61; d) N. T. Anh, *Top. Curr. Chem. 88* (1980) 145; e) N. G. Rondan, M. N. Paddon-Row, P. Caramella, K. N. Houk, *J. Am. Chem. Soc. 103* (1981) 2436; f) P. Caramella, N. G. Rondan, M. N. Paddon-Row, K. N. Houk, *ibid. 103* (1981) 2438; g) G. A. Jeffrey, K. N. Houk, M. N. Paddon-Row, N. G. Rondan, J. Mitra, *ibid. 107* (1985) 321.

[4] A. Wong, J. A. Gladysz, *J. Am. Chem. Soc. 104* (1982) 4948.

[5] See a) J. W. Faller, K.-H. Chao, *Organometallics 3* (1984) 927; b) J. W. Faller, C. Lambert, *Tetrahedron 41* (1985) 5755; c) W. E. VanArsdale, R. E. K. Winter, J. K. Kochi, *Organometallics 5* (1986) 645, and references cited therein.

[6] For a theoretical treatment of the electronic effects of asymmetry at a transition metal on the reactivity of its ligands, see B. E. R. Schilling, R. Hoffmann, J. W. Faller, *J. Am. Chem. Soc. 101* (1979) 592. For a more general discussion, see A. Gutiérrez, J. E. Jackson, K. Mislow, *ibid. 107* (1985) 2880.

[7] K. Mislow, J. Siegel, *J. Am. Chem. Soc. 106* (1984) 3319.

[8] All new compounds gave satisfactory analytical and/or spectral data. For example **1**: ^{1}H-NMR (200 MHz, CD_3CN): $\delta = 6.13$ (br. s, 1H), 5.48 (hr. s, 2H), 3.52 (s, 3H), 2.04 (s, 3H). **3**: IR (neat): $\tilde{\nu} = 2020$, 1965, 1720 cm^{-1}. **5**: m.p. = 89–90 °C; IR (neat): $\tilde{\nu} = 1724$, 1575 cm^{-1}; ^{1}H-NMR (200 MHz, $CDCl_3$): $\delta = 5.37$ (br. s, 1H), 5.18 (d, $J = 2.8$ Hz, 1H), 5.12 (dd, $J = 2.3$, 1.5 Hz, 1H), 4.99 (d, $J = 2.8$ Hz, 1H), 4.96 (br. s, 1H), 3.78 (s, 3H), 2.08 (s, 3H), 0.24 (s, 9H), 0.22 (s, 9H). **9a**: 73%, red oil, IR (neat): $\tilde{\nu} = 2958$, 1707, 1438, 1353, 1250, 836 cm^{-1}; MS (70 eV): *m/z* 532 ($M^{\oplus}$, 16), 517 (5), 473 (13), 459 (100), 73 (40); HRMS: *m/z* 532.1678 (calculated: 532.1695); ^{1}H-NMR (300 MHz, C_6D_6) for major isomer: $\delta = 5.15$ (br. s, 1H), 5.09 (br. s, 1H), 4.85 (br. s, 1H), 3.63 (s, 6H), 3.24 (d, $J = 2.7$ Hz, 1H), 2.26 (d, $J = 2.7$ Hz, 1H), 1.57 (s, 3H), 0.45 (s, 9H), 0.42 (s, 9H), 0.19 (s, 9H); for minor isomer: $\delta = 5.73$ (br. s, 1H), 5.07 (br. s, 1H), 4.21 (br. s, 1H), 3.63 (s, 3H), 3.53 (s, 3H), 3.22 (d, $J = 2.7$ Hz, 1H), 2.27 (d, $J = 2.7$ Hz, 1H), 1.98 (s, 3H), 0.47 (s, 9H), 0.41 (s, 9H), 0.19 (s, 9H).

[9] P. Hart, D. W. Macomber, M. D. Rausch, *J. Am. Chem. Soc. 102* (1980) 1196.

[10] E. R. F. Gesing, J. P. Tane, K. P. C. Vollhardt, *Angew. Chem. 92* (1980) 1057; *Angew. Chem. Int. Ed. Engl. 19* (1980) 1023.

[11] The fully coupled (FUCOUP) two-dimensional ^{13}C-^{1}H chemical shift correlation spectrum [12] of **6** shows $^3J_{C,H}$ couplings between the methyl group hydrogens and one quaternary and one hydrogen-bearing cyclopentadienyl carbon, respectively. This finding establishes **6** as being the 1,2-disubstituted isomer. The 1,3 isomer would give $^3J_{C,H}$ couplings between the methyl group hydrogens and two hydrogen-bearing Cp carbons.

[12] a) A. A. Maudsley, R. R. Ernst, *Chem. Phys. Lett. 50* (1977) 368; b) G. Bodenhausen, R. Freeman, *J. Am. Chem. Soc. 100* (1978) 320; c) H. Bleich, S. Gould, P. Pitner, J. Wilde, *J. Magn. Reson. 56* (1984) 515; d) R. L. Halterman, N. H. Nguyen, K. P. C. Vollhardt, *J. Am. Chem. Soc. 107* (1985) 1379; e) A. L. Waterhouse, I. Holden, J. E. Casida, *J. Chem. Soc. Perkin Trans. 2 1985*, 1011.

[13] Crystal system: monoclinic $P2_1$ (polarity not determined), $a = 13.061(2)$, $b = 7.342(1)$, $c = 23.151(5)$ Å, $\alpha = \gamma = 90$, $\beta = 92.34(2)°$, $V = 2218.4(7)$ Å^3, $Z = 4$, $\rho = 1.259$ g cm^{-3}, $\mu = 8.90$ cm^{-1}, no absorption correction; $Mo_{K\alpha}$ radiation (graphite monochromator); scan range $3° \le 2\theta \le 45°$; reflections collected 5769; 5307 treated as observed [$F_0 \ge 3.5\sigma(F)$], $R = 0.055$, $R_w = 0.058$. Further details of the crystal structure investigation may be obtained from the Fachinformationszentrum Energie, Physik, Mathematik GmbH, D-7514 Eggenstein-Leopoldshafen 2 (FRG), on quoting the depository number CSD-52700, the names of the authors, and the journal citation.

[14] J. H. Bieri, A. S. Dreiding, T. C. C. Gartenmann, E. R. F. Gesing, R. W. Kunz, R. Prewo, *J. Organomet. Chem. 306* (1986) 241.

[15] This statement also applies to crystal packing effects, the closest intermolecular contacts C13-O21 (2.417 Å) and C33-O1 (2.374 Å) being too weak to cause such changes. See also: P. Dauber, A. T. Hagler, *Acc. Chem. Res. 13* (1980) 105.

[16] J. P. Tane, K. P. C. Vollhardt, *Angew. Chem. 94* (1982) 642; *Angew. Chem. Int. Ed. Engl. 21* (1982) 617; *Angew. Chem. Suppl. 1982*, 1360.

[17] a) J. E. Sheats, *J. Organomet. Chem. Libr. 7* (1979) 461; see also b) H. Lehmkuhl, H. F. Nehl, *Chem. Ber. 117* (1984) 3443.

[18] D. W. Slocum, C. R. Ernst, *Adv. Organomet. Chem. 10* (1972) 79.

Real-Time Atomic-Resolution Imaging of Polymorphic Changes in Ruthenium Clusters**

By *Jan-Olle Malm, Jan-Olov Bovin,* Amanda Petford-Long, David J. Smith, Günter Schmid,* and *N. Klein*

A knowledge of the microstructure including free surfaces and defects of small particles, and of any variations of these properties with time, is of great importance for an understanding of the mechanisms involved in heterogeneous catalysis, and in surface reactions such as corrosion. The activity and selectivity of small metal crystal catalysts depend on the surfaces involved in the reaction. It has been shown, for example, that the (111) surface of iron is about four hundred times more active than the (110) surface during ammonia synthesis.[1] The abundance and extent of a specific surface is a direct function of the crystal structure, shape and size, as well as of any structural rearrangements with time. This means that catalytic reactions involve not only the dynamics of any surface atoms of the metal but also the dynamics of the total structure. Consequently, it is desirable to study the behavior of different metals at temperatures relevant for catalytic reactions.

It has recently been shown[2,3] that the atomic structure of small metal particles (≈ 1–10 nm) can be imaged directly by means of modern high-resolution electron microscopes (HREM). Dynamic in situ HREM observations at TV rate, using low-light-level, silicon-intensified target cameras, have revealed structural rearrangements,[4] crystal growth,[5] and surface structures[6] associated with small metal crystals of gold,[7] platinum, rhodium, ruthenium, and zinc.[5] We demonstrate here that video recordings made at atomic resolution with an HREM can yield important information on the morphology and atomic structure of small ruthenium particles.

Novel preparation methods[8] have made it possible to obtain ruthenium metal clusters $[Ru_{55}(PtBu_3)_{12}Cl_{20}]$, with constant size and reasonable stability for transportation into the electron microscope.

The Ru cluster compound is easily oxidized in air and is dispersed in methanol and transferred onto a holey carbon support film in an inert gas (N_2) atmosphere. The sample is then loaded into the microscope while still wet with methanol, and the high vacuum ($\approx 5 \times 10^{-7}$ torr) inside the microscope column is used to evaporate the solvent. The organic ligands and chlorine atoms that cover the 55-atom metal core are removed when the electron beam (typical current density of 20–40 A cm^{-2}) irradiates the area of observation, leaving bare metal particles exposed on the substrate of amorphous carbon. Electron microscopy was performed with a JEM-4000 EX, which was operated at an electron accelerating voltage of 400 kV and could achieve

[*] Dr. J.-O. Bovin, M. Sc. J.-O. Malm
National Center for High Resolution Electron Microscopy
Inorganic Chemistry 2, Chemical Center
P.O. Box 124, S-221 00 Lund (Sweden)

Dr. A. K. Petford-Long [+], Prof. D. J. Smith
Center for Solid State Science, Arizona State University
Tempe, AZ 85287 (USA)

Prof. Dr. G. Schmid, Dipl.-Chem. N. Klein
Institut für Anorganische Chemie, Universität-Gesamthochschule
Postfach 103764, D-4300 Essen 1 (FRG)

[+] Present address:
Department of Metallurgy and Science of Materials
Parks Road, Oxford OX1 3PH (England)

[**] This work was supported by the Swedish National Science Research Council (K-KU3914-120), the National Swedish Board for Technical Development (81-5366), the Swedish National Energy Administration (276332-1), and the American Office for Naval Research, and made use of facilities within the National Facility for High Resolution Electron Microscopy at Arizona State University, funded by the U. S. National Science Foundation (grant DMR-8306501).

a structural resolution of better than 0.17 nm. The typical electron-optical magnification used was 800000×. A fiber-optically coupled TV system, equipped with an yttrium-aluminum-garnet (YAG) detector and an intensifier, was used for video recordings. The recorded images were treated with a Quantex DS-30 digital video processor for noise reduction using a resolution of 512×512×256. It was possible to freeze individual frames (1/30 s recording time) at any time with the processor in order to take photographs of the images visible on the TV monitor.

X-ray diffraction studies[9] of ruthenium metal from room temperature to 1300°C suggest that its crystal structure is hexagonal close-packed (hcp) over the whole range, with a unit cell described by $a = 0.2713$ nm and $c = 0.4303$ nm at 500°C. The existence of only one phase in this temperature range does not agree with earlier specific heat measurements[10] between 0°C and 1600°C which showed two different phases up to 1200°C and an additional two at higher temperatures. The structures of these phases have not been determined. The precise structural arrangements of the 55 ruthenium atoms in the center of the clusters studied here is not known, although we have observed one very small crystal containing approximately 50–60 atoms (Fig. 1), which displays structural characteristics similar to a hexagonal close-packed structure when compared with a computer-simulated image projected along ⟨100⟩ (see Fig. 5a). (The main problem with recording genuine crystal structure images of small crystals[7] is the occurrence of structural rearrangements which are faster than the frame rate of 1/30 s per frame.)

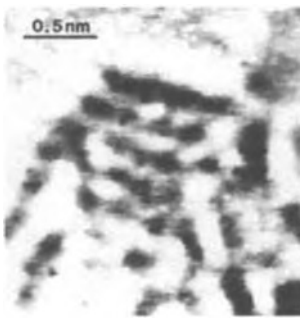

Fig. 1. Ruthenium crystal, containing approximately 50–60 atoms, which originates from the cluster molecule $[Ru_{55}(PtBu_3)_{12}Cl_{20}]$ and which could be regarded as the metal core of the molecules. Comparison with image simulations confirms that the crystal has roughly hcp characteristics (cf. Fig. 5a).

The Ru crystals were found to be randomly oriented and dispersed over the substrate. Those located along the edges of holes in the carbon film were chosen for observation to avoid their images being obscured by contrast from the underlying amorphous carbon support film. Similar to the clusters of gold, platinum and rhodium studied previously,[7] the 55-atom clusters of Ru start to grow under the influence of temperature increases generated by the electron beam as it irradiates the substrate. This growth results in crystals with typical sizes in the range of 2–5 nm. Crystals of this approximate size change their structure rather slowly, with the rate of change also dependent on the size of the contact area with the support. With better contact, the rearrangements usually become slower.

Video recordings of these Ru crystals reveal that their structure is not solely restricted to the known bulk hcp structure. The cubic close-packed (ccp) structure was often seen and a crystal was occasionally observed made up of half ccp and half hcp structures (Fig. 2). It has been known for a long time[11, 12] that the hcp structure could be described as ccp with regular twinning along the ⟨111⟩ direction. The crystal structure image shown in Figure 2 reveals that the lower right part of the crystal is ccp for five atomic planes, viewed here along $\langle 110\rangle_{ccp}$, and the upper half of the crystal contains regularly twinned planes (ten in all) along $\langle 111\rangle_{ccp}$. This results in the normal hcp structure being obtained, viewed here along $\langle 100\rangle_{hcp}$.

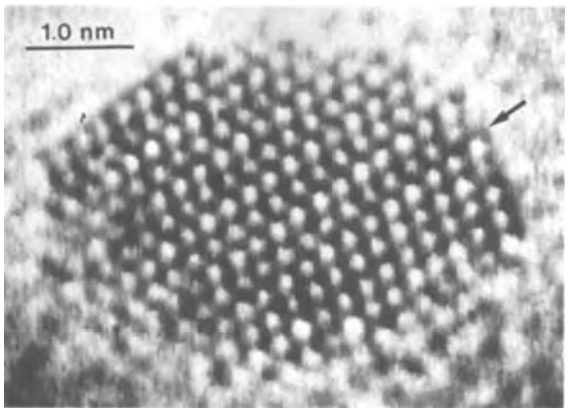

Fig. 2. Structure image confirming the coexistence of hexagonal close-packing and cubic close-packing in the same ruthenium crystal. At the upper left of the image is the characteristic hcp structure, viewed along $\langle 100\rangle_{hcp}$. The five ⟨111⟩ planes at lower right are clearly ordered ccp. The ⟨111⟩ plane that separates the hexagonal structure from the cubic is marked with an arrow.

The calculated structural energy difference between ccp and hcp has been reported to be higher for Ru than for any other 4d element.[13] Experimental enthalpy differences derived from phase diagrams give values which are smaller by about a factor of 10.[14] Moreover, since the same crystal of Ru contains both ccp and hcp structures at the same time, it might be concluded that the energy levels for ccp and hcp stacking are very close to each other. If the atomic volume is considered to be the same for the two types of atomic stacking in ruthenium, as in cobalt metal,[15] the cubic lattice parameter can be calculated to be $a = 0.379$ nm. The projected interatomic distances of Ru viewed along $\langle 110\rangle_{ccp}$ would be 0.232 nm, almost identical to the corresponding distances (0.235 nm) known from images (cf. Fig. 2) recorded of hcp crystals. The image in Figure 2 is the first experimental micrograph that verifies the coexistence of ccp and hcp structures in the same Ru crystal, with both interatomic distances approximately 0.27 nm.

The rearrangements of the small ruthenium crystals not only involved hcp and ccp structures. The video recordings revealed that body-centered cubic (bcc) and icosahedral packing existed for short periods, ranging from 1/30 s (lower limit of recording for one TV frame) to several seconds. The crystal shown in Figure 3 was observed continuously for more than 30 min while it was constantly changing its structure without noticeably growing. Irregular twinning of the ccp structure gives rise to a disordered hcp structure, as reported earlier for hcp cobalt,[16] and such defect twinning also occurs for ruthenium (see Fig. 3b). The stacking sequence of close-packed (111) atom planes from left to right can be represented as

B C A C A B A B A B A

if the white dots are counted as atomic columns, starting from the plane marked with an arrow. This same crystal

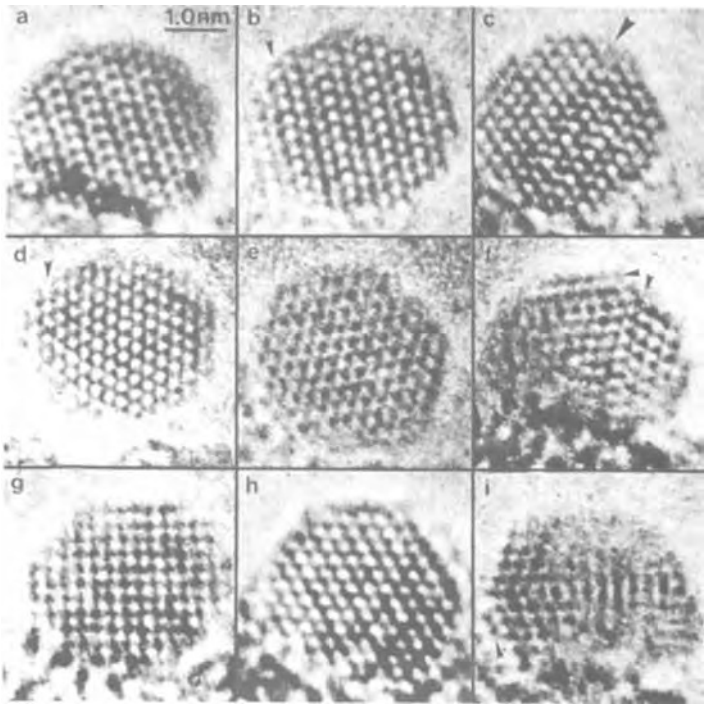

Fig. 3. Images of the same 3-nm ruthenium crystal, recorded during a 30-min period, which show rearrangements in the crystal structure and the occurrence of four basic structure types. a) The hcp structure viewed along ⟨100⟩. b) Disordered hcp structure which can be derived from irregularly twinned ccp. See text for details of stacking sequence of ⟨111⟩ planes. c) Half hcp and half ccp structure: the ⟨111⟩ plane separating the two structure types is marked with an arrow. d) Mostly ccp, except for three/four planes (at left) which show hcp stacking. See text for details of stacking sequence. e) Entire structure is ccp. f) Defects and twinning (marked with an arrow) are common in the ccp state. g) The bcc structure, viewed along ⟨100⟩. h) The bcc structure, viewed along ⟨111⟩. i) The multiply twinned isosahedral stacking. The two outer atomic columns (marked with an arrow) are not located in the expected positions compared with the bulk structure.

also had a structural state of half ccp and half hcp (Fig. 3c), and states having only a minor hcp region were also recorded (see Fig. 3d). The stacking sequence of the (111) atomic planes from left to right in this case is

A C B A B C A B C A B C
hcp ccp

under the same conditions as above. The cubeoctahedral crystal shape in the ccp structure was just as frequently seen as hcp, and one example is shown in Figure 3e. Twinning and antiphase boundaries were very common, as reported earlier for Au.[4] A typical defect in the ccp crystal packing is shown in Figure 3f: two defect planes are visible.

The third basic structural type for metals, namely body-centered cubic (bcc) packing, was imaged several times along different crystallographic axes (Fig. 3g, h). Energy calculations for different structures,[13] as well as experimental enthalpy measurements,[14] indicate that bcc packing should be unlikely for ruthenium. However, theoretical calculations do not predict the existence of the experimentally well-established bcc structure for the corresponding 3d element iron. The very early specific heat experiments for Ru and Fe[10] indicated the close resemblance between the curves of the two elements. Like iron, molybdenum is also reported as adopting both ccp and bcc structures.[17] The atomic radius for iron is 0.130 nm for ccp and 0.126 nm for bcc structures, which is a difference of about 3%. The corresponding difference for molybdenum is about 8% ($r_{ccp} = 0.147$ nm and $r_{bcc} = 0.136$ nm). If the corresponding difference for ruthenium is assumed to be about 5%, then the bcc radius is calculated as 0.130 nm for the unit-cell parameter $a = 0.300$ nm. The projected distances between atomic columns of small bcc Ru crystals, when imaged in the ⟨100⟩ direction, should then be 0.212 nm (in a square net), which is in agreement with the distances measured in the image in Figure 3g. When the same crystal is viewed along the ⟨111⟩ direction (Fig. 3h), a hexagonal net of atomic columns should be seen with a separation of 0.245 nm between the black dots. Note that a hexagonal contrast pattern would appear for an hcp crystal viewed along the c axis, but the shortest distance between the atom columns would be 0.117 nm, which is beyond the structural resolution of the particular microscope used in this study. Computer simulations indicate that the unit cell repeat of 0.271 nm should be visible in the image, and that it should be easily differentiated from the 0.245-nm distance occurring along ⟨111⟩ for bcc Ru.

Icosahedral packing of atoms is expected to be favorable for very small metal clusters ($N \leq 14$ atoms) when the energy of configuration is taken into account.[18] When a third layer of atoms is added, the proper coordination number and bond distances can no longer be obtained. Surface and internal defects are thus introduced as the crystal grows. Defects of this type have been observed previously by HREM for larger silver crystals (≈ 10 nm).[19] Small gold crystals (≈ 3.5 nm) can sometimes attain an icosahedral structure during rearrangements:[5,6] the image in Figure 3 shows that this structural type also occurs for Ru. This structure is, however, not very common—only a couple of cases were observed during the entire recording period. (Note that the two outermost columns of atoms at one surface (arrow) are not located in the expected positions relative to the bulk structure.)

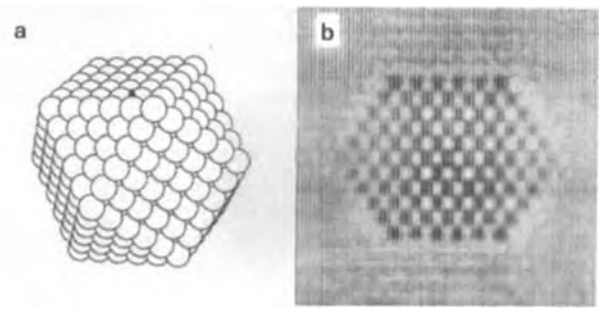

Fig. 4. a) Model for an ideal cubeoctahedron, containing 561 atoms, of the same approximate size as the crystal shown in Fig. 3a. b) Corresponding image simulation, viewed along ⟨110⟩, using the electron-optical parameters of the JEM-4000 EX.

Image simulations, taking into account the microscope imaging conditions, were used to confirm the appearances expected for the various structural types adopted by the Ru clusters. A model for a ccp cubeoctahedron containing 561 atoms, viewed along ⟨110⟩, is shown in Figure 4a, with the corresponding image simulation shown in Figure 4b. This computer simulation can be compared with the experimental micrograph (Fig. 3e). The hcp state of the same crystal (Fig. 3a) can be compared with the image simulation shown in Figure 5a. In this case, the computation was

done for a much smaller (54-atom) crystal of the same shape in order to minimize computation time. Figure 5b shows the computation for an ideal cubeoctahedron containing 55 atoms as viewed along ⟨110⟩. Finally, Figures 5c and 5d show the image simulations for the bcc structure as viewed along ⟨100⟩ and ⟨111⟩, respectively, which should be compared with the experimental images shown in Figures 3g and 3h, respectively.

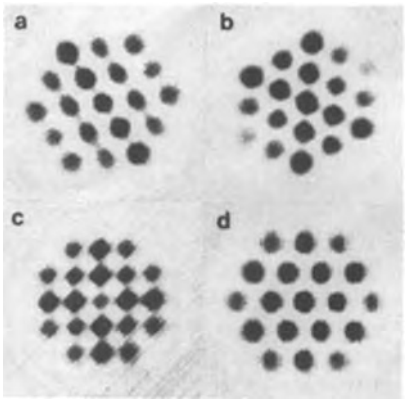

Fig. 5. Computer simulations of various structural types for comparison with the experimental micrographs: a) hcp along ⟨100⟩ containing 54 atoms; b) ccp along ⟨110⟩ containing 55 atoms (ideal cubeoctahedron); c) bcc along ⟨100⟩ containing 59 atoms; d) bcc along ⟨111⟩ containing 59 atoms.

These observations of the important catalyst ruthenium show that its overall crystal structure, and hence its surface structure, change very rapidly under the influence of the electron beam. Earlier studies of small gold crystals[4] indicated that the local temperature in the vicinity of the illuminated area was probably above 500 °C. This constantly changing nature of the metal clusters could well be a quasi-liquid state previously not shown to exist because of the difficulties involved in observing or recording it. Recent results from time-resolved NMR spectroscopy[20] could be interpreted to mean that the small metal clusters with ligands surrounding them altered their structure in solution even at room temperature. These results are of crucial importance for future research on the mechanisms involved in catalytic reactions on metal surfaces.

Received: October 30, 1987 [Z 2490 IE]
German version: *Angew. Chem. 100* (1988) 580

CAS Registry number:
$[Ru_{55}(PtBu_3)_{12}Cl_{20}]$, 104619-09-2.

[1] N. D. Spencer, R. C. Schoonmaker, G. A. Somorjai, *J. Catal. 74* (1982) 129.
[2] L. D. Marks, D. J. Smith, *Nature (London) 303* (1983) 316.
[3] J.-O. Bovin, *ORDO 16* (1982) 13.
[4] D. J. Smith, A. K. Petford-Long, L. R. Wallenberg, J.-O. Bovin, *Science (Washington) 233* (1986) 872, and references cited therein.
[5] A. K. Petford-Long, D. J. Smith, L. R. Wallenberg, J.-O. Bovin, *J. Cryst. Growth 80* (1987) 218, and references cited therein.
[6] J.-O. Bovin, *Proc. XI Int. Cong. Electron Microsc., Jpn. Soc. Electron Microsc. Tokyo 1986*, Abstr. p. 83, and references cited therein.
[7] A. K. Petford-Long, N. J. Long, D. J. Smith, L. R. Wallenberg, J.-O. Bovin in P. Jena, B. K. Rao, S. N. Khanna (Eds.): *Physics and Chemistry of Small Clusters*, Plenum, New York 1987, p. 127, and references cited therein.
[8] G. Schmid, W. Huster, *Z. Naturforsch. B41* (1986) 1028.
[9] E. O. Hall, J. Crangle, *Acta Crystallogr. 10* (1957) 240.
[10] E. M. Jaeger, E. Rosenbohm, *Proc. Acad. Sci. Amst. 34:2* (1941) 808.
[11] W. Barlow, *Nature (London) 24* (1883) 205 (December 27th issue).
[12] G. Aminoff, B. Bloom, *Z. Kristallogr. Kristallgeom. Kristallphys. Kristallchem. 80* (1931) 355.
[13] N. L. Skriver, *Phys. Rev. B31* (1985) 1909.
[14] A. R. Miedema, K. A. Niessen, *CALPHAD Comput. Coupling Phase Diagrams Thermochem. 7* (1983) 27.
[15] A. R. Troiano, J. L. Takich, *Met. Technol. (N. Y.) 15* (1947) 3.
[16] O. S. Edwards, H. Lipsom, *Proc. R. Soc. A180* (1947) 268.
[17] P. S. Aggarwal, A. Goswami, *Proc. Phys. Soc. 70B* (1957) 708.
[18] M. R. Hoare, P. Pal, *Nature (London), Phys. Sci. 230* (1971) 5.
[19] D. J. Smith, L. D. Marks, *Ultramicroscopy 16* (1985) 101.
[20] G. Schmid, U. Giebel, W. Huster, A. Schwenk, *Inorg. Chim. Acta 85* (1984) 97.

Unsaturated Hydrindanone Derivatives from Arenes by Hetero-Claisen Rearrangement**

By *Annegrit Bosum* and *Siegfried Blechert**

The Claisen rearrangement of aromatic compounds proceeds via olefinic intermediates and thus releases the latent functionalities of the arene. The preparative use of these functionalities is usually not possible, however, owing to spontaneous rearomatization, e.g., in the case of *ortho*-substituted arenes, by a second [3,3]-sigmatropic rearrangement to give *para*-substituted products.[1] For carbanion-accelerated hetero-Claisen rearrangement of *N*-aryl-*O*-vinyl systems, very mild reaction conditions may be employed,[2] thereby excluding a subsequent hetero-Cope rearrangement, since the essential driving force for the hetero-Claisen rearrangement—a weak N–O bond and the formation of a C=O bond—is no longer present. Thus, imines may be generated by rearrangement of *ortho*-substituted *N*-phenylhydroxylamine derivatives. These imines, in turn, may be trapped intramolecularly by nucleophiles, leading to the formation of novel five-membered rings.[3]

We have used this strategy to synthesize unsaturated hydrindanone derivatives or other cyclic olefins directly from arenes. In order to avoid regioselectivity problems in the hetero-Claisen rearrangement, we initially employed symmetrically substituted compounds. Reaction of the lithium salt **1**[4] with the readily accessible, acceptor-substituted allenes **2**[5] in tetrahydrofuran at room temperature resulted in Michael addition, rearrangement, and cyclization, leading to formation of the hydrindanone derivatives **5**,[6] in preparatively useful yields, which could be purified by chromatography (for spectroscopic data of the compounds **5a**, **6**, and **7**, see Table 1). The intramolecular trapping reaction is highly stereoselective for the *N*-acylated imine **4**.[7] Intermediates could not be detected.

Because of its position (tertiary allylic), the *N*-acyl group of **5** proved to be a sufficiently good leaving group, so that, by retro-Michael addition, an unsaturated five-membered ring ketone could readily form, which, in turn, leads to material losses upon chromatographic purification of **5**. It is best, therefore, to use unpurified **5** (one-pot reaction) in subsequent reactions. Thus, for studies of the synthesis of terpenes, **5** was hydrogenated with H_2 in the presence of Pd on $BaSO_4$, whereby only the less substituted double bond was attacked. Filtration over neutral Al_2O_3 resulted in amide cleavage. Thus, **7**[6] was obtained from **5a** in 65% overall yield (based on **1**) in a one-pot reaction.

[*] Prof. Dr. S. Blechert, Dipl.-Chem. A. Bosum
Institut für Organische Chemie und Biochemie der Universität
Gerhard-Domagk-Strasse 1, D-5300 Bonn 1 (FRG)

[**] Hetero-Cope Rearrangement, Part 7. This work was supported by the Deutsche Forschungsgemeinschaft and the Fonds der Chemischen Industrie.—Part 6: J. Wilkens, A. Kühling, S. Blechert, *Tetrahedron 43* (1987) 3237.

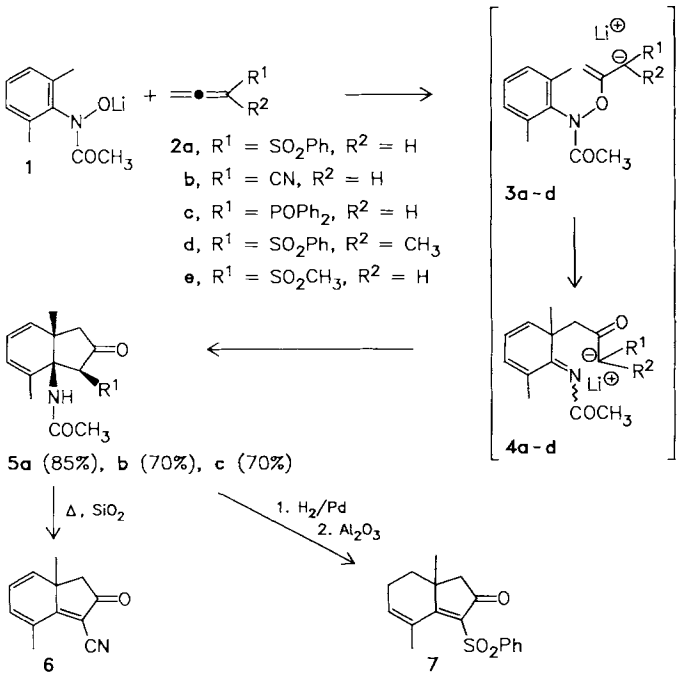

When unpurified **5b** was transferred to a silica surface and heated at 100°C for 5–10 min, **6**,[6,7] as retro-Michael product, was obtained in nearly quantitative yield upon elution with diethyl ether. Compound **6** should be of interest as a readily accessible derivative of the unstable 3a-methyl-3a*H*-indene.[8] Although retro-Michael additions of **5** can also be accomplished by heating in a solvent, indene derivatives of type **6** undergo rapid dimerization and can be handled in solution even at room temperature for only a few minutes.

Table 1. Selected spectroscopic data for the compounds **5a**, **6**, and **7**. 200-MHz ^{1}H-NMR in $CDCl_3$, *J* in Hz.

5a: IR (CCl_4): $\tilde{\nu}$ [cm^{-1}] = 3380, 1750, 1700. — ^{1}H-NMR: δ = 7.9 (dd, *J* = 7.5, 2.0, 2H), 7.4–7.7 (m, 3H), 7.39 (br. s, 1H), 5.9 (m, 2H), 5.35 (dd, *J* = 7.5, 2.0, 1H), 4.2 (s, 1H), 3.0 (d, *J* = 16.5, 1H), 2.8 (d, *J* = 16.5, 1H), 2.19 (s, 3H), 2.15 (s, 3H), 1.2 (s, 3H)

6: UV (CH_3OH): λ_{max} = 354 nm. — IR ($CHCl_3$): $\tilde{\nu}$ [cm^{-1}] = 1725, 1635, 1600. — ^{1}H-NMR: δ = 6.43 (dd, *J* = 9.0, 1.5, 1H), 6.35 (dd, *J* = 6.0, 1.5, 1H), 6.11 (dd, *J* = 9.0, 6.0, 1H), 2.58 (s, 2H), 2.35 (s, 3H), 1.36 (s, 3H)

7: IR ($CHCl_3$): $\tilde{\nu}$ [cm^{-1}] = 1720, 1620. — ^{1}H-NMR: δ = 8.05 (dd, *J* = 8.0, 1.5, 2H), 7.55 (m, 3H), 6.25 (br. s, 1H), 2.44 (d, *J* = 8.0, 1H), 2.43 (d, *J* = 8.0, 1H), 2.35 (s, 3H), 2.34 (dt, *J* = 8.0, 4.0, 2H), 1.80 (t, *J* = 8, 2H), 1.18 (s, 3H)

The conjugated *N*-acylated imines **4**, formed by hetero-Claisen rearrangement, can also be trapped by vinylogous attack, leading to hydrindanone derivatives having a different pattern of substitution. This goal is easy to attain with sterically demanding carbanions such as **4d**. Instead of direct cyclization with the imine moiety, which would lead to the formation of three neighboring quaternary centers, stereochemically uniform formation of **8**[6,7] is observed (78% yield after chromatographic purification on silica gel). Because of the low nucleophilicity of the carbanionic center of **4d**, water as a competing nucleophile can attack the imine group vinylogously. When **1** is allowed to react with **2d** at 40°C in the presence of a small amount of water, the main product obtained (55% yield) is the diastereomerically pure allyl alcohol **9**,[6] which is unstable and undergoes ready transformation to **8**.

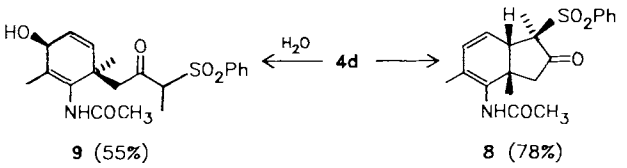

Hetero-Claisen rearrangements of mono-*ortho*-substituted arenes can lead to cyclic olefins or to arenes. We investigated possibilities to control the regioselectivity of the rearrangement in order to selectively synthesize hydrindanone derivatives.[9] The studies of regioselectivity revealed, among other things, a pronounced steric effect of substituents on the arenes as well as on the nitrogen atom. In some cases, this can be used to control the regioselectivity of the rearrangement and of the subsequent cyclization. The hetero-Claisen system generated by reaction of **10** and **2e** rearranges preferentially with involvement of the methyl-substituted position; the formation of the apparently sterically unfavored tetrasubstituted arene is thereby avoided. The vinylogous trapping reaction of the imine is stereochemically unambiguous and affords, after chromatography on silica gel, the functionalized unsaturated hydrindanone derivative **11**.[6,7]

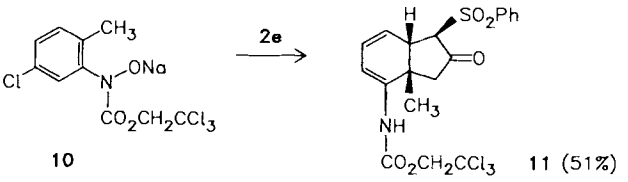

Experimental Procedure

5, **8**, **11**: Hydroxamic acid (2 mmol) was deprotonated in 10 mL of dry tetrahydrofuran with 2 mmol of NaH as a 50% suspension in mineral oil. Water-free lithium fluoroacetate (2.5 mmol) and allene **2** (2.2 mmol) were then added. After the reaction had ended (20 min, monitored by TLC), the mixture was neutralized with formic acid, poured into 60 mL of water, and extracted with 60 mL of dichloromethane. After distillation of the solvent, the crude product was worked up further or—for characterization—purified by flash chromatography.

Received: November 11, 1987 [Z 2497 IE]
German version: *Angew. Chem. 100* (1988) 596

[1] a) G. B. Bennett, *Synthesis 1977*, 589; b) S. Jolidon, H.-J. Hansen, *Helv. Chim. Acta 60* (1977) 978.
[2] S. Blechert, *Helv. Chim. Acta 68* (1985) 1835.
[3] Reviews on cyclopentene annelation: a) M. Ramaiah, *Synthesis 1984*, 529; b) B. M. Trost, *Angew. Chem. 98* (1986) 1; *Angew. Chem. Int. Ed. Engl. 25* (1986) 1.
[4] Compound **3** is an ambident hetero-Claisen system [2]. The use of Na or K salts can lead in some cases to other rearrangement products.
[5] L. Brandsma, H. D. Verkruijsse: *Synthesis of Acetylenes, Allenes and Cumulenes*, Elsevier, Amsterdam 1981.
[6] All new compounds gave correct elemental analyses and/or molecular weights in the high-resolution mass spectrum.
[7] The configurations were determined on the basis of NOE difference spectra, C,H correlations, as well as COSY and NOESY experiments. We thank Dr. *B. Steffan* for the NMR investigations.
[8] For example, A. C. Gibbard, C. J. Moody, C. W. Rees, *J. Chem. Soc. Perkin Trans. 1 1986*, 145.
[9] S. Blechert, unpublished results.

Redox-Active Thieno[3,2-*b*]thiophene as a Novel, Three-Color Electrochromic System

By *Toyonari Sugimoto, Toshio Nagatomi, Hiroshi Ando,* and *Zen-ichi Yoshida**

Organic materials exhibiting electrochromism, a phenomenon of reversible coloration change induced by electrochemical redox reactions,[1] are of current interest in the development of organic electrochromic display devices, the main advantages of which are low-voltage (0.5–5 V) operation, wide-angle vision, and vivid multicoloration. However, except for viologens,[2] such electrochromic systems are limited to metal complexes such as rare-earth metal phthalocyanines[3] and tris(bipyridyl)ruthenium(II) complexes.[4] We have now prepared a metal-free organic electrochromic system displaying three colors and exhibiting high durability, which is composed of 2,3,5,6-tetrakis (3,5-di-*tert*-butyl-4-hydroxyphenyl)thieno[3,2-*b*]thiophene **1** and its two- and four-electron oxidized partners.

A benzene solution of bis(3,5-di-*tert*-butyl-4-hydroxyphenyl)cyclopropenethione **2**[5] and 1.1 equivalents of tri-*n*-butylphosphane was refluxed for 4 h under argon atmosphere. After evaporation of the solvent, the residue was chromatographed on silica gel with CH_2Cl_2/hexane (1 : 4), followed by recrystallization from benzene/hexane, to afford **1** as pale yellow crystals (m.p. >300 °C) in 35% yield.[6] This is the first case of thieno[3,2-*b*]thiophene formation by thermal dimerization of cyclopropenethiones,

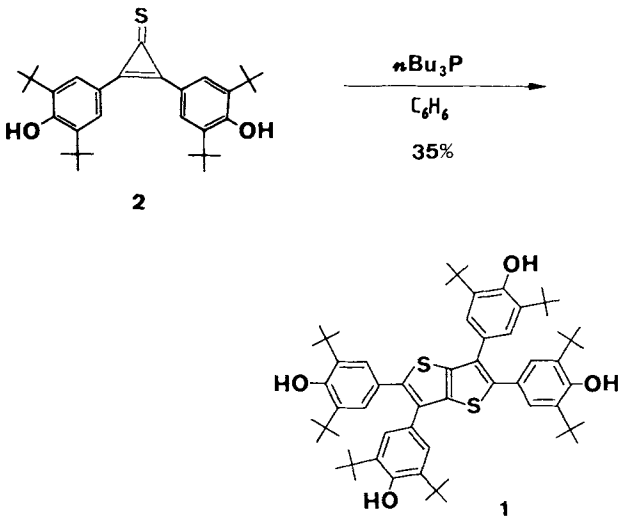

although its photochemical counterpart is already known.[7] When other trivalent phosphorus compounds, such as triphenylphosphane, trimethylphosphite, and hexamethylphosphorous triamide were used, **1** was not formed at all.[8] The structure of **1** was determined from the ^{1}H- and ^{13}C-NMR spectral data (see Table 1).[9] The ^{1}H-NMR spectrum showed the presence of two magnetically different aryl groups. In the ^{13}C-NMR spectrum 15 signals appeared, of which those at $\delta = 138.41$, 137.85, and 131.12 are assigned to the thieno[3,2-*b*]thiophene skeletal carbons.[10]

[*] Prof. Dr. Z. Yoshida, Dr. T. Sugimoto, T. Nagatomi, H. Ando
Department of Synthetic Chemistry, Kyoto University
Yoshida, Kyoto 606 (Japan)

Table 1. Characteristic spectroscopic data for **1**, **3**, and **4**.

Compd	λ_{max}[nm](lgε) (CH_2Cl_2)	IR (KBr) $\tilde{\nu}$ [cm^{-1}]	^{1}H-NMR ($CDCl_3$) δ value
1 [a]	263 (4.41), 303 (4.31), 348 (4.42)	3620, 2940, 2900, 2850, 1425, 1360, 1310, 1230, 1150, 1110, 895	7.24 (s, 4H), 7.13 (s, 4H), 5.17 (s, 2H), 5.16 (s, 2H), 1.35 (s, 36H), 1.33 (s, 36H)
3	279 (3.78), 304 (3.52), 395 (3.47), 634 (4.71)	3620, 2950, 2910, 2850, 1740, 1580, 1450, 1360, 1340, 1130	7.25 (d, J = 2.7 Hz, 2H), 7.24 (s, 4H), 7.01 (d, J = 2.7 Hz, 2H), 5.52 (s, 2H), 1.47 (s, 36H), 1.29 (s, 18H), 0.94 (s, 18H)
4	266 (4.54), 398 (4.78), 516 (4.77), 620 (4.28), 782 (4.54)	2980, 2940, 2900, 2850, 1590, 1570, 1480, 1450, 1390, 1360, 1250, 1120, 1090, 1030	7.29 (br. s, 8H), 1.33 (br. s, 36H), 1.28 (br. s, 36H)

[a] δ(^{13}C) = 153.29, 152.92, 138.41, 137.85, 135.99, 135.92, 131.12, 126.64, 126.56, 126.48, 125.91, 34.38, 34.25, 30.35, 30.21.

By choosing appropriate oxidizing agents, **1** was separately converted into two oxidized products, which were successfully isolated and characterized. Thus, treatment of **1** with iodine, copper(II) chloride, or silver oxide in CH_2Cl_2 containing triethylamine gave almost quantitatively the thieno[3,2-*b*]thiophene **3** (m.p. >300 °C), which contains two quinonoid groups, as dark green crystals after recrystallization from ether. For **3** another structure (**3'**) is

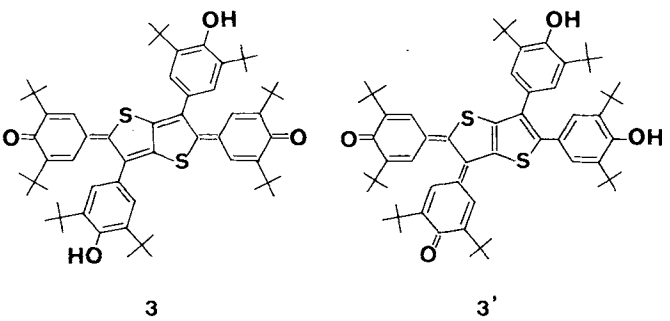

conceivable, but can be excluded by the ^{1}H-NMR spectral data (Table 1). The aryl protons appear as only one singlet,[11] and the two protons on each 4-oxocyclohexadienylidene group are observed as two doublets at $\delta = 7.25$ and 7.01, the former doublet being shifted to lower field than the latter by the anisotropic effect of the neighboring phenyl group. Conversely, this effect causes the high-field shift of the protons of the *tert*-butyl group neighboring the phenyl group. On the other hand, after oxidation of **1** in benzene or CH_2Cl_2 with excess $K_3Fe(CN)_6$ in aqueous 0.1 N NaOH, we isolated a 2,3,5,6-tetrakis(3,5-di-*tert*-butyl-4-oxocyclohexadienylidene)thieno[3,2-*b*]thiophene **4** as a dark brown solid (m.p. ≈260 °C (dec.)) in almost quantitative yield. The redox behavior of **4** was investigated by using cyclic voltammetry.[12] Two pairs of quasi-reversible waves appeared at +0.42 and +0.95 V vs. Ag/AgCl,[13] both of which involve simultaneous transfer of two electrons.[14] Furthermore, **4** could also be reconverted into **3**

and **3** into **1** in quantitative yield by chemical reduction, e.g., with *p*-hydroquinone in benzonitrile.

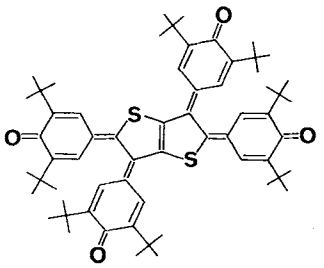

4

The electronic spectra of **1**, **3**, and **4** were measured in CH_2Cl_2 (Table 1). In agreement with the positions of the absorption maxima, the solution of **1** is very pale yellow and that of **3** is very vivid blue. However, **4** exhibits faint brownish-red coloration because of stronger absorption at 516 nm. Most noteworthy is the fact that **1**, **3**, and **4** show very distinct and different coloration. Accordingly, this stable and reversible redox system might provide the basis for developing a new type of three-color electrochromic device.

Received: November 17, 1987 [Z 2503 IE]
German version: *Angew. Chem. 100* (1988) 597

[1] J. R. Platt, *J. Chem. Phys. 34* (1961) 862.
[2] C. J. Schoot, J. J. Ponjeé, H. T. van Dam, R. A. van Doorn, P. T. Bolwijn, *Appl. Phys. Lett. 23* (1973) 64; D. C. Bookbinder, M. S. Wrighton, *J. Electrochem. Soc. 130* (1983) 1080.
[3] I. S. Kirin, P. N. Moskalev, Yu. A. Makashev, *Russ. J. Inorg. Chem. (Engl. Transl.) 10* (1965) 1065; M. M. Nicholson, F. A. Pizzarello, *J. Electrochem. Soc. 126* (1979) 1490.
[4] C. M. Elliott, *J. Chem. Soc. Chem. Commun. 1980*, 261; C. M. Elliott, J. G. Redepenning, *J. Electroanal. Chem. 197* (1986) 219.
[5] The corresponding cyclopropenone was prepared according to the method of *West* et al. (R. West, D. C. Zecher, K. Koster, D. Eggerding, *J. Org. Chem. 40* (1975) 2295). Compound **2** was obtained as pale yellow crystals (m.p. = 221–222 °C) in 80% yield by the reaction of the cyclopropenone with phosphorus(V) pentasulfide in refluxing benzene. IR (KBr): $\tilde{\nu}$ = 3620, 2950, 1595, 1340, 1255, 1240, 1120, 1025, 890 cm^{-1}. ^{1}H-NMR (60 MHz, $CDCl_3$): δ = 1.53 (s, 36H, $C(CH_3)_3$), 5.92 (s, 2H, OH), 8.03 (s, 4H, H_{aryl}).
[6] The present result makes a marked contrast with a recent report on the exclusive formation of another isomeric thieno[3,4-*c*]thiophene by the reaction of bis(*tert*-butylthio)cyclopropenethione with tri-*n*-butyl- or triphenylphosphane: S. Yoneda, K. Ozaki, T. Inoue, A. Sugimoto, K. Yanagi, M. Minobe, *J. Am. Chem. Soc. 107* (1985) 5801.
[7] A. Schönberg, M. Mamluk, *Tetrahedron Lett. 1971*, 4993; S. Singh, M. M. Bhadbhade, K. Venkatesan, *J. Org. Chem. 47* (1982) 3550.
[8] When triphenylphosphane was used, no reaction occurred, and uncharacterized tarry materials were only obtained in the reaction with trimethylphosphite. The reaction of **2** with hexamethylphosphorous triamide afforded a fairly unstable blue material, whose structure is now being characterized.
[9] The mass spectrum and elemental analysis gave satisfactory results.
[10] For the ^{13}C-NMR spectral data of thieno[3,2-*b*]thiophene and its derivatives see S. Gronowitz, I. Johnson, A. Bugge, *Acta Chem. Scand. B 30* (1976) 417.
[11] Assuming the structure **3'**, the *ortho* protons should give rise to six signals in the ^{1}H-NMR spectrum.
[12] The measurement was carried out at 20 °C in benzonitrile containing 0.1 M $(n\text{Bu})_4\text{NClO}_4$ as supporting electrolyte by using platinum working and counter electrodes and a standard Ag/AgCl reference electrode (scan rate: 100 mV s^{-1}).
[13] Both two-electron redox potentials of **4** are comparatively high. Thus, the lower redox potential is almost the same as the first one-electron reduction potential (+0.47 V vs. Ag/AgCl) of 2,3-dichloro-5,6-dicyano-*p*-benzoquinone, a commonly used electron acceptor (M. E. Peover, *J. Chem. Soc. 1962*, 4540). On the other hand, the higher redox potential is comparable to the first one-electron reduction potentials of a *p*-benzoquinodimethane bearing eight cyano substituents (+1.19 V vs. SCE) (L. Bucsis, K. Friedrich, *Chem. Ber. 109* (1976) 2469), a [3]radialene bearing six cyano substituents (+1.13 V vs. SCE) (T. Fukunaga, *J. Am. Chem. Soc. 98* (1976) 610; T. Fukunaga, M. D. Gordon, P. J. Krusic, *J. Am. Chem. Soc. 98* (1976) 611), and tetracyano-*p*-benzoquinone (+1.00 V vs. SCE) (K. Wallenfels, G. Bachmann, *Angew. Chem. 73* (1961) 142). Consequently, **4** (and also **3**) can be used as potent oxidizing agents.
[14] The number of transferred electrons in each pair of waves was determined from the dependence of the peak currents on sample concentrations.

Tris(2,3-di-*tert*-butylcyclotriphosphanyl)stibane—A Compound Containing Three P_3 Rings Linked by an Antimony Atom**

By *Marianne Baudler** and *Loert de Riese-Meyer*

Functionalized cyclotriphosphanes of the type $(PR)_2PX$ (X = functional group) are suitable building blocks for the synthesis of novel compounds containing P_3 rings. For instance, reaction of 1,2-di-*tert*-butyl-3-trimethylstannylcyclotriphosphane **1**[1] with $(t\text{BuP})_2\text{PCl}$ (1:1) and with MePCl_2 (2:1) gave the 1,1'-bicyclotriphosphane $(t\text{BuP})_2\text{P}-\text{P}(t\text{BuP})_2$[2] and the bis(cyclotriphosphanyl)methylphosphane $(t\text{BuP})_2\text{P}-\text{P(Me)}-\text{P}(t\text{BuP})_2$,[3] respectively. However, reaction of **1** with PCl_3 (3:1) leads to partial ring rearrangement and the formation of a 1,2-bis(cyclotriphosphanyl)cyclotetraphosphane $[(t\text{BuP})_2\text{P}]_2t\text{Bu}_2\text{P}_4$.[4] In order to link three P_3 rings through *one* atom, a central atom larger than phosphorus is apparently necessary. We report here on the condensation reaction of **1** with antimony(III) chloride, which leads to the new phosphorus-antimony compounds bis(2,3-di-*tert*-butylcyclotriphosphanyl)chlorostibane **2** and tris(2,3-di-*tert*-butylcyclotriphosphanyl)stibane **3**.

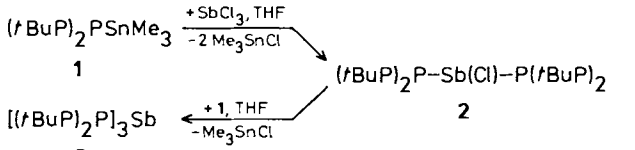

Compound **1** reacts with $SbCl_3$ even in a molar ratio of 1:1 (−78 °C) to give almost exclusively **2** as a mixture of the two configurational isomers **2a** and **2b** (Table 1). No evidence was found for the intermediate $(t\text{BuP})_2\text{P}-\text{SbCl}_2$, which is thus appreciably more reactive than $SbCl_3$.

Increasing the reactant ratio to 3:1 results in the almost exclusive formation of **3** as the two configurational isomers **3a** and **3b** (approx. 1:1). Whereas the symmetric isomer **3a** precipitates from the reaction mixture and can be isolated in analytically pure form at low temperature,[5] the asymmetric isomer **3b** has only been characterized in solution by ^{31}P-NMR spectroscopy. Evidence was not observed for an interconversion between the two diastereomers under conditions where **3** is stable.

Compound **3a** is a yellow solid, which is stable below −30 °C in the absence of air and light. At higher tempera-

[*] Prof. Dr. M. Baudler, Dr. L. de Riese-Meyer
Institut für Anorganische Chemie der Universität
Greinstrasse 6, D-5000 Köln 41 (FRG)

[**] Contributions to the Chemistry of Phosphorus, Part 186. This work was supported by the Deutsche Forschungsgemeinschaft and the Fonds der Chemischen Industrie.—Part 185: M. Baudler, S. Akpapoglou, D. Ouzounis, F. Wasgestian, B. Meinigke, H. Budzikiewicz, H. Münster, *Angew. Chem. 100* (1988) 288; *Angew. Chem. Int. Ed. Engl. 27* (1988) 280.

Table 1. $\delta(^{31}P)$ values [a] and assignment [b] to the P atoms of **2a** and **2b** (both in THF, −80°C).

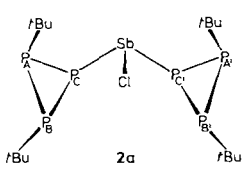

2a

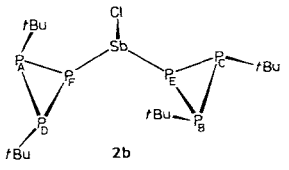

2b

δ Value	Assignment	δ Value	Assignment
− 83.3	P_A, $P_{A'}$	− 73.8	P_A
−108.8	P_B, $P_{B'}$	− 77.0	P_B
−177.5	P_C, $P_{C'}$	−104.0	P_C
		−112.1	P_D
		−177.2	P_E or P_F
		−185.0	P_F or P_E

[a] Estimated from the center of gravity of the signal group. [b] The assignment of the signals to the individual P atoms as well as the configurations of **2a** and **2b** were determined in analogy to the corresponding isomers of $(t\mathrm{BuP})_2\mathrm{P}-\mathrm{P(Me)}-\mathrm{P}(t\mathrm{BuP})_2$ [3].

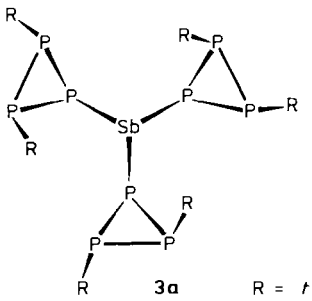

3a R = *t*Bu

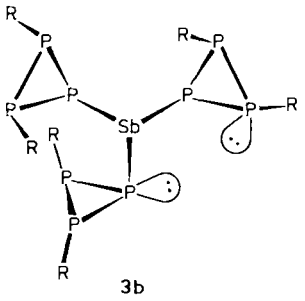

3b

tures or upon exposure to daylight, ring rearrangement and disproportionation reactions occur, leading mainly to the 1,1′-bicyclotriphosphane[2] as well as to phosphorus–antimony polycycles and elemental antimony. In the mass spectrum, the group of peaks for the $M^{\oplus}$ ion (*m/z* 742–746) displays the calculated isotope distribution.

Table 2. $\delta(^{31}P)$ values [a] and assignment to the P atoms of **3a** and **3b** [in THF, −80°C (**3a**) and $[D_8]$THF, −50°C (**3b**)].

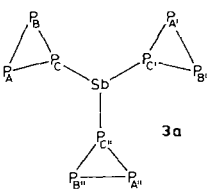

3a

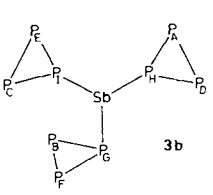

3b

δ Value	Assignment	δ Value	Assignment
− 79.8	P_A, $P_{A'}$, $P_{A''}$	− 74.6	P_A
−106.4	P_B, $P_{B'}$, $P_{B''}$	− 83.3	P_B
−188.2	P_C, $P_{C'}$, $P_{C''}$	− 88.3	P_C
		−101.5	P_D
		−106.4	P_E
		−108.2	P_F
		−171.7	P_G
		−182.3	P_H
		−184.0	P_I

[a] Determined from the center of gravity of the signal groups in the 1D NMR spectrum of **3a** and in the 2D NMR spectrum of **3b**.

Proof of the constitutions of **3a, b** is provided by the ^{31}P-NMR data (Table 2); in addition, a 2D $^{31}P\{^1H\}$-NMR spectrum (COSY 45)[6] was recorded for **3b**. The chemical shifts of all P atoms lie in the high-field region characteristic of phosphorus three-membered ring compounds,[7] the atoms bonded to antimony exhibiting the largest upfield shift in both isomers. The relative arrangement of the *trans*-oriented tert-butyl groups at the three rings is revealed by the spin systems and by the relative magnitudes of the chemical shifts of the respective P atoms. Thus, in **3a**, the downfield position of $\delta(^{31}P_A)$ with respect to $\delta(^{31}P_B)$ indicates that the substituents on P_A, $P_{A'}$, and $P_{A''}$ are in *cis* positions with respect to the exocyclic phosphorus–antimony bond. The analogous facts for **3b** show that the *tert*-butyl groups on P_A, P_B, and P_C are in the corresponding *cis* positions. According to all the NMR spectroscopic findings,[5] **3a** has C_3 symmetry, whereas **3b** has no symmetry element. The two isomers are present as pairs of enantiomers.

The conformations of **3a, b** may be derived from the large P,P long-range couplings, which indicate that the lone pairs on the respective P atoms are directed toward each other.[8] Thus, in the case of **3a**, the absence of fine structure in the upfield group at $\delta = -188$ has to be ascribed to large ^2J couplings between the nuclei P_C, $P_{C'}$, and $P_{C''}$. For **3b**, significant ^2J couplings between P_G and P_H as well as between P_H and P_I are revealed by corresponding cross peaks in the 2D NMR spectrum. The $^3J(P_GP_D)$ coupling constant, which can additionally be observed by variation of the filter function, confirms, in agreement with model considerations, that the three-membered ring $P_BP_FP_G$ is twisted around the exocyclic bond owing to steric interactions between the *t*Bu groups on P_B and P_C.

The first tris(cyclotriphosphanyl) compound, **3**, owes its existence to the relatively large covalent radius of antimony (1.41 Å[9]). Because of its "open" structure, **3** exhibits a high reactivity, which tends to result in a preferred elimination of the central atom.

Received: November 20, 1987 [Z 2507 IE]
German version: *Angew. Chem. 100* (1988) 579

CAS Registry numbers:
1, 113705-86-5; **2**, 113705-87-6; **3**, 113774-75-7; $SbCl_3$, 10025-91-9.

[1] M. Baudler, B. Makowka, *Z. Anorg. Allg. Chem. 528* (1985) 7.
[2] M. Baudler, B. Makowka, *Angew. Chem. 96* (1984) 976; *Angew. Chem. Int. Ed. Engl. 23* (1984) 987.
[3] M. Baudler, L. de Riese-Meyer, *Z. Naturforsch. B 41* (1986) 399.
[4] M. Baudler, L. de Riese-Meyer, C. Wiaterek, *Z. Naturforsch. B*, in press.
[5] *Experimental Procedure:* **3a**: $SbCl_3$ (1.12 g, 4.91 mmol) in THF (9 mL) was added over 10 min under inert atmosphere in the dark to a stirred solution of **1** (5.76 g, 15.53 mmol) in THF (30 mL) at −78°C. The reaction solution immediately turned red; after 2–5 min, a yellow-orange solid began to precipitate. Stirring was continued for 1 h at −78°C, after which the solution was siphoned off in the cold and the precipitate was redissolved in 30 mL of cold THF at −30°C. The solid that precipitated after allowing the solution to stand for 2 d at −78°C was recrystallized again in the same way from 13 mL of *n*-pentane; yield 0.98 g (27%, based on $SbCl_3$) of yellow, isomerically pure **3a**. — $^1H\{^{31}P\}$-NMR ($[D_8]$toluene, −50°C): $\delta = 1.23$ ($P_A t\mathrm{Bu}$), 1.11 ($P_B t\mathrm{Bu}$). — $^{13}C\{^1H,^{31}P\}$-NMR ($[D_8]$toluene, −50°C): $\delta = 32.4$ ($P_A C$), 31.9 ($P_A CC$), 29.9 ($P_B CC$), 29.4 ($P_B C$).
[6] Review: R. Benn, H. Günther, *Angew. Chem. 95* (1983) 381; *Angew. Chem. Int. Ed. Engl. 22* (1983) 350.
[7] Reviews: a) M. Baudler, *Pure Appl. Chem. 52* (1980) 755; b) *Angew. Chem. 94* (1982) 520; *Angew. Chem. Int. Ed. Engl. 21* (1982) 492; c) *Z. Chem. 24* (1984) 352.
[8] a) M. Baudler, G. Reuschenbach, J. Hahn, *Chem. Ber. 116* (1983) 847; b) M. Baudler, T. Pontzen, *Z. Naturforsch. B 38* (1983) 955; c) M. Baudler, J. Hellmann, T. Schmidt, *ibid. B 38* (1983) 537.
[9] Holleman-Wiberg: *Lehrbuch der Anorganischen Chemie*, 91–100th ed., de Gruyter, Berlin 1985, p. 133.

A Pt_2AgH_2 Complex**

By *Alberto Albinati, Francesco Demartin, Luigi M. Venanzi,* and Martin K. Wolfer*

Recent studies have shown that the monocations of the Group 11 metals easily form heterometallic hydrido-bridged complexes.[1-3] Remarkable among them are those formed by Ag^I where a variety of coordination geometries at silver are observed. One frequently occurring type contains a single M-H-Ag bridge arising from the coordination of a mononuclear hydrido complex such as *trans*-$[PtH(C_6X_5)(PEt_3)_2]$ **1** to a $Ag^{\oplus}$ ion, the coordination at silver being completed by a phosphane ligand. In compounds of this type (e.g., **2**), one can describe the bonding in the Pt-H-Ag moiety in terms of a three-center, two-electron interaction of "closed" type.[4]

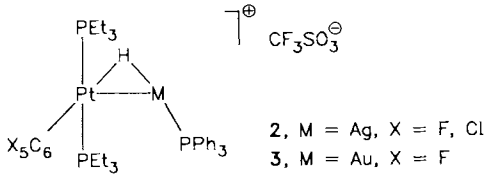

2, M = Ag, X = F, Cl
3, M = Au, X = F

We now find that the phosphane ligand in complexes of type **2** can be replaced by a molecule of **1** resulting in the formation of compounds such as **4**.[5] Related compounds

$[(PEt_3)_2(C_6Cl_5)Pt(\mu\text{-}H)Ag(\mu\text{-}H)Pt(C_6Cl_5)(PEt_3)_2][CF_3SO_3]$ **4**

(e.g., where C_6Cl_5 has been replaced by C_6F_5 and PEt_3 by PMe_3) have also been obtained.[6] Figure 1 shows the metal and donor atom arrangement in the cation of **4** which consists of two square-planar *trans*-$[PtH(C_6Cl_5)(PEt_3)_2]$ units joined by a $Ag^{\oplus}$ ion, the dihedral angle between the two planes being 83.5°.[7]

Both Pt-H-Ag units are similar to the Pt-H-Au unit found in the cation of **3**.[1] Thus relatively short Pt-M distances and small Pt-H-M angles are observed [**4**: Pt-Ag = 2.791(1) Å; Pt-H-Ag = 107(2)°; **3**: Pt-Au = 2.714(1) Å; Pt-H-Au = 103(4)° (average values)]. The other distances and angles, including Pt-H and Ag-H, fall in the expected range for compounds of this type.[1]

The coordination polyhedron around silver can be visualized in different ways depending on the bonding scheme used to describe the Pt-H-Ag interaction. Thus, using a three-center, two-electron model of closed type,[4] i.e., one including a significant, direct Pt-Ag interaction, the coordination at silver can be considered as pseudo-tetrahedral with a spirane-like arrangement of Ag, H, and Pt atoms. On the other hand, if one describes the Ag/Pt-H interaction as arising from the donation to silver of the Pt-H σ-bonding electrons, the coordination at silver can be visualized as being digonal. These two models are qualitatively equivalent to those used to describe $M(H_2)$ interactions given the isolobality of H_2 and the Pt-H fragment.[8] Both models are in agreement with the known coordination chemistry of Ag^I where digonal and tetrahedral geometries are of frequent occurrence.

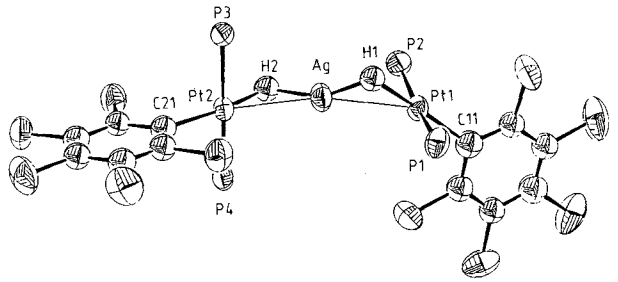

Fig. 1. ORTEP drawing of the cation of **4** with the alkyl groups of the phosphane ligands omitted for clarity. Selected bond lengths [Å] and angles [°] are: Ag-Pt(1) 2.791(1), Ag-Pt(2) 2.790(2), Pt-H 1.75(9), Ag-H 1.70(12) (average values), Pt(1)-P(1) 2.311(5), Pt(1)-P(2) 2.330(5), Pt(2)-P(3) 2.334(6), Pt(2)-P(4) 2.306(6), Pt(1)-C(11) 2.07(1), Pt(2)-C(21) 2.06(2); Pt(1)-Ag-Pt(2) 166.05(4), Ag-H(1)-Pt(1) 106(4), Ag-H(2)-Pt(2) 109(5), H(1)-Ag-H(2) 152(2), P(1)-Pt(1)-P(2) 171.95(6), P(3)-Pt(2)-P(4) 171.91(7), Ag-Pt(1)-C(11) 149.7(1), Ag-Pt(2)-C(21) 147.3(2).

It is noteworthy that small amounts of cations of the type $[(PR_3)_2(C_6X_5)Pt(\mu\text{-}H)Ag(\mu\text{-}H)Pt(C_6X_5)(PR_3)_2]^{\oplus}$ (R = Me, Et; X = Cl, F) together with equivalent amounts of the cations $[Ag(PR'_3)_2]^{\oplus}$ are in equilibrium with a bimetallic species of the type $[(PR_3)_2(C_6X_5)Pt(\mu\text{-}H)Ag(PR'_3)]^{\oplus}$ when solid samples containing the latter cations are dissolved in solvents such as dichloromethane.[1,6]

Received: November 23, 1987 [Z 2510 IE]
German version: *Angew. Chem. 100* (1988) 571

[*] Prof. L. M. Venanzi, Dr. M. K. Wolfer
Laboratorium für Anorganische Chemie der
Eidgenössischen Technischen Hochschule, ETH-Zentrum
Universitätstrasse 6, CH-8092 Zürich (Switzerland)
Prof. A. Albinati, Dr. F. Demartin
Istituto di Chimica Farmaceutica dell'Università di Milano
Viale Abruzzi 42, I-20141 Milano (Italy)

[**] *L. M. V.* and *M. K. W.* gratefully acknowledge the support of the Swiss National Science Foundation and *A. A.* that of the MPI and CNR (Italy).

[1] a) M. Green, A. G. Orpen, I. D. Salter, F. G. A. Stone, *J. Chem. Soc. Dalton Trans. 1984*, 2497; b) H. Lehner, D. Matt, P. S. Pregosin, L. M. Vanenzi, A. Albinati, *J. Am. Chem. Soc. 104* (1982) 6825; c) L. F. Rhodes, J. H. C. Huffman, K. G. Caulton, *ibid. 106* (1984) 6874; d) F. Bachechi, J. Ott, L. M. Venanzi, *ibid. 107* (1985) 1760; e) P. Braunstein, T. M. Gomes Carneiro, D. Matt, A. Tiripicchio, M. Tiripicchio Camellini, *Angew. Chem. 98* (1986) 721; *Angew. Chem. Int. Ed. Engl. 25* (1986) 748; f) A. Albinati, H. Lehner, L. M. Venanzi, M. Wolfer, *Inorg. Chem. 26* (1987) 3935.

[2] B. R. Sutherland, K. Folting, W. E. Streib, D. M. Ho, J. C. Huffman, K. G. Caulton, *J. Am. Chem. Soc. 109* (1987) 3489.

[3] P. D. Boyle, B. J. Johnson, B. D. Alexander, J. A. Casalnuovo, P. R. Gannon, S. M. Johnson, E. A. Larka, A. M. Mueting, L. H. Pignolet, *Inorg. Chem. 26* (1987) 1346.

[4] B. Bau, R. G. Teller, S. W. Kirtley, T. F. Koetzle, *Acc. Chem. Res. 12* (1979) 176.

[5] *Experimental Procedure:* Colorless, air-stable **4** is obtained by adding one equivalent of $AgCF_3SO_3$ to two equivalents of **1** dissolved in diethyl ether. Satisfactory microanalytical data were obtained for this compound which is somewhat photosensitive. IR (Nujol): ν(Pt-H-Ag) = 1680 (br.) and 1725 (br.) cm^{-1}. ^{1}H-NMR (250 MHz, CD_2Cl_2, 233 K): $\delta = -7.97$ (^1J(Pt,H) = 570, $^1J(^{107}Ag,H) = 115$, $^1J(^{107}Ag,H) = 134$ Hz). ^{31}P-NMR (36.43 MHz, CD_2Cl_2, 233 K): $\delta = 11.4$ (^1J(Pt,P) = 2290, $^3J(^{107,109}Ag,P) = 4.2$ Hz). ^{195}Pt-NMR (53.75 MHz, K_2PtCl_4 ext., CD_2Cl_2, 233 K): $\delta = -4851$ ($J(Pt,^{107}Ag) = 475$, $J(Pt,^{109}Ag) = 540$ Hz).

[6] M. K. Wolfer, *Dissertation No. 8151*, ETH Zürich 1986.

[7] **4**: Triclinic, $P\bar{1}$, $a = 13.853(3)$, $b = 14.214(2)$, $c = 15.611(3)$ Å, $\alpha = 94.64(2)$, $\beta = 90.48(2)$, $\gamma = 110.39(2)°$, $V = 2869.7$ Å^3, $Z = 2$. Data were collected at room temperature on a CAD4 diffractometer ($Mo_{K\alpha}$) up to $2\theta \leq 45°$ using an $\omega/2\theta$ scan, with variable scan speed to insure constant statistical precision of the collected intensities. 7090 reflections (corrected for absorption and decay) were collected of which 5235 were considered as observed ($F_o \geq 2.5\sigma(F_o)$) and used for the solution (Patterson and Fourier methods) and refinement of the structure using anisotropic temperature factors for the Pt, P, and F atoms of the cation and for the atoms of the anion. At this stage a Fourier difference showed two strong peaks that were assigned to the bridging hydrogen ligands and refined satisfactorily. The final R is 0.049 (obs. refl.). Further details of the crystal structure investigation are available on request from the Fachinformationszentrum Energie, Physik, Mathematik GmbH, D-7514 Eggenstein-Leopoldshafen 2 (FRG), on quoting the depository number CSD-52845, the names of the authors, and the journal citation.

[8] a) J. K. Burdett, M. R. Pourian, *Organometallics 6* (1987) 1684; b) J. K. Burdett, J. R. Phillips, M. R. Pourian, M. Poliakoff, J. J. Turner, R. Upmacis, *Inorg. Chem. 26* (1987) 3054.

NOESY-TOCSY, an Advantageous 2D NMR Technique for the Analysis of Peptide Sequences**

By *Horst Kessler,** *Gerd Gemmecker,* and *Stefan Steuernagel*

With the introduction of two-dimensional NMR techniques, the problems in the interpretation of spectra resulting from overlapping lines have been greatly reduced. Nonetheless, difficulties are still encountered with increasing molecular size, especially for molecules of biological interest. Here we describe a new variant of the Relayed-NOESY experiment that is particularly suitable for solving these problems in the case of biopolymers.

If a second coherence-transfer step through scalar J coupling is included in a two-dimensional NMR experiment, it is possible to transfer the cross peaks between two nuclei to the resonance frequencies of other nuclei in less crowded regions of the spectrum. In the H-Relayed H,H-COSY experiment[1] two equivalent coherence-transfer steps in which nuclei are correlated by J coupling are combined. *G. Wagner* showed that even the combination of an incoherent transfer step (i.e., one caused by NOE effects) with a coherent transfer step leads to useful information (Relayed-NOESY experiment[2]). Difficulties in phase correction to pure absorption, which is especially advantageous for signals near the diagonal, can be overcome by the introduction of a double-quantum filter (DQF).[3]

We recently showed that in such pulse sequences the two different successive transfer steps can also be replaced by spin-lock periods in the rotating frame;[4] hence this technique, in contrast to Relayed NOESY, is now also applicable to medium-sized molecules with vanishing NOEs (owing to $\omega_0 \tau_c \approx 1$) because the NOE transfer is replaced by an ROE (rotating frame NOE) transfer,[5] which is relatively insensitive to molecular tumbling rates.

All the latter techniques having two different transfer steps afford unsymmetric spectra, since the mixing sequences are not symmetric (i.e., not invariant with respect to time and phase reversal[6]). This important feature is best exemplified by the analysis of peptide and protein sequences, a particularly interesting application of these techniques (Fig. 1). The non-symmetry results from the fact that, across the peptide bond, NOE but no scalar coupling of protons is observed. Thus, the peptide sequence can be "read" directly from the spectrum by means of the unsymmetric cross peaks.[3,4]

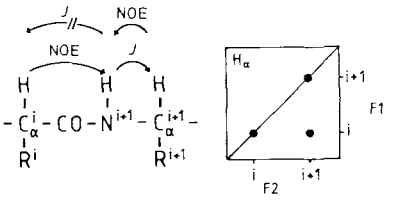

Fig. 1. The formation of cross peaks between the α protons of neighboring amino acids in peptides and proteins via two transfer steps: First step via NOE, second step via J coupling (NOESY-TOCSY). It can be seen that in this experiment a transfer from H_α^i (in the F1 dimension, vertical) to H_α^{i+1} (in the F2 dimension, horizontal) is possible. Since the reverse pathway is blocked due to the absence of J coupling through the peptide bond, the two-dimensional spectrum is unsymmetric. If the sequence of transfer steps is reversed (TOCSY-NOESY), the cross peak appears on the other side of the diagonal.

We now describe two new variants of these unsymmetric pulse sequences and their application to the analysis of a nonadecapeptide which shows strongly negative NOEs. The new pulse sequences (Fig. 2) combine the NOESY experiment with an additional J-coupling transfer step consisting of an MLEV-17 spin-lock period,[7] like that used for TOCSY spectra.[8] The mixing time for the TOCSY transfer is kept so short (ca. 20 ms) that coherences are only transferred to the next nucleus (the transfer pathways thereby remain unambiguous). In analogy to the Relayed-NOESY experiment, we call this technique TOCSY-NOESY or NOESY-TOCSY, depending on the sequence of the two transfer steps.

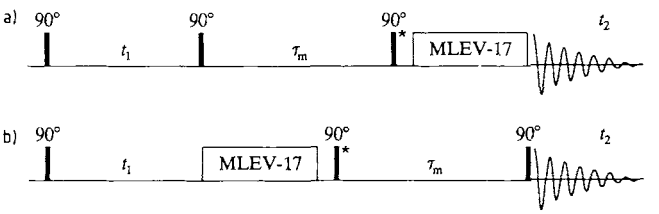

Fig. 2. Pulse sequence for NOESY-TOCSY (a) and TOCSY-NOESY (b). The phase difference between the marked 90° pulse (asterisk) and the spin-lock field must be ±90°. The rest of the phase cycle is fully analogous to that of the NOESY experiment [12].

In many respects, these new techniques are superior to those already described:[2,3,4] Large molecules (like most biopolymers) show strongly negative NOEs. Because the signals in ROESY spectra always contain ROE *and* NOE components with differing signs, which can partially cancel each other, the analysis of pure NOE effects is preferred for such molecules.[9] However, since the signals of these molecules are relatively broad owing to short T_2 times, antiphase structure in the cross peaks leads to their partial cancellation. Hence, some interesting cross peaks in conventional Relayed-NOESY and DQF-Relayed-NOESY spectra can be completely lost. Recording a Relayed-NOESY spectrum with the NOE transfer as the second step would be of little advantage, on the other hand, since, due to the low resolution in F1, increased cancellation of the antiphase signals in this dimension would occur. Replacement of the Relayed step by a TOCSY transfer solves this problem, since the cross peaks then contain only in-phase components. Furthermore, it is now possible to employ an NOE transfer after a TOCSY transfer (in the TOCSY-NOESY version), since only signals with in-phase components are present.

As an example, we show in Figure 3 part of the NOESY-TOCSY spectrum of the polycyclic peptide RO 09-0198.[3] Compared to the DQF-Relayed-NOESY spectrum (Fig. 8a in Ref. [3]), a significantly improved signal-to-noise ratio is attained under identical measurement conditions (same sample, same instrument, same recording time), as shown by the cross sections of the two spectra in Figure 4.

Since pure NOESY signals as well as pure TOCSY signals cannot be suppressed in spectra with combined NOE and J transfer,[2] it is desirable to process the spectra further so that the true "relayed" signals are easier to recognize.

Two methods for reducing the number of cross peaks in these unsymmetric spectra were recently described.[4,6] An *asymmetrization*[4] removes all symmetric contributions from a two-dimensional spectrum and can be easily ob-

[*] Prof. Dr. H. Kessler, Dipl.-Chem. G. Gemmecker, Dipl.-Chem. S. Steuernagel
Institut für Organische Chemie der Universität
Niederurseler Hang, D-6000 Frankfurt am Main 50 (FRG)

[**] This work was supported by the Deutsche Forschungsgemeinschaft and the Fonds der Chemischen Industrie.

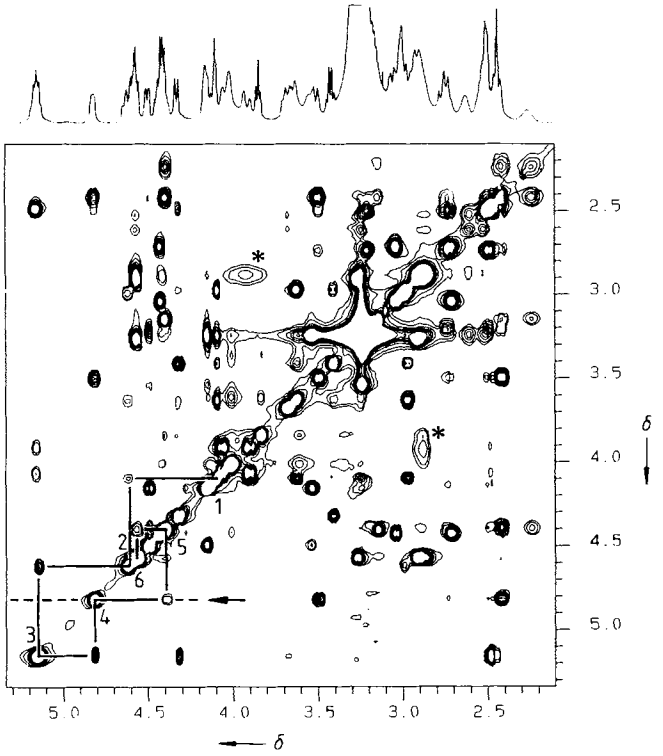

Fig. 3. Part of the 500-MHz NOESY-TOCSY spectrum of RO 09-0198 [3]. Relaxation delay, 2.5 s; 90° pulse, 19 μs; spin-lock field, 5 kHz over 20 ms; NOE mixing time, 300 ms (±20 ms for suppression of zero quanta [13]); sample concentration, 50 mmol. The H_α region is shown; the sequence analysis for the fragment H-Lan^1-Arg^2-Gln^3-Lan^4-Lan^5-Xaa^6 (Lan = one-half of a lanthionine, Xaa = alanine part of lysinoalanine) via H_α-H_α cross peaks is shown (the numbers correspond to the positions of the α protons in the peptide sequence). Peaks appearing symmetrically with respect to the diagonal are caused by pure NOESY or pure TOCSY transfer (e.g., the TOCSY peak marked with an asterisk between H_α and H_β of Phe^{10}). The cross section along the dashed line (arrow) is shown in Figure 4.

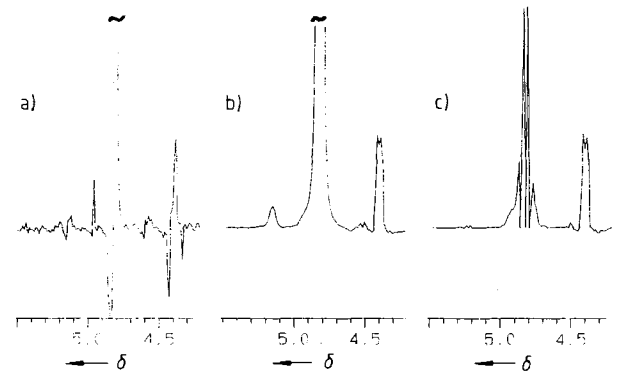

Fig. 4. Cross sections from the 2D NMR spectra of Figure 8a in [3] and from Figures 3 and 6; the part chosen is also marked there. a) DQF Relayed-NOESY [3]. b) NOESY-TOCSY. This spectrum shows the improved signal-to-noise ratio obtained under the same conditions of measurement as for (a). The signal at $\delta = 5.15$ is due to a nonsuppressed pure NOESY transfer. c) NOESY-TOCSY after asymmetrization. The NOESY signal at $\delta = 5.15$ is fully suppressed by this way of data processing.

tained by subtraction of a symmetrized copy of the original data matrix (Fig. 5a). This procedure is very easy to employ, since the symmetrization with commercially available NMR program packages can be carried out very quickly on an array processor.[10] However, this procedure requires

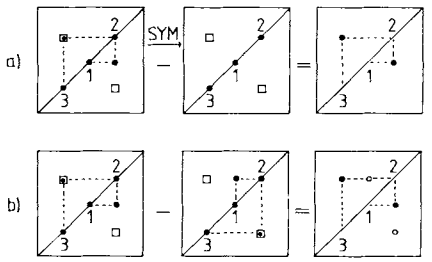

Fig. 5. Schematic drawing of the asymmetrization (a) and anti-symmetrization (b) of a NOESY-TOCSY spectrum in order to eliminate the symmetric components (see text). The square symbolizes a pure NOESY cross peak (symmetric with respect to the diagonal) which overlaps with the unsymmetric NOESY-TOCSY peak (filled circle). SYM = symmetrization [10].

the same line shapes and the same resolution in the two dimensions. Since, in general, the resolution in F2 feasible from the raw data is significantly greater than that in F1, the resolution in F1 is the limiting factor. If the resolution of the recorded FIDs is not reduced to that in F1, then the asymmetrization leads to residual signals having a characteristic "fine structure." This is clearly seen in the asymmetric version of the NOESY-TOCSY spectrum of Figure 3 (Fig. 6).

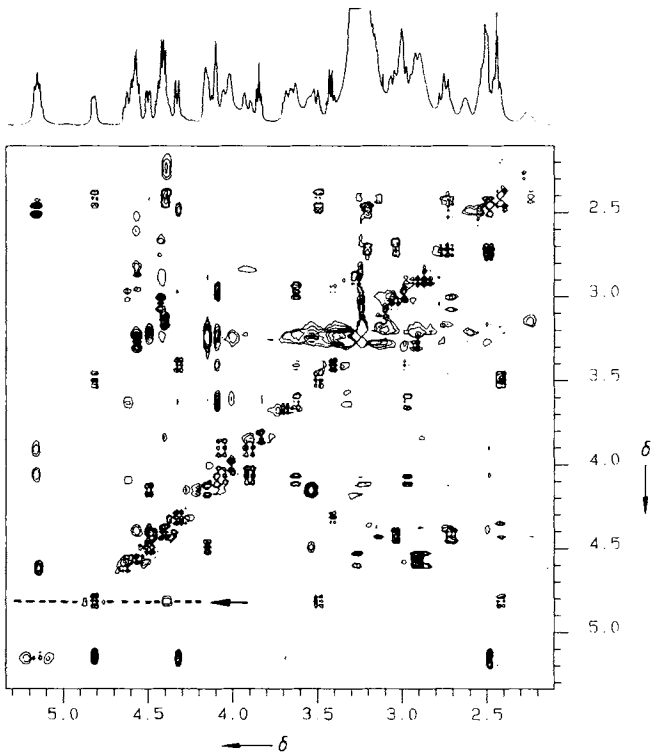

Fig. 6. NOESY-TOCSY spectrum of Figure 3 (same part) after asymmetrization. The cross section along the dashed line (arrow) is shown in Figure 4.

Another possibility of spectral simplification is *anti-symmetrization*,[6] which also removes all symmetric signals from the 2D matrix. However, *both* spectra (namely, TOCSY-NOESY and NOESY-TOCSY) are required, and they must be recorded under identical conditions and processed with the same parameters (apodization, zero-filling, scaling), in order to ensure the same line shapes and intensities in the two spectra. On the other hand, the same resolution in F1 and F2 is no longer necessary, since the

two spectra are substracted row by row. One obtains a "spectrum" with the originally unsymmetric components of the cross peaks on *both* sides of the diagonal but having *different* signs (Fig. 5b). Figure 7 shows the results of this anti-symmetrization carried out for the spectrum of the nonadecapeptide RO 09-0198.[11]

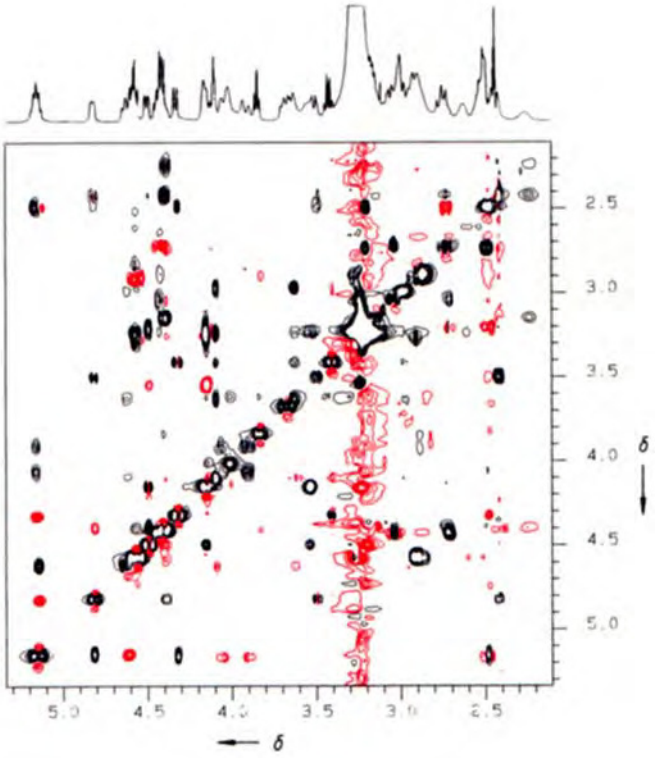

Fig. 7. NOESY-TOCSY spectrum of Figure 3 after antisymmetrization by combination with a TOCSY-NOESY spectrum (same section as in Fig. 3) recorded under the same conditions. Negative signals are shown in red.

The advantages of the NOESY-TOCSY and TOCSY-NOESY techniques presented here are, above all, an improved signal-to-noise ratio, especially in the case of broad signals, and the possibility of reversing the sequence of transfer steps without loss of sensitivity. The methods of data processing described here facilitate the interpretation of these spectra. The NOESY-TOCSY experiment is primarily attractive for larger molecules, which give rise to strongly negative NOEs and broad lines, owing to short relaxation times.

Received: December 7, 1987;
supplemented: January 28, 1988 [Z 2526 IE]
German version: *Angew. Chem. 100* (1988) 600

[1] G. Eich, G. Bodenhausen, R. R. Ernst, *J. Am. Chem. Soc. 104* (1982) 3731.
[2] G. Wagner, *J. Magn. Reson. 57* (1984) 497.
[3] H. Kessler, S. Steuernagel, D. Gillessen, T. Kamiyama, *Helv. Chim. Acta 70* (1987) 726.
[4] H. Kessler, G. Gemmecker, B. Haase, *J. Magn. Reson.*, in press (probably April 1988).
[5] A. A. Bothner-By, R. L. Stephens, J. Lee, C. D. Warren, R. W. Jeanloz, *J. Am. Chem. Soc. 106* (1984) 811.
[6] O. W. Sørensen, C. Griesinger, R. R. Ernst, *Chem. Phys. Lett. 135* (1987) 313.
[7] A. Bax, D. G. Davis, *J. Magn. Reson. 65* (1985) 355.
[8] L. Braunschweiler, R. R. Ernst, *J. Magn. Reson. 53* (1983) 521.
[9] C. Griesinger, R. R. Ernst, *J. Magn. Reson. 75* (1987) 261.
[10] The algorithm used ("SYMA" routine in the DISNMR programs of BRUKER GmbH) reintroduces into the 2D matrix on both sides of the diagonal the smaller value of the two points lying symmetrically with respect to the diagonal with the sign of the smaller value. In the subsequent difference formation with the unprocessed 2D matrix, one therefore always obtains zero for the smaller contribution and the difference of the two original values for the point on the other side of the diagonal. The spectrum so obtained is called the *asymmetrized* spectrum and contains only that component of the magnetization that has passed the desired NOESY-TOCSY transfer. Difficulties in the interpretation of the asymmetrized spectrum can arise when the symmetric and asymmetric components in the original 2D NMR spectrum have different signs, since in that case (dependent on the relative magnitudes of the two components) a signal can appear on the opposite side of the diagonal in the asymmetrized spectrum, albeit with opposite sign. The TOCSY transfer, however, retains the sign, and the pure NOESY signals therefore have the same sign as the NOESY-TOCSY signals, so that the problem can be ignored in this case, particularly, since pure TOCSY signals cannot appear between different amino acid residues (moreover, in the case of large molecules with always negative NOEs ($\omega_0 r_c \gg 1$), they exhibit the same sign as that of the NOESY components).
[11] A single NOESY-TOCSY spectrum can also be decomposed into a symmetric and an antisymmetric component if the symmetrization routine is so modified that every value in the 2D matrix is replaced by the difference between it and the mean value of the two values lying symmetrically with respect to the diagonal. However, this procedure is just as sensitive as an *asymmetrization* toward different line shapes in F1 and F2. Furthermore, this decomposition into a symmetric and an antisymmetric spectrum has no physical meaning, since none of the possible transfer pathways in the NOESY-TOCSY experiment leads to an antisymmetric contribution. The information content of the antisymmetric component, however, would be the same as that of the asymmetrized spectrum.
[12] G. Bodenhausen, H. Kogler, R. R. Ernst, *J. Magn. Reson. 58* (1984) 370.
[13] S. Macura, Y. Huang, D. Suter, R. R. Ernst, *J. Magn. Reson. 43* (1981) 259.

C_5O_2 (1,2,3,4-Pentatetraene-1,5-dione), a New Oxide of Carbon

By *Günther Maier,* Hans Peter Reisenauer, Ulrich Schäfer,* and *Heinz Balli*

The amazing fact that cyclopropenylidene[1] is one of the most common interstellar molecules[2] inspired us to search for further compounds that might be found to exist as "molecules between the stars." Based on the experience gathered so far,[3] possibilities include systems with polycumulated double bonds. Our first investigations in this direction have led to the isolation of the surprisingly stable carbon oxide C_5O_2, the longest such molecule known.

The tris(diazo) ketone **1**,[4] which may be prepared easily by diazo group transfer from phloroglucinol, affords the carbon oxide **2** as sole product upon irradiation (254 nm) in an argon matrix at 12 K. Compound **2** exhibits the IR absorptions shown in Table 1. The same species is obtained when **1** is subjected to pyrolysis in the gas phase (700 °C) and the fragments (in addition to the major component **2**, carbon suboxide is also formed) are condensed along with argon on a window at 12 K.

In agreement with the prognosis[5] that carbon oxides C_nO_2 having an odd number of C atoms should be more stable than those having an even number, it is also possible to prepare **2** on a preparative scale. If **2**, prepared at 10^{-3} torr and 600 °C, is condensed with a low-melting solvent on a cold finger cooled with liquid nitrogen, a solution of **2** may be obtained after thawing in which the compound

[*] Prof. Dr. G. Maier, Dr. H. P. Reisenauer, Dr. U. Schäfer
Institut für Organische Chemie der Universität
Heinrich-Buff-Ring 58, D-6300 Giessen (FRG)
Prof. Dr. H. Balli
Institut für Farbenchemie der Universität
St. Johannsvorstadt 10, CH-4056 Basel (Switzerland)

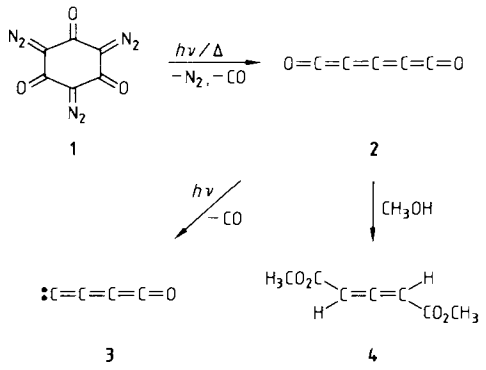

Table 1. IR bands of **2** (Ar matrix, 12 K).

$\tilde{\nu}$ [cm^{-1}] (rel. int.)	Assignment
3717.7 (0.030)	combination mode
3418.3 (0.018)	combination mode
3327.7 (0.003)	combination mode
2759.7 (0.042)	combination mode
2213.0 (1.000)	asymmetric stretching mode
2058.7 (0.340)	asymmetric stretching mode
1144.1 (0.026)	asymmetric stretching mode [a]
1049.6 (0.011)	combination mode [a]
539.0 (0.029)	asymmetric deformation mode
470.0 (0.007)	asymmetric deformation mode

[a] Indefinite assignment.

remains unchanged even after several days at room temperature. Pure **2**, on the other hand, is only stable to about -90 °C (yellow solid). At this temperature, it polymerizes to give a black solid having the composition C_5O_2.

Proof of the structure of **2** was based, on the one hand, on the observation that the yellow solution lost its color immediately upon addition of methanol and the known dimethyl allenedicarboxylate **4**[6] was formed, as shown by comparison of its spectra with those of authentic material. On the other hand, the spectroscopic data establish unequivocally the presence of **2**: In the ^{13}C-NMR spectrum [CH_2Cl_2, -60 °C, Cr(acac)$_3$] three signals are observed at $\delta = 119.0$ (C1/5), 101.2 (C3), and 15.2 (C2/4) in a ratio of 2:1:2.[7] The UV spectrum (cyclohexane) displays an extremely strong absorption at 231 nm ($\log\varepsilon = 5.38$) and a second, weaker band ($\log\varepsilon = 2.18$) at 435 nm. In the mass spectrum, the "correct" molecular ion peak is found at $m/z = 91.9899$ (calcd 91.9898). Finally, the IR spectrum (Table 1 and Fig. 1, top) is in qualitative agreement with the spectrum calculated by the MNDO method[8] [bands at 2493 ($I_{rel.} = 1.00$), 2358 (0.50), 1285 (<0.01), 719 (0.03), 537 (<0.01), and 99 (<0.01) cm^{-1}]. At least, this comparison shows that—as experimentally found[9]—two predominant absorptions in an intensity ratio of about 2:1 should appear in the ketene region.[10]

When matrix-isolated **2** is irradiated with 230-nm light (irradiation at the wavelength of the intense UV band), CO is cleaved off and a new species with IR absorptions at 2221.7 (1.00), 1922.7 (0.65), 1431.5 (0.04), 774.8 (0.01), and 484.0 (0.06) cm^{-1} is formed (Fig. 1, bottom). This spectrum is clearly that of 1,2,3-butatrien-1-one. The calculated IR spectrum[8] for **3** requires—as found—the presence of two strong bands, one in the ketene region [2549 (0.88)] and one in the allene region [2208 cm^{-1} (1.00)].[11]

Received: January 11, 1988 [Z 2569 IE]
German version: *Angew. Chem. 100* (1988) 590

CAS Registry numbers:
1, 33406-97-2; **2**, 51799-36-1; **3**, 112022-61-4; **4**, 1712-36-3.

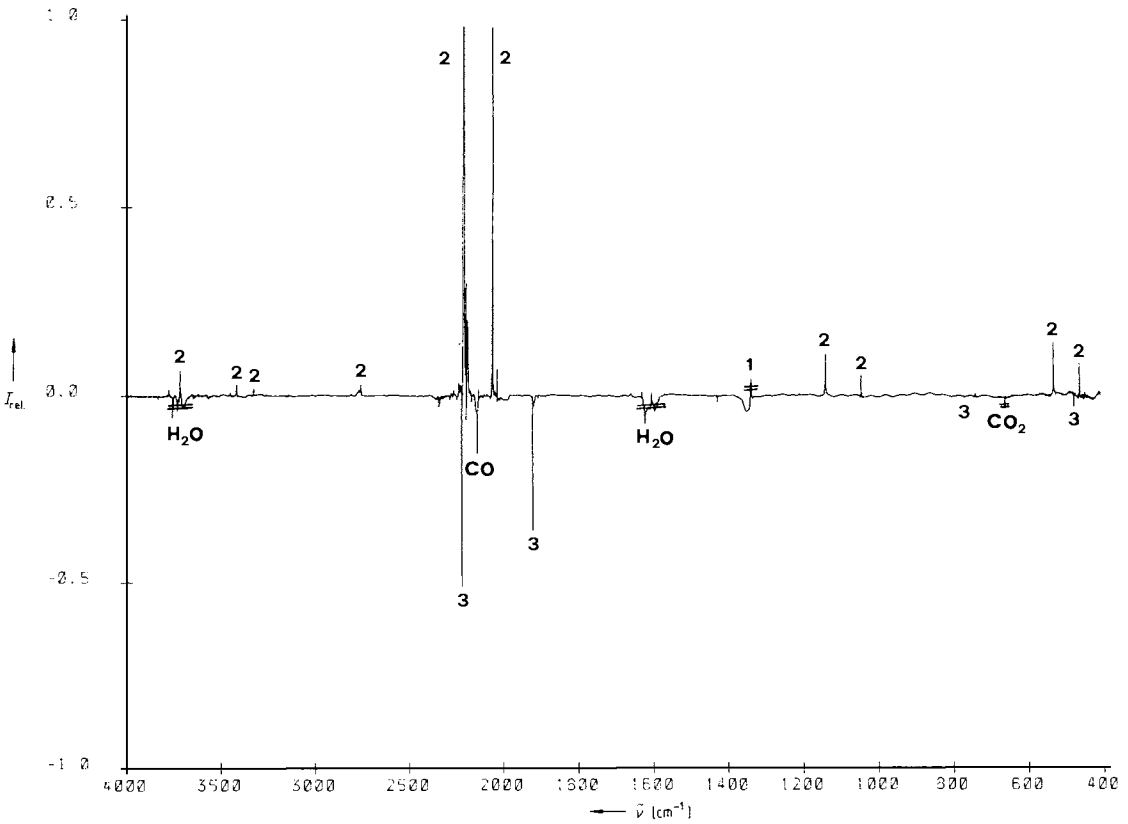

Fig. 1. IR spectra (Ar matrix, 12 K) of **2** (top) and **3** (bottom), obtained by subtraction (spectrum of the thermally generated, nonirradiated sample minus the spectrum after irradiation with 230-nm light).

[1] G. Maier, H. P. Reisenauer, W. Schwab, P. Čársky, B. A. Hess, Jr., L. J. Schaad, *J. Am. Chem. Soc. 109* (1987) 5183.
[2] P. Thaddeus, J. M. Vrtilek, C. A. Gottlieb, *Astrophys. J. 299* (1985) L63.
[3] G. Winnewisser, E. Herbst, *Top. Curr. Chem. 139* (1987) 119.
[4] H. Balli, V. Müller, A. Sèzen-Gezgin, *Helv. Chim. Acta 61* (1978) 104, and references cited therein.
[5] L. D. Brown, W. N. Lipscomb, *J. Am. Chem. Soc. 99* (1977) 3968.
[6] a) J. Cymerman Craig, M. Moyle, *J. Chem. Soc. 1963*, 5356; b) W. Runge, J. Firl, *Ber. Bunsenges. Phys. Chem. 79* (1975) 913.
[7] Carbon suboxide C_3O_2 exhibits ^{13}C-NMR signals at $\delta = 129.7$ (C1/3) and -14.6 (C2): E. A. Williams, J. D. Cargioli, A. Ewo, *J. Chem. Soc. Chem. Commun. 1975*, 366.
[8] QCPE program No. 506 (AMPAC). The spectrum is calculated on the basis of a linear structure for **2**. Ab initio (SCF/4-31G) calculations indicate as minimum a nonlinear molecule with IR bands at 2506 (0.00), 2396 (1.00), 2232 (0.50), 1827 (0.00), 1216 (0.02), 781 (0.02), 726 (0.01), 615 (0.00), 605 (0.00), 586 (0.01), 568 (0.01), 181 (0.00), 61 (0.00) cm^{-1} (B. A. Hess, Jr., L. J. Schaad (Nashville, TN, USA), personal communication).
[9] Preliminary results of *F. Holland* and *M. Winnewisser*, Giessen, have established that the molecule possesses inversion symmetry, since the separation of the rotational lines is $4B$ (B = rotational constant). A decision as to the linearity or quasi-linearity of the molecule can only be made after a detailed analysis of the rotational-vibrational spectrum has been carried out.
[10] Only one ketene band would have been expected for the originally expected compound C_6O_3 (three-membered ring with a ketene unit at each corner), which would have been formed by three Wolff rearrangements.
[11] Note added on February 17, 1988: According to an ESR spectroscopic analysis, C_4O is also formed by photoaddition of CO to matrix-isolated graphite vapor: R. J. Van Zee, G. R. Smith, W. Weltner, Jr., *J. Am. Chem. Soc. 110* (1988) 609. We have repeated the irradiation of **2** under our conditions and have observed the same ESR signal for our product **3**.

A Simple Route to Furo[3,4-*b*]furans, Compounds with a New Diheteropentalene System**

By *Wolfgang Eberbach,* Hans Fritz,* and *Norbert Laber*

Dedicated to Professor Edward Taylor on the occasion of his 65th birthday

Diheteropentalenes **1** are isoelectronic with the pentalene dianion **2**.[1] According to calculations, the resonance stabilization of this 10π-electron system is slightly smaller than that of its analogues with the heteroatoms in 1,4 and 1,6 position;[2a-c] experimental evidence for its expected higher reactivity is available for derivatives with X, Y = S, S or S, N.[2b-d]

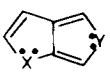

1

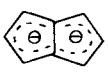

2

Although much work has been done with the structurally related 3,4-benzoannelated pyrroles,[3] thiophenes,[4] and furans[5]—also with respect to preparative applications—relatively few investigations with derivatives of **1** have been described.[6] The series of known diheteropentalenes was recently extended by thieno[3,4-*b*]furan (**1**, X = O, Y = S)[7] and by a thieno[2,3-*c*]furan derivative (**1**, X = S, Y = O).[8] We now report on the preparation of two furo[3,4-*b*]furan (**1**, X = Y = O) derivatives. For the synthesis, we took advantage of the observation that the thermal isomerization of (*Z*)-1,2-epoxy-3-hexen-5-ynes affords 2-vinylfurans, usually in high yields.[9] As starting compounds, the two (alkynylfuryl)oxiranes **5a** and **5b** were used, which are accessible from **3**[10] via the intermediate **4** (and **6**) in 66 and 55% yield, respectively.

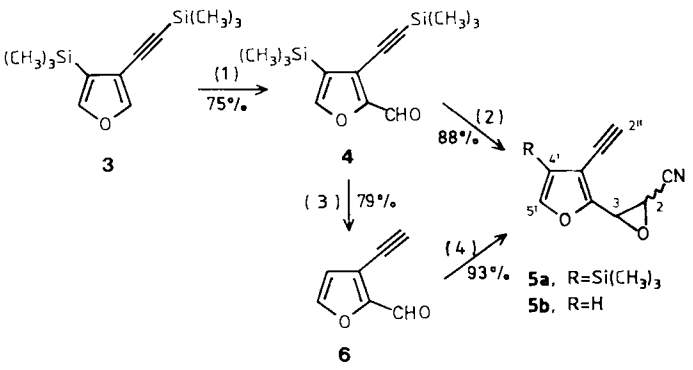

3 **4** **6**

Scheme 1. Synthesis of **5a** and **5b**. (1) a) *n*BuLi, THF; b) *N*-formylmorpholine. (2) Chloroacetonitrile, NaOH, triethylbenzylammonium chloride, acetonitrile. (3) a) Ethylene glycol, *p*-TosOH, benzene; b) NaOH, triethylbenzylammonium chloride, acetonitrile; c) Bu_4NF, THF; d) acetone/H_2O, *p*-TosOH. (4) Chloroacetonitrile, KO*t*Bu, *t*BuOH/ether.

When **5a** or **5b** are heated under short-time or flash vacuum thermolysis conditions (STT: 350°C, ca. 10 s; FVT: 450°C, ca. 10^{-6} torr), a crude reaction mixture is formed containing 60–70% of the two *E*/*Z*-isomeric furofurylacrylnitriles **7** and **8** as the only monomeric reaction products [yields after chromatographic separation: 26% **7a**, 23% **8a** and 31% **7b**, 21% **8b** (average values)]. The *E* isomers, **7a** and **7b**, which were isolated as stable yellow crystals, exhibit intense, relatively long-wavelength UV absorption maxima at 347 ($\varepsilon = 30\,100$) and 345 nm (27 800), respectively (for other data see Table 1).[11]

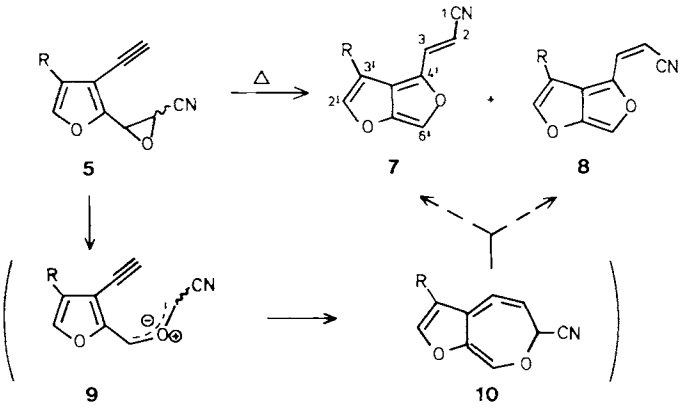

The reaction pathway leading to **7** and **8** presumably proceeds via the carbonyl ylide **9** and its 1,7-dipolar cyclization to the cycloallene derivative **10**, which is subsequently transformed into the furo[3,4-*b*]furan via a pathway involving diradical and/or carbene intermediates.[9]

[*] Prof. Dr. W. Eberbach, Dipl.-Chem. N. Laber
Institut für Organische Chemie und Biochemie der Universität
Albertstrasse 21, D-7800 Freiburg (FRG)
Prof. Dr. H. Fritz
Ciba-Geigy AG
CH-4002 Basel (Switzerland)

[**] This work was supported by the Deutsche Forschungsgemeinschaft and the Fonds der Chemischen Industrie.

Table 1. Selected data for the compounds **5**, **7**, **8**, **12**, and **14** [a]. See the structural formulas for the numbering of the compounds.

5a: (3:2 mixture of *E*/*Z* isomers): IR (CCl_4): $\tilde{\nu}$ = 3310, 2250, 2220, 2115, 1510 cm^{-1}; ^{1}H-NMR (*E*/*Z* mixture): δ = 7.17/7.28 (s; 5'-H), 4.49/4.41 (d; 3-H), 4.10/3.89 (d; 2-H), 3.36/3.34 (s; 2''-H), 0.28/0.30 (s; $SiMe_3$), $J(2,3)$ = 2.1/3.8 Hz

5b: IR (KBr, *Z* isomer): $\tilde{\nu}$ = 3280, 3150, 2250, 2120, 1510 cm^{-1}; ^{1}H-NMR (*E*/*Z* mixture): δ = 7.35/7.46 (d; 5'-H), 6.49/6.52 (d; 4'-H), 4.51/4.42 (d; 3-H), 4.11/3.90 (d; 2-H), 3.31/3.29 (s; 2''-H), $J(2,3)$ = 1.9/3.8, $J(4',5')$ = 1.8/1.8 Hz

7a: m.p. = 107°C (ether/petroleum ether); IR (CCl_4): $\tilde{\nu}$ = 2215, 1700, 1635, 1590 cm^{-1}; ^{1}H-NMR: δ = 7.38 (d; 6'-H), 7.24 (s; 2'-H), 7.05 (d; 3-H), 5.66 (dd; 2-H), 0.29 (s; $SiMe_3$), $J(2,3)$ = 16.5, $J(2,6')$ = 0.7 Hz; ^{13}C-NMR: δ = 158.6 (C-2'), 152.7 (C-6'a), 135.7 (C-4'), 134.2 (C-3), 131.0 (C-3'a), 120.7 (C-6'), 118.8 (C-1), 110.7 (C-3'), 90.5 (C-2), −1.3 ($SiMe_3$); UV (CH_3CN): $\lambda_{max}(\varepsilon)$ = 347 (30100), 267 nm (3900)

7b: m.p. = 144°C (ether/petroleum ether); IR (KBr): $\tilde{\nu}$ = 3160, 3140, 3120, 2210, 1750, 1650, 1600, 1550 cm^{-1}; ^{1}H-NMR: δ = 7.48 (d; 2'-H), 7.45 (s; 6'-H), 7.17 (d; 3-H), 6.50 (dd; 3'-H), 5.63 (dd; 2-H), $J(2,3)$ = 16.5, $J(2',3')$ = 2.5, $J(2,3')$ = 0.6 Hz; UV (CH_3CN): $\lambda_{max}(\varepsilon)$ = 345 (27800), 263 nm (3900)

8a: IR (CCl_4): $\tilde{\nu}$ = 2215, 1695, 1670, 1635, 1585 cm^{-1}; ^{1}H-NMR: δ = 7.58 (d; 6'-H), 7.29 (s; 2'-H), 6.80 (d; 3-H), 5.15 (dd; 2-H), 0.34 (s; $SiMe_3$), $J(2,3)$ = 11.2, $J(2,6')$ = ca. 0.3 Hz

8b: ^{1}H-NMR: δ = 7.45 (d; 2'-H), 7.52 (s; 6'-H), ca. 7.0 (3-H and 3'-H), 5.24 (dd; 2-H), $J(2,3)$ = 13, $J(2',3')$ = 3, $J(2,3')$ = 1 Hz

exo-**12**: m.p. = 300°C (dec., ether/acetone); IR (KBr): $\tilde{\nu}$ = 2220, 1770, 1725, 1600 cm^{-1}; ^{1}H-NMR: δ = 7.5–7.2 (m; Ph–H), 7.25 (d; 3'-H), 5.84 (d; 2'-H), 5.66 (s; 8-H), 5.61 (s; 4-H), 3.78 (d; 9-H), 3.30 (d; 10-H), 3.26 (d; 6-H), 3.14 (d; 5-H), 0.30 (s, $SiMe_3$), $J(2',3')$ = 16.5, $J(9,10)$ = 7, $J(5,6)$ = 6.5 Hz

endo-**12**: m.p. = 300°C (dec., ether/acetone); IR (KBr): $\tilde{\nu}$ = 2230, 1780, 1720, 1600 cm^{-1}; ^{1}H-NMR: δ = 7.5–7.2 (m; Ph–H), 7.13 (d; 3'-H), 6.04 (d; 2'-H), 5.66 (d; 8-H), 5.57 (s; 4-H), 4.00 (dd; 9-H), 3.74 (d; 10-H), 3.32 (d; 6-H), 3.06 (d; 5-H), 0.01 (s, $SiMe_3$), $J(2',3')$ = 16.5, $J(9,10)$ = 10, $J(5,6)$ = 6.5, $J(8,9)$ = 6.5 Hz

14: m.p. = 86°C (ether/hexane); IR (CCl_4): $\tilde{\nu}$ = 2230, 1740, 1670, 1600 cm^{-1}; ^{1}H-NMR: δ = 7.84 (s; 5'-H), 6.77 (d; 6-H), 6.45 (s; 2-H), 5.91 (d; 7-H), 3.80 and 3.81 (OCH_3), 0.12 ($SiMe_3$), $J(6,7)$ = 16 Hz; ^{13}C-NMR: δ = 161.5 and 161.9 (3'-CO/4'-CO), 160.7 (3-CO), 160.6 (4-CO), 153.6 (C-2'), 149.0 (C-6), 147.5 (C-5'), 138.7 (C-4), 134.8 (C-3), 118.9 (C-4'), 116.7 (C-3'), 115.8 (C-8), 102.0 (C-7), 97.1 (C-10), 96.8 (C-9), 84.2 (C-5), 78.5 (C-2), 52.73, 52.68, 52.1 and 51.8 (OCH_3), −0.8 ($SiMe_3$)

[a] ^{1}H-NMR spectra: 250 and 400 MHz, $CDCl_3$; ^{13}C-NMR spectra: 100 MHz, $CDCl_3$.

As expected, the isoannelated furans **7** and **8** display a high Diels–Alder reactivity: **7a** reacts with *N*-phenylmaleimide (NPMI) or dimethyl acetylenedicarboxylate (DMAD) already at 20°C. In both cases—even when using an excess of dienophile—only the 1:2 addition compounds **12** and **13**, respectively, are formed via the corresponding 1:1 adducts (**11** in the case of NPMI); the two stereoisomers *exo*-**12** and *endo*-**12** are obtained in a 7:3 ratio[12] (77% yield; the configuration of **12** was established by detailed NMR experiments). The DMAD addition product **13** is not stable under the reaction conditions and undergoes a Diels–Alder reversion providing the furyldihydrofuran derivative **14** (yield 70%).[14]

The route to furo[3,4-*b*]furans described here should be applicable to the preparation of other isoannelated heteroarenes.

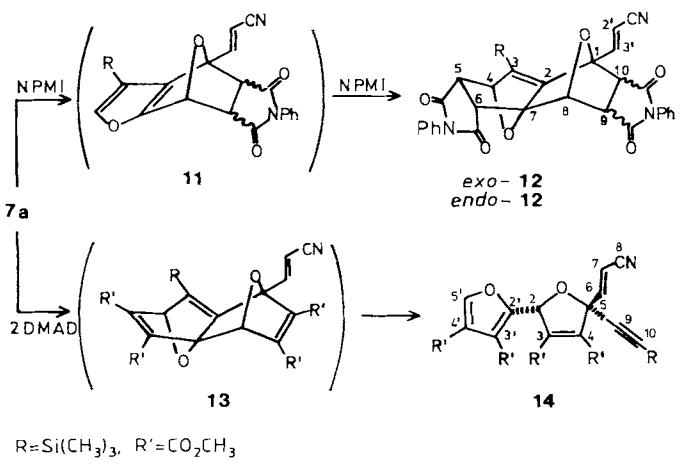

Received: December 7, 1987 [Z 2529 IE]
German version: *Angew. Chem. 100* (1988) 599

[1] Review: P. J. Garratt, M. V. Sargent in J. P. Snider (Ed.), *Org. Chem. (NY) Vol. 16-II* (1971) 252.
[2] a) I. Gutman, M. Milun, N. Trinajstić, *J. Am. Chem. Soc. 99* (1977) 1692; b) M. Milun, N. Trinajstić, *Croat. Chim. Acta 49* (1977) 107; c) B. M. Gimarc, *J. Am. Chem. Soc. 105* (1983) 1979; d) J. Elguero, R. M. Claramount, A. J. H. Summers, *Adv. Heterocycl. Chem. 22* (1978) 183.
[3] Review: R. Bonnett, S. A. North, *Adv. Heterocycl. Chem. 29* (1981) 342.
[4] Review: B. Iddon, *Adv. Heterocycl. Chem. 14* (1972) 331.
[5] W. Friedrichsen, *Adv. Heterocycl. Chem. 26* (1980) 135; U. E. Wirsum, *Aldrichimica Acta 14* (1981) 53; J. G. Smith, P. W. Dibble, R. E. Sandborn, *J. Org. Chem. 51* (1986) 3762; W. C. Christopfel, L. L. Miller, *ibid. 51* (1986) 4169; R. Rodrigo, S. M. Knabe, *ibid. 51* (1986) 3973; Y. Yamaguchi, H. Yamada, K. Hayakawa, K. Kanematsu, *ibid. 52* (1987) 2040; D. Tobia, B. Rickborn, *ibid. 52* (1987) 2611.
[6] Review: M. P. Cava, M. V. Lakshmikantham in A. R. Katritzky, C. W. Rees (Eds.): *Comprehensive Heterocyclic Chemistry. Vol. 4*, Pergamon, Oxford 1984, p. 1037.
[7] J. Moursounidis, D. Wege, *Tetrahedron Lett. 27* (1986) 3045.
[8] W. Friedrichsen, A. Schöning, *Heterocycles 24* (1986) 307.
[9] W. Eberbach, J. Roser, *Heterocycles 23* (1985) 2797; *Tetrahedron 42* (1986) 2221; *Tetrahedron Lett. 28* (1987) 2685.
[10] D. Liotta, M. Saindane, W. Ott, *Tetrahedron Lett. 24* (1983) 2473.
[11] All new products gave correct elemental analyses.
[12] From a stereochemical point of view it is interesting to note that not only does the addition to the primary product **11** proceed with *exo* selectivity (thus differing from the results obtained with the corresponding isodicyclopentadienes[13]), but also that **7a** is predominantly attacked from the *exo* side; in both cases, thermodynamic control of the reaction should be excluded.
[13] P. D. Bartlett, C. Wu, *J. Org. Chem. 50* (1985) 4087.
[14] In the case of the reaction of DMAD with **7b**, the corresponding diadduct **13** (R = H) is stable and can be detected by NMR spectroscopy together with **14** (R = H) as a 4:1 mixture. However, the overall reaction is less clean.

Coupling Metal Centers with Linearly Bridging, Delocalized, π-Bonded Ligands: *p*-Phenylenediimido Dimolybdenum Complexes**

By *Eric A. Maatta** and *David D. Devore*

Transition-metal complexes in which the metal atoms are linked by a bridging group containing a delocalized π system have been the subjects of intense research activity in recent years, perhaps most notably in studies of intervalent electron transfer in dimeric systems and in the construction of polymeric materials of low dimensionality.[1] In the majority of such applications, the bridging ligands employed have been difunctional σ donors, as exemplified by pyrazine in the archetypal Creutz–Taube ion[2] and in various bridged polymers containing metal phthalocyanine[3] or metal porphyrin[4] subunits. While the use of pyrazine and related bridging groups has led to a variety of interesting and important developments, the use of conjugated difunctional σ-donor ligands as bridging groups imposes certain limitations on the kinds of metal fragments that can be interconnected. In particular, it is often observed that coordination of a metal complex to one end of

[*] Prof. Dr. E. A. Maatta, D. D. Devore
Department of Chemistry, Kansas State University
Manhattan, KS 66506 (USA)

[**] This work was supported by the National Science Foundation (USA).

the difunctional σ-donor bridge results in a diminished binding constant for coordination of the remaining donor site; thus, dissociation into mononuclear species is often observed in solution.[5] Second, since metal-to-ligand π backbonding is an integral feature of the ligand–metal interactions in these systems, the majority of studies have focused on rather low-valent metal systems with high d-electron counts.

We wish to report our preliminary studies involving the use of *p*-phenylenediimido ligands as bridging units. In these systems, the ligand binds to the metal via formal M≡N triple bonds, thus obviating any dissociation behavior. Furthermore, since imido-type ligands prefer to bind to high-valent metal fragments, studies of high-oxidation-state systems can be accommodated.

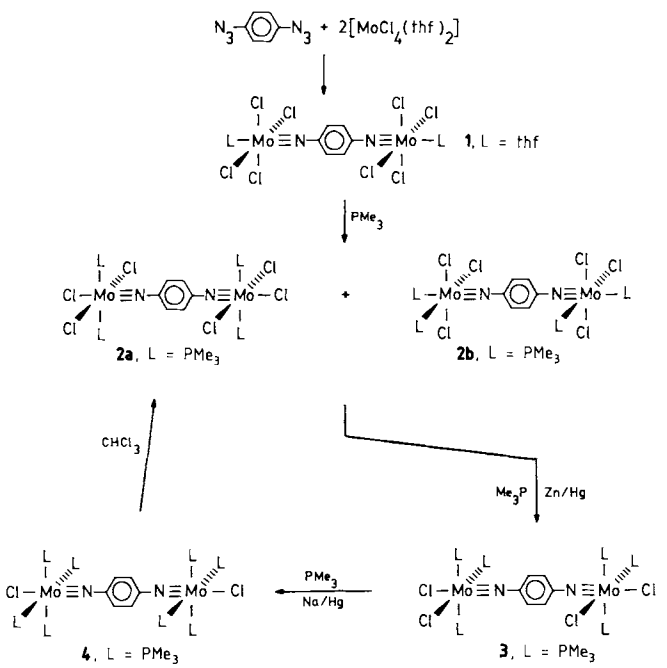

Scheme 1.

The Mo_2^{VI} *p*-phenylenediimido complex **1**[6] is obtained as shown in Scheme 1. The structure indicated is consistent with the observation of a singlet at $\delta = 6.95$ in the 400-MHz ^{1}H-NMR spectrum and is analogous to that determined crystallographically for the related *p*-tolylimido complex $[Mo(NC_6H_4CH_3)Cl_4(thf)]$.[7]

In the presence of PMe_3 in toluene solution, **1** undergoes reduction to yield the 17-electron d^1–d^1 Mo^V dimer **2**.[8] ESR evidence indicates that **2** is formed as a mixture of two geometric isomers: isomer **2a** (major) displays a *trans*-phosphane, *mer*-trichloride configuration at each Mo site and isomer **2b** displays a *cis*-phosphane, *mer*-trichloride configuration at each Mo site of the dimer. Taking the *z* axis as being coincident with the Mo–N bond vectors, the unpaired electron on each Mo^V center will reside in a formally nonbonding d_{xy} orbital. Species **2** undergoes reduction by Zn amalgam in the presence of PMe_3 to form the 18-electron d^2–d^2 Mo^{IV} dimer **3**.[9] The ^{1}H-NMR spectrum of **3** is similar to that of the structurally characterized *p*-tolylimido analogue *cis, mer*-$[Mo(NC_6H_4CH_3)Cl_2(PMe_3)_3]$[10] and supports the assignment of a *cis, mer* geometry for **3**; although **3** is drawn with overall C_{2v} symmetry in Scheme 1, a C_{2h} configuration is also possible.

Treatment of **3** (or **2**) with Na amalgam in toluene in the presence of PMe_3 induces further reduction to yield a lustrous green solid, tentatively identified as the d^3–d^3 Mo^{III} dimer **4**.[11] Complex **4** is paramagnetic, thermally unstable, and extremely air-sensitive. Its formulation as a symmetrical *p*-phenylenediimido-bridged species is supported by its ready reaction with chloroform to afford the Mo^V dimer **2a**.

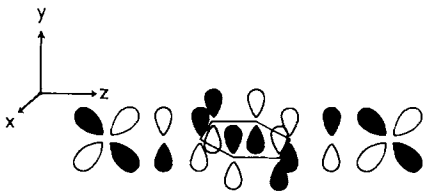

Fig. 1. HOMO for complex **4** as obtained from extended Hückel calculations.

The nature of the bridge bonding in **4** has been investigated by extended Hückel techniques and the nature of the HOMO is as shown in Figure 1. Significantly, it is seen that this orbital consists of a continuously conjugated π system comprising the d_{yz} orbitals on each Mo center and the p_y orbitals of nitrogen and carbon in the *p*-phenylenediimido ligand. This result suggests that the incorporation of d^3–d^3 dimetallo(*p*-phenylenediimido) units into an appropriate polymer network could result in novel types of conducting materials.

Received: October 19, 1987 [Z 2480 IE]
German version: *Angew. Chem. 100* (1988) 583

[1] a) C. Creutz, *Prog. Inorg. Chem. 30* (1983) 1; b) A. Haim, *ibid. 30* (1983) 273; c) T. J. Meyer, *ibid. 30* (1983) 389; d) T. J. Meyer in D. B. Brown (Ed.): *Mixed-Valence Compounds*. Reidel, Dordrecht 1980, p. 75; e) J. S. Miller, *Adv. Chem. Ser. 150* (1976) 18.

[2] a) C. Creutz, H. Taube, *J. Am. Chem. Soc. 91* (1969) 3988; b) L.-T. Zhang, J. Ko, M. J. Ondrechen, *ibid. 109* (1987) 1666, and references cited therein.

[3] a) O. Schneider, M. Hanack, *Angew. Chem. 92* (1980) 391; *Angew. Chem. Int. Ed. Engl. 19* (1980) 392; b) O. Schneider, J. Metz, M. Hanack, *Mol. Cryst. Liq. Cryst. 81* (1982) 273; c) B. N. Diel, T. Inabe, N. K. Jaggi, J. W. Lyding, O. Schneider, M. Hanack, C. R. Kannewurf, T. J. Marks, L. H. Schwartz, *J. Am. Chem. Soc. 106* (1984) 3207.

[4] J. P. Collman, J. T. McDevitt, C. R. Leidner, G. T. Yee, J. B. Torrance, W. A. Little, *J. Am. Chem. Soc. 109* (1987) 4606.

[5] a) R. Ernhoffer, R. E. Shepherd, *J. Chem. Soc. Chem. Commun. 1978*, 859; b) M. S. Haddad, D. N. Hendrickson, J. P. Canady, R. S. Drago, D. S. Bieksza, *J. Am. Chem. Soc. 101* (1979) 898; c) A. J. Lees, J. M. Fobare, E. F. Mattimore, *Inorg. Chem. 23* (1984) 2709; d) R. Gross, W. Kaim, *ibid. 25* (1986) 498.

[6] *Experimental Procedure* for **1**: A mixture of $[MoCl_4(thf)_2]$ (1.12 g, 2.93 mmol) and *p*-phenylenediazide (0.235 g, 1.47 mmol) was refluxed in CH_2Cl_2 (40 mL) under N_2 for 14 h. After cooling to 0°C, the dark purple solid was collected by filtration, washed with pentane, and dried in vacuo (70%). Correct elemental analysis. ^{1}H-NMR (400 MHz, C_6D_6, 25°C): $\delta = 6.95$ (s, 4H; C_6H_4), 4.53 (br., 4H; OCH_2), 1.33 (br., 4H; CH_2).

[7] C. Y. Chou, J. C. Huffman, E. A. Maatta, *J. Chem. Soc. Chem. Commun. 1984*, 1184.

[8] *Experimental Procedure* for **2**: A mixture of **1** (0.74 g, 1.02 mmol) and PMe_3 (0.433 g, 5.7 mmol) in toluene (50 mL) was heated for 24 h at 55°C. After cooling to room temperature, the tan solid product was collected by filtration and dried in vacuo to yield the toluene monosolvate of **2** (75%). Correct elemental analysis. ESR ($CDCl_3$, 25°C): triplet ($g = 1.98$; $A(^{31}P) = 25.9$ G; **2a**); doublet ($g = 1.96$; $A(^{31}P) = 25.0$ G; **2b**).

[9] *Experimental Procedure* for **3**: A solution of **2** (0.82 g, 0.91 mmol) in toluene (80 mL) was stirred with an excess of Zn amalgam under N_2 at 55°C for 36 h and then filtered, and the filtrate was taken to dryness. The residue was extracted with CH_2Cl_2, filtered, and taken to dryness to

yield the yellowish solid product (63%). Correct elemental analysis. ^{1}H-NMR (400 MHz, CD_2Cl_2, 25°C): $\delta = 6.89$ (s, C_6H_4), 1.56 (d, $^2J_{PH} = 8.04$ Hz, *cis*-PMe_3), 1.51 (t, $^2J_{PH} = 3.57$ Hz, *trans*-PMe_3).

[10] a) C. Y. Chou, J. C. Huffman, E. A. Maatta, *Inorg. Chem. 25* (1986) 822; b) C. Y. Chou, D. D. Devore, S. C. Huckett, E. A. Maatta, J. C. Huffman, F. Takusagawa, *Polyhedron 5* (1986) 301.

[11] *Experimental Procedure* for **4**: A mixture of **2** (1.50 g, 1.66 mmol) and PMe_3 (1.05 g, 13.8 mmol) in toluene (60 mL) was stirred with an excess of 2% Na amalgam at 55°C for 3 d. The intensely blue-green solution was filtered, and the filtrate was taken to dryness to yield the lustrous green solid product. ESR (C_6H_6, 25°C): broad singlet ($g = 1.980$).

Cobalt-Catalyzed Reactions of Octamethyl-[4]-radialene and 2,5-Dimethyl-2,3,4-hexatriene with Ethene

By *Ludwig Stehling* and *Günther Wilke**

Dedicated to Professor Emanuel Vogel on the occasion of his 60th birthday

We recently reported[1] the cyclodimerization of 2,5-dimethyl-2,3,4-hexatriene **1** to octamethyl-[4]-radialene **2** on nickel(0). The intermediate **3** with a nickelacyclopentane structure could be isolated and was characterized by a crystal structure analysis. **2** is the result of a reductive elimination with ring closure from **3** (cod = 1,5-cyclooctadiene, MAA = maleic acid anhydride).

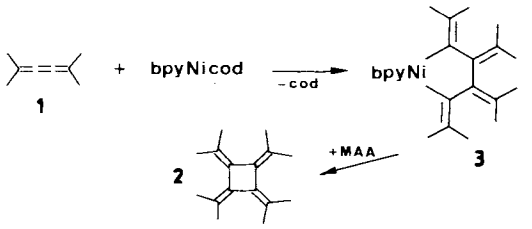

It is already known from the cobalt-catalyzed synthesis of pyridine from acetylene and nitriles[2] that cobaltacyclopentanes are formed as intermediates. This suggested investigating whether the reaction of **1** with $[CpCo(C_2H_4)_2]$ **4** would afford a complex similar to **3**. The components react at room temperature in the ratio 1:1 to give, in almost quantitative yield, the complex **5**, whose structure has been determined X-ray crystallographically.[3] Apparently, **1** and an ethene ligand of **4** initially react at the CpCo moiety to give a cobaltacyclopentane **6**, which after β-H elimination and hydrogen transfer is converted into **5**.

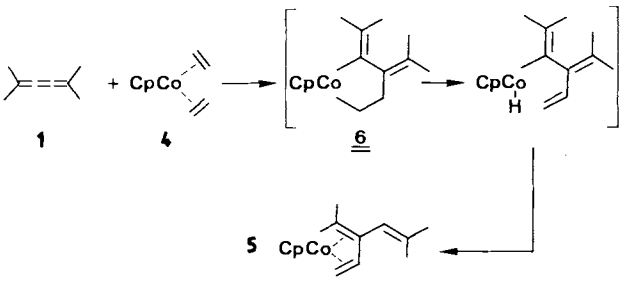

Under ethene pressure at 50°C a catalytic codimerization of **1** with ethene takes place, and the 2,5-dimethyl-3-vinyl-2,4-hexadiene **7**, which is bonded as a 1,3-diene in **5**, is obtained; i.e. **1** and ethene facilitate extrusion of **7** from **5**, with the CpCo moiety functioning as catalytically active species.

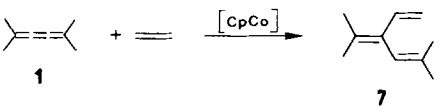

2 cannot be prepared using **4** as the catalyst. Surprisingly, however, in attempts to convert **2** (a bis-1,3-diene) with **4** into a complex with loss of ethene, a catalytic rearrangement of **2** to 2-isopropenyl-1,3-diisopropyl-5-methylbenzene **8** was observed. **8**, which was previously unknown, was unequivocally characterized on the basis of ^{1}H- and ^{13}C-NMR spectra and a crystal structure analysis.[3]

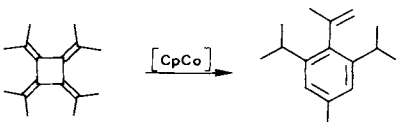

The catalytic rearrangement is presumably initiated by the initial tendency of **2** to undergo complexation with formation of **9**. The crystal structure of **2**[3] suggests that the H atoms of a CH_3 group of **9** lie in close proximity to the Co atom and sterically favor the formation of an alkylcobalt hydride **10**. This, however, adds to the neighboring

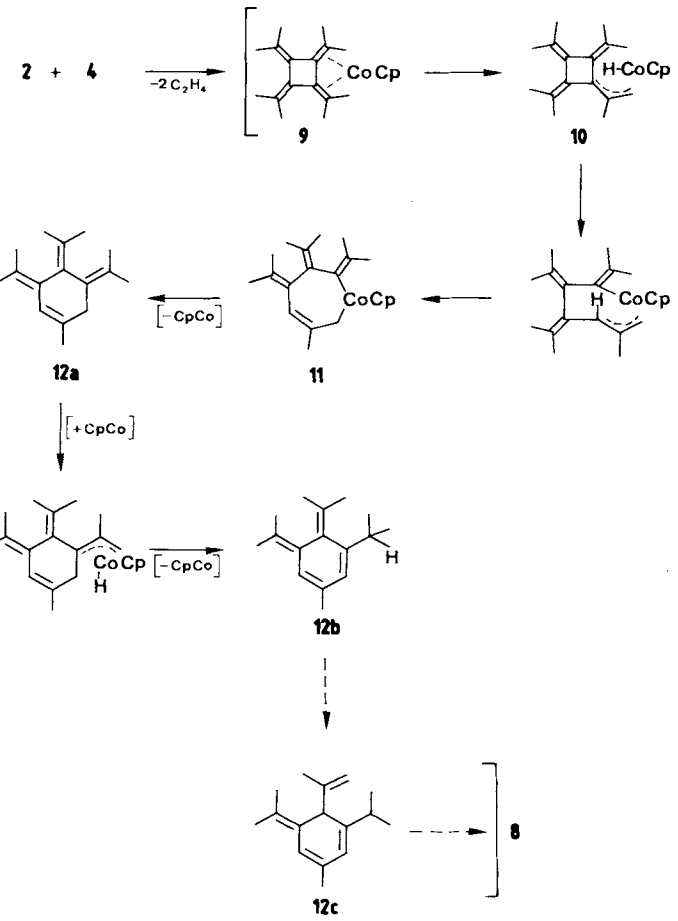

[*] Prof. Dr. G. Wilke, L. Stehling
Max-Planck-Institut für Kohlenforschung
Kaiser-Wilhelm-Platz 1, D-4330 Mülheim a. d. Ruhr (FRG)

C-C bond of the four-membered ring to give a seven-membered cobaltacycle **11**. If a reductive elimination now follows, then a six-membered ring derivative **12** is formed which is converted by several cobalt-induced 1,3-hydrogen shifts into the arene **8**.

This catalytic rearrangement occurs in toluene at 60 °C. Under these conditions no intermediates could be isolated; the reaction course shown can only be regarded as tentative. In THF at 60 °C, however, an isolable complex which may be regarded as an intermediate, namely **13**, is formed.[4]

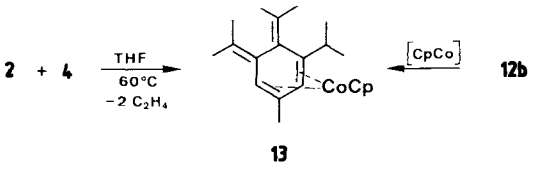

13

Surprisingly, dodecamethyl-[6]-radialene, which can be obtained catalytically from **1** with nickel(0), does not react with **4** under analogous conditions. The crystal structure of dodecamethyl-[6]-radialene[3] shows that the six-membered ring which contains six sp^2-hybridized C-atoms adopts a chair conformation, since neighboring isopropylidene groups strongly hinder each other sterically, thereby blocking the C=C bonds and making them inaccessible for a catalyst.

In this connection the behavior of a diisopropylidenecyclobutene **14**[4] towards **4** is also interesting. Even at room temperature a 1:1 adduct **15**,[5] which was characterized on the basis of ^{1}H- and ^{13}C-NMR spectra and a crystal structure analysis, is formed.[3] After displacement of the ethene molecules and possible complexation of the ring double bond, an oxidative addition to the bond on the opposite side of the ring takes place. In the resulting product **15**, the delocalized π-system is η^4-bonded to the CpCo moiety.

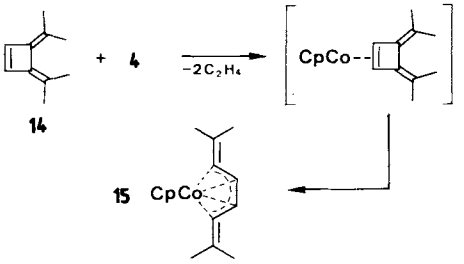

Thus, **15** is in a sense related to **3**, although only two of the four ring C-atoms in **3** are bonded to the Ni atom.

Experimental

5: A solution of **1** (1.31 g, 7.29 mmol) in THF (60 mL) was treated under argon at −78 °C with a solution of **4** (0.799 g, 7.29 mmol) in THF (20 mL). The mixture was warmed slowly to room temperature and, after 12 h, the THF was removed. Yield 1.84 g (7.07 mmol, 96.8%) of pure **5**. Recrystallization from ether furnished 1.4 g (5.38 mmol, 74%) of **5**. ^{1}H-NMR (200 MHz, [D$_6$]benzene): δ = 6.38 (s, 1 H), 4.94 (dd, 1 H), 4.50 (s, 5 H), 1.76 (dd, 1 H), 1.74 (s, 3 H), 1.61 (s, 3 H), 1.20 (s, 3 H), 1.00 (dd, 1 H), 0.60 (s, 3 H). ^{13}C-NMR (75.5 MHz, [D$_6$]benzene): δ = 134.97, 127.61, 96.78, 81.86, 81.14, 53.18, 32.35, 30.92, 25.77, 23.06, 19.65. MS: *m/z* 260 ($M^{\oplus}$, 100%). The structure of **5** was determined X-ray crystallographically.

7: A solution of **1** (30 g, 277 mmol) and **4** (0.46 g, 2.53 mmol) in THF (270 mL) was heated in an autoclave at 50 °C for 24 h under 60 bar ethene. The THF was then removed at 0.1 bar and 50 °C. According to a GC analysis the residue contained 7.82 g (57.8 mmol) of **7** together with unchanged **1** and 5.49 g (33.48 mmol) of C_{12}-hydrocarbons. The conversion of **1** was 33%; 33 cycles. **7** was characterized by combined GC/MS, hydrogenation, and MS (*m/z* 136, $M^{\oplus}$, 45%).

8: A solution of **2** (1.06 g, 5.84 mmol) in toluene (50 mL) was treated under argon with a solution of **4** (1.26 g, 5.84 mmol) in toluene (20 mL) and the mixture heated in a sealed ampoule at 60 °C for 48 h. After removal of the toluene, the residue was taken up in hexane and chromatographed on silica gel. Sublimation of the eluate after removal of hexane furnished 0.76 g (3.51 mmol, 60%) of **8**, which was recrystallized (m.p. 61 °C) from pentane. ^{1}H-NMR (200 MHz, [D$_6$]benzene): δ = 1.20 (d, 6 H), 1.22 (d, 6 H), 1.92 (s, 3 H), 2.22 (s, 3 H), 3.14 (sep. 2 H), 4.84 (dq, 1 H), 5.21 (dq, 1 H), 6.98 (s, 2 H). ^{13}C-NMR (75.5 MHz, CD_2Cl_2): δ = 20.6, 21.7, 24.4, 25.6, 26.4, 115.7, 123.9, 136.9, 138.5, 145.2, 146.1. MS: *m/z* 216 ($M^{\oplus}$, 56%). The C,H analysis agrees with the calculated values. The structure of **8** was unequivocally confirmed by an X-ray crystallographic analysis.

15: 171.7 mg (1.28 mmol) of **14** and 231.7 mg (1.28 mmol) of **4** were dissolved in benzene (50 mL) under argon and the reaction vessel partially evacuated several times over a period of 4 h at room temperature. After removal of the benzene there remained 270 mg of a reddish-brown product, which on recrystallization from ether at −78 °C furnished golden brown crystals. Yield 110 mg (0.42 mmol, 33%) of **15**. ^{1}H-NMR (80 MHz, [D$_6$]benzene): δ = 1.81 (s, 6 H), 1.95 (s, 6 H), 4.36 (d, 2 H), 4.85 (s, 5 H). ^{13}C-NMR (75.5 MHz, [D$_6$]benzene): δ = 23.6, 26.5, 63.4, 82.5, 117.8, 153.1. The NMR spectra of the crude product and the crystals are identical. The structure of **15** was determined X-ray crystallographically.

Received: December 14, 1987;
revised: January 18, 1988 [Z 2537 IE]
German version: *Angew. Chem. 100* (1988) 575

CAS Registry numbers:
1, 2431-31-4; **2**, 88919-66-8; **4**, 69393-67-5; **5**, 113687-26-6; **7**, 113687-24-4; **8**, 113687-25-5; **14**, 3642-14-4; **15**, 113687-27-7; ethene, 74-85-1.

[1] L. Stehling, G. Wilke, *Angew. Chem. 97* (1985) 505; *Angew. Chem. Int. Ed. Engl. 24* (1985) 496.
[2] H. Bönnemann, *Angew. Chem. 97* (1985) 264; *Angew. Chem. Int. Ed. Engl. 24* (1985) 248.
[3] C. Krüger, G. Wilke et al., unpublished.
[4] M. Yalpani, unpublished.
[5] D. J. Pasto, D. K. Mitra, *J. Org. Chem. 47* (1982) 1381.

4-Oxo-2,5-Cyclohexadienylidene — a Carbene with a Stable Triplet and Metastable Singlet State?**

By *Wolfram Sander,** *Wolfgang Müller,* and *Reiner Sustmann*

Of crucial importance in carbene chemistry is the rate of singlet-triplet interconversion (k_{ST}), which, in many cases, might determine the product distribution. A study of diphenylmethylene has shown an ultrafast interconversion rate ($k_{ST} = 3.2 \times 10^9\ s^{-1}$) and equilibration between carbene spin states in a time that is short compared to most reactions.[1]

In this paper we report the generation and matrix isolation of 4-oxo-2,5-cyclohexadienylidene **1**. This carbene can be converted by visible light irradiation in a completely reversible manner from the stable triplet state **1** into a metastable singlet species. The slow thermal conversion of this metastable compound back to **1** at low temperatures (9–60 K) shows a pronounced external heavy-atom effect.

Carbene **1** was generated in solid argon at 9 K by irradiation of 4-diazo-2,5-cyclohexadienone **3**[2] with visible light

[*] Dr. W. Sander
Organisch-Chemisches Institut der Universität
Im Neuenheimer Feld 270, D-6900 Heidelberg (FRG)
Prof. Dr. R. Sustmann, Dipl.-Chem. W. Müller
Institut für Organische Chemie der Universität
Universitätsstr. 5, D-4300 Essen (FRG)

[**] This work was supported by the Deutsche Forschungsgemeinschaft. We thank Prof. Dr. *R. Gleiter* for supporting this work and for helpful discussions.

($\lambda > 495$ nm, 30 min). The IR-, UV-, and ESR-spectra of **1** are in accordance with an electronic structure described by resonance structures **1a**–**1c**.[3]

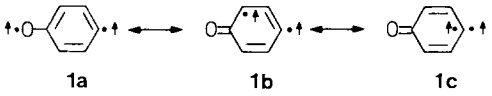

1a **1b** **1c**

In the IR spectrum of **1** the ν(CO) mode is found at 1496 cm^{-1} (Table 1), which indicates a bond order of the C–O bond considerably less than 2. The UV/VIS spectrum[3] shows a long wavelength band [UV (Ar, 10 K): $\lambda = 508$, 521, 535, 551, 566 nm] of medium intensity typical for triplet carbenes.[4] The ESR spectrum of **1**, measured in argon at 23 K, is in good agreement with the reported spectrum of a powder sample at 4 K.[5]

Table 1. IR spectroscopic data of **1**, [D_4]-**1**, **2**, and [D_4]-**2**, matrix isolated in argon at 9 K.

1	[D_4]-1	2	[D_4]-2
1496 s	1487	1720 s	1718
1375 m	1298	1713 vs	1709
1362 w		1679 w	1652
1260 m		1663 w	
1076 m		1520 w	
937 w	929	1305 w	1157
819 s	706	1005 m	
		896 w	876
		892 w	826
		843 m	816
		799 m	766
		741 m	
		583 s	493

Carbene **1** shows the low-temperature chemistry of a triplet carbene. Warming a matrix containing both **1** and carbon monoxide (1% in Ar) to 35 K (softening point of the argon matrix) generates a keto-ketene which is tentatively assigned the structure **4** [IR (Ar, 10 K): $\tilde{\nu} = 2110$ s, 1635 s, 1158 m, 851 m, 707 m cm^{-1}]. If the argon matrix is doped with 1% O_2, *p*-benzoquinone *O*-oxide (**5**) is formed under the same conditions.[3]

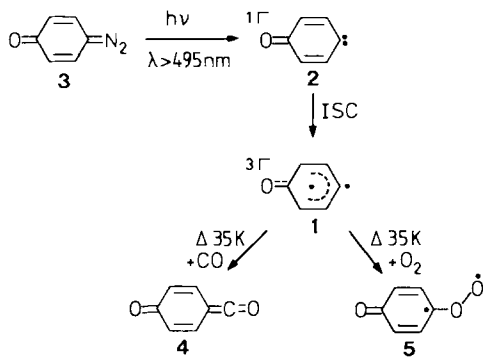

3 **2** **1** **4** **5**

Irradiation (543 ± 10-nm interference filter, 500W mercury high pressure arc lamp) into the long wavelength transition of **1** readily produces a new species **2** (Table 1, Fig. 1) (UV: $\lambda = 440$ (br), 337 nm). After several hours irradiation the conversion of **1** into **2** is >90%; other products are not observed IR spectroscopically.[6]

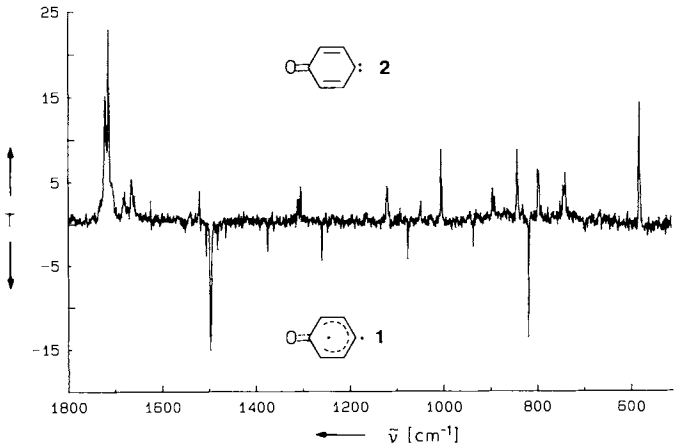

Fig. 1. Difference IR spectrum of the photochemistry of **1**. Bottom: bands assigned to **1**, vanishing on irradiation ($\lambda = 543 \pm 10$ nm). Top: bands assigned to **2**, appearing on irradiation.

Compound **2** is very labile and rearranges back to **1** (>99%) under the following conditions:

- Broad band irradiation ($\lambda > 495$-nm cut-off filter, several min).
- Infrared irradiation (Nernst glower, visible light blocked by using a germanium filter). The disappearance of **2** and appearance of **1** obeys first order kinetics if a constant IR source (IR spectrometer) is used. In Ar, Kr, and Xe matrices the relative rates are 1 : 2.7 : 5.8.
- Standing in the dark. In Ar at 9 K, $t_{1/2} = 165 \pm 30$ h; in Xe at 9 K, $t_{1/2} = 10 \pm 2$ h.[7]

When **1** was irradiated ($\lambda = 543 \pm 10$ nm, Ar, 23 K) in the cavity of the ESR spectrometer, the signal intensity decreased by about 60% within 70 min. No other signal appeared. On standing in the dark the signal intensity increased again slowly, in agreement with the results from the IR experiments. This process was faster in Xe than in Ar matrix. On broad band irradiation ($\lambda > 475$ nm, 1 min), 92% of the original ESR intensity was restored.

The pronounced external heavy atom effect observed both for the IR induced and the thermal rearrangement is evidence for a spin-forbidden intersystem crossing (ISC) step determining the rate constants.[8]

Compound **2** is a carbonyl compound with a singlet ground state energetically lying above the triplet ground state of **1**. The most likely structures for **2** are a singlet carbene **a**, bicyclo[3.1.0]hexa-3,5-dien-2-one **b**, bicyclo-[3.1.0]hexa-2,3-dien-6-one **c**, and cyclohexa-2,3,5-trien-1-one **d**. Although structures **b**–**d** cannot be rigorously excluded, the IR spectrum of **2** (Table 1, Fig. 1) differs from what would be expected for these compounds.

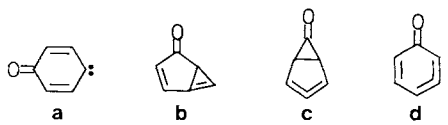

a **b** **c** **d**

Cyclopropene **b** should show a ring vibration in the region 1700–1800 cm^{-1}, exhibiting a characteristic 45 cm^{-1} shift on deuteration of the olefinic position,[9] which is not observed (Table 1). For cyclopropanone **c**, a ν(C=O)

 © VCH Verlagsgesellschaft mbH, D-6940 Weinheim, 1988 0570-0833/88/0404-0573 $ 02.50/0

mode $\approx 1820\ cm^{-1}$ is expected,[10] and allene **d** should show an allene band (1800–1900 cm^{-1}). There are no IR bands in the range 1750–2500 cm^{-1}, and thus structures **c** and **d** are unlikely. In addition, the rearrangement of **b**, **c**, or **d** to **1** requires the rupture of C–C or C–H bonds, and it is not reasonable to assume that these processes occur with such a low activation barrier (kT at 10 K is only 20 cal/mol).

The extremely slow intersystem crossing rate for the conversion of **2** into **1** might be explained in terms of the different structures of **1** and **2**. Whereas **1** is best described as a diradical with a phenyl type σ-system and a phenoxyl type π-system (partially "aromatic" ring system), **2** has a more localized cyclohexadienone structure.

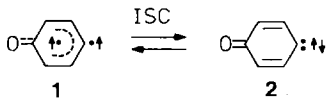

1 **2**

The intersystem crossing thus requires a large geometric change of the molecule, although no covalent bands are rearranged. This new kind of isomerism was first predicted by *Dewar* and *Narayanaswami*[11] and recently postulated in the case of cycloheptatrienylidene.[12] Clearly, more experimental and theoretical studies are necessary to elucidate the factors determining the intersystem crossing rates in carbene reactions.

Received: December 7, 1987 [Z 2527 1E]
German version: *Angew. Chem. 100* (1988) 577

[1] K. B. Eisenthal, N. J. Turro, E. V. Sitzmann, I. R. Gould, G. Hefferon, J. Langan, Y. Cha, *Tetrahedron 41* (1985) 1543.

[2] a) **3** was prepared by treating *p*-hydroxybenzenediazonium chloride with silver oxide: M. Puza, D. Doetschmann, *Synthesis 1971*, 481; b) the educt for the synthesis of [D_4]-**3** was synthesized by H/D exchange. For a general procedure see: N. H. Werstiuk, T. Kadai, *Can. J. Chem. 52* (1974) 2169.

[3] For some spectroscopic data of **1** and a detailed discussion of the reaction of **1** and O_2 see: W. Sander, *J. Org. Chem.*, in press.

[4] R. J. McMahon, O. L. Chapman, *J. Am. Chem. Soc. 109* (1987) 683.

[5] E. Wasserman, R. W. Murray, *J. Am. Chem. Soc. 86* (1964) 4203.

[6] UV irradiation ($\lambda > 345$ nm) of **1** rapidly produces a ring-opened compound containing both a ketene and a terminal acetylene functional group [IR (Ar, 10 K): $\tilde{\nu}$ = 3316 m, 2134 s, 1755 m, 1594 m, 1423 m, 1383 w, 1067 w, 819 w, 648 m, 592 w, 580 w cm^{-1}]. The acetylenes **6a** and **6b** are possible structures; however, an assignment has not been possible so far.

6a **6b**

[7] Rate constants were measured by IR spectroscopy. Both the disappearance of **2** and the appearance of **1** were observed with several bands. To measure the thermal interconversion, the IR beam was turned on for only a short period of time. Due to IR photolysis there is still a systematic error in the rate constants.

[8] J. J. Fischer, J. Michl, *J. Am. Chem. Soc. 109* (1987) 583.

[9] P. R. West, A. M. Mooring, R. J. McMahon, O. L. Chapman, *J. Org. Chem. 51* (1986) 1316.

[10] G. Socrates: *Infrared Characteristic Group Frequencies*, John Wiley, Chichester 1980, p. 62.

[11] a) M. J. S. Dewar, K. Narajanaswami, *J. Am. Chem. Soc. 86* (1964) 2422; b) M. J. S. Dewar, K. M. Merz, jr., *ibid. 107* (1985) 6111.

[12] Both cycloheptatrienylidene (triplet carbene) and cycloheptatetraene (singlet carbenoid species) have been generated (from different precursors) and characterized in low-temperature matrices. In contrast to **1** and **2**, an interconversion of these species has not been observed: a) R. J. McMahon, C. J. Abelt, O. L. Chapman, J. W. Johnson, C. L. Kreil, J.-P. LeRoux, A. M. Mooring, P. R. West, *J. Am. Chem. Soc. 109* (1987) 2456; b) C. L. Janssen, H. F. Schaefer III, *ibid. 109* (1987) 5030.

The Crystal Structures of the Superconducting Oxides $Bi_2(Sr_{1-x}Ca_x)_2CuO_{8-\delta}$ and $Bi_2(Sr_{1-y}Ca_y)_3Cu_2O_{10-\delta}$ with $0 \le x \le 0.3$ and $0.16 \le y \le 0.33$**

By *H. G. von Schnering,* L. Walz, M. Schwarz, W. Becker, M. Hartweg, T. Popp, B. Hettich, P. Müller,* and *G. Kämpf*

The enthusiasm awakened by the epoch-making discovery of *Bednorz* and *Müller*[1] did not pass our laboratories without leaving its trace. Based on earlier experiences with ternary oxides and with the considerable number of variants of the perovskite structure,[2] having in mind especially the $BiO^{\oplus}$ derivatives as investigated by *Aurivillius*[3] and *Sillén*,[4] we started in February 1987 to deal with complex oxides of the type $(Bi_2O_2)M'_{m-1}M_mO_{3m+1}$ with $m = 1, 2, \ldots$ In principle, all metal atoms are eligible to be the cation M′ or the central atom M if the condition $d(M'\text{-}O)/d(M\text{-}O) \simeq \sqrt{2}$, $d(M\text{-}O) = 185\text{–}205$ pm is approximately fulfilled. We assumed—admittedly without further scientific foundation—that the expected strong electron-phonon coupling is due to a 'virtual valence instability' of M, associated with a 'virtual change of the coordination' (cf. Ref. [5]). M should have an odd number of electrons and there should be a strong antiferromagnetic spin coupling. From chemical experience $Cu^{2\oplus}$ was considered most promising for a quick success.

Already in April 1987 we obtained a superconducting phase, and a single crystal X-ray analysis yielded the principal arrangement of the positions of the metal atoms. However, the positions of the oxygen atoms remained unclear. The exact identification as

$Bi_2(Sr_{1-x}Ca_x)_2CuO_{8-\delta}$ **1**

and its reproducible synthesis failed until October 1987.[6] The complications were due to strong absorption effects and to the existence of additional phases, at least to that of

$Bi_2(Sr_{1-y}Ca_y)_3Cu_2O_{10-\delta}$ **2**

Recently *Maeda* et al.[7] and *Chu* et al.[8] reported on the results of investigations of **2**. We are sure that the compound "$Bi_2Sr_2Cu_2O_{7-\delta}$" described by *Michel* et al.[9] is identical to $Bi_2(Sr_{1-x}Ca_x)_2CuO_{8-\delta}$ **1**.

Compounds **1** and **2** can be obtained by reaction of the metal oxides or carbonates at $1070\ K \le T \le 1225\ K$ in air (corundum crucibles). Homogeneous powder samples are obtained by sintering at 1070–1100 K for a few hours. At

[*] Prof. Dr. H. G. von Schnering, Dr. L. Walz, Dr. M. Hartweg, Dipl.-Min. T. Popp
Max-Planck-Institut für Festkörperforschung
Heisenbergstrasse 1, D-7000 Stuttgart 80 (FRG)
Dr. M. Schwarz, Dr. W. Becker, Dr. B. Hettich, Dr. G. Kämpf
Hoechst AG
D-6000 Frankfurt am Main 80 (FRG)
Dr. P. Müller
Institut für Anorganische Chemie der Technischen Hochschule
Professor-Pirlet-Strasse, D-5100 Aachen (FRG)

[**] This work was supported by the Fonds der Chemischen Industrie. We thank Prof. Dr. *Dachs*, Berlin, for the possibility to carry out the neutron diffraction measurements at the TAS1, Risø National Laboratories, Denmark.—These results were presented at the International Conference on High T_c Superconductors and Materials and Mechanisms of Superconductivity (HTSC-M^{2}S) that was held in Interlaken (Switzerland) on February 29.

about 1150 K the reaction mixtures begin to melt, and after a few minutes, crystals can be drawn from the molten phases. **1** and **2** form black glossy plate-like crystals with well-developed faces. They grow up to 5 mm in length along [010]. The ratio of **1** to **2** is influenced less by the stoichiometry of the reactants than by the thermal treatment. Reactions at $T \geq 1070$ K, followed by slow cooling or annealing at 970 K, lead to **1**, whereas **2** is preferably formed if the molten reaction mixture is quenched. It would seem that an excess of CuO is necessary for a successful synthesis of **2**. We assume that an excess of CuO prevents the formation of by-products. The reaction product near the side of the crucible is colorless and chemical analyses show distinct presence of Al, while the clearly separated superconducting material is free of Al.

An important observation is the change in color (black→dark brown) of samples of **1** as a function of the thermal treatment and of the O_2 partial pressure. The structure remains unchanged, although the oxidation activity varies (formation of Cl_2 from HCl). This is related to the number of defects δ within the $(Bi_2O_{4-\delta})^{2\oplus}$ partial structure, and is in agreement with the results obtained from neutron scattering experiments.

The crystal structures of **1** and **2** were determined by X-ray single crystal methods and by powder neutron diffraction measurements. The compounds crystallize orthorhombically in the space group *Amaa* (No. 66), with four formula units per unit cell (Table 1). In both cases reflections of the type $h+k$, $h+l=2n+1$ are very weak, but it must be emphasized that they are essential for the orthorhombic symmetry and the resulting atomic arrangement, and that the fast weakening of the intensities with increasing order of h is of great importance. These effects are due to: a) An unusual anisotropy of the bismuth atoms parallel to [100] that can be described with $U_{11}=0.18$ Å^2 or split positions $x=\pm 0.06 \neq 0$ for **1**, and 0.11 Å^2 or $x=\pm 0.04 \neq 0$ for **2**, respectively. b) A distinct displacement of the bismuth atoms parallel to [010] with $x=0.275 \neq 1/4$. If one neglects these facts, the impression arises that **1** and **2** crystallize tetragonally in the space group $F4/mmm$ ($\triangleq I4/mmm$ with $a'=b'=a/\sqrt{2} \simeq 385$ pm). Indeed, we have also found crystals for which the reflections mentioned above are diffuse. Furthermore, we obtained crystals which exhibit a five-fold, incommensurate superstructure along [100], which is coupled to a twofold one along [001]. It is likely that these superstructures are due to a longitudinal modulation of the parameter x (Bi) along [100]. An exact determination of the oxygen atoms based on X-ray data presents great difficulties, as also indicated in a recent study of **2** by *Subramanian* et al.[10] Only the oxygen atoms within the CuO_2 layers (see Fig. 1) can be localized, while the re-

Table 1. Crystallographic data [11] for **1** and **2** in the space group *Amaa* (No. 66) with $a, b, c = 539.2, 539.4, 2453.7$ pm and 539.5, 539.3, 3062.8 pm, respectively.

Atom	x	y	z	U [Å^2]
Bi	0 [a]	0.272	0.0658	0.083 [a]
Sr [b]	0	0.755	0.1802	0.030
Cu	0	1/4	1/4	0.050
O1	1/4	0	0.245	0.04
O3	0	0.25	0.156	0.10
O4	1/4	0	0.055	0.2
O5 [d]	1/4	1/2	0.055	(0.2) [d]
Bi	0 [a]	0.273	0.0522	0.058 [a]
Sr [b]	0	0.750	0.1408	0.016
Ca [c]	1/2	1/4	1/4	0.030
Cu	0	0.250	0.1966	0.023
O1	1/4	0	0.196	0.03
O2	1/4	1/2	0.198	0.03
O3	0	0.250	0.123	0.10
O4	1/4	0	0.043	0.2
O5 [d]	1/4	1/2	0.043	(0.2) [d]

[a] $U_{11}=0.18$ (0.11) Å^2 and $U_{22} \simeq U_{33}=0.035$ Å^2; using alternatively split positions yields $x(\mathrm{Bi})=\pm 0.06$ (± 0.04). [b] Without Ca. [c] $Sr_{1-x}Ca_x$, $x=0.5$. [d] Site occupation $=0.2 \triangleq \delta=1.6$.

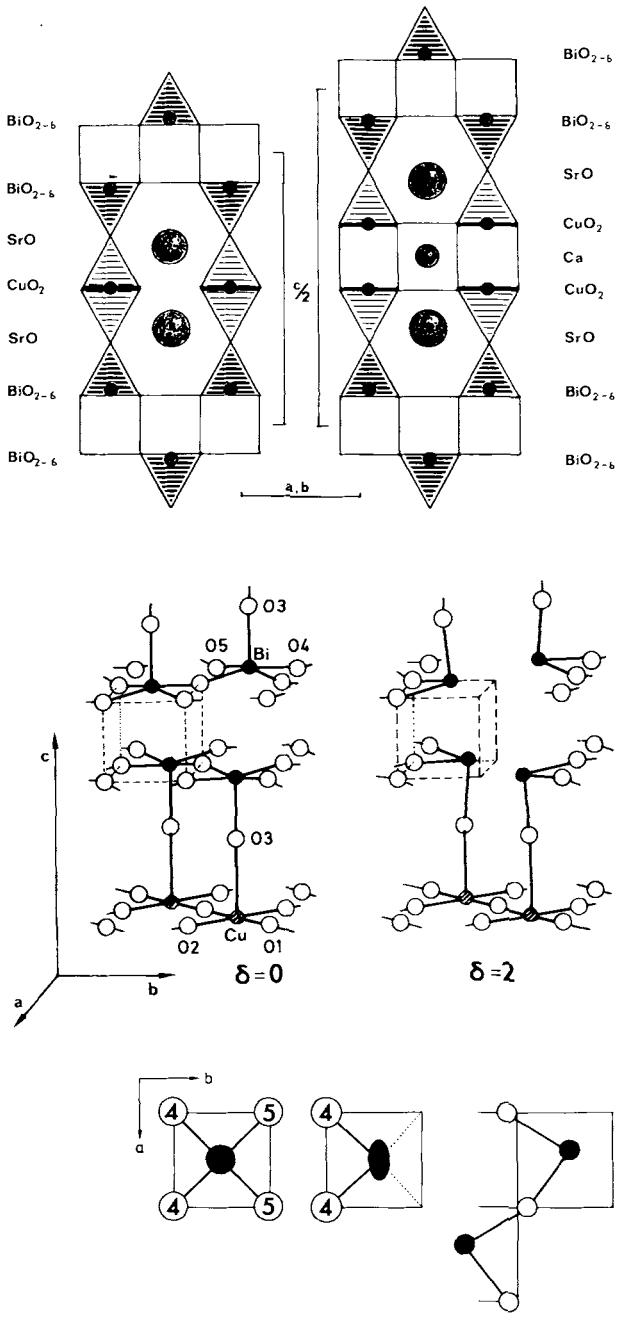

Fig. 1. Top: Schematic and idealized representation of the structures **1** and **2** ($a/2$ in projection). The O atoms occupy all crossing points of the polygons. The small, but significant displacements of the Bi atoms are marked by an arrow. Center: Perspective view showing the Bi-O-Cu-O connection; left part: $\delta=0$, right part: $\delta=2$. Bottom: Section of the $(Bi_2O_{4-\delta})$ plane with $\delta=0$, $x(\mathrm{Bi})=0$, and $y(\mathrm{Bi})=1/4$ (left); $\delta=2$, $y(\mathrm{Bi})=0.275$, and $U_{11}=0.18$ Å^2 (center) and an ordering model (right) with a structure modulated along [100] ($\delta=2$, $x(\mathrm{Bi})=0.05$, $y=0.275$). The size of the atoms (Bi = black) is in agreement with the thermal parameters.

maining ones, especially those in the $Bi_2O_{4-\delta}$ region are considerably displaced together with the Bi atoms. However, the neutron scattering experiments allow an exact determination (cf. Table 1).

The results are given in Figure 1. The structures of **1** and **2** are the first members of the homologous series $Bi_2M'_2M''_nM_{n+1}O_{8+2n-\delta}$ ($n=0, 1$) with $d(M'\text{-}O) \geq d(M''\text{-}O)$ and $d(M'\text{-}O)/d(M\text{-}O) \simeq \sqrt{2}$. The structure of **1** exists with M = Cu and $M' = Sr_{1-x}Ca_x$ ($0 \leq x \leq 0.3$). On varying x, the lattice constants are changed only very little. The single crystal investigated contained only Sr. The structure of **2** exists with M = Cu, M' = Sr, and $M'' = Sr_{1-x}Ca_x$ ($0.5 \leq x \leq 1$; corresponding to $0.16 \leq y \leq 0.33$). The single crystal used for the X-ray determination contained $x = 0.5$ Ca. In **1** and **2** the Bi_2O_4 layers frame different sized fragments of the perovskite structure (Fig. 1, top). The adaptation of the two partial structures is rather unusual. It differs essentially from the known $(Bi_2O_2)^{2\oplus}$ derivatives[3] because of direct Bi-O-Cu sequences along [001] (Fig. 1, center). The lowering of the 12-fold coordination of M' and M'' to a square antiprismatic or cubic 8-fold coordination arises, on the one hand, from the (Bi-O-Cu) packing and, on the other, from the absence of Cu-O-Cu bridges along [001] within **2**. In particular, the copper atoms in **1** are linked to 4+2 oxygen atoms with $d(Cu\text{-}O) = 191$ pm (4×) and 231 pm (2×), leading to a typically elongated $^2_\infty[CuO_{4/2}O_2]$ partial structure. The copper atoms in **2**, however, have a 4+1 coordination with $d(Cu\text{-}O) = 191$ pm (4×) and 225 pm (1×). Distorted tetragonal CuO_{4+1} prisms arranged *trans* to each other are connected by $M''O_8$ cubes (Fig. 1). The coordination of the cations, $Sr^{2\oplus}$ and $Ca^{2\oplus}$, are as expected ($d(Sr\text{-}O) \simeq 260$ pm). In contrast, a completely unusual coordination is found for the bismuth atoms. If the positions of O4 and O5 are completely occupied ($\delta = 0$), then bismuth is present as Bi^V and it is likely that four short Bi-O distances (Bi-O4 2×, Bi-O5 2×) of about 192 pm will be obtained assuming $y(Bi) = 1/4$, together with Bi-O3 = 221 pm and 217 pm, respectively. However, Bi^{III} is present if the position of O5 is completely unoccupied ($\delta = 2$). With $y(Bi) = 0.275$, three convenient Bi-O distances result, and an orientation of the lone pair nearly parallel to (001) occurs, an orientation never observed in such structures.

Indeed, the results of the neutron scattering experiments prove that the defects δ occur only on the position of O5 if $y(Bi) \geq 1/4$. The remarkable feature of these structures is that adaptation of all oxidation states $Bi^{q\oplus}$ ($3 \leq q \leq 5$) within the $(Bi_2O_{4-\delta})$ partial structure is possible. It can be expected that formal charge transfer processes of the kind $Bi^V\text{-}O\text{-}Cu^{II} \rightleftharpoons Bi^{IV}\text{-}O\text{-}Cu^{III}$ as well as $Bi^{IV}\text{-}O\text{-}Cu^{II} \rightleftharpoons Bi^{III}\text{-}O\text{-}Cu^{III}$ and $Bi^{IV}\text{-}O\text{-}Bi^{IV} \rightleftharpoons Bi^{III}\text{-}O\text{-}Bi^V$ play an important role concerning the superconducting properties of these materials. In this connection, we mention the superstructure of **1**, which indicates a periodic modulation of the Bi_2O_4 layers (see Fig. 1, bottom). Changes in the Bi-O coordination are qualitatively in agreement with the process $2\,Bi^{IV} \rightleftharpoons Bi^{III} + Bi^V$. There is good reason to believe that this modulation is related to the number of defects δ. For the crystals investigated δ is about 1.5, i.e., formally Bi^{IV} and Bi^{III} are present, but slight variations of the lattice constants for different powder samples confirm a distinct variability of δ. For instance, deep-black samples of **1** yield slightly smaller values for a and b (535.0 pm). In the case of **2**, a comparison of the values given for the length of the c-axis shows that it can also vary over a greater range (3086 pm,[7] 3078 pm,[8] 3090.4 pm,[10] 3062.8 pm [this work]). This may be due to a different Ca content.

Measurements of the resistivity (four-probe technique) and of the Meissner effect (SQUID) carried out on small rods show critical temperatures of 70–85 K (for some samples only 40 K) with broad transition regions and variable parts of superconducting material (5–50%). A knowledge of the thermal behavior and of the structures allows us to explain this by an oxygen content that hitherto has not been completely optimized. Obviously the range of δ (oxygen defects within the Bi_2O_4 partial structure), in which superconductivity occurs, is smaller for **1** than for **2**. In the case of a sample with the approximate composition $Bi_2Sr_2CuO_x$ and only marginal amounts of Ca, we observed on one occasion a sharp decrease in the resistivity at 140 K ($\Delta T \leq 2$ K) down to a very small resistance, which vanished at 80 K. Attempts to reproduce this experiment have thus far failed.

Received: March 4, 1988 [Z 2647 IE]
German version: *Angew. Chem. 100* (1988) 604

[1] J. G. Bednorz, K. A. Müller, *Z. Phys. B64* (1986) 189.
[2] H. G. von Schnering, Dissertation, Münster 1960; Habilitationsschrift, Münster 1964.
[3] B. Aurivillius, *Ark. Kemi 1* (1949) 463; *ibid. 1* (1949) 499; *ibid. 2* (1950) 519; *ibid. 5* (1952) 39.
[4] L. G. Sillén, E. Jörnstad, *Z. Anorg. Allg. Chem. 250* (1942) 173.
[5] A. Simon, *Angew. Chem. 99* (1987) 602; *Angew. Chem. Int. Ed. Engl. 26* (1987) 579.
[6] H. G. von Schnering, W. Becker, M. Schwarz, L. Walz, E. Waldschmidt, J. Adam, *Dtsch. Pat.-Anm. P3739886.5* (November 25, 1987), Hoechst AG.
[7] H. Maeda, Y. Tanaka, M. Fukutomi, T. Asano, *Jpn. J. Appl. Phys. Lett.*, in press.
[8] R. M. Hazen, C. T. Prewitt, R. J. Angel, N. L. Roy, L. W. Finger, C. G. Hadidiacos, P. J. Heaney, P. H. Hor, R. L. Meng, Y. Y. Sun, Y. Q. Wang, Y. Y. Xue, Z. J. Huang, L. Gao, J. Bechtold, C. W. Chu, *Phys. Rev. Lett. 60* (1988) 1174; see also C. W. Chu et al., *ibid. 60* (1988) 941 and D. R. Vehlen et al., *Nature (London) 332* (1988) 334.
[9] C. Michel, M. Hervieu, M. M. Borel, A. Grandien, S. Deslandes, J. Provost, B. Raveau, *Z. Phys. B-Condensed Matter 68* (1987) 421.
[10] M. A. Subramanian, C. C. Torardi, J. C. Calabrese, J. Gopalakrishnan, K. J. Morrissey, T. R. Askew, R. B. Flippen, U. Chowdhry, A. W. Sleight, *Science 239* (1988) 1015.
[11] Plate-like single crystals, $Mo_{K\alpha}$ radiation, 1651 (1338) *hkl* reflections measured, 198 (179) symmetry independent having $F \geq 3\sigma(F)$; $R = 0.12$ (0.12) for all reflections after absorption correction by F_0/F_c comparison.—30 (44) *hkl* from neutron powder diffraction pattern; $\lambda = 2.014$ Å; $R = 0.12$ (0.10) without profile refinement.

Dinuclear Vanadium(II)- and Vanadium(III)-guaiacolato Complexes Related to Vanadium-based Systems for the Reduction of Nitrogen**

By *Carlo Floriani,* Marinella Mazzanti, Angiola Chiesi-Villa,* and *Carlo Guastini*

Vanadium(II) is a powerful reducing agent for a variety of substrates,[1,2] including dinitrogen.[2] In the latter case the reduction is promoted by the heterogeneous $V(OH)_2/Mg(OH)_2$ system[2a,c] or by the homogeneous vanadium(II)-

[*] Prof. Dr. C. Floriani, Dr. M. Mazzanti
I.C.M.A., Université de Lausanne,
CH-1005 Lausanne (Switzerland)
Dr. A. Chiesi-Villa, Dr. C. Guastini
Istituto di Strutturistica Chimica,
Centro di Studio per la Strutturistica Diffrattometrica del CNR,
Università di Parma, I-43100 Parma (Italy)

[**] This work was supported by the Fonds National Suisse de la Recherche Scientifique (S. N. F. 2.131-0.86).

pyrocatechol system.[2b,c] These findings suggest that vanadium(II) in a coordination sphere provided by oxygen donor atoms, and with an undefined molecular complexity may be the required active species.[2c] Any hypothesis at the molecular level, however, is prevented by the paucity of our knowledge concerning the coordination chemistry of vanadium(II) in environments like those mentioned above,[3] information being available only on organometallic derivatives containing a very different class of ligands.[4] So far only a few and very diversified vanadium(II) coordination compounds have been studied.[5]

In the search for unconventional model compounds for dinitrogen activation, we focused our attention on vanadium(II)-vanadium(III) complexes containing only oxygen donor atoms, and with a ligand which can, somehow, modulate the redox potential of the metal. We report here our findings on guaiacolatovanadium(II)/vanadium(III) systems.

Upon reaction of a solution of sodium guaiacolate (NaG) with $VCl_3(thf)_3$ in THF we obtained, depending on the ligand/metal ratio, the complexes **1** or **2**. Reaction (a) was carried out at $-60°C$. After warming the suspension to room temperature, the volatile components were removed by evaporation. The residue dissolved in toluene gave, after removal of NaCl and addition of *n*-hexane, red-brown crystals of **1** (ca. 65%). Reaction (b) was carried out at room temperature. The complex **2** crystallized as violet crystals from the THF solution (ca. 57%).

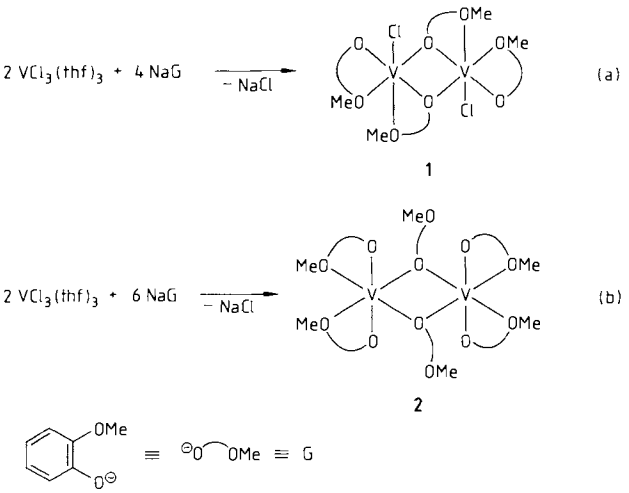

Complexes **1** and **2** are air-sensitive. They have magnetic moments of 2.73 BM and 2.53 BM respectively at 292 K, corresponding to a d^2 high-spin configuration. The magnetic moment of **2**, thus lying lower than the spin-only value, would seem to suggest some coupling between the two vanadium(III) centers. The structures of **1** and **2**[6] have been elucidated by X-ray analyses, but details will be given only for **1** (Fig. 1), which crystallizes with two molecules of toluene.[7]

1 is a centrosymmetric dimer, in which each vanadium exhibits a pseudooctahedral coordination involving a chlorine atom and the oxygen atoms from two guaiacolato anions behaving as chelating ligands. One of the two guaiacolato ions bridges an adjacent centrosymmetric vanadium through the O11 oxygen atom. The distortion of the octa-

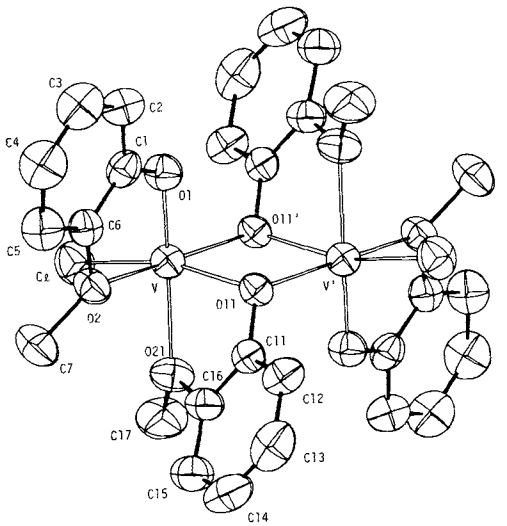

Fig. 1. Crystal structure of the complex **1** (without toluene) (ORTEP). Important bond distances [Å] and angles [°]: V-Cl 2.347(2), V-O1 1.884(5), V-O2 2.133(5), V-O11 2.027(4), V-O11' 2.078(5), V-O21 2.195(6); O1-V-O2 81.5(2), O11-V-O21 75.9(2), O11-V-O11' 77.6(2), O2-V-O11' 169.4(2), O2-V-O11 93.8(2), O1-V-O21 163.4(2), O1-V-O11 94.8(2), Cl-V-O11' 97.7(1), Cl-V-O11 161.0(2), Cl-V-O2 92.5(2), V-O11-V' 102.4(2). Prime indicates a transformation of $-x, -y, -z$.

hedron is mainly due to the bite of the organic ligand [O1-V-O2 81.5(2); O11-V-O21 75.9(2)°] as well as to the bridging mode [O11-V-O11' 77.6(2)°]. The V-O distances range from 1.884(5) to 2.195(6) Å, probably as a consequence of intraligand steric interactions. They are significantly different from those observed in the analogous vanadium(III) complex $[K_3\{V(cat)_3\}]$ [cat ≡ catecholato dianion] ranging from 1.984(1) to 2.036(1) Å.[6] An additional remarkable difference is that **1** is dimeric and $[K_3\{V(cat)_3\}]$ is monomeric. The V-Cl bond length is unexceptional.[8] The two organic ligands are essentially planar, in spite of some distortions in the case of the bridging ligand. However, the five-membered metal-chelate rings assume an envelope conformation, vanadium lying at 0.176(1) and 0.823(2) Å from the planes through O1, C1, C6, O2 and O11, C11, C16, O21, respectively. The V···V separation [3.200(2) Å] rules out any metal-metal interaction. Complex **1** is especially worthy of attention, because of the presence of two potentially reducible and functionalizable vanadium(III) centers.

Compounds **1** and **2** behave in the same way upon reaction with sodium sand, giving the dinuclear vanadium(II) complex **3**. Reduction of **2** was carried out in THF at room temperature, and complex **3** was obtained, after re-

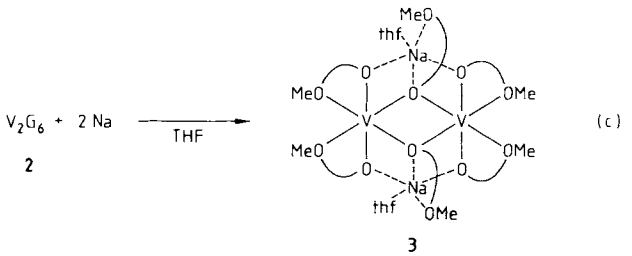

crystallization, as green crystals (ca. 51%). Reduction of **1** leads to formation of a second vanadium complex which has not yet been identified.

 © VCH Verlagsgesellschaft mbH, D-6940 Weinheim, 1988 0570-0833/88/0404-0577 $ 02.50/0

The complex **3** has a magnetic moment significantly lower than expected for a d^3-high spin complex [$\mu = 3.11$ BM at 292 K]; the two bridging oxygens lead to an antiferromagnetic coupling between the two vanadium atoms. The structure of **3** was determined by an X-ray analysis.[9] Figure 2 shows the coordination sphere of the metal ions.

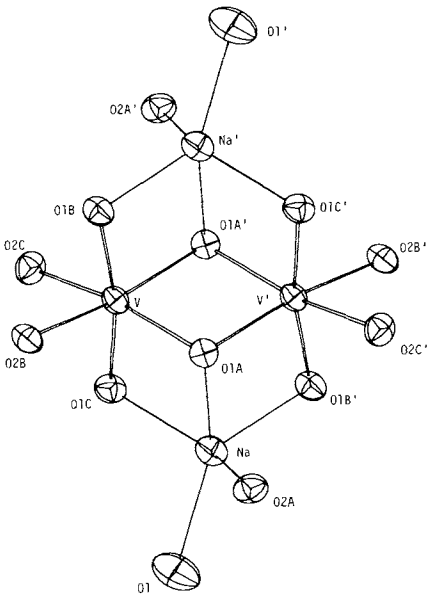

Fig. 2. An ORTEP drawing of the coordination sphere of the metal ions of complex **3**. O1A and O2A, O1B and O2B, and O1C and O2C belong to the guaiacolato ligands A, B and C. Oxygen bearing the methyl group in the guaiacolato ligand is labeled as O2; O1 is the oxygen atom from THF. Important bond distances [Å] and angles [°]: V-O1A 2.104(3), V-O1A' 2.149(4), V-O1B 2.094(5), V-O2B 2.170(5), V-O1C 2.083(4), V-O2C 2.201(4), Na-O1A 2.412(5), Na-O2A 2.393(5), Na-O1B' 2.243(5), Na-O1C 2.251(5), Na-O1 2.371(5); O1B-V-O2B 76.9(2), O1C-V-O2C 76.1(2), O1B-V-O1C 168.9(2), V-O1A-V' 98.2(1). Prime indicates a transformation of $-x, -y, 1-z$.

3 is a centrosymmetric dimer; each vanadium atom is surrounded by three guaiacolato anions (A, B, C) in a pseudo-octahedral environment. The ions B and C act as chelating ligands toward vanadium, while the ion A forms a chelate complex with a sodium atom and, at the same time, bridges the two vanadium atoms through O1A. A very close relationship exists between the structures of **2** and **3**; the reduction in the oxidation state of vanadium and the coordination of $Na^{\oplus}$ affect the parameters of the coordination sphere of vanadium only. The coordination polyhedron around vanadium in **3** is distorted mainly as a consequence of the ligand bite. The V-O distances, ranging from 2.083(4) to 2.201(4) Å, are longer than those found in complexes **1** and **2**[6] as a result of stronger intraligand steric interactions. The Na-O distances vary from 2.243(5) to 2.412(5) Å and have the usual values. The guaiacolate ions B and C are essentially planar, while the anion A, which is greatly influenced by the coordination, shows more significant distortions from planarity, O1 and O2 being at $-0.095(5)$ and 0.043(5) Å from the plane of the aromatic ring. The five-membered chelating rings, like in complex **1**, assume an envelope conformation, the vanadium atoms lying at 0.161(1) and 0.279(2) Å from the planes through the other four atoms for B and C respectively. The sodium atom is displaced 0.239(3) Å from the O1A, C1A, C2A, O2A plane. The V···V separation [3.215(2) Å], like in complex **1**, rules out any metal-metal interaction.

Many characteristics of **3** are worthy of mentioning. It is quite a rare dinuclear vanadium(II) complex having oxygen as unique type of donor atoms. The structure contains both transition metal ions in a low oxidation state as well as a Lewis acid ($Na^{\oplus}$). Such a dianionic structure is a potential ligand for building polynuclear structures.—Studies on the redox properties of complexes **1**-**3** will certainly contribute to an understanding of dinitrogen activation by very similar V^{III}-V^{II} compounds.

Received: December 14, 1987 [Z 2540 IE]
German version: *Angew. Chem. 100* (1988) 587

[1] T. L. Ho, *Synthesis 1979*, 1; T. L. Ho, G. A. Olah, *ibid. 1977*, 170; T. A. Cooper, *J. Am. Chem. Soc. 95* (1973) 4158.

[2] a) A. E. Shilov, N. T. Denisov, O. N. Efimov, N. F. Shuvalov, N. I. Shuvalova, E. Shilova, *Nature (London) 231* (1971) 460; S. I. Zones, T. M. Vickery, J. G. Palmer, G. N. Schrauzer, *J. Am. Chem. Soc. 98* (1976) 1289; G. N. Schrauzer, N. Strampach, L. A. Hughes, *Inorg. Chem. 21* (1982) 2184; S. I. Zones, M. R. Palmer, J. G. Palmer, J. M. Doemeny, G. N. Schrauzer, *J. Am. Chem. Soc. 100* (1978) 2113; b) S. A. Isaeva, L. A. Nikonova, *Izv. Akad Nauk. SSSR 1977*, 1968; N. P. Luneva, L. A. Nikonova, A. E. Shilov, *Kinet. Katal. 18* (1977) 254; *21* (1980) 1041; N. P. Luneva, A. P. Moravsky, A. E. Shilov, *Nouv. J. Chim. 6* (1982) 245; G. N. Schrauzer, M. R. Palmer, *J. Am. Chem. Soc. 103* (1981) 2659; c) R. A. Henderson, G. J. Leigh, C. J. Pickett, *Adv. Inorg. Chem. Radiochem. 27* (1983) 197.

[3] F. A. Cotton, S. A. Duraj, L. E. Manzer, W. J. Roth, *J. Am. Chem. Soc. 107* (1985) 3850.

[4] N. G. Connelly in G. Wilkinson, F. G. A. Stone, E. W. Abel (Eds.): *Comprehensive Organometallic Chemistry, Vol. 3*, Pergamon, Oxford 1982, pp. 656-663.

[5] F. A. Cotton, S. A. Duraj, W. J. Roth, *Inorg. Chem. 24* (1985) 913; P. D. Smith, J. L. Martin, J. C. Huffman, R. L. Bansemer, K. G. Caulton, *ibid. 24* (1985) 2997; R. J. Bouma, J. H. Teuben, W. R. Beukema, R. L. Bansemer, J. C. Huffman, K. G. Caulton, *ibid. 23* (1984) 2715; H. Oumus, C. Lecompte, J. Protas, J. L. Poncet, J. M. Barbe, R. Guilard, *J. Chem. Soc. Dalton Trans. 1984*, 2677; P. Dapporto, F. Mani, C. Mealli, *Inorg. Chem. 17* (1978) 1323; F. A. Cotton, G. E. Lewis, G. N. Mott, *ibid. 22* (1983) 560.

[6] S. R. Cooper, Y. B. Koh, K. N. Raymond, *J. Am. Chem. Soc. 104* (1982) 5092.

[7] **1**, $C_{28}H_{28}Cl_2O_8V_2 \cdot 2C_7H_8$, $M = 849.6$, monoclinic, space group $P2_1/c$, $a = 9.956(2)$, $b = 21.426(3)$, $c = 9.878(2)$ Å, $\beta = 92.86(1)$, $V = 2104.5(7)$ Å^3, $Z = 2$, $\rho_{calcd.} = 1.341$ g cm^{-3}, $Cu_{K\alpha}$ radiation ($\lambda = 1.5418$ Å), $\mu(Cu_{K\alpha}) = 53.6$ cm^{-1}: crystal dimensions $0.32 \times 0.48 \times 0.55$ mm. The structure was solved by the heavy atom method (Patterson and Fourier synthesis) and refined by full-matrix least-squares. For 1901 unique observed structure amplitudes [$I > 2\sigma(I)$, corrected for absorption] collected at room temperature on a Siemens AED diffractometer in the range $7 < 2\theta < 130°$ the R value is 0.072 ($R_w = 0.077$). Most of the hydrogen atoms were located in a difference Fourier map and introduced as fixed contributors in the final stage of refinement [10].

[8] M. Mazzanti, C. Floriani, A. Chiesi-Villa, C. Guastini, *Inorg. Chem. 25* (1986) 4158, and references cited therein.

[9] **2**, $C_{50}H_{58}Na_2O_{14}V_2$, $M = 1030.9$, triclinic, space group $P\bar{1}$, $a = 10.757(2)$, $b = 12.793(2)$, $c = 10.463(2)$ Å, $\alpha = 100.55(3)$, $\beta = 103.87(2)$, $\gamma = 68.08(3)$, $V = 1289.8(5)$ Å^3, $Z = 1$, $\rho_{calcd} = 1.327$ g cm^{-3}, $Mo_{K\alpha}$ radiation ($\lambda = 0.71069$ Å), $\mu(Mo_{K\alpha}) = 3.94$ cm^{-1}: crystal dimensions $0.19 \times 0.42 \times 0.43$ mm. The structure was solved by the heavy atom method (Patterson and Fourier synthesis) and refined by full-matrix least-squares. For 2007 unique observed structure amplitudes [$I > 3\sigma(I)$] collected at room temperature on a Philips PW 1100 diffractometer in the range $6° < 2\theta < 47°$ the R value is 0.050 ($R_w = 0.051$). Most of the hydrogen atoms were located in a difference Fourier map and introduced as fixed contributors in the final stage of refinement. All calculations were carried out using SHELX 76 [10].

[10] Further details of the crystal structure investigations are available from the Director of the Cambridge Crystallographic Data Centre, University Chemical Laboratory, Lensfield Road, Cambridge CB2 1EW (England) on quoting the full journal citation.

Stable Sandwich Complexes with Pentamethylpyrrole Ligands**

By *Norbert Kuhn,* Eva-Maria Horn, Edgar Zauder, Dieter Bläser,* and *Roland Boese*

Very few transition metal complexes of pyrrole are known,[1] and of these, owing to the poor stability of the pyrrole-metal bond, only $[(C_4H_4NMe)Cr(CO)_3]$ has been adequately characterized.[1c,d] The replacement of hydrogen atoms by methyl groups, a strategy which has proven useful for the stabilization of cyclopentadienylmetal complexes,[2] has also been found to be effective in the case of pyrrole coordination. In contrast to the less adequately characterized analogous complex of *N*-methylpyrrole,[1a,b] the complex **3**[5] obtainable by reaction of the sulfane complex **1**[3] with pentamethylpyrrole **2**[4] is stable both in solution and in the solid state up to 80°C.

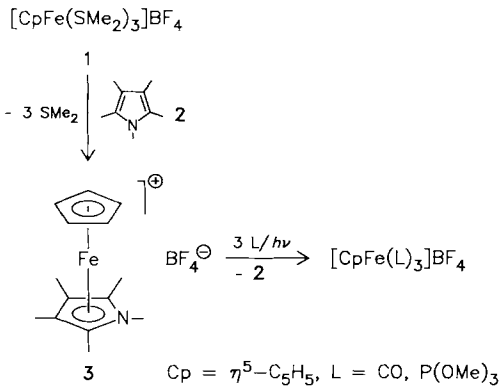

The structure of the cation of **3** in the crystalline state (Fig. 1) reveals its metallocene character;[6] the angle between the "mean" planes of the ring ligands is 3.4°. The pyrrole ring is folded about the C1-N3 axis (angle of fold 12.3°), the cyclopentadienyl ring about the C13-C15 axis (angle of fold 14.5°). The carbon atom C2 is oriented toward the iron atom, while the carbon atom C14 diagonally opposite to C2 is oriented away from the iron atom. The perpendicular from the coordination center to the mean plane of the pyrrole ring forms an angle of only 1.1° with a line joining the iron atom and the geometrical midpoint of the pyrrole ring; i.e. no significant ligand shift is observed. The methyl group bound to the nitrogen atom is located at a distance of 0.31 Å from the ring plane in the direction away from the coordination center. The distances between the centers of the ring ligands and the central metal of 1.65 Å (Fe-C_5H_5) and 1.62 Å (Fe-C_4H_4NMe) are not exceptional.

The cation of **3** not only resembles the ferrocenes, but is also related to arene(cyclopentadienyl)iron cations.[7] The ^{13}C-chemical shift of the C_5H_5 ligand of **3** ($\delta = 76.01$) lies in the usual range (e.g. $\delta = 77.35$ for $[(C_5H_5)Fe(C_6Me_6)]^{\oplus}$[8]). The possible substitution of the pyrrole ligand in **3** by other neutral ligands (e.g. CO, $P(OMe)_3$) by photochemical excitation also correlates with the reaction behavior of the arene complexes.[9]

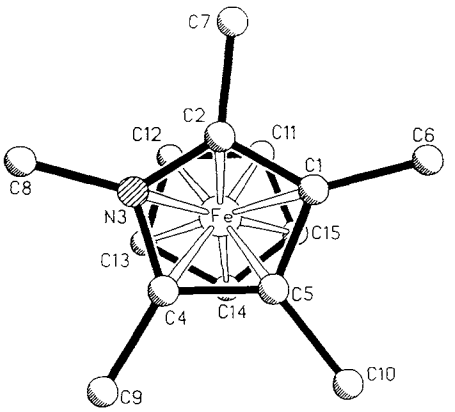

Fig. 1. Crystal structure of **3** (hydrogen atoms omitted). Selected bond lengths [Å] and angles [°]: C1-C2 1.40(1), C1-C5 1.41(3), C2-N3 1.34(2), N3-C4 1.36(3), C4-C5 1.42(3), Fe-C1 2.09(1), Fe-C2 1.88(2), Fe-N3 2.04(2), Fe-C4 2.03(1), Fe-C5 1.96(2), Fe-C11 2.07(1), Fe-C12 2.01(1), Fe-C13 1.94(3), Fe-C14 2.09(1), Fe-C15 2.04(4), Fe-Cp center 1.65, Fe-C_4N center 1.62, $\bar{d}$(C-C(Cp)) 1.40; Cp-center-Fe-C_4N-center 179; the mean torsion angle C(n)-C_4N-center-Cp-center-C(n+10) is 39°.

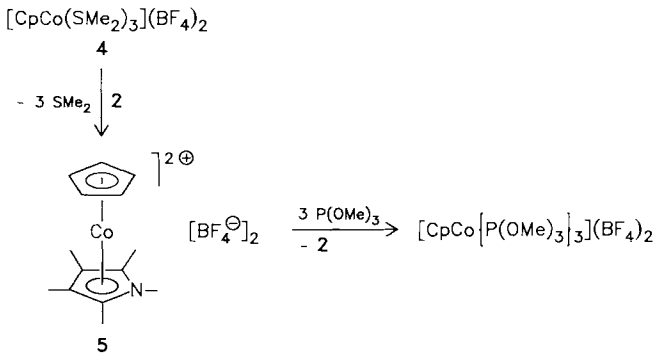

The cobalt complex **5** isoelectronic with **3** is obtained analogously from the sulfane complex **4**.[10,11] **5** is storable for several weeks in nitromethane, but reacts rapidly with trimethyl phosphite with cleavage of the pyrrole ligand to give the $[C_5H_5Co\{P(OMe)_3\}_3]^{2\oplus}$ ion; here also the relationship with the corresponding arene complexes is clearly recognizable on comparing the ^{13}C-NMR data ($\delta(C_5H_5) = 93.27$ (**5**) and 96.8 $[(C_5H_5)Co(C_6Me_6)]^{2\oplus}$[12]).

Received: November 23, 1987;
revised: December 29, 1987 [Z 2508 IE]
German version: *Angew. Chem. 100* (1988) 572

[*] Prof. Dr. N. Kuhn, Dipl.-Chem. E.-M. Horn, Dipl.-Chem. E. Zauder
Fachbereich 6 (Chemie) der Universität-Gesamthochschule
Lotharstr. 1, D-4100 Duisburg 1 (FRG)
Dipl.-Ing. D. Bläser, Dr. R. Boese
Institut für Anorganische Chemie der Universität-Gesamthochschule
Universitätsstr. 5-7, D-4300 Essen 1 (FRG)

[**] This work was supported by the Fonds der Chemischen Industrie. We thank Prof. Dr. *P. Sartori*, Duisburg (FRG) for friendly advice and encouragement.

[1] a) K. K. Joshi, P. L. Pauson, A. R. Quazi, W. H. Stubbs, *J. Organomet. Chem. 1* (1964) 471; b) F. Seel, V. Sperber, *ibid. 14* (1968) 405; c) K. Öfele, E. Dotzauer, *ibid. 30* (1971) 211; d) G. Huttner, O. S. Mills, *Chem. Ber. 105* (1972) 301.

[2] R. B. King, *Coord. Chem. Rev. 20* (1976) 155; P. T. Wolczanski, J. E. Bercaw, *Acc. Chem. Res. 13* (1980) 121.

[3] N. Kuhn, H. Schumann, M. Winter, E. Zauder, *Chem. Ber. 121* (1988) 111.

[4] H. Hart, A. Teuerstein, *Synthesis 1979*, 693.

[5] *Procedure:* A mixture of **1** (0.79 g, 2 mmol), **2** (0.27 g, 2 mmol) and dichloromethane (20 mL) was stirred for 5 min, filtered, and the residue recrystallized from ether with dichloromethane/ether. Yield 0.59 g of **3** (86%), orange-yellow crystals.—^{1}H-NMR (60 MHz, [D$_3$]nitromethane, TMS int.): $\delta = 4.50$ (s, 5H; C_5H_5), 3.41 (s, 3H; N-CH_3), 2.53 (s, 6H; C(2,5)-CH_3), 2.15 (s, 6H; C(3,4)-CH_3). ^{13}C-NMR (75.43 MHz, [D$_6$]ace-

tone, TMS int.): δ=95.21 (C-2,5), 87.53 (C-3,4), 76.01 (C_5H_5), 35.73 (N–CH_3), 10.55 (C(2,5)–CH_3), 9.91 (C(3,4)–CH_3).

[6] **3**: orthorhombic, $Pna2_1$, a=14.978(4), b=7.354(1), c=14.511(4) Å, Z=4, ρ_{calc}=1.4337 g cm^{-3}, $Mo_{K\alpha}$ radiation, scan range $3° \le 2\theta \le 40°$, independent reflections, 1415 observed ($F_0 \ge 4\sigma(F_0)$), R=0.0516, R_w=0.0510. The $BF_4^\ominus$ ion is disordered, and analysis of the "anisotropic temperature parameters" indicates a disorder of the Cp ring and of the pyrrole ring about the C_5 of the cation, similarly as has been observed in the case of ferrocene [13]. Further details of the crystal structure investigation are available on request from the Fachinformationszentrum Energie, Physik, Mathematik GmbH, D-7514 Eggenstein-Leopoldshafen 2 (FRG), on quoting the depository number CSD-52859, the names of the authors, and the journal citation.

[7] H. Schumann, *Chem.-Ztg. 108* (1984) 239, 345; R. G. Sutherland, M. Iqubal, A. Piorko, *J. Organomet. Chem. 302* (1986) 307.

[8] B. R. Steele, R. G. Sutherland, Choi Chuk Lee, *J. Chem. Soc. Dalton Trans. 1981*, 529.

[9] Cf., e.g., T. P. Gill, R. K. Mann, *Inorg. Chem. 22* (1983) 1986.

[10] N. Kuhn, H. Brüggemann, M. Winter, V. M. de Bellis, *J. Organomet. Chem. 320* (1987) 391.

[11] Procedure: A mixture of **4** (2.25 g, 4.65 mmol), **2** (1.28 g, 9.3 mmol), and 1,2-dichloroethane (10 mL) was heated to boiling for 16 h, filtered, and the recovered precipitate purified by recrystallization from nitromethane/ether. Yield 1.73 g of **5** (86%), yellow crystals.—^{1}H-NMR (60 MHz, [D_3]nitromethane, TMS int.): δ=6.23 (s, 5H; C_5H_5), 3.87 (s, 3H; N–CH_3), 2.82 (s, 6H; C(2,5)–CH_3), 2.40 (s, 6H; C(3,4)–CH_3). ^{13}C-NMR (75.43 MHz, [D_3]nitromethane, TMS int.): δ=114.67 (C-2,5), 105.06 (C-3,4), 93.27 (C_5H_5), 38.21 (N–CH_3), 10.91 (C(2,5)–CH_3), 10.04 (C(3,4)–CH_3).

[12] G. Fairhurst, C. White, *J. Chem. Soc. Dalton Trans. 1979*, 1531.

[13] P. Seiler, J. D. Dunitz, *Acta Crystallogr. B35* (1979) 1068, 2020.

Cu^{II} and Cu^{I} Coordination Chemistry of a Novel *O,O,Cl*-Chelate Ligand. Formation of a Stable Carbonylcopper Complex**

By *Wolfgang Kläui** and *Elke Buchholz*

We have already reported in detail on the coordination chemistry of the anionic tridentate ligand $[CpCo\{P(O)(OEt)_2\}_3]^\ominus$.[1a] The complex anion $[(C_6Me_6)RuCl\{P(O)(OMe)_2\}_2]^\ominus$ $[1\text{-}H]^\ominus$, which is accessible via a Michaelis-Arbuzov-type reaction of the trimethyl phosphite complex $[(C_6Me_6)RuCl\{P(OMe)_3\}_2]^\oplus$ with iodide leading to cleavage of iodomethane, also behaves as a chelate ligand toward metal ions.[1b] However, in contrast to the tripodal ligands it can react as a bidentate *O,O*- or tridentate *O,O,Cl*-ligand, depending on the steric and electronic requirements. Noteworthy is its tendency to react with alkali metal salts to give adducts which are readily soluble in apolar solvents. This property, which it shares with other *O,O,X*-chelate ligands of analogous structure, frequently makes its synthesis in pure form difficult.[2] We therefore searched for an alternative synthetic route and have now found a facile entry to $[(C_6Me_6)RuCl\{P(O)(OMe)_2\}\{P(OH)(OMe)_2\}]$ **1**, the protonated form of this *O,O,Cl*-ligand.

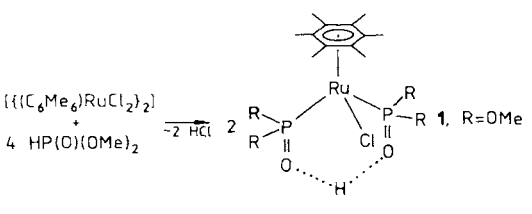

For the reaction of $[\{(C_6Me_6)RuCl_2\}_2]$ with dimethyl phosphite to give **1** it is decisively important to provide an additional driving force in the form of chloride-ion solvation by a good solvating solvent such as methanol. In chloroform, the reaction stops at the stage of $[(C_6Me_6)RuCl_2\{P(OH)(OMe)_2\}]$.

1 is stable toward air and is readily soluble in chlorinated hydrocarbons and THF but only sparingly soluble in diethyl ether, pentane, and water. For use as chelate ligand, **1** can be converted directly into bis(ligand)metal complexes, e.g. with aqueous solutions of metal(II) acetates. For reactions with organometallic compounds that are sensitive to hydrolysis, **1** can be first converted into **2**. This is achieved by reaction with solid potassium hydride in dichloromethane, which leads to evolution of hydrogen.

$K[(C_6Me_6)RuCl\{P(O)(OMe)_2\}_2]$ **2**[3]

2 is readily soluble in dichloromethane. In investigations of the coordination chemistry of copper(I) compounds we have surprisingly found that the bis(ligand)copper(II) complex **3** reacts with copper powder in methanol to give the carbonylcopper complex **4** on introduction of CO.

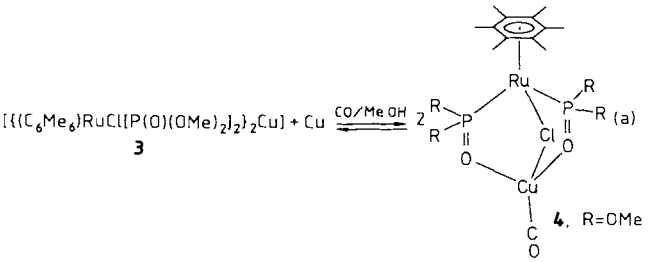

The comproportionation equilibrium (a) is established within a few hours at room temperature, and at 1 atm CO it lies completely on the right-hand side. It is astonishing how rapidly the carbonyl complex **4** is formed, for the copper(II) complex **3** is almost completely insoluble in methanol. The comproportionation takes place significantly more slowly, however, even in dichloromethane. The carbonyl complex **4** is remarkably stable compared to [Cu(CO)Cl] or $[Cu(CO)Cl(H_2O)_2]$.[4] No loss of CO was observed after 1 hours' drying under high vacuum at room temperature.

However, on exposure to air, **4** decomposes with formation of a green compound whose composition is still unknown. **4** reacts immediately with PMe_3 and PPh_3 with extrusion of the CO-ligand. The products that are formed are also sensitive to oxidation. The ν(CO) frequency in the IR spectrum of **4** (2089 cm^{-1} in methanol) is as low as that of the solvent complexes of [Cu(CO)Cl] in methanol and THF.[5] Apparently, the *O,O,Cl*-ligand $[(C_6Me_6)RuCl\{P(O)(OMe)_2\}_2]^\ominus$ $[1\text{-}H]^\ominus$ creates an electronic environment which resembles that in the above mentioned solvent complexes. The high thermal stability of **4**, which is attributed to the chelate effect, is surprising when one considers that the methanol and THF solvent complexes lose CO on isolation, even under a CO atmosphere at 0 °C.[5] The readiness with which the carbonylcopper complex **4** is formed, and its stability, suggest an interesting synthetic potential for this ligand in organometallic chemistry.

[*] Prof. Dr. W. Kläui, E. Buchholz
Institut für Anorganische Chemie der Technischen Hochschule Templergraben 55, D-5100 Aachen (FRG)

[**] This work was supported by the Minister für Wissenschaft und Forschung des Landes Nordrhein-Westfalen (FRG), by the Fonds der Chemischen Industrie, and by Heraeus (gifts of chemicals). We thank Mr. *P. Dharmawan* for valuable assistance with the experiments.

Experimental

1: A mixture of $[\{(C_6Me_6)RuCl_2\}_2]$ (6.60 g, 9.87 mmol) and dimethyl phosphite (40 mL) in methanol (500 mL) was heated under reflux with stirring for 4 d until the initially red solution had turned yellow in color. On subsequent evaporation of the solution under high vacuum a yellow precipitate separated out, which after addition of 100 mL of dichloromethane went into solution again. The solution thus obtained was extracted with 6 × 15 mL of water to remove hydrochloric acid and any unchanged dimethyl phosphite. On removal of the solvent the product precipitated out as a yellow powder. Yield 9.75 g (95%). Recrystallization from dichloromethane/hexane afforded fine yellow crystals. ^{1}H-NMR (80 MHz, $CDCl_3$): $\delta = 2.1$ (t, $^4J(PRuCCH) = 0.9$ Hz, 18 H; CCH_3), 3.59 (virt. t, $^3J(POCH) = 11.1$ Hz, 6 H; OCH_3), 3.72 (virt. t, $^3J(POCH) = 10.3$ Hz, 6 H; OCH_3), 12.7 (br. s, 1 H; PO–H).

3: A suspension of 1.50 g (2.9 mmol) of **1** in 20 mL of water was treated with 570 mg (2.9 mmol) of $Cu(OAc)_2 \cdot H_2O$ and the resulting mixture stirred for 4 h. The product was centrifuged off, washed twice with a small amount of water and dried under high vacuum. Yield 1.49 g (94%). After recrystallization from dichloromethane/pentane, analytically pure yellow crystals were obtained.

4: A mixture of **3** (150 mg, 0.14 mmol) and copper powder (200 mg, 3.15 mmol) in 15 mL of methanol was stirred under a CO-atmosphere until the copper(II) complex had completely dissolved (ca. 3 h). The yellow solution was separated from the excess metal under a CO atmosphere and then evaporated to dryness. The yellow solid product was dried for 1 h under high vacuum. Yield 135 mg (81%). IR (CH_3OH): 2089 cm^{-1} (s, ν(CO)). **4** is readily soluble in methanol and dichloromethane and insoluble in saturated hydrocarbons. It decomposes on exposure to air, rapidly in methanol, but more slowly in dichloromethane and in the solid state.

Received: November 19, 1987 [Z 2504 IE]
German version: *Angew. Chem. 100* (1988) 603

[1] a) W. Kläui, A. Müller, W. Eberspach, R. Boese, I. Goldberg, *J. Am. Chem. Soc. 109* (1987) 164, and references cited therein; b) W. Kläui, E. Buchholz, unpublished.

[2] We have found such adducts of NaI and $NaPF_6$ with $Na[(C_6Me_6)RuCl\{P(O)(OMe)_2\}_2]$ and analogous compounds, e.g. $Na[(C_5Me_5)CoI\{P(O)(OMe)_2\}_2]$ and $Na[(C_6H_6)RuI_2\{P(O)(OMe)_2\}]$. See also the structure determination of $Na[(C_6H_6)OsI\{P(O)(OMe)_2\}_2]$, which crystallizes in a disordered fashion with one equivalent of NaI: U. Schubert, R. Werner, L. Zinner, H. Werner, *J. Organomet. Chem. 253* (1983) 363.

[3] **2**: ^{1}H-NMR (80 MHz, $CDCl_3$): $\delta = 2.0$ (t, $^4J(PRuCCH) = 0.8$ Hz, 18 H; CCH_3), 3.48 (virt. t, $^3J(POCH) = 10.5$ Hz, 6 H; OCH_3), 3.50 (virt. t, $^3J(POCH) = 10.1$ Hz, 6 H; OCH_3).

[4] M. I. Bruce, *J. Organomet. Chem. 44* (1972) 209, and references cited therein.

[5] M. Pasquali, C. Floriani, A. Gaetani-Manfredotti, *Inorg. Chem. 20* (1981) 3382. A value of 2120 cm^{-1} is quoted for the ν(CO) frequency of solvent-free [Cu(CO)Cl] in Nujol.

Diastereo- and Enantioselective Aldol Reactions via α-Silyl Ketones, Asymmetric Synthesis of the Aggregation Pheromone Sitophilure**

By *Dieter Enders** and *Braj Bhushan Lohray*

Dedicated to Professor Helmut Dörfel on the occasion of his 60th birthday

Diastereo- and enantioselective aldol reactions have been the subject of intensive study in recent years.[1] Whereas excellent diastereo- and enantioselectivities have been achieved with aldol-like processes that lead to hydroxycarboxylic acids and their derivatives,[2] direct aldol syntheses of β-hydroxyketones are less widely developed and, in part still unsatisfactory with regard to enantiomeric excesses.[3] We recently reported on a facile entry to highly enantiomerically pure α-trialkylsilyl ketones and α-trialkylsilylaldehydes.[4] We have now found that α-silyl ketones of type **1** can be employed as chiral methylene compounds in aldol reactions and enable the stereoselective synthesis of *syn*-configurated β-hydroxyketones **4** in high diastereomeric and enantiomeric excesses.

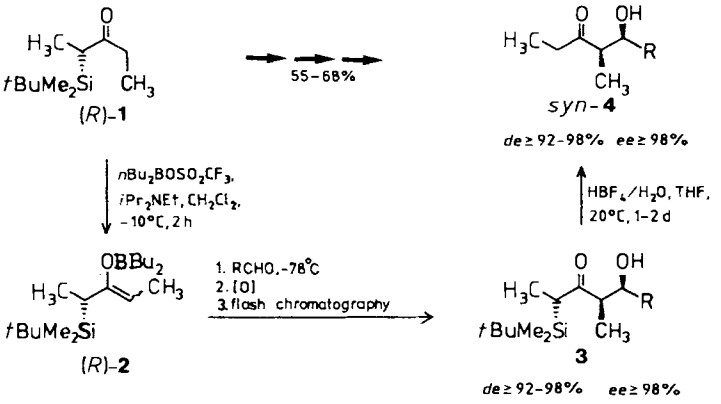

For example, (*R*)-2-(*tert*-butyldimethylsilyl)pentan-3-one, (*R*)-**1**, was converted by reaction with di-*n*-butylboryl triflate in dichloromethane in the presence of Hünig base into the boron enolate (*R*)-**2** and then allowed to react with aldehydes at −78 °C. Subsequent oxidative work-up[5] and flash chromatography furnished the *syn*-aldol adducts **3**, which could be desilylated with 60% aqueous tetrafluoroboric acid in THF to the *syn*-aldol products **4** with high diastereomeric (*de*: 92 to ≥98%) and enantiomeric purity (*ee* ≥ 98%) (Table 1).

Table 1. β-Hydroxy ketones *syn*-**4** prepared by diastereo- and enantioselective aldol reaction with (*R*)- or (*S*)-**1**.

syn-4	R	Total yield [%]	$[\alpha]_D^{22}$ [°] (*c*, solvent)	*de* [%] [a]	*ee* [%] [b]	Configuration [c]
4a	CH_3	55	−30.0 [d] (1.4, ether)	≥98	≥98	(4*R*,5*S*)
4b	C_2H_5	62	−28.0 [e] (1.2, ether)	96	≥98	(4*R*,5*S*)
4b [f]	C_2H_5	58	+26.4 (1.0, ether)	≥98	≥98	(4*S*,5*R*)
4c	i-C_3H_7	62	+33.95 [g] (0.94, $CHCl_3$)	≥98	≥98	(4*R*,5*S*)
4d	$C_6H_5(CH_2)_2$	55	−37.6 (1.0, ether)	92	≥98	(4*R*,5*S*)
4e	C_6H_5	68	−16.0 (1.3, benzene)	≥98	≥98	(4*S*,5*S*) [h]

[a] Determined ^{13}C- and ^{19}F-NMR spectroscopically via the corresponding (*S*)-MTPA ester [7] (MTPA = Ph–C(OCH_3)(CF_3)–CO_2H). [b] Determined as in [a] and also ^{1}H-NMR spectroscopically with Eu(hfc)$_3$ as well as polarimetrically by comparison with literature data [9, 10, 3 h]. [c] Assignment based on a comparison with data in the literature [9, 10, 3 h]. [d] In [9]: $[\alpha]_D^{21} = -30.2$ (c = 1.43, ether). [e] Contaminated with 2% anti-isomer (4*S*,5*S*)-**4b**; in [10]: $[\alpha]_D^{20} = -26.7$ (*c* = 1.52, ether). [f] (*S*)-**1** was used as chiral methylene component. [g] −2.14 (*c* = 1.0, ether); (4*S*,5*R*)-**4c** [3 h]: $[\alpha]_D^{20} = -23.2$ (*c* = 1.8, $CHCl_3$) corresponding to 66% *ee*; the change in sense of rotation on changing the solvent from ether to chloroform is typical for the aldol adducts *syn*-**4**; we thank Dr. *I. Paterson*, Cambridge, for helpful discussions. [h] Confirmed by X-ray structure analysis of the corresponding SAMP-hydrazone [3d, 11].

The simple diastereoselectivity of the aldol C–C coupling can be determined ^{1}H- and ^{13}C-NMR spectroscopically at the stage of the crude adducts **3**. The *syn* : *anti* ratio is ca. 9 : 1, irrespective of the aldehyde employed. From this and from the ^{13}C-NMR spectroscopic and gas-chro-

[*] Prof. Dr. D. Enders, Dr. B. Bhushan Lohray
Institut für Organische Chemie der Technischen Hochschule
Professor-Pirlet-Strasse 1, D-5100 Aachen (FRG)

[**] This work was supported by the Fonds der Chemischen Industrie and by BASF AG, DEGUSSA AG, Bayer AG, and Wacker Chemie GmbH.

matographic monitoring of (*R*)-**2** after conversion into the corresponding trimethylsilyl enol ether[5,6] we derive a *Z*:*E* ratio of ca. 9:1 in the case of (*R*)-**2**. The high enantiomeric purity ($ee \geq 98\%$) of the *syn* adducts **3** and **4** was determined NMR spectroscopically via the corresponding (*S*)-MTPA ester[7] (^{13}C,^{19}F) and by shift experiments [with Eu(hfc)$_3$], as well as polarimetrically (**4**). The agreement in the *de* and *ee* values provides proof of an epimerization-free and racemization-free desilylation. The absolute configurations of the β-hydroxy ketones **4** quoted in Table 1 are based on a comparison of the polarimetric data with data in the literature. As expected, the use of the (*S*)-configurated methylene components (*S*)-**1** leads to the other *syn*-enantiomer (**4b**, Table 1).[8]

The stereochemistry of the diastereo- and enantioselective C–C coupling is consistent with a six-membered transition state in the sense of the Zimmermann-Traxler model.[12] In the case of **4a** and **4b**, the chromatographically separated *anti*-isomers that are formed in small amounts could each be assigned the (4*S*,5*S*)-configuration ($ee \geq 98\%$) on the basis of the ^{13}C-NMR spectra.[11] Accordingly, in the case of aliphatic aldehydes the transition state T_Z leads to the *syn* isomers with (4*R*,5*S*)-configuration, and T_E to the *anti* isomers with (4*S*,5*S*)-configuration.[13] An exception is the benzaldehyde adduct **4e**, which according to an X-ray structure analysis[3d,11] of the corresponding SAMP-hydrazone has the enantiomeric (4*S*,5*S*)-configuration based on T_Z/T_E.[14] The correlation between the *Z*/*E* ratio of the boron enolate and the *syn*/*anti* ratio of **4** (in each case 9:1) indicates a *virtually complete asymmetric induction*.

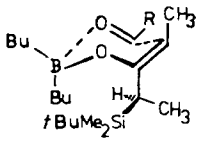

T_Z ⟶ (4*R*,5*S*)-**4** (*syn*)

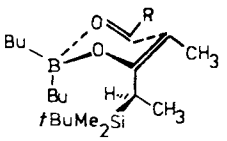

T_E ⟶ (4*S*,5*S*)-**4** (*anti*)

Rice weevils (*Sitophilus oryzae L.*) and maize weevils (*S. zeamis Motsch*) cause some hundreds of millions of dollars worth of damage per annum in the storage of grain. The aggregation-promoting pheromone of these insects was recently identified as *syn*-5-hydroxy-4-methylheptan-3-one (**4b**) (sitophilure) and has been synthesized; its absolute configuration is still unknown.[15,10] Starting from (*R*)-**1** and (*S*)-**1**, we have prepared both enantiomers of sitophilure, (4*R*,5*S*)-**4b** and (4*S*,5*R*)-**4b**, in total yields of 58–62% and high diastereomeric and enantiomeric purity, respectively, thus demonstrating the preparative value of this new variant of the aldol reaction.

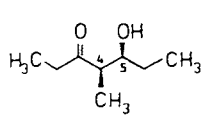

(4*R*,5*S*)-**4b**

$de \geq 96\%$, $ee \geq 98\%$

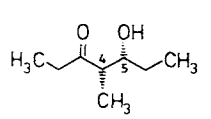

(4*S*,5*R*)-**4b**

$de \geq 98\%$, $ee \geq 98\%$

[*] Note added in proof: Another synthesis of this enantiomer has been reported recently: G. Fuganti, H. E. Höberg, G. Pedrocchi-Fantoni, S. Servi, *Chem. Lett. 1988*, 385.

Experimental

A stirred solution of 12 mmol of ethyl diisopropylamine in 25 mL of dichloromethane was treated under an argon atmosphere at −10°C with 11 mmol of di-*n*-butylboryl triflate **2b**, and then dropwise with a solution of 10 mmol of (*R*)-**1** in 10 mL of dichloromethane. After two hours' stirring at −10°C the reaction mixture, which now contained the boron enolate (*R*)-**2**, was cooled to −78°C and treated with 10 mmol of aldehyde (in the case of enolizable aldehydes: 12–15 mmol dissolved in 20–30 mL of dichloromethane). The mixture was stirred for a further 0.5 h at −78°C and 1 h at 0°C and then subjected as follows to oxidative work-up in analogy to the method used by *Evans* et al.[5], in the case of aromatic aldehydes with 30% H_2O_2 (without sodium hydrogencarbonate solution), in the case of enolizable aldehydes with MoO_5·pyridine·HMPA (MoOPH) [17]: the resulting di-*n*-butylalkoxyborane that was formed was oxidized by addition of 15 mmol of MoOPH at 0°C. The yellow reaction mixture was stirred for 0.5 h at 0°C and 1 h at room temperature and then treated with 100 mL of pH7-buffer solution. After 15 minutes' stirring, the organic phase was separated off and the aqueous phase extracted twice with dichloromethane. The combined organic phases were washed twice with 100 mL of ice-cold 0.5 N HCl and once with saturated NaCl solution, and dried over magnesium sulfate. Removal of the solvent afforded the crude aldol adducts **3** as a *syn*/*anti* mixture (ca. 9:1) which was separated by flash chromatography (silica gel, ether/*n*-pentane 1/4, $R_f(syn) > R_f(anti)$). A stirred solution of 10 mmol of pure *syn*-adduct **3** in 50 mL of THF was treated at room temperature with 10 mL of 60% tetrafluoroboric acid. After 1–2 days stirring the THF was removed and the residue extracted with 3 × 100 mL of ether. The combined ether phases were washed with 5% sodium hydrogencarbonate solution and dried over magnesium sulfate. Removal of the solvent and chromatographic purification (silica gel, ether/*n*-pentane 1/4) furnished *syn*-**4**.

Received: January 8, 1988 [Z 2565 IE]
German version: *Angew. Chem. 100* (1988) 594

CAS Registry numbers:
(R)-1, 107496-27-5; (S)-1, 107496-28-6; (R)-2, 113569-02-1; (S)-2, 113569-08-7; **3a**, 113569-03-2; **3b** (isomer 1), 113569-04-3; **3b**, (isomer 2), 113626-44; **3c**, 113569-05-4; **3d**, 113569-06-5; **3e**, 113569-07-6; **4a** 108161-63-3; **4b** (isomer 1), 108815-20-9; **4b** (isomer 2), 108815-23-2; **4c**, 113626-45-2; **4d**, 113626-46-3; **4e**, 107242-72-8; H_3CCHO, 75-07-0; C_2H_5CHO, 123-38-6; *i*-C_3H_7CHO, 78-84-2; $C_6H_5(CH_2)_2CHO$, 104-53-0; C_6H_5CHO, 100-52-7.

[1] Reviews: a) D. A. Evans, J. V. Nelson, T. R. Taber, *Top. Stereochem. 13* (1982) 1; b) T. Mukaiyama, *Org. React. (NY) 28* (1982) 203; c) C. H. Heathcock in J. D. Morrison (Ed.): *Asymmetric Synthesis, Vol. 3*, Academic Press, Orlando, FL, USA 1984, pp. 111–212; d) S. Masamune, W. Choy, J. S. Petersen, L. R. Sita, *Angew. Chem. 97* (1985) 1; *Angew. Chem. Int. Ed. Engl. 24* (1985) 1; e) M. Braun, *ibid. 99* (1987) 24 and *26* (1987) 24.

[2] Examples: a) S. Masamune, W. Choy, F. A. J. Kerdesky, B. Imperiali, *J. Am. Chem. Soc. 103* (1981) 1566; b) D. A. Evans, J. Bartroli, T. L. Shih, *ibid. 103* (1981) 2127; c) T. Mukaiyama, N. Iwasawa, R. W. Stevens, T. Haga, *Tetrahedron 40* (1984) 1381; d) A. I. Meyers, Y. Yamamoto, *ibid. 40* (1984) 2309; e) G. Helmchen, U. Leikauf, I. Taufer-Knöpfel, *Angew. Chem. 97* (1985) 874; *Angew. Chem. Int. Ed. Engl. 24* (1985) 874; f) C. Gennari, A. Bernardi, L. Colombo, C. Scolastico, *J. Am. Chem. Soc. 107* (1985) 5812; g) W. Oppolzer, J. Marco-Contelles, *Helv. Chim. Acta 69* (1986) 1699; h) S. Masamune, T. Sato, B. M. Kim, T. A. Wollmann, *J. Am. Chem. Soc. 108* (1986) 8279.

[3] a) H. Eichenauer, E. Friedrich, W. Lutz, D. Enders, *Angew. Chem. 90* (1978) 219; *Angew. Chem. Int. Ed. Engl. 19* (1978) 206; b) N. Iwasawa, T. Mukaiyama, *Chem. Lett. 1982*, 1441; c) S. H. Mashraqui, R. M. Kellogg, *J. Org. Chem. 49* (1984) 2513; d) D. Enders, *Chem. Scr. 25* (1985) 139; e) K. Narasaka, T. Miwa, *Chem. Lett. 1985*, 1217; f) H.-F. Chow, D. Seebach, *Helv. Chim. Acta 69* (1986) 604; g) M. T. Reetz, F. Kunisch, P. Heitmann, *Tetrahedron Lett. 27* (1986) 4721; h) I. Paterson, M. A. Lister, C. K. McClure, *ibid. 27* (1986) 4787; i) I. R. Silverman, C. Edington, J. D. Elliott, W. S. Johnson, *J. Org. Chem. 52* (1987) 180.

[4] D. Enders, B. Bhushan Lohray, *Angew. Chem. 99* (1987) 359; *Angew. Chem. Int. Ed. Engl. 26* (1987) 351.

[5] D. A. Evans, J. V. Nelson, E. Vogel, T. R. Taber, *J. Am. Chem. Soc. 103* (1981) 3099, and references cited therein.

[6] In the conversion of (*R*)-**2** into the trimethylsilyl enol ether a partial *Z*/*E* isomerization could not be avoided.

[7] J. A. Dale, H. S. Mosher, *J. Am. Chem. Soc. 95* (1973) 512.

[8] In the meantime we have confirmed the absolute configuration of the α-silyl ketones of type **1** [4] by X-ray structure analysis of a crystalline

SAMP-hydrazone. D. Enders, B. Bhushan Lohray, W. Hesse, M. Jansen, unpublished.
[9] K. Mori, T. Ebata, *Tetrahedron 42* (1986) 4413.
[10] a) K. Mori, T. Ebata, *Tetrahedron 42* (1986) 4421; b) A. Fauve, H. Veschambre, *Tetrahedron Lett. 28* (1987) 5037.
[11] U. Baus, *Dissertation*, Universität Bonn 1985.
[12] H. E. Zimmermann, M. D. Traxler, *J. Am. Chem. Soc. 79* (1957) 1920.
[13] For the mechanism of boron enolate aldol additions, see: R. W. Hoffmann, K. Ditrich, S. Froech, *Tetrahedron 41* (1985) 5517; b) C. H. Heathcock, S. Arseniyadis, *Tetrahedron Lett. 26* (1985) 6009; c) C. Gennari, R. Todeschini, M. G. Beretta, G. Favini, C. Scolastico, *J. Org. Chem. 51* (1986) 612; d) R. W. Hoffmann, K. Ditrich, S. Froech, *Liebigs Ann. Chem. 1987*, 977; e) J. M. Goodmann, I. Paterson, S. D. Kahn, *Tetrahedron Lett.*, in press; we thank Dr. *I. Paterson*, Cambridge, for supplying a preprint.
[14] We have already observed a change in the simple diastereoselectivity in previous studies on changing from aliphatic to aromatic aldehydes in aldol reactions via lithiated SAMP-hydrazones under otherwise the same conditions [11]; an explanation is still lacking.
[15] N. R. Schmuff, J. K. Phillips, W. E. Burkholder, H. M. Fales, C.-W. Chen, P. P. Roller, M. Ma, *Tetrahedron Lett. 25* (1984) 1533.
[16] All the new compounds gave correct elemental analyses and characteristic spectra.
[17] E. Vedejs, D. A. Engler, J. E. Telschow, *J. Org. Chem. 43* (1978) 188.

Synthesis and Structure of $[(OC)_4Fe{=}Si{=}Fe(CO)_4 \cdot 2(Me_2N)_3PO]$— a Complex of Formally Zerovalent Silicon**

By *Christian Zybill,* Dallas L. Wilkinson,* and *Gerhard Müller*

Recently, it has been demonstrated that silanediyl(silylene)-transition metal complexes (**A**) are stable as weak donor adducts.[1] In contrast, μ-Si complexes (**B**) with formally zerovalent silicon and allene-like structure have hitherto defied isolation. Analogous compounds of the higher homologues germanium and lead, on the other hand, are already known.[2] We now present the diiron complex **4** as first example of a donor-stabilized silicon(0) complex of type **B**.

The synthesis of compound **4** was accomplished by reaction of disodiumtetracarbonyl ferrate **1** with silicon tetrachloride **2** in an appropriate donor solvent.[3] The reaction presumably proceeds via the silanediyl complex **3** as intermediate.[1]

After chromatographic separation and crystallization from THF, **4** is obtained as colorless, moderately air- and moisture-sensitive crystals. The silicon complex of type **B** primarily differs from the well-known analogous coordination compounds of germanium and lead[2] with "naked" elements of group 14 by the increase in coordination number of the silicon from 2 to 4 and by the almost tetrahedral

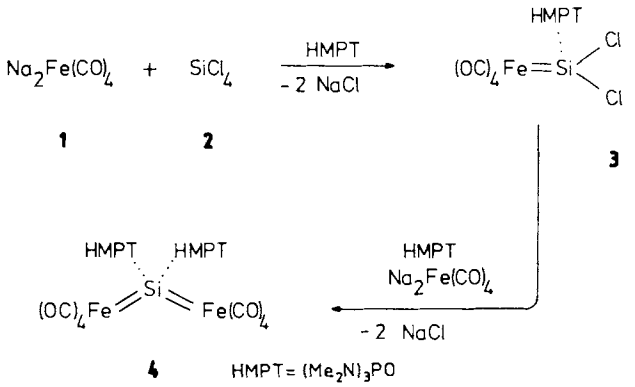

geometry. An indication of the unusual bonding of the silicon is already provided by the increased coupling constant $^3J(^{31}P^1H) = 23.3$ Hz.[4] The vibration spectra show the typical bands for terminal trigonal-pyramidally (tbp) coordinated $Fe(CO)_4$ moieties.[4] Two bands of equal intensity are observed both for the ν_{PO}- as well as for the $\nu_{CO_{ax}}$-vibrations; this is fully consistent with the C_2 symmetry of the complex.[5] The X-ray structure analysis[6] confirms the proposed structure (Fig. 1). The molecule has approxi-

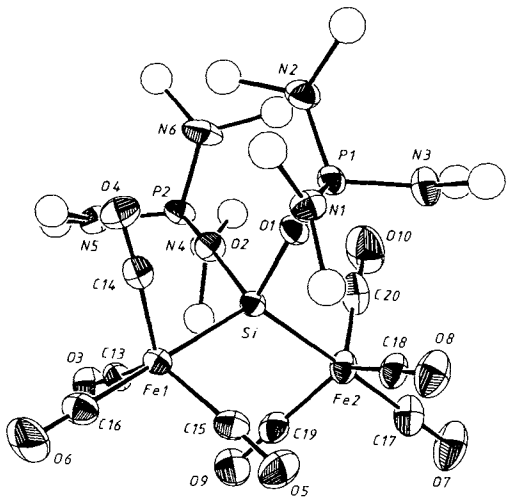

Fig. 1. Crystal structure of **4**·THF (ORTEP, displacement ellipsoids at the 50% probability level, methyl groups with arbitrary radii, without H-atoms and THF). Important bond lengths [Å] and angles [°]: Si-Fe1 2.339(1), Si-Fe2 2.341(1), Si-O1 1.745(2), Si-O2 1.748(3), P1-O1 1.530(2), P2-O2 1.526(3), Fe1-C13 1.769(3), Fe1-C14 1.760(3), Fe1-C15 1.783(4), Fe1-C16 1.788(5), Fe2-C17 1.782(4), Fe2-C18 1.762(4), Fe2-C19 1.787(4), Fe2-C20 1.753(6); Fe1-Si-Fe2 122.6(1), O1-Si-O2 92.1(1), Fe1-Si-O1 110.6(1), Fe1-Si-O2 107.6(1), Fe2-Si-O1 109.2(1), Fe2-Si-O2 110.4(1), Si-O1-P1 160.7(2), Si-O2-P2 167.1(1).

mately C_2 symmetry; the silicon atom is bound to two $Fe(CO)_4$ fragments and occupies an axial position of the tbp-configurated iron atoms. Long donor contacts to the oxygen atoms of the two HMPT molecules complete a distorted tetrahedral coordination of the silicon atom. A striking feature of the structure is that the Fe1-Si-Fe2 angle (122.6(1)°) is significantly widened at the expense of the O1-Si-O2 angle (92.1(1)°), whereas the remaining angles deviate only slightly from the normal tetrahedral angle. The two Fe–Si bonds are almost equal in length (Si-Fe1 2.339(1), Si-Fe2 2.341(1) Å) and somewhat longer than the Si–Fe "double bond" in $[(OC)_4Fe{=}Si(O\,t\mathrm{Bu})_2 \cdot \mathrm{HMPT}]$

[*] Dr. C. Zybill, Dr. D. L. Wilkinson [+], Dr. G. Müller
Anorganisch-chemisches Institut der Technischen Universität München
Lichtenbergstr. 4, D-8046 Garching (FRG)
[+] Permanent address:
Monash University, Clayton, Victoria (Australia)

[**] This work was sponsored by an Alexander-von-Humboldt fellowship *(D. L. W.)*. We thank Prof. *H. Schmidbaur* for support of this work.

(2.289(2) Å).[1a] The approximate tetrahedral coordination and, at least, partial compensation of the electron deficiency at the silicon atom by the oxygen atoms suggest considerable contribution of the zwitterionic resonance structure **4b**.

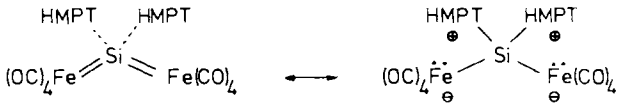

4a **4b**

Received: January 14, 1988 [Z 2574 IE]
German version: *Angew. Chem. 100* (1988) 574

CAS Registry numbers:
1, 14878-31-6; **2**, 10026-04-7; 4·THF, 113584-18-2.

[1] a) C. Zybill, G. Müller, *Angew. Chem. 99* (1987) 683; *Angew. Chem. Int. Ed. Engl. 26* (1987) 669; *Organometallics*, in press; b) D. A. Straus, T. D. Tilley, A. L. Rheingold, *J. Am. Chem. Soc. 109* (1987) 5872.

[2] W. A. Herrmann, *Angew. Chem. 98* (1986) 57; *Angew. Chem. Int. Ed. Engl. 25* (1986) 56; W. A. Herrmann, H. J. Kneuper, E. Herdtweck, *ibid. 97* (1985) 1060 and *24* (1985) 1062; W. Gläde, E. Weis, *J. Organomet. Chem. 213* (1981) 451; for studies on polymetalated silicon see: G. Schmid, V. Bätzel, G. Etzrodt, *ibid. 112* (1976) 345; W. Malisch, H. U. Wekel, I. Grob, F. H. Köhler, *Z. Naturforsch. B37* (1982) 601.

[3] **4**: A suspension of 1.04 g (3.0 mmol) of **1**·1,4-dioxane in 100 mL of THF was treated successively with 255 mg (1.5 mmol) of $SiCl_4$ and 5 mL of HMPT at −40 °C. The dark reddish-brown mixture was stirred for a further 1 h at 0 °C and finally filtered using a G3 frit. The filtrate was concentrated to 10 mL under vacuum, transferred to a water-cooled chromatographic column, and eluted with THF. The rapidly migrating, almost colorless fraction was collected. Colorless crystals of **4**·THF separated out on cooling (0.41 g, 34% yield).

[4] **4**·THF: ^{1}H-NMR (60 MHz, C_6D_6): $\delta = 1.0$ ($^3J(^{31}P^1H) = 23.3$ Hz, 36H, HMPT), 1.36, 3.52 (m, per 4H, THF). IR (KBr): 625, 636 ($\nu_{P=O}$); 1836–1900 ($\nu_{CO_{eq}}$), vs. (E); 2011, 2022 ($\nu_{CO_{ax}}$), s (A_1, local C_{3v} symmetry referred to the Si-Fe axis). A ^{29}Si-NMR spectrum could not be recorded because of the poor solubility of **4**. Correct elemental analysis for C, H, N.

[5] For a discussion of the rotation barriers in compounds isolobal with allene and containing cumulated M=E=M bonding see: N. M. Kostic, R. F. Fenske, *J. Organomet. Chem. 233* (1982) 337.

[6] **4**·THF: Syntex P2$_1$ diffractometer, $Mo_{K\alpha}$ radiation, $\lambda = 0.71069$ Å, graphite monochromator, $T = -45$ °C. $C_{24}H_{44}Fe_2N_6O_{11}P_2Si$, $M_r = 794.38$, triclinic, space group $P\bar{1}$, $a = 10.023(1)$, $b = 10.903(1)$, $c = 18.867(2)$ Å, $\alpha = 95.94(1)$, $\beta = 95.58(1)$, $\gamma = 115.81(1)$°, $V = 1822.7$ Å^3, $Z = 2$, $\rho_{calcd} = 1.447$ g cm^{-3}, $\mu(Mo_{K\alpha}) = 9.7$ cm^{-1}, $F(000) = 828$. 6396 independent reflections, 5816 with $I \geq 1.0\,\sigma(I)$ (ω scan, $\Delta\omega = 0.9$°, $(\sin\theta/\lambda)_{max} = 0.594$ cm^{-1}, $+h$, $\pm k$, $\pm l$). Lp and empirical absorption correction; solution by direct methods (SHELXS-86); $R(R_w) = 0.047$ (0.052), $w = 1/\sigma^2(F_0)$ (anisotropic, H atoms constant, 415 refined parameters, SHELX-76). $\Delta\rho_{fin}$ (max/min) = +0.85/−0.67 e/Å^3. Further details of the crystal structure investigation are available on request from the Fachinformationszentrum Energie, Physik, Mathematik GmbH, D-7514 Eggenstein-Leopoldshafen 2 (FRG), on quoting the depository number CSD-52885, the names of the authors, and the journal citation.

Synthesis and Structure of [{Na(tmeda)}$_3$][LiPh$_4$], an Organometallic Complex Containing Two Different Alkali Metals**

By *Uwe Schümann* and *Erwin Weiss**

As long ago as 1958 *G. Wittig* et al. reported on sodium diphenyllithiate ("diphenyllithium-sodium"), which they formulated as Na[$C_6H_5LiC_6H_5$] **1**.[2] They found that etheral solutions of **1** are capable of stabilizing phenylsodium in any desirable excess, whereas phenylsodium alone is rapidly decomposed by ether. On the other hand, **1** proved to be a more aggressive metalating agent than phenyllithium. So far, however, it has never been fully characterized. In continuation of our systematic investigation of organo(alkali metal) compounds we have now succeeded for the first time in isolating a crystalline ate complex containing two different alkali metals as a tmeda adduct (tmeda = *N,N,N',N'*-tetramethylethylenediamine).

Whereas phenyllithium suspended in hexane can be brought into solution as [{PhLi(tmeda)}$_2$] **2**[3] by addition of an equimolar amount of tmeda, in the case of phenylsodium this is only possible by addition of tmeda in large excess. We have now found that hexane solutions of **1** dissolve suspended phenylsodium at room temperature up to a PhNa/PhLi ratio of about 2.2/1 with a deepening in color of the solution. After filtration the title compound [{Na(tmeda)}$_3$][LiPh$_4$] **3** crystallizes from the 2.2/1 solution at −30 °C in the form of yellow, pyrophoric crystals. Attempts to crystallize a PhLi-PhNa 1/1-complex always gave the Li compound **2** only. ^{7}Li-NMR investigations, however, show that several PhLi/PhNa species are present which undergo partly rapid, partly slow exchange in solution.

The result of an X-ray structure analysis of **3** (Fig. 1)[8] is surprising. The Li atom, which is located in the center of the anion of this ate complex, is pseudo-tetrahedrally coordinated by four phenyl groups and lies approximately at the center of an almost equilateral triangle of tmeda-coordinated Na atoms. Thus, of the two alkali-metal ions, the smaller Li ion is the stronger complexing species. Further, since the coordination number 4 is preferred, there is one lithiate ion to three [Na(tmeda)]$^\oplus$ ions. It thus corresponds to the tetraphenyl- and tetramethylmagnesate ions $[MgPh_4]^{2\ominus}$[4] and $[MgMe_4]^{2\ominus}$[5] which we have previously been able to detect in Li/Mg complexes.

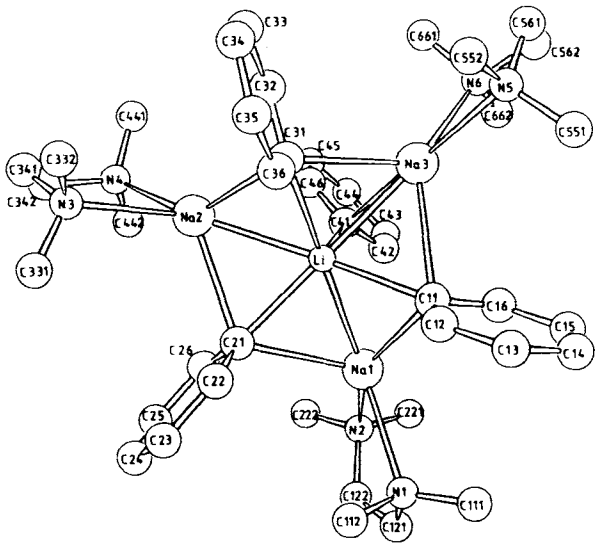

Fig. 1. Crystal structure of **3** with atomic numbering [8]. Important bond lengths [pm] and angles [°]: Li-C11 224(2), Li-C21 225(2), Li-C31 223(2), Li-C41 243(2), Li-Na1 260(2), Li-Na2 261(2), Li-Na3 253(2), Na1-C11 265.8(8), Na1-C21 264.5(8), Na2-C21 256.6(8), Na2-C31 262.7(8), Na3-C11 268.1(8), Na3-C31 271.6(8), Na3-C41 275.6(9), Na1-C41 311(1), Na2-C41 338(1); C11-Li-C21 114.8(7), C11-Li-C31 111.6(6), C11-Li-C41 102.8(6), C21-Li-C31 114.2(6), C21-Li-C41 105.2(6), C31-Li-C41 107.1(6), C11-Na1-C21 91.0(3), C21-Na2-C31 92.7(3), C11-Na3-C31 86.4(2), C12-C11-C16 111.7(7), C22-C21-C26 112.8(8), C32-C31-C36 111.4(7), C42-C41-C46 111.4(10).

[*] Prof. Dr. E. Weiss, Dr. U. Schümann
Institut für Anorganische und Angewandte Chemie der Universität
Martin-Luther-King-Platz 6, D-2000 Hamburg 13 (FRG)

[**] Alkyl- und Arylmetal Compounds, Part 36. This work was supported by the Deutsche Forschungsgemeinschaft and the Fonds der Chemischen Industrie.—Part 35: [1].

Hitherto, only the structure of $[Li(thf)_4][Li\{C(SiMe_3)_3\}_2]$ **4**,[6] an organolithiate complex with twofold linearly coordinated Li ion, was known. Ate complexes are formally formulated with negative charges, but nevertheless they contain positively charged central atoms, as has been shown by MO calculations; the negative charge is delocalized in the organic ligands. In accord with the formula there is also a close relationship between the title compound **3** and the mixed alkali metal-tetramethylguanidino complex $[LiNa_3\{O=P(NMe_2)_3\}_3\{N=C(NMe_2)_2\}_4]$,[7] though a different coordination is found in the latter: the alkali metal atoms and nitrogen atoms of the guanidino ligands are located at the corners of a cube ($LiNa_3N_4$-cubane). Thus, the Li atom is no special coordination center as in **3**.

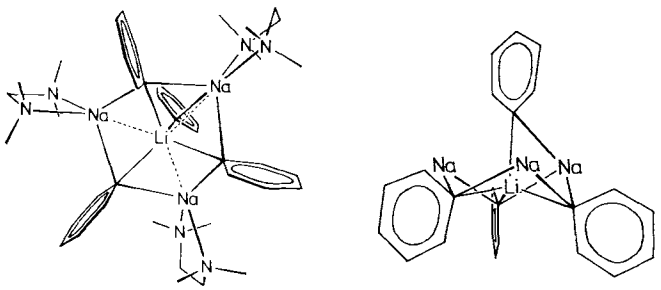

Fig. 2. Line formulas of **3**; right: without tmeda ligands.

The following details about the structure should be mentioned: The Na atoms form an almost equilateral triangle with the Li atom located centrally below the Na_3 plane at a distance of 63 pm. They bridge three of the four phenyl groups and have their shortest contacts to the C atoms bound to the Li atom. These Na-C distances are normal, but vary between 257 and 272 nm. The cause of the remaining deviations of the $LiNa_3Ph_4$-framework from ideal symmetry (C_{3v}) is to be sought in the fourth phenyl group, which bridges Li and Na3. We assume that the metal-carbon interactions are essentially ionic; but a small amount of covalent bonding (multicenter bonds) may be present. The C atoms of the phenyl groups form markedly deformed six-membered rings, as has previously been observed in all phenyl(alkali metal) compounds. The C-C-C angles at the bridging C-atoms are 111 to 113° and thus are clearly smaller than the ideal value of 120°.

Experimental

3: 0.3 g (3.6 mmol) of phenyllithium was dissolved together with 0.6 mL (4.0 mmol) of dry tmeda, in 30 mL of hexane. The stirred solution was then treated dropwise with a suspension of 0.8 g (8.0 mmol) of phenylsodium (prepared from phenyllithium and *t*BuONa[10]) in 30 mL of hexane and 1 mL (6.7 mmol) of tmeda). A considerable part of the phenylsodium immediately goes into solution, which deepens in color from light yellowish-brown to dark brown. The filtered solution was stored for two weeks at −30°C for growing single crystals. Yellow, pyrophoric rectangular parallelepipeds. Yield 63 mg (3%) $C_{42}H_{68}N_6LiNa_3$ (733.0 g mol^{-1}). Elemental analysis: calc. Li 0.95, Na 9.41, C 68.83, H 9.35, N 11.47%; gef. Li 0.92, Na 10.56, C 70.93, H 10.69, N 13.56%.

Received: December 17, 1987 [Z 2543 IE]
German version: *Angew. Chem. 100* (1988) 573

[1] U. Schünemann, E. Weiss, H. Dietrich, W. Mahdi, *J. Organomet. Chem. 322* (1987) 299.
[2] a) G. Wittig, R. Ludwig, R. Polster, *Chem. Ber. 88* (1955) 294; b) G. Wittig, F. Bickelhaupt, *ibid. 91* (1958) 865; c) G. Wittig, E. Benz, *ibid. 91* (1958) 873.
[3] D. Thoennes, E. Weiss, *Chem. Ber. 111* (1978) 3157.
[4] D. Thoennes, E. Weiss, *Chem. Ber. 111* (1978) 3726.
[5] T. Greiser, J. Kopf, D. Thoennes, E. Weiss, *Chem. Ber. 114* (1981) 209.
[6] C. Eaborn, P. B. Hitchcock, J. D. Smith, A. C. Sullivan, *J. Chem. Soc. Chem. Commun. 1983*, 827.
[7] W. Clegg, R. E. Mulvey, R. Snaith, G. E. Toogood, K. Wade, *J. Chem. Soc. Chem. Commun. 1986*, 1740.
[8] $P2_1/a$ (monoclinic), $a = 1445.9(3)$, $b = 1692.0(4)$, $c = 1954.0(4)$ pm, $\beta = 94.41(2)°$, $\rho_{calc} = 1.02$ g cm^{-3}, $Z = 4$, $Mo_{K\alpha}$ radiation, structure determination by direct methods (SHELXS-84 [9]), refinement to $R = 0.069$ (unweighted) with 2246 unique reflections [$|F| > 5\sigma(F)$], measuring range $2° < \theta < 23°$ at 293 K. Anisotropic temperature factors for Li, Na, C, N. The H atoms (common isotropic temperature factors) positioned at calculated positions. Number of refined parameters 472: Further details of the crystal structure investigation are available on request from the Fachinformationszentrum Energie, Physik, Mathematik GmbH, D-7514 Eggenstein-Leopoldshafen 2 (FRG), on quoting the depository number CSD-52874, the names of the authors, and the journal citation.
[9] G. Sheldrick, SHELX: Programs for Crystal Structure Solution, Göttingen 1984.
[10] G. Thirase, E. Weiss, *J. Organomet. Chem. 81* (1974) C 1.

The Cyclohepta[*def*]carbazolium Ion**

By *Beat Freiermuth* and *Jakob Wirz**
Dedicated to Professor Edgar Heilbronner

Cyclohepta[*def*]fluorene (**1**) is the last unknown representative of seven nonalternant pyrene isomers. While the conjugate acid $\mathbf{1H}^{\oplus}$ has been isolated as a salt, all attempts to form **1** by deprotonation of $\mathbf{1H}^{\oplus}$ have failed.[1-3] In 1965, *Heilbronner* et al. drew attention to the biradicaloid nature of the electronic structure of **1** and predicted an unusually low-lying triplet state for this molecule and a strong polarization of charge in the singlet state.[4] This has led us to the expectation that the system should be stabilized by the substitution of an inductive acceptor in the negatively charged position 4. We now report the synthesis of the cyclohepta[*def*]carbazolium ion $\mathbf{2H}^{\oplus}$, the first compound exhibiting the π-topology of **1**.

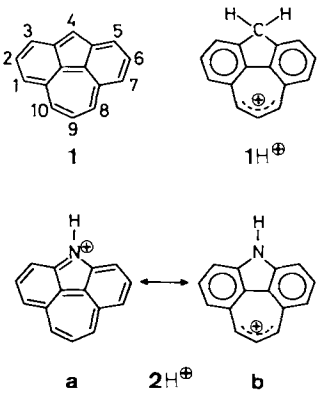

Starting from 2,2′-bis(bromomethyl)-6-nitrobiphenyl (**3**)[5] we have obtained 8,10-dihydrocyclohepta[*def*]carbazol-9(4*H*)-one (**4**) in 14% yield by Thorpe-Ziegler condensation, hydrolysis, and reductive cyclization. After the reduction of the ketone **4**, the dehydration of the resulting alcohol to the somewhat unstable 4,8-dihydrocyclohep-

[*] Prof. Dr. J. Wirz, Dr. B. Freiermuth
Institut für Physikalische Chemie der Universität
Klingelbergstrasse 80, CH-4056 Basel (Switzerland)

[**] This work was supported by the Swiss National Science Foundation (Project No. 2.034-0.86). We thank Mr. *L. Binggeli* for his cooperation.

ta[*def*]carbazole **5** was achieved in moderate yield (ca. 20%) by pyrolysis on alumina. Hydride abstraction finally gave the $BF_4^{\ominus}$ salt of $2H^{\oplus}$ in quantitative yield as a dark

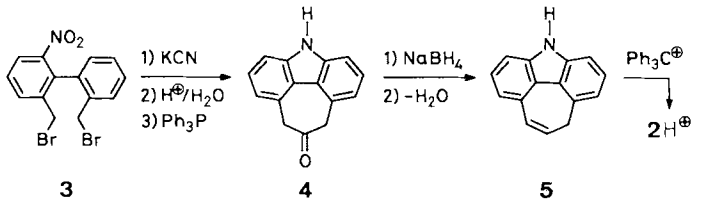

3 **4** **5**

blue solid which decayed within a few days even at $-20°C$ and in the absence of air. Dilute solutions of $2H^{\oplus}$ in 70% perchloric acid were stable for several months. In 1 M aqueous perchloric acid, however, the absorption of $2H^{\oplus}$ disappeared within a few hours, nearly as fast as that of $1H^{\oplus}$ under the same conditions. According to *Munday* and *Sutherland*[1b] the decomposition of $1H^{\oplus}$ in aqueous solution proceeds by hydration of the carbocation at position 8 or 10. We conclude that the high reactivity of $1H^{\oplus}$ towards nucleophilic reagents is hardly reduced in $2H^{\oplus}$ and it is not surprising that our attempts to form the neutral cyclohepta[*def*]carbazole **2** have failed, as with **1**.

A comparison of the ^{1}H-NMR spectra of $1H^{\oplus}$[6] and $2H^{\oplus}$ (see Experimental) confirms that replacement of the CH_2 group ($1H^{\oplus}$) by an NH group contributing two π electrons ($2H^{\oplus}$) does not give rise to a noticeable increase in the charge density at the electrophilic centers C8 and C10; the chemical shifts and coupling constants in the seven-membered ring are very nearly the same in both compounds. The chemical shifts of the ^{1}H-NMR signals may be taken as a reliable measure of the charge distribution,[7] since ring current effects are negligible in $2H^{\oplus}$, as can be seen from a comparison of the chemical shifts of fluorene and $1H^{\oplus}$, and carbazole and $2H^{\oplus}$, respectively.

The above observations correspond precisely to the predictions of an HMO calculation for **1**: the atom-atom polarizabilities $\pi_{4,8}=\pi_{4,10}=-0.0002$ are very small, i.e. the charge distributions q at the atoms 8 and 10 are practically independent of the electronegativity of atom 4 and have the same value of $q_8=q_{10}=0.768$ for all of the compounds **1**, $1H^{\oplus}$, **2**, and $2H^{\oplus}$! Therefore $2H^{\oplus}$ in the electronic ground state is best described by the resonance structure **b**. This is remarkable inasmuch as the resonance structure **a** has one additional π bond; apparently, the latter fact is overruled by the presence of two aromatic sextets in structure b.

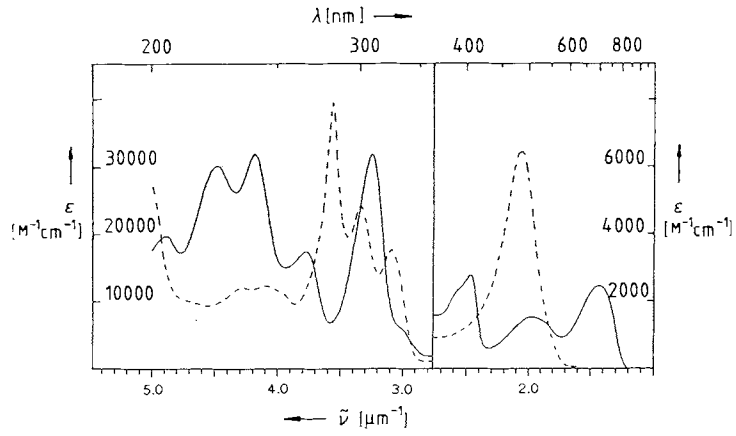

Fig. 1. Absorption spectra of $1H^{\oplus}$ (----) and $2H^{\oplus}$ (——) in 60% $HClO_4$.

In sharp contrast to the ^{1}H-NMR spectra, the UV/VIS absorption spectra of $1H^{\oplus}$ and $2H^{\oplus}$ are entirely different (Fig. 1). As expected, the absorption spectrum of $1H^{\oplus}$ is quite similar to that of the dibenzo[*a*,*c*]tropylium ion.[8] On the other hand, the additional conjugation through the extra lone pair of the nitrogen atom obviously becomes important in the excited states of $2H^{\oplus}$. The predictions of the electronic absorption spectra of $1H^{\oplus}$ and $2H^{\oplus}$ obtained by PPP-SCF-SCI calculations are in satisfactory agreement with experiment.[9] No doubt the first absorption band of singlet **1** lies far in the infrared, as anticipated long ago by *Heilbronner* et al.[4]

Experimental

4: A solution of 28 g (73 mmol) of **3** [5] and 20 g (ca. 300 mmol) of KCN in 2.3 L of MeOH was stirred for 48 h at room temperature and then refluxed for 6 h. Neutralization with dilute HCl, evaporation of the solvent, extraction with ethyl acetate, and chromatography on silica gel (CH_2Cl_2/ether) gave an amorphous yellow solid [6-amino-x-nitro-5*H*-dibenzo[*a*,*c*]cycloheptene-7-carbonitrile, x = 1 or 11, 8.1 g, 40%, m.p. after crystallization from ethyl acetate/hexane 193–197°C; MS (70 eV): *m/z* 277 (100%, $M^{\oplus}$); IR (KBr): $\tilde{\nu}$ = 2184, 1642, 1585, 1524 cm^{-1}], which was dissolved in a mixture of 130 mL ethyl acetate, 35 mL water, and 13.5 mL H_2SO_4 and heated to 150°C for 50 min in an autoclave. Extraction with ether, washing with a bicarbonate solution, and chromatography with CH_2Cl_2 on silica gel furnished 5,7-dihydro-1-nitro-dibenzo[*a*,*c*]cyclohepten-6-one [3.4 g (46%), m.p. 154–155°C (acetate/hexane); MS (70 eV): *m/z* 253 (31%, $M^{\oplus}$), 205 (100%); IR (KBr): $\tilde{\nu}$ = 1710 cm^{-1}; ^{1}H-NMR ($CDCl_3$): δ = 3.5 (s, 2H), 3.6 (m, 2H), 7.2–7.9 (m, 7H)]. Heating the nitro compound with triphenylphosphane following the general procedure of *Ames* et al. [10] (6 d, 160°C) and chromatography with CH_2Cl_2 on silica gel gave 2.2 g (74%) of yellow crystals of **4**, m.p. 229–233°C, correct elementary analysis (C, H, N); IR (KBr): $\tilde{\nu}$ = 3363, 1696, 770, 721 cm^{-1}; UV (EtOH, λ_{max}[nm] (logε) = 246 (4.64), 292 (4.01), 325 (3.59), 340 (3.63); ^{1}H-NMR ($CDCl_3$): δ = 4.4 (s, 4H), 6.9–7.6 (m, 6H), 8.1 (br. s, 1H).

$2H^{\oplus}$: The ketone **4** (200 mg, 0.91 mmol) was reduced with 35 mg (0.93 mmol) of $NaBH_4$ in 6.5 mL of ethanol (30 min, 25°C). Work-up by extraction and sublimation (100°C, 1 Pa) gave 4,8,9,10-tetrahydrocyclohepta[*def*]carbazol-9-ol [197 mg (98%), m.p. 146–148°C; ^{1}H-NMR ($CDCl_3$): δ = 3.4–3.8 (m, 5H), 4.6–4.8 (m, 1H), 6.9–7.4 (m, 6H), 8.1 (br. s, 1H)]. The alcohol (70 mg) was dissolved in CH_2Cl_2 and adsorbed on activated alumina (3 g, Fluka Type 504C, acidic). After evaporation of the solvent, the residue was heated in vacuo (1 Pa), first for 1 h to 200°C and subsequently for 3 h to 250°C. In order to facilitate the evaporation of the product, the alumina, which gradually turned green, was constantly agitated. The sublimate (30 mg) was collected at $-10°C$ on a cold finger and, according to ^{1}H-NMR analysis, contained ca. 80% of **5** and ca. 20% of 4,8,9,10-tetrahydrocyclohepta[*def*]carbazole. The mixture had to be kept in solution (CH_2Cl_2), since **5** polymerizes within a few days when kept as a solid. The above mixture was added dropwise to a stirred solution of 23 mg (0.07 mmol) of tritylium tetrafluoroborate in 1 mL CH_2Cl_2 until the yellow color had disappeared (ca. 14 mg of **5**). The resulting suspension of a dark solid was separated three times by centrifugation and washed with benzene. Upon drying there remained 16.5 mg of dark blue flakes of the $BF_4^{\ominus}$-salt of $2H^{\oplus}$: IR (KBr): $\tilde{\nu}$ = 3375, 3223, 1576, 1477, 1084, 728 cm^{-1}; ^{1}H-NMR (CD_3NO_2, 400 MHz): δ = 8.77 (t, 1H, $J(8,9)$ = 10.3 Hz, H9), 8.80 (dd, 2H, $J(1,2) \cong J(2,3) \cong 7.5$ Hz, H2 and H6), 8.85 (d, 2H, $J(1,2) \cong 7.5$ Hz; H1 and H7 (or H3 and H5)), 8.95 (d, 2H, $J(2,3) \cong 7.5$ Hz, H3 and H5 (or H1 and H7)), 9.95 (d, 2H, $J(8,9)$ = 10.3 Hz, H8 and H10), 11.08 (br. s, 1H, NH).

Received: December 18, 1987 [Z 2547 IE]
German version: *Angew. Chem. 100* (1988) 589

[1] a) D. H. Reid, W. H. Stafford, J. P. Ward, *J. Chem. Soc. 1955*, 1193; b) R. Munday, I. O. Sutherland, *Chem. Commun. 1967*, 569; *J. Chem. Soc. C1969*, 1427; c) K. Hafner, J. Flach, *Erdöl Kohle Erdgas Petrochem. 31* (1978) 89.

[2] *Dissertations:* H. Schaum, Universität München 1964; P. Baumgartner, ETH Zürich 1967; W. Rieper, Technische Hochschule Darmstadt 1968; J. Flach, Technische Hochschule Darmstadt 1976.

[3] In this laboratory we have inter alia attempted in vain to detect **1** by flash photolysis of $1H^{\oplus}$. For similar studies of the azulenium ion, see K. H. Grellmann, E. Heilbronner, P. Seiler, A. Weller, *J. Am. Chem. Soc. 90* (1968) 4238.

[4] P. Baumgartner, E. Weltin, G. Wagniere, E. Heilbronner, *Helv. Chim. Acta 48* (1965) 751; see also R. Zahradnik, J. Michl, J. Pancir, *Tetrahedron 22* (1966) 1355; B. A. Hess, L. J. Schaad, *J. Org. Chem. 36* (1971) 3418; A. DasGupta, N. K. DasGupta, *Theor. Chim. Acta 33* (1974) 177.
[5] D. M. Hall, T. M. Poole, *J. Chem. Soc. B 1966*, 1034.
[6] A 400-MHz ^{1}H-NMR spectrum of the perchlorate salt of $\mathbf{1H}^{\oplus}$ in CD_3NO_2 was recorded for comparison: $\delta = 4.90$ (s, 2H, CH_2), 8.60 (dd, 2H, $J(1,2) \cong J(2,3) \cong 7$ Hz; H2 and H6), 8.85 (t, 1H, $J(8,9) = 11$ Hz; H9), 8.88–8.92 (m, 4H; H1, H3, H5, H7), 9.93 (d, 2H, $J(8,9) = 11$ Hz, H8 and H10).
[7] H. Günther: *NMR-Spektroskopie*, Thieme, Stuttgart 1983, p. 70.
[8] G. Naville, H. Strauss, E. Heilbronner, *Helv. Chim. Acta 43* (1960) 1221.
[9] The standard parameters (R. Zahradnik, *Fortschr. Chem. Forsch. 10* (1968) 1) gave the following predictions for the first absorption band of $\mathbf{1H}^{\oplus}$: $\tilde{\nu} = 2.21$ ($\log\varepsilon = 3.5$), 2.31 (4.2), 3.20 μm^{-1} (3.9); $\mathbf{2H}^{\oplus}$: 1.64 (4.0), 2.26 (3.5), 3.01 μm^{-1} (3.9).
[10] D. E. Ames, K. J. Hansen, N. D. Griffiths, *J. Chem. Soc. Perkin Trans. I 1973*, 2818.

Synthesis and Structure of a Resonance Stabilized (Trimethylphosphonio)metallapropenide**

By *Dimitrios Lappas, David M. Hoffman,* Kirsten Folting,* and *John C. Huffman*

Phosphorus ylides have attracted much research attention due to their frequent application as reagents in organic and organometallic synthesis and a desire to understand the P-C_{ylide} bonding.[1-3] Numerous so-called stabilized ylides have been studied in which the negative charge is resonance delocalized over an organic framework.[3b,4] We describe here the synthesis and structure of a propenide analog, wherein resonance stabilization involves an organometallic moiety (**1**). There is precedent for phos-

$[ReO(\eta^1\text{-}CHCH(PMe_3))(CH_2SiMe_3)_3]$ **1**

phoniopropenide analogs,[5] but all others have a stabilizing substituent at the M-C_α position (e.g., $OSiMe_3$ and $C(=O)OR$[5a]), and **1** is the first structurally characterized example in which the organometallic fragment is in a high oxidation state.[5f] Furthermore, the reaction that yields **1** is unusual because it does not involve a preformed ylide as a reactant.[5e]

The synthesis of **1** is accomplished by reaction of **2** in toluene with an excess of ethyne [Eq. (a)].[6] The reaction

$$\underset{\mathbf{2}}{[ReO(PMe_3)(CH_2SiMe_3)_3]} + C_2H_2 \longrightarrow \underset{\mathbf{1}}{[ReO(\eta^1\text{-}CHCH(PMe_3))(CH_2SiMe_3)_3]} \quad (a)$$

produces a mixture of compounds from which red cubic crystals of **1** can be isolated in 46% first-crop yield. The crystals are analytically pure, but ^{1}H-NMR spectra recorded for the crystals often reveal a trace of another compound.[7]

[*] Prof. D. M. Hoffman, D. Lappas
Department of Chemistry, Harvard University
12 Oxford Street, Cambridge, MA 02138 (USA)
Dr. K. Folting, Dr. J. C. Huffman
Molecular Structure Center, Department of Chemistry
Indiana University
Bloomington, IN 47405 (USA)

[**] This work was supported in part by the Donors of the Petroleum Research fund, administered by the American Chemical Society.

Figure 1 shows the crystal structure of **1**.[8] The complex is square pyramidal with the oxo ligand in the apical position. Re(1) is displaced by 73 pm from the basal plane in the direction of the oxo ligand. The CHCH(PMe_3) ligand

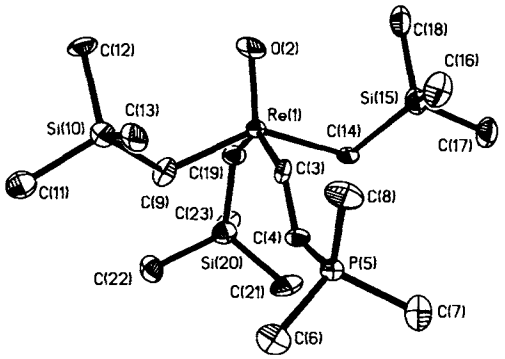

Fig. 1. ORTEP drawing of **1** showing 50% probability ellipsoids and atom-numbering scheme.

is attached to the rhenium via one carbon atom, C(3), such that there is an (*E*)-ReCH=CH(PMe_3) arrangement. The Re-C(3) bond distance of 199.6(9) pm is approximately 13 pm shorter than the alkyl-ligand Re-CH_2 distances, which indicates that the Re-C(3) bond has some multiple bond character. On the other hand, the Re-C(3) bond is not a normal Re-alkylidene bond, because the bond length is 13 pm longer than the Re=C distance in the alkylidene complex **3**.[9]

$[Re(C\mathit{t}Bu)(CH\mathit{t}Bu)I_2(py)_2]$ **3**

The C(3)-C(4) distance, 135.5(13) pm, is typical of an olefin, as is the P(5)-C(4)-C(3) angle of 124.4(8)°. The P-C_{ylide} bond distance, $d(P(5)\text{-}C(4)) = 173.7(10)$ pm, is within 3σ of the average P-Me distance, 178.8(17) pm, and is much longer than the P-C_{ylide} bond distance of 166.1(8) pm reported for the unstabilized ylide Ph_3PCH_2.[10] The P(5)-C(4) distance is comparable to the P-C_{ylide} distances reported for the resonance stabilized ylides (triphenylphosphonio)cyclopentadienide (171.8(2) pm)[4c] and (triphenylphosphonio)dicyanomethanide (175.3(8) pm).[4f]

The structural data for the ReCHCH(PMe_3) fragment suggests that the resonance composite [**1a** ↔ **1b**] best describes the bonding in **1**.[5] Structure **1b** is more important than **1a** since the $P^{\oplus}$-$C^{\ominus}$ interaction in **1a** would be inconsistent with the long P(5)-C(4) bond. Resonance structure **1c** is excluded only on the basis of previously published results that favor a 1,2-zwitterionic description for P-C_{ylide} bonding.[2a,b,3a] In addition, because the Re=O bond distance (170.0(6) pm) and IR stretching frequency (982 cm^{-1}) are normal, resonance structures in which the

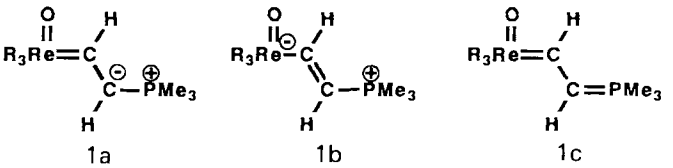

Re=O bond is involved in the delocalization can be excluded.[11] The valence bond description [**1a** ↔ **1b**] represents a resonance stabilized phosphoniometallapropenide.

Further support for the structure and [**1a** ↔ **1b**] bonding description comes from NMR studies of **1**. The chemical shift of the ylide carbon atom ($\delta(C4)=85$) is near the value reported for C_{ylide} in resonance stabilized (triphenylphosphonio)cyclopentadienide ($\delta=78$).[4a] Both shifts are downfield relative to those reported for unstabilized ylides (e.g., $\delta(Me_3P{=}CH_2)=-2.4$).[3b, 4b, 12] The $^{13}C_{ylide}$–H coupling constant, 163 Hz, is similar to the values reported for other ylides,[4b, 12] and the coupling constant across the C=C bond, $^3J_{HH}=17$ Hz, indicates that the (*E*)-ReCH=CH(PMe_3) configuration observed in the solid state is retained in solution. In ReCHCH(PMe_3), the chemical shifts for Re–*C* and Re–C*H* are $\delta=228$ and 12.3, respectively, and $^1J_{CH}=122$ Hz. These values are similar to those reported for Schrock-type rhenium alkylidenes and are further evidence of the Re–C multiple bond character.[9] Overall, the structure and spectroscopic data for **1** are similar to those reported for other phosphoniopropenide analogs.[5]

The molecular orbitals involved in the anion stabilization, excluding any d-orbital contribution from the phosphorus, are **A**–**C**.[3b] The orbitals **A** and **B** are filled, and the HOMO for **1** should be **B**. The orbital **C** is empty and lies just above the empty Re–O π-antibonding MOs in energy. The allyl-like orbitals **A**–**C** are consistent with the

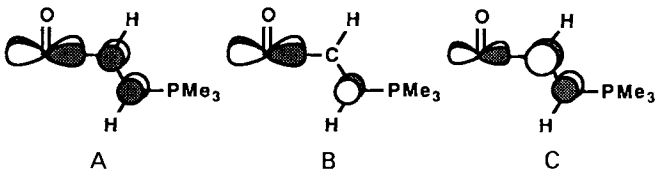

valence bond formulation (**1a**, **1b**). They also explain why the Re=O bond in **1** is not involved in the resonance stabilization: The Re-based orbital involved in the resonance stabilization of the ylides is of the wrong symmetry to interact with the oxo ligand. If the assignment of the HOMO is correct, frontier orbital and steric considerations would suggest that electrophilic attack will occur at the ylide carbon, C(4).[5a, c] Also, the presence of the low-lying MO **C** implies that nucleophilic attack on the CHCH(PMe_3) ligand will occur at C(3), the carbon attached to the Re.

There are three conceivable routes for the formation of **1**: 1. The (*E*)-ReCH=CH(PMe_3) configuration found in **1** suggests that the molecule is formed via attack of external PMe_3 on the coordinated ethyne in a [$ReO(C_2H_2)(CH_2SiMe_3)_3$] intermediate.[5e, 14] 2. It could be formed by insertion of ethyne into the Re–P bond of **2** to yield (*Z*)-ReCH=CH(PMe_3) followed by isomerization.[5a, 14] 3. A dipolar intermediate [$Me_3\overset{\oplus}{P}CH=\overset{\ominus}{C}H$], formed from free PMe_3 and ethyne,[15] could have reacted with **2** or [$ReO(CH_2SiMe_3)_3$]. Further studies concerning the generality of reaction (a) and the reactivity of **1** are in progress.

Experimental

1: In a Schlenk reaction flask, [$ReO(PMe_3)(CH_2SiMe_3)_3$] (0.140 g, 0.26 mmol) was dissolved in toluene (30 mL).[6] The greenish-brown solution was frozen and excess C_2H_2 (2 mmol) was condensed into the flask via a calibrated vacuum manifold. After the mixture was allowed to warm to room temperature, it was stirred for 48 h. The volatiles were then removed under reduced pressure, and the residue was extracted with CH_3CN (5 × 5 mL). The extracts were filtered and the solution was reduced in volume. Upon slowly cooling the solution to −30 °C, red cubic crystals separated out. The crystals were isolated by removing the supernatant liquid via a cannula (yield: 0.068 g, 46%).[13]

Received: November 30, 1987;
Supplemented: January 20, 1988 [Z 2515 IE]
German version: *Angew. Chem. 100* (1988) 585

CAS Registry numbers:
1, 113648-26-3; **2**, 109889-90-9; $ReO(\eta^1\text{-}CHCHPMe_3)(\eta^1\text{-}CHCHCH_2SiMe_3)(CH_2SiMe_3)_2$, 113648-27-4; C_2H_2, 74-86-2.

[1] H. Staudinger, J. Meyer, *Helv. Chim. Acta 2* (1919) 635; G. Wittig, G. Geissler, *Justus Liebigs Ann. Chem. 580* (1953) 44; H. J. Bestmann, O. Vostrowsky, *Top. Curr. Chem. 109* (1983) 85.

[2] a) W. C. Kaska, *Coord. Chem. Rev. 48* (1983) 1; b) H. Schmidbaur, *Angew. Chem. 95* (1983) 980; *Angew. Chem. Int. Ed. Engl. 22* (1983) 907; c) L. Weber in F. R. Hartley, S. Patai (Eds.): *The Chemistry of the Metal–Carbon Bond*, Wiley, New York 1982, p. 91.

[3] a) M. A. Vincent, H. F. Schaefer III, A. Schier, H. Schmidbaur, *J. Am. Chem. Soc. 105* (1983) 3806, and references therein; b) K. A. Ostoja Starzewski, H. Bock, *ibid. 98* (1976) 8486.

[4] a) G. A. Gray, *J. Am. Chem. Soc. 95* (1973) 7736; b) K. A. Ostoja Starzewski, H. tom Dieck, *Phosphorus 6 Relat. Group V Elem.* (1976) 177; c) H. L. Ammon, G. L. Wheeler, P. H. Watts, Jr., *J. Am. Chem. Soc. 95* (1973) 6158; d) P. J. Butterfield, J. C. Tebby, T. J. King, *J. Chem. Soc. Perkin Trans 1 1978*, 1237; e) W. Dreissig, H. J. Hecht, K. Plieth, *Z. Kristallogr. 137* (1973) 132; f) R. Richter, H. Hartung, S. Deresch, J. Kaiser, *Z. Anorg. Allg. Chem. 469* (1980) 179; g) P. J. Wheatley, *J. Chem. Soc. 1965*, 5785; h) A. F. Cameron, F. D. Duncanson, A. A. Freer, V. W. Armstrong, R. Ramage, *J. Chem. Soc. Perkin Trans. 2 1975*, 1030.

[5] a) S. Voran, H. Blau, W. Malisch, U. Schubert, *J. Organomet. Chem. 232* (1982) C33; b) H. Blau, W. Malisch, *Angew. Chem. 92* (1980) 1063; *Angew. Chem. Int. Ed. Engl. 19* (1980) 1019; c) W. Malisch, H. Blau, U. Schubert, *ibid. 92* (1980) 1065 and *19* (1980) 1020; d) W. Malisch, H. Blau, S. Voran, *ibid. 90* (1978) 827 and *17* (1978) 780; e) N. E. Kolobova, L. L. Ivanov, O. S. Zhvanko, I. N. Chechulina, A. S. Batsanov, Yu. T. Struchkov, *J. Organomet. Chem. 238* (1982) 223; f) J. C. Baldwin, N. L. Keder, C. E. Strouse, W. C. Kaska, *Z. Naturforsch. B 35* (1980) 1289; g) W. C. Kaska, C. S. Creaser, *Transition Met. Chem. 3* (1978) 360; h) W. C. Kaska, D. K. Mitchell, R. F. Reichelderfer, W. D. Korte, *J. Am. Chem. Soc. 96* (1974) 2847; i) L. Knoll, *Chem. Ber. 111* (1978) 814.

[6] Synthesis of **2**: S. Cai, D. M. Hoffman, D. Lappas, H.-G. Woo, *Organometallics 6* (1987) 2273.

[7] The other compound has been tentatively identified as [$ReO(\eta^1\text{-}CHCH(PMe_3))(\eta^1\text{-}CHCH(CH_2SiMe_3))(CH_2SiMe_3)_2$].

[8] Crystal data for **1** at −151 °C: $a=1409.7(6)$ pm, $b=1324.2(5)$ pm, $c=1380.7(6)$ pm, $Z=4$, $\rho_{calcd}=1.459$ g cm^{-3}, $V=2577.26\times10^6$ pm^3, $\mu=49.802$ cm^{-1} and space group $P2_12_12_1$. A total of 6032 reflections were collected ($Mo_{K\alpha}$, $6°<2\theta<45°$) of which 3322 were unique and 2905 with $F_o>3.0\sigma(F_o)$ were used in the structure refinement. The structure was solved by a combination of direct methods (MULTAN 78) and Fourier techniques, and refined by full-matrix least squares (383 parameters). All non-hydrogen atoms were refined anisotropically. Hydrogen atoms were located and refined isotropically. Several of the hydrogen atoms behaved poorly during the refinement, but because the positions were qualitatively correct, their positions were not fixed. No absorption correction was deemed necessary. Final residuals were $R(F)=0.0434$ and $R_w(F)=0.0436$ with a final goodness of fit of 0.874. Further details of the crystal structure investigation are available from the Fachinformationszentrum Energie, Physik, Mathematik GmbH, D-7514 Eggenstein-Leopoldshafen 2 (FRG), on quoting the depository number CSD-53039, the names of the authors, and the full citation of the journal.

[9] D. S. Edwards, L. V. Biondi, J. W. Ziller, M. R. Churchill, R. R. Schrock, *Organometallics 2* (1983) 1505.

[10] J. C. J. Bart, *J. Chem. Soc. B 1969*, 350.

[11] Neutral five-coordinate Re^V mono-oxo complexes are rare. **2** [6] has been structurally characterized and found to have $d(Re\text{-}O)=168.8(5)$ pm. The range of Re=O distances in five-coordinate anionic and neutral six-coordinate Re^V complexes is 163–176 pm. P. Stavropoulos, P. G. Edwards, G. Wilkinson, M. Motevalli, K. M. Abdul Malik, M. B. Hursthouse, *J. Chem. Soc. Dalton Trans. 1985*, 2167; M. B. Hursthouse, S. A. A. Jayaweera, A. Quick, *ibid. 1979*, 279; P. J. Blower, J. R. Dilworth, J. P. Hutchinson, T. Nicholson, J. Zubieta, *ibid. 1986*, 1339; C. J. L. Lock, C. Wan, *Can. J. Chem. 53* (1975) 1548; C. J. L. Lock, G. Turner, *ibid. 55* (1977) 333; V. S. Sergienko, M. A. Porai-Koshits, V. E. Mistryukov, K. V. Kotegov, *Koord. Khim. 8* (1982) 230; G. F. Ciani, G. D'Alfonso, P. F. Romiti, A. Sironi, M. Freni, *Inorg. Chim. Acta 72* (1983) 29; P. J. Blower, J. R. Dilworth, J. Hutchinson, T. Nicholson, J. Zubieta, *ibid. 90* (1984)

L27; G. F. Ciani, A. Sironi, T. Beringhelli, G. D'Alfonso, M. Freni, *ibid. 113* (1986) 61; T. Lis, *Acta Crystallogr. Sect. B 35* (1979) 3041; T. Lis, B. Jezowska-Trzebiatowska, *ibid. 33* (1977) 1248; G. Gilli, M. Sacerdoti, V. Bertolasi, R. Rossi, *ibid. 38* (1982) 100; A. C. McDonell, T. W. Hambley, M. R. Snow, A. G. Wedd, *Aust. J. Chem. 36* (1983) 253.

[12] H. Schmidbaur, W. Buchner, D. Scheutzow, *Chem. Ber. 106* (1973) 1251; W. Malisch, D. Rankin, H. Schmidbaur, *ibid. 104* (1971) 145; H. Schmidbaur, W. Tronich, *ibid. 101* (1968) 595; R. Köster, D. Simić, M. Grassberger, *Justus Liebigs Ann. Chem. 739* (1970) 211; K. A. Ostoja Starzewski, M. Feigel, *J. Organomet. Chem. 93* (1975) C 20; K. Hildenbrand, H. Dreeskamp, *Z. Naturforsch. B 28* (1973) 126.

[13] Correct C,H-analysis.—^{1}H-NMR (CD_3CN): $\delta = 12.31$ (dd, 1H, $^3J_{HH} = 17.2$, $^3J_{PH} = 34.2$ Hz; C*H*CHPMe$_3$), 3.42 (dd, 1H, $^3J_{HH} = 17.2$, $^2J_{PH} = 33.6$ Hz; CHC*H*PMe$_3$), 2.36 (s, 2H, C*H*$_2$SiMe$_3$), 2.35 and 1.13 (d of an AB q, 2H, $^2J_{HH} = 8$ Hz; C*H*$_2$SiMe$_3$), 1.65 (d, 9H, $^2J_{PH} = 13.4$ Hz; PMe$_3$), 0.04 (s, 18H; $CH_2Si(CH_3)_3$), −0.17 (s, 9H; $CH_2Si(CH_3)_3$).—^{13}C-NMR (CD_3CN): $\delta = 228.3$ (dd, 1C, $^1J_{CH} = 122$, $^2J_{PC} = 10$ Hz; Re*C*HCHPMe$_3$), 85.0 (dd, 1C, $^1J_{CH} = 163$, $^1J_{PC} = 85$ Hz; CH*C*HPMe$_3$), 38.3 (t, 2C, $^1J_{CH} = 118$ Hz; *C*H$_2$SiMe$_3$), 37.0 (t, 1C, $^1J_{CH} = 117$ Hz; *C*H$_2$SiMe$_3$), 12.9 (dd, 3C, $^1J_{CH} = 111$, $^1J_{PC} = 59$ Hz; PMe$_3$), 4.0 (q, 3C, $^1J_{CH} = 118$ Hz; $CH_2Si(CH_3)_3$), 2.2 (q, 6C, $^1J_{CH} = 118$ Hz; $CH_2Si(CH_3)_3$).—^{31}P{^{1}H}-NMR (CD_3CN): $\delta = 5.78$.—IR (NaCl, Nujol, [cm^{-1}]): $\tilde{\nu}$(Re=O) = 982 (s) [$\tilde{\nu}$(Re=^{18}O) = 921], 1367 (vw), 1359 (vw), 1320 (w), 1299 (s), 1260 (w), 1245 (w), 1239 (s), 1149 (m), 1043 (w), 998 (s), 953 (s), 937 (s), 905 (m), 850 (s), 832 (s), 771 (s), 753 (w), 747 (w), 702 (w), 689 (w), 680 (m), 660 (m), 618 (w), 610 (w).

[14] D. L. Reger, K. A. Belmore, E. Mintz, N. G. Charles, E. A. H. Griffith, E. L. Amma, *Organometallics 2* (1983) 101, and references therein.

[15] W. R. Cullen, D. S. Dawson, *Can. J. Chem. 45* (1967) 2887, and references therein.

Errata

Dinuclear Complexes of Gold(I) Containing Bridging Cyclometalated Arylphosphane or Arylarsane Ligands

By *Martin A. Bennett,* Suresh K. Bhargava, K. David Griffiths, Glen B. Robertson, Wasantha A. Wickramasinghe,* and *Anthony C. Willis*

Following a suggestion by Professor *P. G. Jones*[1] we have reexamined the crystal structure of [Au$_2$(*o*-C$_6$H$_4$PEt$_2$)$_2$][2] and find the space group to be $P\bar{1}$ with two independent centrosymmetric molecules per unit cell (at 0,0,0 and $\frac{1}{2},\frac{1}{2},0$) rather than $P1$ with two independent acentric molecules per cell. For $P\bar{1}$, $R = 0.034$ and $R_w = 0.041$ (cf. 0.032 and 0.038 for $P1$) but refinement is better conditioned and standard error estimates are substantially decreased. The remarked absolute configuration determination in $P1$ (R-factor ratio = 1.022)[3] is apparently an artifact of the overparameterized scattering model. Revised atom coordinates and thermal parameters have been deposited with the Cambridge Crystallographic Data Centre. Revised Au–Au distances [2.8623(5), 2.8493(5) Å] do not differ significantly from the previously quoted values.

Received: February 29, 1988

[*] Dr. M. A. Bennett, Dr. S. K. Bhargava, K. D. Griffiths, Dr. G. B. Robertson, Dr. W. A. Wickramasinghe, Dr. A. C. Willis
Research School of Chemistry, Australian National University
Canberra, A.C.T. 2601 (Australia)

[1] P. G. Jones (Göttingen), private communication (1987).

[2] M. A. Bennett, S. K. Bhargava, K. D. Griffiths, G. B. Robertson, W. A. Wickramasinghe, A. C. Willis, *Angew. Chem. 99* (1987) 261; *Angew. Chem. Int. Ed. Engl. 26* (1987) 258.

[3] W. C. Hamilton, *Acta Crystallogr. 18* (1965) 502.

$[\{Hg_3Co(C_4H_6NO)_6\}(NO_3)_2]_n$: A Macrobicyclic Bimetallic Chain Polymer Incorporating Deprotonated 2-Pyrrolidone Bridges

By *David M. L. Goodgame, David J. Williams,* and *Richard E. P. Winpenny*

Due to a printer's error, Figure 1 in the above mentioned communication (see *Angew. Chem. Int. Ed. Engl. 27* (1988) 261) has been reproduced incorrectly and should be replaced by the correct version depicted below.

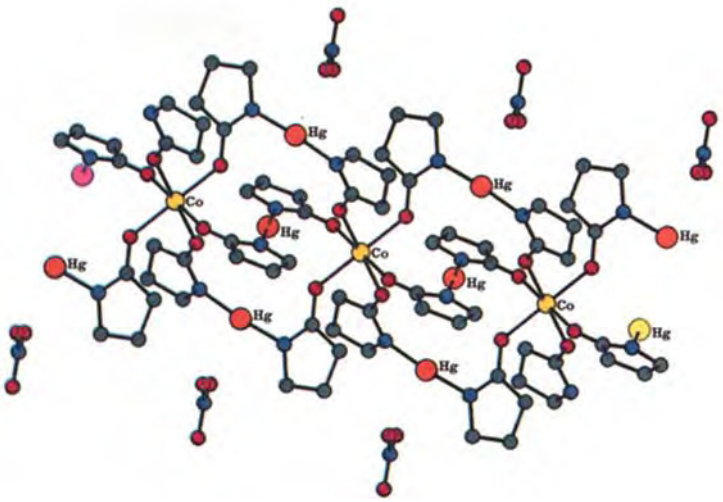

Fig. 1. Part of the contiguous macrobicyclic chain polymer formed by **2** in the crystal.

Hypercarbon Chemistry. By *G. A. Olah, G. K. Surya Prakash, R. E. Williams, L. D. Field,* and *K. Wade.* John Wiley, New York 1987. 311 pp., bound, $ 69.95.—ISBN 0-471-06473-4

Despite the wide occurrence of multicentered two-electron bonds in compounds of elements which lie to the left of carbon in the Periodic System, hypercoordinated carbon (hypercarbon) is often regarded only as an extreme special case. The topic is usually completely ignored in organic chemistry textbooks. What organic textbook is there which even deals with carbaboranes? This monograph gives, for the first time, a coherent account of the many different aspects of the chemistry of compounds containing hypercoordinated carbon atoms.

The first chapter (37 pp., 78 references) introduces the definitions which are essential to the topic, and discusses some typical structures containing hypercoordinated carbon. The different types of localized and delocalized multicentered bonds are described in terms of MO energy diagrams and the isolobal concept. The chapters which follow introduce different types of compounds with hypercoordinated carbon, covering a remarkably wide range. The first to be discussed are a representative selection of bridged and associated alkyl compounds of main group and subgroup metals, which generally involve five- and six-coordinated carbon atoms (32 pp., 96 references).

The next two chapters discuss the importance of hypercoordinated carbon in the extensive area of cluster chemistry. The chapter on carbaboranes and metallacarbaboranes (29 pp., 52 references) includes, in addition to a discussion of structure and bonding, a short account of methods of synthesizing carbaboranes and of their reactions. The following chapter (22 pp., 104 references) reviews the possible types of bonding and coordination of hypercoordinated carbon in mixed metal-carbon cluster compounds and metal carbides. In addition to being of special value to readers who are not very familiar with these more "inorganic" topics, these two chapters form a useful combination with the following chapter on hypercoordinated carbocations (42 pp., 160 references).

Methods for identifying carbocations with hypercoordinated carbon, and experimental results concerning their structures, are summarized here in a similar form to that in the book "Superacids" by *Olah* et al., which appeared from the same publishers in 1985, with some updating of the material. However, in the context of "Hypercarbon Chemistry" this chapter has a different significance. It is made clear to the reader that such carbocations are only one aspect, though an important one, of the broader chemistry of compounds with hypercoordinated carbon atoms. The 2-norbornyl cation, which unfortunately is too often discussed only as an isolated case, is here considered logically along with other hypercoordinated carbocations such as bicyclobutonium ions, bicyclo[2.1.1]hexyl cations, trishomocyclopropenium cations, the Coates cation and the Hogeveen dication. The latest revival of the old controversy about the "nonclassical", i.e. hypercoordinated, structure of the 2-norbornyl cation will be seen as an anachronism after reading this book. The next chapter (20 pp., 45 references) expands on the above topic by dealing with structural analogies and correlations between ^{13}C and ^{11}B NMR chemical shifts, and again brings out very clearly the common features of hypercoordinated carbocations and polyboranes.

The last and longest chapter (64 pp., 192 references) is devoted to short-lived intermediates and transition states involving hypercoordinated carbon atoms. Protolytic reactions of hydrocarbons in superacid media, and reactions between other electrophiles, metal compounds with coordinative unsaturation, carbenes etc. and C–H and C–C σ-bonds are discussed as examples; these provide a contribution to basic understanding of the mechanisms of many organic reactions. This chapter clearly shows that traditional organic chemistry textbooks, in which the chemistry does not begin until after describing the saturated hydrocarbons, are outdated.

There are some problems, which quickly become apparent to the reader, with regard to the different ways of representing bonds to hypercoordinated atoms in structural formulas, using either solid lines or broken lines. For example, one finds two formulas for the μ-hydridoosmium cluster compound $[Os_3H(CO)_{10}CH_3]$, both of which differ from that in the original paper by *Shapley* et al. The method introduced by *Olah* in 1972 of representing a three-centered two-electron bond by broken lines in the middle of a triangle formed by the three coordinated atoms is not always clear, and can easily lead to misunderstanding, as there is no atom at the intersection of the broken lines. The structural formula for the 2-bicyclo[2.2.1]heptyl cation (2-norbornyl cation) on p. 167 is only marginally different from that for the 2-bicyclo[2.1.1]hexyl cation (p. 170). The different ways of writing the same structure are not always formally equivalent. The μ-hydrido bridged cycloalkyl cation $[1,6\text{-}Me_2C_{10}H_{17}]^{\oplus}$ is represented in the introduction with hyper- (two-) coordinated hydrogen and hyper- (five-) coordinated carbon. According to this the cation should have a structure with a closed three-center bond, giving significant transannular C–C interaction. At a later point the formula for the same cation is written with only the μ-hydrogen hypercoordinated. This corresponds to an open three-center bond, a form which was in fact preferred in the original paper by *Sorensen* et al.

The layout and execution of the formulas are not generally up to the normal standard. The diagrams are in some cases too large and in others too small. Some formulas are incorrect. Many of the entries in the subject index (22 pp.) are of little use. For example, how many readers are likely to look up phrases such as "*A*cute Mn-C-Mn bond angles", "*M*athematical explanation", or "*H*ighly stereoregular"?

The book brings together under a unified point of view many items of knowledge from different areas. It not only deals with an aspect of organic chemistry which has hitherto been seriously neglected, but also cuts across the traditional boundaries between inorganic and organic chemistry. It is these qualities which give the monograph its particular value, despite the criticisms of detail mentioned above. In their treatment of hypercarbon chemistry the authors have succeeded in reawakening the reader, who often may have all too easily become a specialist in a narrow field, to the fundamental unity of the many different areas of chemistry.

Hans-Ullrich Siehl [NB 874 IE]
Institut für Organische Chemie
der Universität Tübingen (FRG)

Phosphorus-31 NMR Spectroscopy in Stereochemical Analysis. Edited by *J. G. Verkade* and *L. D. Quin*. VCH Verlagsgesellschaft, Weinheim/VCH Publishers, Deerfield Beach 1987. xvi, 717 pp., hard cover, DM 258.00.—ISBN 3-527-26465-5/0-89573-149-5

In "P-31 NMR Spectroscopy in Stereochemical Analysis," *John Verkade* and *Louis Quin* have provided a thorough coverage of the field involving organophosphorus compounds and phosphorus-metal complexes. The 20 chapters and over 700 pages written by experts in the field cover nearly all aspects of ^{31}P-NMR spectroscopy. A discussion of ^{31}P chemical shifts and their interpretation is presented in the first two chapters. A useful "nuts and bolts" approach to obtaining ^{31}P NMR spectra is provided by *J. C. Tebby* in Chapter 1. A short compilation of representative ^{31}P chemical shifts is also provided. *E. Fluck* and *G. Heckmann* discuss empirical methods for interpreting ^{31}P chemical shifts, largely of compounds with P-heteroatom multiple bonds. These compounds have not often been included in recent reviews of ^{31}P chemical shifts. Chapters 3–6 discuss more detailed theoretical and experimental aspects, including one- and two-dimensional multiple pulse experiments. ^{31}P NMR of oriented phases and theoretical analysis of ^{31}P chemical shifts and coupling constants complete the first section. Both the chapter by *C. B. Chesnut* on ^{31}P chemical shifts and that by *D. J. Jameson* on coupling constants spend considerable time on basic theory. In fact in the later, most of the discussion is directed towards a generalized analysis of coupling between first- and second-row elements, with a minor emphasis on phosphorus.

Chapters 7–10 provide specific applications of the use of ^{31}P chemical shifts in solving structural, conformational, and mechanistic aspects of phosphorus chemistry. The importance of the stereospecificity of ^{31}P coupling constants to all the NMR-active elements is described in Chapters 11–13. The remainder of the book is devoted to stereochemical aspects of metal–phosphorus compounds.

Considering that two other ^{31}P NMR books have recently appeared (D. G. Gorenstein (ed.): *P-31 NMR: Principles and Applications*, Academic Press, New York 1984; C. Tyler Burt: *Phosphorus NMR in Biology*, CRC Press, Boca Raton, FL, USA 1987) and that the *Verkade* and *Quin* book costs \$125, is another book on ^{31}P NMR needed? The answer is a definite yes. The authors have done a really commendable job in minimizing the overlap between the three recent ^{31}P NMR books. The 1984 and 1987 (Tyler) books largely have emphasized theory and applications to biological phosphorus studies and the book by *Verkade* and *Quin* has emphasized organophosphorus and phosphorus–metal complexes. They have provided a highly readable book that researchers in the field will find very useful. It was once possible to largely cover the field of phosphorus NMR in the single volume by *John Van Wazer*. All of the more recent books are needed to adequately cover this enormous field and still have been highly selective in the material they could cover.

There are a few minor typos (*McFarlane*'s equation for line width at half height and a missing third 90° pulse in the NOESY sequence, for example) and a few minor questionable statements (*Gallagher*'s comment about the concentration effect (?) on O-18 isotope shifts on p. 322), but otherwise the book is very well written. The one unfortunate consequence of putting together such a massive undertaking is the time it must have taken for the book to be published. Many of the chapters have references only to 1984 and some even earlier. These are only minor concerns, however, and overall *John Verkade* and *Louis Quin* and the publisher should be commended for putting together a fine volume.

David G. Gorenstein [NB 881 IE]
Chemistry Department, Purdue University
West Lafayette, IN 47907 (USA)

Diazo Compounds. Properties and Synthesis. By *M. Regitz* and *G. Maas*. Academic Press, New York 1986. xvi, 596 pp., bound, \$ 125.00.—ISBN 0-12-585840-X

In addition to their importance as a starting point for preparing carbenes (*G. Maas*, Transition-metal Catalyzed Decomposition of Aliphatic Diazo Compounds—New Results and Application in Organic Synthesis, *Top. Curr. Chem. 137* (1987) 75), diazoalkanes are useful building blocks for cycloadditions (*M. Regitz* and *H. Heydt:* "Diazoalkanes" in *S. Patai* (Ed.): *1,3-Dipolar Cycloaddition Chemistry, Vol. 1*, p. 393, Wiley, New York 1984). Since diazo compounds are so useful in synthesis, everyone who works with them must have felt the lack of an updated account of developments in this area. The comprehensive treatment in the book reviewed here now satisfies this long-standing need. The authors, who have many years of practical experience in this field, intend the treatment to be suitable for final year degree students and preparative chemists in universities and industry.

The book consists of two parts. Part I, "Properties of Aliphatic Diazo Compounds", contains four chapters (structure and spectroscopic properties, thermal properties, reactivity towards acids, and photochemistry). Part II, "Syntheses of Aliphatic Diazo Compounds", has twelve chapters, covering methods which include the diazotization of amines, the Forster reaction, the dehydrogenation of hydrazones, the Bamford-Stevens reaction, the cleavage of *N*-alkyl-*N*-nitroso compounds, the transfer of diazo groups, and substitution reactions of diazoalkanes and isotopically labeled diazo compounds. The reader benefits greatly from the orderly arrangement of the material, and from the carefully prepared formula schemes which can be taken in at a glance, and are in many cases supported by comprehensive tables and bibliography.

The tightly-knit, factual style is pleasing. However, the treatment of the Forster reaction in Chapter 6 is too brief, and on pages 221, 222, and 226 we find three different mechanistic versions of this reaction directly adjacent to each other without any additional discussion. Similarly, virtually no mechanistic interpretation is given for the introduction of diazo groups using the nitroso reaction (Chapter 7).

The book is a mine of information for the specialist, not least because of the literature references, of which there are more than 1800, covering the period up to the end of 1982. The incomprehensibly long delay in the appearance of the book—for which the publishers are no doubt chiefly responsible—has been bridged by the authors' inclusion of an addendum, which is, however, very condensed (it contains no structural formulas!), and therefore makes difficult reading. It contains 184 literature references, for the period up to and including January 1986.

The layout of the monograph is attractive. The text contains scarcely any printing errors. The same is not quite so true of the structural formulas and tables, but this hardly detracts from the excellent overall impression left by this first edition of the work.

In summary, the book is a skilfully written teaching resource, which gives an excellent detailed survey of diazo chemistry, and well represents the present situation in this field of research. In view of the flood of original papers, widely scattered through the various journals, this monograph is a good example of the up-to-date and effective presentation of specialist information. It is certainly well up to the standard required for inclusion in every science library.

Rolf W. Saalfrank [NB 866 IE]
Institut für Organische Chemie
der Universität Erlangen-Nürnberg (FRG)

Catalyst Design. Progress and Perspectives. Edited by *L. L. Hegedus*. Wiley, New York 1987. xi, 288 pp., bound, £ 43.60.—ISBN 0-471-85138-8

Catalysis is a very complex field that has hitherto largely defied all efforts towards a systematic approach to the design of new catalysts—a fact which constantly troubles those engaged in it, especially in industry. It is therefore a welcome initiative when scientists from academic research and industry come together to discuss the possibilities and problems of rational planning for new catalyst development on the basis of the present situation in research. This book contains eight articles by well-known US authors, each discussing the general theme of catalyst design from a different point of view. The topics covered are mainly restricted to heterogeneous catalyst systems; homogeneous catalysis is only touched on briefly in some of the articles, and the area of enzymic catalysis has been omitted.

In the introductory chapter *L. L. Hegedus* (W. R. Grace) briefly discusses the economic importance of catalysis, the technological and scientific progress made in the last 10 to 15 years, and some basic problems in understanding and predicting the effectiveness of catalysts. The article by *G. K. Somorjai* (University of California, Berkeley) deals with the effects of surface morphology and composition on catalyst performance; the various possible ways of controlling the reaction, e.g. by coadsorption or by incorporating structure or bonding modifiers, are clearly described, taking the most recent research results as examples. The starting point for the contribution by *B. C. Gates* (University of Delaware) is organometallic chemistry. The chapter addresses the opportunities in catalyst design by anchoring organometallic complexes to solid surfaces and the stability problems that need to be solved. *A. T. Bell* (University of California, Berkeley) discusses the function of the support and the influence of the method of preparation on the interaction between metal and support, and considers how these effects can be used to increase the performance of metal catalysts. In a more theoretical chapter *M. Boudart* (Stanford University) examines the importance of reaction kinetics in designing new catalysts; for example, he discusses the question of how the selectivity of catalysts can be manipulated in a chosen direction by interfering with the appropriate elementary surface reaction steps which take place sequentially or in parallel in the course of a surface-catalyzed reaction. The article by *R. Aris* (University of Minnesota) discusses quantitative mathematical models of chemical reactivity and transport processes as an aid to optimizing the performance of porous catalysts. Two contributions more closely related to industrial practice are those by *W. O. Haag* and *N. Y. Chen* (Mobil Research and Development) on zeolite catalysts and by *J. Wei* (Massachusetts Institute of Technology) on the design of specific large-scale catalysts for removing metallic impurities from distillation residues in oil refineries.

According to the preface, the book is intended both for academic scientists and for those engaged in industrial catalyst development. The latter will perhaps regret that the book does not give a comprehensive survey of the literature related to more practical aspects of catalyst design or selection. The numerous semiempirical rules for catalyst selection contained in the literature have not been covered here. One might also regret that reaction types and catalyst systems of industrial importance, such as selective oxidation reactions using complex metal oxide catalysts, have not been discussed. When it is stated in the introduction that, in view of the finite number of elements in the Periodic System, future developments in heterogeneous catalysis will lead to multicomponent catalyst systems with complex structures, this is merely describing a trend which has already been evident for a long time in commercial oxidation catalysis. However, apart from these reservations the book gives, on the whole, a realistic survey on the one hand of the advances which have been achieved using modern techniques of investigation and on the other hand of the many different problems which must still be overcome before the eminent empirical work that is required for the development of commercial catalysts can be shortened by a design strategy on a rational basis.

R. Krabetz [NB 872 IE]
BASF Aktiengesellschaft
Ludwigshafen (FRG)

Registered names, trademarks, etc. used in this journal, even when not marked as such, are not to be considered unprotected by law.

© VCH Verlagsgesellschaft mbH, D-6940 Weinheim, 1988.– Printed in the Federal Republic of Germany by Zechnersche Buchdruckerei, Speyer/Rhein.

All rights reserved (including those of translation into foreign languages). No part of this issue may be be reproduced in any form – by photoprint, microfilm, or any other means – nor transmitted or translated into a machine language without written permission from the publishers. Only single copies of contributions, or parts thereof, may be made for personal use. This journal was carefully produced in all its parts. Nevertheless, authors, editors and publisher do not warrant the information contained therein to be free of errors. Readers are advised to keep in mind that statements, data, illustrations, procedural details or other items may inadvertently be inaccurate.

Valid for users in the USA: The appearance of the code at the bottom of the first page of an article in this journal (serial) indicates the copyright owner's consent that copies of the article may be made for personal or internal use, or for the personal or internal use of specific clients. This consent is given on the condition, however, that the copier pay the stated per-copy fee through the Copyright Clearance Center, Inc., for copying beyond that permitted by Sections 107 or 108 of the U.S. Copyright Law. This consent does not extend to other kinds of copying, such as copying for general distribution, for advertising or promotional purposes, for creating new collective works, or for resale. For copying from back volumes of this journal see 'Permissions to Photo-Copy: Publisher's Fee List' of the CCC.

Editorial office: Pappelallee 3, D-6940 Weinheim, Federal Republic of Germany, Telephone (06201) 602315, Telex 465516 vchwh d, Telefax (06201) 602328.

Editor: *P. Gölitz.*

Associate editors: *D. I. Loewus, A. Stimson.* **Editorial assistant:** *E. Schweikart*

Publishers: VCH Verlagsgesellschaft mbH. (Managing Directors: *Prof. Dr. Helmut Grünewald* and *Hans Dirk Köhler*), Pappelallee 3, D-6940 Weinheim, Federal Republic of Germany. Correspondence concerning advertisements should be addressed to VCH Verlagsgesellschaft mbH. (Advertising Manager *R. J. Roth*), Boschstr. 12, P.O. Box 1260/1280, D-6940 Weinheim, Federal Republic of Germany, Telephone Weinheim (06201) 602-0, Telex 465516 vchwh d, Telefax (06201) 602328.

ANGEWANDTE CHEMIE
International Edition in English
Volume 27 · Number 5
May 1988
Pages 593–758

Microscopical Structuring of Solids by Molecular Beam Epitaxy—Spatially Resolved Materials Synthesis

By Klaus Ploog*

Dedicated to Professor A. Rabenau on the occasion of his 65th birthday

Interfaces and heterojunctions which are incorporated into a crystal in well-defined geometrical and spatial arrangements can lead to a structuring or engineering of (semiconducting) solids down to atomic dimensions. The electrical and optical properties are then defined locally, and phenomena related to extremely small dimensions ("quantum size effects") become more important than the actual chemical properties of the materials used. The technique of molecular beam epitaxy allows an atomic layer-by-layer deposition in a two-dimensional growth process, and crystalline materials in alternating layers of arbitrary composition and only a few atomic layers thickness are formed. The synthesis of microscopically structured solids by molecular beam epitaxy affords access to a new class of materials with accurately tailored electrical, optical, magnetic, dielectric, mechanical etc. properties. The semiconductor and metal superlattices described in this article, which are made of alternating thin layers of two different materials, symbolize just the beginning of a new area of materials engineering on a molecular (or atomic) scale. This periodic modulation of the chemical composition normal to the surface imposes an artificial periodicity on the semiconductor or metal crystal, a periodicity of one or two orders of magnitude larger than its natural lattice spacing. The synthesis of other materials combinations, including semiconductor/metal, semiconductor/insulator, metal/insulator, polymers, and magnetic materials, with entirely different properties and for completely different applications will certainly follow. Finally, a large variety of desired combinations of elements can be selected, and even metastable compounds with novel exciting properties can be synthesized by molecular beam epitaxy.

1. Introduction

In modern materials science and materials technology the accurately defined structuring of known solids down to microscopically controlled dimensions is now becoming more important than the continual search for new chemical compounds. Statistically affected preparation techniques, involving e.g. alloying and diffusion, are being replaced more and more by chemically and physically well defined methods, as e.g. epitaxy.[1] This trend is most obvious in the domain of semiconductor research and development, but it also applies to other materials, e.g. ceramics

[*] Dr. K. Ploog
Max-Planck-Institut für Festkörperforschung
Heisenbergstrasse 1, D-7000 Stuttgart 80 (FRG)

 © VCH Verlagsgesellschaft mbH, D-6940 Weinheim, 1988 0570-0833/88/0505-0593 $ 02.50/0

and composites, and in a more general sense even to the most recent developments in the field of high-temperature superconductors.[2] Semiconductor materials required for use in devices must be of extreme purity and their crystal perfection should be as high as possible. Interfaces and accurately defined impurities ("dopants") have to be incorporated into the crystal intentionally and with high spatial resolution, in order to define locally the electrical properties and to adjust the desired potential differences. The important consequence of an accurate structuring of solids in increasingly smaller dimensions is that phenomena related to these restricted small dimensions ("quantum size effects") become more important than the chemical properties of the materials used. A striking example for this postulate is the quantum Hall effect.[3] The numerical value of the Hall resistance depends only on fundamental constants, while the compositions and the dimensions of the crystals become unimportant.

The microscopical structuring of semiconducting solids down to nanometer dimensions is achieved by heterojunctions (i.e. interfaces between two lattice-matched materials of different composition) and by p/n doping interfaces (homojunctions) which are intentionally incorporated into the crystal with high spatial resolution. This process leads to the concept of "band-gap engineering"[4,5] (Fig. 1), the origin of which is already to be found in the patent application for the transitor by *Shockley*[6] and in the later theoretical studies on heterojunctions by *Krömer*.[7] The first experimental confirmation of this concept was accomplished by the successful fabrication of GaAs/$Al_xGa_{1-x}As$ heterojunction lasers[8] which could be operated continuously at room temperature. The real breakthrough for band gap engineering came with the revitalized development of molecular beam epitaxy of III-V compound semiconductors at the Bell Laboratories[9] and with the stimulated efforts to realize artificial semiconductor superlattices in the IBM Thomas J. Watson Laboratories[10] at the beginning of the seventies.

The concept of semiconductor superlattices[10] infers that, by periodic modulation of the chemical composition (e.g. GaAs/$Al_xGa_{1-x}As$) in the direction of growth, an artificial one-dimensional periodicity is imposed on the semiconductor crystal (Fig. 1b). This additional periodicity is one or two orders of magnitude larger than the natural spacing of the lattice planes, but it is smaller than the de Broglie wavelength of electrons, which is about 25 nm in GaAs. The artificial periodicity, which is superimposed on the crystal potential, gives rise to the formation of mini- or sub-bands for electrons and for holes and thus leads to novel electrical and optical properties of the layered material. For many familiar materials the new structures result in unusual electronic properties which open up new technical applications.

The technique of molecular beam epitaxy[9,11] made feasible the first reproducible preparation of multilayer heterostructures with atomically abrupt material transitions at the interfaces and with accurately controlled profiles of composition and doping over regions only a few nanometers wide. Of particular importance is that the single crystalline pattern of the lattice unit in successive layers continues without disruption or distortion across the interfaces between the layers, if lattice matched material systems, such as e.g. GaAs/AlAs, are used.[*]

Table 1. Band gap E_g and lattice constant a of binary III-V compound semiconductors and of the group IV element semiconductors Si and Ge at room temperature. The band-structure type is indicated by d (≙direct) and i (≙indirect). The wavelength λ is calculated according to $\lambda = 1.24/E_g$.

Semiconductor	E_g [eV]	λ [μm]	a [nm]
GaAs	1.425 (d)	0.87	0.5653
AlAs	2.16 (i)	0.57	0.5661
InP	1.35 (d)	0.92	0.5869
InAs	0.36 (d)	3.44	0.6057
GaP	2.26 (i)	0.55	0.5451
GaSb	0.73 (d)	1.70	0.6095
InSb	0.17 (d)	7.29	0.6479
AlSb	1.65 (i)	0.75	0.6135
Si	1.12 (i)	1.10	0.5431
Ge	0.66 (i)	1.88	0.5658

The theoretical concept of semiconductor superlattices and the unique capability of molecular beam epitaxy provided the basis for the successful fabrication of quantum wells, which represent a section out a of a superlattice and thereby form a key element of band-gap engineering (Fig. 1c). The quantum wells are formed by embedding a thin layer of a semiconductor with smaller band gap (e.g. GaAs) between two semiconductor layers with larger band

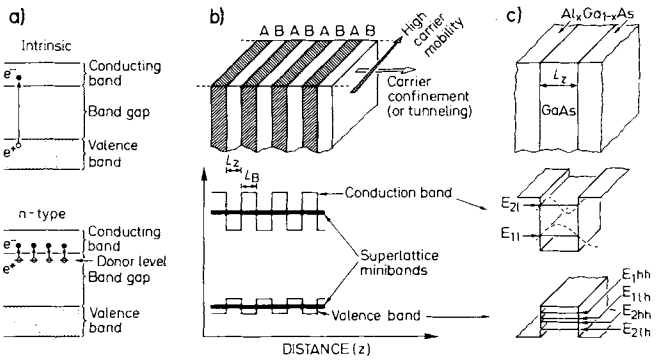

Fig. 1. Schematic illustration of the concept of band-gap engineering in semiconductor superlattices and quantum wells. a) Scheme of conduction and valence band edge in an undoped and in an n-doped semiconductor having a band gap (energy gap) of E_g. b) Periodic modulation of conduction and valence band edge in a superlattice, made of two semiconducting materials with different band gap, and formation of sub-bands for electrons and for holes. c) GaAs quantum well embedded by two $Al_xGa_{1-x}As$ barriers and formation of sub-bands for electrons (E_{1e}) as well as for heavy (E_{1hh}) and light holes (E_{1lh}).

[*] The III-V compound semiconductors are particularly suitable for the fabrication of heterostructures with nearly perfect interfaces because most of them, including GaAs and AlAs, crystallize in the "zinc blende" structure. Within the same group of the periodic table of elements the different constituent elements can be mixed over a wide range, e.g. the Group III elements Al, Ga, In. In this way we can form ternary, quaternary etc. alloy semiconductors without changing the structure type [12]. The lattice constants and the electronic properties of these semiconductors can thus be modified arbitrarily over a wide range simply by the choice of the alloy composition (Table 1). The band gap of the ternary alloy $Al_xGa_{1-x}As$, e.g., increases from 1.42 eV for GaAs (at 300 K) to 1.91 eV for the mole fraction $x = 0.4$. At higher Al content ($x \geq 0.4$) the $Al_xGa_{1-x}As$ alloy transforms from a direct into an indirect-gap semiconductor, where the indirect X-minimum (valley) of the conduction band drops below the direct Γ-minimum [12]. Therefore, for most applications of GaAs/$Al_xGa_{1-x}As$ heterostructures the ternary alloy $Al_xGa_{1-x}As$ of mole fraction $x < 0.4$ is preferred to the binary compound AlAs.

gap (e.g. $Al_{0.3}Ga_{0.7}As$). When the thickness of the embedded GaAs layer is comparable to or smaller than the de Broglie wavelength for electrons, distinct sub-bands for the electrons and holes confined in this potential well are formed. The energy position and the spacing of these subbands depend only on the thickness (width) and on the depth of the quantum well.[13] The depth in turn is given by the energy difference between the conduction band edges (or valence band edges in the case of holes) of the two semiconductors. These energy differences are also called band discontinuities. The wavelength or energy, respectively, of the light emitted or absorbed by the III-V semiconductors in these quantum wells is thus mainly determined by the well width, which is simply a geometric parameter. Similarly to the quantum Hall effect the local chemical composition of the material becomes less important in these layered structures and quantum size effects determine the important features. The preparation and investigation of quantum wells made of III-V semiconductors was crucial for the development of quantum well lasers,[14] which show dramatically improved characteristics as compared to conventional heterostructure lasers, and for the development of novel photodetectors.[15] These two types of devices are decisive for the new technology of photonics, which is based on the optical processing of signals. The application of molecular beam epitaxy for the synthesis of materials with a spatial resolution on an atomic scale has led to a variety of artificially layered semiconductors where the motion of electrons and holes is quantized *in* the layer plane. An important challenge for microstructure materials science lies in the fabrication of quantum wires and quantum dots in which an additional confinement of the carriers in one or two more dimensions *within* the layer plane is required.

In the present review paper we start in Section 2 with an outline of the basic principles of molecular beam epitaxy applied to the growth of III-V semiconductors and discuss the characteristic features of this technique which allow the spatially resolved synthesis of materials. In Section 3, four distinct methods for characterizing artificially layered solids with atomic layer resolution are presented: transmission electron microscopy (TEM), double-crystal X-ray diffraction, luminescence and absorption spectroscopy, and Hall effect measurements. It is shown that improved methods of materials characterization can have a strong impact on the future development of the spatially resolved synthesis of materials. In Section 4 we present some selected examples for the microscopical structuring of solids normal to the crystal surface, and we discuss the exciting electronic properties of the following artificially layered materials: superlattices and quantum well structures made of III-V semiconductors, spatial separation of electrons from their ionized parent impurities in selectively doped III-V heterostructures, $(GaAs)_1(AlAs)_1$ monolayer alloys as example for an ordered alloy of composition $Al_{0.5}Ga_{0.5}As$, monolayer doping in GaAs, combination of a chemical with a structural periodic modulation in Si/Ge superlattices, and finally metal superlattices. In the closing Section 5 a brief outlook on the future developments of spatially resolved materials synthesis and microstructure materials science is given.

2. Fundamentals of Molecular Beam Epitaxy

The controlled fabrication of semiconductor thin films of high crystal perfection requires the application of epitaxial growth techniques, i.e. oriented layer growth on the well ordered surface of a host crystal ("substrate"). The arrangement of the lattice units in the growing layers is predetermined primarily by the structure of the host crystal. Epitaxial growth techniques have been refined dramatically in the past ten years, especially for the III-V semiconductor layers which are now used in the fabrication of optoelectronic (photonic) and high-frequency electron devices. Depending on the scientific and technological requirements, one of the three complementary methods of vapor phase epitaxy, liquid phase epitaxy, or molecular beam epitaxy is used.[16]

Molecular beam epitaxy (MBE) is a method for the fabrication of extremely thin crystalline films of semiconductors and metals as well as artificially layered structures by means of atomic or molecular beams.[11, 17] The specific advantages of this sophisticated technique are that artificially layered solids can be accurately tailored to within atomic dimensions. Distinct atomic layers of a material can be manipulated one by one. Figure 2 shows schematically the basic principle of molecular beam epitaxy for the III-V semiconductors GaAs, $Al_xGa_{1-x}As$, $Ga_xIn_{1-x}As$, and $Al_xIn_{1-x}As$. The growth process is based on the reaction of thermal, non-ionized molecular beams of the constituent elements with a (001) oriented GaAs or InP substrate surface heated to 500–600 °C. At this substrate temperature the impinging species of the molecular beams can react with each other and the atoms can migrate sufficiently fast to their lattice sites so that no defects are formed. The molecular beams are generated by evaporation of the elements Ga, Al, In, and As in small cylindrical effusion cells having a capacity of about 10–100 cm^3. The doping impurities Be for p-type and Si for n-type doping, which are important for adjusting the electrical properties of III-V semiconductors, are incorporated from separate molecular beams into the growing films. Mechanical shutters are

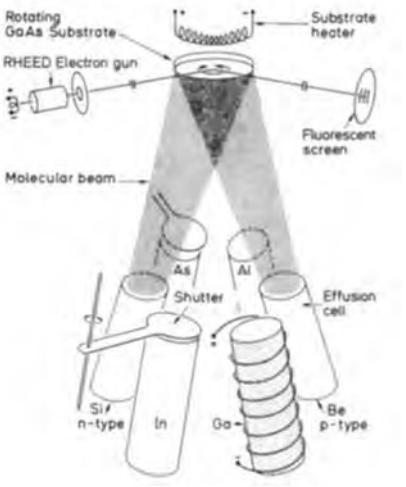

Fig. 2. Schematic illustration of evaporation and deposition process during molecular beam epitaxy of III-V compounds. RHEED = *R*eflection *H*igh-*E*nergy *E*lectron *D*iffraction (see also Fig. 6).

mounted in front of the orifices of the effusion cells. They allow the molecular beams that are directed onto the substrate to be switched on or off within fractions of a second. In this way highly refined layered structures with the composition and/or doping changing over a range of just a few (or even one) atomic layers can be deposited without any deleterious distortion of the crystal growth. The macroscopic electrical and optical properties of the layered structures can be accurately tailored as desired simply by choosing the correct composition and thickness of the constituent layers. In principle, molecular beam epitaxy is a rather elementary synthetic process, since no foreign atoms are present at the gas-solid interface and by-products are not formed.

The basic concepts of the MBE growth process were first developed in the mid-fifties at the Siemens Research Laboratories in Erlangen. Using his so-called "Three-Temperature Method", *Günther*[19] was able to prepare the first stoichiometric thin films of the III-V semiconductors InAs, InSb, and GaAs on glass substrates. The specific difficulty for achieving stoichiometry was that the constituent elements of III-V compounds (i.e. compounds formed from elements of the third and fifth main groups of the periodic table) have largely differing vapor pressures so that these compounds exhibit considerable decomposition at their evaporation temperature (incongruent evaporation). *Günther* used the Group V-element source oven, kept at a low temperature T_1 (e.g. 300°C for As), to maintain a constant vapor pressure in the reaction chamber. The source oven for the Group III element was kept at a much higher temperature T_3 (e.g. 950°C for Ga), thus providing a flux of atoms incident on the substrate that determined the condensation rate of the III-V compounds. The choice of the substrate temperature T_2 was most crucial. This intermediate temperature had to be kept below the incongruent evaporation point, so that a condensation of the III-V compounds could occur, but it had to be increased to a value that ensured re-evaporation of the excess Group V component, which had not reacted, from the substrate surface. The early films prepared by *Günther* were polycrystalline, since they were deposited on amorphous substrates. Furthermore, the vacuum conditions of 10^{-5} torr in the reaction chamber available 30 years ago in the laboratory were not adequate enough for ensuring a reasonable purity of the films. The molecular beam epitaxy of crystalline semiconductor films followed some ten years later in the mid-sixties, when *Arthur*[20] and *Cho*[9] at the Bell Laboratories studied the fundamental aspects of the interaction of Ga atoms and As_2 molecules with crystalline GaAs surfaces under ultrahigh vacuum (UHV) conditions (base pressure 10^{-11} torr). In the author's laboratory, molecular beam epitaxy has been pursued since 1974.

The most characteristic feature of molecular beam epitaxy is its low growth rate of about one lattice plane or monolayer [i.e. one complete layer of Ga plus one complete layer of As on the (001) surface] per second (≙0.3 nm/s). The important consequence of this is that the monocrystalline thin film can be built up atom by atom in a highly controlled manner, and atomically flat growth surfaces are formed. Thus, a high crystal perfection is also achieved for extremely thin films. Owing to the stringent

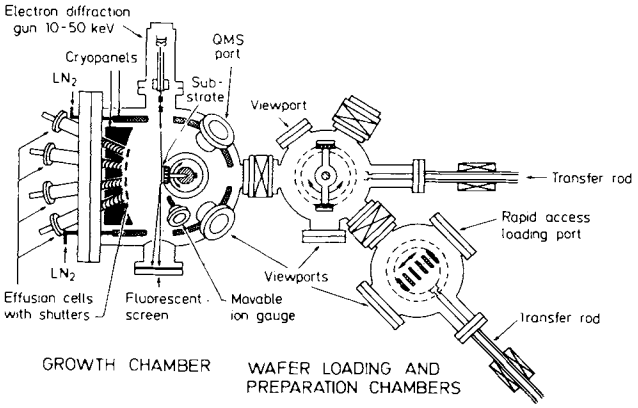

Fig. 3. Schematic cross-section of UHV system used for molecular beam epitaxy of III-V compounds, including reaction chamber, preparation chamber, and load-lock chamber. From the preparation chamber the samples can also be transferred to other processing units or to detailed surface analytical investigations.

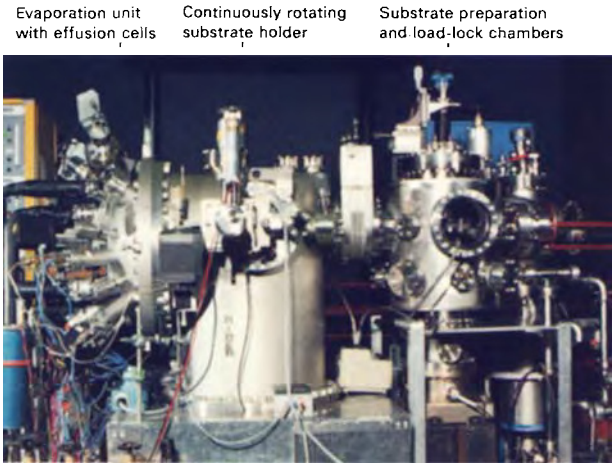

Fig. 4. Side view of a system for molecular beam epitaxy of III-V compounds constructed in the author's laboratory.

purity requirements for semiconductors, the film growth has to be carried out in bakeable UHV systems made of stainless steel and having a base pressure of 10^{-11} torr (this tolerable residual gas pressure is five orders of magnitude lower than in the regions of space traversed by the spacelab). Figure 3 shows a schematic cross-section and Figure 4 a side-view of a three-chamber UHV system for molecular beam epitaxy installed in the author's laboratory. The system consists of the following basic components:

- UHV reaction chamber of 45 cm (≙18 inch) diameter, internally lined with a liquid-nitrogen (LN_2) cooled cryopanel
- evaporator unit with six to ten effusion cells which are thermally isolated from each other by an additional cryopanel
- substrate manipulator for positioning and heating large-area (up to 75-mm diameter) substrate wafers
- load-lock and preparation chamber to introduce and exchange the substrate
- measurement system to control the purity of the system, the molecular beam fluxes, the substrate temperature, and the crystal growth.

Reaction chamber, preparation chamber and load-lock chamber are isolated from each other by large-diameter all-metal gate valves and they are pumped independently of each other. The load-lock chamber is pumped by a closed-loop He cryopump for rapid pump-down cycles, and the two other chambers are each pumped by a combination of ion getter pump and Ti sublimation pump. It is important to make sure that the amount of undesirable hydrocarbons and oxygen-containing compounds in the residual gas of the reaction chamber is kept as low as possible. The substrate wafers mounted on Mo support devices are transferred by magnetically coupled transfer rods from one chamber to the other and they are fixed to the respective heater blocks by a bajonet joint. The material fluxes emerging from the effusion cells are determined by the temperature of each of the cells and monitored by a movable Bayard–Alpert ion gauge which can be moved into the position of the substrate (the central portion of the constituent flux distributions should intersect at this position). The flux measurements by the ion gauge are sufficiently accurate; however, they are not element-specific. To determine accurately the composition of the residual gas and to measure the fluxes specific to the constituent elements, a quadrupole mass spectrometer (QMS) of high sensitivity can be used. For quantitative flux measurements the ionization chamber of the QMS placed in the beam path has to be surrounded by a LN_2 cryopanel, and, owing to material deposits, the spectrometer must be readjusted continuously. The crystal growth on the substrate surface is monitored by electron diffraction under grazing incidence [reflection high-energy electron diffraction (RHEED)]. Details of this important technique for in-situ growth control during MBE will be discussed later (see Fig. 6).

The design of high-quality molecular beam sources fabricated from nonreactive refractory materials is the most important requirement for successful MBE growth. The evaporation sources have to provide stable high-purity molecular beams of the desired intensity and uniformity, and they must withstand operating temperatures up to 1400 °C without themselves contributing to the molecular beams. Precise temperature stability ($\pm 0.1°$ at 1000 °C operating temperature) and reproducibility are essential. For accurate kinetic studies relevant to the growth process, Knudsen (equilibrium) effusion cells with small orifices have been used in the past (Fig. 5a) to produce collision-free thermal energy beams of the constituent elements. The analytical formulas used to calculate the angular intensity distribution of molecular beams emerging from Knudsen cells have been compiled by *Herman*.[21] Unfortunately, only very limited experimental data are available to check the validity of the theoretical approaches. For practical MBE growth, non-equilibrium (Langmuir-type) effusion cells with large orifices are used nowadays (Fig. 5b). In addition to the vapor pressure of the starting materials, the intensity of the molecular beams is also determined by the evaporation geometry. The crucibles made of pyrolytic boron nitride (PBN) are of either cylindrical or conical (tapered) shape, and have a length of about 5 to 10 times greater than their orifice diameter. The crucible capacity of 10 to 100 cm^3 for the different starting materials should be large enough to achieve continuous operating times of several months before recharging is required. The helical Ta wire to heat the crucible is wound in such a way to avoid magnetic stray fields deleterious for the operation of the electron diffraction during growth. Several sheets of thin crimped Ta foil provide a good thermal isolation to keep the heating loss as low as possible. The adjustment and regulation of the temperature is accomplished by continuously operating high-precision regulators having *p*roportional, *i*ntegral and *d*ifferential adjustment (PID regulator). The temperature is measured by a W/Re thermocouple fixed close to the outside bottom of the cylindrical crucible (the W/Re thermocouples do not react with the molecular beams). It is not important to measure the absolute temperature of the melt in the crucible but to detect the temperature at a fixed location of the thermocouple in a reproducible manner. This relative temperature is then related to the molecular beam flux arriving at the substrate surface which is independently determined by the movable ion gauge or by the thickness of the deposited material. *Saito* and *Shibatomi*[22] have recently performed a systematic investigation of the dependence of the uniformity of the molecular beams across the substrate on the geometrical relationship between the Langmuir-type effusion cells and the substrate. Over a substrate diameter of 75 mm they reduced the variation of the composition of $Al_xGa_{1-x}As$ layers to less than $\pm 1\%$ by optimizing the following three geometrical parameters: distance between substrate and effusion cells, taper φ_0 of the conical crucible wall, and diameter of the cell aperture.

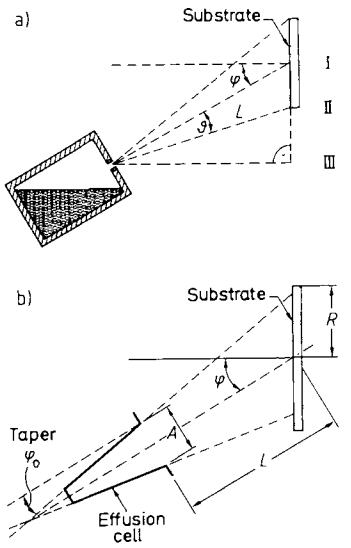

Fig. 5. Schematic illustration of (a) Knudsen (equilibrium) effusion cell and (b) non-equilibrium (Langmuir-type) effusion cell used for molecular beam epitaxy. ϑ = distribution angle of the molecular beam, L = distance between cell orifice and substrate, A = diameter of cell orifice, R = substrate radius, φ = angle of impinging molecular beam with respect to substrate normal, φ_0 = taper of effusion cell wall.

Evaporation of the Group III elements of the periodic table under UHV conditions produces atomic species, i.e. atomic beams emerge from the respective effusion cells. Evaporation of the Group V elements, on the other hand, produces almost exclusively tetrahedrally shaped tetrameric molecules (P_4, As_4, Sb_4) by sublimation. For the preparation of phosphides (GaP, InP, etc.) and for some other special applications dimeric molecules (P_2, As_2, Sb_2) are

required which can be produced by three different methods. First, incongruent evaporation of the binary III-V compounds yields dimeric molecules.[23] Second, the dimeric species are obtained by thermal decomposition of gaseous PH_3 or AsH_3,[24] which, however, also produces a large amount of hydrogen in the UHV system. Third, dimers can be generated from the elements by using a two-zone effusion cell ("cracker cell").[25] A flux of tetramers is first formed in a conventional effusion cell and then passed through an optically baffled high-temperature stage where complete conversion to P_2, As_2, or Sb_2 occurs above 900°C.

The growth of III-V semiconductors during molecular beam epitaxy is essentially determined by the sticking coefficient of the atoms and molecules impinging onto the substrate surface.[23] The substrate temperature is in general chosen to be below the incongruent evaporation temperature of the growing compound. The sticking coefficient of the Group III elements Al, Ga, and In is unity on (001)-oriented GaAs, InP, or GaSb substrates, i.e. each impinging atom sticks. On the other hand, the sticking coefficient of the Group V elements on clean (001) substrate surfaces is zero at the growth temperature. Their condensation occurs only when Al, Ga, or In adatoms have already been deposited on the substrate surface. The growth rate of the films is thus exclusively determined by the arrival rate of the Group III elements. The stoichiometry of most III-V semiconductors during MBE growth is self-regulating as long as excess Group V element molecules are impinging on the growing surface. In practice a two- to tenfold excess is used. The excess species of the Group V elements do not stick on the heated growth surface. As a result, the crystal is built layer-by-layer in the [001] direction, i.e. first a monolayer of GaAs (or InP, AlAs, etc.) is nearly completed before growth of the next monolayer starts. The detailed growth mechanism of III-V semiconductors was first established by *Foxon* and *Joyce*,[26] who studied the surface chemical processes by modulated molecular beam spectroscopy, and it has now been confirmed by investigations of the periodic intensity oscillations of the diffraction features in the RHEED pattern (see Fig. 7).

A good control of the composition of the ternary III-III-V alloys $Al_xGa_{1-x}As$, $Ga_xIn_{1-x}As$, etc. can be achieved by supplying excess Group V species and adjusting the flux intensities of the impinging Group III element beams, as long as the substrate temperature is kept below the congruent evaporation limit of the less stable of the constituent binary III-V compounds (e.g. GaAs in the case of $Al_xGa_{1-x}As$ or InAs in the case of $Ga_xIn_{1-x}As$).[27] At higher growth temperatures, however, preferential desorption of the more volatile Group III element (i.e. Ga from $Al_xGa_{1-x}As$) occurs, so that the final film composition is not only determined by the added flux intensities but also by the differences in the desorption rates. To a first approximation we can estimate the rate of loss of the Group III elements from their vapor pressure data. This assumption is reasonable because the vapor pressure of the element over the compound, e.g. Ga over GaAs, is similar to the vapor pressure of this element over its melt.[28] In Table 2 the rates of loss of Al, Ga, and In are compiled for different substrate temperatures. The surface of alloys grown at high temperatures will thus be enriched by the least volatile Group III element. As a consequence, we expect a significant loss of In in $Ga_xIn_{1-x}As$ films grown above 550°C and a loss of Ga in $Al_xGa_{1-x}As$ films grown above 650°C. For accurate adjustments of the effusion cell temperatures an intermittant calibration based on independently measured film composition, e.g. by X-ray diffraction or photoluminescence measurements (see Section 3), is therefore required. The lower limit of the substrate temperature during MBE growth was in most cases given by the deterioration of the crystal quality owing to the strong increase of the defect density, which occurs, e.g., for GaAs below 450°C. However, *Horikoshi* et al.[29] have recently shown that high quality GaAs and AlAs can be grown at a substrate temperature as low as 300°C, if Ga (or Al) and As_4 are alternately supplied to the growing surface. In an arsenic-free environment, which exists for a short period, the surface migration of Ga and Al is obviously strongly enhanced.

Table 2. Approximate rate of loss of Group III elements (in monolayers per second) from the surface of ternary III-III-V semiconductors estimated from vapor pressure data.

T [°C]	Al	Ga	In
550	—	—	0.03
600	—	—	0.3
650	—	0.06	1.4
700	—	0.4	8
750	0.05	2	30

The growth of ternary III-V-V alloy films such as, e.g., GaP_yAs_{1-y} by MBE is more complicated, since, in particular in phosphorus-containing compounds, the relative amounts of the Group V element incorporated in the growing film are not simply proportional to their relative arrival rates, even at moderate substrate temperatures.[30] In addition, the flux intensity of the Group III element arriving at the growing surface affects the incorporation of the Group V elements. At present the various factors controlling this incorporation behavior are not well understood, and it is difficult to obtain a reproducible composition control of ternary III-V-V alloys during MBE growth. For ternary III-III-V alloys, on the other hand, the simplicity of the MBE process allows composition control from $x=0$ to $x=1$ in $Al_xGa_{1-x}As$, $Ga_xIn_{1-x}As$, etc. with a precision of ± 0.001 and doping control, both n- and p-type, from the 10^{14} to the 10^{19} atoms cm^{-3} range with a precision of a few percent. The accuracy is largely determined by the care with which the growth rate and doping level was previously calibrated in test layers.

In general MBE growth of III-V semiconductors is accomplished on (001) oriented substrate slices of GaAs, InP, or GaSb having thicknesses of 300–500 μm. Before introduction into the growth chamber the substrate surface should be free of crystallographic defects and clean on an atomic scale, so that the crystal film can indeed be built in a two-dimensional growth process. Impurities and defects form nucleation centers for three-dimensional (3D) growth. The substrate preparation always involves treatment with organic solvents and with oxidizing solutions, and the final step consists of chemical etching to produce a

relatively stable oxide on the substrate surface.[11,17] This surface oxide protects the substrate against contamination. After insertion of the substrate into the MBE system the surface oxide is removed by heating to a temperature just below the limit of congruent evaporation, and clean crystallographically well ordered substrate surfaces are obtained. Smaller substrate slices are soldered with liquid In to the circular Mo mounting plate (In becomes liquid at 160°C and it has a high surface tension), and the whole device is then transferred and heated. Larger substrate wafers having a constant diameter of 50 or 75 mm (2 or 3 inches) are fixed without In to a special Mo holder designed for direct-radiation substrate heating. After insertion of one of these Mo holders with the chemically etched substrate into the load-lock chamber and evacuation to a pressure below 10^{-8} torr the substrate is preheated to remove physisorbed gaseous impurities, e.g. H_2O and CO. Then the substrate is transferred to the preparation chamber where the intentionally produced surface oxide is removed by controlled heating. The removal of the surface oxide can also be accomplished in the reaction chamber, in order to observe this process by RHEED. The transfer between the chambers is made by trolleys and magnetically coupled transfer mechanisms. In the growth chamber the Mo mounting plate holding the substrate wafer is fixed by a bayonet joint to the Mo heater block which is originally attached to a special manipulator. This manipulator positions correctly the substrate wafer relative to the evaporation sources, heats it to the required temperature, and continuously rotates it azimuthally for optimum film uniformity.

On using high-purity starting materials (>99.9999%), the purity of the semiconductor films depends crucially on the residual background impurities in the reaction chamber. Recently, unintentionally doped GaAs with an extremely low residual acceptor concentration of 2×10^{13} atoms cm^{-3} was obtained.[31] The residual acceptor is probably due to carbon impurities from the residual gas of the reaction chamber. The application of MBE grown films for fundamental studies as well as in device structures requires the control of the electrical and optical material properties by the deliberate incorporation of small amounts of impurity (dopant) elements from additional effusion cells. The most common dopants used during MBE growth of III-V semiconductors are Be for p-type and Si for n-type doping. Over a large range of growth conditions both elements have a sticking coefficient of unity. Abrupt doping profiles normal to the growth surface can be obtained simply by actuating the shutters in front of the effusion cells. Be substitutes for Ga atoms in the GaAs sublattice and forms a nearly ideal shallow acceptor.[32] For doping concentrations up to 2×10^{19} atoms cm^{-3} each incident Be atom produces one ionized impurity species. By lowering the substrate temperature to 500°C even extremely high acceptor concentrations up to 2×10^{20} cm^{-3} are feasible in Be-doped GaAs with perfect surface morphology. For (001)-oriented substrates, also Si primarily substitutes for Ga atoms in the GaAs sublattice and forms a shallow donor.[33] The electrically measured doping concentration is up to $n=1\times10^{19}$ cm^{-3} directly proportional to the dopant arrival rate, provided care is taken to minimize the background H_2O and CO level during growth. At present, the origin of the upper limit of 1×10^{19} cm^{-3} for the electron concentration in Si-doped GaAs is not exactly clear. Three mechanisms are discussed, (i) autocompensation by incorporation of Si on As sites or on interstitials,[34] (ii) additional impurities evolving from the Si effusion cell heated to above 1300°C,[35] or (iii) formation of Si-vacancy complexes acting as acceptors which lead to a compensation in heavily n-doped GaAs.[36] The possibility of Si migration or diffusion during MBE growth of $Al_xGa_{1-x}As$ films at high substrate temperatures and/or with high donor concentration has been the subject of controversial discussion,[37] because of its deleterious effects on the properties of selectively doped n-$Al_xGa_{1-x}As$/GaAs heterostructures which require abrupt doping profiles. There is some evidence that a migration of Si in $Al_xGa_{1-x}As$ can only occur at high doping concentration ($>2\times10^{18}$ atoms cm^{-3}) as the result of a concentration-dependent diffusion process, which is enhanced at high substrate temperatures. It is finally important to note that the incorporation of Si atoms on either Ga or As sites depends significantly on the orientation of the GaAs substrate.[38] In GaAs grown on (001), (111)B, (211)B, (311)B, (511)A, (511)B, and higher-index orientations, Si atoms predominantly occupy Ga sites and act as donors, while they occupy As sites and act as acceptors on (111)A, (211)A, and (311)A orientations. This different incorporation behavior of Si is now utilized, e.g., to produce a series of lateral p/n junctions in GaAs on graded steps of the (001) substrate surface.[39] Based on this method of spatially resolved synthesis during MBE, semiconductors with a few nanometers wide lateral regions of totally different electrical properties are produced.

Reflection electron diffraction under grazing incidence (RHEED) is the most important technique for in-situ monitoring of the crystal growth during molecular beam epitaxy.[11] The forward scattering geometry with a grazing incidence angle of 1 to 3° schematically shown in Figure 6a implies that also at a primary-beam energy of 10–30 keV the information (penetration) depth is restricted to the out-

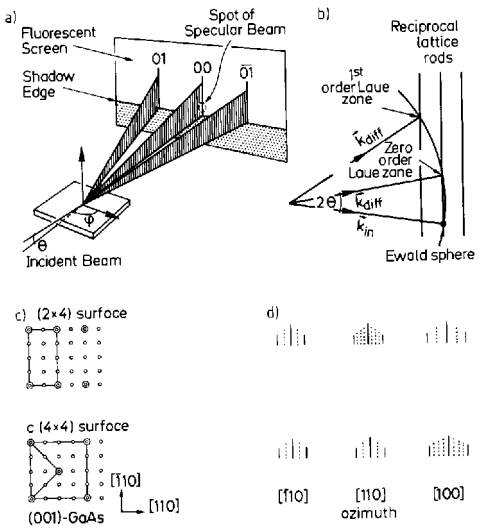

Fig. 6. Geometric arrangement of electron diffraction with grazing-angle incidence (RHEED) used as in-situ analytical tool during molecular beam epitaxy; (b) Ewald construction to interpret the diffraction conditions; (c) and (d) surface unit cell ("mesh") and diffraction patterns of two important reconstructions during molecular beam epitaxy (not to scale).

ermost atomic layers of the growing crystal. This geometry makes RHEED fully compatible with the MBE growth process, and the diffraction pattern can be observed directly on the fluorescent screen ("in-situ"). The diffraction spots are elongated to characteristic streaks normal to the shadow edge. The appearance of streaks instead of spots cannot fully be explained by means of the Ewald construction (Fig. 6b), where in reciprocal space the lattice rods intersect the Ewald sphere tangentially when the diffraction condition is fulfilled. In addition, we have to assume a specific disorder in certain directions of the growing crystal surface.[40] The existence of surface reconstructions characteristic for MBE growth (Fig. 6c) leads to additional features in the RHEED pattern (Fig. 6d) at fractional intervals between the bulk (zinc blende-type) diffraction streaks.[11] The re-ordering of the surface atoms during reconstruction gives rise to a lowering of the symmetry at the surface. In most cases the surface unit cell ("mesh") has a larger periodicity. This rearrangement at the surface results from the rehybridization of binding orbitals in order to minimize the free energy of the surface. The (001) surface of III-V semiconductors exhibits a number of different reconstructions during MBE growth which are directly related to the surface stoichiometry. The surface composition, on the other hand, depends crucially on the growth conditions (substrate temperature, ratio of molecular beam fluxes, etc.).[41] Figure 6d shows (schematically) the diffraction patterns of the two most important surface reconstructions during MBE growth of GaAs, i.e. the arsenic-stable (2×4)- and the (4×4)-reconstruction, taken at different azimuths. From the occurrence of specific surface reconstructions, identified from the diffraction pattern, we can in turn derive the actual reaction conditions, and if necessary we can modify them. The monitoring of the RHEED pattern is of particular importance at the beginning of the epitaxial growth on the chemically etched and thermally heated substrate wafer as well as during the preparation of abrupt material interfaces.

Another characteristic feature of this type of electron diffraction under grazing incidence is the existence of pronounced periodic intensity oscillations of the specularly reflected and of the diffracted beams during MBE growth (Fig. 7, top). The period of these oscillations corresponds exactly to the time required to deposit a monolayer of GaAs (or AlAs, $Al_xGa_{1-x}As$, etc.) on the (001) surface.[42] To explain these features we can to a first approximation assume (Fig. 7, bottom) that the amplitude of the intensity oscillation reaches its maximum when the monolayer is just completed (maximum reflectivity). The formation of the following lattice plane starts with statistically distributed 2D islands having the height of one GaAs monolayer. The intensity of the diffracted (or reflected) electron beam decreases with increasing size of the island. The minimum reflectivity occurs at half-layer coverage ($\theta=0.5$). When the coverage is further increased the islands coalesce more and more, and the reflectivity finally reaches a maximum again at $\theta=1$. The observed damping of the intensity amplitude is probably due to the fact that the individual surface domains probed by the electron beam are not in phase. The damping of the RHEED oscillations can be eliminated when the surface migration of the Group III

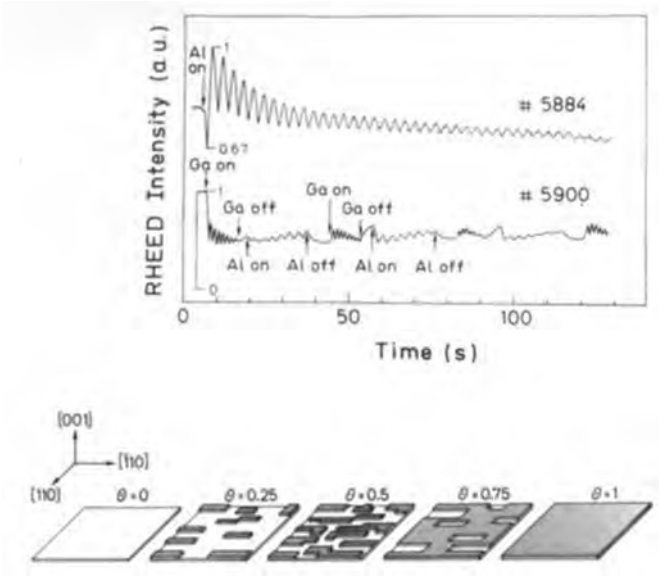

Fig. 7. Top: Periodic intensity oscillation of the specularly reflected electron beam in the RHEED pattern as a function of time during molecular beam epitaxy of GaAs/AlAs layers. Bottom: Formation of 2D growth islands of monolayer height but different lateral size to illustrate the varying reflectivity of the incident electron beam from the growing surface (not to scale).

elements is greatly enhanced by short synchronized cessations of the arsenic flux.[43] In this case only a few large domains are formed on the growing surface. The existence of periodic intensity oscillations in the RHEED pattern is a conclusive confirmation of the assumption that crystals are indeed formed in a 2D layer-by-layer growth mode during molecular beam epitaxy. The RHEED intensity oscillations are now widely used to calibrate and to monitor absolute growth rates in real time and with monolayer resolution and to provide direct real-time evidence of the formation of interfaces on an atomic scale during abrupt deliberate change of the composition.[44] As in the case of the widely used $GaAs/Al_xGa_{1-x}As$ heterointerface, e.g., the sequence of layer growth ternary-to-binary exhibits considerably different properties (structural and electronic) than the sequence binary-to-ternary, since the Ga and Al atoms have a strongly different surface migration rate at normal MBE growth conditions. These differences in the heterointerfaces can be compensated to a certain extent by the interruption of growth at each interface for a short time (10^1–10^2 s, the value depends on the actual growth conditions).

3. Characterization of Microscopically Structured Solids

The characterization of solids which are microscopically structured down to atomic dimensions requires analytical techniques having a high spatial resolution and a high sensitivity and accuracy. The necessity of a detailed characterization stems directly from the historical development of the semiconductor superlattices. In this field, a sound theory made it first possible to predict the intriguing properties of these microscopically structured semiconducting materials. Sophisticated measurement systems were then used to assess the degree to which the predictions have

been fulfilled. It is important to note that the interface perfection experimentally achievable by MBE is now so high that conventional methods of depth profiling analysis, which involve sputtering to section the material combined with some means of composition determination (such as Auger electron spectroscopy or secondary ion mass spectroscopy) are no longer adequate for the required resolution. Therefore, the continuous development of already existing and of new analytical and measurement techniques is an unquestionable requirement. Improved techniques for characterizing materials can in turn also have a strong impact on the development of spatially resolved materials synthesis.

In this paper we briefly introduce four methods for characterizing materials which are routinely used today to assess the specific properties of microscopically structured solids, in particular semiconductors: transmission electron microscopy, double-crystal X-ray diffraction, luminescence and absorption spectroscopy, and Hall effect measurements. In many cases a combination of two or more methods is necessary.

3.1. Transmission Electron Microscopy

The method of cross-section transmission electron microscopy (TEM) with dark-field and lattice imaging was first used by *Petroff*[45] to analyze the periodicity, the degree of order at the interfaces, and the composition in GaAs/AlAs superlattices. This imaging mode requires that the incident electron beam is nearly parallel to the layers of the superlattice, i.e. parallel to the (001) plane in the [110] direction (see Fig. 8, top). To prepare the thin TEM specimen, the (001)-oriented substrate with the epitaxial layer is first cleaved parallel to the (110) plane, and the cleaved fragments are then thinned by chemical etching and ion beam etching down to a thickness of 10–20 nm.[46] The regular layer sequence A, B, A, B, ... in the epitaxial film leads to a periodic array of interfaces which in turn generates a periodic variation of the crystal potential acting as a phase grating for the incident electron beam (provided the coherence length of the electron beam is larger than the grating periodicity). Thus, in addition to the diffraction spots arising from the diffracting lattice planes of the layers A and B, we observe characteristic superlattice spots in the transmission electron diffraction pattern, which represent a Fourier transform of the phase grating. Lattice images are formed either in the bright- or dark-field mode by selecting the transmitted or diffracted beam and one or more of the superlattice diffraction spots with the objective aperture (Fig. 8, top). The intensity distribution in the resulting lattice image shows a periodicity. However, this periodicity represents the true distribution of interfaces in the sample as well as order or disorder at the interfaces only under very crucial imaging conditions. The specimen thickness and the defocussing of the objective lens, for example, strongly affect the periodicity observed in the image.

In Figure 8 (middle and bottom) we show examples for a cross-sectional dark-field TEM image of a 10-nm GaAs/10-nm AlAs superlattice and for a high-resolution lattice image of a 2.8-nm GaAs/2.3-nm AlAs superlattice, respectively. Inspection of the lattice image clearly reveals that the perfect ordering of the lattice units continues without distortion also across the interfaces. The two binary components GaAs and AlAs provide the highest contrast at the interfaces of these superlattices. *Suzuki* and *Okamoto*[47] have recently demonstrated that a high contrast in the lattice plane images can also be obtained for the technologically important $GaAs/Al_xGa_{1-x}As$ superlattices with $x = 0.3$, if the TEM specimens are cut out of the epitaxial layer in (001) orientation so that the electron beam is incident in the [100] direction. However, the specimen preparation for this orientation is rather elaborate because a (100) cleavage plane does not exist for the III-V semiconductors. When the periodicity of the superlattice is larger than several lattice planes it becomes difficult for a microscope of lower resolution to form a dark field image from the superlattice spots, as these spots are then located too

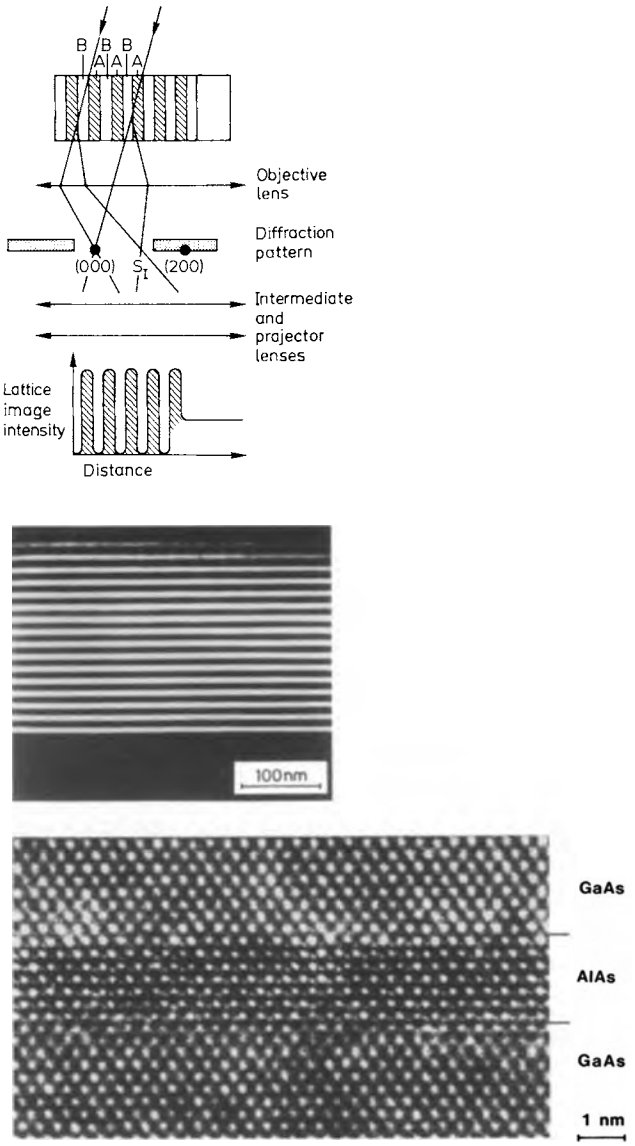

Fig. 8. Top: Geometric arrangement of incident electron beam and constituent layers of a superlattice as well as generation of the imaging conditions for high-resolution transmission electron microscopy (TEM). Middle and bottom: Cross-sectional dark-field TEM image and high-resolution lattice image of GaAs/AlAs superlattices. The TEM micrographs were kindly taken by Dr. *H. Oppolzer*, Siemens AG, Munich.

close to the main lattice reflections. But since the Ga and Al atoms have significantly different scattering factors, the periodic layer sequence can still be imaged as shown in Figure 8 (bottom). In this micrograph the dark bands are GaAs and the light bands are AlAs. It is evident, however, that the resolution is not adequate enough to define the interfaces on an atomic scale.

3.2. Double-Crystal X-Ray Diffraction

Transmission electron microscopy is a destructive analytical method for the wafer, and it calls for an elaborate preparation of suitable specimens. Double-crystal X-ray diffraction, on the other hand, is a non-destructive method and it requires far less experimental effort. X-ray diffraction was already used in the early seventies for the characterization of semiconductor superlattices[48] but it soon lost importance because of its analytical limitations at that time. For about three years the method has experienced a renewed widely spread application, which was initiated by the significantly improved theoretical analysis of the experimentally determined diffraction curves.[49] In a semiconductor superlattice the lattice parameter as well as the scattering power are subject to a one-dimensional periodic modulation in the direction of the layer sequence. As a consequence, the diffraction pattern consists of a series of satellite reflections located symmetrically around the respective Bragg reflection. Figure 9 shows schematically the diffraction geometry of an epitaxial layer grown on a crystalline substrate and the basic principle of a double-crystal X-ray diffractometer operating in a non-dispersive anti-parallel Bragg arrangement. A dislocation-free Ge crystal is used as monochromator and collimator to produce a collimated monochromatic X-ray beam. The appropriate choice of the asymmetry factor of the collimator crystal minimizes the angular divergence of the beam incident on the specimen. In our case the divergence is about 2.35 seconds of arc, and we obtain a very high resolution with such an instrument.[49]

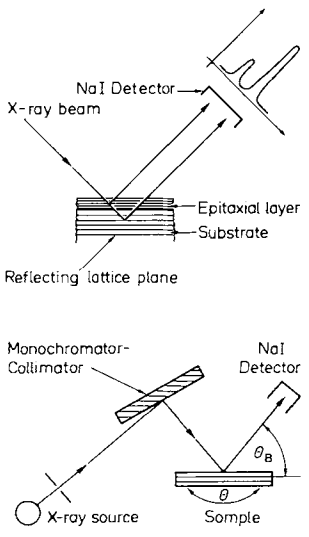

Fig. 9. Schematic illustration of X-ray diffraction from a crystalline epitaxial layer deposited on a crystalline substrate (top) and basic principle of a double-crystal X-ray diffractometer in non-dispersive anti-parallel Bragg arrangement (bottom).

The small difference in the lattice constants between the $Al_xGa_{1-x}As$ epitaxial layer and the GaAs substrate crystal gives rise to a slight distortion of the unit cell of the epitaxy crystal. This distortion of the unit cell can be determined by measuring two reflection curves, one from the lattice planes parallel to the (001) crystal surface and one from lattice planes inclined to the crystal surface. Our measurements have conclusively shown that for this materials system a change of the lattice constant *parallel* to the (001) surface does not exist, while the change of the lattice constant perpendicular to the epitaxial layer surface, i.e. in the [001] direction, depends linearly on the chemical composition of the $Al_xGa_{1-x}As$ layer, i.e. on x. The relative change of the GaAs and AlAs lattice constants perpendicular to the crystal surface amount to $\Delta a = 1.583 \times 10^{-3}$ nm and for a relaxed lattice to $(\Delta a)_{relax} = 0.72 \times 10^{-3}$ nm. After conversion of Δa to $(\Delta a)_{relax}$ using the elastic stiffness constants we can thus determine the composition of the epitaxial $Al_xGa_{1-x}As$ layer very accurately. The thickness of the epitaxial layer can be deduced from the angular spacing of pendellösung fringes,[*] if its total thickness is less than 2 μm (≙ X-ray extinction length).

When very thin layers (thickness < 100 nm) or when layered structures are studied, the diffraction maxima of the epitaxial layer and of the substrate crystal are in general not exactly distinguished, and an unambiguous assessment of lattice distortion and crystal thickness can no longer be made. In this case it is necessary to perform a theoretical treatment of the reflection behavior of the whole crystal (epitaxial layer). We have used a semi-kinematical approach of the dynamical theory of X-ray diffraction for distorted crystals.[49] The theoretical fit of the experimental diffraction curves yields detailed information on the strain profile (lattice distortion), the chemical composition, and the thickness of heterostructures. In Figure 10 we show the comparison between measured and calculated diffraction curves for a ten-period GaAs/AlAs superlattice recorded in the vicinity of the symmetric (004) $Cu_{K\alpha 1}$ reflection. The average Al concentration of the entire superlattice is determined from the angular spacing between the substrate peak and the main epitaxial-layer peak (zeroth-order peak). The angular distance $(\Delta\theta)_{\pm 1}$ between the zeroth-order ("0") peak and the satellite peak "+1" (or "−1") yields the superlattice periodicity T according to the relation

$$T = \frac{\lambda}{(\Delta\theta)_{\pm 1} \sin(2\theta_B)} \tag{1}$$

where λ is the X-ray wavelength and θ_B is the diffraction angle of the zeroth-order peak. Also the thickness of the constituent GaAs and AlAs layers can be determined accurately from these data. The position, the intensity, the half-width, and the number of the satellite peaks are crucial criteria for the layer thickness, the composition, periodicity fluctuations, the inhomogeneity of composition and the in-

[*] Pendellösung fringes = oscillations of the X-ray diffraction curve due to interferences of waves scattered at different depths of the epitaxial layer.

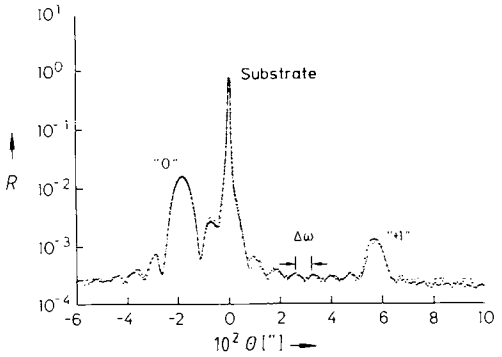

Fig. 10. Experimental (dashed line) and theoretical (solid line) X-ray diffraction curves of a $(GaAs)_{46}(AlAs)_{44}$ superlattice taken in the vicinity of the (004) reflection with $Cu_{K\alpha 1}$ radiation.

terface quality. Figure 11 shows an example for the investigation of interface homogeneity and broadening in GaAs/AlAs superlattices. The diffraction curves were recorded in the vicinity of the quasi-forbidden (002) reflection, because in this geometry the satellite peaks are more pronounced and therefore more sensitive to interface effects. For the (002) reflection the structure factor of AlAs is ten times larger than that of GaAs. The existence of interface disorder (broadening) manifests itself in an increase of the halfwidth and in a decrease of the intensity of the satellite peaks. The two GaAs/AlAs superlattices whose results are depicted in Figure 11 were grown under the same growth conditions and their periodicity is exactly the same, i.e. the maxima of the satellite peaks have the same angular spacing from the zeroth-order peak. The differences between the two superlattices are the following: During growth of sample A the growth was stopped for 10 s at each GaAs/AlAs and AlAs/GaAs interface, while sample B was grown continuously by sequentional opening and closing of the Ga and Al shutters. A detailed quantitative analysis of the diffraction curves in Figure 11 reveals that during continuous growth 2D islands with a

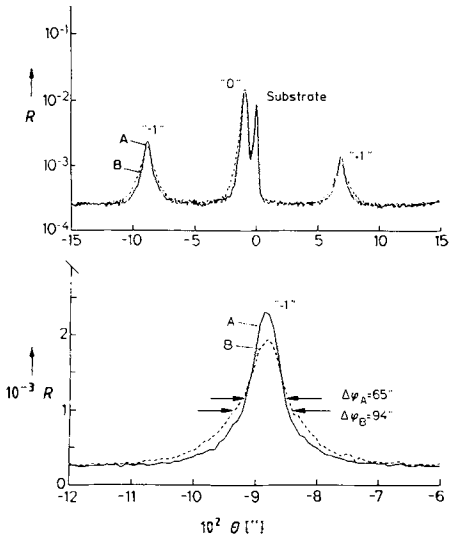

Fig. 11. X-ray diffraction curves of two $(GaAs)_{34}(AlAs)_{42}$ superlattices taken in the vicinity of the quasi-forbidden (002) reflection with $Cu_{K\alpha 1}$ radiation. Sample A was prepared with and sample B without growth interruption at the heterointerfaces.

height of one monolayer (≙lattice plane) are formed which lead to a disorder and thus broadening of the interfaces in the order of a lattice constant (≙0.56 nm). The growth interruption of 10 s is sufficient to smooth the growth surface and to produce abrupt material transitions and extremely sharp interfaces. This result is in accordance with the investigations of the RHEED intensity oscillations.[43,44]

The quantitative analysis of the interface quality by X-ray diffraction becomes even more important when the lattice parameters of the epitaxial layers have to be matched to those of the substrate by appropriate choice of the layer composition, as for $Ga_xIn_{1-x}As$ with $x=0.47$ and $Al_xIn_{1-x}As$ with $x=0.48$ on InP substrates. Therefore, in $Ga_xIn_{1-x}As/Al_xIn_{1-x}As$ superlattices also the chemical composition of the constituent layers has to be evaluated accurately. Deviations of more than one percent from the ideal value cause strain effects which give rise to significant changes in the electronic properties of the material. In some cases the semi-kinematic approach of the dynamical diffraction theory is not sufficient to analyze the measured diffraction curves quantitatively, and the more elaborate dynamical theory must be applied.[50] In Figure 12 (top) we show a comparison between the measured and the calculated diffraction curve of a $Ga_xIn_{1-x}As/Al_xIn_{1-x}As$ superlattice. The capability of both the epitaxial growth method and of the characterization method follows directly from a comparison of data compiled in Table 3 for four superlattices of this type. Finally, it should be pointed out that in an ideally lattice-matched $Ga_{0.468}In_{0.532}As/Al_{0.477}In_{0.523}As$ superlattice on InP substrate the satellite peaks have almost disappeared, as shown in Figure 12 (bottom). The low residual intensity and the pendellösung fringes are caused only by the periodicity of the structure factors in the superlattice. A high intensity of the satellite peaks thus indicates a periodic variation of the strain in

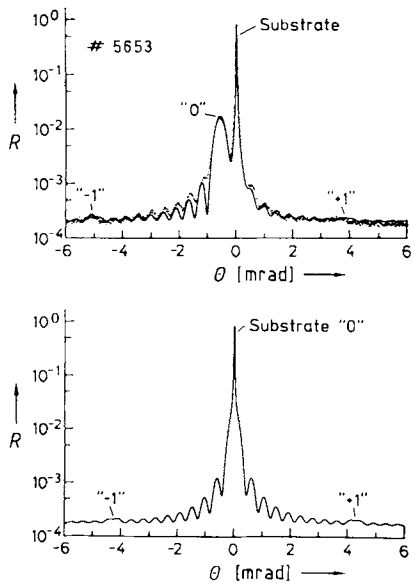

Fig. 12. X-ray diffraction curves of $Ga_xIn_{1-x}As/Al_xIn_{1-x}As$ superlattices on InP substrate taken in the vicinity of the (004) reflection with $Cu_{K\alpha 1}$ radiation. Top: From multilayer sample prepared by molecular beam epitaxy (···· experiment, —— theory). Bottom: Calculated curve for ideally lattice-matched $Ga_{0.468}In_{0.532}As/Al_{0.477}In_{0.523}As$ superlattice.

Table 3. Structural parameters of four different $Ga_xIn_{1-x}As/Al_xIn_{1-x}As$ superlattices determined by double-crystal X-ray diffraction measurements using $Cu_{K\alpha 1}$ radiation.

Thickness of $Ga_xIn_{1-x}As$ layers [nm]	Thickness of $Al_xIn_{1-x}As$ layers [nm]	Average lattice mismatch of superlattice $10^{-4}\,\bar{\varepsilon}_{zz}$	Lattice strain in $Ga_xIn_{1-x}As$ layers $10^{-4}\bar{\varepsilon}_{zz}$	Lattice strain in $Al_xIn_{1-x}As$ layers $10^{-4}\bar{\varepsilon}_{zz}$	Mole fraction x in $Ga_xIn_{1-x}As$ layers	Mole fraction x in $Al_xIn_{1-x}As$ layers
10.6	10.6	−4.5	+6.0	−15.0	0.464	0.487
10.2	10.2	+9.4	+9.5	+ 9.3	0.462	0.470
10.2	10.2	−4.0	+0.0	− 8.0	0.468	0.482
10.2	10.2	−3.5	+7.0	−14.0	0.464	0.486

strained-layer superlattices. However, when the lattice strain of the constituent $Ga_xIn_{1-x}As$ and $Al_xIn_{1-x}As$ layers are of the same magnitude, the satellite peaks also exhibit a weak intensity (see Fig. 12 (top) and Table 3).

3.3. Luminescence and Absorption Spectroscopy

For many III-V semiconductors the specific optical properties[12] play an important role for their application in optoelectronic devices. Methods to evaluate these optical properties are thus ideally also employed for a detailed characterization of microscopically structured solids composed of these materials. The measurement of the luminescence energy of bound excitons (electron-hole pair) $E_0(x)$ in the ternary $Al_xGa_{1-x}As$ alloy at 4 K, which shifts to higher energy with increasing x according to

$$E_0(x) = 1.515\ \text{eV} + x(1.247\ \text{eV}) \quad [\text{for } 0 < x < 0.45] \tag{2}$$

has for long been used to determine the Al content (in GaAs, i.e. $x = 0$, the temperature dependent band gap decreases from 1.515 eV at 4 K to 1.424 eV at 300 K). In the introduction we have already pointed out that the confinement of electrons and holes in the GaAs quantum wells gives rise to the existence of distinct energy levels (sub- or mini-bands) in the conduction and valence bands. The energy spacing between the sub-bands in the conduction and valence bands determines the spectral (energy) position of the light emission (photo- and electroluminescence) and the optical absorption characteristics.[13] In Figure 13a we show schematically the process to create electron-hole pairs by the absorption of photons and the recombination mechanism of electrons and holes, which results in light emission (luminescence). The energy position of the sub-bands depends primarily on the width (thickness) L_z and to a lesser extent on the depth V_0 of the quantum well. The energy for the confinement of electrons, i.e. the spacing between the bottom of the conduction band and the n-th sub-band, assuming infinitely deep wells is to a first approximation given by[13]

$$E_n = (n^2 \pi \hbar^2)/(2 m_e^* L_z^2) \tag{3}$$

with m_e^* = effective mass of conducting electrons[*] and $\hbar$ = Planck's constant divided by 2π. (For more accurate calculations the finite depth of the quantum well has to be taken into account. The allowed sub-bands for the electrons and holes are then given by solutions of the Schrödinger equation normalized by the boundary condition that the wave functions and their derivatives are continuous at the $GaAs/Al_xGa_{1-x}As$ interface.) From Equation (3) it follows that the energy spacing between the allowed sub-band and the band edge is directly proportional to $1/L_z^2$. Consequently, the "optical" band gap which is relevant for luminescence depends primarily on the width of the GaAs quantum well; it becomes larger when the quantum well becomes narrower. This expectation is confirmed

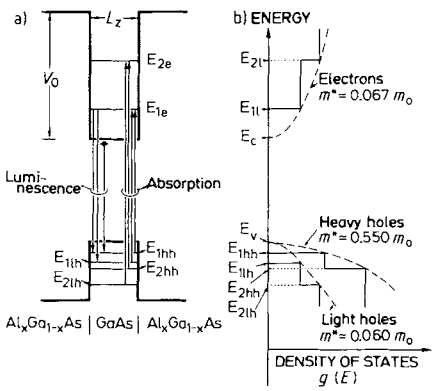

Fig. 13. Schematic illustration of (a) radiative electron-hole transitions during emission or absorption of light in a GaAs quantum well and (b) energy dependence of the density of states $g(E)$ in a homogeneous semiconductor (dotted line) and in a quantum well (solid line).

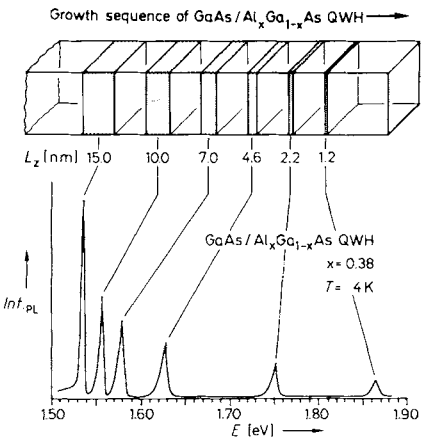

Fig. 14. Photoluminescence spectra of GaAs quantum wells of different well widths L_z. With decreasing well width a strong blue-shift (i.e. to higher energy) of the luminescence is observed. Int. = intensity in arbitrary units.

[*] In semiconductors m_e^* is used instead of the electron mass m_e to account for the influence of the crystal lattice on the conduction electrons ("effective mass approach").

by the photoluminescence measurements on GaAs quantum wells of different widths, the results of which are shown in Figure 14. The luminescence energy $(\hbar\omega)_{PL}$ is given by the energy of the transition between the n=1 electron sub-band E_{1e} and the n=1 heavy-hole sub-band E_{1hh} minus the exciton binding energy E_{ex},[51] according to

$$(\hbar\omega)_{PL} = E_g + E_{1e} + E_{1hh} - E_{ex} \quad (4)$$

(E_g = band-gap energy of GaAs). When the photoluminescence measurements are performed at low temperatures (4 K), also the phenomena arising from defects and impurities and the influence of the interface "roughness" can be studied in detail. The origin of the interface roughness are the 2D growth islands with a height of one monolayer ($a_0/2 = 0.283$ nm) discussed before, which have different lateral extensions. As shown schematically in Figure 15, these islands give rise to different widths of the quantum wells and consequently to different luminescence ener-

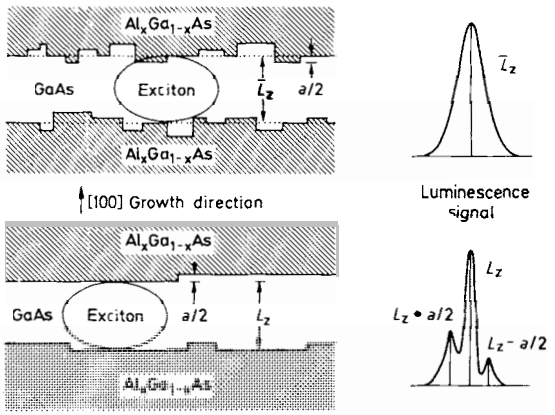

Fig. 15. Influence of the different lateral size of the 2D growth islands at the GaAs/$Al_xGa_{1-x}As$ interface on the effective width L_z of the quantum well and on the localization of excitons.

gies.[52] When the lateral extension W of the growth islands is larger than twice the Bohr radius of the exciton a_B, i.e. $2a_B$ larger than 30 nm (see also Section 4.2), then several peaks appear in the photoluminescence spectrum at different energies corresponding to the distinct islands. However, when W becomes less than $2a_B$ for smaller growth islands, then the exciton "senses" different widths of the quantum well and a spectral broadening $\Delta(\hbar\omega)_{PL}$ of the luminescence occurs,[53] given by

$$\Delta(\hbar\omega)_{PL} = (\hbar^2/m_e^*)(\Delta L_z/L_z^3) \quad (5)$$

In the experiments an increase of the linewidth with decreasing width of the GaAs quantum well was observed, because the relative influence of growth islands of constant height ($a_0/2 = 0.283$ nm) becomes larger. This undesired roughness caused by the small islands ($W < 2a_B$) can be reduced quite markedly by the interruption of growth at the interfaces.[52] Also an enhancement of the surface migration of the Group III elements results in an expansion of the larger islands at the expense of the smaller ones. This discussion emphasizes the importance of actuating the shutters of the effusion cells always at the maximum of the RHEED intensity oscillations.

In the photoluminescence spectra one generally observes electron-hole transitions only between the lowest sub-bands E_{1e} and E_{1hh} (or E_{1lh}, resp.), because the injected carriers relax extremely fast to these levels. Higher sub-band transitions, on the other hand, can be best observed by optical absorption measurements (see Fig. 13a). The absorption spectra of a $Ga_{0.47}In_{0.53}As/Al_{0.48}In_{0.52}As$ superlattice taken at 4 K and at 300 K are shown in Figure 16.[54] The steplike behavior of the absorption coefficient

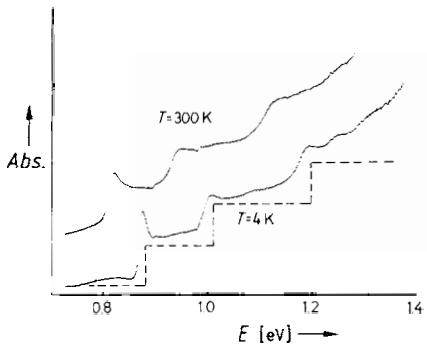

Fig. 16. Absorption spectra of a $Ga_{0.47}In_{0.53}As/Al_{0.48}In_{0.52}As$ superlattice taken at 4 K and 300 K. The dotted line indicates the steplike behavior of the two-dimensional density of states $g(E)$. Abs. = absorption in arbitrary units (logarithmic scale).

as a function of energy is clearly seen. It is caused by the modified density of states in quasi-2D systems. In addition, the absorption edge is shifted by a few meV to lower energies, and distinct excitonic absorption peaks appear (see also Section 4.1.2). For the radiative electron-hole transitions between the higher sub-band levels the selection rule $\Delta n = 0$ holds, i.e. the quantum number n does not change.

The quantization of the wave functions for electrons and for holes in one direction (i.e. in the quantum well) also results in a distinct modification of the energy dependence of the density of states $g(E)$, i.e. the number of the allowed states per energy interval, which now assumes a steplike (staircase) form (Fig. 13b).[13] In bulk semiconductors where the minimum of the characteristic lengths is much larger than the mean free path of an electron, the $g(E)$ curve always exhibits a parabolic shape and it is equal to zero at the minimum energy, i.e. at the band edge. In the case of semiconductor crystals consisting of different elements only the curvature of the parabolic $g(E)$ curve changes. In contrast to bulk material, the steplike $g(E)$ curve of quasi-2D systems has a finite non-zero value of the density of states even at the minimum energy. In addition, the distinct shape of the steplike curve can be adjusted ("tailored") by appropriate choice of the well width L_z and the potential barrier V_0. The artificial arrangement of the constituent atoms leads to a completely different shape of the $g(E)$ curve even for materials made of the most familiar semiconductor crystals, like GaAs and AlAs. To the concept of band-gap engineering mentioned in the introduction we can now add the concept of density-of-states modification. Inspection of Figure 13b further re-

veals that the size quantization also lifts the degeneracy of the light and the heavy holes in GaAs, i.e. two bound states E_{nhh} and E_{nlh} with different energies exist in quantum wells.[13]

For the measurements of the optical absorption of epitaxial layers the substrate must either be a transparent substrate, as is the case for InP in $Ga_{0.47}In_{0.53}As/Al_{0.48}In_{0.52}As$ superlattices,[54] or it must be removed by selective etching, as in the case of the GaAs substrate used to deposit $GaAs/Al_xGa_{1-x}As$ superlattices.[13] The selective removal of the substrate is difficult, and during this treatment strain can be induced in the epitaxial layers. Therefore, instead of absorption measurements, photoluminescence excitation measurements are now frequently used to acquire information on the excitonic resonances and on the energy dependence of the density of states. In this technique the luminescence intensity is measured at a fixed energy (wavelength) while the exciting laser energy is varied across the energy range of interest. Figure 17 shows such a photoluminescence excitation spectrum of a GaAs double quantum well structure. The transitions to higher subbands, which are also observable in the absorption spectrum, are clearly seen.

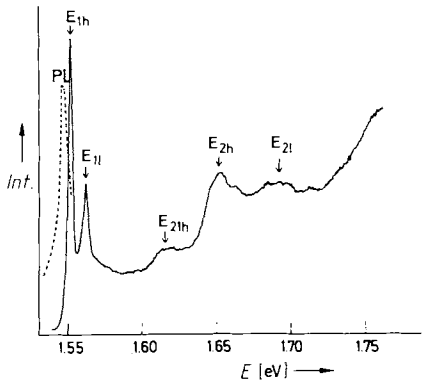

Fig. 17. Photoluminescence excitation spectrum of a 9-nm wide GaAs quantum well taken at 4 K. The dotted curve indicates the position of the photoluminescence line. Int. = luminescence intensity in arbitrary units.

3.4. Hall Effect Measurements

The feasibility of doping semiconductors intentionally with donors (to create free electrons) and with acceptors (to create free holes) and thus to form p/n junctions (or diodes) within a crystal is one of the most important basic requirements for the technical applications of these materials. The measurement of the conductivity (or resistivity, respectively) and of the Hall effect are the most important methods for determining the concentration, the mobility, and the carrier type (electrons or holes) in a semiconductor thin film. When free carriers passing through a crystal are subject to a transverse magnetic field,a phenomenon called the Hall effect appears.[55] Under these conditions an electric field is produced whose direction is perpendicular to the current direction and to the magnetic field vector. The transverse or "Hall" voltage V_H induced by the electric field is proportional to the current I and the magnetic field $\boldsymbol{B}$ and inversely proportional to the thickness of the sample d, as given in equation (6).

$$V_H = R_H \frac{I \cdot \boldsymbol{B}}{d} \tag{6}$$

The proportionality factor R_H, denoted Hall constant or Hall coefficient, is given by

$$R_H = \frac{1}{ne} \tag{7}$$

where e is the electronic charge (negative sign) and n is the electron (carrier) concentration per cm^3. An analogous relation holds for the holes.

Measurement of the Hall coefficient R_H enables determination of the carrier concentration n, which represents a characteristic quantity of semiconducting materials. When electrons as well as holes contribute to the carrier transport in the sample, the Hall coefficient depends also on the respective mobilities. The mobility μ is the proportionality factor in the relation between the drift velocity v of electrons (or holes) in a semiconducting crystal and an applied external electric field $\boldsymbol{E}$. As long as the average drift velocity is small compared to the thermal velocity, the simple relation

$$|\vec{v}| = \mu |\vec{E}| \tag{8}$$

is valid.

The Hall coefficient and the conductivity (or resistivity, respectively) of semiconducting thin films are measured by a method developed by *van der Pauw*.[56] The reciprocal of the mobility determined in this way is a direct measure of the retardation of the free-carrier drift by the influence of the crystal lattice. At low temperatures the scattering of electrons (holes) by ionized donors (acceptors) and by lattice imperfections, such as dislocations, grain boundaries, interstitials, etc., dominates. At higher temperatures, e.g. at room temperature, numerous lattice vibrations are excited so that a strong scattering by lattice vibrations ("phonons") is added to this. The various scattering mechanisms exhibit a different temperature dependence.[57] Further-

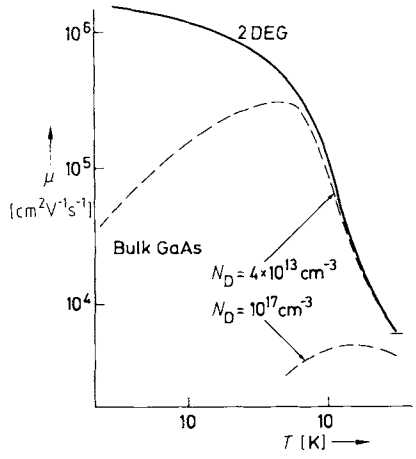

Fig. 18. Dependence of electron mobility on temperature for three different sample configurations determined by Hall effect measurements. The distinct behaviour of each curve indicates a different influence of the various scattering mechanisms in the samples. 2DEG = two-dimensional electron gas. N_D = concentration of dopant atoms.

more, electrons and holes behave differently in the various scattering processes. As a consequence, we often observe a complicated relationship between mobility and sample temperature. Figure 18 shows the dependence of the electron mobility on temperature for three different sample configurations. The highest mobility at low temperatures is obtained from a microscopically structured selectively doped GaAs/$Al_xGa_{1-x}As$ heterostructure. The layer sequence and the properties of this artificially layered structure are described in detail in Section 4.2.

4. Selected Examples for Microscopical Structuring Normal to the Crystal Surface

In the original concept of semiconductor superlattices[10] *Esaki* and *Tsu* in particular elaborated the theoretical possibilities of a carrier transport *perpendicular* to the constituent layers. They proposed the existence of extremely fast so-called Bloch oscillations due to Bragg reflections at the boundaries of the mini Brillouin zone and predicted a negative dynamic conductivity associated with the transfer of electrons into regions of negative mass of the mini Brillouin zone. As yet, however, the Bloch oscillations have never been observed experimentally and today it is anticipated that at the high electric fields required intersubband transitions of the electrons rather than Bragg reflections will occur.[58] A negative differential resistance in the current-voltage characteristics perpendicular to the layers can also be obtained from semiconductor superlattices with thicker barriers owing to "resonant" tunneling phenomena of electrons between adjacent quantum wells. This process requires matching of the energies of the ground state (first sub-band) and of the excited state (second sub-band) in the next well at a certain value of the applied external electric field, i.e. the sub-band levels are in "resonance" (see Fig. 19a for illustration). The first experiments related to this phenomenon, performed in the early seventies,[59] were not unequivocal, because at that time the material quality of the artificially layered structures did not meet the requirements. In particular, the fluctuations of the layer thickness within each quantum well, which are due to the growth islands of monolayer height discussed in Section 3.3 (see also Fig. 15), resulted in fluctuations of the sub-band energy levels of the quantum wells as well as in a destruction of the coherence between the interfering electron waves reflected at the two interfaces. Therefore, fifteen years ago other intriguing properties of the periodically layered semiconductor structures came into the forefront which had not been discussed in the original concept, i.e. the optical (excitonic) properties and the carrier transport parallel to the constituent layers (quasi-2D electron and hole systems). The microscopically structured semiconductors used for the investigation and device application of these phenomena are in general comprised of one or more quantum wells which are isolated from each other by rather thick (>5 nm) barriers. Theoretical calculations have shown that to a good approximation these multiquantum well heterostructures can be treated as if each constituent layer contributes its characteristic electronic properties to the entire system.[60]

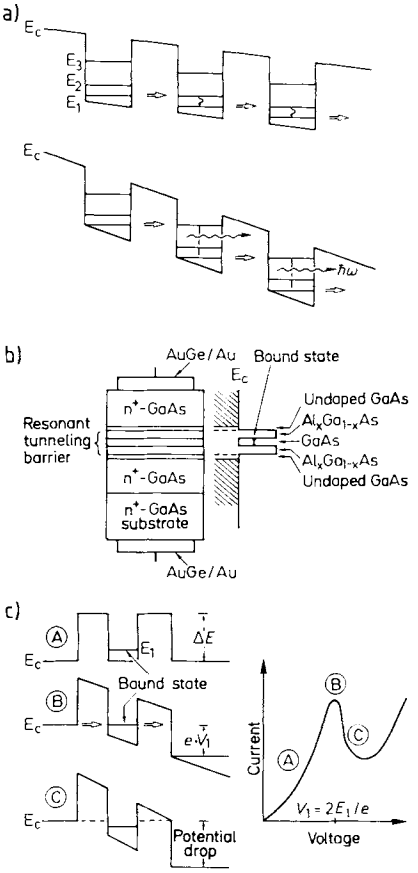

Fig. 19. Schematic illustration of resonant tunneling (i.e. vertical transport perpendicular to the layers) of electrons in GaAs/$Al_xGa_{1-x}As$ superlattices and quantum wells. a) Sequential resonant tunneling in a superlattice occurring when the potential drop across a superlattice period is equal to the energy spacing between a first excited state and ground state or between second excited state and ground state. b) Schematic layer sequence of GaAs/$Al_xGa_{1-x}As$ double-barrier diode for investigating resonant tunneling. c) Process of resonant tunneling in the double-barrier diode and plot of the measured current-voltage characteristics (not to scale).

Before some selected examples for the exciting optical and electrical properties of quasi-2D electron systems will be presented, ist should be pointed out that in the last five years the improvement of the crucial interface quality has inspired a revival of investigations related to resonant tunneling phenomena in microscopically structures semiconductors.[61] The double-barrier structures schematically depicted in Figure 19b are particularly promising for application of the resonant tunneling effect in microwave devices with extremely high switching frequencies. The operating principle of these resonant-tunneling diodes follows directly from the illustrations of Figure 19c. Electrons can tunnel through the double barrier only when the potential (Fermi) energy of the injecting (left) side coincides (is in resonance) with the sub-band energy E_{1e} in the quantum well between the two $Al_xGa_{1-x}As$ barriers by applying an external voltage. The resonant transmission of electrons gives rise to a current maximum in the I/V characteristics at an external voltage of $V = 2E_1e^{-1}$ (the applied voltage is split into two equal voltage drops at each barrier). When the applied voltage is further increased, the current drops steeply ("negative differential resistance"), since the extremely sharp resonance condition is detuned. The potential successful operation of microwave diodes based on the

resonant tunneling effect even at room temperature, imposes stringent requirements, upon the interface quality which can be met only by the application of RHEED intensity oscillation features combined with growth interruption during the spatially resolved synthesis of materials by molecular beam epitaxy.[62] This procedure makes feasible the fabrication of amplifiers and oscillators operating in the submillimeter range with a response time of less than 10^{-13} s. The frequency limit of these diodes is given by the electron tunneling time of $\tau \approx 10^{-13}$ s, which in turn derives from the ultimate limit of the uncertainty relation according to $\tau \leq \hbar/\Delta E$ (ΔE = energy broadening of the tunneling state).

4.1. Optical (Excitonic) Properties of Quasi-2D Electron and Hole Systems

4.1.1. Quantum Well Heterostructure Lasers

In conventional $GaAs/Al_xGa_{1-x}As$ double-heterostructure lasers having a 0.1–0.2 μm thick active layer the energy of the emitted laser light is primarily determined by the band gap of the material forming the active layer ($\simeq 1.42$ eV for GaAs at 300 K).[12] In addition, impurities (or dopants, respectively) of the GaAs layer significantly affect the light emission. The emission energy is always slightly reduced as compared to the band-gap energy, because this "extrinsic" luminescence dominates in doped material. The radiative electron-hole transitions responsible for luminescence change their nature drastically when the thickness of the active GaAs layer is reduced to below 30 nm. At these dimensions the formation of quantum wells with sub-bands for electrons and for holes commences (see Fig. 13). The electrons and holes can still move freely along the layers (i.e. in x- and y-direction), while perpendicular to the layers the impulse, the energy, and the wave function are quantized. It has already been shown in Section 3.3 that under normal excitation conditions the luminescence in these quasi-2D systems is given by the radiative recombination of electrons populating the lowest conduction sub-band E_{1e} with heavy holes populating the uppermost valence sub-band E_{1hh} (transitions from higher populated sub-bands retaining the quantum number selection rules of $\Delta n = 0$ are observable only under high excitation conditions). As a consequence, this "intrinsic" luminescence dominates in (undoped) quantum wells. Since the energy of the sub-bands for electrons and for holes depends primarily on L_z [see Eq. (3)], we have the possibility of adjusting the energy of the emitted light arbitrarily between 1.42 eV (for GaAs) and approximately the band-gap energy of the $Al_xGa_{1-x}As$ barriers (or cladding layers) by matching the appropriate choice of the well width during MBE growth, which is a simple geometric parameter (see Fig. 14).

In addition to the adjustable (or tunable) wavelength of the emitted light, the strongly modified density of states $g(E)$ of these quasi-2D systems was the other important motivation for the development of quantum well laser structures whose layer sequence is schematically shown in Figure 20a. Depending on the requirements for the performance of the laser diode, different configurations of the

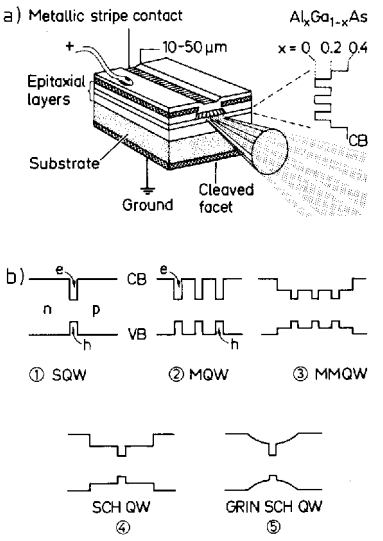

Fig. 20. Schematic layer sequence of quantum well heterostructure laser. a) Layer sequence of a modified multi quantum well (MMQW) laser and real-space energy band diagram. b) Various configurations (layer sequences) of the active region of quantum well lasers illustrated by means of the distinct real-space energy band diagrams (QW = quantum well, MQW = multi QW, SCH QW = separate confinement heterostructure QW, GRIN SCH QW = graded index separate confinement heterostructure QW).

active region are chosen (see Fig. 20b), which result in a modification of the electrical and optical confinement of the injected carriers and of the light, respectively. The simultaneous electrical and optical confinement is only possible because of the reciprocal behavior of direct band gap and refractive index in these semiconductors. However, single quantum wells often do not provide sufficient optical confinement for operation of the laser. Therefore, in the so-called separate confinement heterostructures (SCH), a separate electrical (in the quantum well) and optical confinement (in the superimposed double heterostructure) is accomplished (see Fig. 20b).

The general advantages of quantum well heterostructure lasers can be summarized as follows:[63]

1. The steplike energy dependence of the density of states $g(E)$ in quasi-2D systems gives rise to a narrow bandwidth of the optical gain and a high peak value as compared to the parabolic $g(E)$ behavior in conventional 3D systems. The population inversion required for laser operation is thus achieved at a much lower driving current, and threshold current densities can be obtained which are three to five times lower than in conventional lasers.[14]
2. The characteristic temperature T_0, which is a criterion for the temperature sensitivity of the threshold current I, has a much higher value.[64] The temperature dependence of the threshold current for semiconductor lasers is given by the empirical relation

$$I = I_0 \exp(T/T_0) \tag{9}$$

The steplike function of the density of states $g(E)$ leads to a reduced sensitivity of the energy distribution of the carriers. The resulting decreased temperature sensitivity of the emission wavelength is of particular importance

for $Ga_xIn_{1-x}P_yAs_{1-y}/InP$ and $Ga_xIn_{1-x}As/Al_xIn_{1-x}As$ lasers which operate in the long-wavelength range of 1.3–1.65 μm.

3. The quantum well lasers oscillate more easily in a single longitudinal mode (single wavelength oscillation). The device can thus be operated under direct current modulation up to a very high frequency limit, i.e. at very high bit rates.[65]
4. Quantum well lasers are especially well suited for monolithic integration with other active and passive components on a common substrate,[66] since the absorption coefficient of the non-excited part of the quantum well structure is three to five times lower at the wavelength of the emitted laser light than in conventional laser structures.

At present the best characteristics for GaAs laser diodes are achieved with the parabolic shape of the band edges depicted in Figure 20b ⑤. The parabolic shape is obtained by an appropriate grading of the Al concentration in the $Al_xGa_{1-x}As$ barriers. These so-called GRIN SCH (derived from "*Gr*aded *In*dex *S*eparate *C*onfinement *H*eterostructure) lasers can be operated with threshold current densities as low as 150 A/cm^2.[67] The accurately controlled variation of the composition and of the doping as a function of layer thickness to obtain the symmetric parabolic shape of conduction and valence band edges in these GRIN SCH structures imposes stringent requirements on the spatially resolved materials synthesis.

The wavelength range of minimum optical loss in glass fibers has been shifted from previously 0.85 μm via 1.3 μm to 1.55 μm today. Therefore laser diodes made of $Ga_xIn_{1-x}P_yAs_{1-y}/InP$ and $Ga_xIn_{1-x}As/Al_xIn_{1-x}As$ lattice-matched to InP substrate as well as $GaSb/Al_xGa_{1-x}Sb$ are now used for optical communication systems designed for long distances. The composition of the ternary and quaternary materials and the widths of the quantum wells have to be adjusted accurately such that the lasers emit in the desired wavelength range. The field of application of GaAs quantum well laser diodes is shifting more and more to optical data storage and processing as well as to information transmission and processing in local networks (including computer networks).

4.1.2. *Excitonic Phenomena*

An important consequence of the confinement of electrons and holes is that the excitonic effects have a distinct impact on the optical properties of these microscopically structured semiconductors.[51,68] Excitons are bound electron-hole pairs with a small binding energy, e.g. 4 meV in GaAs; they are created during the absorption of photons. In most homogeneous materials the "fragile" excitons are therefore observable only at low temperatures. The confinement of excitons in quantum wells prevents any dissociation induced by thermal energy, so that excitonic phenomena become observable even at and above room temperature.[69] These effects are now exploited in novel optoelectronic and photonic devices. The enhancement of the binding energy associated with the confinement of the excitons can be understood from the illustrations depicted in Figure 21. The 3D exciton in GaAs has a Bohr radius of about 14 nm. In a quantum well with a width of less than 28 nm the exciton has to shrink and it is squeezed into an elliptic form to fit to the well. The increased interaction between electron and hole induced by the confinement results in an increase of the exciton binding energy by a factor of four in a 5-nm wide GaAs quantum well.[70] In narrower quantum wells and in short-period superlattices the exciton wave function partly penetrates the barriers. The volume of the elliptic exciton thus increases and its binding energy decreases again.

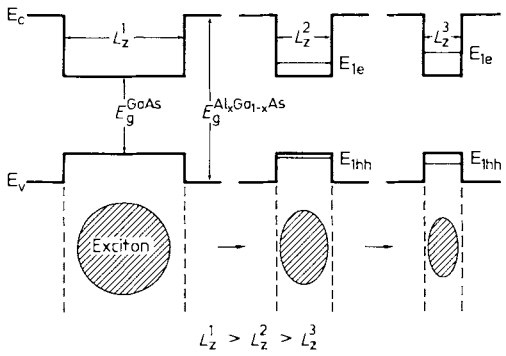

Fig. 21. Schematic illustration of the confinement of excitons in quantum wells of different widths L_z.

As a consequence of the stability of the exciton up to room temperature and higher temperatures, the semiconductor quantum wells and superlattices exhibit pronounced nonlinearities for the absorption coefficient as well as for the refractive index.[71] A saturation of the excitonic absorption is already observed at a very low intensity of the incident radiation because of the screening of the excitons by free carriers. A small increase in the incident light intensity can result in an instantaneous strong increase of the re-emitted intensity.[72] These very pronounced nonlinear optical properties make feasible the application of microscopically structured semiconductors as active elements in photonic circuits used in all-optical computers.[73]

The confinement in quantum wells makes excitons also stable against ionization in an electric field. However, when the electric field is applied perpendicular to the layers, a strong red shift (i.e. shift to lower energy) and a slight decrease in intensity of the excitonic resonances in the absorption and emission spectra is observed.[74] As shown in Figure 22, this electric field in the order of 10 mV per 10 nm (corresponding to several 10^4 V/cm) gives rise to a strong polarization of the electron and hole wave functions in opposite directions towards the interfaces. The electric field pulls the electron-hole pair apart, while the potential barriers hold the two sufficiently close together to remain bound and thus prevent ionization. The ionization can only occur when the electric field is large enough to surmount the confinement energy and the particles can tunnel out of the well.[75] It is, therefore, possible to apply fields about 50 times larger than the classical ionization field and still observe excitonic resonances. In this

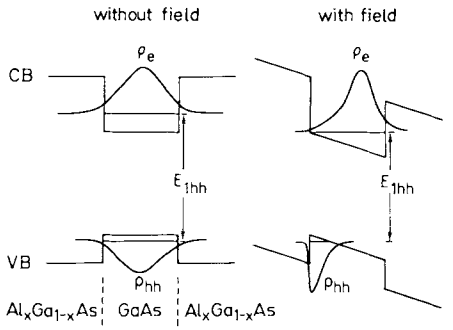

Fig. 22. Opposite polarization of electron and hole wave functions in a GaAs quantum well subject to an external electric field perpendicular to the layers. CB = conduction band edge, VB = valence band edge, ϱ_e and ϱ_{hh} = wave functions for electrons and heavy holes, respectively.

way a red shift of the absorption peak in these structures corresponding to 2.5 times the exciton binding energy is obtained even at room temperature. The pronounced optical nonlinearities and the distinct red shift of the excitonic absorption have provided a basis for the development of extremely fast (131 ps) optical modulators[76] and of self-regulating electro-optical devices (SEED, derived from *S*elf-*E*lectrooptic *E*ffect *D*evice).[77] The latter are promising for application as optical gates requiring a very low switching power, as self-linearized modulators, and as optical switching register.

The red shift of the excitonic features in microscopically structured semiconductors upon application of an electric field is observed not only in absorption but also in emission. The field-induced shift of the excitonic emission energy is particularly pronounced at low temperatures. According to the theory developed by *Brum* and *Bastard*,[78] the low-energy shift ΔE_{1e} of the lowest conduction sub-band in a perpendicular electric field of strength $\boldsymbol{E}$ is given by

$$\Delta E_{1e} \simeq \text{const}\, \boldsymbol{E}^2 L_z^4 \qquad (10)$$

i.e. it is most pronounced in wide GaAs quantum wells. This assumption is fully confirmed by the experimental results shown in Figure 23. Therefore a compromise must be found between the desired large energy shift in the electric field and the necessary confinement when choosing the width of the quantum well. An accurate analysis of the shift of the *absorption* spectra in a perpendicular electric field provides detailed information on the energy structure of the valence sub-bands. This structure is extremely complicated and at present not well understood because of the L_z-dependent partial mixing of sub-bands of heavy and light holes. The method of photocurrent spectroscopy has turned out to be extremely successful, as shown by the data in Figure 24. The observed variation of the photocurrent as a function of energy of the incident light at different electric fields yields a direct replica of the real optical absorption spectrum.[79] The change in the photocurrent can be measured with higher accuracy than the change in the absorption coefficient. The results in Figure 24 demonstrate that the quantum-number selection rules for the radiative electron-hole transitions are no longer

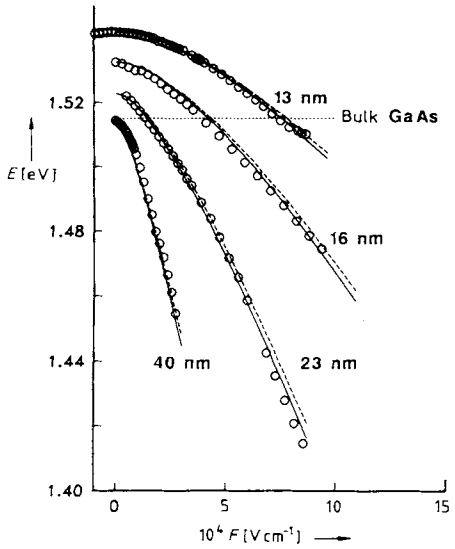

Fig. 23. Shift of the photoluminescence to lower energy (red shift) observed in GaAs quantum wells of different widths L_z subject to a perpendicular electric field. The red shift is most pronounced for the larger L_z values.

valid because of the deformation of the wave function in the electric field, and thus parity-forbidden transitions with $\Delta n \neq 0$ also become possible. These forbidden transitions, in particular, provide the unique possibility of gaining a deeper insight into the energy structure of sub-bands in quantum wells and superlattices. At the close of this section it should be pointed out that the described field-induced effect is comparable to the well-known Stark effect which is observed for atoms in an electric field. Therefore, this effect is now called the quantum confined Stark effect (QCSE).

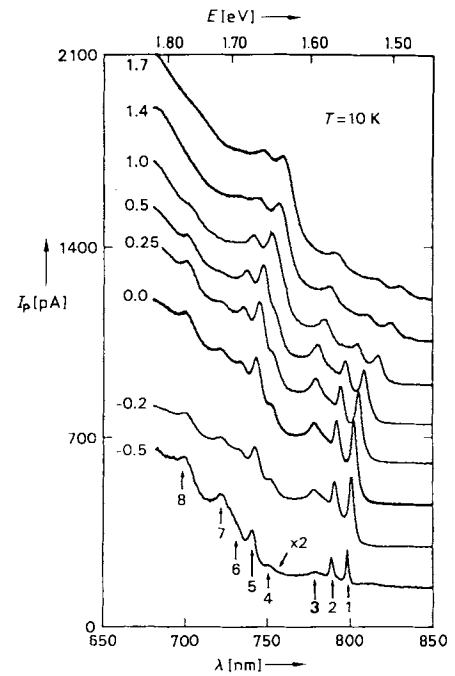

Fig. 24. Photocurrent spectra of a $GaAs/Al_{0.3}Ga_{0.7}As$ superlattice with $L_z = 8.5$ nm subject to different electric fields perpendicular to the layers. For clarity each spectrum is shifted by 150 pA on the vertical axis. At the left-hand side the individual numerical voltage values are indicated.

4.2. Spatial Separation of Free Carriers and Ionized Impurities in Selectively Doped Heterostructures

The unusual electrical properties of quasi-2D electron and hole systems were exploited in an impressive manner in the investigation of the quantum Hall effect and in the development of high electron mobility transistors, both made from selectively doped GaAs/$Al_xGa_{1-x}As$ heterostructures. The fabrication of these microscopically structured semiconductors requires that the abrupt change in composition is synchronized with the abrupt change in doping. The spatially resolved material synthesis during molecular beam epitaxy ensures that only the material with the larger band gap (here: $Al_xGa_{1-x}As$) is selectively doped with Si donors (or acceptors) in an accurately defined region and with a well defined concentration, while the material having the smaller band gap (here: GaAs) is left undoped and is of extreme purity.[80] In Figure 25 we

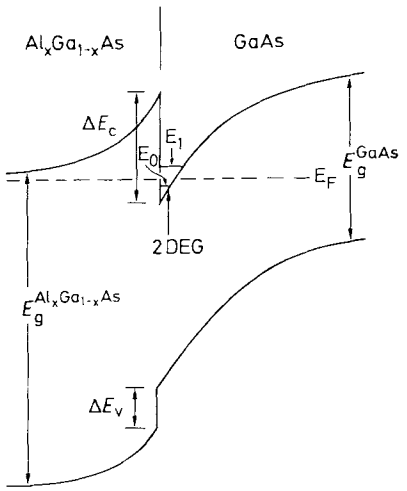

Fig. 25. Schematic plot of conduction and valence band edge in a selectively n-doped GaAs/$Al_xGa_{1-x}As$ heterostructure where only the $Al_xGa_{1-x}As$ is intentionally doped with Si donors. At the interface a quasi two-dimensional accumulation channel for electrons is formed in the GaAs.

show that in this case the free electrons arising from the shallow Si donors are transferred to the energetically more favorable conduction sub-band E_1 in the adjacent GaAs (in an analogous way the holes coming from the shallow Be acceptors would be transferred to the uppermost valence band). The n-$Al_xGa_{1-x}As$ is thus depleted at the interface, while in the GaAs close to the interface a quasi-2D accumulation channel for electrons is formed (a strong band bending towards the interface also exists of course in the GaAs). The band edge discontinuity existing at the GaAs/Al_xGa_{1-x} interface has thus led to a spatial separation of the free carriers from their parent ionized impurities confined to the n- (or p-) $Al_xGa_{1-x}As$. As a result, the ionized impurity scattering for the free carriers confined to the 2D channel in the GaAs is strongly reduced, and extremely high mobilities are observed as compared to homogeneously doped GaAs having an equivalent 3D carrier concentration of about 2×10^{17} cm^{-3}, particularly at low temperatures (see Figs. 18 and 26). But even at room temperature, where thermal phonon scattering is the dominant scattering process, selectively n-doped heterostructures exhibit an electron mobility enhanced by a factor of two.[57]

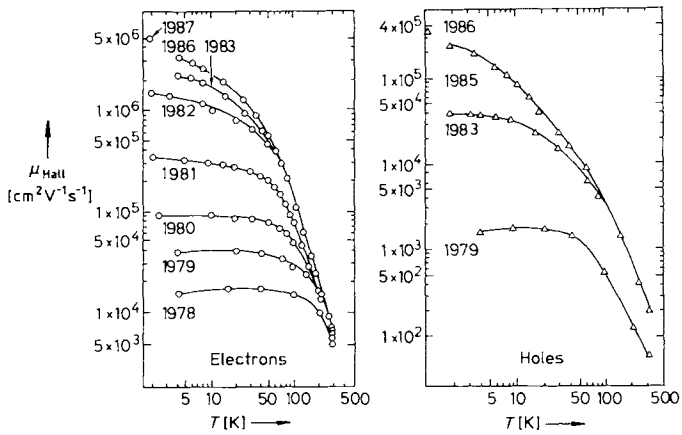

Fig. 26. Improvement of the Hall mobility of electrons (left) and of holes (right) as a function of temperature T in selectively doped GaAs/$Al_xGa_{1-x}As$ heterostructures since 1978.

In Figures 18 and 26 we demonstrate the characteristic feature of the Hall mobility μ of the 2D electron gas (2 DEG) as a function of temperature for different samples. With decreasing temperature, a very steep increase in the mobility is observed down to 77 K and then a less pronounced increase further down to liquid-He temperature (4.2 K). The sheet carrier concentrations of the 2 DEG are typically in the range $n_s=(2\text{ to }6)\times10^{11}$ cm^{-2} at 4.2 K, so that only the lowest sub-band in the triangular potential well at the interface is populated (see Fig. 25). Also the continuous increase in the carrier mobility down to very low temperatures is a characteristic feature of selectively doped heterostructures (GaAs/$Al_xGa_{1-x}As$, $Ga_xIn_{1-x}As$/InP, $Ga_xIn_{1-x}As/Al_xIn_{1-x}As$, etc.) with 2 DEG, and it is a direct consequence of the absence (or strong reduction) of scattering at ionized impurities which represents the dominant scattering process in homogeneously doped material at low temperatures. Ever since the first application of selective (or modulation) doping in heterostructures and superlattices by *Dingle* et al.[81] in 1978, every year has seen new records of electron and hole mobilities being reported (Figure 26). This continuous improvement of the carrier mobility has been achieved through taking the following measures during sample preparation:

1. The originally employed superlattice,[81] in which only the $Al_xGa_{1-x}As$ barriers were doped, was replaced by a simple heterostructure having just one heterojunction, as shown in Figure 25.
2. A thin (10–30 nm) undoped $Al_xGa_{1-x}As$ layer ("spacer") was interspersed between the interface and the doped $Al_xGa_{1-x}As$ region,[82] in order to increase the spatial separation between the free carriers in the 2D accumulation channel and their parent ionized impurities.
3. The growth conditions during molecular beam epitaxy were refined such that the residual impurity concentration of the GaAs with the 2 DEG is now in the low 10^{13} cm^{-3} range and that the GaAs/$Al_xGa_{1-x}As$ interface

is, as far as possible, free of defects.[83] When selecting the design parameters of the heterostructure (layer thicknesses, Al composition, and doping concentration) care must be taken that the $Al_xGa_{1-x}As$ layer is totally depleted and all free carriers are confined to the 2 DEG.

Inspection of Figure 26 reveals that the highest mobility achieved at present for electrons is in the order of 5×10^6 $cm^2 V^{-1} s^{-1}$. The mobilities of holes are about one order of magnitude lower because of their larger effective mass.

The selectively doped $GaAs/Al_xGa_{1-x}As$ heterostructures described above are now used worldwide in many research and development laboratories in order to fabricate electron devices having extremely high switching speeds and low power consumption (HEMT, GaAs IC)[84] and to investigate the quantum Hall effect.[3,85] The minimized devices of integrated circuits (ICs) are often based on the field-effect transistor (FET) principle, the arrangement of which is schematically shown in Figure 27. At present, there is a strong demand for shorter and shorter switching times, i.e. for higher frequency limits. The realization of short switching times requires short gate lengths ($L_G < 1$ μm) and high electron mobilities in the active channel, which exist in particular in selectively doped heterostructures. Switching speeds per gate as low as 10 ps at 300 K and 5 ps at 77 K have been obtained from test circuits (ring oscillators) equipped with two series of high electron mobility transistors (HEMTs).[86] These values are comparable to switching speeds previously only reached by the fastest switching Josephson elements which, however, had to be operated at much lower temperatures (4.2 K). The evolution of heterostructures with high-mobility holes and electrons makes feasible the application of a complementary transistor logic based on GaAs. At present the primary applications of transistors and circuits fabricated from selectively doped heterostructures are extremely fast processor units for supercomputers, extremely fast operating digital-analog and analog-digital converters, as well as low-noise analog amplifiers for microwave technology.[84] The latter ones are now commercially available from various manufacturers.

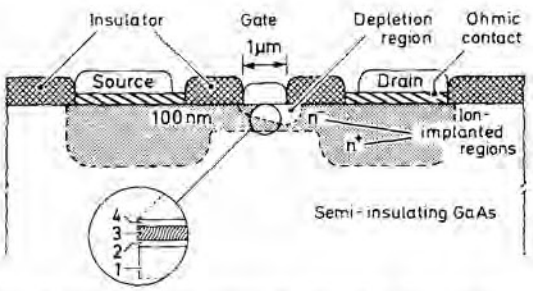

Fig. 27. Schematic configuration of a field-effect transistor ("HEMT") with the active region composed of a selectively doped $GaAs/Al_xGa_{1-x}As$ heterostructure.

The quantization of the Hall resistance in quasi-2D electron and hole systems is of great importance not only for metrology (determination of the unit of the electrical resistance and of Sommerfeld's fine structure constant, α, respectively[87]) but also for fundamental areas of experimental and theoretical solid state physics (localization, Wigner lattice, electron-electron correlation, many body effects, etc.).[3,85] A strong magnetic field ($5 < \boldsymbol{B} < 20$ T) is applied perpendicular to the 2 DEG plane at low temperatures ($T < 4.2$ K) in order to measure these macroscopic quantum phenomena. Under these conditions the electron system is completely quantized. In addition to the electrical quantization of the motion perpendicular to the interface, the magnetic quantization of the motion parallel to the interface is imposed on the carriers; this leads to the formation of the familiar Landau levels, whose energy is characterized by the Landau quantum numbers. Each Landau level can accommodate only a limited number of electrons, and this number depends only on e/h and $\boldsymbol{B}$. Macroscopic quantum phenomena, as e.g. the relative extrema in the electrical resistance of the sample, always occur under the condition that the Fermi level E_F crosses a Landau level. In selectively doped heterostructures having a constant carrier density such quantum oscillations can thus be observed when the transverse magnetic flux density (induction) $\boldsymbol{B}$ is varied continuously from 0 to 20 T. With increasing flux density the Landau levels move across the Fermi level, which on average remains constant, and we observe oscillations in the magnetoresistance (i.e. the longitudinal resistance) R_{xx} (see Fig. 28), which are known as Shubnikov-de Haas oscillations.[57] The measured Hall voltage U_H of the 2 DEG is given by $U_H = R_H I \boldsymbol{B}$ [see also Eq. (6)], where the Hall constant R_H of the 2D carrier system depends only on the (constant) carrier density and on the (constant) elementary charge. When we now introduce the Hall resistance as $R_{H,i} = M_{H,i}/I$ and measure this quantity under the condition that only a certain number i of Landau levels is completely filled, i.e. at certain $\boldsymbol{B}$ values, this gives rise to a quantization of the Hall resistance in rational fractions of (h/e^2).

Figure 28 shows characteristic plots of the magnetoresistance R_{xx} and of the Hall resistance $R_{H,i}$ measured on a selectively doped $GaAs/Al_xGa_{1-x}As$ heterostructure at a

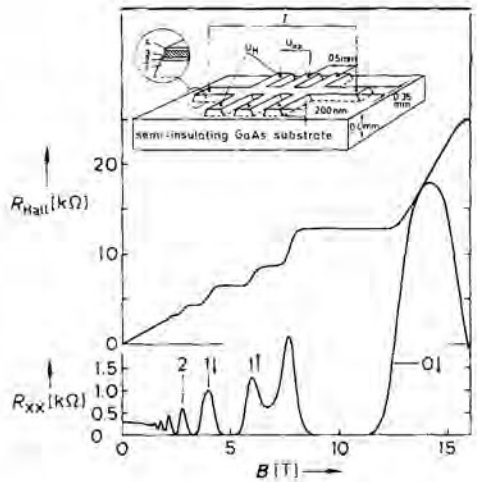

Fig. 28. Hall resistance R_H and magneto- ("longitudinal") resistance R_{xx} of a selectively doped $GaAs/Al_xGa_{1-x}As$ heterostructure as a function of the magnetic flux density $\boldsymbol{B}$. The configuration of the Hall-bar is schematically shown in the upper inset.

temperature of 1.3 K.[3] The curve of the magnetoresistance clearly displays the well-known Shubnikov-de Haas oscillations. Always when a certain number i of Landau levels is completely filled at a well defined magnetic flux density, the Fermi level E_F is just located in the range of the energy gap between two Landau levels and the conductivity σ_{xx} goes to zero with decreasing temperature (since free states in the vicinity of E_F do not exist, a scattering cannot occur). The individual Landau levels are labeled in Figure 28 by the corresponding quantum numbers n. The additional structure for $n \leq 2$ is caused by the additional spin splitting. For magnetic fluxes of $B \geq 3\,T$ the minima of the magnetoresistance are considerably broadened, and in the $R_{H,i}$ curve we observe pronounced regions (plateaus) of constant resistance. These resistance plateaus always appear at values of h/ie^2 and they are totally independent of the specific geometry of the Hall bar and on the design parameters of the heterostructure.[85] The Hall plateaus are extremely flat, and they can therefore be measured with high accuracy. The values of the rational fractions of the quantized Hall resistance are not only independent of the sample employed, but also appear at exactly the same values for many other materials. Thus, the chemical properties of the materials play only a minor role in the existence of these macroscopic quantum phenomena. The explanation for the occurrence of these plateaus is based on the assumption that localized states between the discrete Landau levels exist which are generated by defects or residual impurities in the samples.[3] As a consequence, in samples with higher electron mobility ($\mu > 2 \times 10^5$ cm^2 V^{-1} s^{-1}) the Hall plateaus are observed at lower magnetic flux densities; however, the width of the plateaus decreases drastically in these samples having a lower residual impurity concentration. For fundamental investigations of the quantum Hall effect we have recently incorporated a certain amount of impurities into the 2 DEG region of selectively doped heterostructures with a high spatial resolution.[88]

Based on the results described previously, the Physikalisch-Technische Bundesanstalt (PTB) in Braunschweig has performed precision measurements of the quantized Hall resistance.[89] An accuracy and reproducibility has been obtained for different samples which had never been reached before. The Hall resistance at the step $i = 2$ was determined as $R_{H,2} = 12906.403\ (1 \pm 2.7 \times 10^{-7})$ Ohm, from which a value of $\alpha^{-1} = 137.035992\ (1 \pm 2.7 \times 10^{-7})$ follows for the fine structure constant. During a longer measuring period a standard deviation as low as $s = 4.6 \times 10^{-8}$ was obtained for the ratio of the Hall resistance at the step $i = 2$ to a conventional reference (standard) resistor having nearly the same numerical resistance value. This extremely high precision makes feasible the application of the quantized Hall resistance as a reference resistor for the maintenance of the Ohm preserved in the various national standard laboratories.

4.3. GaAs/AlAs Monolayer Alloys

The control of spatially resolved materials synthesis by molecular beam epitaxy has now reached a standard that makes feasible the reproducible fabrication of periodically layered structures composed of III-V compound semiconductors or of group-IV-elements whose periodicities are equal to or less than the lattice constant of the components of the superlattice.[90] Figure 29 shows schematically the

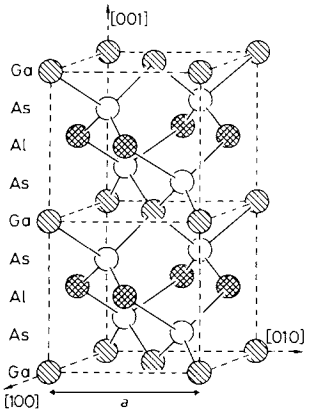

Fig. 29. Schematic arrangement of constituent atoms in a $(GaAs)_1(AlAs)_1$ superlattice ("monolayer alloy") which represents an ordered ternary alloy of composition $Al_{0.5}Ga_{0.5}As$.

arrangement of the atoms in the $(GaAs)_1(AlAs)_1$ superlattice, which is composed of alternating (001) GaAs and (001) AlAs monolayers. The $(GaAs)_1(AlAs)_1$ superlattice is therefore also called monolayer solid solution or monolayer alloy. It has the same composition as the ternary alloy $Al_{0.5}Ga_{0.5}As$ and can thus be considered as an ordered alloy.[91] The motivation for the fabrication of these $(GaAs)_m(AlAs)_n$ superlattices with $(m,n) < 5$ were careful considerations to substitute the ternary $Al_xGa_{1-x}As$ alloy, where the Al and Ga atoms are statistically distributed on the lattice sites of the Group III elements and which exhibits some detrimental structural, electrical, and optical properties. First, the $Al_{0.5}Ga_{0.5}As$ is an indirect-gap semiconductor[12] and the radiative electron-hole recombination requires the assistance of a phonon. Second, the electrical properties of n-type $Al_xGa_{1-x}As$ for $x > 0.2$ are controlled by a deep donor ("DX center") in addition to the hydrogen-like shallow donor due to the peculiar band structure of the alloy.[92] The concentration of the deep donor increases with x and it is the origin of the persistent photoconductivity effect. Third, the interface roughness for growth of binary GaAs or AlAs on the ternary alloy due to the differences in the Ga and Al surface migration yields inferior excitonic and transport properties.[43,44]

During growth of $(GaAs)_m(AlAs)_n$ superlattices with $(m,n) < 5$ by molecular beam epitaxy the growth rate and the interface formation were accurately controlled by monitoring the RHEED intensity oscillations.[90] The growth temperature was lowered to 500 °C to prevent the interdiffusion of Ga and Al across the interfaces, and the growth rate was reduced to one monolayer per 5 s to facilitate the build-up of the crystal atom by atom.[91] At each interface the growth was interrupted for 5 s to produce an atomically flat growth surface before the next monolayer was deposited. Excellent UHV conditions in the MBE system were the most crucial requirements in order to accomplish these growth parameters. The well-ordered periodic layer-by-layer arrangement of Ga and Al atoms on the ap-

propriate lattice sites in the [001] direction in the $(GaAs)_m(AlAs)_n$ superlattices with $m=n$ and $m=1$, 2, 3 manifests itself in the appearance of distinct satellite peaks around the Bragg reflections of the X-ray diffraction patterns shown in Figure 30.[91] As expected, these short-period superlattices exhibit a slight tetragonal distortion in

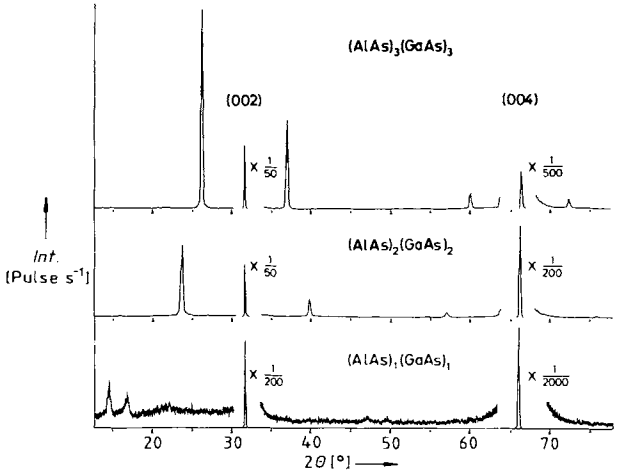

Fig. 30. X-ray diffraction patterns of three short-period $(GaAs)_m(AlAs)_m$ superlattices with $m=1$, 2, 3 taken with $Cu_{K\alpha}$ radiation.

the z-direction. The important structural parameters of the $(GaAs)_m(AlAs)_m$ superlattices compiled in Table 4 were obtained from the position of the satellite peaks and from the angular spacing $\Delta\theta_{0,S}$ between the Bragg reflection of the epitaxial layer and the substrate (not shown in Fig. 30) in a similar manner as described in Section 3.2. The results of Table 4 indicate that the periodicity of the $m=1$ superlattice is about 8% larger than the ideal value of 0.566 nm. However, this deviation does not have any influence on the unique optical properties of this sample.

Table 4. Structural properties of ultrathin-layer $(GaAs)_m(AlAs)_m$ superlattices obtained from X-ray diffraction measurements using $Cu_{K\alpha}$ radiation.

Superlattice configuration	$\Delta\theta_{0,S}$ $\times 10^{-4}$ rad (004)	Average Al content x	Satellite peak position [°] (002)		(004)		Period T [nm]	T/a
$(AlAs)_1(GaAs)_1$	−9.27	0.51	8.43	23.49	24.8		0.6117	1.08
$(AlAs)_2(GaAs)_2$	−9.27	0.51	11.83	19.87	28.45	37.88	1.135	2.01
$(AlAs)_3(GaAs)_3$	−8.81	0.49	13.73	18.55	30.25	36.73	1.714	3.03

This naturally poses the question of the actual differences in the electronic properties between these short-period $(GaAs)_m(AlAs)_n$ superlattices and the ternary $Al_{0.5}Ga_{0.5}As$ alloy having the same composition. To answer this question we have compared the photoluminescence spectra obtained from these samples; the results are compiled in Figure 31 and in Table 5.[91] The luminescence spectrum of the $Al_{0.5}Ga_{0.5}As$ alloy (indirect-gap semiconductor) consists of three bands having approximately the same intensity (the two lower energy lines arise from phonon-assisted transitions), while the $(GaAs)_m(AlAs)_m$ superlattices with $1<m<4$ exhibit only one broad line which strongly shifts in energy as a function of periodicity. It is important to note that the luminescence energy is highest at $m=3$ but then decreases significantly for $m<3$ and $m>3$. According to calculations of the bound states in quantum wells and superlattices, the low-energy shift for $m>3$ is expected, whereas the observed red shift of the luminescence from $m=3$ via $m=2$ to $m=1$ is in contrast to this simple approximation. We can no longer describe the electronic properties of these short-period superlattices with $m=1$, 2, and 3 by the simple assumption that each constituent layer contributes its characteristic properties to the whole system. The shift of the luminescence from the $(GaAs)_1(AlAs)_1$ monolayer alloy by 146 meV to lower energy as compared to the $Al_{0.52}Ga_{0.48}As$ ternary alloy clearly indicates the existence of a new artificial synthetic material. Calculations of the energy band structure of short-period superlattices thus require the treatment of the superlattice crystal as a whole. Recent theoretical calculations performed on this basis are in good agreement with our experimental luminescence results obtained from $(GaAs)_m(AlAs)_m$ superlattices with $m=1$, 2, 3, 4.[93] Also the electrical properties of the $(GaAs)_1(AlAs)_1$ monolayer alloy are possibly of special interest. A pronounced reduction in the alloy scattering is anticipated in doped samples.[94] This additional scattering mechanism results in a significant reduction of the carrier mobilities in random ternary and quaternary alloys.

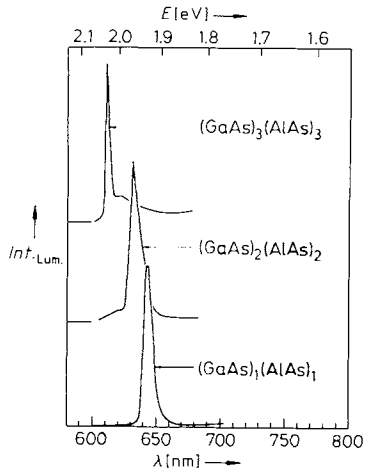

Fig. 31. Low-temperature photoluminescence spectra taken from the short-period $(GaAs)_m(AlAs)_m$ superlattices with $m=1$, 2, 3. Int.$_{Lum.}$ = luminescence intensity in arbitrary units (linear scale).

Table 5. Variation of photoluminescence peak energy as a function of period length observed in ultrathin-layer $(AlAs)_m$-$(GaAs)_m$ superlattices kept at 2 K. For comparison, the energy of the bound-exiton luminescence detected in the ternary $Al_xGa_{1-x}As$ alloy is also listed.

Superlattice configuration	Average Al content x	Luminescence peak energy [eV]
$(AlAs)_1(GaAs)_1$	0.51	1.931
$(AlAs)_2(GaAs)_2$	0.51	1.968
$(AlAs)_3(GaAs)_3$	0.49	2.033
$(AlAs)_4(GaAs)_4$	0.49	1.964
$Al_xGa_{1-x}As$ alloy	0.52	2.077

The short-period superlattices with periodicities down to monolayer alloys have been fabricated not only from lattice-matched components such as GaAs/AlAs, but also from components which exhibit considerable differences in the lattice constants, e.g. GaAs/InAs (7% lattice mismatch)[95] and Si/Ge (4% lattice mismatch).[96] In all cases, successful fabrication was accomplished by spatially resolved synthesis during molecular beam epitaxy.

4.4. Monolayer Doping in GaAs

The concept of monolayer doping, also called delta (δ) or atomic-plane doping and schematically shown in Figure 32, was originally proposed to improve the doping profiles

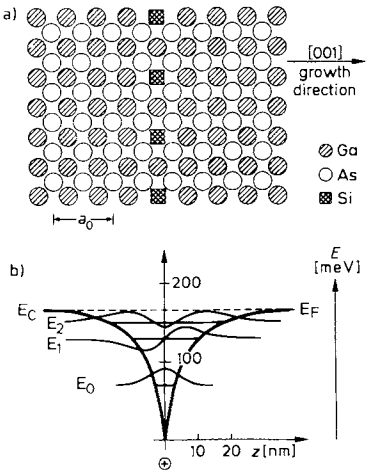

Fig. 32. a) Illustration of the concept of monolayer (delta) doping in GaAs. b) Formation of a V-shaped potential well for electrons by Si monolayer doping (not to scale).

of Ge-doped n-type GaAs layers.[97] We have employed the implementation of monolayer doping profiles with Si donors and Be acceptors in GaAs to generate symmetric, V-shaped potential wells with a quasi-2D carrier gas and to create a new sawtooth doping superlattice having a significantly reduced effective energy gap.[98] The dopant atoms are located in an atomic monolayer parallel to the surface of the (001)-oriented GaAs host material, and the ionized Si donors (or Be acceptors) provide a continuous sheet of positive (or negative) charge. The fractional occupation of the available Ga sites in the (001) plane by dopant atoms can reach several percent. The impurity charge distribution N_D can mathematically be described by the Dirac-delta function according to $N_D = N_D^{2D}\delta(z)$, where N_D^{2D} is the 2D donor concentration. The positive sheet of charge creates a V-shaped potential well. Due to the electrostatic attraction, the electrons remain close to their parent ionized donors and form a quasi-2D electron gas with quantized energy levels (sub-bands) in the narrow potential well. Direct evidence for the existence of a quasi-2D electron system was provided by magnetotransport measurements.[99]

The monolayer doping profiles were obtained during molecular beam epitaxy by interrupting the growth of the GaAs host crystal at the desired position by closing the shutter in front of the Ga effusion cell and leaving the arsenic shutter open. The shutter of the respective dopant effusion cell is opened for a certain time interval (depending on the required doping level up to several minutes). After the intended doping level has been reached, the effusion cell shutter is closed, and the crystal can continue to grow without distortion by opening of the shutter of the Ga source. When the growth temperature is kept below 550°C the distribution of the dopant atoms is indeed restricted to one (001) monolayer. In this way high doping densities of more than 1×10^{13} cm^{-2} in GaAs can easily be achieved with Si as well as with Be dopants. These high densities locally exceed the solubility limit of the respective impurities in GaAs. But nevertheless almost all donors (or acceptors) are ionized and the measured free-carrier concentrations give a realistic picture of the intentionally incorporated impurity atoms.[98] Due to the close proximity of the ionized impurities, the mobilities of the electrons (holes) confined to the V-shaped potential well are comparable to homogeneously doped material, and they are thus much lower than in the selectively doped heterostructures described in Section 4.2.

The concept of monolayer doping during molecular beam epitaxy makes feasible the spatially resolved incorporation of a sheet of electrons and/or holes confined to one lattice plane into a semiconductor crystal. For the reader it is important to note that even at a doping density of 5×10^{12} cm^{-2} not more than one out of one hundred Ga atoms on the (001) plane is replaced by an impurity atom. This explains the crucial purity requirements during growth of the epitaxial layer. We present here two examples for the application of a high-density sheet of electrons in GaAs confined to one (001) monolayer: (i) non-alloyed ohmic contacts having a low contact resistance[98] and (ii) field effect transistors (FETs) having a high transconductance.[100] When the lattice plane doped by an amount of 1×10^{13} cm^{-2} impurity atoms is located just 3 nm beneath the (001) crystal surface, the electrons (or holes) can virtually tunnel without any potential barrier between a metal electrode deposited on the surface and the quasi-2D carrier system. This arrangement thus represents an ohmic contact between the deposited metal and the underlying semiconductor, which exhibits a low specific contact resistance of less than 10^{-6} Ω cm^{-2} without the necessity of alloying (i.e. heating for a short time to 400°C in a stream of hydrogen gas). A (001) GaAs lattice plane having $N_D^{2D} = 4\text{–}6 \times 10^{12}$ cm^{-2} carriers and positioned 25 nm beneath the crystal surface can be employed as current-conducting sheet in a field-effect transistor. Detailed investigations of the HEMTs described in Section 4.2 have demonstrated that, in addition to the enhanced electron mobility, primarily the confinement of the electrons to a quasi-2D channel is responsible for the highly improved characteristics of this device. In the monolayer-doped FET (δ-FET) the electrons are confined to the V-shaped potential well and, thus, during pinch-off below the gate they cannot escape to the undoped semiconductor region. In this way, high transconductances can be achieved in this transistor. In addition, electron densities as high as 6×10^{12} cm^{-2} can be realized in the δ-FET, which are larger by a factor of three than in the HEMT. This higher electron density more than compensates for the lower electron mobility, and the δ-FET exhibits excellent device characteristics.

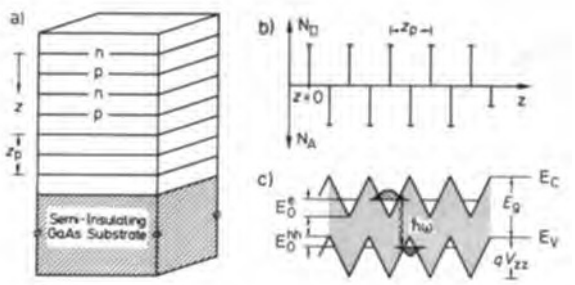

Fig. 33. a) Schematic configuration of a GaAs sawtooth doping superlattice which is composed of a periodic sequence of alternating n- and p-doped monolayers interspersed by undoped GaAs. b) Periodic variation of the doping profile in the direction of layer sequence. c) Sawtooth-shaped modulation of conduction and valence band edge. Also indicated is the radiative electron-hole recombination between the lowest electron and hole subbands.

The layer sequence of GaAs sawtooth doping superlattices is schematically shown in Figure 33a. The structure consists of a periodic sequence of alternating n- and p-type monolayers equally spaced by 5–20 nm undoped GaAs regions.[101] The doping profile (Fig. 33b) can be described by a periodic train of δ-functions. The periodic variation of the positive and negative space charge in the z-direction gives rise to a sawtooth-shaped modulation of conduction and valence band edges (Fig. 33c). In this superlattice the electron-hole recombination important for the emission of light occurs between the lowest electron and hole subbands, E_{1e} and E_{1hh}, in adjacent potential wells. The "optical" band gap given by

$$E_g^{SL} = E_g^0 - qV_z + E_{1e} + E_{1hh} \tag{11}$$

is thus *smaller* than the band gap E_g^0 of the homogeneous material. In Equation (11), q denotes the elementary charge and $V_z = \frac{1}{4}(q/\varepsilon)N^{2D}z_p$ the amplitude of the band-edge modulation (z_p = periodicity of the superlattice and ε = permittivity of the semiconductor). The effective band gap of GaAs sawtooth doping superlattices can thus be shifted by several hundred meV to lower energies by appropriate choice of the monolayer doping density and of the periodicity. We have used this effect to fabricate light emitting diodes and lasers operating in the wavelength range $\lambda > 900$ nm. As a result, we have produced a new material with accurately tailored optical properties by the spatially resolved incorporation of donor- and acceptor-rich lattice planes into a GaAs crystal.

4.5. Strained Si/Ge Superlattices

In the lattice-matched semiconductor superlattices described previously, the lattice constants of the components differ by less than 0.5%. The ordering of the energy band edges at the interfaces is therefore mainly affected by the discontinuity in electron affinity across the heterojunction. However, the strain of the constituent layers in GaSb/AlSb superlattices having a lattice mismatch of only 0.7% can already affect the ordering of the electronic bands.[12] For larger lattice mismatches the strain increases, and it can produce a complete new ordering of the energy band edges. During their investigations of superlattices made of the GaP/GaAs materials system, *Mathews* and *Blakeslee*[103] had recognized already at the beginning of the seventies that semiconductor superlattices almost free of dislocations at the interfaces can be fabricated also from components with a large lattice mismatch, if the constituent layer thicknesses do not exceed a certain critical value of, e.g. 10 nm. Under these conditions the lattice mismatch is totally accommodated by coherent elastic strain and no misfit dislocations are formed at the interfaces. The procedure to build up strained-layer superlattices is schematically shown in Figure 34. The early studies on this subject, which were almost ignored at that time, were revived again at the beginning of the eighties, and today strained-layer superlattices have become the subject of intensive investigations. As a characteristic example of strained-layer superlattices for this review paper we have selected the Si/Ge system, because it is of particular importance for device application.[104]

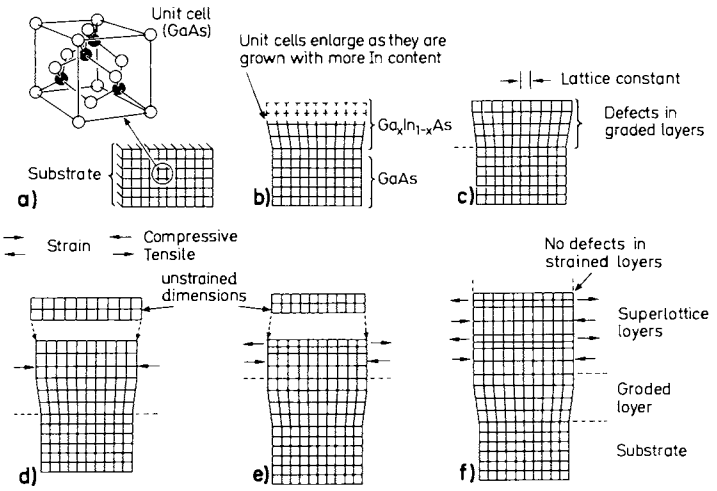

Fig. 34. Schematic illustration of the formation of strained layer superlattices, e.g. GaAs/$Ga_xIn_{1-x}As$ with $x \simeq 0.3$.

According to Vegard's law the lattice mismatch η_0 between Si and Si_xGe_{1-x} is given by $\eta_0 = (a_{SiGe} - a_{Si})/a_{Si} = 0.042x$, where a_{Si} and a_{SiGe} are the respective lattice constants. The successful fabrication of Si/Si_xGe_{1-x} superlattices over the whole composition range was accomplished only after the substrate temperature was reduced during MBE growth to below 600°C (the Si source material is evaporated by electron beam evaporation owing to the high crucible temperature required). In these experiments it has been shown that the upper critical layer thicknesses, at which the formation of misfit dislocation begins, are considerably larger than predicted by the theoretical model of *van der Merwe*.[104]

The aspect of particular importance in strained-layer superlattices is the possibility of modifying the distribution of the strain of the whole epitaxial film on the constituent layers arbitrarily by appropriate choice of the substrate or of the buffer layer (see Fig. 35 for illustration). In this manner the ordering of the conduction and valence band edges across the heterojunctions can be deliberately adjusted.[105] The tetragonal strain existing in the Si/Ge system induces a splitting of the sixfold degenerate conduc-

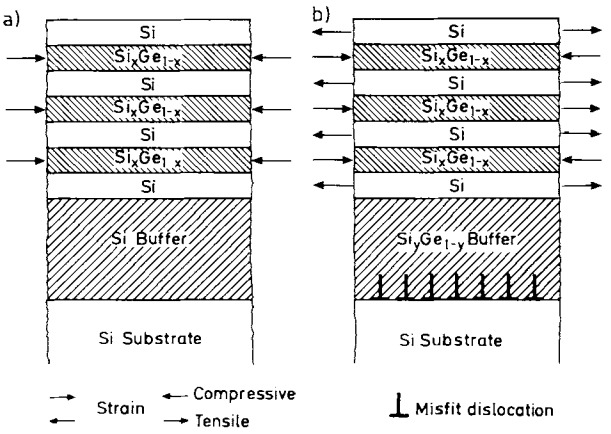

Fig. 35. Schematic illustration of the distribution of the strain of the entire epitaxial film on the constituent superlattice layers by appropriate choice of the buffer layer or of the substrate (for details see text).

tion band into twofold and fourfold degenerate valleys. When the $Si/Si_{0.5}Ge_{0.5}$ superlattice is grown on a Si substrate or buffer layer, as shown in Figure 35a, the constituent Si layers of the superlattice are not strained, whereas the constituent $Si_{0.5}Ge_{0.5}$ layers have to accommodate the total (compressive) strain. This strain, however, can be distributed symmetrically on the two constituent layers when the superlattice is grown on a thick $Si_{0.75}Ge_{0.25}$ buffer layer whose lattice constant is between that of Si and that of $Si_{0.5}Ge_{0.5}$ (see Fig. 35b). In this case the two constituent layers are strained by the same smaller amount, but in opposite directions (i.e. tensile strain in Si and compressive strain in $Si_{0.5}Ge_{0.5}$). These two possibilities of strain distribution result in a completely different position of the energy band edges relative to each other, as schematically shown in Figure 36.

It is important to note that the conduction band edge of the wider-gap material Si can be *lower* in energy than that of $Si_{0.5}Ge_{0.5}$ when a $Si_{0.75}Ge_{0.25}$ buffer layer is employed.[105] As a consequence we can obtain a quasi-2D electron gas with considerably enhanced mobility in the Si layers by selective doping of the constituent $Si_{0.5}Ge_{0.5}$

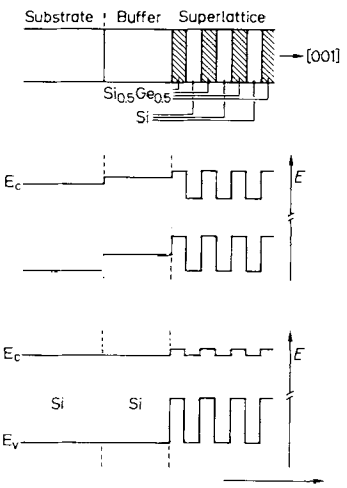

Fig. 36. Variation of the energy position of the band edges in $Si/Si_{0.5}Ge_{0.5}$ superlattices with respect to each other as a function of the distinct distribution of the total strain on the constituent layers by the selection of two different buffer layers.

layers with Sb donor impurities (Fig. 37). A selective n-type doping of the Si layers of the superlattice does not yield a mobility enhancement. On the other hand, also a quasi-2D hole gas of enhanced mobility in the Si layers can be formed by selective doping of the constituent $Si_{0.5}Ge_{0.5}$ layers with Ga acceptor impurites.[106] The significantly enhanced carrier mobilities in these selectively doped Si/Si_xGe_{1-x} superlattices are of great current interest for application in high-speed transistors which operate according to the same principle as the HEMT described in Section 4.2.

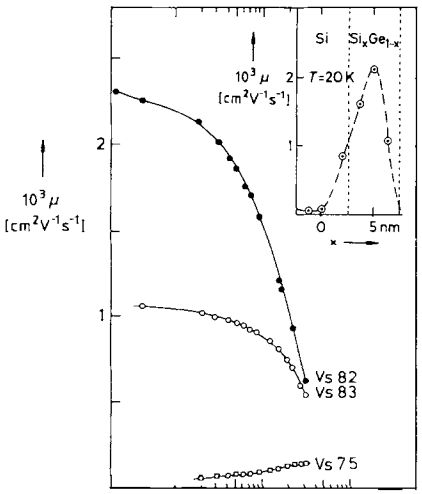

Fig. 37. Temperature dependence of the Hall mobility μ in selectively n-doped strained $Si/Si_{0.5}Ge_{0.5}$ superlattices deposited on $Si_{0.75}Ge_{0.25}$ buffer layers for three samples with different positions of the Sb dopant atoms (Vs 75: center of the Si layer, Vs 82: center of the $Si_{0.5}Ge_{0.5}$ layer, Vs 83: edge of the $Si_{0.5}Ge_{0.5}$ layer). In the upper inset the observed variation of the Hall mobility μ at 20 K as a function of the position of the Sb dopant atoms x is depicted.

In the strained-layer superlattices a structural periodic modulation exists in addition to the chemical modulation in the direction of the layer sequence. This coexistence provides a new degree of freedom to adjust the intriguing custom-tailored electronic properties of these materials. In this field we have just arrived at the very beginning of an exciting stage of development, because the possibilities of combining different materials are far more abundant than in the case of the lattice-matched materials systems.

In metallic materials systems, there are no rigid, directed covalent bonds as in semiconductors. Therefore, the constituent elements for the formation of artificial superlattices always have to be chosen very carefully such that the expected periodic modulation of the chemical composition in the growth direction remains stable at the required growth temperature. Research activities in the field of metal superlattices were very few until 1980, when *Schuller*[107] successfully fabricated a Nb/Cu superlattice. The constituent elements of this superlattice exhibit totally different crystal structures, and they show large differences in their lattice constants. The cubic body-centered Nb grows in the

[110] direction in this superlattice. Since that time the metal superlattices can roughly be devided into two groups: In group 1 superlattices, the two constituent elements have the same crystal structure and they form a continuous series of solid solutions. The periodic modulation of the composition, which is produced during growth, is intrinsically unstable. Examples include the combinations Cu/Ni, Ag/Pd, Nb/Ta, and Gd/Y. In group 2 superlattices, the two constituent elements have a different crystal structure, and their miscibility is rather limited. Therefore, the periodic modulation of the composition in the direction of layer growth exhibits a higher stability. Examples include Nb/Cu, Nb/Al, and Mo/Ni. To a first approximation, geometrical considerations can be taken into account in order to select the two constituent elements suitable for a group 2 superlattice and their orientation with respect to each other.[108] The most common situation for their orientation is that lattice planes of such orientation preferably grow one on top of the other where the packing density of atoms in the plane (atoms per nm^2) is maximized *and* similar for both elements.

Metal superlattices of group 1 have in general been fabricated by molecular beam epitaxy. Carefully synthesized monocrystalline samples, e.g. Nb/Ta superlattices[109] and Gd/Y superlattices,[110] exhibit a coherence length of several hundred nanometer in the periodic modulation, and the broadening at their interfaces amounts to only a few atomic layers. The periodicity of $(Gd)_m(Y)_n$ superlattices could be reduced to 10 atomic layers, i.e. (m, n) is equal to 5. The superlattices of group 2, on the other hand, have as yet been mainly prepared by sputtering techniques,[111] where rather high residual gas concentrations are present in the reaction chamber. It is well established that many metals are excellent getter materials for a number of residual gas constituents. However, at present, any systematic investigations on the influence of impurities on the properties of these artificial multilayer structures do not exist. It is thus most probable that in many cases incoherent periodic multilayer structures were actually obtained or that at least the coherence length was extremely small. In the field of metal superlattices further efforts with respect to preparative aspects are necessary in order to provide a more realistic basis for the numerous investigations of the structural and elastic properties as well as of the electrical and magnetic properties and their correlation to each other.

5. Final Remarks and Future Prospects

Interfaces or heterojunctions, respectively, are incorporated spatially resolved into the crystal. This leads to a microscopical structuring of semiconducting solids. The resulting local discontinuities of conduction and valence band edges provide a basis for the concept of band-gap (or wave-function, or band-structure, respectively) engineering in semiconductors. The electrical and optical properties are locally defined, and phenomena in extremely small dimensions (quantum size effects) become more important than the chemical properties of the employed materials. The microscopical structuring yields novel electronic properties in otherwise familiar semiconducting materials.

The technique of molecular beam epitaxy makes it feasible to build up crystals atom-by-atom to an extremely perfect arrangement. Based on the 2D growth mode the crystal is stacked lattice plane by lattice plane, and atomically flat surfaces are produced. The low growth rate of approximately one monolayer per second allows the accurately controlled regulation of the layer thickness down to one monolayer and the deposition of crystalline materials of arbitrary composition in alternating sheets of only a few atomic layers thick. The comparatively low growth temperature of several hundred °C prevents the interdiffusion of the constituent materials, and extremely abrupt and clean interfaces are formed. The specific advantages of this sophisticated crystal growth technique lie in the unique possibilities to structure solids arbitrarily down to atomic dimensions. In this way superlattices are created by exactly defined periodic modulation of the chemical composition perpendicular to the growth surface. An artificial periodicity in the direction of growth is superimposed on the crystal potential, which is by one or two orders larger than the natural lattice spacing.

The synthesis of periodically modulated structures by molecular beam epitaxy has opened up access to a new class of solids with accurately custom-tailored electrical, optical, magnetic, dielectric, etc. properties. The semiconductor and metal superlattices described in Section 4 constitute just the beginning. The materials combinations semiconductor/metal, semiconductor/insulator, metal/insulator, and magnetic materials having totally different properties and with as yet unpredictable potential applications will certainly follow. It is important to note, however, that in future the materials scientists (chemists) will become engaged more and more in the most profound questions of solid state physics and quantum theory. For example, for the effective prediction of the electronic properties of periodically modulated semiconductor structures, it is not sufficient to be merely aware of the bulk properties of the constituent layers; the electronic phenomena arising from the interfaces must also be understood and explicitly taken into account.

The concept of band-gap engineering is currently seeing significant extension, as evidenced, inter alia, by the first reported efforts to make the locally defined discontinuities of the energy bands adjustable or even tunable by external action. An example for the adjustability of the conduction and valence band discontinuities has already been mentioned with the strained Si/Si_xGe_{1-x} superlattices described in Section 4.5. In this case the various possibilities to distribute the total strain on the constituent layers in a locally well defined manner leads to completely different energy positions of the band edges with respect to each other. A further possibility of adjusting or tuning the band discontinuities locally arises when a fraction of or a monolayer of impurity material is epitaxially incorporated in the vicinity of or directly at the interface. This intermediate layer leads locally to a significant modification of the band discontinuities.[112] Finally, in the case of the third possibility, ultrathin ionized donor and acceptor sheets are incorporated by monolayer doping within a few nanometers of both sides of the heterojunction interface. The electrostatic potential of this double layer of ionized donors and ac-

ceptors ("dipole layer") is either added to or substracted from the potential of the band discontinuity depending on the polarity.[113] When the distance between the sheets of positive and negative charge is in the order of the de Broglie wavelength, the electrons crossing the heterointerface "experience" a new band discontinuity $\Delta E_c \pm e\Delta(\phi)$, where $\Delta\phi$ is the potential of the double layer. These new possibilities of spatially resolved band-gap engineering add a powerful degree of freedom to the investigation and separate tuning of the properties of electrons and holes in accurately defined microscopical regions. These features will certainly establish new electronic functions for electronic and photonic devices which are based on electrical and optical signal processing, respectively.

The application of molecular beam epitaxy to spatially resolved materials synthesis now makes feasible the routine fabrication of a large variety of microscopically structured solids exhibiting a (periodic) modulation in chemical composition perpendicular to the crystal surface down to atomic dimensions. In such artificially layered quasi-2D semiconductors the motion of free charge carriers is quantized within the layer plane. Theoretical considerations have indicated that quantum size effects in low-dimensional semiconductors are significantly enhanced when the dimensionality of the system is further reduced. In order to study the electronic properties of quasi-one-dimensional (1D) and zero-dimensional (OD) systems experimentally, the motion of electrons and holes has to be confined (quantized) not only to *within* the plane but also *perpendicular* to the plane, i.e. the carriers must be confined to a quantum wire or to a quantum box whose relevant dimensions are smaller than one of the characteristic lengths of the carriers. Depending on the properties to be investigated the characteristic lengths can be the de Broglie wavelength of the electron, the elastic scattering length, or the inelastic diffusion length. Although selectively doped $GaAs/Al_xGa_{1-x}As$ heterostructures with electron mobilities of 10^5–10^6 $cm^2\ V^{-1}\ s^{-1}$ at 4 K exhibit comparatively large values of 5 μm for the inelastic diffusion length and of 500 nm for the elastic scattering length, little progress was hitherto made in the fabrication of quantum wires and quantum boxes. Starting from artificially layered quasi-2D semiconductors the following two methods are now preferentially used for lateral patterning in the nanometer range:

a) Optical holography or electron beam lithography combined with reactive ion beam or plasma etching for the distinct local removal of appropriate materials.[114]
b) Selected-area (laterally defined to within a few tens of nanometers) enhanced interdiffusion in $GaAs/Al_xGa_{1-x}As$ quantum wells induced by finely focussed (<50 nm) Ga ion implantation and subsequent rapid thermal annealing.[115]

In addition, attempts are being made to achieve the supplementary confinement of carriers by application of appropriately structured substrates or arbitrarily off-axis oriented substrates during MBE growth.

With respect to the electrical properties, strongly enhanced electron mobilities have been predicted in the case of quantum wires,[116] whereas the quantum boxes should be insulating. The optical properties should also be fundamentally affected, both by the new quantum confinement of excitons and by the modified density of states [in a quantum box, $g(E)$ becomes a periodic sequence of δ-functions].[117] The energy of the sub-bands for electrons and holes, the relaxation of excited carriers, and the interaction of carriers should change drastically. The lower dimensional structures will significantly modify the formation of excitons, the localization of carriers, possible crystallization effects of the electrons, and the saturation of optical absorption. Recently, *Hirayama* et al.[115] were able to confirm the modification of the density of states and the additional quantization, respectively, by the observation of several additional lines in the photoluminescence spectra of $GaAs/Al_xGa_{1-x}As$ quantum wires.

The reproducible fabrication of microscopically structured (semiconducting) solids having quasi-1D and quasi-0D electronic properties remains one of the major challenges in spatially resolved materials synthesis and, moreover, in the entire field of microstructure materials science. Methods must be developed which will enable the removal of materials atom-by-atom or lattice plane-by-lattice plane, respectively, in well-defined spatial and geometrical arrangements without causing any damage to the crystal surface. The etching techniques developed so far are not suitable for this purpose. The necessity for the development of methods and techniques to manipulate the atoms in a crystal one-by-one (growth, removal, displacement)[118] can be justified by a few simple considerations directed far into the future. In today's most advanced commercially available semiconductor memory, the 4 Mbit DRAM (*D*ynamic *R*andom *A*ccess *M*emory), about 10^{13} Si atoms are used for a 1 bit memory cell. In the 1 Gbit DRAM, planned for the end of the nineties, about 10^{11} to 10^{12} Si atoms will be needed for the 1 bit memory. On the other hand, the recently proposed concept of molecular electronics assumes that the molecular or "bio" memory requires only about 10^3 atoms per 1 bit memory. When in the future we also have to try to adopt some important biological principles in (inorganic) semiconductor design in order to further miniaturize the information-processing circuits, the mere diminution of the physical size of materials (or linewidths) will no longer suffice. Totally different operating principles must be realized for transistors and information processing and storage by exploiting "exotic" effects. The imprinting of multifunctional atomic structures onto the (semiconducting) crystal should make it feasible to accomplish the processing of information with a definite selectivity, imitating to a certain degree the unique stereoselectivity of the large biomolecules. Microstructure materials science techniques must be developed for the fabrication and processing of these (inorganic) materials, whose "active" region is shrinking in physical size from micron to subnanometer dimensions.

In conclusion, it is must be emphasized that the aforementioned activities in the field of microstructure materials science represent important contributions to a major branch of *chemistry*. This field of research should also have its established position in the universities, and should not be left almost exclusively to the engineering and physics departments—as was often the case in the past. This

fascinating field of materials science pursues the addition or removal of appropriate materials in accurately defined geometrical and spatial arrangements; it is concerned with the microscopic mechanisms of growth or removal of atoms, ions or molecules, which is essential for developing new materials and new (alternate) processing technologies; it is concerned with the properties of metals, semiconductors, dielectrics (insulators), magnetic materials, ceramics, polymers, and their composites in restricted dimensions; and finally, it is concerned with the interfaces between these materials. With the ever decreasing physical sizes being dealt with, down to subnanometer dimensions, there should ultimately emerge an answer to the fundamental question at which size an agglomeration of a few atoms ("cluster") begins to develop the characteristic properties of crystalline solids.[119]

The author would like to thank his colleagues who were very actively committed to the development of the technique of molecular beam epitaxy and the specific field of microstructure materials science described here, including A. Fischer, H. Fronius, Dr. K. Fujiwara, M. Hauser, Dr. Y. Horikoshi, Dr. T. Isu, Dr. H. Jung, J. Knecht, Dr. H. Künzel, Dr. J. Nagle, Dr. E. F. Schubert, Dr. L. Tapfer, Dr. S. Tarucha, and Mrs. H. Willerscheid. The continuous support of the present research by Prof. Dr. A. Rabenau, Prof. Dr. H. J. Queisser, and Prof. Dr. K. von Klitzing is gratefully acknowledged. The author appreciates the preparation of the line drawings for the figures by Mrs. E. Klasmeier, the typing of the manuscript by Mrs. I. Zane, and the critical reading of the manuscript by Dr. J. Maier. Finally, the financial support of the Bundesministerium für Forschung und Technologie (BMFT) and of the Stiftung Volkswagenwerk is acknowledged. It is through their grants that the author has been able to develop his research in this area.

Received: August 5, 1987 [A 669 IE]
German version: *Angew. Chem. 100* (1988) 611

[1] A. A. Chernov: *Modern Crystallography III. Crystal Growth (Springer Ser. Solid-State Sci. 36)*, Springer, Berlin 1984.
[2] J. G. Bednorz, K. A. Müller, *Z. Phys. B64* (1986) 189; A. Khurana, *Phys. Today 40* (1987) No. 4, p. 17; H. J. Deiseroth, *Nachr. Chem. Tech. Lab. 35* (1987) 488; A. Simon, *Angew. Chem. 99* (1987) 602; *Angew. Chem. Int. Ed. Engl. 26* (1987) 579; T. H. Geballe, J. K. Hulm, *Science 239* (1988) 367.
[3] K. von Klitzing, *Rev. Mod. Phys. 58* (1986) 519.
[4] H. Sakaki, *Proc. Int. Symp. Foundations of Quantum Mechanics*, Tokyo 1983, 94.
[5] F. Capasso, *Science 235* (1987) 172.
[6] W. Shockley, U.S. Pat. 2569347 (1951).
[7] H. Krömer, *RCA Rev. 18* (1957) 332; *Proc. IEEE 51* (1963) 1782.
[8] Zh. I. Alferov, V. M. Andrevev, D. Z. Garbuzov, Yu. V. Zhilyaev, E. P. Morozov, E. L. Portnoi, V. G. Trofim, *Fiz. Tekh. Poluprovodn. (Leningrad) 4* (1970) 1826; *Sov. Phys. Semicond. Engl. Transl. 4* (1970) 1573; I. Hayashi, M. B. Panish, P. W. Foy, S. Sumski, *Appl. Phys. Lett. 17* (1970) 109.
[9] A. Y. Cho, *J. Appl. Phys. 41* (1970) 2780.
[10] L. Esaki, R. Tsu, *IBM J. Res. Dev. 14* (1970) 61.
[11] A. Y. Cho, J. R. Arthur, *Prog. Solid State Chem. 10* (1975) 157.
[12] O. Madelung: *Physics of III-V Compounds*, Wiley, New York 1964; H. C. Casey, M. B. Panish: *Heterostructure Lasers*, Academic Press, New York 1978.
[13] R. Dingle in H. J. Queisser (Ed.): *Festkörperprobleme 15* (1975) 21.
[14] N. Holonyak, R. M. Kolbas, R. D. Depuis, P. D. Dapkus, *IEEE J. Quantum Electron. QE-16* (1980) 170; W. T. Tsang, *Appl. Phys. Lett. 39* (1980) 786.
[15] F. Capasso, W. T. Tsang, G. F. Williams, *IEEE Trans. Electron Devices ED-30* (1983) 381.
[16] Review: J. W. Mathews (Ed): *Epitaxial Growth*, Academic Press, New York 1975.
[17] K. Ploog in H. C. Freyhardt (Ed.): *Crystals, Growth, Properties, and Applications*, Springer, Berlin 1980, p. 73.
[18] A. C. Gossard, *Treatise Mater. Sci. Technol. 24* (1982) 13.
[19] K. G. Günther, *Z. Naturforsch. A 13* (1958) 1081.
[20] J. R. Arthur, *J. Appl. Phys. 39* (1968) 4032.
[21] M. A. Herman, *Vacuum 32* (1982) 555.
[22] J. Saito, A. Shibatomi, *Fujitsu Tech. J. 21* (1985) 190.
[23] C. T. Foxon, B. A. Joyce in E. Kaldis (Ed.): *Current Physics in Materials Science, Vol. 7*, North-Holland, Amsterdam 1981, p. 1.
[24] M. B. Panish, *J. Electrochem. Soc. 127* (1980) 2729.
[25] H. Künzel, J. Knecht, H. Jung, K. Wünstel, K. Ploog, *Appl. Phys. A 28* (1982) 167.
[26] C. T. Foxon, B. A. Joyce, *Surf. Sci. 50* (1975) 434; *ibid. 64* (1977) 293.
[27] C. T. Foxon, B. A. Joyce, *J. Cryst. Growth 44* (1978) 75.
[28] C. T. Foxon, J. A. Harvey, B. A. Joyce, *J. Phys. Chem. Solids 34* (1973) 1693.
[29] Y. Horikoshi, M. Kawashima, H. Yamaguchi, *Jpn. J. Appl. Phys. 25* (1986) L868.
[30] C. T. Foxon, B. A. Joyce, M. T. Norris, *J. Cryst. Growth 49* (1980) 132.
[31] E. C. Larkins, E. S. Hellman, D. G. Schlom, J. S. Harris, M. H. Kim, G. E. Stillman, *J. Cryst. Growth 81* (1987) 344.
[32] M. Ilegems, *J. Appl. Phys. 48* (1977) 1278.
[33] K. Ploog, A. Fischer, H. Künzel, *J. Electrochem. Soc. 128* (1981) 400.
[34] E. Nottenburg, H. J. Bühlmann, M. Frei, M. Ilegems, *Appl. Phys. Lett. 44* (1984) 71.
[35] R. Sacks, H. Shen, *Appl. Phys. Lett. 47* (1985) 374.
[36] J. Maguire, R. Murray, R. C. Newman, R. B. Beal, J. J. Harris, *Appl. Phys. Lett. 50* (1987) 516.
[37] L. Gonzales, J. B. Clegg, D. Hilton, J. P. Gowers, C. T. Foxon, B. A. Joyce, *Appl. Phys. A 41* (1986) 237.
[38] W. I. Wang, E. E. Mendez, T. S. Kuan, L. Esaki, *Appl. Phys. Lett. 47* (1985) 826; H. Nobuhara, O. Wada, T. Fujii, *Electron. Lett. 23* (1987) 35.
[39] D. L. Miller, *Appl. Phys. Lett. 47* (1985) 1309.
[40] B. A. Joyce, J. N. Neave, P. J. Dobson, P. K. Larsen, *Phys. Rev. B 29* (1984) 814; C. S. Lent, P. I. Cohen, *Phys. Rev. B 33* (1986) 8329.
[41] K. Ploog, *J. Vac. Sci. Technol. 16* (1979) 838.
[42] J. H. Neave, B. A. Joyce, P. J. Dobson, N. Norton, *Appl. Phys. A 31* (1983) 1; J. M. van Hove, C. S. Lent, P. R. Pukite, P. I. Cohen, *J. Vac. Sci. Technol. B 1* (1983) 741.
[43] M. Tanaka, H. Sakaki, J. Yoshino, *Jpn. J. Appl. Phys. 25* (1986) L155; F. Voillot, A. Madhukar, J. Y. Kim, P. Chen, N. M. Cho, W. C. Tang, P. G. Newman, *Appl. Phys. Lett. 48* (1986) 1009.
[44] T. Sakamoto, H. Funabashi, K. Ohta, T. Nakagawa, N. J. Kawai, T. Kojima, K. Bando, *Superlattices Microstruct. 1* (1985) 347; B. A. Joyce, P. J. Dobson, J. H. Neave, K. Woodbridge, J. Zhang, P. K. Larsen, B. Bölger, *Surf. Sci. 168* (1986) 423.
[45] P. M. Petroff, *J. Vac. Sci. Technol. 14* (1977) 973.
[46] M. S. Abrahams, C. J. Buiocchi, *J. Appl. Phys. 45* (1974) 3315; S. N. G. Chu, T. T. Sheng, *J. Electrochem. Soc. 131* (1984) 2663.
[47] Y. Suzuki, O. Okamoto, *J. Appl. Phys. 58* (1985) 3456.
[48] A. Segmüller, P. Krishna, L. Esaki, *J. Appl. Crystallogr. 10* (1977) 1.
[49] L. Tapfer, K. Ploog, *Phys. Rev. B 33* (1986) 5565; Y. Kashihara, T. Kase, J. Harada, *Jpn. J. Appl. Phys. 25* (1986) 1834.
[50] L. Tapfer, W. Stolz, K. Ploog, *Ext. Abstracts 1986 ICSSDM* (Jpn. Soc. Appl. Phys., Tokyo 1986) p. 603.
[51] R. C. Miller, D. A. Kleinmann, *J. Lumin. 30* (1985) 520.
[52] R. C. Miller, C. W. Tu, S. K. Sputz, R. F. Kopf, *Appl. Phys. Lett. 49* (1986) 1245.
[53] C. Weisbuch, R. Dingle, A. C. Gossard, W. Wiegmann, *Inst. Phys. Conf. Ser. 56* (1981) 711.
[54] W. Stolz, L. Tapfer, A. Breitschwerdt, K. Ploog, *Appl. Phys. A 38* (1985) 97.
[55] E. H. Hall, *Am. J. Math. 2* (1879) 287.
[56] L. J. van der Pauw, *Philips Res. Rep. 13* (1958) 1.
[57] For a survey on the different scattering mechanisms see: T. Ando, A. B. Fowler, F. Stern, *Rev. Mod. Phys. 54* (1982) 437.
[58] R. O. Grondin, W. Porod, J. Ho, D. K. Ferry, G. J. Iafrate, *Superlattices Microstruct. 1* (1985) 183.
[59] L. L. Chang, L. Esaki, R. Tsu, *Appl. Phys. Lett. 24* (1974) 593.
[60] I. Ivanov, J. Pollmann, *Solid State Commun. 32* (1979) 869.
[61] For a review of the most recent studies see: F. Capasso, K. Mohammed, A. Y. Cho, *IEEE J. Quantum Electron. QE-22* (1986) 1853.
[62] M. Tsuchiya, H. Sakaki, *Jpn. J. Appl. Phys. 25* (1986) L185; *Appl. Phys. Lett. 50* (1987) 1503.
[63] L. C. Chiu, A. Yariv, *J. Lumin. 30* (1985) 551.
[64] N. K. Dutta, *Electron. Lett. 18* (1982) 451; *J. Appl. Phys. 53* (1982) 7211; B. Saint-Cricq, F. Lopez-Dupuy, Vassilieff, *IEEE J. Quantum Electron. QE-22* (1986) 625.
[65] K. Uomi, N. Chinone, T. Ohtoshi, T. Kajimura, *Inst. Phys. Conf. Ser. 79* (1986) 703.

[66] S. Tarucha, H. Okamoto, *Appl. Phys. Lett. 48* (1986) 1; H. Nobuhara, M. Kuno, M. Makiuchi, T. Fujii, O. Wada, *IEEE J. Quantum Electron. QE-23* (1987) 160.

[67] T. Hayakawa, M. Kondo, T. Suyama, K. Takahashi, S. Yamamoto, T. Hijikata, *Jpn. J. Appl. Phys. 26* (1987) L302.

[68] D. S. Chemla, *Helv. Phys. Acta 56* (1983) 607; *Phys. Today 38* (1985) No. 5, p. 57.

[69] T. Ishibashi, S. Tarucha, H. Okamoto, *Inst. Phys. Conf. Ser. 63* (1982) 587.

[70] J. C. Maan, G. Belle, A. Fasolino, M. Altarelli, K. Ploog, *Phys. Rev. B30* (1984) 2253.

[71] Y. Suzuki, H. Okamoto, *J. Electron. Mater. 12* (1983) 397.

[72] H. M. Gibbs, S. S. Tarng, J. L. Lewell, D. A. Weinberger, K. Tsai, A. C. Gossard, S. L. McCall, A. Passner, *Appl. Phys. Lett. 41* (1982) 221.

[73] S. D. Smith, *Appl. Optics 25* (1986) 1550.

[74] D. A. B. Miller, D. S. Chemla, T. C. Damen, A. C. Gossard, W. Wiegmann, T. H. Wood, A. C. Burrus, *Phys. Rev. Lett. 53* (1984) 2173; H. J. Polland, L. Schultheis, J. Kuhl, E. O. Göbel, C. W. Tu, *Phys. Rev. Lett. 55* (1985) 2610; L. Vina, R. T. Collins, E. E. Mendez, W. I. Wang, L. L. Chang, L. Esaki, *Superlattices Microstruct. 3* (1987) 9.

[75] Y. Horikoshi, A. Fischer, K. Ploog, *Phys. Rev. B31* (1985) 7859.

[76] T. H. Wood, C. A. Burrus, D. A. B. Miller, D. S. Chemla, T. C. Damen, A. C. Gossard, W. Wiegmann, *IEEE J. Quantum Electron. QE-21* (1985) 117.

[77] D. A. B. Miller, D. S. Chemla, T. C. Damen, T. H. Wood, C. A. Burrus, A. C. Gossard, W. Wiegmann, *IEEE J. Quantum Electron. QE-21* (1985) 1462.

[78] J. A. Brum, G. Bastard, *Phys. Rev. B31* (1985) 3893.

[79] R. T. Collins, K. von Klitzing, K. Ploog, *Phys. Rev. B33* (1986) 4378.

[80] H. L. Störmer, R. Dingle, A. C. Gossard, W. Wiegmann, M. D. Sturge, *Solid State Commun. 29* (1979) 705; G. Abstreiter, K. Ploog, *Phys. Rev. Lett. 42* (1979) 1308.

[81] R. Dingle, H. L. Störmer, A. C. Gossard, W. Wiegmann, *Appl. Phys. Lett. 33* (1978) 665.

[82] H. L. Störmer, A. Pinczuk, A. C. Gossard, W. Wiegmann, *Appl. Phys. Lett. 38* (1981) 691.

[83] J. J. Harris, C. T. Foxon, K. W. Barnham, D. E. Lacklison, J. Hewett, C. White, *J. Appl. Phys. 61* (1967) 1219; J. H. English, A. C. Gossard, H. L. Störmer, K. W. Baldwin, *Appl. Phys. Lett. 50* (1987) 1826.

[84] M. Abe, T. Mimura, K. Nishiuchi, N. Yokoyama, in *VLSI Electron.: Microstruct. Sci. 11* (1985) 333; T. J. Drummond, W. T. Masselink, H. Morkoc, *Proc. IEEE 74* (1986) 773.

[85] R. E. Prange, S. M. Girvin (Eds.): *The Quantum Hall Effect*, Springer, Berlin 1987.

[86] N. J. Shah, S. S. Pei, C. W. Tu, P. C. Tiberio, *IEEE Trans. Electron Devices ED-33* (1986) 543; P. M. Smith, P. C. Chao, K. H. G. Duh, L. F. Lester, B. R. Lee, *Electron Lett. 22* (1986) 780.

[87] G. Landwehr, *Phys. Bl. 37* (1981) No. 3, p. 59; K. von Klitzing, G. Ebert, *Metrologica 21* (1985) 11. For a compilation of articles on precision measurements of the quantized Hall resistance see also: *IEEE Trans. Instrum. Meas. IM-34* (1986) 301 and *Metrologica 22* (1986) 256.

[88] R. J. Haug, R. R. Gerhardts, K. von Klitzing, K. Ploog, *Phys. Rev. Lett. 59* (1987) 1349.

[89] L. Bliek, E. Braun, F. Melchert, P. Warnecke, W. Schlapp, G. Weimann, K. Ploog, G. Ebert, *Phys. Bl. 39* (1983) 157.

[90] A. C. Gossard, P. M. Petroff, W. Wiegmann, R. Dingle, A. Savage, *Appl. Phys. Lett. 29* (1976) 323; M. Nakayama, K. Kubota, H. Kato, S. Chika, N. Sano, *Solid State Commun. 53* (1985) 493.

[91] T. Isu, D. S. Jiang, K. Ploog, *Appl. Phys. A43* (1987) 75.

[92] E. F. Schubert, K. Ploog, *Phys. Rev. B30* (1984) 7021.

[93] T. Nakayama, H. Kamimura, *J. Phys. Soc. Jpn. 54* (1985) 4726; M. A. Gell, D. Ninno, M. Jaros, D. C. Herbert, *Phys. Rev. B34* (1986) 2416; M. Cardona, T. Suemoto, N. Christensen, T. Isu, K. Ploog, *ibid. 36* (1987) 5906.

[94] T. Yao, *Jpn. J. Appl. Phys. 22* (1983) L680.

[95] Y. Matsui, H. Hayashi, K. Yoshida, *Appl. Phys. Lett. 48* (1986) 1060.

[96] J. Bevk, A. Ourmazd, L. C. Feldman, T. P. Pearsall, J. M. Bonar, B. A. Davidson, J. P. Mannaerts, *Appl. Phys. Lett. 50* (1987) 760.

[97] C. E. C. Wood, G. Metze, J. Berry, L. F. Eastman, *J. Appl. Phys. 51* (1980) 383.

[98] K. Ploog, *J. Cryst. Growth 81* (1987) 304.

[99] A. Zrenner, H. Reisinger, F. Koch, K. Ploog, *Proc. 17th Int. Conf. Phys. Semicond. 1984* (Eds.: J. D. Chadi, W. A. Harrison), Springer, Berlin 1985, p. 325.

[100] E. F. Schubert, A. Fischer, K. Ploog, *IEEE Trans. Electron Devices ED-33* (1986) 625.

[101] K. Ploog, A. Fischer, E. F. Schubert, *Surf. Sci. 174* (1986) 120.

[102] E. F. Schubert, A. Fischer, Y. Horikoshi, K. Ploog, *Electron. Lett. 21* (1985) 411; *Appl. Phys. Lett. 47* (1985) 219.

[103] J. W. Mathews, A. E. Blakeslee, *J. Cryst. Growth 27* (1974) 118.

[104] E. Kasper, *Surf. Sci. 174* (1986) 630.

[105] G. Abstreiter, H. Brugger, T. Wolf, H. Jorke, H. J. Herzog, *Surf. Sci. 174* (1986) 640.

[106] R. People, J. C. Bean, D. V. Lang, A. M. Sergent, H. L. Störmer, K. W. Wecht, R. T. Lynch, K. Baldwin, *Appl. Phys. Lett. 45* (1984) 1231.

[107] I. K. Schuller, *Phys. Rev. Lett. 44* (1980) 1597.

[108] C. M. Falco, *J. Phys. Colloq. 5* (1984) 499.

[109] S. M. Durbin, J. E. Cunningham, C. P. Flynn, *J. Phys. F12* (1982) L75.

[110] K. Kwo, E. M. Gyorgy, D. B. McWhan, M. Hong, F. J. DiSalvo, C. Vettier, J. E. Bower, *Phys. Rev. Lett. 55* (1985) 1402.

[111] I. K. Schuller, C. M. Falco, *Surf. Sci. 113* (1982) 443.

[112] D. W. Niles, G. Margaritondo, P. Perfetti, C. Quaresima, M. Capozi, *Appl. Phys. Lett. 47* (1985) 1092.

[113] F. Capasso, A. Y. Cho, K. Mohammed, P. W. Foy, *Appl. Phys. Lett. 46* (1985) 664.

[114] R. E. Behringer, P. M. Mankiewich, R. E. Howard, *J. Vac. Sci. Technol. B5* (1987) 326; W. Hansen, M. Horst, J. P. Kotthaus, U. Merkt, C. Sikorski, K. Ploog, *Phys. Rev. Lett. 58* (1987) 2586.

[115] H. Okamoto, *Jpn. J. Appl. Phys. 26* (1987) 315; J. Cibert, P. M. Petroff, G. J. Dolan, S. J. Pearton, A. C. Gossard, J. H. English, *Appl. Phys. Lett. 49* (1986) 1275.

[116] H. Sakaki, *Jpn. J. Appl. Phys. 19* (1980) L735.

[117] S. Schmitt-Rink, D. A. B. Miller, D. S. Chemla, *Phys. Rev. B35* (1987) 8113.

[118] A first success has recently been reported: J. S. Foster, J. E. Frommer, P. C. Arnett, *Nature (London) 331* (1988) 324.

[119] T. P. Martin, *Angew. Chem. 98* (1986) 197; *Angew. Chem. Int. Ed. Engl. 25* (1986) 197.

Microbial and Enzymatic Processes for the Production of Biologically and Chemically Useful Compounds

New Synthetic Methods (69)

By Hideaki Yamada* and Sakayu Shimizu*

In recent years, the most significant development in the field of synthetic organic chemistry has been the application of biological systems to chemical reactions. Reactions catalyzed by enzymes and enzyme systems display far greater specificities than more conventional organic reactions. Biological and/or enzymatic syntheses and transformations, that is, "microbial transformations," have great potential. Some of these reactions have already been shown to have useful applications in the fields of synthetic organic chemistry and biotechnology. This article reviews the current status of the rapidly developing field of microbial transformation, the methodology, available technological procedures, and fields of application being described especially in relation to conventional organic synthesis methods.

1. Introduction

During the last ten years, the biochemical reactions performed by microorganisms or catalyzed by enzymes have been extensively evaluated from the viewpoint of synthetic organic chemistry, and as a consequence they have been shown to have a high potential for both theoretical and practical applications to synthetic chemistry. Many attempts to utilize biological reactions for practical synthetic processes have been made; for example, for the preparation of pharmaceuticals, fine chemicals, food additives, and commodity chemicals. Such synthetic technology is called microbial transformation, or, alternatively, "microbial conversion," "biotransformation," "bioconversion," or "enzymation." It is somewhat different from so-called fermentation, another major synthetic technology based on biological reactions, and is a rapidly developing field of synthetic chemistry overlapping both organic chemistry and biochemistry.

A microbial transformation is the conversion of one substance (substrate) to another (product) by a microorganism. It is a chemical reaction catalyzed by a particular cellular enzyme or by an enzyme originally produced within cells. Most such enzymes are necessary for the normal functioning of the life processes of cellular metabolism and reproduction. In microbial transformations, however, these enzymes simply act as catalysts (biocatalysts) for chemical reactions. In addition to their natural substrates, many of these enzymes can utilize other structurally related compounds as substrates and therefore occasionally catalyze unnatural reactions upon addition of foreign substrates to the reaction medium. Thus, microbial transformation constitutes a specific category of chemical synthesis.

Numerous reviews on this topic have been published by both biotechnologists[1-8] and organic chemists.[9-15] In this review, we attempt to evaluate several important aspects of this field and to describe the most recent developments.

[*] Prof. Dr. H. Yamada, Dr. S. Shimizu
Department of Agricultural Chemistry, Kyoto University
Sakyo-ku, Kyoto 606 (Japan)

2. Characteristics of Enzyme Reactions Used in Microbial Transformations

As mentioned in Sections 2.1 and 2.2, microbial transformation is a technique for the synthesis or production of useful compounds which is based fundamentally on both chemical synthesis and fermentation. Therefore, the characteristics of microbial transformation somewhat overlap those of either chemical synthesis or fermentation.

2.1. Microbial Transformation versus Chemical Synthesis

Chemical reactions performed by microorganisms or catalyzed by enzymes are essentially the same as those carried out in conventional inorganic or organic chemistry. The differences in the outcome of a reaction depend on the catalyst used (see Table 1). Enzymes (or biocatalysts) used for microbial transformations increase the reaction rate by lowering the activation energy as normal catalysts do. The most striking differences between enzymes and chemical catalysts, however, lie in their substrate specificities. They catalyze specific reactions involving one or only a few structurally related compounds, distinguishing almost absolutely between stereoisomers or regioisomers. Therefore, only a very specific change in a functional group or bond of a compound is accelerated by the enzyme. As a result, a single product can be expected as long as only one enzyme is involved in a conversion.

High catalytic efficiency is another characteristic property of enzymes. For example, the rate of hydrolysis of an amide by chymotrypsin is about 4000 times higher than that for the corresponding base catalysis.[16] Enzymes increase the catalytic turnover number (moles of product per mole of enzyme per unit time) without a large energy requirement; that is, only a small amount of enzyme is needed to catalyze the conversion of a large amount of substrate. As a result, enzymes exhibit their activity under mild reaction conditions under which normal chemical catalysts hardly function at all, such as atmospheric pressure, temperatures around 20 to 40°C, and pH values near neutrality. These unique properties of enzymes are extremely useful when unstable molecules are to be converted without undesired side reactions.

 © VCH Verlagsgesellschaft mbH, D-6940 Weinheim, 1988 0570-0833/88/0505-0622 $ 02.50/0

Table 1. General characteristics of enzymatic and chemical reactions.

	Enzymatic reaction	Chemical reaction
Reaction conditions		
Temperature	physiological	high
Pressure	physiological	high
Source of the reaction energy	change in enzyme conformation (making and breaking of van der Waals bonds, hydrogen bonds, etc.)	thermal
Solvent	water	water, organic solvents
Specificity		
Substrate specificity	high	low
Stereospecificity	high	low
Regiospecificity	high	low
Concentration of substrate and/or product	low	high

On the other hand, these unique features occasionally make enzymes hard to use as convenient catalysts. For example, the high catalytic activity of enzymes under mild reaction conditions does not mean that they are active under drastic conditions. Indeed, under drastic reaction conditions enzymes are quite inert, whereas normal chemical catalysts often exhibit good activity. Enzymes presumably exhibit their activity *only* under mild reaction conditions because of their delicate protein structures which are maintained, for example, by van der Waals forces and a network of hydrogen bonds. The high selectivity of enzyme catalysis, which is one of the most important characteristics that make enzymes promising as catalysts in synthetic chemistry, may also be a disadvantage, because the selectivity implies limitations. For example, platinum is far superior to a reductase in its ability to reduce a wide variety of compounds.

The International Union of Biochemistry lists more than 2000 enzymes.[17] They are classified according to the reactions they catalyze. Almost all types of chemical reactions also catalyzed by normal chemical catalysts can be found. More than 800 kinds of cell-free enzymes are commercially available.[18] In some cases, therefore, one may easily find an enzyme suitable for a desired conversion.

2.2. Microbial Transformation versus Fermentation

There are two ways of using microorganisms in the production of useful compounds; microbial transformation and fermentation. Fermentation has been performed since ancient times, a good example being alcohol fermentation[19] and it is still a powerful technique for the production of such compounds as organic acids,[20] solvents,[21] antibiotics,[22] amino acids,[23] and nucleic acid-related compounds.[24] In contrast to microbial transformation, fermentation is considered to be a rather biological method, because it is a result of the actual life process of a microorganism. In other words, the product is the result of the complex metabolism of the microorganism involving inexpensive carbon and nitrogen sources. Therefore, living or growing cells are required for fermentation, and the fermentation products are always natural products.

In microbial transformations, on the other hand, it is not so important whether the cells are alive or not. The life process of a microorganism is required only for the production of enzymes and the microorganism itself is simply used as a bag of enzymes or catalysts.

Microbial transformation requires a substrate instead of the carbon and nitrogen sources required for fermentation. A simple and specific change in a substrate molecule occurs under the catalysis of an enzyme. The substrates need not necessarily be natural; unnatural substrates can also undergo a change as long as it is catalyzed by the enzyme. Therefore, not only natural products but also unnatural ones can be produced through microbial transformation.

Table 2. General characteristics of microbial transformation and fermentation.

	Microbial transformation	Fermentation
Microorganism	growing, resting, or treated cells	growing cells
Reaction	simple catalytic reaction (one or several steps)	life process (multistep reaction)
Reaction time	short	long
Starting materials	expensive substrates	inexpensive carbon and nitrogen sources
Product	natural or unnatural	natural
Product concentration	high	low
Product isolation	easy	tedious

The advantages and disadvantages of these two microbial processes are briefly summarized in Table 2. Figure 1 may be useful for imagining the essential differences between microbial transformation and fermentation. However, it is not always possible to draw a clear line between the two categories.

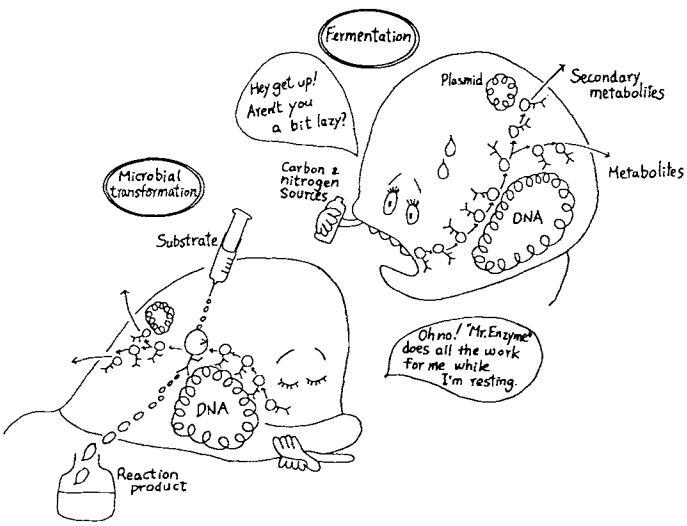

Fig. 1. Illustration of the essential differences between two microbial processes, "microbial transformation" and "fermentation."

3. Historical Background and Present Status of Microbial Transformation

Microbial transformation is an ancient art. The oldest and best known prototype is vinegar production, which has been performed since the dawn of recorded history. The process has been further developed along traditional lines of fermentation without knowledge of the underlying biochemistry. Today, the characteristic oxidation of ethanol to acetic acid by acetic acid bacteria is well understood to proceed by means of two successive dehydrogenations that depend on the cytochrome system for the transfer of electrons to atmospheric oxygen as the ultimate hydrogen acceptor:

$$C_2H_5OH + 1/2O_2 \longrightarrow CH_3CHO + H_2O$$

$$CH_3CHO + 1/2O_2 \longrightarrow CH_3COOH$$

In 1921, a microbial reaction for the stereospecific preparation of D-(−)-ephedrine was described.[25] Yeast cells, actively fermenting glucose to acetaldehyde, were found to condense added benzaldehyde with the acetaldehyde to form optically active L-1-hydroxy-1-phenyl-2-propanone. This product was in turn converted chemically into D-(−)-ephedrine. This was the first example of the successful combination of chemical and enzymatic reactions.

It was only much later, through the discovery of the specific modification of steroids by microorganisms, that microbial transformation obtained the significance it has today.[26,27] Various kinds of steroid modifications, such as hydroxylation, epoxidation, dehydrogenation, isomerization, and hydrolysis, are performed by a wide variety of microorganisms. Many of these reactions cannot be achieved by means of conventional chemical synthesis. Through these microbial reactions, many novel intermediates for the chemical synthesis of new steroid pharmaceuticals became available. In addition to their considerable practical value, the amazing versatility of microorganisms in the transformation of steroids provided an important theoretical background for the application of microbial enzymes to chemical synthesis.[28]

Thousands of microbial transformations involving different types of reactions with organic compounds and natural products are now known; some of them have proved to be very useful for synthetic organic chemistry. It should be noted that remarkable developments in the fields of biochemistry, enzymology, genetics, molecular biology, and microbial cultivation technology also have contributed significantly to the rapid development in this field.

The current technological importance of microbial transformations or enzymatic processes is well recognized in many fields of biotechnology (see Fig. 2). Modification of biologically derived complex molecules (e.g., proteins, polypeptides, lipoproteins, glycoproteins, polysaccharides, and polynucleotides) has high potential for the preparation of pharmaceuticals. For example, various kinds of peptide hormones can be prepared with proteases or peptidases[29] (see also Section 5.2). Conversion of porcine insulin to human insulin has already been commercialized[30–32] (cf. Fig. 9). Enzymatic manipulation is also indispensable for the preparation of DNA and RNA, which are used for genetic engineering.[33]

Enzymes are the best practical catalysts for the preparation of special or fine chemicals. There are many commercial processes for the production of such biological molecules as amino acids, nucleic acid-related compounds, sugars, and lipids. For example, L-alanine (aspartate β-decarboxylase),[34] L-aspartic acid (aspartase),[35] high-fructose corn syrup (glucose isomerase),[36] and 6-aminopenicillanic acid for semisynthetic penicillins (penicillin acylase)[37,38] are produced almost solely through enzymatic processes. A wide variety of chemicals used for analysis and research in clinical chemistry, biochemistry, metabolism, and pharmacology are also produced using enzymes.

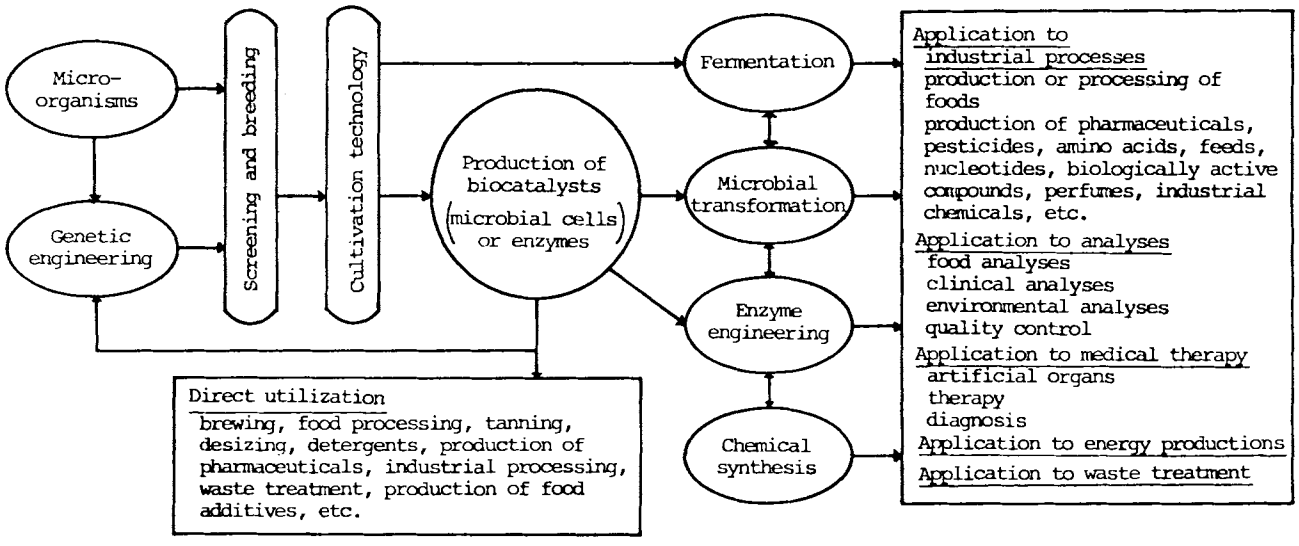

Fig. 2. Area of application of microbial enzymes, microbial transformations, and enzymatic processes in the field of biotechnology.

The production of commodity chemicals is currently one of the fast developing fields of microbial transformation. The use of enzyme reactions in practical processes has been extensively evaluated from the following viewpoints: preparation of high-purity products, energy saving, and environmental acceptability. Acrylamide is now produced commercially from acrylonitrile using nitrile hydratase[39] (see Section 5.6). Oxygenase (or haloperoxidase and halohydrin epoxidase), methanol oxidase, secondary alcohol dehydrogenase, and gallic acid decarboxylase are, respectively, suggested to be useful catalysts for the production of alkene oxides,[40] formaldehyde,[41] ketones,[42] and pyrogallol.[43]

The preparation of chiral synthons using enzyme catalysts is an area of current intense activity in organic and pharmaceutical chemistry. The practical importance of this area has been shown, for example, in the preparation of mevalonolactone,[44] carbapenem antibiotics,[45] nucleoside antibiotics,[46] insect hormones,[47] α-tocopherol,[48] and muscone.[49]

4. Process Designing in Microbial Transformation

In designing a microbial transformation process, many important aspects require careful consideration. They are summarized in Table 3. The selection of the target compound to be synthesized and a survey of available substrates and routes or reactions are especially important.

Table 3. Several important aspects in designing a microbial transformation process.

1. Microbial physiology
2. Microbial metabolism and biosynthesis
New microbial reactions
New synthetic routes
3. Enzyme catalysis
Properties of enzyme
Mechanism of enzyme reaction
Evaluation of potential as catalyst
4. Enzyme production
Mechanism of enzyme formation
... inducer, regulator, etc.
Strain improvement
... screening, mutation, gene engineering, etc.
Optimization
... environmental conditions
5. Enzyme modification
... chemical and/or biochemical modification, immobilization, protein engineering, etc.
6. Microbial or enzymatic synthesis and transformation
Optimization
Process designing

4.1. Evaluation of Enzyme Potential

Occasionally the discovery of a new enzyme or new reaction provides a clue for the designing of a new microbial transformation process. In such a case, the first task is to determine what are the potential characteristics of the new enzyme for practical purposes. The synthetic scheme involving the enzyme or the reaction should be determined through a careful survey of the properties of the enzyme. A typical example is the application of *Achromobacter* protease I; this enzyme specifically hydrolyzes the amide bond at the carboxyl end of L-lysine residues in polypeptides.[50] Therefore, the enzyme can be used to convert porcine insulin into human insulin[31] (cf. Fig. 9).

Another interesting example is the production of L-tyrosine and L-Dopa with bacterial β-tyrosinase.[51] This enzyme had long been believed to be a simple hydrolytic enzyme that catalyzed the α,β-elimination of L-tyrosine to phenol, pyruvate, and ammonia [Eq. (1)].

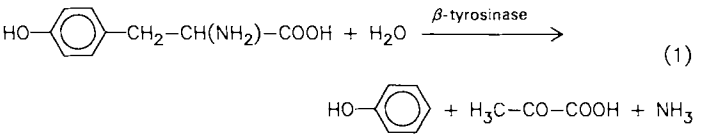

(1)

The enzyme was then found, however, to catalyze the reverse of this α,β-elimination reaction [Eq. (2)], and also the β-replacement reaction of L-tyrosine with phenol derivatives [Eq. (3)].

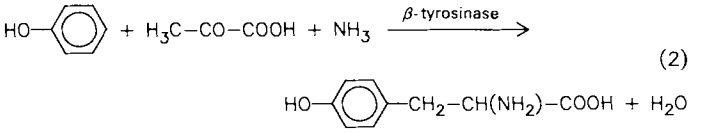

(2)

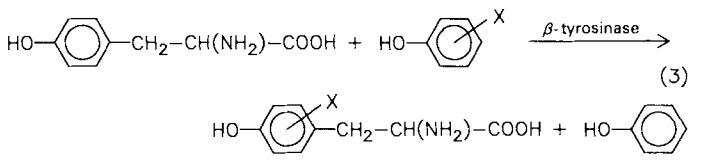

(3)

The application of these reactions to the synthesis of L-tyrosine and L-Dopa did not take long. Subsequently, similar reactions were found to take place under catalysis by various kinds of pyridoxal phosphate-dependent enzymes, and they were successfully applied to the synthesis of optically active aromatic and sulfur-containing amino acids[51-55] (see Section 5.1.2).

These successful examples demonstrate the importance of reassessing the capabilities of well-known enzymes or reactions.

4.2. Searching for New or Suitable Enzymes

Occasionally a synthetic scheme is outlined but the appropriate enzyme(s) or reaction(s) remain unknown. In such a case, it is necessary to search for suitable microbial strains or enzymes. The production of L-lysine from DL-α-amino-ε-caprolactam is a typical example.[56] This process was designed to utilize cyclohexene, a major by-product of nylon production. In this process (Fig. 3), the microorganism or enzyme is required to hydrolyze only the L isomer of α-amino-ε-caprolactam to yield L-lysine. Through a survey of microorganisms capable of catalyzing such a conversion, two microorganisms were found; one of

them hydrolyzes the L isomer of the substrate and the other racemizes the remaining D isomer. As a result, the racemic substrate can be stoichiometrically converted into L-lysine without any optical resolution step.

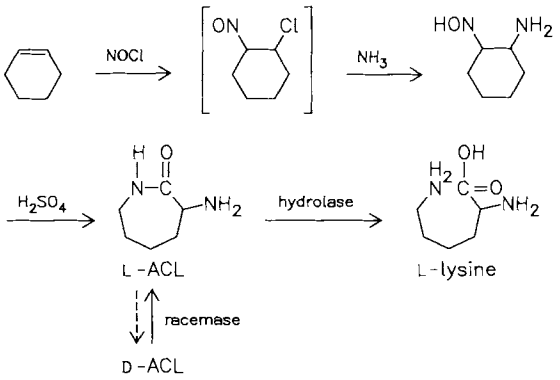

Fig. 3. Chemical and enzymatic process for L-lysine production involving stereoselective hydrolysis of α-amino-ε-caprolactam (ACL) (see text).

The ring-opening hydrolysis of DL 5-substituted hydantoins to yield *N*-carbamoyl-D-amino acids by dihydropyrimidinase is also an interesting example.[53,57,58] This scheme (see Fig. 6) was originally designed for the synthesis of L-methionine from the corresponding DL 5-monosubstituted hydantoin. The scheme itself is very similar to the conventional chemical process of *Bucherer* and *Steiner*[59] for the synthesis of racemic amino acids. In this case, the microorganism is again required for asymmetric hydrolysis of the racemic substrate. Surprisingly, the hydrolysis was found to occur only with the D isomers of various hydantoin compounds. The enzyme catalyzing this hydrolysis was soon revealed to be a known enzyme, dihydropyrimidinase (EC 5.3.2.2), which catalyzes the hydrolytic ring-opening of dihydropyrimidines to *N*-carbamoyl-β-amino acids. These two ring-opening hydrolyses are essentially the same, except for the size of the rings, as shown by Equations (4) and (5).

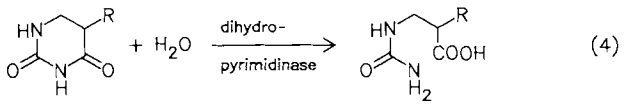

(4)

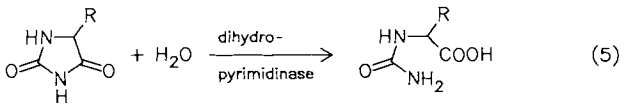

(5)

This finding was a turning point for the strategy. The target product was switched to D-*p*-hydroxyphenylglycine, which is an important intermediate in the synthesis of semisynthetic penicillins and cephalosporins. A new and efficient synthetic route was established to obtain the starting substrate, DL-5-(*p*-hydroxyphenyl)hydantoin. The final results surpassed by far the initial expectations (see Section 5.1.1 for details).

On the conversion of unnatural substrates, it is occasionally uncertain whether the desired reaction takes place or not. The usual way of testing this is by addition of the substrate to be converted to the growth or reaction medium, followed by assaying for the desired reaction products.[60,61] Such a test should be carried out for a wide variety of microorganisms for the following reasons: (1) Enzymes catalyze a variety of chemical reactions as well as chemical catalysts do. We already know of more than 2000 reactions catalyzed by enzymes;[17] some of these enzymes showed better catalysis than chemical catalysts, as seen in the examples described above. (2) There is no limitation as to the number of microorganisms to be tested in nature and they are quite different from one another. They modify or degrade a great variety of complex organic compounds, so at least one of them can be expected to catalyze the desired reaction. Figure 4 shows the diversity of microbial ability as to the reduction of ketopantoyl lactone to pantoyl lactone.[61]

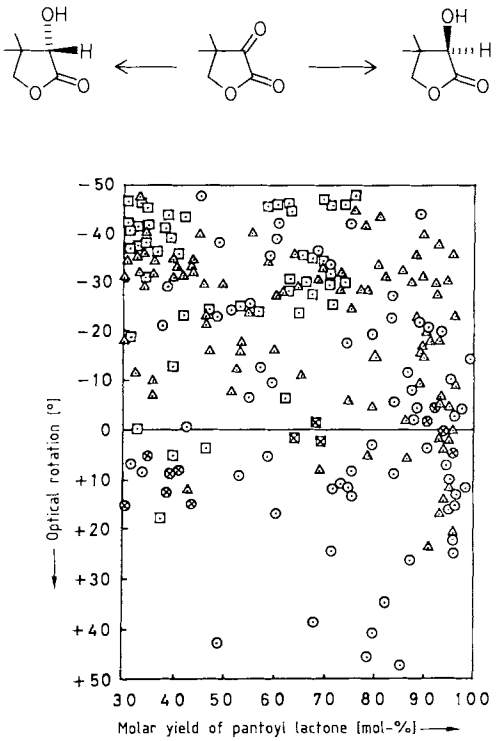

Fig. 4. Diversity of microbial reduction of ketopantoyl lactone to pantoyl lactone (see [61] for details). △, yeasts; ⊙, molds; □, bacteria; ⊗, actinomycetes; ⊠, basidiomycetes.

Many of the tested strains of bacteria, actinomycetes, yeasts, molds, and basidiomycetes exhibit this activity in very different ways; they usually produce mixtures of the D-(−) and L-(+) isomers, but their enantioselectivities vary. Some of them produce predominantly the D-(−) isomer in high yields. On the other hand, there are some strains which produce almost only the L-(+) isomer. Through this test, *Candida parapsilosis* was found to convert 100 g L^{-1} of the added ketopantoyl lactone into D-(−)-pantoyl lactone in a molar yield of nearly 100%[53] (see Section 5.5 for details). Such a test, also called screening, may be one of the most important steps for a successful microbial conversion.[62]

4.3. Substrates

Theoretically any substrate can be used for a microbial transformation, provided the substrate molecules come into contact with the enzyme. Even gases such as methane are effective substrates when bubbled into the reaction medium.[40,63] A substrate should be soluble in the medium and also be able to pass through the cell membrane, unless cell-free enzymes are being used as catalysts. The substrate is usually added to the reaction medium neat or as a concentrated solution.

Only a dissolved substrate is converted. Therefore, slightly soluble substrates must first be dissolved and, after conversion, the products may crystallize from the solution:

substrate (solid) $\rightleftharpoons$ substrate (solution) $\rightleftharpoons$ product (solution) $\rightleftharpoons$ product (solid)

For example, powdered cortisol, at concentrations of up to 500 g L^{-1}, is converted almost stoichiometrically into crystalline prednisolone by *Arthrobacter simplex*.[64] Substrates may also be dissolved in water-miscible organic solvents. The lower alcohols, acetone, dimethylformamide, and dimethyl sulfoxide are suitable solvents. Surfactants can also be used to disperse a substrate. The combination of a water-miscible solvent and a surfactant may have some advantage. In some cases, chemical modification of the substrate may improve its solubility.

When a substrate does not pass through the cell membrane, it is necessary to treat the cells in order to improve the permeability. Grinding with glass beads, air-drying, acetone-drying, lyophilization, autolysis, lysozyme digestion, surfactant treatment, osmotic shock, freezing and thawing, and sonication are usually performed. The use of cell-free enzyme preparations or purified enzymes is also favorable for eliminating the permeability barrier.

If a substrate does not suit the desired conversion, chemical modification of the substrate should be considered. Addition, variation, or removal of a protecting group or modification of a functional group in the substrate molecule sometimes makes it interact with the enzyme more efficiently. In addition, these modifications may protect the substrate from an undesired side reaction or degradation. The systematic assaying for a suitable chloroacetoacetate ester for enantioselective reduction to yield L-4-chloro-3-hydroxybutanoate ester, a promising precursor for the chemical synthesis of L-carnitine, by baker's yeast is an example.[65] A change in the stereoselectivity of a single enzyme, pig liver esterase, on substrate modification was also reported.[45]

In such cases, the potential ability of a microorganism or enzyme is found by screening for the most suitable substrate, instead of screening for the best-suited microorganism or enzyme.

4.4. Types of Catalysts and Reaction Systems

Conventional vegetative cell cultures are most commonly performed. Several alternative systems have been evaluated extensively with regard to, for example, increased yields, control of side reactions, simplification of processes, and improved economy. Advantages and disadvantages of these systems are briefly summarized in Table 4.

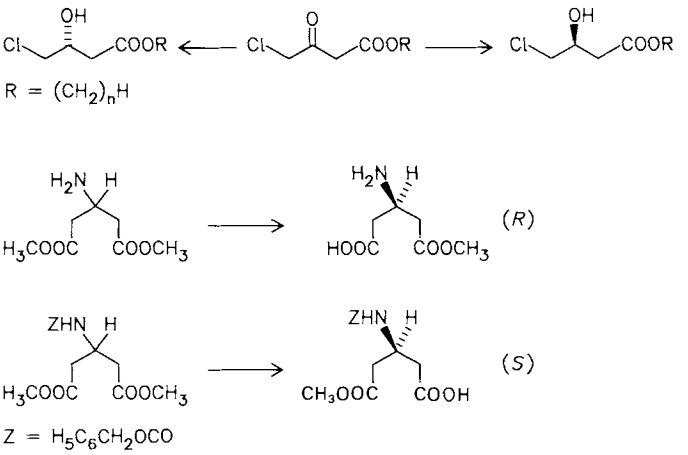

Various types of biocatalysts are useful for microbial transformations. They include whole or treated cells, organelles, cell-free multienzyme systems, and single cell-free enzymes.

Table 4. Types of biocatalysts and reaction systems used in microbial transformations.

Transformation with growing cultures:
The substrate is added to the growth medium during either inoculation or an appropriate phase of growth. The preparation and inoculation of the medium, addition of substrate, and incubation are successively carried out in one flask until the reaction is completed. Because of its extreme simplicity, this procedure is frequently used not only for screening, but also in large-scale production. If high cell densities are required for the transformation, this procedure is not recommended.

Transformation with previously grown cells:
The microorganism is grown under suitable conditions and then cells are collected by centrifugation or filtration. They are resuspended in a simple reaction medium (e.g., a buffer solution or water containing the substrate and appropriate additives if necessary). The reaction is then carried out directly or after suitable treatment of the cells (e.g., washing, improvement of permeability, drying). Growth and reaction steps are controlled independently for optimization.

Transformation with spores [66]:
Many fungal spores have as many useful enzymes as vegetative or grown cells. The spores separated from mycelium can be used as catalysts in a similar way as described above. Usually spores can be stored stably for long periods.

Transformation with immobilized cells [7, 8, 66–72]:
Immobilized cells are cells that have either been fixed or bound to a surface or entrapped in gel matrix. All of the above-mentioned cells can be immobilized. In successful cases, the immobilized calls retain their activities over several months and show a higher operational stability than unsupported cells. Additional advantages are: (1) easy removal of the cells from the reaction mixture, (2) repeated use of the cells, (3) continuous operation of the reaction, (4) cell regeneration by immersion into an appropriate nutrient medium, and (5) easy product isolation. On the other hand, disadvantages must also be considered: (1) The catalytic activity of cells usually decreases during the immobilization procedure. (2) The immobilization itself requires special equipment. The transformation step, especially operated continuously, also requires a special engineering design.

Transformations with cell-free enzymes or purified enzymes [73–75]:
In general, the use of cell-free enzymes or purified enzymes is expensive, because purification of enzymes is often tedious and time-consuming. However, there are several cases in which they are advantageous over systems using cells. Such cases are: (1) poor substrate or product permeability through the cell wall, (2) problems caused by undesired side reactions, (3) availability of the desired enzyme at an acceptable cost. If an extracellular enzyme is used, cells are not involved at all. Cell-free enzymes can also be used as immobilized catalysts.

Multistep reactions with different catalysts are also possible. Any combination of catalysts may be used simultaneously or sequentially for more than two sequential reactions. At present, however, only combinations of catalysts of the same type can be successfully used. Such applications have so far included the continuous production of L-alanine from ammonium fumarate via L-aspartic acid as the intermediate with immobilized *Escherichia coli* (aspartase) and *Pseudomonas dacunhae* (aspartate β-decarboxylase) cells,[76] the complete condensation of racemic homocysteine and adenosine with *Alcaligenes faecalis* (*S*-adenosylhomocysteine hydrolase) and *Pseudomonas putida* (racemase) cells,[77] the production of L-tryptophan from DL-serine and indole (tryptophan synthase and amino acid racemase),[78] complete hydrolysis of racemic α-amino-ε-caprolactam (see Fig. 3),[56] the continuous reduction of benzoylformate to *R*-(−)-mandelic acid by two kinds of cell-free enzymes,[75] and the continuous or batchwise amination of α-keto acids to yield L-amino acids with two kinds of cell-free enzymes.[74,79,80] Current recombinant DNA technology is allowing the combination of such separated enzyme catalysts in a single microorganism.[81]

On the other hand, the synthesis of coenzyme A from pantothenic acid, L-cysteine, and ATP (or AMP), involving five sequential steps, is being commercially performed solely with *Brevibacterium ammoniagenes* cells—a possibility suggested by screening[82] (see Section 5.4.2 for details).

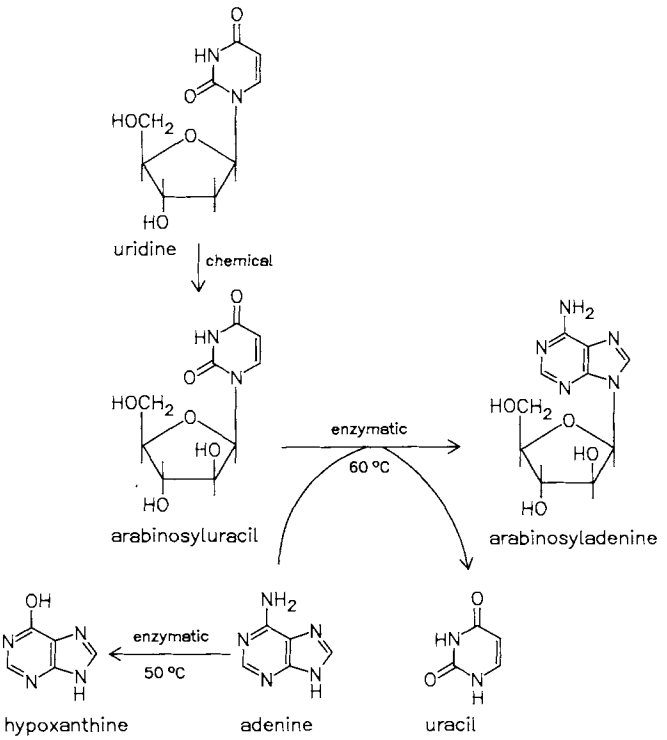

Fig. 5. Chemical and enzymatic process for the synthesis of arabinosyladenine through *trans-N*-arabinosylation by nucleoside pyrophosphorylases at 60°C.

Table 5. Elimination of side reactions by physical or chemical treatment.

Desired reaction	Side reaction	Treatment	Ref.
Ammonium fumarate → L-aspartic acid (*Escherichia coli* aspartase)	Fumaric acid → L-malic acid	Incubation of culture broth at pH 5 and 45°C for 1 h	[76]
Fumaric acid → L-malic acid (*Brevibacterium ammoniagenes* fumarase)	Fumaric acid → succinic acid	Treatment of immobilized cells with 0.6% bile extract	[84]
L-Aspartic acid → L-alanine (*Pseudomonas dacunhae* aspartate β-decarboxylase)	L-Alanine → D-alanine	Incubation of culture broth at pH 4.75 and 30°C for 1 h	[76]
Cholesterol → 1,4-androstadiene-3,17-dione (*Arthrobacter simplex* multistep conversion)	Further decomposition of the steroid ring	Addition of α,α'-bipyridyl (1 mM) to the culture broth for the conversion	[85]
β-Sitosterol → 17-oxosteroids (*Nocardia* sp. multistep conversion)	Further decomposition of the steroid ring	Addition of α,α'-bipyridyl (0.3 mM) to the conversion mixture	[86]
DL-2-Amino-4,5-dihydrothiazole-4-carboxylate → L-cysteine (*Pseudomonas thiazolinophilum* multistep conversion)	Further degradation of L-cysteine	Addition of hydroxylamine or semicarbazide to the reaction mixture	[87]

4.5. Side Reactions

High selectivity is one of the most important characteristics of enzyme catalysts. It means that undesired side reactions are not involved as long as a single purified enzyme is used. The use of purified enzymes, however, is often troublesome owing to their limited availability and instability and for economic reasons. Therefore, usual catalysts (e.g., cells and cell-free enzymes) comprise mixed enzymes or complex enzyme systems, some of which may cause undesired side reactions. Physical or chemical treatment, such as heating, pH changes, and the addition of detergents, organic solvents, or specific inhibitors of a catalyst may lead to specific inactivation of the undesired enzymes. For example, the *trans-N*-arabinosylation of adenine with synthetic arabinosyluracil yielding arabinosyladenine, an antiviral agent, by *Enterobacter aerogenes* cells takes place only at temperatures above 60°C. The reaction does not proceed below 50°C because hypoxanthine is formed by adenine deaminase before the *trans-N*-arabinosylation by the two kinds of nucleoside phosphorylases takes place. Fortunately, these phosphorylases are still active at 60°C, whereas the deaminase is completely inactivated at this temperature (Fig. 5).[83] Other examples are summarized in Table 5.

In some senses, screening for suitable microorganisms and structural modification of a substrate (see Section 4.4) can also be a means of preventing side reactions.

Improvement of the selected microorganism can also successfully overcome such undesired problems. The standard methods of strain improvement include the isolation of single colonies, optionally after mutagenesis, followed by screening for the best-suited isolates. Such conventional genetic manipulation techniques have been de-

veloped during the last 35 to 40 years for the improvement of useful strains. Today, recombinant DNA technology is providing new prospects of strain improvement (see Section 4.6).

4.6. Application of New Biotechnology

At present, several new techniques are rapidly being developed in connection with new biotechnology. One of them is recombinant DNA technology. Plasmids or phage vectors can transfer DNA fragments of microbial, plant, animal, or even synthetic origin into a suitable recipient microorganism. This technology has great potential especially for the construction of new microorganisms,[81] increases in enzyme activity,[88,89] and the improvement of enzyme properties such as stability and substrate specificity. However, it should also be noted that this technology is not so useful for finding new enzymes (e.g., new genes) or new reactions. At present, only in the case of a few microorganisms, such as *Escherichia coli, Bacillus subtilis,* and *Saccharomyces cerevisiae,* for which the genetic background and the appropriate host-vector systems are well-known, has recombinant DNA technology been beneficial. The practical application of this technology to microbial transformations is rare.[81] However, it will undoubtedly provide one of the most important keys for the future development of microbial transformations.

Since their discovery, enzymes have been thought to be inert catalysts in organic solvents. This is basically true, but recent technological advances have made available enzymes that are catalytically active in water-miscible organic solvents. For example, chemically modified peroxidase exhibits its activity well in benzene and *n*-hexane.[90] Polyphenol oxidase converts phenol nearly quantitatively into catechol when the reaction is carried out in chloroform containing only 1–2% water.[91] Such liquid-liquid multiphase systems with low water contents can also be used to shift the hydrolytic equilibrium toward water elimination. The synthesis of esters, amides, and peptides by this method shows great practical potential.[92] The conversion of lipophilic compounds with this system has also been extensively studied.[93]

Microorganisms are undoubtedly the most superior enzyme sources among living organisms. They show high adaptability to new environments and high growth rates. These characteristics are especially useful for easy handling and large-scale cultivation without a high cost. However, there are also many characteristic enzymes and reactions in animals and plants. Use of these organisms has also become more promising with current cell-culture technology.[94,95] Furthermore, protein engineering and cell technology, such as cell fusion, will become useful techniques for microbial transformations in the near future.

5. Specific Applications

A large number of biologically and chemically useful compounds are prepared through microbial transformations. They are briefly summarized in Table 6 together with key references. A brief review of some practical applications follows.

Table 6. Recent advances in microbial transformations.

Transformation of steroids and sterols [28, 96]: Hydroxylation (oxygenases), dehydrogenation (dehydrogenases), side-chain degradation (oxygenases), hydrolysis (hydrolases), peroxidation, reduction (dehydrogenases), isomerization (isomerases), conjugation etc.
Transformation of terpenoids [97]
Transformation of alkaloids [98]
Synthesis of semisynthetic antibiotics [99] (see also Section 5.3): Synthesis of semisynthetic penicillins and cephalosporins (acylases) [100, 101], hydrolysis of penicillins to 6-aminopenicillanic acid (penicillin acylase) [102], modification of carbapenem side chain (acylases) [103]
Synthesis of organic acids (see also Section 5.5): Hydration of fumaric acid (fumarase) [104], α,ω-oxidation of alkenes (oxygenase) [105], asymmetric hydrolysis of epoxysuccinic acid (hydrolase) [106], stereoselective oxidation of isobutyric acid (dehydrogenase) [107], stereoselective reduction of ketopantoyl lactone (reductase) [53, 108], stereoselective reduction of 3-chloroacetoacetic acid ester (reductase) [65], aminolysis of L-histidine (L-histidine amonia-lyase) [109]
Transformation of sugars [110]: Isomerization of glucose (glucose isomerase), hydrolysis of starch (amylases), hydrolysis of cellulose (cellulase), hydrolysis of sucrose (invertase)
Synthesis of peptides and proteins [29, 111, 112] (see also Section 5.2 and Table 8): Synthesis of plastin (proteases) [113], semisynthesis of human insulin (proteases) [30, 31, 114], synthesis of aspartame (protease) [115]
Synthesis of amino acids [23, 116–118] (see Section 5.1 and Table 7)
Synthesis of nucleic acid-related compounds [24, 119] (see also Section 5.4 und Table 9): *trans-N*-Ribosylation and *trans-N*-arabinosylation (phosphorylase) [83], phosphorylation of nucleosides (phosphotransferases) [120], pyrophosphorylation of nucleotides (pyrophosphorylase) [121], synthesis of sugar nucleotides (pyrophosphorylases) [122], nucleosidylation of L-methionine (*S*-adenosylmethionine synthetase) [77], nucleosidylation of L-homocysteine (*S*-adenosylhomocysteine hydrolase) [77], synthesis of coenzymes [119]
Synthesis of amines: Decarboxylation of amino acids (amino acid decarboxylases)
Synthesis of commodity chemicals (see also Section 5.6): Synthesis of alkene oxides (oxygenases) [40], synthesis of ketones (secondary alcohol dehydrogenases) [42], synthesis of aldehydes (alcohol oxidases) [41], synthesis of pyrogallol (decarboxylase) [43], synthesis of amides (nitrile hydratase) [39]

5.1. Optically Active Amino Acids

Numerous useful enzyme reactions are known for the preparation of enantiomerically pure amino acids (Table 7). They can be grouped into four fundamental types; (1) enantioselective hydrolysis of synthetically available racemic precursors (e.g., DL-amino acid esters, *N*-acyl-DL-amino acids, 5-substituted DL-hydantoins), (2) stereospecific condensation of achiral compounds (e.g., ammonia addition to fumaric acid, reverse of α,β-elimination), (3) modification of chiral precursors (e.g., β-replacement), and (4) reductive amination or transamination of α-keto acids).

5.1.1. Use of Hydrolytic Enzymes

The usual enzymatic resolution processes are based on the stereospecific hydrolysis of racemic amino acid derivatives to one enantiomer of an amino acid followed by reracemization of the remaining isomer. Aminoacylase is widely used for this purpose.[139] Esterase, amidase, and ni-

Table 7. Amino acid production by microbial transformations [a].

Amino acid	Reaction	Microorganism und enzyme	Ref.
L-Amino acid	*N*-acyl-L-amino acid + H_2O → L-amino acid + acetic acid	aminoacylase	[123]
S-Adenosylhomocysteine (AdoHcy)	L-Hcy + adenosine → AdoHcy + H_2O	*Alcaligenes faecalis* (*S*-adenosylhomocysteine hydrolase)	[77]
L-Alanine	L-Asp + H_2O → L-Ala + CO_2	*Pseudomonas dacunhae* (Asp β-decarboxylase)	[76]
L-Aspartic acid	fumaric acid + NH_3 → L-Asp	*Escherichia coli* (aspartase)	[60, 76]
	maleic acid + NH_3 → L-Asp	*A. faecalis* (maleate isomerase and aspartase)	[124]
L-Citrulline	L-Arg + H_2O → L-Cit + NH_3	*P. putida* (Arg deiminase)	[125]
L-Cysteine	DL-ATC + $2H_2O$ → L-Cys + NH_3 + CO_2	*P. thiazolinophilum* (ATC racemase, ATC hydrolase, and *S*-carbamoyl-L-cysteine hydrolase)	[87]
	3-chloro-L-Ala + H_2S → L-Cys + HCl	*Enterobacter cloacae* (Cys desulfhydrase) or *Bacillus sphaericus* (Cys synthase)	[52, 55]
L-Cystathionine	L-Cys + *O*-succinyl-L-homoserine → L-cystathionine + succinic acid	cystathionine γ-lyase or cystathionine γ-synthase	[127, 128]
L-Dopa	pyrocatechol + pyruvate + NH_3 → L-Dopa + H_2O	*Erwinia herbicola* (β-tyrosinase)	[51, 52]
	pyrocatechol + DL-Ser → L-Dopa + H_2O		
	L-Tyr + O_2 → L-Dopa + H_2O	*Aspergillus oryzae* (Tyr hydroxylase)	[128]
L-Glutamic acid	DL-5-carboxymethylhydantoin + $2H_2O$ → L-Glu + NH_3 + CO_2	*B. brevis* (hydantoinase and *N*-carbamoyl-L-Glu hydrolase)	[129]
5-Hydroxy-L-tryptophan	5-hydroxyindole + pyruvate + NH_3 → 5-hydroxy-L-Trp	*Proteus rettgeri* (tryptophanase)	[52]
L-Lysine	DL-ACL + H_2O → L-Lys	*Achromobacter obae* and *Cryptococcus laurentii* (ACL racemase and ACL hydrolase)	[56]
L-Phenylalanine	DL-5-benzylhydantoin + $2H_2O$ → L-Phe + NH_3 + CO_2	*Flavobacterium aminogenes* (hydantoinase and *N*-carbamoyl-L-Phe hydrolase)	[130]
	trans-cinnamic acid + NH_3 → L-Phe	*Rhodtorula glutinis* (Phe ammonia-lyase)	[131]
	cinnamate acetamide + amine donor → L-Phe + keto acid	*A. faecalis* (acylase and transaminase)	[132]
	phenylpyruvate + L-Asp → L-Phe + oxaloacetic acid	*E. coli* (Phe transaminase)	[133]
	phenylpyruvate + NH_3 + NADH → L-Phe + NAD	Phe dehydrogenase	[79, 80]
S- or *Se*-substituted L-homocysteine	L-Met + RSH (or RSeH) → *S*- or *Se*-substituted L-Hcy + MeSH	Met γ-lyase	[134]
L-Serine	Gly + HCHO → L-Ser	*Pseudomonas* 3ab, *Sarcina albida*, *Hyphomicrobium methylovorum*, etc. (Ser hydroxymethyltransferase)	[135]
	DL-OOC + H_2O → L-Ser + CO_2	*P. testosteroni* and *B. subtillis* (L-OOC hydrolase and OOC racemase)	[136]
L-Tryptophan	indole + pyruvate + NH_3 → L-Trp + H_2O	*Proteus rettgeri* (tryptophanase)	[52]
	indole + L-Ser → L-Trp	*E. coli* (Trp synthase)	[78, 137]
	DL-IMH + $2H_2O$ → L-Trp + NH_3 + CO_2	*F. amminogenes* (hydantoinase, *N*-carbamoyl-L-Trp hydrolase)	[138]
L-Tyrosine	phenol + pyruvate + NH_3 → L-Tyr + H_2O	*Erwinia herbicola* (β-tyrosinase)	[51, 52]
D-Amino acids	DL-5-substituted hydantoin + H_2O → *N*-carbamoyl-D-amino acid	*P. putida* (dihydropyrimidinase)	[57, 58]
D-Cysteine	3-chloro-D-Ala + NaHS → D-Cys + NaCl	*P. putida* (3-chloro-D-Ala dehydrochlorinase)	[55]
D-*p*-Hydroxyphenylglycine	DL-5-(*p*-hydroxyphenyl)hydantoin + H_2O → *N*-carbamoyl-D-*p*-hydroxyphenylglycine + NH_3 + CO_2	*P. putida* (dihydropyrimidinase)	[57, 58]
D-Phenylglycine	DL-5-phenylhydantoin + H_2O → *N*-carbamoyl-D-phenylglycine	*P. putida* (dihydropyrimidinase)	[57, 58]
D-Valine	DL-5-isopropylhydantoin + H_2O → *N*-carbamoyl-D-Val + NH_3 + CO_2	*P. putida* (dihydropyrimidinase)	[57, 58]

[a] Abbreviations: ATC, 2-amino-4,5-dihydrothiazole-4-carboxylic acid; Dopa, 3,4-dihydroxyphenylalanine; ACL, α-amino-ε-caprolactam; OOC, 2-oxooxazolidine-4-carboxylic acid; IMH, 5-indolylmethylhydantoin.

trilase can also be used. Several other hydrolytic enzymes with more specific substrate specificities are used for the preparation of L-lysine (L-α-amino-ε-caprolactam hydrolase, see Fig. 3),[56] L-cysteine (L-2-amino-4,5-dihydrothiazole-4-carboxylate hydrolase),[87] L-tryptophan and L-phenylalanine (hydantoinase),[130,138] and D-*p*-hydroxyphenylglycine (dihydropyrimidinase/hydantoinase, see Fig. 6).[53,57,58] In contrast to the acylase method, asymmetric hydrolysis is accompanied by reracemization by a specific racemase or under base catalysis in one step in these processes.

D-*p*-Hydroxyphenylglycine[57,58] and its derivatives are important as side-chain precursors for semisynthetic penicillins and caphalosporins. We found that these amino acids can be efficiently prepared from the corresponding 5-substituted hydantoins using bacterial dihydropyrimidi-

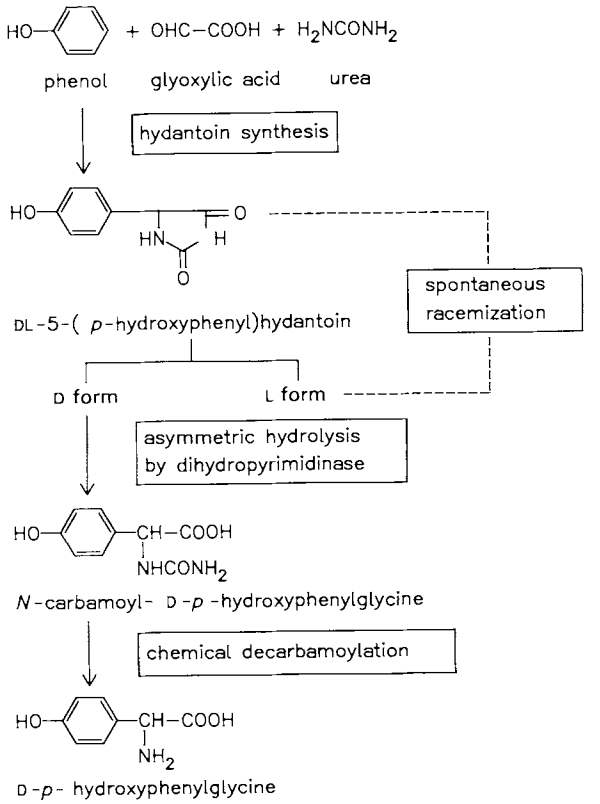

Fig. 6. Chemical and enzymatic process for the production of D-*p*-hydroxyphenylglycine involving stereoselective hydrolysis of DL-5-(*p*-hydroxyphenyl)hydantoin.

nase. High activity of this enzyme is found in a wide variety of bacteria, especially, in *Aerobacter*, *Corynebacterium*, *Agrobacterium*, *Pseudomonas*, *Bacillus*, and *Streptomyces*.[140] The bacterial enzyme has been isolated as crystals from cells of *Pseudomonas putida*. The enzyme shows the highest activity and affinity toward dihydrouracil, but also attacks a variety of aliphatic and aromatic 5-monosubstituted D-hydantoins, yielding the corresponding D-form *N*-carbamoyl-α-amino acids.[141] Thus, the enzyme can be used as a catalyst for the preparation of D-amino acids. The synthetic process involves two chemical steps and one enzymatic step.[142] The substrate hydantoins are generally synthesized by the method of *Bucherer* and *Steiner*[59] with aldehydes as the starting materials. Then, the D-hydantoins are hydrolyzed enzymatically to *N*-carbamoyl-D-amino acids. In practice, bacterial cells exhibiting high enzyme activity can be used directly as the catalyst. Preparation of these cells is carried out by culturing the selected bacterium in a medium supplemented with hydantoin or uracil as the inducer. Under the conditions used for the enzymatic reaction at pH 8 to 10, the L isomers of the remaining hydantoins are racemized rapidly and spontaneously through base catalysis. Therefore, the racemic hydantoins can be converted quantitatively into *N*-carbamoyl-D-amino acids through this step. Decarbamoylation to D-amino acids is performed by treating the *N*-carbamoyl-D-amino acids with equimolar nitrite under acidic conditions.[143] The configuration is completely retained throughout this step, with a nearly quantitative molar yield. Based on these results, a new commercial process for the production of D-*p*-hydroxyphenylglycine has been developed. To avoid the use of expensive *p*-hydroxybenzaldehyde for preparation of the substrate, DL-5-(*p*-hydroxyphenyl)hydantoin, a new and efficient chemical method involving the amidoalkylation reaction of phenol with glyoxylic acid and urea under acidic conditions was developed.[144] Figure 6 shows the overall process for the production of D-*p*-hydroxyphenylglycine. This may be one of the most economical processes for the larger-scale production of this amino acid. In a similar manner, D-phenylglycine and D-valine, which are important intermediates for the synthesis of semisynthetic penicillins and pesticides, respectively, have been commercially produced.

The decarbamoylation step can also be carried out enzymatically.[145] For example, *Pseudomonas* sp. was reported to produce decarbamoylase together with hydantoinase. Therefore, a sequence of two enzyme-catalyzed reactions, the stereospecific hydrolysis of DL-5-(*p*-hydroxyphenyl)hydantoin and subsequent hydrolysis of the D-carbamoyl derivative to D-*p*-hydroxyphenylglycine, is possible.[146] At present, however, enhancement of the activity of the latter enzyme is necessary for practical purposes. Recently, one such decarbamoylase was characterized in detail.[147]

5.1.2. *Use of Pyridoxal Phosphate-Dependent Enzymes*

Most pyridoxal 5′-phosphate-dependent enzymes are involved in the metabolism of amino acids. These enzymes catalyze a variety of reactions, including transamination, racemization, elimination, replacement, decarboxylation, and aldol-type condensation and retrocondensation reactions. Thus, these enzymes are occasionally used for the preparation of a variety of amino acids. Aspartate β-decarboxylase,[76] β-tyrosinase,[51,52] and phenylalanine transaminase[133] are used for the commercial preparation of L-alanine, L-tyrosine, and L-phenylalanine, respectively.

Aromatic Amino Acids and Sulfur-Containing Amino Acids:[51,52,55] β-Tyrosinase (EC 4.1.99.2) and tryptophanase (EC 4.1.99.1) are enzymes which catalyze the degradation of L-tyrosine to phenol, pyruvate, and ammonia, and L-tryptophan to indole, pyruvate, and ammonia, respectively. The properties of the crystalline enzymes prepared from *Citrobacter intermedius* and *Proteus rettgeri*, respectively, were established in some detail.[51,52,148] They catalyze a variety of reactions, e.g., α,β-elimination [Eq. (6)], β-replacement [Eq. (7)], and the reverse of α,β-elimination [Eq. (8)].

$$RCH_2{-}CH(NH_2){-}COOH + H_2O \longrightarrow RH + CH_3{-}CO{-}COOH + NH_3 \quad (6)$$

$$RCH_2{-}CH(NH_2){-}COOH + R'H \longrightarrow R'CH_2{-}CH(NH_2){-}COOH + RH \quad (7)$$

$$R'H + CH_3{-}CO{-}COOH + NH_3 \longrightarrow R'CH_2{-}CH(NH_2){-}COOH + H_2O \quad (8)$$

For β-tyrosinase, R = hydroxyphenyl, OH, SH, Cl, R′ = hydroxyphenyl; for tryptophanase, R = indolyl, OH, Cl, R′ = indolyl.

In the α,β-elimination [Eq. (7)] and β-replacement [Eq. (7)] reactions of β-tyrosinase, L-tyrosine, L-serine, *S*-methyl-L-cysteine, and 3-chloro-L-alanine are substrates. In

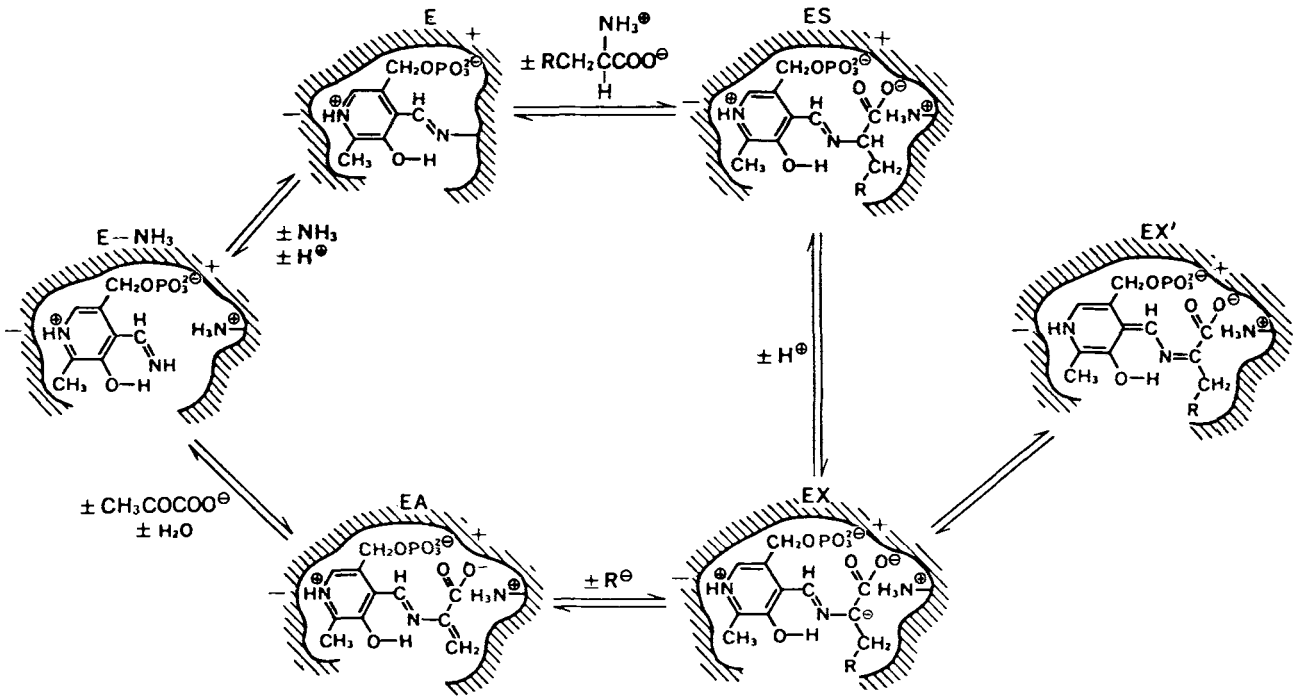

Fig. 7. The mechanism for reactions catalyzed by β-tyrosinase. E, enzyme; S, substrate; ES, EX, EX', and EA, enzyme-substrate complexes; EA, enzyme-α-aminoacrylate complex; E-NH_3, enzyme-ammonia complex.

the β-replacement reaction, phenol is the second substrate for the synthesis of L-tyrosine. When either pyrocatechol, resorcinol, pyrogallol, or hydroxyhydroquinone is the second substrate, instead of phenol, L-Dopa, 2-hydroxy-L-tyrosine, 2,3-dihydroxy-L-tyrosine, and 2,5-dihydroxy-L-tyrosine are synthesized, respectively. L-Tyrosine is also synthesized through the reverse of the α,β-elimination reaction [Eq. (8)] from phenol, pyruvate, and ammonia. As substrates, pyrocatechol, resorcinol, and various kinds of *o*- and *m*-halogenated phenols and alkylated phenols are as good as phenol in the reverse reaction.[51,52,149] These tyrosine derivatives readily crystallize out under the reaction conditions used, thus driving the reaction forward to completion. The mechanism of the tyrosinase-catalyzed reactions can be understood on the basis of the general mechanism for pyridoxal 5'-phosphate-dependent reactions, shown in Figure 7, in which the enzyme-α-aminoacrylate complex (EA in Fig. 7) is the key intermediate for all three reactions.[51]

As in the case of the β-tyrosinase reaction, L-tryptophan and some of its derivatives, such as 5-hydroxy-, 5-amino- and 5-methyl-L-tryptophan, can be synthesized efficiently when tryptophanase is the catalyst.[150]

Based on the results with the crystalline enzymes, simple and efficient enzymatic processes for the production of these aromatic L-amino acids have been developed. In these processes, bacterial cells exhibiting high enzyme activity are directly used as the catalysts. L-Tyrosine, L-Dopa, L-tryptophan, and 5-hydroxy-L-tryptophan can be synthesized in excellent yields.[51,52,151]

Cysteine desulfhydrase (EC 4.1.1.1), *O*-acetylserine sulfhydrolase (EC 4.2.99.8), and 3-chloro-D-alanine dehydrochlorinase (EC 4.5.1.2) catalyze similar reactions. The usefulness of these enzymes for the preparation of L- and D-cysteine and their derivatives has been shown.[52,55,152] Furthermore, γ-replacement reactions catalyzed by cystathionine γ-lyase (EC 4.4.1.1) and cystathionine γ-synthase (EC 4.2.99.9), as well as one catalyzed by methionine γ-lyase (EC 4.4.1.11), have been suggested for the synthesis of L-cystathionine[126,127] and *S*- or *Se*-substituted L-homocysteines.[134]

L-Phenylalanine is an important building block for the low-calorie sweetner aspartame. Various routes to this amino acid have been reported (see Table 7). A recently developed large-scale process involves alkaline hydrolysis of benzylidenehydantoin to phenylpyruvic acid, which in turn is aminated enzymatically (Fig. 8). The enzymatic conversion of phenylpyruvic acid is carried out with L-aspartic acid as the amine donor and L-phenylalanine transaminase as the catalyst.[133,153] When *Escherichia coli* cells immobilized with polyazetidine are used as the catalyst, 30 g L^{-1} of L-phenylalanine can be produced in a molar yield of 98%. The activity of the immobilized cells is quite stable; the half-life has been estimated to be more than

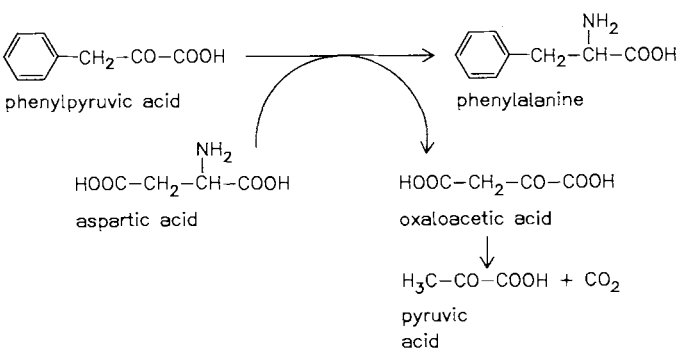

Fig. 8. Chemical and enzymatic process for the production of L-phenylalanine involving enzymatic transamination.

eight months. Although the equilibrium constant for this reaction is approximately one, the reaction is driven to completion by removal of one of the reaction products, oxaloacetic acid, through rapid decarboxylation to pyruvic acid.[133]

5.1.3. *Use of Amino Acid Dehydrogenase*

A recently developed route to L-amino acids of high optical purity is the reductive amination of a series of α-keto acids with amino acid dehydrogenases. The enzymes catalyzing this reaction require NAD(P)H as a cofactor. To avoid an equimolar consumption of the expensive cofactor, a continuous cofactor regeneration system has been suggested. The most successful example is the continuous L-leucine production with leucine dehydrogenase (EC 1.4.1.9) entrapped in a membrane reactor together with formate dehydrogenase and polymer-bound NAD.[74] L-Alanine dehydrogenase (EC 1.4.1.1) and phenylalanine dehydrogenase have been shown to be useful for the production of L-alanine[74] and L-phenylalanine,[79,80] respectively. Such a type of reaction is generally applicable to amino acid production, if suitable dehydrogenases and α-keto acids are available.

5.2. Peptides

The high practical potential of proteolytic enzymes for peptide transformations was recognized in pioneering studies in the 1970s: e.g., the modification of soybean trypsin inhibitor,[154,155] nutritional enrichment of proteins,[113] and synthesis of some biologically active small peptides.[156] The successful semisynthesis of insulin[30–32,114] further emphasized their value as effective catalysts. Since then, various biologically active small peptides including hormones and neuropeptides have been prepared using proteolytic enzymes (Table 8). The application of proteolytic enzymes has recently expanded to include the preparation or modification of large-molecular-weight peptides (e.g., enzymes, antibodies, protein hormones). Other useful enzymes for peptide preparation are nucleoside triphosphate-dependent synthetases. The synthesis of gramicidin S,[166] glutathione and related peptides,[167] and kyotorphin[164] has also been reported.

Human Insulin: Porcine insulin and human insulin differ only in the *C*-terminal amino acid of the B chain. As shown in Figure 9, the selective hydrolysis of the B-chain *C*-terminal alanine residue of porcine insulin and subsequent condensation of the des(AlaB30) insulin with a threonine ester derivative are efficiently catalyzed by a serine protease, *Achromobacter* protease I. The enzyme specifically cleaves the carboxyl side of lysine residues. Although the process involves reactions at pH 8.3 (hydrolysis) and pH 6.5 (condensation) with intermediate isolation and lyophilization of the des(AlaB30) insulin, overall yields of 52% for porcine insulin and 58% for bovine insulin were reported.[31] The unreacted des(AlaB30) insulin can be reused. At present, human insulin is commercially prepared from porcine insulin through such enzymatic transformation and through direct fermentation with an *Escherichia coli* mutant constructed by means of recombinant DNA technology.

Table 8. Enzymatic transformations of biologically important peptides.

Peptide	Enzymes	Ref.
Aspartame	Thermolysin	[115]
(Val^5)-Angiotensin II (1-8)	Papain	[155]
Substance P-related peptide (1-6)-NH_2	Pepsin	[156]
Enkephalin	Papain and chymotrypsin or carboxypeptidase Y	[157] [158]
Caerulein	Chymotrypsin, papain, subtilisin, metalloprotease, and aspartic protease	[159]
Eledoisin-related peptide (1-6)-NH_2	Pepsin	[156]
Salmon calcitonin I (1-32)	Trypsin	[160]
Human insulin	*Achromobacter* protease I or trypsin	[31] [30]
Dynorphin (1-8)	Chymotrypsin, papain, and trypsin	[161]
(Lys^{63})- and (Trp^{63})-soybean-trypsin inhibitors	Chymotrypsin and carboxypeptidase A	[162]
(Arg^{15})- and (Trp^{15})-bovine trypsin-kallikrein inhibitors	Trypsin and carboxypeptidase A, and Chymotrypsin and carboxypeptidase A, respectively	[163]
Kyotorphin	Leucyl-tRNA synthetase or chymotrypsin	[164] [165]
Gramicidin S	Gramicidin S synthetase	[166]
Glutathione	γ-Glutamylcysteine synthetase and glutathione synthetase	[167]
γ-Glutamylpeptides	γ-Glutamyltranspeptidase or γ-Glutamylcysteine synthetase	[167, 168] [167, 169]
Bovine pancreas ribonuclease A	Subtilisin	[170]
(Gly^{48})-*Staphylococcus* nuclease (6-149)	Trypsin	[171]
Plastein	Various proteases	[113]

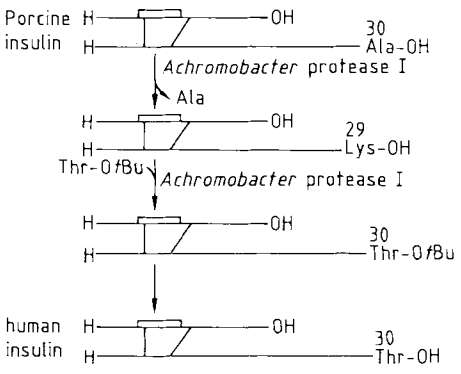

Fig. 9. Enzymatic transformation of porcine insulin to human insulin using *Achromobacter* protease I.

5.3. Antibiotics

A large number of antibiotics have been modified with the use of microorganisms or enzymes. Many of these modifications were based on simple and chemically defined reactions (e.g., hydrolysis, acylation and deacylation,

nucleotidylation, phosphorylation, glycosidation, methylation and demethylation, amination and deamination, oxidation and reduction, isomerization, hydration, halogenation). Some of these reactions have considerable practical significance for the preparation of new semisynthetic antibiotics.

β-Lactam antibiotics have been extensively studied. The deacylation of penicillins and the acylation of 6-aminopenicillanic acid (6-APA), 7-aminocephalosporanic acid, and 7-amino-3-deacetoxycephalosporanic acid are especially important for practical purposes. In general, a single enzyme, penicillin acylase (EC 3.5.1.11), catalyzes the penicillin acylation and deacylation reactions, the directional equilibrium being controlled by pH. Thus, the enzyme can be used for the preparation of either 6-APA or semisynthetic penicillins. The industrial processes for the preparation of 6-APA from penicillin G involve immobilized penicillin acylase[172,173] or immobilized *Escherichia coli* cells containing it.[102] The 6-APA, in turn, serves as a substrate for the preparation of novel semisynthetic penicillins with improved therapeutic properties. Although chemical acylation is usually carried out for this purpose, effective enzymatic acylation reactions are known for the preparation of ampicillin and amoxycillin from 6-APA and, respectively, D-phenylglycine methyl ester and D-*p*-hydroxyphenylglycine ethyl ester.[173] An effective two-step enzymatic process involving the deacylation of benzylpenicillin by *Kluyvera citrophila* at pH 7.5, yielding 6-APA, followed by acylation of the latter with DL-phenylglycine methyl ester at pH 5.5 by *Pseudomonas melagogenum*, yielding ampicillin, has been reported.[174] In this case, the *Pseudomonas* acylase does not attack the benzylpenicillin, which remains unaffected during the acylation step.

5.4. Coenzymes

Some coenzymes are produced on an industrial scale and are used as pharmaceuticals for various diseases. Many methods of preparation, including microbial transformation, fermentation, and chemical synthesis, are known. In addition to their importance as pharmaceuticals, coenzymes are important as cofactors in many enzyme reactions which are useful for microbial transformations. To avoid the stoichiometric consumption of the expensive coenzymes, several systems for their generation or regeneration, especially for ATP and NAD(P)H, have been developed.

5.4.1. Regeneration Systems for Coenzymes and Their Application

ATP: Because ATP is used not only as an energy source but also as a substrate in various enzyme reactions, both regeneration (recycling) and generation (production) must be considered. The generally applicable methods for ATP generation or regeneration are as follows:

(1) Yeast glycolysis system: Ground or dried cells of baker's or brewer's yeast efficiently phosphorylate the added adenosine (or AMP) to ADP and ATP on incubation with high concentrations of glucose and inorganic phosphate.[175] Under suitable conditions using brewer's yeast, 190 μmol mL^{-1} of ATP was produced in a molar yield of 63%.[176] Other yeasts and bacteria are also used for this purpose. In particular, the use of *Saccharomyces cerevisiae* cells, in which hexokinase or glucokinase was enriched by gene technology, led to almost stoichiometric conversion of adenosine (130 mM) to ATP.[177] The mechanism involved in the ATP production is thought to be the substrate-level phosphorylation of AMP or adenosine via ADP using the energy provided by glycolysis, as shown in Figure 10a. An advantage of this method is that readily available baker's yeast can be used as the catalyst.

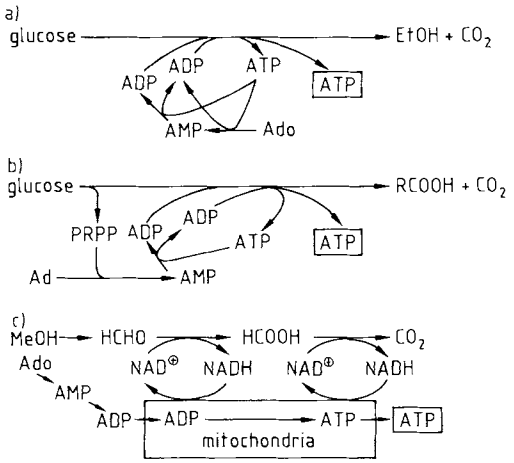

Fig. 10. Schematic representations of the reaction systems for ATP generation through a) yeast fermentation, b) ribotidation of adenine, and c) mitochondrial oxidative phosphorylation. Ad, adenine; Ado, adenosine; PRPP, 5-phosphoribosyl-1-pyrophosphate.

(2) Bacterial ribotidation of adenine. Based on the finding that several coryneform bacteria ribotidate added bases with satisfactory yields,[178] a practical production method for ATP has been developed. Adenine (2 mg mL^{-1}) added to a three-day culture of *Brevibacterium ammoniagenes* was converted into ATP (1.57 mg mL^{-1}), ADP (1.59 mg mL^{-1}), and AMP (2.16 mg mL^{-1}) on further incubation for 24 h.[179] Washed cells of the same bacterium also produced more than 10 mg mL^{-1} of ATP in a molar yield of 83%.[180] Because adenine is one of the cheapest starting substrates, this system is widely applied for the practical preparation of many useful compounds. The formation of phosphoribosyl pyrophosphate from glucose followed by condensation with the added adenine, yielding AMP, and phosphorylation of the AMP to ATP by adenylate kinase are suggested to be key reactions involved in this system (Fig. 10b).

(3) Oxidative phosphorylation: Cells of a methylotrophic yeast, *Kloeckera* sp., which had been treated with a lytic enzyme, zymolyase, or by the addition of sorbitol to the reaction mixture, catalyzed the phosphorylation of adenosine in the presence of methanol as the energy source.[181] Sequential reactions, including the mitochondrial oxidative phosphorylation coupled with the oxidation of methanol to CO_2 and the phosphorylation of adenosine by adenosine kinase and of AMP by adenylate ki-

Table 9. Application of ATP-regenerating systems to syntheses of useful compounds.

Product	ATP-regenerating system	Microorganism or enzyme	Ref.
Nucleoside 5'-triphosphates	Glycolysis [a]	Baker's yeast, etc.	[186]
GTP	Ribotidation [b]	*Brevibacterium ammoniagenes*	[179]
5'-Guanylic acid	Ribotidation [b]	*B. ammoniagenes*	[187]
ppGpp [c] and pppGpp [d]	Ribotidation [b]	*B. ammoniagenes*	[188]
AppppA [e]	Cell-free enzymes	Acetate kinase, adenylate kinase, and leucyl-tRNA synthetase	[189]
Nucleoside diphosphate sugars	Glycolysis [a]	Baker's yeast, etc.	[122, 186]
CDP-choline	Glycolysis [a]	Brewer's yeast, etc.	[190]
NAD	Ribotidation [b]	*B. ammoniagenes*	[191]
	Cell-free enzymes	Acetate kinase, adenylate kinase and NAD pyrophosphorylase	[192]
NADP	Glycolysis [a]	Baker's yeast and *B. ammoniagenes*	[193]
	Cell-free enzymes	Acetate kinase, adenylate kinase, NAD pyrophosphorylase, and NAD kinase	[192]
FAD	Ribotidation [b]	*B. ammoniagenes* or *Sarcina lutea*	[194]
	Glycolysis [a]	Baker's yeast and *Arthrobacter globiformis*	[195]
Coenzyme A	Ribotidation [b]	*B. ammoniagenes* or *S. lutea*	[196]
	Glycolysis [a]	Baker's yeast and *B. ammoniagenes*	[197]
S-Adenosylmethionine	Glycolysis (?) [a]	*Saccharomyces sake*	[198]
	Cell-free enzymes	Pyruvate kinase, adenylate kinase, inorganic pyrophosphatase, and methionine-adenosyltransferase	[199]
Glutamine	Glycolysis [a]	Baker's yeast and glutamine synthetase	[200]
Theanine (N^5-ethylglutamine)	Glycolysis [a]	Baker's yeast and glutamine synthetase	[201]
Glutathione	Glycolysis [a]	Baker's yeast	[202]
	Glycolysis [a]	Baker's yeast, γ-glutamylcysteine synthetase, and glutathione synthetase	[167]
	Cell-free enzyme	Acetate kinase and *Escherichia coli*	[203]
Gramicidin S	Cell-free enzyme	Acetate kinase and gramicidin S synthetase	[166]
Glucose-6-phosphate	Cell-free enzyme	Acetate kinase and hexokinase	[204]
Galactose-1-phosphate	Glycolysis [a]	Baker's yeast and galactokinase	[205]

[a] The general principle of the reaction is illustrated in Fig. 9a. [b] This process involves direct ribotidation of bases or its modification. The general principle of the reaction is shown in Fig. 9b. [c] Guanosine 3',5'-bis(diphosphate). [d] Guanosine 3'-diphosphate-5'-triphosphate. [e] Diadenosine tetraphosphate.

nase, have been proposed as the reaction mechanism (Fig. 10c).[181] The efficient utilization of the energy derived from methanol, a cheap raw material, in this system suggests a general advantage for application to many transformation reactions.

(4) Photophosphorylation: Chromatophores isolated from photosynthetic bacteria grown in the light have been shown to phosphorylate ADP to ATP.[182] ATP generation using isolated thylakoids[183] or chloroplasts[184] has also been reported. These systems are presently of academic interest.

(5) Use of cell-free enzymes: Phosphotransferases (kinases) are enzymes which catalyze the transfer of a phosphate of ATP to their substrates, the ATP being converted into ADP. Some of these enzymes also catalyze the reverse reaction, and are useful for the generation of ATP. Pyruvate kinase (EC 2.7.1.40), carbamoyl kinase (EC 2.7.2.2), creatine kinase (EC 2.7.3.2), phosphoglycerate kinase (EC 2.7.2.3), and aspartokinase (EC 2.7.2.4) are such enzymes. The former three and especially acetate kinase (EC 2.7.2.1) are widely used for this purpose.[185] If the transformation of interest requires a cell-free enzyme, coupling of these enzyme systems is highly recommended.

Applications of the above systems are listed in Table 9. The advantages and disadvantages of (1), (2), and (5) were discussed by *Langer* et al.[206]

NADH and NADPH: Various regeneration systems for NAD(P)H are involved in the complex and regulated metabolism of living cells. For example, the pathway for glucose oxidation via glucose-6-phosphate involves two important reactions yielding NADPH, namely, the oxidation of glucose 6-phosphate by glucose-6-phosphate dehydrogenase followed by the oxidation of 6-phosphogluconate by 6-phosphogluconate dehydrogenase. By means of this system, endogenous NADPH or a catalytic amount of added NADPH can be efficiently regenerated by the simple mixing of microbial cells with glucose in an appropriate reaction mixture. The reductions of various carbonyl compounds by yeast cells occasionally performed in synthetic organic chemistry[15,61,65] are mainly based on this system. Similarly, the reactions involved in the oxidation of methanol to CO_2 by methylotrophic microorganisms are considered to be a very useful system for NADH regeneration (see Fig. 10c).

When cell-free enzymes requiring reduced nicotinamide cofactors are to be used, the construction of a suitable regenerating system is an additional requirement. The generally applicable systems were described by *Whitesides* and *Wong*.[14] Among them, the formate/formate dehydrogenase,[74] glucose/glucose dehydrogenase, and glucose 6-phosphate/glucose 6-phosphate dehydrogenase systems are most widely used, because of the availability of these hydrogen donor substrates and enzymes. In particular, the formate/formate dehydrogenase system is advantageous, because the reaction product from formate, CO_2, causes no problems for the isolation of the desired products. The application of this system has been extensively studied by the group of *Kula* and *Wandley*.[74,79]

5.4.2. *Production of Coenzymes*

Only three coenzymes, for which we developed large-scale production processes, will be described here (for others, see Ref. [119]).

Coenzyme A:[207] The biosynthesis of coenzyme A (CoA) from pantothenic acid, L-cysteine, and ATP is performed through five sequential enzymatic reactions as shown in Figure 11.[208] We found that *Brevibacterium ammoniagenes*

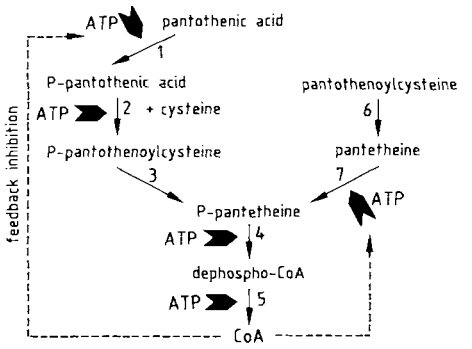

Fig. 11. The pathway for the biosynthesis of coenzyme A (see text).

cells contain all five enzymes necessary for the synthesis of CoA (Fig. 11, route 1-2-3-4-5 or route 7-4-5), all with high activities.[82, 196, 209] Using cells of this bacterium as the catalyst, CoA (2–5 g L^{-1}) can be synthesized from the above substrates efficiently.[82, 196, 207, 210] The CoA biosynthesis from these three substrates or from pantetheine and ATP in this bacterium is mainly regulated by feedback inhibition of pantothenate kinase (EC 2.7.1.33), which catalyzes the phosphorylation of pantothenate or pantetheine, by the end product, CoA. It was therefore difficult to improve the CoA yield, because the overproduced CoA inhibited the CoA synthesis. In order to avoid this feedback inhibition, the enzymatic phosphorylation of pantothenic acid was replaced with a chemical phosphorylation. Under suitable conditions, 1.65 g of CoA was synthesized in 50 mL of a reaction mixture containing *p*-pantothenic acid, L-cysteine, and ATP (molar yield based on ATP, 64.5%).[211] In a similar manner, 115 g L^{-1} of CoA was synthesized from *p*-pantetheine and ATP (quantitative yield).[211]

Another way to improve the CoA yield is to use mutants derepressed as to the feedback inhibition or ones showing elevated pantothenate kinase activity. A mutant strain of *B. ammoniagenes* resistant to oxypantetheine, an oxygen analogue of pantetheine, in which pantothenate kinase activity is threefold higher than in the parent strain, produces 9.3 g L^{-1} of CoA from pantothenic acid (3.6 g L^{-1}), L-cysteine (1.8 g L^{-1}), and AMP (6 g L^{-1}) or 11.5 g L^{-1} of CoA from pantetheine (5 g L^{-1}) and AMP (6 g L^{-1}) with the ATP generation system shown in Figure 10b (molar yield based on AMP, 70–100%).[212] These values are about threefold higher than those in the case of the parent strain.

The reaction conditions for the selective synthesis of *p*-pantothenic acid, *p*-pantetheine, or 3′-dephospho-CoA have also been established.[207, 213]

S-Adenosylmethionine (AdoMet), S-adenosylhomocysteine (AdoHcy)[77, 214] and related nucleosides have recently attracted great interest as key regulator compounds for many biological transmethylation reactions (Fig. 12). Although the great possibilities of these nucleosides in the pharmaceutical and chemotherapeutic fields have been suggested,[215] no process for the practical production of these nucleosides had been established before our current work.

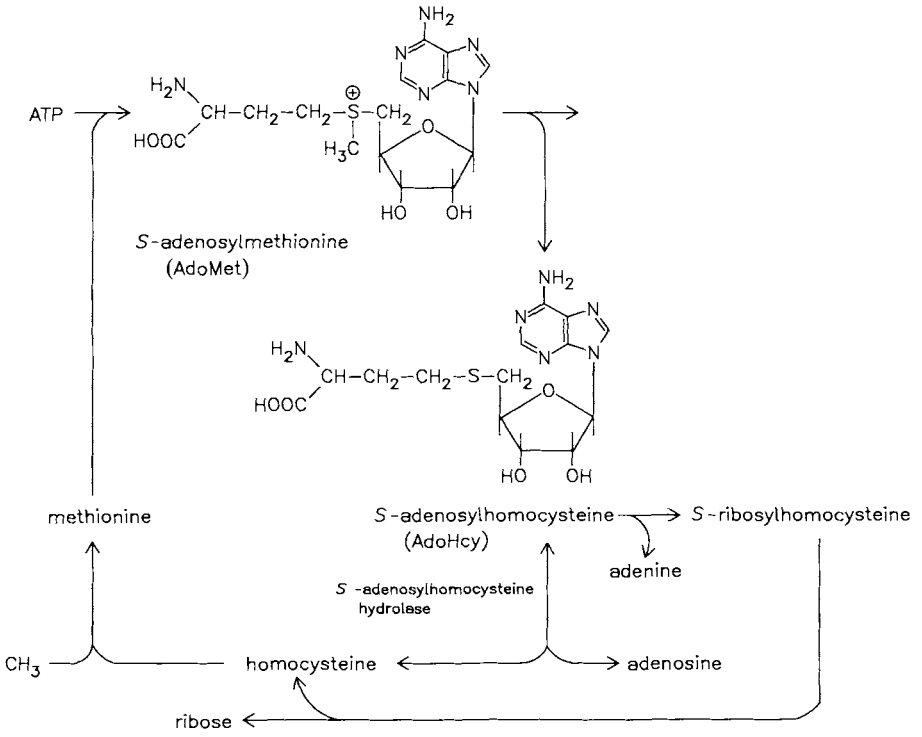

Fig. 12. The activated methyl cycle (*S*-adenosylmethionine).

We have tested a variety of microorganisms as to their ability to accumulate AdoMet derived from L-methionine and found that a group of sake yeasts (*Saccharomyces sake* strains) specifically accumulate the added methionine as AdoMet.[198] *S. sake* Kyokai No. 6, which was selected as the most promising producer, converts about 25% of the added L-methionine (10 g L^{-1}) into AdoMet, when grown with sucrose and urea as the main carbon and nitrogen sources, respectively. Under suitable conditions, 11 g L^{-1} of AdoMet is accumulated in vacuoles in the cells. This amounts to more than 25% of the total dry cell mass, comparing favorably with the commercially available AdoMet-rich yeast which contains only about 20 mg g^{-1} solids. Such abnormal production of AdoMet has been suggested to be mainly due to the significantly high methionine adenosyltransferase (EC 2.5.1.6) activity in this yeast.

AdoHcy is the product of biological transmethylation reactions that utilize AdoMet as the methyl donor. Before our work, two characteristic reactions, the cleavage of the glycosyl linkage of AdoHcy, yielding adenine and *S*-ribosylhomocysteine, followed by the hydrolysis of the *S*-ribosylhomocysteine to L-homocysteine and ribose, had long been believed to be the only reactions for the metabolism of AdoHcy in prokaryotic cells, whereas AdoHcy is directly hydrolyzed to L-homocysteine and adenosine by AdoHcy hydrolase in eukaryotic cells (see Fig. 12 and Ref. [215]). Our screening study for suitable enzymes for the synthesis of AdoHcy revealed that many prokaryotic cells contain AdoHcy hydrolase in considerably high amounts.[216] Prokaryotic AdoHcy hydrolase can easily be purified and crystallized from cells of *Alcaligenes faecalis*, in which the cellular content of this enzyme comprises about 2.5% of the total extractable protein.[216] This value is about 100 times higher than in the case of eukaryotic sources.

Since the synthetic direction is greatly favored for the in vitro hydrolysis of AdoHcy by AdoHcy hydrolase and the enzyme is considered to be a useful catalyst for the synthesis of AdoHcy from L-homocysteine and adenosine, the synthesis of AdoHcy is carried out by incubating adenosine and L-homocysteine with cells of *A. faecalis* (yield, 70–80 g L^{-1}).[217] A problem with this synthetic method was that the D isomer of homocysteine is not recognized by the enzyme. To overcome this, microbial strains capable of synthesizing AdoHcy from D-homocysteine were screened for. *Pseudomonas putida* was found to be such a strain. Although the *P. putida* hydrolase, like the *A. faecalis* enzyme, will only utilize L-homocysteine, the bacterium also produces a racemase which catalyzes the interconversion of the D- and L-homocysteine isomers. On mixing adenosine and DL-homocysteine with a mixture of *A. faecalis* cells (36 g L^{-1}) and *P. putida* cells (4 g L^{-1}) in potassium phosphate buffer, more than 70 g L^{-1} of AdoHcy was obtained in an essentially quantitative yield.[218]

In a similar manner, a number of other novel *S*-nucleosidylhomocysteines can be efficiently synthesized from the corresponding adenosine analogues, e.g., formycin A, neburalin, and adenosine N^1-oxide.[219] These may be promising in the pharmaceutical and chemotherapeutic fields.[215]

5.5. Organic Acids

Optically active α- and β-hydroxycarboxylic acids and their derivatives are important chiral building blocks. Various routes to them have been studied, especially in synthetic organic chemistry. Recently, several useful microorganisms, as described below, were found in screening studies. Other microbial transformations of practical importance yielding organic acids are listed in Table 6.

D-(−)-β-Hydroxyisobutyric acid: Optically active β-hydroxyisobutyric acid has been used as a versatile chiral building block. The L-(+) enantiomer has been used for the synthesis of α-tocopherol,[48] muscone,[49] lasalocid A,[220] calcimycin,[221] and other compounds, while the D-(−) enantiomer is useful for the synthesis of an angiotensin converting enzyme inhibitor, captopril.[222] Several routes to optically active β-hydroxyisobutyric acid have been reported; β-hydroxylation of isobutyric acid,[107,222] hydration of methacrylic acid,[107] enantioselective oxidation of prochiral 2-methyl-1,3-propanediol,[223] and stereoselective reduction of ethyl α-formylpropionate.[224] β-Hydroxylation of isobutyric acid by *Pseudomonas putida* and most other microorganisms yields the L-(+) enantiomer.[107,222] Only a few microorganisms, including *Candida rugosa*, specifically produce the D-(−) enantiomer.[107] A mutant strain derived from *C. rugosa* that lacks β-hydroxyisobutyrate dehydrogenase and is therefore unable to catalyze further oxidation of β-hydroxyisobutyric acid to isobutyraldehyde has been reported to produce 36.6 g L^{-1} of D-(−)-β-hydroxyisobutyric acid in a nearly quantitative yield.[225] This conversion has been applied to the commercial production of captopril (Fig. 13).[222]

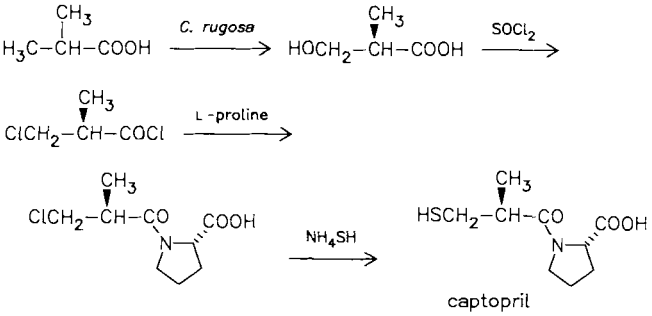

Fig. 13. Synthesis of captopril involving enzymatic oxidation of isobutyric acid.

D-(−)-Pantoyl lactone, the γ-lactone of D-(−)-pantoic acid, is an important starting chiral material for the synthesis of a vitamin, D-(+)-pantothenic acid. The conventional synthesis involves the tedious chemical resolution of racemic pantoyl lactone. We have recently reported two efficient microbial processes that overcome this problem. *Rhodococcus erythropolis* was found to convert only the L-(+) enantiomer in a racemic mixture of pantoyl lactone into the D-(−) enantiomer without any modification of the coexisting D-(−) enantiomer. Under suitable reaction conditions with washed cells as the catalyst, D-(−)-pantoyl lactone in the reaction mixture reached 18.2 g L^{-1} with an optical yield of 94.4% *e.e.* (chemical molar yield, 90.5%).[226] This unique conversion proceeds through the

successive reactions shown in Figure 14: (1) the enzymatic oxidation of L-(+)-pantoyl lactone to ketopantoyl lactone; (2) the rapid and spontaneous hydrolysis of the ketopantoyl lactone to ketopantoic acid; (3) the enzymatic reduction of the ketopantoic acid to D-(−)-pantoic acid. The process is simple and requires no reracemization step, which is necessary for the conventional chemical resolution.

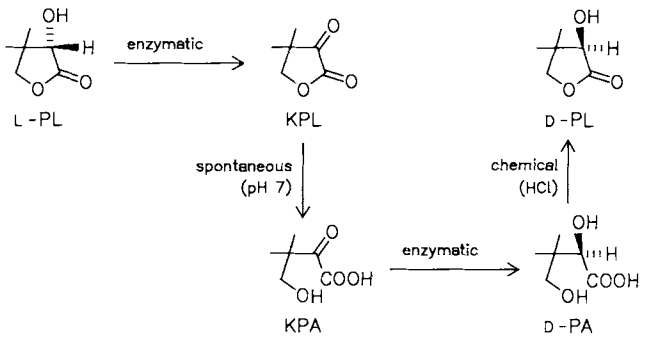

Fig. 14. Stereoselective oxidation and reduction system for the conversion of L-(+)-pantoyl lactone to the D-(−) enantiomer by *Rhodococcus erythropolis* cells. D-PL, D-(−)-pantoyl lactone; L-PL, L-(+)-pantoyl lactone; D-PA, D-(−)-pantoic acid; KPL, ketopantoyl lactone; KPA, ketopantic acid.

Another approach is the enantioselective reduction of ketopantoyl lactone to D-(−)-pantoyl lactone.[53,61,108,227] When *Candida parapsilosis* or *Rhodotorula minuta* cells are incubated with ketopantoyl lactone and glucose, about 100 or 50 g L^{-1}, respectively, of D-(−)-pantoyl lactone is produced in excellent chemical (95–100%) and optical (90–95% *e.e.*) yields.[53,108,227] In this reaction, the asymmetric reduction is catalyzed by a newly found carbonyl reductase specific to conjugated polyketones which requires NADPH as a cofactor.[53] Glucose is thought to be the energy source for the regeneration of NADPH.

5.6. Commodity Chemicals

Microbial transformations in the industrial production of commodity chemicals are rapidly gaining practical significance from several viewpoints (see Section 3). The first successful example, the production of acrylamide by bacterial nitrile hydratase, is described here. Other possible transformations of nitrile compounds are also discussed.

Acrylamide is widely used as a flocculant agent and as a component of synthetic fibers. The conventional synthetic process involves hydration of the nitrile with sulfuric acid or the use of copper salts or palladium complexes as catalysts. From the results obtained in extensive studies on the microbial degradation of nitrile compounds, we have established a new process involving a microbial enzyme, nitrile hydratase, as a catalyst for the hydration of the nitrile.[228]

A novel enzyme, aliphatic nitrile hydratase, which hydrates acetonitrile to acetamide, was highly purified from cells of an acetonitrile-utilizing *Arthrobacter* sp. and characterized in some detail.[229] The enzyme is quite different from nitrilase (EC 3.5.5.1), which catalyzes the formation of acids through hydrolytic elimination of the nitrogen atom to give the ammonium salt [Eq. (9)], in yielding amides through a simple hydration [Eq. (10)].

$$RCN + 2H_2O \longrightarrow RCOOH + NH_3 \quad (9)$$

$$RCN + H_2O \longrightarrow RCONH_2 \quad (10)$$

The proposed reaction mechanisms for nitrilase and nitrile hydratase are shown in Figure 15. A nucleophilic attack by a reactive thiol group of the respective enzyme on the nitrile carbon leads to the formation of an enzyme-bound imine, which is then hydrated to a tetrahedral intermediate (Fig. 15a). This process is the same for both enzymes. In the case of nitrilase catalysis, ammonia is then removed from the intermediate and an acyl-enzyme is formed. The acyl-enzyme is then hydrolyzed to a carboxylic acid (Fig. 15b). On the other hand, the enzyme itself is a leaving group in the case of nitrile hydratase. Thus, an amide is produced (Fig. 15c). The hydratase catalyzes the hydration of a variety of aliphatic nitriles including acrylonitrile and methacrylonitrile. However, when cells of *Arthrobacter* sp. were directly used as the catalyst for amide production, the substrate nitrile compounds were almost completely converted into the corresponding acids. This was due to the simultaneous inducible formation of an amidase (EC 3.5.1.4) showing high activity in the cells.[39] Therefore, screening for microorganisms with high nitrile hydratase and low amidase activities was carried out using various nitrile compounds as growth substrates. *Pseudomonas chlororaphis* B23 was found to be such a strain when grown with isobutyronitrile as the major nitrogen source. Although this bacterium inducibly produces an amidase (which shows some activity toward isobutyronitrile) together with the hydratase during growth, this amidase is, fortunately, almost completely inactive toward acrylamide.[39] This suggests that, theoretically, the stoichiometric conversion of acrylonitrile to acrylamide is possible even when the hydratase preparation is contaminated by amidase.

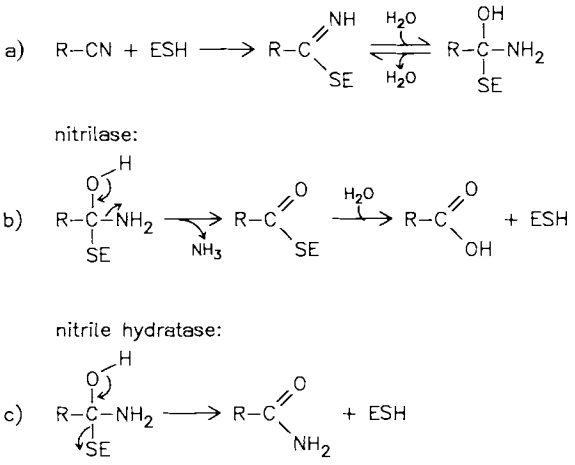

Fig. 15. The proposed reaction mechanism for nitrilase and nitrile hydratase. ESH, enzyme with thiol group (see text).

In practice, the reaction is carried out by incubating acrylonitrile with the *Pseudomonas* cells at low temperature (usually 5 to 10°C). Since acrylonitrile is a specific

modifier of general protein thiol groups, the active site of the nitrile hydratase may be masked by this nitrile at higher temperatures. Under suitable reaction conditions, more than 400 g L^{-1} of acrylamide can be produced in a nearly quantitative yield. In a similar manner, methacrylamide (200 g L^{-1}), acetamide (150 g L^{-1}), propionamide (560 g L^{-1}), *n*-butyramide (160 g L^{-1}), crotonamide (200 g L^{-1}), and isobutyramide (100 g L^{-1}) can be produced.[39]

After optimization of the culture conditions for *Pseudomonas* nitrile hydratase production, the enzyme activity in the culture broth was 900 times higher than that previously reported.[230] The *Pseudomonas* nitrile hydratase has recently been characterized in detail.[231] This process is simple, clean, and rapid, requires no special equipment to provide a source of energy and yields a highly pure product. *P. chlororaphis* B23 was used for the commercial production of acrylamide in 1987.

As suggested by the above example, nitrile converting enzymes such as nitrile hydratase, amidase, and nitrilase constitute a group of enzymes which are expected to have great potential as catalysts in organic chemical processing. In particular, hydratases and amidases are widely distributed in microorganisms. They are usually produced by a single microorganism and show broad substrate specificities. Therefore, these enzymes may be utilized not only for the preparation of amides but also for wide-ranging and more flexible purposes: for example, for the synthesis of optically pure amino acids and hydroxy acids from the corresponding amino nitriles or cyanohydrins, respectively. The enzymatic hydrolysis of a dinitrile, for example, may give rise to five different products, i.e., monoamide mononitrile, monoacid mononitrile, diamide, monoamide monoacid, and diacids, whereas acid- or base-catalyzed hydrolysis gives only diamide and diacid. Furthermore, many other useful compounds may be derived from a nitrile in connection with other chemical or enzymatic reactions (see Fig. 16).[232]

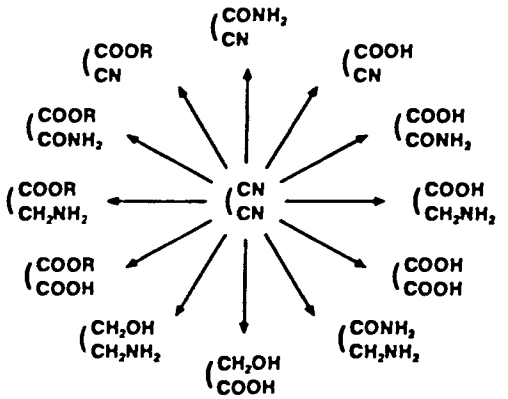

Fig. 16. Possible microbial transformations of dinitriles.

5.7. Lipids

The preparation of oleochemical intermediates such as fatty acids, fatty acid esters, and fatty alcohols involves steps which can also be carried out enzymatically. Lipases are key enzymes in such transformations.[233] They can be used for selective or partial fat splitting, hydrolysis of wax esters to yield fatty alcohols, and ester synthesis and transesterification.

Specific lipases yield valuable triacylglycerol mixtures, depending on their regioselectivity, which cannot be obtained by conventional chemical esterification processes. The transesterification of palm oil with fatty acid methyl esters leading to the cocoa butter equivalent and the hardening of plant oils through interesterification with higher-melting triacylglycerols are interesting examples in this field.[234]

Other examples are the terminal oxidation of fatty acids or *n*-alkanes to dicarboxylic acids,[105] the preparation of prostaglandin synthons, and the modification of prostaglandins.[235]

6. Concluding Remarks

Theoretically, it is possible to perform multistep reactions using microbial transformations, as shown for the synthesis of CoA. Microbial transformations are, however, mostly used in single-step reactions, where their highest potential lies.

Microbial transformation requires a substrate whose structure is closely related to the product, as is the case for conventional chemical synthesis. This is a drawback, because processes such as chemical synthesis and fermentation are required to supply the substrate.

In the production of useful compounds, microbial transformations, fermentative processes, and chemical syntheses seem to compete with each other. However, the best results are obtained with combinations of these methods, as the previous examples have shown.

Microorganisms show great ability to adapt to a wide variety of environments in comparison to higher cells. Therefore, they have a great potential for inducing new or novel enzyme systems capable of converting foreign substrates. It is possible to obtain and cultivate microorganisms that can survive or grow in extraordinary environments, e.g., psychrophilic, thermophilic, acidophilic, and alkalophilic ones. These microorganisms are capable of producing unique enzymes stable toward heat, alkali, and acid. In addition, techniques for cultivation and enzyme purification, as well as gene and enzyme technology, have made great advances. Taking all of these facts into consideration, there must be far more ways than one can imagine of using microorganisms for the production of useful compounds.

Received: April 16, 1987 [A 667 IE]
German version: *Angew. Chem. 100* (1988) 640

[1] H. Rehm, H. Reed (Eds.): a) *Biotechnology, Vol. 6A*, Verlag Chemie, Weinheim 1984; b) *Biotechnology, Vol. 3*, Verlag Chemie, Weinheim 1983; c) *Biotechnology, Vol. 4*, VCH Verlagsgesellschaft, Weinheim 1986.

[2] H. Yamada, S. Shimizu in: *Ullmann's Encyclopedia of Industrial Chemistry, Vol. A4*, VCH Verlagsgesellschaft, Weinheim 1985, p. 150.

[3] J. Tramper, H. C. van der Plas, P. Linko (Eds.): *Biocatalysts in Organic Syntheses (Studies in Organic Chemistry, 22)*, Elsevier, Amsterdam 1985.

[4] J. P. Rosazza (Ed.): *Microbial Transformations of Bioactive Compounds, Vol. 1 and 2*, CRC Press, Boca Raton, FL (USA) 1982.

[5] G. K. Skryabin, L. A. M. Goloveleva: *Microorganisms in Organic Chemistry*, Nauka, Moscow 1976 (Russian); Japanese version (translated by S. Fukui), Gakkai-Shuppan Center, Tokyo 1980.
[6] A. L. Demain, *Science (Washington D.C.) 214* (1981) 987.
[7] I. Chibata (Ed.): *Immobilized Enzymes – Research and Development*, Kodansha, Tokyo 1978.
[8] A. M. Klibanov, *Science (Washington D.C.) 219* (1983) 722.
[9] P. Dunnill, A. Wisman, N. Blakebrough (Eds.): *Enzymic and Non-enzymic Catalysis*, Ellis Horwood, Chichester 1980.
[10] C. J. Suckling in C. J. Suckling (Eds.): *Enzyme Chemistry, Impact and Applications*, Chapman and Hall, London 1984, p. 78; C. J. Suckling, K. E. Suckling, *Chem. Soc. Rev. 3* (1974) 387; C. J. Suckling, H. C. S. Wood, *Chem. Br. 15* (1979) 243; C. J. Suckling, *Chem. Soc. Rev. 13* (1984) 97; *Angew. Chem. 100* (1988) 555; *Angew. Chem. Int. Ed. Engl. 27* (1988) 537.
[11] J. B. Jones, C. J. Sih, D. Perlman: *Applications of Biochemical Systems in Organic Chemistry*, Wiley, New York 1976.
[12] A. R. Battersby, *Chem. Br. 20* (1984) 611.
[13] *Enzymes in Organic Synthesis (Ciba Foundation Symposium 111)*, Pitman, London 1985.
[14] G. M. Whitesides, C. H. Wong, *Aldrichimica Acta 16* (1983) 27; *Angew. Chem. 97* (1985) 617; *Angew. Chem. Int. Ed. Engl. 24* (1985) 617.
[15] C. J. Sih, C. S. Chen, *Angew. Chem. 96* (1984) 556; *Angew. Chem. Int. Ed. Engl. 23* (1984) 570.
[16] D. R. Storm, D. E. Koshland, Jr., *Proc. Natl. Acad. Sci. USA 66* (1970) 445.
[17] International Union of Biochemistry: *Enzyme Nomenclature 1984*, Academic Press, New York 1984.
[18] Sigma catalogue (1988).
[19] N. Kosaric, A. Wieczorek, G. P. Cosentino, R. J. Magee, J. E. Prenosil in [1b], p. 257.
[20] H. Ebner, H. Follmann in [1b], p. 387; K. Buchta in [1b], pp. 409, 467; M. Röhr, C. P. Kubicek, J. Kominek in [1b], pp. 419, 455.
[21] J. G. Zeikus, *Annu. Rev. Microbiol. 34* (1980) 423; T. K. Ng, R. M. Busche, C. C. McDonald, R. W. F. Hardy, *Science (Washington, D.C.) 219* (1983) 733.
[22] J. O'Sullivan, R. B. Sykes in [1c], p. 247; H. Kleinkauf, H. von Döhren in [1c], p. 283; S. Umezawa, S. Kondo, Y. Ito in [1c], p. 309; S. Ōmura, Y. Tanaka in [1c], p. 359; Z. Hošťálek, Z. Vaněk in [1c], p. 393; G. Lancini in [1c], p. 431; J. Bérdy in [1c], p. 465; S. Tsukagoshi, T. Takeuchi, H. Umezawa in [1c], p. 509.
[23] K. Aida, I. Chibata, K. Nakayama, K. Takinami, H. Yamada (Eds.): *Biotechnology of Amino Acid Production*, Kodansha, Tokyo/Elsevier, Amsterdam 1986.
[24] a) K. Ogata, S. Kinoshita, T. Tsunoda, K. Aida (Eds.): *Microbial Production of Nucleic Acid-Related Substances*, Kodansha, Tokyo 1976; b) K. Ogata, *Adv. Appl. Microbiol. 19* (1975) 209; c) A. Kuninaka in [1c], p. 71.
[25] C. Neuberg, J. Hirsch, *Biochem. Z. 115* (1921) 282.
[26] D. H. Peterson, M. C. Murray, *J. Am. Chem. Soc. 74* (1952) 1871.
[27] D. Perlman, E. Titus, J. Fried, *J. Am. Chem. Soc. 74* (1952) 2126.
[28] D. H. Peterson in C. Rainbow, A. H. Rose (Eds.): *Biochemistry of Industrial Micro-organisms*, Academic Press, London 1963, p. 537; Iizuka, A. Naito, *Microbial Transformation of Steroids and Alkaloids*, University of Tokyo Press, Tokyo/University Park Press, State College, PA (USA) 1967; K. Kieslich, O. K. Sebek, *Annu. Rep. Ferment. Processes 3* (1979) 275.
[29] W. Kullmann, *J. Protein Chem. 4* (1985) 1.
[30] K. Morihara, T. Oka, H. Tsuzuki, *Nature (London) 280* (1979).
[31] K. Morihara, T. Oka, H. Tsuzuki, Y. Tochino, T. Kanaya, *Biochem. Biophys. Res. Commun. 92* (1980) 396.
[32] Jap. Pat. Appl. 56-135452.
[33] According to current catalogues of *Takara Reagents for Genetic Engineering Research (1987)* and *New England BioLabs Inc. (1986-1987)* more than 150 enzymes are commercially available.
[34] K. Yamamoto, T. Tosa, I. Chibata, *Biotechnol. Bioeng. 22* (1980) 2045.
[35] T. Sato, Y. Nishida, T. Tosa, I. Chibata, *Biochim. Biophys. Acta 570* (1979) 179; Y. Nishida, T. Sato, T. Tosa, I. Chibata, *Enzyme Microb. Technol. 1* (1979) 95.
[36] Y.-Y. Linko, L. Pohjola, P. Linko, *Process Biochem. 12* (1977) 14.
[37] N. B. Havewala, W. H. Pitcher, *Enzyme Eng. 2* (1974) 315.
[38] T. Sato, T. Tosa, I. Chibata, *Eur. J. Appl. Microbiol. 2* (1976) 153.
[39] Y. Asano, T. Yasuda, Y. Tani, H. Yamada, *Agric. Biol. Chem. 46* (1982) 1183.
[40] H. Dalton in D. E. F. Harrison, I. J. Higgins, R. Watkinson (Eds.): *Transformations by Methane Monooxygenase*, Heyden, London 1980, p. 85; *Chem. Week*, Oct. 1979.
[41] Y. Sakai, Y. Tani, *Agric. Biol. Chem. 50* (1986) 2615.
[42] C. T. Hou, R. N. Patel, A. I. Laskin, N. Barnabe, I. Maarczak, *Appl. Environ. Microbiol. 38* (1979) 135.
[43] H. Yoshida, H. Yamada, *Agric. Biol. Chem. 46* (1982) 2539.
[44] F. C. Huang, L. F. H. Lee, R. S. D. Mittal, P. R. Ravikumar, J. A. Chan, C. S. Sih, *J. Am. Chem. Soc. 97* (1976) 4144.
[45] M. Ohno, S. Kobayashi, T. Iimori, Y.-F. Wang, T. Izawa, *J. Am. Chem. Soc. 103* (1981) 2405; K. Okano, T. Izawa, M. Ohno, *Tetrahedron Lett. 24* (1983) 217; T. Iimori, Y. Takahashi, T. Izawa, S. Kobayashi, M. Ohno, *J. Am. Chem. Soc. 105* (1983) 4049.
[46] Y. Ito, T. Shibata, M. Arita, H. Sawai, M. Ohno, *J. Am. Chem. Soc. 103* (1981) 6739; M. Arita, K. Adachi, Y. Ito, H. Sawai, M. Ohno, *ibid. 105* (1983) 4049.
[47] K. Mori, *Tetrahedron 37* (1981) 1341; K. Mori, M. Matsunaga, *Liebigs Ann. Chem. 1984*, 157.
[48] N. Cohen, W. F. Eichel, R. J. Lopersti, G. Neukom, G. Saucy, *J. Org. Chem. 41* (1976) 3505.
[49] Q. Branca, A. Fischli, *Helv. Chim. Acta 60* (1977) 925.
[50] T. Masaki, T. Fujihashi, K. Nakamura, M. Soejima, *Biochim. Biophys. Acta 660* (1981) 51.
[51] H. Yamada, H. Kumagai, *Adv. Appl. Microbiol. 19* (1975) 249.
[52] H. Yamada, H. Kumagai, *Pure Appl. Chem. 50* (1978) 1117.
[53] H. Yamada, S. Shimizu in [3], p. 19.
[54] H. Yamada, *Enzyme Eng. 6* (1982) 97.
[55] T. Nagasawa, H. Yamada, *Appl. Biochem. Biotechnol. 13* (1986) 147.
[56] T. Fukumura, *Agric. Biol. Chem. 40* (1976) 1687; *41* (1977) 1327.
[57] H. Yamada, S. Shimizu, K. Yoneda, *Hakko to Kogyo 38* (1980) 937.
[58] S. Takahashi in [23], p. 269.
[59] H. T. Bucherer, W. Steiner, *J. Prakt. Chem. 140* (1934) 291.
[60] K. Kitahara, S. Fukui, M. Misawa, *Nippon Nogei Kagaku Kaishi 34* (1960) 44.
[61] S. Shimizu, H. Hata, H. Yamada, *Agric. Biol. Chem. 48* (1984) 2285.
[62] C. T. Goodhue in [4], *Vol. 1*, p. 9.
[63] C. T. Hou, *Annu. Rep. Ferment. Processes 7* (1984) 21.
[64] E. Kondo, E. Masuo, *J. Gen. Appl. Microbiol. 7* (1961) 113.
[65] B. Zhou, A. S. Gopalan, F. Van Middlesworth, W.-R. Shieh, C. J. Sih, *J. Am. Chem. Soc. 105* (1983) 5925; W. Shieh, A. S. Gopalan, C. J. Sih, *ibid. 107* (1985) 2993.
[66] C. Vezina, K. Singh in J. E. Smith, D. R. Berry (Eds.): *The Filamentous Fungi, Vol. 1*, chap. 9, Edward Arnold, London 1975.
[67] K. Venkatsubramanian (Ed.): *Immobilized Microbial Cells*, American Chemical Society, Washington, D.C. 1979.
[68] A. Laskin (Ed.): *Enzymes and Immobilized Cells in Biotechnology*, Addison-Wesley, Reading, MA (USA) 1985.
[69] S. Fukui, A. Tanaka, *Annu. Rev. Microbiol. 26* (1982) 145.
[70] K. Mosbach (vol. ed.), *Methods Enzymol. 44* (1976).
[71] M. D. Trevan: *Immobilized Enzymes: Introduction and Applications in Biotechnology*, Wiley, New York 1980.
[72] I. Chibata (Ed.): *Immobilized Biocatalysts*, Kodansha, Tokyo 1986 (Japanese).
[73] G. M. Whitesides in [13], p. 76.
[74] a) *Third European Congress on Biotechnology, Vol. 1*, Verlag Chemie, Weinheim 1984; b) C. Wandrey, R. Wichmann, W. Berke, M. Morr, M.-R. Kula in [74a], p. 239; C. Wandrey, A. F. Buckmann, M.-R. Kula, *Biotechnol. Bioeng. 23* (1981) 1789.
[75] Y. Yamazaki, H. Maeda, *Agric. Biol. Chem. 50* (1986) 2621, 3213.
[76] S. Takamatsu, I. Umemura, K. Yamamoto, T. Sato, T. Tosa, I. Chibata, *Eur. J. Appl. Microbiol. Biotechnol. 15* (1982) 147.
[77] S. Shimizu, H. Yamada, *Trends Biotechnol. 2* (1984) 137.
[78] DBP 3017861.
[79] W. Hummel, E. Schmid, C. Wandrey, M.-R. Kula, *Appl. Microbiol. Biotechnol. 25* (1986) 175.
[80] Y. Asano, A. Nakazawa, *Agric. Biol. Chem. 49* (1985) 3631; *51* (1987) 2035.
[81] *Newsweek 2* (1986) 17.
[82] K. Ogata, S. Shimizu, Y. Tani, *Agric. Biol. Chem. 34* (1970) 1757; S. Shimizu, Y. Tani, K. Ogata, *ibid. 36* (1972) 370.
[83] T. Utagawa, H. Morisawa, T. Nakamatsu, A. Yamazaki, S. Yamanaka, *FEBS Lett. 119* (1980) 101.
[84] I. Takata, K. Yamamoto, T. Tosa, I. Chibata, *Enzyme Microb. Technol. 2* (1980) 30.
[85] K. Arima, M. Nagasawa, M. Bae, G. Tamura, *Agric. Biol. Chem. 33* (1969) 1636; M. Nagasawa, M. Bae, G. Tamura, K. Arima, *ibid. 33* (1969) 1644.
[86] C. K. A. Martin, F. Wagner, *Eur. J. Appl. Microbiol. 2* (1976) 243.
[87] K. Sano, K. Mitsugi, *Agric. Biol. Chem. 42* (1978) 2315.
[88] H. Mayer, J. Collins, F. Wagner, *Enzyme Eng. 5* (1980) 61; U. Schormer, A. Segner, F. Wagner, *Appl. Environ. Microbiol. 47* (1984) 307.
[89] Y. Asano, K. Endo, A. Nakazawa, Y. Hibino, N. Okazaki, M. Ohmori, N. Numao, K. Kondo, *Agric. Biol. Chem. 51* (1987) 2621.
[90] K. Takahashi, H. Nishimura, T. Yoshimoto, Y. Saito, Y. Inada, *Biochem. Biophys. Res. Commun. 121* (1984) 261.
[91] *Bioprocessing Technology*, Feb. 1985, p. 6.
[92] K. Oyama, K.-I. Kihara, *CHEMTECH 14* (1984) 100; K. Oyama, S. Nishimura, Y. Nonaka, K. Kihara, T. Hashimoto, *J. Org. Chem. 46* (1981) 5241.

[94] N. K. Harakas, *Annu. Rep. Ferment. Processes 7* (1984) 159.
[95] M. Misawa, T. Suzuki, *Appl. Biochem. Biotechnol. 7* (1982) 205; D. A. Evans, W. R. Sharp, P. V. Ammirato, Y. Yamada (Eds.): *Handbook of Plant Cell Culture, Vol. 1*, Macmillan, New York 1983; A. W. Alfermann in [3], p. 225.
[96] W. D. Maxon, *Annu. Rep. Ferment. Processes 8* (1985) 171; L. L. Smith in [1a], p. 31.
[97] K. Krasnobajew in [1a], p. 96.
[98] P. J. Davis in [4], *Vol. 2*, p. 67; in [1a], p. 207.
[99] V. P. Marshall, P. E. Wiley in [4], *Vol. 1*, p. 45; O. K. Sebek in [1a], p. 239.
[100] T. Nara, R. Okachi, M. Misawa, *J. Antibiot. 24* (1971) 321.
[101] T. Takahashi, Y. Yamazaki, K. Kato, M. Isono, *J. Am. Chem. Soc. 94* (1972) 4035.
[102] T. Sato, T. Tosa, I. Chibata, *Eur. J. Appl. Microbiol. 2* (1976) 153.
[103] K. Kubo, T. Ishikura, Y. Fukagawa, *J. Antibiot. 37* (1984) 1394.
[104] K. Kitahara, K. Uchiyama, H. Yamada, *Agric. Biol. Chem. 31* (1967) 200.
[105] R. Uchio, I. Shiio, *Agric. Biol. Chem. 36* (1972) 426, 1169, 1389.
[106] US Pat. 4092220; Jap. Pat. Appl. 54-14191.
[107] J. Hasegawa, M. Ogura, H. Kanema, N. Noda, H. Kawaharada, K. Watanabe, *J. Ferment. Technol. 60* (1982) 501; J. Hasegawa, M. Ogura, S. Hamaguchi, M. Shimazaki, H. Kawaharada, K. Watanabe, *ibid. 59* (1981) 203.
[108] S. Shimizu, S. Hattori, H. Hata, H. Yamada, *Enzyme Microb. Technol.* (1987), in press.
[109] T. Shibatani, N. Nishimura, K. Nabe, T. Kakimoto, I. Chibata, *Appl. Microbiol. 27* (1974) 688.
[110] A. Crueger, W. Crueger in [1a], p. 421.
[111] I. M. Chaiken, A. Komoriya, M. Ohno, F. Widmer, *Appl. Biochem. Biotechnol. 7* (1982) 385.
[112] K. Morihara in E. Ichishima (Eds.): *Proteases*, Gakkai Shuppan Center, Tokyo 1983, p. 237 (Japanese).
[113] M. Fujimaki, S. Arai, M. Yamashita, *Tanpakushitsu Kakusan Koso 20* (1975) 927.
[114] K. Inouye, K. Watanabe, K. Morihara, Y. Tochino, T. Kanaya, J. Emura, S. Sakakibara, *J. Am. Chem. Soc. 101* (1979) 751.
[115] Y. Isowa, M. Ohmori, T. Ichikawa, K. Mori, *Tetrahedron Lett. 1979*, 2611.
[116] K. Soda, H. Tanaka, N. Esaki in [1b], p. 479.
[117] K. Soda, H. Tanaka, N. Esaki, H. Kumagai, H. Yamada, *Biotechnol. Bioeng. 22 Suppl. 1* (1980) 127.
[118] S. Shimizu, H. Yamada, *Yuki Gosei Kagaku Kyokaishi 41* (1983) 1064.
[119] S. Shimizu, H. Yamada in [1c], p. 159.
[120] K. Mitsugi, K. Komagata, M. Takahashi, H. Izuka, H. Katagiri, *Agric. Biol. Chem. 8* (1964) 586.
[121] T. Nishino, S. Murao, *Agric. Biol. Chem. 39* (1975) 1827.
[122] K. Kawaguchi, H. Kawai, T. Tochikura, *Methods Carbohydr. Chem. 8* (1980) 261.
[123] I. Chibata, T. Ishikawa, S. Yamada, *Bull. Agric. Chem. Soc. Jpn. 21* (1957) 300.
[124] Y. Takamura, I. Kitamura, M. Ikura, K. Kono, A. Ozaki, *Agric. Biol. Chem. 30* (1966) 345.
[125] T. Kakimoto, T. Shibatani, N. Nishimura, I. Chibata, *Appl. Microbiol. 22* (1971) 992.
[126] H. Kanzaki, T. Nagasawa, H. Yamada, *Appl. Microbiol. Biotechnol. 25* (1986) 97.
[127] H. Kanzaki, M. Kobayashi, T. Nagasawa, H. Yamada, *Appl. Microbiol. Biotechnol. 25* (1987) 322.
[128] K. Haneda, S. Watanabe, I. Takeda, *Appl. Microbiol. 22* (1971) 721.
[129] R. Tsugawa, S. Okumura, T. Ito, N. Katsuya, *Agric. Biol. Chem. 30* (1966) 27.
[130] K. Yokozeki, K. Sano, C. Eguchi, H. Iwagami, K. Mitsugi, *Agric. Biol. Chem. 51* (1987) 729; K. Yokozeki, Y. Hirose, K. Kubota, *ibid. 51* (1987) 737.
[131] S. Yamada, K. Nabe, N. Izuo, K. Nakamichi, I. Chibata, *Appl. Environ. Microbiol. 42* (1981) 773.
[132] K. Nakamichi, K. Nabe, S. Yamada, T. Tosa, I. Chibata, *Appl. Microbiol. Biotechnol. 19* (1984) 100.
[133] G. J. Calton, L. L. Wood, M. H. Updike, L. Lantz II, J. P. Hamman, *Bio/Technology 4* (1986) 317.
[134] H. Tanaka, N. Esaki, K. Soda, *Appl. Biochem. Biotechnol. 11* (1985) 71.
[135] H. Kune, H. Sahm, F. Wagner, *Eur. J. Appl. Microbiol. 2* (1976) 175; M. Ema, T. Kakimoto, I. Chibata, *Appl. Environ. Microbiol. 37* (1979) 1053; Y. Izumi, H. Takizawa, Y. Tani, H. Yamada, *J. Ferment. Technol. 60* (1982) 269; B. K. Hamilton, H.-Y. Hsiao, W. E. Swann, D. M. Anderson, J. J. Delente, *Trends Biotechnol. 3* (1985) 64.
[138] K. Sano, K. Yokozeki, C. Eguchi, T. Kagawa, I. Noda, K. Mitsugi, *Agric. Biol. Chem. 41* (1977) 819.
[139] a) G. Terui (Ed.): *Fermentation Technology Today (Proc. 4th Int. Fermentation Symp.)*, Soc. Fermentation Technology Jpn., Osaka 1972; b) I. Chibata, T. Tosa, T. Sato, T. Mori, Y. Matsuo in [139a], p. 138.
[140] H. Yamada, S. Takahashi, Y. Kii, H. Kumagai, *J. Ferment. Technol. 56* (1978) 484.
[141] S. Takahashi, Y. Kii, H. Kumagai, H. Yamada, *J. Ferment. Technol. 56* (1978) 492.
[142] S. Takahashi, Y. Kii, H. Kumagai, H. Yamada, *J. Ferment. Technol. 57* (1979) 328.
[143] H. Yamada, S. Shimizu, H. Shimada, Y. Tani, S. Takahashi, T. Ohashi, *Biochimie 62* (1980) 395; S. Shimizu, H. Shimada, S. Takahashi, T. Ohashi, Y. Tani, H. Yamada, *Agric. Biol. Chem. 44* (1980) 2233.
[144] T. Ohashi, S. Takahashi, T. Nagamachi, K. Yoneda, H. Yamada, *Agric. Biol. Chem. 45* (1981) 831.
[145] R. Olivier, E. Fascetti, L. Angelini, L. Degen, *Enzyme Microb. Technol. 1* (1979) 201.
[146] K. Yokozeki, S. Nakamori, S. Yamanaka, C. Eguchi, K. Mitsugi, F. Yoshinaga, *Agric. Biol. Chem. 51* (1987) 715; K. Yokozeki, K. Kubota, *ibid. 51* (1987) 721.
[147] J. M. Kim, S. Shimizu, H. Yamada, *J. Biol. Chem. 261* (1986) 11832.
[148] H. Kumagai, H. Yamada, H. Matsui, H. Ohkishi, K. Ogata, *J. Biol. Chem. 245* (1970) 1767, 1773.
[149] T. Nagasawa, T. Utagawa, J. Goto, C.-J. Kim, Y. Tani, H. Kumagai, H. Yamada, *Eur. J. Biochem. 117* (1981) 33.
[150] H. Yoshida, H. Kumagai, H. Yamada, *Agric. Biol. Chem. 38* (1974) 463; *FEBS Lett. 52* (1975) 157.
[151] H. Enei, H. Matsui, K. Yamashita, S. Okumura, H. Yamada, *Agric. Biol. Chem. 36* (1972) 1861; H. Enei, K. Yamashita, S. Okumura, H. Yamada, *ibid. 37* (1973) 485; H. Enei, H. Matsui, H. Nakazawa, S. Okumura, H. Yamada, *ibid. 37* (1973) 493; H. Enei, H. Nakazawa, S. Okumura, H. Yamada, *ibid. 37* (1973) 725; H. Nakazawa, H. Enei, S. Okumura, H. Yamada, *ibid. 36* (1972) 2523; H. Nakazawa, H. Enei, S. Okumura, H. Yoshida, H. Yamada, *FEBS Lett. 25* (1972) 43.
[152] H. Kumagai, S. Sejima, Y. Choi, H. Tanaka, H. Yamada, *FEBS Lett. 52* (1975) 304; H. Kumagai, H. Tanaka, S. Sejima, Y. Yamada, *Agric. Biol. Chem. 41* (1977) 2071; H. Kumagai, Y. Choi, S. Sejima, H. Yamada, *Biochem. Biophys. Res. Commun. 59* (1974) 789; G. S. Dhillon, T. Nagasawa, H. Yamada, *J. Biotechnol. 1* (1984) 47; H. Yamada, T. Nagasawa, H. Ohkishi, B. Kawakami, Y. Tani, *Biochem. Biophys. Res. Commun. 100* (1981) 1104; T. Nagasawa, H. Ohkishi, B. Kawakami, Y. Yamano, H. Hosono, Y. Tani, *J. Biol. Chem. 257* (1982) 13749; T. Nagasawa, H. Hosono, H. Ohkishi, Y. Tani, H. Yamada, *Biochem. Biophys. Res. Commun. 111* (1983) 809; H. Ohkishi, D. Nishikawa, H. Kumagai, H. Yamada, *Agric. Biol. Chem. 45* (1981) 2397.
[153] H. Ziehr, W. Hummel, H. Reichenbach, M.-R. Kula in [74a], p. 345.
[154] R. W. Sealock, M. Laskowski, Jr., *Biochemistry 8* (1969) 3703.
[155] Y. Isowa, M. Ohmori, M. Satao, K. Mori, *Bull. Chem. Soc. Jpn. 50* (1977) 2766.
[156] Y. Isowa, *Yuki Gosei Kagaku Kyokaishi 36* (1978) 195; see also H.-D. Jakubke, P. Kuhl, A. Könnecke, *Angew. Chem. 97* (1985) 79; *Angew. Chem. Int. Ed. Engl. 24* (1985) 85.
[157] W. Kuhlmann, *J. Biol. Chem. 255* (1980) 8234.
[158] F. Widmer, K. Breddam, J. T. Johansen, *Pept. Proc. Eur. Pept. Symp. 16th 1980 (1981)* 46.
[159] H. Takai, K. Sakato, N. Nakamizo, Y. Isowa in K. Okawa (Eds.): *Peptide Chemistry 1980*, Protein Research Foundation, Osaka 1981, p. 213.
[160] M. Gondo, H. Yamashita, K. Sakakibara, Y. Isowa in T. Shioiri (Eds.): *Peptide Chemistry 1981*, Protein Research Foundation, Osaka 1982, p. 93.
[161] W. Kullmann, *J. Org. Chem. 47* (1982) 5300.
[162] M. Laskowski, Jr. in R. E. Offord, C. DiBello (Eds.): *Semisynthetic Peptides and Proteins*, Academic Press, London 1978, p. 255.
[163] H. Jering, H. Tschesche, *Angew. Chem. 86* (1974) 704; *Angew. Chem. Int. Ed. Engl. 13* (1974) 662.
[164] S. Kitabatake, R. Tsurutani, H. Nakajima, K. Tomita, Y. Yoshihara, H. Ueda, H. Takagi, K. Imahori, *Pharm. Res. 4* (1987) 154.
[165] H. Kumagai, T. Tochikura, S. Kondo, *Abstr. Annu. Meet. Agric. Chem. Soc. Jpn. 1983*, p. 515.
[166] K. J. Skinner, *Chem. Eng. News 53* (1975) No. 33, p. 22.
[167] H. Kumagai in [24a], p. 259.
[168] R. Nakayama, H. Kumagai, T. Tochikura, *J. Bacteriol. 160* (1984) 341; R. Nakayama, H. Kumagai, S. Akashi, H. Sugiura, T. Tochikura, *Agric. Biol. Chem. 49* (1985) 1041.
[169] R. Nakayama, H. Kumagai, T. Maruyama, T. Tochikura, T. Ueno, H. Fukami, *Agric. Biol. Chem. 45* (1981) 2839.

[170] G. A. Homandberg, M. Laskowski, Jr., *Biochemistry 18* (1979) 586; G. A. Homandberg, A. Komoriya, M. Juillerat, I. M. Chaiken in E. Gross, J. Meienhofer (Eds.): *Peptides, Structure and Biological Function*, Pierce Chem. Co., Rockford, IL (USA) 1979, p. 597.
[171] G. A. Homandberg, I. M. Chaiken, *J. Biol. Chem. 255* (1980) 4903.
[172] E. Lagerlof, L. Nathorst-Weltfelt, B. Ekstrom, B. Sjoberg, *Methods Enzymol. 44* (1976) 759.
[173] W. Marconi, F. Cecere, F. Morisi, G. Della Penua, B. Rappuoli, *J. Antibiot. 26* (1973) 228.
[174] R. Okachi, T. Nara, *Agric. Biol. Chem. 37* (1973) 2797.
[175] T. Tochikura, M. Kuwahara, S. Yagi, H. Okamoto, Y. Tominaga, T. Kano, K. Ogata, *J. Ferment. Technol. 46* (1967) 511.
[176] T. Tochikura, Y. Kariya, T. Yano, T. Tachiki, A. Kimura, *Abstr. 5th Int. Congr. Ferment. Symp.*, Berlin 1976, p. 441.
[177] Y. Fukuda, S. Yamaguchi, H. Hashimoto, M. Shimosaka, A. Kimura, *Agric. Biol. Chem. 48* (1984) 2877.
[178] T. Nara, M. Misawa, S. Kinoshita, *Biotechnol. Bioeng. 10* (1968) 277.
[179] H. Tanaka, Z. Sato, K. Nakayama, S. Kinoshita, *Agric. Biol. Chem. 32* (1968) 721.
[180] T. Fujio, A. Furuya, *J. Ferment. Technol. 61* (1983) 261.
[181] Y. Tani, Y. Mitani, H. Yamada, *Agric. Biol. Chem. 46* (1982) 1097; *48* (1984) 431; Y. Tani, T. Yonehara, Y. Mitani, H. Yamada, *J. Biotechnol. 1* (1984) 119; Y. Tani, T. Yonehara, *Agric. Biol. Chem. 49* (1985) 637.
[182] G. W. Pace, H. S. Yang, S. R. Tannenbaum, M. C. Archer, *Biotechnol. Bioeng. 18* (1976) 281; H. S. Yang, K. H. Leung, M. C. Archer, *ibid. 18* (1976) 1425; F. Paul, P. M. Vignais, *Enzyme Microb. Technol. 2* (1980) 281; V. Larreta Garde, G. Gelf, D. Thomas, *Eur. J. Appl. Microbiol. Biotechnol. 14* (1982) 232.
[183] M. F. Cocquempot, D. Thomas, M. L. Champigny, A. Moyse, *Eur. J. Appl. Microbiol. Biotechnol. 8* (1979) 37.
[184] Y. Sawa, K. Kanayama, H. Ochiai, *Agric. Biol. Chem. 44* (1980) 1967.
[185] C. R. Gardner, C. K. Colton, R. S. Langer, B. K. Hamilton, M. C. Archer, G. M. Whitesides, *Enzyme Eng. 2* (1974) 209; D. L. Marshall, *Biotechnol. Bioeng. 15* (1973) 447; K. Sakata, H. Kitano, N. Ise, *J. Appl. Biochem. 3* (1981) 518; H. Kondo, I. Tomioka, H. Nakajima, K. Imahori, *ibid. 6* (1984) 29.
[186] T. Tochikura, H. Kawai, K. Kawaguchi, K. Mugibayashi, K. Ogata in [139a], p. 463.
[187] T. Fujio, Y. Kotani, A. Furuya, *J. Ferment. Technol. 62* (1984) 131.
[188] A. Sato, A. Furuya, *Agric. Biol. Chem. 40* (1976) 465.
[189] S. Kitabatake, M. Dombou, I. Tomioka, H. Nakajima, K. Tomita, *Abstr. Annu. Meet. Soc. Ferment. Technol. Jpn. 1986*, p. 61.
[190] A. Kimura, M. Morita, *Agric. Biol. Chem. 39* (1975) 1469.
[191] K. Nakayama, Z. Sato, H. Tanaka, S. Kinoshita, *Agric. Biol. Chem. 32* (1968) 1311.
[192] D. R. Walt, V. M. Rios-Mercadillo, J. Auge, G. M. Whitesides, *J. Am. Chem. Soc. 102* (1980) 7805.
[193] K. Murata, K. Tani, J. Kato, I. Chibata, *Enzyme Microb. Technol. 3* (1981) 233.
[194] A. Maruyama, A. Ozaki, T. Fujio, *Abstr. Annu. Meet. Soc. Ferment. Technol. Jpn. 1985*, p. 121; T. Sakai, T. Watanabe, I. Chibata, *Agric. Biol. Chem. 37* (1973) 849.
[195] S. Shimizu, K. Yamane, Y. Tani, H. Yamada, *Appl. Biochem. Biotechnol. 8* (1983) 237.
[196] S. Shimizu, K. Miyata, Y. Tani, K. Ogata, *Biochim. Biophys. Acta 279* (1972) 583; N. Nishimura, T. Shibatani, T. Kakimoto, I. Chibata, *Appl. Microbiol. 28* (1974) 117.
[197] K. Ogata, Y. Tani, S. Shimizu, K. Uno, *Agric. Biol. Chem. 36* (1972) 93; H. Samejima, A. Kimura, Y. Ado, Y. Suzuki, T. Tadokoro, *Enzyme Eng. 4* (1978) 237.
[198] S. Shiozaki, S. Shimizu, H. Yamada, *Agric. Biol. Chem. 48* (1984) 2293; *J. Biotechnol. 4* (1986) 345.
[199] A. Gross, S. Geresh, G. M. Whitesides, *Appl. Biochem. Biotechnol. 8* (1983) 415.
[200] T. Tachiki, H. Suzuki, T. Yano, H. Kumagai, T. Tochikura in [74a], p. 313.
[201] T. Tachiki, H. Suzuki, S. Wakisaka, T. Yano, T. Tochikura, *J. Gen. Appl. Microbiol. 32* (1986) 545.
[202] K. Murata, K. Tani, J. Kato, I. Chibata, *Eur. J. Appl. Microbiol. Biotechnol. 11* (1981) 72.
[203] K. Murata, K. Tani, J. Kato, I. Chibata, *Eur. J. Appl. Microbiol. Biotechnol. 10* (1980) 11.
[204] A. Pollaak, R. L. Baughn, G. M. Whitesides, *J. Am. Chem. Soc. 99* (1977) 2366.
[205] Y. Kariya, Y. Owada, A. Kimura, T. Tochikura, *Agric. Biol. Chem. 42* (1978) 1689.
[206] R. S. Langer, B. K. Hamilton, C. R. Gardner, M. C. Archer, C. K. Colton, *AIChE J. 22* (1976) 1079.
[207] S. Shimizu, Y. Tani, K. Ogata, *Methods Enzymol. 62* (1979) 236; S. Shimizu, Y. Tani, H. Yamada in [67], p. 87; H. Yamada, S. Shimizu, Y. Tani, *Enzyme Eng. 5* (1980) 405; S. Shimizu, H. Yamada in [74a], p. 401.
[208] G. M. Brown, *J. Biol. Chem. 234* (1959) 370.
[209] S. Shimizu, K. Kubo, Y. Tani, K. Ogata, *Agric. Biol. Chem. 37* (1973) 2863; S. Shimizu, K. Kubo, H. Morioka, Y. Tani, K. Ogata, *ibid. 38* (1974) 1015.
[210] S. Shimizu, K. Miyata, Y. Tani, K. Ogata, *Agric. Biol. Chem. 37* (1973) 607, 615.
[211] S. Shimizu, R. Komaki, Y. Tani, H. Yamada, *FEBS Lett. 151* (1983) 303.
[212] S. Shimizu, A. Esumi, R. Komaki, H. Yamada, *Appl. Environ. Microbiol. 48* (1984) 1118.
[213] S. Shimizu, S. Satsuma, S. Kubo, Y. Tani, K. Ogata, *Agric. Biol. Chem. 37* (1973) 857; S. Shimizu, K. Kubo, K. Satsuma, Y. Tani, K. Ogata, *J. Ferment. Technol. 52* (1974) 114.
[214] H. Yamada, S. Shimizu, S. Shiozaki, T. Ohshiro in [74a], p. 249.
[215] P. M. Ueland, *Pharmacol. Rev. 34* (1982) 223.
[216] S. Shimizu, S. Shiozaki, T. Ohshiro, H. Yamada, *Eur. J. Biochem. 141* (1984) 385.
[217] S. Shimizu, S. Shiozaki, H. Yamada, *J. Biotechnol. 4* (1986) 81.
[218] S. Shimizu, T. Ohshiro, S. Shiozaki, H. Yamada, *J. Biotechnol. 4* (1986) 91.
[219] S. Shimizu, S. Shiozaki, T. Ohshiro, H. Yamada, *Agric. Biol. Chem. 48* (1984) 1383.
[220] T. Nakata, T. Kishi, *Tetrahedron Lett. 1978*, 2745.
[221] D. A. Evans, C. E. Sacks, W. A. Kleschick, *J. Am. Chem. Soc. 101* (1979) 6789.
[222] M. Shimazaki, J. Hasegawa, K. Kan, K. Nomura, Y. Nose, H. Kondo, T. Ohashi, K. Watanabe, *Chem. Pharm. Bull. 30* (1982) 3139.
[223] H. Ohta, H. Tetsukawa, N. Noto, *J. Org. Chem. 47* (1982) 2400.
[224] P. K. Matzinger, H. G. W. Leuenberger, *Appl. Microbiol. Biotechnol. 22* (1985) 208.
[225] J. Hasegawa, M. Ogura, H. Kanema, N. Noda, H. Kawaharada, K. Watanabe, *J. Ferment. Technol. 60* (1983) 501.
[226] S. Shimizu, H. Hattori, H. Hata, H. Yamada, *Appl. Environ. Microbiol. 53* (1987) 519.
[227] S. Shimizu, H. Yamada, H. Hata, T. Morishita, S. Akutsu, M. Kawamura, *Agric. Biol. Chem. 51* (1987) 289.
[228] H. Yamada, Y. Asano, Y. Tani, *Chemistry and Industry* (Japanese name?) *36* (1983) 101; Y. Tani, Y. Asano, H. Yamada, *Hakko to Kogyo 41* (1983) 382; T. Nagasawa, H. Yamada, *Chemistry and Industry (??) 39* (1986) 666.
[229] Y. Asano, Y. Tani, H. Yamada, *Agric. Biol. Chem. 44* (1980) 2251.
[230] H. Yamada, K. Ryuno, T. Nagasawa, K. Enomoto, I. Watanabe, *Agric. Biol. Chem. 50* (1986) 2859.
[231] T. Nagasawa, H. Nanba, K. Ryuno, K. Takeuchi, H. Yamada, *Eur. J. Biochem. 162* (1987) 691.
[232] S. E. Godtfredsen, K. Ingvorsen, B. Yde, O. Andresen in [3], p. 3.
[233] B. Borgstrom, H. L. Brockman (Eds.): *Lipases*, Elsevier, Amsterdam 1984.
[234] A. R. Macrae in [3], p. 195.
[235] G. P. Peruzzotti in [4], *Vol. 1*, p. 109.

Electron-Transfer Chain Catalysis in Organotransition Metal Chemistry**

By Didier Astruc*

Dedicated to Professor Jean Tirouflet

Parallel to organic electrocatalysis, the field of organotransition metal electrocatalysis has developed explosively since 1980. The theoretical and experimental foundations established by *Feldberg* in 1971 (ECE mechanism) have been applied, using fast electrochemical techniques, to various organometallic reactions such as isomerization, ligand exchange, chelation, decomplexation, and CO insertion and extrusion. Most of the work performed to date concerns ligand exchange reactions of N-donors and P-donors in mononuclear compounds, initiated by oxidants (or anodes) and of carbonyls and P-donors in clusters, initiated by reducing agents (or cathodes). The preparative aspects of electrocatalysis have already been impressively developed in cluster chemistry and indicate that the technique is extremely useful. This review first delineates the principles and characteristics of electrocatalysis applied in organotransition metal chemistry, and then, after outlining the choice of efficient initiating reagents, goes on to describe the systems up to August 1986.

1. Introduction

"Electron-transfer (ET) catalysis" is an exceedingly large branch of chemistry which has its origin in the chlorine exchange reactions carried out in inorganic systems by *Taube* et al.,[1] as well as *Basolo*, and *Pearson* et al. (1954–1960).[2–5] In organic chemistry, its origin traces back to the discovery of catalytic nucleophilic substitution by *Kornblum*, the well documented $S_{RN}1$ mechanism so named and explored by *Bunnett*[8] and by *Russel* et al.[9, 10] The first applications in electrochemistry were reported by *Savéant* and *Amatore* et al.[11–15] Reviews by all these authors are available,[5, 7, 8, 10, 13] and recently critical views on the multiple aspects of ET catalysis have been reported by *Chanon* et al.[16–19] The scope of the present review is restricted to the electrocatalysis of organotransition metal reactions since these have indeed attracted a great deal of interest recently.[20–35] The technique has proven successful for ligand exchange reactions, decomplexations, chelations, isomerizations, insertions and extrusions. As we shall see, the success of all these reactions is due to the extremely fast interconversion of paramagnetic transition metal centers between 17- and 19-valence electron configurations[36–49] and to the ability of transition metal compounds to effect redox processes.[20] Some types of "electron-transfer catalysis" will not be considered here: (i) electrogeneration of transition metal catalysts, which subsequently behave according to pairwise pathways;[50–51] (ii) hydrogen-transfer and alkyl-transfer chain reactions;[21–23] (iii) electron-transfer reactions (as alternatives to electrophilic[40] or nucleophilic attacks[52]) occurring without an external catalytic source of electrons or electron holes.[16–20] Since there is considerable confusion in the literature concerning the nomenclature of redox catalysis and electron-transfer chain (ETC) catalysis (electrocatalysis), we shall start with their definition.

[*] Prof. Dr. D. Astruc
Laboratoire de Chimie Organique et Organométallique
Université de Bordeaux I
351 Cours de la Libération, F-33405 Talence Cedex (France)

2. Distinction between ETC Catalysis (Electrocatalysis) and Redox Catalysis (Mediated Electrochemistry)

It is essential to distinguish between these two types of ET-catalyzed reactions.[53]

ETC catalysis concerns the catalysis of a reaction by an "electron" or by an "electron hole", which, overall, does not result in a redox change (a typical one is ligand exchange), whereas redox catalysis[54] consists in lowering the kinetic barrier of a reduction or of an oxidation which otherwise requires an overpotential (surtension) at the electrode (Scheme 1). For instance, an appropriate redox

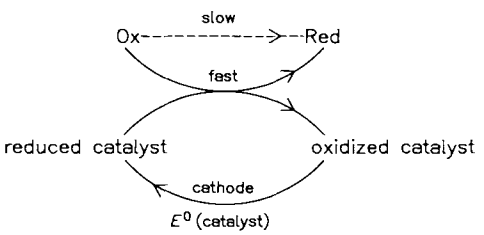

Scheme 1. Principle of redox catalysis.

mediator can lower the potential of reduction of protons at a mercury cathode, or, in other words, diminish the surtension and bring the potential values as close as possible to the thermodynamic potential. In spectacular cases, the redox mediator may effect the reduction of a substrate which is not electroactive under normal working conditions, i.e. given the surtension of reduction of the substrate on the

 © VCH Verlagsgesellschaft mbH, D-6940 Weinheim, 1988 0570-0833/88/0505-0643 $ 02.50/0

cathode in this medium, the solvent or electrolyte would be reduced at a lower potential than the substrate. The redox mediator merely helps to convey the electrons in solution. This task, however, is a major one in saving energy, as is the case in the fuel cell for the photosplitting of water,[54-56] in the reduction of oxygen,[57] and in biological processes.[58]

3. The Principle of Electrocatalysis (ETC Catalysis)

Catalytic amounts of an oxidizing or reducing agent can considerably increase the rate of a reaction. For instance, the substrate A, if neutral, is activated in the form of its radical cation or radical anion and reacts rapidly in this state to give the radical cation or the radical anion of the product. The latter reacts rapidly with the starting material in a "cross redox reaction" to give the product B, which closes the electrocatalytic cycle (Scheme 2).

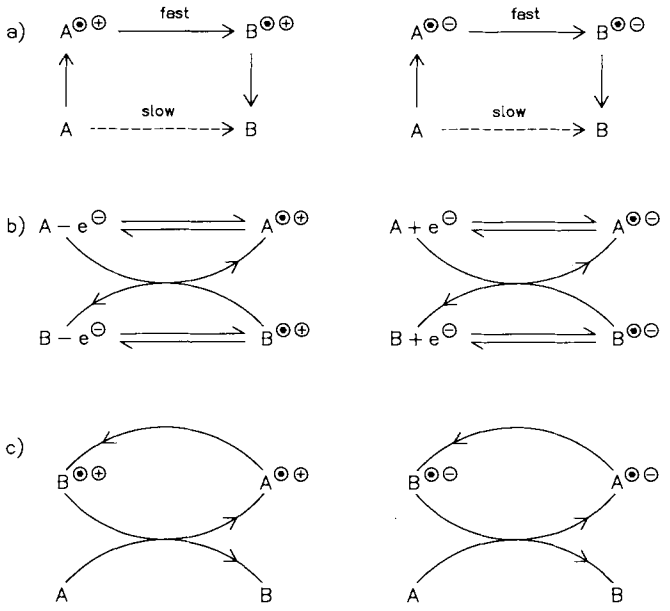

Scheme 2. Schematic representations of the electrocatalysis of reaction A→B. Left: via radical cations. Right: via radical anions. Notation: a) as square; c) cyclic; b) mixture of (a) and (c).

In order to activate the substrate A, one can use a catalytic amount of a redox reagent or an electrode at an appropriate potential. In the case of a soluble redox reagent the ET is homogeneous, whereas in the case of an electrode it is heterogeneous. In both cases, the ET step closing the electrocatalytic cycle (formation of B) can proceed directly, or via the redox reagent or via the electrode, depending on their respective potentials. In the latter case, the redox reagent or the electrode plays a double role: that of initiator and that of electron transfer agent (Scheme 3).

Let us consider the slow reaction of a closed shell, 18-electron transition metal center A to give a product B, of the same 18-electron configuration. The use of a small amount of a suitable oxidant will provide a reactive paramagnetic 17-electron cation $A^{\oplus}$, to give the desired reaction $A^{\oplus} \rightarrow B^{\oplus}$. One may design the system such that the 17-electron complex $B^{\oplus}$ is a better oxidant than $A^{\ominus}$ and A will react with $B^{\oplus}$ in a cross redox reaction to close the electrocatalytic cycle:

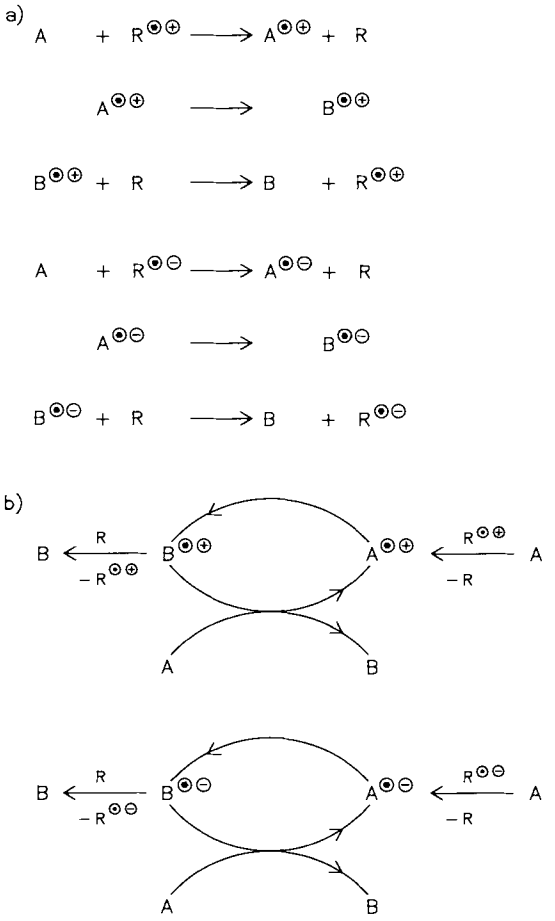

Scheme 3. In the case of an electrode, the redox forms of the electrocatalyst R are replaced by $\vec{E}$ and $\dot{E}$ at this electrode at the appropriate potential. a) Chain mechanism for electrocatalytic cycle where the back ET is mediated by the electrocatalyst R (or electrode). b) Cyclic representation for electrocatalysis where the back ET proceeds either directly by cross redox reaction or via mediation of the redox reagent R (or electrode). In each case reaction via radical cations above, reaction via radical anions below.

$$B^{\oplus}(17e^{\ominus}) + A(18e^{\ominus}) \longrightarrow B(18e^{\ominus}) + A^{\oplus}(17e^{\ominus})$$

This condition becomes indispensible if the reaction $A^{\ominus} \rightleftharpoons B^{\oplus}$ is reversible or shifted to the left; the cross redox reaction is the driving force. Similarly, if one designs a reaction catalyzed cathodically or by a reducing agent, the generation of $A^{\ominus}$, a paramagnetic 19-electron center, induces the reaction $A^{\ominus} \rightarrow B^{\ominus}$. The complex $B^{\ominus}$ is likewise a paramagnetic 19-electron species, which in order to enable the cross redox reaction $B^{\ominus} + A \rightarrow B + A^{\ominus}$ to complete the cycle, must be a better reducing agent than $A^{\ominus}$.

In this way, one is dealing with a catalytic chain process for the overall reaction A→B (Scheme 4). In a way, one may view the electron itself as the catalyst.

Both propagation steps must be very fast in order to limit the competition of side reactions of radical ions and of other intermediates eventually involved in the course of the reaction. If $B^{\oplus}$ is not a better oxidant than $A^{\oplus}$ (or if $B^{\ominus}$ is not a better reducing agent than $A^{\ominus}$), i.e. if the cross

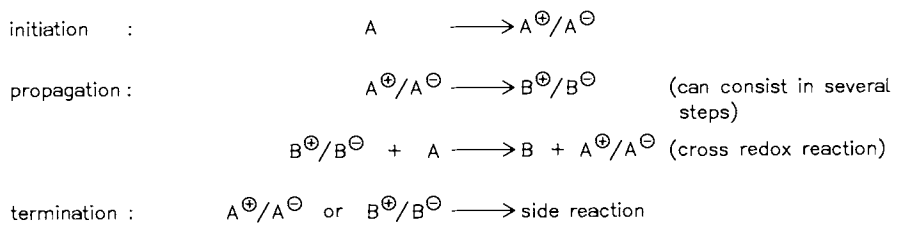

Scheme 4. Chain propagation step of an ETC reaction. The abbreviation $A^{\oplus}/A^{\ominus}$ embraces both oxidatively as well as reductively initiated reactions (cf. Scheme 2).

redox reaction is approximately isoergonic, the only remaining possibility of a driving force for the reactions A→B is the irreversibility of the first chain propagation step.

Electrochemists, who initiate such processes with electrodes, refer to electrocatalysis as an ÊCĒ mechanism (Ê: initiation by ET; C: chemical reaction, the first propagation step; Ē is a "back ET", the second propagation step which can occur in the solution or at the electrode). The ECE (electrocatalytic cycle) was first recognized as such and carefully studied by *Feldberg*[59] in 1972[60] using an organochromium system.[63]

4. How to Initiate a Reaction?

Suppose that one needs to effect a reaction A→B, that the reaction is too slow, and that one wishes to achieve it using electrocatalysis. One may do this either with an electrode or with a redox reagent. The first questions which have to be answered are: (i) Will the reaction be initiated by an oxidizing or a reducing agent? (ii) What is the oxidizing or reducing power needed for the reaction? We have seen in Section 3 (Scheme 4) that there are two propagation steps and that the driving force will be provided by one of these steps. If one does not know "a priori" about the reversibility of the step $A^{\oplus}/A^{\ominus} \rightarrow B^{\oplus}/B^{\ominus}$, which is generally the case, one can envisage gaining the driving force from the ET propagation step $B^{\oplus}/B^{\ominus} + A \rightarrow B + A^{\oplus}/A^{\ominus}$. This means that, if B is more difficult to reduce than A, one can get a driving force in the ET propagation by choosing reduction. Note, however, that the driving force has nothing to do with the strength of the reducing agent which initiates the reaction. On the other hand, if B is more difficult to oxidize than A, one can gain the driving force in the ET propagation step by choosing oxidation. One may be required to guess the relative potentials of reduction and oxidation of A and B, especially if B is not yet a known compound. If oxidation and reduction do not involve the same orbitals (HOMO≠LUMO), it may be that both oxidation and reduction (or neither) provide a driving force. However, since A and B are often closely related compounds, the most frequent case is that only oxidation *or* reduction is suitable for initiation and a choice between the two is essential. If B and an electrochemical setup are available, one may easily check this by recording the cyclic voltammogram (CV) of A and B (if possible in the solvent chosen for the reaction) in order to determine the relative values of their oxidation and reduction potentials. For instance, when one wishes to replace CO by another neutral two-electron ligand, the product B will be more electron-rich than A because CO is one of the most electron withdrawing neutral ligands. One must choose reduction because the expected reaction product B is more difficult to reduce than A. On the other hand, if one wishes to replace MeCN in A by another ligand L, one must choose oxidation because B will be more difficult to oxidize than A (MeCN being one of the most electron releasing ligands; Scheme 5).

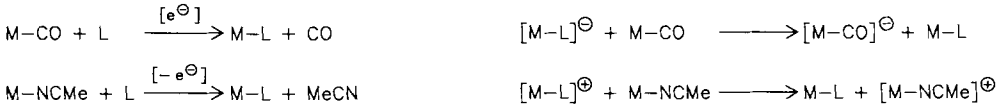

Scheme 5. Initiation of ligand exchange reactions (left) by $[e^{\ominus}]$ or $[-e^{\ominus}]$ to gain a driving force ($\Delta G < 0$) from the cross redox propagation step (right). π-Acidity [62]. CO > L > NCMe; E^0_{ox}: M-CO > M-L > M-NCMe$_3$; E^0_{red}: M-CO < M-L < MNCMe.

One must then choose the nature and strength of the redox reagent (R, $R^{\oplus}$ or $R^{\ominus}$) able to initiate the reaction. For this purpose, one is guided by a simple comparison of the oxidation or reduction potentials of A and of the initiator R. If one initiates the process by reduction, one must choose the reagent R or $R^{\ominus}$ so that its oxidation potential is at least close to (or more negative than) that of A. Conversely, if the initiator R or $R^{\oplus}$ is an oxidant, its reduction potential should be close to (or more positive than) that of A. The ET initiation need not be fast in order to obtain an efficient electrocatalytic cycle. This step can be reversible: $A + R \rightleftharpoons A^{\oplus} + R^{\ominus}$. Thus, there is considerable flexibility in this choice, provided the above condition is fulfilled. When the catalytic efficiency is low because of side reactions, selection of a redox reagent (or of an electrode) with a potential as close as possible to that of A improves the reaction yield since the redox reagent (or the electrode) can then serve as mediator for the "back" ET of $B^{\oplus}/B^{\ominus}$. If the rate of the "back" ET $B^{\oplus}/B^{\ominus} \rightarrow B$ is faster with the redox reagent (or the electrode) than with A (direct cross re-

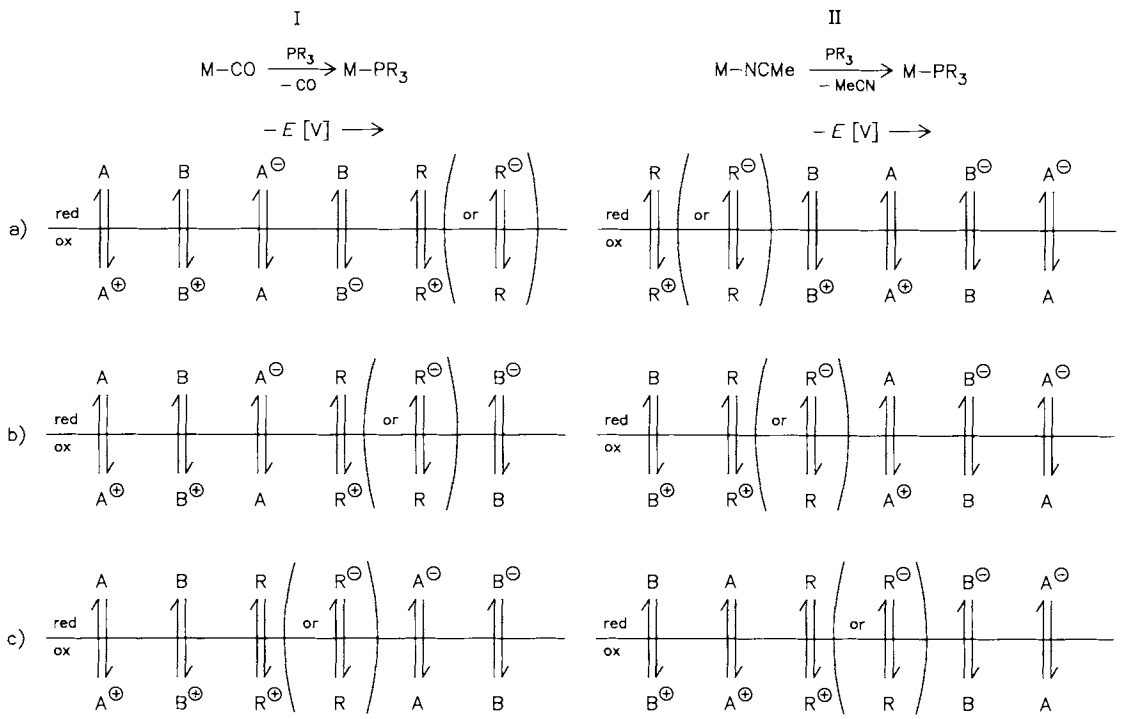

Scheme 6. The redox initiator R is chosen as a function of the relative "electron-richness" of A and B and of the catalytic efficiency. I: B electron-rich, i.e. not as easily reduced as A; reductive initiation with R or $R^{\ominus}$. II: B electron-deficient, i.e. not as easily oxidized as A; oxidative initiation with R or $R^{\oplus}$. The potential of R relative to that of A and of B (a–c) is relatively unimportant in the case of efficient systems, but c > b > a is a good choice in the case of poorly efficient systems. The situation Ic/IIc can be realized best with an electrode as R, but redox reagents could work also.

dox reaction), this efficient process competes better with the side reactions of $B^{\oplus}/B^{\ominus}$ (Scheme 6).

Electrocatalysis has been efficiently practiced using either an electrode or a redox reagent as initiator (electrocatalyst). It is thus extremely useful to have at hand a library of redox reagents and a knowledge of their redox potentials. Table 1 provides a list of the most convenient and commonly used electrocatalytic initiators.[64] Stable, paramagnetic sandwich compounds of iron are very easy to prepare on a large scale: ferrocenium (17-$e^{\ominus}$)[65] is probably the most useful of all the one-electron oxidants and [$Fe^{I}CpC_6Me_6$] (19-$e^{\ominus}$)[47] one of the most useful reducing agents (Scheme 7).

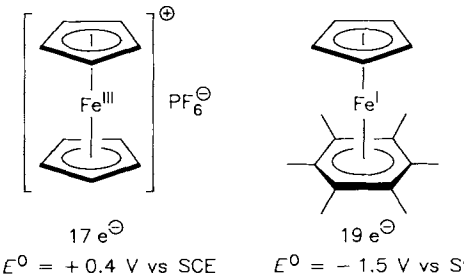

Scheme 7. These two iron sandwiches are perfectly stable redox systems: Fe^{I}/Fe^{II} and Fe^{III}/Fe^{II}. They should be able to electrocatalyze most organometallic reactions dealt with in this review. The Fe^{I} compound has the advantage, over the reagents Na/Ph_2CO and $Na/C_{10}H_8$, in that its corresponding cation is large, so that large organometallic anions are stabilized, thus preventing their undergoing side reactions (cf. clusters).

In summary, one can most simply initiate an electrocatalytic reaction using a redox reagent; a more sophisticated means is the use of an electrode in a preparative electrolytic cell (application of a small current); an occasional means is photochemistry (photoelectrocatalysis), where the initiation is provided by ET between the photoexcited state and a quencher, which then liberates the redox reagent.

5. Coulombic Efficiency

In all cases where electrocatalysis has been used, the desired organometallic reaction was very slow or inefficient in the absence of an electrocatalyst. Low yields were eventually obtainable at high temperatures, typically 100 to 150 °C, but interest in this thermal process is limited, since the selectivity is often a problem and the substrate and products often decompose. In contrast, with an electrocatalyst the same reactions were found to proceed rapidly (typically a few minutes) and in very high yields (90–100%) at room temperature. Even the selectivity problem, when it arose, was easily overcome; for instance in cluster chemistry, the number of ligand exchange reactions can be well controlled. The catalytic chains were often very long. This impressive efficiency of the technique is no doubt due to the combination of two properties of transition metal complexes: their ability to change oxidation state very rapidly[5] (the ET propagation step is very fast) and the high rate of ligand exchange between a 17-electron and a 19-electron valence shell configuration ($17\,e^{\ominus} + L \rightleftharpoons 19\,e^{\ominus}$).[36–46] In spite of their high reactivity, these paramagnetic states turn out to be not too unstable (in many cases, they could be characterized quite well by spectroscopic techniques). Thus, side reactions were rather slower than the

Table 1. Redox reagents [64], candidates for electrocatalysis. Note, the redox potential of sandwich complexes can be finely tuned by modification of the number of ring substituents (only approximate values are given for the redox potentials). DMF = dimethylformamide.

	Redox potential E^0 [V] vs. SCE (25°C)	Solvent
One-electron oxidants		
$[Ru(bpy)_3]^{3\oplus}$ [a]	+1.32	MeCN
$(p\text{-}Br\text{-}C_6H_4)_3N^{\oplus}$	+1.2	DMF
$Ag^{\oplus}$	+1	DMF
$NO^{\oplus}$	+1	DMF
$(Ntol)_3^{\oplus}$ [b]	+0.98	THF
$Fe^{3\oplus}$	+0.53	0.1 M HCl
$I_2(2e^{\ominus})$	+0.3	H_2O
$[FeCp_2]^{\oplus}$ [c]	+0.31	MeCN
	+0.4	DMF
$TTF^{\oplus}$ [d]	+0.30	MeCN
TMPD [e]	+0.21	DMF
TCNQ [f]	+0.127	MeCN
$[Fe(Cp^*)_2]^{\oplus}$ [g]	−0.12	MeCN
$TCNQ^{\ominus\ominus}$ [f]	−0.29	MeCN
O_2	−0.82	MeCN
	−0.87	DMF
One-electron reductants		
Li	−3.28	H_2O
K	−3.16	H_2O
Na	−2.95	H_2O
$NaC_{10}H_8$	−2.5	THF
Na/Hg	−2	DMF
$TBA^{\oplus}Ph_2CO^{\ominus\ominus}$ [h]	−1.88	MeCN
$[Fe^I(Cp^*)(C_6Me_6)]$ [g]	−1.85	DMF
$[Fe^ICp(C_6Me_6)]$ [a]	−1.57	DMF
$[Fe^0(C_6Me_6)_2]$	−1.50	DMF
$[Co^{II}(Cp^*)_2]$ [g]	−1.48	DMF
$[Fe^ICp(C_6H_6)]$ [c]	−1.25	DMF
$[Ru^0(C_6Me_6)](2e^{\ominus})$	−1	MeCN
$[CoCp_27$ [c]	−0.9	DMF
$O_2^{\ominus\ominus}$	−0.87	DMF
$[Mn(Cp^*)_2]$ [g]	−0.56	MeCN

[a] bipy = bipyridine. [b] Tol = o-$C_6H_4CH_3$. [c] Cp = η^5-C_5H_5. [d] TTF = tetrathiafulvalene. [e] TMPD = tetramethylphenylendiamine. [f] TCNQ = tetracyanoquinodimethane. [g] $Cp^* = \eta^5$-$C_5(CH_3)_5$. [h] TBA = tetrabutylammonium.

desired propagation steps ($A^{\oplus}/A^{\ominus} \rightarrow B^{\oplus}/B^{\ominus}$). The catalytic efficiency (chain length) can be measured by determining the number of molecules B formed per electron transferred by the initiator R (redox reagent or electrode). It is also called the "coulombic efficiency." If 2% of one-electron transfer reagent is necessary to obtain an 80% yield, the coulombic efficiency is 40 molecules per electron, a number actually often surpassed. *Kochi* et al. obtained coulombic efficiencies of more than 1000 for ligand exchange reactions in Mn^I complexes initiated by oxidants.[66] Electrochemistry permitted coulometric experiments to be performed at constant intensity, with monitoring of the potential. The end of the reaction is then indicated by a sudden change of potential as in classical potentiometric titrations. If a redox reagent is used, its amount can be varied so as to determine the quantity needed to obtain an optimum yield. These experiments also give an idea of the rate of the reactions.

6. Simple Evidence for Electrocatalysis by Cyclic Voltammetry (CV)

Suppose one wishes to check the electrocatalytic reaction A → B, say a ligand exchange reaction. The CV gives a wave for A which may be reversible or not (at least a certain degree of reversibility should be observable on lowering the temperature and speeding up the scan). In the presence of the entering ligand L^1, the CV of A will show the appearance of a new wave due to the reaction product $B(A \xrightarrow[-L^2]{L^1} B)$. If the wave of A is a cathodic one ($A \rightarrow A^{\ominus}$), setting the potential at or sweeping through this wave generates $A^{\ominus}$ in the vicinity of the cathode. Thus, this initiation having occurred, the electrocatalytic reaction rapidly gives B in the vicinity of the cathode. This explains the observation of a CV wave for B. Meanwhile the CV wave of A is profoundly affected: since $A^{\ominus}$ reacts rapidly with L^1 to give B, its concentration in the neighborhood of the cathode is strongly diminished and can reach zero (depending on the relative rates of the sweep and of the propagation reaction of $A^{\ominus}$ with L^1). Thus, the return anodic wave of A ($A^{\ominus} \rightarrow A$) is much less intense in the presence of L^1. A is also consumed by the cross redox reaction ($A + B^{\ominus} \rightarrow A^{\ominus} + B$); hence, its intensity is also diminished. In this case the wave of B is located at a more negative potential than that of A (Fig. 1). If A can be both oxidized and reduced, one may compare the possibilities of cathodic and anodic electrocatalysis by examining both parts of the voltammogram.

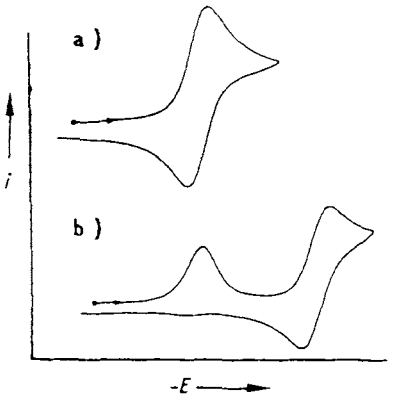

Fig. 1. CV wave of A: a) in the absence of Ligand L^1; b) in the presence of L^1 (appearance of the wave of B at a more negative potential). Electrocatalysis initiated by a cathodic current: $A \xrightarrow[(e^{\ominus})]{L^1} B$.

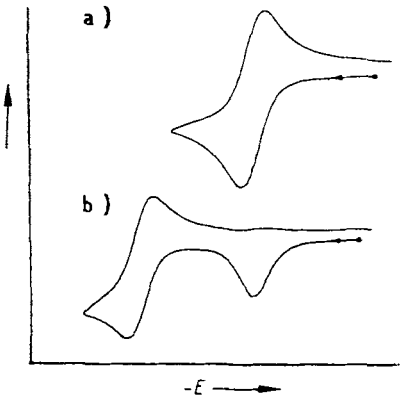

Fig. 2. CV wave of A: a) in the absence of L^1; b) in the presence of L^1 (appearance of the wave of B at a more positive potential). Electrocatalysis initiated by an anodic current $A \xrightarrow[(-e^{\ominus})]{L^1} B$. In the extreme case (fast ETC), the wave of A totally disappears in Figures 1 and 2.

On the other hand, if a ligand exchange reaction is electrocatalyzed by a small anodic current, the CV wave normally observed in the absence of the ligand is modified in the presence of this ligand and a new wave due to the reaction product appears at a more positive potential (Fig. 2).[67]

This behavior is characteristic of electrocatalysis and gives an idea of the rate of both propagation steps.

7. Reaction Mechanism

7.1. Observable Intermediates

On varying the scan rates, CV shows the disappearance of A, $A^{\oplus}/A^{\ominus}$, and $B^{\oplus}/B^{\ominus}$. These experiments can however be performed at room temperature in order to observe the overall electrocatalytic cycle at a reasonable scan rate. Lowering the temperature allows the observation of intermediates by freezing the reaction or effecting each step sequentially. Spectroscopy, especially ESR, enables a structural investigation of the intermediates, in particular the paramagnetic ones $A^{\oplus}/A^{\ominus}$ and $B^{\oplus}/B^{\ominus}$, since the diamagnetic, ESR-silent compounds A and B, although present in solution, are not observed. This type of experiment provides highly valuable information when the reaction studied is not exceedingly simple, i.e. it is important for checking whether other intermediates X and Y are observable besides and between $A^{\oplus}/A^{\ominus}$ and $B^{\oplus}/B^{\ominus}$ [Eq. (a)].

$$A^{\oplus}/A^{\ominus} \xrightarrow{a} X \xrightarrow{b} Y \xrightarrow{c} B^{\oplus}/B^{\ominus} \qquad \text{(a)}$$

7.2. Kinetics

After these important qualitative characterizations, one may proceed to a quantitative treatment of the electrochemical kinetics in order to determine the rate constant of the rate-limiting step. Usually, the ET propagation step is fast and the rate-limiting step concerns the other propagation step $A^{\oplus}/A^{\ominus} \rightarrow B^{\oplus}/B^{\ominus}$, or if there are other intermediates, as assumed in Equation (a), it can be step a, b or c. The rate constants can be determined by theoretical methods, but these will not be dealt with in detail here (construction of theoretical CV,[68-70] computer simulation of the CV by the method of finite differences,[69] a-dimensional analysis).[70] The determination of this rate constant at various temperatures will eventually provide an Arrhenius plot allowing the determination of ΔH and ΔS; additional mechanistic factors can be gleaned therefrom (e.g. a negative activation entropy is consistent with an associative mechanism).[66]

7.3. Thermodynamics

The two chain propagation steps of the catalytic cycle (Scheme 4) can each provide a driving force for the reaction, and the algebraic sum of the two gives the overall free energy ΔG of the reaction A→B (Scheme 8). Overall, ΔG must be negative.

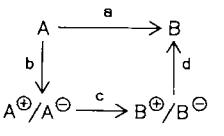

$$\Delta G_{A\rightarrow B} = a = \Delta G_{ET} + \Delta G_{A^{\oplus}/A^{\ominus}\rightarrow B^{\oplus}/B^{\ominus}}$$
$$\Delta G_{ET} = b + d$$
$$\Delta G_{A^{\oplus}/A^{\ominus}\rightarrow B^{\oplus}/B^{\ominus}} = c$$
$$\longrightarrow c = a - (b + d)$$

Scheme 8. Gibbs energy distribution $\Delta G_{A\rightarrow B}$ of the reaction A→B.

The easiest determination is that of ΔG_{ET}, directly provided by the CV of A and of B.

Weller's equation [Eq. (b)][71] holds true when the

$$\Delta G_{ET}[\text{kcal/mol}] = 23(E^{\circ}_{B} - E^{\circ}_{A} + e^2/(\varepsilon_0 r^2)) \qquad \text{(b)}$$

thermodynamic potentials E° are expressed in volts. If the waves are at least partially reversible, then $E^{\circ} \approx 1/2(E^{a}_{p} - E^{c}_{p})$, E^{a}_{p} and E^{c}_{p} being the potential value at the peak for the anodic part and the cathodic part of the wave, respectively.[72] The coulombic term $e^2/(\varepsilon_0 r^2)$ in Equation (b) can be neglected. In the case of total irreversibility of the wave of A or B, ΔG cannot be determined.

The determination of $\Delta G_{A^{\oplus}/A\rightarrow B^{\oplus}/B^{\ominus}}$ is generally impossible, but, if the reaction $A \overset{K_{eq}}{\rightleftharpoons} B$ is somewhat equilibrated, i.e. a small fraction of A is spectroscopically measurable at equilibrium, one may determine the equilibrium constant K_{eq} and thus $\Delta G_{A\rightarrow B}$. Such a case applies only if ΔG is sufficiently small to allow the estimation of the concentration of A. If $\Delta G_{A\rightarrow B}$ and of ΔG_{ET} are known, then $\Delta G_{A^{\oplus}/A^{\ominus}\rightarrow B^{\oplus}/B^{\ominus}}$ can be determined by simple algebraic difference[73] (Scheme 8).

In most cases, in order to ensure a driving force for the reaction one is interested in a large ΔG_{ET} value. In this case the reaction A→B is no longer equilibrated and it is not possible to apply the above technique.

8. Examples of Electrocatalyzed Organometallic Reactions

Feldberg et al. established the theoretical and experimental basis for the electrocatalytic ĒCĒ mechanism[60,61,69] using CV, chronoamperometry and chronocoulometry of the hydrolysis of the chromium–cyano bond in a Cr^{II} complex via the labile Cr^{II} intermediate[60] (Scheme 9).

Almost all of the electrocatalyzed processes studied up to now are similar ligand exchange reactions in mono- and polynuclear complexes, decomplexation and chelation being special examples of this kind. Very few reports have been published concerning other reactions such as isomerization, carbonyl insertion, and extrusion.

8.1. Exchange of a Two-Electron Ligand in Mononuclear Complexes (Oxidation)

The simple exchange of a CO ligand in a mononuclear complex has rarely been reported. The only example in

this sector is an intramolecular chelation[74,75] [see Eq. (e)]. On attempting to replace CO by phosphanes or phosphites in $[Fe(CO)_5]$ *Rieger* et al.[76] observed only a 10% reduction in the current of the first reduction wave and a wave of low intensity corresponding to $[Fe(CO)_4(PP_3)]$. This disappointing result is undoubtedly due to the great tendency of the 17-$e^{\ominus}$ radical anion $[Fe(CO)_4]^{\ominus\ominus}$ to effect side reactions.[24a] In contrast, *Kochi* et al. have shown that mixed complexes, bearing both N-donors (MeCN, pyridine) and carbonyls, exchange the N-donor ligand(s) for other two-electron ligands when a small anodic current is applied, with coulombic efficiencies sometimes reaching 1000 in complexes of the type $[Mn(\eta^5\text{-}C_5H_4Me)(CO)_2L]$[73] and more than 100 in the complexes $[M(CO)_3L_3]$ (n = 3, M = Cr, Mo, W).[77] N-Donors are not π-acids and therefore do not allow much flexibility regarding the oxidation state of the metal. These ligands are poor electron sinks and the strength of the M–N bond must be drastically diminished upon oxidation. However, the Mn^I compounds are reversibly oxidized, giving stable cations at −40 °C, which allows demonstration of their reactivity towards $P(OPh)_3$ at this temperature.[66] This compromise allows high coulombic efficiencies to be obtained (Scheme 10).

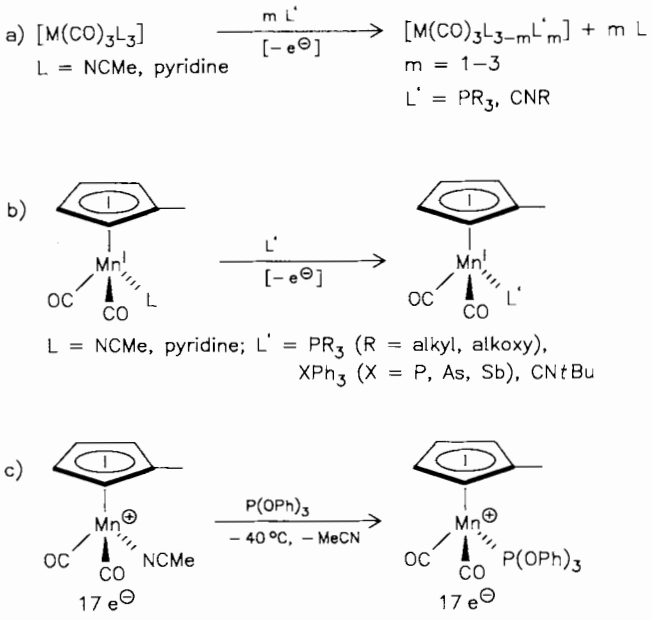

Scheme 10. a) Electrocatalytic exchange of one, two or three N-donor ligands by P- or C- donors, induced anodically in Cr^0-, Mo^0-, W^0-complexes; b) electrocatalytic exchange of a N-donor ligand with a P-, As-, Sb- or C-donor in Mn^I complexes, induced anodically with very high coulombic efficiencies; c) stoichiometric ligand exchange in a 17-electron Mn^{II}-complex.

overall reaction:

$$[Cr^{III}(CN)_6]^{3\ominus} + H_2O \longrightarrow [Cr^{III}(CN)_5(H_2O)]^{2\ominus} + CN^{\ominus}$$

mechanism:

$$[Cr^{III}(CN)_6]^{3\ominus} \xrightarrow[\text{initiation electrode}]{e^{\ominus}} [Cr^{II}(CN)_6]^{4\ominus}$$

$$[Cr^{II}(CN)_6]^{4\ominus} \xrightarrow[-\,CN^{\ominus}]{H_2O} [Cr^{II}(CN)_5(H_2O)]^{3\ominus}$$

$k = 11\ s^{-1}$ at 25 °C

$$[Cr^{II}(CN)_5(H_2O)]^{3\ominus} + [Cr^{III}(CN)_6]^{3\ominus} \longrightarrow [Cr^{III}(CN)_5(H_2O)]^{2\ominus} + [Cr^{II}(CN)_6]^{4\ominus}$$

$$[Cr^{II}(CN)_5(H_2O)]^{3\ominus} \xrightarrow[\text{back ET electrode}]{-\,e^{\ominus}} [Cr^{III}(CN)_5(H_2O)]^{2\ominus}$$

$k = 10^{-4}\ mol^{-1}s^{-1}$

Scheme 9. ÉCÈ mechanism according to *Feldberg* et al. for the substitution of $CN^{\ominus}$ by H_2O in a Cr^{III} complex.

The use of *Savéant*'s a-dimensional analysis[76] allowed *Kochi*'s group to obtain kinetic data ($\Delta S = -25$ u.e. for Scheme 10b, $L' = PPh_3$) which, taken together with the reaction of Scheme 10c, suggest an essentially associative mechanism (S_N2 substitution) for the ligand exchange in the propagation step.[66]

The rate constant k for this step could be related to the Brønsted base strength of the leaving and entering ligands and to the conic angle θ of the entering ligand [Eq. (c)].[78]

$$\lg k_1 = 17 - 0.15\,pK_a^L + 0.28\,pK_a^{L'} - 12\theta \qquad (c)$$

This equation reflects both the electronic and steric factors in the 19-electron intermediates. Thermodynamic data were also obtained in the case of the exchange of MeCN by pyridine, for which the ET propagation step is almost isoergonic ($\Delta E^\circ = 0.01$ V; $\Delta G_{ET} = 0.2$ kcal mol^{-1}). The driving force for the ligand exchange in the cation is thus 2.8 kcal mol^{-1} (Scheme 11).[73]

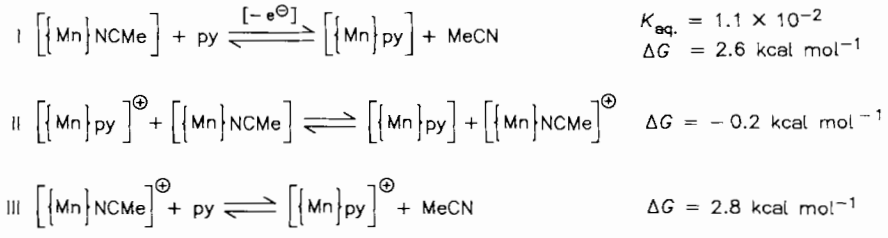

Scheme 11. Thermodynamics of the ligand exchange in Mn^I-complexes according to *Kochi*. {Mn} = $[Mn(\eta^5\text{-}C_5H_4Me)(CO)_2]$, py = pyridine. See Scheme 10 for the structure of the Mn^I-complex (piano-stool) and Scheme 8 for the square representation of the reaction course. ΔG for I from the IR spectra, for II from ΔE°.

In the series $[M(CO)_3L_3]$, it was not possible to find out whether the ligand exchange step is associative (S_N2 via 19-e$^{\circ}$) or dissociative (S_N1 via 15-e$^{\ominus}$, the one-electron oxidation is sometimes irreversible). However, the lack of reactivity of the large entering ligand $P(OPh)_3$ again suggests an associative mechanism.[77]

Brintzinger[79] has recently developed the electrocatalytic carbonylation of a Cr^{II} complex using catalytic amounts of air or of I_2 [Eq. (d)]. One Cp ligand is partly decoordinated, the hapticity shifting from *pentahapto* to *trihapto*. Since the displacement of a hydrocarbon ligand by CO decreases the electron density on the metal (lowers the HOMO), B is less easily oxidized than A and the oxidative initiation thus brings about an exergonic cross redox ET step.

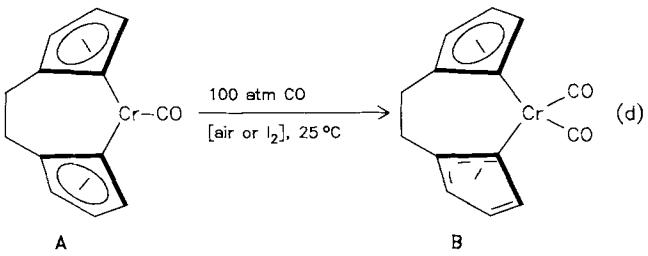

(d)

8.2. Chelation of the Dithiocarbamate (dtc) Ligands in $[Fe(\eta^5\text{-}C_5R_5)(CO)_2(\eta^1\text{-dtc})]$ (Oxidation)

Whereas, the dtc ligand usually prefers the chelating, *dihapto* mode of coordination in mononuclear complexes,[80a] several classical routes lead to the synthesis of the monodentate complexes $[Fp(\eta^1\text{-dtc})]$ ($Fp=[FeCp(CO)_2]$) and $[Fp^*(\eta^1\text{-dtc})]$ ($Fp^*=[FeCp^*(CO)_2]$). We attempted the syntheses of the corresponding chelate complexes, but, for instance, with [Fp(dtc)], only a 5% yield of the desired chelate complex was obtained at 100 °C after several hours, and extensive decomposition was observed.[80b] However, we found that if 10% of $[Cp_2Fe]PF_6$ is added to [Fp(dtc)] or [Fp*(dtc)], 50% yields of chelates are obtained at 20 °C in a few minutes [Eq. (e)].[74]

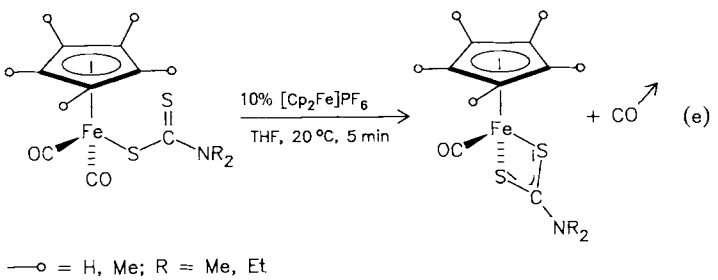

(e)

The mono- and bidentate complexes have oxidation potentials of $E=+1.25$ and $+0.5$ V vs SCE, respectively. Thus, no driving force is obtained from the ET propagation step. However, a driving force is clearly provided here by the irreversibility of the chelation step. In addition, the oxidation of the monodentate dtc complexes is irreversible. Both this and the endoergonicity of the cross redox step take into account the precipitation of the 17-electron chelates limiting the yields of the reactions (Scheme 12).

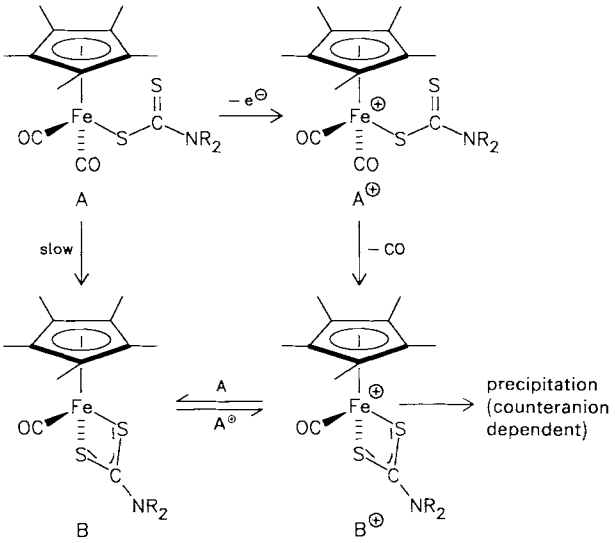

Scheme 12. Square electrocatalytic scheme for the chelation of [Fp(dtc)] with $[Cp_2Fe]PF_6$ as initiator. The endoergonicity of the cross ET and the precipitation of $B^{\oplus}$ limit the yield.

8.3. Decomplexation of Arenes (Reduction)

In the course of extensive studies on the stability and reactivity of 19-electron Fe^I complexes, we found[81] that soluble Fe^I complexes promote an electrocatalytic decomplexation of the otherwise robust[82] 18-electron complexes $[Fe^{II}Cp(arene)]^{\oplus}$ if the arene ligand in these complexes bears less than three methyls group. Thus, the cathodic reduction of $[Fe^{II}Cp(C_6H_6)]PF_6$ in 95% ethanol (Hg pool, 0.1 M LiOH) consumes only 0.3 Faraday to provide quantitatively $Fe^{2\oplus}$, cyclopentadiene and benzene (all species were characterized). In 1981, we proposed an electrocatalytic cycle taking into account this reaction (Scheme 13).[81] The exchange of the arene ligand for solvent molecules in the Fe^I complex **1** provides another Fe^I species, **2**, which reduces the cationic Fe^{II} starting complex and liberates its other ligands.

The stability of the Fe^I complex **1** increases with the number of methyl groups on the arene (k_1), and, when its lifetime is long enough, **1** reduces the medium ($H_2O \rightarrow H_2$). Thus, the unstable redox system **1/1**$^{\oplus}$ with several methyl groups on the arene ligand is also a redox mediator for the electroreduction of water (see Section 2). The cathodic reduction of **1**$^{\oplus}$ as such consumes a large amount of electricity—a trend exactly opposite to that expected from electrocatalysis. Thus, it is not surprising to observe that 0.3 Faraday is necessary to decompose **1**$^{\oplus}$, the apparent coulombic efficiency being 3.3. Similar complexes bearing a small number ($n<3$) of methyl groups can be decomposed in

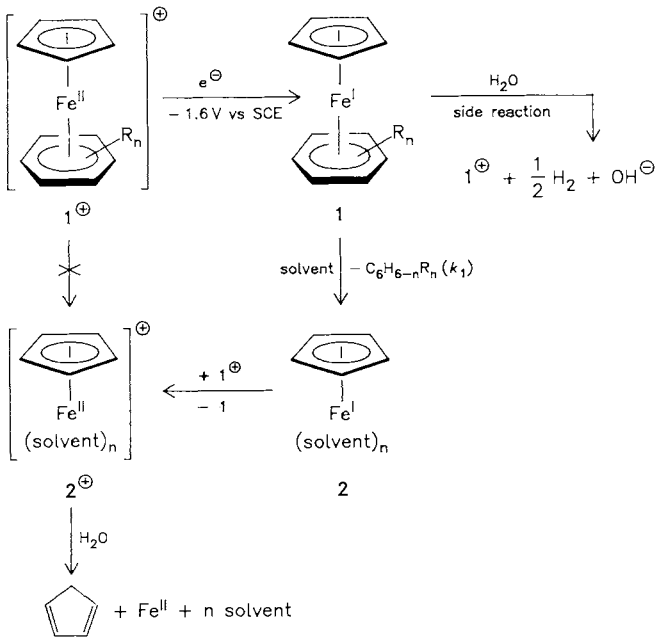

Scheme 13. Electrocatalytic decomplexation of an arene ligand initiated by a Hg cathode. Coulombic efficiency = 3.3 for the quantitative decomplexation of benzene (n = 0) [81]. The side reaction is the reduction of H_2O by the Fe^I-complexes **1** and **2** (redox catalysis). This side reaction dominates when the arene bears more than 3 methyl groups (coulombic efficiency $\ll 1$). Driving forces are provided by both exoergonic propagation steps. R = CH_3; n = 0–6.

this way, but the catalytic efficiency is lower. The durene complex (n = 4) is only half decomplexed after a day (coulombic efficiency $\ll 1$), and the hexamethylbenzene complex (n = 6) is very stable. In this case, the cathodic current in the cell only serves to reduce the medium, a process for which the redox system Fe^{II}/Fe^I is a stable redox mediator.[81] The redox catalysis can be suppressed if no reducible substrate is present in solution. Recently, the electrocatalytic decomplexation of complexes of the type $\mathbf{1}^{\oplus}$ in the presence of $P(OMe)_3$ in DMF or CH_3CN (Scheme 14) has been the subject of a report by other authors. The

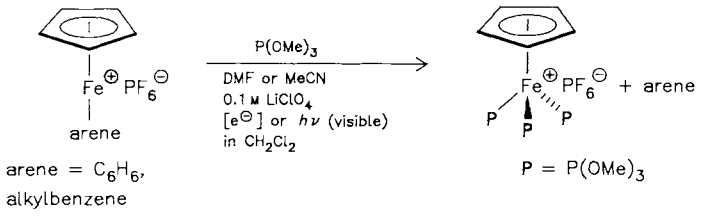

Scheme 14. Exchange of an arene ligand for three phosphite ligands by electrocatalysis or by visible light. (Neither technique works for arene = C_6Me_6.)

coulombic efficiencies were between 0.03 and 0.52, depending on the arene ligand.[83] In fact, it is possible that the variation in the observed coulombic efficiency arises from the differences in purity of the solvents. The latter work opens up a new entry to the compound $[Fe^{II}Cp\{P(OMe)_3\}_3]PF_6$, which can also be obtained in equally good yield from $\mathbf{1}^{\oplus}$ (n = 0) by using visible light.[84] (It is not certain that both methods are unrelated, though this point has not been mentioned yet, see Section 8.4.)

8.4. Initiation of Electrocatalysis by Light: Photoelectrocatalysis (Reduction)

Wrighton et al.[85] found that ligand exchange between MeCN and PPh_3 in $[Re^I(MeCN)(CO)_3(phen)]^{\oplus}$, $\mathbf{3}^{\oplus}$, can be initiated analogously to the reactions described in Section 8.1 by a cathodic current at -1.1 V vs SCE (Scheme 15). The potential for the reduction of $\mathbf{3}^{\oplus}$ is -1.2 V vs SCE (quasi-reversible). The coulombic efficiency is between 6.4 and 45 for quantitative spectroscopic yields.

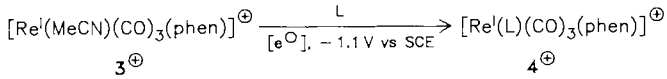

Scheme 15. Electrocatalytic ligand exchange in $\mathbf{3}^{\oplus}$. Catholyte: MeCN, 0.1 M nBu_4NClO_4; L = PPh_3, pyridine; phen = 1,10-phenanthroline.

More interestingly, *Wrighton* et al. showed that the cathode could be replaced by 436-nm irradiation (ca. 2×10^5 einstein), the same result being obtained with quantum yields (number of molecules $\mathbf{4}^{\oplus}$ found per 436-nm photon adsorbed). In order to work, the system needs a quencher, i.e. an oxidizable compound in the medium able to trap the excited state $\mathbf{3}^{\oplus}*$ of $\mathbf{3}^{\oplus}$. The reduction potential of $\mathbf{3}^{\oplus}*$ was estimated to be $+1.5$ V vs SCE. The quencher was *N,N'*-dimethyl-*p*-toluidine or PPh_3 itself. Thus, in the ligand exchange with PPh_3, both the starting complex as well as the entering ligand play a double role (Scheme 16).

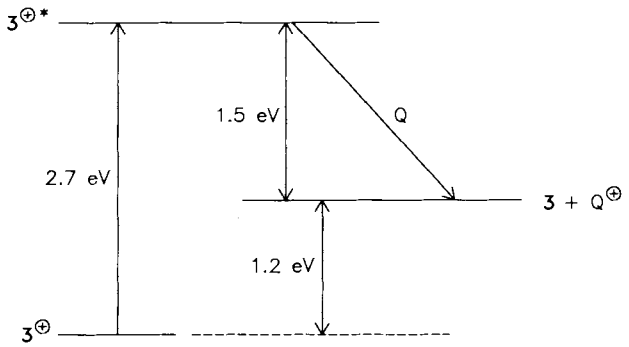

Scheme 16. Energy diagram for the photoreduction of $\mathbf{3}^{\oplus}$ ($\lambda = 436$ nm) in the presence of a quencher Q. Note the redox potential of 1.5 V (vs SCE) of the redox couple $\mathbf{3}^{\oplus}*/\mathbf{3}$.

It is reasonable to assume that the 19-electron species **3** is substitutionally labile and loses MeCN in a dissociative process before combination with PPh_3, which furnishes a strongly reducing 19-electron species **4** (Scheme 17).

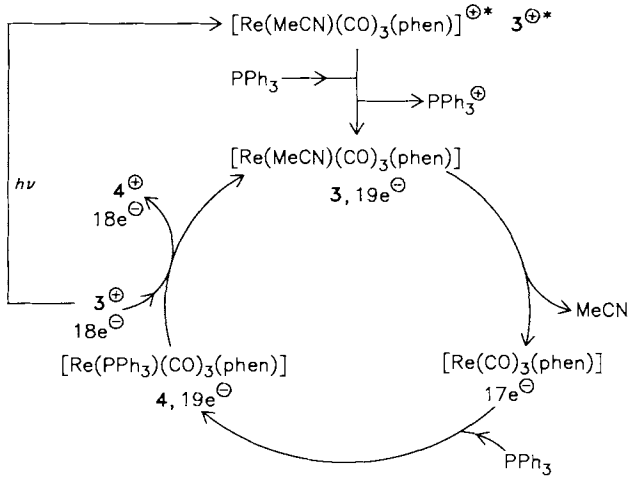

Scheme 17. Photoelectrocatalytic cycle for the exchange of MeCN by PPh_3 in the 18-electron complex $3^{\oplus}$.
Photo-initiation: $3^{\oplus} \xrightarrow{h\nu} 3^{\oplus *} \xrightarrow[-Q^{\oplus}]{Q} 3$;
Chain propagation: $3 \xrightarrow[-MeCN]{} [Re(CO)_3(phen)] \xrightarrow{PPh_3} 4 \xrightarrow[-3]{3^{\oplus}} 4^{\oplus}$

Although *Wrighton* et al. thus had a successfully functioning two-component system, self-activated by visible light, one may also envisage a broader use of photoelectrocatalysis by not restricting it to photoactive complexes. Since the photoprocess is catalytic, one could use an external photocatalyst for the electrocatalysis of reactions of photostable complexes.[86]

8.5. Selective Exchange of Carbonyl Ligands in Bimetallic Complexes and Clusters (Reduction)

Rieger et al. stimulated interest in this area[76] when they showed that CO ligands can be readily replaced by phosphite or phosphane ligands in clusters of the type $[YCCo_3(CO)_9]$ (Y = Ph, Cl) on using a cathodic current. DC polarographic and cyclovoltammetric studies indicated that the current of the first reduction wave drops almost to zero in the presence of the P-ligand while the expected wave appears for the substitution product. A similar behavior[76] was found with the binuclear compound $[(PhCCPh)Co_2(CO)_6]$. *Rieger* et al. judiciously proposed[76] that radical anions of the bi- and trinuclear cobalt complexes have their extra electron in metal-metal antibonding orbitals, which leads to Co–Co bond cleavage. The terminal carbonyl of one of these two Co centers becomes bridging so that one Co center has 18 valence electrons again, while the other Co, bearing the negative charge, has only 17 valence electrons. This latter center is the active one, providing a rapid $17e^{\ominus} \rightleftharpoons 19e^{\ominus}$ interconversion in the same way as mononuclear complexes, so that the P-donor comes in and one of the CO's moves out (Scheme 18). Consistent with this prediction *Rieger* and *Robinson* et al.[87] observed that the ratio i_p^a/i_p^c (anodic/cathodic CV peak) for the primary electrode process, i.e. the lifetime of the primary radical anion, is not affected by the presence of Lewis bases or of CO. Thus, the rate-limiting step involves a reaction of this primary cluster radical anion with a species which reacts rapidly with the Lewis base, but does not involve the Lewis base itself.

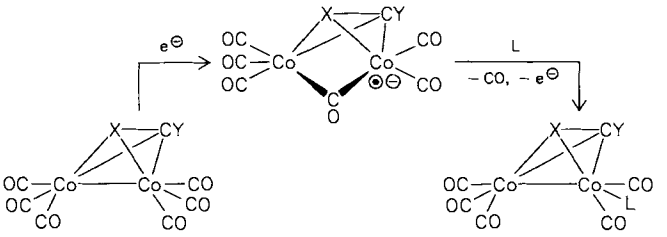

Scheme 18. Mechanism proposed by *Rieger* et al. for the ligand exchange of CO by PR_3 in paramagnetic di- [X = CY; Y = Ph; L = PPh_3, PBu_3, $P(OMe)_3$] and trinuclear Co complexes [X = $Co(CO)_3$; Y = Ph, Cl; L = phosphane, phosphite].

Finally, this system allows the sequential replacement of CO's by one, two and three $P(OMe)_3$ ligands or by one and two PPh_3 ligands in the alkynedicobalt complexes. Good yields were obtained with hexafluorobutyne as alkyne ligand (for example monosubstitution products were obtained for L = MeCN, $P(OMe)_3$, $P(OPh)_3$, PPh_3, $P(C_6H_{11})_3$) and, with other alkyne ligands, the yields were variable, but correlated with the lifetime of the alkyne dicobalt complex radical anions.[88]

A series of papers have recently been published by *Downard, Robinson,* and *Simpson*[88b] in which the ETC-catalyzed replacement of CO by polydentate ligands (dppm, dppe, ttas and tpme) is studied in clusters of the type $[RCCo_3(CO)_9]$ (R = Ph, Me). This is a rare case where the authors find no net advantage in the ETC catalysis over traditional thermal methods. The catalytic efficiency of the first two-electron ligand exchange is independent of the latter but the rate of reaction is solvent-dependent. Subsequent chelation of the dangling ligands in [RC-

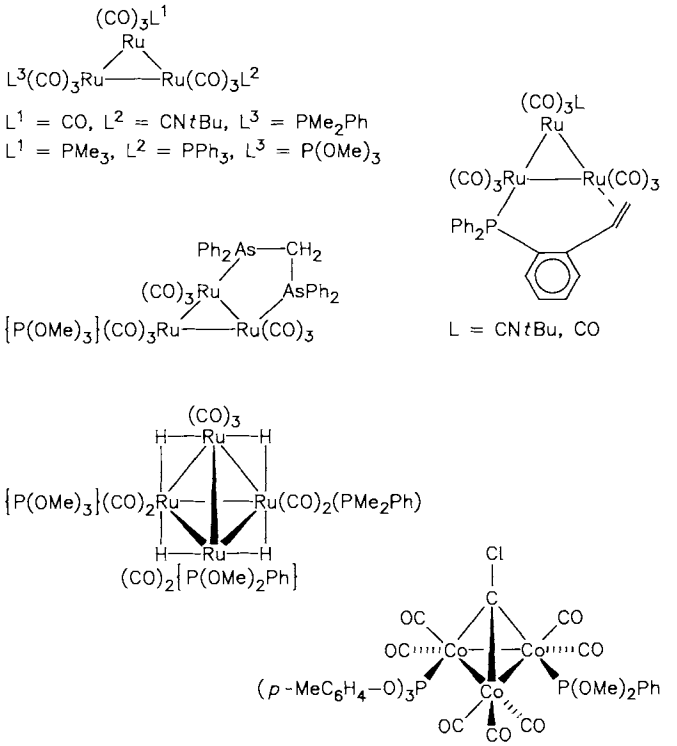

Scheme 19. Clusters obtained by sequential CO-L exchange (selected examples).

$Co_3(CO)_8(L\text{-}L)$] is much slower and of reduced catalytic efficiency. *Bruce* et al. have published[89,90] similar electrocatalytic syntheses of more than 40 clusters (Fe_3, Ru_3, Ru_4, Co_6, and Rh_6) in two reports. Several CO ligands were sequentially replaced by P, As, and C donor ligands. The reactions, initiated by $Na[Ph_2CO]$, were rapid at or just above room temperature. This impressive work demonstrated the efficiency and versatility of the electrocatalytic technique. Since the ligands are so easily and cleanly introduced, the authors[90] effected interesting combinations by sequential introduction of various ligands (Scheme 19). In this way, the first three mixed R_3As/R_3P-substituted Ru-clusters and the first olefin-Ru clusters were synthesized from $[Ru_3(CO)_{12}]$. Unusual olefin-isocyanide-PR_3 clusters of ruthenium were also prepared. Since chiral clusters were also accessible in this study, *Bruce* et al. pointed out[90] that the electrocatalytic route should prove an ideal one for future syntheses of new types of optically active clusters in which the chirality results from a combination of ligands in homometallic clusters, complementary to the known strategy which consisted in designing chiral clusters with different metals[91a] or optically active ligands.[91b]

In several papers,[92-96] *Patin* and *Darchen* et al. have reported the electrocatalytic syntheses of several bi- and trimetallic iron complexes using a cathodic current. These compounds were also obtained by the sequential exchange of CO ligands by $P(OMe)_3$ ligands (Scheme 20). Using this technique or a thermal route, the complex [(RO-C(S)SMe)$Fe_2(CO)_6$] is shown[95] to undergo rearrangement to [(μ_2-RO-CS)(μ_2-SMe)Fe_2CO_6] (R = CH_2-adamantyl).

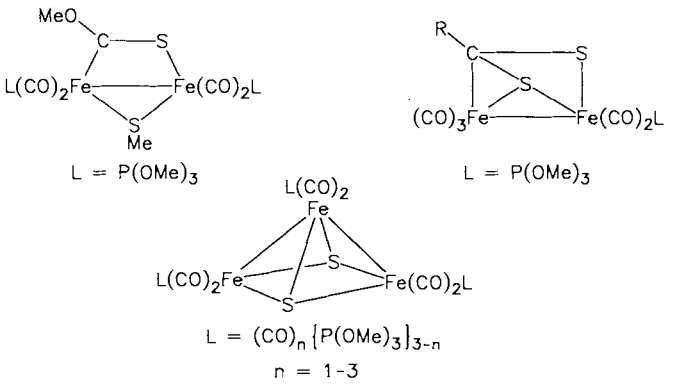

Scheme 20. Examples of electrocatalytically prepared Fe-complexes.

Kochi et al. have recently examined[97,98] the sequential replacement of CO ligands in the phosphanediyl capped clusters **5** and **6** by P donor ligands essentially using a

$[Co_4(CO)_{10}(\mu_4\text{-}PPh)_2]$ **5** $[Fe_3(CO)_9(\mu_3\text{-}PPh)_2]$ **6**

cathodic current.[97] Coulombic efficiencies were found to be low, between 4 and 11, because radical anionic intermediates tend to decompose at competitive rates, as in the alkynedicobalt systems (Scheme 18).[76,87,88] The lifetimes of the primary radical anions are independent of the P donor concentrations, indicating that the rate-limiting step does not involve the nucleophilic attack on the primary radical anion, but the formation of another intermediate which reacts with the P donor molecule. This behavior thus seems general in cluster chemistry; precedents for metal-metal bond breaking prior to substitution were found to exist in closed shell systems by *Vahrenkamp*.[99] However, whether a Co-Co bond or a Co-P bond breaks is not known in the case of **5**. The singly, doubly, and triply $P(OMe)_3$-substituted Co_4 clusters were selectively synthesized by application of a cathodic current at a potential slightly less negative than the E° of **5**; in such short chains, this choice of potential facilitates the formation of the neutral substitution product by heterogeneous ET at the electrode ($\mathbf{ML}^{\odot\ominus} \rightarrow \mathbf{ML}$, Scheme 21: **M** = $Co_4(CO)_9(PPh)_2$; cf. also Scheme 6).

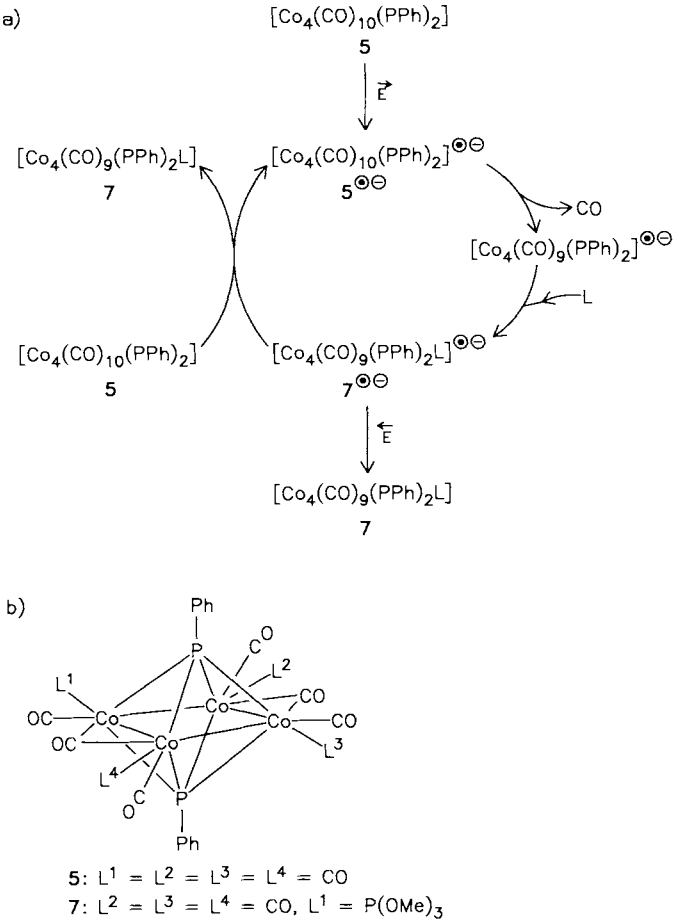

Scheme 21. Electrocatalytic exchange of CO by $P(OMe)_3$ ligands in the bicapped Co_4-cluster **5** [97]. a) Mechanism of electrocatalysis by a cathodic current with low coulombic efficiency (monosubstitution to give **7**); the structures and number of secondary radical anion intermediates is unknown (Co-Co or Co-P bond cleavage?). b) The following holds for the regioselectivity in the case of polysubstitution: disubstitution, $L^1 = L^3 = P(OMe_3)$, $L^2 = L^4 = CO$; trisubstitution, $L^1 = L^2 = L^3 = P(OMe)_3$, $L^4 = CO$. The tetrasubstituted cluster ($L^1 = L^2 = L^3 = L^4 = P(OMe_3)$) is not accessible electrocatalytically but prepared via an alternative route.

In a similar way, the cluster **6** can also exchange one, two or three CO ligands for $P(OMe)_3$ ligands sequentially with coulombic efficiencies of 10 to 20 by applying a cathodic potential.[100-102] Depending on the applied potential, the number of ligand substitutions desired can be achieved as in **5**. This general trend for cluster chemistry is characteristic of short catalytic chains. Note that, if no side

reactions of the paramagnetic intermediates were to occur, i.e. if the electrocatalytic chains were to be as long as are found in the mononuclear Mn^{I} series of Section 8.1, then the stoichiometry of CO substitution would only depend on the relative rates of successive CO substitution and, eventually on the stoichiometry of the P donor introduced in the solution. Thus, in the case of excess phosphane, no selectivity would be obtained with respect to the number of CO substitutions. To our knowledge, this point has thus far never been discussed as origin of the nice selectivity, which all authors have observed in electrocatalytic cluster synthesis. Sometimes the coulombic efficiencies may presumably become very poor when the yields are optimized. In most cases nothing is known concerning the radical anionic intermediates of the electrocatalytic cycles. Whereas oxidative electrocatalysis directly provides the "active 17-electron center", reduction does not, and, by contrast, considerable structural rearrangements, such as those reasonably proposed, are necessary. At each step of these pathways, side reactions may occur and shorten the chain. Fortunately, the recent investigations of *Kochi* and *Ohst*[100-102] on the electrocatalyses of **6** were successful in demonstrating the nature of these paramagnetic intermediates. ^{31}P-coupling provided both by the phosphanediyl caps and the incoming P donor allowed monitoring of the following by EPR: the opening of a Fe-P bond = ($\mu_3 \rightarrow \mu_2$ phosphanediyl slippage), the reaction of PEt_3 on the temporary open cluster anion, and the closure of the phosphane-substituted open cluster anion to the substituted closed one ($\mu_2 \rightarrow \mu_3$ back slippage) (Scheme 22). This unique demonstration,[100] while confirming the need of generating a reactive "17-electron center" by cleavage of one cluster edge, indicates that Fe-P cleavage is preferred over Fe-Fe cleavage and highlights the crucial role of the phosphanediyl cap (Scheme 21), also striking in non-electrocatalyzed paths.[98]

Heteronuclear clusters have been synthesized by *Robinson, Simpson* et al.[103] using the electrocatalytic technique with transition metal anions as nucleophiles (instead of the P donors above). The cluster substrates were $[RCCo_3(CO)_9]$ (R = Me, Ph, H) and the anionic nucleophiles were $[MCp(CO)_3]^{\ominus}$ (Cr, Mo, W) or $Fp^{\ominus}$ (it is likely that the latter reduces the Co_3 cluster; $[HgFp_2]$ gave good results, $Fp^{\ominus}$ did not, Scheme 23). The radical anion $Ph_2CO^{\odot\ominus}$ was the initiator.

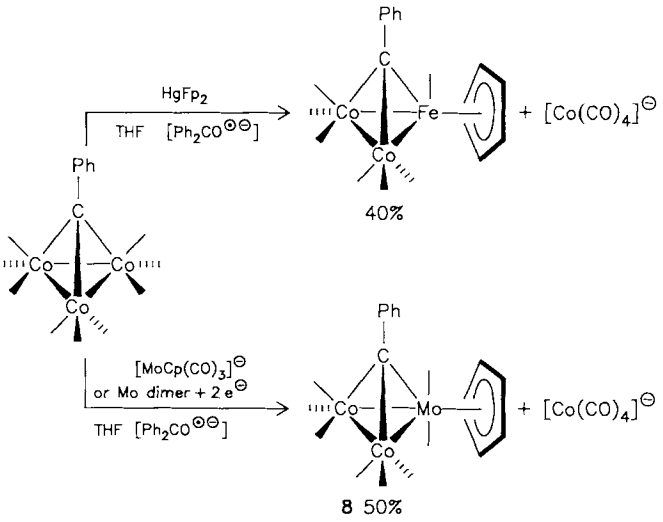

Scheme 23. Electrocatalytic syntheses of heteronuclear clusters using a anionic transition metal species as nucleophilic agent.

The Co_2Mo cluster **8** had already been synthesized by *Vahrenkampf* et al.,[104] but its non-electrocatalytic synthesis necessitates three-days' refluxing in benzene. Thus, both homo- and heteronuclear chiral clusters are now best accessible using electrocatalysis.

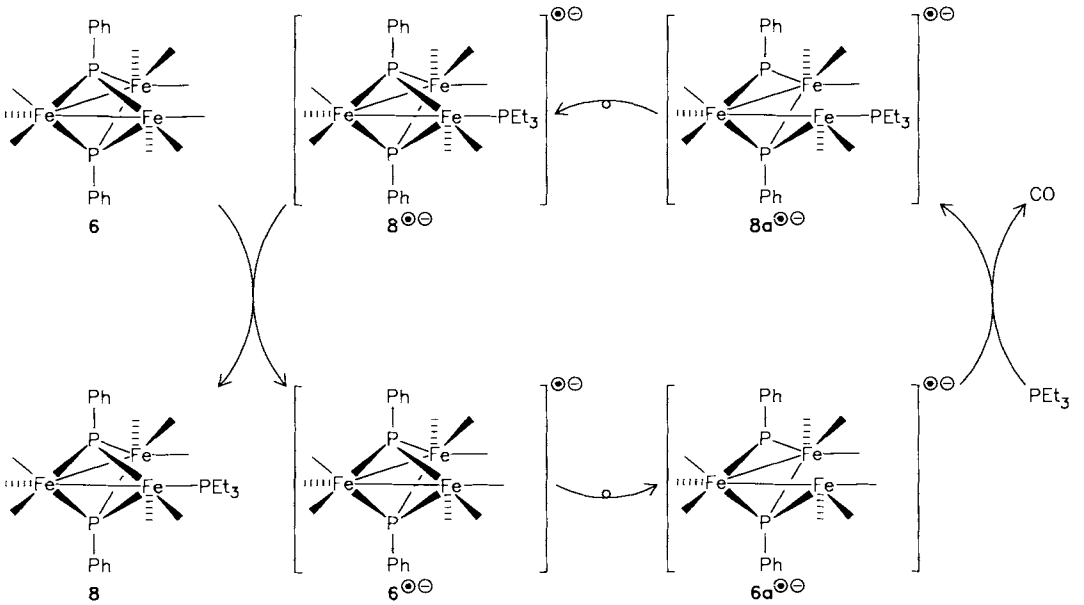

Scheme 22. Electrocatalytic exchange of CO by a P-donor in the bicapped cluster **6**: the four radical anions $\mathbf{6}^{\odot\ominus}$, $\mathbf{6a}^{\odot\ominus}$, $\mathbf{8a}^{\odot\ominus}$, and $\mathbf{8}^{\odot\ominus}$ participating in the propagation cycle have been characterized by EPR (coupling with P ligand(s) in a stepwise sequence at low temperature).

Recently, *Angelici* et al.[104c] reported that the relatively stable bridging thiocarbyne radical, $\mathbf{9}^{\ominus}$, produced by one-electron reduction of cationic precursor $\mathbf{9}^{\oplus}$, catalyzes CO exchange by P-donor ligands in the latter complex [Eq. (f)]. The results of CV studies support the electrocatalytic mechanism, and coulombic efficiencies between 32 and 46 are reported (only in the case of PPh_3 were they poorer: 2.4).

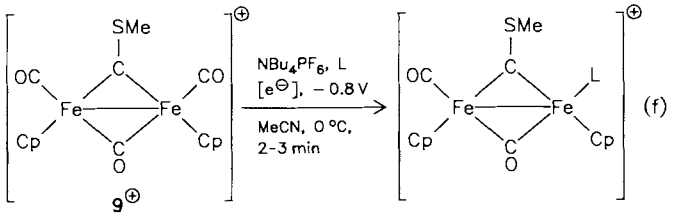

$9^{\oplus}$

L = PEt_3, PMe_2Ph, $PMePh_2$, $CNtBu$

Since the simple and efficient exchange of CO- by a P-donor ligand is not known to proceed electrocatalytically in mononuclear complexes, it is possible that the exchange mechanism in such a bridged dinuclear compound proceeds as in clusters, i.e. involves disruption of the Fe–Fe bond (compare Co–Co cleavage, Scheme 18) or of a Fe–C (carbyne) bond (cf. Fe–P cleavage, Scheme 22).

8.6. Isomerization (Oxidation or Reduction)

The reports by *Rieke, Öfele* et al.[105, 106] of the isomerization of the complexes [M(carbene)$_2$(CO)$_4$] [M = Mo, W, carbene = 2,4-dimethyl-2,4-dihydro-1,2,4-triazol-3-ylidene, 1,3-dimethyl-1,3-dihydroimidazol-2-ylidene (imid) or 1,3-dimethyldihydrobenzimidazol-2-ylidene] are of considerable importance in the electrocatalytic field because they appeared ten years ago, well before the explosion of the 1980's; these pioneering reports include electrochemical as well as preparative aspects and detail the kinetics and thermodynamics of the isomerization processes. The anode catalyzed *trans*→*cis* isomerizations[105] (coulombic efficiencies > 10) were found to occur according to the energy diagram of Scheme 24.

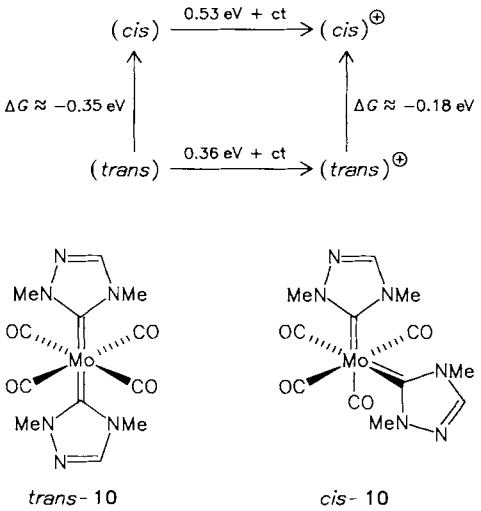

Scheme 24. Energy diagram of the electrocatalytic *trans*→*cis* isomerization of **10**. ct = constant.

Similar carbene complexes of the composition [Mo(imid)$_2$(CO)$_3$L] where L is a C, N, or P donor (cyclohexylisocyanide, triethyl- or triphenylphosphane, pyridine) can exist under the symmetric (*sym*), mericlinal (*mer*), facial (*fac*), or asymmetric (*asym*) *mer* forms. The *sym-mer* complex is electrolyzed in a few minutes with a coulombic efficiency > 10 to give the *fac* complex (Scheme 25); the latter is converted into the cation of the *asym-mer* isomer.[106] The redox process and isomerization were shown to be strongly dependent on the nature of the ligand L.

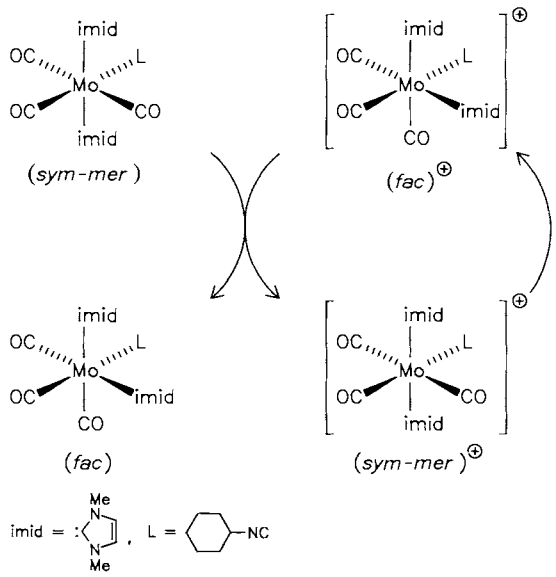

Scheme 25. Electrocatalytic cycle for the anodically initiated isomerization *sym-mer*→*fac* of the biscarbene complexes [Mo(1mid)$_2$(CO)$_3$L] ($k = 0.4\ s^{-1}$ at −20 °C in CH_2Cl_2 for L = cyclohexyl isocyanide).

Robinson, Simpson et al. reported[107] the isomerization of the "flyover" complex **11**. (This complex, as the mono-

[Co_2({(CF$_3$)C}$_6$)(CO)$_2$[P(OMe)$_3$]$_2$] **11**

phosphite analogue, is synthesized by selective electrocatalytic reduction (−0.1 V vs Ag/AgCl) of the parent tetracarbonyl complex; Scheme 26.) The blue bis-phosphite complex isomerizes quantitatively to a purple complex upon application of a cathodic current at −0.7 V (vs Ag/AgCl). The authors explain this process by the cleavage of the Co–Co bond of the primary radical anion while a carbonyl ligand bridges these two metals. Thus, starting from the parent tetracarbonyl complex, either isomer can be synthesized selectively, depending on the applied potential: −0.1 V or −0.7 V vs Ag/AgCl in MeCN or CH_2Cl_2 with Bu_4NClO_4 (Scheme 26).

Connelly et al. have shown[108] that octahedral Mn^I complexes can effect electrocatalytic *trans*→*cis* isomerization quantitatively using a catalytic amount of anodic current (+0.5 V vs SCE) in CH_2Cl_2 (Scheme 27). Interestingly, the

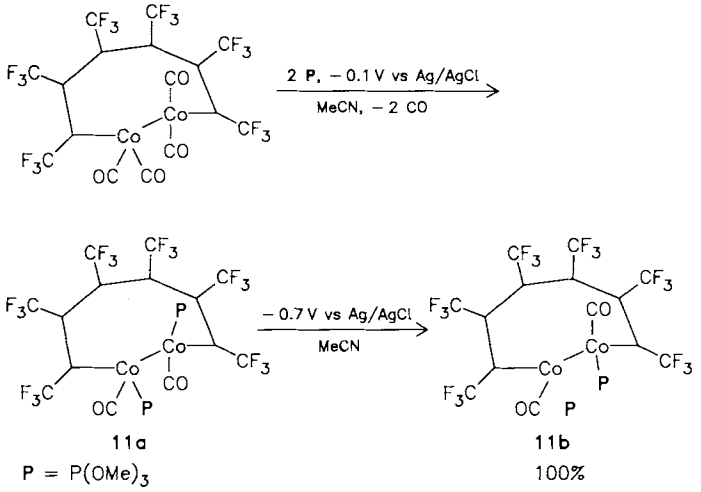

Scheme 26. Electrocatalytic synthesis and isomerization of the "flyover" complex **11** (reductive initiation). For the isomerization **11a** → **11b**, catalytic amounts of reducing agent are required.

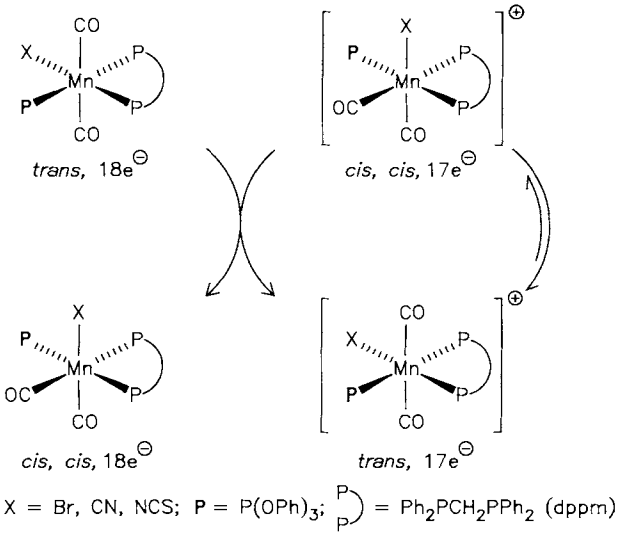

Scheme 27. Electrocatalytic cycle for the anodically induced *trans*→*cis* isomerization of *trans*-[Mn^{I}X(CO)$_2$\{P(OPh)$_3$\}(dppm)]. (Note that the *trans*-configurated complex cation is more stable than the *cis*-configurated.)

trans cation is more stable than its *cis* isomer; indeed, stoichiometric oxidation of the neutral *cis* form leads to the *trans* cation. In the electrocatalytic system, a strong driving force is provided by the favorable difference in the redox potential. Previously, *Bond* had noted[109] that the CV wave shapes of such complexes can only be explained by taking into account the cross redox reaction, as in Scheme 27. Other ETC-catalyzed structural transformations are noted in Section 8.5.[95]

8.7. CO Migratory Insertion (Oxidation or Reduction) and Extrusion (Reduction)

8.7.1. CO Insertion: Oxidative versus Reductive Initiation

The acetyl complex **13** is accessible both by oxidation as well as by reduction (Scheme 28). The subtle difference lies in the nature of one ligand in the educt (PPh_3 in **12**, CO in [$FpCH_3$]). The changeover from PPh_3 to CO is sufficient to invert the relative electron densities on the iron center in the educt and in the product, so that the ET-propagation step is exergonic in both cases. The two studies were published within a span of only a few months by *Vlček* et al. (reductive initiation)[110] and by *Magnuson, Giering* et al. (oxidative initiation).[111]

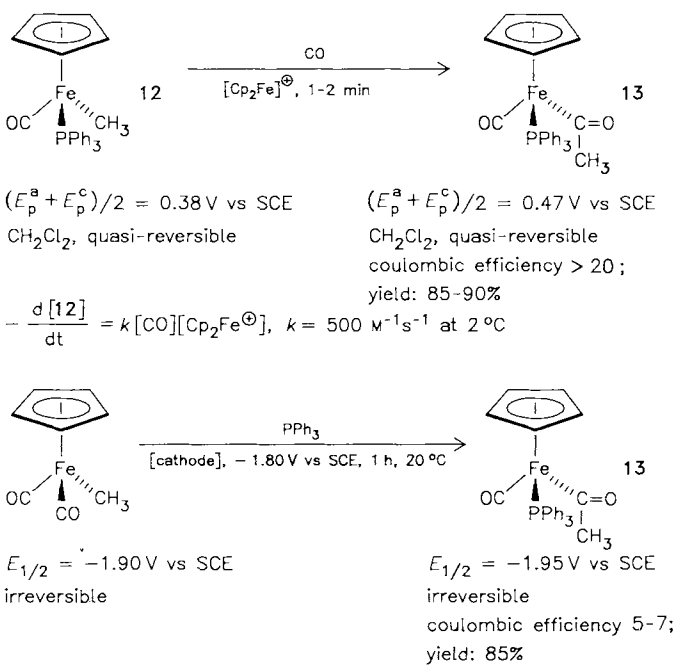

Scheme 28. Electrocatalytic migratory insertion of CO into the iron–methyl bond in **12** and [$FpCH_3$]. By suitable choice of the external ligand and the initiator (oxidizing or reducing), the same product **13** is obtained.

The oxidative process is extremely efficient, one driving force being the cross redox reaction ($\Delta G \simeq 2$ kcal mol^{-1}). The reductive process is less efficient because of side reactions of the radical anions [$FpCH_3$]$^{\odot\ominus}$ and **13**$^{\odot\ominus}$ (neither the reduction of [$FpCH_3$] nor that of **13** being reversible). The driving force provided by the cross redox reaction, although favorable, is also presumably less than that obtained in the oxidation process ($\Delta E_{1/2} = 0.05$ V, but the thermodynamic potentials are unknown).

This duality is of interest because it sheds light on the comparison between oxidative and reductive electrocatalysis. If one hesitates between the two possibilities in the case of an isoergonic cross redox reaction, one should consider the relative reversibilities of the oxidation and reduction CV waves. It is highly probable that the oxidation route is preferable because the catalytic cycle is very short as compared to that of the reduction route. Consistent with this hypothesis, coulombic efficiencies are higher in the oxidation route (see Scheme 28).

8.7.2. CO Extrusion: From Formyl to Hydride (Reduction)

It is well known that formyl complexes are unstable relative to the corresponding hydrides (CO insertion into an M–H bond is unfavorable), but CO extrusion may be slow

$$ArylX \xrightarrow{[e^{\ominus}]} ArylX^{\bullet\ominus} \longrightarrow Aryl^{\bullet} \xrightarrow{Nu^{\ominus}} ArylNu^{\bullet\ominus} \xrightarrow{ArylX} ArylNu$$

$$[M(CO)_n] \xrightarrow{[e^{\ominus}]} [M(CO)_n]^{\bullet\ominus} \longrightarrow [M(CO)_{n-1}]^{\bullet\ominus} \xrightarrow{P} [M(CO)_{n-1}P]^{\bullet\ominus} \xrightarrow{[M(CO)_n]} [M(CO)_{n-1}P]$$

Scheme 30. Close analogy between an $S_{RN}1$ reaction and reductively initiated CO substitution in clusters. $X^{\ominus} = Cl^{\ominus}$, $Nu^{\ominus} = NH_2^{\ominus}$, **P** = PR_3. Both processes suffer from side reactions due to a long catalytic cycle.

and therefore several stable formyl complexes have been isolated.[112] Thus, it is not surprising that electrocatalysis can efficiently facilitate CO extrusion from formyl complexes. Since a hydride ligand is more electron releasing than a formyl ligand, the reductive route should provide the second driving force of an electrocatalytic CO extrusion.

Kochi et al. have shown[113] that the stable anionic formyl complex **14** can be converted into the hydride by ap-

$[cis\text{-}(CO)_5ReRe(CO)_4CHO]^{\ominus}$ **14**

plying a potential of -2.1 V, at which an irreversible reduction is observed (Scheme 29). The process consumes only 0.035 F per mole of formyl complex (coulombic ef-

$$[(CO)_5ReRe(CO)_4(CHO)]^{\ominus} \xrightarrow[\text{yield: 100\%}]{\vec{E}} [(CO)_5ReRe(CO)_4H]^{\ominus} + CO$$

14

$E_{1/2} = -2.1$ V vs SCE (irrev.) $\qquad$ $E_{1/2} = -2.6$ V vs SCE (irrev.)

Scheme 29. Formation of a hydrido ligand from a formyl ligand by extrusion of CO. Both chain propagation steps are strongly exergonic and the electrocatalytic process is efficient.

ficiency = 30). The resulting hydride shows a reduction CV wave at -2.6 V which can be observed in the CV of the formyl complex, as expected for the electrocatalytic extrusion. Anthracenesodium (5 mol%) in THF also gives a 75% yield in 10 min at 25°C. Radical initiators are even more efficient.

9. Concluding Remarks

The field of organometallic electrocatalysis originates from *Feldberg*'s recognition and investigation of the ECE mechanism fifteen years ago using rapid electrochemical techniques. It parallels the electrocatalyzed nucleophilic substitution, $S_{RN}1$ mechanism, discovered by *Kornblum*, researched in aromatic chemistry by *Bennet* and for which *Savéant* and *Amatore* have established the useful a-dimensional analytic technique of kinetic investigation. The kinetic barriers of most classical organometallic reactions can be overcome by the use of this technique. The studies have demonstrated the exceptional reactivities of 17- and 19-electron transition metal centers in mono- and polymetallic compounds and have contributed considerably to the improvement of the syntheses of many known complexes. Some sophisticated chiral cluster syntheses have also already been achieved, the selectivity of which dramatically contrasts with mixtures obtained by tedious classical routes. The limitation of the coulombic efficiency is at the origin of this selectivity, the resulting ET chain being caused by the side reactions of the various radical anionic intermediates in these reductive electrocatalyses. In contrast, oxidative electrocatalysis, to which *Kochi* has made a comprehensive contribution, is most often used for mononuclear compounds; it enables high coulombic efficiencies to be achieved because the catalytic cycle is small (associative mechanisms involving $17e^{\ominus} \rightleftharpoons 19e^{\ominus}$ species). Finally, note that reductive electrocatalytic cluster synthesis curiously resembles aromatic substitution.[114] Both are nucleophilic substitutions encountering the same problem of side reactions of the radical intermediates (Scheme 30). Clearly, the extensive and related organic area developed in the 1970's has been most useful for the advancement of electrocatalytic organometallic chemistry.

It is likely that this field will expand further in the near future, and that this review will be complemented by a large number of reports on investigations of as yet unexplored electrocatalytic mechanisms and catalytic transformations of organic ligands.

I am grateful to Dr. Françoise Moulines and Dr. Marc Lacoste for helpful discussions and assistance, and to the University of Konstanz where this manuscript was prepared during the summer of 1986. Thanks are also due to Professor Hans H. Brintzinger for enjoyable discussions on this topic, and to Professor Gottfried Huttner and his group for enthusiastic scientific collaboration.

Received: December 8, 1986;
revised: February 3, 1987 [A 668 IE]
German version: *Angew. Chem. 100* (1988) 662

Addendum (November 19, 1987)

Since submission of this review, several important papers relevant to this subject have appeared.

J. E. Guerchais et al.[115] have reported electrocatalytic exchange of CO for MeCN (reduction) in a dinuclear Mo complex [Eq. (g)].

$$[Mo_2Cp_2(\mu\text{-}SMe)_2(CO)_4]^{2\oplus} \xrightarrow[-CO]{[e^{\ominus}]\ MeCN} [Mo_2Cp_2(\mu\text{-}SMe)_2(CO)_3(Me_3CN)]^{2\oplus} \quad (g)$$

Lahuerta and *Latorre* et al. have replaced CO by $P(OMe)_3$ in **15** [reduction; Eq. (h), N-N = 2,3-diazanor-

$$[Fe(N{-}N)(CO)_3] \xrightarrow[-CO]{[e^{\ominus}]\ P(OMe)_3} [Fe(N{-}N)(CO)_2\{P(OMe)_3\}] \quad (h)$$

15

bornene]—a rare case of CO exchange in a mononuclear complex.[116a] This study follows the more classical multiple CO exchange by $P(OMe)_3$ in the related trinuclear iron complex $[(N\text{-}N)Fe_3(CO)_9]$[116b] [reduction; Eq. (k), $L = P(OMe)_3$].

$$[(N-N)Fe_3(CO)_9] \xrightarrow{[e^-]} [(N-N)Fe_3(CO)_8L] \xrightarrow{[e^-]} [(N-N)Fe_3(CO)_7L_2] \quad (k)$$

The electrocatalytic exchange of CO by PMe_2Ph or $PMePh_2$ in the cluster $[Co_4(CO)_9(tripod)]$ has been induced cathodically by *Lemoine* et al.[117a] If one Co is replaced by Fe or Ru, ligand exchange of CO by PR_3 (R = Me, Ph) or DMF can be similarly induced in the monoanionic clusters.[117b] *Kotz* and *Garcia* have shown[117c] that electrocatalytic replacement of iodide by a solvent molecule in $[MoCp_2I_2]$ can be induced by the oxidant $[Ru(bipy)_3]^{3\oplus}$.

Photogenerated 19-electron species have been reported by *Tyler* et al.[118] to initiate CO exchange by PMe_2Ph in $[Ru_3(CO)_{12}]$ [Eq. (l)] and by $PnBu_3$ in $[FeCp(CO)_2PnBu_3]^{\oplus}$

$$[Ru_3CO_{12}] + PMe_2Ph \xrightarrow[h\nu]{[Mo_2Cp_2(CO)_6]} [Ru_3(CO)_{11}(PMe_2Ph)] + CO \quad (l)$$

$$[FeCp(CO)_2L]^{\ominus} + L \xrightarrow[h\nu]{[Fe_2Cp_2(CO)_4]} [FeCp(CO)L_2]^{\oplus} + CO \quad (m)$$

[Eq. (m), $L = PnBu_3$]. The reaction (m) substantiates the proposition that electron-rich species are generated by photolysis of $[Fe_2Cp_2(CO)_4]$ in the presence of a P donor.[117, 118]

The disproportionation of the dimeric compounds $[Fe_2Cp_2(CO)_4]$, $[Mo_2Cp_2(CO)_6]$ and $[M_2(CO)_{10}]$ (M = Mn, Re) in the presence of various ligands according to Equation (n) can be induced by a catalytic amount of photons

$$L_nM - ML_n \xrightarrow{P} [ML_nP]^{\oplus} + [L_nM]^{\ominus} \quad (n)$$

(quantum yields $\gg 1$) or of electrons (reduction).[119] This important series of reactions are electrocatalytic in the sense adopted here when initiation is effected by reduction (ET by an initiator and in the propagation); when the initiator is a photon, the first ET transfer intervenes only in the third step but the reaction can still be called electrocatalytic in a broader sense. It is also distinct from the other electrocatalytic reactions reviewed here in that a net overall redox change is involved in the stoichiometry of the reaction.

$$[L_nM - ML_n] \xrightarrow{h\nu} [2\,ML_n]^{\odot}$$

$$[ML_n]^{\odot} + P \longrightarrow [ML_nP]^{\odot}$$

$$[ML_nP]^{\odot} + [L_nM - ML_n] \longrightarrow [ML_nP]^{\oplus} + [L_nM - ML_n]^{\odot\ominus}$$

$$[L_nM - ML_n]^{\odot\ominus} \longrightarrow [L_nM]^{\odot} + [ML_n]^{\ominus}$$

Chanon has published another review on ETC catalysis where organic, inorganic and organometallic exemples are compared; note that the Table of organometallic reactions therein lists electrocatalytic cases having cross ET transfer propagation steps as well as others which have a free radical chain consisting of atom or radical transfers. It is possible to distinguish these two categories of chain mechanism (the latter is not reviewed here).

For instance, CO exchange by a phosphane can proceed easily according to a free-radical chain mechanism when the complex bears a hydride ligand which can be abstracted as a H atom by a radical initiator. Examples are the reactions (o)–(q),[121] for which the radical chain mechanism (r)–(t) holds.

$$cis\text{-}[Os(H)(CH_3)(CO)_4] \xrightarrow[-CO]{PPh_3} [Os(H)(CH_3)(PPh_3)(CO)_3] \quad (o)$$

$$cis\text{-}[Os(H)_2(CO)_4] \xrightarrow[-CO]{PEt_3} [Os(H)_2(CO)_2(PEt_3)_2] \quad (p)$$

$$[Re(CO)_5(H)] \xrightarrow[-CO]{PR_3} [Re(CO)_4H(PR_3)] \quad (q)$$

$$[M(L_n)(H)] \xrightarrow{R^{\odot}} RH + [ML_n]^{\odot} \quad (r)$$

$$[ML_n]^{\odot} \xrightarrow[-L]{PR_3} [M(L)_{n-1}(PR_3)]^{\odot} \quad (s)$$

$$[M(L)_{n-1}(PR_3)]^{\odot} + [M(L)_n(H)] \longrightarrow [M(L)_{n-1}(PR_3)(H)] + [ML_n]^{\odot} \quad (t)$$

Outer-sphere ET proceeds neither in the initiation nor in the propagation (it has been argued that atom or radical transfer is a form of inner sphere ET). Organotransition metal reactions proceeding by such a free-radical chain mechanism were pioneered by *Osborn*'s discovery of oxidative addition to low valent Pt complexes.[122] Recently *Halpern* has found insertion and oxidative addition on Rh porphyrin complexes;[123] photoinduced oxidative addition have also been shown to proceed in this way.[124]

However, metal hydride complexes such as $[VCp(CO)_3H]^{\ominus}$, which are very electron rich, can also initiate ETC ligand exchange in a complex $[ML_n]$ by ET in the initiation step.[125]

Note added in proof: For the coupling of ETC catalysis with organometallic catalysis see Ref. [126].

[1] R. L. Rich, H. Taube, *J. Am. Chem. Soc. 76* (1954) 2608.
[2] F. Basolo, M. L. Morris, R. G. Pearson, *Discuss. Faraday Soc. 29* (1960) 80.
[3] F. Basolo, P. H. Wilks, R. G. Pearson, R. G. Wilkins, *J. Inorg. Nucl. Chem. 6* (1958) 161.
[4] F. Basolo, A. F. Messing, P. H. Wilks, R. G. Wilkins, R. G. Pearson, *J. Inorg. Nucl. Chem. 6* (1958) 203.
[5] F. Basolo, R. G. Pearson: *Mechanismus of Inorganic Reactions*, Wiley, New York 1967.
[6] N. Kornblum, R. E. Michel, R. C. Kerber, *J. Am. Chem. Soc. 88* (1966) 5662.
[7] N. Kornblum, *Angew. Chem. 87* (1975) 797; *Angew. Chem. Int. Ed. Engl. 14* (1975) 734.
[8] J. F. Bunnett, *Acc. Chem. Res. 11* (1978) 413.
[9] G. A. Russel, W. C. Danen, *J. Am. Chem. Soc. 88* (1966) 5663.
[10] G. A. Russel, *Spec. Publ. Chem. Soc. 24* (1970) 271.
[11] J. Pinson, J. M. Savéant, *J. Chem. Soc. Chem. Commun. 1974*, 933.
[12] C. Amatore, J. Chaussard, J. Pinson, J. M. Savéant, A. Thiébault, *J. Am. Chem. Soc. 101* (1979) 6012.
[13] J. M. Savéant, *Acc. Chem. Res. 13* (1980) 323.
[14] C. Amatore, J. M. Savéant, A. Thiébault, *J. Electroanal. Chem. Interfacial Electrochem. 103* (1979) 303; *ibid. 107* (1980) 59, 75.
[15] a) C. Amatore, J. M. Savéant, *J. Electroanal. Chem. Interfacial Electrochem. 85* (1977) 27; *ibid. 86* (1978) 227; *ibid. 102* (1979) 21; *ibid. 107* (1980) 353; b) C. Amatore, J. Pinson, J. M. Savéant, A. Thiébault, *J. Am. Chem. Soc. 104* (1982) 817.
[16] M. Chanon, M. L. Tobe, *Angew. Chem. 94* (1982) 27; *Angew. Chem. Int. Ed. Engl. 21* (1982) 1.

[17] M. Chanon, *Bull. Soc. Chim. Fr. 1982*, 197.
[18] M. Julliard, M. Chanon, *Chem. Rev. 83* (1983) 425.
[19] M. Chanon, *Bull. Soc. Chim. Fr. 1985*, 209.
[20] For major books and reviews concerning the role of ET in inorganic and organometallic chemistry see [5, 16-19, 21-36].
[21] J. K. Kochi: *Organometallic Mechanisms and Catalysis*, Academic Press, New York 1978.
[22] a) J. K. Kochi, *Pure Appl. Chem. 52* (1980) 571; b) in W. A. Pryor (Ed.): *Frontiers of Free Radical Chemistry*, Academic Press, New York 1980, p. 297; c) R. A. Sheldon, J. K. Kochi: *Metal-Catalyzed Oxidations of Organic Compounds*, Academic Press, New York 1981.
[23] J. A. Osborn in Y. Ishii, M. Tsutsui (Eds.): *Organo Transition Metal Chemistry*, Plenum, New York 1975, p. 65.
[24] a) N. G. Connelly, W. E. Geiger, *Adv. Organomet. Chem. 23* (1984) 1; b) W. E. Geiger, N. G. Connelly, *ibid. 24* (1985) 87.
[25] W. E. Geiger, *Prog. Inorg. Chem. 33* (1985) 275.
[26] P. Lemoine, *Coord. Chem. Rev. 47* (1982) 55.
[27] M. F. Lappert, P. W. Lednor, *Adv. Organomet. Chem. 14* (1976) 345.
[28] J. Halpern in M. Tsutsui (Ed.): *Fundamental Research in Homogeneous Catalysis*, Plenum, New York 1979, p. 25; *Q. Rev. Chem. Soc. 15* (1961) 207.
[29] J. Halpern, *Angew. Chem. 97* (1985) 308; *Angew. Chem. Int. Ed. Engl. 24* (1985) 274.
[30] R. D. Cannon: *Electron Transfer Reactions*, Butterworths, London 1980; *Adv. Inorg. Chem. Radiochem. 21* (1978) 179.
[31] A. G. Milaev, O. Yu. Okhlobystin, *Russ. Chem. Rev. (Engl. Transl.) 49* (1980) 893.
[32] H. Bock, W. Kaim, *Acc. Chem. Res. 15* (1982) 9.
[33] H. L. M. Van Gaal, J. G. M. Van der Linden, *Coord. Chem. Rev. 47* (1982) 41.
[34] T. J. Meyer, *ACS Symp. Ser. 211* (1983) 157.
[35] a) N. Sutin, C. Creutz, *J. Chem. Educ. 60* (1983) 809; b) *Adv. Chem. Ser. 168* (1978) 1.
[36] H. Taube, *Angew. Chem. 96* (1984) 315; *Angew. Chem. Int. Ed. Engl. 23* (1984) 329; *Adv. Inorg. Chem. Radiochem. 1* (1959) 1; *J. Chem. Educ. 45* (1968) 452.
[37] A. M. Bond, R. Colton, M. J. McCormick, *Inorg. Chem. 16* (1977) 155.
[38] a) T. L. Brown, *Ann. NY Acad. Sci. 331* (1980) 80; b) B. Byers, T. L. Brown, *J. Am. Chem. Soc. 99* (1977) 2527; *ibid. 97* (1975) 947.
[39] N. W. Hoffman, T. L. Brown, *Inorg. Chem. 17* (1978) 613.
[40] S. B. McCullen, H. W. Walker, T. L. Brown, *J. Am. Chem. Soc. 104* (1982).
[41] Q.-Z. Shi, T. G. Richmond, W. C. Trogler, F. Basolo, *J. Am. Chem. Soc. 104* (1982) 4032.
[42] T. G. Richmond, Q.-Z. Shi, W. C. Trogler, F. Basolo, *J. Chem. Soc. Chem. Commun. 1983*, 650; *J. Am. Chem. Soc. 106* (1984) 76; Q.-Z. Shi, T. G. Richmond, W. C. Trogler, F. Basolo, *ibid. 106* (1984) 71.
[43] J. E. Ellis, R. A. Faltynek, G. L. Rochort, R. E. Stevens, G. A. Zank, *Inorg. Chem. 19* (1980) 1082.
[44] A. Fox, J. Malito, A. J. Poe, *J. Chem. Soc. Chem. Commun. 1981*, 1052.
[45] M. J. Maroney, W. C. Trogler, *J. Am. Chem. Soc. 106* (1984) 4144.
[46] N. G. Connelly in G. Wilkinson, F. G. A. Stone, A. Abel (Eds.): *Comprehensive Organometallic Chemistry*, Pergamon, London 1982, Chapter 22.
[47] a) D. Astruc, E. Román, J. R. Hamon, P. Batail, *J. Am. Chem. Soc. 101* (1979) 2240; b) D. Astruc, J. R. Hamon, E. Román, P. Michaud, *ibid. 103* (1981) 7502; c) J. R. Hamon, D. Astruc, P. Michaud, *ibid. 103* (1981) 758.
[48] P. Michaud, C. Lapinte, D. Astruc, *Ann. NY Acad. Sci. 415* (1983) 97.
[49] a) D. Mandon, L. Toupet, D. Astruc, *J. Am. Chem. Soc. 108* (1986) 1320; b) A. Madonik, D. Astruc, *ibid. 106* (1984) 2437.
[50] a) J. Hennion, J. Nicole, E. Le Roy, F. Petit, *Tetrahedron Lett. 1978*, 2403; b) D. Huchette, J. Nicole, F. Petit, *ibid. 1979*, 1035; c) M. Gilet, J. Nicole, A. Mortreux, F. Petit, *J. Chem. Soc. Chem. Commun. 1979*, 521; d) M. Gilet, A. Mortreux, J. C. Folest, F. Petit, *J. Am. Chem. Soc. 105* (1983) 3876.
[51] a) D. Ballivet-Tkatchenko, M. Riveccie, N. El Murr, *Inorg. Chim. Acta 30* (1978) L289; *J. Am. Chem. Soc. 101* (1979) 2763; b) J. F. Fauvarque, C. Chevrot, A. Jutand, M. François, J. Périchon, *J. Organomet. Chem. 264* (1984) 273; c) J. Périchon, *Actual. Chim. 11* (1982) 25.
[52] P. Michaud, D. Astruc, J. Ammeter, *J. Am. Chem. Soc. 104* (1982) 3755.
[53] C. P. Andrieux, J. M. Dumas-Bouchiat, J. M. Savéant, *J. Electroanal. Chem. Interfacial Electrochem. 87* (1978) 39, 53.
[54] See for instance: R. Dietz, H. Lund in M. Baizer (Ed.): *Organic Electrochemistry*, Dekker, New York 1973, p. 821 and Ref. [19].
[55] a) J. M. Lehn, J. P. Sauvage, R. Ziessel, *Nouv. J. Chim. 3* (1979) 423; b) N. Sutin, *J. Photochem. 10* (1979) 19.
[56] K. Kalyanasundaram, J. Kiwi, M. Grätzel, *Helv. Chim. Acta 61* (1978) 2720.
[57] F. Van den Brink, W. Visscher, E. Barendrecht, *J. Electroanal. Chem. Interfacial Electrochem. 157* (1983) 283.
[58] a) S. Tazuke, N. Kitamura, *Pure Appl. Chem. 56* (1984) 798; b) S. Suzuki, F. Takahashi, I. Satoh, S. Sonobe, *Bull. Soc. Chim. Jpn. 48* (1975) 324; c) B. W. Carlson, L. L. Miller, *J. Am. Chem. Soc. 105* (1983) 7453; d) B. G. Malmström, *Annu. Rev. Biochem. 51* (1982) 21; e) B. Chance, D. C. De Vault, H. Frauenfelder, R. A. Marcus, J. R. Schrieffer, N. Sutin: *Tunneling in Biological Systems*, Academic Press, New York 1979, p. 453.
[59] For an approach, see also: a) N. Tanaka, K. Ebata, *J. Electroanal. Chem. 8* (1964) 120; b) E. Fischerova, O. Dracka, M. Meloun, *Collect. Czech. Chem. Commun. 33* (1968) 473.
[60] S. W. Feldberg, L. Jeftic, *J. Phys. Chem. 76* (1972) 2439; see also Ref. [61].
[61] For previous papers on the ECE mechanism see: a) S. W. Feldberg, *J. Phys. Chem. 75* (1971) 2377; b) M. D. Hawley, S. W. Feldberg, *ibid. 70* (1966) 3459; c) R. N. Adams, M. D. Hawley, S. W. Feldberg, *ibid. 71* (1967) 851; d) G. S. Alberts, I. Shain, *Anal. Chem. 35* (1963) 1959.
[62] J. W. Hershberger, J. K. Kochi, *Polyhedron 2* (1983) 929.
[63] For previous polarographic studies of the chromium systems, see: a) B. R. Baker, B. D. Mehta, *Inorg. Chem. 4* (1965) 848; b) E. Fischerova, O. Fischer, *Collect. Czech. Chem. Commun. 26* (1961) 2570; c) P. J. Elving, B. Zemel, *Can. J. Chem. 37* (1959) 247.
[64] a) A. J. Bard (Ed.): *Encyclopedia of Electrochemistry of the Elements, Vol. 1-14*, Dekker, New York 1980; b) L. Meites, P. Zuman (Eds.): *Handbook Series in Organic Electrochemistry, Vols. 1, 2*, CRC Press, Acron, PA, USA 1974; c) For recent reviews on the electrochemistry (and redox potentials) of transition metal organometallic compounds, see Ref. [24]; d) for redox potentials of stable Fe^{I} compounds, see Ref. [47c] and J. C. Green, M. R. Kelly, M. P. Payne, E. A. Seddon, D. Astruc, J. R. Hamon, P. Michaud, *Organometallics 2* (1983) 211.
[65] a) J. A. Page, G. Wilkinson, *J. Am. Chem. Soc. 74* (1952) 6149; b) For preparation and use, see for instance: D. Catheline, D. Astruc, *J. Organomet. Chem. 266* (1984) C11; c) For review, see Ref. [24a].
[66] J. W. Hershberger, R. J. Klingler, J. K. Kochi, *J. Am. Chem. Soc. 105* (1983) 61.
[67] a) Kochi's papers contain many voltammograms illustrating the CV identification of electrocatalysis. See for instance Ref. [66] and [67b]; b) J. K. Kochi, *J. Organomet. Chem. 300* (1986) 139.
[68] a) R. S. Nicholson, I. Shain, *Anal. Chem. 36* (1964) 706; b) H. Matsuda, V. Ayabe, *Z. Elektrochem. 59* (1955) 494.
[69] Feldberg's papers: a) Refs. [59] and [61a]; b) S. W. Feldberg in A. J. Bard (Ed.): *Electroanalytical Chemistry, Vol. 3*, Dekker, New York 1969, p. 199; in H. B. Mark (Ed.): *Computer Applications in Analytical Chemistry*, Dekker, New York 1972, p. 185.
[70] a) J. M. Savéant, E. Vianello, *Electrochim. Acta 8* (1963) 905; b) J. M. Savéant, *ibid. 12* (1967) 999; c) C. Amatore, J. M. Savéant, *J. Electroanal. Chem. Interfacial Electrochem. 144* (1983) 59.
[71] a) D. Rehm, A. Weller, *Isr. J. Chem. 8* (1970) 259; b) J. Eriksen, C. S. Foote, T. L. Parker, *J. Am. Chem. Soc. 99* (1977) 6455; c) L. E. Manring, C. L. Gu, C. S. Foote, *J. Phys. Chem. 87* (1983) 40; d) V. Balzani, F. Bolleta, M. Ciano, M. Maestri, *J. Chem. Educ. 60* (1983) 447.
[72] a) A. J. Bard, L. R. Faulkner: *Electrochemical Methods*, Wiley, New York 1980; b) Refs. [25] and [69].
[73] a) J. W. Hershberger, J. K. Kochi, *J. Chem. Soc. Chem. Commun. 1982*, 212; b) Ref. [66].
[74] a) D. Catheline, D. Astruc, *Int. Conf. Coord. Chem.* (Budapest 1982), Abstr. Fr. 41; b) D. Catheline, *Thèse de 3e Cycle*, Rennes 1982; *Thèse d'Etat*, Rennes 1985; c) D. Astruc: *Image de la Chimie*, CNRS France, Paris 1982, p. 10; d) C. Amatore, A. Verpeaux, A. Madonik, M.-H. Desbois, D. Astruc, *J. Chem. Soc. Chem. Commun. 1988*, 200.
[75] a) D. Astruc, *Acc. Chem. Res. 19* (1986) 377; *Comments Inorg. Chem. 6* (1987) 61; b) M. Lacoste, M.-H. Desbois, D. Astruc, *New J. Chem. 11* (1987) 561.
[76] G. J. Bezems, P. H. Rieger, S. Visco, *J. Chem. Soc. Chem. Commun. 1981*, 265.
[77] J. W. Hershberger, R. J. Klingler, J. K. Kochi, *J. Am. Chem. Soc. 104* (1982) 3034.
[78] P. M. Zigelman, C. Amatore, J. K. Kochi, *J. Am. Chem. Soc. 106* (1984) 3771.
[79] H. H. Brintzinger, private communication..
[80] a) F. A. Cotton, G. Wilkinson: *Advanced Inorganic Chemistry*, 4th Edit., Wiley, New York 1980; b) E. Román, D. Catheline, D. Astruc, *J. Organomet. Chem. 236* (1982) 229.
[81] C. Moinet, E. Román, D. Astruc, *J. Electroanal. Chem. Interfacial Electrochem. 241* (1981) 121.
[82] a) R. G. Sutherland, M. Igbal, A. Piorkó, *J. Organomet. Chem. 302* (1986) 307; b) D. Astruc, *Tetrahedron 39* (1983) 4027.
[83] A. Darchen, *J. Chem. Soc. Chem. Commun. 1983*, 768.
[84] a) T. P. Gill, K. R. Mann, *J. Organomet. Chem. 216* (1981) 65; b) First synthesis of $[Fe^{II}Cp\{P(OPh)_3\}_3]^{\oplus}$: M. L. H. Green, R. N. Whiteley, *J. Chem. Soc. A 1971*, 1943.
[85] D. P. Summers, J. C. Luong, M. S. Wrighton, *J. Am. Chem. Soc. 103* (1981) 5238.

[86] There is ample precedent in organic chemistry for the photogeneration of electrocatalysts: a) N. J. Turro: *Modern Molecular Photochemistry*, Benjamin Cummings, Menlo Park, CA, USA 1978; b) J. Erikson, C. S. Foote, *J. Phys. 82* (1978) 2659; c) E. G. Blossey, D. C. Neckers, A. L. Thaye, A. P. Shaap, *J. Am. Chem. Soc. 95* (1973) 5820; d) A. J. Bard, *Science 207* (1980) 139; e) For recent examples, see Ref. [19] and the papers by *Schaap* et al.: A. P. Schaap, S. Siddiqui, G. Prasad, E. Palomino, L. Lopez, *J. Photochem. 25* (1984) 167, and references cited therein; A. P. Schaap, L. Lopez, S. D. Gagnon, *J. Am. Chem. Soc. 105* (1983) 663; f) S. L. Mattes, S. Farid in A. Padwa (Ed.): *Organic Photochemistry, Vol. 6*, Dekker, New York 1983, p. 233.

[87] M. Arewgoda, P. H. Rieger, B. H. Robinson, J. Simpson, S. J. Visco, *J. Am. Chem. Soc. 104* (1982) 5633.

[88] a) M. Arewgoda, B. H. Robinson, J. Simpson, *J. Am. Chem. Soc. 105* (1983) 1893; b) A. J. Gownard, B. H. Robinson, J. Simpson, *Organometallics 5* (1986) 1122, 1132, 1140.

[89] M. I. Bruce, D. C. Kehoe, J. G. Matisons, B. K. Nicholson, P. H. Rieger, M. L. Williams, *J. Chem. Soc. Chem. Commun. 1982*, 442.

[90] M. I. Bruce, J. G. Matisons, B. K. Nicholson, M. L. Williams, *J. Organomet. Chem. 236* (1982) C 57.

[91] a) F. Richter, H. Vahrenkamp, *Angew. Chem. 90* (1978) 916; *Angew. Chem. Int. Ed. Engl. 17* (1978) 864; b) M. Bianchi, F. Piacenti, P. Frediani, U. Matteoli, C. Botteghi, S. Gladiali, E. Benedetti, *J. Organomet. Chem. 141* (1977) 107.

[92] A. Darchen, C. Mahé, H. Patin, *J. Chem. Soc. Chem. Commun. 1982*, 243.

[93] A. Darchen, C. Mahé, H. Patin, *Nouv. J. Chim. 6* (1982) 539.

[94] E. K. Lhadi, C. Mahé, H. Patin, A. Darchen, *J. Organomet. Chem. 246* (1983) C 61.

[95] E. K. Lhadi, H. Patin, A. Darchen, *Organometallics 3* (1984) 1128.

[96] A. Darchen, E. K. Lhadi, H. Patin, *J. Organomet. Chem. 259* (1983) 189.

[97] M. G. Richmond, J. K. Kochi, *Inorg. Chem. 25* (1986) 656.

[98] M. G. Richmond, J. K. Kochi, *Inorg. Chem. 25* (1986) 1334.

[99] H. Vahrenkamp, *Adv. Organomet. Chem. 22* (1983) 169.

[100] H. H. Ohst, J. K. Kochi, *J. Chem. Soc. Chem. Commun. 1986*, 121.

[101] H. H. Ohst, J. K. Kochi, *J. Am. Chem. Soc. 108* (1986) 2897.

[102] H. H. Ohst, J. K. Kochi, *Inorg. Chem. 25* (1986) 2066.

[103] S. Jensen, B. H. Robinson, J. Simpson, *J. Chem. Soc. Chem. Commun. 1983*, 1081.

[104] a) H. Beurich, R. Blumhofer, H. Vahrenkamp, *Chem. Ber. 115* (1982) 2409; b) F. Richter, H. Beurich, H. Vahrenkamp, *J. Organomet. Chem. 166* (1979) C 5; c) N. C. Schroeder, R. J. Angelici, *J. Am. Chem. Soc. 108* (1986) 3688.

[105] R. D. Rieke, H. Kojima, K. Öfele, *J. Am. Chem. Soc. 98* (1976) 6735.

[106] R. D. Rieke, H. Kojima, K. Öfele, *Angew. Chem. 92* (1980) 550; *Angew. Chem. Int. Ed. Engl. 19* (1980) 538.

[107] C. M. Arewgoda, B. H. Robinson, J. Simpson, *J. Chem. Soc. Chem. Commun. 1982*, 284.

[108] N. G. Connelly, S. J. Raven, G. A. Garriedo, V. Riera, *J. Chem. Soc. Chem. Commun. 1986*, 992.

[109] R. N. Bagchi, A. M. Bond, G. Brain, R. Colton, T. L. E. Henderson, J. E. Kevekordes, *Organometallics 3* (1984) 4; b) A. M. Bond, S. W. Carr, R. Colton, *Inorg. Chem. 23* (1984) 2343; c) see also A. M. Bond, D. J. Darensbourg, E. Mocellin, B. J. Stewart, *J. Am. Chem. Soc. 103* (1981) 6827.

[110] D. Miholová, A. A. Vlček, *J. Organomet. Chem. 240* (1982) 413.

[111] R. H. Magnuson, R. Meirowitz, S. J. Zulu, W. P. Giering, *Organometallics 2* (1983) 460.

[112] J. A. Gladysz, *Adv. Organomet. Chem. 20* (1982) 1.

[113] B. A. Narayanan, C. Amatore, C. P. Casey, J. K. Kochi, *J. Am. Chem. Soc. 105* (1983) 6351.

[114] The organic counterpart of oxidatively induced electrocatalysis was proposed simultaneously by *Eberson* ($S_{ON}2$) and by *Alder* ($S_{OE}1$, $S_{RE}2$): a) L. Eberson, L. Jönsson, *J. Chem. Soc. Chem. Commun. 1980*, 1187; b) R. W. Alder, *ibid. 1980*, 1184; c) review: L. Eberson, *J. Mol. Catal. 20* (1983) 53.

[115] M. Gueguen, J. E. Guerchais, F. Y. Pétillon, J. Talarmin, *J. Chem. Soc. Chem. Commun. 1987*, 557.

[116] a) F. R. Estenau, P. Lahuerta, J. Latorre, *Inorg. Chim. Acta 116* (1986) L 33; b) P. Lahuerta, J. Latorre, M. Sanau, H. Kisch, *J. Organomet. Chem. 286* (1985) C 27.

[117] a) J. Rimmelin, P. Lemoine, M. Gross, A. A. Bahsoun, J. Osborn, *Nouv. J. Chim. 9* (1985) 181; b) P. Lemoine (Strasbourg), personal communication; c) J. Kotz, M. H. Garcia, in press.

[118] a) A. E. Stiegman, D. R. Tyler, *Comments Inorg. Chem. 5* (1986) 215; b) A. E. Stiegman, A. S. Goldman, D. B. Leslie, D. R. Tyler, *J. Chem. Soc. Chem. Commun. 1984*, 632; c) A. S. Goldman, D. R. Tyler, *Inorg. Chim. Acta 98* (1985) L 47; *Inorg. Chem. 26* (1987) 253.

[119] a) A. E. Steigman, D. R. Tyler, *Coord. Chem. Rev. 1985*, 217; *J. Am. Chem. Soc. 107* (1985) 967; *Inorg. Chem. 23* (1984) 527; b) A. S. Goldman, D. R. Tyler, *J. Am. Chem. Soc. 108* (1986) 89; *ibid. 106* (1984) 4066; c) A. E. Stiegman, M. Stieglitz, D. R. Tyler, *ibid. 105* (1983) 6032.

[120] M. Chanon, *Acc. Chem. Res. 20* (1987) 214.

[121] a) W. J. Carter, J. W. Kelland, S. J. Okasinsky, K. E. Warner, J. R. Norton, *Inorg. Chem. 21* (1982) 3955; b) B. L. Booth, B. L. Shaw, *J. Organomet. Chem. 43* (1972) 369; c) Ref. [38b].

[122] a) J. S. Bradley, D. E. Connor, D. Dolphin, J. A. Labinger, J. A. Osborn, *J. Am. Chem. Soc. 94* (1972) 4043; b) J. A. Labinger, A. V. Kramer, J. A. Osborn, *ibid. 95* (1973) 7908; c) Ref. [23].

[123] R. S. Paonessa, N. C. Thomas, J. Halpern, *J. Am. Chem. Soc. 107* (1985) 4333.

[124] a) D. M. Roundhill, *J. Am. Chem. Soc. 107* (1985) 4354; b) S. Fukuzumi, N. Nishizawa, T. Tanaka, *Chem. Lett. 1982*, 719; c) A. W. Maverick, H. B. Gray, *Pure Appl. Chem. 52* (1980) 2339.

[125] W. D. Jones, J. M. Huggins, R. G. Bergman, *J. Am. Chem. Soc. 103* (1981) 4415.

[126] M. H. Desbois, D. Astruc, *J. Chem. Soc. Chem. Commun. 1988*, 472.

Carbon Dioxide as an Alternative C_1 Synthetic Unit: Activation by Transition-Metal Complexes

By Arno Behr*

The carbon dioxide molecule has been of limited importance as a synthetic unit in organic chemistry. When it is coordinated to transition metals, however, completely new possibilities arise; CO_2 can bond to metal complexes in a variety of ways and can enter into insertion and coupling reactions, or become catalytically attached to other substrates. The formation of C–C bonds between carbon dioxide and unsaturated hydrocarbons under conditions of homogeneous catalysis makes available new synthetic routes to industrially interesting organic compounds.

1. Introduction

Carbon dioxide, whether in free or chemically combined form, is a considerable natural source of carbon. At present it forms 0.034% of the air by volume.[1] The total quantity of carbon present as carbon dioxide, carbonate, and hydrogen carbonate in the atmosphere, hydrosphere, and lithosphere has been estimated as 10^{16} t.[2] Part of the carbon dioxide is subject to natural circulation processes that are influenced to some extent by man. Carbon dioxide and water are converted into carbohydrates and oxygen in plant chloroplasts; this photosynthetic process forms organic compounds from low-energy carbon dioxide by utilizing sunlight [Eq. (1)].[3] A rough estimate has indicated that ca. 200 billion tons of biomass are produced in this way per year. In terms of chemical throughput, therefore, photosynthesis is by far the most important synthetic process.

$$n\,CO_2 + n\,H_2O \rightleftharpoons (CH_2O)_n + n\,O_2 \qquad (1)$$

The respiration of man and animals and the decomposition of organic substances return carbon dioxide to the atmosphere in comparable quantities, and an equilibrium is thus set up. This equilibrium has however been considerably shifted in recent years by the activities of man.[4,5] The increasing demand for energy since the industrial revolution has led to the increased combustion of fossil fuels (coal, oil, gas), forming carbon dioxide; no one can be sure to what extent this increased CO_2 emission will affect our environment. There are many indications that the higher CO_2 concentration in the atmosphere can alter the earth's radiation balance and thus the world climate.[6–12]

A reduction of these negative effects could be achieved by a change in energy policy (a reduction of CO_2 emission by exploiting alternative energy sources). A certain contribution could also be made by chemically converting carbon dioxide into useful products in those places where it is formed in large concentrations, rather than merely allowing it to escape to the atmosphere.

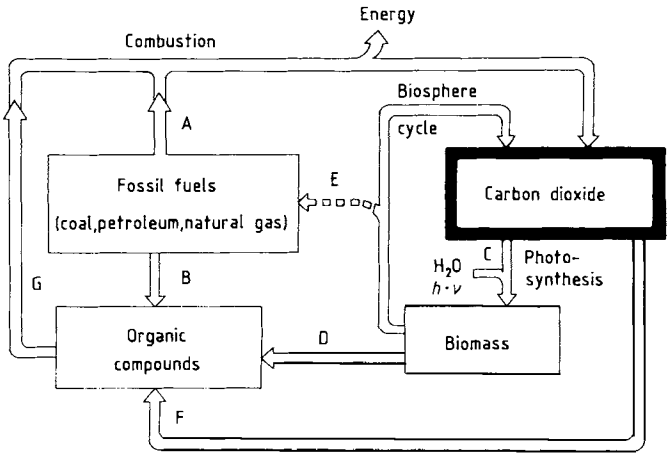

Fig. 1. Carbon dioxide cycle.

Figure 1 depicts the position of carbon dioxide in natural circulation and in processes influenced by man. Until now fossil raw materials (coal, oil, gas) have been used to generate energy (route A) and to synthesize chemicals (route B). The burning of fossil fuels to generate energy forms carbon dioxide, which is converted by photosynthesis (route C) into biomass; this biomass finds little use in chemical synthesis, except for a few special applications (route D). The greater part of the biomass is involved in natural circulation; most plants die and are reconverted into carbon dioxide and water by microorganisms in the soil, but some are eaten by man and animals and converted into CO_2 by respiration. Route E shows the formation of fossil fuels from organic sediments in the course of the earth's history.

Particularly important for industrial organic chemistry is route F, the direct transformation of carbon dioxide into carbon-containing chemicals, which can then be reconverted into CO_2 after use (route G). There are only four important large-scale industrial processes in which carbon dioxide is used for organic syntheses:[13] the synthesis of urea, of cyclic carbonates, of salicylic acid (the Kolbe–Schmitt process), and of methanol (Fig. 2).

[*] Priv.-Doz. Dr. A. Behr [+]
Institut für Technische Chemie und Petrolchemie
der Technischen Hochschule
Worringer Weg 1, D-5100 Aachen (FRG)

[+] New address:
Henkel KGaA
Postfach 1100, D-4000 Düsseldorf 1 (FRG)

 © VCH Verlagsgesellschaft mbH, D-6940 Weinheim, 1988 0570-0833/88/0505-0661 $ 02.50/0

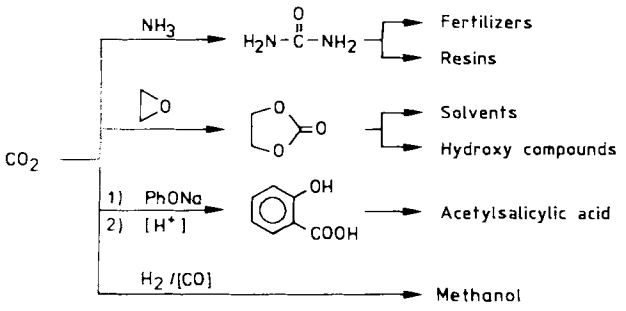

Fig. 2. Industrial organic syntheses with carbon dioxide.

Increased use of carbon dioxide will only be possible if the relatively inert carbon dioxide molecule can be activated. This goal can be achieved with the aid of transition-metal catalysts that lower the activation energy of CO_2 reactions and thus considerably increase the reaction rate. Figure 3 shows (purely schematically) how such a metal catalyst M can influence the bonding of CO_2 to an arbitrary substrate Su. For instance, step I might be the coordination of the substrate to the metal, forming a reactive complex; this could react with the carbon dioxide (step II), followed by elimination of the required molecule Su-[CO_2] (step III) and reformation of the starting complex (step IV). An alternative mechanism is the prior bonding of carbon dioxide to the metal catalyst (step V) and subsequent reaction with the substrate (step VI). Equally possible is the simultaneous coordination of CO_2 and substrate to the metal (step VII).

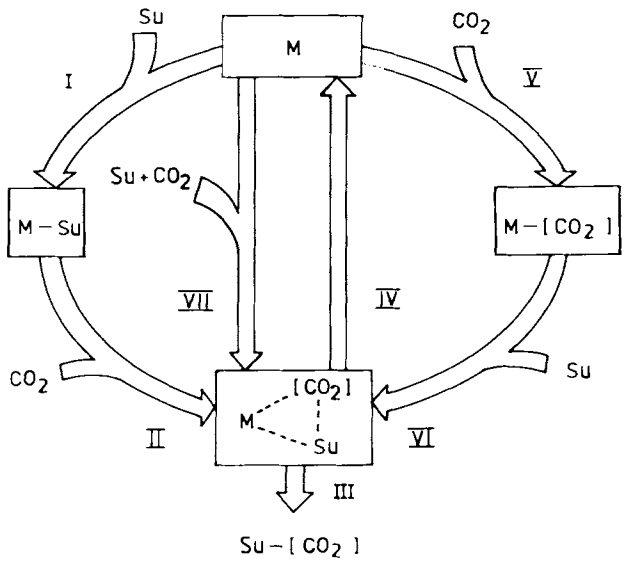

Fig. 3. Possible steps in the reaction of CO_2 with a substrate Su at a transition metal M.

This article will discuss the most important of these reaction steps in more detail:

- the coordination of CO_2 to the transition-metal complex (step V)
- the simultaneous coordination of CO_2 and substrate to the transition-metal complex (step VII)
- the insertion of CO_2 into the M-Su bond (step II)
- the catalytic combination of CO_2 with the substrate (steps III, IV)

2. Coordination of Carbon Dioxide to Transition-Metal Complexes

Carbon dioxide is a molecule with several potential reactive sites: the carbon is a Lewis acid center and the oxygens are weak Lewis bases. The carbon can thus be described as an electrophilic center and the oxygen atoms as nucleophilic centers. In addition, the molecule in its ground state possesses two equivalent C-O π bonds that could also play a role in bonding to a transition-metal center. This polyfunctionality of CO_2 leads to a wide variety of *potential* transition-metal CO_2 complexes (Table 1).

If a metal center reacts with one molecule of carbon dioxide, adducts **1** to **5** can be formed. Type **1**, with a metal-carbon bond, is sometimes termed a metallacarboxylate; electron-rich metal centers should be particularly suitable for forming this sort of bond. Structures **2** and **3** (side-on bonding) are very similar to each other, since the spatial arrangement of the atoms is comparable and only the bonding type (three-membered metallacycle or π complex) varies. Adducts **4** (end-on) seem less probable, because the coordination would be solely through the lone pair of an oxygen atom.

Since carbon dioxide displays up to three potential bonding modes, it is possible that more than one transition-metal center (perhaps different elements) could coordinate to one CO_2 molecule. Table 1 shows some examples (structures **6** to **11**) where two metal centers form adducts with one CO_2 molecule. Conversely, two molecules of CO_2 could in principle bind to one metal center (structures **12** to **19**). A further possibility is that two CO_2 ligands in the coordination sphere of the metal could bond to each other. Structures **20** to **24** are examples where metals and CO_2 combine to form rings or chains.

Many transition-metal CO_2 complexes have been described in the literature. It should however be noted that, especially in the older work, the identification of the complexes was solely on the basis of their IR spectra, which in some cases led to errors. An unambiguous classification of isolated CO_2 complexes according to the structural categories **1** to **24** is usually only possible if an X-ray structure analysis is carried out. Some CO_2 complexes for which this is indeed the case will now be described.

The first example of type **1** was the rhodium complex **25**, isolated by *Herskovitz* and his co-workers.[14,15] It is

[Rh(η^1-CO_2)Cl(diars)$_2$] **25**

likely that the η^1 bonding of CO_2 is stabilized by additional C-H···O interactions with the ligand 1,2-bis(dime-

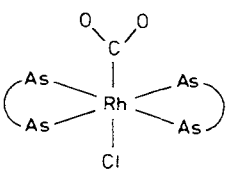

25

Table 1. Potential coordinations of carbon dioxide to transition-metal centers M.

Ratio metal: CO_2	Electron transfer metal → C	Electron transfer metal → C and O → metal	Formation of a π complex	Electron transfer O → metal
1 : 1	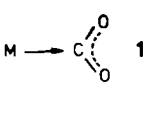 1	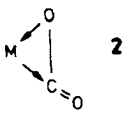 2	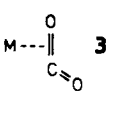 3	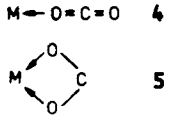 4 5
2 : 1	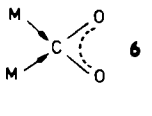 6	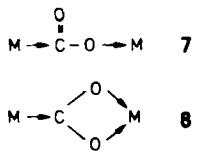 7 8	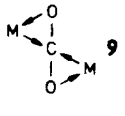 9	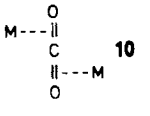 10	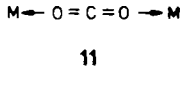 11
1 : 2	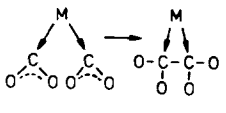 12 13	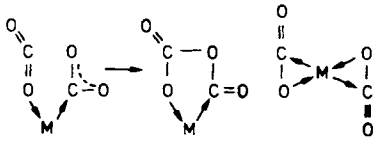 14 15 16	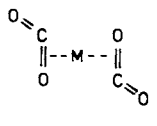 17	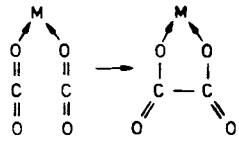 18 19
n : m	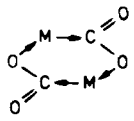 20	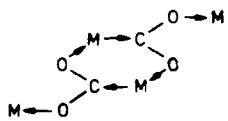 21	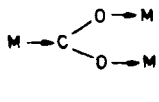 22	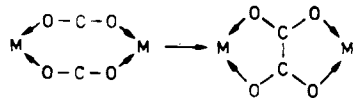 23 24

thylarsino)benzene (diars). In the iridium complex $[Ir(CO)_2Cl(dmpe)_2]$ (dmpe = 1,2-bis(dimethylphosphino)ethane) CO_2 is probably also η^1-coordinated.[16,17] Since the oxygen atoms remain accessible in this type of complex, reactions of the coordinated carbon dioxide are possible, e.g., the addition of a methyl cation [Eq. (2)]. This reaction is an example of step VI shown in Figure 3 with the methyl cation as "substrate."

$$[Ir(CO_2)Cl(dmpe)_2] + FSO_3Me \longrightarrow [Ir(CO_2Me)Cl(dmpe)_2]FSO_3 \quad (2)$$

In 1975 *Aresta* and his co-workers assigned the structure type **2/3** to the nickel complex **26** (Cy = cyclohexyl).[18,19]

$[Ni(CO_2)(PCy_3)_2]$ **26**

The niobium complex $[Nb(CO_2)(C_5H_4Me)_2(CH_2SiMe_3)]$ and the molybdenum complex $[Mo(CO_2)Cp_2]$ (Cp = cyclopentadienyl) also belong to this structure type.[20,21] They are examples of the ability of the earlier "oxophilic" transition metals to form stable CO_2 complexes.

Many structural variants are possible if two transition-metal centers are available for bonding. The structure **7** has been suggested for the iridium-osmium complex **27** (L = pyridine), prepared from Vaska's complex $[IrCl(CO)(PPh_3)_2]$ and osmium tetroxide in the presence of pyridine.[22] In this binuclear complex the bridging CO_2 ligand is formed from CO and oxygen. An X-ray structure analysis is available for the complex obtained by methylation of the exocyclic oxygen of the bridging CO_2 in **27** with methyl trifluoromethanesulfonate.

Fewer cases are known in which two CO_2 molecules are bound to the same transition-metal center. One example is the iridium complex **28** isolated by *Herskovitz* and his coworkers; the carbon of one CO_2 molecule is bonded to the oxygen of the second (structure **15**).[23,24] This type of CO_2 dimerization in the coordination sphere of the transition-metal center is known as "head-to-tail bonding." The authors assume that the uptake of CO_2 occurs stepwise and that the first CO_2 molecule binds to iridium through carbon.

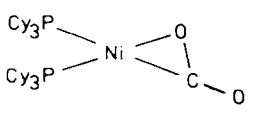

26

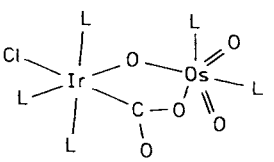

27

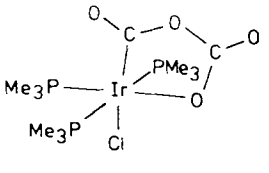

28

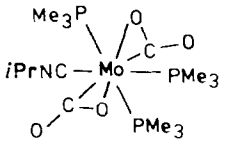

29

A further example is the molybdenum complex **29**, as described by *Carmona* et al.[25,26] Both CO_2 molecules are bonded "side-on" and are *trans* to each other. This structural type can, in simplified form, be represented by formulas **16/17**.

With a view to the use of carbon dioxide in syntheses it is interesting to look for complexes in which two carbon dioxide molecules are bonded "head-to-head" through their carbon atoms. This linkage leads to oxalato complexes and could represent a first step in a catalytic conversion of carbon dioxide to oxalic acid. *Fröhlich* et al. succeeded in 1983 in preparing the binuclear titanium oxalato complex $[Cp_2Ti(C_2O_4)TiCp_2]$ (structure type **24**) via such a dimerization of CO_2.[27] The synthesis of mononuclear oxalato complexes (corresponding to structure **19**) from carbon dioxide has not been reported.

It remains to describe those structural types in which several metal centers combine with carbon dioxide to form ring structures. A μ_3-CO_2 bridge of the type **21** was demonstrated in the rhenium complex **30**.[28] This complex is not formed directly from CO_2, however, but from several "$Re(CO)_5OH$" units by elimination of water. Structure type **22** also contains a μ_3-CO_2 bridge. To this group belongs the cobalt complex **31**, synthesized by *Floriani* and his co-workers, in which the carbon atom is bonded to the transition-metal center and each oxygen enters into interactions with at least one potassium ion.[29-33] This structure is an interesting example of "bifunctional" CO_2 activation by a combination of basic and acid metal centers. It is notable that complex **31** functions as a reversible CO_2 carrier and that the Co-C bond is easily broken. Finally, complex **32** is presented as an example of structure type **22**, in which the metal atom assembly is homonuclear.[34,35]

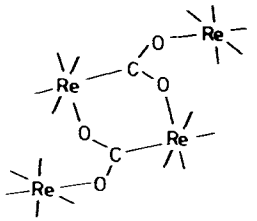

30

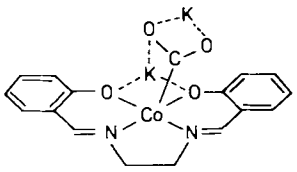

31

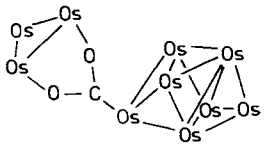

32

By far the most important synthetic reactions of CO_2 complexes are substitution and addition reactions, which also play a decisive role in homogeneous transition-metal catalysis. It is also striking that the synthetic reactions generally occur under mild conditions, nearly always at room temperature and normal pressure. Homogeneous, transition-metal-catalyzed reactions also generally take place at low pressures and temperatures.[36-43] These observations suggest that the use of carbon dioxide in homogeneously catalyzed processes is likely to be successful.

In catalytic reactions of carbon dioxide, the CO_2 molecule bonds to a substrate Su in the coordination sphere of a transition metal (cf. Fig. 3). This can occur by simultaneous oxidative coupling of CO_2 and substrate as they add to the metal (step VII in Fig. 3). It is equally possible that CO_2 inserts into a previously formed M-Su bond (step II in Fig. 3). More detailed investigations of these important potential catalytic steps are presented in Sections 3 and 4.

3. Oxidative Coupling with Carbon Dioxide

Oxidative coupling is an important basic reaction in stoichiometric carbon dioxide chemistry; it leads to products that have been postulated as intermediates in catalytic processes. In the following discussion oxidative coupling is understood to be a reaction of carbon dioxide in which a metal center M, an unsaturated compound X = Y, and CO_2 react together to form a metallacycle [Eq. (3)].

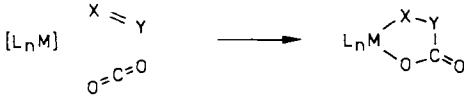

(3)

In all known examples of this type of compound, the oxygen of the CO_2 molecule binds to the metal center, not the carbon. The principle of oxidative coupling has been known for a long time; *Wilkinson* and his co-workers described the reaction of platinum phosphane complexes with oxygen and carbon dioxide in 1967. They obtained a peroxycarbonato complex [Eq. (4)] as well as a carbonato complex[44-48]. Similar reactions have been described for rhodium.[49,50]

(4)

A reaction that has already been presented in Section 2 is the joining of two CO_2 molecules at an electron-rich iridium center, forming the complex **28**.[23,24] This also can be regarded as an oxidative coupling [Eq. (5)].

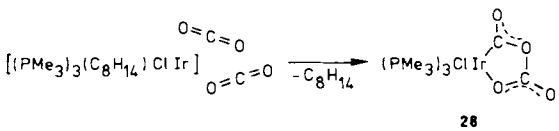

(5)

28

A more detailed investigation of oxidative coupling with CO_2 has been in progress since the beginning of the 1980s. It has been shown that, besides the O-CO_2 bond formation discussed above, N-CO_2 and C-CO_2 bonds can also be formed. The predominant transition-metal compounds were electron-rich Ni^0 complexes.

The reaction of carbon dioxide with aliphatic aldehydes in the presence of (2,2'-bipyridine)(1,5-cyclooctadiene)nickel(0), [Ni(bpy)(cod)], proceeds at room temperature and normal pressure to form an NiC_2O_2 ring [Eq. (6)].[51,52]

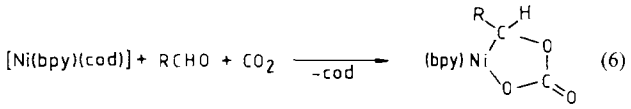

(6)

Analogous reactions, but this time with C–N bond formation, occur with azaolefins RCH=NR'.[53–56] The use of carbodiimides[57] or azadienes[58] also leads to N–C bond formation. *Cenini* and his co-workers observed an oxidative coupling of CO_2 with an η^2-bonded nitrosobenzene ligand [Eq. (7)].[59,60]

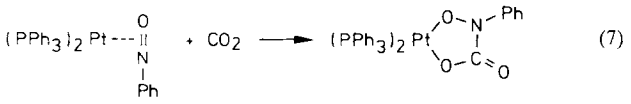

(7)

A C–C bond is formed when alkynes (e.g., acetylene, 2-butyne, or tolane) are allowed to react with carbon dioxide and nickel complexes;[61–63] oxanickelacyclopentene derivatives are formed in yields of between 40 and 90%. Olefins can be used instead of alkynes. Open-chain and cyclic olefins both lead to oxanickelacyclopentanes, which can either be isolated as complexes or identified on the basis of the products obtained by acidic decomposition.[63–67] The oxidative coupling with olefins is exemplified by the following reactions with cycloalkenes.[68] The reaction of the four-membered ring bicyclo[4.2.0]octatriene, which is in equilibrium with cyclooctatetraene, leads to an oxidative coupling of both isomers with CO_2 [Eq. (8)]. A mixture of the nickel complexes **33** and **34** is formed; these are de-

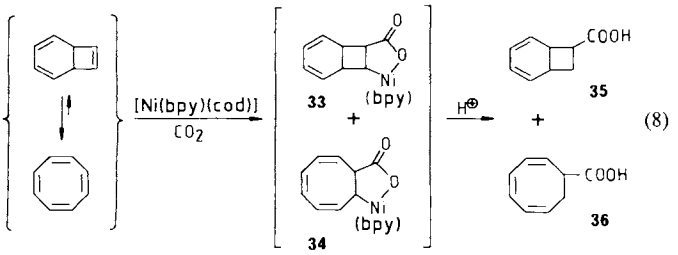

(8)

composed by hydrochloric acid, giving the carboxylic acids **35** and **36**. Dicyclopentadiene was employed as a "five-membered ring molecule"; it possesses two rings with greatly differing reactivities. Equation 9 shows that the norbornene double bond undergoes an oxidative coupling with CO_2 and nickel to form complexes **37** and **38**, which yield the diastereomeric carboxylic acids **39** and **40**

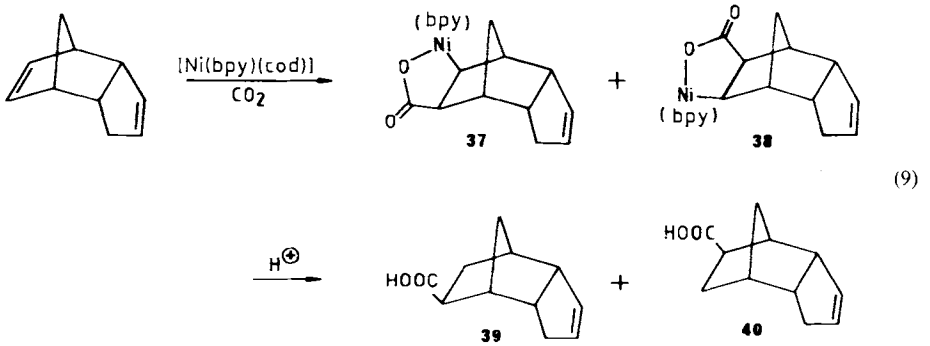

(9)

on treatment with hydrochloric acid. *Walther, Dinjus,* and their co-workers were able to show that conjugated dienes also react with carbon dioxide at nickel(0) complexes.[69–73] In contrast to the five-membered metallacycles described above, complexes with a dianionic ligand are formed, which contain an η^3-coordinated allyl group and a carboxylate group [Eq. (10)]. This C–C bond formation can be explained in terms of an initial η^2 coordination of the 1,3-diene. With L^L = tetramethylethylenediamine and with 2,3-dimethylbutadiene as diene a crystalline complex was obtained; a crystal structure analysis showed[71] that the monodentate carboxylate group, the allyl C atoms, and a nitrogen atom of the chelating ligand coordinate the nickel in a plane, whereas the second nitrogen atom interacts only weakly with the metal.

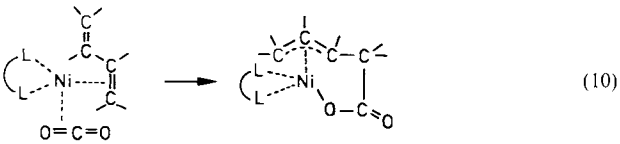

(10)

The hydrolysis of the complexes obtained according to Equation (10) with dilute mineral acids leads to 3-pentenecarboxylic acids. The idea of obtaining carboxylic acids from oxidative coupling of 1,3-dienes and carbon dioxide has formed the basis for intensive study. 1,3-Pentadiene can be converted into sorbic acid[74] (after workup with maleic anhydride) and butadiene into 2,4-pentadienecarboxylic acid.[75] In the presence of pyridine, reaction with a further CO_2 molecule yields an α,ω-dicarboxylic acid.[76]

Since both alkenes and 1,3-dienes can react with carbon dioxide at nickel(0) complexes, it is interesting to consider how a molecule with both functional groups would react. The reaction of 1,3,7-octatriene with (bipyridine)(cyclooctadiene)nickel and carbon dioxide leads to the nickel carboxylato complexes **41** and **42** (Scheme 1).[77] The decomposition of these complexes with HCl in methanol produces the monomethyl ester **43** and the dimethyl diester **44**. The nature of the products is evidence that the reaction takes place at the diene function of the starting material. The carboxylato complex **41a** containing an η^3-allyl group is formed by oxidative coupling of the diene analogously to Equation 10; **41a** is in equilibrium with **41b**, in which a Ni–C η^1 bond is present. A further molecule of CO_2 can insert into this bond, forming the dicarboxylato complex **42**. This reaction is an interesting example of an oxidative coupling and a CO_2 insertion occurring at the same nickel center.

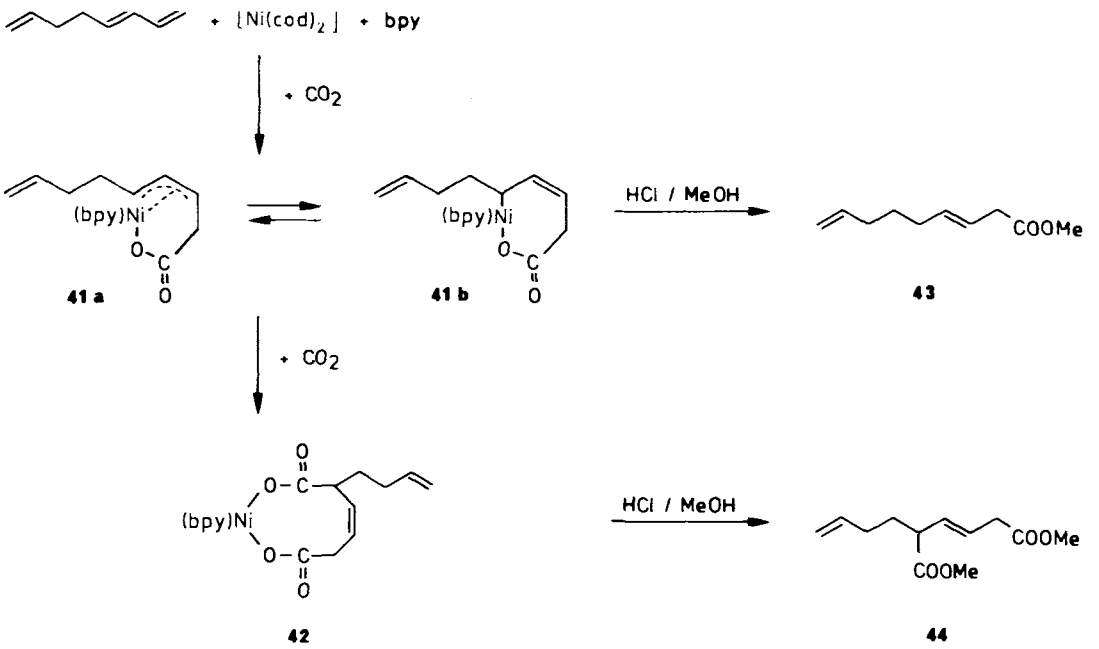

Scheme 1. Coupling of a molecule containing mono- and diene functions with CO_2.

4. Insertion Reactions of Carbon Dioxide

In the last two decades, many insertion reactions of carbon dioxide into M–C, M–H, M–O, and M–N bonds have been described in the literature. Scheme 2 provides a survey of some of the products.

The insertion of CO_2 into the M–C bond generally leads to a carboxylato complex via the formation of a new C–C bond. Insertions in the opposite sense, forming a new C–O bond and thus a 1-metalated formate ester, have only been observed in a few special cases. Similarly, the insertion into M–H bonds can lead to either formato complexes or 1-metalated formic acids. Insertion into M–O bonds preferentially forms alkyl or aryl carbonato complexes; insertion into M–N bonds forms carbaminato complexes.

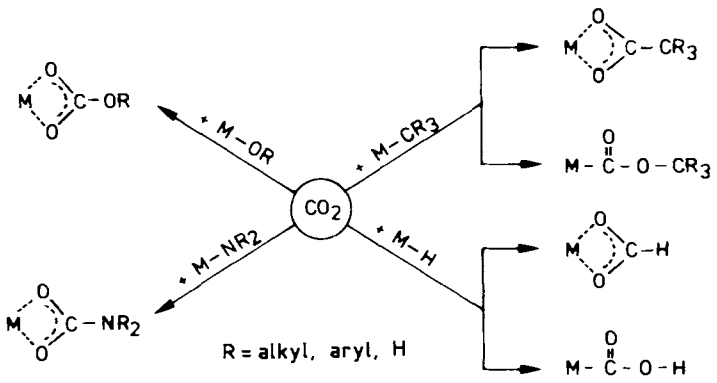

Scheme 2. Adducts formed by insertion of CO_2 into M–X bonds (X = H, O, N, C).

Several review articles covering these insertion reactions have been published.[78–85] Here we shall discuss CO_2 insertion in terms of some typical examples, showing the wide range of applications of this reaction type.

4.1. CO_2 Insertion into the M–H Bond

In insertion reactions the first step is the coordination of CO_2 to the M–X fragment (X = H, O, N, C). In the case of metal hydrido complexes, hydridometal–CO_2 intermediates can be formed (Scheme 3), which then rearrange by hydrogen migration to formato complexes (path A) or 1-metalated formic acids (path B).

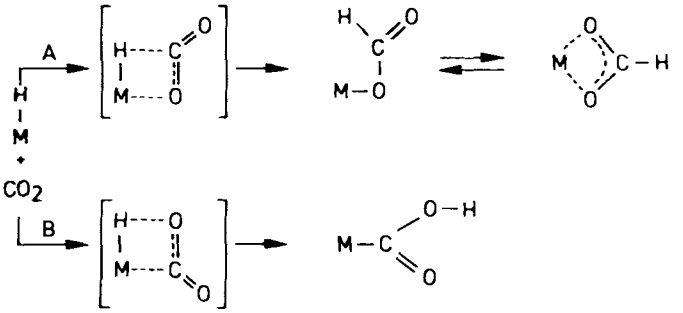

Scheme 3. Insertion of CO_2 into the M–H bond.

Most transition-metal hydrido complexes react with CO_2 to give formato complexes. Important examples are the hydridometal carbonyls $[MH(CO)_5]^{\ominus}$ (M = Cr, Mo, W)[86–88] as well as hydrido complexes of rhenium,[89,90] iron,[91] ruthenium,[92–94] and copper.[95,96] There is only one piece of indirect evidence for the existence of a 1-metalated formic acid: *Kolomnikov, Volpin,* and their co-workers found such a species in a yield of 17% from the reaction of a nitrogencobalt complex with CO_2.[78,97] As seen from Equation 11, the identification was based on the product

$$[Co(N_2)H(PPh_3)_3] + CO_2 \xrightarrow[-N_2]{} [Co(COOH)(PPh_3)_3] \xrightarrow{MeI} \xrightarrow[BF_3]{MeOH} Me-COOMe \quad (11)$$

of subsequent reaction with methyl iodide and methanol/BF_3. However, the reactions of hydridocobalt complexes with CO_2 generally lead to formato complexes.[98,99]

Transition-metal hydrido complexes are not limited to the formation of $M(O_2CH)$ or M-COOH complexes on reaction with CO_2, as demonstrated by the following examples.

The hydridozirconium complex $[ZrCp_2ClH]$ reacts with excess CO_2 to form $[(ZrCp_2Cl)_2O]$ and formaldehyde.[100-102] A reduction of the hydrido complex to the zirconium methanolato complex can be achieved by using the hydrido complex in excess. The different reaction products may be formed via a binuclear intermediate with an $O-CH_2-O$ bridge [Eq. (12)].

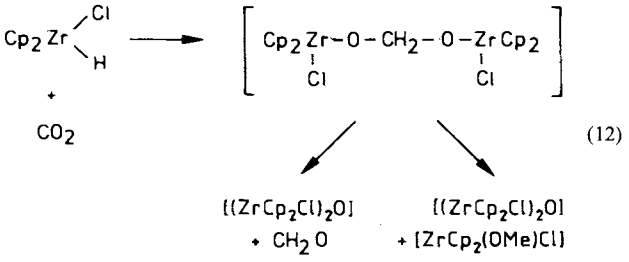

(12)

Another unusual reaction was studied by *Eisenberg* et al.; a hydrido-bridged dirhodium complex reacts with CO_2 to form a dirhodium complex with a formato bridge [Eq. (13)].[103]

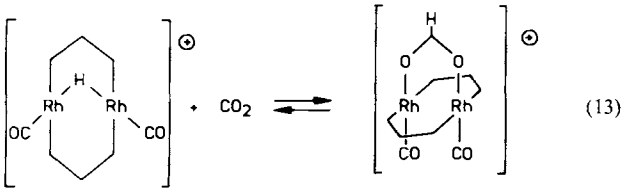

(13)

The reaction of CO_2 with hydridoplatinum complexes allowed an interesting observation; starting from the complexes $[PtH_2L_2]$ in benzene or toluene, a monoformato complex is obtained,[104] whereas in acetone or acetonitrile a binuclear cationic complex with a free formate counterion is formed [Eq. (14), $L = PEt_3$].[105]

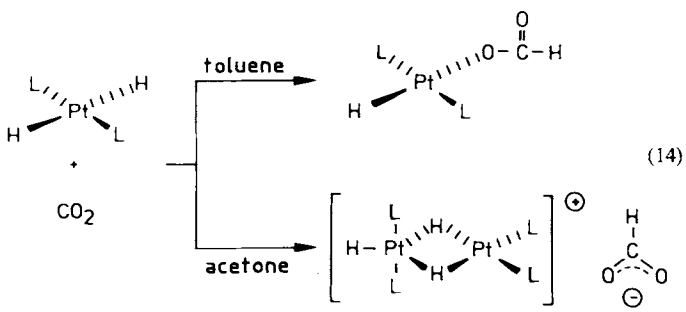

(14)

4.2. CO_2 Insertion into the M-O Bond

A variety of transition-metal complexes with M-OR groups undergo insertion reactions with CO_2. If R is an organic moiety, alkyl or aryl carbonato complexes are formed (cf. Scheme 2); if R is hydrogen, hydrogen carbonato species are obtained. Examples of alkyl carbonato complexes thus obtained are known for zirconium,[106] vanadium,[107] tantalum,[108] molybdenum,[109] and tungsten,[110] and also for the lanthanoids.[111] Alkyl carbonato complexes can be synthesized "in situ" from a suitable precursor complex, an alcohol, and carbon dioxide.[104,112-114] Hydrogen carbonato complexes have been established for (in particular) rhodium and iridium.[115,116] In some cases the formation of metal carbonato complexes was also observed.[117,118] An interesting dimeric carbonato complex, in which the CO_3 ligand functions as an η^1,η^1-bridging group, is obtained from the reaction of the hydroxoplatinum complex $[PtPhL_2(OH)]$ with CO_2 [Eq. (15), $L = P(CH_2Ph)_3$].[119]

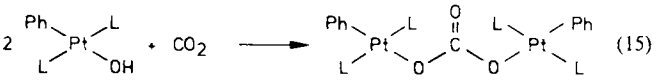

(15)

The insertion of CO_2 into copper alkoxo complexes is worthy of particular attention in this respect. It leads not only to the expected alkyl carbonato complexes,[120,121] but also, by various routes, to a copper hydrogen carbonato complex[122,123] that decarboxylates in water or organic solvents and transfers the released CO_2 to an organic substrate. Scheme 4 shows the reaction with cyclohexanone as an example of such a transcarboxylation. The copper hydrogen carbonato complex functions here as a reversible CO_2 carrier, which could win importance in catalytic reactions.

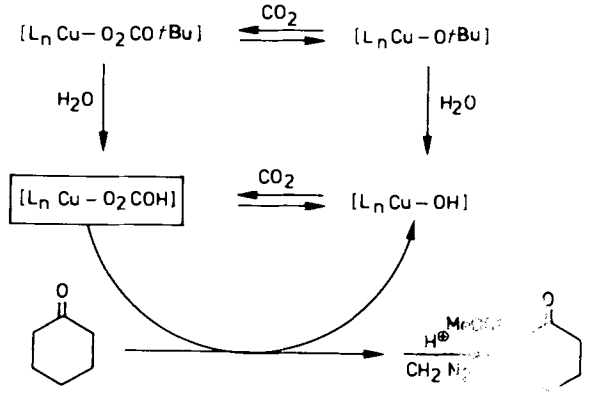

Scheme 4. Insertion of CO_2 into copper alkoxo complexes. L = [illegible]

4.3. CO_2 Insertion into the M-N Bond

Many examples of insertion of CO_2 into M-N bonds are known for the early transition metals (as was also [illegible] to be the case for insertion into M-O bonds). Metal carbaminato complexes are formed in nearly all such reactions (cf. Scheme 2). *Chisholm* and *Extine* investigated CO_2 insertion into dimethylamine complexes of titanium and zirconium and observed a rapid exchange of ^{13}C-labeled carbon dioxide [Eq. (16)].[124,125] The carbon dioxide is obviously only loosely bound; the carbaminato complexes, like the copper hydrogen carbonato species shown in Scheme 4, may be considered to be "CO_2 carriers."

$$[Ti(NMe_2)_4] \xrightarrow{^{13}CO_2} [Ti(O_2{}^{13}C\text{-}NMe_2)_4] \qquad (16)$$
$$\xrightarrow{^{12}CO_2} [Ti(O_2{}^{12}C\text{-}NMe_2)_4]$$

CO_2 insertion into the M–N bond has been investigated not only for metals of the titanium group,[126–128] but also for metals of the vanadium[129] and chromium groups.[130–134] Mechanistic studies show that small amounts of free amine accelerate the reactions markedly. It may thus be assumed that amine and CO_2 form a carbamic acid, which then, in a second step, reacts with the metal amine complex [Eq. (17)]. This would imply that the reaction should strictly be classified as a ligand exchange rather than a CO_2 insertion.

$$Me_2NH + CO_2 \rightleftharpoons Me_2NCOOH \qquad (17)$$
$$\xrightarrow{+[M\text{-}NMe_2]} [M\text{-}O_2CNMe_2] + Me_2NH$$

Reactions of CO_2 with amine complexes are also known for the metals uranium,[135] rhenium,[136] zinc,[113,137] and copper,[121,138–140] but not for the metals of the iron, cobalt, and nickel groups. The carbaminato complexes of the noble metals are however accessible by an indirect synthetic route, namely the reaction of metal complexes with amines and CO_2; the ruthenium hydrido complex $[RuH(PR_3)_5]PF_6$ reacts with dimethylamine and carbon dioxide to form the carbaminato complex $[Ru(O_2CNMe_2)(PR_3)_4]PF_6$ (R = Me, Ph), and the dimethylpalladium complexes $[PdMe_2L_2]$ react similarly to give $[PdMe(O_2CNMe_2)L_2]$ (L = PR_3).[141,142]

4.4. CO_2 Insertion into the M–C Bond

As shown in Scheme 2, there are two modes of CO_2 insertion into complexes with an M–C bond (as already noted for the M–H bond); the "normal" insertion to form a carboxylato complex and the "inverse" insertion to form a 1-metalated formate ester. However, this is a somewhat oversimplified description; CO_2 insertion into the M–C bond will be considered here in more detail.

4.4.1. Insertion into Metal–Aryl and Metal–Alkyl Bonds

The insertion of CO_2 into aryltitanium complexes was investigated in the 1970s.[143–145] *Kolomnikov* et al. observed the formation of the metallacycle **45** (Scheme 5) by the reaction of diphenyltitanocene with CO_2; the product was identified by X-ray structure determination. An arynetitanium complex was assumed to be an intermediate. Treatment of the crude product with methanol/BF_3 leads not only to the expected methyl benzoate but also to small quantities of dimethyl phthalate, the product of a double insertion.

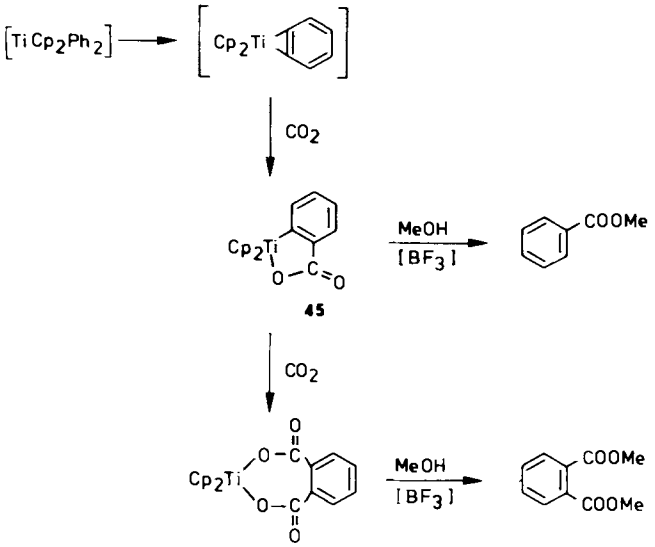

Scheme 5. Insertion of CO_2 into diphenyltitanocene.

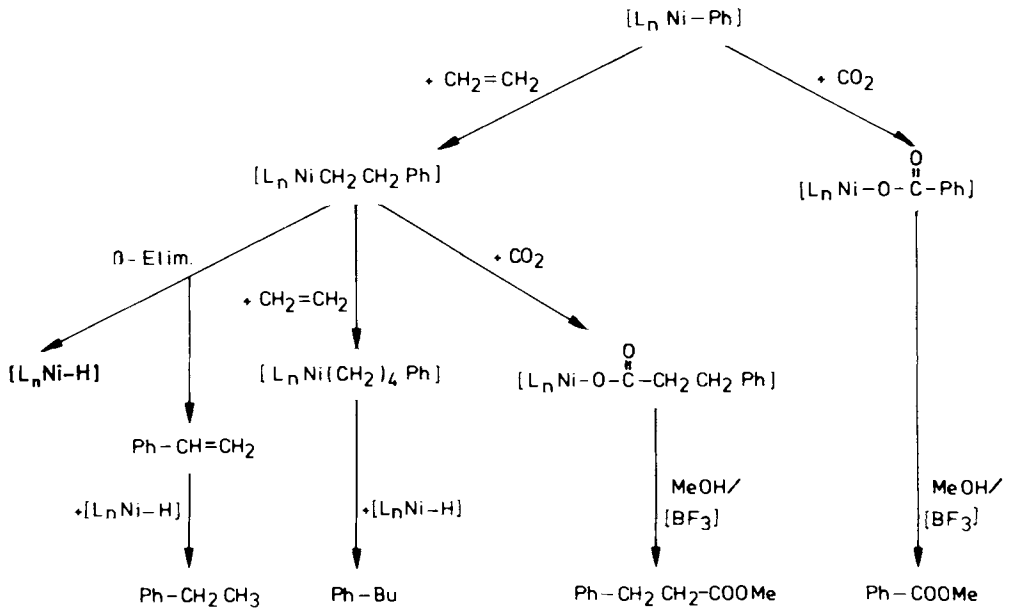

Scheme 6. Reactions with phenylnickel complexes. For L see [146].

Phenylnickel complexes can also undergo CO_2 insertion to form nickel benzoato complexes, which are then esterified to release methyl benzoate (Scheme 6). It is also known that ethene can insert into the nickel–phenyl bond. A (2-phenylethyl)nickel complex is formed, which undergoes β-elimination of styrene. Double insertion leads to a (4-phenylbutyl)nickel complex; the subsequent elimination product, *n*-butylbenzene, was also identified.

Particular attention should be drawn to the first example of a combined insertion of ethene and carbon dioxide.[146] The initial product may be the (2-phenylethyl)nickel complex, into whose Ni–C bond the CO_2 then inserts. The subsequent treatment with methanol/BF_3 releases methyl β-phenylpropionate (Scheme 6).

4.4.2. *Insertion into Metallacycloalkanes*

Insertion reactions of CO_2 into metallacycloalkanes are important because metallacycles are often postulated as intermediates in numerous transition-metal-catalyzed reactions forming C–C bonds, e.g., the dimerization of cyclopropene derivatives and methylenecyclopropane,[147] the oligomerization of allene,[148] and the dimerization of ethene.[149]

The nickelacyclobutane **46** is presented as an example of a metallacycle that undergoes insertion reactions; it is generated "in situ" from (bipyridine)(cyclooctadiene)nickel(0) and quadricyclane (Scheme 7). Its reaction with CO_2 at room temperature forms the nickel carboxylato complex **47** in 92% yield.[68] The decomposition of **47** with acid releases the *endo*-nortricyclane-3-carboxylic acid **48**.

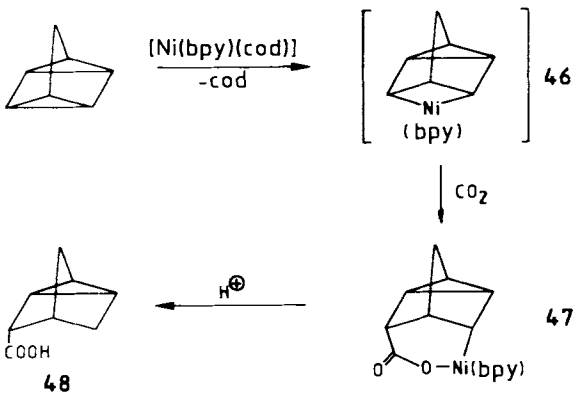

Scheme 7. Insertion of CO_2 into a nickelacycle.

The manganaphosphacyclobutane **49** reacts with CO_2 to form the insertion product **50** in yields of up to 40% [Eq. (18)].[150]

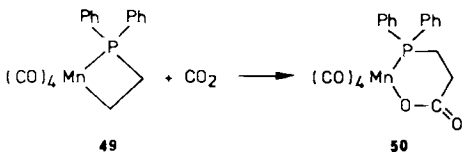

(18)

Whereas the manganacyclobutane forms a six-membered ring on CO_2 insertion, an analogous insertion into the manganaphosphacyclopentane (to form a seven-membered ring) does not occur. However, complexes of other transition metals—e.g., anionic complexes of tungsten [Eq. (19)]—form seven-membered rings of sufficient stability.[151]

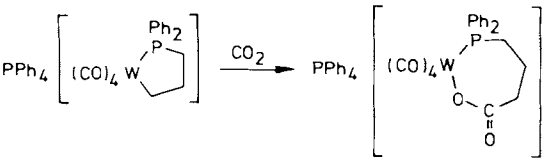

(19)

4.4.3. *Insertion into M–C Bonds Generated in situ*

In Sections 4.4.1 and 4.4.2 carbon dioxide insertion reactions into η^1 transition-metal–carbon bonds of well-defined complexes were described. The possibility of generating the M–C bonds in situ, by oxidative addition of cycloalkanes to transition-metal complexes, was also mentioned (see Scheme 7). Here a further "in situ" method is presented; oxidative addition of compounds with acidic C–H functions can lead to intermediate alkylmetal complexes that then undergo CO_2 insertion.

Ittel, Tolman et al.[152] studied a hydrido-naphthyl complex of iron, to which $^{\ominus}H_2CCN$ (from MeCN) could be added oxidatively, naphthalene being eliminated. The insertion of CO_2 into the resulting Fe–C bond led to a carboxylato complex, which was identified spectroscopically and which reacted with methanol/BF_3 to give methyl cyanoacetate [Eq. (20)]. An analogous reaction in iridium chemistry was described by *English* and *Herskovitz*.[153] These reactions demonstrated the feasibility of forming C–C bonds between acidic hydrocarbons and carbon dioxide in the presence of transition-metal complexes.

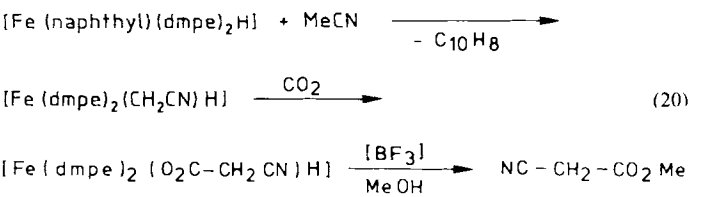

(20)

In order to understand this reaction type better, further experiments were carried out using iridium and rhodium complexes and the strongly C–H-acidic malonodinitrile.[154] The complex **51** can be isolated from the reaction between hydridotetrakis(trimethylphosphane)iridium and equimolar amounts of malonodinitrile and carbon dioxide [Eq. (21)].

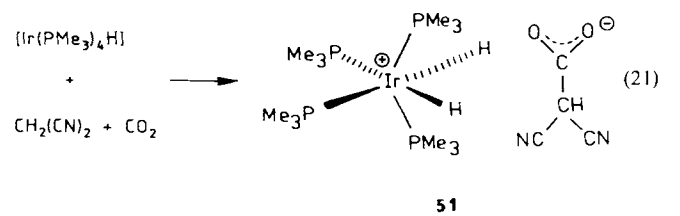

(21)

The distorted tetrahedral arrangement of the phosphane ligands inferred from spectroscopic data was confirmed by an X-ray structure analysis (Fig. 4); this also showed that the dicyanoacetate is dimeric. The central carbon atom,

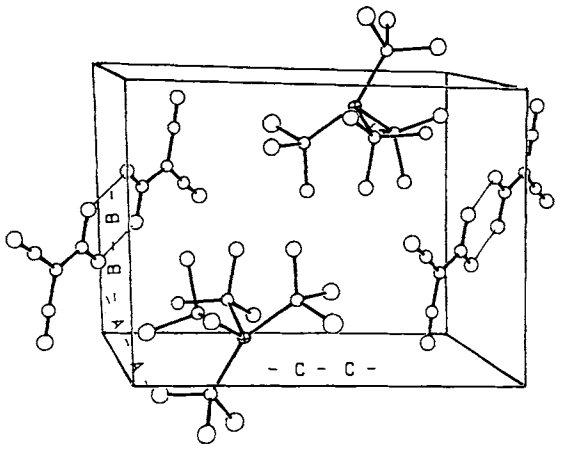

Fig. 4. Unit cell and molecular structure of complex **51**.

which bears the cyano and carboxylate groups, is sp^2-hybridized [see also Eq. (23)], and the distance of 258 pm between oxygen atoms in neighboring monomeric units is typical of carboxylic acid hydrogen bonding.

The formation of C–C bonds between malonodinitrile and CO_2 takes place not only with metal hydrido complexes but also with metal chloro complexes, e.g., $[Ir(depe)_2Cl]$ (depe = bis-1,2(diethylphosphino)ethane). In this case, however, octahedral complexes are formed in which the chloro ligand and the newly added hydrogen atom are mutually *trans* [Eq. (22)].

$$\left.\begin{matrix}[Ir(depe)_2]Cl \\ [Rh(dmpe)_2]Cl\end{matrix}\right\} \xrightarrow[CO_2]{CH_2(CN)_2} \quad (22)$$

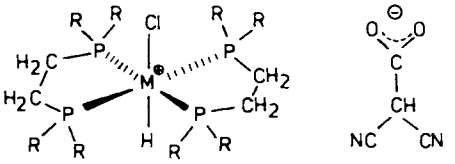

52 : M = Ir, R = Et

53 : M = Rh, R = Me

The generalized Equation (23) summarizes the reactions of the iridium and rhodium complexes with malonodinitrile and carbon dioxide. The first step is the formation of a positively charged metal hydrido complex, stabilized in solution by a dicyanoacetate counterion. Malonodinitrile and CO_2 then undergo the expected C–C bond-forming reaction; however, they do not, as previously assumed, remain bonded to the transition metal as a ligand, but form a free anion in solution. On crystallization, a further remarkable feature is observed; the methine proton of the dicyanoacetate migrates to a carboxylate oxygen and forms a C-deprotonated acid that dimerizes by hydrogen bond formation.

$$[L_nM] + CH_2(CN)_2 + CO_2 \longrightarrow \left[[L_nM\text{-}H]^{\oplus}[(CN)_2CHCOO]^{\ominus}\right] \quad \text{in solution} \quad (23)$$

$$\left[[L_nM\text{-}H]^{\oplus}[(CN)_2CCOOH]^{\ominus}\right]_2 \quad \text{in the crystal}$$

M = Ir, Rh
L = PMe_3, dmpe, depe
n = 2, 4

The question arises as to how the reaction that forms the C–C bond actually proceeds. One possibility (path A in Fig. 5) involves the oxidative addition of the C–H-acidic

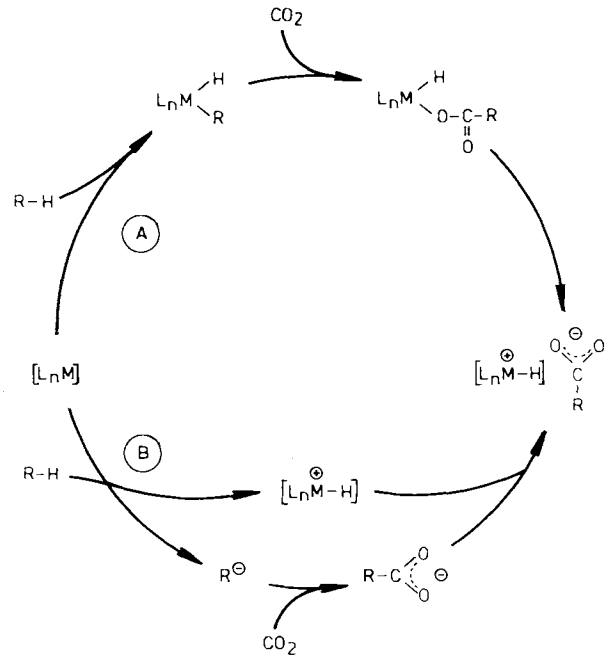

Fig. 5. Possible mechanisms in the reaction of C–H-acidic substrates with CO_2 in the presence of electron-rich transition-metal complexes.

compound R–H to the transition-metal complex L_nM, forming an alkyl-hydrido complex. The insertion of CO_2 into the metal–carbon bond then leads to a carboxylato-hydrido intermediate, which rearranges to the ionic species $[L_nMH]^{\oplus}[RCOO]^{\ominus}$ because of the electron-withdrawing effect of the R group. The second possible reaction path (B in Fig. 5) involves a proton transfer from R–H to the transition-metal complex L_nM, leaving a carbanion $R^{\ominus}$, which then reacts with the electrophilic CO_2 to form the anion $R\text{-}COO^{\ominus}$. Path B, which may be described as a "transition-metal-initiated" C–C bond formation, cannot be considered as a CO_2 insertion; it is however a feasible alternative explanation for the formation of the complexes $[L_nM]^{\oplus}[RCOO]^{\ominus}$.

4.4.4. Insertion into Metal–Olefin Bonds

CO_2 reacts with the bis(ethene)molybdenum complex $[Mo(C_2H_4)_2(PMe_3)_4]$ in a remarkable way.[155] This complex possesses an electron-rich metal center surrounded by labile trimethylphosphane ligands. Carbon dioxide reacts with the coordinated ethene, forming a new C–C bond, and the product is a binuclear molybdenum complex with two bridging acrylic acid ligands (Scheme 8). Hydrogenation leads to a hydrido-propionato complex, which on treatment with *n*-butyllithium and ethene releases lithium propionate and re-forms the starting complex. This reaction sequence is of particular interest because it outlines a possible future catalytic synthesis of industrially important acrylic acid from ethene and carbon dioxide.

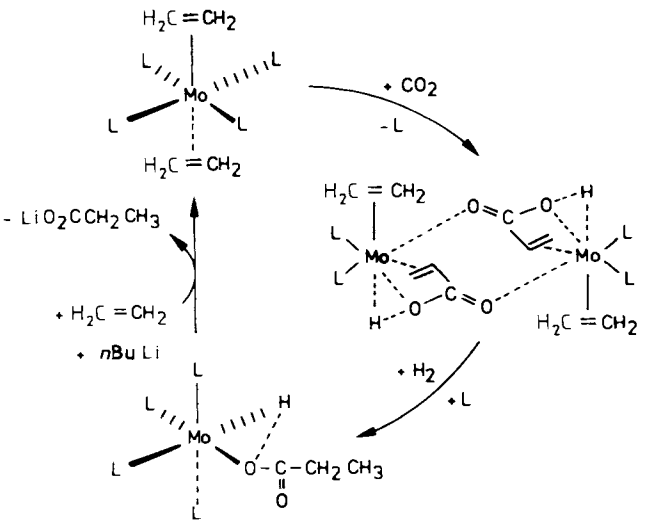

Scheme 8. Insertion of CO_2 into a Mo-ethene bond. L = PMe_3.

4.4.5. *Insertion into Metal–Allyl Bonds*

The insertion of CO_2 into η^3-allyl complexes of titanium has been studied in detail.[156–159] *Sato* et al. prepared the crotyltitanocene complex from $[TiCp_2Cl_2]$, butadiene, and a Grignard reagent (Scheme 9) and allowed it to react with CO_2 yielding a crotonato complex. Subsequent hydrolysis leads to 2-methyl-3-butenoic acid and $[TiCp_2Cl]$, which can be reconverted into $[TiCp_2Cl_2]$. This stoichiometric reaction sequence corresponds to a catalytic synthesis of

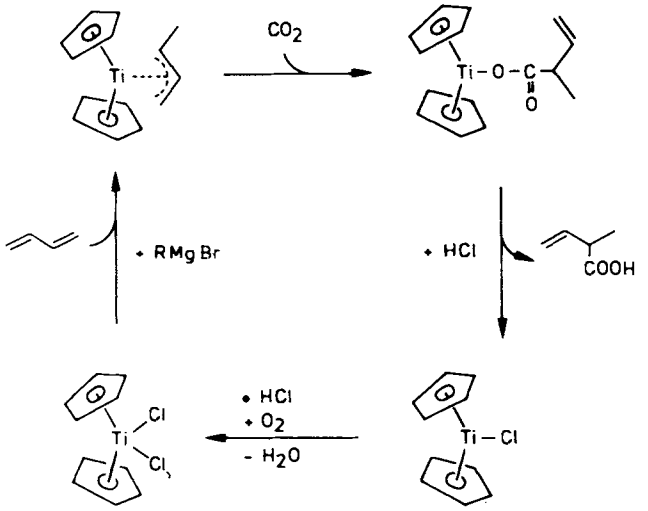

Scheme 9. Insertion of CO_2 into a titanium-allyl bond.

methylbutenoic acid from butadiene and CO_2, although HCl and Grignard reagent are consumed. Particularly notable is the fact that chiral cyclopentadienyl ligands cause an asymmetric insertion of CO_2; by use of a crotyltitanocene complex with a menthyl-substituted cyclopentadienyl ligand, the (*S*)-2-methyl-3-butenoic acid was formed with an optical yield of 18.9%.

Teuben et al. suggest an alternative electrocyclic mechanism, coupled with an allyl migration, for the reaction of the allyltitanium complexes with CO_2 [Eq. (24), R = H, CH_3].

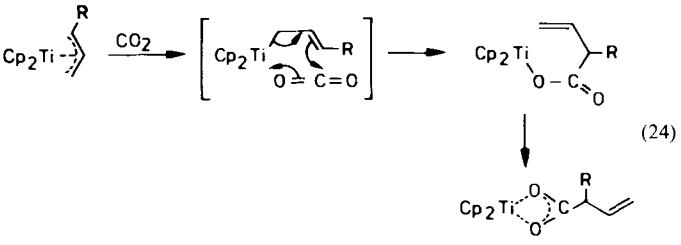

(24)

Bis(η^3-allyl)nickel reacts with CO_2 at room temperature, forming η^3-allyl(vinylacetato)nickel, which releases γ-butyrolactone on heating to 140°C [Eq. (25)].[160]

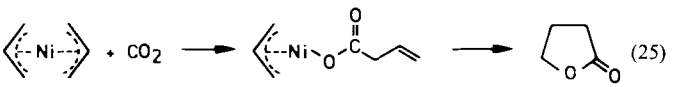

(25)

Jolly, Wilke et al. were able to show that bis(η^3-2-methylallyl)nickel reacts quantitatively with carbon dioxide at −30°C in the presence of basic phosphanes to form a carboxylato complex [Eq. (26)].[161]

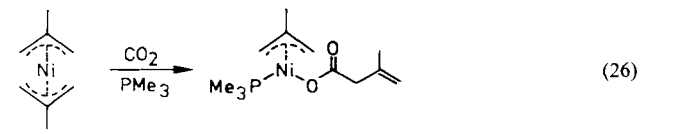

(26)

Allylpalladium complexes have also been treated with CO_2. *Ito* et al. carried out the reaction of bis(η^3-allyl)palladium and bis(η^3-crotyl)palladium with CO_2 and obtained the corresponding carboxylic acids after treatment with mineral acid [Eq. (27a), (27b)].[162]

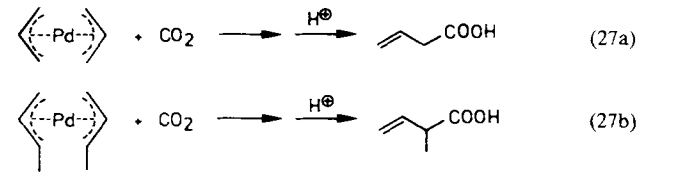

(27a)

(27b)

Jolly, Wilke et al. were able to trap the intermediates in this reaction by adding basic phosphanes.[163] With trimethyl- or tricyclohexylphosphane, complexes were formed that contained both an η^1 and an η^3 allyl ligand. The insertion of CO_2 into the Pd–C σ bond led to an allyl-carboxylato complex, the ligands of which could be displaced by carbon monoxide [Eq. (28), R = Me, Cy].

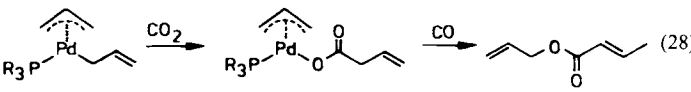

(28)

The binuclear octadienediylpalladium complex **54** displays some remarkable reactions (Scheme 10).[164,165] The addition of one equivalent of triisopropylphosphane leads selectively to complex **55**, in which only one palladium center has acquired a phosphane ligand. Complex **55** reacts with CO_2 to give **56**, which reacts with hydrochloric

acid, releasing 3,8-nonadiene-1-carboxylic acid. The catalytic hydrogenation of this acid yields pelargonic acid.

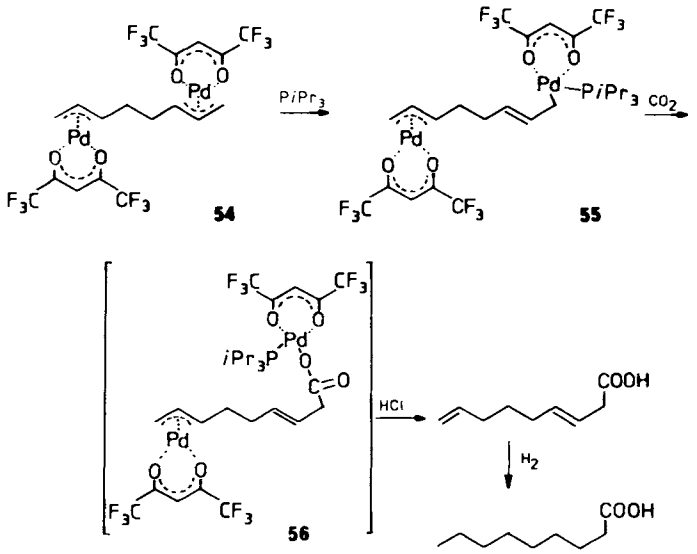

Scheme 10. Insertion of CO_2 into a complex containing two allyl ligands.

The insertion of CO_2 into a Pd–allyl bond, as described in Scheme 10, is unusual. Other insertion reactions into transition-metal allyl complexes with asymmetric allyl ligands always took place at the secondary carbon atom C3 [Eq. (29), path A] (see Scheme 9 for titanium complexes, Eq. (27) for palladium complexes). This necessarily led to branched-chain products. The insertion into complex **55**, however, takes place at the terminal carbon atom C1 [Eq. (29), path B] and the workup leads to a straight-chain product.

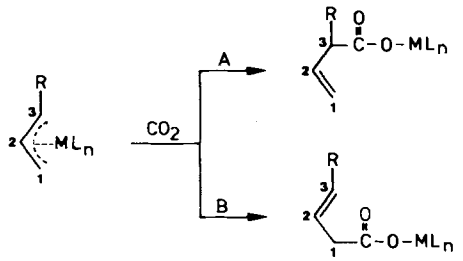

(29)

5. Homogeneously Catalyzed Reactions of Carbon Dioxide with Hydrocarbons[191]

The reaction between carbon dioxide and one or more hydrocarbon molecules can be described as a carboxylation. The well-known carboxylation of aromatic species (the Kolbe–Schmitt synthesis) does not require a transition-metal catalyst.[13] Analogous reactions can be carried out with saturated but C–H-acidic hydrocarbons.[166] Reactions of CO_2 with unsaturated hydrocarbons such as alkynes and mono- and dienes are however generally carried out using homogeneous transition-metal catalysts.

5.1. Reactions with Alkynes

The reaction of alkynes with carbon dioxide was first reported in 1977 by *Inoue* et al.[167] The reaction between 1-hexyne and CO_2 led to 4,6-dibutyl-2-pyrone in 50% yield [Eq. (30)]. Analogous reactions were observed with alkynes bearing nonterminal triple bonds (e.g., 3-hexyne, 4-octyne).[168] Nickel complexes with bidentate phosphane ligands were suitable catalysts.

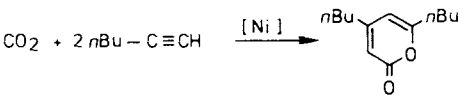

(30)

The mechanism of this reaction type was intensively studied, and two possible reaction paths (A and B in Fig. 6) were discussed. In path A, the first step is the oxidative coupling of two alkyne molecules, forming a nickelacyclopentadiene species. The insertion of CO_2 into a Ni–C bond would then form a cyclic carboxylato complex, which would release the pyrone by reductive elimination. This catalytic cycle could however not be confirmed by comparative stoichiometric studies with nickelacyclopentadiene complexes. Path B involves the reaction of an alkyne and a CO_2 molecule to form an oxanickelacyclopentene complex, which then reacts with a further alkyne, expanding to a seven-membered ring. The use of a stabilizing ligand (e.g., the bidentate, basic *N,N,N',N'*-tetramethylethylenediamine ligand) made possible the isolation of both catalytic intermediates. This is reliable evidence that path B is the actual mechanism of nickel catalysis.

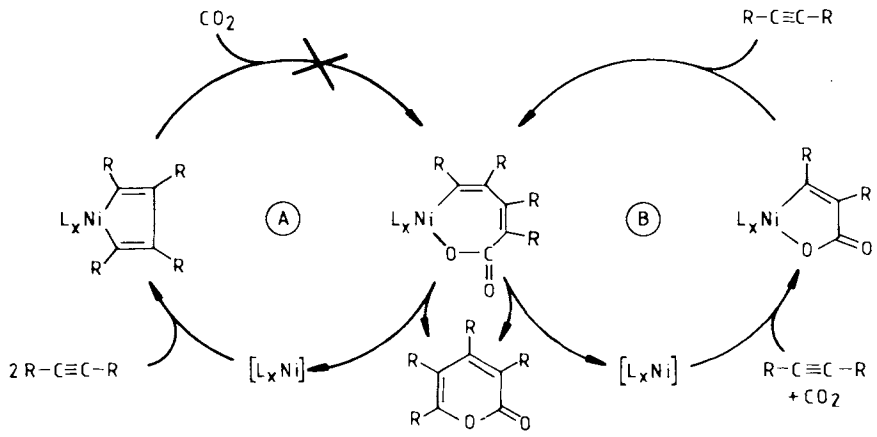

Fig. 6. Suggested mechanisms for the nickel-catalyzed reaction of alkynes with CO_2.

Aresta and *Albano*[169] studied the reaction of CO_2 and propyne with the catalyst [Rh(dppe)(η-BPh_4)] (dppe = 1,2-bis(diphenylphosphino)ethane). They observed the formation of 4,6-dimethyl-2-pyrone in yields of up to 3%. A mechanism was suggested in which the active intermediates were not metallacycles but rhodium complexes with noncyclic substituents.

5.2. Reactions with Monoenes

Transition-metal-catalyzed reactions of carbon dioxide with monoenes are appreciably more difficult than those with alkynes. *Lapidus* et al.[170] reported in 1978 a rhodium-catalyzed reaction of CO_2 and ethene, forming propionic acid and ethyl propionate. Pressures of 700 bar and a catalytic system consisting of Wilkinson's complex and a hydrogen halide were necessary to achieve yields of up to 38%. *Besecke* and *Schröder*[171] patented in 1981 a method of synthesizing esters from propene and carbon dioxide in the presence of ruthenium catalysts and alcohols [Eq. (31)]. Mechanistic studies with ^{13}C-labeled methanol, however, showed that the carbon of the carboxyl group came not from the carbon dioxide but from the alcohol.[172]

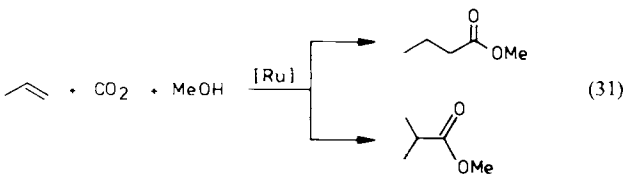

(31)

Methylenecyclopropanes are more reactive than linear olefins. *Inoue* et al. succeeded in 1979 in converting substituted methylenecyclopropanes and carbon dioxide into γ-lactones by using palladium catalysts [Eq. (32)].[173]

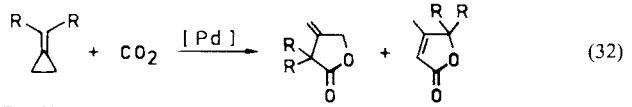

(32)

R = Me
R, R = $-(CH_2)_5-$

In the presence of palladium complexes containing monodentate phosphane ligands, the β-methylene lactone is preferentially formed, whereas the use of [Pd(dppe)$_2$] leads to the α,β-unsaturated lactone as the main product.

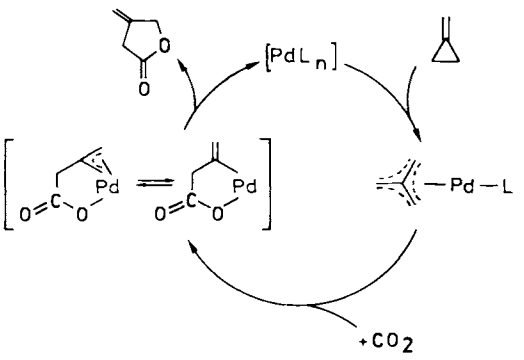

Fig. 7. Suggested mechanism for the reaction of methylenecyclopropane with CO_2.

The suggested mechanism (Fig. 7) involves a trimethylenemethane-palladium intermediate. The CO_2 insertion forms a cyclic carboxylato species from which the lactone is released.

Binger et al.[174] have carried out extensive investigations on the reaction of carbon dioxide with the unsubstituted methylenecyclopropane. Optimum reaction conditions allow the formation of 3-methyl-2-butene-4-olide in 80% yield. In addition to this "co-dimer," however, the further reaction of the lactone with the starting material leads to co-trimers, co-tetramers, and co-pentamers.

5.3. Reactions with Dienes

Both cumulated and conjugated dienes can undergo reactions with CO_2. The palladium-catalyzed reaction of CO_2 with allene leads to the synthesis of two esters and a pyrone [Eq. (33)]. Since pyrones are also formed from al-

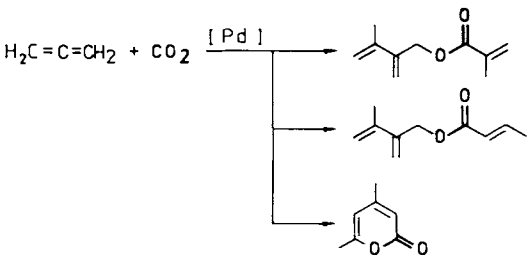

(33)

kynes and CO_2, it was assumed that the allene first isomerized to propyne. Experiments with propyne instead of allene showed, however, that the alkyne does not react with carbon dioxide under comparable reaction conditions.[175]

The optimum catalyst for the allene-CO_2 reaction is a combination of 1,2-bis(η^3-allyl)palladium and bis(cyclohexylphosphino)ethane. The synthesis presumably occurs via metallacyclic intermediates. Cyclic nickel carboxylato complexes were indeed isolated from stoichiometric reactions between allenes and carbon dioxide.[176]

The first studies of the catalytic reactions of 1,3-dienes with CO_2 were carried out by the research groups of *Inoue*[177,178] and *Musco*[179,180] at the end of the 1970s. They succeeded in synthesizing lactones and esters in small quantities from dienes and CO_2, and isolated the products using preparative gas chromatography or column chromatography. Since these first results, preparative methods have been developed that allow the synthesis of a variety of products from dienes and carbon dioxide on an industrial scale.[181-188]

The reaction of butadiene with CO_2 leads to various products, depending on the catalyst. Figure 8 shows that several connected catalytic cycles can be postulated, starting from the transition-metal complex ML_x. Cycle A applies to palladium, ruthenium, or nickel catalysts. The dimerization and addition of two butadiene molecules leads to the bis(η^3-allyl) complex **57**. Carbon dioxide inserts into one allyl bond, forming the allylcarboxylato complex **58**, from which the products **59** to **63** are released, regenerating the catalyst ML_x. Ring closure leads to the δ-lactone 2-ethylidene-6-hepten-5-olide **59** and the γ-lactones **60** and **61**; the esters **62** and **63** are obtained by addition of two further butadiene molecules.

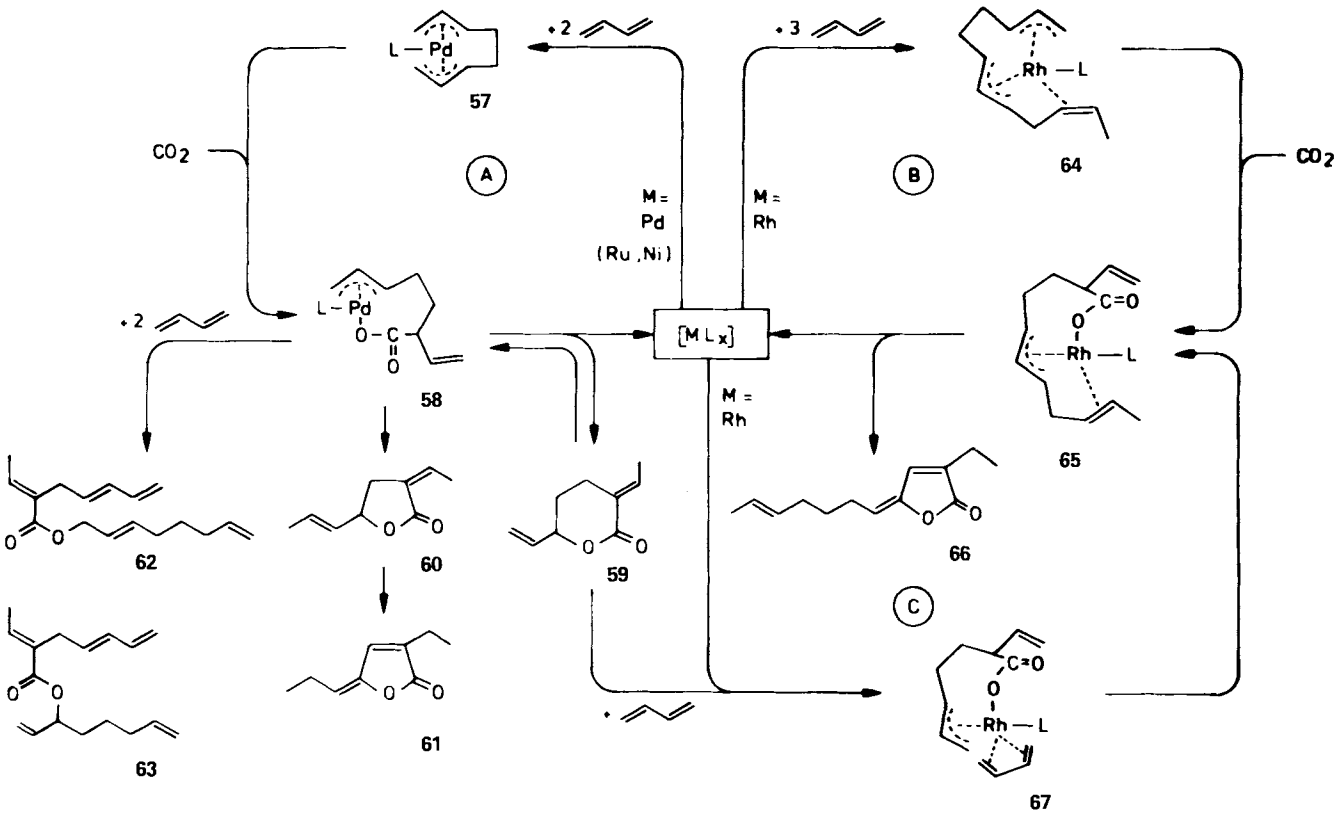

Fig. 8. Catalytic reaction between butadiene and carbon dioxide; products and postulated mechanism with intermediates. L = PR_3.

Cycle B is observed with rhodium catalysts. Three molecules of butadiene coordinate to the metal and form complex **64**; this reacts with carbon dioxide to give the intermediate **65**, from which the γ-lactone **66** is formed.

Cycle C describes a variant of the reaction catalyzed by rhodium. Rhodium compounds can bind the δ-lactone **59**, opening the ring, and simultaneously coordinate a further molecule of butadiene, leading to the intermediate complex **67**; C–C bond formation converts this into another intermediate **65**, the precursor of the γ-lactone **66**.

The crucial intermediates in the reaction of butadiene with CO_2 are carboxylato complexes. To support the proposed mechanisms (Fig. 8), the isolation of such a carboxylato species in a comparable stoichiometric experiment was attempted. The reaction of bis(acetylacetonato)palladium with triisopropylphosphane and the δ-lactone **59** allowed the isolation of the complex bis(2-ethylidene-4,6-heptadienoate)bis(triisopropylphosphane) **68**. The X-ray structure analysis of this complex (Fig. 9) shows that both phosphane ligands and both carboxylato ligands are *trans* at the square-planar-coordinated palladium atom and that the carboxylato ligands are monodentate.

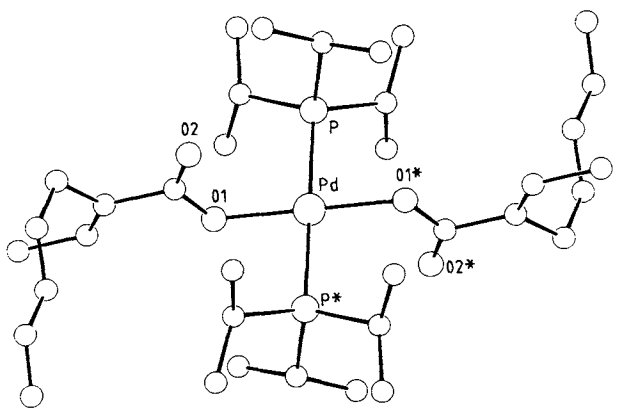

Fig. 9. Molecular structure of complex **68**.

Neither isoprene nor 1,3-pentadiene (piperylene) reacts with CO_2 in the presence of those catalysts that promote good yields (> 50%) with the butadiene-CO_2 reaction. However, it proved possible to react either isoprene or piperylene with butadiene and carbon dioxide; these composite syntheses lead to the lactones **69**, **71**, and **73** (Fig. 10) although the yields from such "three-component systems" are poor (maximum 5%).

The palladium-catalyzed reaction of isoprene with butadiene forms products that result from the linkage of butadiene with either end of the isoprene molecule. The corresponding intermediates should therefore be formulated as bis(η^3-allyl)palladium complexes with the additional methyl group in either the 3- or 2-position. The subsequent insertion of carbon dioxide occurs exclusively in the allyl group generated from butadiene.

The reaction between piperylene, butadiene, and carbon dioxide forms only the "tail-coupling" products **73**. The alternative "head-coupling," to produce the lactones **75** and **76**, is not observed. The CO_2 insertion, in exact analogy to the isoprene reaction, also occurs exclusively at the nonsubstituted allyl group.

Further three-component syntheses have been carried out with dienes, carbon dioxide, and epoxides. These reac-

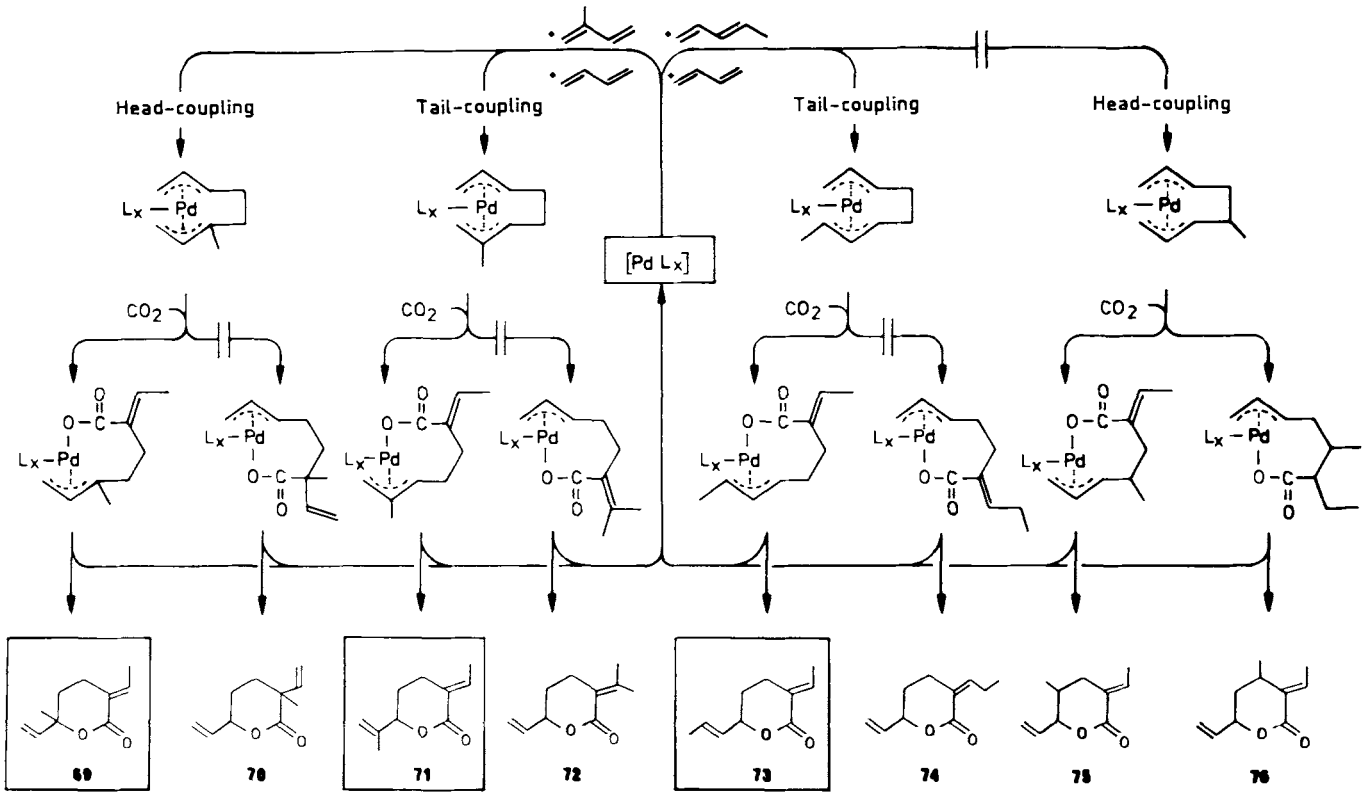

Fig. 10. Reaction combining isoprene or piperylene with butadiene and carbon dioxide. L = PR_3.

tions represent the attempt to extend the catalytic principles formulated in Figure 3 to reactions of carbon dioxide with two entirely different substrates Su.

Butadiene, carbon dioxide, and ethylene oxide react in the presence of palladium catalysts, forming **77**, the glycol ester of 2-ethylidene-4,6-heptadienoic acid [Eq. (34)].[189] The corresponding reaction with propylene oxide is analogous, but produces two isomeric esters **78** and **79** with different positions of the additional methyl group.

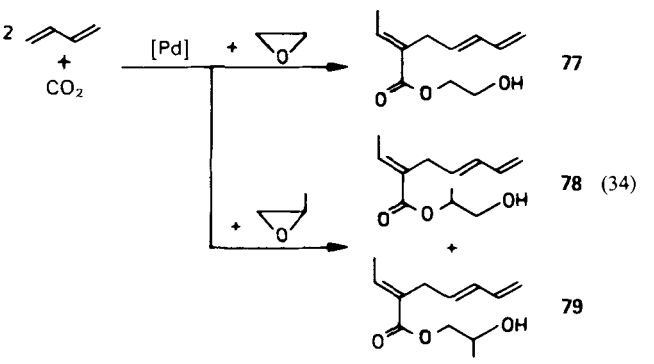

(34)

It is remarkable that the octadienyl esters **62** and **63** and the glycol esters **77** to **79** are derivatives of the same carboxylic acid. It is probable that the mechanisms of their formation are similar (Fig. 11). The first steps in the latter

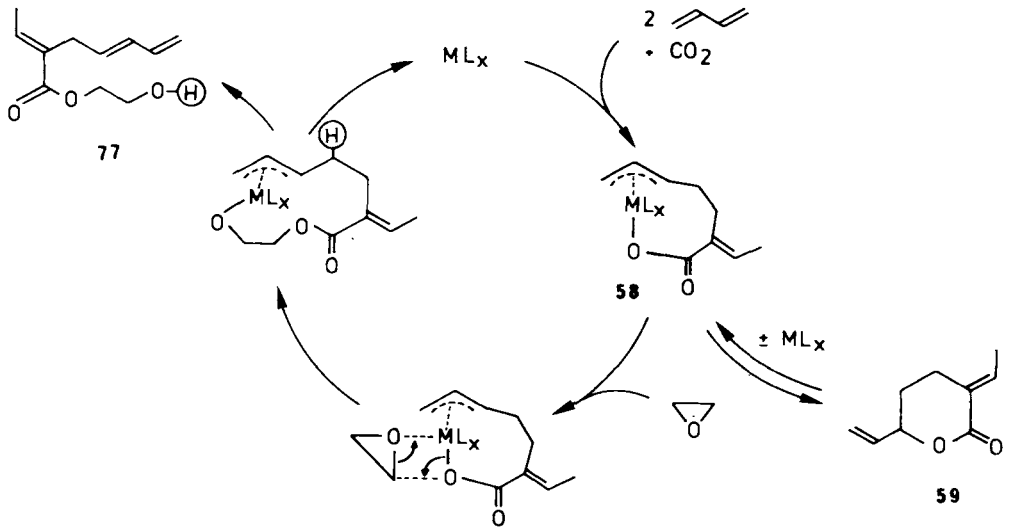

Fig. 11. Suggested mechanism for ester synthesis from butadiene, ethylene oxide, and carbon dioxide. M = Pd, Rh; L = PR_3.

reaction are the oxidative coupling of two butadiene molecules and the insertion of the CO_2, forming the palladium carboxylato complex **58**. The epoxide coordinates to this intermediate product, undergoes ring-opening, and inserts into the Pd-O bond. The catalyst is regenerated by elimination of the glycol ester.

6. Concluding Remarks

How will the chemistry of carbon dioxide develop? A wide variety of different possibilities were recognizable at the "NATO Summer School on Carbon Dioxide," which took place in June 1986 in Pugnochiuso (Italy).[190]

The electrochemical exploitation of CO_2 has become the object of great efforts. The electrochemical reduction of carbon dioxide to carbon monoxide, formic acid, or oxalic acid, and the electrocarboxylation of olefins, aromatic species, and carbonyl and halogen compounds are both being intensively studied. The photochemistry of CO_2 has also made great strides in the last few years, although an industrial application cannot yet be foreseen. A further possibility is that bacteria could be used to convert carbon dioxide into organic products.

Carbon dioxide undergoes a series of industrially important catalytic reactions. The activity and selectivity of heterogeneously catalyzed CO_2 reactions are often higher than those of corresponding reactions with carbon monoxide. The coordination chemistry of CO_2 and the related homogeneous catalysis by transition metals still seem particularly promising areas. "Tailor-made" metal-complex catalysts are able to control the reactions of CO_2 and allow high selectivity in the synthesis of organic chemicals. This interesting research area still has many novelties to be discovered.

Received: August 4, 1986;
revised: January 14, 1987 [A 671 IE]
German version: *Angew. Chem. 100* (1988) 681

[1] H. D. Freyer, *Technik heute 1984*, No. 7, p. 38.
[2] E. Hillenbrand in: *Ullmanns Encyklopädie der technischen Chemie, Band 14*, 4th ed., Verlag Chemie, Weinheim 1977, p. 569.
[3] H. Reichel, U. Harding: *Die Funktionen des CO_2 in der belebten Natur (Physiologie und Biochemie in schematischer Darstellung, Band 3)*, F. K. Schattauer, Stuttgart 1975.
[4] W. C. Clark (Ed.): *Carbon Dioxide Review: 1982*, University Press, Oxford 1982.
[5] W. P. Elliott, L. Machta (Eds.): *Carbon Dioxide Effects Research and Assessment Program*, NTIS: Springfield, VA, USA 1979; *Chem. Abstr. 92* (1980) 168395f.
[6] J. H. Krieger, *Chem. Eng. News 59* (1981) No. 4, p. 34.
[7] N. J. Rosenberg, *Prepr. Div. Pet. Chem. Am. Chem. Soc. 26* (1981) 1026.
[8] R. G. Watts, *Prepr. Div. Pet. Chem. Am. Chem. Soc. 26* (1981) 959.
[9] H. Flohn, *Nachr. Chem. Tech. Lab. 32* (1984) 305.
[10] J. Lemons, *J. Environ. Sci. 28* (1985) 60.
[11] T. M. L. Wigley, P. D. Jones, *Nature (London) 292* (1981) 205.
[12] J. Williams (Ed.): *Carbon Dioxide, Climate and Society (IIASA Proc. Ser. Environ. 1* (1978)).
[13] A. Behr, *Chem. Ing. Tech. 57* (1985) 893; *Chem Eng. Technol. 10* (1987) 16.
[14] J. C. Calabrese, T. Herskovitz, J. B. Kinney, *J. Am. Chem. Soc. 105* (1983) 5914.
[15] T. Herskovitz, *Inorg. Synth. 21* (1982) 99.
[16] T. Herskovitz, *J. Am. Chem. Soc. 99* (1977) 2391.
[17] R. L. Harlow, J. B. Kinney, T. Herskovitz, *J. Chem. Soc. Chem. Commun. 1980*, 813.
[18] M. Aresta, C. F. Nobile, V. G. Albano, E. Forni, M. Manassero, *J. Chem. Soc. Chem. Commun. 1975*, 636.
[19] M. Aresta, C. F. Nobile, *J. Chem. Soc. Dalton Trans. 1977*, 708.
[20] G. S. Bristow, P. B. Hitchcock, M. F. Lappert, *J. Chem. Soc. Chem. Commun. 1981*, 1145.
[21] S. Gambarotta, C. Floriani, A. Chiesi-Villa, C. Guastini, *J. Am. Chem. Soc. 107* (1985) 2985.
[22] J. D. Audett, T. J. Collins, B. D. Santarsiero, G. H. Spies, *J. Am. Chem. Soc. 104* (1982) 7352.
[23] T. Herskovitz, G. W. Parshall, US Pat. 3954821 (Mai 4, 1976); *Chem. Abstr. 85* (1976) 108778d.
[24] T. Herskovitz, L. J. Guggenberger, *J. Am. Chem. Soc. 98* (1976) 1615.
[25] R. Alvarez, E. Carmona, E. Gutierrez-Puebla, J. M. Marin, A. Monge, M. L. Poveda, *J. Chem. Soc. Chem. Commun. 1984*, 1326.
[26] R. Alvarez, E. Carmona, J. M. Marin, M. L. Poveda, E. Gutierrez-Puebla, A. Monge, *J. Am. Chem. Soc. 108* (1986) 2286.
[27] H. O. Fröhlich, H. Schreer, *Z. Chem. 23* (1983) 348.
[28] W. Beck, K. Raab, U. Nagel, M. Steimann, *Angew. Chem. 94* (1982) 556; *Angew. Chem. Int. Ed. Engl. 21* (1982) 526.
[29] C. Floriani, G. Fachinetti, *J. Chem. Soc. Chem. Commun. 1974*, 615.
[30] G. Fachinetti, C. Floriani, P. F. Zanazzi, *J. Am. Chem. Soc. 100* (1978) 7405.
[31] G. Fachinetti, C. Floriani, P. F. Zanazzi, A. R. Zanzari, *Inorg. Chem. 18* (1979) 3469.
[32] S. Gambarotta, F. Arena, C. Floriani, P. F. Zanazzi, *J. Am. Chem. Soc. 104* (1982) 5082.
[33] C. Floriani, *Pure Appl. Chem. 55* (1983) 1.
[34] C. R. Eady, J. J. Guy, B. F. G. Johnson, J. Lewis, M. C. Malatesta, G. M. Sheldrick, *J. Chem. Soc. Chem. Commun. 1976*, 602.
[35] J. J. Guy, G. M. Sheldrick, *Acta Crystallogr. Sect. B 34* (1978) 1718.
[36] G. W. Parshall: *Homogeneous Catalysis*, Wiley-Interscience, New York 1980.
[37] A. Nakamura, M. Tsutsui: *Principles and Applications of Homogeneous Catalysis*, Wiley-Interscience, New York 1980.
[38] C. Masters: *Homogeneous Transition Metal Catalysis*, Chapman and Hall, London 1981.
[39] J. Falbe, H. Bahrmann, *Chem. Unserer Zeit 15* (1981) 37.
[40] W. Keim, *Chem. Ind. (Düsseldorf) 36* (1984) 397.
[41] H. Bönnemann, *Österr. Chem. Z. 85* (1984) 29.
[42] K.-H. Schmidt, *Chem. Ind. (Düsseldorf) 37* (1985) 762.
[43] F. J. Waller, *J. Mol. Catal. 31* (1985) 123.
[44] C. J. Nyman, C. E. Wymore, G. Wilkinson, *Chem. Commun. 1967*, 407.
[45] F. Cariati, R. Mason, G. B. Robertson, R. Ugo, *Chem. Commun. 1967*, 408.
[46] C. J. Nyman, C. E. Wymore, G. Wilkinson, *J. Chem. Soc. A 1968*, 561.
[47] P. J. Hayward, D. M. Blake, G. Wilkinson, C. J. Nyman, *J. Am. Chem. Soc. 92* (1970) 5873.
[48] D. M. Blake, D. M. Roundhill, *Inorg. Synth. 18* (1978) 120.
[49] L. Dahlenburg, C. Prengel, *Organometallics 3* (1984) 934.
[50] M. Aresta, E. Quaranta, A. Ciccarese, *C, Mol. Chem. 1* (1985) 267.
[51] E. Dinjus, J. Kaiser, J. Sieler, D. Walther, *Z. Anorg. Allg. Chem. 483* (1981) 63.
[52] J. Kaiser, J. Sieler, U. Braun, L. Golič, E. Dinjus, D. Walther, *J. Organomet. Chem. 224* (1982) 81.
[53] D. Walther, E. Dinjus, *Z. Chem. 21* (1981) 415.
[54] D. Walther, E. Dinjus, J. Sieler, J. Kaiser, O. Lindqvist, L. Anderson, *J. Organomet. Chem. 240* (1982) 289.
[55] D. Walther, E. Dinjus, V. Herzog, Z. Chem. 22 (1982) 303.
[56] D. Walther, E. Dinjus, V. Herzog, *Z. Chem. 24* (1984) 260.
[57] D. Walther, E. Dinjus, V. Herzog, *Z. Chem. 23* (1983) 188.
[58] D. Walther, E. Dinjus, *Z. Chem. 24* (1984) 298.
[59] P. L. Bellon, S. Cenini, F. Demartin, M. Pizzotti, F. Porta, *J. Chem. Soc. Chem. Commun. 1982*, 265.
[60] S. Cenini, F. Porta, M. Pizzotti, C. Crotti, *J. Chem. Soc. Dalton Trans. 1985*, 163.
[61] G. Burkhart, H. Hoberg, *Angew. Chem. 94* (1982) 75; *Angew. Chem. Int. Ed. Engl. 21* (1982) 76; *Angew. Chem. Suppl. 1982*, 147.
[62] H. Hoberg, D. Schäfer, *J. Organomet. Chem. 238* (1982) 383.
[63] H. Hoberg, D. Schäfer, G. Burkhart, C. Krüger, M. J. Romão, *J. Organomet. Chem. 266* (1984) 203.
[64] E. Dinjus, D. Walther, H. Schütz, *Z. Chem. 23* (1983) 408.
[65] D. Walther, E. Dinjus, J. Sieler, L. Andersen, O. Lindqvist, *J. Organomet. Chem. 276* (1984) 99.
[66] H. Hoberg, Y. Peres, A. Milchereit, *J. Organomet. Chem. 307* (1986) C38.
[67] H. Hoberg, Y. Peres, A. Milchereit, *J. Organomet. Chem. 307* (1986) C41.
[68] A. Behr, G. Thelen, *C, Mol. Chem. 1* (1984) 137.
[69] D. Walther, E. Dinjus, *Z. Chem. 22* (1982) 228.
[70] E. Dinjus, D. Walther, H. Schütz, W. Schade, *Z. Chem. 23* (1983) 303.
[71] D. Walther, E. Dinjus, J. Sieler, N. N. Thanh, W. Schade, I. Leban, *Z. Naturforsch. B 38* (1983) 835.

[72] D. Walther, E. Dinjus, *Z. Chem. 24* (1984) 63.
[73] D. Walther, E. Dinjus, H. Görls, J. Sieler, O. Lindqvist, L. Andersen, *J. Organomet. Chem. 286* (1985) 103.
[74] H. Hoberg, D. Schäfer, *J. Organomet. Chem. 255* (1983) C 15.
[75] H. Hoberg, D. Schäfer, B. W. Oster, *J. Organomet. Chem. 266* (1984) 313.
[76] H. Hoberg, B. Apotecher, *J. Organomet. Chem. 270* (1984) C 15.
[77] A. Behr, U. Kanne, *J. Organomet. Chem. 317* (1986) C 41.
[78] M. E. Vol'pin, I. S. Kolomnikov, *Organomet. React. 5* (1975) 313.
[79] R. Eisenberg, D. E. Hendriksen, *Adv. Catal. 28* (1979) 79.
[80] S. Inoue, N. Yamazaki (Eds.): *Organic and Bio-organic Chemistry of Carbon Dioxide*, Kodansha, Tokyo 1982.
[81] R. P. A. Sneeden in G. Wilkinson (Ed.): *Comprehensive Organometallic Chemistry, Vol. 8*, Pergamon, Oxford 1982, p. 225.
[82] D. J. Darensbourg, R. A. Kudaroski, *Adv. Organomet. Chem. 22* (1983) 129.
[83] A. Behr in W. Keim (Ed.): *Catalysis in C_1-Chemistry*, Reidel, Dordrecht 1983, p. 169.
[84] D. Walther, E. Dinjus, J. Sieler, *Z. Chem. 23* (1983) 237.
[85] R. Ziessel, *Nouv. J. Chim. 7* (1983) 613.
[86] D. J. Darensbourg, A. Rokicki, *Organometallics 1* (1982) 1685.
[87] D. J. Darensbourg, C. Ovalles, *CHEMTECH 15* (1985) 636.
[88] S. G. Slater, R. Lusk, B. F. Schumann, M. Darensbourg, *Organometallics 1* (1982) 1662.
[89] M. G. Bradley, D. A. Roberts, G. L. Geoffroy, *J. Am. Chem. Soc. 103* (1981) 379.
[90] B. P. Sullivan, T. J. Meyer, *J. Chem. Soc. Chem. Commun. 1984*, 1244.
[91] V. D. Bianco, S. Doronzo, N. Gallo, *Inorg. Nucl. Chem. Lett. 16* (1980) 97.
[92] I. S. Kolomnikov, A. I. Gusev, G. G. Aleksandrov, T. S. Lobeeva, Y. T. Struchkov, M. E. Vol'pin, *J. Organomet. Chem. 59* (1973) 349.
[93] I. S. Kolomnikov, T. S. Belopotapova, M. E. Vol'pin, *J. Gen. Chem. USSR (Engl. Trans.) 45* (1975) 1958.
[94] S. Komiya, A. Yamamoto, *Bull. Chem. Soc. Jpn. 49* (1976) 784.
[95] B. Beguin, B. Denise, R. P. A. Sneeden, *J. Organomet. Chem. 208* (1981) C 18.
[96] C. Bianchini, C. A. Ghilardi, A. Meli, S. Midollini, A. Orlandini, *J. Organomet. Chem. 248* (1983) C 13.
[97] I. S. Kolomnikov, G. Stepovska, S. Tyrlik, M. E. Vol'pin, *J. Gen. Chem. USSR (Engl. Transl.) 42* (1972) 1645.
[98] V. D. Bianco, S. Doronzo, N. Gallo, *Inorg. Nucl. Chem. Lett. 17* (1981) 75.
[99] A. Yamamoto, S. Kitazume, L. S. Pu, S. Ikeda, *J. Am. Chem. Soc. 93* (1971) 371.
[100] P. Etievant, G. Tainturier, B. Gautheron, *C. R. Hebd. Seances Acad. Sci. Ser. C 283* (1976) 233.
[101] G. Fachinetti, C. Floriani, A. Roselli, S. Pucci, *J. Chem. Soc. Chem. Commun. 1978*, 269.
[102] S. Gambarotta, S. Strologo, C. Floriani, A. Chiesi-Villa, C. Guastini, *J. Am. Chem. Soc. 107* (1985) 6278.
[103] C. P. Kubiak, C. Woodcock, R. Eisenberg, *Inorg. Chem. 21* (1982) 2119.
[104] A. Immirzi, A. Musco, *Inorg. Chim. Acta 22* (1977) L 35.
[105] R. S. Paonessa, W. C. Trogler, *J. Am. Chem. Soc. 104* (1982) 3529.
[106] M. Hidai, T. Hikita, Y. Uchida, *Chem. Lett. 1972*, 521.
[107] G. A. Razuvaev, L. I. Vyshinskaya, V. V. Drobotenko, G. Ya. Malkova, N. N. Vyshinskii, *J. Organomet. Chem. 239* (1982) 335.
[108] N. A. Ovchinnikova, M. A. Glushkova, Yu. A. Buslaev, *Koord. Khim. 5* (1979) 385.
[109] M. H. Chisholm, F. A. Cotton, M. W. Extine, W. W. Reichert, *J. Am. Chem. Soc. 100* (1978) 1727.
[110] M. H. Chisholm, M. Extine, *J. Am. Chem. Soc. 97* (1975) 5625.
[111] M. N. Bochkarev, E. A. Fedorova, Y. F. Rad'kov, G. S. Kalinina, S. Ya. Khorshev, G. A. Razuvaev, *Dokl. Akad. Nauk SSSR 279* (1984) 1386.
[112] T. V. Ashworth, E. Singleton, *J. Chem. Soc. Chem. Commun. 1976*, 204.
[113] S. Inoue, M. Nukui, F. Kojima, *Chem. Lett. 1984*, 619.
[114] M. Kato, T. Ito, *Inorg. Chem. 24* (1985) 504, 509.
[115] B. R. Flynn, L. Vaska, *J. Am. Chem. Soc. 95* (1973) 5081.
[116] T. Yoshida, D. L. Thorn, T. Okano, J. A. Ibers, S. Otsuka, *J. Am. Chem. Soc. 101* (1979) 4212.
[117] R. van Eldik, D. A. Palmer, H. Kelm, G. M. Harris, *Inorg. Chem. 19* (1980) 3679.
[118] E. Chaffee, T. P. Dasgupta, G. M. Harris, *J. Am. Chem. Soc. 95* (1973) 4169.
[119] R. A. Michelin, G. Strukul, N. Bresciani-Pahor, E. Zangrando, L. Randaccio, *Inorg. Chim. Acta 84* (1984) 229.
[120] T. Tsuda, T. Saegusa, *Inorg. Chem. 11* (1972) 2561.
[121] T. Yamamoto, M. Kubota, A. Yamamoto, *Bull. Chem. Soc. Jpn. 53* (1980) 680.
[122] T. Tsuda, S.-I. Sanada, K. Ueda, T. Saegusa, *Inorg. Chem. 15* (1976) 2329.
[123] T. Tsuda, Y. Chujo, T. Saegusa, *J. Am. Chem. Soc. 102* (1980) 431.
[124] M. H. Chisholm, M. W. Extine, *J. Am. Chem. Soc. 99* (1977) 782.
[125] M. H. Chisholm, M. W. Extine, *J. Am. Chem. Soc. 99* (1977) 792.
[126] G. Chandra, A. D. Jenkins, M. F. Lappert, R. C. Srivastava, *J. Chem. Soc. A 1970*, 2550.
[127] P. Sobota, B. Jezowska-Trzebiatowska, Z. Janas, *J. Organomet. Chem. 118* (1976) 253.
[128] J. N. Armor, *Inorg. Chem. 17* (1978) 213.
[129] M. H. Chisholm, L. S. Tan, J. C. Huffman, *J. Am. Chem. Soc. 104* (1982) 4879.
[130] M. H. Chisholm, F. A. Cotton, M. W. Extine, D. C. Rideout, *Inorg. Chem. 17* (1978) 3536.
[131] M. H. Chisholm, W. W. Reichert, *Inorg. Chem. 17* (1978) 767.
[132] M. H. Chisholm, D. A. Haitko, *J. Am. Chem. Soc. 101* (1979) 6784.
[133] M. J. Chetcuti, M. H. Chisholm, K. Folting, D. A. Haitko, J. C. Huffman, *J. Am. Chem. Soc. 104* (1982) 2138.
[134] T. W. Coffindaffer, I. P. Rothwell, J. C. Huffman, *Inorg. Chem. 23* (1984) 1433.
[135] A. L. Arduini, J. D. Jamerson, J. Takats, *Inorg. Chem. 20* (1981) 2474.
[136] G. La Monica, S. Cenini, F. Porta, M. Pizzotti, *J. Chem. Soc. Dalton Trans. 1976*, 1777.
[137] J. G. Noltes, *Recl. Trav. Chim. Pays-Bas 84* (1965) 126.
[138] J. Vlčková, J. Barton, *J. Chem. Soc. Chem. Commun. 1973*, 306.
[139] T. Tsuda, K. Watanabe, K. Miyata, H. Yamamoto, T. Saegusa, *Inorg. Chem. 20* (1981) 2728.
[140] E. G. Boguslavskii, A. A. Shklyaev, N. G. Maksimov, Z. M. Alaudinova, I. S. Kolomnikov, V. F. Anufrienko, *Izv. Akad. Nauk SSSR Ser. Khim. 1980*, 1231.
[141] T. V. Ashworth, M. Nolte, E. Singleton, *J. Organomet. Chem. 121* (1976) C 57.
[142] F. Ozawa, T. Ito, A. Yamamoto, *Chem. Lett. 1979*, 735.
[143] I. S. Kolomnikov, T. S. Lobeeva, V. V. Gorbachevskaya, G. G. Aleksandrov, Y. T. Struchkov, M. E. Vol'pin, *Chem. Commun. 1971*, 972.
[144] L. E. Manzer, *J. Am. Chem. Soc. 100* (1978) 8068.
[145] M. K. Grigoryan, I. S. Kolomnikov, E. G. Berkovich, T. V. Lysyak, V. B. Shur, M. E. Vol'pin, *Izv. Akad. Nauk SSSR Ser. Khim. 1978*, 1177.
[146] A. Behr, W. Keim, G. Thelen, *J. Organomet. Chem. 249* (1983) C 38.
[147] P. Binger, M. Cetinkaya, M. J. Doyle, A. Germer, U. Schuchardt, *Fundam. Res. Homogeneous Catal. 3* (1979) 271.
[148] P. W. Jolly, C. Krüger, R. Salz, J. C. Sekutowski, *J. Organomet. Chem. 165* (1979) C 39.
[149] J. D. Fellmann, G. A. Rupprecht, R. R. Schrock, *J. Am. Chem. Soc. 101* (1979) 5099.
[150] A. Behr, U. Kanne, G. Thelen, *J. Organomet. Chem. 269* (1984) C 1.
[151] D. J. Darensbourg, R. Kudaroski, T. Delord, *Organometallics 4* (1985) 1094.
[152] S. D. Ittel, C. A. Tolman, A. D. English, J. P. Jesson, *J. Am. Chem. Soc. 100* (1978) 7577.
[153] A. D. English, T. Herskovitz, *J. Am. Chem. Soc. 99* (1977) 1648.
[154] a) A. Behr, E. Herdtweck, W. A. Herrmann, W. Keim, W. Kipshagen, *J. Chem. Soc. Chem. Commun. 1986*, 1262. b) *Organometallics 6* (1987) 2307.
[155] R. Alvarez, E. Carmona, D. J. Cole-Hamilton, A. Galindo, E. Gutierrez-Puebla, A. Monge, M. L. Poveda, C. Ruiz, *J. Am. Chem. Soc. 107* (1985) 5529.
[156] F. Sato, S. Iijima, M. Sato, *J. Chem. Soc. Chem. Commun. 1981*, 180.
[157] J. Blenkers, H. J. de Liefde Meijer, J. H. Teuben, *J. Organomet. Chem. 218* (1981) 383.
[158] E. Klei, J. H. Teuben, H. J. de Liefde Meijer, E. J. Kwak, A. P. Bruins, *J. Organomet. Chem. 224* (1982) 327.
[159] K. Tamao, M. Akita, R. Kanatani, N. Ishida, M. Kumada, *J. Organomet. Chem. 226* (1982) C 9.
[160] T. Tsuda, Y. Chujo, T. Saegusa, *Synth. Commun. 9* (1979) 427.
[161] P. W. Jolly, S. Stobbe, G. Wilke, R. Goddard, C. Krüger, J. C. Sekutowski, Y.-H. Tsay, *Angew. Chem. 90* (1978) 144; *Angew. Chem. Int. Ed. Engl. 17* (1978) 124.
[162] T. Ito, Y. Kindaichi, Y. Takami, *Chem. Ind. (London) 1980*, 83.
[163] T. Hung, P. W. Jolly, G. Wilke, *J. Organomet. Chem. 190* (1980) C 5.
[164] A. Behr, G. von Ilsemann, W. Keim, C. Krüger, Y.-H. Tsay, *Organometallics 5* (1986) 514.
[165] A. Behr, G. von Ilsemann, *J. Organomet. Chem. 276* (1984) C 77.
[166] G. Bottaccio, G. P. Chiusoli, *Chem. Commun. 1966*, 618.
[167] Y. Inoue, Y. Itoh, H. Hashimoto, *Chem. Lett. 1977*, 855.
[168] Y. Inoue, Y. Itoh, H. Kazama, H. Hashimoto, *Bull. Chem. Soc. Jpn. 53* (1980) 3329.
[169] P. Albano, M. Aresta, *J. Organomet. Chem. 190* (1980) 243.
[170] A. L. Lapidus, S. D. Pirozhkov, A. A. Koryakin, *Bull. Acad. Sci. USSR Div. Chem. Sci. (Engl. Transl.)* (1978) 2513.
[171] S. Besecke, G. Schröder, DOS 2948888 (June 11, 1981), Röhm GmbH.
[172] A. Behr, U. Kanne, W. Keim, *J. Mol. Catal. 35* (1986) 19.
[173] Y. Inoue, T. Hibi, M. Satake, H. Hashimoto, *J. Chem. Soc. Chem. Commun. 1979*, 982.

[174] P. Binger, H.-J. Weintz, *Chem. Ber. 117* (1984) 654.
[175] A. Döhring, P. W. Jolly, *Tetrahedron Lett. 1980*, 3021.
[176] H. Hoberg, B. W. Oster, *J. Organomet. Chem. 266* (1984) 321.
[177] Y. Sasaki, Y. Inoue, H. Hashimoto, *J. Chem. Soc. Chem. Commun. 1976*, 605.
[178] Y. Inoue, Y. Sasaki, H. Hashimoto, *Bull. Chem. Soc. Jpn. 51* (1978) 2375.
[179] A. Musco, C. Perego, V. Tartiari, *Inorg. Chim. Acta 28* (1978) L147.
[180] A. Musco, *J. Chem. Soc. Perkin Trans. 1 1980*, 693.
[181] J. A. Daniels, Eur. Pat. Appl. EP 50445 (April 28, 1982); *Chem. Abstr. 97* (1982) 127500w.
[182] A. Behr, K.-D. Juszak, W. Keim, *Synthesis 1983*, 574.
[183] A. Behr, K.-D. Juszak, *J. Organomet. Chem. 255* (1983) 263.
[184] A. Behr, K.-D. Juszak, R. He, *Proc. Int. Congr. Catal. 8th 1984*, Vol. V, p. 565.
[185] A. Behr, R. He, *J. Organomet. Chem. 276* (1984) C69.
[186] W. Keim, A. Behr, K.-D. Juszak, DOS 3317013 (November 15, 1984).
[187] A. Behr, *Bull. Soc. Chim. Belg. 94* (1985) 671.
[188] A. Behr, R. He, K.-D. Juszak, C. Krüger, Y.-H. Tsay, *Chem. Ber. 119* (1986) 991.
[189] A. Behr, U. Kanne, *J. Organomet. Chem. 309* (1986) 215.
[190] *Summer School on Carbon Dioxide: Chemical and Biochemical Uses as a Source of Carbon* (Pugnochiuso, Italy, June 22–July 3, 1986). The main lectures of this meeting have been published in *NATO ASI Ser., Ser. C206* (1987).
[191] Review on transition-metal-catalyzed formation of C–C bonds with CO_2: P. Braunstein, D. Matt, D. Nobel, *Chem. Rev. 88* (1988), in press.

Reduction and Hydrogenation with the System Hydrocarbon/Carbon

New Synthetic Methods (70)

By Toni Dockner*

Dedicated to Professor Helmut Dörfel on the occasion of his 60th birthday

For the synthesis of organic compounds, reduction is an indispensible reaction type which is also widely used on an industrial scale. In industrial processes hydrogen is usually used as reducing agent, since strong reducing agents like alkali metals and hydrides can only be used to a limited extent for safety and economic reasons. Very economical reducing agents that are convenient to handle and have high potential application are hydrocarbons in presence of carbon. Hydrocarbon/carbon systems can be readily used instead of molecular hydrogen and expensive metal catalysts for the hydrogenation of compounds containing, for example, CC-, CO-, or NO-double bonds. Furthermore, these systems can be used for carrying out reductions which hitherto required strong reducing agents such as zinc, tin, alkali metals and hydrides. Especially suitable as economic sources of hydrogen are refinery products such as vacuum gas oil, fuel oil S or vacuum residue oil. Hydrocarbons are dehydrogenated to unsaturated systems and finally to carbon.

1. Introduction

Alkanes[**] are considered as inert under the reaction conditions normally used in organic chemistry. C-C and C-H bonds can be cleaved only at temperatures above 400°C—and even then usually only unselectively. This is the case in the petrochemical industry in processes such as, e.g., steam cracking, re-forming, or hydrocracking.

Recently, there have been numerous studies concerned with "CH activation". Thus, it has been demonstrated, e.g., that hydrocarbons can be incorporated into energy-rich metal-complexes via cleavage of the CH bond.[1]

In 1978, *Laily Bin Din* et al.[2] reported on the reduction of aromatic nitro compounds to anilines with liquid paraffin at 360-390°C, and, already in 1966, *Okamoto* et al.[3] found that predominantly ethylene instead of the expected vinyl chloride is formed in the pyrolysis of 1,2-dichloroethane at 300-400°C in the presence of toluene, benzene or *n*-hexane, and activated carbon as catalyst. Surprisingly, these two publications failed to stimulate further intensive studies on the potential of hydrocarbons as reducing agents. Consequently, the scope of application of the reduction system hydrocarbon/carbon remained unrecognized.

In the following sections a novel, general utilization of hydrocarbons for reduction and hydrogenation in organic chemistry will be outlined.

2. Reduction of Halogeno Compounds

On attempting to cleave 1,2-dichloropropane to allyl chloride and HCl in high-boiling vacuum residue oil at 350°C, we surprisingly found that propene and hydrogen chloride were formed in high yields according to Equation (a)[4] [cf. also Eq. (m)].

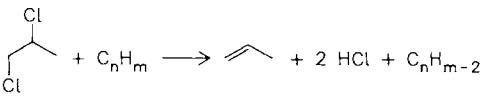

(a)

	Carbon black [%]	Conversion [%]	Selectivity [%]
Vacuum residue oil	23	78	90
Technical white oil	0	<3	—
Techn. white oil-activated carbon	25	78	90

On using other mineral oils such as technical white oil[***] we could not establish any reaction. When activated carbon was added to the white oil, however, the same results as with vacuum residue oil, which contains 23% carbon black, were obtained. Vacuum residue oil, consisting of paraffinic, aromatic and naphthenic hydrocarbons, serves as source of hydrogen. Carbon is formed from the hydrocarbons.

The homologues of 1,2-dichloropropane and also the bromo derivatives are cleaved in good yields, comparable with those obtained in the case of dichloropropane (Table 1). From 1,1,2-trichloroethane, vinyl chloride was obtained in 70% yield with almost quantitative conversion. Allyl chloride, like dichloropropane, is converted into propene. Table 1 permits a further conclusion to be drawn: the higher the degree of halogenation the higher the rate of reaction. Chloro compounds react more rapidly than bromo compounds; i.e. the electron withdrawing effect influences the rate of reaction.

Higher chlorinated hydrocarbons can be cleaved stepwise to yield the halogen-free compounds. Hexachlorocy-

[*] Dr. T. Dockner
BASF Aktiengesellschaft, Ammoniaklaboratorium
D-6700 Ludwigshafen (FRG)

[**] Alkane = paraffin, from the Latin parum affinus = little affinity or inert.

[***] A mixture of high-boiling aliphatic and cycloaliphatic hydrocarbons.

 © VCH Verlagsgesellschaft mbH, D-6940 Weinheim, 1988 0570-0833/88/0505-0679 $ 02.50/0

Table 1. Reductive dehalogenation with vacuum residual oil at 350°C.

Halogeno compound	Product	Conversion [%]	Selectivity [%]
1,2-Dichloropropane	Propene	78	90
1,2-Dibromopropane	Propene	60	60
1,2-Dichlorobutane	1-Butene	90	80
1,2-Dibromobutane	1-Butene	85	50
1,1,2-Trichloroethane	Vinyl chloride	98	70
Allyl chloride	Propene	50	75

clohexane (lindane) already reacts at 200°C with vigorous cleavage of HCl and is reductively dechlorinated at 250°C to monochlorobenzene [Eq. (b)]. The latter can be converted into benzene at 350°C. Perchlorinated biphenyls (PCB) are converted into biphenyl according to reaction (c); in both cases vacuum residue oil serves as reducing system.

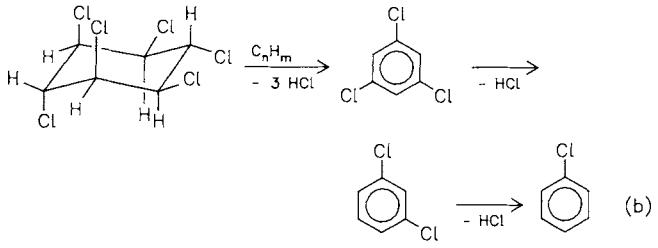

(b)

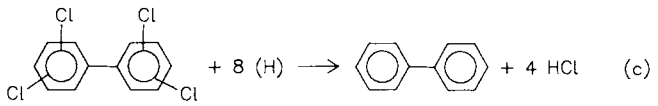

(c)

Aromatic acid chlorides are reduced according to Equation (d) at 350°C in the system technical white oil/activated carbon. As can be seen from Table 2, aldehydes or lactones are formed. Remarkable in this context is the fact that a COCl group of terephthaloyl chloride is even reduced to the methyl group.

Table 2. Reduction of acid chlorides with technical white oil and activated carbon at 350°C.

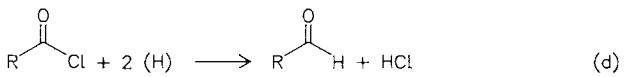

(d)

Acid chloride	Product	Conversion [%]	Selectivity [%]
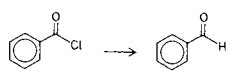		80	50
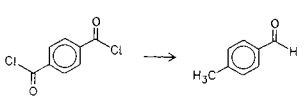		70	80
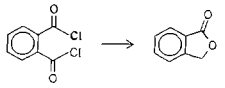		70	40

3. Hydrogenation of CC Double Bonds

The CC double bond of α,β-unsaturated aldehydes can be selectively hydrogenated, in some cases in very good yields[5] [Eq. (e)]. Table 3 lists some examples.

Table 3. Selective hydrogenation of α,β-unsaturated aldehydes with technical white oil and activated carbon at 350°C.

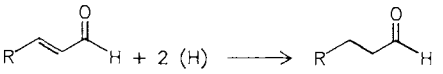

(e)

Aldehyde	Product	Conversion [%]	Selectivity [%]
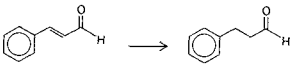		88	50
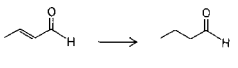		30	90
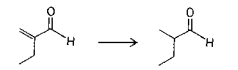		56	85
		52	20

By increasing the pressure, and thus the solubility or residence time, it is possible to hydrogenate ethene, propene, and even arenes. In the case of the stable hydrocarbons the yields are very high at conversion rates which are partially not optimized. An example is reaction (f) in Table 4.

Table 4. Hydrogenation of olefins and arenes with technical white oil and activated carbon (Carboraffin P®) at 350–400°C and 5–35 bar.

Olefin or arene	Product	Conversion [%]	Selectivity [%]
$H_2C{=}CH_2$	$\longrightarrow H_3C{-}CH_3$ (f)	43	95
$H_2C{=}CH{-}CH_3$	$\longrightarrow H_3C{-}CH_2{-}CH_3$	37	90
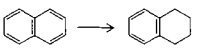		6	90
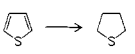		50	20

In the case of hydrogen transfer in the presence of carbon a redox reaction is involved whose equilibrium is dependent on the reduction potential of the H donor and on the oxidation potential of the H acceptor. Thus, for example, naphthalene can be hydrogenated to tetralin with the hydrocarbon mixture technical white oil/activated carbon. Tetralin, however, can be used as source of hydrogen for the reduction of dichloropropane to propene; naphthalene is formed thereby.

The high reduction potential of the system hydrocarbon/carbon manifests itself in the reactions that are collected in Sections 4 to 7.

4. Reduction of Carbonyl Compounds

C=O-functions are reduced to methylene groups. This remarkable reaction takes place at 350°C under normal pressure [see Reaction (g)]. Table 5 contains two examples.

Table 5. Reduction of carbonyl compounds with technical white oil and 10% activated carbon at 350°C.

Carbonyl-compound	Product	Conversion [%]	Selectivity [%]
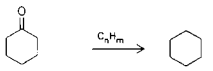		5	>95
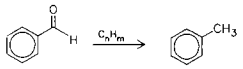	(g)	26	>88

5. Reduction of Sulfur Compounds

The following reaction (h)—the reduction of sulfonic acids or sulfonic acid derivatives to thiols or thiophenols—possibly has some practical importance, especially with regard to aromatic compounds (Table 6). Aromatic sulfonic acid derivatives are known to be readily accessible by sulfonation reactions.

Table 6. Reduction of sulfonic acids and derivatives with technical white oil and activated carbon at 350°C. The yields are based on starting amount of acid or derivative (cf. Table 8).

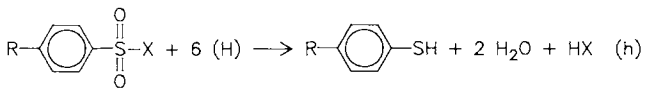

(h)

R	X	Yield [%]	R	X	Yield [%]
H	–OH	78	CH_3	$–OCH_3$	48
H	–Cl	64	CH_3	–Cl	80

These reactions can be easily carried out on an industrial scale in good to very good yields with the system hydrocarbon/carbon without the trouble of ecologically unacceptable salt- or sulfur-containing effluents being formed. Also remarkable is the fact that not only the activated derivatives of the sulfonic acids but also the sulfonic acids themselves are reduced.

Thiols and thiophenols can also be obtained from the disulfides if the latter are treated with technical white oil and activated carbon at 350°C and residence times in the order of seconds [Reaction (i)]. Sulfides can be obtained analogously from sulfoxides according to reaction (k). If R = phenyl the yields are 99 and 66%, respectively.

$$R–S–S–R + 2(H) \longrightarrow 2\,R–S–H \quad (i)$$

$$R–SO–R + 2(H) \longrightarrow R–S–R + H_2O \quad (k)$$

6. Reduction of Phosphorus Compounds

Phosphane oxides, sulfides and dihalides can also be converted into phosphanes with technical white oil and activated carbon[6] [Eq. (l)]. Thus, triphenylphosphane oxide can be reduced to triphenylphosphane with a selectivity of 68%, while triphenylphosphane dichloride is reduced almost quantitatively to triphenylphosphane.

$$R_3PX_2 + C_nH_m \xrightarrow{[C]} R_3P + C_nH_{m-2} + 2\,HX \quad (l)$$

X = halogen; X,X = O,S

The formation of carbon from the saturated hydrocarbon proceeds, as indicated in Equation (l), via mono- or polyunsaturated hydrocarbons.

7. Reduction in the Gas Phase

The reduction reactions presented here, and others, can in principle also be carried out in the gas phase. The substrates are fed with volatile hydrocarbons such as propane, propene, cyclohexane, light petroleum over an activated carbon bed at 300–400°C.

As shown in Table 7, 1,2-dichloropropane was reduced with various saturated hydrocarbons at 400°C on Contarbon BA® according to Equation (m) [cf. also Eq. (a)].

Table 7. Reduction of 1,2-dichlorpropane according to Equation (m) (see text).

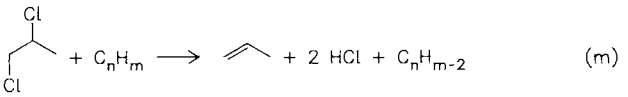

(m)

C_nH_m	Conversion [%]	Selectivity [%]
Methane	98	56
Ethane	98	74
Isobutane	98	88
Cyclohexane	98	91

8. Typical Procedures

Example 1: Reduction of 1,2-Dichloropropane according to Equation (a)

The apparatus employed is shown in Figure 1. 40 mL of 1,2-dichloropropane (1) and 8 L of nitrogen (2) were passed per hour through the 2-L agitator (3) containing 1.2 kg of vacuum residue oil at 350°C. In order to maintain the reaction temperature, unchanged dichloropropane together with volatiles were removed from the reaction mixture by condensation in the flask (4) at 90°C. 12.75 g of condensate (5) together with 80 wt-% dichloropropane were removed per hour, from which a conversion of 78% was calculated. The gaseous reaction products were passed through a washing column (6) for removal of hydrochloric acid. 15 L of exit gas (7) with 43 vol-% propene were collected per hour. This corresponds to a yield of 90% based on the conversion. 217 g of aqueous hydrochloric acid containing 10.5 wt-% HCl were collected in the washing column per hour. This corresponds to 76% of the chlorine contained in the dichloropropane feed.

Example 2: Conversion of Benzaldehyde into Toluene according to Reaction (g)

A mixture of 225 g of technical white oil and 25 g of activated carbon was heated to 350°C in a four-necked flask fitted with stirrer, thermometer, inlet tube and distillation arm. 10.5 g of benzaldehyde and ca. 5 L of nitrogen were then fed into the flask per hour. After 3 h, 33.7 g of condensate was collected, which according to gas chromatographic analysis of the distillate contained 18.6% toluene and 69.3% benzaldehyde. The conversion was thus 25.8%, tbe selectivity 88.6%. Under the same conditions, but without addition of activated carbon, no reaction took place.

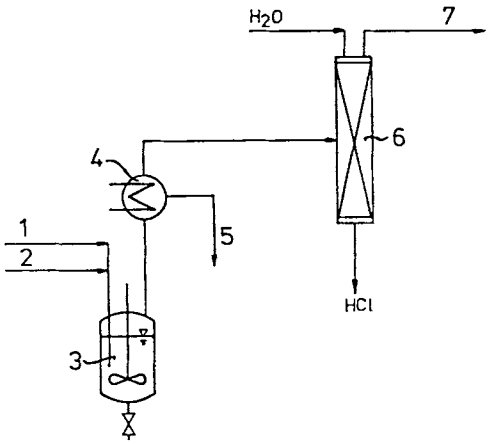

Fig. 1. Apparatus for the reduction of 1,2-dichloropropane according to Equation (a). 1 to 7, see text.

Example 3: Reduction of Aromatic Sulfonic Acids, Sulfonic Acid Derivatives, and Diphenylsulfane according to Reactions (h) and (i)

A mixture of white oil (450 g) and activated carbon (Carboraffin P®) (50 g) was heated to 350 °C and treated with 0.3 mol of the starting material quoted in Table 8 and 30 L of nitrogen per hour: The starting material was added dropwise to the stirred white oil/activated carbon mixture; the vapors leaving the reaction flask were condensed. Solid starting materials were melted at 90 or 140 °C before addition to the mixture. The amounts and yields of the products collected in the condensate after 4 h are listed in Table 8. In the case of *p*-toluenesulfonic acid chloride as starting material (Entry No. 1), the condensate was treated with 20% aqueous caustic soda, and the aqueous phase acidified and extracted with dichloromethane.

Table 8. Reduction of sulfonic acid derivatives and diphenyl disulfide (see text). R′ = *p*-tolyl, R = phenyl (cf. Table 6).

No.	Starting material	Amount [g h^{-1}]	Product	Amount [g] [a]	Yield [%] [b]
1	R′-SO_2Cl	57	R′-SH	131.4	88.3
2	R′-$SO_3H \cdot H_2O$	57	R′-SH	124.0	83.3
3	R′-SO_3CH_3	56	R′-SH	91.4	61.2
4	R-SO_2Cl	53	R-SH	106.8	80.8
5	R-SO_3H	48	R-SH	117.1	87.6
6	R-S-S-R	66	R-SH	263.2	98.8

[a] In examples 2 to 6 the amount of product collected in 4 h was determined by gas chromatographic analysis. [b] Based on amount of starting material.

Example 4: Reduction of Triphenylphosphane Oxide according to Equation (l)

A mixture of technical white oil (250 g) and pulverized activated carbon (25 g) was heated to 350 °C with stirring in a flask and treated with 27.18 g of triphenylphosphane oxide with concomitant passage of nitrogen (5 L per hour). The water formed in the ensuing reaction was continuously distilled off. The reaction was complete after 6 h, and 0.8 g of H_2O had collected in the condenser trap. The reaction mixture was cooled to room temperature and extracted with 5 × 100 mL of glacial acetic acid. After removal of the acetic acid by evaporation, the crystalline residue contained 13.3 g of unchanged triphenylphosphane oxide, 9.2 g of triphenylphosphane, and 6.2 g of acetic acid. The conversion was 52% with a selectivity of 68%.

Example 5: Reduction of 1,2-Dichloropropane in the Gas Phase according to Equation (m)

Figure 2 shows the apparatus employed. The fixed-bed furnace (4) (length 500 mm, diameter 25 mm) was filled with 70 g of activated carbon (Contarbon BA®, special, particle size 4 mm). 15 mL of 1,2-dichloropropane (1) and 15 L of isobutane, preheated to 350 °C via the evaporator (3), were passed at 400 °C over the fixed bed of the furnace per hour. The gases leaving the reactor were fed into the washing column (5) for removal of HCl. 410 g of aqueous hydrochloric acid containing 2.66 wt% HCl were collected per hour. This corresponds to a conversion of 98%. 17.6 L of exit gas containing 16.85 vol-% propene and 0.1 vol-% propane together with smaller amounts of methane, ethane, ethene, and butene were collected per hour. This corresponds to a yield of 88.2% propene based on the conversion.

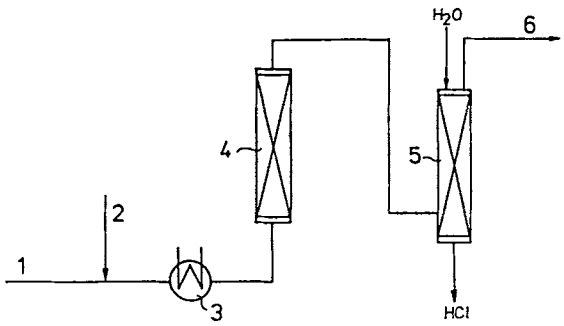

Fig. 2. Apparatus for the reduction of 1,2-dichloropropane in the gas phase according to Equation (m). 1 to 6, see text.

9. Outlook

The current basic raw materials for the chemical industry are petroleum and natural gas, which mainly consist of saturated hydrocarbons. For the synthesis of compounds, the petroleum fractions must be broken down by cracking into alkenes and alkynes or by re-forming into carbon monoxide and hydrogen. The direct functionalization of unsaturated hydrocarbons is still a priority in current research programs. In this context the scission of the C-H bond by incorporation of energy-rich metal-complexes is the correct strategy, yet this method can only be resorted to in industry if the metals are used in catalytic amounts or can be completely and easily recyclized.

The activation by carbon and the use of hydrocarbons as strong reducing agents not only opens up new preparative possibilities, in which the hydrogen from fossil sources can be used directly, but also interesting perspectives regarding radical reactions.

And last but not least, the concept of whether carbon-catalyzed reduction with CH species also plays a role in the formation of petroleum—with removal of oxygen, nitrogen and sulfur—warrants further discussion.

In view of this new potential application of hydrocarbons one is reminded of that intuitive recognition from the years of the oil crisis: "The C-H bond is too good for burning."

Received: February 8, 1988 [A 670 IE]
German version: *Angew. Chem. 100* (1988) 699

[1] R. H. Crabtree, *Chem. Rev. 85* (1985) 245.
[2] Laily Bin Din, J. M. Lindley, O. Meth-Cohn, *Synthesis 1978*, 23.
[3] K. Okamoto, N. Tanaka, K. Adachi, H. Shingu, *Bull. Chem. Soc. Jpn. 39* (1966) 1522.
[4] T. Dockner, H. Krug, H. Nohe, Eur. Pat. 198232 (1985), BASF Aktiengesellschaft.
[5] T. Dockner, H. Krug, M. Sauerwald, Eur. Pat. 233455 (1987), BASF Aktiengesellschaft.
[6] T. Dockner, Eur. Pat. 207432 (1986), BASF Aktiengesellschaft.

When submitting manuscripts, authors of articles intended for publication as "Communications" are requested to read the "Notice to Authors" reproduced in the January issue of the journal following the list of contents; upon request, a copy can be obtained from the editorial office.

Rhodium-Catalyzed Reductive Carbonylation of Methyl Formate to Acetaldehyde**

By *Didier Vanhoye, Serge Melloul, Yves Castanet, André Mortreux,* and *Francis Petit**

The reductive carbonylation of methanol by syngas (CO/H_2) to yield acetaldehyde has been extensively studied.[1] This reaction is catalyzed, at least to some extent, by most Group VIII metals in conjunction with a halogen promoter, the most active system being cobalt salts with an iodide promoter.[2] However, the overall selectivity varies in most cases between 50 and 80% according to the experimental conditions. The main by-products are ethanol, methyl acetate, acetic acid, and 1,1-dimethoxyethane.

In the same way, methyl acetate carbonylation to acetic anhydride[3] (Rh catalysis) or acetaldehyde and acetic acid[4] (Co catalysis) is well known. On the other hand, these systems have been observed to isomerize methyl formate to acetic acid[5] and, upon ruthenium-catalyzed hydrocarbonylation of methyl formate, the nonselective production of acetaldehyde, together with methanol and ethanol, has been reported in the patent literature.[6]

We report here a selective route to acetaldehyde via the reaction of methyl formate with carbon monoxide catalyzed by rhodium complexes.

In a typical reaction, a solution of methyl formate in *N*-methylpyrrolidone (NMP) reacts in an autoclave with CO at 180°C and 80 bar in the presence of $RhCl_3 \cdot 3H_2O$ and LiI to give acetaldehyde and CO_2 in accordance with Equation (1).

$$HCOOCH_3 + CO \xrightarrow[NMP]{RhCl_3 \cdot 3H_2O/LiI} CH_3CHO + CO_2 \qquad (1)$$

Table 1, which lists some typical results obtained under various conditions, shows that different rhodium salts or complexes can be used as catalyst precursor without appreciable change of activity and selectivity for acetaldehyde formation (up to 80% in each case). On the other hand, the presence of an iodide salt $A^{\oplus}I^{\ominus}$ ($A^{\oplus}$ = alkali-metal ion or $[CH_3PPh_3]^{\oplus}$[7]) is absolutely necessary, since in the absence of iodide or in the presence of either I_2 (run 5) or CH_3I (run 6), the activity is very low. In these cases, the addition of triphenylphosphane (runs 4 and 7), which is able to generate a phosphonium iodide salt, results in rate enhancement to give activities which are comparable with those observed in the LiI systems. The addition of PPh_3 also enhances the rates of reactions carried out in the presence of HI. The production of the iodide salt from I_2 is explained according to Equation (3) via CH_3I formation [Eq. (2)], a process which has been already described elsewhere.[8]

Table 1. Acetaldehyde production from methyl formate on rhodium catalysts.

No.	Catalyst [a]	*t* [h]	Conversion [mol-%]	Product selectivity [b] [mol-%] MeCHO	MeOH	$MeCO_2Me$	[c]
1	$RhCl_3 \cdot 3H_2O$	1	29.3	72.9	20.0	—	7.1
	LiI (1.86 mmol)	3	60.5	81.3	11.1	—	7.6
2	$[Rh(CO)Cl(PPh_3)_2]$	1	33.4	82.6	15.6	—	1.8
	LiI (1.86 mmol)	3	58.8	77.0	12.2	—	10.8
3	$[RhCl(CO)_2]_2$	1	33.5	82.7	14.0	—	3.3
	LiI (1.86 mmol)	3	61.5	81.6	8.8	—	9.6
4	$[Rh(CO)Cl(PPh_3)_2]$ I_2 (0.25 mmol) PPh_3 (0.6 mmol)	2	37.9	84.4	1.6	—	14.0
5	$[Rh(CO)Cl(PPh_3)_2]$ I_2 (0.25 mmol)	15	26.0	15.4	76.9	—	7.7
6	$[Rh(CO)Cl(PPh_3)_2]$ CH_3I (0.3 mmol)	15	19.6	17.3	63.8	11.2	7.7
7	$[Rh(CO)Cl(PPh_3)_2]$ CH_3I (0.5 mmol) PPh_3 (0.6 mmol)	1	16.5	66.1	24.8	—	9.1
		3	37.1	81.4	10.2	—	8.4
8	$[Rh(CO)Cl(PPh_3)_2]$ I_2 (0.25 mmol) PPh_3 (0.6 mmol) toluene (50 mL)	15	40	21	3	75	1
9	$[Rh(CO)Cl(PPh_3)_2]$ LiI (1.86 mmol) pyrrolidone (50 mL)	2	75	—	100	—	—
10	$RhCl_3 \cdot 3H_2O$ LiI (1.86 mmol) H_2O (85 mmol)	2	49.6	49.6	48.6	—	1.8

[a] All reactions were conducted with 5 mL (81.2 mmol) of methyl formate in *N*-methylpyrrolidone (50 mL) unless otherwise specified (runs 8 and 9) in the presence of 0.125 mmol of rhodium; $p_{CO} = 80$ bar, $T = 180$°C. [b] In liquid phase. The gas phase contains CO, CO_2, and CH_4; typical $CH_4 : CO_2$ ratios were in the range 1 : 10 to 1 : 5. [c] Formic acid, methyl iodide, acetone, ethanol, butyraldehyde.

$$CH_3I + PPh_3 \longrightarrow [CH_3PPh_3]^{\oplus} + I^{\ominus} \qquad (3)$$

The activity increases with the iodide concentration, in which case however the selectivity for acetaldehyde formation tends to decrease.

The nature of the solvent is also very important, since the use of either pyrrolidone or toluene, instead of *N*-methylpyrrolidone, affects both the reaction rate (which is very low) and again the acetaldehyde selectivity (runs 8 and 9).

A mechanism similar to that envisaged for acetic acid synthesis from methanol and CO might be postulated for this reaction as most probable; the initial step is the cleav-

[*] Prof. Dr. F. Petit, Dr. D. Vanhoye, S. Melloul, Dr. Y. Castanet, Prof. Dr. A. Mortreux
Laboratoire de Chimie Organique Appliquée, UA CNRS 402
Ecole Nationale Superieure de Chimie de Lille
USTL Flandres Artois, BP 108
F-59652 Villeneuve d'Ascq Cedex (France)

[**] This work was supported by USINOR Steel and the Agence Française pour la Maîtrise de l'Energie.

age of methyl formate by LiI,[9] producing the same intermediate CH_3I [Eq. (4)].

$$HCOOCH_3 + LiI \longrightarrow CH_3I + HCOOLi \qquad (4)$$

However, the observation that the same reaction conducted in the presence of water (run 10) does not yield any acetic acid excludes CH_3COI as an intermediate. Further work is in progress to elucidate the mechanism of this reaction.

Received: November 20, 1987 [Z 2506 IE]
German version: Angew. Chem. 100 (1988) 711

CAS Registry numbers:
$RhCl_3$, 10049-07-7; $Rh(CO)Cl(PPh_3)_2$], 13938-94-8; $[RhCl(CO)_2]_2$, 14523-22-9; LiI, 10377-51-2; I_2, 7553-56-2; PPh_3, 603-35-0; H_2O, 7732-18-5; MeOH, 67-56-1; CO, 630-08-0; acetaldehyde, 75-07-0; methyl formate, 107-31-3; pyrrolidone, 616-45-5.

[1] M. Röper, H. Loevenich, J. Korff, *J. Mol. Catal. 17* (1982) 315; G. R. Steinmetz, T. H. Larkins, *Organometallics 2* (1983) 1879.
[2] J. Gauthier-Lafaye, R. Perron: *Methanol et Carbonylation*, Rhône-Poulenc Recherches, Paris 1986, p. 39.
[3] M. Schrod, G. Luft, *Ind. Eng. Chem. Prod. Res. Dev. 20* (1981) 649.
[4] R. Wegman, D. Busby, *J. Chem. Soc. Chem. Commun. 1986*, 332; *J. Mol. Catal. 39* (1987) 261.
[5] N. Isogai, DBP 2026031 (1971), Japon Gas Chemical Co.; E. P. Antoniades, US Pat. 4196056 (1980), Chevron Research Co.
[6] Jap. Pat. 59104329 (1982), Mitsubishi Gas Chemical Co.; *Chem. Abstr. 101* (1984) 191141h.
[7] The activity decreases in the following order: $[CH_3PPh_3]^{\oplus} > Li^{\oplus} \approx Na^{\oplus} \approx K^{\oplus}$.
[8] R. Solly, S. Benson, *Int. J. Chem. Kinet. 1* (1969) 427.
[9] M. Shiina, T. Hashimoto, *Yukagaku 29* (1980) 901.

(Octamethyltetrasila-η^{12}-[2.2]paracyclophane)-chromium—Synthesis, Structure, and Characteristics**

By *Christoph Elschenbroich,* James Hurley, Werner Massa,* and *Gerhard Baum*

The recent synthesis in 1986 of 1,1,2,2,9,9,10,10-octamethyl-1,2,9,10-tetrasila[2.2]paracyclophane **1** provided the first example of a [2.2]paracyclophane containing heteroatoms only in the bridging units.[2] Whereas in [2.2]paracyclophane **3** the inter-ring distances are markedly shorter than in bis(η^6-benzene)chromium **2**, in **1** they are longer as compared to **2**. Since it is possible to introduce a chromium atom into the cavity of **3** by means of cocondensation techniques, we were intrigued by the prospect of *endo* coordination of a transition metal into **1** (complex **5**). The limited availability of **1**, however, suggested that the generation of **5** in a template reaction might be a more promising avenue of approach. In particular, the formation of two Si–Si bonds in a bis(disilyl-η^6-arene)metal precursor should be subject to less compression strain than that encountered in the free arenes [in bis(η^6-arene)metal complexes, the inter-ring distance falls short of the distance governed by the van der Waals radii of free arenes].

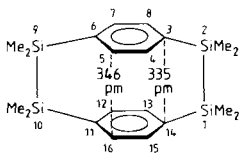

1

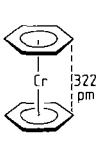

2

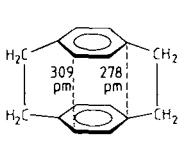

3

We have now found that compound **4**, a precursor to **5**, as well as **6**, which is a precursor to the singly tetramethyldisilano-bridged complex **7**, are accessible by means of metal-atom ligand-vapor cocondensation in relatively good yield. Dechlorinative coupling with lithium/naphthalene in dimethoxyethane (DME) leads to the complexes (1,1,2,2,9,9,10,10-octamethyl-1,2,9,10-tetrasila-η^{12}-[2.2]paracyclophane)chromium **5** and (1,1,2,2-tetramethyldi-1,2-η^6-phenyldisilane)-chromium **7**, respectively. Physical data of the new compounds **4**–**7** are collected in Table 1.

The complexes **5** (red rhombi) and **7** (brown needles) display high thermal stability: **5** melts without decomposition at 310–314 °C and in the EI mass spectrum no peaks, besides those of the molecular ion (100%) and ^{52}Cr (12%), occur with $I > 10\%$. The redox potentials of the couples

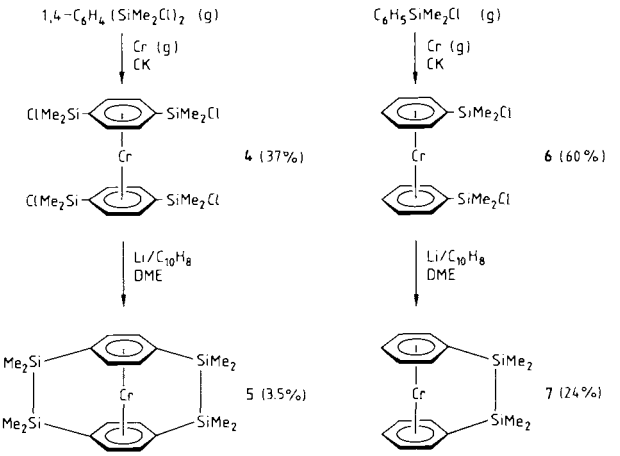

Table 1. Selected physical data for the new compounds **4**–**7**. ^1H-NMR: 300 MHz; ^{13}C-NMR: 75.5 MHz; ESR: X-band; MS: 70 eV; cyclic voltammetry (CV) versus the saturated calomel electrode.

4: ^1H-NMR (C_6D_6): $\delta = 4.63$ (s, 8H; H_{Aryl}), 0.57 (s, 24H; H_{Me}); $^{13}C\{^1H\}$-NMR (C_6D_6): $\delta = 77.35$ (ipso-C), 80.25 (C_{Aryl}), 2.90 (C_{Me}); MS: *m/z* 576 ($M^{\oplus}$, 6.5%), 314 ($[M - C_6H_4(SiMe_2Cl)_2]^{\oplus}$, 100%), 52 ($^{52}Cr^{\oplus}$, 23%)

5: M.p. = 310–314 °C; ^1H-NMR (C_6D_6): $\delta = 4.88$ (s, 8H; H_{Aryl}), 0.38 (s, 24H; H_{Me}); $^{13}C\{^1H\}$-NMR (C_6D_6): $\delta = 80.00$ (ipso-C), 82.60 (C_{Aryl}), −2.43 (C_{Me}); ESR [DMF/$CHCl_3$ (1/1), 20 °C]: $a(^1H_{Aryl}) = 0.275$ mT, $a(^{53}Cr) = 1.75$ mT, $\langle g \rangle = 1.9859$; MS: *m/z* 436 ($M^{\oplus}$, 100%), 378 ($M^{\oplus} - SiMe_2$, 4%), 192 ($Me_2SiC_6H_4SiMe_2^{\oplus}$, 3%), 52 ($^{52}Cr^{\oplus}$, 12%). CV (DME, Bu_4NClO_4, 23 °C): $E_{1/2} = -0.66$ V, $\Delta E_p = 82$ mV, $i_a/i_c = 1.00$, $E_{pa} = 0.94$ V (irreversible, 100 mV s^{-1})

6: ^1H-NMR (C_6D_6): $\delta = 4.35$–4.50 (m, 10H; H_{Aryl}), 0.51 (s, 12H; H_{Me}); $^{13}C\{^1H\}$-NMR (C_6D_6): $\delta = 74.53$ (ipso-C), 78.79, 77.04, 74.53 (C_{Aryl}), 2.63 (C_{Me}); MS: *m/z* 392 ($M^{\oplus}$, 17%), 222 ($[M - PhSiMe_2Cl]^{\oplus}$, 100%), 52 ($^{52}Cr^{\oplus}$, 47%)

7: M.p. = 163–166 °C; ^1H-NMR (C_6D_6): $\delta = 4.73$ (d, 4H; *o*-H), 4.33–4.40 (m, 6H; *m*-, *p*-H), 0.36 (s, 12H; H_{Me}); $^{13}C\{^1H\}$-NMR (C_6D_6): $\delta = 78.48$ (ipso-C), 80.45, 76.63, 76.22 (C_{Aryl}), −2.46 (C_{Me}); ESR [dimethylformamide (DMF)/$CHCl_3$ (1/1), 20 °C]: $a(^1H_{Aryl}) = 0.316$ mT, $a(^{53}Cr) = 1.75$ mT, $\langle g \rangle = 1.9859$; MS: *m/z* 322 ($M^{\oplus}$, 100%), 186 ($[M - PhSiMe_2H]^{\oplus}$, 11%), 135 ($PhSiMe_2^{\oplus}$, 31%), 52 ($^{52}Cr^{\oplus}$, 31%); CV (DME, Bu_4NClO_4, 23 °C): $E_{1/2}(7/7^{\odot\oplus}) = -0.69$ V, $\Delta E_p = 85$ mV, $i_a/i_c = 0.96$, $E_{pa} = 0.93$ V (irreversible, 100 mV s^{-1})

[*] Prof. Dr. Ch. Elschenbroich, J. Hurley M. Phil., Priv.-Doz. Dr. W. Massa, G. Baum
Fachbereich Chemie der Universität
Hans-Meerwein-Strasse, D-3550 Marburg 1 (FRG)

[**] Metal π-Complexes of Benzene Derivatives, Part 32. This work was supported by the Deutsche Forschungsgemeinschaft and by the Fonds der Chemischen Industrie. *J. H.* gratefully acknowledges the award of a scholarship by the Deutscher Akademischer Austauschdienst (DAAD). We thank Dipl.-Chem. *M. Wünsch* for cyclovoltammetric measurements.—Part 31: [1].

neutral complex/radical cation are shifted only marginally relative to bis(benzene)chromium ($E_{1/2} = 0.675$ V). The decreased ESR coupling constants $a(^{53}Cr)$ for the bridged species $\mathbf{5}^{\oplus\ominus}$ and $\mathbf{7}^{\oplus\oplus}$, compared to the corresponding unbridged derivatives bis(trimethylsilyl-η^6-benzene)chromium$^{\oplus}$ [$a(^{53}Cr) = 1.82$ mT] and bis[1,4-bis(trimethylsilyl)-η^6-benzene]chromium$^{\oplus}$ [$a(^{53}Cr) = 1.85$ mT][5] point to a larger degree of metal→ligand spin delocalization in the metallocyclophanes. The high thermal stability of the complexes **5** and **7** contrasts with the solvolytic lability of the radical cations $\mathbf{5}^{\oplus\ominus}$ and $\mathbf{7}^{\oplus\oplus}$: the radical cation $\mathbf{5}^{\oplus\ominus}$, generated through oxidation by 4-pyridinecarbaldehyde, is stable in anhydrous THF for weeks; addition of water (5%) induces quantitative desilylation within a few minutes, however.

Figure 1 presents the structure of **5** in the crystal,[6] which presumably is isotypical to the recently characterized structure of the free ligand **1**.[2] Compound **5**, as well as **1**, possesses a center of inversion; the lattice constants of the metal complex **5** are somewhat decreased, however.[7] The distance between the "best ring planes" in **5** approaches the value for bis(benzene)chromium **2** (324 pm). As compared with the free ligand **1**, the mean C–C bond distances in the coordinated arenes (142.1 pm) are longer by about 3 pm. The boat deformation of the rings is strongly reduced in **5**: the inter-ring distance C1-C4′ [319.8(6) pm] is only slightly shorter than the inter-ring distances C2-C5′ [326.2(6) pm] and C3-C6′ [325.2(6) pm]. Therefore, within a benzene ring and referred to the axes C2···C6 and C3···C5, interplanar angles of only 2.5° and 2.0°, respectively, arise. The Si–Si bond distance in **5** [236.1(4)] is only insignificantly shorter than in **1** [237.6(4)]. The Si–Si–C bond angles are smaller in **5** by about 2.2°. Twisting along the Si–Si axes is not observed: the torsional angle C1-Si1-Si2-C4′ amounts to 0.18(33)°. The bonds C1-Si1 and C4-Si2′, with regard to the planes C1,C2,C6 and C3,C4,C5, form angles of 10.1 and 10.9°, respectively.

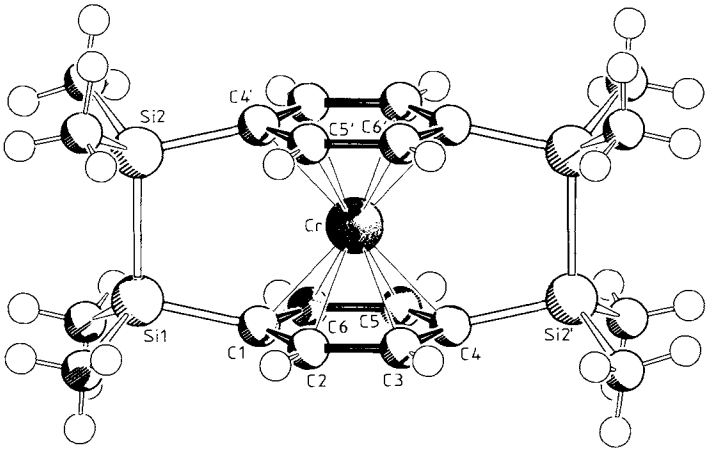

Fig. 1. SCHAKAL plot of a molecule of **5** in the crystal. Important interatomic distances [pm] and angles [°]: Cr-C1 216.3(4), Cr-C2 215.1(4), Cr-C3 214.6(5), Cr-C4 216.5(4), Cr-C5 214.9(5), Cr-C6 214.7(5) (mean Cr-C 215.4), C1-C2 141.7(7), C2-C3 141.3(6), C3-C4 142.0(7), C4-C5 142.8(7), C5-C6 140.9(6), C6-C1 143.6(7) (mean C-C 142.1), Si1-Si2 236.1(4), Si1-C1 188.9(5), Si2′-C4 189.6(5); C2-C1-C6 116.2(5), C1-C2-C3 122.0(5), C2-C3-C4 122.0(5), C3-C4-C5 116.3(5), C4-C5-C6 121.9(5), C5-C6-C1 121.6(5) (mean C-C-C 120.0), C1-Si1-Si2 102.7(3), Si1-Si2-C4′ 102.9(2).

Other chlorobis(organo)silyl derivatives of bis(arene)metal complexes accessible through cocondensation techniques should provide a route to higher-bridged silametallocyclophanes. This technique does not lend itself to the synthesis of carbocyclic metallocyclophanes, however, in that benzyl halides do not yield (η^6-arene)metal complexes under these conditions. Presumably metal insertion into the benzyl–halogen bond interferes.

Experimental Procedure

4: 1,4-bis(chlorodimethylsilyl)benzene (15 g, 26 mmol; internal vaporization) was cocondensed with chromium (0.52 g, 10 mmol) during 2 h at −196 °C/10^{-4} mbar. Extraction with toluene at room temperature, followed by removal of solvent and excess ligand under reduced pressure (70 °C, 10^{-3} mbar), yielded 2.16 g (37%) of **4** as a red-black, sublimable solid.

5: **4** (2.3 g, 4.0 mmol), dissolved in DME (250 mL) was added at −78 °C during 3 h to a solution of $Li^{\oplus}C_{10}H_8^{\ominus}$ (18.4 mmol) in DME (150 mL). After 2 h at −78 °C and warming to RT (12 h), solvent and naphthalene were removed at 50 °C/10^{-2} mbar. Extraction of the residue with toluene (350 mL, 50 °C), filtration through silylated silica gel, and concentration at reduced pressure yielded 60 mg (3.5%) of **5** as red, rhombic crystals.

6: Analogous to **4** by means of external vaporization of (chlorodimethylsilyl)benzene; 2.35 g (60%) of **6** as golden brown, sublimable solid.

7: Analogous to **5** from **6** (1.7 g, 4.3 mmol) in DME (100 mL) and $Li^{\oplus}C_{10}H_8^{\ominus}$ (9.1 mmol) in DME (150 mL). Extraction with petroleum ether (400 mL) and crystallization after concentration yielded 330 mg (24%) of **7** as brown needles.

Received: December 29, 1987 [Z 2561 IE]
German version: *Angew. Chem. 100* (1988) 727

[1] C. Elschenbroich, G. Heikenfeld, M. Wünsch, W. Massa, G. Baum, *Angew. Chem. 100* (1988) 397; *Angew. Chem. Int. Ed. Engl. 27* (1988) 414.
[2] H. Sakurai, S. Hoshi, A. Kamiya, A. Hosomi, C. Kabuto, *Chem. Lett. 1986*, 1781.
[3] C. Elschenbroich, R. Möckel, U. Zenneck, *Angew. Chem. 90* (1978) 560; *Angew. Chem. Int. Ed. Engl. 17* (1978) 531.
[4] The related compound bis(dichloromethylsilyl-η^6-benzene)chromium was synthesized in this way by *P. Timms*: C. G. Francis, P. L. Timms, *J. Chem. Soc. Dalton Trans. 1980*, 1401.
[5] C. Elschenbroich, J. Koch, *J. Organomet. Chem. 229* (1982) 139.
[6] Space group $P2_1/n$, $Z = 2$, $a = 664.9(6)$, $b = 1327.2(4)$, $c = 1270.2(2)$ pm, $\beta = 98.49(4)°$; $\rho_{calcd} = 1.309$ g cm^{-3}; 1648 independent reflections, 1251 with $F_0 > 5\sigma(F_0)$, were collected on a four-circle diffractometer (CAD4, Enraf-Nonius) with $Cu_{K\alpha}$ radiation at 183 K; no absorption correction ($\mu = 61.8$ cm^{-1}), positions of H atoms refined using isotropic temperature factors. 180 parameters, $R = R_w = 0.042$ ($w = 1/\sigma^2(F_0)$). Further details of the crystal structure determination are available on request from the Fachinformationszentrum Energie, Physik, Mathematik GmbH, D-7514 Eggenstein-Leopoldshafen 2 (FRG), by quoting the depository number CSD-52923, the names of the authors, and the journal citation.
[7] The identity of the value of b to that of c, given in [2], is obviously in error; from the density we calculate $b \approx 1330$ pm.

Base-Induced Intramolecular Formation of a Mo–Mo Bond in $[L_2Mo_2^{III}(\mu\text{-}OH)(\mu\text{-}CH_3CO_2)_2]^{3\oplus}$ (L = *N,N′,N″*-Trimethyl-1,4,7-triazacyclononane)**

By *Ademir Neves, Ursula Bossek, Karl Wieghardt,* Bernd Nuber,* and *Johannes Weiss*

Little is known about the mechanism by which complexes containing metal–metal multiple bonds are formed from monomeric complexes in solution.[1] For instance, the monomeric, paramagnetic $[Mo^{III}(OH_2)_6]^{3\oplus}$ is well-

[*] Prof. Dr. K. Wieghardt, Dr. A. Neves, U. Bossek
Lehrstuhl für Anorganische Chemie I der Universität
Postfach 102148, D-4630 Bochum (FRG)
Dr. B. Nuber, Prof. Dr. J. Weiss
Anorganisch-chemisches Institut der Universität
Im Neuenheimer Feld 270, D-6900 Heidelberg (FRG)

[**] This work was supported by the Fonds der Chemischen Industrie. *A. N.* (University of Florianopolis, Brazil) thanks the C.N.Pq. for a fellowship. We thank Dr. *G. Backes-Dahmann* (Oregon Research Center, USA) for preliminary preparative work.

studied,[2] whereas its binuclear, diamagnetic analogue $[Mo_2^{III}(\mu\text{-}OH)_2(OH_2)_8]^{4\oplus}$, containing a Mo–Mo bond, is little investigated.[3] It is surprising that the monomeric aqua ion does not dimerize in aqueous solution and that the reverse process, the formation of the monomer from the dimer, has not been described.

We have now found that the hydrolysis of yellow $[LMo^{III}Br_3]$[4] (L = *N,N',N''*-trimethyl-1,4,7-triazacyclononane) in aqueous solution containing sodium acetate with strict exclusion of oxygen leads to formation of the binuclear cation **1**, which was obtained as a red PF_6 salt.

$[LMo^{III}(\mu\text{-}OH)(\mu\text{-}CH_3CO_2)_2Mo^{III}L]^{3\oplus}$ **1**

Single crystals of $\mathbf{1}(ClO_4)_3 \cdot H_2O$[5] suitable for X-ray structure analysis were obtained from an aqueous solution of $\mathbf{1}(PF_6)_3$ by addition of $NaClO_4$ (*Warning*: $\mathbf{1}(ClO_4)_3 \cdot H_2O$ is very explosive). The structure of **1** is shown in Figure 1. Two Mo^{III} centers coordinated in a distorted octahedral fashion (*fac*-N_3O_3 donor set) are connected by two symmetrical acetate bridges and an OH bridge. The Mo···Mo distance of 3.555(1) Å rules out a direct metal–metal bond—the complex is a classical coordination compound of the Werner type. The two Mo–OH bonds are quite long (average 2.102(7) Å); they correspond to those in $[Mo(OH_2)_6]^{3\oplus}$[6] and in other μ-OH bridged complexes of Mo^{III}.[7] The electronic spectrum of **1** (Fig. 2) is in agreement with these findings; it shows two d–d transitions of low intensity in the visible region, which are characteristic of octahedral Mo^{III} complexes with d^3 configurations, and—interestingly—two spin-forbidden transitions (λ_{max} = 1029, 950 nm). Measurements of the temperature-dependent molar magnetic susceptibility (4–298 K) of solid $\mathbf{1}(ClO_4)_3 \cdot H_2O$ revealed a strong antiferromagnetic spin-spin coupling ($H = -2JS_1S_2$; $S_1 = S_2 = 3/2$; $J = -96$ cm^{-1}); in the analogous Cr_2^{III} dimer, it is significantly weaker ($J = -14$ cm^{-1}[8]).

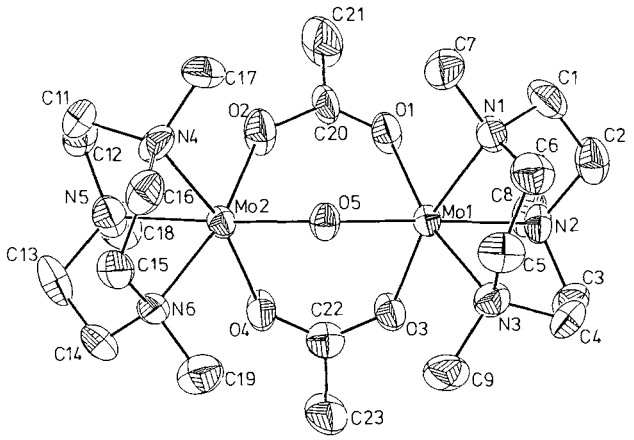

Fig. 1. The molecular structure of **1** in $\mathbf{1}(ClO_4)_3 \cdot H_2O$. Selected distances [Å] and angles [°]: Mo1-N1 2.20(1), Mo1-N2 2.20(1), Mo1-N3 2.19, Mo1-O1 2.100(7), Mo1-O3 2.082(7), Mo1-O5 2.098(7), Mo2-N4 2.18(1), Mo2-N5 2.19(1), Mo2-N6 2.21(1), Mo2-O2 2.092(7), Mo2-O4 2.075(7), Mo2-O5 2.107(7), Mo1-Mo2 3.555(1); Mo1-O5-Mo2 115.4(3).

The cation **1** is a weak acid. Aqueous solutions of **1** containing a small amount of triethylamine afforded brown **2** as crystalline $PF_6^{\ominus}$, $BF_4^{\ominus}$, and $ClO_4^{\ominus}$ salts. After addition of $NaClO_4$, alkaline aqueous solutions of $\mathbf{2}(BF_4)_2$ afforded single crystals of $\mathbf{2}(ClO_4)(BF_4) \cdot H_2O$. Complex **2** is the deprotonated form of **1**, the OH bridge being transformed into an oxo bridge. The pK_a value [Eq. (a)] was determined spectrophotometrically at 25 °C to be 6.8.

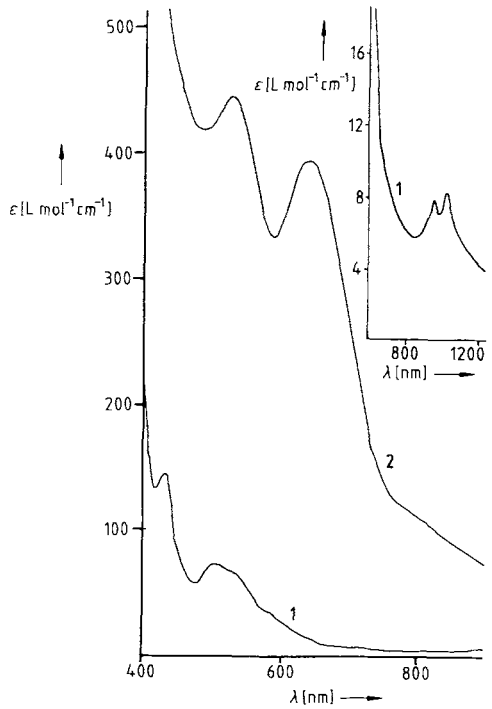

Fig. 2. Electronic spectra of $\mathbf{1}(PF_6)_3$ (insert: spectrum of $\mathbf{1}(PF_6)_3$ in the region 700–1200 nm) and $\mathbf{2}(PF_6)_2$ in acetonitrile (25 °C).

$[LMo^{III}(\mu\text{-}O)(\mu\text{-}CH_3CO_2)_2Mo^{III}L]^{2\oplus}$ **2**

$$\mathbf{1} \overset{K_a}{\rightleftharpoons} \mathbf{2} + H^{\ominus} \qquad \text{(a)}$$

The deprotonation of the OH bridge in **1** leads to a dramatic change in the structure (Fig. 3).[9] Not only is the expected shortening of the Mo–O bond (by 0.156 Å) observed, but, in addition, the distance between the two Mo^{III} centers is reduced by 0.67 Å (!), so that the Mo–Mo distance in **2** is only 2.885(1) Å. The comparable Mo–N and $Mo\text{–}O_{acetate}$ bonds in **1** and **2**, in contrast, are of the same length within the limits of error.

The electronic spectrum (Fig. 2) and the magnetic properties of **2** are significantly different from those of **1**:[10] **2** exhibits two strong intensity absorptions in the visible

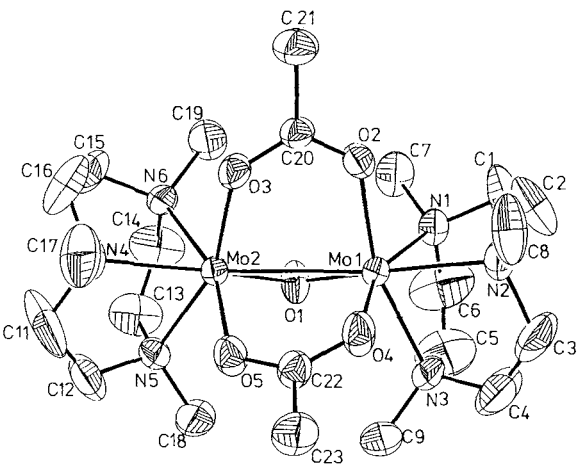

Fig. 3. The molecular structure of **2** in $\mathbf{2}(ClO_4)(BF_4) \cdot H_2O$. Selected distances [Å] and angles [°]: Mo1-O1 1.945(4), Mo1-O2 2.102(4), Mo1-O4 2.097(4), Mo1-N1 2.260(4), Mo1-N2 2.291(5), Mo1-N3 2.243(7), Mo1-Mo2 2.885(1), Mo2-O1 1.946(4), Mo2-O3 2.100(4), Mo2-O5 2.085(4), Mo2-N4 2.298(6), Mo2-N5 2.252(4), Mo2-N6 2.257(5); Mo1-O1-Mo2 95.7(2).

region (Fig. 2) and both $\mathbf{2}(PF_6)_2$ and $\mathbf{2}(ClO_4)_2 \cdot H_2O$ are diamagnetic. These findings point to the existence of a Mo–Mo bond in **2**.

The metal–metal bonding in **2** can be discussed in analogy to that in complexes of the general formula $[X_3M(\mu\text{-}X)_3MX_3]^{2\ominus/3\ominus}$, which have local D_{3h} symmetry,[11] taking into consideration the fact that the formal replacement of two μ-X bridges by two μ-acetate bridges causes a lowering of the symmetry to C_{2v}. The three d orbitals on the two Mo atoms that are available for Mo–Mo bonding are the d_{xy}, d_{yz}, and d_{xz} orbitals, assuming that the $d_{x^2-y^2}$ and d_{z^2} orbitals are mainly required for the Mo–ligand bonds. For D_{3h} symmetry, overlap of the above orbitals leads to one $\sigma(a_1')$ and two degenerate $\pi(e'')$ bonding MOs and to one $\sigma^*(a_1')$ and two degenerate $\pi^*(e'')$ antibonding MOs. For C_{2v} symmetry, the π orbitals are no longer degenerate; three bonding MOs are formed $[\sigma(a_1), \pi_1(a_1), \pi_2(b_1)]$ along with the corresponding antibonding MOs $[\sigma^*(a_1), \pi_1^*(a_2), \pi_2^*(b_2)]$. The Mo–Mo bond in **1** is thus a triple bond ($[\sigma(a_1)]^2[\pi(b_1)]^2[\pi(a_1)]^2$), and the two allowed transitions $\pi(a_1) \rightarrow \pi^*(a_2)$ and $\pi(a_1) \rightarrow \pi^*(b_2)$ are observed in the electronic excitation spectrum (Fig. 2).

The base-induced deprotonation of **1** thus leads to the intramolecular formation of a Mo–Mo bond. This process is completely reversible: protonation of **2** in aqueous solution (0.1 M $HClO_4$) affords **1** quantitatively.

Experimental Procedure

$\mathbf{1}(PF_6)_3$: $[LMoBr_3]$ [4] (0.35 g, 0.7 mmol) was added to an aqueous solution (40 mL) of $NH_4[CH_3CO_2]$ (1.2 g, 16 mmol) through which Ar was being bubbled. After heating for 4 h at reflux under Ar, the resulting reddish-brown solution was treated with $NaPF_6$ (0.2 g, 1.2 mmol) and allowed to stand for 24 h at 0°C. A reddish-brown microcrystalline powder formed which afforded red crystals of $\mathbf{1}(PF_6)_3$ upon recrystallization from H_2O (yield: 0.4 g).—IR (KBr): ν(OH) 3530, ν_{as}(C–O) 1540, ν_s(C–O) 1440, 1455 cm^{-1}; UV/VIS (CH_3CN): λ_{max}(ε per dimer) = 1029(8.6), 950(8.3), 501(66), 431(120) nm.

$\mathbf{2}(PF_6)_2 \cdot 3H_2O$: Triethylamine (1 mL) was added to an aqueous solution (30 mL) of $\mathbf{1}(PF_6)_3$ (0.10 g, 0.09 mmol) through which Ar was being bubbled. The solution turned dark brown. Addition of $NaPF_6$ (0.5 g, 3 mmol) resulted in the precipitation of brown $\mathbf{2}(PF_6)_2 \cdot 3H_2O$ (yield: 0.07 g).—IR (KBr): ν_{as}(C–O) 1510, ν_s(C–O) 1460, 1425 cm^{-1}; UV/VIS (CH_3CN): λ_{max}(ε per dimer) = 644(327), 527(433) nm.

Compounds **1** and **2** are unstable toward oxygen both in solution and in the solid state. The similarly prepared ClO_4 salts are explosive. All salts gave correct elemental analyses (C,H,N).

Received: December 14, 1987;
supplemented: January 26, 1988 [Z 2536 IE]
German version: *Angew. Chem. 100* (1988) 718

[1] F. A. Cotton, R. A. Walton: *Multiple Bonds between Metal Atoms*, Wiley, New York 1982.

[2] a) A. R. Bowen, H. Taube, *Inorg. Chem. 13* (1974) 2245; b) Y. Sasaki, A. G. Sykes, *J. Chem. Soc. Chem. Commun. 1973*, 767.

[3] a) M. Ardon, A. Pernick, *Inorg. Chem. 13* (1974) 2275; b) S. P. Cramer, P. K. Eiden, M. T. Paffett, J. R. Winkler, Z. Dori, H. B. Gray, *J. Am. Chem. Soc. 105* (1983) 799.

[4] G. Backes-Dahmann, W. Herrmann, K. Wieghardt, J. Weiss, *Inorg. Chem. 24* (1985) 485.

[5] a) Crystal structure data for $\mathbf{1}(ClO_4)_3 \cdot H_2O$: orthorhombic, space group D_2^4 ($P2_12_12_1$), $a = 13.047(7)$, $b = 15.769(5)$, $c = 19.116(9)$ Å; $V = 3932.9(10)$ Å^3; $\rho_{calcd} = 1.66$ g cm^{-3} for $Z = 4$; $\mu(Mo_{K\alpha}) = 9.0$ cm^{-1}; Syntex-R3; $Mo_{K\alpha}$ radiation ($\lambda = 0.71069$ Å); 4589 unique reflections ($3° \leq 2\theta \leq 60°$), absorption correction (ψ scans); Patterson method (SHELXTL); anisotropic temperature factors for all non-hydrogen atoms (424 parameters), H atoms in fixed positions; 4509 reflections used in the refinement ($I > 2.5\sigma(I)$), $R = 0.057$, $R_w = 0.056$; $\Delta\rho$(max/min) = 1.4/−0.7 e$^\ominus$/Å^3. b) Further details of the crystal structure investigation may be obtained from the Fachinformationszentrum Energie, Physik, Mathematik GmbH, D-7514 Eggenstein-Leopoldshafen 2 (FRG), on quoting the depository number CSD-52890, the names of the authors, and the journal citation.

[6] M. Brorson, M. Gajhede, *Inorg. Chem. 26* (1987) 2109.

[7] a) K. Wieghardt, M. Hahn, W. Swiridoff, J. Weiss, *Inorg. Chem. 23* (1984) 94; b) G. Kneale, A. Geddes, *Acta Crystallogr. Sect. B31* (1975) 1233.

[8] P. Chaudhuri, M. Winter, H.-J. Küppers, K. Wieghardt, B. Nuber, J. Weiss, *Inorg. Chem. 26* (1987) 3302.

[9] Crystal structure data for $\mathbf{2}(ClO_4)(BF_4) \cdot H_2O$: triclinic, space group $P\bar{1}$, $a = 12.263(6)$, $b = 12.550(5)$, $c = 13.258(6)$ Å, $\alpha = 79.70(3)$, $\beta = 67.64(3)$, $\gamma = 66.56(3)°$; $V = 1730.4(8)$ Å^3; $\rho_{calcd} = 1.69$ g cm^{-3} for $Z = 2$; $\mu(Mo_{K\alpha}) = 8.5$ cm^{-1}; AED-II (Siemens); $Mo_{K\alpha}$ radiation ($\lambda = 0.71069$ Å); 7504 unique reflections ($3° < 2\theta < 65°$), absorption correction (ψ scan); Patterson methods (SHELXTL); anisotropic temperature factors for all non-hydrogen atoms (440 parameters), H atoms in fixed positions; 7192 reflections used in the refinement ($I \geq 2.5\sigma(I)$), $R = 0.058$, $R_w = 0.052$; $\Delta\rho$(max/min) = 0.96/−0.83 e$^\ominus$/Å^3 [5b].

[10] A. B. Lever: *Inorganic Electronic Spectroscopy*, 2nd ed., Elsevier, Amsterdam 1984, pp. 414, 614.

[11] a) R. H. Summerville, R. Hoffmann, *J. Am. Chem. Soc. 101* (1979) 3821; b) R. Saillant, R. A. D. Wentworth, *ibid. 91* (1969) 2174; c) J. L. Templeton, W. C. Dorman, J. C. Clardy, R. E. McCarley, *Inorg. Chem. 17* (1978) 1263.

Carbanions as Intermediates in the Synthesis of Grignard Reagents

By *Henricus J. R. de Boer, Otto S. Akkerman,* and *Friedrich Bickelhaupt**

The mechanism of formation of Grignard compounds from organic halides and magnesium has been intensively investigated.[1–5] A broad consensus exists concerning most of the phases and intermediates shown in Scheme 1. This is especially true for steps (1) and (2); still unclear, among other things, is whether the radical $R^\odot$ formed in step (2) combines directly with the "magnesium subhalide" MgX to form the Grignard reagent $RMgX$[2,5] (3), or whether the reaction occurs initially by reduction of the radical to the carbanion $R^\ominus$ (4), which then reacts with $MgX^\oplus$ to form the Grignard reagent[1] (5). Since step (4) takes place, if at all, after the rate-limiting step,[5b] it cannot be detected at all kinetically and is otherwise difficult to detect. Herein we report a novel rearrangement reaction which provides convincing evidence for a carbanion intermediate $R^\odot$.

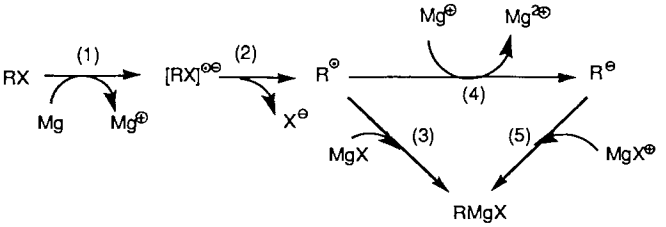

Scheme 1. Proposed mechanism for the formation of Grignard reagents RMgX.

In diethyl ether, *o*-bromobenzyltrimethylstannane **1** does not react with threefold sublimated magnesium. In tetrahydrofuran, on the other hand, rapid reaction occurs, the solution turning yellow (Scheme 2); a white precipitate slowly forms and, after 22 h, **1** is completely consumed. After hydrolysis, titration of the base (with HCl) and of the magnesium (with EDTA) gave values in agreement with a quantitative conversion of **1** to the corresponding Grignard compound **2**. Surprisingly, however, **2** is formed in only 15% yield, as shown by derivatization with chlorotrimethylgermane. Besides the expected **6** (15%), weighing and ^{1}H-NMR analysis showed the presence of **7** (29%), **4** (28%),

[*] Prof. Dr. F. Bickelhaupt, Drs. H. J. R. de Boer, Dr. O. S. Akkerman
Scheikundig Laboratorium, Vrije Universiteit
De Boelelaan 1083, NL-1081 HV Amsterdam (The Netherlands)

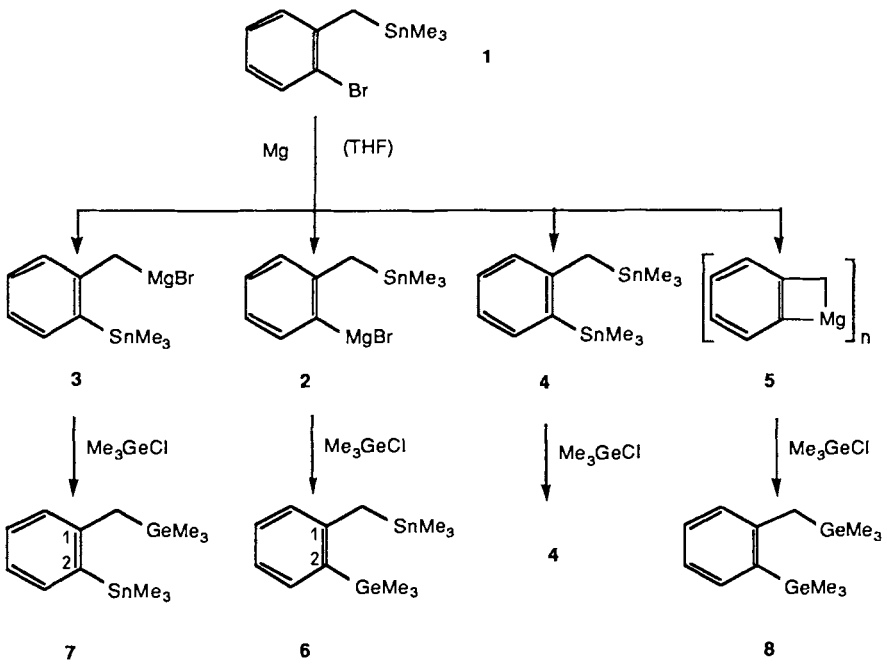

Scheme 2. Products of the reaction of **1** with Mg in THF.

and **8** (28%).[6] Deuterolysis of the reaction mixture afforded, in addition to **4**, the deuterium compounds (D instead of $GeMe_3$) corresponding to **6**–**8**. These findings indicate that, apart from **2**, the isomeric Grignard compound **3**, the distannyl compound **4**, and the (polymeric) magnesacyclobutane **5** are formed. Compound **5** is poorly soluble in THF,[7] which explains the formation of a precipitate. The completely reacted reaction mixture shows no further changes even after 108 h; thus, the unexpected products are only formed during the reaction of the halide with magnesium.

Noteworthy is the migration of the stannyl group from the benzylic position into the aryl position and the reverse migration of the magnesium substituent; this is *formally* (!) a metal-metal exchange reaction, which occurs both intramolecularly (**2** → **3**) and intermolecularly (**2** + **2** → **4** + **5**).

Such exchange reactions are unknown for organomagnesium compounds (except for their reaction with the very reactive stannacyclobutanes[8]), but have been observed for the more strongly carbanionoid organolithium compounds.[9] It is therefore plausible in our case as well to ascribe the extremely rapid and efficient exchange reaction to the carbanion $R^{\ominus}$ formed from **1** (in analogy to Scheme 1). Unequivocal evidence for the existence of this carbanion has not been obtained so far owing presumably to the fact that its lifetime is very short and its stationary concentration very small.

Intermolecular stannyl migrations also occur in other systems. As shown in Scheme 3, reaction of bromobenzene with magnesium in THF in the presence of an equivalent amount of benzyltrimethylstannane **9**, followed by reaction with chlorotrimethylgermane in excess, afforded **11** and **12**, in addition to **9** and **10**, in pairwise equal amounts. A control reaction showed that phenylmagnesium bromide did not react with **9**.

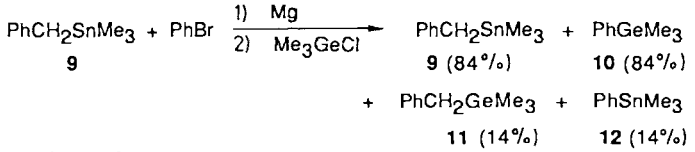

Scheme 3.

In principle, it cannot be ruled out that, instead of $R^{\ominus}$, the radical $R^{\odot}$ in Scheme 1, is responsible for the stannyl migration, since the latter species has been shown to be a true intermediate (!). Homolytic substitutions at stannanes are known, although usually heteroatom-centered radicals (and only in a few cases carbon-centered radicals) have been reported to be the reaction partner.[10] In order to exclude this pathway of reaction for the stannyl migration, it is necessary to investigate how aryl radicals, synthesized independently by a clearly defined route, behave toward benzylstannanes; however, this is not easy under our reaction conditions.[11] The experiments described below indicate, nonetheless, that the reaction of aryl radicals with **1** and **9** is completely different from that of the reactive intermediate involved in the formation of Grignard reagents.

Irradiation of **1** in *n*-pentane (Scheme 4) results not only in the desired cleavage of the carbon-bromine bond[12] but also in that of the carbon-tin bond.[13] At 254 nm, **1** (83%), **9** (4%), and bromotrimethylstannane **13** (13%) were obtained, but not the product of stannyl migration, *o*-trimethylstannyltoluene **14**. Longer irradiation in pentane with a medium-pressure mercury lamp resulted in partial polymerization along with the formation of up to 9% of **14**;[14] however, there are several possible mechanisms for the formation of **14**.[15] If one makes the simplified assumption

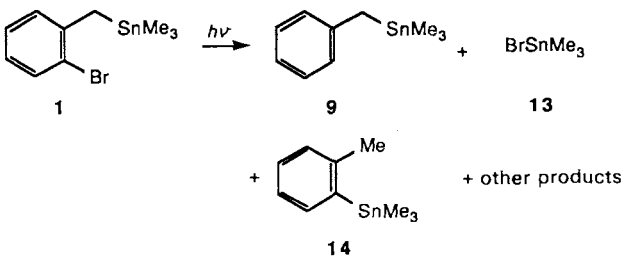

Scheme 4. Photochemical transformation of **1**.

that **14** is formed exclusively by stannyl migration from $R^{\odot}$, then the two alternative reaction modes of $R^{\odot}$, hydrogen abstraction and stannyl migration (i.e., formation of **9** and **14**, respectively), occur in a ratio of 3:1 (15 min[14]). If this product ratio is transferred to the $R^{\odot}$ that occurs with certainty in the formation of Grignard reagents, then it becomes immediately apparent that, in that case, a stannyl migration starting from $R^{\odot}$ can be completely neglected, since even the product of hydrogen abstraction (i.e., **9**) is totally absent (< 1%). In other words, **4** in Scheme 2 must be formed via an intermediate behaving just the opposite of $R^{\odot}$, since this intermediate reacts more quickly with the stannyl group than it is trapped by $MgX^{\oplus}$ (ratio (**3** + **4**) : **2** = 3.8 : 1).

Since a dramatically increased reactivity is not expected for the organotin function in **1**, only the carbanion $R^{\ominus}$, which is otherwise difficult to detect, comes into mind as the factor responsible for the stannyl migration, especially in view of the fact that organolithium compounds exhibit striking parallels in reaction behavior. The radical anion $[RX]^{\odot\ominus}$ can hardly be considered as an alternative, because its lifetime is so short that it is often discussed as a transition state rather than as an intermediate. Moreover, there is the mechanistic problem of how one is to formulate the transfer of the tetracoordinated tin to the radical anion of an organic halide. In further analogy to the reactions of the organolithium compounds, it may be assumed that the rearrangement occurs via stannate complexes.[6,8,16] These also presumably serve as a stabilizing reservoir of carbanions,[17] which would rationalize the surprisingly high proportion of *inter*molecular stannyl transfer.

This stage of the investigation does not permit more detailed statements concerning the identity of the postulated carbanion intermediate. In any case, its reactivity is significantly higher than that of the organolithium compounds: whereas the stannyl transfer requires several hours in the case of organolithium compounds,[9] $R^{\ominus}$ reacts "immediately" despite the presence of its extremely small stationary concentration. This indicates that $R^{\ominus}$ exists in a very reactive form, i.e., presumably as a rather free carbanion. Completely independent evidence for such a species was recently provided by side products obtained in the formation of several crown ether-Grignard compounds.[18]

Received: January 15, 1988 [Z 2577]
German version: *Angew. Chem. 100* (1988) 735

[1] a) C. Prévost, M. Gaudemar, L. Miginiac, F. Bardone-Gaudemar, M. Andrac, *Bull. Soc. Chim. Fr. 1959*, 679; b) M. Andrac, F. Gaudemar, M. Gaudemar, B. Gross, L. Miginiac, P. Miginiac, C. Prévost, *ibid. 1963*, 1385.

[2] B. J. Schaart, C. Blomberg, O. S. Akkerman, F. Bickelhaupt, *Can. J. Chem. 58* (1980) 932, and literature cited therein.

[3] H. M. Walborsky, E. J. Powers, *Isr. J. Chem. 29* (1981) 210, and literature cited therein.

[4] G. Molle, P. Bauer, J. E. Dubois, *J. Org. Chem. 47* (1982) 4120, and literature cited therein.

[5] a) J. F. Garst, J. E. Deutch, G. M. Whitesides, *J. Am. Chem. Soc. 108* (1986) 2490, and literature cited therein; b) H. R. Rogers, R. J. Rogers, H. L. Mitchell, G. M. Whitewides, *ibid. 102* (1980) 231.

[6] Compounds **4** and **8** are known: H. J. R. de Boer, O. S. Akkerman, F. Bickelhaupt, *J. Organomet. Chem. 321* (1987) 291.—**6**: ^{1}H-NMR ($CDCl_3$): δ = 0.11 (s, 9H, ^2J(SnH) = 51 Hz), 0.46 (s, 9H), 2.50 (s, 2H), 7.06–7.42 (m, 4H); ^{13}C-NMR ($CDCl_3$): δ = −9.3 (q, ^1J(CH) = 128.3 Hz; $SnMe_3$), 0.13 (q, ^1J(CH) = 125.5 Hz; $GeMe_3$), 21.8 (t, ^1J(CH) = 125.4 Hz; CH_2), 122.8 (dd, ^1J(CH) = 160.0 Hz, ^3J(CH) = 8.3 Hz; C5), 128.7 (dd, ^1J(CH) = 158.6 Hz, ^3J(CH) = 7.9 Hz; C4), 133.7 (d, ^1J(CH) = 169.7 Hz; C6), 137.6 (br. s; C1), 148.3 (br. s; C2), the signal for C3 apparently coincides with other signals (calcd δ = 126.3 [19]); MS: *m/z* 374 ($M^{\oplus}$, 6%), 359 (6), 240 (3), 225 (3), 209 (3), 194 (15), 179 (17), 165 (100), 150 (8), 135 (15), 120 (4), 119 (16), 91 (8), 89 (7).—**7**: ^{1}H-NMR ($CDCl_3$): δ = 0.16 (s, 9H), 0.35 (s, 9H, ^2J(SnH) = 52 Hz, 54 Hz (^{117}Sn, ^{119}Sn) 2.36 (s, 2H, ^4J(SnH) = 7 Hz), 7.06–7.42 (m, 4H); ^{13}C-NMR ($CDCl_3$): δ = −7.9 (q, ^1J(CH) = 128.3 Hz, ^1J(SnC) = 329.4 Hz; $SnMe_3$), −1.8 (q, ^1J(CH) = 125.5 Hz; $GeMe_3$), 29.3 (t, ^1J(CH) = 125.5 Hz; CH_2), 123.7 (dd, ^1J(CH) = 161.0 Hz, ^3J(CH) = 7.2 Hz, ^3J(SnC) = 48.8 Hz; C4), 127.1 (dd, ^1J(CH) = 154.9 Hz, ^3J(CH) = 6.8 Hz, ^3J(SnC) = 38.1 Hz; C6), 128.4 (dd, ^1J(CH) = 158.6 Hz, ^3J(CH) = 7.5 Hz, ^2J(SnC) = 34.4 Hz; C3), 140.2 (br. s; C2), 148.1 (br. s; C1); MS: *m/z* 374 ($M^{\oplus}$, 5%), 359 (8), 240 (5), 225 (13), 209 (6), 194 (13), 179 (6), 165 (100), 150 (6), 135 (13), 120 (10), 119 (38), 91 (9), 89 (12); high-resolution MS (70 eV): found 372.0116, calcd for $C_{13}H_{24}{}^{72}Ge^{120}Sn$ 372.0106. Correct C,H analyses.

[7] H. J. R. de Boer, O. S. Akkerman, F. Bickelhaupt, G. Erker, P. Czisch, R. Mynott, J. M. Wallis, C. Krüger, *Angew. Chem. 98* (1986) 641; *Angew. Chem. Int. Ed. Engl. 25* (1986) 639.

[8] J. W. F. L. Seetz, G. Schat, O. S. Akkerman, F. Bickelhaupt, *J. Am. Chem. Soc. 105* (1983) 3336.

[9] a) H. Gilman, S. D. Rosenberg, *J. Org. Chem. 24* (1959) 2063; b) D. Seyferth, R. Suzuki, C. J. Murphy, C. R. Sabet, *J. Organomet. Chem. 2* (1964) 431.

[10] K. U. Ingold, B. P. Roberts: *Free-Radical Substitution Reactions*, Wiley-Interscience, New York 1971, p. 96–107.

[11] Phenyl radicals formed upon reaction of bromobenzene with sodium hydride/nickel(II) in *tert*-amyl alcohol (P. Caubère, *Angew. Chem. 95* (1983) 597; *Angew. Chem. Int. Ed. Engl. 22* (1983) 599) attack **9** differently; besides unreacted **9** only benzene (80%), the product of reduction of bromobenzene, was obtained.

[12] G. Lodder in S. Patai, Z. Rappoport (Eds.): *The chemistry of halides, pseudo-halides and azides. Part 2*, Wiley, Chichester 1983, p. 1640.

[13] A. Standt, H. Dreeskamp, *J. Organomet. Chem. 322* (1987) 49, and references cited therein.

[14] A complex mixture of products was obtained; after 15 min, the pertinent products were **1** (71%), **9** (9%), **13** (12%), and **14** (3%); after 60 min, **9** (2%), **13** (64%), and **14** (9%); after 300 min, **13** (72%) and **14** (4%). Cleavage of the C-Br bond and of the benzylic C-Sn bond in **1** is thus fast, whereas that of the aryl C-Sn bond in **14** is slower; it is unclear whether the rapid cleavage of the C-Br bond is caused by photons or by trimethylstannyl radicals.

[15] We assume that the aryl-tin bond of **14** is formed primarily by the reaction of an aryl radical with a trimethylstannyl radical.

[16] H. J. Reich, N. H. Phillips, *J. Am. Chem. Soc. 108* (1986) 2102.

[17] a) G. Wittig, *Angew. Chem. 70* (1958) 65; b) G. Wittig, F. J. Meyer, G. Lange, *Justus Liebigs Ann. Chem. 571* (1951) 167.

[18] P. R. Markies, O. S. Akkerman, F. Bickelhaupt, W. J. J. Smeets, A. L. Spek, *J. Am. Chem. Soc.*, in press.

[19] a) W. Adcock, B. D. Gupta, W. Kitching, D. Doddrell, *J. Organomet. Chem. 102* (1975) 297; b) M. Bullpitt, W. Kitching, W. Adcock, D. Doddrell, *ibid. 116* (1976) 161.

Elementary Reactions at Metal-Sulfur Centers: Base-Induced Substitution of PPh_3 in $[Ru(PPh_3)_2(bmae)]$**

By *Dieter Sellmann** and *Olaf Käppler*

The transition-metal atoms in the active sites of numerous oxidoreductases, from sulfite oxidase to nitrogenase, are surrounded mainly by sulfur ligands and, in some cases, by oxo or amine ligands as well.[1] For practically all these enzymes, however, the molecular course of the elementary reactions is still unknown. This is also true for the mechanism of binding or release of a substrate Y according to

$$M + Y \rightleftharpoons M{-}Y$$

It is commonly assumed that, in the resting state, the metal centers bear protecting ligands L, which must be split

[*] Prof. Dr. D. Sellmann, Dipl.-Chem. O. Käppler
Institut für Anorganische Chemie der Universität
Erlangen-Nürnberg
Egerlandstrasse 1, D-8520 Erlangen (FRG)

[**] Transition-Metal Complexes with Sulfur Ligands, Part 35. This work was supported by the Deutsche Forschungsgemeinschaft and the Fonds der Chemischen Industrie.—Part 34: D. Sellmann, P. Franck, F. Knoch, *J. Organomet. Chem. 339* (1988) 1298. $bmae^{2\ominus}$ = 2,2′-ethylenediiminobis(thiophenolate).

off in precursor reactions in order to generate vacant coordination sites for the binding of Y. A question of fundamental chemical importance concerns the role played by sulfur ligands in such reactions as well as the effect of their replacement, e.g., by amine ligands. We have now found that, in coordinatively saturated thioether dithiolato complexes such as **1** ($dttd^{2\ominus}$ = 2,2′-ethylenedithiobis(thiophenolate)), the π-donor properties of the S atoms are sufficient for the generation of vacant coordination sites (that is, for the release of L), whereas in amino dithiolato complexes such as **2** ($bmae^{2\ominus}$ = 2,2′-ethylenediiminobis(thiophenolate)) the release of L can only be induced by an indirect attack (from the backside) of a base on the NH group of the $bmae^{2\ominus}$ ligand.

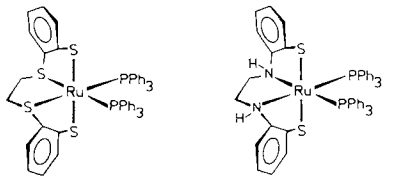

$[Ru(PPh_3)_2(dttd)]$ **1** $[Ru(PPh_3)_2(bmae)]$ **2**

Complexes **1**[2a] and **2**[2b] are isoelectronic and isostructural, but behave completely differently. Complex **1** reacts rapidly already at room temperature and 1 bar CO according to Equation (1); **2**, however, is fully inert under the same or considerably more energetic conditions.

$$\mathbf{1} + CO \xrightarrow[-PPh_3]{THF/RT/1\ bar/10\ min} [Ru(CO)(PPh_3)dttd] \qquad (1)$$

$$\mathbf{2} + CO \xrightarrow{THF/RT/1\ bar} \text{no reaction}$$

$$\mathbf{2} + CO \xrightarrow[-PPh_3]{THF/100\,^{\circ}C/80\ bar} [Ru(CO)(PPh_3)(bmae)] + [Ru(CO)_2(bmae)]$$

3 **4**

Only above 100°C and at 80 bar does complex **2** also undergo reaction with CO, resulting in the simultaneous formation of **3** and **4**.[3]

A comparison of **1** and **2** shows that the high reactivity of **1** is not due to steric factors such as the bulky PPh_3 ligands, but rather due to electronic factors. In the coordinatively unsaturated intermediate **1a** [Eq. (2)], the five-

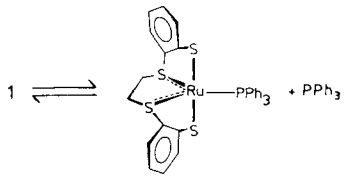

1a

coordinate 16-electron ruthenium center is presumably stabilized by p electrons of the thioether S atoms or by $p_{\pi,S} \rightarrow d_{\pi,Ru}$ bonds.[4]

In order to support this interpretation, we attempted to deprotonate σ-donor amine functions of the unreactive **2**.[5] The resulting σ-π-donor amido centers, like the thioether S atoms in **1**, should stabilize coordinatively unsaturated intermediates (cf. **1a**).

Indeed, in the presence of strong bases such as *n*BuLi or $Na[N(SiMe_3)_2]$, **2** reacts rapidly with CO (room temperature, 1 bar CO). The yellow THF solution of **2** turns deep red on addition of *n*BuLi; stirring for 10 min under CO followed by hydrolysis with MeOH results in the formation of both **3** and **4**.[6]

$$\mathbf{2} + 2\,n\text{BuLi} \xrightarrow[2)\ +MeOH]{1)\ +1\ bar\ CO/THF/RT/10\ min/-PPh_3} \mathbf{3} + \mathbf{4}$$

The deprotonation of the amine functions is shown by IR spectroscopy (absence of the ν_{NH} band of **2** at 3230 cm^{-1}), by $H^{\oplus}/D^{\oplus}$ exchange, which only occurs after addition of *n*BuLi,[7] and by the alkylation behavior of **2**. Whereas **2** reacts with excess MeI to give only the derivative **5**, alkylated on one thiolate S atom,[8] addition of *n*BuLi results in alkylation of both thiolate S atoms, accompanied by simultaneous replacement of PPh_3 by iodide.[9]

$[Ru(PPh_3)_2(bmae(CH_3)_2)]I$ **5**

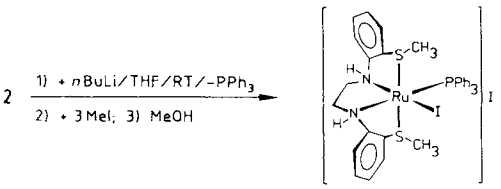

6

The formation of **5** and **6** also shows how the number of alkylation steps is determined by the NH deprotonation. All results indicate the primary formation of the coordinatively unsaturated intermediates **7a** and **7b**, in which the

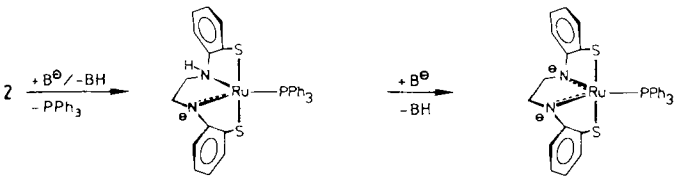

7a **7b**

Ru centers are stabilized by the p electrons of the amido groups.

The introduction of amine ligands into the sulfur coordination sphere of the metal atoms in oxidoreductases can thus lead to pH-dependent substitution, i.e., coordination/decoordination reactions.

Received: November 12, 1987 [Z 2498 IE]
German version: *Angew. Chem. 100* (1988) 706

[1] Cf., e.g.: a) W. E. Newton in A. Müller, B. Krebs (Eds.): *Sulfur, its Significance for Chemistry, for the Geo-, Bio- and Cosmosphere and Technology*. Elsevier, Amsterdam 1984, p. 409; b) T. G. Spiro (Ed.): *Molybdenum Enzymes*, Wiley, New York 1985.

[2] a) D. Sellmann, E. Böhlen, *Z. Naturforsch. B37* (1982) 1026; b) D. Sellmann, U. Reineke, G. Huttner, L. Zsolnai, *J. Organomet. Chem. 310* (1986) 83.

[3] All reactions were carried out under N_2. Reaction of **2** with CO: **2** (200 mg, 0.22 mmol) in THF (30 mL) was stirred for 5 d at 100°C under CO (80 bar). After evaporation of the THF, the products were identified by IR and mass spectroscopy. **3**: ν_{CO} = 1935 cm^{-1}, *m/z* 666 ($M^{\oplus}$, EI); **4**: ν_{CO} = 2050, 1975 cm^{-1}, *m/z* 432 ($M^{\oplus}$, EI).

[4] Concerning the stabilization of coordinatively and electronically unsaturated metal complexes by π-donor S ligands, compare also the properties and structure of $(NEt_4)_2[Cr(CO)_3(S_2C_6H_4)]$: D. Sellmann, W. Ludwig, G. Huttner, L. Zsolnai, *J. Organomet. Chem. 294* (1985) 199.

[5] The deprotonation of amine ligands (formation of σ-π-donor amido ligands) was used to explain the $S_{N1}CB$ mechanism in the substitution reactions of ammine cobalt complexes: cf. a) F. Basolo, R. G. Pearson: *Mechanisms of Inorganic Reactions*, 2nd ed., Wiley, New York 1967; b) J. P. Purzas, R. Nakon, J. L. Petersen, *Inorg. Chem. 25* (1986) 3837. Other authors, however, ascribed the strong labilization effect of $NH_2^{\ominus}$ groups to their basicity: c) D. A. Buckingham, P. A. Marzilli, A. M. Sargeson, *ibid. 8* (1969) 1595.

[6] Reaction of **2** with CO in the presence of *n*BuLi: **2** (200 mg, 0.22 mmol) in THF (30 mL) was treated at −78°C with 0.3 mL (0.48 mmol) of an *n*BuLi solution (1.6 M in hexane). The deep red solution was stirred under CO for 10 min at room temperature and then treated with 5 mL of MeOH. After evaporation of the solvents, the products **3** and **4** were identified by IR and mass spectroscopy (see [3]).

[7] Deuteration of **2**: **2** (45 mg, 0.05 mmol) in THF (20 mL) was treated at −78°C with 0.063 mL (0.1 mmol) of an *n*BuLi solution (1.6 M in hexane) and warmed up to room temperature. After hydrolysis with several drops of D_2O, the solvents were evaporated. The residue was dissolved in CH_2Cl_2, the solution was filtered, and the CH_2Cl_2 was evaporated. IR: $\nu_{N-D} = 2415\ cm^{-1}$.

[8] **5**: **2** (400 mg, 0.44 mmol) in THF (40 mL) was treated with MeI (1 mL, 16 mmol). After stirring for 3 h at room temperature, the precipitated, beige **5** (444 mg = 97% crude product) was separated, dissolved in CH_2Cl_2, and induced to crystallize by addition of a layer of MeOH at room temperature. Yield 295 mg (64%) **5** · MeOH, correct C,H,N analysis. ^{1}H-NMR (60 MHz, $CDCl_3$, TMS int.): $\delta = 2.55$ (s, CH_3), 3.40 (s, MeOH), 1.50–3.60 (m, CH_2-CH_2), 5.05, 5.65 (m, $2\times NH$), 6.20–7.70 (m, $PPh_3 + C_6H_4$). MS: *m/z* 780 ($M^{\oplus} - PPh_3$).

[9] **6**: **2** (400 mg, 0.44 mmol) in THF (40 mL) was treated at −78°C with 0.8 mL (1.3 mmol) of an *n*BuLi solution (1.6 M in hexane) and at room temperature with MeI (0.08 mL, 1.3 mmol). After stirring for 2 h, hydrolysis was carried out with MeOH (5 mL). The solvents were evaporated, the residue was washed with Et_2O (50 mL), and **6** was crystallized from acetone by addition of a layer of pentane. Yield 150 mg (37%, not optimized), analytically pure **6** · acetone. ^{1}H-NMR (60 MHz, CD_2Cl_2, TMS int.): $\delta = 1.45$, 2.70 (s, $2\times CH_3$), 1.00–4.00 (m, CH_2-CH_2), 2.10 (s, acetone), 7.00–8.00 (m, $PPh_3 + C_6H_4$). MS: *m/z* 890 ($M^{\oplus} - CH_3I$). b) The mono- or dialkylation of thiolato complexes is mainly influenced by the charge of the primarily formed species; cf. D. Sellmann, M. Waeber, G. Huttner, L. Zsolnai, *Inorg. Chim. Acta 118* (1986) 49.

Transformation of Open-Chain Thioether-Dithiolato to Cyclic Thioether Ligands by C-S Bond Cleavage and Bond Formation at Ruthenium Centers: Synthesis of the Trithiobenzo[9]crown-3 Complex [Ru(Bzo-9S3)(CO)Br$_2$]**

By *Dieter Sellmann,* Falk Knoch,* and *Christina Wronna*

Sulfur-coordinated transition metals, as the active sites of numerous oxidoreductases, are directly involved in many life processes.[1] A basic understanding of these processes at the molecular level requires a knowledge of the specific properties of the metal centers that are due to the sulfur ligands. These include unusual structures,[2] the coordination, activation, and stabilization of stable or unstable species such as CO, NO, and N_2H_2,[3] and the stabilization of coordinatively and electronically unsaturated metal centers,[4] as well as the ability of many sulfur ligands to make accessible unusual oxidation states of metals.[5] Of equal importance are the reactions of the sulfur ligand framework and the question how the reactivity, for example of coordinated thiolates, is influenced by the metals, their oxidation states, and the coligands. We have now observed specific reaction control by metals for the homologous [M(CO)(dpttd)] complexes of iron and ruthenium (dpttd$^{2\ominus}$ = 2,2′-[thiobis(ethylenethio)]bis(thiophenolate)).[6] Whereas the dpttd$^{2\ominus}$ ligand in [Fe(CO)(dpttd)] undergoes alkylation by bis(2-bromoethyl) sulfide in refluxing THF to give the macrocycle hexathiodibenzo[18]crown-6 (Bzo_2-18S6),[7] [Ru(CO)(dpttd)] **1** only reacts above 120°C (in DMF). However, the reaction proceeds completely differently, leading to a complex containing the new ligand trithiobenzo[9]crown-3 (Bzo-9S3).

Complex **1** is obtained by alkylation of *cis*-[Ru(CO)$_2$(S$_2$C$_6$H$_4$)$_2$]$^{2\ominus}$,via [Ru(CO)$_2$(dpttd)].[8] Complex **1** is thermally so stable that it survives even 5 h of heating at 140°C. Single crystals of **1** · DMF are obtained from these solutions and were shown by X-ray crystallography to have the *meso* form.[9, 10]

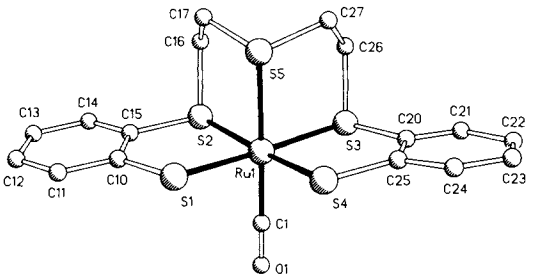

meso-**1**

+ $S(C_2H_4Br)_2$/DMF/140°C
or
1,2-$C_2H_4Br_2$/≈ 6h

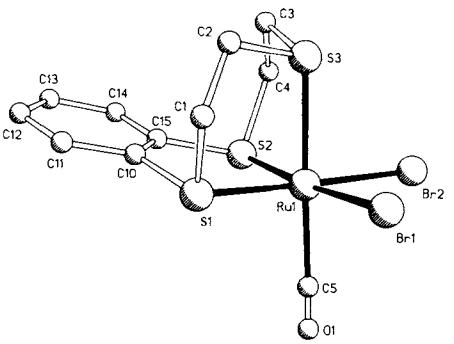

2 + ...

The attempt to alkylate the dpttd ligand in *meso*-**1** with bis(2-bromoethyl) sulfide to give Bzo_2-18S6 yielded a new CO species; however, it was not the expected [Ru(CO)(Bzo_2-18S6)]Br$_2$, but instead the complex [Ru(Bzo-9S3)(CO)Br$_2$] **2**, formed by cleavage of an *o*-benzenedithiolate group. Complex **2** was also characterized by X-ray crystallography.[11]

Although more facile alkylation of the dpttd ligand was expected for **1** as opposed to the Fe analogue, because the [Ru(CO)] fragment is more electron-rich that the [Fe(CO)] fragment, **1** underwent reaction only under considerably more energetic conditions and afforded a different type of product.

In order to interpret the unexpected reaction and the remarkable differences in reactivity between the homologous Fe and Ru complexes, the following findings are important:

(1) The CO ligand of **1**, in contrast to that of [Fe(CO)(dpttd)] is kinetically inert. Therefore, alkylation of **1** with bis(2-bromoethyl) sulfide does not result in release

[*] Prof. Dr. D. Sellmann, Dr. F. Knoch, C. Wronna
Institut für Anorganische Chemie der Universität
Erlangen-Nürnberg
Egerlandstrasse 1, D-8520 Erlangen (FRG)

[**] Transition-Metal Complexes with Sulfur Ligands, Part 36. This work was supported by the Deutsche Forschungsgemeinschaft and the Fonds der Chemischen Industrie. We thank Dr. *M. Moll* for recording the NMR spectra.—Part 35: D. Sellmann, O. Käppler, *Angew. Chem. 100* (1988) 706; *Angew. Chem. Int. Ed. Engl. 27* (1988) 689.

of CO and formation of an intermediate having a vacant coordination site which would favor the formation of new $[MS_2C_2]$ five-membered rings, as is the case for the Fe complex.

(2) Complex **2** is also formed when **1** is allowed to react with 1,2-dibromoethane. Breaking of the C–S bond in the dpttd ligand is therefore probably initiated by attack of the alkylating agent; it still remains an open question whether this reaction occurs by an electrophilic mechanism or by a radical one.

Structurally noteworthy in **1**[10] are the Ru–S distances in the Ru(S1–S4) plane, which have nearly the same values. They lie between 235.9(2) and 237.7(2) and thus in the normal region for Ru^{II} complexes of this type. The Ru–S distance *trans* to the CO ligand, however, is significantly larger (242.4(2) pm). That this is indeed due to the *trans* effect of CO is shown by the corresponding Ru–S distance in the related complex $[Ru(PPh_3)L]$ of only 235.7(2) pm.[8] Here L is a dpttd ligand bearing four *t*Bu groups on the benzene rings. A similar effect is observed for **2**.[11] The two Ru–S distances *trans* to the Br ligands are 230.3(4) pm (average); the Ru–S distance *trans* to the CO ligand is considerably larger, however (242.6(4) pm).

The mirror symmetry of **1** and **2**, which was indicated by X-ray crystallography, is revealed by the ^{13}C-NMR spectra of the two complexes. They show only eight and five signals, respectively, for the sulfur ligands.

Trithiobenzo[9]crown-3 (Bzo-9S3) is the first benzoannelated derivative of trithio[9]crown-3 (or 1,4,7-trithiacyclononane). This ligand has been the object of considerable interest recently, since, owing to its favored rigid *endo* configuration (even in the free state),[13] it exhibits excellent complexation properties;[5b,c] this rigidity of the nine-membered ring should be increased by the presence of the benzene ring. The synthesis of **2** from **1** shows how the formation of such sterically encumbered ring systems can become the main reaction at certain metal centers.

Experimental Procedure

All reactions were carried out in dry solvents under N_2.

a) Single crystals of *meso*-**1** · DMF: A saturated solution of **1** in DMF at 140°C was allowed to cool over 12 h to 20°C. The crystals were filtered, washed with Et_2O, and dried for 3 h under high vacuum. ν_{CO} (IR) [cm^{-1}]: 1960 (in DMF), 1950 (in KBr). $^{13}C\{^1H\}$-NMR (270 MHz, 293 K, in $[D_7]$DMF or CD_2Cl_2): $\delta = 198.1$ (CO); 156.5, 132.7, 130.5, 130.2, 129.5, 122.9 (C_6H_4); 49.7, 35.9 (C_2H_4). MS: *m/z* 498 [$M^{\oplus}$]

b) **2** from **1** and $S(C_2H_4Br)_2$: A solution of **1** · DMF (1.5 g, 2.6 mmol) and $S(C_2H_4Br)_2$ (694 mg, 2.8 mmol) in DMF (50 mL) was heated at 130–140°C until the ν_{CO} absorption of **2** at 1980 cm^{-1} appeared as the most intense band in the IR spectrum of the solution. After complete evaporation of the solvent, the viscous residue was digested with 5 × 10 mL of CH_2Cl_2; the remaining powdery **2** (604 mg, 45%) afforded single crystals of **2** · CH_2Cl_2 (correct elemental analysis) upon recrystallization from CH_2Cl_2 (35→ −20°C). ν_{CO} (IR) [cm^{-1}]: 1985 (in DMF), 2000 (in CH_2Cl_2), 1975 (in KBr). $^{13}C\{^1H\}$-NMR (270 MHz, 293 K, in $[D_6]$DMSO): $\delta = 195.9$ (CO); 137.8, 132.3, 131.9 (C_6H_4); 46.3, 33.8 (C_2H_4). MS: *m/z* 517 [$M^{\oplus}$].

c) **2** from **1** and $C_2H_4Br_2$; **1** · DMF (920 mg, 1.63 mmol) and 1,2-$C_2H_4Br_2$ (0.16 mL, 1.80 mmol) were heated in DMF (60 mL) at 140°C, the reaction being followed by IR spectroscopy. The solvent was evaporated and the viscous residue was extracted with 2 × 20 mL of CH_2Cl_2; the powdery residue was recrystallized from 5 mL of DMF (20→0°C). Dark orange crystals of **2** (180 mg, 22%, not optimized, correct elemental analysis) were obtained.

Received: November 30, 1987 [Z 2517 IE]
German version: *Angew. Chem. 100* (1988) 710

[1] Cf., e.g.: W. E. Newton in A. Müller, B. Krebs (Eds.): *Sulfur, its Significance for Chemistry, for the Geo-, Bio- and Cosmosphere and Technology*, Elsevier, Amsterdam 1984, p. 409–477.
[2] I. G. Dance, *Polyhedron 5* (1986) 1037.
[3] D. Sellmann, G. Binker, J. Keller, M. Waeber, *Rec. Trav. Chim. Pays-Bas (J. R. Neth. Chem. Soc.) 106* (1987) 312.
[4] D. Sellmann, W. Ludwig, G. Huttner, L. Zsolnai, *J. Organomet. Chem. 294* (1985) 199.
[5] Cf., e.g., a) J. A. McCleverty, *Prog. Inorg. Chem. 10* (1968) 49; b) J. Clarkson, R. Yagbasan, P. J. Blower, S. C. Rawle, S. R. Cooper, *J. Chem. Soc. Chem. Commun. 1987*, 950; c) M. N. Bell, A. J. Blake, M. Schröder, H. J. Küppers, K. Wieghardt, *Angew. Chem. 99* (1987) 253; *Angew. Chem. Int. Ed. Engl. 26* (1987) 253; and references cited therein.
[6] This abbreviation was introduced some time ago.
[7] D. Sellmann, P. Frank, *Angew. Chem. 98* (1986) 1115; *Angew. Chem. Int. Ed. Engl. 25* (1986) 1107; for proposals on naming thio crown ethers, etc., see G. A. Melson in G. A. Melson (Ed.): *Coordination Chemistry of Macrocyclic Compounds*, Plenum Press, New York 1979, p. 121.
[8] D. Sellmann, G. Binker, M. Moll, C. E. Campana, *Inorg. Chim. Acta 130* (1987) 221.
[9] Concerning the isomerism of dpttd complexes, see D. Sellmann, G. Binker, M. Moll, E. Herdtweck, *J. Organomet. Chem. 327* (1987) 403.
[10] *meso*-**1** · DMF: *Pna*2_1, $a = 753.5(2)$, $b = 1262.6(2)$, $c = 2399.0(7)$ pm, $V_{calcd} = 2282(1) \times 10^6$ pm^3, $Z = 4$, $T = 213$ K, $\lambda Mo_{K\alpha}$, ω scan, $3.0 < \dot{\omega} < 15°$ min^{-1}, $3 < 2\theta < 50°$. 2497 unique reflections, 2263 with $F > 4\sigma(F)$. 307 LS parameters. Structure solution and refinement using SHELXTL PLUS; $R = 0.031$, $R_w = 0.025$. Important distances [pm] and angles [°]: Ru1-S1 237.2(2), Ru1-S2 235.9(2), Ru1-S3 236.5(2), Ru1-S4 237.7(2), Ru1-S5 242.4(2), Ru1-C1 185.3(7); S5-Ru1-S1 88.3(1), S5-Ru1-S2 86.9(1), S5-Ru1-S3 86.8(1), S5-Ru1-S4 85.8(1), S1-Ru1-S2 87.0(1), S2-Ru1-S3 97.2(1), S3-Ru1-S4 87.2(1), S1-Ru1-S4 87.9(1) [12].
[11] **2** · CH_2Cl_2: $P2_1/c$, $a = 858.0(2)$, $b = 1324.4(4)$, $c = 1625.6(6)$ pm; $\beta = 95.43(2)°$, $V_{calcd} = 1844(1) \times 10^6$ pm^3, $Z = 4$, $T = 200$ K, $\lambda Mo_{K\alpha}$, ω scan, $2.4 < \dot{\omega} < 15°$ min^{-1}, $3 < 2\theta < 54°$. 4008 unique reflections, 2318 with $F > 6\sigma(F)$. 215 LS parameters. Structure solution and refinement using SHELXTL PLUS, direct methods; $R = 0.065$, $R_w = 0.065$. — Important distances [pm] and angles [°]: Ru1-S1 230.0(4), Ru1-S2 230.6(4), Ru1-S3 242.6(4), Ru1-Br1 254.2(2), Ru1-Br2 254.6(2), Ru1-C5 202.3(20); S1-Ru-S2 88.8(1), S1-Ru1-S3 86.3(1), S1-Ru1-Br1 89.4(1), Br1-Ru1-Br2 91.4(1), Br1-Ru1-C5 91.2(4) [12].
[12] Further details of the crystal structure investigations may be obtained from the Fachinformationszentrum Energie, Physik, Mathematik GmbH, D-7514 Eggenstein-Leopoldshafen 2 (FRG), on quoting the depository number CSD 52 794, the names of the authors, and the journal citation.
[13] R. S. Glass, G. S. Wilson, W. N. Setzer, *J. Am. Chem. Soc. 102* (1980) 5068.

Second-Sphere Photochemistry and Photophysics: Luminescence of the $[Pt(bpy)(NH_3)_2]^{2\oplus}$–Dibenzo[30]crown-10 Adduct**

By *Roberto Ballardini,* Maria Teresa Gandolfi, Vincenzo Balzani,* Franz H. Kohnke,* and *J. Fraser Stoddart*

The rapidly expanding availability of a wide range of synthetic molecular receptors[1] is providing the potential for the development of supramolecular chemistry,[2] the chemistry of entities obtained by the appropriate assembly of two or more simple components. Such a trend towards studying more complex chemical systems is clearly emerg-

[*] Dr. R. Ballardini
Istituto FRAE-CNR
I-40126 Bologna (Italy)
Prof. Dr. V. Balzani, Prof. Dr. M. T. Gandolfi
Dipartimento "G. Ciamician" di Chimica
Università degli Studi di Bologna
I-40126 Bologna (Italy)
Dr. F. H. Kohnke [+], Dr. J. F. Stoddart
Department of Chemistry, The University
Sheffield S3 7HF (UK)
[+] Permanent address:
Dipartimento di Chimica Organica e Biologica
dell'Università di Messina
I-98100 Messina (Italy)

[**] This work was supported by the Consiglio Nazionale delle Ricerche, Ministero della Pubblica Istruzione, the Science and Engineering Research Council, and NATO (Grant No. 937/86). We thank Mr. *L. Minghetti* and Mr. *G. Gubellini* for technical assistance.

ing in the field of photochemistry where supramolecular photochemistry[3] has, as its ambitious aim, the design of photochemical molecular devices capable of performing light-induced functions of practical utility. In the field of transition-metal complexes, one way to obtain supramolecular species is via second-sphere coordination, i.e., wrapping up the complex in an appropriate molecular host.[4] So far, however, only a few investigations have been published on the second-sphere photochemistry and photophysics of coordination compounds.[5] Here, we wish to report on the luminescent properties of the 1:1 adduct obtained when $[Pt(bpy)(NH_3)_2]^{2\oplus}$ is encapsulated by dibenzo[30]crown-10 (Fig. 1).[4,6]

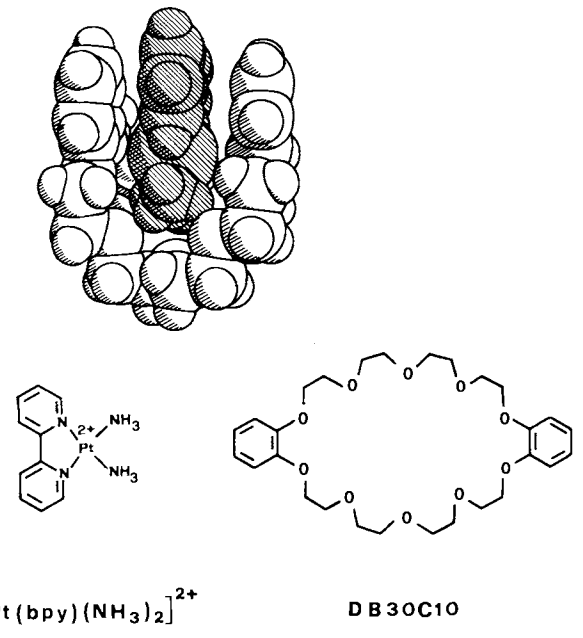

Fig. 1. The supramolecular structure of the $[Pt(bpy)(NH_3)_2]^{2\oplus}$-dibenzo[30]crown-10 (DB30C10) adduct in the solid state. bpy = 2,2'-bipyridine (cf. [6a]).

$[Pt(bpy)(NH_3)_2]^{2\oplus}$ was prepared as its $PF_6^{\ominus}$ salt and dibenzo[30]crown-10 was synthesized as described previously.[6a] In acetonitrile solution at room temperature, $[Pt(bpy)(NH_3)_2]^{2\oplus}$ exhibits a structured luminescence with $\lambda_{max} = 488$ nm (Fig. 2). This luminescence can be attributed to a triplet ligand-centered excited state on the basis of the close similarity to the phosphorescence spectrum of bipyridine and the value of the radiative rate constant at 77 K ($k = 2 \times 10^4$ s^{-1}, obtained from the experimental lifetime, 25 μs, and the luminescence quantum yield of ca. 0.5 at 77 K). $[Pt(bpy)(NH_3)_2][PF_6]_2$ is not soluble in CH_2Cl_2, but it can be solubilized by the addition of dibenzo[18]crown-6, yielding a solution that exhibits a luminescence spectrum which is essentially the same as that of $[Pt(bpy)(NH_3)_2]^{2\oplus}$ in acetonitrile.

In CH_3CN or CH_2Cl_2 solution, dibenzo[30]crown-10 shows an emission band at 308 nm ($\tau < 20$ ns) that can be assigned as the fluorescence emission of its *ortho*-dimethoxybenzene-like units.

The $[Pt(bpy)(NH_3)_2]^{2\oplus}$-dibenzo[30]crown-10 adduct was obtained as pale yellow crystals following a previously reported procedure[6a] or it was prepared in situ by addition of an equimolar amount of dibenzo[30]crown-10 to a CH_2Cl_2 suspension of $[Pt(bpy)(NH_3)_2][PF_6]_2$. In both cases,

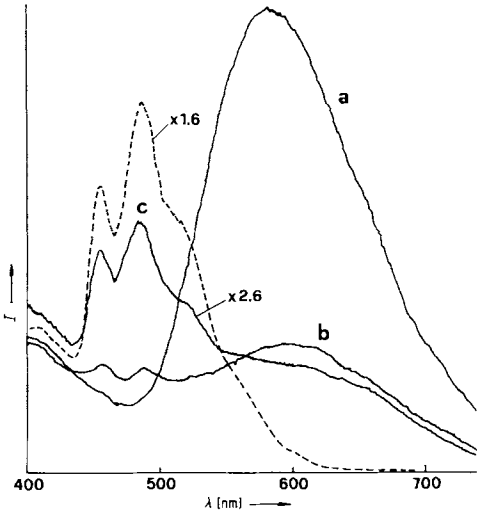

Fig. 2. Dashed line: Emission spectrum of $[Pt(bpy)(NH_3)_2]^{2\oplus}$ in CH_3CN. Full lines: Emission spectra of the $[Pt(bpy)(NH_3)_2]^{2\oplus}$-dibenzo[30]crown-10 adduct in a) CH_2Cl_2, b) CH_2Cl_2-CH_3CN (1:1, v/v), and c) CH_3CN. Intensity I in arbitrary units.

the same properties have been observed. As previously noted,[6] the absorption spectrum of the adduct in CH_3CN or CH_2Cl_2 solution is similar but not identical to the sum of the spectra of the two components. In particular, the intensities of the $\pi \rightarrow \pi^*$ absorptions of the bpy ligand at 306 and 318 nm are reduced significantly while the intensity above 325 nm increases, indicating that a new broad band with maximum at ca. 350 nm is present.

In CH_2Cl_2 solution the adduct exhibits a new broad, relatively weak luminescence band with $\lambda_{max} = 580$ nm (Fig. 2, curve a), while the luminescence intensity in the 308- and 488-nm regions is at least 90% lower than that exhibited by the dibenzo[30]crown-10 and $[Pt(bpy)(NH_3)_2]^{2\oplus}$ components. A comparison among the corrected emission intensities at 580 nm after exciting the adduct at 275 nm (dibenzo[30]crown-10 band), 318 nm ($[Pt(bpy)(NH_3)_2]^{2\oplus}$ band), and 350 nm (adduct band) shows that the level responsible for the emission is populated with the same efficiency in all cases (experimental error ± 15%).

In CH_3CN solution the emission spectrum of the adduct (Fig. 2, curve c) shows a weak band in the 580-nm region and much stronger bands at 308 and 488 nm, indicating that the adduct stability is less in CH_3CN solution than in CH_2Cl_2 solution. This observation is in agreement with a conclusion previously reached on the basis of absorption measurements.[6] In CH_3CN/CH_2Cl_2 (1:1, v/v) mixtures, the 488- and 580-nm bands have comparable intensities (Fig. 2, curve b).

The results obtained show that the $[Pt(bpy)(NH_3)_2]^{2\oplus}$-dibenzo[30]crown-10 supermolecule exhibits absorption properties similar to those of the two components and completely new luminescence properties that arise from the presence of a low-energy "supramolecular" level. The broadness of the emission band suggests that such an energy level can be assigned to a charge-transfer transition, most likely from the π-electron-rich dialkoxybenzene units of dibenzo[30]crown-10 to the empty π* orbitals of bipyridine, i.e., the luminescent level is the triplet counterpart of the singlet charge-transfer excited state responsible for the broad absorption of the adduct in the 350-nm region. In principle, it should be possible to tune the energies of

these levels, and hence the absorption and emission properties of the adduct, by appropriate substitutions on the benzene or pyridine rings.

Received: December 3, 1987 [Z 2522 IE]
German version: *Angew. Chem. 100* (1988) 712

[1] a) C. J. Pedersen, *J. Am. Chem. Soc. 89* (1967) 2495, 7017; C. J. Pedersen, K. H. Frensdorff, *Angew. Chem. 84* (1972) 16; *Angew. Chem. Int. Ed. Engl. 11* (1972) 16; b) J.-M. Lehn, *Pure Appl. Chem. 52* (1980) 2441; c) D. J. Cram, *Angew. Chem. 98* (1986) 1041; *Angew. Chem. Int. Ed. Engl. 25* (1986) 1039; d) F. Vögtle, E. Weber (Eds.): *Host Guest Complex Chemistry/Macrocycles*, Springer, Berlin 1985.

[2] J.-M. Lehn, *Science (Washington, D.C.) 222* (1985) 849; *Angew. Chem. 100* (1988) 91; *Angew. Chem. Int. Ed. Engl. 27* (1988) 89.

[3] V. Balzani (Ed.): *Supramolecular Photochemistry*, Reidel, Dordrecht 1987.

[4] H. M. Colquhoun, J. F. Stoddart, D. J. Williams, *Angew. Chem. 98* (1986) 483; *Angew. Chem. Int. Ed. Engl. 25* (1986) 487.

[5] a) V. Balzani, N. Sabbatini, F. Scandola, *Chem. Rev. 86* (1986) 319; b) B. Alpha, J.-M. Lehn, G. Mathis, *Angew. Chem. 99* (1987) 259; *Angew. Chem. Int. Ed. Engl. 26* (1987) 266; B. Alpha, V. Balzani, J.-M. Lehn, S. Perathoner, N. Sabbatini, *ibid. 99* (1987) 1310 and *26* (1987) 1266.

[6] a) H. M. Colquhoun, J. F. Stoddart, D. J. Williams, J. B. Wolstenholme, R. Zarzycki, *Angew. Chem. 93* (1981) 1093; *Angew. Chem. Int. Ed. Engl. 20* (1981) 1051; b) H. M. Colquhoun, S. M. Doughty, J. M. Maud, J. F. Stoddart, D. J. Williams, J. B. Wolstenholme, *Isr. J. Chem. 25* (1985) 15.

$P_4^{2\ominus}$ Isomers as Complex Ligands**

By *Otto J. Scherer,* Magdalena Swarowsky, Herbert Swarowsky,* and *Gotthelf Wolmershäuser*

Dedicated to Professor Adolf Steinhofer on the occasion of his 80th birthday

Two-electron reduction of white phosphorus (P_4) should result in opening of one edge of the P_4 tetrahedron and formation of the polyphosphide ion $P_4^{2\ominus}$ **A**,[1] which is the dianion of tetraphosphabicyclobutane and has a butterfly-like structure. Opening of two further edges of **A** could result in isomerization to **B**, the dianion of tetraphosphabutadiene.[2] Herein we report that both dianions can be stabilized in the coordination sphere of transition metals.

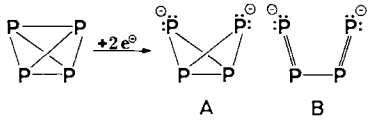

Oxidative addition of white phosphorus to fragments of complexes **1** affords in quantitative yield the "metalated" tetraphosphabicyclobutane derivatives **2**, complexes exhibiting a new type of coordination[3] of the P_4 molecule. In this redox reaction, P_4^0 molecules are formally reduced to polyphosphide ions $P_4^{2\ominus}$ **A** and $M^{2\oplus}$ centers are formally oxidized to $M^{4\oplus}$ centers (M = Zr, Hf).

The air-stable complexes **2** are readily soluble in benzene, toluene, and dichloromethane and moderately soluble in pentane. In contrast to **2a,b**, the Cp* analogue $[Cp_2^*Zr(P_4)]$ **2c**, Cp* = η^5-C_5Me_5, is only stable in solution (^{31}P-NMR[4]). Attempted isolation of **2c** resulted in partial reductive elimination with formation of white phosphorus and "Cp_2^*Zr"[5] ($t_{1/2}$ at 140 °C in xylene: ca. 70 min). The $^{31}P\{^1H\}$-NMR spectra of **2** each show two triplets (A_2X_2 spin system[4]). The X-ray structure analyses[11b] of the isostructural P_4 complexes **2a,b** (disorder problems in the region of the Cp″ ligands prevent a satisfactory structural refinement) confirm the presence of a P_4 butterfly framework with a $Cp_2''M$ bridge. The distances and angles in the P_4 moiety are comparable to those in the tetraphosphabicyclobutane derivatives $P_2(PR)_2$ (R = $N(SiMe_3)_2$,[6a] 2,4,6-$tBu_3C_6H_2$[6b]). The M–P bond lengths are in the expected range.[7]

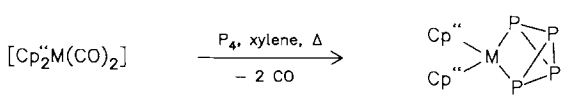

Cp″ = η^5-1,3-$C_5H_3(tBu)_2$; **a**, M = Zr; **b**, M = Hf

If, instead of the "early" transition metals (Zr, Hf), the "late" transition metal rhodium is employed, P_4 can be incorporated into a metallatetraphosphacyclopentadiene,[8] which, in turn, functions as an η^4 ligand in the sandwich complex **4**. Complex **4** forms red crystals, which are stable for only a short time upon exposure to air and are readily soluble in pentane and toluene. Its $^{31}P\{^1H\}$-NMR spectrum displays a complex pattern of signals.[10] The X-ray structure analysis[11a] shows that the planar P_4 fragment and the flat five-membered ring at the Rh1 atom in **4** are nearly parallel (deviation 3.5°) and are mutually oriented in an eclipsed fashion (Fig. 1). The nearly identical P–P distances (average value 2.154 Å) are somewhat shorter than those in the Co complex $[Co(Ph_2PCH_2PPh_2\text{-}P_4\text{-}PPh_2CH_2PPh_2)]BF_4$[12a] containing a zigzag-shaped η^4-phosphabutadiene moiety in the middle of the ligand; however, they are significantly longer than the short P–P distance (2.052(2) Å) in the P_4 rectangle of the sandwich complex **5**.[9] The nearly identically long Rh1–P bonds (average value 2.385 Å) are slightly longer than the Rh2–P bonds (both 2.347(2) Å). The atoms Rh1, P1, Rh2, and P4 form a nearly perfect rhombus (sum of angles in the four-membered ring = 359.4°). The Rh2 atom is displaced by about 55.7° from the plane of a planar five-membered ring. In terms of formal charges, an alternative to $P_4^{2\ominus}$ and d^8,d^6 Rh is $P_4^{4\ominus}$ and d^6,d^6 Rh. Complex **4** could also have been formed from $[(\eta^4\text{-}P_4)RhCp^*]$, a sandwich com-

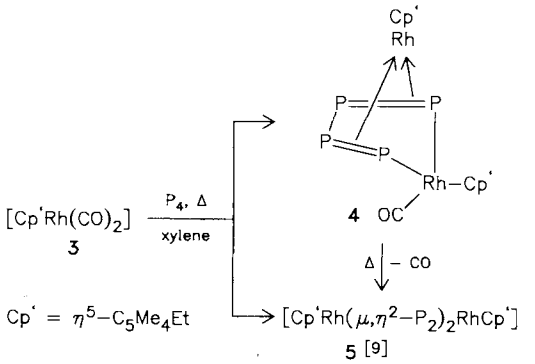

[*] Prof. Dr. O. J. Scherer, Dipl.-Chem. M. Swarowsky, Dipl.-Chem. H. Swarowsky, Dr. G. Wolmershäuser [+]
Fachbereich Chemie der Universität
Erwin-Schrödinger-Strasse, D-6750 Kaiserslautern (FRG)

[+] X-ray structure analysis.

[**] This work was supported by the Fonds der Chemischen Industrie (doctoral fellowship for *H. S.*).

plex containing the phosphorus analogue of cyclobutadiene as ligand, by oxidative addition (opening of a P–P edge).

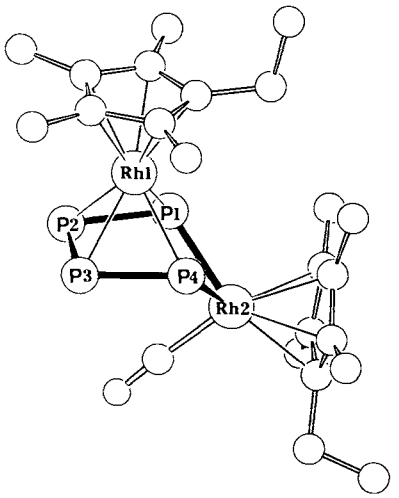

Fig. 1. Molecular structure of **4**. Selected bond lengths [Å] and angles [°]. Rh1-P1 2.381(2), Rh1-P2 2.392(2), Rh1-P3 2.387(2), Rh1-P4 2.381(2), Rh2-P1 2.347(2), Rh2-P4 2.347(2), Rh1-C 2.204(8)-2.263(7), Rh2-C 2.215(11)-2.278(10), Rh2-C(CO) 1.881(11), P1-P2 2.160(3), P2-P3 2.150(3), P3-P4 2.153(3), P1···P4 2.697(3), Rh1-Cp′ (centr.) 1.873, Rh1-P_4 (centr.) 1.749, Rh2-Cp′ (centr.) 1.915; P1-P2-P3 97.1(1), P2-P3-P4 97.4(1), P2-P1-Rh2 112.6(1), P3-P4-Rh2 112.7(1), P1-Rh2-P4 70.1(1), P1-Rh1-P4 69.0(1), Rh1-P1-Rh2 110.1(1), Rh1-P4-Rh2 110.2(1), Cp′ (centr.)-Rh1-P_4 (centr.) 176.1.

Experimental Procedure

2a [**2b**]: A solution of **1a** (505 mg, 1.01 mmol) [13] [**1b** (520 mg, 0.88 mmol) [13]] in xylene (20 mL) was added within 10 min to a refluxing solution of P_4 (166 mg, 1.34 mmol) [152 mg (1.23 mmol)] in xylene (25 mL). The resulting reaction mixture was stirred under reflux for 5 min [25 min] and the solvent was then removed under oil-pump vacuum. The excess phosphorus was removed at 80°C/0.1 mbar. Yield 574 mg **2a** (100%) [577 mg **2b** (100%)]. Both complexes could be recrystallized from hexane.

4: **3** (1000 mg, 3.24 mmol) [13] and P_4 (663 mg, 5.13 mmol) were allowed to stir in ca. 30 mL of xylene in a Schlenk pressure tube at an oil-bath temperature of 200°C. IR spectroscopic control revealed the emergence of the new band of **4** at 2000 cm^{-1} (maximum after ca. 30 min). The red reaction solution containing small amounts of insoluble matter) was evaporated to ca. 10 mL under oil-pump vacuum, then treated with 3 g of Al_2O_3 (basic, activity II) and dried under oil-pump vacuum until freely flowing. In the chromatographic workup (column 25 × 2.5 cm), excess P_4 was eluted with pentane and unreacted **3** (100 mg, 10%) was eluted as a yellow forerun. Pentane/toluene (1:1) afforded **5** [9] (180 mg, 20%) as a yellowish orange fraction; a 1:2 mixture eluted **4** as a red fraction (an intermediary fraction contains both products). After removal of the solvent (oil-pump vacuum), 22 mg (2.3% based on reacted **4**) of pure **5** remained, which—after recrystallization from pentane—afforded red, cube-shaped crystals.

Received: January 27, 1988 [Z 2590 IE]
German version: *Angew. Chem. 100* (1988) 738

[1] Mass-spectrometric evidence for its existence: T. P. Martin, *Angew. Chem. 98* (1986) 197; *Angew. Chem. Int. Ed. Engl. 25* (1987) 197; cf. the mechanism of nucleophilic decomposition of P_4 [C. Brown, R. F. Hudson, G. A. Wartew, *Phosphorus Sulfur 5* (1978) 67; A. Schmidpeter, G. Burget, H. G. von Schnering, D. Weber, *Angew. Chem. 96* (1984) 795; *Angew. Chem. Int. Ed. Engl. 23* (1984) 816] as well as the isoelectronic 22-valence-electron ($P_4^{2\ominus}$) "butterfly anion" $Si_4^{6\ominus}$ [H. G. von Schnering, *ibid. 93* (1981) 44 and *20* (1981) 33, and references cited therein].

[2] Concerning tetraphosphabutadiene/tetraphosphabicyclobutane cf.: E. Niecke, O. Altmeyer, M. Nieger, F. Knoll, *Angew. Chem. 99* (1987) 1299; *Angew. Chem. Int. Ed. Engl. 26* (1987) 1256.

[3] Recent reviews: O. J. Scherer, *Comments Inorg. Chem. 6* (1987) 1; M. Di Vaira, P. Stoppioni, M. Peruzzini, *Polyhedron 6* (1987) 351.

[4] $^{31}P\{^1H\}$ (80.82 MHz, CD_2Cl_2, 293 K, 85% H_3PO_4 ext.) [^1H (200 MHz, 293 K, C_6D_6, TMS int.)] **2a**: $\delta = 166.1$ (t, P_X), -206.5 (t, P_A), $^1J(PP) = 201.7$ Hz [1.22 (s, 36H), 5.27 (t, 2H), 5.47 (d, 4H), $^4J(HH) = 2.6$ Hz]; **2b**: $\delta = 117.5$ (t, P_X), -219.3 (t, P_A), $^1J(PP) = 193.9$ Hz [1.24 (s, 36H), 4.27 (t, 2H), 5.35 (d, 4H), $^4J(HH) = 2.7$ Hz]; **2c**: $\delta = 93.3$ (t, P_X), -214.4 (t, P_A), $^1J(PP) = 201.1$ Hz [1.68 (s, 30H)].

[5] See J. M. Manriquez, J. E. Bercaw, *J. Am. Chem. Soc. 96* (1974) 6229; H.-S. Tung, C. H. Brubaker, Jr., *Inorg. Chim. Acta 52* (1981) 197.

[6] a) E. Niecke, R. Rüger, B. Krebs, *Angew. Chem. 94* (1982) 553; *Angew. Chem. Int. Ed. Engl. 21* (1982) 544; b) R. Riedel, H.-D. Hansen, E. Fluck, *ibid. 97* (1985) 1050 and *24* (1985) 1056. Cf. also $P_2(PCp^*)_2$: P. Jutzi, T. Wippermann, *J. Organomet. Chem. 287* (1985) C5, $[P_2(CtBu)_2ZrCp_2]$: P. Binger, B. Biedenbach, C. Krüger, M. Regitz, *Angew. Chem. 99* (1987) 798; *Angew. Chem. Int. Ed. Engl. 26* (1987) 764 as well as theoretical investigations of $P_2(PX)_2$: W. W. Schoeller, C. Lerch, *Inorg. Chem. 22* (1983) 2992.

[7] Zr–P, e.g., [12b]; Hf–P, e.g., R. T. Baker, J. F. Whitney, S. S. Wreford, *Organometallics 2* (1983) 1049; L. Weber, G. Meine, R. Boese, N. Augart, *ibid. 6* (1987) 2484; E. Hey, S. G. Bott, J. L. Atwood, *Chem. Ber. 121* (1988) 561.

[8] For metallacyclopentadienes as intermediates in alkyne cyclooligomerization see, e.g.: J. P. Collman, L. S. Hegedus, J. R. Norton, R. G. Finke: *Principles and Applications of Organotransition Metal Chemistry*, University Science Books, Mill Valley, CA, USA 1987, p. 509f. For theoretical investigations see: D. L. Thorn, R. Hoffmann, *Nouv. J. Chim. 3* (1979) 39.

[9] O. J. Scherer, M. Swarowsky, G. Wolmershäuser, *Angew. Chem. 100* (1988) 423; *Angew. Chem. Int. Ed. Engl. 27* (1988) 405.

[10] $^{31}P\{^1H\}$-NMR (80.82 MHz, [D_8]toluene, 85% H_3PO_4 ext.). **4**: AA′MNXX′ spin system (AA′ = P2, P3, MN = Rh1, Rh2, XX′ = P1, P4). $\delta(P_{AA'}) = 150.8$, $\delta(P_{XX'}) = 201.5$; $J(P1P2) = J(P3P4) = \pm 300$ Hz, $J(P2P3) = \pm 240$ Hz, $J(P1P4) = \pm 20$ Hz, $J(Rh1P2) = J(Rh1P3) = \pm 21$ Hz, $J(Rh1P1) = J(Rh1P4) = \pm 26$ Hz, $J(Rh2P1) = J(Rh2P4) = \pm 39$ Hz, $J(P1P3) = J(P2P4) = \pm 20$ Hz, $J(Rh1Rh2) = \pm 50$ Hz. ^1H-NMR (200 MHz, C_6D_6, 293 K, TMS int.): $\delta = 1.64$ (s, 6H), 1.59 (s, 6H), Rh1, 2.02 (s, 6H), 1.99 (s, 6H) Rh2, 2.49 (q, 4H) Rh1 and Rh2, 0.86 (t), 0.94 (t) Rh1 and Rh2 (tentative assignment), $^3J(HH) = 7.6$ Hz. We thank Prof. Dr. C. G. Kreiter, Kaiserslautern, for simulation of the ^{31}P-NMR spectrum.

[11] a) **4** forms triclinic crystals, $P\bar{1}$, $a = 9.115(2)$, $b = 17.828(3)$, $c = 8.983(1)$ Å, $\alpha = 97.89(1)$, $\beta = 109.41(1)$, $\gamma = 79.69(1)°$, $Z = 2$, 3803 unique reflections ($Mo_{K\alpha}$, $1.5° < \theta < 25°$), 3261 of which were observed with $F_0^2 \geq 2.0\sigma(F_0^2)$. 302 parameters, $R = 0.046$, $R_w = 0.058$. Further details of the crystal structure investigation may be obtained from the Fachinformationszentrum Energie, Physik, Mathematik GmbH, D-7514 Eggenstein-Leopoldshafen 2 (FRG), on quoting the depository number CSD-52906, the names of the authors, and the journal citation. b) **2a**: monoclinic, $P2_1/c$, $a = 14.287(2)$, $b = 13.501(2)$, $c = 16.725(3)$ Å, $\beta = 114.914(8)°$. **2b**: monoclinic, $P2_1/c$, $a = 14.272(3)$, $b = 13.510(3)$, $c = 16.741(3)$ Å, $\beta = 114.83(2)°$.

[12] a) F. Cecconi, C. A. Ghilardi, S. Midollini, A. Orlandini, *Inorg. Chem. 25* (1986) 1766; b) cf. $[Cp_2\overline{Zr\{P(PR_2)}\underline{P(PR_2)}\overline{P}]$]: E. Hey, M. F. Lappert, J. L. Atwood, S. G. Bott, *J. Chem. Soc. Chem. Commun. 1987*, 597.

[13] M. Swarowsky, H. Swarowsky, O. J. Scherer, unpublished results.

4,6,6-Trimethyl-4-cyclohexene-1,2,3-trione, a Contribution to the Biogenesis of Norcarotinoids**

By *Jürgen Detering* and *Hans-Dieter Martin**

Dedicated to Professor Helmut Dörfel on the occasion of his 60th birthday

The red pigment (3*S*,3′*S*)-actinioerythrin **1**, the ester of actinioerythrol **2** (2,2′-bisnorastaxanthin), is present in the see anemone *Actinia equina*.[1] The benzilic acid rearrangement of a highly oxidized derivative of astaxanthin **3** was suggested as the route of biogenesis.[2,3] This route (Scheme 1) should involve the *vic*-triketone **4** as a reactive intermediate, which could undergo ring contraction to **5**, induced by nucleophilic attack. Subsequent decarboxyla-

[*] Prof. Dr. H.-D. Martin, Dipl.-Chem. J. Detering
Institut für Organische Chemie und
Makromolekulare Chemie der Universität
Universitätsstrasse 1, D-4000 Düsseldorf (FRG)

[**] Small and Medium-Sized Rings, Part 68. This work was supported by the Deutsche Forschungsgemeinschaft, the Fonds der Chemischen Industrie, and BASF AG. Part 67: K. Hassenrück, H.-D. Martin, B. Mayer, *Chem. Ber. 121* (1988) 373.

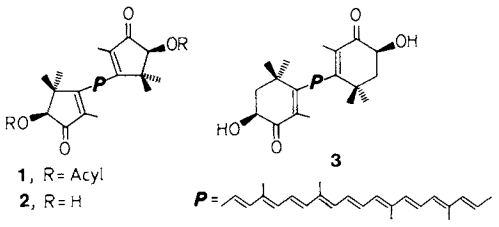

tion could then lead to **2**. In later work, the attack of the nucleophile was indicated to occur at C-2 of **4**.[4]

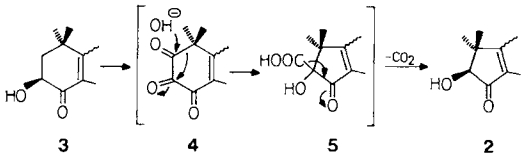

Scheme 1. Proposed route for the biogenesis of **2** from **3**.

This mechanistic proposal gives rise to the following considerations and questions:

(1) The chirality of astaxanthin **3** cannot be transferred to the actinioerythrol **2** according to this mechanism. Since the triketone **4** has not been observed so far, the question arises whether astaxanthin might perhaps remain bound to the same enzyme complex during the entire process.[4]

(2) If the hypothetical triketone **4** is indeed a discrete intermediate, then, in principle, each of the three carbonyl groups could undergo nucleophilic attack, since a priori it should be difficult to decide which of the four electrophilic positions in **4** (the three carbonyl carbon atoms, one Michael-like β position) would be the most reactive, depending on the reaction conditions. In short, what acceptor properties characterize the cyclohexenetrione structure **4**, which, to the best of our knowledge, is still unknown?

(3) As a *vic*-triketone, **4** could in principle undergo redox disproportionation.[5] As applied to the model compound **6**, this means first a benzilic acid rearrangement and then the decarboxylation to give the acyloin **7**, followed by a redox reaction with the excess **6** still present to give the *aci*-reductone **8** and the diketone **9**. The carotinoid terminal group of **2** could thus be formed via a compound of type **9** by enantioselective reduction. This would represent an alternative to formation from **5**.

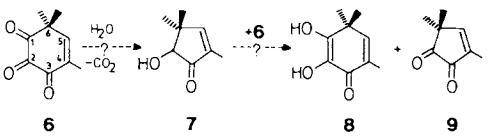

Scheme 2. Possible course of redox disproportionation of the triketone **6**.

Herein we report the first synthesis of a *vic*-cyclohexenetrione, **6**, and describe some of its properties.

The synthesis of **6** started from the diketone **10**,[6a] since this starting compound should also allow the later incorporation of a polyene chain. The steps of the synthesis are shown in Scheme 3: Compound **10** was subjected to acetal formation at position 1 to give **11** (75%), which was then reduced with lithium aluminum hydride in THF. The isomeric mixture **12/13** (3.3 : 1) was formed in 85% yield. The isomer **13** separated out as a crystalline solid and could be isolated. Alcohol **12** can be dehydrated to give **14** (50%) with phosphorus oxychloride. Oxidation of **14** to **15** was achieved with Collins' reagent (40%). Treatment of **15** with SeO_2 affords the acetal-protected triketone **16** in 30% yield. Transformation of **16** to the hydrate **19** has not been accomplished so far. Attempts to remove the acetal group of **16** with mineral acid–THF mixtures resulted in the isolation of up to 80% unchanged acetal. Removal of the acetal group of **15** led to the enolized 1,3-diketone **17**[6b] (85%), which, in chloroform, exists in tautomeric equilibrium between a diketo form and two enol structures. Diazo group transfer afforded the diazoketone **18** (50%). Treatment with *tert*-butylhypochlorite in acetonitrile/water (11 : 1) resulted in formation of the triketone hydrate **19**. Dehydration of **19** by sublimation can be accomplished at 50°C/0.001 torr; triketone **6** was obtained as sticky, deep red crystals (40–50%), which undergo immediate decomposition upon exposure to air to form the hydrate **19**. The structure of **19** was established from the ^{13}C-NMR spectrum and shows that the attack of the nucleophile occurred at the middle carbonyl carbon atom of **6**.

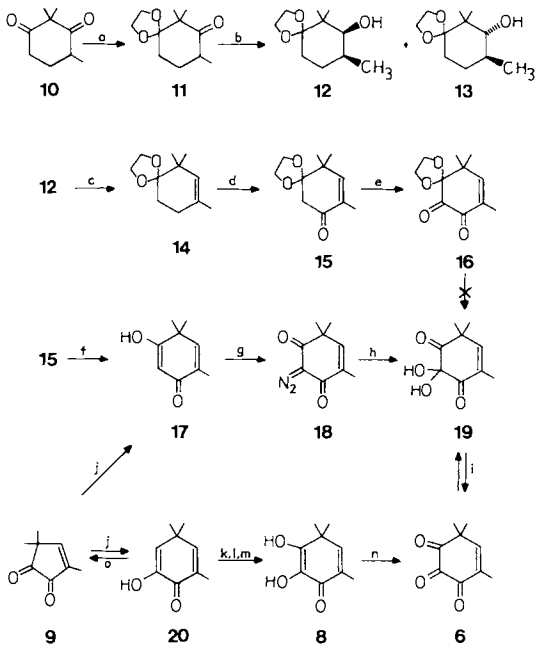

Scheme 3. Synthesis of **6**. Reagents, reaction conditions, and yields: a) 1.5 equiv. ethylene glycol, 1.2 equiv. $HC(OEt)_3$, *p*-TosOH (catalyst), 20°C, 45 min, 75%. b) 0.5 equiv. $LiAlH_4$, THF, 20°C, 4 h, 85%. c) 1.6 equiv. $POCl_3$, pyridine, 20°C, 4 h, 50%. d) 20 equiv. $CrO_3 \cdot 2$pyridine, CH_2Cl_2, 20°C, 50 h, 40%. e) 1.0 equiv. SeO_2, glacial acetic acid, reflux, 3 h, 30%. f) 15% H_2SO_4, 20°C, 4 h, 85%. g) 1.0 equiv. *p*-$TosN_3$, 1.0 equiv. Et_3N, Et_2O/EtOH (1/1), 20°C, 5 h, 50%. h) 1.0 equiv. *t*BuOCl, CH_3CN/H_2O (11/1), 0°C, 20 min, 90%. i) 50°C, 0.001 torr, 40–50%. j) Diazomethane in ether (2 equiv. CH_2N_2)/4% KOH (1.4/1), **9** was added in portions, 20°C, 45 min, 75%. k) 1.3 equiv. Me_3SiCl, 1.0 equiv. pyridine, benzene, 20°C, 3.5 h. l) 1.6 equiv. *m*-chloroperbenzoic acid, *n*-hexane, 20°C, 4 h. m) MeOH, HCl (catalyst), 20°C, 4 h, 45% based on **20**. n) 1.0 equiv. DDQ, benzene, 20°C, 3.5 h. o) 2.0 equiv. SeO_2, glacial acetic acid, reflux, 3.5 h, 20%.

Compound **6** can also be prepared in two ways from the known cyclopentenedione **9**.[7] One of the routes converges with the route described above at **17**, the other utilizes the second ring-expansion product **20**. Compound **9** reacts with diazomethane[8] to afford a mixture of **17** and **20**[9] (2 : 1) in 75% yield. Separation of the two isomers is possible owing to their differing acidities: extraction of the so-

lution of **17/20** in ether with Na_2CO_3 removes **17**. Silylation, epoxidation, and ring opening of **20** gives the *aci*-reductone **8** (45%). Treatment of **8** with dichlorodicyano-*p*-benzoquinone (DDQ) results in formation of slightly impure **6**,[10] which, however, is suitable for further reactions (e.g., for quinoxaline syntheses[11]).

Triketone hydrate **19** does not show the reaction behavior expected for ring contraction accompanied by redox processes[5] as shown in Scheme 2. Compounds **8** and **9** are formed neither thermally nor in alkaline or acidic medium from **19**; only unidentified decomposition products are obtained. On the other hand, ring contraction of **20** to give **9** (20%) is observed upon heating **20** with selenium dioxide in acetic acid. Presumably, **20** undergoes initial oxidation to **6**, which, after ring contraction to **7**, is finally dehydrogenated by selenium dioxide to give **9**. These observations lead to the conclusion that the spontaneous redox disproportionation (i.e., ring contraction and redox behavior according to Scheme 2) plays no or at most only a minor role in the reaction behavior of triketones of structure type **6**. Because of the lability and ready decomposition of **6**, it is unlikely that species **4** exists for any great length of time as a free, achiral intermediate. The suggestion of actinioerythrol formation proposed in Ref. [4] and mentioned at the beginning is a plausible alternative to the route of formation via the free triketone. Besides an attack of the nucleophile as shown in Scheme 1, the attack at the middle carbonyl carbon atom should be considered, in analogy to the hydrate formation (**19**).

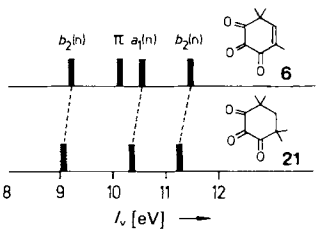

Fig. 1. Comparison of the vertical *n*-ionization energies I_v (He(Iα) PE spectrum) of **6** and **21**. The symmetry notation refers to the C_{2v} symmetry of the $(CO)_3$ structural unit.

In addition to the excitation energies and chemical shifts (Table 1), the ionization energies of **6** are also of interest. They allow conclusions to be drawn concerning the lone-pair splitting (Fig. 1). For saturated six-membered-ring *vic*-triketones, the third lone-pair ionization is often not clearly distinguishable from σ-orbital ionizations, which lie in the same energy region. This is the case for the saturated triketone **21**:[21] A decision as to whether the third n-ionization should be assigned to the band at 11.35 or to that at 12.12 eV in the photoelectron spectrum has not been possible so far. A comparison with the He(Iα) PE spectrum of **6** removes this uncertainty, since, owing to the π bond in **6**, its σ-orbital ionizations lie at higher energies than those of **21**. Only the ionization of **21** at 11.35 eV can be correlated with one of the three lone-pair ionizations of **6**. In this assignment, all three n bands of **21** are thus observed as expected at 0.1–0.2 eV lower ionization energies than those of the corresponding bands of **6**. This is due to the inductive effect of the double bond.[13]

Received: December 4, 1987;
supplemented: February 15, 1988 [Z 2525 IE]
German version: *Angew. Chem. 100* (1988) 714

Table 1. Selected physical and spectroscopic data for compounds **12**–**19**, **6**, and **8**. ^{1}H-NMR: 80 MHz, $CDCl_3$/TMS; ^{13}C-NMR: 25.2 MHz, $CDCl_3$/TMS.

12: b.p. = 62–63 °C (0.06 torr); IR (neat): $\tilde{\nu}$ = 3540, 1440, 1105, 1055, 970 cm^{-1}; ^{1}H-NMR: δ = 0.97 (d, ^3J = 6.5 Hz, 3H), 1.02 (s, 3H), 1.07 (s, 3H), 1.33–2.05 (m, 5H), 2.93 (d, ^3J = 10.2 Hz, 1H; OH), 3.21 (dd, ^3J = 10.2, 2.5 Hz, 1H), 3.95 (mc, 4H); correct C,H analysis

13: m.p. = 103 °C; IR (KBr): $\tilde{\nu}$ = 3400, 1445, 1130, 1045, 985 cm^{-1}; ^{1}H-NMR: δ = 0.98 (s, 6H), 1.00 (d, ^3J = 6.0 Hz, 3H), 1.32–1.78 (m, 5H), 1.80 (d, ^3J = 5.0 Hz, 1H; OH), 3.15 (dd, ^3J = 10.0, 5.0 Hz, 1H), 3.93 (s, 4H); correct C,H analysis

14: b.p. = 40–42 °C (0.07 torr); ^{1}H-NMR: δ = 1.03 (s, 6H), 1.67 (d, ^4J = 1.3 Hz, 3H), 1.80 (mc, 2H), 2.12 (mc, 2H), 3.99 (s, 4H), 5.12 (q, ^4J = 1.3 Hz, 1H); correct C,H analysis

15: m.p. = 83–84 °C; IR (KBr): $\tilde{\nu}$ = 1670, 1635 cm^{-1}; ^{1}H-NMR: δ = 1.18 (s, 6H), 1.77 (d, ^4J = 1.3 Hz, 3H), 2.73 (s, 2H), 4.00 (s, 4H), 6.45 (q, ^4J = 1.3 Hz, 1H); correct C,H analysis

16: m.p. = 88–89 °C; IR (KBr): $\tilde{\nu}$ = 1745, 1672, 1625 cm^{-1}; ^{1}H-NMR: δ = 1.23 (s, 6H), 1.90 (d, ^4J = 1.3 Hz, 3H), 4.05 (s, 4H), 6.70 (q, ^4J = 1.3 Hz, 1H); UV/VIS (*n*-hexane): λ_{max}(lgε) = 442 (1.328), 260 (3.633) nm; correct C,H analysis

17: m.p. = 158–159 °C (159–160 °C [6b]); IR (KBr): $\tilde{\nu}$ = 3300–2200, 1655, 1580, 1525 cm^{-1}; IR ($CHCl_3$): $\tilde{\nu}$ = 3400–2200, 1720, 1665, 1585 cm^{-1}; ^{1}H-NMR: a) 1,3-diketo form: δ = 1.33 (s, 6H), 1.88 (d, ^4J = 1.3 Hz, 3H), 3.55 (s, 2H), 6.63 (q, ^4J = 1.3 Hz, 1H); b) enol form: δ = 1.26 (s, 6H), 1.86 (d, ^4J = 1.3 Hz, 3H), 5.58 (s, 1H), 6.34 (q, ^4J = 1.3 Hz, 1H), 9.80 (br. s, 1H)

18: m.p. = 43–44 °C; IR (KBr): $\tilde{\nu}$ = 2135, 1665, 1650, 1625 cm^{-1}; ^{1}H-NMR: δ = 1.33 (s, 6H), 1.94 (d, ^4J = 1.3 Hz, 3H), 6.42 (q, ^4J = 1.3 Hz, 1H); correct C,H,N analysis

19: IR (CH_2Cl_2): $\tilde{\nu}$ = 1732, 1682, 1635 cm^{-1}; ^{1}H-NMR: δ = 1.44 (s, 6H), 1.93 (d, ^4J = 1.3 Hz, 3H), 4.95 (br. s, 2H), 6.65 (q, ^4J = 1.3 Hz, 1H); ^{13}C-NMR: δ = 15.9 (qd; CH_3 of C-4), 26.2 (qm; 2 × CH_3), 45.8 (m; C-6), 91.2 (s; C-2), 130.6 (m; C-4), 151.5 (dm; C-5), 193.8 (dq; C-3), 204.8 (m; C-1) (numbering as for **6** in Scheme 2; derivative, quinoxaline as described for **6**)

6: melting range 65–75 °C; IR (KBr): $\tilde{\nu}$ = 1715, 1680 (sh), 1670, 1620 cm^{-1}; ^{1}H-NMR: δ = 1.45 (s, 6H), 2.03 (d, ^4J = 1.3 Hz, 3H), 6.91 (q, ^4J = 1.3 Hz, 1H); ^{13}C-NMR: δ = 15.8 (qd; CH_3 of C-4), 25.7 (qm; 2 × CH_3), 49.3 (m; C-6), 136.4 (m; C-4), 153.7 (dm; C-5), 182.4 (m; C-3), 183.5 (s; C-2), 195.1 (m; C-1); MS: *m/z* 166 ($M^{\oplus}$), 138 ($M^{\oplus}$ − CO), 110 ($M^{\oplus}$ − 2CO), 95, 86, 82 ($M^{\oplus}$ − 3CO), 67; UV/VIS (CH_2Cl_2): λ_{max}(lgε) = 537 (1.397), 301 (3.041), 247 (3.903) nm; vertical ionization energies I_v = 9.16, 10.18, 10.51, 11.56 eV; quinoxaline derivative with 4,5-dimethyl-1,2-phenylenediamine: m.p. = 159–161 °C; correct C,H,N analysis

8: **8** was obtained as a highly viscous, readily decomposing oil, which was oxidized directly to **6** without further purification.—IR ($CHCl_3$): $\tilde{\nu}$ = 1640, 1590 cm^{-1}; ^{1}H-NMR: δ = 1.35 (s, 6H), 2.00 (d, ^4J = 1.3 Hz, 3H), 6.17 (q, ^4J = 1.3 Hz, 1H), 6.85 (br. s, 2H); ^{13}C-NMR: δ = 15.5 (qd; CH_3 of C-4), 25.0 (qm; 2 × CH_3), 39.3 (m; C-6), 129.4 (q; C-4), 129.5 (s; C-2), 147.5 (dm; C-5), 161.0 (m; C-1/C-3), 179.8 (m; C-1/C-3) (numbering as for **6**)

[1] S. Hertzberg, S. Liaaen-Jensen, C. R. Enzell, G. W. Francis, *Acta Chem. Scand. 23* (1969) 3290.
[2] S. Hertzberg, S. Liaaen-Jensen, *Acta Chem. Scand. 22* (1968) 1714.
[3] R. Holzel, A. P. Leftwick, B. C. L. Weedon, *J. Chem. Soc. Chem. Commun. 1969*, 128; B. C. L. Weedon in O. Isler (Ed.): *Carotenoids*, Birkhäuser, Basel 1971, p. 40.
[4] R. Buchecker in G. Britton, T. W. Goodwin (Eds.): *Carotenoids Chemistry and Biochemistry*, Pergamon, Oxford 1982, p. 175; T. W. Goodwin, *The Biochemistry of the Carotenoids, Vol. 2*, 2nd ed., Chapman and Hall, London 1984, p. 38.
[5] B. Eistert, G. Bock, E. Kosch, F. Spalink, *Chem. Ber. 93* (1960) 1451; M. B. Rubin, *Chem. Rev. 1975*, 177.
[6] a) J. H. Hargreaves, P. W. Hickmott, B. J. Hopkins, *J. Chem. Soc. C 1968*, 2599; b) C. S. Gibson, A. R. Penfold, J. L. Simonsen, *J. Chem. Soc. 1930*, 1184.
[7] M. Kummer, G. Martin, H.-D. Martin, *Angew. Chem. 98* (1986) 995; *Angew. Chem. Int. Ed. Engl. 25* (1986) 1018; H.-D. Martin, M. Kummer, G. Martin, J. Bartsch, D. Brück, A. Heinrichs, B. Mayer, S. Röver, A. Steigel, D. Mootz, B. Middelhauve, D. Scheutzow, *Chem. Ber. 120* (1987) 1133.
[8] B. Eistert, R. Müller, I. Mussler, H. Selzer, *Chem. Ber. 102* (1969) 2429.
[9] L. De Buyck, Y. Zi-Peng, R. Verné, N. De Kimpe, N. Schamp, *Bull. Soc. Chim. Belg. 94* (1985) 75.
[10] Quantitative separation from unreacted DDQ and the corresponding hydroquinone has not been accomplished so far.

[11] Reaction with 4,5-dimethyl-1,2-phenylenediamine affords two isomeric quinoxalines (35% based on **8**), one of which is obtainable in pure form by fractional crystallization (m.p. = 159–161 °C).
[12] P. Bischof, R. Gleiter, P. Hofmann, *Helv. Chim. Acta 58* (1975) 2130; R. Gleiter, P. Hofmann, P. Schang, A. Sieber, *Tetrahedron 36* (1980) 655.
[13] R. Gleiter, W. Dobler, M. Eckert-Maksic, *Nouv. J. Chim. 6* (1982) 123.

$[\{Cp(CO)_2Mn\}_2SPh]^{\oplus}$, the First Sulfur Analogue of a Phosphanediyl ("Phosphinidene") Complex**

By *Horst Braunwarth, Gottfried Huttner,** and *Laszlo Zsolnai*

Dedicated to Professor Helmut Dörfel on the occasion of his 60th birthday

The chemistry of phosphanediyl complexes[***] $[(L_nM)_2PR]$ (L_n = 16-electron complex fragment, R = monovalent group) has developed into a broad area of research since the synthesis of the first such complex $[\{Cp(CO)_2Mn\}_2PPh]$ **5**.[1] The trigonal-planar coordination of the main-group element P by the two L_nM fragments and the monovalent group, which is characteristic of phosphanediyl complexes, has also been realized for the compounds $[(L_nM)_2XR]$ (X = As, Sb, Bi) involving the heavier elements homologous to phosphorus.[2] However, transfer of this characteristic bonding principle to the $RS^{\oplus}$ fragment as ligand, which is isoelectronic to RP, has not been accomplished so far. Herein we report on the synthesis of $[\{Cp(CO)_2Mn\}_2SPh]PF_6$ **2**, whose complex cation corresponds to that of the isoelectronic phosphanediyl complex **5** in structure and properties.

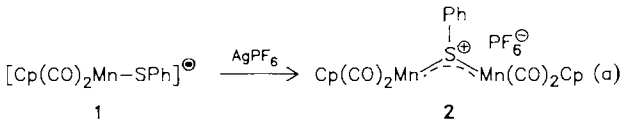

1 2

The mononuclear radical complex **1**[3] can be reversibly oxidized and reduced electrochemically.[4] Its oxidation with $AgPF_6$, however, results in formation of the binuclear compound **2** [Eq. (a)]. Whereas complex **3**, an analogue of

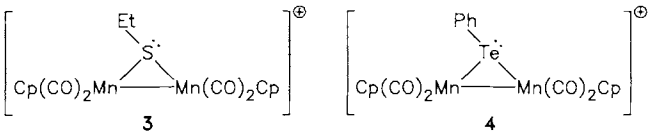

3 4

2 reported by *R. J. Haines* et al.,[5] and the tellurium analogue of **2**,[6] complex **4**, have an Mn–Mn bond and thus display pyramidal coordination around S and Te, respectively, the sulfur atom in **2** is coordinated in a trigonal-planar fashion.[7] The bonding in **2** thus corresponds in all respects to that in the isoelectronic **5**[1,2] (Scheme 1).

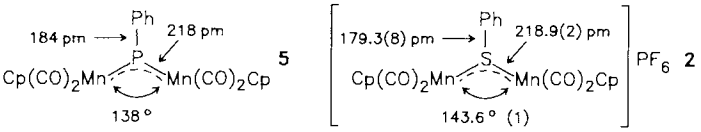

Scheme 1. Comparison of the structures of **2** and **5**.

Accordingly, **2** shows the UV/VIS spectrum characteristic of "diyl" complexes like **5**,[1,2,8] which features an intense long-wavelength absorption at 17860 cm^{-1} (Fig. 1).

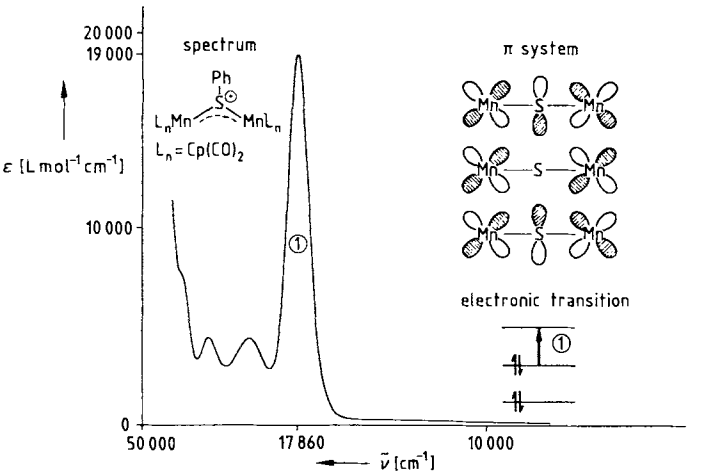

Fig. 1. UV/VIS spectrum of **2** (20 °C, CH_2Cl_2). The intense band at 17860 cm^{-1} is due to a transition in the three-center 4π-electron system Mn=S=Mn.

The fact that compound **2** crystallizes in the open form (Mn=S=Mn), whereas **3** crystallizes in the valence-isomeric closed form (Mn–S–Mn), although the two compounds differ only in the substituents R and S and in the counterion ($ClO_4^{\ominus}$ for **3**), shows that only a small difference in energy exists between the two forms. The valence isomerism between the allyl anion-analogous open form[2,8] and the cyclopropyl anion-analogous closed form in the fifth main group,[2,10] as inferred from trapping reactions for stibanediyl complexes, $[(L_nM)_2SbR]$[2,9] was only demonstrated there in one case.[11] The existence of **2** and **3** leads to the expectation that for the complexes $[(L_nM)_2YR]^{\oplus}$, Y = S, Se, Te, the position of the valence-isomeric equilibrium should be easier to control.

Experimental Procedure

2: **1** (100 mg, 0.35 mmol) (prepared analogously to the procedure described in [3]) was dissolved in toluene (10 mL) under N_2 and the stirred solution was treated with $AgPF_6$ (88 mg, 0.35 mmol). The color turned immediately from blue to violet. After 20 min of stirring, the toluene was removed under high vacuum; the residue was dissolved in 20 mL of CH_2Cl_2 and the resulting solution was filtered under N_2 through 2 cm of silanated silica gel. Crystallization at −30 °C afforded analytically pure **2**. Yield: 27 mg (25% based on Mn).—IR (CH_2Cl_2): $\tilde{\nu}$ [cm^{-1}] = 2051 s, 2015 s, 1986 s, 1935 w; ^{1}H-NMR (293 K, CD_2Cl_2): δ = 5.29 (s, 10H), 6.95–7.55 (m, 5H).

Received: December 7, 1987 [Z 2530 IE]
German version: *Angew. Chem. 100* (1988) 731

CAS Registry numbers:
1, 114095-82-8; **2**, 114095-84-0.

[*] Prof. Dr. G. Huttner, H. Braunwarth, Dr. L. Zsolnai
Anorganisch-chemisches Institut der Universität
Im Neuenheimer Feld 270, D-6900 Heidelberg (FRG)

[**] This work was supported by the Fonds der chemischen Industrie and the Deutsche Forschungsgemeinschaft.

[***] According to IUPAC rules, the ligands RP, RSb, and RB are referred to as "anediyl" ligands. The "inidene" nomenclature is commonly used, however.

[1] G. Huttner, H. D. Müller, A. Frank, H. Lorenz, *Angew. Chem. 87* (1975) 714; *Angew. Chem. Int. Ed. Engl. 14* (1975) 705.
[2] Review: G. Huttner, K. Evertz, *Acc. Chem. Res. 19* (1986) 406.
[3] A. Winter, G. Huttner, L. Zsolnai, P. Kroneck, M. Gottlieb, *Angew. Chem. 96* (1984) 986; *Angew. Chem. Int. Ed. Engl. 23* (1984) 975; A. Winter, G. Huttner, M. Gottlieb, I. Jibril, *J. Organomet. Chem. 286* (1985) 317.
[4] G. Huttner, H. Braunwarth, unpublished results.
[5] J. C. T. R. Burckett-St. Laurent, M. R. Caira, R. B. English, R. J. Haines, L. R. Nassimbeni, *J. Chem. Soc. Dalton Trans. 1977*, 1077.
[6] G. Huttner, S. Schuler, L. Zsolnai, M. Gottlieb, H. Braunwarth, M. Minelli, *J. Organomet. Chem. 299* (1986) C4.
[7] X-ray structure analysis of **2**: $a=678.0(2)$, $b=1316.9(6)$, $c=1303.4(6)$ pm, $\beta=95.16(3)°$, space group $P2_1/m$, $Z=2$. In the space group $P2_1/m$, the $PF_6^\ominus$ ion and the Cp rings are disordered over two rotational positions. In the subgroup $P2_1$, the disorder of the $PF_6^\ominus$ ion remains. The refinement in the space group $P2_1/m$ [EXTL or SHELXTL program system, Sheldrick (Göttingen), 1984] led to the best result ($R=0.074$, $R_w=0.044$). The phenyl ring lies in the crystallographic mirror plane, which makes both $Cp(CO)_2Mn$ fragments symmetry equivalent; i.e., as for phosphanediyl complexes, it is rotated out of the plane of the M=X=M three-center 4π-electron system. Further details of the crystal structure investigation may be obtained from the Fachinformationszentrum Energie, Physik, Mathematik GmbH, D-7514 Eggenstein-Leopoldshafen 2 (FRG), on quoting the depository number CSD-52825, the names of the authors, and the journal citation.
[8] B. Huttner, J. von Seyerl, M. Marsili, H. G. Schmid, *Angew. Chem. 87* (1975) 455; *Angew. Chem. Int. Ed. Engl. 14* (1975) 434.
[9] U. Weber, G Huttner, O. Scheidsteger, L. Zsolnai, *J. Organomet. Chem. 289* (1985) 357.
[10] R. Huisgen, *Angew. Chem. 89* (1977) 589; *Angew. Chem. Int. Ed. Engl. 16* (1977) 572.
[11] A. H. Cowley, N. C. Norman, M. Pakulski, D. L. Bricker, D. H. Rusell, *J. Am. Chem. Soc. 107* (1985) 8211; A. M. Arif, A. H. Cowley, N. C. Norman, A. Guy Orpen, M. Pakulski, *J. Chem. Soc. Chem. Commun. 1985*, 1267.

Synthesis and Structure of (ET)[Ni{SC(CN)=C(CN)S}$_2$], a Radical Cation Salt of Bis(ethylenedithio)tetrathiafulvalene**

By *Walter Reith,* Kurt Polborn,* and *Eberhard Amberger*

The development of inorganic materials having dramatically higher transition temperatures T_c[1] has reawakened hope in increasing the transition temperatures of organic metals as well. Since the discovery of the first organic superconductor $(TMTSF)_2(PF_6)$[2] (TMTSF = tetramethyltetraselenafulvalene) in 1980, numerous radical cation salts of tetrathiafulvalene (TTF) derivatives have been synthesized.[3] The most promising donor at present is bis(ethylenedithio)tetrathiafulvalene (ET), also referred to as BEDT-TTF, whose salts are often superconducting under normal pressure. These salts include the organic superconductor having the highest transition temperature so far reported,[***] $(ET)_2(I_3)$ with $T_c=8$ K.[4,5] The compounds $(ET)_y(X)_z$ are interesting owing to their broad range of structures and their differing ET charge states.[6] Not only can the y/z ratio vary for the same X—for $X=[ReO_4]^\ominus$, $y=1, 2, 3$ and $z=1, 2$;[6] for $X=[TlCl_4]^\ominus$, $y=1, 2$ and $z=1$[7]—but, in addition, different structures occur for the same y/z ratio: α, β, γ, δ, t, z phases of $(ET)_2(I_3)$.[5,8]

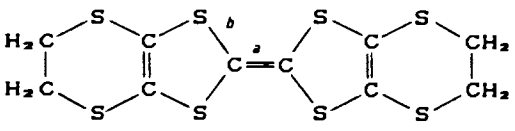

ET

These findings may be explained by several factors. Because of the ethylene moieties, which do not lie in the plane of the molecule, the ET molecules do not stack in a "face over face" fashion, as has been observed for other organic metals containing planar donors and/or acceptors. The "side to side" arrangement typical of ET molecules leads to the formation of two-dimensional layers separated by anions. The resulting sulfur–sulfur contacts are important for the conductivity. So far, ET salts containing small, symmetric inorganic anions have been prepared almost exclusively. A stronger involvement of the anions in the mechanism of conductivity would be desirable and might lead to an increase in the dimensionality. A very promising approach leading to the synthesis of new metals and superconductors is the use of metal complexes as anions. The compound $(TTF)[Ni(dmit)_2]_2$, for example, becomes superconducting at 1.7 kbar and 1.62 K.[9]

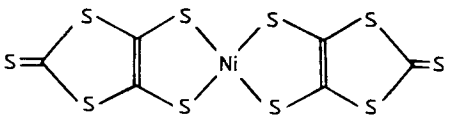

$[Ni(dmit)_2]$

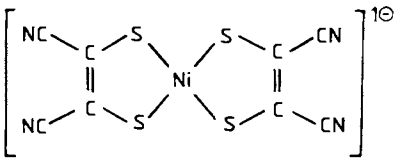

$[Ni(mnt)_2]$

Herein we describe the synthesis and structure of $(ET)[Ni(mnt)_2]$ (mnt = malodinitriledithiolate). Black platelets of $(ET)[Ni(mnt)_2]$ having a metallic luster were obtained from a solution of ET and $(n-Bu_4N)[Ni(mnt)_2]$ in 1,1,2-trichloroethane by galvanostatic oxidation. The structure was determined by X-ray analysis (Fig. 1). Refinement of the structure with incorporation of the hydrogen atoms gave an R value of 0.024.[18]

The angle between the molecular plane of $ET^{\odot\oplus}$ and $[Ni(mnt)_2]^\ominus$ is 49.77(3)°. Four sulfur–sulfur contacts exist between each two Et radical cations; these S–S distances are significantly smaller than the sum of the van der Waals radii (3.70 Å) and the distances from the sulfur atom in the six-membered ring to that in the five-membered ring (3.524 Å) and to that in the six-membered ring (3.528 Å) are nearly identical (see Fig. 1).

The S–S distances between each two, nearly planar $[Ni(mnt)_2]^\ominus$ ions (3.700 Å) correspond exactly to the sum of the van der Waals radii. There are no sulfur–sulfur contacts between the donor and acceptor molecules. A comparison of ET ions in different oxidation states shows that

[*] Dipl.-Chem. W. Reith, Dr. K. Polborn, Prof. Dr. E. Amberger†
Institut für Anorganische Chemie der Universität
Meiserstrasse 1, D-8000 München 2 (FRG)

[**] We thank *Ralf Sieburger*, Sektion Physik der Universität München, for the investigations of superconductivity.

[***] Note added in proof by the editorial staff: A transition temperature of 10.4 K for $(ET)_2Cu(NCS)_2$ was reported in January: H. Urayama, H. Yamochi, G. Saito, K. Nozawa, T. Sugano, M. Kinoshita, S. Sato, K. Oshima, A. Kawamoto, J. Tanaka, *Chem. Lett. 1988*, 55; see also H. Urayama, H. Yamochi, G. Saito, S. Sato, A. Kawamoto, J. Tanaka, T. Mori, Y. Maruyama, H. Inokuchi, *ibid. 1988*, 463, and K. D. Carson, U. Geiser, A. M. Kini, H. H. Wang, L. K. Montgomery, W. K. Kwok, M. A. Beno, J. M. Williams, C. S. Cariss, G. W. Crabtree, M.-H. Whangbo, M. Evain, *Inorg. Chem. 27* (1988) 965.

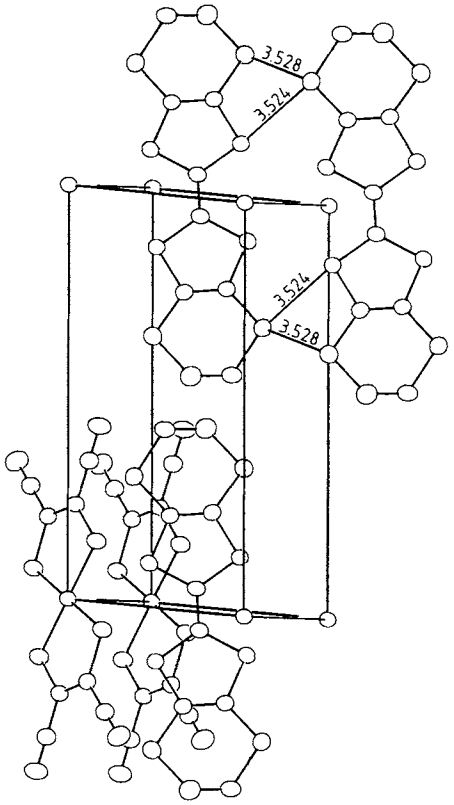

Fig. 1. *A-C* view (rotated by 70° around *B*) of (ET)[Ni(mnt)$_2$]. For the sake of clarity, some of the molecules were omitted. Both the cations and the anions are located on centers of symmetry.

the central C=C bond *a* becomes increasingly longer and bond *b* between these C atoms and the S atoms of the five-membered ring increasingly shorter with increasing oxidation. The ratio *b/a* is plotted against the charge of the cation for several ET compounds in Figure 2. In neutral ET,

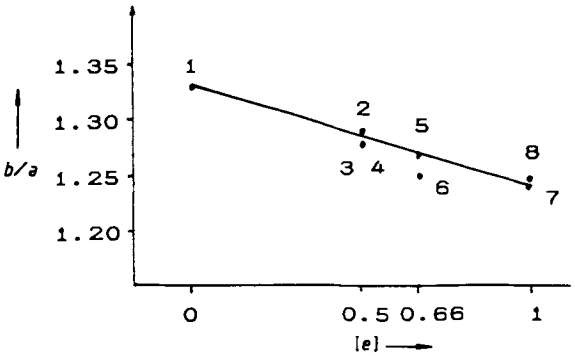

Fig. 2. Ratio of the bond lengths *b* and *a* as a function of the charge |*e*| of ET. For *b*, the mean values of the respective bonds were used. The numbers correspond to the following compounds: 1 = ET [12], 2 = (ET)$_2$[IAuBr] [13], 3 = (ET)$_2$(BrICl) [14], 4 = (ET)$_2$(IBr$_2$) [15], 5 = (ET)$_3$(NO$_3$)$_2$ [16], 6 = α-[(ET)$_3$(ReO$_4$)$_2$] [17], 7 = (ET)[TlCl$_4$] [7], 8 = (ET)[Ni(mnt)$_2$].

bond *a* is 1.32 Å long; in ET with the charges +0.5, +0.66, and +1, it is ca. 1.36, 1.37, and 1.38 Å, respectively. The corresponding values for the four C-S bonds are 1.76, 1.74, 1.73, and 1.72 Å, respectively (averages). With increasing oxidation of the donor ET, the electron density in the central C=C bond decreases.

Experimental Procedure

ET [10] and (*n*Bu$_4$N)[Ni(mnt)$_2$] [11] were prepared as described. Electrocrystallization: Neutral ET (2.34 mmol L^{-1}) and (*n*Bu$_4$N)[Ni(mnt)$_2$] (0.56 mmol L^{-1}) were oxidized galvanostatically in various solvents using a current density of 1 μA cm^{-2}. Black, rhomboid-shaped crystals, whose surfaces have a metallic luster (max. 2 × 1 × 0.5 mm^3), were obtained at a platinum electrode within several days from trichloroethane, acetonitrile, tetrahydrofuran, and dichloromethane. The crystals from trichloroethane were of the best quality. Potentiostatic oxidation ($U \approx 1$–1.5 V) in the same solvent afforded only black, microcrystalline coatings on the electrodes. (ET)[Ni(mnt)$_2$] crystallizes in the triclinic space group *P*-1 with $a = 6.273(1)$, $b = 7.833(1)$, $c = 13.127(2)$ Å, $\alpha = 96.170(15)$, $\beta = 92.591(18)$, $\gamma = 96.218(16)°$, $V = 636.4$ Å^3. Superconductivity was determined by measurement of alternating field susceptibility.

Received: December 16, 1987;
supplemented: February 5, 1988 [Z 2541 IE]
German version: *Angew. Chem. 100* (1988) 722

CAS Registry numbers:
ET, 66946-48-3; (*n*-Bu$_4$N)[Ni(mnt)$_2$], 55401-12-2; (ET)[Ni(mnt)$_2$], 97398-39-5; Pt, 7440-06-4; trichlorethane, 79-00-5; acetonitrile, 75-05-8; tetrahydrofuran, 109-99-9; dichloromethane, 75-09-2.

[1] K. A. Müller, J. G. Bednorz, *Science (Washington) 237* (1987) 1133; H. G. von Schnering, L. Walz, M. Schwarz, W. Becker, M. Hartweg, T. Popp, B. Hettich, P. Müller, G. Kämpf, *Angew. Chem. 100* (1988) 604; *Angew. Chem. Int. Ed. Engl. 27* (1988) 574.
[2] D. Jerome, A. Mazaud, M. Ribault, K. Bechgaard, *J. Phys. Lett. 41* (1980) 95.
[3] K. Bechgaard, *Mol. Cryst. Liq. Cryst. 79* (1982) 1; F. Gross, A. Schenk, K. Andres, F. Wudl, S. D. Cox, J. Brennan, *Phys. Rev. B 20* (1984) 1282; J. M. Williams, T. J. Emge, H. H. Wang, M. A. Beno, P. T. Copps, L. N. Hall, K. D. Carson, G. W. Crabtree, *Inorg. Chem. 23* (1984) 2558; J. M. Williams, K. Carneiro, *Adv. Inorg. Chem. Radiochem. 29* (1985) 249.
[4] V. A. Merkanov, E. E. Kostynchenko, V. N. Lankhin, R. M. Lobhovskaya, R. P. Shibaeva, J. F. Skshegolev, E. B. Yagubskii, *Pis'ma Zh. Eksp. Teor. Fiz. 41* (1985) 146; *Chem. Abstr. 102* (1985) 158855s.
[5] D. Schweizer, P. Bele, H. Brunner, K. J. Keller, E. Gogu, U. Haeberlein, J. Hennig, J. Klutz, R. Swietlik, H. J. Keller, *Z. Phys. B Condens. Matter 67* (1987) 489.
[6] S. S. P. Parkin, *Mol. Cryst. Liq. Cryst. 119* (1985) 357.
[7] W. Reith, K. Polborn, E. Amberger, unpublished results.
[8] R. B. Shibaeva, V. F. Kaminskii, E. B. Yagubskii, *Mol. Cryst. Liq. Cryst. 119* (1985) 361; E. B. Yagubskii, J. F. Skchegoler, V. N. Lankhin, L. J. Boravov, *Pis'ma Zh. Eksp. Teor. Fiz. 39* (1984) 12; *Chem. Abstr. 100* (1984) 113119x; P. C. W. Leung, T. J. Emge, J. M. Williams, A. J. Schultz, M. A. Beno, K. D. Carlson, H. H. Wang, M. A. Firestone, *Solid State Commun. 57* (1986) 93; C. P. Heidmann, K. Andres, H. Veith, H. Fuchs, K. Polborn, E. Amberger, *ibid. 57* (1986) 161; K. Bender, K. Dietz, H. Endres, H. W. Helberg, H. J. Keller, H. W. Schäfer, D. Schweitzer, *Mol. Cryst. Liq. Cryst. 107* (1984) 45.
[9] M. Bousseau, L. Valade, J.-P. Legros, P. Cassou, M. Garbauskas, L. V. Interrante, *J. Am. Chem. Soc. 108* (1986) 1908.
[10] M. Mizuno, A. F. Garito, M. P. Cava, *J. Chem. Soc. Chem. Commun. 1978*, 18.
[11] G. Bähr, G. Schleitzer, *Chem. Ber. 88* (1955) 1771; *ibid. 90* (1957) 438; A. Davison, N. Edelstein, R. H. Holm, A. H. Maki, *Inorg. Chem. 2* (1963) 1227.
[12] H. Kobayashi, A. Kobayashi, Y. Sasaki, G. Saito, H. Inokuchi, *Bull. Chem. Soc. Jpn. 59* (1986) 301.
[13] A. Ugawa, K. Yakushi, H. Kuroda, A. Kawamoto, J. Tanaka, *Chem. Lett. 1986*, 1875.
[14] J. M. Williams, *J. Am. Chem. Soc. 108* (1986) 695.
[15] H. Endres, H. J. Keller, D. Schweitzer, M. Hiller, K. Bender, E. Gogu, I. Heinen, *Z. Naturforsch. B 40* (1985) 1664.
[16] H. Endres, H. J. Keller, A. Weber, *Z. Naturforsch. B 40* (1985) 1658.
[17] H. Kanbara, H. Tajima, S. Aratani, K. Yakushi, H. Kuroda, G. Saito, A. Kawamoto, J. Tanaka, *Chem. Lett. 1986*, 437.
[18] Single crystal ca. 0.3 × 0.15 × 0.2 mm^3. Four-circle diffractometer CAD4, Enraf-Nonius, 28°C, Mo$_{K\alpha}$ radiation ($\lambda = 0.71069$ Å), graphite monochromator. Data collection: $4° < 2\theta < 50°$, $\pm h$, $\pm k$, $+l$, $\omega - 2\theta$ scan, scan width: $0.90° + 0.35 \tan\theta$. Maximum measuring time: 30 s. 2133 measured reflections, 1942 of which were unique and 1815 with $I > 3\sigma(I)$, $R = 0.025$, $R_w = 0.024$, $w = 1/\sigma(F)^2$, 164 parameters. Three intensity control reflections were measured every 3600 s, empirical absorption correction with ψ scans of six reflections ($\mu = 17.32$ cm^{-1}). Solution by Patterson methods. Full-matrix refinement, hydrogen atoms "riding," all non-hydrogen atoms refined anisotropically. Residual peaks: +0.45 and −0.40 *e*/Å. Further details of the crystal structure investigation are available on request from the Fachinformationszentrum Energie, Physik, Mathematik GmbH, D-7514 Eggenstein-Leopoldshafen 2, on quoting the depository number CSD-52771, the names of the authors, and the journal citation.

Multidecker Metallocenophanes**

By *Henning Hopf** and *Jörg Dannheim*

Ferrocene and [2.2]paracyclophane are the most thoroughly investigated double-layer molecules in organometallic[2] and organic chemistry.[3] We suggested earlier[1] that these two prototypes might be linked with each other so as to form multilayer systems having the general structure **1**, in which inorganic and organic structural elements alternate.

–[2.2]phane–ferrocene–[2.2]phane–ferrocene–[2.2]phane– **1**

Oligomers and polymers of this type should have interesting structural, spectroscopic, and chemical properties; their electrochemical behavior is of particular interest. In the meantime, several authors have pointed out that multinuclear complexes derived from ferrocene may function as "electron reservoirs," thereby storing or transferring electrons either stoichiometrically or catalytically.[4]

We consider the carbanions derived from *anti*-[2.2]indenophane **3** to be particularly well-suited as organic structural components for the systems **1**. On the one hand, the benzene rings are separated from each other by only 300 pm, thus guaranteeing the transmission of electronic effects.[3,5] On the other, the *anti* arrangement of the complex-forming cyclopentadienyl rings assures that they do not engage in intramolecular complexation, which would prevent chain formation as shown in **1**.

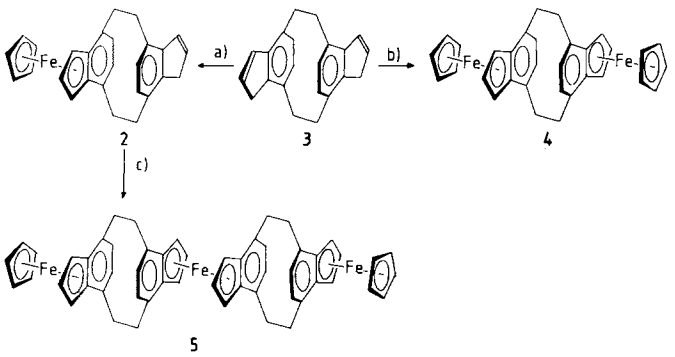

Scheme 1. Synthesis of **2**, **4**, and **5**. a) 1 equiv. CH_3Li, C_5H_5Li, $FeCl_2 \cdot 2THF$. b) 2 equiv. CH_3Li, C_5H_5Li, $FeCl_2 \cdot 2THF$. c) 1 equiv. CH_3Li, $FeCl_2 \cdot 2THF$.

Herein we describe the first complexation experiments involving the carbanions **3**, the synthesis of which was recently reported.[5]

When the monoanion prepared by treatment of **3** with one equivalent of methyllithium in tetrahydrofuran was allowed to react at $-30°C$ with lithium cyclopentadienide in excess and iron(II) chloride·tetrahydrofuran, the monoiron complex **2** was obtained in yields of up to 85% (Scheme 1). Crystallization from petroleum ether afforded **2** as reddish violet needles (m.p. = 215 °C). Pure **2** is indefinitely stable, but, in solution, it is sensitive toward oxidation. Its reactivity toward oxygen increases with increasing solvent polarity. Treatment of **3** with two equivalents of methyllithium (tetrahydrofuran, $-78°C$) transforms it into the dianion,[5] which may be trapped as the diiron complex **4** (63%, reddish violet needles from benzene, dec. above 160 °C) by reaction at $-20°C$ with lithium cyclopentadienide and iron(II) chloride·tetrahydrofuran. Finally, the triferrocenophane **5**—the first "oligomeric section" of the general structure **1**—is obtained when the stable anion, prepared by reaction of **2** with methyllithium in tetrahydrofuran, is dimerized by reaction at $-20°C$ with iron(II) chloride·tetrahydrofuran (60%). The complex affords brownish red rhombic crystals (dec. above 160 °C) from benzene. In crystalline form the complex is stable, but it undergoes oxidation within a few hours in solution upon exposure to air.

The proposed structures for the three new complexes are based on the spectroscopic data. The ^1H-NMR signals of the coordinated cyclopentadienyl rings are particularly revealing (400 MHz, $CDCl_3$, int. TMS; **2**: $\delta = 3.38$ (s, 5H), 3.97 (t, 1H, $J = 2.5$ Hz), 4.35 (d, 2H); **4**: $\delta = 3.33$ (s, 10H), 3.90 (t, 2H, $J = 2.5$ Hz), 4.35 (d, 4H); **5**: $\delta = 3.23$ (s, 10H), 3.53 (ps-s, 6H; "inner" ferrocene moiety), 3.82 (t, 2H, $J = 2.5$ Hz), 4.24 (d, 4H). The structural assignments were unequivocally confirmed for **4** and **5** by X-ray structure analyses,[6] which will be reported together with further metal complexes of **3** and its isomers in a full article.

Received: January 8, 1988 [Z 2566 IE]
German version: *Angew. Chem. 100* (1988) 724

[*] Prof. Dr. H. Hopf, Dr. J. Dannheim
Institut für Organische Chemie der Universität
Hagenring 30, D-3300 Braunschweig (FRG)

[**] Metallocenophanes, Part 5. This work was supported by the Fonds der Chemischen Industrie and by the Stiftung Volkswagenwerk.—Part 4: [1a].

[1] a) H. Hopf, F.-W. Raulfs, D. Schomburg, *Tetrahedron 42* (1986) 1655; b) H. Hopf, F.-W. Raulfs, *Israel J. Chem. 25* (1985) 210; c) S. El-Tamany, F.-W. Raulfs, H. Hopf, *Angew. Chem. 95* (1983) 631; *Angew. Chem. Int. Ed. Engl. 22* (1983) 633; d) A. E. Mourad, H. Hopf, *Tetrahedron Lett. 1979*, 1209.

[2] *Gmelin, Handbook of Inorganic Chemistry, Organoiron Compounds, Part A, Ferrocene, Section 8* and earlier volumes of this series, Springer, Berlin 1986. Review on [m.m]metallocenophanes: U. T. Mueller-Westerhoff, *Angew. Chem. 98* (1986) 700; *Angew. Chem. Int. Ed. Engl. 25* (1986) 702.

[3] P. M. Keehn, S. M. Rosenfeld (Eds.): *The Cyclophanes, Vol. I, II*, Academic Press, New York 1983.

[4] Review: D. Astruc, *Acc. Chem. Res. 19* (1986) 377.

[5] R. Frim, F.-W. Raulfs, H. Hopf, M. Rabinovitz, *Angew. Chem. 98* (1986) 160; *Angew. Chem. Int. Ed. Engl. 25* (1986) 174; J. Dannheim, *Dissertation*, Universität Braunschweig 1988.

[6] We thank Priv.-Doz. Dr. *D. Schomburg* (Gesellschaft für Biotechnologische Forschung, Braunschweig-Stockheim) for carrying out the corresponding measurements.

[1,2,4]Triazolo[1,2-*a*][1,2,4]triazole-1,3,5,7(2*H*,6*H*)-tetrone (Urazourazole), Synthesis and Structure**

By *Edgar Nachbaur,** *Gottfried Faleschini, Ferdinand Belaj,* and *Rudolf Janoschek*

Both the parent compound of the 1,2,4-triazolidine-3,5-diones, urazole **1**, as well as that of the 1,2,4-triazole-3,5(4*H*)-diones,[1] compound **2**, have been known for quite a long time. So far, however, no evidence has been reported for the existence of [1,2,4]triazolo]1,2-*a*][1,2,4]triazole-1,3,5,7(2*H*,6*H*)-tetrone **3** ("urazourazole") as a further parent compound, although the first member of this

[*] Prof. Dr. E. Nachbaur, G. Faleschini, Dr. F. Belaj
Institut für Anorganische Chemie der Universität
Schubertstrasse 1, A-8010 Graz (Austria)
Prof. Dr. R. Janoschek
Institut für Theoretische Chemie der Universität
Mozartgasse 14, A-8010 Graz (Austria)

[**] *F. B.* thanks Prof. *Dr. J. Zemann* (University of Vienna) for the possibility to collect the X-ray data.

class of compounds, namely the 2,6-diphenyl derivative, was prepared already in 1912.[2]

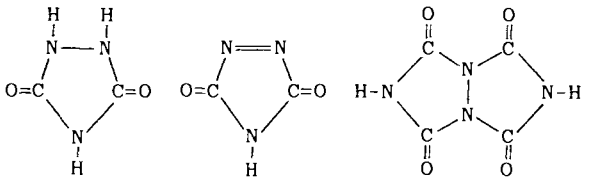

1 2 3

2,6-Dialkyl- or diarylurazourazoles are obtained in good yield by thermolysis of the corresponding 4-substituted 1,2,4-triazole-3,5(4*H*)-diones with loss of N_2.[3] This method fails, however, in the case of the unsubstituted compound **2**, which is stable only in dilute solution at low temperatures.[1b] Otherwise, depending on the conditions, **2** decomposes more or less rapidly to yield N_2, CO, and HNCO,[1a] thus preventing its isolation in pure form.

We have now succeeded in synthesizing **3** starting from persilylated urazole **4**, the structure of which we have been able to elucidate quite recently[4] (Scheme 1).

In the first reaction step all three trimethylsilyl groups are removed from **4** by low-temperature chlorination, and 4-chloro-1,2,4-triazole-3,5(4*H*)-dione **5** is formed. Owing to its lability, **5** could not be isolated, but its formation as an intermediate is supported by the following observation: if the excess of Cl_2 and a part of the solvent is removed at -40 °C by suction under vacuum, dark-red crystals separate, which on further heating react with Me_3SiCl present in the reaction mixture with evolution of Cl_2 to form red 4-trimethylsilyl-1,2,4-triazole-3,5(4*H*)-dione **6**. With the exclusion of water and light **6** is stable at temperatures around 0 °C pure and in solution and could be characterized spectroscopically; the UV/VIS and IR spectroscopic results are consistent with the proposed structure.

The formation of the colorless dideaza dimer **7** in the third reaction step is strongly exothermic and is accelerated still further by addition of donor solvents (dimethylformamide (DMF), pyridine) or by light. This finding is consistent with observations in the thermolysis of the 4-phenyl derivative of **2**.[3a] The hydrolysis of **7** to **3** on standing in a moist atmosphere is quantitative. The highest yield (67%) of **3** is achieved when **7** is not isolated but **6** allowed to stand for at least 48 hours at room temperature in a moist atmosphere.

3 is a colorless substance, crystallizing from water as long, fine needles, and decomposes at 340 °C, without any signs of melting, to yield N_2, CO, and HNCO. The alkalimetrically determined ionization constants of the dibasic acid **3**, $K_1 = 4.0 \times 10^{-4}$ and $K_2 = 1.0 \times 10^{-6}$ are unexpectedly high and indicate the compound as being a much stronger acid than urazole ($K_1 = 5.6 \times 10^{-7}$)[5] and cyanuric acid ($K_1 = 3.1 \times 10^{-7}$).[6]

The X-ray structure of **3** (Fig. 1)[7] shows that the two five-membered rings are significantly non-planar—the deviations of the ring atoms from the best plane being up to 0.043(5) Å—and in contrast to the planar 1,5-diazabicyclo[3.3.0]octane-2,4,6,8-tetrone[8] **8** (2 CH_2 groups instead of the NH groups of **3**) form an angle of 156.0(1)°. In comparison to the derivatives of urazole, the N–N bond is contracted and the N–C–N′ angles are diminished, while the C–N′–C angles are enlarged.[9] Each molecule has two donor and two acceptor hydrogen bonds to neighboring molecules. Since only two facing C=O groups form hydrogen

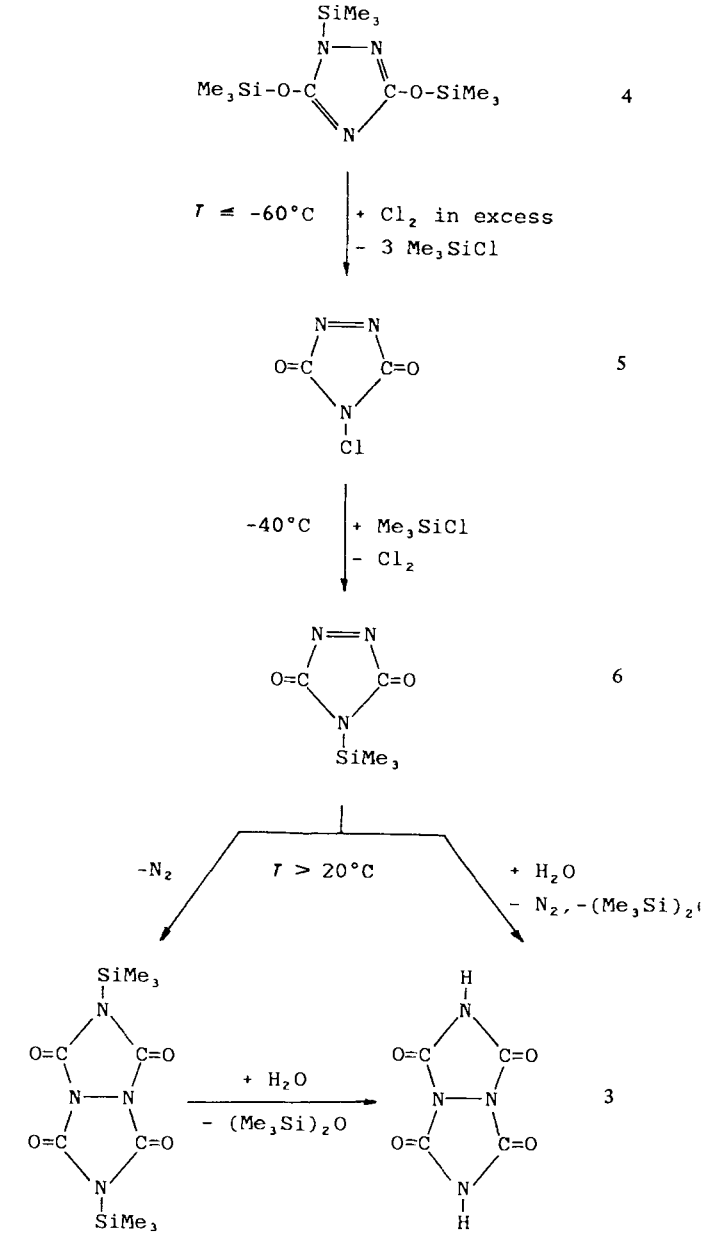

bridges, the C_{2v} symmetry of the molecule is lowered to C_2. Remarkable are the three intermolecular O···C=O contacts with short O···C distances in the range from 2.790(2) to 2.920(2) Å.[10] These, together with the low hydrogen content, contribute to the high density.

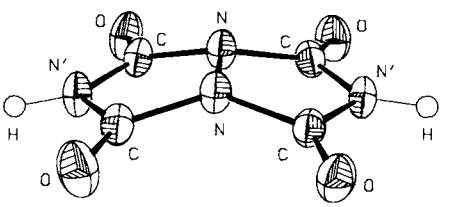

Fig. 1. Crystal structure of **3** (ORTEP), thermal ellipsoids at the 50% probability level (H atoms with arbitrary radii). Important bond lengths [Å] and angles [°] (standard deviations <0.002 Å and <0.1°, resp.): N-N 1.402, N-C 1.395–1.407, C-N′ 1.368–1.387, C-O 1.192–1.204; C-N-C 132.4–134.7, C-N-N 108.4–109.3, N-C-N′ 103.4–104.1, C-N′-C 114.2–114.3, N-C-O 126.0–127.5, N′-C-O 129.1–129.8.

 © VCH Verlagsgesellschaft mbH, D-6940 Weinheim, 1988 0570-0833/88/0505-0702 $ 02.50/0

Quantum chemical ab-initio calculations (SCF, 3-21G-basis set, experimental geometry), were carried out for **3** and the monoanion **3a**, as well as for **1** and its monoanion **1a**, in order to ascertain the reason for the markedly different acidities of the compounds **1** and **3**. The deprotonation energy of **1** was calculated to be 1573 kJ mol^{-1}, and that of **3** to be only 1452 kJ mol^{-1}. This result is understandable on the basis of population analyses according to *Mulliken*, which show a stronger delocalization of the additional electron in the bicyclic **3a** than in **1a**.

The question whether measured structural data (aplanarity of the bicyclic compound) are to be interpreted as molecular properties or must be attributed to packing effects in the crystal, could also be settled by quantum chemical calculations for **3**, the dianion **3b**,[11] and **8**. Comparison of a pyramidal and a planar environment for the nitrogen atom shows that planarity of the central R_2N–NR_2 fragment is more favorable for the molecules **3**, **3b**, and **8**: the relative stabilities for a planar R_2N–NR_2 fragment are +25.3 for **8** (folding angle as in **3**), +15.5 for **3**, and +5.9 kJ mol^{-1} for **3b**. Therefore the folding angles observed in **3** and **3b** in the crystalline state can be attributed to intermolecular interactions and to neighboring cations, respectively.

Experimental

6: A solution of **4** (30 g, 94.4 mmol) in CH_2Cl_2 (50 mL) was cooled to −60°C in the absence of moisture in a three-necked flask fitted with a cooled dropping funnel. 11 g (155.1 mmol) of chlorine (ca. 7 mL at −60°C) were condensed into the dropping funnel and added dropwise within 1 h to the solution of **4**, which turned deep red in color. All volatile components were then removed under vacuum and the temperature slowly raised to 0°C (great care must be taken here: vigorous evolution of Cl_2 takes place spontaneously at ca. −40°C); **6** separated out thereby in the form of red crystals. Yield: 14.4 g (89%). UV/VIS ($CHCl_3$): λ_{max} [nm] = 522 (s), 542 (s), 564 (s); IR (CCl_4): $\tilde{\nu}$(C–H) = 2960 (w), 2925 (w) cm^{-1}, $\tilde{\nu}$(C=O) = 1765 (vs) cm^{-1}, $\tilde{\nu}$(Me_3Si) = 1262 (vs), 850 (vs), 725 (m), 688 (m) cm^{-1}.

7: A solution of **6** (14.4 g, 84.1 mmol) in CH_2Cl_2 (50 mL) was treated with 5 mL of DMF and the mixture heated under reflux for 48 h. After removal of volatile components under vacuum, the pale yellow residue was sublimed at 150°C and 0.01 torr; pure **7** was obtained in the form of colorless needle-shaped crystals. M.p. 168°C: 4.6 g (34%). Correct elemental analysis.—IR (KBr): $\tilde{\nu}$ [cm^{-1}] = 2960 (w), 2910 (vw), 1780 (vs), 1430 (w), 1300 (vs), 1250 (s), 1160 (s), 1060 (s), 850 (vs), 780 (s), 765 (m); ^{29}Si-NMR ($CDCl_3$): δ = 7.69; ^{13}C-NMR ($CDCl_3$): δ = 147.5, −1.10.

3: 14.4 g (84.1 mmol) of **6** was allowed to stand for 48 h at room temperature in the presence of atmospheric moisture and then 24 h at 80°C in a dry box; the color of the substance changed from red to colorless. For purification, the crude product was recrystallized from 50 mL of water, whereby decomposition of **3** by hydrolysis could be essentially reduced by heating to not more than 80°C and rapidly cooling the filtrate to 0°C. Yield: 5.6 g (67%). Decomp. at 340°C. Correct elemental analysis.—IR (KBr): $\tilde{\nu}$ [cm^{-1}] = 3240 (vs), 2750 (sh), 1780 (vs), 1740 (s), 1480 (w), 1430 (s), 1360 (vs), 1180 (s), 1168 (s), 1133 (s), 945 (w), 745 (s); ^{13}C-NMR ([D_6]Me_2SO): δ = 159.79.

Received: November 19, 1987 [Z 2505 IE]
German version: *Angew. Chem. 100* (1988) 703

CAS Registry numbers:
3, 113893-26-8; **4**, 113924-28-0, **6**, 113924-29-1; **7**, 113924-30-4.

[1] a) J. E. Herweh, R. M. Fantazier, *Tetrahedron Lett. 1973*, 2101; b) H. Wamhoff, G. Kunz, *Angew. Chem. 93* (1981) 832; *Angew. Chem. Int. Ed. Engl. 20* (1981) 797.

[2] R. Stollé, *Chem. Ber. 45* (1912) 273.

[3] a) D. W. Borhani, F. D. Greene, *J. Org. Chem. 51* (1986) 1563; b) Le H. Dao, D. Mackay, *Can. J. Chem. 57* (1979) 2727; c) H. Wamhoff, K. Wald, *Chem. Ber. 110* (1977) 1699; d) R. F. Smith, S. B. Kaldor, E. D. Laganis, R. F. Oot, *J. Org. Chem. 40* (1975) 1854.

[4] G. Faleschini, E. Nachbaur, *Monath. Chem. 119* (1988) 457.

[5] J. Bourdais, F. Cugniet, J.-C. Prin, P. Chabrier, *Bull. Soc. Chim. Fr. 1964*, 500.

[6] R. C. Hirt, R. G. Schmitt, *Spectrochim. Acta 12* (1958) 127.

[7] Crystal structure data of **3**: monoclinic, $P2_1/c$, a = 8.2049(4), b = 5.4172(2), c = 13.2406(8) Å, β = 90.28(6)°, V = 588.5(1) Å^3, Z = 4, ρ_{calc} = 1.920 g cm^{-3}, STOE AED 2 four-circle diffractometer, graphite monochromator, $Mo_{K\alpha}$, λ = 0.71073 Å, $2\theta < 60°$, 1725 independent, 1372 significant reflections with $F_0 > 3\sigma(F_0)$. The structure was solved by direct methods (MULTAN), the hydrogen atoms were refined isotropically, the remaining atoms anisotropically. R = 0.0425, R_w = 0.0387 (1372 observables, 118 parameters). Further details of the crystal structure investigation are available on request from the Director of the Cambridge Crystallographic Data Center, University Chemical Laboratory, Lensfield Road, Cambridge CB2 1EW (England), on quoting the names of the authors, and the journal citation.

[8] G. Fritsch, G. Zinner, D. Mootz, M. Scherf, H. Wunderlich, *Arch. Pharm. (Weinheim, Ger.) 319* (1986) 646.

[9] An analysis of the structural data of 64 urazole derivatives from the Cambridge Crystallographic Data File gave as mean values for these parameters 1.432 Å and 105.9° and 110.9°, resp.

[10] H. B. Bürgi, J. D. Dunitz, E. Shefter, *Acta Crystallogr. Sect. B30* (1974) 1517.

[11] An X-ray structure analysis of the dianion **3b** shows that the two best five-membered ring planes form an angle of 140.3(1)° (F. Belaj, unpublished).

Stereoselective Synthesis of *trans*-Decalins via Intramolecular Ene Reactions; Synthesis of the Enantiomerically Pure Cadinane-Sesquiterpene Veticadinol**

By *Lutz F. Tietze,* Uwe Beifuss, Jochen Antel,* and *George M. Sheldrick*

The sesquiterpenes of the cadinane or cadalane series are widely distributed as plant constituents. They are found, inter alia, in vetiver oil, an important olfactory. The cadinanes contain 2,8-dimethyl-5-isopropyldecalin **1** as basic structural unit (numbering as in **2**). They are classified into four groups according to the type of annulation and the position of the isopropyl group: the true cadinanes (cadinane) and the bulgaranes with *trans*-fused rings, and the muurolanes and amorphanes with *cis*-fused rings.[1]

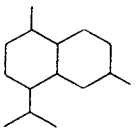

1

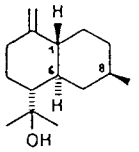

2

Few methods are as yet known for the stereoselective synthesis of both the *cis*- and the *trans*-fused ring systems of the cadinanes.[2] In our studies on the synthesis of terpenoid natural products we developed a novel stereoselective entry to the *trans*-coupled decalin system of the cadinanes which enabled us to synthesize the sesquiterpene veticadinol **2**.[3] From the retrosynthetic analysis it followed that it should be possible to synthesize the decalin system of **2** by two intramolecular cyclizations. The first cyclization is the intramolecular ene reaction of the alkylidenemalonate **5**,[5] which proceeds with high non-induced and induced diastereoselectivity,[4] and the second is the cyclization of **11** (Scheme 1). **5** already cyclizes in 92% yield at −78°C in

[*] Prof. Dr. L. F. Tietze, Dr. U. Beifuss
Institut für Organische Chemie der Universität
Tammannstrasse 2, D-3400 Göttingen (FRG)
Dipl.-Chem. J. Antel, Prof. G. M. Sheldrick
Institut für Anorganische Chemie der Universität
Tammannstrasse 4, D-3400 Göttingen (FRG)

[**] This work was supported by the Deutsche Forschungsgemeinschaft and the Fonds der Chemischen Industrie. We thank Dr. *E. J. Brunke* and Dr. *K. G. Fahlbusch*, Dragoco Holzminden, for kindly supplying us with samples of citronellal and vetiver oil, and Dr. *B. Mauerer*, Firmenich, Geneva (Switzerland) for a gift of vetiver oil.

the presence of $FeCl_3$ on basic aluminum oxide[6] to give the *trans*-substituted cyclohexanes **7** and **6** in the ratio 98.8 : 1.2 (GC; *i-de* 97.6%, *ni-de* > 99%). The $FeCl_3/Al_2O_3$ catalyst newly introduced by us for the ene reaction has great advantages over other Lewis acids in that it is easy to handle, can be used in catalytic amounts and affords very good selectivities and high yields. The absence of almost any side products in the reaction with $FeCl_3/Al_2O_3$ is presumably due in part to the fact that this catalyst acts as a proton scavanger, similarly to alkylaluminum halides.[7]

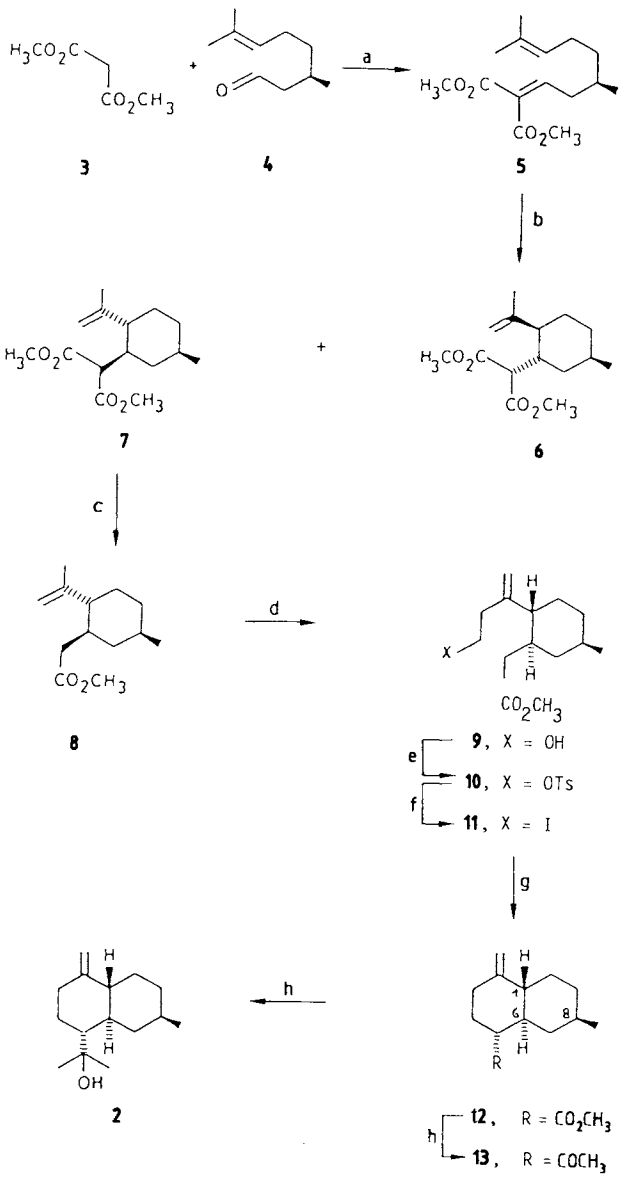

Scheme 1. a) Piperidinium acetate, CH_2Cl_2, 20°C/1 h, 82%. b) $FeCl_3/Al_2O_3$, −78°C/2 h, 20°C/2 h, 92%. c) H_2O, NaCl, Me_2SO, 150°C/4 h, 92%. d) $(CH_2O)_n$, $(CH_3)_2AlCl$, CH_2Cl_2, 0°C, 20°C/4 h, 81%. e) TosCl, pyridine, 0°C/1 h, 5°C/12 h, 93%. f) NaI, acetone, 20°C/12 h, 95%. g) LDA, THF, −78°C, 20°C/2 h, 92%. h) CH_3MgI, Et_2O, 20°C/12 h, 37.5°C/12 h, 12% **13**, 77% **2**, chromatography on silica gel with ethyl acetate/hexane = 1/1. R_f(**13**) = 0.44, R_f(**2**) = 0.10.

The alkylidenemalonate **5** needed for the ene reaction is accessible in 82% yield by condensation of (*R*)-citronellal **4** with **3**.[5] The demethoxycarbonylation[8] of **7** which follows the intramolecular ene reaction furnishes the monoester **8** in 92% yield, which undergoes a Prinz reaction[7] with paraformaldehyde to give the alcohol **9** (81%). For the intramolecular alkylating cyclization,[9] **9** is converted via the tosylate **10** into the iodide **11**, which reacts with lithium diisopropylamide (LDA) in tetrahydrofuran at −78°C via an intermediary ester enolate to give the decalin derivative **12** in 92% yield. The assignment of the structure of **12** follows from the characteristic resonance at $\delta = 0.87$ for an equatorially arranged methyl group, and from the large coupling constants $^3J_{6\text{-H},7\text{-H}} = {}^3J_{7\text{-H},8\text{-H}} = 12$ Hz, indicating *trans* coupling of the rings. The equatorial position of the methoxycarbonyl group is confirmed by the coupling pattern of the signals for 5-H_{ax} at $\delta = 2.24$ with coupling constants $J = 12.3$, 11, and 3.5 Hz.[10] Reaction of **12** with methylmagnesium iodide affords the desired enantiomerically pure veticadinol **2** in 77% yield. In addition, the methyl ketone **13** is obtained in 12% yield in an incomplete reaction, despite the use of a large excess of methylmagnesium iodide. Since the citronellal used for the synthesis is obtainable in both the *R*- as well as *S*-configuration, the enantiomer of **2** can also be prepared in the same way. An X-ray structure analysis was carried out in order to establish unequivocally the relative configuration of **2**.[11]

The synthetic sequence presented here not only enabled the stereoselective preparation of the interesting olfactory veticadinol **2** for the first time,[12] but also provides a general entry to sesquiterpenoid compounds of the decalin type. Moreover, by variation of the aldehyde employed for the Knoevenagel condensation in (a) and of the Grignard reagent in (h), a large variety of compounds of interest for the perfumery industry can be prepared.

Received: December 2, 1987 [Z 2521 IE]
German version: *Angew. Chem. 100* (1988) 739

CAS Registry numbers:
2, 14107-43-8; **3**, 108-59-8; **4**, 2385-77-5; **5**, 106431-76-9; **6**, 106431-82-7; **7**, 106431-81-6; **8**, 114032-14-3; **9**, 114032-15-4; **10**, 114032-16-5; **11**, 114032-17-6; **12**, 114032-18-7; **13**, 114129-01-0.

[1] a) G. Rücker, *Angew. Chem. 85* (1973) 895; *Angew. Chem. Int. Ed. Engl. 12* (1973) 793; b) B. M. Fraga, *Nat. Prod. Rep. 2* (1985) 147; c) B. M. Fraga, *ibid. 3* (1986) 273; d) T. K. Devon, A. I. Scott: *Handbook of Naturally Occurring Compounds, Vol. II*, Academic Press, London 1972; e) W. Karrer: *Konstitution und Vorkommen der organischen Pflanzenstoffe*, Birkhäuser, Basel 1958, 1977, 1981; f) J. S. Glasby: *Encyclopaedia of the Terpenoids*, Wiley, Chichester 1982.

[2] a) C. H. Heathcock in J. ApSimon (Ed.): *The Total Synthesis of Natural Products, Vol. 2*, Wiley, New York 1973, p. 197; b) C. H. Heathcock, S. L. Graham, M. C. Pirrung, F. Plavac, C. T. White in J. ApSimon (Ed.): *The Total Synthesis of Natural Products, Vol. 5*, Wiley, New York 1983, p. 1; c) J. S. Roberts, I. Bryson, *Nat. Prod. Rep. 1* (1984) 105; d) J. S. Roberts, *ibid. 2* (1985) 97; e) M. Vandewalle, P. De Clercq, *Tetrahedron 41* (1985) 1767.

[3] G. Chiurdoglu, A. Delsemme, *Bull. Soc. Chim. Belg. 70* (1961) 5: Veticadinol **2**, whose structure has so far not been unequivocally confirmed, was isolated by *Chiurdoglu* and *Delsemme* from Congolese vetiver oil. An attempt to detect **2** in a sample of "Bourbon" vetiver oil by GC-MS analysis after column chromatographic purification, gave a negative result.

[4] L. F. Tietze, U. Beifuss, *Angew. Chem. 97* (1985) 1067; *Angew. Chem. Int. Ed. Engl. 24* (1985) 1042.

[5] L. F. Tietze, U. Beifuss, *Tetrahedron Lett. 27* (1986) 1767.

[6] Preparation: Portionwise addition of 50 g of basic aluminum oxide (ICN Alumina B-Super I) to a stirred solution of anhydrous iron(III) chloride in 160 mL of dichloromethane under inert atmosphere. After one hours' stirring, removal of the solvent in a vacuum. L. F. Tietze, U. Beifuss, *Synthesis 1988*, 359.

[7] B. B. Snider, D. J. Rodini, T. C. Kirk, R. Cordova, *J. Am. Chem. Soc. 104* (1982) 555.

[8] A. P. Krapcho, *Synthesis 1982*, 805, 893.

[9] D. A. Evans in J. D. Morrison (Ed.): *Asymmetric Synthesis, Vol. 3*, Academic Press, Orlando, FL, USA 1984, p. 1.

[10] **12**: ^{1}H NMR (200 MHz, $CDCl_3$): $\delta = 0.74$ (q, $J = 12$ Hz, 1 H; 7-H_{ax}), 0.87 (d, $J = 6.5$ Hz, 3 H; 8-CH_3), 0.84–1.09 (m, 1 H), 1.19–2.03 (m, 9 H), 2.10 (dddm, $J = 14$, 4.5, 3 Hz, 1 H; 3-H_{eq}), 2.24 (ddd, $J = 12.3$, 11, 3.5 Hz, 1 H; 5-H_{ax}), 2.33–2.47 (m, 1 H), 3.69 (s, 3 H; OCH_3), 4.61 (mc, 1 H; $H_{olef.}$), 4.71 (mc, 1 H; $H_{olef.}$).

[11] Details of the crystal structure investigation are available on request from the Fachinformationszentrum Energie, Physik, Mathematik GmbH, D-7514 Eggenstein-Leopoldshafen 2 (FRG), on quoting the depository number CSD-53 079, the names of the authors, and the journal citation.

[12] a) O. P. Vig, K. L. Matta, G. Singh, I. Raj, *J. Indian Chem. Soc. 43* (1966) 605; b) O. P. Vig, G. Singh, O. P. Chugh, K. L. Matta, *Indian J. Chem. 7* (1969) 434.

Synthesis and Conformational Behavior of Dibenzo[2.2]metaparacyclophanediene**

By *Timothy Wong, Siu Shing Cheung,* and *Henry N. C. Wong**

The preparation of [2.2]metaparacyclophane **1** was reported more than two decades ago by *Cram* et al.[2,3] Variable temperature NMR studies on **1**[4] showed that, due to conformational flipping of the molecule, the signals of the *p*-phenylene protons of **1** coalesced at 146 °C; this corresponds to a $\Delta G_c^{\neq}$ of 87 kJ/mol.[4] On the other hand, [2.2]metaparacyclophane-1,9-diene **2** showed a coalescence temperature $T_c = -96$ °C, thus resulting in $\Delta G_c^{\neq} = 35$ kJ/mol.[5] It was of interest to investigate the conformational behavior[6] of compounds **3**, **4**, and **5**, which are benzoannelated derivatives of **1** and **2**. We report here on the synthesis of **4** and **5** and on the results of variable temperature NMR studies on these compounds.

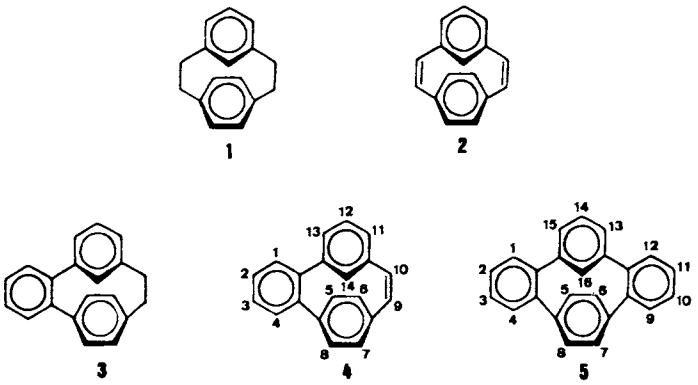

Benzo[2.2]metaparacyclophane **3** was first synthesized by *Vögtle* et al. via several steps starting from 3,4''-bis(bromomethyl)-1,1':2',1''-terphenyl **6**.[7] In the case of **3** $T_c = 116$ °C and $\Delta G_c^{\neq} = 75$ kJ/mol.[7] We were able to prepare compound **3** in one step: phenyllithium-induced coupling of **6**[7,8] resulted in the isolation of **3** in 44% yield. The physical and spectroscopic data of **3** were in accord with the literature data.[7] Bromination[8] of **3** with *N*-bromosuccinimide (NBS) in CCl_4 in the presence of azoisobutyronitrile (AIBN) furnished the monobromide **7** in 43% yield as a mixture of several isomers (m.p. 119–123 °C). The unpurified isomeric mixture was dehydrobrominated with KO*t*Bu, giving benzo[2.2]metaparacyclophan-9-ene **4** in 86% yield as the only isolable product.[8] Compound **4** forms colorless crystals (from hexane), which melt at 90–91 °C.[9]

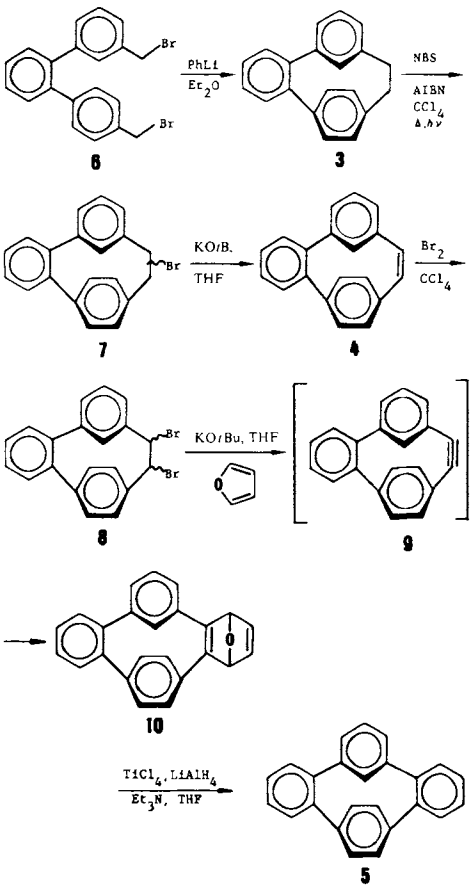

Treatment of **4** with bromine afforded an isomeric mixture of dibromides **8** in 90% yield [MS: *m/z* 412 ($M^{\oplus}$), 414 ($M^{\oplus}+2$), 416 ($M^{\oplus}+4$)]. The dibromides **8** were not separated, but allowed to undergo direct KO*t*Bu dehydrobromination in the presence of furan. The reaction leading to the isomeric epoxides **10** (isolated in 53% yield) presumably proceeds via the species **9**[1,10,11] containing a CC triple bond. The mixture of isomers **10** [m.p. > 300 °C, MS: *m/z* 320 ($M^{\oplus}$)] was not separated, but directly deoxygenated with $TiCl_4$–$LiAlH_4$–Et_3N in THF,[12] to give the title compound dibenzo[2.2]metaparacyclophanediene **5** in 67% yield. Compound **5** forms colorless crystals (from hexane) which decompose at ca. 250 °C. The structure of **5** was established ^{1}H-NMR spectroscopically.[9] In [D_6]acetone at 24 °C, the protons H-5, H-6, H-7, and H-8 gave rise to only a single extremely broad peak at $\delta = 6.95$, which was diffi-

[*] Dr. H. N. C. Wong [1], T. Wong, S. S. Cheung
Department of Chemistry, The Chinese University of Hong Kong
Shatin, New Territories (Hong Kong)

[**] Arene Synthesis by Extrusion Reaction, Part 13. The authors wish to express their sincere thanks to Messrs. *Y. H. Law, K. W. Kwong,* and *C. W. Fung* for their assistance in measuring the 250-MHz ^{1}H-NMR spectra and the mass spectra. *S. S. C.* is grateful to the Croucher Foundation (Hong Kong) for the award of a Croucher Studentship. – Part 12: C. W. Chan, H. N. C. Wong, *J. Am. Chem. Soc. 110* (1988) 462.

cult to detect. This interesting finding clearly indicates that the signals of the four *p*-phenylene protons of **5** coalesce due to flipping of the *p*-phenylene ring.[5,6] In order to prove this, we carried out a series of variable temperature NMR studies on **5** and **4**. Upon heating a $CDBr_3$-solution of **5** from 24°C to 96°C, the broad peak became narrower and narrower until a singlet resulted at $\delta = 6.95$ for H-5, H-6, H-7, and H-8. On cooling a [D_6]acetone-solution of **5** from 24°C to −21°C, however, two singlets appeared at $\delta = 6.51$ and $\delta = 7.50$ for H-5, H-6 and H-7, H-8 respectively. The signal at $\delta = 7.50$ was obscured by that of the *o*-phenylene protons. This situation corresponds to a $\Delta G_c^{\neq}$ of 57 kJ/mol.[13] Similar treatment of **4** (in [D_6]acetone) revealed a $\Delta G_c^{\neq}$ of 44 kJ/mol at $T_c = -41$°C.

In conclusion, the free energy of activation for the flipping process ($\Delta G_c^{\neq}$) and the coalescence temperature (T_c) seem to bear intrinsic relation with the bond distances of the bridges of [2.2]metaparacyclophanes, as can be seen from the aforementioned experimental results. It is thus apparent that the longer the bridge, the larger the values of $\Delta G_c^{\neq}$ and T_c. *Boekelheide* et al.[5] and *Mitchell*[6] have attributed this to the fact that opening of the bridge angle from 109.5° (sp^3) in **1** to 120° (sp^2) in **2** more than compensates for the shorter carbon-carbon double bond length on going from **1** to **2**, making the exchange process much more feasible. Since the length of the CC bonds of benzene lies between that of a single bond and that of a double bond, it is understandable that, in the case of the benzoannelated **5**, $\Delta G_c^{\neq}$ and T_c assume values between those of **3** and **4**: $\Delta G_c^{\neq}$ is 75 (**3**), 57 (**5**), and 44 kJ mol^{-1} (**4**); T_c is 116 (**3**), 24 (**5**), and −41°C (**4**). The values of **5** lie between those of **1** and **2**.

Received: December 7, 1987;
revised: January 25, 1988 [Z 2528 IE]
German version: *Angew. Chem. 100* (1988) 716

CAS Registry numbers:
3, 82388-17-8; **4**, 82733-10-6; **5**, 114032-09-6; **6**, 82388-15-6; **7**, isomer 1, 114032-05-2; **7**, isomer 2, 114032-06-3; **8**, 114032-07-4; **10**, isomer 1, 114032-08-5; **10**, isomer 2, 114129-00-9; furan, 110-00-9.

Alkyne(arene)cobalt, μ-Alkynebis(arenecobalt), and μ-Benzylidynetris(arenecobalt) from Arene/Cobalt Cocondensates**

By *Luis Vasquez, Hans Pritzkow,* and *Ulrich Zenneck**

Arene/cobalt cocondensates have already been used with success for the preparation of bis(2,2'-bipyridyl)cobalt,[2a] reactive organometallic slurries[2b] and catalytically active solutions,[3] but to our knowledge, all attempts have thus far failed to fix the arenes used for reaction with the cobalt as π-ligands in complexes.

We report here on the synthesis of mono-, di-, and trinuclear alkyne(arene)cobalt complexes from the product of the cocondensation of cobalt atoms and arenes.

Reactions of the cocondensates **1** (R = H, CH_3) at −100 to −20°C with alkynes [2-butyne, bis(trimethylsilyl)acetylene] lead, depending on the choice and concentrations of the reactants, to formation of both types of complexes **2** (green) and **3** (red) in varying amounts.

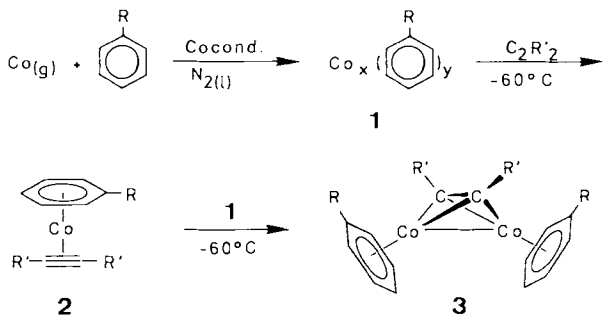

a, R = H, R' = CH_3; **b**, R = R' = CH_3; **c**, R = CH_3, R' = $Si(CH_3)_3$

Scheme 1. Synthesis of alkyne(arene)cobalt complexes via arene/cobalt cocondensation.

When butyne is allowed to react with **1**, R = H, the complex of type **2** is formed [**2a**: 5.6%, m.p. 73°C (decomp.)]. In the system toluene/butyne the type **3** complex is strongly preferred (**3b**: 15.2%, m.p. 90°C), but the amount of **2b** increases (0.4-1.2%, m.p. 55°C) with excess butyne; therefore, the reaction course depicted in Scheme 1 is assumed. With R' = $Si(CH_3)_3$ instead of CH_3 the type **2** complex is again preferred (**2c**: 22%, m.p. 45°C; **3c**: 0.4%, m.p. > 300°C). Thus far, losses have had to be expected in the work-up of the reaction products by fractional vacuum sublimation.

A dimetallatetrahedrane structure analogous to that of the [$Co_2(CO)_6$(μ-alkyne)] clusters[4] can be derived from the analytical data and the NMR spectra of the complexes **3** (Table 1), whereas the molecular structure of complexes of type **2** is without example, as unequivocally demonstrated by the crystal structure analysis of **2a**[5] (Fig. 1).

The butyne methyl groups are bent outwards from the metal center at angles of 35° and 32°, respectively. The plane through C7 to C10 and that through the planar ben-

[*] Dr. U. Zenneck, Dipl.-Chem. L. Vasquez, Dr. H. Pritzkow
Anorganisch-chemisches Institut der Universität
Im Neuenheimer Feld 270, D-6900 Heidelberg (FRG)

[**] Reactive π-Complexes of the Electron-rich Transition Metals. Part 5. This work was supported by the Stiftung Volkswagenwerk.—Part 4: [1].

[1] Also known under the name *Nai Zheng Huang.*
[2] D. J. Cram, R. C. Helgeson, D. Lock, L. A. Singer, *J. Am. Chem. Soc. 88* (1966) 1324.
[3] D. T. Hefelfinger, D. J. Cram, *J. Am. Chem. Soc. 93* (1971) 4754.
[4] D. T. Hefelfinger, D. J. Cram, *J. Am. Chem. Soc. 92* (1970) 1073; *93* (1971) 4767.
[5] T. A. Hylton, V. Boekelheide, *J. Am. Chem. Soc. 90* (1968) 6887; V. Boekelheide, P. H. Anderson, *Tetrahedron Lett. 1970,* 1207; V. Boekelheide, P. H. Anderson, T. A. Hylton, *J. Am. Chem. Soc. 96* (1974) 1558.
[6] R. H. Mitchell in P. M. Keeln, S. M. Rosenfeld (Eds.): *Cyclophanes, Vol. 1,* Academic Press, New York 1983, pp. 239-310.
[7] M. Wittek, F. Vögtle, *Chem. Ber. 115* (1982) 1363.
[8] S. S. Cheung, *M. Phil. Thesis,* The Chinese University of Hong Kong 1986.
[9] ^{1}H-NMR data: **4** ($CDCl_3$): $\delta = 4.79$ (s, H-14), 6.72-6.77 (d, $J = 10$ Hz, H-9), 6.88-6.89 (d, $J_{ortho} = 7.5$ Hz; H-11), 6.93 (s, H-5, 6, 7, 8), 7.03-7.07 (d, $J_{ortho} = 7.5$ Hz, H-13), 7.07-7.17 (t, $J_{ortho} = 7.5$ Hz, 7.5 Hz; H-12), 7.23-7.27 (d, $J = 10$ Hz; H-10), 7.35-7.50 (m, $J_{ortho} = 7.4$ Hz, $J_{meta} = 1.7$ Hz; H-2, 3), 7.50-7.77 (m, $J_{ortho} = 7.4$ Hz, $J_{meta} = 1.7$ Hz; H-1, 4).—**5** ([D_6]acetone, 24°C): $\delta = 5.13$ (t, $J_{meta} = 1.8$ Hz; H-16), 6.95 (br., H-5,6,7,8), 7.08-7.12 (dd, $J_{ortho} = 8.0$ Hz, $J_{meta} = 1.8$ Hz; H-13, 15), 7.25-7.32 (t, $J_{ortho} = 8.0$ Hz, 8.0 Hz; H-14), 7.40-7.55 (m, $J_{ortho} = 7.5$ Hz, $J_{meta} = 1.7$ Hz; H-2, 3, 10, 11), 7.57-7.78 (m, $J_{ortho} = 7.5$ Hz, $J_{meta} = 1.7$ Hz; H-1,4,9,12).
[10] C. W. Chan, H. N. C. Wong, *J. Am. Chem. Soc. 107* (1985) 4790.
[11] H. Psiorz, H. Hopf, *Angew. Chem. 94* (1982) 639; *Angew. Chem. Int. Ed. Engl. 21* (1982) 623.
[12] Y. D. Xing, N. Z. Huang, *J. Org. Chem. 47* (1982) 140.
[13] J. Sandström: *Dynamic NMR Spectroscopy,* Academic Press, New York 1982, pp. 93-123.

Table 1. Spectroscopic data of the compounds **2a–c**, **3b,c**, and **4**.

a) X-band ESR data in toluene.

	g_1 [a]	g_2, g_3 [a, b]	$\langle g \rangle$ [c]	^{59}Co-Hyperfine structure [mT] a_1 [a]	a_2, a_3 [a, b]	$\langle a \rangle$ [c]
2a	2.187	2.00	2.089	12.00	3.5	6.12
2b	2.188	2.00	2.086	12.25	3.5	6.23
2c	2.250	2.00	2.106	11.50	4.5	6.31

b) ^{1}H-NMR data in C_6D_6 [d].

3b: $\delta = 2.04$ (s, 6H), 2.27 (s, 6H), 5.19 (m, 4H), 5.34 (m, 4H), 5.38 (m, 2H)
3c: $\delta = 0.3$ (s, 18H), 2.02 (s, 6H), 5.07 (m, 4H), 5.20 (m, 4H), 5.33 (m, 2H)
4: $\delta = 1.97$ (s, 9H), 5.07 (m, 6H), 5.15 (m, 6H), 5.56 (m, 3H), 7.29 (m, 1H), 7.43 (m, 2H), 7.95 (m, 2H)

[a] Measurement temperature $T = -160$°C. [b] Not accurately estimable, $\Delta g_{2,3} \approx \pm 0.05$, $\Delta a_{2,3} \approx \pm 0.5$ mT. [c] Measurement temperature $T = -60$°C. [d] 200 MHz, relative to TMS.

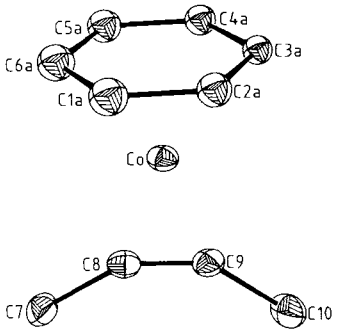

Fig. 1. Molecular structure of **2a**. Some selected bond distances [Å]: C8-C9 1.254(7), Co-C(benzene) 2.08(1)–2.16(1), Co-C8 1.885(4), Co-C9 1.901(5).

zene are almost perpendicular to each other (87°). The benzene ligand is disordered, with the C3a-C6a axis of one of the rotamers (occupation density 0.7) parallel to C8-C9 and that of the second rotamer rotated through ca. 30° to C8-C9. The Co-C8 and Co-C9 distances in particular suggest that all four π-electrons of butyne participate in the bonding to the metal center.[6] The same interpretation results from the ESR spectra (Fig. 2). The ESR data of the complexes **2** (Table 1) are in good agreement with those of anionic 19-valence electron (VE) cobalt complexes of the type [cyclopentadienyl(π^4-ligand)cobalt]$^{\ominus}$.[7,8] The data for the neutral 17-VE complex bis(pentafluorophenyl)(η^6-toluene)cobalt[9] or other 17-VE complexes of cobalt deviate significantly therefrom. Thus, we assume for **2** a HOMO(b_2) which is predominantly localized at the metal center analogous to that for the 19-VE complex anions.[7a] Attempts to oxidize **2a** and **2c** to **2a**$^{\oplus}$ and **2c**$^{\oplus}$ chemically or electrochemically have thus far met without success. The lifetimes of the presumed 18-VE complex cations **2**$^{\oplus}$ are very short. Even at −60°C, purely irreversible oxidations are observed.

In the thermal decomposition of the complexes **2a** and **2b**, small amounts of **3a** and **3b** are formed aside from hexamethylbenzene. At higher temperatures, these also afford the cyclotrimer of 2-butyne.

If the alkyne is replaced by acetonitrile in the reaction with the cocondensate **1**, R = CH_3, the dark-red trimetallatetrahedrane μ_3-benzylidinetris(toluenecobalt) **4** is formed in 0.9% yield together with large amounts of metallic cobalt. Complex **4** could not be observed on thermal decomposition of **1**, R = CH_3.

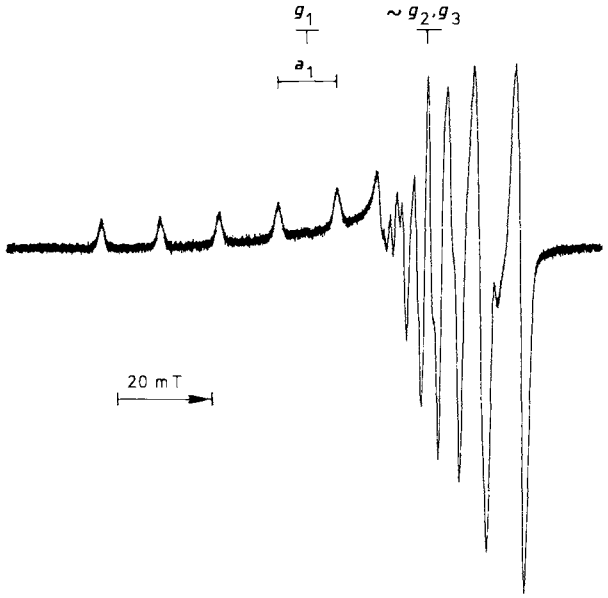

Fig. 2. ESR spectrum (recorded in the X-band of the microwave region) of **2a** in glassy frozen toluene at $T = -160$°C.

The crystal structure analysis[10] affords proof of the molecular structure derivable from the spectra. **4** is closely related to **3** and is formed by formal replacement of an RC fragment by an isolobal arenecobalt moiety (Fig. 3).

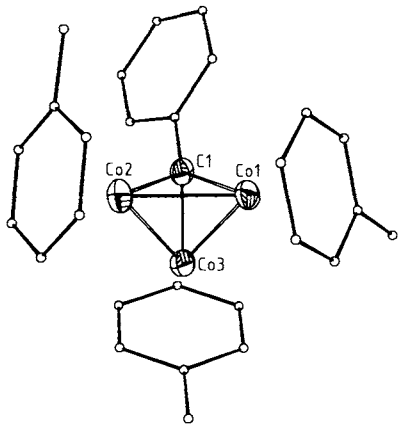

Fig. 3. Molecular structure of **4**.

The unit cell of the crystal contains two crystallographically independent and essentially identical molecules. The three cobalt atoms form an almost equilateral triangle with distances of 2.405(2) to 2.431(2) Å and are symmetrically bridged by the benzylidyne group [C1-Co distances between 1.84(1) and 1.87(1) Å]. The distances of the cobalt atoms from the ring carbon atoms of the toluene ligands are 2.07(2) to 2.18(2) Å. All the structural data thus lie in the expected range of values.[11]

Received: December 10, 1987 [Z 2533 IE]
German version: *Angew. Chem.* *100* (1988) 705

CAS Registry numbers:
2a, 114095-85-1; **2b**, 114095-86-2; **2c**, 114095-87-3; **3b**, 114130-39-1; **3c**, 114130-40-4; **4**, 114095-88-4; C_6H_6, 71-43-2; $C_2(CH_3)_2$, 503-17-3; $C_2[Si(CH_3)_3]_2$, 14630-40-1; Co, 7440-48-4; toluene, 108-88-3; hexamethylbenzene, 87-85-4; acetonitrile, 75-05-8.

[1] M. Driess, D. Hu, H. Pritzkow, H. Schäufele, U. Zenneck, M. Regitz, W. Rösch, *J. Organomet. Chem. 334* (1987) C35.

[2] a) T. G. Groshens, B. Henne, D. E. Bartok, K. J. Klabunde, *Inorg. Chem. 20* (1981) 3629; b) K. J. Klabunde, D. Ralston, R. Zoellner, H. Hattori, Y. Tanaka, *J. Catal. 55* (1978) 213.

[3] G. Vitulli, S. Bertozzi, M. Vignali, R. Lazzaroni, P. Salvatori, *J. Organomet. Chem. 326* (1987) C33.

[4] R. D. W. Kemmit, D. R. Russel in G. Wilkinson, F. G. A. Stone (Eds.): *Comprehensive Organometallic Chemistry, Vol. 5*, Pergamon, Oxford 1982, p. 195.

[5] a) Space group $P2_12_12_1$, $a=5.975(5)$, $b=8.67(1)$, $c=17.32(2)$ Å, $V=897$ Å^3, $Z=4$. 789 observed reflections ($I \geq \sigma_I$). Two-circle diffractometer, $Mo_{K\alpha}$ radiation, ω-scan, rapid decomposition of the crystals during the measurement. Co and butyne C-atoms anisotropic, the disordered benzene ligand was refined with two rigid C_6H_6 rings (C-C 1.395, C-H 0.95 Å) with anisotropic temperature factors for the C atoms, $R=0.046$. b) Further details of the crystal structure are available on request from the Fachinformationszentrum Energie, Physik, Mathematik GmbH, D-7514 Eggenstein-Leopoldshafen 2 (FRG), on quoting the depository number CSD-52910, the names of the authors, and the journal citation.

[6] B. Capelle, M. Dartiguenave, Y. Dartiguenave, A. L. Beauchamps, *J. Am. Chem. Soc. 105* (1983) 4662.

[7] a) T. A. Albright, W. E. Geiger, Jr., J. Moraczewski, B. Tulyathan, *J. Am. Chem. Soc. 103* (1981) 4787; b) H. von Willingen, W. E. Geiger, Jr., M. D. Rausch, *Inorg. Chem. 16* (1977) 581.

[8] W. Siebert, M. El-Din M. El-Essawi, R. Full, J. Heck, *Z. Naturforsch. B40* (1985) 458.

[9] J. H. Ammeter, C. Elschenbroich, T. J. Groshens, K. J. Klabunde, R. O. Kühne, R. Möckel, *Inorg. Chem. 24* (1985) 3307.

[10] Space group $P2_1/c$, $a=17.504(8)$, $b=16.581(6)$, $c=18.130(7)$ Å, $\beta=115.70(3)°$, $V=4741$ Å^3, $Z=8$, 3315 observed reflections ($I \geq \sigma_I$). Four-circle diffractometer, $Mo_{K\alpha}$ radiation, ω-scan. Co and C atoms anisotropic, the toluene rings as rigid rings (C-C 1.425, C-H 0.95 Å), H-atoms with common isotropic temperature factor for each ring, $R=0.058$ [5b].

[11] W. L. Olson, L. F. Dahl, *J. Am. Chem. Soc. 108* (1986) 7675.

Synthesis and Structure of $[(C_5Me_5)_2Rh_2S_8]$, a Dirhodium Complex with Unusual Polysulfide Bridge

By *Henri Brunner, Norbert Janietz, Walter Meier, Bernd Nuber, Joachim Wachter,** and *Manfred L. Ziegler*

Chalcogen-rich transition-metal complexes of the type $L_2M_2X_n$ (L = any substituted cyclopentadienyl ligand; X = S, Se; $n \geq 4$) are currently attracting interest because of their structural variability and versatile chemistry, both of which are strongly influenced by the nature of the metal.[1,2] The reaction of chalcogens with dimeric cyclopentadienylmetal complexes containing metal-metal multiple bonds has proven useful as a general synthetic route for such compounds. The chalcogen chains and rings undergo degradation thereby to mono- or diatomic moieties. Complexes with polysulfide ligands have been postulated as intermediates,[3] but only seldom has it been possible to detect them.[4] We now report on the synthesis and structure of the rhodium dinuclear complex $[Cp^*_2Rh_2S_8]$ **1** ($Cp^* = \eta^5$-C_5Me_5), which contains two unusually coordinated S_4 bridges.

[*] Dr. J. Wachter, Prof. Dr. H. Brunner, N. Janietz, W. Meier
Institut für Anorganische Chemie der Universität
Universitätsstrasse 31, D-8400 Regensburg (FRG)
Dr. B. Nuber, Prof. Dr. M. L. Ziegler
Anorganisch-chemisches Institut der Universität
Im Neuenheimer Feld 270, D-6900 Heidelberg (FRG)

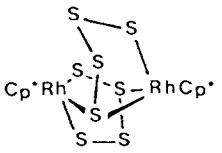

1

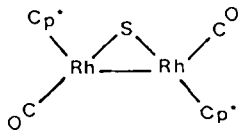

2

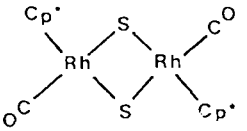

3

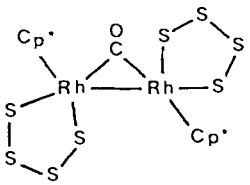

4

The diamagnetic, red-brown complex **1** is obtainable in ca. 62% yield from $[Cp^*_2Rh_2(CO)_2]$ and sulfur (Rh : S 1 : 4, tetrahydrofuran, room temperature). Its composition is confirmed by elemental analysis; the field desorption mass spectrum, however, contains only the molecular ion less one sulfur atom. Contrary to expectation the ^{1}H-NMR spectrum[5] indicates a non-symmetrical structure for the compound. An X-ray structure analysis[6] on a single crystal of **1** (from toluene or CH_2Cl_2) confirms the non-equivalence of the Cp* rings (Fig. 1). The structure is characterized by two RhS_4 chelate rings, which are coupled to each other in such a way that they give the puckered Rh_2S_3 core (envelope conformation) of the molecule. Each S_4 ligand functions as 4e donor. As a consequence of this behavior the length of the S-S bonds varies from 2.032(3) to 2.106(3) Å. The bond angles fall in three ranges: The S-Rh-S angles lie between 78.2(1) and 94.0(1)°, while the other angles in the chelate ring, with exception of Rh1-S1-Rh2 (114.5(1)°) range from 100.1(1) to 109.2(1)°. The "real" chelate angles S1-Rh-S6 and S3-Rh2-S7 are both 94.0(1)°. Both RhS_4 rings have a slightly distorted envelope conformation. Their tips S3 and S4 are 3.539 Å from each other; this could possibly make them suitable for the

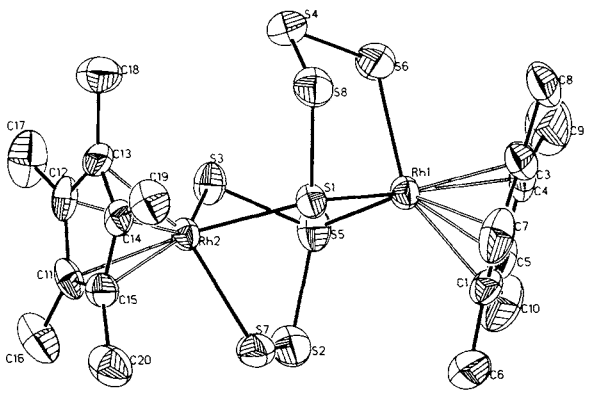

Fig. 1. Crystal structure of **1** (ORTEP). Selected bond lengths [Å] and angles [°]: Rh1-S1 2.384(2), Rh1-S5 2.327(2), Rh1-S6 2.384(2), Rh1-C(Cp^*1)$_{mean}$ 2.197(9), Rh2-S1 2.373(2), Rh2-S3 2.324(2), Rh2-S7 2.407(2), Rh2-C(Cp^*2)$_{mean}$ 2.196(9), S1-S8 2.103(3), S2-S5 2.106(3), S2-S7 2.043(3), S3-S5 2.032(3), S4-S6 2.057(3), S4-S8 2.040(3), Rh1···Rh2 3.999, S1···S5 3.372, S3···S4 3.539; S1-Rh1-S5 91.4(1), S1-Rh1-S6 94.0(1), S5-Rh1-S6 88.3(1), S1-Rh2-S3 91.3(1), S1-Rh2-S7 78.2(1), S3-Rh2-S7 94.0(1), Rh1-S1-Rh2 114.5(1), Rh1-S1-S8 100.1(1), S5-S2-S7 101.5(1), S6-S4-S8 101.7(1), Rh1-S5-S2 108.8(1), Rh1-S5-S3 109.2(1), S2-S5-S3 100.2(1), Rh1-S6-S4 107.4(1), S1-S8-S4 100.7(1).

bidentate coordination of unsaturated complex fragments. To our knowledge the only other bridge-forming S_4 ligands are found in copper(I) polysulfide clusters, in which two copper centers are each bridged by a terminal member of the S_4 chain.[3]

The formation of **1** proceeds via several intermediates. When the dark blue solution of $[Cp_2^*Rh_2(CO)_2]$ in THF is allowed to react with $1/8\,S_8$ at room temperature, the color changes to brown within 15 minutes, and the red-violet **2** can be isolated in 46% yield by column chromatography (Al_2O_3, toluene).[5] The Rh_2S three-membered ring in **2** can be expanded to a four-membered ring by addition of a further S atom. However, there is only IR spectroscopic proof available (ν_{CO} frequency at 2015 cm^{-1}) for the existence of the resulting complex **3**. The Se complex analogous to **3**, on the other hand, can be isolated.[7]

When, however, the reaction of $[Cp_2^*Rh_2(CO)_2]$ with sulfur is carried out at $-25\,^\circ C$ instead of at room temperature, about equal amounts of **1** and **4** can be isolated. The symmetrical compound[5] **4** may contain two RhS_4 chelate rings linked together by a Rh–Rh bond and a μ-CO group.[8] **4** slowly transforms into **1** in solution. The structural changes on going from **3** to **4** are indicated by weak ν_{CO} frequencies temporarily occurring at 1785 and 1980 cm^{-1}, which were observed between -80 and $-60\,^\circ C$. Unfortunately, these absorptions disappear in favor of those of **1** and **4** at higher temperatures, so that they cannot be assigned to specific structures. However, it cannot be ruled out that the monosulfide bridges in **2** and **3** are substitution-labile towards larger sulfur units, e.g. $S_4^{2\ominus}$. An indication in this direction is that the Se analogues of **2** and **3** can be converted into **1** with S_8.[7]

Although rhodium sulfides are of interest as hydrodesulfurization catalysts,[9] **1** is only the third structurally characterized rhodium polychalcogenide complex, after $[Cp_2^*Rh_2Se_5]$[10] and $[Rh(S_5)_3]^{3\ominus}$.[11] From the relatively high number of S–S bonds, a considerable reaction potential can be expected for **1**. Consistent with this prediction three irreversible oxidation waves were found at $E_{1/2} = +0.53$, $+1.38$ and 1.60 V in a cyclovoltammetric experiment (CH_2Cl_2, standard calomel electrode).

Received: December 10, 1087;
supplemented: February 8, 1988 [Z 2534 IE]
German version: *Angew. Chem. 100* (1988) 717

CAS Registry numbers:
1, 114133-33-4; **2**, 114133-34-5; **3**, 114133-35-6; $(C_5Me_5)_2Rh_2(CO)_2$, 69728-343.

[1] For a review of this class of compounds, see J. Wachter, *J. Coord. Chem. 15* (1987) 219.
[2] L. Y. Goh, T. C. W. Mak, *J. Chem. Soc. Chem. Commun. 1986*, 1474.
[3] Transition-metal polysulfides are reviewed in M. Draganjac, T. B. Rauchfuss, *Angew. Chem. 97* (1985) 745; *Angew. Chem. Int. Ed. Engl. 24* (1985) 742; A. Müller, E. Diemann, *Adv. Inorg. Chem. 31* (1987) 89.
[4] M. A. El-Hinnawi, A. A. Aruffo, B. D. Santarsiero, D. R. McAlister, *V. Schomaker, Inorg. Chem. 22* (1983) 1585.
[5] ^{1}H-NMR (60 MHz, $CDCl_3$): $\delta = 1.68$, 1.85 (**1**), 1.93 (**2**), 1.86 (**4**). IR (KBr): $\nu_{CO} = 1955$ (**2**), 1811 (**4**) [8] cm^{-1}. All the compounds gave correct elemental analyses (C, H, S) and were characterized by field desorption mass spectrometry.
[6] **1**: Space group $P2_1/c$, $a = 14.195(7)$, $b = 12.833(8)$, $c = 17.202(6)$ Å, $\beta = 103.30(4)^\circ$, $V = 3049.54$ Å^3, $Z = 4$. AED-II diffractometer ($Mo_{K\alpha}$), $3 < 2\theta < 65^\circ$, 4220 measured reflections with $I > 2.5\sigma(I)$, Patterson and Fourier methods, anisotropic refinement to $R_w = 0.042$. Further details of the crystal structure investigation are available on request from the Fachinformationszentrum Energie, Physik, Mathematik GmbH, D-7514 Eggenstein-Leopoldshafen 2 (FRG), on quoting the depository number CSD-52930, the names of the authors, and the journal citation.
[7] H. Brunner, N. Janietz, W. Meier, J. Wachter, E. Herdtweck, W. A. Herrmann, O. Serhadli, M. L. Ziegler, *J. Organomet. Chem.*, in press.
[8] W. A. Herrmann, C. Bauer, J. Weichmann, *J. Organomet. Chem. 243* (1983) C21.
[9] R. R. Chianelli, T. A. Pecoraro, *J. Catal. 67* (1981) 430.
[10] H. Brunner, W. Meier, B. Nuber, J. Wachter, M. L. Ziegler, *Angew. Chem. 98* (1986) 907; *Angew. Chem. Int. Ed. Engl. 25* (1986) 907.
[11] P. Cartwright, R. D. Gillard, R. Sillanpaa, J. Valkonen, *Polyhedron 6* (1987) 1775.

Reaction of 1,3-Azaarsinines with 2-*tert*-Butyl-1-phosphaethyne—2,9,10-Tri-*tert*-butyl-4,6-diphenyl-1,3,8-triphospha-7-arsatetracyclo[4.4.0.0^{2,8}.0^{3,7}]deca-4,9-diene

By *Gottfried Märkl,* Stefan Dietl, Manfred L. Ziegler,* and *Bernd Nuber*

The 1,3-azaphosphinines **1**[1] and 1,3-azaarsinines **2**[2] recently described by us undergo Diels–Alder reactions with a large variety of alkyne-dienophiles;[1,3,4] the bicycles initially formed rearomatize with elimination of benzonitrile to give the corresponding—in particular also functionally substituted—phosphinines **3**[1,3] and arsinines **4**.[4]

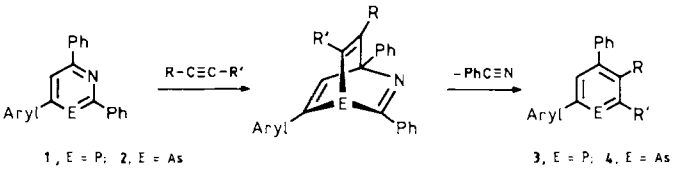

1, E = P; 2, E = As 3, E = P; 4, E = As

We have already reported on the fully unexpected reaction of the azaphosphinines **1** with the heteroalkyne *tert*-butyl-1-phosphaethyne **5** in the molar ratio 1:2; the tetracycles **6** are formed.[5]

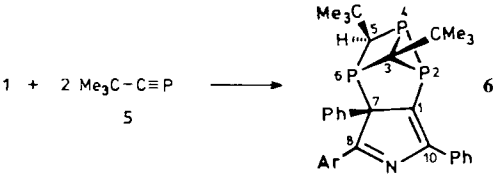

6

We have now been able to show that the 1,3-azaarsinines **2** behave differently again toward **5**. Reaction with **5** in toluene at 120 °C in a Carius tube (48 h) furnishes (after treatment of the residue with ethyl acetate) a colorless, crystalline compound **7a**, m.p. 204–207 °C (from ethyl acetate), which according to an elemental analysis and its mass spectrum is a product formed from **2a** and **5** (in the molar ratio 1:3) with elimination of benzonitrile (Table 1). According to analytical and spectroscopic findings, **2b** reacts analogously to give **7b** (Table 1).

Both the ^{1}H-NMR spectrum, which shows three *tert*-butyl signals, and the ^{31}P-NMR spectrum, with three signals, are consistent with the unsymmetric structure of **7a**. The X-ray structure analysis shows that **7a** has a tetracyclic skeletal framework other than that in **6** and that all P

[*] Prof. Dr. G. Märkl, Dipl.-Chem. S. Dietl
Institut für Organische Chemie der Universität
Universitätsstr. 31, D-8400 Regensburg (FRG)
Prof. Dr. M. L. Ziegler, Dr. B. Nuber
Anorganisch-chemisches Institut der Universität
Im Neuenheimer Feld 270, D-6900 Heidelberg (FRG)

atoms and the As atom of **7a** are located in bridgehead positions.

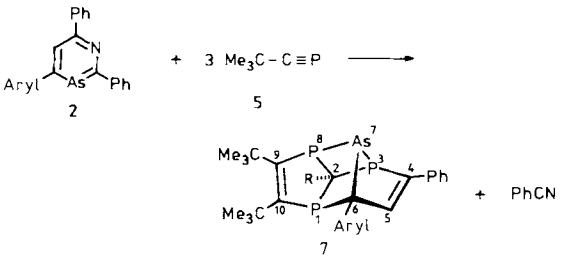

a, Aryl = C_6H_5; b, Aryl = 4-CH_3-C_6H_4

Table 1. Physical and spectroscopic data of **7a** and **7b**.

7a, yield 70%, m.p. 204–207°C (colorless crystals from ethyl acetate).—MS (70 eV): *m/z* 566 ($M^{\oplus\ominus}$, rel. int. 24%), 269 (4,5-di-*tert*-butyl-1,3-diphosphacyclopentadiene fragment, 100%).—^{1}H-NMR (250 MHz, $CDCl_3$): δ = 0.85 (d, J = 2.9 Hz, *t*Bu), 1.13 (s, *t*Bu), 1.45 (s, *t*Bu), 7.17–7.66 (m, Ph), 8.36 (dq, J = 9.2 Hz, 0.9 Hz, CH).—^{31}P{^{1}H}-NMR: we assign the signals as follows: δ = +77.11 (dd, J(P-3/P-8) = 13.5 Hz, J(P-3/P-1) = 6.6 Hz, P-3), +40.96 (dd, J(P-8/P-1) = 99.1 Hz, P-8), −54.87 (dd, J(P-8/P-1) = 99.1 Hz, J(P-3/P-1) = 6.6 Hz, P-1).—UV (CH_3CN): λ_{max} = 330 (sh, 4750), 255 (sh, 20700), 215 (30400) nm

7b, yield 40%, m.p. 234–238°C (colorless crystals from ethyl acetate).—MS (70 eV): *m/z* 580 ($M^{\oplus\ominus}$, 19%), 534 ([$M-C_4H_8$]$^{\oplus\ominus}$, 2%), 269 (4,5-di-*tert*-butyl-1,3-diphosphacyclopentadiene fragment, 100%).—^{1}H-NMR: δ = 0.86 (d, J = 2.9 Hz, *t*Bu), 1.12 (s, *t*Bu), 1.45 (s, *t*Bu), 2.30 (s, CH_3–C_6H_4), 7.09–7.65 (m, Ph), 8.35 (dq, J = 8.9 Hz, 0.8 Hz, CH).—^{31}P{^{1}H}-NMR ($CDCl_3$): δ = +78.95 (dd, J(P-3/P-8) = 13.1 Hz, J(P-3/P-1) = 5.6 Hz, P-3), +43.99 (dd, J(P-3/P-8) = 13.1 Hz, J(P-8/P-1) = 99.0 Hz, P-1), −51.48 (dd, J(P-8/P-1) = 99.1 Hz, J(P-3/P-1) = 5.6 Hz, P-1).—UV (CH_3CN): λ_{max} = 330 (sh, 5100), 257 (sh, 23200), 215 (35900) nm

The chemical shift for P-1 is normal for a P atom in an unstrained tertiary phosphane; P-3 and P-8 in the diphosphaarsacyclobutane ring show downfield shifts of the ^{31}P-resonance signals characteristic for this ring system; the δ(^{31}P) value for P-3, as in similar systems,[6,7] could experience additional downfield shifts due to the proximity of P-3 to the CC double bond. The coupling constant J(P-8/P-1) ≈ 99 Hz lies in exactly the same range as in systems containing the *cis*-≻P–CR=CR′–P≺ structural unit, for which J values of ca. 30–150 Hz are observed.[8,9]

Thus, the azaarsinines **2**, as the higher homologues of **1**, behave quite differently. We interpret this finding in terms of the electrophilicity of the $\lambda^3\sigma^2$-arsenic in **2** being less than that of the $\lambda^3\sigma^2$-phosphorus in **1**, so that a Diels–Alder reaction to give **8** can first take place in the case of **2**. The bicyclic primary adduct **8** decomposes with elimination of benzonitrile to the 1,3-phosphaarsinine **9**.

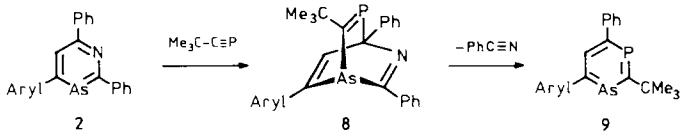

The cycloaddition behavior of **9** toward further phosphaethyne **5** is completely different from that of the 1,3-azaphosphinine **2**. **9a** should furnish the semibullvalene

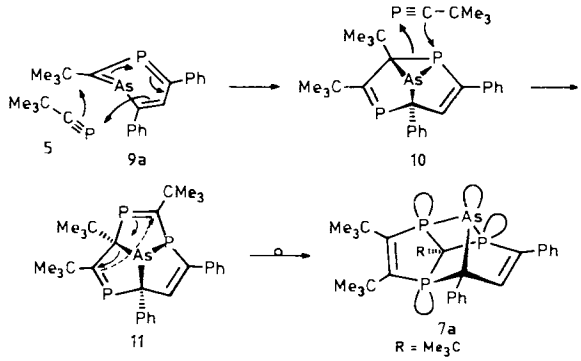

derivative **10** as intermediate, which reacts with further **5** with opening of the three-membered ring to give the "triquinazene derivative" **11**. The driving force for the rearrangement of **11** to **7a** is the conversion of two $\lambda^3\sigma^2$ P-atoms into two $\lambda^3\sigma^3$ P-atoms.

Received: December 14, 1987;
revised: January 22, 1988 [Z 2538 IE]
German version: *Angew. Chem. 100* (1988) 720

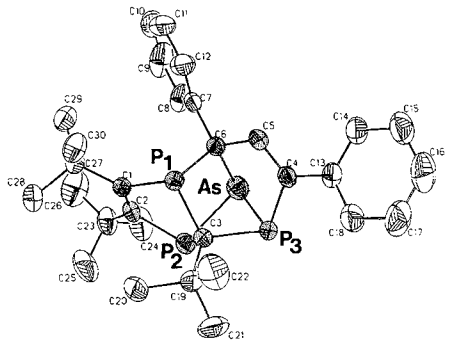

Fig. 1. Crystal structure of **7a** (arbitrary numbering) [10]. Selected bond lengths [Å] and angles [°]: P2-As 2.332(1), P3-As 2.319(1), P3-C3 1.924(3), P2-C3 1.880(4), As-C6 2.037(4), P1-C6 1.908(3), P1-C3 1.859(4), P1-C1 1.873(3), C1-C2 1.347(5), P2-C2 1.856(4), P3-C4 1.846(4), C4-C5 1.346(5), C5-C6 1.504(4); P2-As-P3 73.6(0), As-P3-C3 83.4(1), P2-C3-P3 94.1(2), C3-P2-As 83.4(1), As-C6-P1 108.5(2), C6-P1-C3 94.5(1), P1-C3-P2 111.4(2), P3-As-C6 82.3(1), P1-C1-C2 113.9(2), C1-C2-P2 114.2(2), C2-P2-C3 100.0(2), P2-C3-P1 101.5(2), C3-P1-C1 98.0(2), C3-P3-C4 103.2(2), P3-C4-C5 113.4(2), C4-C5-C6 120.5(3), C5-C6-P1 101.0(2).

[1] G. Märkl, G. Dorfmeister, *Tetrahedron Lett. 28* (1987) 1093.
[2] G. Märkl, S. Dietl, *Tetrahedron Lett. 29* (1988) 535.
[3] T. Riedl, *Diplomarbeit*, Universität Regensburg 1987.
[4] G. Märkl, S. Dietl, *Tetrahedron Lett. 29* (1988) 539.
[5] G. Märkl, S. Dietl, M. L. Ziegler, B. Nuber, *Angew. Chem. 100* (1988) 426; *Angew. Chem. Int. Ed. Engl. 27* (1988) 389.
[6] L. D. Quin, K. C. Caster, J. C. Kisalus, K. A. Mesch, *J. Am. Chem. Soc. 106* (1984) 7021; L. D. Quin, F. C. Bernhardt, *Magn. Reson. Chem. 23* (1985) 929.
[7] G. Märkl, H. J. Beckh, K. K. Mayer, M. L. Ziegler, T. Zahn, *Angew. Chem. 99* (1987) 255; *Angew. Chem. Int. Ed. Engl. 26* (1987) 236; G. Märkl, E. Eckl, U. Jakobs, M. L. Ziegler, B. Nuber, *Tetrahedron Lett. 28* (1987) 2119.
[8] G. Märkl, W. Weber, W. Weiss, *Chem. Ber. 118* (1985) 2365.
[9] A. J. Carty, D. K. Johnson, S. E. Jacobson, *J. Am. Chem. Soc. 101* (1979) 5612.
[10] Crystal data of **7a**: crystal system: triclinic, space group $P\bar{1}$ (No. 2), a = 9.174(2), b = 12.689(2), c = 13.372(6) Å, α = 76.80(3), β = 72.03(3), γ = 86.25(2)°, V = 1441.5 Å^3, Z = 2, ρ_{calc} = 1.30 g cm^{-3}, F(000) = 592, μ($Mo_{K\alpha}$) = 13.6 cm^{-1}. 5601 reflections measured (ω scan) in the region h −14/14, k 0/19, l −20/20; 3° ≤ 2θ ≤ 65°, 5455 independent reflections ($J \geq 2.5\sigma(J)$), Lp and absorption correction (empirical, ψ-scans of 8 reflections with 5.1 ≤ 2θ ≤ 45.4°, transmission factors: min. 0.80, max. 1.0); $Mo_{K\alpha}$ (λ = 0.71069 Å), graphite monochromator, AED II Siemens-Stoe. The structure was solved by Patterson, Fourier, and difference Fourier methods (SHELXTL program), residual electron density: max. 0.86, min. −0.78 e Å^{-3}, R = 0.050, R_w = 0.045; Goof 2.74 shift/esd: max. 0.16, mean 0.02; 334 LS parameters. Further details of the crystal structure investigation are available on request from the Fachinformationszentrum Energie, Physik, Mathematik GmbH, D-7514 Eggenstein-Leopoldshafen 2 (FRG), on quoting the depository number CSD-52847, the names of the authors, and the journal citation.

Solid Phase Synthesis of Peptides and Glycopeptides on Polymeric Supports with Allylic Anchor Groups**

By *Horst Kunz** and *Berthold Dombo*

Merrifield's concept of carrying out the synthesis of peptides on polymeric supports constitutes one of the milestones in modern chemistry.[1] Both in the original[2] as well as in the present day form of this solid-phase peptide synthesis[3] the *C*-terminal amino acid is anchored as substituted benzyl ester to the polymeric support (resin) either via a coupling group ("handle", spacer) or directly. Strong acids are used for detachment of the synthesized peptide from the resin. The *N*-terminal protecting groups and most of the side-chain protecting groups are removed at the same time. Alkoxybenzyl esters[4,5] as anchor groups enable removal of the peptide with trifluoroacetic acid. With dialkoxybenzyl esters as anchor groups,[6,7] even dilute trifluoroacetic acid can be used for removal of the peptide. Then, the fluorenylmethoxycarbonyl (Fmoc) group[8] has to be used as N_α-protecting group, since acid conditions must be carefully avoided during synthesis of the chain with such an acid-labile anchorage.

With the aim of constructing the acid-sensitive and in part also base-sensitive glycopeptides[9] in solid-phase syntheses, we have used the successful strategy of palladium(0)-catalyzed deblocking of peptide- and glycopeptide allyl esters[10] as well as allyloxycarbonyl(Aloc)-peptides and glycopeptides[11] for the development of a polymeric support with allylic anchor groups.[12] Thereby we were able to achieve both an acid- as well as base-stable anchorage of the peptide and glycopeptide chains to be synthesized on a resin, from which, however, they can be detached at room temperature under neutral, weakly acid or weakly basic conditions.[10,11] Suitable for the production of the polymers containing allylic anchor groups such as **3** is the reaction of resins containing aminomethyl groups, e.g. of aminomethylpolystyrene[13] **2** with haloalkenoic acids such as **1a**,[14] which have an allyl halide partial structure. **2** contains 0.8–3.3 mequiv. H_2N-CH_2 per gram resin. This reaction is particularly easy to carry out: **1** and **2** are condensed with dicyclohexylcarbodiimide (DCC) and 1-hydroxybenzotriazole (HOBt)[15] in CH_2Cl_2 to give **3a**.

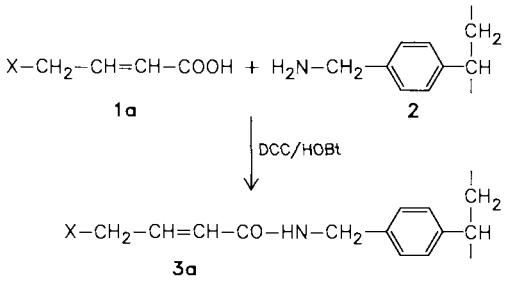

a, X = Br; b, X = OH

A cross-linking alkylation (formation of bromide ions) is not observed in this reaction. Among the possible anchor groups, the polar crotonyl group in **3** has the advantage of being highly acid-stable; therefore the model syntheses of peptides and glycopeptides on the resin **3a** are shown here. The corresponding alcohol **3b** can also be used, but there is the danger of racemization during the esterification with the *C*-terminal amino acids.

Reaction of the allyl halide-resin **3a** with the cesium salts[16] of *N*-protected amino acids **4** (molar ratio 1:1.5) furnishes the [4-(aminoacyloxy)crotonyl]aminomethyl resins **5**. The yields (determined by elemental analysis) of the hitherto unoptimized reactions are 70–82% (Table 1).

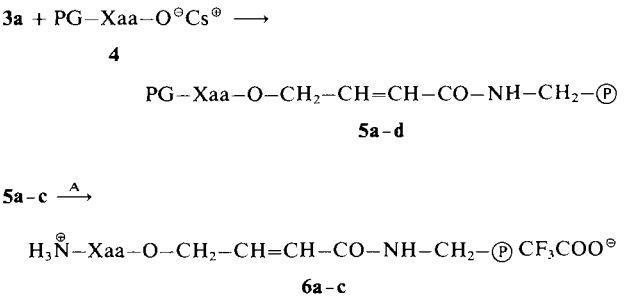

Table 1. Coupling of the amino acid salts **4** with the resin **3a** to protected aminoacyl-Hycram resins **5** and cleavage of the protecting group PG (Step A) with 50% CF_3COOH/CH_2Cl_2 (1 h) to give aminoacyl-hycram resins **6**.

5	PG-Xaa	Yield [%]	6	Xaa
a	Boc-Ala	82	**a**	Ala
b	Boc-Ile	70	**b**	Ile
c	Boc-Leu	73	**c**	Leu
d	Z-Ala	80		

Owing to the high acid-stability of the allylic ester bond, the N_α-Boc group in the protected aminoacyl-Hycram resins **5a–c** is selectively cleavable with trifluoroacetic acid/dichloromethane (step A). The polymer-bound salts **6** thus

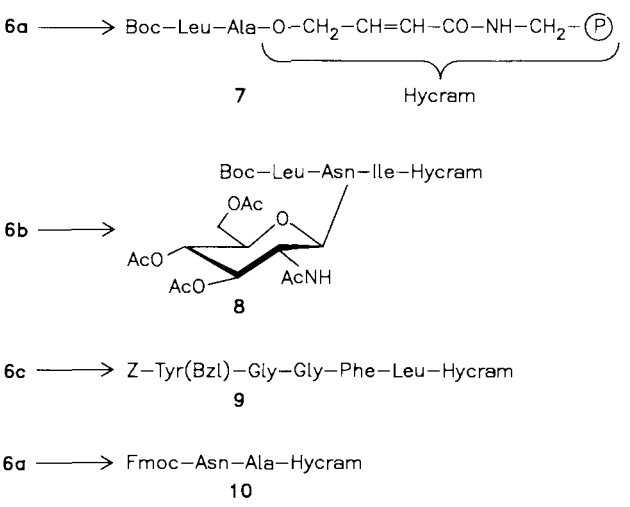

Table 2. Stepwise synthesis of the polymer-bound peptides and glycopeptides **7** to **10**. Normal conditions for step B, see text.

Reaction	Step(s)	Reagents etc.
6a → 7	B1	B1: Boc-Leu-OH, 2 h
6b → 8	B2, A, B3	B2: Boc-Asn(Ac_3GlcNAc)-OH in CH_2Cl_2/DMF, 12 h B3: Boc-Leu-OH, CH_2Cl_2, 8 h
6c → 9	B4, A, B5, A, B5, A, B6	B4: Boc-Phe-OH, 2 h B5: Boc-Gly-OH, 2 h B6: Z-Tyr(Bzl)-OH, 5 h
6a → 10	B7	B7: Fmoc-Asn-OH, DMF, 3 h

[*] Prof. Dr. H. Kunz, Dipl.-Chem. B. Dombo
Institut für Organische Chemie der Universität
J.-J.-Becher-Weg 18–20, D-6500 Mainz (FRG)

[**] This work was supported by the Deutsche Forschungsgemeinschaft and the Fonds der Chemischen Industrie.

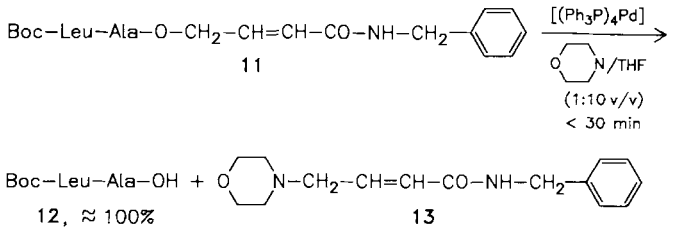

obtained are subjected to the synthesis cycle typical for solid-phase peptide syntheses.[1] In the coupling step B ethyldiisopropylamine, *N*-protected amino acid (PG-Xaa-OH), DCC and HOBt (5:5:6:6) are allowed to react with 1 mequiv. of aminoacyl-Hycram resin **6** with shaking in ca. 50 mL of dichloromethane or dichloromethane/DMF. The same solvent is used for the rewashing. The polymer-bound peptides and glycopeptides **7** to **10** are thus synthesized by stepwise chain lengthening (Table 2).

The coupling with Fmoc-Asn-OH (step B7) is carried out with a small excess of reagent (2:2:2:2) so as to avoid nitrile formation. It is obviously incomplete, since free alanine is found during later cleavage of the resin.

For a better assessment of the cleavage reaction we have synthesized the low molecular counterpart **11** of **7** from the *N*-benzylamide of 4-bromocrotonic acid.[14]

The Pd^0-catalyzed cleavage of **11** proceeds selectively and quantitatively[17,18] in less than 30 min in the way previously described by us.[10,11]

The polymer-bound peptide **7** reacts in a completely analogous way. Almost quantitative cleavage from the resin is achieved within 2 h (step C). Even the glycotripeptide **14** and the Leu-enkephalin **15** protected on the tyrosine are smoothly removed from the Hycram polymer in this way (Table 3).

Because of the incomplete coupling to **10**, the yield of Fmoc-dipeptide **16** is low. But no dipeptide with complete loss of Fmoc is found. Any alanine (formed from unchanged **6a**) and dimedone are separated off chromatographically on a short silica gel column (methanol/dichloromethane). The total yields of glycopeptide **14** and pentapeptide **15** are substantial, considering that no repeated coupling was applied in any of the reactions. It can be concluded therefore that the Pd^0-catalyzed cleavage reaction proceeds very effectively even in the case of the more complex resin-bound products **8** and **9**. The products **15** purified chromatographically with chloroform/methanol or reprecipitated from methanol/chloroform entrain some methanol. Their identity is confirmed by monitoring the 400-MHz ^{1}H-NMR spectra.[20,21]

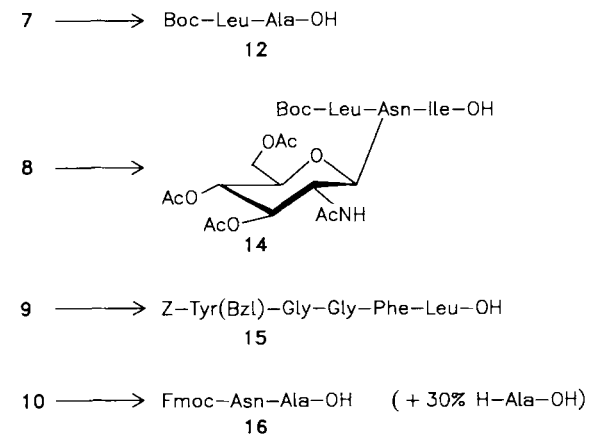

Table 3. Detachment of the peptides and glycopeptides **12** and **14** to **16** from the resin. Normal conditions for step C: 90 mg $(Ph_3P)_4Pd$ per mequiv. peptide or glycopeptide in 50 mL THF and 5 mL morpholine.

Reaction	Step(s)	Reagents etc.	Yield [%]
7 → **12** [19]	C1	see above, 2 h	98 (based on **5a**)
			80 (based on **3a**)
8 → **14** [20]	C1	see above, 10 h	76 (based on **5b**)
9 → **15** [21]	C1	see above, 12 h	63 (based on **5c**)
10 → **16** [22]	C2	see above, but in 30 mL THF and 1 g dimedone, 2 h; from washing **16** with methanol	48 (based on **5a**)

In summary, the polymeric supports such as **3a** with allylic anchor groups have the following advantages:

1. The solid-phase synthesis of peptides and glycopeptides on these supports can be carried out both with acid- as well as base-labile protecting groups.
2. The detachment of the synthesized product from the support can be carried out very effectively under almost neutral conditions.
3. Acid- (Boc) and base-labile (Fmoc or OAc in **14**) protective groups as well as the sensitive glycoside bonds remain intact during the cleavage.

Received: December 18, 1987;
revised: February 9, 1988 [Z 2548 IE]
German version: *Angew. Chem. 100* (1988) 732

[1] Review: G. Barany, N. Kneib-Cordonier, D. G. Mullen, *Int. J. Pept. Protein Res. 30* (1987) 705.
[2] R. B. Merrifield, *J. Am. Chem. Soc. 85* (1963) 2149.
[3] A. R. Mitchell, S. B. H. Kent, M. Engelhard, R. B. Merrifield, *J. Org. Chem. 43* (1978) 2845.
[4] S. S. Wang, *J. Am. Chem. Soc. 95* (1973) 1328.
[5] J. P. Tam, R. DiMarchi, R. B. Merrifield, *Int. J. Pept. Protein Res. 16* (1980) 412.
[6] R. C. Sheppard, B. J. Williams, *Int. J. Pept. Protein Res. 20* (1982) 451.
[7] M. Mergler, *Poster P60, Abstr. 10th Am. Pept. Symp.*, St. Louis 1987.
[8] L. A. Carpino, G. Y. Han, *J. Org. Chem. 37* (1972) 3404.
[9] H. Kunz, *Angew. Chem. 99* (1987) 297; *Angew. Chem. Int. Ed. Engl. 26* (1987) 294.
[10] a) H. Kunz, H. Waldmann, *Angew. Chem. 96* (1984) 49; *Angew. Chem. Int. Ed. Engl. 23* (1984) 71; b) *ibid. 97* (1985) 885 and *24* (1985) 883; c) *Helv. Chim. Acta 68* (1985) 618; d) H. Kunz, H. Waldmann, C. Unverzagt, *Int. J. Pept. Protein Res. 26* (1985) 493.
[11] a) H. Kunz, C. Unverzagt, *Angew. Chem. 96* (1984) 426; *Angew. Chem. Int. Ed. Engl. 23* (1984) 436; b) H. Kunz, H. Waldmann, C. Unverzagt in D. Theodoropoulos (Ed.): *Peptides 1986*, de Gruyter, Berlin 1987, p. 615.
[12] H. Kunz, B. Dombo, Dtsch. Pat.-Anm. 3720269.3 (June 19, 1987).
[13] A. R. Mitchell, S. B. H. Kent, B. W. Erickson, R. B. Merrifield, *Tetrahedron Lett. 1976*, 3795.
[14] K. Ziegler, W. Schumann, E. Winkelmann, *Justus Liebigs Ann. Chem. 551* (1942) 117.
[15] W. König, R. Geiger, *Chem. Ber. 103* (1970) 788.
[16] B. F. Gisin, *Helv. Chim. Acta 56* (1973) 1476.
[17] For reviews on Pd^0-catalyzed allyl transfer for CC bond formation see: a) B. M. Trost, *Acc. Chem. Res. 13* (1980) 385; b) J. Tsuji, *Pure Appl. Chem. 51* (1979) 1235.
[18] For the first observation of reductive allyl ester cleavage by Pd^0-catalyzed hydride transfer see: H. Hey, H.-J. Arpe, *Angew. Chem. 85* (1973) 986; *Angew. Chem. Int. Ed. Engl. 12* (1973) 928; see also b) J. Tsuji, T. Yamakawa, *Tetrahedron Lett. 1979*, 613; c) Pd^0-catalyzed hydrostannylation of allyl carbonates: F. Guibe, Y. Saint M'Leux, *ibid. 22* (1981) 3591; d) allyl carbonate, carboxylate, and carbamate cleavage by Pd^0-catalyzed transesterification with 2-ethyl hexanoate: P. D. Jeffrey, S. W. McCombie, *J. Org. Chem. 47* (1982) 587.
[19] **12**: $[\alpha]_D^{22} = -28.4$ ($c = 1$, MeOH) (W. Danho, C. H. Li, *Int. J. Pept. Protein Res. 3* (1971) 81: $[\alpha]_D^{22} = -29.0$ ($c = 1$, MeOH)), $R_f = 0.21$ (CH_2Cl_2/MeOH 5:1).—400 MHz-^{1}H-NMR ($CDCl_3$): $\delta = 7.13$ (m, 1H, NH, Ala), 5.33 (m, 1H, NH, urethane), 4.53 (m, 1H, α-CH, Ala), 4.22 (m, 1H, α-CH, Leu).
[20] **14**: $[\alpha]_D^{22} = -0.7$ ($c = 0.65$, MeOH), $R_f = 0.29$ (CH_2Cl_2/MeOH 5:1).—400 MHz-^{1}H-NMR ([D$_6$]DMSO): $\delta = 8.72$ (d, $J = 10$ Hz, 1H, β-NH, Asn), 8.32 (m, 1H, α-NH, Asn), 7.99 (d, br., $J = 10$ Hz, 1H, N*H*Ac), 7.08 (m,

1H, NH, Ile), 6.9 (d, $J=10$ Hz, 1H, NH, Leu), 5.25–5.11 (m, 2H, H-1, H-3, GlcNAc), 2.0, 1.95, 1.92 (3 × s, each 3H, OAc), 1.34 (s. br. over multiplet, 9H, CH_3, Boc), 0.88 (m, 12H, CH_3, Leu, Ile).

[21] **15**: $[\alpha]_{578}^{22}=+0.07$, $[\alpha]_{546}^{22}=+0.05$, $[\alpha]_{436}^{22}=-0.07$ ($c=0.7$, MeOH), $R_f=0.48$ (CH_2Cl_2/MeOH 2:1).—400 MHz-^{1}H-NMR ([D$_6$]DMSO): $\delta=8.5$, 8.39, 8.17, 8.08, 7.54 (each 1H, NH), 7.46–7.05 (m, 17H, aromat. H of Phe, Z, Bzl, 2H, Tyr), 6.88 (d, $J=10$ Hz, 2H, Tyr), 5.03 (s, 2H, CH_2, Z); 4.89 (m, 2H, CH_2, Bzl); 0.88 and 0.82 (each d, $J=7$ Hz, each 3H, CH_3, Leu).

[22] **16**: $[\alpha]_D^{22}=-13.4$ ($c=0.8$, DMF), $R_f=0.60$ (CH_2Cl_2/MeOH 1:1).—200 MHz-^{1}H-NMR ([D$_6$]DMSO): $\delta=8.0$–7.25 (m, 11H, Fmoc, amide NH), 6.97 (s, br., 1H, NH, urethane), 3.92–3.70 (m, 4H, α-CH, Asn, $CH-CH_2$, Fmoc), 1.2 (d, $J=7$ Hz, 3H, CH_3, Ala).

Annelation of Carbene Ligands by λ^3-Phosphaalkynes, an Entry to Functionalized Phosphaarenes**

By *Karl Heinz Dötz,* Athanassios Tiriliomis, Klaus Harms, Manfred Regitz,* and *Ulrich Annen*

Following the synthesis of the first stable λ^3-phosphaalkyne[2] under normal conditions, a systematic investigation of this class of compounds became possible. [3+2] and [4+2] cycloadditions[3] as well as metal-induced oligomerizations[4] reveal close parallels with the reaction behavior of alkynes. We were interested in the question of whether phosphaalkynes can also be used for the annelation of carbene ligands. This type of reaction has proven useful for a direct entry to highly substituted hydroquinones[5] and for syntheses in the natural products series.[5,6]

The pentacarbonyl[alkoxy(1-naphthyl)carbene]chromium complex **1** reacts with 2,2-dimethylpropylidynephosphane-**2**, and by coupling of the phosphaalkyne, the carbene and a carbonyl ligand gives the phosphaphenanthrenehydroquinone complexes **3**. The $Cr(CO)_3$ fragment is coordinated to the newly constructed phosphaaromatic ring, whose ^{31}P-NMR signal is characteristically shifted upfield with $\delta=-26.50$ (**3a**) and -24.77 (**3b**), as in the case of the only previously known tricarbonyl(phosphaarene)-chromium complex tricarbonyl(2,4,6-triphenylphosphinine)chromium **5**.[7] Within the limits of NMR detection the incorporation of the P≡C moiety is regiospecific; the coupling constants of $^3J_{P,C}=34.3$ (**3a**) and 35.3 Hz (**3b**), respectively, observed in the ^{13}C-NMR spectrum for the OCH_3- and OCH_2-groups suggest the 3-phosphaphenanthrene structure. As in the carbene annelation with alkynes,[8] the regioselectivity is apparently sterically controlled. By ligand-exchange under CO pressure,[9] the phosphaarene **4** can be liberated almost quantitatively from **3b**; the $Cr(CO)_6$ formed in the reaction can be further used for the synthesis of the carbene complex **1**. As expected, in the ^{13}C- and ^{31}P-NMR spectra of **4** the signals for the ring atoms of the heterocycle are shifted downfield ($\Delta\delta(^{13}C)\approx 30$–40 ppm; $\Delta\delta(^{31}P)\approx 150$ ppm) compared to those of the coordinated phosphaarene **3b**.

In contrast to tricarbonyl(phenanthrene)chromium, in which the metal is coordinated unsymmetrically to the terminal ring,[10] in the phosphaphenanthrene complex **3a** the tricarbonylchromium group is bound centrally to the phosphinine ring (Fig. 1).[11] The metal is in a pseudo-octahe-

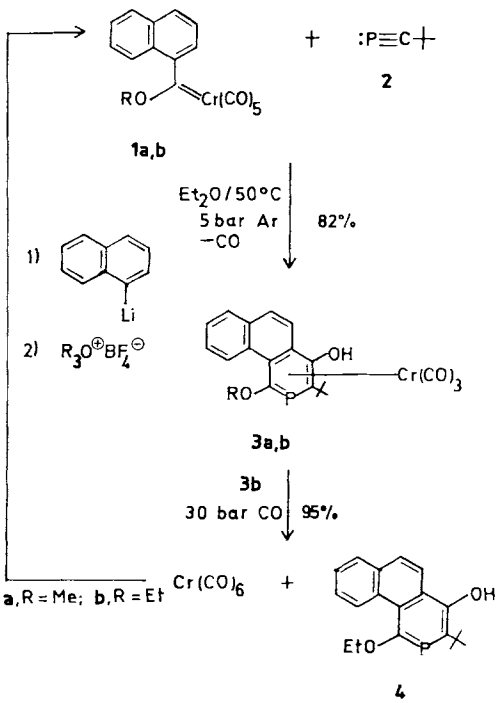

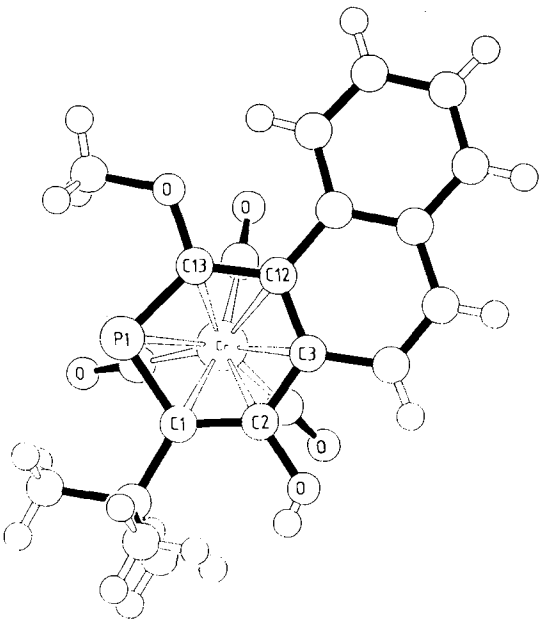

Fig. 1. Structure of **3a** in the crystal. Projection onto the plane of the phosphinine ring. Important bond lengths [Å] and angles [°]: Cr-P1 2.4591(4), Cr-$C_{heterocycle}$ 2.290(1) (mean value), Cr-$C_{carbonyl}$ 1.836(2) (mean value), C1-P1 1.768(1), C13-P1 1.759(1), C1-C2 1.400(2), C2-C3 1.438(2), C3-C12 1.428(2), C12-C13 1.437(2); $C_{carbonyl}$-Cr-$C_{carbonyl}$ 89.5(1) (mean value), Cr-C-$O_{carbonyl}$ 178.2(1) (mean value), C1-P1-C13 101.73(6), P1-C1-C2 121.4(1), C1-C2-C3 126.4(1), C2-C3-C12 124.0(1), C3-C12-C13 117.9(1), P1-C13-C12 128.2(1); torsional angle: C1-C2-C3-C12 0.3(4), C2-C3-C12-C13 4.8(4), C3-C12-C13-P1 −4.2(4), C12-C13-P1-C1 −0.5(3), C13-P1-C1-C2 5.2(2), P1-C1-C2-C3 −5.8(4).

dral environment. On comparison with the only previously X-ray crystallographically investigated phosphaarene-chromium complex **5**,[12] the following differences were noted: the Cr-C_{ring} distances (average: 2.290(1) Å) are somewhat longer and the Cr-P bond (2.4591(4) Å) is

[*] Prof. Dr. K. H. Dötz, Dipl.-Chem. A. Tiriliomis, Dr. K. Harms
Fachbereich Chemie der Universität
Hans-Meerwein-Strasse, D-3550 Marburg (FRG)
Prof. Dr. M. Regitz, Dipl.-Chem. U. Annen
Fachbereich Chemie der Universität
Erwin-Schrödinger-Strasse, D-6750 Kaiserslautern (FRG)

[**] Reactions of Complex Ligands, Part 33. This work was supported by the Deutsche Forschungsgemeinschaft and the Fonds der Chemischen Industrie.—Part 32: [1].

slightly shorter than in **5**. Two carbonyl ligands are staggered with respect to the ring atoms; the third carbonyl group assumes ân almost eclipsed position relative to the phosphorus atom. This conformation apparently corresponds to that with the least steric interactions between the ring substituents and the carbonyl ligands, and rather resembles that in tricarbonyl(2-ethyl-4-methoxy-3-methyl-1-naphthol)chromium,[13] which has a comparable substitution pattern. In the N-, P- and S-heterocyclic complexes investigated so far,[12, 14] however, an approximate *trans*-arrangement of the ring heteroatoms to a carbonyl group was observed.

In contrast to both **5** as well as to uncoordinated phosphinines[15] the heterocycle in **3a** is slightly puckered (largest torsion angles: C13-P1-C1-C2 5.2(2)°, P1-C1-C2-C3 −5.8(4)°, for numbering see Fig. 1); this puckering is still found in the neighboring ring, whereas the third ring, with a maximum torsion angle of 2° at the coupling to the central ring, is almost planar. The C1-P1-C13 angle (101.73(6)°) in **3a** is about 2° larger than that found in **5**, and thus approaches that in uncoordinated phosphinines (ca. 103°). The C-C bond lengths in the heterocycle are significantly different; they also alternate in the neighbouring ring.

Bearing in mind the numerous possible structural variants of carbonyl(carbene) complexes, carbene annelation with phosphaalkynes can be expected to afford direct access to a broad spectrum of functionalized mononuclear and condensed phosphaarenes.[16]

Experimental

3a, **b**: A solution of 7.5 mmol of the carbene complex (2.72 g, **1a**; 2.82 g **1b**) and 0.75 g (7.50 mmol) of **2** in 20 mL of *tert*-butyl methyl ether was heated under an argon pressure of 5 bar for 2 h at 50°C. After removal of the solvent the residue was chromatographed at −25°C with CH_2Cl_2/pentane (1/3 to 1/1) on silica gel. Recrystallization from CH_2Cl_2/pentane (1/1) afforded dark red crystals. Yields: 2.59 g **3a** (82%), 2.41 g **3b** (82%).—**3a**: IR (hexane): $\tilde{\nu}$(C≡O) = 1965 (s), 1885 (s, br) cm^{-1}; ^{1}H-NMR (400 MHz, CD_3COCD_3): δ = 9.35 (dd, 1H; 5-H), 8.55 (s, 1H; OH), 8.32 (d, 1H; 10-H), 7.89 (dd, 1H; 8-H), 7.85 (d, 1H; 9-H), 7.65 (m, 2H; 6,7-H), 4.00 (d, 3H; OCH_3), 1.57 (d, 9H; $C(CH_3)_3$); ^{13}C-NMR (100.4 MHz, CD_3COCD_3): δ = 233.49 ($Cr(CO)_3$), 154.72 (C-2, ^1J(P,C) = 68.0 Hz), 133.04, 133.65, 131.12, 131.04, 130.07, 129.39, 129.19, 128.71, 123.27, 96.97 (C-4a-C-10a), 114.73 (C-4, ^1J(P,C) = 60.1 Hz), 101.06 (C-1, ^2J(P,C) = 7.7 Hz), 58.93 (OCH_3, ^3J(P,C) = 34.3 Hz), 38.01 ($C(CH_3)_3$, ^2J(P,C) = 19.6 Hz), 31.62 ($C(CH_3)_3$, ^3J(P,C) = 14.2 Hz); ^{31}P-NMR (121.4 MHz, CD_3COCD_3): δ = −26.50; MS: *m/z* 434 ($M^{\oplus}$).—**3b**: IR (hexane): $\tilde{\nu}$(C≡O) = 1957 (s), 1887 (s, br) cm^{-1}; ^{1}H-NMR (CD_3COCD_3): δ = 9.50 (d, 1H; 5-H), 7.91, 7.89 (each d, each 2H; 8,9,10-H, OH), 7.66 (m, 2H; 6,7-H), 4.30 (dq, 1H; OCH), 4.09 (dq, 1H; OCH), 1.58 (t, 3H; CH_3CH_2O), 1.57 (d, 9H; $C(CH_3)_3$); ^{13}C-NMR (CD_3COCD_3): δ = 233.67 ($Cr(CO)_3$), 153.72 (C-2, ^1J(P,C) = 68.2 Hz), 115.12 (C-4, ^1J(P,C) = 60.4 Hz), 133.90, 133.70, 131.11, 131.09, 130.17, 129.41, 129.17, 128.60, 123.34, 100.89, 97.04 (C-1, C-4a-C-10a), 70.15 (OCH_2, ^3J(P,C) = 35.3 Hz), 38.03 ($C(CH_3)_3$, ^2J(P,C) = 19.4 Hz), 31.46 ($C(CH_3)_3$, ^3J(P,C) = 14.3 Hz), 15.20 (CH_3CH_2O, ^4J(P,C) = 4.0 Hz); ^{31}P-NMR (CD_3COCD_3): δ = −24.77; MS: *m/z* 448 ($M^{\oplus}$).

4: A solution of **3b** (2 mmol) in ether (40 mL) was heated under a pressure of 30 bar CO for 14 h at 70°C. The solvent was then removed and the almost quantitatively recovered hexacarbonylchromium sublimed under Hg vacuum at 20°C. Column chromatographic purification of the residue on silica gel (10°C, ether/pentane as eluent) and recrystallization (pentane/CH_2Cl_2) afforded yellow crystals. Yield: 95%.—^{1}H-NMR (CD_3COCD_3): δ = 9.80 (d, 1H; 5-H), 8.39 (d, 1H; 10-H), 7.88 (m, 3H; 8,9-H, OH), 7.61 (m, 2H; 6,7-H), 4.48 (q, 2H; OCH_2), 1.71 (t, 3H; CH_3CH_2O), 1.68 (d (^4J(P,H)), 9H; $C(CH_3)_3$); ^{13}C-NMR (CD_3COCD_3): δ = 188.74 (C-2, ^1J(P,C) = 46.6 Hz), 153.97 (C-4, ^1J(P,C) = 47.5 Hz), 149.71, 133.70, 130.57, 129.43, 129.23, 129.16, 128.43, 127.46, 127.29, 122.99, 122.92 (C-1, C-4a-C-10a), 68.61 (OCH_2, ^3J(P,C) = 39.3 Hz), 38.94 ($C(CH_3)_3$, ^2J(P,C) = 23.7 Hz), 31.64 ($C(CH_3)_3$, ^3J(P,C) = 15.4 Hz), 15.39 (CH_3CH_2O), ^4J(P,C) = 4.1 Hz); ^{31}P-NMR (CD_3COCD_3): δ = 125.80; MS: *m/z* 312 ($M^{\oplus}$).

Received: December 23, 1987 [Z 2557 IE]
German version: *Angew. Chem. 100* (1988) 725

[1] K. H. Dötz, R. Noack, G. Müller, *J. Chem. Soc. Chem. Commun. 1988*, 302.

[2] a) G. Becker, G. Gresser, W. Uhl, *Z. Naturforsch. B 36* (1981) 16; b) optimized procedure: W. Rösch, U. Hees, M. Regitz, *Chem. Ber. 120* (1987) 1645.

[3] a) W. Rösch, M. Regitz, *Angew. Chem. 96* (1984) 898; *Angew. Chem. Int. Ed. Engl. 23* (1984) 900; b) W. Rösch, H. Richter, M. Regitz, *Chem. Ber. 120* (1987) 1809 and previous reports of this series.

[4] a) P. Binger, R. Milczarek, R. Mynott, M. Regitz, W. Rösch, *Angew. Chem. 98* (1986) 645; *Angew. Chem. Int. Ed. Engl. 25* (1986) 644; b) P. B. Hitchcock, M. J. Mah, J. F. Nixon, *J. Chem. Soc. Chem. Commun. 1986*, 737; c) P. Binger, R. Milczarek, R. Mynott, M. Regitz, *J. Organomet. Chem. 323* (1987) C35; d) R. Milczarek, W. Rüsseler, P. Binger, K. Jonas, K. Angermund, C. Krüger, M. Regitz, *Angew. Chem. 99* (1987) 957; *Angew. Chem. Int. Ed. Engl. 26* (1987) 908; e) A. R. Barron, A. H. Cowley, *ibid. 99* (1987) 956 resp. *26* (1987) 907; f) M. Driess, D. Hu, H. Pritzkow, H. Schäufele, U. Zenneck, M. Regitz, W. Rösch, *J. Organomet. Chem. 334* (1987) C35.

[5] Reviews: a) K. H. Dötz, *Angew. Chem. 96* (1984) 573; *Angew. Chem. Int. Ed. Engl. 23* (1984) 587; b) K. S. Chan, G. A. Peterson, T. A. Brandvold, K. L. Faron, C. A. Challener, C. Hyldahl, W. D. Wulff, *J. Organomet. Chem. 334* (1987) 9; c) K. H. Dötz, M. Popall, G. Müller, *ibid. 334* (1987) 57; d) K. H. Dötz in H. tom Dieck, A. de Meijere (Eds.): *Organometallics in Organic Synthesis: Aspects of a Modern Interdisciplinary Field*, Springer, Berlin 1988.

[6] Recent examples: a) K. H. Dötz, M. Popall, *Tetrahedron 41* (1985) 5797; b) M. F. Semmelhack, J. J. Bozell, L. Keller, T. Sato, E. J. Spiess, W. D. Wulff, A. Zask, *ibid. 41* (1985) 5803; c) W. D. Wulff, P.-C. Tang, K. S. Chan, J. S. McCallum, D. Y. Yang, S. R. Gilbertson, *ibid. 41* (1985) 5813; d) A. Yamashita, *J. Am. Chem. Soc. 107* (1985) 5823; e) K. H. Dötz, M. Popall, *Angew. Chem. 99* (1987) 1220; *Angew. Chem. Int. Ed. Engl. 26* (1987) 1158.

[7] **5**: ^{31}P-NMR: δ = −4.3; J. Deberitz, H. Nöth, *Chem. Ber. 103* (1970) 2541.

[8] a) K. H. Dötz, J. Mühlemeier, U. Schubert, O. Orama, *J. Organomet. Chem. 247* (1983) 187; b) a predominantly electronic stereocontrol is assumed in the regiospecific [3 + 2]-cycloaddition of 1,3-dipoles to **2**, see, e.g., [2b].

[9] Cf. K. H. Dötz, *J. Organomet. Chem. 140* (1977) 177.

[10] K. W. Muir, G. Ferguson, G. A. Sim, *J. Chem. Soc. B 1968*, 467.

[11] Crystal structure data of **3a**: space group $P2_1/c$, a = 10.334(3), b = 11.834(1), c = 16.445(2) Å, β = 102.33°, Z = 4. CAD-4 (Enraf-Nonius) four-circle diffractometer, $Mo_{K\alpha}$ radiation, graphite monochromator, ω-scans, θ = 2–25°, 3766 measured reflections. Solution by direct methods, refinement to R = 0.030 for 2679 independent reflections with $I \geq 3\sigma(I)$, all non-hydrogen atoms anisotropic, H-atoms riding with fixed isotropic temperature factors. Further details of the crystal structure investigation are available on request from the Fachinformationszentrum Energie, Physik, Mathematik GmbH, D-7514 Eggenstein-Leopoldshafen 2 (FRG), on quoting the depository number CSD-52863, the names of the authors, and the journal citation.

[12] H. Vahrenkamp, H. Nöth, *Chem. Ber. 105* (1972) 1148.

[13] K. H. Dötz, R. Dietz, A. von Imhof, H. Lorenz, G. Huttner, *Chem. Ber. 109* (1976) 2033.

[14] a) G. Huttner, B. Krieg, *Angew. Chem. 83* (1971) 541; *Angew. Chem. Int. Ed. Engl. 10* (1971) 512; b) G. Huttner, O. S. Mills, *Chem. Ber. 105* (1972) 301.

[15] a) W. Fischer, E. Hellner, A. Chatzidakis, K. Dimroth, *Tetrahedron Lett. 1968*, 6227; b) J. C. J. Bart, J. J. Daly, *Angew. Chem. 80* (1968) 843; *Angew. Chem. Int. Ed. Engl. 7* (1968) 811.

[16] So far only very few condensed phosphaarenes have been described. Review: G. Märkl in *Houben-Weyl-Müller, Methoden der Organischen Chemie (4th edit.), Vol. E 1*, Thieme, Stuttgart 1982, p. 72ff.

Inductivity and Bridging in Ammonium and Carbenium Ions

By *Cyril A. Grob,* Alfred Dratva, Martin Gründel,* and *Guangyi Wang*

The reactivities of the cationic centers in ammonium and carbenium ions are fundamentally different. Thus, in the first case the N atom is tetracoordinate and, hence, inert to nucleophiles. In the second case the C-atom is tricoordinate and so electrophilic that it reacts even with weak nucleophiles.

[*] Prof. Dr. C. A. Grob, Dr. A. Dratva, Dr. M. Gründel, Dr. G. Wang
Institut für Organische Chemie der Universität
St.-Johanns-Ring 19, CH-4056 Basel (Switzerland)

The differences are also reflected in the way the inductive (I) effect of substituents control the formation of these cations. This is demonstrated by application of the *Hammett* equation $\lg(K/K_0)=\rho_I\cdot\sigma_I^q$ to the protonation of the bi- and tricyclic amines **1**–**4**, and to the solvolysis rates of the corresponding *p*-toluenesulfonates **5**–**8**. K and K_0 are

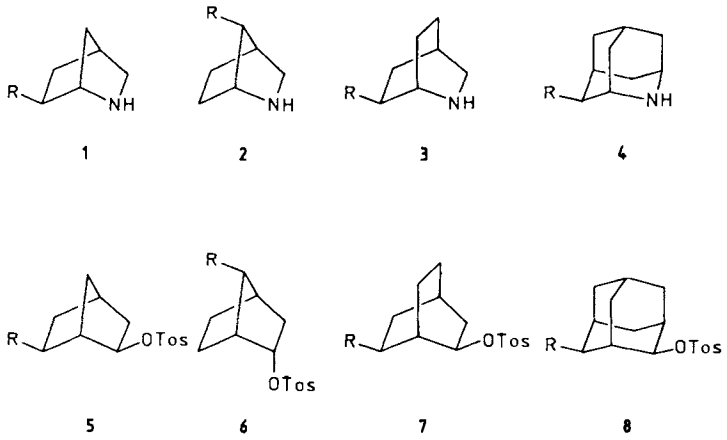

1 **2** **3** **4**

5 **6** **7** **8**

equilibrium or rate constants for the substituted[1] and unsubstituted compounds, respectively; σ_I^q are inductive substituent constants.[2] The reaction constants ρ_I are of primary importance because they serve as a measure of the *inductivity*,[3] i.e. of the intensity with which the I effect of the substituents is transmitted to the reaction center.

The pK_a values of the hydroperchlorates of the amines **1**–**4**[4] as well as the logarithms of the rate constants for the solvolysis of the toluenesulfonates **5**–**8** in 80% ethanol[5] correlate linearly with the corresponding σ_I^q values. Therefore, the protonation of the amines, as well as the ionization of the toluenesulfonates, are determined primarily by the I effect of the substituents. The ρ_I values, as calculated from the slopes of the plots of $\lg K$ vs. σ_I^q, are listed in Table 1. In the case of the amines **1**–**4** they are 1.03 (± 0.02); i.e. the ρ_I values, like the distances between the N atoms and the substituents, are practically the same. Therefore, inductivity is not dependent on the structure of the molecules.

Table 1. Inductivities ρ_I of the amines **1**–**4** and of the toluenesulfonates **5**–**8** (correlation coefficients in brackets). R = general substituent [1] (see formulas).

Compounds	ρ_I
6-*exo*-R-2-azanorbornanes **1**	1.05 (0.994)
7-*anti*-R-2-azanorbornanes **2**	1.01 (0.984)
6-*exo*-R-2-azabicyclo[2.2.2]octane **3**	1.04 (0.994)
4*e*-R-2-azaadamantanes **4**	1.00 (0.999)
6-*exo*-R-2-*exo*-norbornyltoluenesulfonates **5**	−2.00
7-*anti*-R-2-*endo*-norbornyltoluenesulfonates **6**	−0.72
6-*exo*-R-2-*exo*-bicyclo[2.2.2]octyltoluenesulfonates **7**	−1.50
4*e*-R-2*e*-adamantyltoluenesulfonates **8**	−0.80

In contrast, the ρ_I values for the dissociation of the toluenesulfonates **5**–**8** to the ion pairs **9**–**12** differ markedly, although the distances and the partial structures are again practically the same. In these cases then, inductivity depends on the structure of the *whole* molecule. The large variations of ρ_I have been attributed to the varying tendency for dorsal and temporarily pentacoordinate C-atoms to bridge the electrophilic centers in the cations **9**–**12**,[3,5]

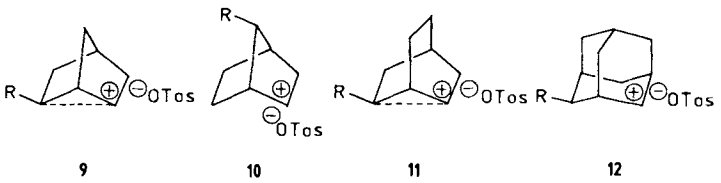

9 **10** **11** **12**

for bridging contributes substancially to the transmission of the I effect. As a directional bonding interaction, bridging generates strain which varies according to the structure of the molecule. Bridging strain is small in the cations **9** and **11**, but considerably larger in **10** and **12**.[6]

As shown by the ρ_I values for protonation of the 2-, 3-, and 4-substituted quinuclidines **13**[7] and for the solvolysis of the corresponding bicyclo[2.2.2]octyl *p*-nitrobenzenesulfonates **14**,[8] inductivity is considerably higher at C2 than at the more remote C atoms in both cases. Furthermore, ρ_I is distinctly higher at C2 in **13** than in **14**. This difference could be due to the presence of the anion in the contact ion pair **15** which partially shields the positive charge at C1 and thereby diminishes the I effect of neighboring substituents. On the other hand, the ρ_I values at C3 and C4 in **14** are slightly larger than at these positions in **13**, an indication that these carbons are weakly bridged.

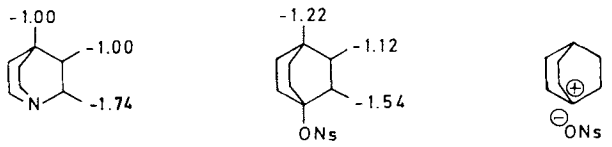

13 **14** **15**

From these results it can be concluded that the transmission of inductive substituent effects in ammonium and carbenium ions differs in that in the first case it involves only structure-*in*dependent polarization, whereas in carbenium ions transmission also involves structure-dependent, short-range bridging. It should be noted, however, that the concept of graded bridging is derived from observed inductivities[3] and differs from the concept of "classical" and "nonclassical" ions, as employed by *Winstein* et al.[9a] and other authors.[9b,c]

Received: December 21, 1987 [Z 2550 IE]
German version: *Angew. Chem. 100* (1988) 723

[1] In each case, eight to twelve different substituents R were introduced.
[2] C. A. Grob, B. Schaub, M. G. Schlageter, *Helv. Chim. Acta 63* (1980) 57.
[3] C. A. Grob, *Acc. Chem. Res. 16* (1983) 426.
[4] The preparation of the amines and the pK_a measurements are described in the dissertations by A. Dratva, M. Gründel, and G. Wang (Universitätsbibliothek Basel, 1987).
[5] W. Fischer, C. A. Grob, R. Hanreich, G. von Sprecher, A. Waldner, *Helv. Chim. Acta 64* (1981) 2298; P. Flury, C. A. Grob, *ibid. 66* (1983) 1971; C. A. Grob, P. Sawlewicz, *ibid. 67* (1984) 1906; C. A. Grob, G. Wittwer, K. Rama Rao, *ibid. 68* (1985) 651.
[6] Strong bridging, as in **9** (R = H), leads to substitution with retention, weak bridging, as in **12** (R = H) to substitution with retention *and* inversion.
[7] C. A. Grob, *Helv. Chim. Acta 68* (1985) 882.
[8] R. Bielmann, C. A. Grob, D. Küry, G. W. Yao, *Helv. Chim. Acta 68* (1985) 2158.
[9] a) S. Winstein, D. S. Trifan, *J. Am. Chem. Soc. 71* (1949) 2953; *ibid. 74* (1952) 1147, 1154; b) P. von R. Schleyer, D. Lenoir, P. Misson, G. Liang, G. K. Surya Prakash, G. A. Olah, *ibid. 102* (1980) 683; c) G. A. Olah, G. K. Surya Prakash, M. Sauders, *Acc. Chem. Res. 16* (1983) 440.

Enzyme-Catalyzed Synthesis of 1-Deoxymannojirimycin, 1-Deoxynojirimycin, and 1,4-Dideoxy-1,4-imino-D-arabinitol**

By *Thomas Ziegler, Alexander Straub,* and *Franz Effenberger**

1-Deoxymannojirimycin (1,5-dideoxy-1,5-imino-D-mannitol) **8**, 1-deoxynojirimycin (1,5-dideoxy-1,5-imino-D-glucitol) **9**, and 1,4-dideoxy-1,4-imino-D-arabinitol **10** are very effective glycosidase inhibitors.[1,2] The piperidine derivatives **8** and **9** have been known for some time,[1] whereas the pyrrolidine derivative **10** was first discovered in 1985 in two types of leguminoses, from which it was isolated.[3]

Because of their great importance as active agents a considerable number of methods have been developed for the synthesis of **8** and **9**, almost all of them starting from naturally occurring carbohydrates so as to introduce as many chirality centers from the very beginning.[4] Recently a synthesis of **9** from L-(+)-tartaric acid was described.[5] In the case of **10**, only one synthesis has been published so far;[6]

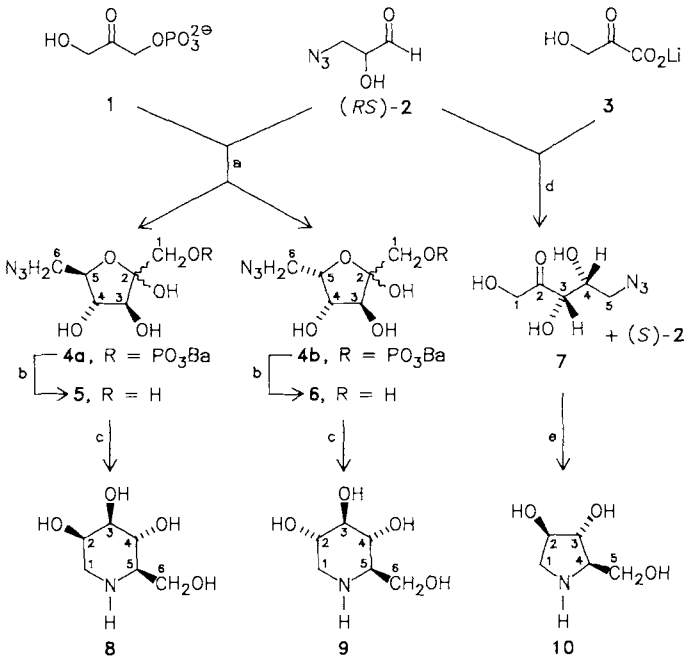

Scheme 1. a) **1** + (*R,S*)-**2**/pH 6/aldolase (EC 4.1.2.13)/12 h/25°C; pH 7/$BaCl_2 \cdot 2H_2O \rightarrow$ **4** (≡ **4a** + **4b**) (70%). b) **4**/phosphatase/pH 4.5/48 h/38°C/chromatography on Dowex 1×8 $HCO_3^{\ominus}$ with $H_2O \rightarrow$ **5** and **6** (each 80%). **5**: $[\alpha]_D^{20} = +52.49°$ ($c = 2.1$, H_2O), **6**: $[\alpha]_D^{20} = -53.78°$ ($c = 2.9$, H_2O). c) **5** or **6**/K_2CO_3/H_2O/Pd/C/80 bar H_2/4 h/50°C/HCl → **8** · HCl and **9** · HCl (each 65%). d) (*RS*)-**2** + **3**/$MgCl_2$/thiamine pyrophosphate/pH 8/transketolase (EC 2.2.1.1)/15 h/30°C/chromatography on Dowex 50 WX8 $Ca^{2\oplus}$ with $H_2O \rightarrow$ (*S*)-**2** (62%) and **7** (71%). (*S*)-**2**: $[\alpha]_D^{20} = -19°$ ($c = 0.4$, D_2O), **7**: $[\alpha]_D^{20} = -13.9°$ ($c = 0.4$, D_2O). e) **7**/K_2CO_3/H_2O/Pd/C/80 bar H_2/12 h/25°C → **10** · HCl and (4*S*)-**10** · HCl (11:1), after recrystallization from methanol/ether **10** · HCl (63%). $[\alpha]_D^{20} = +35.6°$ ($c = 0.4$, H_2O), m.p. 113°C (113–115°C [6]), ^{1}H-NMR-, ^{13}C-NMR-spectra identical with those given in [6].

it starts from D-xylose. Common to all these methods is the involvement of an extensive protecting group technique, which consequently requires a large number of reaction steps and thus leads to low overall yields.

We recently reported on a simple synthesis of dihydroxyacetone phosphate (DHAP) **1** and its use in aldolase-catalyzed aldol additions.[7] We have now used this stereochemically unambiguous CC coupling as key reaction for the synthesis of the compounds **8** and **9** from a chiral precursor (Scheme 1).

In the reaction of **1** with (*R,S*)-3-azido-2-hydroxypropanal **2** catalyzed by rabbit-muscle aldolase we have isolated a diastereomeric mixture **4** of the barium sugar phosphates **4a** and **4b** in 70% yield. The enzymatically determined conversion was >99%. By acid or enzymatic cleavage of phosphate we obtained a diastereomeric mixture which could be readily resolved chromatographically on Dowex 1×8 into the D-fructo- and L-sorbo-compounds **5** and **6**, respectively (each in 80% yield). The purity and composition of the diastereomers **5** and **6** were confirmed by GC-MS analysis of the persilylated compounds (29% α-**5**, 71% β-**5**; 88% α-**6**, 12% β-**6**).

The anomers **5** and **6** were hydrogenated analogously to the method used for the preparation of hydroxypiperidines from 6-aminohexuloses.[4a-c] Thereby we obtained exclusively deoxymannojirimycin **8** from **5** and exclusively deoxynojirimycin **9** from **6**. The diastereomeric purity of **8** and **9** was confirmed by GC-MS analysis of the persilylated compounds; the ^{1}H-NMR, ^{13}C-NMR and MS data are consistent with the published data for **8** and **9**.[4f-h]

For the analogous synthesis of the pyrrolidine derivative **10**, azidoacetaldehyde, which, however, has so far proved impossible to prepare in pure form, had to be used in place of (*R,S*)-**2**. We have now succeeded, however, in preparing the 5-azido-5-deoxy-D-xylulose **7** in good yields from lithium hydroxypyruvate **3** and (*R,S*)-**2** via a transketolase-catalyzed CC coupling (Scheme 1). Upon hydrogenation, the azido sugar **7** furnishes the pyrrolidine derivative **10** in high yields (76%), containing less than 10% of the undesired (4*S*)-diastereomer. The latter byproduct can be removed by simple recrystallization of the hydrochloride from methanol/ether.

Transketolases have thus far found little preparative use.[8] This example demonstrates, not only their utility in the synthesis of sugars, but can also serve for the separation of racemic aldehydes, e.g. (*R,S*)-**2**. The configuration of the aldehyde (*S*)-**2** isolated besides **7** was confirmed

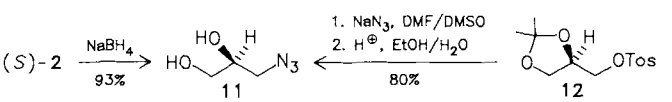

by reduction to the (*S*)-3-azido-1,2-propanediol **11** ($[\alpha]_D^{20} = -15°$). **11** ($[\alpha]_D^{20} = -15.8°$) was prepared via an independent route from the commercially available (*R*)-isopropylideneglycerol tosylate **12**.

Received: January 21, 1988;
revised: February 25, 1988 [Z 2583 IE]
German version: *Angew. Chem. 100* (1988) 737

[*] Prof. Dr. F. Effenberger, Dr. T. Ziegler, Dipl.-Chem. A. Straub
Institut für Organische Chemie der Universität
Pfaffenwaldring 55, D-7000 Stuttgart 80 (FRG)

[**] Enzyme-Catalyzed Reactions, Part 3. This work was supported by the Deutsche Forschungsgemeinschaft, the Fonds der Chemischen Industrie, and the Robert Bosch Stiftung.—Part 2: F. Effenberger, T. Ziegler, S. Förster, *Angew. Chem. 99* (1987) 491; *Angew. Chem. Int. Ed. Engl. 26* (1987) 458.—Part 1: [7].

[1] a) Review: E. Truscheit, W. Frommer, B. Junge, L. Müller, D. D. Schmidt, W. Wingender, *Angew. Chem. 93* (1981) 738; *Angew. Chem. Int. Ed. Engl. 20* (1981) 744; b) L. E. Fellows, *Chem. Br. 23* (1987) 842.

[2] S. V. Evans, L. E. Fellows, T. K. M. Shing, G. W. J. Fleet, *Phytochemistry 24* (1985) 1953.

[3] a) J. Furukawa, S. Okuda, K. Saito, S. I. Hatanaka, *Phytochemistry 24* (1985) 593; b) R. J. Nash, E. A. Bell, J. M. Williams, *ibid. 24* (1985) 1620.
[4] a) H. Paulsen, I. Sangster, K. Heyns, *Chem. Ber. 100* (1967) 802; b) H. Paulsen, K. Todt, *Adv. Carbohydr. Chem. 23* (1968) 115; c) G. Kinast, M. Schedel, *Angew. Chem. 93* (1981) 799; *Angew. Chem. Int. Ed. Engl. 20* (1981) 805; d) A. Vasella, R. Voeffray, *Helv. Chim. Acta 65* (1982) 1134; e) G. Legler, E. Jülich, *Carbohydr. Res. 128* (1984) 61; f) R. C. Bernotas, B. Ganem, *Tetrahedron Lett. 26* (1985) 1123; g) G. W. J. Fleet, L. E. Fellows, D. W. Smith, *Tetrahedron 43* (1987) 979; h) S. Inouye, T. Tsuruoka, T. Ito, T. Nidda, *ibid. 23* (1968) 2125.
[5] H. Iida, N. Yamazaki, C. Kibayashi, *J. Org. Chem. 52* (1987) 3337.
[6] G. W. J. Fleet, S. J. Nicholas, P. W. Smith, S. V. Evans, L. E. Fellows, R. J. Nash, *Tetrahedron Lett. 26* (1985) 3127.
[7] F. Effenberger, A. Straub, *Tetrahedron Lett. 28* (1987) 1641, and references cited therein.
[8] a) A. Mocali, D. Aldinucci, F. Paoletti, *Carbohydr. Res. 143* (1985) 288; b) M. Kapuscinski, F. P. Franke, I. Flanigan, J. K. MacLeod, J. F. Williams, *ibid. 140* (1985) 69; c) J. Bolte, C. Demuynck, H. Samaki, *Tetrahedron Lett. 28* (1987) 5525.

Competition of Endoperoxide and Hydroperoxide Formation in the Reaction of Singlet Oxygen with Cyclic, Conjugated Dienes**

By *Rudolf Matusch,** and *Gerhard Schmidt*

Singlet oxygen ($^1O_2$) usually reacts with cyclic, conjugated dienes in the sense of a [4+2] cycloaddition to give endoperoxides, whereas non-conjugated olefins with allylic hydrogen atoms undergo a double-bond shift with formation of hydroperoxides. In the following we show that both reactions can occur, and that a common intermediate can be formulated in the case of cyclic, conjugated dienes.

In the search for biologically active plant constituents we isolated the two endoperoxides **2** and **3** as active components which are accessible synthetically by reaction of $^1O_2$ with (*R*)-(−)-α-phellandrene **1**[1] and were previously considered to be the sole products of this reaction. To our surprise, however, not only the peroxides **2** and **3** are formed but also all theoretically possible hydroperoxides **4**, **5**, **6**, **7**, and **8**, together with the aromatization product *p*-cymol **9**.[2] Scheme 1 shows the distribution of all products after a preparative HPLC separation (data in wt-%).

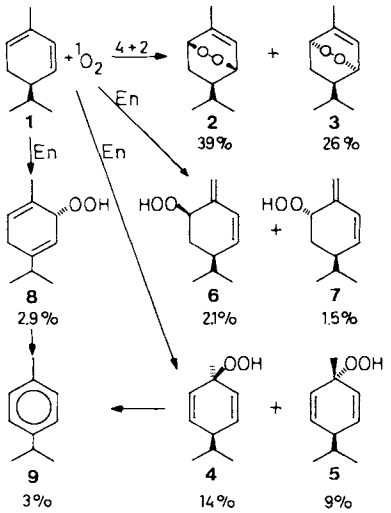

Scheme 1.

Two facts emerge therefrom: First, hydroperooxides are formed to a considerable extent; that is, [4+2] cycloaddition and ene reaction compete. Second, the *cis-trans* ratio (based on the position of the peroxide function to the isopropyl group) is constant for both the endoperoxides as well as the diastereomeric hydroperoxides; it is 3:2.

The latter finding suggests the existence of a common intermediate for endo- and hydroperoxides. *Monroe*[3] has postulated this for the reaction of $^1O_2$ with acyclic dienes; for cyclic dienes, however, he proposed a concerted [4+2] cycloaddition exclusively, since only endoperoxide formation was observed.

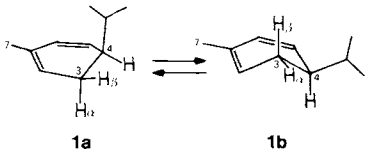

Fig. 1. Conformations **1a** and **1b** of (*R*)-(−)-α-phellandrene **1**.

Dreiding models show that α-phellandrene **1** can assume two conformations (Fig. 1). At room temperature a considerable amount of **1** is present in the conformation **1a**.[4] In a concerted [4+2] cycloaddition with attack of $^1O_2$ from above, steric interactions of the isopropyl group with the dienophile should be considerable for **1a** and negligible for **1b**. On the other hand, both conformers are equally likely to react with $^1O_2$ from below. In summary, therefore, more *trans*-endoperoxide **3** should result. The observed higher proportion of the *cis*-endoperoxide **2** thus contradicts an endoperoxide formation by concerted [4+2] cycloaddition.

Especially interesting concerning the hydroperoxides is the preferred *cis*-conformation of **6** compared to **7**. Since the abstracted H atom here comes from a methyl group, a *cis-trans* ratio of 1:1 would be expected, irrespective of the conformation,[5] if the $^1O_2$ does not preferably approach from above.

How then does this *cis*-directing effect come about? The point is that $^1O_2$ preferably abstracts axial allylic H atoms in an ene reaction, whereas equatorial allylic H-atoms remain undisturbed.[6]

Regarding the *cis* sides of **1a** and **1b** in respect to the formation of **4** and **5**, H-3β being the only proton that could react in an ene reaction has the unreactive equatorial position in the case of **1a** and, additionally, the isopropyl group disfavors abstraction because of unfavorable steric interactions. In contrast this H-3β is axial in the conformer **1b**. Exactly the opposite holds true on the *trans* side for H-3α: in **1a** it is axial, and in **1b** it is equatorial. We therefore presumed that the *cis* products are mainly formed from the conformer **1b** and the *trans* products mainly from the conformer **1a**. To substantiate our assumption we carried out the reaction at −50°C. Since conformer **1a** is the energetically less favorable,[4c] the amount of *trans* products should decrease further. As expected the *cis-trans* ratio increases from 3:2 to 4:2, both in the case of the endo- as well as the hydroperoxides.

According to the above observations the mechanism of the ene reaction must first be considered. In the recent literature[7] a loose complex **10** is proposed in which $^1O_2$ interacts with the olefinic C atoms and with the allylic H atoms to be abstracted. If, as in the present case, both endo- as well as hydroperoxides are formed from a diene,

[*] Prof. Dr. R. Matusch, Dr. G. Schmidt
Institut für Pharmazeutische Chemie der Universität
Marbacher Weg 6, D-3550 Marburg (FRG)

[**] Lecture at the Annual Conference of the Deutsche Pharmazeutische Gesellschaft in Münster, September 10, 1987.

the interactions of the second O atom with the allylic H atom and with the second double bond must compete with each other, as indicated in **11**.

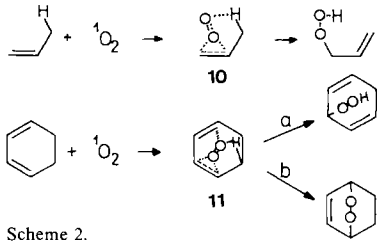

Scheme 2.

The relative strengths of these interactions and thus the electronic and steric factors now decide whether route a (ene reaction) or route b ([4+2]-cycloaddition) will dominate (Scheme 2). If **11** is used as a model for the two conformers **1a** and **1b**, then not only are interactions of the second O-atom with the axial H-3 and with the second double bond possible but also interactions with an H atom of the methyl group (Fig. 2; **1c** and **1d**).

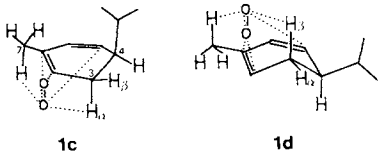

Fig. 2. Postulated intermediates **1c** and **1d** for the interactions of **1a** and **1b**, respectively, with singlet oxygen.

This, however, provides an explanation for the *cis-trans* ratio of the hydroperoxides **6** and **7**. Since a complex in which the second oxygen atom can undergo three interactions is obviously more favorable than a complex with a lower number of interactions, the respective axial H-3 and thus the conformer equilibrium **1a** $\rightleftarrows$ **1b** also directs the formation of **6** and **7**. Finally, enantiomerically pure **8** is formed by $^1O_2$-attack at the other double bond and abstraction of H-4.

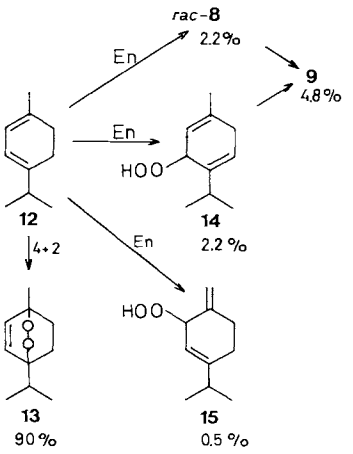

Scheme 3.

The competition between cycloaddition and ene reaction in the case of cyclic, conjugated dienes can also be observed in the reaction of $^1O_2$ with α-terpinene **12**. Here too the endoperoxide, namely ascaridol **13**, was thought to be the only reaction product.[8] And, once again, on closer examination we found the racemic hydroperoxides (**8**, **14**, **15**) depicted quantitatively in Scheme 3.

Received: January 28, 1988;
revised: February 29, 1988 [Z 2593 IE]
German version: *Angew. Chem. 100* (1988) 729

[1] G. O. Schenck, K. Ziegler, *Naturwissenschaften 32* (1944) 157.
[2] For the generation of singlet oxygen we used a sodium vapor lamp as light source, Bengal rose as sensitizer, and methanol as solvent. The reaction time at room temperature was 40 min. To rule out a radical reaction, the radical inhibitor 2,6-*tert*-butyl-*p*-cresol was added. The same product pattern was obtained when using other sensitizers (tetraphenylporphyrin, methylene blue) and other solvents (dichloromethane, isopropyl alcohol). Also no oxidative changes were observed after 40 minutes' treatment with $^3O_2$. Separation of the reaction mixture was accomplished by preparative HPLC (25 × 250 mm column; Li-Chrosorb Si 60, 5 μm, *n*-pentane/diethyl ether 9:1). The amounts of the products (wt-%) in Schemes 1 and 3 are based on the total amount of fractions eluted; the remaining 2.5% (Scheme 1) and 0.3% (Scheme 3) lie in the interstitial fractions. All the products gave correct analytical data.
[3] B. M. Monroe, *J. Am. Chem. Soc. 103* (1981) 7253.
[4] a) W. Burgstahler, H. Ziffer, U. Weiss, *J. Am. Chem. Soc. 83* (1961) 4660; b) A. Moscowitz, E. Charney, U. Weiss, H. Ziffer, *ibid. 83* (1961) 4661; c) H. Ziffer, E. Charney, U. Weiss, *ibid. 84* (1962) 2961.
[5] K. Gollnick, H. J. Kuhn in H. H. Wassermann, R. W. Murray (Eds.): *Singlet Oxygen*, Academic Press, New York 1979, p. 326.
[6] R. W. Denny, A. Nickon, *Org. React. 20* (1973) 133.
[7] a) I. R. Hurst, G. B. Schuster, *J. Am. Chem. Soc. 104* (1982) 6854; b) M. Hotokka, B. Roos, P. Siegbahn, *ibid. 105* (1983) 5263; c) K. Yamaguchi, I. Saito, K. N. Houk, *Tetrahedron Lett. 22* (1981) 749; d) K. N. Houk, J. C. Williams, P. A. Mitchell, K. Yamaguchi, *J. Am. Chem. Soc. 103* (1981) 949.
[8] a) G. O. Schenck, K. Ziegler, DRP 752437 (July 22, 1941); b) see [5], p. 307.

Synthesis of Optically Active Phosphanes via Sharpless Epoxidation**

By *Henri Brunner** and *Adolf Sicheneder*

Optically active phosphanes are the most useful ligands in enantioselective catalysis with transition metal complexes.[2,3] Methods for preparing such phosphanes involve either a resolution step or the transformation of a chiral precursor from the chiral pool.[3] In the present paper we describe a new synthesis of optically active phosphanes making use of the high optical inductions accessible in the Sharpless epoxidation of allyl alcohols.[4-6] Using this methodology, achiral allyl alcohols can be converted in a few steps, via epoxy alcohols and their proper derivatization (Scheme 1), into optically active diphosphanes capable of forming five-membered and six-membered chelate rings.

The allyl alcohols **1a** and **1b** were transformed into the epoxy alcohols **2a** (yield 55%; 93% *ee*) and **2b** (yield 75%; >95% *ee*) as described by *Sharpless* et al.[7,8] The primary alcohol groups of **2a** and **2b** were easily tosylated without affecting the epoxide ring to give **3a** and **3b**. Subsequent reaction with $LiPPh_2$ introduced two PPh_2 substituents, one by tosylate replacement and the other by epoxide ring-opening.

[*] Prof. Dr. H. Brunner, Dipl.-Chem. A. Sicheneder
Fakultät für Chemie und Pharmazie der Universität
Universitätsstr. 31, D-8400 Regensburg (FRG)

[**] Enantioselective Catalysis, Part 42. This work was supported by the Deutsche Forschungsgemeinschaft, the Fonds der Chemischen Industrie, and BASF AG, Ludwigshafen.—Part 41: [1].

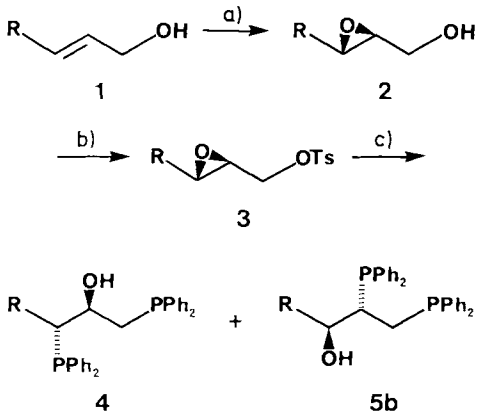

Scheme 1. **a**, R = Ph; **b**, R = *n*Pr. a) Ti(O*i*Pr)$_4$, *t*BuOOH, diethyl tartrate, CH_2Cl_2, −20°C, 3 h. b) *p*-tosylCl, pyridine, −10°C, 20 h. c) $LiPPh_2$, THF, 20°C, 20 h.

The ring-opening of epoxides with strong bases occurs stereospecifically with inversion. However, it may take place at carbon atoms C-2 and C-3, respectively, resulting in a mixture of products. The site of nucleophilic attack can be controlled by steric and electronic effects.[9, 10] We found, that the reaction of **3a** with $LiPPh_2$ is regiospecific, giving exclusively **4a**. In the reaction of **3b** with $LiPPh_2$, however, we isolated a 2.5 : 1 mixture of **4b** and **5b**. All efforts, to separate **4b** and **5b** were unsuccessful.

The tosylates **3a** and **3b** were recrystallized three times. Therefore, we assume that **4a** and the components of **4b/5b** are optically pure. At present, most of the optically active diphosphanes are only accessible in multi-step procedures.[3] The new synthesis presented in this communication is short, operationally simple, and easily employed on a large scale and with a variety of substitution patterns. Moreover, the hydroxy group in **4** and **5** formed upon epoxide ring-opening is suitable for further derivatization.

4a and **4b/5b** served as chiral ligands in the $[Rh(cod)Cl]_2$-catalyzed enantioselective hydrogenation of (*Z*)-α-acetamidocinnamic acid with 1.1 bar H_2 in methanol solution at room temperature. With Rh/ligand ratios between 1 : 1.05 and 1 : 1.10 and Rh/substrate ratios of 1 : 50 the hydrogenation is quantitative within 3 hours. **4a** and **4b/5b** gave (*R*)-(−)-*N*-acetylphenylalanine in 54 and 83% *ee*, respectively, in the usual work-up.[11, 12]. We attribute the high optical induction obtained with the mixture of **4b/5b**, to the component **5b**, which represents a functionalized PROPHOS.[13]

Experimental

3a: The epoxidation of cinnamyl alcohol **1a** was carried out as described [7] to give **2a** in 55% yield, 93% *ee*, containing 15% unreacted **1a**. The pale amber, oily **2a** (6.1 g, 40.6 mmol) was tosylated with *p*-toluenesulfonylchloride (7.75 g, 40.7 mmol) in 40 mL of pyridine at −10°C. After 20 h the mixture was filtered, the filtrate concentrated, treated with 50 mL of 1 M H_3PO_4 and extracted three times with 50 mL CH_2Cl_2. Crystallization of the yellow oil from ether/hexane gave **3a** as colorless crystals: yield 8.6 g (70%). M.p. 68–69°C. $[\alpha]_D = -45°$ ($c = 2.5$, $CHCl_3$). ^{1}H-NMR (250 MHz, $CDCl_3$): $\delta = 7.34$–7.82 (m, 4H, AA'BB'), 7.27 (s, 5), 4.10–4.36 (m, 2), 3.70 (d, 1H, $J = 2$ Hz), 3.10–3.30 (m, 1H), 2.45 (s, 3H).

4a: 8.4 g (27.6 mmol) of **3a** were dissolved in 100 mL of THF and added to a solution of $LiPPh_2$ in 50 mL of THF, prepared by reaction of 10.5 g (56.4 mmol) $HPPh_2$ and 34.5 mL of a solution of BuLi in hexane (1.64 M). After 20 h stirring at room temperature, the mixture was hydrolyzed by addition of 100 mL of acetate buffer (pH 5.1). The aqueous phase was extracted with three 50 mL portions of ether. The combined organic layers were dried over Na_2SO_4, filtered and concentrated to give a pale yellow oil, which crystallized on trituration with cold methanol. Recrystallization from toluene/hexane gave pure **4a** as a colorless powder: yield 9.0 g (65%). M.p. 142–143°C. $[\alpha]_D = -74°$ ($c = 1.0$, $CHCl_3$). CI-MS (isobutane): m/z 505 ($MH^{\oplus}$). ^{1}H-NMR (250 MHz, $CDCl_3$): $\delta = 7.03$–7.57 (m, 25H), 3.85–3.93 (m, 2H), 2.01–2.17 (m, 3H). ^{31}P-NMR (101.257 MHz, $CDCl_3$): $\delta = -5.8$ (d, 1P, $J = 2$ Hz), −20.0 (d, 1P, $J = 2$ Hz). ^{13}C-NMR (22.64 MHz, $CDCl_3$): $\delta = 127.0$–138.0 (m), 68.9 (dd, 1C), 51.3 (dd, 1C), 35.9 (dd, 1C).

Received: January 28, 1988 [Z 2595 IE]
German version: *Angew. Chem. 100* (1988) 730

CAS Registry numbers:
1a, 4407-36-7; **1b**, 928-95-0; **2a**, 104196-23-8; **2b**, 89321-71-1; **3a**, 114395-16-3; **3b**, 114395-17-4; **4a**, 114422-48-9; **4b**, 114422-49-0; **5b**, 114395-18-5.

[1] H. Brunner, J. Kraus, *J. Mol. Catal.*, in press.
[2] H. Brunner, *Top. Stereochem. 18* (1988).
[3] a) J. D. Morrison (Ed.): *Asymmetric Synthesis Vol. 5, Chiral Catalysis*, Academic Press, New York 1985; b) H. B. Kagan in [3a], p. 1.
[4] B. E. Rossiter in [3a], p. 193.
[5] M. G. Finn, K. B. Sharpless in [3a], p. 247.
[6] A. Pfenninger, *Synthesis 1986*, 89.
[7] R. M. Hanson, K. B. Sharpless, *J. Org. Chem. 51* (1986) 1922.
[8] J. G. Hill, K. B. Sharpless, C. M. Exon, R. Regenye, *Org. Synth. 63* (1984) 66.
[9] C. H. Behrens, K. B. Sharpless, *Aldrichimica Acta 16* (1983) 67.
[10] K. B. Sharpless, C. H. Behrens, T. Katsuki, A. W. M. Lee, V. S. Martin, M. Takatani, F. J. Walker, S. S. Woodward, *Pure Appl. Chem. 55* (1983) 589.
[11] H. Brunner, W. Pieronczyk, *J. Chem. Res. Synop. 1980*, 76; *J. Chem. Res. Miniprint 1980*, 1275.
[12] H. Brunner, W. Pieronczyk, B. Schönhammer, K. Streng, I. Bernal, J. Korp, *Chem. Ber. 114* (1981) 1137.
[13] M. D. Fryzuk, B. Bosnich, *J. Am. Chem. Soc. 99* (1977) 6262.

BOOK REVIEWS

The Electronic Structure and Chemistry of Solids. By *P. A Cox*. Oxford University Press, Oxford 1987. 259 pp., paperback, £ 12.50.—ISBN 0-19-855204-1

Solid state research is in vogue. New high temperature superconductors, conducting organic polymers, "heavy fermions", charge and spin density waves—interdisciplinary groups have achieved these and many other advances and discoveries in this field in very recent years. Surface science—a field with close links to both chemistry and physics—has also experienced an explosive growth during the past decade. One result of these developments is the necessity for communication in interdisciplinary fields, since many of the electronic properties of solids are now of interest not merely to a small circle of specialists but also to synthetic chemists. Although there are excellent textbooks available on solid state physics, such as *Kittel*'s "Introduction to Solid State Physics" and "Solid State Physics" by *Ashcroft* and *Mermin*, these standard works, written by physicists for physics students, are not very attractive to chemists for two reasons: first, the presentation of the material is often too mathematically advanced, and

second, the examples chosen are kept very simple and are therefore not of much interest to the chemist who is more concerned with complex substances and structures.

There is quite obviously a gap here, which the present book, derived from a series of lectures to advanced students at the University of Oxford, sets out to fill. In its conception it follows in the steps of the now rather dated "Seven Solid States" by *W. J. Moore*, which in its time familiarized chemists with basic solid state physics, using suitably chosen compounds as examples.

In the first three chapters of the book, basic concepts such as bonding situations in crystals, the free electron gas and optical processes are treated qualitatively and without giving mathematical derivations, illustrated by appropriate examples. Some spectroscopic techniques are outlined as well, with particular emphasis on photoelectron spectroscopy.

The remaining four chapters deal with special topics. An entire chapter is devoted to a "formal" introduction to energy band theory. The concepts needed for the analysis of band structures are worked through with the help of diagrams, without giving involved mathematical derivations, and are tested on simple examples such as graphite and ReO_3. This is followed by a short account of the experimental determination of band structures using angularly resolved photoemission spectroscopy. Two further chapters deal with electron repulsion effects in terms of the Hubbard model, and with lattice distortions and mixed valency compounds. The final chapter is concerned with semiconductors and their uses in photovoltaic cells, transistors etc.

Altogether the conception of the book and the way in which it has been put together make it a useful addition to the literature. The material is arranged in a clear manner, and the individual sections are lucidly written and illustrated by many well chosen examples. Some of the topics are discussed only briefly, but one cannot expect a book of 250 pages to cover every topic of current research in detail. The material included has been well chosen. The references to more detailed review articles and original papers which are included, with comments, at the end of each chapter give the interested reader easy access to further reading, and a short formula index included at the end of the book helps in locating compounds cited as examples.

In summary, the author *P. A. Cox* has brought considerable skill to the task of familiarizing chemists with the electronic structure of solids. At the very attractive price of £ 12.50 in its paperback edition, the book is certainly a worthwhile and useful aid to advanced students and to synthetic chemists.

Wolfgang Tremel [NB 871 IE]
Anorganisch-chemisches Institut
der Universität Münster (FRG)

Symmetry through the Eyes of a Chemist. By *I. Hargittai* and *M. Hargittai*. VCH Verlagsgesellschaft, Weinheim 1986. xii, 458 pp., bound, DM 156.00.—ISBN 3-527-26409-4

I spent the years 1950–51 in *Linus Pauling*'s group at the California Institute of Technology, which was then one of a mere handful of Meccas for theoretical chemists. Together with *Sidney Weinbaum* of $H_2^{\oplus}$ fame (he was—to my knowledge—the first to use an extended basis in a MO-calculation), I was assigned the task of calculating carbon clusters C_n by the then popular valence bond method. We met our Waterloo as soon as we reached the cubical C_8 cluster, not knowing how to factorize the general eigenvalue problem of order 14 into manageable parts. (Those were still the days of the B.C. era, i.e. before computers, even at Caltech.) There was nothing to be ashamed of, since we were in the best of company in our lack of knowledge. Indeed, even in most books on quantum chemistry written for "real" chemists, group theory was conspicuous by its absence. Even in *Streitwieser*'s classic on MO theory written in 1961, symmetry considerations play at best only a Cinderella role.

The situation has changed dramatically since those days. The enormous growth in the use of physical methods, especially spectroscopy, the wide application of quantum mechanics and of a new chemical language derived from it, and the discussion of reaction mechanisms and stereochemical problems in terms of symmetry, have led to a rapid increase of interest in symmetry and group theory. Chemists changed their outlook and began to collect Escher prints, and publishers started to outbid each other in producing introductions to these new fields. One consequence of this is that there is now scarcely a single library which owns a more than half complete collection of all books relating to this area, ranging from advanced mathematical works to those of a popular scientific type. Every newly published book on this theme must therefore be judged against this background of an overabundance of related literature which already exists.

The first thing which strikes one about the book reviewed here is its exorbitant price: a princely DM 156.—for a book which is presumably intended as an introduction. One might therefore ask why the book is so highly priced, and whether this could not have been avoided. One cause of this is a use of space which could scarcely be rivalled in its extravagance. With an approximate page format of $24\ cm \times 17\ cm = 408\ cm^2$, the print area is only about $21\ cm \times 9\ cm = 189\ cm^2$. Admittedly the extremely wide margin—about double the usual width—is partly used for figure legends, but these generally only contain information on the sources for the figures, e.g. the caption "Photograph by the authors", which is repeated about 40 times. The 421 literature references occupy three times as much space as they would in other books, owing to the very large gaps between individual references, allowing only 15 to a page. In addition the number of examples included is wastefully large, many of them scarcely adding anything to the understanding of the material. Or do you believe that the concept of antisymmetry will be made significantly clearer to a novice by having before him a picture showing a McDonald's adjacent to a more up-market restaurant? ("Photograph by the authors"). Likewise "*Eszter Hargittai* in front of a shop window (1980) ("Photograph by the authors") makes only a minimal contribution to the understanding of mirror symmetry. Altogether one gets the impression that the authors have tried, in their understandable enthusiasm for the subject, to include in this book every quotation related to symmetry which they have collected over the years. As a result there are long sections which are more like a family album of personal recollections than a guide through the subject written with the object of instructing the reader. Further, the information content is sometimes appallingly thinly spread. For example, seven pages are needed to explain what a matrix is and how two matrices are multiplied, and ten pages to discuss the symmetry properties of the HMOs in benzene. *Dietrich Stauffer*, in his excellent and wittily written book "Introduction to Percolation Theory", writes: "You may

complain that the square lattice in Figure 1(a) is not very large, but the publishers did not allow me to fill the remaining pages of this book with these squares, ...". One wishes that the authors of the present book had been given similarly valuable advice by the publishers, so that its length—and presumably its price—could have been reduced without difficulty by at least one third, with no sacrifice of information and with a rather more sensible layout.

When we ask the question for whom this book was written, we find that the potential reader must have a very strange, contradictory make-up. It is evidently assumed that he has no knowledge whatsoever of the most elementary matrix operations, nor has he heard of symmetry or crystallography, let alone of group theory, all of which are nowadays obligatory topics in the first semesters of a chemistry course. Is it then a book for the interested layman? By no means! The reader must not only have mastered the formal language of chemistry in all its subtleties, and have a thorough knowledge of much of stereochemistry, in order to understand the significance of the examples, many of which are quite advanced. In addition, this reader, who has just encountered matrices and the simplest types of symmetry considerations for the first time in his life a few pages earlier, must without any previous experience be able to understand and use the operator formalism of the Schrödinger equation, and—without any detailed explanation—be familiar with all relevant concepts of quantum mechanics and molecular orbital theory. In other words, the book is neither fish nor fowl. For the chemistry student who has not been asleep during the first semesters, and who has obtained his knowledge of physical chemistry from a modern book such as the best-selling "Physical Chemistry" by *P. W. Atkins*, some long sections of this work will seem trivial. For the non-chemist, on the other hand, it assumes far too much knowledge, and it is especially at fault in explaining quite simple points at great length, whereas those steps which present real difficulties for the layman are just glossed over. Admittedly, for the reader who already has the necessary previous knowledge, and is interested in the ramifications of symmetry considerations both within and outside chemistry, the book is a fascinating, if over-priced, mine of information, which deserved to be written in a more concise form. The virtually exhaustive bibliography, and the (over)generous selection of examples mentioned earlier, make the book a welcome and useful work of reference for everyone who is seriously involved in teaching the application of symmetry concepts and has so far neglected those aspects not directly related to chemistry. On the other hand, anyone who has already concerned himself with such ideas will get a definite "déjà vu" feeling throughout large sections of the book. Thus it seems worth mentioning that most of the illustrations from art, biology and other fields can be found, for example, at a cost of only DM 40.—, and partly in color, in the excellent, 466-page first volume of the exhibition catalog "Symmetry in Art, Nature and Science" of the Mathildenhöhe in Darmstadt. (Volumes 2 and 3 contain further examples).

However, the publishers, VCH Verlagsgesellschaft, take the view that this book has been written expressly for students. In fact, the same publishers' German translation ("Physikalische Chemie") of the excellent book by *P. W. Atkins* mentioned earlier contains an unexpected innovation: whereas in the original English version the references given for further reading following the chapter on symmetry are to classic works such as *Hermann Weyl*'s "Symmetrie" and the well-known books by *Jaffe, Orchin*, and by *Cotton*, we now find that all these have been deleted from the German edition and replaced by a full-page advertisement for the book reviewed here!

The following quotation is offered to the authors as consolation: "The writer has collected his material together most diligently, and no discovery of importance which became known during the preparation of the work has been omitted. Our only regret is that he tells us indiscriminately and in immense detail everything which he has learned, and thereby unnecessarily increases the cost of his book."—From the 1831 review of the German translation, still well known even today, of the textbook by *Louis Jacques Thénard* (*Neues Journal der Pharmacie 22* (1831) 276).

Edgar Heilbronner [NB 882 IE]
Physikalisch-chemisches Institut
der Universität Basel (Switzerland)

Lasers in Chemistry. Von *D. L. Andrews*. Springer, Berlin 1986. xii, 176 pp., broschiert, DM 68.00.—ISBN 3-540-16161-9

This book with its just 163 pages may be looked upon as a very compact text addressing both the scientist with general interest and the undergraduate student. It is, however, by no means useless to the more advanced reader. It even impresses the reader by the wealth of laser applications mentioned, ranging out to such specialized topics as ceramic powder formation or cancer therapy by lasers. Its general attitude is very positive with regard to the uses of lasers in chemistry and high hopes for the future are expressed. The diligence and the depth of treatment must be viewed differently for the different chapters.

In chapters 1 and 2 attempts are made to provide an introduction into the physics (18 pages) and into the technology (25 pages) of lasers. Doubts are justified if this is really helpful (e.g. one page on the free electron laser). Perhaps the chemist user would benefit more from a simple table of common commercial lasers and their typical performance data. Such a user-oriented survey is indeed provided on page 164, although in rather short form. The strength of the book in the opinion of the referee lies in chapters 3 (Laser Instrumentation in Chemistry) and 4 (Chemical Spectroscopy with Lasers). Especially chapter 4 gives a fair summary of most of the important laser analytic methods in a systematic way. The treatment ranges from specialized absorption techniques over fluorescence and Raman spectroscopies to multiphoton processes and laser mass spectrometry. In the last chapter (Laser Induced Chemistry), which in the preface is said to be most promising among the different laser applications, the following topics are considered: Infrared multiphoton excitation, isotope separation, unimolecular laser induced and bimolecular laser enhanced reactions and—on three pages—surface chemistry with lasers as well as—also very briefly—psec phenomena. This treatment cannot do justice to the laser or to the field of chemical dynamics as such. Lasers are very special energy sources with their combined properties of coherence, high radiation intensity, ultrashort pulses and extreme monochromaticity. Their potential in chemistry cannot easily be realized by traditional chemical thinking and in the language of preparative chemistry. Besides, it should be mentioned that the main success of laser chemistry at present is not so much in synthetic chemistry than in materials research and processing. This is not adequately cov-

ered in the very short paragraph "laser surface chemistry".

All in all this book presents a laser chemistry survey which can only be recommended to the reader with some reservation.

Karl-Ludwig Kompa [NB 862 IE]
Max-Planck-Institut für Quantenoptik,
Garching (FRG)

Photochemistry in Microheterogeneous Systems. By *K. Kalyanasundaram*. Academic Press, New York 1987. xii, 388 pp., bound, $ 49.95.—ISBN 0-12-394995-5

After the many review articles on photochemical processes in microheterogeneous systems which have appeared recently, but have mainly treated special aspects, a general survey of this extensive field can only be welcomed. Further, in *K. Kalyanasundaram* the publishers have engaged the services of an experienced and competent author for this monograph.

Studies on photoreactions in microheterogeneous systems have generally been motivated by a combination of two factors: firstly, photochemical studies provide a uniquely powerful probe for investigating the static and dynamic properties of microheterogeneous systems, and secondly experiments in an organized reaction medium yield especially valuable information about the mechanism of such photoreactions. These two aspects of the motivation for research in this field also determine the topics covered in the book reviewed here, whose main themes are micellar systems and microemulsions (4 chapters), lipids, vesicles and liposomes, monolayers, lipid membranes and liquid crystalline systems, polymers, polyelectrolytes and ion-exchange membranes, inclusion complexes, and surfaces (one chapter each).

A concise but quite adequate introduction serves to familiarize even non-specialists with the many different types of microheterogeneous systems, with the fundamentals of photochemistry, and with some of the most frequently studied photoreactions. Considerable space (about a third of the book) is devoted to photophysical processes and photoreactions in micelles. The author has himself made many contributions to research on this first topic, and is therefore well able to give a comprehensive and authoritative review. This includes separate chapters on singlet and triplet processes. The next chapter describes reactions of photochemically generated radical pairs, with the main emphasis on cage effects, isotope effects and magnetic field effects, together with fragmentation and cycloaddition reactions. Another chapter deals with photochemical processes and reactions in reverse micelles and microemulsions.

The following chapter describes the special properties of vesicles and liposomes. Here again the author deals in turn with singlet processes, the dynamics of exciplex and excimer formation, and energy and charge transfer phenomena. The subject of the next chapter is highly ordered systems such as monolayers, black lipid membranes and liquid crystals. Particular attention is given to energy and electron transfer processes, isomerizations, dimerizations and photochemical fragmentation processes, and photoreactions of metalloporphyrins. The next chapter deals with polymers in solution, polyelectrolytes and ion exchange membranes; these large topics can only be treated in a selective way here. Here too the main emphasis is on studies of the dynamic properties of the systems.

In contrast to micelles, inclusion compounds, for example, cyclodextrins, zeolites, crown ethers and cryptates have well-defined molecular dimensions. For this reason these systems have also become increasingly important in recent years in investigations of selective photochemical processes. Especially detailed studies have been made on cyclodextrins and zeolites, and these are therefore given most space in this chapter. The final chapter discusses photochemical processes and reactions involving molecules adsorbed on colloidal SiO_2, colloidal clays, silica gel, porous vypor glass, and aluminum oxide surfaces. The distribution and the degree of local organization of the adsorbed species greatly influence the reaction behavior, as does the limited diffusion which occurs in the surface layer. For reasons of space it has not been possible to include heterogeneous photocatalysis and colloidal semiconductor systems.

The book is written in a clear style. Each chapter concludes with a comprehensive bibliography, thus enabling the reader to study topics in greater depth. A further useful feature is that the appendix includes an updated bibliography for work published in 1985. The book can be recommended to anyone seeking a survey of the present situation in this area of research.

Jochen Mattay [NB 878 IE]
Institut für Organische Chemie
der Technischen Hochschule Aachen (FRG)

Registered names, trademarks, etc. used in this journal, even when not marked as such, are not to be considered unprotected by law.

© VCH Verlagsgesellschaft mbH, D-6940 Weinheim, 1988. – Printed in the Federal Republic of Germany by Zechnersche Buchdruckerei, Speyer/Rhein.

All rights reserved (including those of translation into foreign languages). No part of this issue may be be reproduced in any form – by photoprint, microfilm, or any other means – nor transmitted or translated into a machine language without written permission from the publishers. Only single copies of contributions, or parts thereof, may be made for personal use. This journal was carefully produced in all its parts. Nevertheless, authors, editors and publisher do not warrant the information contained therein to be free of errors. Readers are advised to keep in mind that statements, data, illustrations, procedural details or other items may inadvertently be inaccurate.

Valid for users in the USA: The appearance of the code at the bottom of the first page of an article in this journal (serial) indicates the copyright owner's consent that copies of the article may be made for personal or internal use, or for the personal or internal use of specific clients. This consent is given on the condition, however, that the copier pay the stated per-copy fee through the Copyright Clearance Center, Inc., for copying beyond that permitted by Sections 107 or 108 of the U.S. Copyright Law. This consent does not extend to other kinds of copying, such as copying for general distribution, for advertising or promotional purposes, for creating new collective works, or for resale. For copying from back volumes of this journal see 'Permissions to Photo-Copy: Publisher's Fee List' of the CCC.

Editorial office: Pappelallee 3, D-6940 Weinheim, Federal Republic of Germany, Telephone (06201) 602315, Telex 465516 vchwh d, Telefax (06201) 602328.

Editor: *P. Gölitz.*

Associate editors: *D. I. Loewus, A. Stimson.* **Editorial assistant:** *E. Schweikart*

Publishers: VCH Verlagsgesellschaft mbH (Managing Directors: *Prof. Dr. Helmut Grünewald* and *Hans Dirk Köhler*), Pappelallee 3, D-6940 Weinheim, Federal Republic of Germany. Correspondence concerning advertisements should be addressed to VCH Verlagsgesellschaft mbH (Advertising Manager *R. J. Roth*), Boschstr. 12, P.O. Box 1260/1280, D-6940 Weinheim, Federal Republic of Germany, Telephone Weinheim (06201) 602-0, Telex 465516 vchwh d, Telefax (06201) 602328.

ADVANCED MATERIALS

Editorial Advisors: E. M. Engler (USA), D. Haarer (FRG), N. Ogata (Japan), G. Petzow (FRG), J. M. Thomas (UK), G. Wegner (FRG)

Editorial

Modern science and technology rely on specialists. Nevertheless, the complexity of many problems is all too often an obstacle to gaining a deeper understanding of physical and chemical phenomena. In particular, the development of advanced materials and new technologies requires the joint efforts of many specialists from a variety of disciplines. The nature of ceramics, polymers, composites and other new materials is such that successful processing must integrate the individual steps of molecular and microstructural design, engineering, testing and manufacturing. The once common distinction between the product, its function in a system, and the material from which it is made has lost its meaning in a context wherein new materials are created on demand to serve special requirements. This implies that a multidisciplinary team of experts is more likely to be successful in the development and application of advanced materials than are individual researchers working within the limits of their special field.

It is always surprising to see that despite the diversity of all the materials in use and under development, the concepts, phenomena and transformations involved in making and using ceramics, metals, polymers and composites are strikingly similar. Important features are phase equilibria, phase transformation mechanisms, defect structures, flow and fracture mechanisms, structures of crystals and glasses and their relationships, internal boundaries and their contribution to macroscopic behavior, the motion or confinement of charge carriers, the statistical mechanics of assemblies of subsystems; these features not only serve to characterize the individual materials in which they were first studied, but also determine the behavior and performance of other materials which at first sight are totally unrelated.

It is this intellectual relationship between the phenomena that are seen in different materials and between the seemingly distinct features that are found in the same material, which has given birth to *Materials Science* as a discipline in its own right. It is also a meeting place of constituent sciences. One of the most challenging tasks is to provide the link between the thinking of the chemist who considers materials mainly in terms of structure and dynamics on the atomic and molecular scale and the concepts of the physicist whose models are often based on the continuous nature of matter. Moreover, materials science integrates important aspects of engineering in so far as certain properties of materials arise solely from the process of manufacturing owing to the physical and chemical methods of handling. The latter is most obvious in modern polymer materials where the supermolecular structure of the constituent chain molecules is entirely determined by the processing methods.

Recent years have witnessed an unprecedented explosion of new structural materials. Today the pace of technological change due to the availability of more and more specialized high performance materials is rapid. We are only begining to realize the opportunities provided by the new materials. In addition to changing the engineering landscape, advanced structural materials have also altered

Contens

Editorial	723
Editorial Advisors	725
C. Razim	
Advanced Materials—A Critical View	726
H. Möhwald	
Controlling the Microstructure of Monomolecular Layers	728
J. G. Bednorz, K. A. Müller	
Nobel Lecture	735
Conference Reports	
High-T_c Superconductors in Interlaken	749
and Bad Nauheim	751
Conducting Polymers, Polyelectrolytes and Ultrathin Polymer Films in Mainz	752
Research News	753
Book Reviews	754
Conference Calendar	756

traditional policies regarding materials. Historically, national interests in materials have centered around the problem of shortages of supply of certain "critical" ores and minerals. The potential of the new materials such as high performance composites goes far beyond substitution. They provide performance and manufacturing advances which cannot be achieved with traditional metals and they are often the key for new technologies. Therefore, an active governmental role in accelerating the development and commercialization of such materials is seen in all major industrialized countries.

Advanced materials are now ranked together with microelectronics and biotechnology as the most promising "high-tech" industries of the future. With the rise of materials science as a recognizable discipline, many new journals covering different aspects of the field have been founded, all of them publishing either original papers or long, in-depth reviews. In addition, there exist book series, a plethora of monographs and even an encyclopedia for this new discipline. What the materials community is still lacking is a truly international journal that provides stimulating short reviews comprehensible to the many subgroups of the discipline, a journal that presents highlights from the recent original literature, conference reports, book reviews, information about funding programs and materials science institutes, as well as other important news, i.e., all those ingredients that make a journal enjoyable and timely. ADVANCED MATERIALS is intended to serve this purpose.

ADVANCED MATERIALS will appear again in July and regularly every month from September on as a distinct addition to both the German and English versions of ANGEWANDTE CHEMIE, the traditional chemistry journal that caters to all chemistry subdisciplines. This journal has, of course, published excellent materials related short communications and reviews in the past—take the molecular beam epitaxy article in this issue as an example—and this practice will not be changed.

ADVANCED MATERIALS will cover all aspects of materials science, but especially genuine new materials and methods for their preparation, modification and investigation; important theoretical concepts will also be discussed. The following list of topics gives examples only and is not intended to be complete:

Development of new materials such as

- organic low and high molecular weight materials with novel electrical, optical, and magnetic properties
- polymers with unconventional mechanical properties
- liquid crystals
- thin films
- colloids
- fibers
- composites as structural materials
- composites for dielectric and electrical/electronics applications
- inorganic materials with applicationally interesting properties
- amorphous metals
- high temperature ceramics
- superconducting ceramics
- intermetallics
- catalysts
- multicomponent alloys
- glasses
- biomedical materials
- sensor materials

Developments in new methods of preparation and characterization

- surface and interface characterization and engineering
- plasma assisted polymerization, etching etc.
- laser methods
- electrochemical methods
- spectroscopic techniques of characterization
- diffraction methods
- modern microscopy techniques
- modern casting and powder metallurgical techniques
- powder technology
- nondestructive testing techniques
- materials modeling

An interdisciplinary approach will be emphasized in all contributions. The key question is, what does the physicist want to know from the chemist and vice versa, and what do both have to communicate with the materials scientists? ADVANCED MATERIALS is planned to stimulate fruitful discussions and to promote cooperation between scientists from different disciplines.

E. M. Engler, D. Haarer,
N. Ogata, G. Petzow,
J. M. Thomas, G. Wegner

Six editorial advisors (see opposite page), together with Dr. Gölitz, the editor of ANGEWANDTE CHEMIE, and Ligia Dominguez, editorial assistant, will shape ADVANCED MATERIALS. We welcome contributions from all over the world, from academia and from industry, from chemists, physicists and materials scientists, provided they are in keeping with the program outlined in the editorial. Authors who are interested in writing short reviews (up to 15 pages of double-spaced manuscript together with an appropriate number of figures and/or formulas) should contact the editor. Please send all manuscripts and inquiries to:

ADVANCED MATERIALS/ANGEWANDTE CHEMIE
Postfach 1260/1280
D-6940 Weinheim
Federal Republic of Germany

Editorial Advisors

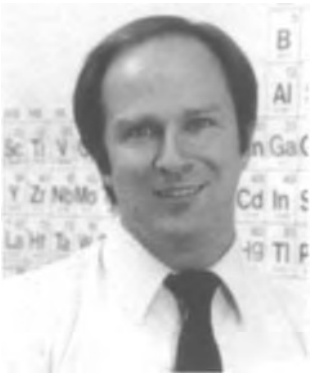

Dr. *Edward M. Engler* is manager of Optical Science and Technology at the IBM Almaden Research Center (650 Harry Road, K32/803D, San Jose, CA 95120-6099, USA). A chemist by training, he received his B.Sc. from Providence College and his Ph.D. from Princeton University. His research has focused on unusual solid-state electronic materials, about which he has published extensively, particularly in the area of organic metals and high temperature superconductors.

Dr. *Naoya Ogata* is Professor of Chemistry at Sophia University, Tokyo (7-1 Kioicho, Chiyoda-ku, Tokyo, Japan). As a chemist he obtained his B.Sc. and his Ph.D. (1961) at Tokyo University. After several postdoctoral years in the USA he started his career at the department of chemistry at Sophia University in 1966. He has written several books and over 250 papers on Langmuir-Blodgett membrane techniques, conducting polymers, and polymeric adsorbents.

Dr. *John M. Thomas*, F.R.S., is Director of the Royal Institution of Great Britain (Davy Faraday Research Laboratory, Royal Institution of Great Britain, 21 Albemarle St., London W1X 4BS, UK). He obtained his Ph.D. in chemistry in 1958 at Queen Mary College in London. After some years as a reader at Bangor, North Wales, he became head of the chemistry department at the University College of Wales in Aberystwyth in 1969. From 1978–1986 he was head of the physical chemistry department at the University of Cambridge. He is author of several books and over 500 papers and his research focusses on the characterization of polycrystalline, quasicrystalline and amorphous solids.

Dr. *Dietrich Haarer* is Professor of Physics at the University of Bayreuth (Lehrstuhl für Experimentalphysik IV, Universitätsstrasse 30, D-8580 Bayreuth, FRG). A physicist by training, he received his Ph.D. in 1969 from the University of Stuttgart. With short interruptions he then worked until 1980 at the IBM research laboratory in San Jose, California, which he left as manager of the Organic Solids Department taking up his current position. His research activities include laser spectroscopy and laser chemistry.

Dr. *Günter Petzow* is Director at the Max Planck Institute for Metals Research in Stuttgart (Max-Planck-Institut für Metallforschung, Institut für Werkstoffwissenschaften, Pulvermetallurgisches Laboratorium, Heisenbergstrasse 5, D-7000 Stuttgart 80, FRG) and a professor at the universities of Stuttgart and Berlin. He studied chemistry and physical metallurgy at the University of Stuttgart and at the Max Planck Institute for Metals Research and received his Ph.D. in 1959. His current research interests are in physical metallurgy, powder metallurgy and ceramics. He has published more than 350 technical papers and four books, and he holds 23 patents.

Dr. *Gerhard Wegner* is Director at the Max Planck Institute for Polymer Research and chemistry professor at the University of Mainz (Max-Planck-Institut für Polymerforschung, Jakob-Welder-Weg 11, D-6500 Mainz, FRG). He obtained his Ph.D. (1965) in chemistry at the University of Mainz. After two postdoctoral years in the USA he started a university career in Mainz. In 1974 he joined the University of Freiburg as professor for polymer chemistry and became Director of the Institute for Macromolecular Chemistry. He has written numerous papers on polymers, especially conducting polymers, and on solid state organic chemistry.

Advanced Materials—a Critical View

By Claus Razim*

Competition in a free market makes ever more exacting demands on all kinds of manufacturers to offer products which are attractive in their performance and price. By using detailed knowledge and experience gained from theoretical and empirical studies, and by the increased application of computer technology in forms such as FEM (finite element methods), CAD (computer aided design), CAM (computer aided manufacturing), data banks, and computer networks, through to the currently much discussed "expert systems" and CIM (computer integrated manufacturing) systems, conventional methods and technologies can be pushed to the full limit of their potential. The urgency of taking advantage of opportunities such as these comes both from economic pressures and from policies on employment.

Further advances, which in many cases open up new markets, can result from increased use of microelectronics, and from putting into practice ideas for new products. Implementing such ideas in many cases gives rise to a desire, or an urgent need, for new materials, further developments of existing materials, or specially treated materials.

In view of this situation, one can understand why a number of countries have intensive research programs on materials science, and why this type of research is emphasized in the media. Although the media reports on modern materials technology are welcome, they are, unfortunately, too often associated with negative side effects. Thus one finds that the media are quite keen to cover aspects of materials technology, but the treatment is often superficial and distorted, owing to well-meaning attempts to present complex facts in a form which can be easily understood. The resulting neglect of scientific and factual consistency confuses the readers, listeners or viewers far more than if they were given a true factual account. In some circumstances this over-simplification can even lead people to draw false conclusions, which may have adverse effects on making special decisions related to work on materials.

For example, the need for progress in developing "revolutionary" materials—e.g., composites, ceramics, and superconductors—is very often emphasized in the media. Even in seriously regarded publications or broadcasts, euphoric reports announce "the end of the iron age", and promote "high tech" as the non-plus-ultra in materials technology. Such one-sided appraisal of unconventional materials developments carries the risk of neglecting the further development of cheap and already familiar conventional materials, which is absolutely essential on overall economic grounds.

The future for materials of very high performance is not restricted to "super-materials", which are certainly very important and which call for intensive efforts to make use of all their potential properties. Equally important is further work on conventional materials and their processing technology. This is made even more urgent by the fact that the relationships between materials properties and treatment processes, and between the properties of a material and the behavior of the components made from it, including their influence on the reliability of the overall assembly, are in many cases not sufficiently known, and have consequently not been formulated in engineering terms.

As an example, Figure 1 shows the remarkably large improvements in fatigue strength which can be obtained in steels through heat and surface treatments. The effects produced by such modifying treatments, and the details of the processes, depend on the type of alloy used, i.e., on its chemical composition, and from a metallurgical standpoint they arise from changes in the microstructure of the material. The ability to produce these changes is the basis for the extremely wide variations that are possible in manufacturing steels with macroscopic properties suited for different engineering uses.

Figure 2 shows the historical development of the different basic types of steels during the last 130 years. From the sigmoid shaped curve found here, which is typical in many different sorts of technological developments, it may be concluded that the development of fundamentally new types of steels is approaching an end! It can be seen that the basic types of steel now known were all developed within a period of about 60 years, and that from 1940 onwards, except for the microalloyed steels, no basically new types of iron alloy materials were "discovered". However, this by no means implies that development has come to a

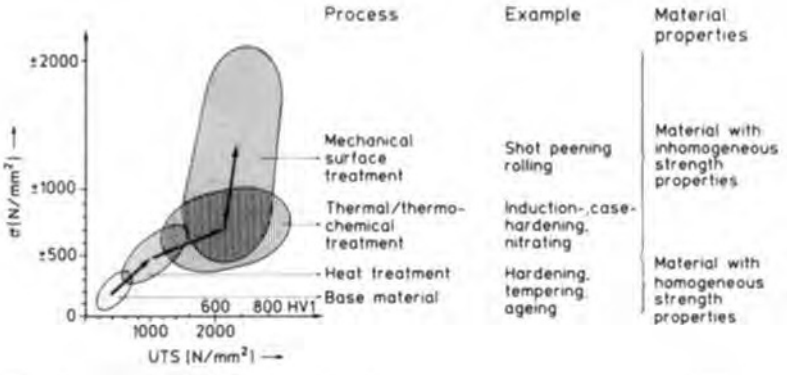

Fig. 1. Improvements in fatigue strength σ of steels by heat and surface treatments. UTS = ultimate tensile strength, HV1 = Vickers hardness.

[*] Prof. Dr.-Ing. C. Razim
Daimler-Benz AG
D-7000 Stuttgart-Untertürkheim (FRG)

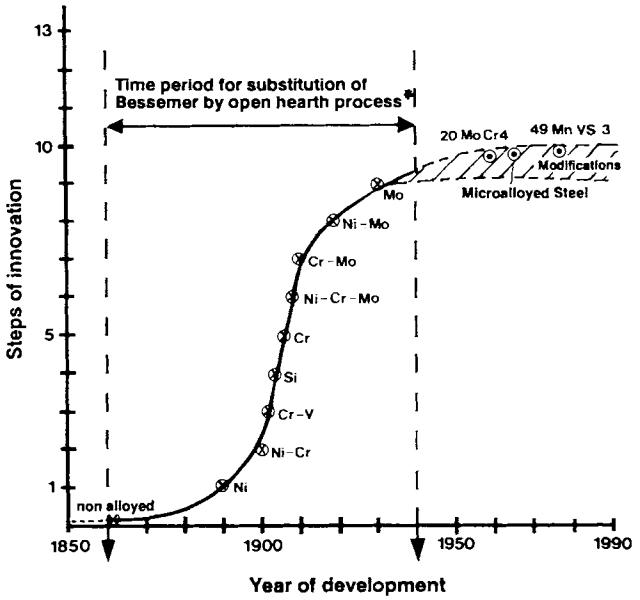

Fig. 2. Steps of development of basic types of steel (*G. H. Robinson*, General Motors Research Center 1980) and use in the automotive industry. *: *C. Marchetti, N. Nakicenovic*, Int. Inst. Appl. Systems Analysis, Laxenburg, Austria 1979.

stop; a wealth of modifications and variations of the known basic types have been developed, bringing about considerable improvements in the performance of these materials.

A remarkably similar development curve, though shifted in time by about 40 years, is found in the case of plastics. Here too, for about the past 15 years, in addition to an intensified use of blending technology, research has been dominated by modifications of already known basic types.

In the application of both the modified old and the new materials, an essential prerequisite is that suitable refined test methods must be developed and made available.

It is only through close interdisciplinary collaboration between chemists, physicists, materials scientists and engineers involved in design and production that new materials and the related treatment technologies for components with desired properties can be developed and successfully introduced into series production.

Irrespective of the choice of particular materials and appropriate treatment methods, the techno-economic aspects of industrial materials technology are of great importance. It is particularly essential to achieve a harmonic optimization of the key parameters of the cost of a material and its behavior during production and use.

Applying these criteria leads to the conclusion that steel and iron, due to their universal suitability, to the relative ease with which their mechanical, corrosion and tribological properties can be varied over a very wide range, and to their generally good processing behavior and ease of working, will continue in the foreseeable future to have great importance in the manufacture of vehicles, machines, and industrial plants. These favorable characteristics are further reinforced by relatively low material costs. An additional factor in favor of these materials, which should not be underestimated, is that of familiarity and long experience.

Depending on the type of application, on needs which are specific to particular business areas, and/or on cost considerations, it may be advantageous or essential to use other materials in place of steel. Those available include the broad palette of non-ferrous metals, ferrous and non-ferrous sintered materials, polymers and composite materials, ceramics, glass, and special materials such as memory metals, amorphous metals and superconductors. However, using materials such as these is not always free of problems, and would be unwise in some cases. For a material to possess just one outstanding property is not generally sufficient in engineering applications; the overall behavior with regard to a range of different properties is usually more important. Here again it may be possible to find solutions through interdisciplinary collaboration of the kind mentioned earlier.

In addition to considerations of function and cost, the choice of materials will become increasingly influenced by ecological factors, waste recycling and conservation of resources, not only for social reasons but equally importantly on economic grounds.

The complexity of the factors involved in finding the "optimal" materials to use in different applications, arising from the numerous aspects which must be considered, indicates a general increase in the importance of materials specialists.

Prof. Dr. Claus Razim, born on March 25, 1930, studied metallurgy at the Technische Universität Berlin and Rheinisch-Westfälische Technische Hochschule Aachen from 1950–1956. He received his Ph.D. from the University of Stuttgart in 1967. After a short employmnet at the Stahlwerke Südwestfalen (1956–1958) he started in 1958 to work for the Daimler-Benz AG in the Central Materials Testing Department. In 1977 he became Head of the Central Materials Department and in 1988 Senior Director of the Research Production Technology Unit. He has authored or co-authored more than 30 publications and received many awards including a Honorary Professorship from the Technische Universität Berlin (1978) and the VDI Gold Metal (1977). Since 1984 he has also been President of the Foundation Institute for Materials Technology in Bremen, FRG, and he is currently President of the International Society for Heat Treatment of Materials.

ADVANCED MATERIALS

Controlling the Microstructure of Monomolecular Layers**

Ultrathin Organic Films
Proteins in Thin Films
Fluorescence Microscopy
X-ray Scattering

By Helmuth Möhwald*

This review reports on the range of lateral structures which have been detected in ultrathin organic films using the newly-developed techniques of fluorescence microscopy and X-ray scattering, together with more conventional methods. A number of unusual low-dimensional ordering processes have been revealed. Hexagonal, lamellar or fractal domain structures are observed and shown to result from an interplay of electrostatic forces due to molecular alignment at interfaces, line energy between different phases and growth kinetics. On a molecular level the microstructure is distinguished by low coherence length of positional order but long coherence length concerning the orientation of crystallographic axes. It is demonstrated that the ideas presented are also relevant to adsorbate structures at interfaces and to the protein arrangement in monolayers.

1. Introduction

In designing a new organic material to perform a given function, it is typically necessary to link many atoms together in the desired spatial arrangement, using well-understood synthetic techniques. For some functions, however, these techniques are not sufficient, as it is also necessary to orient the resulting molecules. A number of different solutions to this problem are known, including crystallization, stretching or extrusion of a loaded polymer, dissolving the functional molecule in a liquid-crystalline matrix, and even the use of lithographically defined nm-sized holes. Here another technique is described, which achieves a very high degree of orientation of densely packed molecules. This technique, involving the principle of self-assembly and orientation of molecules at an interface, was first demonstrated by *Langmuir* and *Blodgett*.[1] It was extensively developed by the elegant work of *Kuhn* and coworkers who demonstrated the feasibility of building molecular machines.[2]

I will show that it is not only possible to design structures consisting of multilayers of ultrathin films with individual thickness of about 2 nm but that the lateral organization of molecules within these films can also be controlled. For this I will concentrate mainly on the monolayer at the air/water interface since the parameters in this system may be varied over a wide range, making it most suitable for understanding the underlying processes. These studies yield insight into new and interesting physics of two dimensions. This was possible by using the novel techniques of fluorescence microscopy and X-ray scattering together with established methods such as film balance and surface potential measurements as well as electron microscopy and spectroscopy. These techniques have become applicable to films as thin as 25 Å mainly due to the development of extremely sensitive TV cameras and of high intensity Synchrotron X-ray sources.

Experimental

Most of the experiments were performed with the phospholipids L-α-dimyristoylphosphatidic acid (DMPA) or L-α-dimyristoylphosphatidylethanolamine (DMPE) (Fluka). Both lipids are highly insoluble in water and form stable monolayers at the air/water interface when spread from solution (3 : 1 chloroform/methanol). The monolayer molecules are oriented, with the hydrophilic head groups pointing towards the water surface and the aliphatic chains towards the air. Varying the subphase ionic conditions by adding NaOH, NaCl (Fluka, p.a.), $CdCl_2$ (Merck), or other divalent ion salts or by binding divalent ions through addition of sodium ethylenediaminetetraacetate (EDTA, Sigma) affects the head group repulsion and thus also alters the microstructure.

As a more simple model compound arachidic acid $CH_3(CH_2)_{18}COOH$ (Fluka) was used. The charge-transfer salt *N*-docosylpyridinium-tetracyanoquinodimethane (Py-TCNQ) was obtained from *A. Barraud, J. Richard, A. Ruaudel-Teixier* and *M. Vandevyver* at Saclay, France; the diacetylenic lipid **1** ("Bronco") was a gift from *H. Ringsdorf*, Mainz. The positively charged surfactant dihexadecyldimethylammonium bromide used for studies of the adsorption of the water soluble disulfonated cyanine dye (Nippon, Kauko, Shikiso, NK 2012) was obtained from *M. Shimomura*, Tokyo, Japan. Concanavalin A (Con A) and dextran were obtained from Sigma. Water was Millipore filtered.

Fluorescence microscopy studies of the monolayer at the air/water interface were performed using a dedicated film balance with an integrated microscope. [3] Contrast is observed in the images leading to Figures 1 and 2 (section 2) since the dye probe NBD-PE **2** (dipalmitoyl-nitrobenzoxadiazolphosphatidylethanolamine) incorporated into the monolayer in a molar con-

[*] Prof. Dr. H. Möhwald
Institut für Physikalische Chemie der Universität
Welder Weg 15, D-6500 Mainz (FRG)

[**] This report is based on the thesis works of my former and present coworkers at the Technische Universität München and Universität Mainz: *M. Flörsheimer, H. D. Göbel, H. Haas, W. M. Heckl, C. A. Helm, S. Kirstein, M. Lösche, A. Miller, R. Steitz* and *P. Tippmann-Krayer*. We enjoyed collaborations with *J. Als-Nielsen, K. Kjaer, W. Knoll, D. Möbius* and *E. Sackmann* and were supported by the Deutsche Forschungsgemeinschaft, Stiftung Volkswagenwerk and the Bundesministerium für Forschung und Technologie. I thank *I. R. Peterson* for critically reading the manuscript.

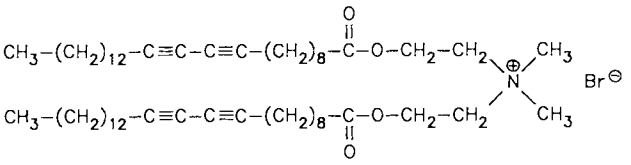

1, Bronco

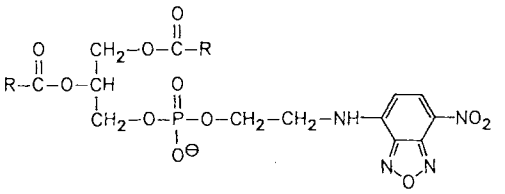

2, R = $(CH_2)_{14}CH_3$

centration below 1% is less soluble in the more ordered phase than in the fluid one. Different solubility in different phases also yields good contrast if a fluorescently labeled protein is used (Fig. 6, section 5). In a third variant of the technique, a water-soluble dye was not incorporated into the main monolayer, but instead formed extensive two-dimensional crystalline layers, or J-aggregates—aggregates of strongly interacting dyes in a coplanar arrangement—adjacent to it and under its influence. These J-aggregates typically had a high fluorescence yield and are shown in Figure 5.

X-ray scattering experiments with monolayers at the air/water interface were performed at the Synchrotron source of HASYLAB, DESY, Hamburg, in collaboration with *K. Kjaer* and *J. Als-Nielsen*, Risø, Denmark. [4-7] For measurements of X-ray diffraction with in-plane wave-vector transfer $Q_{\parallel} = \frac{4\pi}{\lambda} \sin\theta$ ($\lambda = 1.3815$ Å being the wavelength and θ the diffraction angle) the beam enters the surface at glancing incidence. For studies of X-ray reflection (normal wave-vector transfer) as a function of incidence angle α the height of the film balance at the sample stage of the diffractometer is varied. In these experiments the film balance with a pressure measuring system of the *Wilhelmy* type is embedded in a gas-tight housing.

For the electron micrographs, microscope grids were sandwiched between a glass slide and a formvar film, which was coated by vacuum deposition of 100 Å carbon and 50 Å SiO_2. Subsequently, the monolayer was deposited by the Langmuir-Blodgett technique. The observed contrast was due to differential charging of the crystalline and amorphous domains in the Philips EM 400 microscope. [8]

2. Domain Structure at the µm Level

Figure 1 gives a variety of fluorescence microscopic images observed after compression of a monolayer at the air/water interface to achieve a lateral pressure above π_c. The latter is defined from a distinct change in the slope of the isotherm "surface pressure as a function of area per molecule". It corresponds to the onset of the main phase transition of a lipid from a fluid to a more ordered state.[9] The transition is of first order and involves a change in the two-dimensional molecular density by up to 50%. In the denser phase the aliphatic tails are nearly parallel and in the all-*trans* configuration. Thus, the solubility is low for any impurity (e.g., the dye) and the phase appears dark under the fluorescence microscope. It is possible to observe coexistence of phases and to follow domain formation as a function of environmental parameters and time. Until recently, the domain shapes and superstructures presented in Figure 1 were completely unexpected. I will show by qualitative arguments that the periodic structures in Figure 1a, b form due to long-range electrostatic forces, whereas the shapes in Figure 1c, d are kinetically determined.

Electrostatic forces are a peculiar feature of this interfacial system and consist of two contributions: 1. Lipids have dissociable head groups and therefore the monolayer can be charged. The surface charge is counterbalanced either by ions in the subphase (e.g., divalent ions) that strongly bind to the head groups or by ions in the diffuse double layer. Thus, considering long range forces, the monolayer may be viewed as a dipolar sheet. The corresponding dipole moment can be calculated rather satisfactorily on the basis of Gouy-Chapman-Stern theory and varied via pH and ionic milieu.[10-13] 2. A qualitatively similar contribution results from the dipolar nature of the surfactant molecules. As the component of the dipole moment normal to the surface is not compensated due to the partial molecular alignment at the interface a total surface dipole moment results. This contribution is very difficult to assess because a molecule like a phospholipid contains many polar groups and the projection of these groups on the surface normal has to be known. Furthermore, due to the screening by water, the position relative to the water surface is very important. E.g., comparing a polar group above and below the water surface and a change in the dielectric constant from $\varepsilon(\text{water}) \approx 80$ to $\varepsilon(\text{hydrocarbon}) \approx 2$ the contribution of the group under water is reduced by a factor of $\varepsilon^2 \approx 6000$.[13] Therefore this contribution very sensitively depends on the local surface structure.

Despite this difficulty in theoretically quantifying these contributions their sum can be measured rather easily and accurately by surface potential measurements. According

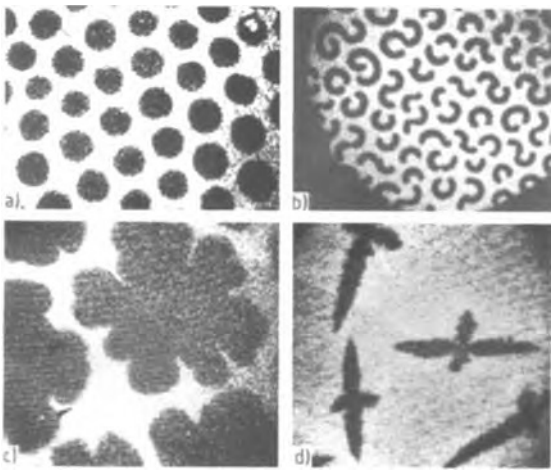

Fig. 1. Fluorescence micrographs of lipid monolayers containing about 1 mol% of the dye NBD-PE **2** in the phase coexistence region of a fluid (bright) and an ordered (dark) phase. The size of an image corresponds to 150 µm. a) DMPA, pH 11.3, 100 mM NaCl, 1 µM $CaCl_2$, $T = 10.5$°C; b) DMPA, 1 mol% cholesterol, pH 11.4, $T = 10$°C; c) DMPA, pH 5.5, $T = 20$°C; d) Bronco after a stepwise pressure increase, pH 5.5, $T = 20$°C.

to the Helmholtz equation the surface potential ΔV and the surface dipole moment are related by

$$\Delta V = \frac{\rho_D}{\varepsilon_0} \quad \text{(a)}$$

$\varepsilon_0 = 8.9 \times 10^{-12}$ C^2 m^{-2} N^{-1} and ρ_D is the dipole density normal to the surface. It is also possible to measure the differences in surface potential of fluid and ordered phases and then to calculate the differences in dipole density. These dipole density differences $\Delta\rho_D$, typically on the order of 100 mDebye nm^{-2} (and due to the difference in molecular density), enter into the calculation of long-range forces. To explain the hexagonal lattice of Figure 1a we have to answer two questions: 1. Why do individual domains repel one another over distances of several 10 μm? 2. Why do these domains exhibit uniform size?

Ad 1: As argued above the condensed phase domain can be considered as a dipolar disc of radius r with dipole moment P given by $P = \pi r^2 \Delta\rho_D$. The repulsive energy of two such discs at a center to center distance d can be estimated as[14]

$$W_{rep} = \frac{1}{4\pi\varepsilon\varepsilon_0 d^3} P^2 \quad \text{(b)}$$

Taking experimental numbers, it is easy to show that W_{rep} is much larger than kT (k = Boltzman const., T = absolute temperature), i.e., the repulsive energy is large enough to overcome any thermal motion.

Ad 2: Usually, for domain sizes above a critical radius r_c, the growth of larger domains is favored at the expense of smaller ones. This is due to the fact that the surface energy per molecule is smaller for a larger domain. The same holds also for a two-dimensional system where changes in surface energy may be ascribed to a line tension in the boundary between the ordered and fluid phases. Uniform domain size in an equilibrium situation therefore requires a force favoring small domains and thus counteracting line tension. Electrostatic forces, being of long range, yield such a contribution, because the energy density of a dipolar disc increases with size due to the dipolar repulsion of the individual molecules. Therefore one expects an equilibrium domain size. The quantitative calculation of the energy density, only logarithmically diverging with r, yields very poor agreement with experiment.[15] Furthermore, the domain dimensions can be varied via nucleation conditions indicating that they are nonequilibrium features.[16] On the other hand, these dimensions can be maintained over hours, and therefore the structure corresponds to a local minimum of free energy.

Hence the most plausible mechanism for formation of hexagonal superstructures is that a certain number of critical nuclei are formed during the initial stages of domain growth. These domains are of uniform size due to identical growth conditions, and they do not split into smaller pieces due to line tension, nor do they fuse due to electrostatic repulsion.

An interesting aspect left for further studies is to determine whether there is an interaction, probably inhibitory, between two growing domains. Electrostatic forces can also be considered to be responsible for formation of elongated domains. In the latter case electrostatic energy would be reduced since the mean distance between interacting molecular dipoles is increased. Elongation, however, requires additional line energy and therefore the balance between these forces determines an equilibrium shape. In the example shown in Figure 1b the electrostatic energy has been increased by increasing the pH (to 11) and reducing the temperature, and the line energy decreased by adding a small amount (1 mol%) of cholesterol.[17, 18] Varying these parameters, one can reversibly change the domain width, which is an apparent equilibrium feature, and induce abrupt changes from lamellar to circular shapes. To understand the spiral shapes one additionally has to take into account molecular chirality.

In many cases domain formation at the air/water interface leads to smooth but irregular shapes that do not become circular even after hours (Fig. 1c). These shapes develop from much more convoluted domains similar to those of Figure 2. The sharpest edges are annealed due to the action of line tension whereas other edges remain.[19] The latter may be due to the presence of impurities which may be enriched in the areas between two protrusions of one domain. This locally reduces line tension, the force responsible for reduction of the domain boundary length.

In special cases one may also observe a pronounced anisotropy of domain morphology which, like in the case of a three-dimensional crystal, reflects the underlying crystallographic lattice.[20] For the case of the diacetylenic lipid Bronco one can show that there is a nearly orthorhombic

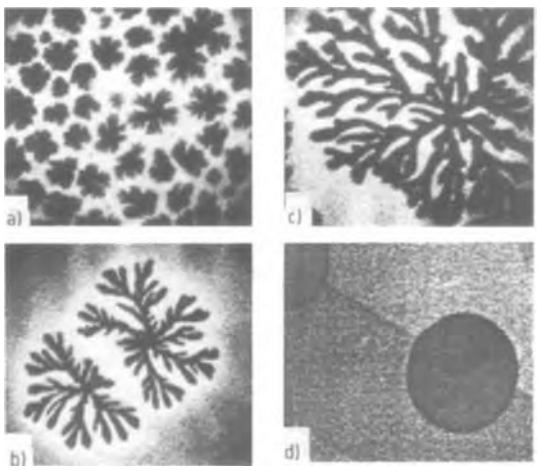

Fig. 2. Fluorescence micrographs of DMPE monolayers containing different concentrations c of a dye probe and at rather fast compression speed (1 Å^2 molecule^{-1} s^{-1}) a) $c = 6$ mol%, b) $c = 1.3$ mol%, c) $c = 0.3$ mol%. The shapes formed at high c do not anneal, whereas they become round at low c; see, e.g., Fig. 2d: $c = 0.7$ mol% after 20 min at constant pressure.

ADVANCED MATERIALS

lattice and that the two axes of preferred growth correspond to diagonals of the unit cell (see Fig. 1d).

These considerations show that the surface morphology strongly depends on growth kinetics, and useful structures may result. Thus it is very important to understand and to control the growth process. One way of doing this is to quickly vary the surface pressure and measure the development of domain size, domain shape, and pressure relaxation. Another possibility is to add impurities, of which the most convenient is the dye probe itself. Via analysis of the images, the impurity distribution can be measured.[19,21]

Typical images at different impurity (dye) concentrations are given in Figure 2. At very low dye concentrations highly convoluted structures are formed (Fig. 2b). These develop within times (<0.1 s) too short to be observed in our experiments. For intermediate dye concentrations (1 mol%) the structures are less intricate but their formation is slow enough to be followed (several seconds, Fig. 2c). For still higher dye concentrations many small domains result, again within very short times (Fig. 2a).

In the intermediate concentration range, where the development of the above mentioned parameters can be measured, the growth kinetics can be described within the framework of constitutional supercooling. During domain growth the impurities are less soluble in the ordered phase and are therefore enriched at the phase boundary.[19] There they reduce the melting temperature and thus inhibit the growth process. For further growth the process is controlled by impurity diffusion away from the interfacial area. The rate of diffusion to a protruding feature will be greater than that to an indentation leading to amplification of any initial roughness and ultimately to a highly folded boundary. Computer simulations on diffusion limited aggregation[22] reveal a self-similar structure with a fractal dimension of $f = 1.5$ in accordance with the value determined by analysis of the images obtained immediately after a pressure jump.[21] f is measured and defined from the equation $M = R^f$, where M is the area of a domain within a radius R about its center. The rounding off at later times (see Fig. 2d) is again due to the influence of line tension. Since the latter is decreased for high impurity concentrations, one understands that structures formed at high dye concentrations never anneal within experimental times. On the other hand, since impurities favor the formation of critical nuclei this could explain the increase in the number of domains with impurity concentrations.

3. Microstructure at the Molecular Level

The variety of domain morphologies presented in Figure 1 is expected to correspond to qualitatively different crystallographic lattice structures. This has indeed been demonstrated in electron diffraction experiments with monolayers on solid supports. The diffraction pattern for a typical phospholipid like DMPE shows a hexagonally symmetric arrangement of rather broad spots and no second order diffraction peak.[12,23] It displays a hexagonal lattice with d_{10} spacings between 4.2 and 4.3 Å typical for vertically oriented aliphatic chains. The local crystallographic axes are parallel within one domain.

In the other extreme when domains with very sharp edges were observed, many narrow diffraction spots with lower than threefold symmetry are encountered. Examples for this are monolayers of the polymerized lipid[24] studied in Figure 1d, of cyanine dyes,[25] and of the Py-TCNQ[26] salt presented in Figure 3. For the latter, electron microscopy shows domains with straight faces and sharp edges. Due to charging by the intense beam applied for diffraction studies, the circular area from which the diffracted intensity was taken could be visualized. The pattern in the insert of Figure 3 shows a variety of spots that are still under more detailed analysis. Apparently in this case the very rigid and well-ordered structure is determined by the extended planar head groups that exhibit no flexibility.

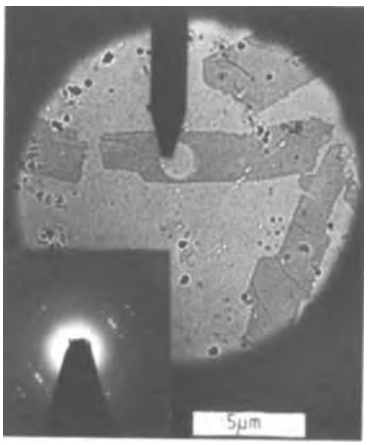

Fig. 3. Electron micrograph and electron diffraction pattern (insert) of a Py-TCNQ bilayer prepared by compression of a monolayer and transferred by the Langmuir-Blodgett technique.

To probe *in situ* the monolayer structure at the air/water interface X-ray diffraction[4,5,7] and reflexion studies[6,7] were performed with different monolayers at various surface pressures, densities, and subphase conditions. As an example, Figure 4 gives data for monolayers of the most frequently studied model compound arachidic acid. Figure 4a gives the intensity as a function of in plane scattering angle on increasing the surface pressure from bottom to top. Considering the variation of intensity and position with surface pressure one clearly observes three different regimes: I: For low surface pressures (high area per molecule, above A_t), the peak position is constant and the intensity increases with pressure. II: For intermediate areas per molecule, $A_s < A < A_t$, the intensity is constant but the position changes. III: Decreasing the area per molecule below A_s, the intensity abruptly increases whereas at higher pressures the line remains virtually unchanged.

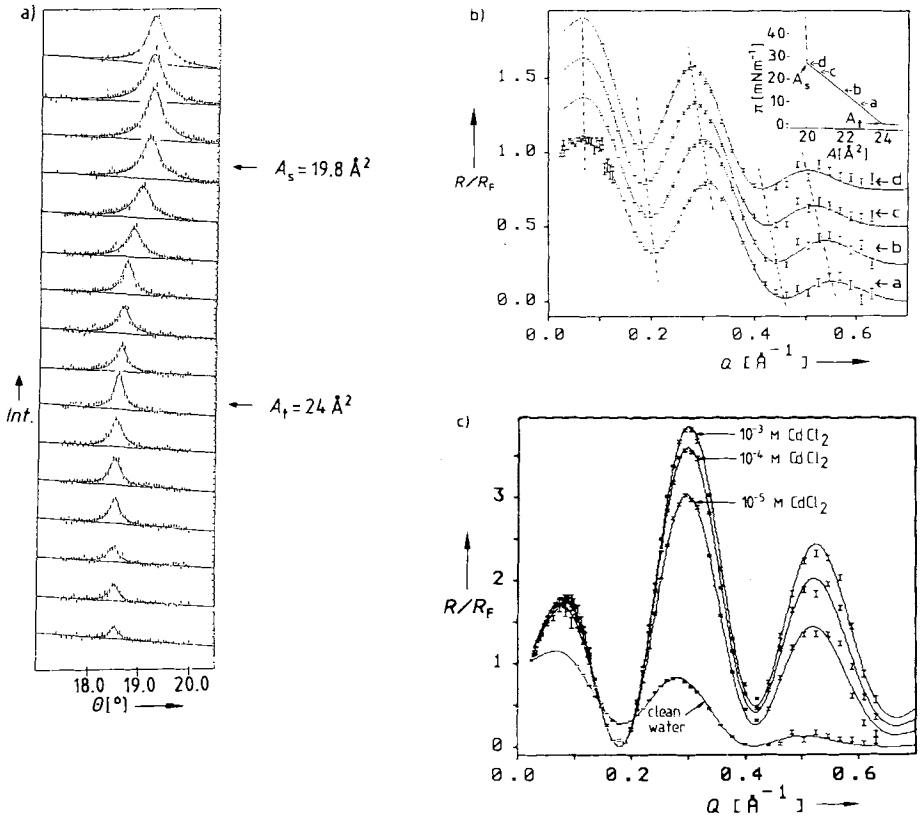

Fig. 4. X-ray scattering data of arachidic acid monolayers at the air/water interface. a) Diffracted intensity as a function of in plane diffraction angle θ for arachidic acid monolayers in the absence of ions and increasing the surface pressure from bottom to top. Indicated are also the areas per molecule A_s, A_t corresponding to breaks in the isotherm slope seen in the insert of b). b) X-ray reflectivity R normalized to the *Fresnel* reflectivity R_F as a function of vertical wave-vector transfer $Q = \frac{4\pi}{\lambda}\sin\alpha$, α being the reflection angle. The lines through the measurement points were obtained from a data fit using the referenced box model. No ions in the subphase, pH 5.5, $T = 20°C$. The measurements are displaced by 0.25 units along the ordinate and correspond to the points indicated on the isotherm in the insert. c) Reflectivity in the absence and presence (concentration indicated) of $CdCl_2$ in the subphase.

These regimes can be correlated with the pressure/area isotherm given in the insert in Figure 4b and interpreted as follows: I corresponds to the coexistence of an expanded disordered with a compressible ordered phase. One measures diffraction of the ordered phase with area fraction decreasing with pressure. Regime II is ascribed to an ordered phase where the structure varies continuously with surface pressure. III is a much less compressible phase normally called the solid phase.[1]

It is especially interesting to study the structural change in regime II in more detail, and this can be done by analysis of X-ray reflection. The reflection intensity R normalized to the value R_F expected for a stepwise density change R_F, as a function of incidence angle α $\left(Q = \frac{4\pi}{\lambda}\sin\alpha\right)$ is given in Figure 4b for various positions along the isotherm. The curves can be simulated using a box model[6,27] where the monolayer consists of two different slabs with defined density and thickness. On the water surface there is the slab containing the head groups (carboxy in this case); it is thus of higher electron density than water. A second slab above the first one contains the hydrocarbon tails and thus exhibits lower electron density. Obviously data have to be analyzed by a sensible combination of simulation and molecular modeling. For a more qualitative approach, however, one may use the fact that the first minimum in the reflectivity curve is due to a destructive interference of reflection at the air/hydrocarbon interface with that from the center of the head groups. The corresponding wave vector Q_{min} is therefore related to the lengths of head group and tail, l_H and l_T, respectively, according to

$$Q_{min} \cdot (l_T + l_{H/2}) = \frac{3}{2}\pi \qquad (c)$$

The shift of the minimum in Figure 4b with surface pressure can therefore be understood as an increase in film thickness. A more detailed analysis shows that within regime II the electron density in the tail region is constant and very high.[28] This demonstrates a uniform alignment of aliphatic tails in the all-*trans* configuration. Comparing the film thickness determined (l_T) with that expected for vertical tail orientation (l_T°) one may calculate the tilt angle φ with respect to the surface normal

$$\cos\varphi = \frac{l_T}{l_T^\circ} \qquad (d)$$

From the reflectivity data one then derives a continuous reduction of the tilt angle from about 30° to 0° in reducing the area per molecule from A_t to A_s. Compression of the monolayer therefore enforces a continuous change of the chain tilt and of the lattice constant.

ADVANCED MATERIALS

To demonstrate the high sensitivity of the X-ray technique to monitor the electron density near the interface Figure 4c compares the X-ray reflectivity measured in the absence and presence of different concentrations of $CdCl_2$ in the subphase for a monolayer in the highly condensed state. One realizes the dramatic influence of the counterion which is almost saturated at the lowest concentration used. This influence is basically due to the increase in electron density in the head group moiety by addition of $1/2\,Cd^{2+}$ per head group.

From a line shape analysis one may derive the positional coherence length. Assuming a grain-like structure one may calculate the grain size L/d from the measured line width Δ according to $L/d = 0.443/\Delta$.

In the example presented above one determines $L/d \approx 100$. This is in marked contrast to the coherence length of crystallographic axes (orientational order) which is larger than $10^5 d$, as determined from electron diffraction[23] and fluorescence polarization data.[29] Similar features were also observed for monolayers of phospholipids[4,5] where in addition a phase transition was found with a drastic change in positional coherence length. Phases with long range positional and short range orientational order are expected theoretically for two-dimensional systems.[30] These calculations also showed the strong influence of trapped impurities on the line shape in accordance with our findings.

4. Structure Formation During Adsorption

The ideas discussed in the preceding sections should not only be valid for surfactant monolayers but more generally for two-dimensional structures at interfaces. An example on this is presented in Figure 5. In a subphase containing a negatively charged dye, it is possible to concentrate the dye near the interface by spreading a positively charged monolayer. If the concentration exceeds the solubility limit the dye crystallizes and in the present example may form brightly fluorescing J-aggregates.[31] Varying the subphase and monolayer conditions various crystal morphologies can be prepared[32] and distinguished by polarization microscopy. On spreading and compressing a monolayer, circular patches of nonoriented aggregates are formed (Fig. 5a). These exhibit dimensions and superstructures similar to those of lipid domains. After some minutes recrystallization becomes observable at the boundary of these domains yielding much brighter linear aggregates (Fig. 5a). On expanding the film the domains disappear and on a second compression the linear aggregates dominate (Fig. c, d). These are of very homogeneous size, which is determined by growth conditions, and repel one another similar to the lamellae of Figure 1. Due to the very high order within these domains sharp electron diffraction spots can be observed.[33]

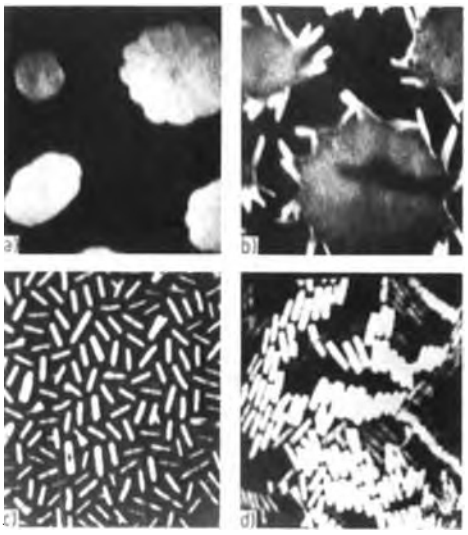

Fig. 5. Fluorescence micrographs of J-aggregates of a water-soluble cyanine dye electrostatically bound to a positively charged monolayer. a) Structure formed immediately after compression and b) about 10 min at a fixed area per molecule. c, d) Second compression with highest molecular density. Different brightnesses are due to the intrinsic polarization of the detection system pH 5.5, $T = 20\,^{\circ}C$, the image size corresponds to 150 μm.

5. Proteins in Thin Films

It has been shown that proteins can be arranged and distributed in a monolayer in a similar way as staining dyes.[34,35] They are generally less soluble in the more condensed phase and therefore concentrated in the fluid environment. This opens new possibilities for increasing local concentrations of reactants and thus to enhance reaction rates. One step further along this line may be to increase protein concentrations at boundaries.

As an example of the latter, Figure 6 presents fluorescence micrographs showing the distribution of fluores-

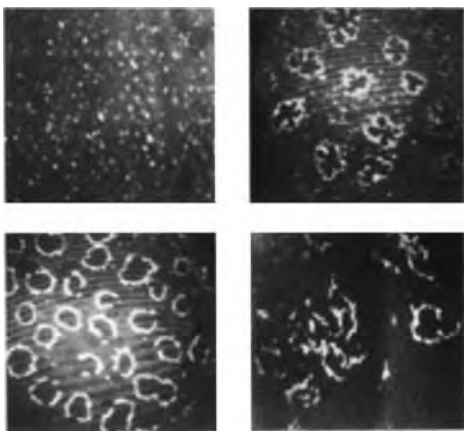

Fig. 6. Fluorescence micrograph of a DMPE monolayer containing aggregated fluorescently labeled Con A. Protein patches already present in the fluid monolayer phase (upper left) are attracted to the fluid/solid domain boundary when the monolayer is in the phase coexistence range (upper right and lower left). On reexpansion the solid (darkest) DMPE domains melt leaving strings of protein (lower right) $T = 20\,^{\circ}C$, pH 7, 100 μM $MnCl_2$, 100 μM $CaCl_2$, 100 mM NaCl.

cently labeled Concanavalin A (Con A) in a DMPE monolayer in the phase coexistence range. One clearly observes the condensed phase DMPE domains (dark) surrounded by a frame of protein patches in those images except in that on the top left where the complete monolayer is fluid. The arrangement of these patches can be understood as follows: According to surface potential data the protein has a normal dipole moment opposite to that of the lipid.[36] Its patches are therefore attracted by the condensed phase domains. Due to the dense packing of the latter, however, they are not incorporated in these domains and therefore remain near the boundary. The protein boundary is a rather loose structure and allows lipid penetration to the interface, since the DMPE domains continue to grow on further compression. On the other hand, on expansion of the monolayer the DMPE domains melt, but the protein patches remain connected to form strings.[37]

6. Concluding Remarks

It is now possible to produce ultrathin films with a periodic arrangement of functional molecules like dyes or proteins. Such control, on an almost molecular level, is a central requirement for any future device fabrication. New ways and physical principles to achieve this were described in this article. Our studies were performed with compounds similar to biological systems. The systems may be considered too artificial by a biologist and too biological by a materials scientist. Nevertheless I tried to demonstrate that part of the ideas presented may be applicable to seemingly different systems like adsorbates or to the fabrication of biosensors requiring oriented arrays of receptor proteins. Beyond that, there are many serious attempts to use this class of organic films for optical, optoelectronic, lubrication, lithographic and other applications, all requiring microstructure control. This report should primarily stimulate more elaborate experimental as well as theoretical studies.

Received: February 11, 1988

[1] G. Gaines: *Insoluble Monolayers at Liquid-Gas Interfaces*, Interscience, New York 1966.
[2] H. Kuhn, D. Möbius, *Angew. Chem. 83* (1971) 672; *Angew. Chem. Int. Ed. Engl. 10* (1979) 620.
[3] M. Lösche, H. Möhwald, *Rev. Sci. Instrum. 55* (1984) 1968.
[4] K. Kjaer, J. Als-Nielsen, C. A. Helm, L. A. Laxhuber, H. Möhwald, *Phys. Rev. Lett. 58* (1987) 2224.
[5] C. A. Helm, H. Möhwald, K. Kjaer, J. Als-Nielsen, *Biophys. J. 52* (1987) 381.
[6] C. A. Helm, H. Möhwald, K. Kjaer, J. Als-Nielsen, *Europhys. Lett. 4* (1987) 697.
[7] K. Kjaer, J. Als-Nielsen, C. A. Helm, P. Tippmann-Krayer, H. Möhwald, *Thin Solid Films*, in press.
[8] A. Fischer, E. Sackmann, *J. Colloid Interface Sci. 112* (1986) 1.
[9] O. Albrecht, H. Gruler, E. Sackmann, *J. Physique 39* (1978) 301.
[10] C. A. Helm, L. A. Laxhuber, M. Lösche, H. Möhwald, *Colloid Polym. Sci. 264* (1986) 46.
[11] A. Miller, C. A. Helm, H. Möhwald, *J. Phys. (Les Ulis, Fr.) 48* (1987) 693.
[12] A. Fischer, E. Sackmann, *J. Phys. (Les Ulis, Fr.) 45* (1984) 517.
[13] D. Andelman, F. Brochard, J.-F. Joanny, *J. Chem. Phys. 86* (1987) 2673.
[14] A. Miller, H. Möhwald, *Europhys. Lett. 2* (1986) 67.
[15] M. Lösche, H.-P. Duwe, H. Möhwald, *J. Colloid Interface Sci.*, in press.
[16] C. A. Helm, H. Möhwald, *J. Phys. Chem.*, in press.
[17] W. M. Heckl, M. Lösche, D. A. Cadenhead, H. Möhwald, *Eur. Biophys. J. 14* (1986) 11.
[18] W. M. Heckl, H. Möhwald, *Ber. Bunsenges. Phys. Chem. 90* (1986) 1159.
[19] A. Miller, H. Möhwald, *J. Chem. Phys. 86* (1987) 4258.
[20] H. D. Göbel, H. E. Gaub, H. Möhwald, *Chem. Phys. Lett. 138* (1987) 441.
[21] A. Miller, W. Knoll, H. Möhwald, *Phys. Rev. Lett. 56* (1986) 2311.
[22] J. Nittman, H. E. Stanley, *Nature (London) 321* (1986) 663.
[23] A. Fischer, M. Lösche, H. Möhwald, E. Sackmann, *J. Phys. Lett. 45* (1984) 785.
[24] H. D. Göbel, H. Möhwald, *Thin Solid Films*, in press.
[25] C. Duschl, W. Frey, W. Knoll, *Thin Solid Films*, in press.
[26] A. Barraud, M. Flörsheimer, H. Möhwald, J. Richard, A. Ruaudel-Teixier, M. Vandevyver, *J. Colloid Interface Sci.*, in press.
[27] J. Als-Nielsen in W. Schommers, P. Blanckenhagen (Eds.): *Structure and Dynamics of Surfaces. Vol. 2*, Springer, Berlin 1986, Chapter 5.
[28] K. Kjaer, J. Als-Nielsen, C. A. Helm, P. Tippmann-Krayer, H. Möhwald, unpublished.
[29] V. T. Moy, D. Keller, H. E. Gaub, H. M. McConnell, *J. Phys. Chem. 90* (1986) 3198.
[30] D. R. Nelson, M. Rubinstein, F. Spaepen, *Phil. Magn. A 46* (1982) 105.
[31] M. Shimomura, T. Kunitake, *J. Am. Chem. Soc. 109* (1987) 5175.
[32] S. Kirstein, *Diplomarbeit*, Technische Universität München 1988.
[33] R. Steitz, *Diplomarbeit*, Universität Mainz 1988.
[34] W. M. Heckl, H. Möhwald, *J. Mol. Electron. 3* (1987) 67.
[35] J. Peschke, H. Möhwald, *Colloids Surf. 27* (1987) 305.
[36] W. M. Heckl, M. Thompson, H. Möhwald, *J. Am. Chem. Soc. 110* (1988), in press.
[37] H. Haas, *Diplomarbeit*, Universität Mainz 1988.

Last minute information:

EUROPEAN SYMPOSIUM ON ADVANCED MATERIALS; THEIR ROLE IN NEW TECHNOLOGIES

MADRID, Congress Center
June 27–29, 1988

Main topics: Semiconductors, Opto-electronics, Ceramic and other Sensor Materials, Magnetic Materials, Superconductivity, Molecular Electronics, Artificially Structured Materials, Composite Materials, Surfaces and Interfaces, Micro Nondestructive Evaluation.
The symposium will be a joint discussion between industry and university researchers. It will be linked directly to the research program of the European Institute of Technology (EIT) in materials science. It is expected that the initial EIT grants under this program to universities and public laboratories will be announced during the symposium.
This symposium will be hosted by AT&T Microelectrónica de España.
The EIT is a major new industrial consortium for scientific and engineering research and education. Founding Members of EIT are: Montedison, Philips, IBM Europe, AT&T and ENICHEM.
For all further information, please contact:

EUROPEAN INSTITUTE OF TECHNOLOGY
TOUR FRANKLIN - CEDEX 11 · 92081 PARIS LA DEFENSE · Tel.: (33)-(1)-49032222

ADVANCED MATERIALS

Perovskite-Type Oxides—the New Approach to High-T_c Superconductivity**

Nobel Lecture

By J. Georg Bednorz* and K. Alex Müller*

Part 1: The Early Work in Rüschlikon

In our lecture, we take the opportunity to describe the guiding ideas and our effort in the search for high-T_c superconductivity. They directed the way from the cubic niobium-containing alloys to layered copper-containing oxides of perovskite-type structure. We shall also throw some light onto the circumstances and the environment which made this breakthrough possible. In the second part, properties of the new superconductors are described.

The Background

At IBM's Zürich Research Laboratory, there had been a tradition of more than two decades of research efforts in insulating oxides. The key materials under investigation were perovskites like $SrTiO_3$ and $LaAlO_3$, used as model crystals to study structural and ferroelectric phase transitions. The pioneering ESR experiments by *Alex Müller (KAM)*[1.1] and *W. Berlinger* on transition-metal impurities in the perovskite host lattice brought substantial insight into the local symmetry of these crystals, i.e., the rotations of the TiO_6 octahedra, the characteristic building units of the lattice.

One of us *(KAM)* first became aware of the possibility of high-temperature superconductivity in the 100 K range from the calculations of *T. Schneider* and *E. Stoll* on metallic hydrogen.[1.2] Such a hydrogen state was estimated to be in the 2-3 Mbar range. Subsequent discussions with *T. Schneider* on the possibility of incorporating sufficient hydrogen into a high-dielectric-constant material like $SrTiO_3$ to induce a metallic state led, however, to the conclusion that the density required could not be reached.

While working on my Ph.D. thesis at the Solid State Physics Laboratory of the ETH Zurich, I *(JGB)* gained my first experience in low-temperature experiments by studying the structural and ferroelectric properties of perovskite solid-solution crystals. It was fascinating to learn about the large variety of properties of these materials and how one could change them by varying their compositions. The key material, pure $SrTiO_3$, could even be turned into a superconductor if it were reduced, i.e., if oxygen were partially removed from its lattice.[1.3] The transition temperature of 0.3 K, however, was too low to cause much excitement in the world of superconductivity research. Nevertheless, it was interesting that superconductivity occurred at all, because the carrier densities were so low compared to superconducting NbO, which has carrier densities like a normal metal.

My (*JGB*'s) personal interest in the fascinating phenomenon of superconductivity was triggered in 1978 by a telephone call from *Heinrich Rohrer*, the manager of a new arrival at IBM Rüschlikon, *Gerd Binnig*. With his background in superconductivity and tunneling, *Gerd* was interested in studying the superconductive properties of $SrTiO_3$, especially in the case when the carrier density in the system was increased. For me (*JGB*), this was the start of a short but stimulating collaboration, as within a few days I was able to provide the IBM group with Nb-doped single crystals which had an enhanced carrier density compared to the simply reduced material. The increase in T_c was exciting for us. In the Nb-doped samples ($n = 2 \times 10^{20}$ cm^{-3}) the plasma edge lies below the highest optical phonon, which is therefore unshielded.[1.4] The enhanced electron–phonon coupling led to a T_c of 0.7 K.[1.5] By further increasing the dopant concentration, the T_c even rose to 1.2 K, but this turned out to be the *limit*, because the plasma edge passes the highest phonon. *Gerd* then lost his interest in this project, and with deep disappointment I realized that he had started to develop what was called a scanning tunneling microscope (STM). However, for *Gerd* and *Heinrich Rohrer*, it turned out to be a good decision, as everyone realized by 1986 at the latest, when they were awarded the Nobel Prize in Physics. For my part, I concentrated on my thesis.

It was in 1978 that *Alex (KAM)*, my second supervisor, took an 18-month sabbatical at IBM's T. J. Watson Research Center in Yorktown Heights, NY, where he started working in the field of superconductivity. After his return in 1980, he also taught an introductory course at the University of Zürich. His special interest was the field of granular superconductivity, an example being aluminum,[1.6]

[*] Dr. J. G. Bednorz, Prof. Dr. K. A. Müller
IBM Research Division
Zürich Research Laboratory
Säumerstrasse 4, CH-8803 Rüschlikon (Switzerland)

[**] Copyright © The Nobel Foundation 1988.—We thank the Nobel Foundation, Stockholm, for permission to print this article.

where small metallic grains are surrounded by oxide layers acting as Josephson junctions. In granular systems, the T_c's were higher, up to 2.8 K, as compared to pure Al with $T_c = 1.1$ K.

Involvement with the Problem

It was in the fall of 1983 that *Alex*, heading his IBM Fellow group, approached me and asked whether I would be interested in collaborating in the search for superconductivity in oxides. Without hesitation, I immediately agreed. *Alex* later told me he had been surprised that he had hardly needed to use any arguments to convince me; of course, it was the result of the short episode of my activities in connection with the superconducting $SrTiO_3$—he was knocking a door already open. And indeed, for somebody not directly involved in pushing T_c's to the limit and having a background in the physics of oxides, casual observation of the development of the increase of superconducting transition temperatures, shown in Figure 1.1, would naturally lead to the conviction that intermetallic compounds should not be pursued any further, as the highest T_c had remained since 1973 at 23.3 K.[1.7] But nevertheless, the fact that superconductivity had been observed in several complex oxides evoked our special interest.

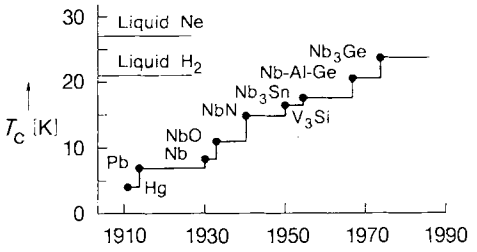

Fig. 1.1. Development of superconducting transition temperatures after the discovery of the phenomenon in 1911. The materials named are metals or intermetallic compounds and gave the highest T_c's at the time.

The second oxide after $SrTiO_3$ to exhibit surprisingly high T_c's of 13 K was discovered in the Li-Ti-O system by *Johnston* et al.[1.8] in 1973. Their multiphase samples contained a $Li_{1+x}Ti_{2-x}O_4$ spinel responsible for the high T_c. Owing to the presence of different phases and difficulties in preparation, the general interest remained low, especially as in 1975 *Sleight* et al.[1.9] discovered the $BaPb_{1-x}Bi_xO_3$ perovskite also exhibiting a T_c of 13 K. This compound could easily be prepared as a single phase and even thin films for device applications could be grown, a fact that triggered increased activities in the United States and Japan. According to the BCS theory[1.10] which gives

$$k \times T_c = 1.13 \hbar \omega_D e^{-1/(N(E_F)) \times V^*}$$

both mixed-valent oxides, having a low carrier density $n = 4 \times 10^{21}$ cm^{-3} and a comparatively low density of states per unit cell $N(E_F)$ at the Fermi level, should have a large electron-phonon coupling constant, leading to the high T_c's. Subsequently, attempts were made to raise the T_c in the perovskite by increasing $N(E_F)$ via changing the Pb : Bi ratio, but the compound underwent a metal-insulator transition with a different structure, and thus all attempts failed.

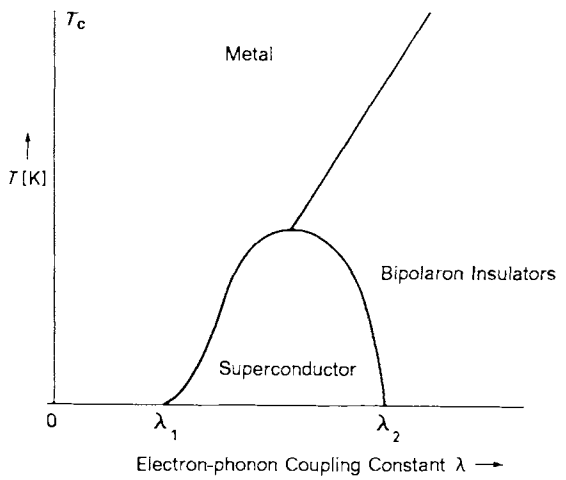

Fig. 1.2. Phase diagram as a function of electron-phonon coupling strength (adapted from [1.11]).

We in Rüschlikon took up this challenge, as we expected other metallic oxides to exist where even higher T_c's could be reached by increasing $N(E_F)$ and/or the electron-phonon coupling. Possibly we could enhance the latter by polaron formation as proposed theoretically by *Chakraverty*[1.11] or by the introduction of mixed valencies. The intuitive phase diagram of the coupling constant $\lambda = N(E_F) \times V^*$ versus T proposed by *Chakraverty* for polaronic contributions is shown in Figure 1.2. There are three phases, a metallic one for small λ and an insulating bipolaronic one for large λ, with a superconductive phase between them, i.e., a metal-insulator transition occurs for large λ. For intermediate λ, a high-T_c superconductor might be expected. The question was, in which systems to look for superconductive transitions.

The Concept

The guiding idea in developing the concept was influenced by the Jahn-Teller (JT) polaron model, as studied in a linear chain model for narrow-band intermetallic compounds by *Höck* et al.[1.12] The Jahn-Teller (JT) theorem is well known in the chemistry of complex states. A nonlinear molecule or a molecular complex exhibiting an electronic degeneracy will spontaneously distort to remove or reduce this degeneracy. Complexes containing specific transition metal (TM) central ions with special valency show this effect. In the linear chain model,[1.12] for small JT distortions with a stabilization energy E_{JT} smaller than the bandwidth of the metal, only a slight perturbation of the

ADVANCED MATERIALS

traveling electrons is present. With increasing E_{JT}, the tendency to localization is enhanced, and for the case where E_{JT} is comparable with the bandwidth, the formation of JT polarons was postulated.

These composites of an electron and a surrounding lattice distortion with a high effective mass can travel through the lattice as a whole, and a strong electron-phonon coupling exists. In our opinion, this model could fit the Chakraverty phase diagram perfectly. Based on the experience from studies of isolated JT ions in the perovskite insulators, our assumption was that the model would also apply to the oxides, our field of expertise, if they could be turned into conductors. We knew there were many of them. Oxides containing TM ions with partially filled e_g orbitals, like Ni^{3+}, Fe^{4+} or Cu^{2+} exhibit a strong JT effect (Fig. 1.3), and we considered these as possible candidates for new superconductors.

Copper Ions in the Oxide Octahedron

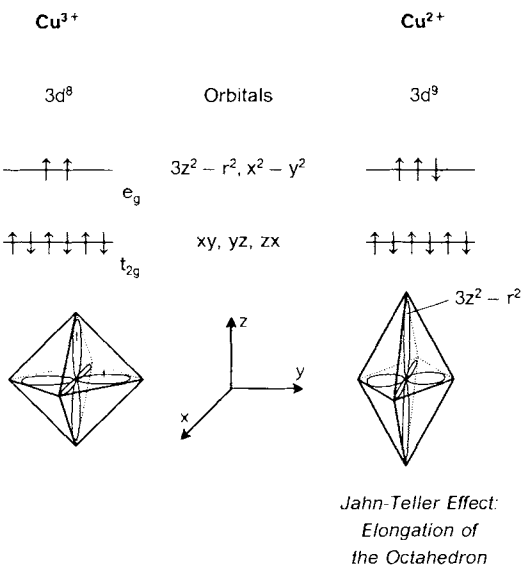

Fig. 1.3. Schematic representation of electron orbitals for octahedrally coordinated copper ions in oxides. For Cu^{3+} with $3d^8$ configuration, the orbitals transforming as base functions of the cubic e_g group are half-filled, thus a singlet ground state is formed. In the presence of Cu^{2+} with $3d^9$ configuration, the ground state is degenerate, and a spontaneous distortion of the octahedron occurs to remove this degeneracy. This is known as the Jahn-Teller effect.

The Search and Breakthrough

We started the search for high-T_c superconductivity in late summer 1983 with the La-Ni-O system. $LaNiO_3$ is a metallic conductor with the transfer energy of the JT-e_g electrons larger than the JT stabilization energy, and thus the JT distortion of the oxygen octahedra surrounding the Ni^{3+} is suppressed.[1,13] However, even the preparation of the pure compound brought some surprises, as the material obtained by our standard co-precipitation method[1,14] and subsequent solid-state reaction turned out to be sensitive not only to the chemicals involved[1,15] but also to the reaction temperatures. Having overcome all difficulties with the pure compound, we started to partially replace Ni^{3+} by Al^{3+} to reduce the metallic bandwidth of the Ni^{3+} ions and make it comparable to the Ni^{3+} Jahn-Teller stabilization energy. With increasing Al^{3+} concentration, the metallic characteristics (see Fig. 1.4) of the pure $LaNiO_3$ gradually changed, first to give a general increase in the resistivity and finally with high substitution leading to a semiconducting behavior with a transition to localization at low temperatures. The idea did not seem to work out the way we had thought, so we considered the introduction of some internal strain within the $LaNiO_3$ lattice to reduce the bandwidth. We achieved this through replacing the La^{3+} ion by the smaller Y^{3+} ion, keeping the Ni^{3+} site unaffected. The resistance behavior changed in a way we had already observed in the previous case, and at that point we started wondering whether the target at which we were aiming really did exist. Would the path we decided to embark upon finally lead into a blind alley?

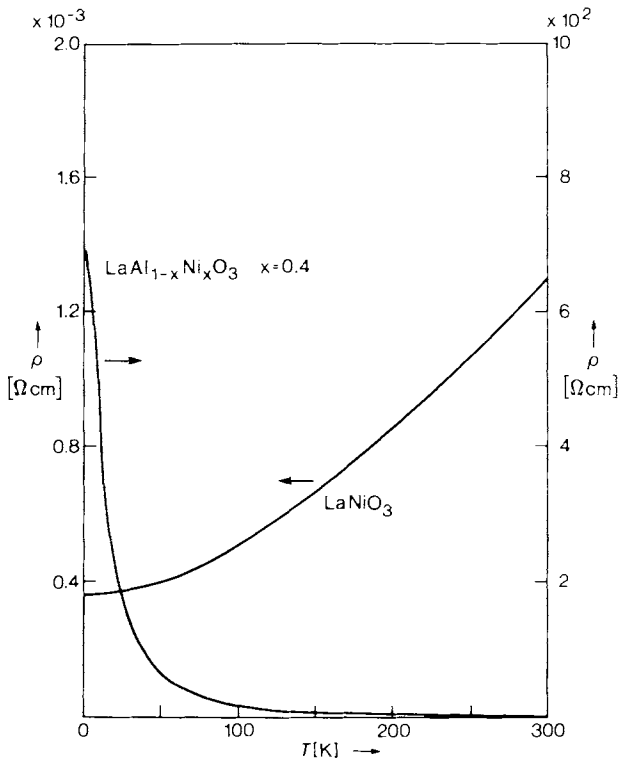

Fig. 1.4. Temperature dependence of the resistivity for metallic $LaNiO_3$ and $LaAl_{1-x}Ni_xO_3$, where substitution of Ni^{3+} by Al^{3+} leads to insulating behavior for $x = 0.4$.

It was in 1985 that the project entered this critical phase, and it probably only survived because the experimental situation, which had generally hampered our efforts, was improved. The period of sharing another group's

equipment for resistivity measurements came to an end as our colleague, *Pierre Guéret*, agreed to my established right to use a newly set up automatic system. Thus, the measuring time was transferred from late evening to normal working hours. *Toni Schneider*, at that time acting manager of the Physics department, supported the plans to improve the obsolete X-ray analytical equipment to simplify systematic phase analysis, and in addition we had some hopes in our new idea, involving another TM element encountered in our search, namely copper. In a new series of compounds, partial replacement of the JT Ni^{3+} by the non-JT Cu^{3+} increased the absolute value of the resistance, although the metallic character of the solid solutions was preserved down to 4 K.[1.13] But again, we found no evidence of superconductivity. The time to study the literature and reflect on the past had arrived.

It was in late 1985 that the turning point was reached. I became aware of an article by the French scientists *C. Michel, L. Er-Rakho* and *B. Raveau*, who had investigated a Ba-La-Cu oxide with perovskite structure exhibiting metallic conductivity between 300 and $-100\,^{\circ}C$.[1.16] That group studied the catalytic properties of oxygen-deficient compounds at elevated temperatures.[1.17] In the Ba-La-Cu oxide with a perovskite-type structure containing Cu in two different valencies, all our concept requirements seemed to be fulfilled.

I immediately went to the ground-floor laboratory and started preparations for a series of solid solutions, since by varying the Ba : La ratio one would have a sensitive tool to continuously tune the mixed valency of copper. Within one day the synthesis was complete, but the measurement had to be postponed, owing to the announcement of the visit of Dr. *Ralph Gomory*, our Director of Research. These visits always kept people occupied for a while, preparing their presentations.

Having lived through this important visit, and returning from an extended vacation in mid-January 1986, I recalled that when reading about the Ba-La-Cu oxide, it had intuitively attracted my attention. I decided to resume my measurements on the new compound. When performing the four-point resistivity measurement, the temperature dependence did not seem to be anything special when compared with the dozens of samples measured earlier. During cooling, however, a metallic-like decrease was first observed, followed by an increase at low temperatures, indicating a transition to localization. My inner tension, always increasing as the temperature approached the 30 K range, started to be released when a sudden resistivity drop of 50% occurred at 11 K. Was this the first indication of superconductivity?

Alex and I were really excited, as repeated measurements showed perfect reproducibility and an error could be ruled out. Compositions as well as the thermal treatment were varied, and within two weeks we were able to shift the onset of the resistivity drop to 35 K (Fig. 1.5). This was an incredibly high value compared to the highest T_c in the Nb_3Ge superconductor.

We knew that in the past there had been numerous reports on high-T_c superconductivity, which had turned out to be non-irreproducible;[1.7] therefore before to the publishing of our results, we asked ourselves critical questions about its origin. A metal-to-metal transition, for example, was unlikely, owing to the fact that with increasing measuring current the onset of the resistivity drop was shifted to

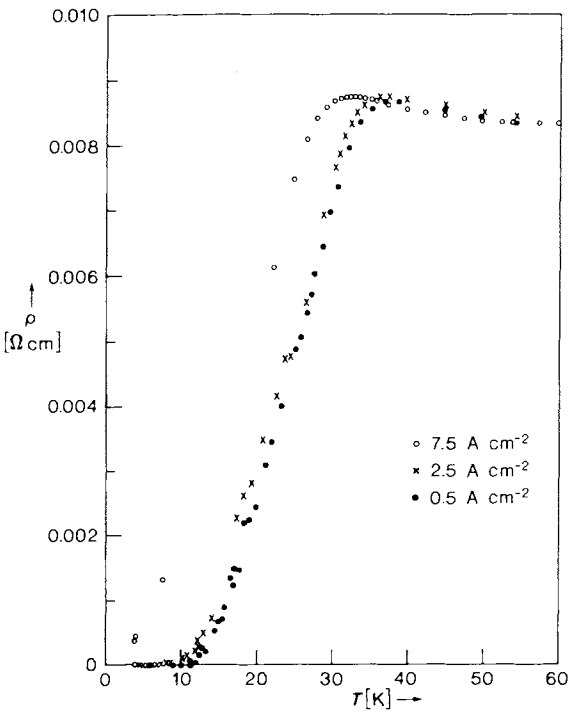

Fig. 1.5. Low-temperature resistivity of a sample with $x(Ba)=0.75$, recorded for different current densities (adapted from [1.19]).

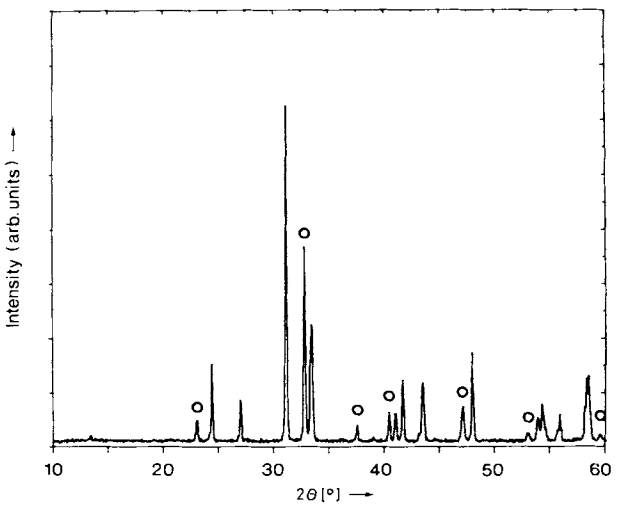

Fig. 1.6. X-ray diffraction pattern of a two-phase sample with Ba : La = 0.08. The second phase occurring together with the K_2NiF_4-type phase is indicated by open circles (adapted from [1.20]).

ADVANCED MATERIALS

lower temperatures. On the other hand, this behavior supported our interpretation that the drop in $\rho(T)$ was related to the onset of superconductivity in granular materials. These are, for example, polycrystalline films of $BaPb_{1-x}Bi_xO_3$[1.18] exhibiting grain boundaries, or different crystallographic phases with interpenetrating grains as in the Li-Ti oxide.[1.7] Indeed, X-ray diffraction patterns of our samples revealed the presence of at least two different phases (see Fig. 1.6). Although we started the preparation process of the material with the same cation ratios as the French group, the wet-chemical process did not lead to the same result. This later turned out to be a stroke of luck, in the sense that the compound we wanted to form was not superconducting. The dominating phase could be identified as having a layered perovskite-like structure of K_2NiF_4-type as seen from Figure 1.7. The diffraction lines of the second phase resembled those of an oxygen-deficient perovskite with a three-dimensionally connected network of octahedra. In both structures, La was partially replaced by Ba, as we learned from an electron microprobe analysis which Dr. *Jürg Sommerauer* at the ETH Zürich performed for us as a favor. However, the question was "which is the compound where the mixed valency of the copper leads to the superconductive transition?"

We had difficulties in finding a conclusive answer at the time; however, we rated the importance of our discovery so high that we decided to publish our findings, despite the fact that we had not yet been able to perform magnetic measurements to show the presence of the Meissner-Ochsenfeld effect. Thus, our report was cautiously entitled "Possible High T_c Superconductivity in the Ba-La-Cu-O System".[1.19] We approached *Eric Courtens*, my manager at the time, who in late 1985 had already strongly supported our request to purchase a dc SQUID magnetometer, and who is on the editorial board of *Zeitschrift für Physik*. In this capacity, we solicited his help to receive and submit the paper, although, admittedly, it did involve some gentle persuasion on our part!

Alex and I then decided to ask Dr. *Masaaki Takashige* whether he would be interested in our project. Dr. *Takashige*, a visiting scientist from Japan, had joined our Laboratory in February 1986 for one year. He was attached to *Alex*'s Fellowship group, and I had given him some support in pursuing his activities in the field of amorphous oxides. As he was sharing my office, I was able to judge his reaction, and noted how his careful sceptical comments changed to supporting conviction while we were discussing the results. We had found our first ally.

Following this, while awaiting delivery of the magnetometer, we tried hard to identify the superconducting

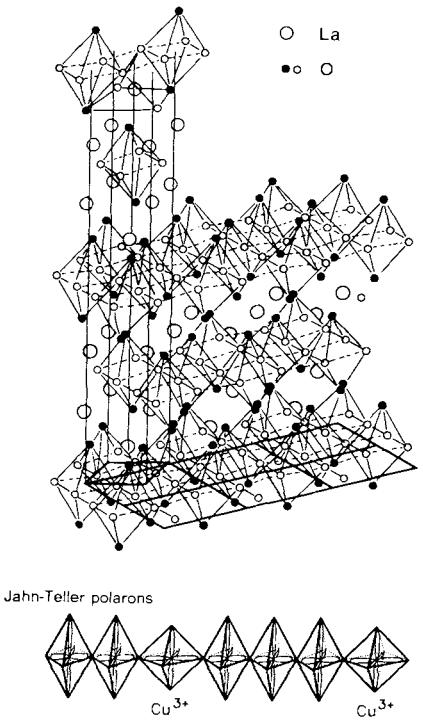

Fig. 1.7. Top: Structure of the orthorhombic La_2CuO_4. Large open circles represent the lanthanum ions, small open and filled circles the oxygen ions. The copper ions (not shown) are centered in the oxygen octahedra (from [1.29], © American Association for the Advancement of Science, 1987). Bottom: It is schematically shown how, in a linear chain, substitution of trivalent La by a divalent alkaline-earth element would lead to a symmetric change of the oxygen polyhedra in the presence of Cu^{3+}.

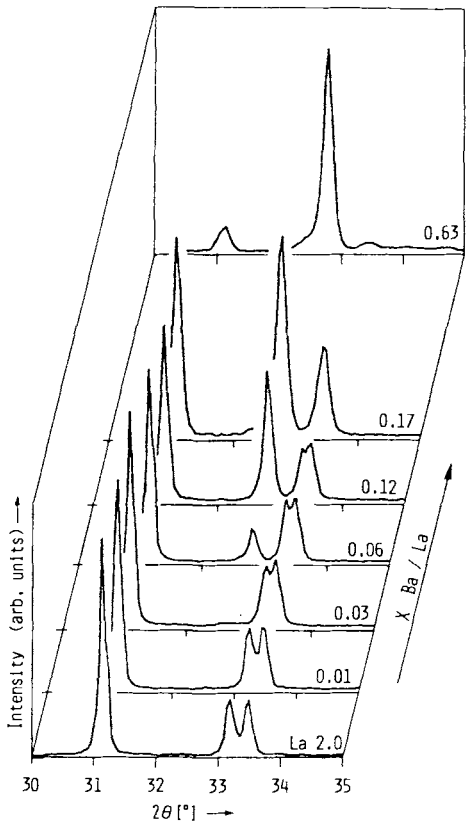

Fig. 1.8. Characteristic part of the X-ray diffraction pattern, showing the orthorhombic-to-tetragonal structural phase transition with increasing Ba : La ratio. Concentration axis not to scale (adapted from [1.20]).

phase by systematically changing the composition and measuring the lattice parameters and electrical properties. We found strong indications that the Ba-containing La_2CuO_4 was the phase responsible for the superconducting transition in our samples. Starting from the orthorhombically distorted host lattice, increasing the Ba substitution led to a continuous variation of the lattice towards a tetragonal unit cell[1.20] (see Fig. 1.8). The highest T_c's were obtained with a Ba concentration close to this transition (Fig. 1.9), whereas when the perovskite phase became dominant, the transition was suppressed and the samples showed only metallic characteristics.

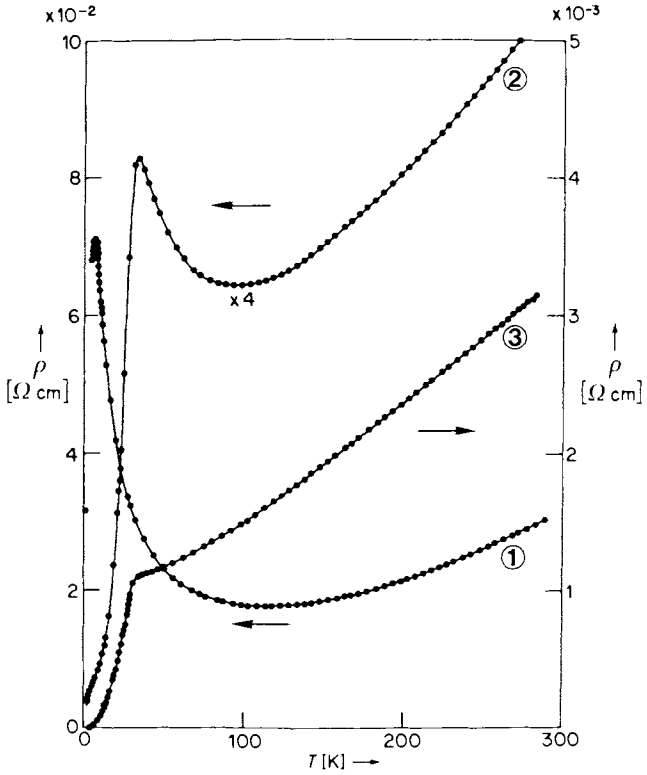

Fig. 1.9. Resistivity as a function of temperature for La_2CuO_{4-y} : Ba samples with three different Ba : La ratios. Curves ①, ②, and ③ correspond to ratios of 0.03, 0.06, and 0.07, respectively (adapted from [1.20]).

Finally, in September 1986, the susceptometer had been set up and we were all ready to run the magnetic measurements. To ensure that with the new magnetometer we did not measure any false results, *Masaaki* and I decided to gain experience on a known superconductor such as lead rather than starting on our samples. The Ba-La-Cu oxide we measured first had a low Ba content, where metallic behavior had been measured down to 100 K and a transition to localization occurred at lower temperatures. Accordingly, the magnetic susceptibility exhibited Pauli-like positive, temperature-independent and Curie-Weiss behavior at low temperatures, as illustrated by Figure 1.10. Most importantly, in samples showing a resistivity drop, a transition from para- to diamagnetism occurred at slightly lower temperatures (see Fig. 1.11) indicating that superconductivity-related shielding currents existed. The diamagnetic transition started below what is presumably the highest T_c in the samples as indicated by theories[1.21, 1.22] describing the behavior of percolative superconductors. In all our samples, the transition to the diamagnetic state was systematically related to the results of our resistivity measurements. The final proof of superconductivity, the presence of the Meissner-Ochsenfeld effect, had been demonstrated. Combining the X-ray analysis, resistivity and susceptibility measurements, it was now possible to clearly identify the Ba-doped La_2CuO_4 as the superconducting compound.

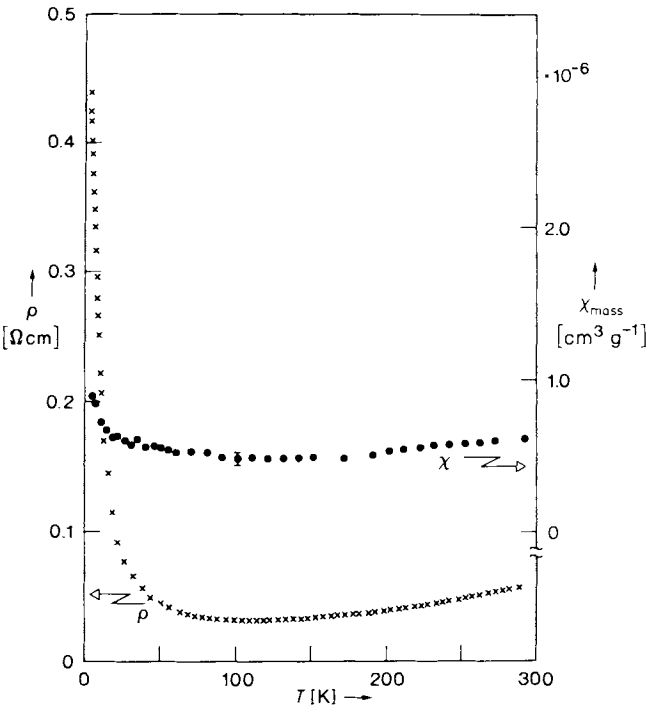

Fig. 1.10. Temperature dependence of resistivity (×) and mass susceptibility (●) of sample ① (adapted from [1.23]).

First Responses and Confirmations

The number of our troops was indeed growing. *Richard Greene* at our Research Center in Yorktown Heights had learned about our results and became excited. He had made substantial contributions in the field of organic superconductors and wanted to collaborate in measuring specific-heat data on our samples. We initiated an exchange of information, telefaxing the latest results of our research and sending samples. Realizing that our first paper had now appeared in the open literature, we rushed to get the results of our susceptibility data written up for publication.

ADVANCED MATERIALS

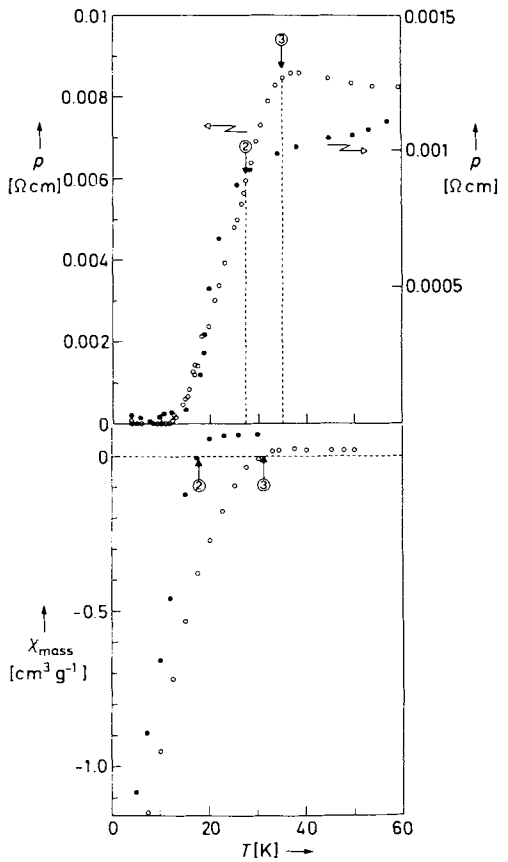

Fig. 1.11. Low-temperature resistivity (top) and mass susceptibility (bottom) of (La-Ba)-Cu-O samples ② (●) and ③ (○). Arrows indicate the onset of the resistivity and the paramagnetic-to-diamagnetic transitions, respectively (adapted from [1.23]).

The day we made the final corrections to our report turned out to be one of the most remarkable days in the history of our Laboratory. *Alex, Masaaki* and I were sitting together, when the announcement was made over our P.A. system that the 1986 Nobel Prize for Physics had been awarded to our colleagues *Gerd Binnig* and *Heinrich Rohrer*. With everything prepared for the submission of our paper,[1.23] for one more day we could forget about our work, and together with the whole Laboratory celebrate the new laureates. One day later we were back to reality, and I started to prepare a set of samples for *Richard Greene. Praveen Chaudhari*, our director of Physical Science in Yorktown Heights, took them with him the same evening.

Later in November, we received the first response to our latest work from Professor *W. Buckel*, to whom *Alex* had send a preprint with the results of the magnetic measurements. His congratulations on our work were an encouragement, as we began to realize that we would probably have a difficult time getting our results accepted. Indeed, *Alex* and I had started giving talks about our discovery and, although the presence of the Meissner effect should have convinced people, at first we were met by a skeptical audience. However, this period turned out to be very short indeed.

We continued with the magnetic characterization of the superconducting samples and found interesting properties related to the behavior of a spin glass.[1.24] We then intensively studied the magnetic field and time dependences of the magnetization, before finally starting to realize an obvious idea, namely, to replace La also by other alkaline-earth elements like Sr and Ca. In particular Sr^{2+} had the same ionic radius as La^{3+}. We started experiments on the new materials, which indicated that for the Sr-substituted samples T_c was approaching 40 K and the diamagnetism was even higher (see Fig. 1.12).[1.25] It was just at that time that we learned from the Asahi-Shinbun International Satellite Edition [28 November 1986] that the group of Professor *Tanaka* at the University of Tokyo had repeated our experiments and could confirm our result.[1.26] We were relieved, and even more so when we received a letter from Professor *C. W. Chu* at the University of Houston, who was also convinced that within the Ba-La-Cu-O system superconductivity occurred at 35 K.[1.27] Colleagues who had not paid any attention to our work at all suddenly became

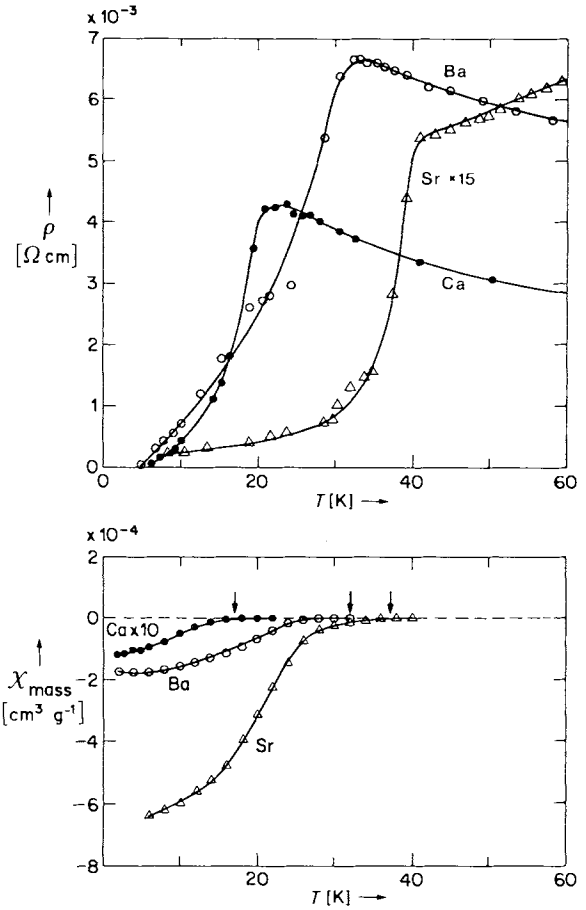

Fig. 1.12. Top: Resistivity as a function of temperature for Ca (●), Sr (△), and Ba (○) substitution with substituent to La ratios of 0.2/1.8, 0.2/1.8, 0.15/1.85, respectively. The Sr curve has been vertically expanded by a factor of 15. Bottom: Magnetic susceptibility of these samples. The substituents are Ca (●), Sr (△), and Ba (○), with total sample masses of 0.14, 0.21, and 0.13 g, respectively. The Ca curve has been expanded by a factor of 10. Arrows indicate onset temperatures (adapted from [1.25]).

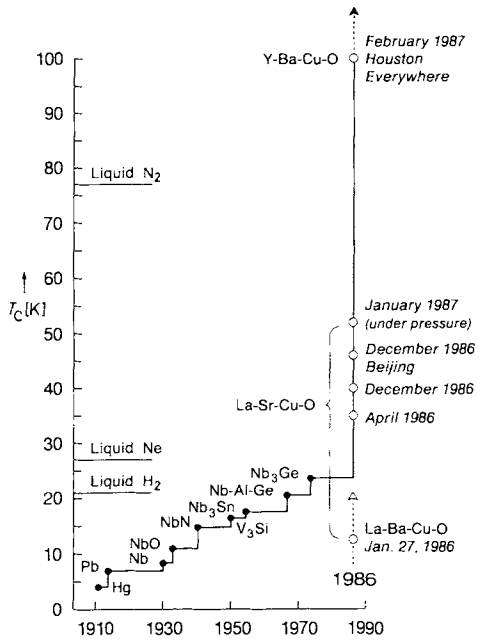

Fig. 1.13. Evolution of the superconductive transition temperature subsequent to the discovery of the phenomenon (adapted from [1.29]).

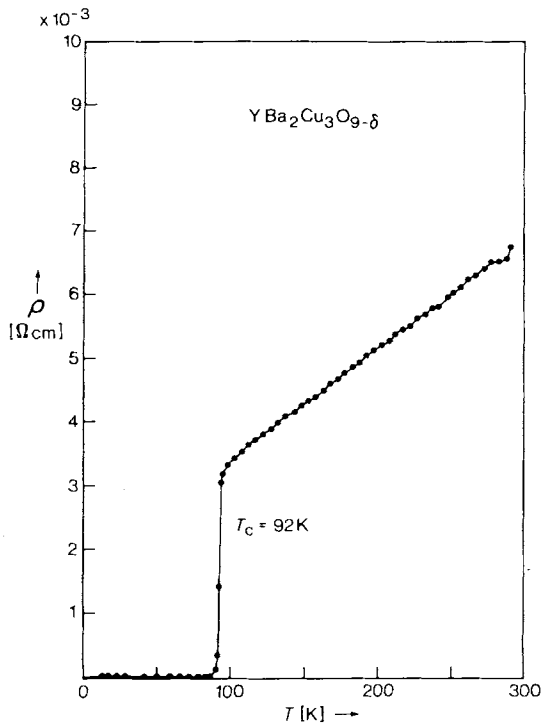

Fig. 1.14. Resistivity of a single-phase $YBa_2Cu_3O_7$ sample ("123 compound") as a function of temperature.

alert. By applying hydrostatic pressure to the samples, Professor *Chu* was able to shift the superconductive transition from 35 to almost 50 K.[1.27] Modification of the original oxides by introducing the smaller yttrium for the larger lanthanum ion resulted in a giant jump of T_c to 92 K in multiphase samples[1.28] (Fig. 1.13). At a breathtaking pace, dozens of groups now repeated these experiments and after an effort of only a few days the new superconducting compound could be isolated and identified. The resistive transition in the new $YBa_2Cu_3O_7$ compound was complete at 92 K (Fig. 1.14), and even more impressive was the fact that the Meissner effect could now be demonstrated without any experimental difficulties with liquid nitrogen as the coolant. Within several months, the field of superconductivity had experienced a tremendous revival, with an explosive development of T_c's such that nobody can predict where it will end.

An early account of the discovery appeared in the September 4 1987 issue of *Science*, which was dedicated to science in Europe.[1.29]

References Part 1

[1.1] K. A. Müller in E. J. Samuelsen, E. Andersen, J. Feder (Eds.): *Structural Phase Transitions and Soft Modes*, Universitetsforlayet, Oslo 1971, p. 85.
[1.2] T. Schneider, E. Stoll, *Physica (Amsterdam) 55* (1971) 702.
[1.3] J. F. Schooley, H. P. R. Frederikse, W. R. Hosler, E. R. Pfeiffer, *Phys. Rev. 159* (1967) 301.
[1.4] A. Baratoff, G. Binnig, *Physica (Amsterdam) 108 B+C* (1981) 1335; A. Baratoff, G. Binnig, J. G. Bednorz, F. Gervais, J. L. Servoin in W. Buckel, W. Weber (Eds.): *Superconductivity in d- and f-Band Metals, Proc. 4th Conf.*, Kernforschungszentrum Karlsruhe 1982, p. 419.
[1.5] G. Binnig, A. Baratoff, H. E. Hoenig, J. G. Bednorz, *Phys. Rev. Lett. 45* (1980) 1352.
[1.6] K. A. Müller, M. Pommerantz, C. M. Knoedler, D. Abraham, *Phys. Rev. Lett. 45* (1980) 832, and references cited therein.
[1.7] M. R. Beasley, T. H. Geballe, *Phys. Today 36* (1984) No. 10, p. 60; J. Mueller, *Rep. Prog. Phys. 43* (1980) 663.
[1.8] D. C. Johnston, H. Prakash, W. H. Zachariasen, R. Viswanathan, *Mater. Res. Bull. 8* (1973) 777.
[1.9] A. W. Sleight, J. L. Gillson, F. E. Bierstedt, *Solid State Commun. 17* (1975) 27.
[1.10] J. Bardeen, L. N. Cooper, J. R. Schrieffer, *Phys. Rev. 108* (1957) 1175.
[1.11] B. K. Chakraverty, *J. Phys. Lett. 40* (1979) L99; *J. Phys. 42* (1981) 1351.
[1.12] K.-H. Höck, H. Nickisch, H. Thomas, *Helv. Phys. Acta 56* (1983) 236.
[1.13] J. B. Goodenough, M. Longo, *"Magnetic and other properties of oxide and related compounds"* in K. H. Hellwege, A. M. Hellwege (Eds.): *Landoldt-Börnstein New Series, Vol. III/4a: Crystal and Solid State Physics*, Springer, Berlin 1970, p. 262, Fig. 73.
[1.14] J. G. Bednorz, K. A. Müller, H. Arend, H. Gränicher, *Mater. Res. Bull. 18* (1983) 181.
[1.15] N. Y. Vasanthacharya, P. Ganguly, J. B. Goodenough, C. N. R. Rao, *J. Phys. C: Solid State Phys. 17* (1984) 2745.
[1.16] C. Michel, L. Er-Rakho, B. Raveau, *Mater. Res. Bull. 20* (1985) 667.
[1.17] C. Michel, B. Raveau, *Rev. Chim. Miner. 21* (1984) 407. It is of interest that back in 1973, J. B. Goodenough, G. Demazeaux, M. Pouchard, P. Hagenmüller (*J. Solid State Chem. 8* (1973) 325) in Bordeaux, and later I. S. Shaplygin, B. G. Kakhan, V. B. Lazarev (*Russ. J. Phys. Chem. 24* (1979) 1478) pursued research on layered cuprates with catalysis applications in view.
[1.18] M. Suzuki, T. Murakami, T. Inamura, *Shinku 24* (1981) 67; Y. Enomoto, M. Susuki, T. Murakami, T. Innukai, T. Inamura, *Jpn. J. Appl. Phys. 20* (1981) L661.
[1.19] J. G. Bednorz, K. A. Müller, *Z. Phys. B64* (1986) 189.

ADVANCED MATERIALS

[1.20] J. G. Bednorz, M. Takashige, K. A. Müller, *Mater. Res. Bull. 22* (1987) 819.
[1.21] D. R. Bowman, D. Stroud, *Phys. Rev. Lett. 52* (1985) 299.
[1.22] C. Ebner, D. Stroud, *Phys. Rev. B31* (1985) 165, and references cited therein.
[1.23] J. G. Bednorz, M. Takashige, K. A. Müller, *Europhys. Lett. 3* (1987) 379.
[1.24] K. A. Müller, M. Takashige, J. G. Bednorz, *Phys. Rev. Lett. 58* (1987) 1143.
[1.25] J. G. Bednorz, K. A. Müller, M. Takashige, *Science 236* (1987) 73.
[1.26] H. Takagi, S. Uchida, K. Kitazawa, S. Tanaka, *Jpn. J. Appl. Phys. Lett. 26* (1987) L123; S. Uchida, H. Takagi, K. Kitazawa, S. Tanaka, *ibid. 26* (1987) L151.
[1.27] C. W. Chu, P. H. Hor, R. L. Meng, L. Gao, Z. J. Huang, Y. Q. Wang, *Phys. Rev. Lett. 58* (1987) 405.
[1.28] M. K. Wu, J. R. Ashburn, C. J. Torng, P. H. Hor, R. L. Meng, L. Goa, Z. J. Huang, Y. Q. Wang, C. W. Chu, *Phys. Rev. Lett. 58* (1987) 908; P. H. Hor, L. Gao, R. L. Meng, Z. J. Huang, Y. Q. Wang, K. Forster, J. Vassilious, C. W. Chu, M. K. Wu, J. R. Ashburn, C. J. Torng, *ibid. 58* (1987) 911.
[1.29] K. A. Müller, J. G. Bednorz, *Science 237* (1987) 1133.

Part 2: Properties of the New Superconductors

In the second part, properties of the new layered oxygen superconductors are described. Since their discovery, summarized in the first part, a real avalanche of papers has appeared; thus it would be beyond the scope of this lecture to review all of them here. A forthcoming international conference in Interlaken, Switzerland, in late February 1988, is intended to fulfill this task and will be chaired by one of us *(KAM)*[*]. Therefore, only a selected number of experiments was discussed in Stockholm—those judged of importance at this time for the understanding of superconductivity in the layered copper oxides. In some of them, the laureates themselves were involved, in others not. Owing to the frantic activity in the field, it may be possible that equivalent work with priority existed unknown to us. Should this indeed be the case, we apologize and propose that the following be read for what it is, namely, a write-up of the lecture given, including the transparencies shown.

After the existence of the new high-T_c superconductors had been confirmed, one of the first questions was "What type of superconductivity is it?" Does one again have Cooper pairing[2.1] or not? This question could be answered in the affirmative. The earliest experiment to come to our knowledge was that of the Saclay-Orsay collaboration. *Estève* et al.[2.2] measured the I-V characteristics of sintered $La_{1.85}Sr_{0.15}CuO_4$ ceramics using nonsuperconducting Pt-Rh, Cu or Ag contacts. In doing so, they observed weak link characteristics internal to the superconductor, to which we shall return later. They then applied microwaves at $\nu = 9.4$ GHz and observed Shapiro steps[2.3] at $V_s = 19\ \mu V$ intervals. From the well-known Josephson formula[2.4]

$$V_s = h\nu/q, \tag{2.1}$$

they obtained $q = 2e$, i.e., Cooper pairs were present. Figure 2.1 illustrates these steps.

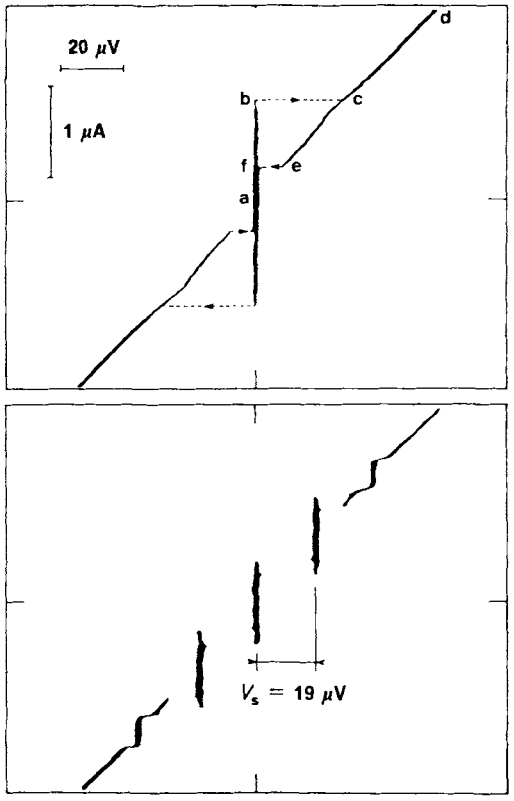

Fig. 2.1. Top: Oscilloscope trace of a current-voltage characteristic obtained at 4.2 K with an aluminum tip on a $La_{1.85}Sr_{0.15}CuO_4$ sample. Letters a through f indicate direction of trace. Dashed lines have been added to indicate the switching between the two branches. Bottom: Steps induced by microwave irradiation at frequency $\nu = 9.4$ GHz; all other experimental conditions identical (adapted from [2.2]).

From the fundamental London equations, the flux ϕ through a ring is quantized:[2.5]

$$\phi = n\phi_0$$
$$\phi_0 = hc/q \tag{2.2}$$

The clearest experiment, essentially following the classical experiments in 1961, was carried out in Birmingham, England, by *C. E. Gough* et al.[2.6] They detected the output of an r.f.-SQUID magnetometer showing small integral numbers of flux quanta ϕ_0 jumping in and out of the ring of $Y_{1.2}Ba_{0.8}CuO_4$ (see Fig. 2.2). The outcome clearly confirmed that $q = 2e$.

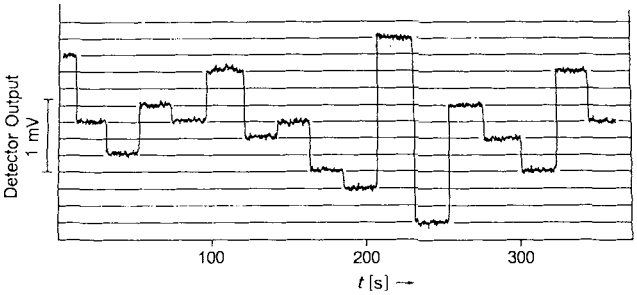

Fig. 2.2. Output of the r.f.-SQUID magnetometer showing small integral numbers of flux quanta jumping in and out of a ring (adapted from [2.6]).

[*] See conference report on page 749 of this issue.

To understand the mechanism, it was of relevance to know the nature of the charge carrier present. In La_2CuO_4 with very little doping, the early measurements[1,23] showed localization upon doping with divalent Ba^{2+} or Sr^{2+} and Ca^{2+}; it was most likely that these ions substituted for the trivalent La^{3+} ions. Thus, from charge-neutrality requirements, the compounds had to contain holes. Subsequent thermopower measurements confirmed this assumption.[2.7] The holes were thought to be localized on the Cu ions. Because the copper valence is two in the stoichiometric insulator La_2CuO_4, doping would create Cu^{3+} ions. Thus a mixed Cu^{2+}/Cu^{3+} state had to be present. By the same argument, this mixed-valence state ought also to occur in $YBa_2CuO_{7-\delta}$ ($\delta \approx 0.1$). Early photoelectron core-level spectra (XPS and UPS) by *Fujimori* et al.[2.8] and *Bianconi* et al.[2.9] in $(La_{1-x}Sr_x)_2CuO_{4-y}$ and $YBa_2La_3Cu_{6.7}$ did not reveal a $\underline{2p}\ 3d^8$ final state arising from a $Cu^{3+}\ 3d^8$ state (the underlining indicates a hole). However, the excitation

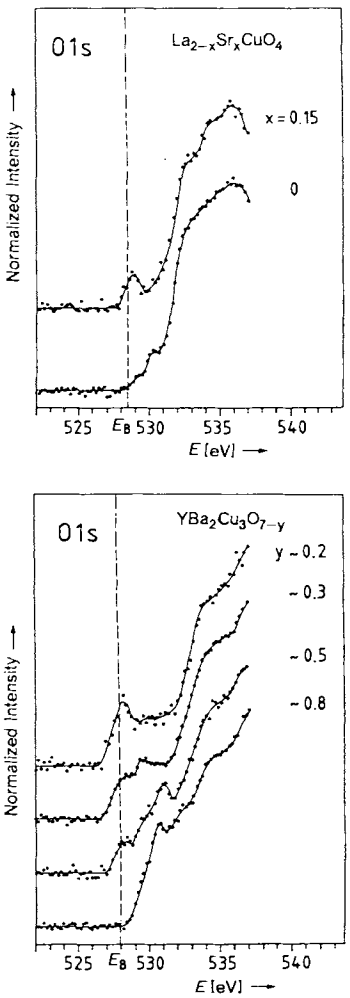

Fig. 2.3. Oxygen 1s absorption edges of $La_{2-x}Sr_xCuO_4$ (top) and $YBa_2Cu_3O_{7-y}$ (bottom) measured by energy-loss spectroscopy. The binding energy of the O 1s level, as determined by X-ray induced photoemission, is shown by the dashed line. In the framework of an interpretation of the spectra in terms of the density of unoccupied states, this line would correspond to the Fermi energy (adapted from [2.11]).

was consistent with the formation of holes $\underline{L}$ in the oxygen-derived band, i.e., a predominant $3d^9\ \underline{L}$ configuration for the formal Cu^{3+} state. Photo-X-ray absorption near the edge structure was also interpreted in the same manner by comparison with other known Cu compounds. Emission spectra by *Petroff*'s group[2.10] pointed in the same direction, since the excitation thresholds were compatible with the presence of holes in Cu–O hybrid bands. From their data, both groups concluded that strong correlation effects were present for the valence carriers. However, these results were challenged by other groups working in the field, partly because the spectra involved the interpretation of Cu-atom satellites. A beautifully direct confirmation of the presence of holes on the oxygen p-levels, like $\underline{L}$, was carried out by *Nücker* et al.[2.11] These authors investigated the core-level excitation of oxygen 1s electrons into empty 2p states of oxygen at 528 eV. This is an oxygen-specific experiment. If no holes are present on the p-level, no absorption will occur. Figure 2.3 summarizes their data on $La_{2-x}Sr_xCuO_4$ and $YBa_2Cu_3O_{7-\delta}$. It is shown that for $x=0$ and $\delta=0.5$, no oxygen p-holes are present and thus no absorption is observed, whereas upon increasing x or reducing δ, a $\underline{2p}$ hole density at the Fermi level is detected in both compounds.

Of considerable interest is the dependence of the transition temperature on the hole concentration. The electron deficiency is hereafter written in the form $[Cu\text{–}O]^+$ as a peroxide complex in which the probability of the hole is about 70% $3d^9\ \underline{2p}$, as discussed above, and 30% $3d^8$ as recently inferred from an XPS study.[2.12] Hall-effect data are difficult to analyze in the presence of two-band conduction, which is possible in these copper oxide compounds, owing to the well known compensation effects. Therefore, *M. W. Shafer, T. Penney,* and *B. L. Olson*[2.13] determined

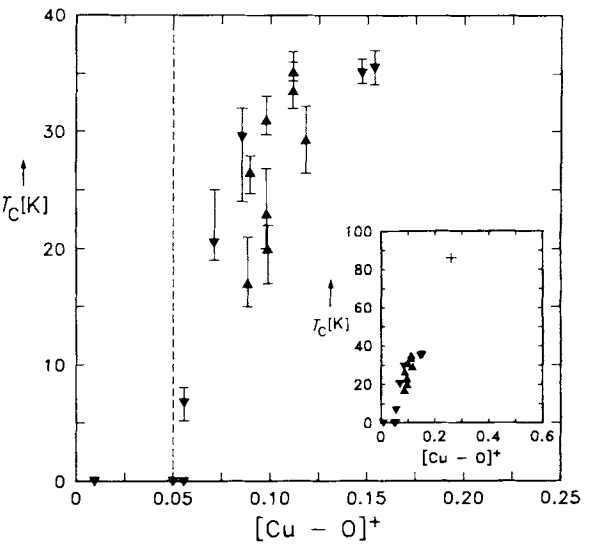

Fig. 2.4. T_c vs the hole concentration $[Cu\text{–}O]^+$, as a fraction of total copper. Down triangles are for compositions with $x<0.15$, up triangles for $x>0.15$. Insert shows same data plus points for a single $YBa_2CuO_{6.6}$ sample as discussed in the text (adapted from [2.13]).

ADVANCED MATERIALS

the concentration by wet chemistry according to the reaction $[Cu-O]^+ + Fe^{2+} \rightleftarrows Cu^{2+} + Fe^{3+} + O^{2-}$ in the $La_{2-x}Sr_xCuO_{4-\delta}$ compound. Figure 2.4 shows a plot of T_c vs $[Cu-O]^+$ concentration with a maximum of 35 K at 15% total copper present. There is also a clear threshold at about 5%. From the study, it is apparent that 15–16% $[Cu-O]^+$ is the maximum number of holes the La_2CuO_4 structure accepts. Beyond this concentration, oxygen vacancies are formed. The relationship between T_c and $[Cu-O]^+$ in $La_{2-x}Sr_xCuO_4$ was extended to $YBa_2Cu_3O_{7-\delta}$. The insert of Figure 2.4 illustrates the results under the assumption that two layers in the 123 compound are active for $\delta \approx 0.1$ and $\delta \approx 0.3$, i.e., T_c's of 92 K and 55 K.[2.14] The latter transition, first reported by *Tarascon* et al., was confirmed by near-room-temperature plasma oxidation of the oxygen-deficient Y-compound.[2.14]

The $La_{2-x}Sr_xCuO_{4-y}$ with its less complicated structure allows easier testing of models. Its magnetic properties below the hole threshold concentration, $x=0.05$, are of special interest. For $x=0$, the susceptibility $\chi(T)=M(T)/H$ exhibits a maximum at low fields of $H=0.05$ T below 300 K. This maximum increases in height and shifts to lower temperatures for higher magnetic fields up to 4.5 T[2.15] as seen in Figure 2.5a. Such behavior is indicative of spin density waves or antiferromagnetic fluctuations. Indeed, neutron diffraction experiments by *Vaknin* et al.[2.16] proved three-dimensional (3-D) antiferromagnetic ordering up to 240 K depending on oxygen stoichiometry (i.e., hole concentration). The structure is shown in Figure 2.5b. Subsequent neutron scattering experiments on a single crystal revealed a novel two-dimensional (2-D) antiferromagnetic correlation well above and also *below* the 3-D Néel temperature T_N as shown in Figure 2.6. This instantaneous (not time-averaged) ordering, seen even above room temperature, was termed a quantum spin fluid (Q.S.F.).[2.17] The existence of antiferromagnetism (A.F.) supports models in which holes lead either to localization or to pairing in the strong-coupling limit as proposed by *Emery*[2.18] and others.[2.19] The resonant valence-band state is also related to the A.F. state.[2.20]

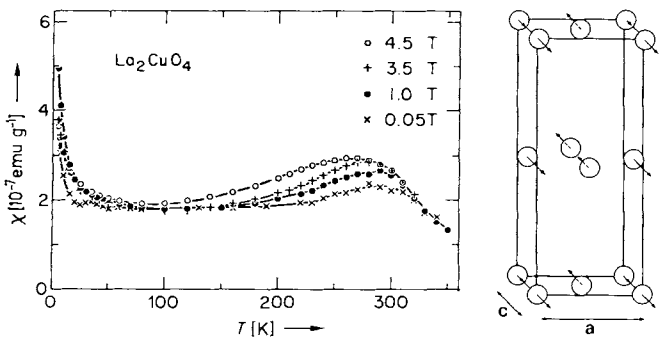

Fig. 2.5. Left: Temperature dependence of the magnetic susceptibility $\chi = M/H$ of La_2CuO_4 in different fields H (adapted from [2.15]). Right: Spin structure of antiferromagnetic La_2CuO_{4-y}. Only copper sites in the orthorhombic unit cell are shown for clarity (adapted from [2.16]).

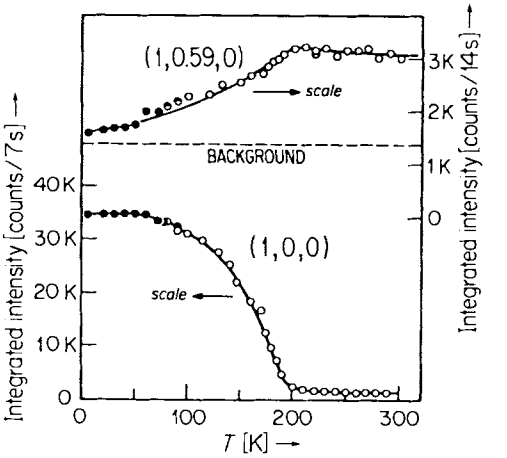

Fig. 2.6. Integrated intensities of the (100) 3-D antiferromagnetic Bragg peak and the (1,0.59,0) 2-D quantum spin fluid ridge. The open and filled circles represent separate experiments (adapted from [2.17]).

From the prevalence of magnetic interactions as a primary cause for the occurrence of high-T_c superconductivity, one would expect the isotope effect to be absent, since it occurs when the Cooper pairing is mediated by phonon interaction, as found in most of the metallic superconductors previously known. Indeed, substituting O^{16} by O^{18} in the $YBa_2Cu_3O_{7-\delta}$ compound at AT&T did not reveal a shift in T_c.[2.21] However, substitution experiments in $La_{2-x}Sr_xCuO_{4-y}$ oxide carried out shortly thereafter did reveal an isotope effect with $0.14 < \beta < 0.35$[2.22] as compared with the full effect of $\beta = 0.5$ deduced from the weak-coupling formula[1.10]

$$T_c = 1.13\,\Theta_D \exp -(1/N(E_F) \times V^*), \tag{2.3}$$

with the Debye temperature $\Theta_D \propto 1/M^{1/2}$, where M is the reduced mass. Thus in the lanthanum compound, oxygen motion is certainly present. As it is highly unlikely that the mechanism is substantially different in the 123 compound, oxygen motion should also be there. This is because absence of the isotope effect does not necessarily exclude a phonon mechanism, which has to be present if Jahn-Teller polarons participate. Indeed, a subsequent, more accurate experiment did show a weak isotope effect in $YBa_2Cu_3O_{7-\delta}$ with $\Delta T_c \approx 0.3$ to 0.5 K.[2.23] From these results, it appears likely that there is more than one interaction present which leads to the high transition temperatures, the low quasi-2D properties certainly being of relevance.

The X-ray and photoemission studies mentioned earlier had indicated strong correlation effects. Cooper pairing having been ascertained, it was therefore of considerable interest whether the new superconductors were of the strong- or the weak-coupling variety. In the latter case, the ratio of the gap 2Δ to kT_c is:[1.10]

$$\frac{2\Delta}{kT_c} = 3.52 \tag{2.4}$$

whereas in the former it is larger.

Tunneling experiments have been widely used to determine the gap in the classical superconductors. However, the very short coherence length yields too low values of 2Δ, as will be discussed later.[2.24] Infrared transmission and reflectivity measurements on powders were carried out at quite an early stage. With the availability of $YBa_2Cu_3O_7$ single crystals, powder infrared data are less relevant, but are quoted in the more recent work. A beautiful example is the reflectivity study by *Schlesinger* et al.[2.25] of superconducting $YBa_2Cu_3O_7$ and a Drude fit to the nonsuperconducting $YBa_2Cu_3O_{6.5}$ data. From the Mattis-Bardeen enhanced peak in the superconducting state, these authors obtained $2\Delta_{ab}/kT_c \approx 8$, i.e., strong coupling in the Cu-O planes (see Fig. 2.7). NMR relaxation experiments by *Mali* et al.,[2.26] although not yet completely analyzed, yield two gaps with ratios 4.3 and 9.3, respectively, the latter being in the range of the infrared data.

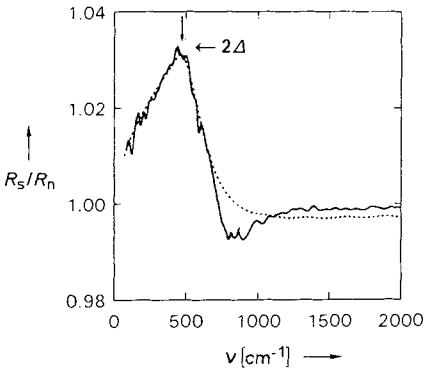

Fig. 2.7. Normalized infrared reflectivity of a single crystal of $YBa_2Cu_3O_7$ and fitted Mattis-Bardeen form of $\delta(\omega)$ (dotted line) in the superconducting state. The arrow shows the peak occurring at $2\Delta \approx 480$ cm^{-1}, hence $2\Delta \approx 8kT_c$ with $T_c = 92$ K (adapted from [2.25]).

NMR relaxation experiments were among the first at the time to prove the existence of a gap.[2.27] They also appear to be important for the new class of superconductors.

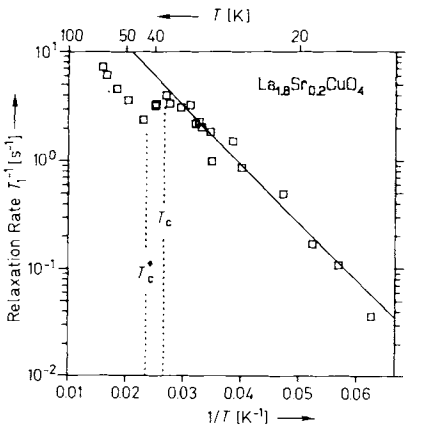

Fig. 2.8. Semilogarithmic plot of $1/T_1$ vs $1/T$. The straight line demonstrates the activated behavior $1/T_1 \sim \exp[-\Delta/kT]$ for $T \ll T_c^*$. An activation energy of $\Delta/k = 135$ K is obtained from this graph (adapted from [2.28]).

Zero-field nuclear spin lattice relaxation measurements on ^{139}La in $La_{1.8}Sr_{0.2}CuO_{4-\delta}$ below T_c follow the relationship $1/T_1 \propto \exp(-\Delta/kT)$ (see Fig. 2.8) with activation energy $\Delta = 1.1$ meV; at low temperatures $kT \ll 2\Delta$ due to a $T_c = 38$ K. A ratio of $2\Delta/kT_c = 7.1$ was obtained.[2.28] Therefore, strong coupling is also present in the La compound. The value of Δ probably has to be attributed to the gap parallel to the planes. In fact, it has been shown that infrared reflectivity data on powders measure the gap along the c-axis, and a ratio of $2\Delta_c/kT_c \approx 2.5$ was given.[2.29] Thus the coupling between the planes appears to be weak. Such a substantial anisotropic property was not previously found in other superconductors.

From the first measurements of resistivity as a function of magnetic field, the slopes dH_{c_2}/dT near T_c could be obtained, and from them very high critical fields at low temperatures were extrapolated. From the many papers published, we quote that of *Decroux* et al.,[2.30] also because this was the first paper to report a specific-heat plateau at T_c. The group at the University of Geneva found $dH_{c_2}/dT = -2.5\,\mathrm{T\,K^{-1}}$, yielding an extrapolated $H_{c_2}(T=0) = 64$ T.

From the well-known formula for the critical field in type-II superconductors

$$H_{c_2} = \frac{\phi_0}{2\pi\xi^2} \tag{2.5}$$

one calculates that the coherence length ζ is of the order of the lattice distances. Actually the coherence lengths evaluated have become smaller; recent results on single crystals by an IBM group in Yorktown Heights[2.31] and on epitaxial layers by the Stanford group [2.32] are of the order $\xi_c \approx 3$–4 Å for the coherence length parallel to c and $\xi_{ab} \approx 20$–30 Å perpendicular to c.

Such short coherence lengths could be expected when one considers the relationship between ξ, the gap and the Fermi energy E_F. *Weisskopf*[2.33] deduced

$$\xi \approx \frac{E_F}{\Delta} d \tag{2.6}$$

from the Heisenberg uncertainty principle. In equation (2.6), d is the screening length, which one can assume to be of the order of a unit cell distance. The ratio E_F/Δ is near unity owing to the large Δ and the small E_F, the latter resulting from the low carrier density and the sizeable electron mass. Therefore in oxides, ξ is considerably smaller than in metals. Because Δ is anisotropic, so is ξ. The comparable size of E_F and Δ indicates that most of the carriers participate in the superconductivity of the new oxides for temperatures $T < T_c$, in contrast to the classical superconductors, where $E_F \gg \Delta \approx 1.7\,kT_c$.

The short coherence lengths in the layered copper oxide superconductors are important theoretically, experimentally, and applicationwise: The short ξ's and carrier concentrations of the order of $n = 10^{21}$ cm^{-3} make one wonder

ADVANCED MATERIALS

whether boson-condensation approaches are not more appropriate, i.e., real-space Cooper pairing in contrast to the wave-vector space pairing of classical BCS theory,[1.10] which applies so well for metals with large ξ's and concentrations n. Actually, *Schafroth*[2.34] back in 1955 was the first to work out a superconducting theory with boson condensation. Referring to *Chakraverty*'s phase diagram in Figure 1.2,[1.11] one may regard the metal superconducting phase line as BCS with weak coupling, and the superconductor-insulator boundary for large coupling constants λ as the Schafroth line.

The short coherence lengths induce considerable weakening of the pair potential at surfaces and interfaces, as emphasized by *Deutscher* and *Müller*.[2.24] Using an expression for the "extrapolation length" b[2.35] for the boundary condition at the superconductor-insulator interface, the $\Delta(x)$ profile was deduced as shown in Figure 2.9 for $T \lesssim T_c$ and $T \ll T_c$.

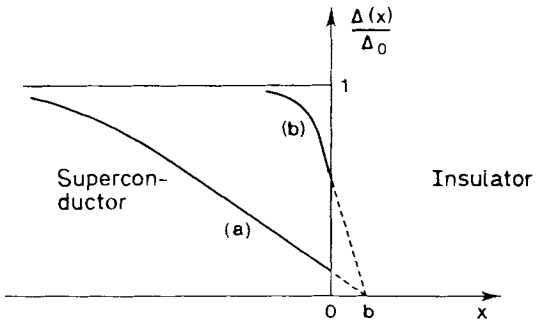

Fig. 2.9. Profile of the pair potential in a short-coherence-length superconductor near a superconductor-insulator boundary. Curve (a): $T \lesssim T_c$; curve (b): $T \ll T_c$ (adapted from [2.24]).

Analogous behavior of $\Delta(x)$ will also be present at superconducting-normal (SN) interfaces. Thus, the depressed order parameter involving experiments of SIS and SNS will result in tunneling characteristics[2.24] with a marked reduction in the observed value of Δ. In consequence, such experiments are less suitable than infrared and NMR studies to determine Δ, and actually lead to erroneous conclusions regarding gapless superconductivity also in point-contact spectroscopy.[2.36] $YBa_2Cu_3O_7$ undergoes a tetragonal-to-orthorhombic phase transition near 700°C. Thus upon cooling, (110) twin boundaries are formed, separating the orthorhombic domains and inducing *intragrain* Josephson or weak-link junctions. These junctions form a network dividing the crystallites into Josephson-coupled domains, with the possibility of fluxon trapping as well. Therefore even single crystals form a superconducting glass *in the presence* of a sizeable magnetic field.

The basic Hamiltonian regarding the phases is[1.22]

$$\beta \mathscr{H} = -\sum J_{ij} \cos(\phi_i - \phi_j - A_{ij}) \tag{2.7}$$

Here, J_{ij} is the Josephson coupling constant between domains. The phase factors $A_{ij} = K_{ij} \boldsymbol{H}$ introduce randomness for $\boldsymbol{H} \neq 0$ because K_{ij} is a random geometric factor. A review of the superconducting glass state has recently appeared.[2.37]

The first evidence indicating the presence of superconducting glassy behavior was deduced from field-cooled and zero-field-cooled magnetization data[1.24,2.38] in $La_{2-x}Ba_xCuO_4$ ceramics. In addition to the twin-boundary-induced *intragrain* junctions, such a material also has junctions resulting from the *intergrain* boundaries. The latter J_{ij}'s are much weaker and uncouple at lower magnetic fields and currents j_c. Consequently, the critical currents observed in the ceramics are more of the order of 10^3 to 10^4 A cm^{-2},[2.39] whereas those in epitaxial layers[2.40] and single crystals[2.1] are of the order of 10^6 to 10^7 A cm^{-2}.[2.41] The latter work, carried out by two IBM groups, is a major breakthrough in the field.

The decay lengths of the superconducting wave functions at SNS and SIS junctions are both of the order of $\xi(0)$. This entails an anomalous temperature dependence $J_c \propto (T - T_c)^2$. Such behavior is seen in the mid-temperature range for $J_c(T)$ in the $YBa_2Cu_3O_{7-\delta}$ epilayer on $SrTiO_3$ of Figure 2.10.[2.40] Such critical currents are acceptable for thin film applications at 77 K for low magnetic fields (Fig. 2.10), whereas in the ceramics the much lower J_c's indicate a need for further development work, or, perhaps better still, the discovery of a new type of high-T_c superconductor that should exist.

The geometrical critical magnetic field $H_{c_1}^*$ is of the order of[1.22]

$$H_{c_1}^* = \phi_0 / 2S \tag{2.8}$$

where S is the projected area of the superconducting loop with uniform phase. In single crystals, the S of domains is of the order of 100 μm^2, whereas that of grains in ceramics is 1–10 μm^2. In agreement with equation (2.8), $H_{c_1}^*$ is of the order of 0.5 G for the penetration of H into twinned crystals, and 5 to 100 G to disrupt intergranular nets in ceramics.

Since the publication on the existence of this new class of materials, the interest and work have far exceeded the expectations of the laureates, whose aim was primarily to show that oxides could "do better" in superconductivity than metals and alloys. Due to this frenzy, progress on the experimental side has been rapid and is expected to continue. This will also assist in finding new compounds, with T_c's reaching at least 130 K (Fig. 2.4). Quantitative theoretical models are expected in the not too distant future, first perhaps phenomenological ones. On this rapidly growing tree of research, separate branches are becoming strong, such as glass aspects, growth techniques for single crystals, epitaxial films, and preparation of ceramics, the latter two being of crucial importance for applications. The former will dominate the small-current microelectronics field, while the latter will have to be mastered in the large-current field. Here the hopes are for energy transport, and

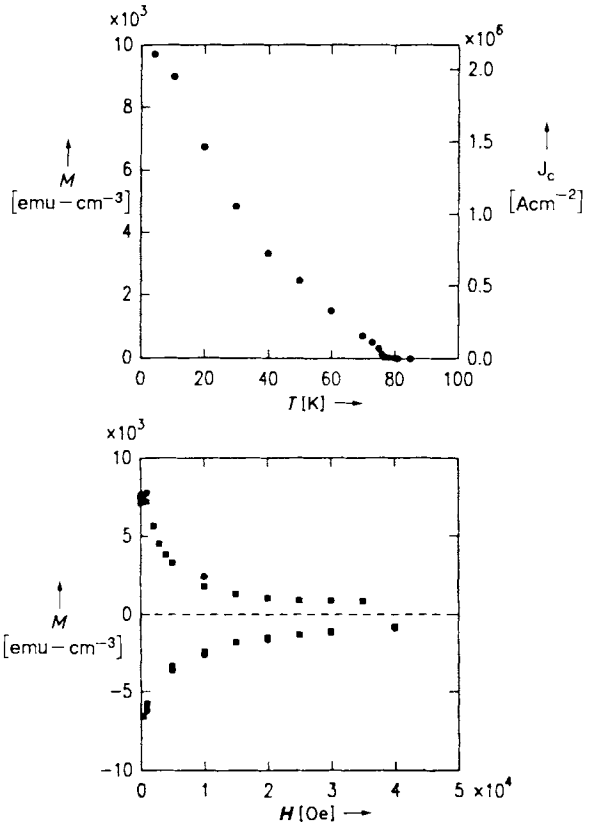

Fig. 2.10. Top: The volume magnetization M vs temperature for an epitaxial sample. The y-axis scale on the right was obtained with the use of the Bean formula $J_c = 30\ M/d$, with the mean radius of the sample $d = 0.14$ cm. Bottom: The volume magnetization M vs applied field H at 4.2 K for two samples (adapted from [2.40]).

later large magnetic field applications, for example in beam bending in accelerators and plasma containment in fusion.

References Part 2

[2.1] L. N. Cooper, *Phys. Rev. 104* (1956) 1189.
[2.2] D. Estève, J. M. Martins, C. Urbina, M. H. Devoret, G. Collin, P. Monod, M. Ribault, A. Revcolevschi, *Europhys. Lett. 3* (1987) 1237.
[2.3] S. Shapiro, *Phys. Rev. Lett. 11* (1963) 80.
[2.4] B. D. Josephson, *Phys. Lett. 1* (1962) 251.
[2.5] F. London: *Superfluids, Vol. 1*, Wiley, New York 1950, p. 152.
[2.6] C. E. Gough, M. S. Colclough, E. M. Forgan, R. G. Jordan, M. Keene, C. M. Muirhead, A. I. M. Rae, N. Thomas, J. S. Abell, S. Sutton, *Nature (London) 326* (1987) 855.
[2.7] F. Steglich, C. D. Bredl, F. R. de Boer, M. Lang, U. Rauchschwalbe, H. Rietschel, R. Schefzyk, G. Sparn, G. R. Stewart, *Phys. Scr. T19* (1987) 253.
[2.8] A. Fujimori, E. Takayama-Muromachi, Y. Uchida, B. Okai, *Phys. Rev. B35* (1987) 8814.
[2.9] A. Bianconi, A. C. Castellano, M. De Santis, P. Delogu, A. Gargano, R. Giorgi, *Solid State Commun. 63* (1987) 1135; A. Bianconi, A. C. Castellano, M. De Santis, C. Politis, A. Marcelli, S. Mobilio, A. Savoia, *Z. Phys. B67* (1987) 307.
[2.10] P. Thiry, G. Rossi, Y. Petroff, A. Revcolevschi, J. Jegoudez, *Europhys. Lett. 5* (1988) 55.
[2.11] M. Nücker, J. Fink, J. C. Fuggle, P. J. Durham, W. M. Temmerman, *Phys. Rev. B*, (1988), in press.
[2.12] P. Steiner, S. Hüfner, V. Kinsinger, I. Sander, B. Siegwart, H. Schmitt, R. Schulz, S. Junk, G. Schwitzgebel, A. Gold, C. Politis, H. P. Müller, R. Hoppe, S. Kemmler-Sack, C. Kunz, *Z. Phys. B69* (1988) 449.
[2.13] M. W. Shafer, T. Penney, B. L. Olson, *Phys. Rev. B36* (1987) 4047.
[2.14] J. M. Tarascon, W. R. McKinnon, L. H. Greene, G. W. Hull, E. M. Vogel, *Phys. Rev. B36* (1987) 226; see also B. G. Bagley, L. H. Greene, J. M. Tarascon, G. W. Hull, *Appl. Phys. Lett. 51* (1987) 622.
[2.15] R. L. Greene, H. Maletta, T. S. Plaskett, J. G. Bednorz, K. A. Müller, *Solid State Commun. 63* (1987) 379.
[2.16] D. Vaknin, S. K. Sinha, D. E. Moncton, D. C. Johnston, J. M. Newsam, C. R. Safinya, H. E. King, Jr., *Phys. Rev. Lett. 58* (1987) 2802.
[2.17] G. Shirane, Y. Endoh, R. J. Birgeneau, M. A. Kastner, Y. Hidaka, M. Oda, M. Suzuki, T. Murakami, *Phys. Rev. Lett. 59* (1987) 1613.
[2.18] V. J. Emery, *Phys. Rev. Lett. 58* (1987) 2794; *Nature (London) 328* (1987) 756.
[2.19] J. E. Hirsch, *Phys. Rev. Lett. 59* (1987) 228; M. Cyrot, *Solid State Commun. 62* (1987) 821, and unpublished results.
[2.20] P. W. Anderson, *Science (Washington) 235* (1987) 1196; P. W. Anderson, G. Baskaran, Z. Zou, T. Hsu, *Phys. Rev. Lett. 58* (1987) 2790.
[2.21] B. Batlogg, R. J. Cava, A. Jayaraman, R. B. Van Dover, G. A. Kourouklis, S. Sunshine, D. W. Murphy, L. W. Rupp, H. S. Chen, A. White, K. T. Short, A. M. Mujsce, E. A. Rietman, *Phys. Rev. Lett. 58* (1987) 2333; L. C. Bourne, M. F. Crommie, A. Zettl, H.-C. zur Loye, S. W. Keller, K. L. Leary, A. M. Stacy, K. J. Chang, M. L. Cohen, D. E. Morris, *ibid. 58* (1987) 2337.
[2.22] T. A. Faltens, W. K. Ham, S. W. Keller, K. J. Leary, J. N. Michaels, A. M. Stacy, H.-C. zur Loye, D. E. Morris, T. W. Barbee III, L. C. Bourne, M. L. Cohen, S. Hoen, A. Zettl, *Phys. Rev. Lett. 59* (1987) 915; B. Batlogg, G. Kourouklis, W. Weber, R. J. Cava, A. Jayaraman, A. E. White, K. T. Short, L. W. Rupp, E. A. Rietman, *ibid. 59* (1987) 912.
[2.23] K. J. Leary, H.-C. zur Loye, S. W. Keller, T. A. Faltens, W. K. Ham, J. N. Michaels, A. M. Stacy, *Phys. Rev. Lett. 59* (1987) 1236.
[2.24] G. Deutscher, K. A. Müller, *Phys. Rev. Lett. 59* (1987) 1745.
[2.25] Z. Schlesinger, R. T. Collins, D. L. Kaiser, F. Holtzberg, *Phys. Rev. Lett. 59* (1987) 1958.
[2.26] M. Mali, D. Brinkmann, L. Pauli, J. Roos, H. Zimmermann, J. Hulliger, *Phys. Lett. A 124* (1987) 112, and references cited therein. It should be noted that analysis of the relaxation data $1/T_c \propto T^3$ is also possible, as one expects in the presence of anisotropic gaps.
[2.27] L. C. Hebel, C. P. Slichter, *Phys. Rev. 113* (1959) 1504.
[2.28] H. Seidel, F. Hentsch, M. Mehring, J. G. Bednorz, K. A. Müller, *Europhys. Lett. 5* (1988) 647.
[2.29] Z. Schlesinger, R. T. Collins, M. W. Shafer, *Phys. Rev. B35* (1987) 7232.
[2.30] M. Decroux, A. Junod, A. Bezinge, D. Cattani, J. Cors, J. L. Jordan, A. Stettler, M. François, K. Yvon, Ø. Fischer, J. Muller, *Europhys. Lett. 3* (1987) 1035.
[2.31] T. K. Worthington, W. J. Gallagher, T. R. Dinger, *Phys. Rev. Lett. 59* (1987) 1160.
[2.32] A. Kapitulnic, M. R. Beasley, C. Castellani, C. Di Castro, *Phys. Rev. B37* (1988) 537.
[2.33] V. F. Weisskopf: *The Formation of Cooper Pairs and the Nature of Superconducting Currents*, CERN, Geneva, Memorandum No. CERN 79-12, Theoretical Studies Division, 21 December 1979.
[2.34] R. Schafroth, *Phys. Rev. 96* (1954) 1149, 1442; *100* (1955) 463.
[2.35] P. G. de Gennes: *Superconductivity of Metals and Alloys*, Benjamin, New York 1968, p. 229.
[2.37] I. K. Yanson, L. F. Rybal'chenko, V. V. Fisun, N. L. Bobrov, M. A. Obolenskii, N. B. Brandt, V. V. Moshchalkov, Yu. D. Tret'yakov, A. R. Kaul', I. É. Graboi, *Fiz. Nizk. Temp. (Kiev) 13* (1987) 557 [*Sov. J. Low Temp. Phys. 13* (1987) 315].
[2.37] K. A. Müller, K. W. Blazey, J. G. Bednorz, M. Takashige, *Physica (Amsterdam) 148B* (1987) 149.
[2.38] F. S. Razavi, F. P. Koffyberg, B. Mitrović, *Phys. Rev. B35* (1987) 5323.
[2.39] J. F. Kwak, E. L. Venturini, D. S. Ginley, W. Fu in S. A. Wolf, V. Z. Kresin (Eds.): *Novel Superconductivity. Proc. Int. Worksh. Novel Mechanisms in Superconductivity*, Plenum, New York 1987, p. 983.
[2.40] P. Chaudhari, R. H. Koch, R. B. Laibowitz, T. R. McGuire, R. J. Gambino, *Phys. Rev. Lett. 58* (1987) 2684.
[2.41] T. R. Dinger, T. K. Worthington, W. J. Gallagher, R. L. Sandstrom, *Phys. Rev. Lett. 58* (1987) 2687.

Received: March 25, 1988

Conference Reports

High-T_c Superconductors in Interlaken

With the discovery of superconductivity in a La-Ba-Cu-O compound just two years ago, the IBM researchers *J. G. Bednorz* and *K. A. Müller* triggered an unprecedented scientific race in laboratories around the world for new superconducting materials with yet higher critical temperatures.[1] The first paper by *Bednorz* and *Müller* received little attention until late 1986, when Japanese and American scientists confirmed the Zürich results at the Materials Research Society meeting in December 1986.[2–4] Early in 1987, the group of *C. W. "Paul" Chu* at the University of Houston announced the existence of superconductivity in a Y-Ba-Cu-O compound with a critical temperature as high as 92 K.[5] This was a dramatic breakthrough because for the first time it was possible to observe superconductivity above liquid nitrogen temperatures. *Paul Chu*'s results were confirmed almost simultaneously by research groups around the world[6,7] and soon the superconducting phase was identified as the black 123-compound $YBa_2Cu_3O_{7-x}$ having an oxygen deficient, perovskite-like structure.[8,9]

Special sessions on High-T_c Superconductivity were scheduled at all major conferences in materials science, physics and chemistry, and scientists from all over the world discussed their views on experimental and theoretical aspects of High-T_c Superconductivity. Since then a flood of publications and numerous conferences and symposia have demonstrated the worldwide impact of *Bednorz* and *Müller*'s discovery. Now, not quite a year after the legendary "Woodstock of the Physicists" at the American Physical Society March Meeting, IBM Rüschlikon, the ETH Zürich, the University of Geneva, the University of Neuchatel, the Swiss National Science Foundation, and the Swiss Academy of Science invited experts to the *International Conference on High-Tc Superconductors and Materials and Mechanisms of Superconductivity (HTSC-M²S)* from February 29 to March 4, 1988, in Interlaken, Switzerland. About 1150 scientists were welcomed by *Alex Müller* of IBM, Rüschlikon. The conference was designed to provide an overview on all current developments of superconductivity in experimental and theoretical physics, chemistry, and applications. About 95 invited lectures were scheduled, 10 of them given in plenary sessions and about 85 in symposia and panel discussions organized in two parallel sessions. Special panel discussions and short talks on very recent results were organized in the evenings. Around 800 contributed papers were presented as posters in three all day sessions, with two hours in the afternoon reserved for the poster discussions and no other scheduled program in parallel. All invited and contributed papers were refereed during the conference and will be published in a special issue of "Physica C—Superconductivity" approximately three months after the conference.

Highlights were certainly the Tuesday and Wednesday evening sessions on new oxide superconductors. Two new groups of superconducting materials with onset temperatures above 100 K, namely Bi-Sr-Ca-Cu-O and Tl-Ba-Ca-Cu-O, were discussed in invited lectures and additionally scheduled five-minute talks. Bi-Sr/Ca-Cu-O compounds were investigated as early as February 1987 by researchers from the Max Planck Institute for Solid State Research and the Hoechst AG.[10] Superconductivity in Bi-Sr-Cu-O compounds was first reported by *Bernard Raveau* of the University of Caen, France, late in 1987.[11] Many other research groups began experimenting with bismuth substitutions into the 123-compound; *Hirshi Maeda* at the National Research Institute for Metals in Tsukuba, Japan, first announced results on January 22, 1988:[12a] superconductivity at 105 K was claimed, however, the group did not succeed in preparing a single phase sample. In his talk during the Tuesday evening session, *Maeda* gave the nominal composition of his sample as $BiSrCaCu_2O_x$. He reported a steep drop in the resistance vs. temperature curve, starting at about 120 K and leveling off near 105 K; $R=0$ was finally reached at 80 K. This behavior was confirmed by other researchers and is considered to be due to a low-T_c phase ($T_c=80$ K) and a high-T_c phase (T_c near 105 K). Other groups, among them *Art Sleight*'s from DuPont and *Bob Cava*'s from Bell Labs, reported $Bi_2Sr_2Ca_1Cu_2O_{8+x}$ as the superconducting compound, again with indications of low- and high-T_c phases.[12b]

More controversial is the structure of the new Bi-compounds. Several groups made proposals for the structure which do not agree with each other on several points. Some more or less common structural features are: The unit cell is made up of two Bi-O layers followed by five perovskite layers (Sr-O, Cu-O, Ca). Most peaks in the X-ray diffraction spectra can be indexed on the basis of a pseudo-tetragonal unit cell with $a=5.40$ Å, $c=30.83$ Å. An incommensurate modulation along the b-axis is observed by some groups, but that could turn out to be a sample and preparation dependent effect. There do not appear to be Cu-O chains in the new Bi-compounds; consequently the Cu-O and Bi-O planar arrangements are considered important for the superconductivity, in the Bi-compounds as well as in the "old" 123-compound. Preparation of samples follows a "shake and bake" recipe similar to the 123-material, but at lower temperatures (between 800 and

850°C). A slow cooling to adjust the oxygen content of the samples does not seem to be necessary with the Bi-compounds.

Superconductivity in Tl-compounds, discovered by scientists of the University of Arkansas,[13] was discussed by *Paul Chu* from the University of Houston and *Paul Grant* from the IBM Almaden Research Center, San Jose, among others. The compounds were synthesized at 950°C and subsequently quenched in air and the composition was given as $Tl_2Ca_2Ba_1Cu_2O_x$. Both *Chu* and *Grant* pointed out that thallium is extremely toxic and great care must be taken in working with these substances. *Grant* presented resistivity curves and magnetometer data that showed complete superconductivity at $T = 118$ K; on Wednesday night he announced that he had obtained new data from his lab via telefax showing bulk superconductivity at $T = 125$ K in the Tl-compounds. Spontaneous applause—and once again a little "Woodstock" atmosphere could be felt. Minutes later, in the conference center lobby, *Paul Grant* was surrounded by reporters, a picture usually associated with politicians rather than scientists.

Even though much was said about the new Bi- and Tl-compounds, most of the invited and contributed papers covered aspects of superconductivity in the "old" 123-compound $YBa_2Cu_3O_{7-x}$. During the symposium on crystal chemistry and structure detailed studies of the interdependence of structure, oxygen content, and superconductivity were presented. A panel discussed oxygen vacancy ordering, oxygen deficiency, and twinning. The role of twinning in the mechanism of superconductivity is still controversial. Processing and preparation of high-T_c superconducting materials were covered by three symposia: growth and properties of single crystals, superconducting glass properties, and thin films. Many posters also addressed the preparation of large single crystals, films of various thicknesses and on a variety of substrates, and dense, polycrystalline samples. Two symposia were scheduled to discuss electronic properties, including panel discussions on thermal and optical properties. Substitutions for Y and Cu, antiferromagnetic ordering, and magnetic flux penetration were presented during the symposium on magnetic properties. An entire evening session was devoted to the discussion of resonance experiments. It became clear that the frequency assignment for the Cu sites in nuclear quadrupole resonance (NQR) experiments will remain controversial until it is possible to reliably calculate the electric field gradient (EFG) at the respective Cu sites. The point charge calculations currently employed were considered insufficient. Various potential uses of high-T_c superconductors were presented and discussed in the symposium on applications. It was pointed out that even for applications such as superconducting connections on circuit boards a critical current density of at least 10^5 A cm^{-2} is absolutely essential. Consequently, many lectures and posters discussed the improvement of the critical current density, the role of grain boundaries for the critical current density, etc. Models on mechanisms, resonant valence bond and related models, bosonic models, and new ideas on theory were presented and debated during two symposia and two evening sessions.

The HTSC-M^{2}S conference demonstrated that one year after the discovery of the 90 K superconductors the interest in these substances is still enormous. Our knowledge of these compounds has grown considerably. Some controversies, e.g., about the existence of a distinct 60 K superconductor with 6.6-6.7 oxygens per formula unit, have been resolved. Great efforts are currently being made to find ways to increase the critical current densities in polycrystalline samples or thin films, predominantly deposited on $SrTiO_3$ substrates, that already exhibit high critical current densities. Particularly interesting work is being conducted at the IBM laboratory in Yorktown Heights, NY, where researchers are working on micro-patterning to "write" superconducting structures in thin films, e.g., loops for use in SQUIDs. New high-T_c superconducting materials will, without doubt, continue to play a significant role in the development of the field. The trend points towards increasingly complex structures. As *Paul Chu* put it "... one layer gives a T_c of 30 K, two give 60 K, three layers give 90 K, and now we have four layers and 120 K". The importance of this lies not only in the higher T_c, but also in the fact that scientists now have different structures available for their studies and so will be able to pin-point the common features in the different substances. This will ultimately help the theorists in their search for the "right" mechanism. *Robert Schrieffer*, summarizing the leading theoretical approaches, talked about conventional phonon mechanisms and charge fluctuations, but also mentioned such exotic concepts as half-fermions and x-ons ("... that's anything you like!"). But after the recent 30% isotope effect found by *Keven Ott* from Los Alamos National Lab, a conventional phonon-mediated mechanism must be re-examined.

A final comment is that, as with other superconductor meetings to date, the HTSC-M^{2}S conference in Interlaken was dominated by physicists and chemists. Only a few materials scientists presented papers or gave talks. There is still a wide gap between basic research and applications, such as interconnects, power transmission lines, or Josephson devices. The future of these applications depends on the materials properties of these substances, and it will be up to the materials scientists to fill the wide gap between basic research and applications.

H. Jaeger, K. Schulze
Max-Planck-Institut für Metallforschung
Stuttgart (FRG)

[1] J. G. Bednorz, K. A. Müller, *Z. Phys. B64* (1986) 189.
[2] C. W. Chu, P. H. Hor, R. L. Meng, L. Gao, Z. J. Huang, Y. Q. Wang, *Phys. Rev. Lett. 58* (1987) 405.
[3] S. Uchida, H. Tagaki, K. Kitazawa, S. Tanaka, *Jpn. J. Appl. Phys. 26* (1987) L 1.

[4] H. Tagaki, S. Uchida, K. Kitazawa, S. Tanaka, *Jpn. J. Appl. Phys. 26* (1987) L123.
[5] M. K. Wu, J. R. Ashburn, C. J. Torng, P. H. Hor, R. L. Meng, L. Gao, Z. J. Huang, Q. Wang, C. W. Chu, *Phys. Rev. Lett. 58* (1987) 908.
[6] Z. Zhao, C. Liquan, Y. Qiansheng, H. Yuzhen, C. Genghua, T. Ruming, L. Guirong, C. Changgeng, C. Lie, W. Lianzhong, G. Shuquan, L. Shanlin, B. Jianqing, *Kexue Tongbao* (1987), No. 6.
[7] P. Ganguly, A. K. Rychaudhuri, K. Sreedhar, C. N. R. Rao, *Pramana-J. Phys. 27* (1987) L229.
[8] P. M. Grant, R. B. Beyers, E. M. Engler, G. Lim, S. S. P. Parkin, M. L. Ramirez, V. Y. Lee, A. Nazzal, J. E. Vazquez, R. J. Savoy, *Phys. Rev. B35* (1987) 7242.
[9] T. Siegrist, S. Sunshine, D. W. Murphy, R. J. Cava, S. M. Zahurak, *Phys. Rev. B35* (1987) 7137.
[10] H. G. von Schnering, L. Walz, M. Schwarz, W. Becker, M. Hartweg, T. Popp, B. Hettich, P. Müller, G. Kämpf, *Angew. Chem. 100* (1988) 604; *Angew. Chem. Int. Ed. Engl. 27* (1988) 574.
[11] C. Michel, M. Hervieu, M. M. Borel, A. Grandin, F. Deslandes, J. Provost, B. Raveau, *Z. Phys. B68* (1987) 421.
[12] a) *Nihon Keizai Shimbun*, morning edition of January 22, 1988, page 1; b) H. Maeda, Y. Tanaka, M. Fukutomi, T. Asano, *Jpn. J. Appl. Phys. Lett.*, in press.
[13] Z. Z. Sheng, A. M. Hermann, *Nature (London) 332* (1988) 138.

... and Bad Nauheim (FRG)

A symposium on the structure and microstructure of high-temperature superconductors was held on April 21–22, 1988, in Bad Nauheim, Federal Republic of Germany. The aim of this comprehensive two-day symposium, organized by the Deutsche Gesellschaft für Metallkunde and chaired by *H. C. Freyhardt*, Göttingen, was to assemble an interdisciplinary group of scientists (physicists, chemists, crystallographers and materials scientists) and provide a forum for discussions devoted to the structure, microstructure, preparation and shaping, and applications of ceramic high-temperature superconductors (HTSCs). Leading scientists from Europe, the United States and Japan were invited to summarize the achievements in the field and to provide an evaluation of recent progress and unresolved problems.

The following lectures were presented: Structural aspects of mixed valence copper oxides and their relationships with superconductivity (*Raveau*, France)/Oxygen stoichiometry in pure and 3d-metal-doped $YBa_2Cu_3O_{7\pm y}$ (*Greene*, USA)/Structural aspects of the new Bi and Tl based high-T_c superconductors (*Batlogg*, USA)/Physical properties of high-T_c superconductors (*Steglich*, FRG)/On the microstructure of high-T_c superconductors (*Heeger*, FRG)/High-resolution transmission electron microscopy; principles and results on $YBa_2Cu_3O_{7-x}$ (*Gruehn*, FRG)/Phase diagrams of non-stoichiometric superconducting oxides (*Hauck*, FRG)/Crystal growth of high-T_c superconductors (*Hosoya*, Japan)/Bulk materials, shaping and prospects for applications (*Krauth*, FRG)/Application of high-T_c thin films in microelectronics (*Rogalla*, Netherlands).

In addition to the ten review talks, the latest results were presented on about 50 posters which were discussed in two plenary sessions. While the structure and properties of HTSCs were at the center of numerous discussions during the first day, the interest on the second day focused on "the real problems", as *H. E. Hoenig* from Siemens put it, namely preparation, shaping and applications. Controversies concerning the structure of the Bi-based superconductors do still exist, as a very lively discussion at the end of the first day showed.

The key quantity for HTSC applications in energy technology and superconducting electronics is the critical current density J_C. Based on magnetization curves of sintered, polycrystalline ceramic superconductors, the critical current density within a single grain was estimated to be of the order of 10^6 Acm^{-2} at $T=4.2$ K. The reason for the much lower J_C in sintered samples—typically 100–1000 Acm^{-2}—is considered to be the *weak links* between the grains in these materials. Defects such as voids, cracks and micro-cracks, second phase, including grain-boundary segregations and oxygen deficiency were also listed as reasons for the degradations of the transport properties. While the critical current densities in sintered HTSC materials are presently too low for most applilcations, J_C values in thin films prepared by a variety of methods are much more promising. However, not only the current carrying capability but also the film morphology must be considered; applications in superconducting electronics require very flat film surfaces for multiple stacked layers. The surface of epitaxially grown films or films made by laser ablation is too rough for applications in superconducting electronics. A further problem associated with thin films of HTSCs is the substrate-film compatibility. Evidence for Mg–Cu interdiffusion of $YBa_2Cu_3O_7$ films on MgO substrates was shown, and the necessity for passivation layers, e.g. silicon nitride on silicon substrates, was suggested. Various methods for the structuring of films were discussed, mostly for the fabrication of Josephson junctions. Because of the small coherence lengths in the HTSC materials, these Josephson junctions are difficult to prepare. Thus superconducting chip-interconnects seem much more likely applications at present than on-chip application of Josephson switching elements.

At this symposium the necessity of an interdisciplinary approach to the problem of high-T_C superconductivity became clear once again. Exact determination of the physical properties of these materials requires samples of higher phase purity and, of course, larger single crystals. Thorough investigations of preparation and shaping of these interesting substances are an important prerequisite for technological applications.

H. Jaeger
Max-Planck-Institut für Metallforschung
Stuttgart (FRG)

Conducting Polymers, Polyelectrolytes and Ultrathin Polymer Films in Mainz (FRG)

At the beginning of 1987, two inter-Nordic projects covering the areas of "molecular electronics" and "conductive polymers" were created and found support by the Nordic Fund for Industrial and Technological Development under the guidance of the Royal Swedish Academy of Engineering Sciences. One of the projects relates to the development of ultrathin organic films for use in electronics and biotechnology while the other involves the production and application of processable conductive polymers. The considerable overlap of these research topics with the current activities at the Max-Planck-Institut für Polymerforschung in Mainz, FRG, stimulated the convening of a one-day symposium held on 21 February 1988 in Mainz.

The symposium served as a platform for the exchange of information between all groups of scientists involved in the projects, i.e. both from the four Nordic countries Denmark, Finland, Norway and Sweden and from the Max Planck Institute, on the state of the art of research in these novel polymer systems including aspects of application in microelectronics, sensor technology and design of devices.

In the opening lecture *J. Böler* (Stockholm) presented an overview of the projects, pointing out that research on conducting ultrathin polymer films is being carried out at the University of Copenhagen (Denmark), Norsk Hydro (Porsbrunn, Norway), Center for Industriforsikring (Oslo, Norway), KSV Chemicals (Helsingfors, Finland), and the Royal Institute of Technology (Stockholm, Sweden). Processable conducting polymers are being studied at Linköping Technical University (Linköping, Sweden), Neste (Kullo, Finland), the Technical Research Center (Helsingfors, Finland), and Chalmers University of Technology (Gothenburg, Sweden).

J. Rühe (Mainz) then discussed hopping conduction in poly(3,4-cycloalkylpyrrole) perchlorates and presented new results on poly(3-alkylpyrroles). *H. Stubb* (Helsinki) described investigations on high-energy ion implantation in polythiophene films and polymer composites containing poly(octylthiophene). The following two lectures dealt with model compounds for conducting polymers. *V. Enkelmann* (Mainz) discussed X-ray structural analysis data of radical cation salts of aromatic hydrocarbons, especially salts of oligophenylenes, which serve as models for poly(*p*-phenylene), while *H. Hjertberg* (Gothenburg) presented some results obtained in synthetic and NMR studies on aniline oligomers.

O. Wennerström (Gothenburg) lectured about NMR studies on conjugated macrocyclophanes and band structure calculations of linear conjugated polymers. *W. Meyer* (Mainz) reviewed the properties of solid polymer electrolytes which might find application in batteries. He concentrated on the properties of ionenes having a constant ion density. The dielectric properties of these polymers were described by *F. Kremer* (Mainz). From the relaxation behavior in an electric field, information is obtained about the transport of charge carriers in these materials. *T. A. Ezquerra* (Mainz) talked about the percolative behavior of spherical poly(pyrrole) particles with a monodisperse distribution in an poly(ethylene oxide) matrix as an example for an insulator-conductor composite. He explained the dc and ac conductivity in such composites in terms of a hopping theory using the random resistor network model of *Miller* and *Abrahams*. Substituted poly(thiophenes) were the subject of two other lectures. *J. Laako* (Kullo) focused on processable conducting polymer blends from poly(alkylthiophenes), which have potential application as shielding materials, and *G. Inganäs* (Linköping) discussed thermochromic effects in these polymers.

The session on ultrathin films began with a lecture by *C. Bubeck* (Mainz) who reviewed briefly the production of ultrathin layers of polymers by the Langmuir-Blodgett (LB) technique. He presented results on LB films consisting of relatively stiff macromolecules like poly(phthalocyaninatosiloxanes) and poly(glutamates). *J. Virtanen* (Helsingfors) and *K. J. Jens* (Oslo) presented results on LB multilayers of conducting compounds, and *J. Raabe* (Mainz) described the determination of structural parameters in ultrathin polymer films by tunneling electron microscopy. The symposium ended with a lecture by *B. Krische* (Stockholm) on oligothiophenes.

In their closing remarks *J. Böler* and *G. Wegner* emphasized the importance of joint research efforts and continuous exchange of information in these novel fields of research which have great future potential in device technology.

Jürgen Rühe
Max-Planck-Institut für Polymerforschung
Mainz (FRG)

Research News

Polymer Liquid Crystals Forming Biaxial Nematic Phases

The field of polymer liquid crystals has experienced an enormous growth over the last years. It is now established that the different types of molecular ordering (nematic, smectic, cholesteric) can also be realized in polymer liquid crystals.[1] Recently it has been demonstrated by *Finkelmann* et al.[2] that polymer liquid crystals with mesogenic groups in the side chain can form biaxial nematic phases. This type of molecular ordering has not yet been observed in low molecular weight liquid crystals.

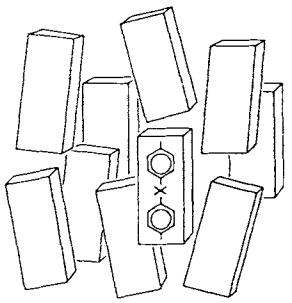

Fig. 1. Biaxial arrangement of lath-like particles [2b].

In a conventional nematic phase the rod-like mesogenic particles rotate around their long axis leading to an optically uniaxial system. For a system of lath-like particles (Fig. 1) orientational correlation may exist not only for their long axis but also for their short axes. The existence of such a biaxial nematic phase was predicted by *Freiser*[3] in 1970. Since then biaxial nematic phases have been the subject of numerous theoretical investigations (see [2b] for further references). A biaxial nematic phase in lyotropic liquid crystals was first observed by *Yu* and *Saupe*[4] in 1980. For thermotropic systems theory predicts[3] that the uniaxial phase should exhibit a second-order transition to the biaxial state upon lowering the temperature. However, this transition has never been observed experimentally for conventional low molecular weight liquid crystals and polymer liquid crystals with mesogenic groups in the side chain, since usually the onset of crystallization or the transition to a smectic phase or to the glassy state intervenes at lower temperatures. *Finkelmann* et al.[2] succeeded in showing that the stability of the biaxial state can be enhanced significantly if the rotation of lath-like mesogens is hindered by lateral attachment to a polymer main chain (Fig. 2, top).

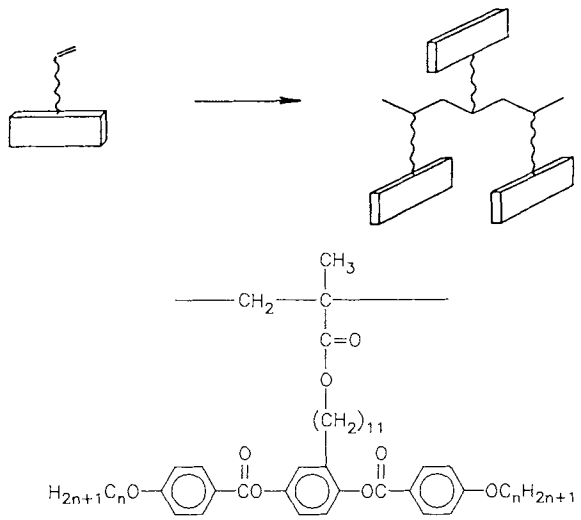

Fig. 2. Polymer liquid crystals with mesogenic groups attached laterally to the polymer backbone [2b]. Top: Schematic drawing; bottom: compounds that exhibit a biaxial nematic phase.

Thus, systems of the type shown in the lower part of Figure 2 exhibit a biaxial nematic phase which transforms into the isotropic state at the clearing temperature. The optical biaxiality was detected directly by conoscopic investigations of aligned samples. This exciting first observation of a thermotropic biaxial nematic phase demonstrates that by means of polymer liquid crystals new types of molecular ordering can be produced which could not be observed in low molecular weight systems. In this context it is important to note that *Ebert* et al.[5] have recently found direct conoscopic evidence for a biaxial nematic phase in a main chain liquid crystal polymer. Here again the stability of the biaxial arrangement was enhanced by long, laterally attached substituents which hinder the rotation around the long axis of the molecule.

[1] Review: H. Finkelmann, *Angew. Chem. 99* (1987) 840; *Angew. Chem. Int. Ed. Engl. 26* (1987) 816; see also *Adv. Polym. Sci. 59–61* (1984).
[2] a) F. Hessel, H. Finkelmann, *Polym. Bull. 15* (1986) 349; b) F. Hessel, R.-P. Herr, H. Finkelmann, *Makromol. Chem. 188* (1987) 1597.
[3] M. Z. Freiser, *Phys. Rev. Lett. 24* (1970) 1041; *Mol. Cryst. Liq. Cryst. 14* (1971) 165.
[4] L. I. Yu, A. Saupe, *J. Am. Chem. Soc. 102* (1980) 4879; *Phys. Rev. Lett. 45* (1980) 1000.
[5] M. Ebert, O. Hermann-Schönherr, J. H. Wendorff, H. Ringsdorf, P. Tschirner, *Makromol. Chem. Rapid Commun.*, in press.

Matthias Ballauff
Max-Planck-Institut für Polymerforschung
Mainz (FRG)

Book Reviews

Materials Research—The Birth of a Science

Advancing Materials Research. Edited by *P. A. Psaras* and *H. D. Langford* (on behalf of the National Academy of Engineering and the National Academy of Sciences). National Academy Press, Washington, D.C., 1987. xvi, 391 pp., bound, $ 47.50.—ISBN 0-309-03697-6

The book is based on presentations and discussions from a symposium held in Washington, D.C., on 28–29 October 1985 under the same heading, celebrating the twenty-fifth anniversary of the "Materials Research Laboratories". These laboratories were and are active in selected areas of materials science and engineering—"polymers, ceramics, metals, catalysis, crystallography, mechanical and microstructural properties of materials, artificially structured materials, electronic and magnetic materials, materials chemistry and surface science, solid state physics, and materials processing", to quote the preface of *T. H. Geballe*, Center for Materials Research, Stanford University, and *D. White*, Laboratory for Research on the Structure of Matter, University of Pennsylvania.

The historical aspects of this very successful chapter of the US funding system can only be appreciated by a true insider of the system—to which the author of this review does not belong. The scientific impact of this funding program, however, and the perspectives which arise after 25 years are of more general importance and point to a competitive future, in which the United States, Japan, and Europe will seek to cover research fields which are considered vital for their economies. The US program was initiated by President *Eisenhower* in 1960, some time after the launch of Sputnik I, on 4 October 1957.

What started in 1960 in three "Interdisciplinary Laboratories" (IDLs, to quote one of the book's many, many abbreviations and acronyms) has grown into a funding scheme which now includes about 15 IDLs and MRLs (Materials Research Laboratories). The first three laboratories were at Cornell, Pennsylvania State, and Northwestern universities; eight laboratories followed in 1961 and six between 1962 and 1982. The funding of the different materials science subdisciplines has certainly changed over the years: Metallurgy, which had originally obtained 31% of the resources, is now funded on a 17% level; the so-called "Materials" showed an almost fivefold increase in funding during the same period (from 11% to 51%). This field of "Materials" will be the main subject of this essay.

Although the book contains a lot of basics in materials science, it does not follow the pattern of a textbook, but rather reflects views of the symposium participants on various basic aspects of materials science. The field is truly interdisciplinary; the book summarizes research projects, most of which were physics (35%) and chemistry related (25%) in 1970, until by 1985 materials science (35%) had caught up with physics (35%), and had left chemistry behind (17%), at least in numbers.

In a list of accomplishments we read on page 44:
- Organic Metals
- Ultralow Temperatures
- Lower-Dimensionality Materials
- Surfaces and Interfaces
- Phase Transitions and
- New Materials

No doubt there would be a different emphasis two years after the discovery of a high-temperature superconductor in a European Laboratory of a US company: Neither organic metals nor ultralow temperatures nor 1-dimensionality was the solution to the dream of high-T_c superconductors—to our surprise (speaking for most of us).

After the historical perspective of materials research has been dealt with in the three articles of part one of the book, a report on "Progress and Prospects in Metallurgical Research" opens the second part. This contribution shows that research in metals is more than a race to increase *Young*'s modulus by investigating sophisticated alloys and by freezing-in non-equilibrium systems, etc.; the article points out that metal alloys play a dominant role as silicides in MOS semiconductor devices, as metallic glasses in power transformers (extrapolated savings of $ 0.7 billion per year), and as magneto-optical layers for optical memories. The second article gives a review of the fundamentals of dislocation theory and of the understanding of the ductile properties of metals. The third article reflects mainly those aspects of metals which are appealing to physicists: Heavy electrons (up to 1000 m_e), quantized *Hall* effect and quantum interference effects in superconducting metals.

In crystallography the advent of quasi-periodic structures with 8-, 10-, and 22-fold diffraction rotation axes has given rise to new excitement in a world where the mathematical boundary conditions of space filling and infinite crystals have so long prevailed.

The short article on "New and Artificially Structured Electronic and Magnetic Materials" covers the field from superionic conductors to quantum well semiconductors, with only brief discussions of the organic 1-dimensional conductors and conducting polymers which have kept many theorists and experimentalists busy after *A. Heeger*'s work on TTF-TCNQ in 1973. I am sure that a similar book in 25 years would feature several articles with headings similar to the one of this chapter.

The article on catalysis is short and emphasizes the EXAFS method, leaving out many aspects of metal-substrate interactions and modern analytical surface characterization tools, e.g., electron spectroscopy and imaging.

The question of "The Role of Chemistry in Materials Science" is treated more like a survey over various topics (new polymers, interface-modifying agents, ..., self assembling systems). It is followed by a short review on "Advanced Ceramics"—too short considering the relevance of these materials. The article on "Organic Polymers" is also very didactically styled. Questions like: How does a very long 'snake-like' molecule diffuse? are treated in enough detail to be understandable.

The last article of the second part, "New Ways of Looking at Surfaces", is more a short presentation of methods and recent applications avoiding details, which would be valuable for the technically interested reader.

The last and shortest part of the book, "Current Topics in Materials Research", reports on facilities and instrumentation, and may therefore be important for people interested in funding practices and politics.

In spite of its inhomogeneous character, with detailed articles describing dislocation theories of metals or the reptation model of polymer diffusion on the one hand, and articles which only give keywords without further explanation on the other hand, the book serves its purpose: It gives a rather complete summary over the first funding period of a gigantic and successful program and it sketches important challenges. Maybe the international competitiveness of today's research in materials science is responsible for the fact that extremely topical research areas such as impact-resistant ceramics, quantum wells, and new aspects of semiconductor research, are only touched upon briefly.

There is no equivalent European or Japanese book on the same topic. The book reflects a good American tradition of formulating and reviewing national goals. I hope that some European programs are stimulating and powerful enough to be the basis for a rewarding book 25 years from now.

Dietrich Haarer
Lehrstuhl für Experimentalphysik IV
der Universität Bayreuth (FRG)

Biosensors

Biosensors International Workshop 1987 (GBF Monographs, Vol. 10). Edited by *R. D. Schmid*. VCH Verlagsgesellschaft, Weinheim 1987, XIV, 346 pp, paperback, DM 128.00, ISBN 3-527-26801-4

In June 1987 the "Gesellschaft für Biotechnologische Forschung (GBF)" invited a representative circle of speakers to a workshop on biosensors in Braunschweig (FRG). The conference proceedings, published late in 1987, offer a good survey of the great variety of lectures held at the GBF. These topical proceedings illustrate, with a well suited mixture of reviews and reports, the broad range of biosensor research as well as the innovative power and the state of the art of this technology.

One of the purposes of this workshop was to define the position of the West German biosensor research in comparison with international activities in the field. In the preface the editor comments on the current situation and describes the position of the FRG by way of analyzing statistical data about biosensor publications and patents. Based on data from 1985, the West German biosensor research has to be placed in the sixth rank, far behind the dominating Japan and even behind the GDR.

Brilliant examples of new biosensors that make use of all important transducer technologies (potentiometric, amperometric, fiber optic and piezoelectric) were presented and their enormous potential, especially in medicine, was illustrated with ion-, enzyme-, and immunosensors. In addition, possible applications of biosensors in process engineering and environmental protection were discussed.

The performance of biosensors is already impressive. Gas sensors for organophophorus compounds with ppb sensitivities and immunosensors with detection limits beyond the picomolar range were reported. The large number of lectures about glucose sensors gives an impression of the topicality and importance of this subject. The long-term goal is an implantable glucose sensor which, combined with an insulin pump, would improve the life of many diabetics. In general, most of the biosensors are developed as diagnostic tools. Because of their excellent performance and cost effectiveness they have already become serious competitors to established methods. Remarkable success in this field is reported from the GDR.

There are many different approaches to reach the long-term goals, i.e., the combination of smale size (mm scale), cheapness (less than 50 cents), high sensitivity (nM–μM) and selectivity (10^5 or better), longevity (years), and high reliability (margin of error less than 1%) in one biosensor. The capabilities of living systems serve as a model. The detection sensitivities of sea animals to minimal water contaminations (down to 10^{-13} M) that are used, for example, to control the quality of drinking-water are still unrivalled. Biosensors with natural receptors are the way to imitate nature in this respect.

The efficient interdisciplinary cooperation of different fields like biology, chemistry, electronics, physics, and medicine is an important key to success and characterizes the internationally leading groups. It should be mentioned that there were also a few interesting contributions from West German researchers, and they demonstrated that a variety of innovations in this field are awaiting a breakthrough. The question remains why biosensor research, which will be an important economic factor in the next decades, has been so long neglected in the FRG. It is estimated that the nineties will see the commercial breakthrough of biosensors. For the year 2000 a study predicts an American biosensor market of $ 200 million for medical applications alone. Biosensors are also important for biotechnology, environmental technology, and the food industry. However, the proceedings of this workshop leave no doubt that medical applications predominate. The current situation in biosensor research in West Germany bears some similarities to the status of microelectronics and gene technology research a few years ago; in both fields, the FRG is now having to undertake enormous efforts to reach international standards. Will biosensor research have a similar fate? Immediate strong support for this interdisciplinary field could help prevent this.

A final word on the workshop proceedings: The editor should have insisted on a better elaboration of some of the abstracts. In a few cases a half-page summary of a lecture is all that is provided. However, the book enables one to rapidly obtain a comprehensive overview of the state of the art in biosensor research. Also, the book gives an impression of the innovative power of this technology.

Norbert Hampp and *Christoph Bräuchle*
Institut für Physikalische Chemie
der Universität München (FRG)

Conference Calendar

June 1988

26-2 **Synthetic Metals**
Los Alamos (USA)
Contact: M. Aldissi, ICSM '88, Los Alamos Natl. Lab., P.O. Box 1663, MS K764, Los Alamos, NM 87545, USA

26-8 **Superconductive Electronics,**
NATO Adv. Study Inst.
Il Ciocco (Italy)
Contact: H. Weinstock, AFOSR/NE Bolling AFB, Washington, DC 20332-6448, USA

29-30 **Organic Materials for Nonlinear Optics (OMNO '88)**
Oxford (United Kingdom)
Contact: Mrs. E. S. Wellingham, OMNO '88, 6 Craig-yr-Haul Drive, Castleton, Cardiff CF3 8SA, UK

July 1988

3-15 **Polymer Colloids III,**
NATO Adv. Study Inst.
Strasbourg (France)
Contact: R. H. Ottewill, Univ. of Bristol, Cantocks Close, Bristol BSB 1 TS, UK

5-8 **Modified Polymers,**
7th IUPAC Int. Conf.
Bratislava (Czechoslovakia)
Contact: A. Romanov, Polymer Inst. CCR, Slovak Acad., Bratislava, CSSR

10-24 **Surfaces and Grain Boundaries of Oxide Ceramics,**
NATO Adv. Study Inst.
Stuttgart (Fed. Rep. Germany)
Contact: Dr. J. Nowotny, Max-Planck-Institut für Festkörperforschung, Heisenbergstraße 1, Postfach 800065, D-7000 Stuttgart 80, FRG

12-15 **Joint Magnetism and Magnetic Materials (MMM)-Intermagn. Conf. (4M3I)**
Vancouver (Canada)
Contact: IEEE, Technical Activities Dept., 345 E 47th St., New York, NY 10017, USA

18-21 **Carbon Fibers and Composites**
Buffalo (USA)
Contact: D. D. L. Chung, Dept. of Mechanical & Aerospace Engineering, SUNY, Buffalo, NY 14260, USA

18-21 **Macromolecules,**
31st Microsymp.
Prague (Czechoslovakia)
Contact: P. M. M. Secretariat, Inst. of Macromol. Chem., 1888 Petriny, Prague 6, CSSR

25-27 **Laser Materials and Laser Spectroscopy**
Shanghai (People's Rep. China)
Contact: Prof. Wang Zhijiang, Chinese Optical Society, P.O. Box 8211, Shanghai, People's Rep. of China

August 1988

1-6 **Macromolecules,**
32nd IUPAC Int. Symp.
Kyoto (Japan)
Contact: Soc. of Polym. Sci. 5-12-8 Ginza, Chuo-ku, Tokyo 104, Japan

8-12 **Superlattices, Microstructure and Microdevices,**
4th Int. Conf.
Trieste (Italy)
Contact: Prof. G. H. Döhler, Univ. Erlangen-Nürnberg, Institut für Technische Physik, Erwin-Rommel-Str. 1, D-8520 Erlangen, FRG

14-19 **Optical and Optoelectronic Applied Sci. and Eng.,**
32nd Annu. Int. Tech. Symp.
San Francisco (USA)
Contact: SPIE, P.O. Box 10, Bellengham, WA 98225, USA

15-19 **Controlled Release of Bioactive Materials,**
15th Int. Symp.
Basel (Switzerland)
Contact: Administrative Office, Controlled Release Soc., 16 Nottingham Dr., Lincolnshire, ILL. 60015, USA

15-19 **Liquid Crystals,**
12th Int. Conf.
Freiburg (Fed. Rep. Germany)
Contact: Dr. G. Baur, Fraunhofer-Institut IAF, Eckerstr. 4, D-7800 Freiburg, FRG

22-25 **Nonlinear Optical Properties of Materials**
Troy (USA)
Contact: OSA, 1816 Jefferson Pl. NW, Washington, DC 20036, USA

22-26 **Ceramic Developments - Past, Present and Future,**
Int. Ceramic Conf. and Fair
Sydney (Australia)
Contact: G. Henness, New South Wales Inst. of Technology, Dept. of Materials Sci., P.O. Box 123, Broadway NSW 2007, Australia

28-1 **Molecular Beam Epitaxy (MBE-5)**
Sapporo (Japan)
Contact: Prof. M. Konagai, Tokyo Inst. Tech., Dept. of Electrical and Electronic Eng., 1-12-1 Okayama, Meguro-ku, Tokyo 152, Japan

28-10 **Structure-Property Relationships in Surface Modified Ceramics**
NATO Adv. Study Inst.
Pisa (Italy)
Contact: C. J. McHargue, Metals & Ceramics Division, Oak Ridge Natl. Lab. P.O. Box 10, Oak Ridge, TN 37831-6118, USA

29-1 **Applications of Polar Dielectrics and Ferroelectrics,**
Int. Symp.
Zürich (Switzerland)
Contact: H. Arend, Swiss Federal Inst. of Tech., Lab. of Solid State Physics, CH-8093 Zürich, Switzerland

29-10 **Ion Beam Analysis of Solids,**
Summerschool
Jena (German Dem. Rep.)
Contact: Prof. G. Götz, Friedrich-Schiller-Univ., Sektion Physik, Max-Wien-Platz 1, DDR-6900 Jena, DDR

September 1988

4-8 **Zeolites as Catalysts, Sorbents and Detergent Builders,**
Int. Symp.
Würzburg (Fed. Rep. Germany)
Contact: Dr. H. G. Karge, Fritz-Haber-Inst. der Max-Planck-Gesellsch., Faradayweg 4-6, D-1000 Berlin 33

4-9 **Metal-Hydrogen Systems, Fundamentals and Applications,**
Int. Symp.
Stuttgart (Fed. Rep. Germany)
Contact: Dr. E. Fromm, Max-Planck-Institut für Metallforschung, Inst. für Werkstoffwissenschaften, Seestraße 92, D-7000 Stuttgart 1, FRG

4-16 **Surfaces and Interfaces on Ceramic Materials,**
NATO Adv. Study Inst.
Oleron (France)
Contact: Dr. L. C. Dufour, Chemie des Materiaux IREQ, CP 1000, Varennes, Quebec JOL 2PO, Canada

4-16 **Plasma Surface Interactions and Processing of Materials,**
NATO Adv. Study Inst.
Alicante (Spain)
Contact: Prof. O. Auciello, NC State Univ., Dept. of Nuclear Eng., Raleigh, NC 27695-7909, USA

5-7 **Electrical, Optical and Acoustic Properties of Polymers**
Canterbury (United Kingdom)
Contact: The Plastics and Rubber Inst., 11 Hobart Pl., London SW1X OHL, UK

5-8 **Surface Science,**
Eur. Conf. (ECOSS-10)
Bologna (Italy)
Contact: Prof. O. Bisi, Univ. di Modena, Dipto. di Fisica, 213/a Via Campi, I-41100 Modena, Italy

10-17 **Electrochemistry of Conductive Polymers**
Sulejow (Poland)
Contact: Janusz Ptocharski, Inst. of Inorganic Technology, ul. Noakowskiego 3, 00664 Warszawa, Poland

12-14 **Materialforschung 1988,**
BMFT Symp.
Hamm (Fed. Rep. Germany)
Contact: Material- und Rohstofforsch., KFA Jülich GmbH, Postfach 1913, D-5170 Jülich, FRG

12-16 **Surface Modification of Metals by Ion Beams,**
6th Int. Conf. (SMMIB '6)
Riva del Garda (Italy)
Contact: Dr. L. Guzman, Technologica in Trento, Istituto per la Ricerca Scientifica, I-38050 Povo, Trento, Italy

12-16 **Properties and Applications of Dielectric Materials,**
2nd Int. Conf. (ICPADM-2)
Beijing (People's Rep. China)
Contact: Prof. Z. Renyu, Tsinghua University, Dept. of Electrical Eng., Beijing, People's Rep. of China

12-15 **Solid State Protonic Conductors IV**
Exeter (United Kingdom)
Contact: Dr. R. C. Slade, Univ. of Exeter, Dept. of Chem., Stocker Rd., Exeter EX4 4QD, UK

12-17 **Evaluation of Adv. Semiconductor Materials by Electron Microscopy,**
NATO Adv. Workshop.
Bristol (United Kingdom)
Contact: Dr. D. Cherns, HH Wills Phys. Lab. Univ. Tyndall Ave., Bristol BSB 1 TL, UK

13-15 **Speciality Polymers,**
3rd Int. Conf.
Cambridge (United Kingdom)
Contact: Monique Heald, Butterworth Scientific Ltd., P.O. Box 63, Westbury House, Bury St., Guilford, Surrey GU2 5BH, UK

13-16 **Structure and Reactivity of Solids**
Trieste (Italy)
Contact: Prof. C. Morterra, Ist. Chimica Fisica, C.so M D'Azeglio 48, I-10125 Torino, Italy

13-16 **Polymers, Laminations & Coatings**
Atlanta (USA)
Contact: Meet. Dept., TAPPI, Technology Park, Atlanta, GA 30348-5113, USA

20-23 **Polymer Surfaces and Interfaces,**
Workshop
Pacific Grove, CA (USA)
Contact: J. Rabolt, IBM, Almaden Research Ctr., 650 Harry Rd., San Jose, CA 95120-6099, USA

21-23 **Solid-State Circuits,**
14th Eur. Conf. (ESSCIRC-14)
Manchester (United Kingdom)
Contact: Dr. P. J. Hicks, UMIST, Dept. of Electrical Eng. and Electronics, P.O. Box 88, Manchester M60 IQD, UK

22-23 **Oxidation of High-Temperature Intermetallics,**
Workshop
Westlake, OH (USA)
Contact: T. Grobstein, NASA Lewis Research Center 2100 Brookpark Rd., M/S49-1 Cleveland, OH 44135-3191, USA

24-30 **World Materials Congress**
Chicago (USA)
Contact: World Materials Congress, Technical Department ASM International, Metals Park, OH 44073, USA

26-30 **Polymer Networks Group,**
9th Mtg.
Freiburg (Fed. Rep. Germany)
Contact: W. Burchard, Inst. für Makromolekulare Chemie, Univ. of Freiburg, Stefan-Meier-Strasse 31, D-7800 Freiburg, FRG

28-30 **Ungewöhnliche Valenzzustände in Festkörpern,**
5. Vortragstagung der Fachgruppe Festkörperchemie der Gesellsch. Dtsch. Chem.
Erlangen (Fed. Rep. Germany)
Contact: GDCh, Abtlg. Tagungen, Postfach 900440, D-6000 Frankfurt am Main 90, FRG

October 1988

3-6 **Farbensymposium,**
10. Int. Symp.
Trier (Fed. Rep. Germany)
Contact: Dr. E. Hahn, BASF AG, D-6700 Ludwigshafen, FRG

9-14 **Ultrafast Phenomena and Nonlinear Optics**
Chicago (USA)
Contact: R. R. Alfano, City College of New York, 138 St. and Convent Ave., New York, NY 10031, USA

12-14 **Ceramic Powder Processing Science,**
2nd Int. Conf.
Berchtesgaden (Fed. Rep. Germany)
Contact: Dtsch. Keram. Gesellsch., Postfach 1226, D-5340 Bad Honnef 1, FRG

18-20 **Deutsche Keramische Gesellschaft,**
Annu. Congr.
Munich (Fed. Rep. Germany)
Contact: Dtsch. Keram. Gesellsch., Postfach 1226, D-5340 Bad Honnef 1, FRG

18-22 **ceramitech '88,**
4th Int. Fair/3rd Int. Symp.
Munich (Fed. Rep. Germany)
Contact: Münchener Messe- und Ausstellungsgesellsch., Postfach 121009 D-8000 München 12, FRG

19-21 **Raw Materials for New Technologies,**
5th Int. Symp. on Mineral Resources
Hannover (Fed. Rep. Germany)
Contact: Dr. Arnt Müller, Bundesanstalt für Geowissenschaften und Rohstoffe, Postfach 510153, D-3000 Hannover 51, FRG

21-24 **Functional and Fine Polymers,**
XISFFP Xian Int. Symp.
Xian (People's Rep. China)
Contact: Prof. Hua Zhao, Xian Modern Chemistry Research Inst., P.O. Box 18, Xian, People's Rep. of China

23-26 **Combustion and Plasma Synthesis of High-Temperatur Materials,**
Int. Symp.
San Francisco (USA)
Contact: Dr. J. B. Holt, Lawrence Livermore Natl. Lab., P.O. Box 808, L-369, Livermore, CA 94550, USA

November 1988

8-10 **European MRS Fall Conference**
Strasbourg (France)
Contact: P. Siffert, Centre de Recherches Nucléaires, Lab. "PHASE", 23, Rue du Loess, F-67037 Strasbourg (France)

9-11 **Perspectives on the New Superconductivity**
Boston (USA)
Contact: D. Berger, Nature Publ. Co., 65 Bleecker St., New York, NY 10012, USA

10-11 **Microstructural and Microanalytic Characterisation of Ceramic Materials**
Bad Nauheim (Fed. Rep. Germany)
Contact: Deutsche Gesellschaft für Metallkunde eV., Adenauerallee 21, D-6370 Oberursel, FRG

19-23 **Multiphase Macromolecular Systems,**
14th Biennial Polymer Symp.
San Diego (USA)
Contact: B. Culbertson, Ashland Chemical Co., P.O. Box 2219, Columbus, OH 43216, USA

27-30 **Ceramic Materials and Components for Engines,**
3rd Int. Symp.
Las Vegas (USA)
Contact: American Ceramic Soc. 757 Brooksedge Plaza Dr., Westerville, OH 43081-6136, USA

28-3 **MRS Fall Meeting**
Boston (USA)
Contact: Materials Research Society, 9800 McKnight Rd., Suite 327, Pittsburgh, PA 15237 (USA)

December 1988

1-4 **Water Soluble Polymers,**
Fuzhou Int. Symp.
Fuzhou (People's Rep. China)
Contact: Hu Bing-huan, Inst. of Polym. Sci., Fujian Teachers Univ., People's Rep. of China

7-8 **Materials Science and Eng. Towards the 21st Century,**
4th Israel Mater. Eng. Conf.
Beer-Sheva (Israel)
Contact: Peltours-Conventions, The Secretariat, 4th Israel Mater. Eng. Conf., P.O. Box 394, 61003 Tel-Aviv, Israel

14-16 **SIMCER 7/ZIRCONIA 88**
7th Int. Symp. on Ceramics
Bologna (Italy)
Contact: Centro Ceramico, Via Martelli, 26
I-43138 Bologna, Italy

If you want to have your conference, symposium, workshop or fair announced in this Calendar, please send all relevant material to

ADVANCED MATERIALS/ ANGEWANDTE CHEMIE
Postfach 1260/1280
D-6940 Weinheim
Federal Republic of Germany

ADVANCED MATERIALS will again appear in the July issue of this journal and from September onwards, monthly.

The July issue will contain short reviews on advanced powder metallurgy *(Petzow/Kaysser)* and polymer synthesis *(Reetz)* as well as contributions to the other sections of ADVANCED MATERIALS.

A number of free reprints of this ADVANCED MATERIALS part of the journal are available.

Please write to:

Reader Service
ADVANCED MATERIALS/ANGEWANDTE CHEMIE
Postfach 1260/1280 · D-6940 Weinheim
Federal Republic of Germany

ANGEWANDTE CHEMIE
International Edition in English
Volume 27 · Number 6
June 1988
Pages 759–864

Tellurium-Rich Tellurides

By Peter Böttcher*

The tellurides represent a class of compounds which exhibit a wide range of physical and chemical properties. In addition to the salt-like compounds, some tellurides show metallic properties while others have strong covalent bonds. Like tellurium itself, many of these are semiconductors, e.g., the II–VI compounds CdTe and MnTe, and in this respect are of special interest. Other tellurides, e.g., $NbTe_4$ and $ZrTe_5$, have low-dimensional electronic transport properties. Some ternary transition metal–main group metal tellurides appear in an amorphous state with spin glass properties. The tellurium-rich tellurides are characterized without exception by directed Te–Te bonds. It turns out that general structural chemical relationships exist between them which allow these different compounds to be treated as a single comprehensive class of substances. They represent a link between the Zintl phases on the one hand, and molecular compounds on the other.

1. Introduction

In recent years the structures of a large number of tellurium-rich tellurides have been reported whose anionic networks are characterized by homonuclear Te–Te bonds. They do not usually follow the structural chemistry of the chalcogen-rich selenides and sulfides, which are found almost exclusively in helical zig-zag chains X_n^{2-} (X = S, Se; n = 4, 5, 6 ...), due to their prevalent two-coordinate covalency. On the other hand, the tellurides reflect the variety of structural possibilities of the element tellurium itself, since the anionic segment can frequently be derived from either known or hypothetical modifications of tellurium in which each atom is more than two-coordinate. The size of the fragment depends on the number of electrons transferred to tellurium, with the most electron-rich anionic components remaining as small, isolated, quasi-molecular fragments. This formal operation of transferring all valence electrons from the more electropositive to the more electronegative atoms is known as the Zintl–Klemm concept, which allows one to predict structural features for distinct classes of compounds.[1–5] In accordance with these ideas, some tellurides show infinite three-dimensional networks of tellurium, while others exhibit infinite two- or one-dimensional anionic building units, as well as those examples that contain only isolated anionic fragments.

2. Some Possible Arrangements of Tellurium

As a Group 6 element, tellurium can bind to a maximum of six neighbors. Several high-pressure experiments have been carried out with the aim of stabilizing a modification with six equivalent bond distances. The α- as well as the β-Po type would show suitable arrangements.[6,7] The close relationships between the α-Po type and the thermodynamically stable modification of Te have already been outlined. The six equivalent Te–Te distances are predicted to be 3.02 Å.[8] All experiments using pressures up to 10 GPa

[*] Prof. Dr. P. Böttcher
Max-Planck-Institut für Festkörperforschung
Heisenbergstrasse 1, D-7000 Stuttgart 80 (FRG)

 © VCH Verlagsgesellschaft mbH, D-6940 Weinheim, 1988 0570-0833/88/0606-0759 $ 02.50/0

have not produced the desired result, although Te undergoes two pressure-dependent phase transformations in this region (at 4.5 and 7 GPa[7, 9]). At 4 GPa one observes a structural change (two-bonded Te→four-bonded Te) together with a semiconductor-to-metal transition. At 7 GPa only a gliding change of the metric occurs (four-bonded $Te_{monoclinic}$→four-bonded $Te_{orthorhombic}$), without any fundamental rearrangement of the tellurium atoms. In addition, some changes in the physical properties are observed.[9] Two further pressure-induced phase transformations have been reported. One of them is said to occur around 3 GPa and results in the gray As structure type (two-bonded Te → three-bonded Te[10]). From this structure the observed modification of Te at 4.5 GPa, which shows four-bonded Te, could indeed arise. The second reported phase transformation was obtained at 7 GPa to give the β-Po structure type.[7] All observations present the following picture (b stands for "bonded"):

Te(2b, trigonal, thermodynamically stable modification) ⟶ [Te(3b, rhombohedral, As type, 3 GPa)] ⟶ Te(4b, monoclinic, 4.5 GPa) ⟶ [Te(6b, rhombohedral, β-Po type, 7 GPa)].

The increase in the bond number with increasing pressure is consistent with expectation.

Table 1 classifies both the existing modifications as well as some selected examples of hypothetical arrangements in a scheme that orders not only by the number of homonu-

Table 1. Structural motifs of tellurium (HP = high pressure).

Electrons per Te bonding	nonbonding pairs	nonbonding deloc.	Example	Neighbors distance [Å] (number) nearest	second nearest	Bond angle [°]	Selected motifs	Fig.	Ref.
6	0	0	—	3.02 (6×)	—	90	$^{3}_{\infty}$[network]	1a	[8]
5	0	1	—	—	—	—	$^{2}_{\infty}$[double sheets]	1i	—
4	1	0	HP-modif. (4–7 GPa)	2.80 (1×) 3.10 (3×)	3.47 (1×) 3.52 (3×)	87.3, 92.7 107.9	$^{2}_{\infty}$[folded nets of squares]	1g	[9]
4	0	2	—	—	—	—	$^{2}_{\infty}$[nets of squares]; 4^4-nets	1h	—
3	1	1	[HP-modif. (~3 GPa)]	2.87 (3×)	3.48 (3×)	94.4	$^{2}_{\infty}$[folded nets of hexagons]	1e, 1f	[10]
3	0	3	—	—	—	—	$^{2}_{\infty}$[nets of hexagons]; 6^3-nets	—	—
2	2	0	stable modif. Te	2.84 (2×)	3.50 (4×)	103.2	$^{1}_{\infty}$[helices]	1b	[11]
2	1	2	—	—	—	—	$^{1}_{\infty}$[planar zig zag chains]	1d	—
2	0	4	—	—	—	—	$^{1}_{\infty}$[linear chains]	1c	—
1	localized double bond		Te_2 (gaseous)	2.56 (1×)	—	—	$^{0}_{\infty}$[dumbbells]	—	[12]

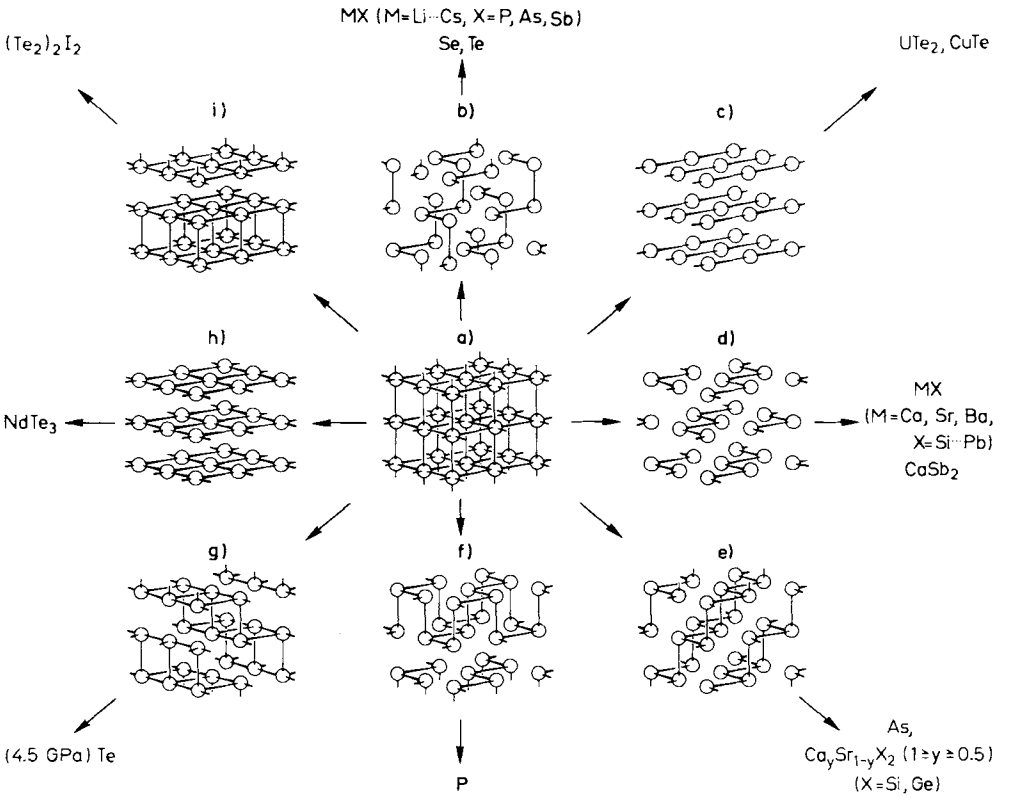

Fig. 1. Selected structural motifs of tellurium illustrating the dependence on the bonding of the Te atoms: a) primitive cubic; b)–i) motifs occurring after bond breaking. Some structural examples that can be derived from each of the motifs are indicated (see Table 1).

clear bonds but also by the localization or the delocalization of the nonbonding electrons that remain. Some of the possible structures are shown in Figure 1.

All modifications in which tellurium has an odd number of bonds should exhibit metallic properties on account of the extra unpaired electron (Fig. 1e: three-bonded Te, As type; Fig. 1i: five-bonded Te, 4^4 double nets). However, in some of the possible structures with an even number of bonds, all of the nonbonding electrons need not be localized into lone pairs. One can imagine four-coordinate Te with two delocalized electrons forming an infinite two-dimensional tetragonal plane (4^4 net). This represents a low-dimensional metal, just as in the two-dimensional double sheets containing five-coordinate Te shown in Figure 1i. Two-coordinate Te arises when four nonbonding electrons occur in two localized lone pairs (found as zig-zag chains—the thermodynamically stable modification). Planar zig-zag chains could arise from divalent tellurium which has one nonbonding pair and two delocalized electrons. Alternatively, divalent Te atoms having four delocalized electrons can produce linear chains. Some examples of such structural variations are realized in Zintl phases with suitable composition in which the electronegative element contains formally six valence electrons. The pressure-induced semiconductor-to-metal transition occurring at 4 GPa also leads to a structure that contains tellurium atoms with an even bond number (4b, cf. Fig. 1g and Fig. 2) in the metallic high-pressure state.

In this phase, which is stable above 4.5 GPa, the pleated 4^4 sheets are not stacked one on top of the other as in α-Po, but are shifted towards one another along the [010] direction by $a/2$ (Fig. 2), whereby the coordination number increases from six to eight (1+3+1+3, Table 1). The bond angle is 108°. Monoclinic behavior remains up to 6.6 GPa. As the pressure increases the monoclinic angle β shifts toward 90° and orthorhombic symmetry occurs. In addition, at 6.6 GPa some of the physical properties change.[9] The distances between the 4^4 nets are not affected with respect to the high pressure. As in the stable modification of Te at ambient pressure as well as in many tellurium-rich tellurides, it is around 3.5 Å.

The operation of bond breaking beginning with highly symmetric arrangements (cf. Fig. 1) has been occasionally discussed.[13–15] For example, it has been shown that 36

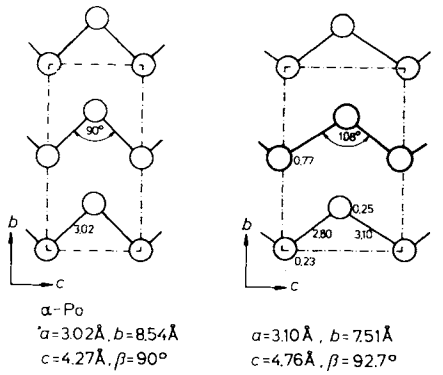

α-Po
a=3.02 Å, b=8.54 Å
c=4.27 Å, β=90°

a=3.10 Å, b=7.51 Å
c=4.76 Å, β=92.7°

Fig. 2. The [100] projection of the structure of the 4.5 GPa HP modification of tellurium. The difference in height along the a-axis of the undulated tellurium nets is denoted by normal and bold lines (right). The corresponding projection of the α-Po structure type (left).

possibilities exist for three-bonded atoms, if the primitive cubic array is used as a starting point. Among these 36 structures, that of gray As and black P have distinct energetic stability with respect to the majority of the alternatives.[13] This result is mirrored in the fact that pressure leads to the transformations P(black) → P(gray As) → P(α-Po) and Sb(As type) → Sb(α-Po).[16]

3. Structures of the Tellurides

According to the Zintl-Klemm concept the valence electrons are transferred from the cations to the more electronegative tellurium. As previously noted, the connectivity within the anionic segment becomes reduced as more electrons are transferred to it. The alkali metal tellurides are examples that clearly follow the expected trends (Table 2). Naturally, no severe correlations exist that would limit one and only one structural type for a given average tellurium oxidation number. Additional effects, such as increasing cation-anion or cation-cation interactions by the introduction of transition metal cations, can influence the structures of the anionic framework.

Table 2. Motifs of the alkali metal tellurides.

General formula	Average oxidation number	Motif of the anionic part	Ref.
MTe_4 (M = Cs)	−0.25	$^2_\infty[TeTe_3^-]$	[17]
MTe_3 (M = Li, Na)	−0.33	$^1_\infty[Te_{1/2}^{0}{}^-(Te_2)_3]$	[18, 19]
$MTe_{2.5}$ (M = Rb, Cs)	−0.40	$^1_\infty[TeTe_4^{2-}]$	[20, 21]
$MTe_{1.5}$ (M = K, Rb, Cs)	−0.67	isolated: Te_3^{2-}	[22, 23]
MTe (M = Na, K)	−1.00	isolated: Te_3^{4-}, Te_2^{2-}, Te^{2-}	[24, 25]
M_2Te (M = Li, Na, K, Rb, Cs)	−2.00	isolated: Te^{2-}	[26, 27]

3.1. Infinite Three-Dimensional Anionic Frameworks

Such frameworks are derived from the α-Po type structure (Fig. 3a) as one systematically removes atoms from its infinite three-dimensional network. Removal of every fourth Te atom results in one of the conceivable structures that contains exclusively four-coordinate Te in which both nonbonding electrons should be delocalized (Fig. 3e). The square planar fragment is marked, which is suitable to build up the network. This framework, which is also observed in the binary compound NbO (Fig. 3d[29]), occurs nearly undistorted in the structure of $AgTe_3$.[28] The bond angles at Te are 89.8° and 90.5° and the Te–Te distance is 3.05 Å. Since the Ag cations occupy the sites of the missing Te atoms (Ag–Te: 3.02 Å and 3.08 Å), the complete structure is essentially an undistorted 1:3 ordered variant of the α-Po type (Fig. 3c). Metallic properties have been confirmed by experiment. $LiTe_3$[18] and $NaTe_3$,[19] both of which are structurally related to $AgTe_3$, have a broken-up infinite three-dimensional anionic network. In these cases only infinite one-dimensional strands are found in which Te is either two- or three-coordinate. The change to the alkali metal cations causes, to some extent, an increased

localization of the nonbonding electrons, in which one recognizes ca. 20% increases in the volume of the anionic structural component over that for $AgTe_3$[26] (see Section 3.3 and Table 4).

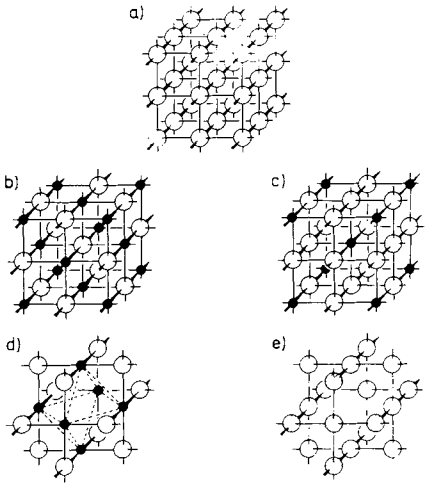

Fig. 3. Two derivatives of the primitive cubic arrangement: a)→b)→d): α-Po type, NaCl type, NbO; a)→c)→e): α-Po type, $AgTe_3$, $^3_\infty[Te_3^-]$.

The 1:3 ordered variant of the α-Po type (≙ $AgTe_3$, Fig. 3c) is compared with the corresponding 1:1 ordered type (≙ NaCl type, Fig. 3b). The same systematic removal of a fourth of all atoms in the case of the NaCl type leads to the NbO structure (Fig. 3d[29]), in the case of $AgTe_3$ there results the anionic structural component $^3_\infty[Te_3^-]$ (Fig. 3e).

3.2. Infinite Two-Dimensional Anionic Networks

The anionic structural component of $CsTe_4$[17] is related to the infinite two-dimensional framework containing five-coordinate Te atoms (Fig. 1i). It can be derived from this two-dimensional section of the α-Po structure through the systematic removal of every third Te atom. The remaining network contains only two and three-coordinate Te atoms, as in the case of the tritellurides $LiTe_3$ and $NaTe_3$. The relationship between the hypothetical double sheet with five-coordinate tellurium (Fig. 1i) and the observed Te network in $CsTe_4$ (Fig. 4) is similar to the relationship between the structure of black phosphorus (Fig. 1f) and pnictide nets in MX_3 materials (M = alkaline earth metal, X = pnicogen).[5,30] Because of the different constituents and oxidation numbers of the cations, puckered X_{14} rings occur within the pnictide nets, while puckered Te_{18} rings are found in $CsTe_4$. The three-coordinate pnicogen atoms in the polyanionic networks (X_3^{2-}) of the pnictides carry just a single nonbonding electron pair, whereas the three-coordinate Te^- ions in the polyanionic sheets of $CsTe_4$ have two nonbonding electron pairs, as does Br in the interhalogen compound BrF_3, due to their function as central atoms for their corresponding fragments. In fact, the interconnected Te_{18} rings can be broken down into 25e-fragments $TeTe_3^-$ (six valence electrons per Te plus one additional electron) analogous to the BrF_3 molecule (Fig. 4,

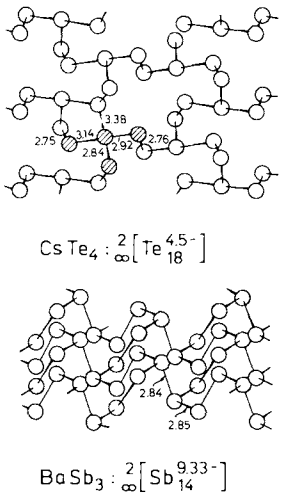

Fig. 4. Top: Anionic part of the $CsTe_4$ structure projected down [30$\bar{2}$]. Bottom: Anionic part of $BaSb_3$.

shaded fragment). On account of the deficiency of three valence electrons compared to BrF_3, the $TeTe_3^-$ units bridge together via the radical centers (the three terminal Te atoms of the T-shaped fragment, in a formal sense) to form 18-membered rings in the infinite two-dimensional sheets. The fragments are distorted: $Te_{central}$–Te_{apical}, 2.92 and 3.14 Å; $Te_{central}$–$Te_{equatorial}$, 2.84 Å; Te_{apical}–$Te_{central}$–$Te_{equatorial}$, 93.6° and 83.6°. As in pseudo trigonal bipyramidal molecules, the apical atoms on average (3.03 Å) lie farther from the central atom than the equatorial atoms. Adjacent fragments are connected via distances of 2.75 and 2.76 Å. When a Te···Te contact of 3.38 Å ($Te_{central}$···Te_{apical}) is included, the T-shaped fragment becomes a heavily distorted square planar structural group $TeTe_4$. In a more undistorted form this represents the preferred arrangement in many Te-rich tellurides.

The closed double sheet fragment of the α-Po structure with five-coordinate Te (Fig. 1i) remains completely maintained in the flat Te double sheets of the remarkable intercalation compound $(Te_2)_2I_2$ (Fig. 5).[31] Independent of whether the remaining nonbonding electrons are localized or delocalized, these nets are not known in any HP modification of Te or in the tellurides. In the compound $(Te_2)_2I_2$, the electronegativities argue against an electron transfer from iodine to tellurium and, therefore, against the formulation of the double nets as anions. Rather, one expects a partial electron loss from the double sheets of the hypothetical five-coordinate Te. Therefore, there are fewer than six electrons per tellurium in the flat double sheets. In a recently published work, both the topological and electronic relationships of this Te framework have been discussed with regard to the structure of β-SnS, which is related to the structure of black phosphorus through a "klassengleich" transformation (Fig. 5).

The bonding characteristics of $(Te_2)_2I_2$ can be qualitatively understood if one derives the band structure of the planar two-dimensional Te double sheets from the slightly puckered SnS double sheets. The differences in the electronic structure are primarily due to the energy difference between S and Sn centered orbitals, as opposed to no en-

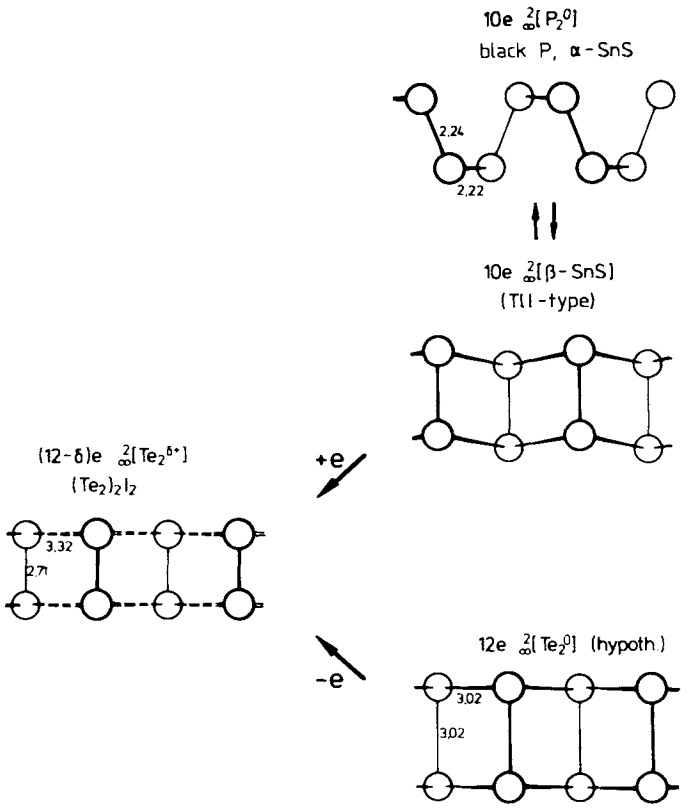

Fig. 5. Relationship between the structures of α- and β-SnS and the 4^4 double nets of $(Te_2)_2I_2$ as well as a double sheet of the hypothetical structure with five-coordinate tellurium.

ergy difference between atomic orbitals in the Te_2 unit, which reflects the relative atomic electronegativities in each material. Analysis of the band structure indicates strong Te–Te interactions perpendicular to the double sheets (Te_2 dimers: 2.71 Å) since the π^* orbitals of the diatomic unit are partially occupied. Parallel to the sheets (Te···Te: 3.32 Å) there is significant occupation of the antibonding region of both the π and π^* bands. Puckering of the Te double sheets is not predicted until significant oxidation of the Te partial structure occurs, which cannot be attained with intercalated halogens. The partial electron transfer expected to proceed from the Te double sheets to iodine leads to fractional occupation of the σ^* levels of I_2 and explains the observed expansion of the I–I distance.[32]

Two-dimensional sheets of Te atoms (4^4 nets cf. Fig. 1h) make up the structures of numerous lanthanoid and actinoid tellurides $LnTe_n$ ($n \geq 1.75$). Only the sesquitelluride $LnTe_{1.5}$ and the monotelluride LnTe are based upon other structural motifs and show no homonuclear Te–Te bonding. The simplest fundamental pattern is the *anti*-Cu_2Sb type,[33] which originates when two mixed lanthanoid/tellurium layers Ln/Te are inserted between every planar 4^4 Te net (stacking sequence: $\cdots 4^4$-(Ln/Te)-(Ln/Te)-$4^4\cdots$). Correspondingly, the ditellurides, $LnTe_2$, do crystallize in the *anti*-Cu_2Sb type. Both compounds of the known phases $LnTe_{2.5} = Ln_2Te_5$ and $LnTe_3$ (see Fig. 6) arise from similar stacking variations of these two types of layers. This has also been found for incompletely characterized compounds ($LnTe_{2.33} = Ln_3Te_7$, $LnTe_{2.75} = Ln_4Te_{11}, \ldots$; cf. Ref. [34]).

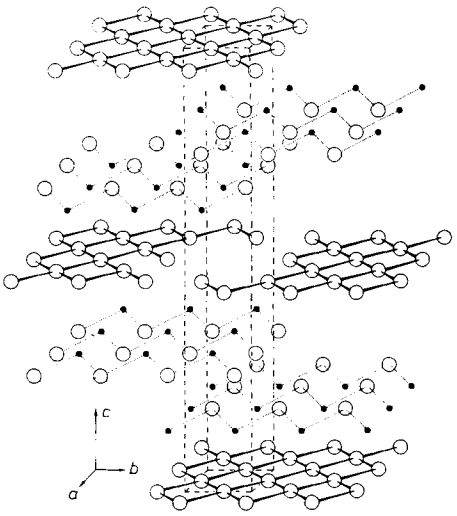

Fig. 6. Structure of $NdTe_3$. The 4^4 tellurium nets become separated from one another through intermediate puckered layers of Nd^{3+}/Te^{2-}

One of the first detailed structural determinations of the tritellurides was carried out for $NdTe_3$.[35] Its basic structure is shown in Figure 6. One recognizes the series of 4^4 tellurium nets, which are either adjacent to one another or are separated by two of the slightly puckered mixed lanthanoid/tellurium layers. The tellurium atoms in adjacent nets are separated by about 3.6 Å. The distances between the tellurium nets and the tellurium atoms in the puckered Ln/Te layers are 4 Å. From their local geometry the tellurium atoms not found in the 4^4 nets can be described as Te^{2-} ions. The compounds in Table 3 are described using an ionic formulation with the lanthanoids as trivalent cations. The examples with the smallest tellurium to metal ratio, $LnTe_2$, show the largest excess of delocalized electrons per 4^4 sheet. The Te–Te distance in the infinite two-dimensional 4^4 nets $^2_\infty[Te^{\delta-}]$ increases with increasing excess charge from 3.07 Å through 3.10 Å to 3.17 Å, which indicates an increasing occupation of antibonding states (Table 3). The *anti*-Cu_2Sb type frequently remains stable even if the 4^4 nets are incompletely occupied, e.g., $LnTe_{2-x}$ for $x \approx 0.25$. However, structures containing only isolated Te^{2-} ions begin with the sesquitellurides, $LnTe_{1.5}$. The 4^4 chalcogen nets of the disulfides and diselenides, LnX_2, are somewhat distorted due to their tendency to form X_2^{2-} dumbbells.[38,54–69] Therefore, they usually crystallize in low symmetry structures which can be derived from the *anti*-Cu_2Sb type (Fig. 7). Materials with incompletely occupied chalcogenide nets, LnX_{2-x}, have been described using the *anti*-Cu_2Sb type and show that a statistically averaged structure is necessary. This has been confirmed by the most recent results with $PrSe_{2-x}$ ($x \approx 0.2$).[69]

Table 3. Lanthanoid and actinoid tellurides $LnTe_n$ ($n \geq 1.75$).

General formula	Ionic description		Average Te-Te distance in the 4^4-nets	Ref.
$LnTe_{2\pm x}$	(Ln^{3+}/Te^{2-})	$^2_\infty[Te^{1/4}_{4/4}]$	3.17 Å	[36-44]
$LnTe_{2.5\pm x}$	(Ln^{3+}/Te^{2-})	$^2_\infty[Te^{0.67-}_{4/4}]_{1.5}$	3.10 Å	[37], [40], [45-48]
$LnTe_{3\pm x}$	(Ln^{3+}/Te^{2-})	$^2_\infty[Te^{0.5-}_{4/4}]_2$	3.07 Å	[35], [37], [40], [41], [49-53]

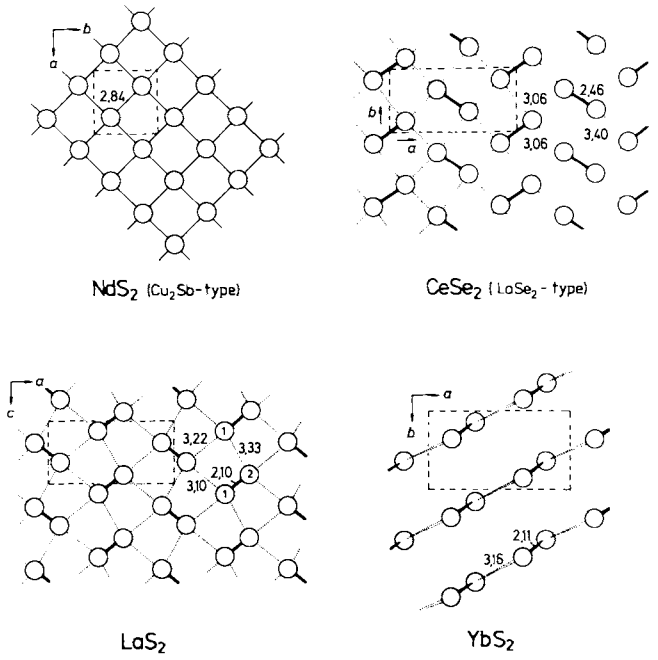

Fig. 7. Section from the anionic structural part of the lanthanoid dichalcogenides, LnX_2.

The electronic relationship between the $^2_\infty[Te_2^{\delta+}]$ double sheets of $(Te_2)_2I_2$ and the 10-electron structure of the β-SnS type has been discussed previously. Planar nets having a tetragonal arrangement of identical atoms occur, for example, in the structure of α-PbO or the $BaAl_4$ family and its ternary variants.[70-72] The oxygen atoms in α-PbO, the aluminum atoms in $BaAl_4$, and the pnicogen as well as the chalcogen atoms in the ternary variants are arranged in 4^4 nets. Over the center of each $M_{4/4}$ square there is an additional atom either of the same type ($AlAl_{4/4}$ of $BaAl_4$) or of a second type ($PbO_{4/4}$ of α-PbO). The band structure for the two-dimensional planar $Al_{4/4}$ net has been described previously. From the selected Al-Al distance of 3.2 Å, one can expect the qualitative results to be equally applicable to tellurium (Fig. 8). Simply, the dispersion of the bands

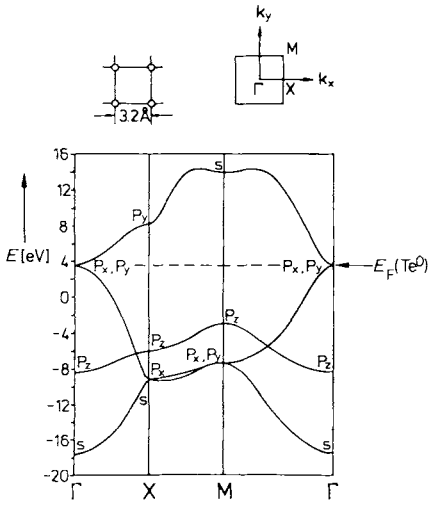

Fig. 8. Band structure for the two-dimensional 4^4 nets of the aluminum atoms in $BaAl_4$ (see [70-72]).

should increase due to the larger size of Te as compared to Al. For the tellurium net, the figure indicates the position of the Fermi level to be the energy of the $5p_x$ and $5p_y$ orbitals at Γ. An interesting consequence of this position of E_F for neutral Te is that an orthorhombic distortion of the square net will stabilize this structure. The band lying energetically higher than $E_F(Te^0)$ is Te-Te antibonding in nature. This agrees with the observation that by increasing the excess charge in the planar nets, the distances become larger (Table 3). In addition, one expects electrical conductivity for $(6+\delta)$ electrons ($\delta < 2$). Although comprehensive measurements are not known, the conductivity increases corresponding to the number of planar nets.[73]

Some further examples are known which suggest the occurrence of two-dimensional arrays of tellurium, if all Te-Te distances up to 3.3 Å are included (cf. $(Te_2)_2I_2$; Fig. 5).

The two tetratellurides $NbTe_4$ and $TaTe_4$ are examples whose structures are rather complicated in detail. The Peierl's distortion in the linear chains of d^1 M^{4+} transition metal cations is the most remarkable feature of the compounds, which leads to further distortions in the structure.[74-78] Theoretical predictions based upon band structure calculations are in agreement with experimental results.[79] Excluding all of the distortions, the structure is similar to that shown in Figure 9. The dimers of tellurium (Te-Te: 2.91 Å) are arranged in such a manner that infinite two-dimensional nets occur. The nets could be constructed from squares (Te-Te: 3.30 Å), which are stacked one on top of the other and twisted by 45° with respect to each other. The transition metals are found in the center of square antiprisms and form chains along [001]. The lower part of Figure 9 shows a 4^4 net from which every fifth atom is removed. It can be placed over the structure of MTe_4 (Fig. 9, top). Under constant unit cell dimensions, this 4^4 net fits best with the net of the tetratelluride structure if a distance of 2.91 Å is used. When the transition metal cations are inserted into the squares, the Te-Te distances increase to 3.30 Å. The Te-Te distances between the squares remain unchanged at 2.91 Å. The tetratellurides, MTe_4, are the first examples in which transition metal cations with incompletely filled d-shells occur. As a result, one may not neglect the cation-anion or the cation-cation interactions. The M^{4+} chains cause marked anisotropy in their electronic transport properties.[80]

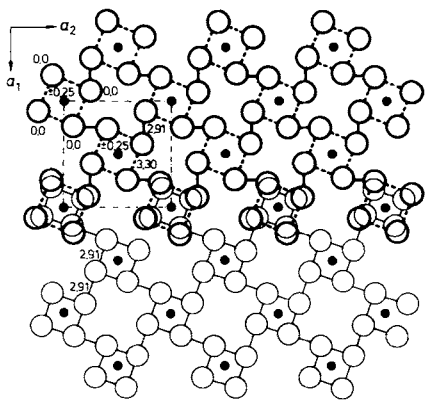

Fig. 9. Section from the structure of the tetratelluride, MTe_4 (M = Nb, Ta) from $z = -0.25$ to $z = 0.25$. In the lower part of the figure, the idealized hypothetical defect 4^4 net that underlies the structure is represented for comparison.

The two pentatellurides $ZrTe_5$ and $HfTe_5$[81] (Fig. 10) also belong to the class of compounds with low-dimensional transport properties. The pentatellurides, MTe_5, are expected to behave similarly to the trichalcogenides ($ZrSe_3$-type, $NbSe_3$-type, TaS_3-type[80]), whose structures are characterized by the description of stacked prisms, and which markedly show one-dimensional transport properties and anomalies. In the structure of the pentatellurides, the Te^{2-} ions (Te1) and the Te_2^{2-} dimers (Te2-Te2: 2.76 Å) assemble along [100] to form an infinite prismatic strand with common triangular faces that are centered by the metal cations (Fig. 10, bottom). The difference from the $ZrSe_3$ type (cf. Fig. 12) occurs only in the observation that the prisms along [001] do not lie directly next to each other, but are bonded to each other through inserted zig-zag chains $^1_\infty[Te_2^0]$: (Te3-Te3: 2.91 Å; Fig. 10). The tellurium atoms of the zig-zag chains (Te3) and the isolated Te1 atoms span a wavy, two-dimensional sheet, in which the average Te-Te distance is 3.17 Å (Fig. 10, top). One therefore expects two-dimensional rather than one-dimensional anisotropic properties. The marked cleavage parallel to the *ac*-plane as well as the missing anisotropy of the electrical resistivities in the *ac*-plane confirm this prediction.[81]

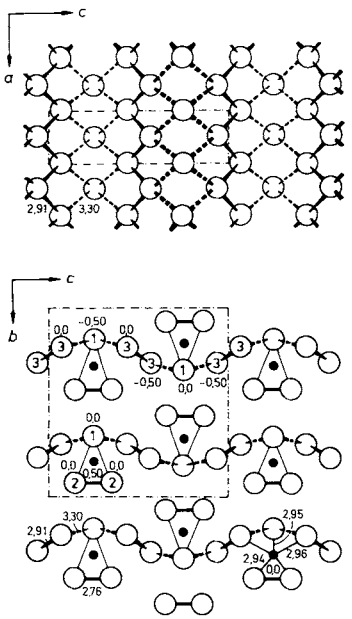

Fig. 10. Bottom: [100] projection of the structure of the pentatellurides MTe_5 (M = Zr, Hf). Top: Projection of the *ac*-plane of the puckered tellurium sheets made up of the Te1 and Te3 atoms.

Both pentatellurides are highly interesting because of the anomaly in their electrical resistivities, which show a maximum at 80 K ($HfTe_5$) and 140 K ($ZrTe_5$). According to the temperature dependence of the electrical resistivity both above and below the maximum, they behave as metals. In spite of many exact measurements, no clear evidence has been obtained for a phase transformation as an indication for the formation of spin or charge density waves.[83] The transport anomalies were also explained by a change in the charge carrier concentration and the fluctuation at the transition point. From the results of band structure calculations no charge density wave instability is expected.[84]

3.3. Infinite One-Dimensional Anionic Strings

The first examples to be considered are the structures of the alkali metal tritellurides, $LiTe_3$[18] and $NaTe_3$,[19] which are closely related to $AgTe_3$ (see Section 3.1). Through the tendency to localize the nonbonding electrons, the three-dimensional framework of the tellurium partial structure divides into one-dimensional strands that run along the [001] direction (Fig. 11, right). In the left part of Figure 11 the arrangement of atoms projected down the [001] direction is shown ($-0.13 < z < 0.13$). One can see the nearly undistorted cubes (shaded) which are in a densest packing arrangement. The corners of the cubes are occupied by six Te3 atoms (Te3-Te3: 3.16 Å) and two Na3 atoms (Na3-Te3: 3.19 Å). The strands along [001] are constructed using these cubes by connecting them via additional tellurium atoms (Te1, Te2). Together with the sodium atoms, Na1 and Na2, the Te1 and Te2 atoms also form cubes, albeit distorted (Te1-Te2: 2.77-3.59 Å; Na-Te: 3.07-3.31 Å). The mean value of the Te-Te distances in such a distorted cube always remains at 3.16 Å, as found in the undistorted ones. If all Te-Te distances are identical and only two different M-Te distances occur, Figure 11, in fact, shows the structure of $AgTe_3$. The resulting differences in the structures can be realized from a comparison of the lattice constants (Table 4). The increase (ca. 20%)[84] in the molar volumes of the tellurium partial structures has already been pointed out for the alkali metal tellurides in Section 3.1.

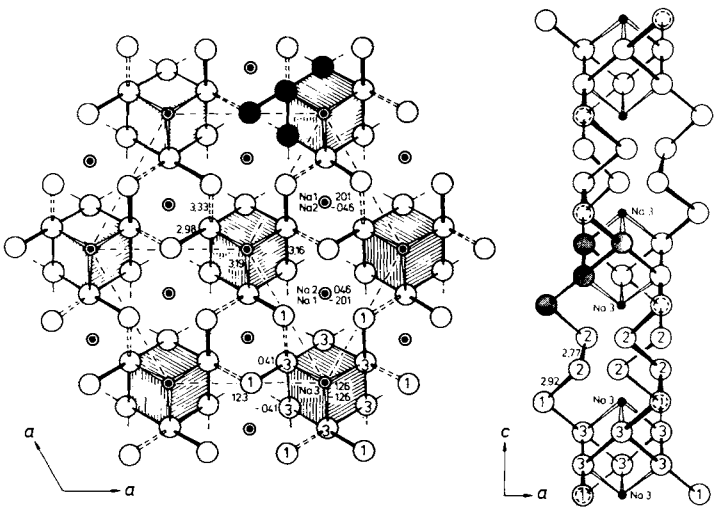

Fig. 11. Left: Section from the structure of the tritellurides MTe_3 (M = Li, Na) from $z = -0.13$ to $z = 0.13$. Right: Projection along [001] showing the tellurium strands.

Table 4. Structural data of the tellurides MTe_3 (M = Li, Na, Ag).

	$AgTe_3$	$LiTe_3$	$NaTe_3$
Space group	$R3m$	$P\bar{3}c1$	$P\bar{3}c1$
a [Å]	8.465	8.714	9.032
c [Å]	5.272	21.35	21.93
V [cm^3 mol^{-1}]	66	70.5	78
V of the Te-anionic part [cm^3 mol^{-1}]	57	69	71

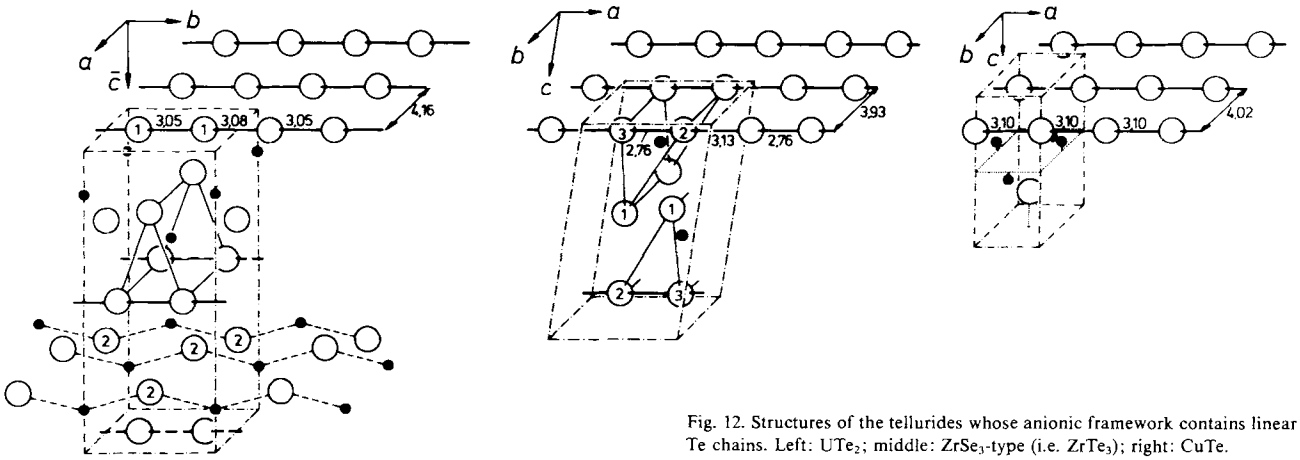

Fig. 12. Structures of the tellurides whose anionic framework contains linear Te chains. Left: UTe_2; middle: $ZrSe_3$-type (i.e. $ZrTe_3$); right: CuTe.

Three Te3 atoms and one Te1 atom form a T-shaped fragment (Fig. 11, shaded) and six of these fragments condense into the Te_{12} cluster ($Na_6^+Te_{12}^{6-}(Te_2^0)_3$). Therefore, the T-shaped fragment can be considered as isotypic to the BrF_3 type as in the case of $CsTe_4$. Furthermore, an additional contact exists (Te1···Te3: 3.33 Å) which produces a distorted square planar unit, $TeTe_4$, from the T-shaped fragment.

Infinite one-dimensional motifs determine the tellurium structural part in UTe_2,[85] in $ZrTe_3$, $HfTe_3$, and UTe_3,[86-88] which crystallize in the $ZrSe_3$-type, as well as in CuTe.[89] As shown in Figure 12, they contain linear tellurium chains with average Te–Te distances of 3.10 Å that are stacked directly above one another. The difference between the two intrachain Te–Te distances is largest for the trichalcogenides with the $ZrSe_3$ structure type (for example US_3 and USe_3). Perpendicular to these tellurium chains are characteristic stacks of trigonal prisms, which share common triangular faces and are centered by the metal cations. In UTe_2 these prismatic stacks actually consist of two metal-centered trigonal prisms which share a common rectangular face. Similarly, the difference in the distances between the directly stacked chalcogen atoms along [100] in the structures of US_3 and USe_3, for example, which crystallize in the $ZrSe_3$-type structure, become so large that they fall apart in a succession of X_2^{2-} dumbbells. Measurements of the magnetic susceptibilities of US_3, USe_3, UTe_3[87] revealed the difference between US_3 and USe_3 on the one hand and UTe_3 on the other.

The structures of both UTe_2 and UTe_3 certainly show a relationship to those of the lanthanoid di- and tritellurides. The linear chains lie approximately 4 Å away from one another and build sheets between which undulated U/Te layers are inserted. The ionic description in Table 5 uses tetravalent uranium (μ_B (spin only, U^{4+}) = 2.83; $\mu_{eff}(UTe_3) = 3.09$[87]). Comparison with the corresponding data for the lanthanoid tellurides in Table 3 suggests that the chains do not form genuine 4^4 nets, because too many excess electrons exist per net. This conclusion is supported by the fact that partial substitution of U^{4+} by Dy^{3+} can lead to the structure type containing 4^4 nets. The structural change only occurs when the excess charge becomes sufficiently reduced by the introduction of M^{3+} ions. Whereas $U_{0.5}Dy_{0.5}Te_2$ crystallizes in the UTe_2 type, $U_{0.5}Dy_{0.5}Te_3$ adopts the $NdTe_3$ type instead of $ZrSe_3$ (Table 5).

Table 5. Uranium tellurides UTe_n.

General formula	Structure type	Ionic description	Average distance in $^n_\infty[Te^{m-}]$	Ref.
UTe_2	UTe_2	$(M^{4+}/Te^{2-})\ ^1_\infty[Te^{2-}]$	3.06 Å	[85]
$U_{0.5}Dy_{0.5}Te_2$	UTe_2	$(M^{3.5+}/Te^{2-})\ ^1_\infty[Te^{1.5-}]$	3.05 Å	[90]
UTe_3	$ZrSe_3$	$(M^{4+}/Te^{2-})\ ^1_\infty[Te^{1-}]_2$	3.05 Å	[87, 88]
$U_{0.5}Dy_{0.5}Te_3$	$NdTe_3$	$(M^{3.5+}/Te^{2-})\ ^2_\infty[Te^{0.75-}_{2/4}]_2$	3.07 Å	[90]

Similar linear chains of two-bonded tellurium atoms are also found in the structure of TlTe[91] (Te3–Te3: 2.91 Å). Additionally, there are chains in the structure that contain two-bonded as well as four-bonded tellurium. These chains arise by crosswise stacking of linear triatomic moieties of tellurium and contain square planar Te_5 units (Te–Te: 3.04 Å and 3.09 Å, cf. Fig. 12).

Similar linear triatomic units as in TlTe are found in UTe_5 to create nonlinear chains[92] (Fig. 13; Te4–Te2: 3.14 Å). Beside the chains, it contains isolated Te_3^{2-} ions (Te3–Te1: 2.80 Å), which condense to form triangular faces (two Te1 and one Te2). As in the $ZrSe_3$ structure type, these triangles stack to produce a one-dimensional chain of face-sharing prisms centered by uranium atoms

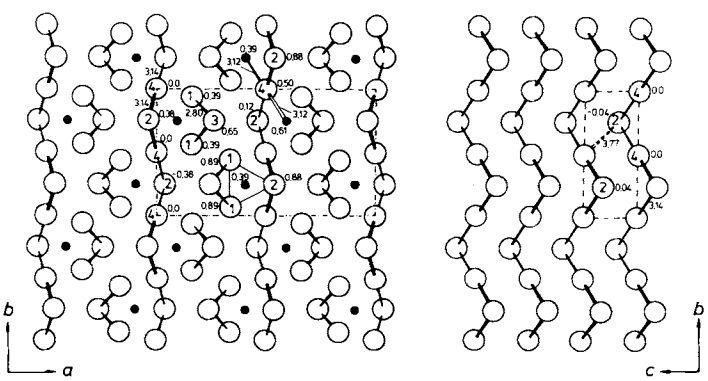

Fig. 13. Left: [001] projection of the structure of UTe_5. Right: The layered units in the *bc*-plane form from the bent chains of Te2 and Te4 atoms.

(Fig. 13 left). The chains are arranged such that a puckered sheet of tellurium atoms occurs (Fig. 13 right).

Finally, Rb_2Te_5 and Cs_2Te_5 belong to the group of infinite one-dimensional tellurium polyanions.[20,21] The partial anionic structure of Cs_2Te_5 arises from a systematic removal of every sixth tellurium atom from the hypothetical infinite two-dimensional double sheets with five-coordinate tellurium atoms. Analogously, another conceivable two-dimensional structural variant with five-coordinate Te is the basis for Rb_2Te_5. Both of the one-dimensional anionic structural motifs in Cs_2Te_5 and Rb_2Te_5 are related to each other just like the nets of black phosphorus and gray arsenic (Fig. 14; cf. also Fig. 1f and 1e).

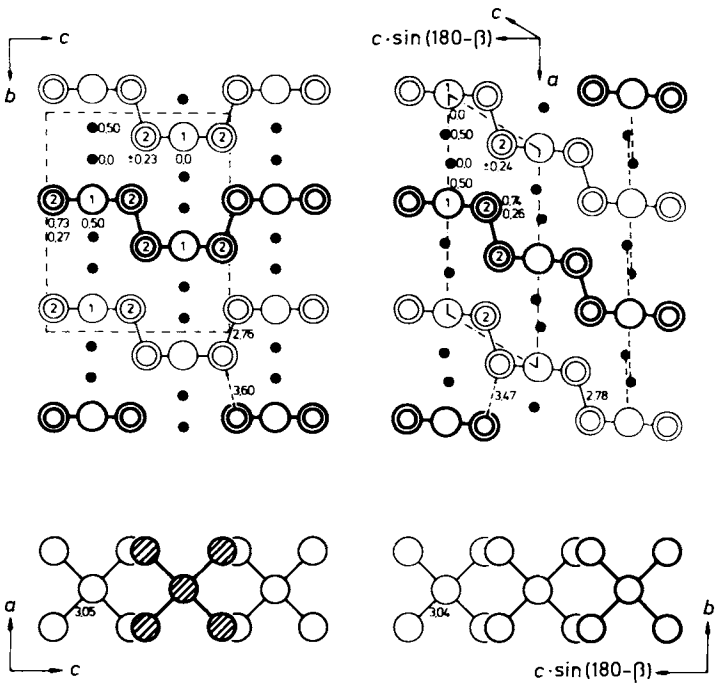

Fig. 14. Top: Projection of the structures of Cs_2Te_5 (left, along [100]) and Rb_2Te_5 (right, along [010]). The different heights of the $^1_\infty[Te_5^{2-}]$ strands above the projection plane are specified by differing line strength. The individual tellurium strands are shown in the lower part.

The quasi-molecular structural building block, $TeTe_4^{2-}$ (32e descendent of the 36e-XeF_4, see Fig. 14, shaded fragment), is fundamental to the structures of the pentatellurides of both Rb and Cs. The bonding distances from the central Te1 atom to the terminal Te2 atom of the fragment are 3.05 Å (Cs_2Te_5) and 3.04 Å (Rb_2Te_5). On account of the relative electron deficiency, the 32e-XeF analogues are connected to neighboring fragments via every terminal Te2 atom to form the infinite one-dimensional strands (Te2–Te2: 2.76 Å in Cs_2Te_5; Te2–Te2: 2.78 Å in Rb_2Te_5, Fig. 14). This corresponds exactly to the effect that has led to the structure of the infinite two-dimensional sheets in $CsTe_4$ from the 25e-$TeTe_3^-$ fragment. The shortest Te···Te contact between the two sheets in $CsTe_4$ (3.51 Å) also corresponds to the shortest Te···Te contact between the strands in Cs_2Te_5 (3.60 Å) and Rb_2Te_5 (3.47 Å).

The question still remains why Cs_2Te_5 and Rb_2Te_5 are not isotypic. When one deducts the volume occupied by the tellurium atoms from the total volume of the elementary cell, a much larger space remains for the cesium atoms in Cs_2Te_5 than for the rubidium atoms in Rb_2Te_5, as required by the larger space requirements of Cs. This occurs solely by the different folding of the strands—all distances and angles in both structures are nearly identical:

Volume	Cs_2Te_5 ($Z=4$)	Rb_2Te_5 ($Z=2$)
Elementary cell [$cm^3\ mol^{-1}$]	703	328
Volume increment of Te_5^{2-} [$cm^3\ mol^{-1}$]	4×120	2×120
Excess volume per M^+ [$cm^3\ mol^{-1}$]	28	22

The molar volume of the Te_5^{2-} ion has been calculated from the increments for four Te^0 atoms and one Te^{2-} ion as described by *Biltz*.[84] In spite of this crude assumption, values for the remaining excess volumes per cation are in good agreement with the values that are known from numerous structures: 26 $cm^3\ mol^{-1}$ and 20 $cm^3\ mol^{-1}$ for Cs^+ and Rb^+, respectively.

The topological similarity between the square planar $TeTe_4^{2-}$ fragments and molecules like XeF_4 is obvious. The same holds for the similarities between T-shaped fragments $TeTe_3$ of $CsTe_4$ and $NaTe_3$ (Section 3.2) with molecules like BrF_3 as well as between the linear fragments $TeTe_2$ of TlTe and UTe_5 with molecules like XeF_2. Only in the most simple cases can one assign an excess negative charge to the fragments, e.g. $TeTe_3^-$ in $CsTe_4$, $TeTe_4^{2-}$ in Rb_2Te_5 and Cs_2Te_5. Then, the deficit of valence electrons of these fragments with respect to the reference molecules (28e-BrF_3/25e-$TeTe_3^-$; 36e-XeF_4/32e-$TeTe_4^{2-}$) may be considered to be responsible for the infinite polyanions. The fragments make as many tellurium bridges to other fragments as the number of valence electrons lost.

It should also be mentioned that planar zig-zag chains with two-coordinate tellurium occur in the monoclinic modification of $AuTe_2$[93] (cf. Fig. 1d; Te–Te: 3.18 Å) and helical zig-zag chains with four- and two-coordinated tellurium in Te_3Cl_2 with partly very short Te–Te distances (2.67 Å).[94]

3.4. Isolated Anions

The previous discussion argues that one can always expect to find isolated, quasi-molecular structural motifs in tellurium-rich tellurides, if these fragments become isoelectronic to familiar reference molecules. This requires that the ionic situation in the sense of Zintl and Klemm holds true and that all other interactions can, in the first instance, be ignored.

3.4.1. XeF_4-Type Square Planar Fragments

The structure of Ga_2Te_5[95] represents an example in which one has the 36 electron $TeTe_4^{6-}$ anionic building block: $(Ga^{3+})_2Te_5^{6-}$ (Fig. 15). The bond distance is 3.03 Å (Te1–Te2) with the anions arranged so that each gallium atom becomes tetrahedrally coordinated. Cations and anions together form a three-dimensional network. The structures of both ternary tellurides, M_2SnTe_5 (M = K, Rb) are characterized by nearly identical 36e-$TeTe_4^{6-}$ ions:[96,97]

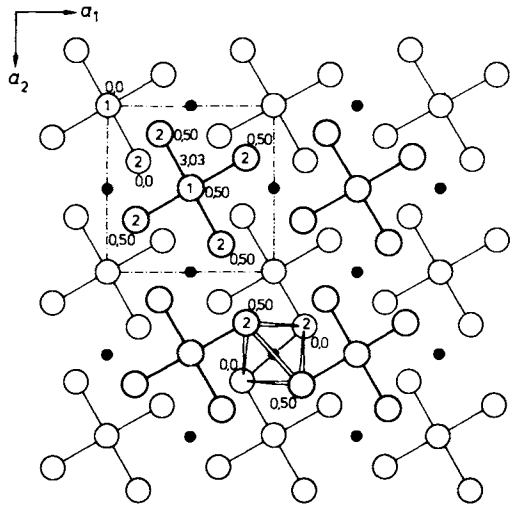

Fig. 15. Section from the structure of Ga_2Te_5. The tetrahedral coordination of the cation is shown.

$(M^+)_2Sn^{4+}Te_5^{6-}$ (Fig. 16). The tin atoms are tetrahedrally coordinated in a similar manner as the gallium atoms in Ga_2Te_5. In this case only infinite one-dimensional $^1_\infty[SnTe_5^{2-}]$ strings parallel to [001] are formed since the additional alkali metal cations must be accomodated. The Te–Te distances of 3.02 Å (Te1–Te3) and 3.05 Å (Te3–Te2)[96] are in good agreement with the analogous distances in Ga_2Te_5.

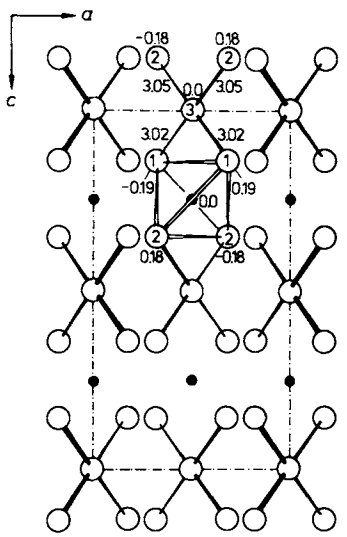

Fig. 16. Section from the structure of the ternary tellurides M_2SnTe_5 (M = K, Rb). The tetrahedral coordination of the tin atom is specified. The alkali metal atoms are not shown.

The third example containing the square planar $TeTe_4$ structural motif is Re_2Te_5.[98] The structure contains Re_6 octahedra whose first coordination sphere has eight tellurium atoms in a cubic arrangement so as to give a Re_6Te_8 cluster. Of the 42 electrons contributed by the six Re atoms, 24 are used to form twelve Re–Re bonds and another 16 are used for Te–Te bonding. The two remaining electrons are donated to the anionic fragment to give the formal structural composition as $Re_6Te_8^{2+}Te_7^{2-}$ ($\cong Re_2Te_5$). The $TeTe_4$ structural motif is the characteristic part of the anion, Te_7^{2-}, with Te–Te distances of 2.98 Å (Te1–Te8) and 3.02 Å (Te3–Te8). Two-coordinate Te2 atoms bridge two opposite pairs of terminal atoms in the $TeTe_4$ fragment to form the butterfly-like Te_7^{2-} ions (Fig. 17).

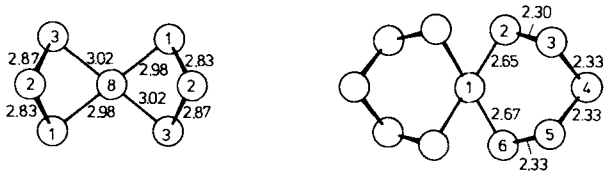

Fig. 17. The Te_7^{2-} anion in Re_2Te_5 (left) and the Se_{11}^{2-} anion in $(PPh_4)_2Se_{11}$ (right).

For comparison, the noteworthy Se_{11}^{2-} anion[99] is shown in Figure 17. It is an exceptional example, which, otherwise, only characterizes the structural chemistry of tellurium-rich tellurides. This anion also contains a central square planar 32e-$SeSe_4$ fragment with expanded distances of 2.65 Å and 2.67 Å. The two-coordinate bridging atoms have distances in the range appropriate for Se–Se covalent single bonds.

Two different structures have been proposed for Tl_5Te_3.[100,101] Assuming the structure proposed by *Man, Imamow* and *Pinsker*[100] to be correct, Tl_5Te_3 contains square planar $TeTe_4$ groups (Fig. 18). There are many more electrons available than required by the 36e-$TeTe_4^{6-}$ ions as well as the additional Te^{2-} ions (Te2). $Tl_{10}Te_6$ may be formally considered as $10\,Tl^+ + Te_5^{6-} + Te^{2-} + 2e$. The Te–Te distances within the $TeTe_4$ groups, which are usually around 3.1 Å, are expanded to a value of approximately 3.3 Å. Additional relatively short contacts form the tellurium sheets (Te1 $\cdots$ Te2 = 3.5 Å).

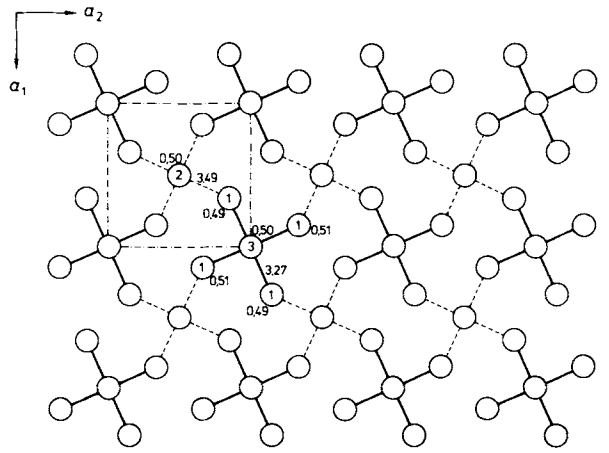

Fig. 18. Section of the structure of Tl_5Te_3 ($0.48 < z < 0.52$; Tl not shown) [100].

3.4.2. *BrF_3-Type T-Shaped Fragments*

Although T-shaped fragments have appeared in some of the previously illustrated structures (25e-$TeTe_3^-$ in $CsTe_4$, 78e-Te_{12}^{6-} fragment in $NaTe_3$), there is no example for the 28e-$TeTe_3^{4-}$ ion (isotypic to BrF_3). Suitable alkali metal tellurides must have a 1:1 composition (M_4Te_4). Since the

structures of NaTe (Section 3.4.3) and K_2Te_2 (Section 2.4.4) are constructed using different structural principles, the question regarding the preparation of simple substances like Rb_2Te_2, Cs_2Te_2, $CaTe_2$, $SrTe_2$, and $BaTe_2$ becomes interesting again.

3.4.3. Linear XeF_2-Type Fragments

There are no known examples in this group of compounds containing the 22e-$TeTe_2^{4-}$ ion isosteric with XeF_2. One expects such species to be preferred in the alkali metal-rich region. In the cesium/tellurium system there is an indication of the compounds, Cs_mTe_n $(m>n)$,[102] whose complete structure in the crystalline form is presently being studied.

NaTe contains isolated Te_5^{4-} ions.[24] A central linear triatomic unit and two additional singly bonded Te^- ions form the Z-shaped anion Te_5^{4-} (Fig. 19). The Te-Te distances behave as expected with distances in the linear part having a value of 3.08 Å, while the distances to each terminal atom are only 2.82 Å. The additional Te4 atoms are assigned as Te^{2-} ions to give the ionic formula, $(Na^+)_6Te_5^{4-}Te^{2-}$ ($\cong$ NaTe). Similar Te_5^{4-} polyanions are also found in Ba_2SnTe_5 $[(Ba^{2+})_6Te_5^{4-}(Sn_3Te_{10})^{8-}]$.[103] They are isoelectronic with the Z-shaped interhalogen cations, $I_3Cl_2^+$[104] and I_5^+.[105]

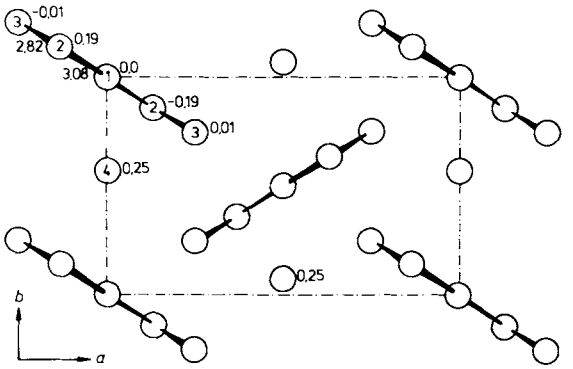

Fig. 19. Section of the structure of NaTe. The Te_5^{4-} ions are packed analogously as the I_2 dimers in elemental iodine.

3.4.4. Pseudotetrahedral Fragments in Te_n^{2-} Ion Chains

The anions of the polytellurides are derived from the infinite chain of the thermodynamically stable modification of the element. Their structural characteristics are analogous to the corresponding selenides and sulfides. Just as in the structures of the elements, the difference between the inter- and intra-chain distances are smaller in the tellurides than in the sulfides or selenides.

There are many known examples containing the dimers, Te_2^{2-}, which include the main group metal tellurides α- and β-K_2Te_2 (Na_2O_2 and Li_2O_2 type[25]), $MgTe_2$ (pyrite type[106]), and the transition metal tellurides $CoTe_2$ and $FeTe_2$ (marcasite type[107]). The Te-Te distances cover a relatively wide range of values (α-K_2Te_2: 2.86 Å; β-K_2Te_2: 2.79 Å; $MgTe_2$: 2.70 Å; $CoTe_2$: 2.91 Å; FeTe-2: 2.93 Å). The number of examples with longer Te_n^{2-} chains ($n=3$, 4, ...) is very small (Table 6). The Te-Te distances correspond exactly to the sum of the covalent radii only when the anions are completely separated by large cations.

Table 6. Zig-Zag chains Te_n^{2-} $(n>2)$.

	Te-Te distances [Å] within the chains	between the chains	Bond angles [°]	Ref.
K_2Te_3	2.80	3.58	104.4	[22]
Rb_2Te_3	2.80	3.72	104.4	[23]
Cs_2Te_3	2.77	3.73	100.1	[23]
$BaTe_3$	2.78	3.68	109.4	[108]
In_2Te_5-I	2.84	3.37	100.1	[109]
In_2Te_5-II	2.86	3.38	101.6	[110]
UTe_5	2.80	3.63	86.7	[92]
Average	2.81	3.58	101.0	
$K_2^{cr}Te_3 \cdot en$ [a]	2.71	7.45	113.1	[111]
$[Ba(en)_3]Te_3$	2.76	4.40	105.7	[112]
$[Ba(en)_{4.5}]Te_3$	2.73	4.48	111.5	[112]
$[PPh_4]_2Te_4 \cdot 2CH_3CN$	2.74	6.20	110.8	[113]
$Na_2^{cr}Te_4$ [a]	2.71	7.65	109.7; 110.0	[114]
$[NBu_4]_2Te_5$	2.73	5.81	110.4; 104.8	[115]
Average	2.73	—	109.2	

[a] $M^{cr} \equiv [M(crypt\text{-}2.2.2)]^+$.

4. Remarks about the Binding Situation in Some Alkali Metal Tellurides

Figure 20 illustrates once again that the square planar $TeTe_4$ moiety represents a prevalent fragment in tellurium-rich tellurides. The chemical bonding in substances with such AB_4 systems has been examined recently.[116, 118]

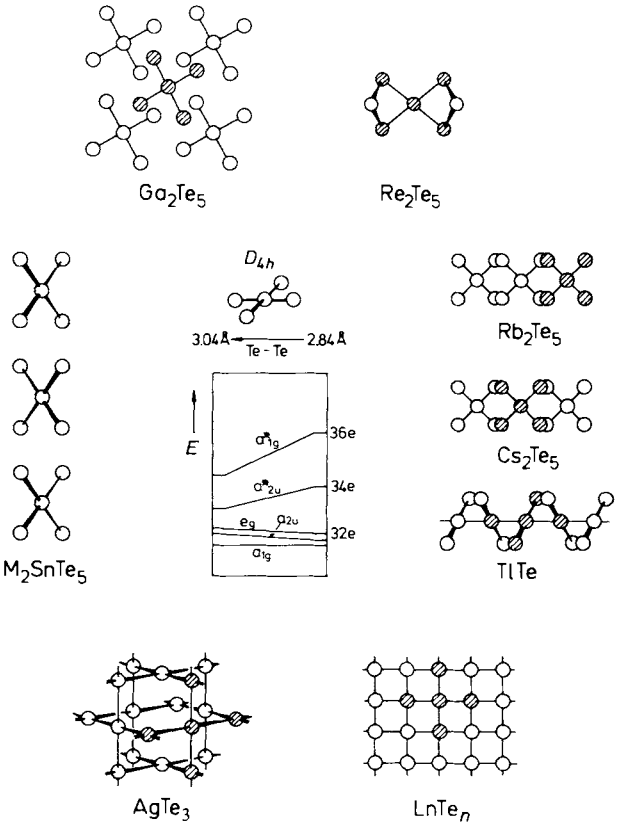

Fig. 20. Schematic trend of the highest occupied states in the $TeTe_4^{n-}$ fragment with D_{4h} symmetry for Te-Te distances ranging from 2.84 Å to 3.05 Å [116].

It is already known that an AB_4 system can possess D_{4h}, C_{4v}, C_{2v}, and T_d symmetry. To a first approximation, the actual observed structure depends upon the number of valence electrons.[117] The 36-electron AB_4 species prefers D_{4h} symmetry. A lengthening of the A–B distances generally leads to a stabilization because both of the highest occupied levels have A–B antibonding character. In cases for which the 36e-$TeTe_4^{6-}$ groups are formally possible (Ga_2Te_5, K_2SnTe_5, and Rb_2SnTe_5), $Te_{central}$–Te_{apical} distances of 3.05 Å ± 0.05 Å are found (the covalent radius of Te is 1.37 Å). For the experimental mean value of the $Te_{central}$–$Te_{terminal}$ distance, 3.04 Å, the a_{1g} and a_{2u} levels become lowered by about 3 eV and 0.5 eV, respectively, relative to the geometry using the distance in elemental tellurium, 2.84 Å. In contrast to ICl_4^- or XeF_4, there is high electron density on the terminal atoms for these two highest occupied antibonding levels due to no electronegativity difference between $Te_{central}$–$Te_{terminal}$. Therefore, in order to attain stability, the 36e-$TeTe_4^{6-}$ fragment will form covalent bonds to strongly electrophilic atoms via their terminal atoms, in order to reduce the electronic charge density at these sites. Such interactions are observed in the structures of Ga_2Te_5 and M_2SnTe_5 (M = K, Rb).

The most important question still remains: why do the 32e-$TeTe_4^{2-}$ species found in both Rb_2Te_5 and Cs_2Te_5 not exist as isolated tetrahedral tetratellurotellurate(VI) anions with T_d symmetry, but instead consist of $^1_\infty[TeTe_4^{2-}]$ fragments with local D_{4h} symmetry connected into chains? Numerous examples including the 32e-AB_4 system have, in particular, T_d symmetry as shown in Table 7. It is plausible that for the special case of the $TeTe_4^{2-}$ species, D_{4h} symmetry is favored for steric and not electronic reasons (the radius ratio r_A/r_B is 1.0). An analogous argument suggests steric in addition to electronic preferences to explain why C_{2v} symmetry is favored over C_{4v} symmetry for the 34e-AB_4 system, e.g., SF_4.[117]

Table 7. Selected examples of tetrahedrally coordinated 32e-AB_4 molecule anions.

Compound	Anion	$\Delta\chi$ [a]	r_K/r_A [119]	Ref.
Fluoroberyllates	BeF_4^{2-}	2.6 (2.50)	0.35	[122]
Silicates	SiO_4^{4-}	1.8 (1.66)	0.32	[123]
Thioantimonates	SbS_4^{3-}	0.6 (0.57)	0.43	[124]
$Ba_5(GaS_4)_2$	GaS_4^{5-}	0.6 (0.26)	—	[125]
M_4SiAs_4	$SiAs_4^{8-}$	0.5 (0.16)	—	[126]
$Ca_{14}AlSb_{11}$	$AlSb_4^{9-}$	0.3 (0.31)	—	[127]
$Ca_{11}InSb_9$	$InSb_4^{9-}$	0.3 (0.35)	—	[128]
Ba_2SiTe_4	$SiTe_4^{4-}$	0.3 (0.20)	0.19	[129]
Na_4SnTe_4	$SnTe_4^{4-}$	0.3 (0.39)	0.33	[130]
$K_3PS_4 \cdot H_2O$	PS_4^{3-}	0.3 (0.29)	0.18	[131]
M_4GeAs_4	$GeAs_4^{8-}$	0.2 (0.20)	—	[132]
Thioarsenates	AsS_4^{3-}	0.2 (0.42)	0.28	[133]

[a] Electronegativity difference according to *Allred* and *Rochow* [120] and *Block* and *Schatteman* [121] (in brackets).

The band structures of Rb_2Te_5 and Cs_2Te_5 are very similar to each another until the Cs_2Te_5 bands are folded back as required on symmetry grounds. Both substances are predicted to be semiconductors with band gaps of the order of 1 eV.[116] The value agrees qualitatively with the results of the photoelectron spectrum of Rb_2Te_5, from which a distance of about 1 eV was found between the highest occupied level to the Fermi edge of the spectrometer.[134] This value is greater than the band gap for elemental tellurium (0.35 eV[135]) and indicates that the emphasis on the quasi-molecular nature of this fundamental structural fragment with nonbonding electrons in localized pairs is not unfounded.

The density of states distribution for K_2SnTe_5 shows the small contribution of the tin orbitals in the neighborhood of the Fermi edge and throughout all occupied bands. This results in the large positive charge calculated for tin,[116] and, therefore, supports the formulation of the tin atoms as Sn^{4+} in the ionic description.

Also, the photoelectron spectra for $NaTe_3$ and NaTe have revealed $NaTe_3$ as metallic (or as a semiconductor with very small band gap) and NaTe as semiconducting.[134] This result reflects the degree of connectivity in the partial anionic structure. It is further supported by observations that the solidified melt of $NaTe_3$ is silvery (the melt: gold color), while the crystals of Rb_2Te_5 and NaTe have dull black surfaces. It confirms again the close structural and electronic relationship of $NaTe_3$ to the metallic $AgTe_3$. The bonding energies of the core electrons have also been measured (Table 8). Succession to further different bonding situations of tellurium atoms (pseudo-noble gases, pseudo-halogens) in the fragments cannot be resolved via chemical shifts.

Table 8. Bond energies [eV] of some alkali metal tellurides.

		NaTe	Rb_2Te_5	$NaTe_3$	Ref. [139]
Tellurium	3p (1/2)	871.2	—	—	873
	3p (3/2)	820.2	—	—	822
	3d (3/2)	583.6	584.0	582.6	585
	3d (5/2)	573.2	573.7	572.2	575
	4s	169.1	—	—	171
	4d	40.6	41.6	40.4	43.5
Sodium	1s	1073.1	—	1071.3	1072
Rubidium	3d	—	110.6	—	110.5
	4s	—	32.5	—	29
	4p (3/2)	—	14.6	—	14

The local symmetry of AB_3 systems depends on the number of valence electrons in a manner analogous to AB_4 systems. In general, 24e-species with D_{3h} symmetry (BX_3; X = halogen), 26e-species with C_{3v} symmetry (PCl_3), and 28e-species with C_{2v} symmetry (T-shaped, BrF_3) are stable. However, there exists a number of exceptions for the AB_3 system with structures that are not predicted by VSEPR theory (26e-NCl_3, pyramidal; 26e-$N(SiH_3)_3$, planar). For the explanation of this problem there must again be both electronic as well as steric arguments.[117] Also noteworthy is the D_{3h} symmetry of the 28e-$SiSi_3^{12-}$ fragments that are found in the solid state structure of $Li_{12}Si_7$.[136–138] In analogy to the electron-rich species containing the $TeTe_4^{m-}$ fragment (Ga_2Te_5, M_2SnTe_5) the destabilization of the highest occupied antibonding state of the $SiSi_3^{12-}$ fragment becomes neutralized through the Li–Si interactions. In this sense, the $^1_\infty[SnTe_5^{2-}]$ strands correspond to the polymeric $Li_{12}Si_4^0$ unit of $Li_{12}Si_7$.

The $TeTe_3^-$ fragments of the infinite two-dimensional sheets of $CsTe_4$ are 25e-AB_3 systems. They are isoelec-

tronic with CX_3^- radicals (X = H, Halogen) and BrO_3. Such species show either D_{3h} symmetry (CH_3) or C_{3v} symmetry (BrO_3). In comparison, the T-shaped geometry of the $TeTe_3^-$ fragments possesses nearly C_{2v} symmetry. Speculations are useless for these fragments, just as they are for the D_{4h}/C_{2v} alternatives for the AB_4 species, $TeTe_4^{m-}$. Again, a delicate balance exists between the obviously frequently occurring and energetically stable C_{3v} structure and the T-shaped structure, which is only observed in this case. The preference of the C_{2v} structure over the C_{3v} structure can be established by the radius ratio of 1.0 and no electronegativity difference between $Te_{central}$ and $Te_{terminal}$.

5. Closing Remarks

In the preceding sections the tellurium-rich tellurides have been discussed with special emphasis on the structural relationships between their tellurium structural components. Details concerning their physical properties have received far less discussion. Also little attention has been paid to factors characterizing structures in individual circumstances, like some cation-anion interactions, packing effects, and similar details. One must always realize, therefore, that with these considerations plus equally powerful generalized arguments (the Zintl-Klemm concept), only a partial understanding of the structural chemical relationships can be accomplished. These arguments cannot express the electronic situation of a compound, because only the number and not the state of the electrons transferred to the anionic part of the structure are considered. Moreover, structural chemical predictability warns against careless application. Substitution of electron donors with one another can lead to a variation in the anionic framework, as illustrated in the structural pairs $NaSbF_4/KSbF_4$[140] and M_4TeO_5 (M = Li, Na)/M'_4TeO_5 (M' = Li).[141,142]

It has been shown that the tellurium-rich tellurides can frequently be treated as a single group of compounds. They also illustrate a smooth transition between the Zintl phases and the molecular compounds of the nonmetals in their structural chemistry and in their physical properties. They are not only of theoretical interest. The transition metal compounds, MTe_4 (M = Nb, Ta), and MTe_5 (M = Zr, Hf), whose low dimensional transport properties have been described, as well as the compounds MTe (M = Pb, Cd, Hg ...) of the group II-VI semiconductors are important structural types. Ternary tellurides of the type M_2SnTe_4 (M = Cr, Mn, Fe, Co), whose representation has proceeded from main group metal tellurides like K_4SnTe_4, show spin-glass properties in amorphous form.[143-146] An extensive understanding of the structures of the tellurides, which can be of great help in the planned synthesis of new compounds, is therefore of importance.

My colleagues U. Kretschmann and R. Keller are gratefully thanked. Support by the Fonds der Chemischen Industrie and the Deutsche Forschungsgemeinschaft has been instrumental to the success of this work and is gratefully acknowledged. Lastly, my thanks go to Herrn K. Kruse for the preparation of the drawings, and also to Dr. G. Miller and Dr. D. Nagaki for their excellent translation of the article. I am also indebted to Dr. G. Miller for many helpful discussions.

Received: November 14, 1986;
revised: February 11, 1988 [A 674 IE]
German version: *Angew. Chem. 100* (1988) 781

[1] H. Schäfer, B. Eisenmann, W. Müller, *Angew. Chem. 85* (1973) 742; *Angew. Chem. Int. Ed. Engl. 12* (1973) 694.
[2] H. G. von Schnering, *Angew. Chem. 93* (1981) 44; *Angew. Chem. Int. Ed. Engl. 20* (1981) 33.
[3] H. Schäfer, B. Eisenmann, *Rev. Inorg. Chem. 3* (1981) 29.
[4] H. Schäfer, *Annu. Rev. Mater. Sci. 15* (1985) 1.
[5] H. Schäfer, *J. Solid State Chem. 57* (1985) 97.
[6] R. J. Desando, R. C. Lange, *J. Inorg. Nucl. Chem. 28* (1966) 1837.
[7] J. Donohue: *The Structures of the Elements*, Wiley, New York 1974, p. 386-392.
[8] A. von Hippel, *J. Chem. Phys. 16* (1948) 372.
[9] K. Aoki, O. Shimomura, S. Mimomura, *J. Phys. Soc. Jpn. 48* (1980) 551.
[10] F. Hulliger, *Phys. Chem. Mater. Layered Struct. 5* (1976) 77.
[11] P. Cherin, P. Unger, *Acta Crystallogr. 23* (1967) 670.
[12] K. P. Huber, G. Herzberg: *Molecular Spectra and Molecular Structure, Vol. IV: Constants of Diatomic Molecules*, van Nostrand-Reinhold, New York 1979.
[13] J. K. Burdett, T. J. McLaman, *J. Chem. Phys. 75* (1981) 5764; J. K. Burdett, P. Haaland, T. J. McLaman, *ibid. 75* (1981) 5774.
[14] J. K. Burdett, *Acc. Chem. Res. 15* (1982) 34.
[15] J. K. Burdett, *Prog. Solid State Chem. 15* (1984) 173.
[16] See [7], p. 295 and 307.
[17] P. Böttcher, U. Kretschmann, *Z. Anorg. Allg. Chem. 523* (1985) 145.
[18] D. Y. Valentine, O. B. Cavin, H. L. Yakel, *Acta Crystallogr. B 33* (1977) 1389.
[19] P. Böttcher, R. Keller, *Z. Anorg. Allg. Chem. 542* (1986) 144.
[20] P. Böttcher, U. Kretschmann, *J. Less-Common Met. 95* (1983) 81.
[21] P. Böttcher, U. Kretschmann, *Z. Anorg. Allg. Chem. 491* (1982) 39.
[22] B. Eisenmann, H. Schäfer, *Angew. Chem. 90* (1978) 731; *Angew. Chem. Int. Ed. Engl. 17* (1978) 684.
[23] P. Böttcher, *J. Less-Common Met. 70* (1980) 263.
[24] P. Böttcher, R. Keller, *J. Less-Common Met. 109* (1985) 311.
[25] R. Keller, *Dissertation*, Technische Hochschule Aachen 1986.
[26] E. Zintl, A. Harder, B. Dauth, *Z. Elektrochem. 40* (1934) 588.
[27] H. Sommer, R. Hoppe, *Z. Anorg. Allg. Chem. 429* (1977) 118.
[28] K.-J. Range, M. Zabel, F. von Krziwanek, R. Marx, B. Panzer, *Angew. Chem. 94* (1982) 717; *Angew. Chem. Int. Ed. Engl. 21* (1982) 706.
[29] A. L. Bowman, T. C. Wallace, J. L. Yarnell, R. G. Wenzel, *Acta Crystallogr. 21* (1966) 843; G. Brauer, *Z. Anorg. Chem. 248* (1941) 1.
[30] H. G. von Schnering, W. Dahlmann, *Naturwissenschaften 58* (1971) 623.
[31] R. Kniep, H.-J. Beister, *Angew. Chem. 97* (1985) 399; *Angew. Chem. Int. Ed. Engl. 24* (1985) 393.
[32] W. Tremel, R. Hoffmann, *Inorg. Chem. 26* (1987) 118.
[33] W. B. Pearson, *Z. Kristallogr. 171* (1985) 23.
[34] See [10], p. 245.
[35] B. K. Norling, H. Steinfink, *Inorg. Chem. 5* (1966) 1488.
[36] R. Wang, H. Steinfink, W. F. Bradley, *Inorg. Chem. 5* (1966) 142.
[37] W. Lin, H. Steinfink, E. J. Weiss, *Inorg. Chem. 4* (1965) 877.
[38] R. Wang, H. Steinfink, *Inorg. Chem. 6* (1967) 1685.
[39] A. A. Eliseew, V. G. Kusnetzow, *Izv. Akad. Nauk SSSR, Neorg. Mater. 1* (1965) 692.
[40] A. A. Eliseew, K. A. Zinchenko, N. Ch. Abrikosow, *Zh. Neorg. Khim. 22* (1977) 238.
[41] E. I. Jarembasch, A. A. Eliseew, E. S. Wigilewa, L. I. Antonowa, *Izv. Akad. Nauk SSSR, Neorg. Mater. 3* (1967) 2184.
[42] K. A. Agajew, R. S. Gamidow, K. S. Mamedow, *Issled. Obl. Neorg. Fiz. Khim. 1970*, 199.
[43] J. F. Cannon, H. T. Hall, *Inorg. Chem. 9* (1979) 1639.
[44] K. Niihara, T. Shishido, S. Yajima, *Bull. Chem. Soc. Jpn. 45* (1972) 1239.
[45] M. P. Pardo, J. Flahaut, *Bull. Soc. Chim. Fr. 1967*, 3658; M. P. Pardo, O. Gorochow, J. Flahaut, L. Domange, *C. R. Acad. Sci. 260* (1965) 1666.
[46] A. A. Eliseew, K. A. Zinchenko, V. M. Semlyanuchina, Nguyen Chin Tam, *Zh. Neorg. Khim. 21* (1976) 2603.
[47] V. I. Chukalin, E. I. Jarembasch, A. I. Willenskij, *Inorg. Mater. (Engl. Transl.) 3* (1967) 1341.
[48] E. I. Jarembasch, E. S. Wigilewa, *Inorg. Mater. (Engl. Transl.) 7* (1971) 1388.
[49] E. I. Jarembasch, *Inorg. Mater. (Engl. Transl.) 10* (1974) 1212.
[50] D. Damien, *J. Inorg. Nucl. Chem. 36* (1974) 307; *Inorg. Nucl. Chem. Lett. 8* (1972) 501; *9* (1973) 453.

[51] D. Damien, A. Wojakowski, W. Müller, *Inorg. Nucl. Chem. Lett. 12* (1976) 441.
[52] D. J. Haase, H. Steinfink, E. J. Weiss, *Inorg. Chem. 4* (1965) 541.
[53] T. H. Ramsey, H. Steinfink, E. J. Weiss, *Inorg. Chem. 4* (1965) 1154.
[54] J. Dugué, D. Carré, M. Guittard, *Acta Crystallogr. B24* (1978) 403.
[55] A. W. Webb, H. T. Hall, *Inorg. Chem. 9* (1970) 1084.
[56] A. A. Eliseew, S. U. Uspenkaja, T. A. Kalganowa, *Russ. J. Inorg. Chem. 17* (1972) 1222.
[57] S. I. Uspenskaja, A. A. Eliseew, *Russ. J. Inorg. Chem. 17* (1972) 1344.
[58] G. M. Kusmichewa, A. A. Eliseew, I. G. Orlowa, B. V. Muchin, *Russ. J. Inorg. Chem. 28* (1983) 755.
[59] Y. Yanagisawa, S. Kume, *Mater. Res. Bull. 21* (1986) 379.
[60] C. L. Teske, *Z. Naturforsch. B29* (1974) 16.
[61] A. B. Webb, H. T. Hall, *Inorg. Chem. 9* (1979) 843.
[62] S. Bénazeth, D. Carré, P. Larueile, *Acta Crystallogr. B38* (1982) 33, 37.
[63] J.-P. Marcon, R. Pascard, *C. R. Acad. Sci. Ser. C266* (1968) 270.
[64] A. A. Eliseew, V. G. Kusnetznow, *Izv. Akad. Nauk SSSR, Neorg. Mater. 2* (1966) 1157.
[65] A. A. Eliseew, J. Laurier, G. Kela, E. I. Jarembasch, M. K. Suleimanow, *J. Struct. Chem. 9* (1968) 464.
[66] S. Benazeth, J. Dugué, D. Carré, M. Guittard, J. Flahaut, *Rare Earths Mod. Sci. Technol. 2* (1980) 223.
[67] A. A. Eliseew, Z. Lorje, G. Kela, E. I. Jarembasch, M. K. Suleimanow, *Zh. Strukt. Khim. 9* (1968) 538.
[68] A. A. Eliseew, S. I. Uspenskaja, A. A. Fedorow, *Russ. J. Inorg. Chem. 16* (1971) 786.
[69] P. Plambeck-Fischer, W. Urland, W. Abriel, *Z. Kristallogr. 178* (1987) 182.
[70] W. Tremel, R. Hoffmann, *J. Am. Chem. Soc. 109* (1987) 124.
[71] G. Trinquier, R. Hoffmann, *J. Phys. Chem. 88* (1984) 6696.
[72] Ch. Zheng, R. Hoffmann, *Z. Naturforsch. B41* (1986) 292.
[73] T. H. Ramsey, H. Steinfink, E. J. Weiss, *J. Appl. Phys. 34* (1963) 2917.
[74] K. Selte, A. Kjekshus, *Acta Chem. Scand. 18* (1964) 690.
[75] E. Bjerkelund, A. Kjekshus, *J. Less-Common Met. 7* (1964) 231; *Z. Anorg. Allg. Chem. 328* (1964) 235.
[76] H. Böhm, H. G. von Schnering, *Z. Kristallogr. 171* (1985) 41.
[77] S. van Smaalen, K. D. Bronsema, *Acta Crystallogr. B42* (1986) 43.
[78] D. Samu, M. B. Walker, *Phys. Rev. B: Condens. Matter 32* (1985) 1643.
[79] a) J. Rouxel (Ed.): *Crystal Chemistry and Properties of Materials with Quasi-One-Dimensional Structures*, Reidel, Dordrecht, Holland 1986; b) M.-H. Wangbo: *Orbital Interaction Analysis for the Electronic Structures of Low-Dimensional Solids*, in [79a], p. 27.
[80] A. Meerschaut, J. Rouxel: *Pseudo-One-Dimensional MX_3 and MX_4 Transition Metal Chalkogenides*, in [79a], p. 205.
[81] T. Sambongi: *Pentachalcogenides of Transition Metals*, in [79a], p. 281.
[82] S. Furuseth, L. Brattas, A. Kjekshus, *Acta Chem. Scand. 27* (1973) 2367.
[83] H. Fjellvag, A. Kjekshus, *Solid State Commun. 60* (1986) 91.
[84] W. Biltz: *Raumchemie der Festen Stoffe*, Verlag L. Voss, Leipzig 1934.
[85] A. J. K. Haneveld, F. Jellinek, *J. Less-Common Met. 21* (1970) 45.
[86] S. Furuseth, L. Brattas, A. Kjekshus, *Acta Chem. Scand. A29* (1975) 623.
[87] H. Noël, *J. Less-Common Met. 121* (1986) 265.
[88] A. Ben Salem, A. Meerschaut, J. Rouxel, *C. R. Acad. Sci. 299* (1984) 617.
[89] See [10], p. 134, and references cited therein.
[90] V. K. Slowianskik, N. T. Kusnetzow, N. V. Gratschewa, *Russ. J. Inorg. Chem. 30* (1985) 314.
[91] J. Weis, H. Schäfer, B. Eisenmann, G. Schön, *Z. Naturforsch. B29* (1974) 585.
[92] H. Noël, *Inorg. Chim. Acta 109* (1985) 205.
[93] G. Tunnell, *J. Wash. Acad. Sci. 25* (1935) 32 (see also [10], p. 228).
[94] R. Kniep, D. Mootz, A. Rabenau, *Z. Anorg. Allg. Chem. 422* (1976) 17.
[95] M. Julien-Pouzol, S. Jaulmes, F. Alapini, *Acta Crystallogr. B33* (1977) 2270.
[96] B. Eisenmann, H. Schwerer, H. Schäfer, *Mater. Res. Bull. 18* (1983) 383.
[97] C. Brinkmann, B. Eisenmann, H. Schäfer, *Mater. Res. Bull. 20* (1985) 299.
[98] F. Klaiber, W. Petter, F. Hulliger, *J. Solid State Chem. 46* (1983) 112.
[99] B. Krebs, Münster, private communication 1986.
[100] L. I. Man, R. M. Imamow, Z. G. Pinsker, *Sov. Phys. Crystallogr. (Engl. Trans.) 16* (1971) 94.
[101] S. Bhan, K. Schubert, *J. Less-Common Met. 20* (1970) 229.
[102] G. Prins, E. H. P. Cordfunke, *J. Less-Common Met. 104* (1984) L1.
[103] C. Brinkmann, B. Eisenmann, H. Schäfer, *IIIrd Eur. Conf. Solid State Chem., Regensburg 1986, Book of Abstracts, Vol. 1*, p. 61.
[104] T. Birchall, R. D. Myers, *Inorg. Chem. 21* (1982) 213.
[105] J. Passmore, P. Taylor, T. Whidden, P. S. White, *Cand. J. Chem. 57* (1979) 968.
[106] S. Yanagisawa, M. Tashiro, S. Anzai, *J. Inorg. Nucl. Chem. 31* (1969) 943.
[107] G. Brostigen, A. Kjekshus, *Acta Chem. Scand. 24* (1970) 1925.
[108] G. Cordier, C. Schwidetzky, H. Schäfer, *Z. Naturforsch. B39* (1984) 833.
[109] H. H. Sutherland, J. H. C. Hogg, P. D. Walton, *Acta Crystallogr. B32* (1976) 2539.
[110] P. D. Walton, H. H. Sutherland, J. H. C. Hogg, *Acta Crystallogr. B34* (1978) 41.
[111] A. Cisar, J. D. Corbett, *Inorg. Chem. 16* (1977) 632.
[112] R. Zagler, B. Eisenmann, H. Schäfer, *Z. Naturforsch. B42* (1987) 151.
[113] J. C. Huffman, R. C. Haushalter, *Z. Anorg. Allg. Chem. 518* (1984) 203.
[114] L. A. Devereux, G. J. Schrobilgen, *Acta Crystallogr. C41* (1985) 1730.
[115] R. G. Teller, L. J. Krause, R. C. Haushalter, *Inorg. Chem. 22* (1983) 1809.
[116] J. Bernstein, R. Hoffmann, *Inorg. Chem. 24* (1985) 4100.
[117] J. K. Burdett: *Molecular Shapes*, Wiley, New York 1980, p. 28.
[118] D. W. Bullet, *Solid State Chem. 51* (1984) 51.
[119] R. D. Shannon, *Acta Crystallogr. A32* (1976) 751.
[120] A. L. Allred, E. Rochow, *J. Inorg. Nucl. Chem. 5* (1981) 264.
[121] A. N. Bloch, G. C. Schatteman in M. O'Keeffe, A. Navrotsky (Eds.): *Structure and Bonding in Crystals, Vol. 1*, Academic Press, New York 1981, p. 49ff.
[122] N. M. Mustafaew, V. V. Iljuschin, N. V. Below, *Sov. Phys. Crystallogr. (Engl. Trans.) 10* (1965) 676.
[123] F. Liebau: *Structural Chemistry of Silicates*, Springer, Berlin 1985.
[124] H. A. Graf, H. Schäfer, *Z. Anorg. Allg. Chem. 425* (1976) 67.
[125] B. Eisenmann, M. Jakowski, H. Schäfer, *Z. Naturforsch. B39* (1984) 27.
[126] B. Eisenmann, H. Jordan, H. Schäfer, *Angew. Chem. 93* (1981) 211; *Angew. Chem. Int. Ed. Engl. 20* (1981) 197.
[127] G. Cordier, H. Schäfer, M. Stelter, *Z. Anorg. Allg. Chem. 519* (1984) 183.
[128] G. Cordier, H. Schäfer, M. Stelter, *Z. Naturforsch. B40* (1985) 868.
[129] C. Brinkmann, B. Eisenmann, H. Schäfer, *Z. Anorg. Allg. Chem. 524* (1985) 83.
[130] B. Eisenmann, H. Schäfer, H. Schrod, *Z. Naturforsch. B38* (1983) 921.
[131] K. Volk, H. Schäfer, *Z. Naturforsch. B34* (1979) 1337.
[132] B. Eisenmann, H. Jordan, H. Schäfer, *Z. Anorg. Allg. Chem. 475* (1981) 74.
[133] G. Cordier, C. Schwidetzky, H. Schäfer, *Z. Naturforsch. B40* (1985) 1.
[134] P. Böttcher, unpublished results, 1986.
[135] C. Gessert, E. Sirtl: *Elektronische Halbleitermaterialien* in H. Harnisch, R. Steiner, K. Winnacker (Eds.): *Chemische Technologie, Vol. 3*, Hanser, München 1983, p. 408ff.
[136] H. G. von Schnering, R. Nesper, J. Curda, K.-F. Tebbe, *Angew. Chem. 92* (1980) 1070; *Angew. Chem. Int. Ed. Engl. 19* (1980) 1033.
[137] R. Ramierez, R. Nesper, H. G. von Schnering, M. C. Böhm, *Chem. Phys. 95* (1985) 17.
[138] M. C. Böhm, R. Ramirez, R. Nesper, H. G. von Schnering, *Ber. Bunsenges. Phys. Chem. 89* (1985) 465.
[139] C. D. Wagner, W. M. Riggs, L. E. Davis, J. F. Moulder, G. E. Muilenberg (Eds.): *Handbook of X-Ray Photoelectron Spectroscopy*, Perkin-Elmer Corp., Eden Prairie (USA) 1978, p. 182ff.
[140] N. Habibi, *J. Fluorine Chem. 12* (1978) 63, 237.
[141] R. Hoppe, U. Untenecker, *IIIrd Eur. Conf. Solid State Chem., Regensburg 1986, Book of Abstracts, Vol. 1*, p. 94.
[142] J. Moret, F. Daniel, W. Loeksmanto, M. Maurin, E. Philipott, *Acta Crystallogr. B34* (1978) 3156.
[143] R. C. Haushalter, L. J. Krause, *Thin. Solid Films 102* (1983) 161.
[144] R. C. Haushalter, *Angew. Chem. 95* (1983) 560; *Angew. Chem. Int. Ed. Engl. 22* (1983) 558; *Angew. Chem. Suppl. 1983*, 766.
[145] R. C. Haushalter, C. J. O'Connor, A. M. Umarji, G. K. Shenoy, C. K. Saw, *Solid State Commun. 49* (1984) 929.
[146] R. C. Haushalter, C. M. O'Connor, J. P. Haushalter, A. M. Umarji, G. K. Shenoy, *Angew. Chem. 96* (1984) 147; *Angew. Chem. Int. Ed. Engl. 23* (1984) 169.

Isoleucyl-tRNA Synthetase: An Enzyme with Several Catalytic Cycles Displaying Variation in Specificity and Energy Consumption

By Wolfgang Freist*

The translation of DNA via the genetic code into protein is a fundamental process carried out by all living systems. The extreme accuracy with which it is performed requires that the enzymes involved operate with extremely high specificity. It is for this reason that the structure and function of these proteins have been of special interest to molecular biologists and biochemists for the last twenty years. The discrimination between the different amino acids present in the cytosol and their esterification with the correct tRNA is the special task of the aminoacyl-tRNA synthetases. One of the most difficult discriminations that has to be performed is the specificity for isoleucine. There are many amino acids in the cell that have a structure similar to isoleucine, in particular valine. To solve this problem, the aminoacyl-tRNA synthetases have evolved unique proofreading mechanisms. The most detailed investigations of these mechanisms have been on the isoleucyl-tRNA synthetases from yeast and from *Escherichia coli*. Both enzymes are single-chain polypeptides with molecular weights of about 110000. Sequence homologies with other aminoacyl-tRNA synthetases seem to occur only within narrow regions, for example in the ATP binding site. The identification of the correct amino acid is achieved in a four-step process. In the first two steps the hydrophobic interaction of the amino acid side chain with the enzyme is utilized for discrimination. The two hydrolytic proofreading steps that follow make use of the steric hindrance associated with the amino acid side chain. The enzymes are characterized by the special property that slight variations in the reaction conditions cause conformational changes that affect the catalytic cycle. In this way the observed specificity of the enzymes can be changed to almost any value. In general, high specificity is associated with high energy cost, which is reflected in high ATP consumption. Under physiological conditions a medium level of specificity and energy consumption seems to be preferred.

1. Introduction

Since the mid-1950s, when the first aminoacyl-tRNA synthetases were discovered and found to be important enzymes of protein biosynthesis,[1-7] more than a hundred of these proteins have been isolated and characterized.[8-12] The quaternary structures and molecular weights of the various purified enzymes are very different. Most consist of a single polypeptide chain (α) or are dimers of two identical subunits (α_2). The molecular weights of the monomeric species range from 40000 to 140000, while the dimers are within the range of 65000 to 240000. A few enzymes have quaternary structures of the type $\alpha_2\beta_2$ ($M_r = 85000$–287000), $\alpha\beta$ ($M_r = 102000$–130000), or α_4 ($M_r = 116000$–380000).[8-12] Generally, these enzymes have one active site per subunit or, in the case of the $\alpha_2\beta_2$ types, one active site per $\alpha\beta$ pair.[9-11,13-21]

The reaction catalyzed by the aminoacyl-tRNA synthetases (E) involves a two-step process, where the amino acid is first activated, then transferred to the tRNA.[9,10] In the *activation step* (a) an aminoacyl adenylate **3** (and pyrophosphate **4**) is formed from the amino acid **1** and adenosine triphosphate (ATP) **2**. This intermediate remains bound to the enzyme and is protected from hydrolysis.

In the *transfer step* (b) the activated amino acid **3** is transferred to a hydroxyl group of the 3′ terminal ribose of the tRNA **5**, resulting in the formation of aminoacyl-tRNA **6** and adenosine monophosphate **7**.

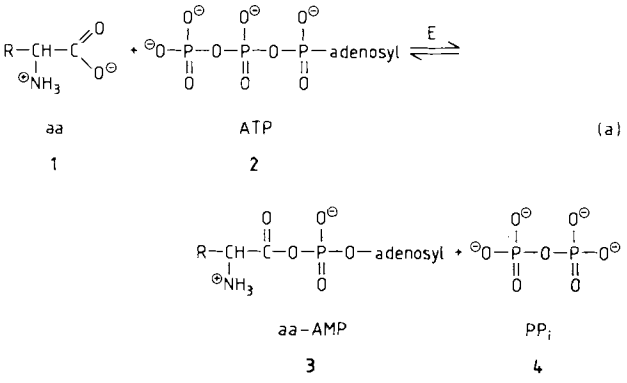

For some synthetases it has been postulated by several workers that perhaps only a one-step mechanism is operating. In these cases a discrete aminoacyl-adenylate intermediate is presumably not formed.[8,22-25]

2. Structure and Reaction Mechanism

The isoleucyl-tRNA synthetases from yeast and *E. coli* are single polypeptide chains of type α. The molecular weight of the synthetase from *E. coli* B is 112000,[26] and

[*] Dr. W. Freist
Max-Planck-Institut für experimentelle Medizin,
Abteilung Chemie
Hermann-Rein-Strasse 3, D-3400 Göttingen (FRG)

 © VCH Verlagsgesellschaft mbH, D-6940 Weinheim, 1988 0570-0833/88/0606-0773 $ 02.50/0

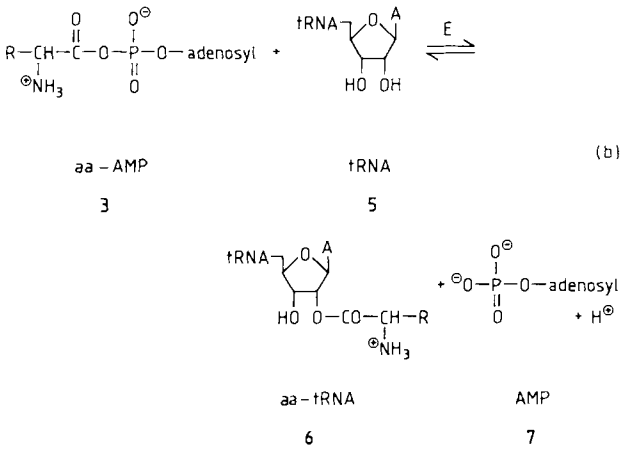

aa-AMP 3 tRNA 5 (b)

aa-tRNA 6 AMP 7

that of the enzyme from *E. coli* MRE600 is 102000.[27] For the synthetase from yeast, $M_r = 115000$.[28,29]

At present, the primary structure of only one isoleucyl-tRNA synthetase has been reported.[30] It was determined from the DNA sequence of the gene isolated from *E. coli* K12 and partly from peptide sequencing of the enzyme from *E. coli* MRE600. The enzyme consists of 939 amino acids and has a molecular weight of 105087. A small region of the sequence, corresponding to eleven amino acids, is homologous with three[31-33] of the seven[31-37] aminoacyl-tRNA sequences that have been determined.[*]

The stoichiometry of adenylate formation shows that isoleucyl-tRNA synthetase forms a 1:1 complex with isoleucyl adenylate **3**, R = *sec*-butyl.[14] This indicates that there is only one active center per peptide chain. The turnover number for aminoacylation of $tRNA^{Ile}$, under optimal reaction conditions, is $k_{cat} \approx 1\ s^{-1}$ for both the *E. coli* and yeast enzymes.[14,38] Compared with other aminoacyl-tRNA synthetases, which have k_{cat} values between 1 and $25\ s^{-1}$,[8,39-42] as well as with other important enzymes of metabolism (cf. Refs. [43-46]), the isoleucyl-tRNA synthetases are "slow" enzymes.

A formal analogy to aminoacylation of tRNA can be found in the activation of fatty acids for β oxidation. The acyl-CoA synthetases catalyze the formation of an enzyme-bound acyl-adenylate intermediate from which the acyl residue is transferred to the thiol group of coenzyme A.

$$R{-}CO_2^{\ominus} + ATP \xrightarrow{E} R{-}CO{-}AMP + PP_i$$

$$R{-}CO{-}AMP + CoA{-}SH \xrightarrow{E} R{-}CO{-}S{-}CoA + AMP$$

The acyl residue can then be easily transferred from the thiol group of CoA to an alcohol; for example, the enzyme carnitine acyltransferase catalyzes the transfer of the acyl group to carnitine **8**.[47,48]

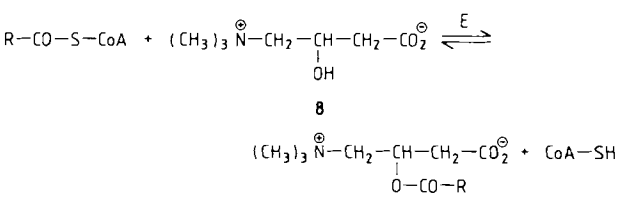

8

The gramicidin S-synthetases and related enzymes that are involved in the biosynthesis of peptide antibiotics also form an aminoacyl adenylate of type **3** from which the amino acid is transferred to a thiol group. The peptide bond is formed by reaction of the thioester.[49-51] It was reasonable to suspect that aminoacyl-tRNA synthetases might also synthesize thioesters of amino acids as intermediates; however, this has still not been unambiguously shown. Of the sixteen cysteine residues of *E. coli* isoleucyl-tRNA synthetase, eleven react with thio-labeling reagents[52] and one reacts very quickly.[52-54] Specific blocking of only this fast-reacting cysteine does not interfere with the activation reaction (a) but completely blocks the aminoacylation of tRNA.[52,54] This observation suggests that the amino acid is indeed transferred from the aminoacyl adenylate **3** to the tRNA via a thioester. However, other authors have found that even with one thiol group blocked there is still a low level of aminoacylation and have concluded that the fast-reacting cysteine may not be essential for catalysis.[55] When the primary structure was elucidated, the fast-reacting cysteine was assigned to position 431 of the peptide chain.[30] This position is 364 amino acid residues away from a group of 11 amino acids believed to make up the ATP binding site.[30] These 11 amino acids (positions 57-67) have direct sequence homology with other aminoacyl-tRNA synthetases. The location of these residues suggests that the active site is located in the *N*-terminal part of the enzyme.[30]

Whereas in the transfer step (b) the existence of a thioester intermediate is not quite clear, stereochemical investigations have shown that the presence of an intermediate in the activation step (a) is unlikely.[56] By using [$^{18}O_2$]isoleucine **1*** and adenosine 5′-[(*R*)-α-^{17}O]triphosphate **2*** as substrates and trapping the isoleucyl adenylate **3*** with hydroxylamine it was established that the reaction proceeds with inversion of configuration at the α-phosphorus atom of ATP, giving ^{17}O-labeled AMP **7***.

This indicates that a direct displacement of the pyrophosphate has occurred and excludes a reaction pathway with *one* intermediate, e.g., an adenylyl enzyme. However, the evidence does not exclude the rather unlikely possibility of *two* intermediates.

Aminoacyl adenylates (**3**) are mixed acid anhydrides and therefore contain both activated aminoacyl and adenylyl moieties. Thus, the aminoacyl-tRNA synthetases can also catalyze reactions in which the AMP residue is transferred to a phosphate moiety.[57-65] The simplest example is the reverse reaction of adenylate formation [reaction (a)]. This is easily followed by monitoring the incorporation of ^{32}P-labeled pyrophosphate into ATP. In another important reaction, the aminoacyl adenylate **3** formed by some aminoacyl-tRNA synthetases can react with ATP to form

[*] After completion of this article, some more primary structures of aminoacyl-tRNA synthetases were elucidated, among which is the amino acid sequence of isoleucyl-tRNA synthetase from yeast. This enzyme consists of 1073 amino acids ($M_r = 123040$) and shows 27% sequence homology with the enzyme from *E. coli*, especially in the supposed regions of the ATP and tRNA binding sites (U. Englisch, S. Englisch, P. Markmeyer, J. Schischkoff, H. Sternbach, H. Kratzin, F. Cramer, *Biol. Chem. Hoppe Seyler 368* (1987) 971).

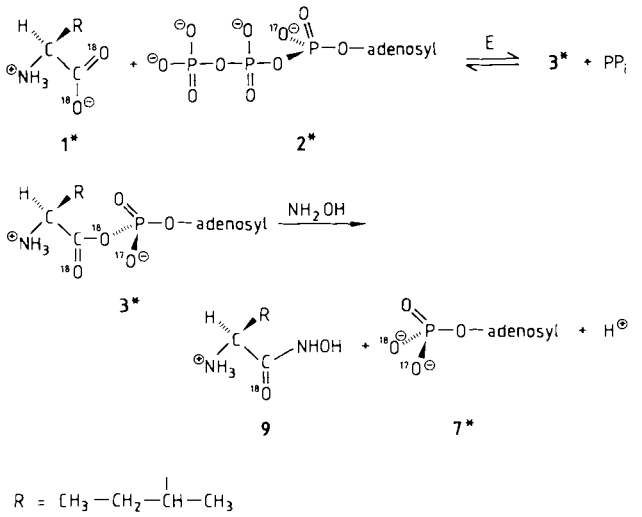

R = $CH_3-CH_2-\underset{|}{CH}-CH_3$

diadenosine-5′,5‴-P^1,P^4-tetraphosphate (AppppA) **10**.[57,58,60–65] AppppA may have important functions in regulation of initiation of DNA replication, cell proliferation, and tRNA synthesis.[66–68] Whereas isoleucyl-tRNA synthetase from *E. coli* catalyzes the formation of AppppA, the enzyme from yeast does not. However, the yeast enzyme does form adenosine 5′-diphosphate (ppA) as a side product.[69] It is possible that this side product is produced by the splitting of AppppA formed in a preceding reaction step.[69]

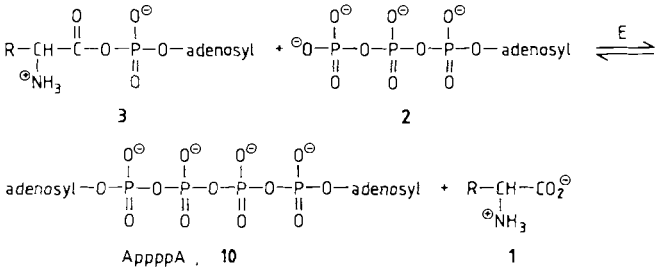

An open question for both enzymes is the possibility that the activity is regulated through phosphorylation by a kinase. Till now such a kinase has only been demonstrated for an isoleucyl-tRNA synthetase from rabbit reticulocytes.[70]

3. Substrate Specificity

3.1. ATP Analogues

Since all aminoacyl-tRNA synthetases have ATP as a substrate, analogues of ATP can be used to investigate the differences in specificity between enzymes. By systematically testing various modified ATP molecules, the topology of the ATP binding site can be determined and the different enzymes arranged in groups showing similar specificities. For the isoleucyl-tRNA synthetases it was possible to elucidate tentative phylogenetic relationships with other aminoacyl-tRNA synthetases.

Difficulties in interpreting the results of these ATP-analogue studies arose from the fact that the real substrate for the synthetases is the ATP·$Mg^{2\oplus}$ complex and not free ATP.[8–11] The exact structure of this complex is still undetermined. Based on studies of the sodium salt of ATP[71] and NMR spectroscopic data,[72–74] a model for the ATP·$Mg^{2\oplus}$ complex, **11**, has been postulated in which the metal ion is coordinated with N-7 of the purine and one oxygen of the β, γ, and possibly also the α phosphate of the triphosphate moiety.[75] In another model, which is based on the affinity of hexokinase for the tetraamminecobalt(III)-ATP complex, the complex is formulated as a bidentate β,γ-complex **12**.[76] The possibility of coordination with the purine N-7 is not discussed in this model.[76]

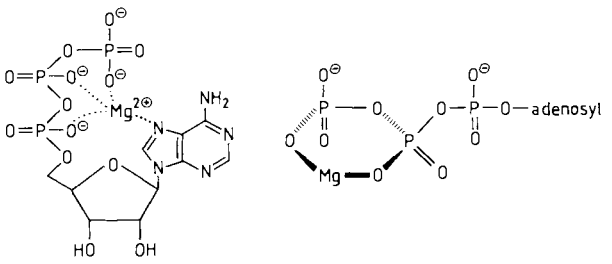

The results obtained using ATP analogues indicate that the aminoacyl-tRNA synthetases use ATP·$Mg^{2\oplus}$ complexes of different structure. The data are consistent with both structural models cited above.

The ATP analogues employed were prepared starting from nucleoside derivatives for which syntheses have been described during the past thirty years[77,78] or from nucleoside antibiotics isolated from microorganisms.[79] In most cases the phosphorylation of the nucleosides **13** was carried out by simple methods such as reaction with $POCl_3$ to form the monophosphate **14** followed by conversion to the phosphate imidazolide **15** and finally reaction with pyrophosphate to give the triphosphate **16**.[80–83]

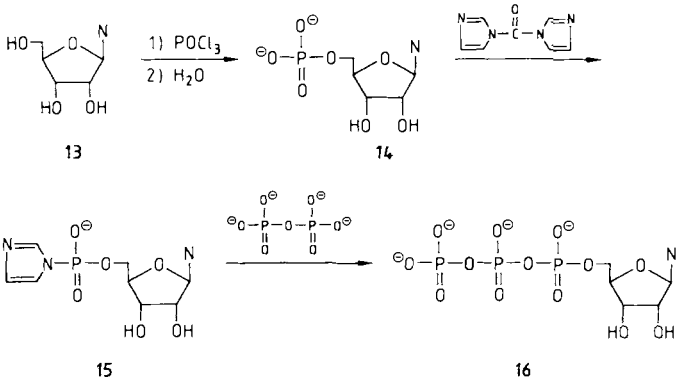

Of the 35 ATP analogues prepared a characteristic set of eight (**17a–h**) were tested as substrates or inhibitors of the aminoacylation reaction.[84–87] These compounds were used to determine the differences between the yeast and *E. coli* aminoacyl-tRNA synthetases.[88] Four of the analogues tested were modified at positions 2, 6, 7, and 8 of the purine ring. The other four were modified at the 2′ and 3′ positions of the ribose.

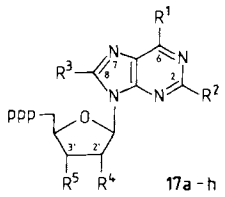

17a - h

	5′-Triphosphate of	R^1	R^2	R^3	R^4	R^5
17a	N^6-methyladenosine (m^6ATP)	NH–CH_3	H	H	OH	OH
17b	2-chloroadenosine (cl^2ATP)	NH_2	Cl	H	OH	OH
17c	8-bromoadenosine (br^8ATP)	NH_2	H	Br	OH	OH
17d	tubercidine =7-deazaadenosine (TuTP)[a]	NH_2	H	H	OH	OH
17e	2′-deoxyadenosine (dATP)	NH_2	H	H	H	OH
17f	3′-deoxyadenosine ($d^{3'}$ATP)	NH_2	H	H	OH	H
17g	2′-methoxyadenosine ($m^{2'}$ATP)	NH_2	H	H	OCH_3	OH
17h	3′-methoxyadenosine ($m^{3'}$ATP)	NH_2	H	H	OH	OCH_3

[a] In position 7, =N– is replaced by =CH–.

The results listed in Table 1 allow the aminoacyl-tRNA synthetases to be arranged in groups. Clearly, two main types of synthetases (I, II) are present in *E. coli* and yeast. However, minor types can also be distinguished. In *E. coli* there are three different groups which are represented by two enzymes each (III–V). Group V is also found in yeast. The histidyl-tRNA synthetases from both organisms are unique and must be regarded as a separate group (VI).

Almost all the enzymes require the amino group in the 6 position of the adenine ring for the binding of ATP (**17a**). Large substituents, such as a bromine atom at the 8 position, that hinder free rotation of the base around the glycosyl bond (see Appendix) and put the nucleotide into the *syn* conformation are not substrates for the aminoacyl-tRNA synthetases (**17c**). In the group I enzymes the nitrogen at position 7 of adenine is essential. This may indicate that these enzymes bind an ATP·$Mg^{2\oplus}$ complex of type **11** in which the $Mg^{2\oplus}$ ion is coordinated to N-7 (**17d**). The ribose hydroxyl groups are not essential for the binding by *E. coli* group I enzymes. In contrast, most of the group I yeast enzymes will not accept dATP or 3′dATP as substrates (**17e, f**). The enzymes from both organisms do not tolerate methoxy substituents at these positions (**17g, h**).

In group II the N-7 does not seem to be necessary for complexation of the $Mg^{2\oplus}$ ion. It is possible that the enzyme binds an ATP·$Mg^{2\oplus}$ complex of type **12** in which the $Mg^{2\oplus}$ ion is only coordinated to the phosphate oxygens (**17d**). The ribose 2′-OH group is not important at least for the *E. coli* enzymes (**17e, f**); *O*-methyl groups are not tolerated (**17g, h**).

The group III and most of the group V enzymes have no requirement for the N-7 of adenosine (**17d**). In the case of the group IV and VI enzymes no conclusions on the structure of the ATP·$Mg^{2\oplus}$ complex can be drawn. Remarkably, the enzymes of group V accept ATP analogues with methylated hydroxyl groups as substrates (**17g, h**).

Using ATP analogues other than the eight described above it is possible to probe more deeply the parts of the ATP molecule important for recognition by the synthetases.[87,89] From the "specificity raster" shown in Table 1, however, the isoleucyl-tRNA synthetase can be grouped with the leucine, valine, methionine, tyrosine, cysteine, glutamate, and glutamine enzymes. In this group, ATP binding sites of similar structure can be expected. Indeed, the amino acid sequence of isoleucyl-tRNA synthetase expected to be associated with ATP binding shows direct homology with the methionyl, tyrosyl, and glutaminyl enzymes.[30]

Table 1. Substrate specificity of 20 aminoacyl-tRNA synthetases from *E. coli* and 13 aminoacyl-tRNA synthetases from yeast with respect to ATP analogues **17a–h** (α_x characterizes the quaternary structure). sss means the compound has more than 50%, ss 10–50%, and s below 10% of the substrate activity of ATP. iii means the compound is active as an inhibitor and diminishes the substrate activity of ATP more than 50%, ii more than 20%, i more than 10% if ATP and inhibitor are present in the same concentration. – means the compound is neither a substrate nor an inhibitor.

Group		I								II					III		IV		V		VI
ATP analogue		Asp	Asn	Lys	Thr	Ser	Gly	Phe	Ile	Leu	Val	Met	Tyr	Cys	Glu	Gln	Ala	Pro	Arg	Trp	His
Aminoacyl-tRNA synthetases from E. coli:		α_2		α_2	α_2	α_2	$\alpha_2\beta_2$	$\alpha_2\beta_2$	α	α	α	α_2	α_2		α ($\alpha\beta$)	α	α_4	α_2	α	α_2	α_2
m^6ATP	**17a**	–	–	ss	–	–	–	–	s	–	–	–	–	–	i	ii	–	–	–	ii	–
cl^2ATP	**17b**	sss	sss	sss	sss	sss	sss	sss	sss	s	sss	s	ss	–	ii	ii	–	–	–	s	ss
br^8ATP	**17c**	–	–	–	–	–	–	–	–	–	–	–	–	–	i	ii	–	–	ii	ii	–
TuTP	**17d**	–	–	–	–	–	–	–	sss	ss	s	sss	sss	sss	sss	sss	–	–	sss	ii	–
dATP	**17e**	ss	ss	ss	ss	sss	sss	ss	–	–	i	–	–	–	ii	ii	–	–	ss	s	–
$d^{3'}$ATP	**17f**	sss	sss	s	s	ss	sss	ss	s	sss	s	s	ss	s	ii	ii	iii	iii	–	s	ii
$m^{2'}$ATP	**17g**	–	–	–	ss	–	–	–	–	–	–	–	–	–	iii	ii	iii	iii	–	s	–
$m^{3'}$ATP	**17h**	–	–	–	–	–	–	–	–	–	–	–	–	–	iii	ii	iii	iii	sss	sss	–
Aminoacyl-tRNA synthetases from yeast:				α_2	α_2	α_2		$\alpha_2\beta_2$	α	α_2	α	α_2							α	α_2	
m^6ATP	**17a**			–	–	–	i	–	iii	–	–	s	iii						iii	–	–
cl^2ATP	**17b**			sss	sss	sss	sss	sss	i	–	s	sss	–						–	sss	ss
br^8ATP	**17c**			iii	–	–	–	–	iii	–	–	–	–						ii	–	i
TuTP	**17d**			ii	ii	–	ii	–	s	sss	ss	sss	–						sss	ss	ii
dATP	**17e**			iii	iii	sss	iii	ss	–	i	–	–	–						sss	s	ii
$d^{3'}$ATP	**17f**			iii	ii	ii	ii	ii	iii	–	iii	–	–						ii	–	ii
$m^{2'}$ATP	**17g**			ii	ii	–	ii	–	–	iii	–	–	–						ss	–	ii
$m^{3'}$ATP	**17h**			iii	ii	–	ii	–	–	iii	–	–	–						ss	s	ii

3.2. Isoleucine Analogues

Precise translation of the genetic code requires high specificity with regard to the selection of the proper amino acid. That this is achieved is illustrated by the difficulty in detecting misacylation of $tRNA^{Ile}$ in the normal aminoacylation assay. In rabbit reticulocytes an error rate of 1:3000 has been determined for misincorporation of valine instead of isoleucine[90] into proteins. Because the misacylation reactions are extremely slow, they can only be measured under special experimental conditions (cf. Section 5).

Higher error rates are found when the aminoacylation reaction is tested with unnatural amino acids. Presumably, the discrimination mechanism is poorer because it does not have the benefits of biological evolution to develop an efficient proofreading system. However, there is some species diversity in regard to misacylation of unnatural amino acids. For example, the yeast isoleucyl-tRNA synthetase accepts γ-hydroxyisoleucine and γ,δ-dehydroisoleucine as substrates but the corresponding *E. coli* enzyme does not.[91]

Detailed binding studies have been performed with the isoleucine derivatives 3-methylpentanoic acid, 2-methylbutylamine, and 2-amino-3-methyl-1-pentanol (isoleucinol). It was concluded that the carboxylate and protonated amino groups of isoleucine may function to open an ion pair on the enzyme surface.[92] A positive charge on the enzyme could act to diminish repulsion between the negatively charged triphosphate moiety of ATP and the carboxylate group.[93] The pH-dependence of the stability of the ATP-enzyme complex suggests that a histidyl or lysyl residue on the enzyme may be involved in binding ATP. Evidence exists as well that implicates a lysyl residue in the binding of isoleucine.[94] It has not been possible, however, to identify the specific histidyl or lysyl residue in the published enzyme sequence.[30]

3.3. tRNA Analogues

For most aminoacyl-tRNA synthetases several isoacceptor tRNAs exist.[95] Two tRNAs that are charged with isoleucine have been isolated from *E. coli*.[96] They consist of 77 and 76 nucleotides of which 27 are different. The *E. coli* $tRNA^{Phe}$ and $tRNA^{fMet}$ are also charged with isoleucine but at rates that are very low and just measureable.[97,98] These latter noncognate tRNAs have sequences that differ in 39 and 40 positions, respectively, when compared with $tRNA^{Ile}$.[96] Mischarging of $tRNA^{Val}$ by yeast isoleucyl-tRNA synthetase has been the subject of extensive kinetic investigations.[99] It is likely that the $tRNA^{Val}$ samples used in these studies contained a number of $tRNA^{Val}$ isoacceptors and the relative proportion of each species varied with each preparation. Despite a comparison of the various tRNA sequences, especially isoacceptors, and experiments with both chemically and enzymatically modified tRNAs, it has not been possible to elucidate the mechanism of tRNA recognition.[100]

Modified tRNAs have been useful in probing the mechanism of aminoacylation; especially important have been the tRNAs altered at the 3′-terminal nucleotide by enzymatic or chemical means.[101,102] The 3′-terminal ribose of the tRNA can be oxidized with periodate to yield the dialdehyde **18**, which in aqueous solution is in equilibrium with the hemiacetal hydrate **19**.[103,104] The generated $tRNA_{oxi}$ (**18**, **19**) can be reduced to the diol ($tRNA_{oxi\text{-}red}$) **20** by $NaBH_4$.[103]

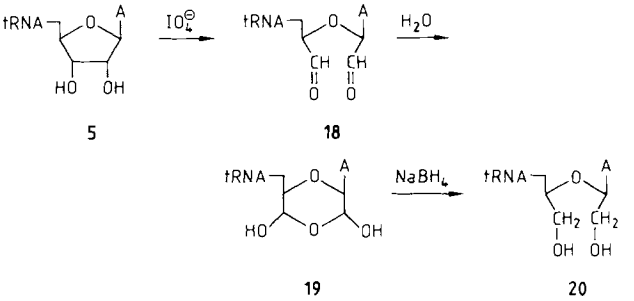

The $tRNA^{Ile}_{oxi\text{-}red}$ **20**, which is missing the bond between C2′ and C3′, is not a substrate for isoleucyl-tRNA synthetase. However, it is an inhibitor of the aminoacylation reaction. The $tRNA^{Ile}_{oxi}$ **19** is also an inhibitor but not a substrate for the enzyme.[29,105] Therefore, an intact terminal ribose is essential for enzymatic acylation of $tRNA^{Ile}$.

Other useful modifications of the C-C-A end of the tRNA can be carried out by enzymatic methods.[101,106-108] The terminal AMP nucleotide of the tRNA can be removed by controlled degradation with snake venom phosphodiesterase and AMP analogues can then be incorporated using tRNA nucleotidyltransferase. An alternative method starts with $tRNA_{oxi}$ **18**, which, when treated with lysine, eliminates the oxidized nucleoside. The terminal 3′ phosphate is removed using alkaline phosphatase and the modified nucleotide incorporated using tRNA nucleotidyltransferase.[109]

By incorporating in turn the 2′- and 3′-deoxyadenosine monophosphate nucleotides into tRNA it was determined which hydroxyl group is aminoacylated by the synthetase. Isoleucyl-tRNA synthetases from both yeast and *E. coli* acylate $tRNA^{Ile}$-C-C-3′dA **21** but not $tRNA^{Ile}$-C-C-2′dA **23**.[106,109,110]

From these results it was concluded that the natural $tRNA^{Ile}$-C-C-A **5** is acylated on the 2′-OH group by the

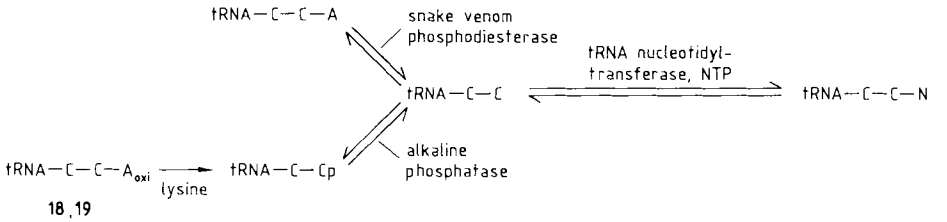

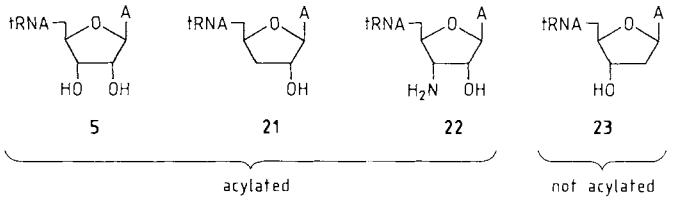

enzyme. However, the 2′-*O*-acyl-tRNA product will isomerize very quickly to a mixture of 2′- and 3′-isoleucyl-tRNA.[111-114] In analogous fashion, incorporation of 3′-deoxy-3′-aminoadenosine monophosphate yields $tRNA^{Ile}$-C-C-A(3′NH_2) **22**, which is also aminoacylated by both yeast and *E. coli* enzymes.[38,115-118] The 2′-*O*-acyl ester product **24** isomerizes by intramolecular aminolysis to the amino acid amide **25** at the 3′ position of the terminal ribose.[118]

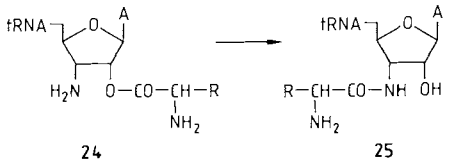

This reaction is important because the product **25** is more stable against hydrolysis than the *O*-acyl ester **24**.[107] As will be described below, this property has made the $tRNA^{Ile}$-C-C-A(3′NH_2) **22** a valuable tool for the investigation of mechanisms which are responsible for the high specificity of the enzymes (see Section 5.1).

4. Substrate Binding and Catalysis

4.1. Determination of Substrate Binding Constants

4.1.1. Activation Reaction

The rate constants for the binding and dissociation of isoleucine and ATP have been determined using stopped flow techniques.[119] For the equilibrium (c)[*]

$$E + Ile \underset{k_{-1}}{\overset{k_1}{\rightleftharpoons}} E \cdot Ile \qquad (c)$$

the dissociation constant is

$$K_d^{Ile} = [Ile][E]/[E \cdot Ile] = k_{-1}/k_1 = 15\,s^{-1}/2.2 \times 10^6\,M^{-1}\,s^{-1} = 6.8 \times 10^{-6}\,M.$$

The rate constant for binding of isoleucine, k_1, is tenfold lower than the diffusion-controlled rate. At low temperatures a two-step process [Eq. (d)] for substrate binding can be detected. The first binding step is fast and is then followed by a slower enzyme isomerization to an active conformation. Perhaps this substrate-induced conformational change plays an important role in the recognition of the proper amino acid (see Section 5.2 for a discussion of the role of this effect in amino acid discrimination).

$$E + Ile \rightleftharpoons (E \cdot Ile)' \rightleftharpoons E \cdot Ile \qquad (d)$$

A standard free energy ($\Delta G°$) of -31.80 kJ mol^{-1} for the binding of isoleucine was determined from the temperature dependence of the dissociation constant.[119] This is now interpreted as being principally due to hydrophobic interactions between the amino acid and the enzyme surface[120] (see Section 5.1).

The dissociation constant for binding of ATP in the presence of $Mg^{2\oplus}$ is $K_d^{MgATP} = 1.75 \times 10^{-4}$ M.[119] Although the individual rate constants could not be determined exactly, it was apparent that ATP binds faster to the enzyme than does isoleucine.

Similar dissociation constants, $K_d^{Ile} = 4.0 \times 10^{-6}$ M and $K_d^{MgATP} = 1.5 \times 10^{-4}$ M, were calculated from kinetic measurements following the incorporation of ^{32}P-labeled pyrophosphate into ATP. This assay monitors the activation reaction (a) from the reverse direction and allows dissociation constants to be calculated by changing the substrate concentration.[121]

The reaction of enzyme-bound ATP and isoleucine to form the activated amino acid complex [Eq. (e)] has been

$$E \cdot Ile \cdot ATP \underset{k_b}{\overset{k_f}{\rightleftharpoons}} E \cdot Ile\text{-}AMP \cdot PP_i \qquad (e)$$

analyzed in detail. The forward rate, k_f, of 135 s^{-1} is slower than the back reaction rate, k_b, of 670 s^{-1}. Therefore, the equilibrium for this step ($K_E = k_f/k_b = 0.2$) favors the reactants Ile and ATP.[119]

The overall equilibrium constant for amino acid activation according to Equation (f)

$$ATP + Ile \rightleftharpoons Ile\text{-}AMP + PP_i \qquad (f)$$

has the low value of

$$K = [Ile\text{-}AMP][PP_i]/([Ile][ATP]) = 4.5 \times 10^{-4}.$$[119]

4.1.2. Aminoacylation Reaction

The dissociation constants K_d for binding of $tRNA^{Ile}$ or the charged Ile-$tRNA^{Ile}$ to the enzyme range from 10^{-6} to 10^{-8} M.[122,123] For the *E. coli* B enzyme the lowest dissociation constant obtained under optimal conditions is 3×10^{-7} M.[124] The equilibrium constant for the overall reaction

$$K_d = [E][tRNA]/[E \cdot tRNA]$$

$$K = [Ile\text{-}tRNA][AMP][PP_i]/([tRNA][ATP][Ile])$$

has a value close to unity.[125]

A comparison of the rate constants for the catalytic process in the *E. coli* B enzyme shows that the release of the acylated tRNA is the rate-determining step.[122] The

[*] In the following analysis a notation will be used that distinguishes between covalently and noncovalently bound complexes. A noncovalent interaction between two species such as the enzyme (E) and isoleucine (Ile) is indicated by a point: E · Ile. Covalent bonds are notated by a dash such as in aminoacyl adenylates: aa-AMP.

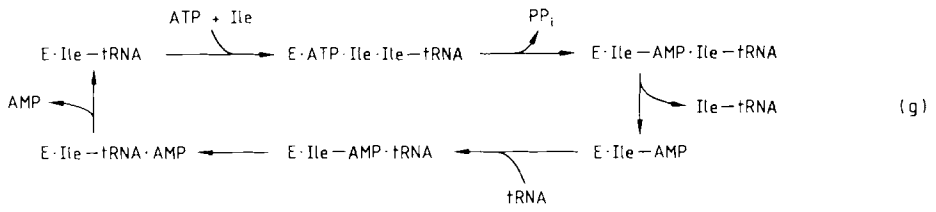

(g)

rate constant for adenylate formation is $<3.5\ s^{-1}$, for the acylation reaction $0.050\ s^{-1}$, and for dissociation of the E·Ile-tRNA complex $0.042\ s^{-1}$. For this enzyme the E·Ile-AMP·Ile-tRNA complex is the main species present in the assumed catalytic cycle (g).[122]

The enzyme from *E. coli* K12, as studied by pulsed quenched flow techniques, has a different rate-determining step.[14, 126] Transfer of the activated amino acid to the tRNA is very slow ($k = 1.47\ s^{-1}$) and follows fast isoleucyl adenylate formation ($k_{cat} = 62\ s^{-1}$ in the ATP/PP_i exchange reaction). The transfer-step rate determines the overall rate and turnover number of the aminoacylation reaction ($k_{cat} = 1.46\ s^{-1}$) [Eq. (h)].[14]

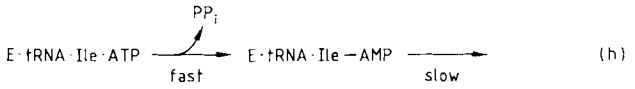

(h)

Thus, the release of the charged tRNA cannot be regarded a priori as rate determining. For the *E. coli* K12 enzyme the E·tRNA·Ile-AMP is the main species present in the catalytic cycle.

4.2. Order of Substrate Addition and Product Release

The order of substrate addition and product release has been determined by investigating the inhibition patterns of substrate analogues of type **17**. The methods for carrying out these initial rate kinetic measurements are well described in the literature and are summarized in the Appendix.[127–134] Analogues of ATP were found to be competitive, noncompetitive, and uncompetitive inhibitors. Modified tRNAs that cannot be charged (see Section 3.3) are competitive or noncompetitive inhibitors.

The first investigation on the order of substrate addition to isoleucyl-tRNA synthetases was performed on the *E. coli* B enzyme.[135] This experiment tested the influence of spermine on the aminoacylation reaction. Spermine, a polyamine, is found in all plant and animal cells.[136] Although not completely characterized, the reaction in the presence of spermine displays sequential substrate addition [see (i)]. In contrast, the reaction in the presence of $Mg^{2\oplus}$ has been postulated to display ping-pong kinetics [see (j)]. According to this mechanism, ATP and isoleucine are bound first and the isoleucyl adenylate is formed with the release of pyrophosphate before the tRNA is bound.

The results obtained from the spermine study have been used to argue that the aminoacyl adenylate is not a discrete intermediate in the reaction. Instead, the reaction mechanism is regarded as concerted and all substrates react in a

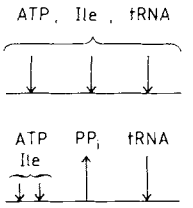

(i) (j)

simultaneous fashion.[8, 135] However, as will be shown below [cf. (l)] a mechanism with sequential addition of substrates can be formulated which includes an aminoacyl-adenylate intermediate. The effect of spermine may be not to affect the enzyme but to change the conformation of the tRNA and thereby make it a poorer substrate.[137]

In detailed investigations of yeast isoleucyl-tRNA synthetase, four reaction mechanisms were elucidated which depend on the assay conditions.[99, 138, 139] As shown in Table 2, the different reaction conditions can be regarded as approaching physiological conditions in a stepwise fashion.

Using an enzyme assay that is optimal for catalysis (pH 7.65, 0.1 M KCl, 15 mM $Mg^{2\oplus}$), the aminoacylation reaction can be shown to follow a sequential mechanism. ATP binds first followed by isoleucine and finally $tRNA^{Ile}$. The products are then released in the order pyrophosphate, Ile-$tRNA^{Ile}$, and AMP. The turnover number under these conditions is $0.83\ s^{-1}$. At pH 8.6 a similar reaction mechanism is observed but the turnover number is reduced to $0.52\ s^{-1}$. In contrast, when the pH is reduced to 6.5, a value also found in yeast cells,[140] the reaction mechanism changes such that the substrates are bound and products released in a random manner. At pH 6.5 the turnover number is $0.47\ s^{-1}$.

Pyrophosphatase (PPase) is present in relatively high amounts in *E. coli*[141] and yeast[142] cells. Addition of this enzyme to the aminoacylation reaction assay performed under optimum conditions changes the mechanism from a sequential to a ping-pong process. ATP and isoleucine bind to the enzyme in a random manner and pyrophosphate is released. Then $tRNA^{Ile}$ binds and the products, AMP and Ile-$tRNA^{Ile}$, are released in an unknown order. The turnover number under these conditions is increased to $1.4\ s^{-1}$. The influence of pyrophosphate on the catalytic pathway has not been investigated in detail; it is possible that this product is also involved in an allosteric interaction.[138]

When the elongation factor complex EF-Tu·GTP is added instead of pyrophosphatase, the reaction pathway remains sequential and the turnover number is reduced to $0.28\ s^{-1}$. It is well known that EF-Tu·GTP forms very specific complexes with acylated tRNAs[99, 143–147] and should thereby increase the turnover number by decreasing the

Table 2. Conditions of aminoacylation, order of substrate addition and product release for isoleucyl-tRNA synthetase from yeast (A = ATP, B = isoleucine, C = $tRNA^{Ile}$, P = pyrophosphate, Q = Ile-$tRNA^{Ile}$, R = AMP), and k_{cat} values; nomenclature of mechanisms according to *Cleland* [130, 134] (for abbreviations see text).

Conditions	Order	Mechanism	k_{cat} [s^{-1}]
pH 6.5, 0.1 M KCl, 15 mM $Mg^{2\oplus}$	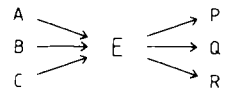	sequential random Ter-Ter	0.47
pH 7.65, 0.1 M KCl, 15 mM $Mg^{2\oplus}$	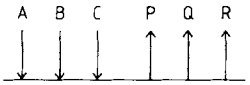	sequential ordered Ter-Ter	0.83
pH 8.6, 0.1 M KCl, 15 mM $Mg^{2\oplus}$	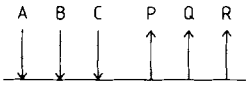	sequential ordered Ter-Ter	0.52
pH 7.65, 0.1 M KCl, 15 mM $Mg^{2\oplus}$, PPase	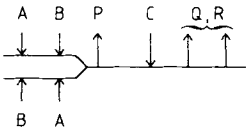	random Bi-Uni Uni-Bi ping-pong	1.40
pH 7.65, 0.1 M KCl, 15 mM $Mg^{2\oplus}$, EF-Tu·GTP	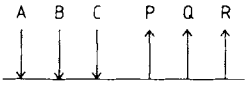	sequential ordered Ter-Ter	0.28
pH 7.65, 0.1 M KCl, 15 mM $Mg^{2\oplus}$, EF-Tu·GTP, PPase	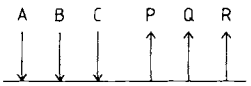	sequential ordered Ter-Ter	0.23
pH 7.65, 0.1 M KCl, 15 mM $Mg^{2\oplus}$, EF-Tu·GTP, PPase, spermine	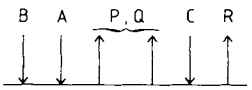	Bi-Bi Uni-Uni ping-pong	0.098
pH 7.65, 0.1 M KCl, 1 mM $Mg^{2\oplus}$, EF-Tu·GTP, PPase, spermine	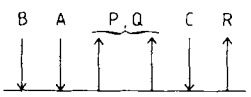	Bi-Bi Uni-Uni ping-pong	0.135

concentration of the free product formed in the reaction. However, up to now no good explanation for the reduced turnover number has been put forward.[148] Remarkably, when both pyrophosphatase and EF-Tu·GTP are present in the assay, turnover number and mechanism remain unchanged.

When spermine, pyrophosphatase, and EF-Tu·GTP are all added to the isoleucyl-tRNA synthetase reaction assay, an unusual ping-pong mechanism is encountered. Isoleucine is bound first and then ATP. Pyrophosphate is the first product released, followed by, remarkably, isoleucyl-tRNA. The kinetic quirk that explains how the product isoleucyl-tRNA can be formed before the $tRNA^{Ile}$ substrate is bound by the enzyme will be given later [cf. (k)]. To complete the catalytic sequence, $tRNA^{Ile}$ is bound next and finally AMP is released from the enzyme. The turnover number for this process (0.098 s^{-1}) is very low. Lowering the $Mg^{2\oplus}$ concentration from 15 mM, used in the "optimal" assay, to 1 mM, which is similar to that found under physiological conditions, increases the turnover number slightly to 0.135 s^{-1}.[149, 150] Even when the best conditions are used, however, the aminoacylation reaction remains about ten times slower than the "optimal" assay where the pyrophosphatase, EF-Tu·GTP, and spermine are omitted.

The *E. coli* MRE600 isoleucyl-tRNA synthetase has been found to display both a sequential and, under slightly different assay conditions, a ping-pong mechanism (Table 3).[151] Addition of the EF-Tu·GTP complex or spermine does not influence the turnover number. In the presence of spermine, however, different reaction mechanisms do occur but have not yet been studied in detail.[146] In total, this enzyme displays a series of reaction mechanisms as diverse as those found for the yeast enzyme and also performs some novel processes not observed in the enzymes from *E. coli* B or yeast.[135]

Table 3. Conditions of aminoacylation, order of substrate addition and product release for isoleucyl-tRNA synthetase from *E. coli* MRE600 (A = ATP, B = isoleucine, C = $tRNA^{Ile}$, P = pyrophosphate, Q = Ile-$tRNA^{Ile}$, R = AMP), and k_{cat} values; nomenclature of mechanisms according to *Cleland* [130, 134] (for abbreviations see text).

Conditions	Order	Mechanism	k_{cat} [s^{-1}]
pH 7.6, 0.15 M KCl, 0.05 mM $Mg^{2\oplus}$	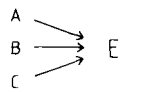	sequential random Ter	0.74
pH 7.6, 0.15 M KCl, 0.05 mM $Mg^{2\oplus}$, PPase	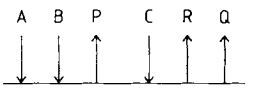	Bi-Uni Uni-Bi ping-pong	1.2
pH 7,6, 0.15 M KCl, spermine	not determined	sequential	0.2
pH 7.6, 0.15 M KCl, spermine, PPase	not determined	sequential	0.4
pH 7.6, 0.15 M KCl, 0.05 mM $Mg^{2\oplus}$, spermine	not determined	ping-pong	0.2
pH 7.6, 0.15 M KCl, 0.05 mM $Mg^{2\oplus}$, spermine, PPase	not determined	ping-pong	0.5

The analysis of "initial rate" kinetics yields information only on the sequence of substrate addition and product release. The type of enzyme–ligand complex associated with each step in a mechanism can only be inferred. It is possible that the enzyme designated as "E" in the schemes of Tables 2 and 3 and in the Appendix is not free enzyme but actually an enzyme–ligand complex formed earlier. Thus, in the special case noted above of the yeast enzyme assay with spermine added, isoleucine must be bound to an enzyme complex with Ile-$tRNA^{Ile}$. The catalytic cycle (k) is purely hypothetical.

Analogously, a sequential-ordered mechanism (l) can be postulated in which ATP and isoleucine are added to an E·Ile-tRNA·AMP complex. From (l) it will be noted

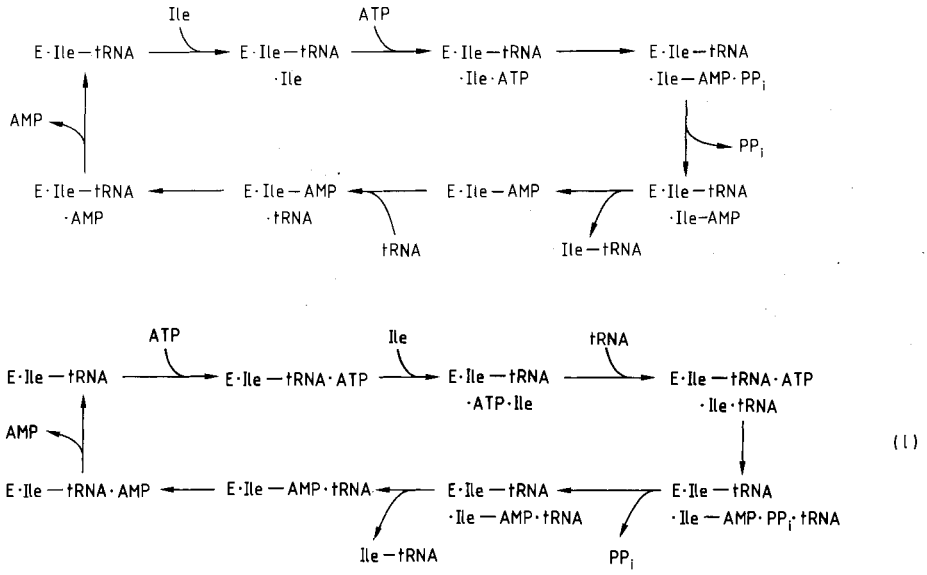

(l)

that ATP, Ile, and $tRNA^{Ile}$ are added in sequential order and an aminoacyl-adenylate intermediate (Ile-AMP) is formed. Similar schemes have been postulated for phenylalanyl-[152] and valyl-tRNA synthetases[153] from yeast; they also involve enzyme–substrate complexes in which two tRNA molecules are bound. Two tRNA binding sites have been suggested for the isoleucyl-tRNA synthetase based on the observation that some tRNA analogues act as noncompetitive inhibitors of the aminoacylation reaction.[29, 105] It is not clear, however, whether the two binding sites reside on a single peptide chain or result from a dimeric enzyme.[148]

The multiplicity of possible reaction pathways found for the isoleucyl-tRNA synthetases from yeast and *E. coli* indicates that the protein cannot be regarded as a rigid construction. Minimal alterations in the environment may cause a different conformation to form and result in a change in mechanism and corresponding change in reaction velocity. The physiological significance of this behavior, which was at first unclear, is apparently related to the specificity of the enzyme.

5. Error Rates in Aminoacylation

Enzyme specificity is characterized as the ratio of the velocities at which the cognate substrate and a noncognate substrate are converted into products. A discrimination factor D can be defined that allows the intrinsic enzyme specificity to be quantified independent of the relative concentrations of cognate and noncognate substrates. For example, the discrimination between isoleucine and valine is given by Equation (m):

$$v_{Ile}/v_{Val} = D \cdot ([Ile]/[Val]) \quad (m)$$

The factor D is related to the kinetic constants k_{cat} and K_m through Equation (n):

$$D = (k_{cat}/K_m)^{Ile}/(k_{cat}/K_m)^{Val} \quad (n)$$

Isoleucyl-tRNA synthetase displays very high specificity and it is therefore very difficult to measure the k_{cat} and K_m values for the noncognate substrates. The rates are very low and the level of radioactivity incorporated, via a radioactive amino acid, into tRNA is only slightly higher than the background radiation. Nevertheless, sufficiently accurate reaction rates can be estimated if the reactions are observed for relatively long periods, the measurements are repeated, and the data analyzed by statistical methods.[145] In this way the following D factor for discrimination of valine by yeast isoleucyl-tRNA synthetase was found:[139]

$$D = (0.83\ s^{-1}/0.02\ mM)/(0.0001\ s^{-1}/0.09\ mM) = 38000$$

The *E. coli* enzyme showed almost twofold higher discrimination:[154]

$$D = (0.82\ s^{-1}/0.006\ mM)/0.00019\ s^{-1}/0.1\ mM) = 71900$$

These values signify that at equal concentrations of the two amino acids only one noncognate valine is transferred to $tRNA^{Ile}$ while 38000 and 71900 isoleucines, respectively, would be incorporated. Both D values are much higher than expected for the difference between the side chains (isobutyl versus isopropyl) and cannot only result from hydrophobic interactions with the enzyme surface. *Pauling* has calculated that such an interaction can only achieve a specificity of 4.3 : 1 and he estimated that for the isoleucine/valine discrimination the upper limit was about 20 : 1.[155] To elucidate the processes that give this 4000-fold higher specificity, important insight was gained using modified tRNAs as tools, especially $tRNA^{Ile}$-C-C-A(3′NH_2) **22**.

5.1. Discrimination between Amino Acids during Aminoacylation of $tRNA^{Ile}$-C-C-A(3′NH_2)

In contrast to $tRNA^{Ile}$-C-C-A **5**, the modified $tRNA^{Ile}$-C-C-A(3′NH_2) **22** can be charged with noncognate amino acids at relatively high rates.[38, 115–118] This allowed the k_{cat}

Table 4. Discrimination factors D und D_2 ($\approx D_1$), stoichiometry of AMP formation in aminoacylation, and factors I_1, I_2, Π_1, Π_2 for discrimination between isoleucine and valine by isoleucyl-tRNA synthetase from yeast (for abbreviations see text).

Conditions	D	AMP per Ile-tRNA	AMP per Val-tRNA	D_2	AMP per Ile-tRNA-C-C-3'dA	AMP per Val-tRNA-C-C-3'dA	I_1	I_2	Π_1	Π_2
pH 6.5, 0.1 M KCl, 15 mM $Mg^{2\oplus}$	8000	3.5	288	48	1.81	13	6.7	14.5	7.2	11.4
pH 7.65, 0.1 M KCl, 15 mM $Mg^{2\oplus}$	38000	5.5	828	180	1.94	96	3.6	70.1	49.5	3.0
pH 8.6, 0.1 M KCl, 15 mM $Mg^{2\oplus}$	14000	6.9	588	94	2.31	71	3.1	53.0	30.7	2.8
pH 7.65, 0.1 M KCl, 15 mM $Mg^{2\oplus}$, PPase	32000	6.3	1165	100	2.63	49	5.4	32.0	18.6	9.9
pH 7.65, 0.1 M KCl, 15 mM $Mg^{2\oplus}$, EF-Tu·GTP	8000	3.0	192	72	1.25	19	4.7	26.6	15.2	4.2
pH 7.65, 0.1 M KCl, 15 mM $Mg^{2\oplus}$, EF-Tu·GTP, PPase	3000	5.1	165	69	2.63	43	4.2	22.1	16.3	2.0
pH 7.65, 0.1 M KCl, 15 mM $Mg^{2\oplus}$, EF-Tu·GTP, PPase, spermine	2000	6.1	118	85	3.12	48	5.5	18.8	15.4	1.3
pH 7.65, 0.1 M KCl, 1 mM $Mg^{2\oplus}$, EF-Tu·GTP, PPase, spermine	10500	3.4	255	105	1.1	20	5.8	24.1	18.2	4.1

and K_m values for misacylation with the nineteen noncognate amino acids occurring in proteins to be determined and the corresponding discrimination factors (D_1) calculated.[120] These D_1 values are much lower than the discrimination factors D for acylation of $tRNA^{Ile}$-C-C-A **5** (cf. Table 4). The yeast enzyme, for example, discriminates against valine with a D value of 38000 but the D_1 value is only 167. However, the D_1 values are still higher than the theoretical results calculated by *Pauling* (e.g., 1 : 10 for valine).[155] The results with $tRNA^{Ile}$-C-C-A(3'NH_2) **22** show that the reaction steps that enhance specificity are considerably restricted during charging of the modified tRNA.

By measuring the stoichiometry of AMP formation [cf. Eq. (a) and (b)] it was found that more than one molecule of AMP was generated per molecule of tRNA acylated.[120] For example, the yeast enzyme hydrolyzes 111 molecules of ATP for each tRNA charged with valine; with the cognate amino acid, isoleucine, only 2.2 molecules of ATP are hydrolyzed. These high rates of AMP formation indicate that a hydrolytic proofreading step is operating. As early postulated,[156, 157] this step must be a "pretransfer proofreading" which acts to hydrolyze the noncognate aminoacyl adenylate. By using $tRNA^{Ile}$-C-C-A(3'NH_2) one can be sure that the measure of AMP formation represents *only* pretransfer proofreading. Although acylation does occur primarily at the 2'-OH group, transacylation to give the hydrolytically more stable 3'-acylamide **25** is much faster[116a, 120] than the rate for the enzymatic hydrolysis of aminoacyl esters.[28] Therefore, no posttransfer proofreading process can operate when using this $tRNA^{Ile}$ analogue. The pretransfer proofreading can be formulated as (o).

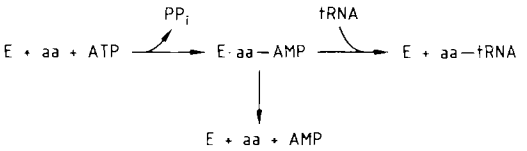

(o)

pretransfer proofreading

It is important to mention that this conclusion is only valid if transacylation of the amino acid from the 2'-OH to 3'-NH_2 (cf. **24**→**25**) is not hindered in the enzyme-tRNA complex. The ratio of the number of AMP molecules formed for each noncognate amino acid to the number formed for isoleucine shows how many more incorrect amino acids are rejected in the proofreading step than isoleucine. For valine this proofreading factor is $\Pi_1 = 111/2.2 = 50$ with the yeast enzyme.

The discrimination factor D_1, described above, is a function of the proofreading factor Π_1 and also of a factor I_1, which corresponds to the difference in Gibbs free energy of binding between cognate and noncognate substrates. Therefore, Equation (p) holds. The complete recognition

$$D_1 = I_1 \cdot \Pi_1 \qquad \text{(p)}$$

process for acylation of $tRNA^{Ile}$-C-C-A(3'NH_2) **22** is shown in (q).

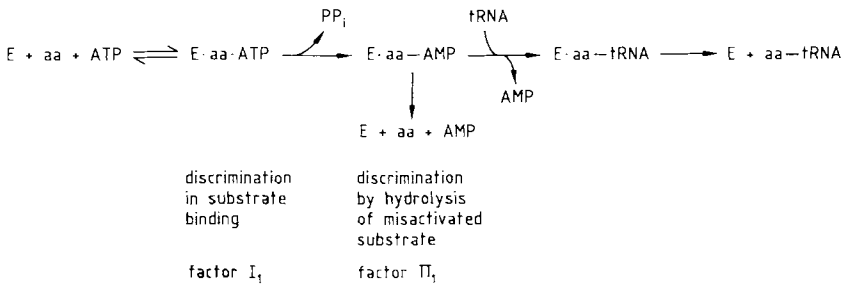

(q)

The difference in Gibbs free energy for binding of a noncognate amino acid and isoleucine is given by Equation (r):[158]

$$\Delta\Delta G_{I_1} = RT\ln I_1 = RT\ln D_1/\Pi_1 \qquad (r)$$

For valine $\Delta\Delta G_{I_1}$ is 3.08 kJ mol^{-1},[139] which corresponds to a value of $I_1 = 3.3$. These values are very similar to those calculated theoretically by *Pauling* ("I" = 4.3, "$\Delta\Delta G$" = 3.77 kJ mol^{-1}).[155] The $\Delta\Delta G_{I_1}$ is consistent with the hydrophobic interaction energy of a methylene group with an enzyme. Values of the same order of magnitude can be estimated from a hydrophobicity scale derived for the transfer of an amino acid side chain from water to an organic solvent.[159]

From the analysis of protein structures it has been found that the accessible surface area of an amino acid is the main determinant in the magnitude of hydrophobic interactions.[160–162] The surface area is defined as the area covered by the center of a water molecule that is placed in van der Waals contact with the atoms of the amino acid without penetrating any of the atoms.[163] Each square angstrom of accessible surface area removed from contact with water contributes 105 J mol^{-1} in energy.[160–162]

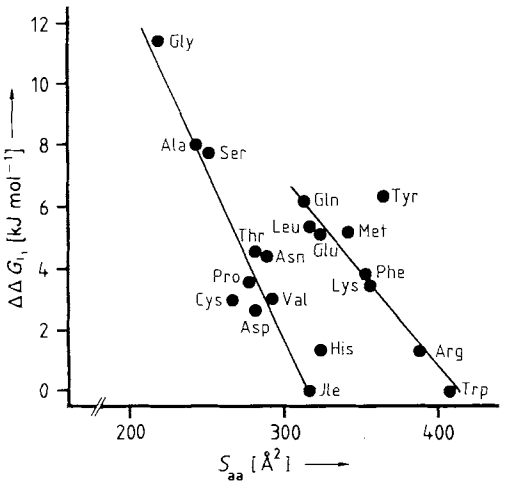

Fig. 1. Relation of differences in Gibbs free energy of binding ($\Delta\Delta G_{I_1}$) to accessible surface areas (S_{aa}) of amino acids.

As shown in Figure 1, a linear relationship exists between the $\Delta\Delta G_{I_1}$ values calculated from misacylation kinetics and the accessible surface of the amino acids (S_{aa}).[164] Strikingly, two groups of amino acids can be distinguished.[120] The first group includes all amino acids with a surface area or side-chain length smaller than isoleucine. The amino acids with side chains longer or with a larger surface area than isoleucine comprise the second group. The slopes of these relationships give the Gibbs free energy values and are 111 J mol^{-1} Å^{-2} and 61 J mol^{-1} Å^{-2}, respectively. Both values are consistent with a hydrophobic interaction. The intersection of the left line in Figure 1 with the ordinate gives the Gibbs free energy for the binding of isoleucine. The value of 34.93 kJ mol^{-1} is of the same order of magnitude as the value for the standard free energy of binding given in Section 4.1.1 ($\Delta G^\circ = -31.80$ kJ mol^{-1}).

A simple model of the amino acid binding site can be used to explain the subdivision of the amino acids into two groups (Fig. 2).[120] The binding cavity can be viewed as having a bulky group that restricts the binding of amino acids larger than isoleucine. The small amino acids are easily bound within the cavity, but for binding of the larger amino acids energy is required to push the bulky group aside. The amount of energy can be estimated from Figure 1 by extrapolating the line for the larger amino acids to the surface area for isoleucine. This yields a value of 6 kJ mol^{-1}.

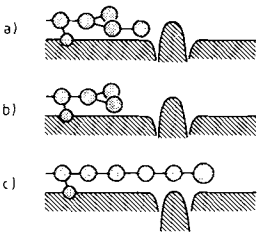

Fig. 2. Initial binding site with a) isoleucine (the binding cavity is completely filled by the isoleucine side chain), b) valine (the binding cavity is only partly filled, the Gibbs free energy of binding is diminished by a value corresponding to the difference in accessible surface area ($\Delta\Delta G_{I_1}$), c) lysine (the side chain of lysine must push aside the "stopper" group in the binding process). For the first group in Fig. 1, $\Delta\Delta G_{I\,1} = 111\ (S_{Ile} - S_{aa})$ [J mol^{-1}]; for the second group in Fig. 1. $\Delta\Delta G_{I\,1} = 61\ (S_{Ile} - S_{aa}) + 6000$ [J mol^{-1}] (S_{Ile} = accessible surface area of isoleucine, S_{aa} = accessible surface area of other amino acids).

A similar result is found for the *E. coli* enzyme[120] with the exception that leucine is included in the group of amino acids from glycine to isoleucine. The $\Delta\Delta G_{I_1}$ values are only slightly higher than those observed for the yeast enzyme (e.g., valine has a $\Delta\Delta G_{I_1}$ value for the *E. coli* enzyme of 3.87 kJ mol^{-1} but only 3.08 kJ mol^{-1} with yeast). This observation indicates that the binding sites of the enzymes from the two sources are similar.

If, in analogy to the $\Delta\Delta G_{I_1}$ values, the $\Delta\Delta G_{\Pi_1}$ values are plotted against the accessible surface area, no significant relation is observed. In general, for both enzymes, the scatter of the $\Delta\Delta G_{\Pi_1}$ values is about 10 kJ mol^{-1}. Therefore, in contrast to binding at the initial binding site, hydrophobic interactions do not seem to play an important role at the hydrolytic site. It remains unclear by which steric influences the cognate isoleucyl adenylate avoids hydrolysis.

5.2. Discrimination between Amino Acids during Aminoacylation of tRNA^{Ile}-C-C-A

The D values calculated from k_{cat} and K_m are 200- to 300-fold higher than the corresponding D_1 values obtained in acylation of tRNA^{Ile}-C-C-A(3'NH$_2$) **22**.[165]

Unexpectedly low D values of 300 to 700 were found for cysteine, aspartic acid, asparagine, and tryptophan. Recently, low error rates have also been found in vivo (cysteine instead of arginine 1 : 1700,[166] lysine instead of arginine 1 : 500[167]). The highest discrimination factors were detected with the yeast enzyme for leucine, serine, methionine, glycine (10000–20000), and valine (38000). The D values for the remaining amino acids range between

2000 and 10000. The *E. coli* enzyme exhibits discrimination factors between 600 and 72000. The lowest values (600–3000) were calculated for cysteine, tryptophan, and arginine. The highest values (≈ 70000) were found for glycine, alanine, and valine. The D values for the other amino acids range from 20000 to 50000.[165]

It is surprising that both *E. coli* and yeast show the highest discrimination for those amino acids which are the most similar to isoleucine and a lower discrimination between the structurally more diverse amino acids cysteine, tryptophan, and arginine.

In parallel with the higher D values found for aminoacylation, higher rates of AMP formation are also observed in the presence of the natural tRNA (tRNA^{Ile}-C-C-A **5**) compared with tRNA^{Ile}-C-C-A(3′NH$_2$) **22** (cf. Table 4). The reason is most probably a second hydrolytic proofreading step which is carried out after transfer of the amino acid to the tRNA ("posttransfer proofreading"). The enzyme-bound aminoacyl-tRNA esters may be in many cases more rapidly hydrolyzed than isoleucyl-tRNA [cf. (s)].[28, 110, 168]

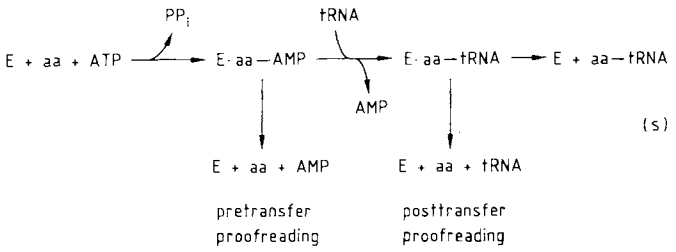

(s)

Proofreading factors for pretransfer (Π_1) and posttransfer proofreading (Π_2) multiply to give the overall proofreading factor Π'. Provided that in the aminoacylation of native tRNA^{Ile}-C-C-A **5** the pretransfer proofreading is of the same magnitude as that found for the acylation of tRNA^{Ile}-C-C-A(3′NH$_2$) **22**, factor Π_2 can be approximately determined as the quotient of Π' and Π_1.

The Π_2 factors calculated for the yeast enzyme are much lower than the Π_1 factors. Only in seven cases does the posttransfer proofreading enhance the discrimination factor D ($\Pi_2 \geqq 1$). Remarkably, the second hydrolytic step gives an improvement of only $\Pi_2 \approx 3$ between isoleucine and valine. For the other eleven amino acids $\Pi_2 \leqq 1$, so there is no discrimination against the proper amino acid.

It should be emphasized that Π_2 observed for valine ($\Pi_2 \approx 3$) corresponds to the Gibbs free energy of binding calculated by *Pauling* for a methylene group. The binding site at which the second hydrolytic proofreading step is carried out seems to serve mainly for discrimination between the isobutyl and isopropyl group. The other amino acids are hydrolyzed slightly faster or slower than isoleucine for steric reasons.

The $\Delta\Delta G_{\Pi_2}$ values, calculated analogously to $\Delta\Delta G_{\Pi_1}$, show no systematic relation to accessible surface areas or other structural properties of the amino acids.

Similarly, as in the case of D_1, the discrimination factor D is the product of the Gibbs free energy for substrate binding (I') and the overall proofreading factor Π' [Eq. (t)].

$$D = I'\Pi' \qquad \text{(t)}$$

Factor I' is calculated from D and Π'. All I' values are higher than the corresponding I_1 values, so for valine a $\Delta\Delta G_{I'}$ value of 14.25 kJ mol^{-1} is found.[165] This value is about fourfold higher than that for the aminoacylation of tRNA^{Ile}-C-C-A(3′NH$_2$) **22**. Similar values were obtained from kinetic measurements of the activation reaction with isoleucine and valine.[157, 158] The reason for the deviation is still unknown. It may be that this phenomenon is related to the conformational change in the enzyme observed during binding of isoleucine (see Section 4.1.1). In the case of phenylalanyl-tRNA synthetase there are considerable differences in the kinetics of complex formation between enzyme·tRNA-C-C-A and enzyme with modified tRNAs.[169, 170] Possibly, in the aminoacylation of tRNA^{Ile}-C-C-A(3′NH$_2$) **22**, a conformational change does not occur which normally with a natural tRNA would be induced by binding of isoleucine and which would enhance hydrophobic interactions. A factor I_2 resulting from this process must multiply with I_1 to give I'. Therefore, the value D is given by Equation (u). Thus, the complete process of amino acid recognition is achieved (Scheme 5) following the scheme for aminoacylation of tRNA^{Ile}-C-C-A(3′NH$_2$) **22** [cf. (q) in Section 5.1].

$$D = I_1 \cdot I_2 \cdot \Pi_1 \cdot \Pi_2 \qquad \text{(u)}$$

$\Delta\Delta G_{I_2}$ calculated analogously to $\Delta\Delta G_{I_1}$ shows a linear relationship to the accessible surface areas of the amino acids. However, in this case the amino acids cannot be arranged into two groups. The most simple scheme requires three groups and is difficult to interpret.[165]

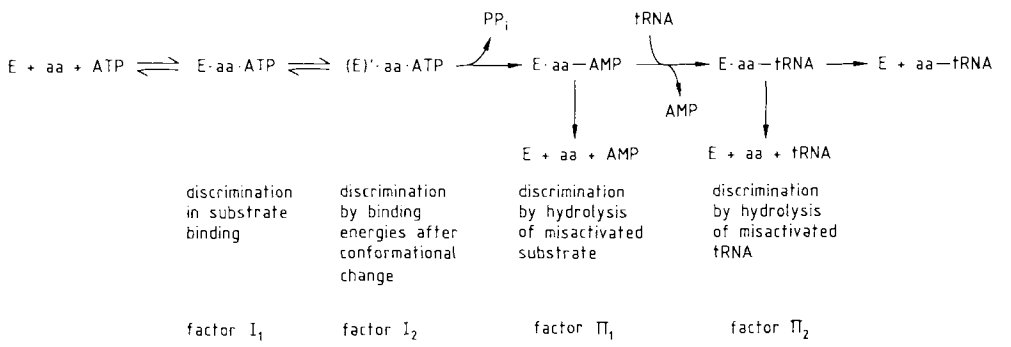

(v)

6. Modulation of Specificity and Energy Consumption

From the different catalytic pathways and reaction conditions listed in Table 2 the turnover numbers can be seen to vary in the range of 0.098 to 1.40 s^{-1}. Since these values determine directly the discrimination factor D it must be expected that isoleucyl-tRNA synthetase exhibits different substrate specificities under the different conditions. In fact, the discrimination factor varies in a range of 2000 to 38000 for the different reaction conditions (Table 4).[139] Consumption of ATP, or generation of AMP, has a stoichiometry of 3.0–6.9 in the synthesis of Ile-$tRNA^{Ile}$-C-C-A as catalyzed by the yeast enzyme and a value of 1.0–1.73 AMP molecules per Ile-$tRNA^{Ile}$-C-C-A for the enzyme from *E. coli*.[139, 165] Formation of the misacylation product Val-$tRNA^{Ile}$-C-C-A causes the release of between 118 and 1165 (*E. coli*) or 530 and 2700 (yeast enzyme) AMP molecules per aminoacyl-tRNA. In parallel with the D values, the discrimination factors D_2 determined for the acylation of $tRNA^{Ile}$-C-C-3′dA vary in a similar fashion (Table 4).[139] Only in the case of valine are these D_2 values practically identical with the D_1 factors observed in acylation of $tRNA^{Ile}$-C-C-A(3′NH_2). They can be used in place of D_1 values in further calculations. The values for AMP formation observed in acylation of $tRNA^{Ile}$-C-C-3′dA can also be used in place of values observed in acylation of $tRNA^{Ile}$-C-C-A(3′NH_2). Factors D_2 ($\approx D_1$) are in the range of 48 to 180, whereas the number of AMP molecules lies in the range of 1.1 to 3.12 for charging with isoleucine and 13 to 96 for charging with valine. The D_1 values determined for the enzyme from *E. coli* are in the range of 100 to 4400. In acylation with isoleucine 1.0–1.7 molecules of ATP are consumed and in acylation with valine 2.6–24.[120] If the single factors I_1, I_2, Π_1, and Π_2 are compared, it is found that, for the yeast enzyme in one case (pH 6.5, 0.1 M KCl, 15 mM $Mg^{2\oplus}$), the proofreading factor Π_2 is higher than Π_1. Under other reaction conditions, however, the reverse is observed. As listed in Table 2 the enzyme displays only at pH 6.5 a random mechanism in which the substrates are added and the products released in any order. This mechanism differs from others in that the enzyme uses a conformation that is more effective in the posttransfer proofreading than in the pretransfer step. A similar result has been found for the reaction pathways of the *E. coli* enzyme. At pH 7.6 this synthetase displays a random mechanism (Table 3) and the proofreading factor Π_2 is twice as high as factor Π_1. These observations confirm that the various pathways for catalysis, which differ in the order of substrate addition and product release, are connected with the overall specificity of the enzyme. The changes in specificity shown by the isoleucyl-tRNA synthetases result from two main causes. First, there may be a change in the catalytic cycle, each cycle being characterized by the different order of substrate addition and product release. Second, each cycle may have a different reaction velocity. Therefore, the specificity of the enzymes can be changed to any degree by changing the reaction conditions. In every case, however, a change in a specificity will be associated with a different energy consumption. Under the conditions which are the closest to the physiological one (pH 7.65, 0.1 M KCl, 1 mM $Mg^{2\oplus}$, EF-Tu·GTP, PPase, spermine) (Table 2), the enzymes work with a medium specificity and medium energy consumption (yeast enzyme: $D = 10500$, 3.4 AMP/isoleucyl-tRNA; *E. coli* enzyme: $D = 40600$, 1.04 AMP/isoleucyl-tRNA).

7. Summary and Outlook

Although in the past twenty years considerable progress has been made in the investigation of the aminoacyl-tRNA synthetases and hundreds of papers have been published, we are still far away from a complete understanding of functions and mechanisms of these enzymes. We do not have a concrete knowledge of the structure of the active site, the identity and reactivity of the functional groups involved in catalysis, or even the exact chemical transformations involved in amino acid activation and transfer to the tRNA.

Kinetic investigations show that the enzyme has many different active conformations and uses different catalytic cycles. No conclusions can be made as to the nature of these conformational differences at this time. Even if X-ray structure analysis could be done, it would be difficult to elucidate these processes, because in the crystals the molecules are in the "frozen" states favorable for crystal formation. Perhaps the conformational changes are connected with a "proteinquake" as postulated for myoglobin.[171]

The high specificity of these enzymes, which was mysterious at first glance, can only be achieved in the four-step process outlined here, because the differences in amino acid structures are insufficient. In the four steps, steric fitting and hydrophobic forces are important. Thus, the high specificity can be explained by simple well-known phenomena. The combination of these known phenomena in aminoacyl-tRNA synthetases results in a type of enzyme which can be adjusted to practically any degree of specificity. High specificity requires high energy consumption. However, in the cell a medium discrimination factor seems to be used (e.g., for valine in yeast, $D = 10000$; in *E. coli*, $D = 40000$) which is associated with medium energy consumption. In the case of the isoleucyl-tRNA synthetases the prokaryotic organism *Escherichia coli* possesses an enzyme which works with more precision than the enzyme from the eukaryotic yeast organism.

Appendix

Comments on Structure and Synthesis of ATP Analogues

N^6-Methyladenosine 5′-triphosphate (m^6ATP) **17a** can be synthesized starting from 6-chloropurine, which is first converted into 6-chloropurineriboside [172, 173]. The chlorine atom in position 6 is then substituted by methylamine [173, 174], and the product is phosphorylated via the monophosphate to the triphosphate.

2-Chloro- (cl^2ATP) and 8-bromoadenosine 5′-triphosphate (br^8ATP), **17b** and **17c**, respectively, exhibit different conformations about the glycosyl bond. cl^2ATP has an *anti* conformation which is also found in the natural substrate ATP in which the adenyl moiety is turned away from the ribose [75, 175, 176]. In the br^8ATP molecule the bromine atom is situated away from the ribose and the purine ring system is turned over the sugar plane [177, 178]; this conformation is called the *syn* conformation [175, 176]. 8-Bromoadenosine can be easily synthesized by bromination of adenosine [179, 180]; 2-chloroadenosine is made by conversion of 2,6-dichloropurine to the riboside and substitution of the chlorine atom in position 6 by ammonia [181].

7-Deazaadenosine, called tubercidine, is isolated from *Streptomyces tubercidicus* [77, 79, 182, 183]. In this molecule the nitrogen atom in position 7 is lacking; therefore, tubercidine 5′-triphosphate (TuTP) **17d** cannot form a $Mg^{2\oplus}$ complex with the $Mg^{2\oplus}$ ion coordinated to this atom. NMR measurements with tubercidine and tubercidine 5′-triphosphate show that the heterocyclic system can rotate around the glycosyl bond and prefers neither the *anti* nor the *syn* conformation [184].

2′- and 3′-deoxyadenosine are both isolated from natural sources; 2′-deoxyadenosine is a component of DNA, 3′-deoxyadenosine (also called cordycepine) a metabolic product of the microorganism *Cordyceps militaris* [77, 79, 185]. 2′- and 3′-methoxyadenosine can be easily prepared by methylation of adenosine with diazomethane [186, 187]. These four nucleoside analogues are also converted into the triphosphates.

Fundamental Principles of Initial Rate Kinetics

If the velocity of aminoacylation of tRNA is measured as a function of the concentration of one of the three substrates, classic linear Lineweaver-Burk plots [188] are obtained by plotting reciprocal velocities against reciprocal concentrations. The plots are related to the well-known Michaelis-Menten equation [189] which gives, by its intersection points with the coordinate axes, the constants K_m (Michaelis constant) and V (maximum velocity). Different inhibitor types are distinguished by the characteristic changes of Lineweaver-Burk plots (Fig. 3) observed when the inhibitor (I) is added to the reaction mixture.

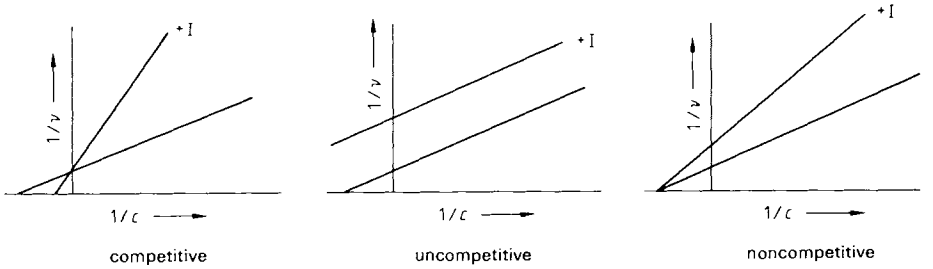

Fig. 3. Lineweaver-Burk plots for enzyme reactions with and without inhibitors. c = substrate concentration, v = reaction velocity (see text).

In the simplest enzymatic reaction [cf. (w)], in which only one substrate is converted, a competitive inhibitor would only change the slope of the plot.

$$E + S \rightleftharpoons E \cdot S \longrightarrow E + P \qquad (w)$$

This inhibitor would form with E an E·I complex which does not react further. If I does not react with E to E·I but with E·S to E·S·I, the slope of the plot is not changed but the intersection point with the $1/v$ axis does change; that means a parallel plot is observed. This inhibitor type is called uncompetitive. If I can react with E and with E·S, slope and intersection point are changed and the inhibitor is called noncompetitive [127, 129].

Whereas in the case of modified tRNAs the observation of noncompetitive inhibitors indicates the existence of a second binding site for this substrate, this conclusion cannot be made in the case of ATP analogues because, for this "small" substrate, binding at the hydrophobic pocket of the amino acid binding site [190] and nonspecific binding to aminoacyl-tRNA synthetases has been found [191].

In the aminoacylation reaction three substrates react instead of only one [cf. (x)]:

$$E + S^1 + S^2 + S^3 \longrightarrow E + P^1 + P^2 + P^3 \qquad (x)$$

Now the inhibitor type depends additionally on which one of the three substrates is chosen to be varied in the Lineweaver-Burk analysis. For example, an inhibitor may be competitive if the reciprocal reaction velocity is plotted against the reciprocal concentration of S^1, but noncompetitive if the velocity is measured at variable concentrations of S^2 or S^3. The way in which the inhibitor type is changed with the variable substrate depends on the reaction mechanism. Therefore, it depends on the order of substrate addition and product release. Inhibitor types that can be expected for nearly all possible mechanisms are listed in tables [127-129].

If three inhibitors are at disposal, each of which shows competitive inhibition with respect to one of the three substrates, characteristic inhibition patterns are observed when the other two substrates are also varied. These typical inhibition patterns allow one to identify the reaction mechanism (order of substrate addition and product release). In Table 5, inhibition patterns corresponding to two mechanisms are listed which have been found for the aminoacyl-tRNA synthetases (cf. Tables 2 and 3). In the first one, the substrates are added in the sequence S^1, S^2, and S^3; the chemical reaction then occurs, and products are released in the sequence P^1, P^2, and P^3. In the commonly used notation [130] it is written as shown in (y).

Table 5. Inhibition patterns of an ordered sequential and an ordered ping-pong mechanism (c = competive, u = uncompetitive, n = noncompetitive).

Sequential, ordered (y)				Ping-pong, ordered (z)			
Inhibitor	Variable substrate			Inhibitor	Variable substrate		
	S^1	S^2	S^3		S^1	S^2	S^3
I^1	c	n	n	I^1	c	n	u
I^2	u	c	n	I^2	u	c	u
I^3	u	u	c	I^3	u	u	c

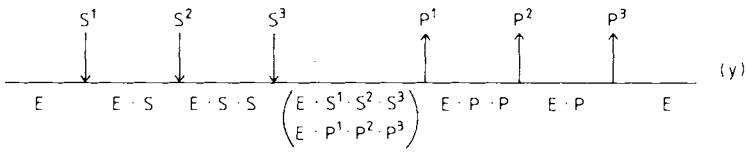

In this scheme the reaction sequence is written from left to right, the enzyme is represented by a horizontal line, and the addition of substrates and release of products are indicated by perpendicular arrows. The numbers of substrates or products that are added or released in one direction are called "uni," "bi," and "tri." If all substrates are added before a product is released, the mechanism is called "sequential"; if one or more products dissociate from the enzyme before all substrates are added, the mechanism is called a "ping-pong" mechanism. If the sequence in which substrates are added or products are released is fixed, then the mechanism is "ordered"; if not, the mechanism is a "random" one. Consequently, mechanism (y) must be called "sequential ordered Ter-Ter."

In the second mechanism, an "ordered Bi-uni Uni-bi ping-pong" mechanism, the substrates S^1 and S^2 are first added, product P^1 is then released, substrate S^3 is added, and, finally, the products P^2 and P^3 dissociate from the enzyme [cf. (z); X = intermediate].

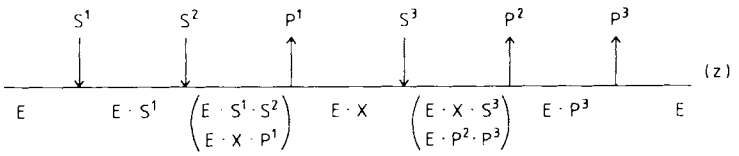

The inhibition patterns which belong to the two mechanisms are given in Table 5; they differ in two positions and thus allow unambiguous classifications of the mechanisms.

Received: December 22, 1986;
revised: June 5, 1987 [A 675 IE]
German version: *Angew. Chem. 100* (1988) 795
Translated by Dr. *Gerald Gish*, Göttingen

[1] M. B. Hoagland, *Biochim. Biophys. Acta 16* (1955) 288.
[2] J. A. DeMoss, G. D. Novelli, *Biochim. Biophys. Acta 18* (1955) 592.
[3] P. Berg, *J. Biol. Chem. 222* (1956) 1025.
[4] M. B. Hoagland, E. B. Keller, P. C. Zamecnik, *J. Biol. Chem. 218* (1956) 345.

[5] M. B. Hoagland, P. C. Zamecnik, M. L. Stephenson, *Biochim. Biophys. Acta 24* (1957) 215.
[6] M. B. Hoagland, M. L. Stephenson, J. F. Scott, L. I. Hecht, P. C. Zamecnik, *J. Biol. Chem. 231* (1958) 241.
[7] P. C. Zamecnik, *Cold Spring Harbor Symp. Quant. Biol. 34* (1969) 1.
[8] R. B. Loftfield, *Prog. Nucleic Acid. Res. Mol. Biol. 12* (1972) 87.
[9] L. L. Kisselev, O. O. Favorova, *Adv. Enzymol. 40* (1974) 141.
[10] D. Söll, P. R. Schimmel in P. D. Boyer (Ed.): *The Enzymes, Vol. 10,* 3rd ed., Academic Press, New York 1974, p. 489.
[11] F. Kalousek, W. Konigsberg, *MTP Int. Rev. Sci. Biochem. Ser. One 7* (1975) 57.
[12] A. Joachimiak, J. Barciszewski, *FEBS Lett. 119* (1980) 201.
[13] D. Kern, R. Giegé, J. P. Ebel, *Biochemistry 20* (1981) 5156.
[14] A. R. Fersht, M. M. Kaethner, *Biochemistry 15* (1976) 818.
[15] R. S. Mulvey, A. R. Fersht, *Biochemistry 15* (1976) 243.
[16] S. Blanquet, M. Iwatsubo, J. P. Waller, *Eur. J. Biochem. 36* (1973) 213.
[17] J. M. Berther, P. Mayer, H. Dutler, *Eur. J. Biochem. 47* (1974) 151.
[18] F. Fasiolo, J. P. Ebel, *Eur. J. Biochem. 49* (1974) 257.
[19] F. Fasiolo, P. Remy, J. Pouyet, J. P. Ebel, *Eur. J. Biochem. 50* (1974) 227.
[20] G. Krauss, A. Pingoud, D. Boehme, D. Riesner, F. Peters, G. Maass, *Eur. J. Biochem. 55* (1975) 517.
[21] G. Krauss, D. Riesner, G. Maass, *Eur. J. Biochem. 68* (1976) 81.
[22] R. B. Loftfield, E. A. Eigner, *J. Biol. Chem. 244* (1969) 1746.
[23] T. N. E. Lövgren, J. Heinonen, R. B. Loftfield, *J. Biol. Chem. 250* (1975) 3854.
[24] M. P. Deutscher, *J. Biol. Chem. 242* (1967) 1132.
[25] R. Parfait, H. Grosjean, *Eur. J. Biochem. 30* (1972) 242.
[26] A. N. Baldwin, P. Berg, *J. Biol. Chem. 241* (1966) 831.
[27] A. Duveković, J. Flossdorf, M.-R. Kula, *Eur. J. Biochem. 36* (1973) 528.
[28] F. von der Haar, F. Cramer, *Biochemistry 15* (1976) 4131.
[29] F. von der Haar, F. Cramer, *Biochemistry 17* (1978) 3139.
[30] T. Webster, H. Tsai, M.-R. Kula, G. A. Mackie, P. Schimmel, *Science (Washington, D.C.) 226* (1984) 1315.
[31] D. G. Barker, J.-P. Ebel, R. Jakes, C. J. Bruton, *Eur. J. Biochem. 127* (1982) 449.
[32] G. Winter, G. L. E. Koch, B. S. Hartley, D. G. Barker, *Eur. J. Biochem. 132* (1983) 383.
[33] P. Hoben, N. Royal, A. Cheung, F. Yamao, K. Biemann, D. Söll, *J. Biol. Chem. 257* (1982) 11644.
[34] G. P. Winter, B. S. Hartley, *FEBS Lett. 80* (1977) 340.
[35] S. D. Putney, N. J. Royal, H. Neumann de Vegvar, W. C. Herlith, K. Biemann, P. Schimmel, *Science (Washington, D.C.) 213* (1981) 1497.
[36] D. G. Barker, C. J. Bruton, G. Winter, *FEBS Lett. 150* (1982) 419.
[37] J. Amiri, H. Mejdoub, N. Hounwanou, Y. Boulanger, J. Reinbolt, *Biochimie 67* (1985) 607.
[38] W. Freist, F. Cramer, *Eur. J. Biochem. 131* (1983) 65.
[39] A. R. Fersht, J.-P. Shi, J. Knill-Jones, D. M. Lowe, A. J. Wilkinson, D. M. Blow, P. Brick, P. Carter, M. M. Y. Waye, G. Winter, *Nature (London) 314* (1985) 235.
[40] F. Fasiolo, A. R. Fersht, *Eur. J. Biochem. 85* (1978) 85.
[41] A. R. Fersht, M. M. Kaethner, *Biochemistry 15* (1976) 3342.
[42] N. Piel, *Dissertation,* Technische Universität Braunschweig 1982.
[43] J. H. Segel: *Enzyme Kinetics,* Wiley-Interscience, New York 1968, S. 80.
[44] A. L. Lehninger: *Biochemie,* 2nd ed., Verlag Chemie, Weinheim 1979, p. 168.
[45] L. Stryer: *Biochemie,* Vieweg, Braunschweig 1979, p. 86.
[46] D. E. Metzler: *Biochemistry,* Academic Press, New York 1977, p. 303.
[47] G. D. Greville, P. K. Tubbs, *Essays Biochem. 4* (1968) 155.
[48] A. L. Lehninger: *Biochemie,* 2nd ed., Verlag Chemie, Weinheim 1979, p. 449.
[49] F. Lipmann, *Science (Washington, D.C.) 173* (1971) 875.
[50] G. S. Laland, T. L. Zimmer, *Essays Biochem. 9* (1973) 31.
[51] W. Schlumbohm, J. Vater, H. Kleinkauf, *Biol. Chem. Hoppe-Seyler 366* (1985) 925.
[52] T. Kuo, M. DeLuca, *Biochemistry 8* (1969) 151.
[53] M. Iaccarino, P. Berg, *J. Mol. Biol. 42* (1969) 151.
[54] M. Kanda, K. Hori, T. Kurotsu, S. Miura, Y. Saito, *J. Biochem. 96* (1984) 701.
[55] P. Rainey, B. Hammer-Raber, M.-R. Kula, E. Holler, *Eur. J. Biochem. 78* (1977) 239.
[56] G. Lowe, B. S. Sproat, G. Tansley, P. M. Cullis, *Biochemistry 22* (1983) 1229.
[57] P. C. Zamecnik, M. L. Stephenson, C. M. Janeway, K. Randerath, *Biochem. Biophys. Res. Commun. 24* (1966) 91.
[58] K. Randerath, C. M. Janeway, M. L. Stephenson, P. C. Zamecnik, *Biochem. Biophys. Res. Commun. 24* (1966) 98.
[59] E. Rapaport, S. K. Svihovec, P. C. Zamecnik, *Proc. Natl. Acad. Sci. USA 72* (1975) 2653.
[60] P. Plateau, J.-F. Mayaux, S. Blanquet, *Biochemistry 20* (1981) 4654.
[61] O. Goerlich, R. Foeckler, E. Holler, *Eur. J. Biochem. 126* (1982) 135.
[62] J. J. Led, W. K. Switon, K. F. Jensen, *Eur. J. Biochem. 136* (1983) 469.
[63] S. P. Harnett, G. Lowe, G. Tansley, *Biochemistry 24* (1985) 2908.
[64] S. Z. Wahab, D. C. H. Yang, *J. Biol. Chem. 260* (1985) 5286.
[65] S. Z. Wahab, D. C. H. Yang, *J. Biol. Chem. 260* (1985) 12735.
[66] E. Rapaport, P. C. Zamecnik, *Proc. Natl. Acad. Sci. USA 73* (1976) 3984.
[67] P. C. Lee, B. R. Bochnev, B. N. Ames, *J. Biol. Chem. 258* (1983) 6827.
[68] A. Varshavsky, *Cell (Cambridge, Mass.) 34* (1983) 711.
[69] W. Freist, unpublished results.
[70] A. M. Pendergast, J. A. Traugh, *J. Biol. Chem. 260* (1985) 11789.
[71] O. Kennard, N. W. Isaacs, J. C. Coppola, A. J. Kirby, S. Warren, W. D. S. Motherwell, D. G. Watson, D. L. Wampler, D. H. Chenery, A. C. Larson, K. A. Kerr, L. R. di Sanseverino, *Nature (London) 225* (1970) 333.
[72] T. A. Glassman, C. Cooper, L. W. Harrison, T. J. Swift, *Biochemistry 10* (1971) 843.
[73] G. P. P. Kuntz, T. A. Glassman, C. Cooper, T. J. Swift, *Biochemistry 11* (1972) 538.
[74] V. Wee, I. Feldman, P. Rose, S. Gross, *J. Am. Chem. Soc. 96* (1974) 103.
[75] M. Sundaralingam, *Biopolymers 7* (1969) 821.
[76] R. D. Cornelius, W. W. Cleland, *Biochemistry 17* (1978) 3279.
[77] Cf. P. Roy-Burman: *Analogues of Nucleic Acid Components,* Springer, Berlin 1970.
[78] Cf. L. B. Townsend, R. S. Tipson (Eds.): *Nucleic Acid Chemistry, Vol. 1, 2,* Wiley, New York 1978.
[79] R. J. Suhadolnik: *Nucleoside Antibiotics,* Wiley-Interscience, New York 1970.
[80] W. Freist, F. Cramer in L. B. Townsend, R. S. Tipson (Eds.): *Nucleic Acid Chemistry, Vol. 2,* Wiley, New York 1978, p. 827.
[81] K. H. Scheit: *Nucleotide Analogs,* Wiley-Interscience, New York 1980.
[82] M. Yoshikawa, T. Kato, T. Takenishi, *Tetrahedron Lett. 1967,* 5065.
[83] D. E. Hoard, D. G. Ott, *J. Am. Chem. Soc. 87* (1965) 1785.
[84] W. Freist, F. von der Haar, M. Sprinzl, F. Cramer, *Eur. J. Biochem. 64* (1976) 389.
[85] W. Freist, F. von der Haar, H. Faulhammer, F. Cramer, *Eur. J. Biochem. 66* (1976) 493.
[86] W. Freist, H. Sternbach, F. von der Haar, F. Cramer, *Eur. J. Biochem. 84* (1978) 499.
[87] W. Freist, H. Wiedner, F. Cramer, *Bioorg. Chem. 9* (1980) 491.
[88] W. Freist, H. Sternbach, F. Cramer, *Hoppe-Seyler's Z. Physiol. Chem. 362* (1981) 1247.
[89] N. Piel, W. Freist, F. Cramer, *Bioorg. Chem. 12* (1983) 18.
[90] R. B. Loftfield, D. Vanderjagt, *Biochem. J. 128* (1972) 1353.
[91] S. Englisch, *Dissertation,* Technische Universität Braunschweig 1984.
[92] E. Holler, P. Rainey, A. Orme, E. L. Bennett, M. Calvin, *Biochemistry 12* (1973) 1150.
[93] E. Holler, B. Hammer-Raber, T. Hanke, P. Bartmann, *Biochemistry 14* (1975) 2496.
[94] E. Holler, G. Schwarze, R. Scheibl, B. Hammer-Raber, *Biochemistry 19* (1980) 5403.
[95] Cf. D. H. Gauss, F. von der Haar, A. Maelicke, F. Cramer, *Annu. Rev. Biochem. 40* (1971) 1045.
[96] M. Sprinzl, D. Gauss, *Nucleic Acids Res. 12* (1984) r1.
[97] M. Yarus, *Biochemistry 11* (1972) 2352.
[98] M. Mertes, M. A. Peters, W. Mahoney, M. Yarus, *J. Mol. Biol. 71* (1972) 671.
[99] W. Freist, H. Sternbach, *Biochemistry 23* (1984) 5742.
[100] Vgl. U. Englisch, D. Gauss, W. Freist, S. Englisch, H. Sternbach, F. von der Haar, *Angew. Chem. 97* (1985) 1033; *Angew. Chem. Int. Ed. Engl. 24* (1985) 1015.
[101] M. Sprinzl, F. Cramer, *Prog. Nucleic Acid Res. Mol. Biol. 22* (1978) 1.
[102] S. M. Hecht, *Tetrahedron 33* (1977) 1671.
[103] F. Cramer, F. von der Haar, E. Schlimme, *FEBS Lett. 2* (1968) 136.
[104] F. Hansske, F. Cramer, *Carbohydr. Res. 54* (1977) 75.
[105] F. von der Haar in J. Augustyniak (Ed.): *Biological Implications of Protein-Nucleic Acid Interactions,* Elsevier/North Holland, Amsterdam 1980, p. 325.
[106] F. Cramer, H. Faulhammer, F. von der Haar, M. Sprinzl, H. Sternbach, *FEBS Lett. 56* (1975) 212.
[107] T. H. Fraser, A. Rich, *Proc. Natl. Acad. Sci. USA 70* (1973) 2671.
[108] M. Sprinzl, H. Sternbach, F. von der Haar, F. Cramer, *Eur. J. Biochem. 81* (1977) 579.
[109] M. Sprinzl, F. Cramer, *Proc. Natl. Acad. Sci. USA 72* (1975) 3049.
[110] F. von der Haar, F. Cramer, *FEBS Lett. 56* (1975) 215.
[111] B. E. Griffin, M. Jarmen, C. B. Reese, J. E. Sulston, D. R. Trentham, *Biochemistry 5* (1966) 3638.
[112] M. Taiji, S. Yokoyama, S. Higuchi, T. Miyazawa, *J. Biochem. 90* (1981) 885.

[113] M. Taiji, S. Yokoyama, T. Miyazawa, *Biochemistry 22* (1983) 3220.
[114] M. Taiji, S. Yokoyama, T. Miyazawa, *Biochemistry 24* (1985) 5776.
[115] F. Cramer, F. von der Haar, G. L. Igloi in P. R. Schimmel, D. Söll, J. N. Abelson (Eds.): *Transfer RNA: Structure, Properties, and Recognition*, Cold Spring Harbor Laboratory, New York 1979, p. 267.
[116] G. Wehmeyer, *Dissertation*, Technische Universität Braunschweig 1980.
[117] G. L. Igloi, F. von der Haar, F. Cramer, *Methods Enzymol. 59* (1979) 282.
[118] T. H. Fraser, A. Rich, *Proc. Natl. Acad. Sci. USA 72* (1975) 3044.
[119] E. Holler, M. Calvin, *Biochemistry 11* (1972) 3741.
[120] W. Freist, H. Sternbach, F. Cramer, *Eur. J. Biochem. 169* (1987) 33.
[121] F. X. Cole, P. R. Schimmel, *Biochemistry 9* (1970) 480.
[122] M. Yarus, P. Berg, *J. Mol. Biol. 42* (1969) 171.
[123] T. N. E. Lövgren, A. Pastuszyn, R. B. Loftfield, *Biochemistry 15* (1976) 2533.
[124] S. S. M. Lam, P. R. Schimmel, *Biochemistry 14* (1975) 2775.
[125] P. R. Schimmel, *Acc. Chem. Res. 6* (1973) 299.
[126] A. R. Fersht, R. Jakes, *Biochemistry 14* (1975) 3350.
[127] See, e.g.: H. I. Fromm: *Initial Rate Enzyme Kinetics*, Springer, Berlin 1975.
[128] I. H. Segel: *Enzyme Kinetics*, Wiley-Interscience, New York 1975.
[129] K. M. Plowman: *Enzyme Kinetics*, McGraw-Hill, New York 1972.
[130] W. W. Cleland, *Biochim. Biophys. Acta 67* (1963) 104.
[131] W. W. Cleland, *Biochim. Biophys. Acta 67* (1963) 173.
[132] C. F. Midelfort, A. H. Mehler, *Methods Enzymol. 29* (1974) 627.
[133] W. W. Cleland, *Biochim. Biophys. Acta 67* (1963) 188.
[134] W. W. Cleland in P. D. Boyer (Ed.): *The Enzymes. Vol. 2*, 3rd ed., Academic Press, New York 1970, p. 1.
[135] Y. Takeda, K. Matsuzaki, *Biochem. Biophys. Res. Commun. 59* (1974) 1302.
[136] T. T. Sakai, S. S. Cohen, *Prog. Nucleic Acid. Res. Mol. Biol. 17* (1976) 15.
[137] T. N. E. Lövgren, A. Petersson, R. B. Loftfield, *J. Biol. Chem. 253* (1978) 6702.
[138] W. Freist, F. von der Haar, F. Cramer, *Eur. J. Biochem. 119* (1981) 151.
[139] W. Freist, I. Pardowitz, F. Cramer, *Biochemistry 24* (1985) 7014.
[140] I. Slavik, A. Kotyk, *Biochim. Biophys. Acta 766* (1984) 679.
[141] J. Josse, S. C. K. Wong in P. D. Boyer (Ed.): *The Enzymes, Vol. 4*, 3rd ed., Academic Press, New York 1971, p. 499.
[142] L. G. Butler in P. D. Boyer (Eds.): *The Enzymes, Vol. 4*, 3rd ed., Academic Press, New York 1971, p. 529.
[143] A. V. Furano, *Proc. Natl. Acad. Sci. USA 72* (1975) 4780.
[144] A. Pingoud, C. Urbanke, G. Krauss, F. Peters, G. Maass, *Eur. J. Biochem. 78* (1977) 403.
[145] A. Pingoud, C. Urbanke, *Biochemistry 19* (1980) 2108.
[146] S. Tanada, M. Kawakami, T. Yoneda, S. Takemura, *J. Biochem. (Tokyo) 89* (1981) 1565.
[147] S. Tanada, M. Kawakami, K. Nishio, S. Takemura, *J. Biochem. (Tokyo) 91* (1982) 291.
[148] W. Freist, F. Cramer, *Biol. Chem. Hoppe-Seyler 367* (1986) 331.
[149] R. B. Loftfield, E. A. Eigner, A. Pastuszyn in D. R. Morris, L. J. Marton (Eds.): *Polyamines in Biology and Medicine*, Marcel Dekker, New York 1981, p. 207.
[150] D. Veloso, R. W. Guynn, M. Oskarsson, R. L. Veech, *J. Biol. Chem. 248* (1973) 4811.
[151] W. Freist, H. Sternbach, F. Cramer, *Eur. J. Biochem. 128* (1982) 315.
[152] R. E. Thiebe, *Nucleic Acids Res. 5* (1978) 2055.
[153] D. Kern, J. Gangloff, *Biochemistry 20* (1981) 2065.
[154] W. Freist, F. Cramer, *Biol. Chem. Hoppe-Seyler 368* (1987) 229.
[155] L. Pauling in: *Festschrift Prof. Dr. Arthur Stoll zum siebzigsten Geburtstag 1957*, Birkhäuser, Basel 1958, p. 597.
[156] J. J. Hopfield, T. Yamane, V. Yue, S. M. Coutts, *Proc. Natl. Acad. Sci. USA 73* (1976) 1164.
[157] A. R. Fersht, *Biochemistry 16* (1977) 1025.
[158] A. R. Fersht: *Enzyme Structure and Mechanism*, Freeman, San Francisco 1977.
[159] Y. Nozaki, C. Tanford, *J. Biol. Chem. 246* (1971) 2211.
[160] C. Chothia, *Nature (London) 248* (1974) 338.
[161] C. Chothia, *Nature (London) 254* (1975) 304.
[162] C. Chothia, *J. Mol. Biol. 105* (1976) 1.
[163] B. Lee, F. M. Richards, *J. Mol. Biol. 55* (1971) 379.
[164] C. Frömmel, *J. Theor. Biol. 111* (1984) 247.
[165] W. Freist, H. Sternbach, F. Cramer, *Eur. J. Biochem. 173* (1988) 27.
[166] P. Edelmann, J. Gallant, *Cell (Cambridge, Mass.) 10* (1977) 131.
[167] N. Mori, Y. Funatsu, K. Hiruta, S. Goto, *Biochemistry 24* (1984) 1231.
[168] E. W. Eldred, P. R. Schimmel, *J. Biol. Chem. 247* (1972) 2961.
[169] G. Krauss, D. Riesner, G. Maass, *Nucleic Acids Res. 4* (1977) 2253.
[170] G. Krauss, F. von der Haar, G. Maass, *Biochemistry 18* (1979) 4755.
[171] A. Ansari, J. Berendzen, S. F. Bowne, H. Frauenfelder, I. E. T. Iben, T. B. Sauke, E. Shyamsunder, R. D. Young, *Proc. Natl. Acad. Sci. USA 82* (1985) 5000.
[172] J. Wempen, J. J. Fox, *Methods Enzymol. 12* (1967) 63.
[173] J. A. Johnson, H. J. Thomas, H. J. Schaeffer, *J. Am. Chem. Soc. 80* (1958) 699.
[174] B. T. Walsh, R. Wolfenden, *J. Am. Chem. Soc. 89* (1967) 6221.
[175] M. Sundaralingam, *Ann. N. Y. Acad. Sci. 255* (1975) 3.
[176] W. Saenger, *Angew. Chem. 85* (1973) 680; *Angew. Chem. Int. Ed. Engl. 12* (1973) 591.
[177] S. S. Travale, H. M. Sobell, *J. Mol. Biol. 48* (1970) 109.
[178] M. Ikehara, S. Vesugi, K. Yoshida, *Biochemistry 11* (1972) 830.
[179] E. J. Reist, D. F. Calkins, L. V. Fisher, L. Goodman, *J. Org. Chem. 33* (1968) 1600.
[180] R. E. Holmes, R. K. Robins, *J. Am. Chem. Soc. 86* (1964) 1242.
[181] J. A. Montgomery, K. Hewson, *J. Heterocycl. Chem. 1* (1964) 213.
[182] K. Anzai, G. Nakamura, S. Suzuki, *J. Antibiot. Ser. A 10* (1957) 201.
[183] G. Nakamura, *J. Antibiot. Ser. A 14* (1961) 90.
[184] F. E. Evans, R. H. Sarma, *Cancer Res. 35* (1975) 1458.
[185] K. G. Cunningham, S. A. Hutchinson, W. Mason, F. S. Spring, *J. Chem. Soc. 1951*, 2299.
[186] J. B. Gin, C. A. Dekker in W. W. Zorbach, R. S. Tipson (Eds.): *Nucleic Acid Chemistry, Vol. 1*, Interscience, New York 1968, p. 207.
[187] D. M. G. Martin, C. B. Reese, G. F. Stephenson, *Biochemistry 7* (1968) 1406.
[188] H. Lineweaver, D. Burk, *J. Am. Chem. Soc. 56* (1934) 658.
[189] L. Michaelis, M. L. Menten, *Biochem. Z. 49* (1913) 333.
[190] C. Monteilhet, D. M. Blow, *J. Mol. Biol. 122* (1978) 407.
[191] G. Engel, H. Heider, A. Maelicke, F. von der Haar, F. Cramer, *Eur. J. Biochem. 29* (1972) 257.

Photochemical Reactions of Ligands in Transition-Metal Complexes

By Anatoli L. Poznyak* and Valeri I. Pavlovski

Three types of photochemical reaction of coordination compounds are well-known and have often been discussed: redox reactions, substitutions, and isomerizations. Less well known is a fourth type of reaction, which occurs fairly frequently: reaction of the ligands themselves. It is the purpose of this article to fill the corresponding gap in the photochemical literature and to summarize our current knowledge of such reactions and of their mechanisms and possible applications.

1. Introduction**

1.1. The Scope of this Article

It can be seen from two monographs[1,2] and from numerous reviews (particular attention should be drawn to Refs. [3–5]) that the irradiation of solutions of transition-metal complexes with visible or ultraviolet light can lead to various types of reaction: (1) a change of oxidation state of the central metal atom, possibly associated with subsequent decomposition of the complex and release of the ligands or their oxidation products (redox reactions); (2) substitution of one of the coordinated ligands by another ligand present in solution or by a solvent molecule (photosubstitution); (3) various isomerization processes (photoisomerization). According to this classification, which is accepted by most photochemists, the photochemistry of coordination compounds should be concerned only with the three above-mentioned reaction types. Examples of photochemical reactions in which the structure or stoichiometry of the coordinated ligand underwent significant changes, but the complex was in all other respects preserved, were regarded as exceptions; they were generally observed in complexes with very complicated organic ligands and were assigned to the realm of organic photochemistry. For this reason, such reactions, although mentioned in articles on photochemistry of coordination compounds (e.g., Refs. [5–7]), have not been extensively discussed. However, the last two decades have seen numerous examples of photochemical reactions of relatively simple ligands in metal complexes and it may fairly be claimed that such reactions occur often enough to merit detailed investigation as a fourth type of photochemical reaction of metal complexes. This prompted us to summarize the current knowledge of this fourth reaction type.

[*] Dr. A. L. Poznyak, Dr. V. I. Pavlovski
Institute for Physics of the
Belorussian Academy of Sciences
Leninskij Prospect 70, 220602 Minsk (USSR)

[**] Abbreviations used in this article: baeg, *N,N*-bis(2-aminoethyl)glycinate; bpy, 2,2′-bipyridyl; chxn, *trans*-1,2-diaminocyclohexane; dtma, diethylenetriamine-1-monoacetate; dtmp, diethylenetriamine-1-monopropionate; diars, *o*-phenylenebis(dimethylarsane); eddp, ethylenediamine-*N,N*-dipropionate; edta, ethylenediaminetetraacetate; edtp, ethylenediaminetetrapropionate; edtra, ethylenediaminetriacetate; edtrp, ethylenediaminetripropionate; en, ethylenediamine; nta, nitrilotriacetate; gly, glycinate; phen, 1,10-phenanthroline; salen, 2,2′-ethylenebis(nitrilomethylidyne)diphenolate; trien, triethylenetetramine; M, transition metal; L, monodentate ligand (e.g., NH_3) or half a bidentate ligand (e.g., 1/2en); LMCT, ligand-to-metal electron transition; S, solvent molecule.

1.2. What are Photochemical Reactions of Coordinated Ligands?

In order to describe the photochemical reactions of coordinated ligands, it is advantageous first to consider the radical pair model proposed by *Adamson* et al. to explain the photochemical reactions of the complexes $[L_5Co^{III}X]^{2\oplus}$ (X = Cl, Br, I, NO_2, SCN, etc.; L = NH_3) on irradiation by light in the region of the LMCT (ligand-to-metal charge-transfer) bands.[8,9] According to this model, the absorption of the light quantum leads to the homolysis of the Co-X bond, forming a radical pair, $\{L_5Co^{2\oplus}, X^{\odot}\}$, surrounded by solvent [Eq. (1)]. Subsequent light-independent pro-

$$[L_5Co^{III}X]^{2\oplus} \xrightarrow[LMCT]{h\nu} \{L_5Co^{2\oplus}, \overset{\odot}{X}\} \quad (1)$$

cesses can be described by Equations (2)–(4) (among others), from which it can be seen how redox reactions [Eq. (2)], substitutions [Eq. (3)], or linkage isomerization of an ambidentate ligand [Eq. (4)] can occur.

$$\{L_5Co^{2\oplus}, \overset{\odot}{X}\} \xrightarrow{+Solv.} [L_5Co^{2\oplus}(Solv.), \overset{\odot}{X}] \longrightarrow Co^{2\oplus} + 5L + Solv. + \overset{\odot}{X} \quad (2)$$
(Redox reaction)

$$\{L_5Co^{2\oplus}, \overset{\odot}{X}\} \xrightarrow{Solv.} [L_5Co^{2\oplus}(Solv.), \overset{\odot}{X}] \longrightarrow [L_5CoSolv.^{3\oplus}] + X^{\ominus} \quad (3)$$
(Solvation)

$$\{L_5Co^{2\oplus}, \overset{\odot}{X}\} \longrightarrow [L_5Co^{III}X]^{2\oplus} \quad (4)$$
(Recombination to re-form the starting complex or to form a complex in which the ligand X (e.g., NO_2, SCN) coordinates to the cobalt through a different donor atom.)

More details of this model can be found in Refs. [6, 10, 11]. Its extension to photochemical reactions of coordinated ligands is based on the assumption that the ligand X is composed of several atoms or groups of atoms (X = ABC) and that the ligand radical $ABC^{\odot}$ in the generated radical pair can either dissociate ($ABC^{\odot} \rightarrow A + BC^{\odot}$) or rearrange ($ABC^{\odot} \rightarrow BCA^{\odot}$). This extended radical pair model would then predict that LMCT excitation could also lead to the elimination of some ligand fragment A [Eq. (5)] or to the rearrangement of the ligand ABC [Eq. (6)].[12,13]

$$[L_5M(ABC)] \xrightarrow{h\nu} [L_5M(BC)] + A \quad (5)$$

$$[L_5M(ABC)] \xrightarrow{h\nu} [L_5M(BCA)] \quad (6)$$

The contraction of a chelate ring (in complexes with polydentate ligands) may be regarded as a special case of elimination of a ligand fragment [Eq. (7)].

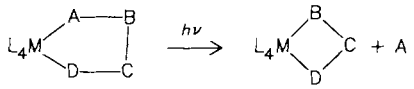

(7)

We may summarize these considerations in the statement that photochemical reactions of coordinated ligands should be understood as those photoinduced processes in which either some ligand fragment is eliminated, the remaining ligand moiety coordinating to the metal, or one of the coordinated ligands undergoes a substantial rearrangement (although retaining its overall stoichiometry) and possibly changes its coordination mode. The complex is, in the wider sense, preserved, although the oxidation state of the central metal atom may change.

The suggested model thus assumes that reactions of the type (5)–(7) occur via the excited LMCT state. It should however be mentioned that photochemical reactions of the ligands may occur in certain circumstances when the irradiation is in the region of the intraligand absorption bands. Well-known examples of such reactions are the photochromic isomerizations of 1,5-diphenylthiocarbazone complexes of a series of divalent metals [Eq. (8); the remaining ligands have been omitted for clarity].[1,4,5]

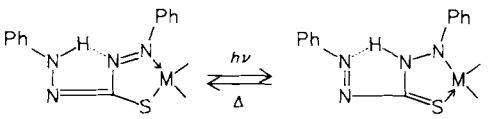

(8)

Equation (8) shows that the photolysis changes the structure of the ligand and thus, necessarily, its mode of coordination to the central metal atom, whereas the stoichiometry of the starting complex and the oxidation state of the central metal atom remain unchanged. Further examples of photochemical reactions of ligands are the *cis–trans* isomerization of dienes coordinated to tungsten(0) carbonyl complexes and the photoinduced rearrangements of ligands in some ferrocene derivatives.[5] However, the reactions proceeding from excited LMCT states according to Equations (5)–(7), in general describable as photoelimination of ligand fragments, are much more varied and interesting. Such reactions (among which photochemical transformations of many carboxylato, aminocarboxylato, ethylenediamine, and azido complexes may be numbered) will play a major role in the following discussion.[*] Analogously to the findings of *Chapman* concerning the photofragmentation of organic substances,[14] it would be expected that elimination of small fragments in the form of stable molecules with large heats of formation (e.g., N_2, CO_2, CO) should predominate. Here we shall discuss only well-studied photochemical reactions of coordinated ligands and shall offer new interpretations of some early work from a modern standpoint.

This article is organized according to the nature of the photolyzed ligand. Most of the examples presented are concerned with cobalt(III) complexes, because the charge-transfer photochemistry of cobalt(III) has been the subject of the most study.

2. Elimination of Molecular Nitrogen in the Photolysis of Azido Complexes

One of the first photoelimination reactions to be discovered was the so-called nitrene pathway in the photolysis of azido complexes.[15] According to Refs. [16–18], the primary step of the photolysis is the loss of a nitrogen molecule from the azido complex, whereupon other species present in solution can add to the nitrene intermediate to form stable end products [Eq. (9)–(11)].

$$[(NH_3)_5Ir^{III}(N_3)]^{2\oplus} \xrightarrow[+H^{\oplus},\,HCl]{h\nu} [(NH_3)_5Ir^{III}(NH_2Cl)]^{3\oplus} + N_2 \quad (9)$$

$$[(CO)_5W^0(N_3)]^{\ominus} \xrightarrow[+CO]{h\nu} [(CO)_5W^0(NCO)]^{\ominus} + N_2 \quad (10)$$

$$[(diars)_2ClRu^{II}(N_3)] \xrightarrow[+O_2]{h\nu} [(diars)_2ClRu^{II}(NO_2)] + N_2 \quad (11)$$

The nitrene pathway has also been demonstrated in the thermal decomposition of azido complexes.[15] It had even earlier been recognized that the thermal decomposition of azido complexes of metals with stable oxidation states $+n$ and $+(n+2)$ led to the formation of nitrido complexes [Eq. (12)]. It was later shown[20,21] that a similar process can

$$[M(N_3)]^{(n-1)\oplus} \xrightarrow{\Delta} [MN]^{(n-1)\oplus} + N_2 \quad (12)$$

be realized photochemically, e.g., with chromium(III) azido complexes of the type $[L_5Cr(N_3)]^{2\oplus}$ [Eq. (13)]. Reaction

$$[L_5Cr^{III}(N_3)]^{2\oplus} \xrightarrow{h\nu} [L_5Cr^{V}N]^{2\oplus} + N_2 \quad (13)$$

type (13) thus allowed the first preparation of a chromium(V) nitrido complex, $[CrN(salen)\cdot H_2O]$, which was obtained in crystalline form.[22] Other authors then used the photochemical method to prepare chromium(V) and manganese(V) nitrides, the structures of which were confirmed by X-ray structure analysis.[23,24] Reaction (13) may thus be considered as a "nitride pathway" for the photolysis of azido complexes (in contrast to the "nitrene pathway"), and the process may be generalized as Equation (14).

$$[L_5M^{n\oplus}(N_3^{\ominus})] \xrightarrow{h\nu} [L_5M^{(n+2)\oplus}(N^{3\ominus})] + N_2 \quad (14)$$

Reaction (14) also has the preparative advantage that it may be used to obtain nitrido complexes that are thermally unstable, because photolysis (unlike the other preparative methods) can be employed at low temperature if necessary.

It has been claimed in several publications[25–28] that the photolysis of $[Cr(NH_3)_5N_3]^{2\oplus}$ with light of wavelength 313 nm leads to the formation of $Cr^{2\oplus}$ ions or coordinated nitrenes. The evidence presented in Ref. [22] shows convincingly, however, that such claims are based on incorrect

[*] Numerous photoelimination reactions are also known for organometallic complexes. This article deliberately omits discussion of the photochemical reactions of ligands in organometallic complexes, because this fascinating photochemical problem has already been reviewed in depth (see, e.g., G. L. Geofroy, M. S. Wrighton: *Organometallic Photochemistry*, Academic Press, New York 1979 or H. G. Alt, *Angew. Chem. 96* (1984) 752; *Angew. Chem. Int. Ed. Engl. 23* (1984) 877).

interpretation of the experimental results. There is no doubt that the photolysis of chromium(III) azides always leads to the formation of chromium(V) nitrido species, even if these are not isolable in the solid state.

3. Photodecarboxylation and Chelate Ring Contraction of Aminocarboxylato Complexes

It is well known that some metal carboxylates can be thermally decarboxylated to form compounds containing σ M–C bonds.[29] Organomercury compounds can also be prepared by photochemical decarboxylation.[30] The photochemical synthesis of σ-organometallic complexes of transition metals, on the other hand, remained unknown for a long time because redox processes had generally been assumed for transition-metal carboxylates (despite the fact that the photolysis of some cobalt(III) oxalates involved organocobalt intermediates.[31] It was also accepted as a fact that cobalt(III) α-aminocarboxylates decomposed to $Co^{2\oplus}$ ions and ligand radicals (with loss of CO_2) in the primary photolytic step [Eq. (15)].[6]

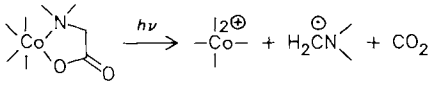

(15)

Our understanding of the photochemical processes of aminocarboxylato complexes underwent a dramatic change when an organocobalt compound was obtained by photodecarboxylation of the corresponding aminocarboxylate.[32–35] The starting materials were cobalt(III) mixed-ligand complexes containing one bidentate glycinate ion and two molecules of bipyridyl or phenanthroline. The X-ray structure analysis of a single crystal of the photolysis product of $[Co(bpy)_2(gly)]^{2\oplus}$ revealed the presence of a three-membered Co–C–N ring.[35] It was thus shown that the primary process of the photolysis consisted of the elimination of carbon dioxide and the simultaneous contraction of the (originally five-membered) glycinate ring to a three-membered ring [Eq. (16)], whereas products corresponding to Equation (15) are formed via photoinduced or thermal decomposition of the primary photolysis product. It should be mentioned that the crystal structure analysis of **1** revealed only one of the presumably two hydrogen atoms at the nitrogen atom of the aminomethyl ligand;[36] however, additional spectroscopic evidence (e.g., ^{1}H-NMR) indicates that both hydrogens are present.[34]

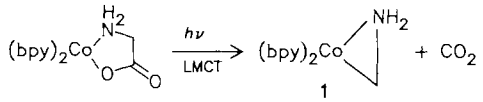

(16)

1

Similar organocobalt compounds, with a three-membered ring substituted at nitrogen, have recently been isolated as crystalline solids from the photodecarboxylation of complexes with ligands such as edta, dtma, and baeg.[37,38] The ^{1}H-NMR spectrum of the decarboxylation product of the baeg complex was easily interpreted and indicated that all the protons of the starting complex and also the mutual orientation of its chelate rings had been preserved.[38]

The photochemical contraction of aminocarboxylate chelate rings is also observed for rings of differing sizes; investigations of complexes with six- and seven-membered rings have demonstrated the validity of the generalized reaction shown in Equation (17), where n = 0, 1, 2 and

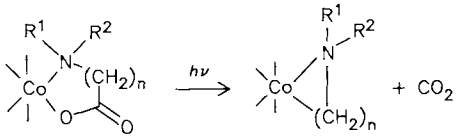

(17)

R^1, R^2 = hydrogen or other substituents. The extension of this principle to the case n = 3 has been prevented by the difficulty in preparing the starting complex with an eight-membered ring.

A comparison of the members of a homologous series of cobalt(III) complexes, each containing two ethylenediamine molecules and one bidentate anion of the amino acids glycine, β-alanine, and γ-aminobutyric acid, provides interesting information on the stability of the metallacyclic photolysis products as a function of chelate ring size. Consistent with Equation (17), the photodecarboxylation of these complexes leads to metallacycles with corresponding three-, four-, or five-membered chelate rings, namely, $[(en)_2\overline{CoCH_2NH_2}]^{2\oplus}$ **2**,[39] $[(en)_2\overline{CoCH_2CH_2NH_2}]^{2\oplus}$ **3**,[37] and $[(en)_2\overline{CoCH_2CH_2CH_2NH_2}]^{2\oplus}$ **4**.[40] In contrast to the photolysis product of $[Co(bpy)_2(gly)]^{2\oplus}$, these products do not contain π-acceptor ligands, which are known to "stabilize" M–C σ bonds,[41] so that their stability is mainly dependent on the chelate ring strain. The photolysis product from **2** contains a highly strained three-membered ring and is thermally not very stable in solution; it is impossible to isolate in the solid state.[39] The products **3** and **4**, on the other hand, possess less strained four- and five-membered rings and are correspondingly more stable; they can be isolated in crystalline form.[36,42] X-ray structure analysis confirms the presence of the four- and five-membered rings.

Stable organocobalt compounds with four-membered chelate rings were recently obtained by photodecarboxylation of a series of cobalt(III) complexes containing various aminopropionate ligands (edtp, eddp, and dtmp); their structures were also confirmed by X-ray analysis.[43–46]

It was once claimed that the metalation of nitrogen-containing donor ligands was impossible if the resulting chelate ring contained less than five atoms.[47] The above examples show that the exploitation of reactions of type (17), which in this case can be described as cyclometalating photodecarboxylations, can successfully lead to numerous cyclometalated complexes, including those with three- and four-membered chelate rings. Most known cyclometalated complexes contain an *ortho*-substituted phenyl group, so they are often termed *ortho*-metalated complexes.[47,48] A further advantage of the photochemical method is that it is also applicable with simple aminoalkyl ligands. Another point worth mentioning is that reactions of type (17) can be carried out in aqueous solution in the presence of air, in contrast to most previously known cyclometalation reac-

tions, which often had to be carried out using organolithium compounds.[49]

The photochemical cyclometalation reactions discussed here can be explained on the basis of the extended radical pair model (Section 1.2). We believe that the excitation of the LMCT state of the cobalt(III) aminocarboxylates leads directly to the formation of a radical pair, **5**, in which the cobalt(II) ion is bonded to the ligand radical via the nitrogen atom of the amino group [Eq. (18)]. Since alkanecarboxyl radicals are extremely unstable with respect to decomposition to carbon dioxide and the corresponding alkyl radical,[50] **5** loses carbon dioxide and is converted into a new radical pair; the subsequent reoxidation of the cobalt(II) ion by the aminoalkyl radical results in formation of the cyclometalated cobalt(III) compound [Eq. (19)].

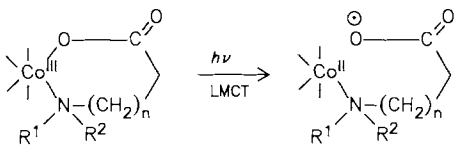

(18)

5

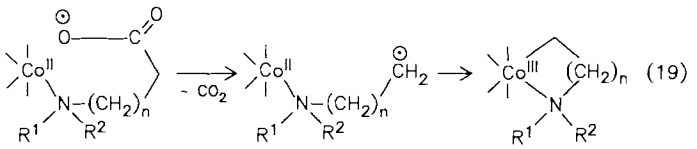

(19)

5

A natural question arising at this point is whether the reaction scheme proposed here is the only deactivation route of the excited LMCT state or whether other processes (e.g., the primary redox process) occur parallel to it. It has been shown[51] that the photoinduced decomposition of $[Co(edta)]^{\ominus}$ involves organocobalt intermediates to the extent of at least 80%, and it might be assumed that this figure really lies nearer to 100%. The photochemistry of cobalt(III) aminocarboxylates is thus the chemistry of the organocobalt products of the primary decarboxylation process. For this reason, a knowledge of the properties of such products is of great importance.

In contrast to the starting materials, the decarboxylation products of cobalt(III) aminocarboxylates are generally stereochemically labile in solution at room temperature, and are thus subject to rapid isomerization or racemization. An interesting exception is furnished by the photodecarboxylation product of $[Co(baeg)(phen)]^{2\oplus}$, in which the geometric configuration of the starting complex is also preserved in solution.[38] The photodecarboxylation products decompose via a spontaneous redox process, apparently by formation of reduced cobalt(II) ions and ligand radicals (homolysis of the Co-C σ bond). In some cases the decarboxylation products show such a marked tendency to undergo redox decomposition that they can only be detected by electronic or CD spectra following photolysis of the solutions at low temperature. Sometimes the products can be chromatographically isolated.[13,39,51-59] It has also been shown that organocobalt products are involved in bimolecular redox reactions in which the starting complexes are reduced.[51,53] However, if the thermal decomposition of the primary decomposition products was restricted to redox processes, this would not alter the mechanism assumed in the literature for the photolysis of cobalt(III) aminocarboxylates.

The photodecarboxylation products of cobalt(III) aminocarboxylates are doubtless also subject to hydrolysis (solvolysis) involving no change of the oxidation state of the central metal atom. This possibility was investigated for photodecarboxylation products isolated in the solid state. For instance, the hydrolysis of the decarboxylation product of $[Co(CN)_2(edta)]^{3\ominus}$ leads to cobalt(III) complexes with edtra as ligand and differing cyanide content, whereas, for the photolysis product of $[Co(edtp)]^{\ominus}$ in solution, a neutral complex, $[Co(edtrp)(H_2O)]$, and a series of unidentified anionic cobalt(III) complexes were demonstrated. This shows that the formation of $[Co(edtrp)(H_2O)]$ by photolysis of $[Co(edtp)]^{\ominus}$, which had already been reported,[60,61] is also to be ascribed to hydrolysis of the primary photodecarboxylation product.

The role of hydrolytic decomposition of primary photodecarboxylation products is clear from the example above, the photolysis of $[Co(edta)]^{\ominus}$. It has been shown[62,63] that the photodecomposition of this complex in neutral aqueous solution at room temperature largely consists in deacetylation [Eq. (20)], whereas the redox decomposition accounts for at most 25% of the entire process. For cobalt(III) complexes with edta and mono- or bidentate ligands such as $Cl^{\ominus}$, $NO_2^{\ominus}$, $CN^{\ominus}$, NH_3, or en, a deacetylation was also observed (as well as the redox decomposition), which was accompanied by a labilization of the second ligand X [Eq. (21)].

$$[Co^{III}(edta)]^{\ominus} \xrightarrow{h\nu} [Co^{III}(edtra)(H_2O)] + CO_2 + \text{other products} \quad (20)$$

$$[Co^{III}(edta)(X)] \xrightarrow{h\nu} [Co^{III}(edtra)(H_2O)] + X + \text{other products} \quad (21)$$

Photodeacetylation has also been observed for copper(II) complexes of nta[64] or edta.[65]

4. Photolysis of Oxalato Complexes

It is logical to assume that the photodecarboxylation reaction takes place not only for cobalt(III) complexes with nitrogen-containing chelate ligands, but also for complexes of other metals, for other heteroatoms in the chelate ring, and for rings with a second carboxyl group (oxalato or malonato complexes) [Eq. (22), where E represents a heteroatom (N, P, S, As, etc.) or a carboxyl group]. Postulations of such a process (based to varying extents on ex-

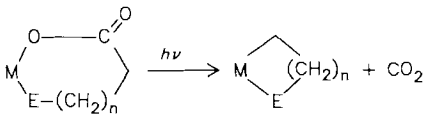

(22)

perimental results) have been published for photolysis of malonato complexes of cobalt(III),[66] manganese(III),[67] and copper(II);[68,69] iron(II) and manganese(III) complexes of ethylenediaminetetraacetate or 1,2-cyclohexanediaminetetraacetate;[70,71] copper(II) complexes with α-hydroxy acids and amino acids;[68,72,73] and a series of transition-metal oxalato complexes.[31,68,74-77]

Here we shall discuss only the photolysis of oxalato complexes, because this photochemical system has proved to be extremely interesting, yet difficult to investigate, and has fascinated photochemists for some decades. So many different, in some cases contradictory, theories as to the nature of the primary photolysis products have been put forward that there is no clear general understanding of the photolysis of such complexes. However, it is our view that the results in the literature (especially those of *Endicott*, *Hoffman*, and co-workers[31,74]) are sufficient to construct a uniform reaction scheme for the photolysis of oxalato complexes.

The so-called long-lived intermediate photolysis products of cobalt(III) complexes of the $[L_4Co(C_2O_4)]^{2\oplus}$ type, where L_4 represents two en or four NH_3 ligands, are almost certainly cobalt(III) complexes with monodentate ligands $CO_2^{2\ominus}$ or the corresponding protonated forms with $CO_2H^{\ominus}$, which are related by the acid-base equilibrium (23). A characteristic of the protonated intermediate

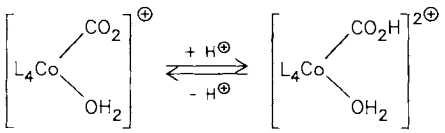

(23)

$[(en)_2Co(CO_2H)(H_2O)]^{\oplus}$ is the $^1A_{1g} \rightarrow {}^1T_{1g}$ band in the electronic spectrum, which is not split and which, in comparison with the corresponding band ($\lambda_{max} = 500$ nm) of the starting complex $[(en)_2Co(C_2O_4)]^{\oplus}$, is strongly shifted to shorter wavelength (421 nm). Similar intermediate photolysis products have been identified for many other cobalt(III) oxalato complexes.[75]

In this context it should be mentioned that a series of relatively stable transition-metal complexes involving the fragment $[M(CO_2)]^{n\ominus}$ have recently been prepared. They are generally regarded as complexes of carbon dioxide, although the formal oxidation state of the central metal atom has not been definitively assigned. X-ray structure analyses of such complexes have shown that the carbon dioxide can be monodentate (η^1-coordination) or bidentate (η^2-coordination).[78-82]

In the photolysis of manganese(III) and copper(II) oxalato complexes, intermediates were observed that presumably contain the fragments $[Mn^{III}(CO_2)]^{\oplus}$ and $[Cu^{II}(CO_2)]$.[68,76,77] We believe that the intermediates observed in the flash photolysis of solutions of $[Fe(C_2O_4)_3]^{3\ominus}$[6,83] and the continuous irradiation of frozen solutions of the same complex[84] may also be regarded as carbon dioxide complexes.

As regards the mechanism of formation of these intermediate photolysis products, it may be assumed that they are formed directly from the excited LMCT state by elimination of carbon dioxide [Eq. (24)], whereby the complex

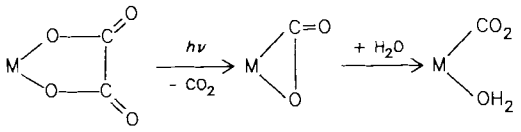

(24)

initially formed (with bidentate carbon dioxide) is converted into a complex with monodentate carbon dioxide and simultaneously aquated. We do not consider it necessary to invoke an "excited ligand state L*"[74] to explain the formation of the intermediate $[M(CO_2)]^{n\oplus}$; such a state was proposed to cause an intramolecular sensitization of the coordinated oxalate ion and to be responsible for the heterolysis of the C-C bond.

For cobalt(III) complexes, the formation of the product $[L_4Co(\eta^2\text{-}CO_2)]^{\oplus}$ in the first photolysis step, and its conversion to $[L_4Co(\eta^1\text{-}CO_2)]^{\oplus}$, can be spectroscopically confirmed by the existence of two distinct forms of the photolysis product of $[Co(C_2O_4)_3]^{3\ominus}$. One of these forms[85] is only stable to 220 K and is characterized (like any low-spin cobalt(III) complex) by two d-d bands, the lower-energy band lying at 505 nm (cf. 600 nm for the starting complex). The other form can only be observed at lower temperatures (163 K); at ca. 200 K it is irreversibly converted into the first form. The electronic spectrum of the second form also shows the characteristics of low-spin cobalt(III) complexes, but the lower-energy band is split into two components at 510 and 633 nm. We believe that this second form corresponds to the complex with η^2-coordinated carbon dioxide, the d-d splitting being due to the low symmetry of this complex. The first, higher-temperature form is thus assignable as the complex with η^1-coordinated carbon dioxide. Finally, it should be noted that a further increase in temperature leads to the redox decomposition of these intermediates, with formation of the products typical of the room temperature photolysis.

5. Decarboxylation and Ligand Rearrangement in the Photolysis of Carboxylato Complexes

The work of *Endicott*, *Hoffman*, and co-workers[31,74] also showed that cobalt(III) complexes with monodentate oxalato ligands, e.g., $[(NH_3)_5Co(C_2O_4H)]^{2\ominus}$, underwent photodecarboxylation with formation of protonated carbon dioxide complexes [Eq. (25), $L_5 = (NH_3)_5$, $(en)_2(H_2O)$].

$$[L_5Co(O_2CCO_2H)]^{2\oplus} \xrightarrow{h\nu} [L_5Co(CO_2H)]^{2\oplus} + CO_2 \qquad (25)$$

It was therefore to be expected that other complexes with monodentate carboxylato ligands would be photolyzed to corresponding σ-organometallic complexes. The flash photolysis of solutions of acetato(pentaammine)cobalt(III) and related complexes, carried out by *Endicott*, *Hoffman*, and co-workers seemed to indicate a simple redox decomposition.[86,87] Our results, however, show that the photolysis of (pentammine)carboxylato complexes leads to organometallic complexes stable at low temperature, and thus

that Equation (26), where R indicates an alkyl or alkylaryl group, is valid for a series of complexes.[12,88]

$$[L_5Co(O_2CR)]^{2\oplus} \xrightarrow{h\nu} [L_5CoR]^{2\oplus} + CO_2 \quad (26)$$

A similar photochemical process has been assumed for copper(II) carboxylates in a series of publications [Eq. (27)].[68,89-91]

$$[Cu(O_2CR)]^{\oplus} \xrightarrow{h\nu} [CuR]^{\oplus} + CO_2 \quad (27)$$

Since the M–C bond in σ-organometallic complexes is thermally labile (especially in the absence of stabilizing π-acceptor ligands) it is understandable that the products in reactions (25) to (27) are unstable at room temperature, decomposing to reduced metal ions and alkyl radicals. It is nevertheless possible to utilize this reaction for the preparation of σ-organometallic complexes. *Roche* and *Endicott* photolyzed cobalt(III) carboxylates in the presence of cobalt(II) complexes of N_4 chelating ligands capable of stabilizing M–C σ bonds; they obtained a series of stable cobalt(III) alkyl complexes that had clearly arisen by oxidation of the cobalt(II) complexes by alkyl radicals formed from the homolysis of the Co–C bond.[92,93] An alternative mechanism would be a ligand exchange between the primary photolysis product $[L_5CoR]^{2\oplus}$ and the kinetically labile cobalt(II) complex.

Cobalt(III) formato complexes, e.g., (pentaammine)formatocobalt(III) complexes, display interesting behavior on photolysis. *Hoffman* and co-workers[31,94] have discovered a reaction of such complexes that can be regarded as a photoinduced ligand rearrangement [Eq. (28)]. It is proba-

$$[L_5Co(OC(O)H)]^{2\oplus} \xrightarrow{h\nu} [L_5Co(C(O)OH)]^{2\oplus} \quad (28)$$

ble that a migration of the labile hydrogen atom in the radical $HC(O)\overset{\odot}{O}$ can take place during the lifetime of the radical pair $(HC(O)\overset{\odot}{O}\rightarrow\overset{\odot}{C}(O)OH)$, which would explain why the photoinduced ligand rearrangement occurs for formato complexes but not for other carboxylato complexes. Furthermore, it cannot be ruled out that a decarboxylation [Eq. (26)] takes place parallel to the ligand rearrangement in the photolysis of formato complexes, but the putative products, the hydrido complexes $[L_5CoH]^{2\oplus}$, have never been detected.

6. The Elimination of Ligand Fragments in the Photolysis of Ethylenediamine Complexes

An interesting case of photoelimination was discovered in the photolysis of cobalt(III) complexes of ethylenediamine.[39] Irradiation in the LMCT region induces a contraction of the five-membered chelate ring to a three-membered ring, with elimination of the $CH_2NH_2^{\oplus}$ ion [Eq. (29)]. The photolysis products should thus be identical with those of the photodecarboxylation of analogous α-aminocarboxylato complexes (i.e., those with the same number of carbon atoms in the chelate ring) [compare Eq. (16) with Eq. (29)]. This has indeed been observed for some

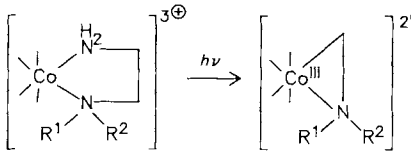

(29)

pairs of complexes, namely, $[Co(en)_3]^{3\oplus}$ and $[Co(en)_2(gly)]^{2\oplus}$,[39] $[Co(trien)(phen)]^{3\oplus}$ and $[Co(dtma)(phen)]^{2\oplus}$,[37] and $[Co(bpy)_2(en)]^{3\oplus}$ and $[Co(bpy)^2(gly)]^{2\oplus}$.[34] Flash photolysis of glycinato and ethylenediamine complexes of copper(II) occurs via the same intermediates, which have been identified as copper complexes with C-bonded methylamine.[72]

The intermediate photolysis product of the complex $[Co(en)_3]^{3\oplus}$, formed in an elimination reaction, is sufficiently stable to allow its chromatographic isolation in solution. It undergoes parallel redox and hydrolysis processes, the relative proportion of the reactions being pH-dependent. The chemically determinable concentration of $[Co(H_2O)_6]^{2\oplus}$ ions in the photolyzed solution of $[Co(en)_3]^{3\oplus}$ is of course dependent on the time elapsed since the onset of irradiation, if this is comparable with the half-life of the intermediate. This explains why the quantum yield of the photoreduction is pH-dependent and why different authors have obtained different quantum yields.[95] It is interesting to note that no such pH-dependence has been observed for the quantum yield of the photoreduction of the $[Co(chxn)_3]^{3\oplus}$ complex, in which a chelate ring contraction is rendered impossible by the nature of the diamine ligand.[96]

The photolysis of ethylenediamine complexes can be explained, analogously to that of aminocarboxylato complexes, using the extended radical pair model.[39] It is assumed that the primary radical pair generated by irradiation in the LMCT region, $[Co^{II}-NH_2CH_2CH_2\overset{\odot}{N}H_2]$, undergoes homolysis of the C–C bond, whereupon the secondary radical pair $[Co^{II}-NH_2\overset{\odot}{C}H_2]$ recombines to form a cobalt(III) complex with a Co–C–N three-membered ring. It is well known from radiochemistry, however, that γ-irradiation of amines leads to radical cations that lose a proton, thereby being converted into uncharged radicals [Eq. (30)]. We have observed a similar process in a hexacyano-

$$RNH_2 \xrightarrow[-e^{\ominus}]{\gamma \text{ or } h\nu} RNH_2^{\odot\oplus} \longrightarrow \overset{\odot}{R}NH + H^{\oplus} \quad (30)$$

ferrate(III)-sensitized oxidation of ethylenediamine.[97,98] The breaking of the C–C bond in the photolysis of ethylenediamine complexes can clearly be ascribed to the influence of the central metal atom on the reactivity of the ligand.

7. Further Elimination Reactions of Complexes

One further example of a photochemical reaction localized at a ligand can be found in the photochemistry of chlorocopper(II) complexes in organic solvents. The photolysis of such complexes occurs via intermediate products, which were first observed by us[99] and later investi-

gated in detail by *Bazhin* and co-workers.[100–104] These intermediates arise on excitation of chlorocopper(II) complexes in the region of the $Cl \rightarrow Cu^{II}$ CT bands; in alcohols they take the form of copper(II) α-hydroxyalkyl derivatives (*Bazhin* and co-workers described them as copper(I) complexes of α-hydroxyalkyl radicals). The intermediates can be assigned one of the two structures presented in Equations (31) and (32). Although it is not yet clear which route is in fact realized, the formation of these intermediates must be regarded as an elimination.

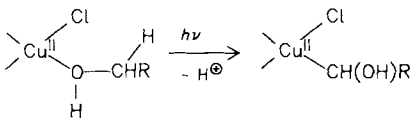

(31)

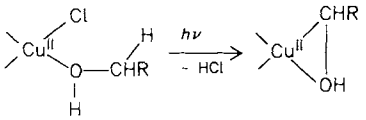

(32)

Another reaction that can be regarded as an elimination is the formation of a ruthenium(IV) *N,N*-dimethylthiocarboxamido complex in the benzophenone-sensitized photolysis of tris(*N,N*-dimethyldithiocarbamato)ruthenium(III) in chloroform [Eq. (33)].[105]

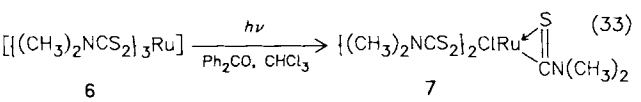

6 7

(33)

8. Conclusions and Prospects

In this article we have presented practically all known examples of photochemical reactions that take place from excited states of the LMCT type and that are localized at relatively simple ligands. Since such reactions are known for a number of complexes (M = Co, Fe, Cu, Cr, Mn, etc.; L = azide, carboxylate, aminocarboxylate, amine), this reaction type is presumably widespread in the photochemistry of coordination compounds. Our sketchy knowledge of the photochemical reactions of ligands is to be attributed to the fact that this area of photochemistry still represents practically "virgin territory." Such reactions—in contrast to other types of photoreaction—have been investigated only for a limited range of metals and ligands; in spite of this it is already possible to utilize them for certain preparative purposes. The photodecarboxylation of aminocarboxylato complexes, for example, allows the synthesis of metallacyclic compounds with simple chelating ligands that would not be attainable using conventional chemical methods. The photoelimination of molecular nitrogen from azido complexes is a simple method of preparing transition-metal nitrides. Particulary promising in this context are photochemical experiments with transition-metal complexes containing bi- or polydentate ligands with various combinations of donor atoms or groups (e.g., N-O, N-S, N-P, S-COO, P-COO, As-COO, S-S); it may be expected that the photolysis of such complexes will proceed via the elimination of various ligand fragments to yield novel metallacyclic complexes. Furthermore, it cannot be ruled out that some photoelimination or photorearrangement reactions might form unusual organic substances as ligands that could be isolated in pure form from their complexes. With a few exceptions (e.g., aliphatic hydrocarbons) almost all classes of organic compounds can be regarded as potential ligands; this would suggest that new kinds of photochemical reactions of coordinated ligands may be discovered in the future.

Received: January 9, 1987 [A 672 IE]
German version: *Angew. Chem. 100* (1988) 812
Translated by Dr. *Peter G. Jones*, Göttingen

[1] V. Balzani, V. Carassiti: *Photochemistry of Coordination Compounds*. Academic Press, London 1970.
[2] A. W. Adamson, P. D. Fleischauer (Eds.): *Concepts of Inorganic Photochemistry*, Wiley, New York 1975.
[3] A. W. Adamson, W. L. Waltz, E. Zinato, D. W. Watts, P. D. Fleischauer, R. D. Lindholm, *Chem. Rev. 68* (1968) 541.
[4] W. L. Waltz, R. G. Sutherland, *Chem. Soc. Rev. 1* (1972) 241.
[5] V. Balzani, *Chim. Ind. (Milan) 55* (1973) 711.
[6] J. F. Endicott in [2], Chap. 3, p. 81.
[7] J. F. Endicott, *Surv. Prog. Chem. 7* (1976) 41.
[8] A. W. Adamson, A. H. Sporer, *J. Am. Chem. Soc. 80* (1958) 3865.
[9] A. W. Adamson, *Discuss. Faraday Soc. 29* (1960) 163.
[10] P. D. Fleischauer, A. W. Adamson, G. Sartori, *Prog. Inorg. Chem. 17* (1972) 1.
[11] J. F. Endicott, G. J. Ferraudi, J. R. Barber, *J. Phys. Chem. 79* (1975) 630.
[12] A. L. Poznyak, V. V. Pansevich, S. I. Arzhankov, *Koord. Khim. 2* (1976) 472.
[13] V. V. Pansevich, A. L. Poznyak, *Koord. Khim. 4* (1978) 745.
[14] O. L. Chapman, *Pure Appl. Chem. 40* (1974) 511.
[15] F. Basolo, *J. Indian Chem. Soc. 54* (1977) 6.
[16] H. D. Gafney, J. L. Reed, F. Basolo, *J. Am. Chem. Soc. 95* (1973) 7998.
[17] P. G. Douglas, R. D. Feltham, H. G. Metzger, *J. Am. Chem. Soc. 93* (1971) 84.
[18] R. M. Dahlgren, J. I. Zink, *Inorg. Chem. 18* (1979) 597.
[19] W. P. Griffith, *Coord. Chem. Rev. 8* (1972) 369.
[20] S. I. Arzhankov, A. L. Poznyak, *Khim. Vys. Energ. 14* (1980) 279.
[21] S. I. Arzhankov, A. L. Poznyak, *Zh. Neorg. Khim. 26* (1981) 1576.
[22] S. I. Arzhankov, A. L. Poznyak, *Z. Anorg. Allg. Chem. 481* (1981) 201.
[23] J. T. Groves, T. Takahashi, W. M. Butler, *Inorg. Chem. 22* (1983) 884.
[24] J. W. Buchler, C. Dreher, *Z. Naturforsch. B39* (1984) 222.
[25] A. Vogler, *J. Am. Chem. Soc. 93* (1971) 5912.
[26] M. Katz, H. D. Gafney, *J. Am. Chem. Soc. 98* (1976) 7458.
[27] R. Sriram, J. F. Endicott, *Inorg. Chem. 16* (1977) 2766.
[28] M. Katz, H. D. Gafney, *Inorg. Chem. 17* (1978) 93.
[29] G. B. Deacon, R. J. Phillips, *Aust. J. Chem. 31* (1978) 1709.
[30] Yu. A. Oldekop, N. A. Mayer: *Synthese metallorganischer Verbindungen durch Decarboxylierung von Metallacylaten* (Russian), Nauka i tekhnika, Minsk 1976.
[31] A. F. Vaudo, E. R. Kantrowitz, M. Z. Hoffman, *J. Am. Chem. Soc. 93* (1971) 6698.
[32] A. L. Poznyak, V. I. Pavlovski, *Z. Chem. 21* (1981) 74.
[33] A. L. Poznyak, V. I. Pavlovski, *Zh. Neorg. Khim. 26* (1981) 539.
[34] A. L. Poznyak, V. I. Pavlovski, *Z. Anorg. Allg. Chem. 485* (1982) 225.
[35] A. L. Poznyak, V. I. Pavlovski, E. B. Chuklanova, T. N. Polynova, M. A. Porai-Koshits, *Monatsh. Chem. 113* (1982) 561.
[36] T. N. Polynova, E. B. Chuklanova, F. G. Kramarenko, M. A. Porai-Koshits, A. L. Poznyak, V. I. Pavlovski, V. E. Stelmashok, *Dokl. Akad. Nauk SSSR 290* (1986) 1399.
[37] V. I. Pavlovski, A. L. Poznyak, *Z. Chem. 25* (1985) 447.
[38] A. L. Poznyak, V. I. Pavlovski, *Koord. Khim. 14* (1988) 801.
[39] A. L. Poznyak, V. V. Pansevich, *Zh. Neorg. Khim. 24* (1979) 713.
[40] A. L. Poznyak, V. I. Pavlovski, *Koord. Khim. 13* (1987) 1381.
[41] D. Dodd, M. D. Johnson, *J. Organomet. Chem. 52* (1973) 1.
[42] V. I. Pavlovski, A. L. Poznyak, *Proc. Vth Symp. Photochem.* (Reinhardsbrunn, DDR, 1986), p. 28.
[43] L. M. Shkolnikova, A. V. Gasparyan, V. K. Belski, A. L. Poznyak, V. E. Stelmashok, N. M. Dyatlova, *Koord. Khim. 13* (1987) 823.
[44] A. V. Gasparyan, L. M. Shkolnikova, V. K. Belski, A. L. Poznyak, V. E. Stelmashok, N. M. Dyatlova, *Koord. Khim. 13* (1987) 1710.
[45] A. L. Poznyak, V. I. Pavlovski, L. M. Shkolnikova, N. M. Dyatlova, A. B. Ilyukhin, *J. Organomet. Chem. 314* (1986) C59.

[46] A. B. Ilyukhin, L. M. Shkolnikova, A. L. Poznyak, V. I. Pavlovski, N. M. Dyatlova, *Koord. Khim. 14* (1988) 705.
[47] M. I. Bruce, *Angew. Chem. 89* (1977) 75; *Angew. Chem. Int. Ed. Engl. 16* (1977) 73.
[48] H. P. Abicht, K. Issleib, *Z. Chem. 17* (1977) 1.
[49] R. Taube, H. Drevs, D. Steinborn, *Z. Chem. 18* (1978) 425.
[50] D. C. Nonhebel, J. C. Walton: *Free-radical chemistry*, University Press, Cambridge 1974.
[51] V. E. Stelmashok, A. L. Poznyak, *Zh. Neorg. Khim. 26* (1981) 2463.
[52] B. A. Budkevich, A. L. Poznyak, G. A. Shagisultanova, N. P. Glukhova in V. V. Sviridov, G. A. Shagisultanova (Ed.): *Photo- und strahlungschemische Prozesse in wässrigen Lösungen und Festkörpern*, Verlag der Belorussischen staatlichen Universität, Minsk 1970, p. 166.
[53] A. L. Poznyak, B. A. Budkevich, S. I. Arzhankov, *Dokl. Akad. Nauk BSSR 17* (1973) 723.
[54] A. L. Poznyak, S. I. Arzhankov, *Dokl. Akad. Nauk BSSR 19* (1975) 439.
[55] A. L. Poznyak, S. I. Arzhankov, V. V. Pansevich, V. E. Stelmashok, *Zh. Neorg. Khim. 23* (1978) 2105.
[56] V. V. Pansevich, A. L. Poznyak, S. I. Arzhankov, N. I. Garbuz, *Dokl. Akad. Nauk BSSR 23* (1979) 43.
[57] A. L. Poznyak, V. E. Stelmashok, *Koord. Khim. 5* (1979) 1670.
[58] A. L. Poznyak, V. I. Pavlovski, *Z. Anorg. Allg. Chem. 465* (1980) 159.
[59] V. I. Pavlovski, A. L. Poznyak, *Dokl. Akad. Nauk BSSR 24* (1980) 1103.
[60] V. E. Stelmashok, A. L. Poznyak, *Koord. Khim. 6* (1980) 144.
[61] V. E. Stelmashok, A. L. Poznyak, *Zh. Neorg. Khim. 29* (1984) 1046.
[62] A. L. Poznyak, V. E. Stelmashok, *Inorg. Chim. Acta 83* (1984) L59.
[63] V. E. Stelmashok, S. A. Mechkovski, A. L. Poznyak, *Zh. Neorg. Khim. 30* (1985) 391.
[64] C. H. Langford, M. Wingham, V. S. Sastri, *Environ. Sci. Technol. 7* (1973) 820.
[65] V. E. Stelmashok, A. L. Poznyak, *Zh. Neorg. Khim. 31* (1986) 805.
[66] A. L. Poznyak, S. I. Arzhankov, *Koord. Khim. 8* (1982) 680.
[67] V. E. Stelmashok, A. L. Poznyak, S. I. Arzhankov, *Koord. Khim. 3* (1977) 524.
[68] V. K. Rumas, A. L. Poznyak, *Dokl. Akad. Nauk BSSR 20* (1976) 1106.
[69] J. Y. Morimoto, B. A. DeGraff, *J. Phys. Chem. 79* (1975) 326.
[70] A. L. Poznyak, S. I. Arzhankov, *Dokl. Akad. Nauk BSSR 23* (1979) 353.
[71] V. E. Stelmashok, A. L. Poznyak, *Koord. Khim. 5* (1979) 1019.
[72] S. Das, G. R. A. Johnson, N. B. Nazhat, R. Saadalla-Nazhat, *J. Chem. Soc. Faraday Trans. 1 80* (1984) 2759.
[73] P. Natarajan, G. Ferraudi, *Inorg. Chem. 20* (1981) 3708.
[74] A. F. Vaudo, E. R. Kantrowitz, M. Z. Hoffman, E. Papaconstantinou, J. F. Endicott, *J. Am. Chem. Soc. 94* (1972) 6655.
[75] A. L. Poznyak, S. I. Arzhankov, B. A. Budkevich, *Dokl. Akad. Nauk BSSR 19* (1975) 905.
[76] V. E. Stelmashok, A. L. Poznyak, *Dokl. Akad. Nauk BSSR 24* (1980) 53.
[77] S. Das, G. R. A. Johnson, *J. Chem. Soc. Faraday Trans. 1 76* (1980) 1779.
[78] M. Aresta, C. F. Nobile, *J. Chem. Soc. Dalton Trans. 1977*, 708.
[79] G. Fachinetti, C. Floriani, P. Z. Zanazzi, *J. Am. Chem. Soc. 100* (1978) 7405.
[80] J. C. Calabrese, H. Herskovitz, J. B. Kinney, *J. Am. Chem. Soc. 105* (1983) 5914.
[81] G. S. Bristow, P. B. Hitchcock, M. F. Lappert, *J. Chem. Soc. Chem. Commun. 1981*, 1145.
[82] S. Gambarotta, C. Floriani, A. Chiesi-Villa, C. Guastini, *J. Am. Chem. Soc. 107* (1985) 2985.
[83] Z. Stasicka, A. Marchaj, *Coord. Chem. Rev. 23* (1977) 131.
[84] A. L. Poznyak, *Khim. Vys. Energ. 3* (1969) 88.
[85] A. L. Poznyak, G. A. Shagisultanova, *Zh. Prikl. Spektrosk. 14* (1971) 334.
[86] E. R. Kantrowitz, M. Z. Hoffman, J. F. Endicott, *J. Phys. Chem. 75* (1971) 1914.
[87] D. D. Campano, E. R. Kantrowitz, M. Z. Hoffman, M. S. Weinberg, *J. Phys. Chem. 78* (1974) 686.
[88] A. L. Poznyak, V. V. Pansevich, *Izv. Akad. Nauk BSSR, Ser. Khim. 1980*, No. 1, 18.
[89] G. Ferraudi, *Inorg. Chem. 17* (1978) 2506.
[90] S. Das, G. Ferraudi, *Inorg. Chem. 25* (1986) 1066.
[91] H. Cohen, D. Meyerstein, *Inorg. Chem. 25* (1986) 1505.
[92] T. S. Roche, J. F. Endicott, *J. Am. Chem. Soc. 94* (1972) 8622.
[93] T. S. Roche, J. F. Endicott, *Inorg. Chem. 13* (1974) 1575.
[94] E. R. Kantrowitz, M. Z. Hoffman, K. M. Schilling, *J. Phys. Chem. 76* (1972) 2492.
[95] D. Valentine, Jr., *Adv. Photochem. 6* (1968) 123.
[96] J. F. Endicott, M. Z. Hoffman, *J. Am. Chem. Soc. 87* (1965) 3348.
[97] A. L. Poznyak, S. I. Arzhankov, G. A. Shagisultanova, *Zh. Fiz. Khim. 46* (1972) 773.
[98] A. L. Poznyak, S. I. Arzhankov, G. A. Shagisultanova, *Biofizika 19* (1974) 233.
[99] A. L. Poznyak, *Khim. Vys. Energ. 3* (1969) 380.
[100] O. B. Kiseleva, V. F. Plyusnin, N. M. Bazhin, *Khim. Vys. Energ. 12* (1978) 87.
[101] V. F. Plyusnin, N. M. Bazhin, O. B. Kiseleva, *Zh. Fiz. Khim. 54* (1980) 672.
[102] V. F. Plyusnin, N. M. Bazhin, O. M. Usov, *Koord. Khim. 6* (1980) 856.
[103] I. V. Khmelinski, V. F. Plyusnin, N. P. Gritsan, N. M. Bazhin, *Khim. Fizika 4* (1985) 1666.
[104] N. P. Gritsan, O. M. Usov, N. V. Shokhirev, I. V. Khmelinski, V. F. Plyusnin, N. M. Bazhin, *Teor. Eksp. Khim. 22* (1986) 32.
[105] G. L. Miessler, L. H. Pignolet, *Inorg. Chem. 18* (1979) 210.

Cyclobutanones and Cyclobutenones in Nature and in Synthesis

New Synthetic Methods (71)

By Daniel Belluš* and Beat Ernst*

Dedicated to Professor Vladimir Prelog

The chemical reactivity of cyclobutanones and cyclobutenones is considerably different from that of cyclic ketones with larger rings; this is due to their ring strain of ca. 25 kcal/mol. Detailed knowledge regarding the influence of this ring strain on regio-, chemo- and stereoselective transformations of four-membered ring ketones is of particular importance. While several reactions, such as the Baeyer–Villiger reaction, the Beckmann and Favorskii rearrangements and *cine*-substitution often proceed in a manner specific to four-membered rings, other reactions such as the facile ring-opening by nucleophiles, the rearrangement to tropolones, the thermal [2+2]-cycloreversion, the isomerization to vinylketenes and the photochemical formation of oxacarbenes are rather specific to cyclobutanones and cyclobutenones. The remarkable selectivity and the excellent yields of such transformations, which are favored or caused by ring strain as the inherent driving force, offer the synthetic chemist fascinating possibilities for the development of new strategies for the synthesis of natural products and biologically active compounds.

1. Introduction

Four-membered ring compounds have definitely developed from academic curiosities to excellent tools in organic synthesis.[1] Cyclobutanones and cyclobutenones are among the most readily available derivatives of cyclobutane. This applies in particular to their substituted derivatives: though a number of syntheses have recently been developed, it is not yet possible to obtain the unsubstituted four-membered ring ketones[2] simply and cheaply in larger quantities.

While up until the mid-1970s interest was focussed on methods for the preparation of cyclobutanones[3,4] and cyclobutenones,[5] the last decade has seen a rapid development of their application as synthetic intermediates. This is certainly no coincidence, because they are in many ways remarkable compounds. Apart from the ready availability already mentioned, their large ring strain,[6] the high electrophilicity of the carbonyl carbon atom, the puckering of the cyclobutanone caused by the repulsion of substituents at C2 and C4,[7] and the high photochemical reactivity all offer interesting preparative and mechanistic aspects. The purpose of this review article is to provide a detailed survey of the synthetic transformations of cyclobutanones and cyclobutenones with particular respect to their regio-, chemo- and stereospecific peculiarities. The cited characteristic examples will take into account in particular the use of cyclobutanones and cyclobutenones as intermediates in the synthesis of naturally-occurring target molecules. Apart from a few important examples from the older literature, only publications which have appeared in the last twelve years will be considered.

[*] Dr. D. Belluš
Research and Development Plant Protection
Agro Division, Ciba-Geigy AG
CH-4002 Basel (Switzerland)
Dr. B. Ernst
Central Research Laboratories, Ciba-Geigy AG
CH-4002 Basel (Switzerland)

For reasons of space it is however not possible to exemplify the syntheses of cyclobutanones and cyclobutenones by formula schemes in all cases. They will be shown only if the method of preparation is new, i.e. it has not been mentioned in previous review articles (e.g. syntheses of **13**, **16**, **124**, **195**, **196**, **1** (from **269**), **274**, **279**, **305**, **321**, **357**, and **417**). It should be mentioned that in the articles cited here and in other papers an enormous amount of spectroscopic, chiroptical and physical data on four-membered ring ketones is published. It would be worthwhile collecting, summarizing, and evaluating these data, since no recent review of this type exists: however, this task would exceed the scope of the present review.

2. Naturally Occurring Cyclobutanones and Cyclobutenones

Numerous compounds with small rings, which occur in nature in an optically active form (e.g. chrysanthemate esters, penicillins, cephalosporins, pinenes) still provide an important (although no longer the exclusive) source for the syntheses of structurally related small ring derivatives. They are used in particular as the starting materials when a product with a certain absolute configuration is required. In contrast, the naturally-occurring four-membered ring ketones presently known (**1**–**4**, **7**, **11**, and **18**) are of no preparative importance, as only their constitution has been described.

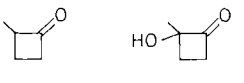

1

2

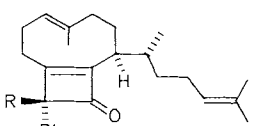

3: R = OCOMe, R' = H
4: R = H, R' = OCOMe

Thus for example no optical rotation values for the simple cyclobutanones **1** and **2** (isolated from the low-molec-

 © VCH Verlagsgesellschaft mbH, D-6940 Weinheim, 1988 0570-0833/88/0606-0797 $ 02.50/0

ular latex fraction of the rubber tree *Hevea brasiliensis*[8]), or for the diterpenes acetylcoriacenone **3** and isoacetylcoriacenone **4** (isolated from the brown sea-alga *Pachydictyon coriaceum*[9]) are known.

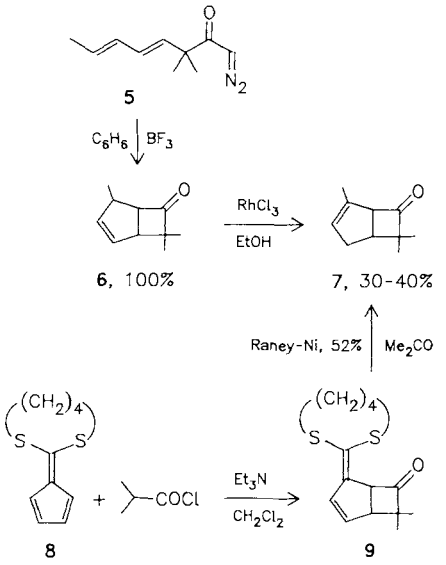

It is interesting that the monoterpene filifolone **7** occurs in nature in both enantiomeric forms. The (1*S*,5*S*)-isomer was isolated from *Artemisia filifolia* Torrey, a sand sage from Arizona, and the (1*R*,5*R*)-isomer from *Ziera smithii* Andrews from Australia.[10,11] **7** was prepared from geranic acid four years prior to its discovery as a natural product.[12] Syntheses from isomeric monoterpenes followed: by photolysis from verbenone **10**,[13] by acid-catalyzed rearrangement of chrysanthenone **11**[14] and by $AlCl_3$-catalyzed cyclization from ocimenone.[15] The (±)-filifolone **7** has recently been prepared by total synthesis starting either from the diazoketone **5**[16] or from 6,6-(tetramethylenedithio)fulvene **8**.[17]

The monoterpene chrysanthenone **11** was isolated in 1957 from the flowers of *Chrysanthemum sinese* Sabin.[18] Its absolute configuration appears to be still unknown, although both enantiomers have now been obtained photochemically from (+)- and (−)-verbenone **10** (though not with clearly defined optical purity).[13]

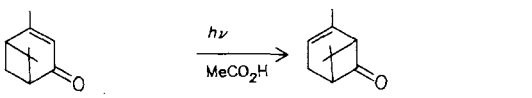

Kulkarni and *Snider*[19] have recently described a simple route to the racemic chrysanthenone **11** via an intramolecular [2+2]-cycloaddition of the vinylketene **12** (from geranyl chloride) to give **13**, followed by a double bond shift.

The mycotoxin moniliformine isolated in 1973 from the maize mold *Fusarium moniliforme*[20] and in 1974 from *Giberella fujikuroi*[21] has a structure which is remarkably simple and unusual for a natural product. It is the potassium salt of **18**. Moniliformine and particularly its esters show

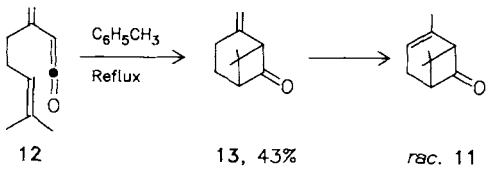

growth-regulating effects on various types of plant. Several syntheses of the strong acid **18** ($pK_a = 0.0 \pm 0.05$[5e,23]) have been described; their common feature is the formation of a hydrolyzable four-membered ring precursor via a [2+2]-cycloaddition (e.g. **14**,[21] **15**,[24] **16**,[25] and **17**[23]).

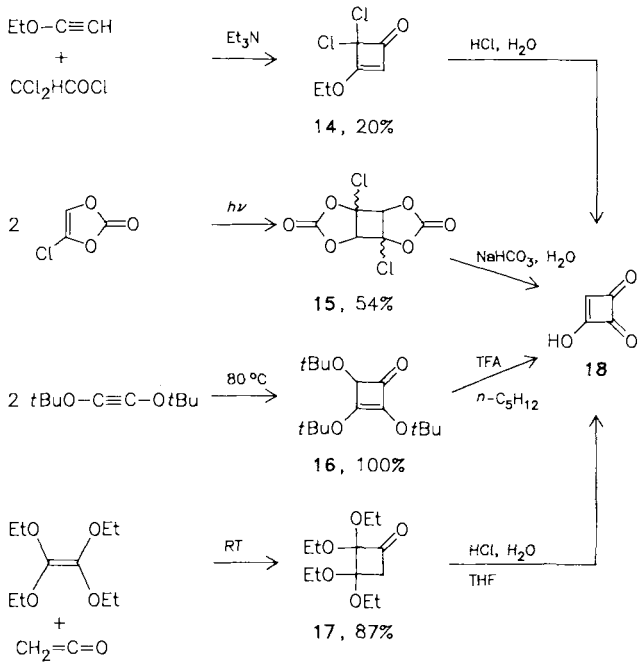

The principle of the latter synthesis, i.e. a [2+2]-cycloaddition of a ketene to a tetraalkoxyethylene as the ring-forming step, can be used for the synthesis of a large series of moniliformine derivatives: thus 2-substituted moniliformines can be prepared from alkyl-, aryl- and vinylketenes;[26] the use of alkoxy-, acetoxy- and chloroketenes allows a very simple synthesis of the dermatologically active[27] squaric acid (2-hydroxy-**18**)[28] or [1-^{14}C]-squaric acid[29] in total yields of up to 90%.

The biosynthesis of moniliformine was recently studied:[30] sodium [2-^{14}C]-acetate was shown to be a precursor of **18**.

3. Ring Enlargements of Cyclobutanones and Cyclobutenones

3.1. γ-Butyrolactones

γ-Butyrolactones are used a great deal as intermediates in synthesis. The Baeyer-Villiger oxidation[31] of cyclobutanones represents an important synthetic route to γ-butyrolactones. A large number of oxidizing agents have already been used for this transformation: H_2O_2;[32] H_2O_2/AcOH;[33] H_2O_2/NaOH;[32,34] NaOBr;[34a] NaOCl/$RuCl_3$;[35] $Me_3SiOOSiMe_3/SnCl_4$[36] or Me_3SiOTf (Tf = tri-

fluoromethanesulfonate);[37] *t*BuOOH/NaOH;[38] *m*-chloroperbenzoic acid;[4b, 15a, 39] trifluoroperacetic acid;[40] alkoxyperformic acid.[39d] The use of $K_2Cr_2O_7/H_2SO_4$ is limited to the oxidation of cyclobutanones to γ-lactones:[41] for example, 2,2,5,5-tetramethylcyclopentanone is recovered quantitatively under these reaction conditions.[42]

The *first central problem* is the chemoselectivity of the oxidizing reagents. A comparison of their reactivity in the oxidation of cyclobutanones, alkenes, and thioethers shows that the substrate specificity can differ from molecule to molecule. Thus the commercially available bicyclo[3.2.0]hept-2-en-6-one **19** (Merck-Schuchardt), which can be used in many ways for the synthesis of prostaglandins,[43] is oxidized mainly to the γ-lactone **20**.[39d]

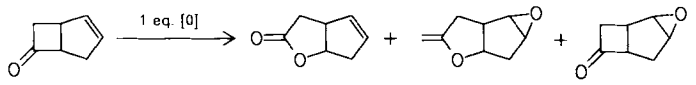

19 **20** **21** **22**

*m*CPBA	95	:	3	:	1
$EtOCO_3H$	69	:	21	:	9
$Cl_3CCH_2OCO_3H$	28	:	40	:	31

In contrast, the double bond and the cyclobutanone carbonyl group in **24** show a remarkable difference in reactivity.[44]

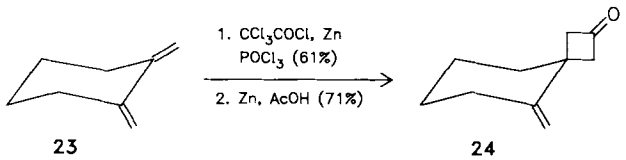

23 **24**

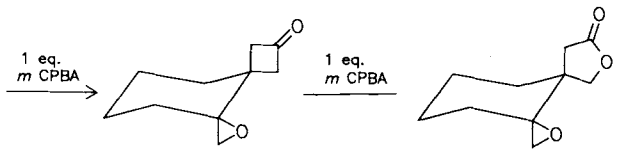

25, 71% **26**, 70%

In cyclobutanone thioethers, the thioether function is oxidized first; thus **27** is converted into **28**:[45]

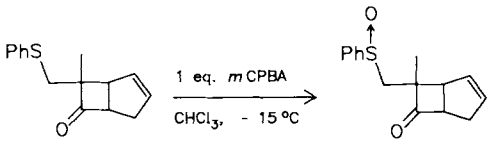

27 **28**, 98%

The *second central problem* is that of the regiospecificity. As in the case of the majority of ketones[31a, b] the oxygen insertion in cyclobutanones occurs between the carbonyl carbon and the more substituted α-carbon or the α-carbon which is not substituted by electronegative groups.[33a, c, 34b, c, 46] Thus, for stereoelectronic reasons the oxidation of **29**[47] gives only **30**.

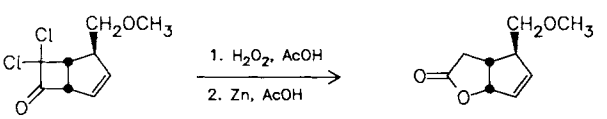

29 **30**, 62%

The Baeyer–Villiger oxidation of the α-chlorocyclobutanone **31** is less specific: the two regioisomeric lactones **32** and **33** are formed in the ratio 19 : 45.[4b]

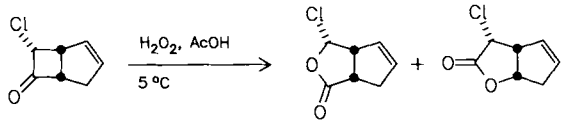

31 **32**, 19% **33**, 45%

In order to insert the oxygen solely on the less substituted side of the four-membered ring ketone, the cyclobutanedione **35** was transformed into the γ-lactone **37** in a two-step process via the anhydride **36**.[48] However, when in a transformation of the type **34** → **35** an unsymmetrical cyclobutane-1,2-dione is formed, this method loses its appeal, since then the regioselectivity problem would reappear at a later stage, i.e. during the reduction of the anhydride.

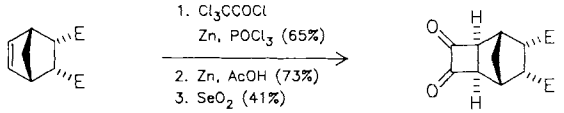

34, E = CO_2Me **35**

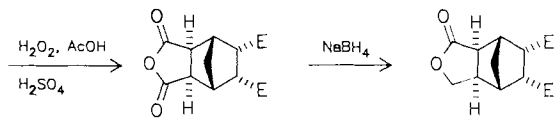

36, 64% **37**, 75%

During his studies on spirolactonization in connection with the synthesis of the widely biologically active lactone plumericine **41**, *Trost* et al. found an unusual influence of selenium substituents on the Baeyer–Villiger oxidation of the cyclobutanone **38**:[32, 49] either **39** or **40** is formed regioselectively, depending on the reaction conditions.

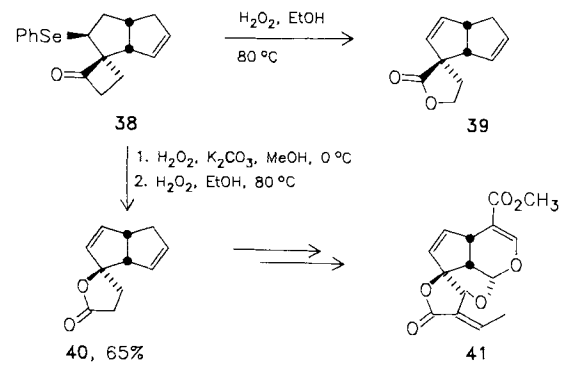

38 **39**

40, 65% **41**

A number of naturally-occurring sesquiterpene-γ-lactones have been investigated with regard to their cytotoxicity.[50] It was shown that the structural element α-methylene-γ-butyrolactone is responsible for the cytotoxicity. This explains the great synthetic interest in this class of

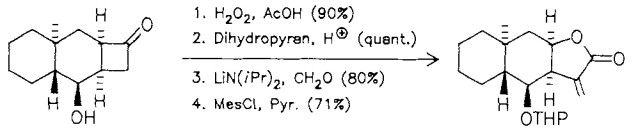

42 43

compounds.[33a,38,51] *Grieco* and *Hiroi*[51a] transformed the cyclobutanone **42** into the α-methylene-γ-lactone **43** by oxidation with H_2O_2/AcOH and subsequent condensation with formaldehyde (Pyr = pyridine, THP = tetrahydropyranyl).

Ali and *Roberts* have shown that the transformation of cyclobutanones into α-methylene-γ-lactones can be shortened to three steps if the methylene carbon is first introduced via chloromethylketene in the [2+2]-cycloaddition step (**44** → **45**)[33c,39a,52] (DBN = diazabicyclononene).

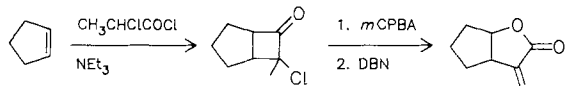

44 45, 77% 46, 80%

The cyclopropyl analogue **49** was prepared using an analogous reaction sequence.[53]

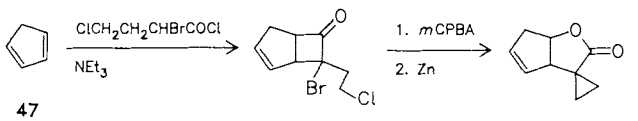

47 48, 70% 49, 65%

3.2. Pyrrolidones

A large number of cyclization reactions are available for the classical synthesis of pyrrolidones.[54] The nitrogen insertion into cyclobutanones, which leads to the corresponding pyrrolidones, has been little used so far. Starting from the cyclobutanone **50**, *Jeffs* et al.[40] found a method for the preparation of the two regioisomeric γ-lactams **51** and **53**. Under the normal Beckmann rearrangement conditions the lactam **51** was formed from the oxime of **50**. The rearrangement of the *N*-methylnitrone **52**, however, afforded the *N*-methyl derivative of the isomeric lactam **53**, a precursor for the alkaloid mesembrine.

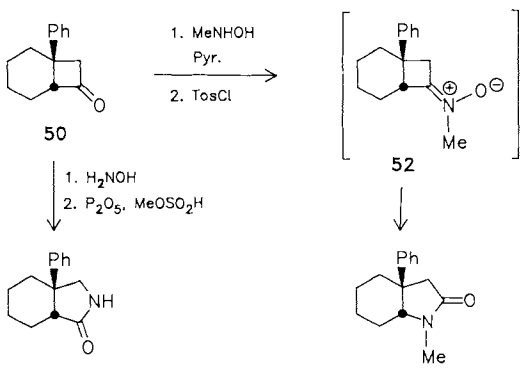

50 52

51, 40% 53, 32%

Greene et al.[55] used the Tamura reagent[56] for the preparation of the lactam-prostanoid **57** via the two cyclobutanones **19** and **56**.

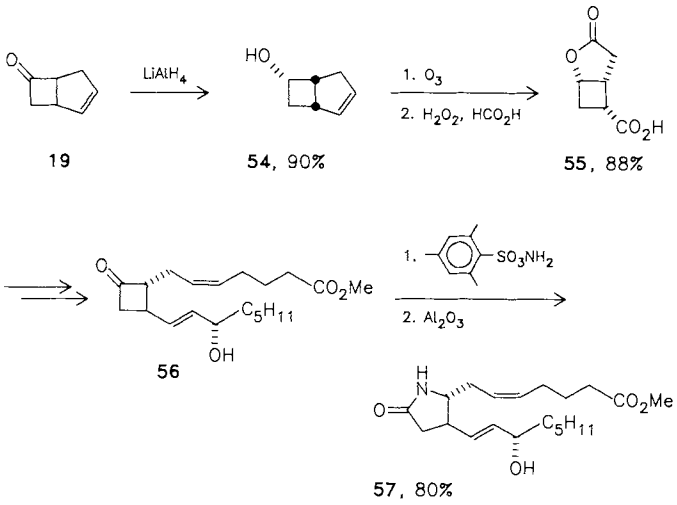

19 54, 90% 55, 88%

56

57, 80%

The Beckmann rearrangement also occurred regioselectively in this case, the nitrogen being inserted on the more substituted side of the four-membered ring ketone. Similar results were obtained by *Bartmann* et al.[57] in a synthesis of prostacyclin analogues. The contribution of *Luh* et al.[58] to the improvement of the regioselectivity of this rearrangement provides a valuable addition to the work cited above: **58** leads to a mixture of **59** and **60** (77 : 15), while **61**, which has electronegative substituents in the α-position, is transformed exclusively into the lactam **62**.

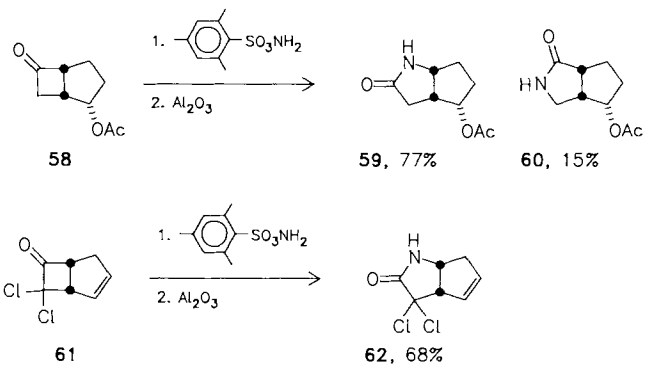

58 59, 77% 60, 15%

61 62, 68%

3.3. Cyclopentanones

Only a few synthetic methods are available for the regioselective annelation of a functionalized cyclopentane ring to an olefin.[59] One of them, the transformation of an olefin into a cyclobutanone derivative, followed by ring enlargement with a diazoalkane[60] to the corresponding cyclopentanone, is broadly applicable. The experiments with the 11-norprostaglandin derivative **56**[55b] clearly demonstrated, however, that in the case of alkyl-substituted cyclobutanones the ring enlargement with diazomethane occurs in a good chemical yield but with only poor regioselectivity.

There are however methods available which permit a regioselective preparation of the required cyclopentanone. *Greene* et al.[61] used an elegant approach for the synthesis

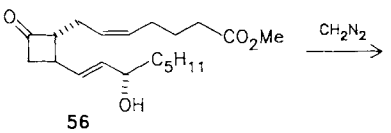

56

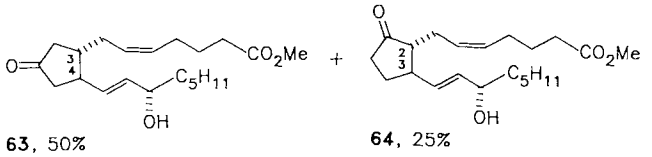

63, 50% 64, 25%

of a 2,3-disubstituted cyclopentanone of type **64**. When the optically active cyclobutanone (−)-**65** is treated with ethyl diazoacetate in the presence of $SbCl_5$, the 2,3-disubstituted cyclopentanone (−)-**67** is formed (via (−)-**66**) almost exclusively (98:2). Diazomethane, however, reacts unselectively, giving rise to both (−)-**67** and the isomeric 3,4-disubstituted cyclopentanone of type **63** in equal amounts.

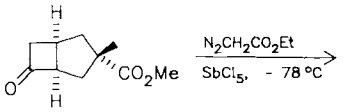

(−)-65

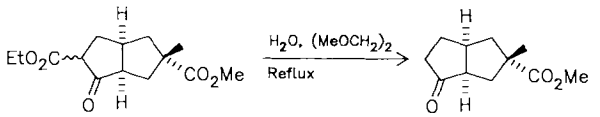

(−)-66 (−)-67, 63%

As can be expected from the electron-withdrawing effects of chlorine substituents, α-chloro- and α,α-dichlorocyclobutanones react faster and more regioselectively in the ring enlargement reaction using diazomethane:[62] no methylene insertion on the halogen-substituted side is observed. This effect can be exploited for the regioselective preparation of a 3,4-disubstituted cyclopentanone (**68** → **69**).[62b]

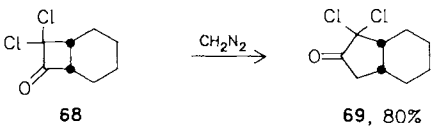

68 69, 80%

The synthetic potential of this regioselective method has already been widely applied in natural product syntheses.[61,63] Thus an elegant synthesis of racemic β-cuparenone **74** has recently been carried out.[64]

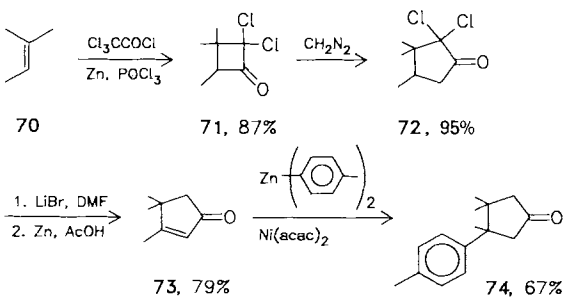

70 71, 87% 72, 95%

73, 79% 74, 67%

Suitably substituted cycloaddition products enable a very short synthesis of α-methylenecyclopentanones,[65] e.g. **77** from the cyclobutanone **76**:

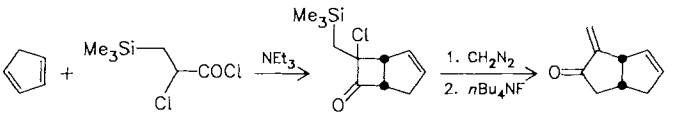

47 75 76, 67% 77, 59%

The racemic aglycon acetate of loganine **82**, a key compound in alkaloid biosynthesis, can be readily prepared by the diazoethane ring enlargement of the cyclobutanone **79**.[66] *Corey* et al.[62] have recently used the same method in their remarkable synthesis of racemic retrigeranic acid.

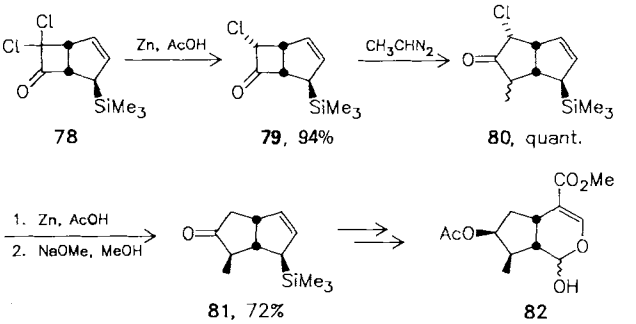

78 79, 94% 80, quant.

81, 72% 82

Fitjer et al.[68] have applied the three-step ring enlargement sequence **83** → **87** (R′ = *p*-$NO_2C_6H_4SO_2$−) in their recent synthesis of [3.3.3]propellanes (32% overall yield). No further preparative applications of this sequence have been reported to date.

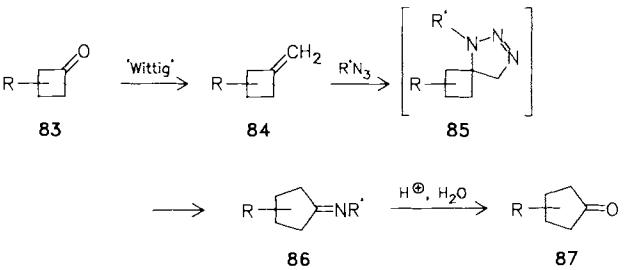

83 84 85

86 87

R′ = *p*-O_2N−C_6H_5−SO_2

Another method for the ring enlargement of cyclobutanones by means of the rearrangement of spiroannelated oxiranes has been developed by *Trost* and *Latimer*.[69] For example, the spirocyclobutanone **89** can be used as the starting material for a synthesis of the gibberellin intermediate **91**.

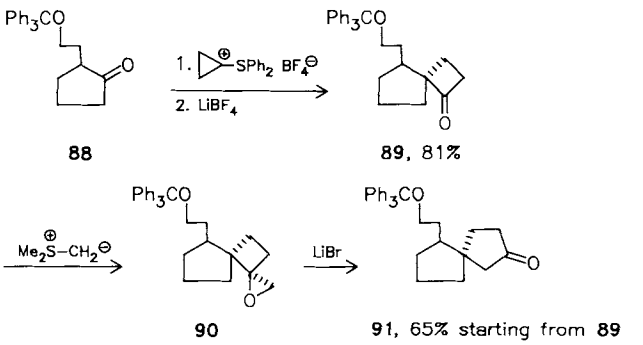

88 89, 81%

90 91, 65% starting from **89**

A similar reaction sequence was used for the synthesis of the sesquiterpene isocomene.[70] A regioselective synthesis of the two cyclopentanones **94** and **96** (carbaprostacyclin precursors) via the spirooxiranes **93** and **95** respectively demonstrate the feasibility of the spiroannelation methodology: both can be synthesized stereoselectively from **92**.[71]

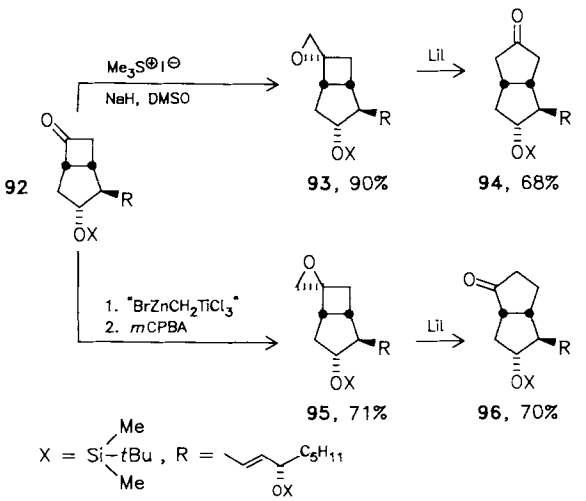

Mechanistically similar ring enlargements of cyclobutanones have been applied in the synthesis of a number of cyclopentanone derivatives using chloride,[72] iodide,[73] ROS–,[70] RSe–,[74] or ROSe–[75] as leaving groups. In addition, the ring enlargement to cyclopentanones is also possible starting from either the readily available cyclobutanone cyanohydrins (e.g. **97**) via a Tiffeneau–Demjanov reaction[76] or starting from cyclobutanols of type **102**.[77] **103** is an intermediate in the synthesis of the cytostatic compound coriolin.

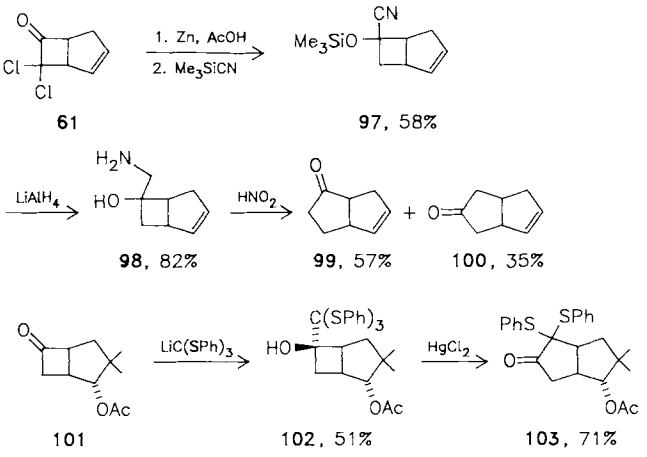

The otherwise unusual carbonylation of a carbon–oxygen double bond functions well with various cyclobutanones: the cobalt-catalyzed insertion of carbon monoxide affords the isolable disilyl ethers of 2-hydroxycyclopentanones in high yields (70–90%). As a specific example **19** affords the pentalene derivative **104**[78] in good yields.

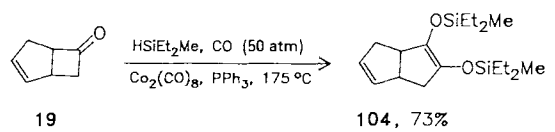

3.4. Cyclopentenones and Cyclohexenones

General methods for the preparation of 2-vinylcyclobutanones have only become available in recent years.[79] This explains why these potentially promising intermediates for the preparation of 5-, 6-, and 8-membered rings have not yet been studied more thoroughly. Thermolysis experiments using the readily available alkylidenecyclobutanones **106** and **107** afforded the first interesting results in this field.[80] The 1,3-rearrangement to **109** occurred at 300 °C via the 2-vinylcyclobutanone **108** as the common intermediate.[81]

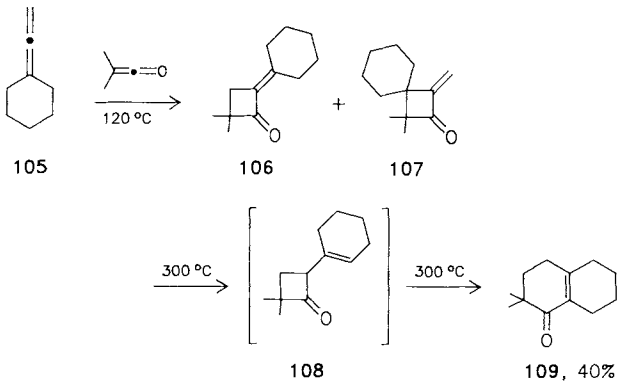

Cohen and *Matz* demonstrated the possibilities of the 1,2- and 1,3-rearrangements under acid conditions.[79d,82] The formation of the cyclohexenone derivative **113** appears to dominate. When however the α-position carries a substituent which can stabilize the carbenium ion, the 1,2-rearrangement to **112** is favored[82] (R'Li = lithium 1-(dimethylamino)naphthalenide).

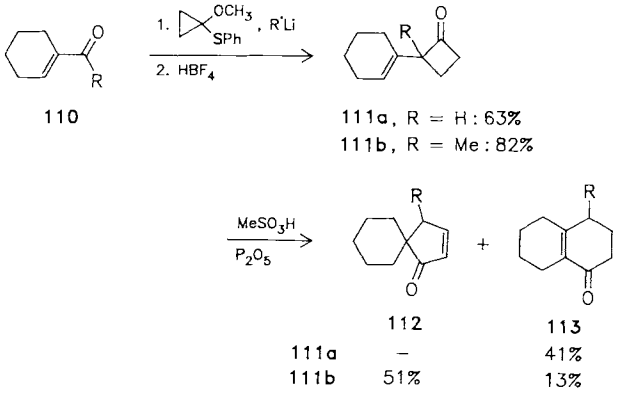

The 1,3-rearrangement can be completely suppressed in the ring enlargement of spirovinyl cyclobutanones.[83] Thus **114** affords solely **115** in a 1,2-rearrangement; a 1,3-rearrangement would in this case violate Bredt's rule.[82]

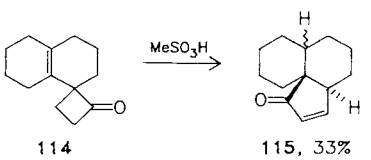

Further studies towards understanding the factors which favor the 1,3-rearrangement were carried out by *Dreiding* et al.[84,85]

The principle found by *Evans* and *Golob*,[86] according to which a correctly positioned alkoxide anion greatly accelerates 3,3-sigmatropic rearrangements, has also been applied to 1,3-rearrangements. While the 1,3-rearrangement of vinylcyclobutanone to cyclohexene requires temperatures of up to 550°,[87] the 1,3-rearrangement of the lithium or potassium salts of 2-vinylcyclobutanols occurs at temperatures as low as 20–70°C. For example, *Danheiser* et al. found that the cyclobutanolate anion of the reduced vinylcyclobutanone **117** rearranges to 4-phenylcyclohex-3-en-1-ol (**118**) merely on warming from −78°C to room temperature.[87]

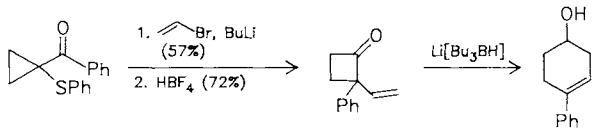

116 117 118, 65%

The potential of this method has also been used in the stereoselective synthesis of the sesquiterpene (−)-β-selinene **122** via the cyclobutanone **120**.[88]

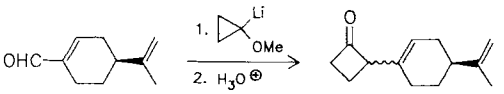

(−)-119 120, 67%

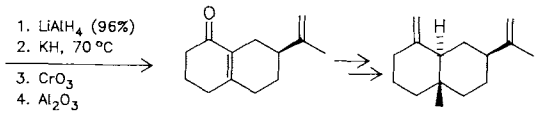

(−)-121, 64% (−)-122

3.5. 1,3-Cyclopentanediones

The disilylated derivative of 2-hydroxycyclobutanone **123**, which can readily be obtained from succinic acid by an acyloin condensation,[89] has a large synthetic potential.[90] Examples in which a cyclobutanone intermediate is involved include the syntheses of cyclopentenones[91] and 1,3-cyclopentadiones.[92] Thus, the condensation of **123** with benzaldehyde affords the cyclobutanone pinacol **124**, which rearranges under acid catalysis to the 2-substituted 1,3-cyclopentanedione **125**.[92b] The release of strain in the four-membered ring is the obvious driving force of this type of rearrangement.

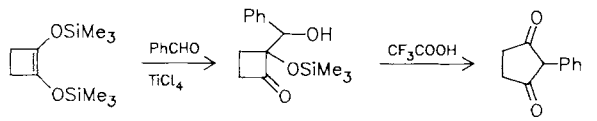

123 124, 78% 125, 97%

Similarly, *Oppolzer* and *Wylie* used **123** (via the cyclobutanone **127**) for the synthesis of the sesquiterpene β-bulnesene **129**.[92c]

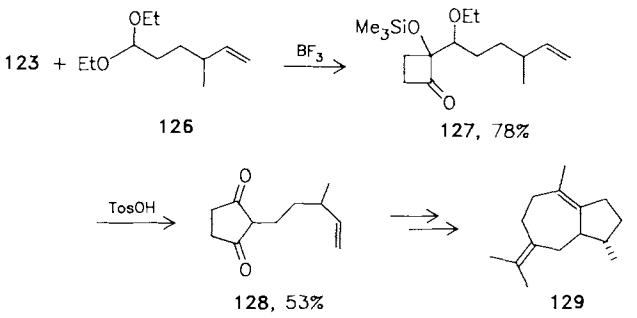

126 127, 78% 128, 53% 129

3.6. Tetralones

Starting from 2-arylcyclobutanones (such as **130**), *Lee-Ruff* et al.[93] found a new approach to tetralone derivatives. However, preparatively useful yields are only obtained when the positive charge which is generated during the reaction at the 3-position of the cyclobutanone can be stabilized by a suitable substituent R. The corresponding tetralone derivative **131** could not be isolated starting from **130**, R = H.

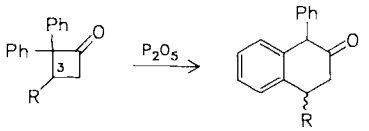

130 131, R = Ph : 85%
131, R = CH=CHCH3 : 85%

This simple method also permits the synthesis of polycyclic dihydrofurans and dihydropyrans, e.g. **133**,[94] as well as steroid-like tetracyclic compounds of type **135**.[95]

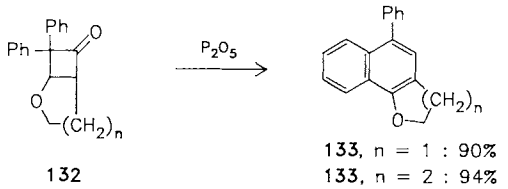

132 133, n = 1 : 90%
133, n = 2 : 94%

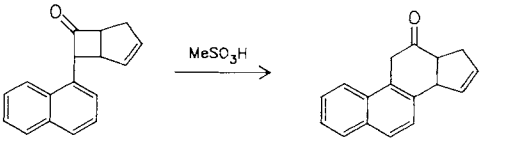

134

3.7. Quinones

Quinones form an important class of compounds which show interesting biological activities.[96] A novel synthetic approach to a wide range of quinone derivatives, starting from cyclobutenediones, was recently reported by *Liebeskind* et al.[97] The key intermediate in his reaction sequence is a maleoylcobalt complex of type **137**:

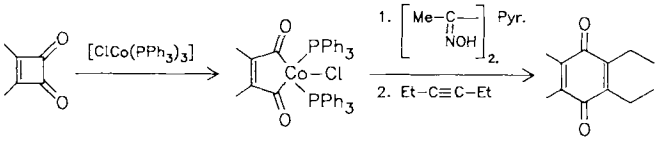

136 137, 90% 138, 65%

Using an intramolecular variant of his own procedure he was able[98] to realize an elegant synthesis of the pyranonaphthoquinone (±)-nanaomycin. Because of their potential antitumor properties, this class of compounds is presently attracting a great deal of attention among research groups engaged in the synthesis of biologically active compounds.

Swenton et al.[99] studied annelation reactions of cyclobutabenzenedione monoketals and found them to be useful for the synthesis of the anthracyclinone (±)-α-citromycinone **141**. The procedure involves reaction of the lithiated *p*-quinone derivative **140** with **139**, which is the equivalent of a 1,4-dipole.

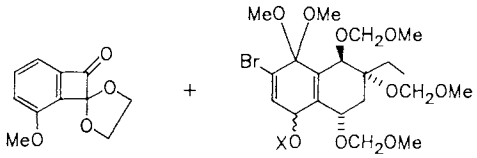

139 **140**, X = $SiMe_2tBu$

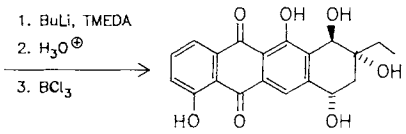

141, 48%

The specific examples mentioned above represent completely new synthetic routes to quinones. Due to the considerably improved accessibility of cyclobutenediones,[97a,100] they may gain broad synthetic acceptance. An additional new synthetic method for highly substituted quinones of type **317** via cyclobutenediones is described in Section 8.

3.8. Bicyclo[2.2.1]heptanones for Prostaglandin Syntheses

It was realized as early as 1960[101] that the tricyclo[3.2.0.$0^{2,7}$]heptan-6-one **143**, which can be generated in situ from dibromobicyclo[3.2.0]heptanone **142** (and was later isolated[102]) constitutes a valuable intermediate for the synthesis of bicyclo[2.2.1]heptan-2-ones of the type **144**.

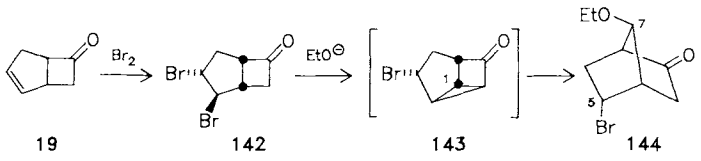

19 **142** **143** **144**

While the above reaction sequence is limited to a substitution of C-1 in **143** by the same nucleophile which is used for its in situ generation, *Roberts* et al.[103] were able to show clearly that the homoconjugated addition to isolated tricyclo[3.2.0.$0^{2,7}$]heptane-6-ones of the type **143** can be carried out with various nucleophiles (halogenide ions, cyanide ions, cuprates, alcoholates). 5-*endo*-7-*anti*-disubstituted bicyclo[2.2.1]heptan-2-ones of the type **144** are formed stereospecifically in all cases. This skeletal rearrangement has been found to be very useful in prostaglandin synthesis: thus the Glaxo synthesis of PGD_2 **148**,[43,104] which starts from the optically active cyclobutanol **54** obtained by a yeast reduction (see Section 7), uses this concept. The 13-azaprostacyclin synthesis of *Collington* et al.[105] represents a further application.

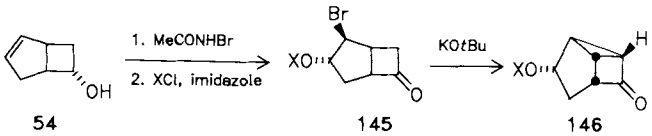

54 **145** **146**

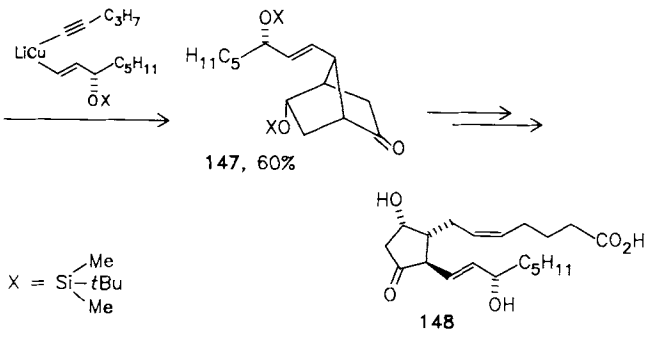

147, 60%

148

Other interesting ring enlargement reactions of cyclobutanones, which begin with the addition of an alkyl- or alkenylmetal compound to the carbonyl group, are described in Section 8 (**292**→**294**, **316**→**317**, **318**) and in Section 10 (**372**→**374**, **377**→**381**, **383**→**384**).

4. The Favorskii Rearrangement

Because of the numerous studies of its mechanism and stereochemistry,[4a-d,107] the rearrangement described by *Favorskii* in 1894[106] has become a reliable tool for the synthetic organic chemist. We know today that the Favorskii rearrangement of α-haloketones to carboxylic acids and their derivatives can proceed by two different mechanisms.

The cyclopropanone mechanism, which was established by *Loftfield* in 1951,[108] is observed for α-haloketones which carry a hydrogen in the α′-position. *Loftfield*'s remarkable experiments with ^{14}C-labeled 2-chlorocyclohexanone show clearly that a symmetrical cyclopropanone intermediate is formed.

α-Haloketones bearing no hydrogen atoms in the α′-position have been suggested to react via a semibenzilic acid mechanism.[109] In experiments with 2-bromocyclobutanone **149**, *Conia* and *Salaun*[110] demonstrated that this

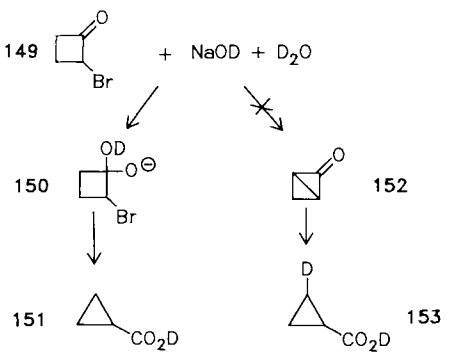

149 **150** **151** **152** **153**

mechanism is also valid for the Favorskii rearrangement of cyclobutanones. The bicyclo[1.1.0]butanone **152** which would be an intermediate in the Loftfield mechanism[108] is apparently avoided because of its very high strain energy content.

Ring opening, *cine*-substitution (see Section 5) and in the case of the [3.2.0]-bicyclic cyclobutanones the formation of tropolones (see Section 5) are all observed as competing reactions in Favorskii rearrangements of α-halocyclobutanones. The ring opening prevails when the α-position of the cyclobutanone is adequately substituted by anion-stabilizing groups, e.g. in **154**[111] and in **156**.[112]

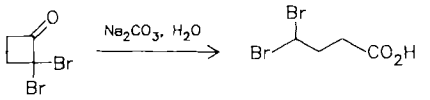

154 **155**, 43%

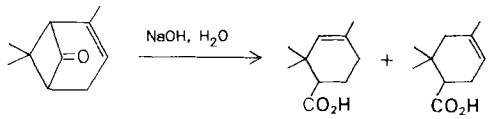

156 **157** 57% **158**
86 : 14

The cyclobutanones **159**[113] and **161**[114] demonstrate very clearly the competitive situation between ring-opening and ring contraction reactions. Since in **159** the negative charge can only be stabilized at C-2, which carries a bromine substituent, an exclusive ring opening to **160** is observed. In contrast, the negative charge generated in the reaction of **161** with an alkoxide anion is apparently better stabilized at the benzylic C-4; thus ring contraction to **163** and **164** occurs preferably.

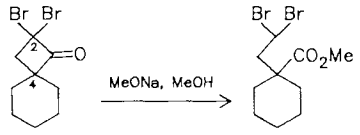

159 **160**, 97%

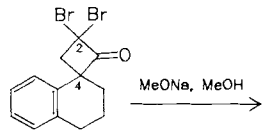

161

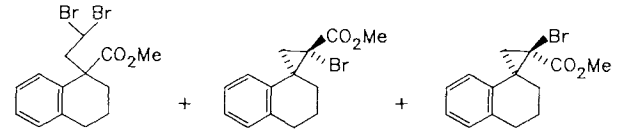

162, 12% **163**, 70% **164**, 18%

A necessary condition for the Favorskii rearrangement in bicyclic systems appears to be the pseudoequatorial position of the α-halogen atom. This was convincingly proven in the case of the two diastereomeric α-chlorocyclobutanones **165** and **167**.[115]

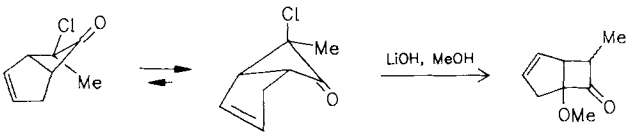

165-ae **165-ax** **166**, quant.

The steric interaction in **165** between the *endo*-methyl group and the five-membered ring forces the chlorine atom into a pseudoaxial position. On treatment with LiOH/MeOH, quantitative reaction to the isomer mixture **166** is observed even at room temperature. The mechanism of this *cine*-substitution is discussed in Section 5. When however a pseudoequatorial position for the chlorine atom is thermodynamically more favored (compare **167**), stereospecific ring contraction to the cyclopropanecarboxylic acid **168** occurs under the same reaction conditions. Many other illustrative examples have been described.[116]

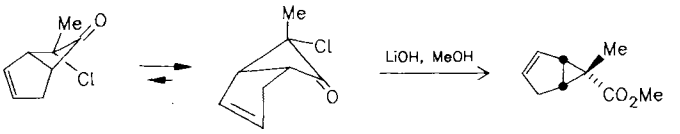

167-ax **167-ae** **168**, 83%

The influence of the leaving group (X = mesyloxy, 4-bromo- or 4-methyl-phenylsulfonyloxy, chloride, bromide; see Table 1), solvent (H_2O, dioxane, toluene, ethanol) and reaction temperature (−10 to +70 °C) on the stereochemical outcome of the Favorskii rearrangement of cyclobutanone **169** has been systematically studied.[117]

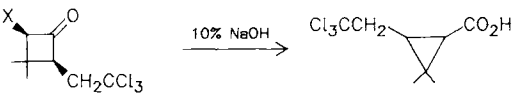

169a-g **170**, 90–95%

Table 1. Influence of the leaving group X on the stereochemical course of the Favorskii ring contraction of **169**.

169	**170**, *cis* : *trans*
a, X = 4-$BrC_6H_4SO_3$	10 : 0
b, X = 4-$MeC_6H_4SO_3$; **c**, X = Br; **d**, X = $MeSO_3$	9 : 1
e, X = Cl	8 : 2
f, X = $MeCO_2$; **g**, X = F	

As far as the nature of the nucleophiles involved is concerned, the potassium enolate **171**[118] and the cyanohydrin anion of **173**[119] are worthy of mention.

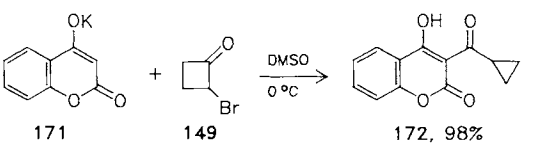

171 **149** **172**, 98%

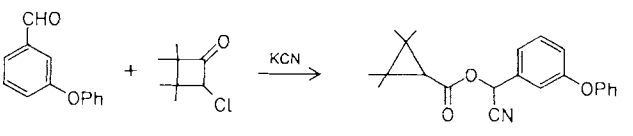

173 **174** **175**, 88%

In addition to the classical Favorskii rearrangement, some of its variations should also be mentioned. Thus the ring contractions of α-halocyclobutanols induced by dehydrohalogenation[120] (e.g. of type **177**[121]) provide a direct access to cyclopropanecarbaldehydes; the cyclobutanols are readily formed from α-halocyclobutanones by reduction with $NaBH_4$.

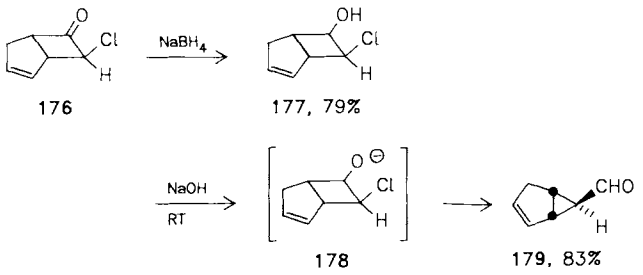

176 **177**, 79% **178** **179**, 83%

Cyclobutane-1,2-diones permit the synthesis of α-hydroxycyclopropanecarboxylic acids;[121] e.g. **182** from **181**:

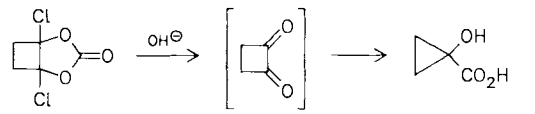

180 **181** **182**, quant.

The silver-ion-assisted ring contraction of α-chlorocyclobutanone **183**[123] was used in the synthesis of the dimethylsesquicarene **185**.[123a]

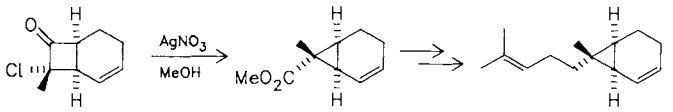

183 **184**, 68% **185**

The photochemical variant of the Favorskii reaction of α-halocyclobutanones, i.e. the photolytic ring contraction to cyclopropanecarboxylic acid derivatives, is also known.[124] A characteristic example, the ring contraction of **169**,[125] is shown in Section 9.

The industrial interest in the Favorskii reaction concentrates on the synthesis of the acid part of chrysanthemates and pyrethroids which show high insecticidal activity. Thus *Van den Brink* et al.[126] have developed an extremely simple synthesis for the racemic chrysanthemic acid **189** via the isomeric cyclobutanones **187** and **188**.

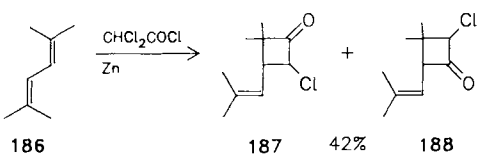

186 **187** 42% **188**

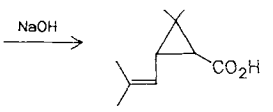

189, 88%

An analogous synthesis[127] starts with the cycloaddition of dichloroketene (generated from trichloroacetyl chloride) to 2,5-dimethyl-2,4-hexadiene **186**. The regioisomeric dichlorocyclobutanone derivatives so obtained are selectively reduced to a 3 : 1 mixture of **187** and **188**.

The dihalovinyl-substituted cyclopropanecarboxylates count among the most active pyrethroids.[128] A very simple entry to them has been developed in the Ciba-Geigy laboratories. Polyhalogenated butyryl chlorides (e.g. **190**) are prepared via Cu(I)-catalyzed addition reactions. These can then be transformed by bases or zinc into haloketenes, which in turn undergo a [2 + 2]-cycloaddition with terminal olefins to give α-halogenocyclobutanones (e.g. **191**). *Cine*-rearrangement (see Section 5) to stereochemically uniform 2,4-*cis*-isomers (e.g. **169e**), followed by Favorskii rearrangement, gives cyclopropanecarboxylic acids containing the required high content of the biologically more active *cis*-isomer. Dichlorovinyl- (**192**),[7d, 124c, 125, 129] dibromovinyl-,[130] and chloroalkylvinyl- or fluoroalkylvinyl-substituted[131] cyclopropanecarboxylic acids have become readily available using such a sequence.

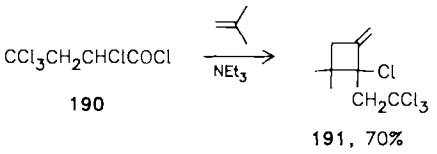

190 **191**, 70%

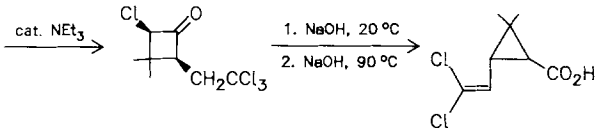

169e, 96% **192**, 89%
cis : *trans* > 4 : 1

A Favorskii rearrangement of the cyclobutanone **196**, which may readily be prepared starting from the chloroenamine **193**, also gives **192**.[132] However, in this case the main product is the undesired *trans*-isomer, since in contrast to **169e** the cyclobutanone **196** is formed in a sterically non-uniform manner. Spiroalkyl-,[131, 133] phenyl-,[134] and phenoxy-substituted[135] cyclopropanecarboxylic acids are also readily prepared from the corresponding cyclobutanones via Favorskii rearrangement.

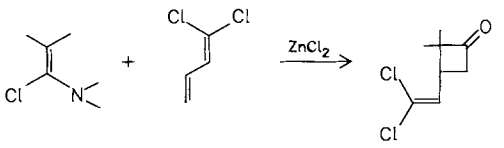

193 **194** **195**, 85%

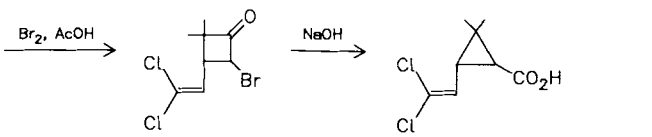

196

192, 65% starting from **195**;
cis : *trans* = 18 : 82

The esters of the two possible enantiomer pairs of the *cis*- and *trans*-cyclopropanecarboxylic acids **189** and **192**

do not show the same biological activity. In order to keep the amount of active substance employed as small as possible, it is worthwhile using only the biologically most active isomers for the ester formation, namely (+)-*trans*-chrysanthemic acid ((+)-*trans*-**189**) and (1*R*,3*R*)-*cis*-3-(2,2-dichlorovinyl)-2,2-dimethylcyclopropanecarboxylic acid ((+)-*cis*-**192**), respectively.

Enantiomerically pure (+)-*trans*-chrysanthemic acid ((+)-*trans*-**189**) has been synthesized starting from the optically active cyclobutanone **197** (see Section 7) via the unstable bromocyclobutanone **198** and subsequent ring contraction.[136] Since the ring contraction occurs stereospecifically (as expected for the semibenzilic acid mechanism[111]) and only the (+)-*trans*-isomer **189** can be isolated, one has to assume that the bromination to **198** also occurs stereospecifically in a *trans* manner.

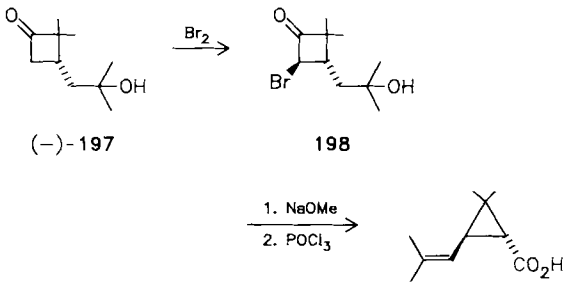

(−)-**197** **198** (+)-*trans*-**189**, 23% starting from (−)-**197**

Enantiomerically pure (+)-*cis*-**192** can be obtained by a Favorskii rearrangement of the optically active cyclobutanone (+)-*cis*-**169e** (Section 7) followed by HCl-elimination.[137]

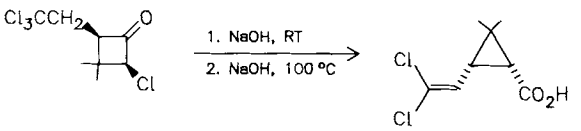

(+)-*cis*-**169e** (+)-*cis*-**192**, 72%

5. *cine*-Substitution, *cine*-Rearrangement

The term *cine*-substitution is used to describe nucleophilic substitution reactions of 2-halogenocyclobutanones of type **199** in which the new substituent enters at the 4-position (**201**). Two possible mechanisms are envisaged: either an enolate/bicyclobutanone mechanism involving intermediates like **200** or an enol/ion pair mechanism via such intermediates as **202**, **203**, and **204**.[7d]

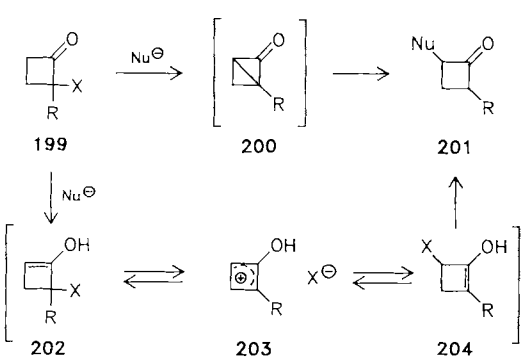

The best-known application of the *cine*-substitution reaction is the synthesis of tropolones, which are of considerable interest because of their antibacterial and fungicidal activity. A principal synthetic approach was described as early as 1965 by *Stevens*,[138] as exemplified by the preparation of the tropolone **206** starting from the dichlorocyclobutanone derivative **61**.

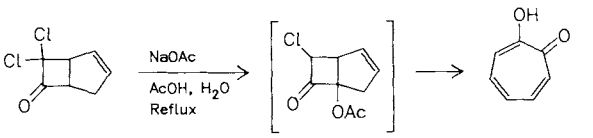

61 **205** **206**, 52%

Bartlett and *Ando*[139] demonstrated by ^{14}C-labeling that the first step is a *cine*-substitution of **61** by acetate anion, which leads to the intermediate **205**. The Stevens tropolone synthesis was later used in the synthesis of α-dolabrine and β- and γ-thujaplicine.[140,141] The use of this type of reaction prior to 1981 has been documented in detail in review articles;[4a-d,i] it has recently been applied to the formation of annelated tropolones.[142]

The *cine*-substitution reaction has also been used as a key step in the syntheses of 3-alkoxy- and 3-aryloxy-2,2-dimethylcyclopropanecarboxylic acids **209** from the simple cyclobutanone **207** (the [2+2]-cycloadduct of dichloroketene and isobutylene).[133b] Several esters of **209** exhibit a strong insecticidal activity.[135]

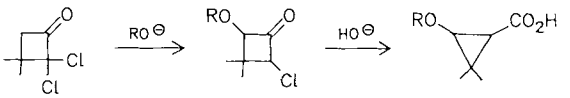

207 **208** **209**

In the presence of a nucleophile, cyclobutanone **191** also undergoes a *cine*-substitution reaction, e.g. to **210**. If the reaction is carried out in the presence of catalytic amounts of a tertiary amine (e.g. Et_3N in toluene under reflux, 68% yield) or a tetraalkylammonium chloride (e.g. nBu_4NCl in the melt, 81% yield), but in absence of an external nucleophile, the *cine*-rearrangement product **169e** can be isolated.[7d]

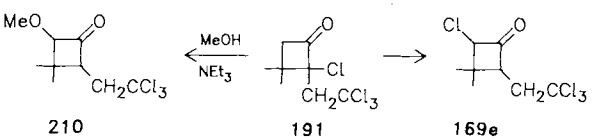

210 **191** **169e**

The experimental results show that the outcome of the *cine*-rearrangement depends on the electronic as well as the steric character of the second α-substituent. The product distribution, which is obtained independent of whether the cyclobutanones **211** or **213** are subjected to a triethylamine-catalyzed *cine*-rearrangement[72,125] indicates a tran-

sition state with a considerable degree of ionic character, e.g., an ion pair of type **212** (Table 2).

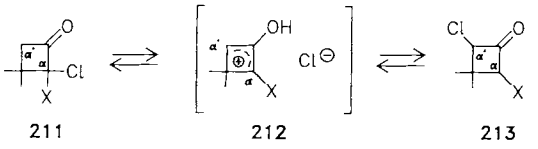

211 **212** **213**

Table 2. Influence of the second α-substituents X on the product pattern in the *cine*-rearrangement of **211** or **213** in presence of triethylamine. **211a ≡ 191**; **213a ≡ 169e**.

	X	211	:	213
a	CH_2CCl_3	0	:	100
b	Cl	0	:	100
c	Me	57	:	43
d	$(CH_2)_2CHMe_2$	15	:	85

The electron-withdrawing groups, such as Cl or CH_2CCl_3, clearly destabilize the positive charge in the α-position of the allyl cation, thus directing the chloride ion completely towards the electronically *and* sterically favored α'-position. α-Alkyl groups, which are able to stabilize the positive charge on the α-carbon, however allow the chloride ion to reenter partially also in the sterically less favored α-position. In terms of stereoselectivity a thermodynamic control of product formation is observed: due to the puckered cyclobutanone ring, the main products of the *cine*-rearrangement, for example cyclobutanones **169** (**213a ≡ 169e**),[7d] exist in the thermodynamically more favorable *cis*-configuration, in which the substituents in α- and α'-position are mutually pseudoequatorial.

Because of the fact that Favorskii ring contractions of α-halocyclobutanones occur with a high stereoselectivity, the *cine*-rearrangement of cyclobutanones of type **191** proved to be an excellent entry to insecticidal *cis*-cyclopropanecarboxylates.[143] An example is the stereoselective synthesis of the *cis*-dichlorovinylcyclopropanecarboxylic acid **192** starting from **191** and proceeding via the *cine*-rearrangement product **169e**[125] (as discussed in Section 4).

6. Ring Opening Reactions of Cyclobutanones and Cyclobutenones

6.1. Monofunctionalization of Double Bonds

Although this synthetic principle has seldom been used so far, it can offer advantages in special cases in which an unambiguous regio- or stereocontrol is required. Thus, *Ficini* et al.[144,145] used the β-monofunctionalization of the α,β-unsaturated ketone **214** via an intermediate cyclobutanone **217** for the first stereospecific synthesis of (±)-juvabione **219**, a sesquiterpene with juvenile hormone activity. The cyclobutanone ring could be annelated to **214** via a [2+2]-cycloaddition of the ynamine **215** to the double bond of **214**. For n=1, the β-diketone **217** could be isolated. With n=2, however, **217** was cleaved directly to give the required diastereomerically pure oxo acid **218**.[145]

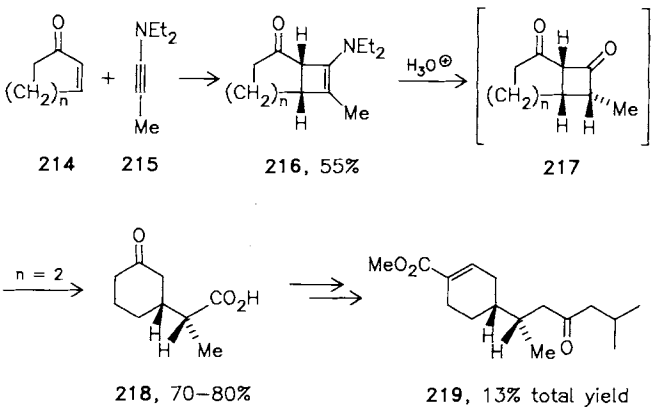

214 **215** **216, 55%** **217**

218, 70–80% **219, 13% total yield**

Other examples of β-monofunctionalization of α,β-unsaturated compounds according to this principle were described later.[146]

The introduction of a 2-cyanomethyl group into the indole **220** via the cyclobutanone oxime **221** under the conditions of a Beckmann rearrangement is also worthy of mention.[147]

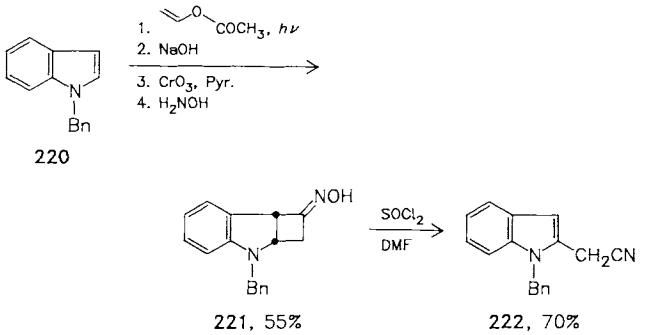

220

221, 55% **222, 70%**

6.2. Vicinal Difunctionalization of Double Bonds

Cyclobutanones are useful intermediates in the conversion of an olefin into the corresponding vicinally disubstituted saturated compound ('vicinal functionalization'). The first step generally involves the addition of a ketene to the double bond which is to be functionalized. Cleavage of the cyclobutanone thus formed by nucleophiles yields regio- and stereoselectively vicinally disubstituted products. Smooth cleavage can be expected if the cyclobutanone ring bears anion-stabilizing substituents in the α-position. Accordingly, it was possible to convert the dichlorocyclobutanone **223** into the cyclopentane derivatives **224** or **225** by correct choice of the reaction conditions.[148]

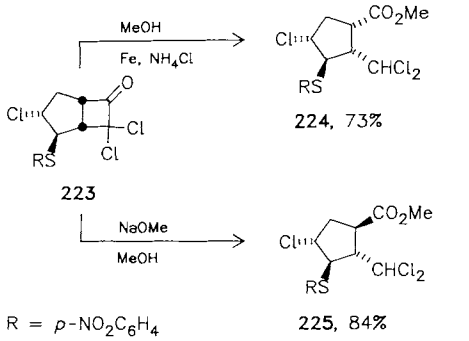

223

224, 73%

R = *p*-$NO_2C_6H_4$ **225, 84%**

Apart from α,α-dichloro-[148, 149] and α,α-dibromosubstituents,[149c, 150] the ring cleavage of cyclobutanones is also favored by other α-substituents with −I and −M effect. Thus a clean cleavage to the vicinally disubstituted product occurred if thioketal,[151] sulfoxide,[151b] ester[152] or aryl substituents[153] were present in the α-position.

The decisive role of the anion-stabilizing substituent was clearly demonstrated by *Ghosez* et al. for the cyclobutanone derivatives **226** and **227**.[151b] Whereas ring opening of **226** takes place only when KOH/*t*BuOK is used, the better stabilization of the carbanion formed during the reaction permits the cyclobutanone ring in **227** to be opened even with 0.5% NaOH.

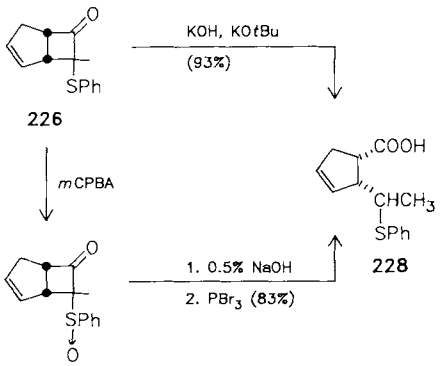

The cleavage of the cyclobutanone ring to give vicinally disubstituted products can also be carried out by C-nucleophiles. Thus the cyclopentene derivative **230** can be prepared from **229** using the dianion of the half-ester of pimelic acid.[151b]

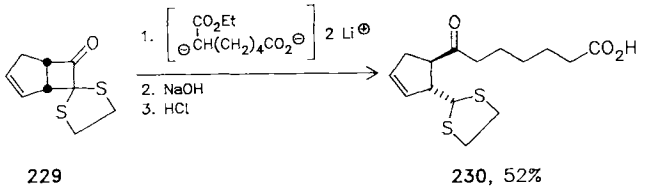

If however the anion-stabilization is not sufficient, the reaction with C-nucleophiles (MeMgI, *n*BuLi) only yields 1,2-addition products. Thus reaction of **226** with methylmagnesium iodide leads exclusively to the tertiary alcohol **231**.[151b] Further examples of such 1,2-additions which do not afford ring-opened products are described in Section 10.

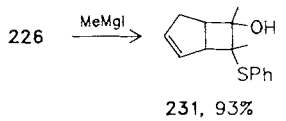

This method of stereoselective vicinal substitution was used for the synthesis of multifidene, a component of the Mediterranean brown alga *Culteria multifida*.[149c, 150a] Starting from the cyclobutanone **232** (one of the two regioisomeric products of cycloaddition of dichloroketene to dicyclopentadiene), the ring cleavage with NaOMe at −20 °C gave only the *cis* ring-opened product **233**. Wittig-olefination (to **234**) followed by pyrolytic elimination of cyclopentadiene (which served in this case as a double-bond protecting group) yielded multifidene (**235**). A more recent but less stereoselective synthesis of multifidene uses the same synthetic methodology, i.e. the vicinal functionalization via a cyclobutanone.[154]

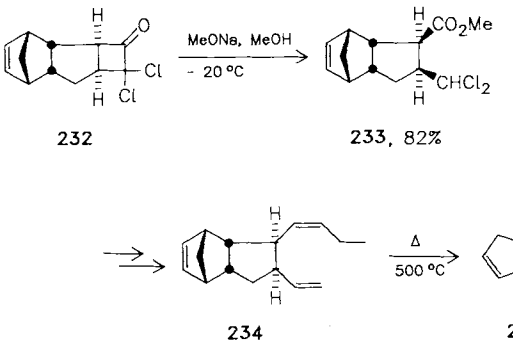

Fragmentation reactions offer a further interesting possibility for vicinal functionalization of double bonds. In a typical example, sulfoxide **28** is smoothly converted into ester **236** by a fragmentation in which a double bond is simultaneously formed.[45]

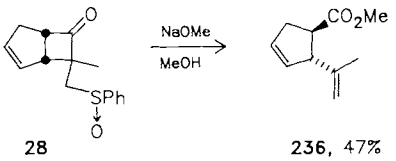

The fragmentation to the acetylene compound **239** is the key step in the synthesis of the macrocyclic lactone hybridalactone (**240**) isolated from the sea alga *Laurencia hybrida*.[155] The reaction of the condensation product **237** with the cyclopropyl nucleophile leads initially to the 1,2-addition product **238**. The cyclobutane ring-opening to the acetylene derivative **239** is carried out with nBu$_4$NF.

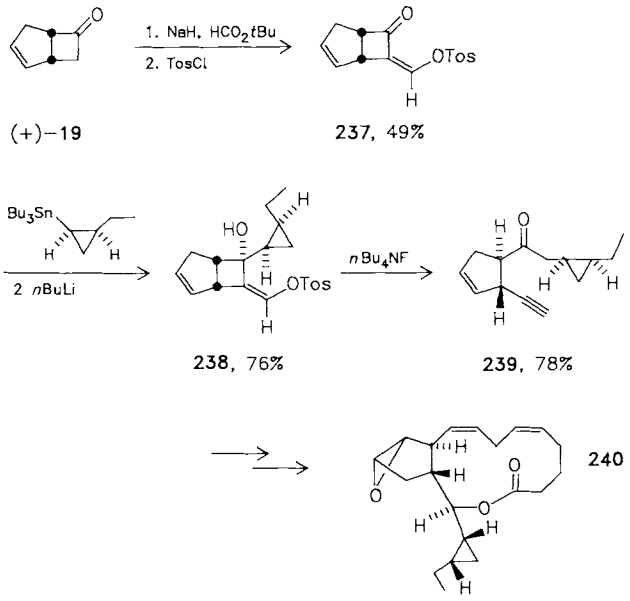

Greene et al.[156] recently reported a stereoselective transformation of olefins into vicinal dicarboxylic acids of type

243. The olefins were first converted into cyclobutanones of the type **241** by means of a [2+2]-cycloaddition with dichloroketene. Conversion into the α-chloroenol acetate **242**, followed by oxidative cleavage of the double bond, afforded the dicarboxylic acid **243** in good yield. This simple methodology was used by the same authors[157] in a short total synthesis of the sesquiterpene bakkenolide A.

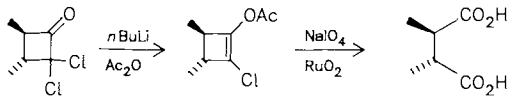

241 242, quant. 243, 76%

A novel variant of vicinal difunctionalization was demonstrated by *Fráter* et al.:[158] the oxime **245** was stereoselectively converted into the bifunctionalized C_5-unit **246** (a macrolide intermediate) under the conditions of the Beckmann rearrangement.

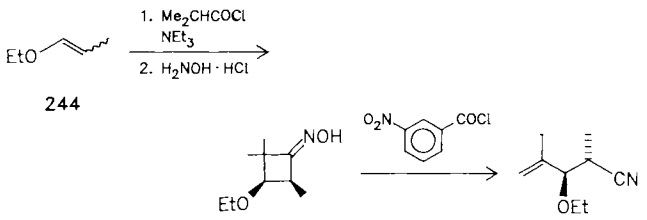

244

245, 74% 246, 61%

Moreover, the γ-lactones, which are readily available via oxidation of cyclobutanones (Section 3.1) or the γ-lactols formed by the reduction of such γ-lactones are de facto cyclic products of a vicinal difunctionalization of double bonds via cyclobutanones.[33a, 66b, 159]

6.3. Special Ring Opening Reactions

Examples of various thermal and photochemical ring opening reactions of cyclobutanones are discussed in Sections 8 and 9. Here we shall only mention two examples which hold promise of becoming preparatively useful reactions because of the simple experimental conditions.

The electrophilic trimethylsilyl iodide can bring about a regioselective ring-opening of the cyclobutanone **247** to the β-iodoketone **248** in the presence of ZnI_2 as a catalyst.[160]

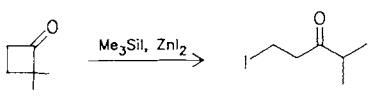

247 248, 83%

It is possible to transform the cyclobutanone **249** in two simple steps (1,2-addition followed by an oxidative ring cleavage of the resulting 1,2-diol) into the γ-oxoaldehyde **250**, which serves as a precursor of dihydrojasmone.[161]

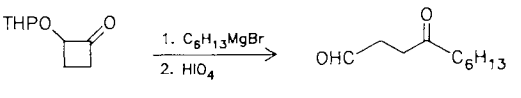

249 250, 45%

7. Optically Active Cyclobutanones: Formation and Applications

Cyclobutanones have proven to be useful starting materials for the synthesis of racemic prostaglandins and pyrethroids. Because of their interesting biological properties, the synthesis of optically active examples appeared worthy of consideration. In order to be able to apply the well established synthetic strategies in the subsequent steps it was first necessary to find methods for the preparation of optically active cyclobutanones.

Three possibilities will be discussed below: the separation of racemates, syntheses of optically active cyclobutanones starting from chiral building blocks, and asymmetric syntheses using chiral auxiliaries. Naturally-occurring cyclobutanones and cyclobutenones are discussed in Section 2.

7.1. Optically Active Cyclobutanones via Separation of Racemates

When a racemic cyclobutanone is allowed to react with an optically active reagent, a new chiral center is generated at the prochiral carbonyl carbon. In principle, four diastereomers can be formed; this appears unattractive for an efficient racemate separation. If however the cyclobutanone to be separated reacts with an optically active reagent under reversible reaction conditions, only the two thermodynamically more stable diastereomeric cyclobutanes are generally formed; this can be explained by the known[162] preference of the two sterically most demanding substituents to occupy 1,3-pseudoequatorial positions in the puckered cyclobutane ring. The separation of diastereomers by recrystallization or chromatography, followed by regeneration of the cyclobutanones, permits the initial racemate to be separated. This method was used successfully by *Kelly* et al.,[163] who converted the racemic cyclobutanone (±)-**251** with either (+)- or (−)-ephedrine into the corresponding oxazolidines. As expected from the consideration of molecular models, steric hindrance led to formation of only two of the possible four diastereomers **252**. Diastereomer separation by recrystallization from methanol, acid hydrolysis and Baeyer-Villiger oxidation afforded the γ-butyrolactone (+)-**253**, which in turn was converted into **254**, prostaglandin $PGF_{2\alpha}$.

The cyclobutanone (+)-*cis*-**169e**, which is a starting material in the synthesis of (1*R*,3*R*)-*cis*-3-(2,2-dichlorovinyl)-2,2-dimethylcyclopropanecarboxylic acid **192** (see Section 4), was also obtained by separation of the racemate.[137] (±)-*cis*-**169e** was first converted into the bisulfite adducts **255** and **256**. With chiral amines (e.g. (*S*)-1-phenylethylamine) only two of the four possible diastereomeric salts were formed. **255** and **256** could be readily separated by fractional crystallization. The optically active cyclobutanone (+)-*cis*-**169e** (2*S*,4*R*) could be obtained either by an acidic (6 N HCl, 60 °C) or a weakly basic ($NaHCO_3$, H_2O) hydrolysis. The enantiomer (−)-*cis*-**169e** (2*R*,4*S*) which cannot be used for the synthesis of the biologically interesting (1*R*,3*R*)-cyclopropanecarboxylic acid **192** racemizes readily with Bu_4NCl and can be utilized again in the sepa-

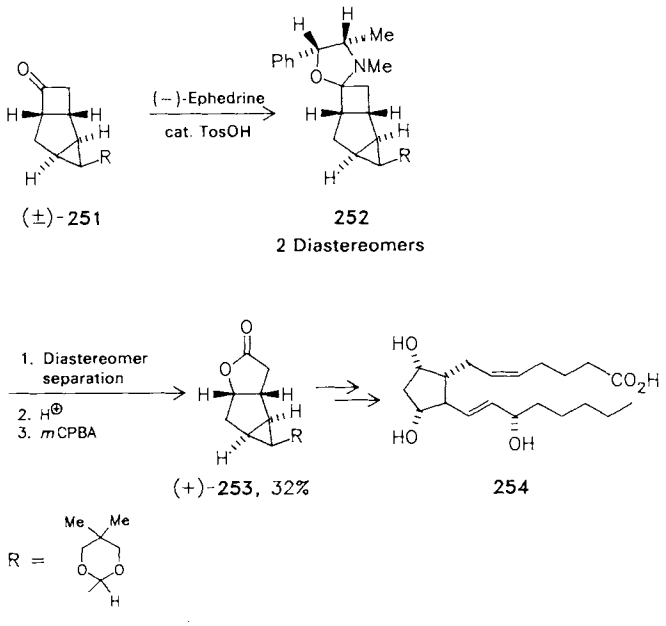

ration steps. Thus the whole procedure represents a chirally economic synthesis.

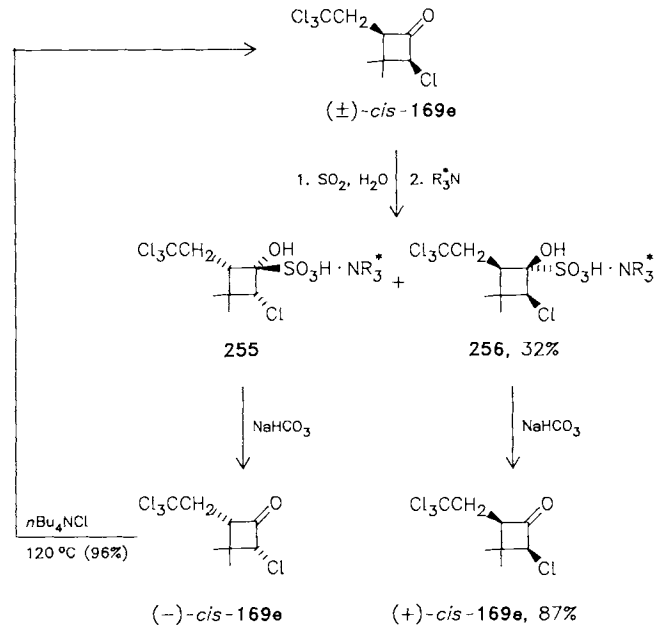

The same principle for obtaining optically active cyclobutanones was applied in the synthesis of prostaglandins E_2 and $F_{2\alpha}$ for the separation of racemic bicyclo[3.2.0]hept-2-en-6-one (±)-(**19**).[164] For the same cyclobutanone, another possibility for racemate separation was demonstrated:[165] because of the preferred *exo*-attack, the reaction of (±)-**19** with an optically active sulfoximine gave only two chromatographically separable α-hydroxysulfoximines (**257** and **258**). Regeneration of the cyclobutanones was carried out by the thermolysis of these adducts at temperatures up to 120 °C. The unusually facile cleavage of a C–C bond in both adducts is no doubt due to the stability of the ylide leaving group.

The enzyme-catalyzed reduction of prochiral cyclobutanones offers an attractive method for the separation of enantiomers. Thus it was possible[159a, 166] to reduce the racemic cyclobutanone (±)-**19** in good optical yield (84 and

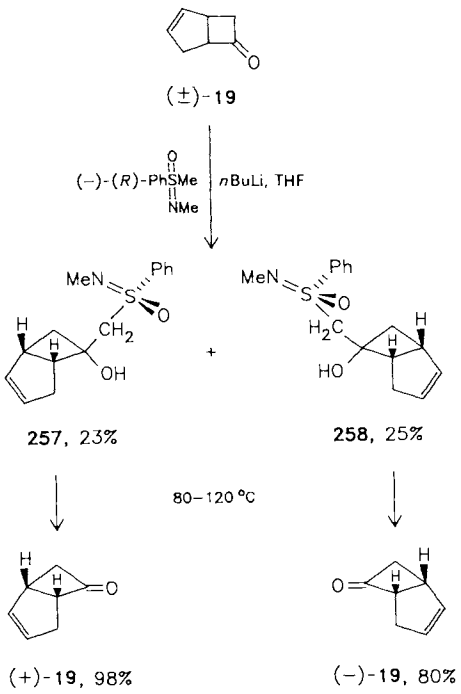

88% *ee* respectively) to the diastereomeric bicycloheptanols (+)-**54** and (−)-**259** using bakers' yeast. Both reduction products have *S*-configuration at the carbon bearing the OH-substituent; they are therefore diastereomers and can be separated by chromatographic methods.

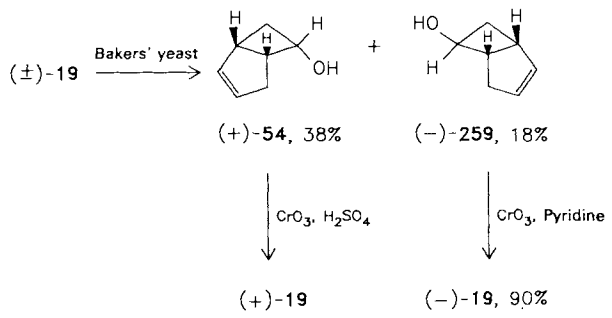

Oxidation of the cyclobutanols (+)-**54** and (−)-**259** affords the enantiomeric cyclobutanones (+)-**19** and (−)-**19**, respectively. Both were used as starting materials in a synthesis of prostaglandin A_2.[167] The advantages of enzymatic separation are (a) the low cost of the chiral catalyst (the enzyme); (b) predictability of the stereochemical outcome of the reaction, since dehydrogenases generally furnish *S*-configurated secondary alcohols;[168] and (c) good separability of the diastereomers. The disadvantage of the low substrate-enantioselectivity was overcome by a broad screening of yeast and other fungus families. Thus starting from racemic (±)-**19**, only (+)-**19** is enantioselectively reduced to the alcohol (+)-**54** by, for example, *Curvularia falcata* or *Martierella ramanniana*. (−)-**19** is recovered unchanged.[166b] Very recently, the enantioselective enzymatic reduction of the 7,7-dimethyl derivative of **19** was reported.[169]

The only method which, in contrast to those described above, allows complete conversion of a racemic cyclobuta-

none into the desired enantiomer was described recently by *Greene* et al.[61] It is based on a conversion of the racemic α,α'-dichlorocyclobutanone (±)-**260** into the prochiral cyclobutene **261**; this in turn is transformed enantioselectively into a cyclobutanol via hydroboration with (+)-diisopinocamphenylborane, followed by Collins oxidation to the cyclobutanone (−)-**65**.

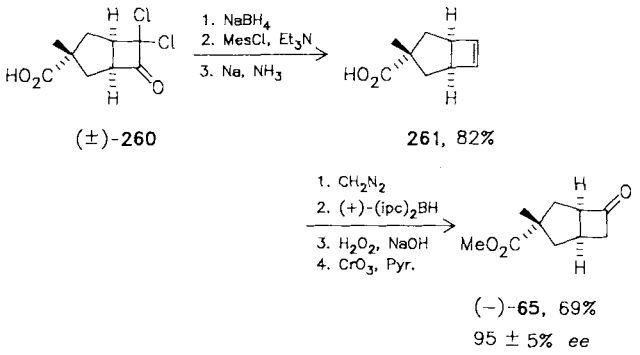

(±)-**260** → **261**, 82%

(−)-**65**, 69%
95 ± 5% *ee*

Since both (+)- and (−)-enantiomerically pure hydroboration reagents are now available,[170] this reaction sequence could develop into a widely applicable synthesis of optically active cyclobutanones.

7.2. Optically Active Cyclobutanones from Chiral Building Blocks

Only few syntheses of this type are mentioned in the literature. (+)-α-Pinene **262** was used as the starting material for the synthesis of the optically active cyclobutanone (−)-**197**;[136] this in turn was converted into (+)-*trans*-chrysanthemic acid **189** by ring contraction (see Section 4).

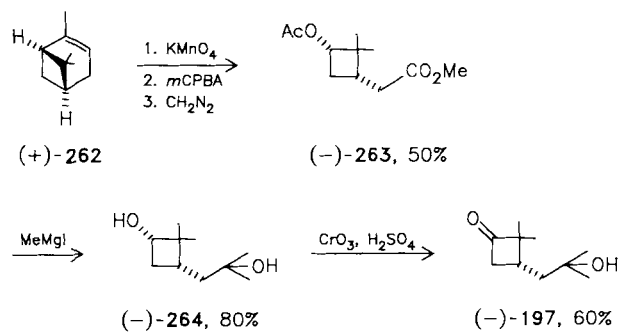

(+)-**262** → (−)-**263**, 50%

(−)-**264**, 80% → (−)-**197**, 60%

Fráter et al. have used the following procedure to obtain the optically active cyclobutanone (−)-**266**.[171] First, the ketone (+)-**265** was prepared from (*S*)-3-hydroxybutyric acid using classical methods. In the next step a base-catalyzed cyclization afforded a 3:4 mixture of the optically active cyclobutanone (−)-**266** and the oxetane (+)-**267**.

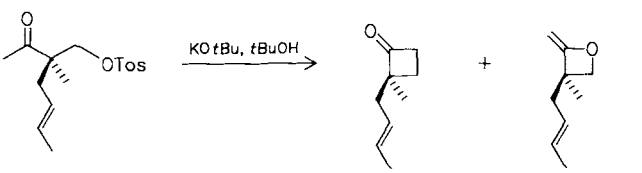

(+)-**265** → (−)-**266**, 34% + (+)-**267**, 43%

7.3. Asymmetric Synthesis of Cyclobutanones using Chiral Auxiliaries

The typical feature of this type of synthesis is the use of a chiral starting material consisting of two parts which are linked by a labile bond. While the first (achiral) part is used for the construction of the cyclobutanone ring, the second (chiral) part induces the required optical activity. After the necessary synthetic steps have been performed, the chiral auxiliary part (terpene, amino acid, phosphane ligand) is removed and recovered.

In analogy to the cycloalkylation of tosylmethyl isocyanide with 1,3-dibromobutane,[2m] (+)-(neomenthylsulfonyl)methyl isocyanide ((+)-**268**) can be used to synthesize a 1:1 mixture of the two masked cyclobutanones **269** and **270**.[172] However, the hydrolysis of the enantiomerically pure **269** is accompanied by considerable racemization, especially on prolonged reaction: at 44% conversion of **269** into **1** the enantiomeric excess is 87%, while at 62% conversion it is only 43%.

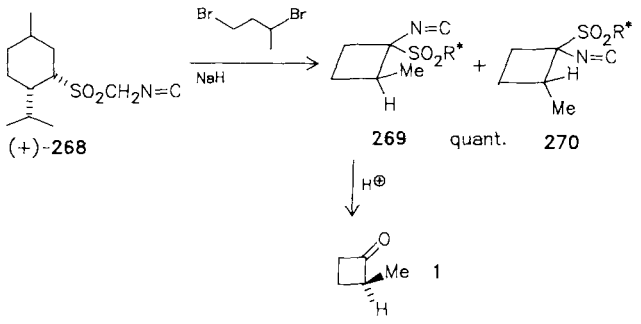

(+)-**268** → **269** quant. + **270** → **1**

Ghosez et al.[173] were the first to study asymmetric induction in [2+2]-cycloaddition reactions. The necessary optically active keteniminium salt **273** was prepared from (2*S*)-methoxymethylpyrrolidine **271** via the chloroenamine **272**. High asymmetric induction (*ee* > 97%) was achieved in the cycloaddition step with cyclopentene. Hydrolysis of the addition product gave the cyclobutanone (−)-**274**. *Greene* and *Charbonnier*[174] recently obtained [2+2]-cycloadducts with optical purities of up to 80% *ee* by reaction of dichloroketene with optically active vinyl ethers.

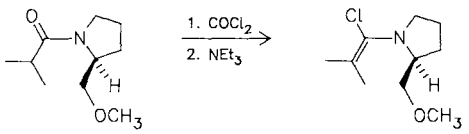

271 → **272**

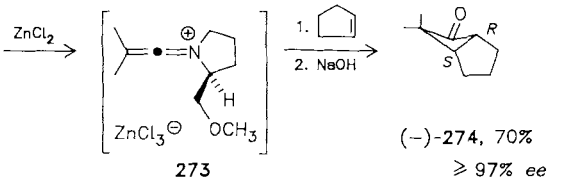

273 → (−)-**274**, 70%
≥ 97% *ee*

Acyl-transition metal complexes offer a further remarkable possibility for the synthesis of optically active cyclobu-

tanones. Thus the metallacycle **275** with the chiral phosphane ligand **276** was converted in 78% yield into a mixture of the acylcobalt complex (−)-**277** and its diastereomer with the opposite configuration at the cobalt atom.[175] Fractional crystallization led to pure (−)-**277**, which was converted by LDA into the lithium enolate, reaction of which with pivaldehyde proceeded with high asymmetric induction. The aldol product (−)-**278** was finally converted by $FeCl_3$ into the required optically pure cyclobutanone **279**.

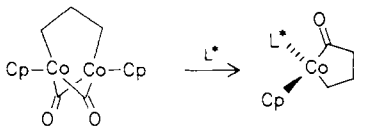

275 **(−)-277**

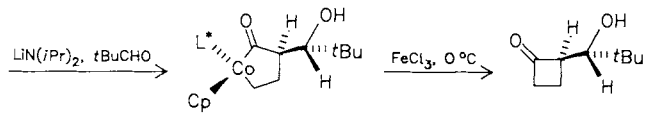

(−)-**278**, 98% **279**, 70%

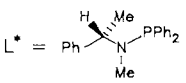

276

8. Thermal Conversions

Cyclobutanones decompose on heating to give ketenes and olefins.[176] These [2+2]-cycloreversions generally occur only at temperatures above 300°C and are therefore of little preparative interest. The concerted nature of the reaction has been demonstrated by *Carless* and *Lee*.[177] They determined stereospecificities of higher than 98% for the thermal cleavage of the stereoisomeric cyclobutanones **280** and **281**.

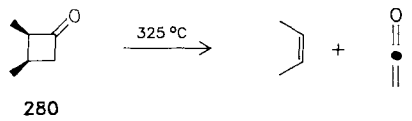

280

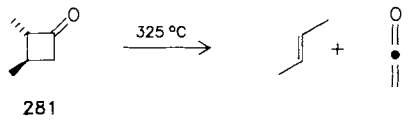

281

Some substituted cyclobutanones can however undergo thermal transformation at much lower temperatures. Thus the cyclobutanones **282**,[178] **283**,[179] and **284**[180] rearrange quantitatively on heating at comparatively low temperatures.

Thermal transformations of cyclobutanone derivatives which contain a 1,5-hexadiene structural element can be used in the synthesis of cyclooctane derivatives. Thus the synthesis of the cyclooctenone **291** is based on a [3,3]-sigmatropic rearrangement of the cyclobutanone **290**.[79e] **290** is readily available via a [2+2]-cycloaddition: the required vinylketene is formed either by electrocyclic ring opening

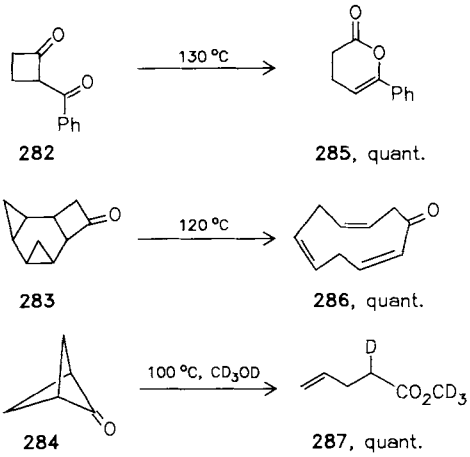

282 **285**, quant.

283 **286**, quant.

284 **287**, quant.

of the cyclobutenone **288** (R = CH_3) or by a 1,4-dehydrochlorination of the tiglic acid chloride **289** (R = H).

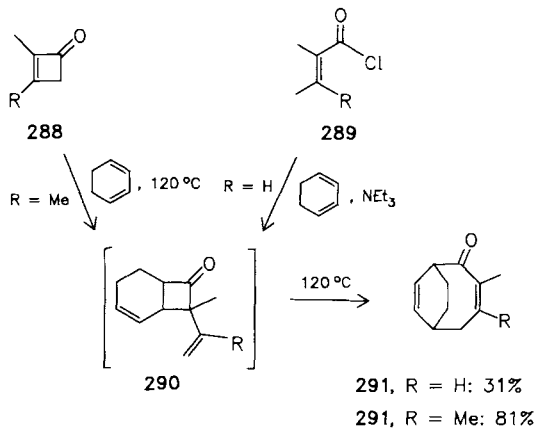

288 **289**

290

291, R = H: 31%

291, R = Me: 81%

Another Cope rearrangement for the synthesis of cyclooctenones has been described by *Dreiding* et al.[84a,181] and *Trahanovsky* et al.[182] The anion-assisted oxy-Cope rearrangement of **292** to **294** via the carbanion adduct **293** can be carried out at much lower temperatures[183] than with **290**. The same strategy was used by *Gadwood* et al.[184] to synthesize the sesquiterpene diols poitediol and 4-epipoitediol and by *Still* et al. to obtain the cytotoxic eucannabinolide.[185]

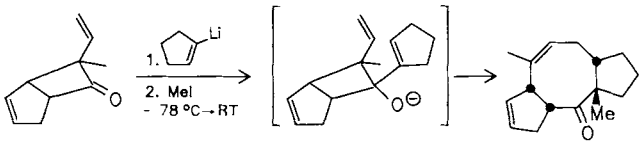

292 **293** **294**, 96%

In contrast to the thermal reactions of cyclobutanones, which are of little preparative use, it has long been known that the thermally labile cyclobutenones can be converted into vinylketenes at temperatures of about 120°C. In this way, they may be used for various preparative purposes. The main reaction modes (a)-(e) are outlined in Scheme 1, and will now be illustrated by some examples.

(a) *Baldwin* and *McDaniel*[186] showed that the electrocyclic ring opening of cyclobutenones occurs stereoselec-

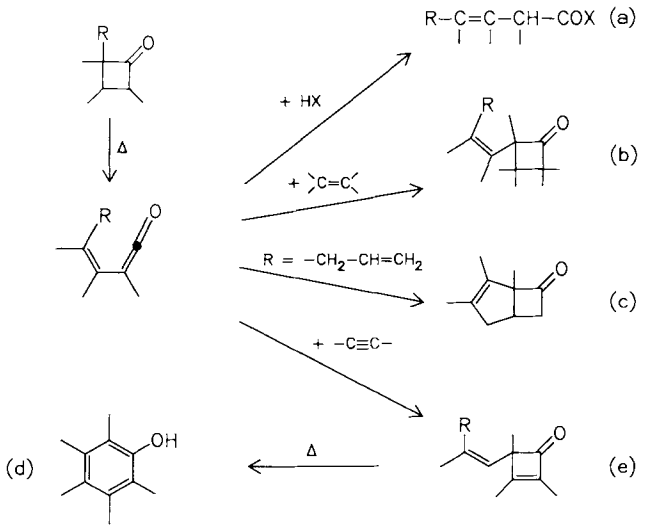

Scheme 1.

tively: thus starting from the cyclobutenone **295**, only the double bond isomer **297** was obtained via the vinylketene **296**.

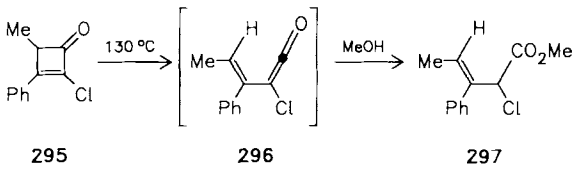

(b) The vinylketenes generated from cyclobutenones by electrocyclic ring opening can undergo an *inter*molecular [2+2]-cycloaddition with olefins. In this manner the trichlorovinyl-substituted cyclobutanone **300** could be obtained from the cyclobutenone **298** via the vinylketene **299**.[124c]

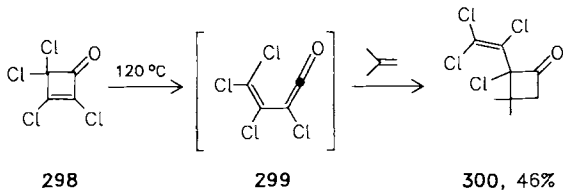

(c) After electrocyclic ring opening of the cyclobutenone **303** to the vinylketene **304**, one allyl side chain acts as ketenophile.[187] The *intra*molecular [2+2]-cycloaddition thus made possible gives the bicyclic cyclobutanone **305** in 80% yield. The elimination of *n*-butanol in **302** is carried out using Me_3SiOTf/NH_3; the conventional methods using Al_2O_3[188] or SiO_2/NEt_3[26b] led in the case of **302** only to complex product mixtures. The cycloadduct **305**, an example of a cyclobutane analog of a β-lactam (a type of compound which has recently been intensively studied[7g, 187, 189]) can also be accomplished in 83% yield from **306**[190] via the same vinylketene **304**.

(d) *Mayr* and *Huisgen* showed in 1975 that geminally diphenyl-substituted cyclobutenones such as **308** can rearrange quantitatively to α-naphthols of type **310**[191]:**308** was converted by thermal ring opening into the arylvinylketene **309** (i.e. a 1,3,5-triene), which cyclized to the naphthol **310**.

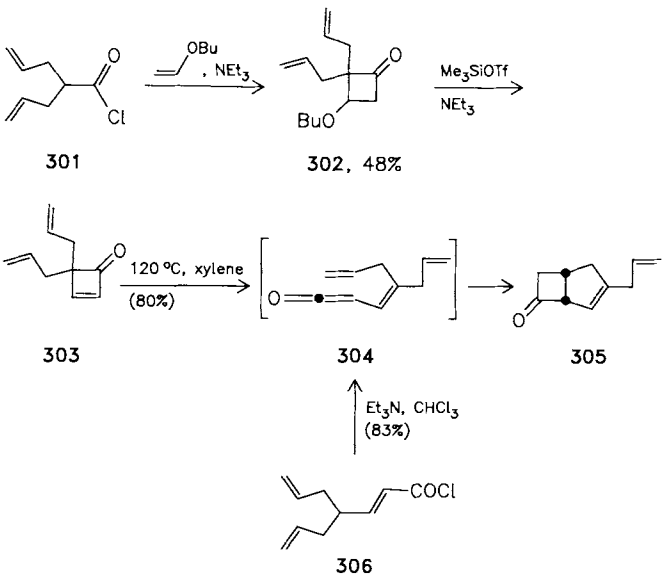

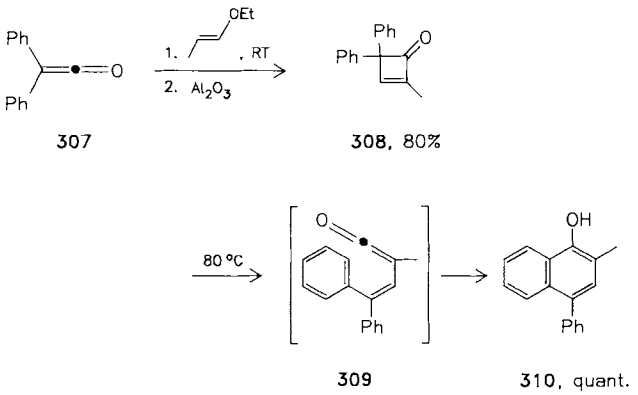

(e) Highly substituted phenols are generally prepared from simple aromatic precursors via electrophilic substitution reactions and/or metalation–alkylation reactions.[192] However, it becomes more difficult to direct the regiochemical course of the substitution reactions as the number of substituents in the ring increases. Annelation strategies in which the aromatic ring is assembled in a single step with all substituents already in place are therefore favorable. This strategy was used by *Danheiser* and *Gee*[193] in a short synthesis of the antibiotic grifolin (**315**): the vinylketene generated thermally from **311** was allowed to react with the acetylene derivative **312** to give the vinyl-substituted cyclobutenone **313**. The latter was not isolated but under the same reaction conditions underwent a thermal ring opening to the butadienyl ketene **314** (i.e. a 1,3,5-triene). Electrocyclic ring closure of this butadienyl ketone, which was also not isolated, and subsequent aromatization led finally to the phenol derivative **315** (i.e. grifolin). The same strategy has recently been used for the synthesis of the antibiotically active mycophenolic acid[194] and cyanophenols.[195]

Moore et al.[196] studied the thermolysis of alkenyl- and alkynyl-substituted cyclobutenones (prepared from the dimethyl ester of squaric acid[197]) in boiling xylene. The vi-

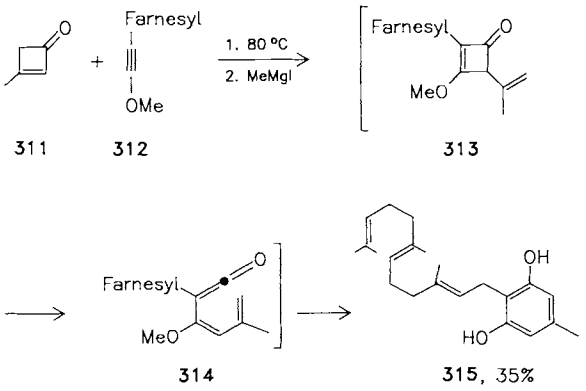

311 312 313

314 315, 35%

nylketene generated from **316** but not isolated, cyclized either to benzoquinones **317** or the cyclopentenediones **318**, depending on the electronic character of the substituent R.

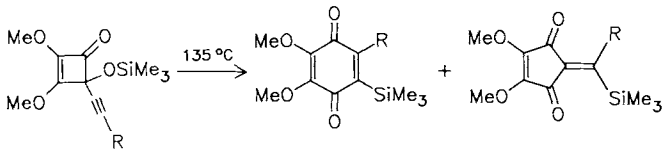

316 317 318

R = CH_2OSiMe_3	80%	0%
R = Ph	13%	52%
R = CO_2Et	0%	43%

A similar approach to highly substituted phenol derivatives was described by *Ficini* et al.[144,198] as early as 1976. In contrast to the approach used by *Danheiser* et al.,[193,194] the electrophilic cyclobutenone **319** was not used as the source for the thermal formation of a vinylketene, but converted at $-50\,^{\circ}C$ in the presence of the heterosubstituted acetylene **215** into the vinyl-substituted cyclobutenone **321** (probably via the bicyclic [2+2]-cycloaddition product **320**). **321** was then thermally rearranged to the phenol **322** at 170°C.

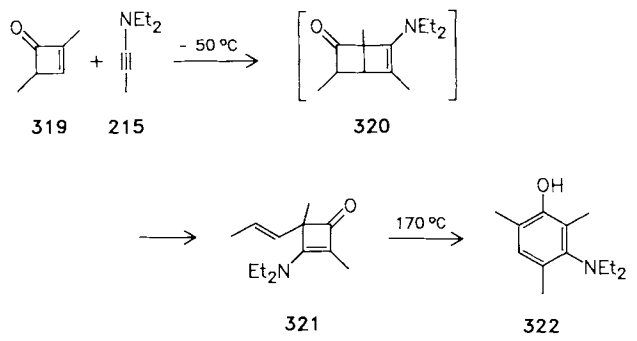

319 215 320

321 322

The synthetic potential of *ortho*-quinoid vinylketenes of type **324**, which can easily be prepared in situ by valence isomerization[199] of readily available benzocyclobutenones[200] of type **323**, was recently indicated by *Schiess* et al.[199b] They found that **324** undergoes facile [4+2]-cycloaddition reactions with various dienophiles (e.g. with chloral to give **325**).

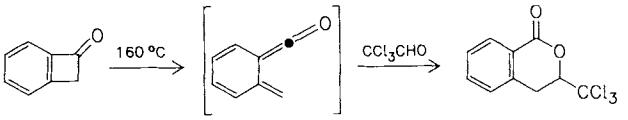

323 324 325, 92%

The great variety of accessible benzocyclobutenones and the simple thermal route to *ortho*-quinoid vinylketenes of type **324** makes it likely that the synthetic potential of this valence isomerization is by no means exhausted by the example **323** → **325**.

9. Photochemical Transformations

On irradiation in solution with UV-light, cyclobutanones can undergo three types of reactions (Scheme 2): *decarbonylation* (leading to cyclopropanes and carbon monoxide; Eq. (f)), [2+2]-cycloreversion (leading to olefins and ketenes; Eq. (g)), and ring enlargement (leading to 2-hydroxy- or 2-alkoxytetrahydrofurans; Eq. (h)). These three competing reactions are preceded by a common photochemical primary process, an α-cleavage to the 1,4-diradical **326**.

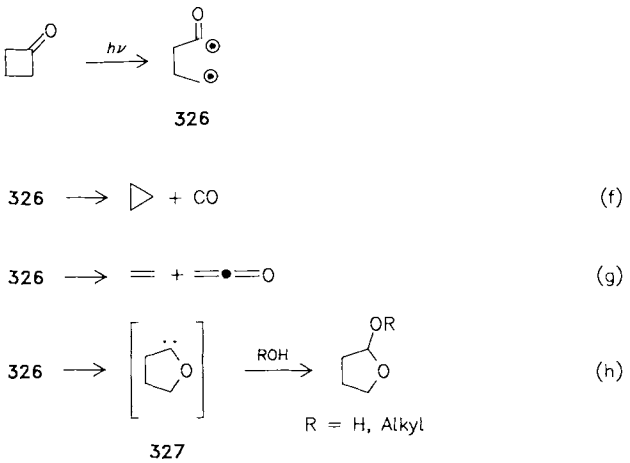

Scheme 2.

All three photoreactions generally occur together, though they are not necessarily of equal importance. Thus, though the photochemical behavior of variously substituted cyclobutanones has been studied in detail,[4k] the chemo-, regio- and stereochemical course of the photolysis of a particular cyclobutanone for preparative purposes is very difficult to predict. The best experimental conditions must be determined in each case, so that until now only a few product-oriented synthetic applications of the photochemistry of cyclobutanones are known.

Cyclic anions ($C_nO_n^{2-}$ are of theoretical interest, since they exhibit a large aromatic stabilization.[201] The first synthesis of the conjugate acid of the compound with n=3, the so-called "deltic acid" **330**, was carried out by *West* and *Eggerding*[202] by the photodecarbonylation of the bistrimethylsilyl ester of the squaric acid **328**. *Dehmlow* had

earlier obtained the diethyl ester of **330** in 10% yield by a similar procedure;[203] however, he did not succeed in hydrolyzing it to the free acid **330**.

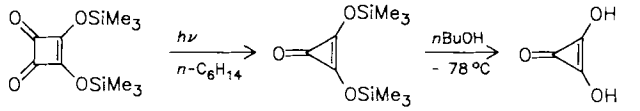

328 **329**, 15% **330**, quant.

Another theoretically interesting molecule, 1,3-dimethylenecyclobutadiene (a new benzene isomer with six π-electrons) was recently prepared by sensitized photodecarbonylation of the dimethylene derivative of **284** at 10°K.[204]

Only a few examples have been described for intramolecular [2+2]-cycloreversions of cyclobutanones annelated to a five-membered ring (e.g. **331** and **334**) which occur in preparatively useful yields.[205] Since cyclobutanones such as **331** and **334** are formed by [2+2]-cycloaddition of ketenes to cycloolefins, the formation of **332** and **335** represents de facto a two-step metathesis of two olefins.[205a]

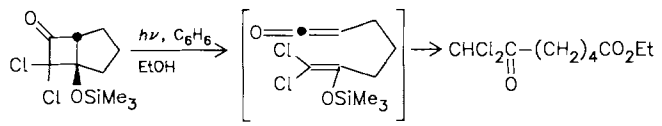

331 **332** **333**, 58%

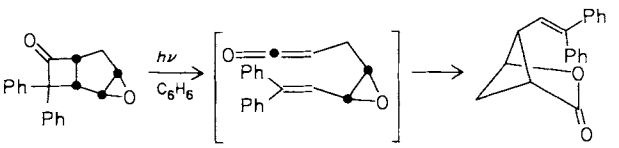

334 **335** **336**, 42%

Photochemical ring enlargement reactions of bicyclic cyclobutanones of type **337** have been used several times by *Roberts* et al. for the synthesis of racemic[206] and optically active[159a] prostaglandins, starting from the readily available adduct **61** of dichloroketene and cyclopentadiene. Apart from the regioselectively formed γ-lactols of type **338**, cyclopentenes of type **339** formed by ketene cleavage according to Eq. (g) were always isolated as by-products.[206c]

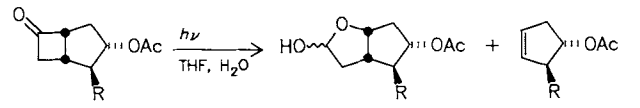

337 **338**, 50% **339**, 15%

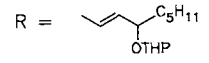

In the conversion of **337** into **338** the intermediate oxacarbene of type **327** was trapped by water. Although the oxacarbene can also be trapped as its dimer, such a process[207] is very unusual and has not yet become preparatively important. Bicyclic acetals can be obtained by an intramolecular trapping reaction in the irradiation of cyclobutanones,[208] e.g. **341** from **340**. Such annelated tetrahydrofuran units form a part of the structure of the aflatoxins and caryoptins.

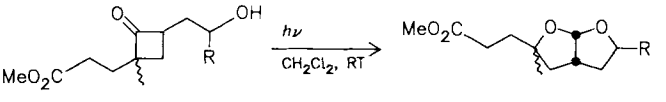

340 **341**, R = H: 70%
341, R = CN: 51%

The products of the direct photolysis of tetraethoxycyclobutanone **342** depend greatly on the solvent used.[209] In all cases 25–30% of the very pleasantly-smelling cyclopropane derivative **343** is isolated; in addition, in *tert*-butanol **344** is obtained (via an oxacarbene of type **327**), in acetone **345** (via cycloaddition of the 1,4-diradical of type **326** to the carbonyl group of acetone), and in methanol the unusual ester **346**. The formation of **346** (possibly also that of **345**) indicate a possible heterolytic α-cleavage of photoexcited **342**.

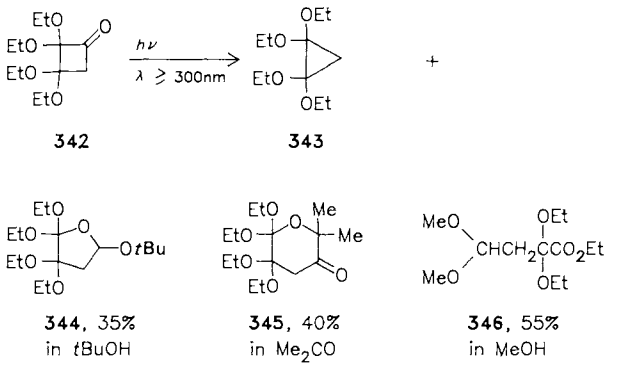

342 **343**
344, 35% in *t*BuOH **345**, 40% in Me_2CO **346**, 55% in MeOH

Depending on the substitution pattern, the irradiation of α-chlorocyclobutanones gives products of a [2+2]-cycloreversion [Scheme 2, Eq. (g)] in competition with the formation of derivatives of cyclopropanecarboxylic acids. The occurrence of a photo-Favorskii reaction was first observed by *Kaplan* and *Turner*[210] and later confirmed by *Jones* and *McDonnell*.[124a,b] The product distribution depends on the stereochemistry of the α-chlorocyclobutanones **165** and **167**.

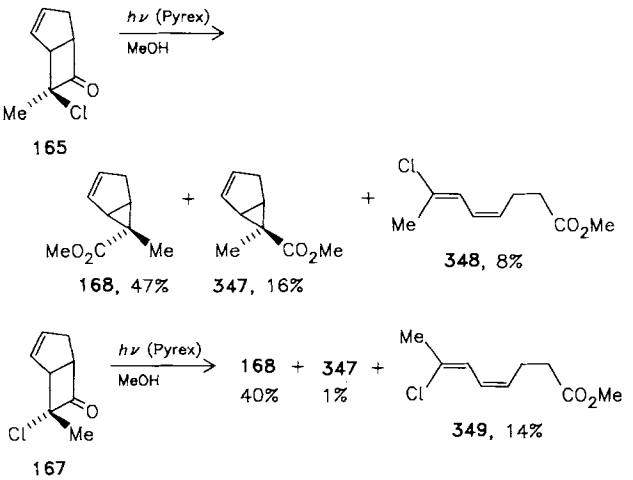

165
168, 47% **347**, 16% **348**, 8%
167
168 40% + **347** 1% + **349**, 14%

In contrast to **165** and **167**, the α-chlorocyclobutanone **169e** affords a complex mixture of products on irradiation in alcohol. However, its photolysis occurs very cleanly in a water/acetone solution (1 : 4).[125] The stereoisomeric cyclopropanecarboxylic acids *cis*-**170** and *trans*-**170** are formed in 97% total yield. While however the stereoselective Favorskii rearrangement of **160** under basic conditions gives an 8 : 2 mixture of *cis*- and *trans*-**170** (Section 4, Table 1), the biologically interesting[133a] *cis*-isomer **170** forms only one third of the product of the photo-Favorskii reaction.

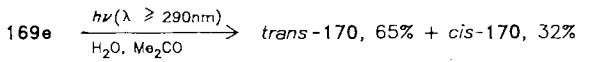

This unfavorable outcome of the photo-Favorskii reaction of **169** can be explained by the mechanism suggested by *Jones* and *McDonnell*.[124a] They assume that the primary step is a heterolytic cleavage of the α-chlorine-carbon bond to provide a trigonal α-oxocyclobutyl cation; this largely rearranges, losing the stereochemical information, to the thermodynamically more stable[211] *trans*-cyclopropylacyl cation, which is then trapped with water to form *trans*-**170**.[125]

In a few cases, photolysis of cyclobutenones leads to products which formally correspond to the primary reactions (f)–(h) (Scheme 2), e.g. the formation of **329** by photodecarbonylation of **328**. The dominant photoreaction of the cyclobutenones is however their valence isomerization to vinylketenes.[212] The few comparative experiments reported indicate that the photochemical and thermal ring openings (Section 8) are stereochemically different (e.g. the reaction of **350** to give either the vinylketene **351** or **353**[186]).

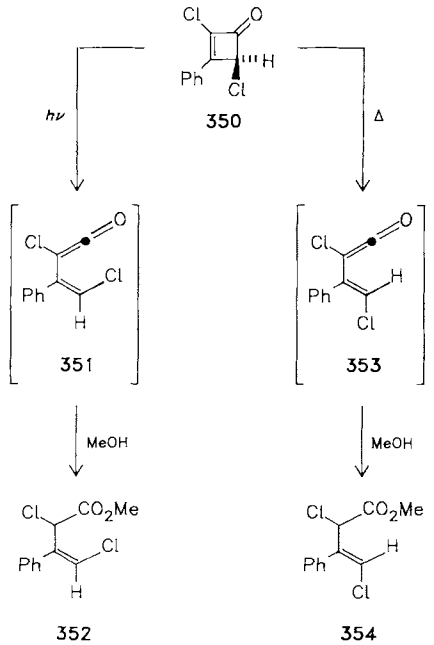

In contrast to the thermal ring opening of cyclobutenones, the photochemical method has until now rarely been used. However, UV-light was used twice in the preparation of the new pyrimidine bases **358** and **359**, first for the cyclobutenone formation **355**→**357** and then for the preparation of **358** via photolysis to the intermediate vinylketene, which was trapped with methanol (**359** is derived from **358**).[213]

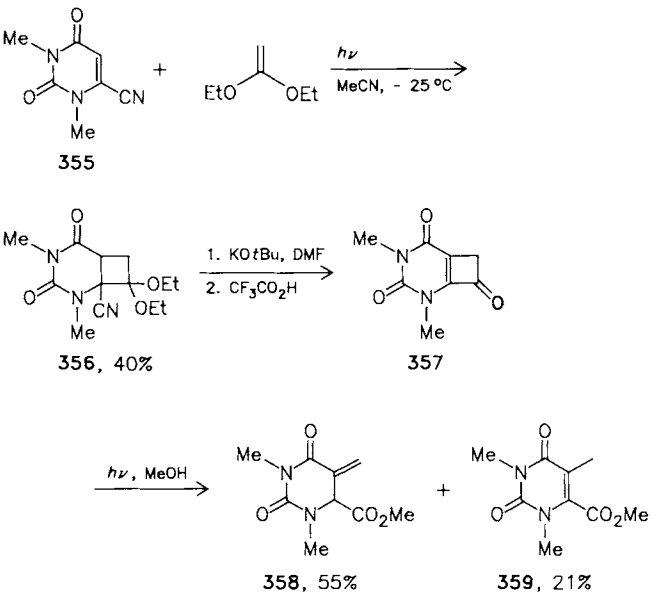

While numerous studies of the photochemical behavior of cyclobutenones[199b,214] and cyclobutenediones[215] have not followed a clear synthetic goal, the efficient formation of **362**, a cyclopentene-1,2,3-trione derivative, could be of preparative interest:[216] the bisketene **361** generated photochemically from **360** was trapped in situ by 2,6-dimethylphenyl isocyanide.

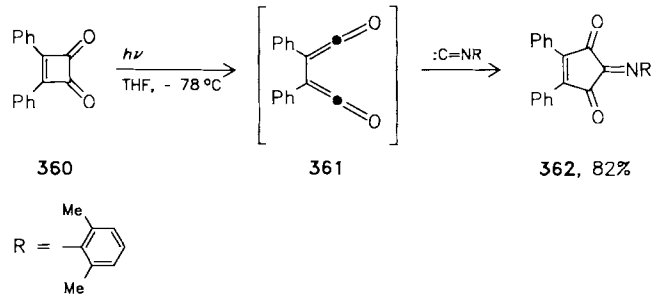

The photochemical behavior of bicyclic α-alkenyl- or α-dienylcyclobutanones (e.g. **363**) was studied by *Frei* et al.[217] Singlet excitation leads to products formed according to Equations (f) and (g) (Scheme 2); however, sensitized triplet excitation gives cyclopentanone derivatives (e.g. **364** and **365**) via a 1,2-acyl shift.

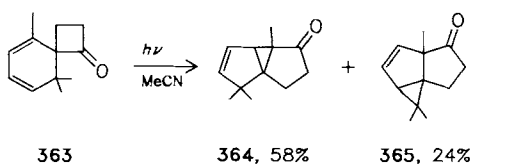

10. Reactions at the Carbonyl Group

10.1. Reactions with Nucleophiles

The bond angle at the carbonyl carbon in cyclobutanone is compressed almost to 90°.[218] Reactions at the carbonyl group in which the sp^2 carbon is converted into an sp^3 carbon therefore lead to a reduction of the angle strain; this explains the unusual reactivity of the carbonyl group in cyclobutanones.[219] It is thus for example possible to convert **366** regioselectively into the thioketal **367**.[220]

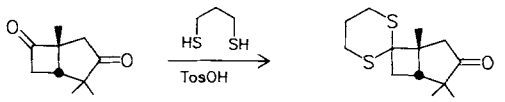

366 **367**, 60%

When the α-positions in a cyclobutanone are substituted with one or more anion-stabilizing groups, the attack of a nucleophile at the carbonyl group leads to ring cleavage (see Section 6). In the absence of anion-stabilizing groups in the α-position, tertiary alcohols are formed; these in turn can be used for the synthesis of interesting target molecules. Of the many examples known,[77,161,221] one in particular should be mentioned: the synthesis of the antibacterially active cyclobutanol derivative **371**. The cyclobutanone (±)-**368** was converted in a Reformatsky reaction into a mixture of the diastereomeric alcohols **369** and **370**. The main component (±)-**369** underwent reaction with Boc-(*S*)-valine to give the amino acid antimetabolite **371**, which had been isolated from *Streptomyces* X-1092.[222]

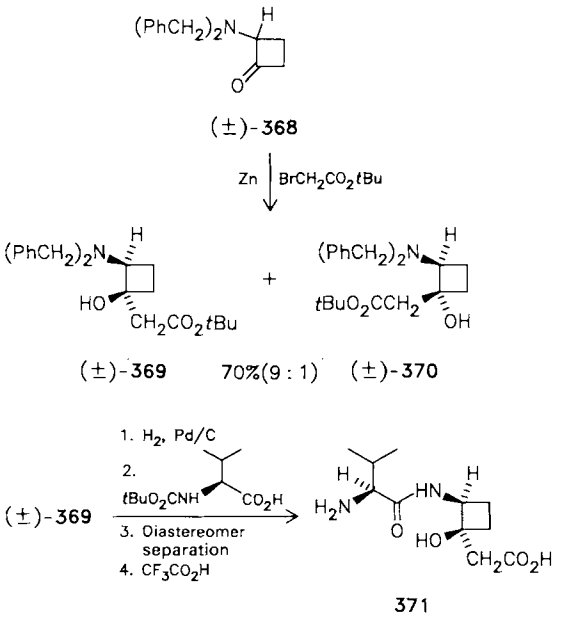

Vedejs and *Larsen*[223] allowed the cyclobutanone **372**, which is readily available from a [2 + 2]-cycloaddition reaction between methylketene and the corresponding silyl enol ether, to react with dibromomethyllithium; the reaction occurs stereoselectively to give the cyclobutanone **373**. Ring enlargement to **374** followed by ring opening afforded the γ-dicarboxylic acid **375**, which was used in the synthesis of fulvine **376**.

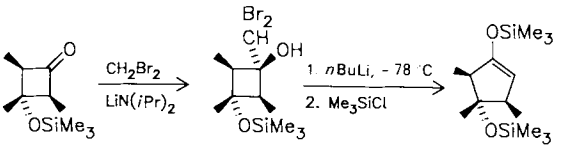

372 **373**, 84% **374**, 85%

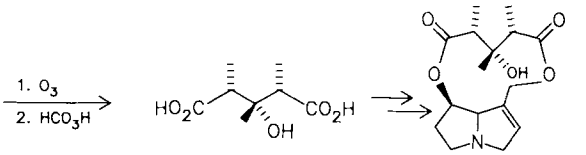

375, 79% **376**

The 1,2-adducts of vinylmetal compounds and cyclobutanones[183b,224] can undergo many useful transformations. When the cyclobutanone contains an additional vinyl substituent in the α-position, a thermal oxy-Cope rearrangement is possible (see Section 8). An example of a $Ag^{\oplus}$-induced aza-Cope rearrangement was reported by *Overman* et al.[224b] Their starting material was the disilylated 2-hydroxycyclobutanone **123**, which reacts with benzylaminoacetonitrile to give the cyclobutanone **377** in good yield.

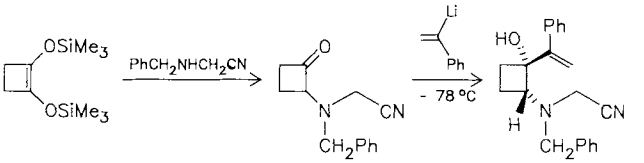

123 **377**, 75% **378**, 58%

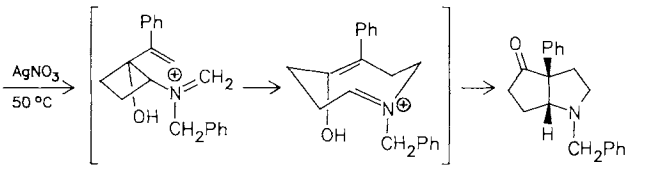

379 **380** **381**, 93%

The attack of 1-phenylvinyllithium on the carbonyl group of **377** occurs exclusively *trans* to the dialkylamino group and leads to **378**. An $Ag^{\oplus}$-catalyzed aza-Cope rearrangement, followed by an intramolecular Mannich cyclization completes the synthesis of pyrrolidine **381**.

The Pd-catalyzed rearrangement of 1-vinyl-1-cyclobutanols (e.g. **383** → **384**) has been studied in some detail.[225] The addition of benzoquinone made it possible to carry out the rearrangement to the cyclopentanone **384** under catalytic conditions.

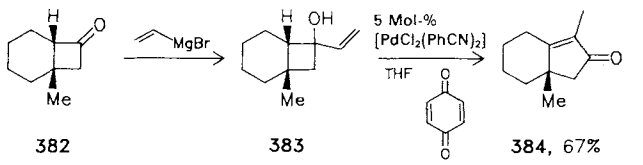

382 **383** **384**, 67%

Starting from cyclobutenones, alkylmetal compounds can be used for the selective synthesis of either 1,2- or 1,4-adducts. *Kraus*[226] showed that the resonance stabilization of the attacking carbanion is not the factor governing its mode of addition to dimethyl squarate (**385**). In fact, the main reason for the regioselectivity appears to be the nature of the metal cation: thus alkyl- and aryllithium compounds favor the 1,2-addition yielding **386** and **387**, while Grignard reagents prefer conjugate addition yielding **388** and **389** (see also Ref. [227]).

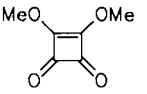

385

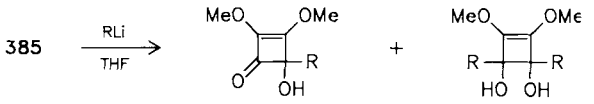

	386	**387**
1.1 eq. MeLi	55%	9%
2.2 eq. MeLi	8%	75%
1.1 eq. PhLi	58%	11%

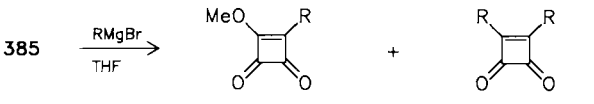

	388	**389**
1.1 eq. MeMgBr	44%	-
2.2 eq. MeMgBr	7%	72%
1.1 eq. PhMgBr	48%	-

The 1,4-addition was applied to the synthesis of jasmolone **393**.[228] The cyclobutenone **390** was first converted via a 1,4-addition of hex-3-ynylmagnesium bromide into **391**. Reduction of the latter with $LiAlH_4$ (a 1,2-addition) and subsequent ozonolysis afforded the α-hydroxy-γ-diketone **392**, which underwent cyclization via an intramolecular Aldol condensation to give jasmolone **393**.

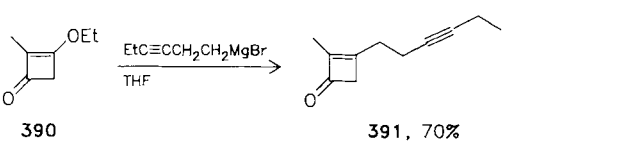

390 **391**, 70%

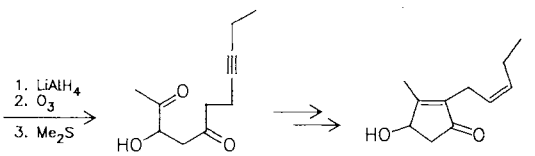

392, 72% **393**

Olefinations of cyclobutanones using the methods of *Wittig* (e.g. [68,91,229]) or *Horner* (e.g. [230]) to give methylenecyclobutane derivatives occur as expected without difficulty.—It was the cyclobutanone **394** which allowed the first ever isolation of an adduct between dichlorocarbene and a carbonyl group: dichlorocarbene, generated under phase transfer conditions, reacts with **394** to give the isomerically pure dichlorooxirane **395**, which on heating rearranges stereospecifically to the *endo*-acid chloride **396**.[231]

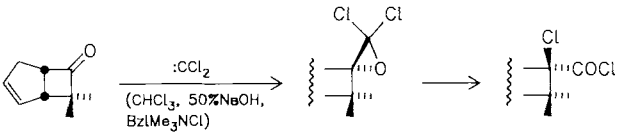

394 **395**, 85% **396**, 97%

10.2. Reductions

The reduction of cyclobutanones to cyclobutanols (i) or cyclobutanes (j) and the reductive amination to cyclobutylamines (k) according to Scheme 3 are all processes which are well documented in the literature:

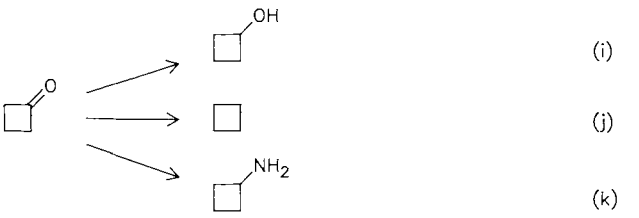

Scheme 3.

(i) Apart from enzymatic reduction[166a,b,232] (see also Section 7), various hydrides have been employed for the reduction of cyclobutanones to cyclobutanols: $LiAlH_4$,[55a,91,154,233] $NaBH_4$,[39b,145b,152,179,234] diisobutylaluminum hydride,[235] $Na[Al(OCH_2CH_2OMe)_2H_2]$,[236] $Li[Al(tBuO)_3H]$,[237] $(iPrO)_3Al/iPrOH$,[238] and $Li[(sBu)_3BH]$.[239] The reduction of cyclobutenones with either $LiAlH_4$[240] or with $NaBH_4$[234i] proceeds chemoselectively to afford the cyclobutenols, while with hydrogen and Ru/C as catalyst[241] only cyclobutanols are obtained.

(j) The reduction of cyclobutanones to cyclobutanes can be accomplished by the usual methods such as Wolff-Kishner reduction,[42,73a,242] reduction of the corresponding tosylhydrazone with $NaBH_4$[2d] or reduction of the corresponding thioketal with Raney nickel.[220,234e]

(k) Several examples of straightforward reductive amination of cyclobutanes to cyclobutylamines via reduction of the corresponding cyclobutanone oximes with sodium in 2-propanol[243] or $LiAlH_4$[244] have been described.

10.3. Syntheses of Cyclobutene Derivatives

Cyclobutene derivatives can be transformed into butadiene derivatives via an electrocyclic ring opening. This method of "in situ" preparation is particularly interesting for butadienes which cannot be isolated due to their high tendency to undergo polymerization. For this reason, the synthesis of the cyclobutenes which serve as starting materials often plays a key role. *Trost* et al. studied in detail the suitability of cyclobutanones for the preparation of 2,3-disubstituted butadienes of type **399**[245] and of 1,4-disubstituted butadienes[234b] via electrocyclic ring opening. The syntheses of carvone **401**[245a] and ipsenol **407**[246] illustrate the underlying synthetic principle: the cyclobutene deriva-

tive **398**, which is readily available from α-bromocyclobutanone **149**, can be transformed via a thermal electrocyclic ring opening into the butadiene **399**. The [4+2]-cycloaddition of **399** with methyl vinyl ketone gives the carvone precursor **400** with high regioselectivity.

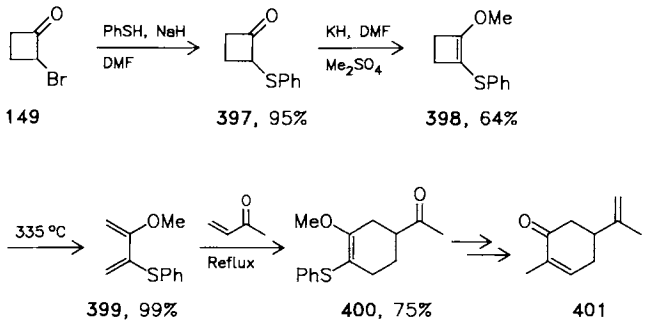

Krief and *Halazy* used the thermal electrocyclic ring opening of the cyclobutene derivative **406** in the synthesis of ipsenol **407**.[246] The former was prepared from cyclobutanone **402** via the 1,1-bis(methylseleno)cyclobutane **403** and the γ-(methylseleno)alcohol **404**.

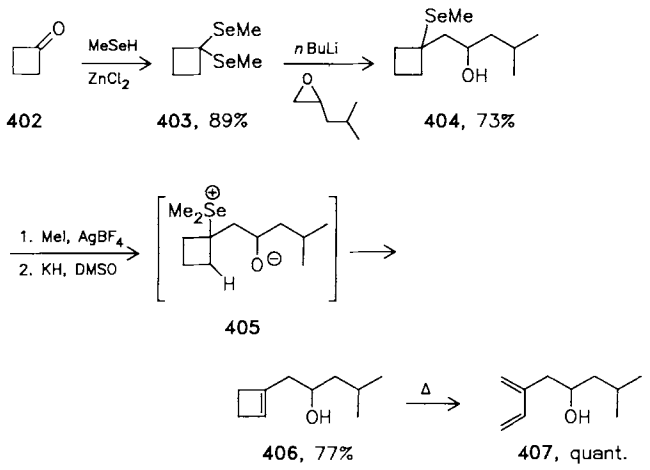

A further method for the preparation of butadiene derivatives was described by *Thummel* et al.[247] During their studies on [4+2]-cycloadditions of 1-vinylcyclobutenes, they prepared the cyclobutene **410** via Grignard addition of **408** to the cyclobutanone **402**.

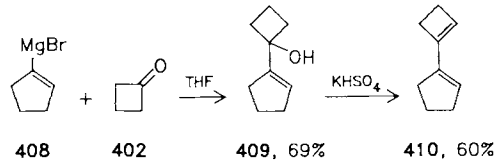

While the silyl enol ethers of cyclobutanones (precursors for synthetically useful electron-rich butadienes) can readily be obtained by a trimethylsilylation under basic conditions,[248] the first successful "in situ" preparation of the cyclobutanone enamine **411** by a modified Mannich–Davidson method has only recently been described.[249] **411** reacts both as a dienophile (→**412**) and as a typical enamine (→**413**).

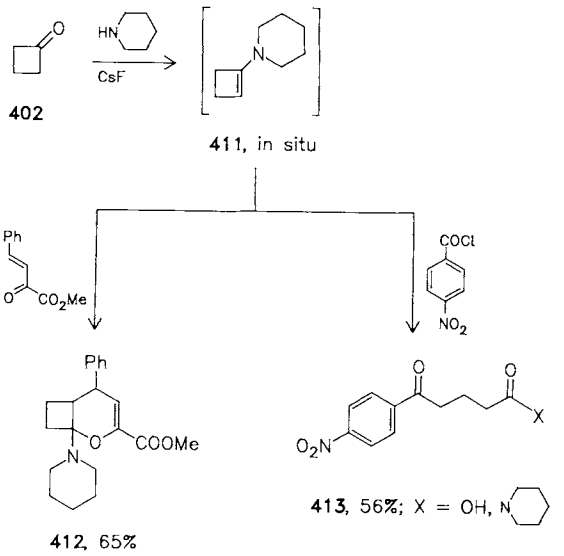

11. Substitution in the α-Position

The numerous methods of transforming α-substituted cyclobutanones which have been presented in the previous sections made it clear that the methods for α-functionalization are of particular synthetic importance. In general, they differ only little from the standard methods for α-functionalization of ketones; however, some reactions (e.g. the use of nucleophilic bases for generating α-anions) are of little use because of the tendency of cyclobutanones to undergo ring opening as well as self-condensation.

11.1. Mono- and Dibromination

Both monobromination in the α-position (e.g. **195**→**196**, see also Ref. [250]) as well as the α,α-dibromination[23,144] of cyclobutanones with bromine are readily carried out. The α-bromocyclobutanones are commonly subjected to the Favorskii ring contraction reactions (see Section 4). In addition, their use may be exemplified by the synthesis of the norephedrine analog **415**:[250b] the α-bromocyclobutanone **149** is allowed to react with dibenzylamine to give the α-aminocyclobutanone derivative **368**. Stereoselective *trans*-addition of phenylmagnesium chloride leads to the amino alcohol **414**, a precursor of **415**.

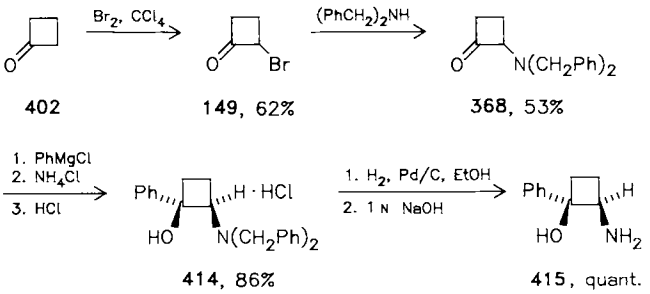

11.2. Oxidation

SeO_2-oxidation at the α-position of cyclobutanones converts them into cyclobutanedione derivatives (compare **34** → **35**). *Inoue* and *Kuwajima*[251] used the oxidation of the cyclobutanone derivative **417** to the 2-(hydroxyimino)cyclobutanone **418** with nitrosyl chloride in the remarkable synthesis of the nucleoside showdomycin **419**. The glycoside linkage to the α-position of the cyclobutanone **417** was formed by reaction of **123** with the β-D-ribose derivative **416** in the presence of $SnCl_4$.

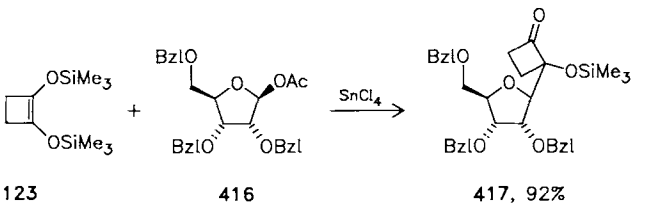

123 416 417, 92%

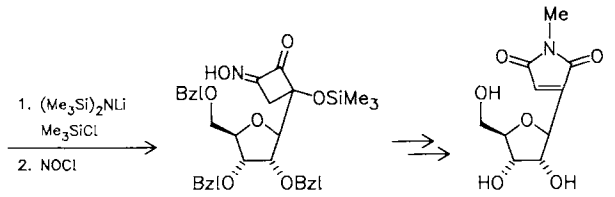

418, quant. 419

11.3. Condensation

The condensation of cyclobutanones with aldehydes via lithium enolates leads either to complex mixtures[252] or to the formation of products of self-condensation of the cyclobutanones.[253] However, *Clark* et al.[252] showed that the enolate prepared from α-chlorocyclobutanone **420** with Me_2CuLi can undergo reaction with a number of aldehydes to give aldol products in good yields.

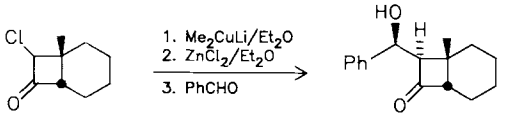

420 421, 83%

A mild alternative is provided by zirconium enolates: thus the zirconium enolate of **422** was used in the synthesis of *N*-acetyl-1-deazathienamycin **424**, an example of a

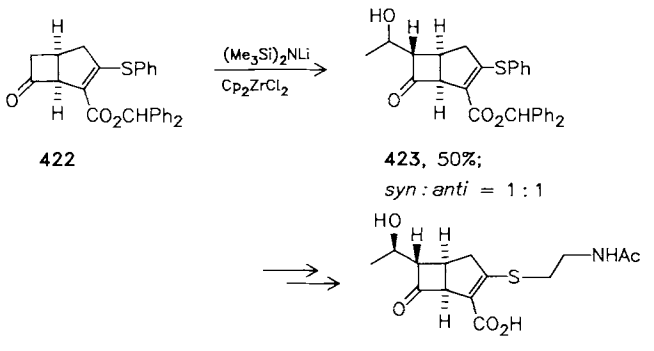

422 423, 50%; *syn* : *anti* = 1 : 1

424

cyclobutanone analogue of β-lactams[79,187,189] to introduce the hydroxyethyl side chain typical for thienamycin.[189d]

The condensation with aldehydes is also possible via boron enolates (e.g. **425** → **426**) or via the Lewis-acid-catalyzed reaction of silyl enol ethers (e.g. **427** → **428**).[253]

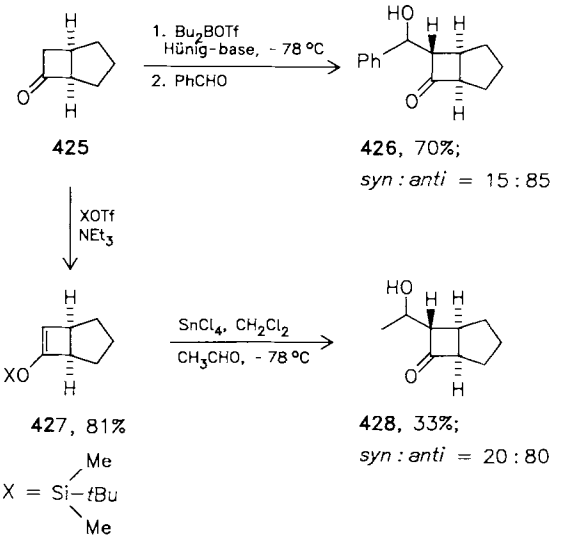

425 426, 70%; *syn* : *anti* = 15 : 85

427, 81% 428, 33%; *syn* : *anti* = 20 : 80

A further possibility for the functionalization of the α-position is provided by the condensation of cyclobutanones with *tert*-butyl formate (e.g. **19** → **237**) or with its equivalent $(Me_2N)_2CHOtBu$.[114,250a,254] In this manner *Greenlee*[254] succeeded in synthesizing the diterpene (±)-trihydroxydecipiadiene **432** starting from the cyclobutanone **429**. The tetracyclic compound **430** was prepared by spiroannelation of **429**[255] using the method of *Trost* et al.[79c,256] The synthesis involves a number of remarkable steps in which the construction and transformation of cyclobutanones play a key role (DMAP = 4-dimethylaminopyridine).

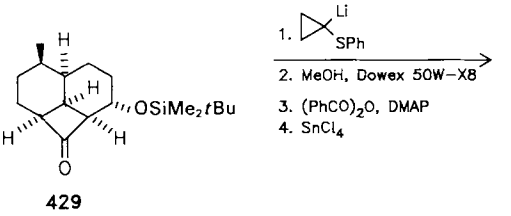

429

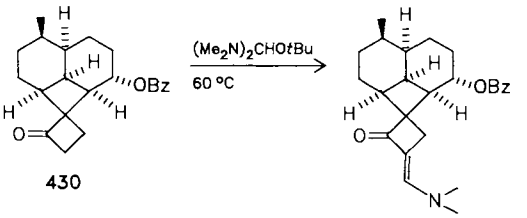

430 431, 52% starting from **429**

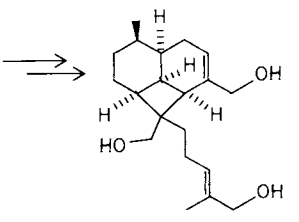

432

11.4. Dehalogenation in α-Position

The mono- and dihalogenocyclobutanones are very readily available via [2+2]-cycloaddition reactions of mono- and dihalogenoketenes[4a-d] to olefins. Thus, they are valuable polyfunctional precursors for a great variety of syntheses. However, since the target molecules are generally halogen-free, countless reductions of α-halogenocycloadducts to halogen-free cyclobutanones have been described. Besides the standard method with Zn/AcOH (e.g. **23**→**24** or **61**→**97**; see also Refs. [7g, 43, 44, 46c, 53, 66b, 76, 127, 189c, 206d, 233b, 234d, 239b]) and with $Zn/NH_4Cl/MeOH$,[33d,235d,254] the following reducing agents have also been employed: n-Bu_3SnH/azoisobutyronitrile (AIBN);[4a,39b,152,257] Ph_3SnH/AIBN[234a] and $CrCl_2$.[141,233c,258]

The selective reduction to monochloro derivatives is also possible: thus for example **61** is reduced selectively by Zn/AcOH[259] or Bu_3SnH/AIBN[257a] to the *endo*-monochloroisomer **31**. However, the exact experimental conditions for a monoreduction must be established in each particular case.

12. Summary and Outlook

Since the first synthesis of a cyclobutane was accomplished by *Perkin* a hundred years ago,[260] the highly-strained four-membered ring compounds have demonstrated their unique usefulness in the interplay between theory and practice[261] as well as in the race to synthesize molecules with the maximum possible strain.[262] However, the inherent strain of the four-membered ring of ca. 25 kcal mol^{-1} was only definitively placed in the service of the preparative chemist in the past twenty years, when it became readily possible to obtain a large variety of substituted cyclobutanones. [2+2]-Cycloaddition reactions between ketenes and olefins and the Trost synthesis of cyclobutanones starting from aldehydes and ketones are broad in scope and now represent the most reliable routes to cyclobutanones and cyclobutenones. Several other methods which have only been mentioned briefly in this review, as well as the routes to optically active cyclobutanones described in Section 7, are certainly capable of considerable extension. They guarantee that the methods for transforming cyclobutanones and cyclobutenones summarized here will render new strategies in synthetic planning possible. One can expect that the complex and unique combination of strain, electrophilicity and puckering in the title compounds will frequently lead to many fascinating surprises. This review is intended to make a contribution towards overcoming the "trial and error" synthetic approach, so that a more precise and faster forecast of the required regio-, chemo-, and stereoselectivity of transformations of cyclobutanones and cyclobutenones can be achieved.

13. Addendum[*]

For the preparation of γ-butyrolactones (cf. Section 3.1) from cyclobutanones, *Matsumo* et al.[263] recommend the use of H_2O_2/2,2,2-trifluoroethanol.

[*] Received: May 6, 1988.

The ring enlargement of cyclobutanones of type **433** to cyclopentanones **434–436** (cf. Section 3.3) with α-lithioalkylaryl sulfoxides and selenoxides enables incorporation of both an unsubstituted as well as a mono- or disubstituted α-carbon atom in one step.[264]

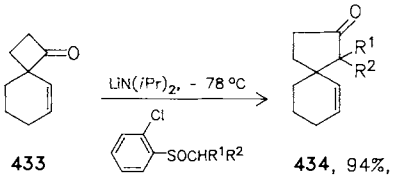

433

434, 94%, $R^1 = R^2 = H$
435, 63%, R^1 = Me, $R^2 = H$
436, 54%, $R^1 = R^2$ = Me

A ring enlargement to the cyclopentanone (cf. Section 3.3) can also be achieved by reaction of cyclobutanones with lithiated thioacetal.[265]

Starting from (*R*)-3-hydroxybutyrates **437**, *Mori* and *Miyake*[266] synthesized the ketene precursors **438**. An intramolecular ketene cycloaddition afforded the two diastereomeric cyclobutanones (+)-**439** and (−)-**440** in the ratio 7:2. The main product (+)-**439** was converted into (+)-grandisol **441**, the pheromone of the boll weevil (cf. Section 7.2).

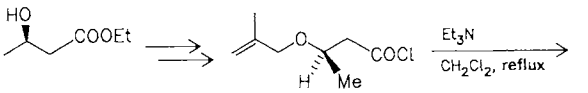

437 **438**

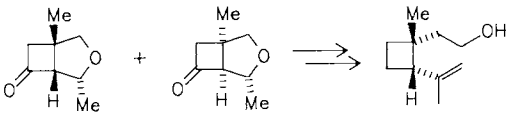

(+)-**439** (−)-**440** (+)-**441**

70% (7:2)

Fráter et al.[267] showed that the [2+2]-cycloaddition of menthyloxymethylketene to (*Z*)-benzyl hexenyl ether **442** leads mainly to the kinetically controlled product **443**. Subsequent refluxing in triethylamine affords the cyclobutanone **445** as major product of a thermodynamically controlled reaction. Finally, (−)-blastamycinone **446** was obtained (cf. Section 7.3).

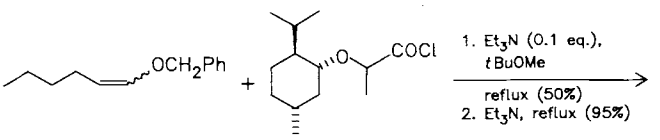

442, *cis* : *trans* = 4 : 1 **443**

≡ Men*OCH(CH3)COCl

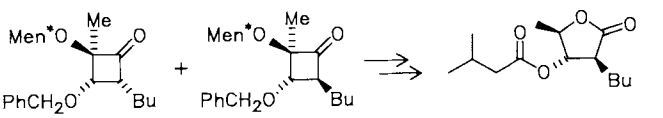

444 (1 : 9) **445** **446**, ≈ 70% *ee*

Pirrung and *Deamicis*[268] investigated many examples for the formation of α-O-, α-S- and α-N-substituted tetrahydrofurans by photolytic ring enlargement of cyclobutanones in the presence of O-, S- and N-nucleophiles (cf. Section 9).

Dreiding et al.[269] used an interesting conversion of the 1,2-adduct of the buta-1,2-dienyltitanium compound (from but-2-yne, *t*-BuLi and $Ti(OiPr)_4$) with the cyclobutanone **447** for the synthesis of (±)-sativene **499** (cf. Section 10.1).

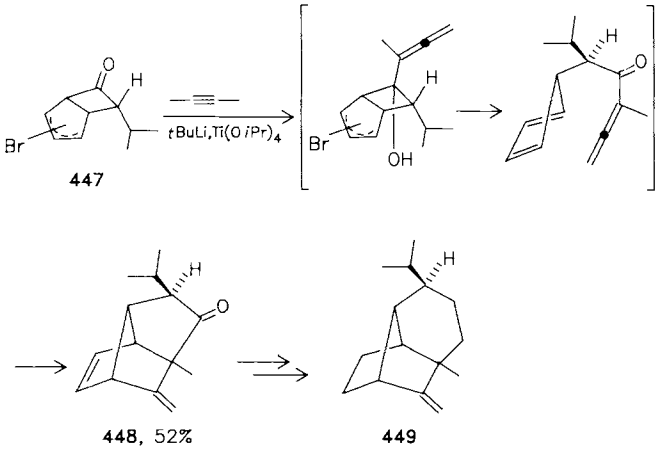

Wakamatsu et al.[270] developed two methods for the 1,2-carbonyl transposition in cyclobutanones (cf. Section 11).

The selective monodehalogenation of 2,2-dichlorocyclobutanones can be carried out in moderate to good yields[271] with magnesium-anthracene (cf. Section 11.4).

Danheiser and *Savariar*[272] have shown that 4,4-dichlorocyclobutenones can be reduced in yields of 70–90% to the corresponding cyclobutenones with zinc/ethanol in the presence of 5 equivalents each of AcOH and TMEDA.

Our own work cited here would not have been possible without the dedicated efforts of many colleagues whose names appear in the literature references; to them we wish to express our heartfelt thanks.

Received: December 12, 1986 [A 673 IE]
German version: *Angew. Chem. 100* (1988) 820
Translated by Professor Dr. *T. N. Mitchell*, Dortmund (FRG)

[1] Recent reviews: a) B. M. Trost, *Top. Curr. Chem. 133* (1986) 3; b) H. N. C. Wong, K.-L. Lau, K.-F. Tam, *ibid. 133* (1986) 83; c) E. Winterfeldt, *Kontakte (Darmstadt) 1986*, 52.

[2] Cyclobutanone: I) from Cyclopropanes: a) J. R. Salaün, J. M. Conia, *Chem. Commun. 1971*, 1579; b) D. H. Aue, M. J. Meshishnek, D. F. Shellhamer, *Tetrahedron Lett. 1973*, 4799; c) J. P. Barnier, B. Garnier, C. Girard, J. M. Denis, J. Salaün, J. M. Conia, *ibid. 1973*, 1747; d) J. R. Salaün, J. Champion, J. M. Conia, *Org. Synth. 57* (1977) 36; e) B. M. Trost, W. C. Vladuchick, *Synthesis 1978*, 821; f) M. Krumpolc, J. Rocek, *Org. Synth. 60* (1981) 20; II) by [2+2]-cycloadditions: g) H. K. Hall, Jr., D. E. Plorde, US-Pat. 3 646 150 (1968), Du Pont; h) J. B. Sieja, *J. Chem. Eng. Data 17* (1972) 108; III) from 1,3-dihalogenopropane and "umpoled" formaldehyde: i) D. Seebach, N. R. Jones, E. J. Corey, *J. Org. Chem. 33* (1968) 300; k) D. Seebach, A. K. Beck, *Org. Synth. 51* (1971) 76; l) K. Ogura, M. Yamashita, S. Furukawa, M. Suzuki, G. Tsuchihashi, *Tetrahedron Lett. 1975*, 2767; m) D. van Leusen, A. M. van Leusen, *Synthesis 1980*, 325; n) K. H. Theopold, R. G. Bergmann, *J. Am. Chem. Soc. 102* (1980) 5694; o) J. W. F. L. Seetz, R. Tol, O. S. Akkerman, F. Bickelhaupt, *Synthesis 1983*, 721; IV) by 1,4-addition: p) K. Hummel, M. Hanack, *Justus Liebigs Ann. Chem. 746* (1971) 211; q) H. Hiraoka, *J. Am. Chem. Soc. 95* (1973) 1664; r) M. Hanack, T. Dehesch, K. Hummel, A. Nierth, *Org. Synth. 54* (1974) 84; s) G. Stork, J. C. Depezay, J. d'Angelo, *Tetrahedron Lett. 1975*, 389; cyclobutenone: t) J. B. Sieja, *J. Am. Chem. Soc. 93* (1971) 2481; 1,2-cyclobutanedione: u) J. M. Denis, J. Champion, J. M. Conia, *Org. Synth. 53* (1973) 158; v) J. P. Barnier, J. M. Denis, J. Salaün, J. M. Conia, *Tetrahedron 30* (1974) 1405; w) J. Salaün, A. Fadel, J. M. Conia, *Tetrahedron Lett. 1979*, 1429; 1,3-cyclobutanedione: x) H. H. Wasserman, J. U. Piper, E. V. Dehmlow, *J. Org. Chem. 38* (1973) 1451; y) M. A. Pericàs, F. Serratosa, E. Valenti, *Synthesis 1985*, 1118; 1,2-cyclobutenedione: z) J. C. Hinshaw, *Chem. Commun. 1971*, 630; aa) A. H. Schmidt, W. Ried, *Synthesis 1978*, 1; ab) H.-D. Martin, A. Oftring, R. Iden, E. Schwichtenberg, H.-J. Schiwek, *Tetrahedron Lett. 23* (1982) 841; ac) B. Albert, C. Heller, R. Iden, G. Martin, H.-D. Martin, B. Mayer, A. Oftring, *Isr. J. Chem. 25* (1985) 74.

[3] Reviews: a) J. M. Conia, J. Gore, *Bull. Soc. Chem. Fr. 1963*, 726; J. M. Conia, J. Gore, *ibid. 1963*, 735; J. M. Conia, J.-P. Sandré, *ibid. 1963*, 744, 752; J. M. Conia, J.-L. Ripoll, *ibid. 1963*, 755, 763, 768, 773; b) F. Effenberger, P. Fischer, G. Prossel, G. Kiefer, *Chem. Ber. 104* (1971) 1987.

[4] Cyclobutanones: I) by [2+2]-cycloaddition of halogenoketenes to multiple bonds: a) W. T. Brady, *Synthesis 1971*, 415; b) S. M. Ali, T. V. Lee, S. M. Roberts, *ibid. 1977*, 155; c) W. T. Brady in S. Patai (Ed.): *The Chemistry of Ketenes, Allenes and Related Compounds*, Interscience, New York 1980, p. 279; d) W. T. Brady, *Tetrahedron 37* (1981) 2949; e) H. W. Moore, M. D. Gheorghiu, *Chem. Soc. Rev. 1981*, 289; II) by ring expansion and ring contraction: f) B. M. Trost, *Top. Curr. Chem. 41* (1973) 1; g) B. M. Trost, *Acc. Chem. Res. 7* (1974) 85; h) B. M. Trost in C. J. M. Stirling (Ed.): *Organic Sulfur Chemistry, Structure, Mechanism, and Synthesis*, Butterworths, London 1975, p. 563; i) J. M. Conia, M. J. Robson, *Angew. Chem. 87* (1975) 505; *Angew. Chem. Int. Ed. Engl. 14* (1975) 473; k) D. R. Morton, N. J. Turro, *Adv. Photochem. 9* (1974) 197.

[5] a) W. Ried, A. H. Schmidt, *Angew. Chem. 84* (1972) 1048; *Angew. Chem. Int. Ed. Engl. 11* (1972) 997; b) A. H. Schmidt, W. Ried, *Synthesis 1978*, 869; c) H. Knorr, W. Ried, *ibid. 1978*, 649; d) A. H. Schmidt, *ibid. 1980*, 961; e) D. Belluš in R. West (Ed.): *Chemistry of Oxocarbons*, Academic Press, New York 1980, p. 169; f) R. West, *Isr. J. Chem. 20* (1980) 300; benzocyclobutenone: g) P. Schiess, S. Rutschmann, *Chimia 39* (1985) 213.

[6] N. L. Allinger, Y. Yuh, J. T. Sprague, *J. Comput. Chem. 1* (1980) 30.

[7] Cyclobutanones are generally puckered in order to relieve strain. A survey of the X-ray structural analyses of 26 cyclobutanones showed that the dihedral angle α between the planes defined by the atoms C(1), C(2) and C(3) and C(1), C(2) and C(4) can reach a value of 41.6° [7a]. In addition, an unexpected deviation β of the carbonyl oxygen atom to the *endo*-side ("Concorde-nose") is demonstrated by the projection **I**. The angles α and β are interdependent: an increase in α is generally also linked with an increase in β: 5-*endo*-(*o*-hydroxyphenoxy)-1,2,5,6-tetramethyltricyclo[2.2.0.$0^{2,6}$]hexan-3-one, $\alpha = 38.2°$; $\beta = 11.3°$ [7b]; 4'-chloro-1',2',3',4'-tetrahydro-3'-oxocyclobuta[1',2':2,3]cholestan-3-yl acetate, $\alpha = 35.4°$; $\beta = 13.5°$ [7c]; 2-chloro-3,3-dimethyl-4-(2,2,2-trichloroethyl)cyclobutanone, $\alpha = 31.5°$; $\beta = 10.6°$ [7d]; 2,2-diphenyltricyclo[4.4.1.$0^{1,4}$]undecan-3-one, $\alpha = 26.2°$; $\beta = 6.3°$ [7e]; 2,2,4,4-tetramethyl-3-pyrrolidinocyclobutanone, $\alpha = 19.4°$; $\beta = 3.0°$ [7f]; 6,6-dichloro-7-

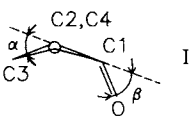

I

oxobicyclo[3.2.0]hept-3-ene-2-carboxylic acid, $\alpha = 16.9°$; $\beta = 1.0°$ [7g]. This O1-*endo*-deviation β allows the p-orbitals at C(1) and O(1) to take a position perpendicular to the C(1) tangential plane of the cyclobutanone "banana" bonds, thus enabling an optimal sp^2-hybridization at C(1) [7d]. – a) C. G. Biefeld, H. A. Eick, *Acta Crystallogr. Sect. B 30* (1974) 1172; b) F. van Bolhuis, *Cryst. Struct. Commun. 10* (1981) 465; c) A. Hassner, J. L. Dillon, Jr., L. R. Krepski, K. D. Onan, *Tetrahedron Lett. 24* (1983) 1135; d) P. Martin, H. Greuter, G. Rihs, T. Winkler, D. Belluš, *Helv. Chim. Acta 64* (1981) 2571; e) K. B. Becker, M. K. Hohermuth, G. Rihs, *ibid. 65* (1982) 235; f) B. Balbach, R. Alt, M. L. Ziegler, *Z. Naturforsch. B 37* (1982) 1005; g) E. M. Gordon, J. Pluščec, M. A. Ondetti, *Tetrahedron Lett. 22* (1981) 1871.

[8] H. Nishimura, R. P. Philip, M. Calvin, *Phytochemistry 16* (1977) 1048.

[9] M. Ishitsuka, T. Kusumi, H. Kakisawa, *J. Org. Chem. 48* (1983) 1937.

[10] a) S. Takahashi, H. Iinuma, T. Takita, K. Maeda, H. Umezawa, *Tetrahedron Lett. 1969*, 4663; b) *ibid. 1970*, 1639.

[11] a) R. B. Bates, M. J. Onore, S. K. Paknikar, C. Steelink, E. P. Blanchard, *Chem. Commun. 1967*, 1037; b) S. J. Torrance, C. Steelink, *J. Org. Chem. 39* (1974) 1068.

[12] J. J. Beerebom, *J. Am. Chem. Soc. 85* (1963) 3525; *J. Org. Chem. 30* (1965) 4230.
[13] W. F. Erman, *J. Am. Chem. Soc. 89* (1967) 3828.
[14] a) W. F. Erman, *J. Am. Chem. Soc. 91* (1969) 779; b) W. F. Erman, R. S. Treptow, P. Bakuzis, E. Wenkert, *ibid. 93* (1971) 657.
[15] a) D. R. Adams, S. P. Bhatnagar, R. C. Cookson, R. M. Tuddenham, *J. Chem. Soc. Perkin Trans. 1 1975*, 1741; b) R. Weyerstahl, W. Zombik, C. Gansau, *Liebigs Ann. Chem. 1986*, 422.
[16] T. Hudlicky, T. Kutchan, *Tetrahedron Lett. 21* (1980) 691.
[17] H. Stadler, M. Rey, A. S. Dreiding, *Helv. Chim. Acta 67* (1984) 1854.
[18] M. Kotake, H. Nonaka, *Justus Liebigs Ann. Chem. 607* (1957) 153.
[19] Y. S. Kulkarni, B. B. Snider, *J. Org. Chem. 50* (1985) 2809.
[20] R. J. Cole, J. W. Kirksey, H. G. Cutler, B. L. Doupnik, J. C. Peckham, *Science (Washington, D.C.) 179* (1973) 1234.
[21] J. P. Springer, J. Clardy, R. J. Cole, J. W. Kirksey, R. K. Hill, R. M. Carlson, J. L. Isidor, *J. Am. Chem. 96* (1974) 2267.
[22] D. Belluš, Hp. Fischer in H. Geissbühler (Ed.): *Advances in Pesticide Sciences, Vol. 2*, Pergamon Press, Oxford 1979, p. 373.
[23] D. Belluš, Hp. Fischer, H. Greuter, P. Martin, *Helv. Chim. Acta 61* (1978) 1784.
[24] H.-D. Scharf, H. Frauenrath, W. Pinske, *Chem. Ber. 111* (1978) 168.
[25] A. Bou, M. A. Pericàs, F. Seratosa, *Tetrahedron Lett. 23* (1982) 361.
[26] a) D. Belluš, *J. Am. Chem. Soc. 100* (1978) 8026; b) D. Belluš, P. Martin, H. Sauter, T. Winkler, *Helv. Chim. Acta 63* (1980) 1130.
[27] R. Happle, K. J. Kalveram, U. Büchner, K. Echternacht-Happle, W. Göggelmann, K. H. Summer, *Dermatologica 161* (1980) 289.
[28] D. Belluš, *J. Org. Chem. 44* (1979) 1208.
[29] J. R. Heys, E. H. Chew, *J. Labelled Compd. Radiopharm. 21* (1984) 409.
[30] B. Franck, G. Breipohl, *Angew. Chem. 96* (1984) 999; *Angew. Chem. Int. Ed. Engl. 23* (1984) 996.
[31] a) C. H. Hassall, *Org. React. 9* (1957) 73; b) B. Plesničar in W. S. Trahanovsky (Ed.): *Organic Chemistry, Vol. 5C*, Academic Press, New York 1978, p. 211.
[32] B. M. Trost, P. Bühlmayer, M. Mao, *Tetrahedron Lett. 23* (1982) 1443.
[33] a) P. A. Grieco, N. Marinovic, M. Miyashita, *J. Org. Chem. 40* (1975) 1670; b) H.-J. Liu, P. C.-L. Yao, *Can. J. Chem. 55* (1977) 822; c) A. Hassner, H. W. Pinnick, J. M. Ansell, *J. Org. Chem. 43* (1978) 1774; d) K. Jarowicki, T. Jaworski, *Monatsh. Chem. 115* (1984) 605.
[34] a) B. M. Trost, M. J. Bogdanowicz, *J. Am. Chem. Soc. 95* (1973) 5321; b) R. D. Miller, D. L. Dolce, V. Y. Merritt, *J. Org. Chem. 41* (1976) 1221; c) B. M. Trost, J. H. Rigby, *ibid. 43* (1978) 2938; d) B. M. Trost, A. Brandi, *J. Am. Chem. Soc. 106* (1984) 5041.
[35] a) R. A. Whitney, *Can. J. Chem. 59* (1981) 2650; b) *ibid. 61* (1983) 1158.
[36] S. Matsubara, K. Takai, H. Nozaki, *Bull. Chem. Soc. Jpn. 56* (1983) 2029.
[37] M. Suzuki, H. Takada, R. Noyori, *J. Org. Chem. 47* (1982) 902.
[38] P. A. Grieco, T. Oguri, S. Gilman, *J. Am. Chem. Soc. 100* (1978) 1616.
[39] a) A. M. Ali, S. M. Roberts, *J. Chem. Soc. Perkin Trans. 1 1976*, 1934; b) W. T. Brady, T. C. Cheng, *J. Org. Chem. 41* (1976) 2036; c) H. G. Heine, A. Hübner, W. Hartmann, DBP 2740849 (1977), Bayer AG; d) L. Ghosez, I. Markó, A.-M. Hesbain-Frisque, *Tetrahedron Lett. 27* (1986) 5211; e) Y. Tsunokawa, S. Iwasaki, S. Okuda, *Chem. Pharm. Bull. 31* (1983) 4578.
[40] a) P. W. Jeffs, G. Molina, *J. Chem. Soc. Chem. Commun. 1973*, 3; b) P. W. Jeffs, G. Molina, N. A. Cortese, P. R. Hauck, J. Wolfram, *J. Org. Chem. 47* (1982) 3876.
[41] R. Jeanne-Carlier, F. Bourelle-Wargnier, *Tetrahedron Lett. 1975*, 1841.
[42] R. Jeanne-Carlier, F. Bourelle-Wargnier, *Bull. Soc. Chim. Fr. 1976*, 297.
[43] S. M. Roberts, R. F. Newton: *Prostaglandins and Thromboxanes*, Butterworths, London 1982.
[44] K. Kakiuchi, Y. Hiramatsu, Y. Tobe, Y. Odaira, *Bull. Chem. Soc. Jpn. 53* (1980) 1779.
[45] Y. Ohshiro, M. Ishida, J. Shibata, T. Minami, T. Agawa, *Chem. Lett. 1982*, 587.
[46] a) L. A. Paquette, M. J. Wyvratt, O. Schallner, J. L. Muthard, W. J. Begley, R. M. Blankenship, D. Balogh, *J. Org. Chem. 44* (1979) 3616; b) U. R. Ghatak, B. Sanyal, G. O. S. V. Satyanarayana, S. Ghosh, *J. Chem. Soc. Perkin Trans. 1 1981*, 1203; c) P. W. Jeffs, G. Molina, M. W. Cass, N. A. Cortese, *J. Org. Chem. 47* (1982) 3871; d) T. Imanishi, M. Inoue, Y. Wada, M. Hanaoka, *Chem. Pharm. Bull. 31* (1983) 1235; e) G. Rosini, R. Ballini, *Tetrahedron 39* (1983) 1085.
[47] B.-W. Au Yeung, I. Fleming, *J. Chem. Soc. Chem. Commun. 1977*, 79.
[48] W. Ried, O. Bellinger, *Liebigs Ann. Chem. 1984*, 1109.
[49] B. M. Trost, J. M. Balkovec, M. K.-T. Mao, *J. Am. Chem. Soc. 105* (1983) 6755.
[50] K.-H. Lee, E.-S. Huang, C. Piantadosi, J. S. Pagano, T. A. Geissman, *Cancer Res. 31* (1971) 1649.
[51] a) P. A. Grieco, K. Hiroi, *Tetrahedron Lett. 1974*, 3467; b) P. A. Grieco, T. Oguri, S. Gilman, *J. Am. Chem. Soc. 102* (1980) 5886; c) N. Petragnani, H. M. C. Ferraz, G. V. J. Silva, *Synthesis 1986*, 157.
[52] S. M. Ali, S. M. Roberts, *J. Chem. Soc. Chem. Commun. 1975*, 887.
[53] S. M. Ali, T. V. Lee, S. M. Roberts, *J. Chem. Soc. Perkin Trans. 1 1979*, 708.
[54] a) R. Livingstone in: *Rodd's Chemistry of Carbon Compounds, Vol. IVa*, Elsevier, Amsterdam 1973, p. 379; b) C. W. Bird, G. W. H. Cheesman in: *Comprehensive Heterocyclic Chemistry, Vol. 4*, Pergamon, Oxford 1984, p. 89.
[55] a) A. E. Greene, J. P. Deprès, M. C. Meana, P. Crabbé, *Tetrahedron Lett. 1976*, 3755; b) A. E. Greene, J. P. Deprès, H. Nagano, P. Crabbé, *ibid. 1977*, 2365.
[56] Y. Tamura, H. Fujiwara, K. Sumoto, M. Ikeda, *Synthesis 1977*, 1.
[57] a) W. Bartmann, G. Beck, *Angew. Chem. 94* (1982) 767; *Angew. Chem. Int. Ed. Engl. 21* (1982) 751; b) W. Bartmann, G. Beck, J. Knolle, R. H. Rupp, *Tetrahedron Lett. 23* (1982) 3647.
[58] T.-Y. Luh, H.-F. Chow, W. Y. Leung, S. W. Tam, *Tetrahedron 41* (1985) 519.
[59] M. E. Jung, *Tetrahedron 32* (1976) 3.
[60] C. D. Gutsche, *Org. React. 8* (1954) 364.
[61] A. E. Greene, M.-J. Luche, A. A. Serra, *J. Org. Chem. 50* (1985) 3957.
[62] a) A. E. Greene, J.-P. Deprés, *J. Am. Chem. Soc. 101* (1979) 4003; b) J.-P. Deprés, A. E. Greene, *J. Org. Chem. 45* (1980) 2036; c) G. D. Annis, L. A. Paquette, *J. Am. Chem. Soc. 104* (1982) 4504; d) G. Mehta, K. S. Rao, *Tetrahedron Lett. 25* (1984) 3481; e) *ibid. 25* (1984) 1839; f) *J. Org. Chem. 50* (1985) 5537.
[63] a) A. E. Greene, *Tetrahedron Lett. 21* (1980) 3059; b) A. E. Greene, M.-J. Luche, J.-P. Deprés, *J. Am. Chem. Soc. 105* (1983) 2435.
[64] A. E. Greene, J.-P. Lansard, J.-L. Luche, C. Petrier, *J. Org. Chem. 49* (1984) 931.
[65] L. A. Paquette, R. S. Valpey, G. D. Annis, *J. Org. Chem. 49* (1984) 1317.
[66] a) B.-W. Au-Yeung, I. Fleming, *J. Chem. Soc. Chem. Commun. 1977*, 81; b) I. Fleming, B.-W. Au-Yeung, *Tetrahedron 37* (1981) 13.
[67] E. J. Corey, M. C. Desai, T. A. Engler, *J. Am. Chem. Soc. 107* (1985) 4339.
[68] L. Fitjer, A. Kanschik, M. Majewski, *Tetrahedron Lett. 26* (1985) 5277.
[69] B. M. Trost, L. H. Latimer, *J. Org. Chem. 43* (1978) 1031.
[70] E. Wenkert, T. S. Arrhenius, *J. Am. Chem. Soc. 105* (1983) 2030.
[71] T. W. Hart, M.-T. Comte, *Tetrahedron Lett. 26* (1985) 2713.
[72] F. Karrenbrock, H. J. Schäfer, *Tetrahedron Lett. 1978*, 1521.
[73] a) M.-L. Leriverend, M. Vazeux, *J. Chem. Soc. Chem. Commun. 1982*, 866; b) V. Reutrakul, C. Panyachotipun, V. Hahnvajanawong, S. Sotheeswaran, *Tetrahedron Lett. 25* (1984) 1825; c) B. F. Riefling, *ibid. 26* (1985) 2063.
[74] a) S. Halazy, A. Krief, *J. Chem. Soc. Chem. Commun. 1982*, 1200; b) S. Halazy, F. Zutterman, A. Krief, *Tetrahedron Lett. 23* (1982) 4385; c) L. Fitjer, H.-J. Scheuermann, D. Wehle, *ibid. 25* (1984) 2329; d) A. Krief, J. L. Labourer, *J. Chem. Soc. Chem. Commun. 1986*, 702.
[75] R. C. Gadwood, *J. Org. Chem. 48* (1983) 2098.
[76] M. Nee, J. D. Roberts, *J. Org. Chem. 46* (1981) 67.
[77] S. Knapp, A. F. Trope, R. M. Ornaf, *Tetrahedron Lett. 21* (1980) 4301.
[78] N. Chatani, H. Furukawa, T. Kato, S. Murai, N. Sonoda, *J. Am. Chem. Soc. 106* (1984) 430.
[79] a) M. Braun, R. Dammann, D. Seebach, *Chem. Ber. 108* (1975) 2368; b) R. W. Holder, H. S. Feiman, M. F. Stefanchick, *J. Org. Chem. 41* (1976) 3303; c) B. M. Trost, D. E. Keely, H. C. Arndt, J. H. Rigby, M. J. Bogdanowicz, *J. Am. Chem. Soc. 99* (1977) 3080; d) T. Cohen, J. R. Matz, *Tetrahedron Lett. 22* (1981) 2455; e) R. L. Danheiser, S. K. Gee, H. Sard, *J. Am. Chem. Soc. 104* (1982) 7670.
[80] M. Bertrand, R. Maurin, J. L. Gras, G. Gil, *Tetrahedron 31* (1975) 849.
[81] a) M. Bertrand, G. Gil, A. Junino, *Tetrahedron Lett. 1977*, 1779; b) M. Bertrand, G. Gil, A. Junino, R. Maurin, *J. Chem. Res. Synop. 1980*, 98.
[82] J. R. Matz, T. Cohen, *Tetrahedron Lett. 22* (1981) 2459.
[83] D. A. Jackson, M. Rey, A. S. Dreiding, *Helv. Chim. Acta 68* (1985) 439.
[84] R. Huston, M. Rey, A. S. Dreiding, *Helv. Chim. Acta 65* (1982) 1563.
[85] D. A. Jackson, M. Rey, A. S. Dreiding, *Tetrahedron Lett. 24* (1983) 4817.
[86] D. A. Evans, A. M. Golob, *J. Am. Chem. Soc. 97* (1975) 4765.
[87] R. L. Danheiser, C. Martinez-Davila, H. Sard, *Tetrahedron 37* (1981) 3943.
[88] T. Cohen, M. Bhupathy, J. R. Matz, *J. Am. Chem. Soc. 105* (1983) 520.
[89] J. J. Bloomfield, J. M. Nelke, *Org. Synth. 57* (1977) 1.
[90] a) I. Kuwajima, T. Azegami, E. Nakamura, *Chem. Lett. 1978*, 1432; b) J. R. Williams, T. J. Caggiano, *Synthesis 1980*, 1024; c) K. W. Anderson, G. E. Lee, *Synth. Commun. 10* (1980) 351; d) I. Nishiguchi, T.

Hirashima, T. Shono, M. Sasaki, *Chem. Lett. 1981*, 551; e) D. de Keukeleire, M. van Audenhove, L. van Hijfte, F. Audenaert, M. Vandewalle, *J. Photochem. 28* (1985) 165.
[91] E. Nakamura, J. Shimada, I. Kuwajima, *J. Chem. Soc. Chem. Commun. 1983*, 498.
[92] a) E. Nakamura, K. Hashimoto, I. Kuwajima, *J. Org. Chem. 42* (1977) 4166; b) E. Nakamura, I. Kuwajima, *J. Am. Chem. Soc. 99* (1977) 961; c) W. Oppolzer, R. D. Wylie, *Helv. Chim. Acta 63* (1980) 1198; d) J. Shimada, K. Hashimoto, B. H. Kim, E. Nakamura, I. Kuwajima, *J. Am. Chem. Soc. 106* (1984) 1759.
[93] a) V. P. Abegg, A. C. Hopkinson, E. Lee-Ruff, *Can. J. Chem. 56* (1978) 99; b) L. H. Dao, A. C. Hopkinson, E. Lee-Ruff, *Tetrahedron Lett. 1978*, 1413.
[94] P. Duperrouzel, E. Lee-Ruff, *Can. J. Chem. 58* (1980) 51.
[95] a) E. Lee-Ruff, A. C. Hopkinson, H. Kazarians-Moghaddam, P. Duperrouzel, B. Gupta, M. Katz, *Tetrahedron Lett. 22* (1981) 4917; b) E. Lee-Ruff, A. C. Hopkinson, L. H. Dao, *Can. J. Chem. 59* (1981) 1675.
[96] a) R. H. Thomson: *Naturally Occurring Quinones*, Academic Press, New York 1971, p. 93; b) W. A. Remers: *Chemistry of Antitumor Antibiotics*. Wiley, New York 1979.
[97] a) L. S. Liebeskind, S. L. Baysdon, *Tetrahedron Lett. 25* (1984) 1747; b) L. S. Liebeskind, J. P. Leeds, S. L. Baysdon, S. Iyer, *J. Am. Chem. Soc. 106* (1984) 6451.
[98] a) M. S. South, L. S. Liebeskind, *J. Am. Chem. Soc. 106* (1984) 4181; b) L. S. Liebeskind, S. L. Baysdon, M. S. South, S. Iyer, J. P. Leeds, *Tetrahedron 41* (1985) 5839.
[99] a) D. K. Anderson, C. E. Coburn, A. P. Haag, J. S. Swenton, *Tetrahedron Lett. 24* (1983) 1329; b) L. A. Spangler, J. S. Swenton, *J. Org. Chem. 49* (1984) 1800; c) L. A. Spangler, J. S. Swenton, *J. Chem. Soc. Chem. Commun. 1986*, 828.
[100] a) A. Herrera, H. Hoberg, *Synthesis 1981*, 831; b) H. Hoberg, A. Herrera, *Angew. Chem. 93* (1981) 924; *Angew. Chem. Int. Ed. Engl. 10* (1981) 876; c) A. Roeding, E. M. Ganns, C. Henrich, H. Schnutenhaus, *Liebigs Ann. Chem. 1981*, 1674; d) N. P. Hacker, J. F. W. McOmie, J. Meunier-Pirel, M. Van Meerssche, *J. Chem. Soc. Perkin Trans. 1 1982*, 19; e) M. S. South, L. S. Liebeskind, *J. Org. Chem. 47* (1982) 3815.
[101] E. Mitch, A. S. Dreiding, *Chimia 14* (1960) 424.
[102] J. C. Gilbert, T. Luo, R. E. Davis, *Tetrahedron Lett. 1975*, 2545.
[103] T. V. Lee, S. M. Roberts, R. F. Newton, *J. Chem. Soc. Perkin Trans. 1 1978*, 1179.
[104] R. F. Newton, S. M. Roberts, *Tetrahedron 36* (1980) 2163.
[105] E. W. Collington, H. Finch, C. J. Wallis, *Tetrahedron Lett. 24* (1983) 3121.
[106] A. E. Favorskii, *J. Russ. Phys.-Chem. Soc. 26* (1894) 559.
[107] a) C. Rappe, L. Knutson, *Acta Chem. Scand. 21* (1967) 163; b) P. J. Chenier, *J. Chem. Educ. 55* (1978) 286; c) A. Baretta, B. Waegell in A. E. Abramowitch (Ed.): *Reactive Intermediates, Vol. 2*, Plenum Press, New York 1982, p. 527.
[108] R. B. Loftfield, *J. Am. Chem. Soc. 73* (1951) 4707.
[109] T. Tchoubar, O. Sackur, *C. R. Hebd. Seances Acad. Sci. 208* (1939) 1020.
[110] J. M. Conia, J. Salaün, *Tetrahedron Lett. 1963*, 1175.
[111] J. M. Conia, J. R. Salaün, *Acc. Chem. Res. 5* (1972) 33.
[112] W. F. Erman, E. Wenkert, P. W. Jeffs, *J. Org. Chem. 34* (1969) 2196.
[113] B. M. Trost, M. J. Bogdanowicz, J. Kern, *J. Am. Chem. Soc. 97* (1975) 2218.
[114] B. M. Trost, M. Preckel, L. M. Leichter, *J. Am. Chem. Soc. 97* (1975) 2224.
[115] D. L. Garin, K. L. Cammack, *J. Chem. Soc. Chem. Commun. 1972*, 333.
[116] a) V. R. Fletcher, A. Hassner, *Tetrahedron Lett. 1970*, 1071; b) W. T. Brady, J. P. Hieble, *J. Org. Chem. 36* (1971) 2033; c) P. R. Brook, J. M. Harrison, *J. Chem. Soc. Chem. Commun. 1972*, 997; d) W. T. Brady, A. D. Patel, *J. Org. Chem. 33* (1973) 4106; e) W. T. Brady, P. L. Ting, *J. Chem. Soc. Perkin Trans. 1 1975*, 456.
[117] a) P. Martin, H. Greuter, D. Belluš, *Pestic. Sci. 11* (1980) 141; b) P. Martin, *Helv. Chim. Acta 66* (1983) 1189.
[118] V. S. Veleževa, V. A. Barkhash, I. V. Machinskaya, *Zh. Org. Khim. 6* (1970) 1788.
[119] M. van den Brink, R. A. Sheldon, Belg. Pat. 857985 (1976), Shell.
[120] a) P. R. Brook, A. J. Duke, *Chem. Commun. 1970*, 652; b) P. R. Brook, A. J. Duke, *J. Chem. Soc. Perkin Trans. 1 1973*, 1013; c) W. Hartmann, H.-G. Heine, D. Wendisch, *Tetrahedron Lett. 1977*, 2263.
[121] R. Huston, M. Rey, A. S. Dreiding, *Bull. Soc. Chim. Belg. 88* (1979) 911.
[122] a) H.-D. Scharf, W. Droste, R. Liebig, *Angew. Chem. 80* (1968) 194; *Angew. Chem. Int. Ed. Engl. 7* (1968) 215; b) A. de Groot, D. Oudman, H. Wynberg, *Tetrahedron Lett. 1969*, 1529; c) H.-D. Scharf, *Angew. Chem. 86* (1974) 567; *Angew. Chem. Int. Ed. Engl. 13* (1974) 520; d) J. P. Barnier, J. M. Denis, J. R. Salaün, J. M. Conia, *Tetrahedron 30* (1974) 1405; e) J. M. Conia, J. M. Denis, *Tetrahedron Lett. 1971*, 2845; f) H. G. Heine, *Chem. Ber. 104* (1971) 2869; g) W. Ried, A. H. Schmidt, H. Medem, *Justus Liebigs Ann. Chem. 1973*, 1530.
[123] a) K. E. Harding, J. W. Trotter, *J. Org. Chem. 42* (1977) 4157; b) A. K. Yagoub, G. M. Iskander, F. Stansfield, *J. Chem. Soc. Perkin Trans. 1 1977*, 697.
[124] a) G. Jones II, L. P. McDonnell, *J. Am. Chem. Soc. 98* (1976) 6203; b) *J. Chem. Soc. Chem. Commun. 1976*, 18; c) P. Martin, H. Greuter, D. Belluš, *Helv. Chim. Acta 64* (1981) 64.
[125] P. Martin, H. Greuter, D. Belluš, *J. Am. Chem. Soc. 101* (1979) 5853.
[126] M. J. van den Brink, H. Austermühle-Bertola, P. A. Kramer, DBP 2539048 (1974), Shell.
[127] W. T. Brady, S. J. Norton, J. Ko, *Synthesis 1983*, 1002.
[128] K. Naumann in R. Wegler (Ed.): *Chemie der Pflanzenschutz- und Schädlingsbekämpfungsmittel, Vol. 7*, Springer, Berlin 1981.
[129] a) P. Martin, H. Greuter, E. Steiner, D. Belluš, US-Pat. 4242278 (1977), Ciba-Geigy AG; b) P. Martin, H. Greuter, D. Belluš, US-Pat. 4255351 (1978), Ciba-Geigy AG; c) H. Greuter, P. Bissig, P. Martin, V. Flück, L. Gsell, *Pestic. Sci. 11* (1980) 148; d) P. Martin, E. Steiner, D. Belluš, *Helv. Chim. Acta 63* (1980) 1947.
[130] P. Martin, H. Greuter, E. Steiner, D. Belluš, S. Afr.-Pat. 78-05960 (1978), Ciba-Geigy AG.
[131] P. Martin, E. Steiner, D. Belluš, DBP 3045768 (1979), Ciba-Geigy AG.
[132] a) H.-G. Heine, W. Hartmann, DBP 2638356 (1976), Bayer AG; b) A. Hübner, H. G. Heine, W. Hartmann, DBP 2918468 (1979), Bayer AG.
[133] a) M. Eliott: *Synthetic Pyrethroids, ACS Symp. Ser. 42* (1977); b) D. Belluš, P. Martin, H. Greuter, E. Steiner, *Chimia 34* (1980) 238; c) T. Kazunori, M. Noritada, H. Makoto, Y. Toshihiko, I. Nobushigo, Eur. Pat.-Appl. 56271 (1981), Sumitomo.
[134] R. Lantzsch, P. Arlt, M. Jautelat, DBP 3220730 (1982), Bayer AG.
[135] P. Bissig, H. Greuter, L. Gsell, Eur. Pat.-Appl. 4316 (1978), Ciba-Geigy AG.
[136] R. B. Mitra, A. S. Khanra, *Synth. Commun. 7* (1977) 245.
[137] H. Greuter, J. Dingwall, P. Martin, D. Belluš, *Helv. Chim. Acta 64* (1981) 2812.
[138] H. C. Stevens, D. A. Reich, D. R. Brandt, K. R. Fountain, E. J. Gaughan, *J. Am. Chem. Soc. 87* (1965) 5257.
[139] P. D. Bartlett, T. Ando, *J. Am. Chem. Soc. 92* (1970) 7518.
[140] T. Asao, T. Machiguchi, T. Kitamura, Y. Kitahara, *Chem. Commun. 1970*, 89.
[141] K. Tanaka, A. Yoshikoshi, *Tetrahedron 27* (1971) 4889.
[142] K. Imafuku, K. Inoue, *Bull. Chem. Soc. Jpn. 55* (1982) 3242.
[143] D. Arlt, M. Jautelat, R. Lantzsch, *Angew. Chem. 93* (1981) 719; *Angew. Chem. Int. Ed. Engl. 10* (1981) 703.
[144] J. Ficini, *Tetrahedron 32* (1976) 1449.
[145] a) J. Ficini, J. d'Angelo, J. Noiré, *J. Am. Chem. Soc. 96* (1974) 1213; b) J. Ficini, J. d'Angelo, A. Eman, A. M. Touzin, *Tetrahedron Lett. 1976*, 683.
[146] a) F. E. Ziegler, G. R. Reid, W. L. Studt, P. A. Wender, *J. Org. Chem. 42* (1977) 1991; b) J. Ficini, A. Guingant, J. d'Angelo, *J. Am. Chem. Soc. 101* (1979) 1318.
[147] M. Ikeda, T. Uno, K. Homma, K. Ohno, Y. Tamura, *Synth. Commun. 10* (1980) 437.
[148] M. G. Bigg, S. M. Roberts, H. J. Suschitzky, *J. Chem. Soc. Perkin Trans. 1 1981*, 926.
[149] a) P. R. Brook, J. M. Harrison, *J. Chem. Soc. Perkin Trans. 1 1974*, 778; b) R. Terlinden, W. Boland, L. Jaenicke, *Helv. Chim. Acta 66* (1983) 466; c) W. Boland, L. Jaenicke, *Chem. Ber. 111* (1978) 3262.
[150] a) W. Boland, L. Jaenicke, *Chem. Ber. 110* (1977) 1823; b) N. Nakamura, K. Sakai, *Tetrahedron Lett. 1978*, 1549.
[151] a) E. Cossement, R. Binamé, L. Ghosez, *Tetrahedron Lett. 1974*, 997; b) P. Michel, M. O'Donnell, R. Binamé, A. M. Hesbain-Frisque, L. Ghosez, J. P. Declercq, G. Germain, E. Ange, M. van Meerssche, *ibid. 21* (1980) 2577.
[152] S. Goldstein, P. Vames, C. Houge, A. M. Frisque-Hesbain, C. Wiaux-Zamar, L. Ghosez, *J. Am. Chem. Soc. 103* (1981) 4616.
[153] W. Friedrichsen, T. Debaerdemaeker, A. Böttcher, S. Hahnemann, R. Schmidt, *Z. Naturforsch. B 38* (1983) 504.
[154] J. E. Burks, Jr., J. K. Crandall, *J. Org. Chem. 49* (1984) 4663.
[155] E. J. Corey, B. De, *J. Am. Chem. Soc. 106* (1984) 2735.
[156] J.-P. Deprés, F. Coelho, A. E. Greene, *J. Org. Chem. 50* (1985) 1972.
[157] A. E. Greene, J.-P. Deprés, F. Coelho, T. J. Brocksom, *J. Org. Chem. 50* (1985) 3943.
[158] G. Fráter, U. Müller, W. Günther, *Tetrahedron Lett. 25* (1984) 1133.
[159] a) J. Davies, S. M. Roberts, D. P. Reynolds, R. F. Newton, *J. Chem. Soc. Perkin Trans. 1 1981*, 1317; b) C. Howard, R. F. Newton, D. P. Reynolds, *ibid. 1981*, 2049.
[160] R. D. Miller, D. R. McKean, *Tetrahedron Lett. 21* (1980) 2639.
[161] A. Murai, M. Ono, T. Masamune, *J. Chem. Soc. Chem. Commun. 1977*, 573.

[162] R. H. Moriarty, *Top. Stereochem. 8* (1974) 271.
[163] a) R. C. Kelly, US-Pat. 3946046 (1970), Upjohn; b) R. C. Kelly, US-Pat. 3966751 (1970), Upjohn; c) R. C. Kelly, V. Van Rheenen, I. Schletter, M. D. Pillai, *J. Am. Chem. Soc. 95* (1973) 2746; d) R. C. Kelly, V. Van Rheenen, *Tetrahedron Lett. 1973*, 1709.
[164] C. J. Wallis, Eur. Pat.-Appl. 74856 (1981), Glaxo.
[165] C. R. Johnson, J. R. Zeller, *J. Am. Chem. Soc. 104* (1982) 4021.
[166] a) R. F. Newton, J. Paton, D. P. Reynolds, S. Young, S. M. Roberts, *J. Chem. Soc. Chem. Commun. 1979*, 908; b) M. J. Dawson, G. C. Lawrence, G. Lilley, M. Todd, D. Noble, S. M. Green, S. M. Roberts, T. W. Wallace, R. F. Newton, M. C. Carter, P. Hallett, J. Paton, D. P. Reynolds, S. Young, *J. Chem. Soc. Perkin Trans. 1 1983*, 2119; c) S. M. Roberts in *Enzymes in Organic Synthesis: Ciba-Foundation Symposium 111*, Pitman, London 1985, p. 31.
[167] R. F. Newton, D. P. Reynolds, J. Davies, P. B. Kay, S. M. Roberts, T. W. Wallace, *J. Chem. Soc. Perkin Trans. 1 1983*, 683.
[168] K. Kieslich: *Microbial Transformations of Chemical Compounds Excluding Steroids and Non-Cyclic Structures*, Thieme, Stuttgart 1976.
[169] S. Butt, H. G. Davies, M. J. Dawson, G. C. Lawrence, J. Leaver, S. M. Roberts, M. K. Turner, B. J. Wakefield, W. F. Wall, J. A. Winders, *Tetrahedron Lett. 26* (1985) 5077.
[170] H. C. Brown, P. K. Jadhav, B. Singram in R. Scheffold (Ed.): *Modern Synthetic Methods*, Springer, Heidelberg 1986, p. 307.
[171] G. Fráter, U. Müller, W. Guenther, *Tetrahedron 40* (1984) 1269.
[172] D. van Leusen, P. H. F. M. Rouwette, A. M. van Leusen, *J. Org. Chem. 46* (1981) 5159.
[173] C. Houge, A. M. Frisque-Hesbain, A. Mockel, L. Ghosez, J. P. Declercq, G. Germain, M. Van Meerssche, *J. Am. Chem. Soc. 104* (1982) 2920.
[174] A. E. Greene, F. Charbonnier, *Tetrahedron Lett. 26* (1985) 5525.
[175] K. H. Theopold, P. N. Becker, R. G. Bergmann, *J. Am. Chem. Soc. 104* (1982) 5250.
[176] a) M. N. Das, F. Kern, T. D. Coyle, W. D. Walters, *J. Am. Chem. Soc. 76* (1954) 6271; b) T. H. McGee, A. Schleifer, *J. Phys. Chem. 76* (1972) 963; c) H. M. Frey, H. Hopf, *J. Chem. Soc. Perkin Trans. 2 1973*, 2016; d) G. Rousseau, R. Bloch, P. Le Perchec, J. M. Conia, *J. Chem. Soc. Chem. Commun. 1973*, 795; e) H. M. Frey, R. A. Smith, *J. Chem. Soc. Perkin Trans. 2 1977*, 752; f) H. M. Frey, R. A. Smith, *ibid. 1977*, 2082; g) J. Indermühle, *Dissertation*, Universität Basel 1978.
[177] H. A. J. Carless, E. K. C. Lee, *J. Am. Chem. Soc. 92* (1970) 4482.
[178] F. Huet, A. Lechevallier, J. M. Conia, *Chem. Lett. 1981*, 1515.
[179] H. Prinzbach, H.-P. Schal, D. Hunkler, H. Fritz, *Angew. Chem. 92* (1980) 575; *Angew. Chem. Int. Ed. Engl. 19* (1980) 567.
[180] M. B. Sponsler, D. A. Dougherty, *J. Org. Chem. 49* (1984) 4978.
[181] R. Huston, M. Rey, A. S. Dreiding, *Helv. Chim. Acta 65* (1982) 451.
[182] W. S. Trahanovsky, B. W. Surber, M. C. Wilkes, M. M. Preckel, *J. Am. Chem. Soc. 104* (1982) 6779.
[183] a) M. Kahn, *Tetrahedron Lett. 21* (1980) 4547; b) S. G. Levine, R. L. McDaniel, *J. Org. Chem. 46* (1981) 2199; c) R. C. Gadwood, R. M. Lett, *ibid. 47* (1982) 2268; d) L. A. Paquette, J. A. Colapret, D. R. Andrews, *ibid. 50* (1985) 201.
[184] R. C. Gadwood, R. M. Lett, J. E. Wissinger, *J. Am. Chem. Soc. 106* (1984) 3869.
[185] W. C. Still, S. Murata, G. Revial, K. Yoshihara, *J. Am. Chem. Soc. 105* (1983) 625.
[186] a) J. E. Baldwin, M. C. McDaniel, *J. Am. Chem. Soc. 89* (1967) 1537; b) J. E. Baldwin, M. C. McDaniel, *ibid. 90* (1968) 6118.
[187] B. Ernst, H. Greuter, S. Veenstra, unpublished works, 1986.
[188] H. Mayr, R. Huisgen, *Angew. Chem. 87* (1975) 491; *Angew. Chem. Int. Ed. Engl. 14* (1975) 499.
[189] a) G. A. Boswell, Jr., A. J. Cocuzza, US-Pat. 4505905 (1982), Du Pont; b) O. Meth-Cohn, A. J. Reason, S. M. Roberts, *J. Chem. Soc. Chem. Commun. 1982*, 90; c) G. Lowe, S. Swain, *ibid. 1983*, 1279; d) A. J. Cocuzza, G. A. Boswell, *Tetrahedron Lett. 26* (1985) 5363; e) G. Lowe, S. Swain, *J. Chem. Soc. Perkin Trans. 1 1985*, 391; f) G. Lange, M. E. Savard, T. Viswanatha, G. I. Dmitrienko, *Tetrahedron Lett. 26* (1985) 1791; g) D. Agathocleous, G. Cox, M. I. Page, *ibid. 27* (1986) 1631.
[190] I. Markó, B. Ronsmans, A.-M. Hesbain-Frisque, S. Dumas, L. Ghosez, B. Ernst, H. Greuter, *J. Am. Chem. Soc. 107* (1985) 2192.
[191] a) H. Mayr, *Angew. Chem. 87* (1975) 491; *Angew. Chem. Int. Ed. Engl. 14* (1975) 500; b) R. Huisgen, H. Mayr, *J. Chem. Soc. Chem. Commun. 1976*, 55.
[192] K. F. Wedemeyer in E. Müller (Ed.): *Houben-Weyl, Methoden der Organischen Chemie, Vol. 6/1c*, Thieme, Stuttgart 1976.
[193] R. L. Danheiser, S. K. Gee, *J. Org. Chem. 49* (1984) 1672.
[194] R. L. Danheiser, S. K. Gee, J. J. Perez, *J. Am. Chem. Soc. 108* (1986) 806.
[195] P. L. Fishbein, H. W. Moore, *J. Org. Chem. 50* (1985) 3226.
[196] a) J. O. Karlsson, N. V. Nguyen, L. D. Foland, H. W. Moore, *J. Am. Chem. Soc. 107* (1985) 3392; b) S. T. Perri, L. D. Foland, O. H. W. Decker, H. W. Moore, *J. Org. Chem. 51* (1986) 3067; c) H. W. Moore, O. H. W. Decker, *Chem. Rev. 86* (1986) 821.
[197] S. Cohen, S. G. Cohen, *J. Am. Chem. Soc. 88* (1966) 1533.
[198] J. Ficini, S. Falou, J. d'Angelo, *Tetrahedron Lett. 1977*, 1931.
[199] a) N. P. Hacker, N. J. Turro, *J. Photochem. 22* (1983) 131; b) P. Schiess, M. Eberle, M. Huys-Francotte, J. Witz, *Tetrahedron Lett. 25* (1984) 2201.
[200] P. Schiess, M. Heitzmann, *Angew. Chem. 89* (1977) 485; *Angew. Chem. Int. Ed. Engl. 16* (1977) 469.
[201] R. West: *Oxocarbons*, Academic Press, New York 1980.
[202] D. Eggerding, R. West, *J. Am. Chem. Soc. 97* (1975) 207.
[203] E. V. Dehmlow, *Tetrahedron Lett. 1972*, 1271.
[204] P. Dowd, Y. H. Paik, *J. Am. Chem. Soc. 108* (1986) 2788.
[205] a) E. Lee-Ruff, A. C. Hopkinson, H. Kazarians-Moghaddam, *Tetrahedron Lett. 24* (1983) 2067; b) H. G. Davies, S. M. Roberts, B. J. Wakefield, J. A. Winders, D. J. Williams, *J. Chem. Soc. Chem. Commun. 1984*, 640.
[206] a) N. M. Crossland, S. M. Roberts, R. F. Newton, *J. Chem. Soc. Chem. Commun. 1978*, 661; b) R. F. Newton, C. C. Howard, D. P. Reynolds, A. H. Wadsworth, N. M. Crossland, S. M. Roberts, *ibid. 1978*, 662; c) N. M. Crossland, D. R. Kelly, S. M. Roberts, D. P. Reynolds, R. F. Newton, *ibid. 1979*, 681; d) R. F. Newton, D. P. Reynolds, N. M. Crossland, D. R. Kelly, S. M. Roberts, *ibid. 1979*, 683.
[207] Y. Fukuda, T. Negoro, K. Kimura, Y. Odaira, *J. Org. Chem. 45* (1980) 177.
[208] a) M. Pirrung, *Angew. Chem. 97* (1985) 1073; *Angew. Chem. Int. Ed. Engl. 14* (1985) 1043; b) S. Butt, H. G. Davies, M. J. Dawson, G. C. Lawrence, J. Leaver, S. M. Roberts, M. K. Turner, B. J. Wakefield, W. F. Wall, J. A. Winders, J. Chem. Soc. Perkin Trans. 1, *1987*, 903.
[209] D. Belluš, unpublished results.
[210] B. E. Kaplan, L. T. Turner, *Abstr. 158th Nat. Meet. Am. Chem. Soc.*, New York, September 1969, ORGN-40.
[211] G. Frenking, J. Schmidt, H. Schwarz, *Z. Naturforsch. B35* (1980) 1031.
[212] O. Kikuchi, *Bull. Chem. Soc. Jpn. 55* (1982) 1669.
[213] I. Saito, F. Kubota, K. Shimozono, T. Matsuura, *Angew. Chem. 95* (1983) 639; *Angew. Chem. Int. Ed. Engl. 22* (1983) 629; *Angew. Chem. Suppl. 1983*, 835.
[214] a) F. Toda, E. Todo, *Chem. Lett. 1974*, 1279; b) T. Nishio, H. Aoyama, Y. Omote, *Heterocycles 3* (1975) 703; c) F. Toda, E. Todo, *Bull. Chem. Soc. Jpn. 49* (1976) 2503; d) E. Toda, Y. Toda, E. Todo, *ibid. 49* (1976) 2645.
[215] G. Maier, W. A. Jung, *Tetrahedron Lett. 21* (1980) 3875.
[216] N. Obata, T. Takizawa, *Bull. Chem. Soc. Jpn. 50* (1977) 2017.
[217] a) K. Murato, B. Frei, W. B. Schweizer, H. R. Wolf, O. Jeger, *Helv. Chim. Acta 63* (1980) 1856; b) T. A. Lyle, B. Frei, *ibid. 64* (1981) 2598; c) T. A. Lyle, H. B. Mereyala, A. Pascual, B. Frei, *ibid. 67* (1984) 774.
[218] The values found in the literature for the bond angle C(2)C(1)C(4) in monocyclic cyclobutanones, which are taken from X-ray structural determinations, vary between 90.4 [218a] and 93.5° [7f]. The corresponding angle in the unsubstituted cyclobutanone was determined by microwave spectroscopy to be 93.1±0.3° [218b]. – a) R. Hoge, J. Jager, K. Fischer, *Cryst. Struct. Commun. 6* (1977) 287; b) L. H. Scharpen, V. W. Laurie, *J. Chem. Phys. 49* (1968) 221.
[219] D. Seebach in E. Müller (Ed.): *Houben-Weyl, Methoden der Organischen Chemie, Band 4/4*, Thieme, Stuttgart 1971, p. 1.
[220] E. Wenkert, D. A. Berges, N. F. Golob, *J. Am. Chem. Soc. 100* (1978) 1263.
[221] a) R. K. Murray, Jr., D. L. Goff, T. M. Ford, *J. Org. Chem. 42* (1977) 3870; b) I. Kuwajima, I. Azegami, E. Nakamura, *Chem. Lett. 1978* 1431; c) I. Kuwajima, I. Azegami, *Tetrahedron Lett. 1979*, 2369; d) B. M. Trost, L. N. Jungheim, *J. Am. Chem. Soc. 102* (1980) 7910; e) M. Fetizon, N. H. T. Huy, *Nouv. J. Chim. 7* (1983) 321; f) G. Wenke, E. N. Jacobsen, G. E. Trotten, A. C. Karydas, Y. E. Rhodes, *Synth. Commun. 13* (1983) 449; g) P. Filip, N. Stefan, F. Chiraleu, I. G. Dinulescu, M. Avram, *Rev. Roum. Chim. 29* (1984) 549; h) A. Fadel, J. Salaün, *Tetrahedron 41* (1985) 413.
[222] a) R. M. Adlington, J. E. Baldwin, R. H. Jones, J. A. Murphy, M. F. Parisi, *J. Chem. Soc. Chem. Commun. 1983*, 1479; b) J. E. Baldwin, R. M. Adlington, M. F. Parisi, H.-H. Ting, *Tetrahedron 42* (1986) 2575.
[223] E. Vedejs, S. D. Larsen, *J. Am. Chem. Soc. 106* (1984) 3030.
[224] a) J. B. Sieja, *J. Am. Chem. Soc. 93* (1971) 130; b) L. E. Overman, M. E. Okazaki, E. J. Jacobsen, *J. Org. Chem. 50* (1985) 2405; c) L. S. Liebeskind, S. Iyer, C. F. Jewell, Jr., *ibid. 51* (1986) 3065.
[225] G. R. Clark, S. Thiensathit, *Tetrahedron Lett. 26* (1985) 2503.
[226] J. L. Kraus, *Tetrahedron Lett. 26* (1985) 1867.
[227] E. V. Dehmlow, H. G. Schell, *Chem. Ber. 113* (1980) 1.
[228] J. Ficini, J. P. Genêt, *Tetrahedron Lett. 1975*, 2633.
[229] J. E. McMurry, D. D. Miller, *Tetrahedron Lett. 24* (1983) 1885.
[230] K. L. Erickson, J. Markstein, K. Kim, *J. Org. Chem. 36* (1971) 1024.
[231] H. Greuter, T. Winkler, D. Belluš, *Helv. Chim. Acta 62* (1979) 1275.
[232] a) T. A. van Osselaer, G. L. Lemière, J. A. Lepoivre, F. C. Alderweireldt, *Bull. Soc. Chim. Belg. 87* (1978) 153; b) J. B. Jones, D. R. Dodds, *Can. J. Chem. 57* (1979) 2533.

[233] a) P. Crabbé, *Inf. Chim. 160* (1976) 229; b) P. Crabbé, E. Barreiro, H. S. Choi, A. Cruz, J. P. Deprés, G. Gagnaire, A. E. Greene, M. C. Meana, A. Padilla, L. Williams, *Bull. Soc. Chim. Belg. 86* (1977) 109; c) K. E. Harding, J. W. Trotter, L. M. May, *J. Org. Chem. 42* (1977) 2715; d) G. R. Lenz, *J. Chem. Soc. Chem. Commun. 1982*, 803; e) A. E. Greene, J. P. Deprés, M. C. Meana, P. Crabbé, *Tetrahedron Lett. 1976*, 3755.

[234] a) L. R. Smith, G. E. Gream, J. Meinwald, *J. Org. Chem. 42* (1977) 927; b) B. M. Trost, S. A. Godleski, J. Ippen, *ibid. 43* (1978) 4559; c) W. T. Brady, R. D. Watts, *ibid. 45* (1980) 3525; d) E. J. Corey, J.-W. Ponder, P. Ulrich, *Tetrahedron Lett. 21* (1980) 137; e) H. Takeshita, I. Kouno, M. Ilno, H. Iwabuchi, D. Nomura, *Bull. Chem. Soc. Jpn. 53* (1980) 3641; f) S. Bernasconi, P. Gariboldi, G. Jommi, M. Sisti, G. Gasparri-Fava, *J. Chem. Soc. Perkin Trans. 1 1981*, 995; g) M. F. Semmelhack, S. Tomoda, *J. Am. Chem. Soc. 103* (1981) 2427; h) D. Bravetti, R. M. Bettolo, *Helv. Chim. Acta 65* (1982) 371; i) J. F. W. Keana, H. R. Taneja, M. Erion, *Synth. Commun. 12* (1982) 167; j) M. Azadi-Ardakani, T. W. Wallace, *Tetrahedron Lett. 24* (1983) 1829; k) M. E. Jung, G. L. Hatfield, *ibid. 24* (1983) 2931.

[235] a) W. R. McKay, J. Ounsworth, P.-E. Sum, L. Weiler, *Can. J. Chem. 60* (1982) 872; b) L. Skatteböl, Y. Stenström, World-Pat. 8403703 (1984), Borregaard; c) L. Skatteböl, Y. Stenström, *Tetrahedron Lett. 24* (1983) 3021; d) B. D. Johnston, K. N. Slessor, A. C. Oehlschlager, *J. Org. Chem. 50* (1985) 114.

[236] M. F. Semmelhack, S. Tomoda, K. M. Hurst, *J. Am. Chem. Soc. 102* (1980) 7567.

[237] J. V. Paukstelis, J. Kao, *J. Am. Chem. Soc. 94* (1972) 4783.

[238] K. E. Harding, J. W. Trotter, L. M. May, *Synth. Commun. 3* (1973) 201.

[239] a) K. T. Mori, T. F. Uematsu, M. T. Sasaki, DBP 3247861 (1981), Sumitomo; b) K. Mori, T. Uematsu, M. Minobe, K. Yanagi, *Tetrahedron Lett. 23* (1982) 1921.

[240] J. Ficini, J.-P. Genet, *Bull. Soc. Chim. Fr. 1975*, 1811.

[241] a) J. C. Martin, US-Pat. 3408344 (1964), Eastman Kodak; b) J. C. Martin, Br. Pat. 1049326 (1962), Eastman Kodak; c) J. C. Martin, US-Pat. 3288854 (1963), Eastman Kodak.

[242] a) T. Sasaki, S. Eguchi, Y. Hirako, *J. Org. Chem. 42* (1977) 2981; b) D. K. Manh, M. Fétizon, S. Lazare, *J. Chem. Res. Synop. 1978*, 22; c) E. J. Corey, M. C. Desai, *Tetrahedron Lett. 26* (1985) 3535.

[243] D. E. Nichols, K. P. Jadhav, R. A. Oberlender, J. E. Zabik, J. F. Bossart, A. Hamada, D. D. Miller, *J. Med. Chem. 27* (1984) 1108.

[244] a) B. Carnmalm, S. Rämsby, A. L. Renyi, S. B. Ross, S.-O. Oegren, N. E. Stjernström, *J. Med. Chem. 21* (1978) 78; b) D. D. Miller, J. F. Bossart, K. Chelekis, *J. Org. Chem. 44* (1979) 4449.

[245] a) B. M. Trost, A. J. Bridges, *J. Am. Chem. Soc. 98* (1976) 5017; b) B. M. Trost, J. Ippen, W. C. Vladuchick, *ibid. 99* (1977) 8116; c) B. M. Trost, W. C. Vladuchick, A. J. Bridges, *ibid. 102* (1980) 3548.

[246] S. Halazy, A. Krief, *Tetrahedron Lett. 21* (1980) 1997.

[247] a) R. P. Thummel, *J. Am. Chem. Soc. 98* (1976) 628; b) E. Heilbronner, B. Kovač, W. Nutakul, A. D. Taggart, R. P. Thummel, *J. Org. Chem. 46* (1981) 5279.

[248] R. W. Aben, H. W. Scheeren, *J. Chem. Soc. Perkin Trans. 1 1979*, 3132.

[249] K. T. Wanner, A. Kärtner, *Arch. Pharm. (Weinheim, Ger.) 318* (1985) 655.

[250] a) B. M. Trost, D. E. Keely, *J. Org. Chem. 40* (1975) 2013; b) D. D. Miller, F.-L. Hsu, K. N. Salman, P. N. Patil, *J. Med. Chem. 19* (1976) 180.

[251] T. Inoue, I. Kuwajima, *J. Chem. Soc. Chem. Commun. 1980*, 251.

[252] G. R. Clark, J. Lin, M. Nikaido, *Tetrahedron Lett. 25* (1984) 2645.

[253] B. Ernst, H. Greuter, S. J. Veenstra, unpublished results, 1985.

[254] M. L. Greenlee, *J. Am. Chem. Soc. 103* (1981) 2425.

[255] W. G. Dauben, G. Shapiro, *J. Org. Chem. 49* (1984) 4252.

[256] B. M. Trost, D. E. Keely, H. C. Arndt, M. J. Bogdanowicz, *J. Am. Chem. Soc. 99* (1977) 3088.

[257] a) W. T. Brady, E. F. Hoff, R. Roe, Jr., F. H. Parry, Jr., *J. Am. Chem. Soc. 91* (1969) 5679; b) R. Montaigne, L. Ghosez, *Angew. Chem. 80* (1968) 194; *Angew. Chem. Int. Ed. Engl. 7* (1968) 221; c) L. Ghosez, R. Montaigne, A. Roussel, H. Vanlierde, P. Mollet, *Tetrahedron 27* (1971) 615; d) D. A. Bak, W. T. Brady, *J. Org. Chem. 44* (1979) 107; e) W. T. Brady, R. M. Lloyd, *ibid. 44* (1979) 2560; f) P. Picard, J. Moulines, M. Lecoustre, *Bull. Soc. Chim. Fr. 1984*, II-65.

[258] K. E. Harding, J. W. Trotter, L. May, *Synth. Commun. 2* (1972) 231.

[259] M. Rey, U. A. Huber, A. S. Dreiding, *Tetrahedron Lett. 1968*, 3583.

[260] W. H. Perkin, Jr., *Ber. Dtsch. Chem. Ges. 17* (1884) 323; *J. Chem. Soc. 1929*, 1347, and references cited therein.

[261] K. B. Wiberg, *Angew. Chem. 98* (1986) 312; *Angew. Chem. Int. Ed. Engl. 25* (1986) 312.

[262] A. de Meijere, *Chem. Unserer Zeit 16* (1982) 13.

[263] M. Matsumoto, H. Kobayashi, *Heterocycles 24* (1986) 2443.

[264] R. C. Gadwood, I. M. Mallick, A. J. DeWinter, *J. Org. Chem. 52* (1987) 774.

[265] W. D. Abraham, M. Bhupathy, T. Cohen, *Tetrahedron Lett. 28* (1987) 2203.

[266] K. Mori, M. Miyake, *Tetrahedron 43* (1987) 2229.

[267] G. Fráter, U. Müller, W. Günther, *Helv. Chim. Acta 69* (1986) 1858.

[268] M. C. Pirrung, C. V. Deamicis, *Heterocycles 25* (1987) 189.

[269] R. Sigrist, M. Rey, A. S. Dreiding, *J. Chem. Soc. Chem. Commun. 1986*, 944.

[270] T. Wakamatsu, N. Miyachi, F. Ozaki, *Heterocycles 26* (1987) 1445.

[271] B. Bogdanović, K. Schlichte, U. Westeppe, *Chem. Ber. 121* (1988) 27.

[272] R. L. Danheiser, S. Savariar, *Tetrahedron Lett. 28* (1987) 3299.

When submitting manuscripts, authors of articles intended for publication as "Communications" are requested to read the "Notice to Authors" reproduced in the January issue of the journal following the list of contents; upon request, a copy can be obtained from the editorial office.

(Mesityl)$_2$Ge(fluorenylidene)—Stabilization of a Ge–C Double Bond by Charge Transfer into an Aromatic System**

By *Mohamed Lazraq, Jean Escudié,* Claude Couret, Jacques Satgé, Martin Dräger,** and *Ralph Dammel**

Multiple bonds to elements of groups 14 and 15 have been the subject of broad interest in recent years.[1] This is especially true for investigations[2] on silaethenes **1** stabi-

$R_2C{=}SiR'_2$ (1) $R_2C{=}GeR'_2$ (2)

lized by bulky groups; the analogous germaethenes **2**, on the other hand, could only be detected until recently by trapping reactions.[3] Newly obtained pure germaethenes **3**

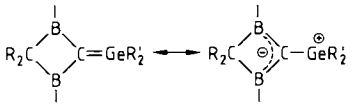

(3)

are stabilized by resonance with an ylide form,[4a] and, for the ether adduct **4b**, we have postulated resonance stabilization involving the fluorenylidene system.[4b] As evidence, we have sought to obtain donor-free **4b** (=**4c**) and to carry out crystal structure analyses of **4c** and of the dihydride **4d** for comparison.

Direct dehydrofluorination of **4a** in a nondonor solvent always gives a nonseparable mixture of **4a/4c/4d**, whereas, in ether, smooth reaction occurs to yield **4b**.[4b] Compound **4b** is very stable thermally; heating it for 15 h at 110°C converts it into **4c**,[5] and reductive hydrogenation of **4b** or **4c** provides **4d**.[4b]

[*] Dr. J. Escudié, M. Lazraq, Dr. C. Couret, Prof. Dr. J. Satgé
Laboratoire de Chimie des Organominéraux
Université Paul Sabatier
118, route de Narbonne, F-31062 Toulouse (France)
Prof. Dr. M. Dräger
Institut für Anorganische Chemie und Analytische Chemie
der Universität
Johann-Joachim-Becher-Weg 24, D-6500 Mainz (FRG)
Dr. R. Dammel
Hoechst Aktiengesellschaft
Hauptlaboratorium G830
D-6230 Frankfurt am Main 80 (FRG)

[**] This work was supported by the Emil and Paul Müller Gedächtnisstiftung, Mainz.

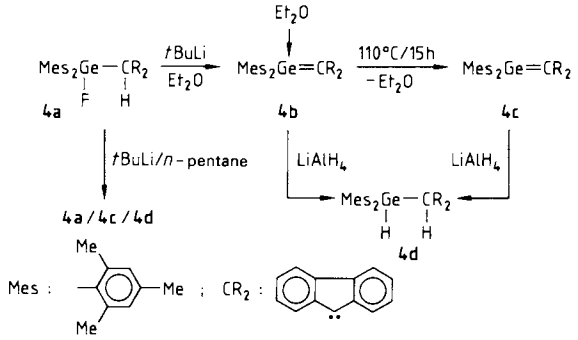

The results of the X-ray structure analyses of **4d** and **4c** are shown in Figures 1 and 2, respectively.[6] The Ge–C1 bond in **4d** (201 pm) is one of the longest known Ge–C

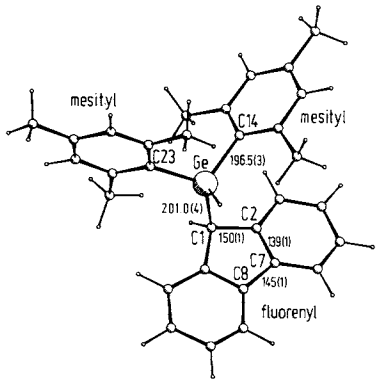

Fig. 1. Structure of **4d** [6] with mean distances [pm] around Ge and in the five-membered ring (with experimental esd's of the individual values Ge–C14 196.4, Ge–C23 196.5; angles around Ge 113.4(2), around C1 105.5(3)°). For a normal fluorenyl group, the mean distances [pm] in the five-membered ring (with standard deviations of the mean value) obtained from analysis of 45 structures [7] are C1–C2 151.9(12), C2–C7 139.5(9), C7–C8 146.3(11) (individual fluctuation C1–C2 148.9–154.1, C2–C7 137.3–142.2, C7–C8 144.0–149.1).

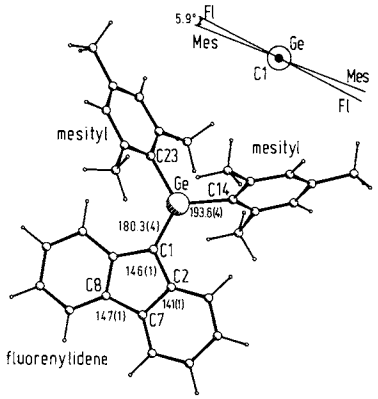

Fig. 2. Structure of **4c** [6] (two crystallographically independent molecules which hardly differ otherwise) with mean distances [pm] around Ge and in the five-membered ring (with experimental esd's of the individual values Ge=C1 180.1 and 180.6, Ge–C14/C23 193.1–194.4; sum of angles around Ge 360.0(2), around C1 360.0(3)°). Above right: Mean twisting around the Ge=C1 bond (variation of the eight torsional angles 4.8–8.6 and 171.0–180.0°). For a normal fluorenylidene group, the mean distances [pm] in the five-membered ring (with standard deviations of the mean values) obtained from analysis of 27 structures [7] are C1–C2 147.2(16), C2–C7 140.5(12), C7–C8 145.9(1) (individual fluctuation C1–C2 144.0–149.6, C2–C7 138.1–143.2, C7–C8 143.6–148.7).

single bonds and, as further evidence for the increased steric encumbrance, differs markedly in length from those of the bonds Ge-C14 and Ge-C23, which lie in the normal range. The Ge atom in **4c** exhibits trigonal-planar coordination (mean deviation ± 1.4 pm). The Ge-C1 distance is 21 pm shorter than in **4d**, and the bonds Ge-C14 and Ge-C23 are also shorter (3 pm) owing to the involvement of sp^2 Ge. In **3**, the length of the Ge=C bond is 183 pm.[4a] Since the mesityl groups in **4c** are twisted to the same extent, it is possible to view the Ge=C bond (= Ge-C1) as a twofold axis.

The fluorene moiety in both compounds corresponds well to the literature data for fluorenyl and fluorenylidene groups. In **4c**, the fluorenylidene moiety is planar (mean deviation ± 2.5 pm), and the planarity extends to the Ge-(C14)-C23 group as well (mean distance of these atoms above the fluorenylidene plane and mean angle made with the plane, +15.1 pm and 7.0°, respectively; mean twisting around Ge=C 6° compared with 36° in **3**). This finding, namely that sixteen atoms lie nearly in the same plane despite higher steric strain than in **4d**, supports our postulate of a stabilization of **4c** by electronic interactions between Ge=C and the fluorenylidene moiety. Similar stabilization of a P-C and of a B-C double bond by the fluorenylidene system is known;[8] for P-C double bonds, interactions with the fluorenylidene π electrons have been proposed.[8a]

Owing to its size, the system **4c** is still too large for the ab initio calculations routinely performed. To study theoretically the above hypothesis, we therefore employed semiempirical (MNDO) calculations, which could provide a satisfactory description of the Ge=C bonding (Table 1), as shown by a comparison of the results obtained for the parent compound $H_2Ge{=}CH_2$ using semiempirical and detailed SCF calculations.[9] The MNDO optimization of the geometric parameters[10a] gave values that, within the limits of error of the method, are in good agreement with the results of X-ray analysis.[10b] The Ge-C double bond is strongly polar; the bond order is significantly less than that of the parent compound (1.50 vs. 1.81). The dipole moment of **4c** is estimated to be 4 Debye. The great importance of a resonance structure $R'_2\overset{\oplus}{G}e{=}C\overset{\ominus}{R}_2$ for describing compounds of type **2** readily explains the better stabilization of **4c** compared with the compounds $R'_2Ge{=}C(Aryl)_2$. The delocalization of the excess negative charge into the fluorenylidene system is much better than in two aryl moieties.[11]

The Raman spectra of finely crystalline **4c** and **4d** hardly differ. To estimate the position of a Ge=C valence vibration, we employed once again ab initio SCF and MNDO calculations.[9, 10c] Such calculations have proved surprisingly reliable for a compound with a Ge-P double bond (Table 1).[12] For **4c**, the Raman- and IR-active valence vibrations of the Ge-C double bond are expected at about 1000 cm^{-1}. In this region, the totally symmetric arene vibrations of the powder sample of **4c** are more strongly structured than those of **4d**, but are not resolved. In order to resolve or decouple further, we recorded single-crystal Raman spectra for several orientations of the two compounds. The only significant difference is a marked emission at 988 cm^{-1} for **4c**, which we assign to the Ge=C valence vibration.

Table 1. Ab initio and MNDO calculated values and experimental values for the distances d(Ge=X) and valence vibrations of compounds containing Ge-X double bonds.

Compound	Calculated		Observed	
	d [pm]	$\tilde{\nu}$ [cm^{-1}]	d [pm]	$\tilde{\nu}$ [cm^{-1}]
$H_2Ge{=}PH$	216.9	481 [a]		
$Mes_2Ge{=}PAryl$ [c]			213.8	503
$H_2Ge{=}CH_2$	177.6	906 [a]		
	172	854 [b]		
4c [d]	177	1018 [b]	180.3	988

[a] Ab initio SCF calculation [9]. [b] MNDO calculation [10]. [c] Aryl = 2,4,6-tri-*tert*-butylphenyl [12]. [d] Twisting of the mesityl groups: calculated according to [b], 72°; observed for the two independent molecules, 63.3 and 65.9(4)°, and 62.6 and 66.0(4)°.

Received: February 9, 1988 [Z 2612 IE]
German version: *Angew. Chem. 100* (1988) 885

CAS Registry numbers:
4a, 108920-25-8; **4b**, 108946-04-9; **4c**, 108946-03-8; **4d**, 108920-31-6.

[1] Recent reviews: R. West, *Angew. Chem. 99* (1987) 1231; *Angew. Chem. Int. Ed. Engl. 26* (1987) 1201; A. H. Cowley, N. C. Norman, *Progr. Inorg. Chem. 34* (1986) 1; S. Lochschmidt, A. Schmidpeter, *Phosphorus Sulfur 29* (1986) 73.

[2] A. G. Brook, K. M. Baines, *Adv. Organomet. Chem. 25* (1986) 1; N. Wiberg, G. Wagner, J. Riede, G. Müller, *Organometallics 6* (1987) 32.

[3] a) J. Satgé, *Adv. Organomet. Chem. 21* (1982) 241; b) N. Wiberg, C. K. Kim, *Chem. Ber. 119* (1986) 2966, 2980.

[4] a) H. Meyer, G. Baum, W. Massa, A. Berndt, *Angew. Chem. 99* (1987) 790; *Angew. Chem. Int. Ed. Engl. 26* (1987) 798; b) C. Couret, J. Escudié, J. Satgé, M. Lazraq, *J. Am. Chem. Soc. 109* (1987) 4411.

[5] *Experimental procedure:* Crude **4b** (2.03 g) prepared from **4a** (2.2 g, 4.4 mmol) [4b] was heated in a sealed tube at 110°C. After 15 h, bound ether could no longer be detected. Recrystallization from pentane at −20°C afforded 1.63 g (3.4 mmol) of air-sensitive, orange crystals (m.p. = 82–83°C; yield based on **4a**, 78%).

[6] Crystal structure analyses: a) **4d**: $P\bar{1}$, $a = 1040.5(5)$, $b = 1189.3(3)$, $c = 1209.1(5)$ pm, $\alpha = 94.00(4)$, $\beta = 110.60(4)$, $\gamma = 110.13(4)°$, $V = 1284(1) \times 10^6$ pm^3, $Z = 2$, 5903 reflections with $I > 3\sigma(I)$, 315 variables, $R = 0.054$; b) **4c**: $P\bar{1}$, $a = 1211.5(4)$, $b = 1306.9(2)$, $c = 1653.9(2)$ pm, $\alpha = 87.61(2)$, $\beta = 77.19(2)$, $\gamma = 78.83(2)°$, $V = 2505(2) \times 10^6$ pm^3, $Z = 4$, 7352 reflections with $I > 2\sigma(I)$, 618 variables, $R = 0.050$. Further details of the crystal structure investigations may be obtained from the Fachinformationszentrum Energie, Physik, Mathematik GmbH, D-7514 Eggenstein-Leopoldshafen 2 (FRG), on quoting the depository number CSD-52981, the names of the authors, and the journal citation.

[7] Cambridge Crystallographic Data Base, update September 1987; inaccurate structure determinations and questionable cases of bonding have not been taken into consideration.

[8] a) T. A. van der Knaap, F. Bickelhaupt, *Chem. Ber. 117* (1984) 915; b) B. Glaser, H. Nöth, *Angew. Chem. 97* (1985) 424; *Angew. Chem. Int. Ed. Engl. 24* (1985) 416.

[9] G. Trinquier, J.-C. Barthelat, J. Satgé, *J. Am. Chem. Soc. 104* (1982) 5931; cf. [3a].

[10] a) AMPAC program package: J. J. P. Steward, QCPE No. 506; 180 internal coordinates, 42 optimized parameters; b) maximal deviation in bond lengths 3 pm, in bond angles 5°; c) for MNDO calculations of force fields, see M. J. S. Dewar, G. P. Ford, M. L. McKee, H. S. Rzepa, W. Thiel, Y. Yamaguchi, *J. Mol. Struct. 43* (1978) 135, and references cited therein.

[11] Compare the pK_a values for fluorene and diphenylmethane (23 and 33.5): A. Streitwieser, Jr., E. Ciuffarin, J. H. Hammons, *J. Am. Chem. Soc. 89* (1967) 63.

[12] M. Dräger, J. Escudié, C. Couret, H. Ranaivonjatovo, J. Satgé, *Organometallics 7* (1988) 1010.

Distorted Triple-Diamond Structure of 3,3-Bis(carboxymethyl)glutaric Acid ("Methanetetraacetic Acid")**

By *Otto Ermer** and *Andreas Eling*

Tetrafunctional organic molecules with tetrahedrally directed substituents are endowed with the fascinating faculty of building novel diamond-like networks in the crystal

[*] Prof. Dr. O. Ermer, A. Eling
Institut für Organische Chemie der Universität
Greinstrasse 4, D-5000 Köln 41 (FRG)

[**] This work was supported by the Fonds der Chemischen Industrie.

("diamondoid" crystal structures). A first and prototypal example is adamantane-1,3,5,7-tetracarboxylic acid **1**,[1]

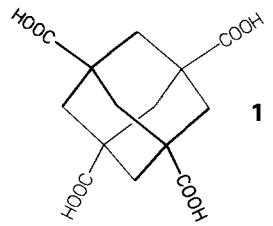

1

which contains tetrahedrally directed carboxyl groups to a good approximation and has a relatively rigid carbon skeleton. The carboxyl groups are interconnected by pairwise hydrogen bonds, such that a molecular architecture results which corresponds to an almost undistorted "super-diamond" structure. However, this highly symmetric, three-dimensional network has very large cavities since the distance between neighboring hydrogen-bonded molecules is appreciable (ca. 10.1 Å). These unfavorable interstices are filled in the crystal in a unique fashion through mutual interpenetration of altogether no less than five translationally equivalent diamondoid networks of **1** (fivefold-diamond structure). The concatenated diamondoid networks are otherwise unconnected; hydrogen bonds occur only within one and the same diamondoid network.[1]

The structure analysis of the adamantanetetracarboxylic acid **1** marked the beginning of a more comprehensive and systematic study of the crystal packing modes of tetrafunctional organic molecules with tetrahedrally directed substituents, especially those capable of forming intermolecular hydrogen bonds. We are particularly interested in the possible capability of such systems to serve as host structures in solid-state inclusion compounds, which may be anticipated in view of the open-meshed three-dimensional networks. Furthermore, diamondoid molecular architectures represent structural models for hypothetical "diamondoid polymers" potentially displaying isotropic high-performance properties.

For the four carboxyl groups of 3,3-bis(carboxymethyl)glutaric acid ("methanetetraacetic acid") **2**[2] tetrahedral directionality may also be envisaged. Accordingly, **2** may also in principle build up diamondoid molecular

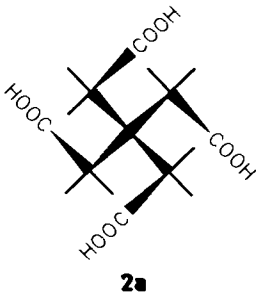

2a

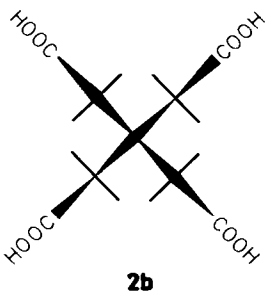

2b

frameworks in the crystal. Model considerations show that diamondoid networks of **2** again involve large cavities (see Fig. 2), yet not as large as in **1**. If **2** indeed forms diamondoid networks, interpenetration of several such architectures thus appears inevitable once again, although the degree of interpenetration (= number of mutually interlocking networks) is expected to be smaller than for **1**. It should be borne in mind, however, that the prerequisites for building up diamondoid structures appear less favorable in the case of **2** than of **1**. On the one hand, the carbon skeleton of **2** is, in contrast to **1**, conformationally flexible, and an approximate tetrahedral orientation of the carboxyl groups is only possible if conformations of type **2a** or **2b** are taken up (highest possible symmetries, S_4 and D_{2d}, respectively).[3] On the other hand, strictly speaking the carboxyl functions in **2a** and **2b** are oriented tetrahedrally merely in a displaced fashion since these groups are not, as in **1**, directed towards a common point, viz. the molecular center. Conversely, however, the conformational flexibility of **2** could also lead to better compliance with diamondoid packing requirements.

These thoughts led us to perform an illuminating crystal structure analysis of **2**, which is reported here. The X-ray measurements show that the molecules of **2**, like those of **1**, do indeed join to build up mutually interlaced, hydrogen-bonded diamondoid networks.

The molecules of methanetetraacetic acid **2** exhibit S_4 symmetry in the tetragonal crystals and adopt the conformation **2a** (Fig. 1).[4] This structure is strained, as evidenced by the angles C(1)-C(2)-C(3), which are opened out to 117.26(8)°. These angle openings may be attributed to four pairs of short intramolecular O···H contacts (2.44 and 2.51 Å) involving the carbonyl oxygen atoms. If the hydroxyl oxygen atoms were involved instead, even stronger O···H repulsions would arise given the preferred bond lengths and angles in carboxyl groups. This reasoning also helps to explain why no orientational disorder of the carboxyl groups is observed, unlike quite frequently in other cases.

In the crystal, **2** forms tetragonally (along the crystallographic axis *c*) elongated diamondoid networks, which are

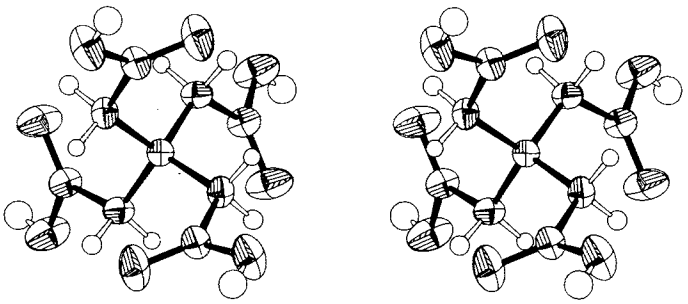

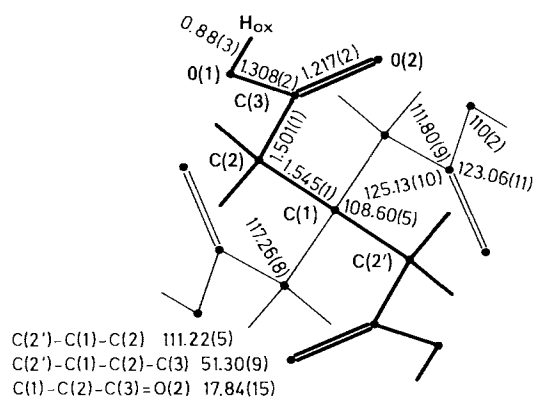

C(2')-C(1)-C(2) 111.22(5)
C(2')-C(1)-C(2)-C(3) 51.30(9)
C(1)-C(2)-C(3)=O(2) 17.84(15)
O(2)=C(3)-O(1)-H_{ox} -5(2)

Fig. 1. Above: Stereoview of **2** along the fourfold rotation-inversion axis S_4; thermal ellipsoids with 50% probability, temperature factors of hydrogen atoms divided by 3. Below: Selected bond lengths [Å], bond and torsion angles [°], and atomic numbering.

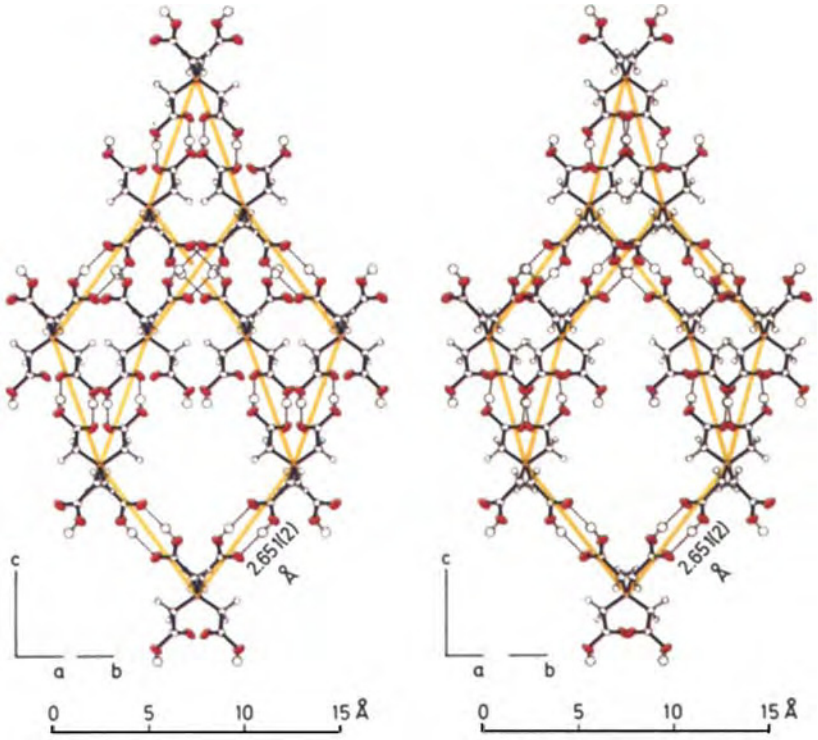

Fig. 2. Stereoview (perpendicular to c axis) of a hydrogen-bonded superadamantane unit of a diamondoid network of **2**. Note the tetragonal elongation along c and the large central cavity, which is filled in the crystal by two equivalent, interpenetrating diamondoid networks. The oxygen atoms are shown in red, and the superadamantane framework is highlighted by yellow lines interconnecting the molecular centers.

held together by pairwise hydrogen bonds between the carboxyl groups; the distance between bridged neighboring molecules is 8.761 Å. A "superadamantane" section of such a network is shown in Figure 2. The distance between opposite molecules along the c axis is $3c$ and that at right angles $\sqrt{2}\,a$, which results in an elongation factor of $3c/(\sqrt{2}\,a) = 1.6914$ (see also Figs. 3 and 4). The corresponding factor for the only slightly distorted diamondoid networks of the adamantanetetracarboxylic acid **1**, which also crystallizes tetragonally, is 0.9376.[1]

The diamondoid networks of **2** are hollow (Fig. 2), although less pronounced than in **1**. The cavities are filled in such a way that each network is interpenetrated by two further ones. Thus altogether three diamondoid networks mutually interpenetrate in **2** (degree of interpenetration = 3), as compared to five in the case of **1**. The distorted triple-diamond structure of **2** is without precedent; only a number of double-diamond structures are known (see Ref. [1]). The three interlaced diamondoid networks of **2** are translationally equivalent and may be merged into each other by shifting them along the c axis by the value of the cell edge $c = 8.962$ Å.[4] This both simple and beautiful mode of interpenetration is illustrated schematically in Figure 3. Three diamondoid networks are shown (black, red, yellow), each consisting of two connected superadamantane frameworks. Only the molecular centers are drawn (small spheres) and interconnected by rods symbolizing hydrogen bonding. The mode of interpenetration of the fivefold-diamond structure of **1** is different and not as simple, although both tetracarboxylic acids crystallize in space group $I4_1/a$.[1,4,6]

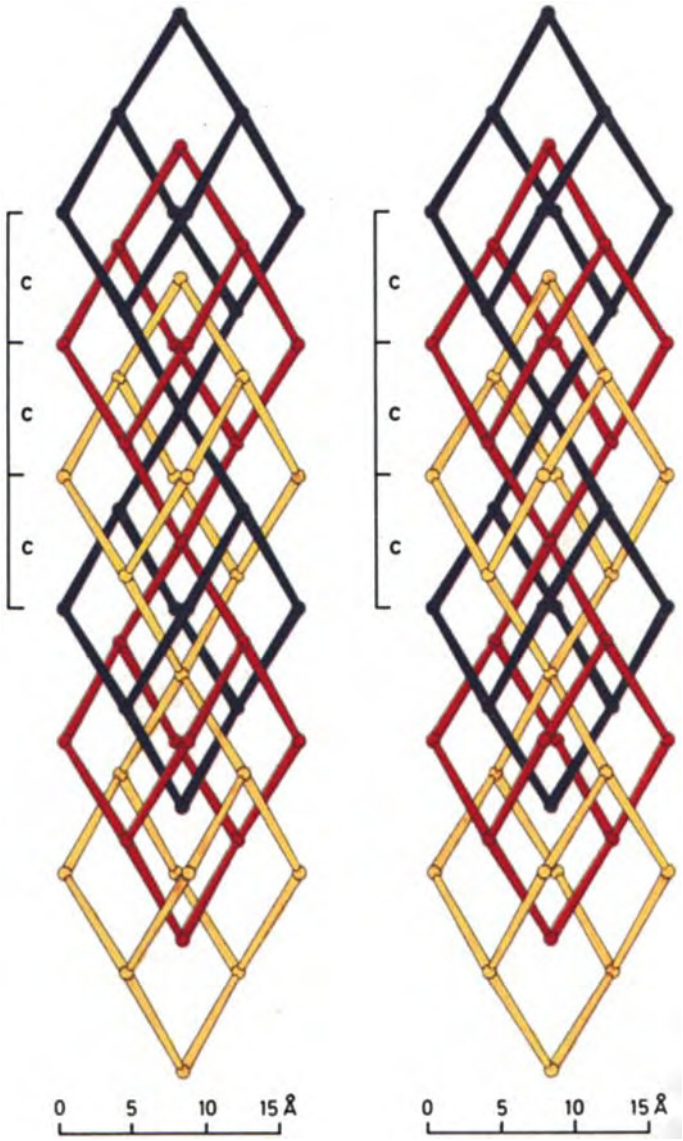

Fig. 3. Schematic stereoview (along the bisector between a and b axes) of the three interpenetrating, tetragonally elongated diamondoid networks of **2** (black, red, yellow), which are each represented by two connected superadamantane frameworks. The translational equivalence of the networks is clearly evident. Only the central carbon atoms of **2** are shown (S_4 axes); the interconnecting rods symbolize the methylene groups and the carboxyl functions tied together by pairwise hydrogen bonds (cf. Fig. 2).

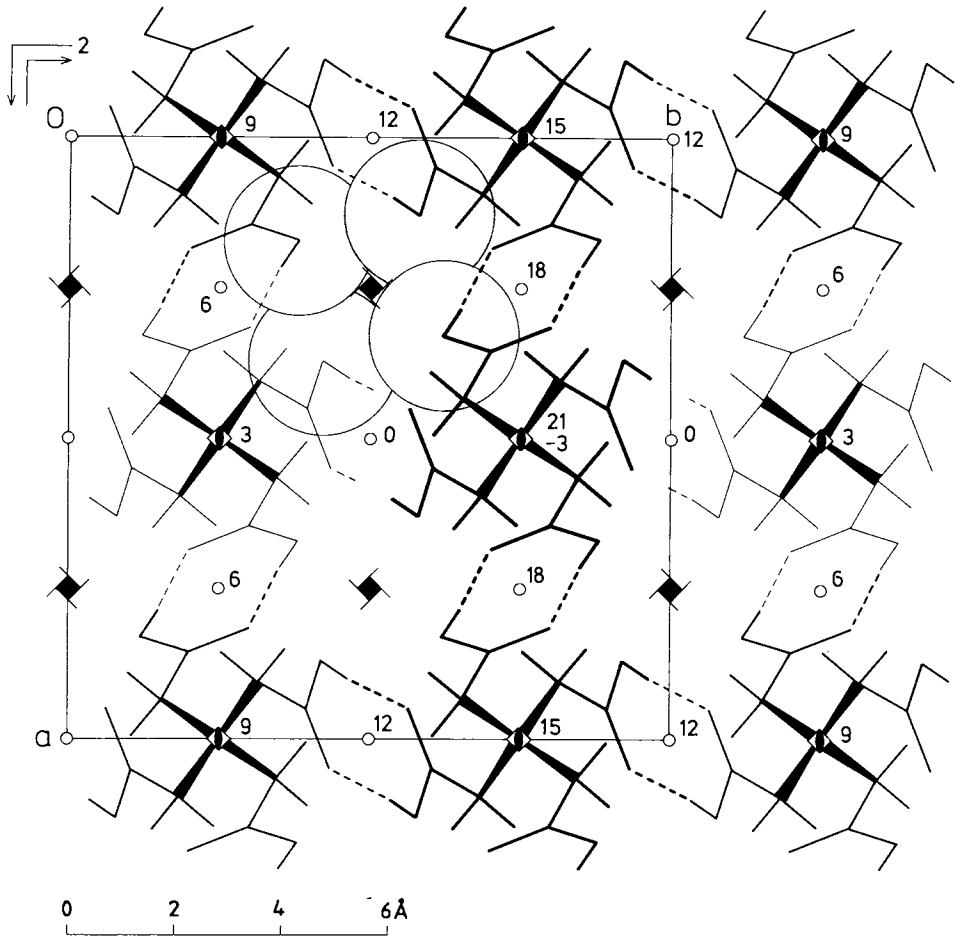

Fig. 4. Space group symmetry diagram of **2**, projected along the tetragonal *c* axis. The symmetry elements of the space group $I4_1/a$ are given, as are the heights of the molecular centers (S_4 axes) in units of $c/8$. Ten molecules of **2** are shown, which build up an elongated superadamantane framework (see Fig. 2). The space required by four hydroxyl oxygen atoms about a fourfold screw axis is indicated by circles with van der Waals radius 1.4 Å, in order to point out that no open channels exist along these symmetry elements (see text). Two molecules in the middle of the diagram are superimposed in this projection.

In the diagram of Figure 4 showing the packing and symmetry of the crystals of **2**, channels are perceptible along the fourfold screw axes, i.e., in the direction of translation of the interlocking diamondoid networks. These channels are not empty, however, but appear adequately filled by the carboxyl groups, such that the formation of solid-state inclusion compounds may hardly be visualized within the triple-diamond structure of **2**. This view is supported by the observation that no uptake of water into the crystals occurs, despite crystallization from aqueous medium.[4] On the other hand, a lower degree of interpenetration, say within a double- or even single-diamond structure, may render feasible the formation of inclusion compounds of **2**.

An interesting structural analogy between methanetetraacetic acid **2** and potassium dihydrogen phosphate KH_2PO_4[7] may be drawn. Above 123 K, KH_2PO_4 crystallizes tetragonally (space group $I\bar{4}2d$), and the $H_2PO_4^{\ominus}$ ions form, like **2**, a diamondoid network held together by hydrogen bonds. Unlike in **2**, however, the $H_2PO_4^{\ominus}$ ions are, for stoichiometric reasons, tied together by single rather than pairwise hydrogen bonds. Averaged over space and/or time, the single O-H···O hydrogen bonds are symmetric (disordered), and, owing to the negative charge, shortened (O···O distance, 2.487(5) Å[7c]). Furthermore, the diamondoid network of the $H_2PO_4^{\ominus}$ ions exhibits a severe tetragonal compression (by a factor of 0.6606) and is less hollow, so that only a single distorted diamondoid anionic architecture is built. Nonetheless, holes are still present, and are occupied by the $K^{\oplus}$ ions in such a way that one $K^{\oplus}$ ion lies in the center of each compressed superadamantane subunit. KH_2PO_4 may thus be considered as a tetragonally compressed diamondoid structure with two interpenetrating networks, one formed by the hydrogen-bonded $H_2PO_4^{\ominus}$ ions and one by the $K^{\oplus}$ ions (distorted "mixed" double-diamond structure).[8]

At 123 K, KH_2PO_4 undergoes a phase change and is polar orthorhombic below this temperature (space group *Fdd*2) with ordered asymmetric O-H···O hydrogen bonds.[7] This ordering process is accompanied by the onset of ferroelectric and piezoelectric properties, which can be utilized technologically. Thus, by straightforward analogy, the appealing possibility emerges that dihydrogen tetracarboxylates with tetrahedral molecular cores of general composition $T(COOH)_2(COO^{\ominus})_2$ may form (interpenetrating) diamondoid networks tied together by single, yet short, charged O-H···O hydrogen bonds. (In the current examples **1** and **2**, T stands for the central adamantane and tetramethylmethane skeletons, respectively.) Singly or multiply charged metal ions could play the role of counter-

 © VCH Verlagsgesellschaft mbH, D-6940 Weinheim, 1988 0570-0833/88/0606-0832 $ 02.50/0

ions, which may be accommodated in the cavities of the interlocked diamondoid anionic networks. Like KH_2PO_4, diamondoid dihydrogen tetracarboxylates could exhibit interesting ferroelectric and piezoelectric properties, provided the short hydrogen bonds are also asymmetric (double-minimum potential).

Received: October 30, 1987;
supplemented: February 23, 1988 [Z 2489 IE]
Publication delayed at authors' request
German version: *Angew. Chem. 100* (1988) 856

CAS Registry number: **2**, 5693-87-8.

[1] O. Ermer, *J. Am. Chem. Soc. 110* (1988), in press.
[2] C. K. Ingold, L. C. Nickolls, *J. Chem. Soc. 1922*, 1638.
[3] Computational estimates applying the MM2 force field (N. L. Allinger, *J. Am. Chem. Soc. 99* (1977) 8127) give practically equal energies for **2a** and **2b**.
[4] Synthesis of **2** according to [2]; tetragonal crystals of compressed octahedral shape (from water); loss of water above about 230°C, presumably with anhydride formation; decomposition accompanied by gas evolution above about 240°C; space group $I4_1/a$ (No. 88), $Z=4$, $a=11.240(1)$, $c=8.962(1)$ Å; $\rho_{calcd}=1.456$, $\rho_{exp}=1.46$ g cm^{-3} [5]; crystallographic molecular symmetry, S_4; intensity measurements on a four-circle diffractometer at room temperature ($\lambda_{Mo}=0.71069$ Å, $\theta_{Mo}(max)=35°$); direct methods; C, O refined anisotropically, H isotropically, including 1046 reflections with $F_0>3\sigma(F_0)$; largest structure amplitude ($\bar{1}\,2\,1$) excluded owing to extinction weakening; $R=0.049$, $R_w=0.054$. We are indebted to Dr. *J. Lex* for performing the intensity measurements. Further details of the crystal structure analysis may be obtained from the Fachinformationszentrum Energie, Physik, Mathematik GmbH, D-7514 Eggenstein-Leopoldshafen 2 (FRG), on quoting the depository number CSD-52952, the names of the authors, and the journal citation.
[5] More than 60 years ago, *Knaggs* reported an axial ratio $a:c=1.786$ for **2** from measurements of dihedral angles between crystal faces (I. E. Knaggs, *J. Chem. Soc. 1923*, 71). This ratio agrees closely with $\sqrt{2}$ times our X-ray value (=1.774), and follows from rotating the axis system about the tetragonal c axis by 45°. Furthermore, *Knaggs* measured a density of 1.460 g cm^{-3}, and the refraction indices $n_e(\parallel c)=1.518$, $n_o(\perp c)=1.487$. The crystal class she gave as holohedral (D_{4h}), whereas it is actually C_{4h}, as evidenced by our measurements. Presumably, this discrepancy is due to the fact that her crystals had no general faces developed. On the whole, there appears to be little doubt that the crystals *Knaggs* examined and ours are the same.
[6] A referee has kindly drawn our attention to theoretical structural studies of *W. Fischer* on interpenetrating tetragonal sphere packings of low density, in particular three- and fivefold interpenetration patterns in space group $I4_1/a$: W. Fischer, *Habilitationsschrift*, Universität Marburg 1970, pp. 40f, 138ff; compare also: W. Fischer, *Acta Crystallogr., Sect. A 25* (1969) S4; *Z. Kristallogr., Kristallgeom., Kristallphys., Kristallchem. 133* (1971) 18; W. Fischer, E. Koch, *Acta Crystallogr., Sect. A 32* (1976) 225. *Fischer* describes the threefold sphere interpenetration in $I4_1/a$ as a system of three coaxial, eight-storeyed screws, and the fivefold interpenetration as five interlocking eight-storeyed screws that do not wind about a common axis. This characterization may readily be carried over to our threefold and fivefold diamondoid interpenetrations, if one bears in mind that the diamond structure may be considered as a framework of interlinked four-storeyed helices winding about the fourfold screw axes. We are grateful to Prof. *Fischer* for providing us with excerpts of his Habilitationsschrift and reprints.
[7] Structure of KH_2PO_4: a) Early X-ray analysis: J. West, *Z. Kristallogr. Mineral. Petrogr. Abt. A 74* (1930) 306; b) structural theory of ferroelectricity: J. C. Slater, *J. Chem. Phys. 9* (1941) 16; c) neutron diffraction of the tetragonal phase at room temperature: G. E. Bacon, R. S. Pease, *Proc. Roy. Soc. London, Ser. A 220* (1953) 397; d) neutron diffraction of the orthorhombic, ferroelectric low-temperature phase (<123 K): G. E. Bacon, R. S. Pease, *ibid. A 230* (1955) 359; e) X-ray diffraction study of the ferroelectric transition: B. C. Frazer, R. Pepinsky, *Acta Crystallogr. 6* (1953) 273.
[8] Related are also the structure types of scheelite $CaWO_4$ (space group, $I4_1/a$, like **2**), and zircon $ZrSiO_4$ (space group, $I4_1/amd$), which may again be described as tetragonally distorted double-diamond structures; see Landolt-Börnstein: *Zahlenwerte und Funktionen aus Physik, Chemie, Astronomie, Geophysik und Technik, Band I, Teil 4*, Springer, Berlin 1955, pp. 59, 73 (types HO_4 and $S1_1$, respectively). A particularly striking example as compared to **2** is ammonium perrhenate, NH_4ReO_4 (scheelite type; G. J. Kruger, E. C. Reynhardt, *Acta Crystallogr., Sect. B 34* (1978) 259), which adopts a tetragonally elongated double-diamond structure, in which both equivalent diamondoid networks are held together by hydrogen bonds.

Mono- and Dinuclear Nickel(0) Complexes of Butadiyne**

By *Werner Bonrath, Klaus R. Pörschke,* Günther Wilke, Klaus Angermund,* and *Carl Krüger*

Dedicated to Professor Klaus Hafner on the occasion of his 60th birthday

In connection with our investigations on nickel(0) complexes containing ethyne and 1-alkynes[1,2] as ligands, we were interested in whether butadiyne could also form complexes with nickel(0). Coordination compounds formed between butadiyne and transition metals have not been described in detail so far.[3] Butadiyne, which is formed in large amounts as a byproduct in the industrial production of acetylene by the electric arc process, readily polymerizes and is potentially explosive in the presence of oxygen. It has therefore not been of commercial value so far. The investigations of the complexation chemistry of butadiyne described here possibly provide a foundation for its catalytic transformations.

Complexes of the type $[L_2M(cod)]$ (M = Ni, Pd, Pt; $L=PR_3$ or $L_2=R_2P(CH_2)_nPR_2$ (n = 2, 3), bpy; cod = 1,5-cyclooctadiene) react with butadiyne with the liberation of cod and the formation of mono- or dinuclear compounds $[(L_2M)_m(HC{\equiv}CC{\equiv}CH)]$, m = 1, 2.[4] Thus, the reactions of **1a** and **1b**,[4] which are prepared from $[Ni(cod)_2]$[5] and $iPr_2PC_2H_4P$-iPr_2 or $iPr_2PC_3H_6P$-iPr_2, respectively, with one or one-half equivalent of butadiyne in pentane at −30°C result in the formation of intensely red solutions, from which the mononuclear complexes **2a** (fine yellow needles) and **2b** (long yellow needles), respectively, or the dinuclear complexes **3a** (long yellow needles) and **3b** (dark yellow needles),[4] respectively, separate in over 90% yield. Complexes **2** are converted into the dinuclear complexes **3** by reaction with the cod complexes **1**. Complexes

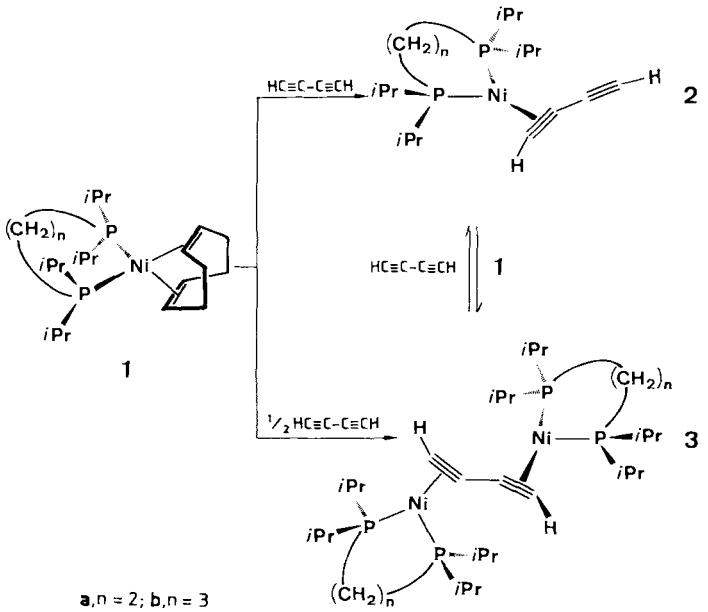

[*] Dr. K. R. Pörschke, Dipl.-Chem. W. Bonrath, Prof. Dr. G. Wilke, Dr. K. Angermund [+], Prof. Dr. C. Krüger [+]
Max-Planck-Institut für Kohlenforschung
Postfach 10 13 53, D-4330 Mülheim an der Ruhr 1 (FRG)

[+] Single-crystal X-ray structure analysis.

[**] We thank Dr. *R. Benn* and Dr. *R. Mynott* for the NMR spectra and Dr. *K. Seevogel* for the IR spectra.

3, in turn, can be converted back into the mononuclear complexes **2** by reaction with butadiyne.

Compounds **1**–**3** are crystalline, stable under inert gas at room temperature, and soluble in pentane. Their spectroscopic data are summarized in Table 1. Reaction with $P(OPh)_3$ results in displacement of all ligands from the nickel(0) center; the butadiyne thereby liberated from **2** and **3** can be identified by gas chromatography (85% of the theoretically expected amount). Reaction of **3b** with four equivalents of CO (pentane, 20°C) results in polymerization of the butadiyne released from the nickel center and the formation of two equivalents of $[(i\mathrm{Pr}_2\mathrm{PC}_3\mathrm{H}_6\mathrm{P}\text{-}i\mathrm{Pr}_2)\mathrm{Ni(CO)}_2]$ (^{31}P-NMR: $\delta = 36.3$). It has not been possible so far to add the butadiyne bound in **2** and **3** to free butadiyne, ethyne, butadiene, or CO_2; coupling with C_2F_4 is under investigation at present.

Table 1. Spectroscopic data for the compounds **1a**, **2a**, **2b**, and **3a** (MS, 70 eV; IR, KBr; ^{1}H-NMR: 200 MHz, [D$_8$]THF, relative to TMS; ^{13}C-NMR, 75.5 MHz, [D$_8$]THF, relative to TMS; ^{31}P-NMR, 32.4 MHz, [D$_8$]THF, relative to 85% aqueous H_3PO_4).

1a: MS (100°C): *m/z* 428 ($M^{\oplus}$, 30% rel. int.), 320 ($[M-\mathrm{cod}]^{\oplus}$, 100); IR: $\tilde{\nu}$ [cm^{-1}] = 3027 (=C–H), 1491 (C=C, cod compl.); ^{1}H-NMR: $\delta = 4.11$ (m, 4H; =CH), 2.35 (m, 4H; CH_2), 2.1 (m, 4H; CH_2), 2.11 (m, 4H; PCH), 1.39 (m, 4H; PCH_2), 1.07 (m, 12H; CH_3), 1.04 (m, 12H; CH_3); ^{31}P-NMR: $\delta = 69.9$

2a: MS (60°C): *m/z* 370 ($M^{\oplus}$, 35% rel. int.), 320 ($[M-\mathrm{C_4H_2}]^{\oplus}$, 80); IR (−30°C): $\tilde{\nu}$ [cm^{-1}] = 3307 (≡C–H free), 3057 (≡C–H compl.), 2068 (C≡C, free), 1669 (C≡C, compl.); ^{1}H-NMR (−30°C): $\delta = 7.44$ (m, 1H, J(PH) = 15.0, J(P'H) = 23.0 Hz; ≡CH compl.), 4.43 (m, 1H, J(PH) = 2.8; ≡CH free), 2.16 ("octet," 2H; PCH), 2.06 ("octet," 2H; P'CH), 1.64 (m, 4H; PCH_2), 1.18, 1.13, 1.06, 1.03 (each: m, 6H; CH_3); ^{13}C-NMR (−30°C): $\delta = 129.5$ (m, 1C, ^1J(CH) = 200.4, J(PC) = 6.1, J(P'C) = 49.3 Hz; ≡CH compl.), 122.1 (m, 1C, ^2J(CH) = 11.2, ^3J(CH) = 5.1, J(PC) = 44.8, J(P'C) = 5.1 Hz; ≡C– compl.), 90.4 (m, 1C, ^1J(CH) = 248, J(PC) = 5.6 Hz; ≡CH free), 81.4 (m, 1C, ^2J(CH) = 50.4, J(PC) = 4.6, J(P'C) = 14.2 Hz; ≡C– free), 25.8 (m, 2C; PCH), 25.8 (d, 2C; P'CH), 22.3 (m, 1C; PCH_2), 22.05 (m, 1C; P'CH_2), 20.0, 19.9, 19.15, 19.1 (each: m, 2C; CH_3); ^{31}P-NMR (38°C): $\delta = 82.2$, 79.6 (d, J(PP) = 40.6 Hz)

2b: MS (70°C): *m/z* 384 ($M^{\oplus}$, 10% rel. int.), 334 ($[M-\mathrm{C_4H_2}]^{\oplus}$, 25), 233 ($i\mathrm{Pr}_2\mathrm{PC}_3\mathrm{H}_6\mathrm{P}\text{-}i\mathrm{Pr}^{\oplus}$, 90), 50 ($C_4H_2^{\oplus}$, 100); IR: $\tilde{\nu}$ [cm^{-1}] = 3305 (≡C–H free), 3057 (≡C–H compl.), 2064 (C≡C free), 1665 (C≡C compl.); ^{1}H-NMR (400 MHz, −40°C): $\delta = 7.24$ (m, 1H, J(PH) = 13.8, J(P'H) = 23.0 Hz; ≡CH compl.), 4.50 (d, 1H, J(HH) = 0.8 Hz; ≡CH free), 2.14 ("octet," 2H; PCH), 1.94 ("octet," 2H; P'CH), 1.92 (m, 2H; CH_2), 1.46 (m, 4H; PCH_2), 1.19, 1.12, 1.08, 1.06 (each: m, 6H; CH_3); ^{13}C-NMR (−30°C): $\delta = 129.2$ (m, 1C, ^1J(CH) = 201, J(PC) = 8.6, J(P'C) = 45.1 Hz; ≡CH compl.), 120.8 (m, 1C, J(PC) = 35.4, J(P'C) = 7.0 Hz; ≡C– compl.), 91.1 (m, 1C, ^1J(CH) = 249, J(PC) = 5.1 Hz; ≡CH free), 81.1 (m, 1C, J(PC) = 13.1, J(P'C) = 4.4 Hz; ≡C– free), 27.3 (m, 2C; PCH), 26.8 (m, 2C; PCH), 24.1 (m, 1C; CH_2), 20.0 (m, 1C; PCH_2), 19.7 (m, 1C; P'CH_2), 20.0, 19.6, 18.7, 18.7 (each: m, 2C; CH_3); ^{31}P-NMR (−30°C): $\delta = 38.9$, 35.7 (d, J(PP) = 3.1 Hz)

3a: MS (130°C): *m/z* 690 ($M^{\oplus}$, 30% rel. int.), 320 ($(i\mathrm{Pr}_2\mathrm{PC}_2\mathrm{H}_4\mathrm{P}\text{-}i\mathrm{Pr}_2)\mathrm{Ni}^{\oplus}$,20); IR: $\tilde{\nu}$ [cm^{-1}] = 3085 (≡C–H), 1757, 1601 (C≡C); ^{1}H-NMR (38°C): $\delta = 6.85$ (m, 2H; ≡CH), 2.05 ("octet," 4H; PCH), 2.01 ("octet," 4H; P'CH), 1.57 (m, 4H; PCH_2), 1.50 (m, 4H; P'CH_2), 1.16, 1.12, 1.05, 1.04 (each: m, 12H; CH_3); ^{13}C-NMR (38°C): $\delta = 132.1$ (m, 2C; –C≡), 116.3 (m, 2C, ^1J(CH) = 202 Hz; ≡CH), 26.12 (m, 4C; PCH), 26.07 (m, 4C; P'CH), 23.0 (m, 2C; PCH_2), 22.95 (m, 2C; P'CH_2), 20.6, 20.15, 19.5, 19.5 (each: m, 4C; CH_3); ^{31}P-NMR (38°C): $\delta = 80.3$, 75.9 (AA'BB', $J(P_AP_B) = 51.4$, $J(P_AP_{A'}) = 7.8$, $J(P_AP_{B'}) = 0$, $J(P_BP_{B'}) = 0.3$ Hz)

The mass spectra of **1**–**3** display peaks for the molecular ions; the mononuclear complexes **2** fragment with elimination of the butadiyne ligand. The IR spectra of **2** exhibit two intense bands at ca. 2060 and ca. 1670 cm^{-1}, which may be assigned to the C≡C stretching vibrations of the free and the coordinated triple bond, respectively. On the other hand, **3**, which contain bridging butadiyne ligands, afford spectra with bands at ca. 1760 and ca. 1600 cm^{-1}, which may be assigned to the coordinated triple bonds. In the Raman spectrum of **3a** we found a C≡C band at 1760 cm^{-1}.

In the ^{1}H- and ^{13}C-NMR spectra of **2**, the signals of the H and C atoms, respectively, of the complexed triple bond (**2b**: $\delta_{H1} = 7.24$, $\delta_{C1} = 129.2$, $^1J_{CH} = 201$ Hz; $\delta_{C2} = 120.8$) are strongly shifted downfield compared with those of the free triple bond ($\delta_{H4} = 4.50$, $\delta_{C4} = 91.1$, $^1J_{CH} = 249$ Hz; $\delta_{C3} = 81.1$). In the dinuclear complexes **3**, the protons and terminal C atoms of the butadiyne ligand are less deshielded and the middle C atoms are more deshielded (**3a**: $\delta_{H2} = 6.85$, $\delta_{C2} = 116.3$, $^1J_{CH} = 202$ Hz; $\delta_{C1} = 132.1$) than in the mononuclear complexes. The coupling constants J_{CH} correspond to those found for bis(phosphane)(ethyne)nickel(0) complexes.[1,2] The NMR spectra of **2** and **3** reveal no evidence for rotation of the complex-bound C≡C groups around the bond axis to the nickel atom at the measurement temperatures (up to 38°C).

The essential results of the crystal structure analyses of **2b**[6] and **3a**[7] are shown in Figures 1 and 2, respectively. As expected, the nickel atoms in the two complexes are coordinated in a trigonal-planar fashion by the two phosphorus atoms and a C≡C group, with the C≡C bond in the P_2Ni plane. The angle P1-Ni-P2 in the PC_3PNi six-membered ring of **2b** is 102.7(1)° and in the PC_2PNi five-membered ring of **3a** it is 92.0(1)°. The complex-bound C≡C bonds in **2b** and **3a** (1.279(9) Å and 1.272(4) Å, respectively) are equally lengthened (uncomplexed C≡C bond of **2b**: 1.19(1) Å). The angles formed upon binding to nickel(0) (**2b**: C1-C2-C3 146.2(6)°; **3a**: C2*-C1*-C1 149.4(3)°) are in accordance with expectations for alkynenickel(0) complexes[1a,b,d] and may be ascribed to partial hybridization change of the C atoms. Particularly noteworthy is the fact that the length of the uncomplexed triple bond in the mononuclear complex **2b** corresponds exactly to the C≡C bond length of free butadiyne.[8] The structure of the dinuclear complex **3a** is characterized by a twofold axis (perpendicular to C1-C1*) determined by the space group. Owing to the torsional angle of 94° (C2-C1-C1*-C2°), the triple-bond π orbitals used for complexation of one part of the butadiyne ligand and those of the neighboring triple bond not used are nearly parallel.

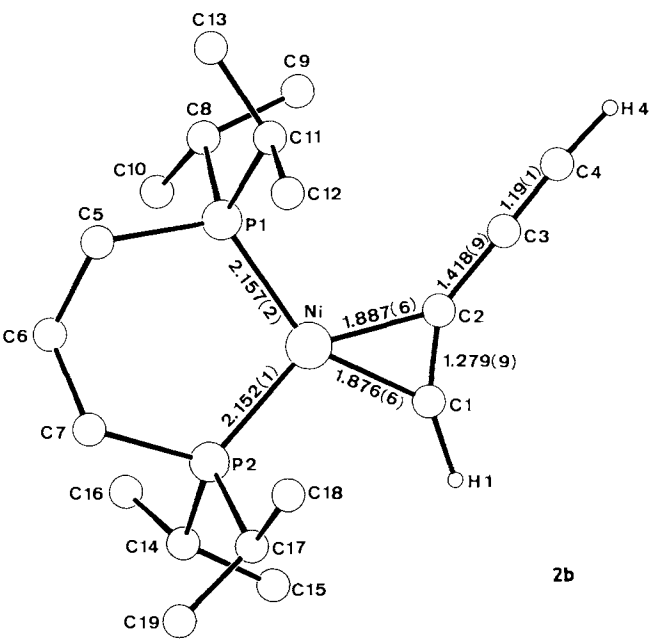

Fig. 1. Molecular structure of **2b** [6]. Bond lengths in Å. Angles [°]: P1-Ni-P2 102.7(1), C1-Ni-C2 39.7(3), C1-C2-C3 146.2(6), C2-C3-C4 177.9(7).

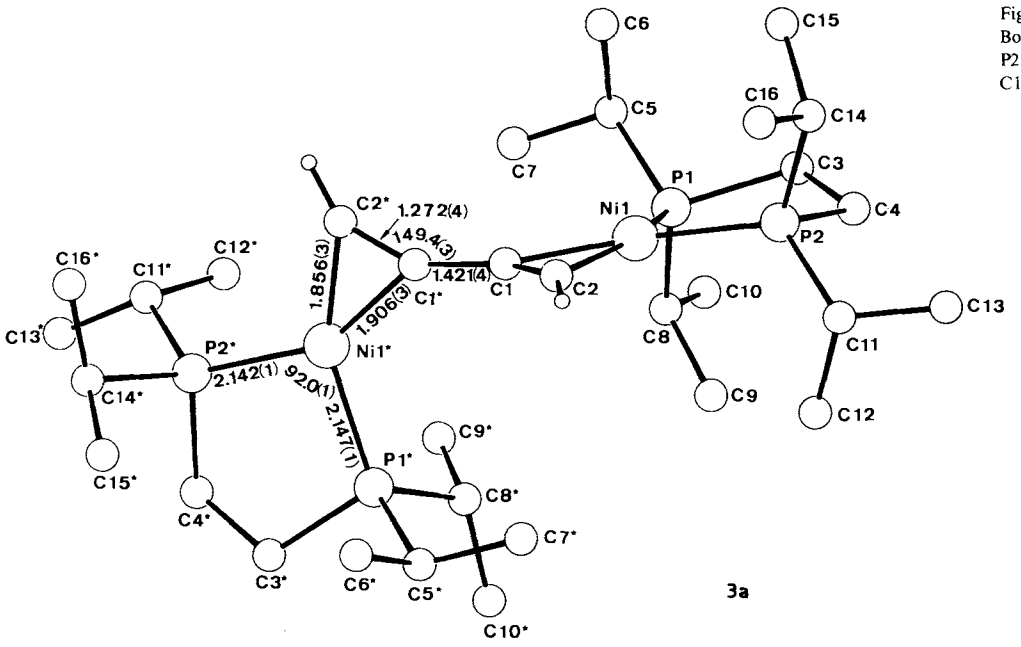

Fig. 2. Molecular structure of **3a** [7]. Bond lengths in Å. Angles [°]: P1-Ni1-P2 92.0(1), C1-Ni1-C2 39.5(1), C2*-C1*-C1 149.4(3).

Experimental Procedure

1a: A suspension of $[Ni(cod)_2]$ (2.75 g, 10.0 mmol) in ether (40 mL) was allowed to react at −20°C with bis(diisopropylphosphino)ethane (2.62 g, 10.0 mmol) in ether (10 mL). Slow warming (16 h) to 20°C resulted in the formation of a clear yellow reaction solution, from which a finely crystalline solid precipitated at −78°C. After removal of the mother liquor with a capillary siphon, the precipitate was washed twice with cold ether and dried under oil-pump vacuum. Yield: 4.0 g (93%); correct elemental analysis: m.p. = 121°C.

2a: A yellow solution of **1a** (1.288 g, 3.0 mmol) in pentane (50 mL) was allowed to react at −78°C with a solution of butadiyne (0.2 mL, 3 mmol) in pentane (10 mL). Upon warming to −30°C, the reaction mixture turned red and, at −78°C, fine yellow needles crystallized and were freed from the mother liquor with a capillary siphon. The crystalline product was washed twice with cold pentane and dried at −30°C under oil-pump vacuum. Yield: 1.02 g (92%); correct elemental analysis.

2b: A solution of **1b** (2.22 g, 5.0 mmol) in pentane (50 mL) was allowed to react at −78°C with butadiyne (0.34 mL, 5.0 mmol) in pentane (10 mL). At −30°C, the initially yellow reaction solution turned burgundy red and long yellow needles slowly crystallized. The crystalline product was isolated as described for **1a** and dried at −30°C. Yield: 1.77 g (92%); correct elemental analysis; m.p. ≈ 45°C (dec.).

3a: a) A clear yellow solution of **1a** (858.5 mg, 2.0 mmol) in pentane (40 mL) was siphoned at −30°C into a yellow solution of **2a** (742.3 mg, 2.0 mmol). The reaction solution was warmed slowly to 20°C; the color turned orange-red (1 h). At −30°C, long yellow needles crystallized. The crystalline product was freed of mother liquor with a capillary siphon, washed twice with cold pentane, and dried under oil-pump vacuum. Yield: 1.27 g (92%). b) A clear yellow solution of **1a** (2.146 g, 5.0 mmol) in pentane (40 mL) was allowed to react at −78°C with butadiyne (0.17 mL, 2.5 mmol) in pentane (10 mL) and the reaction solution was then warmed slowly to −10°C. Yellow needles crystallized from the deep red reaction solution and were isolated as described above. Yield: 1.56 g (90%); correct elemental analysis; m.p. = 112°C.

Received: December 16, 1987 [Z 2542 IE]
German version: *Angew. Chem. 100* (1988) 853

[1] a) K. R. Pörschke, R. Mynott, K. Angermund, C. Krüger, *Z. Naturforsch. B40* (1985) 199; b) K. R. Pörschke, Y.-H. Tsay, C. Krüger, *Angew. Chem. 97* (1985) 334; *Angew. Chem. Int. Ed. Engl. 24* (1985) 323; c) K. R. Pörschke, R. Mynott, *Z. Naturforsch. B42* (1987) 421; d) K. R. Pörschke, W. Bonrath, Y.-H. Tsay, C. Krüger, unpublished results.

[2] a) K. R. Pörschke, *Int. Conf. Organomet. Chem. (Wien) 12* (1985) 207; b) unpublished results.

[3] Irradiation of $[HgCo_2(CO)_8]$ and C_4H_2 affords 1% of $[\{Co_2(CO)_6\}_2(HC{\equiv}CC{\equiv}CH)]$: G. Peyronel, A. Ragni, E. F. Trogu, *Gazz. Chim. Ital. 97* (1967) 1327; *Chem. Abstr. 68* (1968) 22047b.

[4] W. Bonrath, planned dissertation; W. Bonrath, K. R. Pörschke, G. Wilke, unpublished results.

[5] B. Bogdanović, M. Kröner, G. Wilke, *Justus Liebigs Ann. Chem. 699* (1966) 1.

[6] a) Crystal structure analysis of **2b**: space group *Pbca* (No. 61), $a = 13.995(2)$, $b = 14.723(2)$, $c = 21.480(3)$ Å, room temperature, $Z = 8$, $\rho_{calcd.} = 1.16$ g cm^{-3}, $\mu(Mo_{K\alpha}) = 10.19$ cm^{-1}, Enraf-Nonius diffractometer, 5537 measured reflections, averaged to 4983, 2340 observed ($I \geq 2\sigma(I)$); $R = 0.056$, $R_w = 0.055$ ($w = 1/\sigma^2(F_0)$) for 199 parameters. b) Further details of the crystal structure investigations may be obtained from the Fachinformationszentrum Energie, Physik, Mathematik GmbH, D-7514 Eggenstein-Leopoldshafen 2 (FRG), on quoting the depository number CSD-52684, the names of the authors, and the journal citation.

[7] Crystal structure analysis of **3a**: space group $C2/c$ (No. 15), $a = 22.461(3)$, $b = 8.448(1)$, $c = 20.327(2)$ Å, $\beta = 94.85(1)°$, room temperature, $Z = 4$, $\rho_{calcd} = 1.20$ g cm^{-3}, $\mu(Mo_{K\alpha}) = 11.67$ cm^{-1}, Enraf-Nonius diffractometer, 8676 measured reflections, averaged to 4344, 2978 observed ($I \geq 2\sigma(I)$); $R = 0.035$, $R_w = 0.042$ ($w = 1/\sigma^2(F_0)$) for 172 parameters [6b].

[8] L. Pauling, H. D. Springall, K. J. Palmer, *J. Am. Chem. Soc. 61* (1939) 927.

Synthesis and Crystal Structure of a Chiral C_3-Symmetric Monophosphane**

By *Carsten Bolm, William M. Davis, Ronald L. Halterman,* and *K. Barry Sharpless**

Mono- and bidentate phosphanes play an important role in transition metal chemistry.[1] Steric and electronic properties of the ligands markedly affect the stability and reactivity of the complexes.[2] Optically active phosphanes have been extensively used in transition-metal-catalyzed asymmetric syntheses.[3] We now report the preparation of the first C_3-symmetric monophosphane that does not contain a chiral carbon atom.[4]

Compound **2** was synthesized in a one-pot procedure by treatment of the corresponding 2-bromophenol **1** with two

[*] Prof. Dr. K. B. Sharpless, Dr. C. Bolm, Dr. W. M. Davis [+], Dr. R. L. Halterman
Department of Chemistry, Massachusetts Institute of Technology
Cambridge, MA 02139 (USA)

[+] X-ray structure analysis.

[**] *K. B. S.* and *C. B.* thank the John Simon Guggenheim Memorial Foundation, the Deutscher Akademischer Austauschdienst, and NATO for stipends. The authors thank Dr. *D. W. Balogh* (Lilly Research Laboratories) for obtaining mass spectra.

equivalents of *n*-butyllithium[5] followed by successive quenching of the lithium *o*-lithiophenolate with phosphorus trichloride and phosphoryl trichloride (in high dilution) [Eq. (a)].[6] Using analogous reaction conditions the desired [4.4.4]bicyclic product starting from 2-bromobenzyl alcohol could not be obtained.

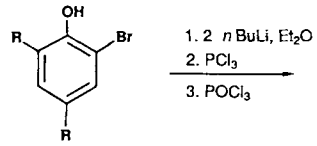

1

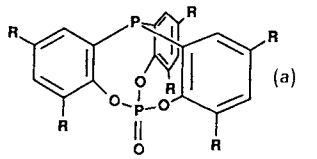

2

a, R = H ; **b**, R = *t*Bu

As determined by X-ray crystallography,[7] compound **2a** is a chiral molecule with a threefold axis of symmetry (Fig. 1).

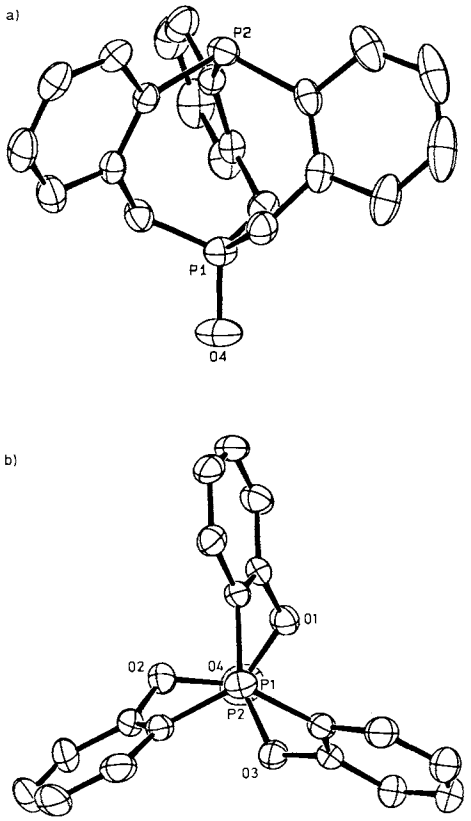

Fig. 1. Structure of **2a** in the crystal (two views, H atoms omitted) [7]. a) Side view. b) Top view, along the P2-P1-O4 axis.

The phosphane–phosphate axis is tilted by about 27° with respect to the planes of the aromatic rings. Both enantiomers are present in the unit cell.

To estimate the energy required for interconversion of the enantiomers (enantiotopomerization), **2a** was converted into the benzylphosphonium bromide **3** (heating of **2a** in pure benzyl bromide, 150°C, 2 h). Via the diastereo-

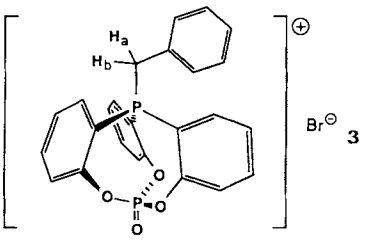

3

topic protons H_a and H_b of the benzyl group in **3**, a mutarotational energy of 11.8 kcal mol^{-1} was determined by variable-temperature NMR experiments. The phosphonium salt of **2b** could not be obtained under the reaction conditions described for the generation of **3**.

Doubly or triply charged ions are commonly found in the mass spectrum of phosphatriptycenes or compounds that contain heteroatoms, on which the positive charge may be localized.[8] No multiply charged ions were observed for **2a** (FD- and EI-MS).

The chemical shift in the ^{31}P-NMR spectrum for the "phosphane" phosphorus in **2a** (P2: $\delta = -33.2$[9]) indicates increased s-character for the lone pair orbital on phosphorus.[10] The "phosphate" phosphorus (P1: $\delta = -15.9$[9]) shows a chemical shift that lies close to the values reported for analogous bicyclic compounds.[11] In the phosphonium salt **3** a strong downfield shift for P2 is observed (^{31}P{^{1}H}-NMR data (CD_3OD, 85% H_3PO_4 ext.): $\delta = -8.1$ (P1), +21 (P2); compare triphenylphosphane, $\delta(^{31}P) = -5.5$, benzyltriphenylphosphonium bromide, $\delta(^{31}P) = +21.4$[12]).

In order to determine the ability of **2** to coordinate to transition metals, **2a** and **2b** were examined by NMR spectroscopy in the presence of $[PdCl_2 \cdot (C_6H_5CN)_2]$ (excess). Complexation was indicated in the ^{31}P-NMR spectrum by the characteristic downfield shift of P2[13] (^{31}P{^{1}H}-NMR data:[9] **2a**/$[PdCl_2 \cdot (C_6H_5CN)_2]$: $\delta = -18.4$ (P1), +15.1 (P2); **2b**/$[PdCl_2 \cdot (C_6H_5CN)_2]$: $\delta = -21.7$ (P1), +23.7 (P2)). Upon complexation the aromatic protons also resonated at lower field.

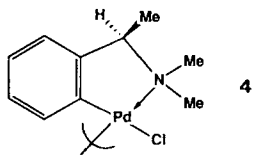

4

2

The optically active palladium complex **4** has been used for the resolution of racemic tertiary phosphanes.[14] In its reaction with **2a** and **2b** no diastereomeric complexes could be distinguished by NMR spectroscopy (^{31}P{^{1}H}-NMR data:[9] **2a/4**: $\delta = -17.3$ (P1), +29.3 (P2); **2b/4**: $\delta = -21.1$ (P1), +37.2 (P2)). Fractional crystallization did not result in a detectable enrichment of one diastereomer.

The concept of C_3-symmetric phosphane ligands is being pursued by the synthesis of compounds which are

structurally related to those described here, but which will hopefully have much greater configurational stability. Optically active C_3-phosphanes might be expected to serve as useful ligands in transition-metal-catalyzed asymmetric processes.

Experimental Procedure

Under argon at -15 °C a solution of **1a** (1.73 g, 10 mmol) in 40 mL of anhydrous ether was treated with 8 mL of a 2.5 M hexane solution of *n*-butyllithium (20 mmol). After 1 h at 0 °C a solution of phosphorus trichloride (457 mg, 3.33 mmol) in 8 mL of ether was added dropwise, forming a white precipitate. The mixture was stirred for 1 h at 0 °C and refluxed for 1 h followed by the addition of 200 mL of anhydrous ether. At 0 °C under vigorous stirring a solution of phosphoryl trichloride (537 mg, 3.5 mmol) in 60 mL of ether was added dropwise (over 4 h). After stirring at room temperature overnight, the mixture was poured into 75 mL of water. The organic layer (including the precipitate) was separated and the aqueous layer extracted twice with 100-mL portions of ether. The precipitate was removed by filtration, and the combined organic layers were dried over $MgSO_4$. After removal of the solvent by evaporation, the residue (0.36 g) was chromatographed (15 g silica gel, petroleum ether : 2-propanol = 20 : 1); yield: 130 mg (11%) of pure **2a**; white crystals, which can be recrystallized using benzene/petroleum ether [6]. The precipitate described above was dissolved in dichloromethane and the solution dried over $MgSO_4$. After evaporation of the solvent another 20 mg (1.7%) of **2a** could be obtained by chromatography.

The same sequence using **1b** (29.2 mmol [15]) yields, after chromatography, 2.49 g (37%) of the analogous product **2b** [6]. No precipitate was formed during the workup.

Received: February 23, 1988 [Z 2626 IE]
German version: *Angew. Chem. 100* (1988) 882

CAS Registry numbers:
1a, 95-56-7; **1b**, 20834-61-1; **2a**, 11449-59-7; **2b**, 114491-60-0.

[1] a) L. H. Pignolet (Ed.): *Homogeneous Catalysis With Metal Phosphine Complexes*, Plenum, New York 1983; b) C. A. McAuliffe, W. Levason: *Phosphine, Arsine, and Stibine Complexes of Transition Metals*, Elsevier, Amsterdam 1979; c) O. Stelzer, *Top. Phosphorus Chem. 9* (1977) 1.

[2] a) J. P. Collman, L. S. Hegedus, J. R. Norton, R. G. Finke: *Principles And Applications Of Organotransition Metal Chemistry*, 2nd ed., University Science Books, Mill Valley, CA, USA 1987; b) A. Yamamoto: *Organotransition Metal Chemistry*, Wiley, New York 1986.

[3] a) H. B. Kagan in J. D. Morrison (Ed.): *Asymmetric Synthesis, Vol. 5*, Academic Press, Orlando, FL, USA 1985, p. 1; b) H. B. Kagan in G. Wilkinson (Ed.): *Comprehensive Organometallic Chemistry, Vol. 8*, Pergamon, Oxford 1982, p. 463; c) B. Bosnich, M. D. Fryzuk, *Top. Stereochem. 12* (1981) 119; d) W. S. Knowles, *Acc. Chem. Res. 16* (1983) 106; e) V. Caplar, G. Comisso, V. Sunjic, *Synthesis 1981*, 85.

[4] Examples of nickel-catalyzed reactions using C_3-symmetric phosphanes *with chiral C-atoms:* a) B. Bogdanović, *Angew. Chem. 85* (1973) 1013; *Angew. Chem. Int. Ed. Engl. 12* (1973) 954; b) B. Bogdanović, B. Henc, B. Meister, H. Pauling, G. Wilke, *ibid. 84* (1972) 1070 and *11* (1972) 1023.

[5] a) U. Schöllkopf in: *Houben-Weyl-Müller: Methoden der Organischen Chemie, 4. Aufl., Bd. XIII/1*, Thieme, Stuttgart 1970, p. 153; b) A. Tzschach, E. Nietzschmann, *Z. Chem. 20* (1980) 341.

[6] **2a**: 12.7%; $R_f = 0.26$ (silica gel, petroleum ether : 2-propanol = 7 : 1); m.p. = 211–212 °C; ^{1}H-NMR (250 MHz, $CDCl_3$): $\delta = 7.23$–7.30 (m, 6H), 7.44–7.49 (m, 3H), 7.83 (ddd, $J = 16$, 7.5, 1.6 Hz, 3H); ^{13}C{^{1}H}-NMR (75 MHz, $CDCl_3$): $\delta = 121.4$ (d, $|J(P,C)| = 7.1$ Hz), 123.6 (d, $|J(P,C)| = 19.7$ Hz), 126.1 (d, $|J(P,C)| = 18.6$ Hz), 132.9 (s), 138.7 (d, $|J(P,C)| = 58.2$ Hz), 154.5 (dd, $|J(P,C)| = 11.5$, 4.5 Hz); ^{31}P-NMR (121.4 MHz, $CDCl_3$, 85% H_3PO_4 ext.): $\delta = -15.9$ (s), -33.2 (q, $J(P,H) = 16$ Hz); IR (CH_2Cl_2): $\tilde{\nu}_{max} = 3060$, 2988, 1440, 1271, 1194, 978 cm^{-1}; MS (FD): *m/z* 354; MS (EI): *m/z* 354 ($M^{\oplus}$, 100%), 199 (21%), 168 (50%); **2b**: 37%; $R_f = 0.5$ (silica gel, petroleum ether : ethyl acetate = 10 : 1); m.p. = 290 °C; ^{1}H-NMR (250 MHz, $CDCl_3$): $\delta = 1.32$ (s, 27H), 1.45 (s, 27H), 7.52 (s, broadened, 3H), 7.70 (dd, $J(P,H) = 18$ Hz, $J(H,H) = 2.5$ Hz, 3H); ^{13}C{^{1}H}-NMR (75 MHz, $CDCl_3$): $\delta = 30.4$ (s), 31.4 (s), 34.7 (s), 35.4 (s), 124.8 (d, $|J(P,C)| = 19.6$ Hz), 128.0 (s), 133.9 (d, $|J(P,C)| = 61.4$ Hz), 140.5 (d, $|J(P,C)| = 7.3$ Hz), 147.2 (d, $|J(P,C)| = 8.4$ Hz), 151.0 (dd, $|J(P,C)| = 10.4$, 4.4 Hz); ^{31}P-NMR (121.4 MHz, $CDCl_3$, 85% H_3PO_4 ext.): $\delta = -20.0$ (s), -23.6 (q, $J(P,H) = 18$ Hz); IR (CH_2Cl_2): $\tilde{\nu}_{max} = 2970$, 1304, 1240, 1110, 982, 738 cm^{-1}; MS (EI): *m/z* 691 ($M^{\oplus}$, 100%), 676 (57%), 191 (52%), 57 (43%); correct elemental analysis (C, H, P).

[7] Crystal data for **2a**: monoclinic, space group *C2/c* (No. 15), $a = 25.260(1)$, $b = 13.592(2)$, $c = 12.027(2)$ Å, $\beta = 116.33(2)°$, $V = 3701(2)$ Å^3, $Z = 8$, $\rho_{calcd} = 1.412$ g cm^{-3}, $F(000) = 1624$, $\mu(Mo_{K\alpha}) = 2.64$ cm^{-1}, 4566 reflections measured, 4467 unique reflections, 2593 observed ($I > 3.00\sigma(I)$), 245 variables, $R = 0.043$, $R_w = 0.057$, Rigaku AFC6R diffractometer, $Mo_{K\alpha}$ ($\lambda = 0.71069$ Å). The title molecule crystallizes with one-half molecule of benzene in the asymmetric unit. Further details of the crystal structure investigation are available on request from the director of the Cambridge Crystallographic Data Centre, Cambridge CB2 1EW (England), on quoting the names of the authors and the full citation of the journal.

[8] a) D. Hellwinkel, W. Schenk, *Angew. Chem. 81* (1969) 1049; *Angew. Chem. Int. Ed. Engl. 8* (1969) 987; b) M. I. Bruce, *J. Chem. Soc. Chem. Commun. 1967*, 593.

[9] ^{31}P-NMR data: 121.4 MHz, $CDCl_3$, 85% H_3PO_4 ext.

[10] E. Fluck, H. Bürger, U. Goetze, *Z. Naturforsch. B22* (1967) 912.

[11] a) J. G. Verkade, R. W. King, *Inorg. Chem. 1* (1962) 948; b) K. J. Coskran, J. G. Verkade, *ibid. 4* (1965) 1655.

[12] S. O. Grim, W. McFarlane, E. F. Davidoff, T. J. Marks, *J. Phys. Chem. 70* (1966) 581.

[13] M. M. Crutchfield, C. H. Dungan, J. H. Letcher, V. Mark, J. R. Van Wazer, *Top. Phosphorus Chem. 5* (1967).

[14] a) K. Tani, L. D. Brown, J. Ahmed, J. A. Ibers, M. Yokota, A. Nakamura, S. Otsuka, *J. Am. Chem. Soc. 99* (1977) 7876; b) S. Otsuka, A. Nakamura, T. Kano, K. Tani, *ibid. 93* (1971) 4301.

[15] Prepared by bromination of 2,4-di-*tert*-butylphenol: D. E. Pearson, R. D. Wysong, C. V. Breder, *J. Org. Chem. 32* (1967) 2358.

Formation of the Diphosphatricyclo[2.1.0.0^{2,5}]pentane Ring System via Phosphaalkyne Dimerization and Carbon Monoxide Incorporation**

By *Andrew R. Barron, Alan H. Cowley,* Stephen W. Hall,* and *Christine M. Nunn*

In principle, the oligomerization of phosphaalkynes represents an excellent synthetic route to a fascinating array of new heterocycles. Indeed, recent research has demonstrated that it is possible to dimerize[1] or trimerize[2] phosphaalkynes within a coordination sphere. However, in each case, the oligomer has remained bound to the transition metal. We report the first instance of the production of an uncoordinated heterocycle starting with a phosphaalkyne and using a transition-metal substrate. Furthermore, the product of this reaction, **1**, constitutes the first example of a new class of phosphorus compound.

The reaction of $[(\eta^5\text{-}C_5H_5)_2Ti(CO)_2]$[3] with *t*BuC≡P[4] in refluxing hexane affords a colorless solid, **1**, with a composition corresponding to $(t\text{BuCP})_2\text{CO}$. The medium-resolution mass spectrum (70 eV) of **1** exhibits a parent peak at *m/z* 228. A fragmentation peak at *m/z* 200 corresponds to the loss of CO, and this is followed by peaks at *m/z* 185, 170, 155, and 143 corresponding to the sequential loss of three methyl groups and one *tert*-butyl group, respectively. The ^{31}P{^{1}H}-NMR spectrum of **1** (121.5 MHz, C_6D_6, 85% H_3PO_4 ext.) exhibits a singlet at $\delta = -346.6$. Such a low-frequency ^{31}P chemical shift is strongly indicative of a tetrahedrane-type phosphorus environment and may be compared with those for P_4 ($\delta = -460$)[5] and **2** ($\delta = -247$).[1c]

The ^{1}H-NMR spectrum of **1** (300 MHz, C_6D_6, TMS ext.) consists of a singlet at $\delta = 0.82$. The ^{13}C{^{1}H}-NMR spec-

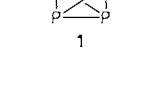

1

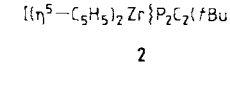

2

[*] Prof. Dr. A. H. Cowley, Dr. A. R. Barron, S. W. Hall, Dr. C. M. Nunn
Department of Chemistry, The University of Texas at Austin
Austin, TX 78712 (USA)

[**] This work was supported by the National Science Foundation (USA) and Robert A. Welch Foundation.

trum of **1** (75.5 MHz, C_6D_6, TMS ext.) shows three resonances assignable as follows: $\delta = 29.35$ (s, $(CH_3)_3C$), 77.56 (t, $^2J_{PC} = 37.7$ Hz, Me_3C), and 178.52 (t, $^1J_{PC} = 15.1$ Hz, C_a). Ring carbon C_b is not detectable by $^{13}C\{H\}$-NMR; nevertheless, the presence of a C=O group is evident from the observation of an IR stretching frequency at 1717 cm^{-1}. The above structure was confirmed by X-ray analysis (Fig. 1).[6] Interestingly, the P-P distance (2.118(3) Å) is 0.09 Å shorter than that of a P-P single bond, thus suggesting a slight multiple-bond character. The complex **2** also features a short P-P bond distance (2.146(1) Å).[1c]

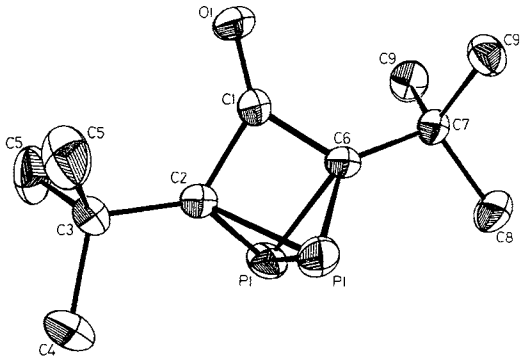

Fig. 1. Structure of **1** in the crystal. Selected bond lengths [Å]: P1-P1 2.118(3), P1-C2 1.897(8), P1-C6 1.895(7), C1-C6 1.514(13), C1-C2 1.511(12), C1-O1 1.200(11). Each molecule of **1** resides on a plane of symmetry perpendicular to the P-P bond.

At present we do not have any direct evidence bearing on the mechanism of formation of **1**. However, it is possible that the sequence of reactions shown in Scheme 1 is involved.

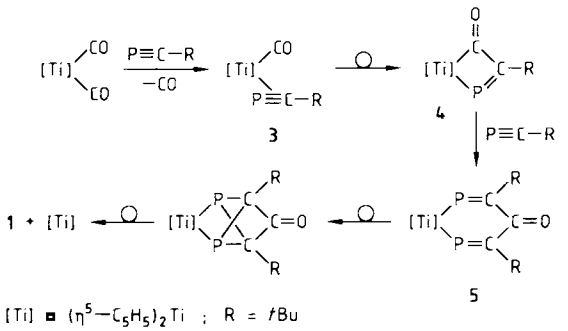

Scheme 1.

The attack of CO on the C atom of coordinated *t*BuC≡P (**3**→**4**) finds precedent in the work of *Nixon* et al.[7] Moreover, the same group has isolated a Rh complex of the P=CR–C(O)–CR=P (R = adamantyl) unit (cf. **5**).

Experimental Procedure

The reaction of $[(\eta^5-C_5H_5)_2Ti(CO)_2]$ [3] (1.0 g, 4.3 mmol) with *t*BuC≡P [4] (1.0 g, 10.0 mmol) in hexane at 25°C results initially in the formation of a bright yellow solid. Upon refluxing for a few hours, the color of the reaction mixture darkens to orange. Filtration results in an orange solid that contains no phosphorus. Evaporation of the filtrate, followed by sublimation of the resulting residue (35°C, 10^{-3} torr) affords colorless, solid **1** in 63.7% yield (0.625 g, 2.74 mmol).

Received: February 9, 1988 [Z 2611 IE]
German version: *Angew. Chem. 100* (1988) 873

CAS Registry numbers:
1, 114491-61-1; $[(\eta^5-C_5H_5)_2Ti(CO)_2]$, 12129-51-0; *t*BuC≡P, 78129-68-7.

[1] a) P. Binger, R. Milczarek, R. Mynott, M. Regitz, W. Rösch, *Angew. Chem. 98* (1986) 645; *Angew. Chem. Int. Ed. Engl. 25* (1986) 644; b) P. B. Hitchcock, M. J. Maah, J. F. Nixon, *J. Chem. Soc. Chem. Commun. 1986*, 737; c) P. Binger, B. Biedenback, C. Krüger, M. Regitz, *Angew. Chem. 99* (1987) 798; *Angew. Chem. Int. Ed. Engl. 26* (1987) 764; d) P. B. Hitchcock, M. J. Maah, J. F. Nixon, *J. Chem. Soc. Chem. Commun. 1987*, 658.

[2] A. R. Barron, A. H. Cowley, *Angew. Chem. 99* (1987) 956; *Angew. Chem. Int. Ed. Engl. 26* (1987) 906; R. Milczarek, W. Rüsseler, P. Binger, K. Jonas, K. Angermund, C. Krüger, M. Regitz, *Angew. Chem. 99* (1987) 957; *Angew. Chem. Int. Ed. Engl. 26* (1987) 908.

[3] D. J. Sikora, D. W. Macomber, M. D. Rausch, *Adv. Organomet. Chem. 25* (1986) 317.

[4] G. Becker, G. Gressner, U. Uhl, *Z. Naturforsch. B 36* (1981) 16; G. Becker, *Z. Anorg. Allg. Chem. 430* (1974) 66.

[5] M. M. Crutchfield, C. H. Dungan, J. H. Letcher, V. Mark, J. R. Van Wazer, *Top. Phosphorus Chem. 5* (1967) 45.

[6] **1**: orthorhombic, space group *Pnma* (No. 62), $Z = 4$, $a = 8.201(2)$, $b = 10.066(4)$, $c = 15.761(3)$ Å, $V = 1301.1$ Å^3; $\rho_{calcd} = 1.165$ g cm^{-3}, $3° < 2\theta < 55°$ ($Mo_{K\alpha}$, $\lambda = 0.71069$ Å, $\mu = 2.98$ cm^{-1}). 1751 unique reflections collected, of which 823 ($I > 3.0\sigma(I)$) were used to solve (direct methods) and refine (full matrix, least squares) the structure of **1**. $R = 0.0658$, $R_w = 0.0859$. Further details of the crystal structure investigation may be obtained from the Fachinformationszentrum Energie, Physik, Mathematik GmbH, D-7514 Eggenstein-Leopoldshafen 2 (FRG), on quoting the depository number CSD-52980, the names of the authors, and the journal citation.

[7] S. I. Al-Resayes, P. B. Hitchcock, J. F. Nixon, *J. Chem. Soc. Chem. Commun. 1987*, 928.

Addition of a Distannene to a Phosphaalkyne. Formation of a Phosphadistannacyclobutene**

By *Alan H. Cowley,* Stephen W. Hall, Christine M. Nunn,* and *John M. Power*

Recently it has been demonstrated that carbenes[1] and silylenes[2] will add to phosphaalkynes, RC≡P, to afford three-membered rings containing phosphorus-carbon double bonds. We have found that the corresponding tin chemistry proceeds in a different fashion.

The stannylidene $[(Me_3Si)_2CH]_2Sn$ exists as a dimer **1b** in the solid state.[3] In solution, however, recent evidence indicates that there is a dynamic equilibrium between the monomer **1a** and dimer **1b**.[4] We find that *t*BuC≡P[5] reacts with this monomer/dimer mixture to afford the first example of a phosphadistannacyclobutene, **2**.

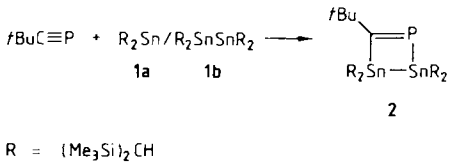

The ^{31}P-NMR chemical shift of **2**[6] falls in the region anticipated for a P=C moiety.[7] Moreover, the presence of two Sn atoms is indicated both by two separate sets of $^{117}Sn/^{119}Sn$ satellites in the $^{31}P\{^1H\}$-NMR spectra and by the observation of two distinct ^{119}Sn resonances. The large Sn/Sn coupling constant of 892.2 Hz is consistent with the presence of a tin-tin bond. The observation of four Me_3Si

[*] Prof. Dr. A. H. Cowley, S. W. Hall, Dr. C. M. Nunn, Dr. J. M. Power
Department of Chemistry, The University of Texas at Austin
Austin, TX 78712 (USA)

[**] This work was supported by the National Science Foundation (USA) and Robert A. Welch Foundation.

resonances in the ^{1}H- and ^{13}C{^{1}H}-NMR spectra is ascribable to the presence of two nonequivalent Sn atoms and to the fact that each $(Me_3Si)_2CH$ group is diastereotopic.

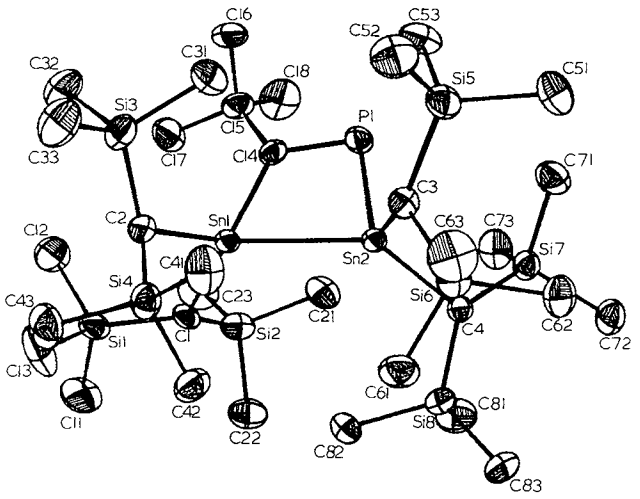

Fig. 1. Structure of **2** in the crystal showing the atom numbering scheme for molecule I. Selected bond lengths [Å] and bond angles [°] for molecule I: Sn1-Sn2 2.878(1), Sn1-C14 2.203(13), Sn2-P1 2.544(4), P1-C14 1.712(15); Sn2-Sn1-C14 76.1(4), Sn1-Sn2-P1 74.78(9), Sn2-P1-C14 94.5(4), Sn1-C14-P1 114.5(6).

The above structure assignment is confirmed by X-ray analysis (Fig. 1).[8] Note that there are two independent molecules per asymmetric unit. Within experimental error, the Sn_2PC ring is planar and the sum of angles at the ring carbon average 359.5°. In contrast to the free distannene **1b**, which adopts a *trans* structure,[3] the conformation of the R_2SnSnR_2 moiety in **2** is *cis*. As expected, the Sn–Sn bond distance in **2** (average 2.886(1) Å) is somewhat longer than that in **1b** (2.768(1) Å) but comparable to that in the distannane, $R_2(Cl)SnSn(Cl)R_2$ (2.844(1) Å).[9] The phosphorus–carbon distance (average 1.697(15) Å) is consistent with a bond order of approximately two.[7]

In principle, the phosphadistannacyclobutene **2** could be formed either by [2+2] cycloaddition of the distannene **1b** to *t*BuC≡P or via the insertion of a second R_2Sn unit into an initially formed phosphastannirene, **3**. However,

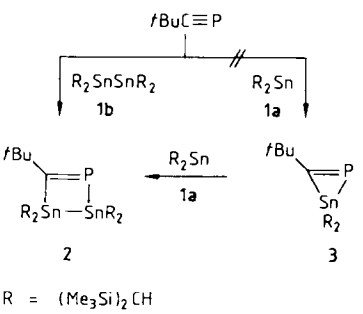

we have found no spectroscopic evidence for the existence of **3** even when an excess of the phosphaalkyne is employed. Moreover, the isoelectronic $[(Me_3Si)_2N]_2Sn$, which exists exclusively as a monomer,[10] fails to react with *t*BuC≡P. This suggests that **2** arises via a distannene/phosphaalkyne reaction.

Experimental Procedure

A magenta solution of $[(Me_3Si)_2CH]_2Sn$ (0.66 g, 0.76 mmol) in *n*-hexane (30 mL) at 25°C was treated via syringe with a dimethoxyethane solution of *t*BuC≡P (1.85 mL of a 0.42 M solution, 0.76 mmol). After 6 h the resulting orange solution was concentrated and microcrystalline **2** was obtained at −20°C. Recrystallization from dichloromethane afforded pure **2** as red-orange crystals. Yield: 0.18 g (24%), m.p. = 136–138°C (dec.).

Received: February 18, 1988 [Z 2624 IE]
German version: *Angew. Chem. 100* (1988) 874

[1] O. Wagner, G. Maas, M. Regitz, *Angew. Chem. 99* (1987) 1328; *Angew. Chem. Int. Ed. Engl. 26* (1987) 1257.
[2] A. Schäfer, M. Weidenbruch, W. Saak, S. Pohl, *Angew. Chem. 99* (1987) 806; *Angew. Chem. Int. Ed. Engl. 26* (1987) 776.
[3] P. J. Davidson, D. H. Harris, M. F. Lappert, *J. Chem. Soc. Dalton Trans. 1976*, 2268; D. E. Goldberg, P. B. Hitchcock, M. F. Lappert, K. M. Thomas, T. Fjelberg, A. Haaland, B. E. R. Schilling, *ibid. 1986*, 2387.
[4] K. W. Zilm, G. A. Lawless, R. M. Merrill, J. M. Millar, G. G. Webb, *J. Am. Chem. Soc. 109* (1987) 7236.
[5] G. Becker, G. Gressner, U. Uhl, *Z. Naturforsch. B36* (1981) 16; G. Becker, *Z. Anorg. Allg. Chem. 430* (1974) 66.
[6] **2**: ^{1}H-NMR (300 MHz, C_6D_6, TMS ext.): δ = 0.26 (s, 18H), 0.30 (s, 18H), 0.31 (s, 18H), 0.34 (s, 18H), 0.64 (s, 2H), 1.47 (s, 9H), 2.06 (s, 2H); ^{13}C{^{1}H}-NMR (75.5 MHz, C_6D_6, TMS ext.): δ = 4.45 (s, $Si(CH_3)_3$), 5.29 (s, $Si(CH_3)_3$), 5.64 (s, $Si(CH_3)_3$), 8.92 (s, $^1J_{SnC}$ = 48.3 Hz, $CH(SiMe_3)_2$), 15.31 (s, $C(CH_3)_3$), 36.2 (d, $^3J_{PC}$ = 12.1 Hz, $C(CH_3)_3$); ^{31}P-NMR (121.5 MHz, C_6D_6, 85% H_3PO_4 ext.): δ = 459.0 (s, $^1J_{SnP}$ = 830.0 (^{117}Sn), 796.0 (^{119}Sn) Hz, $^2J_{SnP}$ = 278.3 Hz); ^{119}Sn-NMR (111.9 MHz, C_6D_6, Me_4Sn ext.): δ = 58.6 (d, $^1J_{PSn}$ = 827.2 Hz), 160.4 (d, $^2J_{PSn}$ = 281.9 Hz, $^1J_{SnSn}$ = 892.2 Hz).
[7] R. Appel, F. Knoll, I. Ruppert, *Angew. Chem. 93* (1981) 771; *Angew. Chem. Int. Ed. Engl. 20* (1981) 731.
[8] **1**: triclinic, space group $P\bar{1}$ (No. 2), Z = 4; a = 20.749(3), b = 22.123(4), c = 12.435(3) Å, α = 105.07(2), β = 93.31(2), γ = 82.15(1)°, V = 5460.2 Å^3, ρ_{calcd} = 1.224 g cm^{-3}; $3° < 2\theta < 45°$ ($Mo_{K\alpha}$, λ = 0.71069 Å, μ = 11.68 cm^{-1}). 14201 unique reflections collected, of which 10513 [$I > 3.0\sigma(I)$] were used to solve (direct methods) and refine (full matrix least squares) the structure R = 0.0602, R_w = 0.0816. Further details of the crystal structure investigation are available on request from the Fachinformationszentrum Energie, Physik, Mathematik GmbH, D-7514 Eggenstein-Leopoldshafen 2 (FRG), by quoting the depository number CSD-53151, the names of the authors, and the journal citation.
[9] T. A. Al-Allaf, C. Eaborn, P. B. Hitchcock, M. F. Lappert, A. Pidcock, *J. Chem. Soc. Chem. Commun. 1985*, 548.
[10] M. J. S. Gynane, D. H. Harris, M. F. Lappert, P. P. Power, P. Riviere, M. Riviere-Baudet, *J. Chem. Soc. Dalton Trans. 1977*, 2004.

Acetylene Polymerization with Ylide–Nickel Catalysts

By *K. Alexander Ostoja Starzewski** and *Josef Witte*

In solution bis(ylide)nickel catalyst systems Ni^0/$Ph_3PCR^1CR^2O$/$R^3_3PCR^4R^5$ (R^1 to R^5 can, for example, be alkyl and aryl groups or heteroatom substituents) preferentially form square-planar phenylnickel complexes containing a phosphinoenolate ligand and a structurally intact coordinated ylide ligand, **1**.[1] These compounds are highly efficient catalysts for ethylene oligomerization and poly-

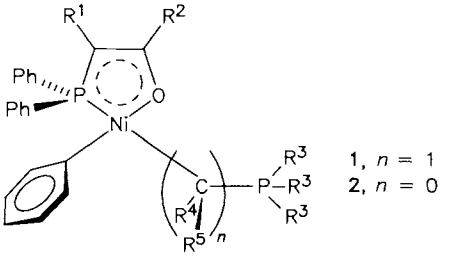

[*] Dr. K. A. Ostoja Starzewski, Dr. J. Witte
Bayer AG, Zentrale Forschung und Entwicklung
Wissenschaftliches Hauptlaboratorium
D-5090 Leverkusen 1 (FRG)

merization[1-3] as well as for the copolymerization of ethylene with α-olefins.[4] Their reactivity exceeds that of the related phosphane complexes **2**.[5]

We have now discovered that complexes **1** and **2** also catalyze acetylene polymerization. Although the *stoichiometric insertion* of diphenylacetylene into the Ni–C_{phenyl} bond of a phosphane complex related to **2** was recently described,[6] no catalytic reactions were reported. The reaction does not proceed beyond the conceivable initial step of the catalytic cycle.

Noteworthy is the catalytic activity of the bis(ylide)nickel catalysts **1** for the polymerization of acetylene in a wide variety of solvents (Table 1). In contrast to the behavior of the phosphane derivatives **2**, the turnover numbers of **1** increase markedly with solvent polarity. The polymerization catalyzed by the complex [NiPh($Ph_2PCHCPhO$)(Me_3PCH_2)] **1a** in dimethyl sulfoxide at 60°C under normal pressure for 1 h results in the conversion of ca. 500 moles of acetylene per mole of nickel·bar.

Table 1. Acetylene polymerization activity of the ylide-nickel catalyst **1a** in various solvents at ca. 60°C and 1 bar acetylene.

Solvent	Activity [a]
Cyclohexane	22
Acetone [b]	31
Acetonitrile	169
Dimethylformamide (DMF)	223
Dimethyl sulfoxide (DMSO)	492

[a] Moles of converted acetylene per mole of nickel. [b] Reflux.

The reaction in DMSO is rapid. After admitting acetylene for 5 min into a solution containing 1 mmol of the catalyst **1a** (single-pulse procedure), 5 g of polyacetylene can be isolated; this corresponds to a conversion of ca. 200 moles of acetylene per mole of nickel. The polymerization is strongly exothermic, and the internal temperature, without cooling, increases from 60 to 110°C.[7] The yield of polyacetylene depends markedly on the reaction temperature. Optimal activity is attained at 60°C, but even at 100°C approximately 300 moles of acetylene per mole of nickel are converted in 1 h.

The normalized activity (mol C_2H_2/mol Ni·bar·h) of the bis(ylide)nickel system thus exceeds, to the best of our knowledge, that of all known acetylene polymerization catalysts based on nickel.[8,9]

The isolable one-component catalysts are especially well suited to study specific ligand effects. With respect to structure/activity relations there are interesting parallels between the polymerization of acetylene and that of ethylene. In both cases, complexes containing intact ylide ligands such as **1** are catalytically more active than related phosphane derivatives **2**.[10] In the case of the acetyl catalysts [NiPh($Ph_2PCHCMeO$)(ylide intact)], benzylidene(triisopropyl)phosphorane effects an especially pronounced increase in activity (Table 2). As observed for ethylene polymerization, the activity increases in the series formyl (R^2 = H) < acetyl (R^2 = Me) < benzoyl (R^2 = Ph), while keeping trimethyl(methylene)phosphorane as structurally intact coordinated ylide ligand.

Table 2. Acetylene polymerization activity of various ylide-nickel catalysts **1**, **2**.

Catalyst [a]	Procedure [b]	Activity [c]
[NiPh($Ph_2PCHCMeO$)(Ph_3P)] **2a**	A	35
[NiPh($Ph_2PCHCMeO$)($NiPr_3PCH_2$)] **1b**	A	215
[NiPh($Ph_2PCHCMeO$)($NiPr_3PCHPh$)] **1c**	A	319
[NiPh($Ph_2PCHCHO$)(Me_3PCH_2)] **1d**	B	73
[NiPh($Ph_2PCHCMeO$)(Me_3PCH_2)] **1e**	B	258
[NiPh($Ph_2PCHCPhO$)(Me_3PCH_2)] **1a**	B	492

[a] 1 mmol in 20 mL of toluene, polymerization in 80 mL of DMSO, polymerization temperature 60°C, polymerization time 1 h. [b] A = single-pulse procedure, B = multi-pulse procedure. [c] Moles of converted acetylene per mole of nickel.

Experimental Procedure

1a (529 mg, 1 mmol) [1] in toluene (20 mL) was added to 80 mL of DMSO at 60°C to which acetylene was being admitted. All operations were carried out with strict exclusion of air and moisture and the catalyst addition was performed at such a rate that, without external heating, the internal temperature was maintained at 60°C. After 1 h at 60°C, black polyacetylene powder was isolated by Schlenk filtration, washed sequentially with ethanol, acetone, and ether, and dried under vacuum. Yield: 12.8 g (93% *trans*, 7% *cis* double bonds, FT-IR).

Received: January 18, 1988 [Z 2580 IE]
German version: *Angew. Chem. 100* (1988) 861

[1] K. A. Ostoja Starzewski, J. Witte, *Angew. Chem. 97* (1985) 610; *Angew. Chem. Int. Ed. Engl. 24* (1985) 599.
[2] K. A. Ostoja Starzewski, J. Witte, *Angew. Chem. 99* (1987) 76; *Angew. Chem. Int. Ed. Engl. 26* (1987) 63.
[3] K. A. Ostoja Starzewski, J. Witte in R. Quirk (Ed.): *Proc. Int. Symp. Transition Metal Catalyzed Polymerizations, Akron, OH, USA 1986*. Cambridge University Press, New York 1988, in press.
[4] K. A. Ostoja Starzewski, J. Witte, K. H. Reichert, G. Vasiliou in W. Kaminsky, H. Sinn (Eds.): *Proc. Int. Symp. Transition Metals and Organometallics as Catalysts for Olefin Polymerization*, Hamburg 1987, Springer, Heidelberg 1988, in press.
[5] W. Keim, F. H. Kowaldt, R. Goddard, C. Krüger, *Angew. Chem. 90* (1978) 493; *Angew. Chem. Int. Ed. Engl. 17* (1978) 466.
[6] W. Keim, A. Behr, B. Gruber, B. Hoffmann, F. H. Kowaldt, U. Kürschner, B. Limbäcker, F. P. Sistig, *Organometallics 5* (1986) 2356.
[7] In order to avoid undesired peaks in temperature in the single-pulse procedure, the polymerization can also be performed according to the multi-pulse method, the desolved catalyst being added parallel to the consumption of acetylene. The temperature of the reaction solution can then be controlled by means of the heat of polymerization.
[8] a) M. L. H. Green, N. Nehme, G. Wilkinson, *Chem. Ind. (London) 1960*, 985; b) L. B. Luttinger, *J. Org. Chem. 27* (1962) 1591; c) W. E. Daniels, *ibid. 29* (1964) 2936; d) L. Porri, M. C. Gallazi, G. Vitulli, *Polym. Lett. 5* (1967) 629; e) J. P. Martella, W. C. Kaska, *Tetrahedron Lett. 1968*, 4889; f) S. Ceriotti, G. Longoni, P. Chini, *J. Organomet. Chem. 174* (1979) C27; g) Shen Zhiquan, Wang Zheng, Wang Guoping, Yu Luping, *Scientia Sinica 30* (1987) 809.
[9] Reviews on the current status of acetylene polymerization: C. Kröhnke, G. Wegner in H. Bartl, J. Falbe: *Houben-Weyl, Methoden der organischen Chemie, Bd. E20, Makromolekulare Stoffe, Teil 2*, Thieme, Stuttgart 1987, p. 1312ff; A. M. Saxman, R. Liepins, M. Aldissi, *Prog. Polym. Sci. 11* (1985) 57.
[10] We have already described the unique features of the electronic structure of ylides: K. A. Ostoja Starzewski et al., *Phosphorus Sulfur 18* (1983) 448; *Inorg. Chem. 18* (1979) 3307; *J. Mol. Struct. 51* (1979) 3307; *J. Am. Chem. Soc. 98* (1976) 8486; *Phosphorus 6* (1976) 177; *Chem. Ber. 109* (1976) 473; *J. Organomet. Chem. 93* (1975) C20; *Angew. Chem. 87* (1975) 197; *Angew. Chem. Int. Ed. Engl. 14* (1975) 173; *J. Organomet. Chem. 65* (1974) 311; *J. Organomet. Chem. 42* (1972) C35.

Synthesis and Properties of a Bridged *syn*-Tricyclo[4.2.0.$0^{2,5}$]octa-3,7-diene: Formation of Propella[3$_4$]prismane**

By *Rolf Gleiter* and *Michael Karcher*

In memoriam David Ginsburg

syn-Tricyclo[4.2.0.$0^{2,5}$]octa-3,7-diene **1** does not isomerize to cubane **2** upon irradiation; the same holds for

[*] Prof. Dr. R. Gleiter, Dr. M. Karcher
Institut für Organische Chemie der Universität
Im Neuenheimer Feld 270, D-6900 Heidelberg (FRG)

[**] This work was supported by the Stiftung Volkswagenwerk, the Fonds der Chemischen Industrie, and the BASF Aktiengesellschaft. We thank Dr. *P. Kunzelmann* and Dr. *G. Schilling* for recording the NMR spectra.

alkyl derivatives of **1**.[1,2] Essentially three reasons have been given to explain this finding: (1) the large difference in strain energy between educt and product;[3] (2) the relatively large separation (3.05 Å) between the two olefinic moieties in **1**;[3] (3) owing to the dominance of through-bond interaction in **1**, π_+ lies above π_- for both sets of π MOs (i.e., reaction (a) is symmetry-forbidden).[4]

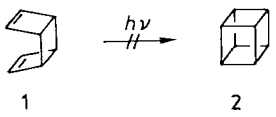

1 2 (a)

Bridging of the two olefinic moieties should favor the photochemical ring closure shown in reaction (a), since, for a sufficiently short bridge, the strain energy of the educt should increase more than that of the product and the separation between the olefinic moieties of the educt should become smaller. With two C_3 bridges, the situation should be especially favorable, since the through-bond effect of two C_3 bridges should nearly compensate that of the C_2 bridges (C1–C2 and C5–C6) in **1**.[5]

Starting from the readily accessible superphane **3**,[6] it was possible to synthesize a tricyclo[4.2.0.0^{2,5}]octadiene bridged by C_3 units (Scheme 1). Oxidation of **3** with Ce^{IV} in aqueous ethanol at 0°C leads smoothly to heptacyclo[10.8.0.0^{2,6}.0^{2,11}.0^{6,17}.0^{7,11}.0^{7,16}]icosa-1(12),16-diene **4**.

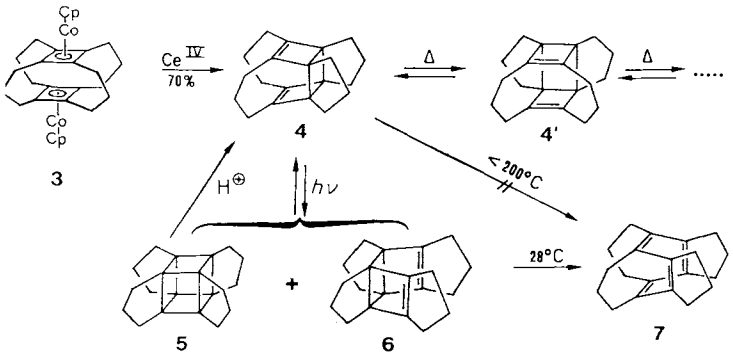

Scheme 1. Synthesis and reactions of **4**.

The reduced separation (ca. 2.6 Å[7]) of the two olefinic moieties in **4**, caused by the bridges, is revealed, for example, by a single signal for the π bands ($I_{v,1}$ = 7.6 eV) in the photoelectron spectrum and by a degenerate Cope rearrangement upon warming. The free energy of activation for the Cope rearrangement can be estimated as 71–76 kJ mol^{-1} from the coalescence temperature (ca. 90°C) for the signals of the CH_2 carbons in the ^{13}C-NMR spectrum.[8] In contrast, **1** undergoes rearrangement at 90–120°C to give cyclooctatetraene,[9] whereas an irreversible valence isomerization at 135°C has been reported for brominated derivatives of **1**.[10]

Irradiation of **4** in degassed *n*-pentane at room temperature with a 500-W high-pressure mercury lamp results in the formation of an equilibrating mixture of **4** and two new products (**5** and **6**) (Scheme 1). At room temperature, the ratio **4** : **5** : **6** is 10 : 1 : 4.

Compounds **5** + **6** can be separated from **4** by chromatography (Al_2O_3/*n*-pentane). Separation of **5** and **6** has only been achieved so far after rearrangement of **6** to **7** at 28°C (Scheme 1) by means of chromatography on Al_2O_3 using *n*-pentane as eluent. The cubane derivative **5** rearranges to **4** in the presence of traces of acid.[11] Irradiation of **5** + **6** affords once again a mixture of **4**, **5**, and **6**. The bridged cyclooctatetraene **7** could not be obtained by thermolysis (< 200°C) of **4**.

Table 1. Spectroscopic data for **4**–**7**.

4: IR (KBr): $\tilde{\nu}$ = 1630 cm^{-1}; UV (*n*-pentane): λ = 225 nm (sh); ^{1}H-NMR (300 MHz, $CDCl_3$): δ = 2.22–2.32 (m, 4H), 2.04–2.09 (m, 4H), 1.56–1.89 (m, 16H); ^{13}C-NMR (75.46 MHz, $CDCl_3$): δ = 144.13 (s), 58.16 (s), 27.36 (t), 25.95 (t), 25.26 (t), 24.48 (t); MS (70 eV): *m/z* 264 (62%, $M^{\oplus}$)

5: ^{1}H-NMR (200 MHz, $CDCl_3$): δ = 1.46–1.70 (m); ^{13}C-NMR (50.32 MHz, $CDCl_3$): δ = 56.72 (s), 31.45 (t), 25.49 (t); high-resolution MS: *m/z* ($M^{\oplus}$) calcd 264.1878, found 264.1851

6: ^{13}C-NMR (50.32 MHz, $CDCl_3$): δ = 153.04 (s), 52.30 (s), 33.64 (t), 29.38 (t), 26.72 (t), 24.13 (t); high-resolution MS: *m/z* ($M^{\oplus}$) calcd 264.1878, found 264.1862

7: IR (KBr): $\tilde{\nu}$ = 1620 cm^{-1}; ^{1}H-NMR (200 MHz, $CDCl_3$): δ = 2.15–2.57 (m), 1.82–2.07 (m), 1.46–1.63 (m); ^{13}C-NMR (50.32 MHz, $CDCl_3$): δ = 142.25 (s), 136.91 (s), 32.57 (t), 25.47 (t), 24.89 (t), 23.70 (t); high-resolution MS: *m/z* ($M^{\oplus}$) calcd 264.1878, found 264.1903

The proposed structures of **5**–**7** are based on analytical data (Table 1), in particular the ^{13}C-NMR spectra. The number of lines in the ^{13}C-NMR spectrum, their multiplicity (DEPT experiment), and their chemical shifts[12] lead to an unambiguous assignment. The cubane derivative **4** can be regarded either as a member of the propella[n$_m$]prismane series (n = 3, m = 4) (point group D_{mh}) having the general formula **8**[13] or as a tetrameric cyclopentyne.[14]

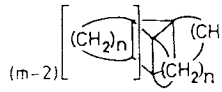

8

Received: November 6, 1987 [Z 2494 IE]
German version: *Angew. Chem. 100* (1988) 851

[1] R. Criegee, *Angew. Chem. 74* (1962) 703; *Angew. Chem. Int. Ed. Engl. 1* (1962) 519; H. Iwamura, K. Morio, H. Kihara, *Chem. Lett. 1973*, 457.
[2] Photolysis of *syn*- and *anti*-perfluorooctamethyltricyclo[4.2.0.0^{2,5}]-octa-3,7-diene gives perfluorooctamethylcubane: L. F. Pelosi, W. T. Miller, *J. Am. Chem. Soc. 98* (1976) 4311.
[3] E. Osawa, *J. Org. Chem. 42* (1977) 2621.
[4] R. Gleiter, E. Heilbronner, M. Hekman, H.-D. Martin, *Chem. Ber. 106* (1973) 28; H. Iwamura, H. Kihara, K. Morio, T. Kunii, *Bull. Chem. Soc. Jpn. 16* (1973) 3248.
[5] R. Gleiter, W. Schäfer, A. Flatow, *J. Org. Chem. 49* (1984) 372; R. Gleiter, W. Sander, *Angew. Chem. 97* (1985) 575; *Angew. Chem. Int. Ed. Engl. 24* (1985) 566; R. Gleiter, M. Karcher, R. Jahn, H. Irngartinger, *Chem. Ber. 121* (1988) 735.
[6] R. Gleiter, M. Karcher, M. L. Ziegler, B. Nuber, *Tetrahedron Lett. 28* (1987) 195.
[7] An X-ray crystal structure analysis of crystals of **4** performed by *M. L. Ziegler* and *B. Nuber* (Heidelberg) revealed strong disorder. An average distance of 2.6 Å was found for the separation between the two olefinic moieties.
[8] H. Günther: *NMR-Spektroskopie*, 2nd ed., Thieme, Stuttgart 1983, p. 229.
[9] H. M. Frey, H.-D. Martin, M. Hekman, *J. Chem. Soc. Chem. Commun. 1975*, 204; R. S. Case, M. J. S. Dewar, S. Kirschner, R. Pettit, W. Slegeir, *J. Am. Chem. Soc. 96* (1974) 7581.
[10] R. Criegee, R. Huber, *Chem. Ber. 103* (1970) 1855.
[11] Gas-chromatographic investigations (Carbowax, OV 101, 180°C) indicate that **5** also undergoes thermal rearrangement to **4**.
[12] The chemical shifts obtained were compared with those of methylcubane (E. W. Della, P. E. Pigou, *J. Am. Chem. Soc. 106* (1984) 1085), strained cyclopentenes (L. Fitjer, U. Kliebisch, D. Wehle, S. Modaressi, *Tetrahedron Lett. 23* (1982) 1661), and bridged cyclooctatetraene derivatives (L. A. Paquette, M. P. Trova, *ibid. 27* (1986) 1895; *ibid. 28* (1987) 2795).
[13] D. Ginsburg: *Propellanes*, Verlag Chemie, Weinheim 1975.
[14] A. Krebs, J. Wilke, *Top. Curr. Chem. 109* (1983) 189, and references cited therein.

1,3,4,6-Tetraamino-2,5-diazapentalenes: Delocalized Antiaromatic Compounds**

By *Fritz Closs, Rudolf Gompper,* Heinrich Nöth,* and *Hans-Ulrich Wagner*

As we have shown through several examples, combinations of donor and acceptor substituents stabilize cyclopolyenes containing (4n) π electrons. They may even take on the properties of arenes (e.g., positive resonance energies).[1] The question of double-bond delocalization in such systems could only be approached so far for diethyl 2,4-bis(diethylamino)cyclobutadiene-1,3-dicarboxylate;[2-4] in contrast to tetra-*tert*-butylcyclobutadiene,[5,6] it exhibits a "benzene-like" double-bond delocalization ("λ_{max}" = 1.24; see below). In continuation of our studies on 2,5-diazapentalenes,[7] we posed the question whether it might also be possible to achieve a delocalization of the double bonds in pentalene by the incorporation of suitable donor–acceptor substituents.

By way of 1,3,5-tri-*tert*-butylpentalene as example it has been shown[8-10] that alkylated pentalenes display bond alternation and that a rapid valence isomerization occurs. These findings are in agreement with the double-bond localization parameter "λ_{max}" (see Table 1) calculated according to *Binsch* and *Heilbronner* et al.;[11,12] its value is significantly higher than the critical value. The "λ_{max}" values of the compounds 1,3,4,6-tetraamino-, 2,5-diaza-, and, above all, 1,3,4,6-tetraamino-2,5-diazapentalene are less than the critical value. This finding and the larger HOMO–LUMO gap lead to the expectation that 1,3,4,6-tetradonor-2,5-diacceptor-substituted pentalenes should exhibit aromatic stabilization and a delocalized π-bonding system (cf. also Ref. [13]).

Table 1. The effect of substituents on the double-bond localization in pentalenes ($\lambda_{crit} \approx 1.7$) [$\alpha_X = \alpha_C + h_X\beta_{CC}$; $h_{NR2} = 1.5$, $h_N = 0.5$]). The ring nitrogen atoms are also regarded here as substituents.

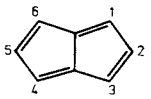

Substituents	$\Delta E_{HOMO-LUMO}$ [β]	"λ_{max}" neutral	radical cation	dication
none (6H)	0.471	2.357	1.358	1.312
1,3,4,6-tetraamino (+2H)	0.918	1.153	6.517	12.393
2,5-diaza (+4H)	0.738	1.677	1.505	2.539
1,3,4,6-tetraamino-2,5-diaza	0.942	0.967	1.094	1.614

In addition to the reaction of succinate esters with aromatic nitriles,[14] the reaction of succinamide **1** with amide acetals[7] offers a simple method for the preparation of pyrrolo[3,4-*c*]pyrrole-1,4(2*H*,5*H*)-diones (e.g., **5**). As amide acetals, we have so far employed a dimethylformamide derivative (cf. **a**) and dimethylbenzamide acetal (cf. **b**).

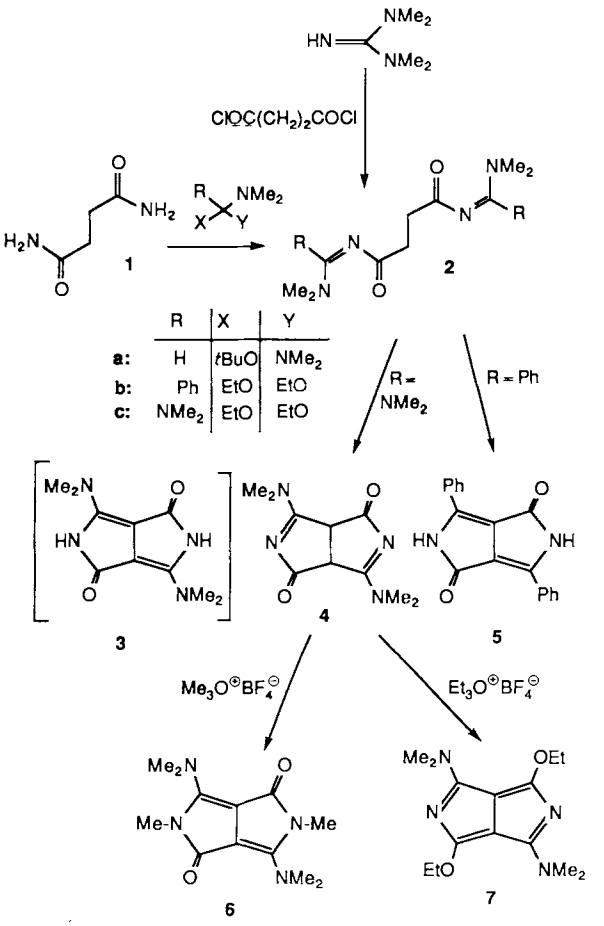

Heating **1** with tetramethylurea diethyl acetal (cf. **c**) affords a high yield of a colorless crystalline compound. The product is not the dione **3**, expected in analogy to the red compound **5**, but rather 3,6-bis(dimethylamino)pyrrolo[3,4-*c*]pyrrole-1,4(3a*H*,6a*H*)-dione **4** (for selected data for all new compounds, see Table 3). The permethylated succinylguanidine **2c**, identified as an intermediate, can also be prepared from tetramethylguanidine and succinyl dichloride and then converted into **4** by treatment with sodium hydride in dimethylformamide. (We are currently investigating the generality of this procedure.)

The readily accessible **4** makes possible the synthesis of numerous 2,5-diazapentalene derivatives. *N*-Methylation with trimethyloxonium tetrafluoroborate yields yellow 3,6-bis(dimethylamino)-2,5-dimethylpyrrolo[3,4-*c*]pyrrole-

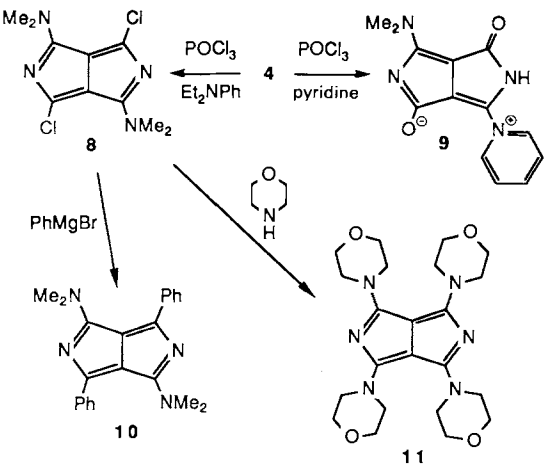

[*] Prof. Dr. R. Gompper, Dipl.-Chem. F. Closs, Dr. H.-U. Wagner
Institut für Organische Chemie der Universität
Karlstrasse 23, D-8000 München 2 (FRG)
Prof. Dr. H. Nöth
Institut für Anorganische Chemie der Universität
Meiserstrasse 1, D-8000 München 2 (FRG)

[**] This work was supported by the Fonds der Chemischen Industrie.

antimonate) has been reported,[16] its structure could not be confirmed. Dications of dibenzopentalene(indenoindenes) have been generated in solution and characterized by NMR spectroscopy,[17] and the radical cation of 1,3,5-tri-*tert*-butylpentalene, which is stable to −77°C, has also been obtained in solution.[18, 19] The tetradonor-substituted diazapentalenes now make possible the simple preparation of a whole series of stable, crystalline dication salts. The double-bond localization parameter "λ_{max}" (Table 1) for **17** is larger than for **11** and **14**. It remains an open question whether **17** is better represented by the structure given or by the delocalized structure **17'** (the Wiberg bond index[20] for C3a–C6a for **17/17'** is 1.852, which almost corresponds to a CC double bond in accordance with **17**). Structure **17** would be analogous to that of the salt **20**.[1] Oxidation of 1,3,5,7-tetrakis(dimethylamino)-2,6-diaza-*s*-indacene[1] to **20** proceeds much more smoothly than that of **14** to **17**, presumably owing to the better spatial separation of the charges in **20** than in **17**.

Tetradonor-substituted 2,5-diazapentalenes are relatively strong bases (pK_a [in 50% EtOH]: **11** = 8.63, 4.28; **14** = 10.35, 6.40; 1,8-bis(dimethylamino)naphthaline = 10.40 [in H_2O = 12.34[21]]; 1,3-bis(dimethylamino)-2-azapentalene[22] = 6.82). It is remarkable that **14** is as basic as "proton sponge,"[21] whereas 1,3-bis(dimethylamino)-2-azapentalene is significantly weaker as a base. This compound also undergoes electrochemical oxidation at 0.62 V to the radical cation; interestingly, the reduction to the radical anion at −1.92 V occurs at practically the same potential as that of **14**. Protonation of **11** and **14** does not occur at the dialkylamino groups, however, as in the case of "proton sponge," but rather at the ring N atoms. Treatment of **11** with tetrafluoroboric acid–ether in dichloromethane leads to the yellow NH salt **18**, which, in the region of its melting point (at ca. 200°C) or in acetonitrile at room temperature, is transformed into the colorless CH salt **19**. Compounds **19**, **20**, and **17** form a series of dications in which two 2-azaallyl moieties are linked increasingly more closely by a CC single bond, a benzene ring, and a CC double bond, respectively.

Table 3. Selected data for the compounds **2c**, **4**, and **6**–**19** (^{1}H-NMR, 80 MHz; ^{13}C-NMR, 20 MHz).

2c: Colorless needles, m.p. = 106°C

4: Colorless needles, m.p. 295–296°C; ^{1}H-NMR ($CDCl_3$): δ = 3.25 (s; 6H, NMe_2), 3.53 (s; 6H, NMe_2), 4.34 (s; 2H, CH); ^{13}C-NMR ($CDCl_3$): δ = 39.98 (q; NMe), 40.53 (q; NMe), 53.01 (d; C3a), 177.83 (s; C1), 183.07 (s; C-3)

6: Yellow needles, m.p. = 185–187°C; UV/VIS ($CHCl_3$): λ_{max} ($\lg\varepsilon$) = 258 nm (4.05), 402 (sh), 417 (4.41); ^{1}H-NMR (C_6D_6): δ = 2.66 (s; 12H, NMe_2), 2.77 (s; 6H, NMe); ^{13}C-NMR (C_6D_6): δ = 29.29, 42.10, 92.41 (C-3a), 149.48 (C-3), 160.17 (C-1)

7: Yellow needles, m.p. = 188°C; UV/VIS (benzene): λ_{max} ($\lg\varepsilon$) = 426 nm (sh), 450 (4.65); ^{1}H-NMR (C_6D_6): δ = 1.16 (t; 6H, OCH_2CH_3), 3.00 (s; 12H, NMe_2), 4.37 (q; 4H, OCH_2CH_3); ^{13}C-NMR (C_6D_6): δ = 15.05, 38.89, 64.21, 99.0 (C-3a), 156.4 (C-1), 163.1 (C-3)

8: Red needles, m.p. = 210°C (dec.); UV/VIS (benzene): λ_{max} ($\lg\varepsilon$) = 470 nm (sh), 499 (4.47); ^{1}H-NMR (C_6D_6): δ = 2.75 (s; 12H, NMe_2); ^{13}C-NMR (C_6D_6): δ = 40.10, 116.2 (C-3a), 148.7 (C-1), 157.2 (C-3)

9: Violet-blue needles, m.p. = 280°C; UV/VIS: λ_{max} ($\lg\varepsilon$) = (in H_2O) 256 nm (3.88), 353 (3.71), 518 (3.59); (in MeOH) 260 (3.15), 357 (3.71), 572 (3.65); (in CH_3CN) 455 (sh), 590 (3.92); (in $CHCl_3$) 363 (4.06), 624 (4.09); ^{1}H-NMR ([D_6]DMSO): δ = 3.06 (s; 6H, NMe_2), 8.07 (mc; 3H, Py-*m,p*), 9.4 (s; 1H, NH), 9.65 (dd, J = 6 Hz, 2 Hz; 2H, Py-*o*)

10: Red needles, m.p. = 228°C (dec.); UV/VIS ($CHCl_3$): λ_{max} ($\lg\varepsilon$) = 251 nm (sh), 286 (4.39), 310 (sh), 508 (4.23); ^{1}H-NMR ($CDCl_3$): δ = 3.18 (s; 12H, NMe_2), 7.50 (mc; 6H, Ph-*m,p*), 7.65 (mc; 4H, Ph-*o*); ^{13}C-NMR ($CDCl_3$): δ = 42.22, 118.07 (C-3a), 127.62, 129.51, 129.96, 134.85, 159.17 (C-1?), 161.45 (C-3?)

11: Orange needles, m.p. = 262°C; UV/VIS (C_6H_6): λ_{max} ($\lg\varepsilon$) = 319 nm (4.41), 458 (sh), 483 (4.38); ^{1}H-NMR (C_6D_6): δ = 3.43 (s, br); ^{13}C-NMR (C_6D_6): δ = 49.55, 66.73, 106.25 (C-3a), 158.84 (C-1)

12: Dark red crystals, m.p. = 330°C (dec.); UV/VIS (DMF): λ_{max} ($\lg\varepsilon$) = 329 nm (4.07), 495 (sh), 525 (4.31); ^{1}H-NMR ([D_6]DMSO): δ = 3.45 (s; 12H, NMe_2), 10.62 (s, br, 2H, NH)

13: Orange needles having a greenish surface luster, m.p. = 251°C; UV/VIS (C_6H_6): λ_{max} ($\lg\varepsilon$) = 326 nm (4.40), 490 (sh), 515 (4.56); ^{1}H-NMR (C_6D_6): δ = 2.49 (s; 6H, SMe), 2.95 (s; 12H, NMe_2); ^{13}C-NMR (C_6D_6): δ = 14.72, 39.89, 119.36 (C-3a), 157.65 (C-3?), 157.78 (C-1?)

14: Orange-red needles, m.p. = 160–162°C; UV/VIS (benzene): λ_{max} = 481 nm; ^{1}H-NMR (C_6D_6): δ = 2.84 (s; 24H, NMe_2); ^{13}C-NMR (C_6D_6): δ = 41.04, 106.51 (C-3a), 160.15 (C-1)

15: Orange-red needles, m.p. = 139–140°C; ^{1}H-NMR (C_6D_6): δ = 2.70 (s; 3H, SMe), 2.76 (s; 6H, NMe_2), 2.89 (s; 6H, NMe_2), 2.97 (s; 6H, NMe_2)

16a, X = BF_4: UV/VIS (CH_3CN): λ_{max} ($\lg\varepsilon$) = 292 nm (4.40), 350 (sh), 529 (sh), 560 (3.99), 595 (3.96)

17a, X = BF_4: Reddish violet powder, m.p. = 208°C (dec.); UV/VIS (CH_3CN): λ_{max} ($\lg\varepsilon$)270 nm (4.49), 362 (3.94), 520 (3.81); ^{1}H-NMR (CD_3CN): δ = 3.5–4.0

18: Yellow crystals, m.p. = 205°C (change in crystal appearance); ^{1}H-NMR (CD_3CN): δ = 3.38 (mc; 16H, NCH_2), 3.63 (mc; 16H, OCH_2); ^{13}C-NMR (CD_3CN): δ = 51.95, 66.82, 96.34, 149.08

19: Colorless needles, m.p. = 288°C; ^{1}H-NMR (CD_3CN): δ = 3.27–3.95 (m; 28H), 4.10–4.50 (m; 4H), 5.42 (s; 2H, CH); ^{13}C-NMR (CD_3CN): δ = 50.83 (t), 51.79 (t), 56.22 (d), 66.51 (t), 66.67 (t), 174.13 (s)

Received: January 27, 1988 [Z 2591 IE]
German version: *Angew. Chem. 100* (1988) 875

CAS Registry numbers:
1, 110-14-5; **2c**, 114491-72-4; **4**, 114491-73-5; **6**, 114491-74-6; **7**, 114491-75-7; **8**, 114491-76-8; **9**, 114491-77-9; **10**, 114491-78-0; **11**, 114491-79-1; **12**, 114491-80-4; **13**, 114504-93-7; **14**, 114491-81-5; **14**·H_2O, 114491-90-6; **15**, 114491-82-6; **16a**, 114491-84-8; **17a**, 114491-86-0; **18**, 114491-87-1; **19**, 114491-89-3; $(Me_2N)_2C(OEt)_2$, 67751-11-5; $HN{=}C(NMe_2)_2$, 80-70-6; $ClCO(CH_2)_2COCl$, 543-20-4.

[1] Cf. F. Closs, R. Gompper, U. Nagel, H.-U. Wagner, *Angew. Chem. 99* (1987) 1068; *Angew. Chem. Int. Ed. Engl. 26* (1987) 1037, and references cited therein.
[2] R. Gompper, G. Seybold, *Angew. Chem. 80* (1968) 804; *Angew. Chem. Int. Ed. Engl. 7* (1968) 824.
[3] H. J. Lindner, B. von Gross, *Chem. Ber. 107* (1974) 598.
[4] R. Gompper, J. Kroner, G. Seybold, H.-U. Wagner, *Tetrahedron 32* (1976) 629.
[5] H. Irngartinger, N. Riegler, K.-D. Malsch, K.-A. Schneider, G. Maier, *Angew. Chem. 92* (1980) 214; *Angew. Chem. Int. Ed. Engl. 19* (1980) 211; H. Irngartinger, M. Nixdorf, *ibid. 95* (1983) 415 and *22* (1983) 403.
[6] O. Ermer, E. Heilbronner, *Angew. Chem. 95* (1983) 414; *Angew. Chem. Int. Ed. Engl. 22* (1983) 402.
[7] F. Closs, R. Gompper, *Angew. Chem. 99* (1987) 564; *Angew. Chem. Int. Ed. Engl. 26* (1987) 552.
[8] K. Hafner, H. U. Süss, *Angew. Chem. 85* (1973) 626; *Angew. Chem. Int. Ed. Engl. 12* (1973) 575.
[9] K. Hafner, *Nachr. Chem. Tech. Lab. 28* (1980) 222; *Pure Appl. Chem. 54* (1982) 939.
[10] B. Kitschke, H. J. Lindner, *Tetrahedron Lett. 1977*, 2511.
[11] G. Binsch, E. Heilbronner, *Tetrahedron 24* (1968) 1215.
[12] E. Heilbronner, Z. Yang, *Angew. Chem. 99* (1987) 369; *Angew. Chem. Int. Ed. Engl. 26* (1987) 360.
[13] M. Kataoka, T. Ohmae, T. Nakajima, *J. Org. Chem. 51* (1986) 358.
[14] L. Cassar, A. Iqbal, A. C. Rochat, Eur. Pat. Appl. 133 156 (July 4, 1983), Ciba-Geigy.
[15] X-ray structure analysis of **14**: Syntex R3 diffractometer, $Mo_{K\alpha}$ radiation, measurement temperature −60°C, single crystal 0.32 × 0.16 × 0.25 mm. Crystal data: $C_{14}H_{24}N_6 \cdot H_2O$, molecular mass 270.38, monoclinic, a = 19.595(11), b = 10.059(5), c = 8.392(4) Å, β = 106.54(3)°, V = 1585(1) Å^3, Z = 4, ρ_{calcd} = 1.133 g cm^{-3}, space group $C2/c$. Data collection, 2θ = 2 to 47° in $hk\pm l$; scan rate, 1.6 to 29.3°/min; ω-2θ scan, 1300 observed, 1123 unique reflections, 983 [$(I) \geq 2.5\sigma(I)$] used for structure determination and refinement. Structure solution: direct methods using the SHELXTL programs. Anisotropic treatment of the nonhydrogen atoms, isotropic treatment of the H atoms. Position of the OH water atom in the subsequent refinement as well as its U_i fixed. R = 0.064, R_w = 0.071. Largest Δ/σ = 0.296, largest residual electron density ρ = 0.24 e Å^{-3}. Further details of the crystal

 © VCH Verlagsgesellschaft mbH, D-6940 Weinheim, 1988 0570-0833/88/0606-0844 $ 02.50/0

1,4(2*H*,5*H*)-dione **6**. Treatment with triethyloxonium tetrafluoroborate, on the other hand, affords the likewise yellow 1,4-diethoxy-3,6-bis(dimethylamino)-2,5-diazapentalene **7**, the first tetradonor–diacceptor pentalene.

Reaction of **4** with phosphorus oxychloride in the presence of diethylaniline gives 1,4-dichloro-3,6-bis(dimethylamino)-2,5-diazapentalene **8**. When pyridine is used as base, this reaction yields the betaine **9**, which is of interest owing, among other things, to its strong solvatochromism. Although **8** should be regarded as an electron-rich compound, it reacts with numerous nucleophiles. Reaction with phenylmagnesium bromide in THF, for example, affords 1,4-bis(dimethylamino)-3,6-diphenyl-2,5-diazapentalene **10**. With respect to the question of bond delocalization discussed at the beginning, the most interesting reaction is that of **8** with morpholine to give 1,3,4,6-tetramorpholino-2,5-diazapentalene **11**.

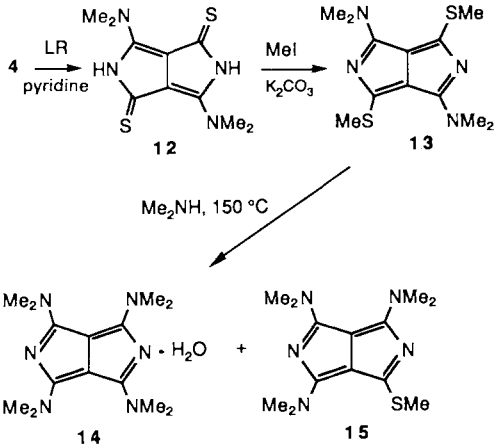

Sulfurization of **4** with Lawesson reagent (LR) yields 3,6-bis(dimethylamino)pyrrolo[3,4-*c*]pyrrole-1,4(2*H*,5*H*)-dithione **12**, which, in contrast to **4**, exists in the enamine form. Methylation of **12** leads to 1,4-bis(dimethylamino)-3,6-bis(methylthio)-2,5-diazapentalene **13**, which, upon heating with dimethylamine in an autoclave, gives **15** and 1,3,4,6-tetrakis(dimethylamino)-2,5-diazapentalene **14**. Compounds **14** and **15** can be separated by fractional crystallization. Compound **14** has C_{2h} symmetry in the localized and D_{2h} symmetry in the delocalized structure.

The X-ray structure analysis of **14** (Fig. 1) shows the double-bond delocalization predicted by theory. It is not possible to rule out completely a rapidly established equilibrium between two localized structures. However, the fact that, in the case of 1,3,5-tri-*tert*-butylpentalene,[8–10] the X-ray structure analysis reveals the theoretically predicted double-bond localization, despite the very rapid valence isomerization, makes it very probable that the double bonds in **14** are delocalized. Accordingly, the compound can be referred to as an "aromatic (4n) π system," since it exhibits the characteristics of an aromatic compound.

Compounds **6**, **7**, **10**, **11**, and **13**–**15** all undergo multistep redox reactions (cf. Table 2). Compound **17a**, X = BF_4, is obtained on a preparative scale as reddish violet crystals by reaction of **11** with trityl tetrafluoroborate in dichloromethane; blue-violet **16a** is obtained by combining **11** with **17a**, X = BF_4, in acetonitrile.

The salts **17** are the first dicationic pentalene derivatives to be isolated and characterized. Although the preparation of a hexachlorodihydropentalenedi(ylium) bis(hexachloro-

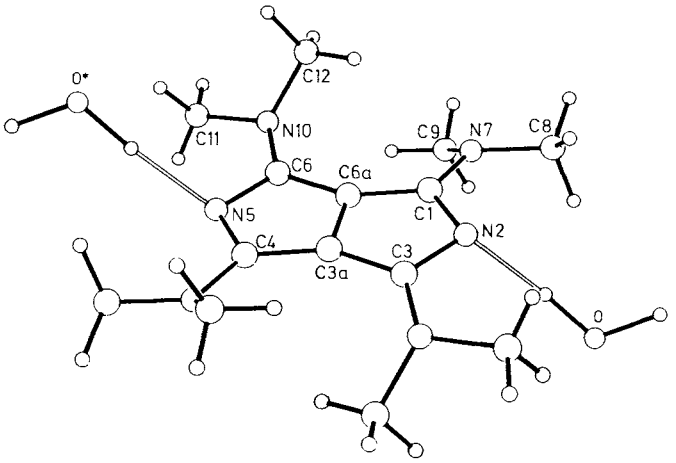

Fig. 1. Molecular structure of **14** (ORTEP) [15]: selected bond lengths [pm]: C1-N2 137.7(3), N2-C3 137.5(3), C1-C6a 142.0(3), C6-C6a 141.5(3), C3a-C6a 142.0(3), C1-N7 136.6(3), C6-N10 137.5(3), O-H 119, N2-H 184; selected bond angles [°]: C1-N2-C3 105.9(2), C6a-C6-N10 127.5(2), C6a-C6-N5 111.4(2), N10-C6-N5 121.0(2), C6-C6a-C1 148.2(2), C6-C6a-C3a 105.7(2), N2-C1-C6a 110.8(2), N2-C1-N7 121.0(2), C6a-C1-N7 128.2(3), C6-N10-C11 118.6(2), C6-N10-C12 117.4(2), C11-N10-C12 113.5(2), C1-N7-C8 119.0(2), C1-N7-C9 118.6(2), C8-N7-C9 114.4(2), H-O-H 118.1; angles between the normals to the planes [°]: N5-C6-C6a-C3a-C4/N10-C11-C12 134.5, N5-C6-C6a-C3a-C4/N7-C8-C9 37.3.

Table 2. Half-wave potentials of **6**, **7**, **10**, **11**, and **13**–**15** determined by cyclic voltammetry ($CH_3CN/Bu_4N^{\oplus}PF_6^{\ominus}$/gold electrode versus $Ag/Ag^{\oplus}$).

	E_2^{Ox} [V]	E_1^{Ox} [V]	E_1^{Red} [V]	E_2^{Red} [V]
6	0.84 [a]	0.17 [a]		
7	0.77	0.17		
10	1.05	0.54	−1.26	−1.70
11	0.47	0.18	−1.74	
13	0.83	0.34	−1.52	
14	0.37	−0.01	−1.95	
15	0.65	0.22	−1.77	

[a] Irreversible in CH_2Cl_2.

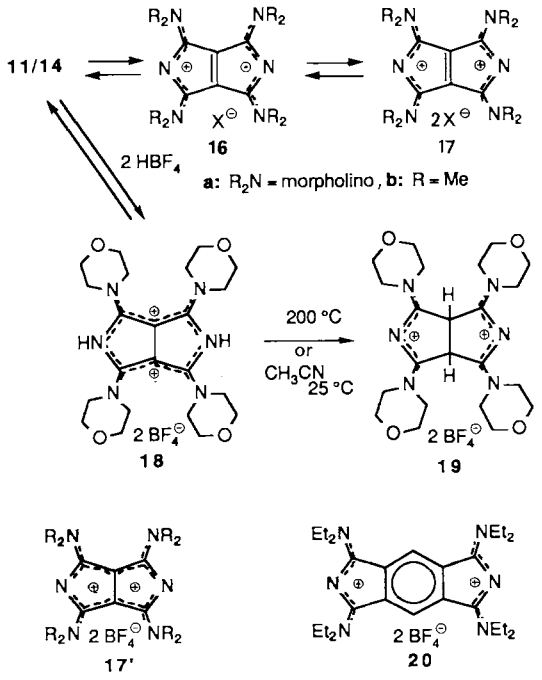

structure investigation may be obtained from the Fachinformationszentrum Energie, Physik, Mathematik GmbH, D-7514 Eggenstein-Leopoldshafen 2 (FRG), on quoting the depository number CSD-53069, the names of the authors, and the journal citation.
[16] K. Kusuda, N. Osaka, *J. Chem. Soc. Chem. Commun. 1972*, 508.
[17] I. Willner, J. Y. Becker, M. Rabinovitz, *J. Am. Chem. Soc. 101* (1979) 395.
[18] R. W. Johnson, *J. Am. Chem. Soc. 99* (1977) 1461.
[19] P. Fürderer, F. Gerson, K. Hafner, *Helv. Chim. Acta 61* (1978) 2974.
[20] M. A. Natiello, H. R. Reale, J. A. Medrano, *J. Comput. Chem. 6* (1985) 108.
[21] a) R. W. Alder, P. S. Bowman, W. R. S. Steele, D. R. Winterman, *Chem. Commun. 1968*, 723; b) F. Hibbert, *J. Chem. Soc. Chem. Commun. 1973*, 463.
[22] H.-J. Gais, K. Hafner, *Tetrahedron Lett. 1974*, 771; K. Hafner, H.-G. Kläs, M. C. Böhm, *ibid. 21* (1980) 41.

Formation of Difluoroethyne as a Ligand by Coupling of Two Fluoromethylidyne Ligands**

By *Dieter Lentz** and *Heike Michael*

Difluoroethyne F–C≡C–F is an extremely unstable molecule,[1] so that its use in the synthesis of difluoroethyne complexes has not been possible so far. We have now succeeded in forming a difluoroethyne ligand by C–C bond formation between the two fluoromethylidyne ligands of **1**[2] in the cluster expansion reaction with **2** [Cp* = $C_5(CH_3)_5$].

$$\underset{\mathbf{1}}{[Fe_3(CO)_9(\mu_3\text{-}CF)_2]} + \underset{\mathbf{2}}{[Cp^*Co(CO)_2]} \xrightarrow[\text{pentane}]{h\nu} \underset{\mathbf{3}}{[Cp^*CoFe_3(CO)_9(\mu_4\text{-}\eta^2\text{-}FC{\equiv}CF)]} + 2\,CO \qquad \text{(a)}$$

The *closo* cluster **1** reacts with **2** in a straightforward fashion with cleavage of two carbonyl ligands to give **3** [reaction (a)].[3] According to the Wade rules,[4] the Cp*Co fragment contributes two framework electrons, so that its incorporation into cluster **1** should yield once again a *closo* structure. The Wade rules provide no information, however, on which of the possible *closo* structures (Fig. 1) is present.

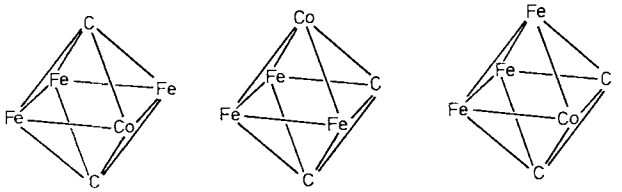

Fig. 1. Schematic drawing of the possible structural isomers of **3**.

The crystal structure investigation (Fig. 2)[5] revealed the presence of two crystallographically independent molecules in the unit cell, which, apart from orientation, display only minor differences. The metal atoms and the difluoroethyne carbon atoms form a severely distorted octahedron. The metal–metal distances lie between 244.5(2) and 265.1(2) pm. The short Co1–Fe1 distance is due to the fact that a carbonyl ligand on Fe1 is directed toward Co1, thus serving as a semi-bridging ligand. The two metal triangles Co1, Fe1, Fe2 and Fe1, Fe2, Fe3 form an angle of 112° (butterfly structure). The distances of the carbon atoms of the difluoroethyne ligands from Fe1 and Fe2 (192(1) pm) are markedly shorter than those to the remaining metal atoms Co1 and Fe3 (196(2) to 208(2) pm). Obviously, the C–C bond of the difluoroethyne ligand is significantly stretched by coordination to the four metal atoms, and the C–C–F structural unit is bent; i.e., the coordinated difluoroethyne has lost its identity and should be viewed as a component of the *closo* cluster.

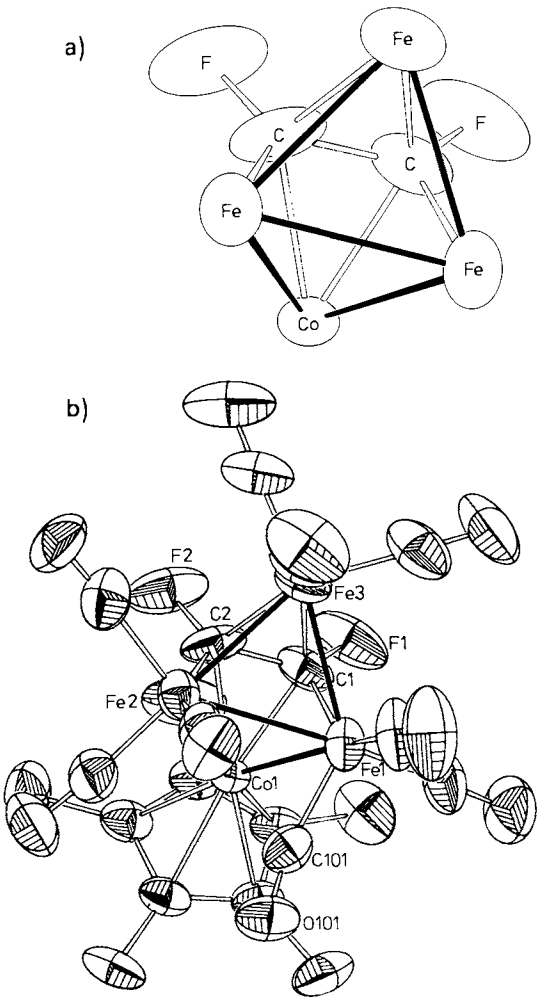

Fig. 2. a) Structure of **3** with ligand spheres omitted. b) Molecular structure of **3** (molecule I). Important bond lengths [pm] and angles [°]. Molecule I/II: Co1-Fe1 244.5(2)/245.7(2), Co1-Fe2 259.1(2)/257.9(2), Fe1-Fe2 263.3(2)/265.1(2), Fe1-Fe3 249.7(3)/251.1(2), Fe2-Fe3 254.2(3)/252.8(2), Co1-C1 196(2)/198.0(8), Co1-C2 202.5(9)/199.4(8), Fe1-C1 192.4(9)/195.0(8), Fe2-C2 192(1)/193.4(9), Fe3-C1 202.1(9)/202.6(9), Fe3-C2 208(2)/207.1(8), Fe1-C101 182(2)/177(1), Co1-C101 243.7(9)/252(1), C1-C2 145(2)/143(2); Co1-Fe1-Fe3 92.1(1)/91.0(1), Co1-Fe2-Fe3 87.8(1)/87.9(1), Fe2-Fe1-C1 72.1(4)/72.2(3), Fe1-Fe2-C2 71.9(4)/71.2(3), Fe1-C1-C2 107.6(7)/106.7(6), Fe1-C1-F1 131.1(8)/132.1(6), Co1-C1-Fe3 126.6(6)/124.5(5), Fe2-C2-C1 108.4(7)/109.8(6), Fe2-C2-F2 131.4(9)/129.2(7), Co1-C2-Fe3 120.2(6)/121.4(4), Co1-C101-O101 124.9(8)/122.4(7), Fe1-C101-O101 165.7(9)/170.3(9).

Although butterfly structures containing alkyne ligands are known for osmium ($[Os_4(CO)_{12}(\mu_4\text{-}\eta^2\text{-}C_2R_2)]$[6]) and ruthenium ($[Ru_4(CO)_{12}(\mu_4\text{-}\eta^2\text{-}C_2R_2)]$[7]), they are formed in a completely different way and no unstable alkynes are stabilized. A similar cluster expansion reaction of $[Fe_3(CO)_9(RC{\equiv}CR)]$ with $[CpRh(CO)_2]$ to give

[*] Priv.-Doz. Dr. D. Lentz, Dipl.-Chem. H. Michael
Institut für Anorganische und Analytische Chemie
der Freien Universität
Fabeckstrasse 34-36, D-1000 Berlin 33

[**] This work was supported by the Fonds der Chemischen Industrie and by BASF AG (donation of pentacarbonyliron). We thank Prof. Dr. *J. Fuchs*, Berlin, for his help in the crystal structure investigation.

$[CpRhFe_3(CO)_9(RC{\equiv}CR)]$ has been reported by *Vahrenkamp* et al.;[8] in that case, however, the formation of an alkyne ligand by C–C bond formation did not occur.

The cleavage and formation of alkynes coordinated to a cluster has been of great recent interest.[9]

Received: February 25, 1988 [Z 2634 IE]
German version: *Angew. Chem. 100* (1988) 871

CAS Registry numbers:
1, 94621-00-8; **2**, 12129-77-0; **3**, 114396-74-6.

[1] W. J. Middleton, US Pat. 2831835 (1958); *Chem. Abstr. 52* (1958) 14658f; J. Heicklen, V. Knight, *J. Phys. Chem. 69* (1965) 2484; L. Kevan, P. Hamlet, *J. Chem. Phys. 42* (1965) 2255; G. Bieri, J.-P. Stadelmann, F. Thommen, J. Vogt, *Helv. Chim. Acta 61* (1978) 357; G. Bieri, A. Schmelzer, L. Åsbrink, M. Jonsson, *Chem. Phys. 49* (1980) 213.

[2] D. Lentz, I. Brüdgam, H. Hartl, *Angew. Chem. 97* (1985) 115; *Angew. Chem. Int. Ed. Engl. 24* (1985) 119.

[3] *Experimental Procedure:* **1** (200 mg, 0.42 mmol) and **2** (150 mg, 0.6 mmol) in *n*-pentane (100 mL) were irradiated in a 100-mL photoreactor (Philips HPK 125-W high-pressure mercury lamp, Pyrex glass) for 60 min. The reaction solution was then filtered through a ca. 5-cm-thick layer of silica gel 60 (Woelm 63–200 μm). Unreacted **1** was eluted with *n*-pentane. Elution with CH_2Cl_2 afforded **3**. The solution was evaporated to dryness under vacuum. The residue was dissolved in *n*-pentane and crystallized at −20°C. Yield: 118 mg (41%) of dark brown to black crystals which decompose above 142°C; MS (80 eV): *m/z* 676 ($M^{\oplus}$), 648 ($[M-CO]^{\oplus}$), 620 ($[M-2CO]^{\oplus}$), 592 ($[M-3CO]^{\oplus}$), 564 ($[M-4CO]^{\oplus}$), 536 ($[M-5CO]^{\oplus}$), 508 ($[M-6CO]^{\oplus}$), 490 ($[M-7CO]^{\oplus}$), 452 ($[M-8CO]^{\oplus}$), 424 ($[M-9CO]^{\oplus}$); high resolution of the molecular ion peak calcd 675.8064, found 675.8048; IR (*n*-pentane): $\tilde{\nu}$ = 2070.2 (vs), 2061.0 (s), 2040.6 (m), 2026.2 (vs), 2016.0 (vs), 2004.0 (w), 1999.2 (w), 1993.6 (w), 1983.6 (vw), 1967.6 (vw), 1959.0 (w), 1926.0 (vw), 1900.8 (vw) cm^{-1}; ^{19}F-NMR (CD_2Cl_2, $CFCl_3$ ext. as standard): $\delta = -22.1$; ^1H-NMR (CD_2Cl_2, $\delta(CHDCl_2) = 5.35$): $\delta = 1.80$.

[4] K. Wade, *Adv. Inorg. Chem. Radiochem. 18* (1976) 1.

[5] Crystals of **3** suitable for crystal structure investigation were obtained by recrystallization from *n*-pentane at −20°C. Monoclinic, $P2_1/c$, $a = 1642.7(5)$, $b = 1938.8(4)$, $c = 1558.1(6)$ pm, $\beta = 99.61(3)°$, $Z = 8$; $\rho_{calcd} = 1.83$ g cm^{-1}; $R = 0.078$ ($Mo_{K\alpha}$, $\lambda = 71.07$ pm, 10792 reflections, 8569 with $I > 2\sigma(I)$, anisotropic temperature factors, no H atom positions, 650 refined parameters, empirical absorption correction using the DIFABS program of *D. Stuart* and *N. Walker* [10]). Further details of the crystal structure investigation may be obtained from the Fachinformationszentrum Energie, Physik, Mathematik GmbH, D-7514 Eggenstein-Leopoldshafen 2 (FRG), on quoting the depository number CSD-53047, the names of the authors, and the journal citation.

[6] R. Jackson, B. F. G. Johnson, J. Lewis, P. R. Raithby, S. W. Sankey, *J. Organomet. Chem. 193* (1980) C1; B. F. G. Johnson, J. W. Kelland, J. Lewis, A. L. Mann, P. R. Raithby, *J. Chem. Soc. Chem. Commun. 1980*, 547.

[7] B. F. G. Johnson, J. Lewis, K. T. Schorpp, *J. Organomet. Chem. 91* (1975) C13.

[8] H. Vahrenkamp, lecture at the 21th GdCh-Hauptversammlung, Berlin 1987.

[9] A. D. Clauss, J. R. Shapley, C. N. Wilker, R. Hoffmann, *Organometallics 3* (1984) 619, and references cited therein; D. Nuel, F. Dahan, R. Mathieu, *ibid. 4* (1985) 1436.

[10] N. Walker, D. Stuart, *Acta Crystallogr. Sect. A 39* (1983) 158.

X-Ray Structure Investigation of 2,2-Diphenyl-1-(phenylsulfonyl)cyclopropyllithium–Dimethoxyethane (2/3): A Sulfonyl "Carbanion" Having an α-C Atom with a Tetrahedral Configuration**

By *Werner Hollstein, Klaus Harms, Michael Marsch,* and *Gernot Boche**

Does the anionic C atom in α-sulfonyl "carbanions" have to display a planar configuration or is a tetrahedral configuration also appropriate for stabilization by an RSO_2 group? The X-ray structure investigations of α-sulfonyl carbanions reported so far do not provide a conclusive answer to this question. In these examples, the environment of the α-C atom is either planar[1a] or does not deviate to a sufficiently large extent from planarity.[1b,c,2] If the "cyclopropyl effect"[3] is taken into consideration in answering this question, one even arrives at contradictory conclusions. Whereas *Zimmerman* et al.[4] and *Cram* et al.[5] found roughly the same equilibrium acidities for cyclopropyl- and isopropylsulfonyl compounds and *DeBoer* et al.[6] and *Kirmse* et al.[7] reported higher kinetic acidities for cyclopropylsulfonyl compounds, *Bordwell* et al.[8] found higher acidities for the isopropyl compounds. *Bordwell* concluded from his results that overlap of the carbon p orbital with a sulfur d orbital was necessary for stabilization of the "anion"; accordingly, α-sulfonyl "carbanions" should be planar like enolate and nitronate ions.[8b] The ^{13}C-NMR investigations of *Marquet* et al.,[9] on the other hand, revealed a hybridization of "between sp^2 and sp^3" for the α-C atom of t-$BuSO_2CH_2Li$. Finally, detailed calculations performed by *Streitwieser* et al.[10] on the stabilization of a negative charge by an RSO_2 group indicated that a p_π–d_π interaction is not important. Thus, the energy difference (3-21G(*)+) between planar $CH_3SO_2CH_2^{\ominus}$ and a $CH_3SO_2CH_2^{\ominus}$ structure in which the H atoms at C_α are bent from planarity by 20° is only +0.57 kcal mol^{-1}. The X-ray crystal structure investigation of (1-phenylsulfonyl)-2,2-diphenylcyclopropyllithium **2**, crystallized as 2,2-diphenyl-1-(phenylsulfonyl)cyclopropyllithium–dimethoxyethane(2/3) **1**, which we describe here, supports those findings

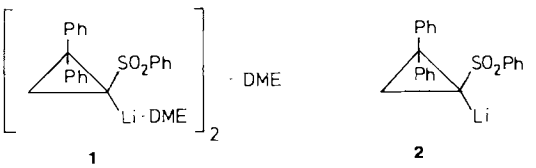

1 **2**

indicating that α-sulfonyl "carbanions" are also stabilized when the α-C atom has a tetrahedral configuration.[20]

Compound **1**[14] is present as a dimer in the crystal (Fig. 1); the lithium atoms are bonded to the O atoms of the sulfonyl groups and to two of the three dimethoxyethane molecules. This results in the formation of the (S-O-Li-O-S-O-Li-O) eight-membered ring characteristic of lithiosulfones.[1,2] The third molecule of dimethoxyethane cocrystallizes. Of special importance is the finding that the $PhSO_2$ group is bent out of the plane of the cyclopropane ring by 61.7(5)° (S1 lies 131.5(3) pm above the plane of the three-membered ring), so that the α-C atom deviates considerably from a planar configuration.[15] The C1–S1 distance (167.6(7) pm) and the S1–O1 distance (148.0(5) pm) are 3.5 and 1.5 pm larger, respectively, than in [α-(phenylsulfonyl)benzyllithium(tmeda)]$_2$.[1a] A salient feature of lithiosulfones is also the additional coordination of the Li atom to the α-C atom (C1–Li1A 244.0(14) pm); this is presumably due to the high charge density in the exocyclic orbital containing the negative charge. The bond axis C1–Li1A is bent by 24.9(6)° out of the plane of the three-membered ring (Li1A lies 103(1) pm below the plane of the three-membered ring). Thus, p_π–d_π interaction indeed plays no role in the stabilization of these (and other) α-sulfonyl "carbanions." Instead, an n–σ* interaction is im-

[*] Prof. Dr. G. Boche, Dipl.-Chem. W. Hollstein, Dr. K. Harms, M. Marsch
Fachbereich Chemie der Universität
Hans-Meerwein-Strasse, D-3550 Marburg (FRG)

[**] This work was supported by the Deutsche Forschungsgemeinschaft and the Fonds der Chemischen Industrie.

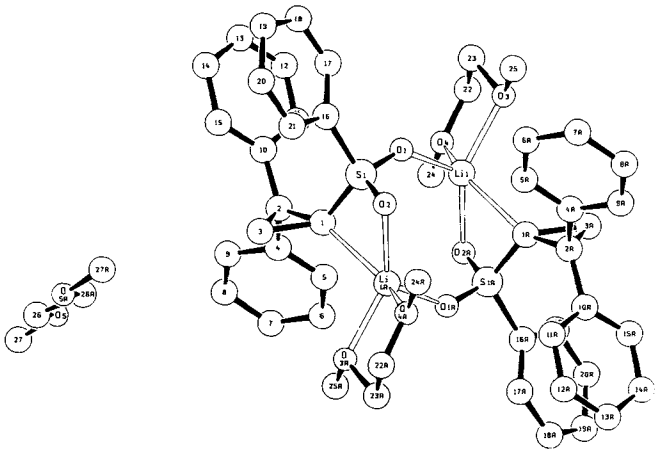

Fig. 1. Crystal structure of **1** [11]. Both the "dimer" and the cocrystallizing molecule of dimethoxyethane have a crystallographic center of symmetry. Symmetry-generated atoms are marked with "A." Crystal structure data of **1**: space group $P\bar{1}$, $a = 1014.7(3)$, $b = 1069.3(2)$, $c = 1191.9(3)$ pm, $\alpha = 86.94(2)$, $\beta = 88.69(2)$, $\gamma = 85.89(2)°$, $Z = 2$ (based on the monomer). Four-circle diffractometer CAD4 (Enraf-Nonius), $Cu_{K\alpha}$ radiation, graphite monochromator, 4059 measured reflections in the range $\theta = 2$–$50°$, 180 K. Solution by direct methods [12], refinement [13] to $R = 0.049$ for 1923 unique reflections with $F > 3\sigma(F)$, all non-hydrogen atoms anisotropic, H atoms, except for those on the three-membered ring, "riding" with a common isotropic temperature factor. Important bond lengths [pm]: C1-C2 152.6(9); C2-C3 154.3(10); C1-C3 152.5(10); C1-S1 167.6(7); S1-O1 148.0(5); S1-O2 147.1(4); C1-Li1A 244.0(14); S1-C16 175.8(8). Further details of the crystal structure investigation may be obtained from the Fachinformationszentrum Energie, Physik, Mathematik GmbH, D-7514 Eggenstein-Leopoldshafen 2 (FRG), on quoting the depository number CSD-52892, the names of the authors, and the journal citation.

portant, as found by means of calculations.[10] Figure 2 shows the configuration at C1 and S1 as well as the conformation around C1-S1.

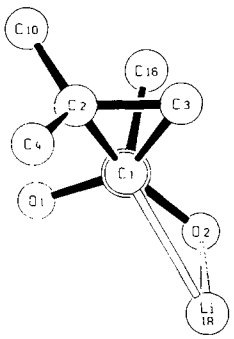

Fig. 2. Configuration at C1 and S1 (not visible) as well as conformation around C1-S1 of **1**. Important bond angles [°]: C2-C1-S1 123.9(5); C3-C1-S1 120.5(5); O1-S1-O2 115.2(3); C10-C2-C4 115.0(6); C2-C1-C3 60.8(5); C1-C2-C3 59.6(5); C1-C3-C2 59.7(5); torsion angles [°]: O1-S1-C1-C2 −72.0(6); O2-S1-C1-C3 90.8(6).

Compound **1** thus differs significantly from cyclopropyl "anions," whose negative charge is stabilized by delocalization, as in ester enolates or nitronates. Accordingly, enolate esters of cyclopropanecarboxylic acids are even highly reactive at −78 °C owing to the additional strain caused by the exocyclic double bond,[16] and cyclopropylnitronate can neither be trapped with an electrophile nor spectroscopically studied.[17] In contrast, 2,2-dimethyl-1-(phenylsulfonyl)cyclopropyllithium—fully in accordance with the above finding—is even stable at 80 °C in THF/DMSO.[5, 18, 19]

Received: January 28, 1988 [Z 2596 IE]
German version: *Angew. Chem. 100* (1988) 868

CAS Registry numbers:
1, 114491-70-2; **2**, 114491-71-3.

[1] a) [(PhCHSO$_2$Ph)Li(tmeda)]$_2$: G. Boche, M. Marsch, K. Harms, G. M. Sheldrick, *Angew. Chem. 97* (1985) 577; *Angew. Chem. Int. Ed. Engl. 24* (1985) 573; b) [(CH$_2$SO$_2$Ph)Li(tmeda)]$_2$: H.-J. Gais, H. J. Lindner, J. Vollhardt, *ibid. 97* (1985) 865 and *24* (1985) 859; c) [(CH$_2$=CHCHSO$_2$Ph)Li(diglyme)]$_2$: *ibid. 98* (1986) 916 and *25* (1986) 939; the deviations from planarity are most striking in this case: the H atom is bent out of the plane by 12°, the C atom by 14° [20].

[2] The structure of [(Me$_3$SiCHSO$_2$Ph)Li(tmeda)]$_2$ corresponds in essential respects to the structure of the compounds mentioned in [1a–c]: G. Boche, W. Hollstein, M. Marsch, K. Harms, unpublished results.

[3] Cyclopropyl effect: If an acceptor substituent X stabilizes a neighboring negative charge mainly by delocalization involving formation of a π bond, then the cyclopropyl compound C_3H_5–X is less acidic than the corresponding isopropyl compound C_3H_7–X, even though cyclopropane is more acidic than propane. Cause: The exocyclic π bond in the three-membered ring "anion" causes an additional strain of ca. 13 kcal mol^{-1}. For a different kind of stabilization, the cyclopropyl compound is more acidic [6].

[4] H. E. Zimmerman, B. S. Thyagarajan, *J. Am. Chem. Soc. 82* (1960) 2505.

[5] A. Ratajczak, F. A. L. Anet, D. H. Cram, *J. Am. Chem. Soc. 89* (1967) 2072; these authors observed dynamic NMR phenomena for dissolved 2,2-dimethyl-1-(phenylsulfonyl)cyclopropyllithium. They emphasized, however, that this is insufficient evidence to assign the α-C atom a tetrahedral configuration, since the dynamic effects might be due to hindered rotation of the sulfonyl group around the C–S axis of an anion having an α-C atom with a planar configuration.

[6] W. T. van Wijnen, H. Steinberg, T. J. DeBoer, *Tetrahedron 28* (1972) 5423, and literature cited therein.

[7] W. Kirmse, U. Mrotzeck, *J. Chem. Soc. Chem. Commun. 1987*, 710.

[8] a) F. G. Bordwell, N. R. Vanier, M. S. Matthews, J. B. Hendrickson, P. L. Skipper, *J. Am. Chem. Soc. 97* (1975) 7160; b) F. G. Bordwell, J. C. Branca, C. R. Johnson, N. R. Vanier, *J. Org. Chem. 45* (1980) 3884.

[9] R. Lett, G. Chassaing, A. Marquet, *J. Organomet. Chem. 111* (1976) C17; see also [1c].

[10] D. A. Bors, A. Streitwieser, Jr., *J. Am. Chem. Soc. 108* (1986) 1397. The stabilization occurs by n-σ* interaction; see also S. Wolfe in F. Bernardi, I. G. Csizmadia, A. Mangini (Eds.): *Organic Sulfur Chemistry (Studies in Organic Chemistry, Vol. 19)*, Elsevier, Amsterdam 1985, p. 133.

[11] E. Keller, SCHAKAL 86, Freiburg 1986.

[12] G. M. Sheldrick, SHELXS-86, Göttingen 1986.

[13] G. M. Sheldrick, SHELX-76, Cambridge 1976.

[14] Preparation of **1**: 2,2-diphenyl-1-phenylsulfonylcyclopropane (100 mg, 0.30 mmol) in dimethoxyethane (2.0 mL) was treated with *n*-BuLi (0.33 mmol) in hexane (0.19 mL) at 0 °C. After 10 min, the solution was evaporated to approximately 0.5 mL under oil-pump vacuum and allowed to stand at −30 °C for ca. 12 h. Crystals suitable for X-ray analysis thereby formed. Yield: 65 mg (46%).

[15] Interestingly, similar bonding is found in triphenylphosphoniocyclopropanide, in which the triphenylphosphane group is bent out of the plane of the three-membered ring atoms by 58°: H. Schmidbaur, A. Schier, B. Milewski-Mahrla, U. Schubert, *Chem. Ber. 115* (1982) 722.

[16] a) I. Reichelt, H.-U. Reissig, *Liebigs Ann. Chem. 1984*, 531, and references cited therein; b) R. Häner, T. Maetzke, D. Seebach, *Helv. Chim. Acta 69* (1986) 1655, and references cited therein; c) G. Boche, H. M. Walborsky in Z. Rappoport (Ed.): *The Chemistry of the Cyclopropyl Group*, Wiley, Chichester 1987, p. 701.

[17] J. Kai, P. Knochel, S. Kwiatkowski, J. D. Dunitz, J. F. M. Oth, D. Seebach, H.-O. Kalinowski, *Helv. Chim. Acta 65* (1982) 137; see also [16c].

[18] We have also found a tetrahedral coordination at an α-C atom and Li coordination to this atom for [1-cyano-2,2-dimethylcyclopropyllithium(THF)]$_\infty$, a cyano-substituted cyclopropyl "anion": M. Marsch, K. Harms, G. Boche, unpublished results. This is in accordance with the observation that the cyano group stabilizes a negative charge primarily through the inductive (field) effect; see also G. Boche, M. Marsch, K. Harms, *Angew. Chem. 98* (1986) 373; *Angew. Chem. Int. Ed. Engl. 25* (1986) 373, and references cited therein.

[19] Reactions with α-sulfonylcyclopropyllithium compounds: A. Padwa, M. W. Wannamaker, A. D. Dyszlewski, *J. Org. Chem. 52* (1987) 4760, and references cited therein.

[20] Note added in proof (May 5, 1988): A remarkably pyramidalized α-C atom has been found in the case of [(phenylsulfonyl)isopropyllithium·diglyme]$_2$, the two methyl groups being bent out of planarity (away from the O atoms of the $C_6H_5SO_2$ group) by 23.6 and 27.1° (H.-J. Gais, J. Vollhardt, G. Hellmann, H. Paulus, H. J. Lindner, *Tetrahedron Lett. 29* (1988) 1259).

A Simple Access to 2-Substituted 3,3,3-Trifluoroalanine Derivatives**

By *Klaus Burger,* Klaus Geith,* and *Karl Gaa*

Of the partially fluorinated amino acids,[2,3,4b] trifluoroalanine[1] and its α-substituted derivatives[5] are of special interest because of the highly increased acidity of the carboxyl function and the greatly reduced basicity of the amino function.[6,7] The lesser known 2-substituted 3,3,3-trifluoroalanine derivatives have been found to be highly specific, irreversible enzyme inhibitors.[4b,8] The incorporation of the fluoro- and/or trifluoromethyl-substituted amino acids into proteins enables further structural studies on proteins by ^{19}F-NMR spectroscopy.[8]

We recently reported on a new method for the synthesis of trifluoroalanine[1] using the readily accessible 5-fluoro-2-phenyl-4-trifluoromethyloxazole **1**[9] as starting material. We have now found that **1** can also be used for the synthesis of 2-substituted 3,3,3-trifluoroalanine derivatives (Scheme 1).

5-Fluoro-4-trifluoromethyl-1,3-azoles[9] readily undergo nucleophilic displacement reactions at the 5-position of the ring.[10] When (allylic) alkenyl alcohols are used as nucleophiles in the presence of KOH as base, a spontaneous exothermic reaction is observed. The products **2** actually expected undergo a hetero-Cope rearrangement under the reaction conditions, yielding the 4-alkenyl-5(4*H*)-oxazalones **3**. The trifluoromethyl group present at position 4 of the ring impedes any further migration of the alkenyl moiety to the 2-position—as *Steglich* et al. have already observed for structurally similar 4-alkyl- and 4-aryl-substituted systems.[11]

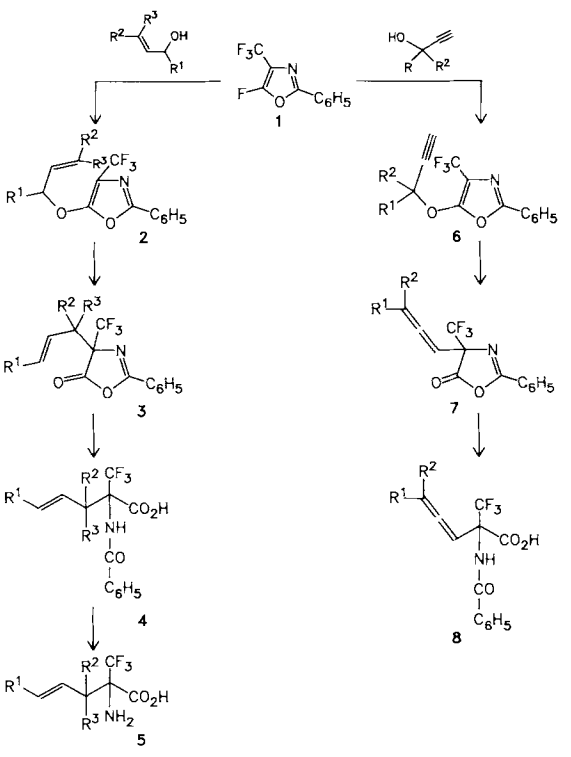

Scheme 1. Substituents R^1–R^3 other than H atoms: **4b**, $R^1=CH_3$; **4c**, $R^1=C_2H_5$; **4d**, $R^1=n\text{-}C_3H_7$; **4e**, $R^1=C_2H_3$; **4f**, $R^2=CH_3$; **4g**, $R^2=n\text{-}C_3H_7$; **4h**, $R^2=R^3=CH_3$; **8b**, $R^1=C_2H_5$; **8c**, $R^1=CH_3$, $R^2=C_2H_5$.

For the synthesis of the 2-substituted 3,3,3-trifluoroalanine derivatives **4**, the isolation of the 5(4*H*)-oxazolones **3** is unnecessary. The ring-opening **3**→**4** is achieved by addition of water to the reaction mixture. The amino function is deblocked by boiling with concentrated HCl. The 5(4*H*)-oxazolones **3**, are amino acid derivatives with protected amino groups and activated carboxyl groups and are suitable for direct use in peptide syntheses.[12]

The substitution pattern (R^1–R^3) of the alkenyl alcohol can be varied within a wide range; even highly substituted alcohols $R^5R^4C{=}CR^3CR^2R^1{-}OH$ have been employed. The CC double bond as well as the CC single bond of the alcohol can be part of a ring system. This opens up an entry to trifluoroalanine derivatives bearing heteroarenes, arenes, heterocycles, and carbocycles as substituents.[13]

Moreover, the double bond introduced by the reaction sequence **1**→**2**→**3**→**4** can be functionalized manyfold, so that polyfunctional trifluoromethyl-substituted amino acids are also accessible by this strategy.[13] When $R^2 \neq R^3$, diastereomeric pairs are formed which can be separated by crystallization.

If alkynyl alcohols are used instead of alkenyl alcohols in the above sequence, the reaction leads via **6** and **7** to 3,3,3-trifluoroalanine derivatives containing an α,β-diene function in the 2-position. When $R^1 \neq R^2$, diastereomeric pairs are formed once again. The ring-opening **7**→**8** presents no problems, whereas all attempts to cleave the *N*-benzoyl protective group have always led to a transformation of the α,β-diene function. To our knowledge, amino acids of type **8** were hitherto unknown; their C=C=C moiety should be useful for syntheses of a broad spectrum of novel trifluoroalanine derivatives. The new compounds were characterized by their melting points, IR, ^{1}H-NMR, ^{13}C-NMR and ^{19}F-NMR spectral data (Table 1), and by mass spectra, and elemental analyses.

Table 1. Data of the compounds **4a** and **8a** (all R = H) [a].

4a: Yield 78%; m.p. 141 °C; IR (KBr): $\tilde{\nu}$ = 3380, 1740, 1730, 1631, 1518 cm^{-1}; ^{19}F-NMR: δ = 4.9 (s); ^{1}H-NMR: δ = 3.07 (1H, dd, $^2J_{gem}$ = 14.2, $^3J_{vic}$ = 7.4 Hz; $-CH_2-$), 3.38 (1H, dd, $^2J_{gem}$ = 14.2, $^3J_{vic}$ = 7.1 Hz; $-CH_2-$), 5.18 (1H, dd, $^2J_{gem}$ = 1.8, $^3J_{cis}$ = 11.0 Hz; $H_2C{=}CH-$), 5.28 (1H, dd, $^2J_{gem}$ = 1.8, $^3J_{trans}$ = 17.1 Hz; $H_2C{=}CH-$), 5.84 (1H, dddd, $^3J_{vic}$(HC−CH$_2$) = 7.1, $^3J_{vic}$(HC−CH$_2$) = 7.4, $^3J_{cis}$ = 11.0, $^3J_{trans}$ = 17.1 Hz; $H_2C{=}CH-$), 7.46-7.59 (3H, m; phenyl-H), 7.86-7.88 (2H, m; phenyl-H) NH and OH not observable; ^{13}C-NMR: δ = 29.81 ($-CH_2-$), 65.67 ($C{-}CF_3$; q, J = 27.7 Hz), 120.63 ($H_2C{=}CH-$), 125.37 (CF_3; q, J = 286.3 Hz), 128.04 (phenyl-C), 129.27 (phenyl-C), 131.20 ($H_2C{=}CH-$), 132.61 (phenyl-C), 134.83 (phenyl-C), 167.01, 167.21 (Ph−CO−, $-CO_2H$)

8a: Yield 64%; m.p. 113-116 °C; IR (KBr): $\tilde{\nu}$ = 3290, 1982, 1762, 1650, 1533 cm^{-1}; ^{19}F-NMR: δ = 4.4 (s); ^{1}H-NMR: δ = 5.18 (2H, dd, $^2J_{gem}$ = 3.3, ^4J = 6.7 Hz; $H_2C{=}C{=}CH-$), 5.84 (1H, t, ^4J = 6.7 Hz; $H_2C{=}C{=}CH-$), 7.44-7.57 (3H, m; phenyl-H), 7.88-7.90 (2H, m; phenyl-H), 8.19 (1H, broad; NH), OH not observable; ^{13}C-NMR: δ = 64.52 ($C{-}CF_3$; q, J = 27.9 Hz), 81.21 ($H_2C{=}C{=}CH-$), 87.91 ($H_2C{=}C{=}CH-$), 124.85 (CF_3; q, J = 285.9 Hz), 128.40 (phenyl-C), 129.18 (phenyl-C), 132.67 (phenyl-C), 134.47 (phenyl-C), 165.89, 167.16 (Ph−CO−, $-CO_2H$), 209.15 ($H_2C{=}C{=}CH-$)

[a] ^{19}F-NMR: 56 MHz, [D$_6$]acetone, trifluoroacetic acid (ext); ^{1}H-NMR: 360.134 MHz, [D$_6$]acetone, TMS (int); ^{13}C-NMR: 90.556 MHz, [D$_6$]acetone, TMS (int), proton broad-band decoupled.

Further possible applications of 5-fluoro-4-trifluoromethyl-1,3-azoles for the synthesis of 3,3,3-trifluoroalanine derivatives and for the synthesis of trifluoromethyl-substituted, medium-sized heterocyclic ring systems will be reported elsewhere.

[*] Prof. Dr. K. Burger, Dipl.-Chem. K. Geith, Dipl.-Chem. K. Gaa
Institut für Organische Chemie der Technischen Universität München, Lichtenbergstrasse 4, D-8046 Garching (FRG)

[**] Synthesis of Naturally Occurring and Synthetic Amino Acids, Part 3. This work was supported by the Deutsche Forschungsgemeinschaft and the Fonds der Chemischen Industrie.—Part 2: [1a].

Experimental

A solution of **1** (2.31 g, 10 mmol) in anhydrous dioxane (30 mL) was treated with 10 mmol of the corresponding alkenyl or alkynyl alcohol and 1.12 g (20 mmol) of solid KOH. After a brief induction period, an exothermic reaction occurs. As soon as the ^{19}F-NMR analysis indicated complete conversion, the reaction mixture was treated with 10 mL of water, and, after complete ring-opening of **3** or **7**, respectively (^{19}F-NMR analysis), evaporated to dryness. The residue was taken up in water/ether (1/1) and the ether phase extracted twice with water. The combined aqueous phases were acidified with half-concentrated HCl (pH 1-2) and extracted twice with ether. The ether extracts were dried over sodium sulfate. After removal of the solvent under reduced pressure, the residue was recrystallized from ether/pentane.

Received: October 6, 1987 [Z 2463 IE]
German version: *Angew. Chem. 100* (1988) 860
Publication delayed at authors' request

CAS Registry numbers:
1, 70276-69-6; **3a**, 114490-65-2; **3b**, 114490-66-3; **3c**, 114490-67-4; **3d**, 114490-68-5; **3e**, 114490-69-6; **3f** (isomer 1), 114490-70-9; **3f** (isomer 2), 114490-71-0; **3g** (isomer 1), 114490-72-1; **3g** (isomer 2), 114490-73-2; **3h**, 114490-74-3; **4a**, 114490-81-2; **4b**, 114490-82-3; **4c**, 114490-83-4; **4d**, 114490-84-5; **4e**, 114490-85-6; **4f** (isomer 1), 114490-86-7; **4f** (isomer 2), 114490-87-8; **4g** (isomer 1), 114490-88-9; **4g** (isomer 2), 114490-75-4; **4h**, 114490-76-5; **5a**, 114490-94-7; **5b**, 114490-95-8; **5c**, 114490-96-9; **5d**, 114490-97-0; **5e**, 114490-98-1; **5f** (isomer 1), 114490-99-2; **5f** (isomer 2), 114491-00-8; **5g** (isomer 1), 114491-01-9; **5g** (isomer 2), 114504-90-4; **5h**, 114491-02-2; **7a**, 114490-77-6; **7b** (isomer 1), 114490-78-7; **7b** (isomer 2), 114490-79-8; **7c** (isomer 1), 114504-89-1; **7c** (isomer 2), 114490-80-1; **8a**, 114490-89-0; **8b** (isomer 1), 114490-90-3; **8b** (isomer 2), 114490-91-4; **8c** (isomer 1), 114490-92-5; **8c** (isomer 2), 114490-93-6; $H_2C{=}CHCH_2OH$, 107-18-6; $H_2C{=}CHCH(CH_3)OH$, 598-32-3; $H_2C{=}CHCH(C_2H_5)OH$, 616-25-1; $H_2C{=}CHCH(n\text{-}C_3H_7)OH$, 4798-44-1; $H_2C{=}CHCH(C_2H_3)OH$, 922-65-6; $H_3CCH{=}CHCH_2OH$, 6117-91-5; $n\text{-}C_3H_7CH{=}CHCH_2OH$, 2305-21-7; $H_3C(H_3C)C{=}CHCH_2OH$, 556-82-1; $HOCH_2C{\equiv}CH$, 107-19-7; $C_2H_5(HO)CHC{\equiv}CH$, 4187-86-4; $C_2H_5(H_3C)(HO)CC{\equiv}CH$, 77-75-8.

[1] a) K. Burger, M. Gold, R. Simmerl, A. Gieren, G. Weber, T. Hübner, *Chem. Ztg. 110* (1986) 422; b) K. Burger, D. Hübl, P. Gertitschke, *J. Fluorine Chem. 27* (1985) 327.
[2] a) W. Steglich, H.-U. Heininger, H. Dworschak, F. Weygand, *Angew. Chem. 79* (1967) 822; *Angew. Chem. Int. Ed. Engl. 6* (1967) 808; b) F. Weygand, W. Steglich, W. Oettmeier, *Chem. Ber. 103* (1970) 818.
[3] G. C. Barrett in R. C. Sheppard (Ed.): *Amino Acids, Peptides and Proteins, Vol. 12*. The Royal Chemical Society, London 1981, p. 11, and references cited therein.
[4] a) R. Filler, Y. Kobayashi (Eds.): *Biomedicinal Aspects of Fluorine Chemistry*. Kodanska, Tokio, Elsevier Biomedical, Amsterdam 1982; b) J. Kollonitsch in [4a], p. 93ff.
[5] J. T. Welch, *Tetrahedron 43* (1987) 3123, and references cited therein.
[6] a) F. Weygand, W. Steglich, W. Oettmeier, A. Maierhofer, R. S. Loy, *Angew. Chem. 78* (1966) 640; *Angew. Chem. Int. Ed. Engl. 5* (1966) 600; b) F. Weygand, W. Steglich, F. Fraunberger, *ibid. 79* (1967) 822 and *6* (1967) 807; c) F. Weygand, W. Steglich, W. Oettmeier, *Chem. Ber. 103* (1970) 1655.
[7] A. Uskert, A. Neder, K. Endre, *Magy. Kem. Foly. 79* (1973) 333; *Chem. Abstr. 79* (1973) 79 147r.
[8] J. T. Greig in [4a], p. 163.
[9] K. Burger, R. Ottlinger, H. Goth, J. Firl, *Chem. Ber. 115* (1982) 2494.
[10] K. Burger, D. Hübl, K. Geith, *Synthesis 1988*, 194.
[11] a) B. Kübel, G. Höfle, W. Steglich, *Angew. Chem. 87* (1975) 64; *Angew. Chem. Int. Ed. Engl. 14* (1975) 58; b) N. Engel, B. Kübel, W. Steglich, *ibid. 89* (1977) 408 and *16* (1977) 394.
[12] F. Weygand, K. Burger, K. Engelhardt, *Chem. Ber. 99* (1966) 1461.
[13] K. Gaa, *Diplomarbeit*, Technische Universität München 1987.

Equipotential Surfaces in Periodic Charge Distributions

By *Alan Lindsay Mackay**

Von Schnering and *Nesper*[1] have produced very beautiful pictures of the zero potential surfaces in various crystal structures by exploiting the capabilities of modern computer graphics. They have thus made it easy to visualize the electrostatics implicit in *Pauling*'s rules for ionic structures and in the electrostatics now recognized as important in proteins (for example by *Sternberg* et al.[2]).

Their method involves the calculation of the potential of an exploratory charge at a test point (x,y,z). This requires the use of the full Ewald-Bertaut algorithm, where part of the calculation is carried out in real space and part in reciprocal space to ensure convergence. As explained most clearly by *Ashcroft* and *Mermin*[3] this slow convergence "is not just a mathematical nuisance. It reflects the physical fact that Coulomb interactions are of such long range that the energy of a collection of charged particles can depend crucially on the configuration of a negligibly small fraction of them on the surface". Computers now make it possible to calculate the energy of small finite clusters of atoms which may comprise real materials.

We have used a microcomputer (Commodore Amiga 1000) to draw some of the same surfaces using a different but related algorithm, which is less exact yet one that gives a good approximation. (We have hitherto used[4] a "finite element analysis" type of algorithm for minimal surfaces, while *Liden* and *Hyde*[5] have recently given another algorithm based on the projection of the normals of a minimal surface onto a sphere to give the Gaussian image.)

Our method was suggested by the standard expressions for the Fermi surfaces of cubic metals which are given (*Kittel*[6]; k = reciprocal lattice vector, a = real lattice vector) as

$$\text{simple cubic: const.} = \cos(\mathbf{k}_x\mathbf{a}) + \cos(\mathbf{k}_y\mathbf{a}) + \cos(\mathbf{k}_z\mathbf{a}) \quad (a)$$

$$\text{body-centred cubic: const.} = \cos(\mathbf{k}_x\mathbf{a}) \times \cos(\mathbf{k}_y\mathbf{a}) \times \cos(\mathbf{k}_z\mathbf{a}) \quad (b)$$

$$\text{face-centred cubic: const.} = \cos(0.5\,\mathbf{k}_x\mathbf{a}) \times \cos(0.5\,\mathbf{k}_y\mathbf{a}) + \cos(0.5\,\mathbf{k}_y\mathbf{a}) \times \cos(0.5\,\mathbf{k}_z\mathbf{a}) + \cos(0.5\,\mathbf{k}_z\mathbf{a}) \times \cos(0.5\,\mathbf{k}_x\mathbf{a}). \quad (c)$$

and are readily seen to be the sum of the Fourier terms:

$$\text{simple cubic: } 100,\ 010,\ 001 \quad (d)$$

$$\text{body-centred cubic: } 111,\ 11\bar{1},\ 1\bar{1}1,\ \bar{1}11 \quad (e)$$

$$\text{face-centred cubic: } 011,\ 01\bar{1},\ 101,\ 10\bar{1},\ 1\bar{1}0,\ 110 \quad (f)$$

If we calculate structure factors for a CsCl structure with a charge of +1 at 000 and a charge of −1 at ½, ½, ½, then the first factors are $F(000)=0$, $F(100)=2$, $F(200)=0$ and, in general, $F(hkl)=1-\cos(2\pi(h+k+l)/2)$. Thus, of the reflections with $N=h^2+k^2+l^2\leq 3$ only those with $hkl=100$, 010, and 001 are non-zero; they are identical with those found for the simple cubic Fermi surface [see (d)].

Similarly, for the NaCl structure with a positive charge at 000 and a negative charge at ½, 0, 0, of the expected first few terms 111, 200, 220, 311, 222 (noting that the reciprocal lattice of a real face-centered cubic lattice is body-centered cubic) only 111 and 311 are non-zero. Thus, of all reflections with $N<11$, only those with $hkl=111$; $11\bar{1}$; $1\bar{1}1$; $1\bar{1}\bar{1}$ are non-zero, as in the body-centered cubic Fermi surface.

For the body-centered cubic structure with a charge of +2 at 000 and ½, ½, ½ and six (doubly) negative charges at ½, 0, 0 plus eight (singly) positive charges at ¼, ¼, ¼ (as suggested by *von Schnering* and *Nesper*) the structure factors (the reciprocal lattice being f.c.c.) are: $F(110)=8$, $F(200)=-8$, $F(211)=8$, $F(220)=0$.

[*] Prof. A. L. Mackay
Department of Crystallography
Birkbeck College (University of London)
Malet Street, London WC1E 7HX (UK)

 © VCH Verlagsgesellschaft mbH, D-6940 Weinheim, 1988 0570-0833/88/0606-0849 $ 02.50/0

If we transform only the reflections 110, as in the calculation of the Fermi surface for a face-centered cubic metal (which has a body-centered cubic reciprocal lattice), then we obtain a surface very similar to that with eight tunnels (*Schoen*'s $I-WP$ surface) described by *von Schnering* and *Nesper*.

Taking the simple cubic surface [cf. Eq. (a)] we see, on taking the second derivatives, that Laplace's equation is satisfied if the constant is zero. Thus, the curve obtained is a solution of Laplace's equation and a zero equipotential.

Our procedure then is to carry out the normal Fourier summation for the electron density, but using only the first very few Fourier terms and concentrating only on plotting the zero potential contour (although other equipotentials can readily be plotted instead). We note that the scattering of electrons in electron microscopy and electron diffraction structure analysis is by the potential and the resultant plot is of that potential (not the electron density as in X-ray structure analysis). If we were calculating structure factors for this purpose from an array of electrons and positrons we would use the form factors which would show the very slow fall off in potential (according to $1/r$). The transform in reciprocal space would thus fall off even more sharply than the Gaussian factor entering into the Ewald-Bertaut method.

If we concentrate on plotting the zero potential this is equivalent to taking more terms, since the partition of space into two regions (positive and negative) by a single sinusoidal wave leads to a square wave which would otherwise be generated by adding up an infinite series of harmonics.

The equipotential surfaces for crystal structures can now be drawn using the tables of charge positions which *von Schnering* and *Nesper* have very usefully collected. First, the structure factors are calculated ($F(000)$ is always zero since there are equal numbers of positive and negative charges). Then the Fourier synthesis is calculated using the first one or two terms only, and finally the zero potential surface is plotted. In simple cases we have plotted contours of this surface directly, by finding, for each pair of y and z coordinates on a grid, the values for x at which the potential is zero. For the simplest cases there is a direct solution but usually the zero of a function of x has been found numerically. Calculations need be made only for the fundamental region which is repeated by the space group to fill space, although a more satisfactory grid is obtained if the whole unit cell is calculated.

For example, to plot the Neovius surface, which corresponds to the NaCl and CsCl charge distributions superimposed in the ratio 1 to 4, we obtain the surface shown (Fig. 1) by adding the Fourier terms of the type 110 and 111. The equipotential surfaces around protein molecules or other ionic structures, can be plotted similarly.

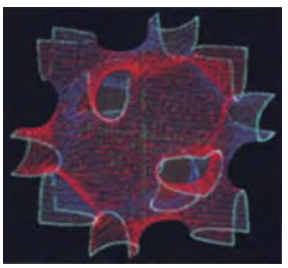

Fig. 1. The cubic unit cell of the zero equipotential surface in the Neovius surface [1].

Thus, the exploration of equipotential surfaces, which *von Schnering* and *Nesper* (as well as *Hyde* and *Andersson*[7]) have shown to be of great importance in understanding chemical properties, is within the compass of comparatively small microcomputers.

Received: January 25, 1988 [Z 2587 IE]
German version: *Angew. Chem. 100* (1988) 867

[1] H. G. von Schnering, R. Nesper, *Angew. Chem. 99* (1987) 1097; *Angew. Chem. Int. Ed. Engl. 126* (1987) 1059.
[2] M. J. E. Sternberg, F. R. F. Hayes, A. J. Russell, P. G. Thomas, A. R. Fersht, *Nature (London) 330* (1987) 86.
[3] N. W. Ashcroft, N. D. Mermin: *Solid State Physics*, Holt-Saunders, Philadelphia 1976, p. 403-404.
[4] A. L. Mackay, *Physica B 131* (1985) 300.
[5] S. Liden, S. T. Hyde, *J. Phys. (Les Ulis Fr.) 48* (1987) 1585.
[6] C. Kittel: *Introduction to Solid State Physics*, 6th Edit., Wiley, New York 1976, p. 231.
[7] S. T. Hyde, S. Andersson, *Z. Kristallogr. 170* (1985) 225.

Synthesis and Structure of $[ClV(OSiMe_3)N_2PPh_2]_2$, the First Cyclodimetallaphosphazene—an Eight-Membered Planar Unsaturated Heterocycle**

By *Michael Witt*,* *Herbert W. Roesky*, *Mathias Noltemeyer*, and *George M. Sheldrick*

Dedicated to Professor Ulrich Wannagat on the occasion of his 65th birthday

We recently reported on the synthesis of six-membered cyclometallaphosphazenes containing a 6π-electron framework.[1] Eight-membered cyclophosphazenes in which one or two phosphorus atoms are replaced by a transition metal were hitherto unknown. Herein we describe the first synthesis of such a cyclodimetallaphosphazene.

Vanadyl chloride **1** reacts with $Me_3SiN{=}PPh_2N(SiMe_3)_2$ **2** in dichloromethane or acetonitrile with cleavage of Me_3SiCl to give $[ClV(OSiMe_3)N_2PPh_2]_2$ **3**,[2] a brick-red

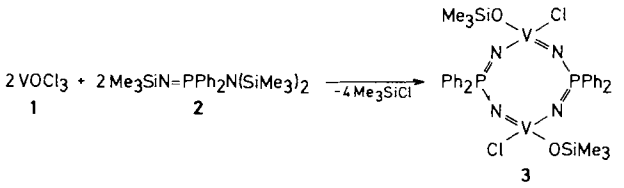

substance that is extremely sensitive to moisture. Crystals of **3** suitable for an X-ray structure analysis were obtained by recrystallization from CH_2Cl_2/CH_3CN at $-30\,^{\circ}C$.

Within the limits of error the single crystal X-ray structure analysis[5] confirms the presence of a planar eight-membered ring. In contrast to the two other cyclic systems containing a N-V-N moiety in the ring, $[S_2N_3VCl_2]_n$[6] and $[(Ph_2P)_2N_3VCl_2]\cdot 2CH_3CN$,[1] which exhibit octahedral coordination at the metal atom, the vanadium atom in **3** shows only tetrahedral coordination, as observed in most open-chain nitrenevanadium compounds.[7] The V-N

[*] Dr. M. Witt, Prof. Dr. H. W. Roesky, Dr. M. Noltemeyer, Prof. G. M. Sheldrick
Institut für Anorganische Chemie der Universität
Tammannstrasse 4, D-3400 Göttingen (FRG)

[**] This work was supported by the Deutsche Forschungsgemeinschaft and the Fonds der Chemischen Industrie.

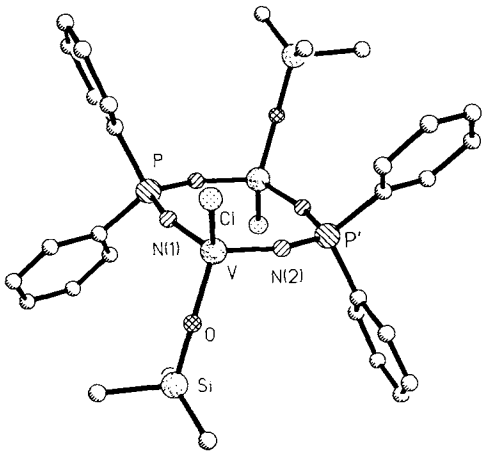

Fig. 1. Crystal structure of **3** (hydrogen atoms omitted). Important bond lengths [pm]: V-N(1) 167.9(5), V-N(2) 166.0(5), V-O 173.5(5), V-Cl 221.4(2), P-N(1) 161.8(5), P'-N(2) 162.1(5), O-Si 162.5(5). Bond angles [°] in the central eight-membered ring at V 110.8(3), N 158.4(3), P 116.9(3). The molecule possesses a crystallographic inversion center.

bonds are ca. 5–15 pm shorter than those in $[S_2N_3VCl_2]_n$,[6] but closely resemble those in open-chain systems.[7]

The P–N bond lengths, on the other hand, lie in the same range as those of similar cyclophosphazene systems.[1,8] The angles at the nitrogen atoms are about 10° greater than those in $P_4N_4F_8$, the only planar eight-membered phosphazene ring thus far reported in the literature.[9]

In mass spectroscopic investigations of **3**, the molecular ion could not be observed. The ^{1}H-decoupled NMR spectra show singlets in the expected regions with extremely large half-widths, which change very little even on lowering the temperature and which cannot be attributed to paramagnetism.[10]

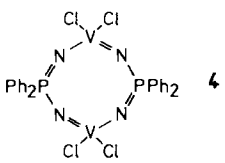

4

Similar effects are observed in the case of **4**, which is accessible from $[Cl_3VNSiMe_3]$[11] and $Me_3SiN{=}PPh_2Cl$. **4** cannot be obtained by reaction of **3** with $SOCl_2$ or PCl_5.[12]

Received: November 16, 1987;
revised: December 23, 1987 [Z 2501 IE]
German version: *Angew. Chem. 100* (1988) 852
Publication delayed at authors' request

CAS Registry numbers:
2, 61500-31-0; **3**, 114490-50-5; **4**, 114490-51-6; $Cl_3VNSiMe_3$, 99589-88-5; $Ph_2PN(SiMe_3)_2$, 13685-61-5; $Me_3SiN{=}PPh_2Cl$, 90413-89-1; Me_3SiN_3, 4648-54-8.

[1] H. W. Roesky, K. V. Katti, U. Seseke, M. Witt, E. Egert, R. Herbst, G. M. Sheldrick, *Angew. Chem. 98* (1986) 447; *Angew. Chem. Int. Ed. Engl. 25* (1986) 477; H. W. Roesky, K. V. Katti, U. Seseke, H. G. Schmidt, E. Egert, R. Herbst, G. M. Sheldrick, *J. Chem. Soc. Dalton Trans. 1987*, 847; K. V. Katti, H. W. Roesky, M. Rietzel, *Inorg. Chem. 26* (1987) 814.

[2] Procedure for **3**: A solution of **1** (1.7 g, 10 mmol) in CH_3CN (20 mL) was added dropwise under N_2 to a solution of **2** (4.3 g, 10 mmol), prepared by oxidation [3] of $Ph_2PN(SiMe_3)_2$ [4] with Me_3SiN_3, in CH_3CN (100 mL). After 24 hours' stirring, the orange-red precipitate was filtered off, washed with a small amount of CH_3CN, dissolved in CH_2Cl_2, and finally treated with a little CH_3CN. Large, brick-red rhombs of **3** crystallized out at −30°C. M.p. 206°C (decomp.), yield 3.1 g (80%). IR: $\tilde{\nu}$ = 1580 w, 1430 s, 1248 m, 1187 vs, 1157 m, 1110 vs, 1065 sh, 1022 m, 995 m, 901 vs, 845 sh, 836 vs, 748 m, 726 s, 704 sh, 680 s, 662 sh, 533 s cm^{-1}.

[3] M. Witt, unpublished; in analogy to $Ph_2P(NSiMe_3)NHSiMe_3$ (K. L. Paciorek, R. H. Kratzer, *J. Org. Chem. 31* (1966) 2426). **2** was first described by *W. Wolfsberger* and *H. Hager* (*Z. Anorg. Allg. Chem. 425* (1976) 169).

[4] H. Nöth, G. Meinel, *Z. Anorg. Allg. Chem. 349* (1967) 225.

[5] Crystal structure analysis of **3**: space group *Pbca*, a = 1162.0(1), b = 1690.4(2), c = 2011.3(8) pm, V = 3.9507 nm^3, Z = 4, μ = 0.7 mm^{-1} ($Mo_{K\alpha}$); 4069 measured intensities, $2\theta_{max} = 45°$, empirical absorption correction, 2499 observed reflections with $F > 4\sigma(F)$ used for the structure solution (Patterson and Fourier methods) and refinement, non-hydrogen atoms anisotropically, H atoms (partly located by difference electron density determination) refined with a riding model, R = 0.067 (R_w = 0.073, $w^{-1} = \sigma^2(F) + 0.0005F^2$). Further details of the crystal structure investigation are available on request from the Fachinformationszentrum Energie, Physik, Mathematik GmbH, D-7514 Eggenstein-Leopoldshafen 2 (FRG), on quoting the depository number CSD-52826, the names of the authors, and the journal citation.

[6] H. W. Roesky, J. Anhaus, H. G. Schmidt, G. M. Sheldrick, M. Noltemeyer, *J. Chem. Soc. Dalton Trans. 1983*, 1207.

[7] For a review of the bonding and bond order of transition metal-nitrogen compounds see: K. Dehnicke, J. Strähle, *Angew. Chem. 93* (1981) 451; *Angew. Chem. Int. Ed. Engl. 20* (1981) 413.

[8] H. R. Allcock: *Phosphorus-Nitrogen Compounds*, Academic Press, New York 1972.

[9] H. McD. McGeachin, F. R. Tromans, *J. Chem. Soc. 1961*, 4777.

[10] ^{29}Si-NMR: δ = 24.0 ($\Delta_{1/2} \approx 30$ Hz); ^{31}P-NMR: δ = −12.6 ($\Delta_{1/2} \approx 1000$ Hz); ^{51}V-NMR: δ = −394.7 ($\Delta_{1/2} \approx 500$ Hz). The lock ($CDCl_3$) signal is sharp. According to ESR studies (Dr. *D. Marsh*, MPI, Biophysikalische Chemie, Göttingen), there are no unpaired electrons in the solid state.

[11] E. Schweda, K. D. Scherfise, K. Dehnicke, *Z. Anorg. Allg. Chem. 528* (1985) 117.

[12] The synthesis and characterization of **4** will be reported elsewhere.

The First "Adamantoid" Alkaline Earth Metal Chelate Complex: Synthesis, Structure, and Reactivity**

By *Rolf W. Saalfrank,* Armin Stark, Karl Peters,* and *Hans Georg von Schnering**

n,n-Dilithioalkanes are of special interest both from the theoretical point of view and because of their remarkable synthetic potential.[1] The same holds true for 1,1-dilithioallyl phenyl sulfone,[2] dilithio(phenylsulfonyl)(trimethylsilyl)methane,[3] and dilithio(tosyl)methyl isocyanide.[4] To our knowledge dilithiomalonate esters have so far never been the subject of a concrete study. The C,C-dialkylation or C,O-diacylation of malonic esters proceeds in two steps via the malonic ester monoanion.[5]

The synthon strategy has proven to be best for the development of new synthetic methods.[6] In this connection we have paid special attention to tetradonor-substituted allenes **1**, which formally react like 1,1-/1,3-dianions **2** of malonic ester ($R^1 = R^2 = OEt$) or malonic amides ($R^1 = R^2 = NR_2$).[7] In extension of the concept developed for the allenes **1** we have also used silyl enol ethers **3** of 1,3-dicarbonyl compounds as 1,3-dianion equivalents **2** (R^1, R^2 = OEt, aryl).[8]

[*] Prof. Dr. R. W. Saalfrank, Dipl.-Chem. A. Stark
Institut für Organische Chemie der Universität
Erlangen-Nürnberg
Henkestrasse 42, D-8520 Erlangen (FRG)
Prof. Dr. H. G. von Schnering, Dr. K. Peters
Max-Planck-Institut für Festkörperforschung
Heisenbergstrasse 1, D-7000 Stuttgart 80 (FRG)

[**] "Adamantoid" Chelate Complexes, Part 1. This work was supported by the Deutsche Forschungsgemeinschaft and the Fonds der Chemischen Industrie.

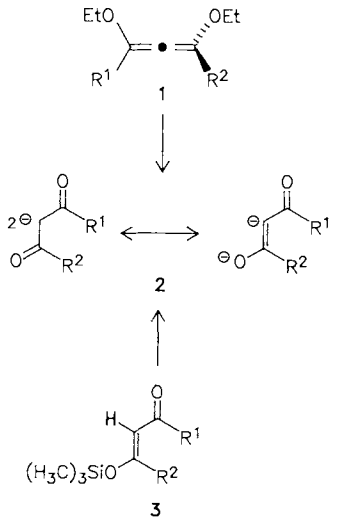

The direct use of doubly metalated 1,3-dicarbonyl compounds $2 \cdot 2\,M^{\oplus}$ could make the circuitous route via tetradonor-substituted allenes **1** or silyl enol ethers **3** superfluous. The malonic ester dianion serves as model species thereby, since it can be regarded as a tetradonor-substituted allene **1** ($R^1 = R^2 = O^{\ominus}$, OM).[9]

Metalation of malonic ester **4** in the presence of two equivalents of methylmagnesium iodide **5** in tetrahydrofuran (THF) at −78 °C followed by addition of a half equivalent of oxalyl chloride **6** and subsequent work-up with aqueous ammonium chloride solution furnished tetraammonium hexakis[tetraethyl-2,3-dioxobutane-1,1,4,4-tetracarboxylato(2−)-$O^{1'},O^2:O^3,O^{4'}$]tetramagnesate(4−) **7** as colorless crystals in ca. 40% yield. If, however, **4**, **5**, and **6** are allowed to react in the molecular ratio 1 : 1 : 0.25, the yield of **7** is increased to 85%. Careful hydrolysis of **7**

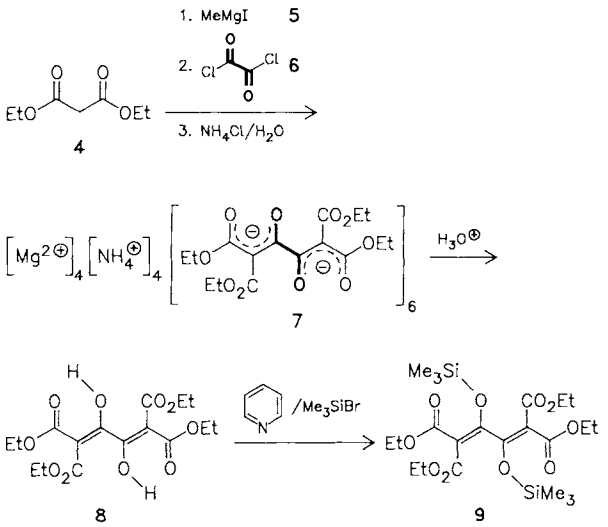

(pH ≈ 5, 20 °C, 2 minutes' ultrasonication) affords tetraethyl 2,3-dihydroxy-1,3-butadiene-1,1,4,4-tetracarboxylate **8** (keto-enol equilibrium). Compounds of type **8** were hitherto unknown. So far **8** could not be obtained in analytically pure form since it readily undergoes an acid cleavage to give two equivalents of malonic ester and one equivalent of oxalic acid. It can be reconverted into **7** by reaction with sodium hydride, magnesium bromide and aqueous ammonium chloride solution. If zinc bromide is used instead of magnesium bromide it is possible to prepare the zinc complex analogue of **7** from **8**. Compound **8** reacts with bromotrimethylsilane/pyridine to give tetraethyl 2,3-bis(trimethylsilyloxy)-1,3-butadiene-1,1,4,4-tetracarboxylate **9**.

When the ratio of the reactants **4** : **5** : **6** = 1 : 1 : 0.25, **7** is formed in a two-step mechanism via the malonic ester monoanion. Evidence against formation of the "dianion **1**" ($R^1 = R^2 = OMgI$) as intermediate is provided by the finding that only one volume equivalent of methane is formed upon reaction of **4** and **5** in the molar ratio 1 : 2 at −78 °C. Liberation of the second volume equivalent of methane (based on the yield of **7**) is first observed upon dropwise addition of **6**. This is consistent with participation of the system monoanion/methyl-Grignard reagent in the formation of **7**.

The ^{1}H- and ^{13}C-NMR spectra of **7** are impressively simple [empirical formula of **7**: $C_{96}H_{120}O_{60}Mg_4(NH_4)_4$; T_d symmetry, eight (!) ^{13}C-NMR signals] and thus provide no detailed information whatsoever about its structure. We therefore carried out an X-ray structure analysis of **7**; this revealed that **7** is present in the crystal in the form of a tetraammonium salt of the first known adamantoid tetramagnesium chelate complex. [Graphical representation of

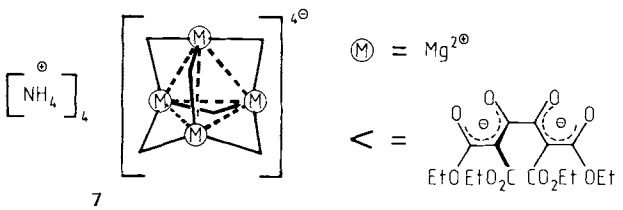

Fig. 1. Graphical representation (schematic) of **7**.

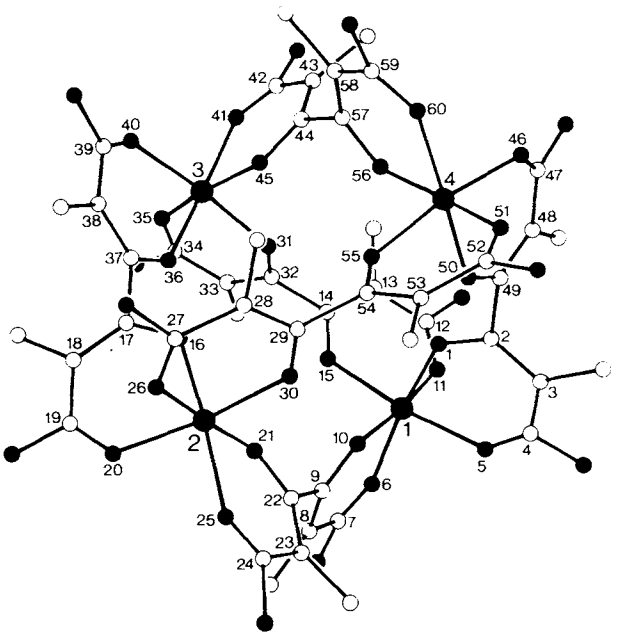

Fig. 2. Stereographic projection of the chelate complex anion of **7** with crystallographic labeling of the skeletal atoms. Large and small black dots indicate Mg and O atoms respectively, circles C atoms. Unlabeled C and O symbols stand for CO_2Et and OEt respectively. The atomic positions of the terminal groups are very inaccurate and were only isotropically refined. The compound crystallizes with one equivalent of 2,3-dihydroxy-2,3-dimethylbutane [14] in the triclinic system, $P\bar{1}$, $a = 1875.6(12)$, $b = 2007.2(7)$, $c = 1777.1(9)$ pm, $\alpha = 103.93(3)$, $\beta = 93.50(5)$, $\gamma = 90.45(4)°$, $Z = 2$, $\rho_{calcd} = 1.169$ g cm^{-3}, 8508 *hkl* with $F > 3\sigma(F)$, $R = 0.144$. Further details of the crystal structure investigation are available on request from the Fachinformationszentrum Energie, Physik, Mathematik GmbH, D-7514 Eggenstein-Leopoldshafen 2 (FRG), on quoting the depository number CSD-52856, the names of the authors, and the journal citation.

the chelate complex (schematic) in Fig. 1; stereographic projection of the chelate complex in Fig. 2].[10] The core of the chelate complex anion of **7** forms a tetrahedron of four magnesium ions; these are coupled via each of the six edges of the tetrahedron by a tetradentate tetraethyl-2,3-dioxobutane-1,1,4,4-tetracarboxylato(2−) bracket such that each of the four magnesium ions is octahedrally surrounded by six oxygen atoms.

The spectroscopic data of the zinc chelate complex differ only slightly from those measured for the corresponding magnesium chelate complex **7**.

Experimental

7: A suspension of **5** (60 mmol) in anhydrous THF (150 mL) was treated (under N_2, −78 °C) within 30 min with a solution of **4** (9.6 g, 60 mmol) in THF (50 mL) and the resulting mixture stirred for 2 h at −78 °C. It was then treated dropwise within 1 h with a solution of oxalyl chloride (1.9 g, 15 mmol) in THF (50 mL), heated to 20 °C within 18 h, and worked-up with aqueous ammonium chloride solution. Yield: 5.1 g (85%), decomp. 180 °C (from acetone).—IR (KBr): $\tilde{\nu}$ = 1690 (C=O), 1635 cm^{-1} (C=C).—^{1}H-NMR (400 MHz, CD_3OD): δ = 1.19 and 1.28 (each t, 72 H; 24 CH_3), 3.95, 4.06, 4.17, and 4.27 (each mc, 48 H; 24 CH_2), 4.84 (s, 16 H; 4 $NH_4^{\oplus}$).—^{13}C-NMR (100.5 MHz, CD_3OD): δ = 14.56 and 14.60 (24 CH_3), 61.22 and 61.71 (24 OCH_2), 96.10 (12 =C), 169.57, 172.01, and 186.31 (24 C=O, 12 C=O).

9: A suspension of **7** (1.2 g, 0.5 mmol) in water (100 mL) was treated with a solution of aluminum sulfate (15 g) in water (50 mL) and the mixture ultrasonicated for 2 min. The aqueous phase was extracted twice with 100 mL of dichloromethane and the combined extracts dried over sodium sulfate. After removal of solvent the remaining enol **8** (reddish oil) was dissolved in 20 mL of diethyl ether (under N_2) and treated with 0.5 g (6 mmol) of pyridine and 4.6 g (30 mmol) of bromotrimethylsilane. The mixture was then stirred for 1 h at 20 °C and filtered. After removal of solvent, the remaining silyl enol ether **9** (orange colored oil) was freed of all volatile impurities at 20 °C under vacuum. Yield: 1.5 g (95%). Decomp. ≈ 55 °C.—IR (film): $\tilde{\nu}$ = 1725 (C=O), 1630 cm^{-1} (C=C).—^{1}H-NMR (400 MHz, $CDCl_3$): δ = 0.20 (s, 18 H; 2 $Si(CH_3)_3$), 1.17 (t, 6 H; 2 CH_3), 1.23 (t, 6 H; 2 CH_3), 4.09 (q, 4 H; 2 OCH_2), 4.18 (q, 4 H; 2 OCH_2).—^{13}C-NMR (100.5 MHz, $CDCl_3$): δ = 0.35 (2 $Si(CH_3)_3$), 13.75 (2 CH_3), 14.01 (2 CH_3), 60.79 (2 OCH_2), 60.97 (2 OCH_2), 113.25 (2 =C), 156.46, 163.59, and 164.11 (O−C=O and =C−O).—MS (70 eV): *m/z* 518 ($M^{\oplus}$).

Received: February 1, 1988;
supplemented: March 9, 1988 [Z 2600 IE]
German version: *Angew. Chem. 100* (1988) 878

CAS Registry numbers:
4, 105-53-3; **5**, 917-64-6; **6**, 79-37-8; **7**, 114446-10-5; **7** analogous zinc complex, 114466-56-7; **7**·2,3-dihydroxy-2,3-dimethylbutane, 114446-11-6; **8**, 114446-12-7; **9**, 114446-13-8; Me_3SiBr, 2857-97-8.

[1] Reviews: A. Maercker, M. Theis, *Top. Curr. Chem. 138* (1987) 1; P. von R. Schleyer, *Pure Appl. Chem. 56* (1984) 151.
[2] J. Vollhardt, H.-J. Gais, K. L. Lukas, *Angew. Chem. 97* (1985) 607; *Angew. Chem. Int. Ed. Engl. 24* (1985) 610.
[3] J. Vollhardt, H.-J. Gais, K. L. Lukas, *Angew. Chem. 97* (1985) 695; *Angew. Chem. Int. Ed. Engl. 24* (1985) 696; for further 1,1-dilithioalkyl phenyl sulfones cf.: J. J. Eisch, S. K. Dua, M. Behrooz, *J. Org. Chem. 50* (1985) 3674; M. C. Mussatto, D. Savoia, C. Trombini, A. Umani-Ronchi, *ibid. 45* (1980) 4002; A. Roggero, T. Salvatori, A. Proni, A. Mazzei, *J. Organomet. Chem. 177* (1979) 313; K. Kondo, D. Tunemoto, *Tetrahedron Lett. 16* (1975) 1397; J. B. Evans, G. Marr, *J. Chem. Soc. Perkin Trans. 1 1972*, 2502; E. M. Kaiser, L. E. Solter, R. A. Schwarz, R. D. Beard, C. R. Hauser, *J. Am. Chem. Soc. 93* (1971) 4237; cf. also 1,*o*-dilithiobis(trimethylsilyl)methyl phenyl sulfone: W. Hollstein, K. Harms, M. Marsch, G. Boche, *Angew. Chem. 99* (1987) 1279; *Angew. Chem. Int. Ed. Engl. 26* (1987) 1287.
[4] S. P. J. M. van Nispen, C. Mensink, A. M. van Leusen, *Tetrahedron Lett. 21* (1980) 3723.
[5] W. Carruthers: *Some Modern Methods of Organic Synthesis*, 2nd edit., University Press, Cambridge 1978, p. 1 ff.
[6] E. J. Corey, *Pure Appl. Chem. 14* (1967) 19; D. Seebach, *Angew. Chem. 91* (1979) 259; *Angew. Chem. Int. Ed. Engl. 18* (1979) 239; T. A. Hase: *Umpoled Synthons, A Survey of Sources and Uses in Synthesis*, Wiley, New York 1987.
[7] R. W. Saalfrank, W. Rost, *Angew. Chem. 97* (1985) 870; *Angew. Chem. Int. Ed. Engl. 24* (1985) 855; R. W. Saalfrank, F. Schütz, U. Moenius, *Synthesis 1985*, 1062; R. W. Saalfrank, K. Hilbig, F. Schütz, K. Peters, H. G. von Schnering, *Chem. Ber. 121* (1988), in press.
[8] R. W. Saalfrank, M. Hanek, *Tetrahedron 44* (1988), in press.
[9] Cf. also P. Knochel, J. F. Normant, *Tetrahedron Lett. 27* (1986) 1043.
[10] For the topology of the chelate complex anion of **7** and its potential applications, cf. the spherical tricycles **I** [11, 12] and **II** [12, 13].

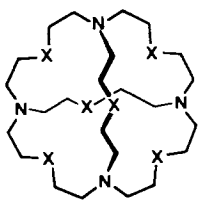

I: x = $(CH_2)_2$; O

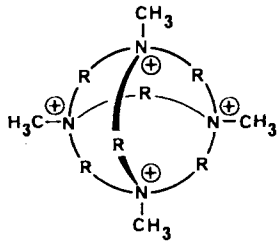

II: R = $(CH_2)_6$

[11] J. M. Lehn, *Angew. Chem. 100* (1988) 91; *Angew. Chem. Int. Ed. Engl. 27* (1988) 89; *Pure Appl. Chem. 49* (1977) 857; E. Graf, J. M. Lehn, *J. Am. Chem. Soc. 97* (1975) 5022.
[12] E. Weber, F. Vögtle, *Kontakte 1981*, No. 1, p. 24; E. Weber: *Phase Transfer Catalysts, Properties and Applications* (Merck-Schuchardt 1987), p. 33.
[13] F. P. Schmidtchen, *Angew. Chem. 89* (1977) 751; *Angew. Chem. Int. Ed. Engl. 16* (1977) 720; *Nachr. Chem. Tech. Lab. 36* (1988) 8.
[14] 2,3-Dihydroxy-2,3-dimethylbutane is formed as by-product in the synthesis of **7** from oxalyl chloride **6** and methyl-Grignard reagent **5**.

Preparative UV-Laser Photochemistry: A Biscarbene Intermediate in the Synthesis of a 5,6-Dihydrodibenzo[*a,e*]cyclooctene Containing a *trans*-Double Bond**

By *Klaus Hannemann** and *Jakob Wirz*

The extremely high light intensities of laser light sources enable multiphoton processes to be achieved which cannot be initiated with conventional lamps. These multiphoton processes were hitherto primarily investigated spectroscopically;[1] in some cases new products have been isolated.[2] Depending upon the time interval between the absorption processes, multiphoton processes range from quasi-simultaneous multiphoton absorption to secondary excitation of singlet and triplet states[2a–f] to photochemical reactions of reactive intermediates.[2g–j] A further interesting case is the photolysis of dichromophores.[4] If both chromophores of a dichromophoric molecule are excited with high-intensity light, a difunctionally reactive intermediate can be formed which may lead to new products. As an example of a dichromophoric system we chose the bis(diazomethane) **1**, and describe here the preparative laser photolysis of **1** as compared to its conventional photolysis.

The bis(diazo) compound **1**[5] was prepared from the bishydrazone of *o,o'*-dibenzoyl(bibenzyl)[2j] by oxidation with activated manganese(IV) oxide. As shown in Scheme 1 conventional irradiation of the starting compound **1** leads to the hydrocarbons **7**–**9**[6] and to small yields of the novel cyclic azine **10**, which is formed via an intramolecular carbene addition to the remaining diazo group of **2**. The formation of the hydrocarbons **7**–**9** can be readily

[*] Dr. K. Hannemann [+], Prof. Dr. J. Wirz
Institut für Physikalische Chemie der Universität
Klingelbergstrasse 80, CH-4056 Basel (Switzerland)
[+] New address: Ciba-Geigy AG—K410.4.02—
Postfach, CH-4002 Basel (Switzerland)

[**] This work was supported by the Fonds der Chemischen Industrie (Liebig Stipendium für *K. H.*), by the Schweizerischer Nationalfonds zur Förderung der wissenschaftlichen Forschung (Project No. 2.034-086) and by the Ciba Stiftung.

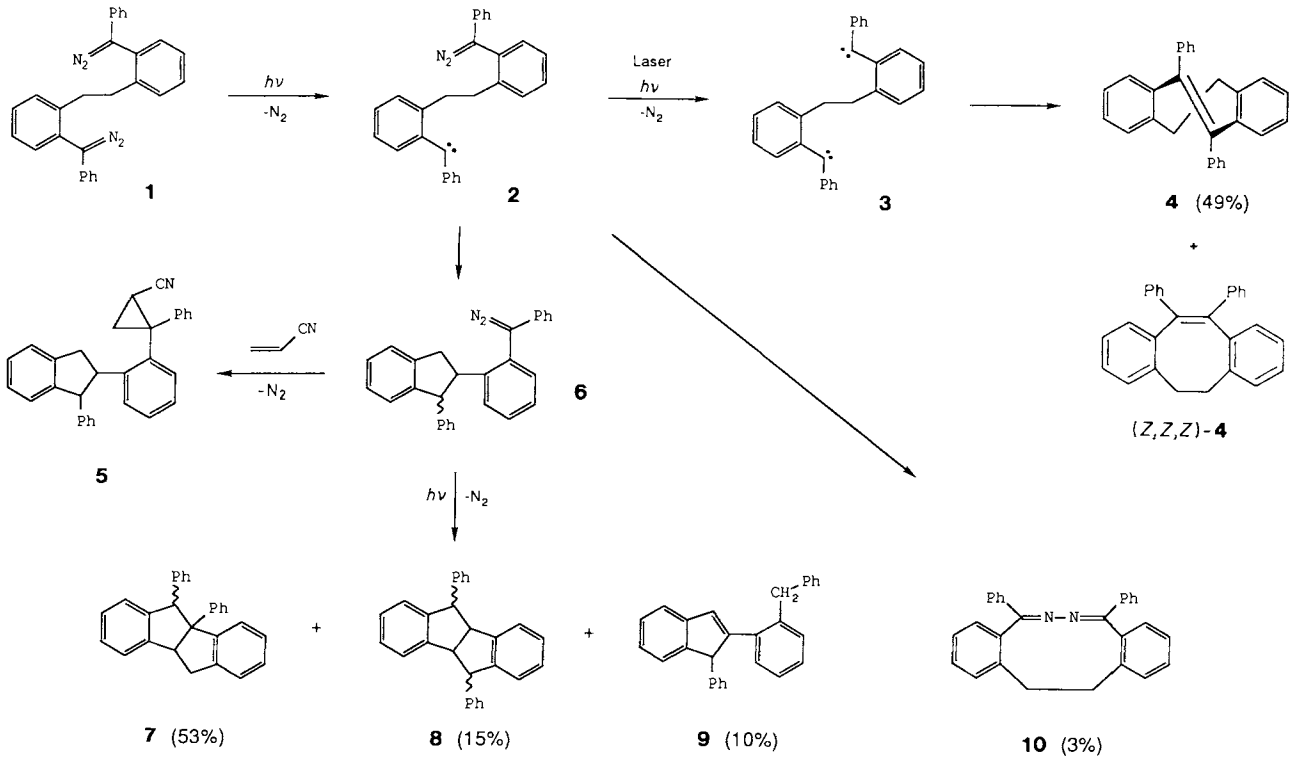

Scheme 1.

explained in terms of sequential cleavage of the diazo groups: elimination of one molecule of nitrogen leads to formation of the diazocarbene **2**, which reacts by way of an intramolecular 1,5-H abstraction[7] via a 1,5-diradical and ring closure to give the diazomethane **6**. The carbene formed from **6** by photochemical elimination of nitrogen cyclizes after a further 1,5-H abstraction to give the hydrocarbons **7** and **8**; disproportionation of **6** furnishes the indene derivative **9**. The existence of the intermediary diazomethane **6** could be demonstrated by trapping with acrylonitrile to give the cyclopropane derivative **5**.

Irradiation of the bis(diazomethane) **1** with a pulsed excimer laser at 248 nm[8] leads to formation of a new compound which is not detectable in a conventional irradiation (254 nm) experiment. The compound could be isolated in 49% yield by chromatography on silica gel and was identified as (*Z,E,Z*)-5,6-dihydro-11,12-diphenyldibenzo[*a,e*]cyclooctene **4**.[9] Control experiments showed that the cyclooctatriene **4** is not formed on laser photolysis of the photoproducts **7**–**10**. Compound **4** is already clearly detectable in the reaction mixture after a single laser pulse on the basis of its strong absorption at 365 nm; its concentration increases linearly with the number of laser pulses. The product-determining reaction steps for the formation of **4** must therefore take place within the laser pulse of 20 ns.

On the basis of the known dimerization of carbenes to olefins[10] it may be assumed that the dicarbene **3** is the precursor of the main product **4**. As could be demonstrated by time-resolved spectroscopy,[11] diphenylcarbene is formed from diphenyldiazomethane within a nanosecond. There is thus sufficient time to excite the diazocarbene **2** formed from **1** once more within the same laser pulse and thereby eliminate the second nitrogen. A thermal denitrogenation of **2** can be ruled out, since conventional photolysis furnishes no **4**. It is noteworthy that intramolecular carbene-dimerization of **3** yields primarily the isomer **4** with a *trans* double bond. (*Z,Z,Z*)-**4**[12] could be detected to the extent of 7% in the photolysis mixture by NMR spectroscopy; the possibility that **4** is formed by photochemical *cis/trans* isomerization of (*Z,Z,Z*)-**4** within a laser pulse, can, however, be ruled out, since the laser photolysis of pure (*Z,Z,Z*)-**4** furnishes far less of the (*Z,E,Z*)-compound **4** than does photolysis of the bis(diazomethane) **1** under the same conditions. As other photochemical studies have already shown,[13] the conformation of an intermediate can decisively influence the further course of the reaction. The biscarbene **3** could exist in a conformation which strongly favors the reaction leading to the (*Z,E,Z*)-olefin **4**. Moreover, it can be assumed that the dimerization of two triplet carbenes does not lead directly to the ground state of the olefin, but mainly proceeds via its triplet state. From molecular models it can be deduced that a hypothetical triplet state twisted by 90° is geometrically more similar to the (*Z,E,Z*)-olefin in the ground state than to the (*Z,Z,Z*)-olefin. We presume, therefore, that a deactivation of the triplet state preferably leads to the (*Z,E,Z*)-isomer **4**.

As we have shown here, the high light intensity of the laser light fundamentally changes the photochemical behavior of the dichromophoric bis(diazomethane) **1**. The main product **4**, the first (*Z,E,Z*)-cyclooctatriene derivative, is preparatively accessible in good yields by laser photolysis.

Received: February 22, 1988 [Z 2627 IE]
German version: *Angew. Chem. 100* (1988) 880

CAS Registry numbers:
1, 114491-62-2; **3**, 114491-64-4; **4** (*Z,E,Z*), 114491-65-5; **4** (*Z,Z,Z*), 114504-92-6; **7**, 67784-51-4; **8**, 67761-48-2; **9**, 114491-66-6; **10**, 114491-67-7; bishydrazone of *o,o'*-dibenzoyl-(bibenzyl), 114491-63-3.

[1] Reviews: a) S. Kimel, S. Speiser, *Chem. Rev. 77* (1977) 437; b) J. I. Steinfeld: *Laser Induced Chemical Processes*, Plenum Press, New York 1981; c) V. S. Letokhov: *Nonlinear Laser Chemistry*, Springer, Berlin 1983; d) W. M. Jackson, A. B. Harvey (Eds.): *Lasers as Reactants and Probes in Chemistry*, Howard University Press, Washington, DC 1985; e) J. C. Scaiano, L. J. Johnston, W. G. McGimpsey, D. Weir, *Acc. Chem. Res. 21* (1988) 22.

[2] a) N. J. Turro, M. Aikawa, J. A. Butcher, Jr., G. W. Griffin, *J. Am. Chem. Soc. 102* (1980) 5127; b) M. Zandomeneghi, M. Cavazza, L. Moi, F. Pietra, *Tetrahedron Lett. 21* (1980) 213; c) V. Malatesta, C. Willis, P. A. Hackett, *J. Org. Chem. 47* (1982) 3117; d) F. Lemaire, R. Stringat, C. Bertaina, R. Fellous, *Tetrahedron Lett. 27* (1986) 5847; e) G. Kaupp, J. A. Döhle, *Angew. Chem. 98* (1986) 814; *Angew. Chem. Int. Ed. Engl. 25* (1986) 828; f) W. G. McGimpsey, J. C. Scaiano, *J. Am. Chem. Soc. 109* (1987) 2179; g) L. J. Johnston, J. C. Scaiano, *ibid. 109* (1987) 5487; h) J. C. Scaiano, P. J. Wagner, *ibid. 106* (1984) 4626; i) L. J. Johnston, J. C. Scaiano, *ibid. 108* (1986) 2349; j) R. M. Wilson, K. Hannemann, K. Peters, E.-M. Peters, *ibid. 109* (1987) 4741.—For examples of preparative studies exploiting the monochromaticity of the laser, see [3].

[3] a) V. Malatesta, C. Willis, P. A. Hackett, *J. Am. Chem. Soc. 103* (1981) 6781; b) R. M. Wilson, S. W. Wunderly, T. F. Walsh, A. K. Musser, R. Outcalt, F. Geiser, S. K. Gee, W. Barbender, L. Yerino, Jr., T. T. Conrad, G. A. Tharp, *ibid. 104* (1982) 4429, and references cited therein; c) W. Adam, U. Kliem, V. Lucchini, *Tetrahedron Lett. 27* (1986) 2953; d) W. Adam, K. Hannemann, R. M. Wilson, J. Am. Chem. Soc. 108 (1986) 929, and references cited therein.

[4] a) J. A. Butcher, Jr., H. R. Hinz, N. Tsou, S. Shah, *Tetrahedron Lett. 25* (1984) 5483; b) W. Adam, K. Hannemann, E.-M. Peters, K. Peters, H. G. von Schnering, R. M. Wilson, *Angew. Chem. 97* (1985) 417; *Angew. Chem. Int. Ed. Engl. 24* (1985) 421.

[5] **1**: red needles, m.p. 117–119°C (decomp., hexane); ^{1}H-NMR ($CDCl_3$): $\delta = 2.81$ (s, 4H), 6.77–7.03 (m, 4H), 7.04–7.15 (m, 2H), 7.15–7.45 (m, 12H); ^{13}C-NMR ($CDCl_3$): $\delta = 34.76$ (t), 59.16 (s), 122.41 (d), 123.97 (d), 127.06 (s, d), 128.98 (d), 129.11 (d), 130.31 (d), 131.84 (s, d), 142.30 (s); UV (hexane): $\lambda(\lg\varepsilon)$ 285 (4.56), 510 (2.20) nm.

[6] The yields in Scheme 1 refer to the compounds isolated by chromatography. All the new compounds were fully characterized.

[7] A 1,5-hydrogen abstraction via a favorable six-membered transition state is preferred over a 1,4-abstraction; a) C. D. Gutsche, H. E. Johnson, *J. Am. Chem. Soc. 77* (1955) 5933; b) T. A. Baer, C. D. Gutsche, *ibid. 93* (1971) 5180.

[8] A Lambda Physik EMG 101 MSC excimer laser (KrF, 20 ns, 200 mJ per pulse) was at our disposal. 50 mL of a degassed 3×10^{-3} M solution of **1** in benzene was irradiated for 12 min at 10 Hz repetition frequency.

[9] (*Z,E,Z*)-5,6-Dihydro-11,12-diphenyldibenzo[*a,e*]cyclooctene **4**: yellow crystals, m.p. 173–174°C (EtOH); ^{1}H-NMR ($CDCl_3$): $\delta = 2.82$, 2.91 (AA'BB', $J = 9.8$, −16.5, 0.6, 9.4 Hz, $-CH_2-CH_2-$), 6.91 (d, $J = 7.7$ Hz, 2 arom. H), 7.05 (m, 6 arom. H), 7.13 (m, 6 arom. H), 7.23 (t, $J = 7.3$ Hz, 2 arom. H), 7.44 (d, $J = 7.3$ Hz, 2 arom. H); ^{13}C-NMR ($CDCl_3$): $\delta = 33.91$ (t), 126.43 (d), 127.27 (d), 127.34 (d), 127.90 (d), 130.42 (d), 130.86 (d), 131.89 (d), 143.59 (s), 144.79 (s), 146.22 (s), 146.57 (s); UV (hexane): $\lambda(\lg\varepsilon) = 363$ (4.16), 265 (4.25), 247 (4.20).—The structure of **4** could be unequivocally confirmed by an X-ray structure analysis (*A. Riesen*, Institut für Anorganische Chemie der Universität Basel). Structural data: K. Hannemann, J. Wirz, A. Riesen, *Helv. Chim. Acta*, in press.

[10] a) W. Kirmse: *Carbene Chemistry*, 2nd Edit., Academic Press, New York 1971; b) M. Jones, Jr., R. A. Moss (Eds.): *Carbenes*, Wiley, New York 1973.

[11] a) K. B. Eisenthal, N. J. Turro, E. V. Sitzmann, I. R. Gould, G. Hefferon, J. Langan, Y. Cha, *Tetrahedron 41* (1985) 1543; b) D. Griller, A. S. Nazran, J. C. Scaiano, *Acc. Chem. Res. 17* (1984) 283; c) *Tetrahedron 41* (1985) 1525.

[12] (*Z,Z,Z*)-**4** was prepared via an independent route for comparison purposes. Whether it is formed directly form **3** or by isomerization of **4** cannot be decided on the basis of the available data.

[13] a) J. C. Scaiano, *Tetrahedron 38* (1982) 819, and references cited therein; b) Y. Ito, T. Matsuura, *J. Am. Chem. Soc. 105* (1983) 5237.

Reduction of Epoxides, α,β-Unsaturated Aldehydes, and Vicinal Diketones with "Reactive Titanocene"

By *Rainer Schobert**

When titanocene dichloride **1** is reduced with one equivalent of magnesium in tetrahydrofuran under argon, deep-green solutions are formed which according to *Brintzinger* et al.[1] and *van Tamelen* et al.[2] contain THF adducts of "reactive titanocene" $[Cp_2Ti]_{1-2}$. These solutions, which decompose within a few hours to brown titanocene alkoxide complexes, have been intensively investigated with regard to their suitability as nitrogen and hydrogen activators[4,5] in the same way as the hydrido species obtainable from **1** with other reducing agents and solvents.[3] *Rausch* and *Herberhold* et al.[6] recently developed a convenient method for the in situ synthesis of stable titanocene derivatives using **1**, magnesium, and an excess of ligand.

As can be seen in Table 1 it has now been found that such solutions of "reactive titanocene" in tetrahydrofuran deoxygenate equivalent amounts of epoxides **2** smoothly and in high yields to the alkenes **3**. *trans*-Epoxides lead exclusively to *trans*-alkenes, *cis*-epoxides furnish predominantly *cis*-alkenes. Even sensitive epoxides such as 2-methyl-2-phenyloxirane **2e**, which form only little olefin with other reducing agents,[7] react here in satisfactory yields.

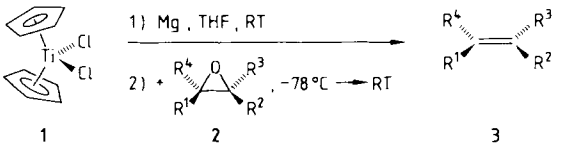

Table 1. Alkenes **3** by reduction of epoxides **2** with "reactive titanocene".

	R^1	R^2	R^3	R^4	Yield [%] [a]	*E/Z* [b]
a	C_6H_5	H	H	H	95	—
b	*n*-C_5H_{11}	H	H	H	92	—
c	$C_6H_5OCH_2$	H	H	H	90	—
d	$H_2C{=}C(Me)COOCH_2$	H	H	H	87	—
e	C_6H_5	H	H	CH_3	60[c]	—
f	CH_3	CH_3	H	CH_3	94	—
g	$-(CH_2)_4-$		H	H	89	—
h	C_6H_5	H	C_6H_5	H	96	100/0
i	*n*-C_5H_{11}	H	CH_3	H	93	100/0
j	*n*-C_5H_{11}	CH_3	H	H	89	20/80
k	*n*-C_7H_{15}	CH_3	H	H	90	23/77
l	$Me_2CH(CH_2)_4$	*n*-$C_{10}H_{21}$	H	H	94	19/81

[a] Based on purified, isolated product. [b] Gas chromatographically determined isomeric ratio. [c] 20% 2-phenylpropanal as by-product when reduced at −78°C; 24% cumol as by-product when reduced at 20°C.

Many methods described hitherto for the synthesis of alkenes by reduction of epoxides use either non-stereoselective reducing agents such as titanium(III) chloride/$LiAlH_4$,[7] zinc/copper couple,[8] sodium amalgam/transition-metal complex,[9] magnesium amalgam,[10] or are evidenced by only a single example, such as the reduction with dibenzenetitanium[11] or triphenylphosphane selenide.[12] Zinc bromide/phosphorus oxide chloride,[13] tungsten(VI) chloride/alkyllithium,[14] alkali metal (dicarbonylcyclopentadienyl)ferrate,[15] iron(III) chloride/butyllithium,[16] lithium diphenylphosphane,[17] and chromium(II) perchlorate/ethylenediamine[18] have proven to be good stereoselective reducing agents.

Under the conditions described here, both simple carbonyl functions, esters, olefins as well as ethers and acetals are inert. Saturated aldehydes are reduced to the alcohols only after 24 h at room temperature without coupling products being formed. α,β-Unsaturated aldehydes **4**, however, react rapidly at −78°C to give the corresponding vicinal bis(allyl alcohols) **5**, which are formed as a diastereomeric mixture with a diastereomeric excess of 30% in favor of the *threo*-racemates.[19] At room temperature, **4** is

[*] Dr. R. Schobert
Institut für Organische Chemie der Universität Erlangen-Nürnberg
Henkestrasse 42, D-8520 Erlangen (FRG)

reduced to the bis(allyl) ethers **6**. Presumably the initially formed radical allyloxytitanium species is so stable at low temperatures that it can dimerize with formation of pinacol, whereas at room temperature the rapid reaction with free aldehyde with CO-bond formation and deoxygenation is preferred (Scheme 1).

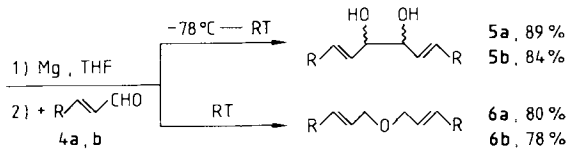

Scheme 1. **a**: $R=CH_3$; **b**: $R=n\text{-}C_3H_7$. Compound **6b** is new; b.p. 50 °C/0.1 torr. Structure proven on the basis of ^{1}H-NMR and GC/MS spectra; correct elemental analyses were obtained.

Vicinal diketones **7** react rapidly with "reactive titanocene" in tetrahydrofuran at room temperature to give deep-green chelate complexes **8**,[20] which, as shown in Scheme 2, furnish: acyloins **9** on work-up with trimethylchlorosilane/water; surprisingly and so far unexplainably saturated monoketones **10** upon treatment with anhydrous hydrogen chloride; and vinylene carbonates **11** on treatment with phosgene. In all cases **1** can be re-formed quantitatively.

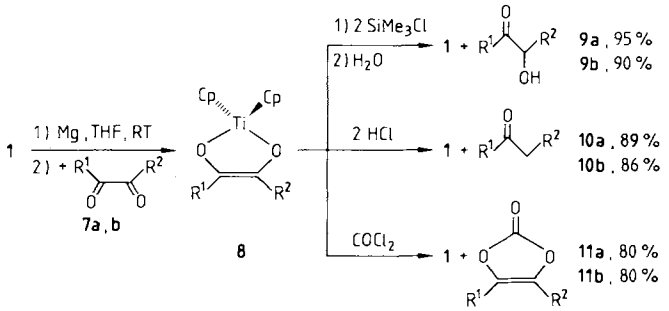

Scheme 2. **a**: $R^1=R^2=C_6H_5$; **b**: $R^1=C_6H_5$, $R^2=C_6H_5CH_2$. Compound **11b** is new, b.p. 111 °C/0.04 torr. Confirmation of structure based on ^{1}H-NMR and GC/MS spectra; correct elemental analyses were obtained.

Further investigations with difunctional carbonyl compounds are presently under way.

Experimental

3: A suspension of **1** (2.49 g, 10 mmol) and magnesium (0.24 g, 10 mmol) in 50 mL of anhydrous tetrahydrofuran was stirred at room temperature until a clear deep-green solution was formed. This was cooled to −78 °C and treated dropwise with a solution of 10 mmol of **2** in 20 mL of tetrahydrofuran. After allowing to stand for 12 h at room temperature and evaporation of the solvent, the residue was filtered through 20 g of silica gel with 200 mL of hexane/ether (1/1) and the filtrate purified by distillation or recrystallization.

Received: February 5, 1988;
revised: March 15, 1988 [Z 2608 IE]
German version: *Angew. Chem. 100* (1988) 869

[1] J. E. Bercaw, R. H. Marvich, L. G. Bell, H. H. Brintzinger, *J. Am. Chem. Soc. 94* (1972) 1219.
[2] E. E. van Tamelen, W. Cretney, N. Klaentschi, J. S. Miller, *J. Chem. Soc. Chem. Commun. 1972*, 481.
[3] M. E. Vol'pin, A. A. Belyi, V. B. Shur, Y. I. Lyakhovelskii, R. V. Kudryartsev, N. N. Bubnov, *J. Organomet. Chem. 27* (1971) C5.
[4] E. E. van Tamelen, H. Rudler, *J. Am. Chem. Soc. 92* (1970) 5253.
[5] E. Bayer, V. Schung, *Chem. Ber. 102* (1969) 3378.
[6] a) L. B. Kool, M. D. Rausch, H. G. Alt, M. Herberhold, U. Thewalt, B. Wolf, *Angew. Chem. 97* (1985) 425; *Angew. Chem. Int. Ed. Engl. 24* (1985) 394; b) L. B. Kool, M. D. Rausch, H. G. Alt, M. Herberhold, U. Thewalt, B. Honold, *J. Organomet. Chem. 310* (1986) 27.
[7] J. E. McMurry, M. G. Silvestri, M. P. Fleming, T. Hoz, M. W. Grayston, *J. Org. Chem. 43* (1978) 3249.
[8] S. M. Kupchan, M. Maruyama, *J. Org. Chem. 36* (1971) 1187.
[9] M. Berry, S. G. Davies, M. L. H. Green, *J. Chem. Soc. Chem. Commun. 1978*, 99.
[10] F. Bertini, P. Grasselli, G. Zubiani, G. Cainelli, *Chem. Commun. 1970*, 144.
[11] H. Ledon, I. Ikatchenko, D. Young, *Tetrahedron Lett. 1979*, 173.
[12] D. L. J. Clive, C. V. Denyer, *J. Chem. Soc. Chem. Commun. 1973*, 253.
[13] J. W. Cornforth, R. H. Cornforth, K. K. Mathew, *J. Chem. Soc. 1959*, 112.
[14] K. B. Sharpless, M. A. Umbreit, M. T. Nieh, T. C. Flood, *J. Am. Chem. Soc. 94* (1972) 6538.
[15] W. P. Giering, M. Rosenblum, J. Tancrede, *J. Am. Chem. Soc. 94* (1972) 7170.
[16] T. Fujisawa, K. Sugimoto, H. Ohta, *Chem. Lett. 1974*, 883.
[17] E. Vedejs, P. L. Fuchs, *J. Am. Chem. Soc. 93* (1971) 4070.
[18] J. R. Hanson, *Synthesis 1974*, 1.
[19] Determined by 400-MHz ^{1}H-NMR analysis. According to a comparison with an authentic *threo/erythro* isomeric mixture the resonance of the proton in the α-position to the hydroxy group in the *threo* isomer lies at 0.2 ppm higher field than that of the corresponding proton in the *erythro* isomer. For the pinacolization of α,β-unsaturated aldehydes cf. also Y. Handa, J. Inanaga, *Tetrahedron Lett. 28* (1987) 5717.
[20] Cf. C. Floriani, G. Fachinetti, *J. Chem. Soc. Chem. Commun. 1972*, 790.

A Novel Tetranuclear Copper(I) Cluster with Alternate Bridging Halide and Triazolopyrimidine Ligands**

By *Jaap G. Haasnoot,* T. Loek F. Favre, Winfried Hinrichs,* and *Jan Reedijk*

The ligand 5,7-dimethyl[1,2,4]triazolo[1,5-*a*]pyrimidine (dmtp) has three potential donor atoms. Coordination through the sterically least hindered N3 nitrogen is normally observed,[1] and it appears that the two methyl groups prevent coordination through the other two nitrogens. Only recently has a coordination through N1 been observed[2] in derivative ligands without the methyl substituent at C7. In this communication coordination through the sterically unfavorable N4 is reported.

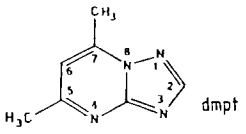

In principle, one could expect coordination through both N3 and N4, in a way similar to the coordination found in dimeric copper(II) species like **1**[3] and in the well-known copper(II)-adenine compounds like **2**.[4] Nevertheless, various attempts with several copper(II) salts yielded only compounds with N3 coordination.[5]

$[Cu_2(1,8\text{-naphthyridine})_2Cl_4]$ **1**

$[Cu_2(ade)_4Cl_2]Cl_2\cdot 6H_2O$ **2**

$[Cu_4(dtmp)_4Cl_2]^{2\oplus}[Cu_2Cl_4]^{2\ominus}$ **3**

[*] Dr. J. G. Haasnoot, T. L. F. Favre, Dr. W. Hinrichs, [+], Prof. Dr. J. Reedijk
Department of Chemistry, Gorlaeus Laboratories, Leiden University
P.O. Box 9502, NL-2300 RA Leiden (The Netherlands)
[+] Present address:
Fachbereich Chemie, Institut für Kristallographie der Freie Universität
Takustrasse 6, D-1000 Berlin 33

[**] The authors are indebted to Dr. *R. Prins* and Mr. *M. J. Suijker* for valuable contributions to this work.

However, when copper(II) chloride was used and allowed to react with dmtp at elevated temperature in ethanol a product **3** of composition $[Cu(dmtp)_{2/3}Cl]$ was obtained.[6] The same product could be obtained directly, starting from CuCl. According to an X-ray structure analysis,[7] **3** consists of a unique tetranuclear cation and the rare anion di(μ-chloro)dichlorodicuprate(I) (Fig. 1). In the

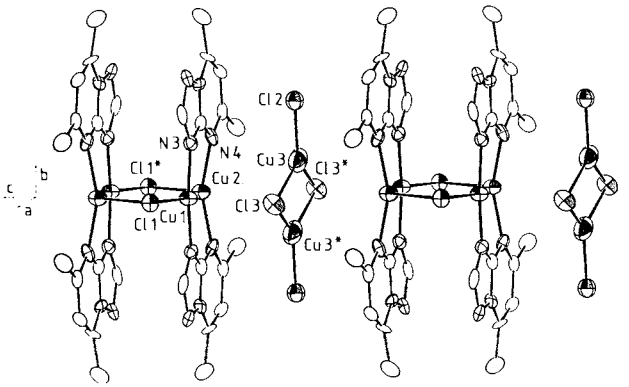

Fig. 1. Structure of $[Cu_4(dmtp)_4Cl_2]^{2\oplus}[Cu_2Cl_4]^{2\ominus}$ **3** in the crystal (ORTEP plot, view on the *bc*-plane). * denotes symmetry-related atoms [7].

cation two $Cu_2(dmtp)_2$ units are bridged by two chloro ligands. The distance between the N-C-N-bridged Cu atoms in the $Cu_2(dmtp)$ units (290.9 pm) is significantly larger than the Cu···Cu distance in other oligonuclear Cu(I) compounds with comparable bridges. For instance, in $[Cu_4(6\text{-methylpyridin-2-olate})_4]$, N-C-O bridge 266–271 pm;[8] in $[Cu_4(MeN_3Me)_4]$, N-N-N bridge 264–268 pm.[9] This enlargement can be attributed to the geometrical demands of the annelated triazole ring, by which its coordinating electron pair is directed away from the pair of the pyrimidine ring. The same effect is found on comparing the $Cu^{II}\cdots Cu^{II}$ distances in acetate bridges (258–262 pm[10]) or in the N-C-N bridge of **1** (266 pm[3]) with those in adenine bridges (cf. **2**, ca. 300 pm[4]).

The distance between the chloride-bridged Cu atoms of the cation, which with 310.7 pm lies in the usual range for Cu^{I}-Cl-Cu^{I} bridges, may be influenced by intraionic stacking interactions of the dmtp ligands.

The Cu···Cu distance in the anionic Cu-Cl-Cu bridge is only 243.3 pm, which is extremely short and only comparable with the bridges in polymeric copper iodides like $[NMe_4][Cu_2I_3]$.[11] All Cu-Cl bonding distances match those of an earlier observation,[12] a difference occurring only in the Cl-Cu-Cl endocyclic angle (118.2° in the present case and 96.8° in the reported one). It is possible that packing effects on the exocyclic chloride distort the ring angle and thus indirectly influence the anionic Cu···Cu distance (Fig. 1). All metal-to-ligand distances lie in the range expected for copper(I) compounds.[13]

The dmtp ligands are arranged in pairs of parallel planes. The distance between these planes within a pair corresponds to the distance between the almost parallel ligands in the cations (320 pm). This means that stacking effects of the rings contribute to the stability of the structure. The packing between the pairs of ligand planes is through contacts via layers of anions; the exocyclic chlorides are thereby "sandwiched" between dmtp ligands (the distance between the anion plane and dmtp plane is 337 pm). No other close contacts have been found.

The dianion $[Cu_2Cl_4]^{2\ominus}$, a member of a series of polynuclear copper(I) chloride anions,[14] has hitherto only been prepared[2] as the anion of the likewise very large cation $[VO(salen)(H_2O)]^{\oplus}$; it is the chloride analogue of $[Cu_2Br_4]^{2\ominus}$[15] and $[Cu_2I_4]^{2\ominus}$.[16]

The cation could also be crystallized with other anions. Under slightly different experimental conditions, yellow needles of the composition $[Cu(dmtp)_{1/2}Cl]$ (Cu, Cl, C, H, N analysis) were obtained. As the IR spectrum of this product is nearly identical to that of **3**, the composition **4** (or **4** with $\{[Cu_2Cl_3]^{\ominus}\}_2$ as anion) is proposed for this product.

$[Cu_4(dmtp)_4Cl_2]^{2\oplus}[Cu_4Cl_6]^{2\ominus}$ **4**

$[Cu_4(dmtp)_4Cl_2]^{2\oplus}[PtCl_4]^{2\ominus}$ **5**

Addition of $K_2[PtCl_4]$ in water to a solution of **3** gave an orange precipitate whose elemental analysis (Cu, C, H, N, Cl, and Pt) is consistent with the composition **5**. The IR spectrum of **5** is likewise identical to that of **3**, apart from in the FIR region where the absorption of the $[PtCl_4]^{2\ominus}$ ion is obvious.

The compounds **3**, **4**, and **5** appear to be quite stable on exposure to air; no change in crystal habit is observed upon storage in open vessels for several months. Oxidation to copper(II) compounds is observed, however, after several days in water/ethanol solutions. Addition of L-ascorbic acid stabilizes the copper(I) state.

Starting from CuBr or CuI and dmtp, substances of the composition $[Cu(dmtp)_{1/2}X]$ (X = Br, I) could be obtained, the IR spectra of which are almost identical to those of the analogous chloride; we therefore suppose that it likewise has tetranuclear cations.

The compounds described here add to the great variety of structural types for copper(I) clusters and illustrate once more the extensive coordinating properties of (de)azapurines, the study of which is of major importance to bioinorganic chemistry.

Received: February 24, 1988 [Z 2633 IE]
German version: *Angew. Chem. 100* (1988) 884

[1] J. Dillen, A. T. H. Lenstra, J. G. Haasnoot, J. Reedijk, *Polyhedron 2* (1983) 195.
[2] M. Biagini-Cinqui, A. M. Manotti-Lanfredi, A. Tiripicchio, J. P. Cornelissen, J. G. Haasnoot, J. Reedijk, *Inorg. Chim. Acta 127* (1987) 189.
[3] C. Mealli, F. Zanobini, *J. Chem. Soc. Chem. Commun. 1982*, 97.
[4] P. de Meester, A. C. Skapski, *J. Chem. Soc. A 1971*, 2167.
[5] T. L. F. Favre, J. G. Haasnoot, J. Reedijk, *Polyhedron 5* (1986) 1405.
[6] **3**: A solution of $CuCl_2 \cdot 2H_2O$ (359 mg, 2 mmol) in ethanol (50 mL) was treated at 75°C with dmtp (592 mg, 4 mmol) in boiling ethanol (30 mL). After cooling to 30°C the solution turned light green, and orange crystals started to separate. Any green precipitate was dissolved by briefly boiling in ethanol. The crystals were collected by filtration.
[7] **3**, crystal dimensions $0.18 \times 0.08 \times 0.10$ mm, space group $C2/m$, $a = 1202.0(3)$, $b = 1650.5(9)$, $c = 992.0(7)$ pm, $\beta = 104.31(4)°$, $V = 1901.9 \times 10^6$ pm^3, $Z = 2$. Enraf-Nonius CAD-4 diffractometer ($Mo_{K\alpha}$, graphite), $T = 115$ K, $\omega/2\theta$ scan, $2° \leq \theta \leq 24°$, 752 independent reflections with $I > 2\sigma(I)$, 801 with $I < 2\sigma(I)$, $F(000) = 590.3$. Combined Patterson and direct methods and subsequent difference Fourier methods, anisotropic refinement, hydrogen atoms by difference Fourier methods, coupled symmetrically to parent C at 96 pm and refined with one overall isotropic thermal parameter to $R(R_w) = 0.046$ (0.039); programs used SHELX-76, MULTAN. Selected distances [pm] and angles [°], cation: Cu1-Cl1 243.3(4), Cu1-N3 191.8(8), Cu2-Cl1* 245.8(4), Cu2-N4 196.5(8); anion: Cu3-Cl2 211.6(5), Cu3-Cl3 236.9(4), Cl2-Cu3-Cl3 120.90(8), Cl3-Cu3-Cl3* 118.2(1), Cu3-Cl3-Cu3* 61.8(1). Further details of the crystal structure determination are available on request from the Fachinformationszentrum Energie, Physik, Mathematik GmbH, D-7514 Eggenstein-Leopoldshafen 2 (FRG), on quoting the depository number CSD-53129, the names of the authors, and the journal citation.

[8] M. Berry, W. Clegg, C. D. Garner, I. H. Hillier, *Inorg. Chem. 21* (1982) 1342.
[9] J. E. O'Connor, G. A. Janusonis, E. R. Corey, *Chem. Commun. 1968*, 445.
[10] V. M. Rao, H. Manohar, *Inorg. Chim. Acta 34* (1979) L213.
[11] S. Andersson, S. Jagner, *Acta Chem. Scand. A 39* (1985) 181, and references cited therein.
[12] L. Banci, A. Bencini, A. Dei, D. Gatteschi, *Inorg. Chim. Acta 84* (1984) L11.
[13] B. J. Hathaway in G. Wilkinson (Ed.): *Comprehensive Coordination Chemistry, Vol. 5*, Pergamon Press, Oxford 1987, Chap. 53, p. 551.
[14] S. Andersson, S. Jagner, *Acta Chem. Scand. A 40* (1986) 52.
[15] S. Andersson, S. Jagner, *Acta Chem. Scand. A 39* (1985) 423.
[16] M. Asplund, S. Jagner, *Acta Chem. Scand. A 38* (1984) 411.

Synthesis of Peptides Containing (*S*)-α-Methylserine**

By *Eva Altmann, Karl-Heinz Altmann*, and *Manfred Mutter**

A large number of chiral α-alkyl-α-amino acids have become accessible by asymmetric synthesis during the last years;[1a,b] however, only a few attempts have been made to incorporate such potential helix-inducing residues into peptides.[2–4]

Our ongoing studies on the design and synthesis of artificial proteins[5a,b] made it highly desirable to have access to a *hydrophilic* helix-inducing amino acid; consequently, we have directed our interest to the chemistry of α-methylserine. Herein we report on the solution synthesis of (*S*)-α-methylserine(α-MeSer)-containing peptides without side chain protection, and on the synthesis of H-α-MeSer(O*t*Bu)-OH as a key intermediate in the future synthesis of larger α-MeSer-peptides.

H-α-MeSer **1** was synthesized according to the procedure of *Seebach* et al.;[1a,6,7] for its use in peptide synthesis, **1** was converted into the methyl ester hydrochloride HCl·H-α-MeSer-OMe **2**.

Table 1. Yields and melting points of α-MeSer-containing peptides [a].

Peptide	Yield [%]	M.p. [°C]
Boc-Ala-α-MeSer-OMe **3**	56	113.7–114.2
Boc-Val-α-MeSer-OMe **4**	55	104.0–107.0
Z-Ala-α-MeSer-OMe **5**	58	oil
Boc-Ala-α-MeSer-OH **6** [b]	90	162.3–163.8
Z-Ala-α-MeSer-OH **7** [b]	92	136.2–137.9

[a] Typical reaction conditions for the preparation of methyl esters **3**–**5**: 2.5 mmol of N_α-protected amino acid; 2.4 mmol of **2**; 2.6 mmol BOP; 5 mmol DIPEA, 35 mL DMF, RT, 15 h. [b] **6** and **7** were obtained by alkaline saponification of **3** and **5**, respectively.

The dipeptide methyl esters **3**–**5** (Table 1) were obtained by BOP (benzotriazol-1-yloxytris(dimethylamino)hexafluorophosphate)[8] mediated couplings of N_α-Boc (*tert*-butyloxycarbonyl) or Z (benzyloxycarbonyl) protected Val or Ala with **2** in DMF with DIPEA (diisopropylethylamine) as neutralizing base. The yields varied between 55% and 58% after chromatographic purification and subsequent crystallization (except for **5**, which could not be crystallized). In contrast, preactivation of Boc-Ala-OH with DCC/HOBt (*N,N'*-dicyclohexylcarbodiimide/1-hydroxybenzotriazole)[9] (1 h at 0°C, 1 h at RT) provided **3** in only 37% yield.

Alkaline saponification (2.5 h, RT) of **3** and **5** with 2 equivalents of NaOH in MeOH provided the corresponding acids **6** and **7** in excellent yields and crystalline form. Boc-cleavage (1.2 N HCl/AcOH, 0.5 h, RT) from **3** and reaction with Boc-Ala-Ala-OH (DCC/HOBt activation) afforded the tetrapeptide Boc-Ala-Ala-Ala-α-MeSer-OMe **8** in 37% yield after chromatographic purification and crystallization from acetone/ether (m.p. 164–165.1°C).

In contrast to the synthesis of peptides in solution, side chain protection of α-MeSer becomes mandatory for its use in polymer supported peptide synthesis.[10] We have therefore explored the synthesis of the side chain protected derivative H-α-MeSer(O*t*Bu)-OH **12**, which is of particular importance in the stepwise synthesis of peptides according to the Fmoc/*t*Bu strategy.[11] **12** represents the key intermediate for the synthesis of Fmoc-α-MeSer(O*t*Bu)-OH and of protected dipeptides of the type Fmoc-Xxx-α-MeSer(O*t*Bu)-OH (Xxx, any amino acid).[12] The synthesis of **12** was accomplished in four steps (starting from **1**) in an overall yield of 42% (Scheme 1), similarly to the synthetic scheme developed by *Wünsch* and *Jentsch* for the synthesis of *tert*-butyl ethers of common hydroxy α-amino acids.[14]

Studies on the conformational properties of α-MeSer containing peptides[15] synthesized by the techniques outlined here indicate that this residue exerts a helix inducing effect, thus representing a valuable building block in the design of new proteins.[5]

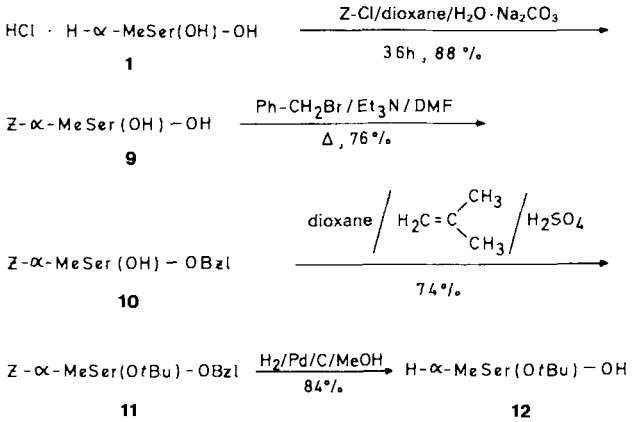

Scheme 1. Synthesis of **12** from **1**.

Experimental

Reaction of (*S*)-α-MeSer with benzyl chloroformate afforded the N_α-Z-protected derivative **9** (88%, oil, $[\alpha]_D^{25} = +8.4°$, $c = 2$ in $CHCl_3$), esterification of which with benzyl bromide in DMF furnished the benzyl ester **10** (76%, oil, $[\alpha]_D^{25} = +13.6°$, $c = 2$ in $CHCl_3$). This was converted into the fully protected derivative **11** by reaction with isobutene/H_2SO_4 in CH_2Cl_2 (74%, m.p. 50.0–51.7°C ($CHCl_3$/pentane), $[\alpha]_D^{25} = +10.0°$, $c = 0.2$ in $CHCl_3$). Simultaneous removal of the Z and benzyl ester moieties from **11** by catalytic hydrogenation over 10% Pd/C in MeOH provided the desired compound **12** as hemihydrate in 84% yield (m.p. 230°C (decomposition) (MeOH/Et_2O), $[\alpha]_D^{25} = +2.7$, $c = 0.4$ in MeOH, $[\alpha]_D^{25} = +1.7$, $c = 0.41$ in H_2O).

Received: February 9, 1988 [Z 2613 IE]
German version: *Angew. Chem. 100* (1988) 855

[*] Prof. Dr. M. Mutter, Dr. E. Altmann, [+], Dr. K.-H. Altmann [+]
Institut für Organische Chemie der Universität
St.-Johanns-Ring 19, CH-4056 Basel (Switzerland)
[+] Present address:
Baker Laboratory of Chemistry, Cornell University
Ithaca, NY 14853 (USA)

[**] This work was supported by the Swiss National Science Foundation. We are also indebted to Prof. *W. A. König*, Hamburg, for performing the gaschromatographic analysis of the optical purity of (*S*)-α-MeSer.

CAS Registry numbers:
1, 114396-62-2; **2**, 114396-63-3; **3**, 114396-64-4; **4**, 114396-65-5; **5**, 114396-66-6; **6**, 114396-67-7; **7**, 114396-68-8; **8**, 114396-69-9; **9**, 114396-70-2; **10**, 114396-71-3; **11**, 114396-72-4; **12**, 114396-73-5; Boc-Ala-OH, 15761-38-3; Boc-Val-OH, 13734-41-3; Boc-Ala-Ala-OH, 27317-69-7; Z-Ala-OH, 1142-20-7.

[1] a) D. Seebach, R. Imwinkelried, T. Weber in R. Scheffold (Ed.): *Modern Synthetic Methods*, Vol. 4, Springer, Berlin, Heidelberg 1986, p. 165; b) U. Schöllkopf, *Top. Curr. Chem. 109* (1983) 65.

[2] F. A. Gorin, T. M. Balasubramanian, T. J. Cicero, J. Schwietzer, G. R. Marshall, *J. Med. Chem. 23* (1980) 1113.

[3] G. R. Marshall, H. E. Bosshard, N. C. E. Kendrick, J. Turk, T. M. Balasubramanian, S. M. H. Cobb, M. Moore, L. Leduc, P. Needleman in A. Loffet (Ed.): *Peptides 1976*, Editions de l'Université de Bruxelles, Brussels 1976, p. 361.

[4] T. M. Balasubramanian, A. S. Redlinski, G. R. Marshall in D. H. Rich, E. Gross (Eds.): *Peptides 1981*, Pierce Chemical Company, Rockford, USA 1981, p. 61.

[5] a) M. Mutter in G. R. Marshall (Ed.): *Peptides: Chemistry and Biology, ESCOM*, Leiden 1988, p. 349; b) M. Mutter, *Angew. Chem. 97* (1985) 639; *Angew. Chem. Int. Ed. Engl. 24* (1985) 639.

[6] D. Seebach, J. O. Aebi, M. Gander, R. Naef, *Helv. Chim. Acta 70* (1987) 1194.

[7] The synthesis was performed on a 10 g scale and (*S*)-α-methylserine had an enantiomeric purity of >99% as assessed by gas chromatographic enantiomeric analysis.

[8] B. Castro, J. R. Dormoy, B. Dourtoglou, G. Evin, C. Selve, J. C. Ziegler, *Synthesis 1976*, 751.

[9] W. König, R. Geiger, *Chem. Ber. 103* (1970) 788.

[10] G. Barany, R. B. Merrifield in E. Gross, J. Meienhofer (Eds.): *The Peptides, Vol. 2*, Academic Press, New York 1980, p. 3.

[11] A. N. Eberle, E. Atherton, A. Dryland, R. C. Sheppard, *J. Chem. Soc. Perkin Trans. 1 1986*, 361.

[12] According to our experience peptide chain elongation with α,α-dialkyl amino acids on a polymeric support should be performed by coupling protected dipeptides containing the α,α-dialkyl amino acids as the *C*-terminal residue rather than the N_α-protected α,α-dialkyl amino acid itself. This excludes any difficulties connected with couplings to the hindered *N*-terminus of this type of amino acid [13]. However, attempts to synthesize Fmoc-Ala-(*S*)-α-MeSer(O*t*Bu)-OH by *tert*-butylation of **5**, saponification of the methyl ester, removal of the Z-group by hydrogenation and reprotection with the Fmoc-group gave an overall yield of only 13% (referred to **5**), mainly due to a yield of only 20% in the *tert*-butylation step. Furthermore this strategy would require a new multistep synthesis for each individual dipeptide Fmoc-Xxx-α-MeSer-OH.

[13] M. T. Leplawy, D. S. Jones, G. W. Kenner, R. C. Sheppard, *Tetrahedron 11* (1960).

[14] E. Wünsch, J. Jentsch, *Chem. Ber. 97* (1964) 2490.

[15] M. Mutter, E. Altmann, K.-H. Altmann, K. Nebel, *Int. J. Pept. Protein Res.*, in press.

Oxidative Coupling of Racemic and of Optically Active 3,6-Di-*tert*-butylocta-1,4,7-triyne-3,6-diol

By *Fumio Toda,* Jyōji Okada,* and *Koji Mori**

The differences in behavior of racemic and optically active monomers in oligomerization and polymerization have been the subject of very few reports. One of the few exceptions has reported that the ring-size of macrolides formed by oligomerization after cationic ring-opening of 6,8-dioxabicycli[3.2.1]octan-7-one depends on whether the monomer is racemic or optically active.[1] We have now found very drastic differences in the reaction behavior of racemic and optically active 3,6-di-*tert*-butylocta-1,4,7-triyne-3,6-diol **1** upon oxidative coupling.

[*] Prof. Dr. F. Toda, J. Okada, K. Mori
Department of Industrial Chemistry, Faculty of Engineering,
Ehime University,
Matsuyama 790 (Japan)

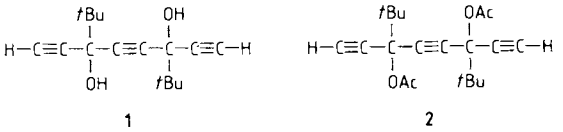

1 **2**

Scheme 1. **a**, racemic; **b**, (−)-form; **c**, (+)-form.

Racemic **1** (= **1a**) was prepared by reaction of methyl pivalate and sodium acetylide in liquid NH_3 using a method which did not furnish any *meso*-isomer.[2] Optical resolution of **1a** was carried out by a complexation method with brucine:[3,4] When a solution of **1a** (7.8 g, 32 mmol) and brucine (12.5 g, 32 mmol) in acetone (190 mL) was kept at room temperature for 12 h, a 1:1 complex of (−)-**1** (= **1b**) and brucine was formed as colorless needles (15.1 g, m.p. 183–184 °C). Decomposition of the complex with dilute HCl afforded **1b** with 94% *ee*, which on recrystallization from ether/petroleum ether furnished **1b** with 100% *ee* [1.8 g, 46%, m.p. 112–113 °C, $[\alpha]_D$ −16.0 (c = 0.3, THF)]. The optical purity of **1b** was determined by measuring the ^{1}H-NMR spectrum of its diacetate (**2b**) (Scheme 1) [m.p. 105–107 °C, $[\alpha]_D$ −7.2 (c = 0.5, THF)] in $CDCl_3$ using $Eu(hfc)_3$ as chiral shift reagent.

Oxidative coupling of **1** was carried out according to the method of *Eglinton* et al.:[5] A solution of **1a** (1 g, 4.1 mmol) and $Cu(OAc)_2 \cdot H_2O$ (12.2 g, 61 mmol) in pyridine (170 mL) was stirred at 55 °C for 4 h and at room temperature for 12 h. The reaction mixture was worked up in the usual way[5] to give a mixture of crude products, which upon treatment with acetone furnished a 1:4 complex of optically inactive cyclic dimer **3** and acetone as colorless prisms (0.31 g, 21%, m.p. > 300 °C), and upon subsequent heating in vacuo gave **3**. The cyclic structure of **3** followed

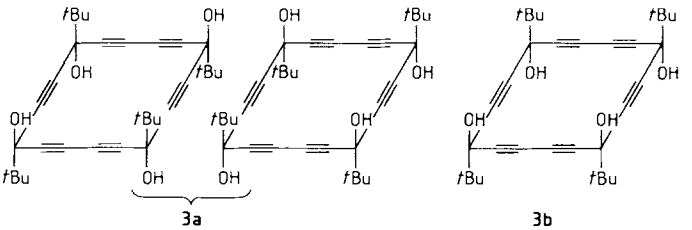

3a **3b**

from its IR spectrum, which does not show any C≡C–H stretching vibrations. The dimeric nature of **3** was ascertained indirectly from a mass spectrum of its hexadecahydrogenation product **4** (**3** is thermally too labile to measure the spectrum). On Pd/C, only the diyne units of **3** are hydrogenated—probably due to steric factors; under the same conditions **1** is hydrogenated to **5**. **3** not only forms 1:4 inclusion complexes with acetone but also with ethanol, 2-propanol, 1-butanol, dimethylformamide, and pyridine. After separation of **3** from the product mixture there remained an oily residue.

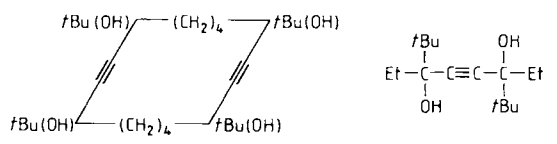

4 **5**

At present, there is no direct evidence of whether **3** is present as racemate (**3a**) or as *meso*-isomer (**3b**). Support for the *meso*-isomer is provided by the fact that optically active **1** does not give any cyclic dimer; the selective formation of **3b** shows that **1b** "recognizes" the enantiomer **1c** precisely, but does not couple with another molecule of **1b**. In contrast, the sole isolable product of the oxidative coupling of **1b** is the optically active polymer **6** [white

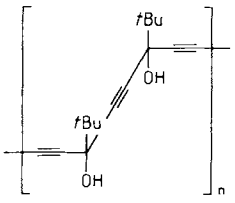

6

powder, yield 75%, m.p. >300°C, $[\alpha]_D$ −191 (c=0.2, THF)]; this polymer (M_n=16700, M_w=35300, M_z=62400, M_w/M_n=2.12, M_z/M_n=3.74) consists of about a hundred monomer units. It is not completely clear whether the high $[\alpha]_D$ value of **6** can be attributed to its asymmetric carbons or its helical structure; high $[\alpha]_D$ values of optically active polymers such as induced asymmetric polymethacrylate have been attributed to helicity.[6,7]

That polymers with a regular structure (e.g. helix) are formed only from an optically active monomer, but not from a racemic one is interesting with respect to the formation of helical polypeptides from optically active amino acids.

Received: February 8, 1988;
revised: March 16, 1988 [Z 2609 IE]
German version: *Angew. Chem. 100* (1988) 872

[1] M. Okada, H. Sumitomo, M. Atsumi, *J. Am. Chem. Soc. 106* (1984) 2101.
[2] R. D. Dillard, D. E. Pavey, *J. Org. Chem. 36* (1971) 749.
[3] F. Toda, K. Tanaka, H. Ueda, *Tetrahedron Lett. 22* (1981) 4669.
[4] F. Toda, K. Tanaka, H. Ueda, T. Ōshima, *Isr. J. Chem. 25* (1985) 338.
[5] G. Eglinton, A. R. Galbraith, *J. Chem. Soc. 1959*, 889.
[6] Y. Okamoto, K. Suzuki, K. Ohta, K. Hatada, H. Yuki, *J. Am. Chem. Soc. 101* (1979) 4763.
[7] D. J. Cram, D. Y. Sogah, *J. Am. Chem. Soc. 107* (1985) 8301.

BOOK REVIEWS

Electrochemistry: Theoretical Foundations, Quantum and Statistical Mechanics, Thermodynamics, the Solid State. By *J. Goodisman*. Wiley, Chichester 1987. ix, 374 pp., bound, £ 50.45.—ISBN 0-471-82850-5

Electrochemistry is predominantly an experimental science; there are only few professional theoreticians in this field, and even fewer books on theoretical electrochemistry. So the appearance of this work—written, significantly, by a quantum chemist—is highly welcome. *J. Goodisman*, well known as the author of a successful introduction to contemporary quantum chemistry, presents his view of the foundations of theoretical electrochemistry in ten chapters, which contain: a general introduction to electrochemistry, the thermodynamics of surfaces, and statistical mechanics (Chapters 1-3); a more detailed discussion of surfaces and interfaces (Chapters 4-6); electrode kinetics from both a classical and a quantum mechanical point of view (Chapters 8-10).

Chapter 7 on diffusion does not really fit into the otherwise well organized presentation. Each chapter is subdivided into smaller, often self-contained units, so that the material may be digested a bit at a time.

While a wide range of topics is covered, certain of these might well have been left to specialist works: the introduction to statistical mechanics, and the derivation of the Gamow tunnelling formula, for example. In many cases the presentation of the material is so condensed that an electrochemist with an average theoretical background will have difficulty in following it. Also, for some of the theoretical results presented, no examples of applications are given. In a revised edition, it would be advisable to shorten the general theoretical material, and devote more space to specific electrochemical problems; this would also give the opportunity to fill in certain gaps: proton transfer reactions, and the foundations of modern spectroscopic methods, for example, are not covered.

Only a few diagrams illustrate the text, and these are badly chosen. Most figures are schematic; only two experimental curves are shown, both for double layer properties. By the end of the second chapter, if not sooner, the reader will notice with regret the absence of a glossary of symbols, a surprising omission in a work of which some 40% consists of formulas. That we find the term "electromotive force" outmoded may be attributed to our personal prejudices, but the sign conventions employed defy both electrochemical tradition and common sense: cathodic currents are taken as positive, but cathodic overpotentials as negative.

In summary: a book on a subject of eminent importance, well conceived, with many good ideas, and a number of weaknesses, which should be remedied in a second, revised edition. In its present form most experimental electrochemists will understand large parts of it only after further consultation of the literature.

Ulrich Frese and *Wolfgang Schmickler* [NB 899 IE]
Institut für Physikalische Chemie
der Universität Bonn (FRG)

Solid-State Chemistry: Techniques. Edited by *A. K. Cheetham* and *P. Day*. Clarendon Press, Oxford 1987. xiv, 393 pp., bound, £ 35.00.—ISBN 0-19-855165-7

The first volume ("Techniques") of a two-volume account of solid state chemistry has now appeared (the second volume is to be subtitled "Compounds"). The work, which is edited by two Oxford experts, is intended to fill a gap. According to the editors it is aimed at final-year undergraduates and first-year post-graduates who are studying solid state chemistry for the first time. Considering this in relation to the requirement for a basic training in solid state chemistry in the German Federal Republic situation, the work is suitable for use by advanced students about to take their final examinations, and by diploma students who wish to prepare themselves for their chosen special area of study. In addition it would be a valuable resource for preparing lectures, and it is also suitable for use by chemists whose specialization is outside the solid state area and who seek information and an extension of their knowledge. In brief: it should be in every library.

This first volume provides a survey of the experimental methods of solid state chemistry. It begins with a chapter on "Synthesis of Solid State Materials" (author: *J. D. Corbett*), which occupies 38 of the 393 pages (a mere 10%!). This is excellent, and shows that, 15 years after *H. Schäfer*'s plea in this journal for more attention to be given to the preparative aspects of solid state chemistry,[*] the learning process then begun is now also bearing fruit in book form. It is clear from this chapter that solid state chemists involved in preparative work (a description which is almost a pleonasm!) are much better than is suggested by their reputation as bakers using powder mixtures.

This is followed by the (one might almost say, unavoidable) chapters on *physical* techniques which the solid state chemist must use to characterize his materials: Diffraction methods *(A. K. Cheetham)*, X-ray photoelectron spectroscopy and related methods *(G. K. Wertheim)*, Magnetic measurements *(W. E. Hatfield)*, Optical techniques *(R. G. Denning)*, High-resolution solid-state MAS NMR investigations of inorganic systems *(C. A. Fyfe* and *R. E. Wasylishen)*, Computational techniques and simulation of crystal structures *(C. R. A. Catlow)*, Transport measurements *(A. Hamnett)* and Vibrational spectroscopy *(D. M. Adams)*. The book concludes with a chapter by *A. Navrotsky* on "Thermodynamic aspects of inorganic solid-state chemistry."

The index, consisting of only four pages, is rather scanty, but since the book is by no means intended to be an encyclopedia but rather is a textbook, this shortcoming can be excused. The fact that all the authors are from the English-speaking world has no doubt made the editorial work easier, but this should not be taken as an indication that solid state chemistry work going on elsewhere is not of the highest standard.

To summarize, this is an indispensable book. This reviewer looks forward with keen anticipation to reading the second volume, which will be of greater interest to him in view of the declared intention to cover "Compounds".

Gerd Meyer [NB 886 IE]
Institut für Anorganische und Analytische Chemie
der Universität Giessen (FRG)

[*] *H. Schäfer:* Zur Situation der präparativen Feststoffchemie—The Present Situation in Preparative Solid-State Chemistry (*Angew. Chem. 83* (1971) 35; *Angew. Chem. Int. Ed. Engl. 10* (1971) 43).

Radiation Chemistry. Principles and Applications. Edited by *Farhataziz* and *M. A. J. Rodgers*. VCH Verlagsgesellschaft, Weinheim/VCH Publishers, New York 1987. 641 pp., bound, DM 208.00.—ISBN 3-527-26197-4/0-89573-127-4

Radiation chemistry is concerned with chemical reactions which are triggered by ionizing radiations. Its importance extends very much further than is often supposed. For example, ionizing radiation makes it possible for the chemist to create free radicals independently of the temperature, color and state of aggregation of the medium, which is not usually possible with other methods, and pulsed radiolysis allows one to investigate the kinetics of free-radical reactions (and also of some non-radical reactions) in a way which is almost unique. Radiation chemistry also provides the basis for a better understanding of the primary chemical processes involved in radiation biology and radiation medicine (the killing of cells by radiation, radiation-induced mutagenesis, tumor therapy etc.). Radiation-chemical techniques have now also become well established in industry.

Various monographs on radiation chemistry have appeared over the years. That most familiar to German readers is the excellent book by *Henglein, Wendenburg,* and *Schnabel* (Einführung in die Strahlenchemie, Verlag Chemie, Weinheim 1967), which is not outdated in its essentials even today. The book reviewed here differs from most of its predecessors in what it sets out to do. It is not so much a textbook as a collection of review articles. It contains contributions from more than twenty authors, although, surprisingly, neither of the two editors has written an article themselves. The fact that it is a multi-author work gives it both its strengths and its weaknesses. The editors have tried to indicate the broadness of the range of areas where radiation chemistry makes an important contribution. Since the number of such areas is too great to be adequately covered, even in more than 600 pages, the editors have had to be highly selective in what has been included. In accordance with their own bias of interest, they have mainly included authors who are active in work on primary radiation-chemical processes. For example, there are detailed discussions of energy absorption and theoretical aspects of radiation chemistry *(A. Chatterjee, J. L. Magee,* and *N. V. Klassen)*, the properties of the electron *(R. A. Holroyd* and *N. R. Kestner)*, reaction kinetics *(A. Hummel)*, and evidence for short-lived transient species, in which the various different pulse radiolysis techniques *(L. K. Patterson)* will be of great interest to many readers. Other topics covered are the special features of the radiation chemistry of gases *(D. A. Armstrong)*, aqueous solutions *(G. V. Buxton)*, organic liquids *(A. J. Swallow)* and solids *(J. E. Willard)*, colloidal aggregates *(J. K. Thomas)*, alkali halides *(V. J. Robinson* and *M. R. Chandratillake)*, and polymers *(A. Charlesby)*.

These chapters, which are mainly oriented towards physical chemistry and theory, make up almost 80% of the book. In contrast the chapter on biopolymers *(L. M. Mee)* is short and consequently unsatisfying, dealing in 22 pages with the radiation chemistry of nucleic acids, chromatin, proteins, lipids and polysaccharides. The excellent chapter by *P. Wardman* on some applications of radiation chemistry in biochemistry and radiation biology gives some indication of the great potential of radiation chemistry beyond its usual domain. It would have been desirable to give non-radiation chemists a wider picture of the many possibilities offered by radiation chemistry techniques for elucidating

free radical, and also non-radical, reactions in organic and inorganic chemistry. Instead of this the editors have included two chapters on the radiation biology of microorganisms *(D. Ewing)* and of mammalian cells *(J. E. Biaglow)*, both of which are very specialized and fail to give any more detailed information about, for example, radiation risks and radiation-induced mutagenesis. The book ends with a chapter by *M. Takehisa* and *S. Machi* on the engineering applications of radiation chemistry (with emphasis on the situation in Japan).

The book will be of interest to readers oriented towards physical chemistry. Because of the articles of a fundamental nature which it contains, it should be included in the library of every academic chemistry department or research institute.

Clemens von Sonntag [NB 867 IE]
Max-Planck-Institut für Strahlenchemie,
Mülheim/Ruhr (FRG)

Ab-initio Molecular Orbital Theory. By *W. J. Hehre, L. Radom, P. von R. Schleyer,* and *J. A. Pople.* Wiley, Chichester 1986. xviii, 548 pp., bound, £ 81.80.—ISBN 0-471-81241-2

After a very brief introduction to the quantum-mechanical basis of ab-initio MO theory, the program packages available under the name "GAUSSIAN-*n*" (where *n* is one of the years 70, 76, 80, 82, or 85) are described. Several of the authors played a considerable part in the development of these programs, which are introduced in a rather pragmatic manner. Most of the book is devoted to applications of the GAUSSIAN-*n* programs, though calculations using other systems are also considered, especially when no GAUSSIAN-*n* calculations are available for the purpose in hand.

This compilation of numerical results is extremely valuable. It spares the reader a tiresome search through the original literature, and since all the calculations carried out with the GAUSSIAN program satisfy certain standardizing criteria, results from various groups can be compared. The wealth of material itself makes the book exceedingly useful. The things that can be done today with ab-initio MO calculations are most impressive—from determination of equilibrium molecular structures, calculation of vibrational spectra, rotation and inversion barriers, bond and reaction energies and intermolecular interactions, to the elucidation of reaction mechanisms. The results concerning carbocations and carbodications deserve special mention, as do those on lithium-carbon compounds. Reading this book should convince any organic chemist that the study of his subject is no longer conceivable without ab-initio MO theory. For anyone who is interested in this type of calculation, an indispensable reference work is now available, including also a good introduction to the use of the GAUSSIAN programs. The book is not, and does not claim to be, an account of the current state of ab-initio quantum-chemical methodology (in this sense the title of the book is misleading). Although it is oriented too much towards GAUSSIAN-*n*, and does not explore fundamental questions sufficiently (for example electron-correlation, and non-adiabatic or relativistic effects), the majority of readers will hardly see this as a disadvantage.

Werner Kutzelnigg [NB 891 IE]
Fakultät für Chemie
der Universität Bochum (FRG)

Dynamics of Proteins and Nucleic Acids. By *J. A. McCammon* and *S. C. Harvey.* Cambridge University Press, Cambridge 1987. 234 pp., hard cover, £ 25.00.—ISBN 0-521-30750-3

The aim of this book is to provide the reader with a self-contained introduction to the theoretical aspects of proteins and nucleic acid dynamics. It is intended for graduate students as well as for research workers in the fields of physical biochemistry and molecular biotechnology. The principal goal of the authors is threefold: (1) to outline theoretical methods and their capabilities, (2) to provide an insight into the nature and biological significance of biomolecular dynamics, mainly by summarizing of and reference to theoretical studies, and (3) to indicate prospects and directions of future work in this area.

The books definitely meets these goals. It is organized as follows: The first three chapters (34 pages) contain a brief introduction to the function, structure and dynamics of proteins and nucleic acids. Chapter 4 (44 pages) discusses the theoretical methods that have been used to describe and model the dynamics of these molecules. On this basis the next four chapters (88 pages) deal with dynamical behavior by reviewing the literature of the last decade. Ordered according to the time scale and spatial scale of the different types of motions, the following are discussed: short time dynamics, local structural transitions, global structural changes, and the dynamics of molecular association. The last chapter (16 pages) stands a bit apart from the rest of the book. It mentions a number of new developments in the field of computer simulation of biomolecules. The book is completed by three appendices (21 pages) discussing some technical details of computer simulation, a list of references, and a subject index.

The authors have done a good job. They have reached the goals they set out. Starting from basic data the book summarizes the literature on theoretical studies of protein and nucleic acid dynamics. The referencing is done very carefully, many numerical examples are given and also the influence of solvent surroundings on the structure and dynamics of biomolecules is not neglected. It may be best characterized as an overview of the theoretical work in the field of biomolecular dynamics up till 1986. Perhaps due to its descriptive style the book is not very critical of the various studies, and space spent on the description of applications is not allotted according to the scientific value of the methods used, but more according to the number of published applications. An example is the relatively exhaustive attention given to normal mode calculations of proteins, which are—as the authors admit (p. 91)—of rather limited value because of the very anharmonic character of protein motion. The most promising practical applications of simulation techniques are only mentioned in the last chapter; the use of molecular dynamics simulation in the refinement of the spatial structures of proteins based on nuclear magnetic resonance atom-atom distance data or on crystallographic X-ray intensities; the thermodynamic cycle integration technique to obtain relative binding constants is briefly but not critically discussed.

The book does not provide sufficient information for the chemist who wishes to use theoretical methods in the study of biomolecular structure and dynamics. It lacks a critical evaluation of the various force fields in use for biomolecules. When discussing the limitations of simulation methods (p. 66) the yet insufficient accuracy of force fields is not even mentioned, whereas a critical discussion of factors contributing to accuracy is essential for a proper as-

sessment of the value of simulation techniques to a specific application. From a critical and detailed comparison with experimental data one would obtain an impression of the predictive power of the methods that are used.

Although chapter 4 and the three appendices contain some more detailed technical information on simulation methods, the level of detail is not sufficient to guide newcomers in the field. Metric tensor corrections which arise from transformations from cartesian to internal coordinates, are not mentioned. The Beeman algorithm for integrating equations of motion is said to be more efficient than the Verlet one (p. 175), whereas it has been proven in the literature that both algorithms generate *exactly* identical atomic trajectories.

However, to be fair to the authors, they did not intend to write a users guide to simulation techniques, nor a critical assessment of the various techniques and applications. They have written a book that nicely summarizes the various studies of the past. It definitely is an enrichment for a library, since new developments in certain areas tend to be rather scattered over a variety of journals. I would strongly recommend this book to any non-specialist who wishes to know more about the application of theoretical methods to the description of the dynamics of proteins and nucleic acids.

Wilfried F. van Gunsteren [NB 879 IE]
Laboratory of Physical Chemistry,
University of Groningen (The Netherlands)

A Pictorial Approach to Molecular Bonding. By *J. G. Verkade*. Springer, Berlin 1986. xiii, 282 pp., bound, DM 125.00.—ISBN 3-540-96271-9

We have here an old set of lecture notes from the early seventies, which has just come into print and is available at the price given above. It is well known, however, that not all wines improve with the years. The pictorial treatment of chemical bonding which is given here is not only free from all considerations of energy, but also completely ignores the different sizes of atoms and atomic orbitals.

Starting from these assumptions, there has been no problem in arranging the contents of the book in a clear and orderly way. The part which deals with general principles is short, and is concerned with hydrogen orbitals and with the formal representation of the idea of hybridization. Since the author, as has already been made clear above, regards only the directional properties of the hydrogen orbitals as important, all radial-dependent factors are neglected from the start. It is true that there are some belated short comments regarding the sizes and energies of the hydrogen orbitals, but no use is made of these subsequently when discussing chemical bonding. Before one has learned anything at all about atoms other than hydrogen, the discussion of chemical bonding begins. This is systematically illustrated using familiar examples. It starts off with diatomic molecules, followed by triatomic molecules. The molecules are classified according to their geometrical shapes. Thus, the chapters which follow deal in turn with tetrahedral molecules, ring molecules, octahedral molecules, bipyramidal molecules and prismatic molecules. The aim in each case is to give the topological shape of the molecular orbitals and qualitative MO correlation diagrams. Those who wish to follow the author in this must familiarize themselves with unusual methods of depicting orbitals and with new abbreviations. Atomic orbitals are represented not by contour lines but by arrows, with the phase having positive sign at the tip of the arrow and negative sign at the tail. Accordingly also molecular orbitals are represented not as LCAOs but as LCVOs (linear combination of vector orbitals). All molecular orbitals are made up of GOs (generator orbitals), which are fictional atomic orbitals in the centers of the molecules. The VOs on central atoms are SOs (symmetry orbitals).

A further aspect of the viewpoint adopted deserves special mention. Wherever possible, in addition to the canonical, delocalized molecular orbitals, localized orbitals are also given. These too are made up from a special set of GOs. This idea is useful and successful, provided that the molecules have sufficient symmetry.

The slightly dated origins of the book, mentioned at the start, occasionally show up rather drastically, as when cyclobutadiene is mentioned as having been discovered only recently and having a triplet ground state, or when prismane is described as a still unknown molecule. A set of exercises is given at the end of each chapter. Some readers may pick up useful ideas from this book regarding the construction of molecular orbitals.

Rudolf Janoschek [NB 875 IE]
Institut für Theoretische Chemie
der Universität Graz (Austria)

Spectroscopy with Polarized Light. Solute Alignment by Photoselection, in Liquid Crystals, Polymers, and Membranes. By *J. Michl* and *E. W. Thulstrup*. VCH Verlagsgesellschaft, Weinheim/VCH Publishers, New York 1986. xvi, 573 pp., bound, DM 265.00.—ISBN 3-527-26516-3/0-89573-346-3

In recent years sophisticated NMR techniques have sometimes led to the impression that other spectroscopic methods of structure determination are obsolete. The book reviewed here, dealing in great detail mainly with the UV and IR spectroscopy of (partially) oriented molecular ensembles, demonstrates that such a view is far from correct.

The book begins with a concise and mathematically rigorous account of the theoretical basis of optical spectroscopy (the nature of light, stationary and time-dependent wave functions, the interaction between light and molecules, and the effects of externally applied fields on absorption). Formulas are derived for the circular dichroism (CD) of (partially) oriented molecules in field-free space and in magnetic or electric fields, including a detailed description of the rotatory strength tensor. The reasons for the appearance of fine structure in CD spectra, and the associated difficulties in determining the rotatory strength, are also thoroughly discussed.

The second chapter is devoted to a detailed treatment of transition moments, dealing with electric dipole and quadrupole transitions and magnetic dipole transitions, and to the description of (symmetry and multiplicity) allowed and forbidden transitions in both absorption and emission. The theoretical concepts are put to the test using partially oriented pyrene as a practical example; the conclusions which can be derived from spectra of this kind are worked through in detail, and reference is made to situations where approximations break down.

A separate chapter is devoted to the practical aspects of recording spectra, especially the stretching of films which are used as sample supporting media. Since it is not possi-

ble by this means to obtain perfect orientation as, for example, in single crystals, it is still essential to average over many orientations. The quantitative description of the degree of this averaging is covered in the next chapter, which also discusses alternative orientation techniques. For this description one uses an "orientation triangle", in which molecules of different shapes (cylindrical shapes, flat disks, rectangular prisms of small height, etc.) are characterized according to different positions.

The fifth chapter discusses absorption and emission processes which arise solely as a result of changes in the electric transition moment. These are described by tensors of rank 2, but in general there are not enough equations available to determine the independent tensor components. They can be determined only in three special cases, namely for disk-shaped or rod-shaped molecules, or for those in which the component of the electric transition moment in one particular direction is practically zero, as is the case in most aromatic molecules for example. However, the molecules must have either at least two C_2 axes or two mutually perpendicular planes of symmetry. This TEM model (an acronym for *Thulstrup/Eggers/Michl*, a fact not mentioned anywhere in this book by the authors *Michl* and *Thulstrup*!), which is limited to uniaxial molecules, is compared with the other three frequently used approximations of *Fraser* and *Beer*, of *Tanizaki*, and of *Popov*, and it is shown that these latter three may all give incorrect results in cases whose occurrence is not always predictable.

The next (very brief) chapter deals with phenomena which can be analyzed by reducing to tensors of rank 2, such as magnetic dipole allowed transitions and the circular dichroism (of optically active compounds, or induced by a magnetic field). The last of the theoretical chapters is devoted to processes which can only be described by tensors of rank 4, such as electric quadrupole absorption and emission, and two-photon processes, e.g. photoluminescence and photodichroism. Here one can only obtain unambiguous information in cases of high molecular symmetry; for less symmetrical molecules the discussion is limited to spectra in which the individual bands do not overlap.

The final, very long, chapter gives many examples which illustrate the application of the methods described. Whilst most of the examples are of aromatic and heteroaromatic systems, some inorganic complexes, free radicals and biopolymers are also included. The use of such measurements to determine molecular conformations is exemplified by results on some steroids, aniline derivatives, peptides and DNA, and reference is also made to a few molecular complexes of biochemical importance. Finally there is a short account of the possibility of storing information in permanent or erasable form using birefringent polymers.

The book is completed by three appendices which give a very compact summary of the fundamentals of group theory and its applications to spectroscopy, Cartesian tensors, and the Mueller-Stokes formalism for describing the interaction between polarized light and anisotropic materials.

This is the first complete monograph on the subject to be published. It is very clearly presented in a good style of language, despite the difficulties of the mathematical formalism which will often be unfamiliar to the experimentalist. Also all the important formulas are thoroughly explained, allowing one to use them correctly even when one has had to gloss over their derivation. Constant warnings are given against over-interpretation of data, and the limitations of the methods are frequently pointed out; these aspects are often overlooked by epigones. The authors have also taken great care to give the units for all important quantities. The coverage of published work extends to quite recent papers. Occasionally when quoting from work by other authors their less exact language is also carried over. The reviewer noticed only a few printing errors (to substantiate this two are noted here: in Equation 1.43 the symbol $\hat{p}$ is missing, and in Equation 5.5, which can be deciphered only with difficulty owing to its very small print, h appears instead of $\hbar$). On page 213 the definition of pseudorotation is different from that generally accepted in stereochemistry, and in redrawing Fig. 8.37 some methyl groups have been overlooked.

This monograph can be warmly recommended to anyone who wishes to gain a greater knowledge of one or more of the topics mentioned. The authors have applied a considerable amount of self-criticism in writing the book. Its very high price will regrettably discourage the wide readership which it deserves.

Günter Snatzke [NB 883 IE]
Fakultät für Chemie
der Universität Bochum (FRG)

Registered names, trademarks, etc. used in this journal, even when not marked as such, are not to be considered unprotected by law.

© VCH Verlagsgesellschaft mbH, D-6940 Weinheim, 1988 – Printed in the Federal Republic of Germany by Zechnersche Buchdruckerei, Speyer/Rhein.

All rights reserved (including those of translation into foreign languages). No part of this issue may be be reproduced in any form – by photoprint, microfilm, or any other means – nor transmitted or translated into a machine language without written permission from the publishers. Only single copies of contributions, or parts thereof, may be made for personal use. This journal was carefully produced in all its parts. Nevertheless, authors, editors and publisher do not warrant the information contained therein to be free of errors. Readers are advised to keep in mind that statements, data, illustrations, procedural details or other items may inadvertently be inaccurate.

Valid for users in the USA: The appearance of the code at the bottom of the first page of an article in this journal (serial) indicates the copyright owner's consent that copies of the article may be made for personal or internal use, or for the personal or internal use of specific clients. This consent is given on the condition, however, that the copier pay the stated per-copy fee through the Copyright Clearance Center, Inc., for copying beyond that permitted by Sections 107 or 108 of the U.S. Copyright Law. This consent does not extend to other kinds of copying, such as copying for general distribution, for advertising or promotional purposes, for creating new collective works, or for resale. For copying from back volumes of this journal see 'Permissions to Photo-Copy: Publisher's Fee List' of the CCC.

Editorial office: Pappelallee 3, D-6940 Weinheim, Federal Republic of Germany, Telephone (06201) 602315, Telex 465516 vchwh d, Telefax (06201) 602328.

Editor: *P. Gölitz.*

Associate editors: *D. I. Loewus, A. Stimson.* **Editorial assistant:** *E. Schweikart*

Publishers: *VCH Verlagsgesellschaft mbH. (Managing Directors: Prof. Dr. Helmut Grünewald and Hans Dirk Köhler),* Pappelallee 3, D-6940 Weinheim, Federal Republic of Germany. Correspondence concerning advertisements should be addressed to VCH Verlagsgesellschaft mbH. (Advertising Manager *R. J. Roth*), Boschstr. 12. P.O. Box 1260/1280, D-6940 Weinheim, Federal Republic of Germany, Telephone Weinheim (06201) 602-0, Telex 465516 vchwh d, Telefax (06201) 602328.

ANGEWANDTE CHEMIE
International Edition in English
Volume 27 · Number 7
July 1988
Pages 865–1008

"Proton Sponges" and the Geometry of Hydrogen Bonds: Aromatic Nitrogen Bases with Exceptional Basicities**

By Heinz A. Staab* and Thomas Saupe

Certain aromatic diamines (the "proton sponges") are found to have exceptionally high basicity constants: this is due to spatial interaction of the basic centers, which are in close proximity. The two factors which are most important in causing this effect are, on the one hand, the extreme steric strain in these systems and the destabilizing effect of the overlap of the nitrogen lone pairs of the neutral diamines and, on the other, the strong N···H···N hydrogen bonds which are formed on *mono*protonation and which lead to a considerable relaxation of the steric strain. By the systematic variation of the structures of such aromatic diamines we have been able to study these effects as a function of steric factors, in particular of the geometry and the bond length of the N···H···N hydrogen bonds, by means of X-ray structural analysis. The hydrophobic shielding of the basic centers and the N···H···N hydrogen bonds, which was characteristic of the "proton sponge" compounds studied previously, is indeed responsible for the extremely low rate of protonation and deprotonation of these compounds; however, it apparently has no influence on their high thermodynamic basicity. The recent synthesis and basicity determination of a new type of "proton sponge" with no hydrophobic shielding whatever show that not only very strong but also kinetically active bases are accessible using the "proton sponge" concept. Their unusual properties, which are discussed here as the result of steric interactions between two basic centers, provide examples of the fact that cooperative steric interactions of reactive structural elements can lead to properties which cannot be derived from an isolated consideration of the various functional groups. Such "proximity effects" are certainly of general importance in chemistry and biochemistry; the study of their structure-function relationships is worthy of closer consideration.

1. Introduction

Acidity and basicity are two of the properties of chemical compounds which have been a source of particular interest since chemistry became a real science. The amount of quantitative information on the dissociation constants of organic acids and bases which has been available for many years has in the last decades played a deciding role in the theoretical understanding of bonding in organic compounds. Our knowledge of the dependence of acidity and basicity on structural and electronic factors such as inductive and mesomeric effects thus appeared to rest on such a secure basis[2] that surprising new results could hardly be expected in this area. The report by *Alder* et al.[3] in 1968 on the unusually high basicity of a relatively simple organic compound was therefore the subject of con-

[*] Prof. Dr. H. A. Staab, Dr. T. Saupe
Abteilung Organische Chemie
Max-Planck-Institut für Medizinische Forschung
Jahnstrasse 29, D-6900 Heidelberg (FRG)

[**] New "Proton Sponge" Compounds, Part 5.—Part 4: [1].

 © VCH Verlagsgesellschaft mbH, D-6940 Weinheim, 1988 0570-0833/88/0707-0865 $ 02.50/0

siderable attention: whereas aniline **1** and 1,8-diaminonaphthalene **2** have similar basicities typical of aromatic amines ($pK_a \approx 4.6$), 1,8-bis(dimethylamino)naphthalene **4** ($pK_a = 12.1$[4]) has a basicity ten million times higher than that of *N,N*-dimethylaniline **3** ($pK_a \approx 5.1$).

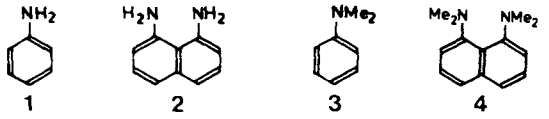

1 **2** **3** **4**

Detailed investigations were carried out in the following years in order to determine the reasons for the high basicity of **4**, particularly by the groups of *Alder*[5-7] and *Hibbert*.[4,5] However, they remained essentially limited to compounds which, like **4**, belong to the class of the *peri*-disubstituted naphthalenes. During the past five years we ourselves have synthesized "proton sponges" with other, more varied basic aromatic structures and carried out basicity and structure determinations for these compounds; we have been able to show that unusually high basicities are also observed for other aromatic diamines with closely neighboring nitrogen atoms. In this way we were able to study this effect on a wider basis as a function of the distance between and the spatial orientation of the basic centers.

Our interest in the title compounds started from the assumption that the high basicity of **4** and its analogues is determined mainly by the formation of a particularly stable N···H···N hydrogen bond in the *mono*protonated bases (see Section 2). The great general importance of hydrogen bonds in chemistry and biochemistry is clearly recognized today; for example, it is well known that hydrogen bonds determine the secondary structures of proteins and are responsible for the base pairing in nucleic acids. It is hence even more surprising that the experimentally available information on the dependence of the bond strength of hydrogen bonds on geometric factors is still so sparse. The questions as to how the bond energy of a hydrogen bond X–H···Y depends on the distance X···Y and whether a linear X–H···Y geometry and an orientation in the direction of the lone pair of the hydrogen bond acceptor Y are energetically particularly favorable have often been discussed in the literature;[8] however, completely convincing experimental answers to these questions could not be given until now.[9] This is due to the fact that in such investigations the crystal structures of compounds with *inter*molecular hydrogen bonds have been used: however, these do not of necessity correspond to optimal hydrogen bond geometries but represent a compromise between the sum of all the lattice forces. In contrast, the *mono*protonated forms of the "proton sponges" have *intra*molecular hydrogen bonds which in turn influence a molecular property which can be measured independently, i.e. the basicity. By systematically varying the geometrical arrangement of the two basic centers it should therefore be possible in principle to obtain information on the dependence of the strength of the hydrogen bonds on geometric factors via the basicity constants. This corresponds to the concept of the simulation of *inter*molecular interactions by structurally clearly defined *intra*molecular bonding systems, a concept which we have used, for example, to determine the structure dependence of charge transfer and excimer interactions.[10,11]

The present review will first deal with the situation of research on "proton sponges" at the beginning of the 1980's. It will continue with an account dealing mainly with our own contributions to this area during the last five years; these are by no means completed, so that quite a number of questions, particularly with respect to the goals formulated above, still remain unanswered.

2. "Proton Sponge" Compounds with Naphthalene Structure

Table 1 shows the pK_a values for some substituted 1,8-diaminonaphthalenes. While increasing *N*-methylation of **3** results in the case of the bis(methylamino) compound **5** and even in the *N,N,N'*-trimethyl derivative **6** in only a small increase in basicity (this being mainly the result of inductive effects), the introduction of the fourth *N*-methyl group to give **4** causes a sudden increase in basicity by nearly six powers of ten.

Table 1. Basicities of some substituted 1,8-diaminonaphthalenes [5]. For further basicity values see Table 3 in Section 6.

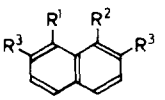

	R^1	R^2	R^3	pK_a	Ref.
2	NH_2	NH_2	H	4.61	[3]
5	NHMe	NHMe	H	5.61	[3]
6	NMe_2	NHMe	H	6.43	[3]
4	NMe_2	NMe_2	H	12.1	[3, 4]
7	NEt_2	NEt_2	H	12.7	[3, 4]
8	NMe_2	NMe_2	OMe	16.1	[5]
9	NEt_2	NEt_2	OMe	16.3	[5]

The way in which the basicity increases with increasing *N*-methylation of **2** suggests that steric effects play a very important role. This assumption is supported by the observation that the replacement of dimethylamino by diethylamino groups (compound **7**) leads to a further increase in basicity. Introduction of methoxy groups in positions 2 and 7 is particularly effective in increasing the basicity (compounds **8** and **9** in Table 1): these groups are suggested to exert "buttressing" steric effects.[5,6]

The increase in basicity on increasing the steric hindrance around the two amino groups in the *peri*-positions is considered to be due to two factors which work in the same direction: firstly the dialkylamino groups are increasingly forced into an arrangement in which the repulsion between the nitrogen lone pairs has a destabilizing effect on the free bases, and secondly protonation yields a monocation in which a particularly stable intramolecular hydrogen bond is formed because of the structurally fixed short N···N distance. The latter removes the destabilizing "lone pair" interaction and thus causes a considerable decrease in the steric strain.

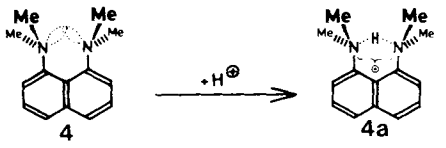

The stability of the monocation (e.g. **4a**) is responsible for the fact that "proton sponges" such as **4** undergo only *mono*protonation even in the presence of an excess of such strong acids as perchloric and tetrafluoroboric acid; under such conditions **2** is doubly protonated. The basicity difference between the first and second protonation steps has been estimated to be at least 20 pK_a units for "proton sponges" of type **4**,[7] although for diamino compounds this difference normally lies between 1 and 5 pK_a units, depending on their structure.

The high basicity of the "proton sponges" is accompanied by an extremely low rate of proton transfer, the latter decreasing in the series **4** > **7** > **8** > **9** as the basicity increases. While the deprotonation of ammonium ions by hydroxide ion is generally diffusion-controlled ($k \approx 10^{10}$ L mol^{-1} s^{-1}),[12] the rate constants for the proton transfer reaction are several orders of ten lower for "proton sponges". Table 2 shows this for the deprotonation of **4a** and some analogues by the hydroxide ion.

Table 2. Rate constants for the reaction of protonated "proton sponges" with the hydroxide ion (DMSO = dimethyl sulfoxide) [13].

	R	X	Solvent [v/v]	k [L·mol^{-1}·s^{-1}]
4a	Me	H	water	$1.9 \pm 0.4 \times 10^5$
			30% DMSO/water	$6.1 \pm 0.5 \times 10^5$
7a	Et	H	30% DMSO/water	$1.6 \pm 0.2 \times 10^4$
8a	Me	OMe	60% DMSO/water	$4.4 \pm 0.5 \times 10^2$
9a	Et	OMe	60% DMSO/water	3.3 ± 0.4

The main reasons for the low rates of proton transfer are the stable intramolecular hydrogen bonds and their shielding by hydrophobic groups. This would apply for both a one-step deprotonation mechanism via direct attack by the base at the bridge proton and a two-step process in which the hydrogen bond is first broken and the "open form" subsequently deprotonated. It is difficult to decide unambiguously which of these mechanisms is correct, though various observations point to the latter two-step mechanism.[13, 14]

The high thermodynamic basicity of the 1,8-bis(dialkylamino)naphthalenes combined with their kinetic inactivity has led to the name "proton sponges", as their behavior has been compared with that of a sponge with regard to water: "Sponges are not kinetically active in seeking water, they merely mop it up when it is presented to them".[6] The kinetic inactivity of the "proton sponges" described above has the consequence that in spite of their high basicity and their extremely low nucleophilicity these compounds have so far found hardly any use as auxiliary bases in organic syntheses.[15]

Because of the paramount importance of steric effects in determining the properties of the "proton sponges", exact information on the molecular structures of both the free base and the *mono*protonated salts is of particular interest. In the series of 1,8-bis(dialkylamino)naphthalenes, X-ray structural determinations have been made for **4** and **4a**. The structure of **4**[16] makes it clear that the steric strain induced by the two dimethylamino groups in *peri*-position leads to a clear deviation of the naphthalene skeleton from planarity. The central C4a–C8a bond is twisted so that the dimethylamino groups are on different sides of the naphthalene plane: their nitrogen atoms then lie 40 pm above and below this plane. The angle C1–C8a–C8 is widened to 125.8°, so that the C1···C8 distance is increased to 256 pm (naphthalene: 245 pm): this results in a further increase of the distance between the dimethylamino groups, the N···N distance of 279 pm being much larger than the fictitious distance of 245 pm which would result for a planar naphthalene system with parallel C_{aryl}–N bonds. Via rotation about the C_{aryl}–N bonds the dimethylamino groups assume a conformation such that one methyl group of each lies almost in the plane of the ring and the lone pairs on nitrogen avoid the destabilizing overlap as far as possible.

The relief of the steric strain which occurs on protonation of **4** is immediately evident from the structure of the *mono*protonated cation **4a**. Although the results of structure determinations for **4a** (one for copper(II) and magnesium tris(hexafluoroacetylacetonates),[17] the other for a bromide dihydrate[18]) conflict to some extent, the two structures do agree in one respect: the deviation of the naphthalene system from planarity is much less in **4a** than in **4**. The N···N distance in **4a** (260 and 265 pm[17] or 255.4 pm[18]) is correspondingly considerably shorter than in **4**. Because of the formation of a stable intramolecular hydrogen bond and the resulting elimination of the lone pair repulsion the dimethylamino groups are twisted towards one another about the C_{aryl}–N bond. However, the hydrogen bonds cannot lie in a straight line because of the spatial arrangement of the molecule: the N···H···N angles are 141°[17] and 153°.[18] The positions of the atoms of **4a** other than hydrogen are symmetrical within the limits of error with respect to the hydrogen bridge: however, the X-ray structural analyses do not allow us to decide whether the bridge itself is symmetric (see Section 3).

The ^{1}H-NMR spectrum of **4a** shows the proton of the N···H···N group as a broad singlet with an unusual low-field shift: $\delta = 18.31$ (in dimethyl sulfoxide) and $\delta = 19.5$ (in trifluoroacetic acid).[3] Coupling with this proton causes the twelve protons of the two dimethylamino groups to be split into a doublet: thus the methyl protons in **4a** are magnetically equivalent, just as are the naphthalene protons in corresponding positions. However, this information is also not sufficient to establish a structural equivalence in the sense of a symmetric N···H···N hydrogen bridge:[19] the expected rapid exchange of the bridging proton between the two positions of an unsymmetrical hydrogen bridge would also explain the observed magnetic equivalence.

However, the ^{2}H isotope effect on the chemical shift of the bridging hydrogen in **4a** ($\Delta\delta(^1H,^2H) = +0.6$ ppm)[20] and the theoretical arguments offered by *S. Forsén* et al.[21]

are in favor of a very strong but unsymmetrical hydrogen bridge. ESCA studies on **4a**-tetrafluoroborate also support the presence of two non-equivalent nitrogen atoms in **4a**, thus pointing to the presence of an unsymmetrical N···H···N hydrogen bridge.[22]

3. "Proton Sponge" Compounds with Fluorene Structure

It is remarkable that after the discovery of the unusual basicity of the 1,8-bis(dimethylamino)naphthalene **4**[3] the search for new, more basic "proton sponges" was limited for a considerable time to the modification of the 1,8-diaminonaphthalene system by introducing various substituents. This is particularly surprising since for structural reasons the two effects responsible for the "proton sponge" properties cannot function in these systems in an optimum manner: firstly the repulsive interaction between the lone pairs, which destabilizes the free bases, whould be smaller for amino groups in *peri*-positions of naphthalene than in systems in which these lone pairs are more strongly directed towards each other along the line joining the nitrogens; and secondly, as is shown by the X-ray structure of **4a**, it is not possible in the case of protonated "proton sponges" of the naphthalene type to form N···H···N bridges with the linear geometry generally considered to be optimal[8]. The consideration of simple molecular models shows that these factors should both be more favorable in the case of fluorenes with dialkylamino groups in 4- and 5-positions: the N···N distance would be smaller (on the basis of the fluorene structure it would be 231 pm in a fictitious planar molecule compared to 245 pm in *peri*-substituted naphthalenes), and in particular it was to be expected that in a 4,5-bis(dialkylamino)fluorene, in contrast to **4**, the lone pairs would be directed nearly along the N···N line, so that an almost linear N···H···N bridge would be formed on monoprotonation.

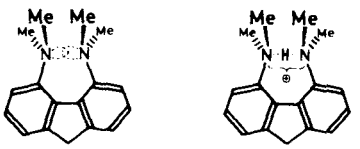

10 **10a**

On the basis of these considerations we synthesized the 4,5-bis(dimethylamino)fluorene **10**.[23] In this synthesis it was remarkable that 4,5-diaminofluorene easily underwent fourfold *N*-methylation on treatment with dimethyl sulfate in the presence of sodium hydride[24] (in tetrahydrofuran, 3 h at reflux); in spite of the considerable steric strain built up during this procedure, the yield was 90%.

10 exhibits typical "proton sponge" behavior in that it is not doubly protonated by excess perchloric acid: only the *mono*protonated **10a**-perchlorate is formed. In the ^{1}H-NMR spectrum of the latter the bridging proton absorbs at very low field ($\delta = 18.25$ in [D$_6$]DMSO, 360 MHz) as a broad singlet. The four methyl groups give one single signal at $\delta = 3.19$ ppm, split into a doublet by coupling with the bridging proton; the coupling constant of $J = 2.03$ Hz is significantly larger than for the perchlorate of **4a** ($J = 1.92$ Hz).

The greater basicity of **10** in comparison with **4** is shown by simple transprotonation experiments: when **4a**-perchlorate was added to a solution of **10** in [D$_6$]DMSO in a molar ratio of 1 : 1, integration of the Me$_2$N signals in the ^{1}H-NMR spectrum (**4**: $\delta = 2.73$; **10**: $\delta = 2.62$; **4a**: $\delta = 3.11$; **10a**: $\delta = 3.19$; 360 MHz) showed that **4a** had undergone almost complete deprotonation by **10**. The determination of the pK_a value of **10** on the basis of the UV/VIS spectroscopic measurement of the ratio of **10** to **10a** in 35% (v/v) dimethyl sulfoxide/water (I = 0.1 mol L^{-1}, 25 °C) gave a value of 12.8 ± 0.1,[32] compared with that of 12.1 ± 0.1 obtained for **4** under analogous conditions.[25,32]

It follows from the X-ray structural analysis of the perchlorate of **10a**[23] that the **10a** moiety of the molecule has C_2-symmetry with a C_2 axis through C9 and the midpoint of the central C–C bond of the five-membered ring (Fig. 1); the C_2 axis lies in the direction of the crystallographic *b* axis. The atoms C4 and C4i (≡C5) are displaced 10 pm in opposite directions out of the median plane formed by the remaining carbon atoms of the fluorene skeleton; this is a result of the steric interactions between the two dimethylamino groups, the nitrogen atoms of which lie 23 pm above and below the median molecular plane, respectively. The deviations from planarity as a result of the steric strain in **10a** are similar to those of the naphthalene system in **4a**. However, in contrast to **4a** the

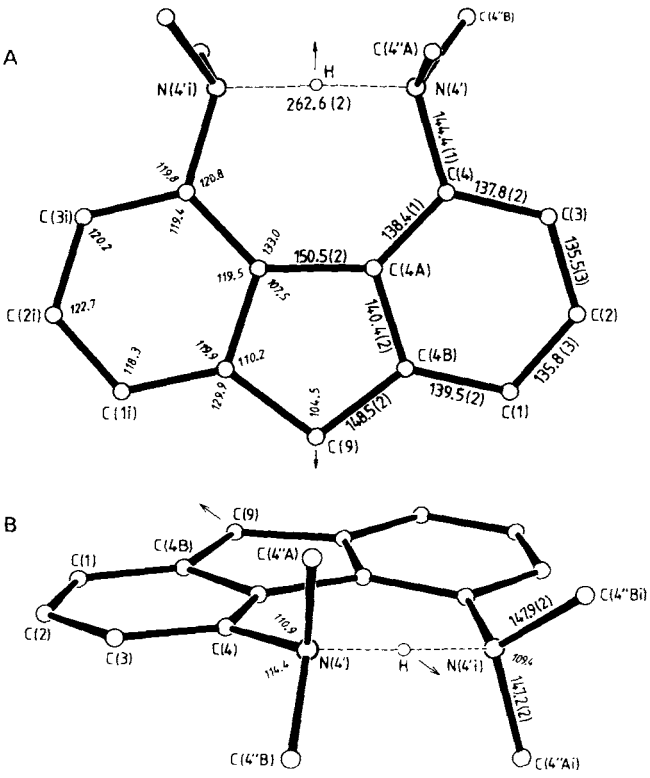

Fig. 1. Molecular structure of the **10a** part of **10a**-perchlorate (A) looking directly down on the fluorene plane, (B) looking sideways on from a position just above the fluorene plane (bond angles in degrees, distances in pm; standard deviations in brackets) [23].

N···H···N hydrogen bridge is nearly linear (N···H···N angle: 178°). When the hydrogen bridge is included, the bond angles at the nitrogen atoms correspond very closely to a tetrahedral arrangement, as was expected from the models referred to above. The N···N distance is unusually short for a linear N···H···N hydrogen bridge: the value is 262.6(2) pm compared with normal N···N distances in N···H—N bridges of 290–320 pm[8] (which, however, don't carry a positive charge on nitrogen).

The C_2-symmetry of **10a** could correspond to a symmetrical hydrogen bridge with a single potential minimum; however, the X-ray structural analysis does not allow us to conclude that this is in fact the case, since such an analysis cannot distinguish between a symmetrical hydrogen bridge and a short unsymmetrical bridge with very close double potential minima. A 1 : 1 disorder effect could also give an apparent C_2-symmetry. The deuterium isotope effect for **10a**-perchlorate ($\Delta\delta(^1H,^2H)$ is $+0.50\pm0.03$ ppm ([D$_6$]-DMSO, 360 MHz, 33 °C) and thus according to *Forsén* et al.[21] suggests a very strong but still unsymmetrical hydrogen bridge.

The considerations which formed the basis for the synthesis of **10** as an effective "proton sponge" are also confirmed by its He(I) photoelectron spectrum.[26] The assignment of this spectrum, which is supported by those for model substances and corresponding MO calculations, shows a splitting of $\Delta E = 2.2$ eV between the two lone pair orbitals n_+ and n_- of the dimethylamino groups. This splitting, which is a measure of the through-space interaction between the lone pairs of the nitrogen atoms, is significantly larger than for **4** ($\Delta E = 2.0$ eV[27]). This suggests that the destabilizing interaction between the two dimethylamino groups in the free base **10**, which in addition to the hydrogen bridge in the *mono*protonated salt is considered to lead to the "proton sponge" properties, differs from that in **4** in the sense of an increase in basicity.

In contrast to the ready synthesis of the bis(dimethylamino) compound **10**, the sterically more demanding fourfold *N*-ethylation of 4,5-diaminofluorene did not occur as originally hoped. Even under conditions where only a threefold ethylation at nitrogen took place (ethyl iodide, sodium hydride, 3 h in refluxing tetrahydrofuran) the 9-position of fluorene was completely ethylated: the product obtained in 70% yield was 4-diethylamino-5-ethylamino-9,9-diethylfluorene **11**.[28] Both the extreme downfield shift of the amino proton ($\delta = 9.5$ rather than the usual range of $\delta = 3.0$–3.5 for aryl NH protons) and the infrared spectrum show that in this compound there is a strong intramolecular N···H···N hydrogen bridge. It can be assumed that the introduction of the fourth *N*-ethyl group is hindered by this hydrogen bridge, particularly since the attack of the auxiliary base sodium hydride at this proton and the subsequent reaction with ethyl iodide are made more difficult by the efficient shielding by the three space-filling ethyl groups. Attempts to introduce the fourth *N*-ethyl group into **11** using excess sodium hydride and ethyl iodide to give **12** failed: even after 15 h in refluxing THF, **11** remained unchanged. However, **12** was obtained in 74% yield by the reaction of 4,5-diaminofluorene with excess diethyl sulfate in the presence of sodium hydride (4 d in refluxing THF).[29]

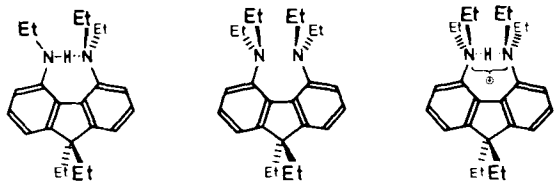

11 **12** **12a**

As expected, **12** formed the corresponding **12a**-monoperchlorate with perchloric acid, even when the latter was in excess. ^{1}H-NMR transprotonation experiments between **4** and **12** indicated the latter to be more basic than **10**. The determination of the pK_a-value in the solvent mixture used previously (35% (v/v) dimethyl sulfoxide/water) was not possible, since the six ethyl groups in **12** make the molecule so hydrophobic that a sufficient solubility requires the mixture to contain 60% DMSO. The UV-spectroscopic determination of the **12/12a** equilibrium via extrapolation with respect to compound **9**, which was also studied in such a solvent mixture (see Table 1)[5] gave a pK_a-value of 13.6 ($\pm$0.2).[28] Thus the increase in basicity with respect to **10** (p$K_a = 12.8\pm0.1$) corresponds within the limits of error to that determined in the naphthalene series when the bis(diethylamino) compound **7** and the bis(dimethylamino) compound **4** were compared.

A comparison between **13** (p$K_a = 13.6$)[30] and **14** (p$K_a = 14.1\pm0.1$)[29] also shows that with corresponding substituents the "proton sponges" of the fluorene series are stronger bases than those of the naphthalene series. In this connection we are interested in 3,6-dimethoxy-4,5-bis(dialkylamino)fluorenes **15** and have commenced work on their synthesis:[31] they are expected to be the most basic "proton sponges" in the naphthalene and fluorene series.

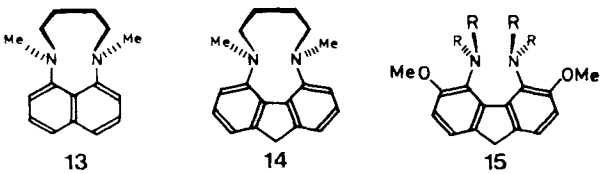

13 **14** **15**

4. "Proton Sponge" Compounds with Phenanthrene Structure

The results obtained in the fluorene series suggested that 4,5-bis(dialkylamino) derivatives of phenanthrene would be suitable candidates for the role of even more potent "proton sponges": molecular models such as those which had led to the choice of the fluorene system indicated the N···N distance to be even shorter in 4,5-bis(dimethylamino)phenanthrene **16** than in the fluorene compound **10**, so that an even greater steric hindrance of the dimethylamino groups with unfavorable overlap of the nitrogen lone pairs would be expected. In addition, the monocation **16a** should form an approximately linear N···H···N hydrogen bridge with an N···N distance shorter than in **10a**.

The synthesis of this molecule was extremely difficult because of its extreme steric strain. Among the various

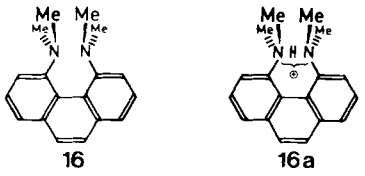

16 16a

routes tried[28] we will mention only the following: starting from 2,2'-bis(bromomethyl)-6,6'-dinitrobiphenyl one can obtain the dibenzo[*c*,*e*]thiepin **17** using sodium sulfide. Reduction of **17** with zinc dust and acetic acid gave the diamino compound **18**, which underwent methylation to the bis(dimethylamino) compound **19** on treatment with dimethyl sulfate and sodium hydride in THF. Oxidation with peroxytrifluoroacetic acid led to the cyclic sulfone **20**; gas phase vacuum pyrolysis of which gave 4,5-bis(dimethylamino)-9,10-dihydrophenanthrene **21** in satisfactory yield.[32] We shall discuss the "proton sponge" properties of **21** in Section 6 in connection with its non-planar structure.

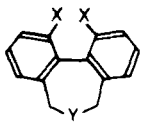

17, X = NO_2, Y = S
18, X = NH_2, Y = S
19, X = NMe_2, Y = S
20, X = NMe_2, Y = SO_2

None of the various dehydrogenation methods applied was successful in converting the 9,10-dihydrophenanthrene compound **21** into **16**, apparently because of the necessary introduction of an extremely large steric strain. However, the synthesis of **16** was possible starting from **20** using a Ramberg-Bäcklund rearrangement as modified by *Meyers* et al.:[33] in spite of its high steric requirements, this procedure gave the 4,5-bis(dimethylamino)-9,10-dichlorophenanthrene **22** in the surprisingly high yield of 53%. Halogen-metal exchange (lithium, THF, 1.5 h, −55 °C to −35 °C) followed by treatment with methanol led to **16** in 55% yield.[32]

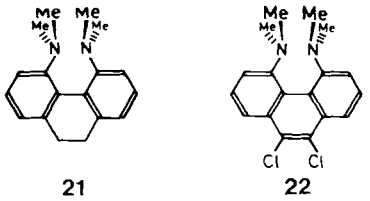

21 22

As expected, **16** gives only a *mono*protonated derivative, even with an excess of acid: thus perchloric acid gives the perchlorate of **16a**, in the proton NMR spectrum of which ([D_6]dimethyl sulfoxide, 360 MHz) the proton forming the N···H···N bridge absorbs at $\delta = 18.37$. The large positive isotope effect observed for this proton [$\Delta\delta(^1H,^2H) = +0.47 \pm 0.03$ ppm] suggests that the hydrogen bridge is in this case also very strong but still unsymmetrical. The variation in the coupling between the bridging proton and the *N*-methyl protons also indicates the presence of a particularly strong hydrogen bridge (**4a**: $J = 1.92$; **10a**: 2.03; **16a**: 2.17 Hz).

While the deviations of the aromatic skeleton from planarity were not very marked in the *mono*protonated systems **4a** and **10a**, the considerable increase in the steric interaction in **16a** (Fig. 2) leads to a drastic deformation of the aromatic system (because of the two-atom bridge, **16a** is of course much more readily able to undergo deformation than are **4a** or **10a**). The structure of **16a** is characterized by a large helical twist (23°) of the phenanthrene system along the C12–C13 axis (Fig. 2). This causes C4 and C5 to lie 30 and 29 pm, and N4' and N5' to lie 75 and 72 pm above or below the plane of the phenanthrene ring. The increase of the bond angles at C12 and C13 to 128° decreases the interaction between the two dimethylamino groups still further: even so, the N···N distance of 254.4 pm in **16a** is significantly shorter than that in **10a** (262.6 pm), and is one of the shortest distances for an approximately linear N···H···N bridge which has yet been found. The small deviation of the hydrogen bridge from

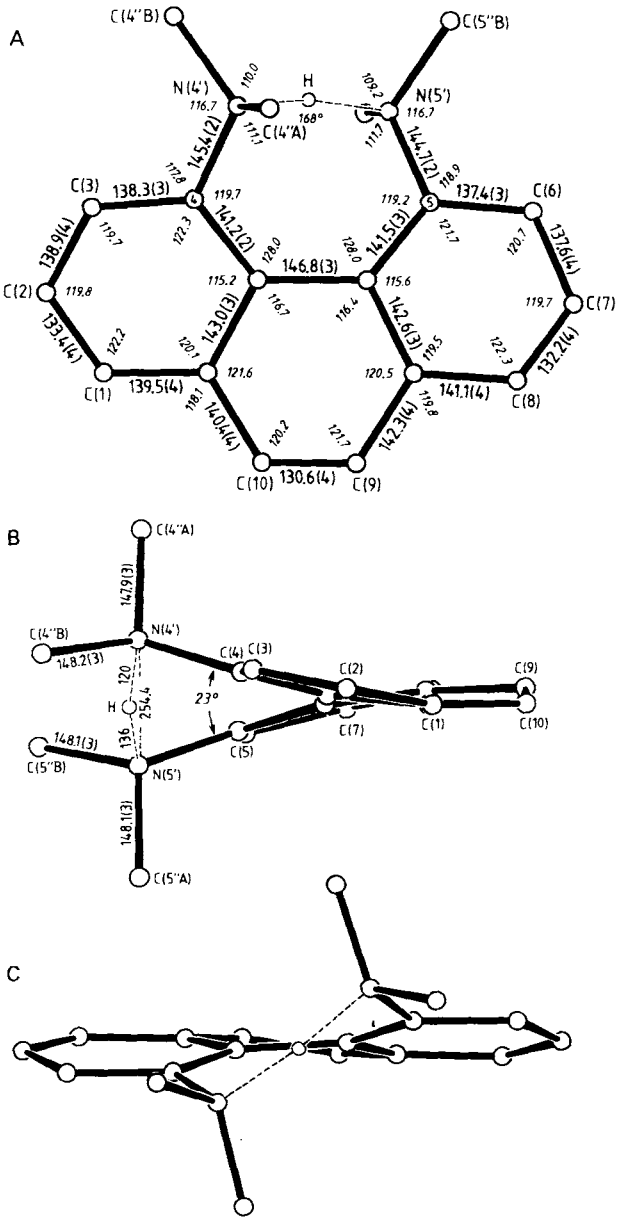

Fig. 2. Molecular structure of the **16a** part of **16a**-perchlorate looking down on the phenanthrene system (A), from the side along the C2–C7 axis (B), and looking along the (approximate) C_2-axis (C) (bond angles in degrees, distances in pm; standard deviations in brackets) [32].

linearity (the angle N···H···N is 168°) is in agreement with the retention of a nearly tetrahedral geometry at the two nitrogen atoms.

The X-ray structural analysis of **16a**-perchlorate and the ^{1}H-NMR results allow us to assume the existence of a strong N···H···N hydrogen bridge. In addition the free base **16** was expected to have a shorter N···N distance than that in **4** or **10**, leading in turn to a more strongly destabilising interaction between the nitrogen lone pairs; this is in agreement with preliminary PE-spectroscopic results ($\Delta E = 2.6$ eV for the n_+/n_- splitting).[34] Both effects led us to expect the basicity of **16** to be considerably higher than that of **10**; experimentally we do find **16** to have the high basicity typical of a "proton sponge", but the exact determination of its pK_a-value under the conditions used for **10** (see above) shows it to have a basicity which is not higher but in fact *lower* than that of **10** ($pK_a = 11.5 \pm 0.1$)[32] (see Table 3 in Section 6).

Various structural factors could be responsible for the observed variation in basicity in the series **4** ($pK_a = 12.1$), **10** (12.8), **16** (11.5). A possible explanation for the reduced basicity of **16** compared to **10** could be that the N···H···N hydrogen bridge in **16a** is, as a result of the particularly large steric strain in this system, compressed beyond the energetically optimal N···N distance of such a hydrogen bridge. Also a plausible assumption, however, would be that the steric strain in **16** is so much stronger than in **4** and **10** that the protonation can not bring steric relief corresponding to that shown by a comparison of the molecular structures **4/4a** and the systems **24/24a** and **25/25a** (Figs. 4 and 5) described later. The strong deformation of **16a** compared to **4a** and **10a**, which follows from the X-ray structure analysis, would appear to support this thesis. The recent successful structure analysis of **16**[35] (Fig. 3) shows that the torsion of the "biphenyl unit" about the central CC bond of the phenanthrene in this compound is 36° and that the C4–N4′ and C5–N5′ bonds form an angle of 44° (Fig. 3B). Besides the twisting about the central CC bond, there is a noticeable bending of the peripheral six-membered rings of the phenanthrene moiety towards each other, whereby the atoms C2, C12, C13, and C7 no longer lie on an axis (Fig. 3C). This, in addition to the widening of the C5–C13–C12 and C4–C12–C13 angles, leads to a mean deviation of C4 and C5 of about 53 pm and for N4′ and N5′ of about 104 pm in opposite directions from the mean plane of the atoms of the central six-membered ring. The result of these deformations is an N···N distance of 278.3 pm for the dimethylamino groups, which—as the structure of **16a** shows (Fig. 2)—is reduced to 254.4 ppm by the *mono*protonation of **16**. Hence the protonation of **16** obviously leads to a reduction in the steric repulsion of the dimethyl groups. However, the ensuing stronger planarization of the phenanthrene system is accompanied by steric deformations at other sites, as shown for example by the additional widening of the external angles at C12 and C13. A quantitative estimation of the net relief of steric strain is therefore hardly possible.

In connection with this result we should finally note the following structural difference between **4a** and **10a** on the one hand and **16a** on the other: because of the small deviation from planarity of the aromatic skeletons in **4a** and **10a** the dimethylamino groups are so arranged that they hydrophobically shield the N···H···N bridge considerably from all sides (see Fig. 1 and Refs. [17, 18]). However, in **16a** the extreme steric strain displaces the dimethylamino groups so far in opposite directions from the median phenanthrene plane and twists them so far about the C_{aryl}–N bonds to obtain a linear N···H···N bridge that this bridge is no longer hydrophobically shielded in all directions as it is in **4a** and **10a** (see Figs. 1B and 2C). If it is indeed the case that the strength of the hydrogen bridge (and thus the basicity of the "proton sponges") is determined not only by the N···N distance and the geometric arrangement (linear or non-linear) of the N···H···N hydrogen bridge but also by the hydrophobic shielding of the

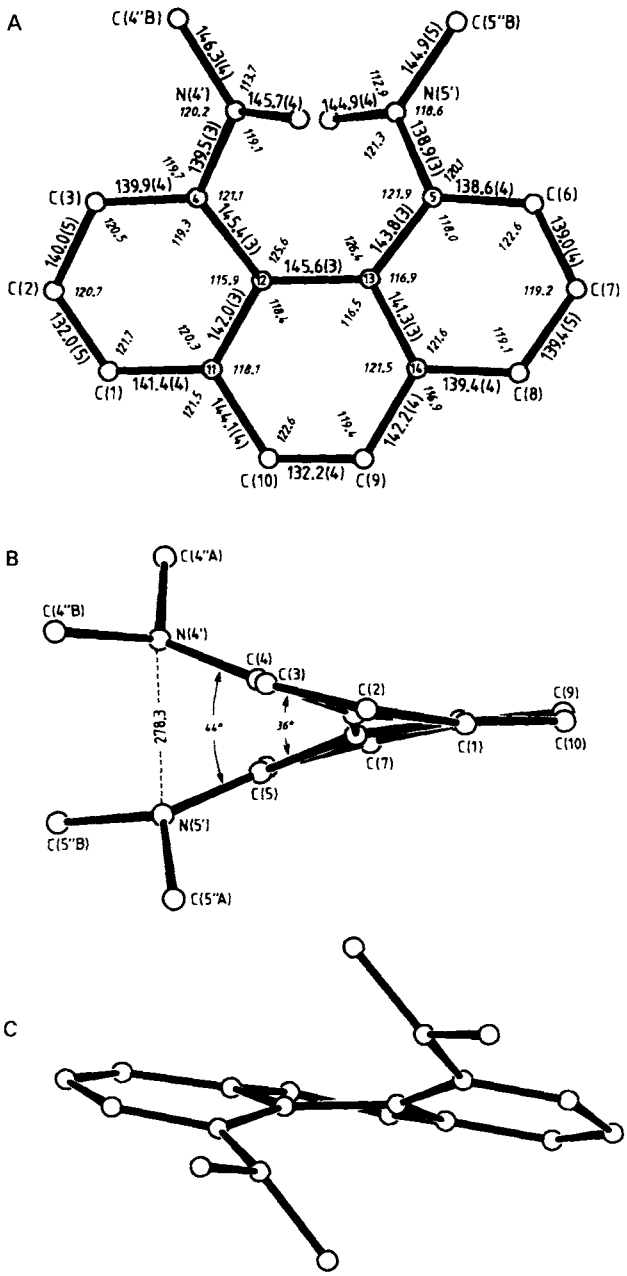

Fig. 3. Molecular structure of **16**, (A) looking down on the phenanthrene plane, (B) side view, (C) view along the (approximate) C_2 axis (bond angles in degrees, bond distances in pm; standard deviations in brackets) [35].

latter, then the observed basicity difference between **16a** and **10a** (or **4a**) could find an explanation on this basis (for a further discussion of this point see Section 8).

These attempts at explaining the variations in basicity in the series **4/10/16** show that several different factors must be taken into account, even within this series of very similar and relatively simple compounds. Our goal of being able to differentiate better between these factors led us to the syntheses of the systems described in Sections 5 and 6.

The 9,10-dichloro compound **22** also forms a monoperchlorate, as expected: in the proton NMR spectrum the N···H···N proton absorbs at $\delta = 17.7$ ([D$_6$]DMSO, 360 MHz); the coupling between this proton and the neighboring *N*-methyl protons is ca. 1.5 Hz. The NMR spectroscopic determination of the transprotonation equilibrium with **4** gave a pK_a-value for **22** of ca. 10.4: the reduction compared to the pK_a-value of **16** (11.5) is probably due to the inductive effect of the chlorine substituents in positions 9 and 10.—The basicity of the 4,5-bis(dimethylamino)-9,10-dihydrophenanthrene **21** will be discussed in Section 6 together with that of related biphenyl systems.

5. "Proton Sponge" Compounds with Dibenzofuran, Dibenzothiophene and Dibenzoselenophene Structures

The preceding comparison of the basicities of the "proton sponges" with naphthalene, fluorene and phenanthrene structures (**4/10/16**) showed that in this series a maximum was observed for the fluorene system **10**. Attempts to prepare and determine the basicities of the fluorene analogues **23**–**26** in which the heteroatom in the central five-membered ring is varied from oxygen via sulfur and selenium to tellurium were therefore of interest: in this series we can expect a stepwise change in the interaction between the dimethylamino groups in positions 1 and 9. On the basis of the X-ray structural analyses for dibenzofuran, dibenzothiophene, dibenzoselenophene and dibenzotellurophene and with the fictitious assumption that the bis(dimethylamino) compounds are planar we can expect the N···N distance to decrease on going from **23** via **24** and **25** to **26**: the fluorene derivative **10** should lie between **24** and **25**, while the phenanthrene derivative **16** has the shortest N···N distance and thus should follow **26**. This order did not change when this crude model based on the assumption of planar structures was replaced by force field calculations;[36] these take into account the deformation of the molecule resulting from the interactions between the dimethylamino groups and thus provide a more realistic basis for the interpretation of the protonation equilibria.

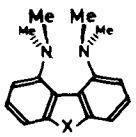

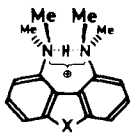

23, X = O ; **24**, X = S; **25**, X = Se; **26**, X = Te **23a**, X = O ; **24a**, X = S; **25a**, X = Se; **26a**, X = Te

The synthesis of the 1,9-bis(dimethylamino)benzofuran **23** has not as yet been completed. However, attempts to synthesize it afforded compound **27**;[36] in contrast to those of the "proton sponges" discussed previously, the basic centers of this compound are unsymmetric, but their arrangement in space corresponds roughly to that in **23**. With tetrafluoroboric acid **27** forms a tetrafluoroborate **27a** · BF_4, the proton NMR spectrum of which ([D$_6$]-DMSO, 500 MHz) shows a resonance at 13.34 ppm characteristic of a strong N···H···N hydrogen bridge. ^{1}H-NMR-spectroscopic determination of the transprotonation equilibrium with **4a** gives an unexpectedly high pK_a-value for **27a** of 12.3 ± 0.1. This result leads us to expect particularly marked "proton sponge" properties for the symmetrical fourfold *N*-methylated 1,9-dibenzofuran **23**.

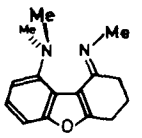

27

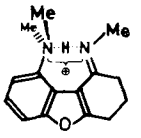

27a

The following route was used in the synthesis of the 1,9-bis(dimethylamino)dibenzothiophene **24**:[37] 2,2′-dibromo-6,6′-dinitrobiphenyl **28** (from 1,2-dibromo-3-nitrobenzene via an Ullmann reaction) was reduced by iron(III) chloride and hydrazine to afford 2,2′-diamino-6,6′-dibromodiphenyl **29**. Fourfold methylation (dimethyl sulfate, sodium hydride, tetrahydrofuran) to give the bis(dimethylamino) compound **30** was followed by treatment with *n*-butyllithium (tetrahydrofuran, −78 °C) to yield the dilithio compound **31**; this gave the desired dibenzothiophene **24** when treated with bis(phenylsulfonyl) sulfide.

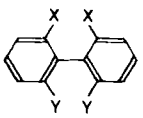

28, X = Br, Y = NO_2
29, X = Br, Y = NH_2
30, X = Br, Y = NMe_2
31, X = Li, Y = NMe_2

With excess tetrafluoroboric acid **24** forms the *mono*protonated **24a**-tetrafluoroborate, the bridging proton of which absorbs at extremely low field ($\delta = 19.06$ ppm, [D$_6$]-DMSO, 500 MHz). The transprotonation equilibrium with **4a** was studied by comparing the intensities of the *N*-methyl signals in the proton spectra: a pK_a-value for **24a** of 11.9 was obtained. Thus the basicity of the dibenzothiophene compound lies between those of the fluorene and phenanthrene "proton sponges" **10** and **16** (see Table 3 in Section 6).

X-ray structure analyses have been carried out for both **24** and **24a** (Fig. 4).[37] The extreme steric strain caused by the interactions between the dimethylamino groups is shown by a very definite deviation from planarity: this is demonstrated particularly by the torsion around the central C9a–C9b bond (21.3°), which causes C1 and C9 to be displaced in opposite directions by 33.1 and 30.3 pm respectively from the median plane of the five-membered ring. N1′ and N9′ are thus displaced 74.8 and 65.6 pm above and below this plane, so that the N···N distance is 286.1 pm.

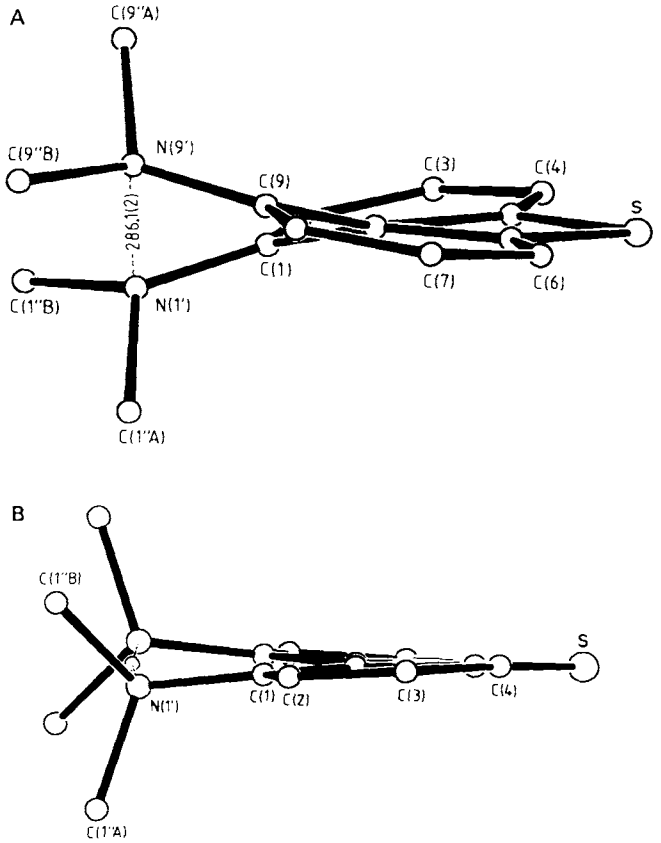

Fig. 4. Structures of **24** (A) and the **24a** part of **24a**-tetrafluoroborate (B) seen from the side along the C3···C7 axis [37].

A comparison of the molecular structures of **24** and **24a**-tetrafluoroborate (Fig. 4) from the side, looking along the C3···C7 axis) shows directly how much the protonation of **24** and the concomitant introduction of a strong N···H···N hydrogen bridge leads to a relief of the steric strain: in **24a** the torsion angle about the central CC bond referred to above is only 7.7° (instead of 21.3° in **24**); C1 and N1′ are displaced only by 9.9 and 24.9 pm respectively out of the plane of the five-membered ring, so that the N···N distance is reduced by 27.4 to 258.7 pm. The N···H···N bridge is almost linear, the angle being 175°.

The 1,9-bis(dimethylamino)dibenzoselenophene **25** was obtained by treating **31** with selenium powder. **25** also gives a monotetrafluoroborate **25a** · BF_4, the N···H···N proton of which absorbs at 19.28 ppm ([D_6]DMSO, 500 MHz). The structures of **25** and **25a**[37] correspond very closely to those of the analogous sulfur compounds **24** and **24a**. The comparison between **25** and the *mono*protonated cation **25a** (Fig. 5) makes clear the reduction in the steric strain which results on protonation, just as in the case of **24/24a**. The N···N distance is reduced from 282.3 to 257.3 pm, and the N···H···N bridge is here again almost linear (175°).

In view of the extremely similar structures of **24** and **25** and their monocations **24a** and **25a** it is not surprising that the basicities of the sulfur and selenium compounds are very similar: estimation of the pK_a of **25**, carried out as for **24** by NMR-spectroscopic determination of the transprotonation equilibrium with **4a** ([D_6]DMSO, 500 MHz), gave a value of 11.8 (within the limits of experimental error the same as that for **24** (11.9)).

Treatment of **31** with elemental tellurium gave the corresponding dibenzotellurophene **26**, from which a tetrafluoroborate was obtained on treatment with tetrafluoroboric acid. Both compounds have been clearly characterised by their mass and proton NMR spectra; however, they have not until now been obtained in sufficient quantities to permit basicity and structural studies.

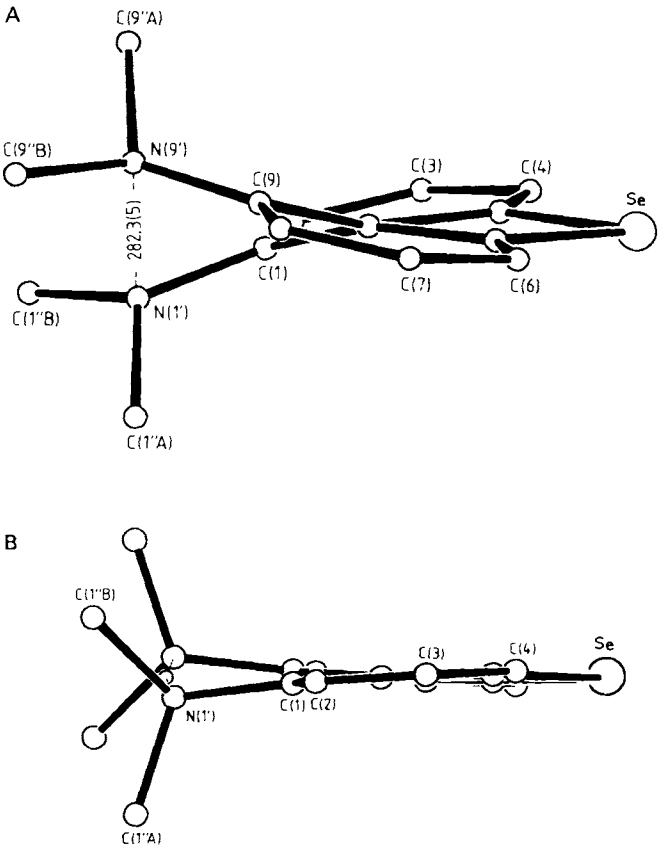

Fig. 5. Structures of **25** (A) and the **25a** part of **25a**-tetrafluoroborate (B) seen from the side along the C3-C7 axis [37].

6. "Proton Sponge" Compounds with Biphenyl Structure; *ortho*-Bis(dimethylamino)benzenes

The bis(dimethylamino)arenes discussed previously are inflexible systems with a large degree of steric strain; they are derivatives of arenes with planar parent structures. The compounds to be described below are however conformationally flexible and sterically less strained, and are derived from non-polar parent structures. Thus one of the two factors discussed above which are responsible for the high basicity of the "proton sponges", the destabilizing interaction of the lone pairs of the dimethylamino groups, should have little or no influence because the latter can more readily move apart; however, the preconditions for forming stable, nearly linear hydrogen bridges are still present. Thus a comparison of these two types of compound was of interest for the purpose of differentiating between and estimating the relative importance of these two factors.

A compound which with respect to its steric situation lies between the actual biphenyl derivatives and the systems derived from planar parent structures is 4,5-bis(dimethylamino)-9,10-dihydrophenanthrene **21**, the synthesis of which has been mentioned in Section 4. As in biphenyls the two aromatic rings in 9,10-dihydrophenanthrene are twisted away from one another around the central C_{aryl}–C_{aryl} bond. The dimethylamino groups in positions 4 and 5 enforce a further deviation from planarity, but the steric strain in **21** should be considerably lower than that in the corresponding phenanthrene derivative **16**.

However, **21** still has the typical properties of a "proton sponge", though these are less pronounced than in the corresponding phenanthrene derivative **16**: with perchloric acid, **21** forms **21a**-*mono*perchlorate, the N···H···N proton of which absorbs at 16.50 ppm ([D6]DMSO, 360 MHz). The pK_a-value was estimated from transprotonation experiments with **4a** to be ca. 10.9.[32]

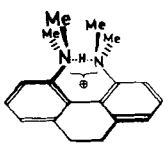

21a

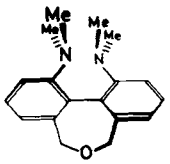

32

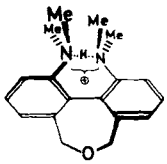

32a

Structural analyses of **21** and its monoprotonation product **21a** have not yet been carried out; however, information on the steric interactions in **21** and **21a**[38] can be obtained from the proton NMR spectra of **21** and **21a**-perchlorate and in particular from a comparison of the temperature-dependence of these spectra. At room temperature (360 MHz, [D2]dichloromethane) the protons of the *N*-methyl groups of **21** give a singlet at $\delta = 2.50$, while the methylene protons at C9 and C10 give an AA'BB'-multiplet with $\delta_A = 2.54$, $\delta_B = 2.77$ and J_{AB} ca. 9.7 Hz. On lowering the temperature the *N*-methyl signal is continually broadened until the coalescence temperature $T_C = 243$ K is reached; at 163 K these protons give two sharp singlets (1:1 intensity ratio) at $\delta = 2.01$ and 2.99. The dynamic process leading to an equivalence of the two pairs of *N*-methyl groups is apparently a nitrogen inversion with concomitant rotation about the C_{aryl}–N bond; $\Delta G^{\ddagger}_{T_c} = 45.7$ kJ mol^{-1}. A "flip" of the twisted ring system by means of a rotation about the central "biphenyl" bond, which would also lead to magnetic equivalence of the *N*-methyl protons, can be excluded because the absorption of the methylene protons at C9 and C10 remains unchanged over the above range of temperature: this multiplet undergoes broadening only above 400 K, though coalescence is still not observed at 423 K (in [D6]DMSO).

In contrast, the temperature-dependence of the proton spectrum of **21a**-perchlorate ([D3]acetonitrile, 360 MHz) shows a completely different dynamic behavior. At 243 K the two singlets for the two pairs of *N*-methyl protons ($\delta = 2.50$ and 3.23) and the splitting of the methylene protons (AA'BB' with $\delta_A = 2.64$, $\delta_B = 2.95$ and J_{AB} ca. 9.2 Hz) show that the two possible motional processes are "frozen" with regard to the NMR time scale, while on raising the temperature coalescence is observed for the methylene protons at 273 K and for the *N*-methyl protons at 283 K; at 353 K both the methylene and the *N*-methyl protons give a singlet ($\delta = 2.79$ and 2.88, respectively). The barriers to rotation for both groups of signals are in agreement ($\Delta G^{\ddagger}_{T_c} = 54.5 \pm 0.4$ and 54.3 ± 0.4 kJ/mol), indicating that the magnetic equivalence is caused by the same process, the flip of the 9,10-dihydrophenanthrene system. Thus this process occurs much more readily for the monocation **21a** than for **21**, due to its closer approach to planarity and the reduction of the steric hindrance of the dimethylamino groups by the N···H···N hydrogen bridge. On the other hand the nitrogen inversion in **21a** is not so facile as in the unprotonated diamine **21**; this again can be plausibly explained as a result of the formation of the strong N···H···N hydrogen bridge.

The 1,11-bis(dimethylamino)-5,7-dihydrodibenzo[*c*,*e*]oxepin **32** is a compound which has an even more twisted biphenyl unit than does **21**, so that the steric interactions between the two dimethylamino groups should be even further reduced. **32** was prepared starting from 2,2'-bis(hydroxymethyl)-6,6'-dinitrobiphenyl via 1,11-dinitro-5,7-dihydrodibenzo[*c*,*e*]oxepin: the diamino compound obtained from the latter by catalytic hydrogenation gave **32** on fourfold *N*-methylation.[38] **32** also shows "proton sponge" properties, even though these are considerably reduced: with excess perchloric acid in acetonitrile or chloroform one obtains **32a**-*mono*perchlorate, the N···H···N proton of which is much less low-field shifted than those of the "proton sponge" compounds discussed previously ($\delta = 11.76$; [D6]DMSO, 360 MHz). NMR-spectroscopic determination of the transprotonation equilibrium between **32a** and **4** gave a pK_a-value of ca. 9.4: this is still surprisingly high, but considerably lower than those of typical "proton sponges" and also lower than that of **21** (10.9).

As in the case of **21** and **21a**, the temperature dependence of the proton NMR spectra provides information on the steric situation in **32** and the monocation **32a** derived therefrom.[38] The spectrum of **32** is unchanged between 163 and 303 K; the twelve dimethylamino protons give a singlet at 2.46 ppm, while the benzylic protons of the dihydrooxepin ring form an AB-system with $\delta_A = 4.45$, $\delta_B = 4.17$ and $J_{AB} = 11.2$ Hz (CD_2Cl_2, 360 MHz). This indicates that the inversion-rotation process undergone by the dimethylamino groups in **32** occurs more readily here than in **21** because of the reduced steric interaction. However, the temperature-invariant AB-spectrum of the benzylic protons shows that the rotation about the central bond of the "biphenyl unit" is also strongly hindered in **32**, as in **21**. In spite of the reduction of the interaction of the dimethylamino groups caused by protonation, this flip of the dibenzooxepin skeleton in **32a** is in contrast to **21a** so slow that no change is observed for the AB-system formed by the benzylic protons of the dibenzooxepin ring between 273 and 353 K ($\delta = 3.81$ and 4.59 (each 2H), $J_{AB} = 11.4$ Hz; [D6]DMSO, 360 MHz). Apparently the seven-membered ring raises the barrier to the approach of the molecule to planarity, the necessary precondition for the flip process. On the other hand, in contrast to **21a**, the inversion/rotation of the dimethylamino groups can be observed in isolation in **32a**: the latter give two signals of equal intensity at 273 K ($\delta = 2.50$ and 3.19 ppm; [D3]acetonitrile, 360 MHz),

which coalesce at 338 K and give a single sharp line ($\delta = 2.82$ ppm) in [D$_6$]DMSO at 363 K. The barrier for the inversion-rotation process undergone by the dimethylamino groups in **32a** is $\Delta G_{T_c}^{\ddagger} = 65.4 \pm 0.4$ kJ mol^{-1}.

Compounds **21** and **32**, which differ from the "proton sponges" with a rigid arene structure and fixed dialkylamino groups by their greater conformational flexibility, lead over to systems in which no steric strain whatever due to interactions between the dialkylamino groups is to be expected. A simple example of such a compound is the 2,2′-bis(dimethylamino)biphenyl **33**: a steric interaction between the two *ortho*-substituents can be avoided by rotation of the aryl rings about the central C–C bond, while on the other hand these substituents are arranged in such a manner that they can be brought together by monoprotonation (to **33a**) to give an N···H···N hydrogen bridge of the type found in the "proton sponges".

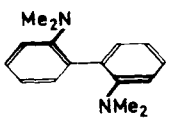

33

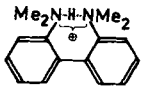

33a

33 had already been described in the literature;[39] we have obtained it in good yield from 2,2′-diaminobiphenyl using the methylation procedure[24] used successfully in the "proton sponges" (sodium hydride/dimethyl sulfate, tetrahydrofuran).[40] The molecular structure of **33** is shown in Figure 6A looking in the direction of the longitudinal axis of the molecule. The aryl rings are twisted by 57° around the central C–C bond and the dimethylamino groups in the two *ortho*-positions are arranged in an "*anti*-conformation" (i.e. far away from each other). The N···N distance is 473.8 pm, so that in contrast to all other bis(dimethylamino)arenes discussed previously there is obviously no steric interaction between the two dimethylamino groups. However, **33** also gives a *mono*hydrobromide with hydrogen bromide in *n*-hexane; the structure of this cation **33a** as determined by an X-ray analysis is shown in Figure 6B. The intramolecular N···H···N bridge formed on protonation brings the dimethylamino groups together so that the N···N distance is 265.0 pm; the hydrogen bridge is almost linear (175°).

NMR-spectroscopic determination of the transprotonation equilibrium with 1,8-dimorpholinonaphthalene[6] gave a pK_a-value of 7.9 ± 0.1 for **33**.[40] The observed increase of the basicity constant by almost three orders of ten compared with *N,N*-dimethylaniline must in this case be due solely to the formation of an N···H···N hydrogen bridge with a favorable geometry, since the destabilization of the free base by steric interactions between the dimethylamino groups discussed above as an additional effect for the actual "proton sponges" cannot exist for the reasons stated. It appears justified to regard the basicity increase for **33** as the *minimum* contribution made by the hydrogen bridge to the basicity increase in the actual "proton sponges". However, this value cannot be used in a quantitative classification of the energetic factors which lead to the unusual basicities of these compounds, since in "proton sponges" such as **4**, **10**, **16**, **24**, or **25** the formation of the hydrogen

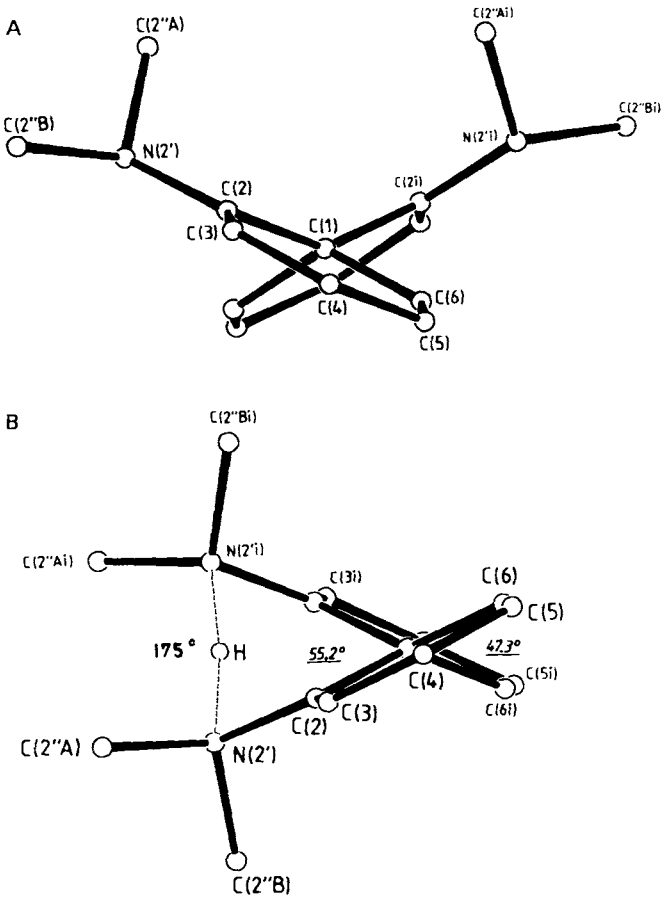

Fig. 6. Molecular structures of **33** (A) and the **33a**-part of **33**- monohydrobromide (B), looking in each case along the longitudinal axis of the biphenyl system [40].

bridge is inseparably connected with the decrease in steric strain resulting from the planarization of the aromatic rings and a normalization of bond lengths and angles. Some data for "proton sponges" are collected in Table 3.

The examples of bis(dimethylamino)arenes with conformational flexibility show that there is a gradual transition from the typical "proton sponges" with rigid structures and strong interactions between the dimethylamino groups

Table 3. Basicities of some "proton sponges"; N···N-distances and angles NHN in the corresponding monocations. For individual details see text.

Cpd.	Skeleton	pK_a	Cation	N···N [pm]	NHN [°]
4	Naphthalene	12.1	**4a**	260, 265	141
				255.4	153
10	Fluorene	12.8	**10a**	262.6	178
12	Fluorene	13.6			
13	Naphthalene	13.6			
14	Fluorene	14.1			
16	Phenanthrene	11.5	**16a**	254.4	168
21	Phenanthrene	10.9			
22	Phenanthrene	10.4			
24	Heterofluorene	11.9	**24a**	258.7	175
25	Heterofluorene	11.8	**25a**	257.3	175
27	Heterofluorene	12.3			
32	Dibenzooxepin	9.4			
33	Biphenyl	7.9	**33a**	265.0	175
34	Benzene		**34a**	271.6	119 [a]
35	Quinoquinoline	12.8			

[a] Additional coordination to water molecules (forked hydrogen bonds).

to compounds in which this steric strain is increasingly reduced until it disappears completely. Part of the "proton sponge" behavior will be retained as long as the geometrical preconditions for the formation of a strong N···H···N bridge are fulfilled. The last example in this series will show that on the other hand rigid arene systems with dimethylamino groups situated very close together do *not* show this unusual behavior when the steric preconditions for both a destabilizing interaction between the lone pairs of the free base and a stable N···H···N hydrogen bridge in the *mono*protonated system are unfavorable. For other reasons, in this case because of its unusual properties as an extremely strong *two*-electron donor, we recently synthesized 1,2,4,5-tetrakis(dimethylamino)benzene **34**, which contains two pairs of dimethylamino groups in positions *ortho* to one another. The steric interaction between the dimethylamino groups in **34** is shown by the fact that the unusually easy release of two electrons ($E_{ox}^{1,2} = -0.266$ V) is connected with the transition of the planar aromatic system into a dication **34a** with two polymethine units, which according to the X-ray structural analysis are tilted away from one another by 49°, thus causing a *twist* arrangement of the six-membered ring.[41]

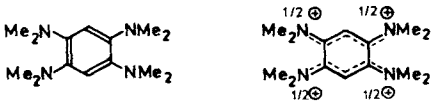

34 **34a**

Although **34** has two pairs of dimethylamino groups in *ortho* positions to one another, the preconditions for "proton sponge" properties are not favorable; because of the diverging C_{aryl}–N bonds the dimethylamino groups must have a larger N···N distance than in the "proton sponges" discussed above. For the same reason the lone pairs cannot be directed towards each other, and of course linear N···H···N hydrogen bridges cannot be formed along the preferred directions of the nitrogen lone pairs.

A **34**-dihydrobromide dihydrate is, however, in fact obtained when a 48% aqueous solution of hydrogen bromide is added to a concentrated solution of **34** in ether; thus each pair of dimethylamino groups undergoes only a monoprotonation. The structure of the dication of **34** is shown in Figure 7A looking down on the benzene ring, and in Figure 7B from the side.[42] The four nitrogens of the dimethylamino group are almost coplanar with the aromatic ring, and the N···N distance of 271.6 pm is so short that relatively strong hydrogen bonds could in fact have been formed if a linear arrangement were possible. However, this is hindered by the preferred directions of the N1-H bonds and the lone pairs on the neighboring nitrogens, so that two very unsymmetrical N–H···N bridges with an angle of 119° are formed. These hydrogen bridges appear to be so labile that their stabilization requires the additional coordination to water molecules in a bifurcated hydrogen bridge, as shown in Figure 7A. Thus, **34** does *not* exhibit the typical properties of "proton sponge" compounds in spite of the close approach of the dimethylamino groups within each pair.

7. Mass Spectra of "Proton Sponge" Compounds

The small distance between the dialkylamino groups, which is so important in determining the "proton sponge" properties of the compounds discussed here, also causes these compounds to exhibit a characteristic behavior under mass spectrometric conditions. Table 4 gives the relative intensities of the most important ions observed in the mass spectra of a series of bis(dimethylamino)arenes on electron impact (EI) ionization. The most prominent fragment ion, which forms the base peak in all these spectra, is formed from the molecular ion by the cleavage of a fragment of

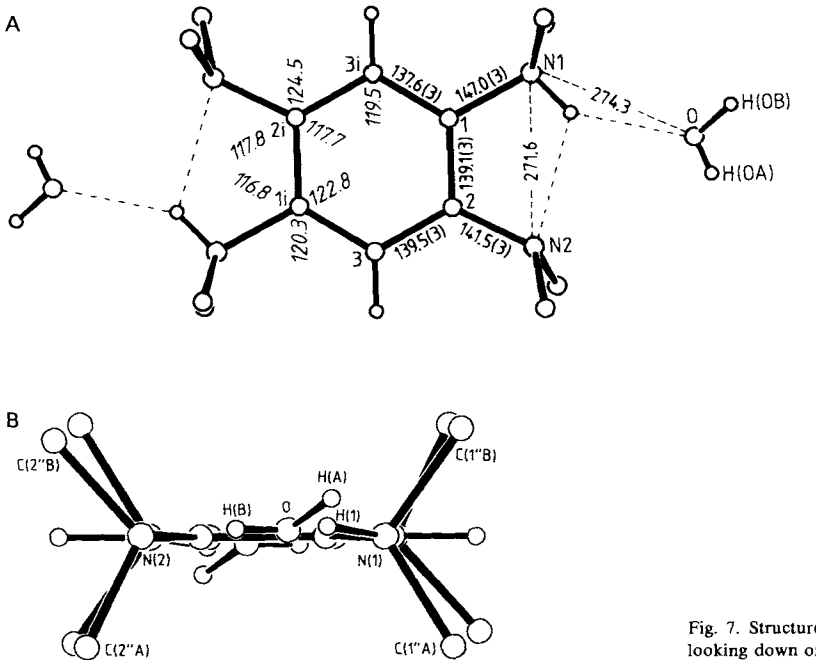

Fig. 7. Structure of the **34**-dication part of **34**-dihydrobromide dihydrate looking down on the benzene plane (A) and from the side (B) [42].

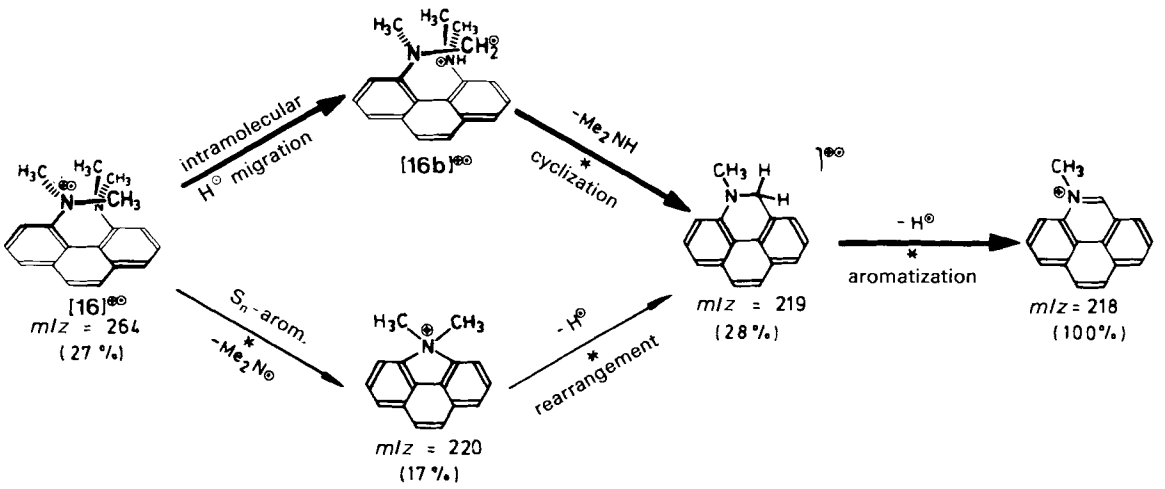

Scheme 1. Main fragmentation routes for 4,5-bis(dimethylamino)phenanthrene **16** under the conditions of EI mass spectrometry [43].

mass 46, which is formally equivalent to dimethylamine plus one hydrogen. Detailed mass-spectrometric studies showed that this fragmentation behavior is the result of rearrangement, cleavage and cyclization processes which are all due to the short distance between the two dimethylamino groups.[43,44]

The driving force in this process is the formation of stable ions with aromatic bonding systems. This is shown in Scheme 1 for the fragmentation of the phenanthrene "proton sponge" **16**.

Similar fragmentation processes have been documented for the other compounds in Table 4,[43,44] and analogous mass-spectrometric decomposition mechanisms have also been found to apply for 1,8-bis(dimethylamino)naphthalene **4** and 4,5-bis(dimethylamino)fluorene **10**.[45]

Table 4. Relative intensities of the most important ions in the EI mass spectra of several "proton sponge" compounds (corrected for their ^{13}C and ^{37}Cl content) [43, 44].

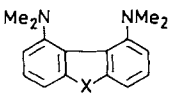

	–X–	$[M]^{\oplus\odot}$	$[M-Me_2NH]^{\oplus\odot}$	$[M-Me_2NH-H]^{\oplus}$
16	–CH=CH–	27	28	100
19	$-CH_2-S-CH_2-$	73	43	100
21	$-CH_2-CH_2-$	25	25	100
22	–CCl=CCl–	25	22	100
24	–S–	69	33	100
25	–Se–	63	24	100
26	–Te–	40	12	100
32	$-CH_2-O-CH_2-$	70	36	100
33	–H H–	66	46	100

8. Quino[7,8*h*]quinoline, a "Proton Sponge" of a New Type

All the "proton sponge" compounds discussed so far are bis(dialkylamino)arenes in which the basic centers, and thus the N···H···N hydrogen bridges of the monoprotonated species, are hydrophobically shielded. It is not yet clear how the bond strength of hydrogen bridges is influenced by such hydrophobic surroundings, but it is certainly the case that the very low rates of proton transfer found for presently known "proton sponges" are connected with this hydrophobic shielding (see Table 2).

In this context a compound which was of interest to us was quino[7,8*h*]quinoline **35**, a compound in which such a hydrophobic shielding is not present but in which two nitrogen atoms are arranged in a manner similar to that in 1,8-bis(dimethylamino)naphthalene **4**, the prototype of a "proton sponge".

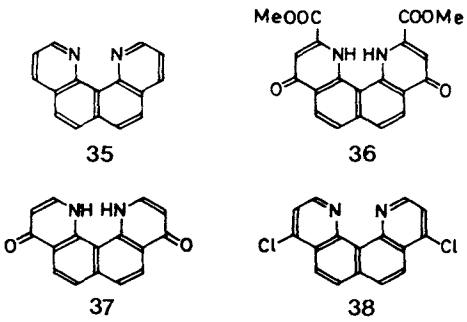

Several reports on the preparation and properties of **35** have appeared in the last four decades:[46,47] however, these reports have in all cases been later shown to be incorrect. In one case the compound reported as **35** was a structural isomer[48] and in a second a Skraup synthesis which should yield **35**[47] actually gave 2-methyl-1,3-diazapyrene.[49] Thus quino[7,8-*h*]quinoline was hitherto unknown.

In our recently reported synthesis of **35**[1] we treated **3** with dimethyl acetylenedicarboxylate to give 2,2'-(1,8-naphthylenediimino)di(methylfumarate),[50] which was thermally cyclized to **36**. Alkaline hydrolysis and thermal decarboxylation (335–370 °C/10^{-5} torr) led to **37**, which was treated with phosphoryl chloride to give 4,9-dichloro[7,8*h*]quinoline **38**. Catalytic hydrogenation (Pd/C, glacial acetic acid, sodium acetate) yielded **35**, the structure of which was determined analytically and spectroscopically, and confirmed by a recent X-ray structure analysis.[51]

Like other "proton sponge" compounds, **35** forms only a *mono*perchlorate with excess perchloric acid; its struc-

ture **35a** follows from the proton NMR spectrum, which shows an absorption at $\delta = 19.38$ (in DMSO), the most strongly downfield-shifted signal yet observed for an N···H···N hydrogen bridge. **37** similarly forms **37a**-perchlorate, for which the absorption of the hydrogen bridge proton is observed at $\delta = 19.34$ (in DMSO).

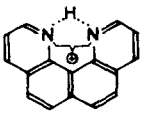

35a

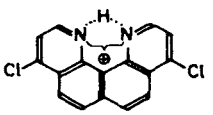

38a

On the basis of transprotonation experiments of **35** with **4a** and of **35a** with **4** the pK_a-value of **35** was estimated by proton NMR spectroscopy (500 MHz, [D$_6$]DMSO) to be ca. 12.8. Thus the basicity of **35** is increased by nearly eight powers of ten compared to that of quinoline ($pK_a = 4.91$), slightly exceeding the increase in basicity of **4** compared with *N,N*-dimethylaniline (cf. Section 1). Thus, the hydrophobic shielding of the N···H···N hydrogen bridge apparently plays no part in determining the high thermodynamic basicity of the "proton sponge" compounds. It does, however, have a great influence on the kinetics of proton transfer: ^{1}H-NMR spectra of mixtures of **35** and **35a** in [D$_6$]DMSO at room temperature already show coalesced signals for the different groups of protons at mean values corresponding to the ratio **35/35a**, so that in contrast to the other types of "proton sponge" discussed above the proton exchange between **35** and **35a** is apparently fast. These results show that according to the "proton sponge" concept not only strong but also kinetically active bases are available when the hydrophobic shielding of the basic centers and the N···H···N hydrogen bridge are avoided. Compounds such as **39** and **40**, the syntheses of which are at present in progress,[52] are of interest since the basicity of **39** at least is expected to be greater than that of **35**.

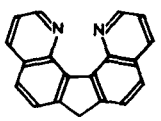

39

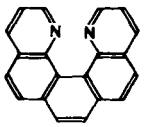

40

9. Future Prospects

The present report on "proton sponge" compounds should make it clear that we are dealing here with a fascinating group of compounds which is of interest not only because of the unusual basicity of its members: it is in fact the combination of the basic properties with steric structural factors and the question of the optimum geometry of hydrogen bridges which makes this area of chemistry so intriguing for us.

In this report we have concentrated on work which has been done in our own group in Heidelberg and have drawn thematic boundaries by restricting ourselves to *aromatic* diamines. Although we are also working in the interesting area of the *mono-* and *bi*cyclic *aliphatic* diamines[29] we have excluded these from the present report, since reviews on this area already exist, even if they are somewhat dated.[53]

Peculiar properties, such as those discussed above which result from steric interactions between basic centers, are certainly also of importance outside the narrow area of the compounds discussed here.[54] We consider them to be examples of cooperative spatial interactions between reactive structural elements which can lead to unusual and gradually varying properties which could not be expected from an isolated treatment of the various functional groups. Such "proximity effects" are indeed of greater importance in chemistry and biochemistry than is reflected by the amount of work so far put into their systematic study.

We thank Dr. Marina Rentzea, Claus Krieger, Dr. Matthias Höne, Dr. Wolfgang Brox, Dipl.-Chem. Michael A. Zirnstein and Dipl.-Chem. Klaus Oberdorf for their engaged and very successful cooperation in dealing with the problems discussed here.

Received: February 10, 1988 [A 680 IE]
German version: *Angew. Chem. 100* (1988) 895
Translated by Prof. Dr. *T. N. Mitchell*, Dortmund (FRG)

[1] M. A. Zirnstein, H. A. Staab, *Angew. Chem. 99* (1987) 460; *Angew. Chem. Int. Ed. Engl. 26* (1987) 460.
[2] Cf., e.g., H. A. Staab: *Einführung in die theoretische organische Chemie*, 4. Edit., Verlag Chemie, Weinheim 1964, Chap. 4; and references cited therein.
[3] R. W. Alder, P. S. Bowman, W. R. S. Steele, D. R. Winterman, *J. Chem. Soc. Chem. Commun. 1968*, 723.
[4] F. Hibbert, *J. Chem. Soc. Perkin Trans. 2 1974*, 1862. Here and in the following ([5a,b]) the basicity is as usual denoted by the acidity constant K_a of the corresponding acid.
[5] a) R. W. Alder, N. C. Goode, N. Miller, F. Hibbert, K. P. P. Hunte, H. J. Robbins, *J. Chem. Soc. Chem. Commun. 1978*, 89; b) F. Hibbert, K. P. P. Hunte, *J. Chem. Soc. Perkin Trans. 2 1983*, 1895.
[6] R. W. Alder, M. R. Bryce, N. C. Goode, N. Miller, J. Owen, *J. Chem. Soc. Perkin Trans. 1 1981*, 2840; the term "proton sponge" was introduced by Aldrich Chemicals Co., Milwaukee, as a tradename for **4**.
[7] R. W. Alder, M. R. Bryce, N. C. Goode, *J. Chem. Soc. Perkin Trans. 2 1982*, 477.
[8] See, e.g., G. C. Pimentel, A. L. McClellan: *The Hydrogen Bond*, W. H. Freeman, San Francisco 1960; S. N. Vinogradov, R. H. Linnell: *Hydrogen Bonding*, Van Nostrand Reinhold, New York 1971; P. Schuster, G. Zundel, C. Sandorfy (Eds.): *The Hydrogen Bond*, North-Holland, Amsterdam 1976.
[9] R. Taylor, O. Kennard, *Acc. Chem. Res. 17* (1984) 320, and references cited therein.
[10] H. A. Staab, W. Rebafka, *Chem. Ber. 110* (1977) 3333; H. A. Staab, U. Zapf, *Angew. Chem. 90* (1978) 807; *Angew. Chem. Int. Ed. Engl. 17* (1978) 757; H. A. Staab, C.-P. Herz, A. Döhling, C. Krieger, *Chem. Ber. 113* (1980) 241; H. A. Staab, C.-P. Herz, C. Krieger, M. Rentea, *ibid. 116* (1983) 3813; H. A. Staab, C. Krieger, P. Wahl, K.-Y. Kay, *ibid. 120* (1987) 551; and references cited therein.
[11] H. A. Staab, N. Riegler, F. Diederich, C. Krieger, D. Schweitzer, *Chem. Ber. 117* (1984) 246; P. Wahl, C. Krieger, D. Schweitzer, H. A. Staab, *ibid. 117* (1984) 260; and references cited therein.
[12] M. Eigen, *Angew. Chem. 75* (1963) 489; *Angew. Chem. Int. Ed. Engl. 3* (1964) 1; M. Eigen, W. Kruse, G. Maass, L. De Maeyer, *Prog. React. Kinet. 2* (1964) 285.
[13] Cf. F. Hibbert, *Acc. Chem. Res. 17* (1984) 115, and references cited therein.
[14] A. J. Kresge, M. F. Powell, *J. Am. Chem. Soc. 103* (1981) 972.
[15] R. J. Saxton, L. J. Wilson, *J. Chem. Soc. Chem. Commun. 1984*, 359; F. Terrier, J.-C. Halle, M.-J. Pouet, M.-P. Simonnin, *J. Org. Chem. 51* (1986) 409.
[16] H. Einspahr, J.-B. Robert, R. E. Marsh, J. D. Roberts, *Acta Crystallogr. Sect. B29* (1973) 1611.
[17] M. R. Truter, B. L. Vickery, *J. Chem. Soc. Dalton Trans. 1972*, 395.
[18] D. Pyźalka, R. Pyźalki, T. Borowiak, *J. Crystallogr. Spectrosc. Res. 13* (1983) 211.
[19] Cf. also R. L. de Groot, D. J. Sikkema, *Recl. Trav. Chim. Pays-Bas 95* (1976) 10.

[20] L. J. Altman, D. Laungani, G. Gunnarsson, H. Wennerström, S. Forsén, *J. Am. Chem. Soc. 100* (1978) 8264; cf. also S. I. Chan, L. Lin, D. Clutter, P. Dea, *Proc. Natl. Acad. Sci. USA 65* (1970) 816.
[21] G. Gunnarsson, H. Wennerström, W. Egan, S. Forsén, *Chem. Phys. Lett. 38* (1976) 96.
[22] E. Haselbach, A. Henriksson, F. Jachimowicz, J. Wirz, *Helv. Chim. Acta 55* (1972) 1757.
[23] H. A. Staab, T. Saupe, C. Krieger, *Angew. Chem. 95* (1983) 748; *Angew. Chem. Int. Ed. Engl. 22* (1983) 731.
[24] H. Quast, W. Risler, G. Döllscher, *Synthesis 1972*, 558.
[25] Cf. also [5b].
[26] R. Gleiter, W. Schäfer, H. A. Staab, T. Saupe, *J. Org. Chem. 49* (1984) 4463.
[27] J. P. Maier, *Helv. Chim. Acta 57* (1974) 994.
[28] T. Saupe, H. A. Staab, unpublished; see also T. Saupe, *Dissertation*, Universität Heidelberg 1985.
[29] W. Brox, *Dissertation*, Universität Heidelberg 1987.
[30] F. Hibbert, G. R. Simpson, *J. Chem. Soc. Perkin Trans. 2 1987*, 613; see also R. W. Alder, R. B. Sessions in S. Patai (Ed.): *The Chemistry of Functional Groups, The Chemistry of Amino, Nitroso, and Nitro Compounds*, Wiley, Chichester 1982, p. 763.
[31] K. Oberdorf, *Diplomarbeit*, Universität Heidelberg 1986 and unpublished results.
[32] T. Saupe, C. Krieger, H. A. Staab, *Angew. Chem. 98* (1986) 460; *Angew. Chem. Int. Ed. Engl. 25* (1986) 451.
[33] C. Y. Meyers, A. M. Malte, W. S. Matthews, *J. Am. Chem. Soc. 91* (1969) 7510; C. Y. Meyers, W. S. Matthews, G. J. McCollum, J. C. Branca, *Tetrahedron Lett. 1974*, 1105; but see the negative results reported by L. A. Paquette, *J. Am. Chem. Soc. 86* (1964) 4085; *Acc. Chem. Res. 1* (1968) 209, for the synthesis of 4,5-disubstituted phenanthrenes via a Ramberg-Bäcklund rearrangement.
[34] R. Gleiter, private communication.
[35] M. Höne, C. Krieger, T. Saupe, H. A. Staab, *Tetrahedron Lett.*, in press.
[36] M. Höne, *Dissertation*, Universität Heidelberg 1987; Programm MM2 (82)/MMP2 from Molecular Design Ltd., Hayward, CA (USA).
[37] H. A. Staab, M. Höne, C. Krieger, *Tetrahedron Lett. 29* (1988) 1905.
[38] H. A. Staab, T. Saupe, unpublished results.
[39] F. R. Shaw, E. E. Turner, *J. Chem. Soc. 1933*, 135.
[40] H. A. Staab, M. Höne, C. Krieger, *Tetrahedron Lett.*, in press.
[41] K. Elbl, C. Krieger, H. A. Staab, *Angew. Chem. 98* (1986) 1024; *Angew. Chem. Int. Ed. Engl. 25* (1986) 1023.
[42] H. A. Staab, K. Elbl, C. Krieger, *Tetrahedron Lett. 27* (1986) 5719.
[43] M. Rentzea, T. Saupe, H. A. Staab, *Tetrahedron Lett. 27* (1986) 5715.
[44] M. Rentzea, M. Höne, H. A. Staab, unpublished results.
[45] M. Rentzea, T. Saupe, W. Brox, H. A. Staab, unpublished results.
[46] I. Iwai, S. Hara, *Yakugaku Zasshi 70* (1950) 32; K. Shibata, *Bull. Chem. Soc. Jpn. 24* (1951) 187.
[47] M. Dufour, N. P. Buu-Hoi, P. Jacquignon, *J. Chem. Soc. C1967*, 1415.
[48] I. Iwai, S. Hara, S. Sayegi, *Yakugaku Zasshi 71* (1951) 1152; S. V. Nekrasov, A. V. El'tsov, *J. Org. Chem. USSR (Engl. Transl.) 7* (1971) 186.
[49] A. Edel, P. A. Marnot, J. P. Sauvage, *Tetrahedron Lett. 26* (1985) 727; H. A. Staab, I. Newsom, unpublished results.
[50] Cf. also K. Honda, H. Nakanishi, A. Yabe, *Bull. Chem. Soc. Jpn. 56* (1983) 2338.
[51] C. Krieger, M. A. Zirnstein, H. A. Staab, *Tetrahedron Lett.*, in press.
[52] H. A. Staab, M. A. Zirnstein, unpublished results.
[53] R. W. Alder, R. B. Sessions in S. Patai (Ed.): *The Chemistry of Functional Groups, The Chemistry of Amino, Nitroso, and Nitro Compounds*, Wiley, Chichester 1982, Chap. 18; R. W. Alder, *Acc. Chem. Res. 16* (1983) 321.
[54] Cf., e.g. R. Schwesinger, M. Missfeldt, K. Peters, H. G. von Schnering, *Angew. Chem. 99* (1987) 1210; *Angew. Chem. Int. Ed. Engl. 26* (1987) 1165.

Atomic Motions in Molecular Crystals from Diffraction Measurements

By Jack D. Dunitz,* Emily F. Maverick,* and Kenneth N. Trueblood*

The information provided by modern crystal structure analyses is not limited to the atomic arrangement. It also includes, for each atom, a set of quantities known as anisotropic Gaussian displacement parameters (ADP's), which provide information about averaged displacements of atoms from their mean positions. From analysis of these quantities, conclusions can be drawn about the rigid-body motion of molecules, about large-amplitude internal molecular motions, and about the identification of any disorder present in the crystals as being mainly dynamic or mainly static in nature. For some crystals, such analyses yield energy barriers to rotation of rigid molecules or molecular fragments that are in good agreement with values obtained by other physical methods.

1. What this Article Is About

The atoms in a crystal are not stationary; they move appreciably about their mean positions. From diffraction studies one obtains information not only about the mean atomic positions but also about the probability density functions of the individual atoms, a measure of their time-averaged displacements from their mean positions, averaged again over all the repeating units in the crystal. Both kinds of information are expressed in the innumerable pictures in the chemical and crystallographic literature where atoms are conventionally represented by "vibration ellipsoids".[1] From such pictures it is not difficult to recognize qualitative features of the atomic motions; in Figure 1, for example, it is apparent that the atoms vibrate preferentially in definite directions and by different amounts. Analysis of the numerical parameters on which such pictures are based often makes it possible to obtain quantitative information about the rigidity of molecules in crystals, about the nature and degree of rigid-body molecular motions, and even about internal motions of supposedly rigid fragments in nonrigid molecules. With the aid of a few rather simple additional assumptions, it is then in principle possible to derive quantities such as force constants or rotation barriers that are normally associated with the realm of spectroscopic methods. The purpose of this article is to describe to chemists and other scientists what can be learned about atomic motions in crystals from the interpretation of diffraction data.

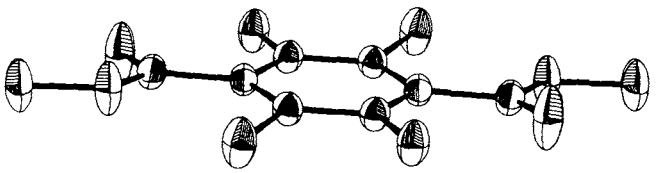

Fig. 1. Vibration ellipsoids for all atoms except hydrogens in the molecule of dimethyl 3,6-dichloro-2,5-dihydroxyterephthalate (see formula **3** in Section 6).

[*] Prof. J. D. Dunitz
Organic Chemistry Laboratory,
Swiss Federal Institute of Technology, ETH-Zentrum
Universitätsstrasse 16, CH-8092 Zürich (Switzerland)
Prof. E. F. Maverick
Department of Chemistry,
Los Angeles City College
Los Angeles, CA 90029 (USA)
Prof. K. N. Trueblood
Department of Chemistry and Biochemistry,
University of California, Los Angeles, CA 90024 (USA)

2. Preliminaries

In most modern X-ray or neutron crystallographic studies of small-molecule structures, it is assumed that the probability density function (pdf) of each individual atom can be represented by a Gaussian. In one dimension, this would be Equation (1), where u^2 is the second moment

$$D(x)=(2\pi u^2)^{-1/2}\exp(-x^2/2u^2) \quad (1)$$

(sometimes known as the variance or dispersion) of the pdf. In three dimensions, the corresponding equation looks more complicated, but it is exactly analogous [Eq. (2)]. Here $\boldsymbol{x}$ is now a vector with three components

$$D(\boldsymbol{x})=(2\pi)^{-3/2}(\det \boldsymbol{U}^{-1})^{1/2}\exp(-\boldsymbol{x}^{\mathrm{T}}\boldsymbol{U}^{-1}\boldsymbol{x}/2) \quad (2)$$

(x_1, x_2, x_3), and $\boldsymbol{U}^{-1}$ is the inverse of the symmetric second-moment matrix $\boldsymbol{U}$. The equiprobability surfaces of this pdf are ellipsoids, and its second moment in an arbitrary direction defined by a unit vector $\boldsymbol{n}(n_1, n_2, n_3)$ is $u^2=\boldsymbol{n}^{\mathrm{T}}\boldsymbol{U}\boldsymbol{n}$, corresponding to the mean-square displacement amplitude (MSDA) in that direction.[2] It must be emphasized that these pdf's are *not* the functions that describe the electron density of the stationary atoms; rather, they approximate the ways in which these electron densities are further spread out (Fig. 2) by the diffuseness in the nuclear positions resulting from lack of perfect periodicity in the crystal. In the real crystal, the atoms are vibrating about their equilibrium positions (dynamic disorder), and they may also be distributed at random over different sets of equilibrium positions from one unit cell to another (static disorder). The pdf's approximate the distributions obtained by averaging the instantaneous atomic positions over time and over all unit cells in the crystal.

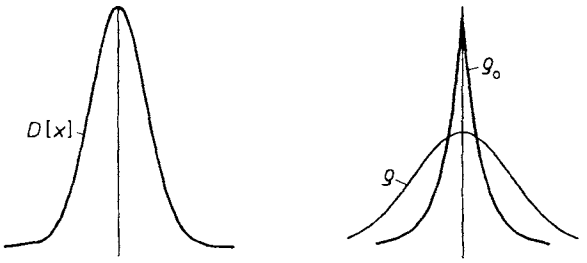

Fig. 2. The one-dimensional electron-density distribution $\rho(x)$ is the convolution of the static density $\rho_0(x)$ with the probability distribution function $D(x)$. The second moment of $D(x)$ (u^2) corresponds to the MSDA of the atom from its average position.

The scattering power (or form factor) of a stationary atom is given by the Fourier transform of its electron density distribution. For a vibrating atom, this form factor has to be multiplied by the Fourier transform of the corresponding pdf. One advantage of the Gaussian description is that the Fourier transform of a Gaussian is also a Gaussian. In three dimensions, this is given by Equation (3),

$$T(\boldsymbol{h}) = \exp(-2\pi^2 \boldsymbol{h}^T \boldsymbol{U} \boldsymbol{h}) \tag{3}$$

where $\boldsymbol{h}(h_1, h_2, h_3)$ is the scattering vector (of length $2\sin\theta/\lambda$) and $\boldsymbol{U}$ is the second-moment matrix mentioned. The quantity $T(\boldsymbol{h})$ is traditionally known as the "temperature factor", here the *anisotropic* temperature factor since it has different values in different directions. It may, or it may not, however, have anything to do with the temperature; it will, if the pdf associated with $\boldsymbol{U}$ is due mainly to dynamic disorder. On the other hand, if the pdf is due mainly to static disorder, some components of $\boldsymbol{U}$ will show little or no temperature dependence.

The components of $\boldsymbol{U}$ (in general, six for each atom) are usually included as parameters, together with the atomic positional parameters, in the least-squares refinement stages of a crystal structure analysis. They have sometimes been called "vibration parameters" and sometimes "thermal parameters", but we prefer a description that is more neutral concerning the possible physical significance of these quantities; we shall therefore refer to them simply as anisotropic displacement parameters (ADP's). Isotropic, one-parameter pdf's are usually assumed in X-ray analysis for hydrogen atoms, and sometimes also for other light atoms in the presence of heavy ones. This is not because the corresponding motions are thought to be really isotropic, but rather because the weak relative scattering power of these atoms calls for extreme economy in the number of parameters involved in the description of their pdf's.

For organic crystals at room temperature, typical MSDA's are around 500 to 1000 pm^2, corresponding to root-mean-square (rms) displacement amplitudes in the range 25 to 30 pm. At 100 K the MSDA's would be reduced to about a third of their room-temperature values. Nominal standard deviations in atomic positions obtained from carefully measured diffraction data are often 1 pm or less. Thus the breadth of an atomic pdf (the rms displacement) is many times larger than the uncertainty in the position of its centroid and is an appreciable fraction of a typical interatomic distance.

A Gaussian atomic pdf would correspond to motion of the atoms in a quadratic potential. In principle, the additional terms (higher cumulants) required for the description of non-Gaussian pdf's could also be determined by including appropriate parameters in the least-squares analysis. In addition to the six parameters describing the second moments, one might include ten cubic terms, fifteen quartic ones, and so on. The main problem is that these higher terms are only likely to be important when the second moments are large. However, the larger the second moments, the more rapidly the scattering from the atom in question falls off with scattering angle. Thus, it is just when the higher terms become important that they become virtually impossible to measure.

The "vibration ellipsoids" that adorn so many crystallographic publications are surfaces given by Equation (4)

$$\boldsymbol{x}^T \boldsymbol{U}^{-1} \boldsymbol{x} = \text{constant} \tag{4}$$

that enclose some specified probability (usually 50%). Although one can obtain a vivid impression of the directions and relative magnitudes of the atomic motions from the ellipsoids, a more quantitative interpretation requires a detailed analysis of the numbers from which they are obtained, the ADP's themselves.

3. Problems in the Interpretation of ADP's

Before we discuss the potentialities of ADP's for the study of atomic motion in crystals, we have to mention some difficulties. First, there is the problem that the ADP's associated with a given atomic center in a crystal structure refer to the motion of an *averaged* atom and not to the motion of any individual one. Thus, although a Gaussian pdf for an individual atom could be regarded as evidence for a harmonic potential for its motion, it is by no means obvious how far this would apply to the motion of the averaged one, where the averaging has been made over all the unit cells in the crystal. (There is a sense in which we can say that this averaged atom does not exist, any more than the average family with 1.743 children exists.) In the second place, the displacements of the individual atoms are highly correlated, and the ADP's provide no information whatsoever about the nature of these correlations; an important part of the information necessary to describe the atomic motions has therefore been lost. The assumption that particular groupings of atoms, e.g., molecules or molecular fragments, are rigid can be very helpful here. It is equivalent to assuming certain types of correlations involving amplitude and phase relationships among the atomic displacements, and we shall make considerable use of it. But even with this assumption, we still have to ignore all forms of correlation between the displacements of atoms belonging to neighboring molecules or between rigid groupings within the same molecule.

We can circumvent these problems to some extent by adopting what can be described as a mean-field model. We assume that the motion of a given atom (or molecule) in the crystal is governed by the effective potential imposed by its averaged environment. If a suitable force field is

available, this potential can be calculated by summing all relevant interatomic interactions, assuming one atom (or molecule) to be displaced while all neighboring atoms (or molecules) remain fixed in their average positions.[3] Although this model is vastly oversimplified, it nevertheless helps us to visualize important aspects of the real, more complex situation, and, as we shall see later, it often even leads to conclusions that agree remarkably well with the experimental observations.

4. The Rigid-Body Model

Most interpretations of ADP's are based on the assumption that the crystal contains more-or-less rigid groupings of atoms. Except for certain kinds of constrained refinement, the U^{ij} parameters, the components of the atomic $\boldsymbol{U}$ matrices, are treated as independent variables. However, it is clear that for a perfectly rigid molecule of known geometry, the values of these U^{ij} parameters would be completely determined by the molecular translational and librational oscillations—under the given conditions, they are the only types of motion possible. Even if the molecule is not perfectly rigid, the amplitudes of the individual atomic motions resulting from its internal vibrations can generally be expected to be much smaller than those from its overall translational and rotational motions. It is therefore often reasonable to use the rigid-body model, at least as a first approximation, and attempt to fit the parameters that describe its translational and rotational motions to the observed U^{ij} values. To describe the translational motion we need six numbers, the components $\langle t^i t^j \rangle$ of a symmetric matrix $\boldsymbol{T}$, analogous to $\boldsymbol{U}$ but now referring to the molecule as a whole. The translational contribution to the ADP's is necessarily the same for all the atoms in the rigid body. The librational motion is more complicated, but it can also be described by the components $\langle \lambda^i \lambda^j \rangle$ of a symmetric matrix $\boldsymbol{L}$. The fitting of the components of $\boldsymbol{T}$ and $\boldsymbol{L}$ to the observed atomic U^{ij} values can be accomplished by a straightforward linear least-squares procedure.

The pioneering work in this direction was done more than thirty years ago by *Cruickshank*[4] who showed how the room-temperature ADP's of the individual carbon atoms in anthracene[5] and naphthalene[6] could be analyzed in terms of the overall molecular translational and librational oscillations. Within rather large experimental uncertainty (the data were decidedly poor by present-day standards), the principal axes of the motion were found to coincide with the principal inertial axes of the molecule. Both the largest translational vibration (mean-square amplitude $\langle t^2 \rangle$ ca. 380 pm^2) and the major librational axis ($\langle \lambda^2 \rangle$ ca. 15(°)^2) were found to be roughly parallel to the long axis of the molecule, as seems reasonable.

Cruickshank assumed that the librational axes intersect at a point (for anthracene and naphthalene, the molecular center of symmetry). However, unless such a molecular center is imposed by the space-group symmetry, there is no reason to suppose that the molecular libration axes intersect at all. The more general case, analyzed in detail by *Schomaker* and *Trueblood*,[7] requires additional parameters to allow for the quadratic correlation between the pure translational and pure librational motions—the most general motion of a rigid body is rotation about an axis, coupled with a translation parallel to this axis, a screw rotation. The additional parameters, nine in number, are of the type $\langle \lambda^i t^j \rangle$ and form the elements of a new matrix $\boldsymbol{S}$, which is unsymmetrical, since $\langle \lambda^i t^j \rangle$ is different from $\langle \lambda^j t^i \rangle$. In the general case, the elements of $\boldsymbol{T}$, $\boldsymbol{L}$, and $\boldsymbol{S}$ can be found by a linear least-squares fit to the observed ADP's, except that the diagonal elements of $\boldsymbol{S}$ cannot be determined completely in this way; only their differences can be obtained. In the computer program THMA[8] (several versions abroad, the latest available being THMA11[9]), the sum of the diagonal elements is arbitrarily set to zero. Except for very small molecules, the minimum of 20 independent U^{ij} values required to fix the 20 determinable elements of $\boldsymbol{T}$, $\boldsymbol{L}$, and $\boldsymbol{S}$, is usually comfortably exceeded. However, there are a few special cases where the least-squares equations may be ill-conditioned because of the particular geometrical arrangement of the atoms.

During the last thirty years, the rigid-body model has been applied, often rather indiscriminately, to the analysis of ADP's from thousands of crystal structures. Where the assumption of reasonable molecular rigidity seems justified, e.g., carbon skeletons of polycyclic molecules, the model usually gives a very good account of itself. For example, applied to the centrosymmetric isomer of tetramethyltetraasterane **1**[10] or to the tricyclic ketal **2** at 96 K,[11] the rigid-body analysis yields calculated ADP's in almost perfect agreement with the observed values.

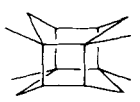

1

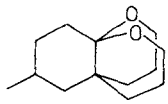

2

Another way of assessing the physical significance of the quantities derived from the rigid-body analysis is to compare them with results of a calculation. In principle, given the equilibrium positions of the atoms in a crystal, together with a suitable set of atom–atom potentials, the elements of the $\boldsymbol{T}$, $\boldsymbol{L}$, and $\boldsymbol{S}$ matrices for the oscillatory motions of rigid molecules can be obtained from lattice-dynamical calculations. These are basically similar to the type of calculation employed to obtain the vibrational frequencies and normal vibrations of free molecules, but involve infinite, periodic arrays of molecules. For crystals of several aromatic hydrocarbons (e.g., benzene, naphthalene, anthracene, pyrene)[12] the matrices calculated by lattice dynamics are in at least fair agreement with those obtained by analysis of the experimental ADP's, even when the latter were not of the highest quality. This serves to show that, whatever uncertainties there may be in the interpretation of these quantities, they cannot be entirely devoid of physical significance.

5. The Rigid-Molecule and Rigid-Bond Tests

For a perfectly rigid molecule, the interatomic distances do not change by definition, no matter how the individual atoms may move when the molecule is translated or rotated. Furthermore, because the individual atoms necessar-

ily move in phase, the mean-square displacement amplitudes (MSDA's) for every pair of atoms A, B must be equal along the interatomic direction [Eq. (5)], where $\boldsymbol{n}$ is the unit

$$\Delta_{A,B} = u_A^2 - u_B^2 = \boldsymbol{n}^T \boldsymbol{U}_A \boldsymbol{n} - \boldsymbol{n}^T \boldsymbol{U}_B \boldsymbol{n} = 0 \quad (5)$$

vector in the A,B direction. Note that the converse does not necessarily hold; for example, $\Delta_{A,B}$ will not differ appreciably from zero for planar or linear molecules with modest vibrations perpendicular to the molecular plane or line. Nevertheless, Equation (5) provides a simple method of testing whether the ADP's obtained for a given molecule are compatible with the rigid-body model.[13] It is also often useful as a test of the overall quality of the ADP's. Bond-stretching vibrations are generally of much smaller amplitude than other kinds of internal motion; for pairs of bonded atoms, therefore, the Δ's should be small, according to *Hirshfeld*,[14] not greater than 10 pm^2 for typical bonds in organic molecules, such as C–C, C–N, and C–O, but excluding bonds involving hydrogen atoms. Thus, if the Δ's for the bonds in an organic molecule are appreciably larger than 10 pm^2, there is ground for suspicion that the ADP's are not of the highest quality.

Mere inspection of the matrix of $\Delta_{A,B}$ values can often reveal relative motion of more or less rigid subgroups in a nonrigid molecule. Within the subgroups, the Δ values should not differ significantly from zero, while relative motion of the subgroups will be manifested by much larger deviations of some of the intergroup Δ's. Table 1 shows Δ values obtained by X-ray analysis for the triphenylphosphine oxide[*] molecule in its orthorhombic crystal modification at 100 K.[15] The triangles labeled A, B, and C contain Δ values for the three phenyl rings (Fig. 3); the three rectangular blocks AB, AC, and BC contain Δ values for pairs of atoms belonging to different rings. The estimated standard deviation (esd) of these Δ values is about 7 pm^2, and the root-mean-square (rms) Δ values for the three individual rings are 11, 6, and 8 pm^2, respectively. Thus, each ring is essentially rigid (ignoring any out-of-plane deformations, which would not be revealed by this test). On the other hand, there is clear evidence of significant motion of the rings *relative* to one another, especially of ring A relative to rings B and C; the rms Δ values for blocks AB and AC are four to five times as large as those within the rings. A calculation of the torsional librational amplitude of each ring about its P–C bond (see Section 6) is consistent with these qualitative conclusions; ring A shows a mean-square libration amplitude of 42(°)^2, almost an order of magnitude larger than those of rings B and C. With data taken at 150 K for the same crystal, the picture is qualitatively similar, the Δ values and mean-square libration amplitudes

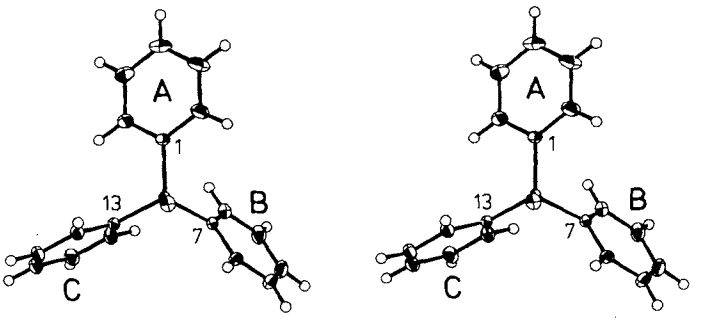

Fig. 3. Stereoview of triphenylphosphine oxide molecule. The rings A, B, and C, attached to the phosphorus at atoms 1, 7, and 13 respectively, correspond to the triangular blocks in Table 1.

[*] Note added by the editorial staff: Since the *systematic* name of PH_3 is phosphane according to IUPAC rule 2.3 (inorganic nomenclature) and IUPAC rule D-5.11 + footnote (organic nomenclature), the editorial staff prefers the use of the -ane nomenclature but has allowed the use of the name triphenylphosphine oxide for Ph_3PO at the authors' request. Indeed, rule 2.3 permits the use of phosphine as an alternative while rule D-5.11 retains only this trivial name.

Table 1. Matrix of Δ values [pm^2] for triphenylphosphine oxide at 100 K. For atom numbering see Figure 3. Positive Δ's mean that the MSDA along the interatomic vector $\overrightarrow{A_1A_2}$ is larger for A_2 than for A_1; negative Δ's mean the reverse.

A_1 \ A_2	C18	C17	C16	C15	C14	C13	C12	C11	C10	C9	C8	C7	C6	C5	C4	C3	C2	C1	P1
O1	0	− 8	−15	− 6	− 6	−19	18	8	10	35	32	9	2	−15	−22	9	48	−10	−20
P1	33	31	23	25	31	10	38	32	22	31	35	22	29	25	16	24	41	13	
C1	48	28	− 2	−11	− 5	− 9	40	44	11	− 5	− 3	0	11	5	5	10	21		
C2	15	5	−23	−44	−46	−34	−73	−89	−100	−77	−57	−61	− 2	− 7	5	−6			
C3	49	26	−22	−45	−38	−20	−21	−31	− 74	−78	−57	−42	−11	−22	2				
C4	56	12	−53	−59	−34	−25	36	67	12	−31	−29	−15	−10	−16		**A**			
C5	14	−32	−78	−68	−41	−47	−25	2	− 25	−40	−29	−33	−11						
C6	17	−10	−34	−32	−18	−30	−50	−34	− 51	−49	−32	−44							
C7	35	42	23	20	19	3	2	− 1	0	1	− 6								
C8	19	13	−19	−23	−23	−36	8	− 9	− 9	1									
C9	19	12	−27	−32	−30	−36	5	− 5	− 3										
C10	27	44	13	4	− 1	−12	− 5	− 8		**B**									
C11	−2	21	1	− 3	− 5	−17	− 7												
C12	6	24	4	− 1	− 1	−11													
C13	7	16	13	7	3														
C14	0	5	7	2															
C15	−8	−13	−11																
C16	2	4		**C**															
C17	−5																		

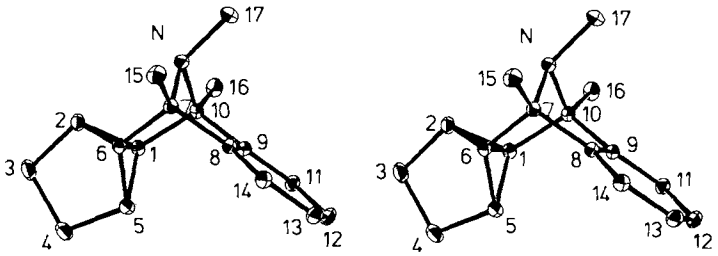

Fig. 4. Stereoview of [3.1.1]propellane derivative, showing atomic numbering used in Table 2. The propellane moiety comprises the atoms C1, C6, C2, C5, C7, N, and C10.

being about 50% larger, as expected for the higher temperature.

Our second example involves an internal motion that can be identified as incipient inversion of the pyramidal amino nitrogen atom in the [3.1.1]propellane derivative shown in Figure 4. The Δ values obtained from an X-ray analysis at 95 K[16] are shown in Table 2 and have esd's of about 7 pm^2 for all bonded pairs and only 6 pm^2 for *all* $15 \times 14/2$ atom pairs of the hexacyclic skeleton (the atoms C1–C14 and N in Figure 4), an indication of how remarkably rigid most of this molecule is. Inspection of Table 2 shows that all Δ values larger than 18 pm^2 involve the *N*-methyl carbon atom (C17); the four largest (25–39 pm^2) are for the vectors between this atom and the phenyl carbons C11–C14. The signs of these four largest Δ's in the column headed C17 are all positive, indicating that this atom has a perceptible motion relative to the others. The pattern of Δ's indicates that the excess motion of C17 is almost normal to the N–C17 bond and in the molecular mirror plane, that is, along the path that would ultimately lead to inversion at the nitrogen atom. (This direction of motion is indeed suggested by the ellipsoid of C17 in Figure 4, but the effect is shown more convincingly by the Δ's in Table 1[17]).

Because of the ever-present internal molecular vibrations, the rigid-body model can be expected to apply tolerably well only for groupings composed of atoms of comparable mass. In organic molecules, the hydrogen atoms are expected to have quite substantial motions relative to the carbon skeleton; consequently, they have to be excluded from the scope of a rigid-body model calculation, or else their ADP's have to be corrected for the effect of the internal vibrations. The best way of making such corrections would be on the basis of a complete normal-mode calculation for the molecule in question, but this is seldom possible.

The Δ matrix calculated from the ADP's taken from a very recent, highly accurate neutron-diffraction study of perdeuterobenzene at 15 K[18] clearly shows the relative motion of the deuterium atoms in the molecular plane (Table 3a). At this temperature we are seeing mainly the zero-point motion. Fortunately, a complete normal-mode calculation has been made for benzene.[19] When the calculated zero-point vibration amplitudes for the molecule are subtracted from the observed U^{ij} values (expressed in an appropriate molecular coordinate system), the corrected Δ matrix (Table 3b) is essentially that expected for a rigid body.

Table 3. C_6D_6 at 15 K. For explanation of signs see Table 1.

a) Matrix of Δ values [pm^2] along interatomic vectors.

A_1 \ A_2	D3′	D2′	D1′	C3′	C2′	C1′	D3	D2	D1	C3	C2
C1	54	42	33	− 1	− 4	0	46	55	33	1	1
C2	45	40	44	1	0	4	57	40	55	2	
C3	38	45	52	0	− 1	1	38	53	42		
D1	−3	1	0	−52	−44	−33	2	−4			
D2	−1	0	−1	−45	−40	−42	3				
D3	0	1	3	−38	−45	−54					

b) Matrix of Δ values corrected for internal motion.

A_1 \ A_2	D3′	D2′	D1′	C3′	C2′	C1′	D3	D2	D1	C3	C2
C1	1	−1	−3	−6	0	0	2	−2	−3	5	−4
C2	5	−1	−5	1	0	0	5	−1	7	2	
C3	−1	2	0	0	−1	6	−1	4	−3		
D1	0	4	0	0	5	3	0	−7			
D2	3	0	−4	−2	1	1	0				
D3	0	−3	0	1	−5	−1					

Table 2. Matrix of Δ values [pm^2] for the [3.1.1] propellane derivative (Fig. 4) at 95 K. For atom numbering see Figure 4. For explanation of signs see Table 1.

A_1 \ A_2	N	C17	C16	C15	C14	C13	C12	C11	C10	C9	C8	C7	C6	C5	C4	C3	C2
C1	−11	−5	16	1	− 2	2	4	5	2	− 5	− 6	−10	−7	5	6	4	4
C2	0	2	7	3	6	8	6	5	0	0	− 2	− 6	−3	0	2	2	
C3	− 3	0	10	3	− 3	0	1	− 2	−1	− 5	− 6	− 7	−7	−2	0		
C4	− 6	−3	6	3	−17	−14	−10	−14	−3	−13	−11	− 6	−7	−1			
C5	− 7	−3	4	6	−11	− 5	− 2	− 8	−3	−12	−10	− 3	−1				
C6	−10	−4	8	17	4	4	1	0	−1	− 2	− 6	− 1					
C7	− 4	5	10	6	8	5	1	1	−1	4	− 3						
C8	4	17	6	8	6	7	3	0	−5	0							
C9	4	21	12	1	3	7	4	0	2								
C10	− 2	6	9	10	7	6	4	5									
C11	4	33	8	6	0	3	1										
C12	8	39	7	9	0	1											
C13	4	38	6	8	− 1												
C14	− 2	25	6	7													
C15	−18	−3	1														
C16	−17	−3															
C17	− 3																

The zero-point vibration amplitude of an atom depends on its mass and should therefore be sensitive to isotopic substitution.[20] The mass effect is largest for the isotopes of hydrogen. From *Johnson*'s values for the internal vibration amplitudes of the atoms in the benzene molecule,[21] the difference between the MSDA's of protium and deuterium can be estimated to be about 16, 36, and 60 pm^2 in the radial, tangential, and perpendicular directions, respectively. The difference in the spherically averaged MSDA's is thus about 37 pm^2.

Although the X-ray scattering powers of different isotopes are identical, we can consider the possibility of distinguishing between protium and deuterium by X-ray analysis on the basis of the difference in their MSDA's. (This distinction is no problem for neutron diffraction, where the scattering power depends on the nuclear structure and is very different for different isotopes.) An attempt in this direction has been carried out for isotopically labeled (2*S*)-malic acid obtained by enzymatic addition of D_2O to fumaric acid. From parallel X-ray analyses of the monoammonium salts of the unlabeled and labeled acids at 93 K,[22] the isotropic MSDA of one of the two methylene hydrogen atoms was found to decrease by about 40 pm^2 (as expected for the switch from protium to deuterium), while the other hardly changed. The configuration of the malate was thereby indicated as (2*S*,3*R*). Since the esd's of the hydrogen MSDA's in this experiment were about 20 pm^2, the statistical significance of the result is certainly not overwhelming. Nevertheless, it was encouraging that the relative configuration indicated by the X-ray experiment was in agreement with that established by other methods (including neutron diffraction of the corresponding phenylethylammonium salt[23]). At any rate, the experiment shows that the use of X-ray diffraction for distinguishing between deuterium and protium should not be dismissed, especially in cases where a neutron-diffraction analysis seems impracticable.

In coordination complexes where the ligand atoms may have an appreciably smaller mass than the metal atom to which they are bonded, the Hirshfeld rigid-bond postulate is again to be interpreted in a somewhat relaxed form; for such ligand–metal bonds, Δ values of the order of 30 pm^2 are to be expected (the MSDA of the lighter atom being the larger). Gross violations of this less stringent test have been exploited to detect spin crossover in crystalline $[Fe^{III}(S_2CNR_2)_3]$ complexes[24] and to estimate the magnitude of dynamic Jahn–Teller distortions in crystals of Cu^{II} and Mn^{III} complexes.[25] For example, for five octahedral $[Cu^{II}L_6]$ complexes expected to show dynamic distortion the average Δ along the Cu–L direction was 210 pm^2, whereas for analogous $[Ni^{II}L_6]$ complexes the average was 25 pm^2. The larger value in the Cu complexes is satisfactorily explained in terms of a statistical distribution of distorted octahedra, each having four short Cu–L bonds of 205 pm and two long ones of 233 pm.

The spin-crossover analysis[24] contains an interesting correlation of Δ values against bond distance. The Fe–S distance is about 230 pm^2 in low-spin $[Fe^{III}(S_2CNR_2)_3]$ complexes and about 245 pm^2 in high-spin ones. For a sample of more than 30 crystal structure analyses, it was noticed that complexes with Fe–S distances close to these extreme values had relatively small Δ(Fe–S) values (ca. 20–30 pm^2), whereas intermediate Fe–S distances were associated with Δ(Fe–S) values of up to 100 pm^2. Indeed, the Δ(Fe–S) versus d(Fe–S) plot was an approximately parabolic curve with its maximum Δ at an Fe–S distance of about 238 pm. These observations can be explained by assuming that for the intermediate range of Fe–S distances, the crystals contain disordered arrangements of molecules in both spin states. For fraction p of the molecules in the low-spin state, and fraction $(1-p)$ in the high-spin one, the apparent Fe–S distance (in pm) would be approximately $230p+245(1-p)$ and it would be associated with a Δ value (in pm^2) of approximately $(15)^2p(1-p)$ over and above the "normal" Δ(Fe–S) value. This is roughly what was found.

6. Internal Molecular Motion in Crystals

Breakdown of the rigid-body model for molecules in crystals may be evident from a casual glance at the displacement ellipsoids (Fig. 1) or from inspection of the matrix of Δ values (Tables 1–3). In general, for free molecules, vibrations involving mainly torsional motions have lower frequencies (and larger amplitudes) than those involving changes in bond distances and angles. For molecules in a crystal, internal and external modes of motion will be strongly coupled, so that no rigorous separation is possible. Nevertheless, as we saw in Section 5, internal motions estimated for free perdeuterobenzene, subtracted from the raw ADP's, were quite adequate to correct for the effect of internal motions in the crystal.

For more flexible molecules with reasonably large-amplitude torsional motions of semirigid groups (e.g., triphenylphosphine oxide, Fig. 3, Table 1), the magnitudes of such motions can be estimated by a slight modification of the usual ***T***, ***L***, ***S*** analysis. In the simplest version, due to *Dunitz* and *White*,[26] an additional parameter, $\langle\phi^2\rangle$, a mean-square torsional amplitude, is added for each group suspected of undergoing appreciable torsional motion. In this approach, the torsional axis needs to be specified in advance, the group undergoing the torsional motion is assumed to be rigid, and all correlations between the internal motion and the overall motion are neglected.

In spite of its simplicity, the Dunitz–White model has been shown to yield essentially the same $\langle\phi^2\rangle$ values as those derived from more elaborate models for the internal molecular motion.[8] Nevertheless, there are problems that cannot be ignored.

First, there is the problem of specifying the correct kind of internal motion to be included in the model. There is no rigorous way to do this, as all information about the relative motions of the different atoms has been lost. Chemical experience and intuition may be valuable guides here, but they can also occasionally lead us astray. A poor guess about the nature of the internal motion is sometimes detectable in that it leads to a $\langle\phi^2\rangle$ value not significantly different from zero, or to a physically unreasonable result, for example, a negative value of $\langle\phi^2\rangle$. Moreover, the impossibility of distinguishing between types of internal molecular motion that differ only with respect to the relative phases of the atomic displacements leads to unavoidable ambigui-

ties. The torsional and out-of-plane bending motions of a nitro group provide us with an example (Fig. 5). In the torsional motion of such a group about the ONO bisector, the two oxygen atoms move by equal amounts in opposite directions. In the corresponding out-of-plane bending distortion (which may be simulated by torsion about an axis perpendicular to the ONO bisector and in the plane of the group), the two oxygen atoms move by equal amounts but in the same direction. From the ADP's alone, we cannot distinguish between these two types of motion.

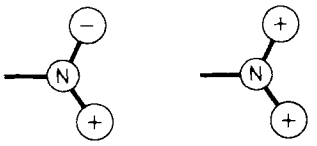

Fig. 5. Rotation (left) and out-of-plane bending (right) of the nitro group differ only in the relative signs (or phases) associated with the displacements of the oxygen atoms (see text).

A second problem concerns the total disregard in the Dunitz–White model of the correlations among the different types of motion. Just as, in the rigid-body model, the components of the S matrix were needed to allow for the quadratic correlation between the pure translational and pure librational motions, so similar terms are called for to allow for the analogous correlations among different types of internal motion and between them and the overall translations and rotations. It is not always easy to decide in advance whether these correlation terms are important or not; in the computer program THMA11,[8,27] they can be included if the nature of the problem seems to make this desirable. Correlations between motions of groups that have no atom in common cannot be determined from the U^{ij}'s.

Even when the extra correlation terms are included in the least-squares fitting, an unavoidable indeterminacy remains concerning the value of $\langle\phi\lambda^{\parallel}\rangle$, where $\lambda^{\parallel}$ denotes the overall libration about an axis parallel to the internal torsion axis. A mathematical analysis, not given here,[27] shows that only $\langle(\lambda^{\parallel})^2\rangle$ and the sum $\langle\phi^2\rangle+2\langle\phi\lambda^{\parallel}\rangle$ can be determined from the U^{ij}'s. This means that when $\langle\phi^2\rangle$ is determined by the Dunitz–White method, the value is only meaningful when it is very large compared with the parallel component of L. Since, usually, we are interested in the internal molecular motions only when they do have fairly large amplitudes, this restriction is often fairly innocuous. Similarly, when the quantity $\langle\phi^2\rangle+2\langle\phi\lambda^{\parallel}\rangle$, as obtained in the model including correlation, is large compared with the parallel component of L, it may be regarded as a good approximation to $\langle\phi^2\rangle$ itself.

Correlations between internal and overall molecular motions can sometimes be important. In one of the three known crystal modifications of dimethyl 3,6-dichloro-2,5-dihydroxyterephthalate **3**, the torsional motion of the carboxyl groups about the exocyclic C–C bonds is extremely large ($\langle\phi^2\rangle\approx 150(^\circ)^2$ at room temperature), corresponding to rms displacements of the carboxyl oxygen atoms of about 25 pm from the mean molecular plane.[28] (This is the molecule illustrated in Figure 1 with its vibration ellipsoids). The molecular libration axes in the molecular plane also produce displacements of these oxygen atoms perpendicular to this plane (Fig. 6). As mentioned above, correlation of the torsion with the parallel libration axis is indeterminate, but correlation with the perpendicular libration axis adds to the out-of-plane displacement of one of the two oxygen atoms and subtracts from the other, leading to unequal rms displacements, as observed in the crystal structure analysis. The introduction of these correlation terms into the internal motion analysis gave a dramatic improvement in the agreement between observed and calculated U^{ij}'s, the R factor[29] decreasing by a factor of 4, from 0.126 to 0.032.

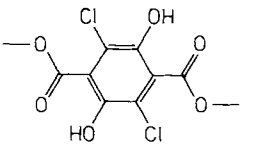

3

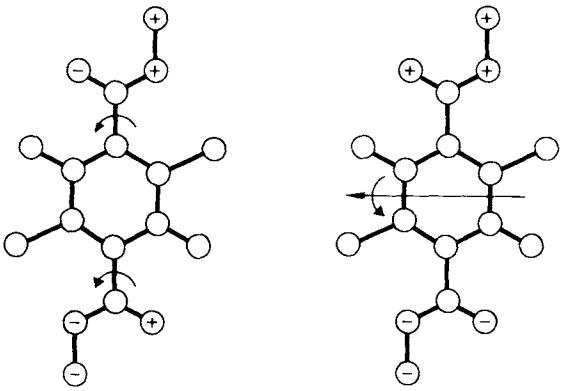

Fig. 6. Torsional rotation of the carboxyl group about the exocyclic C–C bond (left) and libration of the entire molecule about the horizontal axis (right) lead to different relative out-of-plane displacements of the carboxyl oxygen atoms.

7. Relations between Mean-Square Amplitudes and Potential Energy

For a particle in a one-dimensional quadratic potential, $V(x)=fx^2/2$, the classical Boltzmann distribution of displacements from equilibrium is given by Equation (6),

$$p(x)=(2\pi kT/f)^{-1/2}\exp(-fx^2/2kT) \tag{6}$$

which can be recognized as a Gaussian with second moment $\langle x^2\rangle$ given by Equation (7). For many crystals, the sec-

$$\langle x^2\rangle = kT/f \tag{7}$$

ond moments of the atomic pdf's are indeed approximately proportional to the absolute temperature over a considerable range. At sufficiently low and sufficiently high temperatures, however, deviations from this linear dependence are to be expected. At 0 K, it would lead to a zero value of $\langle x^2\rangle$, i.e., to an infinitely sharp pdf, in contradiction to the uncertainty principle. The classical Boltzmann averaging is clearly invalid here. When the averaging is made over the energy levels of a quantized harmonic os-

cillator, the expression for the second moment of the distribution is given by Equation (8), where ν is the frequency

$$\langle x^2 \rangle = (h/8\pi^2\mu\nu)\coth(h\nu/2kT) \quad (8)$$

and μ the reduced mass (or, for a rotational oscillation, the moment of inertia, I). For $h\nu \gg 2kT$, the coth factor is unity, and the expression reduces to Equation (9), corresponding to the zero-point motion. On the other hand, for $h\nu \ll 2kT$, the coth factor becomes $2kT/h\nu$, leading back to the same linear dependence of $\langle x^2 \rangle$ on T as was obtained with the classical Boltzmann averaging (with f set equal to $4\pi^2\mu\nu^2$). The temperature dependence of $\langle x^2 \rangle$, as given by Equations (7) and (8), is shown in Figure 7.

$$\langle x^2 \rangle = h/8\pi^2\mu\nu \quad (9)$$

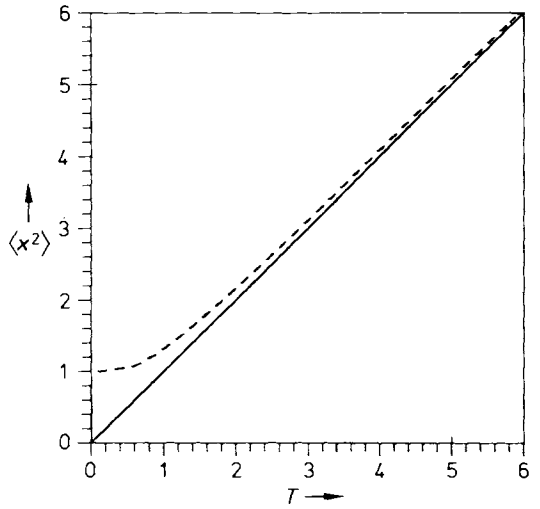

Fig. 7. Variation of MSDA $\langle x^2 \rangle$ (in units of $h/8\pi^2\mu\nu$) with temperature (in units of $h\nu/2k$) for a one-dimensional harmonic oscillator. The linear dependence depicted by the full line is based on the assumption of a classical Boltzmann distribution, while the dashed curve corresponds to a quantized distribution.

For many crystals, the effective mean-field potential in which the atoms move seems to be reasonably quadratic, as judged by the observed temperature dependence of the ADP's or of quantities derived from them, such as $\boldsymbol{T}$ and $\boldsymbol{L}$ components. A fairly thorough study has been made for naphthalene.[30] The main deviation from the behavior expected for a quadratic potential is that experimental ADP's tend to increase with temperature rather more steeply than implied by the linear dependence. This can be explained as a consequence of the general softening of the effective potential as the crystal expands on warming. In a more realistic model—the quasi-harmonic model[31]—the effective force constant of Equation (7) is *not* constant but decreases with increasing temperature. For a diverse set of inorganic solids, the ADP's are found to be approximately proportional to $T^{1.5}$,[32] and a similar relationship has been shown to hold for lithium hydrogen phthalate monohydrate,[33] with ADP's estimated by neutron diffraction at 15, 100, and 298 K.

As mentioned earlier in Section 3, the experimental ADP's refer to the motion of an averaged atom or molecule. From experimental values of $\langle x^2 \rangle$ and a knowledge of the temperatures at which they were measured, Equations (7) or (8) provide estimates of effective quadratic force constants (or frequencies) for the mean-field motions in question. The mean-field potential associated with a given type of motion can be obtained, at least conceptually, by following the potential energy variation when one atom (or molecule) is gradually displaced from its equilibrium position or orientation, all neighboring atoms (or molecules) being held in their equilibrium positions. This is an oversimplified picture. A more realistic model should contain some means of allowing for the ways in which the instantaneous displacements of different atoms (or molecules) are correlated. This is achievable from a complete lattice-dynamical treatment, but only at the cost of considerable additional mathematical complexity and loss of conceptual simplicity. In lattice dynamics,[34] a suitable force field is used to solve the equations of motion for the whole periodic ensemble of molecules that constitute the crystal structure. The calculation yields the frequencies of all the normal modes of vibration of the crystal. The MSDA's of the atoms (or molecules) are then obtained by summing contributions from these normal modes. For each type of motion, say, a molecular libration about a particular axis, characterized by a single frequency in the mean-field model, we now have a range of frequencies, a so-called branch of the frequency spectrum. However, the calculations show that the frequency dispersion within a given branch is usually not very large.

Thus, although the precise physical significance of the effective mean-field force constants and frequencies derived from Equations (7) and (8) may be open to question, the numerical values should generally not differ too much from analogous quantities that appear in more complete dynamical models. In fact, as shown in Table 4, experimental ADP's for a variety of librating rigid groups (such as methyl and *tert*-butyl) yield quadratic force constants and corresponding cosine-function rotation barriers (see Section 8) that are at least in the same range as those derived by other physical methods.[35]

Table 4. Some cosine-function torsional barriers derived from ADP's.

Group	Attached atom	Range of barriers [kJ mol^{-1}] From ADP's	Other methods [a]
CH_3	C, N (trigonally coordinated)	1.5–9.6	(s) 1.2–8.5
	C, N, P (tetrahedrally coordinated)	4–26	(g) 12–22
	O	1–9	CH_3OH (g) 4.5 other (s) 15–19
$NH_3^{\oplus}$	C	14–62 (well correlated with H-bonding)	
CF_3	C (trigonally coordinated)	4–10	(g) 4–7
	C (tetrahedrally coordinated)	9–66	(g) 13–25
$C(CH_3)_3$	C, N, P	7–112	(g) 2–27

[a] s = solid; g = gas.

8. Rotation Barriers in Crystals from ADP's

Consider an individual molecule in crystalline benzene. The molecule, assumed rigid for the moment, will oscillate about its mean orientation, and, as shown by NMR methods, will also from time to time carry out 60° rotational jumps that turn it from one orientation to an equivalent one. The energy barrier hindering such a rotation must have sixfold periodicity in the angular coordinate and, to a first approximation, it can be represented by Equation (10), where B is the barrier height per mole and $n=6$. For

$$V(\phi)=B(1-\cos n\phi)/2 \tag{10}$$

small excursions from the equilibrium orientation at $\phi=0°$, we have $\cos n\phi=1-n^2\phi^2/2$, and hence Equation (11). In this approximation, the potential energy is a quadratic function of ϕ. With the help of Equation (7), derived on the basis of a classical Boltzmann distribution, relationship (11) is converted into Equation (12), where ϕ^2 is replaced by its mean value. Thus, the barrier may be estimated from a knowledge of $\langle\phi^2\rangle$, which is obtainable from analysis of the ADP's. This is the approximation used by *Trueblood* and *Dunitz*[35] in the study leading to the results shown in Table 4; it is valid only when $\langle n^2\phi^2\rangle$ is much smaller than unity, i.e., when the barrier B is at least several times larger than RT.

$$V(\phi)=Bn^2\phi^2/4 \tag{11}$$

$$B=2RT/n^2\phi^2 \tag{12}$$

When this condition is not satisfied, $V(\phi)$ can no longer be approximated as a quadratic function and the probability distribution for ϕ is no longer Gaussian. By analogy with Equation (6), however, the dependence of this probability distribution on B/RT can be obtained from (13),

$$p(\phi)=N\exp\{-B(1-\cos n\phi)/2RT\} \tag{13}$$

where N is a normalization factor. This function is shown in Figure 8, where the gradual change from nearly Gaussian for $RT\ll B$ to nearly flat distribution for $RT>B$ is clearly seen.

A more accurate relationship giving $\langle\phi^2\rangle$ as a function of B and RT [Eq. (14)] is obtained by integrating the classical Boltzmann expression (13). Numerical integration of Equation (14) for various values of RT/B leads to the solutions shown graphically (for $n=5$) in Figure 9, where the linear dependence expected for the quadratic potential described by Equation (11) is also shown. At very low values of RT/B, the classical averaging leading to Figure 9 cannot be expected to hold. The value of $\langle\phi^2\rangle$ must then be estimated from an expression analogous to Equation (8), based on quantum mechanical averaging.

$$\langle\phi^2\rangle=\frac{\int\phi^2\exp\{-B(1-\cos n\phi)/2RT\}\,d\phi}{\int\exp\{-B(1-\cos n\phi)/2RT\}\,d\phi} \tag{14}$$

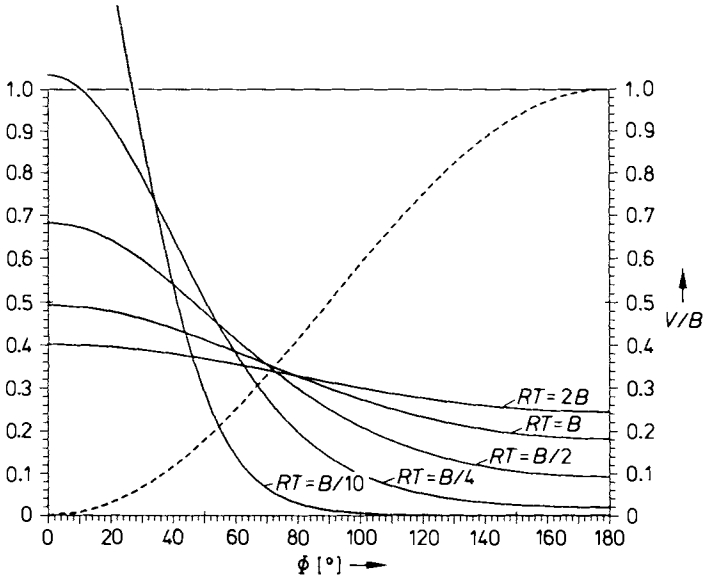

Fig. 8. One-dimensional probability distribution functions [Eq. (13)] for a sinusoidal potential (dashed curve) with barrier height B at various temperatures.

The estimation of a rotation barrier with the help of Figure 9 is quite simple. From an observed value of $\langle\phi^2\rangle$ for a given librating group in a crystal, one reads off the corresponding value of RT/B. A knowledge of the temperature T at which the measurement was carried out then leads directly to the barrier B.

The method has been applied[36] to a series of crystalline metallocenes, for which extensive diffraction data are available over a wide temperature range, and for which barriers for rotation of the cyclopentadienyl rings have also been estimated by NMR spectroscopy (mainly from ^1H spin-lattice relaxation times), by incoherent quasi-elastic neutron scattering (IQENS), and by Raman and IR

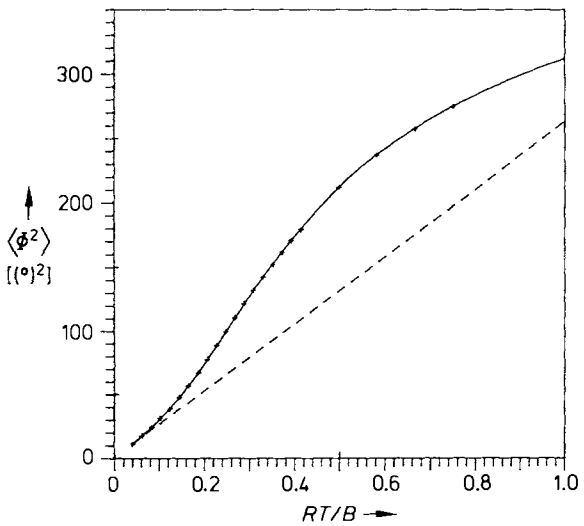

Fig. 9. Full curve: Variation of mean-square libration amplitude $\langle\phi^2\rangle$ with RT/B for a fivefold periodic sinusoidal restricting potential with barrier height B. Dashed curve: $\langle\phi^2\rangle$ for harmonic oscillator potential with the same quadratic force constant. At very low temperatures, both curves should run parallel to the horizontal axis at the nonzero value of $\langle\phi^2\rangle$ corresponding to the zero-point motion, as indicated in Figure 7.

spectroscopy. A comparison of the results obtained by the different methods is given in Table 5.

Table 5. Apparent barriers to ring rotation [kJ mol^{-1}] (esd's in parentheses) in crystalline metallocenes by various methods. (Diffraction results yield individual barriers for symmetry-independent rings at the measurement temperature.)

Compound	Diffraction			Other methods: NMR unless mentioned (see [36] for detailed references)
Ferrocene (triclinic)	101 K	123 K	148 K	
	7.6(7)	6.4(4)	5.9(5)	7.5(8); 10.3(5), 11(2); 8.3;
	12(2)	10.2(5)	10(2)	≈9 (IQENS)
	8.4(6)	6.8(7)	7.0(6)	
	9(2)	8.5(8)	8(1)	
Ferrocene (orthorhombic)		98 K		
		23(20)		24.8(1.0)
		33(16)		
Ferrocene (monoclinic)	173 K	293 K		
	2.7(5)	4.7(8)		5.4(5); 4.4(5) (IQENS)
Nickelocene (monoclinic)	101 K	293 K		
	6.5(6)	5.2(5)		5.0 (Raman); 6.3 (IQENS)
Ruthenocene (orthorhombic)	101 K	293 K		
	25(10)	24(7)		9.6(8); 18.9
	>50	38(13)		

The most extensive diffraction results[37] are for triclinic ferrocene, stable or at least metastable below 164 K. There are four symmetry-independent cyclopentadienyl rings, and the crystal structure was determined at three temperatures (101, 123, 148 K). Table 6 shows that the $\langle\phi^2\rangle$ values increase with temperature and also vary from ring to ring.

Table 6. Mean-square libration amplitudes $\langle\phi^2\rangle$ [(°)^2] (with esd's in parentheses) in crystalline metallocenes at various temperatures.

Compound	Triclinic			Orthorhombic			Monoclinic	
Ferrocene	101 K	123 K	148 K		98 K		173 K	293 K
ring 1A	35(4)	55(5)	78(8)	ring 1	9(7)		231(27)	220(30)
1B	20(4)	30(3)	37(5)	2	7(3)			
2A	31(3)	47(6)	63(6)					
2B	26(3)	38(5)	47(9)					
Nickelocene							101 K	293 K
							45(4)	199(18)
Ruthenocene					101 K	293 K		
				ring 1	9(3)	32(9)		
				2	2(2)	17(5)		

The first trend may be explained by the thermal expansion of the crystal, which will increase intermolecular distances and thus lower the intermolecular contribution to the barrier. The variation from ring to ring is also probably genuine, arising from differences in packing of the individual rings. This is supported by packing energy calculations,[38] using atom-atom potentials, which reproduce the general pattern.[39] From Table 5 it is seen that for triclinic ferrocene, the barrier heights derived from $\langle\phi^2\rangle$ values agree as well as can be expected with those from NMR and IQENS, considering that the latter values refer to averages over a considerable temperature range and that differences among the individual rings are not resolved by the spectroscopic methods.

In monoclinic ferrocene,[40] there is only one symmetry-independent cyclopentadienyl ring. Although the room-temperature result appears to agree well with the spectroscopic values, this is almost certainly fortuitous. From Table 6, it is seen that $\langle\phi^2\rangle$ for the monoclinic modification is virtually constant between 173 and 293 K, a strong indication of static disorder in the ring orientations. Indeed, both X-ray[42] and neutron diffraction[41] analyses have shown that the centrosymmetric, staggered arrangement of the cyclopentadienyl rings, which appears to be demanded by the space-group symmetry of monoclinic ferrocene,[42] is actually a result of static disorder. Since Figure 9 is based on the assumption that the $\langle\phi^2\rangle$ value in question is due to genuine librational motion and not to static disorder, little confidence can be placed in the barriers derived by this method for monoclinic ferrocene. Although a rotation barrier can be obtained from a $\langle\phi^2\rangle$ value at a single temperature, this example illustrates the advisability of multiple-temperature measurements, if only to detect the presence of disorder masquerading as vibration. For nickelocene, too, the good agreement indicated in Table 5 between the different methods should perhaps also be regarded with a certain reserve, as there are indications that an order-disorder phase change may possibly occur in this crystal at some intermediate temperature.

For orthorhombic ferrocene and ruthenocene, the low-temperature values of $\langle\phi^2\rangle$ are so small that they may be due mainly to zero-point motion, in which case the use of Figure 9 (based on classical averaging) to estimate the barriers may lead to inaccuracies. Besides, the low relative precision of $\langle\phi^2\rangle$ leads to further uncertainties in the derived values of the barriers. In view of these difficulties, the agreement (Table 5) between the barriers obtained from $\langle\phi^2\rangle$ and from spectroscopic methods seems eminently satisfactory.

The solid-state barriers are considerably larger than those found for the free molecules. In the gas phase, ferrocene is eclipsed, with a barrier to rotation of the cyclopentadienyl rings of about 3.8 kJ mol^{-1};[43] the barrier in nickelocene is probably still lower.[44] For free ruthenocene, no experimental value is available, but a theoretical study[45] suggests that the barrier is about 2 kJ mol^{-1} higher than that in ferrocene. The increase in the barriers in the solid state is due to intermolecular packing effects and is reproduced nicely by force-field calculations.[38]

The recent highly accurate neutron-diffraction study of crystalline perdeuterated benzene C_6D_6[18] offers another opportunity to test the $\langle\phi^2\rangle$ method of obtaining rotation barriers. Here the crystallographically imposed molecular symmetry is a center of inversion. For the libration of the molecule in its own plane, $\langle\phi^2\rangle$ is estimated to be 2.6(°)^2 at 15 K and 11.0(°)^2 at 123 K. The latter value corresponds to a sixfold rotation barrier of 17 kJ mol^{-1}, well within the range (16.5–18.4 kJ mol^{-1}) obtained by solid-state NMR measurements.[46] The barrier obtained from the 15 K analysis is only 8 kJ mol^{-1}, but here again the use of Figure 9

(adapted for $n=6$) is probably impermissible because of quantum effects at this low temperature; the 17 kJ mol^{-1} barrier would actually correspond to a zero-point libration of about $4(°)^2$, not too different from the observed $\langle\phi^2\rangle$ at 15 K.

It seems quite remarkable that barrier heights obtained from $\langle\phi^2\rangle$ values agree so well on the whole with those estimated by spectroscopic methods. After all, the underlying assumptions behind the two kinds of analysis are so very different. Spectroscopy provides frequencies, relaxation times, and correlation or residence times, which, in turn, can be used to yield rotation barriers by assuming an Arrhenius type of dependence of rate or time on temperature. Starting from $\langle\phi^2\rangle$, on the other hand, we use classical Boltzmann averaging for a cosine type potential (which can be, at best, the leading term in the Fourier expansion of the periodic potential) to estimate the barrier height at a given temperature. In a sense, one can say that spectroscopy sees the rate at which molecules cross the barrier, while diffraction sees the bottom of the potential well; we derive roughly the same barrier height as long as the potential is approximately sinusoidal. The two methods are thus nicely complementary for studies of molecular motion in the solid state.

9. Vibration or Static Disorder?

Among crystallographers, disorder is usually regarded as a nuisance, occasionally as an opportunity to test some potential improvement in refinement techniques, but only seldom as a phenomenon interesting in its own right. Yet disorder is ubiquitous, even in the "ordered" crystalline state, and the physical properties of solids usually depend just as much on the nature and number of the defects from the idealized, perfectly ordered, periodic structure, as on the structure itself. It also has to be admitted that, although diffraction methods are highly successful in establishing the averaged structure of the crystal unit cell, they have much less to say about the nature of the fluctuations from this averaged structure. This is because the influence of all types of disorder on the main Bragg reflections is summed up in the atomic pdf's. However, as we have seen, it is possible from temperature-dependence studies to distinguish disorder that is mainly dynamic (vibrational) from that which is mainly static in origin. Beyond that, the most we can do is to enquire whether a given set of atomic pdf's is compatible with a proposed disorder model or not. Such enquiries sometimes lead to interesting answers.

The room-temperature X-ray analysis of tetra-*tert*-butylcyclobutadiene **4**[47] led to a structure in which the sides of

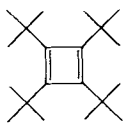

4

the slightly nonplanar four-membered ring were almost equal (146.4 and 148.3 pm), in contrast to results for other cyclobutadiene derivatives where much larger differences (up to 26 pm) between the ring bonds were observed. *Ermer* and *Heilbronner*[48] proposed that the nearly square ring found at room temperature did not correspond to the actual molecular structure but to averaged atomic positions resulting from disorder among two rectangular structures. This was confirmed by a subsequent low-temperature analysis at 123 K,[49] where the ring bond lengths were found to differ significantly (144.1 and 152.7 pm), but still not as much as might have been expected. This raises the question whether residual disorder may not still be present at the lower temperature. To answer this, we can postulate a model, calculate a set of ADP's for it, and examine the pattern of discrepancies between the observed ADP's and those calculated for the model.

The crystallographically imposed molecular symmetry is here a C_2 axis (although the effective molecular symmetry in the crystal is D_2). An analysis of the ADP's in terms of the ***T,L,S*** model with allowance for internal libration of the two independent *tert*-butyl groups about the exocyclic C–C bonds[50] leads to $\langle\phi^2\rangle$ values of 14 and 23 $(°)^2$ for the two internal motions, several times larger than the overall molecular librations. Among the discrepancies between observed U^{ij} components and those calculated for this model, the excess apparent motion of the ring atoms in the tangential directions (by 51 and 31 pm^2 for the two symmetry-independent atoms) is striking and is in qualitative agreement with the disorder model proposed by *Ermer* and *Heilbronner*[48] (Fig. 10). In the crystal it is not necessary that the two perpendicular orientations of the rectangular ring have a common center, as shown in Figure 10, and,

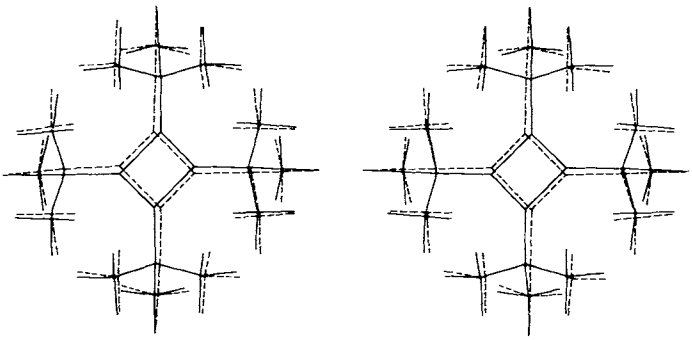

Fig. 10. Disorder model for **4** as proposed by *Ermer* and *Heilbronner* [48] and confirmed by analysis of experimental ADP's from the 123 K crystal structure analysis [50]. In the crystal, one orientation is about four to five times more frequent than the other.

indeed, there are indications that their centers do not quite coincide. The observed excess apparent motion indicated by this analysis is compatible with the presence of two perpendicular orientations of a rectangular ring with sides 134 and 160 pm, with one orientation about four to five times more frequent than the other.

On the other hand, a quite different result is obtained from a comparable analysis of the ADP's from the low-temperature (100 K) crystal structure analysis of 1,3,5,7-tetra-*tert*-butyl-*s*-indacene **5**.[50] In solution, the twelve C atoms of the ring system give only four ^{13}C-NMR signals that show no perceptible line broadening down to -130 °C;[51] this is consistent either with a very low energy

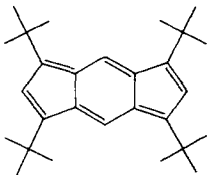

5

barrier between the two valence isomers or with a completely delocalized 12-electron π system. In agreement with this, the X-ray analysis at 100 K (and at room temperature) shows effective D_{2h} symmetry of the carbon skeleton, even though the crystallographically imposed molecular symmetry is only C_i. Here again the ***T,L,S*** analysis with allowance for torsional motion of the *tert*-butyl groups leads to a systematic pattern of discrepancies between calculated and observed U^{ij} components, but the indications are now such that any additional motion required to improve the agreement must be perpendicular to the molecular plane, as would be produced by an out-of-plane bending or buckling of the ring skeleton. There is no indication of disorder between two sets of atomic positions for the skeletal atoms in the molecular plane, as found in **4**. Either the equilibrium structure of **5** has D_{2h} symmetry with a delocalized π-eletron system, or, possibly, the set of atomic positions found in this crystal does not correspond to the ground-state molecular structure but rather to the transition state for the valence isomerization. In the crystal, such a transition state could be stabilized relative to the ground state by packing forces. As a precedent, in a somewhat analogous conformational isomerization, we are reminded of the example of biphenyl, planar in its crystal structure, nonplanar as a free molecule.[52]

The low-temperature (99 K) X-ray analysis of crystalline hexaisopropylbenzene **6**[53] provides another carefully

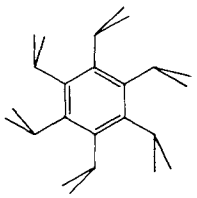

6

studied example of a disordered structure resulting from the presence of two molecular orientations at crystallographically equivalent sites. In the final structural model (Fig. 11), based on a combination of X-ray evidence and force-field calculations, the two orientations are present in about 2 : 1 ratio, and distances between positions of corresponding atoms are 35.7, 76.9, and 11.5 pm for the aromatic, methine, and methyl carbon atoms, respectively. In the standard least-squares refinement, only the two methine carbons were assigned individual positions and ADP's, the aromatic and methyl atom pairs being treated as single scatterers. The "vibration ellipsoids" for the aromatic carbon atoms, based on this model, clearly show the additional motion in the tangential direction, corresponding to the unresolved disorder between the two atomic sites. Since the homomerization energy of **6** is calculated to be about 150 kJ mol^{-1}, the disorder in this crystal is to be classed as static, in contrast to the previous examples.

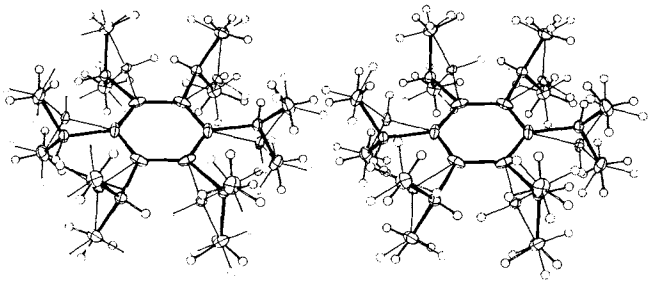

Fig. 11. Disorder model (stereoview) for **6** as deduced from the crystal structure analysis at 99 K and from force-field calculations [53]. The major and minor orientations (thick and thin lines) are present in a ratio of approximately 2 : 1.

10. Corrections to Interatomic Distances

The rigid-body model has been applied in the analysis of ADP's from thousands of crystal structures.[54] Usually, the main objective has been to obtain libration corrections to interatomic distances. As first noted by *Cruickshank*,[55] rotational oscillations of molecules cause the apparent atomic positions to be slightly displaced from the true positions towards the rotation axes. For a mean-square libration $\langle\phi^2\rangle$, the radial displacement $\overline{PB}$ is given approximately by $r\phi^2/2$, where r is the distance of the atom from the axis (Fig. 12). Errors from librational motions about orthogonal axes are additive.

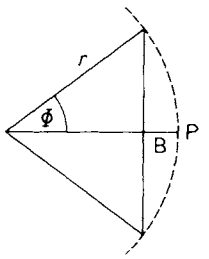

Fig. 12. The displacement $\overline{PB}=r-r\cos\phi\approx r\phi^2/2$, caused by libration.

More generally, X-ray and neutron diffraction analyses locate the centroids of pdf's, and separations computed from these centroids cannot be interpreted directly as average interatomic distances[56] (Fig. 13). To determine the corrections required to convert such separations into interatomic distances, we need information about the correlations between the instantaneous atomic displacements, and this information is usually unavailable. Any estimate of the corrections must then depend on assumptions about the

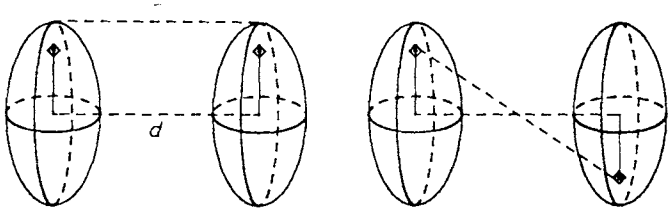

Fig. 13. The distance d between the atomic pdf centroids equals the interatomic distance for in-phase motion of the two atoms. For out-of-phase motion the mean interatomic distance is larger than d.

relative phases of the motions of different atoms.[57] In the rigid-body model, molecular libration corresponds to a correlated motion that makes the molecule appear to shrink slightly.

In room-temperature structures, errors in interatomic distances derived from centroids of atomic pdf's without corrections may amount to more than 5 pm, considerably greater than all the other errors put together. Bond distances derived from such structures should be regarded as highly unreliable, because even when corrections are made they are often based on assumptions whose validity is by no means assured. In particular, estimates of libration amplitudes obtained with the ***T,L,S*** analysis may be wildly in error when the implicit assumption of molecular rigidity is not warranted. In the *riding model*, it is assumed that one atom, the "riding" atom, has all the motion of the atom to which it is bonded, plus an additional uncorrelated motion. This model is particularly appropriate for hydrogen atoms (in cases where the ADP's are available from neutron diffraction studies), and X-H bond distance corrections from this source alone can amount to 5 pm.[58]

Uncorrected bond distances tend to become shorter with increasing temperature. In reasonably accurately determined structures, however, the motional corrections lead to fairly constant values. For example, the mean apparent (uncorrected) C–C distance in triclinic ferrocene[37] decreases from 142.6(1) to 141.5(1) pm as the temperature increases from 101 to 148 K, but the motional corrections lead to much more nearly equal values, 143.3 and 143.0 pm, respectively. Similarly, for naphthalene at five temperatures between 92 and 239 K, the trend towards shorter C–C bonds virtually disappears when corrections are made for the effects of rigid-body librational motion.[30]

Nevertheless, when bond distances are to be determined with the highest possible accuracy, it is best to reduce libration corrections by performing the crystal structure analysis at as low a temperature as possible. This also has the advantage that all the other types of atomic motions, where motional corrections are more difficult to apply, are reduced as well. But even bond distances obtained by low-temperature X-ray analysis and corrected for residual libration may be in error if the centroids of the atomic pdf's are displaced from the nuclear positions by contamination with the nonspherical bonding electron density. This depends on the resolving power of the experiment and brings us to the discussion of the experimental problems involved in the measurement of pdf's, a topic that we have avoided so far.

11. Experimental and Computational Aspects

The quality of the ADP's obtained in a crystal structure analysis obviously depends in the first place on the quality and range of the experimental observations—how accurately the intensities of the Bragg reflections were measured, and how many observations were made. This, in turn, depends on many factors, the quality of the crystals, their chemical and physical stability under the measurement conditions, the temperature at which the measurements were made, the wavelength of the radiation, the mechanical and electronic stability of the diffractometer, the appropriateness of the measurement protocol to the particular problem at hand, and many other factors besides. Important aspects of these problems, particularly in the context of X-ray analysis, have been recently examined by *Seiler*,[59] who has discussed strategies for reducing the errors in the measurement of Bragg reflections. The ADP's obtained in an analysis are also quite sensitive to the way in which the numerical data are treated, especially to details of the least-squares procedures used in the refinement of the structure. Since this article is aimed at the chemist, not at the practicing crystallographer, we mention only a few points that seem particularly relevant.

We are often interested in the precision and accuracy of the ADP's as well as in their particular values. The nominal standard deviations associated with the ADP's depend on the extent as well as on the quality of the experimental data.[60] With a given set of diffraction data, the ADP's of atoms of stronger scattering power will be the more precisely determined; for atoms of the same type, esd's of diagonal U^{ii} components appear to be roughly proportional to the U^{ii} values themselves.[22] An independent estimate of the precision of the ADP's can sometimes be made by examining the Δ values [Eq. (5)] for parts of molecules, such as carbon skeletons of benzene rings, that can reasonably be assumed to behave as rigid bodies; the rms Δ for a supposedly rigid body should be roughly $\sqrt{2}$ times the average esd of the atomic U components. At the lower end of the quality spectrum, a minimal criterion for the physical significance of the ADP's is that the U matrices must be positive definite; i.e., the constant probability surfaces of Equation (4) must correspond to ellipsoids and not to other quadratic surfaces, such as hyperboloids.

Apart from the random errors of measurement, most kinds of experimental error affect the ADP's in a systematic way; i.e., they tend to make the ADP's of *all* the atoms too large, or too small, or too large in one direction and too small in another. In the rigid-body model, these systematic errors affect mainly the description of the translational motion; the librational motion, and also the $\Delta_{A,B}$ values [Eq. (5)], are relatively unaffected. This means that estimates of rigid-body librational motion or of internal torsional motion may still be reasonable, even when the experimental data are seriously flawed.[61]

In X-ray analysis (not in neutron diffraction), one of the main problems in obtaining accurate ADP's (and atomic positions as well) is the fact that the electron-density distribution in the crystal differs slightly from the superposition of the electron densities of the isolated, spherically averaged atoms. This difference, known as the deformation density or bonding density, is of interest in the study of chemical bonding and is a subject for itself.[62] The standard, spherically symmetrical, atomic scattering factors used in the analysis of X-ray diffraction data from crystals take no account of these deformations. This neglect leads to a bias in the atomic positions (and also in the ADP's), the amount of which depends in a complicated way on the nature of the atom, its environment, and the extent of the data set. For example, carbonyl oxygen centroids tend to be drawn towards the lone-pair region, away from the car-

bon atom to which they are bonded, and C=O bond lengths tend therefore to be slightly (about 1 pm) too long. Similarly, the pdf's of carbon atoms in benzene rings tend to be slightly too large in the direction perpendicular to the plane of the ring, because the atomic vibration in this direction is not resolved from the π-electron density.

One way to reduce the free-atom bias is to use exclusively high-order reflections in the least-squares refinement[63] or to assign artificially large weights to these reflections.[64] This is because the valence electrons lie mainly in the outer part of the charge distribution around an atom, so that their contribution to the X-ray scattering falls off more rapidly with increasing scattering angle than that of the inner, core electrons. In fact, not inconsiderable errors in the positional parameters (up to 1–2 pm) and ADP's (up to 50 pm^2) may be introduced by refining only with low-order reflections (say, within the limit of $Cu_{K\alpha}$ radiation) or even with more extensive data sets that include low-order reflections.[65]

Probably the best way of reducing such errors is to model the deformation density by a suitable set of multipole terms centered at each atom. The free-atom scattering factors are augmented by the Fourier transforms of the multipole deformation terms,[66] and the coefficients of these additional terms are then obtained, together with the positional parameters and ADP's, in a special kind of least-squares refinement. However, the additional computational effort can be quite formidable and is only justified when the experimental data are of the very highest quality.

In spite of all the above-mentioned difficulties, reasonably accurate ADP's have been measured for thousands of crystal structures. The main problem today is that much of the information has disappeared, some of it, we fear, irretrievably. For some time now, nearly all published numerical data describing crystal structures have been restricted to a list of atomic positional coordinates with "isotropic" or "equivalent" displacement parameters; the information expressed by the six components of U has been compressed into a single scalar quantity. The ADP's have been relegated to supplementary information, which is sometimes deposited in libraries or other institutions and sometimes not. Deposited ADP's can in principle be retrieved (but often only at the cost of considerable delay, inconvenience, and expense). Numerical data that are not printed are rarely checked. As a result, deposited ADP's, when they can be found at all, are riddled with errors that are difficult to detect and sometimes impossible to correct. Some journals lack a deposition scheme altogether, so that data supplementary to papers published in them are simply lost. One can sympathize with the reluctance of editors of scientific journals to publish long lists of numbers (six per atom for the usual Gaussian ADP's), but at the same time steps have to be taken to secure the information and make it more easily accessible. Data bases probably offer the best solution to the problem. At present, the Inorganic Crystal Structure Data Base (ICSD)[67] contains ADP's for about half of its 25 000 entries. The Cambridge Structural Data Base (CSD),[68] dealing with organic crystal structures, has yet to include them,[69] but we are assured that this omission will be remedied very soon.

12. Macromolecules

The ideas and applications outlined in this article should be particularly relevant to the study of biological macromolecules, proteins, and nucleic acids. Experimental evidence and theoretical arguments agree that these are fluctuating systems that exist in a very large number of conformational substates.[70] In the "equilibrium structure" of such biological macromolecules, some atoms should have very diffuse, anisotropic pdf's, while others should be fairly well localized. For an understanding of the detailed mechanisms of biomolecular recognition processes and enzymatic reactions, a knowledge of the relative flexibility and rigidity of different parts of these molecules will certainly be needed, and it is this information that can be provided, in principle at least, by analysis of the ADP's.

Unfortunately, however, when it comes to the measurement and interpretation of ADP's from crystalline proteins and oligonucleotides, the problems mentioned in the earlier sections become vastly more severe. In the first place, the experimental resolution attainable for most macromolecular crystals is so limited that refinement of ADP's is usually out of the question. There are simply not enough experimental data. In most analyses of crystalline proteins, only isotropic atomic U's have been determined, leading in some cases to deductions about the general rigidity or looseness of different parts of the structures. The second main problem concerns the interpretation, which is even less straightforward than for small-molecule structures. In protein crystals, the atomic MSDA's are compounded of displacements arising from several sources: the multiplicity of conformational substates, diffusion (as in fluid-like regions of the structure), lattice disorder, and genuine vibration. These will all have different kinds of temperature dependence, and it is almost impossible to separate their contributions to the total mean-square displacements.

In a few cases, the temperature dependence of the isotropic U's has been followed; myoglobin is probably the best studied example.[71] In macromolecules, where the excursions of the atoms from their mean positions are much larger than in small-molecule structures, the potential energy associated with such displacements will not necessarily be quadratic, and the temperature dependence of U expressed in Equation (7) cannot be expected to hold. In myoglobin, different types of temperature dependence were observed for atoms in different regions of the molecule, and attempts were made to interpret these results in terms of the functionality.

More recently, ADP's have been obtained by refinement of more extensive diffraction data for several small proteins, including carp muscle calcium binding protein,[72] rubredoxin (for atoms in 30 of its 54 amino acids),[73] and avian pancreatic polypeptide (for atoms in all 36 of its amino acids.[74] No very striking conclusions have been drawn, but many of the results could be interpreted in terms of models involving concerted motions of groups of atoms in distinct regions of each molecule.

A model in which biomolecules are regarded as being built from semirigid groups of atoms, each of which moves more or less independently of the others, is the basis for what has been termed[75] the "segmented rigid-body model

of thermal motion".[76] With this model, in the refinement of the overall structure, the 20 components of T, L, and S are determined for each of a number of assumedly rigid subgroups in the macromolecule, as if each were an independent unit. Refinement of a dodecanucleotide with this model helped to improve the agreement between calculated and observed diffraction intensities and thus reduced the noise level of the difference Fourier map, allowing additional low-occupancy water molecules to be identified. In the analysis of bovine pancreatic ribonuclease A, a model of this kind was applied to the 13 aromatic side-groups (histidine, tyrosine, phenylalanine).[77] The resulting L components were small and inconclusive, the greater part of the group motions being derived from translation. The pattern of results again suggested collective motions of atoms in regions larger than single residues.

Advances in measurement techniques (synchroton radiation, area detectors) and in constrained refinement procedures will undoubtedly soon lead to ratios of data to adjustable parameters large enough to permit a determination of anisotropy for at least some of the atoms in many other macromolecules. Together with the kind of information about structure and dynamics that is becoming available from high-resolution two-dimensional NMR studies,[78] these advances should eventually lead to a better understanding of structure-function relationships in biological macromolecules.

Much of this article was written while E. F. M. and K. N. T. were on sabbatical leave in Zürich. The work described here has been supported over the years by the Swiss National Science Foundation.

Received: October 16, 1987 [A 676 IE]
German version: *Angew. Chem. 100* (1988) 910

[1] C. K. Johnson: *ORTEP II: A FORTRAN Thermal Ellipsoid Plot Program for Crystal Structure Illustrations (Report ORNL-5138)*, Oak Ridge National Laboratory, Oak Ridge, TN, USA 1976.
[2] J. D. Dunitz, V. Schomaker, K. N. Trueblood, *J. Phys. Chem. 92* (1988) 856.
[3] U. Shmueli, P. A. Kroon, *Acta Crystallogr. Sect. A 30* (1974) 768.
[4] D. W. J. Cruickshank, *Acta Crystallogr. 9* (1956) 754.
[5] D. W. J. Cruickshank, *Acta Crystallogr. 9* (1956) 915.
[6] D. W. J. Cruickshank, *Acta Crystallogr. 10* (1957) 504.
[7] V. Schomaker, K. N. Trueblood, *Acta Crystallogr. Sect. B 24* (1968) 63.
[8] K. N. Trueblood, *Acta Crystallogr. Sect. A 34* (1978) 950.
[9] Available on application to *K.N.T., UCLA*, or to Dr. *W. B. Schweizer*, Organic Chemistry Laboratory, Swiss Federal Institue of Technology, ETH-Zentrum, CH-8092 Zürich.
[10] J. P. Chesick, J. D. Dunitz, U. von Gizycki, H. Musso, *Chem. Ber. 106* (1973) 150.
[11] K. L. Brown, G. J. Down, J. D. Dunitz, P. Seiler, *Acta Crystallogr. Sect. B 38* (1982) 1241.
[12] a) G. Filippini, C. M. Gramaccioli, M. Simonetta, G. B. Suffritti, *J. Chem. Phys. 59* (1973) 5088; b) *Acta Crystallogr. Sect. A 30* (1974) 189; c) C. M. Gramaccioli, G. Filippini, M. Simonetta, *ibid. 38* (1982) 350.
[13] R. E. Rosenfield, Jr., K. N. Trueblood, J. D. Dunitz, *Acta Crystallogr. Sect. A 34* (1978) 828.
[14] F. L. Hirshfeld, *Acta Crystallogr. Sect. A 32* (1976) 239.
[15] C. P. Brock, W. B. Schweizer, J. D. Dunitz, *J. Am. Chem. Soc. 107* (1985) 6964.
[16] P. Chakrabarti, P. Seiler, J. D. Dunitz, A.-D. Schlüter, G. Szeimies, *J. Am. Chem. Soc. 103* (1981) 7378.
[17] An alternative to qualitative inspection of the matrix of Δ values is to make a half-normal probability plot of the ratios of these Δ values to their esd's against their statistical expectation values. When the slope of this line is significantly smaller than unity, nonrigidity of the group (or serious underestimation of the esd's) is indicated. See C. Kratky, H. Falk, U. Zrunek, *Monatsh. Chem. 116* (1985) 607.
[18] G. A. Jeffrey, J. R. Ruble, R. K. McMullan, J. A. Pople, *Proc. R. Soc. (London) A 414* (1987) 47.
[19] S. J. Cyvin: *Molecular Vibrations and Mean Square Amplitudes*, Elsevier, Amsterdam 1968, p. 245.
[20] At high enough temperature, Equation (7) (Section 7) applies, and the mean-square vibration amplitude is independent of the mass and depends only on the temperature and the force constant.
[21] C. K. Johnson in B. T. M. Willis (Ed.): *Thermal Neutron Diffraction*, University Press, Oxford 1970, p. 132.
[22] P. Seiler, B. Martinoni, J. D. Dunitz, *Nature (London) 309* (1984) 435.
[23] R. Bau, I. Brewer, M. Y. Chiang, S. Fujita, J. Hoffman, M. I. Watkins, T. F. Koetzle, *Biochem. Biophys. Res. Commun. 115* (1983) 1048.
[24] K. Chandrasekhar, H. B. Bürgi, *Acta Crystallogr. Sect. B 40* (1984) 387.
[25] a) J. H. Ammeter, H. B. Bürgi, E. Gamp, V. Meyer-Sandrin, W. P. Jensen, *Inorg. Chem. 18* (1979) 733; b) M. Stebler, H. B. Bürgi, *J. Am. Chem. Soc. 109* (1987) 1395.
[26] J. D. Dunitz, D. N. J. White, *Acta Crystallogr. Sect. A 29* (1973) 93.
[27] V. Schomaker, K. N. Trueblood, *Acta Crystallogr. Sect. A 40 Suppl.* (1984) C-339; a fuller paper is promised and should appear in *Acta Crystallogr. Sect. A*.
[28] Q.-C. Yang, M. F. Richardson, J. D. Dunitz, *J. Am. Chem. Soc. 107* (1985) 5535.
[29] Sometimes known as the agreement factor, sometimes as the disagreement factor, here defined as $\{\sum w[U^{ij}(\text{obs}) - U^{ij}(\text{calcd})]^2 / \sum w[U^{ij}(\text{obs})]^2\}^{1/2}$, with w a weighting factor, usually taken as inversely proportional to the variance of U^{ij}.
[30] C. P. Brock, J. D. Dunitz, *Acta Crystallogr. Sect. B 38* (1982) 2218.
[31] B. T. M. Willis, A. W. Pryor: *Thermal Vibrations in Crystallography*, Cambridge University Press, London 1975, p. 142.
[32] T. J. Bastow, S. L. Mair, S. W. Wilkins, *J. Appl. Phys. 48* (1977) 494.
[33] H. Küppers, F. Takusagawa, T. F. Koetzle, *J. Chem. Phys. 82* (1985) 5636.
[34] G. S. Pawley, *Phys. Status Solidi 20* (1967) 347.
[35] K. N. Trueblood, J. D. Dunitz, *Acta Crystallogr. Sect. B 39* (1983) 120.
[36] E. F. Maverick, J. D. Dunitz, *Mol. Phys. 62* (1987) 451.
[37] P. Seiler, J. D. Dunitz, *Acta Crystallogr. Sect. B 35* (1979) 2020.
[38] C. P. Brock, E. Maverick, J. D. Dunitz, unpublished results.
[39] As these calculations take no account of cooperative motions, it comes as no surprise that the barriers obtained with them are uniformly too high.
[40] P. Seiler, J. D. Dunitz, *Acta Crystallogr. Sect. B 35* (1979) 1068.
[41] F. Takusagawa, T. F. Koetzle, *Acta Crystallogr. Sect. B 35* (1979) 1074.
[42] a) J. D. Dunitz, L. E. Orgel, *Nature (London) 171* (1953) 121; b) J. D. Dunitz, L. E. Orgel, A. Rich, *Acta Crystallogr. 9* (1956) 373.
[43] A. Haaland, J. E. Nilsson, *Acta Chem. Scand. 22* (1968) 2653.
[44] L. Hedberg, K. Hedberg, *J. Chem. Phys. 53* (1970) 1228.
[45] S. Carter, J. N. Murrell, *J. Organomet. Chem. 192* (1980) 399.
[46] W. E. Sanford, R. K. Boyd, *Can. J. Chem. 54* (1976) 2773.
[47] H. Irngartinger, N. Riegler, K.-D. Malsch, K.-A. Schneider, G. Maier, *Angew. Chem. 92* (1980) 214; *Angew. Chem. Int. Ed. Engl. 19* (1980) 211.
[48] O. Ermer, E. Heilbronner, *Angew. Chem. 95* (1983) 414; *Angew. Chem. Int. Ed. Engl. 22* (1983) 402.
[49] H. Irngartinger, M. Nixdorf, *Angew. Chem. 95* (1983) 415; *Angew. Chem. Int. Ed. Engl. 22* (1983) 403.
[50] J. D. Dunitz, C. Krüger, H. Irngartinger, E. F. Maverick, Y. Wang, M. Nixdorf, *Angew. Chem. 100* (1988) 415; *Angew. Chem. Int. Ed. Engl. 27* (1988) 387.
[51] K. Hafner, B. Stowasser, H.-P. Krimmer, S. Fischer, M. C. Böhm, H. J. Lindner, *Angew. Chem. 98* (1986) 646; *Angew. Chem. Int. Ed. Engl. 25* (1986) 630.
[52] See a) H. Bonadeo, E. Burgos, *Acta Crystallogr. Sect. A 38* (1982) 29 for a lattice-dynamical treatment of biphenyl and b) W. R. Busing, *Acta Crystallogr. Sect. A 39* (1983) 340 for an analysis of packing effects in this crystal.
[53] J. Siegel, A. Gutiérrez, W. B. Schweizer, O. Ermer, K. Mislow, *J. Am. Chem. Soc. 108* (1986) 1569.
[54] ... including many where its applicability is highly questionable, to say the least.
[55] D. W. J. Cruickshank, *Acta Crystallogr. 9* (1956) 757.
[56] W. R. Busing, H. A. Levy, *Acta Crystallogr. 17* (1964) 142.
[57] In principle, information about correlations among the atomic motions is available from the generalized mean-square displacement matrix computed in a complete lattice-dynamical calculation. See, for example, C. Scheringer, *Acta Crystallogr. Sect. A 28* (1972) 512, 616. Corrections to interatomic distances have sometimes been made in this way: for example, C. M. Gramaccioli, G. Filippini, *ibid. A 41* (1985) 356 and [52a].
[58] A correction due to anharmonicity in the X-H stretching vibration may amount to half of this, in the opposite direction, and so may cancel out much of the riding correction. See a) J. A. Ibers, *Acta Crystallogr. 12* (1959) 251; b) G. A. Jeffrey, J. R. Ruble, *Trans. Am. Crystallogr. Assoc. 20* (1984) 129; c) B. M. Craven, S. Swaminathan, *ibid. 20* (1984) 133.

[59] a) P. Seiler in A. Domenicano, I. Hargittai, P. Murray-Rust (Eds.): *Lecture Notes, International School of Crystallography, Static and Dynamic Implications of Precise Structural Information*, Erice, Italy 1985, pp. 79–94; b) *Chimia 41* (1987) 104.
[60] When ADP's are transformed from one coordinate system to another, the variances of the transformed coordinates depend not only on the variances in the initial system but also on the covariances. This information is routinely calculated in most least-squares programs but it is usually ignored.
[61] For example, *Cruickshank*'s 1956 estimates of rigid-body librational amplitudes in anthracene [5] were based on data that are very poor by present standards although exemplary for the time (visually estimated three-dimensional set of reflection intensities from Weissenberg photographs obtained several years earlier by A. McL. Mathieson, J. M. Robertson, V. C. Sinclair, *Acta Crystallogr. 3* (1950) 245).
[62] a) P. Coppens, M. B. Hall: *Electron Distributions and the Chemical Bond*, Plenum, New York 1982; b) K. Angermund, K. H. Claus, R. Goddard, C. Krüger, *Angew. Chem. 97* (1985) 241; *Angew. Chem. Int. Ed. Engl. 24* (1985) 237.
[63] P. Coppens, *Isr. J. Chem. 16* (1977) 159.
[64] J. D. Dunitz, P. Seiler, *Acta Crystallogr. Sect. B29* (1973) 589.
[65] P. Seiler, W. B. Schweizer, J. D. Dunitz, *Acta Crystallogr. Sect. B40* (1984) 319.
[66] a) R. F. Stewart, *Isr. J. Chem. 16* (1977) 124; b) F. L. Hirshfeld, *ibid. 16* (1977) 198.
[67] G. Bergerhoff, R. Hundt, R. Sievers, I. D. Brown, *J. Chem. Inf. Comput. Sci. 23* (1983) 66.
[68] F. H. Allen, S. Bellard, M. D. Brice, B. A. Cartwright, A. Doubleday, H. Higgs, T. Hummelink, B. G. Hummelink-Peters, O. Kennard, W. D. S. Motherwell, J. R. Rodgers, D. G. Watson, *Acta Crystallogr. Sect. B35* (1979) 2331.
[69] As electronic transfer of numerical information becomes more common, direct submission of parameter files containing atomic coordinates and ADP's to databases, such as the ICSD [67] or the CSD [68], should become standard practice. This will avoid the present tedious and error-prone stages of copying from printed records.
[70] G. Careri, P. Fasella, E. Gratton, *Crit. Rev. Biochem. 3* (1975) 141.
[71] a) H. Frauenfelder, G. A. Petsko, D. Tsernoglou, *Nature (London) 280* (1979) 558; b) D. Ringe, J. Kuriyan, G. A. Petsko, M. Karplus, H. Frauenfelder, R. F. Tilton, I. D. Kuntz, *Trans. Am. Crystallogr. Assoc. 20* (1984) 109.
[72] J. H. Konnert, W. A. Hendrickson, *Acta Crystallogr. Sect. A36* (1980) 344.
[73] K. D. Watenpaugh, L. C. Sieker, L. H. Jensen, *J. Mol. Biol. 138* (1980) 615.
[74] I. Glover, I. Haneef, J. Pitts, S. Wood, D. S. Moss, I. Tickle, T. Blundell, *Biopolymers 22* (1983) 293.
[75] S. R. Holbrook, R. E. Dickerson, S.-H. Kim, *Acta Crystallogr. Sect. B41* (1985) 255.
[76] An unfortunate turn of phrase, since it will almost inevitably lead to confusion with the similarly named model due to *Johnson* [21] in which the segments form parts of an overall molecule for which ***T***, ***L***, and ***S*** are determined together with the torsional amplitudes about the intersegmental links.
[77] D. S. Moss, I. Haneef, B. Howlin, *Trans. Am. Crystallogr. Assoc. 20* (1984) 123.
[78] K. Wüthrich: *NMR of Proteins and Nucleic Acids*, Wiley, New York 1986.

The Pentazadienide Ion as a Ligand in Metal Complexes

By Johannes Beck* and Joachim Strähle

The pentazadienide ion is a surprisingly versatile ligand. The planar, zigzag N_5 chain can utilize its atoms N1, N3, and N5 to complex one, two, or three metal atoms in a monodentate or bidentate fashion. Of particular interest is the ligand's ability to promote short metal-metal contacts in complexes with d^{10} metal ions.

1. Introduction

Nitrogen can form chains of from two to eight atoms. The only stable nitrogen-hydrogen compounds at room temperature are hydrazine, H_2N-NH_2, and hydrazoic acid, HN_3. 2-Tetrazene, $H_2N-N=N-NH_2$, decomposes at $T<0°C$. Organic substituents are necessary to stabilize longer chains; 1,5-diphenyl-3-methyl-1,4-pentazadiene **1a** does not decompose until 112°C. However, the 3-unsubstituted analogue, 1,5-diphenyl-1,4-pentazadiene explodes on

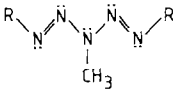

1a, R = phenyl
b, R = tolyl

gentle warming. It may be stabilized by using tolyl rather than phenyl substituents. 1,5-Diaryl-1,4-pentazadienes were first obtained by *P. Griess*[1] in 1866 by the reaction of aryldiazonium salts with amines; the constitution of these compounds was not deduced correctly until 1894 by *H. von Pechmann* and *L. Frobenius*.[2]

Whereas hydrazido, diimido, azido, and triazenido complexes have been known for some time and in considerable variety, 1,4-tetrazadiene complexes have only recently been synthesized and structurally investigated.[3-5] Prior to our investigations, no complexes of pentazadiene or the pentazadienide ion had been reported.

We first attempted to use the more stable **1a** as a ligand, but obtained no metal complexes, because the N_5 chain was always cleaved; for example, the reaction with $MoCl_5$ gives phenyldiazonium hexachloromolybdate(v) as the main product.[6,7]

The 3-unsubstituted 1,5-ditolyl-1,4-pentazadiene **2** has acid character; we have succeeded in synthesizing a large number of novel complexes with the corresponding anion **3**, which displays an astonishing versatility in its role as a ligand.

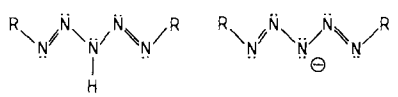

2 **3**

R = *p*-tolyl

[*] Dr. J. Beck
Institut für Anorganische Chemie der Universität
Engesserstrasse, D-7500 Karlsruhe (FRG)
Prof. Dr. J. Strähle
Institut für Anorganische Chemie der Universität
Auf der Morgenstelle 18, D-7400 Tübingen (FRG)

2. The Ligand 1,5-Ditolyl-1,4-pentazadienide 3

2.1. Synthesis and Properties

The intense yellow pentazadiene **2** can be synthesized in aqueous solution from tolyldiazonium chloride and NH_3.[2] In pure form it is extremely explosive and must therefore be handled with the greatest care, preferably while still moist. In alkaline solution **2** functions as an acid and is converted into its anion **3**, which crystallizes from aqueous ammonia, with $Cs^{\oplus}$ as counterion, as Cs(tolN_5tol) **4**.

2.2. Structure of the Pentazadienide Ion 3

The anions **3** are essentially uncoordinated in the cesium salt **4**. The structure analysis[8] reveals a planar, all-*trans* N_5 zigzag chain with symmetry C_2 (Fig. 1). The all-*trans* configuration is also found in all metal complexes of **3**. The tolyl substituents are twisted away from the N_5 plane in **3** and also in most of the metal complexes; the interplane angle in **4** is 25.5°. The N-N bond lengths in **4** indicate slightly lengthened double bonds N1-N2 (127.8 pm) and appreciably shortened single bonds N2-N3 (136.9 pm). The $Cs^{\oplus}$ ions are each surrounded by four N_5 chains, leading to a distorted square antiprismatic coordination with Cs-N contacts between 314.4 and 365.8 pm.

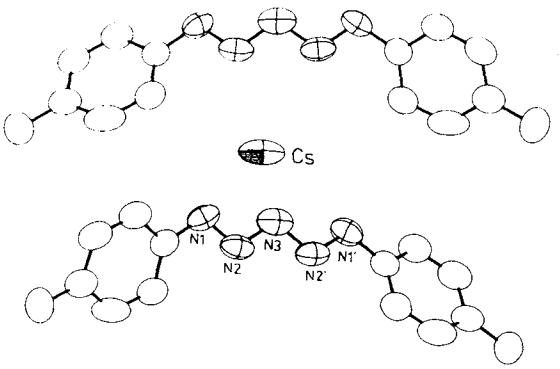

Fig. 1. Molecular structure of **4** projected parallel to [010]. The $Cs^{\oplus}$ ion and the N3 atom of the anion occupy special positions on twofold axes at $y=0.25$ (Cs) and $y=-0.25$ and 0.75 (N3).

[Tl(tolN_5tol)] **13** is a compound with a strongly polar metal-nitrogen bond (Fig. 10 in Section 3.3.6). The partial saltlike character of **13** is evident from the long Tl-N bonds (271.5-279.5 pm) and the lack of coplanarity between the Tl-N bonds and the N_5 plane. Compound **13** is

the only example so far in which all N–N bond lengths are approximately equal (129.6–131.7 pm; Table 1). The extended conjugation indicated by these bond lengths is probably associated with the partial saltlike character of **13**. The observation that the N–N bonds in the cesium salt **4** are of differing lengths (Table 1, N4 = N2′, N5 = N1′) can be explained in terms of a polarization of the anion **3** by the $Cs^{\oplus}$ ion; whereas the distances Tl-N1, Tl-N3, and Tl-N5 are roughly equal, the $Cs^{\oplus}$ ion in **4** is involved in a short contact to the central atom N3 (314.4 pm) but in longer contacts to the outer atoms N1 and N5 (349.6, 410.1 pm). This leads to a concentration of negative charge at N3 and thus to the observed differences in bond length.

Table 1. N-N bond lengths [pm] in **3** (see Scheme 1 in Section 3.2 for details of the compounds).

	N1-N2	N2-N3	N3-N4	N4-N5
uncoordinated **3** in				
4	127.8	136.9	136.9	127.8
symmetrically coordinated **3** in				
1b	126.7	136.2	136.2	126.7
5	122.8	132.7	140.0	119.8
8	129.1	134.9	135.4	128.2
9	127.0	134.2	133.1	128.2
unsymmetrically coordinated **3** in				
6	126.1	128.8	137.2	126.2
7	128.5	132.7	137.1	124.8
10	131.0	132.6	136.0	126.6
(N1,N3)-η^2-, (N5)-η^1-coordinated **3** in				
11	128.2	134.5	135.5	127.9
12	129.0	132.9	136.3	127.5
13	131.7	129.6	130.3	131.6
14	127.9	134.7	133.1	128.6

The unperturbed free anion **3** in solution presumably possesses N–N bonds of differing lengths. However, the difference in energy between the two forms would appear to be small.[8]

3. Metal Complexes of 3

3.1. Synthesis and Properties

The metal complexes of the pentazadienide **3** are synthesized most simply from **2** and soluble metal ammine complexes in aqueous ammonia [Eq. (a)]. In this way we

$$[M(NH_3)_x]^{n\oplus} + n\,\mathbf{3} \longrightarrow [M(tolN_5tol)_n] + x\,NH_3 \qquad (a)$$

obtained the complexes $[Ag(tolN_5tol)]_2$ **8**,[9] $[M^{II}(tolN_5tol)_2]$ (M = Cu (**6**),[10b] Ni (**11**),[7] Co,[11] Zn,[6] Cd,[6] and Pd[6]), and $[Co(tolN_5tol)_3]$,[13] which are precipitated as sparingly soluble complexes. $[Pt(NH_3)_4]^{2\oplus}$, $[Rh(NH_3)_5Cl]^{2\oplus}$, and $[Ru(NH_3)_5Cl]^{2\oplus}$ do not react with **3** in this manner.

[Tl(tolN$_5$tol)] **13** can be prepared in alkaline aqueous solution from TlOH and **2**.[12] AuI, which is insoluble in aqueous NH_3, reacts with **2** in liquid NH_3 to give $[Au(tolN_5tol)]$.[6] $[Mo(\eta^5\text{-}C_5H_5)(CO)_2(tolN_5tol)]$ **10** is formed from $[Mo(\eta^5\text{-}C_5H_5)(CO)_3Br]$ and **2** in ethanol in the presence of NaOH.[10a] $[(Ph_3PAu)]ClO_4$ reacts with **13** in toluene to give $[Au(PPh_3)(tolN_5tol)]$ **5** and $TlClO_4$.[10b]

A further method of synthesizing metal complexes of **3** is to react **8** with halogen–metal compounds in organic solvents [Eq. (b)]. $[Ru(CO)_4I_2]$ reacts under the same con-

$$[Fe(CO)_4I_2] + 2\,\mathbf{8} \longrightarrow [Fe(tolN_5tol)_2] + 2\,AgI + 4\,CO \qquad (b)$$

14

ditions to give $[Ru(CO)_3(tolN_5tol)]_2$ **7**,[13] the ruthenium being reduced. The reducing properties of **3** also result in the formation of $[Cu(tolN_5tol)]_3$ **9** when a solution of **6** is refluxed in organic solvents.[7]

Alcohols replace one pentazadienido ligand in $[Co(tolN_5tol)_2]_2$ to form the hexameric $[Co(OR)(tolN_5tol)]_6$ [Eq. (c)].[11]

$$\mathbf{6}\,[Co(tolN_5tol)_2] + 6\,CH_3OH \longrightarrow [Co(OCH_3)(tolN_5tol)]_6 + 6\,Tol_2N_5H \qquad (c)$$

12

The pentazadienido complexes are all more intensely colored than **3**, **2**, or **1**, which are orange or yellow. The intense color can presumably be attributed to charge-transfer transitions from the metal to the ligand. The molar extinction coefficient of **11**, for example, is 5.6×10^7 cm^2 mol^{-1} at $\lambda = 415$ nm.[6] The absorption maxima lie in at 252 and 415 nm.

The metal complexes generally deflagrate at higher temperatures. They are however not as explosive as the pentazadiene **2**.

3.2. The Coordination Patterns of the Ligand 3

Scheme 1 presents a summary of the six modes of coordination that we have found for the ligand **3**. The atoms N1, N3, and N5 can function as donors.

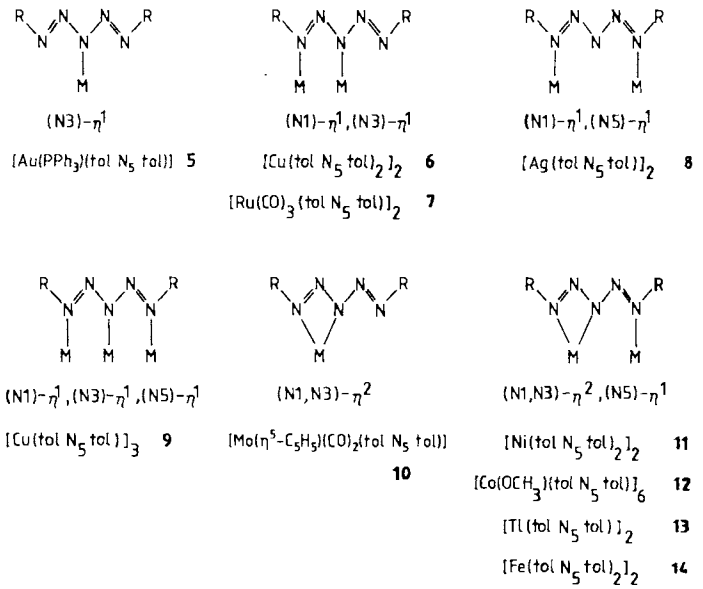

Scheme 1. Observed modes of coordination of **3**.

3.3. Structures of Metal Complexes of 3

3.3.1. 3 as an (N3)-η^1 Ligand: [Au(PPh$_3$)(tolN$_5$tol)]$_5$ 5

In the pentazadienes **1** and **2**, a methyl group or a hydrogen atom is bonded to the atom N3 in the N_5 chain. It is therefore not surprising that the $(Ph_3P)Au$ group, which is isolobal to both the methyl group and the hydrogen atom, also binds to N3. The structure of **5** is shown in Figure 2a,[10b] and corresponds to the structure of **1b** (Fig. 2b).[10b] Another reason for preferential bonding through N3 is that it possesses the highest basicity, the negative charge of **3** being largely localized at N3.

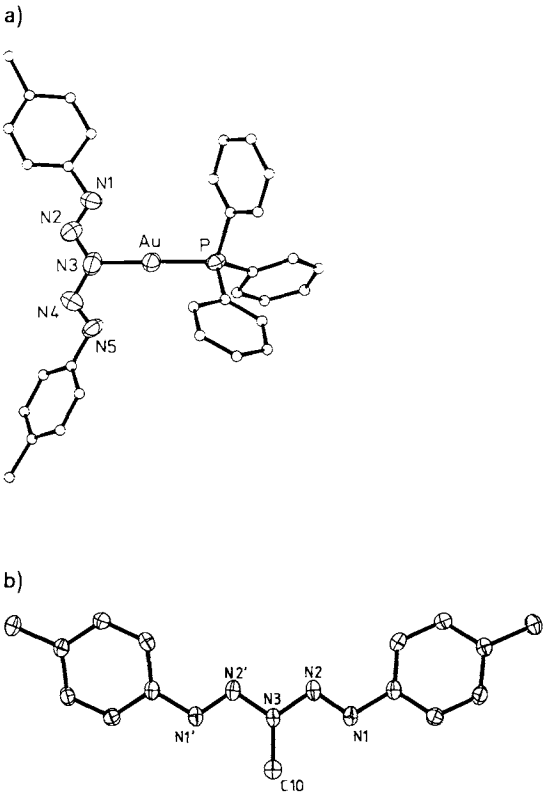

Fig. 2. Molecular structure of a) **5** and b) **1b**.

The Au–N bond length (208.2 pm) corresponds to a single covalent bond. The N–N bond lengths are 121.3 pm (average) for N1-N2 and N4-N5 and 136.4 pm (average) for N2-N3 and N3-N4 (Table 1).

The analogy between **1** and **5** can also be seen in the N–N bond lengths of **1b**, which are 126.7 pm for N1-N2 and 136.2 pm for N2-N3 (Table 1).

3.3.2. 3 as an (N1)-η^1,(N3)-η^1 Ligand: [Cu(tolN$_5$tol)$_2$]$_2$ 6 and [Ru(CO)$_3$(tolN$_5$tol)]$_2$ 7

The anion **3** can behave like the triazenido ligand $RN_3R^{\ominus}$ and bridge two metal atoms. This leads to short metal–metal contacts, since the N1–N3 bite is only ca. 223 pm. Complexes containing **3** as an (N1)-η^1,(N3)-η^1 ligand are therefore preferentially formed by metals that tend to display metal–metal interactions.

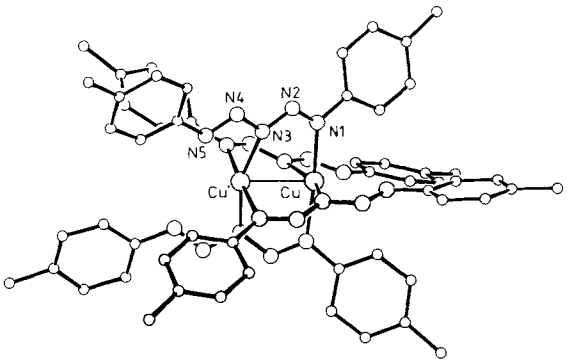

Fig. 3. Molecular structure of **6**. The complex has D_2 symmetry.

In the Cu^{II} complex **6** (Fig. 3),[10b] a structure similar to those of $[Cu(PhN_3Ph)_2]_2$[14] and carboxylato complexes[15] is attained. The crystal structure analysis shows that the complex **6** possesses crystallographic symmetry 222 (D_2), which is a point symmetry seldom observed. The Cu–Cu distance is 253.0 pm, comparable to those in $[Cu(PhN_3Ph)_2]_2$ (245 pm) and the Cu^{II} carboxylato complexes. The Cu–N bond lengths (202 pm) correspond to single bonds. The N–N bond lengths differ from those in **3** because of the unsymmetrical coordination; those in the Cu_2N_3 ring are approximately equal (N1-N2 126.1, N2-N3 128.8 pm), whereas those in the noncoordinating part of the N_5 chain differ appreciably (N3-N4 137.2, N4-N5 126.2 pm; Table 1).

Just as the complex **6** is related to Cu^{II} carboxylato complexes, so the complex **7**[13] is analogous to the Ru^{I} benzoato and acetato complexes $[Ru(CO)_3(O_2CR)]_2$ ($R = CH_3$, Ph).[16] The structure of **7** is shown in Figure 4. In contrast to the eclipsed conformation of the equatorial ligand atoms in the carboxylato complexes, the RuC_2N_2 equatorial planes in **7** are rotated with respect to each other, resulting in a staggered geometry. The Ru–Ru bond length (267.5 pm) is essentially equal to those in $[Ru(CO)_3(O_2R)]_2$ ($R = CH_3$, 268.9 pm; R = Ph, 270.4 pm),

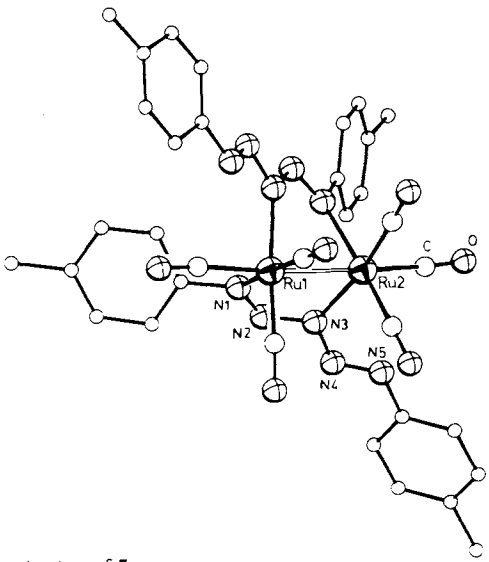

Fig. 4. Molecular structure of **7**.

and is consistent with the assumption of a single bond. The average Ru–N bond length is 212.5 pm. The unsymmetrical coordination has the same effect on the N–N bond lengths as in **6** and **10** (Table 1): N1-N2 128.5, N2-N3 132.7, N3-N4 137.1, N4-N5 124.8 pm.

3.3.3. 3 as an (N1)-η^1,(N5)-η^1 Ligand: [Ag(tolN$_5$tol)]$_2$ 8

In **8** the two silver atoms are coordinated approximately linearly by the outermost N atoms of two pentazadienide ions arranged with their long axes parallel (Fig. 5).[9] A planar Ag_2N_{10} ring results; the tolyl substituents also lie approximately in this plane, so that the overall symmetry is close to D_{2h}. The Ag–N bond lengths of 217 pm lie in the expected range for single bonds. As in **4**, **5**, and **9**, the N–N bond lengths differ appreciably; N1-N2 and N4-N5 (average) 128.7 pm, N2-N3 and N3-N4 (average) 135.2 pm (Table 1).

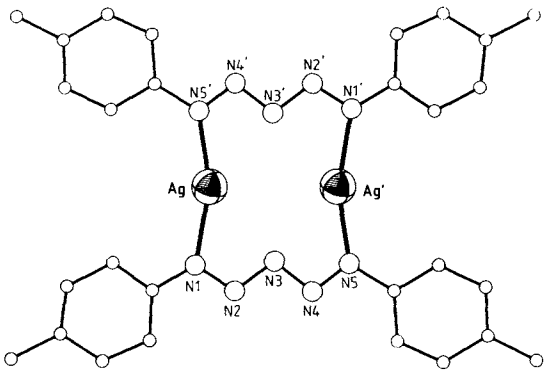

Fig. 5. Molecular structure of **8**.

3.3.4. 3 as an (N1)-η^1,(N3)-η^1,(N5)-η^1 Ligand: [Cu(tolN$_5$tol)]$_3$ 9

The (N1)-η^1,(N3)-η^1,(N5)-η^1 coordination of **3** in **9** gives rise to a linear $Cu_3^{3\oplus}$ chain with extremely short Cu–Cu contacts of 235.2 pm (Fig. 6). This value is lower than that in the Cu^{II} complex **6** (253 pm); it corresponds to twice the covalent radius of copper (234 pm[17]) and can thus be attributed to bonding interactions, although none would be formally expected for the closed d^{10} shells. Hückel MO calculations for d^{10} systems suggest a purely antibonding interaction if only the nd orbitals are considered, but the interaction becomes bonding if the empty

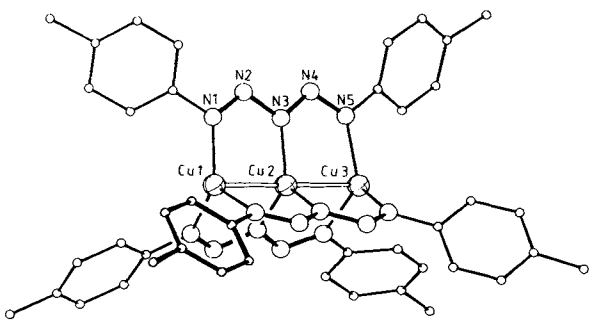

Fig. 6. Molecular structure of **9**.

(n+1)s and (n+1)p orbitals are mixed in.[18–20] The same result has been reached by *K. M. Merz, Jr.* and *R. Hoffmann* for **9**.[21]

Short metal–metal contacts are also observed in [Ag(PhN$_3$Ph)]$_2$[9] and [Au(PhN$_3$Ph)]$_4$,[22] complexes of the related triazenido ligand; we therefore assume that both the triazenido and the pentazadienido ions are capable of promoting d^{10}–d^{10} interactions.

The average Cu–N bond lengths in **9** correspond to those in **6**. The bond to the more strongly basic central N3 atom is somewhat shorter (194.5 pm) than those to the outermost atoms N1 and N5 (203.6 pm). The N–N bond lengths in **9**, like those in **4**, **5**, and **8**, fall into two groups; two shorter bonds of ca. 127.6 pm and two longer ones of ca. 133.7 pm.

3.3.5. 3 as an (N1,N3)-η^2 Ligand: [Mo(η^5-C$_5$H$_5$)(CO)$_2$(tolN$_5$tol)] 10

The structure of the Mo^{II} complex **10** is shown in Figure 7.[10a] The pentazadienide ion coordinates through the atoms N1 and N3 and functions as a chelating bidentate ligand. The N–N bond lengths in the chelate ring are similar (131.0 and 132.6 pm); in the noncoordinating part of the chain, however, they differ appreciably (as in complexes **6** and **7** with (N1)-η^1,(N3)-η^1 coordination: N3-N4 136.0, N4-N5 126.6 pm; Table 1), corresponding to a shortened single bond and a largely localized double bond. The Mo–N bond lengths (Mo-N1 214.9, Mo-N3 211.3 pm) again demonstrate clearly the higher basicity of the atom N3.

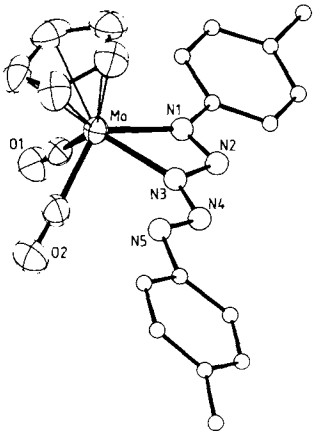

Fig. 7. Molecular structure of **10**.

The Co^{II} complex [Co(tolN$_5$tol)$_2$] is monomeric in solution; (N1,N3)-η^2 coordination by both ligands may be assumed, the $Co^{2\oplus}$ ion thus being tetrahedrally coordinated.[11]

3.3.6. 3 as an (N1,N3)-η^2,(N5)-η^1 Ligand

(N1,N3)-η^2,(N5)-η^1 coordination by the ligand **3** is the most frequently observed. It may also be assumed in the complexes [Zn(tolN$_5$tol)$_2$] and [Cd(tolN$_5$tol)$_2$], the structures of which have not been determined, but which should be analogous to those of the Ni complex **11** and the Fe complex **14**. Three crystalline modifications of **11**

have been studied; a monoclinic, solvated form **11** · THF[7] and two unsolvated forms, one triclinic and one tetragonal. The crystal structures of the monoclinic and tetragonal modifications have been determined. Figure 8 shows the

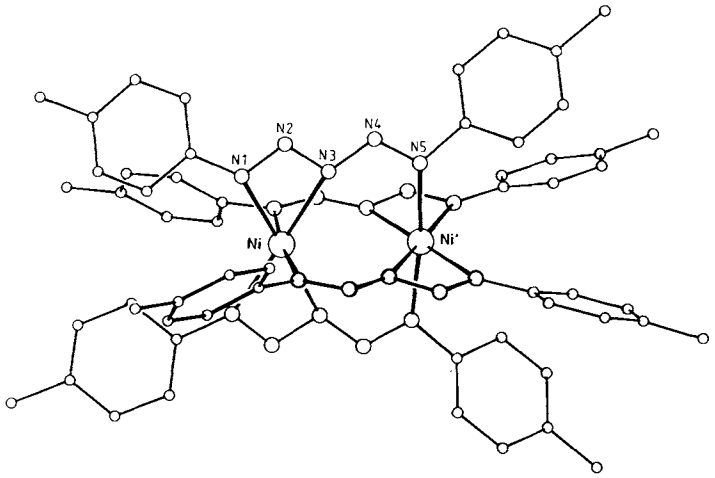

Fig. 8. Molecular structure of **11**. The complex has S_4 symmetry.

structure of tetragonal **11**;[23] the complex possesses crystallographic point symmetry $\bar{4}$ (S_4). In monoclinic **11** · THF this symmetry is only approximately fulfilled because of a rotation of the tolyl groups. The same structure is observed for **14**.[13] In **11** and **14** four parallel zigzag N_5 chains coordinate two $M^{2\oplus}$ ions in a distorted octahedral fashion; the equatorial planes of the octahedra are defined by two chelating N_3 fragments. The Ni–N bond lengths in these planes are 213.5 pm, whereas those to the apices of the octahedra are 206.4 pm. They correspond to single coordinate bonds. The N–N bond lengths in **11** are analogous to those associated with symmetric coordination; the outer, shorter N–N bonds are ca. 128 pm (Table 1); the inner, longer ones are ca. 135 pm. Similar values are observed in **14**; Fe-N 224.7, 215.8, N-N 128.3, 133.9 pm.

The central structural unit of the hexanuclear Co complex **12**[11] is a twelve-membered ring of six $Co^{2\oplus}$ ions and six methoxy O atoms (Fig. 9). The $Co^{2\oplus}$ ions lie in a plane, with the O atoms alternately above and below the plane, giving the ring the approximate symmetry D_{3d}. The pentazadienide ions each bridge two Co atoms, one being chelated and the other singly coordinated. In this way, half the cobalt atoms acquire tetrahedral coordination geometry from two monodentate N atoms (of two pentazadienide ligands) and two methoxy groups; the other half are coordinated octahedrally by two chelating pentazadienides and two methoxy groups. The Co–N bond lengths in the octahedra are longer than in the tetrahedra (221.4, 206.3 pm). The N–N bond lengths (Table 1) suggest the presence of double (128.2 pm) and shortened single (134.6 pm) bonds.

The structure of the Tl^{I} compound **13** is shown in Figure 10.[12] If **13** is regarded as a coordination compound, the coordination mode (N1,N3)-η^2,(N5)-η^1 applies. However, we have already indicated (Section 2.2) that **13** displays a partial saltlike character with markedly polar Tl–N bonds.

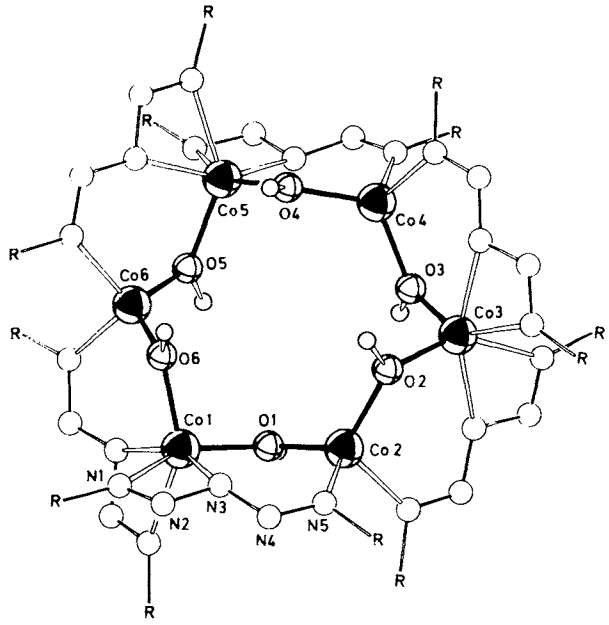

Fig. 9. Molecular structure of **12**.

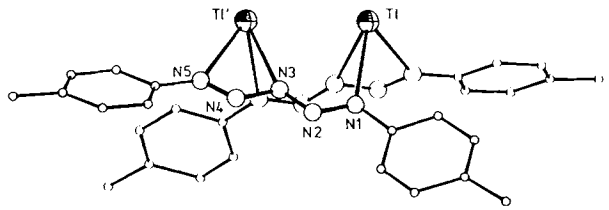

Fig. 10. Molecular structure of **13**.

4. Summary and Prospects

We have presented here several examples of recent structure determinations of metal complexes of the pentazadienide anion and have thus demonstrated its surprising versatility as a ligand. It is probable that we have not yet exhausted all possibilities, because our studies have mostly centered on metals in oxidation states +1 and +2; future investigations with transition metals in oxidation states 0 or higher than +2 would seem worthwhile. Furthermore, initial studies have shown that substituents on the organic groups of **3** can alter the electronic properties of the ligand and thus, for example, permit the control of its influence on d^{10}–d^{10} interactions. The chemistry of derivatives of **3** not involving metals is also clearly an interesting field.

We wish to thank Dipl.-Chem. R. Schmid for his enthusiastic assistance in these studies. The work was financially assisted by generous grants from the Deutsche Forschungsgemeinschaft and the Fonds der Chemischen Industrie.

Received: March 17, 1987;
supplemented: September 1, 1987 [A 678 IE]
German version: *Angew. Chem. 100* (1988) 927

[1] P. Griess, *Ann. Chem. Pharm. 137* (1866) 80.
[2] H. von Pechmann, L. Frobenius, *Chem. Ber. 27* (1894) 899.
[3] M. Denker, G. R. Knox, *Chem. Commun. 1967*, 1243.
[4] M. E. Gross, W. C. Trogler, J. A. Ibers, *J. Am. Chem. Soc. 103* (1981) 192.
[5] P. Overbosch, G. van Koten, O. Overbeek, *Inorg. Chem. 21* (1982) 2373, 3908; *J. Am. Chem. Soc. 102* (1980) 2091.
[6] J. Beck, *Dissertation*, Universität Tübingen 1986.
[7] J. Beck, J. Strähle, *Angew. Chem. 97* (1985) 419; *Angew. Chem. Int. Ed. Engl. 24* (1985) 409.
[8] R. Schmid, J. Beck, J. Strähle, *Z. Naturforsch. B43* (1988) 529.
[9] J. Beck, J. Strähle, *Z. Naturforsch. B41* (1986) 4.
[10] a) J. Beck, *Z. Naturforsch.*, in press; b) J. Beck, unpublished results.
[11] R. Schmid, J. Beck, J. Strähle, *Z. Naturforsch. B42* (1987) 911.
[12] J. Beck, J. Strähle, *Z. Naturforsch. B41* (1986) 1381.
[13] R. Schmid, J. Strähle, *Z. Naturforsch.*, in press.
[14] M. Corbett, B. F. Koskins, N. J. McLeod, B. P. O'Day, *Austr. J. Chem. 28* (1975) 2377.
[15] J. Catterick, P. Thornton, *Adv. Inorg. Chem. Radiochem. 20* (1977) 291.
[16] M. Spohn, T. Vogt, J. Strähle, *Z. Naturforsch. B41* (1986) 1373.
[17] L. Pauling: *Die Natur der chemischen Bindung*, Verlag Chemie, Weinheim 1968; The Nature of the Chemical Bond, Cornell University Press 1960.
[18] A. Dedieu, R. Hoffmann, *J. Am. Chem. Soc. 100* (1978) 2074.
[19] P. K. Mehrotra, R. Hoffmann, *Inorg. Chem. 17* (1978) 2187.
[20] J. Yuansheng, S. Alvarez, R. Hoffmann, *Inorg. Chem. 24* (1985) 749.
[21] K. M. Merz, Jr., R. Hoffmann, unpublished results.
[22] J. Beck, J. Strähle, *Angew. Chem. 98* (1986) 106; *Angew. Chem. Int. Ed. Engl. 25* (1986) 95.
[23] J. Beck, J. Strähle, *Acta Crystallogr. Sect. C43* (1987) 1293.

Surfactants, Micelles and Fascinating Phenomena

By Heinz Hoffmann* and Gerlinde Ebert

In this article we shall describe processes and phenomena which may appear startling and unusual for someone who is familiar with the behavior of solutions of low molecular weight solutes. Some of these phenomena might even be surprising for someone who works with surfactants. The authors still remember their astonishment when they first became aware of a viscoelastic surfactant solution. This was many years after our group had started investigations on surfactants. But all of the solutions we had encountered until that time had behaved normally. Some of the phenomena which will be discussed are also encountered in solutions of polymers. Due to their high molecular weight one expects to find properties which are different from the properties of low molecular weight solutions and does not find them so surprising. Surfactant solutions, however, are aqueous solutions of small molecules with typical molecular weights of 200 to 400. For some of our experiments even dilute solutions were used which contained only up to one percent of surfactant.

1. Introduction

Most of the phenomena described here arise from the ability of the surfactant molecules to form large aggregates of different shapes. In a thermodynamic sense these aggregates—even though they consist of many molecules—can be treated as *single* particles or large molecules that exert forces on each other. For this reason, micelles can be considered as a van-der-Waals-gas, and like real gases, they are capable of condensation or can convert into the crystalline—(in this case the liquid crystalline) state.

The forces of interaction between the particles are determined by the size and the number of charges on the particles. One of the fascinating aspects of these systems is the fact that slight changes in the system on a microscopic level can lead to dramatic changes in the macroscopic properties of the system. Surfactant molecules have in many ways similar properties as membrane-forming lipids. They exist as single chain and double chain molecules. It is therefore likely that nature uses some of the processes which are described here with simple surfactant molecules in the functioning and control of life processes.

One of our goals is to bring these fascinating control mechanisms to the attention of a larger audience which is not directly involved with research in surfactant chemistry. All the experiments mentioned in the text can easily be carried out without the need for elaborate equipment. The chemicals required for such experiments are commercially available and can be purchased at low cost. In principle the phenomena described here are well suited for high-school experiments. We might also mention that some of the described effects are of considerable interest and practical importance from the technological point of view.

Inspite of how startling and unexpected the phenomena may seem, they are nevertheless based on a few rather simple principles; they are always reproducible and can be described quantitatively.

[*] Prof. Dr. H. Hoffmann, Dipl.-Chem. G. Ebert
Physikalische Chemie I der Universität
Universitätsstrasse 30, D-8580 Bayreuth (FRG)

2. Viscoelastic Surfactant Solutions

Many surfactants, in particular commercially produced detergents, dissolve readily in water and form Newtonian solutions up to high concentrations. In these solutions the surfactant molecules aggregate into globular micelles and the solutions are optically isotropic and of low viscosity. Micelles can however grow into rodlike or disklike aggregates, and these structures can be so large that they can form entanglements. The shape of the micelles is controlled by the packing parameters of the surfactant molecule in the micellar assembly. The situation is shown schematically in Figure 1.

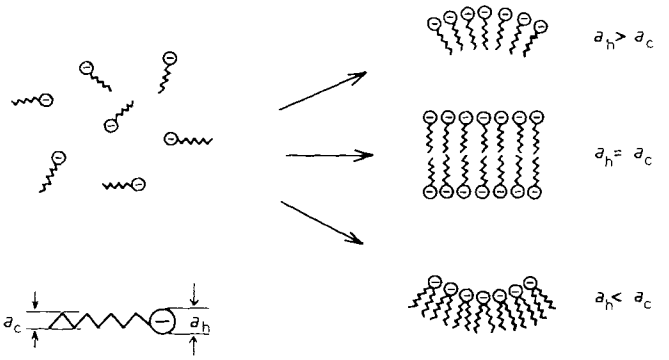

Fig. 1. Schematic illustration of the importance of the natural radius of curvature for micellar structures. The radius of curvature is controlled by the ratio of the required headgroup area a_h of a surfactant molecule at the interface and the cross section of the chain a_c.

If the hydrophobic head at the micellar interface requires an area a_h which is larger than the cross section a_c of the chain in its average surrounding, the system will form aggregates with a convex curvature. If both areas are of the same size, planar structures are favored and if $a_c > a_h$ the system prefers to form inverse structures if this is possible by other constraints.[1]

Surfactant solutions with rodlike micelles can be highly viscoelastic,[2] i.e. exhibit both viscous as well as elastic behavior. Such systems can be prepared by mixing two nor-

 © VCH Verlagsgesellschaft mbH, D-6940 Weinheim, 1988 0570-0833/88/0707-0902 $ 02.50/0

mal micellar solutions or a micellar solution and a salt solution which contains a particular counter-ion that strongly binds to the surfactant-ion. The starting solutions are optically clear and have a viscosity which is close to the viscosity of water. Upon mixing two such solutions one obtains almost instantaneously—with perhaps a few seconds delay after the mixing process— a highly viscoelastic system. The new solution, which in its properties is reminiscent of a gel, is optically clear and has single phase character. Its consistency reminds one of gelatine or fruit jelly. Bubbles which are trapped in the starting solutions during the mixing and shaking process recoil when rotation of the flask or test-tube in which the solution is held is abruptly stopped. The elasticity of the system can be so high that the bubbles do not only show a single recoil but oscillate a few times. Test-tubes with a cross section of 2–3 cm are particularly well suited for demonstrating this phenomena. When we try to empty the test-tube it can be turned almost upside down before the liquid starts flowing; and even then it does not flow smoothly. The solution can even be pulled back into the glass tube after it has already crossed the rim of the glass by abruptly turning the tube again with the open-end pointing upward.

This phenomena is best demonstrated by mixing two equal volumes of a 50 mM cetyltrimethylammonium bromide solution (CTAB) with a 30 mM sodium salicylate solution (NaSal), both of which are Newtonian solutions. The effect can also be observed at other surfactant/salt ratios and other concentrations but is optimized at this surfactant/salt ratio.[3]

The same behavior can be observed on mixing other surfactants. Table 1 lists some surfactants which are suitable for preparing viscoelastic solutions.

Table 1. Surfactants which form viscoelastic solutions.

N-$C_{16}H_{33}$–pyridinium + salicylate
$C_{16}H_{33}-\overset{\oplus}{N}(CH_3)_3$ + salicylate
$C_{16}H_{33}-\overset{\oplus}{N}(CH_3)_3$ + trichloroacetate
$C_{16}H_{33}-\overset{\oplus}{N}(CH_3)_3$ + $SCN^{\ominus}$
$C_{16}H_{33}-\overset{\oplus}{N}(CH_3)_3$ + *p*-chlorobenzoate
$C_{16}H_{33}-\overset{\oplus}{N}(CH_3)_3$ + perfluorobutyrate
$C_{14}H_{29}-\overset{\oplus}{N}(CH_3)_2-O^{\ominus}$ + $C_{12}H_{25}SO_4Na$
$C_{14}H_{29}-\overset{\oplus}{N}(CH_3)_2-O^{\ominus}$ + $C_7F_{15}CO_2Na$
$C_{14}H_{29}-\overset{\oplus}{N}(CH_3)_2-(CH_2)_3CO_2^{\ominus}$ + $C_{12}H_{25}SO_4Na$
$N(C_2H_5)_4^{\oplus}C_8F_{17}SO_3^{\ominus}$
$N(CH_3)_4^{\oplus}C_9F_{19}CO_2^{\ominus}$

What happens in these experiments? In surfactant solutions exhibiting normal behavior, globular micelles are present; these are charged and are surrounded by an electric double layer. The mean distance between neighboring micelles is much greater than their size and the solutions are in this sense dilute and behave like a dilute dispersion. The counterions which are added with the salt bind more strongly to the micellar interface than the original counterions and displace the latter from the micellar interface. As a consequence of this the surfactant headgroups can pack more tightly and form rodlike micelles. The rods grow rapidly in size until their lengths are greater than the intermicellar distance and the system can now be called semidilute. In this situation the rods can—like polymer chains—form entanglements, or they actually may even form a three-dimensional network because the system strives to achieve a state in which global micelles and thus also end caps of the rods are no longer present (Fig. 2).

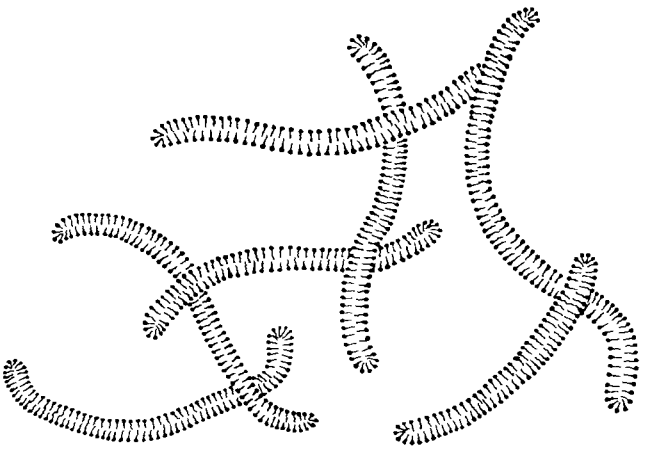

Fig. 2. Schematic drawing of a network of rodlike micelles in a viscoelastic surfactant solution.

Very recently *Hirata* et al. successfully obtained some electron micrographs of networks in viscoelastic surfactants.[3c] These pictures show that the micellar rods can be rather stiff. Depending on the systems and conditions their mean radius of curvature can be more than 1000 Å. Networks possess an entropy of elasticity when they are deformed. The deformation leads to a preferential orientation of the branches of the network and hence to an increase of order and a concomitant decrease of the entropy in the system. Elasticity occurs because of the tendency to increase the entropy of the system. Any deformation is coupled with a strong birefringence.[4] The surfactant network, however, is not a permanent one like the network in a rubber, which is formed by cross-linking of polymers; rather, the situation in the case of surfactant networks is similar to that in entanglement networks.[5]

Any shear stress which has been built up by a deformation of the network relaxes again with a characteristic time constant. In entanglement networks this time constant is determined by diffusional processes. In the case of surfactant networks, the stress can also relax through breakage of the long rods. The network is a temporary one which is continuously broken and reformed by Brownian motion. The dynamic properties of such a network are characterized by the structural relaxation time τ_s. In systems in which the viscoelastic behavior is obvious, the structural relaxation time can be as long as 10 s, sometimes even longer. It is noteworthy however that this time constant can be shortened for the same system by many orders of magnitude by other additives without the network properties being lost. This will be discussed separately in Section 3.1).

For experiments in which a strain is effective for a duration $t < \tau_s$ the system has mainly elastic properties and for experiments in which $t > \tau_s$ the viscous properties dominate. Viscoelastic surfactant solutions do not have a yield point. This can easily be observed with trapped bubbles, which always move slowly upward when the solution is at

rest. In water they need only a few seconds to rise several centimeters, whereas in viscoelastic systems they can need many hours for the same distance. It should be noted however that surfactant systems with yield points do indeed exist. In such systems the bubbles do not rise at all. Such systems are of practical interest for the preparation of stable emulsions and dispersions because these systems rule out any sedimentation.

As in the case of rubbers the elastic properties of a surfactant network can be characterized by an elasticity modulus or a shear modulus G_0. This is defined as the force which acts on a face of a cubic volume element when the volume element is deformed. It has therefore the dimension of a pressure and is normally given in the SI unit Pascal. The value of this modulus is mainly determined by the volume fraction of surfactant in the solution. On the other hand, it is essentially independent of parameters like excess salt concentration, temperature, and type and even chain length of the surfactant.[6] As long as the system remains in the viscoelastic region these parameters have little influence on G_0. They do however strongly influence the characteristic time constant τ_s. The zero-shear viscosity of viscoelastic systems is given by the product of G_0 and τ_s and therefore also depends on both of these parameters. As far as the value of the modulus for the surfactant networks is concerned the situation is analogous to that in the case of polymer networks, where the modulus is independent of the molecular weight of the macromolecules when the coils of the molecules overlap and the solution is in a semidilute state.[7] Furthermore, the modulus is dependent upon the number of entanglements in the system, but independent of the number of free ends in the network. A 100 mM viscoelastic surfactant solution has a typical shear modulus of 10^4 mPa. Polymer solutions containing the same volume fraction of polymers have similar shear moduli. Since the shear stress is given by the modulus of the system and the deformation, it is clear that the restoring forces in sheared viscoelastic solutions can be quite large. This is even more so in the case of normal stress differences which are proportional to the square of the shear rate. The shear modulus is related to the volume fraction ϕ as given in Eq. (a).

$$G_0 \approx \phi^{2.3} \tag{a}$$

From network theories G_0 is directly proportional to the number density c of entanglements [Eq. (b), k = Boltzmann constant].[8]

$$G_0 \approx ckT \tag{b}$$

Viscoelastic networks can even be formed at extremely small surfactant concentrations; they have been observed at volume concentrations of less than 0.1% of surfactant. These systems represent cases in which both the hydrocarbon chains of the surfactants and the water form continuous phases. They are therefore examples of bicontinuous phases with an extremely low hydrocarbon/water-ratio. The networks can be swollen to some extent by further hydrocarbon molecules, and the charge density of the rodlike micelles can be varied without destroying the network structure.

3. Breakdown of Elasticity by Solubilization

3.1. Solubilization of Alcohols

While a viscoelastic surfactant system can be built up by mixing an additive to a micellar solution it is likewise possible to destroy the viscoelastic properties again by the addition of a third component.[9] When 0.5 mL of pentanol is added to 100 mL of the viscoelastic system described in Section 2, the viscoelasticity of the system disappears as soon as the two solutions are mixed. Although the elasticity of the system seems to have completely disappeared—the solution flows again like water or a normal surfactant solution—the situation is actually more complicated than it appears. Detailed scattering experiments on such solutions revealed that the surfactant network is still present and has actually suffered little change upon addition of the alcohol. That is, the alcohol influences the structural relaxation time without having any great effect on the structure of the network. Actually, most of the alcohol is not adsorbed at the network but is in a molecularly dispersed form in the bulk state.[10] Only a fraction of it is adsorbed at the micellar interface. The alcohol molecules act as local lubricants and accelerate the breaking and reforming process of the networks; this shortens the structural relaxation time of the network by three to four orders of magnitude.[11] The dynamics of the system is now so rapid that in the normal handling of the solution the network is not deformed and the elasticity is therefore not observed. However, when such solutions are exposed to high shear rates, deforming forces become apparent again and it is possible under such conditions to orient the network and to observe flow birefringence in the system. Some of the amphiphilic alcohol molecules adsorb at the micellar interface. Their hydrophobic nature is small and for this reason they can quickly adsorb and desorb whenever a new hydrophobic interface is formed. This is the reason why they can be so efficient in accelerating dynamic processes in micellar solutions.

3.2. Solubilization of Hydrocarbons

In Section 3.1 it has been shown how it is possible to apparently destroy the elastic properties; in reality, however, the elastic effect is only diminished. Nevertheless it is indeed also possible to destroy the networks. In a way this is even more spectacular because it can occur with fewer added molecules per surfactant molecule than in the previous situation where the pentanol/surfactant ratio was approximately 8/1.

Surfactant solutions have a general tendency to solubilize a certain amount of hydrocarbon. Surfactant systems with rodlike micelles can actually solubilize rather large amounts of hydrocarbons.[9] For hydrocarbons which have a somewhat shorter chain length than the surfactant, the hydrocarbon/surfactant ratio in a saturated solution has a value of about one. For systems with globular micelles this number is typically at least one order of magnitude smaller.

When the network is monitored while more and more hydrocarbon is solubilized we find that it is transformed

into globular aggregates long before the solution is saturated with the hydrocarbon. The situation is shown schematically in Figure 3.

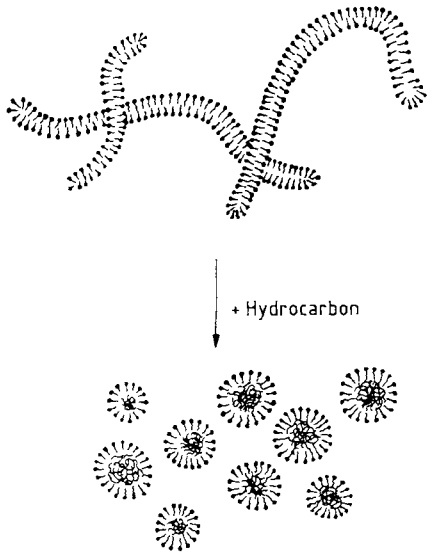

Fig. 3. Illustration of the transformation of rodlike micelles into globular structures by the solubilization of hydrocarbon in the surfactant solution.

The transition from the network to globular aggregates can easily be monitored by light-scattering measurements. Typical results are shown in Figure 4. For the same amount of dissolved surfactant the scattering intensity of light is proportional to the volume of the scattering particles. The scattering intensity R_θ of rodlike particles is very high. While the solutions are still completely transparent to the naked eye their scattering intensity is actually typically 1000 times larger than the scattering intensity of water. The volume of the globular micelles which form in the transformation process is much smaller—in extreme cases the volume ratio of rods and globules can be between

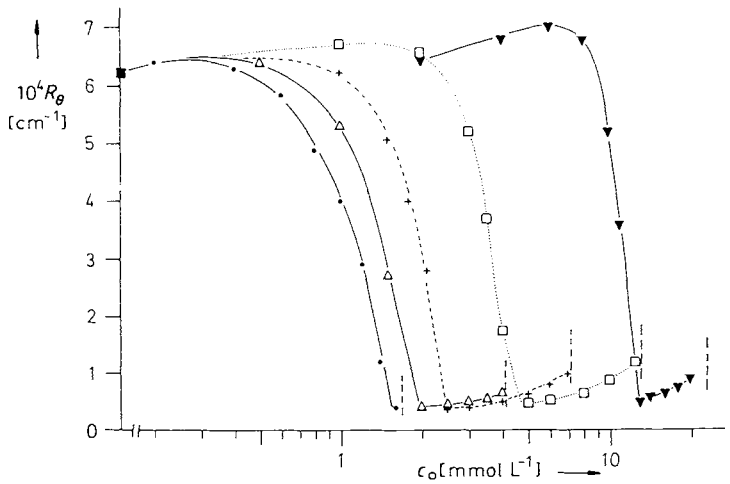

Fig. 4. Plot of the light scattering intensity R_θ of a mixture of a 10 mM solution of trimethyltetradecylammonium salicylate and a 10 mM NaBr solution against the concentration c_0 of solubilized hydrocarbon. The broken perpendicular lines indicate the phase boundaries (maximum solubilization capacity is reached). Note that the breakdown concentration of the rods shifts with decreasing chain length of the hydrocarbon to higher hydrocarbon concentrations. The following hydrocarbons were used (T=25°C): ● tetradecane; △ dodecane; + decane; □ octane; ▼ hexane.

10:1 and 100:1. The transformation therefore leads to a large drop in the scattering intensity. The curve plotted in Figure 4 shows that the transition is rather sharp and that the transformation can already be complete at a hydrocarbon/surfactant ratio of 0.1/1.

With the breakdown of the network the viscoelastic properties disappear and the solution behaves like a normal Newtonian liquid with a shear-independent viscosity and a viscosity like that of water. The solubilization of hydrocarbons in a surfactant solution does not proceed instantaneously but requires time because of their very low solubility in water. Depending on the chain length of the hydrocarbon, several hours' stirring may be necessary in order to achieve solubilization. This makes it difficult to demonstrate the breakdown of the viscosity; it is therefore advisable to prepare the solutions in advance for demonstration purposes. This experiment shows quite dramatically that the aggregation behavior of surfactants which leads to different micellar shapes is dominated by severe packing constraints by the surfactant and the hydrocarbon.

The observed transformation can be explained as follows: The hydrocarbon molecule with no polar headgroup is solubilized in the interior of the rodlike micelles (Fig. 5); the transformation of the rods can only be understood in terms of a simple geometrical model. In the rods the surfactant headgroups are rather tightly packed with a packing parameter of p=2 ($p=a_h l/v$, where l=chain length of the surfactant, v=volume of the hydrocarbon chain). With the solubilization of the hydrocarbon the cross section of the rods begins to increase. As soon as the inner core reaches a size which allows the packing parameter to be the same as in globular particles, the system undergoes transformation because the higher number of globular particles which can be formed from a single long rod are entropy favored.

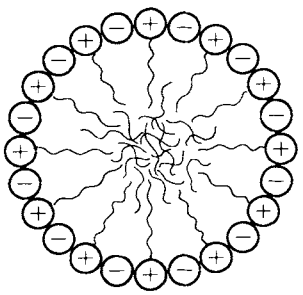

Fig. 5. Schematic view of a microemulsion droplet. The greater part of the solubilized hydrocarbon is located in the interior of the micelle. The interface is covered by the surfactant molecules. There is probably some penetration of the hydrocarbon into the micellar interface.

Figure 4 also shows that the transformation of the network into globular micelles by shorter hydrocarbons is first realized at higher concentrations. The reason for this is that smaller hydrocarbons can better penetrate the palisade layer of the surfactants and are therefore not restricted to the interior of the micelles. We can therefore find situations in which the saturation concentration is reached before the transition concentration. Under these conditions the network is not destroyed by the solubilization but is swollen by the hydrocarbon and typical bicontinuous

phases result.[12] Such systems exhibit very remarkable phenomena and fully unexpected properties.

From Figure 4 it is also clear that saturation of the micellar solution with hydrocarbon is in no way achieved when the transformation is complete, but that the small globules formed now increase in size until saturation is finally reached. Under optimized conditions for the solubilization, the diameters of the globules can become as large as 1000 Å. Extremely high values have been reported by *Strey* et al.[12b] A schematic drawing of micellar globules is shown in Figure 5. By varying the external conditions, the radii of these globules can be continuously changed from 20 to 500 Å. For the very large droplets it becomes increasingly difficult to differentiate between microemulsion droplets which are thermodynamically stable and emulsion droplets which are not stable.

4. From Turbid to Clear Solutions by Solubilization of Hydrocarbons

4.1. From a Condensed Network to Swollen Globular Micelles

If more hydrocarbon than can be solubilized is added to a surfactant solution, then a turbid emulsion is formed which on prolonged standing separates into two distinct macroscopic phases. This is common experience. But with a network system the situation may be more complicated. Such solutions very often separate into two macroscopic phases when excess salt is added or the charge of the rods is neutralized by hydrophobic counterions. The separation into two phases corresponds in the thermodynamic sense to a condensation of the network. We obtain a dilute phase and a more dense phase, as shown schematically in Figure 6.

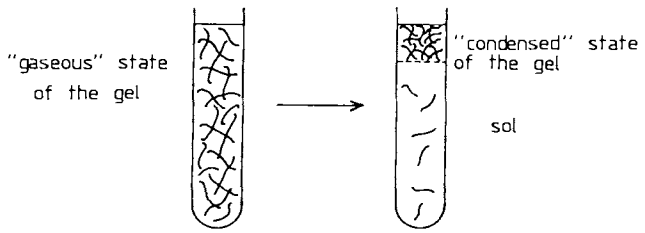

Fig. 6. Schematic representation of the transformation of a viscoelastic network in the "gaseous state" into a condensed state and a sol.

In the literature such phase separations are referred to as coacervation.[13] They are brought about by increased attractive forces between the branches of the network. Increased attraction is also brought about by the solubilization of the hydrocarbons. Coacervation is therefore sometimes observed upon solubilization of a hydrocarbon. Such an example is shown in Figure 7.

Upon addition of ethylbenzene to the starting solution the solution becomes turbid; two phases are formed. When addition of ethylbenzene is continued, however, the turbidity disappears and the system becomes transparent again and now has a much lower scattering intensity than the starting solution. The explanation: The condensed network has undergone a rod-sphere transition and the attractive forces between the smaller globules are not large enough to induce a phase separation.

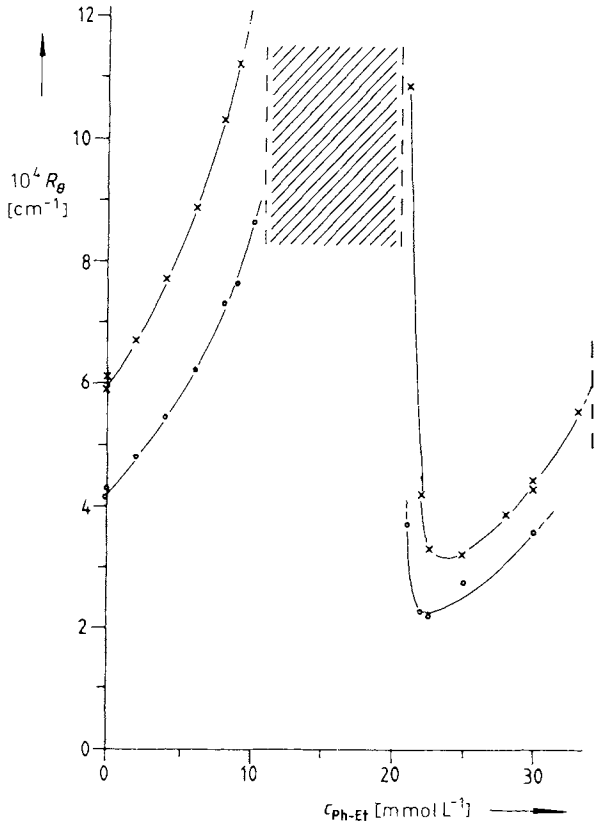

Fig. 7. Light scattering data during the solubilization of ethylbenzene in a solution of 10 mM TAB and 10 mM NaSal (T=25 °C). The hatched area is a turbid two-phase region. Symbols used: × R_δ^{45-7}; ○ R_θ^{180}; the broken lines are ⋮ phase boundaries.

4.2. From Lamellar Phases to Microemulsions

In this Section we present an example of other biphasic systems which are converted into single phase systems by solubilization. We have seen (Section 3.2) that systems with rodlike micelles have a relatively large capacity for the solubilization of hydrocarbons. Rodlike micelles can be formed by adding intermediate chain length alcohols like decanol to nonionic or ionic surfactants containing globular micelles. At a certain alcohol/surfactant ratio characteristic for the surfactant a situation is reached when rods are formed. When the alcohol/surfactant ratio is increased further, phase separation is observed. This may be due to a coacervation, as described in Section 4.1.

The more concentrated phase can also be a lamellar liquid crystalline phase.[14] In this case we have again a turbid two-phase system. Such systems can be again converted back into single phase isotropic systems by solubilization of hydrocarbon. Results for a particular case are shown in Figure 8. Here, the saturation concentration of the hydrocarbon increases continuously with the alcohol/surfactant ratio until appearance of the liquid crystalline phase region. This example also demonstrates that whenever it is of interest to use systems with a high hydrocarbon/surfactant ratio it is of advantage to start from surfactant systems which form lamellar phases in the dilute bi-

nary system. Hydrocarbon/surfactant ratios may easily reach values of over 10/1 in such systems.

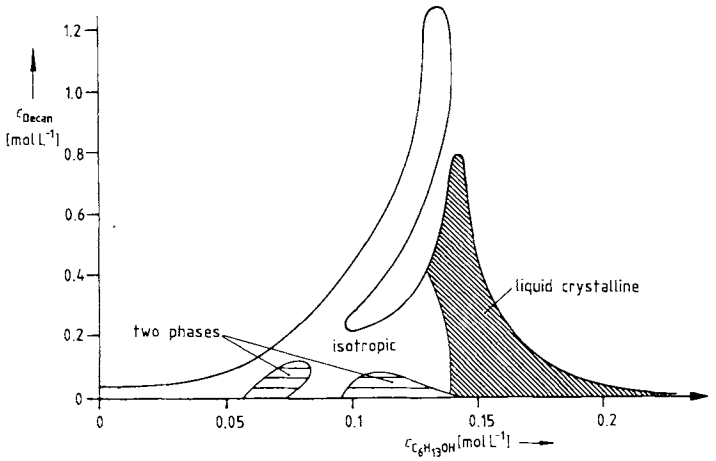

Fig. 8. Dependence of the solubilization capacity of a 0.1 M surfactant solution of (tetradecyl)dimethylamine oxide for decane as a function of the concentration of hexanol (T=20°C). Note that the region of the binary system in which a liquid crystalline phase is in equilibrium with a micellar solution has a much larger solubilization capacity than the isotropic solution. The liquid crystalline phase is however transformed into an isotropic phase by the solubilization.

One of the decisive parameters for the solubilization of the hydrocarbon in surfactant solutions is the mean curvature of the interfaces in the micellar assembly.[15] As seen from the hydrocarbon the mean radius of curvature increases on going from the globular micelle to the rodlike micelle to the lamellar phase. The solubilization capacity also increases, and reaches a maximum when the mean radius of curvature approaches infinity.

5. Inverse Systems: Breakdown of the Conductivity with Increasing Water Content in the System

In the previously mentioned examples the surfactant was always dissolved in the solvent water. Some surfactants, in particular double-chain systems, also have a high solubility in organic solvents like octane, especially in the presence of small amounts of water. It is therefore conceivable that we can expect to find phenomena in these system which are related to networks and structure transformations. This is indeed the case.

F. Evans et al. have shown that didodecyldimethylammonium bromide is soluble in organic solvents.[16] In the presence of less than 10% water such solutions have a high electric conductivity. When the water content in these systems is increased to about 40%—which is possible only with particular solvents—the conductivity decreases by several orders of magnitude (Fig. 9).

This is a very surprising effect, since we are going from a hydrocarbon solvent with a very low dielectric constant to a solvent which should be more water-like. Recent studies on the system have shown that this situation is analogous to the situation in Section 2: it is merely reversed in as much as the organic phase is now the bulk phase and the water and the surfactant form continuous channels which enable the transport of electric current. In a viscoelastic

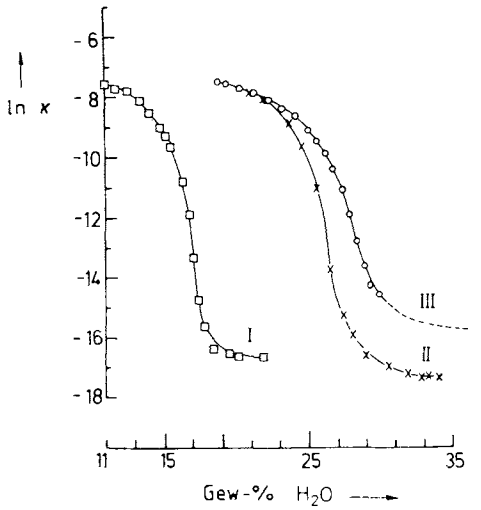

Fig. 9. Breakdown of the electric conductivity k of a microemulsion of didodecyldimethylammonium bromide and water in hydrocarbons with increasing water content [16]. Hydrocarbons used: I=octane; II=decane; III=dodecane.

system with water as solvent the network was destroyed by the solubilization of a hydrocarbon, whereas now the network in the organic phase breaks down by addition of water. With the transformation of the aqueous channels into globular water droplets the conducting channels disappear and the conductivity breaks down. The reason for the transformation of networks into isolated globules is the same in the normal as well as in the inverse case.

6. Large pH-Changes by the Mixing of Two Neutral Surfactants

When two neutral surfactant solutions are mixed we usually do not expect the solution to turn acidic or basic. This behavior, however, has actually been observed and such an example will be described below.

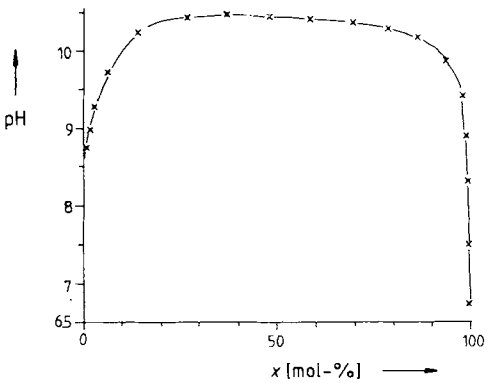

Fig. 10. Plot of the pH of surfactant solutions against the mixing ratio of the two surfactants $C_{14}H_{29}N(CH_3)_2O$ and $C_8F_{17}COON(CH_3)_4$. x=mole fraction of the perfluorononoate. The total concentration is 25 mM.

In Figure 10 the pH of a mixture of 100 mM solutions of perfluorononanoate and dimethyltetradecylamine oxide is plotted against the molar fraction of the perfluorononoate. The solution of the perfluoro compound is neutral, while that of the amine oxide is weakly basic due to the basicity

of the oxygen atom. In the mixture the pH is several orders of magnitude higher.

A similar effect is also observed for other combinations.[17] The perfluorononanoate can be replaced by other anionic surfactants including normal hydrocarbon surfactants, and the amine oxide can be replaced by other amines or by alkylethoxyamines. The effect always occurs when an anionic surfactant is combined with a weakly basic surfactant. It is caused by the change in basicity of the amine oxide group due to neighboring negative charges. The two surfactants form mixed micelles in which the amine oxide is surrounded by negative charges. The combined electric fields of these charges increase the basicity of the N–O groups, which become protonated by water, and OH-ions are released.

This effect of negative charges is also responsible for the fact that pK_{a1} and pK_{a2} of a dibasic acid differ considerably.

This effect, which has already been described in the literature by *Rosen* et al.,[18] can be resorted to for the determination of electric fields in electric double layers of micellar aggregates by incorporating dye indicators into the micelles.[19] The conclusion which we have to draw is that charged micellar interfaces can shift the pK-values of incorporated molecules by several orders of magnitude. The effect is also responsible for an astonishing phenomenon in perfluorocarboxylic acids: Perfluorocarboxylic acids are strong acids and are thus completely dissociated in the monomeric state; the micellar assemblies of these surfactants are however practically completely associated.[20] This is not true however in the case of the perfluoroalkylsulfonic acids. The protonation of the carboxyl groups in the micellar state is probably due to an increase of the acidity constants by the formation of micellar aggregates. The pK_a of the acids in the assemblies is shifted to a value around the pH of the solution, and this is sufficient to bring about protonation of the micellar carboxylates.

7. Gelification of Hydrocarbons by Surfactants

Hydrocarbons like pentane or hexane are highly volatile liquids with low viscosity. By addition of small amounts of surfactants they can be transformed into transparent isotropic gels with viscoelastic properties whose yield points are large enough to prevent flow under gravitational forces. Such a system is shown in Figure 11. A glass vessel containing the hydrocarbon gel was turned in the upside down position. The system can be kept in this position for many hours without any significant motion of the gel being observable. Such systems can contain up to 99.5% of the hydrocarbon, the rest being surfactant and water. The trick in obtaining such systems lies in their preparation. They do not automatically form when we try to dissolve or emulsify a small amount of an aqueous surfactant solution in a relatively large amount of a hydrocarbon phase. They are not even formed spontaneously on using high speed emulsifiers. Rather, such highly mechanical procedures may actually lead to the breakdown of gel systems that may be realizable otherwise. Such systems were first described in the literature by *K. J. Lissant*.[22] *G. Platz* and *G. Ebert* have recently carried out intensive investigations on these systems.[22] They have determined the amounts of different hydrocarbons which can be gelified by this procedure by various surfactants, and have also investigated the viscoelastic properties of the systems as a function of the composition. These investigations have shown that such gel systems consist of polyhedra of surfactant layers filled with the hydrocarbon; the water is contained in the spaces between the polyhedra. They have the same structure as the polyhedral structure of foams. The continuous phase-type character of the small amount of water is expressed in the relatively high conductivities of the systems.

Fig. 11. Transparent hydrocarbon gels; glass vessel in the up-side down position to demonstrate the gel properties. The gel consists of 99% of pentane. SDS (sodium dodecyl sulfate) was used as surfactant.

The polyhedra have typical dimensions of around 5 μm. They can be made visible under the microscope if the gel is swollen by dilution with a small amount of water. To increase the visibility of the phase boundaries, the water layers can be colored by addition of water soluble dye molecules. A typical micrograph with the visible structures is shown in Figure 12.

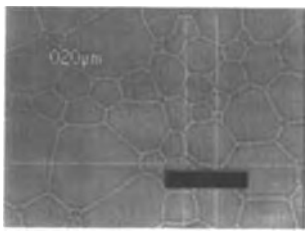

Fig. 12. Micrograph of the structure of a hydrocarbon gel. Note that the angles where two layers meet are always about 120°. The figure 0.20 μm refers to the distance between the two vertical lines.

The gels are of particular high transparency when the amount of water in the system is very small and the refractive index of the surfactant/water mixture is matched to that of the hydrocarbon. For the formation of the gel systems it is necessary to start with a concentrated aqueous surfactant solution. Particularly well suited for this purpose are surfactant solutions whose compositions lie between those of the liquid crystalline hexagonal phase and those of the lamellar phase. Small amounts of the hydro-

carbon can be added to equally small amounts of the surfactant solution; the concentrated gel thus obtained can then be diluted by continuous addition of more hydrocarbon. While these systems in their final form are probably still two-phase systems in the thermodynamic sense it is interesting to note that there is an upper limit for the solubility of the hydrocarbons in the system. If too much hydrocarbon is added an excess phase of the hydrocarbon separates which is in equilibrium with the highly viscous system. It is also noteworthy that the transparent viscous system in this state is flowable and does not exhibit a yield point if it is not shaken too vigorously during its preparation. When such a purely viscous system is given a vigorous jerk, however, it gelifies immediately and remains gelified for a long time. On the other hand, the gel can be completely broken by ultrasonic treatment. Upon sonication, the system separates into two liquid phases. Both cationic and anionic surfactants may be used for the preparation of the gels. If a gel prepared from a cationic surfactant is brought into contact with a gel prepared from an anionic surfactant, the gel structure is destroyed—due to mutual neutralization of the oppositely charged surfactant molecules. Hydrocarbon separates from both systems.

The elastic properties of the gels can be described by equations which were originally developed by *Princen* for the elasticity of foams.[23] The essential parameters are the interfacial tension and the size of the polyhedra. Under a shear deformation the interfacial area of the lamella is increased; this leads to a restoring force. For the shear modulus, *Princen* derived the following equation (σ = interfacial tension, R_{32} = mean drop radius).

$$G_0 = 1.769\sigma\phi^{1/3}(\phi - 0.712)/R_{32} \qquad (c)$$

On the basis of the polyhedra model it is also possible to explain the term 'yield point'. The system starts to flow when the deformation is large enough to allow two neighboring volume elements to pass each other. The situation is shown schematically in Figure 13.

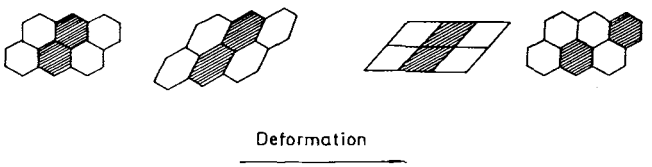

Fig. 13. Schematic representation of the yield value in hydrocarbon gels. The polyhedra are deformed under strain until two neighboring structures can slide past each other. The yield value is therefore determined by the shear modulus and a critical strain.

Platz, *Ebert*, and *Rehage* have shown that the experimentally determined elastic constants and yield values are in good agreement with the theoretically predicted values using this simple model.[24] One of the most remarkable features of these hydrocarbon gels is the fact that the hydrocarbon does not form a continuous phase even though the system consists of 99% of hydrocarbon. All the hydrocarbon is compartmented into small volume elements which are separated by thin aqueous layers and which are stabilized by the surfactant.

This poses the question of the possible existence of inverse gels, i.e. systems which consist of 99% of water, a small amount of surfactant, and possibly some hydrocarbon. The water would be compartmented in polyhedric cells, and the hydrocarbon would form the continuous phase. The walls of the cells would be formed by the surfactant. It is likely that such systems can indeed be formed. There are indications that the L_3-phase in the phase diagram of alkyl polyglycol ethers may indeed represent such a system. *B. Lindman* et al. have shown that the surfactants in these systems form a continuous phase even when the amount of surfactant is very small.[25] The aggregates in the L_3-phase are disklike and they could conceivably form a three-dimensional network. In the presence of salt such systems should have a low conductivity.

8. Microemulsion Gels (Ringing Gels)

We have learned so far that even small amounts of surfactants can, under certain conditions, gelify both water as well as hydrocarbons. It is therefore not surprising to find that gels are indeed formed at higher surfactant concentrations. There is however a particular kind of gel that is formed which exhibits very remarkable properties, and it is therefore only fitting to include such a system in our summary on fascinating phenomena in surfactant systems. Such a gel occurs, e.g., at high concentrations of surfactant in the systems surfactant-water-hydrocarbon. Usually the volume fraction of water is around 50–60% and the sum of the volume fraction of surfactant plus hydrocarbon makes up the remaining part. The volume fraction of hydrocarbon can vary between 0 and 30%. The systems are optically isotropic, transparent, and have a "pudding-like" consistency. Their yield value is high enough to suspend even large, high density particles (Fig. 14). Their most fascinating property, however, is their ability to give off a ringing sound when the vessel in which they are contained is tapped with a soft object like a piece of rubber. For a vessel with a cross section of a few centimeters the sound is in the audible frequency range of around 1000 Hz and decreases with a time constant of about 1 s. All the other gels which

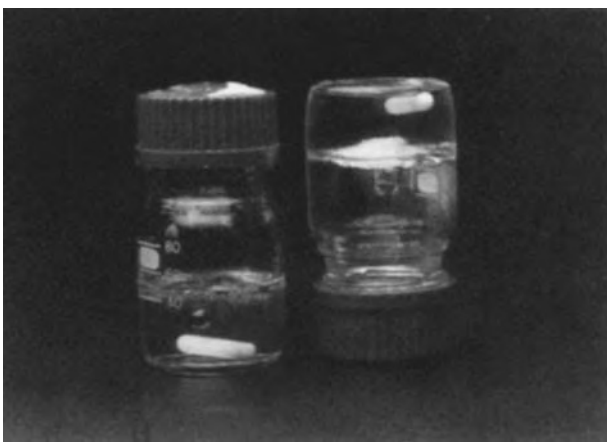

Fig. 14. View of a microemulsion or ringing gel with suspended steel ball bearings.

have been mentioned so far behave very differently in this respect, despite the fact that any gel can be deformed and therefore excited to the point of oscillation. However, the elastic energy is transformed into heat after only a few oscillations, because the elasticity of such gel systems is an entropy elasticity. The network is deformed and the entropy is thereby reduced. When the force which has stretched or deformed the network is released, the network relaxes back to its original state. The system may overshoot its equilibrium position a few times before reaching its final state. During this relaxation the branches of the network slide past solvent molecules; this leads to friction, and hence to dissipation of energy. It is for this reason that the stored energy is rapidly converted into heat. The slowly decreasing sound in the ringing gels indicates that the situation in these systems must be different. The elasticity cannot be caused by entropy but must have the same origin as the vibrations in solids like crystals or glasses. Both situations actually seem to occur in surfactant systems.

The ringing gels were first discovered in ternary systems of alkyl polyglycol ethers, paraffin-oil, and water. The phases with these peculiar properties were called microemulsion gels. It was assumed that hydrogen bonds between the ethoxy groups and water play a key role in the properties. *Führer* et al. and *Nürnberg* et al. carried out intensive investigations on both the microscopic structures in these samples and their elastic properties.[26] Electronmicrographs revealed the presence of globular aggregates with dimensions of up to about 300 Å. The dimensions were also in agreement with SAXS (small angle X-ray structure) data. According to these data the systems must consist of closely packed globular aggregates; the globules are filled with the hydrocarbon, and water forms the continuous phase.[26c]

The SAXS data for some of these systems show a strong correlation peak but no indication of long range order. The situation therefore corresponds to a microemulsion phase, formed from globular particles which are so densely packed that translational motion of the particles is no longer possible. The system seems to be rigidified to a glassy state. A similar conclusion was very recently reached by *A. Junginger* and *Joosten* et al. on the basis of SAXS data.[26c] The diffraction pattern obtained for the gel phases provided little information about the structure.

Systems with similar properties were recently observed by *H. Hoffmann* and *G. Oetter*.[27] In these systems an alkyldimethylamine oxide was used as surfactant. This means that the hydrogen bonds of the ethoxy groups cannot be the main reason for the elastic properties of the aforementioned systems. The phenomenon seems therefore to be a general one in surfactant chemistry and ringing gels can presumably be prepared from many different surfactants. It seems, however, that a few conditions must be fulfilled if they are to be formed. One such condition is that the surfactant in the isotropic binary surfactant solution is capable of forming rodlike micelles. When these rods undergo a rod-sphere transition with increasing solubilization of a hydrocarbon, the resulting little droplets behave like hard core globules in diffraction experiments and can form ringing gels, when the surfactant/hydrocarbon ratio which is necessary for the rod-sphere transformation is kept constant and the total amount of the mixture is increased.

In systems where the surfactant is saturated with hydrocarbons before the transition the microemulsion gels are not formed. It seems therefore that globular aggregates in the dilute solution are a prerequisite for the formation of microemulsion gels. Equally important is the interaction of globular aggregates. This means, moreover, that the surfactant layers and the hydrocarbon core of the globules are not connected to a continuous phase but that the alkyl chains are compartmentalized in small cells.

Densely packed globular particles can however also form cubic phases if all the globules have the same size. Such phases have recently been observed by *Fontell* et al. in the system didodecyldimethylammonium bromide/water/decane.[28] This binary surfactant/water system forms a lamellar phase. After solubilization of a hydrocarbon in the liquid crystalline phase, which contains between 30–40% surfactant, a cubic phase is formed. Obviously the hydrocarbon enforces the transformation of the surfactant layers into globular aggregates. The cubic phase for this system has been characterized by SAXS experiments. Its macroscopic properties are very similar to those of the previously described microemulsion gels. It seems therefore that ringing gels can occur both in the glassy state as well as in the more ordered liquid crystalline state with cubic symmetry.

9. Increase of Viscosity with Increasing Temperature

From experience with normal solutions, a decrease of the viscosity will usually be observed with increasing temperature. This is also the situation with many surfactant solutions, in particular with ionic surfactants. In some of the surfactant systems which are mentioned at the beginning of this article the viscosity decreases many orders of magnitude between 20°C and 80°C. However, the situation can also be the other way around. In solutions of nonionic surfactants like ethoxyalkanes the viscosity increases with increasing temperature.[29] The effects are usually not very large, but can however be dramatic in systems containing alkyl polyether sulfonates (Fig. 15).

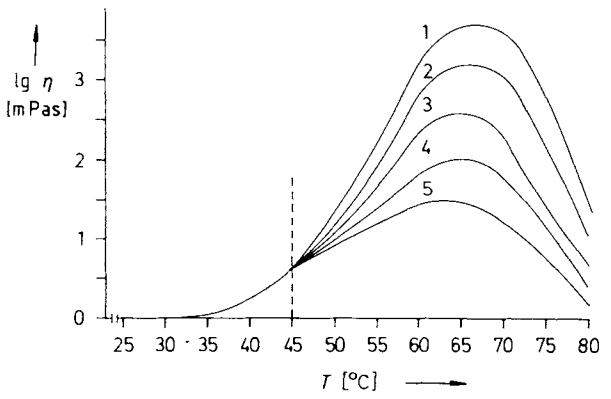

Fig. 15. Increase of the viscosity η with temperature for a surfactant solution of 0.01 M $C_{18}-C_6H_4-P_5-E_{11}-SO_3Na$ in the presence of 3.5% NaCl solution. The curves were recorded at different shear rates [s^{-1}]: 0.10 (1), 0.47 (2), 2.24 (3), 10.60 (4), 50.00 (5).

Recently, data on such a system have been published by *M. J. Greenhill-Hooper* et al.[30] A 2% solution of $C_{18}H_{37}-C_6H_4-(CH(CH_3)-CH_2-O)_5(CH_2-CH_2-O)_{11}SO_3Na$ ($=C_{18}-C_6H_4-P_5-E_{11}-SO_3Na$) in the presence of 3.5% NaCl solution has the same viscosity as water at room temperature. With increasing temperature, the viscosity increases by four orders of magnitude and reaches a maximum at 60°C. At higher temperatures it decreases again.

This effect is due to the transformation of globular micelles into rodlike micelles and finally into networks with increasing temperature. At low temperatures the ethoxy groups are strongly solvated and thus hydrophilic. They occupy a large interfacial area at the micellar interface; this forces the micelles into the globular state. With increasing temperature, the solvation is reduced and the ethoxy groups become more hydrophobic and require less space at the interface. The micelles can grow to rods and the viscosity begins to rise. Other nonionic systems like alkyldimethylamine oxide or phosphine oxide show a similar behavior. These examples show that it is possible to design systems in which the viscosity can increase or decrease with temperature. By exploiting the underlying principle of this effect it is possible to design systems with a very high viscosity over a large temperature range.

10. Phenomena under Shear or during Flow

The emphasis has so far been on phenomena occurring in surfactant systems at rest. For the most part the transient nature of the structures in these systems has not been considered. We have, however, to keep in mind that all these structures are permanently broken and reformed by thermal energy. The micellar structures are in a kind of stationary state. All network systems formed from rodlike or disklike micelles require a certain time to recover when the equilibrium distribution is perturbed by external forces which can be of mechanical, electric or magnetic origin. The systems can also form new equilibrium structures in the presence of these force fields and we can therefore expect to observe unusual phenomena when these parameters are varied.

One variable which plays an important role in surfactant chemistry is the shear rate which acts on flowing systems. All solutions flowing through pipes or which are stirred or pumped are under the influence of shear gradients which may or may not be constant in the whole phase. The shear gradients can have the same effect as a thermodynamic variable like temperature or pressure and contribute to a shift of phase boundaries. In addition, shear may affect systems differently than the temperature since shear is connected with a directional force while temperature is not. Orientational effects can therefore play an important role in surfactant systems under shear.

Many of these effects have not yet been studied in detail. We shall for this reason only mention them briefly in the following description of one particular phenomenon which has been studied extensively because of its industrial importance, namely the "drag reduction" phenomenon.[31] Some dilute surfactant systems suppress flow resistance in the region of turbulent flow. The effect can therefore be used to save energy in the transport of large quantities of water. Detailed studies on effective systems have shown that only those surfactant solutions are effective in which small rodlike micelles are present. Above a critical threshold shear rate these small rods form strings of rods and the strings then align in the direction of flow[32] (Fig. 16). As a consequence of this, small eddies which are present in turbulent flow are, to some extent, suppressed and the flow is laminarized; this leads to a reduction of friction.

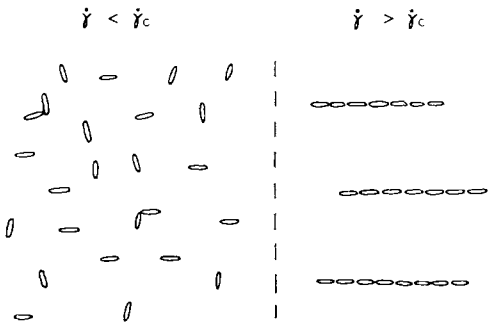

Fig. 16. Schematic view of the build up of large micellar structures under shear above a critical shear rate $\dot{\gamma}_c$. Note that the shear-induced structures are completely aligned, while for $\dot{\gamma} < \dot{\gamma}_c$ the solution is optically isotropic [32].

Viscoelastic surfactant solutions in the semidilute concentration range can also become turbid under flow.[33] It has been shown by flow birefringence measurements that the turbidity develops when the shear rate is high enough to align the large rodlike micelles. It is conceivable that the orientation of the rods reduces the mutual repulsion between them and that the attractive forces between the rods can become dominant, thus resulting in phase separation.

On the other hand, situations are possible in which two phase systems are transformed into an isotropic single phase solution by shear. If, e.g., a solution of 20 mM $C_{16}H_{33}(O-CH_2-CH_2)_3OSO_3Na$ is mixed with a solution of 20 mM $C_{14}H_{29}-NMe_3Br$ in the ratio 4:6, the solution becomes turbid and separates into two distinct macroscopic phases. If this system is vigorously shaken, a clear viscoelastic system is formed which separates into phases again upon standing.[34]

This phenomena is also observed in the case of ternary systems, e.g. the system 2-butanol/water/SDS/hexane.[35] This system separates into two clear phases which are transformable into a single phase by shaking or stirring. In systems of this kind, it would seem that the size of the structures is reduced by the shearing forces and as a consequence the attractive forces between the structures become smaller. The system is thereby transformed from a "condensed two phase equilibrium state" into the "gaseous" state.

11. Summary

The phenomena which have been described in this article are related to the formation or breakdown of surfactant networks. The network can be formed both in the aqueous phase and in a hydrocarbon phase if small quantities of water are present. In water, the networks are formed from entangled, long rodlike micelles, whereas the networks in

hydrocarbons consist of connected channels of water which form the interior of inverse rodlike micelles. Both types of systems can be considered as examples of bicontinuous phases. Under suitably optimized conditions such systems can contain as little as 0.1% of surfactant. In binary systems the diameter of the rods is determined by the chain length of a fully stretched surfactant molecule. In the aqueous phase the micelles can be swollen by solubilization of a hydrocarbon in the network, while in the hydrocarbon phase a swelling of the structure is possible by solubilization of water.

If too much hydrocarbon or water is solubilized the network of long cylindrical aggregates is transformed into globular structures. The network character thereby disappears, as does also the elastic properties and various phenomena associated with network formation. Under certain conditions the network can be saturated with hydrocarbon before the transformation into globular aggregates takes place. Surfactant networks are generally formed by modifying the chemistry of the surfactant, but they can also be formed by increasing the temperature. In systems in which they are formed by increasing temperature, a marked increase of the viscosity with increasing temperature is observed. Under very specific conditions, networks can even be formed under shear. These effects can be used to control the flow behavior of solutions. As a rule, viscoelastic surfactant solutions do not exhibit a yield point. The networks are of a temporary nature. Systems with high yield values are observed in microemulsion gels. These systems consist of densely packed globular structures and have yield values that can be so high that large metal particles can be suspended in them.

Networks do not however always consist of one-dimensional, more or less flexible rods; they can also be formed from two-dimensional planar structures. In such cases the solvent is compartmented in closed cells which are surrounded by sheets of surfactants. The buildup of such structures can lead to a complete gelification of the solvent. In contrast to networks of one-dimensional structures those made up of two-dimensional layered aggregates seem to be thermodynamically unstable; once they are mechanically destroyed, they cannot be reformed. A system in the gel state, however, can be stored for many weeks without fear of its special properties being lost.

Received: December 30, 1987 [A 679 IE]
German version: *Angew. Chem. 100* (1988) 933
Translated by Professor Dr. *H. Hoffmann*, Bayreuth (FRG)

[1] C. Tanford: *The Hydrophobic Effect*, Wiley, New York 1973.
[2] a) S. Gravsholt in R. M. Fitch (Ed.): *Polymer Colloids II*, Plenum, New York 1980; b) J. Ulmius, H. Wennerström, L. B.-A. Johansson, G. Lindblom, *J. Phys. Chem. 83* (1979) 2232; c) H. Hoffmann, H. Rehage, K. Reizlein, H. Thurn in D. O. Schah (Ed.): Proceedings of the ACS Symposium on Macro- and Microemulsions - Theory and Practice, *Am. Chem. Soc.* (1985).
[3] a) U. Olsson, O. Söderman, P. Guering, *J. Phys. Chem. 90* (1986) 5223; b) H. Rehage, H. Hoffmann, unpublished; c) Y. Sakaiguchi, T. Shikata, H. Urakami, A. Tamura, H. Hirata, *J. Electron Microsc. 36* (1987) 168.
[4] M. Löbl, H. Thurn, H. Hoffmann, *Ber. Bunsenges. Phys. Chem. 88* (1984) 1102.
[5] A. Baumgärtner, K. Kremer, K. Binder, *Faraday Symp. Chem. Soc. 18* (1983) 37.
[6] H. Hoffmann, M. Löbl, H. Rehage, I. Wunderlich, *Tenside Deterg. 22* (1985) 290.
[7] W. W. Grassley, *Faraday Symp. Chem. Soc. 18* (1983) 7.
[8] P. G. de Gennes: *Scaling Concepts in Polymer Physics*, Cornell University Press, Ithaca, NY, USA 1979.
[9] H. Hoffmann, W. Ulbricht, *Tenside Surfactans Deterg. 24* (1987) 1.
[10] a) S. Backlund, J. Bakken, A. M. Blokhus, H. Hoiland, I. Vikholm, *Acta Chem. Scand. Ser. A 40* (1986) 241; b) E. Sjöblom, B. Jönsson, A. Jönsson, P. Stenius, P. Sans, L. Ödberg, *J. Phys. Chem. 90* (1986) 119.
[11] J. Lang, R. Zana, *J. Phys. Chem. 90* (1986) 5258.
[12] a) L. E. Scriven, *J. Chem. Phys. 79* (1983) 11; b) F. Lichterfeld, T. Schmeling, R. Strey, *J. Phys. Chem. 90* (1986) 5762; c) R. Nagarajan, M. A. Chaiko, E. Ruckenstein, *ibid. 88* (1984) 2916.
[13] A. E. Vassiliades, *Surfactant Sci. Ser. 4* (1970) 387.
[14] B. Jönsson, H. Wennerström, *J. Phys. Chem. 91* (1987) 338.
[15] W. Helfrich, *J. Phys. (Les Ulis Fr.) 46* (1985) 1263.
[16] D. F. Evans, D. J. Mitchell, B. W. Ninham, *J. Phys. Chem. 90* (1986) 2817.
[17] F.-H. Haegel, H. Hoffmann, *Prog. Colloid Polym. Sci.* Proceedings of ECIS (1987) in Como (1988), in press.
[18] M. J. Rosen, D. Friedman, M. Gross, *J. Phys. Chem. 68* (1964) 3219.
[19] P. Fromherz, B. Masters, *Biochim. Biophys. Acta 356* (1974) 270.
[20] H. Hoffmann, W. Ulbricht, *Z. Phys. Chem. (Wiesbaden) 106* (1977) 167.
[21] K. J. Lissant, *J. Colloid Interface Sci. 22* (1966) 462.
[22] G. Platz, G. Ebert in K. H. Reichert, W. Geiseler (Eds.): *Polymer Reaction Engineering*, Hüthig, Heidelberg 1986, p. 95.
[23] a) H. M. Princen, *J. Colloid Interface Sci. 91* (1983) 160; b) *ibid. 105* (1985) 150; c) *ibid. 112* (1986) 427.
[24] H. Rehage, G. Platz, G. Ebert, unpublished.
[25] P. G. Nilsson, H. Wennerström, B. Lindman, *Chim. Scr. 25* (1985) 67.
[26] a) E. Nürnberg, W. Pohler, *Prog. Colloid Polym. Sci. 69* (1984) 64; b) W. Jettka, *Dissertation*, Technische Universität Braunschweig 1984; c) H. Jousma, J. G. H. Joosten, G. S. Gooris, H. E. Junginger, *Coll. a. Polym. Sci.*, in press.
[27] G. Oetter, H. Hoffmann, unpublished.
[28] K. Fontell, A. Ceglie, B. Lindman, B. Ninham, *Acta Chem. Scand. Ser. A 40* (1986) 247.
[29] M. Corti, C. Minero, *J. Phys. Chem. 88* (1984) 309.
[30] M. J. Greenhill-Hooper, T. P. O'Sullivan, D. A. Wheeler, *J. Colloid Interface Sci.*, in press.
[31] D. Ohlendorf, W. Interthal, H. Hoffmann, *Rheol. Acta 25* (1986) 468.
[32] I. Wunderlich, H. Hoffmann, H. Rehage, *Rheol. Acta 26* (1987) 532.
[33] H. Rehage, H. Hoffmann, I. Wunderlich, *Ber. Bunsenges. Phys. Chem. 90* (1986) 1071.
[34] a) H. Kuhn, *Chimia 38* (1984) 198; b) A. Silberberg, W. Kuhn, *J. Polym. Sci. 13* (1954) 21.
[35] G. Ebert, *Diplomarbeit*, Universität Bayreuth 1986.

Catalytic Activity of Enzymes Altered at Their Active Sites**

By Emil Thomas Kaiser*

Protein engineering has as its goals the design and construction of new peptides and proteins with novel binding and catalytic properties. In one approach to protein engineering, new active sites have been introduced into naturally occurring proteins either by site-directed mutagenesis or by chemical modification. Providing that important changes in the tertiary structures do not result from such alterations, at least a portion of the binding site of the original protein should be available for the formation of complexes between the altered enzyme and its substrates. Many examples of active-site mutations have been described, including the generation by us of a cysteine mutant of alkaline phosphatase. A fundamental limitation of the site-directed mutagenesis methodology is that replacements of residues are restricted to the twenty naturally occurring amino acids. The alternative, chemical modification, is difficult to carry out for the specific replacement of one amino acid by another. However, we have shown that through such modification coenzyme analogues can be introduced covalently into appropriate positions in proteins, allowing us to produce semisynthetic enzymes with catalytic activities radically altered from those of their precursor proteins. In another approach to protein engineering efforts have focused on the construction of systems where, as a first approximation, folding can be neglected and the preparation of secondary structural units is the target. Examples of the successful design of biologically active peptides and proteins along such lines, taken from our own work, include molecules mimicking apolipoproteins, toxins, and many hormones. In recent studies we have progressed to the stage where we are starting to combine the two general approaches to protein engineering we have described and are able to construct small enzymes like ribonuclease T_1 and its structural analogues.

1. Introduction

An important goal of our research in the field of protein engineering is the design of new enzymatic catalysts starting from the constituent amino acids. This is a daunting challenge, particularly since there are, at the present time, no reliable procedures for predicting tertiary or folded structures from primary amino acid sequences. Accordingly, a number of years ago when we began our protein engineering efforts we decided to proceed along two different routes. In one route, we elected to start with naturally occurring folded structures and to introduce new active sites by either chemical modification[1-3] or site-directed mutagenesis.[4] As long as major changes in the tertiary structure do not result from such alterations, this route should allow us to utilize at least part of the binding site of the original protein for the formation of complexes between the modified enzymes and substrates.

Our second approach to the construction of new proteins focuses on the design of structural regions, holding active sites constant where they occur. In contrast to tertiary structures, it appears quite feasible to predict amino acid sequences which form well-defined secondary structures, particularly in cases where peptides or proteins bind at biological interfaces. Thus, for surface-active peptides and proteins ranging in their biological activity from apolipoproteins through chemotactic agents and peptide toxins to peptide hormones, we believe that amphiphilic secondary structures (that is, secondary structures which are hydrophilic on one face and hydrophobic on the other) are readily induced when binding occurs to amphiphilic surfaces such as those found at biological interfaces.[5-7] We have developed design principles permitting the construction of model peptides and polypeptides which simulate the biological and physical properties of the naturally occurring amphiphilic systems. For example, careful examination of a space-filling model of salmon calcitonin, a peptide hormone with high hypocalcemic activity, led us to propose that the biologically active structure of this hormone consists of three parts[8,9] (Fig. 1A). First, there is the "active site" comprising residues 1-7 which are contained in a disulfide loop. The second structural region consists of residues 8-22 which have the potential to form an amphiphilic α-helix (Fig. 1B). When one examines this helix, it is striking that only one residue, the glutamic acid at position 15, violates the hydrophobic-hydrophilic segregation. The final region consists of residues 23-32, a region which serves as a kind of hydrophilic spacer. The proline amide residue at the C-terminus is crucial for the biological activity of the hormone, and perhaps it should be considered to be part of the active site of the hormone in addition to the N-terminal region (residues 1-7). In our model building, we have focused our attention on testing the importance of

[*] Prof. E. T. Kaiser
Laboratory of Bioorganic Chemistry and Biochemistry
The Rockefeller University
1230 York Avenue, New York, NY 10021-6399 (USA)

[**] For other relevant reviews see: D. L. Oxender, C. F. Fox (Eds.): *Protein Engineering*, Alan R. Liss, New York 1987; A. R. Fersht, J.-P. Shi, A. J. Wilkinson, D. M. Blow, P. Carter, M. M. Y. Waye, G. P. Winter, *Angew. Chem. 96* (1984) 455; *Angew. Chem. Int. Ed. Engl. 23* (1984) 505; J. R. Knowles, *Science (Washington, D.C.) 236* (1987) 1252.

A)

```
                                5                  10                  15
SCT-I   H2N-Cys-Ser-Asn-Leu-Ser-Thr-Cys-Val-Leu-Gly-Lys-Leu-Ser-Gln-Glu-Leu-
MCT-II  H2N-Cys-Ser-Asn-Leu-Ser-Thr-Cys-Leu-Leu-Gln-Gln-Leu-Gln-Lys-Leu-Leu-
MCT-III H2N-Cys-Ser-Asn-Leu-Ser-Thr-Cys-Leu-Leu-Gln-Gln-Leu-Gln-Lys-Glu-Leu-

                    20                  25                  30
His-Lys-Leu-Gln-Thr-Tyr-Pro-Arg-Thr-Asn-Thr-Gly-Ser-Gly-Thr-Pro-NH2
Gln-Lys-Leu-Lys-Gln-Tyr-Pro-Arg-Thr-Asn-Thr-Gly-Ser-Gly-Thr-Pro-NH2
Gln-Lys-Leu-Lys-Gln-Tyr-Pro-Arg-Thr-Asn-Thr-Gly-Ser-Gly-Thr-Pro-NH2
```

B)

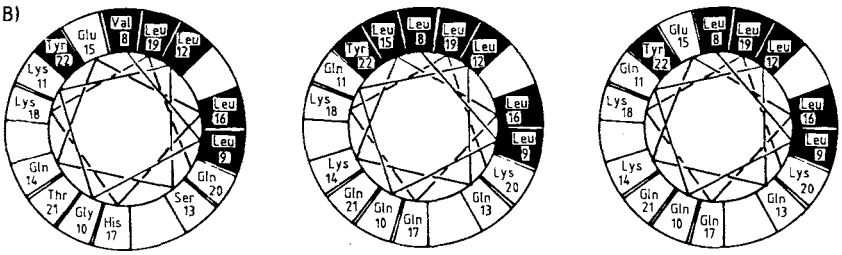

SCT-I MCT-II MCT-III

Fig. 1. A) Sequences of salmon calcitonin I (SCT-I) and model calcitonins MCT-II and MCT-III. MCT-II differs from MCT-III in having a leucine residue at position 15 and has hypocalcemic activity roughly comparable to that of SCT-I, while MCT-III is somewhat more active. B) α-Helical projections of the 8-22 sequences of SCT-I, MCT-II, and MCT-III. The amino acid residues in the shaded areas are hydrophobic and the unshaded residues are hydrophilic. The segregation of the faces of the helices into hydrophobic and hydrophilic regions can be clearly seen.

the amphiphilic secondary structure (residues 8–22) through the construction of analogues. The N-terminal active-site region has been maintained constant, but the putative helical region has been replaced by sequences which have an accentuated potential for forming amphiphilic α-helical structures but differ very significantly from the natural sequence in the region 8–22. The hydrophobic face of salmon calcitonin's helical region consists of a considerable number of leucine residues which are very good aliphatic α-helix formers. In designing our replacement helices, we have found that the most active analogue structures preserve, in large part, the sequence and distribution of residues on the hydrophobic face of the salmon calcitonin helix but have a radically different sequence with increased α-helical potential on the hydrophilic face (Fig. 1B). Our most recent analogue, MCT-III, has a hydrophilic face quite different from that of natural salmon calcitonin but preserves, except for a very minor change, the residues present in the natural hormone's hydrophobic face (Fig. 1). This latest analogue shows about 2½ to 3 times the hypocalcemic activity of the naturally occurring hormone.[10] Studies in which we have designed and constructed models along similar lines have shown that for many hormones, like β-endorphin, corticotropin-releasing hormone, glucagon, growth hormone releasing factor, neuropeptide Y, and vasoactive intestinal peptide, amphiphilic secondary structures play an important role in the biological and physical properties of the hormone.[11]

In this article we are going to concentrate on the approach in which new active sites are introduced into existing tertiary structures. However, as will be seen later, we are now proceeding from the design of secondary structural systems in molecules like calcitonin, where, to a first approximation, tertiary structure has been neglected, to cases in which tertiary structure is crucial. As we learn an increasing amount about the redesign of secondary structural regions in molecules where tertiary structure is all important, we are moving closer to the time when it will be possible to put together what we have learned about building molecules in regions outside the active site with the work which we have done on the active sites so that we can consider the construction of whole enzymatic systems with new structural features and catalytic functions.

2. Choice of Protein Templates for Introduction of New Catalytic Functionalities

In choosing protein structures in which to introduce new catalytic sites, we have felt that it was important to start with systems where the tertiary structure was well defined through X-ray crystallographic studies. Another important consideration is that the proteins being altered be readily available and easily purified. Since we wanted to make the conceptual development of the design of active sites the focal point of our work, we have tried to avoid working on systems where technical difficulties in obtaining purified and well-characterized modified enzymes will occur. The four main proteins whose active sites we have altered are *E. coli* alkaline phosphatase,[12] glyceraldehyde-3-phosphate dehydrogenase (rabbit skeletal muscle[13] and *Bacillus thermophilus*[14]), hemoglobin,[15] and papain.[16–22] In the case of alkaline phosphatase, the active site has been altered by site-specific mutagenesis and for the other three enzymes alterations have been made by chemical modification to produce what we have termed "semisynthetic" enzymes. For each of the proteins where we have redesigned the active site through model building and the use of computer graphics based on the X-ray coordinates, we have examined whether the active-site modifications we have proposed will permit the productive binding of potential substrates. We have found that such model building has been enormously useful in helping us to predict what sorts of substrates we might employ for the study of the mutated enzymes.

3. Choice of Residues for Modification

When site-specific mutagenesis is used as the technique for altering an enzyme's active site, there is a great deal of flexibility in picking a residue to be altered. Although steric and electrostatic considerations are important, there is no restriction on which residues might be altered except for problems which can be encountered in the expression of the mutant gene. In altering enzyme active sites by chemical modification, on the other hand, nucleophilic groups in the enzyme are usually the most convenient targets since most of the reagents with which stoichiometric modifications can be performed contain electrophilic centers. Thus, in our generation of semisynthetic enzymes by the chemical modification of glyceraldehyde-3-phosphate dehydrogenase, hemoglobin, and papain, we have utilized uniquely reactive sulfhydryl groups in these proteins for modification by coenzyme analogues.[13-22] Of course, an important factor in our choice of residues for modification is the apparent accessibility of the modified active site to the binding of appropriate substrates, as judged from model building.

4. Approaches to the Introduction of New Active Site Groups in Proteins

4.1. Chemical Methodology

The first example of the conversion of one active-site nucleophilic residue to another was studied independently by *Bender*[23] and *Koshland*[24] and their co-workers. They found that the treatment of subtilisin with α-toluenesulfonyl fluoride, followed by displacement of the resulting sulfonate group using thiolacetate and subsequent hydrolysis of the acetyl group, gave rise to thiolsubtilisin, a mutated enzyme containing cysteine in place of serine at its active site. Because thiolsubtilisin contains a histidine residue in close proximity to the new cysteine, it seemed possible that the enzyme would show proteolytic activity in much the same way as the naturally occurring thiol enzyme papain does. It was found, however, that thiolsubtilisin was an extremely poor endopeptidase, although it retained the ability to undergo acylation at the active-site thiol group by activated derivatives such as active esters and acyl imidazoles. Subsequent to the thiolsubtilisin work, we explored the consequences of introducing new potential nucleophilic groups into enzyme active sites through modification with highly reactive cyclic esters.[25-28] We were able to show, for example, that the phenolic hydroxyl group introduced into papain by modification of the enzyme's active-site sulfhydryl group (Cys-25) with the sultone 1 could act as an effective intramolecular nucleophile, resulting in the desulfonylation of the enzyme accompanied by re-formation of the cyclic sulfonate (k_{-2} of Scheme 1). Of course, this reaction did not involve generation of a new catalytic nucleophile, but it did show that a nucleophilic group different from that originally in the enzyme active site could be introduced and could function effectively in the enzyme template.

Active-site nucleophiles have been altered in a number of enzymes involved in acyl transfer reactions.[4,29-31] In

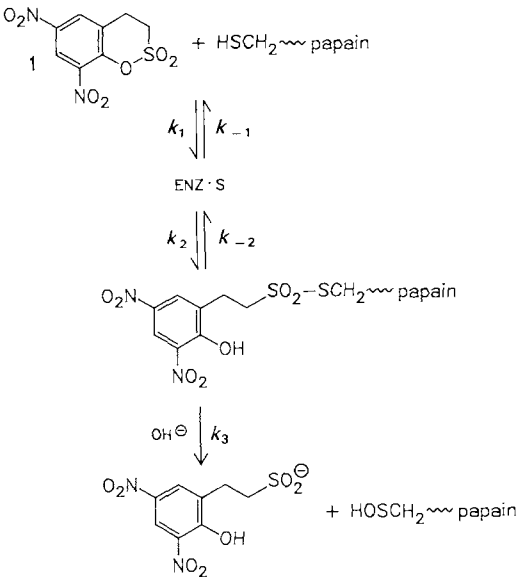

Scheme 1.

general, the mutations result in enzymes possessing low activity towards all but the more highly activated substrates, just as had been observed with thiolsubtilisin. The catalytic pathway for most acyl transfer reactions involves the formation and decomposition of tetrahedral intermediates (except possibly in those cases where very good leaving groups are involved) and requires a series of rapid proton transfers. The replacement of a nucleophilic residue at the active site of a proteolytic enzyme by a new nucleophile may result in the retardation of some proton transfer steps causing a bottleneck in the overall catalytic process. If this hypothesis is correct, then it is possible that to obtain effective new active-site nucleophiles in acyl transfer enzymes there may have to be accompanying alterations of the active-site environment through additional mutations.

4.2. Site-Directed Mutagenesis

The possibility that alteration of active-site nucleophiles may have less deleterious effects in enzymes catalyzing other types of group transfer reactions where proton transfers may not be a requirement for effective catalysis has led us to studies on *E. coli* alkaline phosphatase.[12,31] Conversion of the active-site serine to cysteine by site-directed mutagenesis in alkaline phosphatase results in a mutated enzyme which shows high catalytic activity towards substrates such as 4-nitrophenyl phosphate and 2,4-dinitrophenyl phosphate. Unlike the wild-type enzyme, which shows for many substrates an invariant k_{cat} with changes in the leaving-group tendency, the "thiol alkaline phosphatase" exhibits a marked dependence of its k_{cat} values on the leaving-group tendency. Furthermore, when experiments were done using Tris as a trapping nucleophile, in the case of the wild-type enzyme the amount of trapping of the phosphoryl group by the nucleophile did not, in general, depend upon the nature of the leaving group in the phosphate monoester used. However, for the thiol enzyme there was a strong dependence of the trapping reaction upon the nature of the leaving group. Attempts to titrate

the active-site thiol group in thiol alkaline phosphatase with sulfhydryl reagents such as 5,5'-dithiobis(2-nitrobenzoic acid), DTNB, were unsuccessful. The lack of success could conceivably be due either to steric problems in binding the DTNB in the active site or, alternatively, to the binding of the thiol group by the active-site zinc ion in the mutant enzyme. Only when the active-site metal ion had been removed by treatment of the enzyme at low pH could the sulfhydryl group be titrated. An attempt to detect the formation of a phosphoryl enzyme in the action of the thiol alkaline phosphatase by the use of stopped-flow spectrophotometry employing 2,4-dinitrophenyl phosphate under conditions where a "burst" could be observed in a similar experiment with the wild-type enzyme[32] revealed no such burst for the mutant species.[33] The interpretation of these various results was ambiguous. In particular, one possible explanation seemed to be that coordination of the thiol group of thiol alkaline phosphatase to the active-site zinc resulted in a mutant enzyme which reacted by a new pathway, namely a carbonic anhydrase mechanism, involving the attack by either water or hydroxide ion coordinated to zinc on the phosphate monoester substrates (Scheme 2A). Alternatively, it seemed quite possible that no change

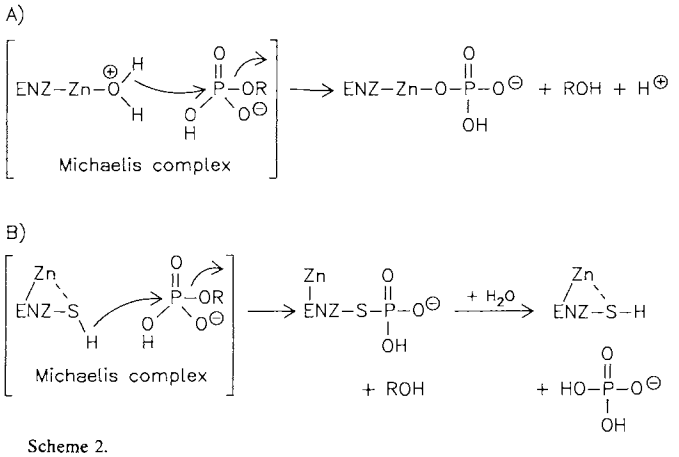

Scheme 2.

in mechanism had occurred but that only a change in the rate-limiting step of the reaction to give rate-limiting phosphorylation of the mutant enzyme had happened (Scheme 2B). To differentiate between these possibilities we performed an experiment with 4-nitrophenyl phosphate chirally labeled with different isotopes of oxygen in the phosphoryl group (**2**). If the mechanism had changed to a zinc-hydroxide or a zinc-water type (Scheme 2A), then we would expect that the reaction would involve a single displacement and, if we transferred the phosphoryl group to a suitable acceptor, we would expect to see stereochemical inversion by such a route. On the other hand, if the thiol group was acting by the usual mechanistic pathway involving the transient formation of a phosphoryl enzyme (Scheme 2B), the stereochemical outcome should be one of retention, due to the expected inversion in the phosphoryl enzyme-forming step and another inversion in the decomposition of the phosphoryl enzyme.[34,35] We found that retention occurred when we followed the course of reaction with the thiol enzyme using (*S*)-propane-1,2-diol as the

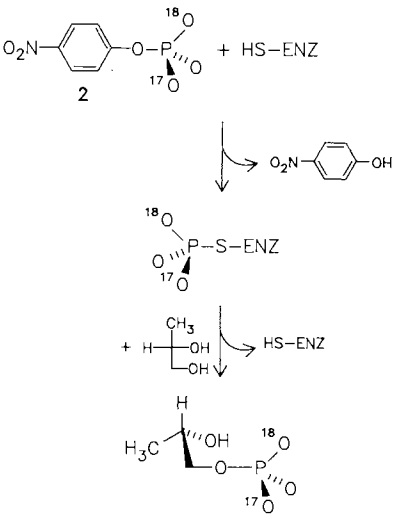

phosphoryl group acceptor.[33] Thus, it appears that the mechanism of attack of the thiol alkaline phosphatase on phosphate monoester substrates involves a normal pathway (Scheme 2B) with a change, however, in what is the rate-limiting step. For the thiol enzyme under the conditions we have employed, it appears that rate-limiting phosphorylation occurs in contrast to the situation for the wild-type species where, depending upon the pH, dephosphorylation or release of product inorganic phosphate is rate-controlling.

4.3. Semisynthetic Enzymes Obtained by Covalent Modification of Active Sites Using Coenzyme Analogues

In view of the results on proteolytic enzymes showing that the replacement of nucleophiles at the active site was not a strategy which readily produced highly active mutated enzymes, a number of years ago we decided to focus on the construction of modified enzymes which we termed semisynthetic enzymes where effective catalysis should not require a series of rapid proton transfer steps.[1,3,13-22] In our approach, we produced semisynthetic enzymes by chemical modification of an amino acid residue of an appropriate protein template with a reactive coenzyme analogue. We postulated that, if properly designed, the hybrid species could exhibit a combination of the general binding properties of the original protein template and the catalytic activity of the covalently bound coenzyme. Flavin cofactors have proved to be particularly good prosthetic groups in our work, although many other cofactors remain to be examined. Such isoalloxazine derivatives are readily synthesized, act as good model compounds for the biological cofactors FAD and FMN and catalyze in solution many of the same reactions promoted by naturally occurring flavoenzymes, although with lower rates and selectivities. To date, we have successfully used a series of isoalloxazine derivatives to modify three templates: papain, glyceraldehyde-3-phosphate dehydrogenase, and hemoglobin. These systems, all of which can function as efficient flavin-dependent oxidoreductases, will be discussed in turn.

4.3.1. *Flavopapain*

Among the most successful targets for our approach to the preparation of semisynthetic enzymes has been the hydrolytic enzyme papain. On the basis of both X-ray crystallographic investigations[36,37] and solution studies, it is known that there is an extended groove approximately 25 Å long in the vicinity of the active-site residue Cys-25. Furthermore, this residue is highly reactive to modification with reagents containing electrophilic centers, and the course of modification can be readily monitored by a variety of techniques including sulfhydryl titration and the loss of the enzyme's proteolytic activity. Using the X-ray structural data it is possible to show with appropriate models that modification of the Cys-25 sulfhydryl group with various flavin coenzyme analogues should permit the extended binding groove near the Cys residue to remain accessible to potential substrates which might interact with the flavin moiety. Our choice of the flavins as the coenzyme analogues for the modification experiments was motivated by the knowledge that these compounds are fairly effective even in the absence of enzyme in catalyzing various oxidation–reduction reactions.[38] Therefore, we felt that it might be sufficient to bind a potential substrate in a geometrically favorable fashion in the vicinity of the enzyme-bound flavin in order to achieve a rapid rate of reaction. In other words, unlike hydrolysis reactions where it seems likely that amino acid functional groups from the protein have to be placed correctly to enhance proton transfer reactions, for the enzyme-bound-flavin reactions to occur it might be sufficient to utilize the binding cavity of the enzyme without requiring specific participation of any enzyme-bound functional groups.[1,13,16–20,36,37] Because our earlier work on flavopapain has been reviewed rather extensively,[1,39] only the more recent studies will be described here.

The most effective flavopapain prepared, **3**, was obtained by alkylation with 8-bromoacetyl-10-methylisoalloxazine **4**. This modified enzyme reacts rapidly with a variety of hydrophobic *N*-alkyl-1,4-dihydronicotinamides. The k_{cat}/K_m value measured for the oxidation of the best of the substrates examined, *N*-hexyl-1,4-dihydronicotinamide, is in the vicinity of $10^6\ M^{-1}\ s^{-1}$ in air-saturated buffer at pH 7.5 and 25 °C.[20,21] Comparison of this rate parameter to the second-order rate constant for the corresponding oxidation reaction catalyzed by the simple model compound 8-acetyl-10-methylisoalloxazine shows that there is more than a 10^3-fold rate acceleration for the enzymatic system. Using anaerobic conditions and the stopped-flow technique, we have investigated the individual steps in the oxidation of *N*-alkyl-1,4-dihydronicotinamides catalyzed by 8-acetylflavopapain **3**. The kinetic results obtained are consistent with Scheme 3.

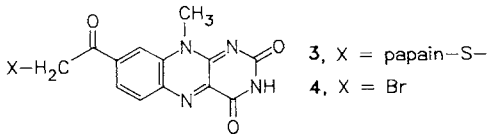

3, X = papain–S–
4, X = Br

$$E_{ox} + NRNH \underset{K_s}{\rightleftharpoons} E_{ox} \cdot NRNH \xrightarrow{k_2} EH_2 + NRN$$

Scheme 3. E_{ox} = the oxidized form of flavopapain **3**, EH_2 = the reduced form of flavopapain **3**, $E_{ox} \cdot NRNH$ = the Michaelis complex, NRNH = *N*-alkyl-1,4-dihydronicotinamide, NRN = *N*-alkylnicotinamide.

For three dihydronicotinamides, *N*-hexyl-, *N*-benzyl-, and *N*-propyl-1,4-dihydronicotinamide, very high values of k_2, the rate constant for the conversion of the Michaelis complex to the reduced dihydroflavopapain species, were obtained ($370 \pm 70\ s^{-1}$, $29 \pm 5.5\ s^{-1}$, and $31 \pm 11\ s^{-1}$, respectively). Indeed, for the *N*-hexyl compound the k_2 value ($\approx 400\ s^{-1}$) was sufficiently large that even using a very efficient stopped-flow instrument only an estimate of this rate constant could be calculated.

Because oxygen is a relatively poor oxidant for the dihydro form of flavopapain **3**, under the turnover conditions used for the aerobic reactions of the dihydronicotinamides, the reaction with dihydroflavopapain was found to be largely rate-limiting over the substrate concentration range employed.[21] Therefore, to achieve turnover conditions where the reduction step rather than the oxidation of the dihydroflavopapain is rate-limiting, it is necessary to employ an acceptor that reacts more rapidly than oxygen. We found that 3-(4,5-dimethylthiazol-2-yl)-2,4-diphenyltetrazolium bromide (MTT), was an especially effective acceptor for achieving high turnover rates in the action of flavopapain **3**. With MTT at about 400 μM, we obtained k_{cat} values for the oxidation of *N*-benzyl- and *N*-propyl-1,4-dihydronicotinamides ($31.5 \pm 1.0\ s^{-1}$ and $62.5 \pm 9.5\ s^{-1}$, respectively) which corresponded reasonably well to the rate constants k_2 (Scheme 3) obtained under anaerobic conditions for the reduction of 8-acetylflavopapain **3** by these substrates. This work demonstrates that a flavoenzyme exhibiting high catalytic efficiency both in terms of k_{cat}/K_m and of the value of the turnover number can be constructed by utilizing the active and binding sites of the hydrolytic enzyme papain. The naturally occurring coenzyme NADH is a relatively poor substrate for flavopapain **3**; this is understandable since the structure of papain indicates that the binding region of the enzyme is quite hydrophobic and should, therefore, interact much better with the *N*-alkyl-1,4-dihydronicotinamides than with NADH.

We have also shown that flavopapains can mediate the oxidation of thiols to disulfides.[22,40] Once again, 8-acetylflavopapain **3** was found to be an effective catalyst for such reactions. Under anaerobic conditions the k_2/K_s values (cf. Scheme 3) for the reduction of the flavopapain by DL-dihydrolipoamide and DL-dihydrolipoic acid were 4400 and $3400\ M^{-1}\ s^{-1}$, respectively. These rate parameters were 126 and 200 times larger than the second-order rate constants for the corresponding reactions of DL-dihydrolipoamide and DL-dihydrolipoic acid with the model compound 8-acetyl-10-methylisoalloxazine. With the dye MTT as an electron acceptor we obtained k_{cat} and K_m values for the oxidation of dihydrolipoamide by flavopapain **3**, under turnover conditions, which were in approximate agreement with the k_2 and K_s values measured under anaerobic conditions, demonstrating that the rate-limiting step of the catalytic cycle is substrate oxidation rather than oxidation of dihydroflavin.[22]

4.3.2. Studies with Flavo-Glyceraldehyde-3-phosphate Dehydrogenase (Flavo-GAPDH)

Recently, we have worked extensively with a new enzyme template, GAPDH, a readily available tetrameric enzyme for which both the primary and tertiary structures are available.[41] The active site contains a binding site for $NAD^{\oplus}$/NADH adjacent to Cys-149 and the catalytic region where glyceraldehyde-3-phosphate binds. Alkylation, even by sterically demanding groups, of this sulfhydryl group, which is essential for catalysis, does not prevent nicotinamide binding.[42,43] Computer graphics modeling (Evans and Sutherland PS-300) using the X-ray coordinates for the thermophilic enzyme from *Bacillus stearothermophilus*[44] suggested that GAPDH might be a good template for the rational design of flavin-dependent oxidoreductases selective for NADH rather than for the hydrophobic *N*-alkyl-1,4-dihydronicotinamides which are oxidized preferentially by flavopapain **3**. At first, we employed GAPDH from rabbit muscle tissue[13] but most of our more recent work has been done on the thermophilic enzyme from *Bacillus stearothermophilus*[14] which is much more stable than the muscle protein. Modification of apo-GAPDH from the respective species with 7-bromoacetyl-10-methylisoalloxazine **5** resulted in incorporation of only one flavin molecule per subunit of these tetrameric enzymes.

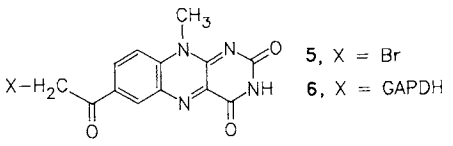

5, X = Br
6, X = GAPDH

Our HPLC and gel filtration data indicate that the initially formed 7-acetylflavo-GAPDH **6** is tetrameric. However, in a process that is apparently irreversible the bacterial semisynthetic enzyme subsequently undergoes dissociation (approximately 1 day at 4 °C) into dimers. For the thermophilic enzyme we have principally studied the dimer. The rabbit muscle flavoenzyme is far less robust, losing 40–60% of its activity within about 12 h.[13] Therefore, in the latter case, only the tetramer was studied. In examining the reactivity of the dihydronicotinamides with the flavo-GAPDH species, we found that, as expected, NADH is the optimal substrate for both proteins. The data obtained with the tetrameric rabbit muscle enzyme are readily fit by standard Michaelis-Menten kinetics. However, pronounced negative cooperativity is observed with the bacterial dimer. We cannot conclusively rule out trivial explanations for the apparent cooperativity (a population of heterogeneous active sites, for instance) at this time. Still, since half-of-the-sites reactivity is well documented for GAPDH itself, cooperative catalysis by bacterial **6** may not be an unreasonable possibility.

The second-order rate constant, k_2, for the oxidation of NADH by 7-acetyl-10-methylisoalloxazine at 25 °C in air-saturated buffer is only 12.9 $M^{-1} s^{-1}$. Under these conditions, the rate enhancement observed in the case of the rabbit muscle enzyme as judged from the rate constant k_{cat}/K_m is 83-fold[13] and for the bacterial flavoprotein it is nearly 6000-fold (under circumstances where negative cooperativity is minimal).[14] Clearly, the magnitude of k_{cat}/K_m for bacterial 7-acetylflavo-GAPDH **6** at low substrate concentrations is in the range of k_{cat}/K_m values observed for naturally occurring flavoenzymes that oxidize NADH. As we have seen for 8-acetylflavopapain **3**, turnover of 7-acetylflavo-GAPDH **6** under aerobic conditions is limited by the rate of reoxidation of the dihydroflavin generated during each catalytic cycle. For this reason, the value of k_{cat} measured depends explicitly on the oxygen concentration and does not reflect the true efficiency of the hydride transfer step. Therefore, we used rapid mixing techniques under anaerobic conditions to determine the rates of reduction of the flavin in the enzyme-substrate complex. In contrast to the situation with rabbit muscle 7-acetylflavo-GAPDH **6**, which is too fragile for stopped-flow experiments, the bleaching of the enzyme-bound flavin cofactor in the bacterial **6**, which followed biphasic kinetics in the presence of excess NADH, could be readily observed by stopped-flow methodology. Approximately half of the isoalloxazines are reduced in a very rapid step and the remainder at a much slower rate, behavior typical of negatively cooperative enzymes that exhibit half-of-the-sites activity.[45] Saturation kinetics are observed for the rate data in the fast phase step of the reduction of bacterial **6**. A rate constant of $k_1 = 1.14\ s^{-1}$ for the reduction of the rapidly reacting subunit proceeding from the corresponding Michaelis complex and an apparent dissociation constant for the Michaelis complex of 12.4 μM were obtained from kinetic measurements on the fast phase. Thus, the apparent second-order rate constant for the reduction of the rapidly reacting subunit of the enzyme is 91900 $M^{-1} s^{-1}$, a value only slightly larger than the steady-state value of k_{cat}/K_m (75600 $M^{-1} s^{-1}$) determined for NADH with this enzyme and comparing very favorably with k_{cat}/K_m obtained for naturally occurring flavoenzymes that oxidize NADH. If a suitable electron acceptor reacting much more rapidly than oxygen to reoxidize dihydroflavo-GAPDH could be found, the turnover number for this bacterial flavoenzyme could approach $1\ s^{-1}$, a value comparable to numbers seen for several natural systems. The work that we have done to date amply demonstrates that GAPDH is an excellent choice as a template for the construction of artificial enzymes.

4.3.3. Studies on Flavohemoglobin

Recently, we have generated a new type of semisynthetic enzyme, flavohemoglobin, in which the heme group is maintained in the protein but a flavin molecule is added by covalent modification.[15] Heme proteins like cytochrome P-450, which carry out redox reactions, function typically by means of single electron transfers in each step.[46] When they operate with the usual biological electron donors like NADPH, which act by two electron transfers, there is a requirement for an electron-transport system. In a typical P-450-like electron-transport system consisting of NADPH, O_2, and NADPH-cytochrome P-450 reductase, a major flavoprotein in the microsomal electron-transport system,[47] hemoglobin has been found to catalyze a wide variety of monooxygenase reactions.[48–52] We sought to de-

termine whether hemoglobin could be modified in a fashion such that it might react directly with two electron donors without the intervention of the full electron transport system. Accordingly, we attached an isoalloxazine residue covalently to hemoglobin in the vicinity of the heme with the hope that the flavin moiety could mediate electron transfer, obviating the need for the P-450 reductase (EC 1.6.2.4). We have found that the flavohemoglobin species did indeed serve as a hydroxylase for aniline in the absence of the reductase protein.[15] The chemical modification was carried out by reaction of a derivative of 7-cyanoisoalloxazine **7**, containing a reactive disulfide group attached through a tether to the N-3 position, with the thiol group of cysteine β-93 in carbon monoxide-hemoglobin ($COHb^{2\oplus}$). Subsequently, ferric flavohemoglobin (Fl-$Hb^{3\oplus}$) **8** was prepared by the oxidation of the covalently modified species Fl-$COHb^{2\oplus}$ with potassium ferricyanide.

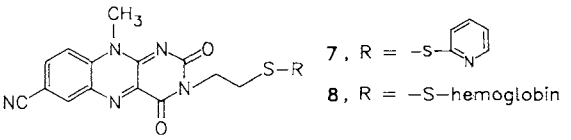

Kinetic measurements on the aniline hydroxylase activity of Fl-$Hb^{3\oplus}$ at pH 7.5 showed that the apparent K_m values for aniline observed were essentially the same as those for ferric hemoglobin, $Hb^{3\oplus}$, assayed in the presence and absence of NADPH-cytochrome P-450 reductase. The apparent k_{cat} for $Hb^{3\oplus}$ was increased considerably when we reconstituted that system with P-450 reductase.[48-52] Still, the apparent k_{cat} for $Hb^{3\oplus}$ in the reconstituted system was smaller than that seen for Fl-$Hb^{3\oplus}$ by itself. Thus, it is clear that the flavin covalently bound to hemoglobin in Fl-$Hb^{3\oplus}$ is able to substitute effectively for the reductase. Electron transfer between the neighboring prosthetic groups in Fl-$Hb^{3\oplus}$ proceeds even more efficiently than that in the combined $Hb^{3\oplus}$–reductase system.

Since a free model flavin does not catalyze the *p*-hydroxylation of aniline in the absence of hemoglobin, it is clear that the heme group is directly involved in the reaction of flavohemoglobin with aniline. The predominance of *p*-hydroxylation over *o*-hydroxylation ($p/o > 4/1$) suggests also that the active oxygen species is likely to be bound to heme and is probably not freely diffusible as in the case of aniline hydroxylation mediated by Fenton's reagent where *o*-aminophenol is the major product. It thus may be that flavohemoglobin acts in a fashion analogous to the cytochrome P-450 system (microsomal mixed-function oxidase). However, there are ambiguities in the detailed mechanism for oxygen activation by flavohemoglobin that need to be resolved, and this is a problem to which we are currently addressing ourselves.

5. Synthetic Applications of Enzymes Altered at Their Active Sites

Recently, we initiated studies on the first practical application of a semisynthetic enzyme to synthesis.[53] In work which will be described briefly here, we have been engaged in the total synthesis of small proteins such as ribonuclease T_1 and its structural analogues. In principle, we could have approached the synthesis of this enzyme through genetic engineering utilizing either the naturally occurring gene or a synthetic gene,[54] and we could consider making the various structural mutants that we would like to design through either site-directed mutagenesis on the natural gene or through alterations in the synthesis of the gene itself. We have chosen, however, to carry out the preparation of the enzyme by a peptide segment synthesis-condensation approach.[55] There are several reasons why we have done this rather than using the genetic methodology. First, of course, we can avoid the problem of expression when we make mutant structures. It is already known that in making some mutants of ribonuclease T_1 the expression has been rather poor because the mutants have had a deleterious effect on the bacteria in which they are being produced.[54] Another point where the synthetic methodology has an advantage is that we can introduce labeled or unnatural amino acids at specific locations where we wish to incorporate them. This ability to introduce labels specifically has great advantages in terms of possible use in fluorescence and NMR studies. Further, we can not only introduce unnatural amino acids at various points in the protein structure by synthesis, but also we have the possibility even of introducing nonpeptidic linkages. This means that we may be able to engineer modified proteins containing structural regions where the use of nonpeptidic segments might prevent degradation by proteolysis, which might normally occur in a biological milieu. A case in point where we have already achieved such a replacement is in our work on models for the peptide hormone β-endorphin[56] where we have replaced the part of the sequence from residue 6 to 13, which we believe to function as a hydrophilic linker region, with a repeating unit of four γ-hydroxymethyl-γ-aminobutyric acid residues hooked together through amide linkages. While this redesigned region still contains amide bonds, the linkages are not the usual peptide linkages, and yet we have found that the β-endorphin model so generated is still very effective, for example, as an analgesic agent.

In carrying out the segment synthesis-condensation methodology, for the preparation of small proteins, the first problem that we had to solve was to develop an efficient synthesis of peptide segments with the protecting groups intact so that the segments could be readily coupled further after purification. The method that we have used for the peptide segment synthesis is based on our development of an oxime polymer[57-59] and is illustrated in Scheme 4. Briefly, the generation of the polymer involves treatment of a polystyrene–1% divinylbenzene copolymer with *p*-nitrobenzoyl chloride. The resultant ketone species is treated with hydroxylamine to generate the corresponding oxime. Subsequently, the first amino acid is attached to the resin using dicyclohexylcarbodiimide as the coupling agent and employing protection such as the Boc group on the α-amino function and appropriate groups on potentially reactive side chains. Once the first amino acid has been attached, a series of deprotection and coupling reactions is performed leading to the formation of a protected peptide derivative attached to the polymer through the ox-

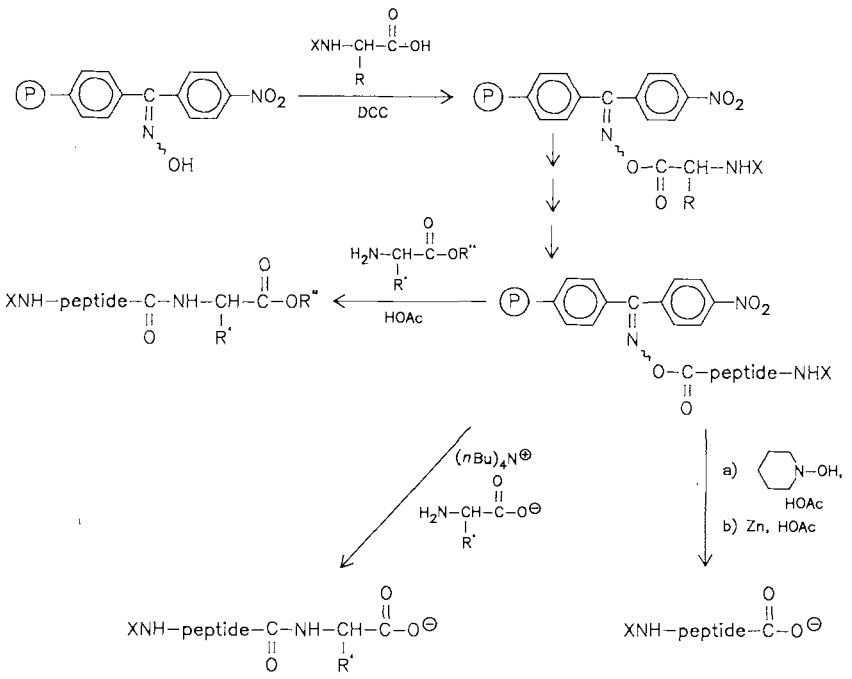

Scheme 4. The three downward pointing arrows represent repetitive deprotection and coupling. X = protecting group.

ime ester linkage. Because the linkage is more labile than the usual linkages such as the benzyl group used in the stepwise Merrifield synthesis, peptides substantially longer than ten amino acid residues are not usually prepared on the oxime resin since losses from the resin start to mount with increases in the length of the peptide. A great advantage of the oxime polymer is, however, that the growing peptide chain can be removed in a variety of ways which can afford a protected peptide segment containing either a free C-terminal carboxyl group or a free C-terminal ester function. An exhaustive list of the methods for removing the peptide from the polymer will not be given here. However, it should suffice to indicate that the peptide chain can be removed by treatment with *N*-hydroxypiperidine, an α-nucleophile, resulting in the formation of the protected peptide ester of *N*-hydroxypiperidine. This peptide ester can be then converted into the protected peptide with a free carboxyl group by the use of zinc and acetic acid, a treatment which is quite general, except for peptides containing sulfur functions, as in the case of methionine. Alternatively, the protected peptide can be removed from the resin by the use of the tetra-*n*-butylammonium salt[60] of the amino acid or by treatment of the resin-bound peptide with an amino acid ester having a free amino group, several equivalents of acetic acid being employed to catalyze the reaction. These procedures result in the insertion at the C-terminus of either the amino acid or the amino acid ester used for the displacement reaction.

In our synthesis of ribonuclease T_1[55] we have used a strategy in which the molecule has been divided into three major fragments chosen both for their synthetic accessibility and because they contain structural features of the enzyme on which we want to focus. For example, from the known X-ray structure of the enzyme the segment corresponding to residues 1–34 can be seen to contain a helical region from residue 12 to 29 which has amphiphilic character.[61] One of the objectives of our current work is to synthesize a helix replacement preserving the amphiphilic characteristics of the natural system but utilizing a significantly different sequence of amino acids. The objective of this work is to establish whether or not incorporation of such a redesigned helix into the ribonuclease T_1 structure will still allow the enzyme to fold properly and function effectively in catalysis.

We have utilized segments prepared by the oxime polymer method to assemble each of the three major segments of ribonuclease T_1. This assembly has been achieved by taking the smaller segments, which have been purified and fully characterized by standard chemical methodology including NMR, mass spectroscopy, and amino acid analysis, and coupling the segments sequentially on a polymeric support. The coupling has typically been carried out using dicyclohexylcarbodiimide and *N*-hydroxybenzotriazole to suppress racemization. We have tried as much as possible to avoid segment couplings where racemization is likely to be an important problem, but the possibility of racemization is one which cannot be totally avoided by our procedures. Of course, after we have assembled the segments we have taken the major segments off the resin and purified them extensively. The final coupling of the three major segments (Scheme 5) has been carried out in solution.

While the synthesis of small proteins such as ribonuclease T_1 is now accessible through fragment synthesis–coupling, it is clear that this approach suffers by comparison with DNA synthesis in an important way. While our syntheses of protected peptide segments by the oxime ester approach are quite convenient, there are still many difficulties in the subsequent condensation of the segments. Yields are not always high, one must be on guard against the possibility of racemization, and sometimes, because protected peptides are used, solubility problems can be en-

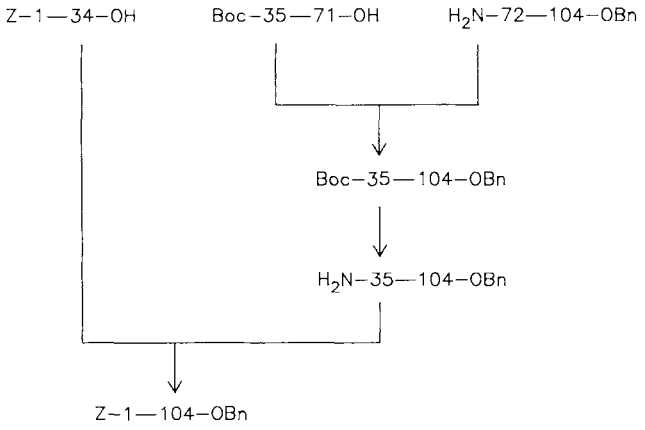

Scheme 5. Synthesis of ribonuclease T_1.

countered. A major difference between the synthesis of small proteins by the methodology outlined here and the synthesis of genes by DNA methodology is that in the case of the DNA synthesis ligases are available which can connect DNA segments. It is true that, in many instances, peptides have been coupled utilizing enzymatic catalysis.[62-69] However, these reactions, which generally involve the use of endopeptidases or exopeptidases, necessitate finding conditions where the equilibrium between peptide-bond synthesis and peptide-bond hydrolysis favors the former process. Sometimes, reactions can be driven by the decreased solubility of the product obtained from coupling. In other cases, solvent conditions, including solvent composition and pH, can be varied to favor peptide-bond synthesis. The difficulty is that each case of a peptide-bond synthesis by the use of a proteolytic enzyme involves determining the optimal conditions for the coupling process. In other words, peptide-bond synthesis using enzymes usually requires finding a new set of conditions for each reaction which is run. Ideally, one would be able to find peptide ligases where a general set of conditions could be developed for coupling peptide segments. One can ask the question, at this point, whether or not it is realistic to consider that such ligases can be found or developed. In work with the semisynthetic enzyme, thiolsubtilisin, we have obtained data which suggest that we have found a beginning to the solution of the problem of developing peptide ligases. As mentioned near the beginning of this article, when *Bender*[23] and *Koshland*[24] described thiolsubtilisin they found that the endopeptidase activity of the enzyme was poor but that the nucleophilic SH group at the active site still did accept acyl groups from activated derivatives such as active esters and acyl imidazoles. We have recognized that just these properties are suitable for the use of an enzyme as a peptide ligase. Specifically, thiolsubtilisin can be acylated at its active site thiol group by an *N*-protected peptide segment containing a C-terminal active ester group, the *p*-chlorophenyl ester function. Since the acyl derivative formed is a thiol ester, it is very susceptible to aminolysis by appropriate amino components. Thus, thiolsubtilisin should be able to catalyze an amide-bond-forming reaction between an *N*-protected peptide active ester and a free N-terminal amino group of another peptide segment. The driving force for the peptide-bond-forming step is the reaction of an active ester with an amino component, and once the peptide bond is formed, we do not have to concern ourselves with rapid hydrolysis because thiolsubtilisin is a damaged endopeptidase. We have carried out numerous peptide syntheses using this approach, and the syntheses of [Leu]^5-enkephalin amide (Scheme 6A) and the segment of ribonuclease T_1 corresponding to residues 12–23 (Scheme 6B) by the enzyme-catalyzed procedure have been accomplished.

A) Z-Tyr-Gly_2-Phe-OR + Leu-NH_2 ⟶

Z-Tyr-Gly_2-Phe-Leu-NH_2 + HOR

67% yield of pure product

B) F_{moc}-Ser_3-Asp-Val-Ser-Thr-Ala-OR + Gln-Ala_2-Gly ⟶

F_{moc}-Ser_3-Asp-Val-Ser-Thr-Ala-Gln-Ala_2-Gly + HOR

47% yield of pure product

R = C_6H_4Cl-*p*

Scheme 6. A) Synthesis of (Leu)^5-enkephalin amide. Conditions: pH 8.0, 0.1 M phosphate buffer/DMF (50/50, v/v), room temperature, 5 h. B) Synthesis of segment 12–23 of ribonuclease T_1. Conditions: pH 7.0, 0.01 M phosphate buffer/DMF (50/50, v/v) room temperature, 30 min. Thiolsubtilisin was used as catalyst in A and B.

Of course, thiolsubtilisin will be useful in coupling peptide segments which have specificities appropriate to the binding pocket of the enzyme. To broaden the scope of the enzyme-catalyzed ligation, it will be necessary to utilize other enzymes with different specificities in a related fashion. Furthermore, although the cysteine mutants of other serine proteases seem appropriate targets for further work on peptide ligases, the possibility that other types of mutants will be found exhibiting reactivity with active esters and lack of reactivity with peptides must be considered. Also, it seems likely that solvent conditions can be utilized where unmutated endopeptidases show reactivity to peptide esters but do not catalyze at rapid rates the hydrolysis of peptide bonds.

6. Future Prospects

At the beginning of this article we saw that the properties of the first semisynthetic enzyme, thiolsubtilisin, did not appear to augur well for the development of the field. However, the low activity of this mutated enzyme may reflect the importance of achieving rapid proton transfer in several steps involved in the overall catalysis process, steps which could be affected by the difference in the acidity of the original nucleophile, the hydroxyl group in the native enzyme, from that of the sulfhydryl group in the mutated species. Through attachment of flavin analogues to suitable locations in several proteins, we have shown that we can obtain highly efficient semisynthetic enzymes which can perform reactions such as oxidation-reduction and hydroxylation. In these reactions it seems unlikely that the precise positioning of enzyme-bound functional groups, which would be involved in proton transfer reactions, is required. Rather, the effectiveness of our semisynthetic en-

zymes is likely to be due to the ability of these species to bind substrates in close proximity to the reactive coenzyme functions. In future studies it will be important to increase the range of the coenzymatic species utilized. Also, the catalytic versatilities of semisynthetic enzymes such as flavohemoglobin have not been explored fully, and this is an important pursuit of our laboratory at the present time. To increase the flexibility of the chemical modification approach, we contemplate in the future to combine it with site-specific mutagenesis. In particular, we are initiating research in which we will place, by site-directed mutagenesis, appropriate "handles" in locations where chemical modification with the coenzyme analogue is likely to result in a species with desirable binding properties for substrates. The semisynthetic enzyme approach will be far more powerful if we will rely not only on the presence of suitable sites for chemical modification which are available in the natural protein systems but also if we can utilize sites which we can introduce by genetic engineering. In closing, it should be noted that very interesting activities have been obtained through the generation of catalytic antibodies[70-72] and that a promising route for the application of the semisynthetic concept will be to apply reactions to the modification of the antibodies similar to those which we have employed with the semisynthetic enzymes.

The experimental efforts and conceptual contributions of my co-workers whose names are given in the various articles cited here are gratefully acknowledged. This research was supported in part by the National Science Foundation (CHE-8418878).

Received: December 21, 1987 [A 677 IE]
German version: *Angew. Chem. 100* (1988) 945

[1] E. T. Kaiser, D. S. Lawrence, *Science (Washington, D.C.) 226* (1984) 505.
[2] E. T. Kaiser, *Ann. N. Y. Acad. Sci. (Enzyme Eng. 8) 501* (1987) 14.
[3] D. Hilvert, E. T. Kaiser, *Biotechnol. Genet. Eng. Rev. 5* (1987) 297.
[4] E. T. Kaiser, *Nature (London) 313* (1985) 630.
[5] E. T. Kaiser, F. J. Kezdy, *Proc. Natl. Acad. Sci. USA 80* (1983) 1137.
[6] E. T. Kaiser, F. J. Kezdy, *Science (Washington, D.C.) 223* (1964) 249.
[7] E. T. Kaiser, *Trends Biochem. Sci. (Pers. Ed.) 12* (1987) 305.
[8] G. R. Moe, R. J. Miller, E. T. Kaiser, *J. Am. Chem. Soc. 105* (1983) 4100.
[9] G. R. Moe, E. T. Kaiser, *Biochemistry 24* (1985) 1971.
[10] F. R. Green III, B. Lynch, E. T. Kaiser, *Proc. Natl. Acad. Sci. USA 84* (1987) 8340.
[11] J. W. Taylor, E. T. Kaiser, *Pharmacol. Rev. 38* (1986) 291.
[12] S. S. Ghosh, S. C. Bock, S. E. Rokita, E. T. Kaiser, *Science (Washington, D.C.) 231* (1986) 145.
[13] D. Hilvert, E. T. Kaiser, *J. Am. Chem. Soc. 107* (1985) 5805.
[14] D. Hilvert, Y. Hatanaka, E. T. Kaiser, *J. Am. Chem. Soc. 110* (1988) 682.
[15] T. Kokubo, S. Sassa, E. T. Kaiser, *J. Am. Chem. Soc. 109* (1987) 606.
[16] H. L. Levine, Y. Nakagawa, E. T. Kaiser, *Biochem. Biophys. Res. Commun. 76* (1977) 64.
[17] H. L. Levine, E. T. Kaiser, *J. Am. Chem. Soc. 100* (1978) 7670.
[18] E. T. Kaiser, H. L. Levine, T. Otsuki, H. E. Fried, R. M. Dupeyre, *Adv. Chem. Ser. 191* (1980) 35.
[19] J. T. Slama, S. R. Oruganti, E. T. Kaiser, *J. Am. Chem. Soc. 103* (1981) 182.
[20] J. T. Slama, C. Radziejewski, S. R. Oruganti, E. T. Kaiser, *J. Am. Chem. Soc. 106* (1984) 6778.
[21] C. Radziejewski, D. P. Ballou, E. T. Kaiser, *J. Am. Chem. Soc. 107* (1985) 3352.
[22] K. D. Stewart, C. Radziejewski, E. T. Kaiser, *J. Am. Chem. Soc. 108* (1986) 3480.
[23] L. Polgar, M. L. Bender, *J. Am. Chem. Soc. 88* (1966) 3153.
[24] K. E. Neet, D. E. Koshland, *Proc. Natl. Acad. Sci. USA 56* (1966) 1606.
[25] E. T. Kaiser, *Acc. Chem. Res. 3* (1970) 145.
[26] J. H. Heidema, E. T. Kaiser, *J. Am. Chem. Soc. 92* (1970) 6050.
[27] P. Campbell, E. T. Kaiser, *Bioorg. Chem. 1* (1971) 432.
[28] P. Campbell, E. T. Kaiser, *J. Am. Chem. Soc. 95* (1973) 3735. The products in the last step of Scheme 1 are those which would result from the normal first step in thiol sulfonate hydrolysis. Although the existence of the enzyme sulfenic acid is speculative, there is some evidence that sulfenic acids may be stable at the active sites of enzymes. See: A. N. Glazer, *Annu. Rev. Biochem. 39* (1970) 101.
[29] I. S. Sigal, B. G. Harwood, R. Arentzen, *Proc. Natl. Acad. Sci. USA 79* (1982) 7157.
[30] G. Dalbodie-McFarland, L. W. Cohen, A. D. Riggs, C. Morin, K. Itakura, J. H. Richards, *Proc. Natl. Acad. Sci. USA 79* (1982) 6409.
[31] D. A. Kendall, E. T. Kaiser in A. Torriani-Gorini, F. G. Rothman, S. Silver, A. Wright, E. Yagil (Eds.): *Phosphate Metabolism and Cellular Regulation in Microorganisms*, American Society for Microbiology, Washington, D.C. 1987, pp. 115-117.
[32] S. H. D. Ko, F. J. Kezdy, *J. Am. Chem. Soc. 89* (1967) 7139.
[33] J. Butler-Ransohoff, personal communication.
[34] S. R. Jones, L. A. Kindman, J. R. Knowles, *Nature (London) 257* (1978) 564.
[35] J. R. Knowles, *Annu. Rev. Biochem. 49* (1980) 877.
[36] J. Drenth, J. N. Jansonius, R. Koekoek, B. G. Wolthers, *Adv. Protein Chem. 25* (1971) 79.
[37] J. Drenth, K. H. Kalk, H. M. Swen, *Biochemistry 15* (1976) 3731.
[38] T. C. Bruice, *Prog. Bioorg. Chem. 4* (1976) 1.
[39] H. L. Levine, E. T. Kaiser, *J. Am. Chem. Soc. 102* (1980) 343.
[40] H. E. Fried, E. T. Kaiser, *J. Am. Chem. Soc. 103* (1981) 182.
[41] J. L. Harris, M. Waters in P. Boyer (Ed.): *The Enzymes, Vol. 13*, Academic Press, New York 1976, pp. 1-49.
[42] G. N. Rafter, S. P. Colowick, *Arch. Biochem. Biophys. 66* (1957) 190.
[43] L. V. Benitez, W. S. Allison, *Arch. Biochem. Biophys. 159* (1973) 89.
[44] G. Biesecher, J. L. Harris, J. C. Thierry, J. E. Walker, A. J. Wonacott, *Nature (London) 266* (1977) 328.
[45] A. Levitzski, *J. Mol. Biol. 90* (1974) 451.
[46] R. Sato, T. Omura (Eds.): *Cytochrome P-450*, Kodansha/Academic Press, Tokyo/New York 1978.
[47] R. W. Estabrook, *Methods Enzymol. 52* (1978) 43.
[48] J. J. Mieyal, R. S. Ackerman, J. L. Blumer, L. S. Freeman, *J. Biol. Chem. 25* (1976) 3436.
[49] I. Golly, P. Hlavica, *Biochim. Biophys. Acta 760* (1983) 69.
[50] O. Takikawa, R. Yoshida, O. Hayaishi, *J. Biol. Chem. 258* (1983) 6808.
[51] B. L. Ferraiolo, G. M. Onady, J. J. Mieyal, *Biochemistry 23* (1984) 5528.
[52] D. W. Starke, K. S. Blisard, J. J. Mieyal, *Mol. Pharmacol. 25* (1984) 467.
[53] T. Nakatsuka, T. Sasaki, E. T. Kaiser, *J. Am. Chem. Soc. 109* (1987) 3808.
[54] M. Ikehara, E. Ohtsuka, T. Tokunaga, S. Nishikawa, S. Uesugi, T. Tanaka, Y. Aoyama, S. Kilyodani, K. Fujimoto, K. Yanase, K. Fuchimura, H. Morioka, *Proc. Natl. Acad. Sci. USA 83* (1986) 4695.
[55] T. Sasaki, M. Findeis, personal communication.
[56] B. Rajashekhar, E. T. Kaiser, *J. Biol. Chem. 261* (1986) 13617.
[57] W. F. DeGrado, E. T. Kaiser, *J. Org. Chem. 45* (1980) 1295.
[58] W. F. DeGrado, E. T. Kaiser, *J. Org. Chem. 47* (1982) 3258.
[59] S. H. Nakagawa, H. S. H. Lau, F. J. Kezdy, E. T. Kaiser, *J. Am. Chem. Soc. 107* (1985) 7087.
[60] P. Lansbury, personal communication.
[61] U. Heinemann, W. Saenger, *Nature (London) 299* (1982) 27.
[62] M. Bergmann, J. S. Fruton, *Adv. Enzymol. 1* (1941) 63.
[63] J. S. Fruton, *Adv. Enzymol. 53* (1982) 239.
[64] Y. V. Mitin, N. P. Zapevalova, E. V. Gorbunova, *Int. J. Pept. Protein Res. 23* (1984) 528.
[65] W. Kullmann, *J. Org. Chem. 47* (1982) 5300; *J. Biol. Chem. 255* (1980) 8234.
[66] P. Luthi, P. L. Luisi, *J. Am. Chem. Soc. 106* (1984) 7285.
[67] H.-D. Jakubke, P. Kuhl, A. Könnecke, *Angew. Chem. 97* (1985) 79; *Angew. Chem. Int. Ed. Engl. 24* (1985) 85.
[68] K. Nakanishi, R. Matsuno, *Eur. J. Biochem. 161* (1986) 533.
[69] J. B. West, C.-H. Wong, *J. Chem. Soc. Chem. Commun. 1986*, 417; *J. Org. Chem. 51* (1986) 5728.
[70] A. D. Napper, S. J. Benkovic, A. Tramontano, R. A. Lerner, *Science (Washington, D.C.) 237* (1987) 1041.
[71] J. W. Jacobs, P. G. Schultz, R. Sugasawara, M. Powell, *J. Am. Chem. Soc. 109* (1987) 2187.
[72] R. A. Lerner, A. Tramontano, *Trends Biochem. Sci. (Pers. Ed.) 12* (1987) 427.

When submitting manuscripts, authors of articles intended for publication as "Communications" are requested to read the "Notice to Authors" reproduced in the January issue of the journal following the list of contents; upon request, a copy can be obtained from the editorial office.

Catalytic Fixation of Nitrogen by the Photocatalytic $CdS/Pt/RuO_2$ Particulate System in the Presence of Aqueous $[Ru(Hedta)N_2]^{\ominus}$ Complex

By *Mirza M. Taqui Khan,* Ramesh C. Bhardwaj,* and *C. Bhardwaj*

The reduction of coordinated dinitrogen to ammonia under ambient conditions has been the subject of active research in recent years.[1-3] In every case, the reduction of dinitrogen to NH_3 or N_2H_4 was achieved either in a stoichiometric manner or at the expense of large quantities of reducing agents such as sodium dihydronaphthylide,[4] metallic Al,[5] $Ti(OH)_2$, V^{II}, Mo^{III}, Nb^{III}, and Ta^{III}[6,7] or was carried out electrolytically.[8] Recently, small quantities of ammonia and hydrazine were obtained[9,10] by a protonation/electrolysis cycle involving the complex $[W(N_2)_2(Ph_2PCH_2CH_2PPh_2)_2]$. Catalytic fixation of nitrogen to NH_3 by ruthenium on active carbon with 32 wt% metallic potassium at ambient conditions has also been reported.[11] The amount of NH_3 obtained was 0.011 mmol per gram of catalyst per day.[11] Photoreduction of nitrogen to NH_3 has been achieved using TiO_2 or iron-doped TiO_2[12] or a gallium phosphide[13] photocathode and an oxidizable anode. In all these photoreductions, N_2 was reduced to NH_3 through a complicated, poorly understood mechanism with the expenditure of large quantities of the anode materials.

A truly catalytic fixation of dinitrogen at room temperature and atmospheric pressure, however, has not been realized so far. An obvious obstacle has been the nonavailability of redox electrons at the desired potential for the reduction of coordinated dinitrogen. These electrons have only been obtained at the expense of large inputs of energy (electrolytic) or costly reducing agents.[2] A possible solution of the problem seems to be the selection of a proper photocatalytic system which could generate photoelectrons for the reduction of coordinated dinitrogen.

Herein we report the photochemical fixation of N_2 to NH_3 in aqueous solution under ambient conditions (30°C and 1 atm of N_2) in the presence of a semiconductor particulate system, $CdS/Pt/RuO_2$, excited by visible light ($\lambda = 505$ nm) and catalyzed by the Ru(II) dinitrogen complex **1**. The yield of ammonia was 6.8 moles of NH_3 per mole of catalyst per hour. In the absence of **1**, the particulate system $CdS/Pt/RuO_2$ brings about the photodecomposition of water.[14] In the absence of $CdS/Pt/RuO_2$, there was no reduction of dinitrogen to NH_3. The catalyst **1** was recovered unchanged from the reaction cell after 24 hours. This was confirmed by the elemental analysis, the electronic and vibrational spectra of the complex, and the cyclic voltammograms before and after the nitrogen fixation experiments.

$[Ru(Hedta)N_2]^{\ominus}$ **1**
Hedta = trianion of ethylenediaminetetraacetic acid

The experiments on the photocatalytic reduction of N_2 to NH_3 were conducted in a water-jacketed glass cell in aqueous solution at 30°C. About 100 mg of $CdS/Pt/RuO_2$ powder was suspended in 25 mL of an aqueous solution of **1** in a glass cell of 100-mL capacity and the system was irradiated at 505 nm, which corresponds to the band gap of 2.2 eV for the particulate system, with a 250-W xenon lamp equipped with a 505-nm filter. Nitrogen gas freed from carbon dioxide was bubbled through the system at a constant rate of 150 mL min^{-1}, fast enough to ensure complete saturation of the solution with respect to dissolved nitrogen at any instant. During the reaction N_2 was dispersed uniformly through the solution by stirring. Most of the ammonia produced was dissolved before escaping into HCl traps. The total amount of ammonia produced was calculated both from the traps and the cell by *Nessler*'s spectrophotometric method. The rate of ammonia production versus time for different concentrations of dinitrogen complex **1** is shown in Figure 1. The yield of ammonia

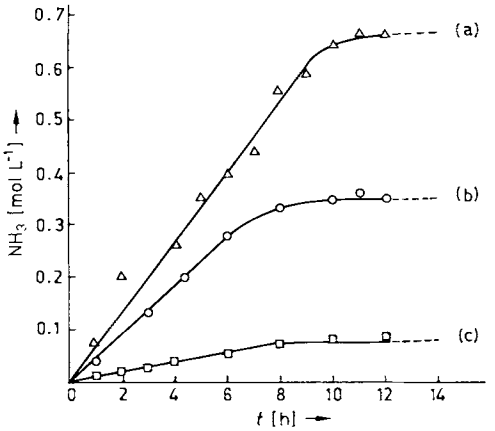

Fig. 1. Amount of NH_3 produced vs. time for different concentrations of $[Ru(Hedta)N_2]^{\ominus}$ **1**: (a) 7.82×10^{-3} mol L^{-1}, (b) 3.91×10^{-3} mol L^{-1}, and (c) 1.96×10^{-3} mol L^{-1}. For conditions see text.

attains a maximum after 12 hours and the reaction continues with only slight change up to 24 hours. After the absorption of NH_3 in the traps the gases contain a mixture of O_2 and excess N_2. The gases were allowed to collect in a column for an hour at the peak of NH_3 production (8th hour). The amount of oxygen in the mixture was determined by absorption in a known volume of alkaline pyrogallol. The amount of O_2 absorbed was about 0.7 mole per mole of NH_3 produced, confirming the stoichiometry of the reaction:

[*] Prof. Dr. M. M. Taqui Khan, R. C. Bhardwaj, C. Bhardwaj
Coordination Chemistry and Catalysis Group
Central Salt & Marine Chemicals Research Institute
Bhavnagar-364002 (India)

$$N_2 + 3H_2O \xrightarrow[cat.]{h\nu} 2NH_3 + 3/2\,O_2$$

The rate of ammonia production for different concentrations of the dinitrogen complex **1** is shown in Figure 2. One observes a first-order dependence of the rate of NH_3 production on the catalyst concentration at lower concentration of the catalyst. The pseudo-first-order rate constant of $2.8 \times 10^{-3}\ s^{-1}$ was calculated from the slope of the plot in Figure 2.

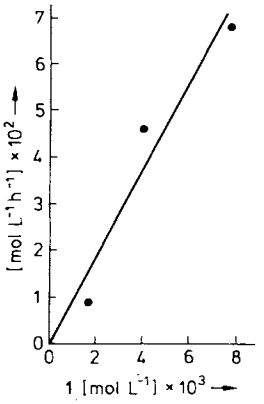

Fig. 2. Amount of NH_3 produced per hour vs. concentration of $[Ru(Hedta)N_2]^{\ominus}$ **1**. For conditions see text.

In order to confirm the source of NH_3 isotopic studies were conducted with $^{15}N_2$ (25% enrichment) as the source of N_2. The NH_3 obtained was absorbed in HNO_3 and the NH_4NO_3 was carefully dried and subjected to mass spectrometric analysis. Peaks were obtained at m/z 44 and 45 in the ratio of 3:1 corresponding to the formation of $^{14}N_2O$ and $^{14}N^{15}NO$, respectively. The reaction did not show any isotopic effect in D_2O.

Based on the kinetics of the reaction, a first-order dependence on the concentration of **1**, the following mechanism is proposed for the photocatalytic reduction of N_2 to NH_3 (the photolysis of water is not shown):

$$\underset{\mathbf{2}}{[Ru(L)H_2O]^{\ominus}} + N_2 \overset{K_1}{\rightleftharpoons} \underset{\mathbf{1}}{[Ru(L)N_2]^{\ominus}} + H_2O$$

$$CdS \xrightarrow{h\nu} h^{\oplus} + e^{\ominus} + \cdots$$

$$\underset{\mathbf{1}}{[Ru(L)N_2]^{\ominus}} + e^{\ominus} \xrightarrow[slow]{k} \underset{\mathbf{3}}{[Ru(L)N_2]^{2\ominus}}$$

$$\underset{\mathbf{3}}{[Ru(L)N_2]^{2\ominus}} + 6H^{\oplus} + 5e^{\ominus} + H_2O \xrightarrow{fast} 2NH_3 + \underset{\mathbf{2}}{[RuL(H_2O)]^{\ominus}}$$

L = Hedta

The irradiation of $CdS/Pt/RuO_2$ in aqueous solution excites an electron from the valence band to the conduction band and a hole is created in the valence band. The holes trap the electrons released in the RuO_2-catalyzed photooxidation of water to $2H^{\oplus}$ and $1/2\,O_2$. The RuO_2 in this system thus acts as a hole scavanger. There is a competition between $H^{\oplus}$ and the dinitrogen complex **1** for electrons in the conduction band. Because of the negative potential of the Ru^{II}/Ru^{I} couple (-0.46 V), the complex is a stronger oxidizing agent than the protons and competes successfully with the latter for the electron.

The electron is transferred in a rate-determining step to **1** to form an intermediate species **3**, where the extra electron can be accommodated on either the metal ion or the dinitrogen ligand. Fast protonation and successive electron transfer to **3** produces NH_3 as the end product and species **2**, which reacts with dinitrogen in the preequilibrium step to form **1** and continue the catalytic cycle. The lack of a deuterium isotope effect rules out a coupled proton transfer in the rate-determining step.

Electrochemical reduction of **1** in the presence of N_2 in the pH range 4–7 at the controlled potential of -0.20 to -0.40 V, corresponding to the redox potential of the Ru^{II}/Ru^{I} couple, gave 5×10^{-4} moles of NH_3 in three hours. The yield then droped rapidly.[15] This confirms the role of the metal ion in the electron transfer to N_2.

A blank experiment in the absence of **1** (see above) produced only hydrogen by the photodecomposition of water.[14] This indicates the role of **1** in the activation of N_2 and its reduction to NH_3. The same experiment conducted in the presence of H_4edta again results in the photodecomposition of water. This rules out the possibility of formation of NH_3 from the decomposition of H_4edta. This is further confirmed by the isotopic studies with $^{15}N_2$; the products contain the label in the same ratio as the dinitrogen employed. The composition of the dinitrogen complex **1** did not change even after 12 hours of experiment, as confirmed by elemental analysis and spectrophotometry. The experiments conducted in the presence of **1** and nitrogen but in the absence of the particulate system also failed to produce NH_3 even after 48 hours. These experiments indicate that the redox electron from the photoexcitation of the particulate system is essential for the reaction. The photocatalytic cycle is shown in Figure 3.

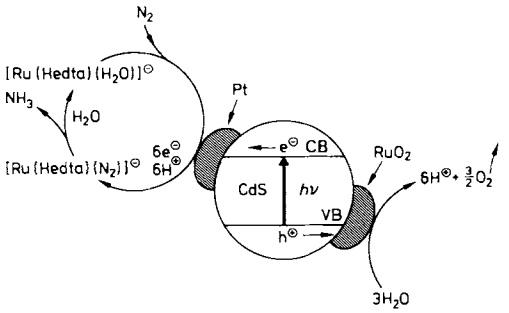

Fig. 3. Mechanism of photocatalytic ammonia production. CB = conduction band, VB = valence band.

The decrease in the yield of NH_3 after 12 hours can be attributed to the photocorrosion of the semiconductor:

$$CdS \xrightarrow{h\nu} CdS(h^{\oplus}_{VB} + e^{\ominus}_{CB})$$

$$2h^{\oplus}_{VB} + CdS \longrightarrow S + Cd^{2\oplus}$$

Thus the photocorrosion takes place only when the rate of the electron transfer is inadequate for the number of holes generated in the system. This may be partly due to the inefficient scavanging of the holes by RuO_2 particles loaded on the semiconductor. The main cause, however, is presumably the poisoning of the CdS by O_2 which is generated in the system.[16]

In conclusion, we feel that efficient reduction of N_2 to NH_3 at ambient conditions is possible if a proper photocatalyst is used and dinitrogen is activated by coordinating to a suitable metal center.

Experimental Procedure

1: $[Ru^{III}(Hedta)Cl]^{\ominus}$ was reduced to $[Ru^{II}(Hedta)(H_2O)]^{\ominus}$ **2** using hydrogen over platinum black under an atmosphere of hydrogen.[17] The photocatalyst $CdS/Pt/RuO_2$ was prepared by the published procedure [18]. Complex **2** exhibits LMCT peaks at 283, 332, and 296 nm. On passing N_2 through dilute solutions of **2** ($\approx 10^{-4}$ M), the peaks corresponding to **2** decrease with the appearance of a new peak at 221 nm, which was taken as a marker peak for the calculation of the stability constant of **1**. The equilibrium constant for the formation of **1** is given by the following expression:

$$\underset{\mathbf{2}}{[Ru(Hedta)(H_2O)]^{\ominus}} + N_2 \overset{K_1}{\rightleftharpoons} \underset{\mathbf{1}}{[Ru(Hedta)(N_2)]^{\ominus}} + H_2O$$

From the solubility of N_2 in water at 25° (7.81×10^{-4} mol L^{-1}) the equilibrium constant for the formation of **1** at 25° was calculated as $\log K_1 = 2.90 \pm 0.02$.

Complex **1** exhibits the $\nu(M-N_2)$ band at 2040 cm^{-1}. Differential pulse polarography (DPP) of **1** gives a single peak at −0.48 V corresponding to the redox couple Ru^{II}/Ru^{I}. The cyclic voltammogram of **1** gives reversible peaks at −0.24 and −1.0 V for the Ru^{III}/Ru^{II} and $H^{\oplus}/H$ potentials, respectively. The peak corresponding to Ru^{II}/Ru^{I} cannot be observed because of the crossover of the cathodic-potential and anodic-potential curves in this region.

Received: January 7, 1987;
revised: November 27, 1987 and April 7, 1988 [Z 2040 IE]
German version: *Angew. Chem. 100* (1988) 1000

CAS Registry numbers:
NH_3, 7664-41-7; N_2, 7727-37-9; CdS, 1306-23-6; Pt, 7440-06-4; RuO_2, 12036-10-1; $[Ru(Hedta)(N_2)]^{\ominus}$, 76058-13-4.

[1] M. M. Taqui Khan, A. E. Martell: *Homogeneous Catalysis by Metal Complexes. Vol. 1*, Academic Press, New York 1974.
[2] M. E. Volpin, V. B. Shur: *New Trends in the Chemistry of Nitrogen Fixation*, Academic Press, New York 1980.
[3] J. Chatt, J. R. Dilworth, R. L. Richards, *Chem. Rev. 78* (1978) 589.
[4] E. E. van Tamelen, *Acc. Chem. Res. 3* (1970) 361.
[5] E. E. van Tamelen, B. J. Akermark, *J. Am. Chem. Soc. 90 (1968)* 4492; N. H. Liu, N. Shanpach, J. G. Palmer, G. N. Schrauzer, *Inorg. Chem. 23* (1984) 2772.
[6] N. T. Denisov, E. M. Burbo, N. I. Shuvalova, A. E. Shilov, *Kinet. Katal. 23* (1982) 874; E. M. Burbo, M. I. Lebedeva, N. T. Denisov, *ibid. 27* (1986) 1504.
[7] N. T. Denisov, N. I. Shuvalova, A. E. Shilov, *Kinet. Katal. 26* (1985) 1493.
[8] C. R. Dickson, A. J. Nozik, *J. Am. Chem. Soc. 110* (1978) 8007.
[9] C. J. Pickett, J. Talarmin, *Nature (London) 317* (1985) 651.
[10] C. J. Pickett, K. S. Ryder, J. Talarmin, *J. Chem. Soc. Dalton Trans. 1986*, 1453.
[11] K. Aika, *Angew. Chem. 98* (1986) 556; *Angew. Chem. Int. Ed. Engl. 25* (1986) 558.
[12] G. N. Schrauzer, T. D. Guth, *J. Am. Chem. Soc. 99* (1977) 7189.
[13] M. Koizumi, H. Yoneyama, H. Tamura, *Bull. Chem. Soc. Jpn. 54* (1981) 1682.
[14] M. M. Taqui Khan, R. C. Bhardwaj, C. Bhardwaj, *J. Chem. Soc. Chem. Commun. 1985*, 1690.
[15] M. M. Taqui Khan, G. Ramachandraiah, unpublished.
[16] K. Kalayanasundaram, E. Borgarello, D. Duonghong, M. Grätzel, *Angew. Chem. 93* (1981) 1012; *Angew. Chem. Int. Ed. Engl. 20* (1981) 987.
[17] A. A. Diamantis, J. V. Dubrawski, *Inorg. Chem. 20* (1981) 1142.
[18] J.-M. Lehn, J. P. Sauvage, R. Ziessel, K. Hilaire, *Isr. J. Chem. 22* (1982) 168.

The First *closo*-Diphosphahexaborane $P_2B_4Cl_4$**

By *Wolfgang Haubold,* Willi Keller,* and *Gisela Sawitzki*

Dedicated to Professor Heinrich Nöth on the occasion of his 60th birthday

Higher boranes have often been prepared by pyrolysis of smaller boranes. If appropriate mixtures of boranes and hydrocarbons are used, carboranes are obtained.[1] Both synthetic principles can be extended to haloboranes.

[*] Prof. Dr. W. Haubold, Dr. W. Keller, Dr. G. Sawitzki
Institut für Chemie der Universität Hohenheim
Garbenstrasse 30, D-7000 Stuttgart 70 (FRG)

[**] This work was supported by the Deutsche Forschungsgemeinschaft and the Fonds der Chemischen Industrie.

Tetrahalodiborane(4) molecules B_2X_4 are transformed upon heating into trihaloboranes and short-lived BX species[2] or into stable cage molecules B_nX_n (X = Cl, Br; n = 8–12).[3] Copyrolysis of halogenated hydrocarbons and B_2X_4 results in the formation of perhalogenated carboranes;[4] little is known about the reaction course. The investigation described here was motivated by the question whether other heteroatoms could be incorporated into halogen-substituted boron clusters.

Pyrolysis of a mixture of B_2Cl_4 and PCl_3 at 330 °C resulted in the formation of *closo*-3,4,5,6-tetrachloro-1,2-diphosphahexaborane(4) **1** as a hygroscopic, colorless, crystalline solid, in addition to small amounts of side products. B_2Cl_4 is apparently not only the source of "BCl" units but acts at the same time as a reducing agent. The idealized formulation of the reaction is given in Equation (a). In the mass spectrum of the crude product, additional signals are observed which have to be assigned to a molecule having the composition $P_2B_5Cl_5$.

$$7\,B_2Cl_4 + 2\,PCl_3 \longrightarrow \underset{\mathbf{1}}{P_2B_4Cl_4} + 10\,BCl_3 \qquad (a)$$

The composition and structure of the phosphaborane **1** are derived from the spectroscopic data (Table 1). Since the two phosphorus atoms can each contribute three electrons to the framework bonds, a *closo*-hexaborane is to be expected according to the Wade rules. Its structure should be derivable from an octahedron. The structure of the cluster is derived from the values for the chemical shift of the boron atoms, and the *cis* arrangement of the phosphorus atoms from the fact that two ^{11}B-NMR signals (1:1 ratio) are observed. The X-ray structure analysis confirms the interpretation of the spectra (Fig. 1).[5]

Table 1. Spectroscopic data for **1**.

^{11}B-NMR (relative to $BF_3 \cdot OEt_2$, 25.67 MHz, C_6D_6, room temperature (RT)): $\delta_1 = 2.5$, $\delta_2 = 22.1$ (intensity ratio 1:1, halfwidth 128 Hz).—^{31}P-NMR (relative to 85% H_3PO_4, 32.2 MHz, C_6D_6, RT): $\delta = -187$.—MS (70 eV); calculated and measured pattern of $^{35}Cl/^{37}Cl/^{11}B/^{10}B$ isotope distribution are in agreement): $M^{\oplus}$ (rel. intensity 84%), $B_4Cl_3^{\oplus}$ (7), $B_3Cl_3^{\oplus}$ (7), $[M-BCl_3]^{\oplus}$ (100), $P_4^{\oplus}$ (30), $PB_2Cl_2^{\oplus}$ (27), $P_2B_2Cl^{\oplus}$ (12), $B_2Cl_2^{\oplus}$ (8), $BCl_2^{\oplus}$ (17)

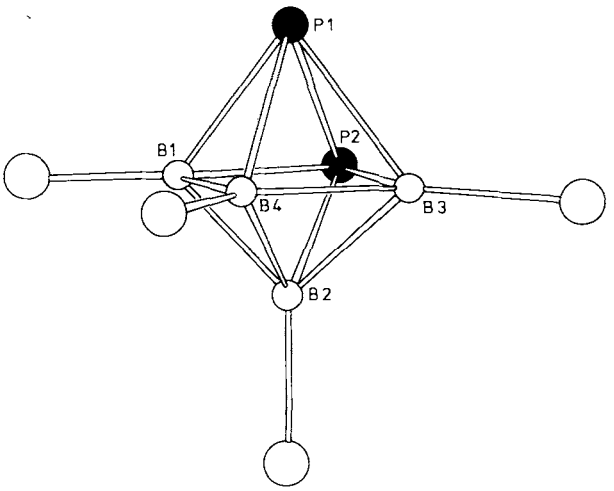

Fig. 1. Molecular structure of **1**. Selected distances [pm] and angles [°]: P1-P2 222.2(3), B2-B4 167.8(12), other B-B(average) 173, B-P(average) 200, B-Cl(average) 176; B1-P1-B3 76.8(4), B1-P2-B3 77.6(4), P1-P2-B2 81.9(3), P2-P1-B4 82.3(3), P2-B2-B4 98.2(5), B1-B2-B3 94.0(6), P1-B4-B2 97.6(5), B1-B4-B3 92.3(6).

The distances and angles reveal the distortion of the octahedron caused by the large phosphorus atoms. The angles at the phosphorus atoms are reduced by displacement of these atoms from the ideal octahedral positions. Those at the boron atoms B2 and B4, in *trans* positions, are increased. The P–P distance corresponds to that of a single bond. The B2–B4 bond on the opposite side (168 pm) is shorter than usual for B–B bonds in clusters. The B–P and the remaining B–B bonds are, as expected for **1**, longer than corresponding two-center bonds. In phosphane–boranes $R_3P{-}BR'_3$, the B–P bonds, with one exception, are shorter than 190 pm; in the diphosphaborirane three-membered ring of $(t\mathrm{BuP})_2\mathrm{BNEt}_2$, the B–P distance is 189.3 pm,[6] and in one of the few known clusters containing phosphorus atoms in the framework, the phosphacarborane $CHPB_{10}H_8Cl_2$, it is 202 pm.[7]

Experimental Procedure

B_2Cl_4 (1.5 g, 9.2 mmol) and PCl_3 (1.0 g, 7.2 mmol) were condensed into a 250-mL thick-walled flask equipped with a break seal. After melting and thawing, the mixture was heated to 330 °C for 1 h and then cooled over ca. 12 h to room temperature. The volatiles were removed at 0 °C and the ocher-colored residue remaining was extracted several times with ca. 5 mL of BCl_3. The solvent was removed and the colorless solid was sublimed by gentle warming onto the cooled neck of the flask and then washed with a small amount of BCl_3 into another pyrolysis flask. Boron trichloride was removed under vacuum. After heating for a short time at 240 °C and slowly cooling, 50 to 100 mg of **1** separated out as colorless, moisture-sensitive needles. In a sealed, evacuated tube, the compound melts at 74–75 °C. Yield: 15–25% [reaction according to Eq. (a)].

Received: September 30, 1987 [Z 2450 IE]
Publication delayed at authors' request
German version: *Angew. Chem. 100* (1988) 958

[1] *Gmelin Handbuch der Anorganischen Chemie, Ergänzungswerk zur 8. Auflage, Band 15 (Borverbindungen 2, Carborane 1)*, Springer, Berlin 1974.
[2] R. Weinmann, *Dissertation*, Universität Stuttgart 1985.
[3] T. Davan, J. A. Morrison, *Inorg. Chem. 25* (1986) 2366.
[4] W. Keller, *Dissertation*, Universität Stuttgart 1987.
[5] X-ray structure analysis: orthorhombic, space group *Pbna* (No. 60), $a = 600.2(2)$, $b = 1240.1(3)$, $c = 2270.6(8)$ pm, $Z = 8$; $\rho_{calcd} = 1.941$ cm^{-3}, $\mu = 16.93$ cm^{-1} ($Mo_{K\alpha}$); $T \approx 170$ K; 2471 unique reflections ($2\theta < 60°$), 1825 observed with $F > 3\sigma(F)$; $R = 0.073$. Further details of the crystal structure investigation may be obtained from the Fachinformationszentrum Energie, Physik, Mathematik GmbH, D-7514 Eggenstein-Leopoldshafen 2 (FRG), on quoting the depository number CSD-52767, the names of the authors, and the journal citation.
[6] M. Fehér, R. Fröhlich, K.-F. Tebbe, *Z. Anorg. Allg. Chem. 474* (1981) 31.
[7] H. S. Wong, W. N. Lipscomb, *Inorg. Chem. 14* (1975) 1350.

Synthesis and Structure of a 1,2,5,6-Tetrahydro-1,2,5,6-tetraborocine**

By *Albrecht Krämer, Hans Pritzkow,* and *Walter Siebert**

Dedicated to Professor Heinrich Nöth on the occasion of his 60th birthday

Dehalogenation of (*Z*)-1,2-diborylethenes **1** with Na/K alloy furnishes 1,2- and 1,3-dihydrodiboretes (**1a** → **2**;[1a] **1b** → 1,3 isomer[1b]) or carbaboranes (**1c** → $(CEt)_4(BCl)_4$[1c]), but no eight-membered ring derivatives.[2] Attempted dimerization of planar **2** to give the diene **3** was also unsuccessful; instead, an intramolecular rearrangement occurred, giving the puckered 1,3 isomer of **2**.[1a] A metal-dependent ring formation reaction is observed upon dehalogenation of [2-(bromomethyl)phenyl]chloro(diisopropylamino)borane;[3] reaction with lithium leads to the formation of 1-(diisopropylamino)dihydrobenzoborete (30%) and reaction with Na/K alloy to 5,11-bis(diisopropylamino)tetrahydrodibenzo[*b,f*][1,5]diborocine (9%).

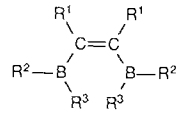

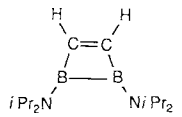

2

1	R^1	R^2	R^3
a	H	$NiPr_2$	Cl
b	*t*Bu	NMe_2	Cl
c	Et	Cl	Cl
d	H	$NiPr_2$	H

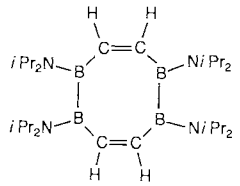

3

Herein we report the synthesis of the 1,2,5,6-tetrahydro-1,2,5,6-tetraborocine derivative **3** from **2** in the presence of hydrogen and Lindlar catalyst. In addition to **3** (27%) and the starting material **2**, **1d** could be isolated in low yield.

In the dimerization of **2**, hydrogen (via PdH_2?) serves an activating function, since no **3** is formed in the presence of Lindlar catalyst alone. Our initial assumption that **1d**, formed by hydrogenation of **2**, might be the intermediate involved in the formation of **3** was not confirmed when we treated **1d** with the catalyst. The mechanism of formation of **3** is still unclear.

The constitution of **3** was established by the NMR and mass spectra. In the ^{11}B-NMR spectrum a signal at $\delta = 51.4$, which is characteristic of diborane(4) derivatives with alkenyl and dialkylamino substituents, was found.[4] Owing to the BN π bond, the two *i*Pr groups on each of the N atoms are nonequivalent [$\delta(^1\mathrm{H})$ of **3** = 1.09 (d, $J = 7.0$ Hz, 24 H), 1.25 (d, 24 H), 3.35 (m, 8 H), 6.65 (br. s, 4 H)]. In the mass spectrum, the molecular ion peak, with an isotope distribution characteristic of four boron atoms, appears at *m/z* 496 (14.9%).

The X-ray structure analysis shows that **3** is present in the crystal as a nonplanar eight-membered ring (Fig. 1).[5] The molecule displays a crystallographically determined twofold axis. Four ring atoms (B1, C1, C2′, B2′, and B2, C2, C1′, B1′) are located in a plane (±0.03 Å). The two planes form an angle of 42° and the bonds B1B2 and B1′B2′ are nearly perpendicular to each other (82°). The distances in **3** differ slightly, but significantly, from those in **2**:[1a] the B–B distance is shorter (1.718 vs. 1.749 Å); the B–N distances (1.412 vs. 1.377 Å) and C=C distances (1.346 vs. 1.312 Å) are longer. Better agreement is found upon comparison with the distances in the 1,2,4,5-tetraborinane ring.[6]

Compound **3** is the first organoborane belonging to the $(CR^1)_4(BR^2)_4$ class; three further compounds having this general formula ($R^1/R^2 = CH_3/H$,[7] C_2H_5/CH_3,[8] C_2H_5/Cl[1c]) exist as carbaboranes owing to their electron deficiency at the boron atoms. In **3**, the diisopropylamino groups satisfy the electron demand of the boron atoms and

[*] Prof. Dr. W. Siebert, Dipl.-Chem. A. Krämer, Dr. H. Pritzkow
Anorganisch-chemisches Institut der Universität
Im Neuenheimer Feld 270, D-6900 Heidelberg 1 (FRG)

[**] This work was supported by the Deutsche Forschungsgemeinschaft, the Fonds der Chemischen Industrie, and BASF.

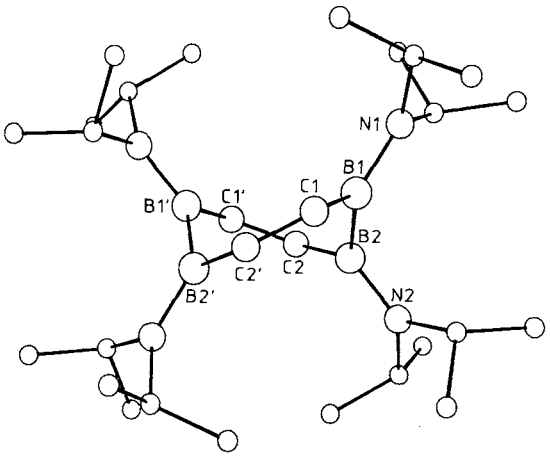

Fig. 1. Molecular structure of **3**. Selected bond lengths [Å] and angles [°] (standard deviations 0.002 Å and 0.1°): B1-B2 1.718, B-N 1.409, 1.412, B-C 1.570, 1.579, C1-C2' 1.346; B-B-C 118.3, 118.7, B-C-C 126.3, 127.2, N-B-B 119.3, 119.4, N-B-C 122.4, 121.8.

so stabilize the organoborane skeleton relative to the carbaborane skeleton.

The relative stabilities of *cyclo*-organoborane/carbaborane compounds (*nido* and *closo*) have been studied in detail for $(CR^1)_4(BR^2)_2$, $(CR^1)_2(BR^2)_3$, and $(CR^1)_2(BR^2)_4$ using PRDDO calculations.[9]

Experimental Procedure

2 (520 mg, 2.1 mmol) was dissolved under nitrogen in 30 mL of pentane, and Lindlar catalyst (130 mg, 5% Pd) and H_2 (47 mL, 2.1 mmol) were then added. After stirring for 6 d, the reaction mixture was filtered at 20°C and the concentrated filtrate (10 mL) was allowed to stand at −20°C, resulting in the crystallization of colorless **3** [(134 mg, 27.0%, m.p. = 196°C (dec.)]. From the mother liquor, 46 mg of **1d** [8.6%, m.p. = 132°C (benzene)] along with the starting material **2** were isolated.

Spectroscopic data for **1d**: ^{1}H-NMR (C_6D_6): δ = 1.10 (d, 12H, ^3J(HH) = 7.6 Hz), 1.18 (d, 12H), 3.29 (sept, 2H), 3.98 (sept, 2H), 6.78 (br. s, 2H), BH signals not identifiable; ^{11}B-NMR ($CDCl_3$): δ = 35.3 (d, ^1J(BH) = 120 Hz); EI-MS: *m/z* 250 ($M^{\oplus}$, 9.7%), 235 (($M^{\oplus} - CH_3$, 15.2%), 207 ($M^{\oplus} - i$Pr, 83.8%), 43 (*i*Pr, 100%).

Received: January 28, 1988 [Z 2594 IE]
German version: *Angew. Chem. 100* (1988) 963

CAS Registry numbers:
1d, 115032-29-6; **2**, 97826-19-2; **3**, 115032-30-9.

[1] a) M. Hildenbrand, H. Pritzkow, W. Siebert, *Angew. Chem. 97* (1985) 769; *Angew. Chem. Int. Ed. Engl. 24* (1985) 759; b) M. Hildenbrand, H. Pritzkow, U. Zenneck, W. Siebert, *ibid. 96* (1984) 371 and *23* (1984) 371; c) M. Hildenbrand, W. Siebert, unpublished results.

[2] See also R. Wehrmann, H. Klusik, A. Berndt, *Angew. Chem. 96* (1984) 369, 810; *Angew. Chem. Int. Ed. Engl. 23* (1984) 369, 826.

[3] W. Schacht, D. Kaufmann, *J. Organomet. Chem. 339* (1988) 33.

[4] H. Nöth, B. Wrackmeyer: *NMR-Spectroscopy of Boron Compounds*, Springer, Berlin 1978.

[5] **3**: space group *P2/n*, a = 7.983(1), b = 10.038(2), c = 21.323(4) Å, β = 96.50(3)°, V = 1698 Å^3, Z = 2; R = 0.062 for 2356 unique reflections (two-circle diffractometer, $Mo_{K\alpha}$ radiation, ω scan, $I \geq \sigma_I$); B,C,N anisotropic, H isotropic. Further details of the crystal structure investigation may be obtained from the Fachinformationszentrum Energie, Physik, Mathematik GmbH, D-7514 Eggenstein-Leopoldshafen 2 (FRG), on quoting the depository number CSD-53075, the names of the authors, and the journal citation.

[6] H. Fisch, H. Pritzkow, W. Siebert, *Angew. Chem. 96* (1984) 595; *Angew. Chem. Int. Ed. Engl. 23* (1984) 608.

[7] T. Fehlner, *J. Am. Chem. Soc. 99* (1977) 8356.

[8] W. Siebert, M. El-Din. El-Essawi, *Chem. Ber. 112* (1979) 1480.

[9] R. D. Camp, D. S. Marynick, G. D. Graham, W. N. Lipscomb, *J. Am. Chem. Soc. 100* (1978) 6781.

Silica-Supported Fe-Pd Bimetallic Particles: Formation from Mixed-Metal Clusters and Catalytic Activity**

By *Pierre Braunstein,* Robert Devenish, Pierre Gallezot, Brian T. Heaton,* Colin J. Humphreys, Jacques Kervennal,* Suzanne Mulley,* and *Michel Ries*

Improved selectivity and stability are found for bi- and multimetallic heterogeneous catalysts when compared with their monometallic counterparts,[1,2] but there is still much to be done in order to understand why these improvements occur.

Previous work has shown that nitrobenzene may be catalytically converted into phenyl isocyanate (240°C/200 atm CO) using the heterogeneous catalyst resulting from impregnation and thermal decomposition and activation of complex **1** on γ-Al_2O_3.[3] This reaction has been extended to the reductive carbonylation of *o*-nitrophenol **3** to benzoxazol-2(3*H*)-one, using **2** on silica as catalyst precursor.[4]

$[Mo_2Pd_2Cp_2(CO)_6(PPh_3)_2]$ Cp = η^5-C_5H_5

1

$[FePd_2(CO)_4(dppm)_2]$ dppm = μ-$Ph_2PCH_2PPh_2$

2

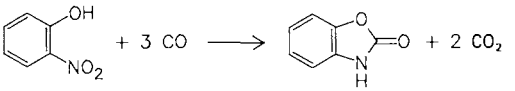

3

We report now that complex **4**[4b,5] also leads to a heterogeneous catalyst having significantly improved properties over those of a conventional catalyst prepared by coimpregnation of iron oxalate and palladium acetate (Table 1, No. 1). Using analytical electron microscopy (AEM) to investigate the catalysts prepared from **2** and **4**, we have shown (1) that bimetallic particles are present at the start of the reaction, (2) that their composition closely parallels that of the metal core in **2** and **4**, and (3) that metal segregation occurs during this reaction. This appears to be the first report addressing, in a combined manner, the formation, catalytic activity, and fate of bimetallic, cluster-derived particles.

[*] Dr. P. Braunstein, Dr. M. Ries
Laboratoire de Chimie de Coordination, UA 416 CNRS,
Université Louis Pasteur
4 rue Blaise Pascal, F-67070 Strasbourg Cédex (France)
Prof. B. T. Heaton, S. Mulley
Department of Inorganic, Physical and Industrial Chemistry,
University of Liverpool
Liverpool L69 3BX (UK)
Dr. J. Kervennal
Centre de Recherches Rhône-Alpes, Atochem
F-69310 Pierre-Bénite (France)
R. Devenish, Prof. C. J. Humphreys
Department of Materials Science and Engineering,
University of Liverpool
Liverpool L69 3BX (UK)
Dr. P. Gallezot
Institut de Recherches sur la Catalyse-CNRS
F-69626 Villeurbanne (France)

[**] We thank C.N.R.S. (ATP Chimie Fine 4384), S.E.R.C., and Atochem for supporting this work and S.E.R.C. for a studentship (to *S. M.*).

Table 1. Catalytic reductive carbonylation of *o*-nitrophenol **3** to benzoxazol-2(3*H*)-one at 200°C. Total volume: 100 mL. Pyridine (1 g) was added in all experiments. Initial CO pressure: 200 atm. 500-mL Hastelloy C reactor with magnetic stirring.

No.	Catalyst [a]	**3** [g]	Catalyst Amount [g]	Fe [b] [mmol]	Pd [b] [mmol]	Mole ratio **3** : Fe	**3** : Pd	Solvent	*t* [h]	Conversion [%]	Selectivity [%] [c]
1	$Pd(OAc)_2 + Fe_2(C_2O_4)_3/SiO_2$	6.95	3.7	0.34	0.53	151 : 1	96 : 1	*o*-$Cl_2C_6H_4$	5	40	90
2	$[FePd_2(CO)_4(dppm)_2]$ **2**$/SiO_2$	6.95	2.75	0.25	0.52	203 : 1	97 : 1	ClC_6H_5	4	98.5	95
3	$[Fe_2Pd_2(CO)_5(NO)_2(dppm)_2]$ **4**$/SiO_2$	13.9	6.68	1.07	1.00	93 : 1	99 : 1	*o*-$Cl_2C_6H_4$	6	99.3	96

[a] The impregnation was carried out by the spray method [3]. Catalysts for Nos. 1 and 2: see [4]. For No. 3, **4** (1.38 g) in THF (40 mL) was used to impregnate 9.7 g of SiO_2 (Shell), which was then dried at 450°C for 16 h. [b] Determined by analysis. [c] Ratio of benzoxazol-2(3*H*)-one produced to **3** reacted.

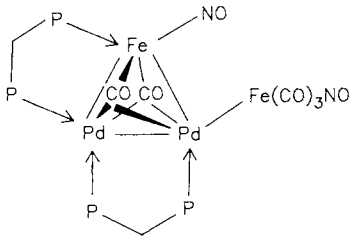

4

The catalytic experiments suggest that a more intimate interaction between Fe and Pd results from the use of a mixed-metal cluster precursor and is, at least in part, responsible for the improved properties of the catalytic system. Indeed, the individual metal particles resulting from **2** have been analyzed by energy-dispersive X-ray analysis (EDX) with a field-emission-gun scanning transmission microscope (FEG-STEM) giving a 1-nm spatial resolution of analysis (0.5-nm spot size). Before catalysis, the particles have a diameter of ca. 20–50 Å (Fig. 1) and are all bimetallic. No Fe or Pd signal is observed outside these particles. The atomic composition of these particles (29.6–38.7 atom% Fe, 70.4–61.3 atom% Pd) is in very good agreement with the theoretical stoichiometry (33.3 atom% Fe and 66.6 atom% Pd).

Particles resulting from **4** have been analyzed with a conventional transmission electron microscope (TEM) and, because of the larger electron probe size (500 nm), EDX analysis encompasses many particles. Before catalysis, the particles are very uniformly distributed on the support. EDX data on 10 different areas were obtained (53.8 ± 2.7 atom% Pd, 45.9 ± 5.3 atom% Fe, 0.2 ± 0.25 atom% Ni), and apart from the presence of Ni, which is probably there as a contaminant from the reactor vessel, these values are very close to that required for **4**.

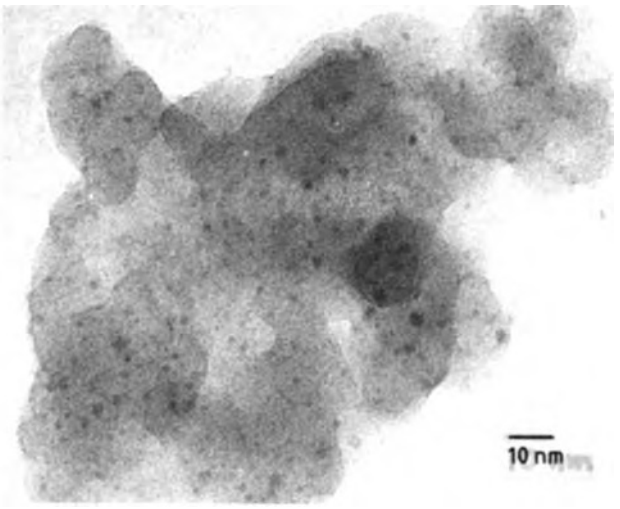

Fig. 1. Transmission electron microscope (TEM) view of the catalyst derived from **2** before catalytic reaction (Fe–Pd clusters).

In contrast, no small bimetallic particles are detected in the conventional, coimpregnated catalyst. Large, micron-size agglomerated particles are observed, whose composition analyzed with the FEG-STEM is variable from one to the other and which appear to be iron-rich in the center. Small particles (30–40 Å) containing only Pd are also observed.

After 4 h of reaction with the catalyst derived from **2**, small bimetallic particles similar to those observed before catalysis were still present. However, large 100–300-Å particles of palladium were formed (Fig. 2). In the case of **4**, we find that 200–500-Å particles are now present on the silica and these particles are either pure Pd or pure Fe. Therefore, there are only slight differences in the fate of the two cluster-derived catalysts after reaction.

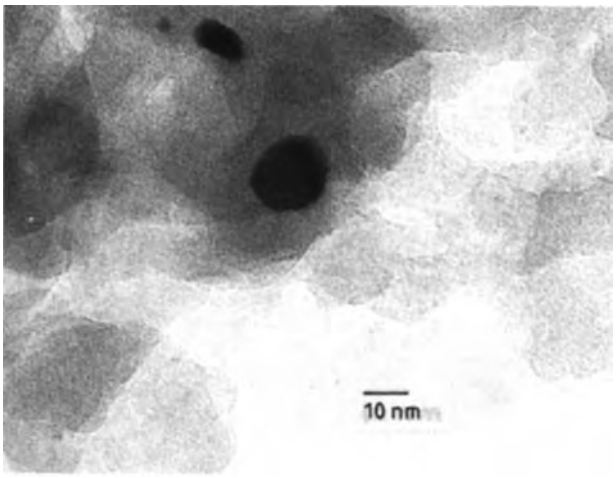

Fig. 2. TEM view of the catalyst derived from **2** after catalytic reaction (Pd particles issued from segregation and sintering of Fe–Pd clusters).

Although Fe and Pd have different crystal structures (bcc and fcc, respectively), up to ca. 75 atom% Pd is found in FePd phases below 600°C[6] and this appears to be the first report of metal segregation occurring during catalysis with a heteropolynuclear carbonyl-cluster-derived heterogeneous[7] catalyst. It is probably induced by the redox character of the reaction studied, the reductive carbonylation of **3**, and/or by the presence of CO, since it is already known from surface science studies that CO adsorption onto bimetallic alloy films causes surface enrichment of one metal, which in some cases is reversible upon desorbing the CO.[10] Interestingly, it has been reported recently that deposition of the mixed-metal clusters **5**, **6**, or **7** onto a partially hydroxylated magnesia support, followed by H_2

treatment at 400°C, gives very small bimetallic particles that have the same bulk metal composition as that of the cluster precursor.[11] Information about their fate under catalytic conditions is not yet available.

$[H_2FeM_3(CO)_{13}]$ $[HFeCo_3(CO)_{12}]$

5, M = Ru; **6**, M = Os **7**

Received: January 15, 1988;
supplemented: March 29, 1988 [Z 2576 IE]
German version: *Angew. Chem. 100* (1988) 972

[1] J. H. Sinfelt: *Bimetallic Catalysts*, Wiley, New York 1983.
[2] P. Braunstein, J. Rosé in I. Bernal (Ed.): *Stereochemistry of Organometallic and Inorganic Compounds, Vol. III*, Elsevier, Amsterdam 1988, in press.
[3] a) P. Braunstein, R. Bender, J. Kervennal, *Organometallics 1* (1982) 1236; b) J. Kervennal, J.-M. Cognion, P. Braunstein, Fr. Pat. 2515640 (1981), Produits Chimiques Ugine Kuhlman; *Chem. Abstr. 99* (1983) 139487.
[4] a) P. Braunstein, J. Kervennal, J.-L. Richert, *Angew. Chem. 97* (1985) 762; *Angew. Chem. Int. Ed. Engl. 24* (1985) 768; b) P. Braunstein, J. Kervennal, J.-L. Richert, M. Ries, Fr. Pat. 2558074 (1984), Atochem; *Chem. Abstr. 104* (1986) 19681.
[5] P. Braunstein, C. de Méric de Bellefon, M. Ries, J. Fischer, *Organometallics 7* (1988) 332.
[6] C. J. Smithels, E. A. Brandes: *Materials Reference Book*, Butterworths, London, 5th ed. 1976, p. 610.
[7] Segregation of physisorbed or surface-bound Fe-Os or Os-Rh clusters is known to occur under CO + H_2 or thermally, respectively [8, 9].
[8] J. R. Budge, B. F. Lücke, B. C. Gates, J. Toran, *J. Catal. 91* (1985) 272.
[9] A. Choplin, M. Leconte, J.-M. Basset, S. G. Shore, W.-L. Hsu, *J. Mol. Catal. 21* (1983) 389.
[10] W. M. H. Sachtler, *Appl. Surf. Sci. 19* (1984) 167.
[11] A. Choplin, L. Huang, A. Theolier, P. Gallezot, J. M. Basset, *J. Am. Chem. Soc. 108* (1986) 4224.

Synthesis of TiNF and Structure Determination by Powder Diffraction using Synchrotron Radiation**

By *Claus Wüstefeld, Thomas Vogt, Ulrich Löchner, Joachim Strähle,* and *Hartmut Fuess**

Owing to its high intensity and low divergence, synchrotron radiation allows powder diagrams to be recorded with high resolution. Herein we report on the synthesis and structure analysis of TiNF, which, according to *Andersson*,[1] is a pseudooxide because of $N^{3\ominus}$ and $F^{\ominus}$ formally replacing two $O^{2\ominus}$. X-ray diffraction using synchrotron radiation suggested itself as a method of structure determination since only a small amount of the substance was available and since very small deviations of the lattice symmetry from that of a high-symmetry oxide structure were possible. Furthermore, the excellent signal-to-noise ratio was expected to permit the observation of weak superstructure reflections in case of an ordering of N and F ions in the anion lattice. Moreover, the mathematical description of Bragg reflections allows structure refinement from powder data by the Rietveld method.[4]

TiNF was synthesized by ammonolysis of activated $(NH_4)_2TiF_6$.[2] To activate the fluorometalate, two reaction steps are necessary. First, $(NH_4)_2TiF_6$ is heated to 400°C with an equimolar amount of NH_4Cl in a sealed system (welded Pt crucible, inert gas) for ca. 12 h to form $(NH_4)_2TiF_6 \cdot NH_4Cl$. The NH_4Cl adduct is then thermally decomposed at 280°C under inert gas. Thus activated, $(NH_4)_2TiF_6$, by subsequent ammonolysis in a dry and oxygen-free stream of NH_3, yields TiNF. Without activation, TiN is the main product.[3] TiNF is a light green to olive green substance and, like TiO_2, thermally stable and largely chemically inert.

The compound could be indexed in analogy to anatase ($a = 3.785$ Å, $c = 9.514$ Å)[5] on a body-centered tetragonal cell with $a = 3.7891(4)$ Å and $c = 9.4863(9)$ Å.[6] Line-shape analysis of the Bragg reflections showed that the line shape did not correspond to a pure Gaussian curve but contained appreciable Lorentz components. Use of the pseudo-Voigt function[7] gave 53% Gaussian line shape. This is due to the method of sample preparation which leads to a small average particle size. The Rietveld refinement[8] led to the atomic parameters Ti(0; 3/4; 1/8), $B = 0.58(6)$ Å^2; N/F(0; 1/4; 0.0833(4)), $B = 0.04(11)$ Å^2.

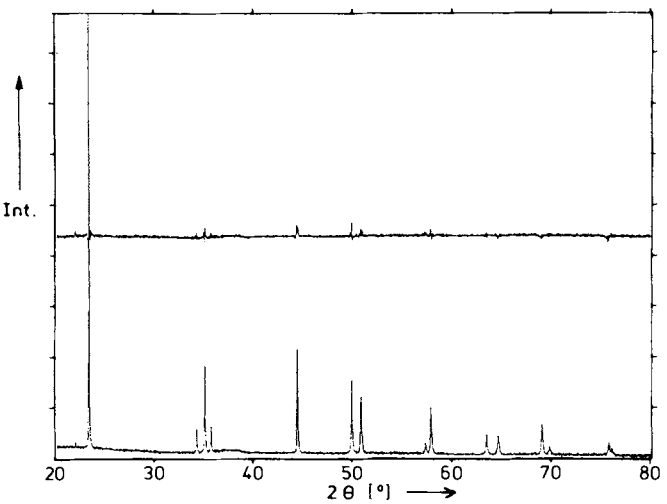

Fig. 1. Measured diffraction pattern (below) and difference between measured and calculated [8] diffraction pattern (above) of TiNF.

Figure 1 shows the measured intensities (below) and the difference between measured and calculated diffraction patterns (above). The refinement was carried out in space group $I4_1/amd$. Refinements in isomorphic subgroups did not lead to better residual figures-of-merit. Since high-resolution electron diffraction and electron microscopic analysis showed no superstructure either,[9] only neutron diffraction powder spectra, where the scattering contributions of F and N are different, can answer the question of a possible order in the anion lattice.

Experimental Procedure

The powder pattern was recorded at the beamline F1 of Hasylab at the Deutsches Elektronen Synchrotron (DESY) in Hamburg. An oil smear of TiNF on a Si(711) plate was fitted into a swinging sample holder, the assembly corresponding to the Cox diffraction geometry [10, 11]. Conditions: Ge(111) monochromator and analyzer, NaI(Tl) scintillation counter, wavelength 1.4358 Å, 2θ steps of 0.01, average measuring time per step 5.2 s. The

[*] Prof. Dr. H. Fuess, Dr. U. Löchner
Institut für Kristallographie der Universität
Senckenberg-Anlage 30, D-6000 Frankfurt am Main (FRG)
Dipl.-Chem. C. Wüstefeld, Prof. Dr. J. Strähle
Institut für Anorganische Chemie der Universität
Auf der Morgenstelle 18, D-7400 Tübingen (FRG)
Dr. T. Vogt
Institut Max von Laue-Paul Langevin
Avenue des Martyrs, F-38042 Grenoble (France)

[**] This work was supported by the Deutsche Forschungsgemeinschaft, the Fonds der Chemischen Industrie, and the Bundesminister für Forschung und Technologie.

background was determined by a linear extrapolation through 10 points without Bragg components. Polarization was set at 100% because of the vertical scattering geometry. Scattering factors and values for anomalous dispersion were taken from the International Tables [12]. No correction for absorption and extinction. Parameters of refinement: zero-point shift: -0.105; U, V, W, [13]: $U=0.129(12)$; $V=0.033(8)$, $W=0.006(1)$; $R_{wp}=0.0145$ (expected: 0.0089). The structure factor table is available on request from the Fachinformationszentrum Energie, Physik, Mathematik GmbH, D-7514 Eggenstein-Leopoldshafen 2 (FRG), on quoting the depository number CSD-53 152, the names of the authors and the journal citation.

Received: February 22, 1988 [Z 2629 IE]
German version: *Angew. Chem. 100* (1988) 1013

[1] S. Andersson, *Ark. Kemi 26* (1967) 521.
[2] C. Wüstefeld, Dissertation, Universität Tübingen 1988.
[3] H. Funk, H. Böhland, *Z. Anorg. Allg. Chem. 334* (1964) 155.
[4] H. M. Rietveld, *J. Appl. Crystallogr. 2* (1969) 65.
[5] D. T. Cromer, K. Herrington, *J. Am. Chem. Soc. 77* (1955) 4708.
[6] Tripled numerical standard deviations in parentheses.
[7] D. Louer, *Chem. Scr. 26A* (1986) 17.
[8] R. A. Young, D. B. Wiles, *J. Appl. Crystallogr. 15* (1982) 430.
[9] E. Schweda, personal communication.
[10] P. Thompson, D. E. Cox, J. B. Hastings, *J. Appl. Crystallogr. 20* (1987) 79.
[11] T. Wroblewski, Hochaufgelöste Pulverdiffraktometrie am Messplatz F1. Ein wegweisender Aufbau (High-resolution Powder Diffraction. A guiding Setup), Statusseminar Synchrotronstrahlung, Berlin, December 10–11, 1987.
[12] K. Lonsdale (Ed.): International Tables for X-ray Crystallography, Vol. III, Kynoch Press, Birmingham 1972.
[13] G. Caglioti, A. Paoletti, F. P. Ricci, *Nucl. Instrum. 3* (1958) 223.

A Topologically Chiral [2]Catenand**

By *Dennis K. Mitchell* and *Jean-Pierre Sauvage**

Chemical interest in nonplanar molecular graphs has increased dramatically with the advent of synthetic strategies allowing easy access to entwined and interlocked molecules. The first topologically nonplanar molecule to be synthesized was reported in 1981.[1,6] It corresponds to *Kuratowski*'s $\mathbf{K_5}$ figure[1,2] (complete graph on five vertices). Another example of a molecule whose graph is nonplanar was recently described by *Walba* et al.[7] It consists of a Moebius strip with three rungs and is isomorphic to $\mathbf{K_{3,3}}$ (complete bipartite graph on two sets of three vertices).

Molecular graphs of interlocked rings (catenanes) and knots[3–5] are nonplanar when embedded in three-dimensional space. Nonplanar graphs can be labeled so as to retain their chirality over all presentations. The term "topological chirality" was coined for this property and has been applied to molecules as well as molecular graphs.[8,10]

Topological chirality requires that mirror image presentations be topologically distinct.[8] As a consequence, it is necessary (but not sufficient) that the molecular graph be nonplanar in three-dimensional space. Although chemical chirality of the K_5 and $K_{3,3}$ nonplanar molecules mentioned above was proven previously,[1,7] it is only recently that their topological chirality was demonstrated.[9]

[*] Dr. J.-P. Sauvage, Prof. D. K. Mitchell [+]
Laboratoire de Chimie Organo-Minérale
Institut de Chimie, Université Louis Pasteur
F-67000 Strasbourg (France)
[+] Permanent address: Los Angeles City College
855 North Vermont Ave., Los Angeles, CA 90029 (USA)

[**] We thank the CNRS for financial support. *D. K. M.* thanks the Ministère des Affaires Etrangères for a fellowship. Stimulating discussions with Dr. *C. O. Dietrich-Buchecker* are also gratefully acknowledged.

Oriented linked rings are the prototypical topologically chiral objects. We now report the synthesis of the first isolated topologically chiral catenane,[10] containing *two interlocked directed* rings (Fig. 1).

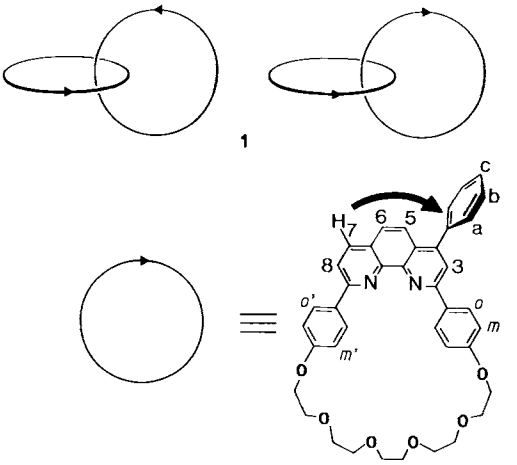

Fig. 1. Principle of construction of topologically chiral [2]catenands **1** and structure of the individual rings showing their directed nature.

We have taken advantage of the previously developed templated synthesis of catenates and catenands.[11] Compound **1** was prepared in five steps from 4-phenyl-1,10-phenanthroline **2**.[12] Compound **2** was reacted with 4-lithioanisole as previously described for 1,10-phenanthroline,[11] leading to **3** in 35% yield. Demethylation of **3** (pyridine, HCl, 210°C) gave a 90% yield of **4**, which, in the presence of 0.5 equivalent of $[Cu(CH_3CN)_4^{\oplus}][BF_4^{\ominus}]$, furnished quantitatively the complex $\mathbf{5}^{\oplus}$, consisting of two ligands **4** entwined around a copper(I) center. Cyclization of $\mathbf{5}^{\oplus}$ to $\mathbf{6}^{\oplus}$ was performed under high-dilution conditions (DMF, 70°C), with a stoichiometric amount of the diiodo derivative of pentaethylene glycol, $ICH_2(CH_2OCH_2)_4CH_2I$, in the presence of a large excess of Cs_2CO_3. Racemic $[\mathbf{6}^{\oplus}][BF_4^{\ominus}]$ was obtained from methanol as a deep red crystalline solid (m.p. 176–183°C), in 12% yield.[13]

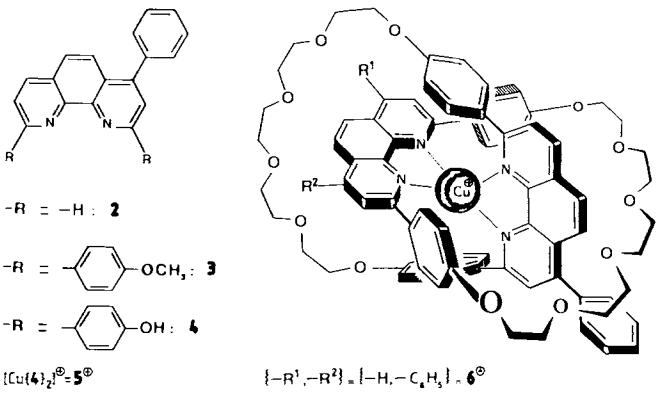

The chirality of $\mathbf{6}^{\oplus}$ was supported by ^{1}H-NMR spectroscopy in the presence of *Pirkle*'s chiral reagent **7** (Fig. 2). Contrary to what was observed with another chiral catenate differing from $\mathbf{6}^{\oplus}$ in its graph-theoretical description,[14] the *entire spectrum* of $\mathbf{6}^{\oplus}$ was split, with the exception of the peaks corresponding to H-3, H-5, and H-6.

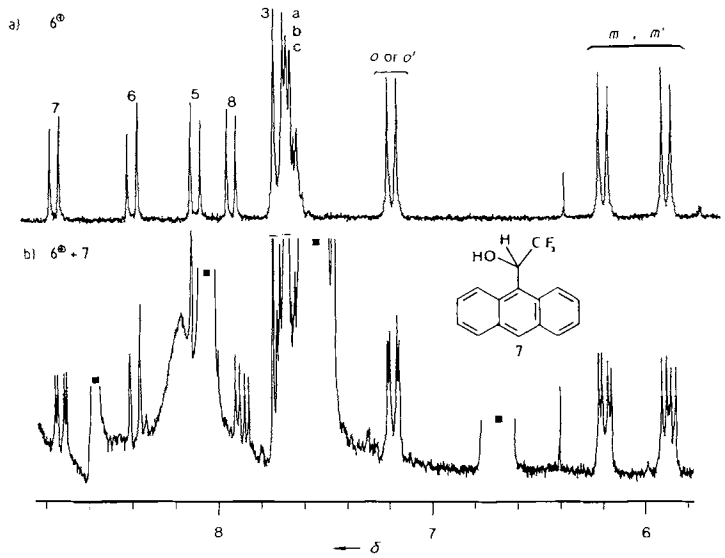

Fig. 2. Part of the ^{1}H-NMR spectra (200 MHz, CD_2Cl_2) of a) $6^{\oplus}$ and b) $6^{\oplus}$ plus ten equivalents of *Pirkle*'s reagent (*S*)-(+)-**7**. Peaks indicated by 7,8, *o* or *o'*, *m*, or *m'* in spectrum (a) (labeling given in Fig. 1) are split in spectrum (b). The signals corresponding to the chiral reagent are marked by a black square.

Those protons might be hidden by the 4-phenyl group and the pentaoxyethylene link so that their chemical shift is not sensitive to the particular environment induced by *Pirkle*'s reagent.

Spectrum 2b indicates that the topological chirality of $6^{\oplus}$ is accompanied by easy recognition of its enantiomers by a chiral reagent. This observation might be related to the high rigidity of the molecule. Demetalation of $6^{\oplus}$ (KCN in H_2O/CH_2Cl_2, 78% yield) leads to an extremely flexible system **1**, whose two rings can easily glide within one another. The catenane nature of **1** was supported by its mass spectrum (*m/z* 1284 (*M*) and 642 (*M*/2)). Its *topological chirality* is obvious from the directed nature of the starting compound **2** and the synthetic route followed. In contrast to $6^{\oplus}$, no clear enantioselective interaction with *Pirkle*'s reagent could be observed in the NMR spectra of **1**.

The present templated synthesis of chiral catenands indicates that separation of their enantiomers will be easiest at the stage of their intermediate rigid copper(I) catenates. These enantiomerically pure complexes are expected to show enantioselectivity in both photoinduced electron transfer and interaction with DNA helices.[15]

Received: February 15, 1988;
revised: March 25, 1988 [Z 2620 IE]
German version: *Angew. Chem. 100* (1988) 985

CAS Registry numbers:
1, 114861-89-1; **2**, 62366-01-2; **3**, 114861-87-9; **4**, 114861-88-0; $5^{\oplus}\cdot BF_4^{\ominus}$, 114928-54-0; $6^{\oplus}\cdot BF_4^{\ominus}$, 114928-56-2; $ICH_2(CH_2OCH_2)_4CH_2I$, 76871-59-5; 4-lithioanisole, 14774-77-7.

[1] H. E. Simmons, III, J. E. Maggio, *Tetrahedron Lett. 22* (1981) 287; S. A. Benner, J. E. Maggio, H. E. Simmons, III, *J. Am. Chem. Soc. 103* (1981) 1581. The graph of a molecule can be defined as formed by its atoms taken as vertices and its chemical bonds as edges. See A. T. Balaban (Ed.): *Chemical Applications of Graph Theory*, Academic Press, New York 1976.

[2] A nonplanar graph cannot be drawn in the plane in such a way that no two edges intersect geometrically except at a vertex to which they are both incident. See R. J. Wilson: *Introduction to Graph Theory*, Oliver Boyd, Edinburgh 1972.

[3] H. L. Frisch, E. Wasserman, *J. Am. Chem. Soc. 83* (1961) 3789.

[4] G. Schill: *Catenanes, Rotaxanes and Knots*, Academic Press, New York 1971.

[5] Catenanes have nonplanar graphs except if the restriction to *connected* graphs is made. In that case the "mechanical" link between the interlocked rings must be ignored: K. Mislow, *Bull. Soc. Chim. Belg. 86* (1977) 595.

[6] L. A. Paquette, M. Vazeux, *Tetrahedron Lett. 22* (1981) 291.

[7] D. M. Walba, R. M. Richards, R. C. Haltiwanger, *J. Am. Chem. Soc. 104* (1982) 3219.

[8] D. M. Walba in R. B. King (Ed.): *Chemical Applications of Topology and Graph Theory*, Elsevier, New York 1983; *Tetrahedron 41* (1985) 3161.

[9] J. Simon, *Topology 25* (1986) 229. We thank Professor *Simon* for sending us a reprint of his work.

[10] As discussed in [8], *Schill* et al. obtained a mixture of catenanes containing one or several topologically chiral catenanes, formed as byproducts. However, no such compound was isolated or characterized: G. Schill, G. Doerjer, E. Logemann, W. Vetter, *Chem. Ber. 113* (1980) 3697. The chirality of catenanes containing oriented rings has been evoked in the past. Important theoretical discussions can be found in [3] and [4]. See also V. I. Sokolov, *Russ. Chem. Rev. (Engl. Transl.) 42* (1973) 452.

[11] C. O. Dietrich-Buchecker, J. P. Sauvage, J. P. Kintzinger, *Tetrahedron Lett. 24* (1983) 5095; C. O. Dietrich-Buchecker, J. P. Sauvage, J. M. Kern, *J. Am. Chem. Soc. 106* (1984) 3043.

[12] F. H. Case, *J. Org. Chem. 16* (1951) 1541.

[13] ^{1}H-NMR and electronic spectra as well as elemental analysis (C, H, N) of compounds **2** to $6^{\oplus}$ were consistent with their structure.

[14] C. O. Dietrich-Buchecker, A. Edel, J. P. Kintzinger, J. P. Sauvage, *Tetrahedron 43* (1987) 333.

[15] B. Nordén, F. Tjerneld, *FEBS Lett. 67* (1976) 368; J. K. Barton, *Science 233* (1986) 727, and references cited therein.

Conjugated and Nonconjugated Cyclopentenones by a Reaction Cascade from Methyl 6-Oxo-5-phenyl-1,3,4-oxadiazine-2-carboxylate and 1,3-Butadienes**

By *Joachim Hegmann, Manfred Christl,* Karl Peters, Eva-Maria Peters,* and *Hans Georg von Schnering*

Five-membered carbocycles are structural components of numerous natural products and therefore attractive synthetic goals.[1] Since synthetic procedures with a broad scope of application are still unknown, new methods are of interest. Herein we report on reactions of the title heterocyclic compound **1** with 1,3-butadienes **2**; these reactions, although multistep processes, afford conjugated and nonconjugated cyclopentenones in a one-pot procedure and also allow the annelation of these five-membered rings.

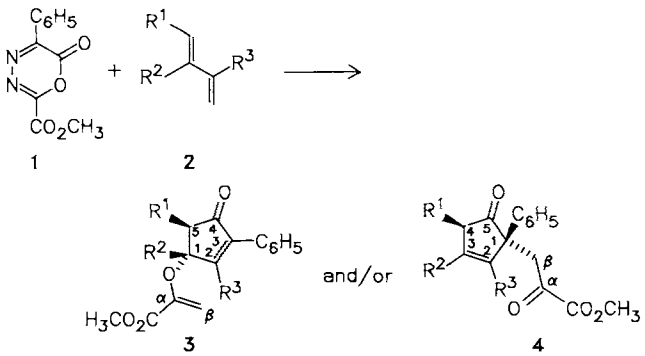

[*] Prof. Dr. M. Christl, Dipl.-Chem. J. Hegmann
Institut für Organische Chemie der Universität
Am Hubland, D-8700 Würzburg (FRG)
Dr. K. Peters, E.-M. Peters, Prof. Dr. H. G. von Schnering
Max-Planck-Institut für Festkörperforschung
Heisenbergstrasse 1, D-7000 Stuttgart 80 (FRG)

[**] Cycloadditions of 1,3,4-Oxadiazin-6-ones (4,5-Diaza-α-pyrones), Part 8. This work was supported by the Deutsche Forschungsgemeinschaft and the Fonds der Chemischen Industrie.—Part 7: M. Christl, J. Hegmann, H. Reuchlein, K. Peters, E.-M. Peters, H. G. von Schnering, *Tetrahedron Lett. 28* (1987) 6433.

Table 1. Reaction conditions, yields, and melting points of some products for the reactions of **1** with **2** (50% excess).

2	R^1	R^2	R^3	Solvent	t_1 [a]	(T [°C])	t_2 [a]	(T [°C])	Product [b]	Yield [%]	M.p. [°C]
a	H	H	H	CCl_4	7	(40)	340	(80)	**3a**, **4a**	20	oil
b	H	CH_3	H	CH_2Cl_2		120 (20)			**3b**	13	80–82
	H	CH_3	H	CCl_4	2	(80)	480	(80)	**4b**	19	oil
	H	H	CH_3						**3b'**	15	oil
c	H	CH_3	CH_3	CCl_4		240 (20)			**3c** [c]	11	oil
				CCl_4		3 (80)			**4c**	51	oil
d [d]	CH_3	CH_3	H	CCl_4	3	(80)	48	(80)	**4d**	46	oil
e	CH_3	H	CH_3	CCl_4	7	(80)	340	(80)	**3e**	27	96–97
f	$(CH_2)_3$		H	CH_2Cl_2	4	(20)	48	(20)	**3f**	54	60–61
g	$(CH_2)_4$		H	CCl_4	2	(80)	48	(80)	**4g**	43	97–100
h	$(CH_2)_5$		H	CH_2Cl_2		48 (20)			**4h**	41	61–62

[a] Reaction times in h; t_1 refers to the complete conversion of **1** and t_2 to that of the corresponding γ-oxoketene, e.g., **5** in Scheme 1. [b] The products were isolated by flash chromatography (SiO_2, petroleum ether/ethyl acetate 4 : 1) or by crystallization (**3f**, **4g**, **4h**). Their structures are in agreement with the elemental analyses and the spectroscopic data (for several examples see Table 2). [c] Along with 38% of **7**, which was separated by crystallization and chromatography. [d] Dimethylbutadiene **2d** (200% excess) was used as a 3 : 1 mixture with its (*Z*) isomer, which reacts appreciably more slowly.

Thus, treatment of **1** with 1,3-butadiene **2a** in tetrachloromethane at 40°C, followed by heating at reflux, gave a 3 : 1 mixture of the conjugated cyclopentenone derivative **3a** and the nonconjugated isomer **4a** in a yield of ca. 20%. Products analogous to **3a** were formed from (*E*)-2-methyl-1,3-pentadiene **2e**, 1-vinylcyclopentene **2f**, 2,3-dimethyl-1,3-butadiene **2c** (at 20°C), and, in part, from isoprene **2b**. On the other hand, the reactions of **1** with (*E*)-3-methyl-1,3-pentadiene **2d**, 1-vinylcyclohexene **2g**, 1-vinylcycloheptene **2h**, 2,3-dimethyl-1,3-butadiene **2c** (at 80°C), and, in part, with isoprene **2b** afforded nonconjugated cyclopentenone derivatives **4**. The results are summarized in Table 1 and selected spectroscopic data are collected in Table 2. The relative configurations of C-1 and C-5 indicated in the formula were confirmed for **3f** by NOE experiments and are therefore plausible for the other compounds **3** as well. From those and from mechanistic considerations (see below) the relative configurations of C-1 and C-4 of compounds **4** were derived.

The reaction cascades presumably begin with the cycloaddition of a CC double bond of **2** to the diazabutadiene system of **1**. In the case of the nonsymmetric butadienes **2**, the unsubstituted vinyl group is expected to be the more reactive and the orientation should correspond to that observed in the addition of styrene to **1**.[2] As found for normal reactions of olefins with **1**,[2] the Diels–Alder adducts could not be observed. However, the products

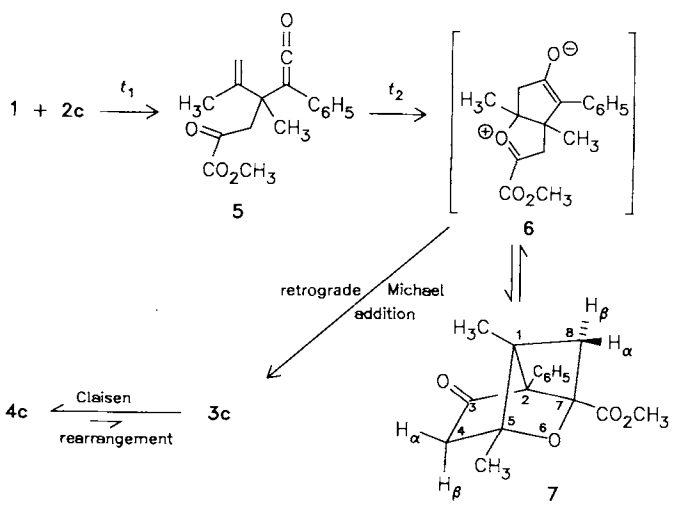

Scheme 1.

Table 2. Selected spectroscopic data for **3a**, **3c**, **4c**, and **7**; NMR ($CDCl_3$, δ values, coupling constants in Hz).

3a: IR (CCl_4): $\tilde{\nu}$ = 1750 (sh), 1738, 1728 (ketone and ester carbonyl), 1629 cm^{-1} (C=C)

3c: ^{1}H-NMR: 1.71 and 2.19 (each s; 1-CH_3, 2-CH_3), 2.64 and 3.16 (each d, $J_{5,5}$ = 18.5; 5-H_2), 3.80 (s; OCH_3), 4.70 and 5.55 (each d, $J_{\beta,\beta}$ = 2.5; β-H_2), 7.31 (*o*-H), 7.36 (*p*-H), 7.42 (*m*-H).—^{13}C-NMR: 12.4 (q; 2-CH_3), 24.7 (lq; 1-CH_3), 45.7 (t; C-5), 52.4 (q; OCH_3), 83.7 (s; C-1), 100.8 (t; C-β), 140.9 (s; C-3), 147.5 (s; C-α), 164.0 (s; CO_2CH_3), 171.1 (s; C-2), 201.4 (s; C-4), 128.3 (especially strong signal, d; *m*-C, *p*-C), 129.1 (d; *o*-C), 130.6 (s; *ipso*-C)

4c: IR (CCl_4): $\tilde{\nu}$ = 1753, 1734, 1710 cm^{-1} (C=O).—^{1}H-NMR: 1.54 (tq, *J* with 3-CH_3 ≈ 1.0, *J* with 4-H_2 ≈ 2.0; 2-CH_3), 1.90 (sext, *J* with 4-H_2 ≈ 1.0; 3-CH_3), 2.96 and 3.06 (each dqq, $J_{4,4}$ = 22.5; 4-H_2), 3.70 and 3.75 (each d, $J_{\beta,\beta}$ = 18.5; β-H_2), 3.84 (s; OCH_3), 7.21–7.26 (*o*-H, *p*-H), 7.32 (*m*-H).—^{13}C-NMR: 10.7 and 14.0 (each q; 2-CH_3, 3-CH_3), 43.2 and 46.4 (each t; C-β, C-4), 53.1 (q; OCH_3), 61.9 (s; C-1), 131.0 (s; C-3), 132.7 (s; C-2), 160.8 (s; CO_2CH_3), 190.9 (s; C-α), 214.7 (s; C-5), 126.2 (d; *o*-C), 127.4 (d; *p*-C), 128.9 (d; *m*-C), 138.5 (s; *ipso*-C)

7: IR (KBr): $\tilde{\nu}$ = 1745 cm^{-1} (ketone and ester carbonyl).—^{1}H-NMR: 1.30 and 1.51 (each s; 1-CH_3, 5-CH_3), 2.20 (d, $J_{8,8}$ = 8.5; 8α-H), 2.63 (d; $J_{4,4}$ = 17.5; 4α-H), 2.64 (dd, $J_{4\beta,8\beta}$ = 1.3; 8β-H), 2.87 (dd, 4β-H), 3.73 (s; OCH_3), 7.12 (*o*-H), 7.27–7.38 (*m*-H, *p*-H).—^{13}C-NMR: 11.8 and 16.4 (each q; 1-CH_3, 5-CH_3), 40.4 and 51.7 (each t; C-4, C-8), 52.5 (q; OCH_3), 59.0 (s; C-1), 77.4 (s; C-2), 85.7 and 86.4 (each s; C-5, C-7), 167.1 (s; CO_2CH_3), 208.2 (s; C-3), 127.6 (d; *p*-C), 128.4 and 129.0 (each d; *o*-C, *m*-C), 131.7 (s; *ipso*-C)

formed from them, γ-oxoketenes such as **5**, could be detected in every case owing to an IR band of the reaction mixture at ca. 2100 cm^{-1}.

In the case of 2,3-dimethylbutadiene **2c**, we were able to identify a second intermediate in addition to the γ-oxoketene **5** (Scheme 1). This intermediate could be isolated (67% yield, m.p. = 133–136°C) when the reaction was carried out in dichloromethane at 20°C (1 d). According to the X-ray structure analysis, it is the tricyclic compound **7**. The bonds C1-C2 and C2-C7 (159.8 and 160.5 pm) in the four-membered ring are significantly lengthened, whereas the lengths of all other endocyclic CC bonds lie between 151.2 and 154.1 pm.[3] Heating of **7** in tetrachloromethane at 80°C resulted in the formation of **4c**, with **3c** being observed as an intermediate.

The zwitterion **6** appears to be a logical intermediate for the conversion of **5** into **3c** and **7**. Intramolecular addition of the enolate group to the carbenium-oxonium moiety would lead to **7**. This reaction is apparently reversible at elevated temperatures, so that **6** can undergo a retrograde Michael addition generating the more stable **3c**. Claisen rearrangement of **3c** then gives rise to **4c**.

Whether the reactions at 80°C lead to the pyruvic ester enol ethers **3** or to the pyruvic esters **4** presumably de-

pends on their relative thermodynamic stability. We draw this conclusion from the finding that alkyl substituents R^2 favor the formation of **4** in each case, at least at 80 °C. The exception, **3f**, might be due to the fact that it has a lower strain energy than **4f**, since the latter contains a CC double bond to a bridgehead.

The reaction **5**→**6** is an electrophilic attack of the ketene functionality at the α-vinyl group with participation of the γ-oxo oxygen atom. Out of a number of conceivable alternatives, the reaction times t_2 (Scheme 1, Table 1) lead us to prefer a two-step process involving a zwitterionic intermediate whose five-membered ring contains a carbocationic center in addition to the enolate moiety. In the second step, the oxo group acts as a nucleophile toward the cationic center. The slow conversion of the ketene intermediate for R^2 = H (compare t_2 in Table 1 for **2a**, **b**, **e**) and its rapid disappearance for R^2 = alkyl (compare t_2 for **2c**, **d**, **f**–**h**) indicate that secondary and tertiary carbocationic centers, respectively, are generated.

Received: February 3, 1988;
revised: March 30, 1988 [Z 2602 IE]
German version: *Angew. Chem. 100* (1988) 969

[1] L. A. Paquette, A. M. Doherty: *Polyquinane Chemistry*, Springer, Berlin 1987, and references cited therein.
[2] M. Christl, *Gazz. Chim. Ital. 116* (1986) 1.
[3] Further details of the crystal structure investigation may be obtained from the Fachinformationszentrum Energie, Physik, Mathematik GmbH, D-7514 Eggenstein-Leopoldshafen 2 (FRG), on quoting the depository number CSD-52845, the names of the authors, and the journal citation.

μ-Hydroxo- and μ-Oxobis(μ-acetato)diruthenium Complexes with Weak Intramolecular Ru···Ru Interactions**

By *Peter Neubold, Karl Wieghardt,* Bernhard Nuber,* and *Johannes Weiss*

The electron-spectroscopic, magnetic, and electrochemical properties of binuclear transition-metal complexes containing the structural unit $[M_2^{III}(\mu\text{-O})(\mu\text{-}CH_3CO_2)_2]^{2\oplus}$ are the subject of intensive investigation, in particular because the complexes of iron and manganese are model complexes for metalloproteins in which the metal centers are held together by μ-oxo and μ-hydroxobis(μ-carboxylato) bridges.[1,2] We recently showed that, in the case of the analogous molybdenum(III) complexes, a Mo≡Mo bond ($\sigma^2\pi^4$) is formed when a μ-hydroxo-bridged complex is deprotonated, giving $[Mo_2(\mu\text{-O})(\mu\text{-}CH_3CO_2)_2]^{2\oplus}$.[3] The mixed-valence Mo^{III}–Mo^{IV} complex, which we also prepared, contains a weaker Mo–Mo bond with a bond order of 2.5 ($\sigma^2\pi^3$).[3b] It was therefore of interest to investigate the corresponding chemistry of ruthenium, since, in this case, only a Ru^{III}–Ru^{III} single bond ($\sigma^2\pi^4\pi^{*4}$) is expected and oxidation to the Ru^{III}–Ru^{IV} complex should result in an *increase* in the bond order to 1.5 ($\sigma^2\pi^4\pi^{*3}$).

[*] Prof. Dr. K. Wieghardt, Dipl.-Chem. P. Neubold
Lehrstuhl für Anorganische Chemie I der Universität
Postfach 102148, D-4630 Bochum (FRG)
Dr. B. Nuber, Prof. Dr. J. Weiss
Anorganisch-chemisches Institut der Universität
Im Neuenheimer Feld 270, D-6900 Heidelberg (FRG)

[**] This work was supported by the Fonds der Chemischen Industrie. We thank Degussa, Hanau, for a generous donation of $RuCl_3 \cdot H_2O$.

Hydrolysis of $LRuCl_3 \cdot H_2O$ (L = *N,N',N''*-trimethyl-1,4,7-triazacyclononane) in aqueous NaOAc solution results in the formation of a deep violet solution, which, after addition of $NaPF_6$, affords violet crystals of **1** in 85% yield. Complex **1** undergoes protonation in 2 M hydrochloric acid, yielding dark green microcrystals of **2**. Dissolution of **2** in H_2O results in deprotonation and quantitative re-formation of **1**. The dissociation constant of **1** at 20 °C ($pK_a = 1.9$) was determined spectrophotometrically.

1 $[L_2Ru_2^{III}(\mu\text{-O})(\mu\text{-}CH_3CO_2)_2][PF_6]_2 \cdot 0.5\,H_2O$

2 $[L_2Ru_2^{III}(\mu\text{-OH})(\mu\text{-}CH_3CO_2)_2][PF_6]_3$

3 $[L_2Ru^{III}Ru^{IV}(\mu\text{-O})(\mu\text{-}CH_3CO_2)_2][PF_6]_3$

Complex **1** was oxidized in aqueous solution with $Na_2S_2O_8$ to the mixed-valence $Ru^{III}Ru^{IV}$ dimer **3**, which was isolated as the orange-brown $PF_6^\ominus$ salt. The electronic spectra of the new complexes are shown in Figure 1.

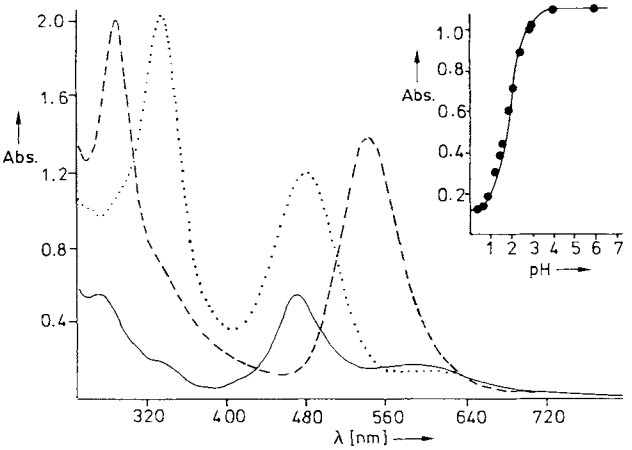

Fig. 1. Electronic spectra of **1** (H_2O), **2** (5 M HCl) and **3** (H_2O). ([1] = 2.15×10^{-4} M (----); [2] = 2.15×10^{-4} M (——); [3] = 2.15×10^{-4} M (·····); 1-cm cuvette); the inset shows the absorption of **1** at 540 nm as a function of pH.

The cyclovoltammogram of **1** in CH_3CN (0.1 M nBu_4NPF_6; Pt electrode) shows a reversible electron transfer at $E_{1/2} = +0.59$ V versus the normal hydrogen electrode (NHE)[4] as well as an irreversible reduction at −0.88 V versus NHE. Coulometry gave 1.0 ± 0.1 electron/dimer for the reversible transition.

Measurement of the molar magnetic susceptibility between 100 and 293 K using the Faraday method showed that **1** is diamagnetic, whereas **2** has a temperature-dependent magnetic moment per dimer of $\mu_{eff} = 0.68\,\mu_B$ (98 K) and $1.82\,\mu_B$ (293 K). Complex **2** exhibits intramolecular, antiferromagnetic coupling of the two low-spin Ru^{III} centers ($H = -2JS_1S_2$, $S_1 = S_2 = 1/2$, $J = -218$ cm^{-1}, $g = 2.4(1)$). For **3**, a weak temperature-dependent moment of $\mu_{eff} = 1.85\,\mu_B$/dimer (98 K) and $2.04\,\mu_B$ (293 K) was found, as expected for a $Ru^{III}Ru^{IV}$ complex containing one unpaired electron per dimer.

Figures 2 and 3 show the structures of the complex cations in **1** and **3** as determined by X-ray crystal structure analysis.[5] Important structural parameters of complexes containing $[M_2(\mu\text{-OH})(\mu\text{-}CH_3CO_2)_2]^{n\oplus}$ and $[M_2(\mu\text{-O})(\mu\text{-}CH_3CO_2)_2]^{m\oplus}$ frameworks are collected in Table 1. The structures of the cations in **1** and **3** are similar. Two Ru

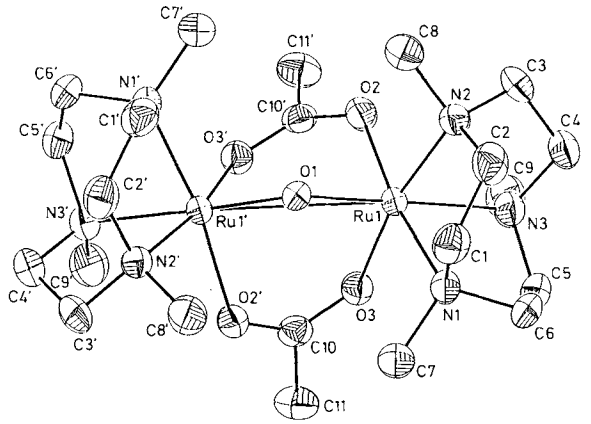

Fig. 2. Molecular structure of the cation of **1**. Selected distances [Å]: Ru1-N1 2.112(4); Ru1-N2 2.109(4); Ru1-N3 2.168(4); Ru1-O1 1.884(2); Ru1-O2 2.072(3); Ru1-O3 2.091(3); Ru1-Ru1'A 3.258(1).

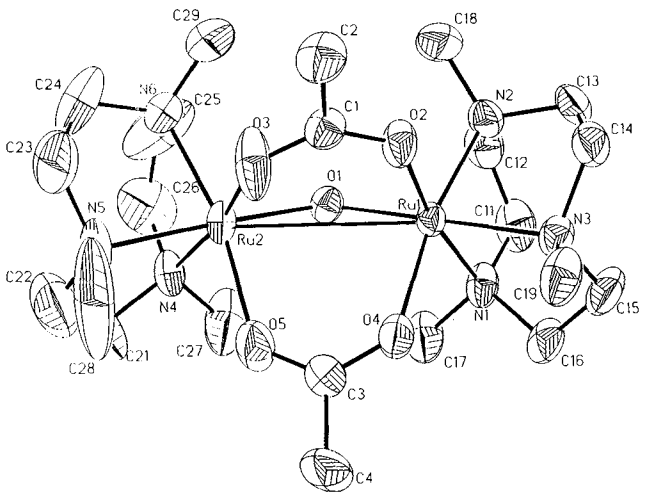

Fig. 3. Molecular structure of the cation of **3**. Selected distances [Å]: Ru1-N1 2.098(5); Ru1-N2 2.086(7); Ru1-N3 2.137(7); Ru2-N4 2.089(6); Ru2-N5 2.143(8); Ru2-N6 2.105(7); Ru1-O1 1.837(5); Ru1-O2 2.059(4); Ru1-O4 2.070(6); Ru2-O1 1.849(5), Ru2-O3 2.039(5); Ru2-O5 2.051(5); Ru1-Ru2 3.342(1).

centers are linked by one oxo and two acetato bridges (face-sharing octahedra having idealized C_{2v} symmetry of the $[N_6Ru_2(\mu\text{-}O)(\mu\text{-}CH_3CO_2)_2]$ skeleton), and all Ru centers are coordinated facially to an amine ligand. The corresponding Ru–N and Ru–O distances in **3** are identical within the limits of experimental error for both of the Ru centers. This is not due to crystallographic symmetry; it points to a delocalization of the valences in **3**.[14] The one-electron oxidation of **1** to **3** leads to a small but significant shortening of all Ru–O and Ru–N distances (0.041 and 0.022 Å, respectively); *however, the Ru–Ru distance increases by 0.084 Å*. This is remarkable and is not in accordance with expectations based on a simple model of bonding (see above). The same effect was observed in the molybdenum complexes **5** and **6** (Δ(Mo···Mo) = 0.084 Å) (Table 1). In these cases, however, the presence of a Mo–Mo bond is unambiguously supported by the metal–metal distance, which is 0.37 Å shorter in each case than those in the Ru complexes **1** and **3**.

According to the bonding analyses of *McCarley* et al.,[6] *Hoffmann* et al.,[7] and *Cotton* et al.,[8] overlapping of the t_{2g} metal orbitals in face-sharing octahedra leads to the formation of one σ and two π bonds (*non* degenerate in C_{2v})

4 $[L_2Mo_2(\mu\text{-}OH)(\mu\text{-}CH_3CO_2)_2][ClO_4]_3 \cdot H_2O$
5 $[L_2Mo_2(\mu\text{-}O)(\mu\text{-}CH_3CO_2)_2][ClO_4][BF_4] \cdot H_2O$
6 $[L_2Mo_2(\mu\text{-}O)(\mu\text{-}CH_3CO_2)_2][ClO_4]_3 \cdot H_2O$
7 $[\{HB(pz)_3\}_2Fe_2(\mu\text{-}OH)(\mu\text{-}CH_3CO_2)_2][ClO_4] \cdot 0.5\,CH_2Cl_2$
8 $[L_2Fe_2(\mu\text{-}O)(\mu\text{-}CH_3CO_2)_2][ClO_4]_2 \cdot H_2O$

Table 1. Structural parameters of selected complexes containing $[M_2(\mu\text{-}O)(\mu\text{-}CH_3CO_2)_2]^{n\oplus}$ and $[M_2(\mu\text{-}OH)(\mu\text{-}CH_3CO_2)_2]^{m\oplus}$ structural elements [a].

Complex	M-$O_{oxo/hydroxo}$ [Å]	M-N_{trans} [Å] [b]	M-N_{cis} [Å] [c]	M-O-M [°]	M-M [Å]	Ref.
2	1.884	2.168	2.110	119.7	3.258	this work
3	1.843	2.140	2.094	130.1	3.342	this work
4	2.090	2.197	2.196	115.4	3.555	[3]
5	1.945	2.294	2.253	95.7	2.885	[3]
6	1.920	2.256	2.208	101.3	2.969	[3b]
7	1.956	2.102	2.102	123.1	3.439	[12]
8	1.800	2.268	2.198	119.7	3.120	[1a]

[a] Bond lengths are average values except for the M–M distance. [b] M–N distance *trans* to M-$O_{oxo/hydroxo}$ bond. [c] M–N distance *cis* to $O_{oxo/hydroxo}$ bond.

between the two metal centers. In the molybdenum complexes **5** and **6** (see Table 1), Mo–Mo bonds of bond order 3 ($\sigma^2\pi^4$) and 2.5 ($\sigma^2\pi^3$), respectively, are present. Complex **1** has a Ru–Ru single bond ($\sigma^2\pi^4\pi^{*4}$); **3** should have a bond order of 1.5 ($\sigma^2\pi^4\pi^{*3}$). On going from **1** to **3**, a shortening of the Ru–Ru bond should therefore be observed. On going from **4** to **5**, a lengthening of the Mo–Mo distance was found, as expected.

The Ru···Ru interactions in **1** and **3** are weak. The diamagnetism of **1** is unusual and may be regarded as an indication for a Ru···Ru bond ($\sigma^2\pi^4\pi^{*4}$), since the known Ru^{III}–O–Ru^{III} complexes show antiferromagnetic coupling.[9] Complexes **1** and **3** are borderline cases for direct metal–metal bonds. It is not easy to explain why the Ru–Ru distance in **3** is greater than in **1**.[10]

In the protonated form **2**, the Ru-$O_{hydroxo}$ bonds are probably longer than the Ru-O_{oxo} bonds in **1**. In the analogous hydroxo/oxo complexes of Mo^{III}, **4** and **5**, as well as of Fe^{III}, **7** and **8**, a lengthening of the M–O bonds by 0.145 and 0.156 Å, respectively, is observed (Table 1). Lengthening of the Ru–O bond in **2** leads to a greater Ru–Ru distance in **2** than in **1** and the weak Ru–Ru bond in **1** is broken upon protonation to give **2**. Accordingly, an intramolecular antiferromagnetic coupling of the two Ru^{III} centers is observed in **2**.

Interestingly, the Os···Os distance in *Walton*'s diamagnetic complex cation $[Os_2^{IV}(\mu\text{-}O)(\mu\text{-}CH_3CO_2)_2]^{4\oplus}$ is 3.440 Å;[13] it is thus 0.098 Å longer than the Ru–Ru bond in **3**. Therefore, an Os–Os double bond ($\sigma^2\pi^4\pi^{*2}$) is ruled out.

Experimental Procedure

$LRuCl_3 \cdot H_2O$: *N,N',N''*-Trimethyl-1,4,7-triazacyclononane(L) (0.8 g, 8 mmol) was added to a suspension of $[Ru^{II}Cl_2(dmso)_4]$ in 25 mL of absolute ethanol. The reaction solution was stirred at 60°C for 30 min and then heated at reflux for 2 h. After removal of the solvent, the red-orange residue was dissolved in 20 mL of concentrated hydrochloric acid and heated at reflux for 30 min, resulting in the formation of orange microcrystals of the product. After combination of the filtrates, additional product was obtained (yield: ca. 60%).—UV/VIS (CH_3CN): $\lambda = 397$ nm ($\varepsilon = 2260\ M^{-1}\ cm^{-1}$), 340 (sh), 300 (1300). Magnetic moment: $\mu_{eff}(293\ K) = 2.35\,\mu_B$.

1: A suspension of $LRuCl_3 \cdot H_2O$ (0.25 g, 0.6 mmol) in 15 mL of an aqueous solution containing 1 g of NaOAc was heated at reflux for 30 min. $NaPF_6$ (0.75 g) in 20 mL of H_2O was then added to the violet, hot solution. At 0°C, violet crystals of **1** formed. Recrystallization from H_2O (yield: 85%).

2: **1** (0.10 g, 0.1 mmol) was dissolved in 5 mL of 2 M HCl at 20°C, whereby the reaction solution turned from violet to green. After addition of $NaPF_6$ (0.15 g) in 5 mL of 2 M HCl, green **2** precipitated at 0°C (yield: 95%).

3: $Na_2S_2O_8$ (0.10 g) in 2 mL of H_2O was added to a solution of **1** (0.15 g, 0.15 mmol) in 10 mL of H_2O, whereby the reaction solution turned from violet to brown. After addition of $NaPF_6$ (0.20 g) in 3 mL of H_2O, brown **3** precipitated (yield: 94%). Single crystals of $[L_2Ru(\mu\text{-}O)(\mu\text{-}CH_3CO_2)_2][ClO_4]_2[PF_6]$ suitable for crystal structure analysis were grown from aqueous solutions of **3** following addition of $NaClO_4 \cdot H_2O$.

All complexes gave correct elemental analyses (C, H, N, Ru).

Received: March 23, 1988 [Z 2676 IE]
German version: *Angew. Chem. 100* (1988) 990

CAS Registry numbers:
1 $[PF_6]_2 \cdot 0.5\ H_2O$, 115140-45-9; **2** $[PF_6]_3$, 115140-47-1; **3** $[PF_6]_3$, 115140-49-3; **3** $[PF_6][ClO_4]_2$, 115140-51-7; $LRuCl_3$, 115140-50-6; $[RuCl_2(dmso)_4]$, 89395-66-4; Ru, 7440-18-8.

[1] a) J. R. Hartman, R. L. Rardin, P. Chaudhuri, K. Pohl, K. Wieghardt, B. Nuber, J. Weiss, G. C. Papaefthymiou, R. B. Frankel, S. J. Lippard, *J. Am. Chem. Soc. 109* (1987) 7387; b) S. J. Lippard, review: *Angew. Chem. 100* (1988) 353; *Angew. Chem. Int. Ed. Engl. 27* (1988) 344.

[2] a) K. Wieghardt, U. Bossek, D. Ventur, J. Weiss, *J. Chem. Soc. Chem. Commun. 1985*, 347; b) K. Wieghardt, U. Bossek, J. Bonvoisin, P. Beauvillain, J. J. Girerd, B. Nuber, J. Weiss, J. Heinze, *Angew. Chem. 98* (1986) 1026; *Angew. Chem. Int. Ed. Engl. 25* (1986) 1030; c) J. E. Sheats, R. S. Czernuszewicz, G. C. Dismukes, A. L. Rheingold, V. Petrouleas, J. Stubbe, W. H. Armstrong, R. H. Beer, S. J. Lippard, *J. Am. Chem. Soc. 109* (1987) 1435.

[3] a) A. Neves, U. Bossek, K. Wieghardt, B. Nuber, J. Weiss, *Angew. Chem. 100* (1988) 718; *Angew. Chem. Int. Ed. Engl. 27* (1988) 685; b) K. Wieghardt, U. Bossek, A. Neves, B. Nuber, J. Weiss, unpublished.

[4] Redox potentials were measured versus an Ag/AgCl reference electrode (sat. LiCl, C_2H_5OH) and referred to NHE by subtraction of 140 mV.

[5] **2**: Syntex R3 diffractometer, $Mo_{K\alpha}$ radiation, graphite monochromator. Orthorhombic space group *Ibca* (D_{2h}^{27}, No. 73), $a = 13.631(4)$, $b = 14.992(8)$, $c = 35.465(14)$ Å, $V = 7247.5$ Å^3, $\rho_{calcd} = 1.79$ g cm^{-3}, $Z = 8$, $T = 22$°C, $\mu(Mo_{K\alpha}) = 10.1$ cm^{-1}. 2880 unique reflections with $I \geq 2.5\sigma(I)$, empirical absorption correction based on ψ scans of seven reflections with $6.6 < 2\theta < 44°$ for a relative transmission of 0.80–1.00, anisotropic temperature factors for all non-hydrogen atoms, H atoms in calculated positions. $R = 0.041$, $R_w = 0.038$, $w = 1/\sigma^2(I)$ for 239 parameters. – **3**: Syntex R3 diffractometer, $Mo_{K\alpha}$ radiation. Monoclinic space group $C2/c$ (C_{2h}^6), $a = 35.270(6)$, $b = 10.661(2)$, $c = 21.650(4)$ Å, $\beta = 114.43(1)°$, $V = 7411$ Å^3, $\rho_{calcd} = 1.83$ g cm^{-3}, $Z = 8$, $T = 22$°C, $\mu(Mo_{K\alpha}) = 10.8$ cm^{-1}. 5243 unique reflections with $I \geq 2.5\sigma(I)$, empirical absorption correction based on ψ scans of seven reflections with $2.7 < 2\theta < 20.4°$ for a relative transmission of 0.82–1.00, anisotropic temperature factors for all non-hydrogen atoms, H atoms in calculated positions. $R = 0.052$, $R_w = 0.047$, $w = 1/\sigma^2(I)$ for 488 parameters.–Further details of the crystal structure investigation may be obtained from the Fachinformationszentrum Energie, Physik, Mathematik GmbH, D-7514 Eggenstein-Leopoldshafen 2 (FRG), on quoting the depository number CSD-53092, the names of the authors, and the journal citation.

[6] J. L. Templeton, W. C. Dorman, J. C. Clardy, R. E. McCarley, *Inorg. Chem. 17* (1978) 1263.

[7] R. H. Summerville, R. H. Hoffmann, *J. Am. Chem. Soc. 101* (1979) 3821.

[8] F. A. Cotton, D. A. Ucko, *Inorg. Chim. Acta 6* (1972) 161.

[9] See, for example: a) T. R. Weaver, T. J. Meyer, S. A. Adeyemi, G. M. Brown, R. P. Eckberg, W. E. Hatfield, E. C. Johnson, R. W. Murray, D. Untereker, *J. Am. Chem. Soc. 97* (1975) 3039; b) D. W. Phelps, E. M. Kahn, D. J. Hodgson, *Inorg. Chem. 14* (1975) 2486.

[10] Similar behavior was observed for the complexes $[Tc_2Cl_8]^{3\ominus}$ and $[Tc_2Cl_8]^{2\ominus}$. The Tc–Tc distance in the reduced form ($\sigma^2\pi^4\delta^2\delta^{*1}$ Tc–Tc bond) is 0.030 Å *shorter* than in the oxidized form ($\sigma^2\pi^4\delta^2$ Tc–Tc bond), although in $[Tc_2Cl_8]^{3\ominus}$ one electron occupies an antibonding δ^* MO [11].

[11] F. A. Cotton, L. Daniels, A. Davison, C. Orvig, *Inorg. Chem. 20* (1981) 3051.

[12] W. H. Armstrong, S. J. Lippard, *J. Am. Chem. Soc. 106* (1984) 4632.

[13] J. E. Armstrong, W. E. Robinson, R. A. Walton, *Inorg. Chem. 22* (1983) 1301.

[14] A statistical disorder of the cations in **3** is also possible. This would lead to apparent equivalence of the delocalized Ru^{III}/Ru^{IV} valences. In the electronic spectrum of **3** an intervalence absorption is observed at 1590 nm ($\varepsilon = 276$ L mol^{-1} cm^{-1}). Therefore, a delocalized description with two Ru centers in the oxidation state +3.5 is preferable.

"Wittig Reactions" of Unsaturated Silicon Compounds >Si=Y: Isolation and Structure of Possible Intermediates**

By *Nils Wiberg,** *Klaus Schurz, Gerhard Müller,** and *Jürgen Riede*

Dedicated to Professor Heinrich Nöth on the occasion of his 60th birthday

When unsaturated silicon compounds >Si=Y of the type >Si=C< (silaethenes) or >Si=N– (silanimines) are generated in the presence of nonenolizable aldehydes or ketones, mutual exchange of Y and O occurs to give polysiloxanes and ethenes >C=C< or imines >C=N–, respectively (Scheme 1), the reaction possibly proceeding via a pseudo-Wittig mechanism involving **1** or **2**, respectively, and >Si=O (silanones).[2–4]

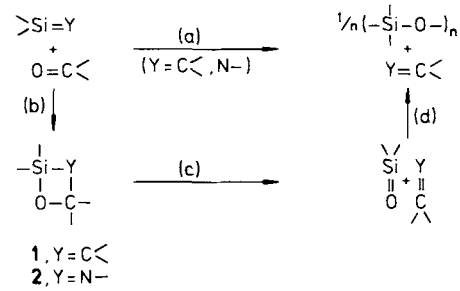

Scheme 1.

Attempts to prove the existence of the postulated intermediates **1** and **2** (oxasila- and oxaazasilacyclobutanes) were initially unsuccessful.[5,6] Several years ago, however, we obtained, for the first time, an oxasilacyclobutane as the [2+2] cycloadduct of benzophenone with the unstable silaethene $Me_2Si{=}C(SiMe_3)_2$.[7] By reaction of the sterically congested and therefore metastable silanimine $tBu_2Si{=}N{-}SitBu_3$[11] with benzaldehyde in pentane at –125°C, we have now also succeeded in preparing an oxaazasilacyclobutane, **2a**.[12]

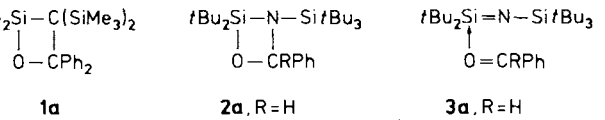

1a | **2a**, R = H; **2b**, R = Ph | **3a**, R = H; **3b**, R = Ph

The question then arose as to the mechanism of formation of **1** and **2** (Eq. (b) in Scheme 1).[13] The [2+2] cycloaddition reaction of carbonyl compounds with >Si=Y compounds can occur in one or two steps,[2,3] the initial step in the latter case being possibly the formation of a bond between Si and O or between Y and C. We obtained evidence supporting the two-step mechanism with initial formation

[*] Prof. Dr. N. Wiberg, Dr. K. Schurz
Institut für Anorganische Chemie der Universität
Meiserstrasse 1, D-8000 München 2 (FRG)
Dr. G. Müller, J. Riede
Anorganisch-chemisches Institut der
Technischen Universität München
Lichtenbergstrasse 4, D-8046 Garching (FRG)

[**] Unsaturated Silicon Compounds, Part 29, and Compounds of Silicon and Its Group Homologues, Part 81.—Parts 28 and 80: [1].

of a Si–O bond when we allowed tBu$_2$Si=N–SitBu$_3$[11] to react with benzophenone in diethyl ether. A potential precursor of **2** having constitution **3b**, according to the X-ray structure analysis (see below), was thereby isolated.

Adduct **3b** forms dark red, hydrolytically labile crystals from pentane at -78 °C;[14] it is readily soluble in diethyl ether and moderately soluble in pentane and benzene, but dissolves in tetrahydrofuran (THF) only with replacement of Ph$_2$C=O by THF. There are obvious steric reasons why **3b** is stable toward transformation to the [2+2] cycloadduct at room temperature, whereas other addition compounds such as Me$_2$Si=C(SiMe$_3$)$_2$·Ph$_2$C=O and **3a**[15] undergo spontaneous transformation to the corresponding [2+2] cycloadducts even at very low temperatures.

Gentle warming (60–80 °C) of a dark red benzene solution of **3b** results in dissociation of **3b** to form a lighter solution of the educts tBu$_2$Si=N–SitBu$_3$ (pale yellow) and Ph$_2$C=O. Thus, **3b** does not rearrange to the [2+2] cycloadduct **2b**. Cooling of the solution results once again in the formation of **3b**. When benzophenone is used as solvent, the thermal dissociation is suppressed so that such solutions remain initially dark red even at 90 °C. Since, under these conditions, **3b** is transformed slowly into uncharacterized products, however, solutions of **3b** in benzophenone also turn lighter within a few hours. In this case, cooling does not result in reappearance of the dark red color.

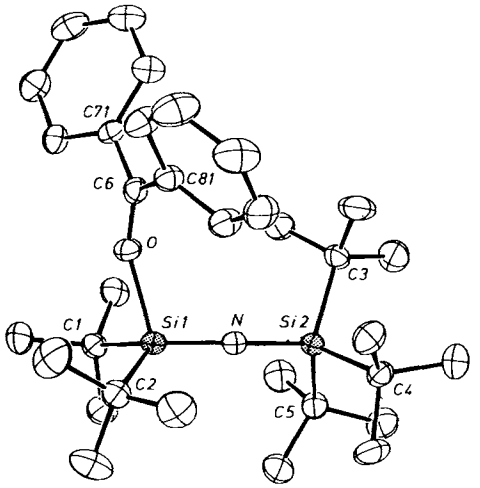

Fig. 1. Molecular structure of **3b** (ORTEP, displacement ellipsoids 50%, without H atoms). The silyl group Si2 is slightly displaced backwards out of the plane of the figure (Si1-N-Si2 169.3(2)°). Important distances [Å] and angles [°]: Si1-N 1.601(2), Si2-N 1.678(2), Si1-O 1.927(2), Si1-C1 1.930(3), Si1-C2 1.923(3), Si2-C3 1.950(3), Si2-C4 1.961(3), Si2-C5 1.961(3), O-C6 1.254(3); O-Si1-N 106.9(1), O-Si1-C1 91.3(1), O-Si1-C2 102.5(1), N-Si1-C1 120.4(1), N-Si1-C2 117.5(1), C1-Si1-C2 112.4(1), Si1-O-C6 153.7(2).

The X-ray structure analysis[16] reveals that **3b** may be regarded as a loose benzophenone adduct at the unsaturated Si atom of the silanimine tBu$_2$Si=N–SitBu$_3$ (Fig. 1). This is shown especially by the unusually long Si–O bond (1.927(2) Å, compared with a normal value of 1.55–1.75 Å[17]), the comparably short C–O distance (1.254(3) Å, compared with 1.231 Å in Ph$_2$C=O[18]), and the incompletely attained tetrahedral geometry of the unsaturated Si atom Si1 (trigonal-planar geometry in free silanimine[11]). The addition is associated with a slight lengthening of the N=Si1 bond (from 1.568(3) Å to 1.601(2) Å); on the other hand, the N–Si2 bond becomes somewhat shorter and the valence angle at the N atom decreases from 177.8(2)° to 169.3(2)°.

Received: December 18, 1987;
revised: February 12, 1988 [Z 2546 IE]
Publication delayed at authors' request
German version: *Angew. Chem. 100* (1988) 979

[1] N. Wiberg, K. Schurz, *Chem. Ber. 121* (1988) 581.
[2] Reviews: L. E. Gusel'nikov, N. S. Nametkin, V. M. Vdovin, *Acc. Chem. Res. 8* (1975) 18; L. E. Gusel'nikov, N. S. Nametkin, *Chem. Rev. 79* (1979) 529; G. Raabe, J. Michl, *ibid. 85* (1985) 419.
[3] Silaethenes + oxo compounds: D. N. Roark, L. H. Sommer, *J. Organomet. Chem. 66* (1974) 29; R. D. Bush, C. M. Golino, G. D. Homer, L. H. Sommer, *ibid. 80* (1974) 37.
[4] Silanimines + oxo compounds: C. M. Golino, R. D. Bush, L. H. Sommer, *J. Am. Chem. Soc. 96* (1974) 614; D. R. Parker, L. H. Sommer, *J. Organomet. Chem. 110* (1976) C 1.
[5] Review: T. J. Barton, *Pure Appl. Chem. 52* (1980) 615.
[6] T. J. Barton, G. P. Hussmann, *Organometallics 2* (1983) 692.
[7] A compound synthesized later than **1a** [8] and falsely reported as the first oxasilacyclobutane [9] has in the meantime been placed in doubt by other researchers [6]. For other known oxasilacyclobutanes, cf. [10].
[8] Preliminary communication: N. Wiberg, G. Preiner, O. Schieda, *Chem. Ber. 114* (1981) 3518.
[9] W. Ando, A. Sekiguchi, T. Sato, *J. Am. Chem. Soc. 104* (1982) 6830.
[10] G. Märkl, M. Horn, *Tetrahedron Lett. 24* (1983) 1477; A. G. Brook, W. J. Chatterton, J. F. Sawyer, D. W. Hughes, K. Vorspohl, *Organometallics 6* (1987) 1246.
[11] N. Wiberg, K. Schurz, G. Reber, G. Müller, *J. Chem. Soc. Chem. Commun. 1986*, 591.
[12] **2a**: M.p. = 104 °C; dec. > 150 °C; ^{1}H-NMR (C_6D_6): δ = 1.10 (s, SitBu$_3$), 1.36/1.41 (s/s, SitBu$_2$), 6.58 (s, CH), 7.12/7.77 (m, Ph); ^{13}C{^{1}H}-NMR (C_6D_6): δ = 23.9 (3 *C*Me), 26.1/28.4 (2 *C*Me$_3$), 29.1/30.8 (2 C*Me*$_3$), 31.8 (3 C*Me*$_3$), 95.0 (CH), 127.7/129.1/129.8/145.3 (Ph); ^{29}Si-NMR (C_6D_6): δ = 2.40 (SitBu$_3$), 26.2 (SitBu$_2$).
[13] Remark on the mechanism of decomposition of **1** and **2**: Increasing bulkiness of the substituents of **1** and **2** increases the stability of the compounds. This is evidence against the intermediary formation of silanones in the transformation of **1** and **2** to polysiloxanes: N. Wiberg, K. Schurz, unpublished results.
[14] **3b**: ^{1}H-NMR (C_6D_6): δ = 1.14 (s, SitBu$_2$), 1.36 (s, SitBu$_3$), 7.08/7.69 (m/m, 2 Ph); ^{13}C{^{1}H}-NMR (C_6D_6): δ = 23.5 (5 *C*Me$_3$), 29.6 (2 C*Me*$_3$), 31.5 (3 C*Me*$_3$), 128.3/130.2/132.1/138.3 (2 Ph), 196.0 (CO); ^{29}Si-NMR (C_6D_6): δ = −9.6 (SitBu$_3$), 54.2 (SitBu$_2$).
[15] Evidence for the formation of an intermediate **3a** during the reaction of tBu$_2$Si=N–SitBu$_3$ with PhHC=O is provided by the deep blue color, which appears immediately after the addition of the first drop of PhHC=O to a pentane solution of the silanimine at −125 °C and disappears shortly after addition of the last drop.
[16] Crystal structure data: $C_{33}H_{55}NOSi_2$, monoclinic, space group $P2_1/n$, a = 13.247(2), b = 15.689(2), c = 17.073(2) Å, β = 110.53(1)°, V = 3323.0 Å^3, ρ_{calcd} = 1.075 g cm^{-3}, μ(Mo$_{K\alpha}$) = 1.3 cm^{-1}, Z = 4. 5179 unique reflections up to (sinθ/λ) = 0.571, 3789 with $F_0 \geq 2.0\sigma(F_0)$ (Enraf-Nonius CAD4, Mo$_{K\alpha}$ radiation, λ = 0.71069 Å, T = −45 °C). Solution by direct methods (SHELXS-86). $R(R_w)$ = 0.050 (0.039), $w = 1/\sigma^2(F_0)$ for 379 refined parameters (anisotropic, H constant, CH$_3$ as rigid groups, SHELX-76). $\Delta\rho_{fin} = \pm 0.27$ e Å^{-3}. Further details of the crystal structure investigation may be obtained from the Fachinformationszentrum Energie, Physik, Mathematik GmbH, D-7514 Eggenstein-Leopoldshafen 2 (FRG), on quoting the depository number CSD-52884, the names of the authors, and the journal citation.
[17] Cf. N. Wiberg, G. Wagner, G. Müller, J. Riede, *J. Organomet. Chem. 271* (1984) 381, and references cited therein.
[18] E. B. Fleischer, N. Sung, S. Hawkinson, *J. Phys. Chem. 72* (1968) 4311.

Diisocyanogen**

By *Thomas van der Does* and *Friedrich Bickelhaupt**

The cyano radical CN$^\odot$ could combine with other radicals R$^\odot$ by bond formation at C or N, resulting in either nitriles RCN or isonitriles RNC.[1,2] It dimerizes only

[*] Prof. Dr. F. Bickelhaupt, Drs. T. van der Does
Scheikundig Laboratorium, Vrije Universiteit
De Boelelaan 1083, NL-1081 HV Amsterdam (The Netherlands)

[**] We thank *R. F. Schmitz*, Amsterdam, for carrying out the difficult recording of the mass spectrum.

through carbon, however, to give cyanogen **1**, which has been known since 1815;[3] to the best of our knowledge, the isomeric cyanoisocyanide NCNC **2** and diisocyanogen CNNC **3** have been prepared neither by $CN^{\ominus}$ dimerization nor via other routes. Theoretical calculations[4] may provide an explanation for these observations; **2** and **3** are about 17 and 65 kcal mol^{-1}, respectively, less stable than **1**. Our research on phosphaalkenes,[5a] in particular 7-norbornadienylidenephosphane,[5b] prompted us to investigate the corresponding nitrogen analogues. This work led to the first synthesis of **3**, the least stable by far of the three isomers, namely by cheletropic elimination from the azine **6**.

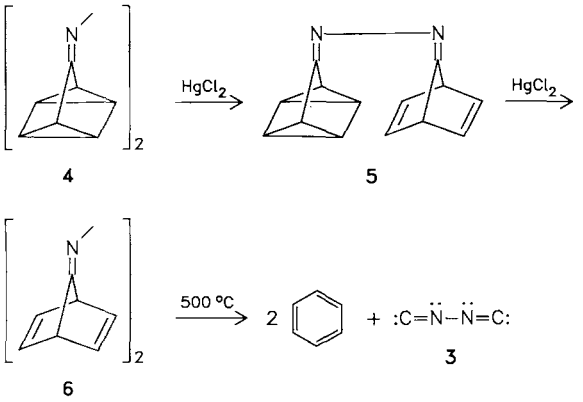

Cheletropic eliminations proceed extremely smoothly for norbornadienes if, in addition to benzene, a second stable fragment is formed.[6] In the case of norbornadienones, the second species is the extremely stable carbon monoxide and the fragmentation occurs even below −70°C. In contrast, aryl isocyanides are eliminated from *N*-arylnorbornadien-7-ylidenamines at 20–80°C[5b,6d] and from benzonorbornadiene derivatives at ca. 120°C.[7] This approach can be used to synthesize **3** from **6** as starting material. We obtained **6** in 65% yield by catalytic isomerization of **4**;[6d,8] the catalyst employed, sublimate, was reported by *Rood* and *Klumpp* to be particularly well-suited for the rearrangement of quadricyclanes to norbornadienes.[9] As expected, the isomerization of **4** to **6** proceeds stepwise via **5**, which could be detected in the reaction mixture by ^{1}H-NMR spectroscopy.

In solution ([D_8]toluene) **6** decomposes above 80°C with polymerization; neither benzene nor other soluble products are formed. Therefore, **6** was subjected to flash vacuum pyrolysis and the products were collected in a trap cooled with liquid nitrogen. At 300–450°C a nearly quantitative mixture of **6**, benzene, and **3** was obtained. The monofragmentation product *N*-isocyanonorbornadien-7-ylidenamine was not found. Above 500°C the reaction of **6** was complete. Since **3** decomposes above −30°C with formation of a brown polymer,[10] the volatile products were condensed at low temperature along with [D_8]toluene in an NMR tube cooled with liquid nitrogen. At −65°C, only the resonance of benzene ($\delta = 7.07$) was observed in the ^{1}H-NMR spectrum; in the ^{13}C-NMR spectrum the resonance of benzene ($\delta = 128.5$) was observed along with a resonance at $\delta = 172$, which vanished at −30°C. We assign this signal to the C atoms of **3**, since it lies in the region characteristic of isocyanides.[13] The ^{13}C-NMR resonance of **1**, which, to the best of our knowledge, has not been previously measured, was found at $\delta = 93$. The ^{13}C-NMR signal of **3** is sharp ($\Delta\nu_{1/2} = 1.2$ Hz) and does not exhibit the ^{14}N coupling usually observed for isocyanides.[14] In the ^{14}N-NMR spectrum,[14] **3** ($\delta = -239$, external standard $MeNO_2$ ($\delta = 0$)) also differs in a characteristic fashion from **1** ($\delta = -118$);[15] here, too, the signal of **3** vanishes above −30°C. The identity of **3** was corroborated by mass spectroscopy (see Experimental Procedure). The molecular ion $C_2N_2^{\odot\oplus}$ is the base peak and the intensities of the fragment ions differ significantly from those observed for $\mathbf{1}^{\odot\oplus}$.[16]

Owing to its high volatility, its ready decomposition in solution, and its spectral data, the new compound can be unambiguously identified as diisocyanogen **3**. The reactivity of this new species is currently being investigated. Noteworthy, however, is the high thermal stability of **3** in the gas phase. Normally, isonitriles undergo rearrangement at temperatures above 200°C to the corresponding nitriles;[17] in contrast, **3** affords no **1**, even at 500°C. This surprising stability of the N–N bond of **3** can be explained by its theoretically predicted double-bond character.[4]

Experimental Procedure

6: A solution of **4** (340 mg, 1.63 mmol) [6d, 8] and $HgCl_2$ (200 mg, 0.74 mmol) in 25 mL of chloroform was stirred for 24 h. After removal of the solvent under vacuum, the residue was extracted with toluene and the filtrate was evaporated. The residue was sublimed (50–60°C, 10^{-5} mbar) and afforded 222 mg (1.07 mmol, 65%) of **6** as colorless crystals (m.p. = 140–142°C (dec)).—MS (70 eV): *m/z* 208 (5%; high resolution, found 208.1005, calcd 208.1000), 130 (8%), 104 (30%), 78 (100%), 77 (32%).—^{1}H-NMR ($CDCl_3$, 250 MHz): $\delta = 6.88$ (m, 4H), 6.79 (m, 4H), 4.47 (m, 2H), 4.01 (m, 2H).—^{13}C-NMR ($CDCl_3$, 62.89 MHz): $\delta = 180.1$ (s), 139.7 (d, $^1J(CH) = 178.5$ Hz), 138.5 (d, $^1J(CH) = 178.5$ Hz), 51.6 (d, $^1J(CH) = 153$ Hz), 47.6 (d, $^1J(CH) = 156$ Hz). ^{1}H–^{13}C double resonance experiments confirmed the expected couplings.—Correct C,H,N analyses.—If the reaction mixture is evaporated after about 3 h, and the residue dissolved in $CDCl_3$, then, in addition to the signals of **4** and **6**, those of **5** are observed in the ^{1}H-NMR spectrum: **5**: $\delta = 6.95$ (m, 2H), 6.89 (m, 2H), 4.76 (m, 1H), 4.09 (m, 1H), 2.05 (br. s, 5H), 1.57 (m, 1H).

3: **6** (100 mg, 0.48 mmol) was heated at 50–60°C and 10^{-5} mbar in a flash vacuum pyrolysis apparatus [18] and underwent sublimation over ca. 30 h through a hot tube (aluminum oxide, 25-cm length, 1.5-cm diameter, 500°C). The products were collected in a cold trap (liquid nitrogen). The cold trap was then removed from the cooling bath and the volatile products (**3**, benzene) were distilled into a second trap cooled with liquid nitrogen. *n*-Pentane was distilled into the trap and the mixture was slowly heated. At −30°C brown flakes began to separate out; this process was complete after several hours at 0°C. After removal under vacuum of pentane and benzene, 14 mg of a brown powder (assumed to be $(CN)_x$ [10], 60% yield) was obtained. In order to record the NMR spectra, the volatile products were collected (as described above) in an NMR tube sealed to the apparatus, followed by distillation of [D_8]toluene into the tube, which was then sealed.—In order to carry out the mass spectral studies, the pyrolysate was distilled into a tube (see above) cooled with liquid nitrogen and connected via a capillary with the direct inlet of a Varian MAT CH-5-DF mass spectrometer, followed by warming of the pyrolysate using a cryostat. Above −140°C the signals of **3** (without benzene signals) were recorded; above −100°C the signals of benzene were also observed. MS (70 eV): *m/z* 52 (100%; high-resolution; found 52.0059, calcd 52.0061), 53 (2.7%), 38 (2.7%), 26 (14%), 24 (23%).

Received: February 8, 1988;
supplemented: March 21, 1988 [Z 2610 IE]
German version: *Angew. Chem. 100* (1988) 998

CAS Registry numbers:
3, 114861-40-4; **4**, 53414-44-1; **5**, 114861-38-0; **6**, 114861-39-1; benzene, 71-43-2.

[1] Z. Rappoport (Ed.): *The Chemistry of the Cyano Group*, Wiley, London 1970.
[2] G. Tennant, *Compr. Org. Chem. 1979*, No. 2, p. 385.
[3] L. J. Gay-Lussac, *Ann. Chim. (Paris) 95* (1815) 175.
[4] M. Sana, G. Leroy, *J. Mol. Struct. 76* (1981) 259.
[5] a) T. van der Does, F. Bickelhaupt, *Phosphorus Sulfur 30* (1987) 515; b) T. van der Does, unpublished results.
[6] a) R. B. Woodward, R. Hoffmann, *Angew. Chem. 81* (1969) 797; *Angew. Chem. Int. Ed. Engl. 8* (1969) 781, and references cited therein; b) R. W. Hoffmann, *Angew. Chem. 83* (1971) 595; *Angew. Chem. Int. Ed. Engl. 10* (1971) 529; C. W. L. Mock in A. P. Marchand, R. E. Lehr (Eds.): *Pericyclic Reactions, Vol. B*, Academic Press, New York 1977, p. 141; d) A. Riemann, R. W. Hoffmann, *Chem. Ber. 118* (1985) 2544; e) R. W. Hoffmann, W. Barth, R. Schüttler, B. Mayer, *ibid. 119* (1986) 3297.

[7] R. S. Atkinson, M. J. P. Harger, *J. Chem. Soc. Perkin Trans. 1 1974*, 2619, and references cited therein.
[8] H. Sauter, H.-G. Hörster, H. Prinzbach, *Angew. Chem. 85* (1973) 1106; *Angew. Chem. Int. Ed. Engl. 12* (1973) 991.
[9] I. D. C. Rood, G. W. Klumpp, *Recl. J. R. Neth. Chem. Soc. 103* (1984) 303.
[10] The elemental analysis (found C 50.16, H 2.12, N 41.37; $(CN)_x$ calcd C 46.14, N 53.86) merely reveals that the ratio C : N (1.4 : 1) roughly corresponds to the value expected; possibly, other substances are present. The brown paracyanogen $(CN)_x$ [11] formed from **1** at higher temperatures is also difficult to analyze [11b]. It should be noted here that diisocyanomethane $CH_2(NC)_2$, like **3**, polymerizes at $-30°C$ [12].
[11] a) T. K. Brotherton, J. W. Lynn, *Chem. Rev. 59* (1959) 841; b) L. L. Bircumshaw, F. M. Tayler, D. H. Whiffen, *J. Chem. Soc. 1954*, 931.
[12] R. Neidlein, *Angew. Chem. 76* (1964) 440; *Angew. Chem. Int. Ed. Engl. 3* (1964) 382.
[13] R. W. Stephany, M. J. A. de Bie, W. Drenth, *Org. Magn. Res. 6* (1974) 45.
[14] B. E. Mann in R. K. Harris, B. E. Mann (Eds.): *NMR and the Periodic Table*, Academic Press, London 1983, S. 96, and references cited therein.
[15] D. Herbison-Evans, R. E. Richards, *Mol. Phys. 8* (1964) 19.
[16] *NBS Library Compilation*, disk library number 55, Finnigan Corporation, San José, CA, USA 1984.
[17] a) See [1], p. 859; b) W. Reichen, C. Wentrup, *Helv. Chim. Acta 59* (1976) 2618; c) C. Wentrup, U. Stutz, H. J. Wollweber, *Angew. Chem. 90* (1978) 731; *Angew. Chem. Int. Ed. Engl. 17* (1978) 688, and references cited therein.
[18] P. A. Kraakman, E. T. J. Nibbering, W. H. de Wolf, F. Bickelhaupt, *Tetrahedron 43* (1987) 5109, and references cited therein.

Carboxime (Isofulminic Acid)**

By *Günther Maier,* Joaquim Henrique Teles, B. Andes Hess, Jr.,* and *Lawrence J. Schaad*

When, after some controversy (1823–1826),[1] it became clear that silver fulminate (*Liebig*) and silver cyanate (*Wöhler*) have the same composition but different chemical properties, the theoretical interpretation followed inevitably: the phenomenon of isomerism had been observed (*Berzelius*, 1830[1]). The order of the C and N atoms in the two salts is interchanged.[2]

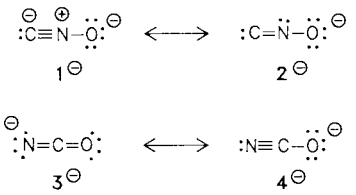

The discussion concerning the free acids **1**–**4** related to the fulminates ($\mathbf{1}^{\ominus} \leftrightarrow \mathbf{2}^{\ominus}$) and cyanates ($\mathbf{3}^{\ominus} \leftrightarrow \mathbf{4}^{\ominus}$) has continued until today: For fulminic acid only dimeric structures were considered initially.[3] *Nef*,[4] in 1894, was the first to recognize the monomeric constitution and ascribed to it the carboxime formula **2**. Seventy more years were to pass until fulminic acid was unequivocally characterized, on the basis of its spectroscopic data (IR[5a,b] and microwave spectrum[5c]), as formonitrile oxide **1** (instead of **2**).

Upon acidification the fulminates furnish exclusively formonitrile oxide **1**, whereas the cyanates give only isocyanic acid **3** (Raman[6a] and IR[6b] spectrum). In agreement with these observations the structural data indicate that resonance structure $\mathbf{1}^{\ominus}$ is the most important one in the case of silver fulminate and that the canonical form $\mathbf{3}^{\ominus}$ is the main contributor in the case of silver cyanate.

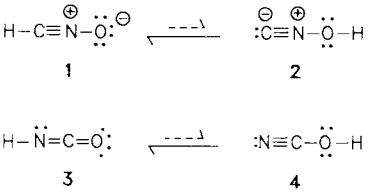

Only with the help of the matrix isolation technique has it been possible to demonstrate the existence of cyanic acid **4** directly.[7] Herein, we report that the last and only missing isomer, namely the real carboxime **2** (isofulminic acid)[8]—altogether there are four "chemically reasonable" linear arrangements (cf. formulas **1**–**4**) for a compound of the formula CHNO—is detectable by the same technique.

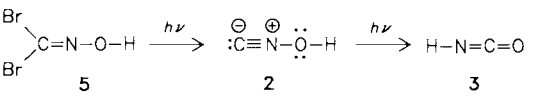

Irradiation of dibromoformoxime **5**[9] in argon at 12 K with a low-pressure mercury lamp leads to disappearance of all IR bands of **5** within 20 minutes, and one obtains the IR spectrum shown in Figure 1, which we assign to the carboxime **2**. Our arguments in support of this assignment are: 1. The new species shows a spectrum different from that of fulminic acid, and even more different from that of isocyanic acid or cyanic acid. 2. The asymmetric stretching vibration of the ONC unit in **2** appears at 2190 cm^{-1}. This

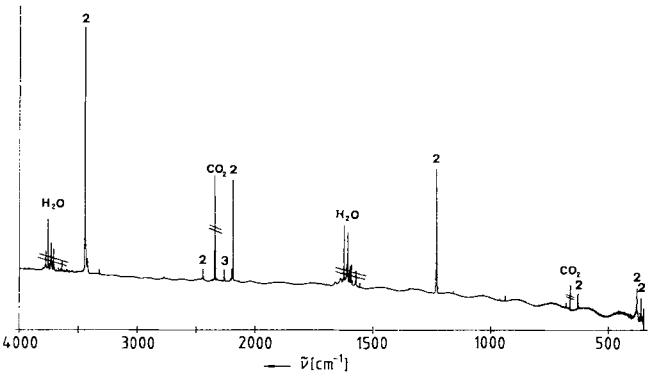

Fig. 1. IR spectrum of isofulminic acid in an Ar matrix at 12 K.

position almost coincides with the position of the corresponding band of fulminic acid **1** (2193 cm^{-1}), but is located at much lower wavelength than the corresponding absorption of isocyanic acid **3** (2260 cm^{-1}) or cyanic acid **4** (2286 cm^{-1}). Calculations also predict that carboxime **2** should show the smallest wave number for this vibration. 3. The difference of 96 cm^{-1} between the wavelengths at

[*] Prof. Dr. G. Maier, Dipl.-Chem. J. H. Teles
Institut für Organische Chemie der Universität
Heinrich-Buff-Ring 58, D-6300 Giessen (FRG)
Prof. Dr. B. A. Hess, Jr., Prof. Dr. L. J. Schaad
Department of Chemistry, Vanderbilt University
Nashville, TN 37235 (USA)

[**] This work was supported by the Deutsche Forschungsgemeinschaft and the Fonds der Chemischen Industrie.—*B. A. H.* and *L. J. S.* thank the National Science Foundation (Grant CHE 8605951) for financial support.

which these absorptions of **4** and **2** appear has also been observed in the spectra of the corresponding esters; the *O*-alkyl derivatives of **2** prepared by *Wentrup* et al.[10] absorb at 2108–2160 cm^{-1}, the cyanates at about 2250 cm^{-1}. 4. The experimental and calculated IR spectra of **2** and its isotopomer [*D*]**2** (Table 1) are in satisfactory agreement, even though the difference is greater than in other cases.[12] 5. On prolonged irradiation (254 nm), the photoproduct of **5** is converted into isocyanic acid.

Table 1. Comparison of the experimental (Ar matrices, 12 K; relative integrated intensities) and calculated IR spectra of **2** and [D]**2**; ν- and δ-absorptions in cm^{-1}.

Assignment	Symmetry	**2**, exp.	**2**, calcd	[D]**2**, exp.	[D]**2**, calcd
$\nu_{OH(OD)}$	A′	3444(1.00)	3803(1.00)	2545(1.00)	2770(1.00)
ν^{as}_{ONC}	A′	2190(0.15)	2139(0.03)	2190(0.13)	2135(0.03)
$\delta_{HON(DON)}$	A′	1232(0.30)	1416(0.69)	903(0.22)	1059(0.88)
ν^{s}_{ONC}	A″	628(0.03)	1001(0.37)	623(0.04)	998(0.52)
δ_{ONC}	A″	379(0.05)[a]	319(0.02)	—	315(0.00)
δ_{ONC}	A′	361(0.03)[a]	274(0.06)	362(0.09)[a]	267(0.10)
$2\times\delta_{HON(DON)}$	A′	2444(0.04)[b]	—	1794(0.03)[b]	—

[a] Assignment may have to be changed. [b] Assignment based on the matrix splitting.

A conceivable alternative is that **5** loses only one halogen atom upon irradiation, resulting in formation of the isomer **6**. This type of reaction has recently been described by us for iodine-containing dihalomethanes.[13a] Dibromomethane **7** could analogously be isomerized to **8**.[13b] This photoisomer shows a strong characteristic UV band at 360 nm. In contrast, no absorption is observed between 250 and 800 nm in the photolysis of **5**. In other words: irradiation of **5** does not lead to **6** but to carboxime **2**.

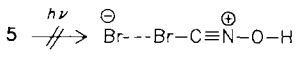

6

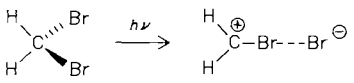

7 **8**

It is no wonder that compound **2** has hitherto evaded direct detection, since it has the highest energy of the four isomers **1**–**4**.

Received: March 7, 1988 [Z 2652 IE]
German version: *Angew. Chem. 100* (1988) 1014

[1] R. Winderlich in G. Bugge (Ed.): *Das Buch der grossen Chemiker, Vol. 2*, Verlag Chemie, Weinheim 1955, p. 6.
[2] X-ray structure analyses of silver fulminate and silver cyanate: a) D. Britton, J. D. Dunitz, *Acta Crystallogr. 19* (1965) 662; b) *ibid. 18* (1965) 424.
[3] Summary: C. Grundmann, P. Grünanger: *The Nitrile Oxides*, Springer, New York 1971, p. 3 ff.
[4] J. U. Nef, *Justus Liebigs Ann. Chem. 280* (1894) 291.
[5] a) W. Beck, K. Feldl, *Angew. Chem. 78* (1966) 746; *Angew. Chem. Int. Ed. Engl. 5* (1966) 722; W. Beck, P. Swoboda, K. Feldl, R. S. Tobias, *Chem. Ber. 104* (1971) 533; b) B. P. Winnewisser, M. Winnewisser, F. Winther, *J. Mol. Spectrosc. 51* (1974) 65; c) M. Winnewisser, H. Bodenseh, *Z. Naturforsch. A 22* (1967) 1724; *ibid. A 24* (1969) 1966, 1973.
[6] a) J. Goubeau, *Chem. Ber. 68* (1935) 912; b) G. Herzberg, C. Reid, *Discuss. Faraday Soc. 9* (1950) 92. In many textbooks the free acid is, as previously, given the wrong structure **4**.
[7] a) M. E. Jacox, D. E. Milligan, *J. Chem. Phys. 40* (1964) 2457; b) V. E. Bondybey, J. H. English, C. W. Mathews, R. J. Contolini, *J. Mol. Spectrosc. 92* (1982) 431.
[8] This molecule is not only of interest in a "local" sense—*Liebig* carried out his investigations on fulminic acid here in Giessen—but also because this species, in analogy to **3**, could occur in intersteller space: G. Winnewisser, E. Herbst, *Top. Curr. Chem. 139* (1987) 119; M. Winnewisser, *Chem. Unserer Zeit 18* (1984) 1, 55.
[9] G. Maier, J. H. Teles, *Angew. Chem. 99* (1987) 152; *Angew. Chem. Int. Ed. Engl. 26* (1987) 155.
[10] C. Wentrup, B. Gerecht, D. Laqua, H. Briehl, H.-W. Winter, H. P. Reisenauer, M. Winnewisser, *J. Org. Chem. 46* (1981) 1046.
[11] Within the context of the naming of the free acids (**1**: fulminic acid, formonitrile oxide; **2**: isofulminic acid, carboxime; **3**: isocyanid acid, cyanic acid) and salts ($\mathbf{1}^{\ominus}\leftrightarrow\mathbf{2}^{\ominus}$: fulminates, $\mathbf{3}^{\ominus}\leftrightarrow\mathbf{4}^{\ominus}$: cyanates) it would be logical to name the esters $R-C\equiv N^{\oplus}-O^{\ominus}$ of fulminic acid fulminates or nitrile oxides and the esters of isofulminic acid isofulminates (and not fulminates [10]) or *O*-alkylcarboximes.
[12] G. Maier, H. P. Reisenauer, W. Schwab, P. Cársky, B. A. Hess, Jr., L. J. Schaad, *J. Am. Chem. Soc. 109* (1987) 5183.
[13] a) G. Maier, H. P. Reisenauer, *Angew. Chem. 98* (1986) 829; *Angew. Chem. Int. Ed. Engl. 9* (1986) 819. The UV spectra of **2a** and **2c** depicted therein (in Fig. 2) must be interchanged; b) G. Maier, H. P. Reisenauer, unpublished.
[14] a) MP2/6-31G** calculations (*B. A. H., L. J. S.*); sequence of the stabilities: **3** > **4** > **1** > **2**; b) cf. also: D. Poppinger, L. Radoc, J. A. Pople, *J. Am. Chem. Soc. 99* (1977) 7806 (**3** > **4** > **1** > **2**); c) A. D. McLean, C. H. Loew, D. S. Berkowitz, *J. Mol. Spectrosc. 64* (1977) 184 (**3** > **4** > **1** ≈ **2**).

Stepwise Synthesis and Crystal Structure of Tricarbonyl[pentakis(methylthio)cyclopentadienyl]-manganese $[\{C_5(SMe)_5\}Mn(CO)_3]$**

By *Karlheinz Sünkel** and *Doris Motz*

Complexes containing cyclopentadienyl ligands substituted with functional groups are an interesting class of compounds.[2] Owing to both their electronic effect and their ability to coordinate further metal fragments, the functional groups can be of great importance for the reactivity, in particular the catalytic activity, of the complex.[3,4] Whereas a large number of metal complexes containing *one* functional group on the cyclopentadienyl ring are known, relatively few examples containing five such substituents R (R = Cl,[5] Br,[6] CO_2Me[7]) have been reported. Although the anions $[C_5(CN)_5]^{\ominus}$[8] and $[C_5(SMe)_5]^{\ominus}$[9] have been known for some time, it has not been possible so far to incorporate them into π complexes. In view of the increased interest in mono- and dichalcogen-substituted ferrocenes,[10] we have developed a stepwise synthesis of the complexes **5** starting from **1**, which is obtainable from $[(C_5Cl_4Br)Mn(CO)_3]$.[1]

By successive halogen–metal exchange and reactions with dimethyldisulfane, it is possible to prepare each member of the series $[\{\eta^5\text{-}C_5Cl_{5-x}(SMe)_x\}Mn(CO)_3]$ with x = 1–5.

The reaction of **1** with BuLi/Me_2S_2 can afford in principle two stereoisomers of **2**. An X-ray crystal structure analysis showed that the 1,3-disubstituted isomer was formed.[11]

[*] Dr. K. Sünkel, D. Motz
Institut für anorganische Chemie der Universität
Meiserstrasse 1, D-8000 München 2 (FRG)

[**] Complexation Chemistry of Perhalogenated Cyclopentadienes and Alkynes, Part 2. We thank Prof. Dr. *W. Beck* for his interest in and support of this work.—Part 1: [1].

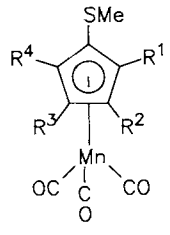

1 - 5

$$\mathbf{1} \xrightarrow[2.\ Me_2S_2]{1.\ BuLi} \mathbf{2} \xrightarrow[2.\ Me_2S_2]{1.\ BuLi} \mathbf{3} \xrightarrow[2.\ Me_2S_2]{1.\ BuLi} \mathbf{4} \xrightarrow[2.\ Me_2S_2]{1.\ BuLi} \mathbf{5}$$

	R^1	R^2	R^3	R^4
1	Cl	Cl	Cl	Cl
2	Cl	SMe	Cl	Cl
3	Cl	SMe	SMe	Cl
4	SMe	SMe	SMe	Cl
5	SMe	SMe	SMe	SMe

The crystal structure of compound **5**, containing five methylthio substituents, could also be solved (Fig. 1).[12] Whereas in the free ligand (in the form of its $AsPh_4$ salt[9]), four methyl groups are situated on one side of the ring plane, in the complex three SMe groups (but four S atoms) are located on the side of the ring facing away from manganese. The deviations of the atoms in the five-membered ring from planarity (maximally +0.31 pm for C13 and −0.37 pm for C14) are small. The sulfur atoms whose methyl groups point toward manganese (S12 and S15) are significantly displaced from the ring plane away from the metal (by about 19.8 and 18.1 pm, respectively) and also exhibit the largest angle C_{ring}-S-C_{methyl} (104.2(4) and 104.4(4)°, respectively). The average distances Mn-C_{ring} and C-C are 214.7(9)±1.8 pm and 142.7(12) pm (142±2 pm in the free ligand[9]); only the short distance C11-C12 (140.4(12) pm) is notable.

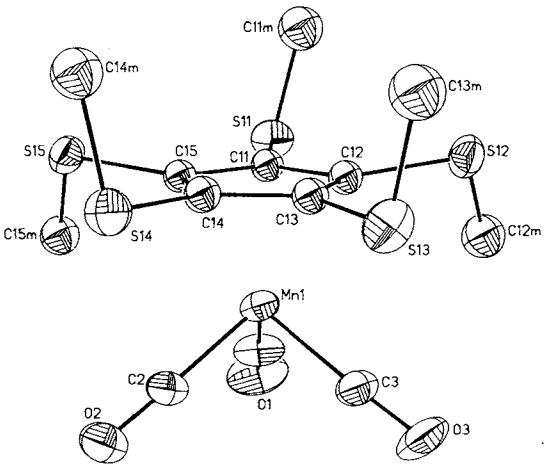

Fig. 1. Molecular structure of **5** (thermal ellipsoids at 20% probability) without H atoms. Selected bond lengths [pm] and bond angles [°]: Mn1-C11 216.5(9), Mn1-C12 215.3(8), Mn1-C13 213.5(9), Mn1-C14 213.1(9), Mn1-C15 215.0(8), C11-C12 140.4(12), C11-C15 143.4(12), C12-C13 143.7(12), C13-C14 142.6(12), C14-C15 143.5(12); C12-C11-C15 109.0(7), C11-C12-C13 108.3(7), C12-C13-C14 107.4(7), C13-C14-C15 108.5(7), C11-C15-C14 106.8(7), C11-S11-C11m 101.3(5), C12-S12-C12m 104.2(4), C13-S13-C13m 101.1(5), C14-S14-C14m 99.9(5), C15-S15-C15m 104.4(4).

The structures of **2** and **5** reveal that the sulfur substituents in **3** are probably in positions 1, 3, and 4 with the methyl groups directed away from manganese,[11b] whereas one methyl group in **4** points toward manganese. The spectroscopic data for **1**–**5** show that the electron density at sulfur decreases and that at the metal increases with increasing number of methylthio substituents: the methyl signals are shifted downfield in the ^{1}H-NMR spectrum and the ν(CO) frequencies are shifted to lower wave numbers. Interestingly, the methyl groups (except for those of **4**) always give only one signal in the 90-MHz ^{1}H-NMR spectrum. Even if a rapid inversion at sulfur at room temperature can be assumed, leading to averaging of the signals for the "*cis*" or "*trans*" methyl groups, it still remains unclear why the different nature of the neighboring groups leads to two absorptions in the case of **4** but not in that of **3**.

The compounds were also examined with respect to their ability to serve as complex ligands for other metals. The preliminary results reveal that they engage in reactions typical of thioethers. For instance, **3** reacts with $[Pd(PhCN)_2Cl_2]$ to form a compound in which the two neighboring methylthio groups are coordinated in a chelate fashion to a $PdCl_2$ moiety. In the ^{1}H-NMR spectrum, two singlets in a ratio of 2:1 appear; the first singlet is significantly shifted downfield in comparison with that of **3**.

Experimental Procedure

All operations were carried out under dry N_2. Correct C,H,S analyses were obtained for **2** to **5**.

2: $[(C_5Cl_4Br)Mn(CO)_3]$ (1.45 g, 3.47 mmol) was dissolved in 20 mL of Et_2O and the solution was cooled to −60°C. The solution was then treated successively with a 1.6 M BuLi solution in hexane (2.17 mL, 3.47 mmol), Me_2S_2 (0.3 mL, 3.47 mmol), BuLi solution (2.17 mL), and Me_2S_2 (0.3 mL). The temperature was allowed to rise to −30°C over 3 h and the solvent was then removed under vacuum. The residue was extracted twice with 20 mL of hexane. The extracts were then concentrated to about 1 mL and cooled to −78°C, resulting in the precipitation of yellow, crystalline **2**. Yield 1.02 g (74%), m.p. = 65–67°C. IR: ν(CO) (hexane): 2044, 2040, 1978, 1969 cm^{-1}. 90-MHz ^{1}H-NMR (C_6D_6): δ = 1.84 (SCH_3). ^{13}C-NMR (C_6D_6): δ = 111.5, 104.0, 89.8 (C_5R_5); 20.3 (SCH_3).

3: Yellow crystals of **3** were obtained from **2** (930 mg, 2.14 mmol), BuLi solution (1.34 mL, 2.14 mmol) and Me_2S_2 (0.19 mL, 2.14 mmol) in 10 mL of Et_2O as described for the synthesis of **2**. Yield 630 mg (66%), m.p. = 70–71°C. IR: ν(CO) (hexane): 2038, 2033, 1975, 1967 cm^{-1}. 90-MHz ^{1}H-NMR (C_6D_6): δ = 1.92 (SCH_3). ^{13}C-NMR (C_6D_6): δ = 112.0, 97.8, 91.6 (C_5R_5), 20.3 (SCH_3).

Likewise, **4** was obtained from **3** and **5** from **4**.

4: Yield 57%, m.p. = 59–60°C. IR: ν(CO) (hexane): 2037, 2033, 1965 cm^{-1}. 90-MHz ^{1}H-NMR (C_6D_6): δ = 2.06, 2.04 (SCH_3). ^{13}C-NMR (C_6D_6): δ = 113.2, 105.2, 99.2 (C_5R_5), 20.8, 20.1 (SCH_3).

5: Yield 32%, m.p. = 93–94°C. IR: ν(CO) (hexane): 2030, 2026, 1958 cm^{-1}. 90-MHz ^{1}H-NMR (C_6D_6): δ = 2.15 (SCH_3). ^{13}C-NMR (C_6D_6): δ = 106.6 (C_5R_5), 20.4 (SCH_3).

Received: February 11, 1988;
revised version: March 24, 1988 [Z 2614 IE]
German version: *Angew. Chem. 100* (1988) 970

CAS Registry numbers:
1, 111998-40-4; **2**, 114928-66-4; **3**, 114928-67-5; **4**, 114928-68-6; **5**, 114944-19-3; $[(C_5Cl_4Br)Mn(CO)_3]$, 56282-22-5.

[1] K. Sünkel, D. Motz, *Chem. Ber. 121* (1988) 799.
[2] D. W. Macomber, W. P. Hart, M. D. Rausch, *Adv. Organomet. Chem. 21* (1982) 1.
[3] a) H. Bönnemann, *Angew. Chem. 97* (1985) 264; *Angew. Chem. Int. Ed. Engl. 24* (1985) 248; b) K. Abdullah, B. L. Booth, C. Stacey, *J. Organomet. Chem. 293* (1985) 103.
[4] B. D. Zwick, A. M. Arif, A. T. Patton, J. A. Gladysz, *Angew. Chem. 99* (1987) 921; *Angew. Chem. Int. Ed. Engl. 26* (1987) 910.
[5] a) F. L. Hedberg, H. Rosenberg, *J. Am. Chem. Soc. 95* (1973) 870; b) K. J. Reimer, A. Shaver, *Inorg. Chem. 14* (1975) 2707; c) W. A. Herrmann, M. Huber, *Chem. Ber. 111* (1978) 3124; d) review: W. A. Herrmann, *Angew. Chem. 90* (1978) 855; *Angew. Chem. Int. Ed. Engl. 17* (1978) 800.

 © VCH Verlagsgesellschaft mbH, D-6940 Weinheim, 1988 0570-0833/88/0707-0940 $ 02.50/0

[6] a) V. A. Nefedov, *Zh. Org. Khim. 9* (1973) 719; b) W. A. Herrmann, M. Huber, *J. Organomet. Chem. 140* (1977) 55.
[7] a) C. Arsenault, P. Bougeard, B. G. Sayer, S. Yeroushalmi, M. J. McGlinchey, *J. Organomet. Chem. 265* (1984) 283; b) M. I. Bruce, R. C. Wallis, M. L. Williams, B. W. Skelton, A. H. White, *J. Chem. Soc. Dalton Trans. 1983*, 2183.
[8] a) O. W. Webster, *J. Am. Chem. Soc. 88* (1966) 4055; b) R. E. Christopher, L. M. Venanzi, *Inorg. Chim. Acta 7* (1973) 489.
[9] F. Wudl, D. Nalewajek, F. J. Rotella, E. Gebert, *J. Am. Chem. Soc. 103* (1983) 5885.
[10] a) M. Herberhold, P. Leitner, *J. Organomet. Chem. 336* (1987) 153; b) R. Broussier, A. Abdulla, B. Gautheron, *ibid. 332* (1987) 165; c) R. V. Honeychuck, M. Okoroafor, L. Shen, C. H. Brubaker, Jr., *Organometallics 5* (1986) 482; d) B. McCulloch, D. L. Ward, J. D. Woolins, C. H. Brubaker, Jr., *ibid. 4* (1985) 1425.
[11] a) K. Sünkel, D. Motz, unpublished results; b) we were able to determine such a structure for the complex $[\{C_5Cl_2(SPh)_3\}Mn(CO)_3]$, which is analogous to **3**.
[12] **5**: Crystal data: crystal dimensions, $0.45 \times 0.36 \times 0.10$ mm^3 (from methylcyclohexane); monoclinic $P2_1/c$, $Z=4$; $a=933.2(5)$, $b=1525.2(7)$, $c=1312.9(6)$ pm; $\beta=92.017(37)°$; $V=1867.5(14) \times 10^6$ pm^3; $4 \le 2\theta \le 35°$ ($Mo_{K\alpha}$, $\lambda=71.069$ pm); ω scan, $\Delta\omega=\pm0.8°$, $8 \le \dot{\omega} \le 29.3°$ min^{-1}; measured $\pm h$, k, $\pm l$, 2434 reflections measured, of which 988 were unique reflections ($I \ge 2\sigma(I)$); empirical absorption correction ($\mu=12.23$ cm^{-1}). Structure solution using SHELXTL 4.1 via direct methods followed by multiple difference Fourier analysis, Mn, S, and CO-s refined anisotropically; positions of the hydrogen atoms calculated for idealized geometries with $U_H=1.2 \times U_C$; $R=0.0543$, $R_w=0.0568$. Further details of the crystal structure investigation may be obtained from the Fachinformationszentrum Energie, Physik, Mathematik GmbH, D-7514 Eggenstein-Leopoldshafen 2 (FRG), on quoting the depository number CSD-52947, the names of the authors, and the journal citation.

Stabilization of 1,2,4,5-Tetradehydrobenzene by Complexation at Two Nickel(0) Centers

By *Martin A. Bennett,* James S. Drage, K. David Griffiths, Nicholas K. Roberts, Glen B. Robertson,* and *Wasantha A. Wickramasinghe*

1,2-Didehydrobenzene, (C_6H_4) **1**, is a short-lived compound that can be observed only by spectroscopic methods in an argon matrix at 8 K or at low pressures in the gas phase;[1] however, it forms stable η^2-transition metal complexes.[2-4] A recent theoretical study[5] predicts that retrocyclization of 1,2,4,5-tetradehydrobenzene **2** and 1,2,3,4-tetradehydrobenzene **3** to HC≡C–C≡C–C≡CH is much more favored energetically than the corresponding ring-opening of 1,2-didehydrobenzene to HC≡CH and HC≡C–C≡CH. We show here that **2** can be stabilized as a dinickel(0) complex **4**.[6] During the preparation of this manuscript, *Buchwald* et al.[7] reported the synthesis and structural characterization of a related zirconium complex **5**.

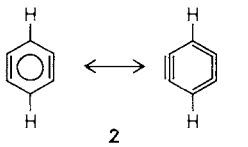

2

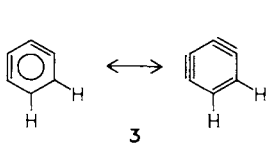

3

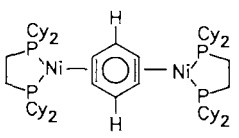

4

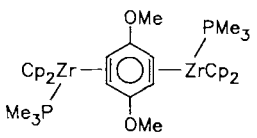

5

Treatment of a mixture of $[NiCl_2(PPh_3)_2]$, 1,2-dichloro-4-fluorobenzene, and a trace of 2,2′-azobis(2-methylpropionitrile) (AIBN) in THF at 45 °C with ultrasound-activated zinc powder affords a 10:1 mixture of the isomeric 2-chloro-4-fluoro- and 2-chloro-5-fluorophenylnickel(II) complexes **6** and **7**[8,9] (Scheme 1). Displacement of the PPh_3 ligands in **6** and **7** by $Cy_2PCH_2CH_2PCy_2$ (Cy = cyclohexyl) in boiling toluene gives a mixture of isomeric (chlorofluorophenyl)nickel(II) complexes **8** and **9**[10] which are reduced to the 4-fluoro-1,2-didehydrobenzene-nickel(0) complex **10** by treatment with two equivalents of potassium graphite (KC_8).[11-13]

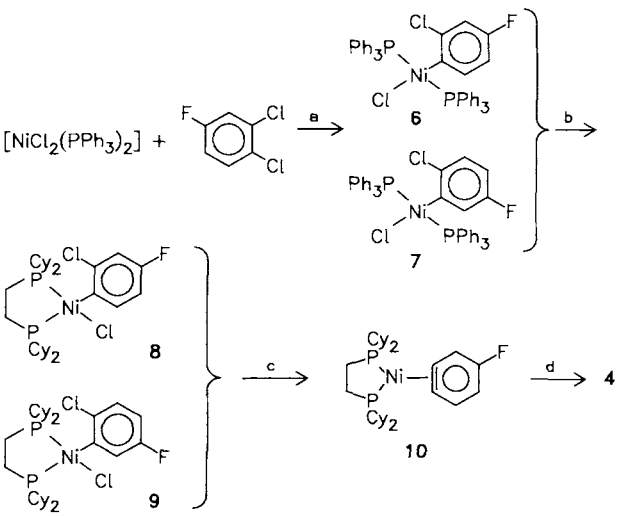

Scheme 1. a) Zn powder, AIBN, ultrasound, 45 °C; b) $Cy_2PCH_2CH_2PCy_2$, toluene, 110 °C; c) KC_8 (2 equiv.), THF; d) $[Ni(C_2H_4)(Cy_2PCH_2CH_2PCy_2)]$, LiTMP, THF.

The last step required to form **4** relies on the fact that 1,2-didehydrobenzene generated by treatment of chlorobenzene with the strongly basic but weakly nucleophilic compound lithium 2,2,6,6-tetramethylpiperidide (LiTMP) can be intercepted by added nucleophiles such as PhSLi[14] [Eq. (a)] or by Diels–Alder reagents such as 1,3-diphenylisobenzofuran[15] [Eq. (b)], or even the nickel(0) complex **11**.[4,16] Thus, treatment of an equimolar mixture of fluorobenzene and **11** in THF at 20 °C with an excess of LiTMP gives **12** in 15–20% yield, together with other unidentified

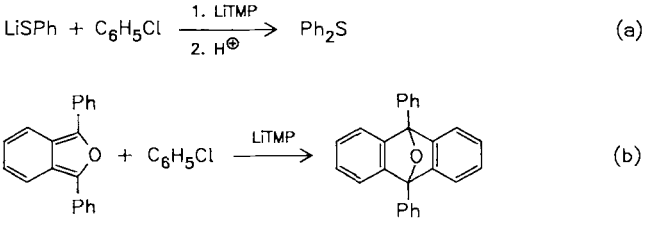

(a)

(b)

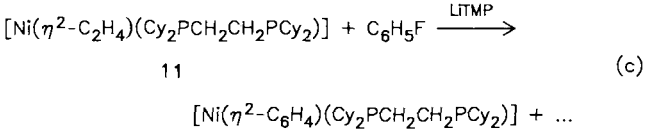

(c)

[*] Dr. M. A. Bennett, Dr. J. S. Drage, K. D. Griffiths [+], Dr. N. K. Roberts, Dr. G. B. Robertson [+], Dr. W. A. Wickramasinghe [+]
Research School of Chemistry, Australian National University
Canberra, A.C.T. 2601 (Australia)
[+] X-ray structure analysis

products [Eq. (c)]. Similarly, addition of an excess of LiTMP to an equimolar mixture of **10** and **11** in THF gives the required tetradehydrobenzene complex **4** in surprisingly good yield and with few byproducts (Scheme 1).[17, 18]

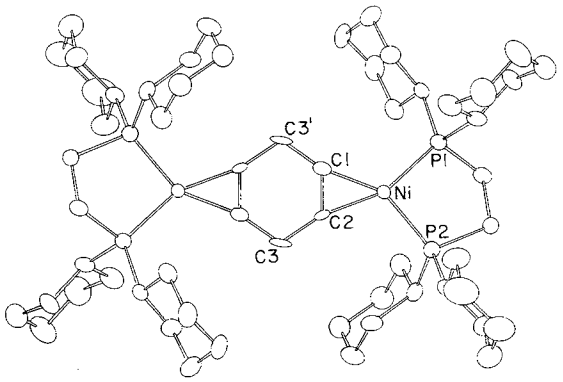

Fig. 1. Molecular structure of **4** (ORTEP [21]). 30% ellipsoids, hydrogen atoms omitted for clarity.

The structure of **4** has been determined by single-crystal X-ray diffraction analysis[19] (Fig. 1). The $(C_6H_2)Ni_2$ moiety is planar to within experimental error [Δ_{max} = 0.003(10) Å] but the nickel atoms are displaced 0.08(2) Å from their (PPCC) coordination planes. Bond lengths and bond angles in the six-membered ring indicate substantial π-electron localization at the ligating carbon atoms.[19] Surprisingly, the very substantial angle deformations in the C_6H_2-ring [e.g. C2-C3-C1′ = 112.2(8)°] are not observed in the analogous zirconium compound **5**.[7]

Received: February 29, 1988 [Z 2639 IE]
German version: *Angew. Chem. 100* (1988) 1002

CAS Registry numbers:
4, 114907-46-9; **6**, 114907-47-0; **7**, 114929-01-0; **8**, 114907-48-1; **9**, 114907-49-2; **10**, 114907-50-5; **11**, 91513-98-3; **12**, 114907-51-6; $NiCl_2(PPh_3)_2$, 14264-16-5; $Cy_2PCH_2CH_2PCy_2$, 23743-26-2; C_6H_5F, 462-06-6; C_6H_5Cl, 108-90-7; 1,2-dichloro-4-fluorobenzene, 1435-49-0; 1,3-diphenylisobenzofuran, 5471-63-6; 9,10-diphenyl-9,10-epoxyanthracene, 19061-38-2.

[1] O. L. Chapman, C. L. McIntosh, J. Pacansky, G. V. Calder, G. Orr, *J. Am. Chem. Soc. 95* (1973) 4061; O. L. Chapman, C-C. Chang, J. Kolc, N. R. Rosenquist, H. Tomioka, *ibid. 97* (1975) 6586; I. R. Dunkin, J. G. MacDonald, *J. Chem. Soc. Chem. Commun. 1979*, 772; R. F. C. Brown, N. R. Browne, K. J. Coulston, L. B. Danen, F. W. Eastwood, M. J. Irvine, A. D. E. Pullin, *Tetrahedron Lett. 27* (1986) 1075; R. D. Brown, P. D. Godfrey, M. Rodler, *J. Am. Chem. Soc. 108* (1986) 1296.

[2] S. J. McLain, R. R. Schrock, P. R. Sharp, M. R. Churchill, W. J. Youngs, *J. Am. Chem. Soc. 101* (1979) 263; M. R. Churchill, W. J. Youngs, *Inorg. Chem. 18* (1979) 1697.

[3] S. L. Buchwald, B. T. Watson, J. C. Huffman, *J. Am. Chem. Soc. 108* (1986) 7411.

[4] M. A. Bennett, T. W. Hambley, N. K. Roberts, G. B. Robertson, *Organometallics 4* (1985) 1992.

[5] L. Radom, R. H. Nobes, D. J. Underwood, W-K. Li, *Pure Appl. Chem. 58* (1986) 75.

[6] Presented as a poster (D9) at a conference of the Inorganic Division of the Royal Australian Chemical Institute, University of Melbourne, January 28-31, 1986, and mentioned briefly in Ref. [5].

[7] S. L. Buchwald, E. A. Lucas, J. C. Dewan, *J. Am. Chem. Soc. 109* (1987) 4396.

[8] *Procedure* for **6** and **7**: A three-neck, round-bottom flask fitted with a nitrogen inlet, mechanical stirrer and solids addition tube was charged under nitrogen with zinc powder (2.7 g) and THF (30 mL) and partially immersed in an ultrasound water bath at 45 °C. After 40 min the vigorously stirred and ultrasonicated mixture was treated successively with 1,2-dichloro-4-fluorobenzene (3.8 mL, ca. 34.5 mmol), $[NiCl_2(PPh_3)_2]$ (18 g, 27.5 mmol) and AIBN (0.36 g). Within 1-2 min the color of the mixture changed from deep blue-green to orange. After 10 min the mixture was filtered through Kieselguhr and the product was washed through with dichloromethane. Concentration under reduced pressure and addition of methanol gave yellow crystals of **6**/**7** (14.1 g, 69%), m.p. 162-165 °C (dec.).

[9] **6**/**7**: ^{1}H-NMR (CD_2Cl_2): δ = 9.70 (12H), 7.40 (18H), 6.59 (1H), 6.00 (1H), 5.93 (1H) (each m; aromatic). $^{31}P\{^1H\}$-NMR (CD_2Cl_2, external standard 85% H_3PO_4): δ = 21.70 (d, J(PF) = 1.95 Hz, major isomer), 21.15 (d, J(PF) = 3.42 Hz, minor isomer) (10:1 ratio).

[10] **8**/**9**: ^{1}H-NMR (CD_2Cl_2): δ = 6.91 (2H), 6.46 (1H) (each m; aromatic), 2.5-1.0 (m, 48H, CH_2 and CH). $^{31}P\{^1H\}$-NMR (CH_2Cl_2): δ = 66.45 (apparent s). Satisfactory C,H-elemental analysis.

[11] Preparation and applications of potassium graphite and of other metals dispersed in graphite: D. Savoia, C. Trombini, A. Umani-Ronchi, *Pure Appl. Chem. 57* (1985) 1887. Naphthalenesodium or 1-methylnaphthalene sodium can also be used for this reduction but it is difficult to remove the aromatic hydrocarbon completely during work-up. Sodium amalgam (1%) does not work well in contrast to its use in the preparation of **12**.

[12] *Procedure* for **10**: A suspension of **8**/**9** (4.0 g, 70 mmol) and KC_8 (1.67 g, 8.1 mmol) in THF (100 mL) was stirred under argon for 30 min. Solids were removed by centrifugation and the solution was concentrated in vacuo to an oil. Trituration with hexane (10 mL) gave a yellow powder which was washed with hexane (3 × 10 mL) and dried in vacuo overnight. The product was spectroscopically but not analytically pure, and was used directly in the next step of the synthesis.

[13] **10**: IR (KBr): ν = 1592 cm^{-1} (s, C=C). ^{1}H-NMR (C_6D_6): δ = 7.87 (1H), 7.76 (1H), 7.18 (1H) (each m; aromatic), 1.95-1.70 (m, 48H, CH_2 and CH). $^{31}P\{^1H\}$-NMR (THF): δ = 79.60 (dd, J(PP′) = 21.97 Hz, J(PF) = 8.90 Hz), 79.00 (dd, J(PP′) = 21.97 Hz, J(PF) = 1.75 Hz). $^{13}C\{^1H\}$-NMR (CH_2Cl_2; aromatic region only): δ = 163.90 (dd, J/CF) = 147.08 Hz, J(CP) = 10.26 Hz; CF), 148.04, 137.92 (each m; dehydrobenzene C), 124.39, 114.33, 110.35 (all m; CH).

[14] R. A. Olofson, C. M. Dougherty, *J. Am. Chem. Soc. 95* (1973) 582.

[15] K. L. Shepard, *Tetrahedron Lett. 1975*, 3371.

[16] K. Jonas, *J. Organomet. Chem. 78* (1974) 273.

[17] *Procedure* for **4**: A solution of LiTMP (680 mg, 4.62 mmol) in THF (10 mL) was added under argon to a well-stirred solution containing **10** (549 mg, 0.954 mmol) and **11** (509 mg, 1.00 mmol). After 20 h the solution was filtered and evaporated in vacuo to give a gummy solid which was triturated with hexane (10 mL). The resulting golden-yellow solid was collected on a frit, washed with hexane (4 × 5 mL), and dried in vacuo. Yield: 700 mg (68%). **4** could be recrystallized from benzene/hexane or from hot dioxane and gave a satisfactory analysis for C, H.

[18] **4**: ^{1}H-NMR (C_6D_6): δ = 8.13 (s, 2H), 2.00-1.70 (m, 96H). $^{31}P\{^1H\}$-NMR (THF): δ = 75.23 (s). $^{13}C\{^1H\}$-NMR (C_6D_6; aromatic region only): δ = 156.00 (m, dehydrobenzene C), 120.64 (t, CH).

[19] **4**: $C_{58}H_{98}P_4Ni_2$, M = 1036.7. Triclinic, space group $P\bar{1}$, a = 13.318(5), b = 11.651(5), c = 9.980(3) Å, α = 80.72(3), β = 85.68(2), γ = 72.23(3)°, V = 1448.6 Å^3, Z = 1, ρ_{calcd} = 1.18 g cm^{-3}, F(000) = 562, $\mu(Mo_{K\alpha})$ = 7.94 cm^{-1}; specimen crystal from benzene/hexane solution, dimensions 0.07 × 0.12 × 0.28 mm^3; cell dimensions and esd's from a least-squares fit to 25 low angle reflections [Philips PW1100 diffractometer, $8 < 2\theta < 18°$, $\lambda(Mo_{K\alpha})$ = 0.71073 Å, T = 20 ± 2 °C]; 5462 measured reflections [$\pm h \pm k + l$, $3 < 2\theta < 50°$]; 3 standards [$\bar{1}04$, $4\bar{2}1$, 451], average degradation rate 0.1928 × 10^{-4} per measured reflection; data corrected for crystal degradation and specimen absorption (transmission factor range 0.901-0.947) but not for extinction; 1748 retained reflections [$I \geq 3\sigma(I)$], $\Sigma\sigma(F_0)/\Sigma|F_0| = 0.059$; structure solved by Patterson and Fourier techniques, refined by full-matrix least-squares analysis; function minimized = $\Sigma w(|F_0| - |F_c|)^2$, with $w = [\sigma(F_0)^2 + 0.002\,F_0^2]^{-2}$; 289 parameters; H-atoms located by calculation [d_{C-H} = 0.95 Å, $B_H = 1.1\,B_C$]; scattering factors with anomalous dispersion corrections from Ref. [20]; molecule drawn with ORTEP [21]; final R = 0.058, R_w = 0.055, G.O.F. = 1.25, shift/esd ratios < 0.1 and difference Fourier map excursions < ± 0.5 e Å^{-3} everywhere; atom coordinates available on request from the Cambridge Crystallographic Data Centre, University Chemical Laboratory, Lensfield Road, Cambridge, CB2 1EW, U.K. Important bond lengths [Å] and angles [°]: Ni-P1 2.120(3), Ni-P2 2.137(3), Ni-C1 1.863(10), Ni-C2 1.859(10), C1-C2 1.313(12), C2-C3 1.402(13), C3-C1′ 1.417(13), P1-Ni-P2 90.9(1), C1-Ni-C2 43.1(**4**), C3′-C1-C2 123.6(9), C1-C2-C3 124.1(9), C2-C3-C1′ 112.2(8).

[20] J. A. Ibers, W. C. Hamilton (Eds.): International Tables for X-ray crystallography, Vol. 4, Kynoch Press, Birmingham 1974, pp. 99-101, 149-150.

[21] C. K. Johnson: ORTEP II, Report ORNL-5138, Oak Ridge National Laboratory, TN, USA 1976.

Higher Thermostability and Selectivity of Köbrich Reagents by Transmetalation**

By *Thomas Kauffmann,* Rolf Fobker,* and *Michael Wensing*

Can the stability of extremely thermolabile organolithium compounds be increased by complexation to transition metals without drastically decreasing the nucleophilicity? We have now checked this using the Köbrich reagents **1** (decomp. $-65\,^{\circ}C$)[2] and **2**–**4** (decomp. $-100\,^{\circ}C$ and below)[2,3] as examples and indeed have found, in some cases, considerable increases in stability. The more closely investigated transmetalation products **5**–**7** proved to be good dichloromethylating reagents exhibiting high chemoselectivity.[4]

Cl_2CHLi	Br_2CHLi	I_2CHLi	Cl_3CLi
1	**2**	**3**	**4**

Transmetalations: It was found that the decomposition temperature of the transmetalation products obtained from **1**–**4** according to or analogously to Scheme 1 can be determined optically: the solutions remain clear and intensely colored until decomposition sets in; at the limiting temperature of stability they become turbid and simultaneously

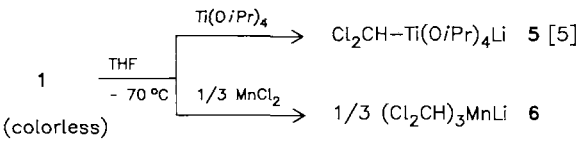

Scheme 1.

turn deep-brown to black in color. The reactions of the transmetalation products with aldehydes and ketones, which proceed in good yields only at temperatures ca. $10\,^{\circ}C$ below the so determined decomposition temperature, demonstrated that this change is a reliable stability criterium.

Table 1. Color in solution and decomposition temperature of the transmetalation products prepared in situ according to Scheme 1 (structures hypothetical).

	Color	Decomp. temp. [°C]		Color	Decomp. temp. [°C]
5 [5]	yellow-green	+10	$Cl_2CHTa(OEt)_5Li$	yellow-green	−30
$I_2CHTi(OiPr)_4Li$	yellow-green	−10	$Cl_2CHNb(OEt)_5Li$	red-brown	−30
$Cl_2CHTi(OnPr)_4Li$	yellow	−15	$Cl_2CHTi(OEt)_4Li$	green	−40
$Br_2CHTi(OiPr)_4Li$	yellow	−20	$Cl_2CHTi(OiPr)_3$ **7**	yellow-green	−60
$Cl_2CHHf(OEt)_4Li$	colorless	−20	$Cl_3CTi(OiPr)_4Li$ **8**	yellow	−80
$Cl_2CHHf(OEt)_3$	yellow	−30	$(Cl_2CH)_2CuLi$	yellow	−60
$Cl_2CHTi(NEt_2)_4Li$	yellow	−30	$Cl_3CTi(OiPr)_3$	red	< −90
				yellow	< −110

[*] Prof. Dr. T. Kauffmann, R. Fobker, Dr. M. Wensing
Organisch-chemisches Institut der Universität
Corrensstrasse 40, D-4400 Münster (FRG)

[**] Transition Metal-Activated Organic Compounds, Part 26. This work was supported by the Deutsche Forschungsgemeinschaft, the Stiftung Volkswagenwerk, and the Fonds der Chemischen Industrie.—Part 25: [1].

As a rule, the transmetalations carried out in situ yielded more stable reagents (Table 1). On the other hand, the reactions of **1** with $Ti(OiPr)_3Cl$, and especially with CuCl, led to marked destabilization. The most noticeable increase in the decomposition temperature was achieved by complexation with $Ti(OiPr)_4$: For the reagents Hal_2CHLi the increase in the order Hal = Cl, Br, I was about 75, 80, and 90 K, respectively. The ate complexes are, in each case, more stable than the corresponding neutral complexes along the series Hal = Cl, Br, I.

Aldehyde vs. ketone selectivity: As shown in Table 2, in the 1:1:1 competition experiment (Scheme 2) **1** reacts

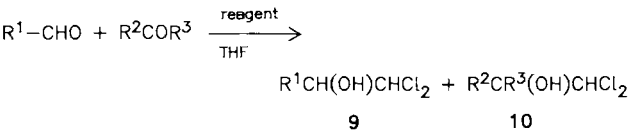

Scheme 2.

Table 2. Reactions according to Scheme 2 with a molar ratio of 1:1:1; after dropwise addition of the THF-solution of the carbonyl compound to the organometallic reagent at the given starting temperature the reaction mixture was warmed within ca. 12 h to room temperature [6].

R^1	R^2	R^3	Reagent	Starting temp. [°C]	Yield [%] **9**	**10**
Ph	Ph	Me	**5**	0	76	0
Ph	Ph	Me	**5**	−78	81	0
Ph	Ph	Me	**6**	−40	68	trace
Ph	Ph	Me	**7**	−90	46	2
Ph	Ph	Me	**1**	−90	48	32
n-C_6H_{13}	Et	Et	**5**	0	54	3
n-C_6H_{13}	Et	Et	**6**	−40	46	2
n-C_6H_{13}	Et	Et	**7**	−90	59	4
Ph	$-(CH_2)_5-$		**8** [a]	−110	91	8
Ph	$-(CH_2)_5-$		**4** [a]	−110	39	61

[a] Here, products analogous to **9** and **10** with CCl_3 instead of CH_2Cl_2 groups were obtained.

with the substrate pair benzaldehyde/acetophenone quite unselectively at $-90\,^{\circ}C$ to give the dichloromethylation products **9** and **10**. In contrast, the transmetalation products **5**–**7** investigated for the same substrate pair proved to be largely aldehyde-selective. High aldehyde-selectivity

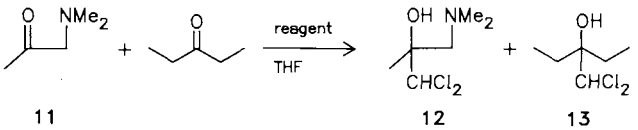

Scheme 3.

Table 3. Reactions according to Scheme 3 with a molar ratio of 1:1:1; conditions as in the reactions according to Scheme 2 (Table 2) [6].

Reagent	Starting temp. [°C]	Yield [%] **12**	**13**
5	−30	71	trace
6	−40	66	trace
7	−90	71	trace
1	−80	33	34

was also achieved in competition reactions of **5**–**7** with the substrate pair heptanal/3-pentanone. In non-competition experiments acetophenone could be dichloromethylated in good yields with **5**–**7**; but only at 0 °C however in the case of **5** (enolate formation at −78 °C).

Grouping selectivity:[7] The reagents **5**–**7** dichloromethylate the α-dimethylaminoketone **11** completely grouping selectively in the presence of 3-pentanones (Scheme 3, Table 3), whereas the lithium compound reacts unselectively.

In contrast to **13** and the products of type **9** and **10** obtained according to Scheme 2, **12** has, to our knowledge, thus far never been described. Spectroscopic data for this oily, readily decomposable substance, which could not be obtained in analytically pure form, are listed in Table 4.

Table 4. Spectroscopic data of **12**.

^{1}H-NMR (300 MHz, $CDCl_3$, TMS): $\delta = 1.65$ (s, 3H; CCH_3), 2.34 (s, 6H; NCH_3), 2.38 (d, 1H; C*H*H), 2.75 (d, 1H; CH*H*), 5.70 (s, 1H; $CHCl_2$); OH signal not observed

^{13}C{^{1}H}-NMR (75 MHz, $CDCl_3$): $\delta = 21.3$ (CCH_3), 47.7 (NCH_3), 64.1 (CH_2), 75.0 (COH), 79.1 ($CHCl_2$)

GC/MS: *m/z* 174 (0.05%), 172 (0.35), 170 (0.55), 149 (0.25), 102 (18), 58 (100), 44 (10), 42 (10); an exact determination was made of the mass from the $(M+H)^{\oplus}$ peak of a CI (isobutane) measurement (resolving power 5000): $M_{exp} = 186.0442$; $M_{calcd} = 186.045245$ for $C_6H_{14}Cl_2ON^{\oplus}$.

Received: March 2, 1988 [Z 2643 IE]
German version: *Angew. Chem. 100* (1988) 1005

CAS Registry numbers:
1, 2146-67-0; **2**, 37555-63-8; **3**, 31103-52-3; **4**, 2146-66-9; **5**, 114885-52-8; **6**, 114885-53-9; **7**, 114885-54-0; **8**, 114885-55-1; **9** (R′ = Ph), 2612-36-4; **9** (R′ = *n*-C_6H_{13}), 99706-66-8; **10** (R^2 = Ph, R^3 = Me), 4773-32-4; **11**, 15364-56-4; **12**, 114838-68-5; **13**, 4773-54-0; PhCH(OH)CCl_3, 2000-43-3; $(CH_2)_5C(OH)CCl_3$, 3508-84-7; $I_2CHTi(OiPr)_4Li$, 114885-56-2; $Cl_2CHTi(OPr)_4Li$, 114885-66-4; $Br_2CHTi(OiPr)_4Li$, 114885-57-3; $Cl_2CHHf(OEt)_4Li$, 114885-58-4; $Cl_2CHHf(OEt)_3$, 114885-59-5; $Cl_2CHTi(NEt_2)_4Li$, 114885-60-8; $Cl_2CHTa(OEt)_5Li$, 114885-61-9; $Cl_2CHNb(OEt)_5Li$, 114885-62-0; $Cl_2CHTi(OEt)_4Li$, 114885-63-1; $(Cl_2CH)_2CuLi$, 114885-64-2; $Cl_3CTi(OiPr)_3$, 114885-65-3; $Ti(OiPr)_4$, 546-68-9; $Ti(OPr)_4$, 3087-37-4; $Hf(OEt)_4$, 13428-80-3; $Hf(OEt)_3Cl$, 101803-59-2; $Ti(NEt_2)_4$, 4419-47-0; $Ta(OEt)_5$, 6074-84-6; $Nb(OEt)_5$, 3236-82-6; $Ti(OEt)_4$, 3087-36-3; $Ti(OiPr)_3Cl$, 3712-48-9; $MnCl_2$, 7773-01-5; CuCl, 7758-89-6; benzaldehyde, 100-52-7; heptanal, 111-71-7; acetophenone, 98-86-2; 3-pentanone, 96-22-0; cyclohexanone, 108-94-1.

[1] T. Kauffmann, T. Abel, M. Schreer, D. Wingbermühle, *Tetrahedron 43* (1987) 2021.
[2] G. Köbrich, *Angew. Chem. 79* (1967) 15; *Angew. Chem. Int. Ed. Engl. 6* (1967) 41.
[3] According to *J. Villieras* et al. (J. Villieras, R. Tarhouni, B. Kirschleger, M. Rambaud, *Bull. Soc. Chim. Fr. 1985*, 825; *ibid. 1986*, 470) the addition of lithium salts to Köbrich carbenoids leads to a reasonable increase in thermal stability; consequently, better yields are achieved in additions to carbonyl compounds.
[4] These results are mainly taken from the Dissertation by *M. Wensing* (Universität Münster 1987).
[5] At −10 °C, the ^{1}H-NMR spectrum (300 MHz) of the hypothetical ate complex **5** dissolved in [D_8]THF shows a singlet at $\delta = 5.31$, which disappears at +10 °C and is therefore assigned to the proton of the Cl_2CH group. In the ^{13}C-NMR spectrum (75 MHz; THF; [D_6]benzene as internal standard) a singlet appears at $\delta = 91.2$ at −30 °C; this disappears on warming to +10 °C and is therefore likewise assigned to the Cl_2CH group. A band at 495 cm^{-1} in the IR spectrum (THF, −10 °C), which disappears at +10 °C, is assigned to a Ti–C vibration, since Ti–C vibrations have already been observed in the range 427–530 cm^{-1} for Ti-methyl complexes (G. L. Karapinka, J. J. Smith, W. L. Carrick, *J. Polym. Sci. 50* (1961) 143; G. W. A. Fowles, D. A. Rice, J. D. Wilkins, *J. Chem. Soc. A 1971*, 1920).
[6] Up to 85–95% of the unchanged carbonyl compounds was recovered.
[7] "Grouping" = combination of functional groups; see T. Kauffmann, T. Möller, H. Rennefeld, S. Welke, R. Wieschollek, *Angew. Chem. 97* (1985) 351; *Angew. Chem. Int. Ed. Engl. 24* (1985) 348.

In-Situ Blocking of an Aldehyde Function by Formation of (α-Triphenylphosphoniumalkoxy)-titanium or -niobium Complexes**

By *Thomas Kauffmann,* Thomas Abel,* and *Martin Schreer*

Investigations of the influence of electron donor compounds on the nucleophilicity of [$MeTiCl_3$] **1** toward aldehydes and ketones revealed that the nucleophilicity decreases as shown in Scheme 1,[2,3] i.e. the circumstances are the reverse to those observed in the case of lithium com-

[$MeTiCl_3$] **1** in CH_2Cl_2, Et_2O, THF, DME, TMEDA
⟶ decreasing nucleophilicity
AlkylLi in TMEDA, DME, THF, Et_2O, C_6H_{12}

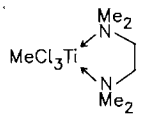

2a [$MeTiCl_3(PPh_3)$] **2b**
[$MeTiCl_3(PPh_3)_2$] **2c**

Scheme 1. [4].

pounds. In these investigations it was found[3] that, in reactions with aldehyde/ketone pairs, the triphenylphosphane complexes **2b** and **2c** preferably methylate the ketone, that is in complete contrast to the tmeda-complex **2a**, which methylates aldehydes in CH_2Cl_2 and is almost inert toward ketones (Table 1).

Table 1. Reactions of phosphane complexes of the compound **1** as pure substances with substrate pairs in $CHCl_2$ at −25 °C (6 h).

Substrates A/B	Ligand	Molar ratio Ligand : **1** : A : B	Methylation product [%] of A	of B	Recovery [%] A	B
Heptanal/ 2-hexanone	—	0 : 1 : 1 : 1	74	3	22	97
	PPh_3	2 : 2 : 1 : 1	10	67	88	30
	PPh_3	4 : 2 : 1 : 1 [a]	9	81	87	5
	dppe	2 : 2 : 1 : 1	4	51	90	44
	dppe	2 : 2 : 1 : 1 [a]	27	95	73	2
Heptanal/ cyclohexanone	—	0 : 1 : 1 : 1	60	19	30	70
	PPh_3	2 : 2 : 1 : 1 [a]	4	89	84	0
Cyclohexane-carbaldehyde/ 2-hexanone	—	0 : 1 : 1 : 1	89	6	9	90
	PPh_3	2 : 2 : 1 : 1 [a]	3	69	94	26
Cyclohexane-carbaldehyde/ cyclohexanone	—	0 : 1 : 1 : 1	45	30	53	69
	PPh_3	2 : 1 : 1 : 1	3	62	94	34
	PPh_3	4 : 2 : 1 : 1	1	74	98	25
	PPh_3	4 : 2 : 1 : 1 [a]	3	95	94	4
	dppe	1 : 1 : 1 : 1	17	61	81	39

[a] Reaction at 0 °C instead of at −25 °C (6 h).

An analogous ketone selectivity was found, albeit somewhat less pronounced, in the case of the complex formed from *P,P′*-ethylenebis(diphenylphosphane) (dppe) and **1** (Table 1).

The ketone selectivity of the complex **2b** can be attributed (and the same holds true for **2c**) to the fact that a

[*] Prof. Dr. T. Kauffmann, Dipl.-Chem. T. Abel, Dipl.-Chem. M. Schreer
Organisch-chemisches Institut der Universität
Corrensstrasse 40, D-4400 Münster (FRG)

[**] Transition Metal-Activated Organic Compounds, Part 27. This work was supported by the Deutsche Forschungsgemeinschaft, the Stiftung Volkswagenwerk, and the Fonds der Chemischen Industrie.—Part 26: [1].

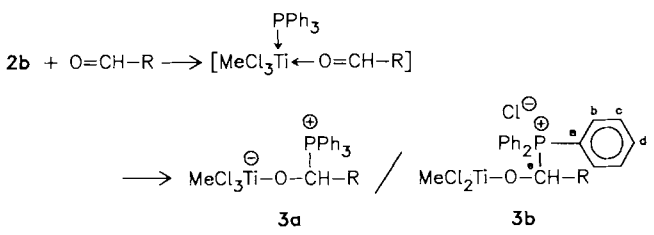

Scheme 2. R = *n*-hexyl.

phosphoniumalkoxy complex of type **3a** or **3b** is formed in reactions with aldehydes according to Scheme 2, whereby the aldehyde function is blocked. In the case of ketones, on the other hand, it is not the phosphane ligand but the methyl group that is transferred. Since 2-hexanone is still methylated to the extent of 28% in the reaction of **2b** with heptanal/2-hexanone in the molar ratio 1:1:1 (instead of 2:1:1) it can be assumed that not only **2b** but also the phosphoniumalkoxy complexes **3a** or **3b** formed therefrom are effective methylating agents.

The assumption of phosphoniumalkoxy compounds such as **3a** or **3b** as intermediates is supported by the following findings:

a) In the IR spectrum of the complex prepared from **2b** and heptanal in CH_2Cl_2 the carbonyl band expected to appear at ca. 1720 cm^{-1} is absent, but several strong bands are observed at ca. 1120 cm^{-1} that can be assigned to C–O vibrations, since transition metal alkoxides strongly absorb in the 1000–1200 cm^{-1} region.

b) The ^{31}P-NMR signal of the complex formed from **2b** and heptanal in $CDCl_3$ is shifted markedly downfield ($\delta = 20.0$) compared to that of PPh_3 ($\delta = -6.0$) and **2b** ($\delta = 10.0$), clearly indicating a triphenylphosphonium group (for comparison: **4b**: $\delta = 17.6$).

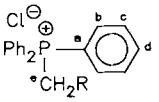

4a, R = Alkyl
b, R = OMe
c, R = Cl

c) In the ^{13}C-NMR spectrum of the complex formed from **2b** and heptanal in $CDCl_3$ the δ values for the phenyl C-atoms are very similar to those for the phosphonium salt **4**.[5] The same holds true for the coupling constants $^1J_{^{31}P^{13}C}$ (Table 2).

Table 2. $\delta(^{13}C)$ and coupling constants $^1J(^{31}P,^{13}C)$ [Hz] (in brackets) of the complex **3** formed from **2b** and heptanal in $CDCl_3$ (20 °C) and of the compounds **4** [5].

Compound	Indexing according to **3b** and **4**				
	[a]C	[b]C	[c]C	[d]C	[e]C
Complex **3a/3b**	116.9 (80.0)	134.0 (9.0)	130.0 (12.0)	135.0 —	85 (56)
4a	117–119 (80–89)	134 (9–11)	131 (12–13)	135 (3)	11–35
4b	117.0 (85.9)	136.6 (10.0)	131.1 (12.8)	135.9 (3.1)	66.2 (69.4)
4c	116.5 (88.3)	134.6 (10.2)	130.9 (13.0)	136.0 (3.0)	33.8 (56.8)

Table 1 shows that on using **1** + dppe (the known complex **2d**[6] may be formed thereby) aldehyde groups are less effectively blocked. This is understandable since **2d** contains a five-membered ring, whereas the complex **5** analogous to **3a** contains a seven-membered ring.

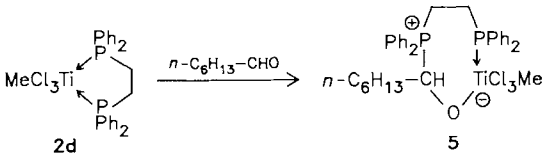

Complexes analogous to **3a/3b** have also been detected spectroscopically in reactions of $[MeNbCl_4(PPh_3)]$ **6**, $[TiCl_4(PPh_3)]$ **7**, and $[NbCl_5(PPh_3)]$ with aldehydes. The niobium complex **6** blocks the aldehyde group of heptanal, but (in contrast to **2b**) not that of benzaldehyde. This enabled the selective methylation of benzaldehyde according to Scheme 3. The complexes analogous to **6** with NPh_3 or $AsPh_3$ instead of PPh_3 did not block the aldehyde group of heptanal.

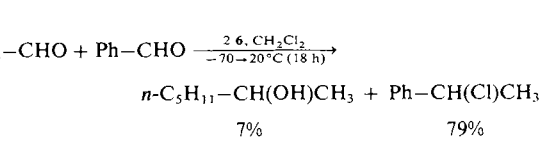

Scheme 3. [7].

Methylation according to Scheme 4 could be achieved with the complex **7**. The scope of application of this particularly convenient ketoselective alkylation method is presently under investigation.

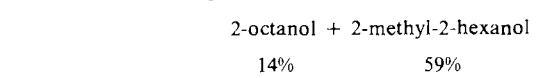

Scheme 4 [3]. Reaction temperature 0 °C (6 h).

Reetz et al.[8] reported comparable possibilities of the reversal of selectivity by in-situ blocking of aldehyde groups: The reagent $[(allyl)Ti(NMe_2)_4MgCl]$ can be used for the selective allylation of a keto function in presence of an aldehyde function (one step method), whereas in the corresponding alkylations the aldehyde function must be chemoselectively blocked by addition of $[Ti(NEt_2)_4]$ and the keto function must be alkylated with moderately nucleophilic reagents (two-step method). The reversal of selectivity by use of phosphane complexes described here could be preparatively attractive because of the very easy access of the reagents.

Received: March 7, 1988 [Z 2650 IE]
German version: *Angew. Chem. 100* (1988) 1006

[1] T. Kauffmann, R. Fobker, M. Wensing, *Angew. Chem. 100* (1988) 1005; *Angew. Chem. Int. Ed. Engl. 27* (1988) 943.
[2] T. Kauffmann, T. Abel, M. Schreer, D. Wingbermühle, *Tetrahedron 43* (1987) 2021, footnote [7b].
[3] T. Abel, T. Kauffmann, unpublished.
[4] The decreasing nucleophilicity of **1** in the given sequence is due to the increasing blocking of coordination sites without heterolysis of the Ti–CH_3 bond taking place.
[5] C. A. Gray, *J. Am. Chem. Soc. 95* (1973) 7736.
[6] G. W. A. Fowles, D. A. Rice, J. P. Wilkins, *J. Chem. Soc. A 1971*, 1920.
[7] As observed in the reaction of Me_2NbCl_3 with benzaldehyde (J. D. Wilkins, *J. Organomet. Chem. 80* (1974) 357), the reaction of **6** with benzaldehyde causes, besides methylation, the exchange of the oxygen function for chlorine. This chlorination process occurs via radicals: M. Schreer, T. Kauffmann, unpublished.
[8] M. T. Reetz, B. Wenderoth, *Tetrahedron Lett. 23* (1982) 5259; M. T. Reetz, B. Wenderoth, R. Peter, *J. Chem. Soc. Chem. Commun. 1983*, 406; M. T. Reetz, *Top. Curr. Chem. 106* (1982) 1.

Alkyne Coordination to Organorhenium Oxides with Rhenium in High Oxidation States**

By *Josef K. Felixberger, Josef G. Kuchler, Eberhardt Herdtweck, Rocco A. Paciello,* and *Wolfgang A. Herrmann**

Dedicated to Professor Heinrich Nöth on the occasion of his 60th birthday

It was hitherto uncertain whether very electron-deficient transition metals in organometal oxides are capable of complexing alkynes, especially as more recent MO theoretical results rather suggested the contrary.[1] Consistent with these theoretical results, it has proved impossible to oxidize the isolable Re^{III} complexes **1a** (R = alkyl, aryl) to the still unknown oxygen-rich Re^{V} derivatives **1b**.[2] And in all the alkynerhenium complexes known to date, the maximum oxidation state exhibited by the metal atom is +3.[3] However, since alkynes can be oxidatively coupled with organorhenium oxides to give furan derivatives,[4] we have directed our attention to the synthesis of suitable model compounds, and now report on a new, simple class of compounds of pentavalent rhenium.

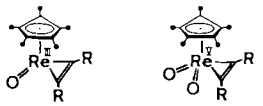

1a **1b**

Triphenylphosphane has proven to be a mild, selective deoxidizing reagent for trioxo(η^5-pentamethylcyclopentadienyl)rhenium(VII) **2** in the directed synthesis of functionalized Re^{V} derivatives.[5] Thus, the tetrachloro complex **3** is accessible according to Scheme 1 with triphenylphosphane/trimethylchlorosilane, whereas the dinuclear oxide **4** is formed on reaction of **2** with the phosphane alone.[5]

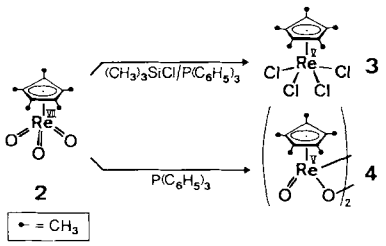

Scheme 1.

It now emerges that none of the mentioned reactions can be extended to the methylrhenium(VII) oxide **5**.[6] In the presence of Lewis base ligands, this compound, in contrast to the π-complex **2**, is prone to an increase in coordination number, because the methyl group is much less sterically demanding than the π-ligand with its additional nine C atoms. Thus, reaction of triphenylphosphane/trimethylchlorosilane with **5** according to Scheme 2 leads to formation of only the dinuclear rhenium(VI) complex **6** in 70% yield, which according to a single-crystal X-ray structure analysis (Fig. 1) has a centrosymmetric molecular structure.[7] As a result, the two slightly distorted octahedra are joined linearly via an oxygen bridge (O2). Electronic d^1-d^1 "superexchange" in the Re,O2,Re′ structural moiety with its shortened metal-oxygen bonds (184.7(< 1) pm) explains the diamagnetism of this Re_2^{VI} compound.

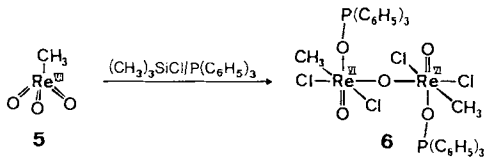

Scheme 2.

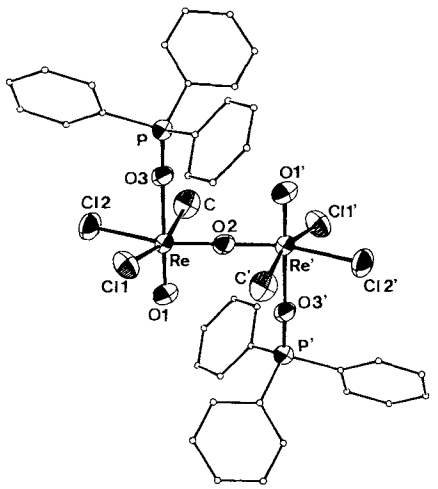

Fig. 1. Molecular structure (ORTEP) of **6**, which crystallizes from methylene chloride/*n*-pentane (1 : 1) at −25°C in the monoclinic space group $P2_1/c$. Selected bond lengths [pm] and angles [°]: Re-Cl1 242.9(2), Re-Cl2 234.2(2), Re-C 213.0(6), Re-O1 165.5(4), Re-O2 184.7(< 1), Re-O3 211.5(4), P-O3 152.4(4); ReO2Re′ 180.0(0), O2ReCl1 95.03(5), O2ReCl2 168.74(5), CReCl1 161.7(2), ReO3P 171.7(3) [12].

Unlike **2**, the complex **5** forms adducts with simple nitrogen bases; thus, on reaction with 1-azabicyclo[2.2.2]octane (quinuclidine) it forms a complex of the composition $CH_3ReO_3 \cdot NC_7H_{13}$.[8]

The complexation of the reducing agent triphenylphosphane, which is disadvantageous for the further use of complexes of type **6**, also hindered attempts to deoxygenate **5** in the presence of other ligands. This problem could be overcome, however, by the use of polymer-bound triphenylphosphane Ⓟ; the polymeric phosphane oxide formed during the reduction is insoluble and is removed from the reaction system, thus allowing for the synthesis of the new compounds **7** according to Scheme 3. Independent of the substituents of the alkynes the reaction is complete at room temperature within hours. The products can be recovered in pure form from the filtered reaction solutions by simple crystallization.

An X-ray structure analysis was carried out on the tolan complex **7h** (Fig. 2).[7] This revealed that the compounds **7** are derived from the educt **5** by reductive substitution of

[*] Prof. Dr. W. A. Herrmann, J. K. Felixberger, J. G. Kuchler, Dr. E. Herdtweck, Dr. R. A. Paciello
Anorganisch-chemisches Institut der Technischen Universität München
Lichtenbergstrasse 4, D-8046 Garching (FRG)

[**] Multiple Bonds between Main Group Elements and Transition Metals, Part 55. This work was supported by the Deutsche Forschungsgemeinschaft, the Fonds der Chemischen Industrie, Degussa AG, the Merck'sche Gesellschaft für Kunst und Wissenschaft e.V. (grant for *J. K. F.*), and the Alexander von Humboldt-Stiftung (grant for *R. A. P.*).— Part 54: J. Kulpe, E. Herdtweck, G. Weichselbaumer, W. A. Herrmann, *J. Organomet. Chem.*, in press.

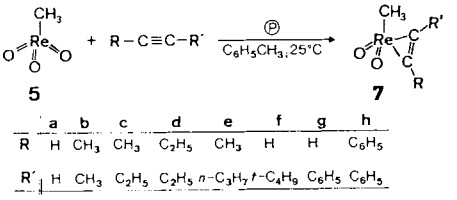

Scheme 3.

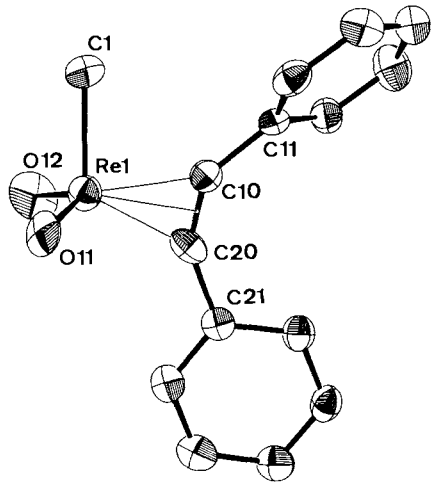

Fig. 2. Molecular structure (ORTEP) of the tolan complex **7h** in the crystal at −80 °C. The compound crystallizes from *n*-hexane at −25 °C in the monoclinic space group $P2_1/c$. The unit cell contains two crystallographically independent molecules A and B which differ only slightly in structure. Selected bond lengths [pm] and angles [°] for molecule A: Re-C1 209.2(7), Re-O11 171.0(4), Re-O12 174.0(4), Re-C10 205.7(7), Re-C20 201.2(7), C10-C20 128.0(9), C10-C11 146.8(9), C20-C21 148.8(9); C1ReO11 102.0(3), C1ReO12 102.2(3), O11ReO12 119.5(2), C11C10C20 141.8(7), C10C20C21 146.9(7) [12].

an oxo-group by the corresponding alkyne ligand without an alkyne/oxygen coupling taking place. The acetylene moiety, the rhenium atom, and the carbon atom of the methyl group lie in a plane that bisects the angle between the two oxo groups. The distances between the metal atom and the methyl group determined for molecule A (209.2(7) pm) and molecule B (203.4(6) pm) correspond to that of a single bond, whereas the Re–O bonds (171.0(4) and 174.0(4) pm for A; 166.8(5) and 172.3(5) pm for B) are typical double bonds. The C–C bond length of the alkyne (128.0(9) pm) for A, 130.1(9) pm for B) corresponds to that of a double bond; the distance between the metal and the center of the acetylene-ligand bond is 193.1 pm in A and 193.6 pm in B.

The observation of two independent molecules in the solid state can be attributed exclusively to packing effects. Molecule A and molecule B differ significantly only in the torsional angles of the acetylene moiety.

According to the ^{13}C-NMR data (Table 1), the alkynes in the d^2-Re^V complexes **7** function as 2e ligands.[9] A rapid rotation of the alkyne ligands around the bonding axis to the metal is not detectable by NMR spectroscopy, not even in the sterically undemanding parent compound **7a**. According to the ^{1}H- and ^{13}C-NMR spectra, **7a** has a rigid framework: the methyl group attached to rhenium couples with only *one* proton of the C_2H_2 ligand ($^4J_{H,H} = 1.8$ Hz), which in turn exhibits a ^3J-coupling of 0.25 Hz with the other CH unit. NOE experiments show that the methyl group attached to the metal couples with that half of the acetylene turned away from it (cf. Fig. 2). A similar NOE difference is observed for the alkyne methyl groups in **7b**. Two non-interconvertable isomers are formed in each of the cases **7c** (2-pentyne) and **7e** (2-hexyne). They can be distinguished by means of their NMR data (Table 1), and their existence is due to the opposite orientation of the alkyne ligands relative to the pyramidal, C_{2v}-symmetric CH_3ReO_2 fragment (see Scheme 3).

With further polymer-bound triphenylphosphane in boiling toluene (2 d), the Re^V complex **7b** can be reduced to the dinuclear Re^{IV} derivative **8**.[10] Alkyne complexes of tetravalent rhenium were hitherto unknown.

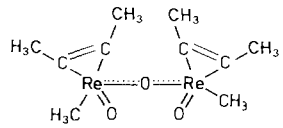

Table 1. Spectroscopic data of the alkyne complexes **7a–d** and **7f–h**.

Cpd.	^{1}H-NMR (270 MHz, $CDCl_3$, 25 °C) [a]	^{13}C{^{1}H}-NMR (68 MHz, $CDCl_3$, 25 °C)	IR (KBr) [cm^{-1}] ν(C≡C)	ν(Re=O)
7a	2.71 (CH_3; d, 3H; ^4J(H,H) = 1.8) 9.33 (CH; d, 1H; ^3J(H,H) = 0.25) 9.51 (*CH*; dq)	6.2 (CH_3), 129.0/138.7 (C≡C) [b]	1629 m	975 vs, 965 vs, 926 vs, 896 vs
7b	2.47 ($ReCH_3$; s, 3H), 2.72, 2.87 (CH_3C; 2 × q, 2 × 3H; ^5J(H,H) = 1.0)	5.3 ($ReCH_3$), 8.7, 14.3 (CH_3C), 131.0, 138.0 (C≡C)	1835 w	968 vs, 933 vs
7c	Isom. I Isom. II [c] 2.48 2.47 ($ReCH_3$; s, 3H) 1.37 1.44 (CH_2CH_3; t, 3H; ^3J = 7.3) 2.74 2.92 (CCH_3; t, 3H; ^5J = 1.0) 3.14 2.99 (CH_2CH_3; qq, 2H; ^3J = 7.3, ^5J = 1.0)	4.3, 5.1 ($ReCH_3$), 9.0, 13.2, 13.5, 14.6, 18.3, 22.0 (CH_2/CH_3), 131.2, 235.9, 136.8, 142.4 (C≡C)	1826 w	970 vs, 931 vs
7d	2.48 ($ReCH_3$; s, 3H), 1.35, 1.41 (CH_2CH_3; 2 × t, 6H; ^3J(H,H) = 7.5), 3.01, 3.20 (CH_2; 3 × tq, 4H; ^3J(H,H) = 7.5, ^5J(H,H) = 1.0)	4.1 ($ReCH_3$) [d], 13.6, 13.9 ($(CH_2)_3$), 18.1, 21.9 (CH_2), 136.1, 140.9 (C≡C)	1821 w	973 vs, 935 vs
7f	2.65 ($ReCH_3$; s, 3H), 1.41 ($C(CH_3)_3$; s, 9H), 8.75 (CH; s, 1H)	5.1 ($ReCH_3$), 30.0 ($C(CH_3)_3$), 33.8 ($C(CH)_3$), 125.3 (C≡*C*H), 153.5 (C≡*C*tBu)	1733 w	975 vs, 936 vs, 904 m
7g	2.78 ($ReCH_3$; s, 3H), 9.37 (C≡CH; s, 1H), 7.53 (C_6H_5; m, 3H), 7.82 (C_6H_5; m, 2H)	6.3 ($ReCH_3$), 126.7, 129.2, 132.0, 133.2 (C_6H_5), 131.5, 140.9 (C≡C)	1735 w	970 vs, 933 vs, 921 vs
7h	2.63 ($ReCH_3$; s, 3H), 7.52 (C_6H_5; m, 8H), 7.83 (C_6H_5; m, 2H)	7.9 ($ReCH_3$), 127.8, 129.0, 129.1, 129.5, 129.9, 130.3, 131.6, 132.0 (C_6H_5), 135.1, 143.1 (C≡C)	—	968 vs, 934 vs, 908 vs

[a] Coupling constants in Hz. [b] CH coupling constants [Hz]: $ReCH_3$ 135.1; C_2H_2 226.0 [^1J(CH)] and 13.0 [^2J(CH)] (mean value). [c] I/II = 65/35 (NMR spectroscopically). [d] ^1J(C,H) = 135.5 Hz.

These results show that the methylrhenium(VII) compound **5** can be reduced stepwise by polymer-bound triphenylphosphane with retention of the methylrhenium partial structure to derivatives of hexa-, penta-, and tetravalent rhenium. That alkyne complexes of type **7** are stable substances, whereas the analogous C_5Me_5-complexes **1b** do not exist, could be attributed to the missing π-donor effect of the methyl as compared to the pentamethylcyclopentadienyl ligand or to a steric effect.

Experimental

7a: A solution of 500 mg (2.01 mmol) of **5** in 20 mL of toluene saturated with acetylene was treated with 700 mg (2.14 mmol) of polymer-bound $P(C_6H_5)_3$ [11] and the mixture stirred for 16 h in a C_2H_2 atmosphere. The mixture was then filtered over celite and the filtrate evaporated to dryness under vacuum. Recrystallization of the residue from *n*-hexane at -30°C furnished 130 mg (25%) of yellow crystals. M.p. 79°C.

7b–h: The procedure was the same as for the synthesis of **7a**, except that a twofold excess of the corresponding alkyne (referred to **5**) was used. Yields 60–95%. All compounds gave correct elemental analyses.

Received: January 8, 1988;
revised: February 2, 1988 [Z 2568 IE]
German version: *Angew. Chem. 100* (1988) 975

[1] B. E. Bursten, R. H. Clayton, *Organometallics 6* (1987) 2004.
[2] a) W. A. Herrmann, R. A. Fischer, E. Herdtweck, *J. Organomet. Chem. 329* (1987) C1; b) W. A. Herrmann, R. A. Fischer, unpublished.
[3] a) J. M. Mayer, T. H. Tulip, *J. Am. Chem. Soc. 106* (1984) 3878; b) J. M. Mayer, D. L. Thorn, T. H. Tulip, *ibid. 107* (1985) 7454; c) E. Valencia, B. D. Santarsiero, S. J. Geib, A. L. Rheingold, J. M. Mayer, *ibid. 109* (1987) 6896.
[4] E. J. M. de Boer, J. de With, A. G. Orpen, *J. Am. Chem. Soc. 108* (1986) 8271.
[5] Review articles: a) W. A. Herrmann, *J. Organomet. Chem. 300* (1986) 111; b) W. A. Herrmann, *Angew. Chem. 100* (1988), in press; *Angew. Chem. Int. Ed. Engl. 27* (1988), in press.
[6] W. A. Herrmann, J. Kuchler, J. K. Felixberger, E. Herdtweck, W. Wagner, *Angew. Chem. 100* (1988) 420; *Angew. Chem. Int. Ed. Engl. 27* (1988) 394.
[7] **6**: reddish-brown prisms; monoclinic, $P2_1/c$ (No. 14); $a = 1201.4(2)$, $b = 986.3(1)$, $c = 1741.8(4)$ pm, $\beta = 100.02(2)°$; $V = 2032 \times 10^6$ pm^3, $Z = 2$; $M = 1148.9$; $T = 24$°C; ρ(X-ray) = 1.877 g·cm^{-3}; $F_{000} = 1104$; CAD4 (Enraf-Nonius), graphite monochromator, $\lambda = 0.7107$ Å ($Mo_{K\alpha}$), data collection range: $2° \leq \theta \leq 20°$, t(max) = 90 s, $h(0/11)$, $k(0/9)$, $l(-16/16)$; 2153 recorded reflections, 1877 independent reflections, 1474 independent reflections with $I > 1.0\sigma(I)$ used for the refinement; solution of structure by the Patterson method; full matrix least-squares refinement; all non-hydrogen atoms refined anisotropically, H atoms at calculated ideal positions and used for calculation of the structure factors; empirical absorption correction, $\mu = 64.2$ cm^{-1}; $R = \Sigma(\|F_0| - |F_c\|)/\Sigma|F_0| = 0.024$; $R_w = [\Sigma w(|F_0| - |F_c|)^2/\Sigma w F_0^2]^{1/2} = 0.016$; GOF = $[\Sigma w(|F_0| - |F_c|)^2/(\text{NO-NV})]^{1/2} = 1.355$ ($w = 1/\sigma^2(F_0)$); $\Delta e_0/$Å$^3 = 0.47$ besides Re; shift/error = 0.00.
7h: colorless prisms; monoclinic, $P2_1/c$ (No. 14); $a = 950.8(3)$, $b = 2083.5(8)$, $c = 1411.1(6)$ pm, $\beta = 100.70(2)°$, $V = 2747 \times 10^6$ pm^3, $Z = 8$; $M = 411.5$; $T = -80$°C; ρ(X-ray) = 1.990 g·cm^{-3}; $F_{000} = 1552$; CAD4 (Enraf Nonius), graphite monochromator, $\lambda = 0.7107$ Å ($Mo_{K\alpha}$), data collection range $2° \leq \theta \leq 22.5°$, t(max) = 60 s; $h(-10/10)$, $k(0/22)$, $l(-15/15)$; 7335 measured reflections, 3552 independent reflections, 3061 independent reflections with $I > 0.5\sigma(I)$ used for the refinement; solution of structure by the Patterson method; full matrix least-squares refinement; all non-hydrogen atoms refined anisotropically, H atoms at calculated ideal positions and used for calculation of the structure factors; empirical absorption correction, $\mu = 89.6$ cm^{-1}, $R = \Sigma(\|F_0| - |F_c\|)/\Sigma|F_0| = 0.039$; $R_w = [\Sigma w(|F_0| - |F_c|)^2/\Sigma w F_0^2]^{1/2} = 0.026$; GOF = $[\Sigma w(|F_0| - |F_c|)^2/(\text{NO-NV})]^{1/2} = 2.117$ ($w = 1/\sigma^2(F_0)$); $\Delta e_0/$Å$^3 = 1.33$ besides rhenium, shift/error = 0.00.
[8] Yellow needles, m.p. 123.5°C (decomp., formation of **5**); yield 100%.—IR: ν(ReO) = 925 cm^{-1} (vs); ^{1}H-NMR (270 MHz, 25°C, $CDCl_3$): $\delta(CH_3) = 1.40$ (s, 3H), $\delta(CH_2, \alpha) = 2.48$ (t, 6H), $\delta(CH_2, \beta) = 1.51$ (dt, 6H), $\delta(CH, \gamma) = 1.80$ (sept, 1H); ^{13}C-NMR (68 MHz, 20°C, $CDCl_3$): $\delta(ReCH_3) = 24.36$, $\delta(CH_2, \alpha) = 47.81$, $\delta(CH_2, \beta) = 26.18$, $\delta(CH, \gamma) = 20.61$; EI-MS (70 eV): m/z 361 (parent ion, ^{187}Re); correct C,H,N,Re analyses; according to an X-ray structure analysis trigonal-bipyramidal with equatorial oxo ligands.
[9] J. L. Templeton, B. C. Ward, *J. Am. Chem. Soc. 102* (1980) 3288.
[10] Orange colored crystals, m.p. = 185°C (decomp.); yield 90%.—IR (KBr): ν(ReO) = 964 (sst), ν(ReORe) = 720 cm^{-1} m; ^{1}H-NMR (270 MHz, 25°C, $CDCl_3$): $\delta(ReCH_3) = 2.76$ (s, 6H), $\delta(CCH_3) = 2.88$, 3.25 (2 q, 12 H; $^5J(H,H) = 1.0$ Hz); ^{13}C-NMR (68 MHz, 20°C, $CDCl_3$): $\delta(CH_3) = 10.8$, 15.9, 23.6; $\delta(C{\equiv}C) = 143.3$, 148.5; EI-MS (70 eV): m/z 558 (parent ion, ^{187}Re); correct C,H,O analysis.
[11] Polystyrene-bound triphenylphosphane (Aldrich) with 9.5% P, cross-linking by 1,4-divinylbenzene; 3.06 mmol triphenylphosphane/g polymer.
[12] Further details of the crystal structure analyses are available on request from the Fachinformationszentrum Energie, Physik, Mathematik GmbH, D-7514 Eggenstein-Leopoldshafen 2 (FRG), on quoting the depository number CSD-52902, the names of the authors, and the journal citation.

Synthesis of Octahedral Hydrido(vinyl)iridium(III) Complexes by C–H Activation: An Example of a Thermodynamically Favored Rearrangement [M(CHR=CHX)]→[M(H)(CR=CHX)]**

By *Helmut Werner,* Thomas Dirnberger,* and *Michael Schulz*

Dedicated to Professor Heinrich Nöth on the occasion of his 60th birthday

During the course of intensive investigations into C–H activation,[1] *Stoutland* and *Bergman* reported in a much referenced paper in 1985 that not only aliphatic and aromatic hydrocarbons but also olefins such as ethylene react with a coordinatively unsaturated metal center by oxidative addition.[2] They concluded on the basis of the results summarized in Scheme 1, which have later been supported by MO calculations,[3] that in the thermal reaction of $[C_5Me_5(PMe_3)IrH(C_6H_{11})]$ with C_2H_4 the ethylene metal complex **2** is the thermodynamically favored product and thus is *not* an intermediate in the formation of **1**. Shortly thereafter, *Perutz* et al. demonstrated spectroscopically that photolysis of $[C_5H_5Ir(C_2H_4)_2]$ in an argon matrix leads to formation of the hydrido(vinyl)iridium compound $[C_5H_5(C_2H_4)IrH(C_2H_3)]$, which isomerizes at 0°C to regenerate the starting material $[C_5H_5Ir(C_2H_4)_2]$.[4]

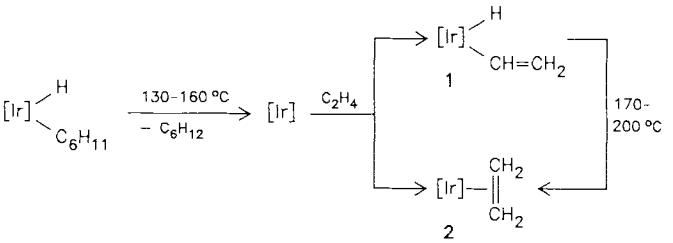

Scheme 1. [Ir] = $[C_5Me_5(PMe_3)Ir]$.

In the present work, we report that the order of thermodynamic stability found by *Bergman* et al. and *Perutz* et al., [Ir](H)(CH=CHR) < [Ir](η^2-CH_2=CHR), is reversed if the coordination geometry at the iridium center is changed and if the hydrido(vinyl)metal moiety is stabilized by an additional linkage to the metal atom.

[*] Prof. Dr. H. Werner, Dipl.-Chem. Th. Dirnberger, Dipl.-Chem. M. Schulz
Institut für anorganische Chemie der Universität
Am Hubland, D-8700 Würzburg (FRG)

[**] This work has been supported by the Deutsche Forschungsgemeinschaft, the Fonds der Chemischen Industrie and by Degussa AG.

Complex **4**, which is formed *in situ* from **3** and $PiPr_3$, reacts with H_2 and benzene to give the five-coordinated iridium(III) compounds **5** and **6**.[5] The osmium complex $[OsHCl(CO)(PiPr_3)_2]$, which is related in structure to **5** and **6**, reacts with olefins such as **7a** and **7b** (see Scheme 2) at room temperature to afford the corresponding adducts $[OsHCl(CO)(CH_2{=}CHX)(PiPr_3)_2]$ (X = CO_2Me, COMe);[6] by contrast, under the same conditions the iridium compounds **5** and **6** are inert toward the olefins **7a–c**. At higher temperature (C_6H_6, 80°C), a slow reaction occurs which leads to the formation of the hydrido(vinyl)metal complexes **9a–c** in excellent yield. The octahedral structure proposed for these compounds with *trans* phosphane ligands, metal-bound hydride and coordination of the C=O group is strongly supported by the NMR and IR data.[7] Participation of a carbene-type resonance form $[\overline{Ir}{=}C(R^1){-}C(R^2){=}C(R^3){-}\overline{O}$ ([Ir] = $IrHClL_2$) is ruled out primarily on the basis of the chemical shift of the α-C atom of the vinyl ligand in the ^{13}C-NMR spectrum of **9b**.[8]

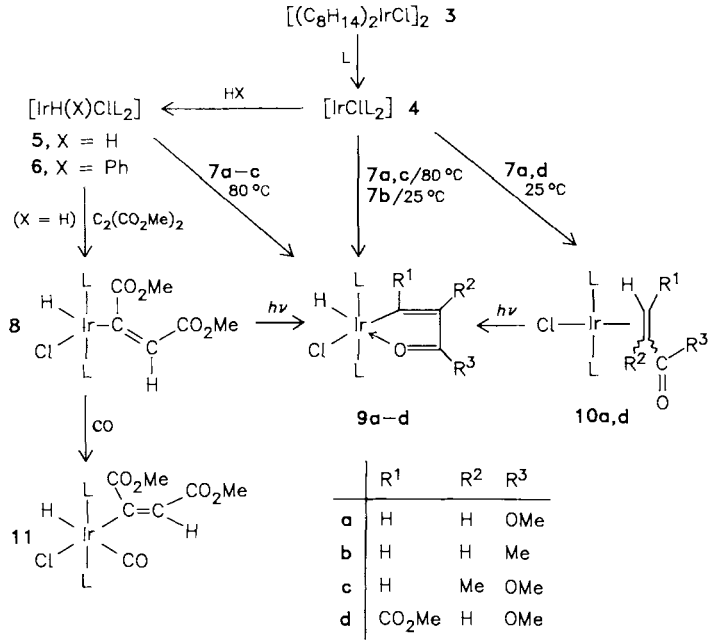

	R^1	R^2	R^3
a	H	H	OMe
b	H	H	Me
c	H	Me	OMe
d	CO_2Me	H	OMe

7a, $CH_2{=}CHCO_2Me$
7b, $CH_2{=}CHCOMe$
7c, $CH_2{=}C(CH_3)CO_2Me$
7d, (E)-$CH(CO_2Me){=}CH(CO_2Me)$

Scheme 2. L = $PiPr_3$.

In contrast to **7a–c**, dimethyl acetylenedicarboxylate reacts with **5** even at room temperature. The coordinatively unsaturated compound **8** is almost quantitatively formed by insertion of the alkyne into one of the Ir–H bonds. It is remarkably stable in the solid state and in solution, but rearranges on photolysis in benzene to give the hydrido(vinyl) complex **9d**. We assume that in presence of UV light a π-π* transition takes place which leads to a weakening of the C=C double bond of the vinyl ligand and, after rotation through 180°, to ring closure.

In the reactions of **5** and **6** with the olefin **7b**, the only other products besides **9b** which can be detected by GC/MS are 2-butanone and benzene. This finding supports the reaction mechanism shown in Scheme 3, which includes the olefin iridium complex **10b**, an isomer of **9b**, as an important intermediate. An attempt to prepare **10b** from **4** and **7b** in benzene at room temperature, however, led quantitatively to the formation of **9b**. By contrast, the olefins **7a** and **7d** react with **4** (C_6H_6, 25°C) to give the olefin–iridium compounds **10a** and **10d** (Scheme 2). The spectroscopic data of **10d**[7] provide no indication of whether the substituents at the C=C double bond are *cis* or *trans* oriented.

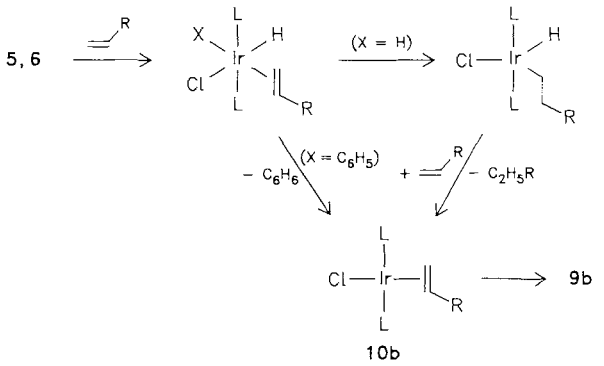

Scheme 3. L = $PiPr_3$; R = COMe.

On irradiation in benzene, the complexes **10a** and **10d** rearrange quantitatively to give the isomers **9a** and **9d**. The solvent is not involved in this process, as in C_6D_6 the deuterium-free products are also formed. The rearrangement can be easily followed visually as the olefin compounds are red whereas the hydrido(vinyl) compounds are colorless (**9a**) or yellow (**9d**), respectively.

Complex **9a** is also obtained by heating a solution of **4** and **7a** in refluxing benzene. Under similar conditions, treatment of **4** with **7c** gives the corresponding hydrido(vinyl) compound **9c**. We assume that, also in these reactions, an olefin complex (**10a** or **10c**) is most probably formed as an intermediate, which, however, reacts very rapidly at 80°C by intramolecular oxidative addition to afford **9a,c**.

A regeneration of **10a,d** from **9a,d** does not occur, either on heating or on photolysis. The stabilization of the hydrido(vinyl)iridium moiety caused by the chelate formation also manifests itself in the compounds **9a–d** being inert towards CO. Under a CO atmosphere, no opening of the chelate ring by breaking of the Ir–O bond takes place. On the contrary, the hydrido(vinyl) complex **8**, which is an isomer of **9d**, smoothly reacts with CO to give **11**, consistent with the behavior of other five-coordinated hydridoiridium(III) compounds.[5b,9]

The present results do not, of course, answer the question as to whether substituted olefins $CH_2{=}CHX$ or $CH_2{=}C(R)X$ (X = COMe, CO_2Me) *in general* react with coordinatively unsaturated transition-metal compounds to form hydrido(vinyl)metal complexes. It has already been shown in recent investigations by *Yamamoto* et al.[10] that the reaction of $[H_2Ru(PPh_3)_4]$ with methacrylic acid esters $CH_2{=}C(CH_3)CO_2R$ (R = Me, Et, *i*Pr, *n*Bu) leads to the formation of metallacyclic compounds of the type $[H(PPh_3)_3Ru{-}\overline{CH{=}C(CH_3){-}C(OMe){=}O}]$ by elimination of PPh_3 and H_2. Therefore, it is *not* new that a hydrido(vinyl) compound is formed from a reactive intermediate such as **4** and an olefin but it is now *evident* that this process occurs via an olefin-metal complex as an intermediate. The high energy barrier which had previously been observed for most of the reactions involving a C–H activation

of a coordinated olefin[2,3] is obviously reduced if the C=C double bond bears an electron-withdrawing substituent and if a chelate linkage of the generated vinyl group is possible. Various examples illustrating the highly facile formation and thermodynamic stability of five-membered rings of the general type $\overline{M-C(R)=C(R')-C(R'')=O}$ are already known.[11] The isolation of the complexes **10a,d** and their rearrangement to give **9a,d** supports the assumption that the C-H activation of benzene[5b] and other arenes[9b] with **4**, functioning as an electron-rich ligand-metal fragment, takes place via adduct formation, i.e., via a primary $[Ir(\eta^2\text{-}C_6H_{6-n}R_n)]$ intermediate.

Experimental

8: A solution of **5** (100 mg, 0.18 mmol) in benzene (7 mL) was treated with $C_2(CO_2Me)_2$ (26 mg, 0.18 mmol) with stirring at room temperature. Stirring was continued for 5 min, and the solution then concentrated to ca. 2 mL in vacuo, and chromatographed on Al_2O_3 (neutral, activity grade V) with hexane/benzene (4:1). After removal of the solvent the residue was washed with cold pentane to give an orange-red, moderately air-stable crystalline powder; m.p. 118°C (decomp.); yield 90%; correct elemental analysis.

9a-c: a) A suspension of **3** (120 mg, 0.13 mmol) in benzene (10 mL) was treated successively with $PiPr_3$ (86 mg, 0.54 mmol) and **7a-c** (0.26 mmol). The suspension was stirred 1) for 3 h under reflux (**7a**), 2) for 20 min at 25°C (**7b**), and 3) for 6 h under reflux (**7c**). After removal of the solvent in vacuo the oily residue was dissolved in hexane/benzene (2:1), and the solution was chromatographed on Al_2O_3 (neutral, activity grade V). Further work-up as for **8**; yield 80-90%.—b) A solution of **5** or **6** (0.18 mmol) in benzene (5 mL) was treated with **7a-c** (0.40 mmol) and heated under reflux for 12 h (**7a, b**) or 4 days (**7c**), respectively. Work-up as for **8**; yield 75-85%. White (**9a, c**) or light yellow (**9b**), moderately air-stable crystals; m.p. (decomp.) 167°C (**9a, b**), 192°C (**9c**); correct elemental analyses.

9d: A solution of **8** (80 mg, 0.12 mmol) in benzene (5 mL) was irradiated for 12 h (Hanovia 450 W). Work-up as for **9a-c**; yield 80%; yellow air-stable crystals, m.p. 175°C (decomp.); correct elemental analysis.

10a,d: A suspension of **3** (110 mg, 0.12 mmol) in benzene (10 mL) was treated successively with $PiPr_3$ (79 mg, 0.49 mmol) and **7a,d** (0.24 mmol) and stirred for 10 min at room temperature. After removal of the solvent the residue was recrystallized from pentane (25°C→−78°C); yield 70-80%. Red, moderately air-stable crystals; m.p. (decomp.) 110°C (**10a**), 121°C (**10d**); correct elemental analyses.—On irradiation in benzene (**10a**: 3 h; **10d**: 12 h) a rearrangement to **9a,d** occurs; yield 80%.

Received: March 22, 1988 [Z 2673 IE]
German version: *Angew. Chem. 100* (1988) 993

[1] Leading references: A. H. Janowicz, R. A. Periana, J. M. Buchanan, C. A. Kovac, J. M. Stryker, M. J. Wax, R. G. Bergman, *Pure Appl. Chem. 56* (1984) 13; W. D. Jones, F. J. Feher, *J. Am. Chem. Soc. 106* (1984) 1650; M. L. H. Green, D. O'Hare, *Pure Appl. Chem. 57* (1985) 1897; J. Halpern, *Inorg. Chim. Acta 100* (1985) 41; R. H. Crabtree, *Chem. Rev. 85* (1985) 245; I. P. Rothwell, *Polyhedron 4* (1985) 77; W. A. G. Graham, *J. Organomet. Chem. 300* (1986) 81.

[2] P. O. Stoutland, R. G. Bergman, *J. Am. Chem. Soc. 107* (1985) 4581.

[3] J. Silvestre, M. J. Calhorda, R. Hoffmann, P. O. Stoutland, R. G. Bergman, *Organometallics 5* (1986) 1841.

[4] D. M. Haddleton, R. N. Perutz, *J. Chem. Soc. Chem. Commun. 1986*, 1734. A further example for the rearrangement $MH(CH=CHR)\rightarrow M(\eta^2\text{-}CH_2=CHR)$ (M = Fe) has been reported: M. V. Baker, L. D. Field, *J. Am. Chem. Soc. 108* (1986) 7433.

[5] a) H. Werner, J. Wolf, A. Höhn, *J. Organomet. Chem. 287* (1985) 395; b) H. Werner, A. Höhn, M. Dziallas, *Angew. Chem. 98* (1986) 1112; *Angew. Chem. Int. Ed. Engl. 25* (1986) 1090.

[6] M. A. Esteruelas, H. Werner, *J. Organomet. Chem. 303* (1986) 221.

[7] Spectroscopic data (without NMR data for the $PiPr_3$ ligands); **8**: M_r = 692 (MS); IR (KBr): ν(IrH) = 2374, ν(CO) = 1741, 1706, ν(C=C) = 1571 cm^{-1}; ^{1}H-NMR ($CDCl_3$, 200 MHz): δ = 5.88 (s, br, =CH), 3.53 and 3.45 (both s, CO_2Me), −38.49 (t, J_{PH} = 13.1 Hz, IrH); ^{13}C-NMR ($CDCl_3$, 200 MHz): δ = 50.65 and 50.91 (both s, OCH_3), 129.66 (s, *C*H), 143.80 (s, br, IrC), 166.65 and 174.36 (both s, CO_2Me).—**9a**: M_r = 634 (MS); IR (KBr): ν(IrH) = 2262, ν(CO) = 1574 cm^{-1}; ^{1}H-NMR (C_6D_6, 90 MHz): δ = 10.51 (d, J_{HH} = 7.3 Hz, α-CH), 6.63 (d, J_{HH} = 7.3 Hz, β-CH), 3.65 (s, OMe), −26.83 (t, J_{PH} = 15.4 Hz, IrH).—**9b**: M_r = 618 (MS); IR (KBr): ν(IrH) = 2230; ν(CO) = 1539 cm^{-1}; ^{1}H-NMR ($CDCl_3$, 200 MHz): δ = 10.72 (d, J_{HH} = 7.3 Hz, α-CH), 6.80 (d, J_{HH} = 7.3 Hz, β-CH), 2.24 (s, br, COMe), −23.67 (t, J_{PH} = 15.8 Hz, IrH); ^{13}C-NMR ($CDCl_3$, 200 MHz): δ = 24.89 (s, CH_3), 133.18 (s, β-CH), 198.81 (t, J_{PC} = 6.1 Hz, α-C), 207.05 (s, *C*CH$_3$).—**9c**: M_r = 648 (MS); IR (KBr): ν(IrH) = 2259, ν(CO) = 1593 cm^{-1}; ^{1}H-NMR (C_6D_6, 90 MHz): δ = 9.95 (s, α-CH), 3.65 (s, OMe), 1.80 (s, br, CMe), −26.50 (t, J_{PH} = 15.4 Hz, IrH).—**9d**: M_r = 692 (MS); IR (KBr): ν(IrH) = 2306, ν(CO) = 1709, 1589 cm^{-1}; ^{1}H-NMR ($CDCl_3$, 200 MHz): δ = 6.72 (t, J_{PH} = 1.3 Hz, β-CH), 3.82 and 3.57 (both s, CO_2Me and OMe), −27.86 (t, J_{PH} = 15.1 Hz, IrH); ^{13}C-NMR ($CDCl_3$, 68 MHz): δ = 51.22 and 52.95 (both s, OCH_3), 122.26 (s, β-CH), 176.39 and 182.08 (both s, *C*O$_2$Me and *C*OMe), 178.92 (t, J_{PC} = 6.8 Hz, α-C).—**10a**: M_r = 634 (MS); IR (KBr): ν(CO) = 1716 cm^{-1}; ^{1}H-NMR (C_6D_6, 200 MHz): δ = 3.58, 2.51 and 1.76 (always m, =CH), 3.42 (s, CO_2Me).—**10d**: IR (KBr): ν(CO) = 1704 cm^{-1}; ^{1}H-NMR ($CDCl_3$, 200 MHz): δ = 3.82 (t, J_{PH} = 6.3 Hz, =CH), 3.45 (s, CO_2Me); ^{13}C-NMR ($CDCl_3$, 200 MHz): δ = 51.43 (s, OCH_3), 133.33 (s, br, *C*HCO$_2$Me), 174.01 (s, *C*O$_2$Me).

[8] For ^{13}C-NMR data of octahedral carbeneiridium complexes see: A. J. Hartshorn, M. F. Lappert, K. Turner, *J. Chem. Soc. Dalton Trans. 1978*, 348; M. A. Gallop, W. R. Roper, *Adv. Organomet. Chem. 25* (1986) 121; J. M. O'Connor, L. Pu, A. L. Rheingold, *J. Am. Chem. Soc. 109* (1987) 7578.

[9] a) A. Höhn, *Dissertation*, Universität Würzburg 1986; b) M. Dziallas, *Dissertation*, Universität Würzburg 1988.

[10] S. Komiya, T. Ito, M. Cowie, A. Yamamoto, J. A. Ibers, *J. Am. Chem. Soc. 98* (1976) 3874.

[11] Recent results: H. G. Alt, H. E. Engelhardt, U. Thewalt, J. Riede, *J. Organomet. Chem. 288* (1985) 165; H. Werner, R. Weinand, H. Otto, *ibid. 307* (1986) 49; M. Cariou, M. M. Kubicki, R. Kergoat, J. E. Guerchais, P. L'Haridon, *ibid. 304* (1986) 127; M. I. Bruce, A. Catlow, M. G. Humphrey, G. A. Koutsantonis, M. R. Snow, E. R. T. Tiekink, *ibid. 338* (1988) 59.

Tetraphosphafulvalenes

By *Nicole Maigrot, Louis Ricard, Claude Charrier,* and *François Mathey**

The search for new synthetic metals and superconductors is currently a very active field of research.[1] The polymeric backbones of most of these superconducting materials are based upon the tetrathiafulvalene (TTF)[2] or the tetraselenafulvalene structure.[3] Recently, tetratellurafulvalene was prepared,[4] and now extends the range of available building blocks for the construction of such materials. A further extension can be envisaged if phosphorus is used as a substitute for sulfur. Using the tetraphosphafulvalene moiety, it is indeed possible to build three structures which are isoelectronic to TTF and its cations (**A-C**). Of course, the redox and coordinating properties of these species could be different from those of their TTF counterparts.

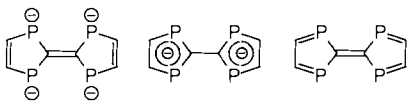

As starting compound for the synthesis of the previously unknown tetraphosphafulvalene moiety we chose the 1,2-dihydro-1,2-diphosphete system **1**, which is now available with a wide range of substituents.[5] The cleavage of the P-P bond of this ring system by lithium in THF has already been described.[6] The dianions **2** thus obtained react with tetrachloroethylene to give the desired tetraphosphafulvalenes **3** (≙ type **A**) in modest but acceptable yields [Eq. (a)].

[*] Prof. F. Mathey, Dr. N. Maigrot, Dr. L. Ricard, Dr. C. Charrier
Laboratoire de Chimie du Phosphore et des Métaux de Transition
DCPH Ecole Polytechnique,
F-91128 Palaiseau Cedex (France)

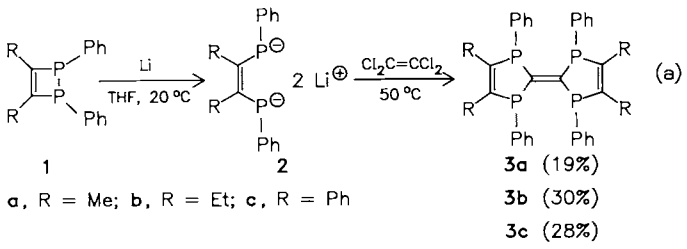

Table 1 shows the spectroscopic data of **3a-c**. In order to characterize this new structure more completely, we also carried out an X-ray crystal structure analysis of the tetra-

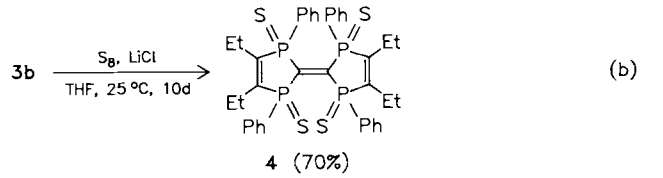

sulfide **4** (Fig. 1),[7] which is obtained as depicted in equation (b). The carbon–carbon double bonds are completely localized. The two five-membered rings are almost perfectly planar but are slightly tilted (interplanar angle 4.22(7)°). The torsion of the central C=C bond is, no doubt, due to steric congestion. The "all-*trans*" disposition of the sulfur atoms is also noteworthy.

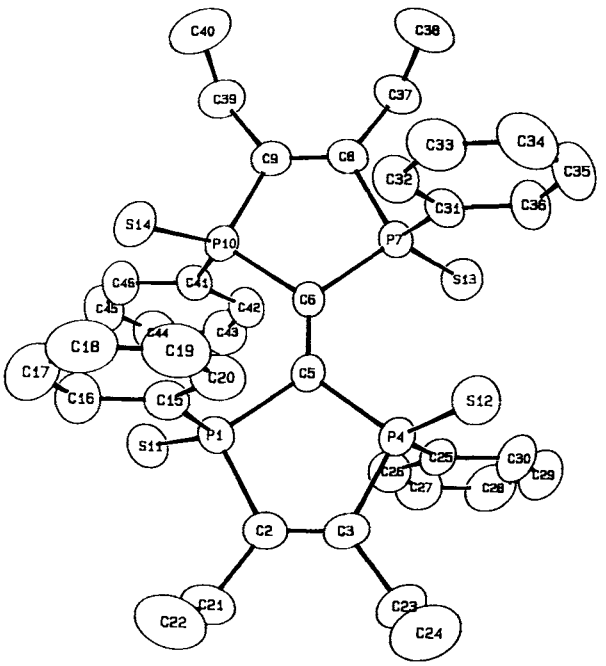

Fig. 1. Structure of 4 in the crystal [7]. Ellipsoids are scaled to enclose 50% of the electronic density. Hydrogen atoms are omitted for clarity. Important bond distances [Å] and angles [°]: S11-P1 1.934(1), S12-P4 1.932(1), S13-P7 1.937(1), S14-P10 1.936(1), P1-C2 1.815(3), P1-C5 1.862(3), P1-C15 1.812(3), P4-C3 1.796(3), P4-C5 1.846(3), P4-C25 1.813(4), P7-C6 1.853(3), P7-C8 1.800(3), P7-C31 1.811(3), P10-C6 1.856(3), P10-C9 1.809(3), P10-C41 1.815(3), C2-C3 1.325(4), C2-C21 1.520(4), C3-C23 1.529(5), C5-C6 1.342(4), C8-C9 1.340(4), C8-C37 1.502(4), C9-C39 1.511(4), ⟨C-H⟩ 0.97(13); C2-P1-C5 98.7(1), C3-P4-C5 99.2(1), C6-P7-C8 99.4(1), C6-P10-C9 98.9(1), P1-C2-C3 116.8(2), P4-C3-C2 117.9(2), P1-C5-P4 107.2(1), P1-C5-C6 125.6(2), P4-C5-C6 127.2(2), P7-C6-P10 107.2(1), P7-C6-C5 126.3(2), P10-C6-C5 126.5(2), P7-C8-C9 117.0(2), P10-C9-C8 117.3(2).

Table 1. Main spectroscopic data of **3a-c** and **4** (NMR spectra in CD_2Cl_2).

3a: ^{31}P-NMR: $\delta = 47.4$; ^{13}C-NMR: $\delta = 15.03$ (m, CH_3), 142.47 (s, MeC=CMe), 157.7 (s, $P_2C{=}CP_2$); MS (EI, 70 eV): *m/z* 565 ($M^{\oplus}+1$, 100%)

3b: ^{31}P-NMR: $\delta = 44.0$; ^{13}C-NMR: $\delta = 14.23$ (s, CH_3), 23.17 (m, CH_2), 149.45 (s, EtC=CEt), 157.7 (s, $P_2C{=}CP_2$); MS (EI, 70 eV): *m/z* 620 ($M^{\oplus}$, 100%)

3c: ^{31}P-NMR: $\delta = 63.2$; ^{13}C-NMR: $\delta = 148.30$ (s, PhC=CPh), 156.76 (s, $P_2C{=}CP_2$); MS (EI, 70 eV): *m/z* 812 ($M^{\oplus}$, 100%)

4: ^{31}P-NMR: $\delta = 48.9$; MS (EI, 70 eV): *m/z* 748 ($M^{\oplus}$, 20%), 716 ($M^{\oplus}-S$, 15%), 684 ($M^{\oplus}-2S$, 21%), 639 ($M^{\oplus}-PhS$, 60%), 607 ($M^{\oplus}-PhS_2$, 55%), 576 ($M^{\oplus}+H-PhS_3$, 51%), 431 (100%)

Experimental

All reactions were carried out under argon in Schlenk tubes.

3a-c: A mixture of **1** (8 mmol) and lithium (17 mmol) in THF was stirred at room temperature for 3 h. The lithium was completely dissolved. The mixture was heated to 50 °C and treated dropwise with 0.41 mL (4 mmol) of C_2Cl_4. The reaction is almost instantaneous. After evaporation of the THF, the residue was chromatographed on silica gel with a degassed hexane/toluene mixture (80/20).

4: A mixture of **3b** (0.5 g, 0.8 mmol), S_8 (0.15 g), and LiCl (0.1 g) in 15 mL of THF was stirred for 10 days at 25 °C. After evaporation of the solvent, the residue was chromatographed on silica gel with toluene. Yield 0.4 g (70%). The crystallization can be carried out in dichloromethane.

Received: April 6, 1988 [Z 2694 IE]
German version: *Angew. Chem. 100* (1988) 997

CAS Registry numbers:
1a, 114862-86-1; **1b**, 75600-53-2; **1c**, 42451-95-6; **3a**, 114862-87-2; **3b**, 114862-88-3; **3c**, 114862-89-4; **4**, 114862-90-7; $Cl_2C{=}CCl_2$, 127-18-4.

[1] For recent reviews of this field, see: D. O. Cowan, F. M. Wiygul, *Chem. Eng. News 64* (1986) No. 29, p. 28; J. M. Williams, M. A. Beno, H. H. Wang, P. C. W. Leung, T. J. Emge, U. Geiser, K. D. Carlson, *Acc. Chem. Res. 18* (1985) 261; R. L. Greene, G. B. Street, *Science (Washington, D.C.) 226* (1984) 651; M. R. Bryce, L. C. Murphy, *Nature (London) 309* (1984) 119. The most striking recent development in this area is the discovery of κ-$(ET)_2[Cu(NCS)_2]$ (ET = bis(ethylenedithio)tetrathiafulvalene), with a superconducting transition temperature of 10.4 K at ambient pressure, see: H. Urayama, H. Yamochi, G. Saito, K. Nozawa, T. Sugano, M. Kinoshita, S. Sato, K. Oshima, A. Kawamoto, J. Tanaka, *Chem. Lett. 1988*, 55; K. D. Carlson, U. Geiser, A. M. Kini, H. H. Wang, L. K. Montgomery, W. K. Kwok, M. A. Beno, J. M. Williams, C. S. Cariss, G. W. Crabtree, M.-H. Whangbo, M. Evain, *Inorg. Chem. 27* (1988) 965.

[2] F. Wudl, G. M. Smith, E. J. Hufnagel, *Chem. Commun. 1970*, 1453; F. Wudl, D. Wobshall, E. J. Hufnagel, *J. Am. Chem. Soc. 94* (1972) 670; D. L. Coffen, *Tetrahedron Lett. 1970*, 2633; D. L. Coffen, J. Q. Chambers, D. R. Williams, P. E. Garrett, N. D. Canfield, *J. Am. Chem. Soc. 93* (1971) 2258; R. Zahradnik, P. Carsky, S. Hünig, G. Kiesslich, D. Scheutzow, *Int. J. Sulfur Chem. 6* (1971) 109; S. Hünig, G. Kiesslich, H. Quast, D. Scheutzow, *Justus Liebigs Ann. Chem. 1973*, 310.

[3] E. M. Engler, V. V. Patel, *J. Am. Chem. Soc. 96* (1974) 7376; *J. Chem. Soc. Chem. Commun. 1975*, 671; *J. Org. Chem. 40* (1975) 387.

[4] R. D. McCullough, G. B. Kok, K. A. Lerstrup, D. O. Cowan, *J. Am. Chem. Soc. 109* (1987) 4115.

[5] L. Ricard, N. Maigrot, C. Charrier, F. Mathey, *Angew. Chem. 99* (1987) 590; *Angew. Chem. Int. Ed. Engl. 26* (1987) 548.

[6] C. Charrier, J. Guilhem, F. Mathey, *J. Org. Chem. 46* (1981) 3; C. Charrier, N. Maigrot, F. Mathey, F. Robert, Y. Jeannin, *Organometallics 5* (1986) 623.

[7] Suitable single crystals of **4** were grown by slow evaporation of CH_2Cl_2 solutions at room temperature. Space group $P\bar{1}$ with $a = 9.635(2)$, $b = 11.391(2)$, $c = 20.917(3)$ Å, $\alpha = 79.58(1)$, $\beta = 87.61(1)$, $\gamma = 65.48°$, $V = 2052.78(85)$ Å^3, $Z = 2$, $\rho_{calc} = 1.372$ g/cm^3, $\mu = 5.4$ cm^{-1}, $F_{000} = 884$. Data were collected at room temperature (18 ± 1 °C) using graphite monochromated $Mo_{K\alpha}$ radiation ($\lambda = 0.71073$ Å) and an Enraf-Nonius CAD4 diffractometer. The crystal structure was solved by direct methods using the Enraf-Nonius SDP program package. An ill-defined CH_2Cl_2 molecule co-crystallizes with the product. Hydrogen atoms were refined with fixed isotropic temperature factors equal to 1.3 times that of the attached carbon atom. 5641 unique reflections, $R = 0.050$, $R_w = 0.075$, GOF = 1.52. Further details of the crystal structure investigation are available on request from the Fachinformationszentrum Energie, Physik, Mathematik GmbH, D-7514 Eggenstein-Leopoldshafen 2 (FRG), on quoting the depository number CSD-53 125, the names of the authors, and the journal citation.

Reversible Coupling and Opening of a Boron–Carbon Bond

By *Günter Schmid,* Wolfgang Meyer-Zaika, Roland Boese,* and *Norbert Augart*

Dedicated to Professor Heinrich Nöth on the occasion of his 60th birthday

Lithium salts of 2,5-dihydro-1*H*-1,2-azaboroles[1] serve in a variety of ways as starting compounds for the synthesis of transition metal complexes and main group metal complexes.[2–4] As a rule, groups such as $E(CH_3)_3$ (E = Si, Ge, Sn, Pb) are σ-bonded to the C3 atom of the anion, thus leading to formation of 2,3-dihydroazaboroles.[5] Reaction (a), in which the 1-*tert*-butyl-2,3-dihydro-2-methyl-3-(4-pentenyl)-1*H*-1,2-azaborole **1** is formed as a colorless liquid ($b.p._{20\,torr}$ = 126–127 °C; 65% yield), proceeds in the same way.[6]

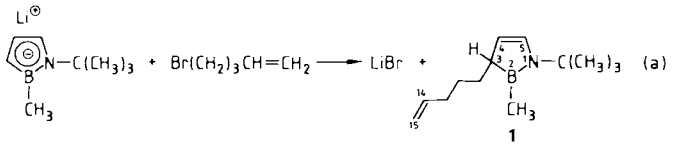

(a)

1

1 can easily be characterized ^1H-, ^{11}B- and ^{13}C-NMR spectroscopically.[6] It is readily isolable by distillation, but, surprisingly, slowly rearranges on cooling below about 80 °C to give the tricyclic crystalline compound **3**,[8a] in which the original olefinic carbon atoms C14 and C15 of the pentenyl group are coupled to the ring atoms C4 and B2, respectively. The process is reversible; i.e. **3** rearranges to the pentenyl compound **1** again at temperatures above 80 °C, and rapidly so upon distillation. **1** vitrifies upon rapid cooling, but does not crystallize.

Scheme 1 outlines our interpretation of the rearrangement process; **1a**–**1c** are merely model representations of the possible changes of conformation of the pentenyl residue on going from **1** to **3**. We visualize the rearrangement as arising from a donor–acceptor interaction between the π-electron pair of the pentenyl group and the electrophilic boron atom, which finally leads to the formation of the B2–C15 σ-bond. The coupling of the B2–C15 and C4–C14 bonds is associated with rehybridizations of the B2 and C4 atoms from sp^2 to sp^3. This results in the five-membered heterocycle no longer being planar. The B2–C15 interaction renders the C14 atom strongly electrophilic, so that this can now interact with the π-electron pair of the C4=C5 double bond of the heterocycle. These unusual bonding situations are verified in **2** (see below). Formation of the C5=N1 double bond takes place concomitantly with that of the B2–C15 and C4–C14 bonds.

Although **2** is not the most thermodynamically stable product, it is a crystallographically independent structure. During the transition from **2** to **3** the disorders in the crystal disappear, since in **3** there are "normal" bonds between C4 and C14 and B2 and C15, and puckering of the heterocycle is terminated.

Dihydroazaboroles themselves neither tend to undergo dimerization nor to react, e.g., with alkenes. The processes depicted in Scheme 1 are not observed even with analogues of **1** which bear a butenyl or hexenyl group on the C3 atom. The unusual behavior of **1** can therefore be attributed to the fact that the reaction **1** ⇄ **3** with the pentenyl group as substituent group can proceed essentially free of strain.

The transition from **1** to **3** and vice versa can be readily monitored by ^{11}B-NMR spectroscopy. For example, when a solution of **3** in toluene is heated to 80 °C the signal of **3** at $\delta = 4.6$ decreases with time and that of **1** at $\delta = 50.2$ increases. After 1 h the intensity ratio of the signals is about 1 : 1 and after 3 h the conversion is quantitative. **2** is only crystallographically detectable, but not in solution. The in-

Scheme 1. Possible course of the reversible reaction 1⇄3. The inset shows, a "stroboscopic recording" of the postulated reaction.

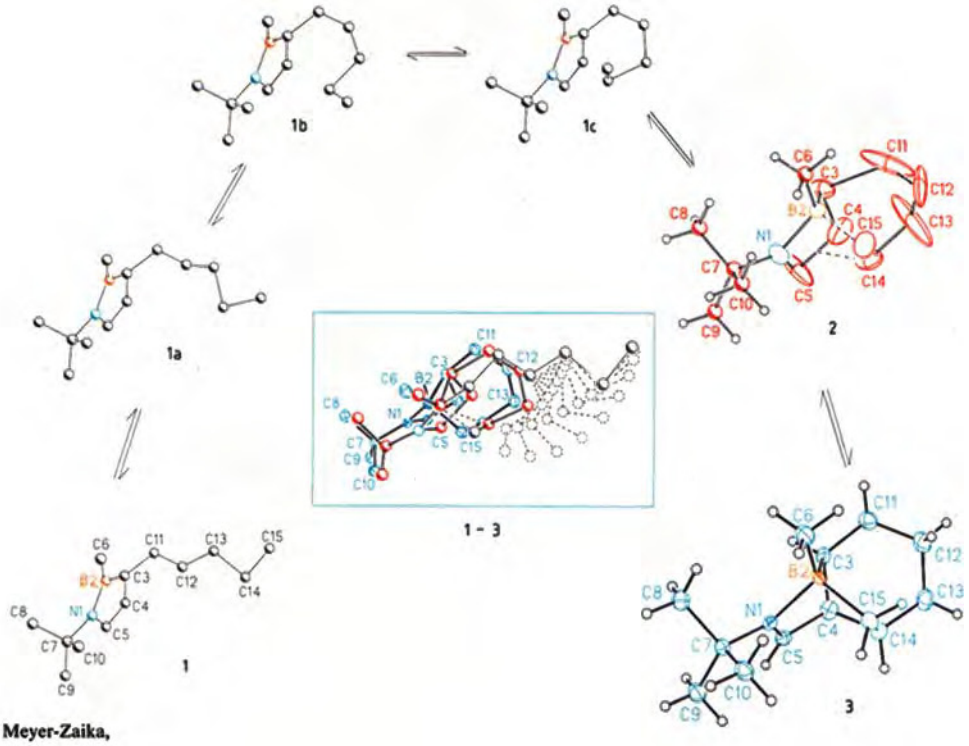

[*] Prof. Dr. G. Schmid, Dipl.-Chem. W. Meyer-Zaika, Dr. R. Boese, Dipl.-Chem. N. Augart
Institut für Anorganische Chemie der Universität
Universitätsstr. 5-7, D-4300 Essen 1 (FRG)

teraction of a ring boron atom with an olefinic C–C bond was first presumed in 1964 on the basis of IR data.[7]

Crystals of **3**[8b,c] (triclinic, $P\bar{1}$) were obtained on allowing the liquid compound to stand for several days in a refrigerator. Data collections at 303 K for two crystals, one of which had been annealed just below the melting point (308 K) for two weeks, furnished comparable structural data, as did also further measurements at 260 K, 180 K and 100 K. The vibration amplitudes of the anisotropically refined atomic parameters increase almost linearly from 100 to 303 K. Thus, in the case of **3**, disorders can be ruled out even just below the melting point. There were also no indications of a phase transition in the crystal in the polymorphic structure of **2**[9] (monoclinic, $P2_1/n$), cylindrical crystals of which were drawn from the melt between 301 K and 317 K in a Lindemann capillary (diameter 0.3 mm) using the Bridgeman technique.[10] Also several crystals of **2** prepared in this way gave comparable structural data. Data collections and refinements at 298 K, 288 K and 248 K gave, especially for the atoms C11, C12, C13, C4 and C5, anisotropic vibration amplitudes with highly disordered structures at the measurement temperatures. The direction of the disorders follows from the illustration of **2** in Scheme 1. As to whether dynamic or static disorders are involved cannot be decided, but the electronic patterns in **2** are consistent with dynamic effects. The disorders were not resolvable, as also indicated, inter alia, by electron density maps. Consequently the atomic positions could not be determined accurately, and the R values and standard deviations are correspondingly high. Determination of the structure of **2** at $T<248$ K was not possible because of broadening of the reflections.

Received: October 20, 1987 [Z 2481 IE]
German version: *Angew. Chem. 100* (1988) 956
Publication delayed at authors' request

CAS Registry numbers:
1, 114738-68-0; **3**, 114738-69-1; $Br(CH_2)_3CH{=}CH_2$, 1119-51-3; 2,5-dihydro-1*H*-1,2-azaborolene (lithium salt), 84356-32-1.

[1] G. Schmid, D. Kampmann, U. Höhner, R. Boese, *Chem. Ber. 117* (1984) 1052.
[2] G. Schmid, *Comments Inorg. Chem. 4* (1985) 17.
[3] G. Schmid, D. Zaika, R. Boese, *Angew. Chem. 97* (1985) 581; *Angew. Chem. Int. Ed. Engl. 24* (1985) 602.
[4] G. Schmid, O. Boltsch, R. Boese, *Organometallics 6* (1987) 435.
[5] G. Schmid, D. Zaika, J. Lehr, N. Augart, R. Boese, *Chem. Ber.*, in press.
[6] **1**: Synthesis by dropwise treatment of a solution of 16.3 g (110.1 mmol) of the lithium salt in 150 mL of THF with 17.0 g (110.1 mmol) of $Br(CH_2)_3CH{=}CH_2$ at −78 °C. After warming to room temperature and removal of the solvent under vacuum all products volatile up to 200 °C and 10^{-5} torr were condensed in a trap which was cooled with liquid nitrogen. On fractional distillation 13.4 g (65%) of **1** were collected as a water-clear liquid at 126–127 °C, (20 torr); correct elemental analysis; MS: m/z 205 ($M^{\oplus}$); ^{1}H-NMR ([D$_8$]toluene): $\delta=2.38$ (br, 1H; H3), 5.43 (dd, $^3J=4$, $^4J=2$ Hz, 1H; H4), 6.53 (dd, $^3J=4$, $^4J=2$ Hz, 1H; H5), 0.72 (s, 3H; B–CH_3), 1.19 (s, 9H; $C(CH_3)_3$), 1.45, 1.78, 2.10 (each m, each 2H; 3 CH_2), 5.82 (m, 1H; H14), 5.01 (dd, m, $^3J_{cis}=8.85$, $^3J_{trans}=19.5$ Hz, 2H; H15); ^{11}B-NMR ([D$_8$]toluene): $\delta=50.2$; ^{13}C{^{1}H}-NMR ([D$_8$]toluene, 373 K): $\delta=41.8$ (br; C3), 114.1 (C4), 139.1 (C5), 53.6 ($C(CH_3)_3$), 31.5 ($C(CH_3)_3$), 1.53 (br; B–CH_3), 28.3, 29.1, 34.4 (3 CH_2), 136.7 (C14), 115.8 (C15).
[7] R. Köster, *Prog. Boron Chem. 1* (1964) 314.
[8] a) **3**: ^{1}H-NMR ([D$_8$]toluene): $\delta=2.38$ (br, 1H; H3), 2.00 (m, 1H; H4), 7.09 (d, $^4J=7$ Hz, 1H; H5), 0.55 (s, 3H; H6), 0.96 (s, 9H; H8–H10), 1.46, 1.65, 1.88 (each m, each 2H; H11–H13), 0.03 (dd, 1H; H14), 1.98 (m, 2H; H15); ^{11}B-NMR ([D$_8$]toluene): $\delta=4.6$; ^{13}C{^{1}H}-NMR ([D$_8$]toluene, 298 K): $\delta=46.7$ (br; C3), 55.7 (C4), 171.2 (C5), 59.8 (C7), 28.9 (C8–C10), 2.6 (br: C6), 18.5, 26.9, 32.4 (C11–C13), 35.3 (C14), 22.6 (br; C15). b) Cell data (100 K): $a=6.065(3)$, $b=7.064(3)$, $c=14.960(10)$ Å, $\alpha=99.27(5)$, $\beta=94.82(5)$, $\gamma=97.01(4)°$, $P\bar{1}$, $Z=2$; 1644 independent reflections, 1266 observed ($F_0>4\sigma(F)$), ω data collection, $2\theta_{max}=45°$, $Mo_{K\alpha}$ radiation, $R=0.048$; maximum residual electron density 0.20 e Å^{-3}. Selected bond lengths [Å] and angles [°]: N1-B2 1.668(3), C5-N1 1.282(3), C4-C5 1.482(3), C3-C4 1.535(4), B2-C3 1.642(4), C4-C14 1.571(4), C14-C15 1.547(3), C15-B2 1.646(4), B2-C6 1.595(4), C3-C11 1.528(3), C11-C12 1.528(4), C12-C13 1.525(4), C13-C14 1.533(3); N1-B2-C3 94.0(2), N1-B2-C15 98.6(2), C15-B2-C3 101.7(2), B2-C15-C14 103.0(2), C4-C14-C15 103.3(2), C13-C14-C15 112.0(2), N1-C5-C4 112.2(2), C5-C4-C3 101.9(2), C4-C3-B2 93.3(2), B2-N1-C5 105.9(2). c) Further details of the crystal structure investigation are available on request from the Fachinformationszentrum Energie, Physik, Mathematik GmbH, D-7514 Eggenstein-Leopoldshafen 2 (FRG) on quoting the depository number CSD-52789, the names of the authors, and the journal citation.
[9] **2**: cell data (288 K): $a=6.493(3)$, $b=18.035(8)$, $c=11.638(5)$ Å, $\beta=101.61(3)°$, $P2_1/n$, $Z=4$; 1250 independent reflections, 983 observed ($F_0>4\sigma(F)$), ω data collection, $2\theta_{max}=45°$, $Mo_{K\alpha}$ radiation, $R=0.135$; maximum residual electron density 0.58 e Å^{-3} [8c].
[10] D. Brodalla, D. Mootz, R. Boese, W. Osswald, *J. Appl. Crystallogr. 18* (1985) 316.

Enzymes and Curvature

By *Zoltan Blum,* Sven Lidin,* and *Sten Andersson*

Numerous proteins and enzyme structures consist of two building units—the α-helix and the β-sheet. Many of these structures seem to belong to two spatial arrangements of the β-sheets—the barrel and the twisted sheet arrangement. Recently *Louie* and *Somorjai*[1] have shown that the barrel, i.e., its inside, is catenoid-like and the twisted sheet is helicoid-like, and that such surfaces are adjoint, which means one can be transformed into the other isometrically (Bonnet transformation, Fig. 1). Figure 2 schematically shows a

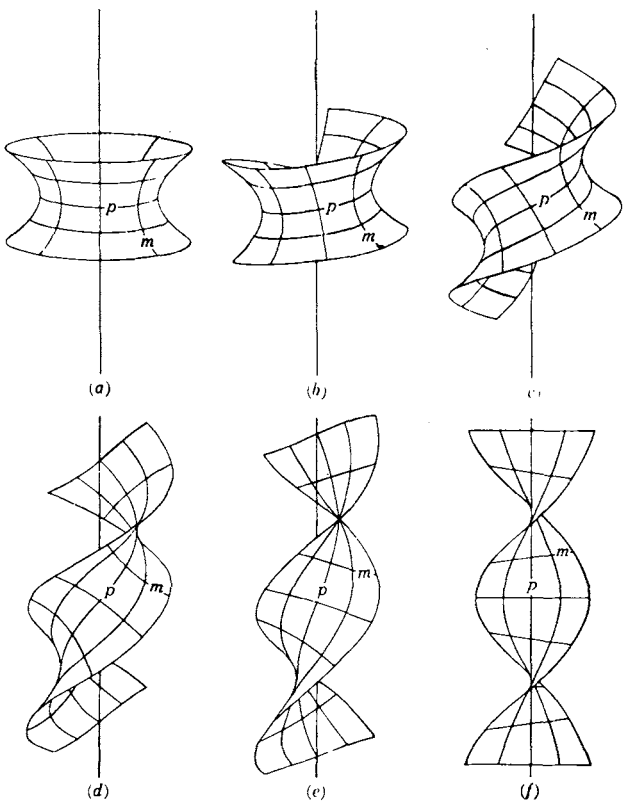

Fig. 1. The Bonnet transformation.

[*] Dr. Z. Blum, S. Lidin, Prof. Dr. S. Andersson
Chemical Center, University of Lund
Inorganic Chemistry 2
Box 124, S-221 00 Lund (Sweden)

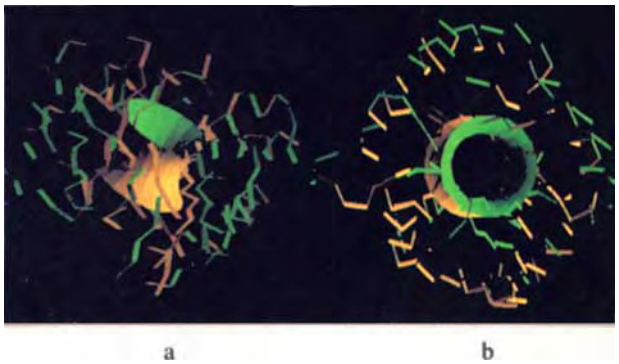

Fig. 2. α-Carbon representation of triose phosphate isomerase fitted to a catenoid; a) side view; b) view down the central "hole."

barrel protein with the catenoid fitted to the structure. The complete topology of the molecule can be approximated by a torus which has negative Gaussian curvature on the inside and positive on the outside. *Louie* and *Somorjai* also showed that the Bonnet transformation can be used to explain leading features of the much debated protein folding problem. They further propose that the Stieltjes integral, $\int F\mathrm{d}A$, describes the enzyme-substrate interaction. A is given by the equation $A = I + \mathrm{i}II$, where I and II are the first and second fundamental forms of equations of surfaces describing the enzyme structure, and F is a function describing the shape of the substrate. The Stieltjes integral is complex; therefore, projections onto the real plane are needed and they claim this is a way to understand catalysis, recognition, etc.

We find the propositions of *Louie* and *Somorjai* of extreme interest. Our approach, however, is different (see below) and also of direct use. It is allied in some ways to the DTE (*d*ynamic *t*ransduction of *e*nergy) theory[2] and, in fact, it seems to unify the static geometrical theory of *Louie* and *Somorjai* with the dynamic DTE theory.

In a number of articles we have demonstrated the use of differential geometry and especially minimal surfaces in chemistry.[3–7] It has also been shown that solids have periodic equi- or zero-potential surfaces, which are identical, or nearly so, with periodic minimal surfaces.[8] In two recent articles we have explained the adsorption properties of two different zeolites in terms of their integral curvature.[9, 10] The peculiar shape of the curves of differential heat versus initial adsorbed amount was explained by assuming a quasi-liquid state of molecules moving in the electrostatic field of the zeolite structure.[10] The initial heat developed at very low charge is often extremely high (Fig. 3).

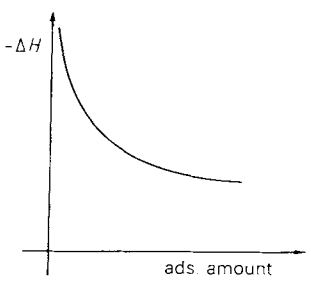

Fig. 3. Schematic representation of heat of adsorption versus loading on a zeolite.

We have explained the adsorptive properties of zeolites in terms of curvature [Eq. (1)]:

$$\Delta H = \mathrm{const}_1 K_{av} N \qquad (1)$$

K_{av} is the integral Gaussian curvature per surface area, ΔH the heat of adsorption, and N an interaction parameter. The first few molecules feel strong force fields focussed (van der Waals lens) via saddle rings of high intrinsic curvature, and high intrinsic heat is developed. This is obviously one of the reasons why zeolites are catalysts; molecules transform or crack even at room temperature owing to the intrinsic heat developed during their interaction with the zeolite surface structure of high curvature.

A unifying description of protein and enzyme structures, giving them negative Gaussian curvature, provides a simple explanation of their role in biosystems. We have estimated their negative average integral curvature to be 0.01–0.03 Å^{-2}. Therefore, according to Equation (1), intrinsic heats of adsorption high enough to start various reactions are easily developed.

The following description of protein action thus emerges; the substrate, conveniently viewed as a freely moving entity, reaches the vicinity of the protein. The latter can be either freely moving or bonded to some kind of biological matrix or "contrivance," e.g., a membrane. At a certain distance the substrate is influenced by attractive forces originating from the highly curved domain of the protein. The α-helices distending the β-sheets can be envisaged as providing discrimination, allowing access for substrates of proper size and/or configuration only. The substrate, so accepted, then enters the space close to the surface set up by the β-sheets. Each van der Waals active structural unit of the β-sheets contributes to a force field, which, owing to the curvature, is focussed, thereby enabling relatively remote units to act upon the substrate. A barrel protein can thus be conceived as a van der Waals lens. As the substrate is intercepted by the protein, kinetic energy is transformed into potential energy; i.e., the deceleration furnishes thermal excitation. Thus, intramolecular electron movement is substantially increased and bonding integrity may be regarded as partially lost. Explicit manipulations on the substrate can then be undertaken.

The model of van der Waals focussing is also valid in twisted sheet proteins because the surface set up by the twisted sheet, the helicoid, is isometric (curvature intact) to the inside of a barrel, the catenoid. Thus, when the substrate is located close to the highly curved surface of the protein it feels strong attractive forces from the entire protein.

Moreover, the relatively high flexibility of proteins permits a dynamic interaction with substrate molecules, thereby tuning the curvature; i.e., the energy "release" is partly governed by the entering substrate.

Other points of utmost importance in enzymatic reactions are concentration and extension. A serious shortcoming of the ordinary lock and key model is its failure to allow fully for the exceedingly low physiological concentrations of many enzyme substrates. Furthermore, a keyhole can only be arrived at by means of highly precise docking procedures; i.e., the reach of a keyhole into "space" is essentially nil. In view of the extraordinarily high turnover numbers often encountered in enzymatic processes it seems highly inexpedient to have a feeding mechanism that requires a low-concentration substrate to interact with the enzyme under conditions of extreme spatial ordering.

A saddle surface, i.e., a catenoid or a helicoid, on the other hand, has none of the keyhole restrictions. It could be regarded as infinite in terms of interactive impact. Any point on a saddle surface is the bull's-eye; the substrate would be intercepted and guided to the region of maximum curvature even though the preliminary encounter was of a random nature.

These ideas can be illustrated by a few examples; only enzymes describable as barrels or twisted sheets have been selected.[11] We have concentrated on enzymes displaying nonsophisticated chemical transformations and where a minimum of atom or group transfer is involved. Nevertheless, we believe that enzymes partaking in complex chemical transformations can be accounted for analogously; i.e., the major energy component is provided by the enzyme–substrate interaction.

Carboxypeptidase: a typical enzyme with the helicoid arrangement. It is a catabolic enzyme, degrading proteins by detaching amino acids starting from the carboxylic end. If we analyze the reaction in a strictly chemical sense, it is obviously a hydrolysis of an amide bond. Normally (i.e., in vitro) we accomplish this by heating an amide in water, adding a basic catalyst. The heat serves to energize the amide bond, i.e., to propagate the transient presence of high-energy entities and to confer additional thrust to the entering nucleophile (water). The catalyst simply transforms water into a more reactive form (hydroxide ion). If we assume that, by means of efficiently focussed van der Waals forces, carboxypeptidase imparts substantial thermal stress to the entering peptide, the free carboxylic end of which serves as an electron-rich target for nonbonding interactions, the transient existence of vibrationally excited entities coupled with heating of surrounding water molecules should provide the impetus necessary to bring about hydrolysis.

Triose phosphate isomerase; an archetypal catenoid enzyme. The reaction catalyzed by this enzyme is the transformation of dihydroxyacetone phosphate to glyceraldehyde-3-phosphate. Chemically this could be viewed either as a redox reaction, i.e., oxidation of an alcohol to an aldehyde and reduction of a ketone to an alcohol, or a re-enolization. Obviously there is no sophisticated chemistry involved and simple thermal excitation furnished by the van der Waals lens (triose phosphate isomerase) could be envisaged to propel the reaction. By analogy to the carboxylate in the example above the phosphate group could serve as an electron-rich target. In fact, one could seriously speculate that the presence of phosphate in biological systems, apart from buffering capacity, is explained by the need for a nontoxic, reasonably electron-rich van der Waals acceptor. Consequently, the role of phosphate esters as biochemical energy-carriers could be due to van der Waals targeting and the ease of hydrolysis of phosphate esters.

Pyruvate kinase; a catenoid enzyme. This enzyme catalyzes the detachment of phosphate from phosphoenolpyruvate yielding pyruvate. The phosphate group is concomitantly transferred to ADP. Chemically, the reaction is once again rather simple; hydrolysis of a phosphate ester followed by re-enolization. Again one can expect that thermal excitation in the presence of water and ADP is the major factor necessary for reaction.

Lactate dehydrogenase; a helicoid enzyme with the redox cofactor NADH. The reaction is a reduction of pyruvate to lactate. NADH is bound to the protein close to the curved arrangement of the β-sheets. Thermal excitation assists the entering hydride supplied by NADH.

Albumin; a carrier protein that cannot be described as either catenoid or helicoid. We have only been able to find clear representatives of the structure of prealbumin. Assuming that the curved nature of prealbumin is essentially preserved during its transformation to albumin, some interesting conclusions can be drawn. The structure can be characterized as an arbitrary part of a minimal surface. The curvature of the β-sheet arrangement appears to be lower than in the aforementioned proteins. Considering the function of albumin as a carrier of fatty acids, the relatively low curvature seems most reasonable. According to Equation (1), the impact of a curved surface on an entering molecule is dependent on the curvature of the surface. Obviously a carrier protein should have a curvature high enough to retain the molecules that are carried but not so high that damage is inflicted on the protein or that release of the molecules is too energy consuming. It is interesting to note that longer-chain fatty acids bind more readily to albumin than shorter-chain fatty acids. Furthermore, unsaturated fatty acids bind with higher affinity than saturated ones. If van der Waals interception is at work, one would indeed expect such behavior.

In this context it is tempting to propose that the extreme toxicity of 2,3,7,8-tetrachlorodibenzo[1,4]dioxin (TCD) might be a result of its interactions with highly curved proteins. If the interacting molecule is electron-rich and stable (both characteristics of TCD), the heat developed owing to the interaction could be sufficient to seriously damage the protein. The resulting collapse of structural integrity would release the TCD, undamaged and free to move to the next protein—the function of the dioxin becomes that of a more or less eternal projectile. Other chlorinated dioxins differ in toxicity, with TCD being the most toxic; owing to the arrangement of chlorine atoms, the slim, symmetrical TCD molecule should provide the best general fit to an arbitrary protein.

Extension of the latter proposal suggests an unprecedented approach to antiviral agents. It has been recently shown that the protein coat of polio viruses is compiled of four discrete proteins. Three of these are barrels. It is our opinion that these barrels are employed by the virus when a host cell is attacked. After binding to the surface of the cell, cell membrane components are attracted into the barrel thereby creating a hole in the cell membrane. Through this passage the virus can then inject the genetic material, the action of which finally proves fatal for the cell.

If this model of virus action is valid, it should be possible to exploit it advantageously in the treatment of viral diseases. By careful molecular design, it may be possible to prepare substances with the ability to interfere with the protein coat of viruses. These substances might irreversibly block the holes in the barrels, or, analogously to the proposed activity of dioxin, they might cause total destruction of the discrete proteins in the coat.

We feel that the recognition of highly curved protein structures represents a totally novel appreciation of protein function. Curvature-induced focussing of nonbonded interactions could also help to account for the energetics of many other biochemical events, such as transport across membranes, antigen-antibody interactions, splicing of mRNA precursors, action of tRNA in protein synthesis, and oxygen interception by hemoglobin.

Received: October 5, 1987;
revised: March 21, 1988 [Z 2459 IE]
German version: *Angew. Chem. 100* (1988) 995

[1] A. H. Louie, R. L. Somorjai, *J. Theor. Biol. 98* (1982) 189; *J. Mol. Biol. 168* (1983) 143; *Bull. Math. Biol. 46* (1984) 745.
[2] J. A. McCammon, P. G. Wolynes, M. Karplus, *Biochemistry 18* (1979) 927.
[3] S. Andersson, S. T. Hyde, H. G. von Schnering, *Z. Kristallogr. 168* (1984) 1.
[4] S. T. Hyde, S. Andersson, *Z. Kristallogr. 168* (1984) 221; *170* (1985) 225; *174* (1986) 225.
[5] S. T. Hyde, S. Andersson, B. Ericsson, K. Larsson, *Z. Kristallogr. 168* (1984) 213.
[6] A.-C. Eliasson, K. Larsson, S. Andersson, S. T. Hyde, R. Nesper, H. G. von Schnering, *Starch/Stärke 39* (1987) 147.
[7] S. T. Hyde, S. Andersson, K. Larsson, *Z. Kristallogr. 174* (1986) 237.
[8] R. Nesper, H. G. von Schnering, *Z. Kristallogr. 170* (1985) 138; *Angew. Chem. 98* (1986) 111; *Angew. Chem. Int. Ed. Engl. 25* (1986) 110.
[9] R. Thomasson, S. Lidin, S. Andersson, *Angew. Chem. 99* (1987) 1056; *Angew. Chem. Int. Ed. Engl. 26* (1987) 1017.
[10] Z. Blum, S. Lidin, R. Thomasson, *J. Solid State Chem.*, in press.
[11] J. S. Richardson, *Adv. Protein Chem. 34* (1981) 167.

$[Cu_8(iPrPCH_2PiPr)_2Cl_4(py)_5]$, a Novel Cu^I Cluster Containing Pentacoordinated Phosphorus in μ_3-PRR′ Bridges (R = *i*Pr, R′ = CH_2PiPr)**

By *Franjo Gol, Peter C. Knüppel, Othmar Stelzer,** and *William S. Sheldrick**

Dedicated to Professor Ulrich Wannagat on the occasion of his 65th birthday

Methylenebisphosphanes $HRPCH_2PRH$[1] can be transformed by oxidative addition[2] into difunctional phosphido-bridges $RPCH_2PR$, bonding up to four transition-metal atoms (**A**–**C**).

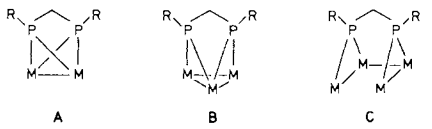

A B C

Attempts to synthesize tetranuclear complexes of monovalent copper by reaction of copper chloride in the presence of pyridine with dianionic PCP ligands formed by cleavage of the P–Si bonds in $(Me_3Si)iPrPCH_2PiPr(SiMe_3)$[3] [reaction (a)] resulted in the formation of a product mixture. When excess CuCl (CuCl: phosphane ligand 4:1) was used, however, a smooth reaction occurred which afforded $[Cu_8(iPrPCH_2PiPr)_2Cl_4(py)_5]$ [reaction (b)].

The diamagnetic Cu_8 complex **2** is a nonelectrolyte in CH_2Cl_2 solution and exhibits a singlet at $\delta = -61.1$ in the $^{31}P\{^1H\}$-NMR spectrum (CH_2Cl_2, 25 °C), which is broad (half-width ca. 50 Hz) owing to the quadrupole effect of $^{63}Cu/^{65}Cu$. Molecular weight determinations (osmometric in CH_2Cl_2) gave lower values (ca. 850) than that expected for **2** (1369.95). These findings indicate that one of the five pyridine ligands (see below the discussion of the X-ray structure) dissociates from the complex [equilibrium reaction (c)].

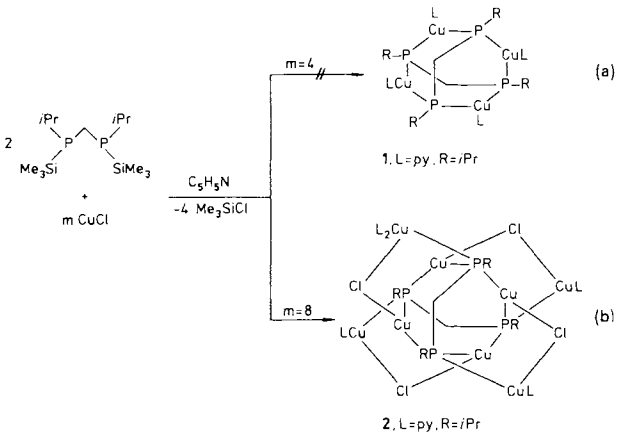

1, L = py, R = *i*Pr

2, L = py, R = *i*Pr

$$2 \rightleftharpoons [Cu_8(iPrPCH_2PiPr)_2Cl_4(py)_4] + py \qquad (c)$$

According to the results of the X-ray structure analysis,[4] the structure of **2** is based on a central $[Cu_4(iPrPCH_2PiPr)_2]$ unit, to which four $CuCl(py)_x$ units ($x = 1, 2$) are joined through Cu–Cl–Cu and Cu–P–Cu bridges (Fig. 1). The Cu atoms Cu1, Cu3, Cu5, and Cu7 and the P atoms P2, P4, P6, and P8 form an eight-membered ring having a distorted boat conformation. P2 and P4 as well as P6 and P8 are linked in a strain-free fashion by CH_2 bridges (P2-C11-P4 105.1(4)°, P6-C72-P8 105.3(4)°, P2-C11 188.7(8), P4-C11 187.7(8), P6-C72 187.5(8), P8-C72 188.2(8) pm). With the exception of Cu6, the arrangement of ligands around the copper atoms is distorted trigonal-planar (sum of the bond angles 358.3 to 359.8°). Of the two pyridine ligands on Cu6, one (N51) is more loosely bound, as shown by a comparison of the bond lengths Cu6-N51 (214.8(8) pm) and Cu6-N61 (205.2(8)). It is presumably this pyridine ligand which dissociates from **2** in solution [cf. equilibrium (c)].

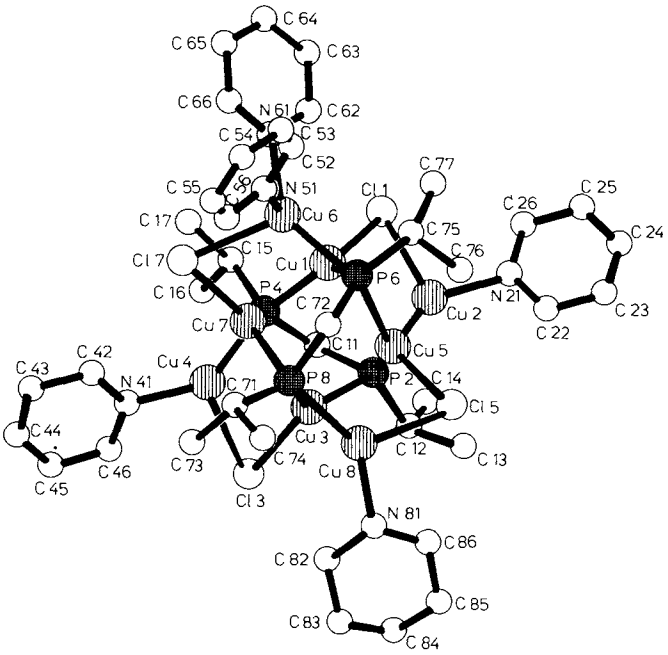

Fig. 1. Molecular structure of **2** [4].

[*] Prof. Dr. O. Stelzer, Dipl.-Chem. F. Gol, Dipl.-Chem. P. C. Knüppel
FB 9 (Anorganische Chemie) der Universität-Gesamthochschule
Gaußstrasse 20, D-5600 Wuppertal 1 (FRG)
Prof. Dr. W. S. Sheldrick
Fachbereich Chemie der Universität
Erwin-Schrödinger-Strasse, D-6750 Kaiserslautern (FRG)

[**] Linear Oligophosphaalkanes, Part 22. This work was supported by the Deutsche Forschungsgemeinschaft and the Fonds der Chemischen Industrie.—Part 21: [5].

A novel structural feature of **2** is provided by the $[Cu_3PRR']$ units (R = *i*Pr, R' = CH_2), which display a distorted trigonal-bipyramidal arrangement of the ligands around the P atoms. Two C atoms and a Cu atom together with the P atom form thereby a coordination plane. The two "axial" P–Cu bonds are bent toward each other in the direction of the "equatorial" P–Cu bond (Fig. 2). The μ_3 coordination of secondary phosphido ligands PRR' observed in **2** has only been reported so far in the complexes **3** recently described by us.[5]

$[Cu_4\{iPrPCH_2P(iPr)_2\}Cl_3(py)_2]$ **3**

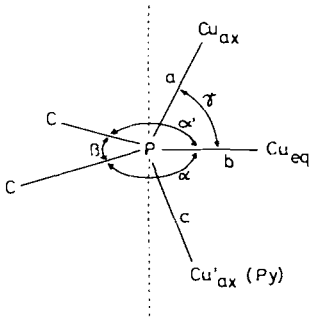

Fig. 2. μ_3-PRR' unit: average value $\bar{a}$ = 233.1 pm, $\bar{b}$ = 232.9 pm, $\bar{c}$ = 226.0 pm; $\bar{\alpha}$ = 128.3°, $\bar{\alpha}'$ = 128.5°, $\bar{\beta}$ = 103.1°, $\bar{\gamma}$ = 67.0°.

Only two electron pairs are available for bonding of the three Cu^I ions in the $[Cu_3PRR']$ units. If, in each case, one pair is used for coordination of the exocyclic $CuCl(py)_x$ groups ($x = 1, 2$), one pair remains for bonding of the four Cu^I ions in the central eight-membered ring. Analogous bonding is found in the electron-deficient system of organocopper(I) compounds of type **D**,[6] in which, instead of the $[PRR'CuClL]^{\ominus}$ units **E**, the isoelectronic bridging ligands $[CH_2SiMe_3]^{\ominus}$ **F** are present.

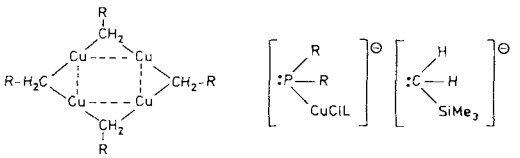

D, R = Me_3Si E, L = py F

In accordance with this formal description of the Cu–P bond in the $[Cu_4(PCH_2P)_2]$ core of **2** as an electron-deficient bond, the endocyclic Cu–P distances ($\bar{a}$, $\bar{b}$, Fig. 2) are up to 10 pm longer than the exocyclic distances (Cu(n)–P(n); n = 2, 4, 6, 8; $\bar{c}$, Fig. 2).

The two orthogonal PCP bridges in **2** hold the Cu^I ions close together and thereby create a favorable situation for interaction of the $3d^{10}$ systems.[6] The separations of the PRR'-bridged Cu atoms (265.0(2)–247.1(2) pm) are correspondingly short and are similar to those in copper (255.6 pm).[7] The μ_2-PPh_2 bridges in the complex $[Cu_2(PPh_2)_2(Ph_2PCH_2CH_2PPh_2)_2]$ **4**, on the other hand, result in considerably larger separations of the Cu atoms (333.0(1) pm).[8]

Complexes **2** and **3**, which exhibit novel bonding at the PRR' bridges, complement the small number of characterized phosphido complexes of the coinage metals. Complex **2** is the first cluster compound of a transition metal to be made up of M_3PRR' units.

Experimental Procedure

$(Me_3Si)iPrPCH_2PiPr(SiMe_3)$ (3.08 g, 10 mmol) was added over 10 min to a solution of CuCl (3.96 g, 40 mmol) and pyridine (6.32 g, 80 mmol) in 10 mL of acetonitrile at 0°C. The reaction mixture was then warmed to room temperature and allowed to stir for 16 h. The yellow crystals of **2** that formed were collected on a suction filter and washed with 2 mL of cold (0°C) acetonitrile. Yield 3.71 g (54%). Additional **2** could be isolated from the reaction solution.

Received: January 5, 1988;
revised: March 9, 1988 [Z 2564 IE]
German version: *Angew. Chem. 100* (1988) 1008

[1] S. Hietkamp, H. Sommer, O. Stelzer, *Chem. Ber. 117* (1984) 3400.
[2] D. J. Brauer, G. Hasselkuss, S. Hietkamp, H. Sommer, O. Stelzer, *Z. Naturforsch. B40* (1985) 961.
[3] F. Gol, G. Hasselkuß, P. C. Knüppel, O. Stelzer, *Z. Naturforsch. 43b* (1988) 31.
[4] Monoclinic, $P2_1/c$, $a = 14.055(3)$, $b = 17.252(4)$, $c = 21.673(4)$ Å, $\alpha = \gamma = 90.00°$, $\beta = 93.42(2)°$, $V = 5245.7(34)$ Å^3, $Z = 4$, $\rho_{calcd} = 1.73$ g cm^{-3}; $Mo_{K\alpha}$ radiation, scan range $3° \leq 2\theta \leq 45°$, 6725 measured reflections, 4315 observed ($F_0^2 \geq 2\sigma(F_0^2)$), $R = 0.054$, $R_w = 0.047$. Further details of the crystal structure investigation may be obtained from the Fachinformationszentrum Energie, Physik, Mathematik GmbH, D-7514 Eggenstein-Leopoldshafen 2 (FRG), on quoting the depository number CSD-53201, the names of the authors, and the journal citation. Important bond lengths [pm] and bond angles [°]: Cu1-Cu5 265.0(2), Cu1-Cu6 256.6(2), Cu1-Cu7 251.7(2), Cu4-Cu7 253.7(2), Cu2-Cu5 247.1(2), Cu3-Cu5 256.2(2), Cu3-Cu7 259.9(2), Cu3-Cu8 251.6(2), P2-Cu2 225.5(3), P2-Cu3 234.2(3), P2-Cu5 231.7(3), P4-Cu1 234.7(3), P4-Cu4 223.8(3), P4-Cu7 234.5(3), P6-Cu1 229.4(3), P6-Cu5 231.8(3), P6-Cu6 228.9(3), P8-Cu3 236.2(3), P8-Cu7 231.7(3), P8-Cu8 226.0(3); Cu2-P2-Cu5 65.41(7), Cu5-P2-Cu3 66.72(7), Cu2-P2-Cu3 128.1(1), Cu5-P2-C11 129.1(3), Cu5-P2-C12 126.7(3), C11-P2-C12 104.2(4).
[5] D. J. Brauer, P. C. Knüppel, O. Stelzer, *J. Chem. Soc. Chem. Commun. 1988*, 551.
[6] P. K. Mehrotra, R. Hoffmann, *Inorg. Chem. 17* (1978) 2187.
[7] L. E. Sutton in: *Tables of Interatomic Distances and Configuration in Molecules and Ions, Supplement 1956-1959*, Chem. Soc. Spec. Publ. No. 18, The Chemical Society, London 1965, p. 59.
[8] T. Graser, E. Weiss, *Chem. Ber. 111* (1978) 516; G. van Koten, J. G. Noltes, A. L. Spek, *J. Organomet. Chem. 159* (1978) 441.

The First Triphosphabicyclobutane—Evidence for a 1,2,3-Triphosphabutadiene**

By *Rolf Appel,** *Bärbel Niemann,* and *Martin Nieger*

Dedicated to Professor Heinrich Nöth on the occasion of his 60th birthday

Compounds derived from butadiene by replacement of one or two C atoms by twofold coordinated P atoms were first reported only a few years ago.[1] They are good complexing agents and—like the pure carbon compounds—are suitable for cycloadditions.[2]

Following the successful synthesis of a 1,2,4-triphosphabuta-1,3-diene,[3] we now attempted the preparation of a 1,2,3-triphosphabuta-1,3-diene. We found however that reaction of the dichlorophosphane **1**[4] with the bis(trimethylsilyl)phosphino-substituted phosphaalkene **2**[5] does not lead to the open-chain triphosphabutadiene **5** but to the triphosphabicyclobutane **6**. The condensation according to (b) likewise furnishes **6**. We explain the formation

[*] Prof. Dr. R. Appel, Dipl.-Chem. B. Niemann, M. Nieger
Anorganisch-chemisches Institut der Universität
Gerhard-Domagk-Strasse 1, D-5300 Bonn 1 (FRG)

[**] Lower Coordinated Phosphorus Compounds, Part 67.—Part 66: R. Appel, J. Hünerbein, M. Nieger, *J. Organomet. Chem.*, in press.

[***] A triphosphabicyclobutane system, $(Me_3Si)_2N-N(SiMe_3)_2$ instead of aryl in **6**, can be obtained on reaction of $R^2NN(R)-P=P-R$ with $Cl-P=CR_2$ (R = $SiMe_3$): E. Niecke, O. Altmeyer, M. Nieger, *Chem. Commun.*, in press.

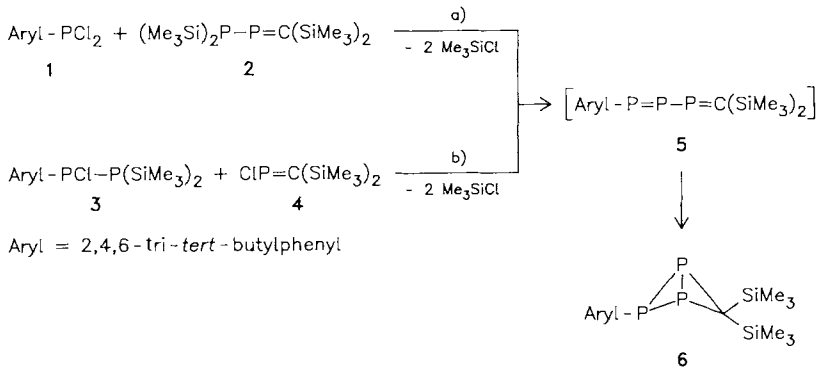

of the bicycle in terms of an intramolecular [2+2]-cycloaddition of **5**.[***]

The ^{31}P-NMR spectrum of **6** shows an AX_2 system with $\delta_A = -65.8$ and an X-part shifted strongly upfield for the bridgehead P atoms ($\delta_X = -244.3$). Similar shifts are quoted for tetraphosphabicyclobutane derivatives.[6] The empirical formula of **6** is confirmed by the ^{31}P- and ^{1}H-NMR spectroscopic data and by the high resolution mass spectrum as well as by a correct elemental analysis.[7] The structure was confirmed by an X-ray diffraction analysis[8] (Fig. 1).

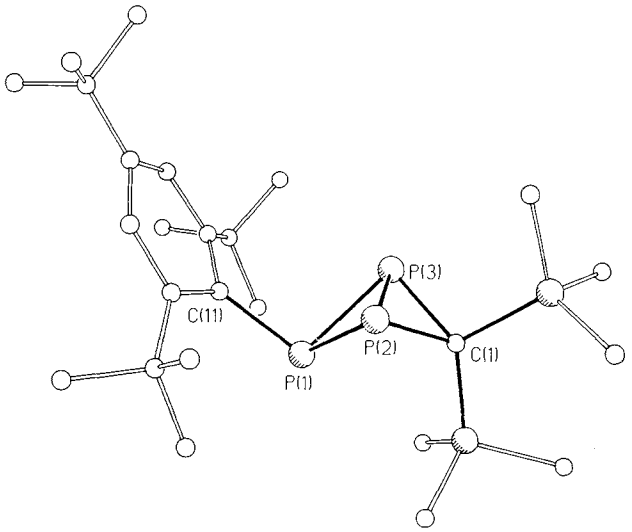

Fig. 1. Crystal structure of **6**. Important bond lengths [Å]: P(1)-P(2) 2.231(2), P(1)-P(3) 2.223(2), P(2)-P(3) 2.136(1), P(2)-C(1) 1.881(4), P(3)-C(1) 1.883(4).

The bond between the bridgehead P atoms in the bicycle is exceptionally short (2.136(1) Å), whereas the P-C bonds are longer than the P-P and P-C bonds in acyclic compounds. The angle between the P(1)-P(2)-P(3) and P(2)-P(3)-C(1) planes is 105°.

Experimental

6: a) A solution of **1** (1.8 g, 5 mmol) in toluene (10 mL) was treated with 1.7 g (5 mmol) of **2** and the mixture stirred for 24 h at room temperature. After removal of volatile components under vacuum the residue was crystallized several times from pentane. M.p. 152°C; yield 0.5 g (20%). b) A solution of **1** (1.7 g, 5 mmol) in ether (20 mL) was treated dropwise at −80°C with a solution of $LiP(SiMe_3)_2 \cdot 2\,THF$ (1.6 g, 5 mmol) in ether. The mixture was allowed to warm to room temperature, the solvent removed under vacuum, and the residue taken up in pentane. The resulting solution was filtered free of LiCl and the filtrate treated dropwise with 0.12 g (5 mmol) of **4**. The mixture was stirred for several hours and then worked up as in (a).

Received: November 30, 1987 [Z 2516 IE]
German version: *Angew. Chem. 100* (1988) 957

CAS Registry numbers:
1, 79074-00-3; **2**, 114032-10-9; **3**, 114032-11-0; **4**, 79454-85-6; **5**, 114032-13-2; **6**, 114032-12-1; $LiP(SiMe_3)_2$, 59624-91-8.

[1] a) R. Appel, H. Kunze, F. Knoch, *Chem. Ber. 117* (1984) 3151; b) R. Appel, V. Barth, F. Knoch, *ibid. 116* (1983) 938; c) R. Appel, U. Kündgen, F. Knoch, *ibid. 118* (1985) 1352; d) R. Appel, P. Fölling, W. Schuhn, F. Knoch, *Tetrahedron Lett. 27* (1986) 1661; e) G. Märkl, H. Sejpka, *ibid. 27* (1986) 171; f) R. Appel, J. Hünerbein, N. Siabalis, *Angew. Chem. 99* (1987) 810; *Angew. Chem. Int. Ed. Engl. 26* (1987) 779.

[2] N. Hoa Tran Huy, J. Fischer, F. Mathey, *J. Am. Chem. Soc. 109* (1987) 3475.

[3] R. Appel, B. Niemann, W. Schuhn, F. Knoch, *Angew. Chem. 98* (1986) 934; *Angew. Chem. Int. Ed. Engl. 25* (1986) 932.

[4] M. Yoshifuji, I. Shima, N. Inamoto, K. Hirotsu, T. Higuchi, *J. Am. Chem. Soc. 103* (1981) 4587.

[5] K. H. Dunker, *Dissertation*, Universität Bonn 1987.

[6] a) E. Niecke, R. Rüger, B. Krebs, *Angew. Chem. 94* (1982) 553; *Angew. Chem. Int. Ed. Engl. 21* (1982) 544; b) R. Riedel, H.-D. Hansen, E. Fluck, *ibid. 97* (1985) 1050 and *24* (1985) 1056.

[7] NMR data: $^{31}P\{^1H\}$-NMR (32.2 MHz, H_3PO_4 extern, C_6D_6): AX_2 system with $\delta_A = -65.8$, $\delta_X = -244.3$, $J_{AX} = 174.7$ Hz; ^{1}H-NMR (90 MHz, C_6D_6): $\delta = -0.06$ (t, $^4J = 1.05$ Hz, 9H; $Si(CH_3)_3$), 0.45 (d, $^4J = 2.4$ Hz, 9H; $Si(CH_3)_3$), 1.18 (s, 9H; *p*-*t*Bu), 1.79 (d, $^5J = 0.9$ Hz, 18H; *o*-*t*Bu), 7.45 (d, $^4J = 2$ Hz, 2H; Aryl-H); MS (70 eV, 300 μA, 80°C): *m/z* (selection) 496.2432 ($M^{\oplus}$), 481 ($M^{\oplus} - CH_3$), 439 ($M^{\oplus} - C(CH_3)_3$), 351 ($M^{\oplus} - 2\,Si(CH_3)_3$).

[8] X-ray structure analysis of **6**: pale yellow crystals from pentane. Crystal dimensions: $0.5 \times 0.5 \times 0.5$ mm^3, monoclinic, space group $P2_1/n$. $a = 9.083(2)$, $b = 28.237(9)$, $c = 12.881(3)$ Å, $\beta = 109.14(2)°$, $V = 3.121$ nm^3, $Z = 4$, $\rho_{calcd} = 1.06$ g cm^{-3}; $\mu = 0.24$ mm^{-1} ($Mo_{K\alpha}$); 4896 symmetry independent reflections ($2\theta_{max} = 48°$), 3725 with $|F| > 4\sigma(F)$ used for the structure solution (direct methods) and refinement (266 parameters). Non-hydrogen atoms anisotropic (C(32) isotropic), H atoms (located by difference electron density) refined with a riding model. $R = 0.057$ ($R_w = 0.059$, $w^{-1} = \sigma_F^2 + 0.0005\,F^2$). Further details of the crystal structure investigation are available on request from the Fachinformationszentrum Energie, Physik, Mathematik GmbH, D-7514 Eggenstein-Leopoldshafen 2 (FRG), on quoting the depository number CSD-52796, the names of the authors, and the journal citation.

Synthesis and Structure of $[Cp_2NbH(tBuB{\equiv}NtBu)]$, a Compound with Side-on Coordinated Iminoborane**

By *Ece Bulak, Gerhard E. Herberich, Ian Manners, Horst Mayer,* and *Peter Paetzold**

Dedicated to Professor Heinrich Nöth on the occasion of his 60th birthday

Iminoboranes RB≡NR′ are isoelectronic with acetylenes; in their structure and reactivity they especially resemble

[*] Prof. Dr. P. Paetzold, E. Bulak, Prof. Dr. G. Herberich, Dr. I. Manners, Dr. H. Mayer
Institut für Anorganische Chemie der Technischen Hochschule Templergraben 55, D-5100 Aachen (FRG)

[**] This work was supported by the government of Nordrhein-Westfalen. *I. M.* thanks the Royal Society (England) for a fellowship grant.

polar acetylenes (e.g. RC≡CF).[1] In the coordination sphere of transition-metal atoms, iminoboranes can dimerize to tetrahapto-bonded BNBN four-membered ring compounds analogous to cyclobutadiene, or they can bridge two metal atoms in the orthogonal position to the metal–metal bond.[1] A third structural type known for acetylenes, namely that with side-on bonding to transition metal atoms, has hitherto not been reported for iminoboranes. We therefore attempted, in analogy to a known reaction of acetylenes,[2] to couple the iminoboranes **1a,b**[3] side-on to niobium; by treatment with Cp_2NbH_3 we obtained the air-sensitive, brown, crystalline products **2a,b**.

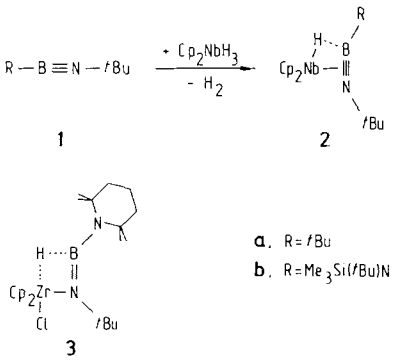

The constitution of **2a,b**, as 1:1 adduct of **1a,b** and Cp_2NbH, follows from the NMR and mass spectra.[4] We assign the broad weak IR bands at 1680 (**2a**) and 1650 cm^{-1} (**2b**) (in hexane) to the Nb–H stretching vibration; its long wavelength position compared to that of $[Cp_2NbH(C_2Pr_2)]$ (1720 cm^{-1})[2a] could be due to an interaction with the B atom. An X-ray structure analysis of **2a** confirmed the side-on bonding between **1** and the niobium atom (cf. Fig. 1).[5]

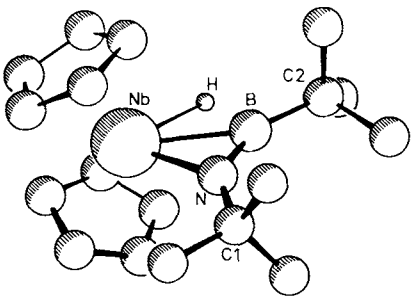

Fig. 1. Molecular structure of **2a** in the crystal (without C-bonded hydrogen atoms). Selected bond lengths and angles ([Å] and [°], resp.; standard deviations in parentheses): Nb-B 2.399(3), Nb-N 2.159(3), B-N 1.294(5), Nb-H 1.80(3), B-H 1.37(3), Nb-C_x 2.058(1), Nb-C_y 2.050(1), N-C1 149.6(5), B-C2 155.9(6), average C-C values of 2Cp 135.4, 136.8; B-Nb-N 32.5(1), Nb-N-B 84.0(2), Nb-B-N 63.5(2), Nb-H-B 98(2), Nb-N-C1 138.7(3), B-N-C1 137.3(4), Nb-B-C2 151.7(3), N-B-C2 144.8(4), C_x-Nb-C_y 133.9, (C_x, C_y: projections of Nb onto the Cp planes).

2a is a bent metallocene (133.9°). The central moiety of **2a** comprises the Nb-N-B triangle and the neighboring coplanar arrangement of the atoms H, C1 and C2. Compared to the typical NbC distances of 2.18–2.25 Å in niobocene-acetylene derivatives,[6] distances of 2.159(3) (NbN) and 2.399(4) Å (NbB) suggest strong bonding between the niobocene and the iminoborane **1a**. In **3**, the corresponding distances are 2.211(2) (ZrN) and 2.627(2) Å (ZrB) and indicate at most a weak ZrB interaction.[7] The BN distance of **1a** (1.258(4) Å) is only slightly expanded on coordination to the niobium; in **3**: 1.360(3) Å). The CBN and BNC angles in linear **1a** are only moderately narrowed (namely to 155.9(6) and 149.6(5)° respectively; in **3**: 140.3(3) and 130.5(2)°), whereas the corresponding CCC angles in niobocene-acetylene derivatives are found between 140 and 146°.[6] Thus, the back-bonding in the iminoborane complex **2a** is weaker than in the comparable acetylene complexes. Compared to the usual range of BH bond lengths of 1.10–1.35 Å,[8] the BH distance of 1.37(3) Å in **2a** suggests at most a very weak BH interaction; the NbH bond is not significantly lengthened (1.80(3) Å; cf. Cp_2NbH_3: 1.69 Å (average)[9]). Whereas **3** can be regarded as an *N*-metalated aminoborane, **2a,b** are side-on coordinated transition-metal complexes of iminoboranes.

Experimental

2a (η^2-[*tert*-Butyl(*tert*-butylimino)borane]bis(η^5-cyclopentadienyl)hydridoniobium): A solution of 0.22 g of **1a** and 0.23 g of Cp_2NbH_3 in 5 mL of toluene was heated to 85 °C for 90 min. Toluene was then removed by distillation under vacuum at room temperature and the residue taken up in pentane containing a trace of toluene. On cooling the solution to −80 °C, **2a** crystallized out (0.25 g, 68%); **2b** was prepared analogously (yield 73%).

Received: December 23, 1987 [Z 2556 IE]
German version: *Angew. Chem. 100* (1988) 964
Publication delayed at authors' request

CAS Registry numbers:
1a, 89786-99-2; **1b**, 93109-75-2; **2a**, 114860-28-5; **2b**, 114860-29-6; Cp_2NbH_3, 11105-67-2.

[1] P. Paetzold, *Adv. Inorg. Chem. 31* (1987) 123.
[2] a) J. A. Labinger, J. Schwartz, *J. Am. Chem. Soc. 97* (1975) 1596; b) J. E. Bercaw, R. S. Threlkel, *ibid. 103* (1981) 2650; c) J. Sala-Pala, J. Amaudrut, J. E. Guerchais, R. Mercier, J. Douglade, J. G. Theobald, *J. Organomet. Chem. 204* (1981) 347; d) G. E. Herberich, B. Hessner, H. Mayer, *ibid. 314* (1986) 123.
[3] P. Paetzold, C. von Plotho, G. Schmid, R. Boese, B. Schrader, D. Bougeard, U. Pfeiffer, R. Gleiter, W. Schäfer, *Chem. Ber. 117* (1984) 1089; P. Paetzold, E. Schröder, G. Schmid, R. Boese, *ibid. 118* (1985) 3205.
[4] **2a**: NMR (C_6D_6): $\delta(^1H) = -8.5$ (1H), 1.05 (9H), 1.08 (9H), 4.65 (10H); $\delta(^{11}B) = 17.9$; $\delta(^{13}C) = 29.9$ (q), 33.5 (q), 53.1 (s), 90.7 (d); the generally broad BC-^{13}C singlet is not traceable. MS: *m/z* 363 (66%, $M^{\oplus}$), 306 (29%, $M^{\oplus} - C_4H_9$), 224 (100%, $Cp_2NbH^{\oplus}$), 223 (90%, $Cp_2Nb^{\oplus}$) etc. — **2b**: NMR (C_6D_6): $\delta(^1H) = -8.25$ (1H), 0.18 (9H), 1.13 (9H), 1.20 (9H), 4.82 (10H); $\delta(^{11}B) = 10.7$; $\delta(^{13}C) = 5.1$ (q), 32.3 (q), 32.6 (q), 53.6 (s), 54.9 (s), 91.7 (d). MS: *m/z* 450 (68%, $M^{\oplus}$), 435 (11%, $M^{\oplus} - CH_3$), 393 (60%, $M^{\oplus} - C_4H_9$), 336 (40%, $M^{\oplus} - 2C_4H_9$), 224 (100%, $Cp_2NbH^{\oplus}$), 223 (100, $Cp_2Nb^{\oplus}$).
[5] Single crystal from pentane; $a = 29.932(8)$, $b = 8.053(5)$, $c = 15.676(5)$ Å, $\beta = 94.19(3)°$, $V = 3768$ Å^3, $Z = 8$, $\rho_{calcd} = 1.28$ g cm^{-3}, *C2/c* (No. 15); crystal dimensions $0.9 \times 0.6 \times 0.3$ mm^3, range of measurement $0.01 < \theta < 30°$; 6667 measured reflections, 2874 independent with $I > \sigma(I)$ and 2117 with $I > 3\sigma(I)$; anisotropic temperature factors for the non-hydrogen atoms; 196 refined parameters; $R = 0.046$. Further details of the crystal structure analysis are available on request from the Fachinformationszentrum Energie, Physik, Mathematik GmbH, D-7514 Eggenstein-Leopoldshafen 2 (FRG), on quoting the depository number CSD-51403, the names of the authors, and the journal citation.
[6] a) J. A. Labinger in G. Wilkinson, F. G. A. Stone, E. W. Abel (Eds.): *Comprehensive Organometallic Chemistry*, Pergamon Press, Oxford 1982, Vol. 3, p. 705; b) A. Antiñolo, P. Gómez-Sal, J. M. de Ilarduya, A. Otero, P. Royo, S. M. Carrera, S. G. Blanco, *J. Chem. Soc. Dalton Trans. 1987*, 975.
[7] D. Männig, H. Nöth, M. Schwartz, S. Weber, U. Wietelmann, *Angew. Chem. 97* (1985) 979; *Angew. Chem. Int. Ed. Engl. 24* (1985) 998.
[8] T. J. Marks, J. R. Kolb, *Chem. Rev. 77* (1977) 263.
[9] R. D. Wilson, T. F. Koetzle, D. W. Hart, Å. Kvick, D. L. Tipton, R. Bau, *J. Am. Chem. Soc. 99* (1977) 1775.

Lewis-Base Adducts of Methyleneboranes**

By *Heidi Lukasch, Günter Schmidt-Lukasch, Uwe Lippold,* and *Armin Berndt**

Dedicated to Professor Heinrich Nöth on the occasion of his 60th birthday

Jutzi pointed out already in 1975 that the dicoordinated boron atom of methyleneboranes **1** exhibits pronounced Lewis acid character.[1] In the stable[2] methyleneboranes

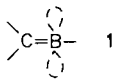

1

2–**4**[3–6] described in the meantime the vacant p-orbital at the boron atom is filled up *intra*molecularly, in **2**[3] non-classically by a neighboring borirane ring, in **3**[5] and **4**[6] classically by an electron pair from the nitrogen substituents on the boron atom.

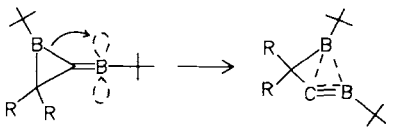

2, R = $Si(CH_3)_3$

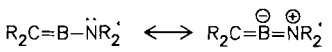

3, R_2C = fluorenylidene, HNR'_2 = 2,2,6,6-tetramethylpiperidine

4, R = $Si(CH_3)_3$, R' = *i*Pr

We have now prepared methyleneboranes in which the vacant p-orbital at the boron atom is occupied *inter*molecularly by Lewis bases (tetrahydrofuran, pyridine derivatives).

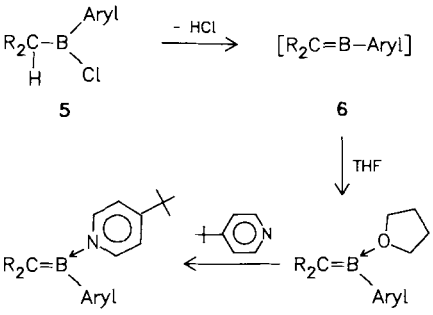

5 **6** **8** **7**

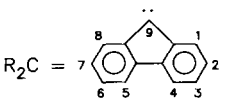

a, Aryl = 2,4,6-triisopropylphenyl;

b, Aryl = 2,3,5,6-tetramethylphenyl;

c, Aryl = 2,4,6-trimethylphenyl

The arylchlorofluorenylboranes **5a** and **5b** can be prepared analogously to chlorofluorenylmesitylborane **5c**[7] from fluorenylsodium and the corresponding aryldichloroboranes in pentane. Reaction of **5a** and **5b** with *tert*-butyllithium in THF at −78°C furnishes the methyleneborane-tetrahydrofuran adducts **7a** and **7b**, respectively (**7a** crystallizes out). **7c** is obtained by reaction of **5c** with 2,4,6-tri-*tert*-butylphenyllithium as base. The coordinated THF in **7a**–**7c** can be easily replaced by 4-*tert*-butylpyridine to give deep-blue[8] **8a** and red[8] **8b** and **8c**, respectively. The non-classically stabilized **2** is inert toward THF, but reacts with 2,4,6-trimethylpyridine[9] to give the red adduct **10**. The formation of deep-colored adducts with pyridine derivatives can thus be used as a reaction for the detection of methyleneboranes.

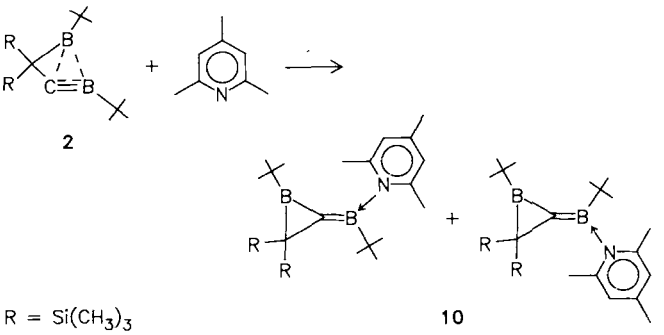

2

R = $Si(CH_3)_3$ **10**

7a and **8a** add methanol with formation of the methoxyborane **9a**, while **7b**, **7c**, and **8b** are cleaved by methanol into fluorene and the corresponding aryldimethoxyboranes. **9a** can be reconverted into **5a** by reaction with BCl_3. The reactions of **7a** and **8a** with HCl lead to product mixtures which do not contain **5a**.

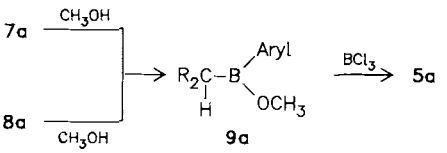

9a

The structures of the compounds **5** and **7**–**10** follow from the ^1H-, ^{13}C- and ^{11}B-NMR spectra[10] and from the described reaction cycle. The double-bond character of the C–B bond in **7** and **8** manifests itself in the different chemical shifts of the atoms C1–C4 and C8–C5 as well as C4a, C9a and C4b, C8a of the fluorene framework, which reflect the unsymmetric substitution at the boron atom. In **10**, both ends of the partial C–B double bond are unsymmetrically substituted, so that *Z,E*-isomers are to be expected; they are recognizable by a doubling of the number of signals in the ^{13}C-NMR spectrum. At room temperature, the second isomer is just recognizable; on cooling a saturated solution in CD_2Cl_2 to −40°C the isomer present in higher concentration partially crystallizes out, in solution both isomers are then present in comparable amounts. The chemical shifts of the C9 atoms of **7** and **8** ($\delta = 108$–110)[12] and that of the C atom doubly bonded to boron in **10** ($\delta = 92.8$) indicate an excess of electrons corresponding to resonance formula **B**.[12]

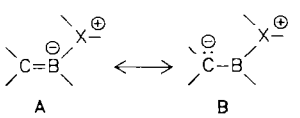

A **B**

[*] Prof. Dr. A. Berndt, Dr. H. Lukasch,
Dipl.-Chem. G. Schmidt-Lukasch, U. Lippold
Fachbereich Chemie der Universität
Hans-Meerwein-Strasse, D-3550 Marburg (FRG)

[**] This work was supported by the Deutsche Forschungsgemeinschaft and the Fonds der Chemischen Industrie.

Delocalization of this charge leads to a shielding of the quasi *ortho* and *para* C atoms 1, 3, 6, 8, 4a, and 4b of the fluorene skeleton in **7** and **8** and of the boron atom in the three-membered ring of **10** ($\delta(^{11}B)=37$ compared to 80 in boriranes).

All attempts to convert **7a–c** into the Lewis base-free methyleneboranes **6a–c** led to decomposition of the compounds.

Experimental

7a: A stirred solution of **5a** (13.1 g, 31.5 mmol) in THF (130 mL) was treated dropwise and very slowly (ca. 1.5 h) at −78 °C with 75.0 mL of a 0.42 molar solution (31.5 mmol) of *tert*-butyllithium in pentane. The orange colored reaction mixture was slowly warmed to −10 to 0 °C, whereupon the precipitated product went completely into solution. At −40 °C, **7a** crystallized out quantitatively and in spectroscopically pure form.

8a: A suspension of 1.36 g (2.45 mmol) of **7a** in 20 mL of pentane was treated dropwise at −20 °C with 0.41 g (3.03 mmol) of 4-*tert*-butylpyridine. After slowly warming the mixture to room temperature it was stirred for 3 h, the solvent was removed by pipette, and the deep-blue precipitate was washed with 2 × 10 mL of pentane and dried in an oil-pump vacuum. **8a** is sparingly soluble in hydrocarbons and ethers, and decomposes rapidly in $CDCl_3$ and slowly in CD_2Cl_2.

10: A solution of **2** (1.68 g, 5.5 mmol) in pentane (20 mL) was treated dropwise at −40 °C with 0.73 mL (5.5 mmol) of 2,4,6-trimethylpyridine. The mixture was warmed to room temperature, stirred for 30 min, and treated with sufficient ether until the precipitated product **10** was redissolved (ca. 30 mL); **10** crystallized out on cooling the solution to −30 °C.

Received: January 13, 1988 [Z 2570 IE]
German version: *Angew. Chem. 100* (1988) 959

CAS Registry numbers:
2, 87556-27-2; **5a**, 114981-27-0; **5b**, 114981-29-2; **5c**, 114981-30-5; **7a**, 114981-20-3; **7b**, 114981-22-5; **7c**, 114981-23-6; **8a**, 114981-21-4; **8b**, 114981-24-7; **8c**, 114981-25-8; **9a**, 114981-28-1; **10** (isomer 1), 114981-26-9; **10** (isomer 2), 114995-31-2; 4-*tert*-butylpyridine, 3978-81-2; 2,4,6-trimethylpyridine, 108-75-8.

[1] P. Jutzi, *Angew. Chem. 87* (1975) 269; *Angew. Chem. Int. Ed. Engl. 14* (1975) 232.
[2] Unstable methyleneboranes were observed in a matrix: G. Maier, J. Henkelmann, H. P. Reisenauer, *Angew. Chem. 97* (1985) 1061; *Angew. Chem. Int. Ed. Engl. 24* (1985) 1065.
[3] H. Klusik, A. Berndt, *Angew. Chem. 95* (1983) 895; *Angew. Chem. Int. Ed. Engl. 22* (1983) 877.
[4] P. H. M. Budzelaar, P. von R. Schleyer, K. Krogh-Jespersen, *Angew. Chem. 96* (1984) 809; *Angew. Chem. Int. Ed. Engl. 23* (1984) 825; G. Frenking, H. F. Schaefer III, *Chem. Phys. Lett. 109* (1984) 521.
[5] B. Glaser, H. Nöth, *Angew. Chem. 97* (1985) 424; *Angew. Chem. Int. Ed. Engl. 24* (1985) 416; B. Glaser, E. Hanecker, H. Nöth, H. Wagner, *Chem. Ber. 120* (1987) 659.
[6] R. Boese, P. Paetzoldt, A. Tapper, *Chem. Ber. 120* (1987) 1069.
[7] C. Pues, G. Baum, W. Massa, A. Berndt, *Z. Naturforsch. B43* (1988) 275.
[8] The pyridine adducts of borabenzene and boranaphthalene are also colored: R. Boese, N. Funke, J. Henkelmann, G. Maier, P. Paetzold, H. P. Reisenauer, G. Schmid, *Chem. Ber. 118* (1985) 1644.
[9] The adduct of **2** and 4-*tert*-butylpyridine is too unstable for a spectroscopic characterization.
[10] NMR spectra in $CDCl_3$ (**5a**, **9a**, **10**), [D$_8$]THF (**7a**), and CD_2Cl_2 (**8a**). If not otherwise quoted, 100-MHz ^{13}C-NMR, 300-MHz ^{1}H-NMR, 96-MHz ^{11}B-NMR.
5a: orange colored oil, b.p. 250 °C (0.001 torr), yield 47%.—^{1}H-NMR: $\delta=7.81$, 7.44 (each d, each 2H; $H_{1,8}$ and $H_{4,5}$), 7.35, 7.21 (each t, each 2H; $H_{2,7}$ and $H_{3,6}$), 6.91 (s, 2H; *m*-H), 4.45 (s, 1H; H_9), 2.87 (m, 1H; *p*-C*H*(CH$_3$)$_2$), 2.18 (m, 2H; *o*-C*H*(CH$_3$)$_2$), 1.25 (d, 6H; *p*-CH(C*H*$_3$)$_2$), 1.13 (br. d, 12H; *o*-CH(C*H*$_3$)$_2$); ^{13}C-NMR: $\delta=150.4$ (s, 1C; *p*-C), 148.2 (s, 2C; *o*-C), 143.3, 141.1 (each s, each 2C; $C_{8a,9a}$ and $C_{4a,4b}$), 137.1 (br. s, 1C; *i*-C), 126.5, 126.4, 125.9 (each d, each 2C; $C_{2,7}$, $C_{3,6}$ and $C_{1,8}$), 120.4, 119.8 (each d, each 2C; *m*-C and $C_{4,5}$), 52.9 (br. d, 1C; C_9), 35.8 (d, 2C; *o*-*C*H(CH$_3$)$_2$), 34.4 (d, 1C; *p*-*C*H(CH$_3$)$_2$), 25.4, 23.1 (each br. q, each 2C; *o*-CH(*C*H$_3$)$_2$) [11], 24.0 (q, 2C; *p*-CH(*C*H$_3$)$_2$); ^{11}B-NMR: $\delta=78$.
7a: orange colored crystals, m.p. 102 °C (decomp.).—^{1}H-NMR: $\delta=8.76$ (d, 1H; fluorenyl-H), 7.78–6.53 (m, 7H; fluorenyl-H), 6.95 (s, 2H; *m*-H), 3.58 (t; THF), 3.40 (m, 2H; *o*-C*H*(CH$_3$)$_2$), 2.89 (m, 1H; *p*-C*H*(CH$_3$)$_2$), 1.75 (m; THF) (2.5 molecules THF per molecule of **7a**), 1.30, 1.16, 0.94 (each d, each 6H; CH(C*H*$_3$)$_2$); ^{13}C-NMR: $\delta=149.6$ (s, 2C; *o*-C), 148.6, 147.2 (each s, each 1C; $C_{8a,9a}$), 146.7 (s, 1C; *p*-C), 133.3, 132.3 (each s, each 1C; $C_{4a,4b}$), 123.4, 122.4 (each d, each 1C; $C_{2,7}$), 122.4, 121.8 (each d, each 1C; $C_{4,5}$), 119.9 (d, 2C; *m*-C), 117.7 (d, 2C; $C_{1,8}$), 116.3, 116.1 (each d, each 1C; $C_{3,6}$), 108.5 (br. s, 1C; C_9), 68.1 (t; THF–$C_{2,5}$), 35.3 (d, 1C; *p*-*C*H(CH$_3$)$_2$), 34.6 (d, 2C; *o*-*C*H(CH$_3$)$_2$), 26.2 (t; THF-$C_{3,4}$), 25.4, 24.9, 24.7 (each q, each 2C; CH(*C*H$_3$)$_2$) [11]; the signal for the *ipso* C atom could not be observed, in C_6D_6 it appears as a broad singlet at $\delta=146$; ^{11}B-NMR: $\delta=46$.
8a: deep blue crystals, m.p. 260 °C, yield 81%.—^{1}H-NMR: $\delta=8.76$ (d, 1H; arom. H), 7.84–6.66 (m, 13H; arom. H), 3.15 (m, 2H; *o*-C*H*(CH$_3$)$_2$), 2.88 (m, 1H; *p*-C*H*(CH$_3$)$_2$), 1.35 (s, 9H; C(CH$_3$)$_3$), 1.64, 0.94, 0.85 (each d, each 6H; CH(C*H*$_3$)$_2$); ^{13}C-NMR: $\delta=168.8$ (s, 1C; pyridine-C_4), 150.6 (s, 2C; *o*-C), 149.2 (s, 1C; *p*-C), 146.3 (d, 2C; pyridine-$C_{2,6}$), 147.6, 143.0 (each s, each 1C; $C_{8a,9a}$), 139.4 (br. s, 1C; *i*-C), 134.5, 133.4 (each s, each 1C; $C_{4a,4b}$), 123.9 (d, 2C; pyridine-$C_{3,5}$), 123.7, 123.6 (each d, each 1C; $C_{2,7}$), 121.0 (d, 2C; *m*-C), 121.6, 119.7 (each d, each 1C; $C_{4,5}$), 119.5, 119.4 (each d, each 1C; $C_{1,8}$), 119.3, 118.5 (each d, each 1C; $C_{3,6}$), 109.6 (br. s, 1C; C_9), 36.2 (s, 1C; *C*(CH$_3$)$_3$), 35.4 (d, 2C; *o*-*C*H(CH$_3$)$_2$), 34.3 (d, 1C; *p*-*C*H(CH$_3$)$_2$), 29.8 (q, 3C; C(*C*H$_3$)$_3$), 24.7, 24.3, 24.0 (each q, each 2C; CH(*C*H$_3$)$_2$) [11]; ^{11}B-NMR: $\delta=42$.
9a: colorless crystals, m.p. 88 °C, yield 61%.—^{1}H-NMR: $\delta=7.78$–6.91 (m, 10H; arom. H), 3.93 (s, 1H; H_9), 3.76 (s, 3H; OCH$_3$), 2.32 (m, 1H; *p*-C*H*(CH$_3$)$_2$), 2.08 (m, 2H; *o*-C*H*(CH$_3$)$_2$), 1.25, 1.06, 0.80 (each d, each 6H; CH(C*H*$_3$)$_2$) [11]; ^{13}C-NMR: $\delta=149.5$ (s, 1C; *p*-C), 149.0 (s, 2C; *o*-C), 145.2 (s, 2C; $C_{8a,9a}$), 140.7 (s, 2C; $C_{4a,4b}$), 133.7 (br. s, 1C; *i*-C), 125.9 (d, 4C; $C_{2,7}$ and $C_{3,6}$), 125.4 (d, 2C; $C_{1,8}$), 120.1 (d, 2C; *m*-C), 119.2 (d, 2C; $C_{4,5}$), 56.5 (q, 1C; OCH$_3$), 47.1 (br. d, 1C; C_9), 35.3 (d, 2C; *o*-*C*H(CH$_3$)$_2$), 34.3 (d, 1C; *p*-*C*H(CH$_3$)$_2$), 25.4, 24.1, 23.5 (each q, each 2C; CH(*C*H$_3$)$_2$) [11]; ^{11}B-NMR: $\delta=50$.
10: dark red crystals, m.p. 174 °C (partial decomp.), yield 58%.—^{1}H-NMR: $\delta=7.30$ (s, 2H; arom. H), 2.97 (s, 6H; *o*-CH$_3$), 2.62 (s, 3H; *p*-CH$_3$), 1.23, 0.91 (each s, each 9H; C(CH$_3$)$_3$), 0.23 (s, 18H; Si(CH$_3$)$_3$); ^{13}C-NMR ([D$_8$]THF, −60 °C): $\delta=155.0$ (s, 2C; *o*-C), 153.5 (s, 1C; *p*-C), 125.9 (d, 2C; *m*-C), 92.8 (br. s, 1C; CB_2), 32.1, 29.8 (each q, each 3C, C(*C*H$_3$)$_3$), 24.5 (q, 2C; *o*-CH$_3$), 22.2, 22.0 (each br. s, each 1C; *C*(CH$_3$)$_3$), 20.8 (q, 1C; *p*-CH$_3$), 17.0 (s, 1C; CSi_2), 3.7 (q, 6C; Si(CH$_3$)$_3$); (CD_2Cl_2, −40 °C): $\delta=154.3$, 154.1 (each s, each 2C; *o*-C), 152.0, 151.7 (each s, each 1C; *p*-C), 125.0, 124.8 (each d, each 2C; *m*-C), 32.3, 31.3, 29.7, 29.0 (each q, each 3C; C(*C*H$_3$)$_3$), 24.3, 23.7 (each q, each 2C; *o*-CH$_3$), 21.0, 20.9 (each q, each 1C; *p*-CH$_3$), 16.4 (s, 2C; CSi_2), 2.8, 2.6 (each q, each 6C; Si(CH$_3$)$_3$); signals for CB_2 and *C*(CH$_3$)$_3$ were not observed; ^{11}B-NMR: $\delta=63$, 37.
[11] For the diastereotopism of the methyl groups of an isopropyl group cf. H. Kessler, D. Leibfritz, *Chem. Ber. 104* (1971) 2143.
[12] For the corresponding C atom (C-9) in fluorenyllithium a value of $\delta(^{13}C)=82.6$ is found: D. H. O'Brien in E. Buncel, T. Durst (Eds.): *Comprehensive Carbanion Chemistry, Vol. A*, Elsevier, Amsterdam 1980, p. 303.

Compounds with Partial Boron–Carbon Triple Bonds**

By *Ralf Hunold, Jürgen Allwohn, Gerhard Baum, Werner Massa,* and *Armin Berndt**

Dedicated to Professor Heinrich Nöth on the occasion of his 60th birthday

Compounds containing a boron–carbon triple bond, i.e. borataalkyne ions[1] **1**, which are isoelectronic with alkynes **2**, have so far not been reported in the literature.[2] Herein

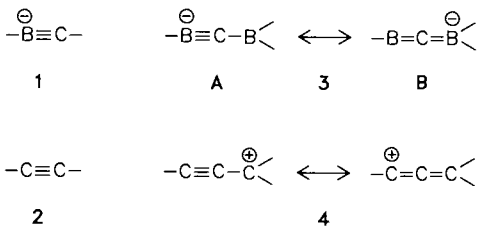

[*] Prof. Dr. A. Berndt, Dr. R. Hunold, J. Allwohn, G. Baum, Priv.-Doz. Dr. W. Massa
Fachbereich Chemie der Universität
Hans-Meerwein-Strasse, D-3550 Marburg (FRG)

[**] This work was supported by the Deutsche Forschungsgemeinschaft and the Fonds der Chemischen Industrie.

we present the first examples of compounds containing a partial boron-carbon triple bond, namely the diboro compounds **3**, which are isoelectronic with propargyl/allenyl cations **4**.[1,3]

The dianion **3a**[4] lithiated in the boryl residue is formed upon reaction of the 1,1-bis(boryl)ethene **5**,[5] or the compound **6** accessible therefrom with K/Na alloy in pentane, with an excess of lithium in diethyl ether. The crucial step in the conversion of **6** into **3a** is the reductive cleavage of the C-C bond of the C_2B_2 framework.

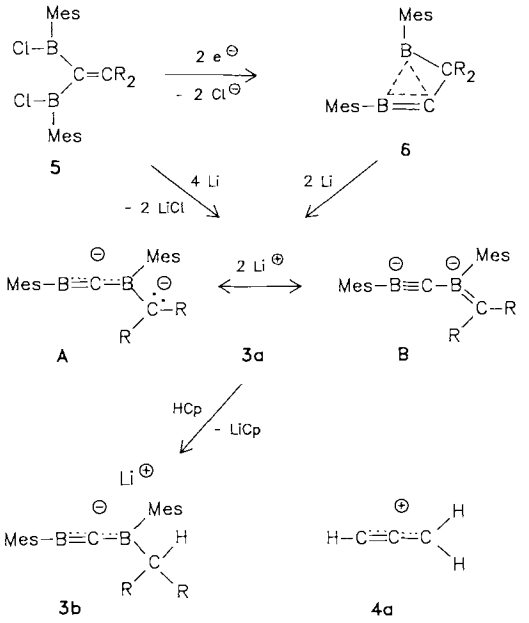

Mes = 2,4,6-trimethylphenyl; R = $Si(CH_3)_3$

Monoprotonation of **3a** with cyclopentadiene HCp leads to the lithium salt of the borylborataalkyne ion **3b**,[4] which crystallizes from pentane with one equivalent of diethyl ether. The result of an X-ray structure analysis[7] of **3b** is shown in Figure 1.

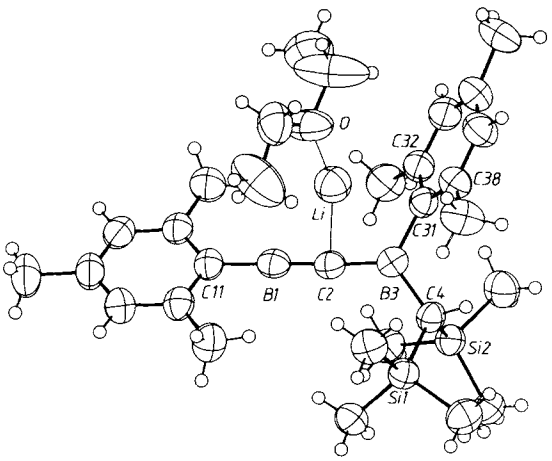

Fig. 1. Crystal structure of **3b** (ORTEP). The thermal ellipsoids are drawn at the 50% probability level. Projection approximately onto the C2-C4-C31 plane. Important distances [pm] and angles [°]: B1-C2 133.9(6), C2-B3 149.2(6), B1-C11 154.3(6), B3-C4 159.9(6), B3-C31 161.2(6), B1-Li 249.3(9), C2-Li 209.4(9), B3-Li 249.0(9), C31-Li 234.5(9); B1-C2-B3 176.5(5), C2-B1-C11 178.0(5), C2-B3-C4 122.6(4), C2-B3-C31 118.9(4), C4-B3-C31 118.4(4), B1-C2-Li 90.4(4), B3-C2-Li 86.3(4), C2-Li-O 155.9(5); Li-C2-B3-C31 −23.3(5), B3-C2-Li-O −143.7(12), C2-B3-C4-Si1 −39.3(6), C2-B3-C4-Si2 92.7(5), C2-B3-C31-C32 −65.7(6), C2-B3-C31-C38 112.9(5).

The BCB moiety is almost linear (BCB bond angle 176.5°, boron atoms bent toward Li). Values of 176.4° and 179.6°, respectively, have been determined for the NBC bond angles in **7**[8] and **8**.[9]

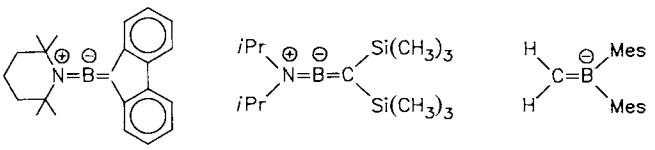

The plane of the mesityl ring attached to the sp-hybridized B1 forms an angle of 41° with the plane through the bonding partners of the sp^2-hybridized B3; B3 itself does not deviate significantly from this plane (0.5(5) pm), and the mesityl ring attached to B3 is twisted through about 66°.

The lithium ion coordinated through the O-atom of a diethyl ether molecule has additional short contacts: to the central carbon atom C2 (209.4(9) pm) bound to the two boron atoms, to C31, the *ipso*-C-atom of the mesityl ring attached to B3 (234.5(9) pm), and to both boron atoms (each about 249 pm). The C2-Li connecting line is not perpendicular to, but almost in the B3-C2-C4-C31 plane.[10]

At B3, the B-C bond lengths to the substituents are 161.2(6) and 159.9(6) pm, i.e. in the range typical for B-C single bonds (158-162 pm);[11] B1-C11 (154.3(6) pm) is markedly shorter. This may be due to the absence of steric hindrance and the increased s-character of the bond to B1. The B3-C2 distance (149.2(6) pm) is distinctly shorter than that of a B-C single bond, even if the sp hybridization of the carbon atom is taken into account;[12] however, in spite of the sp-hybridized C atom, it is noticeably longer than the B_{sp^2}–C_{sp^2} double bond in **9** (144 pm).[11] This indicates partial double-bond character of the C2-B3 bond in **3b** corresponding to resonance formula **3B**. The B1-C2 distance of 133.9(6) pm is the shortest so far measured for a B-C bond. It is markedly shorter than that of the B_{sp}–C_{sp^2} double bond in **7** (142 pm)[8] and **8** (139 pm).[9] About 2 pm of the difference of 5-8 pm can be attributed to sp hybridization of C2, as a comparison of the C=C distances in ethene (133.2 pm) and allene (131.2 pm) shows. The remaining difference of 3-6 pm indicates partial triple-bond character of the B1-C2 bond in **3b** corresponding to resonance formula **3A**.

Both C2-B bonds in **3b** are longer by the same amount (13 pm) than the corresponding C-C bonds in the propargyl cation **4a**, thus verifying the electronic similarity of **3** and **4**.

Since **3a** and **3b** show similar IR bands in the heteroallene region[8] (**3a**: $\tilde{\nu}$ = 1765 and 1810 cm^{-1}; **3b**: $\tilde{\nu}$ = 1765, 1790 and 1830 cm^{-1}), we conclude that the electronic structure of **3a** resembles that of **3b**, despite the additional negative charge. The chemical shift of the quaternary C atom of the $LiC(Si(CH_3)_3)_2$ group (δ = 58.3) shows that the negative charge is essentially localized on this C atom (resonance formula **3a A**). Also consistent with such a localization is the low rotation barrier about the Si_2C=B bond (resonance formula **3a B**) of 13.5 kcal mol^{-1}, which can be determined from the temperature dependence of the ^{13}C-NMR signals of the $Si(CH_3)_3$ groups. A barrier of 57 kcal mol^{-1} has been calculated for $H_2C{=}\overset{\ominus}{B}H_2$.[13]

Received: February 5, 1988 [Z 2607 IE]
German version: *Angew. Chem.* *100* (1988) 961

CAS Registry numbers:
3a, 114958-96-2; **3b**, 114978-53-9; **5**, 114958-95-1; **6**, 114958-97-3; bis(trimethylsilyl)acetylene, 14630-40-1; 1,2-dichloro-1,2-dimesityldiborane, 114978-52-8; *mesityllithium*, 5806-59-7; *1,2-dichloro-1,2-bis(dimethylamino)diborane* (4), 114958-98-4.

[1] Systematically, the systems **1**, **3** and **4** are named as follows: **1**: alkylidyneborate, **3A**: (borylmethylidyne)borate, **3B**: (boranemethylene)borate, 4: 2-propynyl cation ↔ propadienyl cation.

[2] The iminoboranes $\overset{\oplus}{B}\equiv\overset{\ominus}{N}-$ isoelectronic with **1** and **2**, on the other hand, have been studied in great detail: P. Paetzold, *Adv. Inorg. Chem. 31* (1987) 123.

[3] Ab-initio calculations gave C-C distances of 136.0 and 121.4 pm for the propargyl cation **4a**: L. Random, P. C. Hariharan, J. A. Pople, P. von R. Schleyer, *J. Am. Chem. Soc. 98* (1976) 10.

[4] **3a**: yellow crystals, m.p. 120°C, yield ^{13}C-NMR spectroscopically quantitative.—^{1}H-NMR (C_6D_6): $\delta=0.29$ (s, 18H; $Si(CH_3)_3$), 2.10, 2.17 (each. s, each 3H; *p*-CH_3), 2.68, 2.75 (each s, each 6H; *o*-CH_3), 6.77, 6.85 (each s, each 2H; *m*-H); ^{13}C-NMR ([D$_8$]THF, −40°C): $\delta=6.0$, 6.2 (each 3C; $Si(CH_3)_3$), 21.3, 21.5 (each 1C; *p*-CH_3), 24.0, 24.4 (each 1C; *o*-CH_3), 24.8 (2C; *o*-CH_3), 58.3 (1C; CSi_2), 109.6 (br, 1C; CB_2), 126.9 (2C; *m*-C), 127.6, 128.5 (each 1C; *m*-C), 132.1 (1C; *i*-C), 134.0, 135.0 (each 1C; *p*-C), 139.3, 140.0 (each 1C; *o*-C), 142.7 (2C; *o*-C), 150.9 (1C; *i*-C); ^{11}B-NMR (Et_2O): $\delta=26$, 46 (each $\nu_{1/2}\approx670$ Hz). **3b**: yellow crystals, m.p. 122°C (decomp.), yield ^{13}C-NMR spectroscopically quantitative.—^{1}H-NMR (C_6D_6): $\delta=0.56$ (s, 18H; $Si(CH_3)_3$), 1.19 (s, 1H; $CHSi_2$), 2.07, 2.20 (each s, each 3H; *p*-CH_3), 2.66, 2.67 (each s, each 6H; *o*-CH_3), 6.71, 6.83 (each s, each 2H; *m*-H); ^{13}C-NMR ([D$_8$]THF, −40°C): $\delta=3.7$ (q, 6C; $Si(CH_3)_3$), 21.4, 21.7 (each q, each 1C; *p*-CH_3), 24.5, 24.6 (each q, each 2C; *o*-CH_3), 27.4 (d, 1C; $CHSi_2$), 127 (br. s, 1C; CB_2), 126.8, 128.8 (each d, each 2C; *m*-C), 132.6 (s, 1C; *i*-C), 134.8, 135.4 (each s, each 1C; *p*-C), 139.0, 140.8 (each s, each 2C; *o*-C), 147.6 (s, 1C; *i*-C); ^{11}B-NMR [D$_8$]toluene, 90°C): $\delta=41$, 54 (each $\nu_{1/2}\approx660$ Hz).

[5] **5** is obtained upon heating a pentane solution of bis(trimethylsilyl)-acetylene and 1,2-dichloro-1,2-dimesityldiborane(4), which is accessible from mesityllithium and 1,2-dichloro-1,2-bis(dimethylamino)diborane(4) analogously to 1,2-di-*tert*-butyl-1,2-dichlorodiborane(4) [6], for three days.

[6] H. Klusik, A. Berndt, *J. Organomet. Chem. 234* (1982) C 17.

[7] X-ray structure analysis of **3b**: space group $P2_1/c$, $Z=4$, $a=1169.4(7)$, $b=1553.4(16)$, $c=1869.8(6)$ pm, $\beta=95.10(4)°$; 3586 independent reflections with $F_0>5\sigma(F)$ measured on a four-circle diffractometer (CAD4, Enraf-Nonius) with $Cu_{K\alpha}$ radiation at −67°C; no absorption correction ($\mu=10.7$ cm^{-1}); H atoms at calculated positions using a "riding" model and refined groupwise with common isotropic temperature factors. Anisotropic factors used for all other atoms except Li. 452 parameters, $R=0.0711$, $R_w=0.0865$ ($w=1/\sigma^2(F_0)$). Strong anisotropic vibration and/or disorder of the ether molecule could be responsible for these moderate residual indices. Further details of the crystal structure investigation are available on request from the Fachinformationszentrum Energie, Physik, Mathematik GmbH, D-7514 Eggenstein-Leopoldshafen 2 (FRG) on quoting the depository number CSD-52921, the names of the authors and the journal citation.

[8] B. Glaser, E. Hanecker, H. Nöth, H. Wagner, *Chem. Ber. 120* (1987) 659.

[9] R. Boese, P. Paetzold, A. Tapper, *Chem. Ber. 120* (1987) 1069.

[10] All five close neighbors of the Li ion lie approximately in one plane. Above and below this plane there are in each case three additional methyl groups in a distorted trigonal prismatic arrangement which sterically almost completely shield the Li ion.

[11] M. M. Olmstead, P. P. Power, K. J. Weese, *J. Am. Chem. Soc. 109* (1987) 2541, and references cited therein.

[12] A distance of 155 pm was measured for the C_{sp}-B_{sp^2} bond of a bis(boryl)alkyne: A. Meller, W. Maringgele, G. Elter, D. Bromm, M. Noltemey, G. M. Sheldrick, *Chem. Ber. 120* (1987) 1437.

[13] A. Pross, D. J. DeFrees, B. A. Levi, S. K. Pollack, L. Radom, W. J. Hehre, *J. Org. Chem. 46* (1981) 1693.

1,4-Di-*tert*-butyl-2,6-bis(trimethylsilyl)silabenzene, the First Silabenzene Stable in Solution at −100°C

By *Gottfried Märkl** and *Werner Schlosser*

In the past few years *A. G. Brook* et al.[1] and *N. Wiberg* et al.[2] have reported the synthesis of a number of kinetically stabilized silaethenes which, under inert gas, are stable even at room temperature. In contrast, no comparable stable silabenzene derivatives have been described as yet. Silabenzene and 1-methylsilabenzene[3–5] have been identified IR-, UV- and PE-spectroscopically in an argon matrix at 10 K, 1-methylsilabenzene[6] and 1,4-di-*tert*-butylsilabenzene have been detected by trapping reactions with hexafluorobutyne[6] or 1,3-dienes and by dimer formation.[7]

We report here on 1,4-di-*tert*-butyl-2,6-bis(trimethylsilyl)silabenzene (**1**), which is stable up to ca. −100°C.

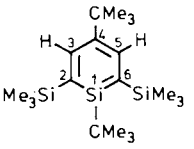

1

Recently, we described the photochemical and thermal elimination of N_2 from 6-diazo-1-methoxy-1,2-bis(trimethylsilyl)-4-*tert*-butyl-1-sila-2,4-cyclohexadiene **2**.[8a] On the basis of the product pattern we postulated that the initially formed carbene is transformed via a 1,2-silyl shift into the silabenzene **3** and via rearrangement of the skeletal framework into the silafulvene **4**, both of which can be trapped as reactive intermediates, e.g. with methanol and 2,3-dimethylbutadiene, respectively.

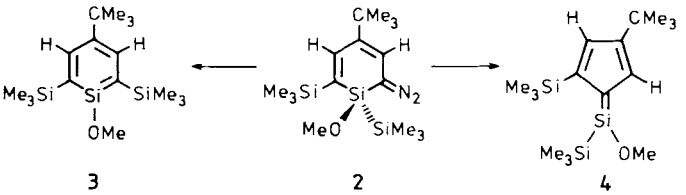

3 **2** **4**

We have now investigated the photochemical behavior of the diazo compound **6**, which is accessible in 5–10% yield from 1,4-di-*tert*-butyl-1,2-bis(trimethylsilyl)-1-sila-2,4-cyclohexadiene **5**[8b] via the lithium compound. Irradiation (3 h) of **6** in anhydrous methanol/THF (1/1) with a halogen lamp ($\lambda>410$ nm) at room temperature leads to elimination of N_2 and formation of the 1-*tert*-butyl-1-methoxysilacyclohexadiene **8**, which can be isolated in 45% yield by chromatographic work-up on silica gel 60 with petroleum ether/benzene (6:1). The formation of **8** can only be interpreted in terms of the carbene **7**, formed as intermediate from **6**, rearranging via a 1,2-Me_3Si-shift to the silabenzene **1**, which then adds methanol to give the stable *syn*-adduct **8**. The physical and spectroscopic properties of **5**, **6** and **8** are listed in Table 1.

Whereas the carbene generated from 4-diazo-1,1-dimethyl-1-sila-2,5-cyclohexadiene by thermolysis at 400°C does not rearrange—via 1,4-methyl-shift—into 1,4-dimethylsilabenzene but dimerizes to the ethene derivative,[9] the strong tendency of the silyl residue in **7** to migrate effects rearrangement to the silabenzene **1**.

After three hours' irradiation of **6** in a Trapp mixture (THF/ether/petroleum ether 4/1/1) at −110°C to −120°C, the reaction solution affords the methanol adduct **8** in 35–40% yield on addition of methanol, even 30 or 60 mins after completion of N_2-elimination. Since **8** is still formed in almost the same yield even after 4–5 h irradiation, a subsequent fast photochemical secondary reaction of **1** under these conditions can be ruled out. And since **8**

[*] Prof. Dr. G. Märkl, Dipl.-Chem. W. Schlosser
Institut für Organische Chemie der Universität
Universitätsstrasse 31, D-8400 Regensburg (FRG)

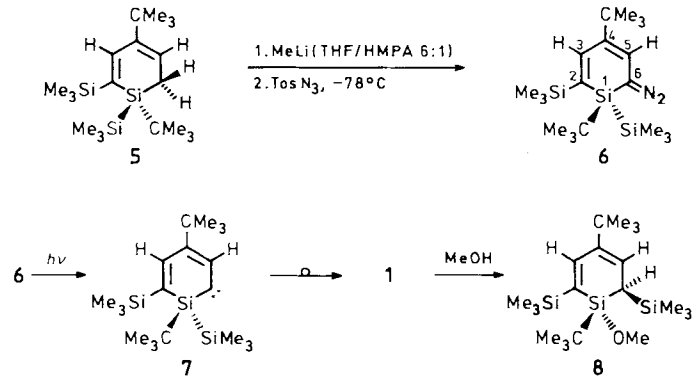

Table 1. Physical and spectroscopical data of **5**, **6** and **8**.

5: Colorless oil, b.p. 160°C/0.01 torr; ^{1}H-NMR (250 MHz, $CDCl_3$, δ-values): 1- and 2-$SiMe_3$: 0.12 (s), 0.15 (s), 1- and 4-CMe_3: 0.91 (s), 1.04 (s), H-6: 1.57 (d), J(H-5/H-6) = 6.9 Hz, H-5: 5.84 (dd), J(H-3/H-5) = 1.6 Hz, H-3: 7.25 (d); MS (70 eV), $M^{\oplus}$: m/z = 352 (6%), $[M-CH_3]^{\oplus}$: 337 (4%), $[M-C_4H_9]^{\oplus}$: 295 (80%), $[295-SiMe_3]^{\oplus}$: 222 (25%), $[SiMe_3]^{\oplus}$: 73 (100%)

6: Non-distillable, viscous red oil; IR (film): ν(C=N_2) = 2050 cm^{-1}; UV (*n*-hexane): λ_{max} = 380 nm; ^{1}H-NMR: 1- and 2-$SiMe_3$: 0.20 (s), 0.27 (s), 1- and 4-CMe_3: 1.10 (s), 1.11 (s), H-5: 6.14 (d), J(H-3/H-5) = 1.5 Hz, H-3: 7.41 (d); ^{13}C-NMR ($CDCl_3$): C-3: 151.9 ppm; C-2: 137.9 (128.1); C-4: 128.1 (137.9); C-5: 116.5; C-6: 24.6; CMe_3: 35.6, 26.4; $SiMe_3$: 1.3, 1.0; [10]; MS: $M^{\oplus}$: m/z = 378 (2%), $[M-N_2]^{\oplus}$: 350 (5%), $[350-CH_3]^{\oplus}$: 335 (12%), $[350-C_4H_9]^{\oplus}$: 293 (80%), $[SiMe_3]^{\oplus}$: 73 (100)

8: Colorless oil, b.p. 180°C/0.01 torr; ^{1}H-NMR: 2- and 6-$SiMe_3$: 0.13 (s), 0.18 (s), 1- and 4-CMe_3: 0.90 (s), 1.07 (s), H-6: 1.35 (d), J(H-5/H-6) = 4.0 Hz, H-5: 5.81 (dd), J(H-3/H-5) = 2.0 Hz, H-3: 7.31 (d), OCH_3: 3.41 (s); MS: $M^{\oplus}$: m/z = 382 (8%), $[M-CH_3]^{\oplus}$: 367 (6%), $[M-C_4H_9]^{\oplus}$: 325 (100%), $[M-Me_3SiOMe]^{\oplus}$: 278 (30%), $[278-C_4H_9]^{\oplus}$: 221 (41%)

is formed only in 45% yield from **6**, even in the presence of methanol, it must be assumed that further products, which so far could not be isolated, are formed upon irradiation of **6**. No clearly identifiable products are formed upon irradiation of **6** in THF in the absence of trapping rearrangements at 25°C, 0°C, −30°C and −60°C; subsequent addition of methanol to these irradiated solutions no longer leads to the adduct **8**.

The assumption that the silabenzene **1** is stable up to ca. −100°C is further substantiated by low-temperature spectroscopy. The ^{29}Si-NMR spectrum of the diazo compound **6** in the Trapp mixture at −100°C shows three signals, at δ = −2.6 and −15.3 (Me_3Si) and at δ = −24.8 (ring Si). On irradiation of **6** in a Trapp mixture ($c \approx 60$ mg/mL) under pure nitrogen in a sealed NMR tube at −110°C to −120°C, the ^{29}Si-NMR signals of **6** disappear within 3 h; a new signal at δ = −17.8 is assigned to the $SiMe_3$-substituents in the 2,6 position, one at δ = +26.8 to the sp^2 ring-Si atom of the silabenzene **1**. On warming the solution to −70°C, these signals disappear. On addition of methanol to the NMR sample solution at $T \leq -110$°C, the methanol adduct is again obtained in 40% yield. The δ(^{29}Si) values for acyclic silaalkenes[11] in C_6D_6 lie between δ = +40 and δ = +144; it appears, however, that THF as donor ligand at the sp^2 silicon leads to a high-field shift of this signal. Thus, e.g., the ^{29}Si-NMR signal for the silanediyl complex $[(CO)_4Fe{=}Si(OtBu)_2 \cdot Do]$ appears at δ = 7.1 (Do = HMPT) and δ = −9.4 (Do = THF).[12]

The signals of the educt also almost completely disappear in the ^{13}C-NMR spectrum recorded at ca. −105°C three hours after irradiation of the solution of **6** ($c \approx 70$ mg/mL); new signals appear for C-2 to C-5 which we assign on the basis of off-resonance measurements to the ring C-atoms of **1** as follows ([D_8]THF/Et_2O/petroleum ether): δ = 166.8 (C-3, C-5), 126.0 (139.5) (C-2, C-6), 139.5 (126.0) (C-4).[13, 14] On briefly warming the solution to −10°C, these signals disappear.[15]

The C=N_2 vibration at 2050 cm^{-1} in the IR spectrum of **6** (Trapp mixture, c = 3 mg/mL, layer thickness 0.2 mm) at −120°C has almost completely disappeared after 6 min. In the UV spectrum (HBO 200, monochromator) after this time under the same conditions the absorption band of **6** at 380 nm has disappeared; the absorption band of **1**, which is to be expected in the same region, cannot be observed.[16] This observation is consistent with the results of *G. Meier* et al.[4] according to which the absorption bands of the silabenzene disappear upon brief irradiation, even in an argon matrix at 10 K.

At concentrations of **6** of ca. 100-fold less than that required for the ^{29}Si- and ^{13}C-NMR measurements, possible photochemical secondary steps or reactions with traces of moisture or oxygen (during irradiation times of 6 min) can lead to complete degradation of **1**. Upon irradiation of **6** in the 1-cm cuvette, the absorption band at 375–390 nm disappears much more slowly at −120°C than at room temperature. Thawing of the solutions of **6** after irradiation at −120°C for 5 min shows that the decreasing extinction accompanying the degradation of **6** is compensated by the synthesis of **1**: the extinction of the band decreases rapidly with increasing temperature. This finding is best explained in terms of the broad band observed at 375–390 nm for the solutions of **6** after irradiation for 5 min being caused by the concomitant presence of **1** and **6**.

From our findings we can conclude that the silabenzene **1** obtainable photochemically from **6** is stable up to about −100°C. Above this temperature, well-defined secondary products of **1** can no longer be isolated in the absence of trapping reagents. The formation of dimers, such as takes place in the case of the short-lived 1,4-di-*tert*-butylsilabenzene,[7] is not observed with **1** — obviously for steric reasons.

Some time ago, the possibility of a photochemical valence isomerization of silabenzene to the Dewar-silabenzene was discussed on the basis of MO calculations.[17]

The assumption made therefrom that silabenzene and silatoluene generated in the matrix already isomerize to Dewar-benzenes upon brief irradiation (rapid disappearance of the bands in the UV spectra) cannot be excluded by our results; the secondary reactions occurring under our conditions, however, must be so slow that unequivocal detection of **1** is possible in the concentration range required for NMR measurements at −100°C. δ(^{29}Si) values of −50 to −100 would be expected for a Dewar-isomer of **1**, in analogy to the values already known for silacyclobutenes and silacyclopropenes.[18] It is surprising that even silabenzene derivatives which should be kinetically highly stabilized, are not stable at room temperature.

Received: January 13, 1988;
supplemented: March 4 and April 25, 1988 [Z 2572 IE]
German version: *Angew. Chem. 100* (1988) 1009

CAS Registry numbers:
1, 114564-38-4; **5**, 114564-39-5; **6**, 114564-40-8; **8**, 114581-47-4.

[1] A. G. Brook, A. Abdesaken, *J. Chem. Soc. Chem. Commun. 1981*, 246.
[2] N. Wiberg, G. Wagner, *Angew. Chem. 95* (1983) 1027; *Angew. Chem. Int. Ed. Engl. 22* (1983) 1005.
[3] B. Solouki, P. Rosmus, H. Bock, G. Maier, *Angew. Chem. 92* (1980) 56; *Angew. Chem. Int. Ed. Engl. 19* (1980) 51.
[4] G. Maier, G. Mihm, H. P. Reisenauer, *Angew. Chem. 92* (1980) 58; *Angew. Chem. Int. Ed. Engl. 19* (1980) 52; G. Maier, G. Mihm, R. Baumgärtner, H. P. Reisenauer, *Chem. Ber. 117* (1984) 2337.
[5] H. Bock, R. A. Bowling, B. Solouki, T. J. Barton, G. T. Burns, *J. Am. Chem. Soc. 102* (1980) 429; C. L. Kreil, O. L. Chapman, G. T. Burns, T. J. Barton, *ibid. 102* (1980) 841.

[6] T. J. Barton, G. T. Burns, *J. Am. Chem. Soc. 100* (1978) 5246.
[7] G. Märkl, P. Hofmeister, *Angew. Chem. 91* (1979) 863; *Angew. Chem. Int. Ed. Engl. 18* (1979) 789.
[8] a) G. Märkl, W. Schlosser, W. S. Sheldrick, *Tetrahedron Lett. 29* (1988) 467; b) W. Schlosser, *Dissertation*, Universität Regensburg 1988.
[9] T. J. Barton, D. S. Banasiak, *J. Organomet. Chem. 157* (1978) 255.
[10] The assignment is supported by a comparison with the ^{13}C-NMR spectra of 1-sila-2,5-cyclohexadienes and 1-sila-2,4-cyclohexadiene (G. Märkl, C. Soper, P. Hofmeister, H. Baier, *J. Organomet. Chem. 174* (1979) 305; P. Jutzi, G. Otto, T. Wippermann, *Chem. Ber. 117* (1984) 1885; see also [8b]. In the Trapp mixture at -105°C, the δ-values for C-2 to C-5 differ only slightly.
[11] A. G. Brook, K. M. Baines, *Adv. Organomet. Chem. 25* (1986) 1.
[12] C. Zybill, G. Müller, *Angew. Chem. 99* (1987) 683; *Angew. Chem. Int. Ed. Engl. 26* (1987) 669.
[13] The remaining signals fall in the range of the solvent signals; a silaalkene that can be used for comparison is **9**, in which the C-2 signal lies at $\delta = 118.1$ [11].

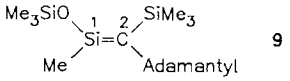

9

[14] After further irradiation at -110°C to -120°C the signals of the educt have completely disappeared; the intensity of the signals of **1** is greater.
[15] Ten new signals appear at $\delta = 126$-163, which likewise disappear after 16 h at 0°C in favor of broader unspecific signals. A further signal appearing at $\delta = 150.5$ upon low-temperature irradiation is still observable even at 0°C, from which the photochemical formation of a stable product can be concluded.
[16] We thank Prof. Dr. *G. Meier* and Dr. *H. P. Reisenauer* for the low-temperature UV and IR measurement.
[17] J. Chandrasekhar, P. von R. Schleyer, R. O. W. Baumgärtner, M. T. Reetz, *J. Org. Chem. 48* (1983) 3453.
[18] D. Seyferth, D. C. Annarelli, S. C. Vick, *J. Organomet. Chem. 272* (1984) 123.

Reaction of [NiCp(PPh$_3$)Cl] with E(SiMe$_3$)$_2$; the Structures of [Ni$_4$Se$_2$Cp$_4$] and [Ni$_4$E$_2$Cp$_4$(PPh$_3$)$_2$] (E = Se, Te)**

By *Dieter Fenske,* Achim Hollnagel,* and *Kurt Merzweiler*

Dedicated to Professor Heinrich Nöth on the occasion of his 60th birthday

Transition-metal halides react with E(SiMe$_3$)$_2$ (E = S, Se, Te) in the presence of phosphane ligands to give metal-rich clusters.[1] Frequently, mixtures of substances are obtained and the structures of the clusters are dependent on the properties of the solvent. But the properties of the phosphane ligands may possibly also have an influence on the cluster size. For example, we also found that multinuclear complexes containing maximally six metal atoms are formed upon reaction of the cyclopentadienyl-transition-metal halides [TiCp$_2$Cl$_2$], [TiCpCl$_3$], [TaCpCl$_4$], [FeCp(CO)$_2$Br] and [VCp$_2$Cl$_2$] with E(SiMe$_3$)$_2$.[2,3]

When, however, [NiCp(PPh$_3$)Cl] is allowed to react with E(SiMe$_3$)$_2$ in THF as solvent a rapid change in color of the solution from violet to dark brown is observed, and a fine crystalline, black precipitate of **1** separates, which is readily soluble in THF. On covering this solution with heptane, **1** is obtained in the form of black platelets, and upon addition of hexane to the filtrate black needles of **2** can be isolated. **2a** and **2b** can also be obtained by reaction of **1a** and **1b**, respectively, with PPh$_3$.

[*] Prof. Dr. D. Fenske, Dipl.-Chem. A. Hollnagel, Dr. K. Merzweiler
Institut für Anorganische Chemie der Universität
Niederurseler Hang, D-6000 Frankfurt am Main 50 (FRG)

[**] This work was supported by the Deutsche Forschungsgemeinschaft and the Fonds der chemischen Industrie.

$$[NiCp(PPh_3)Cl] \xrightarrow{E(SiMe_3)_2} \underset{\mathbf{1}}{[Ni_4E_2Cp_4]} + \underset{\mathbf{2}}{[Ni_4E_2Cp_4(PPh_3)_2]}$$

a, E = Se; **b**, E = Te

The molecular structures of **1a**, **2a** and **2b** were confirmed by crystal structure analyses.[4] **1a** (Fig. 1) contains a square planar Ni$_4$ cluster ($\bar{1}$ symmetry) in which each Ni atom is bound to an η^5-C$_5$H$_5$(Cp) ring and to two μ_4-Se ligands. If one assumes that Se$^{2\ominus}$ and Cp$^{\ominus}$ ligands are present in **1a**, then the Ni has the formal oxidation number +2. The Ni-Ni bond lengths resemble those in other Ni clusters containing Ni-Ni bonds.[1-5] Assuming that four Ni-Ni single bonds exist in the 68e cluster **1a**, it must contain four electrons more than would be expected according to the 18-electron rule.

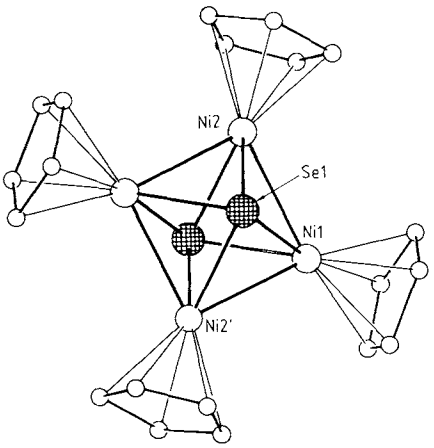

Fig. 1. Structure of **1a** in the crystal. Important bond lengths [pm] and angles [°]: Ni1-Ni2 257.0(1), Ni1-Ni2' 258.1(1), Ni-Se 237.2-238.4(1), Ni-C(Cp) 212.4-217.2(6), C(Cp)-C(Cp) 135.0-141.8(8); Ni-Ni-Ni 89.85-90.15(10), Ni-Se-Ni 65.4-80.0(1), Ni-Ni-Se 57.1-57.5(1), C(Cp)-C(Cp)-C(Cp) 106.0-110.2(4).

The distance between the two μ_4-bridging Se-ligands (305.3(1) pm) is significantly less than the van-der-Waals distance that has been found in Se and $Se_8^{2\oplus}$.[6] This could be due to a weak interaction between the Se ligands. However, it must be taken into account that there is a direct relationship between the Ni-Ni bond lengths and the Se-Se distance for a given Ni-Se distance. A similar situation has already been observed in $[Ni_3Se_2(PEt_3)_6]^{2\ominus}$ and $[Co_4(CO)_8(\mu_2\text{-}CO)_2(\mu_4\text{-}E)_2]$ (E = S, Te, PPh).[7,8]

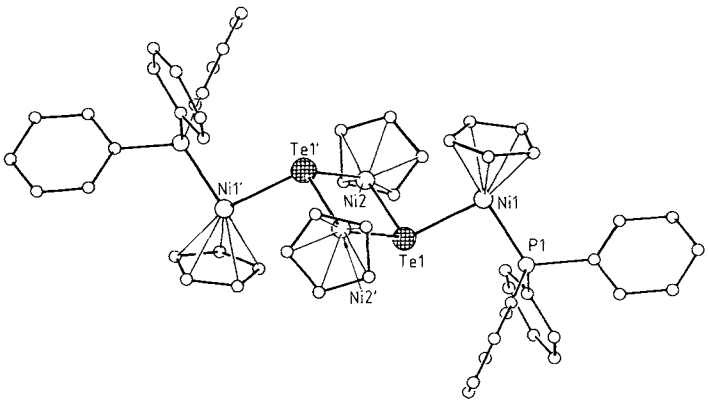

Fig. 2. Structure of **2b** in the crystal (without THF molecules). Important bond lengths [pm] and angles [°]: Ni1-Te1 251.9(1), Ni2-Te1 245.7(1), Ni1-P1 214.5(2), Te1···Te1' 327.7(1), P1-C 183.7-184.2(4), Ni-C(Cp) 208.3-216.3(5), C(Cp)-C(Cp) 138.0-142.0(9); P1-Ni1-Te1 93.1(1), Te1-Ni2-Te1' 83.7(1), Ni2-Te1-Ni1 107.5(1), Ni2-Te1-Ni2' 95.7(1), Ni1-Te1-Ni2' 106.6(1).

Figure 2 shows the molecular structure of **2b**.[4] **2b** ($\bar{1}$ symmetry) contains four NiCp units which are bridged by μ_3-Te ligands; two Ni atoms (Ni1, Ni1') are also bound to PPh_3, and the Ni–Te bonds are different in length. Diamagnetic **2b** contains 72 valence electrons and obeys the 18-electron rule. Accordingly, there are no bonding interactions between the Ni atoms (Ni···Ni2 398, Ni2···Ni2' 362 pm).

Similarly as in **1a**, the distances between the bridging E-ligands in **2b** (Te···Te 327.7(1) pm) and in the isostructural **2a** (Se···Se 311.7(1) pm) point to bonding interactions. The formation of **2** in the reaction of PPh_3 with the Ni_4 cluster of **1** is consistent with a cluster opening, for which further examples have already been found in other multinuclear complexes.[9] Thus, $[Ru_4(CO)_{11}(PPh_2)]$ reacts with CO with opening of a Ru–Ru bond to give $[Ru_4(CO)_{13}(PPh_2)]$.[10]

Experimental

1a/2a: A solution of $[NiCp(PPh_3)Cl]$ (1.5 g, 3.5 mmol) in THF (40 mL) was treated dropwise with a solution of $Se(SiMe_3)_2$ (0.38 mL, 1.75 mmol) in THF (10 mL). The solution turned dark brown in color within a few minutes. After 24 h the reaction mixture was filtered, yielding 0.4 g of **1a** (68% yield). Treatment of the residue with 30 mL of THF and covering of the mixture with heptane led to separation of crystalline **1a**. The filtered reaction solution was covered with a layer of hexane. This led to crystallization of 0.30 g of **2a** (29% yield).

1b and **2b** were obtained analogously by reaction of 2.8 g (6.6 mmol) of $NiCp(PPh_3)Cl$ with 0.91 g (3.3 mmol) of $Te(SiMe_3)_2$ in 40 mL of THF.

Received: January 20, 1988 [Z 2582 IE]
German version: *Angew. Chem. 100* (1988) 978

CAS Registry numbers:
1a, 114836-88-3; **1b**, 114820-40-5; **2a**, 114860-54-7; **2a**·2THF, 114925-31-4; **2b**, 114820-41-6; **2b**·2THF, 114883-97-5; $Se(SiMe_3)_2$, 4099-46-1; $Te(SiMe_3)_2$, 4551-16-0; $NiCp(PPh_3)Cl$, 31904-79-7.

[1] D. Fenske, J. Hachgenei, J. Ohmer, *Nachr. Chem. Tech. Lab. 34* (1986) 432; *Angew. Chem. 97* (1985) 684; *Angew. Chem. Int. Ed. Engl. 24* (1985) 706; D. Fenske, J. Ohmer, J. Hachgenei, *ibid. 97* (1985) 993 bzw. *24* (1985) 993; D. Fenske, J. Ohmer, *ibid. 99* (1987) 155 and *26* (1987) 148; D. Fenske, J. Ohmer, K. Merzweiler, *Z. Naturforsch. B42* (1987) 803.

[2] D. Fenske, P. Maue', *Z. Naturforsch.*, in press.

[3] D. Fenske, P. Maue', K. Merzweiler, *Z. Naturforsch. B42* (1987) 928.

[4] X-ray structure analyses: 293 K; Siemens AED II, $2\theta < 56°$, ω scan, empirical absorption correction, $\lambda = 0.71069$; all atoms except H anisotropically refined; Patterson method. **1a**: space group $P2_1/n$, $a = 986.4(4)$, $b = 779.7(2)$, $c = 1357.5(4)$ pm, $\beta = 105.99(3)°$; $Z = 2$; $\mu(Mo_{K\alpha}) = 72.9$ cm^{-1}. 5129 reflections, 2036 with $I > 2\sigma(I)$. $R_1 = 0.043$, $R_2 = 0.038$. — **2a** (crystallizes with two molecules of THF per formula unit): space group $P\bar{1}$, $a = 1025.2(4)$, $b = 1107.5(7)$, $c = 1403.0(6)$ pm, $\alpha = 102.19(3)$, $\beta = 104.75(4)$, $\gamma = 102.30(3)°$; $Z = 1$; $\mu(Mo_{K\alpha}) = 26.01$ cm^{-1}, 7370 reflections, 4883 with $I > 2\sigma(I)$. $R_1 = 0.068$, $R_2 = 0.059$. — **2b** (crystallizes with two molecules of THF per formula unit): space group $P\bar{1}$, $a = 1020.1(7)$, $b = 1103.9(7)$, $c = 1451.4(5)$ pm, $\alpha = 77.65(4)$, $\beta = 83.87(4)$, $\gamma = 65.46(4)°$; $Z = 1$; $\mu(Mo_{K\alpha}) = 23.34$ cm^{-1}. 7649 reflections, 5169 with $I > 2\sigma(I)$. $R_1 = 0.049$, $R_2 = 0.042$. Further details of the crystal structure investigations are available on request from the Fachinformationszentrum Energie, Physik, Mathematik GmbH, D-7514 Eggenstein-Leopoldshafen 2 (FRG), on quoting the depository number CSD-52940, the names of the authors, and the journal citation.

[5] M. S. Paquette, L. F. Dahl, *J. Am. Chem. Soc. 102* (1980) 6621; H. Vahrenkamp, V. A. Uchtmann, L. F. Dahl, *ibid. 90* (1968) 3272; J. C. Calabrese, L. F. Dahl, A. Cavalieri, P. Chini, G. Longoni, S. Martinengo, *ibid. 96* (1974) 2616.

[6] E. H. Henninger, R. C. Buschert, L. Heaton, *J. Chem. Phys. 46* (1967) 586; R. K. McMullan, D. J. Prince, J. D. Corbett, *Inorg. Chem. 10* (1971) 1749.

[7] F. Cecconi, C. A. Ghilardi, S. Midollini, *Inorg. Chem. 22* (1983) 3802.

[8] R. C. Ryan, L. F. Dahl, *J. Am. Chem. Soc. 97* (1975) 6904; C. H. Wei, L. F. Dahl, *Cryst. Struct. Commun. 4* (1975) 583.

[9] H. Vahrenkamp, *Adv. Organomet. Chem. 22* (1983) 169; G. Huttner, J. Schneider, H. D. Müller, G. Mohr, J. von Seyerl, L. Wohlfahrt, *Angew. Chem. 91* (1979) 82; *Angew. Chem. Int. Ed. Engl. 18* (1979) 76; M. Müller, H. Vahrenkamp, *Chem. Ber. 116* (1983) 2311; J. Schneider, L. Zsolnai, G. Huttner, *ibid. 115* (1982) 989.

[10] J. S. Field, R. J. Haines, D. N. Smit, K. Natarajan, O. Scheidsteger, G. Huttner, *J. Organomet. Chem. 240* (1982) C23; J. S. Field, R. J. Haines, D. N. Smit, *ibid. 224* (1982) C49.

Towards the Making of [12]Collarene**

By *Peter R. Ashton, Neil S. Isaacs, Franz H. Kohnke, Alexandra M. Z. Slawin, Catriona M. Spencer, J. Fraser Stoddart,** and *David J. Williams*

[12]Cyclacene **1** ($n = 12$), a constitutional isomer of kekulene,[1] is a challenging and intriguing target on account of the mystery surrounding[2,3] its molecular and supramolecular properties. While unsaturated hydrocarbons, such as **1** ($n = 12$), are of considerable theoretical interest,[4] their extended conjugated π-systems could confer upon them high reactivities,[5] thus rendering them possibly less easy to prepare and handle than the partially-hydrogenated analogues, [12]beltene **2** ($n = 12$)[3] and [12]collarene **3**

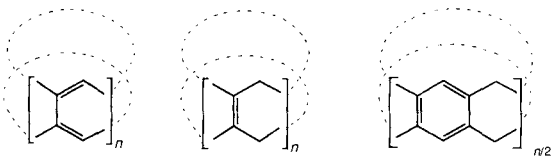

1 **2** **3**

($n = 12$).[6] In this communication, we report the synthesis of the hydrocarbon **7**, which is a common and immediate precursor of [12]cyclacene **1** ($n = 12$) and [12]beltene **2** ($n = 12$) as well as of [12]collarene **3** ($n = 12$): in so doing, we describe how the octahydro[12]cyclacene derivative **7** can be prepared in two steps (Scheme 1) from **4**[7] via a dideoxy derivative **5**: also, we discuss the X-ray structure of the water complex formed by **5** in the solid state.

Deoxygenation[8] (Scheme 1) of **4** at the 3 and 9 o'clock positions[9] afforded[10] **5** in 43% yield. The X-ray crystal structure[11] of **5** (Fig. 1) reveals that, as expected, the four oxygen atoms at 1, 5, 7, and 11 o'clock in **5** lie on the outside of the macropolycycle whilst the four pairs of methine hydrogen atoms at 1:30, 4:30, 7:30, and 10:30[9] are directed into the center of the rigid molecular cavity. The most striking feature of this structure is the Celtic cross-like cavity within which the water molecule is trapped. The cavity has an approximately square cross-section with distances between the mean planes of the parallelly-disposed aromatic rings of 8.9 Å (3 to 9 o'clock) and 9.6 Å (6 to 12 o'clock). This geometry contrasts with the oval-like cavity present[7] in **4** in its solid state where the equivalent 6 to 12 o'clock distance is 7.9 Å. The water molecule which resides on the crystallographic center of symmetry at the center of the macropolycyclic ring in **5** does not enter into any hy-

[*] Dr. J. F. Stoddart, Dr. F. H. Kohnke [+], Dr. C. M. Spencer, P. R. Ashton
Department of Chemistry, The University
Sheffield S3 7HF (UK)
Dr. N. S. Isaacs
Department of Chemistry, The University
Whiteknights, PO Box 224
Reading RG6 2AD (UK)
Dr. D. J. Williams, A. M. Z. Slawin
Chemical Crystallography Laboratory
Department of Chemistry, Imperial College
London SW7 2AY (UK)
[+] Permanent address:
Dipartimento di Chimica Organica e Biologica
dell'Università di Messina
Contrada Papardo, Salita Sperone, 98100 Messina (Italy)

[**] This work was supported by the Agriculture and Food, and Science and Engineering Research Councils in the United Kingdom and by the University of Messina in Italy.

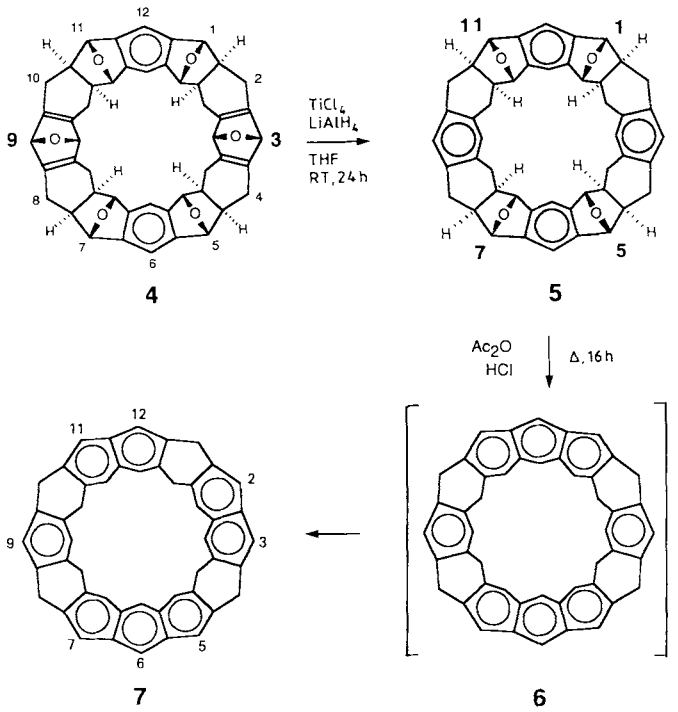

Scheme 1. Synthesis of **7** from **4** via **5** and (possibly) **6**.

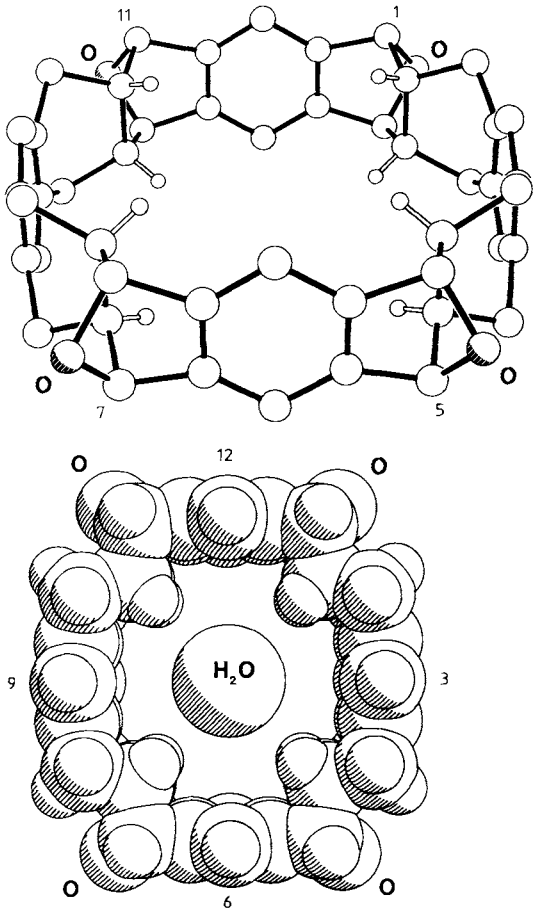

Fig. 1. Top: Structure of **5** in the crystal. Crystal data: orthorhombic, $a=12.026(10)$, $b=12.511(10)$, $c=23.890(15)$ Å, $V=3594$ Å^3, space group *Pbca*, $Z=4$ (the structure has a center of symmetry), $\rho=1.29$ g cm^{-3}, $\mu(Cu_{K\alpha})=6$ cm^{-1}, 1043 independent observed reflections [$|F_o| \geq 3\sigma(|F_o|)$], $\theta \leq 50°$], $R=0.128$. A disordered water molecule sits on the center of symmetry about which **5** is disposed. Bottom: Space-filling representation of the structure of **5**. In view of the disorder in the positions of the hydrogen atoms, the water molecule has been represented as a sphere with radius equivalent to the envelope of a water molecule.

drogen bonding, the water hydrogen atoms being >2.7 Å away from any potential interactive sites within the cavity.[12]

Dehydration[13] of **5** at 1, 5, 7, and 11 o'clock (Scheme 1)[9] gave a mixture of isomeric hydrocarbons (all displaying molecular ions with *m/z* 608 in their EIMS) from which **7** was isolated as the major component after chromatography on much silica gel using a lot[14] of benzene as eluant! The constitution of **7**, which comprises *one benzene, one anthracene,* and *two naphthalene* units was confirmed by (*i*) the identification of *four anisochromous AB systems* in the ^{1}H-NMR spectrum (400 MHz) recorded in $C_6D_5CD_3$ ($\delta_{A1}=3.94$, $\delta_{B1}=3.49$; $\delta_{A2}=3.73$, $\delta_{B2}=3.37$; $\delta_{A3}=3.68$, $\delta_{B3}=3.31$; $\delta_{A4}=3.63$, $\delta_{B4}=3.35$)[15] arising from the *four constitutionally-heterotopic 1,4-cyclohexadiene units* uniquely present[16] in **7** and (*ii*) the ^{1}H-NMR chemical shifts in CD_2Cl_2 (400 MHz) at $\delta=6.91$ and 7.77 respectively for the protons on the benzene ring at 9 o'clock and for the protons[17] associated with the central aromatic ring of the anthracene unit located between 5 and 7 o'clock in **7**.

Hydrocarbon **6**, which is very likely the initial product of the dehydration of **5**, undergoes acid-catalyzed isomerization[18] to octahydro[12]cyclacene **7**. This hydrocarbon, which is expected to be thermodynamically more stable[18] than **6** on account of (*i*) the ability of **7** to attain[16] a higher resonance energy than **6** and (*ii*) the lower macroring strain energy present in **7** compared with **6**. The low solubility[14] and high thermal stability (m.p. >600 °C)[13] are reminiscent of the properties of kekulene.[1] The EIMS of **7** shows intense $M^{\oplus}$ and $M^{2\oplus}$ ions at *m/z* 608 and 304 respectively with the characteristic pattern for loss of hydrogen observed in the EIMS of compounds such as 1,2-dihydronaphthalene and 9,10-dihydrophenanthrene. This observation augurs well for the preparation of [12]cyclacene **1** ($n=12$).

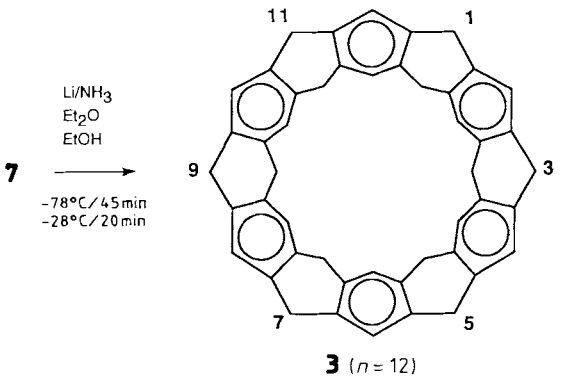

Scheme 2. The conversion of **7** into the [12]collarene **3** ($n=6$) using Birch reduction conditions.

Preliminary investigations of the Birch reduction of **7** (Scheme 2), with [12]beltene **2** ($n=12$) as the synthetic objective, have revealed the presence in the desorption electron impact mass spectrum (with *m/z* 612) of a dodecahydro[12]cyclacene which probably has the constitution **3** ($n=12$). In view of the maximization of the resonance energy achieved[16] by the six alternating benzene rings in **3** ($n=12$), [12]collarene most likely occupies a global energy minimum along the reaction pathway between **7** and [12]beltene **2** ($n=12$).

Experimental

5: A suspension of **4** (315 mg, 0.44 mmol) in THF (15 mL) was added at 0°C to the reagent system previously prepared by refluxing THF (110 mL) containing $TiCl_4$ (1.9 mL, 17.3 mmol) and $LiAlH_4$ (350 mg, 9.21 mmol) for 5 min. The reaction mixture was stirred at room temperature for 18 h and then worked up by adding Et_3N then 20% aqueous K_2CO_3 solution before extracting the crude product with CH_2Cl_2 to yield, after chromatography (SiO_2/$CHCl_3$-MeOH), **5** [128 mg, 43%, crystallized from $CHCl_3$, m.p. > 250°C, *m/z* (positive ion FABMS) 680 for $M^{\oplus}$: ^{1}H-NMR ($CDCl_3$): $\delta = 1.11$ (m, 8H), 2.62 (m, 8H), 2.64 (m, 8H), 5.09 (s, 8H), 6.69 (s, 4H), 6.84 (s, 4H); ^{13}C-NMR ($CDCl_3$): $\delta = 31.8$, 47.0, 83.5, 110.6, 125.6, 138.1, 146.2]. Single crystals, suitable for X-ray crystallography, were grown by the vapor diffusion method ($CHCl_3$/MeOH).

7: **5** (100 mg, 0.147 mmol) was suspended (ultrasonication) in 5:1 Ac_2O:conc. HCl (30 mL) and heated under reflux (Ar) for 16 h. Work-up involved neutralization ($NaHCO_3$–H_2O/5 mL), liquid-liquid extraction (ultrasonication with boiling C_6H_6/80 mL), and chromatography (SiO_2) using hot C_6H_6 as eluant! Yield of **7**, 50.4 mg, 56%, sublimed at 450°C/10^{-3} torr, m.p. > 600°C, *m/z* (EIMS) 608.2501 for $M^{\oplus}$: ^{1}H-NMR (CD_2Cl_2): $\delta = 3.57$–4.23 (4AB, 16H), 6.91 (m, 2H), 7.25 (m, 8H), 7.40 (m, 4H), 7.77 (m, 2H).

3 ($n = 12$): A suspension of **7** (5 mg) in Et_2O (3 mL) was added to Li (150 mg) in NH_3 (50 mL) and EtOH (5–6 drops). The reaction mixture was stirred at −78°C for 45 min before allowing it to warm up so that the NH_3 evaporated. Excess of Li was destroyed (EtOH) and the product was partitioned between C_6H_6 and H_2O. The organic layer yielded a product which exhibited a λ_{max} at 235 nm in CH_2Cl_2 and gave *m/z* (positive ion FABMS) 613 for $(M+H)^{\oplus}$; desorption electron impact mass spectrometry carried out over the temperature range 400–900°C at 50°C/s indicated a mixture of compounds with the most intense peak emerging at *m/z* 612: this conclusion was confirmed by the ^{1}H-NMR (CD_2Cl_2) spectrum which revealed a prominent AB system ($\delta_A = 3.67$, $\delta_B = 3.48$ with $J_{AB} = 15$ Hz) and a prominent singlet ($\delta = 6.92$).

Received: January 28, 1988;
revised: March 24, 1988 [Z 2592 IE]
German version: *Angew. Chem. 100* (1988) 981

CAS Registry numbers:
3, 114907-42-5; **4**, 110330-18-2; **5**, 114907-40-3; **7**, 114907-41-4.

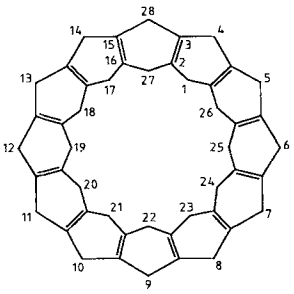

2 ($n = 12$)

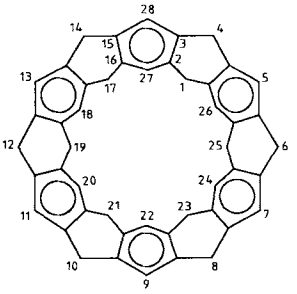

3 ($n = 12$)

which are comprised of alternating fused benzo and fused cyclohexa-1,4-diene as [*n*]collarenes. Thus, [12]collarene is represented by the full structural formula **3** ($n = 12$) shown in Scheme 2 and has the systematic name, 1,4,6,8,10,12,14,17,19,21,23,25-dodecahydro-2,16:3,15-dimethanoundecacene.

[7] The real advances in synthetic chemistry occur at the laboratory bench and not on the office desk. In personal recognition of the talent and tenacity shown by Dr. *Kohnke* in the synthesis (F. H. Kohnke, A. M. Z. Slawin, J. F. Stoddart, D. J. Williams, *Angew. Chem. 99* (1987) 941; *Angew. Chem. Int. Ed. Engl. 26* (1987) 892) of **4**, the senior author of this communication proposes (J. F. Stoddart, *J. Incl. Phenom.*, in press) to call **4**–the first macropolycyclic compound of its kind to be isolated and characterized—*kohnkene*. The systematic name for kohnkene **4** is *rel*-(1*R*,4*S*,4a*S*,7a*R*,8*R*,10*S*,10a*S*,13a*R*,14*R*,17*S*,17a*S*,20a*R*,21*R*,23*S*,23a*S*,26a*R*)-1,4:6,25:8,23:10,21:12,19:14,17-hexaepoxy-1,4,4a,5,6,7,7a,8,10,10a,11,12,13,13a,14,17,17a,18,19,20,20a,21,23,23a,24,25,26,26a-octacosahydro-2,16:3,15-dimethanoundecacene; we thank Dr. *A. D. McNaught* (The Royal Society of Chemistry, London) for his assistance in deriving systematic names for **2**–**4**.

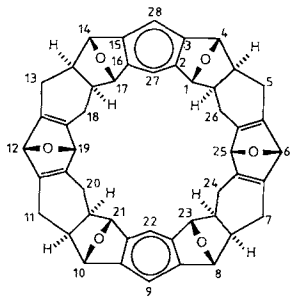

4

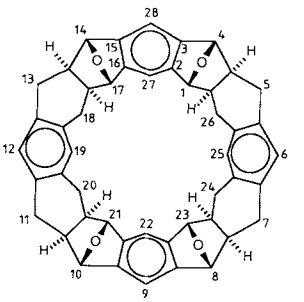

5

[8] Deoxygenation of **4** to give **5** is *not* a trivial reaction. Before successfully employing the conditions reported in Scheme 1, we had established that PPh_3, PI_3, and P_2I_4 were unsuitable. These findings accord with those of others (H. Hart, G. Nwokogu, *J. Org. Chem. 46* (1981) 1251; Y. D. Xing, N. Z. Huang, *ibid. 47* (1982) 140) who have investigated the deoxygenation of 1,4-epoxyarenes. Using $TiCl_4$–$LiAlH_4$, *Xing* and *Huang* have prepared tetraphenylene from 1,4:9,12-diepoxy-1,4,9,12-tetrahydrotetraphenylene in 50% yield. Thus, the 43% yield obtained under identical conditions for the conversion (Scheme 1) of **4** into **5** compares favorably with results reported in the literature for less exotic compounds.

[9] We find the clock numbering system particularly useful when discussing the molecular structures, chemical modifications, and physical properties of derivatives of [12]cyclacene **1** ($n = 12$). While rings can be identified as occurring on the hour at 1, 2, 3, ... o'clock, the ring junctions correspond to half-past the hour and so can be identified at 1:30, 2:30, 3:30, ... etc. After this article was submitted for publication, a communication appeared in the literature (C. B. Knobler, F. C. A. Gaeta, D. J. Cram, *J. Chem. Soc. Chem. Commun. 1988*, 330) where a clock numbering system has been employed in discussing the solid state structure of a 1:1 complex between phenylglycine and a chiral crown ether.

[10] While **4**, when dissolved in CH_2Cl_2 or $CHCl_3$ solutions, undergoes a certain amount of decomposition on standing, possibly as a result of retro Diels–Alder reactions, this problem did not arise even when **5** was allowed to stand in CH_2Cl_2 or $CHCl_3$ solutions for many months.

[11] Nicolet R3m diffractometer, *w* scans, $Cu_{K\alpha}$ radiation (graphite monochromator). The structure was solved by direct methods and refined anisotropically: the high value for *R* is a result of the limited and poor quality data obtained for a very small partially-twinned crystal. Further details of these structural investigations can be obtained from the Director of the Cambridge Data Centre, University Chemical Laboratory, Lensfield Road, Cambridge CB2 1EW (England). Any request should be accompanied by the full literature citation for this communication.

[12] Although disordered about the crystallographic center of symmetry, the positions of the individual hydrogen atoms in the water molecule have been determined and are directed principally towards the pairs of methine protons at 1:30 and 7:30. The water oxygen atom is > 3.5 Å removed from any of the four pairs of inward pointing methine hydrogen atoms.

[13] See, for example, H. Hart, N. Raja, M. A. Meador, D. L. Ward, *J. Org. Chem. 48* (1983) 4357.

[14] Whilst **4** and **5** are moderately soluble in both CH_2Cl_2 and $CHCl_3$, as expected, the hydrocarbon **7** is much less soluble in these solvents but is sparingly soluble in both C_6H_6 and $C_6H_5CH_3$, which do not dissolve **4** or **5**.

[1] F. Diederich, H. A. Staab, *Angew. Chem. 90* (1978) 383; *Angew. Chem. Int. Ed. Engl. 17* (1978) 372; H. A. Staab, F. Diederich, *Chem. Ber. 116* (1983) 3487; H. A. Staab, F. Diederich, C. Krieger, D. Schweitzer, *ibid. 116* (1983) 3504.

[2] F. Vögtle, *Top. Curr. Chem. 115* (1983) 157.

[3] R. W. Alder, R. B. Sessions, *J. Chem. Soc. Perkin Trans. 2 1985*, 1849. Compounds of the type **2** have been referred to in this paper as [*n*]beltenes. For more background to this trivial nomenclature system, see A. Nickon, E. F. Silversmith: *Organic Chemistry: The Name Game*. Pergamon Press, New York 1987, p. 110. Since this communication was submitted, a paper has been published in which the beltenes are referred to as columnenes: R. O. Angus, Jr., R. P. Johnson, *J. Org. Chem. 53* (1988) 314.

[4] S. Kivelson, O. L. Chapman, *Phys. Rev. B 28* (1983) 7236.

[5] Linear acenes from naphthalene to heptacene have been synthesized. See, for example, E. Clar, *Polycyclic Hydrocarbons, Vol. 1*, Academic Press, New York 1964, Ch. 10 and W. J. Bailey, Chien-Wei Liao, *J. Am. Chem. Soc. 77* (1955) 992. Higher homologues ($n > 7$) in the $(C_4H_2)_n$ series have proved to be too reactive to isolate using ordinary laboratory techniques.

[6] The systematic name for [12]beltene **2** ($n = 12$) is 1,4,5,6,7,8,9,10,11,12,13,14,17,18,19,20,21,22,23,24,25,26-docosahydro-2,16:3,15-dimethanoundecacene. We propose to refer to compounds of the general type **3**,

[15] The separate AB systems (J_{AB} = 12.5–13.5 Hz) were identified by a series of double irradiation experiments.

[16] If it is assumed that there are no more than *three* contiguous aromatic rings (i.e. there is no more than *one* fused cyclohexa-1,4-diene unit insulating the four aromatic residues) in the hydrocarbon resulting from complete dehydration of **5**, then **7** is the only constitution which can give rise to the observed ^{1}H-NMR spectroscopic data. If A ≡ anthracene, B ≡ benzene, N ≡ naphthalene and, if, to a first approximation, resonance energies (RE) of 84, 36, and 61 kcal mol^{-1} are assumed for A, B, and N respectively, then a constitution, e.g. the octahydro[12]cyclacene **7**, of [A + B + 2 N] units has a RE of 242 kcal mol^{-1}, which is more stable than a constitution, e.g. octahydro[12]cyclacene **6**, of [2 A + 2 B] units with 240 kcal mol^{-1} RE, but it is less stable than a constitution of [4 N] units with a RE of 244 kcal mol^{-1}. Thus, **7** may be an intermediate en route to the octahydro[12]cyclacene containing *four* naphthalene units. Following on this argument, it is recognized that **7** may not be the most thermodynamically-stable isomer: the acid-catalyzed dehydration of **5** merits detailed investigation to establish (a) if **6** can be isolated and (b) if **7** can be equilibrated to any other isomer, e.g. the octahydro[12]cyclacene containing *four* naphthalene units. Also, on the assumption that there are no more than three contiguous aromatic rings, the RE (kcal mol^{-1}) for the dodecahydro[12]cyclacenes containing different combinations of aromatic residues are [2 A] (168); [1 A + 1 B + 1 N] (181); [3 N] (183); [1 A + 3 B] (192); [2 B + 2 N] (194); [4 B + 1 N] (205); [6 B] (216). It follows that [12]collarene **3** (n = 12) has the highest possible RE of all the possible constitutional isomers that contain *six* aromatic and six insulating fused cyclohexa-1,4-diene rings.

[17] Note that the chemical shift for these central protons resonate ca. 0.63 ppm upfield from those in anthracene.

[18] Isomerizations of this type have been observed previously (E. Clar: *Polycyclic Hydrocarbons, Vol. I*, Academic Press, New York 1964, p. 65) in partially hydrogenated polyacenes. If a reshuffle of the aromatic rings can lead to a higher RE for the molecule, this will occur even under very mild conditions, e.g. the recently reported isomerization of I → II during the attempted crystallization of I: J. Luo, H. Hart, *J. Org. Chem. 52* (1987) 4833.

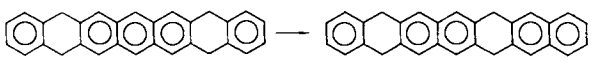

I II

Extremely Short Non-Bonding Oxygen–Oxygen Distances: The Crystal Structures of $NbBO_4$, $NaNb_3O_8$, and $NaTa_3O_8$**

By *Klaus-Jürgen Range*,* *Manfred Wildenauer*, and *Anton M. Heyns*

Dedicated to Professor Heinrich Nöth on the occasion of his 60th birthday

The distances between oxygen atoms not directly bound to each other in oxidic compounds can vary over a wide range.[1] Apart from some small anions in which very short O–O distances follow directly from very short central atom-oxygen distances,[2] only two examples have thus far been reported for O–O distances < 2.30 Å (Stishovite (high-pressure SiO_2): O–O 2.29 Å;[3] andalusite (Al_2SiO_5): O–O 2.25 Å[4]). We have now found unusually short oxygen-oxygen distances of around 2.20 Å in the compounds $NbBO_4$, $NaNb_3O_8$ and $NaTa_3O_8$ synthesized under high pressures in our laboratory.

$NbBO_4$ was first observed as a by-product in the high-pressure reaction of K_2CO_3 and Nb_2O_5 in a BN crucible.[5] It is a colorless substance and can be prepared in pure form by reaction of a stoichiometric mixture of H_3BO_3 and Nb_2O_5 at $p > 25$ kbar and $T > 800$ °C followed by quenching to ambient conditions.[6] $NbBO_4$ is metastable under normal pressure, and, on tempering (1 bar, 700 °C, 12 h), transforms into a mixture of γ'-Nb_2O_5 and amorphous B_2O_3.

$NbBO_4$ is the first structurally well characterized orthoborate of the type MBO_4[7] and concomitantly the only compound so far in the Nb_2O_5–B_2O_5 system with a definite composition.[8] Cations and anions occupy the respective positions of the zircon($ZrSiO_4$) structure,[9] although all coordination polyhedra are more strongly distorted than in $ZrSiO_4$.[10] Boron is coordinated tetrahedrally by oxygen (distances: B–O 1.469(2) Å (4×); O–O 2.222(3) Å (2×), 2.484(3) Å (4×), while niobium is surrounded by eight oxygen atoms in the form of a dodecahedron (distances: Nb–O 2.095(2) Å (4×), 2.037(2) Å (4×); O–O distances, see Table 1). The structure is determined by chains of edge-shared BO_4 tetrahedra and NbO_8 dodecahedra parallel to [001], which in turn are linked together by edge-shared dodecahedra. The common edges of tetrahedra and dodecahedra are markedly shortened (2.222 Å; Fig. 1 and Table 1). This drastic shortening cannot be explained electrostatically.

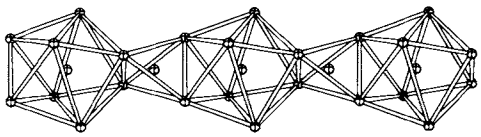

Fig. 1. Edge-shared NbO_8 dodecahedra and BO_4 tetrahedra in the crystal structure of $NbNO_4$. The O–O distance in the sharing edges is 2.222 Å.

The NbO_8 dodecahedra in $NbBO_4$ (Fig. 2) show characteristic distortions compared to the "most favorable dodecahedron" described by *Hoard* and *Silverton*[11] (Table 1). That these distortions cannot be attributed to the edge-sharing with BO_4-tetrahedra follows from the fact that NbO_8 dodecahedra with almost the same dimensions likewise occur in a high-pressure phase of $NaNb_3O_8$.

The synthesis of HD-$NaNb_3O_8$ was accomplished by high-pressure reaction of a mixture of $NaNbO_3$ and Nb_2O_5 in a modified Belt apparatus[6b] (pyrophyllite pressure capsule,[12] 30 kbar, 1100 °C, 30 min) followed by quenching to ambient conditions. The colorless compound is metastable at atmospheric pressure; after tempering (1 bar, 800 °C,

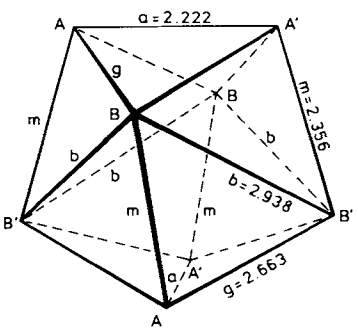

Fig. 2. The NbO_8 dodecahedron in $NbBO_4$ (Nb not shown, designation of the corners and edges according to *Hoard* and *Silverton* [11]).

[*] Prof. Dr. K.-J. Range, Dipl.-Chem. M. Wildenauer
Institut für Anorganische Chemie der Universität
Universitätsstrasse 31, D-8400 Regensburg (FRG)
Prof. Dr. A. M. Heyns
Department of Chemistry, University of Pretoria
Pretoria 0002 (South Africa)

[**] This work was supported by the Fonds der Chemischen Industrie. *K.-J. R.* thanks the University of Pretoria for financial support. We thank Dr. *U. Klement* for the collection of diffraction data.

Table 1. The NbO_8 polyhedra in $NbBO_4$ and $NaNb_3O_8$.

Distance [a]	NbO_9 in $NbBO_4$ [b]	[c]	NbO_8 in $NaNb_3O_8$ [b]	[c]	"Most favorable" dodecahedron [11] [c]
$\overline{Nb\text{-}O(A,B)}$	2.066(2)	1	2.076(2)	1	1
Nb-O(A) (4×)	2.095(2)	1.04	(4×) 2.081(2)	1.003	
Nb-O(B) (4×)	2.037(2)	0.986	(4×) 2.070(2)	0.997	
Nb-O(A)/Nb-O(B)	1.028	1.028	1.005	1.005	1.03
O(A)-O(A') a (2×)	2.222(3) [d]	1.075	a (2×) 2.218(3) [e]	1.067	1.17
O(A)-O(B) g (8×)	2.663(3)	1.289	g (4×) [f] 2.714(2)	1.308	1.24
			g' (4×) 2.721(3)	1.311	
O(A)-O(B') m (4×)	2.356(3) [e]	1.140	m (4×) 2.307(2) [g]	1.112	1.17
O(B)-O(B') b (4×)	2.938(2)	1.422	b (2×) [f] 2.948(2)	1.420	1.49
			b' (2×) 2.991(2)	1.441	

[a] Designation of corners and edges (Fig. 2) after *Hoard* and *Silverton* [11]. [b] In Å. [c] Referred to $\overline{Nb\text{-}O(A,B)} = 1$. [d] Edge-sharing between dodecahedra and tetrahedra. [e] Edge sharing between two dodecahedra. [f] Owing to the different point symmetries of the NbO_8 dodecahedra ($\bar{4}2m$ in $NbBO_4$ and 222 in $NaNb_3O_8$), splitting of the bonds takes place. [g] Edge sharing between dodecahedra and pentagonal bipyramids.

12 h), a Guinier photograph shows the reflections of the normal-pressure modification of $NaNb_3O_8$.[13,14] So far it has been impossible to clarify unequivocally whether the normal-pressure phase formed by reconversion has the ideal composition (Na : Nb = 1 : 3) or the deviating composition (Na : Nb = 1 : 2.7) postulated by *Craig* et al.[15]

HD-$NaNb_3O_8$[16] crystallizes in a novel tunnel structure. The structure[17] comprises two crystallographically independent niobium atoms, Nb(1) and Nb(2), which form different coordination polyhedra, namely dodecahedra $Nb(1)O_8$ (Nb-O distances: 4 × 2.070(1) Å, 4 × 2.081(1) Å) and distorted pentagonal bipyramids $Nb(2)O_7$ (Nb-O distances: 1.834(3) Å, 1.947(2) Å, 1.948(2) Å, 1.959(2) Å, 2.212(3) Å, 2 × 2.367(2) Å). Structurally decisive are chains of edge-shared $Nb(1)O_8$ dodecahedra (Fig. 3) and edge-

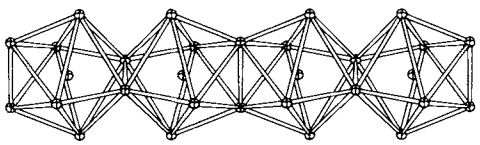

Fig. 3. Edge-shared $Nb(1)O_8$ dodecahedra in the structure of $NaNb_3O_8$. The O-O distance in the sharing edges is 2.218 Å.

shared pentagonal $Nb(2)O_7$ bipyramids parallel to [001]; the chains are connected to each other via common edges and corners. The special arrangement of the chains leads to the formation of channels having an elongated hexagonal cross-section, running along the *c* axis (Fig. 4), in which the $Na^{\oplus}$ ions are accomodated. Although the temperature factors indicate a relatively high mobility of the $Na^{\oplus}$ ions in these channels, we have thus far been unable to exchange the $Na^{\oplus}$ ions for other cations. Once again a

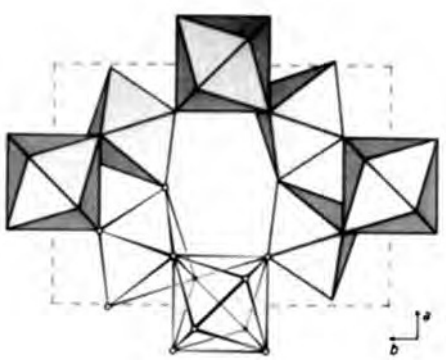

Fig. 4. $NaNb_3O_8$: projection of the crystal structure on the *a,b* plane.

remarkable structural feature is the drastic shortening of every opposite pair of dodecahedron edges, resulting in an oxygen–oxygen distance of 2.218 Å. To the best of our knowledge these are the shortest non-bonding oxygen–oxygen distances found so far in transition metal–oxygen polyhedra.

As shown in Table 1, the dimensions of the NbO_8 dodecahedra in $NbBO_4$ and HD-$NaNb_3O_8$, that is two compounds adopting completely different crystal structures, are almost identical. We are therefore convinced that MO_8 polyhedra, specifically MO_8 dodecahedra (M = Nb, but maybe also Ta, Mo, W), can be structure-determining to a much greater extent than has hitherto been assumed.[18]

$NaTa_3O_8$, which can be synthesized at 35 kbar and 1100 °C from $NaTaO_3$ and Ta_2O_5, is isotypic with $NaNb_3O_8$.[19] Because of the very similar ionic radii of $Nb^{5\oplus}$ and $Ta^{5\oplus}$, the lattice dimensions and bond lengths for $NaNb_3O_8$ and $NaTa_3O_8$ hardly differ from each other (shortest O-O distance in the $Ta(1)O_8$ dodecahedra: 2.225 Å).

Received: February 4, 1988;
supplemented: March 14, 1988 [Z 2605/2606 IE]
German version: *Angew. Chem. 100* (1988) 973

CAS Registry numbers:
$NbBO_4$, 115162-73-7; $NaNb_3O_8$, 12306-18-2; $NaTa_3O_8$, 115204-05-2.

[1] R. D. Shannon, C. T. Prewitt, *Acta Crystallogr. Sect. B 25* (1969) 925.
[2] a) Examples are, inter alia, $CaCO_3$ (aragonite, C–O 1.282 Å, O–O 2.220 Å) [2b] and Na_3NO_4 (N–O 1.384 Å, O–O 2.260 Å) [2c]; b) J. P. R. de Villiers, *Am. Mineral. 56* (1971) 758; c) M. Jansen, *Angew. Chem. 91* (1979) 762; *Angew. Chem. Int. Ed. Engl. 18* (1979) 698.
[3] R. J. Hill, M. D. Newton, G. V. Gibbs, *J. Solid State Chem. 47* (1985) 185.
[4] a) C. W. Burnham, M. J. Buerger, *Z. Kristallogr. 115* (1961) 269; J. K. Winter, S. Ghose, *Amer. Mineral. 64* (1979) 573. The O–O distance of 2.25 Å is not undisputed and could also be simulated by a disorder [4b]; b) E. Eberhard, S. Hamid Rahman, *Z. Kristallogr. 178* (1987) 56.
[5] Commercially available sintered BN contains ca. 2% B_2O_3 as sintering agent.
[6] Modified Belt apparatus [6b], BN crucible, 30 min; b) K.-J. Range, R. Leeb, *Z. Naturforsch. B 30* (1975) 889.
[7] a) According to older works [7b, c] $TaBO_4$ appears to be isotypic with $NbBO_4$. Accurate structure data, however, are as yet unknown. We are currently attempting the growth of single crystals of $TaBO_4$; b) A. I. Zaslavskij, R. A. Zvincuk, *Dokl. Akad. Nauk SSSR 90* (1953) 781; c) M. E. Mrose, W. J. Rose, *Am. Min. Soc. Prog. 1961*, 111 A.
[8] E. M. Levin, *J. Res. Nat. Bur. Stand. Sect. A 7* (1966) 11.
[9] K. Robinson, G. V. Gibbs, P. H. Ribbe, *Am. Miner. 56* (1971) 782.
[10] Crystal structure data of $NbBO_4$: Enraf-Nonius CAD4 diffractometer, $Mo_{K\alpha}$ radiation, $\lambda = 0.71073$ Å, graphite monochromator, $T = 24$ °C; tetragonal, space group $I4_1/amd$, $a = 6.2141(6)$ Å, $c = 5.476(1)$ Å, $V = 211.46$ Å^3, $\rho_{calc} = 5.27$ g cm^{-3}, $Z = 4$. $\mu(Mo_{K\alpha}) = 52$ cm^{-1}, 2308 measured intensities, 1980 observed with $I > 2\sigma(I)$, 308 independent ($R_{int} = 0.028$), ω-2θ scan, $\Delta\omega = 0.7 + 0.34\tan\theta$, $(\sin\theta/\lambda)_{max} = 1.08$,

$-13 \le h \le +13$, $0 \le k \le 13$, $-11 \le l \le +11$. Heavy atom method, anisotropic refinement of all atoms (Program system SHELX 76): 4Nb in 4a, 4B in 4b, 16 O in 16h with $x = 0.0712(3)$, $z = 0.1994(4)$, $R = 0.025$, $R_w = 0.021$ (including unobserved reflections), 12 parameters, $\Delta\rho_{max} = 2.0$ e/Å^{-3}.

[11] J. L. Hoard, J. V. Silverton, *Inorg. Chem. 2* (1963) 235.

[12] Single crystals are obtainable on using a Pt crucible and some H_2O as mineralizer.

[13] S. Andersson, *Acta Chem. Scand. 21* (1967) 1777.

[14] Y. Bouilland, *Bull. Soc. Chim. Fr. 1968*, 112.

[15] D. C. Craig, N. C. Stephenson, *J. Solid State Chem. 3* (1971) 89.

[16] Referred to the normal pressure phase [13], $\Delta V/V_0 = -0.119$.

[17] Crystal structure data for $NaNb_3O_8$: Enraf-Nonius CAD4 diffractometer, $Mo_{K\alpha}$ radiation, $\lambda = 0.71073$ Å, graphite monochromator, $T = 24$°C; orthorhombic, space group *Ibam*, $a = 7.3244(4)$, $b = 10.3100(5)$, $c = 7.0426(4)$ Å, $V = 531.82$ Å^3, $\rho_{calcd} = 5.37$ g cm^{-3}, $Z = 4$, $\mu(Mo_{K\alpha}) = 62$ cm^{-1}. 2782 measured intensities, 1010 with $F > 3\sigma(F)$ independent ($R_{int} = 0.019$). ω-2θ scan, $\Delta\omega = 0.8 + 0.38 \tan\theta$, $(\sin\theta/\lambda)_{max} = 1.08$, $0 \le h \le +15$, $0 \le k \le +22$, $-15 \le l \le +15$. Empirical absorption correction via ψ scans of selected reflections. Heavy atom method, anisotropic refinement of all atoms (Program SDP 3.0): 4 Na in 4a, 4 Nb(1) in 4b, 8 Nb(2) in 8j with $x = 0.25239(4)$, $y = 0.26430(2)$, 8 O(1) in 8j with $x = 0.9833(3)$, $y = 0.1670(2)$, 8 O(2) in 8j with $x = 0.1067(3)$, $y = 0.4237(2)$, 16 O(3) in 16k with $x = 0.1985(2)$, $y = 0.3611(1)$, $z = 0.2996(3)$. 34 parameters, $R = 0.040$, $R_w = 0.035$, $S = 0.769$.

[18] a) Indications of this are also found in complex compounds, e.g. $W(C_9H_5NOBr)_4 \cdot C_6H_6$ [18b] and $[Nb(C_7H_5O_2)_4]_2(O(HCl)_3) \cdot CH_3CN$ [18c]; b) W. D. Bonds, R. D. Archer, W. C. Hamilton, *Inorg. Chem. 10* (1971) 1764; c) A. R. Davis, F. W. Einstein, *ibid. 14* (1975) 3030.

[19] Crystal structure data of $NaTa_3O_8$: Enraf-Nonius CAD4 diffractometer, $Mo_{K\alpha}$ radiation, $\lambda = 0.71073$ Å, graphite monochromator, $T = 24$°C; orthorhombic, space group *Ibam*, $a = 7.242(2)$, $b = 10.462(3)$, $c = 7.001(3)$ Å, $V = 530.44$ Å^3, $\rho_{calcd} = 8.69$ g cm^{-3}, $Z = 4$, $\mu(Mo_{K\alpha}) = 652$ cm^{-1}. 3299 measured intensities, 894 with $F > 3\sigma(F)$ independent ($R_{int} = 0.037$). ω-2θ scan, $\Delta\omega = 0.75 + 0.34 \tan\theta$, $(\sin\theta/\lambda)_{max} = 1.15$, $0 \le h \le +16$, $-24 \le k \le +24$, $0 \le l \le +16$. Empirical absorption correction via Ψ scans of selected reflections. Heavy atom method, anisotropic refinement of all atoms (Program system SHELX 76): 4 Na in 4a, 4 Ta(1) in 4b, 8 Ta(2) in 8j with $x = 0.23846(6)$, $y = 0.26424(4)$, 8 O(1) in 8j with $x = 0.9902(13)$, $y = 0.1742(7)$, 8 O(2) in 8j with $x = 0.1183(10)$, $y = 0.4322(7)$, 16 O(3) in 16k with $x = 0.1926(8)$, $y = 0.3570(5)$, $z = 0.2971(8)$. 34 parameters, $R = 0.042$, $R_w = 0.031$. Further details of the crystal structure analyses of $NbBO_4$, $NaNb_3O_8$ and $NaTa_3O_8$ are available on request from the Fachinformationszentrum Energie, Physik, Mathematik GmbH, D-7514 Eggenstein-Leopoldshafen 2 (FRG), on quoting the depository number CSD-52988, the names of the authors, and the journal citation.

Synthesis of Strictosidine Analogues by Hetero-Diels–Alder Reaction and Their Biomimetic Transformation to Indole Alkaloids**

By *Lutz-F. Tietze,* Jürgen Bachmann,* and *Wolfgang Schul*

The glucoside strictosidine **1a**, which is formed in plants from secologanin[1] and tryptamine in a reaction catalyzed by strictosidine synthase,[2] is the first nitrogen-containing precursor of the over one thousand monoterpenoid indole alkaloids[3] as well as of the cinchona and pyrroloquinoline alkaloids. Many of these compounds exhibit pronounced biological activity[4] and are used as pharmaceuticals, for example the dimeric indole alkaloid vincristine.[5]

Enzymatic glycolysis[6] of strictosidine **1a** leads to the highly reactive aglycone **1b**, which can react in vivo via the dialdehyde form **1c** by reductive amination to give a large variety of products such as corynantheine **2**. A direct extension of this principle to the in vitro synthesis of indole alkaloids, however, encounters considerable difficulties owing to the small difference in reactivity of the aldehyde groups in **1c**; furthermore, the formation of **1b** from **1a** is limited to enzymatic cleavage in an aqueous system.[7] Accordingly, an efficient biomimetic synthesis of indole alkaloids[8] requires a simple route to strictosidine analogues that, instead of a glucosyl group as in **1a**, contain a readily removable protecting group and exhibit different reactivities at C-17 and C-21 in the aglycone. Moreover, the in vitro transformation of such strictosidine analogues should afford new insights into the so far only partially understood biosynthetic transformation of **1a** to indole alkaloids.

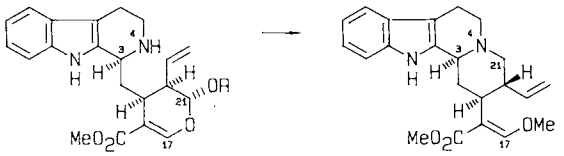

1a: R = β-D-glucose
1b: R = H
1c: dialdehyde form of **1b**

2

The synthesis of the strictosidine analogues **8** was achieved in a simple fashion in 92% yield by tandem Knoevenagel/hetero-Diels–Alder reaction[9] of the aldehyde **3a**, which is obtainable from tryptamine and a mixed malondialdehyde acetal,[10,11] *N,N*-dimethylbarbituric acid **4** and (*E*)-benzyl 1-butenyl ether **6**[12] (Scheme 1). The initially formed 2-alkylidene-1,3-dicarbonyl compound **5** reacts with **6** even at 20°C, since the heterodiene moiety in **5** has a low-lying LUMO[9] owing to the electron-accepting substituent in the α position. The stereoselectivity is less pronounced than for the intramolecular reactions, whose *i-de* and *ni-de* values[13] are greater than 90%. Compounds **8a**, **8b**, **8c**, and **8d** are thereby obtained in a ratio of 3 : 3.6 : 1 : 1.2 (HPLC); separation could be carried out by chromatography on silica gel. The diastereoselectivity induced by the stereogenic center C-3 is relatively high for a 1,3-induction in an acyclic system (**8a** + **8b** : **8c** + **8d** = 3 : 1); on the other hand, the *endo/exo* selectivity is low (**8b** : **8a** = 1.2 : 1; **8d** : **8c** = 1.2 : 1).

A discussion of the transition structures leading to the diastereomers is extremely difficult; thus, **8a** — and, similarly, **8b**–**d** — can be formed either via an *exo-E-syn* geometry[14] with attack occurring from above (*Re*)[15] or via an *endo-Z-syn* arrangement with attack occurring from below (*Si*), since two heterodiene systems (*E* and *Z*) are present in **5**. (*Z*) Heterodienes are generally less reactive.[16] We therefore propose the following transition-state structures: *Re-exo-E-syn* for **8a**, *Re-endo-E-anti* for **8b**, *Si-exo-E-syn* for **8c**, and *Si-endo-E-anti* for **8d**. The preferred attack from the *Re* side in **5** can be explained by steric shielding of the *Si* side of the (*E*)-heterodiene system by the substituent on nitrogen.

The subsequent cleavage of the protecting groups on C-21 and N-4 in **8** and the reductive amination proceed as a cascade reaction by hydrogenation with Pd/C as catalyst. The initially formed aglycone **9**, which was not isolated, undergoes transformation to the iminium salt **10** after initial opening to **7**; under the reaction conditions, **10** is immediately hydrogenated to **11**. Thus **8a**, which at all stereogenic centers has the same relative configuration as strictosidine **1a**, reacts to give **11a** in 86% yield.[17] Under the same conditions, **8b** affords a 1 : 1 mixture of **11a** and **11b** in 76% yield, whereas **8c** and **8d** each selectively lead in 72% yield to **11c**. The isomeric mixture of **8** can also be

[*] Prof. Dr. L. F. Tietze, Dipl.-Chem. J. Bachmann, Dr. W. Schul
Institut für Organische Chemie der Universität
Tammannstrasse 2, D-3400 Göttingen (FRG)

[**] Inter- and Intramolecular Hetero-Diels–Alder Reactions, Part 24. This work was supported by the Fonds der Chemischen Industrie.—Part 23: L. F. Tietze, T. Hübsch, E. Voss, M. Buback, H. Tost, *J. Am. Chem. Soc. 110* (1988) 4065.

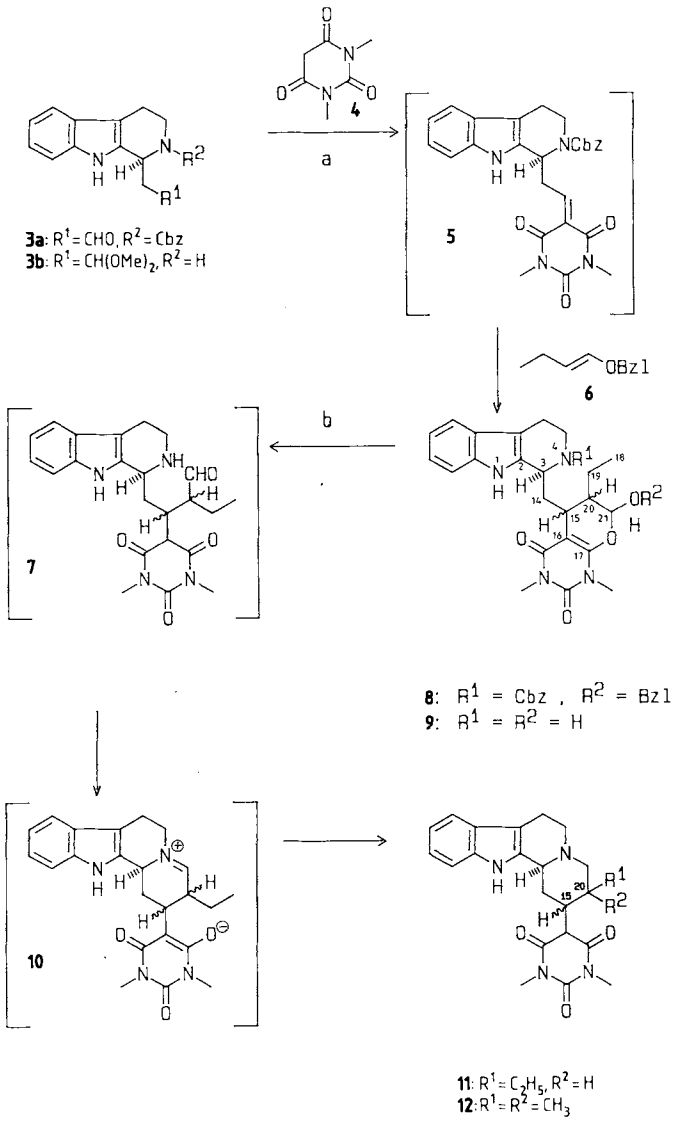

7–9	C-15	C-20	C-21	10–12	C-15	C-20
a	*S*(α-H)	*R*(α-H)	*R*(β-H)	**a**	*S*(α-H)	*R*(β-H)
b	*S*(α-H)	*S*(β-H)	*S*(α-H)	**b**	*S*(α-H)	*S*(α-H)
c	*R*(β-H)	*S*(β-H)	*S*(α-H)	**c**	*R*(β-H)	*S*(α-H)
d	*R*(β-H)	*R*(α-H)	*R*(β-H)			

Scheme 1. a: Ethylenediammonium diacetate (catalytic amount), tenfold excess of **6**, sonic bath, 50–60°C/4 h, 92% **8**; separation by chromatography on silica gel with dichloromethane/*tert*-butyl methyl ether/pentane = 1:1:1. R_f(**8a**) = 0.60; R_f(**8b**) = 0.36; R_f(**8c**) = 0.77; R_f(**8d**) = 0.66.—b: H_2/Pd/C (10%), EtOH, 20°C/8 h. **8a** → **11a**: 86%; **8b** → **11a** + **11b** (ca. 1:1): 76%; **11b** can be obtained in pure form by recrystallization from MeOH; **8c** → **11c**: 72%; **8d** → **11c**: 72%.

employed directly in the hydrogenation to give **11a** in 45% yield. The reaction of **8b** to **11a** and of **8d** to **11c** is associated with an isomerization at C-20 demanding the intermediate formation of an enamine. It has not been possible so far to determine whether the hydrogenation occurs via the enamine or via the iminium salt structure; however, both reaction pathways should lead to the same distribution of products.[18] Also, the formation of an enamine is not necessary for the course of the reaction: use of benzyl 2-methyl-1-propenyl ether, instead of **6**, in the reaction sequence resulted in an 85% yield of the indole alkaloid derivatives **12a** and **12c** (2.7:1).

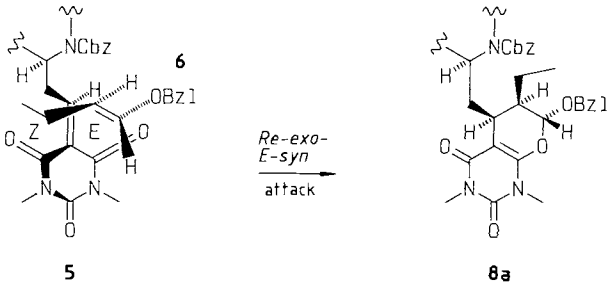

Compounds **11a** and **11b** are present as *trans*-quinolizidines (3-H(**11a**): $\delta = 3.90$), whereas **11c** displays a *cis*-quinolizidine structure (3-H: $\delta = 4.70$). The X-ray data reveals that the dimethylbarbituric acid group in **11b** is arranged axially and forms an intramolecular salt structure with N-4.[19]

The investigations have shown that the tandem Knoevenagel/hetero-Diels–Alder/hydrogenation sequence opens up a simple and general approach to the synthesis of indole alkaloids of the corynanthé type. By variation of the 1,3-dicarbonyl compound **4** and the enol ether **6**, it should be possible to obtain a wide range of products. The experiments described here were carried out with *rac*-**3b**; the reaction sequence can also be used, however, for the synthesis of enantiomerically pure indole alkaloids, since the acetal **3b** can be prepared in >95% *ee* from tryptophan.[20]

Received: February 11, 1988 [Z 2615 IE]
German version: *Angew. Chem. 100* (1988) 983

[1] L. F. Tietze, *Angew. Chem. 95* (1983) 840; *Angew. Chem. Int. Ed. Engl. 22* (1983) 828; A. R. Battersby, A. R. Burnett, P. G. Parson, *Chem. Commun. 1968*, 1280.

[2] J. F. Treimer, M. H. Zenk, *Eur. J. Biochem. 101* (1979) 225; H. Mizukami, H. Nordlöv, S. L. Lee, A. I. Scott, *Biochemistry 18* (1979) 3760.

[3] J. D. Phillipson, M. H. Zenk (Eds.): *Indole and Biogenetically Related Alkaloids*, Academic Press, London 1980; Atta-ur-Rahman, A. Basha: *Biosynthesis of Indole Alkaloids*, Clarendon Press, Oxford 1983; G. A. Cordell, *Lloydia 37* (1974) 219.

[4] W. A. Creasey in A. Weissberger, E. C. Taylor (Eds.): *The Chemistry of Heterocyclic Compounds, Vol. 25, Part 4*, Wiley, New York 1983, p. 783; M. Suffness, G. A. Cordell in A. Brossi (Ed.): *The Alkaloids, Chemistry and Pharmacology, Vol. 25*, Academic Press, Orlando, FL (USA) 1985, p. 1.

[5] G. A. Cordell, J. E. Saxton in R. G. A. Rodrigo (Ed.): *The Alkaloids, Chemistry and Physiology, Vol. 20*, Academic Press, New York 1981, p. 192; P. Potier, *J. Nat. Prod. 43* (1980) 72; J. Kutney, *Lect. Heterocycl. Chem. 4* (1978) 59; Atta-ur-Rahman, A. Basha, M. Ghazala, N. Waheed, *Z. Naturforsch. B31* (1976) 1416.

[6] T. Hemscheidt, M. H. Zenk, *FEBS Lett. 110* (1980) 187.

[7] a) R. T. Brown in W. Bartmann, E. Winterfeldt (Eds.): *Stereoselective Synthesis of Natural Products*, Excerpta Medica, Amsterdam 1979, p. 62; b) A. I. Scott, S. L. Lee, W. Wan, *Biochem. Biophys. Res. Commun. 75* (1977) 1004; c) J. Stöckigt, H. P. Husson, C. Kan-Fan, M. H. Zenk, *J. Chem. Soc. Chem. Commun. 1977*, 164; d) C. Kan, S. K. Kan, M. Lounasmaa, H. P. Husson, *Acta Chem. Scand. B35* (1981) 269.

[8] For recent syntheses of indole alkaloids, see C. Szántay, G. Blaskó, K. Honty, G. Dörnyei in A. Brossi (Ed.): *The Alkaloids, Chemistry and Pharmacology, Vol. 27*, Academic Press, Orlando, FL (USA) 1986, p. 131; E. Winterfeldt in W. Bartmann, B. M. Trost (Eds.): *Selectivity—a Goal for Synthetic Efficiency*, Verlag Chemie, Weinheim 1984, p. 349; P. Magnus in T. Lindberg (Ed.): *Strategies and Tactics in Organic Synthesis*, Academic Press, New York 1984, p. 83.

[9] L. F. Tietze in W. Bartmann, B. M. Trost (Eds.): *Selectivity—a Goal for Synthetic Efficiency*, Verlag Chemie, Weinheim 1984, p. 299.

[10] L. F. Tietze, K. H. Glüsenkamp, W. Holla, *Angew. Chem. 94* (1982) 793; *Angew. Chem. Int. Ed. Engl. 21* (1982) 787; L. F. Tietze, H. Meier, E. Voss, *Synthesis 1988*, 274.

[11] Four-step reaction: 1) tryptamine hydrochloride, 2-(2,2-dimethoxyethyl)-5,5-dimethyl-1,3-dioxane, CH_3CN/H_2O/HCl, pH 3, 60°C/6 h, 60%. 2) MeOH/HCl, 20°C/6 h, 60%. 3) $ClCO_2Bzl$, Et_3N, CH_2Cl_2, 0°C/0.5 h, 20°C/4 h, 98%. 4) 50% CF_3COOH, CH_2Cl_2, 20°C/15 min, 94% **3a**.

[12] The use of (*Z*)-benzyl 1-butenyl ether gave the corresponding cycloadducts in comparable yield but with lower selectivity.
[13] L. F. Tietze, U. Beifuss, *Angew. Chem. 97* (1985) 1067; *Angew. Chem. Int. Ed. Engl. 24* (1985) 1042.
[14] *exo/endo*, position of the OR group relative to the heterodiene; *E/Z*, configuration of the reacting heterodiene, the reacting CO group hereby has a higher priority than the nonreacting CO group; *anti/syn* position of the H atoms at the prostereogenic centers between which C–C bonds are to be formed.
[15] The descriptors *Re* and *Si* refer to the absolute configuration of **5** given in the formulas. Cf. V. Prelog, G. Helmchen, *Angew. Chem. 94* (1982) 614; *Angew. Chem. Int. Ed. Engl. 21* (1982) 567.
[16] L. F. Tietze, T. Brumby, M. Pretor, G. Remberg, *J. Org. Chem. 53* (1988) 810; G. Desimoni, G. Golombo, P. P. Righetti, G. Tacconi, *Tetrahedron 29* (1973) 2635; cf. also L. F. Tietze, S. Brand, T. Pfeiffer, J. Antel, K. Harms, G. M. Sheldrick, *J. Am. Chem. Soc. 109* (1987) 921.
[17] **8a**: ^{1}H-NMR (200 MHz, $C_2D_2Cl_4$, 100°C, TMS): $\delta = 0.93$ (t, $J = 7$ Hz; 3H, 18-H$_3$), 1.0–3.0 (m; 8H, 6-H$_2$, 14-H$_2$, 15-H, 19-H$_2$, 20-H), 3.19 (s; 3H, N–CH$_3$), 3.37 (s; 3H, N–CH$_3$), 3.43 (m; 1H, 5-H$_{ax}$), 4.43 (dd, $J = 13.5$ Hz, $J = 4.5$ Hz; 1H, 5-H$_{eq}$), 4.75 (d, $J = 12.5$ Hz; 1H, OCH$_2$Ph), 4.85 (d, $J = 12.5$ Hz; 1H, OCH$_2$Ph), 5.10 (m; 2H, OCOCH$_2$Ph), 5.26 (d, $J = 5.2$ Hz; 1H, 21-H), 5.81 (dd, $J = 7.0$ Hz, $J = 3.5$ Hz; 1H, 3-H), 6.97–7.46 (m; 14H, phenyl-H), 8.83 (s; 1H, NH). The structural assignment of **8c** and **8d** is based on the signal for 21-H in **8c** ($\delta = 5.30$, $J_{20\text{-H},21\text{-H}} = 9.0$ Hz) and **8d** ($\delta = 5.39$, $J_{20\text{-H},21\text{-H}} < 1$ Hz). Thus, H-20 and H-21 occupy *trans*-diaxial positions in **8c** and *trans*-diequatorial positions in **8d**. Since the substituent at C-15 always is in a pseudoaxial position, the ethyl group and the substituent at C-15 in **8c** must have a *cis* arrangement and those in **8d** a *trans* arrangement. **11a**: ^{1}H-NMR (200 MHz, $CDCl_3/CD_3OD$, 20°C, TMS): $\delta = 0.81$ (t, $J = 7.0$ Hz; 3H, 18-H$_3$), 0.9–3.8 (m; 13H), 3.24 (s; 3H, N–CH$_3$), 3.34 (s; 3H, N–CH$_3$), 3.90 (t br, $J = 7.5$ Hz; 1H, 3-H), 7.00–7.51 (m; 4H, phenyl-H), 10.52 (s br; NH); ^{13}C-NMR (50 MHz, CD_3OD, 20°C, TMS): $\delta = 11.17$ (C-18), 20.30 (C-6), 24.88 (C-19), 27.74 (N–CH$_3$), 28.50 (N–CH$_3$), 32.64 (C-14), 38.03 (C-15), 53.74 (C-5), 59.98 (C-21), 63.04 (C-3), 88.92 (C-16), 106.35 (C-7), 112.52 (C-12), 119.11 (C-9), 120.66 (C-11), 123.43 (C-10), 127.34 (C-8), 130.60 (C-2), 138.38 (C-13), 154.74 (CO), 164.60 (CO), 165.90 (CO). The assignment of the signals was made in analogy to the work of *E. Wenkert* et al. as well as of *F. W. Wehrli* and *T. Nishida:* E. Wenkert, J. S. Bindra, C.-J. Chang, D. W. Cochran, F. U. Schell, *Acc. Chem. Res. 7* (1974) 46; F. W. Wehrli, T. Nishida, *Fortschr. Chem. Org. Naturst. 36* (1979) 1.
[18] P. Deslongchamps: *Stereoelectronic Effects in Organic Synthesis*, Pergamon Press, Oxford 1983, p. 209ff.
[19] G. M. Sheldrick, J. Antel, J. Bachmann, L. F. Tietze, unpublished results.
[20] L. F. Tietze, J. Bachmann, unpublished results.

N-Aryl-*O*-acylhydroxylamines: Preparation by *O*-Acylation or *N*→*O* Transacylation and Reaction with Amines; Model Reactions for Key Steps Connected with the Carcinogenicity of Aromatic Amines**

By *Gernot Boche,* Ferdinand Bosold,* and *Stefan Schröder*

The following reaction steps are considered to be important for the transformation of an aromatic amine into the active metabolite (ultimate carcinogen) and its decisive further reaction with bionucleophiles:[1]

After oxidation of the amine **1** to the hydroxylamine **3** or of the acetamide **2** to the hydroxamic acid **4**, *O*-acetylation of **3** or *N*→*O* transacetylation of **4**[2] should lead to the *N*-aryl-*O*-acetylhydroxylamine **5**, an active metabolite. It is assumed that such compounds react in the next step as electrophilic aminating reagents with bionucleophiles like DNA to give "adducts".[1] Herein we report on the in-vitro preparation of *o*-acyl derivatives of type **5** from **3** or from acylhydroxyamic acids such as **4**, and on the reaction of **5** with nucleophiles.

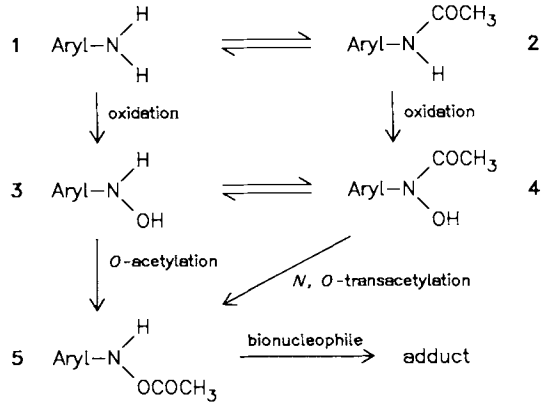

First of all we prepared the *O*-acylhydroxylamines **5aα**, **5aβ**, **5bα**, and **5bβ** by *O*-acylation of the corresponding hydroxylamines **3**[3–5] and investigated their reactivity towards the amines **6** and **7**. The hydrazines[4,6] **8** and **9**, respectively, are formed. The results are summarized in Table 1.[7]

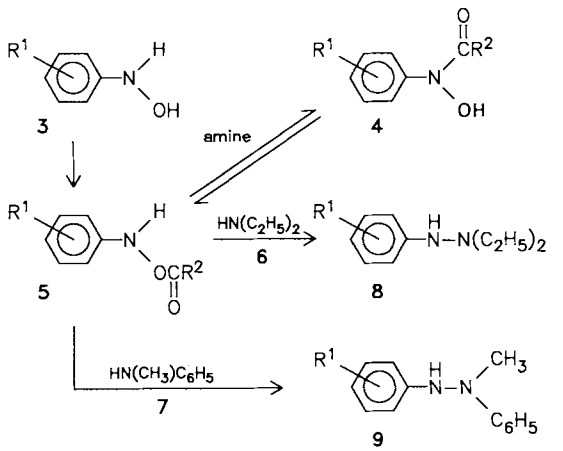

a: R^1 = *m*-Br α: R^2 = CH_3
b: R^1 = H β: R^2 = $C(CH_3)_3$

Table 1. Reactions of the *O*-acyl compounds **5** with the amines **6** (**5**: 1.0 M in **6**) or **7** (**5**: 0.93 M in **7**) to give the hydrazines **8** and **9**, respectively.

No.	5	R^1	R^2	Amine	Hydrazine [%]	*T* [°C]	*t* [h]	Byproduct **A** [%] [a]
1	**5aα**	*m*-Br	CH_3	**6**	**8**, 40	55	0.5 [b]	55
2	**5aα**	*m*-Br	CH_3	**6**	**8**, 16	20	20	77
3	**5aα**	*m*-Br	CH_3	**7**	**9**, 88	80	1 [c]	—
4	**5aβ**	*m*-Br	$C(CH_3)_3$	**6**	**8**, 67	55	1 [c]	14
5	**5aβ**	*m*-Br	$C(CH_3)_3$	**7**	**9**, 85	20	72	—
6	**5bα**	H	CH_3	**6**	**8**, 27	20	5	73
7	**5bα**	H	CH_3	**7**	**9**, 90	20	5	—
8	**5bβ**	H	$C(CH_3)_3$	**6**	**8**, 20	20	16	72
9	**5bβ**	H	$C(CH_3)_3$	**7**	**9**, 50	20	16	45

[a] **A** = azoxy compound $R^1–C_6H_4–N{=}N^{\oplus}(O^{\ominus})–C_6H_4–R^1$ [5b, 9]. [b] **5aα** was added in **6**, which had been heated to 55°C. [c] The reaction partners were heated together.

The amination of *N*-nucleophiles by *O*-acylhydroxylamines **5**, especially by the *O-acetyl* compounds **5aα** and **5bα**, thus affords an in-vitro proof for the in-vivo reaction of this class of compounds with bionucleophiles.[1,10]

In addition, we were able to simulate in vitro the enzymatic *N*→*O*-transacetylation **4α**→**5α**[2] by amine catalysis.

[*] Prof. Dr. G. Boche, F. Bosold, Dipl.-Chem. S. Schröder
Fachbereich Chemie der Universität
Hans-Meerwein-Strasse, D-3550 Marburg (FRG)

[**] This work was supported by the Fonds der Chemischen Industrie, by the Deutsche Forschungsgemeinschaft, and by BASF AG.

To this end hydroxamic acids **4** were allowed to react with *diethylamine* **6** ($pK_a = 18.75$[11]) and the intermediary *O*-acylhydroxylamines **5** were trapped by the same amine to give the hydrazines **8**. In a second series of experiments the hydrazines **9** could likewise be obtained from the corresponding hydroxamic acid **4** by reaction with the less basic *N*-methylaniline **7** (pK_a ca. 11[11]), but only after *triethylamine* ($pK_a = 18.46$[11]) had been introduced for the catalysis of the $N \rightarrow O$-transacylation (see Table 2).

Table 2. Reactions of hydroxamic acids **4** with the amines **6** (**4**: 1.0 M in **6**) or **7** (**4**: 0.83 M in a 1:1 mixture of **7** and triethylamine) to give the hydrazines **8** and **9**, respectively.

No.	4	R^1	R^2	Amine	Product [%]	T [°C]	t [h]	Byproduct E [%] [a]
1	**4aα**	*m*-Br	CH_3	**6**	**8**, 84	55	40	—
2	**4aα**	*m*-Br	CH_3	**7**	**9**, 85	80	68	15
3	**4aβ**	*m*-Br	$C(CH_3)_3$	**6**	**8**, 92	55	8	—
4	**4aβ**	*m*-Br	$C(CH_3)_3$	**7**	**9**, 94	80	2	—
5	**4bα**	H	CH_3	**6**	**8**, 49	55	30	50
6	**4bα**	H	CH_3	**7**	**9**, 62	80	30	35
7	**4bβ**	H	$C(CH_3)_3$	**6**	**8**, 80	55	20	15
8	**4bβ**	H	$C(CH_3)_3$	**7**	**9**, 95	80	2	—

[a] E = Educt.

If the rate of formation of the *O*-acylhydroxylamine **5** is rapid, i.e. compared to its back reaction to the hydroxamic acid **4** and to any further reaction, it can be isolated. Thus, on treatment of the hydroxamic acid **4aβ** with triethylamine at 80°C for 1 h the *O*-pivaloylhydroxylamine **5aβ** is obtained in 95% yield.[5c] The higher stability of the *O-pivaloyl* derivative compared to the *N-pivaloyl* derivative was confirmed by MNDO calculations: according to the enthalpies of formation ΔH_f^0, **5bβ** (-25.2 kcal mol^{-1}) is preferred over **4bβ** (-20.1 kcal mol^{-1}) by $\Delta\Delta H_f^0 = 5.1$ kcal mol^{-1}.

Contrary to this finding, in the case of the *acetyl* compounds occurring in vivo the *hydroxamic acid* isomers are more stable. This was demonstrated by the reaction of **5aα** with two molar equivalents of 1,8-diazabicyclo[5.4.0]undec-7-ene (DBU), the most effective amine catalyst ($pK_a = 24.32$[11]),[12] in triethylamine, which led after 10 min at 20°C to **4aα** in 98% yield. This experiment also proves the presence of an equilibrium, at least between **5aα** and **4aα**. The preferred formation of the acetylhydroxamic acid compared to the *O*-acetyl compound was again confirmed by the MNDO enthalpies of formation: **4bα** ($\Delta H_f^0 = -21.0$ kcal mol^{-1}) is 5.7 kcal mol^{-1} stabler than **5bα** ($\Delta H_f^0 = -15.3$ kcal mol^{-1}). It is therefore not surprising that all attempts to convert **4aα** and **4bα** with DBU (in triethylamine) into **5aα** and **5bα** respectively, were in vain.[13] In view of the in-vivo finding mentioned at the outset, however, it is decisive that acetylhydroxamic acids such as **4aα** and **4bα** can react via small equilibrium concentrations of the active metabolites **5aα** and **5bα** respectively with nucleophiles to give adducts.[14]

Summary: The *N*-aryl-*O*-acylhydroxylamines **5** described here can be prepared in vitro by *O*-acylation of the corresponding hydroxylamines **3** and by $N \rightarrow O$-transacylation from the corresponding hydroxamic acids **4**; they react with amines to give hydrazines such as **8** and **9**. Hence, reactions which are of fundamental importance for the carcinogenicity of aromatic amines could be simulated in vitro.

Received: February 11, 1988;
supplemented: April 20, 1988 [Z 2617/2618 IE]
German version: *Angew. Chem. 100* (1988) 965

CAS Registry numbers:
4aα, 38373-20-5; **4aβ**, 114838-67-4; **4bα**, 1795-83-1; **4bβ**, 111750-22-2; **5aα**, 114838-63-0; **5aβ**, 107986-35-6; **5bα**, 71825-04-2; **5bβ**, 114838-64-1; **6**, 109-89-7; **7**, 100-61-8; **8a**, 114838-65-2; **8b**, 39837-50-8; **9a**, 114838-66-3; **9b**, 37682-91-0; **Aa**, 23377-24-4; **Ab**, 495-48-7.

[1] a) J. A. Miller, *Cancer Res. 30* (1970) 559; b) E. Kriek, *Biochim. Biophys. Acta 335* (1974) 177; c) E. Miller, *Cancer Res. 38* (1978) 1479; d) E. C. Miller, J. A. Miller, *Cancer (Amsterdam) 47* (1981) 2327; e) S. S. Thorgeirsson in H. Greim, R. Jung, M. Kramer, H. Marquard, F. Oesch (Eds.): *Biochemical Basis of Chemical Carcinogenesis*, Raven Press, New York 1984, p. 47.

[2] a) G. Booth, *Biochem. J. 100* (1966) 745; b) F. A. Beland, W. T. Allaben, F. E. Evans, *Cancer Res. 40* (1980) 834; c) W. T. Allaben, C. C. Weiss, N. F. Fullerton, F. A. Beland, *Carcinogenesis (London) 4* (1983) 1067; d) C. M. King, N. R. Traub, Z. M. Lortz, M. R. Thissen, *Cancer Res. 39* (1979) 3369; e) V. C. Marhevka, N. A. Ebner, R. D. Sehon, P. E. Hanna, *J. Med. Chem. 28* (1985) 18, and references cited therein; f) see [1e], and references cited therein; g) W. Lenk, Lecture at the 2nd European Meeting of the International Society for the Study of Xenobiotics, Frankfurt, March 21–April 3, 1987.

[3] Details on the preparation of **5aα**, **5aβ**, **5bα**, and **5bβ** as well as other *N*-aryl-*O*-acylhydroxylamines by acylation of hydroxylamines **3** with acetyl or pivaloyl cyanide will be given in a full paper.

[4] All the new compounds were characterized analytically (C,H,N), mass spectroscopically and IR spectroscopically or by their 400-MHz ^{1}H-NMR spectra.

[5] Numerous attempts have been made to synthesize *N*-aryl-*O*-acylhydroxylamines because of their importance in connection with the carcinogenicity of aromatic amines, but very few have been successful: a) *N*-acetoxy-2,4-dinitrophenylamine: W. Borsche, *Chem. Ber. 56* (1923) 1494; A. C. Huggett, J. L. Cone, S. S. Thorgeirsson, P. P. Roller, *J. Org. Chem. 52* (1987) 4933; b) the *O*-acylation of the arylhydroxylamines **3** with arylcarbonyl or acetyl cyanides has so far been the favored general method: S. Prabhakar, A. M. Lobo, M. M. Marques, *Tetrahedron Lett. 23* (1982) 1391; A. M. Lobo, M. M. Marques, S. Prabhakar, H. S. Rzepa, *J. Chem. Soc. Chem. Commun. 1985*, 1113; *J. Org. Chem. 52* (1987) 2925; c) *N*-(3-bromophenyl)-*O*-pivaloylhydroxylamine **5aβ**: M. Novak, L. H. Rovin, M. Pelecanou, J. J. Mulero, R. K. Lagerman, *ibid. 52* (1987) 2002; see also: d) T. R. Juneja, H. Dannenberg, *Tetrahedron 31* (1975) 701; e) E. S. Hand, W. W. Paudler, *J. Heterocycl. Chem. 12* (1975) 1063; f) Y. Kawazoe, O. Ogama, G.-F. Hung, *Tetrahedron 36* (1980) 2933; g) L. Christensen, P. E. Iversen, *Acta Chem. Scand. B33* (1979) 352; h) Y. Hashimoto, K. Shudo, T. Okamoto, *J. Am. Chem. Soc. 104* (1982) 7636; i) T. R. Juneja, A. Ojha, R. L. Gupta, *Indian J. Chem. 23B* (1984) 60; j) M. Demeunynck, M.-F. Lhomme, J. Lhomme, *J. Org. Chem. 48* (1983) 1171; k) M. Demeunynck, N. Tohme, M.-F. Lhomme, J. M. Mellor, J. Lhomme, *J. Am. Chem. Soc. 108* (1986) 3539.

[6] a) Hydrazines have also been observed in reactions of *N*-aryl-*O*-(diphenylphosphinoyl)hydroxylamines with amines: see G. Boche, R. H. Sommerlade, F. Bosold, *Angew. Chem. 98* (1986) 563; *Angew. Chem. Int. Ed. Engl. 25* (1986) 562; b) see also [5h].

[7] *Ortho* rearrangement products such as frequently occur in the case of *N*-aryl-*O*-acylhydroxylamines, or products in which the amine is in the phenyl ring [8], were not observed under the above reaction conditions.

[8] See [5b, c], and references cited therein.

[9] The formation of the azoxy compounds **A** in reactions of arylhydroxylamine derivatives is sufficiently well known; see also P. A. Smith: *Open Chain Nitrogen Compounds, Vol. 2*, W. A. Benjamin, Menlo Park 1966, p. 4.

[10] P. D. Lotlikar, M. B. Wasserman, *Biochem. J. 120* (1970) 661, and references cited therein.

[11] The pK_a values of diethylamine and triethylamine in *acetonitrile* are quoted in J. F. Coetzee, G. R. Padmanabhan, *J. Am. Chem. Soc. 87* (1965) 5005. The pK_a value for *N*-methylaniline in *acetonitrile* has not yet been determined; it therefore had to be estimated from that for aniline (10.56). We thank Dr. *R. Schwesinger*, Universität Freiburg, for his help. The pK_a value for DBU in *acetonitrile* has already been reported: R. Schwisinger, *Angew. Chem. 99* (1987) 1209; *Angew. Chem. Int. Ed. Engl. 26* (1987) 1164.

[12] Catalysis by DBU, cf. [3].

[13] If one assumes that $\Delta\Delta H_f^0 = 5.8$ kcal mol^{-1} corresponds to the ΔG^0 value at 25°C, only 6×10^{-3}% of the *O*-acetyl compound **5bα** is present in the equilibrium besides acetylhydroxamic acid **4bα**.

[14] The amine-catalyzed transacylation proceeds intramolecularly, as demonstrated by crossover experiments and kinetic investigations.

 © VCH Verlagsgesellschaft mbH, D-6940 Weinheim, 1988 0570-0833/88/0707-0974 $ 02.50/0

Chirality Solely Due to the Presence of an Excited State**

By *E. W. Meijer** and *Hans Wynberg*

One of the most fascinating challenges in the study of optical activity is the synthesis of a compound in which the optical activity is solely due to the presence of an excited state. This property is available in *meso* compounds with two identical chromophores, in which one of the chromophores is selectively excited. In the case of diketones with a plane of symmetry in the ground state, the chirality in the excited state is due to the out-of-plane geometry of one of the two carbonyl groups. We have focused our attention on 2,4-adamantanedione **1**, whose chiral excited state is **1***.

1 **1***

The only way to obtain **1*** in a high enantiomeric excess is by selective excitation of one of the two carbonyl groups of **1** by chemical conversion. The enantiomeric excess via a photochemical process is expected to be low, since the difference in absorption of right (or left) circular polarized light by the two carbonyls is governed by the dissymmetry factor in absorption. Obviously, resolution of an excited-state diketone belongs in the realm of fantasy.

Chemiexcitation of ketones is well known to occur via the decomposition of 1,2-dioxetanes.[1-3] A high yield of singlet-excited-state adamantanone is obtained from the 1,2-dioxetane of 2-(methoxymethylene)adamantane.[4] The chemical route towards optically active **1*** via the optically active 1,2-dioxetane **3** is based on our previous work.[5-8]

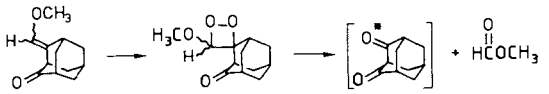

2 **3** **1***

The optically active precursor of **3** is enol ether **2**. The latter is prepared in several steps from adamantanone via the resolution of *endo*-bicyclo[3.3.1]non-6-ene-3-carboxylic acid.[8] A photooxygenation with $^1O_2$ at -50 °C, followed by rapid low-temperature column chromatography, afforded a solution of 1,2-dioxetane **3** in dichloromethane.

The ketodioxetane **3** was not stable enough to allow a structure determination. However, dilute solutions of **3** in *n*-heptane yielded chemiluminescence, ($\lambda_{max} = 420$ nm, characteristic of ketone fluorescence) when heated. The product, which could be isolated in almost quantitative yield proved to be 2,4-adamantanedione **1**. It is reasonable to assume that the chemiluminescence is obtained from the decomposition of **3**, which generates **1** in the excited state (**1***). The enantiomeric excess of **3** is assumed to be identical to that of the resolved starting material, to wit $ee = 69\%$. Therefore it is expected that in the formation of **1*** one of the two carbonyls is excited in favor over the other in an enantiomeric excess of 69%.

This synthesis of chiral **1*** is, to the best of our knowledge, the first example of a chemical route to a chiral compound (with high *ee*) whose chirality is solely due to the presence of an excited state.

The synthesis of **1*** is one challenge, the detection of optical activity in this short-lived molecule is another. It seemed obvious to measure the circular polarization of chemiluminescence (CPCL) in the thermal activation of **3**.[9] However, the CPCL measurements of **3** (10^{-3}-10^{-6} mol L^{-1} in *n*-heptane) showed complete lack of optical activity at the moment of emission ($g_{chemlum} = 0 \pm 3 \times 10^{-3}$).

This is probably caused by a fast racemization in the singlet-excited state. This racemization occurs by an energy transfer between the two carbonyls in the rigid conformation of **1***. This fast energy transfer in **1*** is reasonable due to the close proximity of the two carbonyls. The UV spectrum of **1** and the CD spectrum of its mono-^{18}O analogue even indicate some π overlap of these chromophores.[7] The intramolecular n,π^* energy transfer is fast relative to the lifetime of a singlet-excited-state ketone, pointing to a rate of energy transfer of $k_{ET} = 1 \times 10^{10}\ s^{-1}$. Energy transfer between carbonyl n,π^* excited states is a very intriguing phenomenon and several systems have been investigated,[10-13] showing both efficient and slow processes. Recently, the circular polarization in fluorescence was studied after excitation of *meso* diketones with circular polarized light,[13] indicating a very efficient energy transfer for carbonyl groups in close proximity to each other. Although triplet-triplet annihilation can be regarded as another source of racemization in the excited state, it is assumed to be of minor importance. This is based on both the reaction conditions used and the fact that up to now the occurrence of this phenomenon in 1,2-dioxetane chemiluminescence has not been reported.

From the preliminary results presented here we can conclude that a synthesis of a compound that is chiral solely in its excited state can be performed by chemiexcitation of a *meso* diketone via an optically active 1,2-dioxetane. In order to obtain stability with respect to racemization it is necessary to increase the distance between the two chromophores. This type of compound would enable us to investigate the rate of intramolecular energy transfer.

Received: February 29, 1988 [Z 2637 IE]
German version: *Angew. Chem. 100* (1988) 1004

[*] Dr. E. W. Meijer
Philips Research Laboratories
P.O. Box 80000, NL-5600 JA Eindhoven (The Netherlands)
Prof. Dr. H. Wynberg
Dept. of Organic Chemistry, University of Groningen
NL-9747 AG Groningen (The Netherlands)

[**] The authors gratefully acknowledge Dr. *H. P. J. M. Dekkers* and Dr. *P. H. Schippers* for measuring the CPCL spectra and for stimulating discussions.

[1] T. Wilson, *Int. Rev. Sci. Phys. Chem. Ser. Two 9* (1976) 265.
[2] P. D. Bartlett, M. E. Landis in H. H. Wasserman, R. W. Murray (Eds.): *Singlet Oxygen*, Academic Press, New York 1979, p. 243.
[3] A. L. Baumstark in A. A. Frimer (Ed.): *Singlet O_2, Vol. II*, CRC Press, Boca Raton, FL, USA 1985, p. 1.
[4] E. W. Meijer, H. Wynberg, *Tetrahedron Lett. 1979*, 3997.
[5] H. Wynberg, H. Nyman, *J. Am. Chem. Soc. 99* (1977) 603.
[6] H. Numan, H. Wynberg, *J. Org. Chem. 43* (1978) 2232.
[7] E. W. Meijer, H. Wynberg, *J. Am. Chem. Soc. 104* (1982) 1145.
[8] H. Numan, C. B. Troostwijk, J. H. Wieringa, H. Wynberg, *Tetrahedron Lett. 1977*, 1761.
[9] H. Wynberg, H. Numan, H. P. J. M. Dekkers, *J. Am. Chem. Soc. 99* (1977) 3870.
[10] P. J. Wagner, T. Nakahira, *J. Am. Chem. Soc. 95* (1973) 8474.
[11] P. Lechtken, N. J. Turro, *Angew. Chem. 85* (1973) 300; *Angew. Chem. Int. Ed. Engl. 12* (1973) 314.
[12] E. A. Lissi, M. V. Encinas, F. Castaneda, F. A. Olea, *J. Phys. Chem. 84* (1980) 251.
[13] P. H. Schippers, H. P. J. M. Dekkers, *J. Am. Chem. Soc. 105* (1983) 145.

Influence of Chromophore Orientation on the Circular Dichroism of Isomeric Helical Molecules**

By *Klaus Jürgen Przybilla, Fritz Vögtle,* Martin Nieger,* and *Sybille Franken*

How does the circular dichroism of the helical[1] pyridinophane **1** change when the nitrogen atom in the six-membered ring successively moves further away from the O-atom (as in **2**-**4**)? The "rotation" of the pyridine chromophore in the plane of the six-membered ring systematically generates structural isomers—with retention of the rigid helical chiral molecular framework. The pyridinophanes **1**-**4** synthesized for the first time in connection

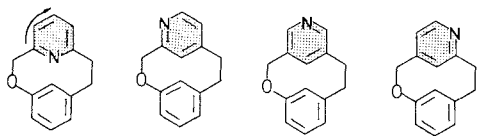

1 **2** **3** **4**

with our studies of this phenomenon differ only in the orientation[2] of the transition dipole moments of the two arene moieties with otherwise formally the same chromophores (e.g. **2** and **4**). In the pyridine-chromophores **1** and **3** the permanent dipole moments are in opposite directions.

Figure 1 shows the circular dichroism curves of the isomeric molecules after enantiomeric separation or enrichment on poly(diphenyl-2-pyridylmethylmethacrylate).[3] The isomers **1**-**4** show comparable curves: on going from right to left, i.e. from larger to smaller wavelengths, a strong negative Cotton effect is followed by a positive one and then a negative one again. All Cotton effects of **2**-**4** are shifted bathochromically, in the sequence $\mathbf{2} < \mathbf{4} < \mathbf{3}$, compared to those of **1**, and the distance between first and second maximum becomes progressively smaller in the same sequence.

The transition from pyridinophane to pyridiniophane by merely changing the measurement conditions (0.1 N aqueous HCl) leads to a significant bathochromic shift and broadening of the longest wavelength negative Cotton effect (Fig. 1b) and to a loss in structure of the curves. Thus, e.g., the weak maximum of **1** ($\Delta\varepsilon = +1.4$) at 293 nm disappears. In the short wavelength region, the CD curves are changed to such a significant extent that they cannot be correlated with those of the corresponding unprotonated molecules.[4] A comparison of the chiroptical properties of the pyridinophanes **1**-**4** with those of the likewise helical 1-oxa[2.2]metacyclophane **5** (see Scheme 2)[5] (Fig. 1a), whose resolution has now been successfully accomplished on cellulose-tris(3,5-dimethylphenyl)carbamate[6] in our laboratories, shows that, despite the simplicity of the molecular structures, a detailed analysis according to the exciton-chirality method[7] or the MO model[8] is necessary for the structure-chiroptic correlation.

The oxa[2.2]metacyclophane **5**,[5] with such a short C-O bond, is the narrowest-bracketed [2.2]metacyclophane

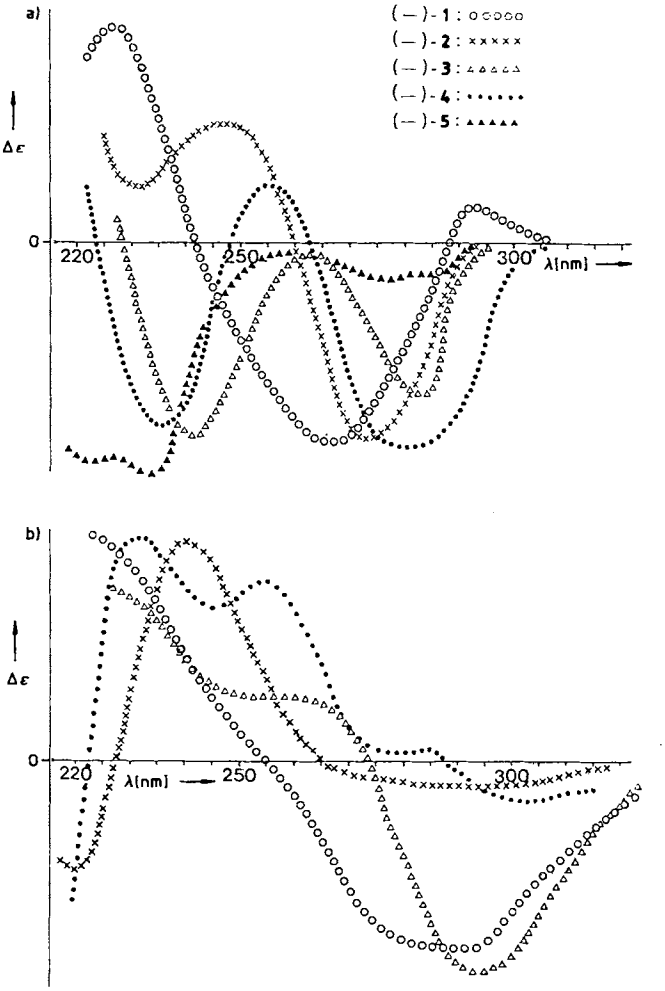

Fig. 1. Circular dichroism curves of the (enriched) (−)-enantiomers of **1**-**5**. a) In methanol, b) in 0.1 N HCl (**1** and **5** enantiomerically pure). **1**: $\Delta\varepsilon_{293} = +1.4$, $\Delta\varepsilon_{267} = -10.8$, $\Delta\varepsilon_{226} = +11.4$; **5**: $\Delta\varepsilon_{285} = -2.2$, $\Delta\varepsilon_{277} = -2.3$, $\Delta\varepsilon_{234} = -14.6$. (The CD curves of **2**-**4** are adjusted to the curve for **1**.)

known so far, as evidenced by the extreme, hitherto highest upfield shift found for an internal aromatic proton ($\delta(H_{i(a)}) = 3.86$) and the high racemization barrier of 131 kJ mol^{-1}. Figure 2 shows the result of the first X-ray crystal structure analysis of an oxa[2.2]phane. The C(3)-O(2) bond length is 138.5 pm, and is thus 11.6 pm shorter than the opposite C(7)-C(9) bond (150.1 pm). The CH_2-O bridge is likewise shorter (by 7.3 pm) than the CH_2-CH_2 bridge. As a result of these two short distances the planes of the arene rings are tilted at an angle of 3.6° to each other. The special case of the oxa[2.2]metacyclophanes also follows from

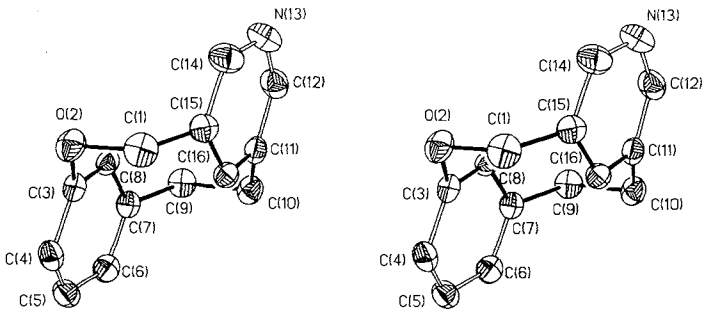

Fig. 2. Crystal structure of **3** (stereoview) ($\alpha = 2.00$, $\beta = 4.50$, $\gamma = 3.20$, $\delta = 3.60°$; for the definition of the "helicity angle" see [1]).

[*] Prof. Dr. F. Vögtle, Dipl.-Chem. K. J. Przybilla
Institut für Organische Chemie und Biochemie der Universität
Gerhard-Domagk-Strasse, D-5300 Bonn 1 (FRG)
M. Nieger, Dr. S. Franken
Anorganisch-chemisches Institut der Universität
Gerhard-Domagk-Strasse 1, D-5300 Bonn 1 (FRG)

[**] This work was supported by the Deutsche Forschungsgemeinschaft. *K. J. P.* thanks the Fonds der Chemischen Industrie for a graduate fellowship.

the fact that the shortest intramolecular distance known so far [C(8)–C(6) 257.9 pm] is observed in **3** (for comparison: 268.9 pm in [2.2]metacyclophane).

The synthesis of **5** has already been reported, but the method used involved several steps and the yields were low (only milligram amounts were isolated).[5] To obtain the pyridinophanes **1**–**4** in the required gram amounts we have developed a new, generally applicable two-step synthesis for heteroarenes: a bis(halogenomethyl)-substituted arene or heteroarene is cyclized with 3-(mercaptomethyl)phenol under dilution conditions[9] and in the presence of cesium carbonate[1] in ethanol to a [3.2]phane as precursor in good yields (up to 45%) (Scheme 1). Subsequent desulfurization[10] in a thiophilic solvent [$P(OMe)_3$ or $P(OEt)_3$] (Scheme 2) leads to the narrow-bracketed product in remarkably good yields (up to 40%), considering the hitherto narrowest [2.2]phane ring.

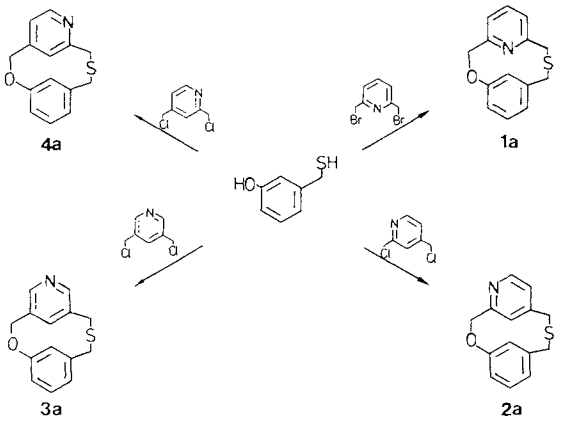

Scheme 1.

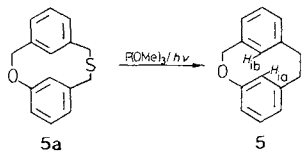

Scheme 2.

For the determination of the ring-inversion barriers of the [3.2]phanes **1a**–**5a** we have used the coalescence of the ^{1}H-NMR signals of the CH_2–O group: the free enthalpy of activation for **3a** is 95 kJ mol^{-1}. **1a** shows no coalescence up to −55 °C (90 MHz) because of the small steric demands of the lone pair of the nitrogen atom;[11] the corresponding barriers for **2a**, **4a** and **5a** all lie at 88 kJ mol^{-1}.

To gain a better insight into the influence of chromophore orientation on the circular dichroism we are currently studying further helical molecules with formal clockwise rotation of the chromophore in the molecule.

Experimental

Cyclization: The solutions of bis(halogenomethyl)arene [e.g. 1,3-bis(bromomethyl)benzene] (10.0 mmol) in ethanol (250 mL) and of 3-(mercaptomethyl)phenol (10.0 mmol) and potassium *tert*-butoxide (11.0 mmol) in 85% ethanol (250 mL) were added dropwise within 10 h to 1 L of boiling ethanol (dilution principle apparatus [12]). The cyclization was noticeably favored by addition of a spatula-tip of Cs_2CO_3. After a further 3 hours' boiling the reaction mixture was worked up column chromatographically [silica gel, dichloromethane/acetone mixture (20/1 to 10/1)].

Desulfurization: the [3.2]phane (3.00 mmol) was dissolved in $P(OMe)_3$ (freshly distilled over sodium) and irradiated in a quartz flask with a high-pressure mercury lamp (HQ 600; 15 h, argon, 30 °C). $P(OMe)_3$ was removed under vacuum and the residue chromatographed on silica gel [dichloromethane/acetone mixture (20/1 to 10/1)] [14].

Crystal structure analysis of **3** [14]: colorless crystals; crystal dimensions: $0.15 \times 0.25 \times 0.5$ mm^3; $M_r = 211.2$, space group $P2_12_12_1$, $a = 589.1(4)$, $b = 784.0(3)$, $c = 2336.8(13)$ pm. $V = 1.079$ nm^3, $Z = 4$, $\rho_{calcd} = 1.30$ g cm^{-3}, $\mu(Mo_{K\alpha}) = 0.08$ mm^{-1}; 1886 symmetry independent reflections ($2\theta_{max} = 50°$); 1617 reflections with $|F| > 3\sigma(F)$ were used for the structure solution (direct methods) and refinement (145 parameters); non-hydrogen atoms anisotropically, H atoms (located by difference electron density determination) refined with a riding model; $R = 0.055$ [$R_w = 0.053$, $w^{-1} = \sigma^2(F) + 0.005F^2$]. The absolute configuration could not be determined.

Received: February 15, 1988 [Z 2621 IE]
German version: *Angew. Chem. 100* (1988) 987

[1] Regarding the helicity of the phanes substituted unsymmetrically in the bridge see: a) K. Meuer, F. Vögtle, A. Mannschreck, G. Stühler, H. Puff, A. Roloff, *J. Org. Chem. 49* (1984) 3483; b) F. Vögtle, K. J. Przybilla, A. Mannschreck, N. Pustet, P. Büllesbach, H. Reuter, H. Puff, *Chem. Ber. 121* (1988) 823.

[2] Cf. a) H. A. Staab, W. Rebafka, *Chem. Ber. 110* (1977) 3333; b) H. A. Staab, C. P. Herz, *Angew. Chem. 89* (1977) 839; *Angew. Chem. Int. Ed. Engl. 16* (1977) 799.

[3] Y. Okamoto, K. Hatada, *J. Liq. Chromatogr. 9* (1986) 369.

[4] Cf. V. Buss, M. Klein, *Chem. Ber. 121* (1988) 89. We thank Prof. Dr. *V. Buss* and Prof. Dr. *G. Snatzke* for helpful discussions.

[5] F. Vögtle, J. Struck, H. Puff, P. Woller, *J. Chem. Soc. Chem. Commun. 1986*, 1248.

[6] a) Y. Okamoto, K. Hatada, *Chem. Lett. 1986*, 1237; b) *J. Chromatogr. 363* (1986) 173.

[7] a) K. Nakanishi, N. H. Park, R. Takeda, J. T. Vazquez, W. T. Wiesler in W. Bartmann, K. B. Sharpless (Eds.): *Stereochemistry of Organic and Bioorganic Transformations, Workshop Conference Hoechst, Vol. 17*, VCH Verlagsgesellschaft, Weinheim 1986; b) N. Harada, K. Nakanishi: *Circular Dichroic Spectroscopy, Exciton Coupling in Organic Stereochemistry*, University Press, Oxford 1983.

[8] G. Snatzke, *Angew. Chem. 91* (1979) 380; *Angew. Chem. Int. Ed. Engl. 18* (1979) 363.

[9] a) F. Vögtle, *Chem. Ztg. 1972*, 396; b) L. Rossa, F. Vögtle, *Top. Curr. Chem. 113* (1983) 1.

[10] a) V. Boekelheide, I. D. Reingold, M. Tuttle, *J. Chem. Soc. Chem. Commun. 1973*, 406; b) J. Bruhin, W. Kneubühler, W. Jenny, *Chimia 27* (1973) 277.

[11] H. Förster, F. Vögtle, *Angew. Chem. 89* (1977) 443; *Angew. Chem. Int. Ed. Engl. 16* (1977) 429.

[12] Manufacturer Normag, Otto Fritz GmbH, 6238 Hofheim/Taunus (FRG).

[13] The compounds **1**–**5** have been characterized by their ^{1}H-NMR spectra, mass spectra (high resolution), and elemental analyses.

[14] Further details of the crystal structure investigation are available on request from the Fachinformationszentrum Energie, Physik, Mathematik GmbH, D-7514 Eggenstein-Leopoldshafen 2 (FRG) on quoting the depository number CSD-52919, the names of the authors, and the journal citation.

Blocking of the Retro-Diels–Alder Reaction by Complex Formation: [(η^5-Cyclopentadienyl)(η^5-dicyclopentadienyl)iron]**

By *Janet Blümel, Frank H. Köhler,* Gerhard Müller,* and *Dallas L. Wilkinson*

The retro-Diels–Alder reaction is part of the standard repertoire[1,2] of the preparative chemist; nonetheless, a great deal of work is being invested towards the improvement of this reaction—for example, to circumvent the usually dras-

[*] Prof. Dr. F. H. Köhler, Dr. G. Müller,
Dr. D. L. Wilkinson [+], Dipl.-Chem. J. Blümel
Anorganisch-chemisches Institut der Technischen Universität München
Lichtenbergstrasse 4, D-8046 Garching (FRG)

[+] Fellow of the Alexander von Humboldt Foundation. Permanent address: Monash University, Clayton, Victoria (Australia).

[**] This work was supported by the Fonds der Chemischen Industrie.

tic conditions required by pyrolysis. Recent chemical approaches have included the acceleration of the reaction by the incorporation of silyl groups,[2a] by acid catalysis in the aza variant,[2b] and by reducing the molecular strain[2c] or the basicity[2d-k] on going from the educt to the products. With regard to the latter variant, we recently found that the retro-Diels–Alder reaction can even proceed so rapidly that the actual starting compound cannot be observed.[3] For instance, the reaction of the stannylated dicyclopentadiene **1** with methyllithium leads to dicyclopentadiene **2** and cyclopentadienyllithium even at −78 °C. We have not yet been able to detect the proposed intermediate **1a**.

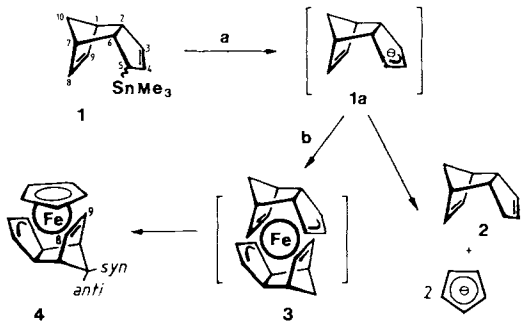

Scheme 1. a) MeLi/Et_2O, THF, −78 °C; b) $Fe_2Cl_4(THF)_3$, −78→25 °C; the counterions are $Li^{\oplus}$.

We have now found that **1a** may be trapped with solvated iron(II) chloride; the title compound η^5-cyclopentadienyl-(η^5-dicyclopentadienyl)iron,[4] **4**, the only isolable iron compound, is thereby formed in a yield of 20% (not optimized, based on **1**; Scheme 1). The identity of **4** ("DicpFeCp") follows from the correct elemental analysis and the spectroscopic data.[5] Important features include the following: The number of NMR signals corresponds to C_s symmetry in solution. The $\delta(^1H)$ and $\delta(^{13}C)$ data indicate the formation of an allylic system; the bonding of C8/9 to the iron is not supported by δ(H8/9), since a signal shift of only ca. −0.4 ppm is observed on going from **2** or **1**[3] to **4**. For the same transformations, however, the signal for C8/9 is shifted by ca. −60 ppm, which does reflect coordination of C8/9 to iron. ^1J(C8-H8) [^1J(C9-H9)][5,6] thereby decreases by only ca. 3 Hz; the rehybridization and a conceivable charge transfer from the allylic moiety to C8/9 thus have little effect. Noteworthy are the coupling constants ^1J(CH)[5,6] of **4**, which are 5–8 Hz smaller for C1/7 and C2/6 than those of **2**; this indicates a reduction in the angles at the corresponding carbon atoms owing to the binding to iron (compare below). Comparison of **4** with ferrocene reveals that the position of the ^{13}C-NMR signal of C_5H_5 at $\delta \approx 80$ is unusual; we ascribe this to a transannular effect of the Dicp ligand on Cp, which is much larger than that observed for ferrocenes.[7,8]

The X-ray structure analysis[9] of **4** (cf. Fig. 1) confirms the findings outlined above. A ferrocene analogue is present in which a Cp ligand is replaced by Dicp, with the Dicp forming a basketlike ligand. Both the olefinic and allylic moieties of the Dicp coordinate to the Fe atom. As a result, the double bond C8-C9 (1.420(4) Å) is characteristically lengthened[10] and the allyl plane (C3, C4, C5) is bent away from iron by 27.0° with respect to the plane A (C2, C3, C5, C6). The interplanar angle A/D (cf. caption to Figure 1) is 117.0°, and B/D is only 108.8°, so that the distances of the olefinic C atoms (C8/9) from the termini of the allylic moiety (C5/3) are only 2.69 and 2.67 Å, respectively. The Fe-C distances for Dicp and Cp are thus similar (except for Fe-C4, 2.017(2) Å). The Fe-C bond lengths lead to a distance of only 1.21 Å between the best plane E through C3, C4, C5, C8, and C9 and the iron, whereas the Fe-Cp(center) distance is 1.73 Å. The two planes form an angle of 3.6° and are thus ca. 0.4 Å closer in **4** than the corresponding planes in ferrocene;[11] this is revealed as a transannular effect in the ^{13}C-NMR data. These results and the absence of ferrocene (cf. Scheme 1) make the following route for the formation of **4** plausible: **3** is initially formed; the mutual steric hindrance of Dicp ligands in **3** is so large, however, that one of the two ligands cleaves off cyclopentadiene. The retro-Diels–Alder reaction is therefore only partially blocked. Thus, a general route[12] is now possible to complexes of the (Cp-metal) type, which are strongly perturbed owing to formal separation of the olefinic and allylic moieties.

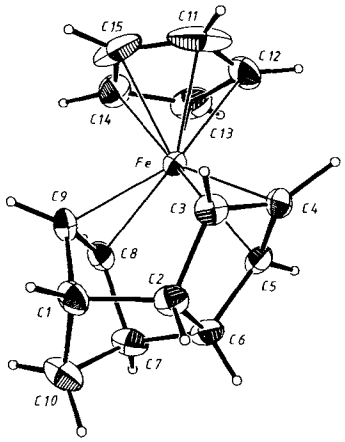

Fig. 1. Molecular structure of DicpFeCp **4** (ORTEP, displacement ellipsoids 50%, H atoms with arbitrary radii). Selected distances [Å]: Fe-C3 2.091(2), Fe-C4 2.017(2), Fe-C5 2.092(2), Fe-C8 2.077(2), Fe-C9 2.081(2), Fe-C11 2.109(3), Fe-C12 2.106(3), Fe-C13 2.101(3), Fe-C14 2.084(2), Fe-C15 2.111(3), C3-C4 1.413(4), C4-C5 1.421(4), C8-C9 1.420(4), C2-C6 1.573(3); interplanar angles [°]: A/D 117.0, B/D 108.8, B/C 127.2, C/D 124.1 with A = C2, C3, C5, C6, B = C1, C7, C8, C9, C = C1, C7, C10, D = C1, C2, C6, C7.

The redox behavior of **4** is similar to that of ferrocene. Cyclovoltammetry[13] shows a reversible ($I_{pa}/I_{pc} = 0.94$) oxidation, the half-wave potential of which is cathodically shifted by 260 mV relative to internal ferrocene. This finding is apparently typical[14] of the perturbation of ferrocenes, either by alkylation or by interruption of the cyclic conjugation in the ligands.

Received: February 16, 1988;
revised: March 28, 1988 [Z 2622 IE]
German version: *Angew. Chem. 100* (1988) 1011

[1] a) J.-P. Ripoll, A. Rouessac, F. Rouessac, *Tetrahedron 34* (1978) 19; b) A. Ichihara, *Synthesis 1987*, 207.

[2] a) P. Magnus, P. M. Cairus, J. Moursounidis, *J. Am. Chem. Soc. 109* (1987) 2469; b) P. A. Grieco, D. T. Parker, W. F. Fobare, R. Ruckle, *ibid. 109* (1987) 5859; c) R. D. Miller, D. L. Dolce, *Tetrahedron Lett. 1977*, 3329; d) E. S. Bowman, G. B. Hughes, J. B. Grutzner, *J. Am. Chem. Soc. 98* (1976) 8273; e) W. Neukam, W. Grimme, *Tetrahedron Lett. 1978*, 2201; f) O. Papies, W. Grimme, *ibid. 21* (1980) 2799; g) J. V. N. Vara Prasad, P. Iyer, C. N. Pillai, *J. Org. Chem. 47* (1982) 1380; h) T. V. Rajanbabu, D. F. Eaton, T. Fukunaga, *ibid. 48* (1983) 652; i) S. Knapp, R. M. Ornaf, K. E. Rodrigues, *J. Am. Chem. Soc. 105* (1983) 5494; k) H. Hart, K. Shahlai, *Tetrahedron Lett. 28* (1987) 5437.

[3] J. Blümel, F. H. Köhler, *J. Organomet. Chem. 340* (1988) 303.

[4] Abbreviation for η^5-cyclopentadienyl-(3,4,5,8,9-η^5-tricyclo-[5.2.1.$0^{2,6}$]-deca-3,8-dien-5-yl)iron: DicpFeCp is used here as an acronym.

[5] EI-MS (70 eV): *m/z* (rel. int.) 252 ($M^{\oplus}$, 43), 186 ([$M-C_5H_6$]$^{\oplus}$, 100), 121 ($CpFe^{\oplus}$, 65), 56 ($Fe^{\oplus}$, 38).—^{1}H-NMR (C_6D_6, 270 MHz, 30°C): $\delta=1.36$ (dt, $^2J=8.8$ Hz, $^3J=1.2$ Hz, *syn*-H10), 1.96 (m, H2/6), 1.98 (dt, partially overlapped, $^3J=1.2$ Hz, *anti*-H10), 2.72 (m, H1/7), 3.69 (s, C_5H_5), 4.42 (m, incl. $^3J=3.4$ Hz, H4), 5.06 (m, incl. ^3J(H3/5-H4)=3.4 Hz, H3/5), 5.52 (m, H8/9); assignment by selective homodecoupling.—^{13}C-NMR (C_6D_6, 67.8 MHz, 30°C): $\delta=50.60$ (^1J(CH)=140.9 Hz, C1/7), 55.67 (^1J(CH)=127.9 Hz, C2/6), 56.59 (^1J(CH)=127.8 and 133.3 Hz, C10), 67.95 (^1J(CH)=163.1 Hz, ^2J(CH)=9.5 and 5.1 Hz, C3/5), 73.23 (^1J(CH)=165.1 Hz, C8/9), 79.92 (^1J(CH)=174.6 Hz, ^2J(CH)≈^3J(CH)=6.6 Hz, C_5H_5), 84.63 (^1J(CH)=167.5 Hz, C4); assignment by selective ^{13}C{^{1}H} experiments.

[6] In **2**, the ^1J(Cn-Hn) values for n=1...10 are: 146.7, 135.7, 159, 159, 128 (*exo*- and *endo*-H), 135.2, 145.0, 167.3, 168.2, 131.1/135.3 (*syn*- and *anti*-H, respectively) Hz; J. Blümel, F. H. Köhler, unpublished results.

[7] a) A. N. Nesmeyanov, P. V. Petrovskii, L. A. Fedorov, V. I. Robas, E. I. Fedin, *J. Struct. Chem. (Engl. Transl.) 14* (1973) 42; b) S. Gronowitz, I. Johnson, A. Maholanyiova, S. Toma, E. Solčániová, *Org. Magn. Reson. 7* (1975) 372.

[8] If, on the other hand, **4** is viewed as a half-sandwich complex, $\delta(^{13}C)\approx 80$ is normal for the C_5H_5 ligands: compare, e.g., A. O. Gansow, D. A. Schexnayder, B. Y. Kimura, *J. Am. Chem. Soc. 94* (1972) 3406.

[9] Reddish brown crystals were obtained by slow cooling of a pentane solution of **4**. Crystal data: $C_{15}H_{16}Fe$, $M_r=252.14$, monoclinic, space group $P2_1$ (No. 4), $a=6.004(1)$, $b=7.257(1)$, $c=12.867(2)$ Å, $\beta=97.55(1)°$, $V=555.8$ Å^3, $Z=2$, $\rho_{calcd}=1.507$ g cm^{-3}, $\mu(Mo_{K\alpha})=13.2$ cm^{-1}, $F(000)=264$, $T=-40$°C. 2338 unique reflections up to $(\sin\theta/\lambda)_{max}=0.639$ Å^{-1} ($+h$, $\pm k$, $\pm l$, ω scan, $\Delta\omega=0.8°$, Syntex $P2_1$ diffractometer, $Mo_{K\alpha}$ radiation, $\lambda=0.71069$ Å). Lp and empirical absorption correction (rel. transmission: 0.75–1.00), solution by automated Patterson methods (SHELXS-86). $R(R_w)=0.026$ (0.033), $w=1/\sigma^2(F_0)$ for 144 refined parameters and all reflections (anisotropic, H constant with $U_{iso}=0.05$ Å^2, inverse set of coordinates: $R_w=0.049$, SHELX-76). $\Delta\rho_{fin}$(max/min) $=0.41/-0.46$ e Å^{-3}. The centrosymmetric space group $P2_1/m$ can be ruled out, since the approximate mirror plane through the molecule is not parallel to the *ac* plane. Further details of the crystal structure investigation may be obtained from the Fachinformationszentrum Energie, Physik, Mathematik GmbH, D-7514 Eggenstein-Leopoldshafen 2 (FRG), on quoting the depository number CSD-52974, the names of the authors, and the journal citation.

[10] Cf. C2-C3 1.34 Å in norbornadiene; E. E. Burnell, P. Diehl, *Can. J. Chem. 50* (1972) 3566. Cf. C6-C7 1.35 Å in bicyclo[3.2.1]octa-2,6-dienyllithium·TMEDA; N. Hertkorn, F. H. Köhler, G. Müller, G. Reber, *Angew. Chem. 98* (1986) 462; *Angew. Chem. Int. Ed. Engl. 25* (1986) 468.

[11] P. Seiler, J. D. Dunitz, *Acta Crystallogr. Sect. B 36* (1979) 2020, and references cited therein.

[12] Special routes have been reported by a) J. Lewis, A. W. Parkins, *J. Chem. Soc. A 1969*, 953; b) C. White, S. J. Thomson, P. Maitlis, *J. Chem. Soc. Dalton Trans. 1978*, 1305.

[13] **4** was 9.9×10^{-4} M (plus ferrocene 9.9×10^{-4} M) in THF/[(nBu)$_4$N]PF$_6$ at 25°C, 50 mV/s.

[14] C. Elschenbroich, E. Bilger, R. D. Ernst, D. R. Wilson, M. S. Kralik, *Organometallics 4* (1985) 2068.

Modified Cyclodextrins— Novel, Highly Enantioselective Stationary Phases for Gas Chromatography**

By *Wilfried A. König,* Sabine Lutz,* and *Gerhard Wenz*

Capillary gas chromatography on chiral stationary phases[1] is being employed increasingly for the determination of the configuration of natural products, for investigating the enantiomeric purity of chiral pharmaceuticals, and for determinating enantiomeric excesses of asymmetric syntheses or enzymatic transformations, ever since suitable columns with thermostable phases have become commercially available[2] and new methods of derivatization[3] have enabled the separation of a large number of substances.

In most cases "chiral recognition" can be attributed to diastereomeric associates formed by hydrogen bonding between chiral substrate and stationary phase.[4] Hence, with few exceptions, only derivatives capable of such interactions (amides, carbamates, oximes, some alcohols) are separable in this way.

In the case of cyclodextrins, which are employed in liquid chromatography as chiral supports,[5] it is known that inclusion effects play an important role in the separation of enantiomers. A separation is achieved when the enantiomers differ in their ability to be accomodated in the cavity of the macrocyclic cyclodextrin molecule. *Sybilska* et al.[6] recently showed that this type of intermolecular interaction is also suitable for gas chromatographic enantiomeric separations. Due to their high melting points, however, the free cyclodextrins are suitable only as stationary phases for gas-solid chromatography. It was therefore thought worthwhile attempting to lower the melting point and increase the thermal stability by introducing hydrophobic moieties. This was achieved both by complete alkylation as well as by partial alkylation and acylation of the hydroxy functions of the cyclodextrins.[7]

It emerged that, e.g., per-*n*-pentylated α-cyclodextrin (Phase I) as well as the β-cyclodextrin pentylated at the hydroxy groups in position 2 and 6 and acetylated in position 3 (Phase II) exhibit a marked selectivity toward enantiomers. Especially high separation factors are obtained in the case of the enantiomers of trifluoroacetylated carbohydrates, methylglycosides, and the 1,5-anhydroalditols[9] as obtained on reductive degradation of polysaccharides.[8] Moreover, derivatives of many other chiral molecules are separated, including building blocks for natural product syntheses, e.g. hydroxy acids (Fig. 1), polyols, triols, vicinal diols, alcohols (Fig. 2), amino alcohols, amines and amino acids. The separation factors for trifluoroacetylated α-chi-

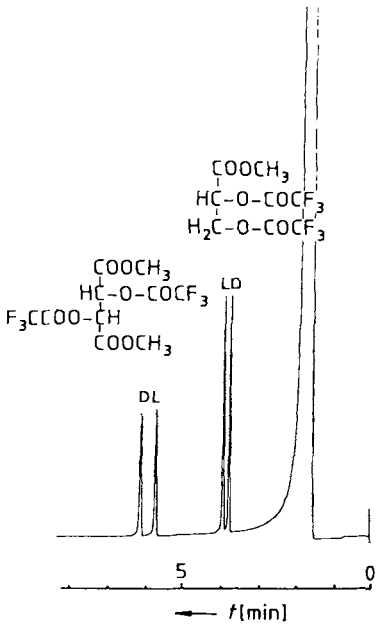

Fig. 1. Enantiomer separation of glyceric acid and of tartaric acid after esterification with methanol and trifluoroacetylation. 40-*m* glass capillary with perpentylated α-cyclodextrin. Column temperature 90°C; Carrier gas: 1 bar H_2.

[*] Prof. Dr. W. A. König, Dipl.-Chem. S. Lutz
Institut für Organische Chemie der Universität
Martin-Luther-King-Platz 6, D-2000 Hamburg 13 (FRG)
Dr. G. Wenz
Max-Planck-Institut für Polymerforschung
Jakob-Welder-Weg 11, D-6500 Mainz (FRG)

[**] This work was supported by the Bundesminister für Forschung und Technologie in connection with the Project "Polysaccharidforschung" (Project No. 0319134A).

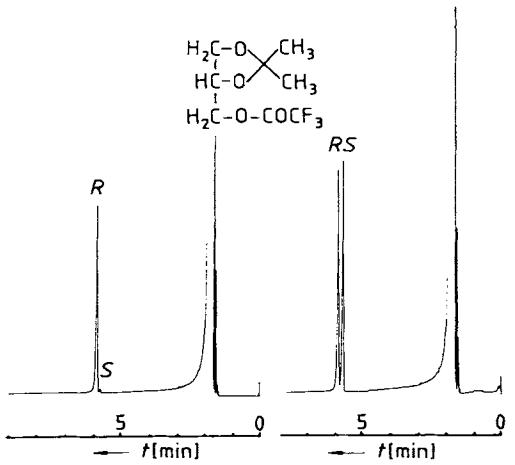

Fig. 2. Right: Enantiomer separation of 1,2-isopropylideneglycerol after trifluoroacetylation. Left: Monitoring of the enantiomeric purity of a sample prepared from D-mannitol. 40-m glass capillary with perpentylated α-cyclodextrin. Column temperature 70°C; carrier gas: 1 bar H_2.

ral amines with values between 1.2 and 1.3 at retention times of a few minutes on Phase II are exceptionally high.

An overview of the separation results is given in Table 1.

Table 1. Separation factors (α) for a selection of gas-chromatographic enantiomer separations on modified cyclodextrins.

Compound (trifluoracetyl derivate)	α-Value	First eluted enantiomer	Phase [a]	Column temp. [°C]
Glyceraldehyde	1.021	D	I	72
Erythrose	1.033	D	I	80
α-Ribopyranose	1.064	D	I	115
β-Ribopyranose	1.150	L	I	115
α-Glucopyranose	1.117	L	I	115
β-Glucopyranose	1.166	L	I	115
α-Methylgalactopyranoside	1.070	D	I	110
β-Methylgalactopyranoside	1.106	D	I	110
1,5-Anhydrogalactitol	1.080	D	I	120
Arabitol	1.111	D	I	110
Sorbitol	1.033	L	I	110
Methyl lactate	1.151	D	I	55
2-Hydroxybutyric acid methyl ester	1.048	?	I	62
3-Hydroxybutyric acid methyl ester	1.034	?	I	62
Dimethyl tartrate	1.071	L	I	90
Methyl galactate	1.087	D	I	100
Isopropylideneglycerine	1.034	*S*	I	70
1-Phenylethanol	1.028	*R*	I	70
trans-Cyclohexane-1,2-diol	1.037	?	I	90
Phenylglycol	1.023	*S*	I	100
1,2-Butanediol	1.021	?	I	45
1,2-Octanediol	1.063	?	I	90
1,2,4-Butanetriol	1.028	*S*	I	70
1-Phenylethylamine	1.200	*R*	II	120
2-Pentylamine	1.250	*R*	II	90
2-Octylamine	1.279	?	II	90
2-Aminobutan-1-ol	1.049	*R*	I	80
Valinol	1.120	*R*	II	90
Threonine	1.074	D	I	95
Alanine	1.036	D	I	80
Phenylalanine	1.028	D	I	130

[a] 40-m glass capillary for Phase I; 11-m glass capillary for Phase II.

Since, in all cases, the highly volatile and readily accessible *O*- or *N*-trifluoroacetylated derivatives can be used, most of the separations are possible with short retention times and at low temperatures, i.e. in the region of particularly high separation efficiency of the gas chromatographic column.

A broader application of the permethylated β-cyclodextrin described as stationary phase for gas chromatographic enantiomer separation[10, 11] failed because of the high melting point of this derivative (> 155°C). By mixing with polysiloxanes it was possible, however, to use permethylated β-cyclodextrin at temperatures below 100°C for enantiomer separation.[12]

Particularly interesting in the case of the cyclodextrins are their different ring sizes and the numerous functional groups, which should enable the preparation of stationary phases that are tailor-made for specific separation problems.

Received: February 16, 1988 [Z 2623 IE]
German version: *Angew. Chem. 100* (1988) 989

CAS Registry numbers:
3, 114551-48-3; **4**, 114551-50-7; **5**, 114551-51-8.

[1] a) V. Schurig, *Angew. Chem. 96* (1984) 733; *Angew. Chem. Int. Ed. Engl. 23* (1984) 747; b) W. A. König: *The Practice of Enantiomer Separation by Capillary Gas Chromatography*, Hüthig, Heidelberg 1987.

[2] "Fused Silica" capillaries with the chiral phases Chirasil-val® and XE-60-L-valine-(*S*)-α-phenylethylamide are available from Chrompack, Middelburg (The Netherlands).

[3] a) I. Benecke, W. A. König, *Angew. Chem. 94* (1982) 709; *Angew. Chem. Int. Ed. Engl. 21* (1982) 709; b) W. A. König, E. Steinbach, K. Ernst, *ibid. 96* (1984) 516 and *23* (1984) 527.

[4] a) B. Feibush, A. Balan, B. Altman, E. Gil-Av, *J. Chem. Soc. Perkin Trans. 2 1979*, 1230; b) B. Koppenhoefer, E. Bayer, *J. Chromatogr. Libr. 32* (1985) 1.

[5] D. W. Armstrong, T. J. Ward, R. D. Armstrong, T. E. Beesley, *Science (Washington) 232* (1986) 1132, and references cited therein.

[6] T. Koscielski, D. Sybilska, S. Belniak, J. Jurczak, *Chromatographia 21* (1986) 413.

[7] α-Cyclodextrin was allowed to react with a threefold excess of *n*-pentyl bromide and NaOH in dimethyl sulfoxide (as described by I. Ciucanci, F. Kerek, *Carbohydr. Res. 131* (1984) 209). The cyclodextrins pentylated in position 2 and 6 of the glucose building block are obtained in almost quantitative yield. The pentylation of the 3-positions could be achieved in THF with NaH/*n*-$C_5H_{11}Br$ by boiling under reflux for four days. The cyclodextrins acetylated in position 3 were prepared from the 2,6-dipentylated derivatives, acetic anhydride/triethylamine (3 molar equivalents each) and 5 mol-% 4-dimethylaminopyridine by 24 hours' boiling under reflux.

[8] J. G. Jun, G. R. Gray, *Carbohydr. Res. 163* (1987) 247.

[9] W. A. König, P. Nischnick-Lübbecke, B. Brassat, S. Lutz, *Carbohydr. Res.*, in press.

[10] Z. Juvancz, G. Alexander, J. Szeijtli, *J. High Res. Chromatogr. Chromatogr. Commun. 10* (1987) 105.

[11] J. Szejtli, *Starch/Stärke 39* (1987) 357.

[12] V. Schurig, H.-P. Nowotny, *J. Chromatogr. 441* (1988) 155.

Accurate Determination of the Redox State in High-T_c Superconductor Oxides

By *J. Maier, P. Murugaraj*, C. Lange,* and *A. Rabenau*

Although little is absolutely clear as to the mechanism of conduction in the high temperature superconductors, it can be said with certainty that the redox state of the elements, at a given molar ratio of metal to oxygen content per formula unit, plays a significant role.[1] In this communication two methods will be described for the determination of the oxygen excess (δ) and experimental results will be presented for the prototypic superconductor $YBa_2Cu_3O_{6.5+\delta}$.[2] Here, $\delta = 0$ corresponds to the reference

[*] Dr. J. Maier, Dr. P. Murugaraj, C. Lange,
Prof. Dr. A. Rabenau
Max-Planck-Institut für Festkörperforschung
Heisenbergstr. 1, D-7000 Stuttgart 80 (FRG)

composition of the "normal compound" as determined from the oxidation states of the ions $Cu^{2\oplus}$, $Ba^{2\oplus}$, $Y^{3\oplus}$, $O^{2\ominus}$. Alternately, these average values may be compensated for by corresponding fractions of oxidation states (e.g. $Cu^{1\oplus}$, $Cu^{3\oplus}$ and/or $O^{2\oplus}$). Moreover, the real degree of covalency and delocalization does not enter into the theme presented here.[3]

For the sake of simplicity and without limiting the general validity of the method, we shall describe the redox process purely in terms of valence changes of the copper. The molar ratios of the metals are assumed to be established by spectroscopic or wet chemical analysis. In the case of $YBa_2Cu_3O_x$, ICP analysis (plasma excited atomic emission spectrometry) accomplishes this, e.g., with relative inaccuracies of $\leq 3\%$. Determination of the oxygen content merely from the difference in the mass balance is not accurate enough. Typically two methods have been used to determine the oxygen content: 1. Reduction of the compound at high temperatures (e.g. 1000 °C in the case of $YBa_2Cu_3O_x$) with CO or H_2, whereby Y_2O_3, BaO and metallic copper are formed, and determination of the change in mass by thermogravimetry.[1,6] With CO as reductant, the CO_2 that is formed can be advantageously detected by IR spectroscopy. (Commercially available O-analysis apparatus for the determination of the O-content of oxides are based on this method; temperatures up to 3000 K.) 2. Determination by redox titration with iodide/thiosulfate.[7]

In the first method the main sources of error inherently stem from the working technique used at high temperatures (temperature gradients, possible crucible reactions etc.). If one does not work at extremely high temperatures a further difficulty is encountered—in the subsequent (generally room temperature) phase analysis. Since not only the "excess oxygen" (i.e. the δ value) is determined, non-stoichiometric oxide in the compound and in the products as well as general instrumental errors also contribute significantly (see below).

The primary disadvantage of the second method arises from the fact that the redox potential of the $I^{\ominus}/I_2$ equilibrium lies not only below that of $Cu^{3\oplus}/Cu^{2\oplus}$, but also below that of $Cu^{2\oplus}/Cu^{\oplus}$ (see Table 1). Thus two measurements are necessary (before and after annihilation of the higher oxidized states), and δ is obtained as the difference of two comparably large numbers.

We report here on two very accurate methods from which δ is determined directly: A) determination of the shift of the $Fe^{2\oplus}/Fe^{3\oplus}$ concentration ratio (redox potential) and B) measurement of the O_2-pressure after reaction with H_2O.

In method A the superconducter is dissolved in a sulfuric acid solution of $[Fe(NH_4)_2(SO_4)_2(H_2O)_6]$ or $FeSO_4$ (previously stored over Fe) and transferred to a gas-tight quartz vessel. The final state ($BaSO_4$ + solution) must correspond to the oxidation states of the ions $Y^{3\oplus}$, $Ba^{2\oplus}$, $Cu^{2\oplus}$, and $O^{2\ominus}$. Under these conditions no evolution of oxygen is observed.[9] The $Fe^{3\oplus}$ that is formed is detected photometrically at 520 nm using salicyclic acid (buffering with $(NH_4)_2SO_4$/HOAc; pH 3).[10] At higher concentrations the natural color of the $Cu^{2\oplus}$-complex interferes somewhat but this can be compensated for in the calibration. $Fe^{2\oplus}$ does not interfere. Owing to the position of the redox potential (see Table 1). $Cu^{3\oplus}$ (representing the higher oxidation state) is reduced in this method, but not $Cu^{2\oplus}$. Anions such as $SCN^{\ominus}$, $I^{\ominus}$ (or even $OH^{\ominus}$) shift the redox potential above that of the introduced redox pair, because of the formation of sparingly soluble Cu^{I} compounds (see Table 1).

Table 1. Standard potentials referred to pH 3 [a] for some relevant redox equilibria.

Redox equilibria	E^0 [mV] [a]
$Cu^{2\oplus} + BaSO_4 \rightleftharpoons (Cu^{3\oplus} + Ba^{2\oplus}) + SO_4^{2\ominus} + e^{\ominus}$ [b]	> 1640
$Cu^{2\oplus} \rightleftharpoons (Cu^{3\oplus}) + e^{\ominus}$ [c]	> 1050 [d]
$H_2O \rightleftharpoons 1/2\,O_2 + 2e^{\ominus} + 2H^{\oplus}$	1050
$CuI \rightleftharpoons Cu^{2\oplus} + e^{\ominus} + I^{\ominus}$	840
$CuSCN \rightleftharpoons Cu^{2\oplus} + e^{\ominus} + SCN^{\ominus}$	800
$Fe^{2\oplus} \rightleftharpoons Fe^{3\oplus} + e^{\ominus}$	770
$Fe^{2\oplus} + 3\,SCN^{\ominus} \rightleftharpoons Fe(SCN)_3 + e^{\ominus}$	560
$I^{\ominus} \rightleftharpoons 1/2\,I_2 + e^{\ominus}$	540
$Cu^{\oplus} \rightleftharpoons Cu^{2\oplus} + e^{\ominus}$	170
$1/2\,H_2 \rightleftharpoons H^{\oplus} + e^{\ominus}$	− 180

[a] pH 3; other ionic activities in the redox equilibria normalized to 1. [b] Symbolic notation (see text); referred to the dissolution in H_2SO_4. [c] Symbolic notation (see text); verified by dissolution in HOAc. [d] *Rosamilia* et al. [8] quote a potential for $YBa_2Cu_3O_7$ in 1 M NaCl which lies ca. 100 mV above that of H_2O/O_2.

This precludes, for example, the use of the thiocyanate method for the determination of $Fe^{3\oplus}$ and of $I^{\ominus}$ as reducing agent.

The value of δ is obtained from equation (a) (M^* = molecular mass of the normal compound, $M_0 = 16$ g mol^{-1}; m_s = mass of sample).

$$\delta = \frac{M^* \Delta n}{2m_s - \Delta n M_0} \simeq \frac{M^*}{2m_s} \Delta n \qquad \text{(a)}$$

$\Delta n = n^{\infty}_{Fe^{3\oplus}} - n^{0}_{Fe^{3\oplus}}$, $n^{\infty}_{Fe^{3\oplus}}$ is the final number of gram molecules in solution, $n^{0}_{Fe^{3\oplus}}$ the $Fe^{3\oplus}$ content at the beginning of the measurement. Normally ($\delta \geq 0$), $n^{0}_{Fe^{3\oplus}}$ is simply the blank value, which is determined more accurately in a parallel blank experiment. A definite amount of ($n^{0}_{Fe^{3\oplus}}$) can be used at the beginning also, so as to oxidize any $Cu^{\oplus}$ that is present. Thus, a negative Δn corresponds to a negative δ value. As a rule, the absolute accuracy of detection is limited by the blank value.

In equation (a) it is seen that when $M_0\delta \ll M^*$ (typical error 0.5%) the expression for δ reduces to a proportionality.

In method B the compound is dissolved in H_2SO_4 (10 vol-%) in a gas-tight vessel, i.e. H_2O/O_2 acts as the redox pair. The oxygen evolved by $Cu^{3\oplus}$-reduction is detected by the increase in pressure in a sealed Hg manometer. There is no reduction of $Cu^{2\oplus}$, and any $Cu^{\oplus}$ present will be oxidized by O_2, so that negative δ values can also be determined. Since the dissolution kinetics are not known it is essential not to remove the evolved oxygen. Any CO_2 present can be removed by use of an appropriate filter.

A similar volumetric method[11] and mass spectrometric method[12] for the determination of the evolved oxygen have been described, however without any analytical details.

Correspondingly, we find (neglecting the change of volume compared to the total volume V, error typically 0.5%; Δp: pressure increase):

$$\delta = \frac{\Delta p V M^*}{RTm_s/2 - \Delta p V M_0} \approx \frac{2\Delta p V M^*}{RTm_s} \quad \text{(b)}$$

In this approximation, as in equation (a), a proportionality is found between δ and the measuring effect. This is important for the accuracy of both methods, since the relative errors are simply additive.

Assuming that by X-ray analysis a second phase ($\leq 5\%$) with "normal" valencies ($Cu^{2\oplus}$, $Ba^{2\oplus}$, $Y^{3\oplus}$) will be overlooked, then an error of up to 5% in δ can occur. In the case of $YBa_2Cu_3O_x$ a typical value for δ is ca. 0.2, i.e. $\Delta\delta = 0.01$, being negligible in all cases. Similarly, this will also hold true for "active" second phases. If the total oxygen as in the CO/H_2 method (typical value for x: 6.7) or the oxygen content beyond that of Y_2O_3 and BaO (typically 3.2) is measured, then the error increases by more than an order of magnitude; this argument also applies in the case of the determination of oxygen by difference in mass balance. Since, on the one hand, very small $Fe^{3\oplus}$-contents (> 0.1 ppm) can be measured by the salicylate method and blanks can be kept very small, and, on the other hand, pressure increases of ca. 1 torr are easy to measure, we estimate the accuracy for δ to be ca. 2% from method A and ca. 4% from method B. This corresponds to an accuracy of the δ value to the third decimal place, which is more than satisfactory in practice, where the accuracy is already influenced considerably by the uncertainty in the determination of the ratios of the metals (e.g. $\Delta M^*/M^* = 1\%$ for 3% accuracy in the Ba-content).

Table 2. Determination of the oxygen content δ in $YBa_{2-y}CuO_{6.5-y+\delta}$ by the methods A and B described in the text.

Ceramic	Remarks	δ		
		Method A	Method B	
			[b]	[c]
$YBa_2Cu_3O_{6.5+\delta}$	unannealed	0.18	0.17	0.18
$YBa_2Cu_3O_{6.5+\delta}$	annealed [a]	0.22	0.20	0.21
$YBa_{1.9}Cu_3O_{6.4+\delta}$	unannealed	0.17	0.15	0.16
$YBa_{1.9}Cu_3O_{6.4+\delta}$	annealed [a]	0.21	0.19	0.20
$YBa_{1.8}Cu_3O_{6.3+\delta}$	unannealed	0.15	0.14	0.15
$YBa_{1.8}Cu_3O_{6.3+\delta}$	annealed [a]	0.22	0.20	0.21

[a] 600°C, 10 h, $p(O_2) = 1$ atm. [b] Uncorrected. [c] Increased solubility of gas taken into account on increasing the pressure (the pressure coefficient of pure H_2O was used.

Table 2 shows the excellent agreement between the two values obtained for conventional $YBa_2Cu_3O_{6.5+\delta}$-ceramics and for the BaO-substoichiometric ceramics prepared by us,[13] of which $YBa_{2-y}Cu_{6.5-y}$ is the "normal compound." An obviously slight systematic deviation is partially eliminated (cf. Table 2) if, in the O_2-method, the pressure dependence of the gas absorption[14] is taken into account ($\Delta\delta = 0.012$ if, for lack of data, the pressure coefficient in water is used).[15]

An additional advantage of method B is the possibility of being able to easily determine the overall dissolution kinetics. We have always observed the existence of a maximum Δp; whether this can be attributed to intermediate formation of a $Cu^{\oplus}$ compound[16] which is then reoxidized or whether this simply reflects a slow O_2 absorption as a result of the increased pressure, is still unclear. Consistent with the latter mentioned effect is the fact that the subsequent small decrease in pressure corresponds exactly to the deviation in the uncorrected results between the two methods.

Received: May 16, 1988 [Z 2667 IE]
German version: *Angew. Chem. 100* (1988) 967

[1] a) P. K. Gallagher, H. M. O'Bryan, Jr., S. A. Sunshine, D. W. Murphy, *Mater. Res. Bull. 22* (1987) 995; b) R. J. Cava, B. Batlogg, C. H. Chen, E. A. Rietman, S. M. Zahurak, D. Werder, *Nature (London) 329* (1987) 423; c) A. Manthiram, J. S. Swinnea, Z. T. Sui, H. Steinfink, J. B. Goodenough, *J. Am. Chem. Soc. 109* (1987) 6667.

[2] a) R. Kanno, Y. Takeda, M. Hasegawa, O. Yamamoto, M. Tanaka, Y. Ikeda, Y. Bando, *Mater. Res. Bull. 22* (1987) 1525; b) J. D. Jorgensen, A. Beno, G. D. Hinks, L. Soderholm, K. J. Volin, R. L. Hitterman, J. D. Grace, I. K. Schuller, C. U. Segre, K. Zhang, M. S. Kleefisch, *Phys. Rev. B36* (1987) 3608.

[3] On the basis of photoelectron spectroscopic findings it appears most meaningful to ascribe the excess positive charge to the Cu-O sublattice [4]. Furthermore, the interplay between localization-delocalization and correlation effects is presumably important [5].

[4] a) A. P. Malozenoff, P. M. Granz, *Z. Phys. B67* (1987) 3608; b) F. Baudelet, G. Collin, E. Dartyge, A. Fountaine, J. P. Kappler, G. Krill, J. P. Itie, J. Jegoudez, M. Maurer, Ph. Monod, A. Revcolevschi, H. Tolentino, G. Tourillon, M. Verdauger, *ibid. 69* (1987) 141.

[5] W. Urland, *Angew. Chem. 99* (1987) 1316; *Angew. Chem. Int. Ed. Engl. 26* (1987) 579.

[6] E. Schönherr, *Mater. Res. Bull.*, in press.

[7] D. C. Harris, T. A. Hewston, *J. Solid State Chem. 69* (1987) 182.

[8] J. M. Rosamilia, B. Miller, L. F. Schneemeyer, J. V. Waszcak, H. M. O'Bryan, Jr., *J. Electrochem. Soc. 134* (1987) 1863.

[9] F. D. Snell, C. T. Snell: *Colorimetric methods of analysis, Vol. IIA*, Van Nostrand, Princeton, NJ, USA 1959, p. 321.

[10] Evolution of O_2 occurs as a side reaction only in very dilute H_2SO_4, where also the oxygen is reduced again by $Fe^{2\oplus}$ in a closed system.

[11] H. Eickenbusch, W. Paulus, R. Schöllhorn, R. Schlögl, *Mater. Res. Bull. 22* (1987) 1505.

[12] J. Chunlin, C. Chuanmeng, L. Sulan, W. Kuihan, F. Zhanguo, Z. Guofan, *Int. J. Mod. Phys. B1* (1987) 285.

[13] P. Murugaraj, J. Maier, A. Rabenau, *Solid State Commun. 66* (1988) 735.

[14] *Gmelins Handbuch der Anorganischen Chemie (8th Edit.), Sauerstoff, Vol. 3*, Verlag Chemie, Weinheim 1958.

[15] A remark on the use of other methods is warranted: Isothermal degradation of oxygen has been attempted, but from the kinetics appears problematic. An electrochemical determination, by coulometric titration, can in principle be very accurate but requires a detailed knowledge of a series of parameters which are not available at present.

[16] A different rate of reaction of $Cu^{3\oplus}$ and $Cu^{\oplus}$ in the superconductor structure as a possible explanation appears unlikely in view of the reaction times.

***Ab Initio* Methods in Quantum Chemistry, Part I and Part II (Series: Advances in Chemical Physics, Vols. 67 and 69).** Series editors: *I. Prigogine* and *S. A. Rice*; volume editor: *K. P. Lawley*. Wiley, Chichester 1987. Part I: 556 pp., bound, £ 65.00.—ISBN 0-471-90900-9; Part II: 588 pp., bound, £ 59.95.—ISBN 0-471-90901-7

To the series "Advances in Chemical Physics", well known for its high quality, two extensive new volumes devoted to *ab initio* quantum chemistry have now been added, increasing the number of volumes in the series to 69. The aim of the editors of this series is to bring together in a single work review articles on specialist topics by internationally known experts, so as make new ideas in chemical physics accessible to a wide readership. The authors are encouraged to bring to task their own individual evaluations and viewpoints. Here once more those aims have been fulfilled very successfully. The books contain a wealth of new and highly interesting information and ideas, not only for theoreticians but also for experimentalists who need theory to help in guiding their work.

The first contribution in Part I (by *Bruna* and *Peyerimhoff*) is on electronic excited states, and comes from the Bonn group which is very active in this field; it contains a detailed survey of calculated properties, mainly of diatomic and triatomic molecules. It is clearly presented, and the schematic layout contributes to rapid assimilation of the ideas. This article will be greatly welcomed not only by quantum chemists but also by all who have an interest in the spectroscopic properties of small molecules. The article by *Amos* deals with the calculation of functions describing molecular properties, with special emphasis on methods for directly calculating dipolar properties and polarizabilities. The power of the theory is illustrated by numerous examples of calculations of IR and Raman intensities. In another contribution *Bernardi* and *Robb* have undertaken the important task of giving a critical summary of theoretical knowledge on mechanisms of typical reactions, mainly organic. Such studies would not be possible without using numerical methods to locate the extrema on multidimensional potential energy surfaces. The algorithms used for this purpose are described in a clear and comprehensible fashion in the article by *Schlegel*. *Balasubramanian* and *Pitzer* give details of the methods now available for calculations of relativistic effects, and describe various applications of relativistic quantum chemistry, mainly to spectroscopic problems. *Durand* and *Malrieu* have undertaken a detailed study of effective Hamiltonian operators and their physical significance. *Jones* describes methods and results based on the formalism of density functions. *Wilson* deals with the question of choosing between different basis sets and applying them. Lastly, *Ahlrichs* and *Scharf* give a concise description of methods based on coupled pairs approximations. In this important and interesting contribution, the various methods are critically compared and their advantages and disadvantages are discussed with the help of examples.

It seems impossible now to escape the increasing flood of new abbreviations to describe ever more detailed aspects of solutions of the Schrödinger equation for the motions of electrons and nuclei. Not only will most scientists working in the field be unaware, for example, that CEPA is also a botanical abbreviation defining the edible onion family, they are also likely to have difficulty with creations which they are often assumed to be familiar with such as WNR (wavefunction Hessian matrix Newton-Raphson), APT (atomic polar tensors), or SAC (symmetry adapted cluster approach). In view of the large number of new abbreviations, it would have been sensible to include in both volumes a glossary of these terms with explanations, and perhaps also literature references. In contrast, the index of cited authors contained in the book does not seem particularly useful, as each article has its own separate bibliography. In my opinion neither book is really suitable as an introduction to *ab initio* methods in quantum chemistry, which was the declared intention of the editors.

Taken as a whole, the first volume can be recommended to all readers who have some knowledge of or interest in *ab initio* methods in quantum chemistry. They will find much new material here, and in addition to its other merits the book is an extremely useful up-to-date work of reference on specialized aspects of theoretical chemistry. These are qualities which the "Advances in Chemical Physics" series has now been providing in an outstanding way for nearly thirty years, covering many fields of research.

The second volume is mainly concerned with modern algorithms of quantum chemistry. Five of the nine contributions deal with multi-configurational methods and their applications. Advanced *ab initio* methods of this kind are indispensable in, for example, exact calculations of dissociation energies, for calculations on near-degenerate electronic states, for dealing with regions in which a crossover of potentials is just avoided, and for spin coupling effects. The last few years have seen the introduction of new numerical methods, largely based on group theory considerations, which allow efficient handling of multi-reference problems. The application of these methods has been greatly helped by progress in computer technology, with the advent of large capacity vector-processing computers and super-minicomputers. These methods make it possible to solve problems formulated in more and more general terms. The appearance of this book is very much to be welcomed, since it deals with the latest developments and will undoubtedly have a stimulating effect.

The book begins with an article by *Werner* on direct methods for the solution of multi-reference problems involving configurational interaction. The author begins by describing his recent work on MCSCF methods which give fast and certain convergence, and on direct methods for the solution of the MCSCF-CI problem. All the algorithms described are especially suitable for vector computers. The article is very well written from a teaching standpoint, contains many new ideas, and can be warmly recommended to all who are interested in modern MCSCF methods. *Shepard*, in a very detailed contribution (134 pages!), reviews the development of MCSCF methods and discusses the different ways in which they can be formulated. *Roos* deals with the special case of the MCSCF method in which one considers all configurations for a given number of molecular orbitals. Valence bond methods, although they are based on a different theoretical model, are used for the same purposes as MCSCF methods. The present state of knowledge on these methods is reviewed by *Cooper*, *Gerratt*, and *Raimondi*. The theoretical treatment of transition metal compounds usually requires multi-reference methods. *Salahub* gives an excellent overview of methods ap-

plied to transition metal atoms and their dimers. This contribution can be recommended as a source of information for readers interested in the theory of chemical bonding involving metals. The calculation of potential energy surfaces for weakly bonded systems continues to present a great challenge for *ab initio* quantum chemical methods, as discussed in the contribution by *van Lenthe, van Diujneveldt,* and *van de Rijdt,* with particular attention to the basis superposition effect. A very competent article on analytical derivation methods in quantum chemistry is provided by *Pulay*, one of the pioneers in this highly topical area of research. As well as reviewing these methods, the author gives a critical appraisal and indicates possibilities for further developments. This contribution too is very valuable from a teaching standpoint. *Oddershede* deals with the propagator methods, which are especially useful for electronic excited states and applications such as calculation of dynamic polarizabilities. Everyone interested in previous work based on this formalism will find here a useful review and commentary on the methods. Finally, *Dunlop* discusses symmetry and degeneracy in the theory of $X\alpha$ functions and density functions.

This second volume, containing articles which are more oriented towards methodology, is aimed at the specialist to an even greater extent than is the first volume. The individual articles are of excellent quality, and they deal with topical research themes which are still rapidly developing. Consequently, the book will not only be indispensable for libraries, but will also provide theoreticians with a starting point for further developments in their armory of techniques.

Pavel Rosmus [NB 859 IE]
Institut für Anorganische Chemie
der Universität Frankfurt/Main (FRG)

Principles and Applications of Organotransition Metal Chemistry. By *J. P. Collman, L. G. Hegedus, J. R. Norton,* and *R. G. Finke.* Oxford University Press, Oxford 1987. xii, 989 pp., bound, £ 40.00.—ISBN 0-935702-51-2

When the first edition of *Collman* and *Hegedus* appeared on the market seven years ago it did not seem very impressive. It was made by direct reproduction of a typescript, with a result which was not altogether attractive to the eye, and it also contained many errors, especially in structural formulas and equations. However, even then a closer study of the book revealed its merits: for the first time it attempted, in a skilful and instructive way, to bridge the gulf between fundamental knowledge of organotransition metal chemistry and its importance for catalytic process technology, and also to show how this knowledge could be applied in organic synthesis. The success of the textbook was therefore already assured, despite the unsatisfactory manner of its production.

The second edition is now available; it has, naturally, turned out to be somewhat larger, and the involvement as co-authors of a further two organometallic chemists, *J. R. Norton* and *R. G. Finke*, who have a more inorganic bias, has remedied some weak points of the first edition. The text is divided into three parts: I. Basic Principles, II. Catalytic Processes and III. Applications to Organic Synthesis; their respective lengths of 500, 140 and 270 pages seem appropriate to the subject matter.

The longest, Part I, begins by discussing structure and bonding, then continues with a survey of the various types of organotransition metal complexes, arranged according to the nature of the ligands. This is followed by a very thorough treatment of the most important types of reactions which the previously listed complexes are known to undergo, discussed under the headings of ligand exchange processes, oxidative additions and reductive eliminations, intramolecular insertion reactions, and lastly nucleophilic and electrophilic attack of ligands. The majority of the examples are well chosen, and the sections on individual topics include details even of very recent and highly topical results, e.g. on electron transfer catalysis in substitution reactions, the oxidative addition of Si–H and C–H bonds to transition metals, carbene insertions, MHC three-centre bonding, and complexes containing SO, SO_2, CO_2, NS or diazoalkanes as ligands. Part I is concluded by a chapter on metallacycles, including discussions of olefin metathesis and other important reactions which involve metallacyclobutanes.

In Part II the discussion of catalytic processes begins with homogeneous catalytic hydrogenation, hydrosilylation and hydrocyanation, then continues with the metal-catalyzed polymerizations of olefins and acetylenes, and concludes with a concise survey of catalytic reactions involving carbon monoxide. In this chapter the Roelen oxo synthesis (hydroformylation), the Monsanto acetic acid process, and, of course, the Fischer-Tropsch synthesis are discussed. Commendable features of the treatment are that modern variations of well-known processes are also described in detail (e.g. the manufacture of ethylene glycol by the Fischer-Tropsch process), and that up-to-date figures relating to industrial production are given.

Part III, covering applications in organic synthesis, has without doubt undergone the greatest changes since the first edition, thereby reflecting one of the most important current trends affecting organometallic chemistry in recent years. Several monographs on the theme of organometallic compounds for organic synthesis have recently appeared in rapid succession, and it is also no accident that since 1981 a series of conferences on this topic has been set up. Here the authors have arranged the material according to the types of organometallic compounds used, i.e. metal hydride complexes, compounds with M–C σ-bonds, carbonyl and carbene complexes, metallacycles, olefin, diolefin, and dienyl compounds, alkyne and allyl complexes, and finally sandwich complexes formed by arene ligands. One can fairly confidently predict that in the next edition of the book Part III will again grow in size.

What are the good and bad features of "Collman, Hegedus, Norton and Finke"? The overall concept of the book is undoubtedly good, as is the balance between the different types of compounds and reactions, the way in which the chemistry is related to applications, and the topicality of content. The presentation, the reproduction of structural formulas and the typography are better than in the first edition. Regrettably many printing errors have again crept in (despite proof-reading by four authors). These appear as early as the first page of the contents list ("Formal-Metal Bonds" instead of Formal Metal-Metal Bonds, "Isolabal" instead of Isolobal), and continues through the tables (Historical Landmarks: "Reppe describes the catalytic cyclotrimerization of acetylene to cyclooctatetraene") to the individual chapters. Especially displeasing are incorrect formulas, as uninitiated readers at least will be confused by these; examples: p. 78, bottom left: this should read five-coordinate osmium(*0*)-complex, p. 106 bottom left: positive charge missing, p. 153: $PtCl_2(COD)$—not $PtCl_2(COD)_2$, p. 160: $Ru\text{-}PPh_3$—not $Ru\text{-}PPh_2$, p. 171: **154**

has not been synthesized by this method, p. 294, line 5: $(CO)_2$, p. 298, Eq. 5.31: the product is $[CpIrHL_2]^{\oplus}$, p. 317, middle left: negative charge missing, p. 321, Eq. 5.67: should be C_5Me_5, p. 380: C_6Me_6Ru—not Cp*Ru, and p. 890, Eq. 19.19: $MoO_2(acac)_2$ instead of $Mo(O_2)(acac)_2$. Also it is regrettable (and a little disappointing) to find that the historical milestones are in some cases viewed through "USA-tinted" spectacles. For example, in the chapter on "Historical Perspectives" there is no mention of *Walter Hieber* and his pioneering work on metal carbonyl complexes, and no reference is made reflecting the very important publications by *Dewar, Chatt,* and *Duncanson* on bonding in olefin–metal complexes. Again, the false impression is given that the structure of ferrocene was correctly proposed only by *Wilkinson, Rosenblum* and *Woodward,* whereas it also came simultaneously from *Fischer* and *Pfab*. Other omissions: when mention is made of the Monsanto process, why not also of the Wacker process, which is equal in technological importance? When, in connection with the discovery of the intermolecular oxidative addition of saturated hydrocarbons to transition metals, mention is correctly made of *Bergman*, why not also of *Graham* in the same breath? An opportunity has been missed here to present an objective picture (acceptable throughout the world) of the historical development of the subject; this is especially regrettable when one considers that students also need to be educated in the history of science.

However, taken as a whole the positive impressions given earlier outweigh these criticisms, and the textbook can be strongly recommended for reading by advanced students. Fortunately the price is also reasonable, something which is nowadays much appreciated.

Helmut Werner [NB 885 IE]
Institut für Anorganische Chemie
der Universität Würzburg (FRG)

Nitroazoles. The *C*-Nitro Derivatives of Five-Membered *N*- and *N,O*-Heterocycles. By *J. H. Boyer*. VCH Publishers, Deerfield Beach 1986. xv, 368 pp., bound, DM 185.00.—ISBN 0-89573-138-7

In the fifties and sixties, nitro compounds interested chemists primarily as propellants and explosives. Since then, however, this most easily introduced of functions, the nitro group, has been recognized to have an activating effect on numerous organic reactions, and to be easily convertible into other useful nitrogen functional groups. This is emphasized by the commencement of a new series, "Organic Nitro Chemistry", of which Volume 1, "Nitroazoles", has now appeared.

The 368-page work is divided into sections on nitration, chemical, physical (spectroscopic) and biological properties, reactions, and references. Inside this framework, nitropyrroles, nitroimidazoles, nitropyrazoles, nitrotriazoles and nitrotetrazoles are described, as are the nitro derivatives of isoxazoles, oxazoles, oxadiazoles and the heterocyclic systems derived from these by annelation of further rings. The table of contents, though very detailed, could have been more clearly laid out.

The bibliography contains 1501 original citations, and an extensive list of references is also appended to each chapter (the names of German, Austrian and Swiss workers are unfortunately often misquoted). While many classic heterocycle monographs, series, reviews, and articles are cited, one seeks in vain for the newest standard work, "Comprehensive Heterocyclic Chemistry" (published 1984). The author earns special praise for having analyzed and evaluated the overwhelming number of Soviet publications on the subject of nitroazoles. In doing so, he has made an area that has been intensively studied in the Soviet Union available in the West for the first time.

The first five chapters deal extensively with the most favorable reagents and methods for nitration of the various heterocycles. Where direct nitration is difficult, ring closure or ring transformation reactions often give the desired result. The sections on chemical reactivity include alkylation, acylation and arylation at both nitrogen and carbon, halogenation, reduction (including electrochemical methods), oxidation, decarboxylation, rearrangements, exchange of the nitro group for side-chains, nucleophilic and electrophilic substitution and addition, metallation, ring cleavage, free radical reactions, thermo- and photochemistry (degradation) and glycosylation. For important key reactions the yields are always reported, and stereochemical aspects are taken into account. Biotechnological conversions of amino- into nitroheterocycles are also described (p. 95). The sections on physical properties offer much information, and the biological properties of the nitroazoles and their derivatives are described in separate sections.

While the computer-drawn structural formulas are clear and informative in every respect, for a book in this price range they display numerous flaws and deficiencies. Bond lengths are too short or too long, heteroatoms are superimposed on bonds, substituents are cramped, rings are set out crookedly (e.g. pp. 190, 191, 227), carbonyl groups are distorted (p. 331), and substituents are twisted (p. 131). Many less expensive textbooks are able to offer more than this! The consistent numbering of formulas with the chapter number as prefix is very practical.

All in all, this monograph is a valuable addition to the chemical literature, and is highly recommended for anyone who comes in contact with the topic of azoles.

Heinrich Wamhoff [NB 888 IE]
Institut für Organische Chemie und Biochemie
der Universität Bonn (FRG)

Biohalogenation. Principles, Basic Roles, and Applications. By *S. L. Neidleman* and *J. Geigert*. Ellis Horwood, Chichester 1986. 203 pp., bound, £ 25.00.—ISBN 0-85312-984-3

Halogens and halogen compounds play an important role in many areas of chemistry. It therefore seems at first surprising that not very much is known about halogenation in biochemistry. Certainly many halogen compounds occur in nature, but there is no precise knowledge about their formation and importance. It has only recently become possible to detect and characterize halogenating enzymes in prokaryotic organisms, whereas they had already been recognized long before this in eukaryotic organisms (molds and algae). These enzymes were given the name "haloperoxidases", since in addition to halide ions they also need hydrogen peroxide in order to halogenate an organic compound.

The present state of knowledge on biohalogenation is reviewed for the first time in the book by *Neidleman* and *Geigert*. The nine chapters deal with some of the halogen compounds which occur in nature, the organisms producing them, the halogenating enzymes that have so far been isolated, and their importance to the organisms concerned.

A list of the halogen compounds produced by a wide range of different organisms gives impressive evidence of the large number of such compounds formed in nature. The chapters on halogenating enzymes include, in addition to a rather too detailed compilation of schemes for the purification of those haloperoxidases which have so far been isolated, a summary of the reactions catalyzed by these enzymes. The section on the mechanism of enzymatic halogenation deals with the various theories currently being considered, from which it is evident that it has not yet been possible to unambiguously clarify the mechanism. The importance of halogenating enzymes and of naturally occurring halogen compounds is discussed in terms of their enhanced biological activity compared with the corresponding non-halogenated compounds, with reference to a number of examples. One chapter deals with the relationship between halogenating enzymes and defence mechanisms in mammals. For example, hypochlorite can act as an antiseptic. Chapter 8 discusses biological dehalogenation, which is not simply a reversal of the halogenation process. This environmentally important topic is, however, not treated fully.

This book is indispensable for scientists involved in work on biological halogenation, and for others it undoubtedly makes interesting reading.

Franz Lingens, Karl-Heinz van Pée [NB 894 IE]
Institut für Mikrobiologie
der Universität Hohenheim (FRG)

Nonlinear Optical Properties of Organic Molecules and Crystals. Edited by *D. S. Chemla* and *J. Zyss*. Academic Press, Orlando, FL (USA) 1987. xiii, 482 pp., bound, $ 67.50.—ISBN 0-12-170611-7

Optical techniques are becoming increasingly important in the storage, transfer and processing of information. The demands for miniaturization and faster processing of data are forcing the adoption of technologies which make use of the unique properties of organic molecules. This book begins with a short introduction by *R. Silbey* ("The Structure and Properties of the Organic Solid State", 18 pp.), which gives a survey of the physics and chemistry of solid organic compounds in relation to their optical properties and electrical conductivity.

In the article "Quadratic Nonlinear Optics and Optimization of the Second-Order Nonlinear Optical Response of Molecular Crystals" (169 pp.) *J. Zyss* and *D. S. Chemla* deal with the physical and mathematical aspects of quadratic nonlinear optics in molecules and molecular crystals. *D. Pugh* and *J. O. Morley*, in the chapter "Molecular Hyperpolarizabilities of Organic Materials" (33 pp.), show how quantum theoretical models can be used to calculate polarizabilities and hyperpolarizabilities. The chapter "Design and Synthesis of Organic Molecular Compounds for Efficient Second-Harmonic Generation" (70 pp.) by *J. F. Nicoud* and *R. J. Twieg* continues the theme of the second chapter by treating the chemical and physicochemical aspects of "optical materials", with numerous examples and literature references. The contribution "Growth and Characterization of Molecular Crystals" (60 pp.) by *J. Badan, R. Hierle, A. Perigaud,* and *P. Vidakovic* deals with these important techniques as applied to organic crystals and waveguide structures. *A. Barraud* and *M. Vandemeyer*, in the chapter "Growth and Characterization of Organic Thin Films (Langmuir-Blodgett Films)" (27 pp.), discuss the preparative aspects and characterization of such films. "Properties and Applications of Urea" (20 pp.) by *J.-M. Halbout* and *C. L. Tang* is a well researched contribution dealing with the nonlinear optical properties of crystalline urea. Next, in the chapter "Nonlinear Optical Properties of Guest-Host Polymer Structures" (31 pp.), *D. J. Williams* discusses the physical properties of structures of this kind with organic molecule "guests", in which the host materials may be thermoplastic polymers, thermoplastic liquid crystal polymers, or polar polymer chains in an isotropic medium. The final chapter "Electro-Optic Organic Materials" (32 pp.) by *K. D. Singer, S. L. Lalama, J. E. Sohn,* and *R. D. Small* deals with electro-optical processes in organic materials; applications to optical integrated circuits are described with a number of examples.

Each chapter is followed by a detailed bibliography extending up to 1986. A comprehensive subject index enables one to find information on specialized topics. Certain equations and facts are frequently repeated in different chapters; cross-referencing here could have saved a few pages. The editors come out firmly against making a distinction between linear and nonlinear optics, pointing out that optics is in essence nonlinear. One can only agree with this statement and commend it to all authors who adopt too narrow a definition of nonlinear processes. The book can be recommended unreservedly to physicists, chemists and advanced students who are concerned with the optical properties of organic compounds.

Manfred Dieter Lechner [NB 873 IE]
Institut für Physikalische Chemie
der Universität Osnabrück (FRG)

Registered names, trademarks, etc. used in this journal, even when not marked as such, are not to be considered unprotected by law.

© VCH Verlagsgesellschaft mbH, D-6940 Weinheim, 1988. - Printed in the Federal Republic of Germany by Zechnersche Buchdruckerei, Speyer/Rhein.

All rights reserved (including those of translation into foreign languages). No part of this issue may be be reproduced in any form - by photoprint, microfilm, or any other means - nor transmitted or translated into a machine language without written permission from the publishers. Only single copies of contributions, or parts thereof, may be made for personal use. This journal was carefully produced in all its parts. Nevertheless, authors, editors and publisher do not warrant the information contained therein to be free of errors. Readers are advised to keep in mind that statements, data, illustrations, procedural details or other items may inadvertently be inaccurate.

Valid for users in the USA: The appearance of the code at the bottom of the first page of an article in this journal (serial) indicates the copyright owner's consent that copies of the article may be made for personal or internal use, or for the personal or internal use of specific clients. This consent is given on the condition, however, that the copier pay the stated per-copy fee through the Copyright Clearance Center, Inc., for copying beyond that permitted by Sections 107 or 108 of the U.S. Copyright Law. This consent does not extend to other kinds of copying, such as copying for general distribution, for advertising or promotional purposes, for creating new collective works, or for resale. For copying from back volumes of this journal see 'Permissions to Photo-Copy: Publisher's Fee List' of the CCC.

Editorial office: Pappelallee 3, D-6940 Weinheim, Federal Republic of Germany, Telephone (06201) 60 23 15, Telex 465 516 vchwh d, Telefax (06201) 602 328.

Editor: *P. Gölitz.*

Associate editors: *D. I. Loewus, A. Stimson.* **Editorial assistant:** *E. Schweikart*

Publishers: VCH Verlagsgesellschaft mbH. (Managing Directors: *Prof. Dr. Helmut Grünewald* and *Hans Dirk Köhler*), Pappelallee 3, D-6940 Weinheim, Federal Republic of Germany. Correspondence concerning advertisements should be addressed to VCH Verlagsgesellschaft mbH. (Advertising Manager *R. J. Roth*), Boschstr. 12. P.O. Box 1260/1280, D-6940 Weinheim, Federal Republic of Germany, Telephone Weinheim (06201) 602-0, Telex 465 516 vchwh d, Telefax (06201) 602 328.

ADVANCED MATERIALS

Editorial Advisors: E. M. Engler (USA), D. Haarer (FRG), N. Ogata (Japan), G. Petzow (FRG), J. M. Thomas (UK), G. Wegner (FRG)

Liquid Crystals—State of the Art

By Heino Finkelmann*

A century ago, in 1888, the liquid crystalline state of matter was discovered. One might suppose from this that liquid crystals have begun to grow old. Actually the reverse holds: liquid crystals have increased our possibilities for producing advanced materials par excellence. The realization of super-molecular organization in the liquid crystalline state offers additional dimensions for tuning the physical properties of organic or organometallic materials including macromolecular systems. Therefore the molecular design of liquid crystals to create materials with exceptional properties is a challenging task for chemists in cooperation with physicists, materials scientists and engineers.

What are the main aspects of liquid crystalline materials currently under investigation? Although the different basic molecular geometries and constitutions causing the formation of the liquid crystalline state are known, so far only systems built up by rigid rod-like molecules have proven to be suitable for new applications. This holds for low molar mass as well as for polymeric liquid crystals.

Low molar mass liquid crystals in the nematic phase, in which the rigid rod-like molecules are ordered with respect to their long molecular axis, have been intensively studied both experimentally and theoretically during the last few decades. This was mainly due to their potential applications in optoelectronics, especially for low energy consuming displays: by applying an electric field the preferred orientation of the molecules can be altered (due to the liquid state), which causes a change in the (anisotropic) optical properties. Although this process had already been developed early in the seventies, remarkable progress in the layout of the display cell and in thin film transistor (TFT) technology calls for new designs of liquid crystals. Their chemical constitution has to be optimized with respect to the anisotropic phase properties such as viscosity, dielectric and elastic constants. Several new classes of nematics have been designed, which give a increased output in display technology: super-twisted-nematic (STN) displays are available having high resolution (e.g. for computers) and TFT displays give excellent picture quality for pocket color TV sets or for projection of TV pictures.

Liquid crystals research currently focuses not only on nematics but also on the ferroelectric chiral smectic phases, especially the chiral smectic-C phase. In this phase the rod-like molecules also have long range positional order within layers, with the long molecular axis tilted relative to the layer normal. These ferroelectric liquid crystals allow the production of very fast switching displays, which compete with TFT displays for TV screens. Only a few years ago little was known about these smectics, especially with regard to the relationship between the chemical constitution of the molecules and the temperature regime of the smectic-C phase. Since then intensive research by chemists and physicists has allowed the systematic synthesis and blending of smectics, which can serve technological demands, especially of the optoelectronics industry.

Polymeric liquid crystals have attracted much attention during the last few years. The combination of polymer-specific properties with the anisotropic physical properties of the liquid crystalline state offers wide-ranging possibilities for the design of new materials. Two different types of polymers—both based on rigid rod-like monomer units, yet completely different in application—have been examined: the "LC-main-chain polymers", where the rod like monomer units are within the polymer backbone, and the "LC-side-chain polymers", where the rod like moieties are attached as side groups to the backbone.

Contents

H. Finkelmann
Liquid Crystals—State of the Art 987
W. A. Kaysser, G. Petzow
Advanced Materials by Powder Metallurgy 989
M. T. Reetz
Anionic Polymerization of α-Activated Olefins 994
Conference Report 998
Research News 999
Book Reviews 1001
Conference Calendar 1005

[*] Prof. Dr. H. Finkelmann
Institut für Makromoleculare Chemie der Universität
Stefan-Meier-Strasse 31, D-7800 Freiburg (FRG)

LC-main-chain polymers exhibit an orientational long range order of the polymer main chains in the nematic state. A shear gradient—e.g. during a spinning process—causes a macroscopic alignment of the preferred orientation of the macromolecules. Fibers can be easily obtained, where the polymer main chains are highly ordered in the direction of the fiber axis. This yields outstanding mechanical properties. Due to the orientation of flow the (anisotropic) viscosity was also observed to be lower than the viscosity of amorphous melts, which makes the processing of these materials easier. Furthermore, injection molded samples have very small thermal expansion coefficients in the solid (partially crystalline) state and, as a result, can be used as construction elements, since they hardly change their dimensions with temperature.

For LC-side-chain polymers the most remarkable property is the vitrification process of the liquid crystalline polymer melt. Liquid crystalline polymers—smectic or nematic—do not change their structure when frozen in the glassy state and consequently become *anisotropic glasses*. This means that the liquid crystalline polymer melt can be macroscopically or locally aligned by external electric or magnetic fields and vitrified to the ordered, anisotropic glass, giving solid materials with anisotropic physical properties. The vitrification of ordered ferroelectric chiral smectic-C polymers, for example, might give a completely new class of materials. Furthermore their non-centrosymmetric phase structure makes them suitable for applications in nonlinear optics. Research in this field is, however, still in its infancy.

The enormous potential of LC-side-chain polymers, especially for optical applications, is demonstrated by an example recently developed in our laboratory. The chemical crosslinking of the linear LC-side-chain polymers yields liquid crystalline elastomers ("rubbers"). Mechanical deformation of these elastomers by stretching or compressing causes a macroscopic orientation of the liquid crystalline molecules similar to the electric field orientation of low molar mass liquid crystals. Elastomer films can be prepared, whose macroscopic optical properties are similar to the optical properties of an anisotropic single crystal having the same dimensions. There is, however, an additional feature to these elastomers: a local deformation of the macroscopically aligned film causes a local change of the optical properties. This is schematically shown in Figure 1. If the plane surface of the film is brought into contact with a

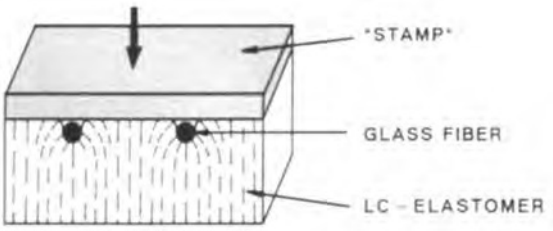

Fig. 1. Schematic drawing of the local deformation of the optical axis of an LC-elastomer by a "stamp" for application as planar light conductor for integrated optics. In this example a smooth stamp presses a glass fiber (10 μm diameter) into the elastomer surface. The arrow indicates the viewing direction parallel to the optical axis (of the undisturbed elastomer) as shown in Figure 2.

"stamp", which has a defined pattern of micron dimensions, the pattern deforms the elastomer surface and consequently the local direction of the optical axis. This can be directly observed in a polarizing microscope with crossed polarizers as shown in Figure 2. It is obvious that this offers a relatively simple technique for producing elements for the integrated optics. Light conducting pathways can be mechanically pressed into the liquid crystalline elastomer film (similar to the production of a record) and durably stored in the glassy state.

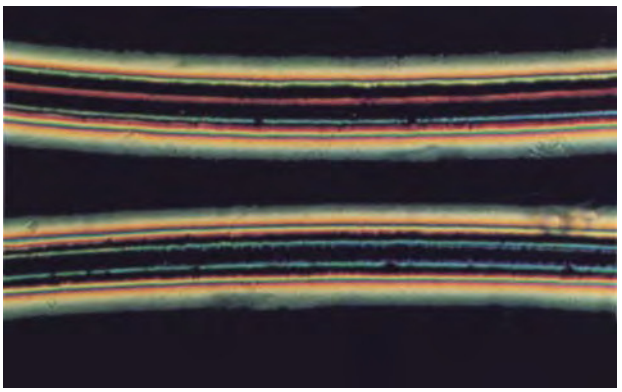

Fig. 2. Polarizing photomicrograph (crossed polarizers) of a locally deformed LC-elastomer. The local change of the birefringence is indicated by the interference pattern. The black area denotes regions where the optical axis of the elastomer is parallel to the viewing direction.

Although the liquid crystalline state of matter was discovered one hundred years ago, it was for many decades regarded only as a laboratory curiosity. The developments in the last twenty years impressively demonstrate the outstanding potential of liquid crystals as technologically relevant advanced materials.

Prof. Dr. Heino Finkelmann is Professor of Polymer Chemistry at the University of Freiburg, FRG. Born in 1945 in Gronau/Alfeld, he first became an engineer. Starting in 1969, he then studied chemistry at the Technical University of Berlin (Diplom in 1972) and at the University of Paderborn, where he earned his PhD under the supervision of H. Stegemeyer. He spent three postdoctoral years with H. Ringsdorf at the University of Mainz, and moved to the Technical University of Clausthal in 1978. Immediately after the Habilitation in 1984 in Clausthal he was offered his current position. He has been awarded the Carl-Duisberg-Gedächtnispreis of the Gesellschaft Deutscher Chemiker and the "Dozentenstipendium" of the Fonds der Chemischen Industrie. Professor Finkelmann is a member of the Scientific Committee of the 12th International Liquid Crystals Conference to be held in Freiburg from 15–19 August 1988.

Advanced Materials by Powder Metallurgy

Ceramics/Intermetallics
Hot Isostatic Pressing
Dispersion Hardening
Rapid Solidification

By Wolfgang A. Kaysser* and Günter Petzow

1. Introduction

One of the techniques which have an inherent potential to produce some of the future's tailored, high-tech materials is powder metallurgy (PM). The efficient use of powder metallurgy depends both on a scientific understanding of the complex physical and chemical problems of powder production, handling, forming and consolidation and on highly developed complex engineering capabilities. The interaction between materials science and engineering is a characteristic feature of the new powder metallurgy.

From the ancient powder forged pillar of Delhi to the present, powder metallurgy has shown itself to be a potent method for forming special, artificial materials when no other techniques are available due to high melting points or bad machinability of the materials or microstructures not obtainable by other techniques. PM high-tech materials must be fine grained and completely free of pores. Mechanisms of powder densification and simultaneous microstructural changes are therefore of major technical and scientific interest.

The basic steps of conventional powder metallurgy are powder preparation, handling, shaping, and consolidation.[1] Powders may be produced by chemical reactions from precursors or by disintegrating solid or liquid bulks. The powders are shaped in dies under uniaxial load or put into thin-walled capsules and isostatically pressed. The shaped compacts contain pores between the individual particles which amount to porosities between 60 and 10 vol-%. One of the purposes of the subsequent sintering, a heat treatment below the melting temperature of the major constituents, is to eliminate the pores; the process is driven by a reduction in solid–vapor interface area. Porosity reduction requires an increasing fraction of solid material in each unit volume cell by rearrangement or by shape change of the particles (Fig. 1 top).

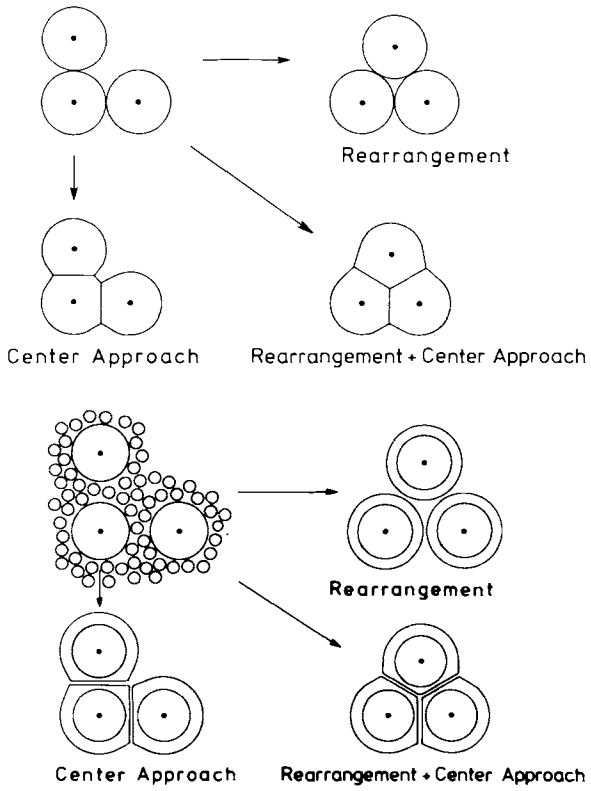

Fig. 1. Shrinkage by rearrangement and center approach (shape change) during sintering. Top: Monosized grains without coarsening. Bottom: Grains with broad size distribution and coarsening.

2. Advanced PM Materials by Pressureless Sintering

Shape change or center to center approach during solid state sintering occurs in a quantified way when vacancies diffuse from pores into the grain boundaries where they are subsequently eliminated. Unfortunately, the transport of vacancies to the grain boundary sinks by bulk diffusion or by grain boundary diffusion does not provide complete densification in metal powders of sizes between 1 and 100 μm. In the final stage of sintering, when the porosity is below 6%, the continuous pore channels transform into isolated pores which lie at grain boundaries. If the pores are too small to hold the grain boundaries, but too large, and therefore too immobile, to move along with the grain boundaries, grain boundaries and pores separate during regular grain growth (Fig. 2). Pores that are trapped inside the grains shrink at much lower rates than pores at grain boundaries, and they are therefore deleterious for densification. Powders can be sintered to full density if the diffusion mechanism controlling the vacancy transport from the

[*] Dr. W. A. Kaysser, Prof. Dr. G. Petzow
Max-Planck-Institut für Metallforschung
Institut für Werkstoffwissenschaften
Pulvermetallurgisches Laboratorium
Heisenbergstrasse 5, D-7000 Stuttgart 80 (FRG)

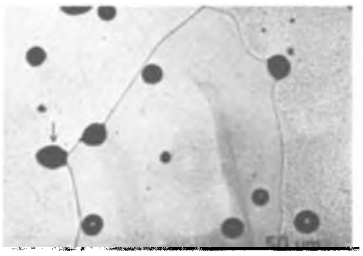

Fig. 2. Microstructure showing pore drag (asterisk) and pore/grain boundary separation (arrow) after final stage sintering of W – 0.15 wt.-% Ni at 1400°C for 3 h.

pores to the grain boundaries is enhanced and if the grain boundary mobility is decreased by additives. These basic principles were successfully applied to obtain translucent ceramic materials for sodium vapor pressure lamps. The dense alumina (Lucalox) can be produced by pressureless sintering when the bulk diffusivity is enhanced and the grain boundary mobility is reduced by doping the powder with less than 1000 ppm magnesia.[2]

The bulk diffusivity of metals, which controls a major transport path for vacancies from the pore to the grain boundary via diffusion through the bulk, can only be moderately increased by doping with small amounts of an alloying metal additive. The enhancement of the grain boundary self-diffusion, which controls a second major transport path for vacancies, as in W doped with Ni,[3] however, also increases the grain growth rate leading to increased pore/grain boundary separation.

The metallic materials produced by pressureless sintering, such as hard metals, heavy metal alloys and permanent magnets, are all sintered in the presence of a liquid phase, which reflects the problems of sintering to a pore-free material in the solid state, but also indicates the ability to obtain dense materials by liquid phase sintering. The microstructural development and the shrinkage during sintering in the presence of a liquid phase are governed by a number of basic principles.[4] At sintering temperatures in all materials one or more phases are solid and at least one phase is liquid. After processing the microstructure consists often of two solid (sometimes interpenetrating) networks. Densification during liquid phase sintering is also based on rearrangement and shape change of the solid constituent particles (Fig. 1 bottom). The driving force for both phenomena results from a decrease in energy caused by changes in the areas of the liquid/vapor, liquid/solid and solid/vapor interfaces during rearrangement and/or shape change. Melt may originate from low melting point particles or areas which have built low melting point compositions by diffusion during heating. With good wetting, the liquid phase is pulled by capillary forces into particle necks and small pores. As a reaction to the capillary forces, particles are rearranged if their mobility allows it. This rearrangement of the solid particles is a necessary prerequisite for effective densification throughout the sintering process even during later sintering stages, when, for example, the rates of particle shape change also limit the rearrangement rate. Shrinkage due to the shape change of the solid constituents always involves solution-reprecipitation processes, e.g., when during coarsening by diffusion controlled Ostwald ripening the grains accommodate their shape to a changing environment.[5] This is shown in Figure 3 for liquid phase sintering of Mo-Ni by internal etching boundaries. A major part of the shrinkage results from rearrangement when small particles are dissolved making way for the movement of larger particles (see also Fig. 1 bottom).

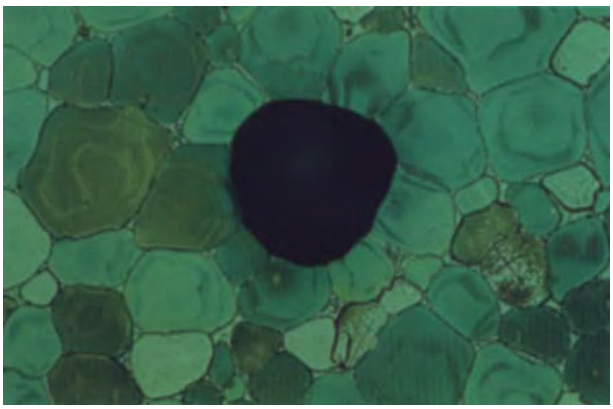

Fig. 3. Microstructure of Mo-4wt.-% Ni after cyclic liquid phase sintering between 1300 and 1460°C (Held at 1460°C for 30 min in each cycle). Etched with *Murakami*'s solution. [5] The bulk material is densely packed; the center is a pore. Scale: 24 mm equal 10 μm.

Due to the effective shrinkage mechanisms liquid phase sintering yields dense PM materials. As shown above, densification requires grain growth and rearrangement. Complete elimination of pores is thus limited to systems where either powders are fine initially or where large amounts of a suitable liquid phase are available. Typical examples of liquid phase sintered high performance materials are hard metals (e.g. WC-Co cutting tools) or hard magnets (e.g. Fe-Nd-B shown in Figure 4[6]).

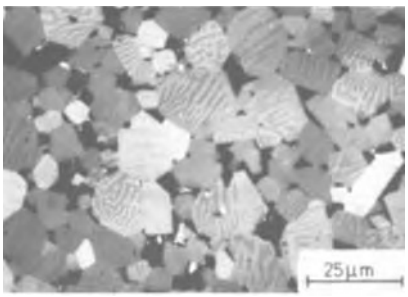

Fig. 4. Pore free microstructure of liquid phase sintered Fe-18.5Nd-6.5B. The magnetic grains are indicated by line patterns (Kerr effect). The black areas are solidified eutectic melt.

3. Advanced PM Materials by Pressure Assisted Consolidation

For most of the complex alloy systems fine powders and suitable melt phases are not available. The powder metal

lurgical production of these advanced materials of great commercial interest only became possible when, mainly in the early eighties, modern engineering provided production facilities for powder consolidation where heat (as during sintering) and pressure (as during compaction) could be applied simultaneously. The simultaneous application of pressure and heat allows the use of comparatively coarse, prealloyed powders with complex microstructures and high yield strength. Densification is readily attained without solid state sintering additives and without the presence of a liquid phase. The processes most frequently used are hot isostatic pressing and hot extrusion.

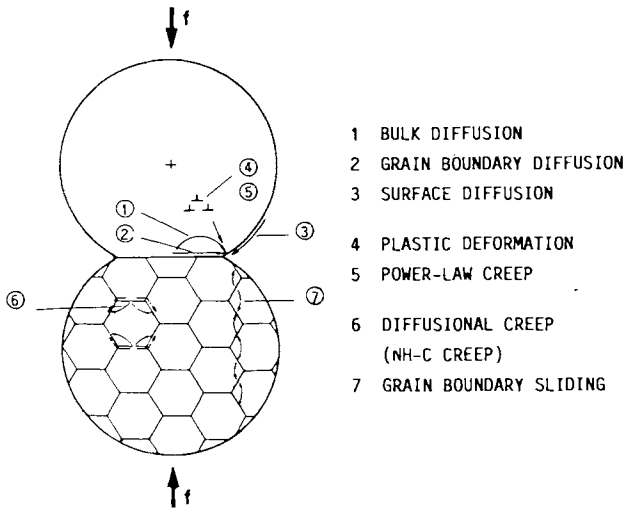

Fig. 5. Transport mechanisms during hot isostatic pressing. f = force.

During *hot isostatic pressing* (HIPing) plastic flow and a number of creep mechanisms contribute to densification (Fig. 5).[7,8] Which one of these mechanisms dominates shrinkage and neck growth rate depends on a number of powder parameters (size, grain size, current geometry, bulk material properties, interface properties) and processing parameters (pressure, temperature, time). The neck growth and center approach rates are described by analytical equations but can also be predicted from the deformation of single powder particles under a well controlled load in a dilatometer.[8] These experiments indicate power-law creep as the dominant densification mechanism for most metal alloys.

During normal HIPing the powders must be encapsulated in closed thin-walled preforms, a tedious and costly operation. In 1985 a new method, sinter-HIPing, started to come into use.[9] The development became possible through the construction of improved HIP equipment with pressure vessels which allow dewaxing of binders, often added to the initial powder mixtures for superior handling, vacuum sintering and subsequent HIPing in one cycle. The vacuum sintering is performed to closed porosity (porosity below 6%), i.e. to a state where all pores are separated from each other and completely enclosed in a dense material matrix. The sources for the closed pores are not limited to the usual porosity remaining from the starting porosity in dense randomly packed powder arrangements, but may also stem from undestroyed initial powder agglomerates, inhomogeneous flow of powder particles during mould filling or inhomogeneous drying in slip cast greens. The elimination of these larger pores, which constitute critical defects in the final material, during HIPing or sinter-HIPing makes the PM materials often superior to cast materials which frequently contain casting porosity. Figure 6 shows the collapse of a large pore during HIPing of presintered Al_2O_3-anorthite by a combined flow of Al_2O_3 grains and the anorthite glass.[9]

Fig. 6. Closing artificial pore in presintered Al_2O_3-10 vol-% anorthite after HIPing at 10 MPa for 30 min. The arrows indicate the formation of special boundaries by coalescence of the Al_2O_3 grains.

As mentioned above, the use of HIPing or hot extrusion provides dense materials also from unsinterable particulate combinations, such as short-fiber reinforced composites and oxide dispersion strengthened high-temperature alloys. Mixtures of fibers of high strength and high stiffness with fine powders are consolidated at temperatures low enough to avoid fiber decomposition by chemical reactions with the matrix, but sufficient to allow adequate bonding of the fibers to the matrix. Whereas reinforcement of metals and ceramics with long fibers was found economically unviable, *short-fiber reinforcement*, particularly with SiC whiskers, is seen to offer a more favorable cost property-improvement ratio.[10] At present the most frequently investigated systems are SiC-whisker reinforced Al_2O_3, Si_3N_4, and Al alloys.[10] A number of technical and economic problems are, however, still unsolved. The SiC whiskers are too expensive. The distribution of the whiskers in the fine powder matrix and sintering to closed porosity as well as chemical reactions between the whiskers and the matrix require further research.

Oxide dispersion hardened Al alloys or superalloys are produced by reaction milling in an attritor. During milling, surface oxides on the powder are destroyed and finely distributed in the interior of the powders together with other intentionally added fine oxide powders due to a continuing fracture and rejoining sequence.[11] A modification of this method is the reaction milling of a mixture of Al and graphite powder which provides an extremely homogeneous distribution of fine graphite inclusions in the Al matrix.[12] During tempering of the hot extruded milled blends, fine Al_4C dispersoids form at the sites of the fine graphite inclusions (Fig. 7). The tensile strength of this material at 400 °C is 50% of the room temperature tensile strength.

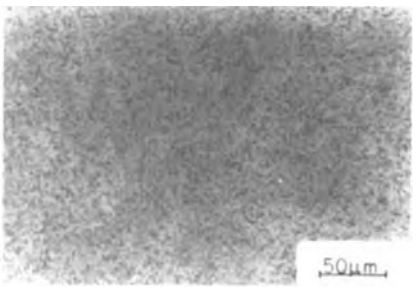

Fig. 7. Microstructure of a dispersion hardened Al alloy (DISPAL 1 Si 12 transv.).

HIPing and other new consolidation methods such as hot extrusion also allow fast densification and defect healing of coarse, unsinterable powders with unusual microstructures. Such powders are produced by *rapid solidification*; high cooling rates and high undercooling result in refined microstructures, decreased segregation, metastable and new phases, as well as in increased solid-solubility ranges. Gas or water atomization are valuable methods for producing rapidly solidified powders for high-performance materials in large quantities. With these methods a thin falling stream of the molten alloy is disintegrated into fine droplets by the impact of high pressure gas or water jets.[1]

An important aspect of the *microstructural refinement* is the cooling rate of the droplets which determines the velocity of the solidification front. The cooling rate is governed by the convective heat transfer from the droplet to the surrounding flowing gas. The cooling rates range from 10^4 to 10^7 K s^{-1} for droplets of 50 µm (argon) to 5 µm (helium) in diameter, respectively. For a special group of advanced PM materials fine microstructures are not sufficient, but *segregation-free microstructures* are required. They allow the formation of highly supersaturated solid solutions yielding a large amount of extremely fine precipitates during ageing. These are often stable against further coarsening due to a low equilibrium solid solubility of the alloying elements in the solvent at service temperatures. Segregation-free solidification is only possible if the growth velocity of the solidification front is larger than the diffusion speed of the solute atoms.[13] In Cu-7wt.-%Sn a solidification-front velocity of about 4 m s^{-1} is required for segregation-free solidification, which is high compared to the velocity of 0.02 m s^{-1} obtained during cooling of an atomized 5 µm droplet. To attain a sufficiently fast solidification-front movement in fine melt droplets, considerable undercooling of the liquid is necessary. Undercooling is possible if potent heterogeneous nuclei are absent. The probability of a potent heterogeneous nucleus being present in a droplet decreases rapidly with decreasing droplet volume. The percentage of powder particles which have solidified after considerable undercooling increases rapidly with decreasing particle size. Due to extensive engineering efforts and the application of advanced principles of fluid mechanics, facilities are now available for producing the required fine powders in large quantities.

From the abundance of recent developments of materials from rapidly solidified powders, three examples are presented. The first example, the aluminides, illustrates the beneficial use of high cooling rates to obtain finer microstructures. The other two examples, a dispersion strengthened Cu-Sn alloy and a Cu-Ti-B alloy, are indicative of the advantages of high undercooling.

Iron aluminide and nickel aluminide *intermetallics* have recently been the object of considerable interest as potential structural materials for high temperature applications. The cubic DO_3 (Fe_3Al), $L1_2$ (Ni_3Al), and B2 (FeAl, NiAl) lattice structures yield special properties such as a low density (compared to the superalloys), high strength and high elastic moduli which make them interesting for lightweight applications in the aerospace industry. Excellent corrosion resistance up to 800 °C with high yield strength at elevated temperatures open a wide field in coatings, especially in oxygen-rich hot gases, with an optimum relation of price to performance. A major problem of coarse-grained intermetallics is their extreme brittleness, whereas single crystals and polycrystals with grain sizes smaller than 20 µm display considerable ductility at room temperature.[14] The reasons for the failure of coarse-grained materials are the weak grain boundary structures and the sensitivity of grain boundaries to segregation of impurity atoms. Several remedies exist to improve the unfavorable properties, the most promising one being the use of rapid solidification to obtain fine-grained materials. Figure 8 top shows Ni_3Al powder with an average grain size below 15 µm which was obtained by Ar atomization.[15]

A homogeneous distribution of fine oxides, giving a *dispersion strengthened material*, can be obtained directly from rapidly solidified melts. The Ar-atomized Cu-7Sn particle shown in Figure 8 bottom has an area where segregation-free solidification occurred. Undercooling was increased by minimizing the number of potent nuclei. With the addition of Al, the metal oxides which were the initial potent nuclei of the melt were transformed into fine, dispersed Al_2O_3 particles of low potency. A homogeneous distribution of Al_2O_3 particles was obtained in areas which

ADVANCED MATERIALS

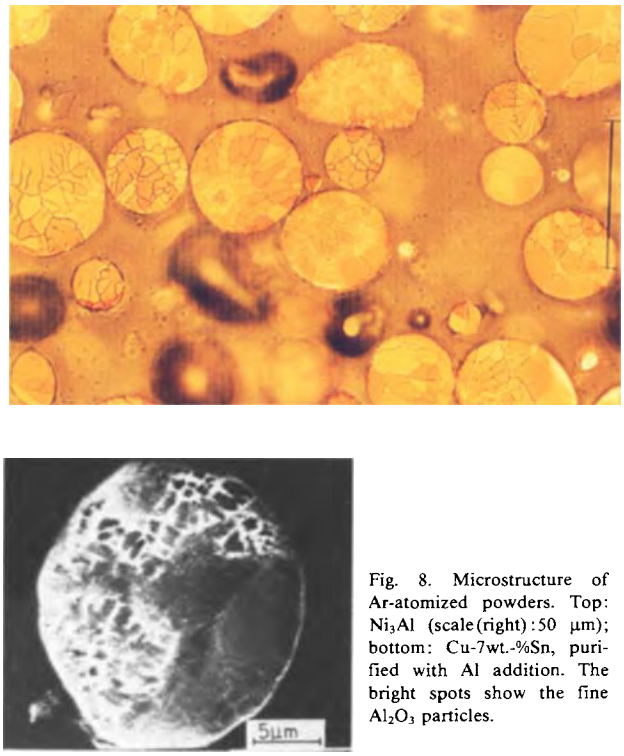

Fig. 8. Microstructure of Ar-atomized powders. Top: Ni_3Al (scale(right): 50 µm); bottom: Cu-7wt.-%Sn, purified with Al addition. The bright spots show the fine Al_2O_3 particles.

solidified segregation-free[16] (small bright spots in Fig. 8 bottom).

Cu-Ti alloys are mainly used as electric conductors and contact materials with increased microhardness and only slightly reduced electrical conductivity compared to unalloyed Cu.[17] The mechanical and electrical properties of Cu-Ti can be further improved by the addition of boron resulting in *dispersion hardened copper alloys* for welding machines, where a high microhardness is obtained by additional dispersion strengthening. If suitable amounts of B and Ti are added to Cu, extremely stable TiB_2 precipitates form during ageing with a negligible amount of Ti and B remaining in the solid solution, providing an increased hardness at high electrical conductivity. However, during cooling of ternary Cu-Ti-B melts at rates below 10^4 K s^{-1} the primary solidification of TiB_2 yields precipitates, which are too coarse for effective precipitation hardening. In atomized powders the primary precipitation of TiB_2 during solidification is suppressed due to undercooling and a high cooling rate. Ti and B remain in a supersaturated Cu solid solution, which provides a hardness of more than 500 $HV_{0.1}$ after ageing the powders at moderate temperatures.[18]

4. Outlook

Powder metallurgy (PM) is now recognized by most of the governments of the industrial nations to be key technology in the development of advanced materials. For example, in 1987, the Bundesministerium für Forschung und Technologie invested no less than 60 million DM in support of the German PM research and development program. Faith in the potential of powder metallurgy rests on two factors:

- PM can satisfy the demands of specific material requirements. The inherent flexibility of PM materials, as compared to cast materials, results from an almost unlimited number of workable phase combinations, which include ceramics, polymers and metals. PM is one of the most promising techniques for the production of complex composites.
- PM enables the production of refined, homogeneous and highly supersaturated materials. New classes of materials can be used, which require small grain sizes, such as the intermetallic phases.

Powders are increasingly being used for the production of thin layers and layered structures. The plasma spraying of powders has already established itself as one of the most important methods for the production of high quality surface coatings. The spray deposition of atomized liquid droplets onto substrates is increasingly serving the same purpose. Fine droplets form a rapidly solidifying thin liquid layer on a substrate. The latter method smoothly bridges the gap between PM and casting technology.

Received: March 28, 1988

[1] *Metals Handbook, 9th Ed., Vol. 7, Powder Metallurgy*, coordinator E. Klar, American Society for Metals, Metals Park, OH, USA 1984.
[2] W. A. Kaysser, M. Sprissler, C. A. Handwerker, J. E. Blendell, *J. Am. Ceram. Soc. 70* (1987) 339-343.
[3] W. A. Kaysser, M. Hofmann-Amtenbrink, G. Petzow in G. C. Kuczynski, D. P. Uskokovic, H. Palmour III, M. M. Ristic (Eds.): *Sintering '85*, Plenum Press, New York 1987, p. 121-132.
[4] W. A. Kaysser, G. Petzow, *Powder Metall. 28* (1985) 145-150.
[5] S.-J. L. Kang, W. A. Kaysser, G. Petzow, D. N. Yoon, *Acta Metall. 33* (1985) 1919-1926.
[6] G. Schneider, E.-Th. Henig, H. H. Stadelmaier, G. Petzow, *Proc. 5th Int. Symp. Magn. Alloys*, Bad Soden, FRG 1987, p. 347-362.
[7] E. Arzt, M. F. Ashby, K. E. Easterling, *Metall. Trans. A 14* (1983) 211.
[8] W. A. Kaysser, M. Aslan, E. Arzt, M. Mitkov, G. Petzow, *Powder Metall.*, in press.
[9] W. A. Kaysser, M. Aslan, G. Petzow in H. Kolaska (Ed.): *Sinter/HIP-Technologie*, Schmid-Verlag, Freiburg, FRG 1987, p. 67-86.
[10] R. F. Singer, M. J. Couper in W. J. Huppmann, W. A. Kaysser, G. Petzow (Eds.): *Powder Metallurgy 1986—State of the Art*, Schmid-Verlag, Freiburg, FRG 1986, p. 177-204.
[11] J. S. Benjamin, M. J. Bonaford, *Metall. Trans. A 8* (1977) 1301.
[12] G. Jangg, F. Kutner, G. Korb, *Powder Metall. Int. 9* (1977) 24-26.
[13] W. J. Boettinger, S. R. Coriell in P. R. Sahm, H. Jones, C. M. Adam (Eds.): *Science and Technology of the Undercooled Melt (NATO ASI Series E, No. 114)* Martinus Nijhoff, Dordrecht 1986, p. 81-110.
[14] E. M. Schulson, *J. Powder Metall. 23* (1987) 1.
[15] R. Laag, W. A. Kaysser, G. Petzow, *Proc. VIIIth Yugoslav-German Meeting on Materials Science and Development, 18-21 May*, Brdo pri Kranju, Yugoslavia, in press.
[16] K. Rzesnitzek, W. A. Kaysser, G. Petzow, *Proc. VIIIth Yugoslav-German Meeting on Materials Science and Development, 18-21 May*, Brdo pri Kranju, Yugoslavia, in press.
[17] H. Schreiner, *Powder Metall. Int. 17* (1985) 195-198.
[18] D. Bosic, R. Laag, W. A. Kaysser, M. Mitkov, G. Petzow, *Proc. VIIIth Yugoslav-German Meeting on Materials Science and Development, 18-21 May*, Brdo pri Kranju, Yugoslavia, in press.

ADVANCED MATERIALS

New Methods for the Anionic Polymerization of α-Activated Olefins

Group Transfer Polymerization
Metal-free Polymerization
Living Polymers

By Manfred T. Reetz*

1. Introduction

One of the exciting developments in current polymer research concerns the controlled polymerization of monomers with formation of macromolecules having a defined molecular weight and a narrow molecular weight distribution. If a given process has the additional feature of yielding living polymers, such interesting reactions as functionalizations of the chain end and/or block and graft polymerizations are possible. The costs of these polymerizations may be higher than those of traditional processes lacking such characteristics. However, in certain applications this may be offset by the favorable properties of the polymers.

In recent years several different types of polymerizations have been developed with the aim of fulfilling some or all of the above mentioned requirements. These include cationic polymerizations of isobutylene and other electron rich olefins,[1] polymerization of cyclic olefins using olefin metathesis,[2] and anionic polymerizations of α-activated olefins such as acrylic and methacrylic acid esters.[3-12] This report deals with the latter area, with emphasis on the author's own research.

2. Group Transfer Polymerization

In 1983 *Webster* and co-workers at Du Pont startled the scientific community by introducing the so-called group transfer polymerization (GTP) of methacrylic acid esters **2** and other α-activated olefins.[3] Accordingly, the *O*-silyl ketene ketal **1** functions as the initiator in combination with a nucleophilic or electrophilic catalyst, e.g., fluorides or Lewis acids, respectively. It turned out that the former are better suited. Such fluorides as HF_2K, $FNnBu_4$ or $[Me_3SiF_2][S(NMe_2)_3]$ induce the quantitative polymerization of **2** at *room temperature* with formation of polymers having a narrow molecular weight distribution, i.e., *D* values of <1.3 ($D = M_w/M_n$; ratio of the weight average molecular weight to the number average molecular weight). Such results are significant because the classical anionic polymerization of methacrylates using hindered alkyllithium initiators requires low temperatures (-20 to -70 °C),[4] which is uneconomical.

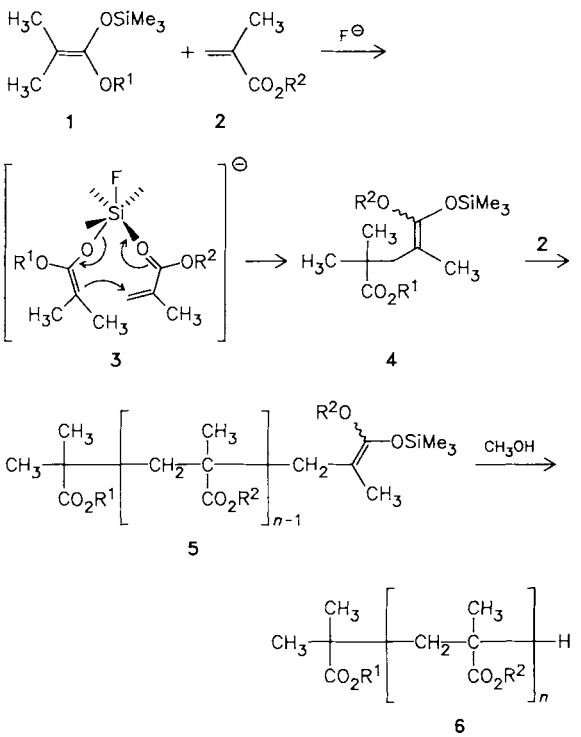

R^1 = CH_3, *n*-alkyl, $CH_2CH_2OSiMe_3$
R^2 = CH_3, *n*-alkyl, allyl

The mechanism of GTP involves activation of the initiator by fluorides to form a pentavalent silicon species which then undergoes Michael addition to the monomer via the hexacoordinated intermediate **3**. Although the details of this step are still being studied,[5] it became clear that the silyl group migrates to the oxygen atom of the monomer, forming a new *O*-silyl ketene ketal **4** which in turn undergoes another Michael addition. Labeling experiments

[*] Prof. Dr. M. T. Reetz
Fachbereich Chemie der Universität
Hans-Meerwein-Strasse, D-3550 Marburg (FRG)

ADVANCED MATERIALS

show that the silyl groups remain attached to the growing chain, i.e., they do not jump to other chains.[6]

The molecular weight can be controlled by the amount of monomer added relative to the quantity of initiator used. Most of the reported molecular weights M_n lie between 1000 and 20000. There appear to be very few chain transfer or terminating events, which means that in a practical sense the polymers are living. Following the termination of a given polymerization, the same or a different methacrylic acid ester can be added, resulting in the continuation of polymerization.

Since the R^1 group in the initiator **1** can contain a protected functional group (e.g., $CH_2CH_2OSiMe_3$), one end of the polymer may bear a functional group (e.g., OH following hydrolytic deprotection) which can be used as an anchor point for the formation of graft polymers. Such functionalized polymers (chelic polymers) are useful for the production of dispersing agents and ABA block polymers.[7] Functionalization, coupling and dimerization at the chain end have also been reported.[3,7]

Since the details of the Dupont process have been delineated elsewhere,[7] no further information is given here, except to point out that *acrylic* acid esters were reported to cause problems.[7,8] Nucleophilic catalysts lead to broad molecular weight distributions. Lewis acid catalysts, especially ZnX_2, are better suited. They activate the monomer by coordinating at the carbonyl function. However, it was reported that the polymers are no longer living at room temperature, i.e., renewed addition of monomer following the termination of polymerization did *not* lead to a continuation of polymerization.[8]

It is generally accepted that the anionic polymerization of acrylates is more difficult than that of methacrylates.[4,7] Not only are the former monomers more reactive, but also the polymer chain contains C–H acidic positions which undergo undesirable deprotonations (metalations). In spite of this, we attempted the GTP of acrylic acid esters at room temperature using silylated thiols **7** as initiators. We were pleased to discover that ZnI_2 as catalyst (only 1% with respect to the *initiator*!) induces the quantitative polymerization of **8** in toluene with formation of *living* acrylates having excellent *D*-values (≈ 1.1).[9] Functionalized initiators (e.g. **7b**) behave similarly. This paves the way for preparing block, graft, chelic and telechelic polymers. In the polymerization of **8b** with **7b**/ZnI_2, further monomer was added at room temperature three hours after termination of polymerization; this led to a continuation of the polymerization with quantitative formation of a polymer having a molecular weight distribution which is only slightly broadened ($D = 1.25$). Following aqueous work-up, the isolated polymers are stable at higher temperatures, e.g., heating at 260 °C for three hours causes no loss of sulfur.[10]

The success of group transfer polymerization rests upon the migration of covalently bonded *O*-silyl groups along the polymer chain under mild conditions,[3,9] in contrast to the highly polar lithium enolates in classical anionic polymerization. The reactivity is expected to increase in the following sequence: Si-enolates < Li-enolates < K-enolates < NR_4-enolates. At first glance the ionic end of the scale, i.e., a metal-free system with ammonium as the counterion, might be expected to lead to disastrous results at room temperature. Nevertheless, we decided to venture into this area.

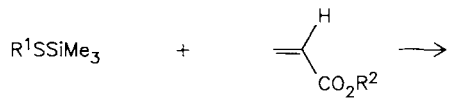

7a, $R^1 = CH_3$ **8a**, $R^2 = CH_3$
7b, $R^1 = CH_2CH_2OSiMe_3$ **8b**, $R^2 = n$Bu
7c, $R^1 = Ph$

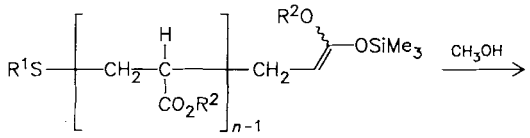

9

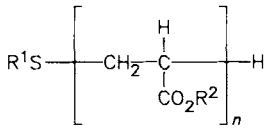

10

3. Metal-free Anionic Polymerization

We turned first to ammonium thiolates RSN*n*Bu$_4$ as initiators for the anionic polymerization of acrylic acid esters.[11] They are accessible by deprotonation of the corresponding thiols by HON*n*Bu$_4$ or by treating the sodium thiolates with ClN*n*Bu$_4$.

Upon adding methyl or *n*-butyl acrylates to the initiators at *room temperature* in the absence of catalysts, essentially quantitative formation of polyacrylates was observed! Equally surprising is the discovery that under proper conditions the molecular weight distribution is very narrow.[11] The best results are obtained in acetonitrile, nitrobenzene or mixtures of nitrobenzene and THF, whereas dimethyl sulfoxide (DMSO) should be avoided. Typically, the initiator **11a** induces the polymerization of *n*-butyl acrylate at room temperature in acetonitrile, *D* being 1.15 (M_n(calc.) = 1.37; M_n(obs.) = 1.28; $M_w = 1.47$).

Mechanistically, the ammonium thiolates undergo rapid Michael additions to form an ammonium enolate **12** which in turn sets the stage for further Michael additions. In the case of the functionalized initiator **11c** the polymer has a hydroxy group on one end following acidic work-up, the *D* value being 1.14. In spite of the above positive aspects, the method has several limitations. The initiators are generally not stable for long periods of time due to decomposition via dealkylation of the ammonium ion. Moreover,

when aiming at molecular weights of >2000, the M_n(obs.) values are much too low. This can be attributed to a side reaction involving thiolate elimination at one end of the polymer chain, a chain terminating process that is induced by the basic nature of the chain end.[11] The eliminated thiolate then starts a new chain. Since the *D* values are also poor in such cases, the process is limited to the synthesis of low molecular weight polymers. It is nevertheless important to note that sodium and lithium *n*-butylthiolates in acetonitrile are inefficient initiators, leading to incomplete polymerization and broad molecular weight distributions ($D > 3$).[11]

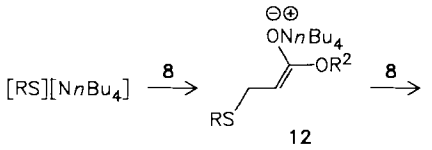

12

11a, R = *n*Bu

11b, R = Ph

11c, R = $CH_2CH_2OSiMe_3$

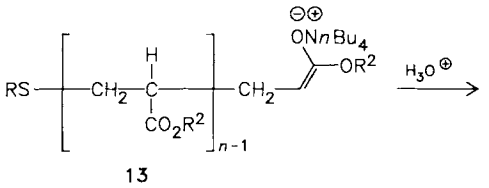

13

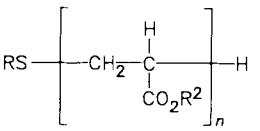

14

In order to eliminate the above drawbacks, we explored the possibility of employing metal-free carbon nucleophiles as initiators.[12] In particular, C-H-acidic compounds were deprotonated with $HONnBu_4$ or their sodium salts treated with $ClNnBu_4$ to form the resonance-stabilized compounds **15**–**17**. They are stable at 0°C for months and can be handled at room temperature without any decomposition.

$[RC(CO_2R')_2][NnBu_4]$

15a, R = R' = C_2H_5

15b, R = C_2H_5, R' = CH_3

$[CH_3C(CN)_2][NnBu_4]$

16

$[(CH_3)_2CNO_2][NnBu_4]$

17

Although a number of ammonium carbanions have been reported, they were generally not fully characterized.[13] In the present case the compounds were studied by NMR and IR spectroscopy.

Upon adding *n*-butyl acrylate to solutions of **15** at room temperature, a spontaneous exothermic reaction was observed with formation of polyacrylate (>95% conversion to **19** after aqueous workup). Thus, the doubly stabilized initiators **15** add in a Michael fashion to form less stabilized carbanions **18** which then continue chain growth until no more monomer is added. It is possible to add a different *n*-alkyl acrylate immediately following the consumption of monomer and to continue the polymerization with formation of a polymer having two well defined blocks.

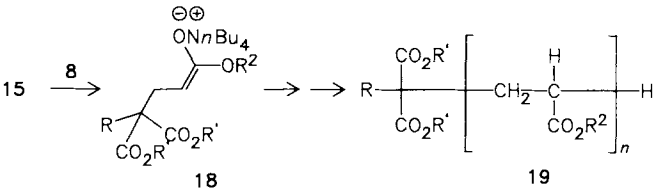

18 **19**

In contrast to the previous oligomerizations induced by thiolate anions, this new method allows the synthesis of polymers having molecular weights of >2000.[12] Moreover, the molecular weight distributions are surprisingly good (Table 1). For example, when aiming for a molecular weight of ca. 20000, M_n(calc.) and M_n(obs.) agree well, and the *D* value is 1.3 (entry 10 of Table 1). The other initiators also induce the polymerization of *n*-butyl acrylate, although the nitrostabilized initiator appears to be less efficient (entries 15 and 16 of Table 1).

Table 1. Polymerization of *n*-butyl acrylate **8b** at room temperature [a].

Entry	Initiator	Solvent	M_n(calc.) [kg mol^{-1}]	M_n(obs.) [kg mol^{-1}]	*D*
1	**15a**	THF	1.15	0.90	1.16
2	**15a**	THF	5.32	3.13	1.36
3	**15a**	THF	10.44	7.42	1.25
4	**15b**	THF	1.44	1.51	1.50
5	**15b**	Toluene	1.44	0.64	1.37
6	**15b**	THF	5.29	5.86	1.30
7	**15b**	Toluene	5.29	6.82	1.36
8	**15b**	Toluene	10.41	10.92	1.30
9	**15b**	THF	20.67	17.43	1.38
10	**15b**	Toluene	20.67	20.39	1.30
11	**16**	THF	1.36	0.61	1.14
12	**16**	Toluene	1.36	0.71	1.61
13	**16**	THF	5.21	2.59	1.43
14	**16**	Toluene	5.21	4.21	1.34
15	**17**	THF	1.37	0.85	2.71
16	**17**	Toluene	1.37	1.25	2.18

[a] During polymerization the temperature rises by 10–20°C.

In a similar manner, dianions such as **20** are effective initiators in the polymerization of *n*-butyl acrylate (e.g., M_n(calc.) = 1717; M_n(obs.) = 1624; $D = 1.1$).[12]

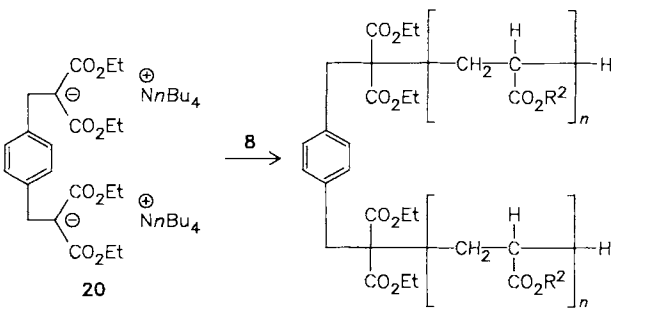

20 **21**

ADVANCED MATERIALS

It is difficult at present to explain why the ammonium carbanions are such excellent initiators at room temperature. One of the major chain-terminating processes of the classical anionic polymerization of acrylates and methacrylates is the "back-biting" reaction.[4] This intramolecular Claisen condensation requires a metal ion such as $Li^{\oplus}$ or $Na^{\oplus}$ for the activation of the ester group and the ready expulsion of alkoxide ions (cf. **22** → **23** + **24**). In the case of the present system, metal complexation is not possible. Even if the (reversible) addition step were to occur, it is likely that elimination of "naked" alkoxide is a kinetically and thermodynamically unfavorable process, certainly in comparison to chain propagation involving electrophilic monomers. Nevertheless, it remains to be tested how long the chain end survives following the complete consumption of monomer and prior to the addition of electrophiles (e.g., more monomer or $H_3O^{\oplus}$). It should be mentioned that the sodium salts of the above initiators are inefficient, leading to incomplete conversion and poor D values (>3).[12]

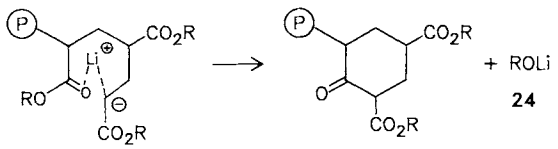

P = Polymer

Although detailed studies remain to be carried out, it is interesting to speculate about the mechanism. Strong electrostatic attractive forces between the anionic chain end and the ammonium counterions are likely to be involved.[11, 12] Molecular orbital calculations on tetraalkylammonium ions show that the positive charge is *not* localized on the nitrogen atom as indicated by the traditional representation **25**, but rather on the four α-carbon atoms, see **26**.[10] This means that a tetraalkylammonium ion has a tetrahedral distribution of charge.

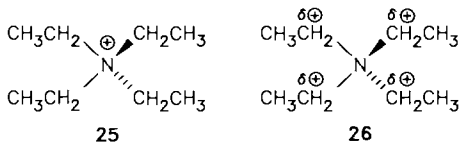

The monomer may well approach one corner of the tetrahedron; this process might be looked on as a kind of solvation. As the Michael addition then proceeds, the ester function turns into the new enolate chain end. Concomitantly, the previous enolate becomes an ester function along the chain, perhaps solvating intramolecularly until the next monomer approaches. In line with these speculations is the observation that bulky ammonium ions such as tetraoctylammonium are not well suited for metal-free polymerizations.[10] The reactions are often sluggish, leading to polymers with broad molecular weight distributions. The long groups pointing from the tetrahedral positions probably prevent a tight and ordered transition state.

Experiments directed toward the synthesis of ammonium malonates having protected functional groups are in progress.[10] A different strategy for the preparation of chelic polymers pertains to the reaction of the carbanion **27** bearing a hydrogen atom at the reactive center. We discovered that in 1 : 1 reactions with various Michael acceptors smooth exothermic additions occur. Following the complete consumption of the reaction components at room temperature, the crude product was quenched with methyl iodide. The products turned out to be **31** and **33**, which means that proton transfer occurs (e.g. **29** → **30**) prior to alkylation.[10] Thus, the initiator **30** can be prepared without undesired polymerization of the very reactive acrylonitrile! This chemistry also suggests that an easily hydrolyzable ester (e.g., **8**, R^2 = *tert*-butyl) should react in the same manner, i.e., the *in situ* preparation of initiators of the type **32** (R^2 = *tert*-butyl) is probably an easy task. In experiments already performed, the nucleophilic *end* of the chain was *O*-silylated with Me_3SiCl.[10]

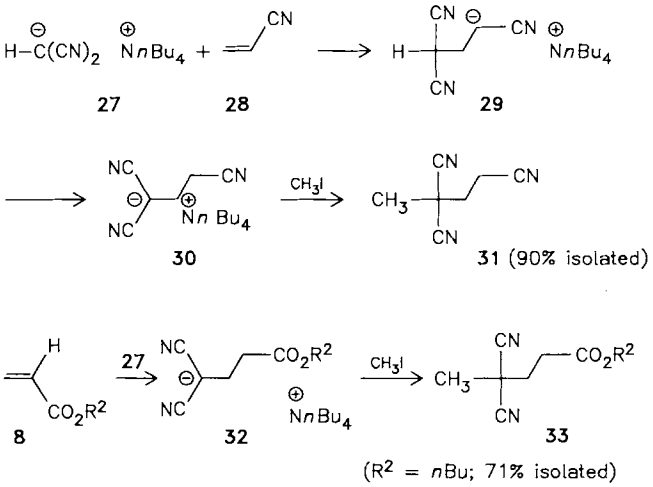

Finally, other α-activated olefins such as the extremely reactive acrylonitrile[10] as well as the less reactive methacrylates[12] can also be polymerized in a controlled manner. In the latter case the nitro-stabilized carbanion **17** is the best initiator, although an induction period of 30–60 s is generally observed.

4. Conclusions and Applications

Free radical initiation remains the method of choice for the production of high molecular weight homopolymeric acrylates and methacrylates. However, GTP with formation of living polymers results in a number of structural features generally not accessible by radical processes: narrow molecular weight distribution, controlled introduction of end groups, segmentation of chains in blocks, and accurate control of molecular weight in the range 1000 to

20000. GTP also produces polymers with linear backbones, in contrast to free radical polymerization in which branching may occur. One of the problems yet to be solved in GTP and metal-free polymerizations is the control of tacticity.[14]

As far as industrial applications are concerned, Dupont has invested great efforts towards developing such products as star polymers for use in toughening plastics and coatings, e.g., for the automobile industry. It remains to be seen whether the customer will pay a higher price for a more durable product. Other potential applications include thermoplastic elastomers, non-aqueous dispersions for the control of rheological properties,[7] and liquid crystalline polymers.[15] Chiral polymers made by GTP have also been reported.[16]

Although metal-free polymerization has only recently been developed, similar applications are in principle possible. The mechanism and theoretical basis also need to be explored. Finally, the question arises whether other types of anionic polymerizations (e.g., ring opening processes) can also be performed using metal-free initiators.

The author thanks Bayer AG for financial support. Discussions with D. Arlt, K. E. Piejko and B. Bömer are highly appreciated.

Received: May 20, 1988

[1] T. Higashimura, M. Miyamoto, M. Sawamoto, *Macromolecules 18* (1985) 611; R. Faust, J. P. Kennedy, *Polym. Bull. 15* (1986) 317.
[2] L. R. Gillion, R. H. Grubbs, *J. Am. Chem. Soc. 108* (1986) 733.
[3] O. W. Webster, W. R. Hertler, D. Y. Sogah, W. B. Farnham, T. V. Rajan-Babu, *J. Am. Chem. Soc. 105* (1983) 5706.
[4] M. Morton: *Anionic Polymerization, Principles and Practice*, Academic Press, New York 1983; M. van Beylen, S. Bywater, G. Smets, M. Szwarc, D. J. Worsfold, *Adv. Polym. Sci. 86* (1988) 87.
[5] F. Bandermann, H. D. Speikamp, *Makromol. Chem. Rapid Commun. 6* (1985) 336; A. H. E. Müller in M. Fontanille, A. Guyot (Eds.): *Recent Advances in Mechanistic and Synthetic Aspects of Polymerization*, Reidel, Dordrecht 1987, p. 23.
[6] W. B. Farnham, D. Y. Sogah, *ACS Polymer Preprints 27* (1986) 167.
[7] O. W. Webster, D. Y. Sogah in M. Fontanille, A. Guyot (Eds.): *Recent Advances in Mechanistic and Synthetic Aspects of Polymerization*, Reidel, Dordrecht 1987, p. 3.
[8] W. R. Hertler, D. Y. Sogah, O. W. Webster, B. M. Trost, *Macromolecules 17* (1984) 1417.
[9] M. T. Reetz, R. Ostarek, K. E. Piejko, D. Arlt, B. Bömer, *Angew. Chem. 98* (1986) 1116; *Angew. Chem. Int. Ed. Engl. 25* (1986) 1108.
[10] M. T. Reetz, T. Knauf, U. Minet, R. Ostarek, unpublished results.
[11] M. T. Reetz, R. Ostarek, *J. Chem. Soc. Chem. Commun. 1988*, 213.
[12] M. T. Reetz, T. Knauf, U. Minet, C. Bingel, *Angew. Chem. 100* (1988), in press; *Angew. Chem. Int. Ed. Engl. 27* (1988), in press.
[13] See e.g.: W. Schlenk, J. Holtz, *Chem. Ber. 49* (1916) 603; G. Wittig, M. Heintzeller, M. W. Wetterling, *Justus Liebigs Ann. Chem. 557* (1947) 201; E. B. Troughton, K. E. Molter, E. M. Arnett, *J. Am. Chem. Soc. 106* (1984) 6726.
[14] Poly(ethyl acrylate) of molecular weight 4000 (initiator: **15a**) is atactic, but solvent effects remain to be studied.[10] The thiolate induced polymerization of methyl acrylate (MW 1400) leads to an isotactic product as judged on the basis of ^{1}H-NMR studies.[11] GTP generally gives atactic polymers.
[15] W. Kreuder, O. W. Webster, H. Ringsdorf, *Makromol. Chem. Rapid Commun. 7* (1986) 5.
[16] J. Suenaga, D. M. Sutherlin, J. K. Stille, *Macromolecules 17* (1984) 2913.

Conference Report

Photovoltaic Solar Energy in Europe

More than 750 materials scientists, physicists, engineers, marketing specialists, and government officials from 45 countries met from 9–13 May 1988 at the "8th European Photovoltaic Solar Energy Conference and Exhibition" in Florence, the largest European Conference ever held on this topic. Photovoltaic (PV) energy has now reached maturity. Crystalline and polycrystalline silicon modules have proven to be the most reliable decentralized source of energy. Their still rather high cost limits their applications at present to the electrification of isolated sites, which are however abundant. Performance and reliability of standalone PV systems in the 10 W to 60 kW range have been evaluated during the past ten years by the US Army, several American and European agencies, and by Third World organizations.

Whereas the reliability of crystalline and polycrystalline silicon modules complies with military standards, many peripherical components such as inverters and battery regulators still have reliability problems. For most household applications, low voltage direct current is therefore preferable to 220 V alternating current, in spite of the high price and poor choice of dc household appliances. The storage of electrical energy has turned out to be a crucial problem for photovoltaics. According to *E. Voss* (Varta, Kelkheim), the lead-acid battery is at present the only viable system for power applications. Possible alternative storage systems for the future are Zn–Br and Cr–Fe batteries, whereas Ni–Cd batteries will not be cost-competitive.

Progress in photovoltaics is intimately linked with the development of new materials and processing technologies. Amorphous hydrogenated silicon, discovered as an electronic material by *Spear* and *Lecomber* (University of Dundee) in 1975, is today a $ 200 million per year business in non-PV applications, and has become one of the leading thin film solar cell materials.

Progress that has recently been made in the production of silicon cells is mainly due to the minimization of optical and recombination losses. Crystalline cells with recombination-free interfaces have been developed by *M. A. Green* in Kensington, Australia (passivated emitter and laser-

grooved buried contact), and by *R. Swanson* of Stanford University (point contact cell). Light trapping is used now in all kinds of silicon solar cells, and has given a spectacular improvement in conversion efficiency. It enhances the optical path of poorly absorbed red or near-infrared light and allows one to make cells thinner. Thin amorphous silicon cells show less light-induced degradation than thicker ones.

The search for a low band-gap a-Si alloy for solar cells has not yet given conclusive results, as pointed out by *J. Bullot* (Orsay University), since the reproducibility and electronic quality of silicon-germanium alloys are not yet satisfactory. The recent improvement in conversion efficiency of a-Si p-i-n cells is mainly related to the p-doped window layer: microcrystalline a-$Si_{1-x}C_x$:H layers, doping with $B(CH_3)_3$ instead of B_2H_6, and superlattice p-layers. Efficiencies of 10% (active area) for $10 \times 10\ cm^2$ modules were announced by Sanyo (Osaka). *D. Carlson* (Solarex, Newtown, PA) reviewed in-line processing technology for large area a-Si modules. Initial efficiencies of 8% on 1000 cm^2 modules are currently achieved by several American and Japanese companies. Stability of a-Si cells has greatly improved. Light-induced degradation can be reduced to 15% in very thin (0.2 to 0.3 μm) cells.

Polycrystalline cells have seen spectacular progress, too, both in fundamental research (*L. L. Kazmerski*'s (SERI, Denver)talk on the analysis of hydrogen at grain boundaries by scanning tunneling microscopy was one of the highlights of this conference) and on the technological side. *A. Barnett* (University of Delaware) reported efficiencies of over 12.5% with small polycrystalline cells processed on low-cost ceramic substrates.

Non-silicon materials are outsiders in PV technology. In spite of the high price of indium, $CuInSe_2$ continues to attract much attention, especially due to progress in material processing (sputter and spray methods). Stacked a-Si/$CuInSe_2$ cells were described by ARCO. Economic criteria will determine the future of this technology.

It remains an open question whether crystalline, polycrystalline or amorphous silicon will be the leading material for the solar cell technology in the next century. Amorphous silicon seems to have the highest potential for cost reduction. However, this requires large scale plants (well above 1 MW/year), since the initial investment is very high.

The vigorous financial effort of the Commision of the European Comunity and national governments (especially in West Germany) to encourage photovoltaics research and development in Europe has so far been a success. 35 companies exhibited PV modules and systems and showed that photovoltaics is already an industrial reality.

Martin P. Schmidt
Paris (France)

Research News

Lord Kelvin Updated

William Thompson, better known to science as Lord *Kelvin*, demonstrated theoretically as long ago as 1853 that the rate of temperature change in a cyclically loaded body is directly related to the rate of change of the sum of the principal stresses, if conditions are adiabatic. If a specimen is stressed inhomogeneously, in cyclic fashion, then the distribution of stresses is expressed by a distribution of mean ΔT (relative to the undisturbed temperature of the sample). The ΔT oscillate with the same frequency as the applied cyclic stress. (An increasing tensile stress gives a temperature fall, an increasing stress, a temperature rise.)—Kelvin's principle can be thought of as the thermoelastic analogue of Faraday's principle of electromagnetic induction, established at roughly the same time.

Kelvin's principle has been exploited for some years now to map the distribution of stresses in an inhomogeneously stressed thin flat body—for instance, a sheet containing a hole or a notch—by measuring the time-averaged temperature change at each point by means of a scanning infrared emission camera: the camera is electronically controlled to read ΔT at each test point in synchrony with the frequency of the applied stress. The strategy has been used for non-destructive examination (NDE) of an object's resistance to fatigue damage. Here the cyclic stress is used to modify the state of the material rather than as a mere probe to examine stress distributions. Incipient fracture, or delamination of a fibre-reinforced composite, leads to enhanced local temperature changes, and such damage sites show up in *vibrothermography*—as the technique is sometimes called—long before they can be detected by any other NDE method.[1] The method has been found especially favourable for NDE of fibre-reinforced composites.[1]

However, vibrothermography can do more than provide NDE: given sufficiently sensitive equipment and appropriate theory, the distribution of stresses which would result from an applied steady load can be determined by a ΔT scan with a low-frequency cyclic load which itself is far too small to damage the specimen in any way. A new instrument based on a design by SIRA in England, named

SPATE (for *S*tress *P*attern *A*nalysis by measurement of *T*hermal *E*mission) can be used in this way. (Spatial resolution is 0.25 mm^2 and temperature resolution, 0.001 °C). The infrared signal at each point the specimen at the peak of the stress cycle is averaged over many cycles to achieve an accurate estimate of the stress distribution.

Recent work[2-4] at the Aeronautical Research Laboratory in Melbourne, Australia, has now advanced the technique to new and unexpected level of subtlety. *Machin* et al.[2] found experimentally that, contrary to Kelvin's theory, not only the cyclic stress amplitude but also the mean stress affect the output of the SPATE instrument. Sustained attempts to develop the theory to account for this finding led to an expression[3] in which ΔT is linearly related to the mean stress when measured at the primary frequency, but is modified by a second term with a coefficient proportional to the square of the stress range when measured at the second harmonic (twice the primary frequency). This new theoretical relationship was obtained by taking into account the variation of Young's modulus with temperature, something that *Kelvin* omitted to do. This new analysis offers the prospect of using vibrothermography to separate out oscillating stress amplitudes (which mimic the distribution of stress which would be created by an externally applied load) from a fixed, *residual* stress distribution which exists in the absence of any external load.

In another recent paper,[4] the Australian team has demonstrated that such separation is indeed feasible. For this purpose, the electronic processor which filters out non-primary frequencies has to be by-passed so that any component of thermal response at twice the primary frequency can be separated out. *Wong* and his coworkers[4] prepared an aluminum alloy plate which was plastically loaded to create a predetermined distribution of residual stresses across the plate width. These stresses were also measured with an array of strain gauges cemented to the plate before the plastic loading. The plate was then cyclically loaded, well inside the elastic range, with a non-zero mean load. Use of SPATE with the electronic bypass referred to then allowed the ΔT distribution at each of the two key frequencies to be determined, and from this the residual stress distribution could be calculated. (This was straightforward because the cyclic stress distribution was uniform across the plate). The Figure 1 taken from reference[4] compares the stress distribution obtained in this way, with error bars, with that directly determined by means of the array of strain gauges (solid line). The agreement is very satisfactory.

A few points are not quite clear in the published paper. The ordinate of the graph is simply labelled "residual stress": presumably the sum of the principal stresses is meant. Also, it is not clear whether the use of a non-zero mean load in the cyclic loading regime is essential in order to be able to determine the residual stresses, presumably a non-zero mean load helps in separating out the weak double-frequency term from the background noise.

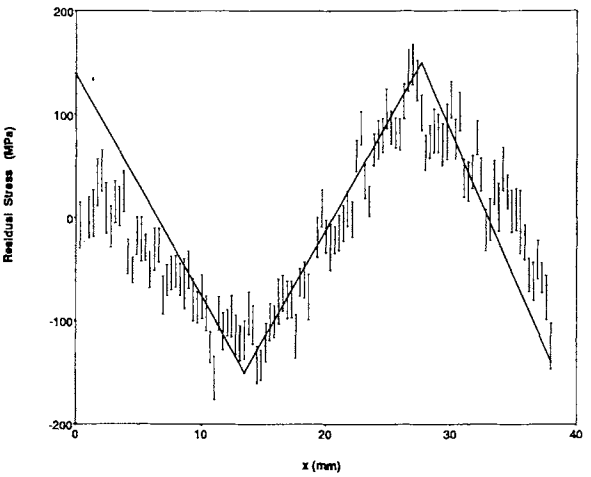

Fig. 1. Residual stress profile for a four-point straightened specimen.

The authors point out that their demonstration was conducted under artificially simple circumstances: the simple rectangular shape of the sample, without holes or other disturbances, meant that the cyclic stress was uniform throughout the specimen. (However, the technique, in this simplified form, could be applied to difficult cases such as that of a glass sheet; the only extant NDE method of estimating residual stresses involves X-ray diffraction and this cannot be used with a non-crystalline material.)—With more realistic specimens of more complex shape, the cyclic stress as well as the residual stress will vary from point to point. To separate out such variables, the sensitivity of SPATE will need to be greatly enhanced, and microstructural features such as grain boundaries and preferred crystallographic orientation of the grains, would also need to be taken into account in these interpretations. Meanwhile, Lord *Kelvin* is well on the way to becoming the most frequently cited nineteenth century physical scientist: his paper on the theory of the instability of liquid jets is already a firm current favourite, and now the even earlier paper on the thermoelastic effect may well join it in its lonely eminence.

Robert W. Cahn
Dept. of Materials Science & Metallurgy
Cambridge University (UK)

[1] E. G. Henneke III in M. B. Bever (Ed.): *Encyclopedia of Materials Science and Engineering*, Pergamon Press, Oxford 1986, pp. 5245-5249.
[2] A. S. Machin, J. G. Sparrow, M. G. Stimson, *Strain 23* (1987) 27-30.
[3] A. K. Wong, R. Jones, J. G. Sparrow, *J. Phys. Chem. Solids 48* (1988) 749-753.
[4] A. K. Wong, S. A. Dunn, J. G. Sparrow, *Nature (London) 332* (1988) 613-615.

Book Reviews

Materials Engineering for Nobody

The Technology and Applications of Engineering Materials. By *M. S. Ray*. Prentice Hall, Englewood Cliffs, N. J., USA 1987. xxv, 736 pp., paperback, $ 27.95.—ISBN 0-13-902081-0

Many years ago, a review of another book on materials opened with the words: "Of books on Shakespeare's plays, the Malaise of Modern Man, and materials science, there is no end. No blinding new insights are to be expected on any of these topics: selection, clarity and economy must be our touchstones." Since I wrote those despairing words in 1974, my shelf of such books has grown to bend increasingly under the burden of several dozens of such volumes (see the book under review, pp. 458–60, 'Bending of Beams'). Any new general text on the science and technology of materials has to be of exceptional quality to succeed in a crowded market place. *Martyn Ray*'s book, I regret to say, fails the tests of selection, clarity and economy: I cannot give it even a qualified welcome.

Texts for students of Materials Science and Engineering (MSE) set out with different objectives. At one extreme is the physics-centered, fundamental interpretative approach, setting out to explain properties in terms of atomic and crystal structure, quantum mechanics and statistical mechanics. The first such book was Cottrell's *Theoretical Structural Metallurgy* of 1948, followed some years later by Wert and Thomson's *Physics of Solids* (1964). Another, even earlier, and extremely influential physics-based book was Barrett's *Structure of Metals* (1943), which has lasted well in the form of successive editions. The same fundamental approach is possible in regard to the chemical approach to materials. The classic here is Darken and Gurry's *Physical Chemistry of Metals* of 1953. Midway between the physical and chemical approaches one finds Swalin's *Thermodynamics of Solids* (1962).

The fundamental approach to polymers was a little slower in coming and probably began with Treloar's 1958 book, *The Physics of Rubber Elasticity*. Since then, the polymer scientists have also been well served with fundamentally biased texts, with a strong undertow of statistical mechanics. From the 1970s on, basic texts began to use the term *materials science*. Notable examples include Ruoff's *An Introduction to Materials Science* of 1972 and Hornbogen's *Werkstoffe* of 1973.

At the other extreme there are texts aimed at the engineer who selects materials for incorporation in his designs, and also at the materials processing specialist who converts materials into semi-finished or finished products. These have been, if anything, even more numerous than the science-centered texts. Early ones had titles such as *Metallurgy for Engineers* (Rollason, 1939) and *Physical Metallurgy for Engineers* (Clarke and Varney, 1952). Later titles covered a broader range of materials; among the better are *Engineering Materials* by Jastrzebski (1959), *The Principles of Engineering Materials* by Barrett, Nix and Tetelman (1973), *Structure and Properties of Engineering Materials* by Harris and Bunsell (1977), as well as the comprehensive *Metals, Ceramics and Polymers* by Wyatt and Dew-Hughes (1974), which was the volume that drew forth the reviewer's words cited at the outset.

A good example of a book aimed specifically at processes is Alexander and Brewer's *Manufacturing Properties of Materials* (1963). More recently still have come some splendid texts aimed directly at developing for fledgling engineers a systematic approach for selecting materials during the design process: *Engineering Materials—An Introduction to their Properties and Applications*, by Ashby and Jones (1980) is a good example.

The titles cited here are only a small selection and include some of the best and most durable. Some of them, especially in the "engineering" group, are really broad treatments that succeed in marrying the S and E of MSE: the books by *Wyatt* and *Dew-Hughes* and by *Harris* and *Bunsell* are examples. The engineers who are to learn from these books are paid the compliment of being supposed intelligent and curious, of wanting to understand complex facts rather than to learn them by rote (and then promptly forget them). By contrast, *Ray*'s book (the volume under review) assumes that his readers do not want to understand—or, perhaps, are incapable of understanding? I am sorry to have to add that this attitude may well stem from a frequent and unmistakable lack of understanding by the author himself. A diet of bare uninterpreted fact, often so vague as to be unintelligible even as fact, has to substitute for insight.

A few quotations will give the flavor: "The molecular weight used to characterize a polymer may be based upon several criteria. The most popular are the viscosity average, number average and weight average molecular weights. For a molecular weight distribution these averages have different values, although they would be identical if the polymer possessed a unique molecular weight." That is all on this subject. Another quotation: "The creep process occurs because of two mechanisms; these are grain boundary sliding and dislocation movement by climbing past obstacles." That is all there is in the book on the role of dislocations in plastic deformation ... yet the cover is decorated by a large diagram of an edge dislocation! Another: "The TTT diagrams described so far are obtained by cooling a

steel isothermally at a series of temperatures." One of the illustrations in the chapter on joining consists of a variety of screw heads!

Several features of the book, especially the very extensive lists of standard specifications and numerous tables of numerical values of properties, betray a measure of confusion between the roles of a textbook and a handbook (such as the *Metals Reference Book*). 100 pages are devoted to elementary school mechanics, which have no place in a book of this kind, supposedly directed at professional engineers-to-be. According to the preface, the book is in fact directed not only at these but also at technicians taking pre-degree courses. But these, also, need and deserve understanding, not just a diet of undigested and sometimes erroneous fact.

Ray also has the peculiar habit of providing a list of keywords for each chapter, apparently in the hope that the reader can check for himself whether he has learned key concepts. In a chapter on engineering design, the list of keywords includes, inter alia, "perseverance, willpower, scientific knowledge, conceptual ability". The author has demonstrated the first two but not, alas, the last two.

Robert W. Cahn
Dept. of Materials Science & Metallurgy
Cambridge University (UK)

Liquid Crystals

Thermotropic Liquid Crystals. Edited by *G. W. Gray*. Wiley, New York 1987. 178 pp., £ 38.00.—ISBN 0-471-91504-1

As long ago as 1962, *G. W. Gray* published the book "Molecular Structure and the Properties of Liquid Crystals", which was a classic for a long time. Display technology has stimulated the synthesis of thousands of new liquid crystal compounds; many of the technologically relevant ones come from *Gray*'s laboratory. Usually, a purely physical approach is chosen for the presentation of the field of thermotropic and lyotropic liquid crystals. This is convenient because it is necessary to describe precisely the properties of anisotropic fluid systems. Furthermore, a great variety of physical measurement techniques directly related to technological applications has to be mastered. Chemists, however, will be more familiar with the approach chosen in this book that has been edited by *G. W. Gray*; it contains six articles written by different authors.

The wealth of mesomorphic phases in organic compounds, and in particular the recently discovered phases, require a refinement of the classification scheme. This is outlined by *A. J. Leadbetter* (27 pages) with special regard to structural analysis by X-ray and neutron diffraction. The phases are characterized essentially by positional order, orientational order, and molecular orientation. This makes it possible to distinguish between different smectic phases and, more generally, between a liquid crystal and a true (though disordered) crystal; such a clear cut distinction has not always been made in the literature. Discotic phases are briefly mentioned. They are not formed exclusively by aromatic compounds, as is erroneously stated.

K. Toyne (36 pages) presents a detailed discussion of the influence of individual structural elements of the rigid backbone and the terminal or lateral substituents on transition temperatures, especially for the nematic to isotropic phase transition. The correlation of this temperature with the length/breadth ratio and the packing density is outlined. The influence of the chemical structure of a compound on properties relevant for technological applications is only briefly mentioned. However, *I. Sage* (35 pages) describes the known correlations with optical and dielectric anisotropy, elastic constants and viscosity. The structures and modes of operation of the most important types of displays employing nematic phases are also discussed.

The requirements for compounds and mixtures with smectic A and C phases are considered by *D. Coates* (21 pages). In this chapter the reader is familiarized with displays that make use of these smectic phases. *D. G. McDonnell* (25 pages) gives a survey on the current state of development of thermochromic cholesteric liquid crystals. He outlines clearly the influence of different parameters on the selective reflection of light. The description of the influence of chemical structure on the optical rotatory power and the sign of rotation of the helix characteristic for the cholesteric phase is particularly interesting to read. *H. Finkelmann* (26 pages) gives a good overview of the synthesis, the phase behavior (as influenced by the molecular structure), and the properties and applications of liquid crystalline linear and branched polymers. This contribution contains many details that are important for a deeper understanding.

All the articles are written with great care, and focus on the essentials of this rapidly progressing field. An extensive up to date reference list is also provided. Thermotropic liquid crystals are discussed with particular regard to their application potential in display technology. For this reason the book treats almost exclusively calamitic, as opposed to discotic or other recently discovered molecular assemblies of fluid systems. The figures, chemical formulas, tables and physical equations are well selected and useful. The book can be recommended as a reference work to chemists active in the field, as well as to physicists having a basic knowledge of chemistry. It will also be valuable for newcomers.

R. Eidenschink,
Nematel, Mainz (FRG)

ADVANCED MATERIALS

Molecular Crystals and Organic Solids

Molecular Crystals. By *J. D. Wright.* Cambridge University Press, Cambridge 1987. VIII, 178 pp., bound, £ 32.50.—ISBN 0-542-26460

Twenty years ago the three volumes entitled "Physics and Chemistry of the Organic Solid State", edited by *Fox, Labes* and *Weissberger* and published between 1963 and 1967 provided an excellent introduction to the subject, which was then covered by some 30 authors in 26 chapters, encompassing more than 2300 pages. The series was as successful as such books can be, and many of the chapters are still well worth reading. Since then the subject has grown enormously; some of the then existing areas have been developed beyond anything that could have been foreseen: crystal growth, the effect of solvents and impurities on crystal morphology, organic solid-state reactions, to name only a few. At the same time important new areas have been added: force field calculations and lattice dynamics (made possible by computer developments), organic metals and superconductors, second-harmonic generators, the study of molecular motion in crystals by solid-state NMR as well as diffraction methods. Also, since the mid-60s the number of molecular crystal structures available, so to say, for detailed scrutiny has increased from around 2000 to more than 70000.

As Dr. *Wright* correctly points out in his preface, there is a serious gap in the teaching of this subject in that most of the current solid-state chemistry and physics textbooks scarcely mention molecular crystals. There are excellent advanced texts covering limited areas, but apart from their specialized coverage they tend to be difficult for newcomers.

In this book, Dr. *Wright* has made a brave attempt to cover the whole subject, single-handed, in less than 180 pages. There are short chapters on purification and crystal growth (10 pages), intermolecular forces (9 pages), crystal structures (12 pages), impurities and defects (24 pages), molecular motion in crystals (22 pages), optical properties of molecular crystals (20 pages), chemical reactions in molecular crystals (23 pages), and, finally, electrical properties (the pièce de résistance with 46 pages). The author whisks us briskly through all these topics, in one door, out of another, and it is all a little like being taken on a ten-minute tour of the Louvre. Thus the book does provide an overall impression of the richness and variety of the subject matter. There are many illuminating explanations and comments, as well as a few slips and other mishaps, but the pace is so breathtaking that they do not really matter. On almost every topic, the beginner is likely to be dazed as much as enlightened, and the research worker will find the treatment far too superficial for his needs.

As an example, take the chapter on crystal structures. Dr. *Wright* considers a few very simple structures out of the 70000 available and has some sensible things to say about them. But he gives the impression that a classification of molecular crystal structures into three groups (nonpolar molecules, molecules with polar substituents, and intermolecular donor-acceptor or charge-transfer complexes) provides genuine insight into the complexity of this enormously intricate subject. Such a classification could at best serve as a basis for defining three special types of interaction that could be invoked in the discussion of crystal structures, but in the vast majority of actual structures all three types of interaction come into play. We are still very far from an understanding of why particular molecules crystallize as they do. We may understand the general principles, but there are far too many details. It is true that when energy calculations based on fairly simple types of force field are made for an *observed crystal structure*, they usually produce an energy minimum at or close to the structure in question, but they give no hint of what other molecular arrangements may be possible. Nearly all the structures discussed here are built from planar aromatic molecules, a very small sample of the real, messy world. More stereodiagrams (I found only one) would have helped the reader, in this chapter and in others, to visualize the three-dimensional packing of the molecules.

In my opinion, Dr. *Wright* has undertaken a hopeless task in his effort to provide an elementary textbook on molecular crystals in such a short book. Perhaps it is the publishers who are to be blamed for imposing this limitation (as well as for the price, which will surely drive much of the prospective readership to the photocopier). Solid-state NMR in less than five pages! Lattice dynamics in three! It is difficult to see how a student can benefit from such superficial coverage. Many of the topics that are compressed here into a few pages would take an entire book to do them justice. His publishers should encourage him to expand one or two of his chapters into such a book. That would be a really worthwhile venture!

Organic Solid State Chemistry. Edited by *G. R. Desiraju.* Elsevier Science Publishers, Amsterdam 1987. xx, 550 pp., hard cover, Hfl 360.00.—ISBN 0-444-42844-5

This book is a collection of 14 review articles that describe developments in solid state chemistry during the last two decades. First a description of the contents: The book opens with five chapters on "Organic solid state reactions: topochemistry and mechanism". The reactions discussed are mainly photochemical intramolecular hydrogen abstractions *(Scheffer)* and [2+2] additions *(Theocharis* and *Jones,* and *Hasegawa),* there is a chapter on the prediction of reactivity using geometric criteria *(Kearsley)* and one on phonon spectroscopy *(Prasad).* The middle section consists of four chapters on the theme "Some stereochemical questions: pure and applied chemistry". *J. M. Thomas* and *Harris* discuss experimental and computational techniques for studying the structure and properties of molecules em-

bedded within solid hosts. This is followed by a long, informative chapter on clathrates *(Tsoucaris)* and one on the structural complexities of phenols and their expression in different types of solid state reactivity *(Perrin, Lamartine, Perrin,* and *Thozet).* A chapter by *Paul* and *Curtin* on gas–solid reactions and polar crystals concludes this section. The five chapters of the final section entitled "Intermolecular interactions: from crystallography to chemical physics" form what is perhaps the most interesting part of the book. *Rao* summarizes what is known about phase changes in molecular crystals, *Gavezzotti* and *Simonetta* discuss the nature and magnitude of molecular motions in solids, and *Ramdas* and *N. W. Thomas* take up again the problem of modeling the packing energy in terms of inter- and intramolecular interactions. *Bernstein* provides a wealth of examples of conformational polymorphism—structural relationships that a physicist would describe as phase transformations, a chemist as conformational isomerizations—and finally *Desiraju* takes up the question of why some planar chloro aromatic molecules crystallize with a 4 Å translation and others not.

In a way, this book is a tribute to the memory of *G. M. J. Schmidt* and *A. I. Kitaigorodskii*, who did so much to pioneer the systematic study of organic chemical crystallography and whose names are mentioned in nearly every chapter. For the non-specialist the book provides a useful survey of current research in a complex, rapidly developing field, and also the experienced researcher in solid-state organic chemistry will find many fascinating snippets of information even in his own speciality besides an introduction to less familiar areas.

Yet I do not think the editor has succeeded in the attempt to produce "a reference work for specialists and non-specialists alike". As in many other multi-authored books, there is a sad lack of coordination among the various chapters. There seems to have been little agreement about the level of knowledge to be taken for granted in the imaginary reader; in one chapter, for example, this shadowy person knows all about the Metropolis algorithm but needs to be reminded that inversion of the cyclohexane ring interchanges axial and equatorial substituents. A work of reference needs a better index than the one provided. The end result is not much more than a collection of disconnected essays. Even visually, the book makes a disjointed impression as it was obviously prepared from camera-ready copy with a noticeable lack of agreement even about such matters as the choice of fonts, styles, literature citations, etc.

There are advantages to a type-set book. If this one had been type-set it could have benefited from the services of a copy editor, who would have corrected most of the spelling mistakes and noticed, for example, that Figures 10 and 11 of Chapter 2 are not mentioned in the text, besides other minor blemishes, such as, in one place, 10^{16} s (for 10^{-16} s). Moreover, the authors themselves would have had a second chance to correct undetected errors and mishaps at the galley proof stage. All this costs time and money, it must be assumed. The advantages of making a book from camera-ready copy would then, one might suppose, be cheapness and speed of publication. But there is no evidence that this volume was produced with any remarkable alacrity, and the price of 360 Hfl is certainly not cheap but rather seems outrageously expensive for a book produced from camera-ready copy.

Jack D. Dunitz
Laboratorium für Organische Chemie der
Eidgenössischen Technischen Hochschule
Zürich (Switzerland)

Zeolites

Synthesis of High-Silica Aluminosilicate Zeolites. By *P. A. Jacobs* and *J. A. Martens*. Elsevier, Amsterdam 1987. xvi, 390 pp., bound, Hfl 280.00.—ISBN 0-444-42814-3

For about 15 years high-silica zeolites have been attracting much interest. Meanwhile, they have become important especially as catalysts for petrochemical processes, although their application potential is not limited to this field. The variety of possible applications can be demonstrated with the best-known example of this class of compounds, the zeolite ZSM-5.

The intense research activity, especially on the synthesis of high-silica zeolites, is documented by a large number of publications, a very important fraction of which is patent literature. The great variety of zeolites makes it difficult, even for the expert, to keep up with the literature. Who, for instance, is familiar with the classification of the zeolite ZETA-1?

Therefore, it was time for a comprehensive account, such as the one *P. A. Jacobs* and *J. A. Martens* now present as volume 33 of the series "Studies in Surface Science and Catalysis". The authors restrict their topic to zeolites which can be synthesized directly as high-silica zeolites, and which have potential uses as shape-selective catalysts. They exclude zeolites that can be obtained by isomorphic replacement of aluminum lattice atoms by other elements. There may be some controversy about this restrictive interpretation of the term "high-silica zeolites", but not about the great usefulness of this monograph, in spite of the mentioned limitations.

The first part ("experimental", 40 pages) gives detailed and tested recipes for the preparation of 14 high-silica zeolites. The resulting materials are characterized by X-ray diffraction, electron microscopy, and IR spectroscopy. These instructions will be welcomed, and not only by newcomers.

The much larger second part of the book is devoted to zeolites having the structures MFI (ZSM-5), MEL (ZSM-11), TON, MTT, MTW, and FER (ferrierite). In addition

to the discussion of experimental conditions for their synthesis, information on structure and crystal morphology can be found in the individual chapters. As expected, the authors put the main emphasis on the various preparation methods of ZSM-5. For this zeolite they also briefly discuss molding methods, a topic highly relevant to applications. The book concludes with a short third part on zeolites with unknown structures.

The keyword "synthesis of zeolites" provokes a comparison with *R. M. Barrer*'s classic "Hydrothermal Chemistry of Zeolites" (Academic Press, London 1982). Such a comparison is, however, difficult because the two monographs follow completely different approaches: While *Barrer* focuses on the general principles of zeolite synthesis, *Jacob* and *Martens* present a collection of facts, especially on high-silica zeolites. The authors have critically reviewed the literature up to and including 1985. They have succeeded in giving a clear and understandable presentation of their topic, which is partly due to a large number of well presented diagrams and figures. In particular, the numerous X-ray diffraction data may often save the reader a lot of tedious literature searching. In summary, this book will be a valuable tool for the expert as well as for novices in the field of high-silica zeolites.

Eckehart Roland
Degussa AG, ZN Wolfgang,
Hanau (FRG)

Conference Calendar

August 1988

15–19 **Controlled Release of Bioactive Materials,**
15th Int. Symp.
Basel (Switzerland)
Contact: Administrative Office, Controlled Release Soc., 16 Nottingham Dr., Lincolnshire, ILL. 60015, USA

15–19 **Solid State Studies in Ceramics,**
Gordon Conf.
Meridan (USA)
Contact: A. M. Cruickshank, Gordon Res. Ctr., Univ. Rhode Island, Kingston, RI 02881-0801, USA

15–19 **Physics of Semiconductors,**
19th Int. Conf.
Warsaw (Poland)
Contact: J. Kossut, Inst. of Physics, Polish Academy of Sci., Al. Lotnikow 32/46, 02-668 Warsaw, Poland

15–19 **Liquid Crystals,**
12th Int. Conf.
Freiburg (Fed. Rep. Germany)
Contact: Dr. G. Baur, Fraunhofer-Institut IAF, Eckerstr. 4, D-7800 Freiburg, FRG

16–19 **Critical Currents in High-Temp. Superconductors**
Snowmass Village (USA)
Contact: J. R. Clem, A 517 Physics, Iowa State Univ. Ames, IA 50011, USA

18–22 **Synchrotron Radiation,**
(SR-88)
Novosibirsk (USSR)
Contact: A. N. Skrinsky, USSR Academy of Sci., Siberian Div., Inst. of Nuclear Physics, 11 Lavrentyer, USSR-630090 Novosibirsk, USSR

21–25 **Applied Superconductivity**
San Francisco (USA)
Contact: C. Henning, L-644, LLNL, Livermore, CA 94550, USA

22–25 **Nonlinear Optical Properties of Materials**
Troy (USA)
Contact: OSA, 1816 Jefferson Pl. NW, Washington, DC 20036, USA

22–26 **Ceramic Developments – Past, Present and Future,**
Int. Ceramic Conf. and Fair
Sydney (Australia)
Contact: G. Henness, New South Wales Inst. of Technology, Dept. of Materials Sci., P.O. Box 123, Broadway NSW 2007, Australia

22–27 **Phase Interaction in Composite Materials**
Patras (Greece)
Contact: Prof. S. A. Paipetis, Univ. of Patras, Patras 26001, Greece

23–27 **Interface Phenomena – Adhesion and Friction: Microscopic Concepts**
Halifax (Canada)
Contact: H. J. Kreuzer, Phys. Dept., Dalhousie Univ., Halifax, Nova Scotia, B3H 3Y5 Canada

24–26 **Solid State Devices and Materials**
Tokyo (Japan)
Contact: Business Center for Academic Societies Japan, Yamazaki Bldg. 4F, 40-14 Hongo 2-chome, Bunkyo, Tokyo 113, Japan

28–1 **Molecular Beam Epitaxy (MBE-5)**
Sapporo (Japan)
Contact: Prof. M. Konagai, Tokyo Inst. Tech., Dept. of Electrical and Electronic Eng., 1-12-1 Okayama, Meguro-ku, Tokyo 152, Japan

28–10 **Structure-Property Relationships in Surface Modified Ceramics**
NATO Adv. Study Inst.
Pisa (Italy)
Contact: C. J. McHargue, Metals & Ceramics Division, Oak Ridge Natl. Lab. P.O. Box 10, Oak Ridge, TN 37831-6118, USA

29–1 **Applications of Polar Dielectrics and Ferroelectrics,**
Int. Symp.
Zürich (Switzerland)
Contact: H. Arend, Swiss Federal Inst. of Tech., Lab. of Solid State Physics, CH-8093 Zürich, Switzerland

29–1 **Semiconductor Lasers,**
11th IEEE Conf.
Boston (USA)
Contact: R. T. Wangeman, IEEE Leos, 345 East 47th St., New York, NY 10017, USA

29-2 **Defects in Insulating Crystals**
Parma (Italy)
Contact: Dr. R. Capelletti, Dipt. di Fisica, Univ. di Parma, Via M. D'Azeglio 85, 43100 Parma, Italy

29-1 **E-MRS Polycrystalline Semiconductors '88—Phys. Prop. of Grain Boundaries and Interfaces**
Malente (Fed. Rep. Germany)
Contact: H. J. Möller; H. P. Strunk, Tech. Univ. Hamburg-Harburg, Eissendorfer Str. 42, 2100 Hamburg 90, FRG

29-2 **Electrical Transport and Optical Properties in Inhomogeneous Media,**
2nd Int. Conf.
Paris (France)
Contact: J. Lafait, Lab. d'Optique des Solides, Univ. Pierre and Marie Curie, 4 Place Jussieu, 75252 Paris Cedex 05 France

29-10 **Ion Beam Analysis of Solids,**
Summerschool
Jena (German Dem. Rep.)
Contact: Prof. G. Götz, Friedrich-Schiller-Univ., Sektion Physik, Max-Wien-Platz 1, DDR-6900 Jena, GDR

September 1988

1-3 **Electrets,**
6th Int. Symp.
Oxford (United Kingdom)
Contact: Dr. D. K. Das-Gupta, School of Electronic Eng. Sci., Univ. College of North Wales, Bangor, Gwynedd, LL57 1UT, UK

4-8 **Zeolites as Catalysts, Sorbents and Detergent Builders,**
Int. Symp.
Würzburg (Fed. Rep. Germany)
Contact: Dr. H. G. Karge, Fritz-Haber-Inst. der Max-Planck-Gesellsch., Faradayweg 4-6, D-1000 Berlin 33

4-9 **Electron Microscopy,**
9th Eur. Congr. (EUREM 88)
York (United Kingdom)
Contact: EUREM 88, The Royal Microscopical Soc., 37-38 St. Clements, Oxford OX 4 1AJ, UK

4-9 **Metal-Hydrogen Systems, Fundamentals and Applications,**
Int. Symp.
Stuttgart (Fed. Rep. Germany)
Contact: Dr. E. Fromm, Max-Planck-Institut für Metallforschung, Inst. für Werkstoffwissenschaften, Seestraße 92, D-7000 Stuttgart 1, FRG

4-16 **Surfaces and Interfaces on Ceramic Materials,**
NATO Adv. Study Inst.
Oleron (France)
Contact: Dr. L. C. Dufour, Chemie des Materiaux IREQ, CP 1000, Varennes, Quebec JOL 2PO, Canada

4-16 **Plasma Surface Interactions and Processing of Materials,**
NATO Adv. Study Inst.
Alicante (Spain)
Contact: Prof. O. Auciello, NC State Univ., Dept. of Nuclear Eng., Raleigh, NC 27695-7909, USA

5-7 **Electrical, Optical and Acoustic Properties of Polymers**
Canterbury (United Kingdom)
Contact: The Plastics and Rubber Inst., 11 Hobart Pl., London SW1X OHL, UK

5-8 **Surface Science,**
Eur. Conf. (ECOSS-10)
Bologna (Italy)
Contact: Prof. O. Bisi, Univ. di Modena, Dipto. di Fisica, 213/a Via Campi, I-41100 Modena, Italy

6-9 **Physics of Semiconductors**
Frankfurt an der Oder (German Dem. Rep.)
Contact: Kammer der Technik, Ebertusstr. 2, DDR-1200 Frankfurt an der Oder, GDR

6-9 **Fiber Optics, Optoelectronics, and Laser Applications in Sci. and Eng.,**
Int. Symp. and Exhibition
Boston (USA)
Contact: SPIE, P. O. Box 10, Bellingham, WA 98227-0010, USA

7-9 **Techniques and Mechanisms in Polymer Degradation and Stabilisation**
Brighton (United Kingdom)
Contact: Dr. N. S. Allen, Dept. of Chemistry, John Dalton Faculty of Technol., Manchester Polytechnic, Chester St., Manchester M15GD, UK

10-17 **Electrochemistry of Conductive Polymers**
Sulejow (Poland)
Contact: Janusz Ptocharski, Inst. of Inorganic Technology, ul. Noakowskiego 3, 00664 Warszawa, Poland

12-14 **Materialforschung 1988,**
BMFT Symp.
Hamm (Fed. Rep. Germany)
Contact: Material- und Rohstofforsch., KFA Jülich GmbH, Postfach 1913, D-5170 Jülich, FRG

12-16 **Industrial Applications of the Mößbauer Effect,**
Int. Symp. (ISIAME '88)
Parma (Italy)
Contact: Prof. M. Carbucicchio, Univ. di Parma, Dipto. di Fisica, Viale delle Scienze, I-43100 Parma, Italy

12-16 **Surface Modification of Metals by Ion Beams,**
6th Int. Conf. (SMMIB '6)
Riva del Garda (Italy)
Contact: Dr. L. Guzman, Technologica in Trento, Istituto per la Ricerca Scientifica, I-38050 Povo, Trento, Italy

12-16 **Properties and Applications of Dielectric Materials,**
2nd Int. Conf. (ICPADM-2)
Beijing (People's Rep. China)
Contact: Prof. Z. Renyu, Tsinghua University, Dept. of Electrical Eng., Beijing, People's Rep. of China

12-15 **Solid State Protonic Conductors IV**
Exeter (United Kingdom)
Contact: Dr. R. C. Slade, Univ. of Exeter, Dept. of Chem., Stocker Rd., Exeter EX4 4QD, UK

12-17 **Evaluation of Adv. Semiconductor Materials by Electron Microscopy,**
NATO Adv. Workshop
Bristol (United Kingdom)
Contact: Dr. D. Cherns, HH Wills Phys. Lab. Univ. Tyndall Ave., Bristol BSB 1 TL, UK

13–15 **Speciality Polymers,**
3rd Int. Conf.
Cambridge (United Kingdom)
Contact: Monique Heald, Butterworth Scientific Ltd., P.O. Box 63, Westbury House, Bury St., Guilford, Surrey GU2 5BH, UK

13–16 **Modern Optics,**
3rd Int. Symp. (OPTIKA '88)
Budapest (Hungary)
Contact: Optical, Acoustical and Filmtechnical Soc., Secretariat of OPTIKA '88, Foe u. 68, H-1027 Budapest, Hungary

13–16 **Structure and Reactivity of Solids**
Trieste (Italy)
Contact: Prof. C. Morterra, Ist. Chimica Fisica, C.so M D'Azeglio 48, I-10125 Torino, Italy

13–16 **Polymers, Laminations & Coatings**
Atlanta (USA)
Contact: Meet. Dept., TAPPI, Technology Park, Atlanta, GA 30348-5113, USA

19–23 **Plasma Surface Engineering,**
1st. Int. Conf.
Garmisch-Partenkirchen (Fed. Rep. Germany)
Contact: Dtsch. Gesellsch. für Metallkunde e.V., Adenauerallee 21, D-6370 Oberursel, FRG

19–23 **Optical Sci. and Eng.,**
Int. Conf. and Exhibition (EUROPTIKA 88)
Hamburg (Fed. Rep. Germany)
Contact: SPIE, P.O. Box 10, Bellingham, WA 98227-0010, USA

20–23 **Polymer Surfaces and Interfaces,**
Workshop
Pacific Grove, CA (USA)
Contact: J. Rabolt, IBM, Almaden Research Ctr., 650 Harry Rd., San Jose, CA 95120-6099, USA

21–23 **Solid-State Circuits,**
14th Eur. Conf. (ESSCIRC-14)
Manchester (United Kingdom)
Contact: Dr. P. J. Hicks, UMIST, Dept. of Electrical Eng. and Electronics, P.O. Box 88, Manchester M60 1QD, UK

22–23 **Oxidation of High-Temperature Intermetallics,**
Workshop
Westlake, OH (USA)
Contact: T. Grobstein, NASA Lewis Research Center 2100 Brookpark Rd., M/S49-1 Cleveland, OH 44135-3191, USA

24–30 **World Materials Congress**
Chicago (USA)
Contact: World Materials Congress, Technical Department ASM International, Metals Park, OH 44073, USA

26–30 **Polymer Networks Group,**
9th Mtg.
Freiburg (Fed. Rep. Germany)
Contact: W. Burchard, Inst. für Makromolekulare Chemie, Univ. of Freiburg, Stefan-Meier-Str. 31, D-7800 Freiburg, FRG

26–30 **Welding and Melting by Electron and Laser Beams,**
4th Int. Colloq.
Cannes, France
Contact: Commissariat a l'Energie Atomique, DTECHSTA, 91191 Gif-sur-Yvette Cedex, France

28–30 **Ungewöhnliche Valenzzustände in Festkörpern,**
5. Vortragstagung der Fachgruppe Festkörperchemie der Gesellsch. Dtsch. Chem.
Erlangen (Fed. Rep. Germany)
Contact: GDCh, Abtlg. Tagungen, Postfach 900440, D-6000 Frankfurt am Main 90, FRG

October 1988

3–6 **Farbensymposium,**
10. Int. Symp.
Trier (Fed. Rep. Germany)
Contact: Dr. E. Hahn, BASF AG, D-6700 Ludwigshafen, FRG

3–7 **Laser Interaction with Matter,**
19th Eur. Conf.
Madrid (Spain)
Contact: G. Velarde, Inst. de Fusion Nuclear, ETS Ingenieros Industriales, José Gutiérrez Abascal n. 2, 28006 Madrid, Spain

9–14 **Ultrafast Phenomena and Nonlinear Optics,**
Chicago (USA)
Contact: R. R. Alfano, City College of New York, 138 St. and Convent Ave., New York, NY 10031, USA

12–14 **Ceramic Powder Processing Science,**
2nd Int. Conf.
Berchtesgaden (Fed. Rep. Germany)
Contact: Dtsch. Keram. Gesellsch., Postfach 1226, D-5340 Bad Honnef 1, FRG

12–14 **Electrochemistry and Electronics**
Basel (Switzerland)
Contact: Dr. W.-D. Luz, Metallgesellschaft AG, D-6000 Frankfurt am Main 1, FRG

13–14 **Laser-Materialbearbeitung,**
Eur. Conf.
Bad Nauheim (Fed. Rep. Germany)
Contact: Dtsch. Verband für Schweißtechnik e.V., Postfach 2725, D-4000 Düsseldorf 1, FRG

13–15 **Berliner Polymeren-Tage 1988**
West-Berlin
Contact: Bundesanstalt für Materialforschung und -prüfung (BAM), Abt. 3 - Organische Stoffe, Unter den Eichen 87, D-1000 Berlin 45, FRG

18–20 **Deutsche Keramische Gesellschaft,**
Annu. Congr.
Munich (Fed. Rep. Germany)
Contact: Dtsch. Keram. Gesellsch., Postfach 1226, D-5340 Bad Honnef 1, FRG

18–21 **Schichtsysteme für neuartige Bauelemente der Mikro-, Opto-, Bioelektronik und Optik**
Karl-Marx-Stadt (German Dem. Rep.)
Contact: Technische Univ. Karl-Marx-Stadt, Abt. Zentrale Veranstaltungen, Postfach 964, DDR-9010 Karl-Marx-Stadt, GDR

18–22 **Ceramitech '88,**
4th Int. Fair/3rd Int. Symp.
Munich (Fed. Rep. Germany)
Contact: Münchener Messe- und Ausstellungsgesellsch., Postfach 121009, D-8000 München 12, FRG

19–21 **Raw Materials for New Technologies,**
5th Int. Symp. on Mineral Resources
Hannover (Fed. Rep. Germany)
Contact: Dr. Arnt Müller, Bundesanstalt für Geowissenschaften und Rohstoffe, Postfach 510153, D-3000 Hannover 51, FRG

21–24 **Functional and Fine Polymers,**
XISFFP Xian Int. Symp.
Xian (People's Rep. China)
Contact: Prof. Hua Zhao, Xian Modern Chemistry Research Inst., P.O. Box 18, Xian, People's Rep. of China

23–26 **Combustion and Plasma Synthesis of High-Temperatur Materials,**
Int. Symp.
San Francisco (USA)
Contact: Dr. J. B. Holt, Lawrence Livermore Natl. Lab., P.O. Box 808, L-369, Livermore, CA 94550, USA

23–26 **High Technology Materials Characterization**
San Francisco (USA)
Contact: W. S. Young, IBM Corporation, 5600 Cottle Rd., San Jose, CA 95193, USA

November 1988

8–10 **European MRS Fall Conference**
Strasbourg (France)
Contact: P. Siffert, Centre de Recherches Nucléaires, Lab. "PHASE", 23, Rue du Loess, F-67037 Strasbourg (France)

9–11 **Perspectives on the New Superconductivity**
Boston (USA)
Contact: D. Berger, Nature Publ. Co., 65 Bleecker St., New York, NY 10012, USA

10–11 **Microstructural and Microanalytic Characterisation of Ceramic Materials**
Bad Nauheim (Fed. Rep. Germany)
Contact: Dtsch. Gesellsch. für Metallkunde eV., Adenauerallee 21, D-6370 Oberursel, FRG

17–18 **Projection Plasma Spraying**
Paris (France)
Contact: IITT-International, 40 promenade Marx Dormoy, F-93460 Gournay-Sur-Marne, France

19–23 **Multiphase Macromolecular Systems,**
14th Biennial Polymer Symp.
San Diego (USA)
Contact: B. Culbertson, Ashland Chemical Co., P.O. Box 2219, Columbus, OH 43216, USA

27–30 **Ceramic Materials and Components for Engines,**
3rd Int. Symp.
Las Vegas (USA)
Contact: American Ceramic Soc. 757 Brooksedge Plaza Dr., Westerville, OH 43081-6136, USA

28–3 **MRS Fall Meeting**
Boston (USA)
Contact: Materials Research Society, 9800 McKnight Rd., Suite 327, Pittsburgh, PA 15237 (USA)

December 1988

1–4 **Water Soluble Polymers,**
Fuzhou Int. Symp.
Fuzhou (People's Rep. China)
Contact: Hu Bing-huan, Inst. of Polym. Sci., Fujian Teachers Univ., People's Rep. of China

5–9 **Lasers and Applications,**
11th Int. Conf.
Lake Tahoe (USA)
Contact: Prof. H. J. Eichler, Techn. Univ. Berlin, Optisches Inst., Straße des 17. Juni 135, D-1000 Berlin 12, FRG

7–8 **Materials Science and Eng. Towards the 21st Century,**
4th Israel Mater. Eng. Conf.
Beer-Sheva (Israel)
Contact: Peltours-Conventions, The Secretariat, 4th Israel Mater. Eng. Conf., P.O. Box 394, 61003 Tel-Aviv, Israel

12–17 **Advances in Holography and Speckle Phenomenon and their Industrial Applications,**
Int. Workshop
Madras (India)
Contact: Prof. R. S. Sirohi, Indian Inst. of Technology, Physics Dept., Madras 600036, India

14–16 **SIMCER 7/ZIRCONIA 88**
7th Int. Symp. on Ceramics
Bologna (Italy)
Contact: Centro Ceramico, Via Martelli, 26
I-43138 Bologna, Italy

ADVANCED MATERIALS will again appear in the September issue of this journal and from then onwards, monthly.

A number of free reprints of the first ADVANCED MATERIALS part of the journal that appeared in the May issue are still available.

Please write to:

ADVANCED MATERIALS/ANGEWANDTE CHEMIE
Postfach 1260/1280 · D-6940 Weinheim
Federal Republic of Germany

ANGEWANDTE CHEMIE
International Edition in English
Volume 27 · Number 8
August 1988
Pages 1009–1112

The Design of Molecular Hosts, Guests, and Their Complexes (Nobel Lecture)**

By Donald J. Cram

Origins

Few scientists acquainted with the chemistry of biological systems at the molecular level can avoid being inspired. Evolution has produced chemical compounds exquisitely organized to accomplish the most complicated and delicate of tasks. Many organic chemists viewing crystal structures of enzyme systems or nucleic acids and knowing the marvels of specificity of the immune systems must dream of designing and synthesizing simpler organic compounds that imitate working features of these naturally occurring compounds. We had that ambition in the late 1950's. At that time, we were investigating π-complexes of the larger [m.n]paracyclophanes with $(NC)_2C{=}C(CN)_2$, and envisioned structures in which the π-acid was sandwiched by two benzene rings. Although no intercalated structures were observed,[1,2] we recognized that investigations of *highly structured complexes* would be central to simulation of enzymes by relatively simple organic compounds.

In 1967, *Pedersen*'s first papers appeared[3,4] which reported that alkali metal ions bind crown ethers to form highly structured complexes. We immediately recognized this work as an entree into a general field. The 1969 papers on the design, synthesis, and binding properties of the cryptands by *J.-M. Lehn, J.-P. Sauvage,* and *B. Dietrich*[5,6] further demonstrated the attractions and opportunities of complexation chemistry. Although we tried to interest graduate students in synthesizing *chiral crown ethers* from 1968 on, the efforts were unsuccessful. In 1970 we insisted that several postdoctoral co-workers enter the field. During 1973, we published five Communications on the subject.[7–11] In 1974 with *Jane M. Cram*, we published a general article entitled "Host-Guest Chemistry", which defined our approach to this research.[12]

Aeschylus, the Athenian Poet-Dramatist, wrote 2500 years ago, "Pleasantest of all ties is the tie of host and guest."[13] Our research of the past 17 years has dealt with the pleasant tie between host and guest at the organic molecular level. The terms *host, guest, complex,* and their binding forces were defined in 1977 as follows:[14] "Complexes are composed of two or more molecules or ions held together in unique structural relationships by electrostatic forces other than those of full covalent bonds ... molecular complexes are usually held together by hydrogen bonding, by ion pairing, by π-acid to π-base interactions, by metal-to-ligand binding, by van der Waals attractive forces, by solvent reorganizing, and by partially made and broken covalent bonds (transition states) ... high structural organization is usually produced only through multiple binding sites ... a highly structured molecular complex is composed of at least one host and one guest component ... a host-guest relationship involves a complementary stereoelectronic arrangement of binding sites in host and guest ... the host component is defined as an organic molecule or ion whose *binding sites converge* in the complex ... the guest component is defined as any molecule or ion whose *binding sites diverge* in the complex ..." In these definitions, hosts are synthetic counterparts of the receptor sites of biological chemistry, and guests, the counterparts of substrates, inhibitors, or cofactors. These terms and concepts have gained broad international acceptance.[15] A new field requires new terms which, if properly defined, facilitate the reasoning by analogy on which research thrives.

[*] Prof. D. J. Cram
Department of Chemistry and Biochemistry
University of California at Los Angeles
Los Angeles, CA 90024 (USA)

[**] Copyright © The Nobel Foundation 1988.—We thank the Nobel Foundation, Stockholm, for permission to print this lecture.

From the beginning, we used Corey-Pauling-Koltun (CPK) molecular models,[16] which served as a compass on an otherwise uncharted sea full of synthesizable target complexes. We have spent hundreds of hours building CPK models of potential complexes, and grading them for desirability as research targets. Hosts were then prepared by my co-workers to see if they possessed the anticipated guest-binding properties. Crystal structures of the hosts and their complexes were then determined to compare what was anticipated by model examination with what was experimentally observed. By the end of 1986, Drs. *K. N. Trueblood, C. B. Knobler, E. F. Maverick,* and *I. Goldberg,* working at UCLA, had determined the crystal structures of over 50 complexes, and those of another 25 hosts. These crystal structures turned our faith into confidence. Scheme 1 traces the steps involved in linking the structures of *biotic complexes* of evolutionary chemistry with our *abiotic complexes* designed with the aid of CPK molecular models.[17]

In molecular modeling, we made extensive use of the self-evident principle of complementarity: "to complex, hosts must have binding sites which cooperatively contact and attract binding sites of guests without generating strong nonbonded repulsions."[18] Complexes were visualized as having three types of common shapes: 1) perching complexes, resembling a bird perching on a limb, an egg

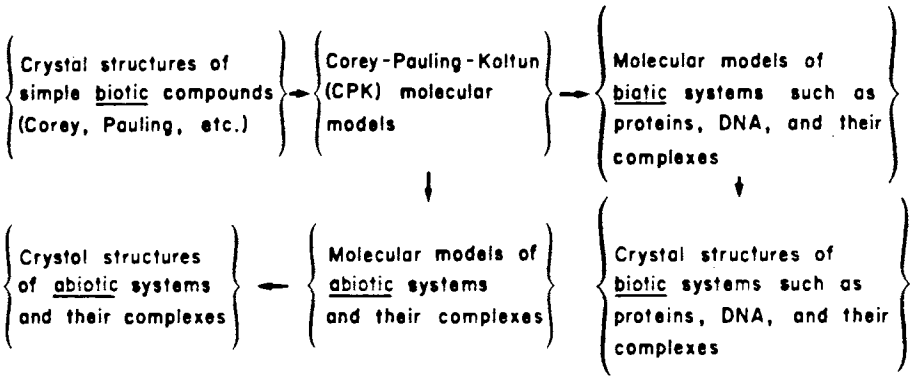

Scheme 1. Crystal structures of biotic compounds are correlated with those of abiotic compounds through CPK models.

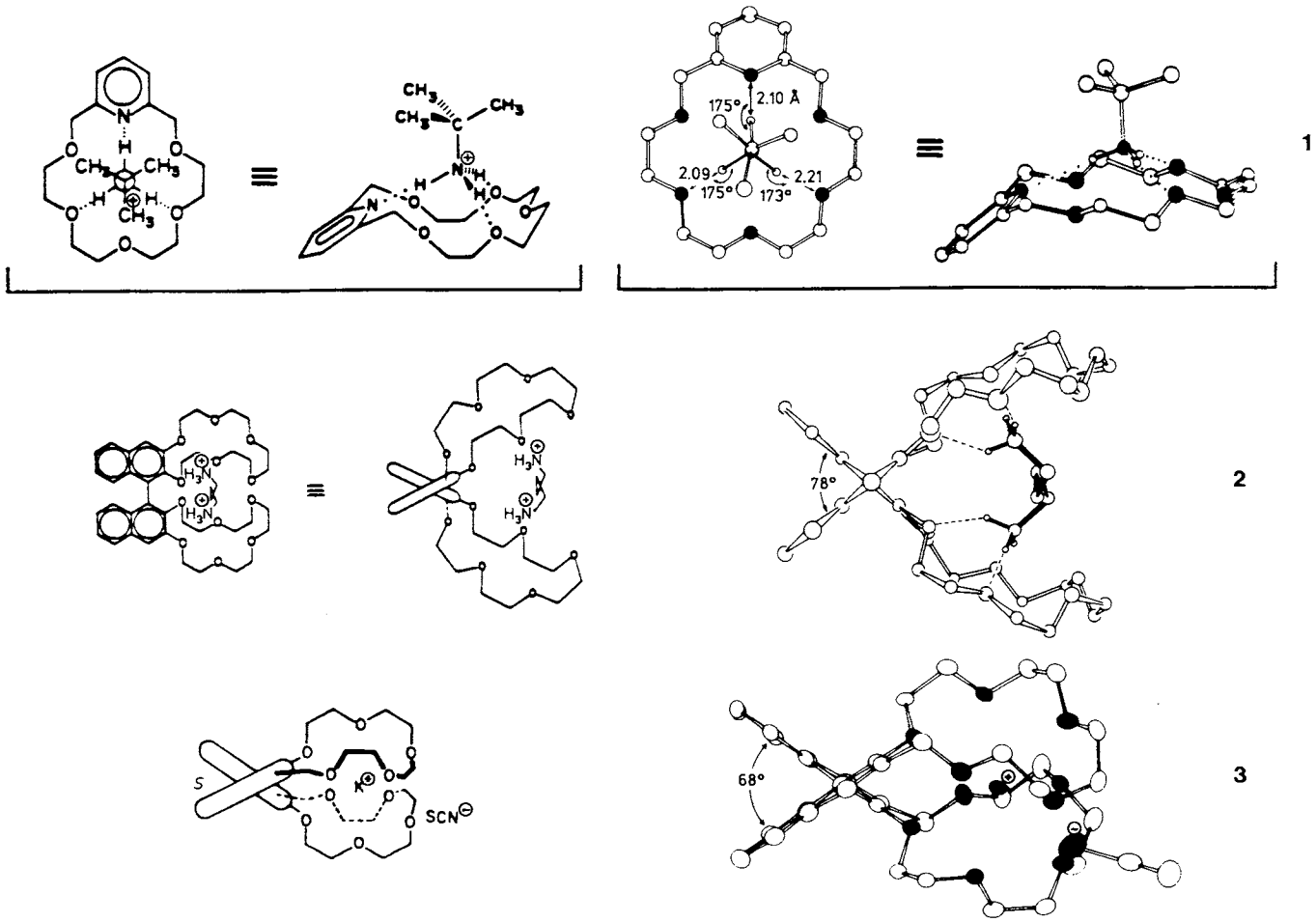

Scheme 2. Three types of complexes. **1** is a perching complex, **2** is a nesting complex, and **3** is a capsular complex. Left: CPK models; right: crystal structures.

protruding from an egg cup, or a scoop of ice cream sitting on a cone; 2) nesting complexes, similar to an egg resting in a nest, a baby lying in its cradle, or a sword sheathed in its scabbard; 3) capsular complexes, not unlike a nut in its shell, a bean in its pod, or a larva in its cocoon. Scheme 2 provides a comparison of CPK models of the three types of complexes (**1**, **2**, and **3**) and their actual crystal structures.[19,20]

Principle of Preorganization

Crystal structures of *Pedersen*'s [18]crown-6[21] and *Lehn*'s [2.2.2]cryptand[22,23] show that in their uncomplexed states, they contain neither cavities nor convergently-

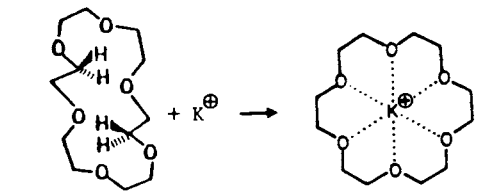

4 **5**

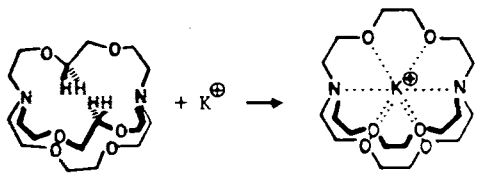

6 **7**

arranged binding sites. Comparisons of the crystal structure of host **4** with that of its $K^{\oplus}$ complex **5**, and of host **6** with that of its $K^{\oplus}$ complex **7** indicate that the complexing act must be accompanied by host reorganization and desolvation.

With the help of CPK molecular models, we designed ligand system **8**, whose oxygens have no choice but to be octahedrally arranged around an enforced spherical cavity complementary to $Li^{\oplus}$ (**9**) and $Na^{\oplus}$ ions (**10**). We have given the family name, *spherand*, to completely preorganized ligand systems, and the name, *spheraplex*, to their complexes, which like **7**, are capsular.[24] The syntheses of **8**–**10** and their structures **11**–**13** have been reported.[25] As expected, **11** contains a hole lined with 24 electrons, which are shielded from solvation by six aryl and six methyl groups. The snowflake-like structures **11**, **12**, and **13** are nearly identical. Thus **8** is the first ligand system to be designed and synthesized which was completely organized for complexation during synthesis, rather than during complexation.

A method was developed for determining the binding free energies of lipophilic hosts **H** toward guest picrate salts of $Li^{\oplus}$, $Na^{\oplus}$, $K^{\oplus}$, $Rb^{\oplus}$, $Cs^{\oplus}$, $NH_4^{\oplus}$, $CH_3NH_3^{\oplus}$, and *t*-$BuNH_3^{\oplus}$. The guest salts **G**Pic were distributed between $CDCl_3$ and D_2O at 25 °C in the presence and absence of host. From the results, K_a [mol^{-1}] and $-\Delta G^0$ values [kcal mol^{-1}] were calculated [Eq. (a)]. This method was rapid

$$\mathbf{H} + \mathbf{G}\,\mathrm{Pic} \underset{k_{-1}}{\overset{k_1}{\rightleftharpoons}} \mathbf{H}\cdot\mathbf{G}\cdot\mathrm{Pic} \qquad K_a = k_1/k_{-1};\ -\Delta G^0 = RT\ln K_a \quad \text{(a)}$$

and convenient for obtaining $-\Delta G^0$ values at 25 °C ranging from about 6 to 16 kcal mol^{-1} in $CDCl_3$ saturated with D_2O.[26] Higher values (up to 22 kcal mol^{-1}) were obtained by equilibration experiments between complexes of known and those of unknown $-\Delta G^0$ values.[18,27,28] Others were determined from measured k_{-1} and k_1 values, all in the same medium at 25 °C.[18] Spherand **8** binds LiPic with

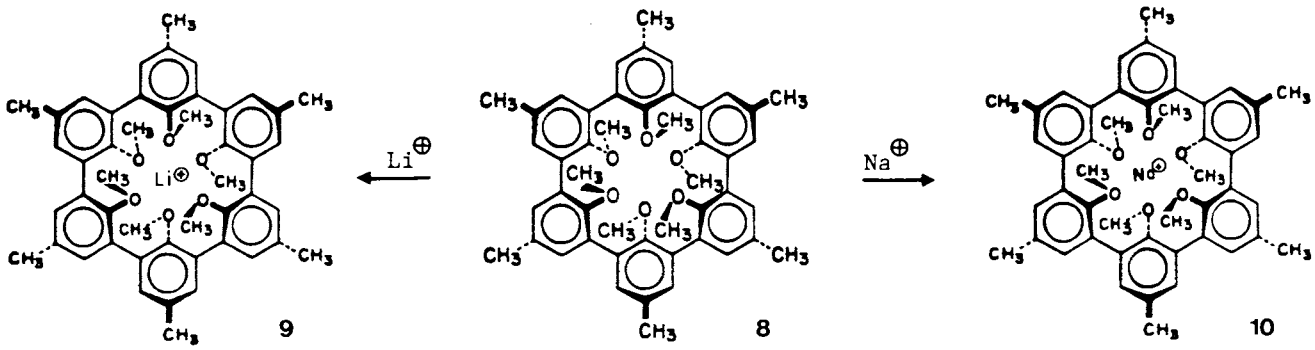

9 **8** **10**

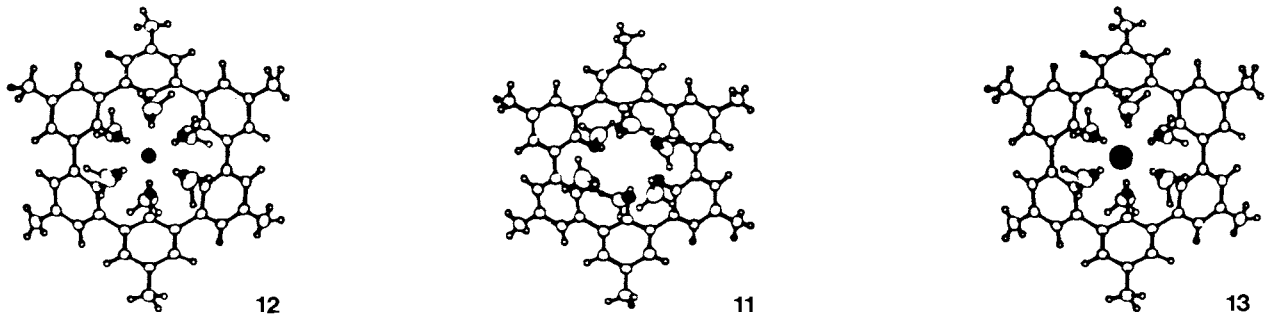

12 **11** **13**

>23 kcal mol^{-1}, NaPic with 19.3 kcal mol^{-1}, and totally rejects the other standard ions, as well as a wide variety of other di- and trivalent ions.[18] The open-chain counterpart of **8**, podand **14**, binds LiPic and NaPic with $-\Delta G^0 < 6$ kcal mol^{-1}.[29] *Podand* is the family name given to acyclic hosts.[15]

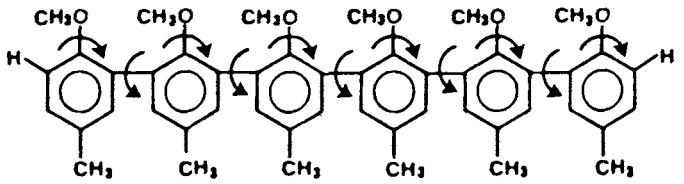

14

Podand **14** differs constitutionally from spherand **8** only in the sense that **14** contains two hydrogen atoms in place of one Ar–Ar bond in **8**. The two hosts differ radically in their conformational structures and states of solvation. The spherand possesses a single conformation ideally arranged for binding $Li^{\oplus}$ and $Na^{\oplus}$. Its oxygens are deeply buried within a hydrocarbon shell. The orbitals of their unshared electron pairs are in a microenvironment whose dielectric properties are between those of a vacuum and of a hydrocarbon. No solvent can approach these six oxygens, which remain unsolvated. The free energy costs of organizing the spherand into a single conformation and of desolvating its six oxygens were paid for during its synthesis. Thus spherand **8** is preorganized for binding.[30] The podand can, in principle, exist in over 1000 conformations, only two of which can bind metal ions octahedrally. The free energy for organizing the podand into a binding conformation and desolvating its six oxygens must come out of its complexation free energy. Thus the podand is not preorganized for binding, but is randomized to maximize the entropy of mixing of its conformers, and to maximize the attractions between solvent and molecular parts.

The difference in $-\Delta G^0$ values for spherand **8** and podand **14** binding $Li^{\oplus}$ is >17 kcal mol^{-1}, corresponding to a difference in K_a of a factor of $>10^{12}$. The difference in $-\Delta G^0$ values for **8** and **14** binding $Na^{\oplus}$ is >13 kcal mol^{-1}, corresponding to a difference in K_a of a factor of

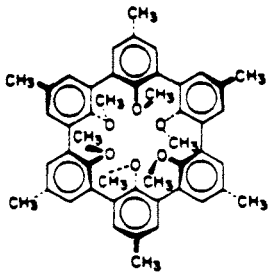

8, spherand

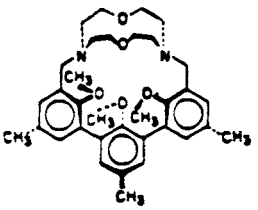

15, cryptaspherand

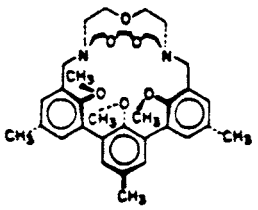

16, cryptaspherand

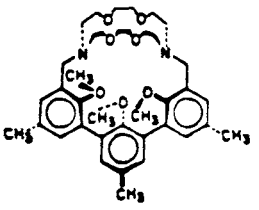

17, cryptaspherand

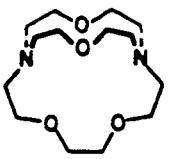

18, cryptand

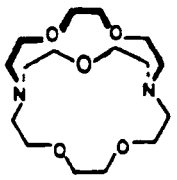

19, cryptand

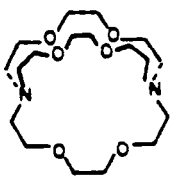

6, cryptand

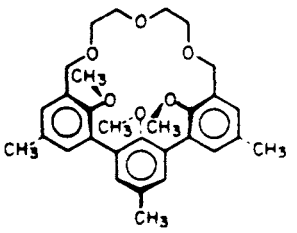

20, hemispherand

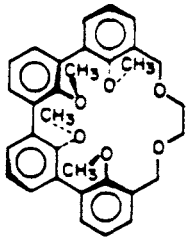

21, hemispherand

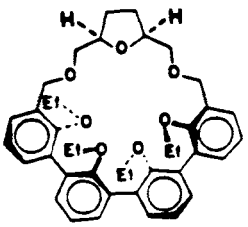

22, hemispherand

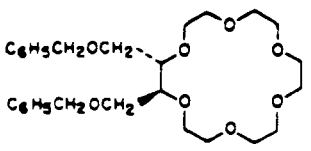

23, corand

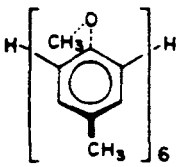

14, podand

Scheme 3. Host structures arranged in the order of decreasing $-\Delta G^0$ values for binding their most complementary guest picrate salts at 25°C in $CDCl_3$ saturated with D_2O.

$> 10^{10}$. These differences are dramatically larger than any we have encountered that are associated with other effects on binding power toward alkali metal ion guests. We conclude that *preorganization is a central determinant of binding power*. We formalized this conclusion in terms of what we call the principle of preorganization, which states that "the more highly hosts and guests are organized for binding and low solvation prior to their complexation, the more stable will be their complexes." Both enthalpic and entropic components are involved in preorganization, since solvation contains both components.[29] Furthermore, binding conformations are sometimes enthalpically rich. For example, the benzene rings in spherand **8** and spheraplexes **9** and **10** are somewhat folded from their normal planar structures to accommodate the spacial requirements of the six methoxy groups.[30] The anisyl group is an intrinsically poor ligand.[31,32] That **8** is such a strong binder provides an extreme example of the power of preorganization.

Families of hosts generally fall into the order of their listing in Scheme 3 when arranged according to their $-\Delta G^0$ values with which they bind their most complementary guests: spherands > cryptaspherands > cryptands > hemispherands > corands > podands. Corand is the family name given to modified crown ethers.[33] Spheraplex **9** (= **8** · $Li^{\oplus}$) provides a $-\Delta G^0$ value of > 23 kcal mol^{-1}. Cryptaspheraplexes **15** · $Na^{\oplus}$, **16** · $Na^{\oplus}$, and **17** · $Cs^{\oplus}$[34] give values of 20.6, 21.0, and 21.7 kcal mol^{-1}, respectively.[27] Cryptaplexes **18** · $Li^{\oplus}$, **19** · $Na^{\oplus}$, and **6** · $K^{\oplus}$ give respective values of 16.6, 17.7, and 18.0 kcal mol^{-1}.[27] Hemispheraplexes **20** · $Na^{\oplus}$, **21** · $Na^{\oplus}$, and **22** · $K^{\oplus}$ are bound by 12.2, 13.5, and 11.6 kcal mol^{-1}.[35,36] Coraplex **23** · $K^{\oplus}$ has a $-\Delta G^0$ value of 11.4[26,37] and podaplexes **14** · $M^{\oplus}$ values of < 6 kcal mol^{-1}.[29] Although the numbers of binding sites and their characters certainly influence these values, the degree of preorganization appears to be dominant in providing this order.

Structural Recognition

Just as preorganization is the central determinant of binding power, complementarity is the central determinant of structural recognition. The binding energy at a single contact site is at most a few kilocalories per mole, much lower than that of a covalent bond. Contacts at several sites between hosts and guests are required for structuring of complexes. Such contacts depend on complementary placements of binding sites in the complexing partners.

The most extensive correlations of structural recognition with host-guest structure involve the K_a values with which the spherands, cryptaspherands, cryptands, and hemispherands associate with the various alkali metal picrate salts at 25 °C in $CDCl_3$ saturated with D_2O. Scheme 4 lists the $K_a^A/K_a^{A'}$ ratios for various hosts binding two alkali metal ions A and A′ that are adjacent to each other in the periodic table.[33] Notice that factors as high as $> 10^{10}$ are observed for the spherands binding $Na^{\oplus}$ better than $K^{\oplus}$.

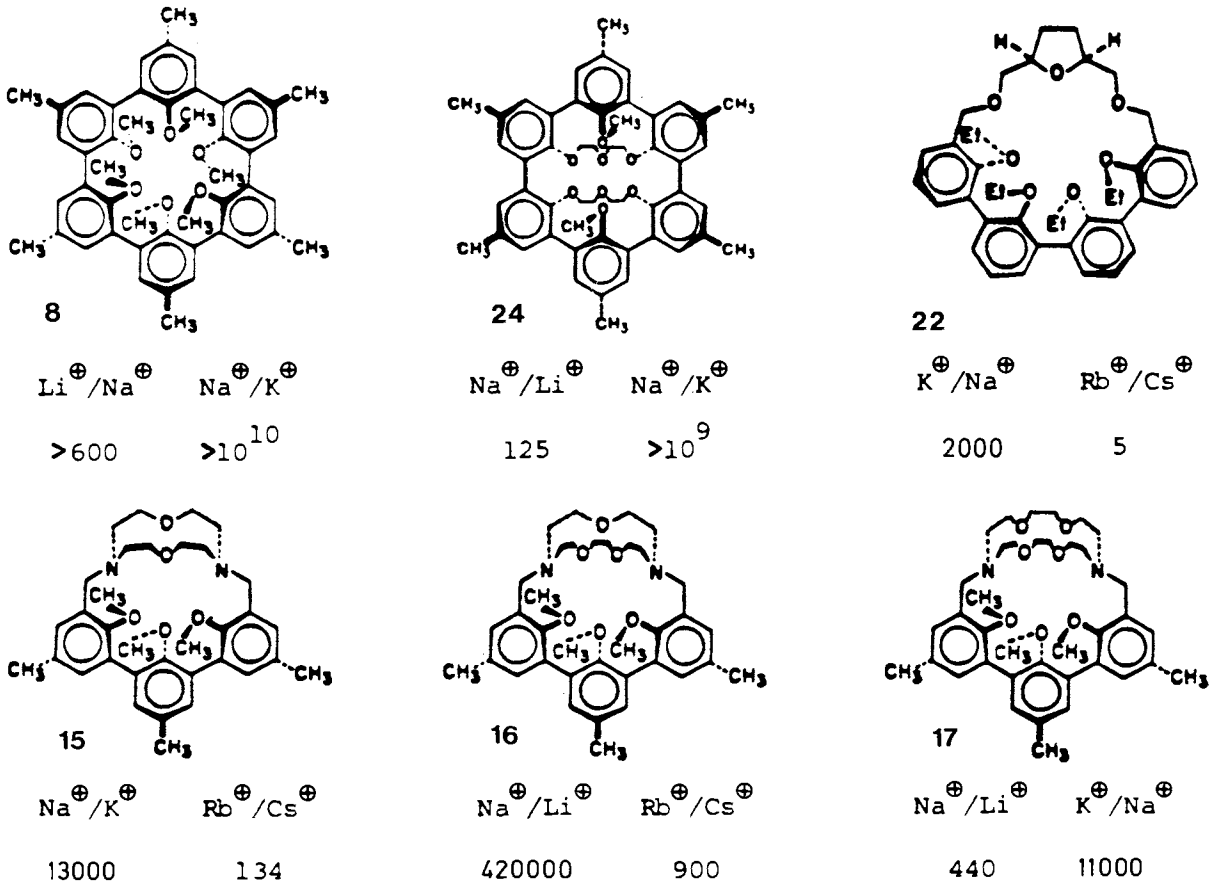

Scheme 4. Structural recognition measured by $K_a^A/K_a^{A'}$ values for alkali metal picrates at 25 °C in $CDCl_3$ saturated with D_2O.

Cryptaspherand **15** provides a factor of 13000. The highest factors for hosts binding $K^{\oplus}$ better than $Na^{\oplus}$ are observed for cryptaspherand **17** (11000) and hemispherand **22** (2000). The highest factors for a host binding $Li^{\oplus}$ over $Na^{\oplus}$ are found for cryptand **18** (4800). These particular selectivities are important because of the physiological importance of these ions. These hosts, or modifications of them, are being developed for commercial use in the medical diagnostics industry.

Scheme 5 provides stereoviews of crystal structures of capsular complexes **15** · $Na^{\oplus}$, **17** · $Na^{\oplus}$, and **17** · $K^{\oplus}$. Notice that in **15** · $Na^{\oplus}$ and **17** · $K^{\oplus}$ the metal ions contact all of the heteroatoms, whereas in **17** · $Na^{\oplus}$, the $Na^{\oplus}$ ion does not. Here is a visual example of complementarity vs. noncomplementarity. The $K_a^A/K_a^{A'}$ ratio for **17** · $K^{\oplus}$/**17** · $Na^{\ominus}$ = 11000.[34]

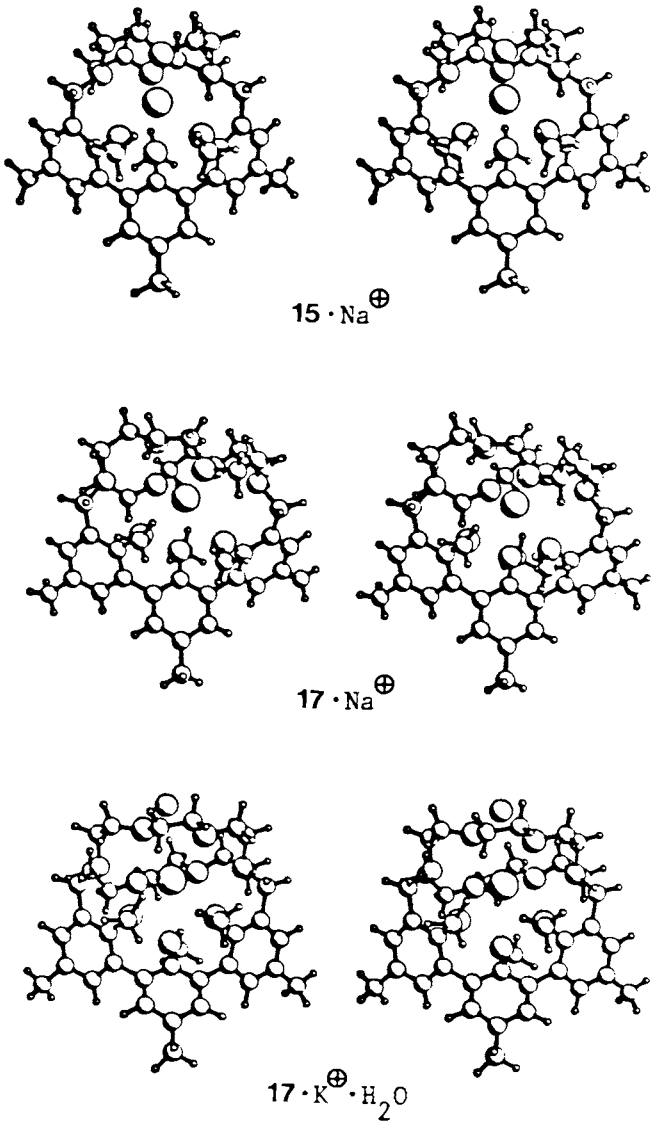

Scheme 5. Stereoviews of crystal structures of cryptaspheraplexes.

Arrangement of the classes of hosts in decreasing order of their ability to select between the alkali metal ion guests provides spherands > cryptaspherands ~ cryptands > hemispherands > corands > podands. This order is similar but less rigidly followed than that for host preorganization. In some cases, rather small changes in structure provide a substantial spread in $-\Delta G^0$ values for binding under our standard conditions.[33]

Chiral recognition in complexation is a fundamental aspect of structural recognition in complexation in the biotic world. We synthesized host **25** in an enantiomerically pure form to study its ability to distinguish between enantiomers in the complexation of amino acids and ester salts in solution. We were careful to design a system containing at least one C_2 axis of symmetry, a tactic that made the hosts *nonsided* with respect to perching guests. A solution of (*R,R*)-**25** in $CDCl_3$ at 0°C was used to extract D_2O solutions of racemic amino acid or ester salts. As predicted in advance by CPK molecular models, the D-enantiomers were extracted preferentially into the organic layer. Chiral recognition factors ranged from a high of 31 for $C_6H_5CH(CO_2CH_3)NH_3PF_6$ to a low of 2.3 with $CH_3CH(CO_2H)NH_3ClO_4$. These factors represent free energy differences between diastereomeric complexes of 1.9 kcal mol^{-1} and 0.42 kcal mol^{-1}, respectively. Other amino acid and ester salt guests ranged between these values. We interpreted these results in terms of the complementarity between host and guest of the (*R,R*)-D-configurations as visualized in the complex **26**, and the lack of complementarity in those of the (*R,R*)-L-configurations, which were designed not to form.[38,39]

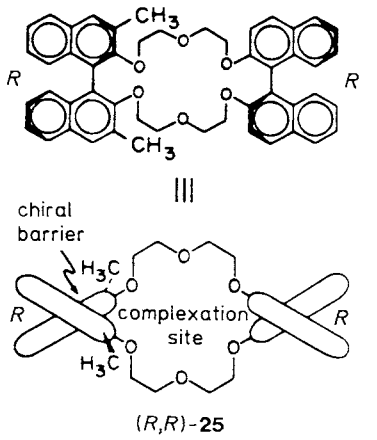

(*R,R*)-**25**

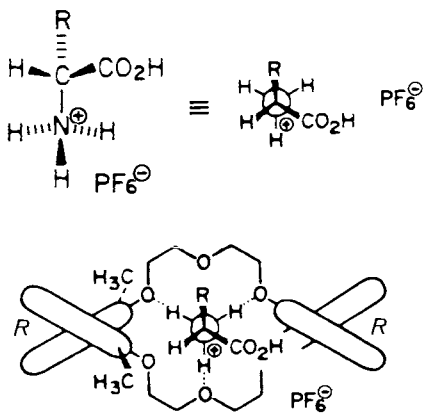

26

An amino acid and ester resolving machine was designed, built, and tested, which is pictured in Figure 1. It made use of chiral recognition in transport of amino acid or ester salts through lipophilic liquid membranes. From the central reservoir of the W-tube containing an aqueous

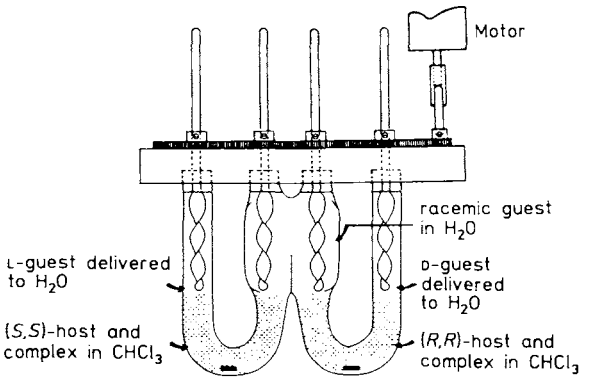

Fig. 1. Enantiomer resolving machine.

solution of racemic salt, the L-enantiomer was picked up by (*S,S*)-**25** in the-left hand chloroform reservoir and delivered to the left-hand aqueous layer, while the D-enantiomer was transported by (*R,R*)-**25** in the right-hand chloroform reservoir and delivered to the right-hand aqueous layer. The thermodynamic driving force for the machine's operation involved exchange of an energy-lowering entropy of dilution of each enantiomer for an energy-lowering entropy of mixing. To maintain the concentration gradients down which the enantiomers traveled in each arm of the W-tube, fresh racemic guest was continuously added to the central reservoir, and L- and D-$C_6H_5CH(CO_2CH_3)NH_3PF_6$ of 86–90% enantiomeric excess were continuously removed from the left- and right-hand aqueous reservoirs, respectively.[40]

In another experiment, we covalently attached the working part of (*R,R*)-**25** at a remote position of the molecule to a macroreticular resin (polystyrene-divinylbenzene) to give immobilized host of ~18000 mass units per average active site. This material (the host part of **27**) was used to give complete enantiomeric resolution of several amino acid salts. The behavior in the chromatographic resolution paralleled that observed in the extraction and transport experiments, and was useful both analytically and preparatively. Separation factors ranged from 26 to 1.4, the complexes of the (*R,R*)-D- or (*S,S*)-L-configurations always being the more stable. The structure envisioned for the more stable complex is formulated in **27**.[41]

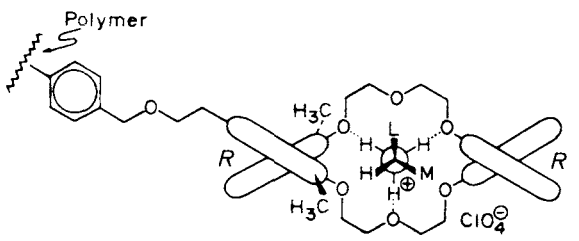

27

Partial Transacylase Mimics

The design and synthesis of enzyme-mimicking host compounds remains one of the most challenging and stimulating problems of organic chemistry. We chose to examine transacylase mimics first because the mechanism of action of these enzymes had been so thoroughly studied.

The active site of chymotrypsin combines a binding site, a nucleophilic hydroxyl, an imidazole, and a carboxyl group in an array preorganized largely by hydrogen bonds as indicated in **28**. With the help of molecular models, we designed **29** as an "ultimate target" host possessing roughly the same organization of groups as that of **28**.

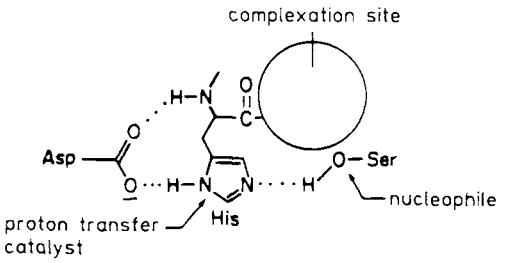

28

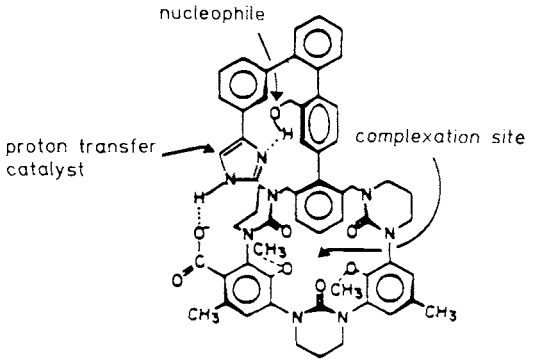

29

Compound **29** is much too complicated to synthesize without getting encouragement from simpler model compounds. An incremental approach to **29** was employed. We first prepared **30**, and found that it binds *t*-$BuNH_3Pic$ in $CDCl_3$ saturated with D_2O with $-\Delta G^0 = 13.2$ kcal mol^{-1}. The complex, **30** · $tBuNH_3^{\oplus}$, had the expected crystal structure.[42] Accordingly, **31** was prepared, and found to bind CH_3NH_3Pic and NaPic under our standard conditions with $-\Delta G^0 = 12.7$ and 13.6 kcal mol^{-1}, respectively.[43] Host **31** was acylated by **32** to give **33** and *p*-nitrophenol. The kinetics of formation of **33** were measured in $CHCl_3$, and found to be first order in added Et_3N/Et_3NHClO_4 buffer ratio. Thus the alkoxide ion is the nucleophile. The rate constant for acylation of **31** by **32** was calculated to be ~10^{11} higher valued than the rate constant for the noncomplexed model compound, 3-phenylbenzyl alcohol.[44] This high factor demonstrates that collecting and orienting reactants through highly structured complexation can result in an enormous rate acceleration. When $NaClO_4$ was added to the medium, the acylation rate of **31**

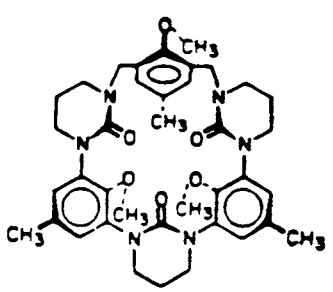

30

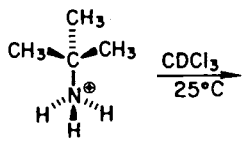

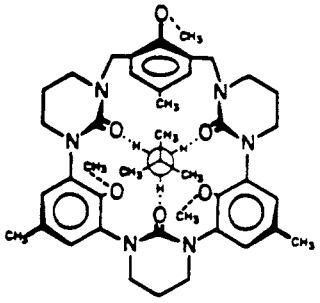

30 · $(CH_3)_3CNH_3^{\oplus}$

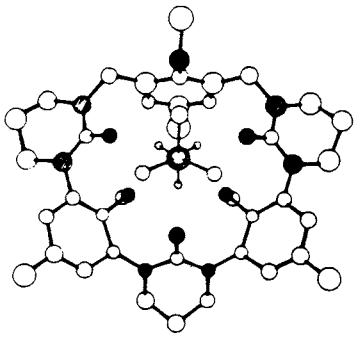

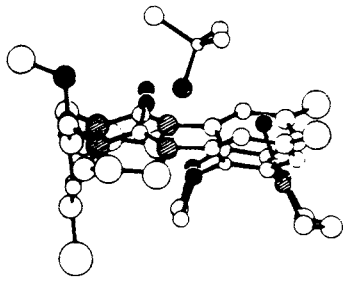

30 · $(CH_3)_3CNH_3^{\oplus}$

was depressed by several powers of ten. Thus the acylation of **31**, like that of the serine esterases, is subject to competitive inhibition.

gave **36**. In $CHCl_3$ in the absence of any added base, the observed rate constant for acylation of **34** by **32** was higher by a factor of 10^5 than that for acylation of an equal

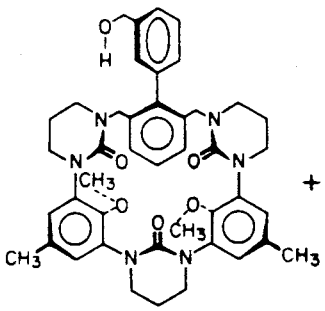

31

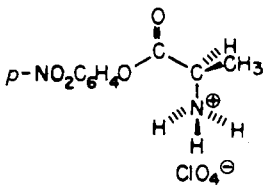

32

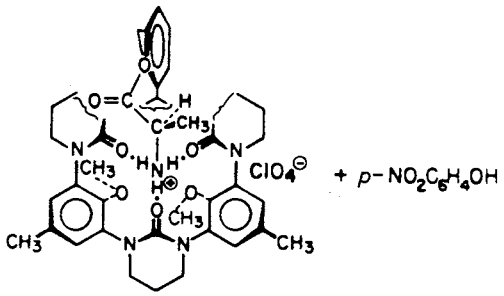

33

A thirty-step synthesis of **34** was then devised, and about 0.5 g of the compound prepared.[45] This compound combines the binding site, the nucleophilic hydroxy group, and the imidazole proton-transfer agent in the same molecule, lacking only the carboxylate group of final target compound **29**. Compound **34** complexed CH_3NH_3Pic and NaPic with respective $-\Delta G^0$ values of 11.4 and 13.6 kcal mol^{-1} in $CDCl_3$ saturated with D_2O at 25°C. In pyridine-chloroform, amino ester salt **32** instantaneously acylated the imidazole group of **34** to give **35**, which more slowly

molar mixture of noncomplexing model compounds **39** or **40** under the same conditions. The same ratio was obtained when **37** was substituted for **34**. Thus the imidazole groups of **34** and **37** are the sites of acylation. Introduction of $NaClO_4$ into the medium as a competitive inhibitor of complexation destroyed much of the rate acceleration. When **32** added to **38** was substituted for **34**, the resulting complex acylated imidazole **40** with a 10 rate-constant factor increase. Thus complexed **32** is a better acylating agent than **32** alone.

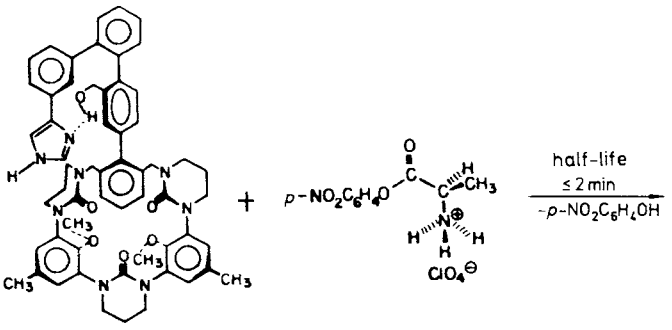

34 32

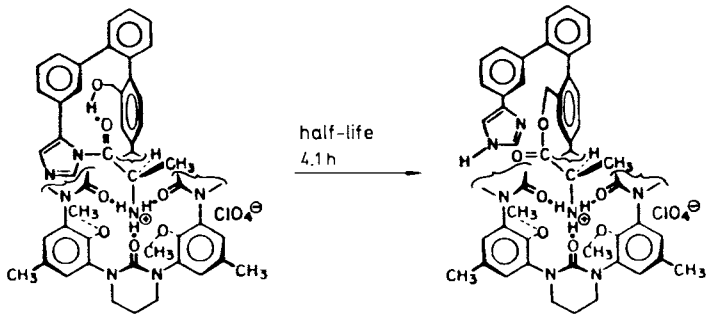

35 36

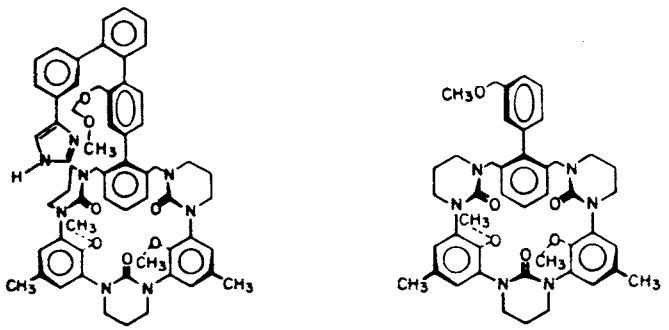

37 38

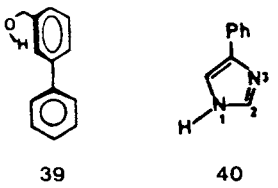

39 40

The disadvantages of comparing rate constants for reactions with different molecularities are avoided by referring to uncomplexed **34** or **37**, noncomplexing imidazole **40**, and uncomplexed acylating agent **32** as standard starting states, and the rate-limiting transition states for transacylation as standard final states. This treatment introduces K_a into the second order rate constant expression when complexation precedes acylation. The resulting second order rate constants for **32** acylating **34** or **37** are higher by factors of 10^{10} or 10^{11} than the second order rate constant for **32** acylating **40**. This work clearly demonstrates that complexation of the transition states for transacylation can greatly stabilize those transition states to produce large rate factor increases over comparable noncomplexed transition states.[46] Others have shown that the imidazole of chymotrypsin is acylated first by esters of nonspecific substrates.[47]

These investigations demonstrate that totally synthetic systems can be designed and prepared which mimic the following properties of enzymes: the ability to use complexation to vastly enhance reaction rates and the sensitivity to competitive inhibition. In a different, chiral system, we demonstrated that a synthetic host was capable of distinguishing between enantiomeric reactants.[48,49] We anticipate that as the field matures, many of the other remarkable properties of enzyme systems will be observed in designed, synthetic systems. Our results illustrate some of the strategies and methods that might be applied in this expanding field of research.

Cavitands—Synthetic Molecular Vessels

Although enforced cavities of molecular dimensions are frequently encountered in enzyme systems, RNA, or DNA, they are almost unknown among the seven million synthetic organic compounds. In biological chemistry such cavities play the important role of providing concave surfaces to which are attached convergent functional groups which bind substrates and catalyze their reactions. If synthetic biomimetic systems are to be designed and investigated, simple means must be found of synthesizing compounds containing enforced concave surfaces of dimensions large enough to embrace simple molecules or ions. We applied the name cavitand to this class of compound.[50]

Cavitands designed and studied include compounds **42**–**45**, many of which were prepared from **41**. The structure and conformational mobility of **41** had been established by *A. G. S. Högberg*.[51] The substance is prepared in good

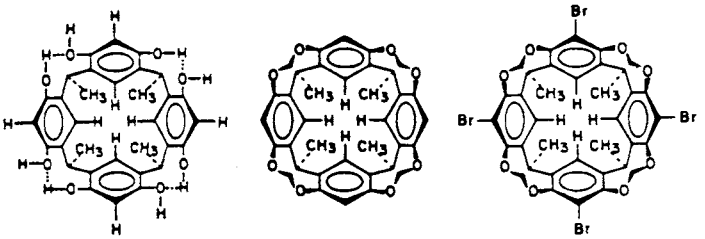

41 42 43

yield by treatment of resorcinol with acetaldehyde and acid. We rigidified **41** and its derivatives by closing four additional rings to produce **42**–**45**.[50,52]

As anticipated by molecular model examinations, **42**–**45** crystallize only as solvates because these rigid molecules taken alone are incapable of filling their voids either intermolecularly or intramolecularly. They are shaped like bowls of differing depth supported on four methyl "feet." Compound **42** forms crystallates with SO_2, CH_3CN, and CH_2Cl_2, molecules to which it is complementary (molecu-

lar model examination). Cavitand **43**, whose cavity is deeper, crystallizes with a mole of $CHCl_3$. Crystal structures of **42** · CH_2Cl_2 and **43** · $CHCl_3$ show they are caviplexes, as predicted.[53] Cavitand **44** is vase-shaped. It crystallizes with one mole of $(CH_3)_2NCHO$, which is just small enough to fit into the interior of **44** in models. Although the amide cannot be removed at high temperature and low pressure, it is easily displaced with $CHCl_3$, one and one-half moles of which appear to take the place of the $(CH_3)_2NCHO$ in the crystallate.[50]

Treatment of octol **41** with R_2SiCl_2 gave a series of cavitands, of which **45** is typical. In molecular models, **45** has

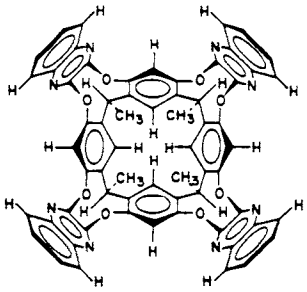

44

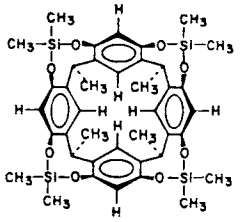

45

a well-shaped cavity, defined by the bottoms of four aryls and by four inward-turned methyl groups. In molecular models, this well is complementary to small, cylindrical molecules such as S=C=S, $CH_3C{\equiv}CH$, and O=O, but not to larger compounds such as $CDCl_3$ or C_6D_6. Cavitand **45** and its analogues when dissolved in $CDCl_3$ or C_6D_6 complex guests such as those mentioned above, whose external surfaces are complementary to the internal surface of the host cavity. Association constants were determined for **45** and its analogues binding S=C=S. Values of $-\Delta G^0$ as high as 2 kcal mol^{-1} have been observed. A crystal structure of **45** · CS_2 shows that CS_2 occupies the well in the expected manner. Compound **45** in $CDCl_3$ was also shown to bind dioxygen reversibly.[52] Dissolution of **45** in solvents such as $CDCl_3$ or C_6D_6 is the equivalent of dissolving "holes" in a medium into which appropriately shaped solutes fall. The discrimination shown by the holes for the guests exemplifies the principle of complementarity as applied to cavitand complexation.

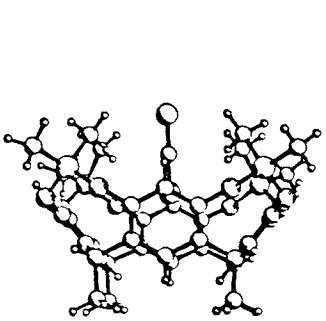

45·CS_2 (side view)

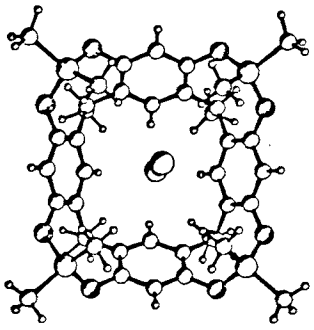

45·CS_2 (top view)

The next steps in research on these cavitands is to append to them water-solubilizing and catalytic groups. The former will provide them with hydrophobic driving forces to complex nonpolar guests, and the latter to catalyze reactions of such guests.

Carcerands—Synthetic Molecular Cells

Absent among the millions of organic compounds hitherto reported are closed-surface hosts with enforced interiors large enough to imprison behind covalent bars, guests the size of ordinary solvent molecules. After much thought and molecular model examination, we chose **48** as the target for synthesis of the first molecular cell. The term *carcerand* was applied to this class of compound. The synthesis involved treating Cs_2CO_3 with a solution in $(CH_3)_2NCHO$–$(CH_2)_4O$ of equal molar amounts of cavitands **46** and **47** under an atmosphere of argon. The first question to be answered was: what guest compounds would be trapped inside during the shell closure? This

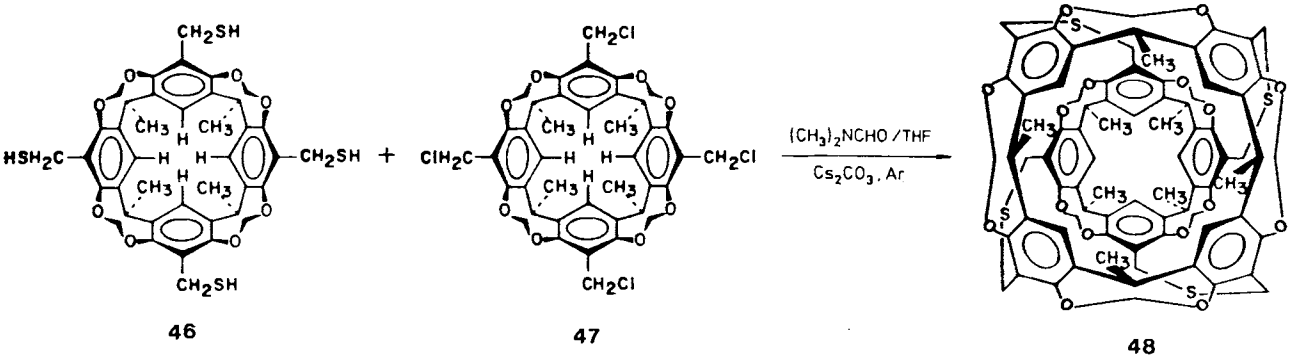

46 **47** **48**

question is akin to asking whether two soup bowls closed rim-to-rim under the surface of a kettle of stew would net any stew. The answer was that **48** "contained" essentially every kind of component of the medium present during ring closure.[54]

The product (**48** and guests) was very insoluble in all media, and was purified by extracting it with the most powerful solvents of each type. The remaining material was subjected to elemental analysis for C, H, S, O, N, Cl, and Cs. Nitrogen analysis and an IR spectrum of the substance revealed that $(CH_3)_2NCHO$ had been entrapped. The presence of equivalent amounts of Cs and Cl demonstrated that one or the other ion or both had to be encapsulated in the host.

A fast atom bombardment mass spectrum of **48**·**G** showed the presence of the following host-guest combinations, the species trapped in the interior of **48** being enclosed by parentheses:

48 (no guest)	**48**·$(Cs^{\oplus})\cdot Cl^{\ominus}$
48·$[(CH_3)_2NCHO]$	**48**·$(Cs^{\oplus} + H_2O)\cdot Cl^{\ominus}$
48·$[THF + H_2O]$	**48**·$[(CH_3)_2NCHO + Cs^{\oplus}]\cdot Cl^{\ominus}$
48·$(Cs^{\ominus} + Ar)\cdot Cl^{\ominus}$	**48**·$(Cs^{\oplus} + H_2O + Cs^{\oplus})\cdot 2Cl^{\ominus}$
48·$(Cs^{\oplus} + Cl^{\ominus})$	**48**·$(Cs^{\ominus} + Cs^{\ominus} + Cl^{\ominus})\cdot Cl^{\ominus}$

No peaks were found at molecular masses above that of the last carcaplex listed. None were observed that could not be interpreted in terms of appropriate host-guest combinations. When highly dried **48** was boiled with D_2O, the **48**·$(Cs^{\oplus} + H_2O)$ peak was substantially replaced by a **48**·$(Cs^{\oplus} + D_2O)$ peak. Models suggest that **48** has two small portals lined with methyl groups through which molecules as small as H_2O can pass.

Molecular models of **48** show that its interior surface is complementary to the outer surface of *anti*-$ClCF_2CF_2Cl$. Shell closure of **46** and **47** in the presence of this Freon resulted in entrapment of a small amount of this gas in the interior of **48**.

The FAB-MS coupled with the elemental analyses indicated that about 5% of the mixture was noncomplexed **48**, about 60% encapsulated $Cs^{\oplus}$, about 45% encapsulated $(CH_3)_2NCHO$, 15% encapsulated $(CH_2)_4O$, but only 1–2% encapsulated $Cl^{\ominus}$. Thus $Cs^{\oplus}$ was mainly inside and $Cl^{\ominus}$ mainly outside the carcaplex. Models show that if the final covalent bond leading to **48**·**G** involves an intramolecular SN_2 linear transition state as in **48**, any $Cs^{\oplus}$ ion-paired to the $S^{\ominus}$ is trapped inside the cavity and the $Cl^{\ominus}$ must be external to the cavity.[54]

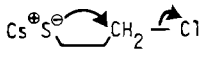

49

We anticipate that unusual physical and chemical properties will provide unusual uses for carcaplexes, particularly when their design renders them soluble and separable.

I warmly thank the following co-workers for carrying out the research described here: L. A. Singer, R. H. Bauer, M. G. Siegel, J. M. Timko, K. Madan, S. S. Moore, T. L. Tarnowski, G. M. Lein, J. L. Toner, J. M. Mayer, S. P. Ho, M. P. de Grandpre, S. P. Artz, G. D. Y. Sogah, S. C. Peacock, L. A. Domeier, H. E. Katz, I. B. Dicker, J. R. Moran, and K. D. Stewart as graduate students; E. P. Kyba, L. R. Sousa, K. Koga, R. C. Helgeson, G. W. Gokel, D. M. Walba, J. M. Cram, T. Kaneda, S. B. Brown, K. E. Koenig, P. Stückler, G. D. Y. Sogah, G. R. Weisman, Y. Chao, F. C. A. Gaeta, M. Newcomb, P. Y. S. Lam, S. Karbach, A. G. S. Högberg, Y. H. Kim, and M. Lauer as postdoctoral fellows. The crystal structure work of colleagues K. N. Trueblood, C. B. Knobler, E. F. Maverick, and I. Goldberg was indispensable.

I gratefully acknowledge the financial support of the following granting agencies: the Division of Basic Energy Sciences of the Department of Energy for the work on the metal ion binding; the National Science Foundation for the work on structural recognition; the National Institutes of Health for research on catalysis. I warmly thank all former and present co-workers, over 200 in number, and the many others whose results and discussions have stimulated and instructed me over the years. My long-time colleague, Roger C. Helgeson, has not only provided me with excellent ideas and results, but also with continuity. The artwork displayed here and in my slides and publications for the last twelve years was done by Mrs. June Hendrix, to whom I am much indebted.

Received: February 24, 1988 [A 683 IE]
German version: *Angew. Chem. 100* (1988) 1041

[1] D. J. Cram, R. H. Bauer, *J. Am. Chem. Soc. 81* (1959) 5971–5977.
[2] L. A. Singer, D. J. Cram, *J. Am. Chem. Soc. 85* (1963) 1080–1084.
[3] C. J. Pedersen, *J. Am. Chem. Soc. 89* (1967) 2495–2496.
[4] C. J. Pedersen, *J. Am. Chem. Soc. 89* (1967) 7017–7036.
[5] B. Dietrich, J.-M. Lehn, J.-P. Sauvage, *Tetrahedron Lett. 1969*, 2885–2888.
[6] B. Dietrich, J.-M. Lehn, J.-P. Sauvage, *Tetrahedron Lett. 1969*, 2889–2892.
[7] E. P. Kyba, M. G. Siegel, L. R. Sousa, G. D. Y. Sogah, D. J. Cram, *J. Am. Chem. Soc. 95* (1973) 2691–2692.
[8] E. P. Kyba, K. Koga, L. R. Sousa, M. G. Siegel, D. J. Cram, *J. Am. Chem. Soc. 95* (1973) 2692–2693.
[9] R. C. Helgeson, K. Koga, J. M. Timko, D. J. Cram, *J. Am. Chem. Soc. 95* (1973) 3021–3023.
[10] R. C. Helgeson, J. M. Timko, D. J. Cram, *J. Am. Chem. Soc. 95* (1973) 3023–3025.
[11] G. W. Gokel, D. J. Cram, *J. Chem. Soc. Chem. Commun. 1973*, 481–482.
[12] D. J. Cram, J. M. Cram, *Science (Washington) 183* (1974) 803–809.
[13] Aeschylus (525–456 v. Chr.): *Choephoren*.
[14] E. P. Kyba, R. C. Helgeson, K. Madan, G. W. Gokel, T. L. Tarnowski, S. S. Moore, D. J. Cram, *J. Am. Chem. Soc. 99* (1977) 2564–2571.
[15] F. Vögtle, E. Weber (Eds.): *Top. Curr. Chem. 98* (1981); *ibid. 101* (1982); *ibid. 121* (1984).
[16] W. L. Koltun, *Biopolymers 3* (1965) 665–679.
[17] The crystal structures and references to them up to 1980 are gathered in: D. J. Cram, K. N. Trueblood, *Top. Curr. Chem. 98* (1981) 43–106.
[18] D. J. Cram, G. M. Lein, *J. Am. Chem. Soc. 107* (1985) 3657–3668.
[19] J. M. Timko, S. S. Moore, D. M. Walba, P. C. Hiberty, D. J. Cram, *J. Am. Chem. Soc. 99* (1977) 4207–4219.
[20] R. C. Helgeson, T. L. Tarnowski, D. J. Cram, *J. Org. Chem. 44* (1979) 2538–2550.
[21] J. D. Dunitz, M. Dobler, P. Seiler, R. P. Phizackerly, *Acta Crystallogr. Sect. B 30* (1974) 2733–2738; J. D. Dunitz, P. Seiler, *ibid. 30* (1974) 2739–2741; M. Dobler, J. D. Dunitz, P. Seiler *ibid. 30* (1974) 2741–2743; P. Seiler, M. Dobler, J. D. Dunitz, *ibid. 30* (1974) 2744–2745; M. Dobler, R. P. Phizackerley, *ibid. 30* (1974) 2746–2748; 2748–2750.
[22] R. Weiss, B. Metz, D. Moras, *Proc. Int. Conf. Coord. Chem. 13th 2* (1970) 85–86.
[23] B. Metz, D. Moras, R. Weiss, *Acta Crystallogr. Sect. B29* (1973) 1377–1381.
[24] D. J. Cram, T. Kaneda, R. C. Helgeson, G. M. Lein, *J. Am. Chem. Soc. 101* (1979) 6752–6754.
[25] K. N. Trueblood, C. B. Knobler, E. Maverick, R. C. Helgeson, S. B. Brown, D. J. Cram, *J. Am. Chem. Soc. 103* (1981) 5594–5596.
[26] R. C. Helgeson, G. R. Weisman, J. L. Toner, T. L. Tarnowski, Y. Chao, J. M. Mayer, D. J. Cram, *J. Am. Chem. Soc. 101* (1979) 4928–4941.
[27] D. J. Cram, S. P. Ho, *J. Am. Chem. Soc. 107* (1985) 2998–3005.

[28] D. J. Cram, *Science (Washington) 219* (1983) 1177–1183.
[29] D. J. Cram, M. P. deGrandpre, C. B. Knobler, K. N. Trueblood, *J. Am. Chem. Soc. 106* (1984) 3286–3292.
[30] D. J. Cram, T. Kaneda, R. C. Helgeson, S. B. Brown, C. B. Knobler, E. Maverick, K. N. Trueblood, *J. Am. Chem. Soc. 107* (1985) 3645–3657.
[31] J. Mitsky, L. Jaris, R. W. Taft, *J. Am. Chem. Soc. 94* (1972) 3442–3445.
[32] H. W. Aitken, W. R. Gilkerson, *J. Am. Chem. Soc. 95* (1973) 8551–8559.
[33] D. J. Cram, *Angew. Chem. 98* (1986) 1041–1060; *Angew. Chem. Int. Ed. Engl. 25* (1986) 1039–1057.
[34] D. J. Cram, S. P. Ho, C. B. Knobler, E. Maverick, K. N. Trueblood, *J. Am. Chem. Soc. 107* (1985) 2989–2998.
[35] K. E. Koenig, G. M. Lein, P. Stückler, T. Kaneda, D. J. Cram, *J. Am. Chem. Soc. 101* (1979) 3553–3566.
[36] S. P. Artz, D. J. Cram, *J. Am. Chem. Soc. 106* (1984) 2160–2171.
[37] The *cis*-isomer gave a lower $-\Delta G^0_{av}$ value than the *trans*-isomer by 0.7 kcal mol^{-1}.
[38] S. C. Peacock, L. A. Domeier, F. C. A. Gaeta, R. C. Helgeson, J. M. Timko, D. J. Cram, *J. Am. Chem. Soc. 100* (1978) 8190–8202.
[39] S. C. Peacock, D. M. Walba, F. C. A. Gaeta, R. C. Helgeson, D. J. Cram, *J. Am. Chem. Soc. 102* (1980) 2043–2052.
[40] M. Newcomb, J. L. Toner, R. C. Helgeson, D. J. Cram, *J. Am. Chem. Soc. 101* (1979) 4941–4947.
[41] G. D. Y. Sogah, D. J. Cram, *J. Am. Chem. Soc. 101* (1979) 3035–3042.
[42] D. J. Cram, I. B. Dicker, M. Lauer, C. B. Knobler, K. N. Trueblood, *J. Am. Chem. Soc. 106* (1984) 7150–7167.
[43] H. E. Katz, D. J. Cram, *J. Am. Chem. Soc. 105* (1983) 135–137.
[44] D. J. Cram, H. E. Katz, I. B. Dicker, *J. Am. Chem. Soc. 106* (1984) 4987–5000.
[45] D. J. Cram, P. Y. S. Lam, *Tetrahedron 42* (1986) 1607–1615.
[46] D. J. Cram, P. Y. S. Lam, S. P. Ho, *J. Am. Chem. Soc. 108* (1986) 839–841.
[47] C. D. Hubbard, J. F. Kirsch, *Biochemistry 11* (1972) 2483–2493.
[48] Y. Chao, D. J. Cram, *J. Am. Chem. Soc. 98* (1976) 1015–1017.
[49] Y. Chao, G. R. Weisman, G. D. Y. Sogah, D. J. Cram, *J. Am. Chem. Soc. 101* (1979) 4948–4958.
[50] J. R. Moran, S. Karbach, D. J. Cram, *J. Am. Chem. Soc. 104* (1982) 5826–5828.
[51] A. G. S. Högberg, *J. Am. Chem. Soc. 102* (1980) 6046–6050.
[52] D. J. Cram, K. D. Stewart, I. Goldberg, K. N. Trueblood, *J. Am. Chem. Soc. 107* (1985) 2574–2575.
[53] D. J. Cram, J. M. Cram, W. Bartmann, B. M. Trost (Eds.): in *Selectivity—A Goal for Synthetic Efficiency; Proc. Workshop Conf. Hoechst 14th 1983*, VCH Verlagsgesellschaft, Weinheim 1984, p. 42–64.
[54] D. J. Cram, S. Karbach, Y. H. Kim, L. Baczynskyj, G. W. Kalleymeyn, *J. Am. Chem. Soc. 107* (1985) 2575–2576.

The Discovery of Crown Ethers (Noble Lecture)**

By Charles J. Pedersen*

Introduction

In this lecture I would like to discuss the discovery of the crown ethers. I will divide my lecture into three parts.

First, because every discovery takes place in more than a scientific context, I would like to touch on my life and background. In the weeks since it was announced that I would share this year's Noble prize in chemistry, people have expressed as much interest in my early life as they have in my later work. So I think it appropriate to say a few words myself on the matter. It may also be that details of my past have more than casual bearing on my work.

Second, I would like to describe for you my research program and some of the specific events that led to the discovery of the first crown ether. Since I am the only one who knows at firsthand the excitement and pleasure of the discovery, I will devote a portion of my time to sharing this experience with you.

And third, I would like to discuss the properties and preparation of crown ethers. In doing so, I hope I will convey to you that I was always a "hands-on" chemist; I took satisfaction from what I did in the laboratory. Also, I was very much an industrial chemist and was always interested in the potential application of my work. In fact, when I submitted my first major paper on the discovery of the crown ethers, the editor of the Journal of the American Chemical Society, *Marshall Gates*, remarked that my descriptions were replete with industrial jargon. Fortunately he published the paper anyway.

Personal Background

My father, *Brede Pedersen*, was born in Norway in 1865 and trained as a marine engineer. Due to sibling disharmony, he left home for good as a young man and shipped out as an engineer on a steam freighter to the Far East. He eventually arrived in Korea and joined the fleet of the Korean customs, which was administered by the British. He rose in rank and later joined one of the largest Japanese steamship lines and became a chief engineer. Then a tragedy occurred that changed the course of his life. A childhood disease took the life of my elder brother while my father was away from home on a long journey. He abandoned the sea and became a mechanical engineer at the Unsan Mines in what is now the northwestern section of present-day North Korea.

My mother, *Takino Yasui*, was born in 1874 in Japan. She had accompanied her family to Korea when they decided to enter a large-scale trade in soybeans and silkworms. They established headquarters not far from the Unsan Mines, where she met my father.

The Unsan Mines were an American gold and lumber concession, 500 square miles in area. It had been granted by the Emperor of Korea to an American merchant named *James R. Morse* prior to 1870. I was conceived there in mid-winter just before the start of the Russo-Japanese war. Frequent incursions by Cossacks across the Yalu River into the region of the mines were considered to endanger my mother, so she and several American ladies were sent south by carriage to the railhead for safety. I was thus born on October 3, 1904, in the southern Port of Fusan, the largest in Korea. My arrival was doubly welcomed because mother was still grieving the loss of her firstborn. She devoted the next 10 years to overseeing my education and that of my sister, *Astrid*, five years my senior, in foreign language schools.

I spent my first and last winter at the mines when I was 4 years old. The region was known for severe weather due to the confluence of the Siberian steppes, Mongolian Gobi Desert and the mountains of Korea. Large Siberian tigers still roamed the countryside and were frightened away with bells on the pony harnesses. Wolves killed children during the cold winter nights, and foxes slept on rooftops against the chimneys to keep warm.

Because the Unsan Mines were an American enclave—the top management being all Americans—great emphasis was placed on making life as American as possible. The country club was the center of social activities and life was considerably more gentle than at the typical gold mine of the legendary American West. So my contacts with Americans began early, and I spoke English which was the common language at the mines.

I do not know if such an environment had a lifelong influence on me, but I can speculate that perhaps it did. Freedom of the Americans to administer their affairs in taking care of themselves in the wilds, where things could not be ordered for overnight delivery, no doubt taught a certain independent approach to problem solving. As for chemistry, I recall that the gold was recovered by the cyanide process, and the monthly cleanup day was marked by the pervasive odor of the process. The pouring of the molten gold was always a beautiful sight, and that might have started my interest in chemistry. Also, my sister claimed that I loved to play with a collection of colorful Siberian minerals.

Foreign language schools did not exist in Korea then, and so at the age of eight, I was sent to a convent school in Nagasaki. When I was ten years old, my mother took me to Yokohama where she remained with me for a year as I began my studies at St. Joseph College, a preparatory school run by a Roman Catholic religious order of priests and brothers called the Society of Mary. There I received a

[*] C. J. Pedersen
57 Market Street, Salem, NJ 08079 (USA)

[**] Copyright © The Nobel Foundation 1988.—We thank the Nobel Foundation, Stockholm, for permission to print this lecture.

general secondary education and took my first course in chemistry.

When the time came for me to start my higher education, there was no question of where it would be obtained. I had lived among Americans and had determined, with my father's encouragement, to study in America. I selected the University of Dayton in Ohio for two reasons: First, we had family friends in Ohio, and secondly, the same organization, the Society of Mary, ran both St. Joseph College and the University of Dayton.

My four years in Dayton and a year in graduate school at Massachusetts Institute of Technology were pleasant and taken up with activities that made me into an American. This perhaps also molded my scientific character and represented something of a personal metamorphosis. The sequence—Dayton first and then MIT—was also good, making a false start by a young man much less likely. The University of Dayton was a college of 400 men, most of them living in dormitories under strict monastic regimen. Training of the spirit was considered as important as training of the body and soul. I enjoyed all phases of the training. I became vice president of my graduating class, won letters in tennis and track and a gold medal for excellence that reflected my four years of performance there. Excellence in general was encouraged; I was even awarded a gold medal for conduct.

MIT was another matter. Boston, where I lived, is an old city of great charm and a center of the arts. I did not apply myself to my courses as I should, but my extracurricular activities contributed to the formation of my ultimate character. It was while studying at MIT that I first felt the exhilaration of utter freedom. MIT was considered deficient in the humanities, but with a little effort that deficiency could be remedied delightfully by visiting second-hand book stores. Why second-hand books appealed to me more than library books still remains a mystery—thought it possibly was the prospect of finding unexpected treasures. I celebrated my graduation from MIT as a chemist by taking a walking tour of the Presidential Range in New Hampshire.

In spite of the urging of *James F. Norris*—a very prominent professor and my research advisor—I did not remain at MIT to take a Ph.D. My bills were still being paid by my father, and I was anxious to begin supporting myself. In 1927, I obtained employment at Du Pont through the good offices of Professor *Norris*, and I was fortunate enough to be directed to research at Jackson Laboratory by *William S. Calcott*. My career of 42 years had begun.

The research environment at Du Pont during those years was not altogether typical of industrial laboratories of the time. The company had formed the nucleus of a basic research department that in a few years' time would have scientists such as *Wallace Carothers* and the young *Paul Flory* working on the polymer studies that led to nylon and other breakthroughs. And in general, Du Pont was a productive center of research where many interesting and important problems were being solved. For example, one day while visiting *Julian Hill* at the Du Pont Experimental Station in Wilmington, Delaware, I observed him pull the first oriented fiber of polyester. On another occasion, at Jackson Laboratory, across the Delaware River in New Jersey where I worked, I noticed commotion in the laboratory of *Roy Plunkett*, which was across the hall from my own. I investigated and witnessed the sawing open of a cylinder from which was obtained the first sample of Teflon® fluoropolymer. At Jackson Laboratory, during that time, other important advances were taking place in tetraethyllead and new petroleum chemicals, new elastomers, and a new series of fluorocarbons for refrigeration and aerosols. The atmosphere was vibrant and exciting, and success was expected. It was in this atmosphere I began my career.

As a new scientist I was initially set to work on a series of typical problems, the successful solution of which buoyed my research career.[1-5] After a while, I began to search for oil-soluble precipitants for copper, and I found the first good metal deactivator for petroleum products.[6-8] As a result of this work, I developed a great interest in the effects of various ligands on the catalytic properties of copper and the transition elements generally, and I worked in that field for several years. I noticed a very unusual synergistic affect wherein a metal deactivator greatly increased the efficacy of antioxidants.[9, 10]

So more and more, I became interested in the oxidative degradation of the substrates themselves, particularly petroleum products and rubber. As my interests moved in that direction, I left off working on metal deactivators and coordination chemistry. By the mid-1940s, I was in full career, having established myself in the field of oxidative degradation and stabilization.[11-13] I was independent in terms of the problems I might choose and had achieved the highest non-management title then available to a scientist at Du Pont. During the 1940s and 1950s, my interests became more varied. For example, I became interested in the photochemistry of new phthalocyanine adducts and of quinoneimine dioxides. I found some polymerization initiators, discovered that ferrocene was a good antiknock agent for gasoline, and made some novel polymers.[14-23]

Discovery of the Crown Ethers

But then there arose a challenging opportunity that led me back to ligand chemistry. In response to my desire to contribute to the elastomer field, my colleague *Herman Schroeder* suggested that there was an interesting problem in the coordination chemistry of vanadium. This sparked my curiosity, and I began work with the initial goal of understanding factors which govern the catalytic activity of vanadium in oxidation and polymerization. This was a relatively unexplored area, and previous work had been empirical. It was my work in this area that led to the discovery of crown ethers, which I will now describe.

As I have related, I studied for many years the autoxidation of petroleum products and rubber and its retardation by antioxidants. Autoxidation is greatly catalyzed by trace metals, such as copper and vanadium. Hence, I had developed the compounds referred to earlier, namely the "metal deactivators" which suppress the catalytic activity of the metal salts by converting them into inactive multidentate complexes. The first of these was *N,N'*-bis(*o*-hydroxybenzylidene)-1,2-propanediamine (Fig. 1), an excellent deactivator for copper which has been used industrially for many years.

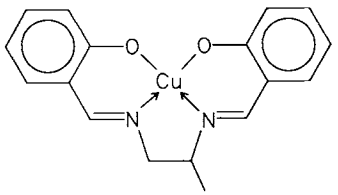

Fig. 1. Copper complex of *N,N'*-bis(*o*-hydroxybenzylidene)-1,2-propanediamine.

In 1960, when I returned to investigations in coordination chemistry, I decided to study the effects of bi- and multidentate phenolic ligands on the catalytic properties of the vanadyl group, VO.[24] The multidendate ligand I selected was bis[2-(*o*-hydroxyphenoxy)ethyl] ether **3**, whose synthesis is depicted in Figure 2. As I proceeded, I knew

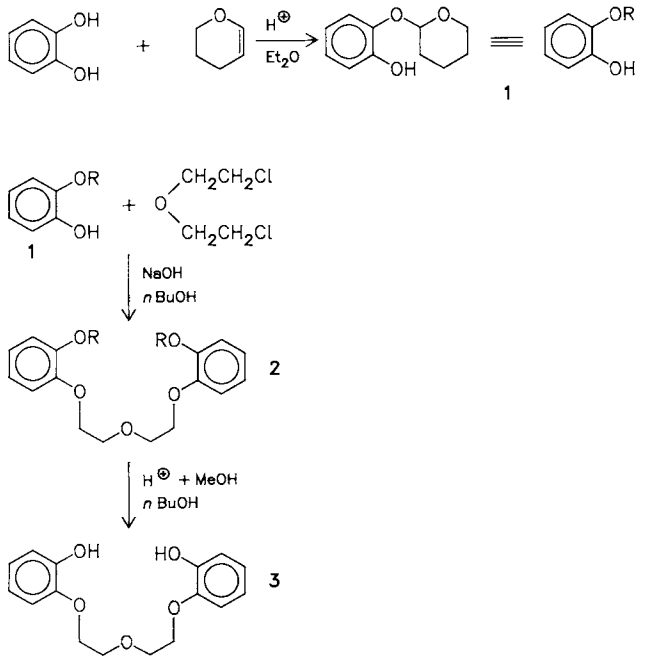

Fig. 2. Synthesis of **3** from catechol and dihydropyran. **1** is a partially protected catechol.

that the partially protected catechol **1** was contaminated with about 10 percent unchanged catechol. But I decided to use this mixture for the second step anyway since purification would be required at the end. The reactions were carried out as outlined and gave a product mixture in the form of an unattractive goo. Initial attempts at purification gave a small quantity (about 0.4 percent yield) of white crystals which drew attention by their silky, fibrous structure and apparent insolubility in hydroxylic solvents.

The appearance of the small quantity of the unknown should have put me in a quandary. It probably was not the target compound because that would be obtained in a higher yield. My objective was to prepare and test a particular compound for a particular purpose. Had I followed this line, I would have doomed the crown ethers to oblivion until such a time as another investigator would retrace my steps and make the better choice at the critical moment. Crown ethers, however, were in no danger, because of my natural curiosity. Without hesitation, I began to study the unknown substance.

It was fortunate that I used an ultraviolet spectrophotometer to follow the reactions of the phenols. These compounds and their ethers in neutral methanol solutions absorb in the region of 275 mμ. On treatment with alkali, the absorption curve is not significantly altered if all the hydroxy groups are covered, but it is shifted to longer wavelengths and higher absorption if one or more hydroxy groups are still free, as shown by the dashed curve in Figure 3.

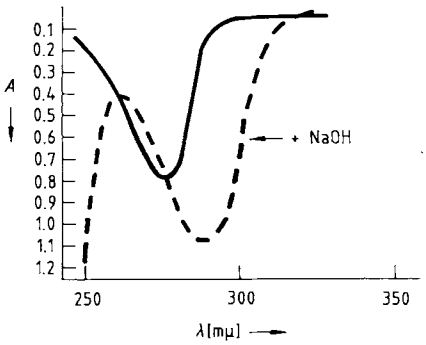

Fig. 3. Influence of NaOH on the UV spectrum of free or only partially protected catechol. *A* = absorption.

The unknown product was very sparingly soluble in methanol, and the neutral solution gave an absorption curve characteristic for a phenolic compound (Fig. 4, left). The solution was rendered alkaline with sodium hydroxide with the expectation that the curve would either be unaffected or shifted to longer wavelengths. The resulting spectrum, however, showed neither effect, but rather the one shown in Figure 4. At the same time, I noticed that the

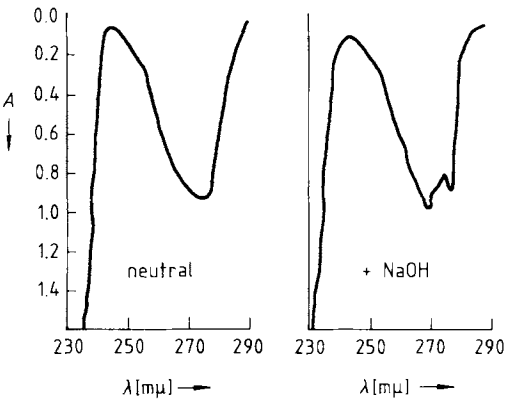

Fig. 4. Influence of NaOH on the UV spectrum of the unknown compound formed in the reaction shown in Fig. 2 in methanol.

fibrous crystals were freely soluble in methanol in the presence of sodium hydroxide. This seemed strange since the compound did not contain a free phenolic group, a fact confirmed by its infrared and NMR spectra. I then found that the compound was soluble in methanol containing any soluble sodium salt. Thus, the increased solubility was not due to alkalinity but to sodium ions. But there was no

obvious explanation for the behavior of the compound because its elementarly analysis corresponded with that of 2,3-benzo-1,4,7-trioxacyclonon-2-ene **4** (Fig. 5), a plausible

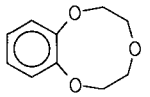

4

Fig. 5. 2,3-Benzo-1,4,7-trioxacyclonon-2-ene **4**.

product from the reaction of catechol and bis(2-chloroethyl) ether in the presence of sodium hydroxide. However, the moment of revelation came when I learned that its molecular weight was exactly twice that of the above compound. The true structure was that of an 18-membered ring, dibenzo[18]crown-6 (**5**), the first and most versatile of the aromatic crown compounds (Fig. 6). The shape is that of a torus or a doughnut.

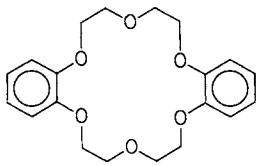

5

Fig. 6. Structural formula of the first crown ether 2,3,11,12-dibenzo-1,4,7,10,13,16-hexaoxacyclooctadeca-2,11-diene **5**.

It seemed clear to me now that the sodium ion had fallen into the hole in the center of the molecule and was held there by the electrostatic attraction between its positive charge and the negative dipolar charge on the six oxygen atoms symmetrically arranged around it in the polyether ring. Tests showed that other alkali metal ions and ammonium ion behaved like the sodium ion so that, at long last, a neutral compound had been synthesized which formed stable complexes with alkali metal ions. Up to that point, no one had ever found a synthetic compound that formed stable complexes with sodium and potassium.

My excitement, which had been rising during this investigation, now reached its peak and ideas swarmed in my brain. One of my first actions was motivated by esthetics more than science. I derived great esthetic pleasure from the three-dimensional structure as portrayed in the computer-simulated model in Figure 7. What a simple, elegant

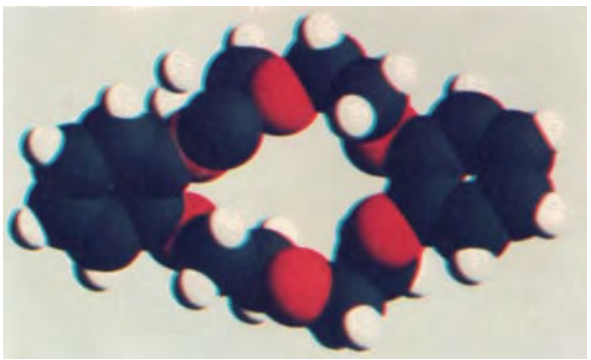

Fig. 7. Computer-simulated space-filling model of **5**.

and effective means for the trapping of hitherto recalcitrant alkali cations! I applied the epithet "crown" to the first member of this class of macrocyclic polyethers because its molecular model looked like one and, with it, cations could be crowned and uncrowned without physical damage to either, as shown for the potassium complex in Figure 8. As my studies progressed, I created the system of

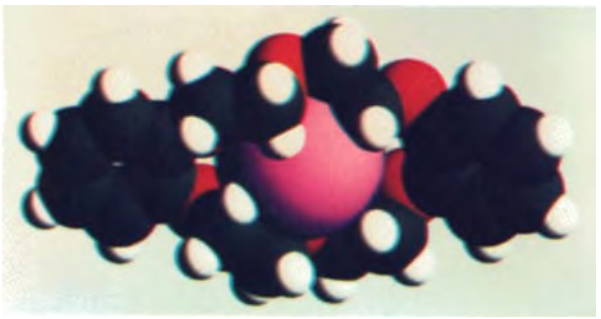

Fig. 8. Computer-simulated space-filling model of the potassium complex of **5**.

crown nomenclature chiefly because the official names of the crown ethers were so complex and hard for me to remember. It is a source of special satisfaction to me that this system of abbreviated names, devised solely for the ready identification of the macrocyclic polyethers, has been retained by the scientific establishment. In Figure 9 I have illustrated how the nomenclature system is made up of the side-ring substituents, the total number of oxygen atoms in the main ring and the size of the ring.

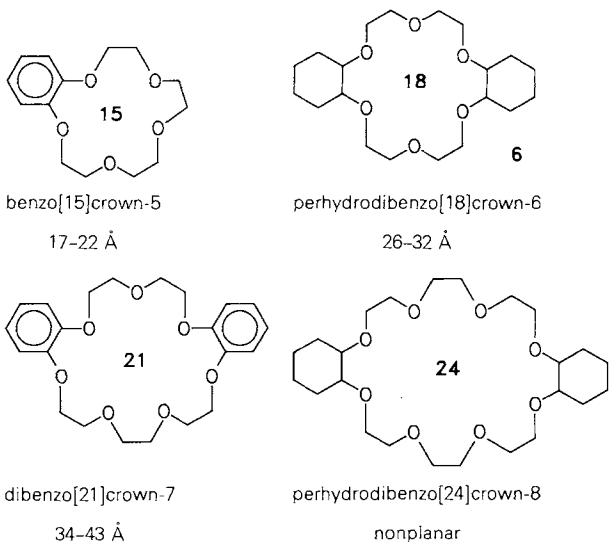

Fig. 9. Some macrocyclic polyethers. The numbers within the diagrams are the numbers of atoms in the polyether rings. The numbers under the names are the estimated diameters of the holes in Å. Cyclohexane rings of crown ethers are referred to here as perhydrobenzo rings; they are usually, but misunderstandingly, referred to as cyclohexyl rings.

Another aspect of this discovery filled me with wonder. In ordinary organic reactions only rings of 5, 6, or 7 members form easily. Here a ring of 18 atoms had been formed in a single operation by the reaction of two molecules of catechol, which was present as a minor impurity, with two

molecules of bis(2-chloroethyl) ether. Further experiments revealed that **5** can be synthesized from these intermediates in a 45 percent yield without resorting to high dilution techniques. This was most unexpected and some good reason must exist for such an unusual result. I concluded that the ring-closing step, either by a second molecule of catechol or a second molecule of bis(2-chloroethyl) ether, was facilitated by the sodium ion which, by ion–dipole interaction, "wrapped" the molecular pieces around itself to form a three-quarter circle and disposed them for the final ring closure in much the same fashion as is involved in the synthesis of the porphyrins and phthalocyanines. Later experiments appear to support this hypothesis. The yields of **5** are higher when it is prepared with sodium or potassium hydroxide than when lithium or tetramethylammonium hydroxide is used. Lithium and the quaternary ammonium ions are not strongly complexed by the polyether. The best complexing agents are rings of 15 to 24 atoms including 5 to 8 oxygen atoms. They are formed in higher yields than smaller or larger rings, or rings of equal sizes with only four oxygen atoms. Finally, even open-chain polyethers such as **7** (Fig. 10) were found to form complexes with sodium and potassium ions.

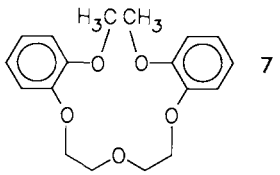

7

Fig. 10. The open-chain polyether 3,4,12,13-dibenzo-2,5,8,11,14-pentaoxapentadeca-3,12-diene **7** complexing sodium and potassium ions.

Thus did I discover dibenzo[18]crown-6 **5**, the first crown ether and the first neutral synthetic compound capable of complexing the alkali metal cations.[25,26]

With the realization that I had something very unusual and with the utmost curiosity and anticipation, I devoted all my energies over the next several years to the study of this fascinating class of ligands and their interaction with inorganic cations. Every successful experiment produced a significantly novel result and led to new thoughts on what to synthesize and also as to the many potential uses of these extraordinary substances.

I was especially interested in the stability of the "complexes" and the reason for their behavior. For example, I found that for maximum stability of its salt complex, each cation has an optimum size of the ring of the polyether. A complex can form even if the fit is not the best by forming a sandwich complex consisting of two molecules of polyether per cation. The thermal stability of some salt complexes, for example that with KCNS, is attested to by their having melting points higher than those of the components.

Preparation and Properties of Macrocyclic Polyethers

Spurred by curiosity regarding the factors involved in the stability of the salt complexes (such as the relative sizes of the hole and the cation, and the number and symmetrical arrangement of the oxygen atoms in the polyether ring), I initiated an extensive program of syntheses. Ultimately, about 60 macrocyclic polyethers were prepared containing 12 to 60 atoms to a polyether ring including 4 to 10 oxygen atoms and some with nitrogen and sulfur atoms. Many of these compounds were found to be useless as complexing agents, but they served to define the effective ones which are compounds containing 5 to 10 oxygen atoms in the ring, each separated from the next by 2 carbon atoms. I also noted that even whole molecules such as the thioureas formed complexes with some crown compounds. I accomplished all this working alone with the help of my able technician, *Ted Malinowski.*

Some of the general properties of the aromatic macrocyclic polyethers are as follows: They are neutral, colorless compounds with sharp melting points, and are sparingly soluble in water and alcohols, moderately soluble in aromatic solvents, and very soluble in methylene chloride and chloroform. They undergo substitution reactions characteristic for aromatic ethers (halogenation, nitration, etc.), and form formaldehyde resins when treated with paraformaldehyde under acid conditions. They are decomposed by reactions which cause the scission of ethers.

The saturated macrocyclic polyethers are obtained most simply by catalytically hydrogenating the aromatic compounds using ruthenium catalyst. Bridge-bond isomers are obtained from compounds containing two or more aromatic side-ring substituents. For example, dibenzo-[18]crown-6 **5** gives a mixture of stereoisomers of perhydrodibenzo[18]crown-6 **6** (see Fig. 9). The saturated polyethers are colorless, viscous oils or solids with low melting points. They are thermally stable, but, like the aromatic compounds, must be protected from oxygen at high temperatures. They are, as a group, very much more soluble than the aromatic compounds in all solvents, and most of them are even soluble in petroleum ether.

The unique property of the macrocyclic polyethers as complexing agents is their preference for alkali metal ions, which do not form complexes with the numerous ligands used for the transition metal ions. The crown compounds form stable crystalline complexes and solutions of the complexes with some or all of the cations of alkali and alkaline earth metals plus ammonium ions and others. Some of them, for example **6**, form complexes with Co^{II}, and some other transition metal ions. The saturated compounds are better complexing agents than the corresponding aromatic compounds.

Three criteria have been used for the formation of complexes between macrocyclic polyethers and salts: (a) isolation of the complexes as crystals; (b) characteristic changes in the ultraviolet spectra of the aromatic compounds; and (c) changes in the solubilities of the polyethers and salts in different solvents.

As is evident from Table 1, these compounds have holes of different diameters in the center of the polyether rings. The uncomplexed cations also differ in size, given in Table 2 in Ångström units: sodium 1.94, potassium 2.66, ammonium 2.86, rubidium 2.94, and cesium 3.34. Depending, therefore, on the relative sizes of the hole and the cation, crystalline complexes with polyether/cation ratios of 1 : 1,

Table 1. Hole diameter d of [m]crown-n compounds.

m	14	15	18	21
n	4	5	6	7
d [Å]	1.2–1.5	1.7–2.2	2.6–3.2	3.4–4.3

Table 2. Complexable cations and their diameters in Å.

Group I		Group II		Group III		Group IV	
$Li^{\oplus}$	1.36						
$Na^{\oplus}$	1.94						
$K^{\oplus}$	2.66	$Ca^{2\oplus}$	1.98				
$Cu^{\oplus}$	1.92	$Zn^{2\oplus}$	1.48				
$Rb^{\oplus}$	2.94	$Sr^{2\oplus}$	2.26				
$Ag^{\oplus}$	2.52	$Cd^{2\oplus}$	1.94				
$Cs^{\oplus}$	3.34	$Ba^{2\oplus}$	2.68	$La^{\oplus}$	2.30		
$Au^{\oplus}$	2.88	$Hg^{2\oplus}$	2.20	$Tl^{\oplus}$	2.80	$Pb^{2\oplus}$	2.40
$Fr^{\oplus}$	3.52	$Ra^{2\oplus}$	2.80				
$NH_4^{\oplus}$	2.86						

3 : 2, and 2 : 1 have been prepared as illustrated in Table 3. The aromatic macrocyclic polyethers tend to give high melting complexes which are not readily soluble in aprotic solvents, while the saturated compounds give lower melting complexes which are more soluble. Most of the pure complexes are decomposed by water, the rate and extent of decomposition depending on the proportion of water and the temperature.

Table 3. Crystalline complexes of polyethers and alkali-metal salts.

	Mole Ratio Polyether : Salt
Benzo[15]crown-5 + NaI	1 : 1
Benzo[15]crown-5 + KSCN	2 : 1
Dibenzo[15]crown-5 + KSCN	2 : 1
Dibenzo[18]crown-6 + KSCN	1 : 1
Dibenzo[18]crown-6 + NH_4SCN	1 : 1
Dibenzo[18]crown-6 + RbSCN	1 : 1
Dibenzo[18]crown-6 + RbSCN	2 : 1
Dibenzo[18]crown-6 + CsSCN	2 : 1
Dibenzo[18]crown-6 + CsSCN	3 : 2
Perhydrodibenzo[18]crown-6 + KI_3	1 : 1
Perhydrodibenzo[18]crown-6 + CsI_3	3 : 2
Dibenzo[24]crown-8 + KSCN	1 : 1
Dibenzo[24]crown-8 + KSCN	1 : 2
Dibenzo[30]crown-10 + KSCN	1 : 1
Dibenzo[30]crown-10 + NaSCN	1 : 2

It was postulated from the beginning that complexes of macrocyclic polyethers containing less than seven oxygen atoms consisted of a cation surrounded by the oxygen atoms arranged symmetrically in a single plane. The essential correctness of this view of the structure has been confirmed by Professor *M. R. Truter* and her collaborators who have been the first to determine the structures of a number of crystalline salt complexes of crown compounds by X-ray diffraction methods.[27]

All macrocyclic polyethers containing one or more benzo groups have a characteristic absorption maximum at 275 mμ in methanol, and the shapes of the curves are altered by the addition of complexable salts as shown in Figure 4. The spectral evidence is nearly always confirmed by the other two criteria.

Macrocyclic polyethers and complexable salts mutually increase their solubilities in solvents wherein the complexes are soluble. Sometimes these effects are spectacular; for instance the solubility of the potassium thiocyanate complex is about 0.1 mol L^{-1}, a 100-fold increase. Some of the saturated polyethers, e.g. **6**, have the useful property of solubilizing alkali metal salts, particularly those of potassium, in aprotic solvents. Crystals of potassium permanganate, potassium *tert*-butoxide, or potassium tetrachloropalladate ($PdCl_2 + 2KCl$) can be made to dissolve in liquid aromatic hydrocarbons merely by adding **6**. This is dramatic for the crown complex of potassium permanganate which colors toluene purple. Benzylpotassium is rendered soluble in *n*-heptane by the polyether, but the polyether ring is gradually decomposed by this organometallic compound. The solubilizing power of the saturated macrocyclic polyethers permits ionic reactions to occur in aprotic media. It is expected that this property will find practical use in catalysis, enhancement of chemical reactivity, separation and recovery of salts, electrochemistry, and in analytical chemistry.

The complexing efficiencies of saturated macrocyclic ethers can be ranked numerically by measuring the relative distribution of a colored alkali metal salt (such as picrate) between an immiscible organic solvent and water in the presence of the crown ether as depicted. If the polyether is ineffective, the organic phase will be colorless; if the polyether is very powerful, most of the color will be in the organic phase. The efficiencies of the polyether will lie between these two limits as shown in Table 4.[28–35]

Table 4. Extraction results [a].

Polyether	Picrate Extracted [%]			
	$Li^{\oplus}$	$Na^{\oplus}$	$K^{\oplus}$	$Cs^{\oplus}$
Perhydrodibenzo[14]crown-4	1.1	0	0	0
Perhydrobenzo[15]crown-5	1.6	19.7	8.7	4.0
Dibenzo[18]crown-6 **5**	0	1.6	25.2	5.8
Perhydrodibenzo[18]crown-6 **6**	3.3	25.6	77.8	44.2
Perhydrodibenzo[21]crown-7	3.1	22.6	51.3	49.7
Perhydrodibenzo[24]crown-8	2.9	8.9	20.1	18.1

[a] Two-phase liquid extraction: dichloromethane and water.

Dr. *K. H. Frensdorff* has determined the stability constants for 1 : 1 complexes of many macrocyclic polyethers with alkali metal ions by potentiometry with cation-selective electrodes. Selectivity toward the different cations varies with polyether ring size, the optimum ring size being such that the cation just fits into the hole, that is, 15–18 for sodium ion, 18 for potassium ion, and 18–21 for cesium ion.[33]

That concludes my remarks on the discovery, properties and preparation of the crown ethers. It remains only for me to mention certain individuals who contributed to the success of my research and to add a few words concerning my interest and hope for the future of research in this area.

First, I want to remember on this occasion my wife *Susan* who died in 1983. It would have been wonderful to share with her all that has happened to me of late as we shared everything else during our marriage of 36 years.

Next, I would like to thank the Du Pont Company, They encouraged me to pursue my research on crown ethers, even when it was evident that, at least initially, my work might not have a significant practical impact. At another company, I might not have met with such encouragement and latitude.

Within the company I received support from certain individuals. I appreciate the advice and counsel of my close friend, Dr. *Herman Schroeder*, who was always interested in my research and whose companionship has meant so much to me during the many years we have known each other. I also thank my friend Dr. *Rudolph Pariser*, who has been tireless in his efforts to assure recognition for my accomplishments.

Finally, I want to thank the analytical groups of the company for making all their resources available to me; my technical colleagues for their scientific consultation; and our academic friends for their interest.

Of course, I must mention my respect and admiration for the two scientists with whom I share this year's prize. If I may use an analogy reflecting my youth at the Unsan gold mines, I see the discovery of the crown ethers as comparable to the finding of a new field with a lot of action in it. Professor *Cram* and Professor *Lehn* staked claims to particular veins of rich ore and went on to discover gold mines of their own.

I know that the crown ethers continue to create great interest among biologists for studying the mechanism of transport of ions across cell membranes.[36] But whether it be in biology or some other field, it is my fervent wish that before too long it matters not by whom the crown ethers were discovered but rather that something of great benefit to mankind will be developed about which it will be said that were it not for the crown compounds it could not be.

Received: February 23, 1988 [A 681 IE]
German version: *Angew. Chem. 100* (1988) 1053

[1] F. B. Downing, A. E. Parmalee, C. J. Pedersen, US-Pat. 2004160 (1935), Du Pont.
[2] F. B. Downing, C. J. Pedersen, US-Pat. 2008753 (1935), 2087103 (1937), Du Pont.
[3] R. G. Clarkson, C. J. Pedersen, US-Pat. 2054282 (1936), Du Pont.
[4] L. Spiegler, C. J. Pedersen, US-Pat. 2087098 (1937), Du Pont.
[5] F. B. Downing, C. J. Pedersen, US-Pat. 2121397 (1938), Du Pont.
[6] F. B. Downing, C. J. Pedersen, US-Pat. 2181121 (1939), Du Pont.
[7] C. J. Pedersen, *Oil Gas J.* (1939) 97.
[8] C. J. Pedersen, *Ind. Eng. Chem. 41* (1949) 824.
[9] C. J. Pedersen, *Del. Chem. Symp.*, December 1948 (Prooxidant Catalytic Activity of Metal Chelates).
[10] C. J. Pedersen, *Adv. Chelate Chem. 1954*, 113.
[11] C. J. Pedersen, *Del. Chem. Symp.*, January 1950 (Mechanism of Decomposition of Perbenzoic Acid Compared with Benzoyl Peroxide).
[12] C. J. Pedersen, *Encyclopedia Britannica 1953* (Antioxidants).
[13] C. J. Pedersen, *J. Org. Chem. 22* (1957) 127; US-Pat. 2662895-7 (1953), 2681347 (1954), 2741531 (1956), 2831805 (1958), Du Pont.
[14] C. J. Pedersen, *Ind. Eng. Chem. 48* (1956) 1881.
[15] C. J. Pedersen, *J. Am. Chem. Soc. 79* (1957) 2295.
[16] C. J. Pedersen, *J. Am. Chem. Soc. 79* (1957) 5014; US-Pat. 2681918 (1954), 2741625 (1956), 2831805 (1958), Du Pont.
[17] C. J. Pedersen, US-Pat. 2867516 (1959), Du Pont.
[18] C. J. Pedersen, US-Pat. 3341311 (1967), Du Pont.
[19] C. J. Pedersen, US-Pat. 3038299-300 (1962), Du Pont.
[20] C. J. Pedersen, *J. Org. Chem. 23* (1958) 252, 255.
[21] J. Diekmann, C. J. Pedersen, *J. Org. Chem. 28* (1963) 2879; D. N. Dhar, *Chem. Rev. 67* (1967) 611.
[22] C. J. Pedersen, US-Pat. 3232914 (1966), Du Pont.
[23] C. J. Pedersen, US-Pat. 3320214 (1967), Du Pont.
[24] C. J. Pedersen, US-Pat. 3361778 (1968), Du Pont.
[25] C. J. Pedersen, *J. Am. Chem. Soc. 89* (1967) 2495, 7017.
[26] C. J. Pedersen, *Aldrichimica Acta 4* (1971) 1.
[27] M. R. Truter, C. J. Pedersen, *Endeavour 30* (1971) No. 111, p. 142.
[28] C. J. Pedersen, *Fed. Proc. Fed. Am. Soc. Exp. Biol. 27* (1968) 1305.
[29] C. J. Pedersen, *J. Am. Chem. Soc. 92* (1970) 386.
[30] C. J. Pedersen, *J. Am. Chem. Soc. 92* (1970) 391.
[31] C. J. Pedersen, *J. Org. Chem. 36* (1971) 254.
[32] C. J. Pedersen, *J. Org. Chem. 36* (1971) 1690.
[33] C. J. Pedersen, H. K. Frensdorff, *Angew. Chem. 84* (1972) 16; *Angew. Chem. Int. Ed. Engl. 11* (1972) 16.
[34] C. J. Pedersen, *Org. Synth. 52* (1972) 66.
[35] C. J. Pedersen, US-Pat. 3562295 (1971), 3622577 (1971), 3686225 (1972), 3687978 (1972), 3856813 (1974), 3873569 (1975), 3987061 (1976), 3998838 (1976), Du Pont; C. J. Pedersen, M. Bromels, US-Pat. 3847949 (1974), 4031111 (1977), Du Pont.
[36] C. J. Pedersen, H. E. Schroeder, *Curr. Top. Macrocycl. Chem. Jpn. 1987*, 1, 5.

Somatic Generation of Immune Diversity (Nobel Lecture)**

By Susumu Tonegawa*

One day in the fall of 1970, I received an airmail letter from *Renato Dulbecco*, who was traveling in Europe. At that time I was a postdoctoral fellow in his laboratory at the Salk Institute. The letter, written on stationery of the Hotel Hassler in Rome said:

> Dear Susumu,
>
> I don't know what arrangements you have made for after your departure from La Jolla at the end of the year but I would like to mention to you another possibility. The Institute of Immunology in Basel, Switzerland, will start operating in a month. They already have an excellent collection of immunologists, but have not yet built an adequate background in molecular biology. I talked about you to Niels Jerne, the Director, and they are interested in having you there ... There are many immunologically interesting phenomena obtained with crude RNA preparations but they are unreliable because RNA is not characterized. In general, it seems the best system for understanding development at a molecular level and you may like to get into such a field. If you are interested, write to Niels K. Jerne, Basel Institute for Immunology, 487 Grenzacherstrasse ...

Thanks partly to the remarkably prophetic letter and partly to the U.S. immigration law that prevented me from remaining in the USA, in February 1971 I found myself in this cozy Swiss town almost completely surrounded by immunologists. For someone who had no formal training in immunology whatsoever and had never even visited Switzerland, it was a rather drastic change. Indeed, the first twelve months at the Basel Institute were not easy.

After I arrived in Basel I initially attempted to continue the project of my days in *Dulbecco*'s laboratory, namely, the transcriptional control of the simian virus 40 genes. However, I soon realized that this was not a subject that aroused great interest in an Institute almost entirely staffed by immunologists nor one that allowed me to take full advantage of my many talented colleagues. I therefore decided to learn immunology by talking to them, reading papers, and asking questions. An immunologist, *Ita Askonas*, and a geneticist, *Charlie Steinberg*, became my tutors and were most helpful to me in getting into a new field. It was during this process that I was introduced to the problem of the origin of antibody diversity.

[*] Prof. S. Tonegawa
Center for Cancer Research and Department of Biology
Massachusetts Institute of Technology
Cambridge, MA 02139 (USA)

[**] Copyright © The Nobel Foundation 1988.—We thank the Nobel Foundation, Stockholm, for permission to print this lecture.

The Problem

Immunologists agreed that an individual vertebrate synthesizes many millions of structurally different forms of antibody molecules even before it encounters an antigen. Moreover, *Gerald Edelman* and *Rodney Porter* had shown that a typical antibody molecule is composed of two identical light chains and two identical heavy chains.[1,2] It had also been found that each of these two types of chain exhibits great sequence variability in the amino terminal region between one antibody molecule and the next and no sequence variability in the carboxyl terminal regions.[3] These two regions were then referred to as the variable, or V, and the constant, or C, regions. However, immunologists and geneticists were divided for many years into two schools of thought with respect to the issue of whether the genetic diversity required for the synthesis of these proteins is generated during evolution and is carried in the germ line or during development, in which case it would be present in somatic but not germ-line cells. One school of thought held that the germ line must include a separate gene for every polypeptide that ultimately appears in an antibody molecule.[4] In this germ-line theory, antibody or immunoglobulin genes are expressed in exactly the same way as those for any other protein, and no special gene-processing mechanisms are needed. On the other hand, the model requires an enormous number of immunoglobulin genes inherited from the parents. While the four-chain structure of an immunoglobulin molecule allows diversity to be generated by chain pairing, the number of genes required for both light and heavy chains is still very large. One major difficulty for germ-line theories of antibody diversity was the observation that all antibody polypeptide chains of a given type share a common genetic marker (allotype) that segregates as a single Mendelian gene. If there were many thousands of light- and heavy-chain genes, how could the same genetic marker in all of these genes have been maintained?

The second theory supposed that there are only a limited number of antibody genes in the germ line, and that these genes somehow diversify as the antibody-forming B lymphocytes emerge from their stem cells. In other words, the diversification of antibody gene sequences takes place in specialized somatic, or body, cells rather than being carried from generation to generation by the germ cells.[5-7] One attraction of this latter theory is that it relieves the host of the need to commit a disproportionately large fraction of the inherited genes to code for antibodies, but the theory demands an unprecedented mechanism for diversifying the inherited genes somatically.

Arguments for and against these contrasting ideas were made both vocally and in written form for many years. However, all of these arguments were based on the inter-

pretation of amino acid sequences of immunoglobulin polypeptide chains or on the generally accepted principles of evolution and genetics. No direct evidence for either view had been obtained. This was because no technique was available that would allow an analysis of the fine structure of specific genes from higher organisms.

Gene Counting

In the early seventies the technology for purifying a specific eukaryotic mRNA was just becoming available. Furthermore, a method to determine the number of copies of a specific gene by kinetic analysis of nucleic acid hybridization had already been established.[8,9] These technical developments led some scientists, including myself, to think that one can experimentally determine the number of immunoglobulin genes contained in a germ-line genome and thereby decide which of the two major theories of antibody diversity is correct. The validity of this approach is based in part on the fact that the V region of a given chain type, while being different, exhibits a high degree of amino acid sequence homology. It was therefore thought that an mRNA coding for a specific immunoglobulin polypeptide chain would hybridize not only with its own gene but also with many other immunoglobulin genes, if they existed in a germ-line genome.

I thus obtained mouse myeloma cells and put my effort to purifying immunoglobulin mRNA and carrying out the hybridization studies. However, the initial studies focusing on the mouse κ-light-chain and heavy-chain genes gave ambiguous results. The difficulty was primarily due to uncertainty about the purity of the mRNA used as the hybridization probe as well as a lack of knowledge on the extent to which a probe will hybridize with the related but not identical genes and the precise effect of sequence differences on hybridization kinetics. Thus it turned out to be nearly impossible to make a convincing interpretation of the data obtained in these early studies in relation to the issue of the evolutionary versus somatic generation of antibody diversity.

One subsequent series of experiments that I carried out on genes coding for the mouse λ light chains, however, was very encouraging.[10] Using an mRNA preparation that was more than 95% pure, I could show that the mouse λ-light-chain gene is reiterated no more than the β-globin gene. The latter gene had been shown to be essentially unique. Fortunately, *Weigert*, *Cohn* et al. had identified at least eight different V_λ-region sequences among BALB/c-derived myelomas.[11] Since these V regions were highly homologous, differing by only one, two, or three amino acid residues, it was very likely that the corresponding genes would cross-hybridize extensively if they existed separately in the germ-line genome. Furthermore, statistical analysis of λ-light-chain-secreting myelomas strongly suggested that a BALB/c mouse has the capacity to synthesize many more than the eight different V_λ regions identified. Thus the number of the mouse λ genes determined experimentally (no more than a few) was far smaller than the number of different V_λ regions (at least eight, most probably many more) detected in proteins. On the basis of these results I was convinced that a somatic diversification occurs in this gene system.

Rearrangement

In the meantime I became aware that some immunologists had been speculating that immunoglobulin polypeptide chains may be encoded by two separate DNA segments, one each for the V and C regions. Drawing an analogy from the elegant Campbell model[12] on the integration and excision of a phage λ genome, *Dreyer* and *Bennett* had further suggested that one of many "V genes" may be excised from the original chromosomal position and joined with the single "C gene" in an immunoglobulin-producing B cell.[13] This model successfully explained the maintenance of the common genetic marker in all immunoglobulin polypeptide chains of a given type by postulating a single C gene for that chain type. Although a somatic recombination between the "V and C genes" is an inherent aspect of the model it is clearly a version of the germ-line theory of antibody diversity because the model assumed that the germ-line genome carries many "V genes", one for every V region that an organism can synthesize.

When the Dreyer and Bennett model was published in 1965, it was not accepted widely by biologists. This is understandable because the model was built on two hypotheses, both of which violated the then current dogmas of biology. These are the principles of one gene encoding one polypeptide chain and the constancy of the genome during ontogeny and cell differentiation. My personal reaction to the model when I learned of it in the early nineteen seventies was also that of skepticism. At the same time, however, I thought that the model might be testable if one were to use restriction enzymes. While in *Dulbecco*'s laboratory I had heard of *Daniel Nathan*'s breakthrough in the analysis of the SV40 genome by an application of the then newly discovered restriction enzymes.[14] As one who used to struggle to define the transcriptional units of this DNA virus, I was keenly aware of the power of these enzymes for the analysis of DNA structure. However, an extension of the restriction enzyme analysis from a viral genome of 5×10^3 base pairs to the 2×10^9 base-pair genome of a eukaryote as complex as a mouse required the use of an additional trick for the detection of a specific DNA fragment in a vast array of irrelevant fragments. An obvious solution seemed to lie in the combination of an electrophoretic separation of enzyme-digested DNA and the sensitive technique of nucleic acid hybridization. I discussed with *Charlie Steinberg* the need for developing a method that allows an in situ detection of a specific DNA sequence among the electrophoretically fractionated DNA fragments, but we really could not come up with a good idea worthy of exploring. As we all now know, a very simple and elegant method ideal for this purpose was later developed by *Edward Southern*.[15]

A few weeks passed before I accidentally saw in one of the Institute's cold rooms a huge plexiglass tray in which someone was fractionating serum proteins by starch gel electrophoresis. I thought one may be able to fractionate a sufficient amount of digested DNA in a gel of such dimen-

sions, so that the DNA eluted from gel slices could be used for liquid-phase hybridization. A quick calculation seemed to indicate that the experiment was feasible. *Nobumichi Hozumi*, a postdoctoral fellow in my laboratory, and I therefore decided to give it a try although we were keenly aware of the intense labor required by this type of experiment. As hybridization probes we used purified κ or λ light-chain mRNA (V+C probe) and its 3'-half fragment (C probe) that had been radioiodinated to a high specific activity. The rationale of the experiment was as follows: first, if an immunoglobulin polypeptide chain is encoded by two "genes" (V and C) in the germ-line genome, it is highly probable that treatment with a restriction enzyme will separate these DNA sequences into fragments of distinct size, thus allowing their electrophoretic separation. Second, if a somatic rearrangement joins the V and C "genes" it is also highly probable that the myeloma DNA digested with the same restriction enzyme will contain a DNA fragment carrying both V and C "genes".

The results obtained were clear-cut: To our pleasant surprise the patterns of hybridization of the embryo DNA (a substitute of germ-line DNA) and a κ-myeloma DNA were not only drastically different but also perfectly consistent with the occurrence of separate V and C "genes" and a joined V plus C gene, respectively.[16] We were of course aware of the alternative interpretations of the results, such as a fortuitous modification of the enzyme cleavage sites in one of the two types of DNA. However, we considered these alternative explanations of the results unlikely because they all required multiple fortuitous events. Our confidence was fortified soon afterwards as the development of Southern blot techniques allowed us to carry out more extensive analyses using a variety of restriction enzymes and myeloma cells.

Joining of Gene Segments

While the experiments with restriction enzymes were informative, details of the rearrangement were difficult to come by with this approach. Fortunately, recombinant DNA technology was just becoming available and was the ideal means for this purpose. Debates on the possible hazards of this type of research were flaring, initially in the United States and, shortly afterwards, in European countries. In order to make sure that our research would not become a target of controversy, *Charlie* and I got in touch with *Werner Arber* at the University of Basel who was coordinating recombinant DNA research activities in Switzerland. A small informal work group was set up by the local researchers interested in this technique. The consensus of the group, which was supported by most of the other Swiss researchers, was that we should all follow the practices and guidelines being adopted in the United States. We met about once a month and exchanged information regarding both ethical and practical aspects of the technology.

On the basis of the previous experiments attempting to count immunoglobulin genes, I thought that it would be wise to start with the mouse λ-light-chain system, the simplest of all chain types that had been studied. Our goal was to clone the V_λ and C_λ "genes" in the germ-line state from embryonic cells, as well as the rearranged V plus C "genes" from a λ myeloma, and to determine the relationship between these genomic DNA clones by electron microscopy and DNA sequencing. No precedent existed at that time for cloning "unique" eukaryotic genes. We therefore had to devise a few tricks as we attempted to clone the first immunoglobulin gene. For instance, our available probe at that time was again 95% pure mRNA rather than a cDNA clone. This situation made the screening of a large number of DNA clones difficult because of the high background. To avoid this problem, we pre-enriched the λ-gene-containing genomic DNA fragments as much as possible using preparative R-loop formation,[17,18] so that the DNA library constructed would have the clone of interest at a high frequency.

Starting with the embryonic DNA, we could isolate a clone that clearly hybridized specifically with the λ mRNA.[18] When an electron microscopist, *Christine Brack*, who had just joined us from the Biozentrum of the University of Basel, examined the mixture of this clone and λ mRNA that had been annealed under appropriate conditions, she found a beautiful R-loop from which about half of the mRNA strand protruded. This and additional analysis convinced us that we had cloned a V_λ "gene" to which no C "gene" was contiguously attached, thus confirming at the DNA clone level that the V and C "genes" are indeed separate in the germ-line genome. A subsequent DNA sequencing study carried out in collaboration with *Allan Maxam* and *Walter Gilbert* of Harvard University revealed that this DNA clone corresponded to the V "gene" for the λ_2 subtype.[19]

In the meantime *Minoru Hirama*, another postdoctoral fellow, succeeded in preparing λ and κ cDNA clones. Once these probes became available, isolation of the genomic clones became much easier. My assistant *Rita Schuller* and I isolated a number of genomic DNA clones from λ- and κ-chain-synthesizing myelomas as well as from embryos.[20,21] Analysis of these DNA clones by electron microscopy, by restriction enzyme mapping, and by DNA sequencing not only confirmed the somatic rearrangement of immunoglobulin genes but also revealed some striking features of their arrangement and rearrangement (Fig. 1). These can be summarized as follows:

1. Although the V and C "genes" are rearranged and are much closer to each other in myeloma cells than in embryo cells, they are not contiguous and are separated by a few kilobases of DNA sequence that does not participate in coding of the polypeptide chain. This untranslated DNA sequence present within the rearranged, complete immunoglobulin gene was unanticipated and was also among the first demonstrations of an intron in eukaryotic genes.[22]
2. The V "gene" found in the germ-line genome is about 13 codons short when it is compared to the length of the conventionally defined V region. The missing codons were found in a short stretch of DNA referred to as a *J* (or joining) gene segment that is located many kilobases away from the incomplete V "gene" (referred to as a *V* gene segment) and a few kilobases upstream of the C

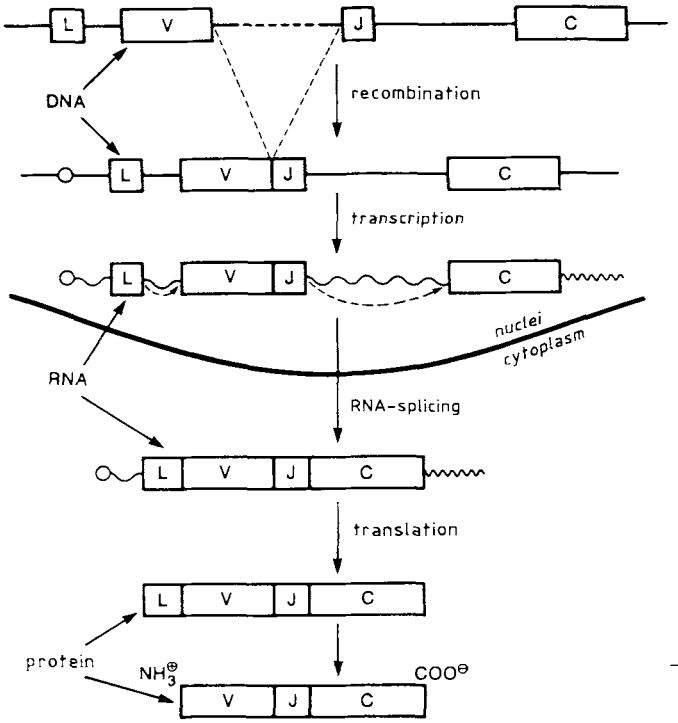

Fig. 1. The basic scheme for rearrangement and expression of an immunoglobulin light-chain gene. At top is an arrangement of the gene segments on a germ-line genome. Somatic rearrangement links the *V* and *J* gene segment and generates a complete light-chain gene shown just below the germ-line genome. The entire gene containing the leader exon (L), the V-region exon (V and J), the C-region exon (C), and the introns present between these exons are transcribed into a pre-mRNA in the nuclei of the B cell. The pre-mRNA is processed by RNA splicing as it is transported from the nuclei to the cytoplasm. The resulting mRNA devoid of introns is translated in the endoplasmic reticulum into a nascent polypeptide chain from which a mature λ light chain is generated after cleavage of the signal peptide.

"gene" (also referred to as a *C* gene segment). In myeloma cells the rearrangement event attaches the *J* gene segment to the *V* gene segment and thereby creates a complete V-region "gene".[20,23]

3. The signal peptide is encoded in yet another DNA segment referred to as the *L* (or leader) exon which is separated from the *V* gene segment by a short intron.[19,23]

Finding that the V_λ "gene" was split into two gene segments, V_λ and J_λ, in the germ-line genome was completely unexpected. But as soon as this discovery was made its implication for the somatic generation of antibody diversity was obvious. If the germ-line genome carries multiple copies of different *V* and *J* gene segments, the number of complete V "genes" that can be generated by random joinings between these two types of gene segments would be much greater than the total number of the inherited gene segments. Thus, contrary to the original concept of *Dreyer* and *Bennett*, DNA rearrangement can provide a major means for the somatic diversification of antibody molecules. The amino acid sequence data of the κ light chains and heavy chains were consistent with this concept.[24,25] Indeed, the nucleotide sequence analysis of the mouse κ-chain gene complex carried out both in my laboratory and in *Phillip Leder*'s laboratory at the United States National Institutes of Health confirmed that a germ-line genome contains multiple *V* and *J* gene segments and that these gene segments are joined in different combinations in each myeloma cell.[20,26] Four different J_κ gene segments were found several kilobases upstream of the C_κ gene segment. The exact number of V_κ gene segments is unknown even today, but it is estimated to be two to three hundred.[27]

Heavy-Chain Genes

Inasmuch as an immunoglobulin heavy chain is also composed of V and C regions, it was reasonable to expect that its gene also would undergo the type of DNA rearrangement described for the light-chain genes. This supposition was confirmed by *Leroy Hood* et al. at California Institute of Technology and by ourselves (Fig. 2).[28,29] As in κ genes, four *J* gene segments were found several kilobases upstream of the *C* gene segments coding for the C region of the μ-class heavy chain. Multiple *V* gene segments were also identified.

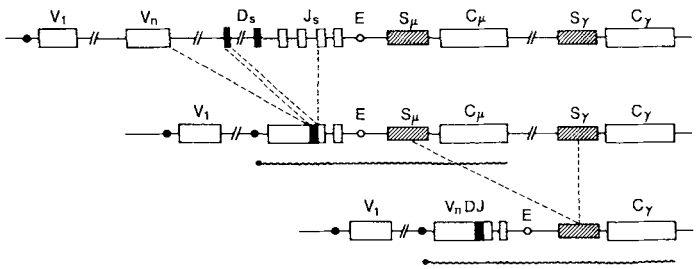

Fig. 2. Organization of the immunoglobulin heavy-chain gene family. At top, middle, and bottom are the organization in a germ-line genome, in a genome of B cells synthesizing a μ-class heavy chain, and in a genome of a plasma cell synthesizing a γ-class heavy chain, respectively. A mouse haploid genome carries several hundred different *V* gene segments, about a dozen *D* gene segments, four *J* gene segments, and one copy of a *C* gene segment for each of the eight different classes or subclasses of immunoglobulin heavy chains. In a virgin B cell one copy each of the *V*, *C*, and *J* gene segment pools have been linked up and the joined *VDJ* DNA sequence is transcribed into a pre-mRNA together with the C_μ gene segment. In different B cells of the same organism a different set of *V*, *D*, and *J* gene segments are usually hooked up and expressed. As the virgin B cell differentiates either to a plasma cell or to a memory B cell (see Fig. 5), the second type of somatic recombination, called "switch recombination", often occurs between a region (S_μ) located upstream of the C_μ gene segment and another region (S_γ) located upstream of the C_γ gene segment. As shown at the bottom, the switch recombination replaces the C_μ gene segment with the C_γ gene segment without changing the *VDJ* exon. Filled circles designate transcriptional promoters present upstream of every *V* gene segment. The open circle designates the transcriptional enhancer [102, 103] which, together with the promoter, activates the rearranged heavy-chain gene for a high-level expression.

While these features of the organization of heavy-chain genes are essentially the same as those of the light-chain genes, one observation made during these studies suggested that the somatic assembly of gene segments plays an even more prominent role in the diversification of heavy chains than of light chains. It was found that from one or two to a dozen amino acid codons that are present in the V–J junction region of the assembled gene are not found in either of the apparently corresponding germ-line *V* or *J* gene segments.[30,31] This suggested that a third type of short gene segment, referred to as *D* (or diversity), might participate in the somatic assembly of a heavy-chain gene. Indeed, *Hitoshi Sakano* and *Yoshi Kurosawa*, two postdoctoral fellows in my laboratory, soon discovered about a

dozen D gene segments,[32,33] which were subsequently mapped in a region upstream of the J cluster in the germline genome.[34,35] Thus the construction of a complete heavy-chain V "gene" requires two DNA-recombination events, one joining a V with a D gene segment and the other the same D with a J gene segment.

Recombination Rule

The joining of V-J or V-D-J gene segments involves a site-specific recombination. It might therefore be expected that these gene segments would carry sequences in the vicinity of the joining ends that are recognized by a putative site-specific recombinase. Furthermore, such recognition sequences are likely to be common for all gene segments of a given type (e.g., V_κ's), because they all seem to be capable of joining with the common set of gene segments of the appropriate type (e.g., J_κ's). There indeed are a heptamer and a nonamer that are conserved in the region immediately downstream of each V_κ gene segment (Fig. 3).[36,37]

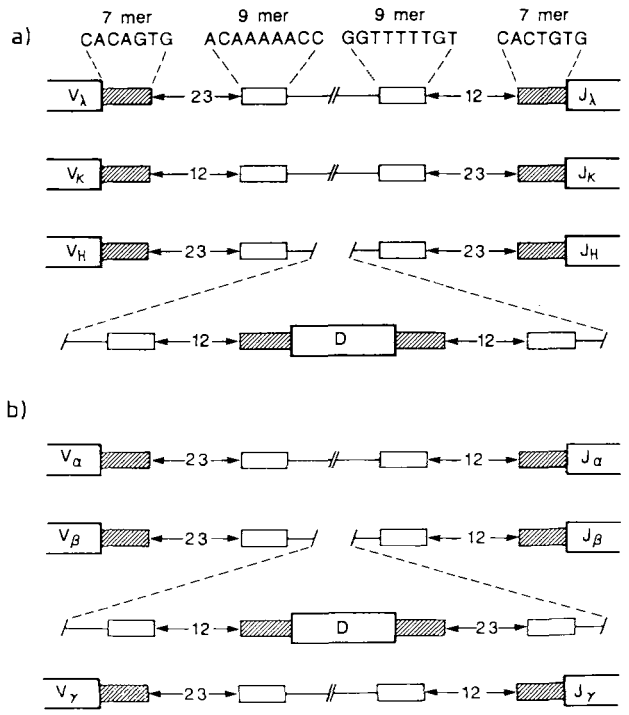

Fig. 3. Putative recognition sequences for the rearrangement of immunoglobulin and T-cell receptor genes. The conserved heptamer and nonamer sequences and the length of the spacer between these sequences are schematically illustrated for immunoglobulin (a) and for T-cell-receptor (b) gene families. The sequences shown on top are consensus sequences. Individual sequences may deviate from these consensus sequences by a few nucleotides.

Sequences complementary to the V_κ heptamer and nonamer were also found in the region immediately upstream of each of the four J_κ gene segments. The same sets of sequences were also found in the corresponding regions of the V_λ and J_λ gene segments.[36] When the heavy-chain V and J gene segments were analyzed subsequently, they too had the common conserved sequences.[30,31] Furthermore, D gene segments carry the heptamer and nonamer sequences both upstream and downstream.[32,33] Another interesting feature of these putative recognition sequences is the fact that the length of the spacer between the heptamer and nonamer is either 12 or 23 base pairs.[30,31] Furthermore, a gene segment carrying a recognition sequence with one type of spacer is able to join only with a gene segment with the spacer of the other type. This 12/23 base-pair spacer rule seems to be adhered to strictly. Little is currently known about the recombinase, but proteins with an affinity for the heptamer or nonamer have been identified in the extract of Abelson-virus-transformed pre-B-cell lines in which the rearrangement occurs in vitro at a relatively high frequency.[38,39]

Diversity Generated at the Joining Ends

When the deduced amino acid sequence of a germ-line J_κ gene segment was compared with the determined amino acid sequences of those κ chains that are encoded in part by that J_κ gene segment, it was noticed that the 5′ end of the J_κ gene segment is not prefixed but rather shifts upstream or downstream by several base pairs in different joining events.[36,37] This flexibility in the precise site of the joining was subsequently found to be a characteristic of the joining ends of other gene segments rather than of just J_κ gene segments.[31] It applies even when the same pair of gene segments were joined in different B-cell precursors, such that the completed V "genes" are likely to have slightly different codons in the junction regions.

The V-D and D-J junctions exhibit diversity of yet another type. We found that up to a dozen base pairs of essentially random sequence are inserted in these junctions apparently without a template during the breakage and reunion of the recombining gene segments.[32,33] While the precise mechanism is yet unknown, the terminal deoxynucleotide transferase that is found in early B-lymphatic nuclei or an enzyme with similar characteristics is thought to play a role in this phenomenon.[40]

The part of the V region affected by the above two diversification mechanisms is limited. But this does not mean that they do not play a significant role in the determination of antibody specificity. On the contrary, the junctions encode the most variable two of the six loops of polypeptides that make up the antigen binding region of the antibody molecule (Fig. 4). Furthermore, specific cases are known where the affinity of an antibody for a defined antigen is drastically altered by a slight change in one junctional sequence.[41] Thus the junctional variation also is a potent somatic generator of antibody diversity.

Somatic Mutation

When *F. Macfarlane Burnet* proposed the clonal selection theory, he recognized the need for some kind of random genetic process in order to generate antibodies able to bind specifically to the vast variety of antigens.[42] He considered somatic mutations as the most plausible mechanism. Subsequently, this idea was adopted and forcefully presented by many, including *Joshua Lederberg*, *Niels Kaj Jerne*, and *Melvin Cohn*.[5,6,7]

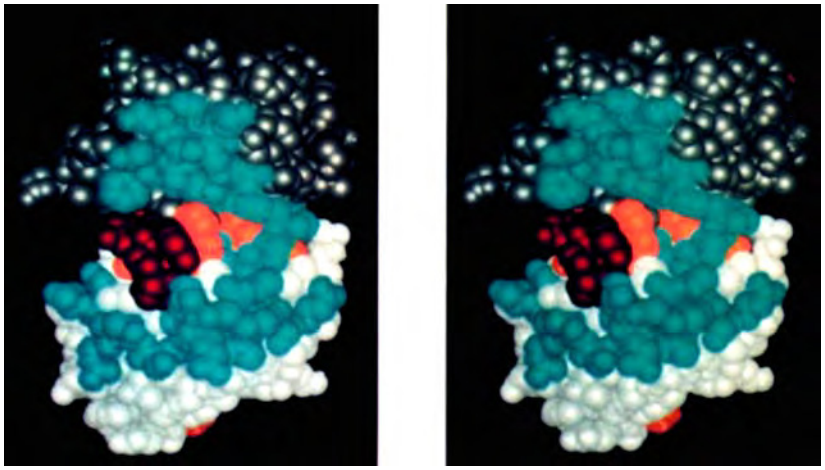

Fig. 4. Space-filling, stereo image of an antibody combining site. Atomic coordinates of mouse immunoglobulin MOPC 603 [104] were used to produce the picture. The heavy-chain variable domain is color-coded dark grey, the light-chain variable domain light grey. The hypervariable regions (except the VH third hypervariable region) are blue, the heavy-chain segment coded for by the D gene is red, and the heavy- and light-chain segments coded for by the J genes are yellow. The D segment corresponds virtually exactly to the third heavy-chain hypervariable region; hypervariable regions were defined as in *Novotney* et al. [105] except for the second heavy-chain hypervariable region, which is marked as defined by *Kabat* et al. [25]. The antigen of this particular immunoglobulin, phosphorylcholine, binds into the cavity in the middle of the picture in between the VH and VL domains, making contacts to amino acid residues belonging to the VH and J segments of the heavy chain and the VL segment of the light chain. The importance of the D segment is well illustrated in the two crystallographic structures of antibodies which bind the protein antigen lysozyme [106, 107]. There, the contact areas contributed by the D segment amount to 60% and 24%, respectively, of the total heavy-chain contact area. This image was computer-generated by *Jiri Novotny* using the program SPHERE of *Robert Bruccoleri*.

The amino acid sequence data accumulated by *Martin Weigert* in *Melvin Cohn*'s laboratory at the Salk Institute provided an excellent opportunity to examine directly the role of somatic mutations in antibody diversity.[7, 11] They had analyzed the λ_1 light chains derived from 18 myelomas. All the mice were of an inbred strain, BALB/c, and so should have been genetically identical. They found that twelve of the $V_{\lambda 1}$ regions were identical but that the other six differed both from the majority sequence and from one another by only one, two, or three amino acid residues. They proposed that BALB/c mice may carry only one germ-line $V_{\lambda 1}$ "gene" which codes for the majority sequence, and that all the other $V_{\lambda 1}$ regions observed are encoded by somatic mutants of this single $V_{\lambda 1}$ "gene" that arose in B-cell development. As I already mentioned in the section on gene counting, the hybridization kinetics suggested that the germ-line BALB/c genome carries no more than a few $V_{\lambda 1}$ "genes". This number was reduced to one when we reevaluated the copy number by the more reliable Southern blotting method.[20] The final proof of somatic mutation in $V_{\lambda 1}$ came when we cloned and sequenced the sole germ-line $V_{\lambda 1}$ gene segment and the rearranged λ_1 genes expressed in a myeloma.[23] As *Weigert* and *Cohn* guessed, the nucleotide sequence of the germ-line $V_{\lambda 1}$ gene segment corresponded to the major amino acid sequence, while the λ_1 gene expressed in the myeloma had been altered by single base changes.

Since this work, several subsets of κ light chains and heavy chains and their germ-line *V* gene segments have been analyzed by cloning and sequencing.[43–46] These results have all confirmed that somatic mutations further amplify the diversity encoded in the germ-line genome. Particularly revealing was the analysis carried out by *Patricia J. Gearhart, Leroy Hood* et al. for the V_H regions associated with the binding of phosphorylcholine (PC). They demonstrated that the single base changes can be extensive and yet are restricted to the joined VDJ sequences and the immediately adjacent regions.[47, 48]

Developmental Control of Rearrangement and Hypermutation

Why have two extraordinary somatic genetic mechanisms, recombination and hypermutation, evolved in the immune system in order to carry out what appears to be one task, namely, to diversify antibodies?

I believe that the answer may be the differential roles of these two genetic mechanisms. Thanks to the efforts of several independent groups of cellular and molecular immunologists, a general picture is emerging that describes the relationship between the stages of B-cell development and the occurrence of somatic recombination or mutation (Fig. 5).[49–55] Somatic recombinations contributing to diversity are initiated first for the heavy chain and then for the light chain during the differentiation of progenitor cells, and the completion of somatic recombination is accompanied by the appearance of virgin B cells.[56–58] These B cells form clones, each of which is composed of cells bearing homogeneous IgM molecules as surface receptors. Thus, somatic recombination is completed *prior to* any possible interaction of a B cell with antigens.

When an antigen enters the lymphatic system for the first time, it will be screened by these virgin B cells. The

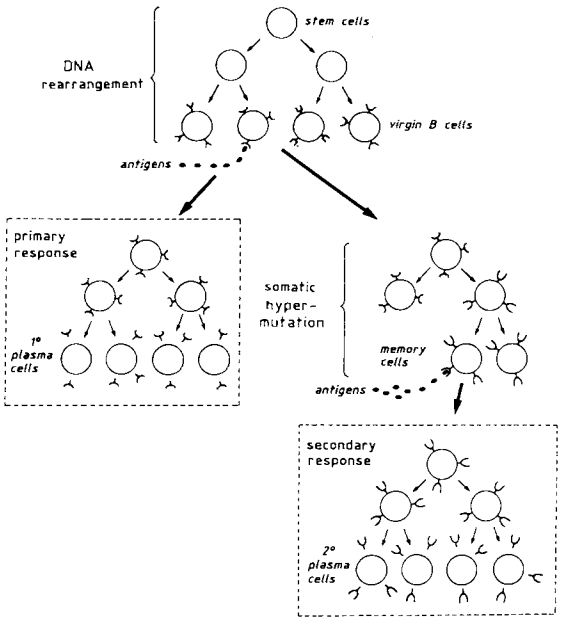

Fig. 5. Differentiation of B cells. Note that the receptors present on the memory cells and the antibody molecules secreted by the plasma cells of the secondary response have a tighter fit to the antigen than the receptors on the ancestral virgin B cells or the antibodies secreted by the plasma cells of the primary response. See text for the full explanation.

small fraction of these B cells that happen to have sufficient affinity for the antigenic determinants in question will respond and follow either of two pathways: they will produce the primary antibody response, or they will contribute to the generation of memory B cells. In the former pathway, the selected B cells will proliferate and differentiate into antibody-secreting plasma cells. During this process, the C region of the heavy chain can switch from μ to another class, but mutation is rare in either the heavy- or the light-chain V region. Consequently, the antibodies secreted by plasma cells in the primary response would largely have the same V regions as the immunoglobulin receptors on the virgin B cells from which they derive.

By contrast, immunoglobulin remains in the cell surface receptor form during the other pathway taken by the antigen-activated virgin B cells, namely, the generation of memory B cells. During this process the hypermutation apparatus appears to be most active and the rate of the mutation approaches 10^{-3} base substitution per cell per generation. Antigen selects, in a stepwise fashion, better and better fitting mutants so that the immunoglobulins on the surface of memory B cells achieve a substantially higher affinity than the immunoglobulins on the ancestral virgin B cells. Switch recombination also occurs frequently during this process. When the same antigen as the one that elicited the primary response reenters the body, the memory B cells are selectively propagated and differentiate into plasma cells. This is the so-called secondary antibody response, which, therefore, consists of high-affinity antibodies of "mature" isotype showing extensive somatic mutation in their V regions. Somatic mutations appear to cease after memory cells are generated, and little or no further mutation takes place during the secondary antibody response.

This scheme of B-cell differentiation can be rephrased as follows. An organism is prepared for infection by pathogens bearing virtually any antigens with a large variety of resting B cells. These B cells bear unique immunoglobulin receptors encoded by one copy each of complete light- and heavy-chain genes that have been constructed by a random or quasi-random assembly of the inherited gene segments. Since the assembly occurs independently of antigens and since the inherited gene segments are not usually selected during evolution for precise fit to particular antigens, the antibodies secreted by the plasma cells derived directly from the selected resting virgin B cells during a primary antibody response usually have a relatively low affinity. By contrast, the frequent single base changes that occur during the generation of memory B cells provide the organism with a great variety of finely altered immunoglobulin receptors from which only those with the best fit to the antigen in question will be selected. Since the plasma cells generated during the secondary antibody response are mostly direct descendants of these memory B cells having no further alterations in the antigen-combining sites, these antibodies usually exhibit a much higher affinity for antigen than do primary antibodies. This explains the long-known phenomenon of affinity maturation of antibodies during the course of repeated immunizations.[59]

Thus somatic creation of antibody genes can be viewed as a two-step process. In the first step, blocks of gene segments are employed to build, in an antigen-independent fashion, a set of genes coding for antibodies of great diversity but with low affinity. In the second step, once the antigen is defined, a small selected set of B cells bearing low-affinity antibodies as cell surface receptors undergo somatic mutations with the result that a fraction of them develop a higher affinity for that antigen and can be selected for further expansion. This process improves the ability of the immune system to detect a low concentration of antigens. One wonders what happens to those cells in which mutation did not improve affinity. A recent study suggests that at least some of these cells may be set aside for selection by different antigens.[54] Thus somatic mutation may also contribute to the repertoire of receptors specific for antigens not previously introduced into an immune system.

T-Cell Receptors

As the mystery of the genetic origins of antibody diversity was unraveled at least in its basic outlines, it seemed natural to extend our research to "the other half" of the lymphoid system, namely, T cells. Although we often discussed the idea of research on the nature of antigen recognition by T cells in the laboratory in the late seventies while I was still in Basel, the real work did not start until the early eighties in my new laboratory at MIT. Although T cells were known to recognize and distinguish antigens as precisely as B cells, nothing was known about the biochemical nature of the molecules responsible for this task, namely, T-cell receptors (TCR). This lack of information was in stark contrast to the wealth of information about antibodies. Much debate took place among cellular immunologists on the nature of these molecules. Some argued that T-cell receptors are just another class of immunoglobulins. Others thought T-cell receptors would have to be

quite different from immunoglobulins. Indeed, studies carried out in the late seventies had shown that the way in which a T cell recognizes an antigen is quite different from the way a B cell does: The T cell reacts to antigens on a cell surface, and the T-cell receptor simultaneously recognizes both an antigen and a determinant present on a glycoprotein encoded by a gene in the major histocompatibility complex (MHC).[60-62] This discovery raised another issue: Does a T cell recognize two determinants with one receptor or does it have two receptors, one for antigen and the other for an MHC product?

The receptor protein was first detected in 1983 in experiments carried out by three independent groups of scientists headed by *James P. Allison, Ellis L. Reinherz,* and *Phillipa Marrack* and *John Kappler.*[63-65] They prepared antibodies that bind to a protein on the T-cell surface: Since these proteins were similar but exhibited clonally distributed structural diversity, they were thought to be a good candidate for the receptor. Furthermore, the antibodies they prepared were T-cell clone-specific and they could show that these antibodies blocked activation of the T-cell clone in a clone-specific fashion. The receptor identified by these experiments was composed of two polypeptide subunits, designated α and β, which are held together by a disulfide bond. These studies were critical in the sense that the receptor was finally identified, its overall structure defined, and its predicted structural variability confirmed. However, the paucity of the protein on the T-cell surface and the absence of the secreted form of the receptor made it very difficult to obtain further information about the structure of this molecule, especially its amino acid sequence.

α and β Genes

In the meantime, molecular biologists were attempting to identify the genes coding for the T-cell receptor. This turned out to be a much more difficult endeavor than the cloning of immunoglobulin genes. Although T-cell lines and hybridomas expressing a homogeneous receptor were becoming available, these cells were more difficult to grow than myelomas and the amount of the receptor made was at least two orders of magnitude less than the amount of immunoglobulin produced by a myeloma cell. In 1984, *Mark Davis* et al. at Stanford University and *Tak Mak* et al. at the University of Toronto independently made a breakthrough.[66-68] Their experimental strategy depended on two assumptions: first, that mRNAs coding for the α and β polypeptide chains are present in a T-cell hybridoma or T-cell tumor but are absent in B-cell tumors; second, that the α- and β-chain genes are rearranged in T cells in a manner similar to that of the immunoglobulin genes in B cells. Thus, they made a library from the fraction of T-cell cDNA that did not hybridize with B-cell-derived mRNA and tested each T-cell-specific cDNA clone for rearrangement of the corresponding gene in T cells. As the source of T cells, *Davis'* group used a hybridoma obtained by fusing a mouse helper T cell recognizing antigen plus self class II MHC molecules with a T-cell tumor while *Mak*'s group used a human T-cell tumor. The two groups came up with one common class of cDNA clones that satisfied the above criteria. The nucleotide sequence showed that the corresponding polypeptide chain is significantly (30–35%) homologous to immunoglobulin chains. Furthermore, the cDNA clones contained sequences homologous to V and C regions in the correct orientation. Thus it seemed certain that the gene represented by this class of cDNA clones codes for one of the two subunits of the T-cell receptor. That this gene encodes the β-subunit was soon confirmed by determination of the partial amino acid sequence of the human β chain.[69]

In my laboratory at MIT *Haruo Saito* and I collaborated with *David Kranz* and *Herman Eisen* to isolate both α and β cDNA clones from another type of T cell, namely, a cytotoxic T-cell clone specific for class I MHC molecule. In 1984, using a modified subtractive cDNA library method, we identified two classes of cDNA clones that also satisfied the criteria for a T-cell receptor gene.[70] One class of these clones represented the β-subunit. Taken together with the earlier finding by *Davis'* group, this demonstrated that the two major classes of T cells, helper T cells and cytotoxic T cells, employ the same set of genes at least for the β subunit. The same conclusion was drawn subsequently for the α subunit. This point is significant because the two types of T cell are specific for two distinct subclasses of MHC gene products. Thus, the same T-cell receptor genes mediate recognition of both class I and class II MHC.

The polypeptide chains encoded by the other class of rearranging T-cell-specific cDNAs isolated by *Saito* and myself was also homologous to immunoglobulin chains by 30–35%. These cDNA clones were, however, clearly distinct from β cDNA clones because the polypeptide chains encoded by the two sets of cDNAs were homologous by only 30–35% not only in the V regions but also in the C regions. Since only two subunits, α and β, were known for the T-cell receptor, we initially proposed that this second class of cDNAs represented the α gene.[70] However, even before the work was published a question arose about the assignment of this gene as encoding the α chain. The putative α cDNAs do not carry codons for N-linked glycosylation sites, while unpublished studies from *Charlie Janeway*'s laboratory at Yale University and *Jim Allison*'s at Berkeley indicated that both α and β subunits of at least some T cells carry N-linked carbohydrates. While it was still possible that the apparent discrepancy in glycosylation could be explained by differences in the type of T cell or in the mouse strains used, continued screening of our subtracted cDNA library yielded within a few weeks a third class of clones whose genes also rearrange specifically in T cells.[71] This gene not only was as homologous to immunoglobulin genes as the first two classes of T-cell-specific genes, but also had two potential sites for N-linked glycosylation, and therefore was a better candidate for the α gene. This proposition was soon confirmed by comparing its nucleotide sequence with the partial amino acid sequence of the human α subunit.[72] Furthermore, the α gene was also cloned at about the same time from a helper hybridoma.[73]

Once cDNAs encoding the α and β chains were identified, it was straightforward to determine the organization of

the corresponding genes in genomic DNA. These studies demonstrated that both α and β genes are organized in the germ-line genome and rearranged in T cells in a way remarkably similar to that of the immunoglobulin genes.[74-77] Thus, the organism inherits the genetic information for these polypeptide chains as V_α and J_α gene segments or V_β, D_β, and J_β gene segments, and a random assembly of these gene segments occurs exclusively during T-cell development to generate a diversity comparable to that of immunoglobulins for receptors expressed on the surface of mature T cells. Even the presumed recognition sequences for the site-specific recombinase, the so-called heptamers and nonamers with a 12- or 23-base-pair spacer, seem to be common for both the immunoglobulin and T-cell receptor genes (see Fig. 3).

The complete primary structure of a T-cell receptor can be deduced from the nucleotide sequences of the α and β cDNA clones. Its comparison with the primary structure of an immunoglobulin molecule suggests that the external part of the receptor is composed of four compact, immunoglobulin-like globular domains associated in two noncovalently bound pairs V_α-V_β and C_α-C_β, and further stabilized by an interchain disulfide bond between the C domain and the transmembrane region. This extracellular part of the receptor is anchored on the membrane lipid bilayer through two transmembrane peptides, one each from the α and β chains (Fig. 6).[70]

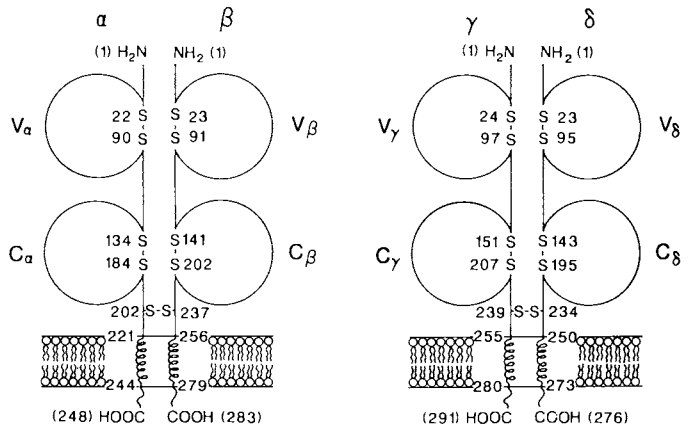

Fig. 6. Diagram showing the subunit structures of T-cell receptors αβ (left) and γδ (right) as deduced from the nucleotide sequences of cDNA clones. The αβ receptor is from an alloreactive cytotoxic mouse T-cell clone, 2C, and the γδ receptor from a mouse thymocyte hybridoma, KN6, prepared by *Osami Kanagawa* of Lilly Research Laboratories, La Jolla, California. Intra- and interchain disulfide bonds are indicated. The receptors are thought to be anchored on the membrane lipid bilayer by transmembrane peptides. The invariant CD3 complex associated with the heterodimers is not shown.

Determining the structure and organization of genes encoding the T-cell receptors settled the issue of their relationship with immunoglobulins and accounted for the genetic origins of their diversity. However, these studies did not illuminate the mechanism by which these receptors can accomplish the dual recognition of an antigen and an MHC determinant. This last issue is particularly tantalizing because recent studies using a technique for injecting T-cell receptor genes into cloned, functional T cells confirmed that the αβ heterodimer alone is sufficient to mediate this dual specificity.[78] In order to understand how the heterodimer simultaneously recognizes the two determinants, much more information is needed as to the structure of the receptor and of its compound ligand. It seems that the ultimate solution has to come from X-ray crystallographic analysis of the receptor protein.

A New T-Cell Receptor, γδ

Since it was established that the third T-cell-specific rearranging gene discovered was for the α subunit, the second one became an orphan. This gene is so closely related to the other two genes, however, that it seems certain that it must have some role in recognition by T cells. Nevertheless, previous immunochemical studies did not reveal any polypeptide chain that might be considered as a candidate for the protein product of this gene. The γ gene is also assembled somatically from *V*, *J*, and *C* gene segments and shares a number of characteristics with the α and β genes as well as with immunoglobulin genes.[79,80]

A number of possibilities were considered initially as firsthand roles for the putative γ chain. For instance, it was thought that the γ chain may be a subunit for a second T-cell receptor coexpressed with the αβ heterodimer. This hypothesis is in line with the two-receptor model of dual recognition of antigen and MHC by T cells. Another possibility proposed was that there may be a switch in the subunits of the T-cell receptor during T-cell development. A model was proposed in which a T-cell receptor composed initially of an γβ heterodimer switches to an αβ heterodimer as T cells differentiate in the thymus.[81,82] This model, which seemed to be supported by the time-course kinetics of appearance of α-, β-, and β-specific RNA in developing thymocytes, was an attempt to explain an apparent dilemma in the intrathymic selection of the T-cell repertoire (for instance, see Ref. [83]).

Subsequent studies carried out in my and several other laboratories, however, revealed a number of features of the γ gene and its expression which are not necessarily consistent with these hypotheses. First, the γ gene is not rearranged in some T-cell clones or hybridomas. Furthermore, even in many of those T cells in which this gene is rearranged, the joining of the *V* and *J* gene segments does not allow the *J*-region codons to be translated in phase with the *V*-region codons.[84-86] Thus, the γ gene product does not seem to be universally expressed in conventional, αβ-receptor-positive cytotoxic and helper T cells. Second, the γ polypeptide chain is expressed on the surface of a small (less than 0.5%) subset of peripheral T cells as a component of a heterodimer referred to as γδ.[87-89] The majority of these T cells exhibit none of the CD4 or CD8 glycoproteins of conventional αβ-receptor T cells on their surface, and therefore belong to a distinct cell population. Third, like the αβ heterodimer, the γδ heterodimer is associated relatively tightly with another glycoprotein, CD3.[87] The invariant CD3-protein complex contains a subunit that seems to play a critical role in the transmission of the signal received by the variable heterodimer into the cell.[90] Thus, the similarity between the γδ- and αβ-receptor heterodimer includes both their structure and transmembrane

signal transmission. Fourth, γδ-bearing cells are relatively abundant in the $CD4^-$, $CD8^-$ fraction of fetal and adult thymocytes.[91-94] For instance, thymocytes of 16-day-old fetal mice, which are mostly double-negative (i.e., $CD4^-$ and $CD8^-$) cells, are a relatively rich source of γδ-bearing cells. Since double-negative thymocyte populations contain precursors for mature, functional, αβ-bearing T cells,[95] a natural question that arises is whether γδ-bearing thymocytes are precursors for αβ-bearing T cells. Fifth, another major site of expression of the γδ receptor is epidermal tissues. It was recently found by two groups that this tissue contains Thy-1^+ (another cell surface marker shared by all types of T cells), $CD3^+$, $CD4^-$, and $CD8^-$ cells bearing γδ heterodimers.[96,97] Unlike conventional T cells, these cells look more like dendritic cells and are therefore referred to as dendritic epidermal cells (DEC). Finally, the δ gene also undergoes rearrangement. *D*, *J*, and *C* gene segments for δ polypeptide chains have recently been mapped within the α gene family between V_α and J_α gene segments.[98] The nested configuration of α and δ gene segments is intriguing and provokes curiosity about the possible relationship of gene organization to the regulation of the rearrangement and expression of the two types of genes. Another intriguing question is whether and to what extent the pool of V_α and V_δ gene segments overlap.

Despite the rapid progress made in the characterization of the γ and δ genes and their products, the most intriguing problem, namely, the physiological role of the γδ-receptor-bearing cells, is currently unknown. One can only speculate on this matter using the currently available information. As to the ligand of this new receptor, it is probably correct to emphasize the fact that the receptor shares with the immunoglobulin B-cell and the αβ T-cell receptors the same genetic basis for somatic diversification. It therefore is likely that the ligand in question will also exhibit structural diversity. In this respect it is interesting that recent studies by us and others suggest that at least part of the ligand is encoded in the MHC.[99,100] The effector function of the cells bearing γδ receptors has not yet been defined with certainty, but recent studies using human and mouse γδ-cell clones suggest that many of these cells have cytotoxic capacity.[89,100,101] The finding of a new type of T cell with an apparently distinct set of T-cell receptors in epidermal tissues stimulates one's imagination. It may be that occurrence of this type of T cell is not restricted to the outer epithelial tissues but extends to all epithelial layers including the lining of various internal organs (*C. Janeway*, personal communication). If so, these cells may have evolved to protect the part of the body that is most vulnerable to infection, namely, its external and internal epithelial surfaces that are in direct contact with the environment. However, the prominence of γδ cells in the thymus suggests an intrathymic role of these cells as well. An exciting possibility that has not been ruled out is a role for these cells in the intrathymic selection of appropriate αβ T cells.

Concluding Remarks

Use of restriction enzymes and recombinant DNA methods allowed resolution of a long-standing and central issue in immunology, the genetic origins of antibody diversity. It turned out that an organism does not inherit even a single complete gene for antibody polypeptide chains. Rather, the genetic information is transmitted in germ line as no more than several hundred gene segments. Through a series of specialized somatic recombinations occurring specifically during the differentiation of B lymphocytes, these gene segments are assembled into tens of thousands of complete genes. Somatic hypermutation occurring in these assembled genes further diversifies antibody polypeptide chains, so that B cells displaying immunoglobulin receptors having a better fit to a given antigen can be selected in a later phase of B-cell differentiation. Thus, in the immune system, organisms have exploited two major processes for modification of DNA, recombination and mutation, as a means to diversify somatically the limited amount of inherited genetic information in order to cope with the vastly diverse antigen universe.

Why has somatic diversification been necessary in the evolution of the immune system? Microorganisms and substances produced by them are the primary source of biologically relevant antigens against which vertebrates need to produce antibodies for survival. Since the generation time of microorganisms is several orders of magnitude shorter than that of vertebrates, the former can produce genetic variants much faster than the latter. Thus, if genetic alterations in the germ-line genome were to be the only source of antibody diversity, vertebrates would be unable to deal effectively with the rapidly changing world of antigens. Somatic diversification allows the individual organism to generate a virtually limitless number of lymphocyte variants. Like organisms in an ecosystem, these lymphocytes are subject to selection by antigens and the fittest will survive. Thus, as *Jerne* and *Burnet* were aware, the individual immune system can be conceived of as a kind of Darwinian microcosm.

The molecular biological approach played an even more fundamental role in the analysis of the T-cell receptor in that very little structural information existed prior to the cloning of the receptor genes. It was demonstrated that the polypeptide chains composing the receptor protein are encoded by genes that share a common ancestor with the immunoglobulin genes. Like immunoglobulins, T-cell receptors are diversified by somatic recombination, but unlike immunoglobulins, these receptor proteins have not been observed to undergo further diversification by somatic mutation. The reason for this difference is unknown, but it seems likely that the explanation will be as follows. First, unlike immunoglobulins, T-cell receptors function exclusively as cell surface receptors which are specialized for interacting with cell-bound antigens. Since both ligand and receptor are distributed in two-dimensional space when a T cell interacts with an antigen-presenting cell, and since T cells have mechanisms for transiently adhering to other cells, these receptor–ligand interactions occur under conditions of high local concentration. Thus, improvement of the affinity beyond the one accomplished by somatic rearrangement may not be necessary in T-cell recognition.

Second, the ligand consists in part of an essentially invariant component, self MHC. As the T-cell receptor is selected both during development and during immunization

for self-MHC recognition, the extreme variability available via somatic mutation may not only be unnecessary but even disadvantageous. Finally, and probably more important, T cells appear to be selected early in development for self tolerance, the inability to recognize self antigen. Somatic mutation during antigenic stimulation, as occurs in B lymphocytes, could lead to the development of autoreactivity. While autoreactive B cells depend upon the additional presence of autoreactive helper T cells to generate autoimmunity, this is not true of autoreactive T cells, which can directly produce disease. Thus, *Ehrlich*'s famous concept of "honor autotoxins", originally developed for antibodies, is probably critical only for T cells. It will be interesting to examine autoreactive T-cell receptors for any evidence of post-thymic somatic diversification.

Finally, it is interesting to notice that during the fifteen years in which I have studied the immune system, the role of molecular genetics in immunological research has altered radically. When I started investigating the problem of antibody diversity, there was abundant information about the structure and function of antibody molecules, while virtually nothing was known about their genes. By contrast, in the most recent study on T-cell recognition no gene product was known at all when the rearranging gene γ was discovered. From the structure of the gene and its rearranging behavior, it was deduced to be a receptor gene, and this discovery has led directly to new insights into T-cell development and T-cell biology. This short history of research in one area, lymphocyte receptors, is yet another witness to the power of DNA technology, and to the ability of this approach not only to explain known biological phenomena, but also to contribute to the discovery of new biological systems.

The work summarized in this article is the result of collaboration with many colleagues, students, and technical assistants. I wish to extend my sincere thanks to every one of them. I also extend my thanks to Hoffman La Roche which so generously supported my work in Basel. My special thanks are extended to Charles A. Janeway, Jr., Nancy Hopkins, and Yohtaroh Takagaki for many useful comments on the manuscript, to Jiri Novotny for preparing Figure 5, and to my secretary, Eleanor Lahey Basel, for her tireless devotion.

Received: February 24, 1988 [Z 684 IE]
German version: *Angew. Chem. 100* (1988) 1060

[1] R. R. Porter, *Science 180* (1973) 713-716.
[2] G. M. Edelman, *Science 180* (1973) 830-840.
[3] N. Hilschmann, L. C. Craig, *Proc. Natl. Acad. Sci. USA 53* (1965) 1403-1409.
[4] L. Hood, D. W. Talmage, *Science 168* (1970) 325-334.
[5] J. Lederberg, *Science 129* (1959) 1649-1653.
[6] N. K. Jerne, *Eur. J. Immunol. 1* (1971) 1-14.
[7] M. Cohn, B. Blomberg, W. Geckeler, W. Raschka, R. Riblet, M. Weigert in E. E. Sercarz, A. R. Williamson, C. F. Fox (Eds.): *The Immune System: Genes, Receptors, Signals*, Academic Press, New York 1974, p. 89ff.
[8] A. H. Gelderman, A. V. Råke, R. J. Britten, *Proc. Natl. Acad. Sci. USA 68* (1971) 172-176.
[9] J. O. Bishop, *Biochem. J. 126* (1971) 171-185.
[10] S. Tonegawa, *Proc. Natl. Acad. Sci. USA 73* (1976) 203-207.
[11] M. Weigert, M. Cesari, S. J. Yonkovich, M. Cohn, *Nature (London) 228* (1970) 1045-1047.
[12] A. Campbell, *Adv. Genet. 11* (1962) 101.
[13] W. J. Dryer, J. Bennett, *Proc. Natl. Acad. Sci. USA 54* (1965) 864-869.
[14] J. J. Danna, G. H. Sack Jr., D. Nathans, *J. Mol. Biol. 78* (1973) 363.
[15] E. Southern, *J. Mol. Biol. 98* (1975) 503.
[16] N. Hozumi, S. Tonegawa, *Proc. Natl. Acad. Sci. USA 73* (1976) 3628-3632.
[17] M. Thomas, R. L. White, R. N. Davis, *Proc. Natl. Acad. Sci. USA 73* (1976) 2294-2298.
[18] S. Tonegawa, C. Brack, N. Hozumi, R. Schuller, *Proc. Natl. Acad. Sci. USA 74* (1977) 3518-3522.
[19] S. Tonegawa, A. M. Maxam, R. Tizard, O. Bernard, W. Gilbert, *Proc. Natl. Acad. Sci. USA 75* (1978) 1485-1489.
[20] C. Brack, M. Hirama, R. Lenhard-Schuller, S. Tonegawa, *Cell 15* (1978) 1-14.
[21] R. Lenhard-Schuller, B. Hohn, C. Brack, M. Hirama, S. Tonegawa, *Proc. Natl. Acad. Sci. USA 75* (1978) 4709-4713.
[22] C. Brack, S. Tonegawa, *Proc. Natl. Acad. Sci. USA 74* (1977) 5652-5656.
[23] O. Bernhard, N. Hozumi, S. Tonegawa, *Cell 15* (1978) 1133-1144.
[24] M. Weigert, L. Gatmaitan, E. Loh, J. Schilling, L. Hood, *Nature (London) 276* (1978) 785-789.
[25] E. A. Kabat, T. T. Wu, H. Bilofsky, M. Reid-Miller, H. Perry, U. S. Dept. of Health and Human Services Publication, 1983.
[26] J. G. Seidman, A. Leder, M. Nau, B. Norman, P. Leder, *Science 202* (1978) 11-16.
[27] S. Cory, B. M. Tyler, J. M. Adams, *J. Mol. Appl. Genet. 1* (1981) 103-116.
[28] M. M. Davis, K. Calame, P. W. Early, D. L. Livant, R. Joho, I. L. Weisman, L. Hood, *Nature (London) 283* (1980) 733-738.
[29] R. Maki, A. Traunecker, H. Sakano, W. Roeder, S. Tonegawa, *Proc. Natl. Acad. Sci. USA 77* (1980) 2138-2142.
[30] P. W. Early, H. Huang, M. M. Davis, K. Calame, L. Hood, *Cell 19* (1980) 981-992.
[31] H. Sakano, R. Maki, Y. Kurosawa, W. Roeder, S. Tonegawa, *Nature (London) 286* (1980) 676-683.
[32] H. Sakano, Y. Kurosawa, M. Weigert, S. Tonegawa, *Nature (London) 290* (1981) 562-565.
[33] Y. Kurosawa, H. von Boehmer, W. Haas, H. Sakano, A. Traunecker, S. Tonegawa, *Nature (London) 290* (1981) 565-570.
[34] Y. Kurosawa, S. Tonegawa, *J. Exp. Med. 155* (1982) 201-218.
[35] C. Wood, S. Tonegawa, *Proc. Natl. Acad. Sci. USA 80* (1983) 3030-3034.
[36] H. Sakano, K. Hüppi, G. Heinrich, S. Tonegawa, *Nature (London) 280* (1979) 288-294.
[37] E. E. Max, J. G. Seidman, P. Leder, *Proc. Natl. Acad. Sci. USA 76* (1979) 3450-3454.
[38] B. D. Halligan, S. V. Desiderio, *Proc. Natl. Acad. Sci. USA 84* (1987) 7019-7023.
[39] R. J. Aguitera, S. Akira, K. Okagaki, H. Sakano, *Cell*, in press.
[40] F. W. Alt, D. Baltimore, *Proc. Natl. Acad. Sci. USA 79* (1982) 4118-4122.
[41] T. Azuma, V. Igras, E. B. Reilly, H. N. Eisen, *Proc. Natl. Acad. Sci. USA 81* (1984) 6139-6143.
[42] F. M. Burnet: *The Clonal Selection Theory of Acquired Immunity*. Cambridge University Press, London 1959.
[43] A. L. M. Bothwell, M. Paskind, M. Reth, T. Imanishi-Kari, K. Rawesky, D. Baltimore, *Cell 24* (1981) 624.
[44] S. Crews, J. Griffin, H. Huang, K. Calame, L. Hood, *Cell 25* (1981) 59-66.
[45] D. Givol, R. Zakut, K. Effron, G. Rechavi, D. Ram, J. B. Cohen, *Nature (London) 292* (1981) 426-430.
[46] E. Selsing, U. Storb, *Nucleic Acids Res. 9* (1981) 5725-5735.
[47] P. J. Gearhart, N. D. Johnson, R. Douglas, L. Hood, *Nature (London) 291* (1981) 29-33.
[48] S. Kim, M. Davis, E. Sinn, P. Patten, L. Hood, *Cell 27* (1981) 573-580.
[49] B. A. Askonas, A. R. Williamson, *Eur. J. Immunol. 2* (1972) 487-493.
[50] C. Berek, G. M. Griffiths, C. Milstein, *Nature (London) 316* (1985) 412-418.
[51] D. McKean, K. Hüppi, M. Bell, L. Standt, W. Gerhard, M. Weigert, *Proc. Natl. Acad. Sci. USA 81* (1984) 3180-3184.
[52] K. Okumura, M. H. Julius, T. Tsu, L. A. Herzenberg, *Eur. J. Immunol. 6* (1976) 467-472.
[53] M. Sablitzberg, C. Kocks, K. Rajewsky, *EMBO J. 4* (1985) 345-350.
[54] M. Sickevitz, C. Kocks, K. Rajewsky, R. Dildrop, *Cell 48* (1987) 757-770.
[55] L. J. Wysocki, T. Manser, M. L. Gefter, *Proc. Natl. Acad. Sci. USA 83* (1986) 1847-1851.
[56] R. Maki, J. Kearney, C. Paige, S. Tonegawa, *Science 209* (1980) 1366-1369.
[57] R. P. Perry, D. E. Kelley, C. Coleclough, J. F. Kearney, *Proc. Natl. Acad. Sci. USA 78* (1981) 247-251.
[58] M. G. Reth, P. A. Ammirati, S. J. Jackson, F. W. Alt, *Nature (London) 317* (1985) 353-354.

[59] H. N. Eisen, G. W. Siskind, *Biochemistry 3* (1964) 996-1000.
[60] A. S. Rosenthal, E. M. Shevach, *J. Exp. Med. 138* (1973) 1194-1212.
[61] D. H. Katz, T. Hamaoka, M. E. Dorf, B. Benacerraf, *Proc. Natl. Acad. Sci. USA 70* (1973) 2624-2628.
[62] R. M. Zinkernagel, P. C. Doherty, *J. Exp. Med. 141* (1975) 1427-1436.
[63] J. P. Allison, B. W. McIntyre, D. Bloch, *J. Immunol. 129* (1982) 2293-2300.
[64] S. C. Meuer, O. Acuto, R. E. Hussey, J. C. Hodgdon, K. A. Fitzgerald, S. F. Schlossman, E. L. Reinherz, *Nature (London) 303* (1983) 808-810.
[65] K. Haskins, R. Kubo, J. White, M. Pigeon, J. W. Kappler, P. Marrack, *J. Exp. Med. 157* (1983) 1149-1169.
[66] S. M. Hedrick, D. I. Cohen, E. A. Nielsen, M. M. Davis, *Nature (London) 308* (1984) 149-153.
[67] S. M. Hedrick, E. A. Nielsen, J. Kavaler, D. I. Cohen, M. M. Davis, *Nature (London) 308* (1984) 153-158.
[68] Y. Yanagi, Y. Yoshikai, K. Leggett, S. P. Clark, I. Aleksander, T. W. Mak, *Nature (London) 308* (1984) 145-149.
[69] O. Acuto, M. Fabbi, J. Smart, C. B. Poole, J. Protentis, H. D. Royer, S. F. Schlossman, E. L. Reinherz, *Proc. Natl. Acad. Sci. USA 81* (1984) 3851-3855.
[70] H. Saito, D. M. Kranz, Y. Takagaki, A. C. Hayday, H. N. Eisen, S. Tonegawa, *Nature (London) 309* (1984) 757-762.
[71] H. Saito, D. M. Kranz, Y. Takagaki, A. C. Hayday, H. N. Eisen, S. Tonegawa, *Nature (London) 312* (1984) 36-39.
[72] T. H. Hannum, J. W. Kappler, I. S. Trowbridge, P. Marrack, J. H. Freed, *Nature (London) 312* (1984) 65-67.
[73] Y-h. Chien, D. M. Becker, T. Lindsten, M. Okamura, D. J. Cohen, M. M. Davis, *Nature (London) 312* (1984) 31-35.
[74] Y-h. Chien, N. Gascoigne, J. Kavaler, N. E. Lee, M. M. Davis, *Nature (London) 309* (1984) 322-326.
[75] G. Siu, M. Kronenberg, E. Strauss, R. Haars, T. W. Mak, L. Hood, *Nature (London) 311* (1984) 344-350.
[76] A. C. Hayday, D. J. Diamond, G. Tanigawa, J. S. Heilig, V. Folsom, H. Saito, S. Tonegawa, *Nature (London) 316* (1985) 828-832.
[77] A. Winoto, S. Mjolsness, L. Hood, *Nature (London) 316* (1985) 832-836.
[78] Z. Dembić, W. Haas, S. Weiss, J. McCubray, H. Kiefer, H. von Boehmer, M. Steinmetz, *Nature (London) 320* (1986) 232-238.
[79] D. M. Kranz, H. Saito, M. Heller, Y. Takagaki, W. Haas, H. N. Eisen, S. Tonegawa, *Nature (London) 313* (1985) 752-755.
[80] A. C. Hayday, H. Saito, S. D. Gillies, D. M. Kranz, G. Tanigawa, H. N. Eisen, S. Tonegawa, *Cell 40* (1985) 259-269.
[81] D. H. Raulet, R. D. Garman, H. Saito, S. Tonegawa, *Nature (London) 314* (1985) 103-107.
[82] B. Pernis, R. Axel, *Cell 41* (1985) 13-16.
[83] R. Schwarz in W. Paul (Ed.): *Fundamental Immunology*, Raven Press, New York 1984, p. 379-438.
[84] E. B. Reilly, D. M. Kranz, S. Tonegawa, H. N. Eisen, *Nature (London) 321* (1986) 878-880.
[85] F. Rupp, G. Frech, H. Hengartner, R. M. Zinkernagel, R. Joho, *Nature (London) 321* (1986) 876-878.
[86] J. S. Heilig, S. Tonegawa, *Proc. Natl. Acad. Sci. USA 84* (1987) 8070-8074.
[87] M. B. Brenner, J. McLean, D. P. Dialynas, J. L. Strominger, J. A. Smith, F. L. Owen, J. G. Seidman, S. Ip, F. Rosen, M. S. Krangel, *Nature (London) 322* (1986) 145-149.
[88] L. L. Lanier, N. A. Federspiel, J. J. Ruitenberg, J. H. Phillips, J. P. Allison, D. Littman, A. Weiss, *J. Exp. Med. 165* (1987) 1076-1094.
[89] J. Borst, R. J. Van de Griend, J. W. van Oostveen, S-L. Ang, C. J. Melief, J. G. Seidman, R. L. H. Bolhuis, *Nature (London) 325* (1987) 683-688.
[90] J. P. van Wauve, J. R. de Mey, J. G. Goosens, *J. Immunol. 124* (1980) 2708-2812.
[91] I. Bank, R. A. DePinho, M. B. Brenner, J. Cassimeris, F. W. Alt, L. Chess, *Nature (London) 322* (1986) 179-181.
[92] A. M. Lew, D. M. Pardoll, W. L. Maloy, B. J. Fowlkes, A. Kruisbeck, S-F. Cheng, R. N. Germain, J. A. Bluestone, R. H. Schwartz, J. E. Coligan, *Science 234* (1986) 1401-1405.
[93] N. Nakanishi, K. Maeda, K. Ito, M. Heller, S. Tonegawa, *Nature (London) 325* (1987) 720-723.
[94] D. M. Pardoll, B. J. Fowlkes, J. A. Bluestone, A. Kruisbeck, W. L. Maloy, J. E. Coligan, R. H. Schwartz, *Nature (London) 326* (1987) 79-81.
[95] B. J. Fowlkes, *Thesis*, George Washington University Graduate School of Arts and Sciences, Washington DC 1984.
[96] F. Koning, G. Stingl, W. M. Yokoyama, W. L. Maloy, E. Tschachler, E. M. Shevach, J. E. Coligan, *Science 236* (1987) 834-837.
[97] W. A. Kuziel, A. Takashima, M. Bonyhadi, P. R. Bergstresser, J. P. Allison, R. E. Tigelaar, P. W. Tucker, *Nature (London) 328* (1987) 263-266.
[98] Y-h. Chien, M. Iwashima, K. B. Kaplan, J. F. Elliott, M. M. Davis, *Nature (London) 327* (1987) 677-682.
[99] K. Maeda, N. Nakanishi, B. L. Rogers, W. G. Haser, K. Shitara, H. Yoshida, Y. Takagaki, A. A. Augustin, S. Tonegawa, *Proc. Natl. Acad. Sci. USA 84* (1987) 6536-6540.
[100] L. A. Matis, R. Cron, J. A. Bluestone, *Nature (London) 330* (1987) 262-264.
[101] P. Moingeon, S. Jitsukawa, F. Faure, F. Troalen, F. Triebel, M. Graziani, F. Forestier, D. Bellet, C. Bohuon, T. Hercend, *Nature (London) 325* (1987) 723-726.
[102] S. D. Gillies, S. L. Morrison, V. T. Oi, S. Tonegawa, *Cell 33* (1983) 717-728.
[103] J. Banerji, L. Olson, W. Schaffner, *Cell 33* (1983) 729-739.
[104] Y. Satow, G. H. Cohen, E. A. Padlan, D. R. Davies, *J. Mol. Biol. 190* (1986) 593-604.
[105] J. Novotny, R. E. Bruccoleri, J. Newell, D. Murphy, E. Haber, M. Karplus, *J. Biol. Chem. 258* (1983) 14433-14437.
[106] A. G. Amit, R. A. Mariuzza, S. E. V. Phillips, R. Poljak, *Science 233* (1986) 747-752.
[107] S. Sheriff, E. W. Silverton, E. A. Padlan, G. H. Cohen, S. J. Smith-Gill, B. C. Finzel, D. R. Davies, *Proc. Natl. Acad. Sci. USA 84* (1987) 8075-8079.

Protein Phosphorylation in Bacteria—Regulation of Gene Expression, Transport Functions, and Metabolic Processes

By Josef Deutscher* and Milton H. Saier, Jr.

The importance of protein phosphorylation to the regulation of physiological processes in eukaryotic cells has been known for almost half a century. In contrast, the first conclusive evidence for functionally relevant protein phosphorylation in bacteria was obtained less than a decade ago. To date, only five functionally well-characterized bacterial proteins have been shown to be regulated by reversible phosphorylation. (1) Phosphorylation of isocitrate dehydrogenase in *Escherichia coli* controls the relative flux of carbon through the Krebs cycle and the glyoxylate shunt. (2) In gram-positive bacteria, phosphorylation of HPr, a phosphoryl carrier protein of the phosphoenolpyruvate-dependent sugar phosphotransferase system, regulates carbohydrate uptake via this system. (3) Phosphorylation of glycerol kinase in *Streptococcus faecalis* probably serves to regulate the degradation of glycerol. (4) Phosphorylation of the nitrogen regulatory protein I (NR_I) in *E. coli* controls expression of genes encoding the enzymes which participate in nitrogen metabolism. (5) Phosphorylation of citrate lyase ligase in *Clostridium sphenoides* regulates the conversion of citrate lyase from the inactive sulfhydryl form to the active acetylated form. Recent investigations have shown that more than one hundred proteins in *E. coli* are phosphorylated. It can therefore be anticipated that protein phosphorylation will prove to be as important to the regulation of physiological processes in bacteria as it is in eukaryotes.

1. Introduction

The activities of numerous enzymes are controlled by protein-modifying reactions which occur post-translationally. Covalent, reversible derivatization of a protein requires both the enzyme-catalyzed transfer of the modifying group from a donor molecule to the protein as well as the enzymatic cleavage of this group from the protein (Fig. 1). These two opposing activities are frequently regulated by so-called second messengers (cAMP, cGMP, $Ca^{2\oplus}$) or by cellular metabolites. The coordination of these two activities determines the ratio of the free to the derivatized form of the protein. Since the modified and unmodified enzyme derivatives frequently (but not always) exhibit different K_m or V_{max} values, functional regulation of the enzyme results. When the enzyme is also subject to allosteric regulation, modification can alter its affinity for the effector. Another, recently described mechanism by which protein modification can control enzymatic reactions, the so-called zero-order ultrasensitivity, will be discussed in detail in Section 2.

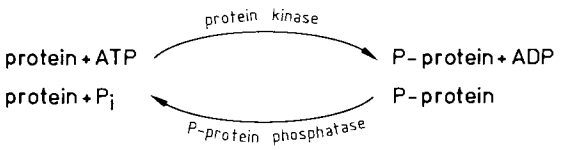

Fig. 1. Generalized reactions for reversible protein modification illustrated by protein phosphorylation.

Among the various reversible, post-translational protein modification reactions (Table 1), protein phosphorylation is by far the most prevalent. In 1943, *Cori* and *Green* observed that glycogen phosphorylase, which degrades glycogen with the formation of glucose-1-P, exists in two interconvertible forms which they designated "a" and "b".[1] Twelve years later phosphorylase a was shown to be a phosphorylated derivative of the enzyme while phosphorylase b was the free form.[2,3] Thus, glycogen phosphorylase was the first protein for which a phosphorylation/dephos-

Table 1. List of the most frequently occurring, reversible protein modification reactions, the respective donor molecules, and the amino acids in the protein that are modified.

Modification	Donors	Modified amino acids
phosphorylation	ATP, GTP, PEP	serine threonine tyrosine histidine
methylation	*S*-adenosylmethionine	aspartate glutamate lysine histidine glutamine
acetylation	acetyl-CoA	lysine cysteine
sulfation	3-phosphoadenosine 5-phosphosulfate	tyrosine
ADP-ribosylation	$NAD^{\oplus}$	arginine lysine glutamate
nucleotidylation (adenylylation, uridylylation)	ATP, UTP	tyrosine serine
tyrosylation	tyrosine	carboxyl terminus

[*] Dr. J. Deutscher
Max-Planck-Institut für Systemphysiologie
Rheinlanddamm 201, D-4600 Dortmund 1 (FRG)
Prof. Dr. M. H. Saier, Jr.
Department of Biology, C-016
University of California, San Diego
La Jolla, CA 92093 (USA)

phorylation cycle was demonstrated. Since the phosphorylated and unphosphorylated forms of the enzyme differed in their activities, and since they were differentially activated by adenosine monophosphate, the enzyme derivatization process was shown to be functionally significant.[4] Subsequently, it was found that phosphorylase kinase, the enzyme that catalyzes the phosphorylation of glycogen phosphorylase,[5] and glycogen synthetase, which synthesizes glycogen,[6] were also regulated by reversible phosphorylation. Although it was initially assumed that the phenomenon of reversible protein phosphorylation was limited to the proteins of glycogen metabolism, the activities of other enzymes, such as the mitochondrial pyruvate dehydrogenase complex,[7] were subsequently shown to be similarly regulated. Phosphorylase kinase is phosphorylated by a cAMP-dependent protein kinase which also phosphorylates numerous other protein substrates. This observation partly explains the many physiological effects exerted by cAMP.[8,9] Today, we know that protein phosphorylation in eukaryotes regulates such widely differing processes as protein, carbohydrate, lipid, and nucleic acid metabolism, DNA repair, gene expression, muscle contraction, receptor functions, and transmembrane transport. In all of these processes, phosphorylation of the relevant proteins occurs most frequently on serine residues and less frequently on threonine residues (Fig. 2).

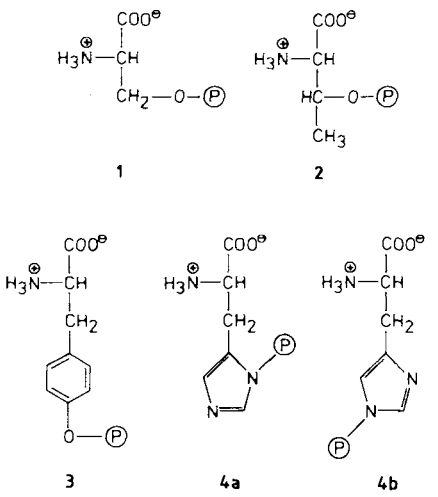

Fig. 2. Structural formulas of the most frequently found phosphorylated amino acids in phosphoproteins (serine **1**, threonine **2**, tyrosine **3**, and histidine **4a** and **4b**). More than one amino acid can be phosphorylated in a single protein.

At the end of the 1970s, it was discovered that $pp60^{v\text{-}src}$, the protein responsible for the transforming properties of Rous sarcoma virus, possessed protein kinase activity.[10] In contrast to the previously known protein kinases, $pp60^{v\text{-}src}$ phosphorylated tyrosine residues in proteins.[11] Viral oncogenes are probably derived from cellular protooncogenes, the products of which fulfill normal regulatory functions in the cell. They are believed to exhibit alterations which give rise to the transformed state after successful viral infection. Thus, identification of the physiologically relevant protein substrates of oncogene-encoded protein-tyrosine kinases should lead to an understanding of growth regulation and the mechanisms of cancerous transformation.[*]

In contrast to the situation in eukaryotes and their viruses, it was long doubted that protein phosphorylation represented a significant bacterial regulatory mechanism. In 1964, *Roseman* et al. discovered the bacterial phosphotransferase system (PTS), a transport system for sugars and sugar alcohols in *Escherichia coli*,[12] and they demonstrated that one of the proteins of this system was phosphorylated. Other enzymes of the PTS were subsequently shown to be phosphorylated. Each of these proteins was phosphorylated either on N-3 of a histidine residue or on N-1 (**4b** and **4a**, respectively, in Fig. 2). The phosphorylation of these proteins did not fulfill a regulatory role but instead served a catalytic function, since the proteins comprise a phosphoryl transfer chain in which the phosphoryl group is transferred from phosphoenolpyruvate (PEP) to the sugar via the various phosphoprotein intermediates (cf. Fig. 4). Although the PEP-dependent phosphorylation of the proteins of the PTS does not fall into the category of the reversible protein phosphorylations discussed here, which do serve regulatory functions, it is discussed in detail in Sections 3 and 4.

In 1969, *Kuo* and *Greengard* reported the presence of a cAMP-dependent *E. coli* protein kinase which phosphorylated histones from calf thymus,[13] but this report has never been confirmed. In fact, the existence of cAMP-regulated, bacterial protein kinases is still in question. A few years later, *Rahmsdorf* et al. observed protein phosphorylation in *E. coli* after infection with the bacteriophage T7.[14] It was soon realized that the protein kinase was encoded by one of the early phage genes.[15] This protein kinase was found to be synthesized shortly after successful infection and phosphorylates 40 to 50 different *E. coli* proteins. These proteins include ribosomal proteins and the β and β′ subunits of the *E. coli* RNA polymerase.[16] The phosphorylation of these proteins presumably halts synthesis of *E. coli* host proteins and promotes synthesis of bacteriophage T7 proteins.

The first unambiguous evidence for a functionally active, prokaryotically encoded protein kinase was obtained by *Wang* and *Koshland* using *Salmonella typhimurium*.[17] By pulse-labeling cells with [^{32}P]phosphate, they detected four phosphorylated proteins and subsequently provided evidence for four protein kinases with differing substrate specificities and sensitivities towards inhibitors.[18] The first bacterial protein to be identified as the target of a protein kinase was isocitrate dehydrogenase from *E. coli*.[19] The regulation of this protein is discussed together with the phosphorylation of isocitrate lyase in Section 2. In Section 3, we concern ourselves with the ATP-dependent phosphorylation of HPr of the bacterial phosphotransferase system in gram-positive bacteria, and then, in Section 4, we consider the unusual regulation of the dihydroxyacetone/glycerol kinase from *Streptococcus faecalis*. This latter process occurs by reversible, PTS-mediated phosphorylation. Thereafter, we discuss in Section 5 the phosphory-

[*] Protein phosphorylation in eukaryotes has been comprehensively reviewed in P. D. Boyer, E. G. Krebs (Eds.): *The Enzymes, Vol. 17* (1986) and *Vol. 18* (1987), Academic Press, New York.

lation of the nitrogen regulatory protein I (NR_I) by the nitrogen regulatory protein II (NR_{II}), a process that controls transcription of genes involved in nitrogen utilization in *E. coli*. In the final section, we mention several additional, less well characterized bacterial protein phosphorylation reactions and discuss future research directions.

2. Regulation of Isocitrate Dehydrogenase in *E. coli* by Reversible Phosphorylation

Isocitrate dehydrogenase (ICDH) is an enzyme of the tricarboxylic acid (TCA) cycle that converts isocitrate into α-ketoglutarate in a reaction involving the $NADP^{\oplus}$-dependent oxidation of the substrate followed by its decarboxylation. The degradative route via the TCA cycle serves to provide energy and biosynthetic precursors. Isocitrate can also be cleaved to glyoxylate and succinate by isocitrate lyase in the first step of the glyoxylate cycle. Glyoxylate is then condensed with acetyl-CoA to yield malate, and the glyoxylate bypass thus merges with the TCA cycle to yield two C_4 acids from one C_6 acid and acetyl CoA (Fig. 3).[20] The succinate and malate formed can be used for biosynthetic purposes.

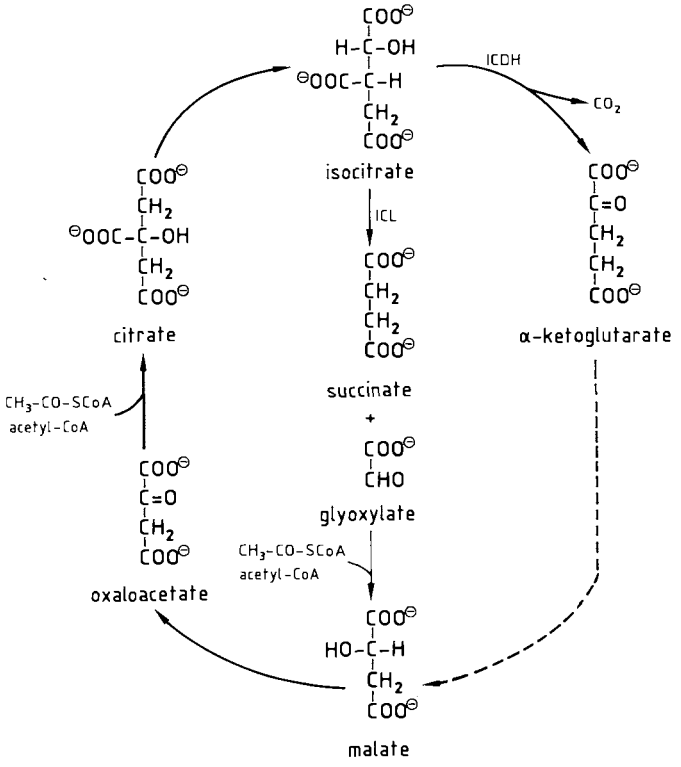

Fig. 3. Depiction of the degradative pathways for isocitrate by *E. coli* illustrating the glyoxylate bypass (involving isocitrate lyase, ICL) and the TCA cycle (involving isocitrate dehydrogenase, ICDH). The succinate formed from isocitrate via the glyoxylate cycle can be used for biosynthetic purposes.

The enzymes of the glyoxylate bypass are inducibly synthesized. They are produced in enhanced amounts when the cells are grown on acetate, ethanol, or a fatty acid as the sole source of carbon. Under these conditions, the glyoxylate cycle is required for the synthesis of cellular building blocks. Isocitrate must be metabolized, therefore, via both the TCA cycle (for the production of energy) and the glyoxylate cycle (for the formation of biosynthetic precursors) in order for cells to grow at the sole expense of a C_2 compound.

Garnak and *Reeves* first observed that reduction of the ICDH activity during growth of *E. coli* on acetate as the sole carbon source occurred concomitantly with phosphorylation of the enzyme.[19] The phosphorylated form of the enzyme could be purified after growth of the cells in a medium containing [^{32}P]phosphate. Partial acid hydrolysis of the purified, [^{32}P]phosphate-labeled protein and subsequent separation of the hydrolysis products established that phosphorylation of ICDH had occurred on a serine residue. Phosphorylation of ICDH led to almost complete loss of activity.[21,22]

Cleavage of the phosphorylated, radioactively labeled ICDH by trypsin[23] or chymotrypsin[24] gave rise to a single radioactively labeled peptide that was isolated and sequenced. The sequence around the phosphorylated serine residue at position 113 in ICDH is shown in Table 2. This

Table 2. Amino acid sequences of the phosphorylation sites in isocitrate dehydrogenase (ICDH) from *E. coli* as well as the HPr proteins from *S. aureus*, *S. faecalis*, and *B. subtilis*. The asterisks indicate the amino acid phosphorylated in each protein. ATP-dependent phosphorylation of HPr from *E. coli* could not be demonstrated.

ICDH	-Pro-Val-Gly-Gly-Gly-Ile-	-Arg-Ser*-Leu-Asn-Val-Ala-Leu-Arg-
(E. coli)	106	119
HPr	-Gly-Lys-Lys-Val-Asn-Leu-Lys-	Ser*-Ile-Met-Gly-Val-Met-Ser-
(S. aureus)	39	52
HPr	-Gly-Lys-Ser-Val-Asn-Leu-Lys-	Ser*-Ile-Met-Gly-Val-Met-Ser-
(S. faecalis)	39	52
HPr	-Gly-Lys-Thr-Val-Asn-Leu-Lys-	Ser*-Ile-Met-Gly-Val-Met-Ser-
(B. subtilis)	39	52
HPr	-Gly-Lys-Ser-Ala-Ser-Ala-Lys-Ser-Leu-Phe-Lys-Leu-Gln-Thr-	
(E. coli)	39	52

sequence does not show homology with the phosphorylation sites of known eukaryotic phosphoproteins. It is of interest to note that the sequence around the phosphorylated serine residue (Arg-Ser-Leu-Asn) is also present in another $NADP^{\oplus}$-dependent enzyme, dihydrofolate reductase from chicken liver.[25] Since this sequence is near the $NADP^{\oplus}$ binding site in dihydrofolate reductase, it was suggested that phosphorylation of ICDH might lead to loss of coenzyme binding. In fact, as demonstrated by fluorescence titration experiments, NADPH does not bind to phosphorylated, inactive ICDH although it binds stoichiometrically to the nonphosphorylated enzyme.[26] The negative charge of the phosphate group is apparently responsible for this effect. When the serine residue at position 113 in ICDH is replaced by an aspartate residue, complete inactivation of the enzyme results.[114]

ICDH kinase, the enzyme that catalyzes the phosphorylation of ICDH, was first purified by *LaPorte* and *Koshland*.[27] This enzyme, with a molecular mass of 66000 daltons, possessed not only ICDH kinase activity but also P-ICDH phosphatase activity. Thus, two enzyme activities with opposing actions were found in a single polypeptide chain. A similar observation had been made previously for other regulatory enzymes including 6-phosphofructo-2-kinase/phosphatase and glutamine synthetase adenylyltransferase.[28]

Regulation of ICDH kinase/phosphatase is effected by a variety of intracellular metabolites. Isocitrate, ADP, pyruvate, phosphoenolpyruvate, 3-phosphoglycerate, and oxaloacetate all inhibit the kinase while stimulating the phosphatase. The latter activity is inhibited by NADPH.[29] Citrate, fructose 6-phosphate, and glyoxylate inhibit the kinase but have no effect on the phosphatase.[30] Under in vivo conditions, pyruvate stimulates ICDH both in wild-type strains and in strains unable to metabolize pyruvate.[30] The latter observation suggests a direct interaction between ICDH kinase/phosphatase and pyruvate. However, isocitrate appears to be the most important effector of this regulatory enzyme. During growth of *E. coli* on acetate, high concentrations of isocitrate (up to 0.6 mM) accumulate. Higher levels of isocitrate allow its metabolism via the glyoxylate bypass since isocitrate lyase possesses relatively low affinity for isocitrate ($K_m = 1$ mM). They also lead to dephosphorylation of P-ICDH and thus to increased ICDH activity.[31]

In connection with the regulation of ICDH by reversible phosphorylation, the phenomenon of "zero order" ultrasensitivity has been discussed.[32] Although it had been previously formulated mathematically, the first experimental evidence for this type of regulatory mechanism was obtained in experiments with ICDH kinase/phosphatase. This phenomenon is based on the fact that a relatively small increase in the activity of a converter enzyme (in this case, ICDH phosphatase or ICDH kinase) can lead to a substantial shift in the ratio of the modified to free form of the protein.[33]

The importance of ICDH phosphorylation to the regulation of carbon flux through the glyoxylate bypass is emphasized by the fact that the gene encoding the ICDH kinase/phosphatase, together with those encoding the enzymes specific to the glyoxylate bypass (isocitrate lyase and malate synthase), comprise the glyoxylate (*ace*) operon. Thus, synthesis of these three enzymes must be coordinately regulated.

Regulation of the two competing metabolic pathways is further complicated by the recent observation that isocitrate lyase (cf. Fig. 3) can also be phosphorylated in vitro.[34] The phosphorylation of this enzyme takes place at N-1 of a histidine residue (cf. **4a** in Fig. 2) and not on serine, threonine, or tyrosine.[115] Unlike ICDH, the phosphorylated form of the isocitrate lyase appears to be the more active form. While the significance of isocitrate lyase phosphorylation is not known, it is clear that regulation of branch-point enzymes is of prime importance to all living organisms. The ability to utilize a wide variety of substrates, one of the more conspicuous features of bacteria, requires the integration of all requisite metabolic processes into a coordinated whole. Section 3 further illustrates this fact employing a second highly complex regulatory system dependent on protein phosphorylation.

3. Regulation of Carbohydrate Uptake via the Phosphotransferase System in Gram-Positive Bacteria

Anaerobic and facultatively anaerobic bacteria possess a transport system for carbohydrates which was first described in 1964 by *Kundig, Ghosh,* and *Roseman* and designated the bacterial phosphotransferase system (PTS).[12] An essential feature of this transport system is that a sugar or sugar alcohol is phosphorylated during transport in a tightly coupled process.[35] The energy and phosphate donor for sugar transport and phosphorylation is phosphoenolpyruvate. The phosphate group is transferred to the incoming sugar via a chain of three or four phosphorylated proteins (Fig. 4). Sugars transported via the PTS include

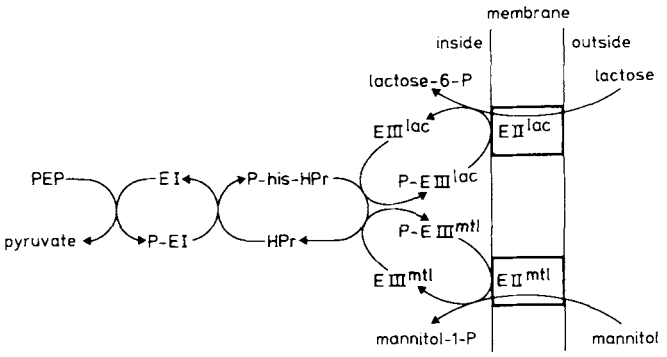

Fig. 4. Schematic representation of phosphoryl transfer via the phosphotransferase system in *S. aureus*. The phosphate group is transferred from phosphoenolpyruvate (PEP) to the sugar via the proteins enzyme I (EI), HPr, enzyme III (EIII), and enzyme II (EII). There is a specific enzyme II/enzyme III pair for each sugar. Lactose and mannitol are transported across the membrane in a process coupled to sugar phosphorylation.

glucose, fructose, mannose, mannitol, glucitol, lactose, and sucrose. Enzyme I and HPr are the general protein components of the PTS and are not sugar-specific. Enzymes II and the enzyme II/III pairs exhibit sugar-specificity as illustrated in Figure 4 for lactose and mannitol. Enzyme I, HPr, and enzymes III are water-soluble proteins while enzymes II are integral membrane proteins. The polypeptide chains of enzymes II pass through the lipid bilayer of the membrane several times.[36]

As mentioned in Section 1, the phosphoryl groups in all PTS proteins are bonded at N-1 (HPr, enzymes II) or N-3 (enzyme I; enzymes III) of histidine residues. In connection with the phenomenon of inducer expulsion, it was discovered that HPr is subject to ATP-dependent phosphorylation.[37] Inducer expulsion is a regulatory mechanism by which sugars taken up via the PTS and accumulated as phosphorylated derivatives are expelled from the cell as the free sugars upon addition of a metabolizable PTS sugar.[38,39] In vivo experiments revealed that the process was probably dependent on cytoplasmic ATP and a glycolytic intermediate. Possibly, the sugar phosphate phosphatase that cleaves the phosphoryl group from the intracellular sugar phosphates is activated by protein phosphorylation.[40]

Under the conditions of inducer expulsion in *Streptococcus pyogenes*, a protein of low molecular weight was found to be phosphorylated,[40] but it did not possess the expected sugar phosphate phosphatase activity. It was subsequently identified as HPr of the PTS.[37] Although the exact mechanism of inducer expulsion remains unclear, the ATP-dependent phosphorylation of HPr was found to be important to the regulation of the PTS in gram-positive

bacteria. In addition to HPr from *S. pyogenes*, HPr's from *Streptococcus faecalis, Streptococcus lactis, Streptococcus mutans, Streptococcus salivarius, Staphylococcus aureus, Staphylococcus carnosus, Bacillus subtilis, Bacillus stearothermophilus, Clostridium histolyticum, Lactobacillus casei,* and *Lactobacillus brevis* have all been found to undergo ATP-dependent phosphorylation. HPr from gram-negative bacteria such as *E. coli* was not phosphorylated.[41-44,62]

In contrast to the PEP-dependent, enzyme I-catalyzed phosphorylation of HPr, which occurs on a histidine residue, a serine residue was shown to be modified in the ATP-dependent phosphorylation reaction. The phosphorylated protein, P-Ser-HPr, was not able to transfer its phosphate group to a sugar.[37] Phosphorylated, radioactively labeled peptides were isolated from [^{32}P]Ser-HPr of *S. faecalis*[45] and *S. aureus*[*] and sequenced (Table 2). Because the amino acid sequences of the two proteins were known, the phosphorylated serine residue could be identified as serine-46. The regions around serine-46 in the three gram-positive HPr proteins of known amino acid sequences (those from *S. aureus, S. faecalis,* and *B. subtilis*[46,47]) showed striking sequence identity (Table 2). In contrast, HPr from *E. coli* showed much less homology around serine-46, possibly explaining why this protein was not phosphorylated by the HPr kinases from gram-positive bacteria.

ATP-dependent HPr kinases, which catalyze the formation of P-Ser-HPr, have been purified from *S. faecalis*,[41] *S. pyogenes*,[42] *L. brevis*,[**] and *B. subtilis*.[***] The activities of these enzymes are stimulated by metabolites such as gluconate-6-P, 2-P-glycerate, and fructose-1,6-diphosphate (FDP), and they are inhibited by phosphate. P-Ser-HPr phosphatase has been purified from *S. faecalis*.[48] The enzyme requires high phosphate concentrations (about 50 mM) for optimal activity.

The ATP-dependent phosphorylation of HPr at serine-46 inhibited the PEP-dependent enzyme I-catalyzed phosphorylation reaction by about three orders of magnitude,[49] and a reciprocal effect was also observed.[41,42] Thus, formation of doubly phosphorylated P_2(ser,his)HPr occurs very slowly.

The PEP-dependent phosphorylation of P-Ser-HPr was found to be accelerated by the presence of any one of the various enzymes III.[49] The physiological significance of this observation is still not clear. It is possible that some PTS sugars are transported preferentially over others and that the formation of P-Ser-HPr serves to regulate the PTS-mediated uptake of carbohydrates. Phosphorylation of *o*-nitrophenylgalactoside, a lactose analogue[48] and of mannitol[****] by the PTS proteins of *S. aureus* was found to occur 150-fold slower in the presence of P-Ser-HPr compared with HPr. Since growth of staphylococcal cells on lactose or mannitol as well as other PTS sugars led to elevated levels of intracellular P-Ser-HPr, this was additional evidence that the formation of P-Ser-HPr serves to regulate the PTS-mediated uptake of carbohydrates. In this context, investigations on the regulation of pyruvate kinase by intracellular metabolites in *S. lactis*[50] are of interest. This enzyme is regulated in practically the same way as the HPr kinases from *S. faecalis* and *S. pyogenes*; i.e., it is inhibited by phosphate (>3 mM) and stimulated by FDP (25 mM). Investigations on the changes in the concentrations of FDP, PEP, and phosphate that occur when resting cells of *S. lactis* are transferred to a medium containing glucose revealed that the FDP concentration increased (from 1 mM to about 25 mM) while the concentrations of phosphate and PEP decreased (from 50 mM to about 3 mM and from 5-10 mM to about 1 mM, respectively).[50,51] Similar effects would be expected for other carbohydrates degraded via the Embden-Meyerhof pathway and thus for virtually all PTS sugars.

The uptake of a PTS sugar into the cell and the associated changes in the concentrations of glycolytic intermediates probably lead to the formation of P-Ser-HPr by the mechanism proposed in Figure 5. A high concentration of

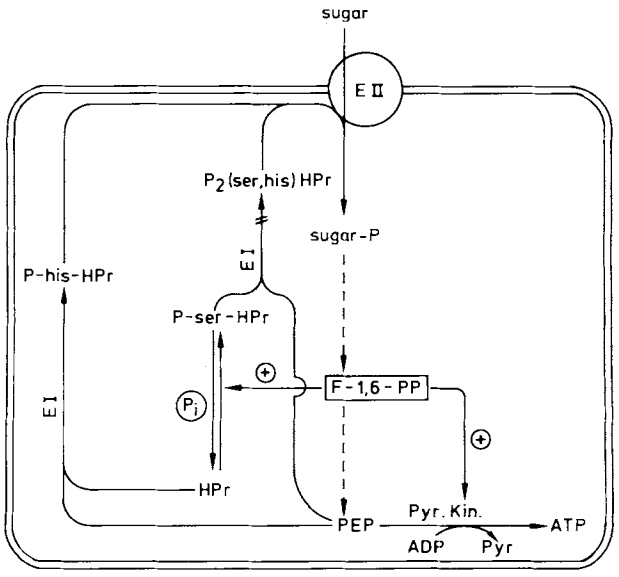

Fig. 5. Effect of HPr (Ser) phosphorylation on sugar uptake by the phosphotransferase system in gram-positive bacteria. Abbreviations are as follows: EI, enzyme I; EII, enzyme II; P-Ser-HPr, HPr phosphorylated at serine-46; P-His-HPr, HPr phosphorylated at histidine-15; P_2(ser,his)HPr, HPr phosphorylated at serine-46 and histidine-15; Pyr. Kin., pyruvate kinase; F-1,6-DP, fructose-1,6-diphosphate; Pyr, pyruvate; ⊕, stimulation.

cytoplasmic phosphate inhibits the HPr kinase and stimulates the P-Ser-HPr phosphatase so that free HPr predominates. When a PTS sugar is taken up, its degradation leads to a rapid increase in the FDP concentration and to a decrease in the phosphate concentration. FDP stimulates the HPr kinase, and the formation of P-Ser-HPr results in a depressed rate of uptake. Simultaneously, FDP stimulates pyruvate kinase, giving rise to an increased rate of ATP synthesis and depletion of the PEP concentration. The activities of HPr kinase, pyruvate kinase, and P-Ser-HPr are thereby adjusted so that the uptake of a carbohydrate via the PTS correlates with its consumption.

Recently, serine-46 in HPr from *B. subtilis* was replaced by alanine by site-specific mutagenesis. The mutant pro-

[*] W. Hengstenberg, unpublished results.

[**] J. Reizer, A. Peterkofsky, A. Romano, unpublished results.

[***] J. Reizer, M. H. Saier, unpublished results.

[****] N. Meyer, J. Deutscher, unpublished results.

tein possessed about 50% of wild-type HPr activity.[47][*] Use of this HPr, which no longer can be phosphorylated by the HPr kinase, in appropriate gram-positive HPr mutant bacteria should permit estimation of the significance of P-Ser-HPr formation to the regulation of the PTS and to inducer expulsion.[47]

In *S. salivarius*, the ATP-dependent phosphorylation of HPr at N-3 of a histidine residue has been reported.[43] Nothing is yet known about the physiological significance of this reaction, and it has not been determined whether histidine-15 is the site of phosphorylation. Nor are the consequences of this ATP-dependent phosphorylation event with respect to PTS activity known.

4. Regulation of Glycerol Kinase from *Streptococcus faecalis* by P-His-HPr-Mediated Phosphorylation

Glycerol is believed to be taken up into bacteria by facilitated diffusion.[52] This process is catalyzed by the glycerol facilitator, which forms a pore specific for glycerol and dihydroxyacetone.[53] Glycerol is then converted by glycerol kinase into glycerol phosphate or by glycerol dehydrogenase and dihydroxyacetone kinase into dihydroxyacetone phosphate. These phosphorylated metabolites are trapped in the cell. In the gram-negative bacteria *E. coli* and *Salmonella typhimurium* the activity of glycerol kinase is regulated by allosteric interactions with fructose-1,6-diphosphate and enzyme III^{glc} of the PTS.[54,55] In the course of a search for a gram-positive enzyme III^{glc} it was found that a protein from *S. faecalis* with a relative molecular mass of 55000 daltons can be phosphorylated in the presence of PEP and the two energy-coupling proteins of the PTS, enzyme I and HPr[56] (Fig. 4). No enzyme III activity was found to be associated with this protein. Attempts to demonstrate a regulatory function for this protein similar to that of the enzyme III^{glc} in gram-negative bacteria led to its identification as glycerol kinase.[57] Dihydroxyacetone (DHA), however, proved to be a better substrate for this enzyme (lower K_m and higher V_{max} values), and thus it was designated DHA/glycerol kinase.

Depending on the oxygen supply, glycerol can either be phosphorylated to glycerol phosphate by *S. faecalis* (under aerobic conditions) or it can be oxidized to DHA and then phosphorylated (under anaerobic conditions).[58] Phosphorylation of both DHA and glycerol is presumably catalyzed by the DHA/glycerol kinase. The PEP-dependent phosphorylation of the DHA/glycerol kinase by P-His-HPr occurs at N-3 of a histidine residue and leads to a tenfold increase in activity.[57] Phosphorylation of the kinase by P-His-HPr takes place slowly in comparison to phosphorylation of an enzyme III, but the process is apparently reversible.

The uptake of a PTS sugar in *B. subtilis* has been shown to inhibit glycerol uptake.[59] Furthermore, it was observed that mutants without enzyme I activity took up glycerol very slowly. Based in part on earlier work,[60] a dependence of glycerol uptake on the PTS was proposed.

When the results described above for both *S. faecalis* and *B. subtilis* are considered, a potential regulatory mechanism can be proposed. When the PTS proteins are phosphorylated, DHA/glycerol kinase will also be phosphorylated, and it will show high activity. However, when a PTS sugar is added to the medium, the PTS proteins will become dephosphorylated,[61] and, consequently, DHA/glycerol kinase will also be dephosphorylated.[57] This model can explain both the decreased rate of glycerol uptake in the presence of a PTS sugar and the dependence of glycerol uptake on a functioning PTS.

Phosphorylation of the *S. faecalis* DHA/glycerol kinase is unusual in three respects. First, a phosphorylated protein (P-His-HPr), in which the phosphate group originates from PEP rather than from a nucleoside triphosphate, is the phosphate donor. Second, there is no P-protein phosphatase which cleaves the phosphate group from P-DHA/glycerol kinase. Third, the phosphate group is bonded to N-3 of a histidine residue in P-DHA/glycerol kinase. This last fact should render phosphoryl transfer between HPr and DHA/glycerol kinase fully reversible. In spite of these peculiarities, the phosphorylation of DHA/glycerol kinase by the PTS fulfills the criteria of a reversible protein modification which serves to regulate an enzyme activity. The relevance of this phosphorylation reaction to the regulation of glycerol uptake in intact cells has yet to be determined.

Also worthy of note is the recent demonstration that glycerol kinase of *Bacillus stearothermophilus* is phosphorylated by PEP, enzyme I, and HPr.[62] However, no results indicative of an increase of the enzyme activity or of reversibility are available. It is possible that the regulation of glycerol kinase in *B. subtilis* may utilize a mechanism involving allosteric interaction with enzyme III^{glc}, as has been demonstrated for *E. coli* and *S. typhimurium*.[62]

5. Transcriptional Regulation of *glnA* Gene Expression by Protein Phosphorylation in Enteric Bacteria

Enteric bacteria such as *E. coli*, *S. typhimurium*, and *Klebsiella aerogenes* can grow on a variety of inorganic nitrogen compounds such as N_2, NH_3, and $NO_3^{\ominus}$ as sole sources of nitrogen. They can also utilize organic nitrogen compounds such as histidine, proline, and arginine. As a result of work in several laboratories, a molecular mechanism accounting for the regulation of the various anabolic and catabolic reactions of nitrogen metabolism is emerging.[63] For the regulation of the activity of glutamine synthetase, allosteric interactions with several effectors have been demonstrated.[63-66] This enzyme is a dodecahedron, built of twelve identical subunits. It is subject to cumulative feedback inhibition by various end products of nitrogen metabolism such as histidine, tryptophan, alanine, glycine, AMP, CTP, carbamoyl phosphate, and glucosamine 6-phosphate. This mechanism in part enables bacteria to adjust the rate of nitrogen metabolism to their needs.

The activity of glutamine synthetase is also controlled by reversible, covalent protein modification. Adenylylation of glutamine synthetase at a tyrosine residue within each subunit results in reduced enzyme activity and altered allo-

[*] J. Reizer, unpublished results.

steric regulation. The enzyme that catalyzes the adenylylation of glutamine synthetase is itself subject to allosteric regulation by a tetrameric protein designated P_{II}.[67] P_{II}, in turn, is subject to uridylylation, a reaction analogous to adenylylation.[68] Both the adenylyl transferase and the uridylyl transferase are bifunctional enzymes which, like the ICDH kinase/phosphatase, catalyze both the modification and demodification reactions. Intracellular metabolites, such as α-ketoglutarate, glutamine, and glutamate, the concentrations of which reflect the availability of nitrogen in the medium, regulate the activities of these two enzymes by allosteric interactions.[66,69] Indicators of energy availability (ATP and inorganic phosphate) also regulate their activities, allowing the coordination of nitrogen metabolism with carbon utilization.

In addition to the regulation of glutamine synthetase by allosterism and protein modification, transcription of the *glnA* gene, which encodes the enzyme, is subject to regulation. The direct participation of glutamine synthetase was initially assumed,[70–72] but subsequent investigations demonstrated that the products of two regulatory genes (*ntrB* and *ntrC*), adjacent to the *glnA* gene, as well as the product of an additional regulatory gene (*ntrA* or *rpoN*) function in *glnA* regulation (Fig. 6).[73,74] The products of the *ntrA, B,* and *C* genes coordinately control expression of *ntrB* and *ntrC*[75] since the latter two genes together with the *glnA* gene comprise an operon.

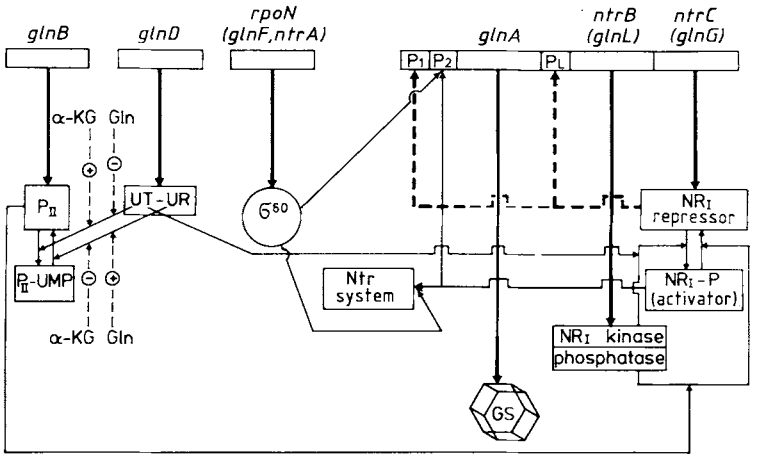

Fig. 6. Suggested mechanism for regulation of the expression of genes encoding enzymes participating in nitrogen metabolism in *E. coli* [63]. The thick unbroken arrows point to the respective gene products; the thin unbroken arrows signify protein-protein interactions; the thick broken arrows signify protein-DNA interactions, and the thin broken arrows signify interactions of metabolites with proteins (⊕, stimulatory; ⊖, inhibitory). Abbreviations are as follows: GS, glutamine synthetase; UT-UR, uridylyltransferase-uridylyl removing enzyme; P_{II}-UMP, uridylylated P_{II}; NR_I-P, phosphorylated NR_I; α-KG, α-ketoglutarate; Gln, glutamine; *rpoN*, additional regulatory gene; P_1, P_2, and P_L, promoters (binding sites for RNA polymerase on the DNA). For further explanation, see the text.

In the last few years, the products of the three regulatory *ntr* genes were identified and partially characterized. This accomplishment has resulted in a clearer understanding of the molecular processes involved in the transcriptional regulation of the *glnA* gene. The product of the *ntrA* gene is a sigma factor (σ^{60}) with a molecular mass of 60000 daltons. It binds to RNA polymerase to displace other sigma factors. RNA polymerase with bound σ^{60} preferentially transcribes operons whose protein products participate in nitrogen metabolism.[75]

The *ntrC* gene encodes a DNA-binding protein, designated NR_I,[76,77] which, in addition to the σ^{60}-loaded RNA polymerase, is necessary for the in vitro transcription of the *glnA* gene.[78] The product of the *ntrB* gene, designated NR_{II},[79] changes the activity of NR_I from a transcriptional repressor to a transcriptional activator by means of reversible protein modification. This modification reaction has been identified as the ATP-dependent phosphorylation of NR_I.[80] NR_{II} is a bifunctional enzyme that catalyzes both the phosphorylation and the dephosphorylation of NR_I and has, therefore, been termed NR_I kinase/phosphatase.

The previously mentioned proteins P_{II} and uridylyl transferase, which are encoded by the genes *glnB* and *glnD*, respectively, are also involved in transcriptional regulation of the glutamine synthetase gene. A series of protein-modification reactions, which lead to altered protein-protein and protein-DNA interactions, enable the bacterium to enhance rates of synthesis of the nitrogen biosynthetic enzymes under conditions of nitrogen insufficiency. This mechanism is illustrated schematically in Figure 6. The activity of the NR_I kinase/phosphatase is regulated by P_{II} and the enzyme that catalyzes the uridylylation and deuridylylation of P_{II}, the uridylyltransferase/uridylyl-removing enzyme (the UT/UR enzyme).

UT, which catalyzes synthesis of P_{II}-UMP, is stimulated by α-ketoglutarate and inhibited by glutamine whereas UR is stimulated by glutamine and inhibited by α-ketoglutarate.[66] A nitrogen insufficiency, which effects a high intracellular concentration of α-ketoglutarate and a low glutamine concentration, consequently leads to conversion of P_{II} to P_{II}-UMP, whereas a sufficient supply of nitrogen gives rise to unmodified P_{II}. Genetic data indicate that P_{II} not only controls the adenylylation of glutamine synthetase but also controls the activity of the NR_I kinase/phosphatase. P_{II}-UMP apparently exerts no influence on this enzyme. Thus, mutants that lack P_{II} (due to mutations in the *glnB* gene) exhibit an increased transcriptional rate of the *glnA-ntrB-ntrC* operon when the nitrogen supply is adequate.[81] Conversely, loss of UT-UR activity (by mutation of the *glnD* gene) causes a low rate of *glnA-ntrB-ntrC* operon transcription even under conditions of nitrogen deficiency.[82] The effects observed for both mutants require an active NR_I kinase/phosphatase since *ntrB* mutants are not responsive to mutations in the *glnB* and *glnD* genes.[83] This observation permits the conclusion that P_{II} and UT-UR exert their effects on gene expression by way of the NR_I kinase/phosphatase.

Some *ntrB* mutants specifically exhibited loss of NR_I phosphatase activity. These mutants always showed an increased rate of transcription of the *glnA* operon regardless of the growth conditions and the presence or absence of

P_{II}.[84] As shown in Figure 6, the effects on expression of the *glnA-ntrB-ntrC* operon caused by widely differing genetic and physiological manipulations can be explained by the assumption that P_{II}, but not P_{II}-UMP, interacts with the NR_I kinase/phosphatase to stimulate the NR_I phosphatase and inhibit the NR_I kinase. Conversely, according to this model, UT-UR inhibits the NR_I phosphatase while stimulating the NR_I kinase. Figure 6 also illustrates the fact that phosphorylation of NR_I leads to altered interactions with the DNA. In contrast to NR_I, which binds to promoter P_1, resulting in inhibition of transcription, P-NR_I binds to promoter P_2, thereby stimulating transcription of the *glnA* operon. Under certain conditions, expression of *ntrB* and *ntrC* are controlled similarly. Expression of these two genes, however, appears to also be controlled by binding of NR_I to the promoter P_L with inhibition of transcription.[85] Expression of amino acid permeases and enzymes involved in nitrogen metabolism is also apparently regulated by the *ntr* gene products.

The Ntr regulatory system represents the first example in which a transcriptional repressor is converted into a transcriptional activator by protein phosphorylation. The participation of protein phosphorylation in the regulation of transcription in eukaryotic cells has been discussed.[86-88] There is substantial genetic evidence that transcription of certain proteins of the bacterial phosphotransferase system is also controlled by protein phosphorylation.[89] It is interesting to note that NR_I exhibits sequence homology to a series of other transcriptional activators, such as the proteins of the genes *phoB* and *ompR* of *E. coli*.[116] By analogy with NR_I, it may be assumed that the proteins PhoB and OmpR are each subject to a reversible protein modification in which the proteins PhoR and EnvZ, respectively, serve as the modifying enzymes. PhoR and EnvZ show homology to NR_{II}, the NR_I kinase/phosphatase.

The protein pair PhoB/PhoR is important for the expression of certain enzymes during growth of the cells under phosphate-limiting conditions. The protein pair OmpR/EnvZ responds to changes in the extracellular osmolarity.[116] Homology of these proteins to the chemotaxis proteins of *E. coli*, Tar, Tsr, and Trg, which likewise respond to extracellular signals, has also been noted.[117] The latter three proteins are integral membrane proteins that function as chemoreceptors for aspartate (Tar), serine (Tsr), and ribose and galactose (Trg). They signal changes in the extracellular concentrations of their respective ligands to the interior of the cell. Reversible protein modification (methylation of glutamyl residues) by the *cheB* and *cheR* gene product plays a major role in this process. It is possible that signal transfer in all of these systems is based on a common principle in spite of the nature of the differing, reversible protein modifications.

6. Less Well Characterized Bacterial Phosphoproteins

The report by *Wang* and *Koshland* on protein phosphorylation in *S. typhimurium*[17] initiated an intensive search for protein phosphorylation in a variety of bacteria. In addition to the work cited in the previous sections, publications have appeared on protein phosphorylation in *Halobacterium halobium*,[90] *Myxococcus xanthus*,[91] *Rhodospirillum rubrum*,[118] *Sulfolobus acidocaldarius*,[92] *Clostridium sphenoides*,[93] *Synechococcus 6301*,[91] *Rhodocyclus gelatinosus*,[95] *Rhodomicrobium vannielii*,[96] *Bacillus subtilis*,[97] and *Mycoplasma gallisepticum*.[98] An apparently distinct protein derivatization reaction, involving ADP ribosylation[103] has been described for *Rhodospirillum rubrum*,[99,100] *Rhodobacter capsulatus*,[101] and *Chromatium vinosum*.[102] Some of the above-mentioned examples are discussed briefly below.

Halobacteria possess light-driven $H^{\oplus}$ and $Cl^{\ominus}$ pumps which lead to the formation of ion gradients that can be used for transport and other energy-dependent processes. When cells of *Halobacterium halobium* that have been labeled in the dark with [^{32}P]phosphate are exposed to light, the dephosphorylation of three phosphoproteins occurs. These proteins are rapidly rephosphorylated during a subsequent dark period.[90,104] Dephosphorylation was found to be dependent on retinal, the chromophore of bacteriorhodopsin and halorhodopsin. It was therefore assumed that these three phosphoproteins are involved in phototransduction.

Light-dependent phosphorylation of two proteins has also been observed in the cyanobacterium *Synechococcus 6301*.[94] One of these proteins is localized in the thylakoid membrane, which also contains photosystems I and II. The functions of these proteins have not been identified.

Myxococcus xanthus and *B. subtilis* are bacteria that are capable of forming spores. In both organisms, the formation of spores from vegetative cells is accompanied by a change in the protein phosphorylation pattern.[91,97] In *Myxococcus xanthus*, the phosphorylation states of two principal membrane proteins are changed after initiation of sporulation by the presence of glycerol.[91] These proteins are possibly of importance for the maintenance of cell shape. A role for a 55000-dalton phosphoprotein in the maintenance of cell shape in *Mycoplasma gallisepticum* has also been suggested.[98]

In *Rhodospirillum rubrum*,[99,100] *Rhodobacter capsulatus*,[101] and *Chromatium vinosum*,[102] nitrogenase, which reduces molecular nitrogen to ammonia, is regulated by a covalent modification reaction that was initially thought to involve phosphorylation. The enzyme consists of two dissimilar subunits, a molybdenum-containing subunit and an iron-containing protein. Interconvertible active and inactive forms of the iron-containing protein have been demonstrated.[99,101] The active form is present when the cells are exposed to conditions of ammonia insufficiency. In the active form, the iron-containing protein of *R. rubrum* is a dimeric protein with a subunit molecular mass of 30000 daltons. The inactive form, however, has two apparently dissimilar subunits with molecular masses of 30000 daltons and 31500 daltons, as determined on SDS-polyacrylamide gels.[99] Labeling experiments with [^{32}P]phosphate indicated that the heavier subunit (31500 daltons) of the inactive complex contained covalently bound phosphate. The derivatizing moiety could be cleaved from this subunit, which was then reconverted into the active form. A similar change in size, as determined by SDS-polyacrylam-

ide gel electrophoresis, was observed upon derivatization of the iron-containing protein of the nitrogenase complex from *Rhodobacter capsulatus* (from 33500 to 38000 daltons). Experiments with the *R. rubrum* enzyme established that the modifying group was adenosine diphosphoribose, and that the guanidinium moiety of an arginine residue was modified.[103] These experiments suggest that the activities of nitrogenase in these bacteria are regulated by reversible ADP ribosylation, rather than phosphorylation, that nitrogen insufficiency produces the active, free form of the iron-containing protein, and that nitrogen sufficiency gives rise to the inactive form. By analogy with other ADP ribosylation reactions, the donor molecule is probably NAD® (see Table 1).

In *Clostridium sphenoides*, the enzyme citrate lyase ligase is reversibly phosphorylated.[93] This enzyme catalyzes the conversion of the inactive, sulfhydryl form of citrate lyase to the active, acetylated form. The phosphorylated derivative of citrate lyase ligase is the active form. Dephosphorylation of the phosphoenzyme leads to inactivation. Glutamate stimulates the conversion of the inactive, unphosphorylated citrate lyase ligase to the active, phosphorylated form. Additionally, glutamate plus citrate are required for the acetylation of citrate lyase by the active, phosphorylated form of citrate lyase ligase.[105] A protein modification cascade evidently operates to regulate the degradation of citrate either to glutamate or to acetate and oxaloacetate.

Autophosphorylation of the *dnaK* gene product from *E. coli* has been observed.[106] This protein is assumed to participate in DNA replication of the bacteriophages λ and M13.[107, 108] Autophosphorylation is frequently a characteristic of protein kinases. Indeed, it was found that the *dnaK* gene product participates in the phosphorylation of glutaminyl tRNA synthetase and threonyl tRNA synthetase.[109] It is interesting to note that infection of *E. coli* cells with phage M13 results in altered phosphorylation of the protein encoded by the *dnaK* gene. Not only was the extent of phosphorylation of this protein considerably increased, but the position of phosphorylation shifted from serine to threonine.[110]

Protein-tyrosine phosphorylation has been found both in *E. coli* and *Rhodospirillum rubrum*.[111, 118] In *E. coli*, a protein associated with the ribosome was phosphorylated.[112] A two-dimensional gel analysis of *E. coli* phosphoproteins was attempted. Separation in the first dimension was performed on the basis of isoelectric point and in the second dimension on the basis of size. Under anaerobic conditions, 20 phosphorylated proteins were found,[113] but under aerobic growth conditions, 128 phosphorylated proteins were detected.[112] Exact knowledge of the isoelectric points and the relative molecular masses of these proteins should facilitate their identification. Recognition of the fact that numerous unidentified proteins in bacteria are reversibly phosphorylated leads to the suggestion that protein phosphorylation plays a central role in the regulation of widely differing cellular processes as has been shown previously for eukaryotic cells.

Received: October 12, 1987 [A 685 IE]
German version: *Angew. Chem. 100* (1988) 1072

[1] G. T. Cori, A. A. Green, *J. Biol. Chem. 151* (1943) 31.
[2] E. H. Fischer, E. G. Krebs, *J. Biol. Chem. 216* (1955) 121.
[3] E. W. Sutherland, U. D. Wosilait, *Nature (London) 175* (1955) 169.
[4] A. A. Green, G. T. Cori, C. F. Cori, *J. Biol. Chem. 142* (1942) 447.
[5] E. G. Krebs, D. J. Graves, E. H. Fischer, *J. Biol. Chem. 234* (1959) 2867.
[6] D. L. Friedmann, J. Larner, *Biochemistry 2* (1963) 669.
[7] T. C. Linn, F. H. Pettit, F. Hucho, L. J. Reed, *Proc. Natl. Acad. Sci. USA 64* (1969) 227.
[8] D. A. Walsh, J. P. Perkins, E. G. Krebs, *J. Biol. Chem. 243* (1968) 3763.
[9] E. W. Sutherland, *Science (Washington, D.C.) 177* (1972) 401.
[10] M. S. Collett, R. L. Erikson, *Proc. Natl. Acad. Sci. USA 75* (1978) 2021.
[11] T. Hunter, B. M. Sefton, *Proc. Natl. Acad. Sci. USA 77* (1980) 1311.
[12] W. Kundig, S. Ghosh, S. Roseman, *Proc. Natl. Acad. Sci. USA 52* (1964) 1067.
[13] J. F. Kuo, P. Greengard, *J. Biol. Chem. 224* (1969) 3417.
[14] H.-J. Rahmsdorf, P. Herrlich, S. H. Pai, M. Schweiger, H. G. Wittmann, *MGG Mol. Gen. Genet. 127* (1973) 259.
[15] H.-J. Rahmsdorf, S. H. Pai, H. Ponta, P. Herrlich, R. Roskoski, Jr., M. Schweiger, F. W. Studier, *Proc. Natl. Acad. Sci. USA 71* (1974) 586.
[16] W. Zillig, H. Fujiki, W. Blum, D. Janekovic, M. Schweiger, H.-J. Rahmsdorf, H. Ponta, M. Hirsch-Kauffmann, *Proc. Natl. Acad. Sci. USA 72* (1975) 2506.
[17] J. Y. J. Wang, D. E. Koshland, Jr., *J. Biol. Chem. 253* (1978) 7605.
[18] J. Y. J. Wang, D. E. Koshland, Jr., *J. Biol. Chem. 256* (1981) 4640.
[19] M. Garnak, H. C. Reeves, *Science (Washington, D.C.) 203* (1979) 1111.
[20] H. L. Kornberg, *Biochem. J. 99* (1966) 1.
[21] G. A. Nimmo, A. C. Borthwick, W. H. Holms, H. G. Nimmo, *Eur. J. Biochem. 141* (1984) 401.
[22] D. C. LaPorte, D. E. Koshland, Jr., *Nature (London) 305* (1983) 286.
[23] P. J. Malloy, H. C. Reeves, J. Spiess, *Curr. Microbiol. 11* (1984) 37.
[24] A. C. Borthwick, W. H. Holms, H. G. Nimmo, *FEBS Lett. 174* (1984) 112.
[25] K. W. Volz, D. A. Matthews, R. A. Alden, S. T. Freer, C. Hansch, B. T. Kaufman, J. Kraut, *J. Biol. Chem. 257* (1982) 2528.
[26] D. Garland, H. G. Nimmo, *FEBS Lett. 165* (1984) 259.
[27] D. C. LaPorte, D. E. Koshland, Jr., *Nature (London) 300* (1982) 458.
[28] H. G. Nimmo, *Trends Biochem. Sci. Pers. Ed. 9* (1984) 475.
[29] H. G. Nimmo, A. C. Borthwick, E. M. T. El-Mansi, W. H. Holms, C. MacKintosh, G. A. Nimmo, *Biochem. Soc. Symp.*, in press.
[30] E. M. T. El-Mansi, H. G. Nimmo, W. H. Holms, *J. Gen. Microbiol. 132* (1986) 797.
[31] E. M. T. El-Mansi, H. G. Nimmo, W. H. Holms, *FEBS Lett. 183* (1985) 251.
[32] D. C. LaPorte, D. E. Koshland, Jr., *Nature (London) 305* (1983) 286.
[33] D. C. LaPorte, K. Walsh, D. E. Koshland, Jr., *J. Biol. Chem. 259* (1984) 14068.
[34] E. F. Robertson, J. C. Hoyt, H. C. Reeves, *Curr. Microbiol. 15* (1987) 103.
[35] P. W. Postma, J. W. Lengeler, *Microbiol. Rev. 49* (1985) 232.
[36] C. A. Lee, M. H. Saier, Jr., *J. Biol. Chem. 258* (1983) 10761.
[37] J. Deutscher, M. H. Saier, Jr., *Proc. Natl. Acad. Sci. USA 80* (1983) 6790.
[38] J. Reizer, C. Panos, *Proc. Natl. Acad. Sci. USA 77* (1980) 5497.
[39] J. Thompson, M. H. Saier, Jr., *J. Bacteriol. 146* (1981) 885.
[40] J. Reizer, M. J. Novotny, C. Panos, M. H. Saier, Jr., *J. Bacteriol. 156* (1983) 354.
[41] J. Deutscher, R. Engelmann, *FEMS Microbiol. Lett. 23* (1984) 157.
[42] J. Reizer, M. J. Novotny, W. Hengstenberg, M. H. Saier, Jr., *J. Bacteriol. 160* (1984) 333.
[43] E. B. Waygood, R. L. Mattoo, E. Erickson, *Can. J. Microbiol. 32* (1986) 310.
[44] C. S. Mimura, F. Poy, G. R. Jacobson, *J. Cell. Biochem. 33* (1987) 161.
[45] J. Deutscher, B. Pevec, K. Beyreuther, H.-H. Kiltz, W. Hengstenberg, *Biochemistry 25* (1986) 6543.
[46] W. Hengstenberg, J. Deutscher in J. Reizer, A. Peterkofsky (Eds.): *Sugar Transport and Metabolism in Gram-Positive Bacteria*, Ellis Horwood, Chichester 1987, p. 215.
[47] R. Eisermann, G. Gonzy-Treboul, J. Deutscher, W. Hengstenberg, *J. Biol. Chem.*, in press.
[48] J. Deutscher, U. Kessler, W. Hengstenberg, *J. Bacteriol. 163* (1985) 1203.
[49] J. Deutscher, U. Kessler, C.-A. Alpert, W. Hengstenberg, *Biochemistry 23* (1984) 4455.
[50] P. W. Mason, D. P. Carbone, R. A. Cushman, A. S. Waggoner, *J. Biol. Chem. 256* (1981) 1861.
[51] J. Thompson, D. A. Torchia, *J. Bacteriol. 158* (1984) 791.
[52] E. C. C. Lin, *Annu. Rev. Microbiol. 30* (1976) 535.

[53] R. Z. Jin, E. C. C. Lin, *J. Gen. Microbiol. 130* (1984) 83.
[54] P. W. Postma, W. Epstein, A. R. J. Schuitema, S. O. Nelson, *J. Bacteriol. 158* (1984) 351.
[55] M. J. Novotny, W. L. Fredericksen, E. B. Waygood, M. H. Saier, Jr., *J. Bacteriol. 162* (1985) 810.
[56] J. Deutscher, *FEMS Microbiol. Lett. 29* (1985) 237.
[57] J. Deutscher, H. Sauerwald, *J. Bacteriol. 166* (1986) 829.
[58] N. J. Jacobs, P. J. VanDemark, *Arch. Biochem. Biophys. 88* (1960) 250.
[59] J. Reizer, M. J. Novotny, I. Stuiver, M. H. Saier, Jr., *J. Bacteriol. 159* (1984) 243.
[60] P. Gay, P. Cordier, M. Marquet, A. Delobbe, *MGG Mol. Gen. Genet. 121* (1973) 355.
[61] S. O. Nelson, A. R. J. Schuitema, P. W. Postma, *Eur. J. Biochem. 154* (1986) 337.
[62] J. Reizer, A. Peterkofsky in J. Reizer, A. Peterkofsky (Eds.): *Sugar Transport and Metabolism in Gram-Positive Bacteria,* Ellis Horwood, Chichester 1987, p. 333.
[63] Y. S. Halpern in S. Sanchez-Esquivel (Ed.): *Nitrogen Source Control of Microbial Processes,* CRC Press, Boca Raton 1988, in press.
[64] E. R. Stadtman, P. B. Chock, *Curr. Top. Cell. Regul. 13* (1978) 53.
[65] R. J. Almassy, C. A. Janson, R. Hamlin, N.-H. Xuong, D. Eisenberg, *Nature (London) 322* (1986) 304.
[66] S. Kustu, J. Hirschman, J. C. Meeks, *Curr. Top. Cell. Regul. 27* (1985) 201.
[67] M. S. Brown, A. Segal, E. R. Stadtman, *Proc. Natl. Acad. Sci. USA 68* (1971) 2949.
[68] S. P. Adler, D. Purich, E. R. Stadtman, *J. Biol. Chem. 250* (1975) 6264.
[69] M. H. Saier, Jr.: *Enzymes in Metabolic Pathways,* Harper and Row, New York 1987, p. 226.
[70] B. Tyler, A. B. Deleo, B. Magasanik, *Proc. Natl. Acad. Sci. USA 71* (1974) 225.
[71] R. A. Bender, B. Magasanik, *J. Bacteriol. 132* (1977) 106.
[72] B. Tyler, *Annu. Rev. Biochem. 47* (1978) 1127.
[73] S. Kustu, D. Burton, E. Garcia, L. McCarter, N. McFarland, *Proc. Natl. Acad. Sci. USA 76* (1979) 4576.
[74] N. McFarland, L. McCarter, S. Artez, S. Kustu, *Proc. Natl. Acad. Sci. USA 78* (1981) 2135.
[75] T. P. Hunt, B. Magasanik, *Proc. Natl. Acad. Sci. USA 82* (1985) 8453.
[76] L. J. Reitzer, B. Magasanik, *Proc. Natl. Acad. Sci. USA 80* (1983) 5554.
[77] L. J. Reitzer, B. Magasanik, *Proc. Natl. Acad. Sci. USA 82* (1985) 1979.
[78] J. Hirschman, P.-K. Wong, K. Sei, J. Keener, S. Kustu, *Proc. Natl. Acad. Sci. USA 82* (1985) 7525.
[79] A. J. Ninfa, S. Ueno-Nishio, T. P. Hunt, B. Robustell, B. Magasanik, *J. Bacteriol. 168* (1986) 1002.
[80] A. J. Ninfa, B. Magasanik, *Proc. Natl. Acad. Sci. USA 83* (1986) 5909.
[81] F. Foor, Z. Reuveny, B. Magasanik, *Proc. Natl. Acad. Sci. USA 77* (1980) 2636.
[82] F. R. Bloom, M. S. Levin, F. Foor, B. Tyler, *J. Bacteriol. 134* (1978) 569.
[83] R. Bueno, B. Magasanik, *Curr. Top. Cell. Regul. 27* (1985) 201.
[84] T. MacNeil, G. P. Roberts, D. MacNeil, B. Tyler, *MGG Mol. Gen. Genet. 188* (1982) 325.
[85] G. Pahel, D. M. Rothstein, N. Magasanik, *J. Bacteriol. 150* (1982) 202.
[86] C. S. Rubin, O. M. Rosen, *Annu. Rev. Biochem. 44* (1975) 831.
[87] E. G. Krebs, J. B. Beavo, *Annu. Rev. Biochem. 48* (1979) 923.
[88] P. Boerner, M. H. Saier, Jr., *J. Cell. Physiol. 122* (1985) 316.
[89] M. H. Saier, Jr., J. Deutscher, *Biol. Unserer Zeit 18* (1988) 9.
[90] J. L. Spudich, W. Stoeckenius, *J. Biol. Chem. 255* (1980) 5501.
[91] T. Komano, N. Brown, S. Inouye, M. Inouye, *J. Bacteriol. 151* (1982) 114.
[92] R. Skórko, *Eur. J. Biochem. 145* (1984) 617.
[93] G. Antranikian, C. Herzberg, G. Gottschalk, *Eur. J. Biochem. 153* (1985) 413.
[94] J. F. Allen, C. E. Sanders, N. G. Holmes, *FEBS Lett. 193* (1985) 271.
[95] B. Averhoff, G. Antranikian, G. Gottschalk, *FEMS Microbiol. Lett. 33* (1986) 299.
[96] A. M. Turner, N. H. Mann, *J. Gen. Microbiol. 132* (1986) 3433.
[97] E. Köhler, G. Antranikian, *Arch. Microbiol.*, in press.
[98] M. W. Platt, S. Rottem, Y. Milner, M. F. Basile, J. Reizer, *J. Biol. Chem.*, in press.
[99] P. W. Ludden, G. G. Preston, T. E. Dowling, *Biochem. J. 203* (1982) 663.
[100] J. W. Gotto, D. C. Yoch, *J. Biol. Chem. 257* (1982) 2868.
[101] Y. Jouanneau, C. M. Meyer, P. M. Vignais, *Biochim. Biophys. Acta 749* (1983) 318.
[102] J. W. Gotto, D. C. Yoch, *Arch. Microbiol. 141* (1985) 40.
[103] M. R. Pope, S. A. Murrell, P. W. Ludden, *Proc. Natl. Acad. Sci. USA 82* (1985) 3173.
[104] E. N. Spudich, J. L. Spudich, *Methods Enzymol. 88* (1982) 213.
[105] G. Atranikian, F. Giffhorn, *FEMS Microbiol. Rev. 46* (1987) 175.
[106] M. Zylicz, J. H. LeBowitz, R. McMacken, C. Georgopoulos, *Proc. Natl. Acad. Sci. USA 80* (1983) 6431.
[107] H. Saito, H. Uchida, *J. Mol. Biol. 113* (1977) 1.
[108] D. I. Friedman, E. R. Olson, C. Georgopoulos, K. Tilly, I. Herskowitz, F. Banuett, *Microbiol. Rev. 48* (1984) 299.
[109] M. Wada, K. Sekine, H. Itikawa, *J. Bacteriol. 168* (1986) 213.
[110] C. Rieul, J.-C. Cortay, F. Bleicher, A. J. Cozzone, *Eur. J. Biochem. 168* (1987) 621.
[111] M. Manai, A. J. Cozzone, *FEMS Microbiol. Lett. 17* (1983) 87.
[112] J.-C. Cortay, C. Rieul, B. Duclos, A. J. Cozzone, *Eur. J. Biochem. 159* (1986) 227.
[113] A. Quentmeier, G. Antranikian, *FEMS Microbiol. Lett. 34* (1986) 231.
[114] P. E. Thorsness, D. E. Koshland, Jr., *J. Biol. Chem. 262* (1987) 10422.
[115] E. F. Robertson, J. C. Hoyt, H. C. Reeves, *J. Biol. Chem. 263* (1988).
[116] G. N. Gussin, C. W. Ronson, F. M. Ausubel, *Annu. Rev. Genet. 20* (1986) 567.
[117] A. Krikos, N. Mutoh, A. Boyd, M. I. Simon, *Cell 33* (1983) 615.
[118] R. H. Vallejos, L. Holuigue, H. A. Lucero, M. Torruella, *Biochem. Biophys. Res. Commun. 126* (1985) 685.

Say It in English, Please!*

By Robert Schoenfeld †

Robert Schoenfeld, managing editor of the *Australian Journal of Chemistry* until his retirement in 1985, was known to countless scientists as the author of *The Chemist's English*. He was widely admired for his outgoing manner, his enlivening humor, and his keen insight into the interplay of language and science, and he will be deeply missed. Shortly before his untimely death on November 24, 1987, he began writing a series of essays directed initially at German-speaking writers of English. As in *The Chemist's English*, he hoped through "Say It in English, Please!" to foster an awareness of good English, this time by pointing out the pitfalls and finer problems awaiting the non-native speaker. His intention was not to dictate usage but rather to entertain and to provoke discussion. By sharing his own joy in language, he wanted to make writing English more enjoyable for others. The nine completed essays are printed here as a fitting tribute to *Bob*, who might have begun the series as follows: "I submit these columns to the kind judgment of my readers."

David Loewus
Angewandte Chemie

1. A Singular Beginning

What's that? What you said just now sounded pretty strange. Of course I understood what you meant: you wanted some help with your written English. I'll be glad to do my best. But one of the words you just used was not quite right. You said: I want *advices*. You should have stuck to the singular: I want *advice*.

It is one of the mysterious features of idiomatic English that *advice*, in the sense of "helpful recommendation", is practically never found in the plural. The word apparently suggests "an ensemble of recommendations", something not countable, therefore not multipliable. In a German–English dictionary *advice* is likely to be given as synonym for both *Rat* and *Ratschlag*. But in spirit it is closer to *Rat*, which in idiomatic German also is seldom found in the plural form. No native German speaker (or am I mistaken?) is likely to say "Geben Sie mir einige Räte". He or she will say "einige Ratschläge". You had this last phrase in mind and let your dictionary betray you into misusing *advice* as its plural. Don't ever ask for "some advices" in an English-speaking country, or you'll be greeted by a condescending smile and a reply in very basic English.

But I have been talking about advice without explaining who I am and what right I have to offer you any. I am the author of a book on the English language that most critics found pretty entertaining. This book dealt mostly with the needs of native English writers, but it provoked surprising interest among those "non-natives" who often publish papers or reports in English. My publisher, VCH, thought that I should try to write some short articles specially for this second group.

Please don't expect miracles, and above all don't believe that you can learn a second language as you learn geometry, by filling your mind with rule after rule. First of all, English is so capricious that, no sooner do you think you have found a general rule, you can think of an exception to it.[**] And then, if you really want to master a language, you must reach a point where you can forget all the rules. In other words, I don't set out to teach, but to entertain. I hope to give you a feeling for the English language, and to communicate some of my love for it.

Just how hard it is to teach the finer points of a language, and to devise rules for them, can be seen from the example I have given. English usage treats *advice*, in most of its meanings, as a "noncount noun". It cannot be divided into units, hence cannot be multiplied, and therefore does not take the plural **advices* (the asterisk is the grammarian's way of telling the reader that what follows is wrong). The same is true of *information*, which the English mind treats as an indivisible continuum (just like the German *Wissen*), and *progress*. A German speaker, thinking of *Informationen*, is apt to write **informations* but an English editor, with a shudder, will cross the plural out.

Now you may well ask: What is the rule concerning noncount nouns?; How do I spot them?; How does English usage differ from German? Sorry, there I cannot help you at all. Noncount nouns are not specially marked in the dictionary. Many nouns (as in German) have a sense in which they are noncount, and another in which they take the plural:

The philosopher seeks after *truth*.
I told him some unpleasant *truths*.

This last pair of sentences is perfectly translatable into German, and so are many others. But in words like *advice* customs differ, and there are no rules to help the nonnative. He has to develop his own feeling for English, until

[*] Reprints of this article are available upon request. Please address all inquiries to Redaktion Angewandte Chemie, Postfach 1260/1280, D-6940 Weinheim (FRG).

[**] Modern linguists, who do not like to lose an argument, do not talk of "exceptions" but of "optional transformation rules".

 © VCH Verlagsgesellschaft mbH, D-6940 Weinheim, 1988 0570-0833/88/0808-1050 $ 02.50/0 Angew. Chem. Int. Ed. Engl. 27 (1988) 1050–1057

he stops using his native language as a crutch. In fact, if you want to learn the finest details of a strange language, you have to proceed exactly as you did when you learned your native language as a child: pay attention to the data base of words and sentences around you, try analogous sentences, be prepared to make the occasional mistake, and figure out where you went wrong.

Let me, to help you get into the right mood, say something in praise of this great love of mine, English. Books on linguistics proclaim that all languages are equally efficient, and that only the known cultural and economic factors have made English into the international language of science. I beg to disagree. English is predestined for its dominant role by its peculiar virtues. It is the perfect language "in between". It is, for instance, easier to learn for a German speaker than is Chinese, and easier for a Chinese speaker than is German.

Let me explain. Linguists would classify German as very strongly "inflected"; that means, the word stems are modified so as to show how the words of the sentence are connected. When you write

Die bekannte Zeitschrift veröffentlichte einen interessanten Artikel

the ending of the verb indicates the third person singular, and the changes to the articles and adjectives show which noun they belong to, which is the subject and which the object.

Chinese is an "isolating" language. The words remain unmodified and sit loosely side by side. Anyone studying such a language does not have to conjugate verbs or decline nouns; all he or she has to do is to pay attention to the order of the words.

English is inflecting (inflect, inflects, inflected) but only weakly so—think of how the adjective sits unmodified beside the noun. Its basic rules of grammar will not seem unduly difficult to a Chinese speaker, and they will seem ridiculously simple to a German speaker. It is easy to get a start in English—the difficulties come afterwards.

2. Caesar's Revenge

I made the point that English was a "weakly inflecting" language and its grammar was about halfway between German and Chinese. Let me follow that thought a little further.

Latin is one of the most heavily inflected languages—I still remember with horror the many endings to nouns and verbs: *amo, amas, amat*, etc. But these endings had a practical use: they served as grammatical labels. This word, so the labels said, will be the verb of the sentence, this the subject, this the direct object, this the indirect object, and so on.

With words so carefully labeled, there is really no need to insist that they be kept in a rigid order. At some stage, every Latin student is asked to translate *Brutus killed Caesar* and he dutifully comes up with *Brutus Caesarem interfecit*. But the endings *-us* and *-em* so clearly indicate killer and victim that the meaning remains the same no matter how the words of the sentence are permuted. In fact, Latin poets shuffle their words about so radically to make them fit their hexameters that the poor student is left dizzy.

Now let us try less inflected languages. If you change the nouns about in *Brutus tötete Caesar* you have changed the meaning: the boot is now on the other foot, or rather the dagger is in the other man's hand. And now remember that English is an even more weakly inflecting language than German—that means, the order of words is even more rigid.

In fact, English is what linguists call an SVO language. In every normal sentence the expectation is that the subject S will precede the verb V and this will then be followed (if the sense permits) by the object O. Every 18-month-old child who lisps *Bobby want banana* or *Daddy drive car* has mastered the SVO principle.

German, being more inflected, is less rigid. It is true that the standard sentence is SVO but there are numerous inversions between S and V. Consider

Sobald ich rufe, *kommt er* gelaufen.
As soon as I call *he comes* running.

In fact, English puts up a furious resistance to this inversion. If it does occur, it inevitably involves an auxiliary verb. Here we go again:

Sprechen Sie Englisch?
Do you speak English?

In the last sentence, the "dummy" auxiliary verb *to do* has been created specially so that you/speak/English will appear in their customary SVO order.

So what is the non-native to do about English word order? If he is not confident, he should stick to SVO and avoid inversions like the plague. But, at the same time, he should develop an eye for exceptions. There *are* some exceptions. For example, they often occur if in a normal sentence the predicate or some part of it is moved to the front for emphasis:

Inversion occurs only in exceptional circumstances.	(normal)
Only in exceptional circumstances *does inversion* occur.	(emphasis)
Of particular importance *were the two peaks* in the high-frequency region.	(emphasis)

Note that the second sentence resorts to the dummy auxiliary *does* and the third has the normal auxiliary *were*. Only in such conditions *will the inversion* be acceptable.

There are some other exceptions, one of which was made famous by the early years of *Time* magazine: "Said President Coolidge ..."; "Spoke J. Edgar Hoover ..."

But these exceptions belong to literary style and not to the plain prose of the simple scientist. Let us draw the conclusion that English is a pretty rigid SVO language, almost as rigid as Chinese. Wenn Sie da etwas ändern wollen, *brauchen Sie (you need)* ein feines Ohr.

3. Where Is the Verb?

German and English, you might think, are closely related languages; their kinship expresses itself in such similarities as *house* and *Haus*. But the differences between the

languages are deep-seated and important. To startle you, I shall now argue that English grammar is nearer to Chinese than to German grammar!

That is so because both Chinese and English are dominated by the SVO word order (English admits some rare exceptions). German is not dominated so absolutely by the SVO pattern. Most of the *Hauptsätze*, it is true, appear in this form, but we have already noted how readily the inversion to VSO occurs. About an even more radical reshuffling of the order, more in a moment.

How did German and English, whose grammars were practically identical through most of the Middle Ages, drift so far apart? Professional philologists will give you a multitude of reasons, but I shall wildly oversimplify and point out the two main ones.

First, when modern high German *(Neuhochdeutsch)* replaced middle high German *(Mittelhochdeutsch)*, there occurred a change in word order. The main clause remained SVO (like Chinese) but the *Nebensatz* took the form SOV (like Japanese!).

Second, an even more fateful development took place in England. Towards the late Middle Ages, its language shed many of its inflected forms, and above all the ending of the infinitive: *werk-en/work-en* and *drink-en* became *work* and *drink*. That meant that noun and verb became formally indistinguishable, and one could be readily formed from the other. Note how easy it is to tell the verb from the noun in German, and how hard in English:

I *drink* (verb). I enjoy my *drink* (noun).
Ich *trinke* (verb). Ich genieße meinen *Trunk* (noun).

In German, you never have any doubt which is which. But as you "enter" an English sentence, you are forced to ask yourself instantly, Where is the verb?

These differences between English and German are so fundamental that I beg my readers to retain this mental image of the two languages:

German has a relatively elastic word order: the verb stands out sharply; the subordinate clauses are neatly distinguished from the main clause. This allows the construction of long sentences, and if the verb appears late at their end, this may be helpful to create emphasis.

English is firmly based on the SVO principle. The effective sentence is the one in which the reader understands immediately what the subject is and where the verb is.

I shall give an example, not infrequently found in the literature, in which a perfectly sound German sentence has been translated all-too-faithfully into English:

With light petroleum 8–10% of a green waxy material and with chloroform 25–27% of a tarry fraction of high molecular weight were obtained.

It is not that the English version is grammatically incorrect, it is just that it is clumsy. First of all, where is the subject S? A careful search reveals the unexpected: the first of two subjects is *8–10%*. And which and where is the verb? It is *were*, and it occurs right near the end of the sentence, miles away from the subject, when the reader has just about given up hope.

Of course, it is easy enough to remedy our limping text. Here are two suggestions:

Chromatography gave, with light petroleum, 8–10% ...
Elution with light petroleum gave 8–10% ...

Here our S is very prominent, V and O follow promptly, and our two versions have the additional advantage that V is in the more colorful active form.

Perhaps a comparison will make the meaning of this essay clear. German and English are two different card games. In German you are free to finesse about, play your weaker cards first and finally, with great effect, throw your trumps on the table. In English the best strategy is to lead with your strong cards.

I said "the *best* strategy". English is flexible enough to permit unorthodox strategies, and often the most brilliant stylists are the ones who defy the rules. If your English is advanced enough to let you read *William Faulkner* or *James Joyce*, you will find that these two obsessed sentence-spinners have turned the English language on its head. But you are not *Faulkner* or *Joyce*, your editors are not *Maxwell Perkins*[*] or *Sylvia Beach*,[**] and these articles are not a guaranteed cookbook for the English sentence. All I can do is to increase your appetite, and to a humble extent improve your taste. Don't give yourself any complexes about being a non-native. Cooking sentences is a delicate art, and "natives" have their troubles, too.

4. That Strange Particle, the Article

What a nice, helpful, user-friendly language English seems at first! Think only of the article. Just *the* one for all genders, and the choice of genders is usually dictated by logic, not custom! One should think no foreigner could have trouble with the English article—unless of course such a foreigner comes from a language like Russian or Japanese, where such particles of speech are unknown. But even with the simplest parts of a sentence there are tricky differences between languages, so let us have *a* look at *the* English article.

German or French speakers will have little trouble with the indefinite article. In their languages, this word (*ein/eine* or *un/une*) means "one". In English, the indefinite article started the same way. "One" became corrupted to *an* and the final *n* of that word then disappeared before consonants.

That gives us an approximate rule for the function of the indefinite article. It pulls a single item or individual, about which or whom nothing definite is known, out of a group. When we say "I saw *a* house", what we mean is that "I saw *one unspecified member of the class* house".

Such a complex explanation for such a simple word! Things now get worse, because we must remember that by saying *a* we have indicated (1) that nothing specific is known about the noun that follows and (2) that the noun belongs to a class that can be divided into units (in other words, it is countable).

[*] *Maxwell Perkins* (1884–1947), editor of many major American writers, including *F. Scott Fitzgerald* and *Ernest Hemingway*.

[**] *Sylvia Beach* (1887–1962), first publisher of *James Joyce*'s *Ulysses*.

Since the indefinite article means one, no such article can occur with plural nouns:

I saw *a* house.
I saw houses.
Among the pyrolysis products were *a* ketone and several olefins.

Notice that here German runs exactly parallel to English.

When do we exchange an indefinite article for the definite article, then? As soon as the noun is either specified beforehand (I saw *a* house; *The* house was large) or will be specified right away (*The* largest house in the street was painted in white). It goes without saying (but does anything ever go without saying in linguistics?) that the definite article can be used with plural nouns (He investigated *the* pyrolysis products).

Back to the indefinite article. Suppose our sentence contains a singular, unspecified noun [condition (1)] but this noun fails condition (2) by not being countable? In that case no article is used at all (modern grammarians say "the zero article is used"). Let us have some examples:

I saw *destruction* everywhere.
We used *chromatography* to separate the mixture.

In the second example, *chromatography* clearly has non-countable status. But this status can be subtly changed:

We separated the components by *a* chromatographic technique.

Thus, chromatography is perceived as an unstructured concept, whereas techniques are countable.

All the above are just rough rules, designed to give the non-native writer a start. In the great English grammars, the rules about articles go on for dozens of pages, and there is no unifying logic that holds them together. For instance, why do we say *a* in "Such *a* technique is helpful"? Surely the use of *such* specifies the noun *technique*? All I can say is that between *such* and a singular noun there occurs either *a(n)* or the zero article (I approve of *such* determination) but never *the*.

German speakers will be relieved to learn how little English differs from their native language. The main problems come with the use of the zero article. The German speaker is a bit hesitant about this, and prefers "*Die* Chemie ist eine noble Wissenschaft" and "*Das* Klettern macht mir Vergnügen". The English speaker just "zeroes" the two articles out (Chemistry is a noble science; I enjoy climbing).

The French language is at one with German and English about the indefinite article, but has a real horror of the zero article. A French speaker says "J'aime *les* chats", but an English speaker says "I love cats". And, alas, *le langage se moque de la logique* translates as *language laughs at logic*.

5. Lest We Forget

Recently, for the first time in my life, I had occasion to help translate a book from the German, and that caused me to wonder about what must have caused multitudes of translators to wonder before me: how hard it is to replace *a single word* in one language with a completely equivalent word in another. If the word is highly scientific or technical, there is generally no trouble: *acetone* is *Aceton* in German, not an electron more or less; and an equally efficient exchange is *Schraubenzieher* for *screwdriver*. But the nearer you get to everyday life, the harder it is to achieve such a perfect match. Words acquire multiple meanings, and each of these meanings resonates with characteristic cultural overtones. For instance, the meaning of English *security* may oscillate between German *Sicherheit* and *Sorgenfreiheit*, and *Sicherheit* may mean *security* in one sentence and *certainty* in another.

Eventually (note that this word means *später* or *schließlich* in German but never *eventuell*) we reach the domain of the so-called untranslatable words—words so characteristic of one language they simply cannot be expressed in another, except perhaps by paraphrasing. It is often said that German *Gemütlichkeit* is such a word, and psychologists generally do not attempt to translate *Schadenfreude* but write it in the original language (along with *Gestalt* and *Angst*). During my recent attempt at translation I had trouble with *Verlauf*; several English words suggested themselves but none was a perfect fit—in the end I had to reword the difficult phrases. And I do believe Italian has the delightful words *magari* and *pure* all to itself. *Cercate pure, cari lettori, magari troverete qualcosa*! ([Go ahead and] look, dear readers, [with some luck] you may find something!)

However, my article is not about these oddities of the vocabulary but about something far more surprising. One expects that nouns, verbs, or adverbs will not match perfectly in translation, but the other day it occurred to me, to my astonishment, that there is no perfect one-to-one correspondence even among conjunctions. These words, after all, are so simple, so impersonal, so devoid of double meanings, that one would assume they must match from language to language, and no vocabulary could exist without a one-word expression for *and, or, but, if,* and the like.

Of simple, one-word conjunctions the English language contains at most three dozen. One should think other languages would have a perfectly matching set of equivalents for these humble and elementary tools of language, but no. *But* no? The commonplace English conjunction *but* translates perfectly into French *mais*, but in German it sometimes means *aber*, sometimes *doch*, sometimes (especially when followed by *instead* or *rather*) *sondern*. In fact, the conjunction *sondern* is rather a specialty of the German language because at times it implies a sharp contrast between two alternatives:

Schweitzer verfolgte seine Konzert-Karriere nicht weiter, *sondern* vergrub sich in Afrika.

In such cases it takes the two words *but instead* to translate one simple conjunction.

I shall now talk about two conjunctions that are highly peculiar to English, and which non-natives are therefore afraid to use. One of these, *lest*, is a rather literary word and more at home in a novel than in a scientific paper. The other, *unless*, is in common and frequent use, and anyone who wants to be confident in the English language should get to the point where he or she employs the word spontaneously.

Unless is the synonym of the two words *if ... not*, and can take the place of *wenn ... nicht*. I shall give a few examples, to make readers familiar with its use:

> You cannot be certain of priority *unless* you check the literature.
> *Unless* conditions are rigorously followed the yields will be low.

And a very vivid poetic example, from *Yeats*:

> An aged man is but a paltry thing,
> a tattered coat upon a stick, *unless*
> soul clap its hands and sing, and louder sing
> for every tatter in its mortal dress.

Such splendid language should make you feel at home with this conjunction, *unless* of course you have no ear for verse. In that case you need not bother with the second conjunction, *lest*, which is a word so literary that it is always used with the subjunctive. In German it can be translated with *damit ... nicht*, but with *lest* there is always an implication that the motive of the action is fear. *Lest* I *be* accused of negligence I shall give you two examples, both from poetry. In the first, *Kipling*, at the height of British imperialism, has a sudden premonition of the crumbling of the Empire:

> Lord God of Hosts, be with us yet,
> *lest* we forget ... *Lest* we forget.

In the second, *Oscar Wilde* imagines a fellow prisoner in Reading Gaol, about to be hanged, under the supervision of warders:

> ... who watched him *lest* himself should rob their scaffold of its prey.

There, *unless* you have hearts of stone, you will not want to forget these two characteristic conjunctions, *lest* they give you bad dreams. There is a lesson in this. If you wish to become confident in scientific English, you will of course read the appropriate scientific books, and learn the required nouns and verbs from these. But *unless* you spare some time for poetry, your sentences will sound creaky, because you will not know how to link them together properly. So study your poets, *lest* you forget your conjunctions.

6. The Great Ugliness Contest

There are some German words, especially simple and honest ones like *gelassen* and *schlicht*, that I love and admire. Indeed, they make me feel envious, like the child who sees an attractive toy in a neighbor's household and complains, "Why can't *we* have that, Daddy?"

On the other hand, there are some German words that get enormously on my nerves, and among these *beziehungsweise* is in the front rank. Such a bumbling, pompous, bureaucratic-sounding word! And how can a modern language tolerate a conjunction five syllables long?

Many writers, in fact, seem to be aware that the word is too long for its grammatical function, and abbreviate it to *bzw.* (I must confess that, when I first saw these letters in a German manuscript, I guessed at Bayerische Zündkerzen-Werke!)

Be that as it may, German speakers, who, after all, are perfectly free to disregard my personal prejudices, have become fond of the word and it may appear not only in official documents, newspaper reports, and scientific texts, but also in serious novels. I found it in one recently, by a respectable Swiss writer. It described a celebration on board a ship whose passengers were of various nationalities, and read:

> Die Deutschen tranken Champagner, *beziehungsweise* Sekt.

Now of course I have no business teaching Swiss novelists their trade. But what does the 15-letter monster right after the comma contribute to the meaning of the sentence? Would not a simple *oder* have been sufficient?

All right, dear readers, I know that the correct use of *beziehungsweise* is a point of contention and apologize for inflicting my personal prejudices on you. You don't have to take the slightest notice of outsiders, and in your own writings you can spark off as many Bayerische Zündkerzen as you like. What concerns me, though, is what happens if you export your BZW into the English language.

It is at this moment that trouble strikes. The German speaker looks at his text and finds that the word *beziehungsweise*, abbreviated to *bzw.*, occurs frequently. He next looks at the English journals on his desk and finds that in these the word *respectively*, abbreviated to *resp.*, is of common occurrence. He then makes the fatal mistake of believing that the two words are equivalent in meaning.

Now it is true that there are occasions when the meanings of *bzw.* and *resp.* overlap, but this does not happen all that often. Let us examine what each word means. German usage may be typified by the following sentence:

> Die beiliegende Tabelle gibt eine Übersicht über die elektropositiven *bzw.* elektronegativen Eigenschaften der Reagentien.

What does the word *beziehungsweise* mean here? Surely only "or, according to circumstances". The word *or* offers a choice. *Beziehungsweise* adds to this the information that the choice obeys certain laws. Let us push semantic analysis one step deeper: in German usage *beziehungsweise* applies to a situation where a certain number of entities will vary in properties or behavior, but this variation is nonrandom. It is not necessary (but it is permissible), in German, to list these entities one by one.

In this lies the key difference to *respectively*. This word means exclusively "in the order named". In other words, it is obligatory to name the members of the set of entities one by one (E_1, E_2, etc.) and then match them, in the same order, to the properties P_1, P_2, etc. An example is provided by the following sentence:

> The percentages of iron, manganese, nickel, and zinc were, *respectively*, 30, 26, 24, and 20.

Here it would indeed be legitimate to translate *respectively* with *beziehungsweise* (if this was placed before the last number). The question is: Is *respectively* in this example really needed?

The two ugly sisters, *beziehungsweise* and *respectively*, so often confused by translators, have this in common: They sound clumsy, and nearly always they are useless. Let German writers ask themselves if, most of the time, they cannot replace *bzw.* by a simple *und* or *oder*. And let English writers ask themselves whether they really need *respectively*—after all, the orderly correspondence of E_1, E_2, etc. to P_1, P_2, etc. emerges generally quite obviously from the text.

I hasten to add that *beziehungsweise* cannot be translated by **relationwise*—thank goodness, nobody has added this ghastly word to the English language yet. Since we are engaged in an interlanguage ugliness contest, and I have mentioned *relation*, let me parade another unlovely word that turns up frequently in everyday and scientific writing, namely *relationship*. Not only is the word unaesthetic but most writers (and especially English-language journalists) misuse it most of the time. A *Beziehung* between two people or things is, in correct English, a *relation*. *Relationship* is, all too frequently, used interchangeably with *relation*, but it should not be; it really means "the nature of a relation". But why should I ask my readers to be careful with words that are daily misused in the Anglo-Saxon press? I shall already be happy if they do not create improper *Beziehungen* between *resp.* and *bzw.*!

7. A Meticulous Investigation into a "Non-Problem"

So you want to submit a paper in English. To a journal of the American Chemical Society? Of the Royal Society of Chemistry? Or an international multilingual journal?

You are probably worried about what "subspecies" of English to write, and how to spell it. No doubt you have been told that there are great differences between British and American usage. I note that in the literary pages of the best West German dailies it is always meticulously stated that the novel reviewed has been translated "aus dem Englischen" or "aus dem Amerikanischen".

There, I think, meticulous Germans are going too far. There is no such thing as a separate "amerikanische" language. Indeed, when it comes to Spoken Everyday English, there will be problems of communications for a resident of Newcastle-on-Tyne who has suddenly decided to settle in Peoria, Illinois. There are also certain differences (but definitely not leading to a communications gap) in The Journalist's English because of the highly personal style of certain popular American columnists.

In The Novelist's English, in our times, the differences have been reduced to the vanishing point (except, naturally, for the spoken word the novelist records). A German publishing house, satisfied with the rendering "aus dem Englischen" of a novel by *Anita Brookner*, may well ask the translator to try his or her hand next on a book by *Joyce Carol Oates*, "aus dem Amerikanischen". There are, of course, the oft-quoted differences in vocabulary, such as (American usage first) *faucet/tap, gas/petrol, trunk/boot,* and *store/shop*. As for differences in grammar, it is very hard to think of any, and in most cases usages overlap. American English has two past participles for the word *to get*: *got* to express a condition or state (you've got a problem there, pal) and *gotten* to express completed action (I've just gotten a new car). Americans also have a preference for the present subjunctive (I suggested that he *take* immediate action) where the British favor the auxiliary verb (... that he *should take* ...). I confess that my sympathies in the matter are with the Americans, for I should hate to see such an interesting verb form as the subjunctive driven out of the language altogether.

If differences in The Novelist's English are small, in The Chemist's English (that is, the English you write your papers in) they are practically nonexistent. These days, if you do not glance at the authors' names and addresses, you have little chance of knowing whether the work originated in the United States, Canada, Great Britain, or Australia (as every editor knows, if the English is particularly faultless, the authors are likely to be Dutch or Scandinavian!).

It was not always so, and when I wrote my first essays on language in 1972 I thought I could detect a slight preference by American authors for the first person plural over the passive voice. But these days we all publish so much, and travel so much, that the "accents" in our writing have disappeared. Moreover, we all dream of writing one day the definitive text on our special subject, and we do not wish to limit the sales of this masterpiece on either side of the Atlantic.

There remains only, really, the question of spelling, and even that is not truly a problem. In the case of ACS or RSC publications, there are efficient copy editors at work, and anyway corrections such as *favor/favour* will almost automatically trip out of the keyboard operator's fingers—as for international journals, they will generally remain neutral. The only thing you really need watch out for is consistency—don't start out the British way and then suddenly opt for the American. Bear in mind the distinctions *meter/metre*, *liter/litre*, and remember that in the United States you might find your lecture theat*re* in the conference cent*er*.

One point you might care to note is the doubling of the last consonant in a verb before *-ing* and *-ed*, if the preceding vowel is spelled with a single letter (so *to seem* is outside the rule). The general rule is: if the last syllable is stressed in pronunciation, double the consonant (*occurring, distilled, pipetting*), otherwise do not (*entering*).

Now the British have a habit of transgressing this rule for the *un*stressed form of final *-l* (*travelled, counselled, cancelled, modelled*); the majority of Americans stay true to the rule. The British also double unstressed *-p* in *worshipping* and many Americans join them in this in *handicapped*.

Note also that the doubling of *-c*, even in unstressed syllables, expresses itself as *-ck* (*panicked*). But, with verbs like *panic* and *worship*, we have already left the realm of the more unemotional Chemist's English. Why *plow/plough* over minuscule differences about how a word is *spelled/spelt*? How about going *picnicking*, everybody?

8. Say It Out Loud

I was recently privileged to help in the translation of a most instructive and entertaining German book. Its author is Professor *Volker Neuhoff* and its German title is *Der Kongress*, which we changed to *Scientists in Conference* because a literal translation might have misled American

readers into thinking of the legislative body in the Capitol. The author and his translator-consultant had a most enjoyably stimulating time and became firm friends. The book, for all its careful coverage of its subject matter, sparkles with human insight and humor and our task was to see that the English paragraphs gave off a similar sparkle. The translation grew almost by itself and wittily annotated drafts flew across the continents. My feeling is that, during a few months of translation, I gained more insight into the German language than I would have acquired during a full-time course in Germanistics at an Australian university. My friend felt similarly enriched.

Anyhow, the book is about scientific conferences; and all the preparatory work that precedes them bears fruit at the moment when a lecturer faces an audience, which is intent on *hearing* his or her words.

This prompts me to take the title of this series literally and to consider the case when you, a native German speaker, deliver a lecture in English to a British, American, or international audience. First of all, are you worried about an accent? Don't be. Audiences at scientific meetings are tolerant. In Australia, most visiting German-speaking scientists, seniors or young postdocs, have gained the admiration of their listeners for their fluency, and the teaching of English in modern *Gymnasien* or *Gesamtschulen* (called *high schools* in the Anglo-Saxon world) deserves the highest praise.

If you are in a higher age group, have not benefited from modern teaching methods, and have ingrained habits of speech, your best allies are the English-speaking research scholars in your department. Read your manuscript to them and ask them to point out recurrent errors, then record the talk again and ask them to be so kind as to check it once more.

If you do not have access to such help, and are worried about how a certain word should be pronounced, consult a good dictionary. Note that certain English words have stresses that are in totally illogical contradiction to etymology: PREFerable, COMParable, PREValent. (My own pet explanation for this phenomenon is that, in the Age of Humanism and in the High English Renaissance under *Elizabeth I*, educated men enriched the vocabulary by borrowing very large numbers of words from Latin and Greek, but were not sure of the pronunciation themselves. What we now stress as PARasite was pronounced as paRAsite by *Shakespeare*.)

The most painful proof of this total lack of logic is the difference between PERjure (swear a false oath) and abJURE (renounce a vice). Consider the difference in how the vowel is pronounced, and you will ask yourself why etymology was ever so trampled on.

If in doubt, stick to etymological logic; pronounce the syllables clearly and you will be understood. Certain stresses vary throughout the Anglo-Saxon world: LABoratory/laBORatory; REsearch/reSEARCH. Let me repeat that the main thing to do is to speak clearly and not to try to solve your problems by mumbling. Your audience will follow you.

Your audience will follow you, anyway, once you are well launched into your talk and showing your slides. There is no greater magic of communication than that between an audience and a lecturer animatedly discussing a slide. It is your opening remarks and historical review you have to worry about. Here take note of cultural gaps, especially at international congresses. Professor *Potapenko* may not be familiar with a quotation from the Bible, and Dr. *Hirakawa* may not know what the "labors of Hercules" were.

I speak as repentant sinner. I once arrived in Vancouver, Canada, at an IUPAC Congress with a prepared speech in which I referred to a certain type of organizational structure as a "hydra-headed monster". I saw a number of Chinese and Japanese faces stare at me in incomprehension, apologized to my colleagues from the Far East, and explained at the blackboard that "hydra" had nothing to do with hydrogen but was a creature from Greek fable, a snake with many heads.

There may be moments of confusion during discussion time after a lecture. Most Japanese laboratory chemists travel frequently and are therefore as good in their spoken as in their written English, but "computer chemists" travel less often (perhaps because there is less need) and there may be difficulties. Or an Indian delegate may address a question to you in excellent but to your ears monotonous English. A little blackboard work may be of help there.

In these and similar circumstances the best way is to turn to the Chair with a smile: "Mr. Chairman, we seem to have a little communications problem there." If your Chairman is good, he will help out ever so tactfully; and he is bound to be good if he has first read the proper chapter in *Volker Neuhoff*'s volume. Not for nothing does this bear the subtitle "The Congress Organizer's Handbook. The Congress Visitor's Companion".

9. No Flamin' Flashbacks!

Students at the University of Melbourne are often required to do a "prac". For this "practical exercise" they have to prepare a compound known from the literature of the thirties and forties and then to characterize it according to modern physical organic methods. And so, during "prac" time, there is often a knock at my door, and a student thrusts a photocopy of a paper at me with the words: "Bob, you know the language. Can you tell me what it means?"

I look and find that the author is someone I used to hero-worship in my youth: *Butenandt, Diels, Ruzicka* ... I say "sure", pick up the copy confidently enough and find myself confronted with a typical specimen of *Geheimratsdeutsch* such as this:

> Die gekühlte und filtrierte Lösung wurde, nach sorgfältigem Auswaschen, in einen Kolben transferiert.

I rattle the words off and I find my student is more perplexed than ever. "So what am I to do first, Bob? Cool? Filter? Wash?"

I laugh. "You know what your problem is, Jim? Your author published his paper before the last chapter of *The Chemist's English* appeared in print."

And indeed, in this last chapter of my book I got ambitious and proposed a "universal stylistic grammar". It took the following form: take the meaning of what you have

written and transcribe it into the script for a silent documentary film. The version in which the images follow in the most logical order, so that the script is shortest, is the best version:

> The solution was cooled. It was then filtered, and the solid material washed.

Now the *Geheimräte* had no way of reading my mind. Their great classical papers are full of "*zuerst* auf eine Aluminiumoxydsäule gegossenen Extrakten" and of such phrases as "*nach* Ausschüttelung" and "*vorher* aufgearbeitet". The *Geheimräte*, in their movie-making, were all too fond of the device known as flashback and used it with the enthusiasm of *Alain Resnais* in *Last Year in Marienbad*. I loved that film, but only because I yielded to its sweet confusion. But for your next chemistry paper, would you go to the scriptwriter *Robbe-Grillet* and ask him for help with its structure?

Now I don't want to be accused of disrespect towards the heroes of my youth. I proudly proclaimed my "documentary" device as a universal grammar. It works pretty well in English; sentence by sentence and paragraph by paragraph it points the way towards the logical order of presentation. But in "heavily inflected" languages it may work less well on the sentence level. The words hang more closely together, and *Die Lösung nach Neutralisierung* or *le précipité après calcination* may well constitute *one* image in the reader's mind.

But such constructions sound pretty awkward in English. This brings me to the following problem: You want to publish a paper in the English language. Do you write in German first, and then translate? Or straight in English?

Here my advice is very firm, and I am sure my readers have no need of it. If you want to be published in English, start writing your first version in that language. If you use your native language as a crutch, your prose will limp. Scholarly readers please correct me if I am wrong, but my guess is that, in the past, the great German-speaking Nobel Prize winners in chemistry were stronger in their French than in their English. Had this not been so, and had they read more *Hemingway* and less *Jules Romains*, then perhaps there might have been a slight movement away from *Geheimratsdeutsch*. Anyhow there is no excuse for you good fellows: you are not *Geheimräte*, and you have my last chapter. So fill that blank sheet with lovely, lively, loosely inflected English. But please (and here comes a vigorous Australian word), no flamin' flashbacks!

When submitting manuscripts, authors of articles intended for publication as "Communications" are requested to read the "Notice to Authors" reproduced in the January issue of the journal following the list of contents; upon request, a copy can be obtained from the editorial office.

Triple Proton Abstraction from a 1-Methylallyl Ligand on Thermolysis: Formation of a $Hf_3(C_4H_4)$ Cluster**

By *Bart Hessen, Anthony L. Spek,* and *Jan H. Teuben**

Transition-metal complexes with 1- or 2-methylallyl ligands can, upon thermolysis, yield butadiene[1] or trimethylenemethane[2] species, respectively. We used this method successfully for the preparation of the butadiene complexes **2** by thermolysis of the 1-methylallyl complexes **1**.[3] While exploring the reactivity and thermolysis of the complex **3**,[4] we observed a unique multiple proton abstraction from the 1-methylallyl ligand.

$$\underset{\mathbf{1}}{[Cp^*M(1\text{-}C_4H_7)_3]} \xrightarrow{\Delta} \underset{\mathbf{2}}{[Cp^*M(C_4H_6)(1\text{-}C_4H_7)]} + C_4H_8$$

$Cp^* = \eta^5\text{-}C_5Me_5$; M = Ti, Zr, Hf;
$1\text{-}C_4H_7$ = 1-methylallyl; C_4H_6 = butadiene

$$4\underset{\mathbf{3}}{[Cp^*Hf(1\text{-}C_4H_7)Cl_2]} \xrightarrow{\Delta} \underset{\mathbf{4}}{[Cp^*_3Hf_3Cl_5(C_4H_4)]} + [Cp^*HfCl_3] + 3\,C_4H_8$$

Thermolysis of **3** (toluene, 90 °C) produced a poorly soluble, orange, crystalline compound, which contains two nonequivalent Cp* groups (ratio 1:2) and four nonequivalent CH groups.[5] An X-ray structure determination[6] showed that the trinuclear species **4** (Fig. 1) had been formed.

Both C_4H_8 (mixture of 1-butene and *trans*-2-butene in a 2:3 ratio, GC) and $[Cp^*HfCl_3]$ (NMR) could be identified in the reaction mixture. Complex **4** contains a *cis*-1,3-butadiene-1,4-diyl unit that is symmetrically η^4-bound to both Hf2 and Hf3 and, at the same time, asymmetrically σ^2-bound to Hf1. Complexes of the unsubstituted 1,3-butadiene-1,4-diyl ligand are very rare. For the early transition metals only the thermally rather labile **5** has been reported.[7] In **4** the fragment is stabilized by being completely incorporated into the trinuclear cluster arrangement. For the late transition metals dinuclear complexes like **6**[8] and **7**[9] are known.

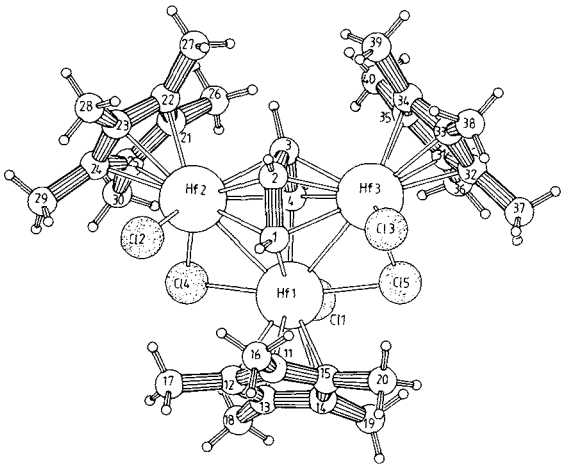

Fig. 1. Crystal structure of **4**. Selected bond lengths [Å] and angles [°]: Hf1-Cl 2.227(9), Hf1-C4 2.36(1), Hf2-C1 2.48(1), Hf2-C2 2.37(1), Hf2-C3 2.40(1), Hf2-C4 2.47(1), Hf3-C1 2.48(1), Hf3-C2 2.38(1), Hf3-C3 2.38(1), Hf3-C4 2.50(1), C1-C2 1.46(2), C2-C3 1.45(1), C3-C4 1.44(1), Hf1-Cl1 2.521(3); Hf1-Hf2-Hf3 81.53(3), C1-Hf1-C4 64.6(3), Hf1-C1-C2 129.2(7), C1-C2-C3 110.9(8), C2-C3-C4 109.5(9), C3-C4-Hf1 125.7(7).

$$\underset{\mathbf{5}}{[Cp_2Ti(C_4H_4)]}$$

$$\underset{\mathbf{6}}{[CpCo(\sigma^2,\eta^4\text{-}C_4H_4)CoCp]}$$[8]

$$\underset{\mathbf{7}}{[(CO)_3Fe(\sigma^2,\eta^4\text{-}C_4H_4)(\mu\text{-}CO)Fe(CO)_2]}$$

The coordination sphere of Hf1 in **4** can be viewed as a severely distorted octahedron with the Cp* group and C4 in the axial positions (C4-Hf1-Cp*(centroid) 170.5(2)°). As in structures of CpZr compounds with distorted octahedral geometry, like $[CpZrCl_3]_x$[10] and $[CpZrCl_3(dme)]$,[11] significant elongation of the axial bond is observed in **4** (Hf1-C4 2.36(1) Å). However, the equatorial bond (Hf1-C1 2.227(9) Å) is normal for a Hf–C σ bond.[12] The fully delocalized π-electron density in the C_4H_4 fragment contrasts with the localized structure in the monomeric 2,3,4,5-tetraphenylhafnacyclopenta-2,4-diene complex $[Cp_2Hf(\sigma^2\text{-}C_4Ph_4)]$.[13] The chlorine-bridged Hf–Hf distances (Hf1-Hf2 3.2261(9) Å, Hf1-Hf3 3.2061(9) Å) are comparable to the hydrido-bridged distances in $[Cp^*Hf(H)_2Cl_4]\cdot C_6H_6$ (average 3.233 Å[14]) and it is unlikely that there is any intermetal bonding interaction in **4**. The strongly asymmetrical chlorine bridges (e.g., Hf1-Cl4 2.610(3) Å, Hf2-Cl4 2.432(2) Å) indicate donation of electron density from Cl4 and Cl5 to the (formally neutral) $Cp^*Hf1(C_4H_4)Cl$ fragment. The overall structure of **4** is probably an average of four resonance structures (Scheme 1), through which the formal quadrivalence of Hf is conserved.

Formation of **2** (albeit in a low isolated yield, 23%) shows that multiple proton abstractions from methylallyl

[*] Dr. J. H. Teuben, Drs. B. Hessen
Department of Inorganic Chemistry, University of Groningen
Nijenborgh 16, NL-9747 AG Groningen (The Netherlands)
Dr. A. L. Spek
Department of Structural Chemistry, University of Utrecht
Padualaan 8, NL-3508 TB Utrecht (The Netherlands)

[**] This work was supported by the Netherlands Foundation for Chemical Research (SON) with financial aid from the Netherlands Organization for Scientific Research (NWO).

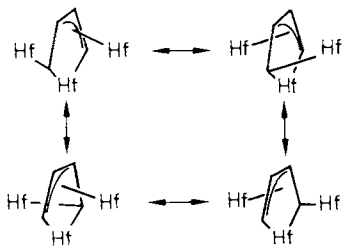

Scheme 1. Resonance structures for the $Hf_3(C_4H_4)$ unit in **4**.

ligands are possible and that Hf can form small organometallic clusters without metal–metal bonds supporting the framework.

Experimental Procedure

3: At 0°C, 19.2 mL of a 0.63 M [(1-C_4H_7)MgBr] solution in ether was added dropwise to a suspension of [Cp*$HfCl_3$] (1.679 g, 4.00 mmol) in ether. After stirring for 2 1/2 h the ether was pumped off and the residue extracted twice with 50 mL of pentane. Evaporation of the pentane yielded **3** as an orange oil [3]. This was dissolved in 25 mL of toluene together with [Cp*$HfCl_3$] (3.310 g, 7.89 mmol) and stirred for 15 h at room temperature. From the yellow solution **3** could be obtained by concentrating and cooling. Yield (after a cold washing with pentane) 3.740 g (8.51 mmol, 71%). Satisfactory elemental analysis.

3, 2-C_4H_7 instead of 1-C_4H_7: According to the same procedure but using instead [(2-C_4H_7)MgCl] in THF, [Cp*$Hf(2\text{-}C_4H_7)Cl_2$] can be prepared as well (74% yield). Satisfactory elemental analysis.

4: **3** (0.390 g, 0.887 mmol) was dissolved in 10 mL of toluene and heated to 90°C for 24 h. A deep red solution with orange crystals was formed. The toluene was pumped off and the residue washed with 5 mL of pentane (to remove red oil) and repeatedly with 10 mL of ether (to remove [Cp*$HfCl_3$]). Orange, crystalline **2** was isolated (0.060 g, 0.051 mmol, 23%). Satisfactory elemental analysis.

Received: March 18, 1988 [Z 2668 IE]
German version: *Angew. Chem. 100* (1988) 1115

[1] A. Zwijnenburg, H. O. Van Oven, C. J. Groenenboom, H. J. De Liefde Meijer, *J. Organomet. Chem. 94* (1975) 23.
[2] a) G. C. Emerson, K. Ehrlich, *J. Am. Chem. Soc. 94* (1972) 2464; b) J. M. Mayer, C. J. Curtis, J. E. Bercaw, *ibid. 105* (1983) 2651.
[3] J. Blenkers, H. J. De Liefde Meijer, J. H. Teuben, *J. Organomet. Chem. 218* (1981) 383.
[4] J. Blenkers, B. Hessen, F. Van Bolhuis, A. J. Wagner, J. H. Teuben, *Organometallics 6* (1987) 459.
[5] **4**: ^{1}H-NMR (300 MHz, [D_8]THF, 23°C): $\delta = 2.00$ (s, 15H, $C_5(CH_3)_5$), 2.09 (s, 30H, $C_5(CH_3)_5$), 5.10 (m, 1H, C*H*), 6.38 (m, 1H, C*H*), 6.9 (m, 2H, C*H*). ^{13}C-NMR (75.4 MHz, [D_8]THF, 23°C): $\delta = 12.10$ (q, 126.5 Hz, $C_5(CH_3)_5$), 12.16 (q, 127.4 Hz, $C_5(CH_3)_5$), 117.77 (d, 164 Hz, *C*H), 120.12 (s, $C_5(CH_3)_5$), 122.49 (s, $C_5(CH_3)_5$), 128.29 (d, 164 Hz, *C*H), 156.00 (d, 138 Hz, *C*H), 188.30 (d, 143 Hz, *C*H).
[6] **4**: A suitable crystal was obtained directly from the thermolysis reaction mixture. Space group $P2_1/n$, $a = 11.374(2)$, $b = 21.137(4)$, $c = 15.017(3)$ Å, $\beta = 95.07(2)°$ (100 K). $Z = 4$, $\rho_{calcd} = 2.162$ g cm^{-1}. Data were collected on an Enraf-Nonius CAD4F diffractometer ($Mo_{K\alpha}$, Zr-filtered, 100 K) and corrected for Lp and absorption ($\mu = 89.6$ cm^{-1}). The structure was solved by direct methods (SHELXS-86) and refined by full-matrix least squares (SHELX-76) to $R = 0.037$ ($R_w = 0.040$) for 4770 reflections with $I \geq 2.5\sigma(I)$. Further details of the structure determination are available from the Director of the Cambridge Crystallographic Data Centre, University Chemical Laboratory, Lensfield Road, Cambridge CB2 1EW (England), by giving the names of the authors and the full journal citation.
[7] a) H. G. Alt, H. E. Engelhardt, M. D. Rausch, L. B. Kool, *J. Am. Chem. Soc. 107* (1985) 3717; b) *J. Organomet. Chem. 329* (1987) 61.
[8] H. Rosenblum, B. North, D. Wells, W. P. Giering, *J. Am. Chem. Soc. 94* (1972) 1239.
[9] a) E. Weiss, W. Hübel, R. Merényi, *Chem. Ber. 95* (1962) 1155; b) G. Dettlaf, E. Weiss, *J. Organomet. Chem. 108* (1976) 213.
[10] L. M. Engelhardt, R. L. Papasergio, C. L. Raston, A. H. White, *Organometallics 3* (1984) 18.
[11] N. J. Wells, J. C. Huffman, K. G. Caulton, *J. Organomet. Chem. 213* (1981) C17.
[12] Typical values for Hf-C σ bonds lie in the region of 2.23–2.29 Å. For example see: W. E. Hunter, D. C. Hrncir, R. V. Bynum, R. E. Pentilla, J. L. Atwood, *J. Chem. Soc. Dalton Trans. 1984*, 399; G. Erker, P. Czisch, C. Krüger, J. M. Wallis, *Organometallics 4* (1985) 2059.
[13] J. L. Atwood, W. E. Hunter, H. G. Alt, M. D. Rausch, *J. Am. Chem. Soc. 98* (1976) 2454.
[14] M. Booij, J. Blenkers, J. C. M. Sinnema, A. Meetsma, F. Van Bolhuis, J. H. Teuben, *Organometallics 7* (1988) 1029.

Alkali-Metal Hydrogen Tetraphosphides, M^IHP_4—the First Salts of Bicyclo[1.1.0]tetraphosphane**

By *Marianne Baudler,* Christoph Adamek, Sylvia Opiela, Herbert Budzikiewicz,* and *Dimitrios Ouzounis*

Dedicated to Professor Heinrich Nöth on the occasion of his 60th birthday

The simplest bicyclic phosphane, tetraphosphane(2), P_4H_2, was identified some time ago during mass spectroscopic investigation of phosphane mixtures.[1,2] The only derivatives of this phosphorus–hydrogen compound so far known are the three covalent compounds $P_4[N(SiMe_3)_2]_2$,[3] $P_4(2,4,6\text{-}tBu_3C_6H_2)_2$,[4] and $P_4(C_5Me_5)_2$[5] as well as the complex $[(\eta^5\text{-}C_5Me_5)_2ZrP_4]$.[6] We have now found the first salts containing the $HP_4^{\ominus}$ ion **1** and report herein on their formation and structural characterization.

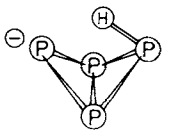

1

One or two electrons should be transferred initially to a P_4 molecule upon reduction with white phosphorus. The resulting radical anion or dianion, respectively, reacts immediately with further P_4 molecules to give P-richer polyphosphide ions such as $P_7^{3\ominus}$, $P_{19}^{3\ominus}$, $P_{26}^{4\ominus}$, $P_{21}^{3\ominus}$, and $P_{16}^{2\ominus}$.[7] Under suitable conditions, however, it is possible to suppress these subsequent reactions and to isolate **1**.

The reaction of white phosphorus with naphthalenesodium/potassium solution in 1,2-dimethoxyethane (DME) has proven particularly advantageous for the preparation of alkali-metal hydrogen tetraphosphides. Fractional extraction of the resulting polyphosphide mixture with the same solvent and separation of the phosphorus-richer compounds by low-temperature crystallization affords a red-orange solution of (Na/K)HP_4, which contains, in addition, only a small amount of phosphorus and possibly some naphthalene.[8] This solution can be stored for approximately 24 h at −78°C without undergoing decomposition. Warming the solution to room temperature results in a transformation to P-richer phosphides, especially $M_2^IP_{16}$ and also some M^IP_5.[9] More stable (Na/K)HP_4 solutions, which can be kept for approximately 70 h at

[*] Prof. Dr. M. Baudler, Dr. C. Adamek, S. Opiela, D. Ouzounis
Institut für Anorganische Chemie der Universität
Greinstrasse 6, D-5000 Köln 41 (FRG)
Prof. Dr. H. Budzikiewicz
Institut für Organische Chemie der Universität
Greinstrasse 4, D-5000 Köln 41 (FRG)

[**] Contributions to the Chemistry of Phosphorus, Part 189. This work was supported by the Deutsche Forschungsgemeinschaft and the Fonds der Chemischen Industrie.—Part 188: M. Baudler, D. Grenz, U. Arndt, H. Budzikiewicz, M. Fehér, *Chem. Ber.*, in press.

$-78\,^{\circ}C$ or for 1 h at room temperature, can be prepared by removing the DME at $0\,^{\circ}C$ under vacuum followed by dissolving the residue in cold dimethylformamide (DMF). Their composition was established by positive-ion FAB mass spectrometry.[10] Besides the ions characteristic of DMF (*m/z* 74, $[DMF+H]^{\oplus}$; 73, $DMF^{\oplus}$; and 58, $[DMF-CH_3]^{\ominus}$), as well as further ions (*m/z* 125, $[P_4+H]^{\oplus}$ and 129 $[C_{10}H_8+H]^{\oplus}$, see above), the most intense peaks correspond to $NaHP_4^{\oplus}$ (*m/z* 148) and $[NaHP_4+DMF+H]^{\oplus}$ (*m/z* 222), and a peak of lower intensity to $[NaHP_4+2\,DMF+H]^{\oplus}$ (*m/z* 295). $HP_4^{\ominus}$ cannot be detected in the negative-ion FAB spectrum. This finding indicates that, under these measuring conditions, $NaHP_4$ is present as a tight ion pair, since, otherwise, desorption of the free ions by the FAB beam should occur.

$LiHP_4$ is formed in the analogous reaction of white phosphorus with naphthalenelithium solution.[8] Furthermore, it is formed upon addition of phosphorus to lithium dihydrogen phosphide (ratio $P_4:LiPH_2\approx 3:2$) in THF followed by addition of DMF to the soluble reaction products.

The alkali-metal hydrogen tetraphosphides are each characterized in the ^{31}P-NMR spectrum by a downfield signal group and two upfield signal groups (intensity ratio 1:1:2). A singlet is observed in the ^{7}Li-NMR spectrum of $LiHP_4$.[11] Proof of the constitution of **1** is provided by the complete analysis of the ^{31}P-NMR spectrum of the $(Na/K)HP_4$ solution (Table 1); the hydrogen atom on P_M

Table 1. ^{31}P- and ^{1}H-NMR data [a] of $(Na/K)HP_4$ (in 1,2-dimethoxyethane, $-20\,^{\circ}C$) [b].

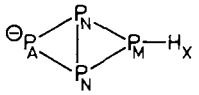

	δ	J(PP)	J(PH)
^{31}P	+ 71.3 (P_A)	−194.4 (P_AP_N)	
	−329.5 (P_M)	−244.2 (P_MP_N)	
	−355.1 (P_N)	+ 12.5 (P_AP_M)	
^{1}H	− 4.54 (H_X)		+129.2 (P_MH_X)
			+ 3.2 (P_NH_X)
			+ 16.5 (P_AH_X)

[a] J [Hz]. [b] RMS value of the spectrum calculation, 0.6; 48 of 64 calculated transitions were assigned.

is also revealed directly in the ^{1}H-NMR spectrum.[11] As shown by the positions of the signals for P_M and P_N as well as by the ^{1}J(PP) coupling constants, **1** has a tetraphosphabicyclobutane framework. Whereas the bridgehead atoms P_N exhibit nearly the same chemical shift as in $P_4(C_5Me_5)_2$ ($\delta=-357$[5]), in the case of the bridging atoms P_A and P_M, only the average of the resonance positions largely agrees with the $\delta(^{31}P)$ values of the organosubstituted nuclei in $P_4(2,4,6\text{-}t\text{Bu}_3C_6H_2)_2$ ($\delta=-130$[4]) and $P_4(C_5Me_5)_2$ ($\delta=-134$[5]). Surprising is the downfield position of the signal for the charge-bearing atom P_A. Since electronegative substituents, especially oxygen, are not present, only electronic effects come into consideration (see below). The value of $J(P_MP_N)$ is characteristic of coupling between three-membered ring atoms having lone pairs in *cis* positions.[12] The hydrogen atom on P_M is therefore arranged in the *endo* position. Further support for this conclusion is provided by the strongly upfield position of the proton signal, which should be due to anisotropy effects. Evidence of a hydrogen exchange between P_M and P_A was not found by ^{31}P-NMR spectroscopy. Noteworthy is the dependence of the chemical shift of the phosphidic atom P_A on the solvent and counterion; by contrast, the positions of the other phosphorus signals are hardly affected.

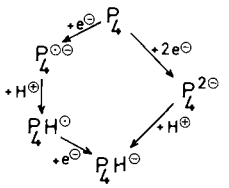

1

Anion **1** is directly related to the unknown initial product formed in the reductive cleavage of P_4; owing to its hyperreactivity, this product is immediately protonated by the solvent. It remains an open question whether the radical anion or the dianion is initially formed. The remarkably downfield position of the ^{31}P-NMR signal for the phosphidic atom P_A of **1** is an indication of an unusual electronic structure as a consequence of change in hybridization (decrease in the s character of the electron pair[13]), partial delocalization of the anionic charge into the phosphorus framework,[14] and interaction between **1** and the counterion.[15]

Received: April 5, 1988;
revised: May 11, 1988 [Z 2687 IE]
German version: *Angew. Chem. 100* (1988) 1110

[1] a) M. Baudler, H. Ständeke, M. Borgardt, H. Strabel, *Naturwissenschaften 52* (1965) 345; b) M. Baudler, H. Ständeke, M. Borgardt, H. Strabel, J. Dobbers, *ibid. 53* (1966) 106; c) M. Baudler, *Pure Appl. Chem. 52* (1980) 755.

[2] Reviews: a) M. Baudler, *Angew. Chem. 94* (1982) 520; *Angew. Chem. Int. Ed. Engl. 21* (1982) 492; b) *Z. Chem. 24* (1984) 352; c) *Angew. Chem. 99* (1987) 429; *Angew. Chem. Int. Ed. Engl. 26* (1987) 419.

[3] E. Niecke, R. Rüger, B. Krebs, *Angew. Chem. 94* (1982) 553; *Angew. Chem. Int. Ed. Engl. 21* (1982) 544.

[4] a) R. Riedel, H.-D. Hausen, E. Fluck, *Angew. Chem. 97* (1985) 1050; *Angew. Chem. Int. Ed. Engl. 24* (1985) 1056; b) E. Fluck, R. Riedel, H.-D. Hausen, G. Heckmann, *Z. Anorg. Allg. Chem. 551* (1987) 85.

[5] P. Jutzi, T. Wippermann, *J. Organomet. Chem. 287* (1985) C5.

[6] O. J. Scherer, *Nachr. Chem. Tech. Lab. 35* (1987) 1140.

[7] See [2c] and references cited therein.

[8] *(Na/K)HP₄ solution:* A naphthalenesodium/potassium solution (11 mL, 6.87 mmol (prepared by reaction of 4 g of naphthalene in 50 mL of DME with 1 mL of Na/K alloy (1:3) at $-78\,^{\circ}C$) was injected as quickly as possible under inert gas with stirring to freshly distilled, finely dispersed white phosphorus (1.01 g, 0.033 g-atom; prepared by dissolution in 250 mL of refluxing THF and subsequent removal of the solvent with stirring at $10\,^{\circ}C$) at $-78\,^{\circ}C$. After 30 min, the reaction mixture was warmed to $-55\,^{\circ}C$. As soon as the color of the reaction solution had turned from green to red, the mixture was cooled once again to $-78\,^{\circ}C$ and stirred for an additional 15 min. The reaction solution was then filtered in the cold and the residue was washed with 50 mL of DME ($-78\,^{\circ}C$), the wash solutions being discarded. Extraction with cold DME (ca. 150 mL) in portions was carried out until the filtrate was colorless. The combined extracts were concentrated under vacuum at $0\,^{\circ}C$ to 30 mL and allowed to stand at $-78\,^{\circ}C$ for 12 h to enable the remaining P-richer polyphosphides to separate. Filtration in the cold gave a largely pure solution of $(Na/K)HP_4$ in DME, which contained, in addition, only a small amount of phosphorus and possibly some naphthalene. Yield (by comparison of the intensities of the ^{31}P-NMR signals of **1** with the singlet of a $(Ph_3P)_2NCl$ solution of known concentration in [D₆]acetone): 4%, based on phosphorus. If the solution is not intended for immediate further use, DME can be completely removed at $0\,^{\circ}C$ without causing decomposition.—*LiHP₄ solution:* White phosphorus (0.94 g, 0.030 g-atom) was allowed to react at $-78\,^{\circ}C$ with naphthalenelithium solution (10 mL, 6.24 mmol; prepared by reaction of 0.3 g of thin Li sheet with a solution of 1.2 g of naphthalene in 15 mL of DME)

and the reaction solution was worked up quickly as described above. The solution of $LiHP_4$ in DME contains, in addition, only a small amount of phosphorus.

[9] a) M. Baudler, D. Düster, D. Ouzounis, *Z. Anorg. Allg. Chem. 544* (1987) 87; b) M. Baudler, S. Akpapoglou, D. Ouzounis, F. Wasgestian, B. Meinigke, H. Budzikiewicz, H. Münster, *Angew. Chem. 100* (1988) 288; *Angew. Chem. Int. Ed. Engl. 27* (1988) 280.

[10] MAT 731 mass spectrometer (acceleration voltage 8 kV, post-acceleration 7.5 kV) equipped with an 11 NF FAB ion source (Ion Tech Ltd., Teddington, UK; 10^{-5} torr Xe, 8 kV, Cu target). The sample was admitted by applying a freshly prepared solution of $(Na/K)HP_4$ in DMF to a target cooled with liquid nitrogen followed by slow warming in the ion source accompanied by continuous recording of the spectra.

[11] $LiHP_4$: ^{7}Li-NMR (dimethylformamide, −40°C, versus 1 M LiCl in H_2O, 116.436 MHz): $\delta = +1.05$.—$(Na/K)HP_4$: ^{1}H-NMR ([D_7]dimethylformamide, −40°C, 300.133 MHz): $\delta = -4.54$; $J = +128.3$ (P_MH), +3.5 (P_NH), +17.1 Hz (P_AH).

[12] M. Baudler, B. Makowka, *Z. Anorg. Allg. Chem. 528* (1985) 7.

[13] J. Hahn, M. Baudler, C. Krüger, Y.-H. Tsay, *Z. Naturforsch. B37* (1982) 797.

[14] See also: M. Baudler, R. Heumüller, *Z. Anorg. Allg. Chem.*, in press.

[15] Preliminary attempts at derivatization have not led to conclusive results so far.

Synthesis and Physical Properties of 3,6-Di-*tert*-butyl-1,4-diazapentalene

By *Shoji Tanaka, Kyosuke Satake, Akira Kiyomine, Tsutomu Kumagai,* and *Toshio Mukai**

The aza analogues of pentalene possessing a planar 8π-electron system are theoretically of interest to predict the degree of antiaromaticity, which appreciably depends on the positions of the nitrogen atoms.[1] Although several aza- and diazapentalenes have been synthesized, all of them are resonance-stabilized by conjugative interactions with substituents.[2] Herein we describe the synthesis of 3,6-di-*tert*-butyl-1,4-diazapentalene **2** from the 1,4-dihydro derivative **1**,[3] and report its physical properties, which provide information concerning the antiaromatic nature of this 8π-electron system.

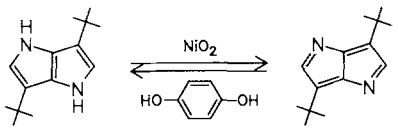

1 **2a**

The oxidation of **1** was carried out with an excess of nickel peroxide in benzene at 20°C, producing a dark red solution. The solvent was removed by the freeze-dry method. The resulting crude material was then purified by high-vacuum sublimation (20°C, 10^{-6} torr) to give red-brown, fine needles (m.p. 93°C) in 68% yield. Compound **2** could be recrystallized from hexane at −70°C, but was not so stable at room temperature in the presence of air. The spectral data are listed in Table 1. Compound **1** was regenerated in 56% yield when a benzene solution of **2** was treated with 1.2 equivalents of hydroquinone at room temperature.

[*] Prof. Dr. T. Mukai [+], A. Kiyomine, Dr. T. Kumagai, Dr. S. Tanaka, Dr. K. Satake
Department of Chemistry, Faculty of Science
Tohoku University, Aramaki, Sendai 980 (Japan)

[+] Present address: Department of Industrial Chemistry, College of Engineering, Nihon University
Koriyama 963 (Japan)

Table 1. Spectroscopic data for **2**. A correct elemental analysis was obtained.

MS (25 eV): m/z 216 ($M^{\oplus}$, 7%); IR (KBr): $\tilde{\nu}$ [cm^{-1}] = 3035, 2945, 2890, 2845, 1617, 1478, 1465, 1450, 1382, 1359, 1350, 1297, 1262, 1210, 1186, 1098, 1041, 975, 967, 924, 905, 808, 696, 628, 543, 470; ^{1}H-NMR (90 MHz, CCl_4, 35°C): $\delta = 7.17$ (s, 2H; H-2,5), 1.20 (s, 18H; 2*t*Bu); ^{13}C-NMR (50 MHz, CD_2Cl_2, 20°C): $\delta = 173.0$ (d; C-2,5), 163.2 (s; C-3a,6a), 145.7 (s; C-3,6), 32.4 (s; CMe_3), 28.5 (q; CH_3); UV (cyclohexane): $\lambda_{max}(\varepsilon) = 245$ (1510), 330 (8620) nm.

In contrast to pentalene **3**,[4] diazapentalene **2** could not be subjected to X-ray analysis, because a single crystal could not be obtained. However, the ^{1}H- and ^{13}C-NMR data indicate that, of the two bond-alternated structures **2a** and **2b**, the structure **2a** is more important. In the ^{13}C-

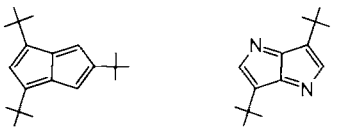

3 **2b**

NMR spectrum of diazapentalene, the signal of C-2(C-5) appears at $\delta = 173.0$, which is at appreciably higher frequency than that of C-3a(C-6a) at $\delta = 163.2$. The ^{13}C-NMR chemical shifts in azaheterocycles are reported to be correlated linearly with the total electron densities of the respective carbons by $\Delta\delta = 60$ ppm per electron.[5] Thus, the electron densities at C-2 and C-3a in structures **2a** and **2b** were calculated by the MNDO method, which gave values of 3.94 and 4.07, respectively, for **2a** and 4.00 and 4.01, respectively, for **2b**. Based on these values, the difference in chemical shift between these positions is predicted to be 7.8 ppm for **2a** and 0.6 ppm for **2b**. The observed difference, 9.8 ppm, is in good agreement with the calculated one for **2a**, but not for **2b**, supporting the existence of double-bond fixation as in the case of pentalene.[6] The MNDO calculation also indicates that the structure **2a** is 7.8 kcal mol^{-1} more stable than **2b**.

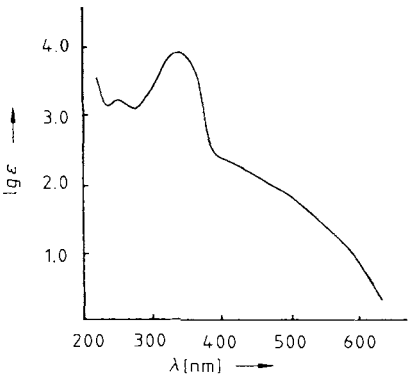

Fig. 1. Electronic spectrum of **2** in cyclohexane. ε in cm^2 mol^{-1}.

The UV/VIS spectrum of **2** (Fig. 1) is characteristic of the pentalene system. The long tail throughout the visible region indicates the existence of a low-energy excited state having potential energy curves appreciably different in shape from the ground state.[7] The low-energy excited state can contribute to inducing the π-orbital paramagnetism.[8] The degree of paramagnetic shielding in the diaza-

pentalene **2** is estimated by comparing the chemical shift of the ring proton with that of the CH=N protons of **4** ($\delta = 7.23$).[9] The extension of the conjugation by introduction of double bonds in **4** should induce a downfield shift

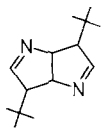

4

of the proton signal. Assuming that the chemical shift difference is the same as that ($\Delta\delta = 0.82$ ppm) for the olefinic protons on going from cyclopentene ($\delta = 5.60$) to cyclopentadiene ($\delta = 6.42$ ppm), the signal for the ring proton of **2** is expected to be located at $\delta = 8.05$ ppm. The difference between the expected and observed value ($\Delta\delta = 0.88$ ppm) can be attributed to the paramagnetic shielding effect in this diazapentalene. The degree of the shielding is comparable to that in 1,4-dihydropyrazines ($\Delta\delta \approx 0.75$ ppm), which is considered to be a typical antiaromatic molecule.[10]

Received: March 15, 1988 [Z 2664 IE]
German version: *Angew. Chem. 100* (1988) 1134

[1] a) B. A. Hess, Jr., L. J. Schaad, C. W. Holyoke, Jr., *Tetrahedron 31* (1975) 295; b) I. Gutmann, M. Milun, N. Trinajstić, *J. Am. Chem. Soc. 99* (1977) 1692.
[2] a) K. Hafner, F. Schmidt, *Angew. Chem. 85* (1973) 450; *Angew. Chem. Int. Ed. Engl. 12* (1973) 418; b) H.-J. Gais, K. Hafner, *Tetrahedron Lett. 1974*, 771; c) W. Treibs, *Naturwissenschaften 46* (1959) 170; d) S. Hünig, H.-C. Steinmetzer, *Justus Liebigs Ann. Chem. 1976*, 1090; e) J. J. Eisch, T. Abraham, *Tetrahedron Lett. 1976*, 1647; f) F. Closs, R. Gompper, *Angew. Chem. 99* (1987) 564; *Angew. Chem. Int. Ed. Engl. 26* (1987) 552.
[3] K. Satake, T. Kumagai, T. Mukai, *Chem. Lett. 1984*, 2033.
[4] a) B. Kitschke, H. J. Linder, *Tetrahedron Lett. 1977*, 2511; b) P. Bischop, R. Gleiter, K. Hafner, K. H. Knauer, J. Spanget-Larsen, H. U. Süss, *Chem. Ber. 111* (1978) 932 and Ref. [20] therein.
[5] W. Adam, A. Grimison, G. Rodriguez, *Tetrahedron 23* (1967) 2513.
[6] G. Binsch, I. Tamir, *J. Am. Chem. Soc. 91* (1969) 2450.
[7] a) K. Hafner, H. U. Süss, *Angew. Chem. 85* (1973) 626; *Angew. Chem. Int. Ed. Engl. 12* (1973) 575; b) T. Nakajima, Y. Yaguchi, R. Kaeriyama, Y. Nemoto, *Bull. Chem. Soc. Jpn. 37* (1964) 272; c) N. C. Baird, R. M. West, *J. Am. Chem. Soc. 93* (1971) 3072.
[8] a) J. H. van Vleck: *The Theory of Electronic and Magnetic Susceptibilities*, Clarendon, Oxford 1932, Chap. 4; b) J. A. Pople, K. G. Untch, *J. Am. Chem. Soc. 88* (1966) 4811.
[9] K. Satake, T. Kumagai, T. Mukai, *Chem. Lett. 1983*, 743; The NMR spectra of **2** and **4** were measured under the same conditions.
[10] W. Kaim, *Angew. Chem. 93* (1981) 620; *Angew. Chem. Int. Ed. Engl. 20* (1981) 599.

Catalytic Isomerization of Methylated 1,5-Cyclooctadienes**

By *Michael Mallien, Erhard T. K. Haupt,* and *Heindirk tom Dieck**

Dedicated to Professor Heinrich Nöth on the occasion of his 60th birthday

1,5-Cyclooctadiene **1**, which is readily accessible by catalytic cyclodimerization of butadiene on nickel complexes, undergoes facile rearrangement in the presence of catalysts to give bicyclo[3.3.0]oct-2-ene **2**. This reaction may be effected in a particularly selective fashion under mild conditions using a catalyst prepared from bis(2-ethylhexanoato)nickel and dichloroethylaluminum, as described by *Farona* et al.[1] The analogous reaction with substituted 1,5-cyclooctadienes can, depending on the pattern of substitution, lead to numerous isomers, analysis of which affords insight into the stereochemical course of the catalytic isomerization.

Isoprene reacts on diazadieneiron(0) catalysts at room temperature to give directly 1,6-dimethyl-1,5-cyclooctadiene **3**, and a 1:1 mixture of isoprene and *trans*-piperylene selectively affords 1,7-dimethyl-1,5-cyclooctadiene **4**.[2] Piperylene and 2,3-dimethylbutadiene also react to give codimers (89%); these consist mainly (70%) of 1,2,4-trimethyl-1,5-cyclooctadiene **5** (62% overall yield). All three cyclooctadienes react on the Farona catalyst to give unexpected products, which depend on the solvent and temperature. The topology and stereochemistry of the products could be elucidated by 2D INADEQUATE experiments[3] and other 2D NMR methods.

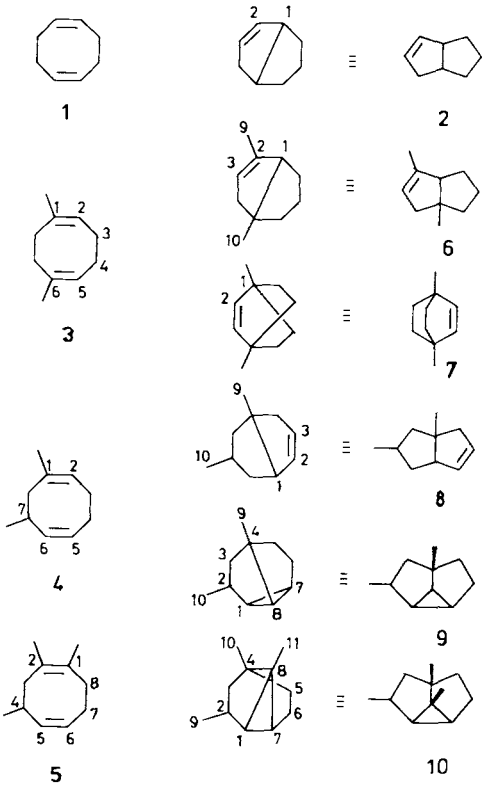

In benzene, **3** reacts at 81 °C to give 2,5-dimethylbicyclo[3.3.0]oct-2-ene **6** as the main product (93% after 4 h); this corresponds to the transformation **1** → **2**. At 69 °C in hexane, on the other hand, 1,4-dimethylbicyclo[2.2.2]oct-2-ene **7** is found (63% after 8 h). Its formation cannot be explained alone by C–C bond formation and hydride shift; C–C bond breaking is also required. Compound **6** does not isomerize to **7** in refluxing benzene.

Reaction of **4** for a longer time in benzene yields primarily 5,7-dimethylbicyclo[3.3.0]oct-2-ene **8**. The reaction appears to be analogous to that of **1** to **2** and of **3** to **6**. However, in contrast to **6**, the methyl group is not located in the unsaturated but rather in the saturated five-mem-

[*] Prof. Dr. H. tom Dieck, Dipl.-Chem. M. Mallien, Dr. E. T. K. Haupt
Institut für Anorganische und
Angewandte Chemie der Universität
Martin-Luther-King-Platz 6, D-2000 Hamburg 13 (FRG)

[**] This work was supported by the Deutsche Forschungsgemeinschaft, the Fonds der Chemischen Industrie, and the Stiftung Volkswagenwerk.

bered ring. Reaction of **4** in refluxing hexane, on the other hand, gives a fully saturated compound as the main product, which was identified as 2,4-dimethyltricyclo[5.1.0.0^{4,8}]octane **9**. The catalytic formation of such a highly strained cyclopropane system may at first seem surprising. Reaction times longer than 2 h, however, result in the slow isomerization of **9** to **8** (50% after 40 h) and the formation of six further, unidentified products having similar retention times upon gas-chromatographic separation. Reaction of **5** in refluxing hexane also results in rapid and exclusive formation of a tricyclic compound, 2,4,8-trimethyltricyclo[5.1.0.0^{4,8}]octane **10**, which, on first sight, resembles **9**. The positions of the methyl groups reveal once again that the route to **10** does not occur only via the formation of C–C bonds but also by bond breaking.

A nickel hydrido complex, which coordinates **1** and **3–5** is presumably the active species involved in the isomerization, since other nickel hydrido systems also allow the isomerization of **1** to **2**.[4] The first step, after coordination of the cyclooctadiene, is a hydrogen transfer from the nickel center to one of the sp^2 carbon atoms. A Ni–C σ bond to a tertiary C atom is thereby formed (**A**, **A'**), since the products **6–10** all have at least one angular methyl group. Because bonds to secondary C atoms should be more favorable, the activation barrier for a product with a Ni–C$_{sec}$ σ bond in the catalytic cycle must be higher and the yield of the corresponding catalysis product lower. Formation of a transannular C–C bond results in transformation of **A** to the bicyclo[3.3.0]octylnickel intermediate **B**, from which **2** or **6** are formed by β-elimination. In the corresponding intermediate involved in the isomerization of **4**, the nickel center would have a methyl group and a bridgehead H atom as neighbors. If the methyl group is *cis* to the nickel atom, then no β-elimination to this side is possible, so that a product containing a double bond to a bridgehead C atom should be formed. This does not occur, but instead **9** is obtained. Its formation can easily be explained by an intermediate containing a methyl group and a nickel center in *endo* positions, **B'**, since γ-elimination from such a species with formation of the cyclopropane ring of **9** should be sterically facile. However, an *endo* Ni atom can only be attained by opening of the eight-membered ring (e.g., **A'** → **F** → **B'**). The Ni–H elimination leading to **9** is apparently reversible, as shown by the isomerization of **9** to **8**. If "Ni–H" adds to **9** in such a way that **G** and not **B'** is formed, a normal β-elimination can readily occur leading to **8**. This mechanism would explain why—in contrast to **6**—compound **8** contains the double bond in the unsubstituted five-membered ring.

The formation of **7** formally requires, among other steps, the opening of the C3–C4 bond of **3** to give **C**. A second hydride transfer would give the new enyl complex **D**. A bicyclo[2.2.2]octylnickel complex can be formed in one step from this species. Ni–H elimination from this complex, in turn, gives **7**. Evidence for the intermediacy of **C** is provided by the appearance of traces of a product having the retention time of a 1,4-dimethyl-4-vinylcyclohexene. However, a catalytic rearrangement of 1,4-dimethyl-4-vinylcyclohexene itself to **7** cannot be detected.

Finally, the formation of the tricyclic compound **10** from **5** is a complete surprise. The INADEQUATE experiment, in connection with a ^{13}C APT spectrum (APT = attached proton test) unambiguously gives, without any presuppositions, the molecular topology. Two of the methyl groups are found at mutually linked quaternary C atoms; the molecule has a three-membered ring containing a quaternary and two tertiary C atoms; the third methyl group is found on a tertiary C atom, the configuration of which cannot be derived with certainty from the ^{1}H-NMR data, and is in proximity to the three-membered ring. Therefore, this tricyclic structure must have been formed by (formal!) breaking of the C1–C8 bond and formation of the bonds C2–C8 as well as C1–C5 and C1–C6 (numbering of **5**). The formation of **9** could also have occurred in a sequence of steps analogous to the path **5** → **10** instead of the "simple" way via **F**, **B'**.

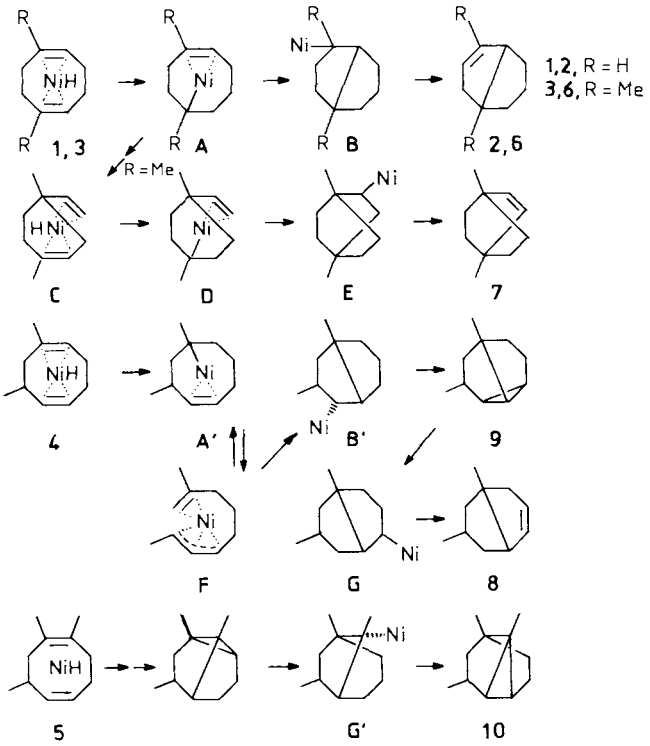

The formation of **7** and **10** clearly shows that the primary coordination of the active nickel species is capable of activating different σ bonds of the eight-membered ring. The formation of methylene-2-vinylcyclopentane, often observed upon dimerization of butadiene to the usual cyclodimers, can also be explained by opening of the C3–C4 bond of **B** and Ni–H elimination. The extremely selective formation of the various types of products as a function of the pattern of substitution and the temperature, however, still remains to be explained.

Experimental Procedure

The ^{13}C-NMR assignment for **2** reported by *Benn* et al. [6a] and by *Whitesell* et al. [6b] could be confirmed.

6, **7**: Bis(2-ethylhexanoato)nickel (0.1 mmol) [1] as a 0.1 M solution in hexane was added to **3** (2.7 g, 20 mmol) in hexane (15 mL) and activated with 2 mL of a 1 M solution of $EtAlCl_2$ (2 mmol) in hexane. After refluxing for 9 h, the reaction was quenched by adding 5 mL of EtOH. **3** had reacted completely, resulting in the formation of **7** (63%), **6** (7%), and three further products in 7–8% yield. The same reaction in benzene yielded **6** (93%) along with three further products (together 7%).—^{13}C-NMR ($CDCl_3$): **6**: δ = 15.45 (C9), 25.90 (C7), 28.92 (C10), 30.80 (C8), 43.05 (C6), 48.25 (C4), 49.07 (C5), 61.14 (C1), 122.71 (C3), 141.80 (C2); the ^{13}C-NMR assignment in [6b], which corrected that in [6c], was confirmed by 2D INADEQUATE NMR experiments. **7**: δ = 25.37 (C9, C10), 33.95 (C1, C4), 35.04 (C5, C6, C7, C8), 138.21 (C2, C3). Hydrogenation afforded 1,4-dimethylbicyclo[2.2.2]octane, whose ^{13}C-NMR spectrum is in agreement with the data given in [5].

8, **9**: The precatalyst and activator were added to **4** (2.7 g, 20 mmol) in 15 mL of hexane as described above. After refluxing for 2 h, 60% of **4** had reacted to give virtually exclusively **9**. After 4–5 h, **4** had undergone complete reaction. Analysis of the products showed the presence of **9** (63%), **8** (10%), and unidentifiable products having similar retention times (16, 5, 5, 3, and 2%). After 40 h, the proportion of **8** had attained 50% and **9** was no

longer present. In addition, isomers were formed in yields of 16, 5, 5, and 4% along with further compounds (<3%). The course of reaction is similar, but faster, in refluxing benzene or heptane. — ^{13}C-NMR ($CDCl_3$): **8**: δ = 19.10 (C10), 29.51 (C9), 33.52 (C7), 41.14 (C8), 48.10 (C5), 49.80 (C4), 52.27 (C6), 58.31 (C1), 129.35 (C3), 134.13 (C2). **9**: δ = 22.19 (C10), 24.29 (C6), 25.27 (C9), 26.97 (C7), 31.35 (C2), 34.08 (C1), 35.70 (C8), 47.40 (C5), 50.99 (C4), 57.06 (C3).

10: **5** was prepared according to the procedure in [2] by reaction of 2,3-dimethylbutadiene and *trans*-piperylene (30 mmol each) with $(dad)_2Fe/AlEt_3$ (dad = 1,4-dicyclohexyl-1,4-diaza-1,3-butadiene; 1 mmol Fe/5 mmol Al) at room temperature for 60 h (after complete conversion: 63% **5**, 22% 1,2-dimethyl-4-propenylcyclohexenes (DMPC), 9% piperylene codimer, and 6% of an unidentified codimer). Reaction of the mixture of **5** and DMPC with the nickel catalyst in refluxing hexane for 2 h resulted in exclusive and complete conversion to **10** together with unreacted DMPC. After 3 additional hours of refluxing, another isomerization occurs which has not yet been identified. **10**: ^{13}C-NMR ($CDCl_3$): δ = 16.59 (C11), 22.50 (C9), 22.98 (C6), 23.24 (C10), 30.18 (C2), 33.76 (C7), 38.72 (C8), 40.79 (C1), 47.21 (C5), 51.66 (C4), 56.76 (C3).

Received: March 7, 1988;
revised version: May 17, 1988 [Z 2648 IE]
German version: *Angew. Chem. 100* (1988) 1091

[1] N. A. Maly, H. R. Menapace, M. F. Farona, *J. Catal. 29* (1973) 182.
[2] H. tom Dieck, J. Dietrich, *Angew. Chem. 97* (1985) 795; *Angew. Chem. Int. Ed. Engl. 24* (1985) 781.
[3] J. Buddrus, H. Bauer, *Angew. Chem. 99* (1987) 642; *Angew. Chem. Int. Ed. Engl. 26* (1987) 625.
[4] W. Keim, *New J. Chem. 11* (1987) 531.
[5] W. Adcock, A. N. Abeywickrema, V. Sankarlyer, G. B. Kok, *Magn. Reson. Chem. 24* (1986) 213.
[6] a) R. Benn, H. Butenschön, R. Mynott, W. Wisniewski, *Magn. Reson. Chem. 25* (1987) 653; b) J. K. Whitesell, R. S. Matthews, *J. Org. Chem. 42* (1977) 3878; c) J. K. Whitesell, R. S. Matthews, P. A. Solomon, *Tetrahedron Lett. 1976*, 1549.

Strongly Bent Naphthalene Units in [2](2,6)Naphthalino[2]paracyclophane and [2](2,6)Naphthalino[2]paracyclophane-1,11-diene

By *Norman E. Blank, Matthias W. Haenel,* Carl Krüger, Yi-Hung Tsay,* and *Heike Wientges*

In the series of [n]paracyclophanes **1**, n = 4–8, the decreasing length of the aliphatic bridge increasingly forces the benzene ring to adopt a deformed boatlike structure. The effects of this deformation on the spectroscopic and chemical properties of the aromatic benzene ring can therefore be investigated.[1–7] In the stable derivatives of [6]paracyclophane **1**, n = 6, the benzene ring is bent by an

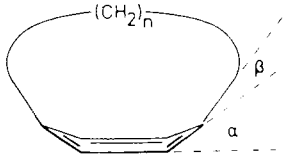

1

angle of $\alpha = 19.4$–$21.1°$, as determined by X-ray crystallography.[4] [5]Paracyclophanes exist only in solution at low temperatures,[5] and, according to calculations, are bent by an angle α of approximately 23°.[6] [4]Paracyclophanes are reactive intermediates which can only be detected by trapping reactions.[7] The deformation of *poly*cyclic arenes, on the other hand, has been little investigated.[8]

We have already described the synthesis of [2](2,6)naphthalino[2]paracyclophane **2** from the dithia[3.3]phanes **4** and **5**, which were ring-contracted by photolytic sulfur extrusion and pyrolytic sulfur dioxide extrusion, respectively.[9] Since, formally, **2** can be viewed as the product in

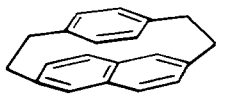

2

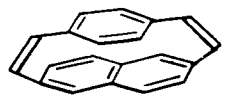

3

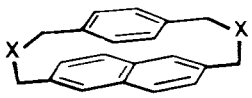

4, X = S
5, X = SO_2

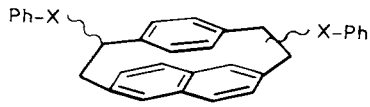

6, X = S
7, X = SO

which the two ends of the longer 2,6-dimethylnaphthalene are linked with the ends of the shorter *p*-xylene, a "bow" (naphthalene) and a "bow string" (benzene) must be formed. Indeed, an X-ray structure analysis of **2** (Fig. 1) reveals an extremely bent naphthalene moiety bridged by a nearly planar benzene ring.[10, 11]

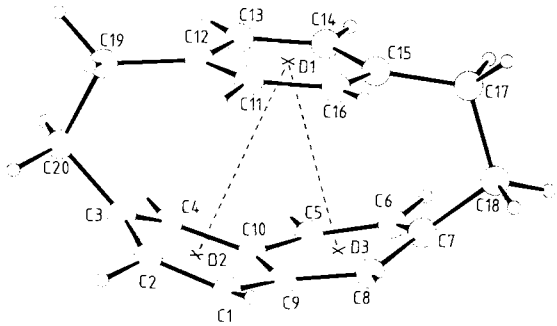

Fig. 1. Molecular structure of **2**.

To bend the "naphthalene bow" still further, we have synthesized the [2](2,6)naphthalino[2]paracyclophane-1,11-diene **3**. Two Stevens rearrangements, accomplished by reaction of **4** with dehydrobenzene (prepared from 1-(2'-carboxyphenyl)-3,3-dimethyltriazene in refluxing xylene[12]) led to the ring-contracted bis(phenylthio)[2.2]phane **6** (isomeric mixture,[13] m.p. 128–135°C, 15–20%), which was oxidized to the disulfoxide **7** (>95%) with *m*-chloroperbenzoic acid. Thermal elimination of phenylsulfenic acid by gas-phase pyrolysis of **7** at 320°C or by heating a solution of **7** in toluene to 160°C in a sealed tube gave **3** together with diphenyl disulfide **8**, which is apparently formed from phenylsulfenic acid.[14] Compound **8**, which could not be separated from **3** by chromatography, was reduced with excess *threo*-1,4-dimercapto-2,3-butanediol (racemate) **9**[15] in ethanol. Thiophenol **10**, thereby formed, was removed by extraction with aqueous sodium carbonate solution, and 4,5-dihydroxy-

[*] Prof. Dr. M. W. Haenel, Dr. N. E. Blank [+], Prof. Dr. C. Krüger, Dr. Y.-H. Tsay, H. Wientges
Max-Planck-Institut für Kohlenforschung
D-4330 Mülheim a. d. Ruhr (FRG)
[+] New address: Teroson GmbH, D-6900 Heidelberg (FRG)

1,2-dithiane **11** was easily separated by chromatography on alumina with cyclohexane as eluent. Colorless crystals of **3** (m.p. 124°C, 15–20%) were thus obtained.[16]

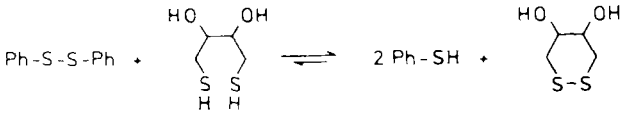

8 9 10 11

The X-ray structure analysis (Fig. 2) shows that the naphthalene moiety in **3**[17] is somewhat more strongly deformed than that in **2**. This is particularly revealed by the dihedral angles C4-C10-C9/C8-C9-C10 (32.8° and 33.1°) in the two crystallographically independent molecules of **3**, compared with that in **2** (28.1°). Most of the other dihedral angles in the naphthalene moiety of **3** are also larger

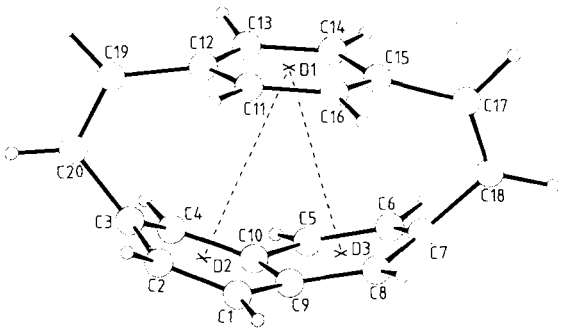

Fig. 2. Molecular structure of one of the two independent molecules of **3**.

(by an average value of 2°) than those in **2**. The large degree of bending is reflected well by the angle between the lines through C20-C3 and C7-C18, which is 94.5° in **2** and 85.0° and 84.5° in **3**. The benzene ring in both compounds is only slightly deformed toward a boatlike structure (dihedral angle between C11-C12-C13 and C11-C13-C14-C16 and between C11-C13-C14-C16 and C14-C15-C16 in **2**: 4.9/2.8°; in **3** (two molecules): 5.0/5.2° and 5.6/4.9°). By contrast, the angle formed at the benzene C atoms C12 and C15 (angle between the line through C19-C12 and the plane C11-C12-C13 and between the line through C17-C15 and the plane C14-C15-C16) is 5.4/5.8° and 5.7/5.7° in **3** (two molecules) and therefore considerably larger than the corresponding angle in **2** (1.4/2.5°). The distance between the center of the benzene ring plane C11-C13-C14-C16 and the center of the central naphthalene bond C9-C10 in **3** (3.423 and 3.432 Å) is slightly longer than that in **2** (3.379 Å). The center of the benzene ring (D1) in **2** is 3.33 Å from the centers D2, D3 of the bent naphthalene moieties; the lines through D2-D1 and D1-D3 form an angle of 41.8°. The corresponding average values in **3** are 3.36 Å and 41.3°.

In the UV absorption spectra of **2**[9] and **3**[16] the three characteristic naphthalene bands (α, p, and β) are shifted by about 20 nm to longer wavelengths compared with those of 2,6-dimethylnaphthalene, the bathochromic shift of the p and β bands of **3** being slightly (3–5 nm) larger than that of **2**. The pronounced vibrational fine structure of the naphthalene α band, which is largely retained for **2**, is completely lost for **3**. Since, additionally, the extinction coefficient of the α band is significantly smaller for **3**, this band is only observed as a shoulder of the p band. Investigations of the emission spectra and of the excited triplet state are now being carried out to differentiate between the effects of deformation, transannular π-electron interaction, and through-bond interaction via the bridges on the electronic properties.

As shown here, condensed polynuclear arenes can be deformed considerably. The structures of **2** and **3** also indicate that molecules such as C_{60}, "Buckminsterfullerene" or "Footballene",[18] should be stable, since, to form this three-dimensional sphere-shaped cluster containing 60 sp^2-hybridized carbon atoms, neighboring six-membered rings must be bent in a similar fashion to the deformations observed in the naphthalene moieties of **2** and **3**.

Received: March 21, 1988 [Z 2669 IE]
German version: *Angew. Chem. 100* (1988) 1096

[1] D. J. Cram, C. S. Montgomery, G. R. Knox, *J. Am. Chem. Soc. 88* (1966) 515; for a recent review see: S. M. Rosenfeld, K. A. Choe in P. M. Keehn, S. M. Rosenfeld (Eds.): *Cyclophanes, Vol. 1*, Academic Press, New York 1983, p. 311.

[2] K.-L. Noble, H. Hopf, L. Ernst, *Chem. Ber. 117* (1984) 455; *ibid. 117* (1984) 474, and references cited therein.

[3] J. Hunger, C. Wolff, W. Tochtermann, E.-M. Peters, K. Peters, H. G. von Schnering, *Chem. Ber. 119* (1986) 2698.

[4] Y. Tobe, K. Kakiuchi, Y. Odaira, T. Hosaki, Y. Kai, N. Kasai, *J. Am. Chem. Soc. 105* (1983) 1376; J. Liebe, C. Wolff, C. Krieger, J. Weiss, W. Tochtermann, *Chem. Ber. 118* (1985) 4144; Y. Tobe, K. Ueda, K. Kakiuchi, Y. Odaira, *Angew. Chem. 98* (1986) 364; *Angew. Chem. Int. Ed. Engl. 25* (1986) 369; Y. Tobe, A. Nakayama, K. Kakiuchi, Y. Odaira, Y. Kai, N. Kasai, *J. Org. Chem. 52* (1987) 2639.

[5] L. W. Jenneskens, F. J. J. de Kanter, P. A. Kraakman, L. A. M. Turgenburg, W. E. Koolhaas, W. H. de Wolf, F. Bickelhaupt, Y. Tobe, K. Kakiuchi, Y. Odaira, *J. Am. Chem. Soc. 107* (1985) 3716; Y. Tobe, T. Kaneda, K. Kakiuchi, Y. Odaira, *Chem. Lett. 1985*, 1301; G. B. M. Kostermans, W. H. de Wolf, F. Bickelhaupt, *Tetrahedron Lett. 27* (1986) 1095; *Tetrahedron 43* (1987) 2955.

[6] J. E. Rice, T. J. Lee, R. B. Remington, W. D. Allen, D. A. Clabo, Jr., H. F. Schaefer III, *J. Am. Chem. Soc. 109* (1987) 2902; cf. also N. L. Allinger, J. T. Sprangue, T. Liljefors, *ibid. 96* (1974) 5100; H. Schmidt, A. Schweig, W. Thiel, M. Jones, Jr., *Chem. Ber. 111* (1978) 1958; L. Carballeira, J. Casado, E. González, M. A. Rios, *J. Chem. Phys. 77* (1982) 5655; R. B. Remington, T. J. Lee, H. F. Schaefer III, *Chem. Phys. Lett. 124* (1986) 199.

[7] G. B. M. Kostermans, M. Bobeldijk, W. H. de Wolf, F. Bickelhaupt, *J. Am. Chem. Soc. 109* (1987) 2471; T. Tsuji, S. Nishida, *J. Chem. Soc. Chem. Commun. 1987*, 1189.

[8] [7](1,4)Naphthalinophanes are discussed in [3].

[9] M. W. Haenel, *Chem. Ber. 115* (1982) 1425; cf. also *Tetrahedron Lett. 1977*, 4191.

[10] **2**: $C_{20}H_{18}$, $P2_12_12_1$, $a=7.915(1)$, $b=11.079(1)$, $c=16.107(2)$ Å, $V=1412.4$ Å^3, $Z=4$, $\rho_{calcd}=1.21$ g cm^{-3}, $\mu(Cu_{K\alpha})=4.80$ cm^{-1}, 3397 measured reflections ($\pm h$, $+k$, $+l$), averaged to 1712 unique reflections, of which 1478 were observed reflections, 253 refined parameters, $R=0.081$, $R_w=0.090$.

[11] Further details of the crystal structure investigation may be obtained from the Fachinformationszentrum Energie, Physik, Mathematik GmbH, D-7514 Eggenstein-Leopoldshafen 2 (FRG), on quoting the depository number CSD-53031, the names of the authors, and the journal citation.

[12] I. D. Reingold, W. Schmidt, V. Boekelheide, *J. Am. Chem. Soc. 101* (1979) 2121; H. Heany, J. M. Jablonsky, C. T. McCarty, *J. Chem. Soc. Perkin Trans. 1 1972*, 2903.

[13] After fractionation and enrichment by HPLC, seven isomers of **6** could be identified by ^{1}H-NMR spectroscopy. R. Benn, A. Rufińska, G. Schroth, unpublished.

[14] F. A. Davis, S. G. Yocklovich, G. S. Baker, *Tetrahedron Lett. 1978*, 97.

[15] U. T. Rüegg, J. Rudinger, *Methods Enzymol. 47* (1977) 111.

[16] **3**: ^{1}H-NMR (400 MHz, CD_2Cl_2): $\delta=7.21$, 7.11, 6.90 (ABC with $J_{AB}=8.4$, $J_{BC}\approx 0.5$ Hz, 6H; naphthalene H); 7.23, 6.75 (AB with $J_{AB}=10.0$ Hz, 4H; olefin H); 6.08, 6.04 (AA'BB', 4H; benzene H).—MS (70 eV): *m/z* 254 (100%, $M^{\oplus}$), 226 (23%).—UV (*n*-hexane): $\lambda_{max}(\lg\varepsilon)=229$ (4.41), 244 (sh 4.17), 291 (3.67), 330 nm (sh 2.41).

[17] **3**: $C_{20}H_{14}$, $P2_1/c$, $a=7.738(1)$, $b=11.242(2)$, $c=31.772(4)$ Å, $\beta=94.34(1)°$, $V=2756.0$ Å^3, $Z=8$, $\rho_{calcd}=1.23$ g cm^{-3}, $\mu(Mo_{K\alpha})=0.64$ cm^{-1}, 6627 measured reflections, ($\pm h$, $+k$, $+l$), averaged to 6211 unique reflections of which 3038 were observed, 361 refined parameters, $R=0.065$, $R_w=0.068$ [11].

[18] H. W. Kroto, J. R. Heath, S. C. O'Brien, R. F. Curl, R. E. Smalley, *Nature (London) 318* (1985) 162; D. J. Klein, W. A. Seitz, T. G. Schmalz, *ibid. 323* (1986) 703.

Kinetics and Stereochemistry of the $SO_4^{\odot\ominus}$-Induced Hydroxylation of Cyclohexenes in Aqueous Solution

By *Günther Koltzenburg,* Eugenie Bastian,* and *Steen Steenken*

Alkyl radicals containing leaving groups such as Cl, OSO_3R, OPO_3R_2 (R = alkyl) in the β position are hydrolyzed in aqueous solution several orders of magnitude faster[1] than alkyl compounds containing the same leaving groups; e.g., $k_{hydrol}((CH_3)_2\overset{\odot}{C}CH_2Cl) = 3.5 \times 10^4\ s^{-1}$, $k_{hydrol}((CH_3)_3CCl) = 6.4 \times 10^{-3} s^{-1}$ at 22 and 15 °C, respectively.[1,2] β-Hydroxyalkyl radicals are thereby formed[1] [Eq. (a)].

$$(CH_3)_2\overset{\odot}{C}-CH_2Cl + H_2O \longrightarrow H^{\oplus} + (CH_3)_2\overset{\odot}{C}-CH_2OH + Cl^{\ominus} \quad (a)$$

Alkyl radicals containing sulfate groups in the β position are presumed to be the first intermediates in the $SO_4^{\odot\ominus}$-induced hydroxylation of olefins in aqueous solution.[3] Such reactions have found preparative applications.[4–6] Their mechanism, however, has not yet been completely determined and details of their kinetics are unknown. The possibility that an olefin radical cation[1,3] might be the first intermediate formed upon hydrolysis of the radicals in water (S_N1 mechanism) remains only speculation so long as an S_N2 mechanism, which would involve a polar transition state and thereby avoid the formation of an intermediate, cannot be ruled out. We were particularly interested in elucidating the mechanism of hydrolysis since the existence of chemical methods for the generation of short-lived olefin radical cations in water is a prerequisite for the comparative investigation of UV- or γ-radiation-initiated ionization processes of olefins and other unsaturated compounds in water.

Using pulse radiolysis and laser flash photolysis, we investigated the kinetics of the two-step reaction of $SO_4^{\odot\ominus}$ with several cyclohexenes [Eq. (b) and (c)]. The SO_4 radical

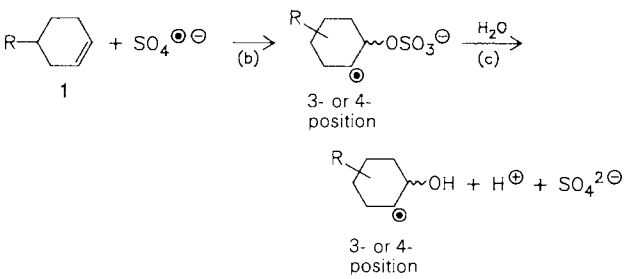

anions were generated from $S_2O_8^{2\ominus}$ either by pulse radiolysis employing a pulse length of 0.2 μs ($e_{aq}^{\ominus} + S_2O_8^{2\ominus} \longrightarrow SO_4^{\odot\ominus} + SO_4^{2\ominus}$) or by photolysis using a 20-ns flash ($S_2O_8^{2\ominus} \xrightarrow{h\nu} 2\,SO_4^{\odot\ominus}$). The formation of protons in reaction (c) was demonstrated by time-resolved conductivity measurements. Starting with low concentrations of cyclohexene, the rate of acid formation initially increases linearly with increasing concentration of cyclohexene, eventually leveling off to a plateau. From the linear part (reaction (b) rate-determining) it is possible to obtain k_b and from the plateau (reaction (c) rate-determining) k_c[7] (Table 1). We found no plateau value for α-terpineol **1d** and 2-methyl-α-terpineol **1e**, because the hydrolysis was too fast for the experimentally possible time resolution.

Table 1. Kinetic data for the reaction of SO_4 radical anions with cyclohexenes **1** (in O_2-free aqueous solutions at 20 °C).

	R	k_b [$M^{-1} s^{-1}$]	k_c [s^{-1}]
1a	H	1.7×10^9 [a]	3.0×10^4
1b	CH_2OH	4.3×10^9	6.5×10^3
1c	$(H_3C)_2COH$	4.6×10^9	8.4×10^3
1d	$(H_3C)_2COH$ [b]	4.6×10^9	$> 5 \times 10^6$
1e	$(H_3C)_2COH$ [c]	1.8×10^9 [a]	
		4.3×10^9 [d]	$> 5 \times 10^6$

[a] In H_2O/acetonitrile 1 : 1. [b] Additional methyl group in 4-position to R. [c] Two additional methyl groups on the CC double bond. [d] In H_2O/acetonitrile 2 : 1.

The k_b values in water are close to those for diffusion-controlled reactions. In water/acetonitrile, they are somewhat smaller, pointing to a polar transition state for the $SO_4^{\odot\ominus}$ addition. Substituent and solvation effects are reflected in the k_c values. The increase of three or more orders of magnitude on going from norterpineol **1c** to α-terpineol **1d**[8–10] indicates a late transition state with pronounced charge separation.

We employed stereochemical criteria to further elucidate the reaction mechanism. The barium salts of *cis*- and *trans*-4-*tert*-butylcyclohexyl sulfate (10^{-2} M) were allowed to react with OH radicals in aqueous solution at pH 5–7 in the presence of dithiothreitol (= *threo*-1,4-dimercapto-2,3-butanediol, 5×10^{-3} M) as H donor (or at pH 3 in the presence of 10^{-2} M ascorbic acid) at room temperature. We generated the OH radicals by exposure of N_2O-saturated solutions to ^{60}Co γ-radiation. The radiation doses caused conversion of 3–10% of the substrate. Together with other H-abstraction radicals, the radical anions **2** and **3** were

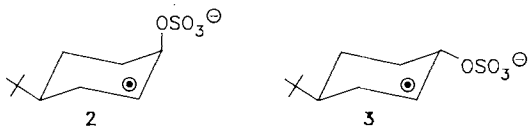

formed with the conformations shown. Hydrolysis results in their conversion to β-hydroxycyclohexyl radicals [Eq. (c), R = *tert*-butyl]. They are then transformed by reaction with H donors (> 95% under our conditions) into the *tert*-butylcyclohexanols **4**–**7** [Eq. (d)].[11]

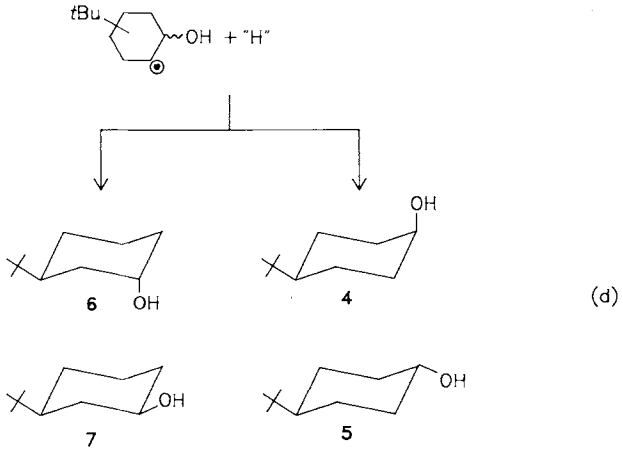

(d)

[*] Dr. G. Koltzenburg, E. Bastian, Dr. S. Steenken
Max-Planck-Institut für Strahlenchemie
Stiftstrasse 34-36, D-4330 Mülheim a. d. Ruhr 1 (FRG)

A conceivable isomerization of the β-hydroxycyclohexyl radicals before the reduction (e.g., by an $H^{\oplus}$-catalyzed 1,2 OH migration[12]) did not take place under our conditions. It requires pH values less than 1. The alcohols **4**–**7** were analyzed by GLC after extraction with ether (Table 2).

Table 2. Product composition after hydrolysis of the radicals **2** and **3** and subsequent reduction by H donors.

Radical	*tert*-Butylcyclohexanol [%]			
	4	**5**	**6**	**7**
2	38±2	4±1	52±2	6±1
3	54±2	6±1	35±2	5±1

The values in Table 2 reveal that alcohols are formed with approximately 90% axial OH groups (**4** + **6**). Alcohols **5** and **6** (56±2% inversion), having *trans* configuration, predominate in the hydrolysis products of the radical **2**, having *cis* configuration. Alcohols **4** and **7** (59±2% inversion), having *cis* configuration, predominate in the hydrolysis products of the radical **3**, having *trans* configuration. The results are in clear agreement with the assumption of a largely solvent-separated 4-*tert*-butylcyclohexene radical cation/sulfate ion pair **8** as intermediate and thus point to an S_N1 mechanism.

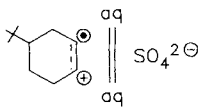

8

Attack of water on the radical cation occurs before the sulfate group has completely departed. Therefore, the sulfate group hinders the approach of water somewhat from one side of the molecule. Otherwise, **2** and **3** afford a radical cation having the same conformation. In terms of kinetics, the attack of water competes with ion recombination and with further separation of the ions by water molecules, namely with processes for which a picosecond time scale has been measured for other cation/anion pairs.[13,14] Presumably, therefore, the radical cation of **8** has a lifetime in this range (10–100 ps). The high stereoselectivity of the water addition is remarkable when compared with the stereoselectivity observed in the direct radical hydroxylation of a cyclohexene with OH radicals (which we have studied here for the first time). As cyclohexene, the water-soluble norterpineol **1c** was used.[15] The results are summarized in Table 3.

Table 3. Product composition [%] after radical hydroxylation of **1c** in water both directly with $^{\circ}OH$ and indirectly with $SO_4^{\odot\ominus}$ followed by reduction with ascorbic acid; R = $(CH_3)_2COH$.

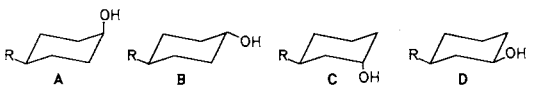

$^{\circ}OH$	29±1	21±1	29±1	21±1
$SO_4^{\odot\circ}$	46±2	4±1	46±2	4±1

In both cases, the hydroxylation is equally effective at either carbon of the double bond [(**C** + **D**) : (**A** + **B**) 1 : 1] and at either face of **1c** [(**A** + **D**) or (**B** + **C**)]. However, clearly evident is the high stereoselectivity in the indirect radical hydroxylation with $SO_4^{\odot\ominus}$ and the low stereoselectivity in the direct radical hydroxylation with $^{\circ}OH$ (**A** : **B**, **C** : **D**).

Received: March 9, 1988 [Z 2653 IE]
German version: *Angew. Chem. 100* (1988) 1113

[1] G. Koltzenburg, G. Behrens, D. Schulte-Frohlinde, *J. Am. Chem. Soc. 104* (1982) 7311; *ibid. 105* (1983) 5168.
[2] P. M. Laughton, R. E. Robertson, *Can. J. Chem. 34* (1956) 1714.
[3] M. J. Davies, B. C. Gilbert, *J. Chem. Soc. Perkin Trans. 2 1984*, 1809.
[4] C. Clerici, F. Minisci, K. Ogawa, J.-M. Surzur, *Tetrahedron Lett. 1978*, 1149.
[5] C. Arnoldi, A. Citterio, F. Minisci, *J. Chem. Soc. Perkin Trans. 2 1983*, 531.
[6] F. Minisci, A. Citterio, C. Giordano, *Acc. Chem. Res. 16* (1983) 27.
[7] The $SO_4^{\odot\ominus}$ addition to the CC double bond dominates, in all cases, over H abstraction from the substrate. The latter is revealed, for high concentrations of the substrate, in a relatively small, non-time-resolved conductivity jump occurring immediately after the laser flash.
[8] Methyl group effects of three or more orders of magnitude have been observed for the hydrolytic cleavage of leaving groups in the β position, for example with Cl as leaving group on alkyl radicals [1] as well as with $OCOCH_3$ [9] or OPO_3R_2 [10] as leaving group on α-alkoxyalkyl radicals.
[9] G. Berhens, G. Koltzenburg, A. Ritter, D. Schulte-Frohlinde, *Int. Radiat. Biol. Relat. Stud. Phys. Chem. Med. 33* (1978) 163.
[10] G. Behrens, G. Koltzenburg, D. Schulte-Frohlinde, *Z. Naturforsch. C37* (1982) 1205.
[11] Pulse radiolysis was used to measure k_{hydrol} values of 2.8×10^4 and $3.2 \times 10^4\ s^{-1}$ for **2** and **3**, respectively. Thus, **2** and **3** are too short-lived to react with H donors employed.
[12] B. C. Gilbert, R. O. C. Norman, P. S. Williams, *J. Chem. Soc. Perkin Trans. 2 1981*, 1401.
[13] J. D. Simon, K. S. Peters, *Acc. Chem. Res. 17* (1984) 277.
[14] J. M. Masnovi, J. K. Kochi, *J. Am. Chem. Soc. 107* (1985) 7880.
[15] For the direct hydroxylation, N_2O-saturated aqueous solutions, containing 10^{-2} M **1c** and 10^{-2} ascorbic acid, were exposed to ^{60}Co γ-radiation; the doses used effect up to 5% conversion of **1c**. For indirect hydroxylation, the above solutions were saturated with argon and treated with ca. 20 mol% $K_2S_2O_8$, resulting in the formation of $SO_4^{\odot\ominus}$ and ascorbate radicals (in addition to $H^{\oplus}$ and $SO_4^{2\ominus}$). The ascorbate radicals do not effect hydroxylation of **1c**. The reaction solutions, after neutralization with NaOH, were analyzed directly by gas chromatography.

Isolation and Structure of $[(Fluorenone^{\odot\ominus})\{Na^{\oplus}(dme)_2\}]_2$—a Touchstone for Radical Contact Ion Pairs?**

By *Hans Bock,* Hans-Friedrich Herrmann, Dieter Fenske,* and *Helmut Goesmann*

Dedicated to Professor Heinrich Nöth on the occasion of his 60th birthday

The formation of contact ion pairs $[M^{\oplus}A^{\ominus}]_{solv}$ in a common solvent cage involves a complex interplay of Coulombic attraction and single-ion solvation $M^{\oplus}_{solv} \cdots A^{\ominus}_{solv}$. The existence of such species, which are known to influence the course of numerous chemical and biochemical reactions,[2] has been firmly established by a variety of measurements.[1–3] Their structure in solution has been probed, for example, by ENDOR investigations[1,3] on radical salts such as that of 1-aminoanthraquinone (cf. **1**),[1] whose experimentally determined positive metal couplings indicate

[*] Prof. Dr. H. Bock, Dipl.-Chem. H.-F. Herrmann, Prof. Dr. D. Fenske, Dr. H. Goesmann
Institut für Anorganische Chemie der Universität
Niederurseler Hang, D-6000 Frankfurt am Main 50 (FRG)

[**] Electron Transfer and Ion-Pair Formation, Part 5. This work was supported by the Deutsche Forschungsgemeinschaft.—Part 4: [1].

a π spin transfer and therefore a "docking" of the cations above the chelate plane.

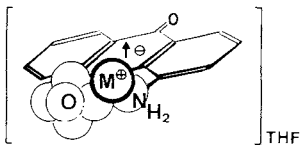

1

We have now succeeded in growing deep red, metallically lustrous needles of the extremely air- and moisture-sensitive sodium salt of the fluorenone radical anion by ultrasound-activated stoichiometric reaction of sodium with fluorenone in pure dimethoxyethane at 260 K under argon followed by slow cooling of the deep red solution to 230 K.[4] The single-crystal X-ray structure analysis[5,6] (Fig. 1) revealed the presence of a dimer **2**.

those in the comparable benzophenone dianion (140.6 pm[7b]). Important structural information is provided by the dihedral angle ω(Na-O-C9-C10) = 76.3° (Fig. 1B, C): accordingly, the $Na^{\oplus}$ ion interacting most strongly with fluorenone$^{\odot\ominus}$ is situated 115 pm above the framework of the radical anion and lies about 28 pm outside of the perpendicular π_{CO} plane.

As a prototype of dimeric metal ketyls $(R_2CO^{\odot\ominus}Na^{\oplus})_2$, the ion quadruplet (fluorenone$^{\odot\ominus}Na^{\oplus})_2$ has been studied repeatedly by ESR spectroscopy,[8a] especially in methyltetrahydrofuran glasses at 100 K,[8b,c] and, on the basis of the observed zero-field (triplet) splitting, a C_{2v} geometry was eventually postulated.[8c] The structure of the tetrakis(dimethoxyethane) solvate **2** (Fig. 1) presented here further refines this prediction, although packing effects in the crystal cannot be ruled out. In solutions of higher concentration, electronic spectra indicate the formation of more highly aggregated ion clusters, especially for alkaline-earth metals,[8b] whereas, in dilute solutions, ENDOR measure-

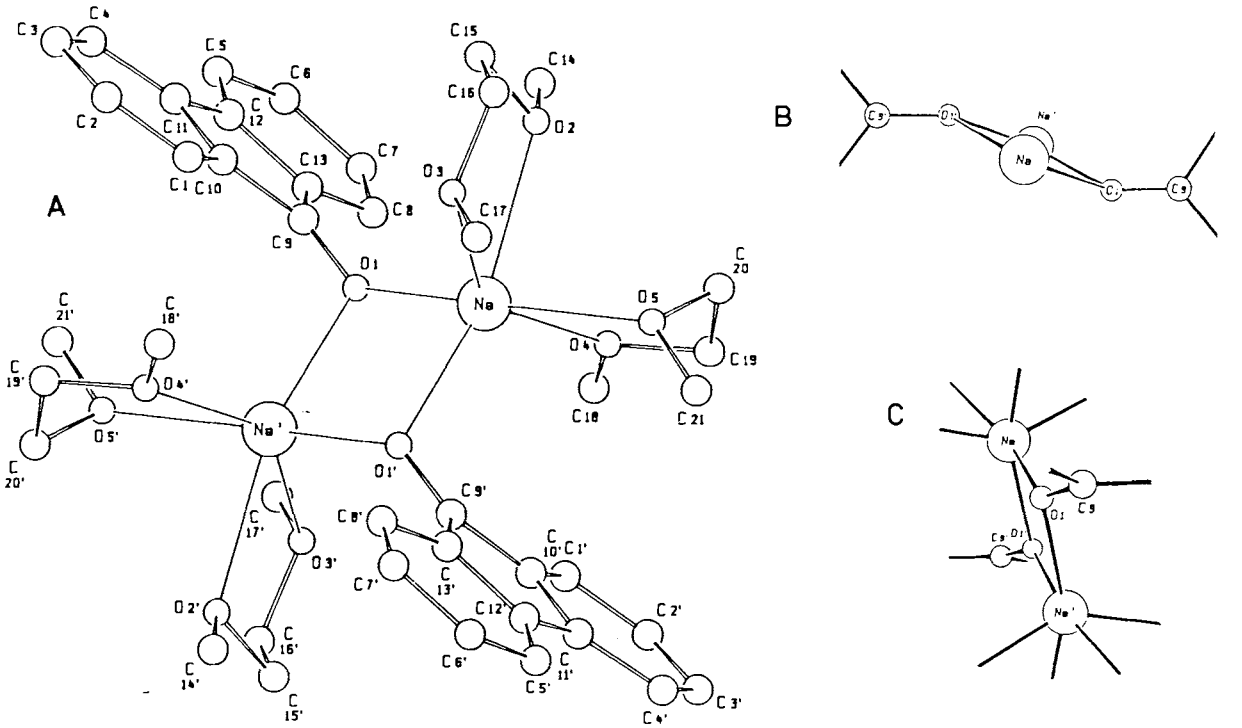

Fig. 1. Molecular structure of [(fluorenone$^{\odot\ominus}$)(Na$^{\oplus}$(dme)$_2$)]$_2$ **2** (A; H atoms omitted) as well as the cross section $Na_2O_2C_2$ perpendicular to the π planes (B) and after rotation by 90° (C). Important distances (±0.3 pm) and angles (±0.2°): Na-O1 228.1, Na-O1' 239.8, Na···Na' 335.0, O1···O1' 326.9, O1-C9 128.2; O1-Na-O1' 88.6, Na-O1-Na' 91.4, Na-O1-C9 141.0, Na'-O1-C9 117.7; Na-O1-C9-C10 76.3, Na-O1-C9-C13 73.3, Na'-O1-C9-C13 57.7. For further details see [6].

The structure of **2**, exhibiting C_i symmetry (Fig. 1A), reveals that the two [fluorenone$^{\odot\ominus}Na^{\oplus}$] moieties are linked by a planar, parallelogram-like Na_2O_2 four-membered ring (d_{NaO} 228.1 and 239.8 pm). The remaining four coordination sites of each $Na^{\oplus}$ ion are "solvated" by two dimethoxyethane molecules (d_{NaO} 245.1 to 252.4 pm). The molecular frameworks of the fluorenone radical anions, deviating slightly from planarity with the oxygens of the CO groups directed out of the plane by 8.5° ≙ 19 pm, are displaced perpendicularly to each other by approximately 100 pm about a center of inversion (Fig. 1C), and their CO axes are shifted parallel to each other by about 150 pm (Fig. 1B). As expected, the CO bonds in **2** (128.2 pm) are longer than those in neutral fluorenone (122.0 pm[7a]) and shorter than

ments prove the existence of only monomeric radical contact ion pairs (fluorenone$^{\odot\ominus}M^{\oplus})_{solv}$.[3] It should also be noted that the reduction of organic carbonyl compounds with, for example, sodium is used on a preparative scale for the synthesis of 1,2-diols HOR_2C-CR_2OH[9] and that dimers formed on the metal surface, in analogy to the generation of **2**, are presumably involved in the redox equilibria in solution.

The question posed in the title should be answered affirmatively—taking into consideration once again the complex processes involved in ion-pair formation and the possible crystallization of configurations favored by packing effects. The position of the most strongly interacting $Na^{\oplus}$ ion in the structure of **2** (Fig. 1)—above the fluorenone$^{\odot\ominus}$

framework and outside of the π_{CO} plane—is in agreement with expectations based on ESR/ENDOR measurements[3] in 10^{-5} M solutions (cf. **1**), in which partially fluxional[10] radical ion pairs are present as monomers in their respective solvent cage.

Received: March 30, 1988;
revised: May 3, 1988 [Z 2685 IE]
German version: *Angew. Chem. 100* (1988) 1125

CAS Registry number: [fluorenone$^{\odot\ominus}$Na$^{\oplus}$(dme)$_2$], 115512-56-6.

[1] H. Bock, B. Hierholzer, P. Schmalz, *Angew. Chem. 99* (1987) 811; *Angew. Chem. Int. Ed. Engl. 26* (1987) 791, and references cited therein.

[2] Cf. e.g.: a) M. Szwarc (Ed.): *Ions and Ion Pairs in Organic Reactions, Vol. 1, Vol. 2*, Wiley-Interscience, New York 1972, 1974; b) Y. Marcus: *Ion Solvation*, Wiley, Chichester 1985, p. 218f.; c) J.-M. Lehn, *Angew. Chem. 100* (1988) 91; *Angew. Chem. Int. Ed. Engl. 27* (1988) 89; cf. references cited therein as well as in [1, 3].

[3] W. Lubitz, M. Plato, K. Möbius, R. Biehl, *J. Phys. Chem. 83* (1979) 3402, and references cited therein.

[4] *Experimental Procedure* (cf. H.-F. Herrmann, *Dissertation*, Frankfurt am Main 1988): Na (76 mg, 3.3 mmol) and sublimed fluorenone (595 mg, 3.3 mmol) were weighed into a Schlenck trap under argon at 260 K and, after evacuation (high vacuum), 30 mL of DME (dried over Na/K) was added by condensation. Following activation with ultrasound (five 5-s treatments at short intervals) and reaction for 3 d, *n*-hexane (2 mL) was condensed into the reaction mixture, which was then cooled in a cryostat to 230 K at a rate of 5°/h. The air-sensitive dark red needles of **2** (dec. >413 K), which grew within 20 h, were characterized as follows: Titration of the sodium hydroxide solution formed after hydrolysis of a weighed sample indicates a formula weight of 366 (calcd for fluorenone·Na·2DME: 383). Quenching of dried crystals (which thereby lose DME) with O_2-saturated $CDCl_3$ and integration of the NMR signal intensities gave a ratio fluorenone : DME = 1 : >1.3. A solid-state ESR spectrum ($g = 2.0034$, compared with $g = 2.00343$ reported in the literature for solutions [3]) indicates that the crystal contains fluorenone radical anions. This is further supported by the decreased IR frequency ($\tilde{\nu}$(CO) = 1540 cm^{-1}) relative to fluorenone (1600 cm^{-1}) and by the absorption spectrum in the visible ($\tilde{\nu}_{max}$ = 19000 cm^{-1}).

[5] Extensive literature search for the structures of other radical-anion salts yielded the following: In [TCNQ$^{\odot\ominus}$Rb$^{\oplus}$] (A. Hoekstra, T. Spoelder, A. Vos, *Acta Crystallogr. Sect. B 28* (1972) 14) the tetracyanoquinodimethane radical anions are stacked on top of one another. In [biphenyl]$^{\odot\ominus}$K$^{\oplus}_{solv}$] or [biphenyl$^{\odot\ominus}$Rb$^{\oplus}_{solv}$] (J. J. Mooij, A. A. K. Klaassen, E. de Boer, H. M. L. Degens, T. E. M. van den Hark, J. H. Noordik, *J. Am. Chem. Soc. 98* (1976) 680; J. H. Noordik, J. Schreurs, R. O. Gouid, J. J. Mooij, E. de Boer, *J. Phys. Chem. 82* (1978) 1105) the countercations, which are embedded in polyethers, are separated from the radical anions. Therefore, the structure presented here (Fig. 1) is presumably the first one in which interactions between the radical anion and its countercation are visible.

[6] **2**, X-ray structure analysis (180 K): space group $P1$, $Z = 1$, $a = 962.4(15)$, $b = 1071.3(15)$, $c = 1114.8(13)$ pm, $\alpha = 93.4(1)$, $\beta = 96.6(1)$, $\gamma = 112.4(1)°$, $\mu(Mo_{K\alpha}) = 0.68$ cm^{-1}. Siemens AED 2, $2\theta \leq 52°$, 4299 reflections, 3470 with $I > 2\sigma(I)$. Direct methods, Na/C/O positions refined anisotropically, H positions isotropically. $R_1 = 0.047$, $R_2 = 0.050$. Further details of the crystal structure investigation may be obtained from the Fachinformationszentrum Energie, Physik, Mathematik GmbH, D-7514 Eggenstein-Leopoldshafen 2 (FRG), on quoting the depository number CSD-53118, the names of the authors, and the journal citation. Further details on distances [pm] and angles [°] (cf. Fig. 1): Na-O2 252.4, Na-O3 245.1, Na-O4 245.3, Na-O5 247.1, Na···C9 320.2, Na···C10 371.9, Na···C13 436.3, C-C in DME 148.9 to 150.8, C-O in DME 141.5 to 143.1, C9-C10 145.1, C10-C11 143.1, C11-C12 145.2, other distances in six-membered rings 137.6 to 140.8; O1-Na-O3 108.5, O1′-Na-O3 93.4, O1-Na-O4 94.5, O1′-Na-O4 115.8, C10-C9-C13 106.0, O1-C9-C10 126.4, O1-C9-C13 127.5, other angles in five-membered ring 107.4 to 109.2. Angles in six-membered ring 119.1 to 120.9.

[7] a) H. R. Luss, D. G. Smith, *Acta Crystallogr. Sect. B 28* (1972) 884. Other differences involve the five-membered ring, which is equalized under constant angles (d_{CC}(fluorenone) = 139.0 to 148.6 pm; d_{CC}(fluorenone$^{\odot\ominus}$) = 142.5 to 147.5 pm); b) B. Bogdanović, C. Krüger, B. Wermeckes, *Angew. Chem. 92* (1980) 844; *Angew. Chem. Int. Ed. Engl. 19* (1980) 817. The salt

$[(Ph_2CO^{2\ominus})\{Li^{\oplus}(thf)\}\{Li^{\oplus}(Me_2NCH_2CH_2NMe_2)\}]_2$

also shows a planar, compressed Li_2O_2 four-membered ring, although with identical LiO bond lengths.

[8] a) N. Hirota, *J. Am. Chem. Soc. 89* (1967) 32; b) S. W. Mao, K. Nakamura, N. Hirota, *ibid. 96* (1974) 5341; c) M. Guerra, P. Palmieri, G. F. Pedulli, *Chem. Phys. 33* (1978) 45. Cf. the literature cited in these references as well as in [2, 3]. A D_{2d} geometry that deviates both from the above quoted and from the crystal structure in Figure 1 has been postulated by H. van Willigen, C. F. Mulks, *J. Chem. Phys. 76* (1981) 2135.

[9] Cf., e.g., J. March: *Advanced Organic Chemistry*, Wiley, New York 1985, p. 1110f. The reaction of fluorenone with Na affords the pinacol in 95% yield (W. E. Bachmann, *J. Am. Chem. Soc. 55* (1933) 1179).

[10] For example, the 2,5-bis(trimethylsilyl)-*p*-benzosemiquinone/K$^{\oplus}$ contact ion pair, according to temperature-dependent ESR measurements attains the slow-exchange region at 223 K (P. Hänel, *Dissertation*, Universität Frankfurt am Main 1987; cf. H. Bock, B. Solouki, P. Rosmus, R. Dammel, P. Hänel, B. Hierholzer, U. Lechner-Knoblauch, H.-P. Wolf in H. Sakurai (Ed.): *Organosilicon and Bioorganosilicon Chemistry*, Ellis Horwood, Chichester 1985, p. 59f). A MNDO study (R. Dammel, *ibid.*, p. 67) yields an activation enthalpy of 30 kJ/mol and a value of 400 pm for the distance of K$^{\oplus}$ above the radical anion molecular plane at the saddle point of the fluxional motion.

ENDOR Spectroscopy in Water: Reductions and Oxidations of Organic Compounds**

By *Hans Bock** and *Bernhard Hierholzer*

Dedicated to Dr. Wolf-Dieter Luz on the occasion of his 60th birthday

Although water-free solutions are frequently advantageous for the generation, detection, and isolation[1] of radical ions and their salts, biological redox processes mostly take place in water.[2] An extension of high-resolution ENDOR spectroscopy,[3] the best method currently available for the structural elucidation of paramagnetic compounds in liquid phase, to the medium water is therefore desirable, despite the disadvantageous temperature-dependent properties of water.[4] By choosing selective one-electron-transfer reagents and working under O_2-free conditions, we have succeeded in detecting and characterizing the organic radical ions **1** to **4** in aqueous solutions by their ENDOR spectra (Fig. 1).

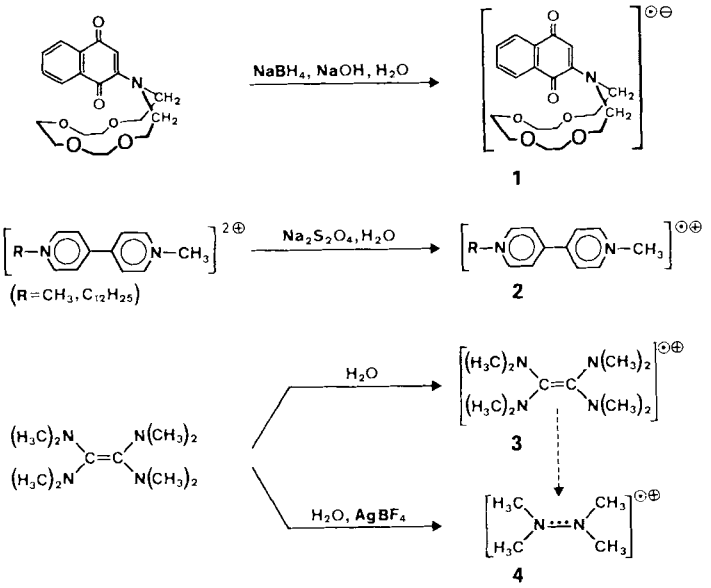

The experimental prerequisites for recording ENDOR spectra exhibiting an acceptable signal-to-noise ratio

[*] Prof. Dr. H. Bock, Dr. B. Hierholzer
Institut für Anorganische Chemie der Universität
Niederurseler Hang, D-6000 Frankfurt am Main 50 (FRG)

[**] Electron Transfer and Ion-Pair Formation, Part 6. This work was supported by the Deutsche Forschungsgemeinschaft, the Fonds der Chemischen Industrie, and the Land Hessen.—Part 5: [1].

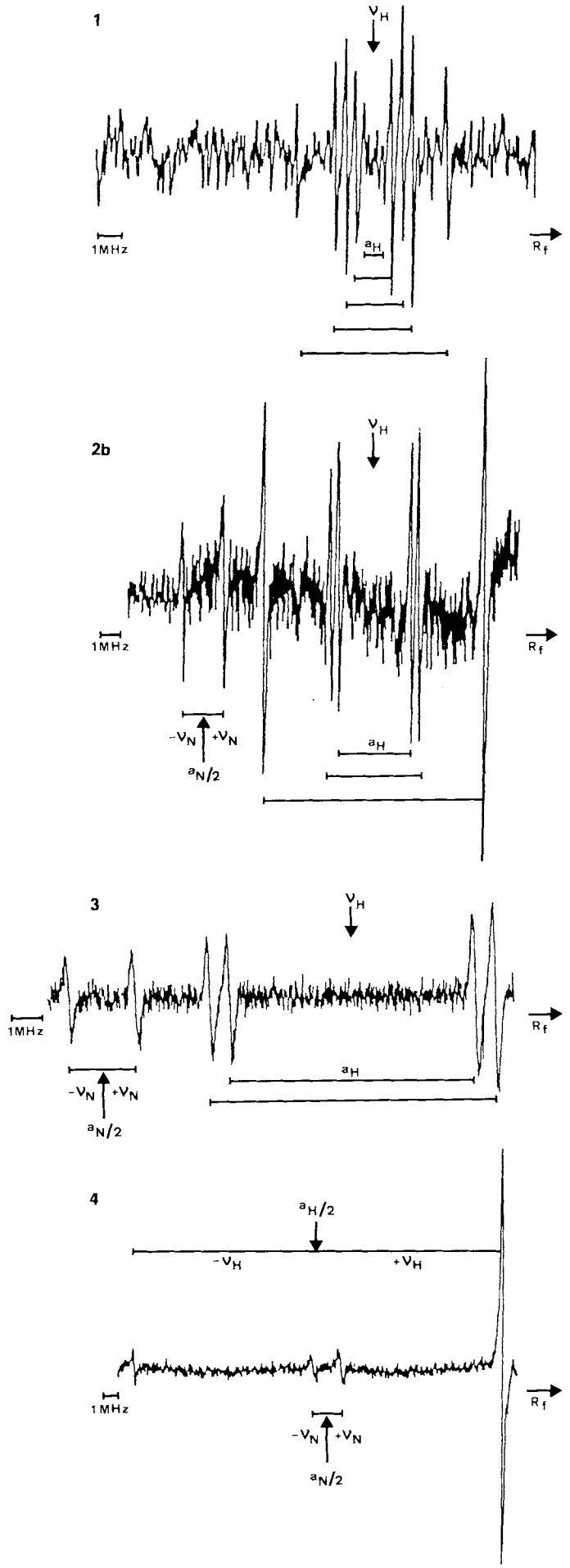

(number of scans $> 10^2$) in aqueous solutions are capillary tubes with walls of constant thickness and diameters < 1 mm as well as optimized concentrations of the redox components of $\approx 10^{-6}$ mol L^{-1}.[5] Concerning both the reactions in conductivity-pure water under argon and the assignment of the ENDOR spectra (Fig. 1), the following comments are added:

1. The ENDOR spectrum of the radical anion **1** (Fig. 1) does not show the ^{23}Na coupling observed under aprotic conditions,[6] indicating the formation of a "solvent-separated" ion pair. Because the ^1H couplings of the five ring hydrogen atoms are comparable to those of the $Cs^{\oplus}$ "contact ion pair" generated in aprotic medium, the countercations $Na^{\oplus}_{aq}$ ($r \approx 270$ pm[6]) and $Cs^{\oplus}$ ($r \approx 170$ pm[6]), surrounded by the flexible monoaza crown, cause similar π spin populations in the naphthosemiquinone radical anion. It should be further noted that the frequently used oxidation of hydroquinones with O_2 in alkaline solution, which is disadvantageous for ENDOR measurements, has been replaced by a one-electron reduction with $NaBH_4$. Generated in this way, the radical anions of biologically important quinones should also be characterizable by ENDOR spectroscopy.
2. Reduction of the dications with dithionite affords the radical cations of *N,N'*-dimethyl- (**2a**) and *N*-dodecyl-*N'*-methylviologen (**2b**). Their ENDOR coupling constants, which were determined in aqueous solution and agree with ESR literature values,[7] are identical, even though sodium dodecyl sulfate in 100-fold excess was added during the measurement of the dodecyl derivative **2b** (Fig. 1). Nonetheless, the demonstrated possibility to record ENDOR spectra of aqueous micellar solutions could be the starting point for obtaining information on aggregation and permeability of these dynamic systems by the addition of appropriate salts.
3. The electron-rich tetrakis(dimethylamino)ethene exhibits a negative oxidation potential < -0.6 V[8] and, therefore, is oxidized even by O_2-free water to the radical cation **3**. The ENDOR coupling constants of **3**[8] are in agreement with ESR values, which were measured after reduction of the dication with zinc in acetonitrile,[8] and can be interpreted in terms of a planar C_2N_4 molecular framework in which rotation around the CN axis is sterically hindered. According to our ENDOR measurements (Fig. 1), the oxidative hydrolysis of $(R_2N)_2C{=}C(NR_2)_2$, which has been the subject of controversy,[9] clearly begins with a one-electron transfer resulting in formation of the radical cation.
4. Upon addition of $AgBF_4$ to an aqueous solution of the ethene radical cation **3**, the ENDOR spectrum of the corresponding hydrazine radical cation **4** (Fig. 1 and Ref. [10]) is obtained, which can also be recorded after oxidation of tetramethylhydrazine with $AgBF_4$ in water. In addition, workup of a preparative run results in the isolation of tetramethylurea and dimethylformamide.[5] These findings suggest that the reaction proceeds by $Ag^{\oplus}$ oxidation of the ethene radical cation **3** to the dication and its nucleophilic hydrolysis to an unstable intermediate, **5**, which must be common to all the subse-

● Fig. 1. ENDOR spectra in water: radical anion **1** of the crown ether derivative 2-(1,4,7,10-tetraoxa-13-aza-13-cyclopentadecyl)-1,4-naphthoquinone at 270 K, radical cation **2b** ($R = C_{12}H_{25}$) of *N*-dodecyl-*N'*-methylviologen (with addition of sodium dodecyl sulfate in 100-fold excess) at 282 K, radical cation **3** of tetrakis(dimethylamino)ethene at 277 K, and radical cation **4** of tetramethylhydrazine at 270 K (for explanation see text).

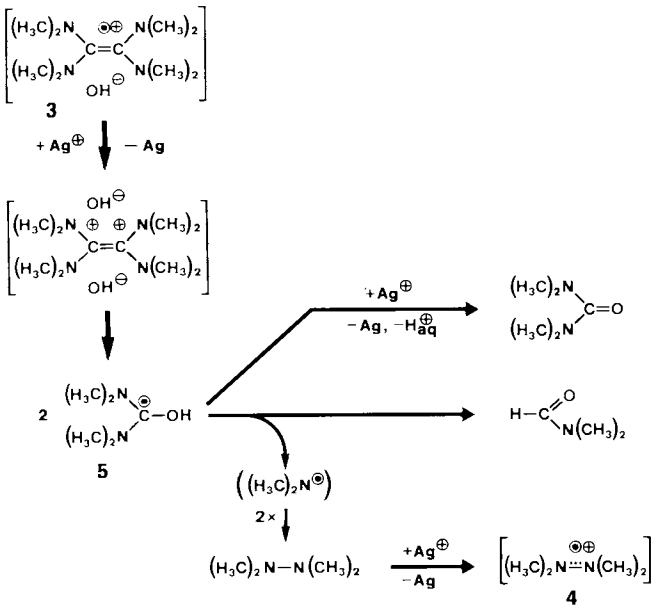

quent products. Both the dimerization of dimethylaminyl radicals[8] and their sole formation upon γ-irradiation of tetramethylurea in a 4 K matrix[11] have been reported.

In summary, the ENDOR experiments in water described here establish the utility of this physiologically important medium for the high-resolution electron/nucleus double-resonance measurement technique and the value of the accessible information on electron-transfer reactions.

Received: April 18, 1988 [Z 2706 IE]
German version: *Angew. Chem. 100* (1988) 1127

CAS Registry numbers:
1, 88288-46-4; **1** (Na complex), 88288-48-6; **2** (R = CH_3), 25239-55-8; **2** (R = $C_{12}H_{25}$), 115483-93-7; **3**, 34525-41-2; **4**, 34504-32-0.

[1] H. Bock, H.-F. Herrmann, D. Fenske, H. Goesmann, *Angew. Chem. 100* (1988) 1125; *Angew. Chem. Int. Ed. Engl. 27* (1988) 1067, and references cited therein.

[2] Cf., e.g., B. Alberts, D. Bray, J. Lewis, M. Raff, K. Roberts, J. D. Watson: *Molekularbiologie der Zelle*, VCH, Weinheim 1986; *Molecular Biology of the Cell*, Garland Publishing, New York 1983.

[3] Cf. the review of H. Kurreck, B. Kirste, W. Lubitz, *Angew. Chem. 96* (1984) 171; *Angew. Chem. Int. Ed. Engl. 23* (1984) 173, and references cited therein. Difficulties in carrying out ENDOR measurements in H_2O are discussed on p. 189 and p. 190, respectively.

[4] Thus, the high melting point of water restricts the ENDOR "window of measurement" to 0 to 50°C, its high dipole moment is responsible for considerable dielectric losses, i.e., demands drastically reduced sample cross sections, and its small, only weakly temperature-dependent viscosity interferes with the establishment of optimal rotation correlation times [3].

[5] Cf. B. Hierholzer, *Dissertation*, Universität Frankfurt am Main 1988. The water used, which was distilled in a BIDEST quartz apparatus, degassed repeatedly at 10^{-5} mbar, and stored under argon, exhibited a conductivity of $< 10^{-7}$ Siemens cm^{-1}.

[6] H. Bock, B. Hierholzer, F. Vögtle, G. Hollmann, *Angew. Chem. 96* (1984) 74; *Angew. Chem. Int. Ed. Engl. 23* (1984) 57. The ^1H coupling constants of **1** are:

$M^{\oplus}$	LM	a_m [mT]	$a_{H,3}$ [mT]	$a_{H,6}$ [mT]	$a_{H,5}$ [mT]	$a_{H,8}$ [mT]	$a_{H,7}$ [mT]
$Na^{\oplus}$	H_2O	—	0.248	0.129	0.092	0.058	0.034
$Na^{\oplus}$	THF [5]	0.024	0.404	0.087	0.055	—	0.037
$Cs^{\oplus}$	THF [5]	0.174	0.260	0.108	0.072	0.045	0.032

The cation radii given were taken from: *Holleman-Wiberg: Lehrbuch der Anorganischen Chemie*, 91st-100th ed., de Gruyter, Berlin 1985.

[7] The ENDOR coupling constants of **2a** and **2b** agree with the ESR values: H. Fischer (Ed.): *Landolt-Börnstein, Gruppe 2, Magnetische Eigenschaften freier Radikale, Bd. I*, Springer, Berlin 1965):

Method	a_N [mT]	$a_{H,2}$ [mT]	$a_{H,3}$ [mT]	$a_H^{CH_3}$ [mT]
ENDOR	0.482	0.159	0.134	0.402
ESR	0.432	0.157	0.133	0.399

For ESR measurements on micelles in frozen solutions, see, e.g.: E. Szajdzinska-Pietek, R. Maldonado, L. Kevan, R. M. Jones, *J. Am. Chem. Soc. 107* (1985) 6467, and references cited therein.

[8] Cf., e.g., cyclovoltammetric measurements in DMF (H. Bock, D. Jaculi, *Angew. Chem. 96* (1984) 298; *Angew. Chem. Int. Ed. Engl. 23* (1984) 305). The coupling constants of **3** are (ESR values: K. Kuwata, D. H. Geske, *J. Am. Chem. Soc. 86* (1964) 2197):

Method	a_N [mT]	a_H [mT]	a_H [mT]
ENDOR	0.484	0.2725	0.3275
ESR	0.484	0.284	0.328

[9] Cf., e.g., S. Patai (Ed.): *The Chemistry of the Amino Group*, Wiley, London 1968; N. Wiberg, J. W. Buchler, *Chem. Ber. 96* (1963) 3000, 3223.

[10] ENDOR coupling constants of **4** (ESR values: S. F. Nelson, G. R. Weismann, P. J. Hintz, D. Olp, M. R. Fahay, *J. Am. Chem. Soc. 96* (1974) 2916):

Method	a_N [mT]	a_H [mT]
ENDOR	1.340	1.290
ESR	1.340	1.270

Concerning the structure, see H. Bock, W. Kaim, *Acc. Chem. Res. 15* (1982) 9, and references cited therein.

[11] M. C. R. Symons, *Chem. Phys. Lett. 117* (1985) 381; *J. Chem. Soc. Chem. Commun. 1987*, 866.

Dications Based on a Hydrotris(phosphonio)borate Skeleton**

By *Hubert Schmidbaur,* Thomas Wimmer, Gabriele Reber,* and *Gerhard Müller*

Phosphane-boranes, containing a P-B bond, are a little investigated class of compounds, despite their noteworthy properties.[1] The presence of one or more formal positive charges in immediate proximity to the boron atom leads to a reduction or even reversal ("umpolung") in the polarity of the B-H bonds. As a result, prototypes having the stoichiometries **A** and **B** are sensitive neither to oxidation nor to hydrolysis. These substances are often stable even toward aqueous acids and alkaline solutions; extremely strong bases attack the alkyl moieties.[2-7] These properties should be more pronounced in the hydrotris(phosphonio)borate dications **C**, the boron atom of which is sur-

[*] Prof. Dr. H. Schmidbaur, Dipl.-Chem. T. Wimmer, Dipl.-Chem. G. Reber [+], Dr. G. Müller [+]
Anorganisch-chemisches Institut der Technischen Universität München
Lichtenbergstrasse 4, D-8046 Garching (FRG)

[+] X-ray structure analyses.

[**] This work was supported by the Deutsche Forschungsgemeinschaft (Leibniz-Programm), the Fonds der Chemischen Industrie, and Hoechst AG. We thank *J. Riede* for preparing the crystallographic data sets.

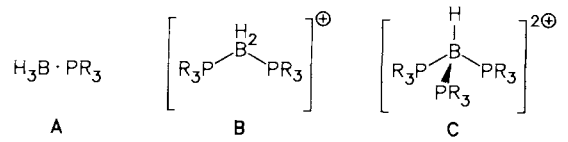

rounded by three phosphonium centers and only one hydrogen atom.

The investigations described here are also of interest in connection with studies on the analogous methane derivatives having one, two, or three phosphonium centers, and on the corresponding ylides,[8] as well as with attempts to use phosphane-boranes as precursors and model compounds for polymers based on boron phosphide (PB, isoelectronic with SiC).

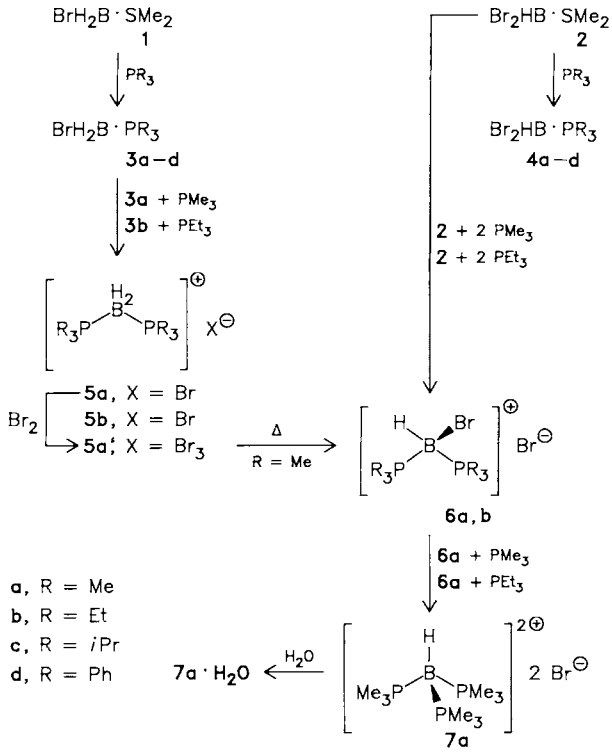

The starting material for the synthesis of the title compounds is the adduct **1**,[9] which reacts with two equivalents of trimethyl- or triethylphosphane to give the salts **5a,b**; compound **5a** has already been well characterized.[10,11] Reaction of **5a** with bromine leads initially only to the sparingly soluble tribromide **5a'**, thereby demonstrating once again the resistance of the BH_2 unit in these molecules toward undergoing reaction. At its melting point (136 °C), **5a'** rapidly evolves HBr with formation of the salt **6a** containing a bromine-substituted boron atom. This salt and its ethyl homologue **6b** are also accessible from the adduct **2**[9] by reaction with two equivalents of PR_3.

Finally, treatment of **6a** with PMe_3 in excess affords the hydrotris(trimethylphosphonio)borate dibromide **7a**, a colorless, air-stable, readily water-soluble salt, in a slow but nearly quantitative reaction.

An X-ray crystal structure analysis was carried out on single crystals of a monohydrate, **7a** · H_2O, obtained from a mixture of dioxane, ethanol, and water (10 : 80 : 1).[12] The

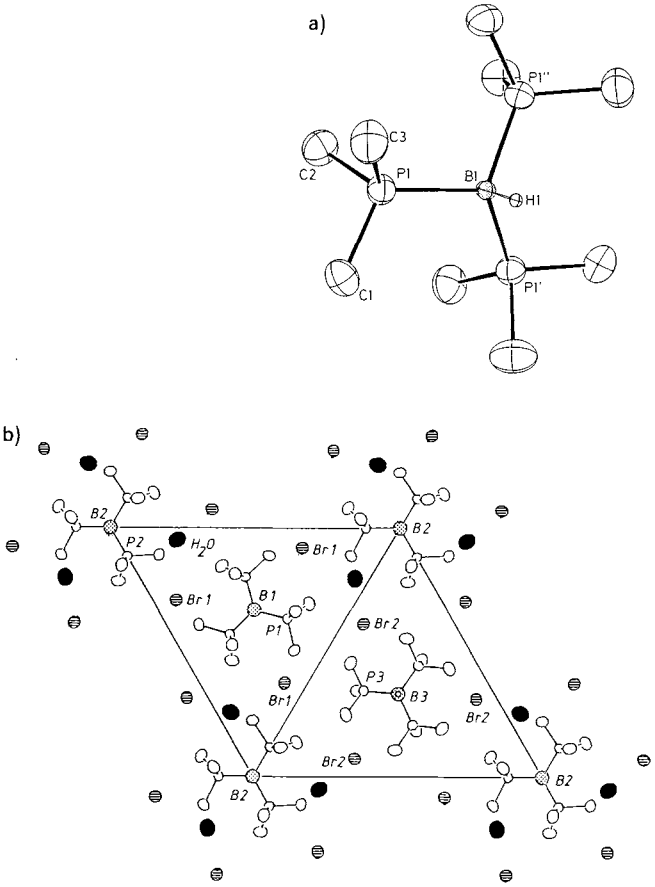

Fig. 1. a) Molecular structure of one of the three crystallographically independent dications of **7a** · H_2O (H atoms on carbons omitted). Important distances [Å] and angles [°] (for numbering see Fig. 1b): P1-B1 1.955(3), P2-B2 1.935(3), P3-B3 1.948(3); P1-B1-P1' 113.1(3), P2-B2-P2' 113.5(2), P3-B3-P3' 114.8(2). b) Arrangement of cations, anions, and hydrate water molecules in the unit cell of **7a** · H_2O (projection onto the *ab* plane).

trigonal unit cell of **7a** · H_2O contains three crystallographically independent formula units (Fig. 1), which differ only with respect to conformation. Each of the cations has crystallographic C_3 symmetry. The threefold axes lie along the B–H bonds. As expected, the C–P–C angles are larger than the tetrahedral norm; the P–B distances agree with expectations. There are no directed interactions between the cations on the one hand and the anions and hydrate water molecules on the other. The ^1H-, ^{11}B-, ^{13}C-, and ^{31}P-NMR spectra, recorded in $(CD_3)_2SO$ or CD_3OD, show that the crystallographic symmetry also holds in solution; particularly noteworthy is a 1 : 3 : 3 : 1 quartet in the $^{11}B\{^1H\}$-NMR spectrum with $^1J(BP) = 95$ Hz, $\delta = -47.1$.

Even under stronger conditions, **6b** does not react with PEt_3. Presumably, steric factors are mainly responsible for this finding, since reaction of the Me_2S precursors **1** and **2** with the more bulky phosphanes $PiPr_3$ or PPh_3 results only in formation of the adducts **3c,d** or **4c,d**, respectively. Surprisingly, treatment of **6a** with PEt_3 for long reaction times also gives **7a**, thereby demonstrating the reversibility of the reaction. The poor solubility of **7a** is certainly one of the reasons for the equilibrium being shifted toward the symmetric tris(phosphonio)borate salt.

The salt **8** and the adduct **9** may be prepared by reaction of **1** and **2**, respectively, with the sterically less demanding chelate ligand "Diphos". Similarly, the sixfold phenyl-substituted ligand "Tripod" reacts with **2** to give

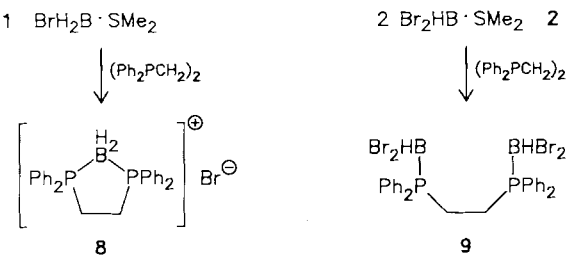

8 9

only the chelate compound **10** containing one noncoordinated PPh_2 function (^{31}P-NMR), instead of the desired cage compound (cf. **11**). Presumably, this finding also is due to steric factors. Use of the spatially less congested hexamethyl analogue of "Tripod" allows facile formation of the salt **11** of a bicyclic dication.

The identity and structure of this new type of phosphane-borane were readily established[13] by the unambiguous analytical and spectroscopic data as well as by an X-ray structure analysis.[14]

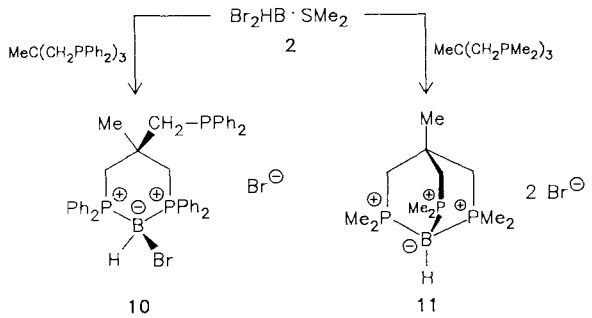

10 11

Compound **11** is poorly soluble in water; the solutions are stable. The NMR spectra (in methanol) are in agreement with a cation structure having C_{3v} symmetry. The cation of **10**, on the other hand, has no symmetry and shows the corresponding signal splittings. The vibrational spectra are each characterized, among other peaks, by a ν(BH) absorption (**10**, 2410; **11**, 2492 cm^{-1}).

Although the dications in the unit cell of crystalline **11** (orthorhombic, space group $P2_12_12_1$, $Z=4$), which have quinuclidine-like configurations, have no crystallographic symmetry, the deviations from point group C_3 are minimal (Fig. 2). The P–B distances correspond to those in **7a** · H_2O, but the P–B–P angles are, on the average, 102.8° and thus appreciably smaller than in the non-cagelike analogue (113.8°). The counterions ($2\,Br^{\ominus}$) have no discrete contacts with the cations. The crystals are solvate-free. In alkaline D_2O, the boron-bound H atom of **7a** and **11** is exchanged against deuterium, indicating protic character.

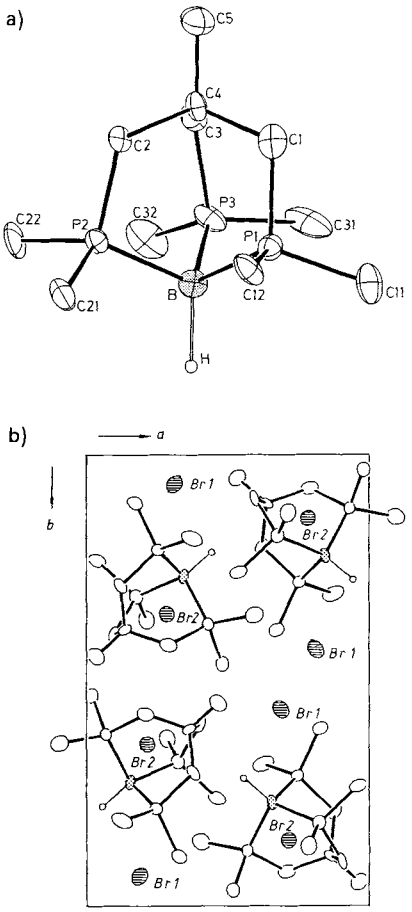

Fig. 2. a) Molecular structure of the dication of **11a** (H atoms on carbons omitted). Important distances [Å] and angles [°]: P1-B 1.94(1), P2-B 1.96(1), P3-B 1.97(1); P1-B-P2 101.3(5), P1-B-P3 104.6(5), P2-B-P3 102.4(5). b) Arrangement of cations and anions of **11a** in the unit cell (projection onto the *ab* plane).

Experimental Procedure

5a: A solution of **1** (3.87 g, 25.0 mmol) in benzene (50 mL) was combined at 5°C with PMe_3 (3.80 g, 50.0 mmol) [15]. After stirring for 1 h at 20°C, the reaction solution was filtered and the product was washed with benzene and dried under vacuum. Yield 5.33 g (87%), m.p. 254°C.

5b: A solution of **1** (3.87 g, 25 mmol) and PEt_3 (5.91 g, 50 mmol) in benzene (50 mL) was allowed to stand at 20°C for 24 h. Yield 7.20 g (88%), m.p. 160°C. ^{31}P-NMR (MeOH): $\delta=13.5$ (q, $J=92$ Hz). ^{11}B-NMR (MeOH): $\delta=-58.3$ (t, $J=92$ Hz). IR (KBr): 2410, 2379 cm^{-1} (νBH_2).

5a': Bromine (1.05 mL, 20.0 mmol) in a small amount of $CHCl_3$ was added dropwise to a suspension of **5a** (4.90 g, 20.0 mmol) in $CHCl_3$ (250 mL). An orange precipitate formed. Yield 7.62 g (94%), m.p. 136°C (dec.).

6a: **5a'** (8.09 g, 20.0 mmol) was heated to 140°C, resulting in the evolution of HBr gas. The colorless melt cake was dissolved in EtOH and the product was precipitated by addition of Et_2O. Yield 5.11 g (79%), m.p. 242°C.—The same product was obtained from **2** (5.84 g, 25 mmol) and PMe_3 (3.80 g, 50 mmol) in benzene (50 mL) at 5–20°C (5 d). Yield 4.05 g (50%). ^{1}H-NMR ([D$_6$]DMSO, 25°C): $\delta=1.80$ ("d", $N=12$ Hz, CH_3). ^{13}C-NMR (EtOH, 25°C): $\delta=6.6$ ("d", $N=56$ Hz, CH_3). ^{11}B-NMR (EtOH): $\delta=-38.9$ (t, $J=91$ Hz). IR (KBr): 2435 cm^{-1} (νBH).

6b: A solution of **2** (3.51 g, 15 mmol) and PEt_3 (3.54 g, 30 mmol) in toluene (25 mL) was refluxed for 5 d. Yield 3.86 g (63%), m.p. 180°C. ^{31}P-NMR (MeOH): $\delta=5.5$ (q, $J=92$ Hz). IR (KBr): 2412 cm^{-1} (νBH).

7a: A colorless precipitate formed over 20 d from **6a** (6.48 g, 20 mmol) and PMe_3 (1.52 g, 20 mmol) in acetonitrile (200 mL) at 20°C. Yield 4.08 g (51%), m.p. 224°C. ^{1}H-NMR ([D$_6$]DMSO): $\delta=1.98$ ("d", $N=12$ Hz, CH_3). ^{13}C-NMR (EtOH): $\delta=12.5$ ("d", $N=47$ Hz, CH_3). ^{31}P-NMR (EtOH): $\delta=-9.8$ Hz (q, $J=94$ Hz). ^{11}B{^{1}H}-NMR (EtOH): $\delta=-47.1$ (q, $J=95$ Hz); (D_2O, ^{1}H-coupled): $\delta=-47.4$ (quin, J(PB)=J(BH)=94 Hz). IR (KBr): 2393 cm^{-1} (νBH).

8: Prepared from $(Ph_2PCH_2)_2$ (7.97 g, 20 mmol) and **1** (3.10 g, 20 mmol) in benzene (50 mL). Yield 5.53 g (56%), m.p. 254°C. ^{1}H-NMR ($CDCl_3$): $\delta=3.30$ ("d", $N=10$ Hz, CH_2); 7.60 (m, Ph). IR (KBr): 2478, 2431 cm^{-1} (νBH_2).

9: Prepared from **2** (2.34 g, 10 mmol) and $(Ph_2PCH_2)_2$ (3.98 g, 10 mmol) in benzene (50 mL). Yield 2.02 g (55%), m.p. 198°C. ^{1}H-NMR ([D$_6$]acetone): $\delta=3.06$ ("d", $N=5$ Hz, CH_2); 7.75 (m, Ph). IR (KBr): 2485 cm^{-1} (νBH).

10: Prepared by refluxing a solution of $MeC(CH_2PPh_2)_3$ (3.12 g, 5.0 mmol) and **2** (1.16 g, 5.0 mmol) in toluene (50 mL) for 6 h. Yield 3.38 g (85%), m.p. 252°C. ^{1}H-NMR ([D$_6$]DMSO): $\delta=0.87$ (s, Me); 3.40 (m, CH_2); 3.69 (t, $J=13$ Hz, CH_2); 7.3–8.0 (m, Ph). ^{31}P-NMR ([D$_6$]DMSO): $\delta=-6.1$ (br, P_2B); -27.7 (s, P). IR (KBr): 2410 cm^{-1} (νBH).

11: Prepared by allowing a solution of $MeC(CH_2PMe_2)_3$ (1.26 g, 5.0 mmol) and **2** (1.16 g, 5.0 mmol) in toluene (140 mL) to react for 16 h at 20°C. Yield 1.72 g (81%), m.p. 342–345°C (dec., recrystallized from EtOH/MeOH (9 : 1)). ^{1}H-NMR (D_3COD): $\delta=1.47$ (q, $J=4$, CMe); 2.07 ("d", $N=12$ Hz, PMe); 2.56 ("d", $N=13$ Hz, CH_2). ^{13}C-NMR (D_3COD): $\delta=13.47$ (m, $N=52$ Hz, PMe); 31.15 (m, $N=42$ Hz, CH_2); 34.26 (q, $J=14$ Hz, *C*Me); 36.25 (s, C*Me*).

^{31}P-NMR (D_3COD): $\delta = 15.0$ (q, $J = 92$ Hz). ^{11}B-NMR (D_3COD): $\delta = -53.5$ (q, $J = 90$ Hz). IR (KBr): 2492 cm^{-1} (νBH).

Received: April 6, 1988 [Z 2695 IE]
German version: *Angew. Chem. 100* (1988) 1135

[1] H. Schmidbaur, *J. Organomet. Chem. 200* (1980) 287.
[2] G. Müller, U. Schubert, H. Schmidbaur, *Chem. Ber. 112* (1979) 3302.
[3] H. Schmidbaur, H.-J. Füller, G. Müller, A. Frank, U. Schubert, *Chem. Ber. 112* (1979) 1448.
[4] H. Schmidbaur, G. Müller, K. C. Dash, B. Milewski-Mahrla, *Chem. Ber. 114* (1981) 441.
[5] H. Schmidbaur, G. Müller, *Monatsh. Chem. 111* (1980) 1233.
[6] G. Müller, D. Neugebauer, W. Geike, F. H. Köhler, J. Pebler, H. Schmidbaur, *Organometallics 2* (1983) 257.
[7] H. Schmidbaur, E. Weiss, W. Graf, *Organometallics 4* (1985) 1233.
[8] H. Schmidbaur, S. Strunk, C. E. Zybill, *Chem. Ber. 116* (1983) 3559.
[9] Aldrich Chemical Co.
[10] H. Schmidbaur, E. Weiss, G. Müller, *Synth. React. Inorg. Met.-Org. Chem. 15* (1985) 401, 415.
[11] G. Müller, *Dissertation*, Technische Universität München 1980.
[12] **7a** · H_2O: $C_9H_{28}BBr_2P_3 \cdot H_2O$, $M_r = 417.88$; trigonal, space group $P\bar{3}$ (No. 143), $a = b = 15.834(1)$, $c = 6.583(1)$ Å, $Z = 3$, $\rho_{calcd} = 1.456$ g cm^{-3}, $\mu(Mo_{K\alpha}) = 44.5$ cm^{-1}, $T = 22$°C. 4586 unique reflections, 3218 "observed" with $F_0 \geq 4.0\sigma(F_0)$ ($+h$, $+k$, $\pm l$, $(\sin\theta/\lambda)_{max} = 0.659$ Å^{-1}, Enraf-Nonius CAD4, $Mo_{K\alpha}$ radiation, $\lambda = 0.71069$ Å). Lp and absorption correction, solution by Patterson methods (SHELXS-86); R (R_w) = 0.041 (0.031), $w = 1/\sigma^2(F_0)$ (anisotropic, CH_3 as rigid groups, H on B constant, SHELX-76). $\Delta\rho_{fin} = +0.85/-0.88$ e/Å^3 [15].
[13] H. Schmidbaur, W. Wolfsberger, *Synth. React. Inorg. Met.-Org. Chem. 4* (1974) 149.
[14] **11a**: $C_{11}H_{20}BBr_2P_3$, $M_r = 423.89$, orthorhombic, space group $P2_12_12_1$ (No. 19), $a = 9.280(1)$, $b = 14.954(2)$, $c = 12.915(2)$ Å, $Z = 4$, $\rho_{calcd} = 1.571$ g cm^{-3}, $\mu(Mo_{K\alpha}) = 47.2$ cm^{-1}, $T = -40$°C. 2766 unique reflections, 2380 "observed" with $F_0 \geq 4.0\sigma(F_0)$ ($+h$, $+k$, $\pm l$, $(\sin\theta/\lambda)_{max} = 0.572$ Å^{-1}, Syntex $P2_1$). Data correction and structure solution as for **7a** · H_2O [12]. R (R_w) = 0.061 (0.059), $w = 1/\sigma^2(F_0)$. $\Delta\rho_{fin} = +2.78/-1.40$ e/Å^3 [15].
[15] The absolute configuration of **7a** · H_2O and **11a** was confirmed by refinement of the inverse set of coordinates. Further details of the crystal structure investigation may be obtained from the Fachinformationszentrum Energie, Physik, Mathematik GmbH, D-7514 Eggenstein-Leopoldshafen 2 (FRG), on quoting the despository number CSD-53250, the names of the authors, and the journal citation.

From the Dilithiooctamethylcyclotetrasilazane to the 1,3,5,7-Tetraaza-2,4,6,8,9-pentasilabicyclo[3.3.1]nonane System**

By *Kerstin Dippel, Uwe Klingebiel,* Mathias Noltemeyer, Frank Pauer,* and *George M. Sheldrick*

Dedicated to Professor Ulrich Wannagat on the occasion of his 65th birthday

The ammonolysis of dichlorodimethylsilane leads to formation of the corresponding cyclotrisilazane **1a** and cyclotetrasilazane **1b**.[1-3]

$$n\,Me_2SiCl_2 + 3n\,NH_3 \longrightarrow (Me_2Si{-}NH)_n + 2n\,NH_4Cl$$

1a, n = 3
1b, n = 4

The reaction behavior of the six-membered ring compound **1a** has recently been the subject of intensive studies.[2] In contrast, no reactions of the eight-membered ring compound **1b** with retention of the ring moiety[4] have been reported since its first synthesis some forty years ago.[1] All attempts to carry out substitution reactions with **1b** have led to formation of isomeric six- and four-membered rings.[4]

Assuming that **1b** isomerizes according to the same rules as **1a**,[2,5] we prepared the dilithium compound **2**.[6] An X-ray structure analysis (single crystals grown from THF) provided information about the ring size and the site of second lithiation (Fig. 1).

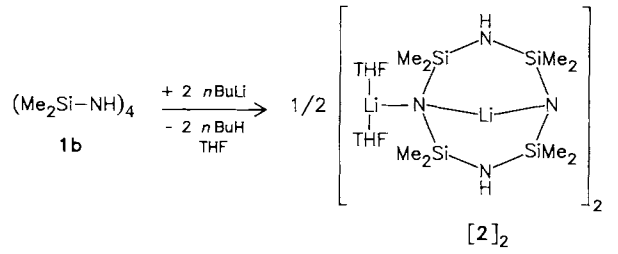

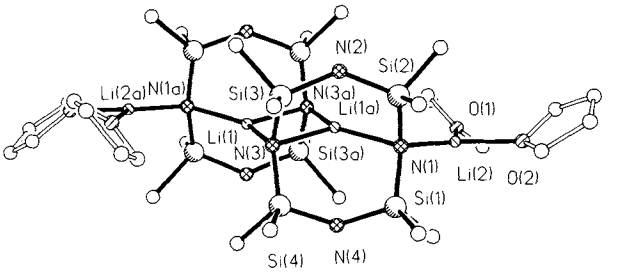

Fig. 1. Molecular structure of the dimer $[2]_2$ of **2** in the crystal (symmetry-independent atoms indicated); symmetry $\bar{1}$. Selected bond lengths [pm] and angles [°]: Si1-N1 168.3(3), N1-Si2 168.6(2), Si2-N2 174.1(2), N2-Si3 175.5(3), Si3-N3 168.7(2), N3-Si4 168.6(3), Si4-N4 174.4(2), N4-Si1 173.2(3), N1-Li2 195.0(6), N3-Li1 210.8(5), N3-Li1a 215.6(6), N1-Li1a 217.3(5), Li2-O1 192.5(5), Li2-O2 193.5(6); Si1-N1-Si2 135.6(1), Si2-N2-Si3 130.6(2), Si3-N3-Si4 130.3(1), Si4-N4-Si1 132.0(2), N1-Li1a-N3 144.7(3), N3-Li1-N3a 104.9(2), Li1-N3-Li1a 75.1(2).

2 crystallizes as the dimer $[2]_2$. The eight-membered rings are bound via a perpendicularly oriented planar, symmetrical $(LiN)_2$ four-membered ring. Li1 and Li1a are not, however, located over the centroids of the eight-membered rings: Li1a is nearer to N2 while Li1 is nearer to N2a; the distance is 241 pm in each case, whereas the distance between Li1a and N4 and between Li1 and N4a is 288 pm. Li1a and Li1 are each bound to two oppositely disposed N atoms of an eight-membered ring, namely with N1 and N3 and with N1a and N3a, respectively. The Li atoms of the four-membered ring are thus threefold coordinated. Li2 and Li2a are each coordinated to two THF molecules. The (H)N–Si bonds are systematically 5–7 pm longer than the (Li)N–Si bonds; this is consistent with ab initio calculations[7] on $(H_3Si)_2NH$ (Si–N calcd. 176 pm) and $(H_3Si)_2N^{\ominus}$ (Si–N calcd. 165 pm).

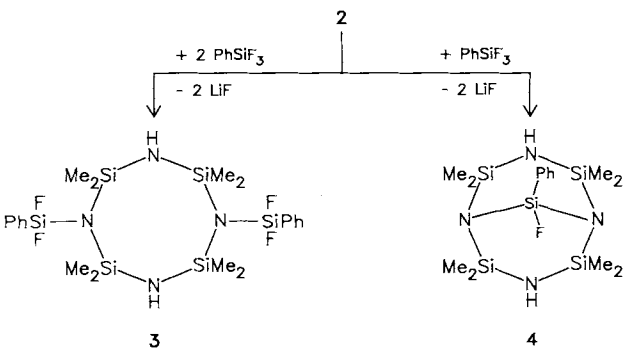

[*] Prof. Dr. U. Klingebiel, K. Dippel, Dr. M. Noltemeyer, F. Pauer, Prof. G. M. Sheldrick
Institut für Anorganische Chemie der Universität
Tammannstrasse 4, D-3400 Göttingen (FRG)

[**] This work was supported by the Deutsche Forschungsgemeinschaft and the Fonds der Chemischen Industrie.

2 reacts with fluorosilanes, e.g. with $F_3SiC_6H_5$, in the molar ratio 1 : 2 to give disubstituted ("monomeric") products containing an eight-membered ring.[8]

Reaction in the molar ratio 1 : 1 leads to a derivative **4** of the novel bicyclic system 1,3,5,7-tetraaza-2,4,6,8,9-pentasilabicyclo[3.3.1]nonane (Fig. 2).[9] The N2–N4–Si2–Si3 and N2–N4–Si4–Si1 planes of the two six-membered rings are inclined towards each other. N2, Si1, N1, Si4, and N4 are coplanar, whereas N3 of the second six-membered ring is bent towards the bridging atom Si5, so that N3, Si2, N4, Si5, N2, and Si3 form a tub-shaped moiety.

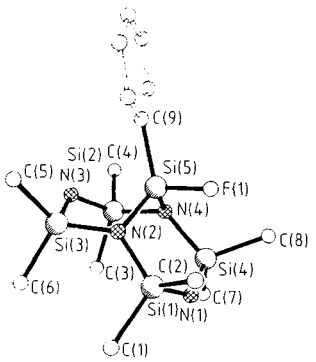

Fig. 2. Molecular structure of **3** in the crystal. Selected bond lengths [pm] and angles [°]: N1-Si1 174.7(15), Si1-N2 173.5(7), N2-Si3 175.3(7), Si3-N3 172.8(13), N3-Si2 172.8(7), Si2-N4 174.3(5), N4-Si4 175.8(8), Si4-N1 171.8(16), N2-Si5 173.2(13), Si5-N4 172.4(12), Si5-F1 160.4(5); Si1-N1-Si4 133.9(5), Si2-N3-Si3 127.1(5), Si1-N2-Si3 131.2(5), Si1-N2-Si5 111.5(6), Si3-N2-Si5 107.5(4), Si2-N4-Si4 126.4(5), Si2-N4-Si5 108.9(6), Si4-N4-Si5 110.8(4), N2-Si5-N4 106.1(5).

Experimental

A solution of **1b** (0.01 mol) in hexane (100 mL) was treated with 0.02 mol of nC_4H_9Li (15% in hexane) in a three-necked flask fitted with an internal thermometer. For complete cleavage of butane, the sludge was heated under reflux for 2 h. THF was then added until the lithium salt dissolved at the boiling temperature. **2** crystallized out at room temperature. For the synthesis of **3** and **4** the solution of **2** was cooled to −20°C. After slow dropwise addition of 0.02 mol and 0.01 mol of $PhSiF_3$, respectively, the solutions were warmed to room temperature for 2 h (^{19}F-NMR monitoring). After removal of lithium fluoride, **3** and **4** crystallized out from the solutions: yields 4.5 g (92%) **2**, 4.8 g (84%) **3**, 2.6 g (63%) **4**.

Received: March 7, 1988;
revised: April 13, 1988 [Z 2651 IE]
German version: *Angew. Chem. 100* (1988) 1093

[1] S. D. Brewer, C. P. Haber, *J. Am. Chem. Soc. 70* (1948) 3888.
[2] U. Klingebiel, *Nachr. Chem. Tech. Lab. 35* (1987) 1042.
[3] J. Haiduc, D. B. Sowerby: *The Chemistry of Inorganic Homo- and Heterocycles*, Academic Press, London 1987.
[4] W. Fink, *Helv. Chim. Acta 52* (1969) 2261.
[5] W. Clegg, U. Klingebiel, G. M. Sheldrick, L. Skoda, N. Vater, *Z. Naturforsch. B35* (1980) 1503. For the disubstitution, **1a** is best dilithiated beforehand. Partial contraction of the six-membered ring is observed in the stepwise disubstitution.
[6] **2**: m.p. 130°C; ^{13}C NMR (THF, C_6D_6): $\delta = 6.58$, 9.17 (coalescence at +50°C, $\delta = 7.62$); ^{29}Si NMR (THF, C_6D_6): $\delta = -21.19$; space group $P\bar{1}$, $a = 1089.6(2)$, $b = 1115.1(2)$, $c = 1241.1(1)$ pm, $\alpha = 79.02(1)$, $\beta = 64.10(1)$, $\gamma = 81.65(1)°$, $Z = 2$ (the two molecules form a dimer $[\mathbf{2}]_2$ via an inversion center). 2878 independent reflections with $F > 3\sigma(F)$ and $2\theta_{max} = 45°$, measured at −80°C with $Mo_{K\alpha}$ radiation, $R = 0.046$ [10].
[7] C. Glidewell, C. Thomson, J. Comput. Chem. 3 (1982) 495.
[8] **3**: m.p. 125°C, MS (70 eV): *m/z* 561 (100, $[M-CH_3]^{\oplus}$), ^{1}H NMR (CH_2Cl_2, TMS int.): $\delta = 0.25$ ($^5J_{HF} = 1.0$ Hz, CH_3), 7.35, 7.68 (C_6H_5); ^{13}C NMR (CH_2Cl_2, C_6D_6, TMS int.): $\delta = 4.93$ ($^4J_{CF} = 1.9$ Hz, SiC_2), 128.54, 130.94 ($^2J_{CF} = 28.4$ Hz), 131.71, 134.57 ($^3J_{CF} = 1.2$ Hz, C_6H_5); ^{19}F NMR (CH_2Cl_2, C_6F_6 int.): $\delta = 36.6$; ^{29}Si NMR (CH_2Cl_2, C_6D_6, TMS int.): $\delta = -47.42$ ($J_{SiF} = 268.8$ Hz, SiPh), −5.72 ($SiMe_2$).
[9] **4**: m.p. 150°C, MS (FI measurement): *m/z* 414 (100, $M^{\oplus}$); ^{1}H NMR (C_6D_6, TMS int.): $\delta = 0.020$, 0.022, 0.223, 0.225, 0.284, 0.286 (6 CH_3), 0.470 ($^5J_{HF} = 3.2$ Hz, CH_3), 0.472 ($^5J_{HF} = 3.2$ Hz, CH_3), 7.5 (C_6H_5); ^{13}C NMR (C_6D_6, TMS int.): $\delta = 4.09$, 6.34 (C-3, C-4, C-5, C-6), 6.46 ($^4J_{CF} = 6.1$ Hz, C-2, C-8), 7.83 ($^4J_{CF} = 1.0$ Hz, C-1, C-7), 127.64, 129.86, 134.31 ($^3J_{CF} = 2.1$ Hz), 137.94 ($^2J_{CF} = 25.0$ Hz, C_6H_5); ^{29}Si NMR ($CDCl_3$, TMS int.): $\delta = -31.91$ ($J_{SiF} = 263.7$ Hz, Si-5), −3.00 ($^3J_{SiF} = 4.7$ Hz, Si-1, Si-4), −1.65 ($^3J_{SiF} = 1.7$ Hz, Si-2, Si-3); space group *Pc*, $a = 909.6(2)$, $b = 1110.1(2)$, $c = 1659.8(3)$ pm, $\beta = 137.96(2)°$, $Z = 2$, 1033 independent reflections with $F > 3\sigma(F)$ and $2\theta_{max} = 45°$ (+21°C, $Mo_{K\alpha}$), $R = 0.060$ [10].
[10] Further details of the crystal structure investigations are available on request from the Fachinformationszentrum Energie, Physik, Mathematik GmbH, D-7514 Eggenstein-Leopoldshafen 2 (FRG), on quoting the depository number CSD-52963, the names of the authors, and the journal citation.

Azirineimine as a Structural Unit in the Side Chain of a Hexofuranose**

By *Wolfgang Meyer zu Reckendorf** and *Norbert Schultz*

A series of theoretical papers on the origin of life in the universe consider reactions of hydrogen cyanide and its derivatives. Azirineimine is discussed as a possible stable intermediate in the formation of peptides from hydrogen cyanide.[1] We obtained a derivative of this previously unknown compound in a completely surprising way.

All previous attempts to lengthen the chain of carbohydrates or to synthesize branched-chain compounds by reaction of sulfonic acid esters with cyanides have failed because the nucleophilicity of the cyanide ion is too low. Only *Grewe* and *Rockstroh*[2] were able to synthesize a D-glucose-6-carbonitrile from 1,2-*O*-isopropylidene-6-*O*-*p*-toluenesulfonyl-α-D-glucofuranose and KCN. However, since this reaction proceeds via the 5,6-epoxide and therefore does not seem to be applicable to compounds without neighboring hydroxy groups, we chose 1,2-*O*-isopropylidene-3,5,6-tri-*O*-*p*-toluenesulfonyl-α-D-glucofuranose **1**[3] for experiments to investigate the reaction capability of the sulfonic acid esters in more detail. Upon reaction of **1** with KCN and tetrabutylammonium chloride in nitromethane/water under phase-transfer conditions[4] (2 d at 50°C) and subsequent chromatographic separation we obtained—besides some unchanged starting material, the hydrolysis product **3**, and difficultly isolable byproducts—a crystalline compound of the composition $C_{26}H_{29}N_3O_{11}S_2$ as the main product (15%), which proved to be the azirineimine derivative **2**.

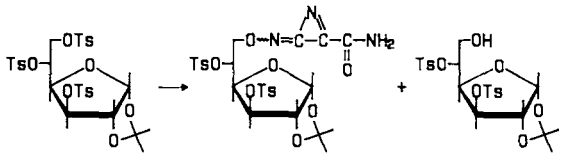

Ts = *p*-toluenesulfonyl.

[*] Prof. Dr. W. Meyer zu Reckendorf, Apotheker N. Schultz
Institut für Pharmazeutische Chemie der Universität
Hittorfstrasse 58-62, D-4400 Münster (FRG)

[**] We thank Dr. *I. Lauterwein*, Organisch-chemisches Institut der Universität Münster (FRG), for invaluable assistance in interpreting the nuclear resonance spectra; we thank the NMR-department for carrying out the measurements.

Table 1. Selected analytical and spectroscopic data of the new compounds **2**, **2a**, **2b**, **4**, **4a**, **4b**, **5**, **6**, **6a**, 7, 7a, **8**, and **8a**. All the compounds listed were characterized by combustion analysis. The ^{1}H-NMR spectra were recorded at 300 MHz, the ^{15}N-NMR spectra at 36.5 MHz, and the ^{13}C-NMR spectra at 75.46 MHz (**4**, **4a**, **4b**, **6**, 7a, **8**) and 90.56 MHz (**2**, **2a**, **2b**, **5**, **6a**, 7).

2: yield 15% (based on reacted **1**).—m.p. 130–131 °C.—$[\alpha]_D^{20} = +13.8$ ($c = 0.2$ in $CHCl_3$).—^{1}H-NMR ($CDCl_3$): $\delta = 6.4$ (s, N*H*H'), 7.28 (s, NH*H'*).—^{13}C-NMR ($CDCl_3$): $\delta = 156.1$ (s, *C*CONH$_2$), 133.5 (s, *C*CONH$_2$), 112.3 (s, *C*CONH$_2$).—^{15}N-NMR ($CDCl_3$, Standard: NH_3): $\delta = 407.7$, 259.4, 105.0.—MS (CI/NH_3): *m/z* [%]: 641 (41, $[M+NH_4]^{\oplus}$), 546 (100, $[M+NH_4-C_3H_2N_3O+1]^{\oplus}$).—MS (FD): *m/z* [%]: 623 (100, $M^{\oplus}$)

2a: yield 15% (based on reacted **1**).—m.p. 130–131 °C.—^{1}H-NMR ($CDCl_3$): $\delta = 6.3$ (dd, ^{15}N*H*H'), 7.28 (dd, ^{15}NH*H'*); $^1J_{^{15}N/H} = 89.6$ Hz, $^1J_{^{15}N/H'} = 93.0$ Hz, $^2J_{H/H'} = 2.1$ Hz.—^{13}C-NMR ($CDCl_3$): $\delta = 155.9$ (d, CCCO^{15}NH$_2$), 132.7 (d, CCCO^{15}NH$_2$), 111.8 (s, *C*CCO^{15}NH$_2$); $^1J_{^{15}N/C} = 18.3$ Hz, $^2J_{^{15}N/C} = 9.5$ Hz.—^{15}N-NMR ($CDCl_3$): $\delta = 102$ (dd, ^{15}NH$_2$): $^1J_{^{15}N/H} = 89.6$ Hz, $^1J_{^{15}N/H'} = 93.0$ Hz.—MS (CI/NH_3): *m/z* [%]: 642 (20, $[M+NH_4]^{\oplus}$)

2b: yield 0.5% (referred to $^{13}CH_3NO_2$).—m.p. 130–131 °C.—^{13}C-NMR ($CDCl_3$): $\delta = 156.0$ (dd, ^{13}C^{13}*C*CONH$_2$), 132.8 (dd + D, ^{13}C^{13}*C*CONH$_2$), 111.7 (dd + D, ^{13}*C*^{13}CCONH$_2$), 76.6 (d, C-6); $^1J_{^{13}C\text{-}3'/C\text{-amide}} = 63.2$ Hz, $^2J_{^{13}C\text{-}2'/C\text{-amide}} = 6.1$ Hz, $^1J_{^{13}C\text{-}2'/^{13}C\text{-}3'} = 100.8$ Hz, $^3J_{^{13}C\text{-}2'/C\text{-}6} = 5.5$ Hz.—MS (CI/NH_3): *m/z* [%]: 643 (50, $[M+NH_4]^{\oplus}$)

4: yield 1.5% (based on reacted **1**), 70% (from **2** in acetone/sodium hydrogencarbonate/water), 50% (from **2** in sodium methoxide at 37 °C), 46% (from **2** in sodium methoxide at 50 °C), 0.7% (on work-up of **6**), 63% (from **6** in sodium methoxide).—m.p. 180–182 °C.—$[\alpha]_D^{20} = +78.1$ ($c = 0.2$ in $CHCl_3$).—^{1}H-NMR ($CDCl_3$): $\delta = 5.65$ (s, N*H*H'), 6.99 (s, NH*H'*).—^{13}C-NMR ($CDCl_3$): $\delta = 158.5$ (s, *C*CONH$_2$), 127.2 (s, *C*CONH$_2$), 106.8 (s, *C*CONH$_2$).—MS (CI/NH_3): *m/z* [%]: 641 (100, $[M+NH_4]^{\oplus}$), 546 (32, $[M+NH_4-C_3H_2N_3O+1]^{\oplus}$).—MS (FD): *m/z* [%]: 623 [100, $M^{\oplus}$]

4a: yield 1.5% (based on reacted **1**), 47% (from **2a** in sodium methoxide at 50 °C), 2% (on work-up of **6a**).—m.p. 180–182 °C.—^{1}H-NMR ($CDCl_3$): $\delta = 5.65$ (dd, ^{15}N*H*H'), 6.99 (dd, ^{15}NH*H'*); $^1J_{^{15}N/H} = 90.2$ Hz, $^1J_{^{15}N/H'} = 92.7$ Hz, $^2J_{H/H'} = 1.8$ Hz.—^{13}C-NMR ($CDCl_3$): $\delta = 158.4$ (d, CCCO^{15}NH$_2$), 127.3 (d, CCCO^{15}NH$_2$), 106.8 (s, CCCO^{15}NH$_2$); $^1J_{^{15}N/C} = 19.6$ Hz, $^2J_{^{15}N/C} = 9.8$ Hz.—MS (CI/NH_3): *m/z* [%]: 642 (100, $[M+NH_4]^{\oplus}$)

4b: yield 27% (1:9 mixture of **4b** and **4**).—^{13}C-NMR ($CDCl_3$): $\delta = 158.3$ (dd, ^{13}C^{13}*C*CONH$_2$), 127.3 (D, ^{13}C^{13}*C*CONH$_2$), 106.8 (D, ^{13}*C*^{13}CCONH$_2$); $^1J_{^{13}C\text{-}3'/C\text{-amide}} = 77.6$ Hz, $^2J_{^{13}C\text{-}2'/C\text{-amide}} = 5.7$ Hz, $^1J_{^{13}C\text{-}2'/^{13}C\text{-}3'} = 86.7$ Hz

5: yield 5%.—m.p. 196–198 °C.—^{1}H-NMR ([D$_6$]acetone): $\delta = 4.27$ (m, 3-H), 4.38 (m, 3-H'), 5.13 (m, 2-H), 7.1 (s, N*H*H'), 7.3 (d, 1 H, arom. H), 7.47 (d, 1 H, arom. H), 7.6 (s, NH*H'*), 8.29 (dd, dd, 2 H, arom. H), 8.95 (d, d, 2 H, arom. H), 9.09 (m, N*H*CH$_2$), 9.25 (d, N'*H*CH); $^3J_{2\text{-}H/3\text{-}H} = 6.3$ Hz, $^3J_{2\text{-}H/3\text{-}H'} = 5.5$ Hz, $^2J_{3\text{-}H/3\text{-}H'} = 14.4$ Hz, $^3J_{2\text{-}H/NH\text{-}C\text{-}2} = 7.24$ Hz, $^3J_{3\text{-}H/NH\text{-}C\text{-}3} = 6.22$ Hz, $^3J_{3\text{-}H'/NH\text{-}C\text{-}3} = 6.07$ Hz.—^{13}C-NMR ([D$_6$]acetone): $\delta = 170.7$ (s, CCCONH$_2$), 149.2 (s, arom. C), 148.0 (s, arom. C), 137.2 (s, arom. C), 136.9 (s, arom. C), 132.1 (s, arom. C), 131.8 (s, arom. C), 130.6 (d, 2 C, arom. C), 124.1 (s, 2 C, arom. C), 115.8 (d, 2 C, arom. C), 56.2 (s, C-2), 45.7 (s, C-3).—MS (CI/NH_3): *m/z* [%]: 453 (4, $[M+NH_4]^{\oplus}$)

6: yield 20% (at 37 °C), 4.5% (at 50 °C).—amorph.—$[\alpha]_D^{20} = +58.8$ ($c = 0.09$ in $CHCl_3$).—^{1}H-NMR ($CDCl_3$): $\delta = 3.82$ (s, OCH$_3$), 5.50 (s, N*H*H'), 6.91 (s, NH*H'*), 7.41 (s, =NH, superposed by arom. H).—^{13}C-NMR ($CDCl_3$): $\delta = 161.8$ (s, CCCONH$_2$), 159.1 (s, *C*CCONH$_2$), 145.5 (s, CCCONH$_2$), 53.1 (s, OCH$_3$).—MS (FD): *m/z* [%]: 655 (100, $M^{\oplus}$)

6a: yield 8% (at 50 °C).—^{1}H-NMR ($CDCl_3$): $\delta = 5.4$ (dd, ^{15}N*H*H'), 6.99 (dd, ^{15}NH*H'*), 7.41 (s, =NH); $^1J_{^{15}N/H} = 89.5$ Hz, $^1J_{^{15}N/H'} = 92.3$ Hz, $^2J_{H/H'} = 2.0$ Hz.—^{13}C-NMR ($CDCl_3$): $\delta = 161.5$ (d, CCCO^{15}NH$_2$), 159.0 (s, CCCO^{15}NH$_2$), 145.3 (d, CCCO^{15}NH$_2$); $^1J_{^{15}N/C} = 19.4$ Hz, $^2J_{^{15}N/C} = 8.3$ Hz.—MS (CI/NH_3): *m/z* [%]: 671 (15, $[M+NH_4-3]^{\oplus}$), 657 (100, $[M+NH_4-CH_3(OCH_3)-H_2(^{15}NH_2)]^{\oplus}$), 642 (70, $[M+NH_4-OCH_3-H(=NH)]^{\oplus}$)

7: yield up to 10% (variable).—m.p. 133–134 °C.—$[\alpha]_D^{20} = +23.9$ ($c = 0.34$ in $CHCl_3$).—^{1}H-NMR ($CDCl_3$): $\delta = 5.50$ (s, NH), 5.87 (s, N*H*H'), 6.65 (s, NH*H'*), 7.10 (s, =NH).—^{13}C-NMR ($CDCl_3$): $\delta = 161.7$ (s, *C*CONH$_2$), 160.7 (s, CCCONH$_2$), 146.3 (s, CCCONH$_2$, together with C–Tosyl).—MS (CI/NH_3): *m/z* [%]: 659 (1, $[M+NH_4]^{\oplus}$), 546 (40, $[M+NH_4-C_3H_4N_3O_2+1]^{\oplus}$).—MS (FD): *m/z* [%]: 641 (100, $M^{\oplus}$)

7a: yield 24%.—m.p. 133–134 °C.—^{1}H-NMR ($CDCl_3$): $\delta = 5.9$ (s, NH), 6.25 (d, ^{15}N*H*H'), 6.65 (d, ^{15}NH*H'*), 7.1 (s, =NH); $^1J_{^{15}N/H} = 88.3$ Hz, $^1J_{^{15}N/H'} = 91.1$ Hz.—^{13}C-NMR ($CDCl_3$): $\delta = 161.9$ (s, *C*CCO^{15}NH$_2$), 160.9 (d, CCCO^{15}NH$_2$), 146.5 (d, CCCO^{15}NH$_2$); $^1J_{^{15}N/C} = 17.2$ Hz, $^2J_{^{15}N/C} = 7.8$ Hz.—MS (CI/NH_3): *m/z* [%]: 660 (1, $[M+NH_4]^{\oplus}$), 643 (100, $[M+NH_4-=NH-H_2(^{15}NH_2)]^{\oplus}$), 546 (40, $[M+NH_4-C_3H_4{}^{15}NN_2O_2+1]^{\oplus}$)

8: yield 7%.—amorph.—$[\alpha]_D^{20} = +6.1$ ($c = 1.0$ in $CHCl_3$).—^{1}H-NMR ($CDCl_3$): $\delta = 3.91$ (s, OCH$_3$), 6.17 (s, N*H*H'), 6.80 (s, NH*H'*).—^{13}C-NMR ($CDCl_3$): $\delta = 160.9$, 160.6 (each s, 2 C, C-amide and C-side chain), 146.5 (s, C-side chain), 53.1 (s, OCH$_3$).—MS (FD): *m/z* [%]: 656 (100, $M^{\oplus}$)

8a: yield 1%.—^{1}H-NMR ($CDCl_3$): $\delta = 5.7$ (d, ^{15}N*H*H'; d, 1 H, 1-H), 6.7 (d, ^{15}NH*H'*); $^1J_{^{15}N/H} = 88.2$ Hz, $^1J_{^{15}N/H'} = 92.7$ Hz.—MS (CI/NH_3): *m/z* [%]: 675 (30, $[M+NH_4]^{\oplus}$), 658 (90, $[M+NH_4-CH_3(OCH_3)-H_2(^{15}NH_2)]^{\oplus}$)

The coupling of the new side chain to C-6 followed from the catalytic hydrogenation of **2** (Pd/carbon/MeOH, 10 h), which led to **3**, and from the NMR spectroscopic data (see Table 1). Isotope labeling experiments afforded unequivocal proof of the structure. Contrary to expectation, in the synthesis with KC^{15}N a product was formed whose molecular weight was greater by only one mass unit. The ^{1}H-NMR spectrum of the compound **2a** shows the two H/^{15}N couplings characteristic for amide groups, which are confirmed in the ^{15}N-NMR spectrum, as well as the H/H' coupling which is not visible in the proton spectrum of the unlabeled substance **2**.[6] The ^{13}C-NMR spectrum, as already known from that of [^{15}N]acetamide,[7] shows a ^{13}C/^{15}N coupling with the amide carbon atom and a ^{13}C/^{15}N coupling with the neighboring C-atom. The structure of the remaining [CN$_2$] group was still unclear at this point.

The product **2b**, which is obtained by synthesis with $^{13}CH_3NO_2$ and KCN, has a molecular weight increased by two mass units. Two C-atoms characterized by two very intense signals in the ^{13}C-NMR spectrum mutually couple with the unusually large coupling constant of $^1J_{^{13}C/^{13}C} = 100.8$ Hz. Accordingly, they form a chain together with the amide carbon. The absorption at relatively high field is thus due to the azirine.

To obtain chemical proof of the structure we investigated the catalytic hydrogenation of **2** in more detail and, after reaction with 1-fluoro-2,4-dinitrobenzene (FDNB), were able to isolate 2,3-bis(2,4-dinitrophenylamino)propionic acid amide **5** in 5% yield.

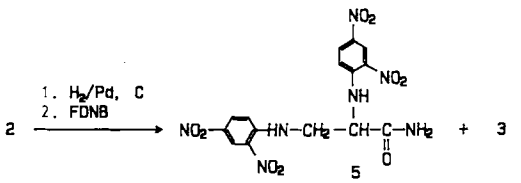

When **2** was allowed to react with $NaHCO_3$ in acetone, the isomeric compound **4** was formed in 70% yield. This substance, which is also present in small amounts in the nitromethane-water reaction mixture, differs markedly from **2** in the chromatogram as well as in its melting point and its optical rotation. Since the IR, ^{1}H-NMR and ^{13}C-NMR data (including the couplings of the ^{15}N nucleus with the investigated nuclei) as well as the mass spectra and elemental analyses of **2** and **4** agree in all essential points, these two compounds can be distinguished only with respect to the geometry of the exocyclic nitrogen atom. Although only slightly deviating values are found in the spectra of the ^{13}C-enriched substances, **2b** and **4b**, both for the couplings of the two C atoms of the azirine ring as well as for the coupling of these atoms to the amide C atom, they nevertheless prove that the two C atoms form a chain with the amide carbon also in the case of **4**. Such isomeric structures have already been reported in the literature.[8]

On attempting to open the azirine ring of the compound **2** with 0.015 M sodium methoxide solution, the geometric isomer **4** was formed once again as the main product after 2 days (37 °C). A significantly stronger polar product with a molecular weight increased by 32 mass units and showing a signal for the methoxy group in the ^{1}H- and ^{13}C-NMR spectra proved to be the methanol addition product **6**.

Two substances were formed on layer-chromatographic work-up of **6**. One had an even lower, the other a considerably higher relative migration rate than **6**. The latter turned out to be the isomer **4** formed by elimination of methanol, which could also be obtained from **6** directly by reaction with methoxide.

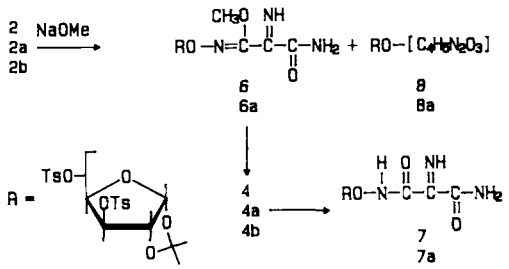

The compound with the smallest R_f value has a molecular weight 18 mass units higher than that of **2**. According to the analytical and spectroscopic data this compound is the hydrolysis product **7**, which is clearly recognizable in the ^{1}H-NMR spectrum of the $CO^{15}NH_2$-labeled substance.

On strongly heating **2** in a sodium methoxide solution the reaction time is reduced to about 1 h, but a further by-product **8** is formed which is only slightly less polar than the starting compound **2**. It has a molecular weight of only one mass unit higher than **6**, and the elemental analysis indicates hydrolysis of the imine function. The structure of **8** has not yet been elucidated.

$^{\ominus}O-N=CH-CH=NO_2^{\ominus}$ **9**

The mechanism of formation of the azirineimine is still unclear. In the first step, nitromethane could form the condensation product **9**;[9] how **9** reacts with KCN, however, remains a matter of speculation.

Received: March 10, 1988 [Z 2657 IE]
German version: *Angew. Chem. 100* (1988) 1094

[1] a) J. H. Clemmons, P. G. Jasien, C. E. Dykstra, *Mol. Phys. 48* (1983) 631; b) B. Bak, O. J. Nielsen, H. Svanholt, *Chem. Phys. Lett. 59* (1978) 330; c) M. Cignitti, M. L. Tosato, *Bioelectrochem. Bioenerg. 4* (1977) 98; d) W. Yang, R. Minard, C. Matthews, *J. Theor. Biol. 56* (1976) 111; e) J. B. Moffat, *J. Chem. Soc. Chem. Commun. 1975*, 888; f) W. Yang, *Diss. Abstr. Int. B 35* (1974) 745; *Chem. Abstr. 81* (1974) 169820a; g) W. Yang, R. D. Minard, C. N. Matthews, *J. Chem. Soc. Chem. Commun. 1973*, 435.
[2] R. Grewe, G. Rockstroh, *Chem. Ber. 86* (1953) 536.
[3] W. P. Shyluk, J. Honeyman, T. E. Timell, *Can. J. Chem. 33* (1955) 1202.
[4] a) Nissan Chemical Industries, Jpn. Kokai Tokkyo JP 5936653 [84,36,653] (Cl.C07C121/66), February 28, 1984, Appl. 82/146,420, August 24, 1982; *Chem. Abstr. 101* (1984) P6855h; b) F. Devinsky, I. Lacko, L. Krasnec, R. Kurillova, Czech. Pat. CS 214154 (Cl.C07C121/16), February 15, 1985, Appl. 80/4,678, July 1, 1980; *Chem. Abstr. 103* (1985) P22179n.
[5] M. Miljkovic, D. Miljkovic, A. Jokic, V. Andrejevic, E. A. Davidson, *J. Org. Chem. 37* (1972) 2536.
[6] B. Sunners, L. Piette, W. G. Schneider, *Can. J. Chem. 38* (1960) 681.
[7] G. C. Levy, R. L. Lichter: *Nitrogen-15 Nuclear Magnetic Resonance Spectroscopy*, Wiley, New York 1979, pp. 120, 126.
[8] H. Quast, E. Schmitt, *Angew. Chem. 82* (1970) 395; *Angew. Chem. Int. Ed. Engl. 9* (1970) 381.
[9] D. Seebach, E. W. Colvin, F. Lehr, T. Weller, *Chimia 33* (1979) 1.

Intramolecularly Stabilized Organogallium Compounds**

By *Herbert Schumann,* Uwe Hartmann, Andreas Dietrich,* and *Joachim Pickardt*

Organometallic compounds are gaining increasing importance in the production of thin films and epitactic layers. Thus, for example, both trimethylgallium as well as its less sensitive adducts with amines and other bases are used for the gas-phase separation of gallium arsenide.[1] In our studies in this area we have prepared the interesting new intramolecularly base-stabilized organogallium compounds **1**–**4** by reaction of dimethylgallium chloride with 3-dimethylamino- or 3-diethylaminopropyllithium,[2] of methylgallium dichloride with 3,3′-methyliminobis(propylmagnesium chloride) or of gallium trichloride with 3,3′,3″-nitrilotris(propylmagnesium chloride).[3]

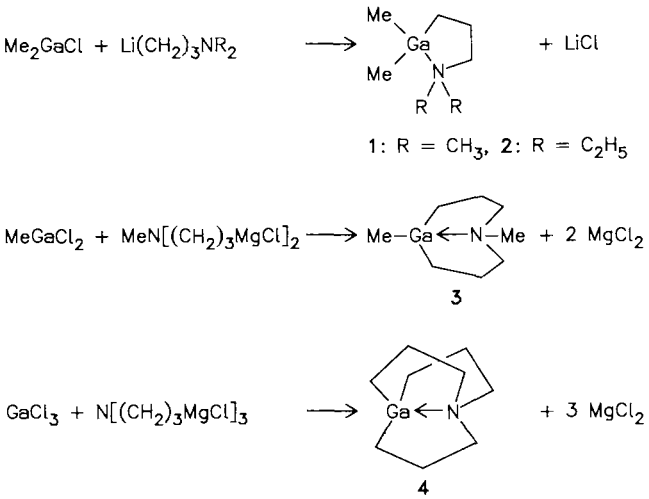

Compounds **1**–**4** are colorless solids which are only slowly attacked by atmospheric oxygen. They are very soluble in ethers and in aliphatic and aromatic hydrocarbons. **1** melts without decomposition at 49 °C under a vapor pressure of 230 Pa. It boils at 192 °C at normal pressure and can be sublimed under vacuum at room temperature; at 270 °C it decomposes with separation of gallium. **2** melts at 43–45 °C. **3** already melts at 34 °C and is just as stable as **1**.[4]

The X-ray structure analysis of **4** shows that the gallium atom is surrounded trigonal-monopyramidally by three CH_2 groups and the amine nitrogen (Fig. 1).[5] The GaC_3 moiety is trigonal planar with angles of 120° at the gallium. The electron deficiency of the metal atom is balanced by the intramolecular coordinative bonding of the nitrogen atom situated at the apex of the pyramid (Ga–N distance 209.5(2) pm). The Ga–N distance lies between that in **5** (197.9(3) pm)[6] and that in the pure donor–acceptor complex **6** (220(3) pm)[7] and, due to the ring strain in the molecular frame-work, is somewhat longer than the sum of the covalent radii of Ga and N (195 pm).

[*] Prof. Dr. H. Schumann, Dipl.-Chem. U. Hartmann, MSc. A. Dietrich, Prof. Dr. J. Pickardt
Institut für Anorganische und Analytische Chemie der Technischen Universität
Strasse des 17. Juni 135, D-1000 Berlin 12

[**] This work was supported by the Fonds der Chemischen Industrie and E. Merck AG, Darmstadt (FRG).

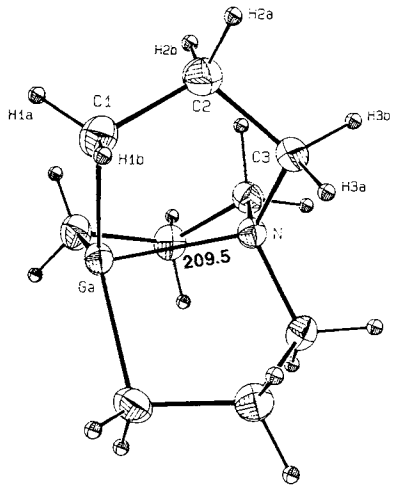

Fig. 1. Crystal structure of 4. Selected bond lengths [pm] and angles [°] (standard deviations in parentheses): Ga-Cl 199.8(2), Ga-N 209.5(2), C1-C2 153.9(2), C2-C3 153.0(2), C3-N 148.6(2); C1-Ga-N 89.2(1), C3-N-Ga 105.2(1), C1-Ga-C1′ 120.0, C3-N-C3′ 113.3(2).

Since the distance of the gallium atom from the nitrogen atom of the neighboring molecule is 409 pm, and an additional intermolecular donor–acceptor interaction can be ruled out, the gallium on this coordinatively unprotected underside of the pyramid should be prone to nucleophilic attack. In the triorganogallium-amine complexes free of steric strain that have so far been investigated X-ray crystallographically, the gallium is coordinated in a distorted tetrahedral fashion with C-Ga-C angles of 116.7° in **6**,[7] 116.6(3)° in **7**[8] and 115.9(4)° in [$Me_3Ga\cdot$(urotropine)].[9] The Ga-C distances (199.8(2) pm) are in good agreement with those in **6** (199.8(4)[7]) and **7** (199(1)[8]).

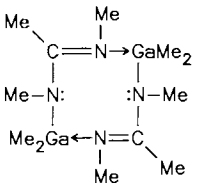

5

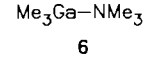

6

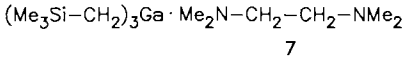

7

Experimental

1: A suspension of $Li(CH_2)_3NMe_2$ (1.5 g, 16 mmol) in pentane (15 mL) was treated dropwise at −78°C in the course of 15 min with a solution of 2.16 g (16 mmol) of Me_2GaCl in 15 mL of pentane. After thawing and 24 hours' stirring at 20°C, the mixture was allowed to stand and the clear solution decanted off. After removal of the solvent the residue was sublimed in a vacuum. Yield 2.1 g (71%). ^{1}H-NMR (C_6D_6, 25°C): $\delta = -0.16$ (s, 6H, $(H_3C)_2Ga$), 0.57 (t, 2H, $-CH_2Ga$, $^3J = 7.01$ Hz), 1.70 (tt, 2H, $-CH_2-$, $^{3,3}J = 7.01$, 6.31 Hz), 1.86 (s, 6H, $(H_3C)_2N$), 1.98 (t, 2H, $-CH_2N$, $^3J = 6.31$ Hz); ^{13}C-NMR (C_6D_6, 25°C): $\delta = -6.15$ (s, $(H_3C)_2Ga$), 9.33 (s, $-CH_2Ga$), 24.35 (s, $-CH_2-$), 45.87 (s, $(H_3C)_2N$), 63.96 (s, $-CH_2N$).

4: The Grignard reagent obtained from 4.9 g (20 mmol) of $N[(CH_2)_3Cl]_3$ and 1.6 g (66 mmol) of Mg in 60 mL of THF and 3.5 g (20 mmol) of $GaCl_3$, dissolved in 60 mL of THF, were added dropwise and synchronously over 3 h into 350 mL of toluene at 60°C. The mixture was then heated under reflux for 2 h, ca. 250 mL of the solvent removed by distillation, and the $MgCl_2$ that separated out was filtered off over a frit. The solution was evaporated to dryness. Sublimation of the residue at 40-60°C under vacuum furnished 0.92 g (22%) of colorless needles of **4**. M.p. 54°C. ^{1}H NMR (C_6D_6, 25°C): $\delta = 0.59$ (t, 6H, $-CH_2Ga$, $^3J = 6.34$ Hz), 1.76 (tt, 6H, $-CH_2-$, $^{3,3}J = 6.34$, 5.72 Hz), 2.14 (t, 6H, $-CH_2N$, $^3J = 5.72$ Hz); ^{13}C NMR (C_6D_6, 25°C): $\delta = 9.84$ (s, $-CH_2Ga$), 26.50 (s, $-CH_2-$), 57.02 (s, $-CH_2N$).

Received: March 16, 1988 [Z 2666 IE]
German version: *Angew. Chem. 100* (1988) 1119

[1] J. P. Mullin, S. J. C. Irvine, R. H. Moss, P. N. Robson, D. R. Wight (Eds.): *Proc. 2nd Int. Conf. Metalorg. Vapor Phase Epitaxy*, Sheffield (England) 1984; *J. Cryst. Growth 68* (1984) 1-790; G. B. Stringfeld (Ed.): *Proc. 3rd Int. Conf. Metalorg. Vapor Phase Epitaxy*, Universal City, CA (USA) 1986; *J. Cryst. Growth 77* (1986) 1-652.

[2] K. H. Thiele, E. Langguth, G. E. Müller, *Z. Anorg. Allg. Chem. 462* (1980) 152.

[3] K. Jurkschat, A. Tzschach, *J. Organomet. Chem. 272* (1984) C 13.

[4] Preliminary gas-phase-epitaxy investigations showed that **1**–**4** are suitable as gallium-containing starting materials for the generation of epitactic gallium arsenide layers.—E. Pohl (E. Merck GmbH, Darmstadt), private communication.

[5] **4**: rhombohedral crystals, space group $R3c$, $a = 787.7(1)$ pm, $\alpha = 95.099(5)°$, $V = 4.826 \times 10^8$ pm^3, $Z = 2$, $\rho_{calcd} = 1.44$ g cm^{-3}. Enraf-Nonius CAD-4 diffractometer, data collection at −134(5)°C, $Mo_{K\alpha}$ radiation, graphite monochromator, $\omega/2\theta$ scans, Lorentz and polarization correction, empirical absorption correction ($\mu = 26.96$ cm^{-1}). The structure was solved by Patterson methods. 1121 independent structure factors; $R = 0.027$, $R_w = 0.024$. Further details of the crystal structure investigation are available on request from the Fachinformationszentrum Energie, Physik, Mathematik GmbH, D-7514 Eggenstein-Leopoldshafen 2 (FRG), on quoting the depository number CSD-53203, the names of the authors, and the journal citation.

[6] H. D. Hausen, F. Gerstner, W. Schwarz, *J. Organomet. Chem. 145* (1978) 277.

[7] L. M. Golubinskaya, A. V. Golubinskii, V. S. Mastryukov, L. V. Vilkov, V. I. Bregadze, *J. Organomet. Chem. 117* (1976) C 4.

[8] R. B. Hallock, W. E. Hunter, J. L. Atwood, O. T. Beachley, *Organometallics 4* (1985) 547.

[9] H. Krause, K. Sille, H. D. Hausen, J. Weidlein, *J. Organomet. Chem. 235* (1982) 253.

Tris(thioxanthen-9-ylidene)cyclopropane, and Its Radical Cation and Dication**

By *Toyonari Sugimoto, Yohji Misaki, Tohru Kajita, Toshio Nagatomi, Zen-ichi Yoshida,** and *Jun Yamauchi**

[3]Radialene (trimethylenecyclopropane), a hydrocarbon composed of a three-membered carbocycle and three exocyclic double bonds, can possess one pair of degenerate highest occupied molecular orbitals (HOMOs) if one assumes it to have C_3 symmetry or higher. Introduction of electron-donating groups into the exocyclic double bonds raises the energy of the HOMOs, and makes the [3]radialene more oxidizable. If the resulting dication has a triplet ground state, the molecule could serve as donor component for the production of donor-acceptor type organic ferromagnets,[1] which are currently attracting a great deal of interest. Indeed, tris(diaminomethylene)cyclopropane has already been proposed by *Miller*, *Epstein* et al. as a promising donor.[2] In spite of much interest in the electron-donating [3]radialenes, to our knowledge there has so far been no report on their synthesis.[3] In this paper we wish to report the first synthesis of **1**, an oxidizable [3]radialene with three electron-donating thioxanthenylidene

[*] Prof. Dr. Z. Yoshida, Dr. T. Sugimoto, Y. Misaki, T. Kajita, T. Nagatomi
Department of Synthetic Chemistry, Kyoto University
Yoshida, Kyoto 606 (Japan)
Dr. J. Yamauchi
College of Liberal Arts and Science, Kyoto University
Yoshida, Kyoto 606 (Japan)

[**] This work was supported by The Ministry of Education, Science and Culture, Japan (Grant No. 62604004).

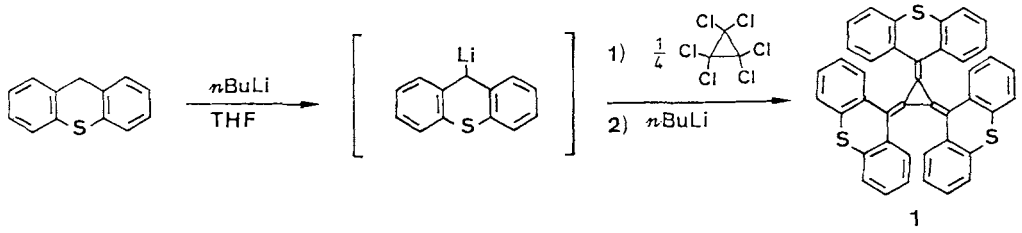

Scheme 1.

groups, and the characterization of its radical cation $\mathbf{1}^{\odot\oplus}$ and dication $\mathbf{1}^{2\oplus}$ by ESR spectroscopy.

A THF solution of thioxanthene[4] was treated with an equimolar amount of *n*-BuLi (1.6 M hexane solution) at −70°C. The resultant dark red solution of lithium thioxanthenide was treated with 1/4 molar equivalent of hexachlorocyclopropane[5] and then with an equimolar amount of *n*-BuLi (Scheme 1). The reaction mixture was stirred for 30 min at −70°C and then warmed to room temperature. After purification of the reaction mixture by column chromatography (silica gel; dichloromethane/hexane (1:4)), and then recrystallization from dichloromethane/acetone/methanol, **1** was obtained as blue crystals (m.p. 269–270°C) in 21% yield.[6] The electronic spectrum of **1** in CH_2Cl_2 showed four absorption maxima at $\lambda = 252$ ($\log\varepsilon = 4.72$), 328 (4.10), 392 (3.48) and 600 nm (4.48).[7] The ^{13}C-NMR spectrum in $CDCl_3$ showed eight signals at $\delta = 116.6$, 119.9, 124.8, 125.1, 127.1, 130.4, 132.7 and 134.9,[8] suggesting that **1** has approximately C_3 symmetry in solution. The cyclic voltammogram of **1** measured in dichloromethane[9] was composed of two pairs of reversible waves at +0.67 and +0.80 V vs. Ag/AgCl, each of which corresponds to a one-electron transfer process.[10] On the other hand, in PhCN solvent only one irreversible wave involving simultaneous transfer of two electrons, was observed at +0.70 V.

By electrochemical oxidation at constant potential, or more conveniently by chemical oxidation with $Tl(CF_3CO_2)_3$, $\mathbf{1}^{\odot\oplus}$ and $\mathbf{1}^{2\oplus}$ were generated or isolated, and characterized by ESR spectroscopy. The degassed CH_2Cl_2 solution of **1** in contact with excess $Tl(CF_3CO_2)_3$ at −78°C showed only a 600-nm absorption band due to **1** itself. At ca. −40°C the band gradually decreased and a new 536-nm band due to $\mathbf{1}^{\odot\oplus}$ increased. On raising the temperature further to −10 to 0°C the 536-nm band rapidly vanished and another new 630-nm band due to $\mathbf{1}^{2\oplus}$ appeared, which was not subject to change in the temperature range. The temperature-dependent formation of $\mathbf{1}^{\odot\oplus}$ and $\mathbf{1}^{2\oplus}$ was also monitored ESR spectroscopically. The first observed ESR spectrum of $\mathbf{1}^{\odot\oplus}$ was composed of quintet lines with ca. 0.23 mT splitting at a relatively large *g* value ($g_{iso} = 2.00638$).[11] On the other hand, for $\mathbf{1}^{2\oplus}$ one sharp ESR signal with a linewidth of 0.40 mT appeared at $g = 2.00414$ whose intensity decreased with lowering temperature (−30 to −100°C) in frozen 1,2,3-trichloropropane,[12] thus suggesting the possibility that $\mathbf{1}^{2\oplus}$ is a thermally accessible triplet. To substantiate this conjecture, isolation of $\mathbf{1}^{2\oplus}$ was attempted, and the $CF_3CO_2^{\ominus}$ salt ($\mathbf{1}^{2\oplus}\cdot 2CF_3CO_2^{\ominus}$) was successfully obtained as a dark blue solid (m.p. 65–66°C).[13] This solid exhibited one slightly broad (linewidth = 0.55 mT) ESR signal with $g = 2.00353$ at 25°C. At −196°C the spectrum exhibited fine structure together with simultaneous appearance of a half-field resonance signal at 164.8 mT (see Fig. 1). From analysis of the spectrum, D, one of the zero-field splitting parameters,

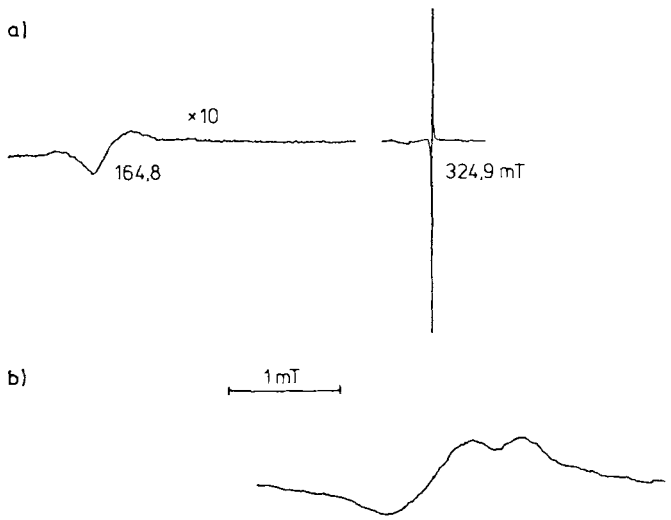

Fig. 1. ESR spectrum of $\mathbf{1}^{2\oplus}\cdot 2CF_3CO_2^{\ominus}$ at −196°C. a) The complete spectrum (the half-field resonance ($\Delta m_s = \pm 2$) signal was measured with tenfold amplification). b) The width-expansion of the central signal at 324.9 mT.

was determined to be ca. 0.7 mT. This very small value strongly suggests that the two unpaired electrons are far removed from each other and probably are located on the three thioxanthenylidene groups. From the similar temperature-dependence of the central broad signal to that of the frozen solution experiment, it was shown that the ground state of $\mathbf{1}^{2\oplus}$ is certainly a singlet and the triplet state lies only 0.07 eV higher in energy.

As is discussed for pentaarylcyclopentadienyl cations, whose ground state is a singlet with a triplet lying 0.002–0.04 eV higher,[14] it seems to be likely also for $\mathbf{1}^{2\oplus}$ that the singlet is favored because the large π electron system decreases electron correlation and the complex structure allows easy symmetry-lowering distortion. However, by choosing appropriate electron-donating substituents other than thioxanthenylidene, a ground state triplet might be produced for dicationic species of the new [3]radialenes.

Received: April 7, 1988 [Z 2697 IE]
German version: *Angew. Chem. 100* (1988) 1129

[1] a) H. M. McConnel, *Proc. Robert A. Welch Found. Conf. Chem. Res. 11* (1967) 144; b) R. Breslow, *Pure Appl. Chem. 54* (1982) 927.

[2] a) J. S. Miller, A. J. Epstein, *J. Am. Chem. Soc. 109* (1987) 3850; b) J. S. Miller, A. J. Epstein, W. M. Reiff, *Chem. Rev. 88* (1988) 201; c) *Science (Washington) 240* (1988) 40; d) *Acc. Chem. Res. 21* (1988) 114.

[3] On the other hand, the unsubstituted and hexamethyl-substituted [3]radialenes, and the derivatives substituted with strong electron-withdrawing hexacyano, tris(2,6-di-*tert*-butyl-4-oxocyclohexadienylidene), and tris(fluorenylidene) groups have already been synthesized: a) A. T. Blomquist, D. T. Longone, *J. Am. Chem. Soc. 81* (1959) 2012; b) E. A. Dorko, *ibid. 87* (1965) 5518; c) G. Köbrich, H. Heinemann, *Angew. Chem. 77* (1965) 590; *Angew. Chem. Int. Ed. Engl. 4* (1965) 594; d) P. A. Waitkus, E. B. Sanders, L. I. Peterson, G. W. Griffin, *J. Am. Chem. Soc.*

89 (1967) 6318; e) R. West, D. C. Zecher, *ibid. 89* (1967) 152; f) T. Fukunaga, *ibid. 98* (1976) 610; g) M. Iyoda, H. Ohtani, M. Oda, *Symp. Org. Chem. Struct. 1985*, Abstract p. 115-117.
[4] A. Mustafa, M. K. Hilmy, *J. Chem. Soc.* (1952) 1343.
[5] S. W. Tobey, R. West, *J. Am. Chem. Soc. 86* (1964) 56.
[6] The mass spectrometric and elemental analysis of **1** gave satisfactory results.
[7] The UV/VIS absorption spectra of tris(2,6-di-*tert*-butyl-4-oxocyclohexadienylidene)- and tris(fluorenylidene)cyclopropanes also revealed absorptions extending into the long wavelength region of 600-800 nm.
[8] The two signals at $\delta = 116.6$ and 119.9 were assigned to the two exocyclic carbons of the three-membered ring.
[9] Cyclovoltammetry in dichloromethane or benzonitrile containing 0.1 M $(n\text{Bu})_4\text{NClO}_4$ as supporting electrolyte, platinum working electrode and counter electrode, and standard Ag/AgCl reference electrode (scan rate: 50 mV/s).
[10] The number of transferred electrons in each step was determined from the dependence of the peak currents on sample concentrations (A. J. Bard, L. R. Faulkner, *Electrochemical Methods: Fundamentals and Applications*; Wiley: New York, 1980, p. 218).
[11] A detailed analysis of the spectrum will be reported elsewhere.
[12] $\mathbf{1}^{2\oplus}$ could also be prepared in 1,2,3-trichloropropane (m.p. -14°C) at -10 to 0°C. Immediately thereafter the solution was frozen.
[13] Although the salt isolated was expected to be pure it gradually decomposed. Consequently, the purity of the salt used in the ESR measurement was not checked by magnetic susceptibility measurements but by the ESR counting method using a stable radical TMPOL (2,2,6,6-tetramethylpiperidin-4-ol-1-oxyl) as a standard. The purity was estimated to be >90%. The error inherent in this method was of the order of about ten percent. On the other hand, we could not isolate the pure $CF_3CO_2^{\ominus}$ salt of $\mathbf{1}^{\odot\oplus}$; it was always contaminated with the salt of $\mathbf{1}^{2\oplus}$.
[14] a) R. Breslow, H. W. Chang, W. A. Yager, *J. Am. Chem. Soc. 85* (1963) 2033; b) R. Breslow, H. W. Chang, R. Hill, E. Wasserman, *ibid. 89* (1967) 1112; c) W. Broser, H. Kurreck, P. Siegle, *Chem. Ber. 100* (1967) 788.

Tris(fluoren-9-ylidene)cyclopropane, a Novel [3]Radialene

By *Masahiko Iyoda,* Hiroyuki Otani,* and *Masaji Oda*

Dedicated to Professor Emanuel Vogel on the occasion of his 60th birthday

Radialenes (polymethylenecycloalkanes) have received considerable attention from both theorists and experimentalists,[1] because they display a particular arrangement of π-electrons and because they can serve as electron donors and acceptors.[2] However, the synthetic methodology for access to these molecules is still very limited and many compounds containing the radialene framework have not yet been synthesized.

We recently reported a novel method for preparing the radialenes **3** by cyclooligomerization of the ate-type complexes **2**, which were obtained from **1**.[3] We report here on

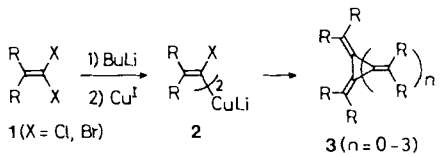

the synthesis and properties of tris(fluoren-9-ylidene)cyclopropane **6** by cyclotrimerization of the ate-type complex **5**, which was obtained from 9-(dibromomethylene)-fluorene **4**.

Reactions of the known metal methylidenecarbenoids were reported to give only dimerized butatrienes like **7** or their metal complexes via coupling of the corresponding carbenoids and/or carbenes.[4] However, reaction of the ate-type complex generated from lithium carbenoid with an appropriate copper(I) complex proceeds formally as a cyclooligomerization of the carbene center.

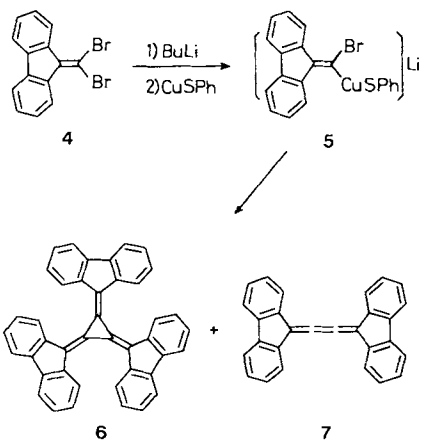

Thus, treatment of **4** with one equivalent of butyllithium (THF, below -90°C), followed by addition of one equivalent of copper(I) phenylthiolate[5] furnished the mixed cuprate **5**. When the solution was allowed to warm to ambient temperature and stirred for 24 h, the desired [3]radialene **6**[6] was obtained in 22% yield, together with the butatriene **7** in 58% yield.[7] With 0.5 equivalents of $CuI \cdot PBu_3$ or $CuBr \cdot SMe_2$ as the Cu^{I} complex, the [3]radialene **6** was formed in 2-3% yield, together with **7** (76-85%); with CuCN, however, the main product was **7** with only trace amounts of **6**.

The reaction of the ate-type complex, derived from **4**, with $CuI \cdot PBu_3$ in the presence of **7** gave the [3]radialene **6** in 3% yield, and no improvement in the yield of **6** was observed. Therefore, addition of the methylidenecarbene to **7** can be ruled out for the formation of **6**. Although the structure and the state of aggregation of the ate-type complex are still uncertain, trimerization of the complex **5** plays an important role in the formation of **6**. Interestingly, neither [4]- nor [5]radialenes were isolated in this reaction, and a steric factor may contribute to oligomerization of carbenoids. In agreement with this steric effect, the copper carbenoid derived from 1,1-dibromo-2-methylpropene forms the corresponding [4]- and [5]radialenes,[3b] and the copper carbenoid derived from 1,1-dibromo-2,2-diphenylethylene results in the formation of octaphenyl[4]radialene.[3a]

The [3]radialene **6** thus obtained is very stable and crystallizes from hexane/dichloromethane in the form of reddish-black crystals with metallic luster, which show no melting point up to 300°C. The electronic spectrum shows a broad, strong absorption tailing at 800 nm, corresponding to the deep-blue color in solution. The ^{1}H- and ^{13}C-NMR spectra reflect its highly symmetrical structure, although molecular models show that **6** cannot have a planar structure with D_{3h}-symmetry. We suggest a propeller-like structure with D_3-symmetry, in analogy with the twisted conformation of 9,9′-bifluorenylidene.[8]

The ethylene, butadiene and butatriene derivatives **8**, **9** and **7**, respectively, can be readily reduced with alkali metals to give stable dianions.[9] Therefore, **6** can be expected to form the dianion **10** by electrochemical reduction. Cy-

[*] Prof. Dr. M. Iyoda, Dr. H. Otani, Prof. Dr. M. Oda
Department of Chemistry, Faculty of Science, Osaka University
Toyonaka, Osaka 560 (Japan)

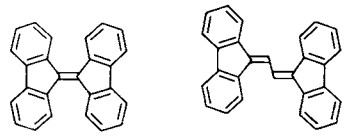

8 9

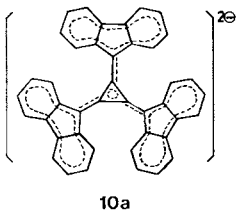

10a

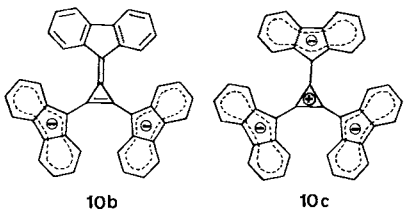

10b 10c

clovoltammetry of **6** displays two reversible one-electron reduction steps, shown in Figure 1. Under analogous con-

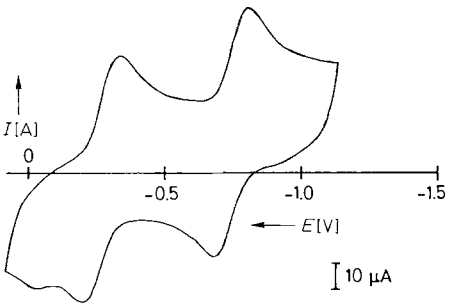

Fig. 1. Cyclovoltammogram of **6**. $c = 3.8 \times 10^{-4}$ M, *N,N*-dimethylformamide/0.1 M tetrabutylammonium perchlorate vs Ag/AgCl reference electrode [12]; scan rate 244 mVs^{-1}.

ditions, compounds **7**, **8**[10] and **9** show similar stepwise, reversible reduction to the corresponding dianions (Table 1). A remarkable feature of these reduction potentials is

Table 1. First and second reduction potentials ($E^1_{1/2}$ and $E^2_{1/2}$) of **6**–**9** [a].

	$E^1_{1/2}$ [V]	$E^2_{1/2}$ [V]	$E^1_{1/2} - E^2_{1/2}$
6	−0.27	−0.75	0.48
7	−0.73	−1.15	0.42
8	−0.92	−1.44	0.52
9	−1.06	−1.39	0.33

[a] The potentials were measured under the conditions given in the caption to Figure 1.

the fact that the $E^1_{1/2}$ and $E^2_{1/2}$ values of **6** are much more positive than those of **7**, **8** and **9**. The dianion of **6** should exist in the delocalized form **10a** but can be formulated as the structure **10b** like calicene.[11] The contribution of the cyclopropenium structure **10c** may therefore explain the extremely low reduction potentials of **6**.

Received: April 18, 1988 [Z 2707 IE]
German version: *Angew. Chem. 100* (1988) 1131

[1] M. J. S. Dewar, G. J. Gleicher, *J. Am. Chem. Soc. 87* (1965) 692; B. A. Hess, Jr., L. J. Schaad, *ibid. 93* (1971) 305; J. Aihara, *ibid. 98* (1976) 2750; A. T. Blomquist, D. T. Longone, *ibid. 81* (1959) 2012; E. A. Dorko, *ibid. 87* (1965) 5518; P. A. Waitkus, E. B. Sanders, L. I. Peterson, G. W. Griffin, *ibid. 89* (1967) 6818; T. Bally, E. Haselbach, Z. Lanyiova, P. Baertschi, *Helv. Chim. Acta 61* (1978) 2488.

[2] R. Breslow, *Pure Appl. Chem. 54* (1982) 927; *Mol. Cryst. Liq. Cryst. 125* (1985) 261; T. J. LePage, R. Breslow, *J. Am. Chem. Soc. 109* (1987) 6412; J. S. Miller, A. J. Epstein, *ibid. 109* (1987) 3850; T. Sugimoto, Y. Misaki, T. Kajita, Z. Yoshida, T. Kai, N. Kasai, *ibid. 109* (1987) 4106, and references cited therein; J. S. Miller, A. J. Epstein, W. M. Reiff, *Science (Washington) 204* (1988) 40; see also T. Sugimoto, Y. Misaki, T. Kajita, T. Nagatomi, Z. Yoshida, J. Yamauchi, *Angew. Chem. 100* (1988) 1129; *Angew. Chem. Int. Ed. Engl. 27* (1988) 1078.

[3] a) M. Iyoda, H. Otani, M. Oda, Y. Kai, Y. Baba, N. Kasai, *J. Am. Chem. Soc. 108* (1986) 5371; b) *J. Chem. Soc. Chem. Commun. 1986*, 1794.

[4] W. Kirmse: *Carbene Chemistry, Vol. 1*, Academic, New York 1964, p. 67; G. Köbrich, *Angew. Chem. 77* (1965) 75; *Angew. Chem. Int. Ed. Engl. 4* (1965) 49.

[5] G. H. Posner, D. J. Brunelle, L. Sinoway, *Synthesis 1974*, 662.

[6] **6**: FD-MS: *m/z* 528 ($M^{\oplus}$); ^{1}H-NMR (500 MHz, $CDCl_3$): $\delta = 7.22$ (t, $J = 7.3$ Hz, 6H, H-3,6), 7.28 (d, $J = 7.3$ Hz, 6H, H-4,5), 7.42 (t, $J = 7.3$ Hz, 6H; H-2,7), 7.88 (d, $J = 7.3$ Hz, 6H, H-1,8); ^{13}C-NMR (125 MHz, $CDCl_3$): $\delta = 118.11$ (s, C-9), 120.39 (d, C-4,5), 124.45 (s, C-10), 126.88 (d, C-1,8), 128.33 (d, C-2,7 or C-3,6), 128.76 (d, C-3,6 or C-2,7), 138.44 (s, C-4a,4b), 140.84 (s, C-8a,9a); UV/VIS (CH_2Cl_2): λ_{max} (log ε) = 250 (4.97), 285 sh (4.63), 383 (4.07), 420 (4.04), 550 sh (4.16), 618 (4.59), 675 nm (4.72); IR (KBr): $\tilde{\nu} = 3030$, 2903, 1604, 1595, 1537, 1468, 1444, 1432, 1356, 1308, 1220, 1145, 1093, 1030, 996, 940, 770, 726, 705, 610 cm^{-1}; Raman (KBr): $\tilde{\nu} = 1754$, 1737 cm^{-1}.

[7] Under the conditions described here, the reproducibility of the yields of **6** and **7** was invariably poor. In other cases, the [3]radialene **6** was obtained in 5% yield.

[8] N. A. Bailey, S. E. Hull, *J. Chem. Soc. Chem. Commun. 1971*, 960; *Acta Crystallogr. Sect. B 34* (1978) 3289.

[9] R. H. Cox, *J. Magn. Reson. 3* (1970) 223; M. Walzak, G. D. Stucky, *J. Organomet. Chem. 97* (1975) 313; Y. Cohen, J. Klein, M. Rabinovitz, *J. Chem. Soc. Chem. Commun. 1986*, 1071; J. M. Edinger, A. R. Day, *J. Org. Chem. 36* (1971) 240.

[10] D. H. Evans, R. W. Busch, *J. Am. Chem. Soc. 104* (1982) 5057.

[11] W. M. Jones, R. S. Pyron, *J. Am. Chem. Soc. 87* (1965) 1608.

[12] Under analogous conditions of measurement, the oxidation potential of ferrocene was found to be $E_{ox} = +0.61$ V.

Is Tetrasilatetrahedrane Kinetically Stable?**

By *Shigeru Nagase** and *Mari Nakano*

Tetrahedrane (C_4H_4) has long counted among the fascinating synthetic targets, largely because of its chemical significance, high strain, and aesthetic appeal.[1] Considerable interest is currently directed toward the preparation and characterization of the silicon analogues of polycyclic carbon compounds.[2]

Clabo and *Schaefer* have recently calculated that tetrasilatetrahedrane **1** is a local minimum on the Si_4H_4 potential energy surface and is an interesting synthetic target.[3] The local minimum T_d structure of **1** is also claimed in a very recent study by *Sax* and *Kalcher*.[4] *Schoeller* et al. have indicated that the fusion of rings is unfavorable in carbon compounds but advantageous in silicon compounds such as **1**.[5] However, none of these studies has dealt with the kinetic stability of the silicon analogues.

By way of contrast, we have shown[6] that polycyclic silicon compounds having only fused three-membered rings

[*] Prof. Dr. S. Nagase, M. Nakano
Department of Chemistry, Faculty of Education
Yokohama National University, Yokohama 240 (Japan)

[**] This work was supported in part by a grant from the Ministry of Education, Science, and Culture in Japan. Calculations were carried out at the Computer Center of the Institute of Molecular Science and the Computer Room of the Faculty of Education of Yokohama National University.

are highly strained[6a,7] and subject to "bond stretch" isomerism[6b,c,8] because of relatively weak Si–Si bonds (compared with C–C bonds).[9] Ab initio calculations[10] now show that **1** isomerizes almost without a barrier, contrary to general expectation.[3-5,11]

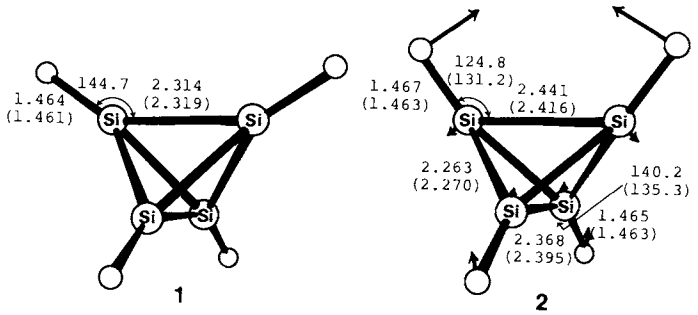

Fig. 1. Bond lengths [Å] and angles [°] of the HF/6-31G(d) and HF/6-31G(2d,p) optimized structures of **1**(T_d) and **2**(C_{2v}). HF/6-31G(2d,p) values are in parentheses. The arrows in **2** indicate the displacement vector of the reaction coordinate (the normal coordinate with an imaginary frequency) at the transition state.

Figure 1 shows the structure of **1** and a transition structure (**2**) of C_{2v} symmetry[12] (characterized by one single imaginary frequency of $325i$ cm^{-1} (a_1)) for its isomerization located at the Hartree-Fock (HF) level with the split-valence d-polarized 6-31G(d) basis set.[10] Unlike the carbon counterparts,[13] **1** and **2** are very similar. Reflecting this "early" transition state, the barrier for the isomerization of **1** is only 1.6 kcal mol^{-1}, as shown in Table 1.

Table 1. Relative Energies [kcal mol^{-1}] of **1**–**4** at various levels.

Method	**1**(T_d) [a]	**2**(C_{2v})	**3**(D_{2d})	**4**(D_{2h})
HF/6-31G(d)	0.0	1.6	−11.3	−4.2
HF/6-31G(2d,p)	0.0	0.4		
HF/6-31G(2df,p) [b]	0.0	0.4		
MP2/6-31G(d) [c]	0.0	−2.3	−39.4	−5.7
MP3/6-31G(d) [c]	0.0	−1.5	−33.5	−7.4
CI/6-31G(d) [c]	0.0	−0.4	−23.6	−4.8
CI/6-31G(d) [c, d]	0.0	−1.3	−33.4	−7.9

[a] The total energies of **1** are −1157.82123 (HF/6-31G(d)), −1157.84191 (HF/6-31G(2d,p)), −1157.85291 (HF/6-31G(2df,p)), −1158.14814 (MP2), −1158.18784 (MP3), −1158.13951 (CI), and −1158.20174 (CI) [d]. [b] Using HF/6-31G(2d,p) optimized geometries. [c] Using HF/6-31G(d) optimized geometries. [d] Values after size-consistency correction due to unlinked clusters (see Ref. [15b]).

Further inclusion of a set of d-type polarization functions on Si and a set of p-type polarization functions on H (i.e., 6-31G(2d,p) basis) brings **2** nearer to **1** and lowers the HF/6-31G(d) barrier to 0.4 kcal mol^{-1}. This barrier height was not changed at the HF level by further inclusion of a set of f-type polarization functions on Si (see HF/6-31G(2df,p) in Table 1). A zero-point correction made with the HF/6-31G(d) harmonic vibration frequencies yields a height of 0.6 kcal mol^{-1} for the classical barrier. This indicates that **1** is very unstable towards isomerization despite the fact that the lowest frequency of **1** is relatively high (277 (e) cm^{-1} at the HF/6-31G(d) level).

To confirm the findings at the HF level, the so-called HF instability problem was checked for **1** and **2** according to the procedure proposed by *Seeger* and *Pople*.[14] All positive eigenvalues of the instability matrices calculated at the HF/6-31G(d) level suggest that both **1** and **2** can be well described in the HF single-determinant treatment. Thus, the effect of electron correlation was imcorporated by means of Møller-Plesset (MP) perturbation theory up to third-order and configuration interaction (CI) calculations with all single and double excitations from the HF single-determinant in the core-frozen approximation.[15] As summarized in Table 1, electron correlation gives a lower energy for **2** than for **1** at all levels of theory.[16] This suggests that most probably **1** cannot be a minimum energy structure and, hence, is not synthesized and isolated.

Along a symmetry-allowed path, **1** collapses via **2** to a D_{2d} puckered ring structure (**3**) with all the hydrogens in axial positions.[17] As Figure 2 shows, the minimum D_{2d}

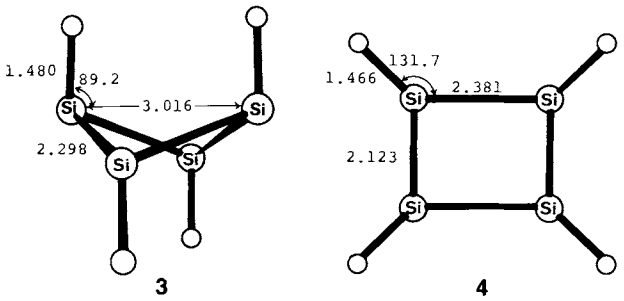

Fig. 2. Bond lengths [Å] and angles [°] of the HF/6-31G(d) optimized structures of **3**(D_{2d}) and **4**(D_{2h}).

structure can be viewed as a "two-bond stretch" isomer and is ca. 33 kcal mol^{-1} more stable than **1**, as shown in Table 1.[18] On the other hand, the symmetry-forbidden rearrangement of **1** to tetrasilacyclobutadiene **4** is ca. 8 kcal mol^{-1} exothermic. However, it should be noted that **4** has two imaginary frequencies and is not a minimum in the planar D_{2h} form.[3,4] We found that **4** leads to a nonplanar C_s structure with one axial hydrogen and three equatorial hydrogens (being 24.8 kcal mol^{-1} more stable than **1** at the CI/6-31G(d) level after size-consistency correction[15b]), as calculated very recently by *Schaefer* et al.[19]

In conclusion, the tetrahedral Si_4H_4 is unlikely to be a local minimum on the potential energy surface, in sharp contrast with the tetrahedral C_4H_4. However, it may be an interesting challenge to find out whether a proper substituent can stabilize the tetrasilatetrahedrane framework.

Received: March 23, 1988;
revised: May 13, 1988 [Z 2674 IE]
German version: *Angew. Chem. 100* (1988) 1098

[1] For reviews, see a) A. Greenberg, J. F. Liebman: *Strained Organic Molecules*, Academic Press, New York 1978; b) N. S. Zefirov, A. S. Koz'min, A. V. Abramenkov, *Russ. Chem. Rev. (Engl. Transl.) 47* (1978) 163; c) G. Maier, *Angew. Chem. 100* (1988) 317; *Angew. Chem. Int. Ed. Engl. 27* (1988) 309.

[2] For the synthesis and characterization of bicyclic silicon compounds, see S. Masamune, Y. Kabe, S. Collins, D. J. Williams, R. Jones, *J. Am. Chem. Soc. 107* (1985) 5552; R. Jones, D. J. Williams, Y. Kabe, S. Masamune, *Angew. Chem. 98* (1986) 176; *Angew. Chem. Int. Ed. Engl. 25* (1986) 173; H. Matsumoto, H. Miyamoto, N. Kojima, Y. Nagai, *J. Chem. Soc. Chem. Commun. 1987*, 1316; H. Matsumoto, H. Miyamoto, N. Kojima, Y. Nagai, M. Goto, *Chem. Lett. 1988*, 629.

[3] D. A. Clabo Jr., H. F. Schaefer III, *J. Am. Chem. Soc. 108* (1986) 4344.

[4] A. F. Sax, J. Kalcher, *J. Chem. Soc. Chem. Commun. 1987*, 809.

[5] W. W. Schoeller, T. Dabisch, T. Busch, *Inorg. Chem. 26* (1987) 4383; T. Dabisch, W. W. Schoeller, *J. Chem. Soc. Chem. Commun. 1986*, 896.

[6] a) S. Nagase, M. Nakano, T. Kudo, *J. Chem. Soc. Chem. Commun. 1987*, 60; b) S. Nagase, T. Kudo, *Organometallics 6* (1987) 2456; c) *J. Chem. Soc. Chem. Commun. 1988*, 54.

[7] The strain energy is as large as 141 kcal mol^{-1} in **1** [6a]. In contrast, silicon compounds consisting of four-membered rings possess consider-

ably smaller strain energies: for example, octasilacubane (being 94 kcal mol^{-1} strained) is 65 kcal mol^{-1} less strained than cubane and forms an interesting synthetic target [6a].

[8] See also P. von R. Schleyer, A. F. Sax, J. Kalcher, R. Janoschek, *Angew. Chem. 99* (1987) 374; *Angew. Chem. Int. Ed. Engl. 26* (1987) 364; P. von R. Schleyer, R. Janoschek, *Angew. Chem. 99* (1987) 1312; *Angew. Chem. Int. Ed. Engl. 26* (1987) 1267; Ref. [5].

[9] Si-Si bonds are ca. 14 kcal mol^{-1} weaker than C-C bonds: R. Walsh, *Acc. Chem. Res. 14* (1981) 246.

[10] The program used is GAUSSIAN 82 developed by *J. S. Binkley, M. J. Frisch, D. J. DeFrees, K. Rahgavachari, R. A. Whiteside, H. B. Schlegel, E. M. Fludre, J. A. Pople*, Department of Chemistry, Carnegie-Mellon University, Pittsburgh, USA. For the basis sets employed, see M. M. Francl, W. J. Pietro, W. J. Hehre, J. S. Binkley, M. S. Gordon, D. J. DeFrees, J. A. Pople, *J. Chem. Phys. 77* (1982) 3654; M. J. Frisch, J. A. Pople, J. S. Binkley, *ibid. 80* (1984) 3265.

[11] For example, see p. 90 in Ref. [1a].

[12] We also located a stationary point for a structure with D_{2d} symmetry which corresponds to the simultaneous breaking of two Si-Si bonds. This stationary point (with two Si-Si bonds stretched to 2.612 Å) was only 3.7 kcal mol^{-1} less stable than **2** at the HF/6-31G(d) level but had two imaginary frequencies; one of these frequencies was associated with distortion to **2**.

[13] H. Kollmar, F. Carrion, M. J. S. Dewar, R. C. Bingham, *J. Am. Chem. Soc. 103* (1981) 5292, and references cited therein.

[14] a) R. Seeger, J. A. Pople, *J. Chem. Phys. 66* (1977) 3045; b) for the current topics of the HF instability problem, see J. Paldus, J. Cizek, *Can. J. Chem. 63* (1985) 1803, and references cited therein.

[15] a) For MP, see J. A. Pople, J. S. Binkley, R. Seeger, *Int. J. Quantum Chem. Symp. 10* (1976) 1; b) for CI, see J. A. Pople, R. Seeger, R. Krishnan, *ibid. 11* (1977) 149.

[16] In order to check the effect of electron correlation on the geometry optimization, the structure of **1** was reoptimized at the MP2 level with the 6-31G(d) basis set. However, the resultant MP2 optimized structure (Si-Si = 2.316 and Si-H = 1.478 Å) differed little from the corresponding HF optimized structure (Si-Si = 2.314 and Si-H = 1.464 Å) and its MP2 energy (−1158.14842 au) was 2.1 kcal mol^{-1} higher than the MP2 energy of **2** calculated even on the HF/6-31G(d) optimized structure of **2**.

[17] An equatorial arrangement of the hydrogens results in a less stable minimum D_2 structure which correlates in symmetry with **4** in Figure 2. On the other hand, a C_{2v} transition structure results by arranging two hydrogens in equatorial positions and two other hydrogens in axial positions, which leads to a C_s structure as described in the text. However, it should be noted that the rearrangements of **3** to the D_2 and C_{2v} structures are both symmetry forbidden.

[18] The stability analyses of **3** and **4** show that the HF solutions (being singlet stable but non-singlet unstable [14b]) are unstable with respect to the spin density wave (SDW) solutions. This suggests that the four-membered rings of **3** and **4** have some tetraradical character (antiferromagnetic electron-spin localization onto each Si) and more sophisticated treatments of electron correlation may be essential for their relative energies. For some hexaradical character and puckering of the six-membered ring in hexasilabenzene, see S. Nagase, H. Teramae, T. Kudo, *J. Chem. Phys. 86* (1987) 4513.

[19] B. F. Yates, D. A. Clabo, H. F. Schaefer III, *Chem. Phys. Lett. 143* (1988) 421.

1,2-Dilithioethane from Ethylene and Lithium

By *Nicolaas J. R. van Eikema Hommes, Friedrich Bickelhaupt,* and *Gerhard W. Klumpp**

So far, simple vicinal dilithioalkanes have eluded generation under conditions of long life.[1] On the one hand, the most accessible routes to organolithium compounds, starting from the corresponding halogen compounds, in the case of *vic*-dihaloalkanes lead to β-halolithioalkanes. These eliminate lithium halide [Eq. (a)] much faster than they exchange the halogen substituent for lithium.[2] On the other hand, calculations have shown that 1,2-dilithioethane **1** should be much less stable than an isomeric complex consisting of vinyllithium **2** and lithium hydride [Eq. (b)].[3]

$$\mathrm{HalCH_2CH_2Hal} \longrightarrow \mathrm{HalCH_2CH_2Li} \longrightarrow \mathrm{H_2C{=}CH_2 + LiHal} \quad \text{(a)}$$

$$\underset{\mathbf{1}}{\mathrm{LiCH_2CH_2Li}} \longrightarrow \underset{\mathbf{2}\cdot\mathrm{LiH}}{\mathrm{H_2C{=}CHLi\cdot LiH}} \quad \Delta H = -29.8\ \mathrm{kcal\ mol^{-1}} \quad \text{(b)}$$

In agreement with the calculational results, ethylene, in the presence of catalysts, reacts with lithium to give mainly **2** and lithium hydride.[4,5] The small amounts of 1,4-dilithiobutane **3** that are also formed may be due to addition of **1** to ethylene.[6] Recently, we were able to generate **1** by reductive coupling of two molecules of iodomethyllithium at −100 to −80 °C.[7] As expected, the elimination of lithium hydride did not occur at this temperature, and the presence of **1** could be demonstrated for the first time by stannylation. Unfortunately, this method of preparation is afflicted with the rapid destruction of **1** (presumably with the formation of ethylene [see Eq. (a)] after exchange of a lithium atom for an iodine atom from the diiodomethane used to generate iodomethyllithium); therefore, the yield of 1,2-bis(trimethylstannyl)ethane **4** is very low (0.5%).[8] We now report that **1** and **3** are formed when lithium vapor is condensed onto a glass composed of ethylene and dimethyl ether at −196 °C in the apparatus described by *Kündig* and *Perret*,[9] after which the glass is allowed to melt and the resulting solution kept at −120 °C for one hour.

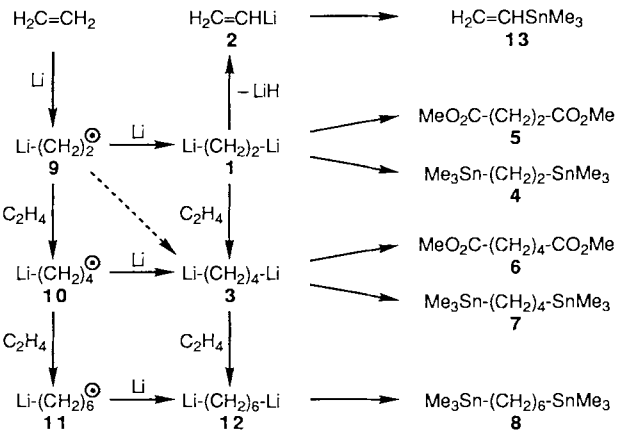

The reaction mixture, consisting of a light brown supernatant and a black sediment, was treated with gaseous CO_2, worked up in the usual way, and subjected to reaction with diazomethane, giving dimethyl succinate **5** and dimethyl adipate **6**, each in ca. 8% yield based on lithium. Treatment of the reaction mixture with chlorotrimethylstannane led to **4** and 1,4-bis(trimethylstannyl)butane **7** in practically the same yield. In one experiment, a small amount of 1,6-bis(trimethylstannyl)hexane **8** could be detected. Hexamethyldistannane was the only other product formed.

Destruction of the unreacted lithium with excess *n*BuCl *before* addition of chlorotrimethylstannane had no effect on the yields of **4** and **7**. This excludes formation of **4** via the following sequence: stannylation of the β-lithioethyl radical **9**, lithium reduction of the β-(trimethylstannyl)ethyl radical thus formed, and stannylation. The presence of **1** and **3** explains the formation of the diesters **5** and **6** and the ditin compounds **4** and **7**, respectively. The following routes of formation are conceivable for **3**: (1) addition of **1** to ethylene in analogy to the known ethylen-

[*] Prof. Dr. G. W. Klumpp, Drs. N. J. R. van Eikema Hommes, Prof. Dr. F. Bickelhaupt
Scheikundig Laboratorium, Vrije Universiteit
De Boelelaan 1083, NL-1081 HV Amsterdam (The Netherlands)

ation of alkyllithium compounds;[10] (2) addition of the β-lithioethyl radical **9** to ethylene to give **10**, followed by reaction of **10** with lithium.[11] Compound **3** may also (in part) result from the dimerization of **9**. The corresponding reactions of **3** and **10** with ethylene give **12** (in the case of **10** via **11**), whose presence is indicated by **8**. In agreement with the earlier results and their interpretation,[4] no **4** was isolated when the mixture of **1**, **3**, and unreacted lithium in pentane was maintained at 0°C for 30 min and then subjected to stannylation. Instead, a corresponding amount of trimethylvinylstannane **13** was found, together with **7**, present in unchanged yield. **13** is the product of stannylation of **2** formed from **1**.[12]

The formation of **1** from ethylene and lithium at a temperature much lower than the one previously required (which caused immediate elimination of lithium hydride) is a consequence of the high activity of the lithium used; i.e., in this form the reduction potential of lithium manifests itself kinetically much more strongly than is the case for lithium shavings[4a] or lithium sand.[4b]

Experimental Procedure

A steel crucible containing lithium (15 mmol) was placed in the evaporator of the Kündig-Perret apparatus. The rotating 1000-mL pear-shaped flask, cooled to −196°C, was then charged with dimethyl ether (12 g) and ethylene (140 mmol) was condensed into the flask. After reducing the pressure to 5×10^{-3} mbar, the crucible was heated to 550°C.

After ca. 30 min, the sublimation of lithium was complete. The contents of the flask were allowed to melt by warming to −120°C. The solution was kept at this temperature for one hour. Then it was cooled to −130°C and gaseous CO_2 was introduced in a rapid stream. After warming to room temperature, diethyl ether was added, the resulting mixture was shaken with several milliliters of 2 N HCl and the organic phase was dried, concentrated, and added to diazomethane in ether at 0°C. After concentration, analysis of the reaction mixture and isolation of the products were performed by gas chromatography [13]. Stannylation was carried out by adding 18 mmol of Me_3SnCl, dissolved in 50 mL of diethyl ether/pentane 1/1, to the reaction mixture at −120°C. The resulting mixture was then allowed to warm to room temperature, shaken with water, concentrated and subjected to gas chromatography for analysis and isolation of the products [13].

Received: March 21, 1988 [Z 2670 IE]
German version: *Angew. Chem. 100* (1988) 1100

[1] A. Maercker, M. Theis, *Top. Curr. Chem. 138* (1987) 1.
[2] R. West, E. G. Rochow, *J. Org. Chem. 18* (1953) 1739.
[3] P. von Ragué Schleyer, A. J. Kos, E. Kaufmann, *J. Am. Chem. Soc. 105* (1983) 7617.
[4] a) V. Rautenstrauch, *Angew. Chem. 87* (1975) 254; *Angew. Chem. Int. Ed. Engl. 14* (1975) 259; b) B. Bogdanović, B. Wermeckes, *Angew. Chem. 93* (1981) 691; *Angew. Chem. Int. Ed. Engl. 20* (1981) 684.
[5] A. Maercker, B. Grebe, *J. Organomet. Chem. 334* (1987) C21; H. Kuus, *Uch. Zap. Tartu Gos. Univ. 193* (1966) 130; *Chem. Abstr. 69* (1968) 67443q.
[6] An alternative interpretation starts from the β-lithioethyl radical **9**, which, on the one hand, can lead to **3** by addition to ethylene [11] or by dimerization and, on the other hand, can lead to **2** by donating a hydrogen atom to the radical anions formed from the catalyst. The lithium compounds formed by the latter route should finally eliminate lithium hydride.
[7] N. J. R. van Eikema Hommes, F. Bickelhaupt, G. W. Klumpp, *Recl. Trav. Chim. Pays Bas 106* (1987) 514.
[8] The yield of **4** increases to 10% if the reaction is carried out in the presence of $MgBr_2$: N. J. R. van Eikema Hommes, F. Bickelhaupt, G. W. Klumpp, *Recl. Trav. Chim. Pays Bas 107* (1988) 393.
[9] E. P. Kündig, C. Perret, *Helv. Chim. Acta 64* (1981) 2606.
[10] See P. D. Bartlett, C. V. Goebel, W. P. Weber, *J. Am. Chem. Soc. 91* (1969) 7425.
[11] We thank a referee for pointing out to us this possibility.
[12] Although its hypothetical gas-phase monomer is considerably less stable than that of its isomer **1**, complete decomposition of 1,1-dilithioethane into **2** and lithium hydride requires standing at room temperature for eight hours. A. Maercker, M. Theis, A. J. Kos, P. von Ragué Schleyer, *Angew. Chem. 95* (1983) 755; *Angew. Chem. Int. Ed. Engl. 22* (1983) 733.
[13] The analytical data of the isolated compounds are in agreement with those of authentic samples.

The Activation of Phenylmagnesium Compounds by Crown Ethers**

By *Peter R. Markies, Tateo Nomoto, Otto S. Akkerman, Friedrich Bickelhaupt,* Wilberth J. J. Smeets,* and *Anthony L. Spek*

Organomagnesium[1b] and organolithium[1c] compounds can be employed interchangeably in a wide range of organometallic reactions. However, certain types of reactions, such as halogen-metal exchange[2] and hydrogen-metal exchange in arenes,[3] are the exclusive province of organolithium compounds and are observed not at all—or only under special conditions—with the less reactive organomagnesium compounds.[4] We have now found that these two types of reactions indeed do occur with phenylmagnesium compounds under very mild conditions if the reactivity of these compounds is enhanced by complexation with crown ether **2**, a derivative of [15]crown-4.

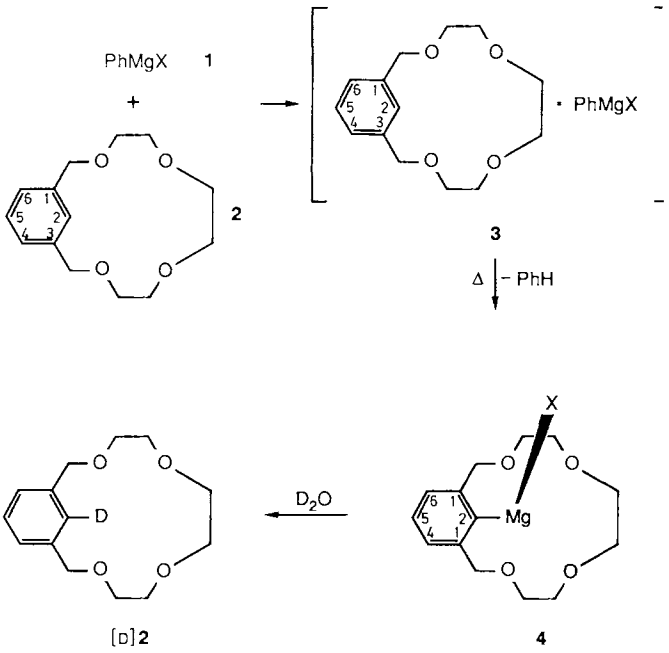

Scheme 1. **a**, X = Ph; **b**, X = Br.

For example, the metalation of **2** with diphenylmagnesium **1a** to give **4a** proceeds stepwise via the complex **3a** (Scheme 1). Using an all-glass apparatus,[5] we added, with stirring, a solution of 1 mmol of **1a** in 10 mL of diethyl ether to 1 mmol of **2**; a colorless precipitate formed and was purified by decanting the mother liquor, washing with redistilled ether, and drying under vacuum. The ^{1}H-NMR spectrum,[6] as well as the HCl and EDTA titration[5] after

[*] Prof. Dr. F. Bickelhaupt, Drs. P. R. Markies, Dr. T. Nomoto, Dr. O. S. Akkerman
Scheikundig Laboratorium, Vrije Universiteit
De Boelelaan 1083, NL-1081 HV Amsterdam (The Netherlands)
Drs. W. J. J. Smeets, Dr. A. L. Spek
Vakgroep Algemene Chemie, Afdeling Kristal- en Structuurchemie, Rijksuniversiteit
Padualaan 8, NL-3584 CH Utrecht (The Netherlands)

[**] We thank *A. J. M. Duisenberg* for collecting the X-ray data. This work was supported by the Netherlands Foundation for Chemical Research (SON) and by the Netherlands Organisation for Scientific Research (NWO) (*P. R. M., T. N., W. J. J. S., A. L. S.*).

hydrolysis, showed the composition to be **3a** · 0.75 Et_2O. Adduct **3a** was unchanged after 24 h in [D_6]benzene at room temperature. In [D_8]toluene at ca. 80 °C, on the other hand, it underwent reaction within 6 h to give **4a** and benzene quantitatively; **4a** was characterized by its ^{1}H-NMR spectrum,[6] by deuterolysis to [D]-**2**,[7] and by X-ray structure analysis.[8] Similarly, we obtained the Grignard compound **4b** from phenylmagnesium bromide **1b** and **2**; we had obtained **4b** earlier from aryl bromide **5** and magnesium.[7] The essential features of the crystal structures of **4a** (Fig. 1) and **4b**[7] are in agreement.

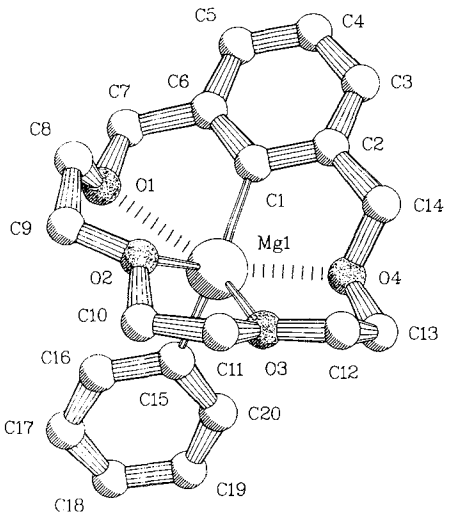

Fig. 1. PLUTON drawing of **4a** in the crystal (only one of the two nearly identical molecules is shown). Selected distances [Å] and angles [°]: Mg1-C1 2.127(4), Mg1-C15 2.154(4), Mg1-O1 2.619(3), Mg1-O2 2.183(3), Mg1-O3 2.209(3), Mg1-O4 2.335(3); C1-Mg1-C15 127.8(1), C1-Mg1-O2 111.2(1), C1-Mg1-O3 125.5(1), C15-Mg1-O2 105.6(1), C15-Mg1-O3 100.5(1), O2-Mg1-O3 71.4(1).

With organolithium compounds, the halogen–metal exchange occurs appreciably more readily than the hydrogen–metal exchange. The same should hold for organomagnesium compounds. Indeed, **1a** reacts with **5** to give **4a** (Scheme 2) faster than it reacts with **2**. After dissolution in [D_8]toluene, the precipitate formed initially from **1a** and **5** in diethyl ether showed immediately, even at room temperature, the ^{1}H-NMR signals of **4a** and bromobenzene; the reaction was quantitative after 24 h at room temperature.

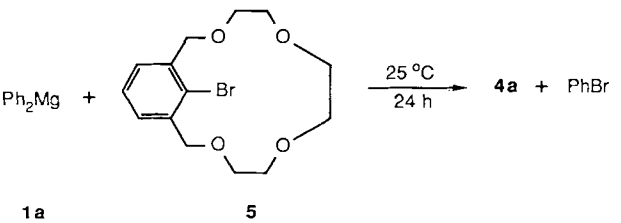

Scheme 2.

Further investigations are necessary to elucidate the mechanism of these reactions. However, several interesting features of the reaction have already emerged: (1) The reaction **1** + **2** → **4** + benzene is certainly favored thermodynamically by the polycoordination of magnesium in **4**. (2) Steric effects play an important role, since reaction of **1a** with the next higher crown ether homologue of **2**, a derivative of [18]crown-5, under comparable conditions, does not lead to hydrogen–metal exchange. Instead, an organometallic rotaxane is formed in which nearly linear but structurally intact **1a** fills the cavity of the crown ether.[9] (3) It is tempting to speculate that, in the reaction of **1** with **2**, an important role is played not only by the carbanionic activation of the phenyl group, which occurs with certainty in the reaction of organolithium compounds, but also by the electrophilic attack of magnesium, activated by polarization of the Mg–C bond, on the benzene ring of **3**. (4) The halogen–metal exchange reveals that the reactivity of organolithium compounds is approached qualitatively but not quantitatively: organolithium reagents exchange the bromine atom in **5** at −78 °C,[10] but **1a** reacts with **5** only at room temperature. Furthermore, the direct metalation of **2** with organolithium reagents is not possible, since ethylene glycol ethers are cleaved under these conditions.[10, 11]

The reactions described here are further characteristic examples for organolithium-like behavior of organomagnesium compounds effected by polycoordination by crown ethers or cryptands; such behavior has also been observed in additions to pyridine[12a] and in ether cleavages.[9, 12b] Such reactions are not only mechanistically but also preparatively interesting, since **2** is appreciably more accessible than the bromide **5**,[7, 10] thereby allowing the facile synthesis of an organometallic compound of type **4** directly from the parent compound **2**.

Received: March 28, 1988 [Z 2679 IE]
German version: *Angew. Chem. 100* (1988) 1143

[1] a) G. Wilkinson, F. G. A. Stone, E. W. Abel (Eds.): *Comprehensive Organometallic Chemistry, Vol. 1*, Pergamon, Oxford 1982; b) W. E. Lindsell in [1a], p. 155; c) J. L. Wardell in [1a], p. 43.

[2] a) R. G. Jones, H. Gilman, *Org. React. NY 6* (1951) 339; b) H. J. S. Winkler, H. Winkler, *J. Am. Chem. Soc. 88* (1966) 696, and references cited therein; c) H. J. Reich, N. H. Phillips, I. L. Reich, *ibid. 107* (1985) 4101, and references cited therein.

[3] a) H. Gilman, *Org. React. NY 8* (1954) 258; b) H. W. Gschwend, H. R. Rodriguez, *ibid. 26* (1979) 1; c) P. Beak, V. Snieckus, *Acc. Chem. Res. 15* (1982) 306; d) G. W. Klumpp, *Recl. Trav. Chim. Pays-Bas 105* (1986) 1, and references cited therein.

[4] a) M. S. Kharash, O. Reinmuth: *Grignard Reactions of Nonmetallic Substances*, Prentice-Hall, New York 1954; b) H. Gilman, S. M. Spatz, *J. Am. Chem. Soc. 63* (1941) 1553; c) H. Gilman, A. H. Haubein, *ibid. 67* (1945) 1033, and references cited therein; d) L. I. Zakharkin, O. Yu. Okhlobystin, K. A. Bilevitch, *J. Organomet. Chem. 2* (1964) 309; e) H. H. Paradies, M. Görbing, *Angew. Chem. 81* (1969) 293; *Angew. Chem. Int. Ed. Engl. 8* (1969) 279.

[5] A. D. Vreugdenhil, C. Blomberg, *Recl. Trav. Chim. Pays-Bas 82* (1963) 453, 461.

[6] **2**: ^{1}H-NMR (260 MHz, C_6D_6, C_6HD_5 (δ = 7.30) as internal standard): δ = 8.51 (s, 1H; H2), 7.26 (t, ^3J = 7.5 Hz, 1H; H5), 7.03 (dm, ^3J = 7.5 Hz, 2H; H4,6), 4.61 (d, ^4J = 0.5 Hz, 4H; aryl-CH_2), 3.62 (s, 4H; C_2H_4), 3.59 (s, 8H; C_2H_4). — **3a** · 0.75 Et_2O: ^{1}H-NMR (90 MHz, C_6D_6, C_6HD_5 (δ = 7.30) as internal standard): δ = 8.30–8.13 (m, 4H; Ph-H2,6), 7.77–7.41 (m, 6H; Ph-H3,4,5), 7.30–7.16 (m, 1H; H5), 6.95 (dm, ^3J = 7 Hz, 2H; H4,6), 4.47 (s, 4H; Aryl-CH_2), 3.50 (s, 4H; C_2H_4), 3.42 (q, ^3J = 7 Hz, 4 × 0.75H; OCH_2CH_3), 3.33 (s, 8H; C_2H_4), 1.26 (t, ^3J = 7 Hz, 6 × 0.75H; CH_3), H2 not identified. — **4a**: ^{1}H-NMR (250 MHz, [D_8]toluene, $C_6D_5CHD_2$ (δ = 2.33) as internal standard): δ = 7.99 (d, ^3J = 7 Hz, 2H; Ph-H2,6), 7.40 (dd, ^3J = ^3J = 7 Hz; Ph-H3,5), 7.28 (t, ^3J = 7 Hz, 1H; Ph-H4*), 7.19 (t, ^3J = 7 Hz, 1H; H5*), 6.84 (dm, ^3J = 7 Hz, 2H; H4,6), 4.44 (AB spectrum, $\Delta\delta$(AB) = 0.49 ppm, ^2J(AB) = 13 Hz, 4H; Aryl-CH_2), 3.32–3.06 (m, 8H; C_2H_4), 2.70–2.63 (m, 4H; C_2H_4)). The assignments marked with an asterisk are uncertain and may have to be interchanged.

[7] P. R. Markies, O. S. Akkerman, F. Bickelhaupt, *J. Am. Chem. Soc.*, in press.

[8] Crystal structure analysis of **4a**: $C_{20}H_{24}O_4Mg$, space group $P2_1/n$, $a = 11.284(1)$, $b = 18.277(2)$, $c = 18.682(2)$ Å, $\beta = 101.50(1)°$, $Z = 8$, $\rho_{calcd} = 1.241$ g cm^{-3}. Enraf-Nonius CAD4F diffractometer (Zr filtered $Mo_{K\alpha}$ radiation, $\lambda = 0.71073$ Å); direct methods (SHELXS86) and difference Fourier techniques, refinement with SHELX76 ($R = 0.0479$, $R_w = 0.0483$ for 3037 reflections with $I > 2.5\sigma(I)$). Hydrogen atoms at calculated positions, all non-hydrogen atoms refined with anisotropic thermal parameters. Further details of the crystal structure determination are available on request from the director of the Cambridge Crystallographic Data Centre, University Chemical Laboratory, Lensfield Road, Cambridge CB2 1EW (England).

[9] P. R. Markies, T. Nomoto, O. S. Akkerman, F. Bickelhaupt, W. J. J. Smeets, A. L. Spek, *J. Am. Chem. Soc. 110* (1988) 4845; cf. A. D. Pajerski, G. L. Bergstresser, M. Parvez, H. G. Richey Jr., *ibid. 110* (1988) 4844.

[10] M. Skowronska-Ptasinska, P. Telleman, V. M. L. J. Aarts, P. D. J. Grootenhuis, J. van Eerden, S. Harkema, D. N. Reinhoudt, *Tetrahedron Lett. 28* (1987) 1937.

[11] a) R. A. Ellison, F. N. Kotsonis, *J. Org. Chem. 38* (1973) 4192; b) J. J. Fitt, H. W. Gschwend, *ibid. 49* (1984) 209.

[12] a) H. G. Richey, Jr., B. A. King, *J. Am. Chem. Soc. 104* (1982) 4672; b) E. P. Squiller, R. R. Whittle, H. G. Richey, Jr., *Organometallics 4* (1985) 1154.

β-Mannosides from β-Glucosides by Intramolecular Nucleophilic Substitution with Inversion of Configuration**

By *Horst Kunz** and *Wolfgang Günther*

Owing to their immunological as well as pharmacokinetic and pharmacodynamic properties, glycoconjugates are attracting increasing attention for the synthesis of selectively active biological substances. A central structural unit of the *N*-glycoproteins, which are widespread as serum and membrane components, is the β-mannosylchitobiose in the core region.[1]

Manβ1–4GlcNacβ1–4GlcNacβ1–Asn
core region

Of the glycoside linkages, the β-mannosidic link is especially difficult to realize, since both the anomeric effect as well as the neighboring group effects in the sense of the Koenigs–Knorr reactions favor only formation of the α-mannosides.[2] The β-mannoside syntheses described hitherto start from 2,3-carbonyl-,[3] 2-*O*-mesyl-,[4] or benzyl-protected mannosyl donors which are activated with silver silicate[5] or silver-zeolite.[6] With silver silicate as reagent, complex oligosaccharides of the *N*-glycoproteins have been synthesized. However, a satisfactory selectivity in the β-mannosidic linkage to the glucosamine is achieved only when glucosamine is employed in the form of reactive 1,6-anhydro-2-azido derivatives.[2] With 3,6-*O*-benzyl-protected *N*-acetylglucosamine derivatives, sometimes the α-mannoside is also formed exclusively by this method.[7,8] A further β-mannoside synthesis in which the benzyl-protected *N*-acetylglucosamine derivatives could be employed involves the epimerization of β-glucosides by oxidation and subsequent reduction in the 2-position.[9] Common to all these methods is that α-mannosides[3,8] or β-glucosides[9] are formed as well as the desired β-mannosides, and consequently a subsequent separation is essential.

Herein we report a method by which the β-mannosides can be obtained from the accessible β-glucosides via an inversion of configuration at C-2 by nucleophilic substitution.[10,11] The S_N2 reaction at C-2 of the glycosides is difficult because the coaxially oriented lone pair on the ring oxygen interferes. We accomplished this reaction by introduction of the oxygen nucleophile intramolecularly in the sense of a neighboring group effect. The neighboring group is formed via the *N*-phenylurethane **2** of the 1,2:5,6-di-*O*-isopropylidene-α-D-glucofuranose **1**, from which the glucosyl donor **5** is synthesized via hydrolysis to **3** and acetylation to **4** by the usual reaction with HBr/glacial acetic acid (see Scheme 1).

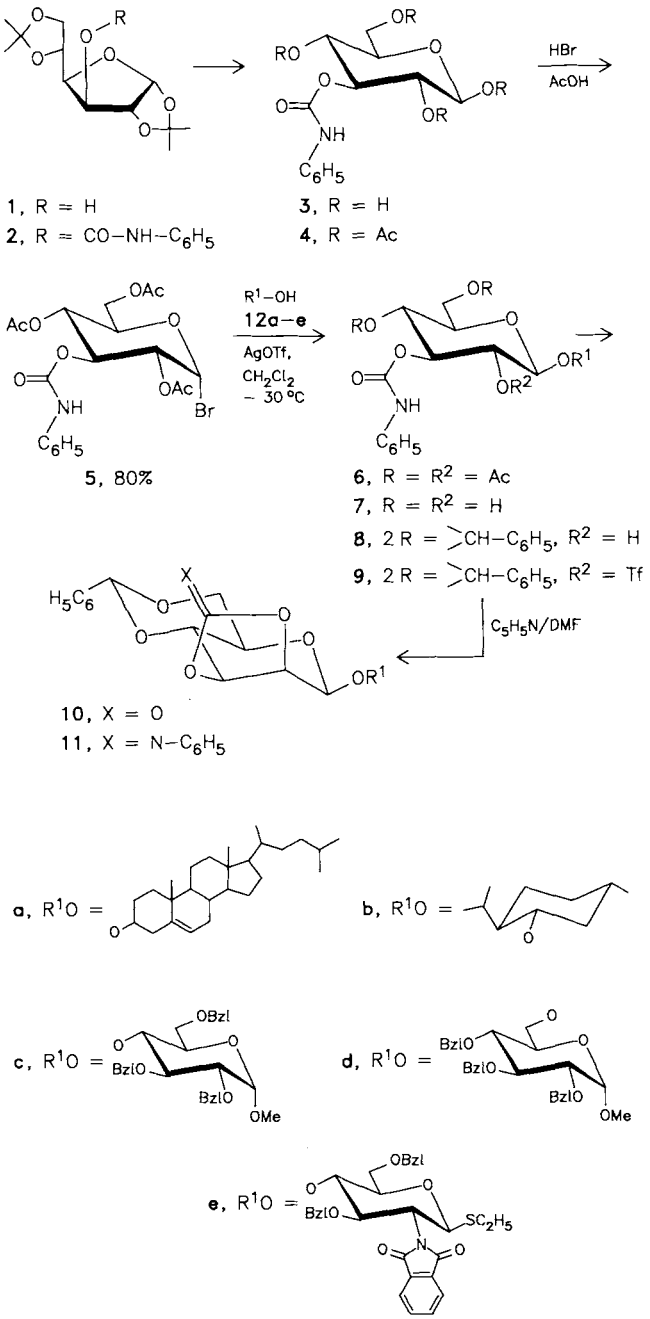

Scheme 1. **1**→**2** [12]: H_5C_6–N=C=O; **2**→**3**: H_2SO_4/H_2O/dioxane; **3**→**4**: Ac_2O/pyridine; **6**→**7**: K_2CO_3, MeOH; **7**→**8**: H_5C_6–$CH(OMe)_2$, HBF_4/Et_2O; **8**→**9**: $(F_3CSO_2)_2O/CH_2Cl_2$/pyridine.—Tf = F_3CSO_2, C_5H_5N = pyridine.

The reactions leading to **4** proceed almost quantitatively. 2,4,6-Tri-*O*-acetyl-3-*O*-(*N*-phenylcarbamoyl)-α-D-gluco-

[*] Prof. Dr. H. Kunz, Dipl.-Chem. W. Günther
Institut für Organische Chemie der Universität
J.-J.-Becher-Weg 18–20, D-6500 Mainz (FRG)

[**] This work was supported by the Deutsche Forschungsgemeinschaft and the Fonds der Chemischen Industrie.

pyranosyl bromide **5** is obtained from **4** in 80% yield. The synthesis of the β-glucosides **6** is carried out according to the silver triflate method[13] and, without exception, leads (not optimized) to 65–80% yields. Losses arise alone by orthoester formation and associated hydrolysis (see Table 1). In no case is the α-glucoside observed.

Table 1. Synthesis of β-mannosides **10** via the inversion of glycosides **6** at C-2 according to Scheme 1.

	β-Glucoside [a]			β-Mannoside **10**		
	Yield [%]	δ(C-1) [b]		Yield [%] [c]	$[\alpha]_D^{23}$ (*c*) [d]	δ(C-1) [b]
6a	40 [e]	99.7	**10a**	65	− 91.8 (0.5)	94.3
6b	65	98.8	**10b**	80	−149.3 (1.0)	92.8
6c	67	100.1	**10c**	67	− 43.3 (1.0)	95.6
6d	69	100.7	**10d**	66	− 32.9 (1.0)	94.9
6e	82	100.1	**10e**	65	− 24.5 (1.0)	96.6
			+ **11e**	10	− 14.6 (0.5)	100.01

[a] The yields (referred to **5**) were not optimized. [b] 100.1-MHz ^{13}C-NMR ($CDCl_3$). [c] Referred to **8**, which is obtained in ca. 75% yield from the respective glucoside **6**. [d] In CH_2Cl_2. [e] Using silver 4-hydroxyvalerate [14].

In particular the sluggishly reactive acceptor **12e** (with benzyl-protective groups in the 3- and 6-position), which cannot be used for direct β-mannosylation,[7] reacts with **5** to give the desired β-glucoside **6e** in 82% yield. For conversion of the β-*gluco*-compounds **6** into the β-*manno*-compounds **10/11** the *O*-acetyl groups are removed with K_2CO_3 in methanol. In the resulting sugar **7**, the 4- and the 6-hydroxy group are protected as the benzylidene acetal (→ **8**). Both reactions proceed in 85–90% yield. The free 2-hydroxy group of the β-glucosides **8** is now activated with trifluoromethanesulfonic anhydride/pyridine for the inversion of configuration to give the isolable triflates **9**, which can be converted directly into the β-mannosides **10** by heating to 75°C in pyridine/dimethylformamide. This inversion at C-2 proceeds smoothly and without side reactions because the intramolecular attack of the carbamoyl oxygen is favored entropically. It initially affords a mixture of the 2,3-*O*-carbonyl-β-mannoside **10** in crude yields of ca. 90% and small amounts of the corresponding iminocarbonate **11**. The latter has been isolated for characterization in the case of the β-mannosylglucosamine derivative **11e**. The iminocarbonates can be easily converted into the carbonates **10** by mild hydrolysis. No carbohydrate derivatives other than the β-mannosides **10/11** are detectable in the thin-layer chromatogram of the reaction mixture. The *gluco*-configurated starting material **8** is completely converted, so a chromatographic isolation of the mannosides **10** was not really necessary. However, in these first syntheses it was carried out in order to obtain analytically pure β-mannosides. The yields of the inversion reactions after chromatographic separation are 65–80% based on the benzylidene-protected *gluco*-derivatives **8**. Thus, the disaccharide β-mannosyl-*N*-acetylglucosamine (with protecting groups: **10e**) contained in the core region of the *N*-glycoproteins is obtained in 75% yield, without having to separate side products with another configuration at C-1 or C-2.

The structure of the β-mannosides **10** has been confirmed ^{1}H-NMR and ^{13}C-NMR spectroscopically. Due to the 2,3-carbonate grouping the β-mannosides **10** show a remarkably large C-1/H-1 coupling with $J \approx 171$ Hz, signals shifted upfield to $\delta = 93$–96.5 for C-1 (see also Table 1), and a relatively large coupling constant $J_{1,2} \approx 3.5$ Hz in the ^{1}H-NMR spectrum.

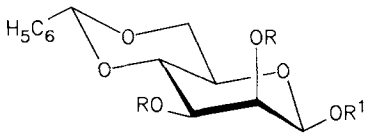

	R	R	δ(C-1)	*J*(C-1/H-1) [Hz]
10a	−CO−		94.3	170.9
13a	H	H	98.0	157.1
10b	−CO−		92.8	172
13b	Ac	Ac	95.9	155

Removal of the CO group from **10b** under basic conditions and acetylation of the 2-OH and 3-OH groups furnishes the corresponding di-*O*-acetyl-β-mannoside **13b**, whose C-1 signal and, in particular, C-1/H-1 coupling confirm the β-mannoside structure. $J_{1,2}$ (≈ 1 Hz) in the ^{1}H-NMR spectrum of **13b** also has the small value typical for β-mannosides.

The reaction sequence shown in Scheme 1 thus enables the difficultly realizable β-mannosidic linkage to be achieved both selectively and efficiently.

Received: March 25, 1988 [Z 2678 IE]
German version: *Angew. Chem. 100* (1988) 1118

[1] For a review see, e.g.: J. Montreuil, *Adv. Carbohydr. Chem. Biochem. 37* (1980) 157.
[2] H. Paulsen, M. Heume, Z. Györgydeak, R. Lebuhn, *Carbohydr. Res. 144* (1986) 57, and references cited therein.
[3] P. A. J. Gorin, A. S. Perlin, *Can. J. Chem. 39* (1961) 2474.
[4] V. K. Srivastava, C. J. Schuerch, *J. Org. Chem. 46* (1981) 1121.
[5] H. Paulsen, O. Lockhoff, *Chem. Ber. 114* (1981) 3102.
[6] P. J. Garegg, P. Ossowski, *Acta Chem. Scand. Ser. B 37* (1983) 249, and references cited therein.
[7] H. Paulsen, R. Lebuhn, *Liebigs Ann. Chem. 1983*, 1047.
[8] T. Ogawa, T. Kitajima, T. Nukada, *Carbohydr. Res. 123* (1983) C 5.
[9] C. Auge, C. D. Wassen, R. W. Jeanloz, *Carbohydr. Res. 82* (1980) 85.
[10] An inversion of the configuration of simple galactosides by external nucleophiles has been reported recently: S. David, A. Fernandez-Mayoralas, *Carbohydr. Res. 165* (1987) C 11.
[11] Intramolecular inversion of the configuration of neuraminic acid derivatives at the 4-position: H.-W. Hagedorn, R. Brossmer, *Helv. Chim. Acta 69* (1986) 2127.
[12] A. F. Bochkov, I. V. Obruchnikov, N. K. Kochetkov, *Izv. Akad. Nauk SSSR Ser. Khim. 1971*, 1282.
[13] S. Hanessian, J. Banoub, *Carbohydr. Res. 53* (1977) C 13.
[14] G. Wulff, J. Wichelhaus, *Chem. Ber. 112* (1979) 2847.

Polycyclic Silylamides of Ge^{II} and Sn^{II} with Different Structures—Bis(germanediyl) versus Distannate**

By *Michael Veith** and *Richard Lisowsky*

Dedicated to Professor Heinrich Nöth on the occasion of his 60th birthday

The differing coordination behavior of homologous elements in compounds of the same type can be due, inter alia, to differences in electronegativity and/or atomic size. We report here on the incorporation of two germanium(II) or tin(II) atoms respectively into the cyclodisilazane **1**; the

[*] Prof. Dr. M. Veith, Dr. R. Lisowsky
Institut für Anorganische Chemie der Universität
D-6600 Saarbrücken (FRG)

[**] Cyclic Diazastannylenes, Part 27.—Part 26: [1].

extreme differences in the structures of the products **2** and **3** are attributed to specific ring-strain effects.

Continuing on the basis of investigations into the chemistry of low valent main group elements[2] we have examined the reaction of the tetralithium salt of **1**[3] with two equivalents of the dioxane adduct of germanium dichloride and with the dichlorides of tin and lead.

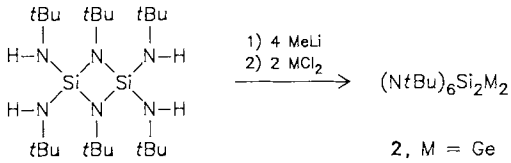

$(NHtBu)_2(NtBu)_4Si_2Pb$ **4**

In the reaction with $PbCl_2$, a compound could be isolated in small yields which contained only one lead atom and, according to an elemental analysis, could be formulated as **4** (owing to its ready decomposition further physical-chemical characterization was not possible).

The compounds **2** and **3**, which are isolated in good yields, have analogous composition, have the expected molecular weights in benzene, and do not decompose in the gas phase under reduced pressure (mass spectra). The ^{1}H-NMR spectra of **2** and **3** consist of two singlets in the integral ratio 2 : 1 (Table 1).

Table 1. Some data for **2** and **3**.

	2	**3**
M_r (exp. in benzene/calc.)	620/628.08	710/720.30
^{1}H-NMR (δ values)	1.49 (18 H, *t*Bu), 1.57 (36 H, *t*Bu)	1.49 (36 H, *t*Bu), 1.52 (18 H, *t*Bu)
Crystal system	tetragonal	monoclinic
space group	$P4_2nm$	$P2_1/c$
a [pm]	957.7(9)	915.1(9)
b [pm]	957.7(9)	1931(2)
c [pm]	1753(2)	994(1)
β [°]	90	111.1(1)
V [$10^6 \cdot pm^3$]	1608	1639
Z	2	2
Measured reflections	775	1952
($F < 2\sigma$)	203	341
Parameters	55	262
R (R_w)	0.056 (0.069)	0.038 (0.029)
Weighting scheme	k_1 1.000	0.7583
$W = k_1/(\sigma_F^2 + k_2 \cdot F^2)$	k_2 0.01819	0.000173

The single-crystal X-ray structure analyses of **2** and **3** (Table 1) show that the structures of the two compounds are fundamentally different despite their similar composition (Fig. 1): **2** is a dispiro system with crystallographic point symmetry *mm*2 (C_{2v}) and is the first example of a species containing two isolated germanediyl units in one molecule (cf. also Refs. [4, 5]; a digermanetetrayl with both germanium atoms of formal oxidation state +1 has been described recently[6]); compound **3**, on the other hand, is a pentacycle with crystallographic point symmetry $\bar{1}$ (C_i) and with three-coordinate tin atoms. The H/Ge exchange in **1** formally proceeds with coupling of the nitrogen atoms bound to the *same* silicon atom; consequently, **2** contains two spiro centers and a linear arrangement of silicon and germanium atoms. In contrast, in the case of the formal H/Sn exchange the nitrogen atoms bridge *different* silicon atoms. The tin atoms thus come in the proximity of the nitrogen atoms N2 and N2', and, consequently, formation of an additional λ^4N-λ^3Sn bond can occur. The pentacyclic $Sn_2N_6Si_2$ skeleton can be described in terms of two face-sharing (Si_2N_2) seco-norcubane units.

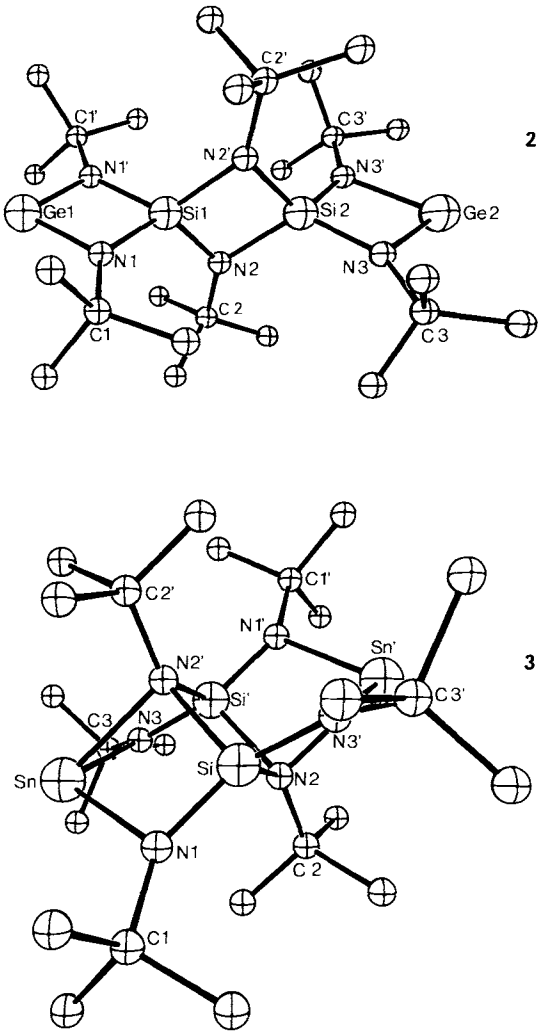

Fig. 1. Molecular structures of compounds **2** and **3**. Some (mainly averaged) bond lengths [pm] and angles [°]: **2**: N-Ge 185.6(6), N1,3-Si 173.4(3), N2-Si 174.9(1); N-Ge-N 80.9(3), N1,3-Si-N1',3' 88.0(2), N2-Si-N2' 85.9(1).—**3**: N-Sn 224.7(9), N1,3'-Si 166.8(1), N2,2'-Si 181.0(4); N1-Sn-N3 110.8(2), N1,3-Sn-N2 70.7(2), N2-Si-N2' 86.7(3), N1-Si-N3' 142.2(9) [10].

With regard to the bond lengths and angles in **2** and **3** the following special features are noteworthy (cf. Fig. 1):

1) The Si–N distances in the central Si_2N_2 four-membered ring are, as expected, shorter in **2** than in **3**, corresponding to the different coordination numbers of N2 in **2** (three, sp^2 hybridization) and in **3** (four, sp^3).

2) The Si1–N1 and Si2–N3 distances in **2** are longer than Si–N1 and Si–N3' in **3**. It can therefore be concluded that the neighboring Sn–N bond is more polar than the neighboring Ge–N bond, consistent with the higher electronegativity of the germanium compared to the tin.[7]

3) The Ge–N bond in **2** is short compared to that in the likewise monomeric bis(2,2,6,6-tetramethylpiperidino)germanium (188.5 pm);[4] this can be explained by additional p$\pi \rightarrow$pπ bonding (N$\rightarrow$Ge). All the Sn–N bonds in **3** are

about the same length; their length compares very well with those of typical λ^3Sn-λ^4N bonds such as are found in $Sn_4(NtBu)_4$ (Sn–N = 220.2 pm).[8]

The N1-Si-N3′ bond angle in **3** (Fig. 1) is extremely large for a four-coordinate silicon atom, thus indicating large steric constraints. **3** is isoelectronic and isostructural with sodium *tert*-butoxystannate **5**.[9] However, whereas

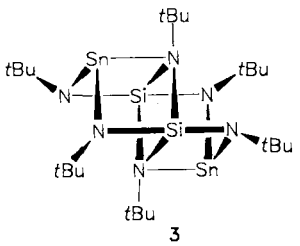

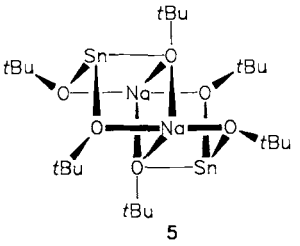

sodium as electropositive element can cope relatively well with the imposed strain in **5** (O-Na-O angle: axial 177.9(2)°, equatorial 103.3(2)°), the electronegative silicon in **3** would prefer a tetrahedral geometry (for comparison: N1-Si-N3′ 142.2°, N2-Si-N2′ 86.7°).

The different structures of **2** and **3** may be directly related to the aforementioned constraints. Since the germanium atom has a smaller radius than the tin atom, the distortion at the silicon atom in **3** should increase on formal exchange of Sn by Ge. The system is apparently no longer stable and changes to the dispiro compound **2**, even though the germanium thereby achieves the electronically less favorable coordination number two.

Experimental

A solution of **1** (1.8 g, 3.7 mmol) [3] in 20 mL hexane/20 mL diethyl ether was treated dropwise with 9.9 mL (15 mmol) of a 1.5 M solution of methyllithium in diethyl ether. After heating under reflux for 3 h the solution was cooled to −78°C and treated with 1.7 g (7.4 mmol) of germanium dichloride-dioxane adduct, [11] 1.4 g (7.4 mmol) of anhydrous tin(II) chloride or 2.06 g (7.4 mmol) of lead(II) chloride, respectively. The reaction mixture was then warmed to room temperature and stirred for a further 4 h. In all three cases the solvent was removed under high vacuum and the resulting residue recrystallized from toluene. Yields: 1.86 g (71%) pale yellow crystals of **2** (150°C, decomp.), 1.63 g (61%) orange-yellow crystals of **3** (decomp. 200°C), and 0.38 g (15%) deep-red crystals of **4**.

Received: March 30, 1988;
revised: May 3, 1988 [Z 2686 IE]
German version: *Angew. Chem. 100* (1988) 1124

[1] M. Veith, R. Lisowsky, *Z. Anorg. Allg. Chem. 560* (1988) 59.
[2] M. Veith, *Angew. Chem. 99* (1987) 1; *Angew. Chem. Int. Ed. Engl. 26* (1987) 1.
[3] R. Lisowsky, *Dissertation*, Universität Saarbrücken 1988.
[4] M. F. Lappert, M. J. Slade, J. L. Atwood, M. J. Zaworotko, *J. Chem. Soc. Chem. Commun. 1980*, 621.
[5] M. Veith, M. Grosser, *Z. Naturforsch. B37* (1982) 1375.
[6] H. H. Karsch, B. Deubelly, J. Riede, G. Müller, *Angew. Chem. 99* (1987) 703; *Angew. Chem. Int. Ed. Engl. 26* (1987) 673.
[7] J. E. Huheey: *Inorganic Chemistry: Principles of Structure and Reactivity*, Harper and Row, New York 1983.
[8] M. Veith, O. Recktenwald, *Z. Naturforsch. B38* (1983) 1054.
[9] M. Veith, R. Rösler, *Z. Naturforsch. B41* (1986) 1071.
[10] Further details of the crystal structure investigations are available on request from the Fachinformationszentrum Energie, Physik, Mathematik GmbH, D-7514 Eggenstein-Leopoldshafen 2 (FRG), on quoting the depository number CSD-53094, the names of the authors, and the journal citation.
[11] W. P. Kolesnikov, V. I. Shiryaev, O. M. Nefedov, *Izv. Akad. Nauk SSSR Ser. Khim. 1966*, 584.

The Enzymic Interconversion of Isobutyryl and *n*-Butyrylcarba(dethia)-Coenzyme A: A Coenzyme-B_{12}-dependent Carbon Skeleton Rearrangement**

By *Günther Brendelberger, János Rétey,** *Doreen M. Ashworth, Kevin Reynolds, Frances Willenbrock,* and *John A. Robinson**

Dedicated to Professor Theodor Wieland on the occasion of his 75th birthday

Coenzyme B_{12} has one of the most complex structures[1] amongst the known coenzymes and in association with various proteins is able to promote several rearrangement reactions that until recently were without clear chemical precedence. Amongst these are three well known carbon skeleton rearrangements[2] in which an organic moiety and a hydrogen atom exchange positions on adjacent carbon atoms [Eq. (a)]. The mechanism of these rearrangements is

(a)

R = CO–SCoA methylmalonyl-CoA mutase
R = $CHNH_2$–COOH glutamate mutase
R = C(=CH_2)–COOH methyl itaconate mutase

still incompletely understood. Recently, evidence was presented for the existence of a novel rearrangement, occurring in the polyether antibiotic producing organism *Streptomyces cinnamonensis*, which involves the interconversion of isobutyryl-CoA **1** and *n*-butyryl-CoA **2**[3] [Eq. (b)]. We describe here evidence that this represents a new type of coenzyme-B_{12}-dependent enzymic rearrangement.

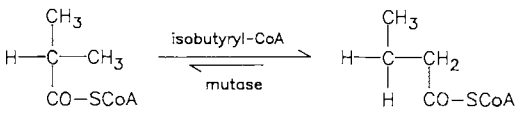

(b)

1 2

It was shown recently that synthetic methylmalonyl-dethia(carba)-coenzyme A (with CH_2CoA partial structure) is an excellent substrate for methylmalonyl-CoA mutase from *Propionibacterium shermanii*.[4] Such CH_2-CoA

[*] Prof. Dr. J. Rétey, Apotheker G. Brendelberger
Lehrstuhl für Biochemie im Institut
für Organische Chemie der Universität
Richard-Willstätter-Allee, D-7500 Karlsruhe 1 (FRG)
Dr. J. A. Robinson, Dr. D. M. Ashworth, Dr. K. Reynolds,
Dr. F. Willenbrock
Department of Chemistry, The University
Southampton SO9 5NH (UK)

[**] This work was supported by the Deutsche Forschungsgemeinschaft, the Fonds der Chemischen Industrie (*G. B.* and *J. R.*) as well as by SERC, Apcell, Beechams, Glaxo and ICI (*D. M. A., K. R., F. W.*, and *J. A. R.*). *G. B.* thanks the Land Baden-Württemberg for a scholarship for graduate students. We are grateful to Dr. *M. Spraul*, Bruker Analytische Meßtechnik GmbH, Rheinstetten/Karlsruhe for the 500-MHz ^{1}H-NMR spectrum.

analogues, unlike their thioester counterparts, are stable to hydrolysis and can be used for mechanistic investigations.[5] In view of this, isobutyryl-CH_2CoA **3** was prepared, starting from isopropyl vinyl ketone,[6] and following the same reaction sequence described already for the synthesis of propionyl-CH_2-CoA.[4] The ^{1}H-NMR spectrum[7] of the product, after chromatography, revealed also the presence, to the extent of about 15%, of the isobutyryl-CH_2-iso-CoA (2′-phospho-CH_2-CoA) isomer, which should not be transformed by the enzyme.

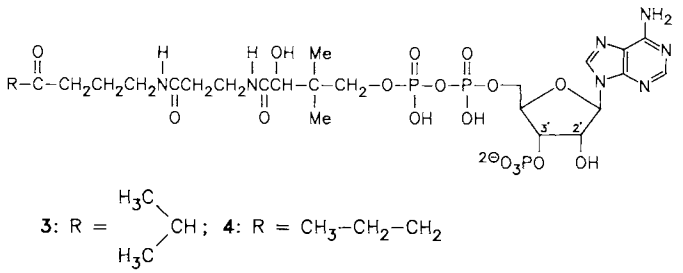

3: R = H_3C–CH(–CH_3)–; **4**: R = CH_3–CH_2–CH_2–

After **3** (5 mg) was incubated, in the presence of coenzyme B_{12} (20 μM),[8] with an ammonium sulfate fraction of a cell-free extract from *Streptomyces cinnamonensis*[9] (ca. 30 mg protein, Tris/HCl buffer, pH 7.3, 30 °C, 60 min), the protein was precipitated by acid and removed, and the products were chromatographed on DE-32 cellulose.

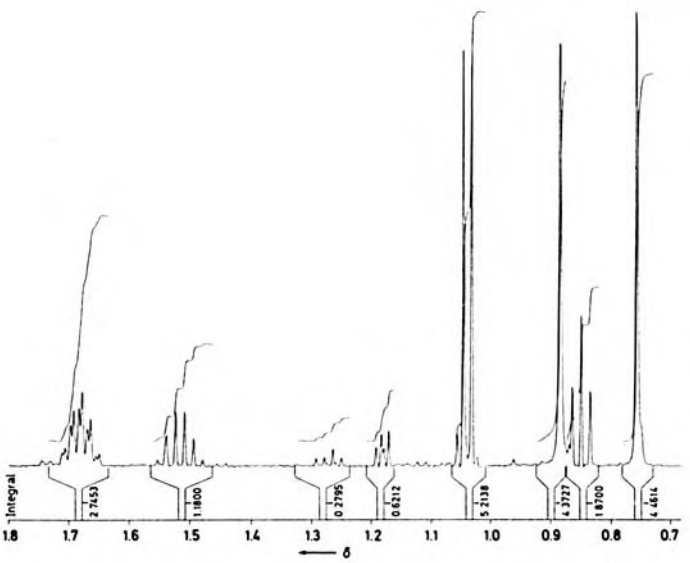

Fig. 1. Part of the 500-MHz ^{1}H-NMR spectrum of the enzymically obtained equilibrium mixture of isobutyryl- (**3**) and *n*-butyryl-carba(dethia)-coenzyme A **4** in deuterium oxide. The triplet and the sextet at $\delta = 0.85$ and 1.52, respectively, arise from the *n*-butyryl portion of **4**, while the two slightly resolved quintets at around $\delta = 1.68$ can be assigned to the middle one of the three adjacent methylene groups of the CH_2CoA moiety in each of **3** and **4** (see structural formulas).

Figure 1 shows a portion of the 500-MHz ^{1}H-NMR spectrum of these materials (3.8 mg). Clearly assignable are the signals from both isobutyryl-CH_2CoA **3** and *n*-butyryl-CH_2CoA **4**,[10] in the ratio 60:40. After taking account of the unreacted[11] isobutyryl-CH_2-iso-CoA (≈8%), the equilibrium ratio of iso- and *n*-butyryl species was 56.5:43.5.[12]

In separate incubations with the *Streptomycetes* extract, the conversion of (1-^{13}C)*n*-butyryl-CoA **2*** into (1-^{13}C)isobutyryl-CoA **1*** could also be detected,[13] and this activity was completely dependent upon the addition of coenzyme-B_{12} to the assay. The same *Streptomyces* extract was also shown to catalyze the rearrangement of methylmalonyl-CH_2CoA to succinyl-CH_2CoA, with the additional decarboxylation of about half the substrate to propionyl-CH_2CoA. However, neither isobutyryl-CH_2CoA nor isobutyryl-SCoA was a substrate for highly purified methylmalonyl-CoA mutase from *P. shermanii*. Whether or not the methylmalonyl-CoA mutase and isobutyryl-CoA mutase activities from *Streptomyces cinnamonensis* are promoted by the same protein is not yet clear. Antibodies raised against the methylmalonyl-CoA mutase from *P. shermanii* failed to inhibit the isobutyryl-*n*-butyryl-CoA rearrangement, although the same antibodies showed a clear reaction with the methylmalonyl-CoA mutase from *Streptomyces cinnamonensis* as seen on a Western Blot (immunoblot) analysis.[14]

It seems most likely that in an evolutionary sense the methylmalonyl-CoA mutase and isobutyryl-CoA mutase will be very closely related, perhaps by a mutation in the active site, in which a basic amino acid residue (for binding $COO^\ominus$) is changed to a lipophilic one (for binding CH_3).

Received: March 28, 1988;
revised: April 29, 1988 [Z 2683 IE]
German version: *Angew. Chem. 100* (1988) 1122

[1] P. G. Lenhert, D. C. Hodgkin, *Nature (London) 192* (1961) 937.
[2] H. A. Barker, H. Weissbach, R. D. Smyth, *Proc. Natl. Acad. Sci. USA 44* (1958) 1093; M. Flavin, S. Ochoa, *J. Biol. Chem. 229* (1957) 965; H. Eggerer, E. R. Stadtman, P. Overath, F. Lynen, *Biochem. Z. 333* (1960) 1; H. F. Kung, S. Cederbaum, L. Tsai, T. C. Stadtman, *Proc. Natl. Acad. Sci. USA 65* (1970) 978.
[3] D. Gani, D. O'Hagan, K. Reynolds, J. A. Robinson, *J. Chem. Soc. Chem. Commun. 1985*, 1002; K. Reynolds, J. A. Robinson, *ibid. 1985*, 1831; K. Reynolds, D. Gani, J. A. Robinson, *ibid. 1986*, 1334.
[4] M. Michenfelder, J. Rétey, *Angew. Chem. 98* (1986) 337; *Angew. Chem. Int. Ed. Engl. 25* (1986) 366.
[5] I. Nikawa, S. Numa, T. Shiba, C. J. Stewart, T. Wieland, *FEBS Lett. 91* (1978) 144; W. E. Hull, M. Michenfelder, J. Rétey, *Eur. J. Biochem. 173* (1988) 191.
[6] P. R. Thomas, G. J. Tyler, T. E. Edwards, A. T. Radcliffe, R. C. P. Cubbon, *Polymer 5* (1964) 525.
[7] **3**: 250-MHz ^{1}H-NMR (^2H_2O): $\delta = 0.74$ (s, 3H), 0.88 (s, 3H), 1.04 (d, $J = 7.0$ Hz, 6H), 1.71 (quint., $J = 7.0$ Hz, 2H), 2.46 (t, $J = 6.3$ Hz, 2H), 2.58 (t, $J = 7.0$ Hz, 2H), 2.71 (sept., $J = 7.0$ Hz, 1H), 3.12 (t, $J = 6.6$ Hz, 2H), 3.46 (t, $J = 6.3$ Hz, 2H), 3.71 (ABX, $J = 9$ Hz, $J_{HP} = 4$ Hz, 2H), 4.02 (s, 1H), 4.26 (m, 2H), 6.19 (d, $J = 6.2$ Hz, 1H), 8.29 (s, 1H), 8.57 (s, 1H).
[8] The dependence on coenzyme B_{12} has been shown only for the conversion of the natural thioester substrate **1**.
[9] Prepared by sonification of the cells, centrifugation, batch adsorption of the supernatant on DEAE cellulose and a final ammonium sulfate precipitation.
[10] **4** (enzymatically prepared): 250-MHz ^{1}H NMR (^2H_2O): $\delta = 0.74$ (s, 3H), 0.84 (t, $J = 7.4$ Hz, 3H), 0.88 (s, 3H), 1.52 (sext., $J = 7.4$ Hz, 2H), 1.71 (quint., $J = 7.0$ Hz, 2H), 2.46 (t, $J = 6.2$ Hz, 2H), 2.48 (t, 2H), 2.53 (t, 2H), 3.12 (t, $J = 7.0$ Hz, 2H), 3.46 (t, $J = 6.2$ Hz, 2H), 3.71 (ABX, $J = 9.4$ Hz, $J_{HP} = 5$ Hz, 2H), 4.02 (s, 1H), 4.26 (m, 2H), 6.19 (d, $J = 6.0$ Hz, 1H), 8.29 (s, 1H), 8.57 (s, 1H).
[11] A small portion of the isobutyryl-CH_2-iso-CoA was separated by chromatography. Its ^{1}H-NMR spectrum showed that it was devoid of *n*-butyryl-CH_2-iso-CoA.
[12] In four separate incubations of between 1 and 16 h duration the same product ratio was obtained each time.
[13] The reaction products were hydrolyzed, extracted with ether and the ratio isobutyric/*n*-butyric acid was determined by gas-liquid chromatography coupled to mass spectroscopy.
[14] H. Towbin, T. Staehelin, J. Gordon, *Proc. Natl. Acad. Sci. USA 76* (1979) 4350.

Isolated, Complex Zintl Molecules in the Gas Phase**

By *Andreas Hartmann* and *Konrad G. Weil**

Intermetallic molecules can be prepared in many different ways. For example, they are formed in high yields by aggregation from the gas phase; they are detected by electron collision ionization and subsequent mass selection. Studies of this sort have been reported, inter alia, by *Martin*.[1] Small, mostly diatomic intermetallic molecules have been detected mass spectrometrically by several groups, and their results have been reviewed in detail by *Gingerich*.[2]

We are especially interested in establishing whether even larger intermetallic aggregates can occur in equilibrium vapors. In the past few years we have carried out a series of mass spectrometric investigations on the composition of vapors over alkali metal/antimony and alkali metal/bismuth mixtures and have in this connection reported on two classes of intermetallic compounds:

a) predominately ionic molecules like Cs_2Sb_2 and Cs_2Sb_4[3]
b) cluster-like alkali-metal-rich particles such as Na_6Sb_4[4] and Cs_6Sb_4[5]

The molecules mentioned under a) can be regarded as aggregates of cesium ions and $(Sb_2)^{2\ominus}$ dumbbells or square-planar $(Sb_4)^{2\ominus}$ ions, while the particles mentioned under b) can be interpreted as alkali-metal octahedra arranged around a tetrahedral Sb_4 nucleus.

We now report on a further class of intermetallic molecules which we will describe as ternary and quaternary isolated Zintl molecules. For investigating the molecular beam emerging from a Knudsen cell we used a sector field mass spectrometer (VG Micromass MM-30K), modified by the incorporation of an ion-counting system and a Hall probe. It was possible to ease the manipulation of the complex spectrometer system still further by incorporating microprocessor controlling with a personal computer (Olivetti M24) and software developed by us.

The controlling of the electromagnet and of the ion counting unit are crucial in facilitating the computer-controlled detection and processing of the mass spectrometric signals. In order to avoid as far as possible any fragmentation effects during the ionization, electrons with an energy of ≤ 12 eV were used.

We investigated alloys of the following components:

cesium/indium/antimony	(2/1/3)
cesium/tin/antimony	(1/1/3)
cesium/tin/antimony/bismuth	(1/1/2/1)

The mixtures corresponding to the compositions shown in parentheses were prepared in a glovebox and sealed in evacuated quartz glass ampules. The ampules were opened under argon and a part of the regulus was transferred to a steel Knudsen cell, which was immediately placed in the mass spectrometer and evacuated. Depending on the combination of elements investigated, the signals of $Cs^{\oplus}$, $Sb_2^{\oplus}$, $Sb_4^{\oplus}$, $Bi^{\oplus}$, $Bi_2^{\oplus}$ and of the monomeric and dimeric ions of indium and tin dominate in the mass spectra. Moreover, molecules corresponding to the known intermetallic compounds of the ternary system cesium/antimony/bismuth are found as minority species. As examples for the identification of ternary molecules Figure 1 shows a section of the mass spectrum that was obtained from vapor over the cesium/indium/antimony mixture. The spectra for Cs_2InSb_3 and Cs_2Sb_4 calculated from the natural isotopic ratios are shown under the mass spectrum in the region $740 \leq m/z \leq 758$ after computer subtraction of background signals. It is immediately apparent that the assignment is unequivocal.

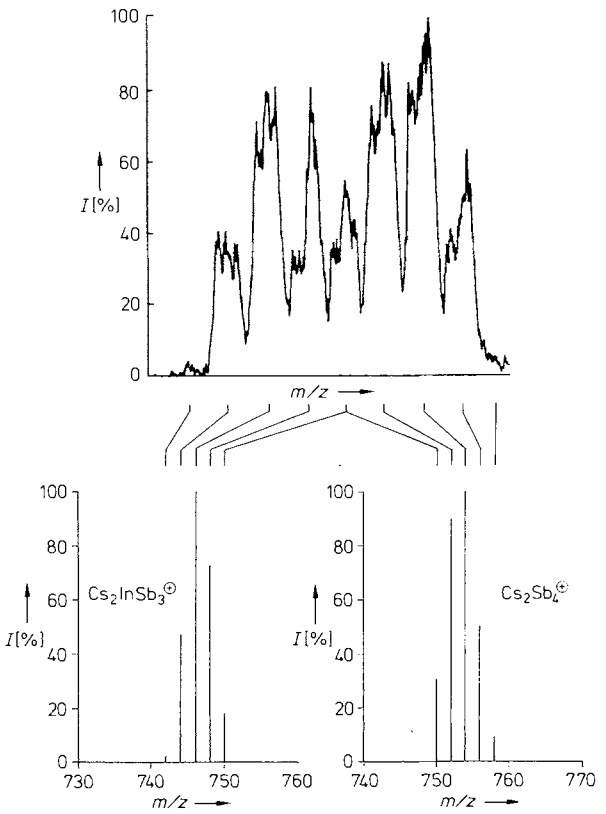

Fig. 1. Comparison of measured and calculated mass spectra for the vapor over a cesium/indium/antimony mixture at $T = 994$ K in the range $740 \leq m/z \leq 758$. I = relative intensity, referred to strongest signal.

The other ternary and quaternary compounds listed in Table 1 could be similarly assigned. The large number of natural tin isotopes makes the identification of tin-containing molecules difficult, since the neighboring mass signals in the mass range under consideration cannot be completely resolved. The comparison between calculated and measured mass spectra nevertheless leads to an unequivocal assignment, as shown for the example $CsSnSb_3$ in Figure 2. The ionization energies of the intermetallic molecules are, as far as they are known, also listed in Table 1. In addition, all the molecules mentioned in Table 1 show a significant shutter effect, thus evidencing their origin from within the Knudsen cell.

The compounds contain aggregates such as $(InSb_3)^{2\ominus}$, $(SnSb_3)^{\ominus}$, $(SnBiSb_2)^{\ominus}$, $(SnBi_2Sb)^{\ominus}$, and $(Sn_2Sb_2)^{2\ominus}$, isoelec-

[*] Prof. Dr. K. G. Weil, Dipl.-Ing. A. Hartmann
Institut für Physikalische Chemie der Technischen Hochschule
Petersenstrasse 20, D-6100 Darmstadt (FRG)

[**] This work is part of the Dissertation by *A. Hartmann*, Darmstadt D 17. It was supported by the Deutsche Forschungsgemeinschaft (Schwerpunkt: Physik anorganische Cluster) and by the Fonds der Chemischen Industrie.

Table 1. Ternary and quaternary intermetallic molecules that have been characterized via their isotopic patterns.

Molecule	Appearance energy [eV]
Cs_2InSb_3	[a]
$CsSnSb_3$	5.6 ± 0.2
$CsSnBiSb_2$	5.3 ± 0.2
$CsSnBi_2Sb$	5.0 ± 0.3
$Cs_2Sn_2Sb_2$	[a]

[a] Not yet determined.

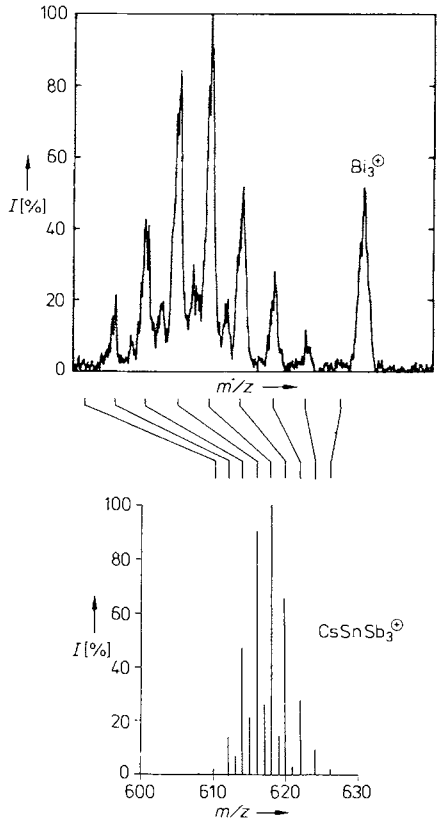

Fig. 2. Comparison of the measured and calculated mass spectra for the vapor over a cesium/tin/antimony mixture at $T = 779$ K in the range $610 \leqslant m/z \leqslant 630$. For clarity only signals with even m/z values are assigned. The signal at $m/z = 627$ contains the signal of $Bi_3^{\oplus}$ as background signal from previous experiments.

tronic with Sb_4 and with one or two $Cs^{\oplus}$ ions respectively for charge equalization.

The incorporation of heteroatoms (In, Sn) into tetrahedral Sb_4-units, not known in the solid state, is thereby made possible, at least formally, by the alkali metals transferring an appropriate number of electrons to the elements of the third and fourth main groups, respectively, such that these satisfy the (8-N) rule. Hence the above-mentioned molecules can be classified according to the concept of *Zintl, Klemm,* and *Busmann*.[6]

Received: April 11, 1988 [Z 2699 IE]
German version: *Angew. Chem. 100* (1988) 1111

[1] T. P. Martin, *Angew. Chem. 98* (1986) 197; *Angew. Chem. Int. Ed. Engl. 25* (1986) 197.
[2] K. A. Gingerich, *Curr. Top. Mater. Sci. 6* (1980) 345.
[3] B. Busse, K. G. Weil, *Ber. Bunsenges. Phys. Chem. 86* (1982) 93.
[4] T. Scheuring, K. G. Weil, *Surf. Sci. 156* (1985) 457.
[5] A. Hartmann, K. G. Weil, *ISSPIC 4*, Aix-en-Provence, France 1988.
[6] H. Schäfer, B. Eisenmann, W. Müller, *Angew. Chem. Int. Ed. Engl. 12* (1973) 694.

A Monomeric Potassium Salt of Bis(trimethylsilyl)methyl Phenyl Sulfone and the Determination of the $^1J(^{13}C,^{29}Si)$ Coupling Constants of Si-Stabilized "Carbanions"**

By *Hans-Joachim Gais,* Jürgen Vollhardt,* and *Carl Krüger*

Dedicated to Professor Ulrich Wannagat on the occasion of his 65th birthday

Crystal structure analyses of dimeric lithium salts of type **I** have afforded important insights into the nature of the stabilization of a carbanion by a sulfonyl group.[1] The structure of their asymmetric α-sulfonyl carbanions ($R^1 \neq R^2$) is essentially that postulated, e.g., in dimethyl sulfoxide solution[2] and calculated in the gas phase.[3a,b] Accordingly, coulombic interaction and negative anionic hyperconjugation ($n_C - \sigma^*_{SR^3}$)[3c] appear to be the dominant mechanisms of charge stabilization.

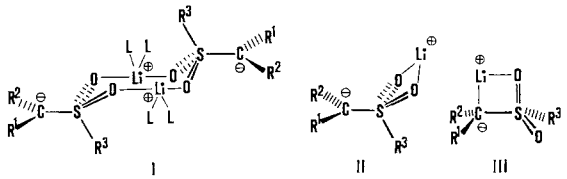

Alkali-metal salts of sulfones in dilute tetrahydrofuran solution (10^{-3} M), however, are not *dimeric* but rather *monomeric* contact ion pairs.[4] Ab initio calculations revealed two monomers (types **II** and **III**) for lithiomethyl methyl sulfone. Type **II** exhibits clear similarities to **I**, whereas **III** is completely different.[3b] What is the structure of monomeric contact ion pairs of metalated sulfones and how reliable are the calculated structures?[5] We hoped that the yet missing crystal structure of such a monomeric species might provide at least a partial answer to this question. We describe here the crystal structure analysis of the monomeric potassium·18-crown-6 salt of bis(trimethylsilyl)methyl phenyl sulfone, **1**, and we report, for the first time, the determination of the $^1J(^{13}C^{29}Si)$ coupling constants in "α-silyl carbanions".

The potassium salt **1** was obtained by metalation of bis(trimethylsilyl)methyl phenyl sulfone with potassium bis(trimethylsilyl)amide in diethyl ether in the presence of an equimolar amount of 18-crown-6. We selected this chelate ligand in order to suppress the dimerization, and the choice of potassium instead of lithium was expected to reveal the possible structural effect of the counterion.

The crystal structure analysis shows that **1**[6] is a monomer of type **II**; i.e., the potassium ion is bonded only to the sulfonyl O atoms of the anion (Figs. 1 and 2). The potassium ion is further coordinated by six O atoms of the

[*] Prof. Dr. H.-J. Gais, Dipl.-Ing. J. Vollhardt
Institut für Organische Chemie und Biochemie der Universität
Albertstrasse 21, D-7800 Freiburg (FRG)
Prof. Dr. C. Krüger
Max-Planck-Institut für Kohlenforschung
Kaiser-Wilhelm-Platz 1, D-4330 Mülheim a. d. Ruhr (FRG)

[**] This work was supported by the Deutsche Forschungsgemeinschaft. We thank Prof. Dr. *H. Fritz*, Dr. *S. Braun*, Dr. *J. Buddrus*, and Dr. *H. Hunkler* for the NMR spectra, Dipl.-Ing. *I. Erdelmeier* for the lithiosulfoximine, Dr. *R. Schwesinger* and Dipl.-Chem. *H. Schlemper* for the phosphazene base, and Prof. Dr. *G. Boche* and Prof. *F. G. Bordwell* for providing us with unpublished results.

crown ether. The anionic atom C1, which is located outside the coordination sphere of the potassium ion, is coordinated in a nearly planar fashion.

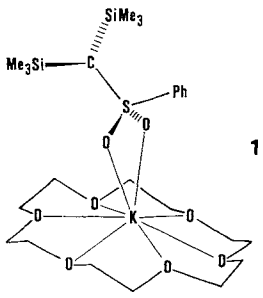

1

Fig. 1. Spatial representation of **1**.

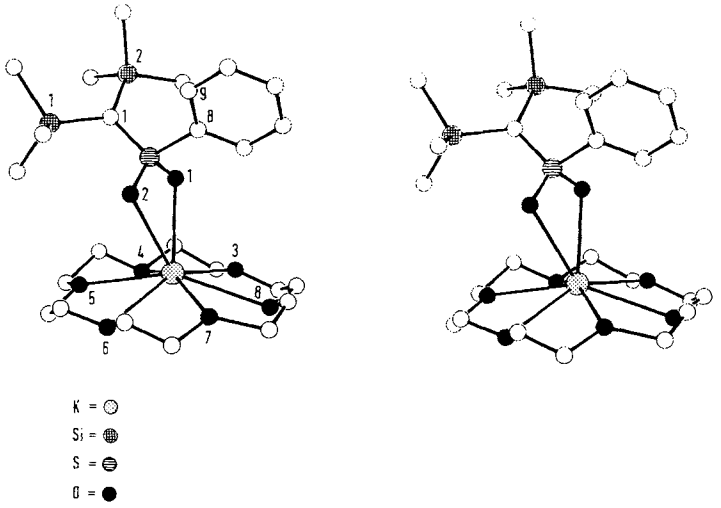

Fig. 2. Stereoprojection of the molecular structure of **1** (H atoms omitted). Important distances [Å] and angles [°]: C1-S 1.648(4), S-O1 1.473(3), S-O2 1.458(3), S-C8 1.802(4), C1-Si1 1.826(4), C1-Si2 1.875(7), K-O1 2.787(3), K-O2 2.880(3), K-O3-K-O8 2.774(4)-2.911(5); O1-K-O2 50.7(1), O1-S-O2 112.0(2), C8-S-C1 109.6(2), Si1-C1-Si2 124.0(2), Si1-C1-S 117.0(2), Si2-C1-S 118.7(2); C8-S-C1-Si1 −116.0, C8-S-C1-Si2 69.6, C1-S-C8-C9 34.3, O1-S-C1-Si2 −45.0, O2-S-C1-Si1 −1.0.

The anion has a conformation in which the lone pair on C1 is *gauche* to the two sulfonyl O atoms; however, it is rotated by ca. 23° from the ideal position[1d] for an $n_C-\sigma^*_{SPh}$ interaction. A similar finding was also made for the dimeric 1,*o*-dilithium salt of bis(trimethylsilyl)methyl phenyl sulfone **10**[7] (Table 1), which still exhibits the characteristic structural element of **I**.[7a] The length of the C1–S bond in bis(trimethylsilyl)methyl phenyl sulfone (1.747 Å)[7a] is decreased by 0.1 Å in **1** (1.648 Å), whereas the S–O bonds are only slightly longer in **1**. *There are no fundamental differences in the structures of the α-sulfonyl carbanions of* **1**, **I**, **II**, *and dimeric* **10**.

The $^1J(^{13}C^1H^\alpha)$ values have proven to be valuable probes of the structures of "carbanions" and ylides in solution:[8] sp^2 hybridization of the anionic C atom correlates with a positive Δ^1J(C,H) value and sp^3 hybridization with a negative value relative to the protonated precursor.[9] The same might hold for the $^1J(^{13}C,^{29}Si)$ coupling[10] in the synthetically important and structurally interesting "α-silyl carbanions",[11] e.g., **1** and α-silyl ylides.[12] In addition, this coupling might provide information on the C^α–Si bond.

Trimethylsilylmethyllithium **2**, which displays C–Li bonds in the crystal and whose anionic C atom is sp^3-hybridized,[13] is characterized by a solvent-dependent decrease in ^1J(C,Si) and ^1J(C,H). In contrast, ^1J(C,Si) increases relative to the protonated precursor for the Si- and S-stabilized "monocarbanions" so far investigated (Table 1). For the lithiated thioethers **3** and **4**,[14a] Δ^1J(C,Si) is smaller than for the SO-stabilized species **5**, **6a–d**, and **7**. Furthermore, the decrease in ^1J(C,H) is significantly less for **3** and **4** than, for example, for lithiomethyl phenyl sulfide, whose anionic C atom is sp^3-hybridized and which exhibits a C–Li bond.[8b,15] In the case of $^6Li/^{13}C$-labeled **4**, no C,Li coupling was observed down to −100 °C in THF; owing to the possibility of rapid exchange even at low temperatures, however, it is not possible to rule out the existence of C–Li bonds. Only a crystal structure analysis can reveal whether, in **3** and **4**, the anionic C atom exhibits partial planarity. In contrast, the SO-stabilized lithium salts **5**,[14b] **6a**,[16,1e] **6b**, and **7**, as well as the phosphazenium salts **6c** and **6d**, are characterized by a marked increase in *both* coupling constants: in the crystal, C1 of **6a** is coordinated in a nearly planar fashion,[1e] and this may be assumed to hold for **5**, **6b–d**, and **7** as well. The Δ^1J

Table 1. $^1J(^{13}C,^{29}Si)$ and $^1J(^{13}C,^1H)$ values of "α-silyl carbanions" and deviations from the corresponding values of the protonated compounds [a].

Compound	Δ^1J(C,Si)	^1J(C,Si)	Δ^1J(C,H)	^1J(C,H)	Experimental conditions [b]
$[Me_3SiCH_2]Li$ **2**	− 2.8	47.9	−17.1	101.1	[D$_8$]THF/27/3.00 [c]
2	−14.0	36.3	−23.8	94.6	C_6D_6/37/1.60 [d]
$[Me_3SiCHSCH_2SiMe_3]Li$ **3**	+21.4	70.0	− 5.6	122.7	[D$_8$]THF/37/1.00 [c]
$[Me_3SiCHSPh]Li$ **4**	+25.5	71.4	− 4.7	126.4	[D$_8$]THF/27/0.50 [e]
$[Me_3SiCHSOPh]Li$ **5**	+42.5	86.0	+15.5	143.4	[D$_8$]THF/27/0.70 [d]
$[Me_3SiCHSO_2Ph]Li$ **6a**	+41.2	79.9	+17.9	144.8	[D$_8$]THF/27/0.35 [e]
6a	+42.6	81.3	+18.7	144.0	[D$_6$]DMSO/22/1.00 [d]
$[Ph_3SiCHSO_2Ph]Li$ **6b**	+47.3	90.1	+19.8	146.4	[D$_8$]THF/22/0.20 [d]
$[Ph_3SiCHSO_2Ph]X$ **6c** [f]	+52.3	95.1	+20.2	146.0	[D$_8$]THF/33/0.20 [c]
$[Me_3SiCHSO_2Ph]X$ **6d** [f]	+47.1	86.0	+18.7	144.0	[D$_8$]THF/33/0.20 [c]
$[Me_3SiC(CH=CH_2)SO_2Ph]Li$ **7**	+42.0	79.0	—	—	[D$_8$]THF/22/0.50 [d]
$[(Me_3Si)_2CSO_2Ph]Li$ **8**	+30.0	64.1	—	—	[D$_8$]THF/37/0.20 [c]
8 · 2 Et_2O	+25.0	59.0	—	—	$C_6D_5CD_3$/79/0.20 [c]
$[(Me_3Si)_2CSO_2Ph]K \cdot Y$ **1** [g]	+33.4	67.5	—	—	[D$_8$]THF/37/0.30 [c]
$[(Me_3Si)_2CSO(NTs)Ph]Li$ **9**	+29.4	61.5	—	—	[D$_8$]THF/24/0.30 [d]
$[(Me_3Si)_2CSO_2C_6H_4Li]Li$ **10**	+29.2	63.3	—	—	[D$_8$]THF/37/0.20 [c]
$[Me_3SiCSO_2Ph]Li_2$ **11**	−22.2	57.0	—	—	[D$_8$]THF/50/0.30 [e]

[a] J and ΔJ in Hz; sign of J not determined. [b] Solvent/temperature [°C]/concentration [mol L^{-1}]. [c] 20 MHz. [d] 100 MHz. [e] 75 MHz. [f] X = $\{[(Me_2N)_3P{=}N]_3P{=}NHtBu\}^\oplus$. [g] Y = [18]crown-6.

values for **6a** in THF and dimethyl sulfoxide are nearly identical, and no C,Li coupling was found for $^6Li/^{13}C$-labeled **6a** down to $-100°C$ in THF; in contrast to lithiated sulfoximines,[17c,d] C-Li bonds in lithiated sulfoxides[17a,b] and sulfones have thus far not been observed.[21] Interestingly, $^1J(C,Si)$ and $^1J(C,H)$ for the phosphazenium salts **6c** and **6d**, prepared by quantitative deprotonation of (triphenylsilyl)- and (trimethylsilyl)methyl phenyl sulfone, respectively, with the phosphazene base $[(Me_2N)_3P{=}N]_3P{=}NtBu$,[18] show a somewhat stronger increase than for the lithium salts **6a** and **6b**.

That the silyl group in **6b** and most likely in the other "α-silyl carbanions" acts as a strong stabilizing group is shown by the acidity of (triphenylsilyl)methyl phenyl sulfone, which is 7.7 pK_a units greater than that of methyl phenyl sulfone.[19,2] An increase in $^1J(C,Si)$ is also found for the doubly Me_3Si-substituted potassium and lithium salts **1** and **8**, respectively, the lithiosulfoximine **9**, and the 1,*o*-dilithio sulfone **10**; in the crystal, Cl of **1** and **10** is coordinated in a nearly planar fashion. However, sp^2 hybridization alone cannot explain the high, positive $\Delta^1J(C,Si)$ values of the Si/S-stabilized "carbanions", as shown by the smaller Δ^1J values of +15.0 Hz (*E*)/ +16.9 Hz (*Z*) for $Me_3SiC(=CHPh)SO_2Ph$ relative to $Me_3SiCH(CH_2Ph)SO_2Ph$. Finally, the lithiation of the monolithium salt **6a** to give the 1,1-dilithium salt **11** is accompanied by a decrease in $^1J(C,Si)$; at least two lithium ions are bound to each dianionic C atom of **11** in the crystal *and* in solution.[20]

Received: March 25, 1988 [Z 2677 IE]
German version: *Angew. Chem. 100* (1988) 1108

[1] a) G. Boche, M. Marsch, K. Harms, G. M. Sheldrick, *Angew. Chem. 97* (1985) 577; *Angew. Chem. Int. Ed. Engl. 24* (1985) 573; b) H.-J. Gais, H. J. Lindner, J. Vollhardt, *ibid. 97* (1985) 865 and *24* (1985) 859; c) *ibid. 98* (1986) 916 and *25* (1986) 939; d) H.-J. Gais, J. Vollhardt, G. Hellmann, H. Paulus, H. J. Lindner, *Tetrahedron Lett. 29* (1988) 1259; e) G. Boche (Marburg), personal communication.

[2] F. G. Bordwell, J. C. Branca, C. R. Johnson, N. R. Vanier, *J. Org. Chem. 45* (1980) 3884, and references cited therein.

[3] a) S. Wolfe, *Stud. Org. Chem. (Amsterdam) 19* (1985) 133; b) D. A. Bors, A. Streitwieser, Jr., *J. Am. Chem. Soc. 108* (1986) 1397; c) D. A. Dixon, T. Fukunaga, B. E. Smart, *ibid. 108* (1986) 4027, and references cited therein.

[4] M. J. Kaufman, S. Gronert, D. A. Bors, A. Streitwieser, Jr., *J. Am. Chem. Soc. 109* (1987) 602.

[5] For the structure of $KC(SO_2R)_3$, which is unproductive in this respect, see J. S. Grossert, J. Hoyle, T. S. Cameron, S. P. Roe, B. V. Vincent, *Can. J. Chem. 65* (1987) 1407.

[6] Crystal structure analysis of $1 \cdot 1/2\,Et_2O$: $P\bar{1}$, $a = 11.557(2)$, $b = 11.847(3)$, $c = 14.284(1)$ Å, $\alpha = 79.29(1)$, $\beta = 83.80(1)$, $\gamma = 70.68(2)°$, room temperature, $Z = 2$, $\rho_{calcd} = 1.18$ g cm^{-3}, $\mu(Mo_{K\alpha}) = 3.04$ cm^{-1}. Enraf-Nonius diffractometer; 8203 measured reflections of which 5556 were observed ($I > 2\sigma(I)$); $R = 0.072$, $R_w = 0.095$ ($w = 1/\sigma^2(F_0)$) for 410 parameters. Ether molecule disordered at the center of inversion. Further details of the crystal structure investigation may be obtained from the Fachinformationszentrum Energie, Physik, Mathematik GmbH, D-7514 Eggenstein-Leopoldshafen 2 (FRG), on quoting the depository number CSD-52970, the names of the authors, and the journal citation.

[7] a) W. Hollstein, K. Harms, M. Marsch, G. Boche, *Angew. Chem. 99* (1987) 1279; *Angew. Chem. Int. Ed. Engl. 26* (1987) 1184; b) H.-J. Gais, J. Vollhardt, *Tetrahedron Lett. 29* (1988) 1529.

[8] a) G. Chassaing, A. Marquet, *Tetrahedron 34* (1978) 1399; b) D. Seebach, J. Gabriel, R. Hässig, *Helv. Chim. Acta 67* (1984) 1083, and references cited therein; c) S. O. Grim, *Methods Stereochem. Anal. 8* (1987) 645, and references cited therein.

[9] $^1J(^{13}C,^{31}P)$ in lithiophosphonates and phosphorus ylides show a hybridization dependence similar to $^1J(C,H)$: T. Bottin-Strzalko, J. Corset, F. Froment, M.-J. Pouet, J. Seyden-Penne, M.-P. Simonnin, *J. Org. Chem. 45* (1980) 1270; [8c].

[10] M. D. Beer, R. Grinter, *J. Magn. Reson. 31* (1978) 187.

[11] a) E. Colvin: *Silicon in Organic Synthesis*, Butterworths, London 1981; b) E. Block, M. Aslam, *Tetrahedron 44* (1988) 281; c) P. von R. Schleyer, T. Clark, A. J. Kos, G. W. Spitznagel, C. Rohde, D. Arad, K. N. Hok, N. G. Rodan, *J. Am. Chem. Soc. 106* (1984) 6467, and references cited therein.

[12] H. Schmidbaur, W. Richter, W. Wolf, F. H. Köhler, *Chem. Ber. 108* (1975) 2649.

[13] B. Tecle, A. F. M. Maqsudur Rahman, J. P. Oliver, *J. Organomet. Chem. 317* (1986) 267.

[14] a) F. A. Carey, A. S. Court, *J. Org. Chem. 37* (1972) 939; b) F. A. Carey, O. Hernandez, *ibid. 38* (1973) 2670.

[15] R. Amstutz, T. Laube, W. B. Schweizer, D. Seebach, J. Dunitz, *Helv. Chim. Acta 67* (1984) 224.

[16] J. Vollhardt, H.-J. Gais, K. L. Lukas, *Angew. Chem. 97* (1985) 695; *Angew. Chem. Int. Ed. Engl. 24* (1985) 696.

[17] a) G. Boche, M. Marsch, W. Massa, G. Baum, *Angew. Chem. 98* (1986) 1004; *Angew. Chem. Int. Ed. Engl. 25* (1986) 1011; b) H.-J. Gais, H. J. Lindner, J. Vollhardt, unpublished. c) H.-J. Gais, I. Erdelmeier, H. J. Lindner, J. Vollhardt, *Angew. Chem. 98* (1986) 914; *Angew. Chem. Int. Ed. Engl. 25* (1986) 938; d) H.-J. Gais, U. Dingerdissen, C. Krüger, K. Angermund, *J. Am. Chem. Soc. 109* (1987) 3775.

[18] R. Schwesinger, H. Schlemper, *Angew. Chem. 99* (1987) 1212; *Angew. Chem. Int. Ed. Engl. 26* (1987) 1167.

[19] F. G. Bordwell (Evanston, IL, USA), personal communication.

[20] H.-J. Gais, J. Vollhardt, H. Günther, D. Moskau, H. J. Lindner, S. Braun, *J. Am. Chem. Soc. 110* (1988) 978.

[21] Note added in proof (June 6, 1988): W. Hallstein, K. Harms, M. Morsch, *Angew. Chem. 100* (1988) 868; *Angew. Chem. Int. Ed. Engl. 27* (1988) 846, found a C^{α}-Li bond in 2,2-diphenyl-1-(phenylsulfonyl)cyclopropyllithium-dimethoxyethane (2/3).

Photolytic Cluster Synthesis: Synthesis and Structure of $[\{(Ph_3P)Au\}_7Mo(CO)_3]OH$**

By *Georg Beuter* and *Joachim Strähle**

In continuation of our studies on the controlled decomposition of azido complexes[1,2] we have also directed our attention to the photochemical degradation of $[(Ph_3P)AuN_3]$. Whereas most azido complexes undergo cleavage at the N_α-N_β bond with formation, e.g., of nitrido, nitrene, or phosphoraneimine complexes, on irradiation of $[(Ph_3P)AuN_3]$ the azide group is reductively eliminated with formation of $(Ph_3P)Au$ radicals, which subsequently unite to form gold clusters. In the presence of carbonyl-transition-metal complexes, heteronuclear metal clusters are formed. As first result of these investigations we report here on the new cluster $[\{(Ph_3P)Au\}_7Mo(CO)_3]^{\oplus}$ **1**, which can also be regarded as a half-sandwich complex of molybdenum(0) in which the C_6H_6 ligand is replaced by a previously unknown icosahedral $\{(Ph_3P)Au\}_7^{\oplus}$ fragment. Most of the gold clusters already known[3] were obtained by reduction of phosphanegold(I) halides $[(R_3P)AuX]$.

$$7[(Ph_3P)AuN_3] + [Mo(CO)_6] + H_2O \longrightarrow [\{(Ph_3P)Au\}_7Mo(CO)_3]^{\oplus}OH^{\ominus} + 3CO + 9N_2 + HN_3 \quad \text{(a)}$$

1 · $OH^{\ominus}$

For the synthesis of **1** [Eq. (a)] a mixture of $[(Ph_3P)AuN_3]$ and excess $[Mo(CO)_6]$ in THF is irradiated for ca. 12 h; after removal of the solvent the residue is taken up in CH_2Cl_2 and the reaction products separated by column chromatography.[4] The new cluster **1** crystallizes as $[(Ph_3PAu)_7Mo(CO)_3]^{\oplus}OH^{\ominus}$ in the form of air-stable red platelets.

The counterion $OH^{\ominus}$ was identified by X-ray structure analysis.[5] It arises as result of hydrolysis. If $[Mo(CO)_6]$ is not used in excess, then predominantly homonuclear gold

[*] Prof. Dr. J. Strähle, Dipl.-Chem. G. Beuter
Institut für Anorganische Chemie der Universität
Auf der Morgenstelle 18, D-7400 Tübingen 1 (FRG)

[**] This work was supported by the Deutsche Forschungsgemeinschaft and the Fonds der Chemischen Industrie.

complexes that have not yet been fully characterized are formed. The IR spectrum of **1** shows two CO stretching vibrations at 1835 and 1895 cm^{-1} characteristic for the local symmetry C_{3v}. The low frequencies point to a pronounced donor behavior of the $\{(Ph_3P)Au\}_7$ residue.

Gold clusters with more than seven Au atoms are characterized by their having a central Au atom and, as a rule, they can be derived from a centered icosahedron.[3,6] A remarkable feature is that the bonds from the central atom to the peripheral Au atoms are always distinctly stronger than the bonds between the peripheral Au atoms. In the cationic cluster **1** (Fig. 1) the seven Au atoms form an icosahedral fragment with Au–Au distances between 283.8 and 303.1 pm, as are typical for bonds between peripheral Au atoms.[6] The Mo atom replaces the central Au atom of the homonuclear Au cluster and is about equidistant from all seven Au atoms (277.1–286.0 pm). With regard to its structure, the Au_7Mo skeleton has so far no analogue among the homonuclear Au_8 clusters.

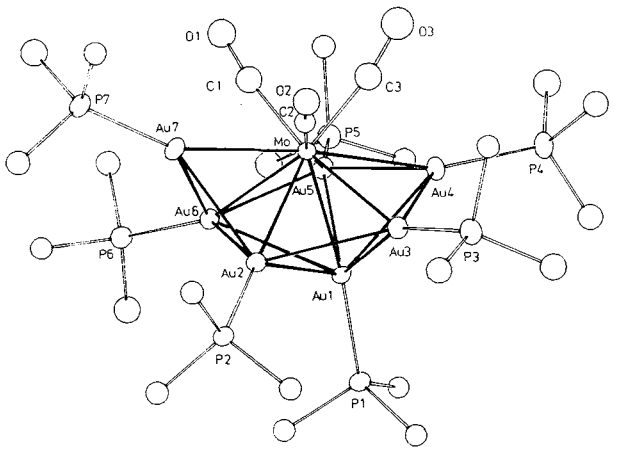

Fig. 1. Structure of **1** in the crystal of $\mathbf{1}\cdot OH^{\ominus}$. Of the phenyl groups of the phosphane ligands, only the bridgehead atoms are shown. Important bond lengths [pm] and angles [°]: Au-Au 283.80(9)–303.09(2), Mo-Au 277.11(1)–285.97(2), Au-P 228.65(4)–234.21(4), Mo-C1 197.4(2), Mo-C2 194.6(2), Mo-C3 193.8(2), C1-O1 119.1(2), C2-O2 120.1(2), C3-O3 121.2(2); Mo-C1-O1 171.8(2), Mo-C2-O2 176.3(1), Mo-C3-O3 168.5(2), C1-Mo-C2 96.90(8), C1-Mo-C3 79.49(8), C2-Mo-C3 78.14(8).

Most of the known hetero-metal-gold clusters contain isolated $(R_3P)Au$ fragments.[6,7] Two of the few examples of clusters with Au–Au bonds and a central hetero-metal atom are $[Au_6Pt(CC\text{-}t\text{Bu})(PPh_3)_7]^{\oplus}$[8] and $[\{(Ph_3P)Au\}_8Pt]^{2\oplus}$.[9] In neither case, however, can the Au_n skeleton be derived from an icosahedron.

The Mo–C–O groups in **1** are slightly bent, presumably for steric reasons; their C atoms are closer to the atoms Au4 and Au7 (C1–Au7 = 265.8(2), C2–Au7 = 280.5(2), C3–Au4 = 248.1(2) pm).

Assuming that the Mo atom has the oxidation state 0 and that only the electrons of the Au atoms contribute to the metal–metal bonds, then there are six electrons available for the skeletal bonding, as is also the case in toroidal Au clusters[3,6] and in the pentagonal-bipyramidal $[Au(PPh_3)]_7^{\oplus}$ cluster.[10] With these six electrons the Mo atom achieves a stable 18-electron configuration.

The cluster synthesis by reductive elimination of azide groups developed by us has the advantage over previously described reduction methods that only N_2 is formed as oxidation product. By variation of the phosphane ligands and the carbonyl components this method should provide access to a wide variety of clusters. Moreover, it can be extended to $[(Ph_3P)_2CuN_3]_2$.

Received: April 20, 1988 [Z 2713 IE]
German version: *Angew. Chem. 100* (1988) 1099

[1] K. Dehnicke, J. Strähle, *Angew. Chem. 93* (1981) 451; *Angew. Chem. Int. Ed. Engl. 20* (1981) 413.
[2] J. Strähle, *Comments Inorg. Chem. 4* (1985) 295.
[3] D. M. P. Mingos, *Gold Bull. 17* (1984) 5.
[4] Procedure: A mixture of 750 mg (1.5 mmol) of $[(Ph_3P)AuN_3]$ and 760 mg (2.5 mmol) of $[Mo(CO)_6]$ in 70 mL of freshly distilled THF was irradiated under a weak stream of nitrogen with UV light for 12 h. The solvent was then removed under vacuum and the residue dissolved in CH_2Cl_2 and chromatographed on a column of Al_2O_3. The red solution of **1** that was separated off was evaporated to dryness and treated with acetonitrile. $\mathbf{1}\cdot OH^{\ominus}$ crystallized in the form of plate-like crystals (yield 10%).—IR (KBr): $\tilde{\nu}_{C\text{-}O}$ = 1835 (s), 1895 cm^{-1} (vs); ^1H NMR ($CDCl_3$, 80 MHz): δ = 6.7–7.5; ^{31}P NMR (CH_2Cl_2, 32.4 MHz): δ = 45.3 (broad).
[5] $\mathbf{1}\cdot OH^{\ominus}$: $P2_1/n$, a = 1446.0(4), b = 3016.6(5), c = 3007.3(8) pm, β = 91.63(2)°, Z = 4, R = 0.047 for 7772 independent reflections with $I > 3\sigma(I)$ and 669 refined parameters (Enraf-Nonius CAD4, SDP-PLUS, $Cu_{K\alpha}$, ω/θ scan $5 \leq \theta \leq 55°$. Empirical absorption corrections, anisotropic temperature parameters for the metal atoms and P atoms; H atoms not considered. Further details of the crystal structure investigation are available on request from the Fachinformationszentrum Energie, Physik, Mathematik GmbH, D-7514 Eggenstein-Leopoldshafen 2 (FRG), on quoting the depository number CSD-53061, the names of the authors, and the journal citation.
[6] K. P. Hall, D. M. P. Mingos, *Prog. Inorg. Chem. 32* (1984) 237.
[7] P. Braunstein, J. Rose, *Gold Bull. 18* (1985) 17.
[8] D. E. Smith, A. J. Welch, I. Treurnicht, R. J. Puddephatt, *Inorg. Chem. 25* (1986) 4616.
[9] J. J. Bour, R. P. F. Kanters, P. P. J. Schlebos, W. P. Bosman, H. Behm, P. T. Beurskens, J. J. Steggerda, *Recl. Trav. Chim. Pays-Bas 106* (1987) 157.
[10] J. W. A. van der Velden, P. T. Beurskens, J. J. Bour, W. P. Bosman, J. H. Noordik, M. Kolenbrander, J. A. K. M. Buskes, *Inorg. Chem. 23* (1984) 146.

Helicates: Tetra- and Pentanuclear Double Helix Complexes of Cu^I and Poly(bipyridine) Strands**

By *Jean-Marie Lehn** and *Annie Rigault*

Dedicated to Professor Edgar Lederer on the occasion of his 80th birthday

The design of molecular species undergoing self-assembling into a well-defined structure opens ways to the spontaneous but directed generation of an organized supramolecular entity, following an "Aufbau plan" contained in the structural elements whose interaction leads to the association process. Such systems may display positive cooperativity and represent prototypes of molecular amplification devices, if, once initiated, the subsequent steps of the assembling process are facilitated.[1] The formation of the double helix of nucleic acids is a cooperative self-assembling of a supramolecular structure held together by the hydrogen bonds between the complementary nucleic bases. In general terms, such properties may be displayed by polytopic receptor molecules in which interaction between the subunits or substrate binding to them, occurs in a way so that each association step sets the stage for the following one.

[*] Prof. Dr. J.-M. Lehn, A. Rigault
Institut le Bel, Université Louis Pasteur
4, rue Blaise Pascal, 67000 Strasbourg (France)

[**] We thank Dr. *Jack Harrowfield* and Dr. *Jay Siegel* for their contribution to the initial stages of this work, which was supported by the CNRS and, in part, by ORIS Industrie.

In continuation of our studies on quaterpyridine pQP[2] we have recently shown that the acyclic ligands BP_2, **2**[3] and BP_3, **3**[3] containing two and three bpy[3] subunits (derived from 6,6′-dimethyl-2,2′-bipyridine **1**) bind Cu^I ions so as to form respectively dinuclear or trinuclear *double stranded helicate* complexes in which two ligand molecules wrap around two or three Cu^I ions (one per bpy site of each ligand) which hold the strands together. The structures of the dinuclear $[Cu_2(pQP)_2]^{2\oplus}$,[2] trinuclear $[Cu_3(BP_3)_2]^{3\oplus}$[3] and dinuclear $[Cu_2(BP_2)_2]^{2\oplus}$[4] complexes were confirmed by X-ray crystallography.[5]

In order to further explore this ability of polybipyridine ligands to spontaneously assemble into double helix complexes, we have synthesized and studied the Cu^I binding properties of the next two members of the series, namely BP_4 **4** and BP_5 **5**, respectively.

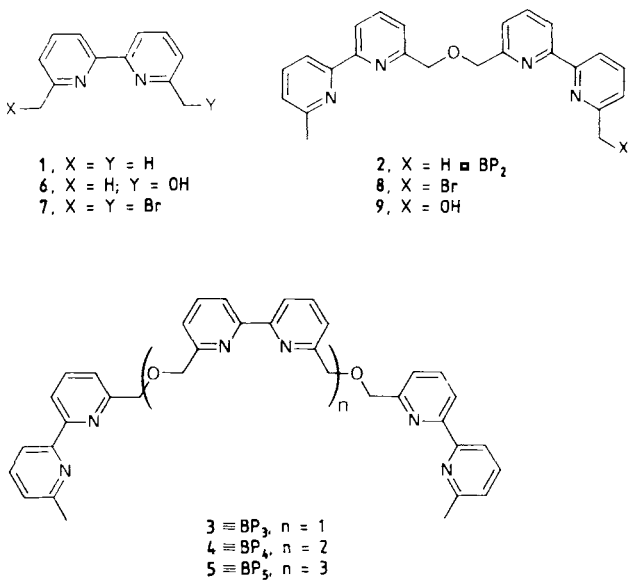

Treatment of the monohydroxymethyl bipyridine derivative **6**[3] with NaH in tetrahydrofuran (THF) at room temperature for 30 min, followed by addition of one equivalent of the bis(bromomethyl) compound **7**[6] and heating at reflux for 3 h gave a mixture from which chromatography on silica (eluent 1% $MeOH/CH_2Cl_2$) enabled isolation of the monobromomethyl dimeric compound **8** in 45% yield (m.p. 152–155 °C) together with 15% of the trimeric substance **3**[3] and 30% of recovered **7**. Reaction of **8** with sodium acetate (in dimethylformamide, 140 °C, 12 h) followed by hydrolysis with NaOH (methanol/water (9/1), 30 min reflux) gave the monohydroxymethyl compound **9** (m.p. 178 °C, 80% yield). Treatment of **9** with one equivalent of potassium *tert*-butoxide in THF (room temperature, 30 min) followed by addition of one equivalent of **8** and heating to reflux for 12 h, gave a precipitate of the tetrameric substance **4** in 65% yield (m.p. > 260 °C). Similar treatment of **9**, followed by addition of 0.5 equivalent of the dibromide **7**[6] and heating at reflux for 3 h gave a precipitate of practically pure pentameric compound **5** in 68% yield (m.p. > 260 °C). The new compounds **4**, **5**, **8**, and **9** gave spectral (^{1}H-NMR, ^{13}C-NMR, FAB-MS) and microanalytical data in agreement with the assigned structures.

Compound **4** and even more so **5** have very low solubility in most common organic solvents. They are however readily soluble in acidic aqueous or organic solution at pH < 2, in which they are protonated. The 400-MHz NMR spectrum of BP_5 **5** measured under such conditions is shown in Figure 1.

The two compounds BP_4 and BP_5 are linear repetitive polybipyridine ligands, which, in view of the rich coordination chemistry of the bpy subunit, should be able to form polynuclear complexes with numerous metal ions. We have at present mainly investigated the complexation of Cu^I ions, which are known to bind bpy units in a distorted tetrahedral geometry, as found both in the case of the parent substance 6,6′-dimethyl-bpy **1**[7] and in the crystal structures of the double helicates formed with BP_3[3] and BP_4.[4]

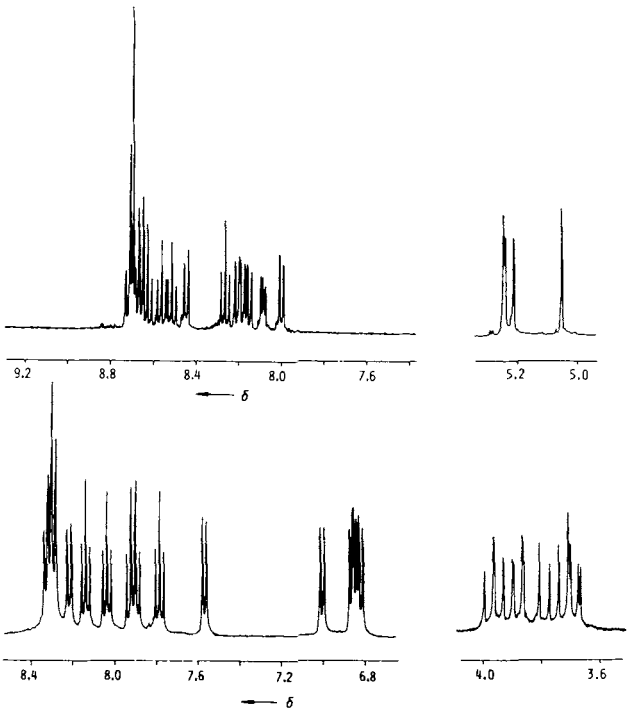

Fig. 1. 400-MHz ^{1}H-NMR spectra of the ligand BP_5 **5** (top) in [D$_6$]acetone + 10% CF_3COOD, and of the complex $[Cu_5(BP_5)_2][CF_3SO_3]_5$ in [D$_3$]acetonitrile (bottom); the signals of the CH_2 protons ($\delta = 3.5$–5.5) are shown with an expanded scale compared to those of the bipyridine protons ($\delta = 6.8$–8.8); the CH_3 signals are not shown.

The Cu^I complexes of BP_4 **4** and BP_5 **5** have been prepared either by addition of a slight excess of an acetonitrile solution of a Cu^I salt (perchlorate, trifluoroacetate, trifluoromethanesulfonate) to a solution/suspension of the ligand in chloroform, or by addition of an aqueous solution of a Cu^{II} salt to a suspension of the ligand in acetonitrile followed by reduction with a slight excess of aqueous hydrazine. The formation of the Cu^I complexes is quantitative and results in the immediate appearance of the deep orange-red color characteristic of $[Cu^I(bpy)_2]^{\oplus}$ and related species.[7] The complexes were crystallized from 50% aqueous acetonitrile as deep-red needles. They are very stable toward oxygen. Their solubility depends on the counteranions, the triflates being soluble in organic solvents such as CH_3CN and $CHCl_3$. Their electronic absorptions correspond to those expected for Cu^I(bpy)-complexes (see Ref. [3] and references cited therein). Titration of the ligands by $[Cu(CH_3CN)_4]BF_4$ monitored by the absorption at 449 nm gave the compositions $[Cu_4(BP_4)_2][BF_4]_4$ and $[Cu_5(BP_5)_2][BF_4]_5$ for the complexes of BP_4 and BP_5 respectively. The following absorption coefficients have been measured

at $\lambda_{max} = 449$ nm under the same conditions (solvent $CH_3CN/H_2O = 4/1$; 20°C): $\varepsilon = 4800$, 10300, 14500, 18900, and 22300 (±10%) for the complexes formed respectively by ligands **1**, BP_2 **2**, BP_3 **3**, BP_4 **4**, and BP_5 **5** with $CuCF_3SO_3$; these values agree with the number of sites present in each complex.

The ^{1}H-NMR spectra of the complexes are very different from those of the ligands, the changes observed being similar to those found on going from BP_3 **3** to $[Cu_3(BP_3)_2](CF_3CO_2)_3$.[3] On complex formation, the bpy proton signals are shifted markedly upfield and, most importantly, the CH_2OCH_2 protons which appear as singlets in the free ligands, shift upfield by more than 1 ppm and split into overlapping AB patterns (Fig. 1, bottom). Thus, the CH_2 protons have become nonequivalent in the complexes and lie in the shielding regions of the bipyridine groups. Furthermore, addition of the optically active NMR shift reagent (Eu(tfc)$_3$ [tfc = 3-(trifluoromethylhydroxymethylene)-(+)-camphorato] to a solution of the complexes formed by BP_4 and BP_5 in CD_3CN, led to splitting of some proton NMR signals, demonstrating the presence of two diastereomeric species; consequently, the complexes must have a chiral structure.

By analogy with the earlier spectral and structural results on the trinuclear Cu^I complex of BP_3 **3**,[3] these properties indicate that the Cu^I complexes of BP_4 and BP_5 are tetranuclear and pentanuclear *double-stranded helicates* of Cu^I, designated by ds-$\mathscr{H}[Cu_4(BP_4)_2]^{4\oplus}$ and ds-$\mathscr{H}[Cu_5(CP_5)_2]^{5\oplus}$.[8] Their overall shape is that of *inorganic double helices*, schematically represented by **I** and **II** and presenting about 2 and 2.5 turns respectively. Their total length may be estimated to lie around 22 Å and 27 Å respectively; they thus are *self-organized nanostructures*, and represent entries into the field of functional nanoscale species and molecular devices.[1] Their structural features should be analogous to those of the trinuclear complex of BP_3 **3**;[3] more accurate data have to await crystal structure determination. From the point of view of coordination chemistry, they represent polynuclear complexes containing a string of metal ions.

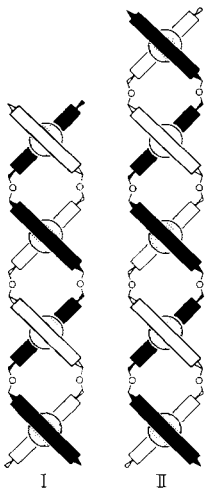

I II

The present results extend the earlier ones[3] and show that inorganic double helices can indeed be generated on the basis of the structural design developed. Further chain length extension will lead to even larger organized nanostructures, eventually up to polymeric repetitive ligands and to double helical polymeric complexes. Numerous studies may be envisaged from the organic, inorganic, physical and biochemical points of view such as: subunit modification, complexation of various other metal ions, binding cooperativity, dynamics of double helix wrapping and unwrapping, interaction with DNA double helices, self-organization and amplification devices, etc.

Received: May 26, 1988 [Z 2781 IE]
German version: *Angew. Chem. 100* (1988) 1121

[1] J.-M. Lehn, *Angew. Chem. 100* (1988) 91; *Angew. Chem. Int. Ed. Engl. 27* (1988) 289.
[2] J.-M. Lehn, J.-P. Sauvage, J. Simon, R. Ziessel, C. Piccini-Leopardi, G. Germain, J.-P. Declercq, M. Van Meersche, *Nouv. J. Chim. 7* (1983) 413.
[3] J.-M. Lehn, A. Rigault, J. Siegel, J. Harrowfield, B. Chevrier, D. Moras, *Proc. Natl. Acad. Sci. USA 84* (1987) 2565.
[4] J. Harrowfield, J.-M. Lehn, B. Chevrier, D. Moras, unpublished results.
[5] For recent examples of helical dinuclear complexes see: E. C. Constable, M. G. B. Drew, M. D. Ward, *J. Chem. Soc. Chem. Commun. 1987*, 1600; J. Libman, Y. Tor, A. Shanzer, *J. Am. Chem. Soc. 109* (1987) 5880; for an earlier case, see: G. Struckmeier, U. Thewalt, J.-H. Furhop, *J. Am. Chem. Soc. 98* (1976) 278; see also references cited in [3].
[6] J.-C. Rodriguez-Ubis, B. Alpha, D. Plancherel, J.-M. Lehn, *Helv. Chim. Acta 67* (1984) 2264.
[7] P. J. Burke, D. R. McMillin, W. R. Robinson, *Inorg. Chem. 19* (1980) 1211 and references cited therein.
[8] The spectroscopic data unequivocally rule out a polymeric complex, which in itself would be very interesting.

Methyl 4-Hydroxy-5-iodo-2,3-dimethoxy-6-methylbenzoate: The Aromatic Fragment of Calichemicin $\gamma^I_{1\alpha}$. Synthesis, X-Ray Crystallographic Analysis, and Properties**

By *K. C. Nicolaou,* T. Ebata, N. A. Stylianides, R. D. Groneberg,* and *P. J. Carrol*

The calichemicins are a new class of naturally occurring compounds with potent biological activities recently isolated by a Lederle group.[1] One of the most prominent members of this class is calichemicin $\gamma^I_{1\alpha}$ **1** isolated from *Micromonospora echinospora ssp. calichencis*. The biological profile of **1** includes: (1) subpicogram potency against gram-positive bacteria, and, in the biochemical induction assay, (2) very high potency against a number of animal tumor models and (3) cleavage of double-stranded DNA with minimal concurrent single-stranded breakage.[1,2] The aromatic fragment of this important biomolecule with its high degree of substitution and unusual pattern presents an interesting synthetic and stereochemical problem due to steric congestion and potential out-of-plane orientations of certain of its appendages. Herein we report (a) the first synthesis of this calichemicin $\gamma^I_{1\alpha}$ fragment as its methyl ester **2**, (b) its spontaneous resolution by crystallization into pure enantiomeric forms, (c) X-ray crystallographic

[*] Prof. K. C. Nicolaou, T. Ebata, N. A. Stylianides, R. D. Groneberg, P. J. Carrol
Department of Chemistry, University of Pennsylvania
Philadelphia, PA 19104 (USA)

[**] This work was supported by Lederle Laboratories, Pearl River, NY, and by the University of Pennsylvania. Stimulating and helpful discussions with Dr. *May Lee* and Dr. *Ving Lee* (Lederle Laboratories), Dr. *David Eaton* (Du Pont de Nemours, Experimental Station, Wilmington, DE), Dr. *R. Huffman* (Indiana University), Prof. *Jay Siegel* (University of California, San Diego), and Prof. *Kurt Mislow* (Princeton University) are acknowledged. We also thank Dr. *George Furst* and *John Dykins* of our Department for their excellent NMR and mass spectroscopic assistance and useful comments.

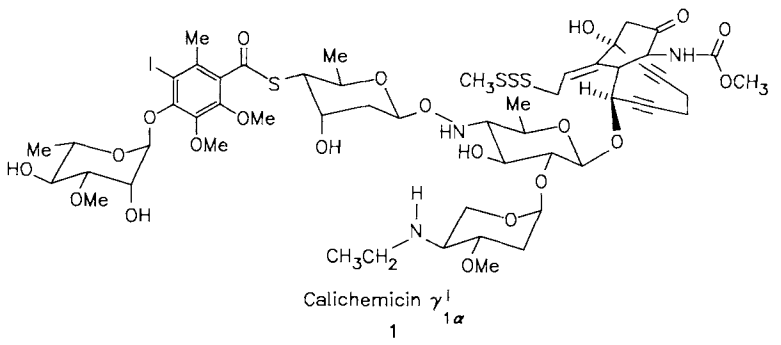

analysis of both enantiomers, and (d) the properties of **2**, including its second harmonic generation (SHG) activity.

For the synthesis of the aromatic segment **2**, we started with 3,4,5-trimethoxytoluene **3** and proceeded as outlined in Scheme 1. Thus, **3** was diiodinated under Suzuki conditions[3] to afford diiodide **4** in 93% yield. Selective monodemethylation of **4** using boron trichloride led to compound **5** (58%), which was then benzyloxymethylated under standard conditions to afford compound **6** in quantitative yield.

Catalytic methoxycarbonylation of **6** under the conditions of *Dolle* et al.[4] furnished the methyl benzoate **7** as the major product (44% yield, accompanied by ca. 11% regioisomer and 6% diester.) Finally, deprotection of **7** under acidic conditions followed by flash chromatography led to the desired calichemicin $\gamma^{I}_{1\alpha}$ fragment **2** in 89% yield as a crystalline solid. Recrystallization from chloroform–petroleum ether afforded colorless monoclinic crys-

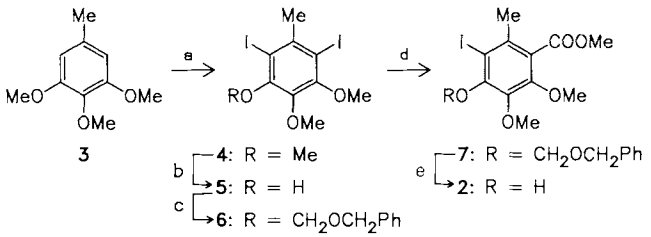

Scheme 1. Synthesis of compound **2**. Reagents and conditions: (a) 1.1 equiv. I_2, 0.56 equiv. HIO_4, AcOH, 53 °C, 24 h, 93%; (b) 6.0 equiv. BCl_3, CH_2Cl_2, 25 °C, 40 h, 58% (plus 13% regioisomer and 12% dihydroxy compound); (c) 1.5 equiv. $PhCH_2OCH_2Cl$, 2.0 equiv. iPr_2NEt, $ClCH_2CH_2Cl$, 70 °C, 18 h, 100%; (d) 0.05 equiv. $Pd(OAc)_2$, 0.05 equiv. $Ph_2P(CH_2)_3PPh_2$, 2.0 equiv. Et_3N, CO atmosphere, DMSO/MeOH (2:1), 70 °C, 24 h, 44% (plus ca. 11% regioisomer plus 6% dimethyl ester); (e) conc. HCl, MeOH, 25 °C, 7 h, 89%. Spectral data of compound **2**: ^{1}H-NMR (250 MHz, $CDCl_3$): $\delta = 6.42$ (s, 1H, OH), 3.88, 3.87, 3.84 (3s, each 3H, OCH_3), 2.32 (s, 3H, CH_3); ^{13}C-NMR (125.0 MHz, $CDCl_3$): $\delta = 167.8$, 150.4, 149.6, 136.5, 134.0, 121.8, 84.0, 61.3, 61.0, 52.4, 25.2; IR ($CHCl_3$): $\tilde{\nu}_{max} = 3519$ (m), 3040 (w), 3020 (m), 2960 (m), 1730 (s), 1575 (m), 1465 (s), 1428 (m), 1364 (m), 1270 (s), 1234 (m), 1099 (m) cm^{-1}; UV (MeOH): $\lambda_{max} = 214$ nm; MS, calculated for $C_{11}H_{14}O_5I$ $[M+H]^{\oplus}$ 352.9886, found $[M+H]^{\oplus}$ 352.9848.

tals (m.p. 134–135 °C). Spectral data for authentic **2** obtained by degradation of calichemicin $\gamma^{I}_{1\alpha}$ **1** were in agreement with those for synthetic **2**, thus proving the identity of the two samples.[5]

Restricting the stereogenic elements in **2** to the three axes C1-COOMe, C2-OMe, and C3-OMe (assuming that the hydroxyl hydrogen lies on the plane of the benzene ring and is H-bonded to the C-3 oxygen), one recognizes the possibility of four diastereomeric pairs, of which only **2a** and **2b** (Scheme 2) need to be seriously considered.[6] MM2 calculations (MacroModel)[7] on **2a** and **2b** placed them rather close in energy. An X-ray crystallographic analysis of **2** was undertaken, therefore, in order to shed light on this stereochemical question. Interestingly, it was

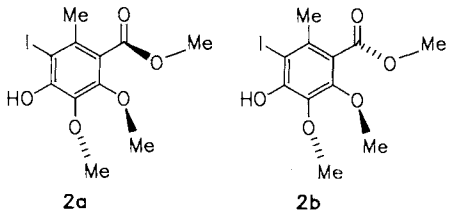

Scheme 2. Two of the four possible diastereomeric pairs of **2** (enantiomers not shown).

found that the crystals obtained as described above were a statistical mixture of two types, each containing pure enantiomer of **2a**.[8]

Table 1. Summary of X-ray data [a].

Crystal No.	I	II
Measured reflections	2654	2702
Reflections used in refinement $[F_0^2 > 3\sigma(F_0^2)]$	2232	2223
c_1	102.7	93.2
c_2	174.3	166.0
R, R_w ((*R,R,R*)-**2a**)	0.023, 0.028	0.030, 0.036 [b]
R, R_w ((*S,S,S*)-**2a**)	0.027, 0.032 [b]	0.019, 0.023

[a] Crystals of **2** were subjected to X-ray diffraction structure determination using an Enraf-Nonius CAD4 diffractometer. $C_{11}H_{13}O_5I$, $M_r = 352.13$, monoclinic, $P2_1$, $a = 8.568(2)$, $b = 6.189(2)$, $c = 12.375(5)$ Å, $\beta = 99.68(3)°$, $V = 646.9$ Å^3, $Z = 2$, $\rho_{calcd} = 1.808$ g cm^{-3}, $\lambda(Mo_{K\alpha}) = 0.071073$ Å, $\mu = 24.5$ cm^{-1}. Data collection was performed for reflection classes *hkl*, *hkl*, $\overline{hkl}$, and $\overline{hkl}$ to provide Friedel pairs of monoclinic data. The absolute configuration was determined by including anomalous dispersion terms in the scattering factors. Data were corrected for Lorentz and polarization effects and a numerical absorption correction was applied. The structure was solved by Patterson methods followed by weighted Fourier syntheses. Hydrogen atoms were found from a subsequent difference Fourier map, but were not refined. Refinement was performed by full-matrix least squares to minimize $\Sigma w(|F_0|^2 - |F_c|^2)$ with $w = 1/(1 + [(F_0 - c_1)/c_1]^2)$. All crystals examined revealed acentric crystal lattices. Further details of the crystal structure determination are available on request from the Director of the Cambridge Crystallographic Data Centre, University Chemical Laboratory, Lensfield Road, Cambridge CB2 1EW (England), on quoting the full literature citation. [b] The fit for the molecule of opposite configuration is not as good, as indicated by the R, R_w values.

Table 1 summarizes the results for two of the structure determinations. Crystal I contained the (*R,R,R*) enantiomer and crystal II the (*S,S,S*) enantiomer of **2a** as determined from the R and R_w values. Figure 1 displays an ORTEP representation of (*R,R,R*)-**2a** and (*S,S,S*)-**2a**. Figure 2 shows an ORTEP drawing of the unit cell of (*R,R,R*)-**2a**.

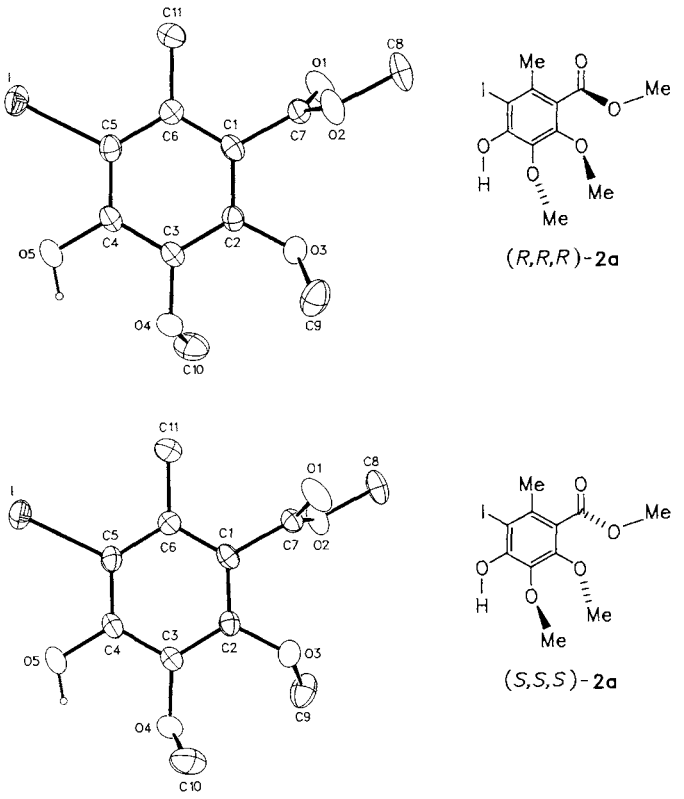

Fig. 1. Molecular structure of (*R,R,R*)-**2a** and (*S,S,S*)-**2a** (ORTEP). Intermolecular hydrogen bonds: O5···O1 2.757 Å, O5-HO5 0.885 Å, HO5···O1 2.045 Å, ∢O5-HO5···O1 140.3°. Intramolecular hydrogen bonds: HO5···O4 2.240 Å, ∢O5-HO5···O4 114.9°. The moiety O4-C3-C4-O5-HO5 is planar within 0.02 Å. Torsion angles [°]: C2-C1-C7-O1 101.0(4), C3-C2-O3-C9 −65.2(5), C6-C1-C7-O1 −76.4(4), C2-C3-O4-C10 −72.0(5), C2-C1-C7-O2 −80.1(4), C4-C3-O4-C10 108.8(4), C6-C1-C7-O2 102.5(4), C3-C4-O5-HO5 3.2(5), C1-C2-O3-C9 119.2(4), C5-C4-O5-HO5 −179.3(3).

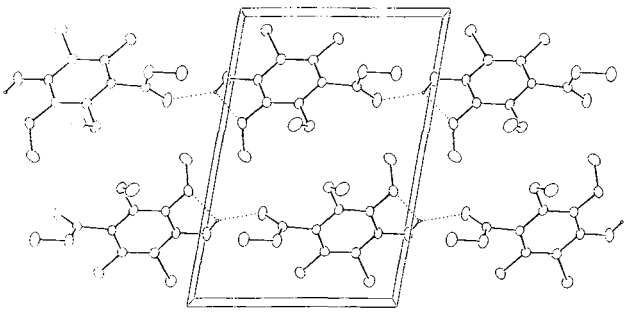

Fig. 2. Unit cell of (*R,R,R*)-**2a** (ORTEP).

In the crystal lattice, the molecules line up in parallel rows with the carbonyl of one molecule facing the free hydroxyl group of the next molecule. The hydroxyl hydrogen atom participates in (1) a weak intermolecular hydrogen bond with the carbonyl oxygen (O1) of a neighboring molecule and (2) a weak intramolecular interaction with methoxy oxygen O4.

Measurements on methanolic solutions of selected crystals of **2a** revealed no optical rotation, thus indicating racemization upon dissolution. It appears, therefore, that special crystal packing forces are responsible for the observed spontaneous resolution of the two enantiomers of **2a** upon crystallization.

Based on the observation of the acentric nature of the crystal lattice of compound **2** and the presence of donor-acceptor substituents on this aromatic system, we were encouraged to investigate its second harmonic generation (SHG) activity.[9] Indeed, the SHG activity of **2** is ca. 50% of that of urea.[10] The crowded aromatic system represents a new concept in the development of SHG-active materials and may prove useful in the preparation of more potent compounds by suitable substituent manipulation on the ring.

In conclusion, we have synthesized, by a short and efficient route, the aromatic segment (**2**) of calichemicin $\gamma^{I}_{1\alpha}$, which was found to crystallize spontaneously into pure enantiomeric forms, (*S,S,S*)-**2a** and (*R,R,R*)-**2a**. X-ray crystallographic studies revealed the acentric nature of the crystal lattice and parallel rows of molecules arranged in a head-to-tail fashion. The phenolic hydrogen was found to be simultaneously engaged in both intramolecular and intermolecular H-bonding. Finally, we have demonstrated that this class of compounds may hold considerable promise as SHG materials.[11]

Received: March 23, 1988 [Z 2675 IE]
German version: *Angew. Chem. 100* (1988) 1138

[1] M. D. Lee, T. S. Dunne, M. M. Siegel, C. C. Chang, G. O. Morton, D. B. Borders, *J. Am. Chem. Soc. 109* (1987) 3464; M. D. Lee, T. S. Dunne, C. C. Chang, G. A. Ellestad, M. M. Siegel, G. O. Morton, W. J. McGahren, D. B. Borders, *ibid. 109* (1987) 3466.

[2] A similar class of compounds, the esperamicins, was reported by a Bristol-Myers group: J. Golik, J. Clardy, G. Dubay, G. Groenewold, H. Kawaguchi, M. Konishi, B. Krishnan, H. Ohkuma, K. Saitoh, T. W. Doyle, *J. Am. Chem. Soc. 109* (1987) 3461; J. Golik, G. Dubay, G. Groenewold, H. Kawaguchi, M. Konishi, B. Krishnan, H. Ohkuma, K. Saitoh, T. W. Doyle, *ibid. 109* (1987) 3462.

[3] H. Suzuki, *Org. Synth. 51* (1971) 94.

[4] R. E. Dolle, S. J. Schmidt, L. I. Kruse, *J. Chem. Soc. Chem. Commun. 1987*, 904.

[5] We thank Dr. *May Lee* of Lederle Laboratories for these spectra.

[6] The other two diastereomeric pairs with *syn* orientation of the methyl groups at C-2 and C-3 suffer from strong nonbonding interactions between these methyl groups.

[7] We thank Professor *W. C. Still* (Columbia University) for making this program available to us.

[8] For some interesting examples and discussions on the subject of spontaneous resolution see: a) J. Jacques, A. Collet, S. H. Wilen: *Enantiomers, Racemates and Resolutions*. Wiley, New York 1981, and references cited therein; b) R. E. Pincork, K. R. Wilson, *Chem. Educ. 50* (1973) 455, and references cited therein; c) E. Havinga, *Biochem. Biophys. Acta 13* (1954) 171; d) I. Bernal, W. Ries, H. Brunner, D. K. Rastogi, *J. Organomet. Chem. 290* (1985) 353; e) I. Bernal (University of Euston), personal communication; f) J. Shaeffer (University of British Columbia), personal communication.

[9] D. J. Williams, *Angew. Chem. 96* (1984) 637; *Angew. Chem. Int. Ed. Engl. 23* (1984) 690, and references cited therein.

[10] We thank Dr. *David Eaton* (Du Pont de Nemours, Experimental Station, Wilmington, DE) for these results. These measurements were done on a powder of **2**; the urea used was 250-μm size. Crystal phase matching has not been investigated as yet.

[11] Synthetic studies on the cyclic enediyne moiety of **1**: K. C. Nicolaou, G. Zuccarello, Y. Ogawa, E. J. Schweiger, T. Kumazawa, *J. Am. Chem. Soc. 110* (1988) 4866.

Pentadienyl, a More Reactive and More Strongly Bound Ligand Than Cyclopentadienyl**

By *Enrique Meléndez, Atta M. Arif, Manfred L. Ziegler,** and *Richard D. Ernst**

Cyclopentadienyl ligands have proven to be invaluable to the field of organometallic chemistry, in large part due

[*] Prof. R. D. Ernst, E. Meléndez, Dr. A. M. Arif
Department of Chemistry, University of Utah
Salt Lake City, UT 84112 (USA)
Prof. Dr. M. L. Ziegler
Anorganisch-chemisches Institut der Universität
Im Neuenheimer Feld 270, D-6900 Heidelberg 1 (FRG)

[**] This work was supported by the National Science Foundation (USA).

to their robust binding to metals, which allows them to function as superb "stabilizing ligands".[1] It has recently become clear that the open pentadienyl ligands also have much promise. Despite arguments that these open ligands could be both more strongly bound and more reactive than their cyclic counterparts,[2] there has to date been no evidence demonstrating such stronger binding, and in an early review it was even concluded that metal-pentadienyl bonding seemed generally weaker.[3] In fact, direct comparisons between seemingly similar "open metallocene" and metallocene systems are not possible due to their differing steric and symmetry environments, and further complications may result from differing spin configurations. In order to circumvent such problems, and therefore to allow for more direct comparisons, we have synthesized a series of "half-open metallocenes", namely, $[M(C_5H_5)(\text{pentadienyl})]$ (M = Cr, Fe, $Co^{\oplus}$, Ru, Os)[4] and $[M(C_5H_5)(\text{pentadienyl})(L)]$ (M = Ti, V, L = phosphane; M = Cr, L = CO)[4,5] in which the above complications have been eliminated. Herein we report details for the "half-open titanocenes", and the unusual observation that, relative to the C_5H_5 ligands in these complexes, the metal-pentadienyl linkages are indeed more reactive, readily taking part in potentially useful carbon-carbon bond-forming reactions, despite the fact that the pentadienyl ligands are surprisingly more strongly bound than the "stabilizing" cyclopentadienyl ligands.

The syntheses of the desired complexes are carried out as in Equation (a), leading to the isolation of analytically

$$\underset{\mathbf{1}}{[Ti(C_5H_5)Cl_2(thf)_2]} + L + 2KL' \xrightarrow{THF} \underset{\mathbf{2}}{[Ti(C_5H_5)LL']} \qquad (a)$$

a, $L' = C_5H_7$, L = PEt_3; **b**, $L' = 2,4\text{-}Me_2C_5H_5$, L = PMe_3, PEt

pure products in reasonable yields. Treatment of the PEt_3 complexes with $P(OMe)_3$ leads to the corresponding phosphite compounds, e.g., $[Ti(C_5H_5)(C_5H_7)P(OMe)_3]$.

In order to compare the pentadienyl and cyclopentadienyl bonding in these species, a single-crystal X-ray diffraction study was undertaken for **2b**, L = PEt_3 (Fig. 1).[6]

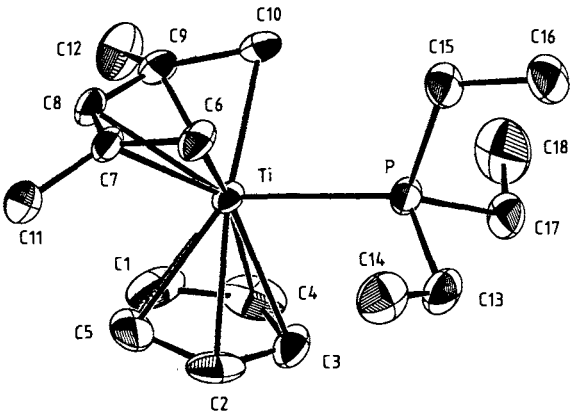

Fig. 1. Perspective view of **2b**, L = PEt_3.

Quite unlike some pentadienyl complexes of chromium, iron, cobalt, and ruthenium, the $Ti\text{-}C_{pentadienyl}$ bonds are dramatically shorter (0.106(5) Å) than the $Ti\text{-}C_{cyclopentadienyl}$ bonds, averaging 2.240(3) vs. 2.346(4) Å, respectively. A similar observation has been made for the complex $[V(C_5H_5)(C_5H_7)PEt_3]$. Hence, it becomes clear that metal-pentadienyl bonding for at least titanium and vanadium is inherently and surprisingly stronger than that for the "stabilizing" cyclopentadienyl ligand, and in complexes such as $[M(2,4\text{-}Me_2C_5H_5)_2]$ (M = Ti, V), one can surmise that this is not simply the result of differing spin configurations.[7]

Despite its remarkably strong binding to titanium, the pentadienyl ligand has retained its greater chemical reactivity relative to cyclopentadienyl. Thus, treatment of **2b**, L = PEt_3, with CH_3CN was expected to bring about a coupling reaction, producing a complex ligand such as in **I**. In

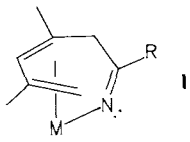

I

fact, such a species, **3**, was isolated in an analytically pure state, and an X-ray diffraction study demonstrated that indeed pentadienyl-acetonitrile coupling had taken place (Fig. 2).[6] Notably, the former pentadienyl portion rearranged to a sickle configuration apparently prior to the coupling step, and a dimeric product resulted via N_2Ti_2 ring formation and loss of PEt_3. Our early studies indicate that pentadienyl ligands are reasonably prone to engage in such coupling reactions and the resulting carbon-carbon bond constructions appear to offer practical applications.[8]

$[\{Ti(C_5H_5)(Me_3C_6H_5N)\}_2]$ **3**

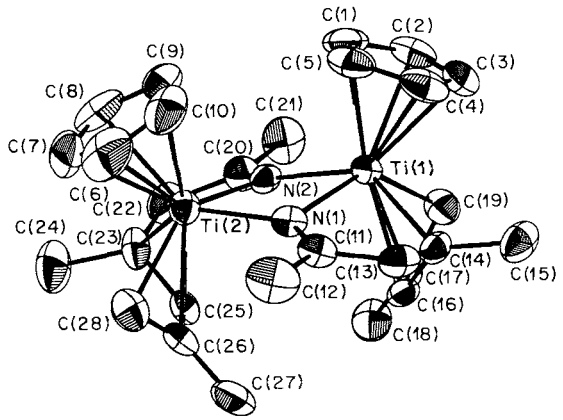

Fig. 2. Perspective view of **3**.

Since metal-pentadienyl and metal-cyclopentadienyl bonding had been found to be so similar for chromium, iron, the cobalt cation, and ruthenium,[2c,4c] there was no reason previously to expect titanium and vanadium to be any different, and shorter V-C bond distances in $[V(2,4\text{-}Me_2C_5H_5)_2]$ compared with $[V(C_5H_5)_2]$ could readily be considered to be an artifact of their differing spin configurations. The isolation of "half-open titanocenes" and "half-open vanadocenes" has now led to a resolution of this problem, with the surprising result that for at least titanium and vanadium, the open ligand may be more strongly bound than even cyclopentadienyl, and this may well account in part for the high thermal stability of "open titanocenes"[9] relative to the unstable complexes $[Ti(C_5H_5)_2]$ and even $[Ti(C_5Me_5)_2]$.[10] While it appears re-

markable that such a strongly bound ligand would be so reactive, it is possible to reconcile these seemingly contradictory observations. The key to this is the extra resonance stabilization experienced by the aromatic cyclopentadienyl unit, which may be regarded as a factor imparting a greater relative tendency to resist change. This readily translates into both a greater reluctance of this ligand to undergo disruption of its π system through coupling reactions (which are, however, known in some cases[11]) and a weaker metal-ligand bonding interaction. Thus, the lower reactivity of the cyclopentadienyl ligand in this case is a reflection of its inherent stability, rather than the strength of its binding to the metal center. However, if one were to deal with a process involving the complete removal of the π ligands, it would be expected that the cyclopentadienyl unit should be lost more readily.[12] Additional experimental and theoretical studies are underway to gain further insight into these observations.

Experimental Procedure

2b, L = PEt_3: A blue-green solution of 1.0 g (3.1 mmol) **1** in 50 mL of THF was cooled under nitrogen to −78 °C and 0.90 mL (6.2 mmol) of PEt_3 was added, yielding a dark-blue solution. To this solution was slowly added 0.9 g (6.6 mmol) of the potassium salt of the 2,4-dimethylpentadienyl anion dissolved in 50 mL of THF, after which the mixture was stirred for 2 h at −78 °C, resulting in a brown solution. The reaction mixture was allowed to warm to room temperature and stirred for about 6 h. The solvent was removed in vacuo and the crude product extracted with several portions of hexane and filtered on a coarse frit. The greenish-brown hexane solution was concentrated under reduced pressure and cooled to −78 °C, yielding a red, air-sensitive crystalline product. Complete IR data (Nujol): $\tilde{\nu}$ [cm^{-1}] = 3170 (m), 1563 (m), 1304 (mw), 1261 (s), 1170 (sh), 1155 (mw), 975 (w), 889 (w), 797 (s).—^{1}H-NMR: δ = 6.01 (s, 1 H), 5.02 (d, 5 H, J = 1 Hz), 1.83 (s, 8 H), 1.26 (m, 6 H), 0.71 (m, 9 H), −0.85 (t, 2 H, J = 6 Hz).—^{13}C-NMR: δ = 112.46 (d, 1 C, J = 156 Hz), 101.37 (s, 2 C), 100.60 (d, 5 C, J = 170 Hz), 53.89 (t, 2 C, J = 150 Hz), 30.91 (q, 3 C, J = 134 Hz), 18.69 (t, 2 C, J = 126 Hz), 7.94 (q, 2 C, J = 128 Hz).—^{31}P-NMR: δ = 41.28.—Correct C,H analysis.

3: To a solution of 0.40 g (1.22 mmol) **2b**, L = PEt_3, in 30 mL of hexane at room temperature was added 0.20 mL (3.6 mmol) of CH_3CN dropwise. Reaction began immediately with the formation of a dard-red solution, followed by the precipitation of an oily dark-brown solid. Upon completion of the addition, the dark-red reaction mixture was stirred for an additional 30 min. Cooling the solution to −78 °C for ca. 12 h yielded a dark-brown air-sensitive product. After removing the supernatant solution, the crystalline product was dried in vacuo. Complete IR (Nujol): $\tilde{\nu}$ [cm^{-1}] = 3170 (m), 1629 (s), 1563 (m), 1311 (mw), 1261 (ms), 1172 (mw), 1157 (m), 977 (w), 890 (m), 800 (s) cm^{-1}.—^{1}H-NMR: δ = 0.89 (d, 1 H, J = 5 Hz), 1.16 (s, 3 H), 1.31 (s, 3 H), 1.52 (d, 1 H, J = 5 Hz), 2.04 (s, 3 H), 2.17 (d, J = 20 Hz), 2.76 (d, 1 H, J = 20 Hz), 5.23 (s, 1 H), 5.89 (s, 5 H).—^{13}C-NMR: d = 21.93 (q, 1 C, J = 122 Hz), 26.37 (q, 1 C, J = 120 Hz), 26.76 (q, 1 C, J = 125 Hz), 60.58 (t, 1 C, J = 124 Hz), 69.97 (t, 1 C, J = 136 Hz), 76.53 (s, 1 C), 111.74 (d, 5 C, J = 170 Hz), 122.33 (d, 1 C, J = 158 Hz), 133.98 (s, 1 C), 174.74 (s, 1 C).—Correct elemental analysis (C, H, N, Ti).

Received: October 20, 1987;
revised: April 15, 1988 [Z 2482 IE]
German version: *Angew. Chem. 100* (1988) 1132

[1] a) J. P. Collman, L. S. Hegedus, J. R. Norton, R. G. Finke: *Principles and Applications of Organotransition Metal Chemistry*, University Science Books, Mill Valley, CA (USA) 1987; b) C. M. Lukehart: *Fundamental Transition Metal Organometallic Chemistry*, Brooks/Cole, Monterey, CA (USA) 1985); c) I. Haiduc, J. J. Zuckerman: *Basic Organometallic Chemistry*, de Gruyter, New York 1985.

[2] a) D. R. Wilson, A. A. DiLullo, R. D. Ernst, *J. Am. Chem. Soc. 102* (1980) 5928; b) D. R. Wilson, J.-Z. Liu, R. D. Ernst, *ibid. 104* (1982) 1120; c) R. D. Ernst, *Acc. Chem. Res. 18* (1985) 56.

[3] I. I. Kritskaya, *Russ. Chem. Rev. (Engl. Transl.) 41* (1972) 1027.

[4] a) J. W. Freeman, D. R. Wilson, R. D. Ernst, P. D. Smith, D. D. Klendworth, M. P. McDaniel, *J. Polym. Sci. Part A 25* (1987) 2063; b) C. Elschenbroich, E. Bilger, R. D. Ernst, D. R. Wilson, M. S. Kralik, *Organometallics 4* (1985) 2068; c) R. D. Ernst, H. Ma, G. Sergeson, T. Zahn, M. L. Ziegler, *ibid. 6* (1987) 848.

[5] R. M. Kowaleski, F. Basolo, W. C. Trogler, R. W. Gedridge, T. D. Newbound, R. D. Ernst, *J. Am. Chem. Soc. 109* (1987) 4860.

[6] **2b**, L = PEt_3, crystallizes in space group $P2_1/c$ with a = 7.986(2), b = 7.960(1), c = 29.129(8) Å, β = 90.18(2)°, Z = 4; R = 0.066, R_w = 0.067 for 1852 independent, observed reflections. **3** crystallizes in space group $P2_1/a$ with a = 14.377(7), b = 10.440(8), c = 16.920(10) Å, β = 90.60(5)°, Z = 4; R = 0.050, R_w = 0.040 for 3344 independent, observed reflections. Further details of the X-ray crystal structure analysis are available on request from the Fachinformationszentrum Energie, Physik, Mathematik GmbH, D-7514 Eggenstein-Leopoldshafen 2 (FRG) on quoting the depository number CSD-53153, the names of the authors, and the full journal citation.

[7] To establish the validity of such a comparison, one can note that even though "open ferrocenes" possess *longer* Fe-C bonds than those of ferrocene, MO studies indicate that the Fe-pentadienyl bonding is actually slightly *stronger*, indicating that the lower stability of the free pentadienyl unit can lead to stronger metal bonding even at slightly longer distances. In a molecule such as **2b**, L = PEt_3, in which the M-pentadienyl bonds are dramatically *shorter* relative to C_5H_5, one must conclude that pentadienyl is more strongly bound, which is quite reasonable given that overlap and steric effects, which could hinder metal-pentadienyl bonding relative to metal-C_5H_5 bonding, should be less important for larger metals such as titanium and vanadium. See M. C. Böhm, M. Eckert-Maksić, R. D. Ernst, D. R. Wilson, R. Gleiter, *J. Am. Chem. Soc. 104* (1982) 2699.

[8] a) M. S. Kralik, J. P. Hutchinson, R. D. Ernst, *J. Am. Chem. Soc. 107* (1985) 8296; b) G. Erker, K. Engel, J. L. Atwood, W. E. Hunter, *Angew. Chem. 95* (1983) 506; *Angew. Chem. Int. Ed. Engl. 22* (1983) 494; *Angew. Chem. Suppl. 1983*, 675; c) H. Yasuda, A. Nakamura, *ibid. 99* (1987) 745 and *26* (1987) 723.

[9] J.-Z. Liu, R. D. Ernst, *J. Am. Chem. Soc. 104* (1982) 3737.

[10] a) H. H. Brintzinger, J. E. Bercaw, *J. Am. Chem. Soc. 92* (1970) 6182; b) J. E. Bercaw, *ibid. 96* (1974) 5087; c) G. P. Pez, J. N. Armor, *Adv. Organomet. Chem. 19* (1981) 1.

[11] G. K. Anderson, *Organometallics 5* (1986) 1903.

[12] An interesting parallel may be noted in some of the work of *Jonas* in which the C_5H_5 anion is readily replaced by other organic anions: K. Jonas, *Angew. Chem. 97* (1985) 292; *Angew. Chem. Int. Ed. Engl. 24* (1985) 295.

Phase Transformations of Lithium Nitride under Pressure

By *Heinz Jürgen Beister,* Sabine Haag, Rüdiger Kniep, Klaus Strössner,* and *Karl Syassen*

Of the binary compounds A_3B of the alkali metals (A = Li, Na, K, Rb, Cs) with an element of the nitrogen group (B = N, P, As, Sb, Bi), lithium nitride Li_3N is unique in that it is so far the only known nitride of the alkali metals. The compound is made up of planar Li_2N-layers and pure Li layers (Fig. 1), and is known to be a rapid conduc-

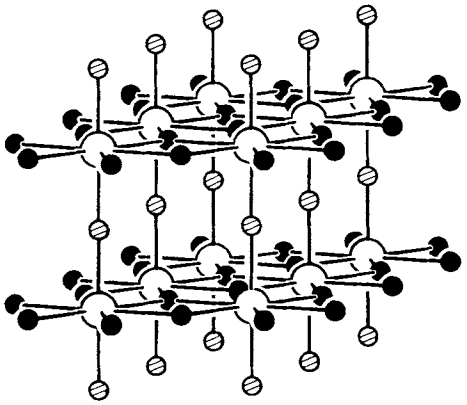

Fig. 1. The crystal structure of α-Li_3N. Large circles: nitrogen; small circles (black or shaded): lithium.

[*] Dr. H. J. Beister, Dipl.-Ing. (FH) S. Haag, Prof. Dr. R. Kniep [+], Dr. K. Strössner, Priv.-Doz. Dr. K. Syassen
Max-Planck-Institut für Festkörperforschung
Heisenbergstr. 1, D-7000 Stuttgart 80 (FRG)

[+] Permanent address: Eduard-Zintl-Institut der Technischen Hochschule Hochschulstr. 4, D-6100 Darmstadt (FRG)

tor of lithium ions;[1,2] its conductivity is caused by lithium vacancies within the Li_2N layers. Due to the elongated cavities between the Li_2N layers the structure of Li_3N is very loosely packed, and, consequently, it could be expected to undergo a pressure-induced phase transformation. Indeed, the first indications of such a transformation have been provided by a recent ^{7}Li-NMR investigation.[3]

Fragments of a Li_3N single crystal grown by the Czochralski method[4] were used for a series of pressure experiments. It was visually established that the red transparent sample became dark opaque at 0.6 ± 0.05 GPa in a pressure cell with diamond window[5] (pressure measurement by the ruby luminescence method[6]). Optical absorption measurements in the region of about 1.85–2.30 eV (Fig. 2)

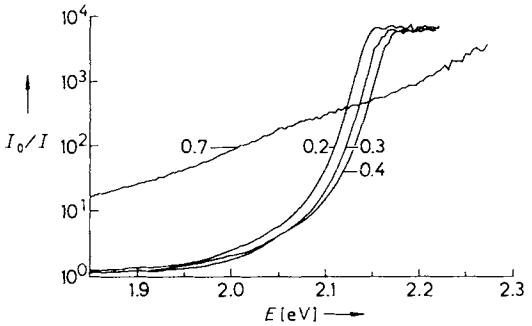

Fig. 2. Absorption spectra (unpolarized light, incident light // c axis) of Li_3N at various pressures p. Given is the inverse transmission I_0/I for samples of about 30 μm thick. p in GPa.

on the normal pressure phase α-Li_3N ($p < 0.6$ GPa) show that the absorption edge shifts to higher energies with increasing pressure. In the high-pressure phase β-Li_3N ($p > 0.6$ GPa) the absorption increases with increasing energy, but has little structure in the spectral range investigated. Raman measurements and X-ray powder investigations show that β-Li_3N is stable up to at least 8 GPa.

Larger amounts (0.3 g) of β-Li_3N were prepared in a Belt apparatus in a graphite crucible at room temperature and 4 GPa in 15 h. After release of pressure the high-pressure phase remained metastable. The results of differential thermal analyses (heating) and subsequent X-ray powder investigations provide evidence for the exothermal transformation of β-Li_3N into α-Li_3N above 200 °C. The X-ray powder diagram of β-Li_3N obtained by the Guinier method ($Cu_{K\alpha}$ radiation, film technique, evaluation with micrometer and densitometer) indicated a hexagonal structure.[7] A more accurate determination of the lattice constants by a least squares calculation gave a c/a ratio of 1.78, thus indicating a structure of the Na_3As type.[8] The X-ray powder diagram calculated for β-Li_3N with the atomic parameters of Na_3As[9] agrees with the observed values for reflection positions and intensities. Thus β-Li_3N and Li_3P are isotypic (Na_3As structure[8]). The crystallographic data of α-Li_3N[10] and β-Li_3N are listed in Table 1.

The crystal structure of β-Li_3N (Fig. 3) consists of planar layers of hexagonal symmetry with a composition $Li_{3/3}N_{3/3} \equiv LiN$ (Li–N distance in the layers 205.5 pm). The layers are stacked in the sequence ABAB ... in the 001 direction. Each nitrogen atom binds two further lithium atoms at a distance of 209.5 pm above and below the plane, thus completing its first coordination sphere to give

Table 1. Crystallographic data for α-Li_3N [10] and β-Li_3N.

	α-Li_3N	β-Li_3N
Space group	$P6/mmm$	$P6_3/mmc$
Lattice parameters [pm]	$a = 364.8(1)$	$a = 355.2(1)$
	$c = 387.5(1)$	$c = 631.1(3)$
Z	1	2
V [pm^3]	44.659×10^6	68.956×10^6
ρ_{calcd} [mg mm^{-3}]	1.295	1.677
Point positions N	1(a) 0, 0, 0	2(c) 1/3, 2/3, 1/4
Li(1)	1(b) 0, 0, 1/2	2(b) 0, 0, 1/4
Li(2)	2(c) 1/3, 2/3, 0	4(f) 1/3, 2/3, 0.583

a trigonal bipyramid $Li_2NLi_{3/3}$. As a result of the interpenetration of the Li_3N layer packets each nitrogen atom in a second coordination sphere is additionally coordinated trigonal prismatically by six lithium atoms further away (231.3 pm). Thus, altogether each nitrogen atom is surrounded by a fully capped trigonal prismatic array of lithium atoms.

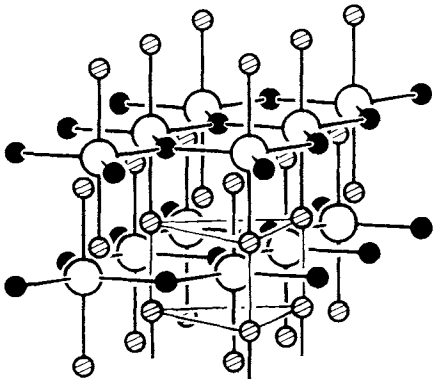

Fig. 3. The crystal structure of β-Li_3N. Large circles: nitrogen; small circles (black or shaded): lithium. The trigonal prismatic coordination in the second sphere is outlined for a nitrogen atom.

Figure 4 shows the relationship between the structure types α-Li_3N and Na_3As. For the transformation of α-Li_3N into β-Li_3N (Na_3As-type) the Li–N bonds marked with ≈ have to be opened and the layer packets shifted towards

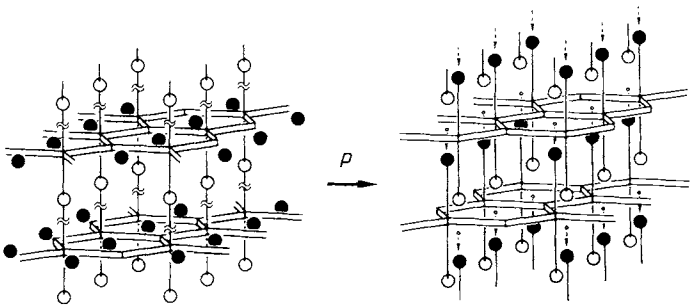

Fig. 4. Structural relationship between α-Li_3N and β-Li_3N. The Li_3N_3 structural unit is represented schematically and simply as a hexagonal network. The small dots indicate the positions from which the lithium atoms have to be shifted in the direction of the arrow. For further details see text.

each other such that the packing of the nitrogen atoms changes from a simple hexagonal arrangement (α-Li_3N) into a hexagonal closest packing arrangement (β-Li_3N). The lithium atoms shown in black then have to be merely

shifted in the direction of the nitrogen atoms of the neighboring layer.

Since the phase transformation takes place at the relatively low pressure of 0.6 GPa, it can hardly be ruled out that at least a partial transformation of α-Li_3N into β-Li_3N takes place on preparing powdered samples by grinding in a mortar, so that X-ray powder photographs of α-Li_3N always show small amounts of β-Li_3N. The observation of "additional reflections" in Li_3N powders was first reported in the literature more than a decade ago.[11]

Depressurized Li_3N samples which had previously been subjected to pressures of more than 10 GPa were investigated by the Gandolfi technique.[12] In one case an X-ray powder diagram was obtained whose reflections were consistent with a cubic structure with extinctions corresponding to an F-centered lattice (observed reflections 111, 200, 220, 311; $a = 427.3(2)$ pm; $Cu_{K\alpha}$ radiation). It is assumed that the highest pressure phase of Li_3N crystallizes in the Li_3Bi-type structure.[13] Dimorphism between Na_3As- and Li_3Bi-type structures is also observed in some higher homologues of Li_3N, e.g. in K_3Bi[14] and Li_3Sb.[13]

Received: March 22, 1988 [Z 2672 IE]
German version: *Angew. Chem. 100* (1988) 1116

[1] A. Rabenau, *Festkörperprobleme 18* (1978) 77.
[2] A. Rabenau, *Solid State Ionics 6* (1982) 24.
[3] M. Mali, J. Roos, D. Brinkmann, *Phys. Rev. B: Condens. Matter 36* (1987) 3888.
[4] E. Schönherr, G. Müller, E. Winkler, *J. Cryst. Growth 43* (1978) 469.
[5] A. Jayaraman, *Rev. Mod. Phys. 55* (1983) 65.
[6] G. J. Piermarini, S. Block, J. D. Barnett, R. A. Forman, *J. Appl. Phys. 46* (1975) 2774.
[7] D. Louer (Laboratoire de Cristallochimie, Université des Rennes I): *DICVOL, Trial and Error Method for the Automatic Indexing of Powder Patterns, 1982.*
[8] G. Brauer, E. Zintl, *Z. Phys. Chem. Abt. B37* (1937) 323.
[9] K. Yvon, W. Jeitschko, E. Parthé (Laboratoire de Cristallographie aux Rayons-X, Université de Genève): *LAZY-PULVERIX, A Program to calculate X-Ray and Neutron-Diffraction Powder Patterns, 1977.*
[10] A. Rabenau, H. Schulz, *J. Less-Common Met. 50* (1976) 155.
[11] B. A. Boukamp, R. A. Huggins, *Phys. Lett. A58* (1976) 231.
[12] G. Gandolfi, *Mineral. Petrogr. Acta 13* (1967) 67.
[13] E. Zintl, G. Brauer, *Z. Elektrochem. Angew. Phys. Chem. 41* (1935) 297.
[14] D. E. Sands, D. H. Wood, W. J. Ramsey, *Acta Crystallogr. 16* (1963) 316.

Functionalized, Enantiomerically Pure [2.1.1]-, [2.2.1]-, and [2.2.2]-Triblattanes**

By *Hermann Müller, Johann-Peter Melder, Wolf-Dieter Fessner, Dieter Hunkler, Hans Fritz,* and *Horst Prinzbach**

We have developed an efficient scheme for the synthesis and resolution of the gyrochiral, D_3-symmetric trishomocubanetrione **1**.[1] Target compounds for which compound **1** should prove useful as starting material include not only the already known D_3-symmetric 1,4,7-trisexomethylene- and 1,4,7-trispiro-derivatives[1] and 1,4,7-triscarbocations,[2] but also variously functionalized as well as variously (hetero)benzoid annelated [2.1.1]- (**A**), [2.2.1]- (**B**) and [2.2.2]-triblattanes (**C**).[3,4] Such structural entities are of interest,

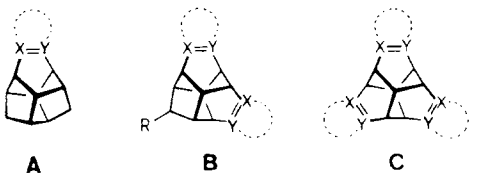

inter alia, as synthetic intermediates for the study of intramolecular interactions[5] between their characteristically oriented X=Y chromophores, because of their chiroptic properties,[3] and because of their potential as "chiralica". Herein we present efficient methods for the synthesis of the prototypical, enantiomerically pure structural entities **A**, **B** and **C** with homonuclear X=Y units (HC=CH, C_6H_4). Their PE, ORD and X-ray structure analyses,[6] preparative extensions (e.g. to X=Y = C–N; R = CO_2H, NH_2), and preparative/analytical applications will be reported elsewhere.[7]

For the synthesis of the C_2-symmetrical dimethanotwistene *rac*-**8** from the [1.1.1]-ketone *rac*-**2**[8] (Scheme 1), several standard methods of homologization and olefination were tested regarding the problems of twofold and threefold functionalization of **10** and **1**, respectively. The ring enlargement of **2** to the [2.1.1]-ketone **5** (according to *Nakazaki* et al. less selective (56%) with CH_2N_2[3]) was accomplished in 75–80% yield, both according to the method of *Schöllkopf* et al.[9] as well as with a modified *Tiffeneau-Demjanov* method (**2**→**3**→**4**→**5**, 82%).[10,11] Several variants of β-elimination for the olefination at the stage of the alcohols (e.g. $-H_2O$, –HOAc, –HOMes) derived

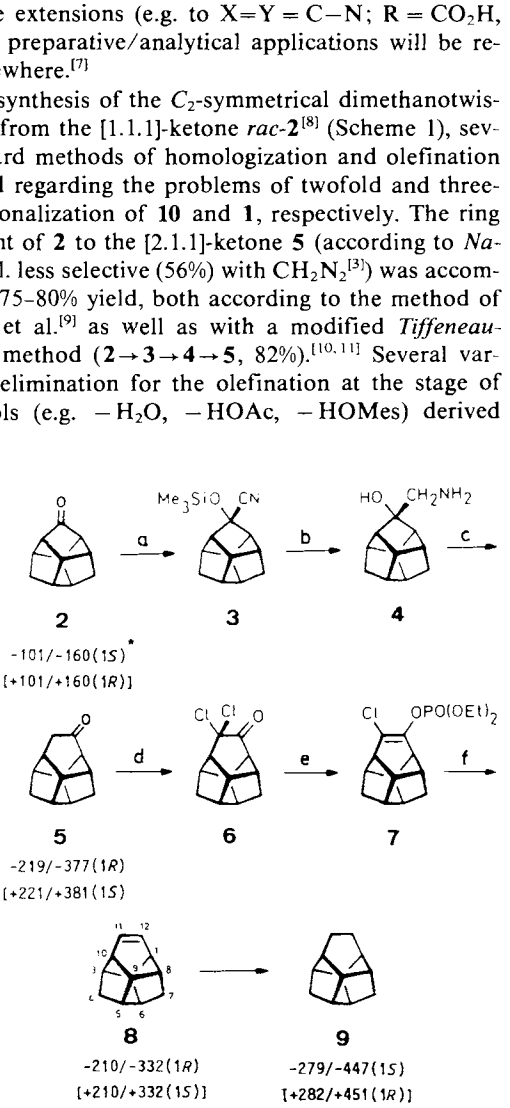

Scheme 1. The numbers quoted here and in the other schemes refer to specific rotations of the pure enantiomers measured at $\lambda = 587$ nm in cyclohexane or chloroform, respectively (**10**, **17**).

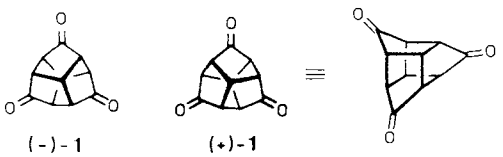

[*] Prof. Dr. H. Prinzbach, Dipl.-Chem. H. Müller, Dipl.-Chem. J.-P. Melder, Dr. W.-D. Fessner, Dr. D. Hunkler, Prof. Dr. H. Fritz
Chemisches Laboratorium der Universität, Institut für Organische Chemie und Biochemie
Albertstr. 21, D-7800 Freiburg (FRG)

[**] This work was supported by the Deutsche Forschungsgemeinschaft, the Fonds der Chemischen Industrie, and BASF AG.

from the ketone **5** proved to be unproductive (the same holds true for attempts with the diols and triols derived from the diketone **12** and the triketone **16**, respectively). We therefore attempted olefination according to the methods of *Bamford, Stevens* and *Shapiro*, of *Fetizon* et al.,[12] and of *Perkow* and *Bianchini* et al.[13] The ^{1}H- and ^{13}C-NMR spectra of the waxy solid substance *rac*-**8** (*rac*-pentacyclo[6.4.0.0^{2,6}.0^{3,10}.0^{5,9}]dodec-11-ene, λ_{max}(cyclohexane) = 210 nm (ε = 1220))[11], isolated according to the last method in 80–85% yield (based on **5**), showed the expected seven and six signals, respectively, for C_2-symmetry (Table 1). The enantiomers of **2**, separated by the method of *Eaton* and *Leipzig*,[14] analogously furnished (+)-**8** and (−)-**8**, thus also establishing their absolute configuration. Hydrogenation of (+)-**8** and (−)-**8** yielded enantiomerically pure (+)- and (−)-[2.1.1]-triblattane **9**, respectively; (−)-**9** has already been described as an optically enriched sample.[3]

Table 1. Melting points, ^{1}H-NMR spectra ($CDCl_3$, 400 MHz) and ^{13}C-NMR spectra ($CDCl_3$, 100.6 MHz) of selected compounds.

8: m.p. 84–86 °C; ^{1}H-NMR (250 MHz): δ = 6.14 (m, 11-, 12-H), 2.20–2.25 (m, 1-, 10-H; m, 3-, 8-H), 1.68 (m, 5-, 6-H), 1.56 (m, 2-, 9-H), 1.48 and 1.28 (AB, 4,4-, 7,7-H$_2$); ^{13}C-NMR: δ = 130.2 (C-11, -12), 50.1 (C-1, -10), 47.3 (C-5, -6), 44.2 (C-3, -8), 36.1 (C-2, -9), 33.6 (C-4, -7)

14: m.p. 47–48 °C; ^{1}H-NMR (250 MHz): δ = 6.35 (ddd, 8-, 13-H), 6.07 (ddd, 7-, 12-H), 2.44 (t, 6-, 11-H), 1.90 (m, 3-, 5-H), 1.80 (t, 1-, 9-H), 1.56 (br. s, 4,4-H$_2$), 1.34 (br. q, 2-, 10-H); ^{13}C-NMR: δ = 133.8 (C-8, -13), 129.1 (C-7, -12), 48.2 (C-3, -5), 46.9 (C-6, -11), 45.1 (C-1, -9), 36.2 (C-4), 29.5 (C-2, -10)

18: m.p. 106–107 °C; ^{1}H-NMR (250 MHz): δ = 6.42 (m, 6 H, H$_{olef.}$), 1.97 (m, 6 H, H$_{aliph.}$), 0.95 (br. q, 2 H, 2-, 11-H); ^{13}C-NMR: δ = 134.3 (6 C), 47.1 (6 C), 20.8 (2 C)

21: ^{1}H-NMR: δ = 3.31 (t, 4-, 8-, 14-H), 3.20 (t, 5-, 9-, 13-H), 2.83 (br. t, 1-, 3-, 7-H), 2.18 (m, 6-, 10-, 11-, 12-H), 1.97 (br. q, 2-H); ^{13}C-NMR: δ = 54.6 (C-4, -8, -14), 48.6 (C-5, -9, -13), 36.0 (C-6, -10, -12), 33.0 (C-2), 29.9 (C-11), 29.7 (C-1, -3, -7)

22: m.p. 189–190 °C; ^{1}H-NMR (250 MHz): δ = 3.46 (t, 1 H), 3.42 (t, 1 H), 3.28 (t, 1 H), 3.24 (t, 1 H), 3.12 (br. t, 2 H), 3.03 (br. t, 1 H), 2.98 (br. t, 1 H), 2.90 (br. t, 1 H), 1.99–2.15 (m, 4 H), 1.94 (br. t, 1 H); ^{13}C-NMR: δ = 54.5, 54.2, 54.1, 49.5, 49.2, 49.0, 35.7, 35.4, 34.9, 31.6, 30.7, 30.6 (2 C), 29.9

23: m.p. 100–101 °C; ^{1}H-NMR: δ = 7.20 (m, 4 H), 2.73 (d, 1-, 10-H), 2.43 (m, 5-, 6-H), 1.90 (br. q, 2-, 9-H), 1.80 (m, 3-, 8-H), 1.63 and 1.47 (AB, 4,4-, 7,7-H$_2$); ^{13}C-NMR: δ = 140.3 (C-11, -12), 125.6 (C-3′, -6′*), 124.4 (C-4′, -5′*), 49.6 (C-5, -6), 47.8 (C-1, -10), 46.4 (C-3, -8), 37.4 (C-2, -9), 34.0 (C-4, -7)

24: m.p. 59–60 °C; ^{1}H-NMR: δ = 7.10–7.19 (m, 4 H), 6.39 (br. t, 13-H), 6.18 (br. t, 12-H), 2.93 (br. d, 6-H), 2.58 (br. t, 11-H), 2.30 (d, 9-H), 2.06 (m, 3-H), 1.93 (m, 5-H), 1.80 (br. t, 1-H), 1.71 and 1.65 (AB, 4,4-H$_2$), 1.62 (m, 2-, 10-H); ^{13}C-NMR: δ = 143.2, 139.9 (C-7, C-8), 133.5 (C-13), 129.7 (C-12), 125.6 (C-3′, -4′), 124.8, 123.4 (C-5′, C-6′), 50.8 (C-6), 49.1 (C-9), 48.0 (C-3), 47.4 (C-5), 46.6 (C-11), 43.9 (C-1), 36.5 (C-4), 31.5, 30.9 (C-2, C-10)

25: m.p. 209–210 °C; ^{1}H-NMR: δ = 7.20 (m, 6 H), 7.08 (m, 2 H), 3.06 (br. d, 6-, 11-H), 2.30 (br. d, 1-, 9-H), 2.08 (m, 3-, 5-H), 1.90 (br. q, 2-, 10-H), 1.82 (m, 4,4-H$_2$); ^{13}C-NMR: δ = 142.5, 139.8 (C-7, -12, C-8, -13), 126.0, 125.8 (C-4′, -4″, C-5′, -5″), 125.0 (C-6′, -6″), 123.4 (C-3′, -3″), 50.4 (C-6, -11), 47.4 (C-1, -9), 47.2 (C-3, -5), 36.9 (C-4), 32.8 (C-2, -10)

26: m.p. 91–93 °C; ^{1}H-NMR: δ = 7.17 (br. s, 4 H), 6.48 (td, 9-, 14-H), 6.44 (td, 8-, 13-H), 2.50 (d, 3-, 6-H), 2.12 (br. t, 1-, 10-H), 1.90 (br. t, 7-, 12-H), 1.27 (br. q, 2-, 11-H); ^{13}C-NMR: δ = 143.8 (C-4, -5), 134.4 (C-9, -14), 133.6 (C-8, -13), 125.3 (C-4′, -5′), 123.8 (C-3′, -6′), 50.4 (C-3, -6), 46.7 (C-7, -12), 45.2 (C-1, -10), 22.8 (C-2, -11)

27: m.p. 178–179 °C; ^{1}H-NMR: δ = 7.22 (m, 4 H), 7.15 (m, 2 H), 7.10 (m, 2 H), 6.51 (m, 13-, 14-H), 2.63 (d, 3-, 10-H), 2.42 (d, 6-, 7-H), 2.05 (m, 1-, 12-H), 1.57 (br. q, 2-, 11-H); ^{13}C-NMR: δ = 143.5, 142.9 (C-4, -9, C-5, -8), 133.7 (C-13, -14), 125.7, 124.5, 125.6 (C-4′, -5″, C-5′, -4″, C-6′, -3″), 123.8 (C-3′, -6″), 50.0 (C-3, -10), 48.6 (C-6, -7), 44.9 (C-1, -12), 24.7 (C-2, -11)

28: m.p. 215–216 °C; ^{1}H-NMR: δ = 7.23 (m, 6 H), 7.17 (m, 6 H), 2.57 (br. d, 6 H), 1.90 (br. q, 2 H); ^{13}C-NMR: δ = 142.7 (6 *ipso*-C), 125.9 (6 *m*-C), 124.0 (6 *o*-C), 48.4 (6 C), 26.7 (2 C)

30: m.p. > 370 °C; ^{1}H-NMR: δ = 8.11 (m, 6 H), 7.80 (m, 6 H), 3.34 (dd, 6 H), 2.87 (br. q, 2 H); ^{13}C-NMR: δ = 155.5 (C-4, -5, -8, -9, -13, -14), 142.2 (6 *ipso*-C), 129.6 (6 *o*-C), 129.1 (6 *m*-C), 47.4 (6 C), 28.2 (2 C)

Because of the relatively rapid formation of higher triblattanes,[3] the CH_2N_2-variant was a priori not taken into consideration for the single ring enlargement of the two cyclopentanone rings in the [1.1.1]-diketone *rac*-**10**[15] which was required on the route to the C_2-symmetric methanoditwistadiene *rac*-**14**. Via the intermediates isolated analogously to **3**/**4** (reaction steps a and b in Scheme 2) in test runs,[11] an impressive yield of 75% of a mixture of the three [2.2.1]-diketones **11** (C_2; *rac*-pentacyclo[7.4.0.0^{2,6}.0^{3,11}.0^{5,10}]trideca-7,12-dione), **12** (C_2; -8,13-dione) and **13** (C_1; -7,13-dione) was achieved. Pure **11** (m.p. 175–176 °C, 18–20%) could be isolated from the product

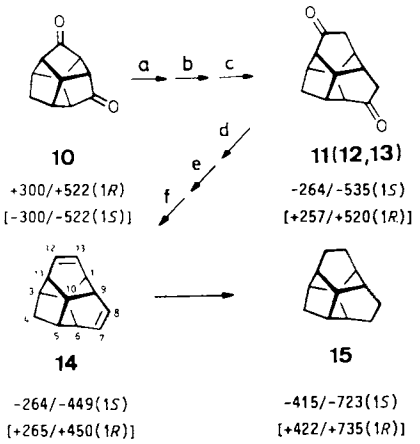

Scheme 2.

mixture by chromatography and pure **12** (m.p. 183–184 °C, 25 °C) by crystallization. The twofold olefination also presented no problems. After extensive preliminary experimentation with pure diketone *rac*-**11**, pure tetrachloro-derivative (step d) and pure bisenol ester (step e), an average yield of 75% of crystalline *rac*-**14** (*rac*-pentacyclo[7.4.0.0^{2,6}.0^{3,11}.0^{5,10}]trideca-7,12-diene) was finally achieved on using the mixture of diketones **11**–**13** via the Perkow route, suitably modified at the chlorination stage (steps d–f).[11] The C_2-symmetry of **14** is confirmed by the ^{1}H-/^{13}C-NMR spectra (Table 1, $J_{1,2} = J_{2,3} = J_{2,6} = 6.0$, $J_{3,4} = 1.5$, $J_{5,6} \approx 0$, $J_{6,7} = 7.0$, $J_{7,8} = 8.0$, $J_{8,9} = 7.0$ Hz; λ_{max}(cyclohexane) = 215 nm (δ = 2720)). After efficient enantiomeric separation of *rac*-**10** with (*R*,*R*)-2,3-butanediol,[1] the pure enantiomers (+)- and (−)-**14** could be prepared and their absolute configuration be confirmed by hydrogenation to (+)- and (−)-**15**, respectively[13] (15% optically pure (−)-**15** has already been described; [α] = −58.6, calculated −404[3]).

A key role in our studies with the unsaturated [2.2.2]triblattanes is played by the D_3-symmetrical $(CH)_{14}$[16] tritwistatriene **18**. The preparative demands associated therefore with the synthesis of **18** from the [1.1.1]triketone **1** could be largely fulfilled (Scheme 3): both the steps a–c leading to the threefold homologization of *rac*-**1**, which afford a 1:2 mixture (53%) of the chromatographically separated triketones **16** (C_3; *rac*-pentacyclo[8.4.0.0^{2,7}.0^{3,12}.0^{6,11}]tetradeca-4,8,14-trione, m.p. 245–247 °C, 17%) and **17** (C_1; -4,8,13-trione, m.p. 236–237 °C, 36%), as well as the steps d–f for the threefold olefination carried out with the ketone mixture according to the Perkow method, which is the only suitable method here, are reduced to economical one-pot reactions. The latter steps had been optimized to an overall yield of 68% using the pure triketones **16** and **17**,

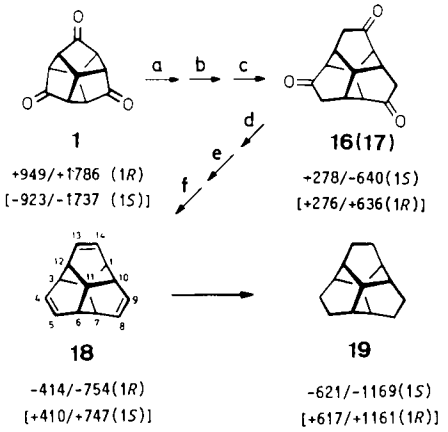

Scheme 3.

the two hexachlorotriketones (step d) and trisenol esters (step e). The yield of crystalline *rac*-**18**[11] (*rac*-pentacyclo[8.4.0.0^{2,7}.0^{3,12}.0^{6,11}]tetradeca-4,8,13-triene, λ_{max}(cyclohexane) = 216 nm (ε = 4240)), based on *rac*-**1**, is an impressive 36% for at least 21 functional changes. The antipodes (+)-**18** and (−)-**18** obtained from the triketones (+)-**1** and (−)-**1** or (+)-**16(17)** and (−)-**16(17)**, respectively, have been correlated by hydrogenation with (+)-**19** and (−)-**19**, respectively, (the known (−)-**19** had an optical purity of 44%; [α] = −250, calculated −567[3]).

The D_3-symmetry of **18** is confirmed by only three ^{1}H- and ^{13}C-NMR signals (Table 1, $J_{1,2}$ = 7.5, $J_{1,14}$ = 4.5 Hz). Despite a strain energy of 49.1 kcal mol^{-1} (force field calculation, MM2; 45.9 (47.7) kcal mol^{-1} for **8** (**14**)), **18** is thermally very stable; it slowly changes on heating in benzene (ca. 10^{-2} M) above 200°C; under dehydrogenating conditions (over Pd/C), mainly phenanthrene (X = HC=CH) (up to 75%) is formed—presumably via [4+2]-cycloreversion (**20**, Scheme 4, cf. basketene and ansaradiene).[17] In an analogous way, **14** furnishes fluorene (X = CH_2) in ca. 75% yield.

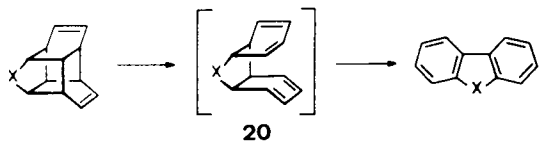

Scheme 4. Isomerization of **14** and **18** over Pd/C.

The preparatively important, in its details still unclear tendency of the [2.2.2]-triblattane skeleton to undergo (acid-catalyzed) isomerization[3] manifests itself in the perepoxidation of *rac*-**18**: even with carbamic peracids, byproducts and secondary products are formed besides the trioxides *rac*-**21** and *rac*-**22** (about 60% as a ca. 1:10 mixture, Table 1).[18]

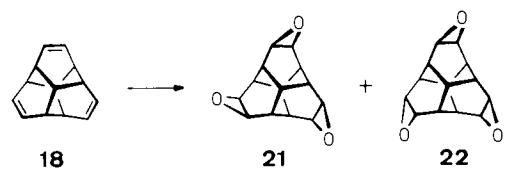

The C=C or C=O functions in the [2.1.1]-, [2.2.1]-, and [2.2.2]-triblattanes presented here can be used in the usual way for the annelation of benzoid or heterobenzoid rings. Thus, the benzoannelated derivatives **23**, **24** and **25** or **26**–**28** could be prepared in good to very good yields from the enantiomerically pure olefins **8**, **14** and **18** via the tetrachlorothiophene dioxide adducts (Table 1).

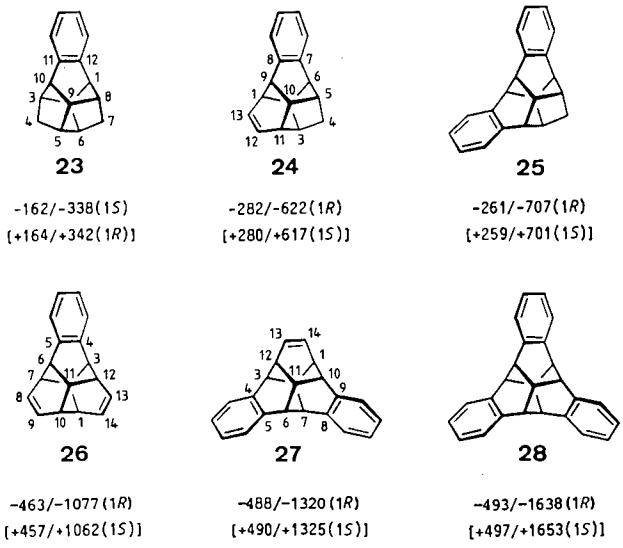

Scheme 5. Benzoannelated derivatives of **8**, **14** and **18**.

The conversion of the ketones **5**, **11** and **17** into the single, double, and triple α-diketones, respectively, presented difficulties. The α-diketones, finally set free by ozonolysis from the respective α-methylene derivatives, proved to be increasingly unstable in the order single > double > triple, but nevertheless could be trapped with *o*-phenylenediamine, e.g. the hexaketone **29** as triquinoxaline **30**, albeit in drastically decreasing yield (95%, 56%, 9%) (Table 1).

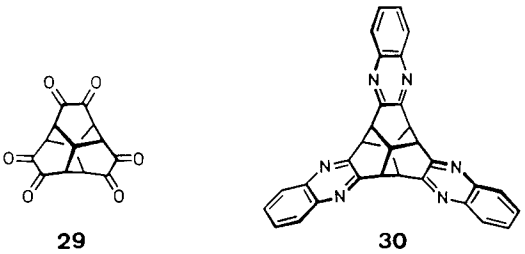

Received: March 28, 1988 [Z 2682 IE]
German version: *Angew. Chem. 100* (1988) 1140

[1] W.-D. Fesser, H. Prinzbach, *Tetrahedron 42* (1986) (on page 1800, the absolute configurations of (−)-**6c** and (+)-**1** must be interchanged (cf. experimental part)). In the meantime the yield of the subsequent triol oxidation has been improved from ca. 50% to 70% (J.-P. Melder, *Diplomarbeit*, Universität Freiburg 1986). In a later work on the synthesis of *rac*-**1** (A. P. Marchand, G. V. M. Sharma, G. S. Annapurna, P. R. Pednekar, *J. Org. Chem. 52* (1987) 4784) the "art of citing references" is remarkable.

[2] These triscations will be reported on in collaboration with *G. Olah* et al.

[3] M. Nakazaki, *Top. Stereochem. 15* (1984) 199, and references cited therein; K. Naemura, Y. Hokura, M. Nakazaki, *Tetrahedron 42* (1986) 1763.

[4] K. P. Meurer, F. Vögtle, *Top. Curr. Chem. 127* (1985) 1.

[5] H.-D. Martin, B. Mayer, *Angew. Chem. 95* (1983) 281; *Angew. Chem. Int. Ed. Engl. 22* (1983) 283.
[6] In collaboration with *G. Snatzke, R. Gleiter, H. Irngartinger.*
[7] The value of other derivatives of the type **I** (R = CO_2H, OH, NH_2; X = O, NR) derived from (−)-**1** ((+)-**1**) as chiral reagents is being investigated.

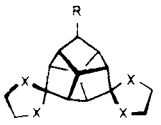

I

[8] P. E. Eaton, R. A. Hudson, C. Giordano, *J. Chem. Soc. Chem. Commun. 1974*, 978.
[9] U. Schöllkopf, B. Banhidai, H. Fresnelli, R. Mayer, H. Beckhaus, *Justus Liebigs Ann. Chem. 1974*, 1767.
[10] D. A. Evans, G. L. Caroll, L. K. Truesdale, *J. Org. Chem. 39* (1974) 914; W. E. Parham, C. S. Roosevelt, *Tetrahedron Lett. 1971*, 923.
[11] All the new compounds are characterized by elemental analyses and spectra (^1H, ^{13}C-NMR, IR, MS). See Table 1.
[12] M. Fetizon, M. Jurion, N. T. Anh, *J. Chem. Soc. Chem. Commun. 1969*, 112.
[13] W. Perkow, *Chem. Ber. 87* (1954) 755; E. M. Gaydou, J.-P. Bianchini, *Can. J. Chem. 54* (1976) 3626.
[14] P. E. Eaton, B. Leipzig, *J. Org. Chem. 43* (1978) 2483.
[15] E. C. Smith, J. C. Barborak, *J. Org. Chem. 41* (1976) 1433.
[16] A. T. Balaban, C. Deleanu, *Rev. Roum. Chim. 32* (1987) 271; cf. J.-P. Melder, F. Wahl, H. Fritz, H. Prinzbach, *Chimia 41* (1987) 426.
[17] H.-D. Martin, P. Pföhler, *Angew. Chem. 90* (1978) 901; *Angew. Chem. Int. Ed. Engl. 17* (1978) 847.
[18] The C_s-symmetrical 3,8,14,18-tetraoxaoctacyclo[8.7.1.$0^{2,4}$.$0^{5,16}$.$0^{6,12}$.$0^{7,9}$.$0^{11,17}$.$0^{13,15}$]octadecane **II** ($C_{14}H_{14}O_4$), formed on cleavage of one of the three bisallylic C–C single bonds, has been identified.

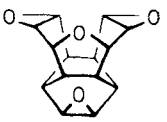

II

BOOK REVIEWS

Organic Chemistry—in Color, and Good

Organic Chemistry. By *K. P. C. Vollhardt*. W. H. Freeman, Oxford 1987. xxii, 1275 pp. + index, paperback, £ 18.95/bound, £ 49.95.—ISBN 0-7167-1915-0/0-7167-1786-1

This textbook by a competent author is evidence of the enormous advantage inherent in a first edition, where, in contrast to revisions of already established textbooks, one is not encumbered with outdated ideas in previous editions which are now getting on in years. Thus, modern organic chemistry terminology and methods (e.g. stereoselective synthesis and retrosynthesis) and instrumental analysis (^1H and ^{13}C NMR) are given adequate coverage rather than being squeezed into whatever space is available. Furthermore, the choice of content is, as a matter of course, up to date, as it is not necessary to clear out unwanted material. The organization chosen here, based on functional groups and their reactions, has been proved by experience to be especially useful, and is a welcome feature. Each chapter deals first with the nomenclature of the relevant class of compounds, followed by structure and physical properties; their reactions and mechanisms are then discussed alongside each other. Each chapter contains a summary of the most important experimental findings. The exercises included are up to the most modern standard as regards selection and type of examples.

The elaborate four color printing, which the author refers to with some pride as having great didactic value ("learning simplified by the use of color"), does in fact seem to be justified. For example, nucleophiles are represented in red and electrophiles in blue, while radicals and leaving groups are shown in green, thus enabling one to see at a glance where the individual fragments of a newly formed molecule have come from. In stereochemistry colors are used to denote the sequence of substitutions according to the Cahn-Ingold-Prelog rules, and in spectroscopy the assignment of individual signals to the corresponding molecular fragments is clearly indicated by using the same color for both. In this consistent use of color it has not always been possible to avoid the risk of gaudiness (e.g. on pages 272 and 1041), but one has to accept this in view of the undeniable advantages of the technique. The typeface is clear and the structural formulas are spaciously set out, and this too is a commendable feature from a learning standpoint. The careful (possibly computer-aided?) processing of the text makes it difficult to detect printing errors, and in any case it would be petty to list them in a work of this quality.

The treatment of spectroscopy is outstandingly good, including both the introduction to the physical fundamentals and the applications to organic chemistry, generously illustrated by reproducing spectra of excellent quality. However, the contribution brought to the understanding of the subject by a photograph of a commercial (NMR) spectrometer, which after all appears as nothing more than a "black box"—decorated, of course, by the inclusion of a pretty female assistant—must remain the author's own secret.

Some examples of the small number of inaccuracies are as follows: the chlorophyll formula (p. 1040) is incorrect (as, incidentally, it also is in *Streitwieser* and *Heathcock*'s "Organic Chemistry"); enantiomerically pure amino acids are obtainable not only by cleavage of racemates and by enzymic synthesis (pp. 1240f.), but also of course by enantioselective synthesis; in connection with the 95% photochemical conversion of norbornadiene (p. 594), it should have been mentioned that a sensitizer was needed; in describing the elegant photoreaction using the matrix isolation technique (p. 1164), it would have been better to formulate a starting material that does not release any cyclobutadiene-complexing CO_2 when irradiated. Or are these points merely splitting hairs? The author's concern with completeness sometimes results in including equations of complex reactions with scarcely any explanation, e.g. in

[*] Editor's comment: But not in ANGEWANDTE CHEMIE, where electron lone pairs are represented by a pair of dots so as to avoid confusion with negative charges—a point which time and again gives cause for discussion.

that of squalene to give a steroid system (p. 492), or that of bioluminescence (pp. 329–330); this is too much of a good thing, and is unlikely to be understood by the student.

The subdivision and choice of titles in some of the chapters call for comment. It seems strange that in Chapter 2, which is entitled "Molecules lacking functional groups", the subsection which follows defines functional groups. In the title of Chapter 17, carboxylic acids are grouped together with the introduction to IR spectroscopy, whose use is by no means restricted to carboxylic acids, while in that of Chapter 18, carboxylic acid derivatives are grouped with the introduction to the equally general topic of mass spectrometry. It would have been better to include these spectroscopic techniques in Chapter 10, which has been reserved for NMR spectroscopy. Even the statement that "... at strategic points throughout the book, the important spectroscopic techniques ... are introduced" does not excuse this arrangement of topics. It is unlikely that any reader will consume this book like a detective novel, starting at page 1 and continuing through to page 1275.

Are there any topics in a work of this length which have been treated too briefly? In the description of electrocyclic reactions, although the distinction between *conrotatory* and *disrotatory* movements is pointed out, the fact that corresponding photochemical and thermal reactions have different stereochemistry is described merely as "curious"; the concepts of orbital symmetry are not explained, but the reader is referred to more advanced papers on the subject. The description of aromaticity according to the Hückel model is quite confusing and lacks conviction. It would have been desirable to include the mnemonic devices introduced by *Frost* and *Musulin* (for Hückel type arenes) and by *Zimmermann* (for Möbius type arenes), which are so useful to organic chemists. At the same time, however, special mention must be made of the very successful detailed treatment of aromatic substitution and of spectroscopic evidence for aromaticity (UV, IR, NMR). From the organic chemist's viewpoint, it would have been useful to augment the satisfying and appropriately detailed coverage of natural products chemistry with a discussion of biochemical questions such as photosynthesis and the respiratory chain, not only because topics such as these are now included in examinations, but, even more importantly, because the discipline of organic chemistry will in the future undoubtedly have (as formerly) a much greater biochemical bias.

These desirable extensions of the work need to be balanced by suggestions as to what might be taken out. Perhaps with the aim of addressing scientists of other specializations, and also possibly arising from the different structure of the education system in the USA, some chapters start from an astonishingly low level (e.g. in the discussion of stereochemistry, or in the introduction to NMR spectroscopy: "... discrete spin packets ... which are also called **quanta** of energy"), but quickly advance to a treatment of appropriate depth. Some shortening would be possible here by raising the starting level and sacrificing some of the section on general chemistry, since the book, by virtue of its declared aim, content and length, is in any case unsuitable for non-chemists.

To these critical comments, some of which are merely personal views, one may add two further sources of annoyance: 1) It is quite incomprehensible why, in a completely new textbook, which after all has been written for the 1990s, consistent use is not made of the SI system of units set up in the early seventies (e.g. kJ/mol rather than kcal/mol). Already in some monographs it is regarded as superfluous to continue including kcal/mol units in parentheses after the kJ/mol units; where this practice is still followed, it is because the older generation undoubtedly still thinks in kcal units. 2) The practice of showing only covalent bonds as dashes, while electron lone pairs are shown as a pair of dots, is now unusual,[*] at least in organic chemistry, and is also unjustified, since the latter electrons too have their spins paired. Representing electrons by dots can indeed sometimes have a confusing effect, as in the formulas of the 1,2-diketones at the top of p. 1008 (the comment on p. 16 that "The writing of electron-dot structures can be cumbersome ..." is meant in a different context, but nevertheless, how true!).

The criticisms made here should not be allowed to detract from the excellent overall impression of the book, but are meant rather as suggestions for a revised edition to follow. The book deserves to be classed as *excellent*, and if the justification for publishing a new textbook is that it should be better than all its predecessors, then "Vollhardt" is, in this reviewer's opinion, very close to reaching that goal! It is to be hoped that a German translation of this textbook will soon appear, even though one might expect today's chemists and chemistry students to have an adequate knowledge of English. Using "Vollhardt" should enable the student to progress, in many aspects of chemistry, through the intermediate examinations and on to the final degree.

Harry Kurreck [NB 895 IE]
Institut für Organische Chemie
der Freien Universität Berlin

PS: Unfortunately, a 'study guide', 'solutions manual,' and "overhead transparencies" were not available when this review was written.

The Chemistry of Inorganic Homo- and Heterocycles. Vol. 1 and 2. Edited by *I. Haiduc* and *D. B. Sowerby*. Academic Press, New York 1987. Vol. 1: xxiv, pp. 1–416, xi, hard cover, individual volume price: £ 60.00.—ISBN 0-12-655775-6; Vol. 2: xxiv, pp. 417–877, xi, hard cover, individual volume price: £ 65.00.—ISBN 0-12-655776-4 (price for two-volume set: £ 104.50)

This two volume work is a comprehensive and much needed review of the title area covering the years 1969–1979. It includes some thirty chapters of varying lengths by an impressive selection of widely recognized authors. Even a cursory glance through the chapter headings will reveal that inorganic ring systems constitute a truly vast area of research. The preface offers reasons for restricting the survey to the period 1969–1979. The main reasons for this are that earlier work was covered by the 1970, two-volume, work "The Chemistry of Inorganic Ring Systems" by *I. Haiduc*. Also, work since 1980 will be covered in a series of annual surveys in "Reviews in Inorganic Chemistry". It should be added that many chapters contain more modern references than 1979 so that many of the more significant recent developments are included. Page number restrictions were also cited for the limitation of the survey to a 10 year period. Valid though all these reasons are, one suspects that many potential individual buyers will be put off by the combination of the inevitably high price and the fact that 1979 is a long time ago as far as chemistry is concerned.

The work is divided into two volumes. In Volume 1, the major emphasis is on compounds involving Main Group 3 and 4 elements. Almost inevitably these rings and cages include some of the main group 5 or 6 elements. However, the main coverage of the rings and cages of these groups is emphasized in Volume 2. The material in Volume 1 involves sixteen chapters. The first five of these deal with various types of rings involving boron. Not surprisingly, Chapter 2 on boron–nitrogen heterocycles by *Maringgele* is by far the most extensive, occupying over 80 pages and over 400 references. In contrast, Chapter 3 by *Sowerby* on boron–phosphorus and boron–arsenic heterocycles involves only six pages and just over twenty references. Their relative lengths accurately reflect the amounts of activity in both fields and will undoubtedly call attention to the lack of existence of several types of B–P and B–As heterocycles which are well known for the B–N analogues. Chapters 4 and 5 by *Haiduc* and *Siebert* deal with B–O and B–S/Se cyclic systems. There is significant overlap between these and review articles covering similar compounds published in 1982 and 1983. Chapter 6 by *Cesari* and *Cucinella* covers the fascinating aluminum–nitrogen rings and cages. Surprisingly, the few known gallium and indium analogue compounds are not mentioned. There are also three short chapters dealing with the homocycles of (i) boron (Ch. 1, *Haiduc*), (ii) germanium and related compounds (Ch. 12, *Haiduc* and *Drägen*) and (iii) tin (Ch. 14, *Harrison*). A somewhat longer chapter (7) by *Hengge* and *Hassler* on silicon homocycles is comprehensive up to 1982. An interesting aspect of this chapter involves the amount of space given to cyclotrisilanes. In the period since it was written, there has been more activity involving these compounds, because they are precursors for the disilenes.

Four chapters, Nos. 8–11, cover silicon heterocycles. The longest (Ch. 8) by *Klingebiel* deals with silicon–nitrogen compounds. The following chapter by *Fritz* and *Härer* covers the phosphorus–silicon analogues and is much shorter, although there has been a considerable amount of work published in the area more recently. The subsequent chapter (10) on Si–O heterocycles by *Chvalovsky* covers material up to 1982 and contains considerable tabular material. This method of presentation, though hardly easy to read, is necessitated by the huge literature (936 references) of the area. In contrast, the corresponding silicon–sulfur compounds (Ch. 11, *Haiduc*) includes only 56 references. The remaining chapters in this volume, 13–15 and 16, cover germanium and tin heterocycles. Chapter 13 covers all germanium heterocycles whereas the more extensive work on tin merits two chapters; one, chapter 16 by *Veith*, on Sn–N and Sn–P and a further one, chapter 17 by *Mathiasch* on tin chalcogenides. These two chapters along with Chapter 6 on Al–N compounds provide convincing proof that main group compounds display a most fascinating variety of molecular architecture and reactivity.

The second volume opens with a chapter (17, *Haiduc*) on nitrogen homocycles. This is predictably short owing to the instability of the compounds. However, the corresponding phosphorus compounds, covered in Chapter 18 by *Baudler* and *Glinka*, involves some 200 references. This chapter, in contrast to some others, is considerably more up to date and contains numerous references from 1983 and 1984. The three following chapters cover the vast area of P–N cyclic compounds. Chapter 19 by *Keat* involves P(III)–N cyclics, Chapter 20 by *Allen* and Chapter 21 by *Schmidpeter* deal with cyclophosph(v)azanes with various phosphorus coordination numbers. Chapter 20 involves over 1000 references alone which the author has managed to squeeze into less than 200 pages. Summary tables for structural data are also provided. A welcome feature of all three chapters is that they contain many references from 1981 and 1982. More recent work is generally available in reviews named in the bibliography. Two somewhat shorter chapters, 22 by *Durif* and 23 by *Sowerby*, cover P–O, P–S, and P–Se rings and cages. These include a considerable amount of structural data as well as numerous references from the early eighties. Chapter 24, by *Haiduc*, treats cycloarsanes, in addition to arsenic heterocycles, and their antimony and bismuth analogues are covered in Chapters 23 and 26 by *Sowerby*. The literature on sulfur homocycles in Chapter 27 by *Steudel* involves some 160 references. The fascinating structures and chemistry of these sulfur species is made very current by the notes added in proof which even include some 1986 references! Equally interesting, but less investigated, are their selenium analogues in Chapter 28 by *Steudel* and *Strauss*. Many important references up to 1986 are also given. Sulfur–nitrogen heterocycles are ably reviewed by *Chivers* in Chapter 29. References from 1984 are included as an integral part of the text. The degree of activity in the area can be gauged from the large number of citations. A much shorter final chapter by *Haiduc* on S–O, Se–O and Se–N heterocycles completes the text.

In summary, these two volumes along with their 1970 precursor represent the classic reference work in the field of inorganic heterocycles. The presentation is excellent, generally error free, and the contents comprehensive within its limits. It could be argued, however, that some of the ring structures involving lithium hetero compounds would fall within the definition outlined by the editors. The style is also uniform despite coming from some twenty-five different authors. The only serious criticism of the work is the fact that many chapters are now out of date although some, particularly those dealing with sulfur compounds, are quite current. This drawback aside, the work is a most valuable one and is indispensible to anyone working in this field.

Philip P. Power [NB 889 IE]
Department of Chemistry,
University of California,
Davis, CA (USA)

Industrielle Aromatenchemie. Rohstoffe, Verfahren, Produkte. By *H.-G. Franck* and *J. W. Stadelhofer*. Springer, Berlin 1987. xiv, 504 pp., bound, DM 128.00.—ISBN 3-540-18146-6

The main factors which shaped the development of the chemical industry after the second world war can be reduced to one very simple common denominator: essentially it flourished due to the availability of cheap aliphatic raw materials for petrochemicals, which led to a spectacular growth in aliphatic chemistry throughout the world. Insofar as the production of large-volume chemicals is now becoming less and less economically attractive for the traditional chemical manufacturing countries, with high-value chemical products coming into the foreground instead, the former supremacy of aliphatic chemicals is being eroded in favor of arenes. Consequently the chemical industry's field of interest is in a sense reverting to its beginnings in the mid-19th century, when the industry took as

its starting point the manufacture of dyestuffs based on the arenes present in coal-tar. In view of this situation the appearance on the market of a competently written book on industrial arene chemistry must be regarded as a welcome development, satisfying a need which has already been felt for a considerable time. Arenes and the products derived from them, which already make up almost a third of basic organic chemicals, have here at last received the comprehensive treatment which they deserve.

After a historical introduction the volume continues by discussing the nature of aromaticity, leading to the modern definition of the term "aromatic" and the boundaries of its applicability. This is followed by a very detailed chapter on sources of feedstocks, emphasizing the special importance of coal-tar and of the products obtained from the catalytic cracking and vapor phase pyrolysis of hydrocarbons. Future possibilities for making increased use of renewable raw materials as alternative feedstocks for arenes are touched on briefly.

The chapters which follow describe the properties of key arenes with reference to their manufacture and uses. The book deals first with the so-called BTX arenes, which come at the top of the production scale in megatonnes per year. These are followed by the poly(alkyl)benzenes, naphthalene, alkylnaphthalenes, anthracene and the rest of the polycyclic arenes. A separate chapter is devoted to the manufacture and uses of carbon-based products made from mixtures of condensed arenes. The final part of the book deals with the manufacture and uses of aromatic heterocycles. These chapters show strikingly that in addition to bulk chemicals with annual production figures of many millions of tonnes, such as ethyl benzene, styrene, cumene, phenol, phthalic anhydride and terephthalic acid derivatives, the field of arene chemistry also includes a large number of well-known products of the chemical, pharmaceuticals, dyestuffs and plant protection industries. Furthermore, other areas of application are discussed, some of them especially topical and others with future potential, e.g. the production of fibers of high carbon content from mesophases of pitch, the use of diisopropylnaphthalenes as solvents for NCR ("no carbon required") duplicating papers, extraction of cellulose from wood using anthraquinone, the manufacture of synthetic pyrethroid insecticides, and the use of a magnesium-anthracene complex as an intermediate in the manufacture of the hydrogen-storing medium magnesium hydride—to name only a few representative examples. A work such as this must, of course, also include a chapter on toxicology and environmental protection. This is augmented by a list giving toxicities and threshold limit values for the most important arenes.

The choice of material and the presentation of the chemical and technical details enable the reader to make a critical evaluation not only of the methods of manufacture in current use, but also of the numerous specialized applications. Economic aspects of arene chemistry are not neglected: data on production in different regions of the world, and on the distribution of the principal uses between the various business sectors, are given for the most important arenes and their derivatives. In a book of this kind the chemical process schemes are an important criterion of quality, and indeed they constitute a sort of touchstone for the technically biased chemist and the process engineer. The instructive, uniformly styled schematic diagrams effectively bring out the essential features of the production processes. In keeping with the textbook character of the work, literature references for further reading are listed in an appendix, classified according to the individual chapters.

Altogether, considering all aspects—text, figures and quality of production—this is a pleasing book, and even at a price which is by no means low, it will definitely find a wide readership in industry, universities, business and administration.

Kurt Dialer [NB 909 IE]
Institut für Technische Chemie
der Technischen Universität München
Garching (FRG)

Advances in Electrophoresis. Vol. 1. Edited by *A. Chrambach, M. J. Dunn* and *B. J. Radola*. VCH Verlagsgesellschaft, Weinheim/VCH Publishers, New York 1987. ix, 441 pp., bound, DM 154.00.—ISBN 3-527-26741-7/0-89573-669-1 (ISSN 0932-3031)

In their preface the editors tackle the problem that is doubtless uppermost in their minds: why they have brought into the world a series which is planned to appear annually, yet—and this is admitted—predominantly contains review articles that have already been published in a similar form in the relevant journals. *Advances in Electrophoresis* is intended as a "review bank", written by experts to help overcome problems which arise from contradictory reports given by various specialists. This aim is not achieved, at least with this volume, and indeed cannot be achieved, for to do so would require the detail needed for practical work to be investigated far more thoroughly. Even in a "cookery-book"—and this is not the aim—this would hardly be possible in reality without continually "stepping on people's toes". In addition, it would first be necessary to introduce binding international definitions and test criteria, DIN-standards of electrophoresis, so to speak, by which results could be judged.

The second aim, to bring together fields of research whose publications would otherwise have to be laboriously collected from many journals, appears by contrast to be a sensible one, and as Volume 1 exemplifies, achievable. The third aim, to indicate the most important of the many, varied applications of electrophoretic methods, and their potential for solving the reader's own research problems (sometimes overestimated, sometimes underestimated), is likewise achievable.

The fourth aim, that the collected reviews should be useful to interested people who have no time to follow the original literature, is commendable. However, there are too many annoying citation errors, and significant references are simply missing, quite apart from factual errors, so this is not really a substitute for reading the original literature. For the attentive reader this shortcoming is remedied to some extent by the fact that the first two articles contain significant (avoidable!) overlaps, so that in the end one finds all the relevant literature references at least once. It is also irritating that in the introduction to the important article on two-dimensional electrophoresis, with its numerous modifications and promising applications which are well described, the historical development is evaluated in a misleading way, even though all the relevant papers are quoted. Those seeking a more accurate picture should therefore take good note of the year of each publication! In any case, not all of the contributions included here are unreservedly suitable as "key references" (the fifth aim in the preface); they could easily lead to a (most irksome) propagation of errors. After all, anyone unacquainted with

the subject will undoubtedly be keen to have review articles by experts to lean on, and on which they can rely (!).

In *Advances in Electrophoresis*, a "balanced mixture" of review articles is to appear, dealing with both methods and applications. From this point of view Volume 1 is a good beginning, with contributions from *M. J. Dunn:* "Two-dimensional polyacrylamide gel electrophoresis" (109 pages, 587 references); *C. R. Merril:* "Detection of proteins separated by electrophoresis" (28 pp., 98 references); *J. M. Gershoni:* "Protein blotting: a tool for the analytical biochemist" (32 pp., 148 references); *Nancy C. Stellwagen:* "Electrophoresis of DNA in agarose and polyacrylamide gels" (49 pp., 155 references); *K. Takeo:* "Affinity electrophoresis" (48 pp., 207 references); *P. Gebauer, V. Dolnik, M. Demel* and *P. Boček:* "Recent trends in capillary isotachophoresis" (76 pp., 239 references); *R. Horuk:* "Preparative polyacrylamide gel electrophoresis of proteins" (17 pp., 30 references); *J. S. Sutton:* "Red cell enzyme markers in forensic science: methods of separation and some important applications" (46 pp., 141 references). The index, so important for a book of this sort, contains ca. 1000 entries (11 pp.), and is therefore adequate for practical use. The numerous, well-reproduced figures and tables are informative throughout.

All in all, the idea of this series as a collection of review articles on various aspects of electrophoresis is a promising one, though the beginning is somewhat clumsy. DM 154.00 is a princely price, for which the editors are of course not responsible; however, with the good presentation overall (and a Coomassie-blue colored band at its head!), it seems justified.

Volker Neuhoff [NB 902 IE]
Max-Planck Institut für experimentelle Medizin,
Göttingen (FRG)

Protein Engineering. Edited by *D. L. Oxender* and *C. F. Fox.* Alan R. Liss, New York 1987. xvii, 365 pp., bound, $ 36.00.—ISBN 0-8451-4300-X

This book, consisting of 30 separate articles, provides the reader with an excellent survey of theoretical and practical aspects of protein structure and stability, and the effects obtained by introducing structural modifications. Our present understanding of structure-activity relationships is mainly based on protein structure determinations by X-ray analysis and (more recently) by high resolution NMR spectroscopy. These two techniques are treated in the first section of the book, which also includes a chapter on the possibilities for theoretically predicting structural modifications produced by mutagenesis. The section which follows consists of seven articles, which on the one hand describe techniques for mutagenesis and for isolating recombinant and mutant proteins, and on the other hand indicate the possibilities for using suitably modified proteins to investigate the principles of protein chain folding and structure. The third section deals, in nine articles, with basic aspects of the structure and stability of proteins in aqueous solution. Several articles are devoted to the hydrophobic effect, hydrogen bonding and amphiphilic structures, and their fundamental importance to stability and chain folding of proteins is clearly explained, taking account of the most up to date views. Other articles in this section describe the application of these principles to peptidomimetics and protein design, e.g. in synthesizing artificial amphiphilic oligopeptides with calcitonic activity. The final section of the book contains eleven articles describing, for example, experiments on regiospecific mutagenesis of individual proteins. These articles have two main objectives: on the one hand to extend understanding of the principles underlying the stability of the native form of a protein with its specific chain folding, and on the other hand to clarify the mechanism of enzymic activity at the molecular level.

This book is an excellent introduction to "protein engineering". The individual articles are, without exception, written by acknowledged experts in their fields. They are well coordinated, and cover in appropriate detail all the important aspects of this area of research. Where there is a small amount of overlapping, as is necessary for a coherent treatment of the topics, this is not a serious drawback, and it is not usually possible to avoid it completely in a collection of individual articles. Detailed descriptions of particular techniques have been deliberately omitted in favor of stressing fundamental principles and experimental procedures of general validity. The adoption of this philosophy will ensure that, even several years hence, this book will not have become much out of date. It is intended mainly for advanced students and non-specialists. Nevertheless, it is undoubtedly also of great value to the expert, whether his background is in biochemistry, biophysics or genetics. Finally, the price of $ 36.00 makes the book attractive.

Franz X. Schmid [NB 893 IE]
Institut für Biophysik und Biophysikalische Chemie
der Universität Regensburg (FRG)

The Chemistry of the Metal-Carbon Bond. Vol. 4: The Use of Organometallic Compounds in Organic Synthesis. Edited by *F. R. Hartley.* Wiley, Chichester 1987. xiv, 1349 pp., bound, $ 420.00.—ISBN 0-471-90888-6

This is (provisionally) the final volume in the series "The Chemistry of the Metal-Carbon Bond", and is aimed primarily at the organic chemist. A clear-cut distinction from Volumes 2 ("The Nature and Cleavage of Carbon-Metal Bonds") and 3 ("Carbon-Carbon Bond Formation using Organometallic Compounds") is not discernible, and according to the editor was also not intended. Those who are interested in the reactivity of organometallic compounds and also wish to use them in organic synthesis would therefore do well to consult not only the present Volume 4, but also Volumes 2 and 3, in order (hopefully) to find what they require.

The contents are divided into two parts, approximately equal in their coverage. The first is concerned with the preparation of main-group metal compounds, and their use in organic synthesis. The first two chapters, on organo-alkali metals (mainly Li; 157 pp., 1247 references) and organoalkaline earth metals (mainly Mg; 148 pp., 539 references) therefore have a broad field to cover, as might be expected. In this section particularly, the material is often presented in tabular form, which undoubtedly makes an overview easier to obtain. Chapters 3-6 are devoted to the synthesis and uses of organoboranes (102 pp., 625 references), organo-aluminum compounds (62 pp., 281 references), organothallium(III) compounds (66 pp., 325 references) and organo-silicon compounds (82 pp., 455 references). In general, the literature is surveyed up to 1984, and so here too it struggles along behind the year of publication, though not so glaringly as in some chapters of the previous volumes. It is not obvious why organo-tin compounds, which are be-

coming more and more important for organic synthesis, are not treated in conjunction with the analogous silicon compounds, but quite separately, in volume 3. This would certainly have been a help in demonstrating the advantages and disadvantages of the use of the two classes of compounds.

Part 2 is devoted exclusively to the use (not the preparation) of certain families of organo-transition metal compounds. Fortunately the individual chapters were almost without exception written by very competent authors, which has been of very great benefit to the quality. The first chapter deals with organo-iron compounds (107 pp., 303 references), and makes brief mention of their significance as electron-transfer catalysts. There is some overlap here with the later chapter on the use of transition metal-stabilized carbocations (90 pp., 151 references), but this is acceptable. Between the two lie expositions of organometallic complexes of rhodium (86 pp., 551 references) and nickel (69 pp., 363 references); here too, some overlap with individual chapters of Volume 3 can be discerned. Chapters 11 ("Hydrogenation", 69 pp., 665 references) and 12 ("Mechanism of homogeneous hydrogenation", 23 pp., 90 references) are devoted to the use of organometallic compounds as hydrogenation catalysts, in which it is not only homogeneous and heterogeneous hydrogenations with H_2 that are discussed, but also catalytic hydrogen transfer, and—though only briefly—enantioselective hydrogenations with the aid of chiral metal complexes. The final chapter deals with the activation of C–H bonds in saturated hydrocarbons, including considerations of biochemical aspects (88 pp., 295 references) and of the fixation of catalytically active organometallic compounds onto oxide and metal supports (62 pp., 479 references). The volume ends with a detailed author index, and a rather less detailed subject index. Whether a continuation volume will follow, to fill the gaps that still exist at the moment, seems to be undecided at present.

Collecting the material presented up till now must have been a herculean task, and the editors earn great respect for it. Apart from the arrangement of the individual chapters, which is not always successful, the presentation of results is almost without exception very effective. It is not only the price, however, that stands in the way of the distribution of this four-volume work, but also the fact that the even more comprehensive work "Comprehensive Organometallic Chemistry" appeared shortly before it. Whether Hartley/Patai can compete with this remains to be seen.

Helmut Werner [NB 903 IE]
Institut für Anorganische Chemie
der Universität Würzburg (FRG)

The Chemistry of the Actinide Elements. 2nd Edition. Edited by *J. J. Katz, G. T. Seaborg,* and *L. R. Morss.* Chapman and Hall, London 1986. Volume 1: xii, pp. 1–886, bound. Volume 2: xii, pp. 887–1674, bound. Price per volume £ 95.00.—ISBN 0-412-10550-0 and 0-412-27370-5

The first edition preceding this two-volume work (published in 1957 and authored by *J. J. Katz* and *G. T. Seaborg* only) dates from the pioneering years of research on the transuranium elements and has since then become by far the best known textbook on the chemistry of the actinide elements. Thirty years ago, not only was the final element of the actinide series (in the sense of *Seaborg*'s now well-established "actinide hypothesis") missing, but also the existence of the preceding element, nobelium, had not yet been fully confirmed. Now, however, in addition to No and Lr, the transactinides with atomic numbers 104 to 110 have also been made. The new edition, notwithstanding its unaltered title, includes not only the 15 elements Ac to Lr but all the translawrencium elements as well.

Without considering the elements Ac, Th, Pa and U (which together account for 430 pages of the present work), *C. Keller* had still managed in 1971 to describe the chemistry of the transuranium elements in a single volume of 675 pages. Obviously the progress which has taken place in almost every sector of actinide chemistry has necessitated a restructuring of the old Katz/Seaborg version (506 pages), into a well-composed collection of 24 chapters written by 33 acknowledged experts from the USA and Western Europe. One of the four European authors is the late *Fritz Weigel* (of the University of Munich).

The very comprehensive division of the material into Part I, which is a systematic description of the individual elements, and Part II which is focusing on specific properties and classes of compounds, respectively, of all the actinides, not only follows the structure of *Keller*'s book, but is already discernible in the 1st Edition. The three editors have themselves written the historically oriented introduction (Chapter 1, 11 pages), along with several other chapters, including one of particular versatility (Chapter 14, 74 pages: Summary and Comparative Aspects of the Actinides). This chapter is intended to be an introduction to Part II, and contains short sub-sections on such varied topics as naturally occurring transuranium elements, superconductivity, oxidation states, organometallic compounds, nuclear reactor wastes, biological effects, and the toxicology of actinide compounds. For non-specialists Chapter 14 might in fact serve as a guide to other parts of both volumes.

More than half of Part I is occupied by Chapters 5 (uranium, 274 pages, by *F. Weigel*) and 7 (plutonium, 388 pages, by *F. Weigel, J. J. Katz,* and *G. T. Seaborg*). These chapters deal in great detail with aspects of high importance for nuclear technology, e.g. the extraction of uranium and plutonium, and chemical reprocessing of nuclear fuels. Separation techniques are described in this chapter too, and are also treated in detail in chapter 21. Some compilations of data in the form of tables extending over several pages, e.g. on structural parameters of selected intermetallic uranium compounds (pages 235 to 241), are perhaps out of place in a book which is intended to also attract a non-specialist readership. The transeinsteinium elements, with atomic numbers 100 to 109, are treated collectively in Chapter 13 (by *R. J. Silva,* 32 pages), while the final chapter (Chapter 24, by *G. T. Seaborg* and *O. L. Keller, Jr.,* 25 pages), is devoted to "elements of the future", including the so-called superheavy elements.

Organoactinide chemistry, which was virtually non-existent in 1957, is here given considerable space, mainly in Part II. For some reason the authors of Chapter 22 (*T. J. Marks* and *A. Streitwieser*) and Chapter 23 (*T. J. Marks*), focus mainly on the 82 pages of these two chapters, on selected, and probably exemplaric, aspects of thorium and uranium chemistry. However, chapters 3, 5, 7, 14, 18, and 20 also each include several pages on organometallic compounds, and some transuranium elements finally feature here. Quite a lot of repetition has crept in here, e.g. on page 368, as a consequence of the renaming of allyl complexes to "allenyl complexes". Other instances of overlap-

ping between chapters in Parts I and II may be found, where the material at the two locations is not mutually complementary.

Nevertheless, the chapters in Part II all deal with important topics: (optical) spectra of the free atoms and ions (Chapter 15, *M. S. Fred* and *J. Blaise*) and of ions in compounds (Chapter 16, *W. T. Carnall* and *H. M. Crosswhite*), thermodynamic and magnetic properties (Chapters 17 and 18, by *L. R. Morss* and by *N. M. Edelstein* and *J. Goffart*, respectively), the metallic state (Chapter 19, *M. V. Nevitt* and *M. B. Brodsky*), structural chemistry (Chapter 20, *J. H. Burns*), and solution chemistry and ionic reaction kinetics (Chapter 21, *S. Ahrland*). Analytical chemistry has not been considered however.

Thermodynamic data of the highly radioactive actinide compounds, which are very difficult to determine, have rarely been presented before as systematically and comprehensively as in Chapter 17. Chapter 18 contains a short introduction to the quantitative magnetochemistry of systems with strong spin-orbit coupling and similarly large crystal field interactions, which appears suitable even for teaching purposes; even special treatments of magnetochemistry seldom include a chapter comparable to this. Chapter 19 deals with systems involving non-localized (itinerant) f-electrons and heavy fermions, two related concepts which are now the subject of intensive studies, and of relevance for an understanding of superconductivity. (One comes across references to the superconducting properties of actinide compounds in several of the chapters). Chapter 20, on structural chemistry, is organized too rigidly along classical lines, and does not mention any modern structural concepts such as those dealing with the coordinative saturation of f-element ions, nor has the structural chemistry of complexes with macrocyclic and/or large polycyclic ligands been considered, a subject of paramount interest at the present time. The only example given, in the section on actinyl complexes, is the "superphthalocyanine" complex formed by template reaction of five phthalodinitrile molecules with the uranyl cation, its structure having been elucidated as long ago as 1975. This structure is presented once more, under its systematic name, in Chapter 5 (page 385), where e.g. crown ether complexes and their structures are also briefly discussed. The section on organometallic compounds in Chapter 20 fails to take into account a number of recent developments (e.g. the uranium complexes with arene ligands which have been reported since 1971), and could, in view of the detailed coverage provided in Chapters 22 and 23, probably be omitted without creating a great loss.

The very comprehensive indexes provided at the end of each of the two volumes (59 pages of author index and 44 of subject index in total) are usually effective in directing one to the desired material (despite there being sometimes not enough cross-references). Admittedly though, in the case of the famous prehistoric nuclear reactor of Gabun, one needs to know the key word "Oklo", or must instead track it down in Chapter 14 (under actinide elements of natural origin). If one is interested in finding examples of 8-coordinate cubic actinide complexes, a ligand arrangement known to be highly unfavorable for d-transition metal ions, some more searching is needed before one finds help in Chapter 18 (page 1373), where the magnetic properties resulting from the special crystal field splitting of the cubic $[U(NCS)_8]^{4-}$ ion is mentioned, and also in Chapter 20 (pages 1447 and 1458). Appendix I (nuclear magnetic dipole and electric quadrupole moments) might lead one into a fruitless search for NMR spectroscopic data, since the first successful ^{235}U NMR experiment carried out in 1983 is nowhere mentioned. Even in Appendix II, with its extensive tables of nuclear properties, we still do not find a chart of common nuclides for atomic numbers ≥ 89, nor *Seaborg*'s popular "coastal landscape" which allegorically depicts the relative stabilities of the heaviest elements. Apart from the inclusion of numerous molecular and crystal structures, the second edition is less richly illustrated than the first, which contained, for example, a color chart showing the colors of individual actinide ions, and full-page photographs of laboratories especially equipped for work on transuranium elements.

Despite the above comments, the transition from the classical Katz/Seaborg to the completely restructured version of this second edition has already reached a remarkably high standard in its first appearance. The books will certainly find their way into every good-sized chemistry library, and will be consulted frequently. The three editors conclude their preface by expressing the hope that this new edition might also serve as a valuable source of information to all those responsible for making far-reaching decisions on the production of nuclear energy and the control of nuclear weapons.

R. Dieter Fischer [NB 863 IE]
Institut für Anorganische und Angewandte Chemie
der Universität Hamburg (FRG)

Registered names, trademarks, etc. used in this journal, even when not marked as such, are not to be considered unprotected by law.

© VCH Verlagsgesellschaft mbH, D-6940 Weinheim, 1988. - Printed in the Federal Republic of Germany by Zechnersche Buchdruckerei, Speyer/Rhein.

All rights reserved (including those of translation into foreign languages). No part of this issue may be be reproduced in any form - by photoprint, microfilm, or any other means - nor transmitted or translated into a machine language without written permission from the publishers. Only single copies of contributions, or parts thereof, may be made for personal use. This journal was carefully produced in all its parts. Nevertheless, authors, editors and publisher do not warrant the information contained therein to be free of errors. Readers are advised to keep in mind that statements, data, illustrations, procedural details or other items may inadvertently be inaccurate.

Valid for users in the USA: The appearance of the code at the bottom of the first page of an article in this journal (serial) indicates the copyright owner's consent that copies of the article may be made for personal or internal use, or for the personal or internal use of specific clients. This consent is given on the condition, however, that the copier pay the stated per-copy fee through the Copyright Clearance Center, Inc., for copying beyond that permitted by Sections 107 or 108 of the U.S. Copyright Law. This consent does not extend to other kinds of copying, such as copying for general distribution, for advertising or promotional purposes, for creating new collective works, or for resale. For copying from back volumes of this journal see 'Permissions to Photo-Copy: Publisher's Fee List' of the CCC.

Editorial office: Pappelallee 3, D-6940 Weinheim, Federal Republic of Germany, Telephone (06201) 602315, Telex 465516 vchwh d, Telefax (06201) 602328.

Editor: *P. Gölitz.*

Associate editors: *D. I. Loewus, A. Stimson.* **Editorial assistant:** *E. Schweikart*

Publishers: VCH Verlagsgesellschaft mbH. (Managing Directors: *Prof. Dr. Helmut Grünewald* and *Hans Dirk Köhler*), Pappelallee 3, D-6940 Weinheim, Federal Republic of Germany. Correspondence concerning advertisements should be addressed to VCH Verlagsgesellschaft mbH. (Advertising Manager *R. J. Roth*), Boschstr. 12. P.O. Box 1260/1280, D-6940 Weinheim, Federal Republic of Germany, Telephone Weinheim (06201) 602-0, Telex 465516 vchwh d, Telefax (06201) 602328.

ANGEWANDTE CHEMIE
International Edition in English

Volume 27 · Number 9
September 1988
Pages 1113–1226

Transition Metals in the Synthesis and Functionalization of Indoles

New Synthetic Methods (72)

By Louis S. Hegedus*

The use of transition-metal complexes as reagents for the synthesis of complex organic compounds has been under development for at least several decades, and many extraordinary organic transformations of profound potential have been realized. However, adoption of this chemistry by the practicing synthetic organic chemist has been inordinately slow, and only now are transition-metal reagents beginning to achieve their rightful place in the arsenal of organic synthesis. Several factors contributed to the initial reluctance of synthetic organic chemists to use organometallic reagents. Lacking education and experience in the ways of elements having d electrons, synthetic chemists viewed organometallic processes as something mysterious and unpredictable, and not to be discussed in polite society. Organometallic chemists did not help matters by advertising their latest advances as useful synthetic methodology, but restricting their studies to very simple organic systems lacking any serious functionality (e.g., the "methyl, ethyl, butyl, futile" syndrome). Happily, things have changed. Organometallic chemists have turned their attention to more complex systems, and more recently trained organic chemists have benefited from exposure to the application of transition metals. This combination has set the stage for major advances in the use of transition metals in the synthesis of complex organic compounds. This review deals with one aspect of this area, the use of transition metals in the synthesis of indoles.

1. Introduction

The indole nucleus **1** is common to a large number and a wide variety of biologically active natural and unnatural compounds,[1] and the synthesis and functionalization of indoles has been the object of research for over one hundred years, beginning with synthetic studies of indole-based dyes.[2] Among the many more recent synthetic targets have been the pharmacologically active ergot alkaloids **2**,[3] the antitumor agents ellipticine **3**[4] and mitomycin C **4**,[5] and the considerably more complex "dimeric" indole alkaloids such as vincristine and vinblastine.[6]

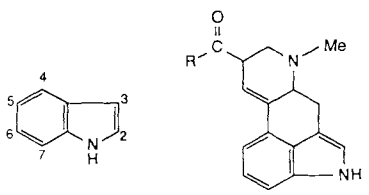

1

2

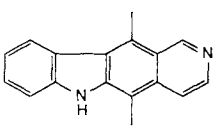

3

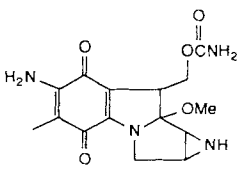

4

[*] Prof. L. S. Hegedus
Department of Chemistry, Colorado State University
Fort Collins, CO 80523 (USA)

Until very recently, indole syntheses relied primarily on well-established methods such as the Fischer indole synthesis, the Madelung cyclization of *N*-acyl-*o*-toluidines, the reductive cyclization of *o*-nitrobenzyl ketones, the Batcho–Leimgruber synthesis of indoles from *o*-nitrotoluenes and dimethylformamide acetal, and the Gassman synthesis of indoles from *N*-halo anilines.[7] All of these approaches involve "classic" organic synthetic methodology and display typical "organic" reactivity patterns and selectivities. Similarly, functionalization of existing indole ring systems relied heavily on well-established electrophilic substitution reactions, typical reactions for π-electron-rich systems.[8]

With the advent and continuing refinement of transition-metal-assisted organic synthetic methodology,[9] a number of new and potentially quite versatile methods for both the synthesis and the functionalization of indoles have been developed. This new methodology is the subject of this review.

Virtually all organic functional groups will coordinate to some transition metal, producing either stable complexes or unstable, but reactive, organometallic intermediates. This complexation is usually quite specific, permitting the activation of a single functional group in the presence of other quite similar ones, thereby reducing the need for protecting groups. Once complexed, the reactivity of the organic functional group is governed by the chemistry of the metal, and the normal reactivity patterns of the functional group are often dramatically altered. Since most transition metals also have associated with them ancillary "spectator" ligands which do not participate directly in reactions at the coordinated functional group but do affect the overall reactivity of the system, it is often possible to "fine-tune" the reactivity of the complexed species. These features, exemplified by the transition-metal-assisted indole syntheses presented below, permit the use of unconventional starting materials with unusual reactivity patterns to produce complex organic compounds with a high degree of efficiency and selectivity.

2. Palladium Complexes in the Synthesis of Indoles

Palladium complexes have been used in the synthesis of organic compounds for over twenty years, starting with the commercially important Wacker process for the oxidation of ethylene to acetaldehyde.[10] A number of palladium complexes are commercially available and can be used as catalysts or catalyst precursors without further processing. Hence, a wide variety of palladium-assisted organic reactions has been developed and applied to the synthesis of complex organic molecules, including indoles. Palladium exists in two stable oxidation states—Pd^{II} and Pd^0—and, as usual, the chemistry of these differs substantially with regard to both substrate specificity and type of reaction promoted.

2.1. Palladium(II) Complex Chemistry

Palladium(II) salts are moderate to strong electrophiles, depending on the counterion. Commercially available salts are $Pd(OAc)_2$, $Pd(CF_3CO_2)_2$, and $[PdCl_2]_n$. The former two are relatively soluble in organic solvents, but $[PdCl_2]_n$ is a chloro-bridged polymer which is quite insoluble. It does form soluble solvates with nitriles or "ate" complexes with lithium or sodium chloride, and it is in these soluble forms that it is normally used in organic synthesis.

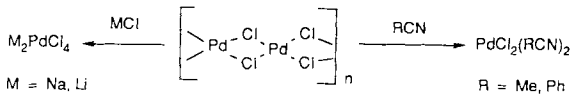

Palladium(II) complexes are electrophiles, and they complex and activate π-electron-rich organic compounds. Arenes are directly metalated by $Pd(OAc)_2$ or $Pd(CF_3CO_2)_2$, forming σ-arylpalladium(II) complexes in a typical electrophilic aromatic substitution. Arenes can be coupled to give biphenyls by treatment with $Pd(OAc)_2$ in acetic acid, in a process that probably involves two successive substitutions followed by a reductive elimination. Unfortunately, this process has not yet been developed into an efficient catalytic one (Ar = aryl).

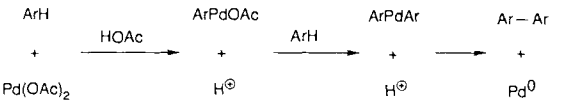

Olefins rapidly and reversibly complex to $PdCl_2$, forming relatively stable but reactive π-olefin complexes. Once complexed, the olefin becomes generally reactive toward *nucleophilic* attack—a reversal of normal olefin reactivity—forming a carbon–nucleophile bond and a palladium(II)–carbon σ bond (Scheme 1). Nucleophiles ranging from $Cl^\ominus$ to $Ph^\ominus$ react, spanning a range of 10^{36} in basicity. Most nucleophiles attack at the more-substituted olefin position. The σ-alkylpalladium(II) complex is generally not stable and can only be isolated in unusual cases. However, it is highly reactive and undergoes transformations typical of σ-alkylpalladium(II) species, regardless of the method of formation. Thus β-hydride elimination ensues at temperatures above about 0 °C, giving the formal product of nucleophilic substitution. Hydrogenolysis (> −20 °C, 1 atm H_2) produces the formal product of nucleophilic addition. Transmetalation from a main-group organometallic—Sn, Hg, Cu, Tl—produces a dialkylpalladium(II) complex which can undergo reductive elimination resulting in overall difunctionalization of the olefin. Difunctionalization of the olefin also results from insertion of carbon monoxide or olefins. The regiochemistry of olefin insertion is governed by steric rather than electronic factors, and alkylation at the less-substituted olefin terminus usually predominates in intermolecular insertion processes. Note that all of these processes produce Pd^0 in the final step, while Pd^{II} is required for the olefin-activation step. Reoxidation of Pd^0 to Pd^{II} is thus required for *catalytic* processes. Oxidants such as $CuCl_2/O_2$, benzoquinone, and $K_2S_2O_8$ are most commonly used for this purpose, the choice of oxidants being dictated by the reactant and product compatibility. All of these processes have been used in the synthesis and functionalization of indoles and will be discussed below.

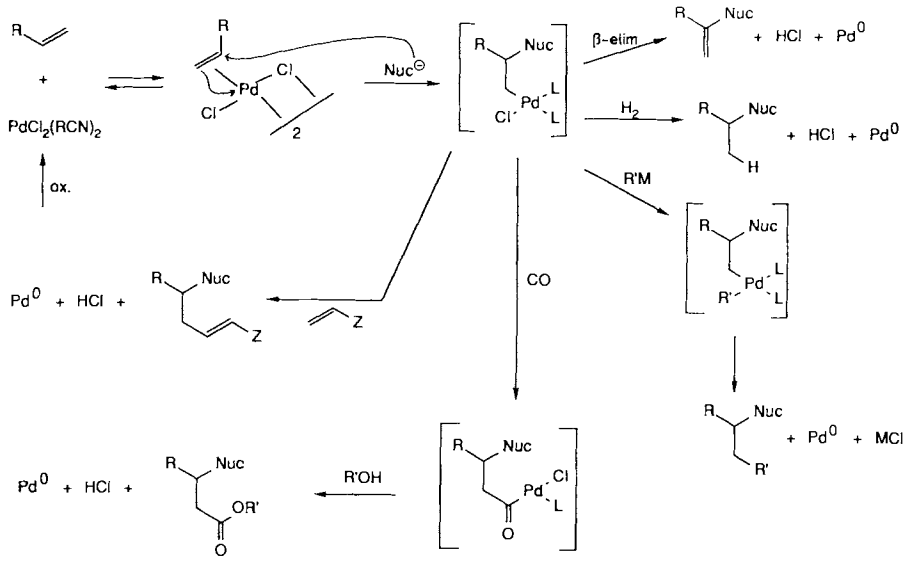

Scheme 1. Reactions of nucleophiles with palladium(II) complexes. Nuc = Cl, OH, AcO, R_2N (from R_2NH), $HC(CO_2R)_2$, Ph; Z = H, R, Ph, CN, CO_2Me, OR, NHAc; L = RCN (not always drawn).

2.1.1. *Coupling of Arenes by Palladation*

Although the coupling of arenes by direct palladation is not an efficient process, it has been used in several cases to synthesize functionalized indole ring systems. The early studies involved the coupling of substituted diphenylamines. Although one to two equivalents of palladium(II) acetate were required, reasonable yields of carbazoles were obtained.[11] Ellipticine **3** was made by this process.[12] Although the yield of the coupling was low, the directness of the approach made it competitive with other synthetic routes.

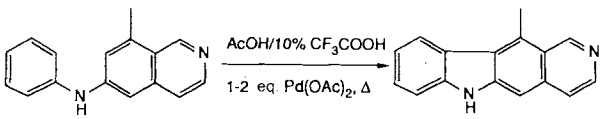

3, 25%

Indole itself undergoes direct palladation at the 2- and 3-positions. This has been used to make fused-ring indole systems—e.g., **5**,[13] **6**, and **7**[14]—as well as to introduce olefinic side chains at the 3-position (cf. **8**) or at the 2-position in 3-methylindole.[15–17] Carbonylation at the 3-position has also been achieved by this method, carbon monoxide being inserted rather than an olefin.[18] Unfortunately, all of these processes require virtually stoichiometric amounts of $Pd(OAc)_2$ even when suitable reoxidants are present, and efficient catalysis has not yet been achieved in these systems.

Finally, in a remarkable reaction, $Pd(OAc)_2$ catalyzed a single-electron-transfer process which combined 4,*N*,*N*-trimethylaniline with tetrahydrofuran to produce dihydroindole **9**.[19] Iodobenzene served as the reoxidant. This unusual process was not general.

Although direct aromatic palladation remains a catalytically inefficient process, palladium(II) is an efficient catalyst for the olefination and alkylation of thallated indoles,

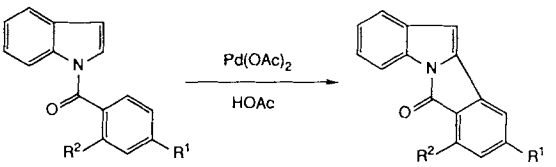

R^1 = H, Cl, Me; R^2 = H, Me, Cl

5, 6-40%

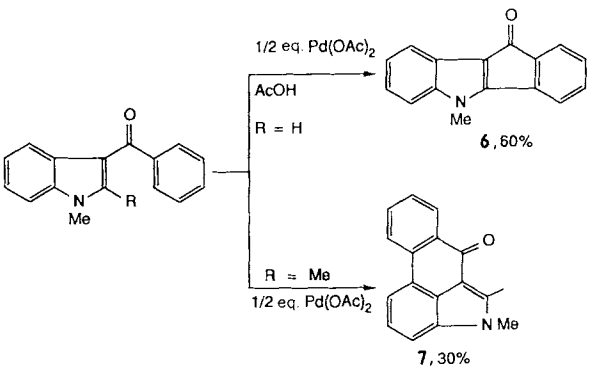

6, 60%

7, 30%

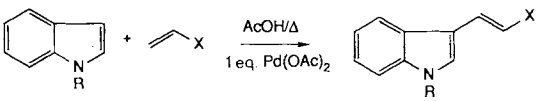

R = CH_3CO, SO_2Ph, $PhCH_2$, H

X = CN, CO_2Me, Ph

8, 40-70%

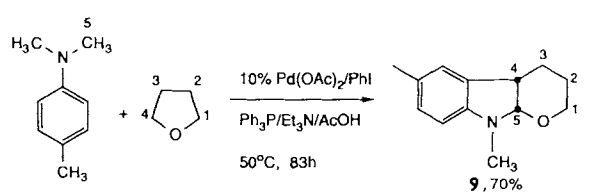

9, 70%

via a transmetalation-insertion-elimination process (Scheme 1). Thus, indole-3-carbaldehyde underwent thallation primarily at the 4-position (→ **10**). In the presence of a $Pd(OAc)_2$ as catalyst, transmetalation to palladium, followed by olefin insertion or reductive elimination, ensued producing 4-alkylated indoles in modest yield (R = CO_2Me, H). Thallium(III) probably serves as the reoxidant for palladium(0). This is a synthetically important reaction for ergot alkaloid synthesis, since ergots require substitution in the normally unreactive 4-position of the indole ring system (TFA = trifluoroacetyl; cat. = catalytic amount).

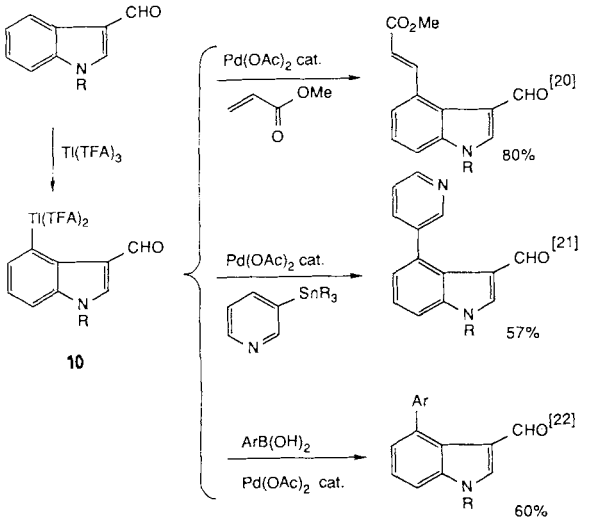

2.1.2. *Palladium(II)-Catalyzed Amination of Olefins*

Palladium(II) chloride catalyzes the amination of olefins (cf. Scheme 1). When the amine and the olefin are in the same molecule, cyclization to give nitrogen heterocycles occurs. *o*-Allylanilines were efficiently converted into 2-methylindoles using palladium(II) catalysis and benzoquinone as reoxidant[23,24] (Scheme 2). The process was

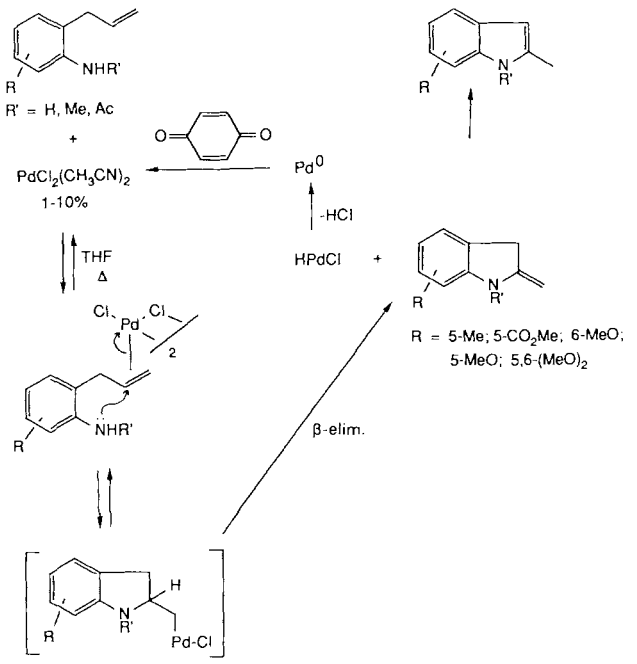

Scheme 2. Palladium(II)-catalyzed cyclization of allylanilines to 2-methylindoles.

thought to involve coordination of the olefin to Pd^{II} followed by intramolecular amination. As expected, attack occurred at the more-substituted position of the olefin, forming the indole ring and an unstable σ-alkylpalladium complex. β-Hydrogen elimination followed by olefin rearrangement produced the indole. When β-hydrogen elimination was suppressed, either by blocking with an alkyl group, or by careful control of conditions, insertion of CO or an olefin ensued, leading to more complex indoles such

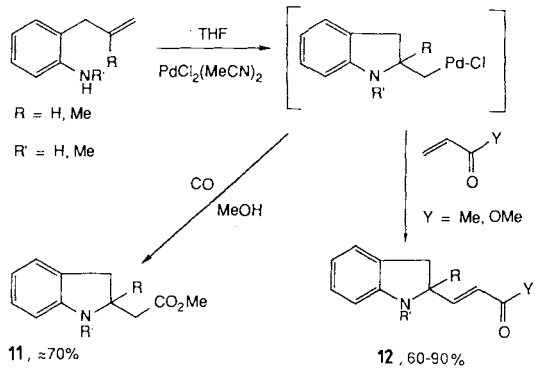

as **11** and **12**.[25] When the olefin was also incorporated into the starting aniline, pyrroloindoles such as **13** were formed efficiently.[25,26] This process was used in the syn-

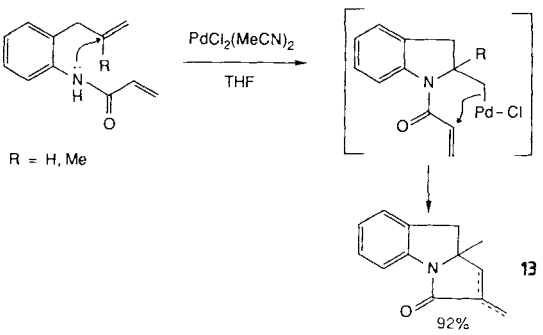

thesis of pyrroloindolequinones such as **14** and **15**, which are related to mitomycin C **4**.[27]

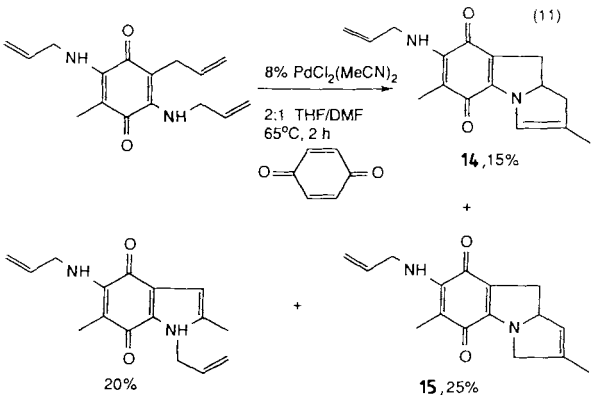

Indoles such as **16** were also produced in a stoichiometric reaction involving most of the processes described in Scheme 1, including transmetalation, insertion, elimination, and amination of olefins.[28]

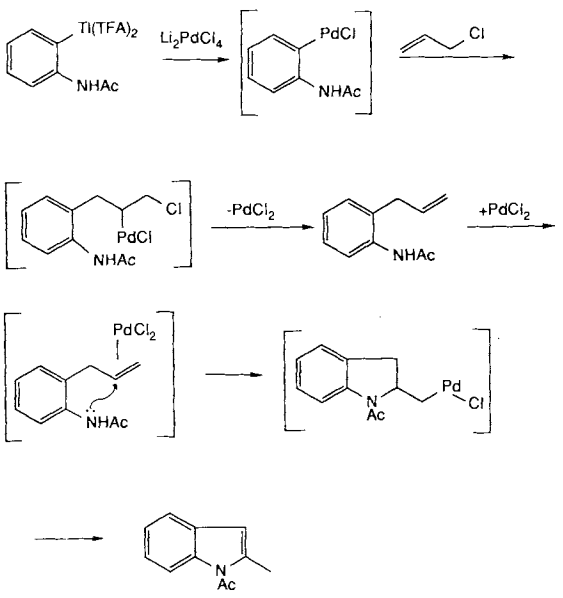

16, 45%

Palladium-assisted amination of olefins was also used to *N*-alkylate indole with olefins, giving *N*-alkylindoles upon reduction, N-vinylindoles upon β-elimination, and 3-(1-indolyl)propionic esters upon carbonylation.[29] This was a stoichiometric process since conditions to carry out the Pd^0 to Pd^{II} redox chemistry in the presence of indole anion could not be found. The strongly electrophilic $Pd(CH_3CN)_4(BF_4)_2$ promoted a Ritter-like reaction between *N*-allyl-3-methylindole and nitriles, giving pyrazino[1,2-*a*]indoles such as **17**.[30] While interesting, this process was neither efficient nor general.

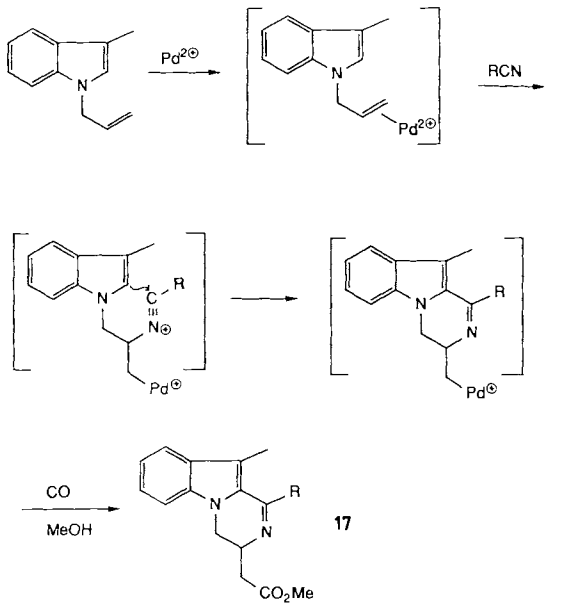

R = Me, 34%; Et, 47%; Ph, 35%

In contrast to alkenes, alkyne aminations assisted by palladium(II) are much less common, primarily because of facile alkyne oligomerization reactions which occur. However, *o*-alkynylated anilides were successfully cyclized to indoles such as **18** by $PdCl_2(MeCN)_2$.[31] The mechanism

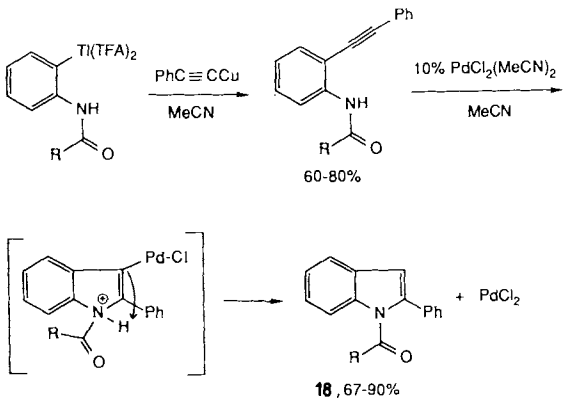

18, 67-90%

must be somewhat different from that observed with olefins, since the σ-vinylpalladium(II) intermediate cannot undergo β-hydride elimination, and protolytic cleavage of the Pd–C bond is assumed. Acetylenedicarboxylates were annelated to anilines to give indole-2,3-dicarboxylic acids in an electron-transfer process requiring stoichiometric amounts of palladium.[32]

2.1.3. Palladium(II)-Catalyzed (and Other Metal-Catalyzed) Reaction of Azirines

Thermolysis of phenylazirines **19** at temperatures above 170 °C produced indoles, presumably via a nitrene intermediate. Palladium(II) chloride catalyzed this process, permitting it to ensue at 30 °C.[33] Rhodium(I), palladium(0),

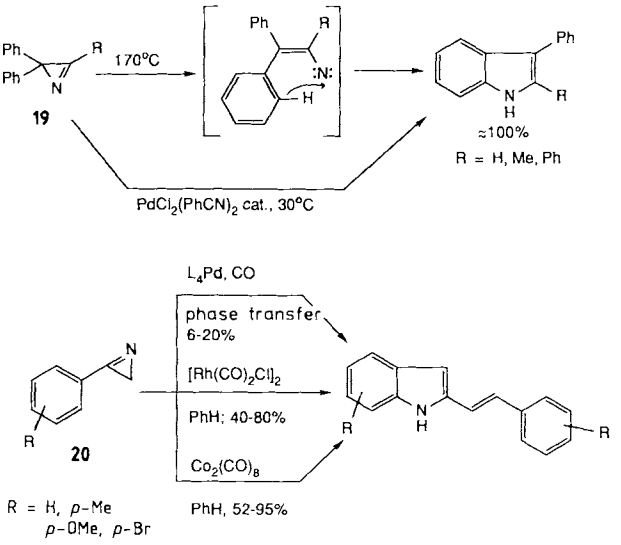

and cobalt(0) complexes catalyzed a puzzling dimerization of azirines **20** to produce indoles in variable yields.[34-36]

2.2. Palladium(0) (and Nickel(0)) Complex Chemistry

While palladium(II) salts are electrophilic reagents which react with olefins and arenes, palladium(0) complexes are strong nucleophiles and are most reactive toward organic halides. The two most common, commercially available complexes for palladium(0) catalysis are $Pd(PPh_3)_4$ and $Pd(dba)_2$ (dba = dibenzylideneacetone),

which is converted into $Pd(PPh_3)_4$ when treated with triphenyl phosphane. Both of these have been extensively used as catalysts in organic synthesis. However, it is frequently more convenient to generate palladium(0) catalysts in situ, by reducing palladium(II) catalyst precursors. Thus, treatment of $Pd(PPh_3)_2Cl_2$ with diisobutylaluminum hydride or with CO or triethylamine (see below) will generate the catalytically active Pd^0 species "PdL_n". Perhaps the most extensively used palladium(0) catalyst precursor, however, is palladium(II) acetate, which is readily reduced in situ by a range of compounds including carbon monoxide, olefins, phosphanes, and tertiary aliphatic amines such as triethyl- or tri-*n*-butylamine.[37] This causes some confusion in the literature, since palladium(0) catalysis is involved but palladium(II) acetate appears in all the equations. Invariably, some reducing agent is present in these systems, and palladium(0) catalysis is indeed involved.

The typical reaction of Pd^0 complexes is the "oxidative addition" of organic halides, wherein the Pd^0 complex is formally oxidized to a σ-alkylpalladium(II) halide complex and the "oxidizing agent" (RX) adds to the metal (Scheme 3). This reaction is limited to halides lacking β hydrogens,

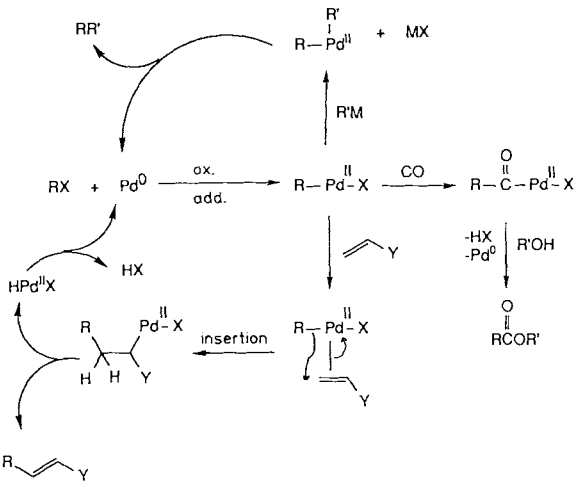

Scheme 3. Palladium(0)-catalyzed reactions of organic halides.

since β-hydride elimination (cf. Scheme 1) prevents the further use of these complexes. The most common substrates are aryl, vinyl, benzyl, and allyl halides. The order of halide reactivity is I > Br ≫ Cl, and iodides will often react in the absence of phosphane ligands while bromides require a phosphane. Chlorides generally are not useful. This "oxidative addition" produces a σ-alkylpalladium(II) complex which undergoes all the reactions described in Scheme 1 for σ-alkylpalladium(II) species produced by nucleophilic attack on olefins. The most extensively used reactions are transmetalation from main-group organometallics, and insertion of CO or olefins. These reactions are summarized in Scheme 3. These processes all re-form Pd^0, which can reenter the catalytic cycle directly, in contrast to Pd^{II}-catalyzed reactions, which require an additional oxidant. This feature, in conjunction with recent advances which permit very high catalyst turnover[38] and very mild conditions,[39] accounts for the extensive use of Pd^0 catalysis in the syntheses and functionalizations discussed below.

2.2.1. Palladium(0)-Catalyzed Alkynylation of Bromoanilines

o-Alkynylanilines such as **21**, made by palladium(0)-catalyzed coupling of alkynes with *o*-haloaniline precursors,[40,41] are readily cyclized to indoles. (Note that a Pd^{II} complex is the precatalyst which is reduced to Pd^0 by triethylamine.) In a related process, hydroboration of

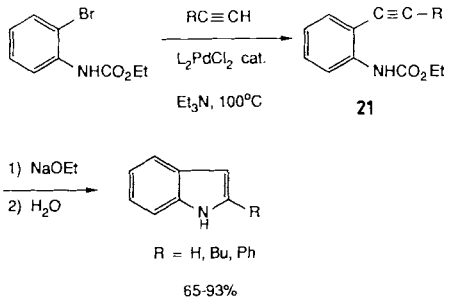

ethoxyacetylene gave a vinylborane, **22**, which underwent Pd^0-catalyzed oxidative addition/transmetalation to produce an indole precursor.[42]

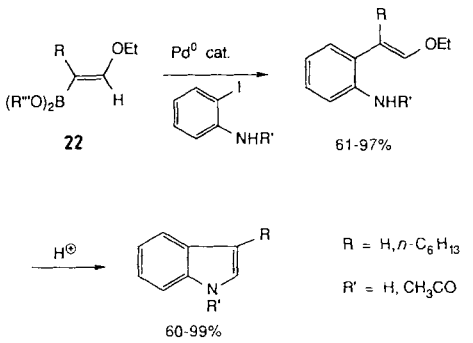

2.2.2. Palladium(0)-Catalyzed Cyclization of 2-Halogenated N-Allyl-, N-Vinyl-, or N-Arylanilines to Indoles

o-Bromoanilines are easily *N*-allylated, producing substrates ideally suited for a Pd^0-catalyzed oxidative addition/olefin insertion approach to the indole ring system. As a consequence, this route has been extensively developed. Both activated[43,44] and simple olefins[45] inserted effi-

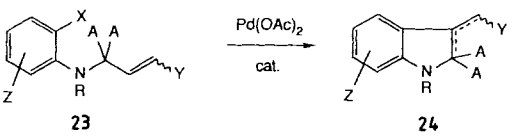

A	R	X	Y	Z	24, Yield [%]
1/2 O=	$PhCH_2$	Br	Ph CO_2Me	H	50–73
H	Ac	Br	CO_2Me	H	73
H	H	I	H	5-Me 5,6-$(MeO)_2$ 5-CO_2Me H	50–87

ciently. The insertion product **23** of simple olefins gave good yields of indoles **24** with catalytic amounts of palladium. This cyclization was even effective with highly substituted arenes and was used to synthesize indolequinones via **25** and **26**.[46] Carbazoles were produced in low yields from 3-anilinocyclohexenones such as **27** (R = H, Et)[47]

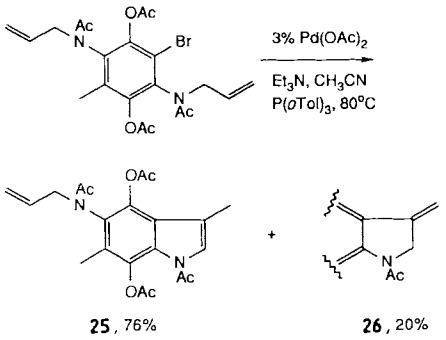

25, 76% **26**, 20%

and in good yield from diphenylamines such as **28**[48] utilizing similar oxidative addition/insertion chemistry. Mi-

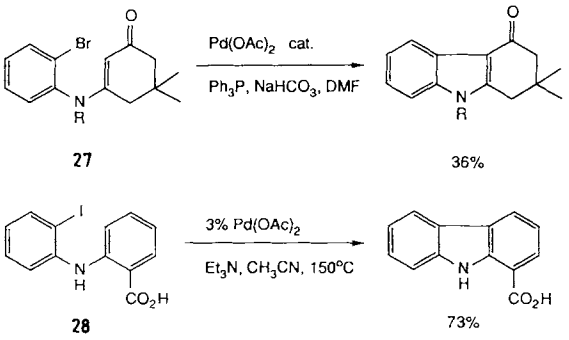

27 36%

28 73%

tomycin analogues (cf. **29**) were prepared very efficiently by the same process,[49,50] although the last cyclization also occurred in the absence of a Pd catalyst. Carbazoles such

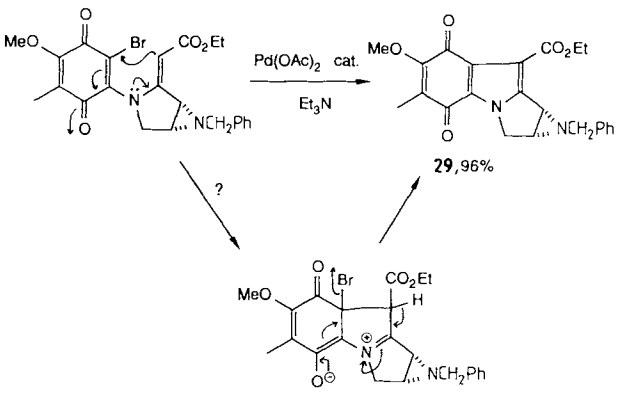

29, 96%

as **30** were also produced by an intramolecular amination of an aryl halide.[51-53] This process required 1.2 equivalents of Pd^0 complex (L = Ph_3P) and its mechanism is not yet understood.

In contrast to nickel(II) salts, which differ dramatically from palladium(II) salts in their chemistry, nickel(0) complexes closely resemble palladium(0) complexes in their reaction chemistry. Thus nickel(0) complexes can also be

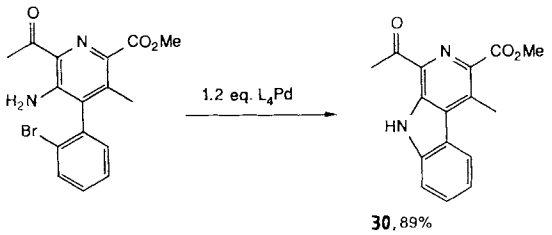

30, 89%

used to cyclize *N*-allyl-2-haloanilines to indoles, although the yields obtained are somewhat lower.[54-59]

The regioselectivity of intramolecular olefin insertion processes warrants comment. As noted in Section 2.1, the regioselectivity in the intermolecular insertion process is strongly governed by steric rather than electronic factors, and alkylation at the less-substituted terminus of the olefin predominates regardless of the electronic nature of the olefin substituents. In intramolecular processes, the effects of developing ring strain may well override those of olefin substituents, making the site of alkylation (e.g., ring size) difficult to predict.

2.2.3. *Palladium(0)-Catalyzed Functionalization of Indoles*

Palladium(0) catalysis has also been used extensively to functionalize indoles. Chloropyrazines **31** coupled to the 2-position of indole in the presence of Pd(0), probably by

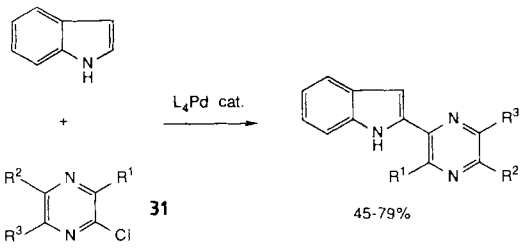

31 45-79%

R^1, R^3 = Me, Et, *i*Pr, Ph, H; R^2 = H, Ph

an oxidative addition/insertion process.[60] The 3-aminoethyl side chains of indoles were elaborated by a Pd^0-catalyzed carbonylation, for example with ring closure to give **32**.[61]

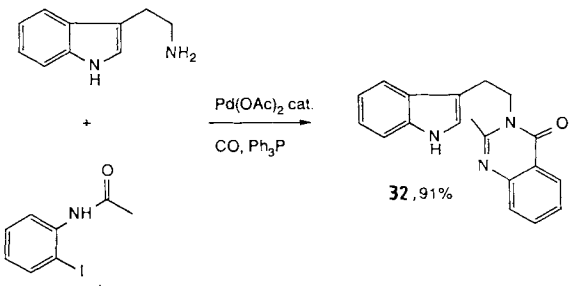

32, 91%

Palladium(0)-catalyzed reactions of haloindoles are among the most synthetically useful processes and have been extensively developed for application in the synthesis of 3,4-disubstituted indole ring systems including ergot alkaloids (see Section 2.2.4). Introduction of functionality at the 4-position of indole using conventional electrophilic indole chemistry is difficult, since the 1-, 2-, and 3-posi-

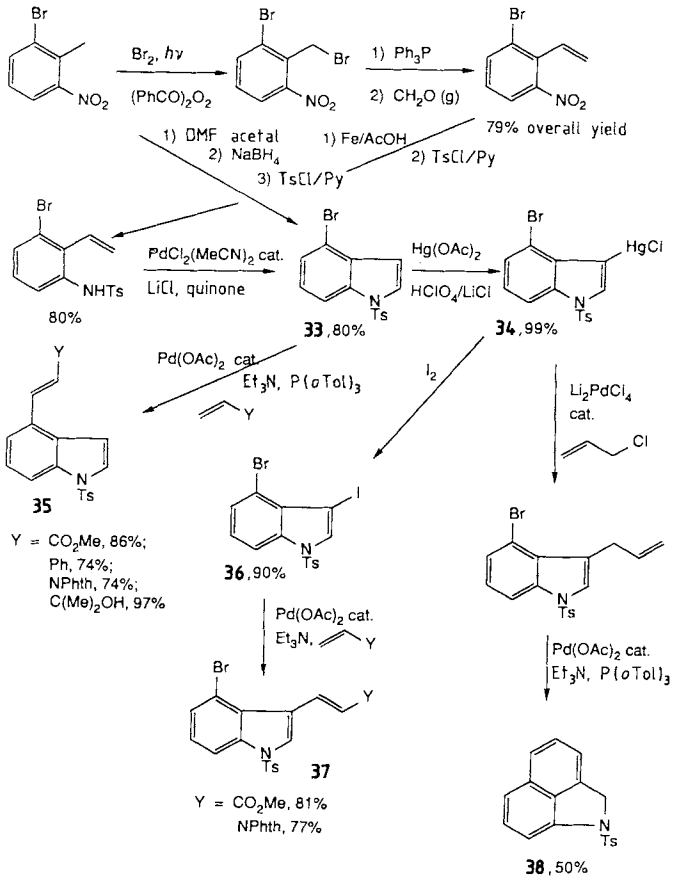

Scheme 4. Palladium(0)-catalyzed synthesis of 3- and 4-substituted indoles. NPhth (cf. **35** and **37**) = phthalylimido, Py = pyridine.

tions are considerably more reactive. Scheme 4 shows one approach to the introduction of functionality at the 3- and 4-positions of indoles.[62] The key compound in all these transformations is 4-bromo-*N*-tosylindole **33**, prepared in good yield by Pd^{II}-catalyzed cyclization of the appropriate *N*-tosyl-*o*-vinylaniline, or, more recently, by the DMF-acetal/reduction/tosylation approach. Compound **33** reacted in typical aryl halide fashion in the Pd^0-catalyzed oxidative addition/insertion process to produce 4-alkylated indoles **35** in excellent yield. Direct electrophilic mercuration at the 3-position produced **34**, which was readily iodinated to give 4-bromo-3-iodoindole **36**. The same Pd^0-catalyzed process permitted facile alkylation of the 3-position as well (cf. **37**). Complete discrimination between the bromide, which requires a phosphane to react, and the iodide, which reacts in the absence of a phosphane, was possible by appropriate choice of conditions. The mercurioindole **34** also underwent a facile Pd^{II}-catalyzed transmetalation/insertion process to give the 3-allyl-4-bromoindole. Cyclization to tricyclic compound **38** was catalyzed by palladium(0). Although **38** had the tricyclic ring system found in ergot alkaloids, rearrangement of the indole to the more stable naphthalene made this specific compound of little synthetic interest. 7-Substituted indoles were available by a related route involving thallation/iodination of the 7-position of an indole followed by Pd^0-catalyzed oxidative addition/olefin insertion.[63,64]

2.2.4. *Palladium Catalysis in the Synthesis of Ergot Alkaloids*

After many years of development, palladium catalysis is finally finding its way into mainstream organic synthesis. Its utility is evident from the ergot syntheses discussed below, as are its limitations. When properly applied, however, palladium catalysis can result in very short and efficient synthetic approaches to complex organic compounds. A fine example of this is seen in Scheme 5, wherein Pd^0-catalyzed functionalization of the 4-position of the indole nucleus provided the key intermediate **39** for the synthesis of

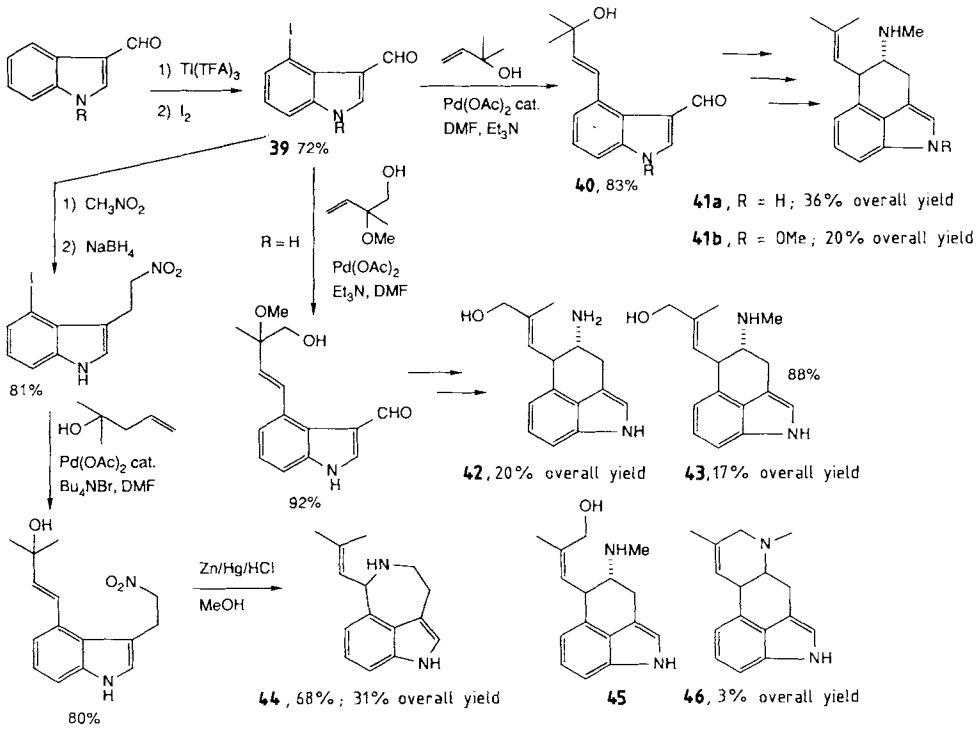

Scheme 5. Palladium-catalyzed synthesis of clavine alkaloids, which belong to the ergot alkaloids. The yields of **39** and **40** refer to R = H, OMe.

a number of ergot alkaloids such as (±)-6,7-secoagroclavine **41a** (via **40**),[65] (±)-1-methoxy-6,7-secoagroclavine **41b**,[66] (±)-norchanoclavine I **42**, (±)-chanoclavine I **43**,[67] (±)-aurantioclavine **44**,[68] (±)-isochanoclavine **45**, and (±)-agroclavine **46**.[67] These all rely on the formyl-directed thallation of indole-3-carbaldehyde, followed by iodination with iodine to give the iodide **39** and Pd^0-catalyzed introduction of the appropriate side chain at the 4-position. The remaining steps involve conventional organic chemistry.

An even more extensive use of palladium catalysis is seen in the total synthesis of the methyl ester of (±)-*N*-acetylclavicipitic acid **49**,[69] which involves as key steps Pd^{II}-catalyzed formation of the indole ring, Pd^0-catalyzed introduction of both C-ring side-chain precursors, and Pd^{II}-catalyzed formation of the seven-membered ring (Scheme 6). This twelve-step synthesis in 18% overall yield from commercially available starting materials is quite efficient.

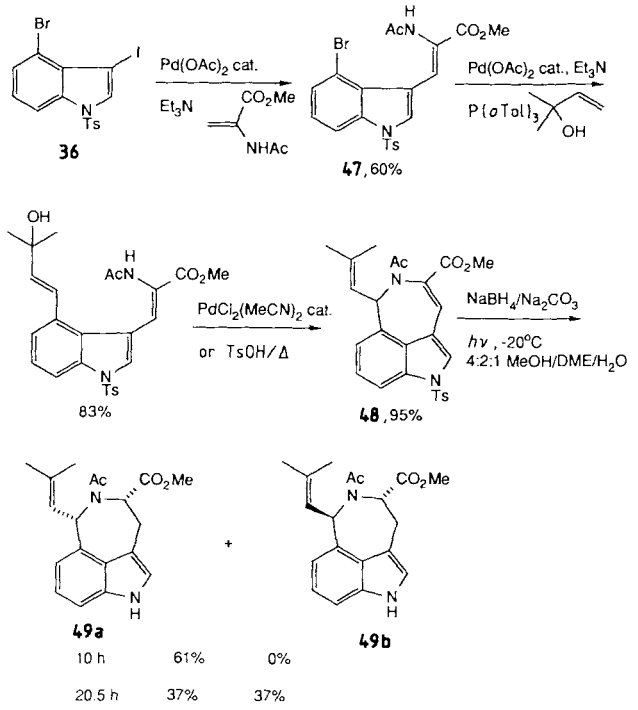

Scheme 6. Palladium-catalyzed synthesis of the methyl ester of (±)-*N*-acetylclavicipitic acid, **49**. Only the isomer shown here is formed from compound **47**.

A related approach was used in the total synthesis of (±)-aurantioclavine **44** (Scheme 7).[70] In this case, oxidative addition to Ni^0 followed by transmetalation from Zr^{IV} proved more reliable than Pd^0-catalyzed oxidative addition/transmetalation from boron for introduction of the enol ether at the 3-position. Pd^0-catalyzed introduction of the 4-alkyl group, followed by acid-catalyzed condensation/cyclization and photolytic reductive decarbonylation, completed the synthesis of compound **44**.

A potential approach to tetracyclic ergot alkaloids involving extensive palladium catalysis is shown in Scheme 8.[71] Acylation of the 3-mercurioindole **34** by acryloyl chloride using Pd^0-catalyzed oxidative addition/transmetalation to give **50**, followed by Pd^0-catalyzed cyclization,

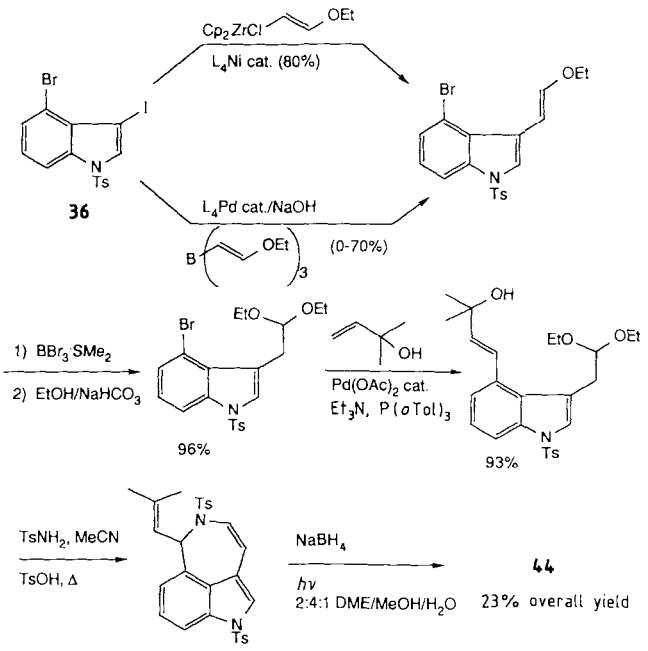

Scheme 7. Palladium-catalyzed synthesis of (±)-aurantioclavine **44**.

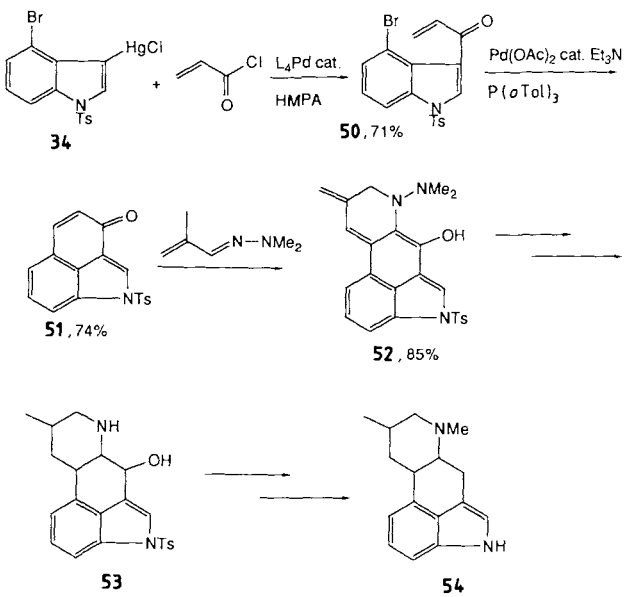

Scheme 8. Palladium-catalyzed synthesis of tetracyclic ergot alkaloids such as **54**. The reaction of **51** was carried out without solvent.

produced tricyclic intermediate **51**, which was prevented from rearranging to the naphthalene (cf. **38** in Scheme 4) by the position of the carbonyl group. Cycloaddition of **51** to an azadiene produced the proper ergot alkaloid skeleton, **52**, in a highly oxidized state. Reduction and removal of heteroatoms are required to produce the proper ergot ring system.

2.3. π-Allylpalladium Complexes in the Synthesis and Functionalization of Indoles

π-Allylpalladium(II) complexes can be prepared by proton abstraction from olefin palladium(II) complexes, by in-

sertion of dienes into σ-alkylpalladium(II) complexes, or by oxidative addition of allylic substrates to palladium(0) complexes. They are yellow, air-stable crystalline solids, quite stable to a variety of reactive species. In the presence of good donor ligands (usually phosphanes), however, these complexes become generally reactive toward nucleophiles such as amines or stabilized carbanions, resulting in allylation of these nucleophiles and production of Pd^0 species (Scheme 9). This forms the basis of a very useful Pd^0-

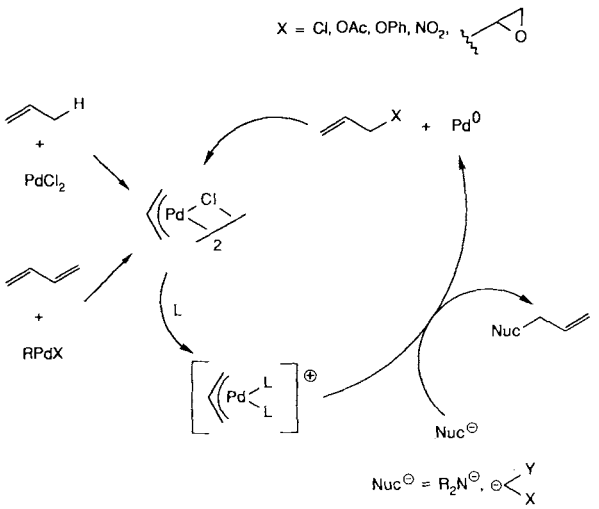

Scheme 9. Synthesis and reactions of π-allylpalladium(II) complexes.

catalyzed allylic activation process which has been extensively developed for use in organic synthesis. Some of these applications involve indoles and are presented below.

Formation of the indole ring via π-allylpalladium(II) intermediates—e.g., **55**[72] and **56**[73]—is relatively uncom-

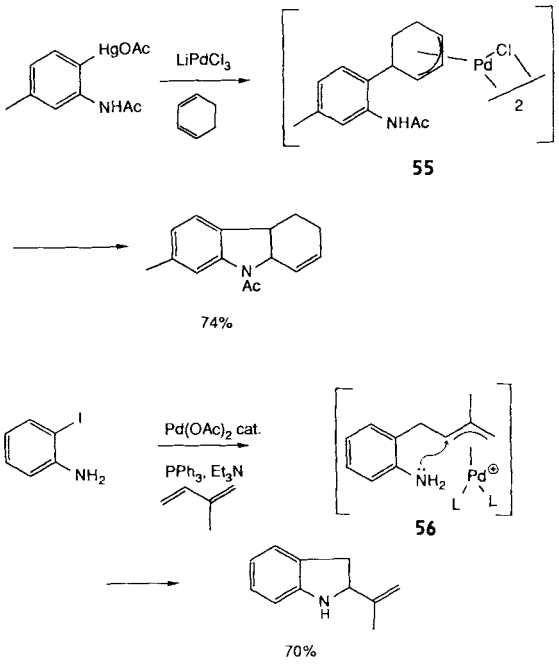

mon. These two examples involve diene insertion into σ-arylpalladium(II) species. π-Allylpalladium(II) chemistry is more commonly used to elaborate existing indole ring systems. The isoquinuclidine ring of ibogamine **57**[76] and cantharanthine **58**[77] were synthesized by a Pd^0-catalyzed

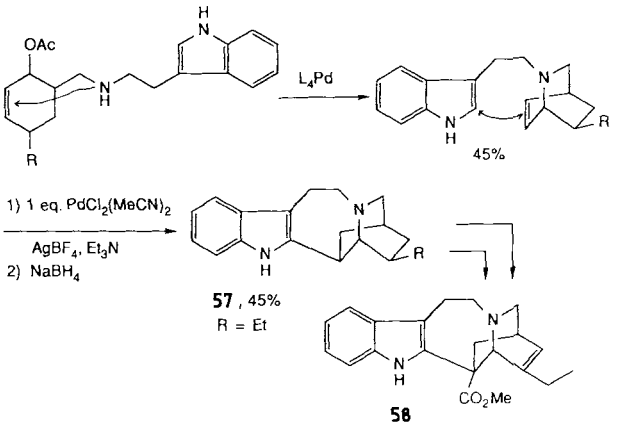

allylic amination.[74-77] Alkylation at the indole 2-position was accomplished using palladium(II) activation.[78] Other indole alkaloid syntheses have used Pd^0-catalyzed allylic alkylation to elaborate nonindolic heterocyclic rings such as **59** and **60**.[78]

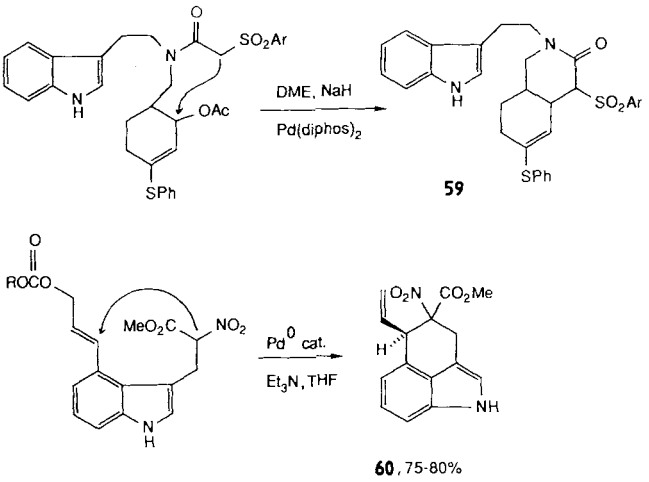

3. Other Transition Metals in the Synthesis and Functionalization of Indoles

3.1. Copper(I)-Catalyzed Cyclization and Condensation

Although palladium is by far the most extensively used transition metal for the synthesis and functionalization of indoles, many others have found at least limited use in this

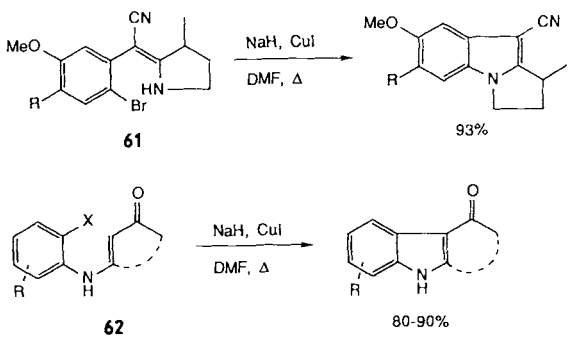

regard. For instance, copper(I) salts have long been known to catalyze the reactions of nucleophiles with aromatic halides (e.g., the Hurtley reaction). With appropriate substrates, indoles can be formed. Thus *o*-haloaryl enamines, such as **61**, R = Me, OMe, H,[81] and **62**,[82] cyclized to indoles in the presence of copper(I) iodide in excellent yield. Under similar conditions enolates condensed with *o*-iodoaniline to produce indoles.[83] *o*-Haloacetamides (e.g. **63**[84]) also cyclized to indole derivatives under these conditions. Copper(I) oxide catalyzed the cyclization of *o*-isocyanophenylacetones to indoles.[85–87]

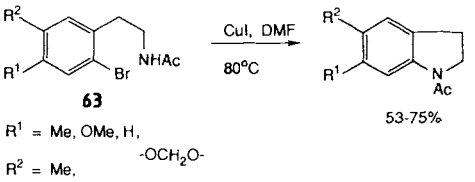

3.2. Reductive Cyclizations using Low-Valent Transition-Metal Compounds

A number of indole syntheses use low-valent transition metals to reduce aromatic nitro groups to amines, which can then cyclize with electrophilic groups in the *ortho* position to form indoles. These typically involve *o*-nitroaryl enamines (cf. **64**) and reducing agents such as iron(0),[88] titanium(III) chloride,[89] or nickel boride.[90] Tryptamine

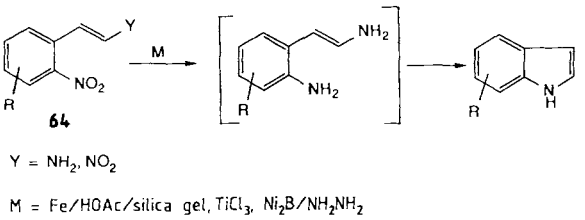

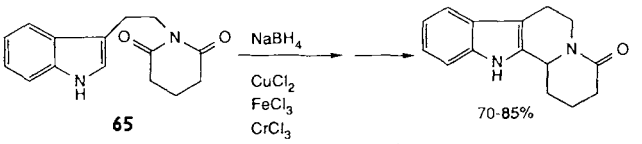

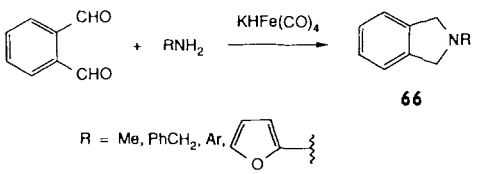

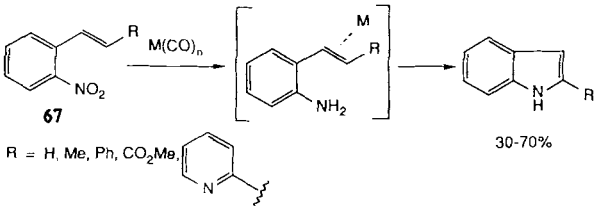

derivatives such as **65** were reductively cyclized to β-carbolines by $NaBH_4$ and copper(II), iron(III), or chromium(III) halides.[91] Dihydroisoindoles **66** were produced in excellent yield by the $KHFe(CO)_4$-promoted reductive amination of *o*-dialdehydes.[92] Finally, *o*-nitrostyrenes such as **67** were reductively cyclized to indoles by metal carbonyls, in a process which must involve olefin activation by the metal, as well as nitro group reduction.[93]

3.3. Ruthenium(II)- or Palladium-Catalyzed Oxidative Cyclization

Ruthenium(II) chloride-catalyzed oxidation of alcohols has been used to form indoles in modest yield, although the conditions are somewhat severe.[94–96] 2,6-Dimethylphenyl isocyanide was converted into 7-methylindole **68** in

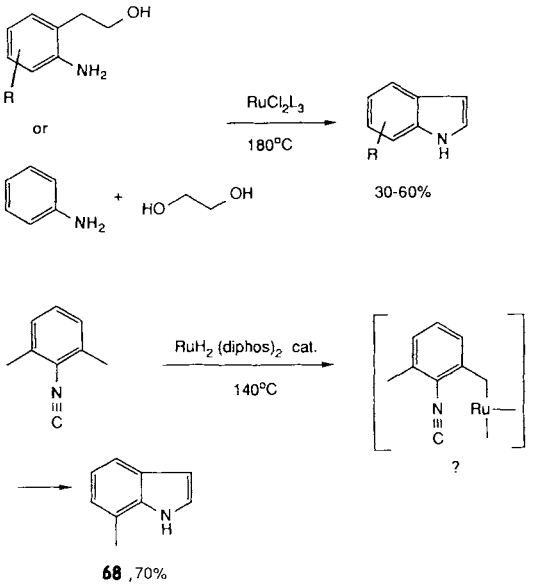

a process which must have involved C–H activation by the ruthenium (four catalytic cycles per $[RuH_2(diphos)_2]$).[97] Palladium on carbon catalyzed oxidative cyclization to **69**.[98]

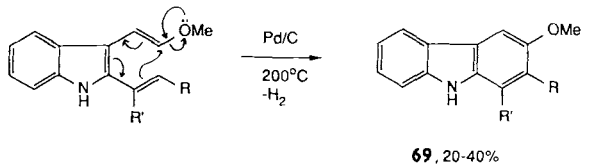

3.4. Cobalt-Catalyzed Cyclotrimerization Reactions

The cobalt(I)-catalyzed cyclotrimerization of alkynes and cocyclotrimerization of alkynes and alkenes have been extensively developed for use in organic synthesis.[99] The synthesis of compounds **70**[100] and **71**[101] exemplify the use of the latter in the synthesis of indoles. Cobalt(I) complexes also catalyzed the addition of alkynes to diazenes to produce *N*-aminoindoles **72**.[102]

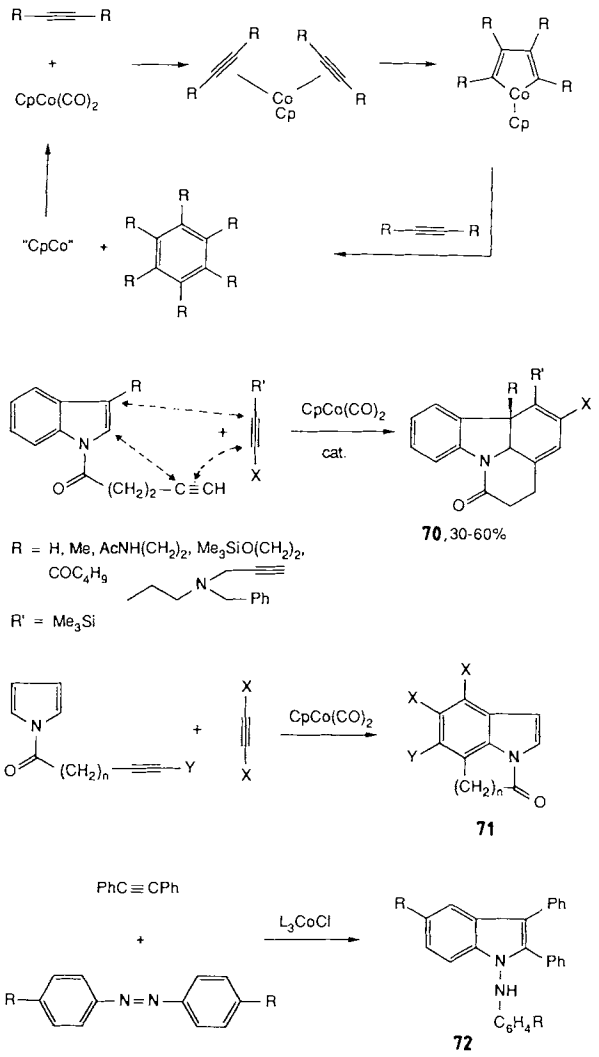

3.5. Arenechromium Tricarbonyl Complexes in Indole Chemistry

Arenes readily form η^6 complexes with chromium hexacarbonyl usually by simply heating the two together. Once complexed to the chromium tricarbonyl fragment, the arene becomes reactive toward nucleophilic attack and toward ring lithiation, the effect of the $Cr(CO)_3$ fragment being comparable to having introduced a nitro group. Thus, direct nucleophilic aromatic substitution and lithiation becomes feasible. This feature has been used to introduce functionality at normally unreactive positions of the indole ring system.

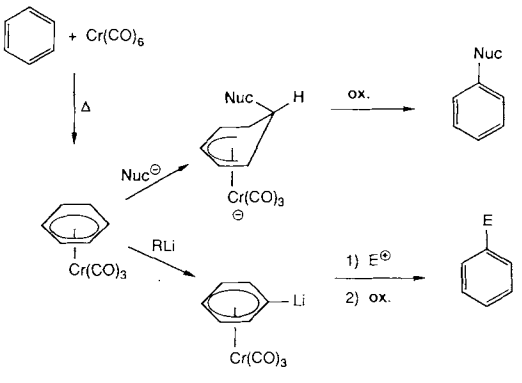

This chemistry allowed 5-chlorodihydroindoles to be converted into 5-methoxydihydroindoles by nucleophilic substitution of chloride by methoxide,[103] and complexed indoles (**73**) were alkylated in the 4- and 7-positions (major and minor product, respectively) by carbanions.[104, 105]

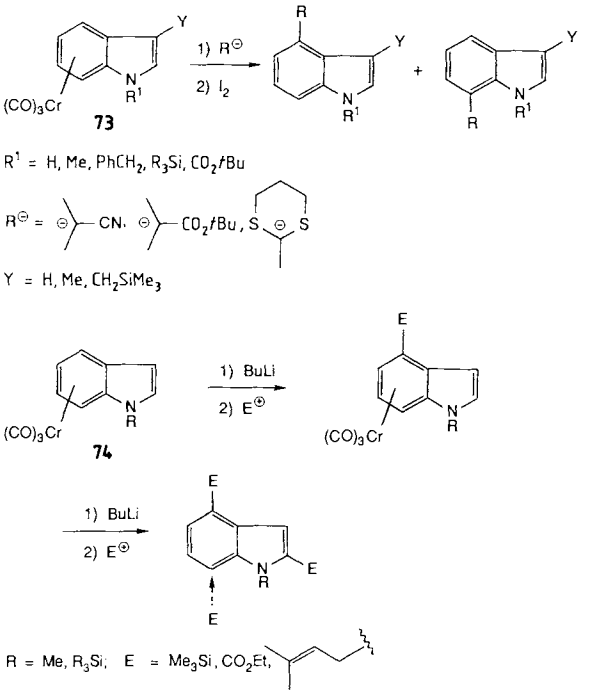

Lithiation of complexed indoles (**74**) occurred at the 4-position when the *N*-substituent was large, but at the 2-, 4-, and 7-positions when it was small.[106, 107]

3.6. Miscellaneous Indole Syntheses

The copper-catalyzed decomposition of aryl azides to produce nitrenes has been used to synthesize a number of pyrroloindolequinones (such as **75**).[108] The site of inser-

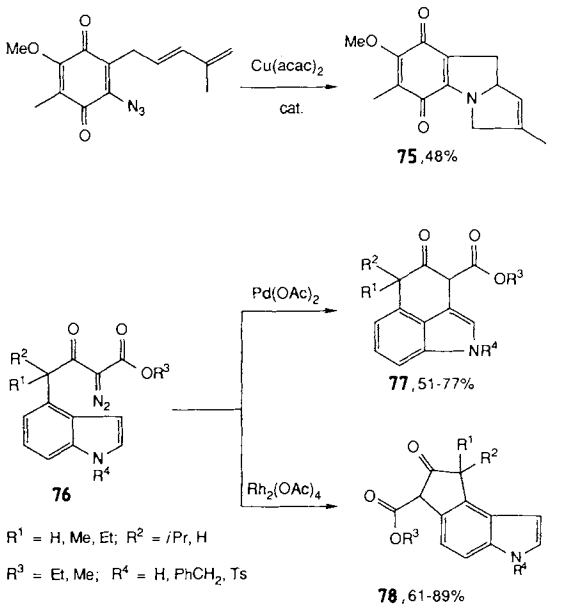

tion of carbenes generated by transition-metal-catalyzed decomposition of α-diazoesters such as **76** depended strongly on the catalyst (cf. **77** and **78**).[109] Aryl isocyanides combined with carbene complexes (M = Cr, Mo, W) to produce indoles, via ketenimine complexes **79**.[110,111]

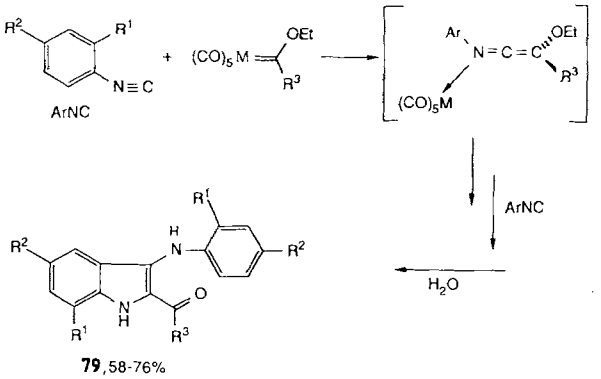

79, 58-76%

4. Outlook

Although most of the fundamental organometallic reaction chemistry utilized in the synthesis of indoles has been known for at least a decade, only recently have these fundamental processes been applied to complex multifunctional organic substrates with the serious intent of accomplishing the total synthesis of a natural product. This extension to more complex systems has vividly brought into focus both the power and the limitations of organometallic chemistry in the synthesis of complex organic compounds. A decade ago only inorganic and "organometallic" chemists ventured into the transition series to find useful organic transformations. Today, transition metals are common in synthetic organic chemistry, and new transition-metal-catalyzed transformations of organic substrates are readily adopted by synthetic chemists. This is expected to continue.

Our research in the area of palladium catalysis in the synthesis and functionalization of indoles was supported by the National Science Foundation and the National Institutes of General Medical Sciences of the Public Health Service, whom we gratefully acknowledge.

Received: November 23, 1987 [A 687 IE]
German version: *Angew. Chem. 100* (1988) 1147

[1] a) R. H. F. Manske (Ed.): *The Alkaloids, Vol. 1-17*, Wiley, New York 1950-1979; b) M. Hesse: *Indolalkaloide in Tabellen*, Springer, Berlin 1964; c) J. S. Glasby: *Encyclopedia of the Alkaloids*, Plenum Press, New York 1975.
[2] W. C. Sumpter, F. M. Miller, *Chem. Heterocycl. Compd. 8* (1954) 171.
[3] D. C. Horwell, *Tetrahedron 36* (1980) 3123.
[4] Y. Oikawa, O. Yonemitsu, *J. Chem. Soc. Perkin Trans. 1 1976*, 1479; *J. Org. Chem. 41* (1976) 1118.
[5] R. W. Fransk, *Prog. Chem. Org. Nat. Prod. 38* (1979) 1.
[6] P. Mangeney, R. Andriamialisoa, N. Langlois, Y. Langlois, P. Potier, *J. Am. Chem. Soc. 101* (1979) 2243.
[7] a) A. R. Katritzky, C. W. Rees (Eds.): *Comprehensive Heterocyclic Chemistry, Vol. 4*, Pergamon, Oxford 1984; b) R. J. Sundberg: *Pyrroles and Their Benzo Derivatives: Synthesis and Applications* in [7a], p. 313-376.
[8] R. A. Jones: *Pyrroles and Their Benzo Derivatives: Reactivity* in [7a], p. 201-312.
[9] J. P. Collman, L. S. Hegedus, J. R. Norton, R. G. Finke: *Principles and Applications of Organotransition Metal Chemistry*, 2nd ed., University Science Books, Mill Valley, CA (USA) 1987.
[10] P. M. Henry: *Palladium Catalyzed Oxidation of Hydrocarbons*. D. Reidel, Dordrecht (Niederlande) 1980.
[11] B. Akermark, L. Eberson, E. Jonsson, E. Pettersson, *J. Org. Chem. 40* (1975) 1365.
[12] R. B. Miller, T. Moock, *Tetrahedron Lett. 21* (1980) 3319.
[13] T. Itahara, *Synthesis 1979*, 151.
[14] T. Itahara, T. Sakakibara, *Synthesis 1978*, 607.
[15] T. Itahara, M. Ikeda, T. Sakakibara, *J. Chem. Soc. Perkin Trans. 1 1983*, 1361.
[16] T. Itahara, K. Kawasaki, T. Ouseto, *Synthesis 1984*, 236.
[17] Y. Murakami, Y. Yokoyama, T. Aoki, *Heterocycles 22* (1984) 1493.
[18] T. Itahara, *Chem. Lett. 1982*, 1151.
[19] T. Sakakibara, S. Karasumaru, I. Kawano, *J. Am. Chem. Soc. 107* (1985) 6417.
[20] M. Somei, Y. Saida, N. Komura, *Chem. Pharm. Bull. 34* (1986) 4116.
[21] M. Somei, F. Yamada, K. Naka, *Chem. Pharm. Bull. 35* (1987) 1322.
[22] M. Somei, H. Amari, Y. Makita, *Chem. Pharm. Bull. 34* (1986) 3971.
[23] L. S. Hegedus, G. F. Allen, E. L. Waterman, *J. Am. Chem. Soc. 98* (1976) 2674.
[24] L. S. Hegedus, G. F. Allen, J. J. Bozell, E. L. Waterman, *J. Am. Chem. Soc. 100* (1978) 5800.
[25] L. S. Hegedus, G. F. Allen, D. J. Olsen, *J. Am. Chem. Soc. 102* (1980) 3583.
[26] S. Danishefsky, E. Taniyama, *Tetrahedron Lett. 24* (1983) 15.
[27] P. R. Weider, L. S. Hegedus, H. Asada, S. V. D'Andrea, *J. Org. Chem. 50* (1985) 4276.
[28] R. C. Larock, C. L. Liu, H. H. Law, S. Varaprath, *Tetrahedron Lett. 25* (1984) 4459.
[29] L. S. Hegedus, P. M. Winton, S. Varaprath, *J. Org. Chem. 46* (1981) 2215.
[30] L. S. Hegedus, T. A. Mulhern, H. Asada, *J. Am. Chem. Soc. 108* (1986) 6224.
[31] E. C. Taylor, A. H. Katz, H. Salgado-Zamora, A. McKillop, *Tetrahedron Lett. 26* (1985) 5963.
[32] T. Sakakibara, Y. Tanaka, S. Yamasaki, *Chem. Lett. 1986*, 797.
[33] K. Isomura, K. Uto, H. Taniguchi, *J. Chem. Soc. Chem. Commun. 1977*, 664.
[34] H. Alper, C. P. Mahatantila, *Heterocycles 20* (1983) 2025.
[35] H. Alper, J. E. Prickett, *J. Chem. Soc. Chem. Commun. 1976*, 483.
[36] H. Alper, J. E. Prickett, *Tetrahedron Lett. 1976*, 2589.
[37] R. McCrindle, G. Ferguson, G. J. Arsenault, A. J. McAlees, D. K. Stephenson, *J. Chem. Res. Synop. 1984*, 360.
[38] A. Spencer, *J. Organomet. Chem. 258* (1983) 101; *270* (1984) 115; *265* (1984) 323; *247* (1983) 117.
[39] T. Jeffrey, *J. Chem. Soc. Chem. Commun. 1984*, 1287; *Tetrahedron Lett. 26* (1985) 2667.
[40] T. Sakamoto, Y. Kondo, H. Yamanaka, *Heterocycles 24* (1986) 31.
[41] A. Tischler, T. J. Lanza, *Tetrahedron Lett. 27* (1986) 1653.
[42] M. Satoh, N. Miyahra, A. Suzuki, *Synthesis 1987*, 373.
[43] M. Mori, K. Chiba, Y. Ban, *Tetrahedron Lett. 1977*, 1037.
[44] M. Mori, Y. Ban, *Tetrahedron Lett. 1979*, 1133.
[45] R. Odle, B. Blevins, M. Ratcliff, L. S. Hegedus, *J. Org. Chem. 45* (1980) 2709.
[46] L. S. Hegedus, T. A. Mulhern, A. Mori, *J. Org. Chem. 50* (1985) 4282.
[47] H. Iida, Y. Yuasa, C. Kibayashi, *J. Org. Chem. 45* (1980) 2938.
[48] D. E. Ames, A. Opalko, *Tetrahedron 40* (1984) 1919.
[49] J. R. Luly, H. Rapoport, *J. Org. Chem. 49* (1984) 1671.
[50] K. J. Shaw, J. R. Luly, H. Rapoport, *J. Org. Chem. 50* (1985) 4515.
[51] D. L. Boger, J. S. Panek, *Tetrahedron Lett. 25* (1984) 3175.
[52] D. L. Boger, S. R. Duff, J. S. Panek, M. Yasuda, *J. Org. Chem. 50* (1985) 5782.
[53] D. L. Boger, S. R. Duff, J. S. Panek, M. Yasuda, *J. Org. Chem. 50* (1985) 5790.
[54] M. Mori, Y. Ban, *Tetrahedron Lett. 1976*, 1803.
[55] M. Mori, Y. Ban, *Heterocycles 9* (1978) 391.
[56] M. Mori, S. Kudo, Y. Ban, *J. Chem. Soc. Perkin Trans. 1 1979*, 771.
[57] J. G. Rodriguez, *J. Heterocycl. Chem. 22* (1985) 1511.
[58] J. G. Rodriguez, L. Canoira, *J. Heterocycl. Chem. 22* (1985) 883.
[59] M. Mori, Y. Hashimoto, Y. Ban, *Tetrahedron Lett. 21* (1980) 631.
[60] Y. Akita, A. Inoue, K. Yamamoto, A. Ohta, *Heterocycles 23* (1985) 2327.
[61] M. Mori, H. Kobayashi, M. Kimura, Y. Ban, *Heterocycles 23* (1985) 2803.
[62] P. J. Harrington, L. S. Hegedus, *J. Org. Chem. 49* (1984) 2657.
[63] M. Somei, Y. Saida, *Heterocycles 23* (1985) 3113.
[64] M. Somei, T. Funamoto, T. Ohta, *Heterocycles 26* (1987) 1783.
[65] M. Somei, F. Yamada, *Chem. Pharm. Bull. 32* (1984) 5064.
[66] M. Somei, H. Ohnishi, Y. Shoken, *Chem. Pharm. Bull. 34* (1986) 677.
[67] M. Somei, Y. Makita, F. Yamada, *Chem. Pharm. Bull. 34* (1986) 948.

[68] F. Yamada, Y. Makita, T. Suzuki, M. Somei, *Chem. Pharm. Bull. 33* (1985) 2162.
[69] P. J. Harrington, L. S. Hegedus, K. F. McDaniel, *J. Am. Chem. Soc. 109* (1987) 4335.
[70] L. S. Hegedus, J. L. Toro, W. H. Miles, P. J. Harrington, *J. Org. Chem. 52* (1987) 3319.
[71] L. S. Hegedus, P. J. Harrington, E. T. Michaelson, M. Sestrick, *J. Org. Chem.*, in press.
[72] R. C. Larock, L. W. Harrison, M. H. Hsu, *J. Org. Chem. 49* (1984) 3665.
[73] J. M. O'Conner, B. J. Stallman, W. G. Clark, A. Y. L. Shu, R. E. Spada, T. M. Stevenson, H. A. Dieck, *J. Org. Chem. 48* (1983) 807.
[74] B. M. Trost, J. P. Genet, *J. Am. Chem. Soc. 98* (1976) 8516.
[75] B. M. Trost, E. Keinan, *J. Am. Chem. Soc. 100* (1978) 7779.
[76] B. M. Trost, S. A. Godleski, J. P. Genet, *J. Am. Chem. Soc. 100* (1978) 3930.
[77] B. M. Trost, S. A. Godleski, J. L. Belletire, *J. Org. Chem. 44* (1979) 2054.
[78] B. M. Trost, J. M. D. Torrunar, *Organometallics 1* (1982) 7.
[79] S. A. Godleski, E. B. Villhauer, *J. Org. Chem. 51* (1986) 486.
[80] J. P. Genet, S. Grisoni, *Tetrahedron Lett. 27* (1986) 4165.
[81] T. Kametani, K. Takahashi, M. Ihara, K. Fukumoto, *Heterocycles 3* (1975) 691.
[82] A. Osuka, Y. Mori, H. Suzuki, *Chem. Lett. 1982,* 2031.
[83] H. Suzuki, S. V. Thiruvikramank, A. Osuka, *Synthesis 1984,* 616.
[84] T. Kametani, T. Ohsawa, M. Ihara, *Heterocycles 14* (1980) 277.
[85] Y. Ito, Y. Inubushi, T. Sugaya, K. Kobayashi, T. Saegusa, *Bull. Chem. Soc. Jpn. 51* (1978) 1186.
[86] Y. Ito, K. Kobayashi, T. Saegusa, *Tetrahedron Lett. 1979,* 1039.
[87] Y. Ito, K. Kobayashi, T. Saegusa, *J. Org. Chem. 44* (1979) 2030.
[88] A. K. Sinhababu, R. T. Borchardt, *J. Org. Chem. 48* (1983) 347.
[89] D. H. Lloyd, D. E. Nichols, *Tetrahedron Lett. 24* (1983) 4561.
[90] D. H. Lloyd, D. E. Nichols, *J. Org. Chem. 51* (1986) 4294.
[91] A. U. Rahman, M. Ghazala, N. Sultana, M. Bashir, A. A. Ansari, *J. Chem. Soc. Pak. 4* (1982) 91.
[92] Y. Watanabe, S. C. Shim, H. Uchida, T. Mitsudo, Y. Takegani, *Tetrahedron 35* (1979) 1433.
[93] C. Crotti, S. Cenini, B. Rindone, S. Tollari, F. Demartin, *J. Chem. Soc. Chem. Commun. 1986,* 785.
[94] Y. Tsuji, K.-T. Huh, Y. Yokoyama, Y. Watanabe, *J. Chem. Soc. Chem. Commun. 1986,* 1575.
[95] Y. Tsuji, K.-T. Huh, Y. Watanabe, *Tetrahedron Lett. 27* (1986) 377.
[96] Y. Tsuji, K.-T. Huh, Y. Watanabe, *J. Org. Chem. 52* (1987) 1673.
[97] W. D. Jones, W. P. Kosar, *J. Am. Chem. Soc. 108* (1986) 5640.
[98] S. Kano, E. Sugino, S. Shibuya, S. Hibino, *J. Org. Chem. 46* (1981) 3836.
[99] K. P. C. Vollhardt, *Angew. Chem. 96* (1984) 525; *Angew. Chem. Int. Ed. Engl. 23* (1984) 539.
[100] D. B. Grotjahn, K. P. C. Vollhardt, *J. Am. Chem. Soc. 108* (1986) 2091.
[101] G. S. Sheppard, K. P. C. Vollhardt, *J. Org. Chem. 51* (1986) 5498.
[102] H. Gstach, H. Kisch, *Z. Naturforsch. B38* (1983) 251.
[103] T. Oishi, M. Fujui, Y. Endo, *Heterocycles 7* (1977) 947.
[104] A. P. Kozikowski, K. Isobe, *J. Chem. Soc. Chem. Commun. 1978,* 1076.
[105] M. F. Semmelhack, W. Wulff, J. L. Garcia, *J. Organomet. Chem. 240* (1982) C 5.
[106] G. Nechvatal, D. A. Widdowson, *J. Chem. Soc. Chem. Commun. 1982,* 467.
[107] G. Nechvatal, D. A. Widdowson, D. J. Williams, *J. Chem. Soc. Chem. Commun. 1981,* 1260.
[108] K. Maruyama, N. Nagai, Y. Naruta, *Chem. Lett. 1987,* 97.
[109] M. Matsumoto, N. Watanabe, H. Kobayashi, *Heterocycles 26* (1987) 1479.
[110] R. Aumann, H. Heinen, *Chem. Ber. 119* (1986) 2289.
[111] R. Aumann, H. Heinen, C. Krüger, Y.-H. Tsay, *Chem. Ber. 119* (1986) 3141.

Molecular Organometallic Chemistry on Surfaces: Reactivity of Metal Carbonyls on Metal Oxides

By H. Henry Lamb, Bruce C. Gates, and Helmut Knözinger*

Metal carbonyls react on metal oxide surfaces to give a wide range of structures analogous to those of known compounds. The reactions leading to formation of surface-bound metal carbonyls are explained by known molecular organometallic chemistry and the functional group chemistry of the surfaces. The reaction classes include formation of acid–base adducts as the oxygen of a carbonyl group donates an electron pair to a Lewis acidic center; nucleophilic attack at CO ligands by basic surface hydroxyl groups or $O^{2\ominus}$ ions; ion-pair formation by deprotonation of hydrido carbonyls to give carbonylate ions; interaction of bifunctional complexes with surface acid–base pair sites such as $\{Mg^{2\oplus}O^{2\ominus}\}$; and oxidative addition of surface hydroxyl groups to metal clusters. The reactions of surface-bound organometallic species include redox condensation and cluster formation on basic surfaces (paralleling the reactions in basic solution) as well as oxidation of mononuclear metal complexes and oxidative fragmentation of metal clusters by reaction with surface hydroxyl groups. Most supported metal carbonyls are unstable at high temperatures, but some, including osmium carbonyl cluster anions on the basic MgO surface, are strongly stabilized in the presence of CO and are precursors of catalysts for CO hydrogenation at 550 K.

1. Introduction

Organometallic chemistry has been extended to the surfaces of metal oxides. The chemistry of analogues of molecular metal carbonyls and related species on metal oxides such as silica, γ-alumina, and magnesia is becoming understood in a detail approaching that attainable in solution chemistry, provided that the surface organometallics are characterized by such techniques as IR, NMR, and EXAFS (extended X-ray absorption fine structure) spectroscopy. Elucidation of this surface chemistry is leading to new understanding of the structures and reactivities of oxide surfaces and to the preparation of new surface structures of interest as catalysts. Carbonyls of the Group VIII metals are the most thoroughly investigated of these surface species. The surface organometallic chemistry is consistent with the known molecular chemistry of the metal carbonyls in solution and with the functional group chemistry of the metal oxide surfaces, particularly the acid–base chemistry of OH groups, $O^{2\ominus}$ ions, and Lewis acidic centers such as $Al^{3\oplus}$ and $Mg^{2\oplus}$.

Knowledge of the organometallic chemistry of molecular metal carbonyls on metal oxide supports is leading to new surface structures and catalysts and to better understanding of conventional supported metal catalysts. This review is concerned with the synthesis and reactivity of well-defined surface-bound transition metal carbonyls on silica, alumina, and magnesia, prototype supports for metal catalysts. Reactions leading to the formation of poorly defined structures, often mixtures, are not considered here. The notation used is given in Table 1. Prototype reactions characterizing the adsorption of metal carbonyls on metal oxides are summarized in Table 2. These and related reactions are discussed in detail following a brief summary of the surface chemistry of the metal oxides. The important high-temperature reactions of surface-bound metal carbonyls are also examined, including the oxidative fragmentation of metal clusters to yield groupings of covalently bound subcarbonyl complexes and the reductive carbonylation of metal ions on basic supports to yield metal clusters.

[*] Prof. B. C. Gates, Dr. H. H. Lamb
Center for Catalytic Science and Technology
Department of Chemical Engineering
University of Delaware
Newark, DE 19716 (USA)
Prof. Dr. H. Knözinger
Institut für Physikalische Chemie der Universität
Sophienstrasse 11, D-8000 München 2 (FRG)

2. Nature and Reactivity of Metal Oxide Surfaces

High-surface-area, microporous metal oxides are used widely as supports for catalysts incorporating highly dispersed metal aggregates (or crystallites). Silica, alumina, and magnesia are commonly used catalyst supports representative of a wide range of surface acid–base properties. Although structure and bonding within the bulk vary greatly among the oxides, there are similarities in their surface chemistries since all the surfaces incorporate hydroxyl groups. The acid–base character of these groups depends on the metal oxide and its pretreatment, typically ranging from mildly Brønsted acidic for silica to strongly Brønsted basic for magnesia. Aprotic functional groups (e.g., $Al^{3\oplus}$ and $O^{2\ominus}$) are also present on surfaces pretreated at elevated temperatures (> 473 K) in vacuo. Regulation of the concentration of surface hydroxyl groups by variation of the pretreatment temperature is the most straightforward and useful method of controlling the surface properties of a metal oxide.

 © VCH Verlagsgesellschaft mbH, D-6940 Weinheim, 1988 0570-0833/88/0909-1127 $ 02.50/0

Table 1. Notation used to represent surface-bound organometallic species.

Notation	Meaning	Examples
{AB}	Denotes species terminating the bulk solid	$\{Mg^{2\oplus}O^{2\ominus}\}$, magnesia surface ion pairs; $\{Al^{3\oplus}-OH\}$ or {Al–OH}, surface hydroxyl groups of alumina
[Organometallic complex]/metal oxide, [OMC]/MO	Denotes supported organometallic complex for which the details of the local interaction with the surface are unknown or uncertain	$[Rh_6(CO)_{16}]/Al_2O_3$, hexarhodium carbonyl absorbed on alumina; $[Os_{10}C(CO)_{24}]^{2\ominus}/MgO$, decaosmium carbide carbonyl ionically bound to magnesia
OMC···{AB}	Denotes a well-established local chemical interaction between a ligand of the organometallic complex and a surface group	$[CpW(CO)_2CO^{\ominus}\cdots\{Mg^{2\oplus}(OH)^{\ominus}\}]$, surface-bound $[CpW(CO)_3]^{\ominus}$ ion-paired through a CO ligand with a surface $Mg^{2\oplus}$ ion
Transition metal (TM)/MO or TM-on-MO	Denotes a supported metal incorporating aggregates or crystallites of the metal on the support	Rh/Al_2O_3, Rh crystallites supported on alumina

Table 2. Molecular metal carbonyls on metal oxide surfaces: prototype syntheses and surface structures.

Synthesis reaction	Adsorbates	Surface structure	Metal oxide [a] SiO_2	Al_2O_3 [b]	MgO
Adduct formation via a bridging CO ligand, involving:					
a) Lewis acidic centers	$[CpFe(\mu_3\text{-}CO)]_4$	$[Cp_4Fe_4(\mu_3\text{-}CO)_3(\mu_3\text{-}CO\cdots\{M^{n\oplus}\})]$	—	HD	—
b) Brønsted acidic centers (H-bond donors)	$Co_2(CO)_8$	$[Co_2(CO)_7(\mu_2\text{-}CO\cdots\{HO-M\})]$	PD	—	—
Nucleophilic attack at a CO ligand, involving:					
a) basic surface hydroxyl groups	$Fe_3(CO)_{12}$	$[HFe_3(CO)_{10}(\mu_2\text{-}CO)]^{\ominus}\{M^{n\oplus}\}$	—	H	H
	$Fe(CO)_5$ [c]	$[HFe_3(CO)_{10}(\mu_2\text{-}CO)]^{\ominus}\{M^{n\oplus}\}$	—	H	H
b) $O^{2\ominus}$ ions of $\{M^{n\oplus}O^{2\ominus}\}$ acid-base pairs	$Fe(CO)_5$	$[Fe(CO)_4(CO_2)^{\ominus}\cdots\{M^{n\oplus}\}]$	—	—	HD
Deprotonation of hydrido carbonyls, involving:					
a) basic surface hydroxyl groups	$[H_4Os_4(CO)_{12}]$	$[H_{4-x}Os_4(CO)_{12}]^{x\ominus}\{M^{n\oplus}\}$ $x = 1$ or 2	—	PD	PD
b) $O^{2\ominus}$ ions of $\{M^{n\oplus}O^{2\ominus}\}$ acid-base pairs	$[HWCp(CO)_3]$	$[CpW(CO)_2CO^{\ominus}\cdots\{M^{n\oplus}(OH^{\ominus})\}]$	—	—	HD
Bifunctional interaction with surface acid-base pairs, involving:					
a) promoted migratory insertion of CO	$[CH_3Mn(CO)_5]$	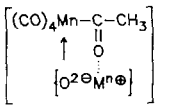	—	PD, HD	—
b) hydrido carbonyls as H-bond donors	$[H_2Os(CO)_4]$	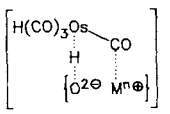	—	PD	PD, HD
Oxidative addition of hydroxyl groups to give covalently bound metal clusters	$Os_3(CO)_{12}$	$[(\mu\text{-}H)Os_3(CO)_{10}\{\mu\text{-}OM\}]$	H, PD	H, PD	H [d]

[a] H, PD, and HD refer to a fully hydroxylated, partially dehydroxylated, and highly dehydroxylated metal oxide, respectively. [b] η and γ phases. [c] $[HFe(CO)_4]^{\ominus}$ is suggested to be the initial surface species formed. [d] The magnesia surface in these cases was highly contaminated with adsorbed CO_2 (surface carbonates).

2.1. Silica[1-3]

Amorphous SiO_2 is often regarded as chemically inert relative to other common metal oxide supports. Weakly acidic hydroxyl groups are usually inferred to be the most reactive native surface species. The building blocks of silica are linked SiO_4 tetrahedra, with each O atom bridging two Si atoms. Bonding within the solid is covalent. At the fully hydrated surface, the bulk structure is terminated by hydroxyl (silanol) groups {Si–OH}. Two types of these groups are usually distinguished: (1) isolated groups giving rise to a sharp IR absorption at 3750 cm^{-1} and (2) hydrogen-bonded vicinal groups identified by a broader band in the 3550-cm^{-1} region. Fully hydrated samples, calcined at temperatures below 473 K, may contain geminal groups, $\{Si(OH)_2\}$. Heating in vacuum removes the vicinal groups by dehydroxylation, i.e., condensation to form H_2O and surface Si-O-Si linkages:

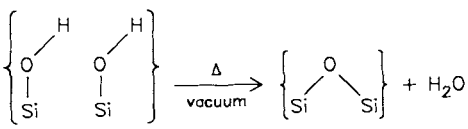

(1)

Complete removal of the surface hydroxyl groups requires treatment at temperatures above 973 K in vacuo and is inferred to result in significant changes in surface morphology.

The surface hydroxyl groups of silica are weakly Brønsted acidic. Hydrogen bonding involving isolated hydroxyl groups results in a decrease in the intensity of the 3750-cm^{-1} ν_{OH} absorption and the appearance of a broad band at lower frequency; the shift relative to the 3750-cm^{-1} band, $\Delta\nu_{OH}$, is indicative of the strength of the interaction and is typically 100–200 cm^{-1}. Strong bases, such as ammonia and amines, are protonated by surface silanol groups. Aprotic sites, present after dehydroxylation at 873–1025 K, are suggested to be highly strained Si-O linkages. Such groups have been identified by IR spectroscopy[4] and inferred to serve as weak Lewis acidic centers.[5]

2.2. Transition Aluminas

Transition aluminas, the most commonly used supports for metal catalysts, are defective, metastable solids formed from aluminum hydroxide as it is heated; at temperatures exceeding about 1400 K, the transition aluminas are converted into stable, crystalline α-Al_2O_3. Two closely related transition aluminas, η-Al_2O_3 and γ-Al_2O_3, which incorporate $Al^{3\oplus}$ ions in both tetrahedral and octahedral coordination, display a wide range of surface acid-base properties that depend on the degree of thermal activation.[6] Acidic and basic sites and acid-base pair sites on the aluminas have been identified by spectroscopic characterization of adsorbed probe molecules.

Both η- and γ-Al_2O_3 have defect spinel structures with cubic close-packed oxygen sublattices; the Al sublattice in each is highly disordered, and irregular occupation of the tetrahedral interstices results in a tetragonal distortion of the spinel structure. There is a higher occupancy of tetrahedral cation positions in γ-Al_2O_3 and a higher density of stacking faults in the oxygen sublattice of η-Al_2O_3. Crystallites are terminated by anion layers, and on the basis of an electrostatics argument, these surface layers are inferred to be occupied by hydroxyl groups. In modeling the alumina surfaces, *Knözinger* and *Ratnasamy*[6] considered the (100), (111), and (110) planes of the spinel lattice and proposed five coordination environments for hydroxyl groups. This estimate of the number of chemically distinct hydroxyls is in agreement with IR spectra.[7]

Heating fully hydroxylated η- or γ-Al_2O_3 in vacuo to temperatures above 473 K results in the evolution of water and elimination of surface hydroxyl groups. This dehydroxylation process leads to the formation of a coordinatively unsaturated $O^{2\ominus}$ ion and an adjacent surface anion vacancy (Fig. 1). Assuming a close-packed (111) surface plane, the anion vacancy is expected to expose either two five-coordinate $Al^{3\oplus}$ ions or one three-coordinate $Al^{3\oplus}$ ion.[6] Thus, during the dehydroxylation process, both Lewis acidic and Lewis basic sites are created.

The acid-base properties have been examined by titration[8] and by the adsorption of organic probe molecules and characterization of the surface species by IR and NMR spectroscopy.[1] The hydroxyl groups of η- and γ-Al_2O_3 act as hydrogen-bond donors to adsorbed benzene, although the interaction is generally weaker than that observed for silica, suggesting very weak Brønsted acidity. IR spectra of adsorbed nitriles and pyridine reveal surface

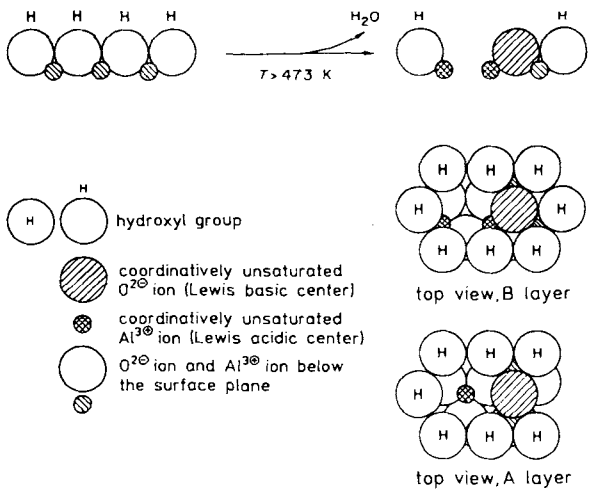

Fig. 1. Schematic representation of the dehydroxylation process for (111) surface planes of the η- and γ-Al_2O_3 structures, showing two possible configurations of the Lewis acid-base sites formed.

Lewis acidic sites.[7] Shifts in the N-H stretching frequency of adsorbed pyrrole provide evidence of strongly basic sites on transition aluminas,[9] but on this basis alone one cannot differentiate between $O^{2\ominus}$ ions and hydroxyl groups as the basic sites. Bifunctional adsorbate molecules interact with acid-base pair sites on these surfaces. For example, dissociative chemisorption of alcohols has been suggested to occur through the precursor state **I**.[2, 10, 11]

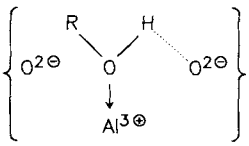

I

2.3. Magnesia

MgO has the simple rock salt structure, with octahedral coordination of magnesium and oxygen. Ab-initio molecular orbital calculations indicate that the electronic structure is highly ionic, with the $Mg^{2\oplus}O^{2\ominus}$ formalism being an accurate representation of both the bulk and surface structures.[12] The lattice is commonly envisioned to terminate in (100) planes incorporating five-coordinate (5C) $Mg^{2\oplus}$ and $O^{2\ominus}$ ions (Fig. 2). This model appears to be physically

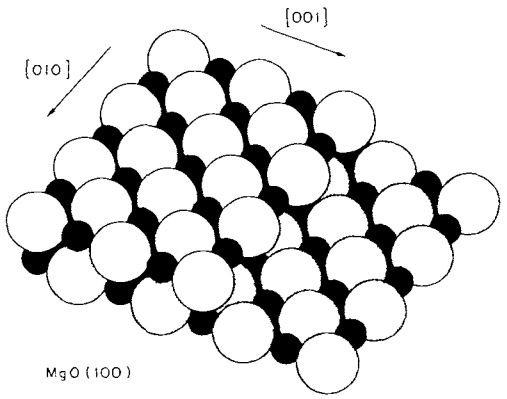

Fig. 2. Space-filling model of the MgO (100) plane, showing a unit atomic step in the [001] direction which exposes a portion of the MgO (200) plane.

accurate for MgO smoke, which may be regarded as a model crystalline metal oxide support. The (100) surface of MgO is electrically neutral, and the presence of surface hydroxyl groups need not be postulated, but *Anderson* et al.[13] demonstrated that hydroxyl groups are present on surfaces of polycrystalline MgO derived from $Mg(OH)_2$. Two absorptions assigned to hydroxyl groups were discerned by IR spectroscopy of samples treated in vacuo at 673–1073 K, and, on the assumption that the surface layers consist of (100) planes, two distinct environments for hydroxyl groups were postulated (Fig. 3).[13] Type A hydroxyl

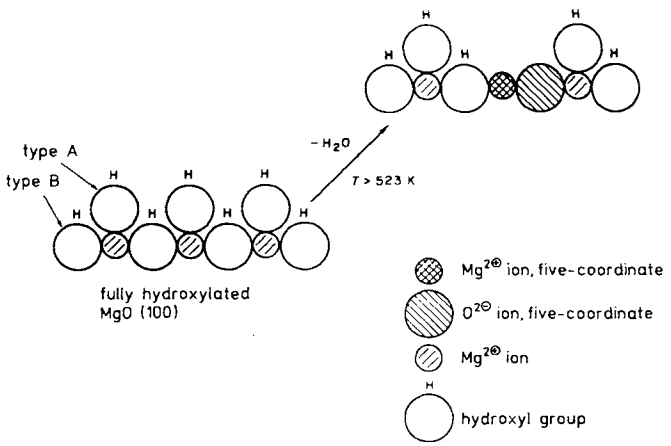

Fig. 3. Simple model of MgO dehydroxylation based on the work of *Anderson* et al. [13], who considered only the MgO (100) plane.

groups occupy the sixth coordination site of a surface $Mg^{2\oplus}$ ion and are associated with the "free" or isolated O–H vibration observed at 3740–3750 cm^{-1}. Type B hydroxyl groups may be formally derived from the protonation of surface $O^{2\ominus}$ ions. The proton could bridge (or hydrogen bond) to neighboring $O^{2\ominus}$ ions on the surface, consistent with the broad absorption observed at 3610 cm^{-1}. The dehydroxylation of this surface layer is expected to proceed by the combination of a type A hydroxyl group with the proton of a type B group to form a water molecule which desorbs, exposing a $\{Mg^{2\oplus}O^{2\ominus}\}$ 5C ion pair (Fig. 3).

The surface chemistry of MgO is dominated by its basicity. Numerous organic Brønsted acids have been shown to chemisorb to form surface-bound carbanions and surface hydroxyl groups.[14,15] These adsorbates are inferred to react dissociatively with surface ion pairs:

$$\{Mg^{2\oplus}O^{2\ominus}\} + XH \longrightarrow \begin{matrix} X^{\ominus} & H^{\oplus} \\ | & | \\ \{Mg^{2\oplus}O^{2\ominus}\} \end{matrix} \qquad (2)$$

The unique nature of highly dehydroxylated MgO originates in its high strength as a solid base, capable of deprotonating even very weak Brønsted acids such as NH_3 ($pK_a = 36$), propene ($pK_a = 35$), and acetylene ($pK_a = 25$); even the heterolytic dissociative adsorption of dihydrogen on polycrystalline MgO has been reported.

Highly coordinatively unsaturated sites appear to be required for the dissociative chemisorption of weak Brønsted acids on MgO.[14] Three- and four-coordinate $Mg^{2\oplus}$ and $O^{2\ominus}$ ions have been detected on the surfaces of polycrystalline MgO, derived from $Mg(OH)_2$, after activation at 1073 K; these sites have been characterized by ultraviolet–visible diffuse reflectance spectroscopy[16] and photoluminescence spectroscopy.[17] The ratio $\{Mg^{2\oplus}O^{2\ominus}\}(5C) : \{Mg^{2\oplus}O^{2\ominus}\}(4C) : \{Mg^{2\oplus}O^{2\ominus}\}(3C)$ has been estimated to be approximately 90 : 10 : 1.[14] The locations of the 4C and 3C sites remain in doubt, but they have been suggested to be at edges and corners of (100) planes.

The surfaces of MgO powders incorporate reducing sites in addition to the sites associated with strong basicity.[18] These are apparently defect sites, possibly surface cation vacancies. The paramagnetic surface species formed from CO adsorbed on highly dehydroxylated MgO have been thoroughly characterized by IR, ESR, and UV/VIS spectroscopy. The chemistry of the reducing sites and that of the basic sites of MgO are inferred to be closely related, since the dissociative adsorption of Brønsted acids blocks the reactivity of the reducing sites.[15a,18c]

3. Chemisorption of Metal Carbonyls on Metal Oxide Surfaces

This section is a summary of the reactions of metal carbonyls with metal oxide surfaces. The reaction classes (Table 2) all have well-established precedents in solution organometallic chemistry.

3.1. Formation of Acid–Base Adducts

One of the simplest chemisorption modes of a metal carbonyl on a metal oxide involves the formation of a Lewis acid–base adduct, the basic oxygen of a carbonyl group interacting with a coordinatively unsaturated metal ion of the surface. Adduct formation is anticipated for binary metal carbonyls adsorbed on dehydroxylated η- and γ-Al_2O_3 (because of the presence of strong Lewis acidic sites) and has been proposed for $M(CO)_6$ (M = Cr, Mo, W) complexes adsorbed on alumina, for example.[19]

This chemistry is well illustrated by the results of *Tessier-Youngs* et al.,[20] who investigated the adsorption of polynuclear carbonyl complexes of iron and nickel on highly dehydroxylated alumina films in a series designed to yield stable *O*-bound surface adducts. Each of the adsorbates chosen for the experiments, $[CpFe(CO)]_4$, $[Cp_3Ni_3(CO)_2]$, and $[CpNi(CO)]_2$, contains only bridging carbonyl groups and would be expected to form adducts readily with surface Lewis acidic centers. These molecules also are expected to have relatively low susceptibilities to nucleophilic attack, which minimizes a possible side reaction, discussed Section 3.2. The carbonyl complexes were deposited on alumina films from solution by evaporation of the solvent (benzene or dichloromethane). Formation of adducts with surface $Al^{3\oplus}$ ions was monitored by IR spectroscopy.

Tessier-Youngs et al. found that $[CpFe(CO)]_4$ forms the most stable adduct with the alumina surface, the proposed structure being shown in Figure 4. The redshift of the IR band assigned to a triply bridging carbonyl ligand of this

complex, bound through its oxygen atom to a surface $Al^{3\oplus}$ ion, is 185 cm^{-1} (compared with shifts of 102 and 257 cm^{-1} observed for the presumably analogous $Al(C_2H_5)_3$ and $AlBr_3$ adducts, respectively). Not surprisingly, the complex could be recovered from the surface by washing with pyridine. A complication in this investigation was that a significant fraction of the complexes were not molecularly dispersed, but instead formed crystallites on the alumina surface during the evaporation of the solvent.

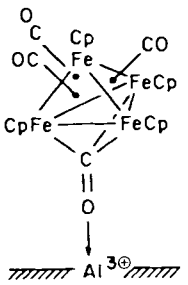

Fig. 4. Proposed structure of adduct formed by the chemisorption of $[CpFe(CO)]_4$ on highly dehydroxylated γ-Al_2O_3 [20].

The chemistry of adduct formation may, alternatively, involve simple hydrogen bonding at the surface and can therefore occur on any of the metal oxides. For example, when $Co_2(CO)_8$ is sublimed onto SiO_2 in the presence of 6.7 kPa of CO, the resulting surface species is the molecularly adsorbed dimer, apparently hydrogen-bonded to silanol groups via bridging carbonyl ligands. The hypothesis of weak hydrogen bonding is supported by the observation of characteristic shifts of IR absorptions in both the ν_{OH} and ν_{CO} regions.[21] When $Co_2(CO)_8$ is sublimed onto SiO_2 (pretreated at 673 K in vacuo) without added CO, $Co_4(CO)_{12}$ forms as the predominant organometallic surface species, as shown by the IR spectrum in the ν_{CO} region. The surface reaction is inhibited by CO, as suggested by Equation (3).

$$2\,Co_2(CO)_8 \longrightarrow Co_4(CO)_{12}/SiO_2 + 4\,CO \qquad (3)$$

3.2. Nucleophilic Attack at a CO Ligand

Adsorption of $Fe(CO)_5$ vapor on highly dehydroxylated MgO (pretreated in vacuo at 1073 K) results in formation of the surface complex $[Fe(CO)_4(CO_2)^{2\ominus}\cdots\{Mg^{2\oplus}\}]$[22a] (Fig. 5), demonstrating that the influence of surface hydration on the reactivity of adsorbed metal carbonyls can be substantial. The novel $[Fe(CO)_4(CO_2)^{2\ominus}\cdots\{Mg^{2\oplus}\}]$ structure was found to be consistent with a complete analysis of the CO and CO_2 stretching bands after ^{13}CO enrichment of the surface species. Similar structures have been proposed

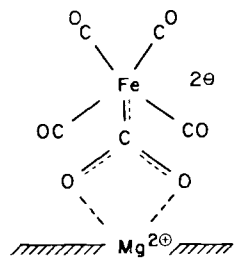

Fig. 5. Schematic representation of the surface structure formed by chemisorption of $Fe(CO)_5$ on highly dehydroxylated magnesia [22a].

for the surface species derived from the adsorption of $M(CO)_6$ (M = Cr, Mo, W) and $Ni(CO)_4$ on the highly dehydroxylated surface of MgO.[22b,c] The bent CO_2 moiety results from the interaction of a carbonyl ligand with a $\{Mg^{2\oplus}O^{2\ominus}\}$ pair. The basic $O^{2\ominus}$ ion evidently acts as a nucleophile toward coordinated CO, and the structure is stabilized by interaction with the neighboring $Mg^{2\oplus}$ ion. As evidenced by the IR data, at least two chemically distinct ion-pair sites are involved in $Fe(CO)_5$ adsorption. Closely related chemistry is discussed in Section 3.4 in the context of interactions of bifunctional organometallic reactants with surface acid–base pair sites. It is evident that the reaction classes listed in Table 2 overlap.

Binary metal carbonyls also react with basic surface hydroxyl groups of alumina and magnesia to form surface-bound anions, the reactivity being analogous to that of metal carbonyls with hydroxide ion in solution:

$$M'_x(CO)_y + \{M^{n\oplus}-OH\} \longrightarrow [HM'_x(CO)_{y-1}]^{\ominus}\{M^{n\oplus}\} + CO_2 \qquad (4)$$

Hugues et al.,[23a] who investigated the adsorption of iron carbonyls on the surfaces of hydrated η- and γ-Al_2O_3 and MgO, concluded that the adsorption of $Fe_3(CO)_{12}$ from hexanes at room temperature results in ionically bound $[HFe_3(CO)_{11}]^{\ominus}$, as evidenced by IR, ^1H NMR, and UV/VIS spectroscopy (Fig. 6). The surface-bound cluster

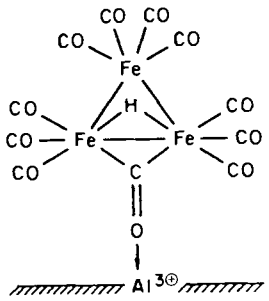

Fig. 6. Structure suggested by *Hugues* et al. [23a] for surface-bound $[HFe_3(CO)_{11}]^{\ominus}$ on η- and γ-Al_2O_3.

could be removed from the surfaces by ion exchange but not by washing with hydrocarbon, halocarbon, or alcohol solvents alone. Extractions with Et_4NCl in CH_2Cl_2 resulted in 60–70% yields of $[Et_4N][HFe_3(CO)_{11}]$. Since only little CO_2 was evolved (ca. 0.05 molecules per cluster) and IR data indicated the formation of surface bicarbonate ions, the following stoichiometry was suggested for chemisorption on alumina:

$$Fe_3(CO)_{12} + 2\{Al^{3\oplus}-OH\} \longrightarrow [HFe_3(CO)_{11}]^{\ominus}\{Al^{3\oplus}\} + \{(Al^{3\oplus})(HCO_3)^{\ominus}\} \qquad (5)$$

An alternative route to the formation of $[HFe_3(CO)_{11}]^{\ominus}$ from $Fe_3(CO)_{12}$ on γ-Al_2O_3 is indicated by results of *Hanson* et al.,[23b] who observed an inhibition of the reaction by CO and the formation of $Fe(CO)_5$ during the adsorption process. Disproportionation reactions of the type reported by *Hieber*[23c] were invoked to explain these results.

Hugues et al.[23a] found that the adsorption of $Fe(CO)_5$ on hydrated η- and γ-Al_2O_3 and hydrated MgO also results in the formation of surface-bound $[HFe_3(CO)_{11}]^{\ominus}$. This result is not surprising, since $Fe(CO)_5$ reacts in aqueous

amine solution at 353 K to give $[HFe_3(CO)_{11}]^{\ominus}$. The initial reaction of $Fe(CO)_5$ with the basic surface sites of alumina should parallel that suggested for $Fe_3(CO)_{12}$:

$$Fe(CO)_5 + 2\{Al^{3\oplus}-OH\} \longrightarrow [HFe(CO)_4]^{\ominus}\{Al^{3\oplus}\} + \{(Al^{3\oplus})(HCO_3)^{\ominus}\} \quad (6)$$

Apparently the chemistry on fully hydroxylated MgO is nearly the same. There are several plausible stoichiometries for subsequent redox condensation processes resulting in the trinuclear cluster anion (see Section 3.4 for an example involving the Os analogue), but since no gas evolution data are available, the stoichiometry of the surface-mediated condensation remains to be determined.

3.3. Deprotonation of Hydrido Carbonyls

One of the most easily defined acid–base reactions that occurs on metal oxide surfaces is the deprotonation of hydrido carbonyl complexes. The reaction class provides one of the most straightforward and easily applied routes for the preparation of molecularly dispersed organometallics on basic surfaces such as those of alumina and magnesia.

The adsorption of weakly acidic hydrido carbonyl clusters on partially dehydroxylated γ-Al_2O_3 results in the formation of surface-bound carbonylate anions. The clusters are believed to be deprotonated by reaction with basic surface hydroxyl groups, in analogy to their reactivity with hydroxide ion in solution.[24] $[H_4Os_4(CO)_{12}]$ ($pK_a = 12.0$ (CH_3OH)[24]), $[H_2RuOs_3(CO)_{13}]$, $[H_4RuOs_3(CO)_{12}]$, and $[H_4Ru_4(CO)_{12}]$ ($pK_a = 11.9$ (CH_3OH)[24]) are all deprotonated when brought into contact with alumina from hydrocarbon solvents.[25] In these experiments, the solids were typically separated from the adsorbate solution by filtration, rather than by evaporation of the solvent, and washed exhaustively. This procedure maximizes the likelihood of direct bonding to the surface and minimizes the likelihood of formation of crystallites of adsorbate on the surface. For example, when $[H_4Os_4(CO)_{12}]$ is adsorbed from refluxing hexanes onto γ-Al_2O_3 pretreated at 673 K, the resulting species is $[H_3Os_4(CO)_{12}]^{\ominus}$, ionically bound to the surface.[25a] The IR spectrum of the surface species (obtained in air) agrees closely with that of $[(Ph_3P)_2N][H_3Os_4(CO)_{12}]$ (Fig. 7), suggesting that, at least in the presence of co-adsorbed (atmospheric) moisture, $[H_3Os_4(CO)_{12}]^{\ominus}$ does not interact through specific chemical bonding with surface $Al^{3\oplus}$ counterions. $[H_3Os_4(CO)_{12}]^{\ominus}$ could be extracted from the surface by ion exchange with $(Ph_3P)_2NCl$ in CH_2Cl_2, but no osmium carbonyls were removed by washing with CH_2Cl_2 alone. Analogous results were obtained when the hydrido metal clusters $[H_2RuOs_3(CO)_{13}]$[25b,c] and $[H_4Ru_4(CO)_{12}]$[25d] were adsorbed on γ-Al_2O_3.

Since the chemistry of MgO is dominated by its strong basicity, the deprotonation of hydrido carbonyls occurs most readily on this surface. Hydrido carbonyl complexes and clusters of Os,[26,27] W,[28] Ru,[25d] and Re[29] chemisorb dissociatively on MgO. The chemisorption of $[H_4Os_4(CO)_{12}]$ on highly dehydroxylated MgO powder (pretreated in vacuo at 1073 K) leads not only to formation of adsorbed $[H_3Os_4(CO)_{12}]^{\ominus}$, the predominant organometallic surface species, but also to adsorbed $[H_2Os_4(CO)_{12}]^{2\ominus}$, as indicated by IR[27a] and ^{13}C NMR spectra[27b] of the surface structures. These anions could be removed from the surface by cation metathesis with $(Ph_3P)_2NCl$ in dry CH_2Cl_2, acetone, or 2-propanol. The formation of the dianion by deprotonation underscores the strong basicity of highly dehydroxylated MgO; even treatment of $[H_4Os_4(CO)_{12}]$ with excess KOH in methanol yields only $[H_3Os_4(CO)_{12}]^{\ominus}$.[30]

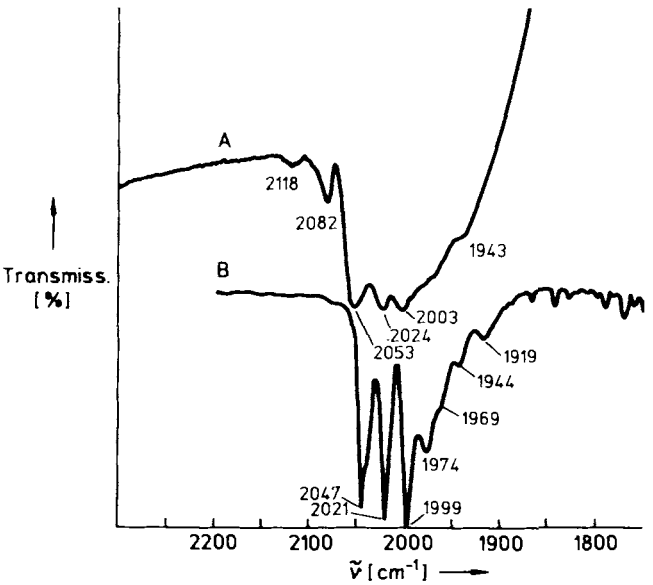

Fig. 7. Comparison of the ν_{CO} bands of surface-bound $[H_3Os_4(CO)_{12}]^{\ominus}$ on γ-Al_2O_3 (A) and the complex $[(Ph_3P)_2N][H_3Os_4(CO)_{12}]$ in CH_2Cl_2 (B) [25a].

The dissociative chemisorption of hydrido carbonyl complexes on highly dehydroxylated MgO can also result in well-defined surface ion pairs. The adsorption of $[HWCp(CO)_3]$ ($pK_a = 9.0$ (CH_3OH)[24]) from dry hexanes or toluene at room temperature results in the formation of surface-bound $[CpW(CO)_3]^{\ominus}$, paired with a surface $Mg^{2\oplus}$ ion:[28]

$$[HWCp(CO)_3] + \{Mg^{2\oplus}O^{2\ominus}\} \longrightarrow [CpW(CO)_2CO^{\ominus}\cdots\{Mg^{2\oplus}(OH^{\ominus})\}] \quad (7)$$

Three IR bands of approximately equal intensity are observed for the complex in the ν_{CO} region, with the low-frequency band at 1711 cm^{-1} indicating a direct $W\text{-}CO\cdots\{Mg^{2\oplus}\}$ interaction. $[CpW(CO)_3]^{\ominus}$ can be extracted from the solid by cation metathesis with $(Ph_3P)_2Cl$ in CH_2Cl_2. The $W\text{-}CO\cdots\{Mg^{2\oplus}\}$ interaction is analogous to that characterizing the tight ion pairs observed for $[CpM(CO)_3]^{\ominus}$ (M = Cr, Mo, W) with $Li^{\oplus}$, $Na^{\oplus}$, $K^{\oplus}$,[31] $Mg^{2\oplus}$(Mo),[32] and $Al^{3\oplus}$(W)[33] in THF solution; the ν_{CO} IR absorptions of the surface species are listed with those of the soluble analogues in Table 3. Figure 8, left, shows a model for the structure of $[CpW(CO)_3]^{\ominus}$ on MgO; the crystal structure of $[(py)_4Mg\{CpMo(CO)_3\}_2]$ (Fig. 8, right) suggests that a magnesium–carbonyl oxygen bonding distance of approximately 0.20 nm should be expected.[32a] The contact ion pairing of $[CpW(CO)_3]^{\ominus}$ complexes with surface $Mg^{2\oplus}$ ions represents the first well-characterized example

Table 3. IR spectroscopic data for surface-bound $[CpW(CO)_3]^{\ominus}$ and analogous contact ion pairs in solution.

Species	ν(CO) [cm^{-1}]			Ref.
$[CpW(CO)_2CO^{\ominus}\cdots\{Mg^{2\oplus}(OH^{\ominus})\}]$ [a]	1884	1766	1711	[28]
$[CpW(CO)_2CO^{\ominus}\cdots Li^{\oplus}]$ [b]	1903	1803	1716	[31]
$[CpW(CO)_2CO^{\ominus}\cdots Na^{\oplus}]$ [b]	1896	1792	1742	[31]
$[CpW(CO)_2CO^{\ominus}\cdots K^{\oplus}]$ [b]	1894	1784	1748	[31]
$[(CpMo(CO)_2CO^{\ominus})_2\cdots Mg^{2\oplus}\cdot 4THF]$ [b]	1912	1815	1680	[32b]
$[(CpW(CO)_2CO^{\ominus})_3\cdots Al^{3\oplus}\cdot 3THF]$ [b]	1942	1854	1655–1548 [c]	[33]

[a] Magnesia disc. [b] THF solution. [c] Bands at 1655, 1591, 1567, and 1548 cm^{-1} are reported.

of this interaction for a surface-bound carbonylate anion. Carbonylate anions appear to be excellent probes of the coordination environment of surface cations, much as they have proved to be useful probes of the coordination of alkali metal ions in solution.[34]

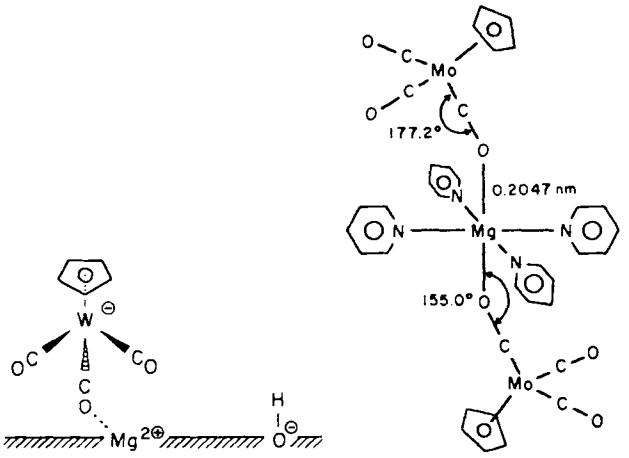

Fig. 8. Left: Proposed structures of surface species resulting from the dissociative chemisorption of $[HWCp(CO)_3]$ on magnesia. Right: Molecular structure of $[(py)_4Mg\{CpMo(CO)_3\}_2]$, a molecular analogue of $[CpW(CO)_3]^{\ominus}$ on magnesia [32a].

3.4. Bifunctional Interactions

Chemisorption of certain organic molecules (e.g., alcohols) on dehydroxylated metal oxide surfaces is believed to involve bifunctional interactions with surface acid–base pairs. Metal complexes can also interact simultaneously with neighboring surface acidic and basic centers owing to the involvement of multiple chemical functionalities (i.e., the metal center and ligands). For example, *Shriver*, *Burwell*, and co-workers used $[(CH_3)Mn(CO)_5]$ and $[CpFe(CH_3)(CO)_2]$ as probes for acid–base pairs on alumina surfaces,[35,36] since "diphilic" Lewis acids such as $AlBr_3$ were known to promote methyl migration in these complexes. *Correa* et al.[35] found that when $[(CH_3)Mn(CO)_5]$ is deposited from pentane solution onto partially dehydroxylated or highly dehydroxylated alumina, an immediate color change occurs, and the IR spectrum of the surface species (obtained after evaporation of the solvent) is in close agreement with that of the $[(CH_3CO)Mn(CO)_4]\cdot AlBr_3$ adduct. Gas evolution during adsorption was negligible. Similar results were obtained for the adsorption of $[CpFe(CH_3)(CO)_2]$. The structure illustrated in Figure 9 was proposed for the surface-bound acyl derivative $[Mn(CO)_4(COCH_3)\{O-Al\}]$. These findings are good evidence for the presence of adjacent Lewis acidic and basic centers on the alumina surface, clearly demonstrating the utility of employing organometallic complexes as probes of metal oxide surface structure and reactivity.

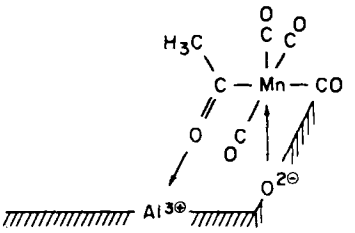

Fig. 9. Schematic representation of the proposed structure of the acyl complex derived from $[CH_3Mn(CO)_5]$ adsorbed on the γ-Al_2O_3 surface [36].

The adsorption of $[H_2Os(CO)_4]$ on the surfaces of SiO_2, Al_2O_3, and MgO has been investigated with the goal of comparing these surfaces on the basis of the acid–base chemistry of adsorption.[26,27] The expected deprotonation product of $[H_2Os(CO)_4]$ adsorption on basic metal oxides is $[HOs(CO)_4]^{\ominus}$, which has been shown to form ion pairs with alkali-metal ions in THF.[26] Adsorption of the weakly acidic $[H_2Os(CO)_4]$ ($pK_a = 14.7$ (CH_3OH)[24]) on the metal oxides was effected from hexanes at room temperature. Adsorption on SiO_2 was weak and reversible (physisorption). In contrast, on MgO and γ-Al_2O_3 pretreated at 1073 and 773 K, respectively, the complex was chemisorbed; the IR band pattern of the parent complex was strongly perturbed, and low-frequency absorptions appeared which are attributable to $Os-CO\cdots\{M^{n\oplus}\}$ interactions. The pattern of the IR bands is similar for $[H_2Os(CO)_4]$ adsorbed on magnesia and on alumina (Fig. 10); however, on magnesia the strong high-wavenumber bands (assigned to terminal carbonyl ligands) appear at lower wavenumbers relative to those of the alumina-supported complex. Significantly, the relative positions of the weak low-wavenumber bands (assigned to isobridging carbonyls, $Os-CO\cdots\{M^{n\oplus}\}$) are re-

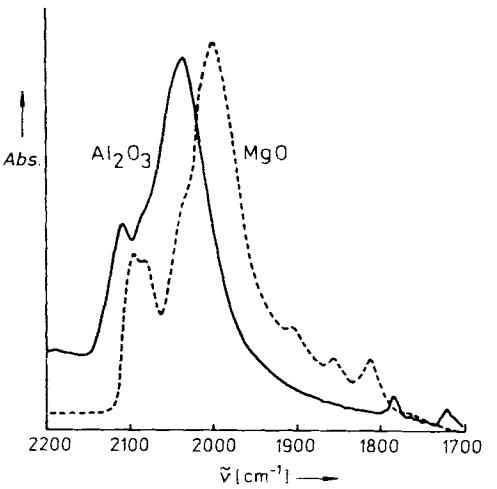

Fig. 10. Comparison of the ν_{CO} bands of the surface species derived from $[H_2Os(CO)_4]$ chemisorption on MgO and γ-Al_2O_3.

versed. Consistent with these results, the ^{13}C NMR spectrum of the MgO-supported complex showed carbonyl groups in two distinct environments, in a 3 : 1 ratio.[27b] Extraction of the species from the MgO surface with $(Ph_3P)_2NCl$ in CH_2Cl_2 resulted in the isolation of $[(Ph_3P)_2N][HOs_3(CO)_{11}]$. The formation of the trinuclear cluster anion is consistent with a redox condensation reaction known from solution chemistry:

$$2[H_2Os(CO)_4] + [HOs(CO)_4]^{\ominus} \longrightarrow [HOs_3(CO)_{11}]^{\ominus} + CO + 2H_2 \quad (8)$$

In contrast, treatment of the structure formed from adsorption of $[H_2Os(CO)_4]$ on γ-Al_2O_3 with $(Ph_3P)_2NCl$ in CH_2Cl_2 yielded predominantly $[H_2Os(CO)_4]$ with only a trace of $[HOs_3(CO)_{11}]^{\ominus}$.

A model for the surface structures formed from $[H_2Os(CO)_4]$ adsorption on the polar alumina and magnesia surfaces is illustrated in Figure 11. The chemistry ob-

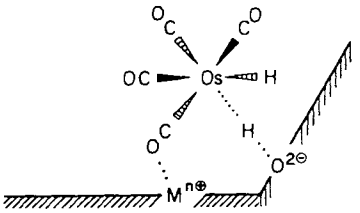

Fig. 11. Proposed structure of surface species formed from the chemisorption of $[H_2Os(CO)_4]$ on highly dehydroxylated MgO and γ-Al_2O_3.

served in the extraction experiments (consistent with the IR spectrum of the surface species) indicates that the Os–H···{$O^{2\ominus}$} interaction (H-bond donation) dominates on MgO, leading to deprotonation and formation of $[HOs(CO)_4]^{\ominus}$. On alumina the interaction with basic sites is weak, the Os–CO···{$Al^{3\oplus}$} interaction dominates, and $[H_2Os(CO)_4]$ is released from the surface by extraction. However, acid–base pairs are evidently the adsorption sites for the hydrido carbonyl on both metal oxide surfaces. Because their reactions are easily monitored with IR spectroscopy and they can engage in a variety of simple acid–base interactions, metal carbonyls are proving to be excellent probes of metal oxide surfaces.

3.5. Oxidative Addition of Surface Hydroxyl Groups

A reaction class common to metal carbonyl clusters adsorbed on hydroxylated metal oxide surfaces is the oxidative addition of surface hydroxyl groups. This chemistry was established for $Os_3(CO)_{12}$ on silica and alumina in early work by *Basset, Psaro, Ugo*, and co-workers.[37] $Os_3(CO)_{12}$ is simply physisorbed from CH_2Cl_2 onto silica surfaces pretreated at 300 and at 773 K, but upon heating to 423 K under argon, the cluster reacts to give covalently bound $[(\mu\text{-H})Os_3(CO)_{10}\{\mu\text{-OSi}\}]$. Two CO molecules are evolved per cluster, with only negligible H_2 production. This stoichiometry is consistent with the simple oxidative addition of a surface hydroxyl group to the cluster:

$$Os_3(CO)_{12} + \{Si{-}OH\} \longrightarrow [(\mu\text{-H})Os_3(CO)_{10}\{\mu\text{-OSi}\}] + 2CO \quad (9)$$

The reaction is most facile on hydrated silica surfaces with high concentrations of hydroxyl groups. A triosmium cluster with two labile nitrile ligands, $[Os_3(CO)_{10}(CH_3CN)_2]$, also chemisorbs on silica at room temperature to form $[(\mu\text{-H})Os_3(CO)_{10}\{\mu\text{-OSi}\}]$; this observation suggests that the thermal treatment of physisorbed $Os_3(CO)_{12}$ serves to labilize the CO ligands, thereby facilitating its chemisorption. The suggested structure of the chemisorbed Os_3 cluster is analogous to that of the crystallographically characterized $[(\mu\text{-H})Os_3(CO)_{10}(\mu\text{-OSiEt}_3)]$[38] (Fig. 12) and of related soluble analogues. The oxidative addition of HX molecules (where X has unshared electron pairs) to $M_3(CO)_{12}$ clusters generally results in structures which have bridging hydrides and bridging X groups.[39]

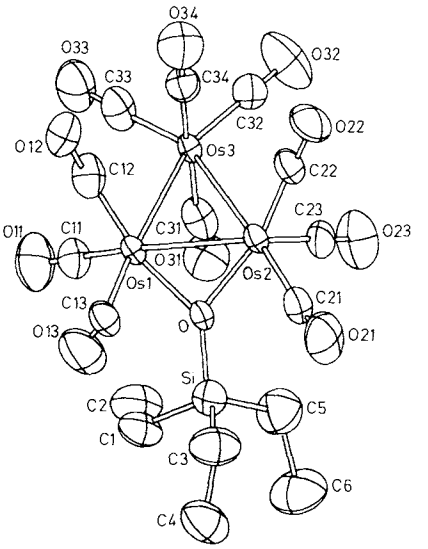

Fig. 12. Molecular structure of $[(\mu\text{-H})Os_3(CO)_{10}(\mu\text{-OSiEt}_3)]$, a soluble analogue of covalently bound supported triosmium clusters [38].

The reactivity of $Ru_3(CO)_{12}$ with the silica surface is similar to that of $Os_3(CO)_{12}$, resulting in the species $[(\mu\text{-H})Ru_3(CO)_{10}\{\mu\text{-O}-\text{Si}\}]$,[40] but this surface-bound cluster is unstable and decomposes even under synthesis conditions.

The surface hydroxyl groups of transition aluminas react similarly to the hydroxyl groups on silica.[37,41] Physisorbed $Os_3(CO)_{12}$ is converted into covalently bound $[(\mu\text{-H})Os_3(CO)_{10}\{\mu\text{-OAl}\}]$ at 353–373 K under argon or in vacuo; this surface species is formed on both fully hydroxylated and partially dehydroxylated η-Al_2O_3 surfaces (the latter pretreated at 673 K). Concomitant with the formation of $[(\mu\text{-H})Os_3(CO)_{10}\{\mu\text{-OAl}\}]$, two molecules of CO are evolved per $Os_3(CO)_{12}$ cluster. The IR spectrum of the supported cluster is closely similar to that of $[(\mu\text{-H})Os_3(CO)_{10}\{\mu\text{-OSi}\}]$ and that of the analogue $[(\mu\text{-H})Os_3(CO)_{10}(\mu\text{-OSiEt}_3)]$ (cf. Fig. 12).[38] The surface-bound cluster has also been prepared by direct reaction of $Os_3(CO)_{12}$ in refluxing *n*-octane solution with γ-Al_2O_3.[41]

$[Os_3(CO)_{10}(C_6H_8)]$ and $[Os_3(CO)_{10}(CH_3CN)_2]$ also chemisorb at room temperature on hydroxylated alumina to form $[(\mu\text{-H})Os_3(CO)_{10}\{\mu\text{-OAl}\}]$. The alumina-supported cluster has been characterized by Raman[42] and extended X-ray absorption fine structure (EXAFS) spectroscopy[43] and observed by high-resolution transmission electron mi-

croscopy.[44] The EXAFS analysis of *Duivenvoorden* et al.[43b] is consistent with the proposed structure of the supported cluster, yielding the structural parameters given in Table 4. *Cook* et al.[43a] found that a bis-oxygen species

Table 4. Characterization of γ-Al_2O_3-supported osmium carbonyls by EXAFS spectroscopy [43b].

Sample	$Os_3(CO)_{12}$ [a]	$[HOs_3(CO)_{10}\{OAl\}]$	$[Os(CO)_x\{OAl\}_3]$
Os–Os distance [nm]	0.288 [b]	0.288 [c]	—
Os–Os coordination number	2 [b]	2 [c]	—
C : Os atomic ratio	4	3.33 [c]	2.8 [c]
$Os–O_{support}$ distance [nm]	—	0.216 [c]	0.217 [c]
$Os–O_{support}$ coordination number	—	0.65 [c]	3 [c]

[a] Reference compound, characterized in the crystalline state. [b] Value determined by X-ray crystallography. [c] Value determined by EXAFS. The coordination numbers have uncertainties of ±15% and the bond distance uncertainties of ± 1%.

such as $[Os_3(CO)_{10}(\mu\text{-}OH)\{\mu\text{-}OAl\}]$ provided a slightly better fit to their EXAFS data than a structure with a single bridging oxygen, and it was suggested[43c] that the Raman data[42] provide evidence of such a structure. However, the formation of such a surface-bound species from $Os_3(CO)_{12}$ should require the oxidative addition of two HX surface groups:

$$Os_3(CO)_{12} + H_2O + \{Al\text{–}OH\} \longrightarrow [Os_3(CO)_{10}(\mu\text{-}OH)\{\mu\text{-}OAl\}] + 2\,CO + H_2 \quad (10)$$

Since *Psaro* et al.[37a] measured only negligible H_2 evolution accompanying the formation of the alumina-supported Os_3 cluster, the original formulation of $[\mu\text{-}HOs_3(CO)_{10}\{\mu\text{-}OAl\}]$ appears to be preferable.

The wide range of characterization methods applied to these samples is exemplary; most informative are the data characterizing the surface stoichiometry, the IR spectra (giving an excellent fingerprint for comparison with the molecular analogues), and the EXAFS data, giving precise structural information.

Oxidative addition involving $Os_3(CO)_{12}$ and the surface hydroxyl groups of hydroxylated MgO also takes place, as on SiO_2 and Al_2O_3, but only when the MgO surface is contaminated with adsorbed CO_2 (which forms surface carbonates at the basic sites); otherwise anion formation occurs.[45]

3.6. Summary

These results provide evidence of the various reactivities of the metal oxide surfaces toward adsorbing metal carbonyls. The silica surface is relatively unreactive toward binary and hydrido metal carbonyls adsorbed under mild conditions. In many cases, simple physisorption occurs. Since a strong chemical interaction with the support is a prerequisite for incorporating isolated molecular complexes for use as catalysts or catalyst precursors, the metal carbonyl/SiO_2 combination is usually not advantageous. Reactions of metal carbonyls with silica under more vigorous conditions, however, can lead to the oxidative addition of surface hydroxyl groups to the adsorbing metal carbonyl. Occasionally, these reactions lead to well-characterized surface-bound complexes, e.g., $[(\mu\text{-}H)Os_3(CO)_{10}\{\mu\text{-}OSi\}]$, but often the products are ill-defined mixtures of surface species.

The reactivity of alumina with metal carbonyls is more complex and varied than that of silica, reflecting the complex nature of the alumina surface, with its Lewis acidic and Lewis basic centers in addition to hydroxyl groups. The surface hydroxyl groups of hydrated alumina are basic in character and react with adsorbed binary metal carbonyls via nucleophilic attack at coordinated CO and with hydrido carbonyls via deprotonation to yield surface-bound carbonylate anions. Alumina surfaces expose $Al^{3\oplus}$ ions, which form adducts with electron-pair donors such as complexes incorporating bridging carbonyl groups, and the acid–base pairs on the surface may interact cooperatively with organometallic reagents. Oxidative addition of surface hydroxyl groups also occurs, as on silica, to yield covalently bound metal clusters.

The reactivity of the MgO surface is dominated by its basicity. Even weakly acidic hydrido metal carbonyls are deprotonated on MgO, and a wide variety of surface-bound anions are thus formed. $M\text{–}CO\cdots\{Mg^{2\oplus}\}$ interactions are important for mononuclear carbonylates and may influence the reactivity of the supported carbonyl anions. Acid–base pairs have been identified as adsorption sites for hydrido carbonyls on MgO (as on γ-Al_2O_3). On MgO surfaces contaminated with adsorbed CO_2, the formation of surface-bound clusters resulting from oxidative addition of hydroxyl groups occurs, as on silica and alumina.

4. Oxidation–Reduction and Fragmentation–Condensation Reactions of Supported Metal Carbonyls

The simple chemisorption of metal carbonyls on metal oxide surfaces discussed in the preceding section was often characterized by one surface reaction giving a single, relatively well-defined surface species. In this section we broaden the scope of surface reactions to emphasize the more complex transformations that occur when supported metal carbonyls are subjected to severe thermal conditions. These reactions often lead to changes in the nuclearity of the surface organometallic species (i.e., aggregation or fragmentation), which are often accompanied by changes in metal oxidation state.

Typically, the thermal activation (or decarbonylation) of an adsorbed metal carbonyl leads to oxidation of the transition metal center via a redox process involving the oxidative addition of surface hydroxyl groups:

$$M'(CO)_x + n\{M\text{–}OH\} \longrightarrow [M'(CO)_{x-y}\{O\text{–}M\}] + \frac{n}{2}H_2 + y\,CO \quad (11)$$

When supported metal clusters are the precursors, fragmentation of the metal framework generally occurs with oxidation of the metal centers. Occasionally, the oxidative fragmentation of chemisorbed metal clusters has been inferred to produce more-or-less unique groupings (or en-

sembles) of low-valent mononuclear surface complexes. Because of the complexity of the reaction sequences, however, the potential for producing mixtures of surface species is great. Only for certain metal carbonyl–metal oxide combinations (in narrow ranges of conditions) are unique surface species obtained.

On basic metal oxide surfaces (e.g., magnesia, alumina), the oxidative fragmentation process can be reversed. Examples are provided by reactions (12) and (13).

$$[Os(CO)_2\{O-Mg\}_4]^{2\ominus} \xrightarrow{CO+H_2} [Os_{10}C(CO)_{24}]^{2\ominus}/MgO \quad (12)$$

$$[Rh(CO)_2\{O-Al\}\{HO-Al\}] \xrightarrow{CO+H_2O} [Rh_6(CO)_{16}]/Al_2O_3 \quad (13)$$

These reactions closely parallel the reductive carbonylation of metal salts in basic solution—an important synthetic route to anionic metal carbonyl clusters.[46] Redox condensation reactions, which are implicated in the reductive carbonylation process, also occur, involving low-valent mononuclear metal carbonyls adsorbed on basic metal oxides. As in solution, such reactions lead to the formation of high-nuclearity molecular metal clusters. As a consequence of these base-promoted condensation processes, the surface organometallic chemistry on basic metal oxides can be molecular chemistry even at elevated temperatures in the presence of $CO + H_2$.

4.1. Oxidation of Supported Mononuclear Metal Carbonyls by Surface Hydroxyl Groups

Burwell, *Brenner*, and co-workers[36,47] employed gas evolution measurements to investigate the stoichiometry of the thermal decomposition of $Mo(CO)_6$ deposited on γ-Al_2O_3. Surface hydroxyl groups play a key role in the surface chemistry, oxidizing the supported metal carbonyl; the average oxidation state of Mo in the decarbonylated products depends directly on the degree of hydroxylation of the alumina. $Mo(CO)_6$ was deposited from pentane solution onto the support, and the complex was inferred to be physically adsorbed. Thermal activation of $Mo(CO)_6$ on partially dehydroxylated γ-Al_2O_3 in He at temperatures up to 373 K results in CO evolution but does not lead to oxidation of the Mo centers. However, activation of $Mo(CO)_6/\gamma$-Al_2O_3 at temperatures above 423 K results in further decarbonylation with concomitant oxidation of the Mo. H_2 and CH_4 are produced, the process evidently initiated by the oxidative addition of surface hydroxyl groups to zerovalent Mo species. From the stoichiometry of these reactions, the average oxidation state of Mo in materials activated at 573 K is indicated to be +2, but the materials are apparently nonuniform, since, after activation at temperatures above 473 K, Mo^V ions were detected by electron paramagnetic resonance (EPR) spectroscopy. Further heating increases the average Mo oxidation state to +3 and then approximately +6. Additional details of this complicated surface chemistry have been elucidated by IR spectroscopy.[19b] Mixtures of surface species are formed, and the spectra do not allow simple interpretations.

By avoiding the oxidation of the zerovalent Mo in the form of $Mo(CO)_6$, it may be possible to prepare metallic molybdenum-on-alumina. A sample prepared using a highly dehydroxylated γ-Al_2O_3 (pretreated at 1223 K) was activated to give material that was inferred to incorporate largely zerovalent Mo; exposure of this material to H_2 at 923 K was inferred to result in supported crystallites of metallic Mo,[36] but this interpretation is controversial.

Brenner et al.[48] established the generality of the redox reactions between surface hydroxyl groups and adsorbed metal carbonyls. The oxidation reactions are common to many metal carbonyls on typical metal oxide supports, but identification and thorough characterization of stable subcarbonyl intermediates have been reported only rarely; typically, during the decomposition of supported metal carbonyls, a mixture of species is present. However, simple surface chemistry is observed occasionally, as exemplified by the decomposition of chemisorbed $[HRe(CO)_5]$ on MgO, which proceeds through the formation of a single covalently bound tricarbonyl species, $[Re(CO)_3\{O-Mg\}\{HO-Mg\}_2]$.

Kirlin et al.[49] investigated the thermal decarbonylation of $[HRe(CO)_5]/MgO$ in flowing He and in flowing H_2. $[HRe(CO)_5]$ is weakly chemisorbed on MgO; interaction with basic surface groups [see (14)] apparently leads to the incipient deprotonation of the following complex:

$$[HRe(CO)_5]/MgO \longrightarrow [(CO)_5Re\cdots H\cdots\{O^{2\ominus}Mg^{2\oplus}\}] \quad (14)$$

The conversion of this species into the complex $[Re(CO)_3\{O-Mg\}\{HO-Mg\}_2]$ at 353 K was established by IR spectroscopy. The covalently bound surface complex was suggested to be equivalent to the well-characterized tricarbonyl species derived from the decomposition of $[H_2Re_3(CO)_{12}]^{\ominus}/MgO$.[29] Although there was no net change in *formal* oxidation state, the oxidative addition of a surface hydroxyl group was suggested to result in a Re–O bond to the surface:

$$[HRe(CO)_5] + 3\{Mg-OH\} \xrightarrow[H_2 \text{ or } He]{353\ K} [Re(CO)_3\{O-Mg\}\{HO-Mg\}_2] + H_2 + 2CO \quad (15)$$

$[Re(CO)_3\{O-Mg\}\{HO-Mg\}_2]$ decomposes at temperatures above 523 K under H_2 or He to give surface species having no ν_{CO} IR absorptions.

4.2. Condensation of Supported Mononuclear Complexes to Give Surface-Bound Molecular Metal Clusters

It is clear from the preceding discussion that attempts to free metal coordination sites by thermal decarbonylation of oxide-supported metal carbonyls often fail because of oxidation of the metal centers by surface hydroxyl groups. This complication, inherent to the activation of metal carbonyls supported on typical metal oxides, has frustrated efforts to use supported molecular metal carbonyls as catalysts. However, in the case of CO hydrogenation and related reactions, high partial pressures of CO can be employed to inhibit decarbonylation (and oxidation) and stabilize the supported clusters. Unfortunately, in most cases, the neutral metal carbonyls are volatile, and the metals are gradually lost from the catalyst.

The key to stabilizing surface-bound molecular metal carbonyls at high temperatures is to use them in the presence of CO and to use basic metal oxide supports such as magnesia, which provide the opportunity to prepare a wide variety of ionically bound carbonylates. Moreover, anionic metal carbonyls are effective homogeneous catalysts or catalyst precursors for alkene hydroformylation, alcohol homologation, the water-gas shift reaction, and other reactions involving CO as a reactant.[50] Until recently, little was known about the reactivity or catalytic activity of metal carbonyls on basic supports under CO or $CO + H_2$ atmospheres at elevated temperatures. However, one should anticipate parallels to the chemistry of metal carbonyls in basic solution. This subject is developed below on the basis of the surface organometallic chemistry of species derived from $[H_2Os(CO)_4]$ chemisorbed on magnesia. In analogy to the reactivity of metal carbonyls in basic solution, a rich chemistry of molecular cluster growth on basic supports is now emerging.

$[H_2Os(CO)_4]$ chemisorbs on MgO to produce surface species described as surface-bound $[HOs(CO)_4]^{\ominus}$; the dominant adsorbate–surface interaction involves a hydride ligand and a basic surface group ($O^{2\ominus}$ ion or hydroxyl group), leading to incipient deprotonation of the complex (Section 3.4). As demonstrated by the extraction of the surface species with $(Ph_3P)_2NCl$ in CH_2Cl_2 to give $[(Ph_3P)_2N][HOs_3(CO)_{11}]$, the supported complexes are susceptible to redox condensation involving $[H_2Os(CO)_4]$ and its conjugate base. The condensation of the supported mononuclear carbonyls to yield anionic clusters bound to the MgO surface is therefore to be expected.

Indeed, samples prepared by adsorption of $[H_2Os(CO)_4]$ on magnesia (pretreated at 673 K) heated at 548 K under 1 MPa of $CO + H_2$ in 1:3 (molar) ratio (conditions under which the catalytic hydrogenation of CO occurs) for more than two days yielded materials incorporating $[H_3Os_4(CO)_{12}]^{\ominus}$ and $[Os_{10}C(CO)_{24}]^{2\ominus}$ as the predominant surface species.[26] Spectroscopic characterization of the samples after reaction gave evidence for the presence of molecular surface-bound clusters, but not metal particles. $[H_3Os_4(CO)_{12}]^{\ominus}$ was extracted from the solids by cation metathesis with $(CH_3)_4NCl$ in 2-propanol. The reddish-brown carbido cluster $[Os_{10}C(CO)_{24}]^{2\ominus}$ remained on the MgO surface after extraction, as evidenced by the IR and UV/VIS spectra of the solid. Elemental analysis of samples before and after reaction indicated that 30% of the osmium initially present had been lost, presumably as the volatile $[H_2Os(CO)_4]$ or as other neutral carbonyls.

The condensation of the original supported mononuclear metal complexes was monitored by high-pressure IR spectroscopy.[51] As in the previous experiments, the sample was heated from 300 to 548 K under flowing 1:1 CO/H_2 at 1 MPa. The initial IR spectrum recorded at 548 K (Fig. 13A) is in excellent agreement with that of surface-bound $[H_{4-n}Os_4(CO)_{12}]^{n\ominus}$ (n = 1, 2) clusters on MgO (Fig. 13B); limited spectroscopic evidence suggests the formation of $[HOs_3(CO)_{11}]^{\ominus}$ as an intermediate condensation product at lower temperatures. (The formation of surface-bound $[H_{4-n}Os_4(CO)_{12}]^{n\ominus}$ (n = 1, 2) appears to be analogous to the reaction of $[HRu_3(CO)_{11}]^{\ominus}$ in solution in the presence of H_2 to yield $[H_2Ru_4(CO)_{12}]^{2\ominus}$.[52]) As the $CO:H_2$ molar ratio of the feed mixture was changed to 1:3, the IR bands characteristic of $[H_{4-n}Os_4(CO)_{12}]^{n\ominus}$ (n = 1, 2) decreased in intensity with time, and a band appeared which was tentatively assigned to $[Os_6(CO)_{18}]^{2\ominus}$, a likely intermediate in the formation of the ultimate product, $[Os_{10}C(CO)_{24}]^{2\ominus}$.[53] Similar results were obtained in an experiment with a sample initially incorporating $[H_{4-n}Os_4(CO)_{12}]^{n\ominus}$ (n = 1, 2) derived from the adsorption of $H_4Os_4(CO)_{12}$ (Section 3.3).

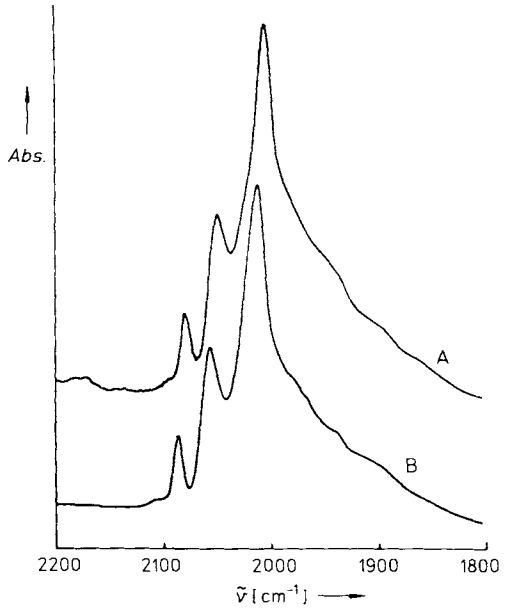

Fig. 13. Comparison of the ν_{CO} bands of surface-bound $[H_{4-n}Os_4(CO)_{12}]^{n\ominus}$ (n = 1, 2) on magnesia derived from chemisorbed $[H_2Os(CO)_4]$ by heating to 548 K under 1 MPa of equimolar $CO + H_2$ (spectrum recorded initially under these conditions) (A) and from the products of the dissociative chemisorption of $[H_4Os_4(CO)_{12}]$ after heating to 473 K under 100 kPa of equimolar $CO + H_2$ (spectrum recorded in vacuo at 300 K) (B).

The observation of $[Os_{10}C(CO)_{24}]^{2\ominus}$ and the tetranuclear hydrido osmium carbonyl anions as the predominant surface species after long reaction times reflects the thermodynamic stability of these clusters under the chosen conditions. The ultimate synthesis of $[Os_{10}C(CO)_{24}]^{2\ominus}$ on the basic MgO surface at high temperatures parallels its synthesis in solution via condensation of lower-nuclearity osmium carbonyls under reducing conditions.[53] The relative stability of the $[H_{4-n}Os_4(CO)_{12}]^{n\ominus}$ (n = 1, 2) clusters is attributed to the high H_2 partial pressures employed and their influence on the equilibrium; the neutral cluster $[H_4Os_4(CO)_{12}]$ has been demonstrated to be the most stable hydrido carbonyl cluster of osmium under similar conditions in solution.[54] The tetranuclear cluster anions have also been observed to form from $Os_6(CO)_{18}$ on MgO.[27c]

In summary, the combination of stable osmium carbonyls with the basic magnesia support allows the extension of the rich molecular chemistry of cluster growth in basic media to surfaces.

4.3. Oxidative Fragmentation of Supported Metal Clusters and Aggregates

This section begins with descriptions of the syntheses of stable mononuclear surface complexes by the oxidative

fragmentation of supported metal clusters, $[(\mu\text{-}H)Os_3(CO)_{10}\{\mu\text{-}OM\}]$ (M = Si, Al, Mg), $[Rh_6(CO)_{16}]/Al_2O_3$, and $[H_2Re_3(CO)_{12}]^{\ominus}/MgO$. Evidence is presented for the existence of ensembles consisting of three mononuclear metal complexes originating from the decomposition of the trinuclear Os and Re clusters. Next, the surface organometallic chemistry of the rhenium-on-alumina system is described as a basis for developing the parallels between the oxidative fragmentation of supported molecular metal clusters and the disruption of small supported aggregates of metal resulting from exposure to CO.

4.3.1. Oxidative Fragmentation of Supported Metal Carbonyl Clusters

Having established the potential for forming stable low-valent subcarbonyl species via the decarbonylation of supported mononuclear carbonyls (Section 4.1), we now turn to the more complex process of oxidative fragmentation of surface-bound metal clusters. Because the metal atoms in supported clusters are initially associated, the thermal decomposition of these species provides the opportunity to synthesize ensembles of subcarbonyl complexes covalently bound to a metal oxide surface. A prerequisite for the synthesis of uniform isolated ensembles is the initial chemisorption of a metal cluster precursor, the goal being to create ensembles having the nuclearity of the cluster. For certain metals (e.g., Rh, Os, Re), the low-valent mononuclear complexes formed by the thermal decomposition of supported metal clusters provide excellent models for the surface structures formed by the analogous CO-initiated oxidative fragmentation of highly dispersed supported metal particles (Section 4.3.2). *Robbins*[55] has proposed that the rhodium(I) dicarbonyl species formed by the disruption of small alumina-supported Rh aggregates remain clustered on the support, the process being analogous to the formation of ensembles by the decomposition of metal clusters.

As described in Section 3.5, $Os_3(CO)_{12}$ reacts with silica, alumina, and magnesia at 333–423 K (the temperature depending on the support and the preparation) to give the surface-bound cluster $[(\mu\text{-}H)Os_3(CO)_{10}\{\mu\text{-}OM\}]$ (M = Si, Al, Mg). Treatment of the supported trinuclear clusters in vacuo or under inert gases at elevated temperatures leads to fragmentation and oxidation to form mononuclear Os^{II} complexes.[37,40,41,45] The temperature required to induce fragmentation depends on the metal oxide support and its pretreatment.

The oxidative fragmentation of $[(\mu\text{-}H)Os_3(CO)_{10}\{\mu\text{-}OAl\}]$ has been investigated by a number of research groups. Treatment of $[(\mu\text{-}H)Os_3(CO)_{10}\{\mu\text{-}OAl\}]$ at temperatures above 373 K in vacuo or under an inert atmosphere induces the irreversible breakup of the triosmium cluster and the formation of mononuclear Os^{II} subcarbonyl complexes bound to the alumina surface.[37,41] *Psaro* et al.[37] found that 3 molecules of H_2 and 1.6 molecules of CO per cluster were evolved upon heating $[(\mu\text{-}H)Os_3(CO)_{10}\{\mu\text{-}OAl\}]$ in argon from 373 to 423 K; the oxidative addition of surface hydroxyl groups (as indicated by the H_2 evolution) occurs concomitantly with the fragmentation of the supported cluster. The H_2 evolution and X-ray photoelectron spectroscopy measurements[44a] are consistent with the formation of Os^{II} surface species. On the basis of the IR spectrum of the surface species (typically, three ν_{CO} bands are observed at 2120–2130, 2030–2050, and 1940–1970 cm^{-1}) and a comparison of the spectrum to those of molecular analogues such as $[Os(CO)_3X_2]_2$ (X = Cl, Br, I) and $[Os(CO)_2I_2]$, the surface composition was inferred to be a mixture of di- and tricarbonyl complexes covalently attached to the alumina surface by Os–O–Al bonds. On the basis of changes in the relative intensities of the IR bands, *Knözinger* and *Zhao*[41b] proposed that the proportions of the di- and tricarbonyl species depend on the severity of the thermal treatment and that the interconversion of the two subcarbonyl species is reversible:

$$[Os(CO)_3L\{O-Al\}_2] \rightleftharpoons [Os(CO)_2L\{O-Al\}_2] + CO \qquad (16)$$
$$L = \{O^{2\ominus}\} \text{ or } \{OH^{\ominus}\}$$

The structure of the mononuclear species resulting from the treatment of $[(\mu\text{-}H)Os_3(CO)_{10}\{\mu\text{-}OAl\}]$ at 423 K in vacuo for five hours has recently been elucidated by EXAFS spectroscopy[43b] (Table 4). The average M–CO coordination number was found to be 2.8, consistent with a mixture of osmium di- and tricarbonyl species. On the average, three oxygen back-scatterers at a distance of 0.217 nm are associated with each osmium complex, consistent with a hypothetical surface species $[Os(CO)_n\{O-Al\}_2\{HO-Al\}]$ (n = 2, 3). Back-scattering suggestive of direct Os–Os bonds was absent. A structural model of a tricarbonyl species situated in a threefold hollow of an alumina surface layer of close-packed $O^{2\ominus}$ ions and hydroxyl groups is presented in Figure 14; analysis of the relative intensities of the IR bands allows additional insight into the local geometry of the carbonyl ligands.[41b]

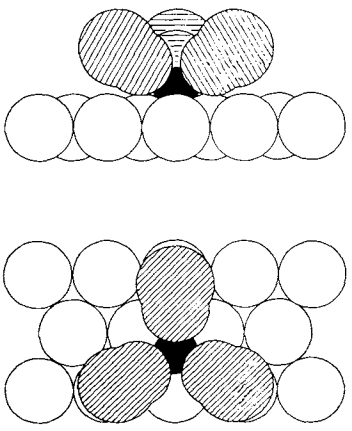

Fig. 14. Suggested model of an Os^{II} tricarbonyl site on a close-packed surface layer of γ-Al_2O_3. Top: Side view. Bottom: top view.

Similar surface complexes are formed by the decomposition of the surface-bound triosmium clusters on silica and magnesia, but there are differences in the surface organometallic chemistry. On silica there is some evidence for intermediate $[HOs(CO)_3\{O-Si\}\{HO-Si\}]$ species, which may be converted (with evolution of H_2) into $[Os(CO)_3\{O-Si\}_2]$ or $[Os(CO)_3\{O-Si\}_2\{HO-Si\}]$.[40] There is

also evidence, in contrast to observations made with alumina-supported samples, that vacuum treatment at temperatures above 523 K produces aggregates of supported Os metal.[40,43a] Also, only on silica has the apparent re-formation of the original surface-bound trinuclear cluster by treatment of the subcarbonyl complexes with CO + H_2O at elevated temperatures been observed.[40,43a] *Psaro* et al.[45b] observed that on magnesia the interconversion of the di- and tricarbonyl species was inhibited. Also, the formation of a unique Os^{II} dicarbonyl complex has been inferred;[45] the proposed structure of this species is illustrated in Figure 15. This highly stable complex forms by the oxidation of magnesia-supported triosmium clusters in the presence of O_2. Its formulation as $[Os(CO)_2\{O-Mg\}_4]^{2\ominus}$ was based on the agreement between the IR spectrum of the surface species and that of the molecular analogues $[Os(CO)_2X_4]^{2\ominus}$ (X = Cl, Br, I).

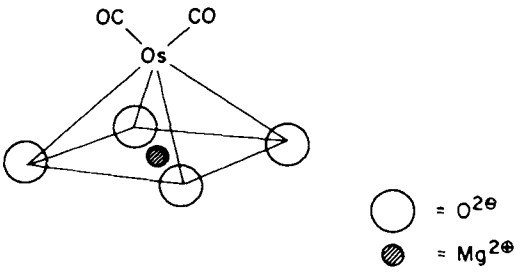

Fig. 15. Proposed structure of $[Os(CO)_2\{OMg\}_4]^{2\ominus}$ [45a].

Well-characterized Rh^I geminal dicarbonyl species are formed by the oxidative fragmentation of $[Rh_6(CO)_{16}]$ on η- and on γ-Al_2O_3.[56] $[Rh_6(CO)_{16}]$ interacts only weakly with the aluminas pretreated at 773 K. However, upon exposure of adsorbed $Rh_6(CO)_{16}$ to small quantities of water (sufficient to hydroxylate the surface completely) at 298 K, the cluster undergoes oxidative fragmentation to yield Rh^I geminal dicarbonyl species anchored to the alumina surface. At the same time, H_2 is evolved (0.5 molecules of H_2 per $Rh_6(CO)_{16}$ cluster). The dicarbonyl complex was suggested to be a 16-electron species, having a square-planar configuration with one covalent Rh–O bond and a single hydroxyl donor ligand. The intensity of the ν_{CO} bands assigned to the dicarbonyl species increased on subsequent exposure of the sample to 40 kPa of CO, which implies that other, totally decarbonylated Rh species (e.g., Rh^{III} ions) had also formed as a result of the fragmentation of $Rh_6(CO)_{16}$. *Basset* et al.[56b] suggested that a mixture of $[Rh(CO)_2\{O-Al\}\{HO-Al\}]$ and $[Rh(H)_2\{O-Al\}\{HO-Al\}]$ complexes form by the breakup of $Rh_6(CO)_{16}/Al_2O_3$ under these conditions, accounting for the observed H_2 evolution (less than required for formation of $Rh^I(CO)_2$ complexes alone) and the CO uptake. The facile fragmentation of $Rh_6(CO)_{16}/Al_2O_3$ is apparently initiated by the electrophilic attack of surface protons at the zerovalent metal centers.

The rhodium dicarbonyl complex decomposes upon treatment at 413 K in vacuo. The exact nature of the Rh species present after complete decarbonylation has not been established; however, the material was reported to chemisorb H_2 (1.2 H/Rh), suggestive of the formation of very small rhodium aggregates or, as *Basset* et al.[56b] proposed, rhodium hydride complexes. The reduction of the Rh^I subcarbonyl species may have occurred via the oxidation of a CO ligand:

$$Rh^I(CO)_2 \longrightarrow Rh^0 + CO + CO_2 \qquad (17)$$

Exposure of the decarbonylated sample to CO at room temperature resulted in the reappearance of the IR bands assigned to the $Rh^I(CO)_2$ species. The regeneration of $Rh_6(CO)_{16}/Al_2O_3$ from $[Rh(CO)_2\{O-Al\}\{HO-Al\}]$ by exposure to CO + H_2O at 298 K is discussed in Section 4.4.

$[Rh(CO)_2Cl]_2$ has been proposed as a molecular analogue of the $Rh^I(CO)_2$ species on alumina. Several researchers have investigated the chemisorbed dimer on alumina as a model for Rh^I geminal dicarbonyl sites produced by the oxidative fragmentation of supported Rh clusters and by the CO-initiated disruption of alumina-supported Rh crystallites (discussed in detail below).[55,56a,57] $[Rh(CO)_2Cl]_2$ chemisorbs on hydroxylated γ-Al_2O_3 by the following reaction:

$$[Rh(CO)_2Cl]_2 + 2\{Al-OH\} \longrightarrow 2[Rh(CO)_2\{O-Al\}] + 2HCl \qquad (18)$$

The IR spectrum of the resulting surface species has the characteristic two-band pattern typically assigned to $[Rh(CO)_2\{O-Al\}\{HO-Al\}]$. *Robbins*[55] used IR, solid-state ^{13}C NMR, and EPR spectroscopy to characterize the surface species. A strong doublet (2098 and 2026 cm^{-1}) was observed in the ν_{CO} IR spectrum, consistent with previous observations. The ^{13}C NMR spectrum (recorded with magic-angle spinning) displayed a doublet centered at $\delta = 180.9$ downfield of tetramethylsilane, indicating the presence of only terminal CO ligands; the splitting can be ascribed to ^{103}Rh–^{13}C coupling. Low-temperature EPR spectroscopy gave no evidence of paramagnetic Rh centers, consistent with the presence of d^8 Rh^I species.

The oxidative fragmentation of trirhenium clusters supported on γ-Al_2O_3 and on MgO has also been demonstrated. The products of the decomposition of $[H_2Re_3(CO)_{12}]^{\ominus}$ on magnesia have been characterized by IR, UV/VIS, and EXAFS spectroscopy.[29,49] The structure of the mononuclear complex $[Re(CO)_3\{O-Mg\}\{HO-Mg\}_2]$, formed by thermal decomposition of $[H_2Re_3(CO)_{12}]^{\ominus}$/MgO in H_2 or in He at 498 K, is illustrated in Figure 16. The subcarbonyl complex was found to be stable (as assessed by IR spectroscopy) at 523 K in H_2 or He.

Evidence for the formation of ensembles of mononuclear Os and Re complexes resulting from the oxidative fragmentation of the surface-bound $[(\mu\text{-}H)Os_3\{CO\}_{10}\{\mu\text{-}O-Al\}]$ and $[H_2Re_3(CO)_{12}]^{\ominus}$/MgO clusters, respectively, comes primarily from transmission electron microscopy (TEM) in the former case[44] and from the results of a structure-sensitive catalytic test reaction (cyclopropane hydrogenolysis)[58] and EXAFS[49] in the latter.

The existence of ensembles of three Os^{II} complexes resulting from the decomposition of $[(\mu\text{-}H)Os_3(CO)_{10}\{\mu\text{-}O-Al\}]$ was first suggested on the basis of electron micro-

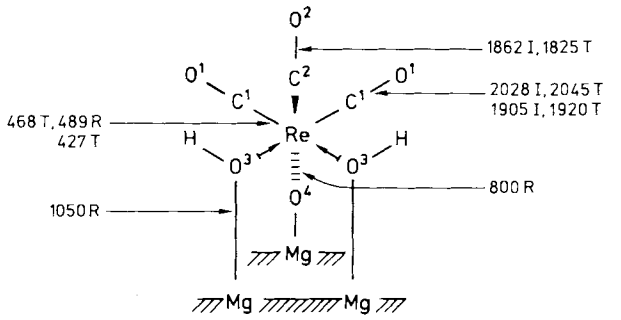

Fig. 16. Structure of rhenium tricarbonyl sites on magnesia as inferred from ν_{CO} IR (I), ν_{Re-O} Raman (R), and inelastic electron tunneling (T) data [29].

graphs of the supported osmium species showing extremely uniform scattering centers less than 1.0 nm in size.[44a] A more detailed high-resolution TEM study of the ensembles was reported by *Schwank* et al.[44b] who observed uniform scattering centers approximately 0.6 nm in size for a sample of $[(\mu\text{-H})Os_3(CO)_{10}\{\mu\text{-O-Al}\}]$ decomposed in argon at 473 K. Because of the size and uniformity of the scattering centers and their resistance to sintering under the electron beam, the surface species were inferred to be groupings of three divalent Os complexes. Further evidence of the presence of small groupings of osmium atoms derived from the oxidative fragmentation of triosmium clusters on alumina and on silica comes from attempts to model the IR spectra of the Os^{II} di- and tricarbonyl species. *Cook* et al.[43a] found that the mixed-isotope ($^{12}CO/^{13}CO$) vibrational spectra of these surface species could not be accounted for by isolated (vibrationally decoupled) $Os(CO)_3$ and $Os(CO)_2$ units. These researchers and others[59] have suggested the retention of direct Os–Os bonding within the supported ensembles. For example, *Collier* et al.[59] derived materials from $Os_3(CO)_{12}$ on alumina that were evidently present in an ill-defined aggregated form rather than as molecularly dispersed clusters.[37b] In this case, it was proposed that groupings containing roughly 12 Os atoms resulted from the decomposition of the supported organometallic precursor at 423 K in He; the ν_{CO} IR spectrum of the material was similar to the spectra reported by others[37,41] for mixtures of Os^{II} di- and tricarbonyl complexes on alumina, and the presence of these species on the surface (as part of a complex mixture) is considered likely.

The presence of groupings of three $[Re(CO)_3\{O-Mg\}\{HO-Mg\}_2]$ complexes following the oxidative fragmentation of $[H_2Re_3(CO)_{12}]^{\ominus}/MgO$ in H_2 or in He has been inferred from the catalytic properties of these materials.[58] Isolated $[Re(CO)_3\{O-Mg\}\{HO-Mg\}_2]$ complexes derived from $[HRe(CO)_5]$ chemisorbed on MgO (Section 4.1) are the precursors of catalysts for propene hydrogenation but not for cyclopropane hydrogenolysis. In contrast, materials derived from the decomposition of $[H_2Re_3(CO)_{12}]^{\ominus}/MgO$ (presumably to give trinuclear ensembles) were effective catalysts for both hydrogenation and hydrogenolysis. Hydrogenolysis is generally classed as a structure-sensitive catalytic reaction requiring the cooperative action of two or more neighboring metal centers.[60]

4.3.2. CO-Induced Fragmentation and Oxidation of Supported Metal Aggregates

The oxidative fragmentation of supported metal clusters, discussed above, further illustrates the pronounced tendency of surface hydroxyl groups to add oxidatively to zerovalent metal centers. A similar oxidative fragmentation process has been proposed to account for the formation of $Rh^{I}(CO)_2$ species when highly dispersed rhodium-on-alumina is brought into contact with CO at 298 K.[61] The breakup of small metal aggregates by CO is not surprising in light of the established tendency of CO to fragment high-nuclearity metal clusters in solution.[46] The CO-induced fragmentation and oxidation of supported Re[49] and Os[62] aggregates to give low-valent mononuclear subcarbonyl species have also been proposed. Obviously, the generation of metal carbonyl intermediates is plausible under such circumstances, and the surface organometallic chemistry described above indicates that these might readily react with surface hydroxyl groups to produce the oxide-bound metal carbonyl complexes typically observed.

Supported rhodium catalysts have received a great deal of attention recently; some of these materials are catalysts for the selective formation of oxygenated products in synthesis gas conversion.[63] The problem of the nature and origin of the dicarbonyl species typically observed following CO chemisorption on highly dispersed rhodium-on-alumina has a long history.[55]

van't Blik et al.[61] investigated a series of rhodium-on-alumina catalysts derived from $\gamma\text{-}Al_2O_3$ impregnated with aqueous $RhCl_3$. Employing temperature-programmed reduction and EPR and X-ray photoelectron spectroscopy, they established that more than 95% of the rhodium in a sample containing 0.57 wt% Rh was reduced to the zerovalent state by treatment with H_2 at 593 K for one hour. The supported Rh aggregates chemisorbed H_2 at 298 K to the extent of 1.7 H atoms/Rh atom, which implies that the rhodium was highly dispersed.

EXAFS spectroscopy was used to characterize the metallic rhodium structures. The average Rh–Rh coordination number was 3.7, which is suggestive of small rhodium entities (the Rh–Rh coordination number of $Rh_6(CO)_{16}$, for example, is 4), but the average Rh–Rh distance was close to that characterizing bulk rhodium metal. Backscattering due to oxygen atoms was observed, with the scatterers placed at an average distance from Rh of 0.274 nm with an average Rh–O coordination number of 1.9. The authors suggested that the oxygen scatterers were associated with the support, since the Rh–O distance was longer than would be expected for a rhodium oxide phase, and other evidence indicated the essentially complete reduction of the rhodium.

The interaction of CO with these ultradispersed rhodium aggregates illustrates the ability of CO to fragment small "naked" clusters of supported metal atoms. CO chemisorption measurements at 298 K gave a value of 1.9 CO molecules/Rh atom, suggesting the formation of a dicarbonyl species. The inference is supported by a comparison of the IR spectrum observed following adsorption of CO with that reported by *Basset* et al. for $[Rh(CO)_2\{O-Al\}\{HO-Al\}]$[56] and by others for geminal di-

carbonyl species derived from alumina-supported Rh;[64] the spectra are quite similar, with strong, sharp bands at approximately 2095 and 2025 cm^{-1}.

van't Blik et al.[61] provided additional characterization of the dicarbonyl surface species by EXAFS spectroscopy and X-ray photoelectron spectroscopy (XPS). By XPS the Rh $3d_{5/2}$ binding energy of a rhodium-on-alumina sample, reduced and exposed to CO in a pretreatment chamber integral with the spectrometer, was found to be equivalent, within experimental error, to that measured for $[Rh(CO)_2Cl]_2$, in which rhodium is in the +1 oxidation state. Analysis of data from in-situ EXAFS measurements indicated an average of 1.8 CO ligands per rhodium atom. Significantly, no Rh nearest neighbors were observed (at least at bonding distances); instead, oxygen backscatterers were identified at a distance of 0.212 nm, which implies oxidation of the rhodium. These results confirm that CO adsorption led to the oxidative fragmentation of the bare metal aggregates present initially.

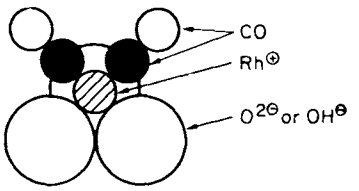

Fig. 17. Structure of Rh^I geminal dicarbonyl sites on γ-Al_2O_3 suggested by *van't Blik* et al. [61].

The structure suggested by *van't Blik* et al. for the geminal dicarbonyl species on alumina is shown in Figure 17. The Rh^I ions are proposed to exist as five-coordinate 18-electron species, associated with the threefold hollows of a close-packed surface layer of oxide ions and hydroxyl groups, in contrast to the 16-electron square-planar configuration suggested by *Robbins*[55] and *Basset* et al.[56] The structural inference of *van't Blik* et al. is based on the EXAFS finding of an average Rh–O coordination number of 3.1.

The interaction of CO with small alumina-supported rhodium aggregates has been monitored over a wide temperature range by in-situ IR spectroscopy.[65] At 77 K the spectra indicate only the presence of CO adsorbed on Rh crystallites. However, at temperatures greater than about 100 K the Rh^I dicarbonyl species is formed. These results suggest that, as expected, the oxidative fragmentation of the supported Rh aggregates is an activated process.

Robbins[55] suggested that the $Rh^I(CO)_2$ complexes remain clustered on the γ-Al_2O_3 surface following particle breakup, consistent with the formation of ensembles from the oxidative fragmentation of supported metal clusters. This view is confirmed in part by transmission electron micrographs showing 0.5–3.0-nm scattering centers after exposure of highly dispersed rhodium-on-alumina catalysts to CO.[64b,65a] However, apparently unlike the Os ensembles described above, the $Rh^I(CO)_2$ species are vibrationally decoupled.[66]

The formation of $Rh^I(CO)_2$ species by the exposure of ultradispersed alumina-supported rhodium aggregates to CO may be explained by considering the well-known tendency of CO to fragment high-nuclearity rhodium clusters in solution and the facile nature of the oxidative addition of hydroxyl groups to zerovalent metal centers. Although the detailed mechanism of the CO-induced oxidation and fragmentation of alumina-supported rhodium aggregates remains in doubt, the analogy to the oxidative fragmentation of $Rh_6(CO)_{16}/Al_2O_3$ is strong. The complementary paths taken by *Basset* and co-workers (who investigated molecular carbonyl clusters) and *van't Blik* and co-workers (who approached a problem in conventional heterogeneous catalysis) demonstrate the excellent consistency between the surface chemistry of conventionally derived supported metal catalysts and the surface organometallic chemistry of supported metal carbonyls. We believe that this work portends a rapid consolidation of the heretofore seemingly disparate fields of surface organometallic chemistry and classical heterogeneous catalysis.

4.4. Reductive Carbonylation of Supported Metal Ions

The oxidative fragmentation of supported molecular metal clusters characterizes the surface organometallic chemistry in the absence of a stabilizing CO atmosphere. However, especially on basic metal oxide surfaces, the low-valent mononuclear metal complexes formed by cluster fragmentation can be reductively carbonylated to regenerate supported molecular clusters, and sometimes this chemistry leads to simple, efficient cluster syntheses.[45c,67,70] The molecular clusters formed usually do not reflect the nuclearity of the original cluster precursor, which suggests a high mobility of the surface reaction intermediates. Generally it appears that the thermodynamically favored molecular cluster is produced; the precise nature and state of aggregation of the precursor complexes appear to be of little importance. Consistent with this view, it was established that surface-bound molecular clusters of Os and Ru are prepared in high yield by the reductive carbonylation of surface structures formed by aqueous impregnation of magnesia with H_2OsCl_6 and $RuCl_3$, respectively.[67] There are clear parallels between reductive carbonylation in basic solution and on basic metal oxide surfaces; in both cases, redox condensation reactions are expected to play a central role. This chemistry is illustrated below with a focus on the synthesis of supported molecular clusters from covalently bound metal carbonyl complexes and supported metal halide salts.

$Rh_6(CO)_{16}/Al_2O_3$ is regenerated from the species $[Rh(CO)_2\{O-Al\}\{HO-Al\}]$ by treatment with $CO + H_2O$ at 298 K and atmospheric pressure.[56] Under optimum conditions, the yield of $Rh_6(CO)_{16}$ is high; the molecular cluster can be extracted from the surface with chloroform. However, when the partial pressure of CO is less than ca. 20 kPa, large Rh crystallites form, as observed by electron microscopy. It was inferred[56b] that $[Rh(CO)_4]^{\ominus}$, a strong nucleophile in typical solvents, was possibly the key intermediate in the reductive carbonylation process. The complex process was suggested to be initiated by the nucleophilic attack of adsorbed H_2O on $[Rh(CO)_2\{O-Al\}\{HO-Al\}]$, generating mobile mononuclear carbonylrhodate ions:

$$[Rh(CO)_2\{O-Al\}\{HO-Al\}] + H_2O \xrightarrow{CO} [Rh(CO)_4]^{\ominus} + \{H^{\oplus}\} + 2\{HO-Al\} + CO_2 \quad (19)$$

Redox condensation to form adsorbed $Rh_6(CO)_{16}$ could then plausibly occur following nucleophilic attack of $[Rh(CO)_4]^{\ominus}$ on a $[Rh(CO)_2\{O-Al\}\{HO-Al\}]$ complex. These hypothetical steps are consistent with metal-metal bond formation being initiated by the generation of carbonyl complexes in different oxidation states.

The reductive carbonylation of Rh ions in the supercages of large-pore zeolites has also been reported.[68] Polynuclear carbonyls are formed by the treatment of Rh^{III} ions in hydrated zeolite Y with $CO + H_2$ at 298 K; molecular Rh carbonyl clusters in zeolite Y are apparently stable at 523 K and 3 MPa ($CO : H_2 = 1 : 2$).

Similar chemistry was observed under more severe conditions by *Deeba* et al.,[45a] who investigated the behavior of materials derived from $Os_3(CO)_{12}$ adsorbed on MgO pretreated at 473 K. The basicity of MgO pretreated in this manner is severely reduced by strongly adsorbed CO_2 (surface carbonates). $[(\mu\text{-}H)Os_3(CO)_{10}\{\mu\text{-}OMg\}]$ was inferred to be the predominant surface species present initially. When the supported triosmium cluster was exposed to air under ambient conditions, a mononuclear surface species formulated as $[Os(CO)_2\{O-Mg\}_4]^{2\ominus}$ (cf. Fig. 15) was formed (see Section 4.3.1). When a sample initially incorporating this surface species was used as a catalyst for CO hydrogenation (573 K, 0.7 MPa, $CO : H_2 = 1 : 4$), molecular osmium carbonyl clusters formed, as evidenced by the IR spectrum of the used catalyst; these clusters are now recognized to be $[Os_{10}C(CO)_{24}]^{2\ominus}$.[26] The decaosmium cluster was evidently produced by reductive carbonylation of the Os^{II} complexes originally present, and this process likely coincided with the development of strong surface basicity under the synthesis conditions. This hypothesis is confirmed by the formation of $[Os_{10}C(CO)_{24}]^{2\ominus}$ from $[H_2Os(CO)_4]$/MgO (Section 4.2).

$[Os_{10}C(CO)_{24}]^{2\ominus}$/MgO has also been synthesized efficiently from MgO impregnated with aqueous H_2OsCl_6 and exposed to CO or $CO + H_2$ at 548 K and 100 kPa.[67] The reactions were monitored by in-situ IR spectroscopy, and Os^{II} subcarbonyls on MgO were observed as intermediate products. By ion exchange with $(Ph_3P)_2NCl$ in acetone, $[(Ph_3P)_2N]_2[Os_{10}C(CO)_{24}]$ was extracted from samples that had been treated with $CO + H_2$ at 548 K and 100 kPa for 5 h; 60–70% of the Os could be removed in this manner. Confirmation of the surface structure was obtained from UV/VIS and EXAFS spectroscopy; and electron microscopy of samples prepared by the surface synthesis gave no evidence of scattering centers larger than 1.0 nm.[69] The surface-mediated synthesis of $[Os_{10}C(CO)_{24}]^{2\ominus}$ and the analogous preparation of $[Ru_6C(CO)_{16}]^{2\ominus}$ from $RuCl_3$-on-magnesia[67] represent the first syntheses of high-nuclearity Ru and Os clusters by reductive carbonylation of metal salts.

In summary, basic metal oxide supports, incorporating highly nucleophilic surface hydroxyl groups, facilitate the formation of molecular metal carbonyl clusters by reductive carbonylation. $[Os_{10}C(CO)_{24}]^{2\ominus}$ and $[Ru_6C(CO)_{16}]^{2\ominus}$/MgO are even produced (in low yields) from the supported metals under conditions of catalytic CO hydrogenation,[67] suggesting that these molecular metal clusters may be the thermodynamically favored surface species under these extreme conditions. Even when the surface-bound molecular clusters are not the most stable surface species, their likely presence in small concentrations (especially on highly ba-

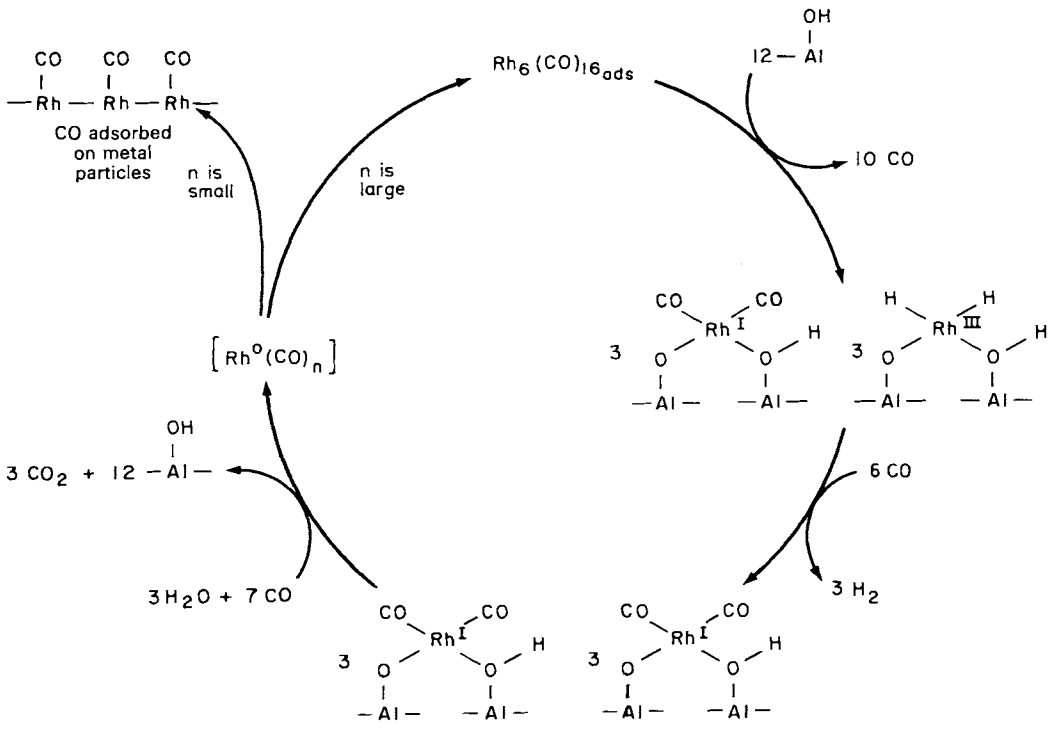

Fig. 18. Catalytic cycle for the water-gas shift reaction ($CO + H_2O \rightleftharpoons CO_2 + H_2$), which is proposed to involve only molecular rhodium complexes on alumina when the partial pressure of CO is maintained in excess of 20 kPa and the CO/H_2O ratio is high [56b].

sic supports like magnesia) suggests a heretofore unexpected role of molecular metal clusters in catalysis of carbonylation reactions. A catalytic cycle (Fig. 18) has been proposed by *Basset* et al. for the water gas shift reaction involving molecular Rh carbonyls on alumina under mild conditions.[56b] Key steps in the hypothetical process have been verified, including the oxidative fragmentation of $Rh_6(CO)_{16}/Al_2O_3$ and its regeneration by the reductive carbonylation of $[Rh(CO)_2\{O-Al\}\{HO-Al\}]$ complexes.

5. Summary and Outlook

The subject of "molecular" chemistry of transition-metal carbonyls on metal oxide surfaces has developed dramatically in just the preceding several years. The chemistry is consistent with that of molecular metal carbonyls in solution, being influenced strongly by the nature of the support, especially the acid-base properties. Some syntheses of organometallic compounds on supports are simpler and more efficient than conventional solution syntheses; we anticipate a rapid growth in the application of surface-mediated organometallic synthesis.[45c, 67, 70] Some "molecular" organometallic species on surfaces are stable even at temperatures approaching 600 K and some have demonstrated catalytic activity. The understanding of this chemistry is developing rapidly, benefiting from surface characterization techniques such as IR, NMR, and EXAFS spectroscopy. There is a compelling opportunity to exploit organometallic chemistry for the creation of materials with novel surface structures and new catalytic properties.[71] These novel catalysts may be expected to include (1) stable surface-bound metal complexes and clusters; (2) unique supported metal aggregates with framework nuclearities the same as those of precursor metal clusters; and (3) ensembles of metal ions on surfaces, with nuclearities tailored to meet the requirements for particular structure-sensitive reactions.

The work was supported by the National Science Foundation (H. H. L. and B. C. G., Grants CBT-8605699 and INT-8304494) and by the Deutsche Forschungsgemeinschaft (H. K.).

Received: March 12, 1987;
revised: December 10, 1987 [A 688 IE]
German version: *Angew. Chem. 100* (1988) 1162

[1] H. P. Boehm, H. Knözinger in J. R. Anderson, M. Boudart (Eds.): *Catalysis - Science and Technology, Vol. 4*, Springer, Berlin 1983, p. 39.
[2] H. Knözinger in P. Schuster, G. Zundel, C. Sandorfy (Eds.): *The Hydrogen Bond*, North Holland, Amsterdam 1976, p. 1263.
[3] H. Winde, P. Fink, A. Kohler, *Z. Chem. 17* (1977) 41.
[4] a) B. A. Morrow, A. Cody, *J. Phys. Chem. 79* (1975) 761; b) F. Boccuzzi, S. Coluccia, G. Ghiotti, C. Morterra, A. Zecchina, *ibid. 82* (1978) 1298.
[5] H. Knözinger, W. Stählin, *Prog. Colloid Polym. Sci. 67* (1980) 33.
[6] H. Knözinger, P. Ratnasamy, *Catal. Rev. Sci. Eng. 17* (1978) 31.
[7] H. Knözinger, *Adv. Catal. 25* (1976) 184.
[8] K. Tanabe: *Solid Acids and Bases*, Academic Press, London 1969.
[9] P. O. Scokart, P. G. Rouxhet, *J. Colloid Interface Sci. 86* (1982) 96.
[10] H. Jeziorowski, H. Knözinger, W. Meye, H. D. Müller, *J. Chem. Soc. Faraday Trans. 1 69* (1973) 2744.
[11] H. Knözinger, B. Stübner, *J. Phys. Chem. 82* (1978) 1526.
[12] E. A. Colbourn, W. C. Mackrodt, *Surf. Sci. 143* (1984) 391.
[13] P. J. Anderson, R. F. Horlock, J. F. Oliver, *Trans. Faraday Soc. 61* (1965) 2754.
[14] E. Garrone, F. S. Stone, *Proc. Int. Congr. Catal. 8th 3* (1984) 441.
[15] a) R. Martinez, M. A. Barteau, *Langmuir 1* (1985) 684; b) R. N. Spitz, J. E. Barton, M. A. Barteau, R. H. Staley, A. W. Sleight, *J. Phys. Chem. 90* (1986) 4067.
[16] A. Zecchina, M. G. Lofthouse, F. S. Stone, *J. Chem. Soc. Faraday Trans. 1 71* (1975) 1476.
[17] S. Coluccia, A. M. Deane, A. J. Tench, *J. Chem. Soc. Faraday Trans. 1 74* (1978) 2913.
[18] a) J. H. Lunsford, J. P. Payne, *J. Chem. Phys. 44* (1966) 1492; b) A. Zecchina, F. S. Stone, *J. Chem. Soc. Faraday Trans. 1 74* (1978) 2278; c) R. M. Morris, K. J. Klabunde, *J. Am. Chem. Soc. 105* (1983) 2633.
[19] a) J. L. Bilhou, A. Theolier, A. K. Smith, J. M. Basset, *J. Mol. Catal. 3* (1977/78) 245; b) A. Kazusaka, R. F. Howe, *ibid. 9* (1980) 183; c) *9* (1980) 199.
[20] C. Tessier-Youngs, F. Correa, D. Ploch, R. L. Burwell, Jr., D. F. Shriver, *Organometallics 2* (1983) 898.
[21] R. L. Schneider, R. F. Howe, K. L. Watters, *Inorg. Chem. 23* (1984) 4593.
[22] a) E. Guglielminotti, A. Zecchina, *J. Mol. Catal. 24* (1984) 331; b) E. Guglielminotti, A. Zecchina, F. Buccuzzi, E. Borello in J. Bourdon (Ed.): *Growth and Properties of Metal Clusters*, Elsevier, Amsterdam 1980, p. 165; c) E. Guglielminotti, A. Zecchina, *J. Chim. Phys. Phys. Chim. Biol. 78* (1981) 891.
[23] a) F. Hugues, J. M. Basset, Y. Ben Taarit, A. Choplin, M. Primet, D. Rojas, A. K. Smith, *J. Am. Chem. Soc. 104* (1982) 7020; b) B. E. Hanson, J. J. Bergmeister III, J. T. Petty, M. C. Connaway, *Inorg. Chem. 25* (1986) 3089; c) W. Hieber, *Adv. Organomet. Chem. 8* (1970) 1.
[24] R. G. Pearson, *Chem. Rev. 85* (1985) 41.
[25] a) T. R. Krause, M. E. Davies, J. Lieto, B. C. Gates, *J. Catal. 94* (1985) 195; b) J. R. Budge, J. P. Scott, B. C. Gates, *J. Chem. Soc. Chem. Commun. 1983*, 342; c) J. P. Scott, J. R. Budge, A. L. Rheingold, B. C. Gates, *J. Am. Chem. Soc. 109* (1987) 7736; d) R. Pierantozzi, E. G. Valagene, A. F. Nordquist, P. N. Dyer, *J. Mol. Catal. 21* (1983) 189.
[26] H. H. Lamb, B. C. Gates, *J. Am. Chem. Soc. 108* (1986) 81.
[27] a) H. H. Lamb, B. C. Gates, to be published; b) L. C. Hasselbring, J. Puga, C. Dybowski, B. C. Gates, *J. Phys. Chem. 92* (1988) 3934; c) H. H. Lamb, T. R. Krause, B. C. Gates, *Proc. Int. Congr. Catal. 9th, Vol. 3* (Calgary 1988), The American Institute of Canada, Ottawa 1988, p. 1378.
[28] H. H. Lamb, M. D. Nagle, B. C. Gates, to be published.
[29] P. S. Kirlin, F. A. DeThomas, J. W. Bailey, H. S. Gold, C. Dybowski, B. C. Gates, *J. Phys. Chem. 90* (1986) 4882.
[30] B. F. G. Johnson, J. Lewis, P. R. Raithby, G. M. Sheldrick, K. Wong, M. McPartlin, *J. Chem. Soc. Dalton Trans. 1978*, 673.
[31] M. Y. Darensbourg, P. Jimenez, J. R. Sackett, J. M. Hanckel, R. L. Kump, *J. Am. Chem. Soc. 104* (1982) 1521.
[32] a) S. W. Ulmer, P. M. Skarstad, J. M. Burlitch, R. E. Hughes, *J. Am. Chem. Soc. 95* (1973) 4469; b) G. B. McVicker, *Inorg. Chem. 14* (1975) 2087.
[33] R. B. Peterson, J. J. Stezowski, Che'ng Wan, J. M. Burlitch, R. E. Hughes, *J. Am. Chem. Soc. 93* (1971) 3532.
[34] W. F. Edgell in M. Szwarc (Ed.): *Ions and Ion Pairs in Organic Reactions Vol. 1*, Wiley, New York 1972, p. 153.
[35] F. Correa, R. Nakamura, R. E. Stimson, R. L. Burwell, Jr., D. F. Shriver, *J. Am. Chem. Soc. 102* (1980) 5112.
[36] R. L. Burwell, Jr., *J. Catal. 86* (1984) 301.
[37] a) R. Psaro, R. Ugo, G. M. Zanderighi, B. Besson, A. K. Smith, J. M. Basset, *J. Organomet. Chem. 213* (1981) 215; b) R. Psaro, R. Ugo in B. C. Gates, L. Guczi, H. Knözinger (Eds.): *Metal Clusters in Catalysis*, Elsevier, Amsterdam 1986, p. 427.
[38] L. D'Ornelas, A. Choplin, J. M. Basset, L.-Y. Hsu, S. Shore, *Nouv. J. Chim. 9* (1985) 155.
[39] H. Vahrenkamp, *Adv. Organomet. Chem. 22* (1983) 169.
[40] J. M. Basset, B. Besson, A. Choplin, F. Hugues, M. Leconte, D. Rojas, A. K. Smith, A. Theolier, Y. Chauvin, D. Commereuc, R. Psaro, R. Ugo, G. M. Zanderighi, *Fundam. Res. Homogeneous Catal. 4* (1984) 19.
[41] a) M. Deeba, B. C. Gates, *J. Catal. 67* (1981) 303; b) H. Knözinger, Y. Zhao, *ibid. 71* (1981) 337.
[42] M. Deeba, B. J. Streusand, G. L. Schrader, B. C. Gates, *J. Catal. 69* (1981) 218.
[43] a) S. L. Cook, J. Evans, G. S. McNulty, G. N. Greaves, *J. Chem. Soc. Dalton Trans. 1986*, 7; b) F. B. M. Duivenvoorden, D. C. Koningsberger, Y. S. Uh, B. C. Gates, *J. Am. Chem. Soc. 108* (1986) 6254; c) V. D. Alexiev, N. Binsted, J. Evans, G. N. Greaves, R. J. Price, *J. Chem. Soc. Chem. Commun. 1987*, 395.
[44] a) H. Knözinger, Y. Zhao, B. Tesche, R. Barth, R. Epstein, B. C. Gates, J. P. Scott, *Faraday Discuss. Chem. Soc. 72* (1981) 53; b) J. Schwank, L. F. Allard, M. Deeba, B. C. Gates, *J. Catal. 84* (1983) 27; c) B. Tesche, E. Zeitler, E. A. Delgado, H. Knözinger, *Proc. 40th Electron Microsc. Soc. Am. Meeting*, Washington 1982, p. 658.
[45] a) M. Deeba, J. P. Scott, R. Barth, B. C. Gates, *J. Catal. 71* (1981) 373; b) R. Psaro, C. Dossi, R. Ugo, *J. Mol. Catal. 21* (1983) 331; c) A. S. Fung, P. A. Tooley, M. J. Kelley, B. C. Gates, *J. Chem. Soc. Chem. Commun. 1988*, 371.

[46] P. Chini, G. Longoni, V. G. Albano, *Adv. Organomet. Chem. 14* (1976) 285.
[47] a) A. Brenner, R. L. Burwell, Jr., *J. Am. Chem. Soc. 97* (1975) 2565; b) R. L. Burwell, Jr., A. Brenner in B. Delmon, G. Jannes (Eds.): *Catalysis: Heterogeneous and Homogeneous, 1974*, Elsevier, Amsterdam 1975, p. 157; c) A. Brenner, R. L. Burwell, Jr., *J. Catal. 52* (1978) 353; d) R. G. Bowman, R. L. Burwell, Jr., *ibid. 63* (1980) 463; e) D. A. Hucul, A. Brenner, *J. Phys. Chem. 85* (1981) 496.
[48] A. Brenner in M. Moskovits (Ed.): *Metal Clusters*, Wiley, New York 1986, p. 249; and references cited therein.
[49] P. S. Kirlin, F. B. M. van Zon, D. C. Koningsberger, B. C. Gates, to be published.
[50] L. Markó, A. Vizi-Orosz in B. C. Gates, L. Guczi, H. Knözinger (Eds.): *Metal Clusters in Catalysis*, Elsevier, Amsterdam 1986, p. 89.
[51] H. H. Lamb, B. C. Gates, to be published.
[52] J. C. Bricker, C. C. Nagel, S. G. Shore, *J. Am. Chem. Soc. 104* (1982) 1444.
[53] T. C. Hayward, J. R. Shapley, *Inorg. Chem. 21* (1982) 3816.
[54] J. N. Nicholls, D. H. Farrar, P. F. Jackson, B. F. G. Johnson, J. Lewis, *J. Chem. Soc. Dalton Trans. 1982*, 1395.
[55] J. L. Robbins, *J. Phys. Chem. 90* (1986) 3381.
[56] a) A. K. Smith, F. Hugues, A. Theolier, J. M. Basset, R. Ugo, G. M. Zanderighi, J. L. Bilhou, V. Bilhou-Bougnol, W. F. Graydon, *Inorg. Chem. 18* (1979) 3104; b) J. M. Basset, A. Theolier, D. Commereuc, Y. Chauvin, *J. Organomet. Chem. 279* (1985) 147.
[57] W. M. Bowser, W. H. Weinberg, *J. Am. Chem. Soc. 103* (1981) 1453.
[58] P. S. Kirlin, B. C. Gates, *Nature (London) 325* (1987) 38.
[59] G. Collier, D. J. Hunt, S. D. Jackson, R. B. Moyes, I. A. Pickering, P. B. Wells, *J. Catal. 80* (1983) 154.
[60] a) M. Boudart, *Adv. Catal. 20* (1969) 153; b) G. A. Somorjai, J. Carrazza, *Ind. Eng. Chem. Fundam. 25* (1986) 63.
[61] H. F. J. van't Blik, J. B. A. D. van Zon, T. Huizinga, J. C. Vis, D. C. Koningsberger, R. Prins, *J. Am. Chem. Soc. 107* (1985) 3139.
[62] E. A. Delgado, B. Tesche, H. Knözinger, to be published.
[63] a) M. Ichikawa, *Bull. Chem. Soc. Jpn. 51* (1978) 2273; b) J. R. Katzer, A. W. Sleight, P. Gajardo, J. B. Michel, E. F. Gleason, S. McMillan, *Faraday Discuss. Chem. Soc. 72* (1981) 121; c) F. Solymosi, I. Tombacz, M. Kocsis, *J. Catal. 75* (1982) 78.
[64] a) D. J. C. Yates, L. L. Murrell, E. B. Prestridge, *J. Catal. 57* (1979) 41; b) D. J. C. Yates, L. L. Murrell, E. B. Prestridge in J. Bourdon (Ed.): *Growth and Properties of Metal Clusters*, Elsevier, Amsterdam 1980, p. 137; c) R. R. Cavanagh, J. T. Yates, *J. Chem. Phys. 74* (1981) 4150; d) C. A. Rice, S. D. Worley, C. W. Curtis, J. A. Guin, A. R. Tarrer, *ibid. 74* (1981) 6487.
[65] a) M. Primet, *J. Chem. Soc. Faraday Trans. 1 74* (1978) 2570; b) M. Zaki, G. Kunzmann, B. C. Gates, H. Knözinger, *J. Phys. Chem. 91* (1987) 1486.
[66] J. T. Yates, K. Kolasinski, *J. Chem. Phys. 79* (1983) 1026.
[67] H. H. Lamb, T. R. Krause, B. C. Gates, *J. Chem. Soc. Chem. Commun. 1986*, 821.
[68] P. Gallezot in M. Moskovits (Ed.): *Metal Clusters*, Wiley, New York 1986, p. 219.
[69] H. H. Lamb, D. C. Koningsberger, B. C. Gates, to be published.
[70] H. H. Lamb, P. A. Tooley, S. A. Fung, J. Puga, T. R. Krause, M. J. Kelley, B. C. Gates, to be published.
[71] Y. Iwasawa, B. C. Gates, *Hyomen (Surface) (Japan)*, in press.

Molecular Mechanisms of Biomineralization in the Formation of Calcified Shells

By Gottfried Krampitz* and Gabriele Graser

Biological calcification processes (calcification, biomineralization) occur in microorganisms, in plants, and in the animal kingdom. Under physiological conditions, the results of mineral deposition in biological systems can be seen in the formation of bones, teeth, mollusc shells, egg shells, pearls, and corals. There are, however, also pathological aspects of biomineralization, including the formation of kidney stones (renal calculus), gallstones (biliary calculus), intravasal depositions (atherosclerosis, calcinosis). Abnormal mineralization processes (demineralization) can be found, e.g., in bone resorption (osteoporosis) and caries. A detailed knowledge of the molecular mechanisms of biomineralization could help considerably toward solving some of the problems encountered in orthopedics, urology, cardiovascular science, dentistry and veterinary medicine. Research in biomineralization is always interdisciplinary. In this article the typical interactions between mineral phase and organic matrix will be demonstrated using two examples—mollusc shells and egg shells.

1. Introduction

Biological calcification processes are of wide occurrence in nature. They occur in microorganisms, in plants, in the animal kingdom and in humans. The results of mineral deposition under physiological conditions can be seen in the formation of bones, teeth, shell material (mollusc shells, egg shells), coccoliths, corals, pearls, etc. The variety of biomineralizates can best be expressed by the fact that, alone, approximately 128000 species of molluscs exist. The majority of them (Conchifera) produce shells and capsules from $CaCO_3$ having different sizes, shapes and color patterns.[1] There are, however, also pathological aspects of biomineralization, e.g. the formation of body stones (kidney, gall-bladder), atherosclerosis. Processes of demineralization (bone resorption, caries) must be regarded as abnormal biomineralization processes.

Biomineralization can be defined as a sequence of events whereby living organisms produce minerals which crystallize and add together to form hard pieces. In spite of their various forms and functions all biomineralizates are formed according to the same principle. The hard pieces are composed of organic and inorganic substances. The organic components are, as a rule, proteins (e.g. collagen, dentin, elastin, conchiolin). Proteoglycans and lipids have been detected, but their function is still unclear. The inorganic (mineralized) components can be found in crystallized form. Although at least twenty different skeletal minerals have thus far been reported to exist in living organisms,[2,3] only four are generally found: aragonite, calcite, hydroxyapatite, and opal.[3] The remaining kinds of minerals are either trace constituents or occur only in a few special species.[4]

Most of the research to date in the field of biomineralization can be classified under the following headings:

1. Morphological studies of the complex relationships between mineral phase and organic macromolecules (matrix).
2. Investigations on the chemical composition of mineralized tissue and minerals.
3. Exploration of ion-transport mechanisms in cellular systems and of mineral deposition on organic substrates.[5]

Despite numerous and diverse studies, our knowledge of the molecular mechanisms of biological calcification is still superficial. Surprisingly, comparatively little is known about the synthesis of organic macromolecules that participate in the processes of biomineralization. The various aspects and problems of biomineralization can be solved and explained only by interdisciplinary cooperation (chemistry, biochemistry, molecular genetics, physical chemistry, physics, biophysics, mineralogy, crystallography, geology, orthopedics, dentistry, cardiovascular science, urology, veterinary medicine, agricultural sciences, nutrition etc.).

In the following an outline is given—using the examples of mollusc shells and egg shells—of the state of our knowledge of the structure and chemical composition of biomineralizates and of our concept of the interactions between organic phase and inorganic crystals. Particular emphasis is placed on the properties of macromolecules which are involved in the formation of biomineralizates and on their functions and their ability to bind calcium.

2. Mechanisms of Biomineralization

Our concepts of biological calcification are based on the assumption that an organic matrix determines the mineralogical and crystallographic properties of the inorganic phase. Nevertheless, opinions on the types and functions of a matrix are divided. The matrix hypothesis implies that

[*] Prof. Dr. G. Krampitz, Dr. G. Graser
Abteilung für Biochemie, Institut für Anatomie,
Physiologie und Hygiene der Haustiere, Universität Bonn
Katzenburgweg 7-9, D-5300 Bonn 1 (FRG)

processes of epitaxis[*] play a predominant role, while the compartment hypothesis regards the formation of ordered matrix compartments as being crucial.

2.1. Matrix Hypothesis

This hypothesis (cf. Fig. 1) has been developed from studies on calcified tissues. It was observed that the nucleation and orientated growth of a substance can take

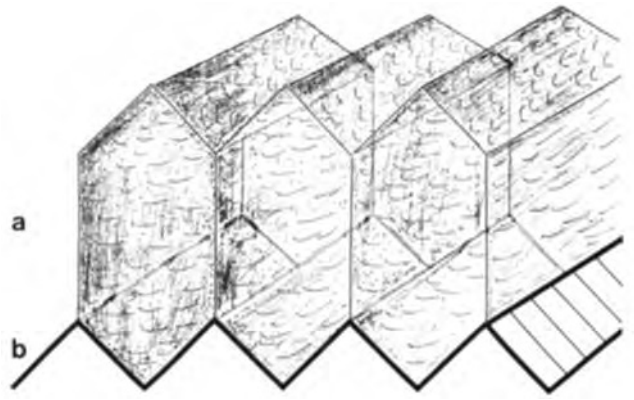

Fig. 1. The matrix hypothesis (simplified model). By its structure, the reactive matrix (b) of organic material determines the form and size of the deposited inorganic crystals (a). In this way a regular growth of the crystals is achieved.

place on the surface of another substance if both have some crystallographic parameter in common. The structure of the substrate-phase dictates the orientation of the superimposed phase. Applied to biomineralization, the organic matrix plays the role of the substrate, i.e. the directing matrix. Nucleation and growth of the inorganic biocrystals take place on the surface of the organic support. The lattice of the nucleate of the growing phase should be dependent on the atomic distances within active centers of the organic matrix. The size and, to some extent, the shape of the growing biocrystals are determined by the matrix. There is no clear understanding about the nature of the functional groups which induce the nucleation, but the simplicity of the matrix hypothesis is attractive.[7] This hypothesis is supported by results obtained from studies on mollusc shells:[8]

1. From the behavior of transplants one could derive that there are calcite-specific and aragonite-specific (conchiolin)matrices within this group of invertebrates.[9, 10]
2. There is a dependence of the orthorhombic *b*-axis in plates of mother of pearl on the direction of the individual fibrils of the conchiolin "membranes" of pelecypodes[11] and a dependence of the *a*-axis on the direction of the "trabecular cords" in the "membranes" of *Nautilus pompilus*.[12, 13]

[*] Epitaxis is defined as a process by which two chemically and/or structurally different crystalline phases grow together. An epitactic system consists of a host crystal (substrate), on which a secondary crystal has developed [6].

2.2. Compartment Hypothesis

Column-like macroprisms of the exterior side of the prism layer of *Pinna nobilis* and *Mytilis edulis* are composed of crystallites which are completely covered with an organic layer.[14, 16] This led to the idea of a hollow space formed by the organic substance ("compartment"),[7, 9] in which the crystallite is formed and in which its habit is shaped by the surrounding organic envelopes. The compartment (cf. Fig. 2) hypothesis negates the existence of reactive matrices.[9]

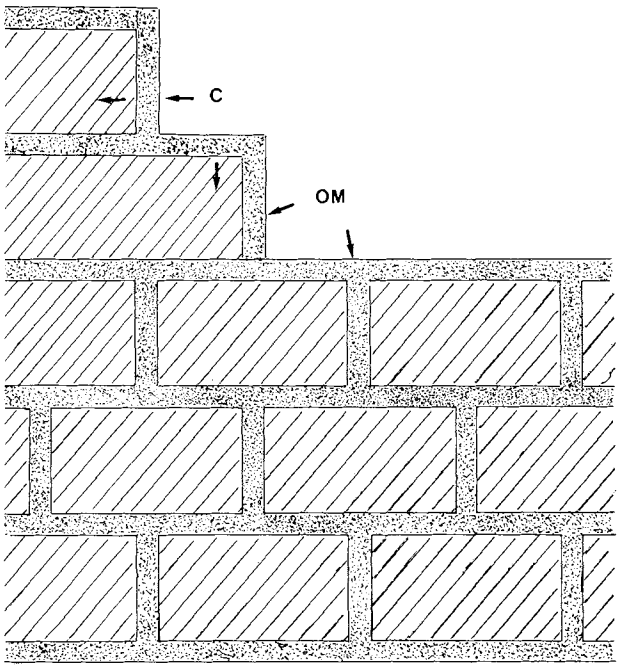

Fig. 2. Compartment hypothesis (simplified model). The mode of synthesis of this type of biomineralizate is also referred to as the "brick-wall" model in which the crystals (C) are compared with bricks and the organic material (OM) with mortar. A reactive matrix is not assumed. The growth of the crystals is irregular, as, e.g. in mother of pearl.

A decision as to whether or not the matrix or the compartment hypothesis applies in invertebrates or in vertebrates or whether both hypotheses must be taken into account has been impossible to make as yet.

2.3. Role of Cells in Biomineralization

A discussion of the cellular aspects of biomineralization immediately poses the question of which evolutionary processes have led to this biological phenomenon. The following points should be considered: The calcium ion is one of the pharmacologically most significant ions. All normal cellular processes can be interrupted by unphysiological $Ca^{2\oplus}$-concentrations. Hence, the intracellular calcium ion concentration is very carefully adjusted in the range of 10^{-6} to 10^{-7} mol/L, and therefore a surprisingly large number of cells deposit intracellular minerals which are rich in calcium.

Since $Ca^{2\oplus}$ in concentrations $> 10^{-6}$ mol/L has a toxic effect on living cells, these ions must be eliminated. There are several possibilities: on conversion from the ionized form into a non-ionized Ca-compound, insoluble substances are often formed. These can either be precipitated within the cell and its compartments or leave the cell as crystals. In other cases the precipitation occurs extracellularly (cf. Fig. 3). The appearance of extracellularly deposited Ca-compounds is nothing else but a detoxification process. It is therefore not surprising that, e.g., in mollusc shells, but also in avian egg shells, various metal-compounds can be detected apart from $CaCO_3$, albeit in trace quantities.[17] It cannot be ignored that the calcification products have originally been formed extracellularly. Moreover they represent a protection for single cells (coccoliths) and for molluscs. The formation of egg shells can be seen as an elimination mechanism for $Ca^{2\oplus}$ and concomitantly as a protection for the vulnerable egg. The evolution from exoskeleton to endoskeleton is then "only" a step from a stiff armor to a somewhat more elastic skeleton of the vertebrates.[17]

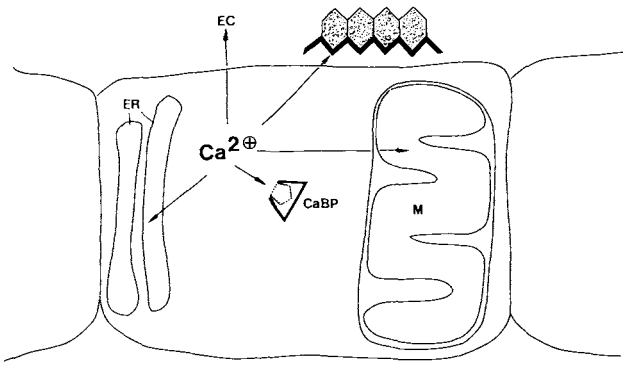

Fig. 3. Biomineralization as cellular detoxifying process. In the cytoplasm the $Ca^{2\oplus}$ concentration is precisely regulated. An excess of $Ca^{2\oplus}$ can be removed intracellulary by Ca-binding proteins (CaBP), storage in mitochondria (M) and in the endoplasmic reticulum (ER), as well as by transport into the extracellular compartment (EC). Insoluble Ca-compounds can crystallize out extracellularly if a suitable matrix is secreted concomitantly.

The contemporary processes of calcification take place in mineral-producing cells. Calcium phosphates—mainly as "inorganic calcium phosphate" $Ca_9(PO_4)_6$—are synthesized in the inner compartment of mitochondria. Amorphous calcium phosphate normally changes autocatalytically into hydroxyapatite if it is not stabilized by $Mg^{2\oplus}$ and ATP within the cells. Stabilized amorphous calcium phosphate is said to be able to cross intracellular membranes in order to serve at other sites of the cell or its surface as a precursor for larger and more stable mineral forms (hydroxyapatite).[18-20]

In unicellular organisms, e.g. protozoa *(Spirostonum ambiguum)*, the formation of $CaCO_3$ is very closely associated with the function of the vacuoles of the Golgi apparatus.[21] In the Golgi apparatus, globular structures (spherical clusters) having a diameter of 0.1 to 1.0 μm are formed, which are then secreted from the cell.[22] Presumably, during special periods of the cell activity, osteocytes and other vertebrate cells produce similar spherical structures, which consist of accumulations of mineralized filaments.[22]

2.4. Bindung of $Ca^{2\oplus}$ to Proteins

Prerequisite for calcification is the possibility to concentrate $Ca^{2\oplus}$ on the organic matrix. In this context Ca-binding properties, especially of the matrix-proteins, are discussed, but there are numerous open questions concerning binding sites. Of the amino acids (and sulfated sugars), whose Ca-binding capacity is known, only a few could actually be of importance in the Ca-binding proteins of biomineralizates. Figure 4 gives an overview.

2.4.1. Binding to Amino Acids with Free Carboxy Groups

Numerous Ca-binding proteins from biomineralizates contain a characteristically unusually high proportion of glutamic and aspartic acids. Although the ability of aminodicarboxylic acids to bind $Ca^{2\oplus}$ has long been known, there arises the question, whether the high proportions of these amino acids in Ca-binding proteins suffices to explain the Ca-binding property. There are proteins which are rich in aspartic and glutamic acids, but do not bind $Ca^{2\oplus}$.[23]

The shell matrices of various species of molluscs contain a high proportion of aspartic acid, as has been shown by amino acid analysis of the HCl-hydrolyzates. On the basis of these findings, a particular amino acid sequence $(Asp-X-)_n$ has been postulated, in which aspartic acid and predominantly serine or glycine residues (X) are arranged alternately, and which should be responsible for the Ca-binding.[24] It is still unclear whether asparagine is hydrolyzed by HCl into aspartate and ammonia. A definite proof, one way or the other, can only be presented after a complete amino acid sequence analysis, which has not been published as yet. For the above mentioned reasons this postulate has been a matter of controversy.[25-28]

In contrast, the strong Ca-binding amino acid γ-carboxyglutamic acid is found in numerous biomineralizates of vertebrates, e.g. in bones,[29] tooth cement and dentin,[30] calcified epiphyseal cartilage,[31] calcified tendons,[32] atherosclerotic plaques, sclerodermia, dermatomyosia and local calciphylaxia.[33] Furthermore, γ-carboxyglutamic acid has been detected as a building block of prothrombin and other proteins of the blood coagulation-system.[34,35] This amino acid has not been found up to now in calcified tissues of invertebrates.[36]

2.4.2. Binding to Phosphorylated Amino Acids

O-Phosphoserine, *O*-phosphothreonine and γ-glutamyl phosphate are also able to bind $Ca^{2\oplus}$. However, thus far it has only been possible to detect these amino acids in biomineralizates of vertebrates.[30,37] It seems that these amino acids do not occur in egg shells and mollusc shells.

Free SH-, OH-, amino- and amido-groups of protein building blocks as well as the spatial structures of polypeptides[38-56] could be essential for the Ca-binding ability of some proteins in biomineralizates. In the formation of mollusc shells and egg shells, however, they play only a subordinate role.

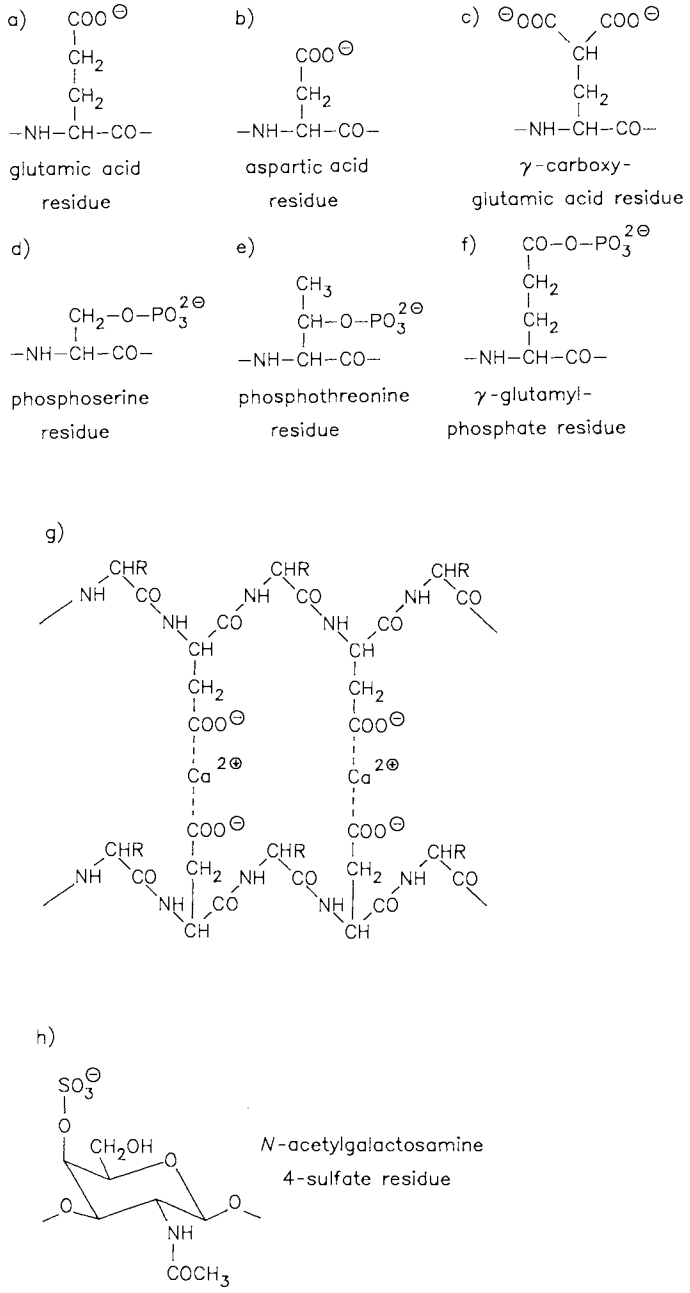

Fig. 4. Ca-binding in organic matrices. A local concentration of $Ca^{2\oplus}$ as prerequisite for crystallization is achieved by appropriate building blocks of proteins and glycoproteins (or proteoglycans) of the matrix. Typical Ca-binders are given in a)-f); they are amino acids in the peptide with negatively charged side chains. By frequent repetition of these building blocks in the polypeptide chain, the Ca concentration can be increased. g) Indicates the possibility of Ca-binding by aspartic acid residues opposite to each other. However, a Ca-binding by neighboring aspartic acid residues is also conceivable (R = H ≙ glycine residue, R = CH_2OH ≙ serine residue). An analogous situation can be constructed for glutamic acid residues. Ca-binding by aspartate has been discussed in connection with the formation of mollusc shells (see text). h) Reflects the possible mode of Ca-binding in avian egg shells. In contrast to examples a)-g) a Ca-binding by sulfated sugars or sugar derivatives is involved here.

2.4.3. Binding to Sulfated Sugars

The Ca-binding properties of the matrices of calcified shells rest primarily on sulfated sugars,[25,26,57] which are building blocks of oligo- or polysaccharides attached to polypeptides.[28,58]

3. Importance of the Matrix in Biomineralizates

Biochemical and micromorphological studies have clearly underscored the importance of matrix components as essential factors for biomineralization processes. The concept of an organic matrix (in each hard part) is based on the hypothesis of a control of deposition of insoluble inorganic material by macromolecular organic components (see Section 2.1). The term "matrix = uterus" is derived from mater and expresses that something is built or formed at a fixed place or in a defined medium. The criteria for a real matrix include:

1. Existence of the matrix before the formation of the product.
2. Participation of the matrix in its formation.
3. Spatial inclusion of the product by the matrix.

Matrices from hard parts are macromolecular polyions; these are primarily proteins and glycoproteins. Occasionally strong basic polycations and polyuronic acids are also observed.[5]

The chemistry of the organic matrices of invertebrates has received greater attention in the last decade. From these studies, functions of the matrices of invertebrate shells can also be derived:[59]

1. Crystal nucleation.
2. Limitation of crystal growth.
3. Crystal orientation.
4. Connection of crystals and crystal layers (influences physical behavior of the shell).

It has been assumed from studies on a large number of organic matrices that the precipitation of calcium ions and phosphate ions from solutions[60-66] by "heterogenous" nucleation is initiated or accelerated by organic matrices.[67-69] Since the mineral is normally deposited in the extracellular space, this observation can contribute to our understanding of the way in which the mineral phase is formed and where it is deposited. Therefore, it was supposed—in analogy to nucleation phenomena in organic chemistry—that such organization of the matrix is an essential characteristic for a matrix, which can influence the rate of crystal formation. This supposition led to inquiries into the chemical structure of the matrices with the aim of explaining relationships between structure and calcification ability. Despite great effort, however, the role of the components of calcifying matrices is still uncertain.[59]

Organic matrices are also detectable in mollusc shells and egg shells. They are found in the biocrystalline layer, i.e. in the real biomineralizate. As already mentioned, it appears that the crystal modification of $CaCO_3$ (calcite, aragonite, etc.) is controlled primarily by the chemical structure of the organic matrix in the corresponding crystal layer.

Although the inorganic components of the shells have been well studied, there is still a considerable lack of information on the chemical structures, and especially about the molecular functions and the synthesis of the (organic) matrix-components and their regulation mechanisms. The

organic matrix of mollusc shells and avian egg shells can easily be prepared by dissolution of $CaCO_3$ crystals (e.g. with EDTA solutions). A fraction that is highly soluble and a fraction that is insoluble in aqueous systems are obtained. The concentration of the total matrix of mollusc shell amounts to 0.01 to 10% depending on the species.[70]

4. Biomineralization Processes in the Formation of Mollusc Shells

4.1. Soluble Matrix

It is assumed that the soluble matrix occurs intracrystalline,[25,71,72] while the insoluble matrix is always localized intercrystalline. The concentration of the soluble matrix components varies remarkably depending on the species of animals (14% to 64% of the total matrix).[26]

The extraction and, in part, purification of a soluble matrix component of *Mercenaria mercenaria* was first reported as late as 1972.[25] It is a water-soluble glycoprotein (M_r ca. 160 kDalton) which is evenly distributed within the shell and exhibits strong negative charges (ester sulfates).[73] The amino acid composition of this sulfated glycoprotein essentially corresponds also to the composition of the insoluble matrix of other mollusc shells (see Refs. [25, 26, 74, 75]).

There is still no information available on the quantity and the relative molecular masses of soluble matrix proteins.[76,77] From our recent observations it can be concluded that, depending upon the age of the shell, very different protein profiles can occur upon gel filtration. The M_r values range from <30 to >5000 kDalton. In freshly shucked oyster shells only two groups of soluble shell proteins (5000 and 500 kDalton) occur. When these proteins are treated with sodium dodecyl sulfate (SDS) solutions they dissociate into subunits (each ca. 15 kDalton) whose amino acid compositions are nearly identical in all the mollusc species studied so far. Accordingly, these high molecular weight, soluble matrix protein aggregates are made up of only a few subunits. The existence of genes which code for 5000-kDalton proteins is very unlikely.[77]

Soluble matrix-proteins bind $Ca^{2\oplus}$ easily. This is understandable because its isoelectric point (I.P.) is about 2. Bicarbonate ions, however, decompose under these conditions into CO_2 and H_2O. Consequently, soluble matrix-proteins cannot be regarded as $CaCO_3$-forming agents. Furthermore, sulfates as well as ester sulfates, are considered as "crystal poisons" (e.g. for $CaCO_3$ crystals). An alternative explanation to circumvent these difficulties of interpretation has been offered by *Wheeler* et al.[78] The soluble, acidic shell proteins could terminate the process of shell formation. These proteins can easily intercept "excessive" amounts of Ca ions; $Ca^{2\oplus}$ ions are then not available for crystal formation. Ca ions that are already excreted cannot be picked up again by a steep $Ca^{2\oplus}$-gradient in the mucosal cells of the mantle epithelium. These ions remain bound to proteins and their charges are thereby neutralized.

Protein chemical studies on fossil mollusc shells are difficult to judge. Very different influences may have altered shell proteins over long periods of time. Therefore, it is never quite clear whether the material examined stems from components of the soluble or the insoluble matrix. Such fossil proteins are often soluble. Even though $CaCO_3$ layers may protect shell proteins from decomposition processes to a certain degree, it is doubtful whether, e.g., after 80 million years glycoproteins are still preserved in their original structure.[79] In this context a thesis has been suggested that during the source of evolution the repeating amino acid sequences $(-Asp-X-)_n$ have been well preserved. This thesis assumes that aspartic acid is the most frequently occurring amino acid next to glycine in shell proteins. This view is based on the assumption that the Ca-binding in soluble shell proteins is determined by the β-carboxy group of aspartic acid.

Other research workers suggest that it is not aspartate,[25,80-82] but asparagine, which has been detected by partial sequence analysis. The repeating sequence in shell protein may rather correspond to $(-Asn-X-)_n$. The Ca-binding is then explained by the presence of ester sulfate.

In spite of various reservations against studies on fossil peptides it is still understandable that the prevailing amino acid sequences are preserved in well conserved fossil oyster shells *(Ostrea carrissima, Lopha diluvianus, Lopha marshi)*. This points to only a small frequency of mutation of the corresponding genes; at the same time it is recognizable that $CaCO_3$ shells have protected "their" proteins from decomposition. Only some amino acid residues differ from the basic pattern. This could be dependent on evolutive or diagenetic processes.[81,82]

Besides the typical soluble shell proteins, polyphenol oxidases have been detected in the soluble matrix of *Crassostrea gigas, Strombus aureus*[59,83] and *Mercenaria mercenaria*.[84] Substrates for these enzymes (tyrosine and other phenolic substances) could be identified in shell matrices. It is possible that the effect of polyphenol oxidases is connected with aggregation or polymerization processes in the insoluble matrix.[83]

4.2. Insoluble Matrix (Conchiolin)

Conchiolin (Span. concha = mussel) has often been described as a group of proteins with an occasionally significant polysaccharide content. The latter seems to be species dependent.[71,80,85] The term "insoluble matrix" has been introduced during the last decade, but it is misleading. Conchiolin can be converted into a soluble form (see Section 5.2.2).

Conchiolin has a high affinity for lipid-staining agents (e.g. sudan black),[86,87] although even after thorough extraction with chloroform-methanol or diethyl ether, no reduced stain and no presence of lipids in the extracts have been detectable.[26] Probably the sudan-black color is due rather to a pigment distribution than to a chemical reaction. Perhaps it is connected with a predominance of aliphatic amino acids in conchiolin.

Studies on conchiolin are relatively scarce. The reason for this is the difficulty of solubilizing this material under mild conditions to give soluble proteins (polypeptides).

Therefore, most studies on the structures of conchiolin have been limited to amino acid data, IR spectra[88] and X-ray diffraction patterns.[85] It can be concluded that antiparallel pleated-sheet structures seem to be predominant.[85] Besides these, low ordered structures have also been reported.[28]

Promising efforts to extract proteins stepwise soon slowed down in the early stages.[89] It has been argued that dissolution of conchiolin proteins by means of aggressive reagents (NaOH, HCl, HCOOH)[89,90] may cause undesirable side-reactions (transformation of lysine into ornithine, deamination reactions, random partial hydrolysis etc.). That conchiolin of oyster shells can be cleaved reproducibly into subunits by SDS-containing solutions was first reported by our working group in 1986.[76] Accordingly, conchiolin is made up of a relatively low number of polypeptides (75 and 40 kDalton). These subunits contain different quantities of sulfated oligosaccharides. From these structures, subunits having I.P. values between >9.3 and 3.1 are derived. Subunits with I.P. values >7.0 simultaneously bind $Ca^{2\oplus}$ and $HCO_3^{\ominus}$. Therefore, they could be regarded as initiation factors of shell formation. Conchiolin subunits with I.P. values <7.0 may rather participate together with soluble matrix proteins in the termination of shell formation. Intact conchiolin of oyster shells in aqueous suspension has an I.P. value of ca. 8.5 and simultaneously binds $Ca^{2\oplus}$ and $HCO_3^{\ominus}$. Sulfate and phosphate ions prevent this binding.[91]

Anti-conchiolin sera not only react positively with soluble proteins of oyster shells, but also with the proteins of the soluble and insoluble matrix of egg shells.[58,76,77,92] This is indicative of relationships between the protein structures of egg shells and mollusc shells.

4.3. Molecular Mechanisms of Mollusc Shell Formation

Based on all the information now available on shell formation in molluscs, the following hypothesis can be proposed: The synthesis of soluble precursor proteins of the shell matrix seems to be localized in the hepatopancreas. Modification reactions of the soluble precursor proteins of the shell (polypeptides), i.e. additions of sulfated oligosaccharides may first take place after transportation into the mantle epithelium. Polypeptides, which occur in the soluble matrix, have relative molecular masses of about 15 kDalton, while polypeptides in the insoluble matrix (conchiolin) have M_r values in the range of ca. 75 kDalton and 40 kDalton.[76]

Figure 5 shows the structure of the mollusc shell. Matrix subunits are accumulated in mucosal cells of the mantle epithelium. $Ca^{2\oplus}$, $HCO_3^{\ominus}$ and conchiolin are excreted into the extrapallial fluid. It is not known whether the aggregation of conchiolin subunits is already accomplished in the mucosal cells or after secretion. The inorganic composition of the extrapallial fluid of marine molluscs is different from that of seawater. In the extrapallial fluid of freshwater molluscs there is less $Ca^{2\oplus}$, but more $HCO_3^{\ominus}$ than in marine molluscs. Furthermore, seasonal fluctuations in the composition of this secretion, and fluctuations which are dependent on physiological conditions of the animal have

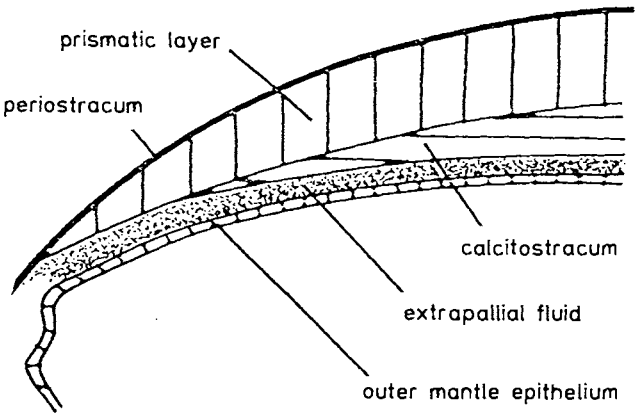

Fig. 5. Structure of the mollusc shell. The prismatic layer and the calcitostracum are made up of biocrystallites. The mantle epithelium secretes the extrapallial fluid (contains all the components for biomineralization). The periostracum is the outer layer of the mollusc shell.

been reported.[26] The contents of organic components have so far rarely been examined.

It must be assumed that aggregates of conchiolin bind $Ca^{2\oplus}$ and $HCO_3^{\ominus}$ simultaneously in vivo, as has been established in vitro.[80] At pH>8.0, precipitation of $CaCO_3$ as primary crystals might be initiated by this mechanism. Since the extrapallial fluid is supersaturated with $Ca^{2\oplus}$ and $HCO_3^{\ominus}$, it is reasonable to assume that further crystal formation is driven by kinetic forces.

Probably the termination of the crystallization process depends on components of the soluble matrix. These are proteoglycan-like, highly-sulfated macromolecules which could serve as Ca scavengers (see Section 5.4). In this way, there is the possibility of separating $Ca^{2\oplus}$ from the reaction with $HCO_3^{\ominus}$. Another function of these substances is understandable in the following context. Proteoglycans are able to inhibit the formation of calcium phosphate crystals[93,94] and calcium oxalate crystals.[56,95,96] The inhibitory effect is explained in terms of simple physical phenomena which are due to interactions of proteoglycans with already existing crystals. These crystals are protected by proteoglycans from a further accumulation of crystals.[93] Moreover high molecular proteoglycans are more effective than the subunits. Depolymerization of high molecular aggregates reduces or even prevents the inhibition effect.[97] Proteolytic enzymes of lysosomal origin are responsible for the deaggregation of high molecular weight proteoglycans, which results in calcification of cartilage.[93,98-103]

Whether both inhibition mechanisms occur during the termination phase of the formation of mollusc shells has not yet been investigated. Nothing is known so far on the regulation of the synthesis of matrix polypeptides and the control of modification reactions. It is possible that hormone-dependent regulation mechanisms exist.[104]

5. Biomineralization Processes in the Formation of Egg Shells

5.1. Function of the Egg Shell

Calcareous egg shells are found in all species of birds, in several reptiles, in monotremata, and in some gastro-

pods.[59, 70] The calcified egg shells protect the contents of the egg from mechanical effects during the extrauterine incubation and permit the exchange of water and gases through the pores. Furthermore, the egg shell prevents desiccation of the egg and the growing embryo in animals, which live in arid areas, particularly in the tropics and subtropics. On the other hand, the relatively thin shell permits exchange of temperature during the incubation period even at very low environmental temperatures (penguins). Eventually the calcareous egg shell is used as a Ca-reservoir for the construction of the embryonic skeleton.[105, 106]

The avian egg shell is morphologically divided into three layers (Fig. 6):

1. Membrana testacea.
2. Biocrystalline layer.
3. Tegmentum (cuticula).

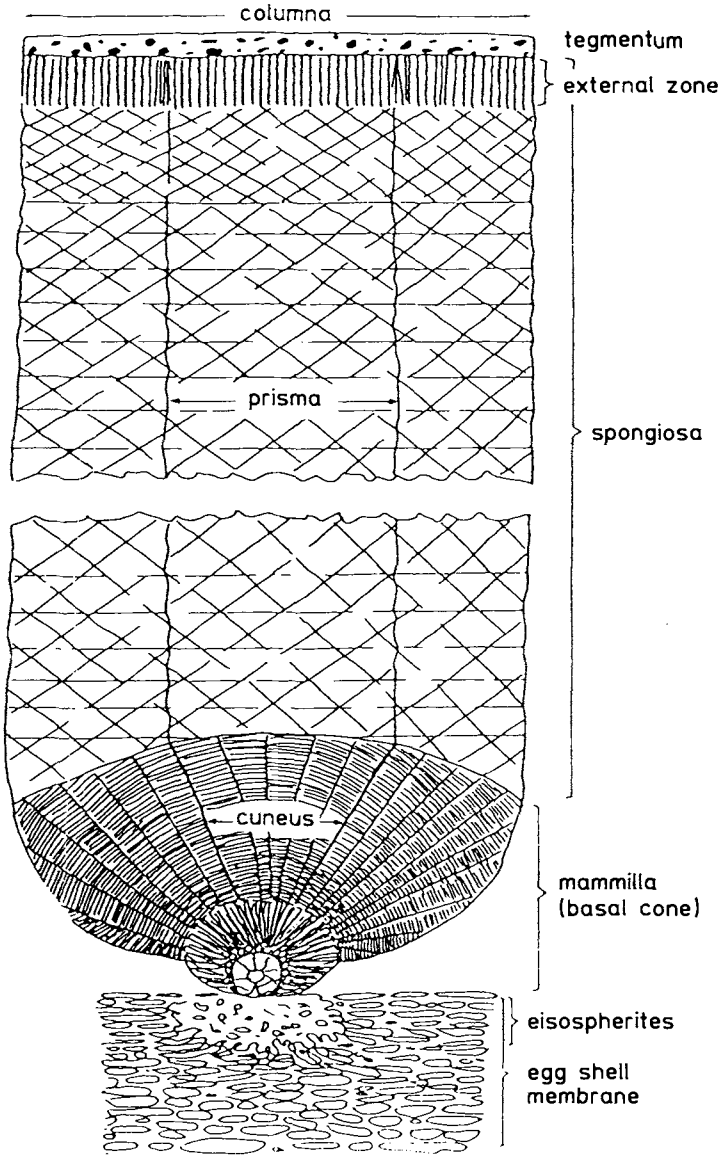

Fig. 6. Structure of the egg shell. The egg-shell membrane (membrana testacea, MT; netlike system of cysteine-rich fiber proteins) serves as elastic support for the process of shell formation. The biocrystallite layer includes the mammilla and spongiosa region as well as the external zone. The tegmentum is the outer layer of the egg shell. Columna, prisma and cuneus describe horizontal limitations of smaller units (biocrystallites) and biocrystals.

5.1.1. *Membrana testacea*

The membrana testacea (MT) of avian egg shells seems to be necessary for the construction of the biocrystalline layer. Under appropriate experimental conditions no egg shell is formed when the membrana testacea is omitted.[107] It is generally accepted that the initial processes of calcification (egg-shell formation) is localized in the mammillary layer of the shell.[105]

The MT can be divided mechanically into two net-like layers. Its biological function is primarily regarded as a filter (microorganisms).

The predominant components of the MT consist of proteins, a very low proportion of which (6%) is soluble in aqueous systems. So far there is considerable uncertainty about the characteristics of insoluble MT proteins.[50, 108–110] Some authors regard them as keratins or ovokeratins;[111] other authors disagree, because the insoluble MT proteins are distinctly different in structure, amino acid composition,[112] and solubility behavior[113] compared to classical keratins. Some consider MT proteins as collagen-like proteins because of the presence of hydroxyproline and hydroxylysine.[114] Others claim to have found elastin-like proteins in the MT.[115]

As long as it is not possible to seggregate MT proteins into soluble subunits under mild conditions and to fractionate these and carefully examine the individual proteins (polypeptides), no further insights can be expected. In this direction experiments have been carried out to study the possibility of an attack of nucleophilic reagents, e.g. $CN^{\ominus}$, on the S atoms of the sterically accessible disulfide bridges. Structure analyses of the fragments (M_r about 3 kDalton) revealed that about 45% of the intact MT is made up of cysteine-rich proteins. The remaining proteins of the MT are linked to sulfated oligosaccharide moieties.[116] Glucose, mannose, xylose, sialic acid[112] and hexosamines[110] were identified as building blocks. Uronic acids seem to be absent.[117] The presence of lipids in MT has been reported[118, 119] (mono-, di- and triacylglycerines, free fatty acids, cholesterol and cholesterol esters, and phospho- and sphingolipids).

Since the MT does not bind any Ca ions it has not been regarded as a factor of the initial phase of calcification. Probably the mesh-system of the MT functions as a support for $CaCO_3$ crystals.[120]

We assume that soluble precursor polypeptides of the MT are synthesized in the liver and in the isthmus section of the laying tract.[82] These precursors are presumably stored in the isthmus portion, from which they are secreted to form aggregates of fiber-like structures.[59] It should be mentioned that soluble precursor polypeptides of cysteine-rich feather proteins are also synthesized in the liver.[127]

5.1.2. *Tegmentum (cuticula)*

The avian egg shell is covered by a cuticula (tegmentum), which is made up of two layers. The tegmentum of freshly layed eggs has a reddish fluorescence, which depends on a so called "ooporphyrin". These layers are es-

sentially composed of glycoproteins. They do not participate in the calcification of the shell.

5.2. Organic Matrix of Avian Egg Shells

The biocrystallite layer of avian egg shell, like mollusc shells, contains organic compounds which collectively have been described as an organic matrix. It consists of a protein–oligo(poly)saccharide complex with a low content of lipids and water.[115] Glucosamine, galactosamine, mannose and fucose have been identified as building blocks of the oligo- or polysaccharides. The presence of chondroitin sulfate A and dermatan sulfate has also been reported.[117] Sialic acids are said to occur in small amounts. The evidence for matrix proteins in avian egg shells rests on amino acid analyses after HCl-hydrolysis of the organic matrix.

The organic matrix of egg shells can be likewise divided into a soluble and a water-insoluble fraction after dissolution of the mineral phase.

5.2.1. Soluble Matrix

Because of their high solubility in water and aqueous salt solutions, those macromolecules of the organic shell matrix have been studied preferentially. Shells of freshly layed eggs, similarly as freshly shucked oyster-shells, yield two groups of soluble protein-containing macromolecules (5000 and 500 kDalton). In hot SDS solution, both high molecular aggregates fall apart into relatively small subunits of about 15 kDalton.[77] With increasing age of egg shell smaller fragments appear (<30 kDalton). The I.P. of these subunits is in the range of 2.2 and enables these substances to bind $Ca^{2\oplus}$. This typical subunit (of about 15 kDalton) contains highly sulfated oligosaccharides, which are attached to the polypeptide structure. Functionally, this 15 kDalton-subunit of the soluble matrix is regarded as a termination factor of shell formation,[58] even though not every observation on shell formation can be explained in this way only.

Another soluble component of the shell matrix is carbonic anhydrase (carbonate-dehydratase) which occurs in the chicken egg shell in the form of two active isoenzymes (M_r ca. 28 kDalton). This enzyme catalyzes the reversible reaction

$$CO_2 + HOH \rightleftharpoons H^{\oplus} + HCO_3^{\ominus}$$

This is probably the primary function of this matrix enzyme, even though it concomitantly exhibits an esterase-activity.[106, 123, 124] The same enzyme occurs in the shell gland of laying hens. Its activity depends on the laying cycle. During molting a low activity is observed in the shell gland,[125, 126] which is influenced by progesterone.[127, 128] The shell gland enzyme is closely related with the formation of the biocrystallite layer of the shell, since acetazolamide and other sulfonamides, as inhibitors of carbonic anhydrase, also reduce the rate of shell formation.

The functions of the shell enzyme probably include the provision of hydrogen carbonate for calcification processes, and also the local dissolution of the shell. Through this phenomenon, which is often observed in the form of resorption-craters in hatched eggs[75, 105, 129–131] calcium of the biocrystalline layer can be provided for the construction of the embryonic skeleton.[59] Participation of carbonic anhydrase in the termination process of the shell formation is very likely. When carbonic anhydrase catalyzes the reaction

$$H_2CO_3 \rightleftharpoons H_2O + CO_2$$

there is no more $HCO_3^{\ominus}$ available for the formation of $CaCO_3$. The presence of so-called globular inclusions in $CaCO_3$ crystals of the egg shell and perhaps pore formation in the egg shell are due to gaseous CO_2.

5.2.2. Insoluble Matrix

The insoluble matrix of egg shells has scarcely been studied as yet. It was merely known that it must be composed of proteins and polysaccharides with low contents of water and lipids.[115]

From our studies on conchiolin,[91] it could be established that the insoluble matrix of egg shells is able to bind $Ca^{2\oplus}$ and $HCO_3^{\ominus}$ simultaneously.[92] The insoluble matrix has a pH of ca. 8.5 in aqueous suspension. This can help to explain the binding properties for $Ca^{2\oplus}$ and $HCO_3^{\ominus}$ and, thus, how primary crystals are formed.

Analogous to studies on conchiolin[76] the insoluble matrix of chicken egg shells could be split by treatment with SDS into subunits and then fractionated.[58] Remarkably, the insoluble matrix of egg shell is made up of only a few polypeptides (discovered so far: 50, 16 and 14 kDalton). However, there are multiple modifications of these polypeptides due to sulfated oligosaccharides, which influence the binding capability for $HCO_3^{\ominus}$. All modified subunits bind $Ca^{2\oplus}$. Nevertheless, only such subunits with I.P. values of >7.0 have an additional affinity for $HCO_3^{\ominus}$.

Subunits of the insoluble matrix of egg shells react positively with anti-conchiolin sera; also positive immunoreactions of anti-shell-matrix sera and subunits of conchiolin have been reported.[58, 77] Anti-shell-matrix sera react very strongly with the cytosol of mucosa cells of the chicken shell gland. This demonstrates the occurrence of components of shell matrix in these cells only.[58]

5.3. Synthesis of Shell Proteins

According to our own studies, soluble precursor polypeptides of egg shell matrix are synthesized in the liver.[58] The primary products of the synthesis include only a few soluble polypeptides (detected so far: 60, 40, 14, 12 kDalton), which are modified in subsequent reactions (limited proteolysis, polysaccharide addition, oligosaccharide addition, and sulfation reactions). The modification steps could take place in the liver or in the shell gland. The transportation of the primary products or secondary products proceeds from the liver through the blood to the shell gland. The modification reactions should occur, at latest, in the shell gland. Two sorts of secondary products exist. The same 12-kDalton polypeptide is attached to sulfated

polysaccharide molecules, which then aggregate to form suprastructures (ca. 5000 kDalton) and resemble proteoglycans. These structures correspond to the soluble matrix. It is unknown whether aggregates or subunits of matrix are accumulated or secreted by mucosal cells of the shell gland. Probably the 50- and the 14-kDalton polypeptides (insoluble matrix) are only slightly modified (oligosaccharide units, no sulfation), stored, and secreted from the mucosal cells. Presumably only modified subunits are secreted since no shell-protein aggregates are detectable in the uterine secretion. Such polypeptides also aggregate to form suprastructures at latest on contact with fibrils of the membrana testacea. These suprastructures correspond to the insoluble matrix (cf. Fig. 7).

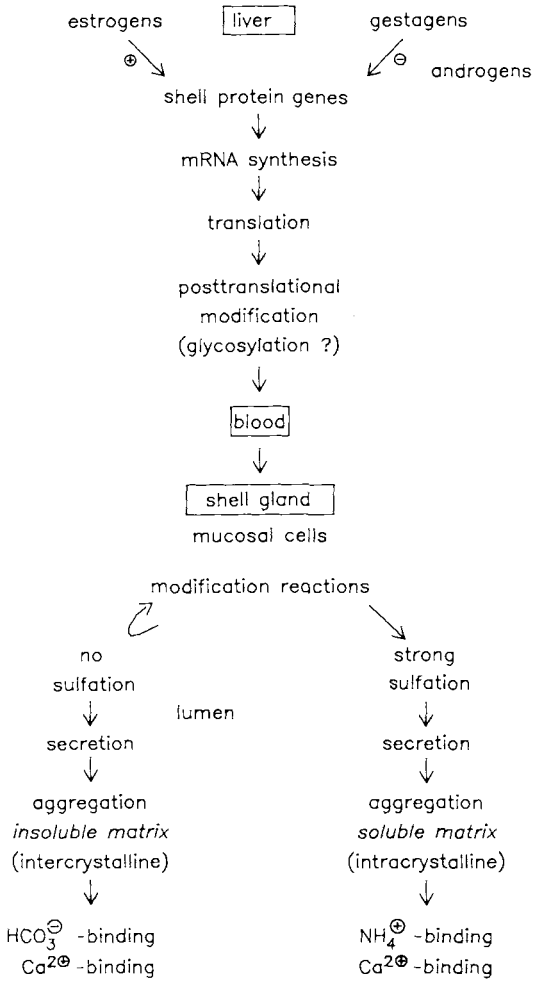

Fig. 7. Schematic representation of egg-shell protein synthesis (for details see text).

A very important question here concerns the regulation mechanisms of the hepatic synthesis of precursor polypeptides of the egg-shell matrix. We have worked on this problem because it is of practical importance and could help to answer questions relating to the formation of thin chicken egg shells (cracked eggs). Present experimental results show that the hepatic shell protein synthesis depends on the estrogen status and functional mechanisms of the liver. Antiestrogens, e.g. tamoxifen, inhibit shell protein synthesis as do androgens, gestagens, and typical liver poisons (α-amanitin and phalloidin).[77] There are direct correlations between high estrogen levels in laying hens and liver damage. Animals with high laying rates and high estrogen production frequently suffer from fatty-liver hemorrhagia syndrome.[132] This is already a pathological situation. Additional adminisitration of estrogens (17β-estradiol or diethylstilbestrol) to animals with high laying rates results in massive liver damage and terminates egg production and the synthesis of shell protein precursors in the liver.[133] These observations can help to explain the reasons for the formation of thin chicken egg shells.

5.4. Molecular Mechanisms of Egg Shell Formation

Although there is little information available about the molecular mechanisms of the formation of egg shells, we will nevertheless try to construct a working hypothesis. All of the components necessary for the formation of the egg shell are accumulated in the shell gland prior to secretion. It is not clear, whether the individual components are stored for a longer period of time in the mucosal cells (MC) of this gland. A signal for the secretion of these substances is apparently triggered by a mechanical stimulation through rotation of the shell-free egg in the gland. This effect can be induced, e.g., with a ping-pong ball whose surface is covered with a layer of membrana testacea. The thus prepared ping-pong balls must not be fixed in the shell gland. Under these conditions (rotating ping pong ball), the deposition of a shell occurs on an artificial support.[107]

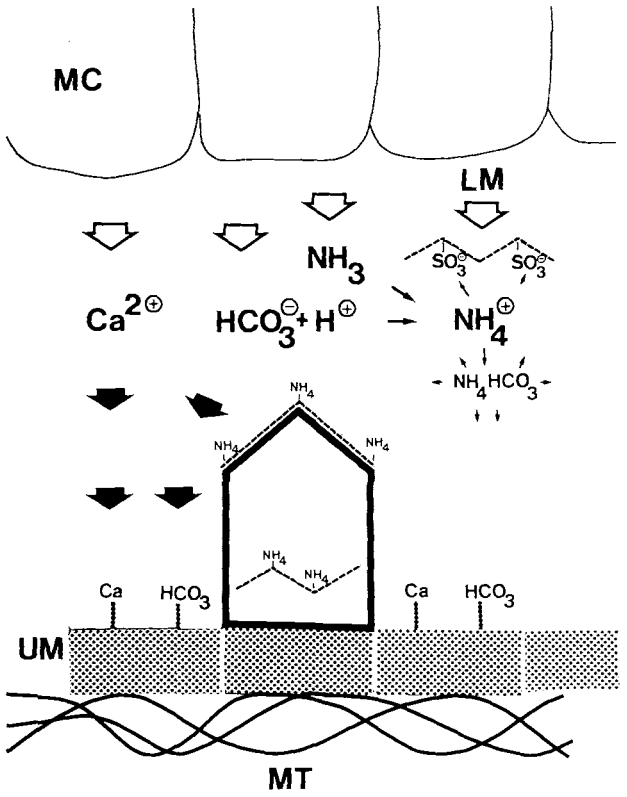

Fig. 8. Molecular mechanisms of shell formation: Initiation phase. Mucosal cells (MC) of the shell gland secrete $Ca^{2\oplus}$, $HCO_3^{\ominus}$, aggregates of the insoluble matrix (UM), aggregates of the soluble matrix (LM) and NH_3. First of all the UM is deposited on the egg shell membrane (MT) and simultaneously binds calcium and hydrogencarbonate ions. Primary crystals ($CaCO_3$) and $H^{\oplus}$ are formed. Protons react with NH_3 to give $NH_4^{\oplus}$. Ammonium ions are bound by sulfate groups of the LM and by hydrogencarbonate ions.

It must be assumed that subunits of insoluble matrix (UM) are first deposited on the membrana testacea (MT) and form the insoluble matrix. These aggregates are able to bind $Ca^{2\oplus}$ and $HCO_3^{\ominus}$ (pH > 8.0) simultaneously, and to form primary crystals (Fig. 8). This is only possible, when the protons that are formed can be eliminated. Ammonia can possibly serve as proton scavenger. Ammonia is produced in relatively high concentrations during shell formation.[134,135] Adenosine-deaminase has been identified as an ammonia producing enzyme in the shell gland. This enzyme obviously deaminates adenosine (uric acid is the final product of protein metabolism in birds) and eliminates NH_3 through the laying tract. Besides NH_3, other poisons, e.g. Be, Hg, Cd, are removed from the organism[136] by egg deposition. NH_3 intercepts protons according to the following equation:

$$Ca^{2\oplus} + HCO_3^{\ominus} + NH_3 \longrightarrow CaCO_3 + NH_4^{\oplus}$$

A reabsorption of $NH_4^{\oplus}$ by mucosal cells is possible but very difficult. Therefore $NH_4^{\oplus}$ must remain at the site of calcification. The situation is understandable if the soluble matrix (LM) is included in this reaction. The soluble matrix produces large quantities of ammonia after HCl hydrolysis (at least 60–80% of the ninhydrin-positive substances of LM). Obviously LM binds $NH_4^{\oplus}$ by means of its large number of ester sulfate residues. Probably a further but smaller portion of $NH_4^{\oplus}$ reacts with $HCO_3^{\ominus}$ to form NH_4HCO_3; this reaction helps to stabilize a slight alkaline milieu and thereby creates favorable conditions for the formation of $CaCO_3$ crystals (pH > 8.0). In addition, the intracrystalline presence of soluble matrix can be explained. The insoluble matrix is always intercrystalline (cf. Fig. 9). Since the proteins of the soluble and insoluble matrices have very similar amino acid compositions, it is very likely that they have similar amino acid sequences. At the positions which determine the crystal shape the sequences may be identical.[*]

Presumably the insoluble matrix is deposited at the latest, when a transition from one morphological layer of the shell to another is necessary, e.g. within the mammilla and within the spongiosa layer (see also Fig. 6).

The termination of egg shell formation is probably initiated by the action of carbonic anhydrase, which forms gaseous CO_2 from H_2CO_3 (Fig. 10). Therefore $HCO_3^{\ominus}$ is available for $CaCO_3$ formation; the interception of $H^{\oplus}$ is unnecessary. This means, that the secretion of NH_3 is not necessary any more. Excess of $Ca^{2\oplus}$ can be bound by the sulfate groups, while a reabsorption of $Ca^{2\oplus}$ by mucosal cells against a steep $Ca^{2\oplus}$-gradient is not possible. The formation of gaseous CO_2 is likely; this might help to explain the occurrence of globular inclusions in $CaCO_3$ crystals. It is still uncertain, however, whether pore formation is due to the production of CO_2. Pores and carbonic anhydrase have been found in egg shells, whereas both are absent in mollusc shells.

[*] Determination of the sequence is very difficult, because the fragmentation is scarcely reproducible. Shell proteins cannot be hydrolyzed by any proteolytic enzymes known thus far. A fragmentation by appropriate chemical reactions is also impossible, because the requisite amino acids (e.g. methionine) do not occur in these proteins.

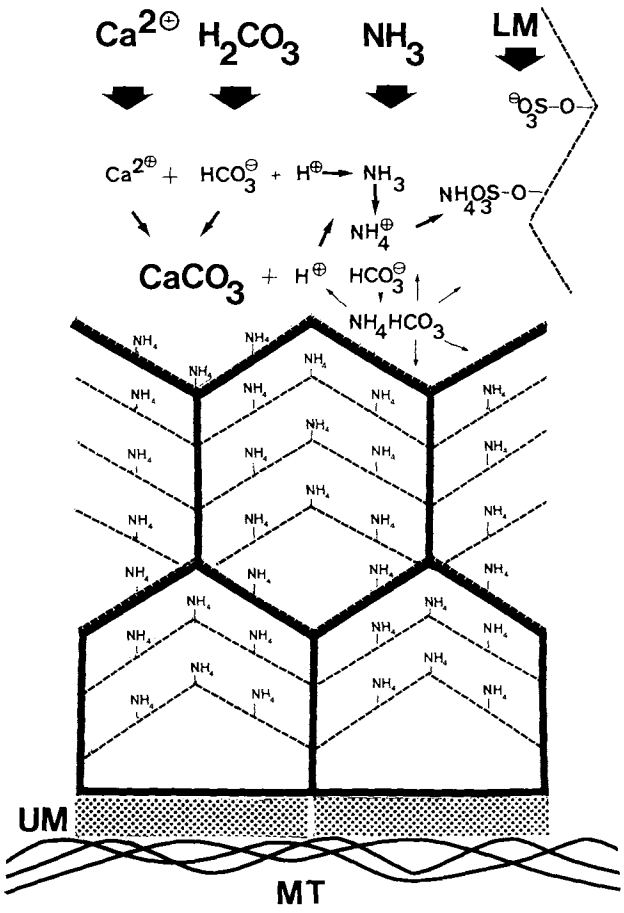

Fig. 9. Molecular mechanisms of shell formation: Elongation phase. The process outlined in Figure 8 continues and leads to crystal growth with intracrystalline inclusion of the soluble membrane (LM) (after reaction with $NH_4^{\oplus}$). The insoluble membrane UM is presumably deposited between crystalline layers (see Fig. 2).

A reduced synthesis of shell proteins automatically leads—according to the above mentioned hypothesis—to a decreased binding of $NH_4^{\oplus}$ to the soluble matrix, even when sufficient amounts of $Ca^{2\oplus}$ and $HCO_3^{\ominus}$ are present. Protons can be only insufficiently intercepted by NH_3, even when a small portion of $NH_4^{\oplus}$ is formed. $HCO_3^{\ominus}$ is then not available at the site of crystal formation. Protons in excess dissolve already existing $CaCO_3$ crystals.

A decreased synthesis of shell proteins results in thin egg shells (cracked egg syndrome). As a supervisory system, the estrogen status controls the rate of synthesis of shell proteins[133] and of carbonic anhydrase,[127] and eventually the shell formation. It is thus clear why the egg shell quality cannot be improved merely by feeding laying hens a diet high in calcium.[137]

The molecular mechanisms of mollusc shell formation may be similar to those described for egg shell formation. Not very much is known about the synthesis of mollusc shell proteins and their regulation.

6. Summary and Prospects

Biomineralization processes are widespread in nature. They differ from geological mineralization processes by

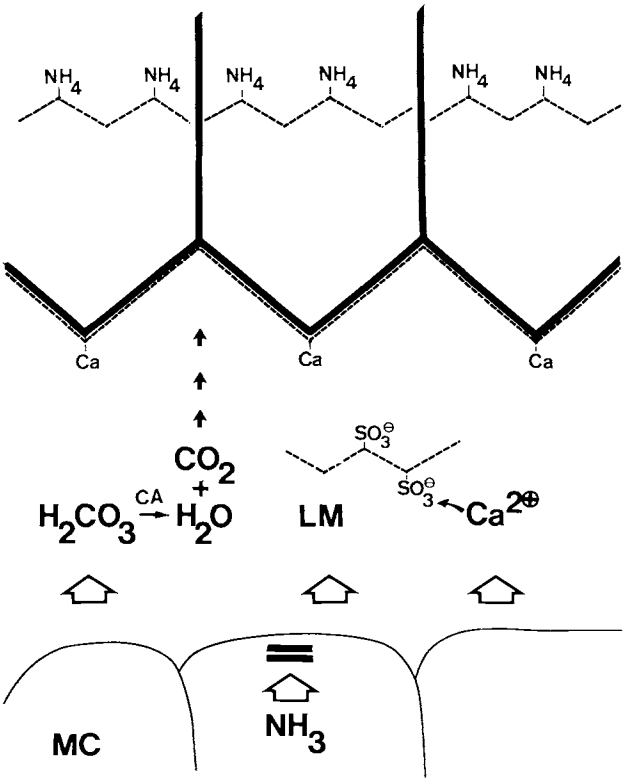

Fig. 10. Molecular mechanisms of shell formation: Termination phase. The mucosal cells (MC) of the shell gland first terminate the secretion of NH_3. In the lumen of the shell gland, secreted carbonic anhydrase (CA) forms gaseous CO_2, while excess Ca ions are bound by sulfate groups of the soluble membrane (LM). This leads to the termination of the secretion process (for details see text).

the existence of organic matrices. Organic matrices frequently include proteins (collagen, dentin, conchiolin, etc.); occasionally they are made up exclusively of polysaccharides (coccoliths). Inorganic crystals are deposited on a matrix (mineral phase), their form and dimensions being determined by the structure of the matrix. The matrix components can, in some cases, be separated into a water-soluble fraction and an insoluble part.

Biological calcification processes may have originally developed from a detoxification mechanism. The Ca ion concentration is carefully regulated because of its pharmacological effects in living cells. An excess of $Ca^{2\oplus}$ is removed from the cytoplasm and transported preferentially into the extracellular space. Appropriate counterions (phosphates, bicarbonate, rarely sulfates) react with $Ca^{2\oplus}$ to form depositions. They can be found to form exoskeletons (mollusc shells) or endoskeletons (vertebrates).

Using the example of egg shell formation, the interactions of organic matrix components with $Ca^{2\oplus}$, $HCO_3^{\ominus}$, and NH_3 can be demonstrated. In this case soluble matrix-precursors (polypeptides) are synthesized in the liver, whereas the secretion of the matrix proteins together with $Ca^{2\oplus}$, $HCO_3^{\ominus}$ and NH_3 takes place in the shell gland of the laying tract. NH_3 serves as proton interceptor and is bound as $NH_4^{\oplus}$ by the ester sulfate residues of the soluble matrix. The latter is intracrystalline. The rate of synthesis is regulated by the estrogen status. A high estrogen level causes liver damage. Decreased liver-function reduces the rate of synthesis and results in thin egg shells. The synthesis of soluble matrix precursors in the liver is regulated by a normal estrogen level and is dependent on a well-functioning liver. These findings should be born in mind in all future animal-breeding programs.

There is already the possibility of examining the structure of shell matrix genes in detail by means of a "gene-library" of the chicken genome. From these studies, information on possible mutations could be obtained.

Our studies mentioned here were generously supported by the Deutsche Forschungsgemeinschaft.

Received: July 7, 1987;
revised: November 6, 1987 [A 689 IE]
German version: *Angew. Chem. 100* (1988) 1181

[1] K. J. Götting: *Malakozoologie: Grundriss der Weichtierkunde*, Gustav Fischer, Stuttgart 1974, p. 1, 39.
[2] H. A. Lowenstam in T. W. Donelly (Ed.): *The Earth Sciences: Problems and Progress in Current Research*, Chicago Press, Chicago 1963, p. 137.
[3] H. A. Lowenstam in R. W. Brauer (Ed.): *Barobiology and the Experimental Biology of the Deep Sea*, University of North Carolina Press, Chapel Hill 1973, p. 19.
[4] E. T. Degens, *Top. Curr. Chem. 75* (1964) 1.
[5] J. E. Eastoe in H. J. J. Blackwood (Ed.): *First European Symposium on Bone and Teeth*, Pergamon Press, Oxford 1964, p. 269.
[6] H. Gebhard, A. Neuhaus: *Epitaxie-Daten anorganischer und organischer Kristalle*, Springer, Berlin 1972.
[7] K. M. Towe, *Biomineralisation 4* (1972) 1.
[8] H. K. Erben, *Biomineralisation 4* (1972) 15.
[9] N. Watabe, K. M. Wilbur, *Nature (London) 188* (1960) 334.
[10] K. Simkiss, *Comp. Biochem. Physiol. 16* (1965) 423.
[11] K. Wada, *Bull. Nat. Pearl Res. Lab. Jpn. 7* (1961) 703.
[12] C. Grégoire, *Bull. Inst. R. Sci. Nat. Belg. 38* (1962) 1.
[13] H. Mutvei, *Acta Univ. Stockh. Stockholm Contrib. Geol. 20* (1969) 17.
[14] C. Grégoire, *Biol. Rev. Cambridge Philos. Soc. 42* (1967) 653.
[15] D. Travis, *J. Ultrastruct. Res. 23* (1968) 183.
[16] D. Travis in H. Schraer (Ed.): *Biological Calcification: Cellular and Molecular Aspects*, North Holland, Amsterdam 1970, p. 203.
[17] a) N. Watabe, K. M. Wilbur (Eds.): *The Mechanisms of Mineralization in Invertebrates and Plants*, University of South Carolina Press, Columbia 1976; b) K. Simkiss in [17a], p. 1.
[18] J. W. Greenawalt, C. S. Rossi, A. L. Lehninger, *J. Cell Biol. 23* (1970) 21.
[19] A. L. Lehninger, *Biochem. J. 119* (1970) 129.
[20] F. Bett, N. C. Blumenthal, A. S. Posner, G. L. Becker, A. L. Lehninger, *Proc. Natl. Acad. Sci. USA 72* (1975) 2088.
[21] F. G. E. Pautard in [17a], p. 33.
[22] R. B. Rucker, D. Ford, W. Goettlich Riemann, K. Tom, *Calcif. Tissue Res. 14* (1974) 317.
[23] W. Dirscherl, H. Dohr, *Hoppe-Seyler's Z. Physiol. Chem. 355* (1974) 1135.
[24] J. Matheja, E. T. Degens, *Neues Jahrb. Geol. Paläont. Monatsh. 4* (1968) 215.
[25] M. A. Crenshaw, *Biomineralisation 6* (1972) 6.
[26] a) G. H. Nancollas (Ed.): *Biological Mineralization and Demineralization*, Springer, Berlin 1982; b) M. A. Crenshaw in [26a], p. 243.
[27] G. Krampitz, J. Engels, M. Hamm, C. Cazaux, *Biomineralisation 9* (1977) 59.
[28] G. Krampitz in [26a], p. 219.
[29] P. V. Hauschka, J. B. Lian, P. M. Gallop, *Proc. Natl. Acad. Sci. USA 72* (1975) 3925.
[30] M. J. Glimcher, B. Lefteriou, D. Kossiva, *Calcif. Tissue Int. 27* (1979) 83.
[31] M. J. Glimcher, D. Kossiva, A. Roufosse, *Calcif. Tissue Int. 27* (1979) 187.
[32] M. J. Glimcher, D. Brickley-Parsons, D. Kossiva, *Calcif. Tissue Int. 27* (1979) 281.
[33] J. B. Lian, M. Skinner, M. J. Glimcher, P. Gallop, *Biochem. Biophys. Res. Commun. 73* (1976) 349.
[34] J. Stenflo, P. Fernlund, W. Egan, P. Roepstorf, *Proc. Natl. Acad. Sci. USA 71* (1974) 2730.
[35] J. Stenflo, J. W. Suttie, *Annu. Rev. Biochem. 46* (1977) 157.
[36] K. King, *Biochem. Biophys. Acta 542* (1978) 542.
[37] L. Cohen-Solal, J. B. Lian, D. Kossiva, M. J. Glimcher, *Biochem. J. 177* (1979) 81.
[38] M. P. Molinari-Tosatti, L. Gotte, *Calcif. Tissue Res. 6* (1971) 329.

[39] D. A. Hall, *Biochem. J. 59* (1955) 459.
[40] R. Eisenstein, J. P. Ayer, S. Papajiannis, G. M. Hass, H. Hellis, *Lab. Invest. 13* (1964) 1198.
[41] M. P. Molinari-Tosatti, L. Galziguan, V. Moret, L. Gotte, *Calcif. Tissue Res. 2* (1968) 88.
[42] B. C. Starcher, G. Saccomani, D. W. Urry, *Biochim. Biophys. Acta 310* (1973) 481.
[43] B. C. Starcher, B. A. Cox, D. W. Urry, *Calcif. Tissue Res. 17* (1974) 1.
[44] D. W. Urry, *Proc. Natl. Acad. Sci. USA 68* (1971) 810.
[45] J. A. Foster, E. Bruenger, W. R. Gray, L. B. Sandberg, *J. Biol. Chem. 248* (1973) 2876.
[46] I. Mandl, R. S. Keller, *Proteins Relat. Subj. 22* (1975) 127.
[47] D. V. Van der Helm, T. V. Willoughby, *Acta Crystallogr. Sect. B25* (1969) 3217.
[48] D. W. Urry, W. D. Cummingham, T. Onishie, *Biochim. Biophys. Acta 292* (1973) 853.
[49] G. Krampitz, H. K. Erben, K. Kriesten, *Biomineralisation 4* (1972) 88.
[50] G. Krampitz, K. Kriesten, R. Faust, *Biomineralisation 7* (1974) 1.
[51] G. Krampitz, U. Koester, W. Fischer, *Z. Zool. Syst. Evolutionsforsch. 13* (1975) 125.
[52] G. Krampitz, W. Boehme, K. Kriesten, H. Hardebeck, *Z. Zool. Syst. Evolutionsforsch. 12* (1974) 1.
[53] H. K. Erben, G. Krampitz, *Biomineralisation 3* (1971) 51.
[54] S. Hunt: *Polysaccharide-Protein Complexes in Invertebrates*, Academic Press, London 1970.
[55] R. W. Wickhoff: *The Biochemistry of Animal Fossils*, Scientechnica, Bristol 1972, p. 71.
[56] H. Wuzel, *Dissertation*, Universität Bonn 1985.
[57] E. Marler, E. A. Davidson, *Proc. Natl. Acad. Sci. USA 54* (1965) 648.
[58] J. Eckert, R. Schade, H. Glock, G. Krampitz, A. Enbergs, J. Petersen, *J. Anim. Physiol. Anim. Nutri. 56* (1986) 258.
[59] G. Krampitz, W. Witt, *Top. Curr. Chem. 78* (1979) 57.
[60] E. Bonucci, *Calcif. Tissue Res. 24* (1977) Abstr. No. 16.
[61] B. Strates, W. F. Neumann, G. J. Levins, *J. Phys. Chem. 61* (1957) 279.
[62] M. S. Santanam, *J. Mol. Biol. 1* (1959) 65.
[63] B. N. Bachra, A. E. Sobel, J. W. Stanford, *Arch. Biochem. 84* (1959) 79.
[64] B. N. Bachra, A. E. Sobel, *Arch. Biochem. 85* (1959) 9.
[65] M. J. Glimcher, A. J. Hodge, F. O. Schmitt, *Proc. Natl. Acad. Sci. USA 43* (1957) 860.
[66] M. J. Glimcher in R. F. Soagnaes (Ed.): *Calcification in Biological Systems*, Am. Assoc. Adv. Sci., Washington DC 1960, p. 421.
[67] W. F. Neumann, M. W. Neumann: *The Chemical Dynamics of Bone Mineral*, University of Chicago Press, Chicago 1958, p. 169.
[68] M. J. Glimcher, L. C. Bonar, E. J. Daniel, *J. Mol. Biol. 3* (1961) 541.
[69] D. R. Taves, W. F. Neumann, *Arch. Biochem. 108* (1964) 390.
[70] a) A. Mehner, W. Hartfiel (Eds.): *Handbuch der Geflügelphysiologie*, VEB Fischer, Jena 1983; b) G. Krampitz in [70a], p. 1050.
[71] V. R. Meenakshi, P. E. Hare, K. M. Wilbur, *Comp. Biochem. Physiol. B Comp. Biochem. 40* (1971) 1037.
[72] N. Watabe, *J. Ultrastruct. Res. 12* (1963) 351.
[73] K. M. Wilbur, K. Simkiss, *Compr. Biochem. 26A* (1968) 229.
[74] S. Weiner, *Calcif. Tissue Int. 29* (1979) 163.
[75] S. Weiner, L. Hood, *Science (Washington) 190* (1975) 987.
[76] R. Schade, *Dissertation*, Universität Bonn 1986.
[77] R. Schade, *Arch. Geflügelkd. 51* (1987) 81.
[78] A. P. Wheeler, J. W. George, C. A. Evans, *Science (Washington) 212* (1981) 1397.
[79] S. Weiner, H. A. Lowenstam, L. Hood, *Proc. Natl. Acad. Sci. USA 73* (1976) 2541.
[80] M. A. Crenshaw, H. Ristedt in [17a], p. 353.
[81] G. Krampitz, *Haliotis 10* (1980) 82.
[82] T. Samata, G. Krampitz, *Malacologia 22* (1982) 225.
[83] T. Samata, P. Sanguansri, C. Cazaux, M. Hamm, J. Engels, G. Krampitz in M. Omori, N. Watabe (Eds.): *The Mechanisms of Biomineralization in Animals and Plants*, Tokai University Press, Tokyo 1980, p. 37.
[84] J. Gordon, M. R. Carriker, *Mar. Biol. (Berlin) 57* (1980) 251.
[85] S. Weiner, W. Traub, *FEBS Lett. 111* (1980) 311.
[86] G. E. Beedham, *Nature (London) 174* (1954) 750.
[87] M. A. Crenshaw, H. Heeley, *J. Dent. Res. 49B* (1967) 65.
[88] S. Hotta, *Earth Sci. Tokyo 23* (1969) 133.
[89] C. Grégoire, *Chem. Zool. 7* (1972) 45.
[90] T. Samata, private communication 1985.
[91] G. Krampitz, H. Drolshagen, S. Hotta, *Experientia 39* (1983) 1104.
[92] R. Schade, H. Glock, D. Röttgen, G. Krampitz, *J. Anim. Physiol. Anim. Nutri. 52* (1984) 1104.
[93] D. S. Howell, J. C. Pita, *Clin. Orthop. 118* (1976) 208.
[94] B. Engfeldt, A. Kulth, O. Westerborn, *Arch. Pathol. 68* (1959) 600.
[95] A. Hesse, H. Wuzel, *Urol. Int. 41* (1986) 81.
[96] A. Hesse, H. Wuzel, G. Krampitz, W. Vahlensieck, *Urol. Res. 15* (1987) 93.
[97] H. Fleisch, R. Felix, R. Schenk in H. Slavkin, R. E. Greulich (Eds.): *Extracellular Matrix Influences on Gene Expression*, Academic Press, New York 1975, p. 368.
[98] G. M. Herring, *Calcif. Tissue Res. 24* (1977) 29.
[99] S. Y. Ali, L. Evans, *Biochem. J. 112* (1969) 427.
[100] A. J. Barrett, *Biochem. J. 117* (1970) 601.
[101] H. B. Fell, T. J. Dingle, *Biochem. J. 87* (1963) 403.
[102] A. I. Sapolsky, R. D. Altmann, J. F. Woessner, D. S. Howell, *J. Clin. Invest. 52* (1973) 624.
[103] J. F. Woessner, R. J. Shamberger, *J. Biol. Chem. 246* (1971) 1951.
[104] A. A. Dogterom, A. Doderer, *Calcif. Tissue Int. 33* (1981) 505.
[105] H. K. Erben, *Biomineralisation 1* (1970) 1.
[106] G. Krampitz, J. Engels, I. Heindl, A. Heinrich, M. Hamm, R. Faust, *Arch. Geflügelkd. 38* (1974) 197.
[107] G. Krampitz, E. Greuel, K. Kriesten, H. Hardebeck, J. Engels, U. Koester, I. Helfgen, F. Arabi, *Berl. Münch. Tierärztl. Wochenschr. 86* (1973) 313.
[108] G. Krampitz, H. K. Erben, K. Kriesten, *Biomineralisation 4* (1972) 88.
[109] J. Wolken, *Anat. Rec. 111* (1951) 79.
[110] J. R. Baker, D. A. Balch, *Biochem. J. 82* (1962) 352.
[111] K. Simkiss, T. G. Taylor, *Phys. Biochem. Domest. Fowl 3* (1971) 1331.
[112] E. Wedral, D. V. Vadehra, R. C. Baker, *Comp. Biochem. Physiol. B Comp. Biochem. 47* (1974) 631.
[113] D. V. Vadehra, K. R. Nath, R. C. Baker, *Poult. Sci. 50* (1971) 1638.
[114] J. K. Candlish, R. G. Scougall, *Int. J. Protein Res. 1* (1969) 299.
[115] K. Simkiss, C. Tyler, *Q. J. Microsc. Sci. 98* (1957) 12.
[116] A. Paul-Gardais, J. Picard, B. Hermelin, *Biochim. Biophys. Acta 354* (1974) 11.
[117] D. A. Balch, R. A. Cooke, *Ann. Biol. Anim. Biochim. Biophys. 10* (1970) 13.
[118] R. J. Hasiak, D. V. Vadehra, R. C. Baker, *Comp. Biochem. Physiol. 37* (1970) 429.
[119] R. J. Hasiak, D. V. Vadehra, R. C. Baker, *Comp. Biochem. Physiol. 35* (1970) 761.
[120] A. Heinrich, *Dissertation*, Universität Bonn 1975.
[121] M. Müller, R. Schade, G. Krampitz, *Arch. Geflügelkd. 51* (1987) 121.
[122] K. Bronsch, T. Diamantstein, *Zentralbl. Veterinärmed. 2* (1964) 323.
[123] G. Krampitz, J. Engels, I. Heindl, *Arch. Geflügelkd. 39* (1975) 189.
[124] G. Krampitz, K. Kriesten, I. Helfgen, *Experientia 30* (1975) 228.
[125] R. S. Bernstein, J. Nevalainen, F. Schraer, H. Schraer, *Biochem. Biophys. Acta 159* (1968) 367.
[126] T. Diamantstein, F. Schlüns, *Acta Histochem. 19* (1964) 269.
[127] A. Potz, G. Krampitz, *Arch. Geflügelkd. 45* (1981) 9.
[128] F. Schlüns, T. Diamantstein, *Nature (London) 209* (1960) 304.
[129] G. Krampitz, J. Engels, *Proteins Relat. Subj. 22* (1975) 355.
[130] W. J. Schmidt, *Z. Zellforsch. Mikros. Anat. 68* (1965) 874.
[131] A. R. Terepka, *Exp. Cell Res. 30* (1963) 183.
[132] W. Hartfiel in [70a], Part II, p. 703.
[133] D. Wieser, G. Krampitz, *Zuchthygiene 22* (1987) 267.
[134] J. W. Campbell, K. V. Speeg, *Nature (London) 224* (1969) 725.
[135] G. Reddy, J. W. Campbell, *Experientia 28* (1972) 530.
[136] G. Krampitz, P. Fischer, *Z. Tierphysiol. Tierernähr. Futtermittelkd. 50* (1983) 113.
[137] K. P. Linn, *Dissertation*, Universität Bonn 1986.

When submitting manuscripts, authors of articles intended for publication as "Communications" are requested to read the "Notice to Authors" reproduced in the January issue of the journal following the list of contents; upon request, a copy can be obtained from the editorial office.

1,4-Diphospha-2-rhodacyclopentadiene—an Isolable Intermediate in the Metal-Induced Cyclodimerization of *tert*-Butylphosphaacetylene**

By *Paul Binger,* Bruno Biedenbach, Richard Mynott, Carl Krüger, Peter Betz,* and *Manfred Regitz*

Cyclodimerizations of *tert*-butylphosphaacetylene **3** in the coordination sphere of a metal atom have only recently been reported. Depending on the metal, one obtains either the 1,3-diphosphacyclobutadiene complexes **1**[1,2] (M = Co, Rh) or the 1,3-diphosphabicyclo[1.1.0]butanediyl complex **2**.[3] 1,4-Diphospha-2-metallacyclopentadienes, formed by oxidative coupling of two phosphaalkynes at the metal center, have been postulated as intermediates in these reactions.[1b] We have now succeeded in isolating and characterizing such a species for the first time. This species was shown to undergo transformation to a corresponding 1,3-diphosphacyclobutadiene complex in solution.

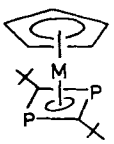

1

M= Co,Rh

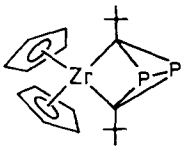

2

Reaction of $[(C_2H_4)_2RhCl]_2$ with trimethylphosphane and *tert*-butylphosphaacetylene **3** in a molar ratio of 1:4:4 at 0°C resulted in the formation of a 1:2 mixture (^{31}P NMR) of the two rhodium complexes **4** and **5**, which could be separated by extraction with pentane and ether. The known rhodium complex $[(Me_3P)_2RhCl]_2$[4] is presumably formed as an intermediate in this reaction, but it was not isolated.

The X-ray crystal structure analyses of the two new rhodium complexes show that **4** is a chlorobis(trimethylphosphane)-1,4-diphospha-2-rhodacyclopentadiene derivative and that **5** is the corresponding 1,3-diphosphacyclobutadiene derivative.[5] The structure of **4** (Fig. 1, top) is

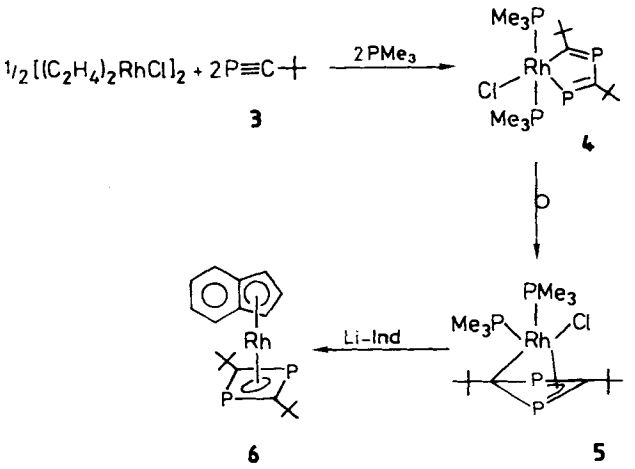

3 **4** **5** **6**

best described as a distorted octahedron, whose base is defined by the atoms P1, C5, Cl, and a fourth, vacant coordination site; the apices are occupied by P3 and P3*. The heterocycle lies in the crystallographic mirror plane of the molecule. The P1–C1 and P2–C5 distances (1.685(4) and 1.710(4) Å, respectively) fall in the range for PC double-bond distances.[6] The Rh–P1 and Rh–C5 distances (2.235(1) and 1.980(3) Å, respectively) also agree with expectations. Furthermore, the spectroscopic data (MS, ^{31}P and ^{13}C NMR)[7] are in agreement with this structure.

Complex **5** has a distorted tetrahedral structure (Fig. 1, bottom). The P_2C_2 four-membered ring is nonplanar, forming a dihedral angle of 5.1° between the two CP_2 planes. Whereas the bonds Rh–P1 and Rh–P2 are roughly of the same length (2.381(1) and 2.397(1) Å, respectively), the distance Rh–C1 (2.179(3) Å) is markedly shorter than Rh–C6 (2.307(3) Å, *trans* effect of the chlorine atom). In agreement with these findings, two sharp multiplets at $\delta = 84.5$ and 149.8 are observed for C1 and C6 in the ^{13}C NMR spectrum of **5**;[7] i.e., no rotation of the ring is apparent at 40°C. A slow exchange of C1 and C6 could only be demonstrated by ^{13}C 2D NMR exchange spectroscopy.[8] The large difference in the chemical shifts of the ring C atoms[9] and the spin–spin coupling constants[7] show that the bonding of the P_2C_2 ring to the Rh atom is best described as η^1,η^2 bonding.

By reaction with indenyllithium, complex **5** can be transformed into the known complex[10] η^4-(2,4-*tert*-butyl-1,3-diphosphacyclobutadiene)-η^5-indenylrhodium **6** (12 h stirring at 20°C in THF, yield 60%; ^{31}P NMR: $\delta = 35.6$ (d, $J_{Rh,P} = 31.3$ Hz)). It can also be shown by ^{31}P and ^{13}C NMR spectroscopy that complex **4** slowly rearranges to **5** in solution at room temperature (in 24 h, 40%). Thus, 1,4-diphospha-2-metallacyclopentadienes are clearly intermediates in the η^4-diphosphacyclobutadiene–metal complex formation (e.g., of **1**). Even the synthesis of the zirconium compound **2** can be interpreted quite well in terms of this intermediate.

Experimental Procedure

$[(C_2H_4)_2RhCl]_2$ (3.24 g, 8.3 mmol) was dissolved in 100 mL of THF at 0°C and trimethylphosphane (2.57 g, 34 mmol) was added to the solution, which was then stirred for 1 h at 0°C. Compound **3** (3.3 g, 33 mmol) dissolved in 30 mL of THF was then added dropwise over 2 h and the resulting reaction solution was stirred for an additional 2 h. All volatiles were removed at 10^{-2}

[*] Prof. Dr. P. Binger, Dipl.-Chem. B. Biedenbach, Dr. R. Mynott, Prof. Dr. C. Krüger, Dr. P. Betz
Max-Planck-Institut für Kohlenforschung
Kaiser-Wilhelm-Platz 1, D-4330 Mülheim an der Ruhr (FRG)
Prof. Dr. M. Regitz
Fachbereich Chemie der Universität
Erwin-Schrödinger-Strasse, D-6750 Kaiserslautern (FRG)

[**] This work was supported by the Stiftung Volkswagenwerk.

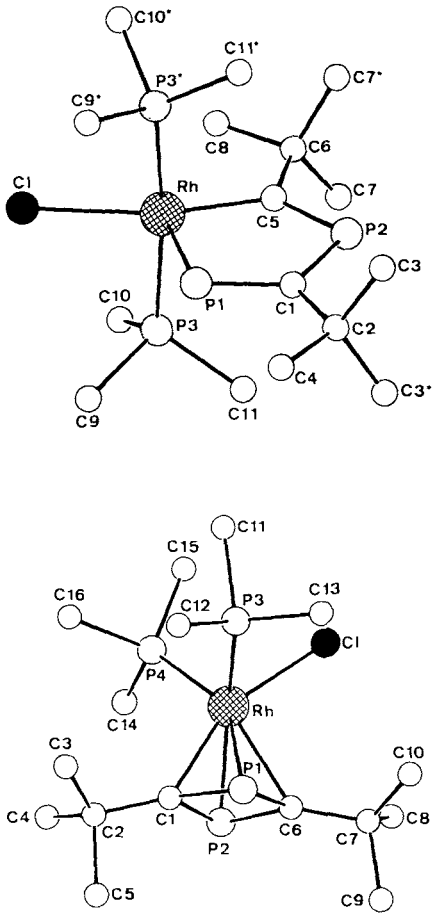

Fig. 1. Top: Molecular structure of **4** (crystallographic numbering). Selected bond lengths [Å] and bond angles [°]: Rh-P1 2.235(1), Rh-P3 2.345(1), Rh-Cl 2.456(1), Rh-C5 1.980(3), P1-C1 1.685(4), P2-C1 1.802(3), P2-C5 1.710(4), C1-C2 1.532(5), C5-C6 1.549(5); P3-Rh-P3* 171.6(1), Cl-Rh-P3 87.3(1), Cl-Rh-P1 110.5(1), Cl-Rh-C5 161.9(1), P3-Rh-P1 88.0(1), P3-Rh-C5 93.6(1), P1-Rh-C5 87.6(1), Rh-P1-C1 107.9(1), P1-C1-C2 122.1(3), P1-C1-P2 118.7(2), C2-C1-P2 119.2(3), C1-P2-C5 100.2(2), P2-C5-C6 118.9(2), P2-C5-Rh 125.6(2), C6-C5-Rh 115.5(2).—Bottom: Molecular structure of **5** (crystallographic numbering). Selected bond lengths [Å] and angles [°]: Rh-Cl 2.473(1), Rh-P1 2.381(1), Rh-P2 2.397(1), Rh-P3 2.325(1), Rh-P4 2.334(1), Rh-C1 2.179(3), Rh-C6 2.307(3), P1-C1 1.802(3), P1-C6 1.766(3), P2-C1 1.819(3), P2-C6 1.792(3); P1-Rh-P2 69.2(1), P1-Rh-C1 46.3(1), P1-Rh-C6 44.2(1), C1-Rh-P2 46.5(1), C6-Rh-P2 44.7(1), C1-Rh-C6 63.0(1), P1-C1-P2 97.1(1), C1-P2-C6 81.1(1), P2-C6-P1 99.3(1), C6-P1-C1 82.3(1).

torr, the residue was extracted with 60 mL of pentane, and the filtered solution was concentrated to one-half of its original volume and then diluted with 15 mL of diethyl ether. Cooling the solution to −60°C resulted in the crystallization of **4** (0.68 g, 8.4%; reddish-brown crystals). The solid residue of the pentane extraction was dissolved in 50 mL of diethyl ether, filtered through Al_2O_3, and kept at −20°C for 24 h. Orange crystals of **5** were thereby obtained (2.3 g, 28%, dec. >146°C).

Received: March 28, 1988 [Z 2680 IE]
German version: *Angew. Chem. 100* (1988) 1219

CAS Registry numbers:
3, 78129-68-7; **4**, 116149-70-3; **5**, 116149-71-4; $[(C_2H_4)_2RhCl]_2$, 12081-16-2.

[1] a) P. Binger, R. Milczarek, R. Mynott, M. Regitz, W. Rösch, *Angew. Chem. 98* (1986) 645; *Angew. Chem. Int. Ed. Engl. 25* (1986) 644; b) P. Binger, R. Milczarek, R. Mynott, E. Raabe, C. Krüger, M. Regitz, *Chem. Ber. 121* (1988) 637.

[2] P. B. Hitchcock, M. J. Maah, J. F. Nixon, *J. Chem. Soc. Chem. Commun. 1986*, 737.

[3] P. Binger, B. Biedenbach, C. Krüger, M. Regitz, *Angew. Chem. 99* (1987) 798; *Angew. Chem. Int. Ed. Engl. 26* (1987) 764.

[4] H. Werner, R. Feser, W. Buchner, *Chem. Ber. 112* (1979) 834.

[5] a) Crystal structure analysis of **4**: $C_{16}H_{36}ClP_4Rh$, space group *Pnma*, $a=17.927(4)$, $b=12.660(2)$, $c=10.712(1)$ Å, room temperature, $Z=4$, $\rho_{calcd}=1.34$ g cm^{-3}, $\mu(Mo_{K\alpha})=10.59$ cm^{-1}, Enraf-Nonius diffractometer; 9318 measured reflections, averaged to 4352, 3083 observed reflections ($I>2\sigma(I)$); $R=0.029$, $R_w=0.038$ ($w=1/\sigma^2(F_0)$) for 115 parameters [5c]; b) crystal structure analysis of **5**: $C_{16}H_{36}ClP_4Rh$, space group $P2_1/n$, $a=9.258(1)$, $b=24.700(3)$, $c=10.602(3)$ Å, $\beta=98.91(1)°$, room temperature, $Z=4$, $\rho_{calcd}=1.36$ g cm^{-3}, $\mu(Mo_{K\alpha})=10.75$ cm^{-1}, Enraf-Nonius diffractometer; 5828 measured reflections, averaged to 5415, 4489 observed reflections ($I>2\sigma(I)$); $R=0.028$, $R_w=0.036$ ($w=1/\sigma^2(F_0)$) for 199 parameters [5c]; c) Further details of the crystal structure investigation may be obtained from the Fachinformationszentrum Energie, Physik, Mathematik GmbH, D-7514 Eggenstein-Leopoldshafen 2 (FRG), on quoting the depository number CSD-52985, the names of the authors, and the journal citation.

[6] a) R. Appel, J. Kochta, F. Knoch, *Chem. Ber. 120* (1987) 131; b) J. Fink, W. Rösch, U.-J. Vogelbacher, M. Regitz, *Angew. Chem. 98* (1987) 265; *Angew. Chem. Int. Ed. Engl. 26* (1987) 280.

[7] Spectroscopic data of **4** (numbering as in Fig. 1): ^{31}P NMR (81.0 MHz, H_3PO_4 ext.): $\delta=494.3$ ($J_{Rh,P1}=45.7$, $J_{P1,P2}=24.6$, $J_{P1,P3}=18.2$ Hz; P1), 318.9 ($J_{Rh,P2}=16.3$ Hz; P2), −10.7 ($J_{Rh,P3}=121.3$ Hz; P3); ^{13}C NMR (75.5 MHz, C_6D_6): $\delta=261.6$ ($J_{P2,C5}=52.5$, $J_{Rh,C5}$ and $J_{P1,C5}=29.8$ and 23.6, $J_{P3,C5}=6.6$ Hz; C5), 231.1 ($J_{P1,C1}=81.7$, $J_{P2,C1}=56.4$, $J_{P3,C1}=3.8$ Hz; C1), 47.8 ($J_{P2,C}=20.1$ Hz; $C(CH_3)_3$ on C5), 43.0 ($J_{P1,C}=19.5$, $J_{P2,C}=11.9$ Hz; $C(CH_3)_3$ on C1), 33.2 ($J_{P,C}=13.3$, 8.1, $J_{P3,C}=2.1$ Hz; $C(CH_3)_3$ on C1), 32.9 ($J_{P2,C}=14.5$ Hz; $C(CH_3)_3$ on C5), 14.1 ($J_{P3,C}+J_{P3*,C}=32.6$, $J_{Rh,C}$ or $J_{P,C}=4.6$ Hz; PCH_3). Assignment supported by ^{31}P,^{1}H, and ^{13}C,^{1}H 2D correlated NMR spectra, optimized for long-range couplings.—**5** (numbering as in Fig. 1): ^{31}P NMR (AA'MM'X spectrum; A, M = ^{31}P, X = ^{103}Rh): $\delta=51.7$ ($J_{P1,P3}$ and $J_{P1,P4}=26.2$ and 23.6, $J_{P1,3,Rh}=17.8$ Hz; P1, P2), 6.6 ($J_{P3,4,Rh}=145.2$ Hz; P3, P4); ^{13}C NMR (75.5 MHz, C_6D_6): $\delta=149.8$ ($J_{P1,2,C6}=61.2$, $J_{Rh,C6}=8.3$, $J_{P3,4,C6}=3.8$ Hz; C6), 84.5 ($J_{P1,2,C1}=49.0$, $J_{Rh,C1}=15.3$, $J_{P3,4,C1}=1.6$ Hz; C1), 37.8 ($J_{P1,2,C}=6.6$ Hz; $C(CH_3)_3$), 33.5 ($J_{P1,2C}=7.2$ Hz; $C(CH_3)_3$), 31.8, 30.5 ($J_{P,C}=5.0$ Hz; $C(CH_3)_3$), 22.1 (PCH_3).

[8] a) B. H. Meier, R. R. Ernst, *J. Am. Chem. Soc. 101* (1979) 644; J. Jeener, B. H. Meier, P. Bachmann, R. R. Ernst, *J. Chem. Phys. 71* (1979) 4546.

[9] P. W. Jolly, R. Mynott, *Adv. Organomet. Chem. 19* (1981) 289.

[10] P. Binger, B. Biedenbach, in press.

Synthesis of Oligomeric and Polymeric Monosaccharides by Aldol Group-Transfer Polymerization**

By *Günter Wulff,* Paul Birnbrich,* and *Achim Hansen*

Following the earlier described group-transfer polymerization of acrylates,[1,2] an aldol group-transfer polymerization (aldol-GTP), involving the Lewis acid-catalyzed reaction of trialkylsilyl vinyl ethers **1** with aldehydes, has recently been reported[3] (see Scheme 1). Cleavage of the silyl groups affords oligomeric or polymeric polyvinyl alcohols **2b**.

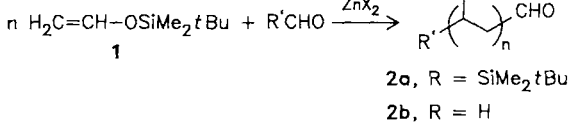

1

2a, R = $SiMe_2tBu$
2b, R = H

We have now succeeded in carrying out an aldol-GTP on the enediolate 2-phenyl-1,3,2-dioxaborole **5** producing oligomeric and polymeric monosaccharides (see also Ref. [2a], p. 74). The dioxaborole **5** was originally prepared via an anthracene adduct through retro-Diels–Alder reaction.[4,5] Now, it can be obtained more readily from 2-phenyl-1,3,2-dioxaborolane **3** (prepared from phenylboronic acid and ethylene glycol) by photochlorination with sulfuryl chloride to give the monochloro derivative **4** and sub-

[*] Prof. Dr. G. Wulff, Dipl.-Chem. P. Birnbrich, Dr. A. Hansen
Institut für Organische Chemie und Makromolekulare Chemie der Universität
Universitätsstrasse 1, D-4000 Düsseldorf (FRG)

[**] This work was supported by the Deutsche Forschungsgemeinschaft and the Fonds der Chemischen Industrie.

sequent thermal elimination of HCl. Dioxaborole **5**, prepared in this manner, contains trace amounts of HCl; however, this is advantageous for catalyzing the aldol-GTP reaction and does not initiate cationic polymerization.

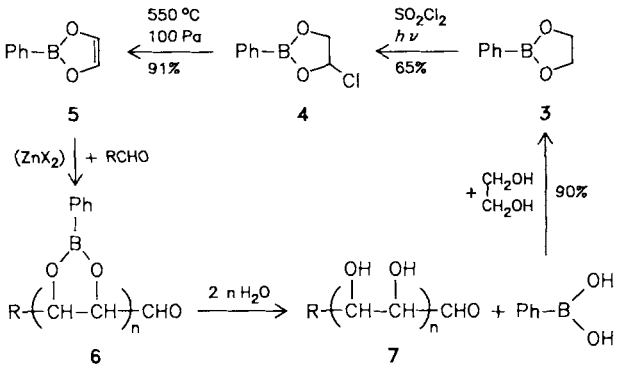

The heterocycle **5** undergoes an aldol reaction with an aldehyde to give, initially, the mono- and diaddition products, both of which could be isolated.[4,5] In both cases, the reaction products still contain a reactive aldehyde group. As a result, in the presence of excess **5**, the reaction directly leads, without addition of a catalyst, to oligomeric and polymeric products **6**.[6] Compound **5** reacts with aldehydes much faster than with silyl enol ethers **1**. This acceleration of the reaction rate may be attributed to the participation of the boron atom in the transition state of the reaction (see Scheme 1). The reaction rate is significantly enhanced by the addition of zinc halides.

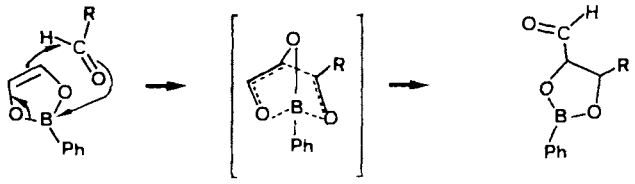

Scheme 1.

The terminal aldehyde group in the polymers **6** and **7** is present in equilibrium with pyranoid and furanoid hemiacetals, as was shown previously for diaddition products.[4,5] However, it can also react as an aldehyde, for example with 2,4-dinitrophenylhydrazine to give the corresponding hydrazone derivative. Furthermore, addition of new monomer, even after several hours, leads to a continuation of the polymerization, resulting in the formation of a high-molecular-weight polymer having monomodal molecular weight distribution; therefore, this process can be described, according to the definition of *M. Szwarc* et al.,[7] as a living polymerization.

Preliminary investigations on the constitution of the polymers indicate that exchange processes occur in the boron-containing polymer **6**. The five-membered 1,3,2-dioxaborolane structures are partially transformed into the six-membered 1,3,2-dioxaborinane structures, similar to the earlier observations made by *R. Köster* et al.[8] in the case of ethylboronates of sugar alcohols. In analogy with the results obtained in the low-molecular-weight range,[5] presumably the chains in the deprotected polymers **7** primarily contain isotactic and heterotactic triads. In the polyvinyl alcohols **2**, on the other hand, a random arrangement is found.

As shown in Table 1, the molecular weight can be controlled by the ratio of initiator to monomer, suggesting the occurrence of a transfer-free polymerization. Furthermore, the polydispersity indices of the polymers (Table 1) reveal a largely non-terminated polymerization. Polymers having molecular weights between 700 and 130000 were prepared. Both mono- and dialdehydes can be employed as initiators, the former producing monofunctional macromers, the later producing bifunctional telechelics. Both types of polymers can be used as building blocks for the construction of complex polymeric materials. This holds particularly true for unsaturated oligomers (Table 1, entries 1 and 2).

The boronic acids can be cleaved hydrolytically from the oligomers and polymers if the phenylboronic acid is removed from the equilibrium. The phenylboronic acid can be reused, so that, in principle, it is possible to synthesize the products **7**[6] starting from ethylene glycol. These are oligomeric or polymeric monosaccharides and can be used directly as macromers or telechelics. Interestingly, the higher-molecular-weight products are no longer water-soluble, as has already been shown for the products obtained by polymerization of vinylene carbonate followed by removal of carbonic acid.[9]

Received: March 21, 1988 [Z 2671 IE]
German version: *Angew. Chem. 100* (1988) 1197

Table 1. The effect of the ratio of initiator to monomer on the molecular weight of **6**.

No.	Initiator [mmol mL^{-1}]	Monomer **5** [mmol mL^{-1}]	Catalyst [mmol mL^{-1}]	M_n (found) [a] [g mol^{-1}]	M_n (calcd) [b] [g mol^{-1}]	$\frac{M_w}{M_n}$ [a]	Yield [%]
1	H_2C=CH–C_6H_4–CHO 1.52	7.6	— —	700	861	1.5	82
2	H_2C=CH–$(CH_2)_8$–CHO 1.3	7.53	— —	1200	1013	1.6	58
3	C_6H_5CHO 0.2	1.5	$ZnCl_2$ 0.078	1100	1200	1.5	90
4	C_6H_5CHO 0.1	1.5	ZnI_2 0.052	2400	2293	1.1	80
5	OHC–C_6H_4–CHO 0.082	3.0	$ZnCl_2$ 0.1	5000	5468	— [c]	75
6	OHC–C_6H_4–CHO 0.04	6.28	$ZnCl_2$ 0.068	12000	23025	2.2	67
7	OHC–C_6H_4–CHO 0.0125	6.33	$ZnBr_2$ 0.058	130000	73967	— [c]	40

[a] Determined by gel chromatography using polystyrene standards [10]. [b] Calculated from the monomer/initiator ratio. All polymerizations were carried out at room temperature. Solvent: THF (diethyl ether for entry 4). [c] Not calculated.

[1] O. W. Webster, W. R. Hertler, D. Y. Sogah, W. B. Farnham, T. V. Rajan Babu, *J. Am. Chem. Soc. 105* (1983) 5706.
[2] a) M. Fontanille, A. Guyot (Eds.): Recent Advances in Mechanistic and Synthetic Aspects of Polymerization, D. Reidel, Dordrecht, Holland 1987, Section I with six articles, pp. 1-76; b) M. T. Reetz, R. Ostarek, K.-E. Piejko, D. Arlt, B. Bömer, *Angew. Chem. 98* (1986) 1116; *Angew. Chem. Int. Ed. Engl. 25* (1986) 1108; see also: M. T. Reetz, *ibid. 100* (1988) 1026 and 994.
[3] D. Y. Sogah, O. W. Webster, *Macromolecules 19* (1986) 1775.
[4] G. Wulff, A. Hansen, *Angew. Chem. 98* (1986) 552; *Angew. Chem. Int. Ed. Engl. 25* (1986) 560.
[5] G. Wulff, A. Hansen, *Carbohydr. Res. 164* (1987) 123.
[6] *General Experimental Procedure:* Compound **5** and the initiator aldehyde were allowed to react at room temperature in the appropriate solvent (in some cases, in the presence of ZnX_2) under inert atmosphere (see Table 1). After 3-24 h the reaction mixture was added dropwise to hexane in order to precipitate the polymer. Purification was accomplished by precipitation from THF in petroleum ether (60-80). Cleavage of phenylboronic acid was achieved by stirring the polymer for several days in a two-phase system of ether/water.
[7] a) M. Szwarc, M. Levy, R. Milkowich, *J. Am. Chem. Soc. 78* (1956) 2656; b) M. Szwarc: *Living Polymers and Mechanisms of Anionic Polymerization (Adv. Polym. Sci. 49* (1983)).
[8] W. Fenzl, W. V. Dahlhoff, R. Köster, *Liebigs Ann. Chem.* (1980) 1176.
[9] a) C. C. Unruh, D. A. Smith, *J. Org. Chem. 23* (1958) 625; b) N. D. Field, J. R. Schaefgen, *J. Polym. Sci. 58* (1962) 533.
[10] P. E. Slade, Jr.: *Techniques and Methods of Polymer Evaluation, Polymer Molecular Weights (Part II)*, Marcel Dekker, New York 1975, p. 298 ff.

Trimethylplatinum-Theophylline Hexamer: A Novel Pt_6 Heterocycle Containing Both Pt-N and Pt-O Bonds**

By *Jörg Lorberth*, Werner Massa, Mohy E.-Essawi,* and *Lilian Labib*

Dedicated to Professor Heinrich Nöth on the occasion of his 60th birthday

In the trimethylplatinum series $[Me_3Pt-X]_n$, the only known compound for $n=1$ is $[Me_3PtC_5H_5]$.[1] Several 1,3-diketone complexes containing Pt-O and Pt-C bonds are known for $n=2$;[2,3] no compounds are known for $n=3$. The largest number of compounds have been reported for $n=4$; these have "cubane-like" frameworks in which halogens, pseudohalogens, and similar ligands bridge three Pt atoms; examples have been reported for X = Cl,[4,5] Br,[6] I,[7,8] N_3,[9] SCN,[10] OH,[11] and SCH_3.[12,13]

Trimeric units have been postulated for trimethylplatinum complexes of the anion of the pharmacologically active purine base theophylline (Hthp) on the basis of NMR

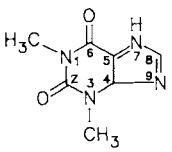

Theophylline (Hthp)

spectroscopic data and osmometrically determined molecular weights.[14] Using modified conditions, we have obtained crystals of Me_3Pt-thp·$2CHCl_3$; its X-ray structure analysis[19] surprisingly revealed the following novel structure: Trimethylplatinum-theophylline is present as hexameric units having symmetry $\bar{3}$ (C_{3i}), in which one Me_3Pt group is coordinated in a *cis* fashion by N7 and N9 of neighboring purine molecules; a Pt-O bond to O6 of a guanine framework completes the distorted octahedral coordination of the Pt atoms. The extent of the slight octahedral distortion is revealed by the "*cis*" bond angles of 82-98° and the "*trans*" bond angles of 172-177° (Fig. 1).

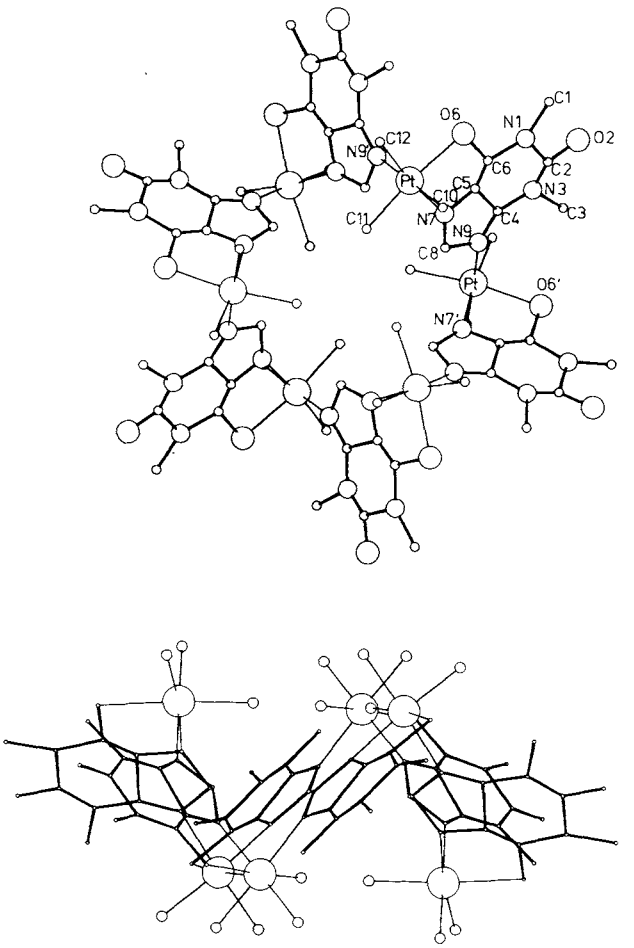

Fig. 1. Molecular structure of the hexamer $[Me_3Pt\text{-thp}]_6$ of $[Me_3Pt\text{-thp}]_6 \cdot 12CHCl_3$. Top: View along the $\bar{3}$ axis (arbitrary atomic radii). Bottom: Side view of the molecule. Important bond lengths [pm] and angles [°]: Pt-N9 221(2), Pt-N7′ 217(2), Pt-O6′ 234(2), Pt-C10 205(2), Pt-C11 207(2), Pt-C12 207(3), N1-C1 148(3), N1-C2 141(3), C2-O2 122(3), C2-N3 139(3), N3-C3 148(3), N3-C4 141(3), C4-N9 133(3), C4-C5 136(3), C5-C6 140(3), C6-O6 129(3), C5-N7 137(3), N7-C8 137(3), C8-N9 138(2), C6-N1 137(3); N9-Pt-N7′ 85.3(6), N9-Pt-O6′ 92.5(7), N9-Pt-C11 94.2(8), N9-Pt-C12 91.2(9), N9-Pt-C10 175.8(9), N7′-Pt-O6′ 78.8(7).

The Pt-N distances (217 and 221 pm) and Pt-O distance (234 pm) are in the range expected from comparable $[Me_3Pt-X]_4$ tetramers (Table 1); the Pt-C distances (205-207 pm) are nearly identical with those in the tetramers. A side view of the hexamer in Figure 1, bottom, shows more clearly the salient features of this structure: the six thp ligands are oriented by a *cis*-arrangement of neighboring guanine rings (as observed in the complexation of Pt^{II} complexes by DNA) and, additionally, by a Pt-O bond (which completes the octahedral coordination of the Pt^{IV} atom) in such a way that they lie in a layer with three Me_3Pt groups on either side.

The presence of a Pt-O bond in addition to the expected Pt-N bonds is new: even in cases where this should, in

[*] Prof. Dr. J. Lorberth, Priv.-Doz. Dr. W. Massa
Fachbereich Chemie der Universität
Hans-Meerwein-Strasse, D-3550 Marburg (FRG)
Dr. L. Labib, Prof. Dr. M. El-Essawi
Chemistry Department, University of Alexandria
Alexandria, A.R.E. (Egypt)

[**] This work was supported by Degussa, Hanau, through donation of chemicals.

Table 1. Comparison of selected structural parameters of the tetramers $[Me_3Pt\text{-}X]_4$ and $[Me_3Pt\text{-}thp]_6$.

X	Pt-X [pm]	Pt-Pt [pm]	X-X [pm]	X-Pt-X [°]	Pt-X-Pt [°]	Pt-C [pm]	Ref.
Cl	248	373	328	81.0	99.0	209	[4]
Br	268	393	363	85.4	94.3	201	[6]
I	281.9	411	385.2	86.2	93.7	202	[8]
OH	222	342.0	278	77.6	101.2	204	[11]
N_3	225	344.9		80.0	100.0	205	[9]
SCN	255 (S) 208 (N)	383		82.4	97.3	203	[10]
SCH_3	247	378	315	79.3	99.1	207	[13]
$[Me_3Pt\text{-}thp]_6$	217 (N) 221 (N) 234 (O)			85.5		206	this work

principle, be possible for Pt^{IV} atoms, e.g., in a *trans*-$[(NH_3)_2Pt^{IV}$(1-methylcytosine)] complex,[15] chelate ring formation through nitrogen atoms is observed exclusively; this problem has been discussed in detail.[16] Chelate complexes of titanocene with xanthine[17] and theophylline[18] show, in the case of xanthine, the unique presence of two N,O-coordinated as well as one N,Cl-coordinated titanocene group, whereas, for theophylline, only a 1 : 1 complex with titanocene (N7-O6 coordination) is formed.

Experimental Procedure

An aqueous solution (20 mL) containing the potassium salt of theophylline (0.38 g, 0.17 mmol) was added dropwise at room temperature to a solution of $[Me_3Pt(H_2O)_3]_2SO_4$ (0.5 g, 0.086 mmol) in 20 mL of water. The resulting solution was refluxed for 5 h and then filtered. The filtrate was concentrated under vacuum and the solid, white residue was recrystallized from dry acetonitrile. White crystals, m.p. >215°C (dec.), were obtained. Yield: ca. 50%. For the X-ray crystal structure analysis, a small sample was recrystallized from dry $CHCl_3$.

Received: February 15, 1988;
revised: May 27, 1988 [Z 2619 IE]
German version: *Angew. Chem. 100* (1988) 1194

CAS Registry numbers:
$[Me_3Pt(H_2O)_3]_2SO_4$, 7270-24-8; $[Me_3Pt\text{-}thp]_6$, 115960-35-5; $[Me_3Pt\text{-}thp]_6 \cdot 12CHCl_3$, 116050-13-6; Hthp-potassium salt, 57533-87-6.

[1] G. W. Adamson, J. C. Bart, J. J. Daly, *J. Chem. Soc. A 1971*, 2616.
[2] A. G. Swallow, M. R. Truter, *Proc. R. Soc. London Ser. A 252* (1960) 205.
[3] A. C. Hazell, M. R. Truter, *Proc. R. Soc. London Ser. A 252* (1980) 218.
[4] R. E. Rundle, J. D. Sturdivant, *J. Am. Chem. Soc. 69* (1947) 1561.
[5] R. N. Hargreaves, M. R. Truter, *J. Chem. Soc. A 1971*, 90.
[6] W. Massa, G. Baum, B. S. Seo, J. Lorberth, *J. Organomet. Chem.* (1988), in press.
[7] G. Donnay, L. B. Coleman, N. G. Krieghoff, D. O. Cowan, *Acta Crystallogr. Sect. B 24* (1968) 287.
[8] R. Allmann, D. Kucharczyk, *Z. Kristallogr. 165* (1983) 227.
[9] M. Atam, U. Müller, *J. Organomet. Chem. 71* (1974) 435.
[10] B. Vance, *J. Organomet. Chem. 336* (1987) 441.
[11] H. S. Preston, J. C. Mills, C. H. L. Kennard, *J. Organomet. Chem. 14* (1968) 447.
[12] G. Smith, C. H. Kennard, T. C. Mak, *J. Organomet. Chem. 290* (1985) C7.
[13] H. Herdtweck, B. S. Seo, H. Donath, J. Lorberth, *J. Organomet. Chem.* (1988), in press.
[14] N. H. Agnew, T. G. Appleton, J. R. Hall, G. F. Kilmister, I. J. McMahon, *J. Chem. Soc. Chem. Commun. 1979*, 324.
[15] R. Beyerle-Pfnür, H. Schöllhorn, U. Thewalt, B. Lippert, *J. Chem. Soc. Chem. Commun. 1985*, 1510.
[16] J. Reedijk, A. M. J. Fichtinger-Schepman, A. T. van Oosterom, P. van de Putte, *Struct. Bonding Berlin 67* (1987) 53.
[17] A. L. Beauchamp, F. Belanger-Gariepy, A. Mardhy, D. Cozak, *Inorg. Chim. Acta 124* (1986) L23.
[18] D. Cozak, A. Mardhy, M. J. Olivier, A. L. Beauchamp, *Inorg. Chem. 25* (1986) 2600.
[19] Crystal structure determination of $C_{10}H_{16}N_4O_2Pt \cdot 2CHCl_3$: space group $R\bar{3}$, $a = 2220.7(8)$, $c = 2231.4(9)$ pm, $Z = 18$, 1322 unique reflections with $F_0 > 5\sigma$ were measured on a four-circle diffractometer (CAD4, Enraf-Nonius) with $Mo_{K\alpha}$ radiation at 163 K; no absorption correction ($\mu = 70.9$ cm^{-1}). Application of anisotropic temperature factors for Pt and Cl (136 parameters, H atoms omitted) gave residual indices of $R = 0.054$, $R_w = 0.049$ ($w = 1/\sigma^2(F_0)$). Despite the low temperature of measurement, the two $CHCl_3$ molecules exhibit in part very high temperature factors, indicating the existence of disorder, which may have affected the results of the refinement. Further details of the crystal structure investigation may be obtained from the Fachinformationszentrum Energie, Physik, Mathematik GmbH, D-7514 Eggenstein-Leopoldshafen 2 (FRG), on quoting the depository number CSD-53 187, the names of the authors, and the journal citation.

Naked Molecule Chemistry: Different Bonding Modes of CO to FeX_2**

By *Ian R. Beattie,* Susan D. McDermott, Elizabeth A. Mathews, Keith R. Millington,* and *Andrew D. Willson*

It is well established that many metal halides isolated in inert gas matrices can interact with dopants such as CO to give species showing ν_{CO} in the IR spectrum to *high* frequency of the isolated CO molecule. *Hauge* et al.[1] have summarized much of this work by showing how $\Delta\nu_{CO}$ (the shift of ν_{CO} in the "complex" from that of free CO) varies as a function of the formal metal charge divided by the square of the "metal to CO distance". Similar data have recently been given for CO on metal oxide surfaces.[2]

When iron(II) halides are cocondensed at 12 K with argon doped with CO, bands are present in the IR spectrum to high frequency of free CO. There are also metal halogen vibrations to low frequency of that of the halide isolated in pure argon. Noting that CO is known to give complexes with the (expected) impurities H_2O[3] or HX,[4] our spectra at low dopant concentrations (1 mol% CO in Ar) show additional features at 2175 cm^{-1} (Cl) and 2169 cm^{-1} (Br). The band for the iodide is apparently too close to the impurity bands for reliable observation. The precise position of these bands and the number of features observed is dependent on dopant concentration.

On annealing these matrices at temperatures of the order of 20 K, major changes occur in the spectra of the chloride, bromide, and iodide. In each case one principal band is observed in the ν_{CO} region characteristic of metal carbonyl halide formation: 2111 (Cl), 2103 (Br), 2088 cm^{-1} (I). The precise position of the bands is again to some extent dependent on dopant concentration. There are also two less-intense bands in the 600-cm^{-1} region (609 and 584 cm^{-1} in the chloride), the higher-frequency band being narrow while that to lower frequency is broader and shows indications of resolution into a doublet in some spectra. The frequency region below 500 cm^{-1} is complex and will be discussed in detail elsewhere.

Isotopic substitution using ^{13}CO gave the expected frequency shift for the ν_{CO} bands. The bands near 600 cm^{-1} both shifted by ca. 15 cm^{-1}, suggesting they are M–C–O

[*] Prof. I. R. Beattie, S. D. McDermott, E. A. Mathews, A. D. Willson
Chemistry Department, Southampton University
Southampton SO9 5NH (UK)
Dr. K. R. Millington
CEGB Berkeley Nuclear Laboratories
Berkeley, Gloucestershire, GL13 9PB (UK)

[**] We thank SERC and AEE Winfrith for financial support for this work, Dr. *A. Brisdon* and Dr. *T. R. Gilson* for helpful discussion, Dr. *P. J. Jones* for experimental help, and Dr. *P. Goggin* for the spectrum of AuCl·CO.

deformation modes. This frequency region is clear of other vibrations and represents a *useful test for the presence of metal carbonyl halides in such systems.*

Partial isotopic substitution ($^{12}CO:{}^{13}CO$ ca. 1:1) suggested for the ν_{CO} region the presence of one degenerate vibration in the parent (all ^{12}CO) compound.[5] Unfortunately, because of the relatively high frequencies of the carbonyl bands, this region is partially obscured by the intense free ^{13}CO band. Attempts to eliminate all free CO by annealing at 35 K using a krypton matrix were not successful. In 20:1:1 Ar:^{12}CO:^{13}CO, however, the narrow δ_{MCO} band at 609 cm^{-1} gave a quintet (Fig. 1). For *trans*-

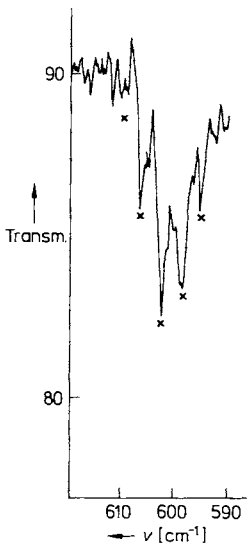

Fig. 1. Effect of ca. 50% ^{13}C isotopic enrichment on 609-cm^{-1} band. × positions for equally spaced quintet.

$[Fe(CO)_4Cl_2]$ the out-of-plane deformation of the planar D_{4h} $Fe(CO)_4$ residue would be of a_{2u} symmetry. In the absence of coupling this nondegenerate vibration must result in a quintet for a 1:1 $^{12}CO:{}^{13}CO$ isotopic ratio. There is strong evidence that molecular $FeCl_2$ is linear[6] so that acquisition of four CO molecules leads to the *trans* adduct if this linearity is retained. The only previously known isomer is the *cis* form.

The bands observed by us for *trans*-$[Fe(CO)_4I_2]$—e_u 2084, a_{2u} 612, e_u 598 cm^{-1}—are close to those proposed for the same compound produced by photolysis of *cis*-$[Fe(CO)_4I_2]$.[7,8] However, our assignments reverse those in the literature for the δ_{MCO} modes. (We also note that in one case the b_{1g} mode is reported as IR active.)

Our results suggest that the initial $FeX_2 \cdot n\,CO$ species at low dopant concentrations has an n value of less than 4.[9] Annealing enables migration of the CO molecules to occur giving a species which can then reorganize to give the iron carbonyl halide. If $FeCl_2$ is cocondensed with *pure* CO, the "π complex" is formed even at 9 K.

It is instructive to contrast the ease of reaction of CO and the *isolated* FeI_2 molecule with a *synthetic* method for *cis*-$[Fe(CO)_4I_2]$ which recommends treatment of FeI_2 with CO at 110 atm for 10 h.[10]

There is no clear-cut evidence for π species containing less than four carbonyl groups. Nor is there evidence for "π-acceptor" behavior with FeF_2. It is possible that the sharp differentiation between the fluoride and the other halides is associated with the spin changes necessary in forming the π adduct and with the "harder" metal center. Certainly the shift of the antisymmetric stretching frequency of FeF_2 from 731 cm^{-1} in Ar to 587 cm^{-1} in CO suggests a strong interaction with CO. A complication in such experiments is the variation in intensity of ν_{CO} with frequency.[7,11]

At least three types of linear CO interaction can occur, the boundaries between them not being clear:

1. van der Waals: high-frequency ν_{CO}[*]; no observed M-C-O skeletal modes. Example: $BF_3 \cdot CO$ with $d(B\text{-}C) = 2.886$ Å[12] and ν_{CO} in an argon matrix at 2150 cm^{-1}.[13]
2. "σ-bonded": high-frequency ν_{CO}; M-C-O skeletal modes present. Example: $AuCl \cdot CO$ with $d(Au\text{-}C) = 1.93$ Å[14] and ν_{CO} in the region of 2157 cm^{-1}.
3. "π-acceptor": lower-frequency ν_{CO}; M-C-O skeletal modes present. Example: $Ni(CO)_4$ with $d(Ni\text{-}C) = 1.84$ Å[15] and ν_{CO} at 2058 cm^{-1}.

Matrix isolation represents a sensitive method for studying such interactions. In particular it may be possible to examine the relationship between van der Waals, σ-bonded, and π-acceptor species by systematically varying the acceptor. It should also be possible to examine the number of CO molecules interacting on one center and possibly dipole-dipole or phonon interactions. $CrF_3 \cdot n\,CO$ would seem to be an appropriate model for the study of surface chromium atoms on $\alpha\text{-}Cr_2O_3$ where the (001) faces at 298 K show a single IR peak for CO, varying from 2185 to 2170 cm^{-1}.[16] Finally, such studies may be relevant to the occurrence of bond-stretch isomers.[17]

Received: April 13, 1988 [Z 2702 IE]
German version: *Angew. Chem. 100* (1988) 1202

[1] R. H. Hauge, S. E. Gransden, J. L. Margrave, *J. Chem. Soc. Dalton Trans. 1979*, 745.
[2] M. I. Zaki, H. Knözinger, *Spectrochim. Acta Part A 43* (1987) 1455.
[3] H. Dubost, *Chem. Phys. 12* (1976) 139; H. Dubost, L. Abouaf-Marguin, *Chem. Phys. Lett. 17* (1972) 269.
[4] L. Andrews, R. T. Arlingham, G. L. Johnson, *J. Chem. Phys. 78* (1983) 6347, and references cited therein.
[5] See, e.g., J. H. Darling, J. S. Ogden, *J. Chem. Soc. Dalton Trans. 1972*, 2496.
[6] M. Hargittai, I. Hargittai, *J. Mol. Spectrosc. 108* (1984) 155.
[7] K. Noack, *Helv. Chim. Acta 45* (1962) 1847.
[8] M. Pankowski, M. Bigorgne, *C. R. Hebd. Seances Acad. Sci. 263* (1966) 239.
[9] C. W. DeKock, D. A. Van Leirsburg, *J. Am. Chem. Soc. 94* (1972) 3235.
[10] W. Hieber, H. Lagally, *Z. Anorg. Allg. Chem. 245* (1940) 305.
[11] C. Morterra, E. Garrone, V. Bolis, B. Fubini, *Spectrochim. Acta Part A 43* (1987) 1577.
[12] K. C. Janda, L. S. Bernstein, J. M. Steed, S. E. Novick, W. Klemperer, *J. Am. Chem. Soc. 100* (1978) 8074.
[13] J. Gebicki, J. Liang, *J. Mol. Struct. 117* (1984) 283.
[14] P. Jones, *Z. Naturforsch. B 37* (1982) 823.
[15] J. Ladell, B. Post, I. Fankuchen, *Acta Crystallogr. 5* (1952) 795.
[16] D. Scarano, A. Zecchina, *Spectrochim. Acta Part A 43* (1987) 1441.
[17] See, e.g., Y. Jean, A. Lledos, J. K. Burdett, R. H. Hoffman, *J. Chem. Soc. Chem. Commun. 1988*, 140.

[*] In all cases there is a kinematic increase of ν_{CO} on coordination which depends on the effective mass of the acceptor and the M-C force constant.

Modification of Hydrophobic and Polar Interactions by Charged Groups in Synthetic Host-Guest Complexes**

By *Hans-Jörg Schneider** and *Thomas Blatter*

The quantification of noncovalent interactions plays an important role in understanding biological processes at the molecular level (for example, for the recognition between substrate and receptor) as well as in planning modifications of enzymes by genetic engineering. Synthetic host-guest complexes, by allowing structurally defined changes in a largely fixed environment, provide a way of obtaining information about the individual interactions. Herein we report on the complexation behavior of cyclobisdiphenylmethane compounds of types **A** and **B** in aqueous solution. In contrast to the earlier investigated,[1] structurally analogous macrocycle **C**, structures **A** and **B** do not have positive charges on the inner surface of the cavity, but instead negative charges that are distant from the binding center.[2]

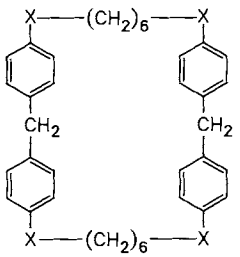

A: 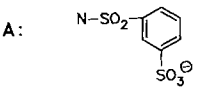

B: X = 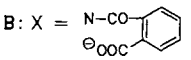

C: X = $^{\oplus}NMe_2$

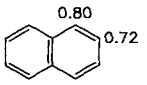

1

A: − 12.9
B: − 13.4
C: − 16.9

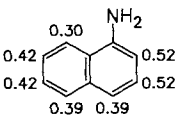

2

A: − 14.7
B: − 11.5
C: − 15.8

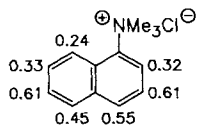

3

A: − 16.0
B: a)
C: − 4.8

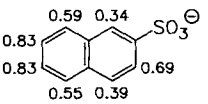

4

A: − 8.9
B: − 7.0
C: − 22.6

Scheme 1. Complexation energies ΔG^0 [kJ mol^{-1}] and selected CIS values [−ppm] of host **A** in D_2O/CD_3OD (80:20). The complexation constants of **3**/**B** were not determined, since the complex is not soluble in water.

The macrocyclic host compounds **A** and **B** are accessible by reaction of the corresponding tetraazacyclobisdiphenylmethane compounds with 1,3-benzenedisulfonyl dihalide and phthalic anhydride, respectively.[3] The cavities of **A** and **C** should have similar geometries, also with respect to the sp^3 hybridization of the N atoms. Indeed, similar results are obtained even for **A** and **B**, although somewhat different conformations are expected for the carboamide **B**. Measurements of the equilibrium constants K were carried out using ^{1}H-NMR-shift titrations with **1** and its naphthalene derivatives **2**–**4** (Scheme 1) as well as computer fitting according to reported procedures.[4] For a positively charged substrate like trimethyldinaphthylammonium ion **3** in methanol/water (20:80 v/v), the K values were, as expected, large compared with electroneutral naphthalene **1** and larger still compared with the negatively charged guest molecule **4**. The contributions of the attractive and repulsive electrostatic interactions, ca. 3 kJ mol^{-1} (ΔG^0 comparison **3/1** for host **A**, Scheme 1) and ca. 4 kJ mol^{-1} (**1/4**, host **A**), respectively, are relatively constant. Comparison of these values with the corresponding ΔG^0 values for the complexation of the same substrate with host **C**, which, while analogous in structure, carries positive charges in the ring, reveals larger ΔG differences of 12 (comparison **3/1**) and 6 kJ mol^{-1} (**1/4**), as expected owing to the greater proximity of the host and guest charges.

The complexation-induced ^{1}H NMR shifts obtained by nonlinear curve fitting (CIS, see Scheme 1 for selected values), which show the expected shielding effects,[5] indicate the pseudoequatorial inclusion of the substrates **1**–**4** in the cavity of **A** and **B**, whereby the ring-current effect of both the host and the guest molecule dominates. The considerably smaller CIS values obtained with the anionic host compounds **A** and **B** in comparison with the shifts observed with the host **C**[1c,5] support our conclusion[5] that the effect of the electric field due to the charges cannot be neglected.[1b] To compare the complexation behavior, it is important to note that the absence of NMR effects due to the anionic phenyl side groups in **A** and **B** (CIS < 0.01 ppm) rules out a significant involvement of these groups through lipophilic interaction with the substrate.

Unexpected results were obtained upon comparing the binding constants K of naphthalene **1** with **A** and **C**; the K value for **A** is five times smaller than that for compound **C**,[1c] which contains four positively charged N atoms on the surface of the cavity. The presence of these four ammonium centers in **C**—which, in addition, make the macrocycle water-soluble—should lead to a *reduction* instead of an increase in the complexation constants, since the ammonium centers are much more hydrophilic[6] than the neutral nitrogen atoms in **A** (and **B**) and since the binding of hydrocarbons to **1** is mainly due to hydrophobic interactions. Moreover, dispersive lipophilic interactions should be assisted rather than weakened by neutral nitrogen atoms. Investigations using other neutral substrates, such as **2**, confirm the unexpected order of stability (Scheme 1), although in these cases smaller differences are possible owing to hydrogen bonds and polar groups. Aza host compounds containing $-NH_2^{\oplus}$ instead of $-NMe_2^{\oplus}$ units exhibit similar complexation constants. Apparently, in contrast to previous assumptions, one should consider the possibility of increased hydrophobic interactions, and possibly special ion-π-system interactions,[2b] instead of hydrophilic interactions, in the vicinity of charged groups.

[*] Prof. Dr. H.-J. Schneider, Dipl.-Chem. T. Blatter
Institut für Organische Chemie der Universität
D-6600 Saarbrücken 11 (FRG)

[**] Host-Guest Chemistry, Part 16. This work was supported by the Deutsche Forschungsgemeinschaft and the Fonds der Chemischen Industrie. Part 15: H.-J. Schneider, D. Güttes, U. Schneider, *J. Am. Chem. Soc.*, in press.

Received: April 21, 1988 [Z 2716 IE]
German version: *Angew. Chem. 100* (1988) 1211

[1] a) K. Odashima, K. Koga in P. M. Keehn, S. M. Rosenfeld (Eds.): *Cyclophanes Vol. 2*, Academic Press, New York 1983, p. 629; b) K. Odashima,

A. Itai, Y. Iitaka, K. Koga, *Tetrahedron Lett. 21* (1980) 4347; c) H.-J. Schneider, K. Philippi, J. Pöhlmann, *Angew. Chem. 96* (1984) 907; *Angew. Chem. Int. Ed. Engl. 23* (1984) 908.

[2] We thank a referee for bringing to our attention recent publications on other systematic investigations on the large effect of changes on host-guest complexes: a) F. Diederich, *Angew. Chem. 100* (1988) 372 (especially p. 382); *Angew. Chem. Int. Ed. Engl. 27* (1988) 362; b) T. J. Shepodd, M. A. Petti, D. A. Dougherty, *J. Am. Chem. Soc. 110* (1988) 1983.

[3] All new compounds gave satisfactory analytical data (^{1}H and ^{13}C NMR, elemental analyses).

[4] H.-J. Schneider, R. Kramer, J. Pöhlmann, U. Schneider, *J. Am. Chem. Soc. 110* (1988), in press.

[5] H.-J. Schneider, R. Pöhlmann, *Bioorg. Chem. 15* (1987) 183.

[6] Compare the hydrophobic increments of $-NHCH_3$, which are roughly five orders of magnitude larger compared with those of $-\overset{\oplus}{N}Me_3$ substituents: C. Hansch, A. Leo: *Substituent Constants for Correlation Analysis in Chemistry and Biology*, Wiley, New York 1979, p. 49ff.

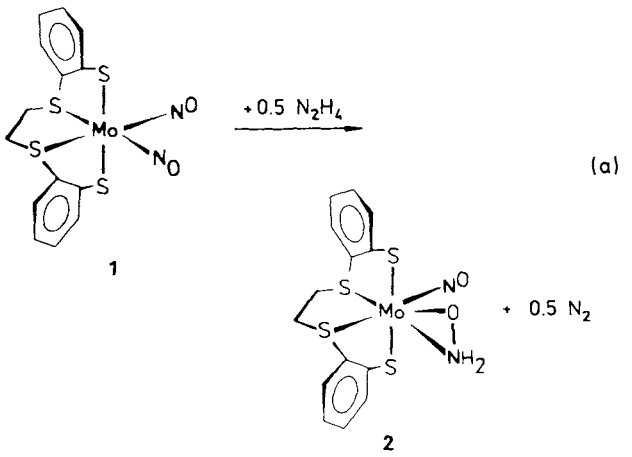

1 2

Transformation of η^1-Nitrosyl to η^2-Hydroxylaminyl Ligands in the Reduction of [Mo(NO)$_2$('S$_4$')] to [Mo(η^2-NH$_2$O)(NO)('S$_4$')]: A Model Reaction for a Partial Step in the Enzymatic [$NO_3^\ominus \rightarrow NH_3$] Conversion**

By *Dieter Sellmann,* Bernd Seubert, Matthias Moll,* and *Falk Knoch*

The transition-metal-catalyzed activation and reduction of NO are important in both industrial[1a] and enzymatic reactions.[1b] In the treatment of exhaust gases, molecular nitrogen is the desired end product; the biological [$NO_3^\ominus \rightarrow NH_3$] conversion, however, avoids the formation of the energetically favored N_2 molecule, and the reduction of NO to the NH_2OH stage becomes the key step. The reduction of NO ligands to NH_2OH ligands in isolable complexes is therefore an important model reaction for understanding the biological nitrogen cycle.

The synthesis of nitrosyl complexes by use of hydroxylamine is well known[2a] and, in one case, the reversible *intramolecular* transformation of NO to NH_2O ligands has been achieved by protonation-deprotonation;[2b] the electrons involved were derived from either the NH_2O ligand or the metal center. The *intermolecular* reduction of NO to NH_2O ligands, however, has not been reported previously.[3] We have now observed such a reaction in the reduction of **1** with hydrazine according to Equation (a) (THF, 20°C, 2 h; see Experimental Procedure).

N_2 evolves and two configurational isomers of the NH_2O complex **2** are formed in equal amounts;[4] they are obtained as **2** · DMF upon recrystallization from DMF/Et_2O. The isomer shown schematically in Equation (a) was characterized by an X-ray structure analysis.[5]

Figure 1 shows that the molybdenum center is sevenfold coordinated by one oxygen, two nitrogen, and four sulfur atoms, forming a distorted pentagonal bipyramid with S3-Mo1-N2 as the main axis. The [Mo(NO)('S$_4$')] fragment of the educt **1** remains intact; the replacement of the η^1-NO ligand by a side-on-bonded η^2-NH_2O ligand leads to a further reduction in the S1-Mo1-S4 angle from 160.1(3)° in **1**[6] to 154.0(1)° in **2** · DMF. The distances in the [Mo(NH_2O)] unit clearly establish the η^2 bonding of the NH_2O ligand; the NO distance of 137.5(5) pm corresponds to a normal NO single bond.[7] One of the two H atoms forms a hydrogen bond to a DMF solvate molecule ($d_{N-H\cdots O}$ = 184.5 pm).

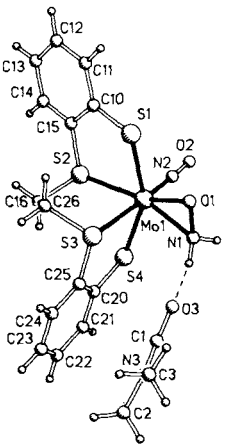

Fig. 1. Molecular structure of **2** · DMF [5].

The formation of two configurational isomers is revealed by NMR spectroscopy. The ^{13}C NMR spectrum (67.940 MHz) shows two sets of fourteen signals each for the fourteen C atoms of the ('S$_4$') ligand; they are also observed at higher temperatures (up to 60°C in [D$_8$]THF and up to 75°C in [D$_6$]DMSO), thus showing that the isomers are configurationally stable up to these temperatures. The ^{1}H NMR spectrum (Fig. 2), too, is in agreement only with the presence of two isomers: Four lines, arising from the two different AB systems, are observed for the NH_2 protons. The temperature dependence of the signals indicates exchange processes.

The ^{95}Mo NMR spectrum (17.061 MHz) exhibits only a broad ^{95}Mo signal at $\delta = -395$ (rel. $(NH_4)_6Mo_7O_{24}$) with a half-width of 760 Hz; on the one hand, the half-width presumably prevents resolution of the expected two Mo signals; on the other, it shows that the two Mo centers have very similar chemical environments and differ only in the position of the NH_2O ligand in relation to the [Mo(NO)('S$_4$')] fragment.

The 1:1 ratio of the two isomers is understandable in terms of the route of formation of **2**: the reduction **1** → **2**

[*] Prof. Dr. D. Sellmann, Dipl.-Chem. B. Seubert, Dr. M. Moll, Dr. F. Knoch
Institut für Anorganische Chemie der
Universität Erlangen-Nürnberg
Egerlandstrasse 1, D-8520 Erlangen (FRG)

[**] ('S$_4$')$^{2\ominus}$ = 2,2'-(ethylenedithio)dibenzenethiolate.—Transition Metals with Sulfur Ligands, Part 39: This work was supported by the Deutsche Forschungsgemeinschaft and the Fonds der Chemischen Industrie.—Part 38: D. Sellmann, H. Kunstmann, M. Moll, F. Knoch, *Inorg. Chim. Acta*, in press.

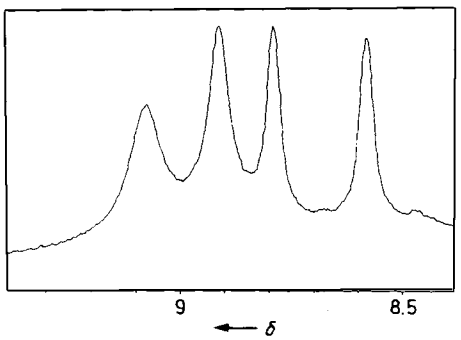

Fig. 2. δ_{NH} region of the ^1H NMR spectrum of **2** at 20°C in [D$_6$]DMSO.

[Eq. (a)] is a proton-coupled two-electron reduction, hydrazine serving as both proton and electron source:

$$N_2H_4 \longrightarrow N_2 + 4H^{\oplus} + 4e^{\ominus}$$

Upon reduction of **1**, bending of one of the two NO ligands is expected to occur,[8] resulting in the formation of **2a** and **2b** with equal probability (Eq. (b)].

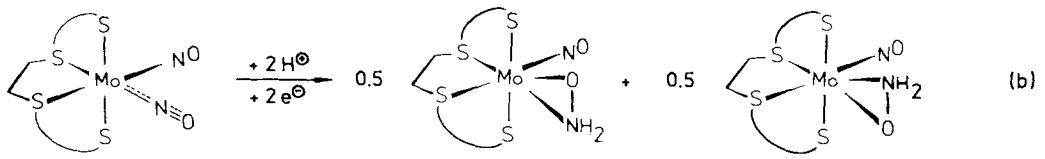

1 **2a** **2b**

Of fundamental importance for understanding the mechanism of reduction and for describing the NH_2O ligand is the question whether electrons of the metal are involved in the NO→NH_2O reduction. The ^{95}Mo shifts of **1** ($\delta = -512$) and **2** ($\delta = -395$) indicate that the reaction according to Equation (a) does not lead to a change in the oxidation state of the Mo center;[9] therefore, in both cases, it can be regarded as an Mo^{II} center. Accordingly, the 15-electron fragment [Mo(NO)('S$_4$')] is stabilized in **1** by the 3-electron donor $:\overset{\odot}{N}\equiv O:$ and in **2**, isoelectronically, by the 3-electron donor $H_2\ddot{N}-\overset{\odot}{\ddot{O}}:$, which is thus to be described as a hydroxylaminyl ligand.[10]

The transformation of **1** to **2** shows that the reduction of NO to the NH_2OH stage in metal oxidoreductases under mild conditions should be favored when the metal center is surrounded by sulfur ligands and can easily change its coordination number.

Experimental Procedure

1 (925 mg, 2.0 mmol) [11] in 70 mL of THF was allowed to react at 20°C with N_2H_4 (0.08 mL, 2.5 mmol). A clear, orange-yellow solution containing a small amount of a brown precipitate was formed over ca. 2 h accompanied by N_2 evolution (GC, MS). The solution was filtered, all volatiles were removed from the filtrate under reduced pressure, and the residue was dissolved in DMF. Addition of a layer of Et_2O (ca. 20 mL) to this yellow-brown solution and cooling to −30°C resulted, after 3 d, in the formation of amber-colored crystals. IR (KBr): $\tilde{\nu}_{NH} = 3240\ cm^{-1}$, $\tilde{\nu}_{NO} = 1635\ cm^{-1}$. FD-MS: *m/z* 468 ($M^{\oplus}$). Yield 85% (correct elemental analysis).

Received: April 5, 1988 [Z 2690 IE]
German version: *Angew. Chem. 100* (1988) 1221

CAS Registry numbers:
1, 97775-39-8; **2a**, 116077-87-3; **2b**, 116179-37-4; **2**·DMF, 116077-88-4; N_2H_4, 302-01-2; NO, 10102-43-9.

[1] a) *Ullmanns Encyklopädie der technischen Chemie, 4. Aufl., Bd. 6*, Verlag Chemie, Weinheim 1981, p. 172; b) M. N. Hughes: *The Inorganic Chemistry of Biological Processes*, 2nd ed., Wiley, New York 1981.

[2] a) Cf. the following review: K. Wieghardt, *Adv. Inorg. Bioinorg. Mech. 3* (1984) 213; b) cf. the reaction

$$[V(NO)(tha)]^{\ominus} + 2H^{\oplus} \rightleftharpoons [V(NH_2O)(tha)]^{\oplus}$$

(H_3(tha) = 1,1',1''-nitrilotri-2-propanol), for which a four-electron transfer $V^I \rightleftharpoons V^V$ is assumed: K. Wieghardt, U. Quilitzsch, *Z. Naturforsch. B36* (1981) 683.

[3] In the electrochemical reduction of $[M(tpy)(bpy)(NO_2)]^{\oplus}$ (M = Ru, Os; tpy = terpyridyl; bpy = bipyridyl), intermediates are observed which can be explained in terms of the formation of $[M^{II}(tpy)(bpy)(L)]^{2\oplus}$ (L = NH_2O, NHO): W. R. Murphy, Jr., K. Takeuchi, M. H. Barley, T. H. Meyer, *Inorg. Chem. 25* (1986) 1041.

[4] Owing to the chiral Mo center, they exist as pairs of enantiomers.

[5] X-ray structure analysis of **2**·DMF: $P2_1/c$, $a = 1204.4(3)$, $b = 1579.7(4)$, $c = 1253.0(4)$ pm, $\beta = 117.44(2)°$; $V_{calcd} = 2114(1) \times 10^6$ pm^3; $Z = 4$. $T = 213$ K, $\lambda Mo_{K\alpha}$; ω-scan; $3.0 < \dot{\omega} < 15°\ min^{-1}$, $4 < 2\theta < 60°$. 5982 unique reflections, 4246 with $F > 6\sigma(F)$. SHELXTL-PLUS, direct methods, $R = 0.056$, $R_w = 0.040$. The two H atoms of the NH_2O ligands were located by difference Fourier synthesis; one of them forms a hydrogen bond to a DMF solvate molecule ($d_{N-H\cdots O} = 184.5$ pm)). Important distances [pm] and angles [°]: Mo1-N1 210.3(3), Mo1-O1 205.3(3), Mo1-N2 176.1(3), Mo1-S1 248.7(1), Mo1-S2 253.8(1), Mo1-S3 258.8(1), Mo1-S4 246.9(1), N1-O1 137.5(5), N2-O2 119.3(4); O1-Mo1-N1 38.6(1), N2-Mo1-O1 99.1(1), S3-Mo1-N2 173.0(1), N2-Mo1-N1 95.7(1), S1-Mo1-S4 154.0(1), S2-Mo1-S3 83.4(1). Further details of the crystal structure investigation may be obtained from the Fachinformationszentrum Energie, Physik, Mathematik GmbH, D-7514 Eggenstein-Leopoldshafen 2 (FRG), on quoting the depository number CSD-53058, the names of the authors, and the journal citation.

[6] D. Sellmann, J. Keller, M. Moll, H. P. Beck, W. Milius, *Z. Naturforsch. B41* (1986) 1551.

[7] Similar distances are also found in other NH_2O complexes [2a]. d_{N-O} is 147(3) pm in NH_2OH and 136.9(7) pm in $[NH_3OH]Cl$ (C. A. Bunton, D. R. Llewellyn, *J. Chem. Soc. 1953*, 1692), and R. Doss, R. van Eldik, H. Kelm, *Ber. Bunsenges. Phys. Chem. 86* (1982) 925).

[8] Cf. J. A. McCleverty, *Chem. Rev. 79* (1979) 53.

[9] For Mo^{II} compounds, the ^{95}Mo shifts extend over a range of ca. 2000 ppm: H. Minelli, J. H. Enemark, R. T. C. Brownlee, M. J. O'Connor, A. G. Wedd, *Coord. Chem. Rev. 68* (1985) 169. Similar δ values are also observed for other $[Mo^{II}('S_4')]$ complexes: D. Sellmann, J. Keller, M. Moll, C. F. Campana, M. Haase, *Inorg. Chim. Acta 141* (1988) 242.

[10] For nomenclature (and nomenclature difficulties) see [2b].

[11] Origin of **1**: D. Sellmann, L. Zapf, J. Keller, M. Moll, *J. Organomet. Chem. 289* (1985) 71.

Mechanism of Ethylene Hydrogenation by the Molecular Hydrogen Complex $[Ir(H)_2(H_2)(PMe_2Ph)_3]^{\oplus}$—Characterization of Intermediates**

By *Eric G. Lundquist, John C. Huffman, Kirsten Folting,* and *Kenneth G. Caulton**

Facile loss of coordinated H_2 is a common characteristic of most dihydrogen (η^2-H_2) complexes.[1] While those who

[*] Prof. K. G. Caulton, Dr. E. G. Lundquist, Dr. J. C. Huffman, Dr. K. Folting
Department of Chemistry and the Molecular Structure Center
Indiana University, Bloomington, IN 47405 (USA)

[**] This work was supported by the National Science Foundation (Grant No. CHE-8707055). We thank Dr. *M. J. Hampden-Smith* for valuable advice and discussions, Johnson-Matthey for material support, and *Scott Horn* for skilled technical assistance.

investigate the structural and physical properties of these complexes might view this occurrence as a nuisance (obligatory manipulations under H_2, low temperatures, etc.), we consider it to be a convenient opportunity to access, under exceptionally mild conditions, the relatively unexplored field of unsaturated hydride complexes. Here we report on the protonation of $[IrH_3p_3]$ ($p = PMe_2Ph$) with HBF_4 to produce the cationic complex $[IrH_4p_3]^{\oplus}$,[2] which we show to contain intact H_2. This complex serves as an effective ethylene hydrogenation catalyst while, at the same time, providing an excellent opportunity to characterize and study the intermediates in a catalytic cycle.

When $[IrH_3p_3]$ is protonated with $HBF_4 \cdot OEt_2$ in CH_2Cl_2, the complex $[IrH_4p_3]^{\oplus}$ **1**[2] is formed. T_1 measurements at $-70\,^{\circ}C$ in CD_2Cl_2[3] support the interpretation that this cation is comprised of an Ir^{III} octahedron with two hydride ligands and a coordinated dihydrogen molecule. We had previously speculated[2] that this was the structure of **1** based upon chemical reactivity studies which suggested the occurrence of the equilibrium (a).

$$\underset{\mathbf{1}}{[IrH_4p_3]^{\oplus}} \underset{kk}{\rightleftharpoons} [IrH_2p_3]^{\oplus} + H_2 \qquad (a)$$

Addition[4] of excess ethylene to **1** in CH_2Cl_2 gives a 97% yield of the BF_4 salt of $[Ir(C_2H_4)_2p_3]^{\oplus}$ **2** as a cream-colored powder. The ^1H NMR spectrum[5] of this material shows resonances for two coordinated ethylene molecules and no remaining hydride ligands. The $^{13}C\{^1H\}$ NMR spectrum of a sample obtained using ^{13}C-enriched ethylene (Fig. 1), is

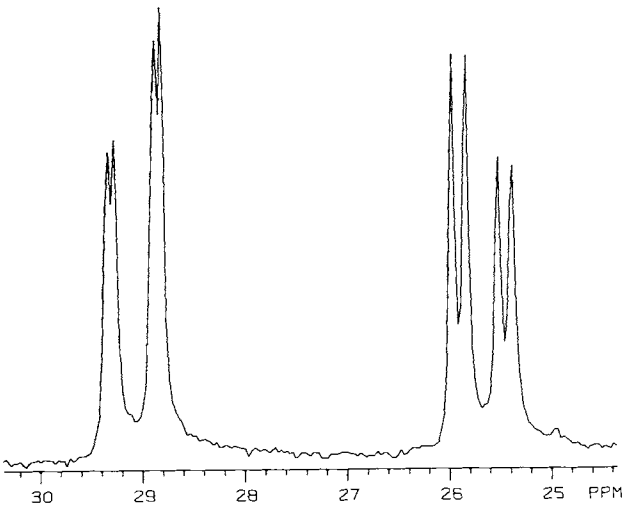

Fig. 1. $^{13}C\{^1H\}$ NMR (90 MHz, 24°C, CD_2Cl_2) of the ethylene carbons in $[Ir(^{13}C_2H_4)_2(PMe_2Ph)_3]^{\oplus}$, showing inequivalent carbons ($\delta = 29.1$ and 25.6), each of which couples to *only* one phosphorus.

invariant with temperature and, together with the $^{31}P\{^1H\}$ NMR spectrum,[5] suggests a rare,[6,7] stereochemically *rigid*, five-coordinate iridium cation with equivalent nonrotating (-80 to $+80\,^{\circ}C$) ethylene ligands: $[Ir(C_2H_4)_2p_3]^{\oplus}$ **2**. The solid-state structure determination of **2**[8] (Fig. 2) is consistent with the spectral parameters and reveals a trigonal-bipyramidal arrangement around iridium with two ethylenes and one phosphane ligand occupying the equatorial sites.

When the reaction of $[Ir(H)_2(H_2)p_3]^{\oplus}$ **1** with excess ethylene is monitored by ^1H NMR at $-50\,^{\circ}C$, *cis,mer*-

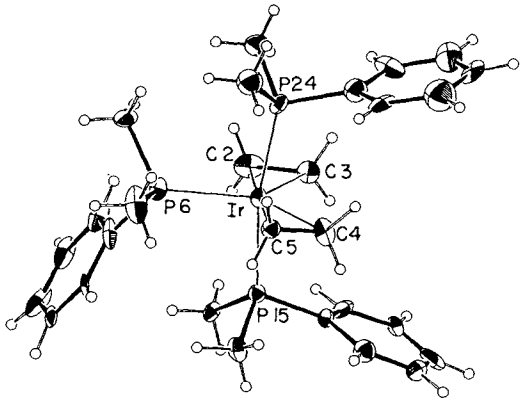

Fig. 2. The molecular structure of $[Ir(C_2H_4)_2(PMe_2Ph)_3]^{\oplus}$ (ORTEP) as the BF_4 salt [8]. Unlabeled ellipses are carbon; open circles are hydrogen. Selected distances [Å] and angles [°]: Ir-P6 2.356(5), Ir-P15 2.363(5), Ir-P24 2.351(5), Ir-C2 2.140(16), Ir-C3 2.164(16), Ir-C4 2.171(15), Ir-C5 2.166(16), C2-C3 1.401(25), C4-C5 1.427(24); P6-Ir-P15 97.11(16), P6-Ir-P24 93.47(16), P15-Ir-P24 169.41(15).

$[IrH_2(C_2H_4)p_3]^{\oplus}$ **3**, a 1:1 adduct of ethylene and $[IrH_2p_3]^{\oplus}$ (formed by loss of H_2 from **1**), can be observed.[9] Over time the resonances of **3** decrease while those of the bis-olefin complex **2** and of ethane appear. However, in the absence of excess ethylene, even at room temperature, the cationic hydrido-olefin complex **3** is stable and does not eliminate ethane. Thus, the reduction of ethylene to ethane is ethylene-promoted. The cationic complex **3** can also be generated by the reaction of **2** with H_2 [Eq. (b)]. The curious elimination of *ethylene* (not ethane) in this reaction,

$$\underset{\mathbf{2}}{[Ir(C_2H_4)_2p_3]^{\oplus}} + H_2 \longrightarrow \underset{\mathbf{3}}{\textit{cis,mer}\text{-}[IrH_2(C_2H_4)p_3]^{\oplus}} + C_2H_4 \qquad (b)$$

together with the fact that an ethylene molecule in **2** exchanges within 30 minutes with ^{13}C-labeled ethylene, implicates the equilibrium (c).[10] Thus, while **2** appears "stat-

$$\underset{\mathbf{2}}{[Ir(C_2H_4)_2p_3]^{\oplus}} \rightleftharpoons [Ir(C_2H_4)p_3]^{\oplus} + C_2H_4 \qquad (c)$$

ic" on the NMR time scale ($\Delta t < 1$ s), it shows unimolecular reactivity on the preparative time scale ($\Delta t > 1$ min). Addition of D_2 to compound **2** initially generates $[IrD_2(C_2H_4)p_3]^{\oplus}$, which shows rapid incorporation of deuterium into the ethylene and points to the rapid reversibility of reaction (d), which again involves a 16-electron $[Ir(H)(R)p_3]^{\oplus}$ species [cf. Eq. (a)].

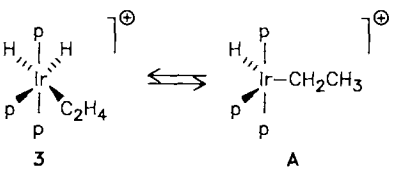

3 A (d)

Equation (d) alone, however, is not sufficient to explain the observed scrambling between *both* the hydrogens in *cis* and *trans* positions and all ethylene hydrogens of $[IrD_2(C_2H_4)p_3]^{\oplus}$, since the hydrides in **3** are stereochemically rigid. However, since **3** exchanges with D_2 (1 atm) at a rate comparable to that of reaction (d), an equilibrium

H_2-elimination from **3** must also occur [Eq. (e)].[11] Note that this equilibrium involves the same 16-electron species implicated in Equation (c).

$$[IrH_2(C_2H_4)p_3]^{\oplus} \rightleftharpoons [Ir(C_2H_4)p_3]^{\oplus} + H_2 \qquad (e)$$

The product-forming hydrido-ethyl (**A**) and hydrido-ethyl ethylene (**B**) species (Scheme 1) "downstream" of reaction (d) have not been observed under a variety of conditions. However, when methyl acrylate is substituted for ethylene, the hydrido-alkyl complex **4** can be isolated in near quantitative yield.[12] This thermally stable complex serves as an ideal model for the proposed hydrido-ethyl ethylene intermediate **B**.

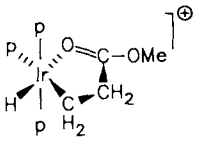

4

Incorporation of all the above experimental evidence leads to the catalytic cycle shown in Scheme 1 for the hydrogenation of ethylene by $[Ir(H)_2(H_2)p_3]^{\oplus}$ **1**. The $BF_4^{\ominus}$ ion

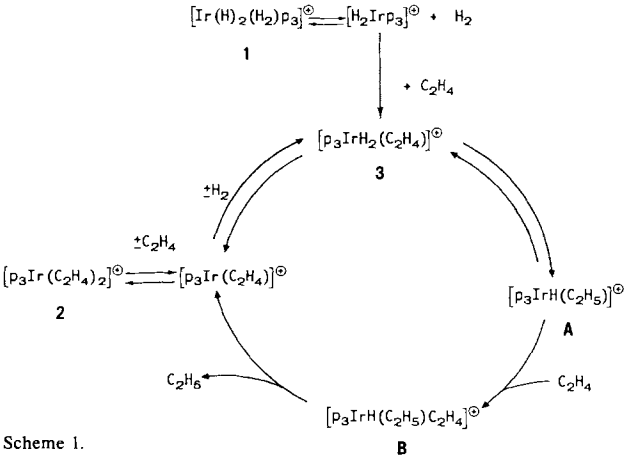

Scheme 1.

and CH_2Cl_2 also play a role as more active participants in the catalytic cycle.[13]

Received: April 14, 1988;
revised: June 3, 1988 [Z 2703 IE]
German version: *Angew. Chem. 100* (1988) 1236

CAS Registry numbers:
1, 115983-32-9; **2**, 115983-34-1; **3**, 115983-35-2; **4**, 115983-37-4; ethylene, 74-85-1.

[1] a) G. J. Kubas, C. J. Unkefer, B. I. Swanson, E. Fukushima, *J. Am. Chem. Soc. 108* (1986) 7000; b) R. H. Crabtree, M. Lavin, L. Bonneviot, *ibid. 108* (1986) 4032; c) H. C. Clark, M. Hampden-Smith, *ibid. 108* (1986) 3829; d) R. H. Morris, J. F. Sawyer, M. Shiralian, J. D. Zubkowski, *ibid. 107* (1985) 5581; e) F. M. Conroy-Lewis, S. J. Simpson, *J. Chem. Soc. Chem. Commun. 1986*, 506; f) R. H. Crabtree, M. Lavin, *ibid. 1985*, 1661.

[2] L. F. Rhodes, K. G. Caulton, *J. Am. Chem. Soc. 107* (1985) 259.

[3] T_1 values, measured by inversion-recovery at 200 K and 360 MHz with a 180°-τ-90° pulse sequence, are 20 ms for $[H_4Ir(PMe_2Ph)_3]BF_4$ in CD_2Cl_2 and 465 ms for *fac*-$[H_3Ir(PMe_2Ph)_3]$ in [D_8]toluene.

[4] Unless stated otherwise, all reactions were run at 25°C and 1 atm. The counterion was $BF_4^{\ominus}$ in each case.

[5] **2**: ^{1}H NMR (360 MHz, 24°C, CD_2Cl_2): $\delta = 1.35$ (vt, J(PMe) = 3 Hz, 12H), 2.05 (d, J(PMe) = 11 Hz, 6H), 2.30 (br. m, $H_2C{=}CH_2$, 4H), 2.45 (br. m, $CH_2{=}CH_2$, 4H), 7.5–8.0 (m, PPh). $^{13}C\{^1H\}$ NMR of the ethylene carbons (Fig. 1): $\delta = 29.1$ (dd, J(C-C) = 41 Hz, J(P-C) = 5 Hz); 25.6 (dd, J(C-C) = 41 Hz, J(P-C) = 12.5 Hz). $^{31}P\{^1H\}$ NMR (146 MHz, 24°C, CD_2Cl_2): $\delta = -42.0$ (d, J(P-P) = 22 Hz, 2P); −55.5 (t, J(P-P) = 22 Hz, 1P).

[6] J. R. Shapley, J. A. Osborn, *Acc. Chem. Res. 6* (1973) 305.

[7] Another stereochemically rigid, five-coordinate complex with nonrotating ethylene ligands is $[Os(PMe_3)_2(C_2H_4)_2(CO)]$. See G.-Y. Kiel, J. Takats, F.-W. Grevels, *J. Am. Chem. Soc. 109* (1987) 2227.

[8] Crystallographic data for $[Ir(C_2H_4)_2(PMe_2Ph)_3]BF_4 \cdot 0.5\,H_2O$ (−155°C): space group $P2_1/c$, $a = 10.580(5)$, $b = 20.332(12)$, $c = 27.771(17)$ Å, $\beta = 93.84(3)°$, $Z = 8$; $R(F) = 0.0693$ for 5950 reflections with $F > 2.33\sigma(F)$. Two independent molecules, statistically identical, were located in the unit cell. Positional and thermal parameters are available from the Director of the Cambridge Crystallographic Data Centre, University Chemical Laboratory, Lensfield Road, Cambridge CB2 1EW (England), by quoting the names of the authors and the journal citation.

[9] **3**: ^{1}H NMR (360 MHz, −50°C, CD_2Cl_2): $\delta = -12.00$ (d, t, J_{trans}(H-P) = 92, J_{cis}(H-P) = 17 Hz, 1H), −9.25 (dt, J_{cis}(H-P) ≈ J_{cis}(H-P) = 14.5 Hz, 1H), 1.00 (vt, J(P-Me) = 3 Hz, 6H), 1.30 (d, J(P-Me) = 9 Hz, 6H), 1.80 (vt, J(P-Me) = 3 Hz, 6H), 2.85 (s, $CH_2{=}CH_2$, 4H), 7.0–8.0 (m, PPh); $^{31}P\{^1H\}$ NMR (146 MHz, 24.0°C, CD_2Cl_2): $\delta = -35.6$ (d, J(P-P) = 19 Hz, 2P), −50.6 (t, J(P-P) = 19 Hz, 1P); $^{13}C\{^1H\}$ NMR (74 MHz, −50°C, CD_2Cl_2): $\delta = 46.9$ (s, $^{13}CH_2{=}{}^{13}CH_2$).

[10] The cation $[Ir(C_2H_4)p_3]^{\oplus}$ has been trapped with MeCN and MeLi (unpublished results) and represents the likely intermediate in forming $[IrH_2(C_2H_4)p_3]^{\oplus}$ from $[Ir(C_2H_4)_2p_3]^{\oplus}$ and H_2.

[11] An alternative mechanism for incorporation of D_2 into **3** involves addition of D_2 to **A**, H/D site-exchange, elimination of HD, then β-hydrogen elimination [Eq. (d)], producing $[D_1]$-**3**. We thank a referee for this suggestion.

[12] **4**: ^{1}H NMR (360 MHz, 24°C, CD_2Cl_2): $\delta = -27.75$ (d, t, J_{cis}(H-P) = 11.8, J_{cis}(H-P) = 17.8 Hz, 1H), 1.20 (m, Ir-CH_2, 2H), 1.40 (overlapping vt, P-Me, 12H), 1.50 (br. d, P-Me, 6H), 2.25 (m, CH_2-CO_2Me, 2H), 3.65 (s, OMe, 3H), 7.5–8.0 (m, PPh). $^{31}P\{^1H\}$ NMR (146 MHz, 24°C, CD_2Cl_2): $\delta = -21.0$ (d, J(P-P) = 19 Hz, 2P), −34.0 (t, J(P-P) = 19 Hz, 1P). IR (Nujol): $\tilde{\nu} = 2240$ (w, Ir-H), 1750 cm^{-1} (m, CO_2Me).

[13] K. G. Caulton et al., to be published.

Synthesis, Structure, and Reactivity of $[Mn_2(\mu\text{-}H)_2(CO)_6(\mu\text{-}Ph_2PCH_2PPh_2)]$**

By *Francisco J. García Alonso, Manuel García Sanz, Victor Riera,* Miguel Angel Ruiz, Antonio Tiripicchio,** and *Marisa Tiripicchio Camellini*

Organometallic transition-metal compounds containing a formally unsaturated $M_2(\mu\text{-}H)_2$ (M = M) moiety are attractive species for the study of the reactions of small molecules at metallic centers, as suggested from the chemistry developed around $[Os_3(\mu\text{-}H)_2(CO)_{10}]$.[1] We report here the preparation, structure, and reactivity of $[Mn_2(\mu\text{-}H)_2(CO)_6(\mu\text{-dppm})]$ **1** (dppm = $Ph_2PCH_2PPh_2$). Only a few manganese analogues of **1** are known—$[Mn_2H_2(CO)_4(dppm)_2]$,[2] $[Mn_2H_2(PPh_2)(CO)_6]^{\ominus}$,[3] and $[Mn_2H_2(CO)_6(tedip)]$[4] (tedip = $(EtO)_2POP(OEt)_2$)—and their reactivity has not been explored in detail.

Reduction of $[Mn_2Cl_2(CO)_6(dppm)]$[5] with four equivalents of $Li[HBEt_3]$ in THF at 0°C affords the red-purple compound **1** in 50–60% yield. The crystal structure analysis (Fig. 1)[6] shows that the Mn–Mn distance (2.699(2) Å) is in agreement with the formal unsaturation predicted for the molecule on the basis of electron counting. Accordingly, **1** reacts under mild conditions with a variety of small molecules (see Scheme 1).

[*] Prof. V. Riera, Dr. F. J. García Alonso, Dr. M. García Sanz, Dr. M. A. Ruiz
Departamento de Química Organometálica, Universidad
E-33071 Oviedo (Spain)
Prof. A. Tiripicchio, Prof. M. Tiripicchio Camellini
Istituto di Chimica Generale ed Inorganica, Università
Centro di Studio per la Strutturistica Diffrattometrica del C.N.R.
Viale delle Scienze, I-43100 Parma (Italy)

[**] This work has been supported by the Spanish Comisión Asesora de Investigación Científica y Técnica and by the Italian Ministero della Pubblica Istruzione.

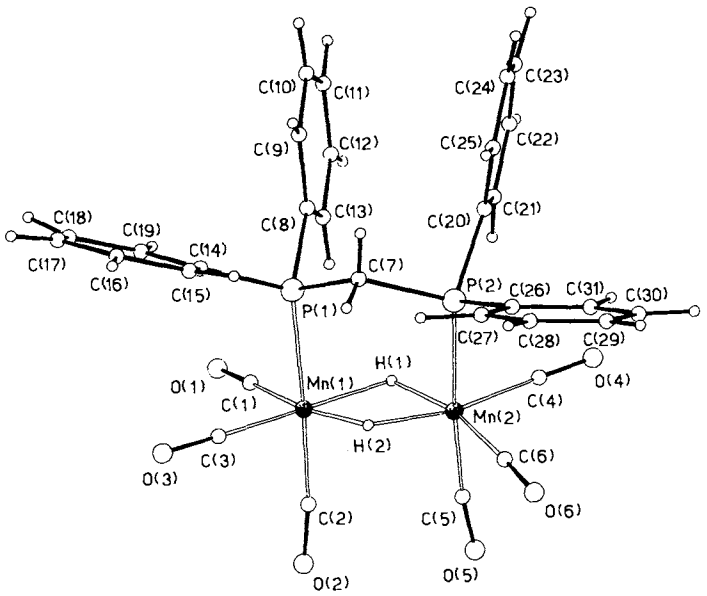

Fig. 1. Perspective view of the structure of $[Mn_2(\mu\text{-}H)_2(CO)_6(\mu\text{-dppm})]$ **1**. Selected bond lengths [Å] and angles [°]: Mn1-Mn2 2.699(2), Mn1-P1 2.308(3), Mn2-P2 2.326(3), Mn1-C1 1.784(6), Mn1-C2 1.818(6), Mn1-C3 1.791(6), Mn2-C4 1.801(6), Mn2-C5 1.804(6), Mn2-C6 1.791(5), Mn1-H1 1.76(5), Mn2-H1 1.59(5), Mn1-H2 1.81(5), Mn2-H2 1.68(5); H1-Mn1-H2 71(2), H1-Mn2-H2 78(2), Mn1-H1-Mn2 107(3), Mn1-H2-Mn2 102(2).

Reaction with *p*-MeC_6H_4SH results in H_2 elimination to give the μ-hydrido,μ-thiolato complex **2a**. On the other hand, reaction of **1** with *t*BuNC or MeCN results in intramolecular H_2 elimination to give the μ-σ,π-isocyanido (**3**) or -nitrilo (**4**) complexes, whereas elemental sulfur inserts into one μ-H bridge to give the μ-mercapto complex **2b**; the latter exists in solution as a mixture of two isomers, differing probably in the orientation of the S-H vector relative to the Mn_2S plane (above or below it).

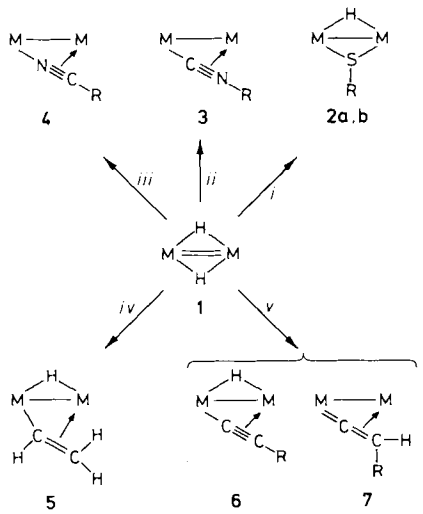

Scheme 1. i: **2a** (R = *p*-MeC_6H_4), 1 equiv. *p*-MeC_6H_4SH, toluene, room temperature, 10 min; **2b** (R = H), 1 equiv. S_8, toluene, room temperature, 5 min. ii: **3** (R = *t*Bu), 1 equiv. *t*BuNC, toluene, room temperature, 5 min. iii: **4** (R = Me), MeCN (excess), toluene, room temperature, 2 h. iv: **5** C_2H_2 (excess), THF, room temperature, 4 h. v: **6** and **7** (R = *t*Bu), *t*BuC_2H (excess), THF, room temperature, 3 d.

Complex **1** also reacts with several alkynes RC_2H (R = H, Ph, *t*Bu) at room temperature, the nature and relative amounts of the products being strongly dependent on the nature of R; thus, when R = H, insertion into a Mn-H bond leads to the μ-σ,π-vinyl complex **5**, whereas for R = *t*Bu the μ-σ,π-acetylide compound **6** is the major species formed. Compounds **5** and **6** appear to be fluxional at room temperature, as concluded from their NMR spectra. Interestingly, for R = *t*Bu, a minor product **7**[7] is also obtained. Compound **7** contains a μ-σ,π-vinylidene ligand, as confirmed by an X-ray structure determination.[8]

Received: April 18, 1988;
revised: June 20, 1988 [Z 2708 IE]
German version: *Angew. Chem. 100* (1988) 1224

[1] a) R. D. Adams, J. P. Selegue in G. Wilkinson, F. G. A. Stone, E. Abel (Eds.): *Comprehensive Organometallic Chemistry, Vol. 4*, Pergamon, Oxford 1982, p. 1032; b) K. Burgess, *Polyhedron 3* (1984) 1175.

[2] H. C. Aspinall, A. J. Deeming, *J. Chem. Soc. Chem. Commun. 1983*, 838.

[3] K. Henrick, J. A. Iggo, M. J. Mays, P. R. Raithby, *J. Chem. Soc. Chem. Commun. 1984*, 209.

[4] V. Riera, M. A. Ruiz, A. Tiripicchio, M. Tiripicchio Camellini, *J. Chem. Soc. Chem. Commun. 1985*, 1505.

[5] V. Riera, M. A. Ruiz, *J. Chem. Soc. Dalton Trans. 1986*, 2617.

[6] **1**: orthorhombic, *Pbca*, $Z=8$, $a=10.519(5)$, $b=19.220(7)$, $c=29.223(9)$ Å; $V=5908(4)$ Å^3; $M_r=664.35$, $\rho_{calcd}=1.494$ g cm^{-3}; Siemens AED diffractometer ($Mo_{K\alpha}$), $\mu=9.68$ cm^{-1}; $3<\theta<28°$, 7902 unique reflections, 4634 observed with $I>2\sigma(I)$, $R=0.0426$, $R_w=0.0632$. Further details of the crystal structure analysis may be obtained from Cambridge Crystallographic Data Centre, University Chemical Laboratory, Lensfield Road, Cambridge CB2 1EW (UK), on quoting the names of authors and the journal citation.

[7] **1**: IR (toluene, [cm^{-1}]): $\tilde{\nu}$(CO) = 2035 s, 2005 s, 1955 s, 1920 br, vs; ^{1}H NMR ($CDCl_3$, *J* in Hz): $\delta=-17.5$ (t, $J_{PH}=21$, Mn(μ-*H*)$_2$Mn). **2a**: IR (CH_2Cl_2): $\tilde{\nu}$(CO) = 2035 s, 2005 s, 1954 m, 1935 sh, 1917 s; ^{1}H NMR (C_6D_6): $\delta=-14.5$ (t, $J_{PH}=21$, Mn(μ-*H*)Mn). **2b**: IR (hexane): $\tilde{\nu}$(CO) = 2035 s, 2005 s, 1960 s, 1940 s, 1927 br, vs; ^{1}H NMR ($CDCl_3$): $\delta=-0.8$ (t, $J_{PH}=20$, Mn(μ-S*H*)Mn, major isomer), -2.3 (t, $J_{PH}=15$, Mn(μ-S*H*)Mn, minor isomer), -15.3 (t, $J_{PH}=20$, Mn(μ-*H*)Mn); ^{31}P NMR (CH_2Cl_2): $\delta=56.5$ (s, minor isomer), 49.1 (s, major isomer). **3**: IR (toluene): $\tilde{\nu}$(CO) = 2028 vs, 1975 vs, 1953 s, 1912 vs, 1890 m; $\tilde{\nu}$(CN) = 1757 m, 1720 w; ^{31}P NMR ($CDCl_3$): $\delta=68.6$ (d, $J_{PP}=80$), 60.36 (d, $J_{PP}=80$); ^{13}C NMR ($CDCl_3$): $\delta=232$, 226.5, 223.7, 217.0, 213.5 (relative intensities 1:2:2:1:1, *C*O and *C*NR). **4**: IR (toluene): $\tilde{\nu}$(CO): 2022 vs, 1968 vs, 1945 s, 1910 vs, 1887 m; ^{31}P NMR ($CDCl_3$): $\delta=56.2$, 54.2 ([AB] system, $J_{PP}=65$); ^{13}C NMR (CD_2Cl_2, −60°C): $\delta=231.5$ (d, $J_{PC}=24$, *C*O), 230.6 (d, $J_{PC}=28$, *C*O), 227.1 (m, *C*O), 222.7 (m, *C*O), 216.4 (d, $J_{PC}=28$, *C*O), 214.7 (d, $J_{PC}=38$, *C*O), 157.2 (m, N*C*CH$_3$). **5**: IR (hexane): $\tilde{\nu}$(CO) = 2041 s, 2005 s, 1970 m, 1935 vs, 1920 s; ^{1}H NMR ($CDCl_3$): $\delta=6.8$ (m, Mn−C*H*=CH$_2$), 5.0 (d, $J_{HH}=9$), 4.6 (d, $J_{HH}=16$, Mn−CH=C*H*$_2$), −17.1 (t, $J_{PH}=19$, Mn(μ-*H*)Mn); ^{31}P NMR ($CDCl_3$): $\delta=62.2$ s; ^{13}C NMR ($CDCl_3$): $\delta=164.4$ (Mn−*C*H=CH$_2$), 83.6 (Mn−CH=*C*H$_2$). **6**: IR (hexane): $\tilde{\nu}$(CO) = 2042 vs, 2012 s, 1961 s, 1943 s, 1931 vs, $\tilde{\nu}$(C≡C) = 1975 sh, w; ^{1}H NMR ($CDCl_3$): $\delta=-14.2$ (t, $J_{PH}=21$, Mn(μ-*H*)Mn); ^{31}P NMR ($CDCl_3$, −80°C): $\delta=52.6$ s; ^{13}C NMR ($CDCl_3$): $\delta=110.3$ (t, $J_{PC}=18$, Mn−*C*≡C−C(CH$_3$)$_3$), 107.2 (s, Mn−C≡*C*C(CH$_3$)$_3$). **7**: IR (THF): $\tilde{\nu}$(CO) = 2028 s, 1962 vs, 1910 s, 1890 m; ^{1}H NMR (C_6D_6): $\delta=3.55$ (m, C=C(*H*)C(CH$_3$)$_3$); ^{31}P NMR ($CDCl_3$, −50°C): $\delta=79.7$ s, ($CDCl_3$, 25°C): $\delta=79.7$, 78.6 ([AB] system, $J_{PP}=122$); ^{13}C NMR ($CDCl_3$): $\delta=84.8$ (C=*C*(H)C(CH$_3$)$_3$).

[8] F. J. García Alonso, V. Riera, M. A. Ruiz, A. Tiripicchio, M. Tiripicchio-Camellini, unpublished results.

The Influence of Polar and Steric Effects on the Selectivity of the β-Cleavage of Alkyl Radicals**

By *Kurt Klenke, Jürgen O. Metzger,** and *Stefan Lübben*

The β-cleavage of radicals plays an important role in the complex reaction mechanisms of pyrolysis, combustion, photooxidation, the thermal degradation of polymers,[1] and increasingly also in preparatively useful reactions.[2] The selectivity of the β-cleavage has been the subject of

[*] Priv.-Doz. Dr. J. O. Metzger, Dr. K. Klenke,
Dipl.-Chem. S. Lübben
Fachbereich Chemie der Universität
Carl-von-Ossietzky-Strasse 9-11, D-2900 Oldenburg (FRG)

[**] This work was supported by the Deutsche Forschungsgemeinschaft.

very few studies. We have therefore carried out experiments aimed at demonstrating the influence of polar and steric effects on the β-cleavage of alkyl radicals.

The radicals **2** were generated by addition of cyclohexyl radicals (c-$C_6H_{11}^{\odot}$) to the alkenes **1**. These fragment in an intramolecular competition reaction to give the products **3** and **4** with cleavage of methyl and ethyl radicals, respectively.[3] The polar effect of X on the selectivity of the radical cleavage can be investigated by variation of the substituents X on the radical carbon atom.[5] The products **3** and **4** are each formed as (*E*)- and (*Z*)-isomers, so that also the polar effect of X on the stereoselectivity can be measured.

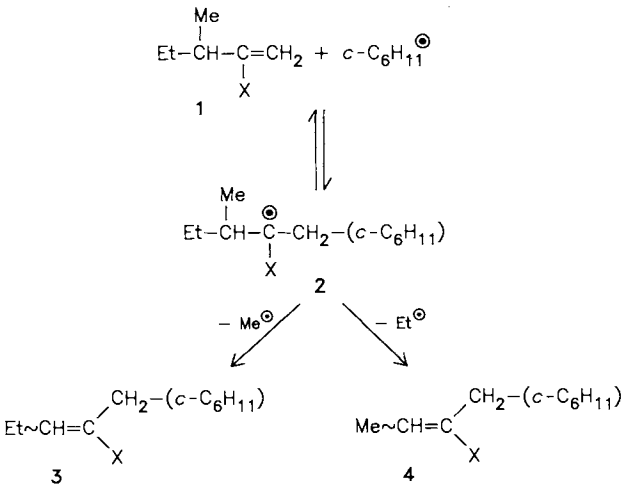

a, X = COOMe; b, X = Ph; c, X = p-MeO–C_6H_4; d, X = p-Cl–C_6H_4

The results (Table 1) are in many respects surprising. The benzyl radical **2b** fragments more slowly than the methoxycarbonylalkyl radical **2a**, since **2b** is about 15 kJ/mol more stable than **2a**.[6] The selectivity of the cleavage of the more reactive radical **2a** is, however, clearly greater. The stereoselectivity is also greater. This reversal of the reactivity-selectivity principle can be explained, in analogy to the radical addition to alkenes, in terms of the polar effect of the leaving radical and of the substituents X in the alkyl radical **2**.[7] The cleavage of the more nucleophilic ethyl compared to the methyl radical is accelerated by the electron-withdrawing substituent X = COOMe. This polar effect is especially evident on considering the difference in the activation energies, which amounts to ca. 18 kJ/mol for the fragmentation of **2a** to **3a** and **4a**. The difference in the stability of the products is only ca. 8 kJ/mol.[8] The polar effect of the methoxycarbonyl group is thus about 10 kJ/mol referred to the two leaving groups in question and increases the selectivity. The converse is true in the case of the nucleophilic radical **2b**, which gives the more electron-rich alkenes **3b** and **4b**. The cleavage of nucleophilic radicals is all the more difficult the more nucleophilic they are. The cleavage of the ethyl radical is more strongly retarded than that of the methyl radical. The difference of 4.5 kJ/mol in the activation energies again makes the polar effect especially noticeable. The transition states lie ca. 3.5 kJ/mol closer together than the ground states of the products that are formed. In this case the polar effect of the phenyl group reduces the selectivity of the β-cleavage.

Table 1. β-Cleavage of the radicals **2** to give the products **3** and **4** at 350°C [3].

2	Yield [a] [mol-%]	[**4**]/[**3**] [b]	[(*E*)-**4**]/[(*Z*)-**4**]	ΔE_a [c] [kJ/mol]	A_4/A_3 [c]
a	14.7	17.8 (1.25)	3	−18.2±2	0.6±0.2
b	6.0	7.3 (0.86)	2.5	− 4.5±0.5	3.0±0.3
c	7.4	8.9 (0.95)	2.3	− 8.4±0.6	1.6±0.2
d	9.0	9.4 (0.97)	2.3	− 7.2±0.8	2.4±0.5

[a] Sum of the β-cleavage products **3** and **4** based on alkene **1** used. [b] In parenthesis: selectivity S = lg([**4**]/[**3**]). [c] $\Delta E_a = E_a(\mathbf{4}) - E_a(\mathbf{3})$; 300–450°C.

Smaller but significant effects are observable on comparing the fragmentation of the radicals **2b**, **2c** and **2d** (Table 1). The electron withdrawal by chlorine in **2d** increases the reactivity and the selectivity compared to **2b**. Surprisingly, the *p*-methoxy group in **2c** apparently reacts only through its −I effect. The selectivity of the ethyl/methyl cleavage is increased significantly compared to **2b**. This is understandable only in terms of the *p*-methoxy group having an electron-attracting effect.

The radicals **6** were obtained by the addition of cyclohexyl radicals to the alkenes **5**. These fragment in a competition reaction to give the products **7** and **8** and a methyl radical.[9] The relative effect of the substituents attached to the carbon atom at which the C–C bond is ruptured on the cleavage of the methyl radical can be determined from the ratio of the products **7** : **8**.

The fragmentation is remarkably selective (Scheme 2): the thermodynamically more stable alkene **7** is formed in only slight excess at 400°C. Normalized to the number of cleavable methyl groups, the methyl radical is even preferentially cleaved from the lesser substituted alkyl group to give the thermodynamically more unstable alkene **8**.

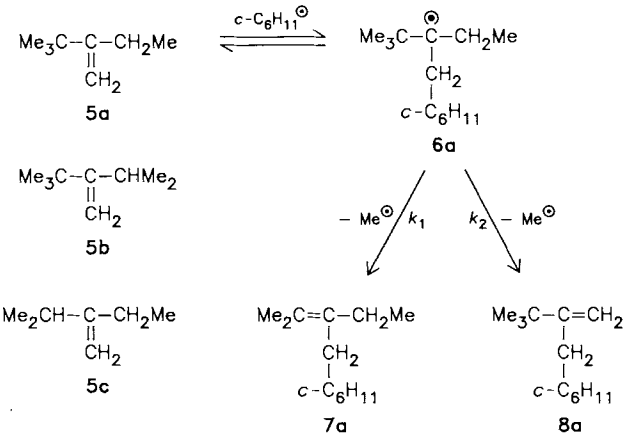

Table 2. Selectivity of the β-cleavage of the radicals **6** at 400°C.

6	[**7**] [mol-%]	[**8**] [mol-%]	$[k_2/k_1]_{norm.}$ [a]	S [b]
a	57	43	2.3	0.36
b	52	48 [c]	1.4	0.15
c	62 [c]	38	1.2	0.08

[a] Relative rate normalized to one methyl group. [b] $S = \lg k_2/k_1$. [c] (*E*)- and (*Z*)-products.

At first sight this result is surprising. One might expect that the stabler alkene is formed with higher selectivity[10] and that the cleavage of the methyl radical preferably occurs at the more substituted alkyl group. However, the result is understandable if the β-cleavage is considered from the point of view of the addition (Fig. 1). Substituents on the C atom that is attacked sterically hinder the addition.[7, 12] The free enthalpy of activation for the addition of the methyl radical to the alkene **7** is raised in comparison

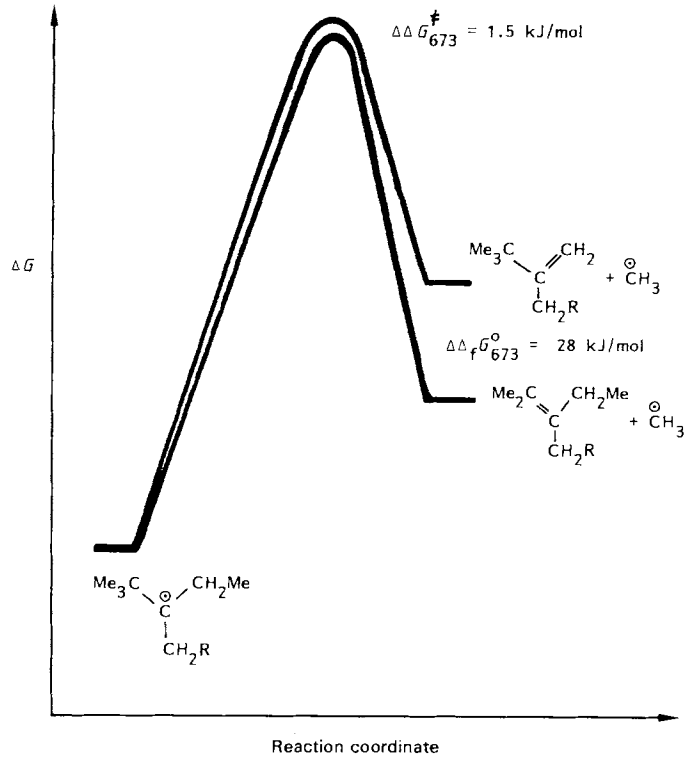

Fig. 1. Reaction coordinate of the β-cleavage of radical **6a**.

to the alkene **8** by the larger number of methyl groups on the C atom that is attacked. This means that the transition state of the β-cleavage is correspondingly also raised and the reaction retarded.[13]

The steric effects of substituents in β-cleavages should also play an important role in α-cleavages. Evidence to this effect is provided, for example, in S_H reactions of alkyltin[14] and alkylboron compounds.[15] Our results show that it is essential that polar and steric effects be taken into account as well the generally dominating influences of product stability[1] when considering the selectivity of β-cleavage.

Received: March 2, 1988;
revised: June 10, 1988 [Z 2645/2646 IE]
German version: *Angew. Chem. 100* (1988) 1195

CAS Registry numbers:
1a, 3070-70-0; **1b**, 26452-86-8; **1c**, 115982-37-1; **1d**, 115982-38-2; **2a**, 115982-39-3; **2b**, 115982-40-6; **2c**, 115982-41-7; **2d**, 115982-42-8; **3a**, 115982-43-9; **3b**, 115982-44-0; **3c**, 115982-45-1; **3d**, 115982-46-2; (*E*)-**4a**, 115982-47-3; (*Z*)-**4a**, 115982-51-9; (*E*)-**4b**, 115982-48-4; (*Z*)-**4b**, 115982-52-0; (*E*)-**4c**, 115982-49-5; (*Z*)-**4c**, 115982-53-1; (*E*)-**4d**, 115982-50-8; (*Z*)-**4d**, 115982-54-2; **5a**, 18231-53-3; **5b**, 20442-64-2; **5c**, 7357-93-9; **6a**, 115982-55-3; **6b**, 115982-56-4; **6c**, 115982-57-5; **7a**, 115982-58-6; **7b**, 115982-59-7; (*Z*)-**7c**, 115982-60-0; (*E*)-**7c**, 115982-61-1; **8a**, 115982-62-2; (*Z*)-**8b**, 115982-63-3; (*E*)-**8b**, 115982-64-4; **8c**, 115982-65-5; cyclohexane, 110-82-7; cyclohexyl, 3170-58-9.

[1] a) E. S. Huyser: *Free Radical Chain Reactions*, Wiley, New York 1970, p. 211; b) J. A. Kerr, A. C. Lloyd, *Q. Rev. London 22* (1968) 549.
[2] M. Ramaiah, *Tetrahedron 43* (1987) 3541.
[3] 0.03 mol/L solutions of the alkene **2** in cyclohexane were heated at 300–450 °C and 200 bar for 2 min in a high-pressure/high-temperature flow reactor [4]. The radical chain reaction was initiated by molecule-induced homolysis [4b]. The product solutions were analyzed by capillary gas chromatography. The products were identified by independent syntheses and/or GC/MS.
[4] a) P. Köll, J. O. Metzger, *Angew. Chem. 90* (1978) 802; *Angew. Chem. Int. Ed. Engl. 17* (1978) 754; b) J. Hartmanns, K. Klenke, J. O. Metzger, *Chem. Ber. 119* (1986) 488.
[5] A steric effect on the β-cleavage in this system can be largely ruled out, since the steric interaction of a methyl radical with an ethyl substituent should be the same as that of an ethyl radical with a methyl substituent.
[6] C. Rüchardt: *Die Bindung zwischen Kohlenstoffatomen, das Rückgrat der Organischen Chemie, und ihre Grenzen*, Springer, Berlin 1984, p. 67.
[7] B. Giese, *Angew. Chem. 95* (1983) 771; *Angew. Chem. Int. Ed. Engl. 22* (1983) 753.
[8] a) $\Delta\Delta H_f^\circ(\mathbf{3}\text{-}\mathbf{4}) \approx -20$ kJ/mol [11]; $\Delta\Delta H_f^\circ(Me^\odot - Et^\odot) = 28$ kJ/mol [8b]; b) J. J. Russel, J. H. Seetula, D. Gutman, *J. Am. Chem. Soc. 110* (1988) 3092.
[9] 0.01 mol/L solutions of the alkene **5** in cyclohexane were heated at 350–450 °C and 200 bar for 20 min as described in [3]. The conversions were maximally 4 mol-%.
[10] As models for examining the stability of the alkenes **7** and **8**, alkenes were chosen in which the $CH_2C_6H_{11}$ group is replaced by the CH_3 group. The thermochemical data of these alkenes are tabulated in Ref. [11] (e.g. $\Delta\Delta G_{600}^\circ = 28$ kJ/mol for 2,3,3-trimethyl-1-butene and 2,3-dimethyl-2-pentene).
[11] R. A. Alberty, C. A. Gehrig, *J. Phys. Chem. Ref. Data 14* (1985) 803.
[12] J. M. Tedder, *Angew. Chem. 94* (1982) 433; *Angew. Chem. Int. Ed. Engl. 21* (1982) 401.
[13] In the selected systems polar effects play only a minor role. Thus, the rate of addition of methyl radicals to alkenes is influenced only slightly by the polar effects of methyl substituents [12].
[14] A. G. Davies, B. Muggleton, B. P. Roberts, M.-W. Tse, J. N. Winter, *J. Organomet. Chem. 118* (1976) 289.
[15] P. J. Baker, J. N. Winter in S. Patai (Ed.): *The Chemistry of the Metal-Carbon-Bond, Vol. 2*, Wiley, Chichester 1985, p. 190.

Biomimetic Synthesis of an Octavinylogous Porphyrin with an Aromatic [34]Annulene System**

By *Georg Knübel* and *Burchard Franck**

Application of the principles of natural products chemistry allows extension of the theoretically and methodologically inspiring field of annulenes[1] to higher ring systems. The series of well-defined, normal annulenes ended previously with the diatropic (aromatic) [22]annulene **2** and the paratropic (antiaromatic) [24]annulene[1] (Scheme 1). Using porphyrin biosynthesis as our model, we recently synthesized a tetravinylogous porphyrin, **7**, containing a [26]annulene system.[2a] Compound **7** displays unusual properties with possible topical applications.[3]

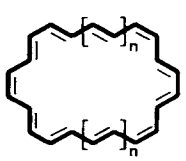

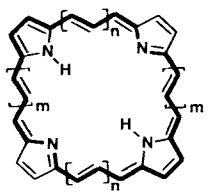

1, n = 0	[18]annulene	**5**, n, m = 0	[18]porphyrin
2, n = 1	[22]annulene	**6**, n = 1, m = 0	[22]porphyrin-[1.3.1.3]
3, n = 2	[26]annulene	**7**, n, m = 1	[26]porphyrin-[3.3.3.3]
4, n = 4	[34]annulene	**8**, n, m = 2	[34]porphyrin-[5.5.5.5]

Scheme 1. Structures of previously reported (above the broken line) and still unknown diatropic annulenes **1**–**4** together with the corresponding vinylogous porphyrins **5**–**8** [5].

Herein we report on the synthesis of an eightfold vinylogously enlarged porphyrin, **17**, containing a cyclic conjugated 34π-electron system. The basic structure of **17**, being a bridged diaza derivative of [34]annulene **4**, is named [34]porphyrin-[5.5.5.5] according to our nomenclature proposal.[5]

To develop a synthesis of the [34]porphyrin **17** involving as few steps as possible, we followed the pathway of porphyrin biosynthesis[6] (Scheme 2). It is known[4, 7] that porphobilinogen **9**, the biogenetic precursor of all porphyrin

[*] Prof. Dr. B. Franck, Dipl.-Chem. G. Knübel
Organisch-chemisches Institut der Universität
Orléansring 23, D-4400 Münster (FRG)

[**] Novel Porphyrinoids, Part 6. This work was supported by the Deutsche Forschungsgemeinschaft and the Fonds der Chemischen Industrie.—Part 5: [2b].

natural products, as well as similar 2-(aminomethyl)- and 2-(hydroxymethyl)pyrroles, can undergo acid-catalyzed condensation in vitro to give porphyrins.

This *biomimetic cyclotetramerization* is even suitable for the synthesis of sterically highly strained *N,N',N'',N'''*-tetraalkylated and *N,N'*-bridged porphyrinogens and porphyrins.[2b,4] Even though such condensations lead to porphyrinogens, which are (still?) unknown as natural products, these reactions are by definition[8] *biomimetic*, since they are closely related to biosynthesis.

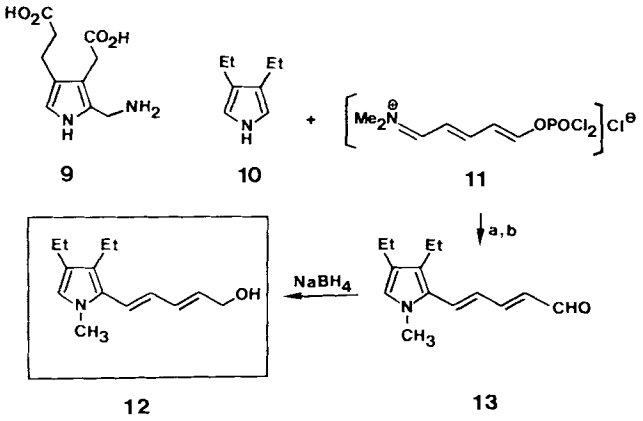

Scheme 2. Porphobilinogens **9** and synthesis of the 5-pyrrylpentadienol **12**. Reaction conditions: a) *N,N*-dimethylaminopentadienal/$POCl_3$, CH_2Cl_2, −40°C, inert gas, 4 h, 44% yield. b) NaH, dry dimethylformamide, CH_3I, 20°C, 30 min, 87% yield; **13**: m.p. 55°C.

The key building block for the biomimetic construction of a [34]porphyrin system **8** is the pyrrylpentadienol **12** (Scheme 2). Owing to its high reactivity, **12** is generated from the stable aldehyde precursor **13** by $NaBH_4$ reduction immediately prior to the acid-catalyzed condensation. Compound **13** was synthesized from 3,4-diethylpyrrole **10**[9] by doubly vinylogous Vilsmeier formylation using the complex **11**, followed by *N*-methylation.

Of decisive importance for the further synthesis of the [34]porphyrin derivative **17** was the question whether, in analogy to the porphobilinogen **9**, a derivative **12** having a doubly vinylogous side chain would also undergo acid-catalyzed condensation. The high selectivity in the biomimetic condensation of suitable monopyrroles to cyclic tetrapyrroles may be ascribed to steric interactions of substituents in the β positions of neighboring pyrrole rings.[2d,4] This effect should be strongly diminished when the bridges linking the pyrrole rings are lengthened, as in **14** and **15**.

Nonetheless, the acid-catalyzed condensation of **12** gave the colorless, cyclically nonconjugated, octavinylogous [34]porphyrinogen **14**[12] (Scheme 3). However, the yield of this reaction (4.1% based on **13**) was, as expected, smaller than that of the tetravinylogous [26]porphyrinogen **15** (27%).[2a] Still, this yield reveals a remarkable selectivity in this complex cyclization when one considers that the yield of **14** refers to a five-step synthesis—comprising reduction and four cyclization steps—and therefore represents an average yield of 53% for each reaction step.

The lesser tendency of **12** to form cyclic tetramers is also revealed in the fact that, in addition to **14**, a more slowly eluting product was isolated by flash chromatography (silica gel, cyclohexane/ethyl acetate 20 : 1) in nearly the same amount. On the basis of its mass spectrum ($M^{\oplus}$ 1005, 25%), it can be assigned the structure of a pentamer, **16**.

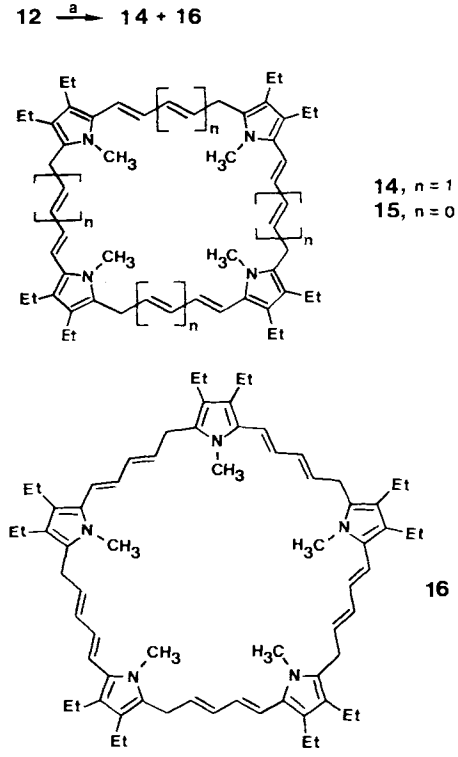

Scheme 3. Acid-catalyzed biomimetic condensation of the 5-pyrrylpentadienol **12**. Reaction conditions: a) *p*-toluenesulfonic acid, acetic acid, MeOH, 50°C, inert gas, 30 min; 4.1% yield; **14**, m.p. 168°C.

The cyclic conjugated target molecule **17** is so stable that the educt **14**—like the [26]porphyrinogen **15**[2a]—can be dehydrogenated by treatment with bromine. The [34]porphyrin-[5.5.5.5] was thereby obtained as the bisquaternary dibromide **17**.

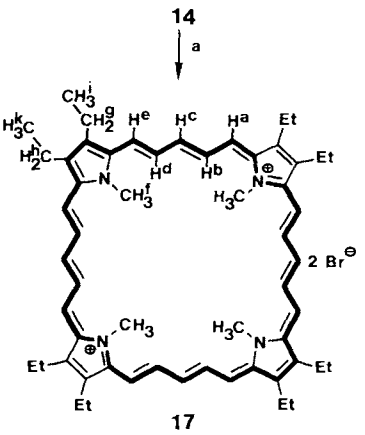

	δ	J [Hz]
H^a, H^e	16.18 d	13.1
H^b, H^d	−14.27 t	13.1
H^c	17.19 t	13.1
H^f	−11.44 s	
H^g, H^h	6.04 br	
H^i, H^k	2.83 t	7.2

Scheme 4. Synthesis of the [34]porphyrin-[5.5.5.5] **17** and ^1H NMR data (in [D_6]DMSO, see Fig. 1). Reaction conditions: a) Br_2/CCl_4, polymer base (diethylaminomethylpolystyrene), 20°C, 5 h; 12.5% yield after chromatographic purification (silica gel, CH_2Cl_2/MeOH 10/1).

The [34]porphyrin **17**, which forms deep blue (λ_{max} = 664 nm) solutions, exhibits an extraordinarily large ring-current effect in the ^1H NMR spectrum (Scheme 4). The maximum shift difference $\Delta\delta$ of the resonance signals between the inner ($\delta = -14.27$) and outer protons ($\delta = 17.19$) is 31.5 ppm. This value indicates that the dia-

magnetic ring-current effect of **17** significantly surpasses the $\Delta\delta$ value (25.3 ppm)[2a] found for the analogous [26]porphyrin and that found for [18]annulene **1** (12.1 ppm).[1] The ^{1}H NMR spectrum of **17** (Fig. 1) is probably the first obtained for a non-organometallic compound in which the measured proton resonances extend over a range of more than 30 ppm. Splitting of the signals for the protons H^a, H^b, and H^c of **17** (Fig. 1a), observed only at extreme dilution, indicates a tendency toward association.

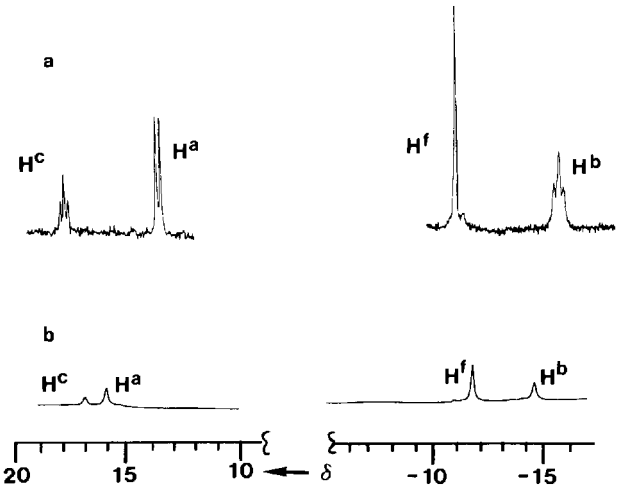

Fig. 1. 300-MHz ^{1}H NMR spectra of [34]porphyrin **17** in [D$_6$]DMSO. Concentrations: a) 0.1 g L^{-1}; b) 3.0 g L^{-1}.

The synthesis of the [34]porphyrin **17** with its high ring-current effect, characterizing its aromaticity,[10] supports—as already shown for the [26]porphyrin system—the validity of the (4n+2) rule for higher annulene systems. That the annulenes so far available exhibit diatropic behavior only in the range of 14–22 π electrons—as experimentally found and as calculated[11]—can no longer be regarded, therefore, as a limitation of the (4n+2) rule.

The diatropic behavior of the vinylogous porphyrins is appreciably more pronounced than for the annulenes. We ascribed this finding to the flattening effect of the pyrrole rings, which hinders inversions of the ring system.[2a] The present results show that this principle is so efficient that even vinylogous porphyrins having the large 34π ring system—that is, C_5 chains between the pyrrole rings—are conformationally more stable that the [18]annulene **1**.

Received: April 25, 1988;
supplemented: June 3, 1988 [Z 2721 IE]
German version: *Angew. Chem. 100* (1988) 1203

[1] a) F. Sondheimer, *Acc. Chem. Res. 5* (1972) 81; b) P. J. Garratt: *Aromaticity*, Wiley, New York 1986, p. 100ff.

[2] a) M. Gosmann, B. Franck, *Angew. Chem. 98* (1986) 1107; *Angew. Chem. Int. Ed. Engl. 25* (1986) 1100; German Pat. Appl. P 3635820 (1986), BASF; b) R. Timmermann, R. Mattes, B. Franck, *Angew. Chem. 99* (1987) 74; *Angew. Chem. Int. Ed. Engl. 26* (1987) 64; c) G. Bringmann, B. Franck, *Liebigs Ann. Chem. 1982*, 1261; d) *ibid. 1982*, 1272.

[3] One possible application is in the phototherapy of tumors. Cf. H. van den Bergh, P. Cornaz, *Nachr. Chem. Tech. Lab. 33* (1985) 582; A. Andreoni, R. Cubeddu: *Porphyrins in Tumor Phototherapy*, Plenum Press, New York 1984.—Since the [26]porphyrin [2a] exhibits more advantageous properties, in terms of the wavelength of its fluorescence emission, its chemical stability, and its solubility, than the derivatives of hematoporphyrin so far employed, it is now being tested in medical applications.

[4] B. Franck, *Angew. Chem. 94* (1982) 327; *Angew. Chem. Int. Ed. Engl. 21* (1982) 343.

[5] For the nomenclature of vinylogous porphyrins, see M. Gosmann, B. Franck [2a]. The compounds are thus named in analogy to annulenes. To describe the structure unambiguously, the number of C atoms between the pyrrole rings is also given. Examples are: [26]porphyrin-[3.3.3.3] or [18]porphyrin-[1.1.1.1] **5** (the "simple" porphyrin).

[6] L. Bogorad in D. Dolphin (Ed.): *The Porphyrins*, Vol. 6, Academic Press, New York 1979, p. 125.

[7] G. H. Cookson, C. Rimington, *Biochem. J. 57* (1954) 476.

[8] R. Breslow, *Q. Rev. Chem. Soc. 1* (1972) 553.

[9] H. W. Withlock, R. Hanauer, *J. Org. Chem. 33* (1968) 2169.

[10] P. J. Garratt in D. H. R. Barton, W. D. Ollis (Eds.): *Comprehensive Organic Chemistry*, Vol. 1, Pergamon, Oxford 1979, p. 224.

[11] M. J. S. Dewar, G. J. Gleicher, *J. Am. Chem. Soc. 87* (1965) 685.

[12] The new compounds **13**, **14**, and **17** have been fully characterized by elemental analysis and spectroscopic data: **14**: MS (EI): *m/z* 804 (64%, $M^{\oplus}$), 775 (26, $M-C_2H_5$), 402 (26, *M*/2); ^{1}H NMR (C_6D_6): δ=2.78 (s, 12H, N–CH_3), 3.15 (d, 8H, =CH–CH_2–pyrrole), 5.60 (dt, *J*=4.8, 15.1 Hz, 4H, =CH–CH_2); IR (KBr): $\tilde{\nu}$=2950, 2920, 2860 (CH), 1605, 960 cm^{-1} (*trans* C=C); R_f=0.41 (silica gel, cyclohexane/ethyl acetate 10/1).—**17**: MS (FD): *m/z* 800 (100%, $M-2Br^{\oplus}$); ^{1}H NMR see Scheme 4 and Fig. 1; FT-IR (KBr): $\tilde{\nu}$=2963, 2926, 2870, 2853 cm^{-1} (CH); UV/VIS/NIR (chloroform): $\lambda_{max}(\varepsilon)$=663 (370000), 997 nm (24000); R_f=0.40 (RP 18, MeOH/THF 5:1, 0.005 M sodium dodecylsulfate).

An Antibody-Mediated Redox Reaction**

By *Kevan M. Shokat, Christian J. Leumann, Renee Sugasawara,* and *Peter G. Schultz**

The advent of monoclonal antibodies makes possible the generation of highly selective receptors to a vast number of structurally diverse ligands.[1] Recently, the high binding affinity and specificity of antibody combining sites has been exploited in the development of selective catalysts for acyl transfer,[2] carbon–carbon bond-forming,[3] and carbon–carbon bond-cleaving reactions.[4] We now report that antibody combining sites can modulate the thermodynamics of redox processes. The use of antibody specificity to alter flavin redox potentials is the first step toward developing antibodies capable of using cofactors to catalyze stereoselective reductions.

Oxidized flavin **1** and the two-electron-reduced 1,5-dihydroflavin **1a** have substantially different electronic and conformational properties.[5] The dipole moment of oxidized flavin is reduced by 40% upon two-electron reduction and the N^1 position becomes an H-bond donor.[6] In fact, the pK_a of the N^1–H bond in **1a** is 6.5, indicating it may exist largely as the anion in solution. In terms of structural differences, a bent (N^5–N^{10} axis) conformation is preferred by reduced flavin, whereas a planar form is favored by the oxidized flavin (however, the calculated energy difference between the two conformations is small, 1–2 kcal mol^{-1}).[6] Consequently, antibodies generated specifically to the oxidized flavin should preferentially bind **1** relative to 1,5-dihydroflavin **1a**. This differential stabilization of the oxidized and two-electron-reduced flavin by the

[*] Prof. P. G. Schultz, K. M. Shokat
Department of Chemistry, University of California, Berkeley
Berkeley, CA 94720 (USA)
Dr. C. J. Leumann
Institut für Organische Chemie der
Eidgenössischen Technischen Hochschule, ETH-Zentrum
Universitätsstrasse 16, CH-8092 Zürich (Switzerland)
Dr. R. Sugasawara
IGEN Incorporated
Rockville, MD 20852 (USA)

[**] The authors gratefully acknowledge support by the Department of Energy, contract C87-101226 *(P. G. S.)*, and the Swiss National Science Foundation *(C. J. L.)*. We thank Dr. *W. McIntire* and Dr. *T. Singer* for helpful contributions to this work.

antibody (Ig) combining site should make the Ig-**1a** complex a substantially stronger reducing agent than free **1a** in solution.

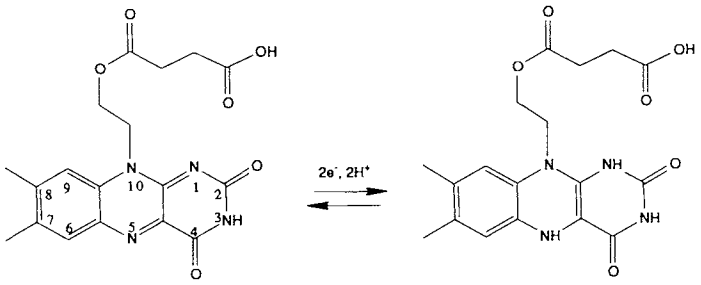

1 **1a**

Periodate oxidation of riboflavin afforded 10-(formylmethyl)riboflavin, which was subsequently reduced with sodium borohydride and reacted with succinic anhydride to afford the acid **1**.[14] Hapten **1** was then coupled to the carrier proteins bovine serum albumin and keyhole limpet hemocyanin using water-soluble carbodiimide,[7] and antibodies were generated according to techniques described elsewhere.[8] Six clones were obtained and purified from mouse ascites fluid by Protein-A chromatography[9] and were judged homogeneous by sodium dodecyl sulfate polyacrylamide gel electrophoresis with Coomassie blue staining.[10]

The binding constant of flavin **1** to one of the monoclonal antibodies was determined by the method of fluorescence quenching[11] (flavin fluorescence is completely quenched upon binding to the antibody). Antibody-ligand dissociation constants of 8×10^{-9} M and 6×10^{-8} M were obtained for **1** and riboflavin, respectively.[12] The UV spectrum of **1** bound to antibody displayed a 15-nm bathochromic shift (443 to 458 nm) and a shoulder appeared at 482 nm; the 375-nm maximum did not shift appreciably. Such spectral perturbations indicate association with aromatic amino acid side chains in the antibody combining site.[13]

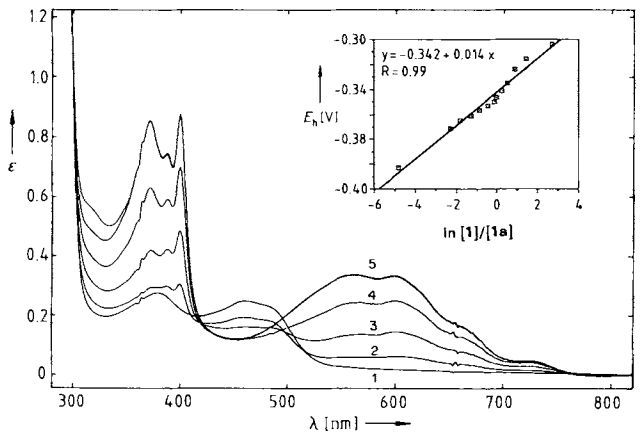

Fig. 1. Anaerobic dithionite (5 mM) titration of **1** (30 μM) bound to antibody (31 μM) in the presence of benzyl viologen (30 μM) in 0.1 M phosphate, pH 7.0; 1, **1** and oxidized benzyl viologen; 2-4, partially reduced **1** and partially reduced benzyl viologen after 0.5, 1.0, and 1.5 equivalents of dithionite were added, respectively; 5, fully reduced flavin and fully reduced benzyl viologen after 2.0 equivalents of dithionite were added. Ig concentration was determined by absorbance at 280 nm by using $E^{0.1\%}_{1cm}=1.37$ [2c]. Inset: E_h [V] vs. ln([**1**]/[**1a**]).

Reduction potentials were measured in anaerobic solutions under an atmosphere of argon by titration of flavin in the presence of redox-active dyes.[13] The antibody-**1** complex was reduced by dithionite titration in the presence of benzyl viologen (E_m(dye) = −358 mV; Fig. 1). Reduction of benzyl viologen resulted in an increase in absorbance at 598 nm where the flavin has no interfering absorption. Flavin reduction was calculated based on its decrease in absorbance at 440 nm. Using the Nernst equation [Eq. (a)],

$$E_h = E_m(\text{dye}) + \frac{RT}{nF}\ln([\text{dye}_{ox}]/[\text{dye}_{red}]) \qquad (a)$$

the potential can be directly evaluated and a plot of E_h vs. ln([flavin$_{ox}$]/[flavin$_{red}$]) allows the determination of E_m(**1**-Ig) (inset, Fig. 1). The reduction potential of flavin **1** bound to antibody is −342 mV, representing a lowering of the reduction potential (E_m(**1**) = −206 mV) by 136 mV. When the antibody-**1** complex was reduced by dithionite in the absence of benzyl viologen, no spectra associated with the protonated blue (λ_{max} = 570 nm) or the deprotonated red (λ_{max} = 480 nm) semiquinone radical species were observed. Using a thermodynamic cycle, the antibody dissociation constant for the dihydroflavin **1a** can be calculated to be 3×10^{-4} M. The antibody exhibits a more than five order of magnitude preference for binding to the oxidized over the reduced flavin.

Because the antibody-**1a** complex is a stronger reducing agent than free **1a**, compounds with reduction potentials in the range −206 to −342 mV should be reduced by Ig-**1a** but not by free **1a** in solution (inset, Fig. 2). To demonstrate this, we studied the reduction of the dye Safranine T (E_m(dye) = −289 mV). The Ig-**1** complex was stoichiometrically reduced by dithionite (no excess dithionite present) and aliquots of Safranine T were subsequently added. Oxidation of Ig-**1a** (increase in absorbance at 375 and 458 nm) occurred rapidly, whereas no absorption due to oxidized Safranine T (510 nm) was observed, indicating that antibody-bound **1a** is in fact able to reduce Safranine T (Fig. 2). Following complete flavin oxidation, O_2 was added in order to oxidize Safranine T (Fig. 2, curve 4). As expected, free **1a** is not a powerful enough reducing agent to reduce Safranine T.

In summary, an antibody binding site has been used to modulate the reduction potential of flavin **1** by preferen-

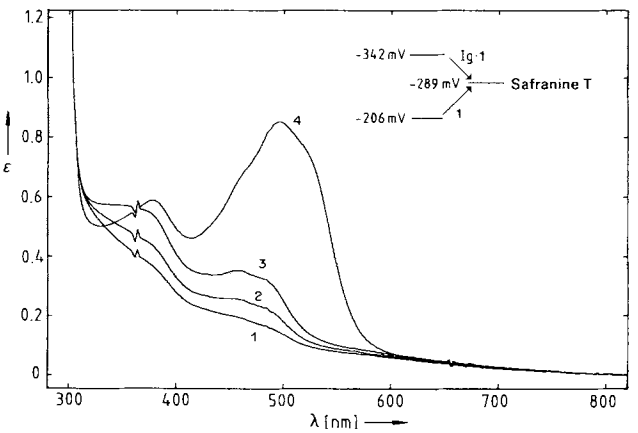

Fig. 2. Anaerobic addition of Safranine T (6 mM) to **1a** (30 μM) bound to antibody (31 μM), same conditions as Fig. 1; 1, **1a**; 2-3, partially oxidized **1a** after addition of 0.3 and 0.8 equivalents of Safranine T respectively; 4, after addition of oxygen.

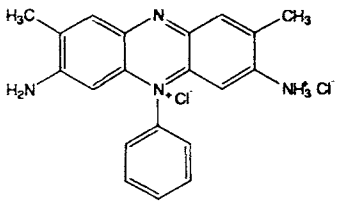

Safranine T

tially binding the oxidized form over the reduced dihydro form. The antibody–flavin complex is able to mediate redox processes not thermodynamically accessible to free flavin. Incorporation of a substrate binding site into these antibodies may lead to catalytic antibodies which can carry out stereocontrolled chemical reductions.

Received: April 26, 1988;
revised: June 7, 1988 [Z 2724 IE]
German version: *Angew. Chem. 100* (1988) 1227

CAS Registry number:
1, 110031-00-0.

[1] D. Pressman, A. Grossberg: *The Structural Basis of Antibody Specificity*, Benjamin, New York 1968.
[2] a) S. Pollack, J. Jacobs, P. G. Schultz, *Science (Washington) 234* (1986) 1570; b) A. Tramantano, K. Janda, R. A. Lerner, *ibid.* 1566; c) J. Jacobs, P. G. Schultz, *J. Am. Chem. Soc. 109* (1987) 2174; d) A. Napper, S. J. Benkovic, A. Tramantano, R. A. Lerner, *Science (Washington) 237* (1987) 1041.
[3] P. G. Schultz, D. Y. Jackson, J. W. Jacobs, R. Sugasawara, S. H. Reich, P. A. Bartlett, *J. Am. Chem. Soc. 110* (1988) 4841.
[4] P. G. Schultz, *Science (Washington) 240* (1988) 426.
[5] a) F. Muller, *Top. Curr. Chem. 108* (1983) 71; b) V. Massey, P. Hemmerich, *Biochem. Soc. Trans. 8* (1980) 246.
[6] L. H. Hall, M. L. Bowers, C. N. Durfor, *Biochemistry 26* (1987) 7401.
[7] B. Erlanger, *Methods Enzymol. 70* (1980) 85.
[8] a) B. Hurn, S. Chantler, *Methods Enzymol. 70* (1980) 104; b) R. Sugasawara, C. Prato, J. Sippel, *Infect. Immun. 42* (1983) 863; c) E. Engvall, J. Perlmann, *J. Immunol. 109* (1972) 129.
[9] G. Kornvall, H. Grey, R. Williams, *J. Immunol. 105* (1970) 1116.
[10] V. Laemmli, *Nature (London) 227* (1970) 680.
[11] M. Nishikimi, Y. Kyodoku, *J. Biochem. 73* (1973) 1233.
[12] Flavin binding antibodies have been previously isolated: a) M. Y. Chang, F. K. Freidman, S. Beychok, J. S. Shyong, E. F. Osserman, *Biochemistry 20* (1981) 2916; b) M. J. Barber, D. C. Eichler, L. P. Solomonson, B. A. Ackrell, *Biochem. J. 242* (1987) 89.
[13] a) D. Edmondson, T. Singer, *J. Biol. Chem. 248* (1973) 8144; b) B. Burleigh, G. Foust, C. Williams, *Anal. Biochem. 27* (1969) 536.
[14] **1**: m.p. 194–198 °C; UV/VIS (0.1 N NaOH): $\lambda(\lg\varepsilon)=269$ (4.71), 355 (4.25), 450 nm (4.26); ^{1}H NMR ([D$_6$]dimethyl sulfoxide): $\delta=2.09$ (t, 2H, $J=11$ Hz), 2.23 (t, 2H, $J=11$ Hz), 2.35 (s, 3H), 2.42 (s, 3H), 4.37 (t, 2H), 4.80 (t, 2H), 7.83 (s, 2H), 11.35 (br. s, 1H); FAB$^+$-MS (high resolution): 387.1305 ($C_{18}H_{19}N_4O_6$, MH$^\oplus$).

A Stable Bis(chelate) Analogue of the Creutz–Taube Ion**

By *Wolfgang Kaim,* Volker Kasack, Herbert Binder, Eberhard Roth,* and *Jeanne Jordanov*

Since its isolation 20 years ago the electronic structure of the mixed-valence ($Ru^{II}Ru^{III}$) "Creutz–Taube ion" **2**[1] has been the subject of numerous theoretical and experimental investigations.[2–4] The controversy has focused, above all, on the extent of (de)localization between the metal centers ($Ru^{II}Ru^{III}$ or $Ru^{2.5}Ru^{2.5}$) and on the role of the bridging ligand.[2,4] Whereas delocalized mixed-valence complexes of class III-A with ruthenium ammine complex fragments have been unambiguously established in protic solvents,[2] the widely used $[Ru(bpy)_2]^{n\oplus}$ fragments, which are important in (photochemical) redox catalysis,[5] gave only mixed-valence compounds exhibiting low stability toward disproportionation ($K_c < 10^3$).[6]

$$2[Ru^{II}Ru^{III}] \overset{K_c}{\rightleftharpoons} [Ru^{II}Ru^{II}] + [Ru^{III}Ru^{III}] \qquad (a)$$

Only recently were we able to prepare binuclear compounds of this fragment which, owing to strong ligand–metal interaction, exhibit large comproportionation constants K_c;[7] however, the mixed-valence species could not be isolated because of the considerable anodic shift of the potential for metal oxidation. Nonetheless, complexes of $[Ru(bpy)_2]^{2\oplus/3\oplus}$ are soluble in aprotic media in contrast to those of $[Ru(NH_3)_n]^{2\oplus/3\oplus}$, so that complications due to acid–base equilibria and hydrogen-bonding interactions can be avoided.

By using reduced forms of very π-electron-deficient bis(chelate) ligands, we have attempted to synthesize stable bis(chelate) analogues of the Creutz–Taube ion that exhibit a high degree of delocalization. When pure N systems[8a] or when *o*- and *p*-semiquinone ligands[9] were used, however, we were able to characterize only ligand-centered (i.e., radical anion-containing) intermediates,[10a] instead of mixed-valence binuclear complexes. Herein we report on a paramagnetic binuclear complex **1** with a largely reduced diethyl azodicarboxylate (adc) bridging ligand; the spectroscopic measurements reveal that **1** can be regarded as a first true, isolable bis(chelate) analogue of the Creutz–Taube ion **2**.

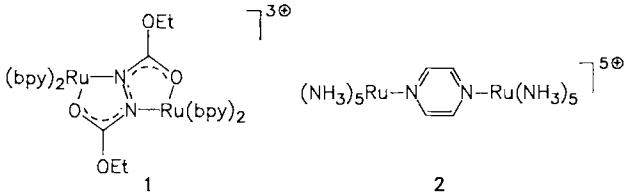

1 **2**

Complex **1** is directly obtained by reaction of the bridging ligand with *cis*-$[Ru(bpy)_2Cl_2]$ in 1,2-dichloroethane (DCE); the neighboring oxidation states are accessible by reduction with Zn or by oxidation with Ag$^\oplus$. Owing to the stereogenicity of the two equivalent metal centers, *meso*/DL diastereomers should be formed;[7,9c] an effect of such isomerism on the spectroscopic data discussed here is not evident, however.

Cyclic voltammetry in DCE/0.1 M Bu_4NClO_4 shows two reversible steps at +0.38 and +0.89 V versus the saturated calomel electrode (SCE); thus, the comproportionation (stability) constant K_c [Eq. (a)] for the intermediate **1** is 4.4×10^8 (cf. $K_c=4\times10^6$ for **2**[1,2]). This high value favors the isolation of the paramagnetic species **1** and, moreover, is in agreement[7] with the large molecular orbital (MO) coefficients at N and O π centers in the lowest unoccupied MO (LUMO) of azodicarboxylic acid derivatives.[9c]

In contrast to numerous mono- and binuclear radical anion complexes of the $[Ru(bpy)_2]^{2\oplus}$ fragment,[8,9] the paramagnetic intermediate **1** does not exhibit an ESR spectrum at room temperature or at 77 K; only below about

[*] Prof. Dr. W. Kaim, Dipl.-Chem. V. Kasack, Prof. Dr. H. Binder
Institut für Anorganische Chemie der Universität
Pfaffenwaldring 55, D-7000 Stuttgart 80 (FRG)
Dr. J. Jordanov, Dipl.-Chem. E. Roth
Département de Recherche Fondamentale,
Centre d'Etudes Nucléaires
85X, F-38041 Grenoble Cedex (France)

[**] This work was supported by the Deutsche Forschungsgemeinschaft, the Stiftung Volkswagenwerk, the Flughafen Frankfurt am Main AG, and the Fonds der Chemischen Industrie. We thank Degussa AG for a donation of chemicals and Prof. *H. Elias* and Dr. *K. J. Wannowius* (Darmstadt) for making the NIR absorption measurements possible.

50 K is a rhombic signal without hyperfine structure observable (Fig. 1). Very rapid relaxation is characteristic of metal-centered paramagnetic transition-metal complexes[3, 10] [Eq. (b) **A**]; also, close-lying excited states with partial ligand localization of the unpaired electron [Eq. (b)

$$[Ru^{II}(L^{2\ominus})Ru^{III}]^{3\oplus} \longleftrightarrow [Ru^{II}(L^{\bullet\ominus})Ru^{II}]^{3\oplus} \quad (b)$$

A **B**

B] may be responsible for this. The relatively small anisotropy of the glass spectrum of **1** (Fig. 1) compared with that of the Creutz-Taube ion **2** ($g = 1.346$, 2.489, 2.799; $\langle g \rangle = 2.30$[3]), which contains only inorganic co-ligands, also indicates a larger contribution of the radical anion resonance structure for **1** than for **2**.[3, 4, 11] However, this anisotropy is appreciably more pronounced than that found for the ligand-centered radicals containing $(bpy)_2Ru$[8–10, 12] which points to considerable involvement[11] of the heavy-metal center with its large spin-orbit coupling factor $(Ru^{II(III)}) = 700$–$1250\ cm^{-1}$,[4] according to formulation **A**.

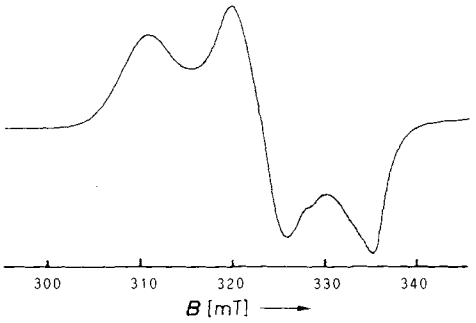

Fig. 1. X-band ESR spectrum of **1** at 3.6 K in acetone (counterions $PF_6^{\ominus}$): $g_x = 2.108$, $g_y = 2.036$, $g_z = 1.963$; $\langle g \rangle_{calcd} = 2.0364$.

In the X-ray photoelectron spectrum (−50 °C, gold foil) of **1**, as in that of the Creutz-Taube ion **2**,[4d] bands for Ru^{II} ($3d_{5/2}$: 283.0 eV) *and* Ru^{III} ($3d_{3/2}$: 290.0 eV) are observed, although they are partially overlapped by the C(1s) signal at 286.2 eV. The (2+) oxidation state, on the other hand, only exhibits a Ru^{II} ($3d_{5/2}$) band. However, this finding cannot be taken as evidence for a Ru^{II}/Ru^{III} localization, as has been discussed in detail for compound **2**.[4d]

In addition to the $d(Ru^{II}) \rightarrow \pi^*(bpy)$ charge-transfer absorption (MLCT)[13] at 450 nm,[12] the electronic spectrum of **1** shows a band with a half-width of $\Delta\nu_{1/2} = 2600\ cm^{-1}$ and an extinction coefficient of $\varepsilon = 7800\ M^{-1}\ cm^{-1}$ in the near-IR region (NIR; maximum at 1410 nm = 7100 cm^{-1}, shoulder at 1180 nm, Fig. 2). These data are very similar to the corresponding values for the Creutz-Taube ion: $\nu_{max} = 6400\ cm^{-1}$, $\varepsilon = 5000\ M^{-1}\ cm^{-1}$, $\Delta\nu_{1/2} = 1250\ cm^{-1}$,[1, 2] so that, in accordance with the formula **A**, these features may be attributed to the expected $Ru^{II} \rightarrow Ru^{III}$ intervalence transition (MMCT)[1, 2] and to an LMCT transition $\pi(adc^{2\ominus}) \rightarrow d(Ru^{III})$.

However, formulation **B** would also explain absorptions in the NIR, which would then be attributed to transitions from Ru^{II} d orbitals to the singly occupied MO of the ($adc^{\bullet\ominus}$) bridging ligand and would be split by metal-metal interactions.[9b, 10a, 12] The CT absorptions[13] of the dication [680 nm (sh; LLCT $\pi(adc^{2\ominus}) \rightarrow \pi^*(bpy)$), 527 nm (MLCT $d(Ru^{II}) \rightarrow \pi^*(bpy)$)] and of the tetracation [369 nm (MLCT $d(Ru^{II}) \rightarrow \pi^*(bpy)$)[12], 900 nm (MLCT $d(Ru^{II}) \rightarrow \pi^*(adc)$ for formula **C**, or LMCT $\pi(adc^{2\ominus}) \rightarrow d(Ru^{III})$ for formula **D**[9b])] are significantly different; values are from solutions in 1,2-dichloroethane (Fig. 2).

$$[Ru^{II}(L)Ru^{II}]^{4\oplus} \longleftrightarrow [Ru^{III}(L^{2\ominus})Ru^{III}]^{4\oplus} \quad (c)$$

C **D**

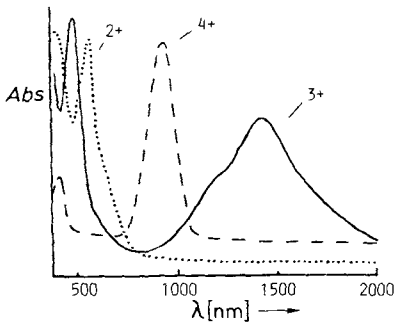

Fig. 2. Absorption spectra of **1** and of its two neighboring oxidation states in 1,2-dichloroethane (absorbance scale different for each spectrum).

The spectroscopic comparison thus shows that **1** occupies an intermediate position between the largely metal-centered, mixed-valence Creutz-Taube ion **2** and clearly ligand-centered radical complexes.[8, 10a, 12] In addition to the metal–metal interaction, the bridging ligand itself can be strongly involved in the electron delocalization, leading to the formation of extensively delocalized multimetal complexes having unusual electronic structures and remarkable physical properties.[14, 15]

Experimental Procedure

1$[PF_6]_3$: *cis*-$[Ru(bpy)_2Cl_2] \cdot 2H_2O$ (100 mg, 0.19 mmol), diethyl diazodicarboxylate (17 mg, 0.10 mmol), and KPF_6 (70 mg, 0.38 mmol) were heated at reflux in 50 mL of 1,2-dichloroethane for 2 d. The product was precipitated from the cooled and concentrated reddish-brown solution by addition of diethyl ether and then recrystallized from acetone/diethyl ether (3 : 1) and from 1,2-dichloroethane/diethyl ether (4 : 1). Yield 30 mg (21%), correct elemental analysis (C,H,N).

The reduced (2+) oxidation state could be obtained from the (3+) ion by column chromatography on basic Al_2O_3 using acetone/water as eluent. The violet compound was recrystallized from acetone/diethyl ether (3 : 1) as the bis(hexafluorophosphate) (75%, C,H,N analysis).

Received: May 5, 1988 [Z 2743 IE]
German version: *Angew. Chem. 100* (1988) 1229

[1] C. Creutz, H. Taube, *J. Am. Chem. Soc. 95* (1973) 1086.
[2] a) C. Creutz, *Prog. Inorg. Chem. 30* (1983) 1; b) D. E. Richardson, H. Taube, *Coord. Chem. Rev. 60* (1984) 107; *J. Am. Chem. Soc. 105* (1983) 40.
[3] A. Stebler, J. H. Ammeter, U. Fürholz, A. Ludi, *Inorg. Chem. 23* (1984) 2764.
[4] a) J. Ko, L. T. Zhang, M. J. Ondrechen, *J. Am. Chem. Soc. 108* (1986) 1712; b) L. T. Zhang, J. Ko, M. J. Ondrechen, *ibid. 109* (1987) 1666; c) M. Ondrechen, J. Ko, L. T. Zhang, *ibid. 109* (1987) 1672; d) P. H. Citrin, A. P. Ginsberg, *ibid. 103* (1981) 3673.
[5] Cf. K. Kalyanasundaram, *Coord. Chem. Rev. 46* (1982) 159; A. Juris, V. Balzani, F. Barigelletti, S. Campagna, P. Belser, A. von Zelewsky, *ibid. 84* (1988) 85.
[6] a) R. W. Callahan, F. R. Keene, T. J. Meyer, D. J. Salmon, *J. Am. Chem. Soc. 99* (1977) 1064; b) D. P. Rillema, K. B. Mack, *Inorg. Chem. 21* (1982) 3849; c) D. P. Rillema, G. Allen, T. J. Meyer, D. Conrad, *ibid. 22* (1983) 1614.
[7] S. Ernst, V. Kasack, W. Kaim, *Inorg. Chem. 27* (1988) 1146.
[8] a) W. Kaim, S. Ernst, S. Kohlmann, P. Welkerling, *Chem. Phys. Lett. 118* (1985) 431; b) D. E. Morris, K. W. Hanck, M. K. DeArmond, *J. Am. Chem. Soc. 105* (1983) 3032.

[9] a) S. Ernst, V. Kasack, C. Bessenbacher, W. Kaim, *Z. Naturforsch. B 42* (1987) 425; b) S. Ernst, P. Hänel, J. Jordanov, W. Kaim, V. Kasack, E. Roth, submitted for publication; c) S. Ernst, *Dissertation*, Universität Frankfurt 1987.
[10] a) W. Kaim, *Coord. Chem. Rev. 76* (1987) 187; b) A. Bencini, D. Gatteschi, *Transition Met. Chem. N. Y. 8* (1982) 1.
[11] For the relation between metal/ligand (de)localization and the *g* factor, see R. Gross, W. Kaim, *Inorg. Chem. 26* (1987) 3596; *J. Chem. Soc. Faraday Trans. 1 83* (1987) 3549.
[12] M. Haga, E. S. Dodsworth, A. B. P. Lever, *Inorg. Chem. 25* (1986) 447.
[13] W. Kaim, S. Ernst, S. Kohlmann, *Chem. Unserer Zeit 21* (1987) 50.
[14] Cf. R. Gross, W. Kaim, *Angew. Chem. 99* (1987) 257; *Angew. Chem. Int. Ed. Engl. 26* (1987) 251.
[15] Note added in proof: In analogy to organic compounds described recently, **1** may be formulated as a 2,5-acceptor-1,3,4,6-donor-substituted pentalene π system: F. Closs, R. Gompper, H. Nöth, H.-U. Wagner, *Angew. Chem. 100* (1988) 875; *Angew. Chem. Int. Ed. Engl. 27* (1988) 842.

Asymmetric Induction in the Replacement of Diastereotopic Bromine Atoms by Lithium Atoms**

By *Reinhard W. Hoffmann,* Martin Bewersdorf, Klaus Ditrich, Michael Krüger,* and *Rainer Stürmer*

In memoriam Gert Köbrich 1929–1974

The formation of new chiral centers by intramolecular asymmetric induction is accomplished almost exclusively by reactions at the diastereotopic *sides* of a prochiral C=C, C=N, or C=O group.[1] The use of diastereotopic *groups* in preparative chemistry, on the other hand, has been reported in only a few special cases.[2] On cyclic systems, the selective replacement of one of two diastereotopic bromine atoms by a metal atom has long been known.[3] Herein we report on the diastereoselective replacement of one of the bromine atoms of open-chain, chiral 1,1-dibromoalkanes **1**. The investigations were carried out on racemic compounds.

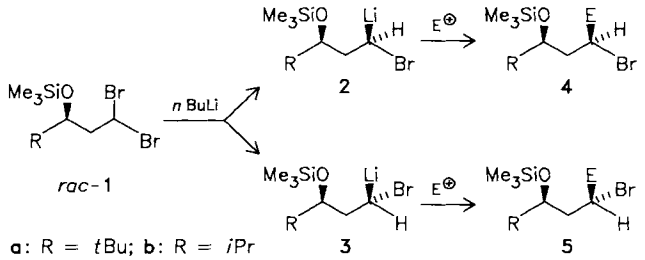

a: R = *t*Bu; b: R = *i*Pr

In a typical experiment, 3.3 mmol of a 1.55 M solution of *n*-butyllithium in hexane was added dropwise to a solution of **1a** (3 mmol)[4] and acetone (6 mmol) as electrophile, $E^{\oplus}$, in 25 mL of Trapp mixture[6] at −120°C. After 1 h at < −90°C, the solution was allowed to reach room temperature and the products were hydrolyzed, affording a 94:6 mixture of the two diastereomeric epoxides **6a** in 90% yield.[5] Similar reaction using the pinacol ester of phenylboronic acid, instead of acetone, gave a 93:7 mixture of the diastereomeric boronates **7a**.[7] Addition of the carbenoids to isobutyraldehyde resulted in a 3:1 mixture of the *cis*- and *trans*-epoxides **8a** and **9a**. Each of these epoxides had a diastereomeric purity of >90:10.

[*] Prof. Dr. R. W. Hoffmann, Dipl.-Chem. M. Bewersdorf, Dr. K. Ditrich, Dipl.-Chem. M. Krüger, R. Stürmer
Fachbereich Chemie der Universität
Hans-Meerwein-Strasse, D-3550 Marburg (FRG)

[**] This work was supported by the Fonds der Chemischen Industrie and the Deutsche Forschungsgemeinschaft (SFB 260).

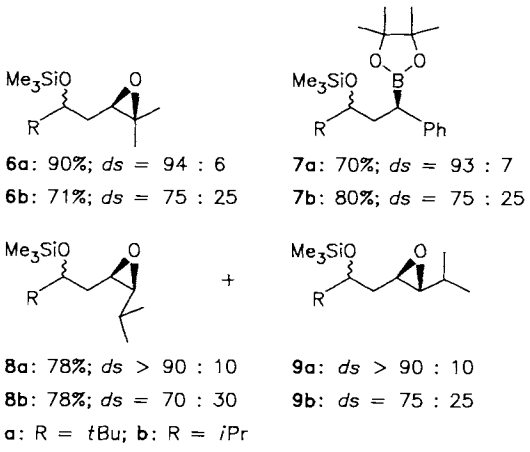

a: R = *t*Bu; b: R = *i*Pr

In the series **1b**,[4] with R = isopropyl, the results were essentially the same, although the diastereoselectivity (of **6b**–**9b**) was less[8] than in the *tert*-butyl-substituted series **1a**.

These findings indicate that the halogen–metal exchange on **1a** takes place with a diastereoselectivity of ca. 93:7 (for **1b**, 75:25), that the carbenoids **2/3** are configurationally stable at −120 to −90°C, and that they are trapped stereospecifically by the electrophiles $E^{\oplus}$ to give **4/5**. This interpretation is based on the fact that the ratio of the isomers **4/5** was independent of the nature of the trapping electrophile in the examples investigated. For a rapid epimerization of **2** and **3**, on the other hand, the product ratio **4/5** would be expected to depend on the nature of the electrophile. Thus, the halogen–metal exchange on **1** is presumably the product-determining step. Preliminary results from experiments in which the organolithium compounds were varied support this conclusion, as shown by the reaction of *rac*-**1b** to give **6b**.

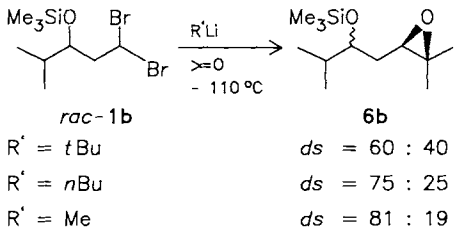

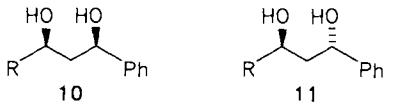

Since the configuration of the product is established during the halogen–metal exchange, it is of interest to determine which of the diastereotopic bromine atoms in **1** is exchanged. To this end, the mixture of diastereomers **7a**, as well as **7b**, was oxidized with alkaline H_2O_2 to afford a mixture of the known diols[9] **10/11**. The main diastereomer in each case had the *threo* configuration **11**. Thus, the *pro-ul* bromine atom[10] in **1** is preferentially exchanged with formation of the carbenoid **2**. The (unproven) notion that coordination of the organolithium compounds to the trimethylsiloxy group might play a role in this process[3] was crucial in selecting **1** for these experiments.

Received: May 9, 1988 [Z 2750 IE]
German version: *Angew. Chem. 100* (1988) 1232

[1] Cf. J. D. Morrison (Ed.): *Asymmetric Synthesis, Vol. 1-5*, Academic Press, New York 1983-1985.
[2] For example, diastereotopic protons in chiral sulfoxides: R. Viau, T. Durst, *J. Am. Chem. Soc. 95* (1973) 1346; G. Solladié, R. G. Zimmermann, *Tetrahedron Lett. 25* (1984) 5769; diastereotopic chlorine atoms in chiral dichloromethaneboronic esters: D. S. Matteson, K. M. Sadhu, M. L. Peterson, *J. Am. Chem. Soc. 108* (1986) 810.
[3] K. G. Taylor, W. E. Hobbs, M. S. Clark, J. Chaney, *J. Org. Chem. 37* (1972) 2436; T. Harada, Y. Yamaura, A. Oku, *Bull. Chem. Soc. Jpn. 60* (1987) 1715.
[4] **Ia** was prepared by reaction of *tert*-butyloxirane with dibromomethyllithium at $-100°C$ in the presence of BF_3-ether, followed by silylation. **Ib** was obtained by reaction of dibromomethyllithium at $-95°C$ with prenyl bromide [5], followed by hydroboration, oxidation, and silylation.
[5] J. Villieras, B. Kirschleger, R. Tarhouni, M. Rambaud, *Bull. Soc. Chim. Fr. 1986*, 470, and references cited therein.
[6] G. Köbrich, H. Trapp, *Chem. Ber. 99* (1966) 670, 680.
[7] Cf. G. Köbrich, H. R. Merkle, *Chem. Ber. 100* (1967) 3371.
[8] The bis(phenylseleno)acetal corresponding to **Ib** gave a diastereomeric ratio of 91:9 upon selenium-lithium exchange and subsequent addition to acetone.
[9] S. Kiyooka, H. Kuroda, Y. Shimasaki, *Tetrahedron Lett. 27* (1986) 3009.
[10] D. Seebach, V. Prelog, *Angew. Chem. 94* (1982) 696; *Angew. Chem. Int. Ed. Engl. 21* (1982) 654.

A Synthetic Heparin-like Compound which still Activates Antithrombin III although It Contains an Open Chain Fragment instead of α-L-Idopyranuronate**

By *Constant A. A. van Boeckel,* Jan E. M. Basten, Hans Lucas,* and *Sjoerd F. van Aelst*

The sulfated pentasaccharide **Ia** (Scheme 1), which is synthetically available,[1] corresponds to a unique antithrombin III (AT-III) binding region of the anticoagulant drug heparin. **Ia** catalyzes the AT-III-mediated inactivation of coagulation factor Xa (anti-Xa activity in an amidolytic assay = 590 U/mg), but not of thrombin. Recently, it has been established[2,5] that most of the charged groups in heparin fragment **Ia** participate in the AT-III-activation process. Moreover, the synthetic analogue **Ic** containing an extra 3-*O*-sulfate at unit 6 elicits higher activity (i.e. anti-Xa activity = 1270 U/mg) than the naturally occurring fragment.[3]

A special role should be ascribed to the rare, flexible carbohydrate α-L-iduronic acid (unit 5) in compound **Ia**.[4] For instance, it has been shown[5] that the carboxylate group of the α-L-idopyranuronate moiety of **Ia** is essential for AT-III activation, while the removal of its 2-*O*-sulfate substituent (Scheme 1, compound **Ib**) leads to a fourfold reduction of activity.[2b] The crucial question remains whether the presence of the complex α-L-idopyranuronate is essential for the biological activity of the heparin fragment.

To answer this question we synthesized a "ring-opened" analogue (i.e. compound **II**), in which α-L-iduronic acid (unit 5) is replaced by an (*R*)-glyceric acid -2-*O*-CH_2- moiety (2,3 *seco*-2,3-di-*nor*-α-L-iduronic acid). In addition, compound **II** contains an extra 3-*O*-sulfate group at unit 6

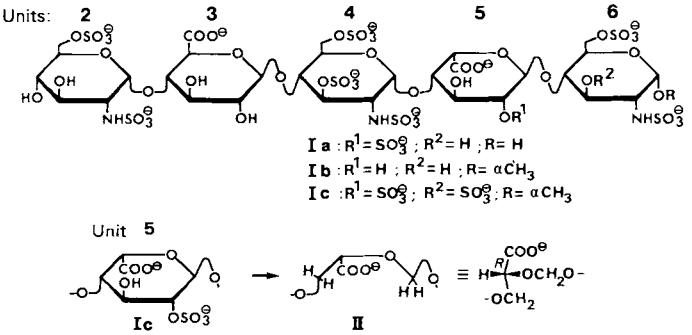

Scheme 1. Compound **Ia** comprises the antithrombin activating region of heparin. Compounds **Ib** and **Ic** are synthetic analogues, which are respectively less and more active than the naturally occurring derivative **Ia**. The synthetic analogue **II** is described in this communication; the α-L-iduronic acid moiety (unit 5) has been replaced by an (*R*)-glyceric acid-OCH_2-moiety.

to compensate for the drop in activity caused by the absence of the 2-*O*-sulfate group at unit 5 (see above).

A key goal in the synthesis of **II** was the preparation of a suitably protected and activated (*R*)-glyceric acid building block (i.e. compound **7**) that could be coupled via a 2-oxymethylene function to the (low reactive) 4-hydroxy group of compound **8**[3a] (see Scheme). Since this coupling reaction is formally identical to a carbohydrate glycosidic bond formation, we adopt a $BF_3 \cdot OEt_2$-catalyzed glycosidation with glycosyl fluorides[6] for coupling of the (*R*)-glyceric acid-2-*O*-CH_2F derivative **7**. The synthesis of **7** started from (*R*)-glyceric acid methyl ester **2**, which was prepared from D-serine (**1**).[7] The primary hydroxy group of **2** was protected selectively with a DMT group,[*] after which the secondary hydroxy group was methoxymethylated to give **3** in high yield. Mild acid treatment afforded compound **4**, which was allylated in a two-step procedure to provide derivative **5** in 58% overall yield. Acetolysis of **5** afforded compound **6** in quantitative yield. The latter was treated with HF/pyridine[8] to give the key building block **7** in 70% yield. Reaction of **7** with **8**, in the presence of $BF_3 \cdot OEt_2$ afforded the corresponding coupled product in 84% yield, from which the temporary allyl protective group was cleaved by $PdCl_2$ treatment to give **9** in 40% yield. The resultant aglycon **9** was then stereoselectively condensed with the known glycon **10**[1c] in 65% yield using $HgBr_2$/$Hg(CN)_2$ as promoter. The α-coupled product **12a** was first de-levulinoylated to give **12b** and then coupled to monosaccharide **11**[9] to give the fully protected pentasaccharide analogue **13** in 50% yield. Compound **13** was converted into the desired analogue **II**[10] in 22% overall yield by the following well-established[1,2c,3a,5] reaction sequence: (i) NaOH; (ii) $Me_3N \cdot SO_3$, DMF; (iii) H_2/Pd; (iv) pyridine·SO_3, H_2O; and gel permeation chromatography.

Analogue **II** displayed prominent AT-III-mediated anti-Xa activity (150 U/mg), thus proving that the biological activity of a heparin-like fragment is retained when the complex carbohydrate α-L-iduronic acid has been replaced by a linear chain that is substituted by a correctly oriented carboxylate group. Preliminary conformational analysis studies reveal that the conformational freedom of the linear moiety of **II** is restricted considerably. Thus, vicinal proton-proton coupling constants and NOE data of com-

[*] Dr. C. A. A. van Boeckel, J. E. M. Basten, H. Lucas, S. F. van Aelst
Organon International B.V.
Scientific Development Group
P.O. Box 20, NL-5340 BH Oss (The Netherlands)

[**] We thank Dr. *J.-R. Mellema* and Mr. *G. N. Wagenaars* for the ^{1}H-NMR spectrum of **II**, Drs. *R. Gebhard* for assistance with the syntheses, Mr. *Th. G. van Dinther* for determining the anti-Xa activities and Dr. *H. C. J. Ottenheijm* for discussions.

[*] Abbreviations: DMT = 4,4'-dimethoxytrityl; All = Allyl; Lev = levulinoyl; Ac = acetyl; Bz = benzoyl; Bn = benzyl; THF = tetrahydrofuran; DMF = *N,N*-dimethylformamide; MS = molecular sieve.

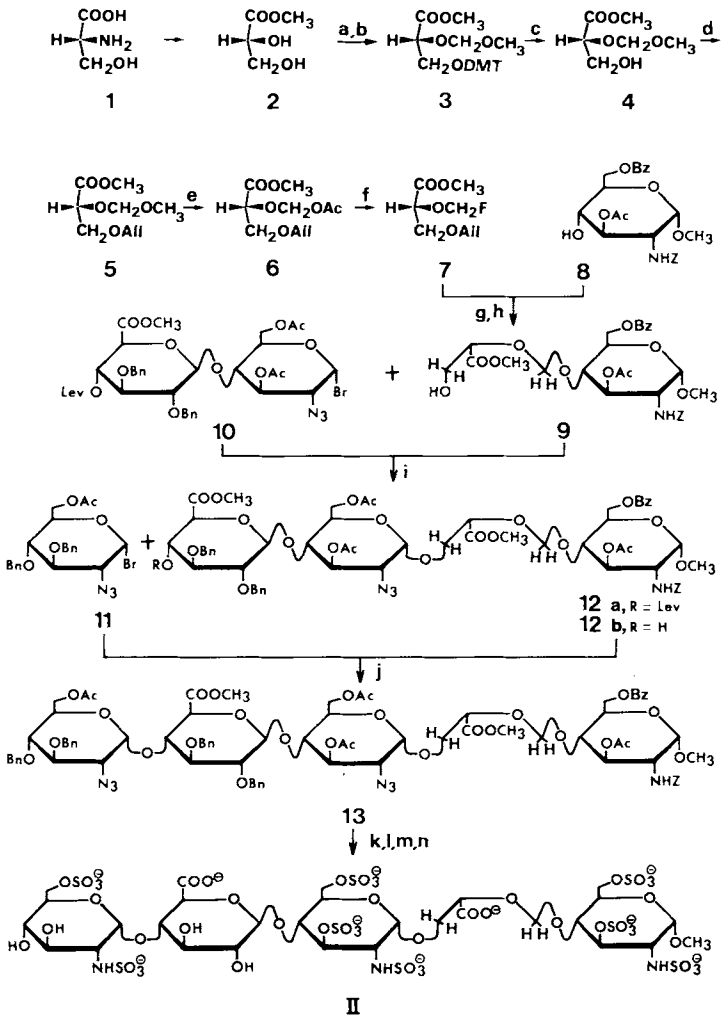

Scheme 2. a) DMT-Cl, THF/pyridine, −5°C, 2 h (90%); b) CH_3OCH_2Cl, ethyldiisopropylamine, 40°C, 20 h (89%); c) AcOH/H_2O, RT, 2 h (89%); d) Allyloxycarbonyl chloride, pyridine/CH_3CN, −35°C, 2 h (79%); $Pd(Ph_3P)_4$, dioxane, 100°C, 0.5 h (82%); e) Ac_2O/CF_3COOH/AcOH, RT, 2 h (99%); f) 70% HF/pyridine, 0°C, 1 h (70%); g) $BF_3 \cdot OEt_2$, CH_2Cl_2, −20°C, 1 h (84%); h) $PdCl_2$, AcOH/AcONa, 16 h, RT (40%); i) $Hg(CN)_2/HgBr_2$, CH_2Cl_2, MS 4 Å, 40 h, RT (65%); j) $AgSO_3CF_3$, MS 4 Å, 2,6-di-*tert*-butylpyridine, CH_2Cl_2, −55°C, 2 h (50%); k) NaOH, $H_2O/CH_3OH/CHCl_3$, RT, 16 h (78%); l) $Me_3N \cdot SO_3$, DMF, 50°C, 24 h (58%); m) H_2, Pd/C, *t*BuOH/H_2O, RT (90%); n) Pyridine $\cdot SO_3/Na_2CO_3/H_2O$, RT (55%).

pound **II** indicate that the glyceric acid $-OCH_2-$ moiety favors a conformation corresponding to that of the backside region (O-4, C-4, C-5, O) of α-L-idopyranuronate in the $^1C_4$ form. Taking the above mentioned results into consideration we believe that the introduction of similar "opened" carbohydrate-like moieties in other biologically active carbohydrates will find an application in broader domains of glycoconjugate research. For that purpose, asymmetrically substituted $-OCH_2O-$ acetal functions can be introduced by the methodology described in this communication.

Received: May 5, 1988 [Z 2745 IE]
German version: *Angew. Chem. 100* (1988) 1217

[1] a) J. Choay, M. Petitou, J. C. Lormeau, P. Sinaÿ, B. Casu, G. Gatti, *Biochem. Biophys. Res. Commun. 116* (1983) 492; b) P. Sinaÿ, J. C. Jacquinet, M. Petitou, P. Duchaussoy, I. Lederman, J. Choay, G. Torri, *Carbohydr. Res. 132* (1984) C 5; c) C. A. A. van Boeckel, T. Beetz, J. N. Vos, A. J. M. de Jong, S. F. van Aelst, R. H. van den Bosch, J. M. R. Mertens, F. A. van der Vlugt, *J. Carbohydr. Chem. 4* (1985) 293; d) Y. Ichikawa, R. Monden, H. Kuzuhara, *Tetrahedron Lett. 27* (1986) 611.

[2] a) M. Petitou, *Nouv. Rev. Fr. Hematol. 26* (1984) 221; b) M. Petitou, J. C. Lormeau, J. Choay, *Thromb. Haemostasis 58* (1987) 7; c) T. Beetz, C. A. A. van Boeckel, *Tetrahedron Lett. 27* (1986) 5889.

[3] a) C. A. A. van Boeckel, T. Beetz, S. F. van Aelst, *Tetrahedron Lett. 28* (1988) 803; b) C. A. A. van Boeckel, S. F. van Aelst, T. Beetz, D. G. Meuleman, Th. G. van Dinther, H. C. T. Moelker, *Ann. N. Y. Acad. Sci.* (1988), in press.

[4] a) D. R. Ferro, A. Provasoli, M. Ragazzi, G. Torri, B. Casu, G. Gatti, J.-C. Jacquinet, P. Sinaÿ, M. Petitou, J. Choay, *J. Am. Chem. Soc. 108* (1986) 6773; b) C. A. A. van Boeckel, S. F. van Aelst, G. N. Wagenaars, J.-R. Mellema, H. Paulsen, T. Peters, A. Pollex, V. Sinnwell, *Recl. Trav. Chim. Pays-Bas 106* (1987) 19; c) H. Paulsen, A. Pollex, V. Sinnwell, C. A. A. van Boeckel, *Liebigs Ann. Chem.* (1988) 411.

[5] a) C. A. A. van Boeckel, H. Lucas, S. F. van Aelst, M. W. P. van den Nieuwenhof, G. N. Wagenaars, J.-R. Mellema, *Recl. Trav. Chim. Pays-Bas 106* (1987) 581; b) S. F. van Aelst, C. A. A. van Boeckel, *ibid. 106* (1987) 593.

[6] K. C. Nicolaou, A. Chucholowski, R. E. Dolle, J. L. Randall, *J. Chem. Soc. Chem. Commun. 1984*, 1155.

[7] C. M. Lok, J. P. Ward, D. A. van Dorp, *Chem. Phys. Lipids 16* (1976) 115.

[8] M. Hayashi, S. Hashimoto, R. Noyori, *Chem. Lett. 1984*, 1747.

[9] H. Paulsen, W. Stenzel, *Chem. Ber. 111* (1978) 2334.

[10] ^{1}H-NMR data (360 MHz, D_2O, ref. HOD): the ^{1}H-NMR spectrum of **II** was completely assigned using 2D-COSY techniques. The following resonances are important: unit 6: 5.03 (d, J=3.6 Hz, 1H, H-1), 3.48 (dd, J=3.6, 9.4 Hz, 1H, H-2), 4.45 (dd, J=9.4, 9.9 Hz, 1H, H-3), 3.42 (s, 3H, OCH_3); unit 5: 4.91, 5.11 (AB, J=7.5 Hz, 2H, $-OCH_2O-$), 3.85, 4.12 (m, 2H, OCH_2C), 4.41 (t, J=2.4 Hz, 1H, $CHCOO^{\ominus}$); unit 4: 5.12 (d, J=3.6 Hz, 1H, H-1), 3.42 (dd, J=3.6 Hz, J=9.4 Hz, 1H, H-2), 4.37 (dd, J=9.4 Hz, J=9.9 Hz, 1H, H-3); unit 3: 4.61 (d, J=7.9 Hz, 1H, H-1); unit 2: 5.61 (d, J=3.6 Hz, 1H, H-1), 3.25 (dd, J=3.6, 9.4 Hz, 1H, H-2), 3.62 (t, J=9.9 Hz, 1H, H-3), 3.56 (t, J=9.9 Hz, 1H, H-4); $[\alpha]_D^{20} = +92.7°$ (c=0.91, H_2O).

Simple Synthesis of KDO α-Glycosides by Anomerically Selective *O*-Alkylation**

By *Richard R. Schmidt** and *Angelika Esswein*

Lipopolysaccharides (LPS) are important components of the outer membranes of gram-negative bacteria.[1] The lipophilic portion of LPS, lipid A, is responsible for anchoring the lipid in the membrane; it determines the toxic and immunostimulatory properties of LPS. Lipid A consists essentially of a β(1–6′)-linked glucosamine disaccharide containing phosphate groups at the C-1 and C-4′ atoms as well as long-chain fatty acids on the N atom and on some of the free O atoms. The hydrophilic portion of LPS consists of a complex oligosaccharide chain, which is linked through KDO (3-deoxy-D-manno-2-octulosonic acid) to the glucosamine disaccharide.[1] According to recent investigations, an α(2–6′)-glycosidic bond is present.[2] The application of the Koenigs-Knorr procedure for α-glycosidic bond formation using KDO halogenoses as glycosyl donors has often given unsatisfactory results owing to elimination of hydrogen halide and, in part, formation of β-glycoside bonds.[3] Good results were recently reported using fluoride as the leaving group.[4]

The anomerically selective *O*-alkylation reported here is an especially simple procedure for saccharide synthesis.[5,6] However, several prerequisites must be satisfied: (1) decomposition reactions in the sugar portion (particularly in the ring-open form) occurring after deprotonation of the hemiacetal hydroxyl group must be avoided; (2) the ano-

[*] Prof. Dr. R. R. Schmidt, Dipl.-Chem. A. Esswein
Fakultät für Chemie der Universität
Postfach 5560, D-7750 Konstanz (FRG)

[**] Anomeric *O*-Alkylation, Part 6. This work was supported by the Deutsche Forschungsgemeinschaft and the Fonds der Chemischen Industrie.—Part 5: [5].

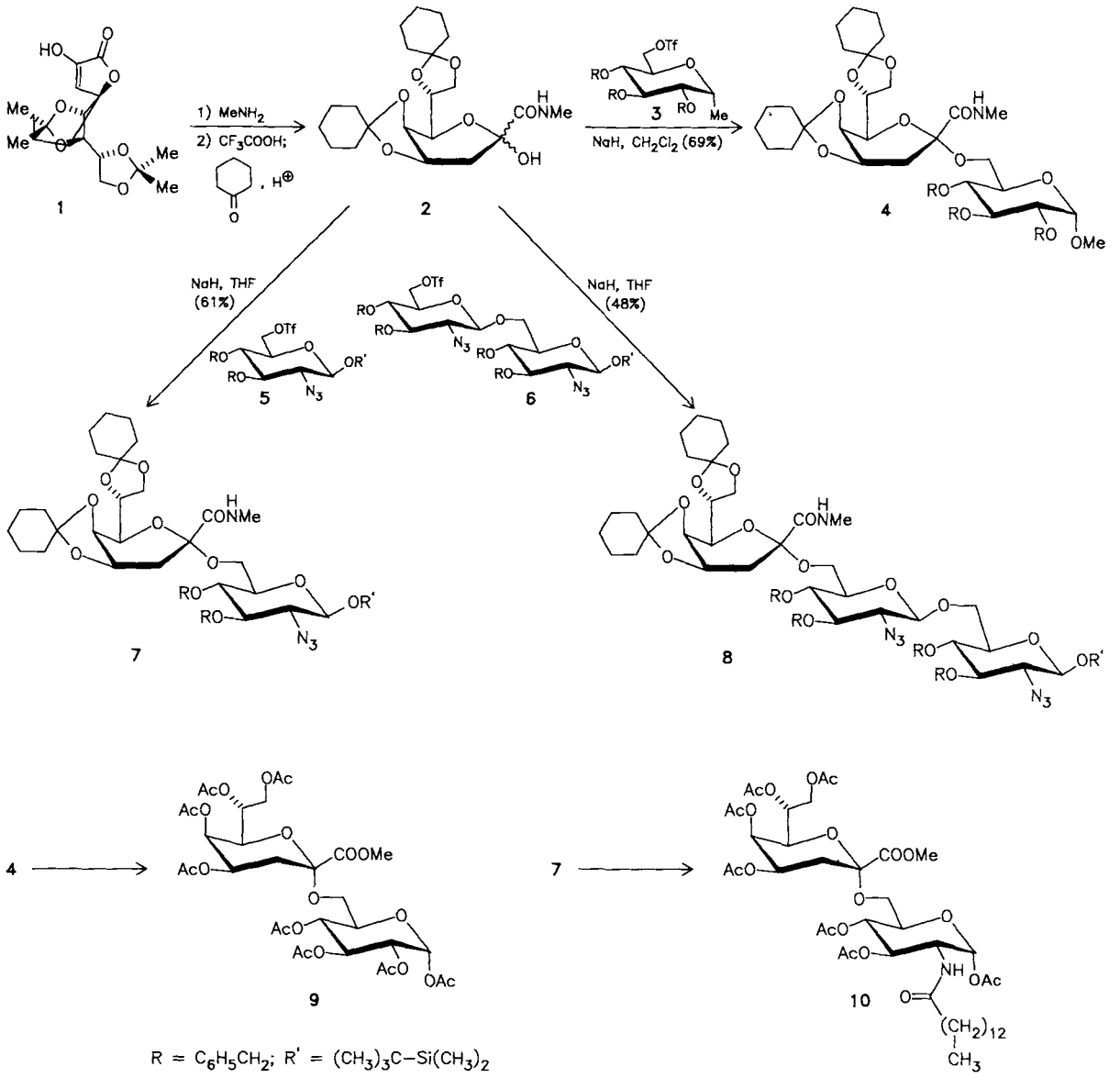

meric oxygen atom must exhibit sufficient nucleophilic reactivity; and (3) stereocontrol in the *O*-alkylation must be achieved.[6] Owing to the 1-carboxyl group and the favoring of the $^5C_2$ conformation in the 4,5,7,8-tetra-*O*-acyl-protected KDO (which is usually employed in glycoside synthesis[3]), the prerequisites are not favorably met with respect to stability and reactivity of the alkoxide intermediate and with respect to α-diastereoselectivity in the *O*-alkylation.[7]

We therefore chose the 4,5:7,8-di-*O*-cyclohexylidene derivative **2** of KDO as our starting material; this compound can be obtained in a few steps from β-lithiated α-alkoxyacrylic acid derivatives and 2,3:4,5-di-*O*-isopropylidene-D-arabinose via compound **1**.[8,9] The ^{1}H NMR data show that compound **2** exists in the boat conformation.[10] Thus, stereomodels show that, through the carboxamide group, the ring oxygen atom, and the oxygen atoms at C-5 and C-8, **2** can serve as a tetradentate chelating ligand for the complexation of a metal ion. Such complexation, accompanied by generation of the dianionic species $\mathbf{2}^{2\ominus}$ (deprotonation of the carboxamide group and of the anomeric hydroxyl group), should have a positive effect on all factors, in particular the nucleophilic reactivity and the desired α-selectivity. Indeed, addition of two equivalents of sodium hydride as base to the KDO derivative **2**, followed by addition of D-glucose-6-*O*-triflate **3** as alkylating agent, led to the isolation of the α(2–6′)-linked disaccharide **4** in 69% yield. No β-linked product was formed. To carry out a structural analysis, **4** was subjected to hydrogenolytic debenzylation, followed by acid-catalyzed cleavage of the protecting groups; per-*O*-acetylation, subsequent treatment with sodium nitrite in acetic anhydride/acetic acid, and immediate thermolysis of the resulting nitroso compound afforded the methyl ester **9**. The ^{1}H NMR data of its KDO portion agree with the corresponding data obtained for other *O*-acetylated KDO α-glycosides[3] and, moreover, satisfy the rule stated by *Unger*[11] for KDO α-glycosides.

The anomerically selective *O*-alkylation was also applied successfully to α(2–6′)-glycosidic bond formation with the glucosamine derivative **5**[9] and to α(2–6′)-glycosidic bond formation with the β(1–6′)-linked diglucosamine derivative **6**.[9] Using sodium hydride as base and THF as solvent, good yields of the desired disaccharide **7** and trisaccharide **8**, respectively, were obtained. The ^{1}H NMR data of the KDO portion of these compounds largely agree

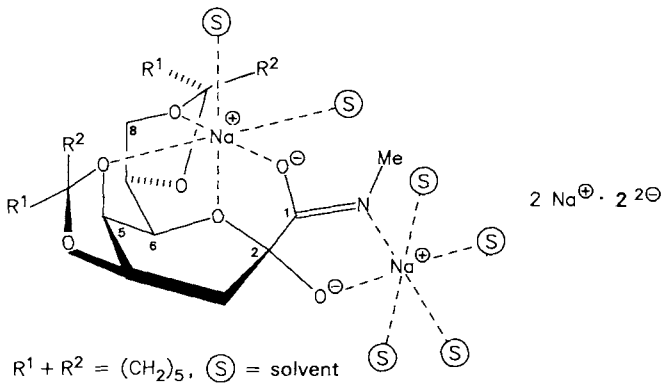

with those of compounds **4**. To carry out a structural analysis, compound **7** was converted into the derivative **10** by amide/ester conversion, azide reduction with hydrogen sulfide/pyridine, acylation of the free amino group with myristic acid, acid-catalyzed cleavage of the cyclohexylidene and *tert*-butyldimethylsilyl groups, *O*-acetylation, hydrogenolytic debenzylation, and, once again, *O*-acetylation. The ^{1}H NMR data for the KDO portion correspond to those obtained for compound **9**.

General Experimental Procedure

4, 7, and **8**: **2** (2 mmol) was dissolved under N_2 in 50 mL of dry dichloromethane (**4**) or tetrahydrofuran (**7**, **8**) and the resulting solution was cooled to -30°C. Sodium hydride (4.2 mmol) was then added and, after 20 min, a solution of the triflate (2.2 mmol; **3**, **5**, and **6**, respectively) in 30 mL of dry dichloromethane, or tetrahydrofuran, was then slowly added dropwise. After standing for 3 h at -30°C, the solution was allowed to warm to -10 to 0°C and then stirred. The reaction was monitored by thin layer chromatography. The reaction mixture was filtered through silica gel and concentrated under vacuum, and the products were chromatographed on silica gel using petroleum ether (30–60°C)/ethyl acetate as eluent.

R_F (petroleum ether/ethyl acetate). **4** (1/1) 0.41; **7** (2/1) 0.60; **8** (2/1) 0.48.

^{1}H NMR (400 MHz, $CDCl_3$): **4**: $\delta = 4.42$ (ddd, $J_{3'eq,4'} = 3.91$, $J_{3'ax,4'} = 4.46$, $J_{4',5'} = 7.33$ Hz, 1 H, 4'-H), 4.30 (ddd, $J_{6',7'} = 6.59$, $J_{7',8'a} = 6.34$, $J_{7',8'b} = 4.88$ Hz, 1 H, 7'-H), 4.17 (dd, $J_{5',6'} = 1.95$ Hz, 1 H, 5'-H), 4.05 (dd, $J_{8'a,8'b} = 8.79$ Hz, 1 H, 8'b-H), 4.00 (dd, 1 H, 8'a-H), 3.75 (dd, 1 H, 6'-H), 2.76 (d, $J = 4.88$ Hz, 3 H, $NHCH_3$), 2.54 (dd, $J_{3'ax,3'eq} = 15.38$ Hz, 1 H, 3'ax-H), 1.90 (dd, 1 H, 3'eq-H).

7: $\delta = 4.43$ (ddd, 1 H, 4'-H), 4.31 (ddd, $J_{6',7'} = 6.34$ Hz, 1 H, 7'-H), 4.16 (dd, $J_{5',6'} = 1.95$, $J_{4',5'} = 7.08$ Hz, 1 H, 5'-H), 4.07 (dd, $J_{8'a,8'b} = 8.55$, $J_{7',8'b} = 6.35$ Hz, 1 H, 8'b-H), 3.94 (dd, $J_{7',8'a} = 5.12$ Hz, 1 H, 8'a-H), 3.74 (dd, 1 H, 6'-H), 2.75 (d, $J = 5.13$ Hz, 3 H, $NHCH_3$), 2.46 (dd, $J_{3'ax,3'eq} = 15.14$, $J_{3'ax,4'} = 5.12$ Hz, 1 H, 3'ax-H), 1.91 (dd, $J_{3'eq,4'} = 3.91$ Hz, 1 H, 3'eq-H).

8: $\delta = 4.30$–4.27 (m, 2 H, 4''-, 7''-H), 4.06 (m, 1 H, 8''b-H), 4.02 (dd, $J_{5'',6''} = 1.96$ Hz, 1 H, 5''-H), 3.94 (dd, $J_{8''a,8''b} = 8.55$, $J_{7'',8''a} = 5.37$ Hz, 1 H, 8''a-H), 3.75 (dd, $J_{6'',7''} = 5.61$ Hz, 1 H, 6''-H), 2.71 (d, $J = 4.88$ Hz, 3 H, $NHCH_3$), 2.46 (dd, $J_{3''ax,3''eq} = 15.38$, $J_{3''ax,4''} = 4.88$ Hz, 1 H, 3''ax-H), 1.82 (dd, $J_{3''eq,4''} = 3.66$ Hz, 1 H, 3''eq-H).

^{1}H NMR (400 MHz, C_6D_5): **9**: $\delta = 5.77$ (s, br, 1 H, 5'-H), 5.68 (ddd, $J_{3'eq,4'} = 5.12$, $J_{3'ax,4'} = 12.2$, $J_{4',5'} = 2.93$ Hz, 1 H, 4'-H), 5.54 (ddd, $J_{7',8'a} = 4.39$, $J_{7',8'b} = 2.44$, $J_{6',7'} = 9.28$ Hz, 1 H, 7'-H), 4.81 (dd, $J_{8'a,8'b} = 12.45$ Hz, 1 H, 8'b-H), 4.51 (dd, $J_{5',6'} = 0.98$ Hz, 1 H, 6'-H), 4.23 (dd, 1 H, 8'a-H), 3.26 (s, 3 H, $COOCH_3$), 2.40 (dd, $J_{3'ax,3'eq} = 12.7$ Hz, 1 H, 3'ax-H), 2.32 (dd, 1 H, 3'eq-H).

8: $[\alpha]_{589}^{20} = +9.0°$ ($c = 0.7$, $CHCl_3$); **9**: $[\alpha]_{589}^{20} = +105°$ ($c = 0.34$, $CHCl_3$); **10**: $[\alpha]_{589}^{20} = +67.7°$ ($c = 0.7$, $CHCl_3$).

Received: May 4, 1988;
revised: June 28, 1988 [Z 2740 IE]
German version: *Angew. Chem. 100* (1988) 1234

[1] E. T. Rietschel, H. Brade, L. Brade, A. Bünsch, A. Tacker, U. Zähringer, *Forum Mikrobiol. 8* (1985) 286; F. M. Unger, *Adv. Carbohydr. Chem. Biochem. 38* (1981) 323, and references cited therein.

[2] M. Imoto, S. Kusumoto, T. Shiba, H. Naoki, T. Iwashita, E. T. Rietschel, H. W. Wollenweber, C. Galanos, O. Lüderitz, *Tetrahedron Lett. 24* (1983) 4017; H. Brade, E. T. Rietschel, *Eur. J. Biochem. 145* (1984) 231; H. Brade, U. Zähringer, E. T. Rietschel, *Carbohydr. Res. 134* (1984) 157; R. Christian, G. Schulz, P. Waldstätten, F. M. Unger, *Tetrahedron Lett. 25* (1984) 3433.

[3] H. Paulsen, M. Schüller, *Liebigs Ann. Chem. 1987*, 249; H. Paulsen, M. Stiem, F. M. Unger, *ibid. 1987*, 273; M. Kiso, M. Fujita, E. Hayashi, A. Hasegawa, F. M. Unger, *J. Carbohydr. Chem. 6* (1987) 691, and references cited therein.

[4] M. Imoto, N. Kusunose, Y. Matsuura, S. Kusumoto, T. Shiba, *Tetrahedron Lett. 28* (1987) 6277.

[5] R. R. Schmidt, M. Reichrath, U. Moering, *J. Carbohydr. Chem. 3* (1984) 67.

[6] R. R. Schmidt, M. Reichrath, *Angew. Chem. 91* (1979) 497; *Angew. Chem. Int. Ed. Engl. 18* (1979) 466; R. R. Schmidt, *ibid. 98* (1986) 213 and *25* (1986) 212, and references cited therein.

[7] Favorable structural prerequisites for α-selective *O*-alkylation are found for neuraminic acids.

[8] R. R. Schmidt, R. Betz, *Angew. Chem. 96* (1984) 420; *Angew. Chem. Int. Ed. Engl. 23* (1984) 430.

[9] A. Esswein, *Dissertation*, Universität Konstanz 1988; A. Enhsen, *Dissertation*, Universität Konstanz 1988.

[10] A corresponding conformation was also observed for a 4,5:7,8-di-*O*-isopropylidene-protected KDO derivative: see [4].

[11] H. Paulsen, Y. Hayauchi, F. M. Unger, *Liebigs Ann. Chem. 1984*, 1270, 1288; F. M. Unger, D. Stix, G. Schulz, *Carbohydr. Res. 80* (1980) 191.

Enantioselective Catalytic Transfer-Hydrogenation of α,β-Unsaturated Carboxylic Acids with Triethylammonium Formate**

By *Henri Brunner*,* and *Walter Leitner*

The hydrogenation of prochiral olefins in the presence of optically active rhodium complexes is the most well-known enantioselective catalysis by transition metal compounds.[1] The decomposition of formic acid to hydrogen and carbon dioxide is also catalyzed by rhodium compounds.[2] We have been able to combine these two processes to provide a simple, effective alternative to the dangerous and frequently impracticable use of gaseous hydrogen. Scheme 1 shows the enantioselective transfer-hydrogenation of (*Z*)-α-acetylaminocinnamic acid **1a** and itaconic acid **1b** to **2a** and **2b**, respectively.

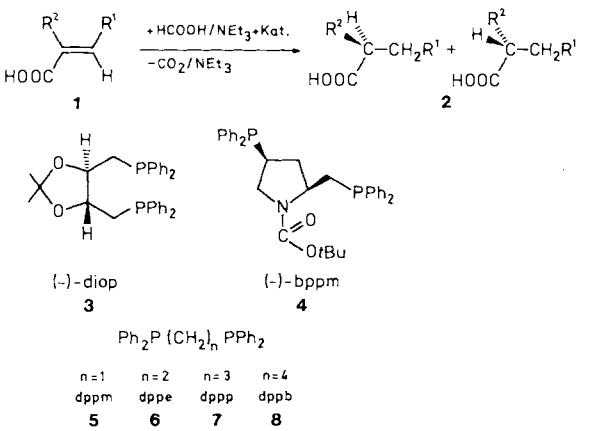

Scheme 1. **a**, R^1 = Ph, R^2 = NHCOMe; **b**, R^1 = H, R^2 = CH_2COOH.

In situ systems of $[Rh(cod)Cl]_2$ (cod = 1,5-cyclooctadiene) and phosphane ligands serve as catalysts, as are also used in the hydrogenation with molecular hydrogen.

[*] Prof. Dr. H. Brunner, Dipl.-Chem. W. Leitner
Institut für Anorganische Chemie der Universität
Universitätsstrasse 31, D-8400 Regensburg (FRG)

[**] Enantioselective Catalysis, Part 43. This work was supported by the Deutsche Forschungsgemeinschaft, the Fonds der Chemischen Industrie, the Stiftung Volkswagenwerk, and BASF AG, Ludwigshafen.—Part 42: H. Brunner, A. Sicheneder, *Angew. Chem. 100* (1988) 730; *Angew. Chem. Int. Ed. Engl. 27* (1988) 718.

Triethylammonium formate (TEAF)[3] has proven to be a useful source of hydrogen. TEAF is a commercially available azeotrope of formic acid and triethylamine (molar ratio 5 : 2).[4] Owing to its solubility in organic solvents, TEAF, in contrast to other formates, furnishes homogeneous reaction mixtures. On using dipolar aprotic solvents, under mild conditions, results are obtained which approach or even surpass those achieved with hydrogen. Even in boiling acetone or ethanol the transfer-hydrogenation leads to complete reduction of the CC double bond, albeit with optical yields of less than 10%. The highest enantiomeric excesses are achieved in DMSO (Table 1).

Table 1. Enantioselective transfer-hydrogenation of (*Z*)-α-acetylaminocinnamic acid **1a** and itaconic acid **1b** with triethylammonium formate (TEAF). The substrates were quantitatively hydrogenated [a].

Substrate	Ligand	Solvent	*T* [°C]	*ee* [%] [b] (conf.)	Number of experiments	*ee* [%] [c]
1a	**3**	DMSO	27	50.0 ± 2.1 (*R*)	10	81 [7]
1a	**4**	DMSO	45	71.7 ± 5.4 (*R*)	11	93 [9]
1a	**3**	DMF	27	37.9 (*R*)	1	
1a	**3**	MPY [d]	45	20.5 (*R*)	1	
1b	**3**	DMSO	27	49.1 ± 1.6 (*S*)	12	45 [8]
1b	**4**	DMSO	45	83.8 ± 1.2 (*S*)	5	94 [9]

[a] Determined ^{1}H-NMR spectroscopically. [b] Determined polarimetrically. Rotations of the pure hydrogenation products: (*S*)-*N*-acetylphenylalanine: $[\alpha]_D^{25} = 46.5°$ ($c = 1$, EtOH) [5], (*R*)-methylsuccinic acid: $[\alpha]_D^{25} = 15.5°$ ($c = 2.82$, EtOH) [6]. [c] For comparison: rhodium-catalyzed hydrogenation with H_2. The data refer only to substrate and ligand, not to solvent and temperature! [d] MPY = *N*-methylpyrrolidone.

In the case of **1a** the transfer-hydrogenation affords somewhat lower values, in the case of **1b**, however, similar values as the rhodium-catalyzed hydrogenation with molecular hydrogen. With the ligand **3**, the optical induction in the transfer-hydrogenation of **1b** is even higher than in the hydrogenation with molecular hydrogen. In all the cases investigated so far the preferred configuration is the same in both types of reaction. The employment of TEAF in DMSO as source of hydrogen is a substantial improvement compared to the transfer-hydrogenation with 80% aqueous formic acid recently described by us.[10]

High enantioselectivities and high reaction rates are achieved in the transfer-hydrogenation with TEAF only when ligands such as **3** or **4** are used which can form seven-membered chelate rings. With the ligands norphos[11] or prophos,[12] which form five-membered chelate rings and have proven useful in hydrogenation, only small enantiomeric excesses, usually with incomplete hydrogenation, are obtained in the transfer-hydrogenation described here. This influence of the chelate ring size is also reflected in the relative rates of reaction for the ligands **5**–**8**. When the decrease in concentration of **1b** during the catalysis is monitored via the decrease in intensity of the peaks of the methylene protons in the ^{1}H-NMR spectrum ($\delta = 6.39$ and 5.90) relative to the internal standard mesitylene ($\delta = 6.69$) curves like those shown in Figure 1 for **8** are obtained. A short induction phase is followed by a linear decrease in the substrate concentration.

A comparison of the slopes of the linear portions of the curves shows that the rate of hydrogenation is lowest with **6**. With **5** it increases by a factor of 4, with **7** by a factor of 77, and with **8** by even a factor of 128. The reason for this behavior could lie in the lack of readiness of five-membered ring forming ligands to act as so-called "dangling ligands",[13] and thus to make coordination sites free at the metal atom.

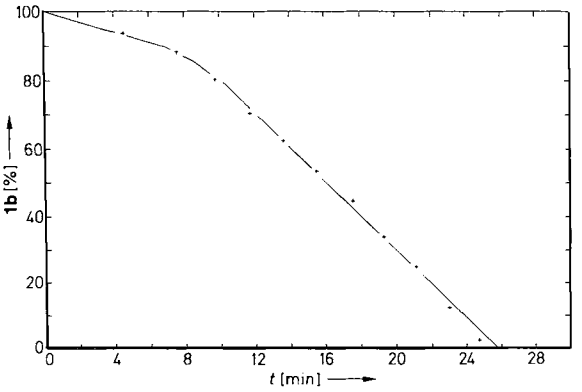

Fig. 1. ^{1}H-NMR spectroscopic monitoring of the transfer-hydrogenation of **1b** with $[Rh(cod)Cl]_2$ in the presence of the ligand **8** as catalyst (see text).

Experimental

500 mg of substrate, 0.7 mol-% of $[Rh(cod)Cl]_2$ and 1.8 mol-% of ligand were dissolved in 3.75 mL of anhydrous DMSO under an atmosphere of nitrogen. After 30 mins' stirring at the given reaction temperature (Table 1) the mixture was treated with sufficient TEAF (Merck; dried over $MgSO_4$ and distilled under N_2) to make the substrate/formic acid ratio 1 : 5. Shortly thereafter a vigorous evolution of gas was observed in the orange solution. The mixture was then stirred for 20 h, rendered alkaline with 10 mL of 2 N NaOH, and filtered. The filtrate was washed with 4 × 30 mL of ether, acidified with 6 mL of 10% HCl, and the product extracted with 4 × 50 mL of ether. After drying over $MgSO_4$ the solvent was removed and the product dried for 5 h at 40°C under vacuum. The yields were quantitative. To avoid the tedious drying necessary for the removal of DMSO residues, the ether extracts of the acid solution can be washed with 3 × 5 mL of 5% HCl. The yields are then about 75%.

Received: May 11, 1988 [Z 2756 IE]
German version: *Angew. Chem. 100* (1988) 1231

[1] J. D. Morrison (Ed.): *Asymmetric Synthesis, Vol. 5*, Academic Press, Orlando 1985; H. Brunner, *Top. Stereochem. 18* (1988) 129.
[2] S. H. Strauss, K. H. Whitmire, D. F. Shriver, *J. Organomet. Chem. 174* (1979) C 59.
[3] L. F. Fieser, M. Fieser (Eds.): *Reagents for Organic Synthesis, Vol. 3*, Wiley, New York 1972, p. 300.
[4] K. Narita, M. Sekiya, *Chem. Pharm. Bull. 25* (1977) 135.
[5] E. J. Eisenbrunn, S. M. McElvain, *J. Am. Chem. Soc. 77* (1955) 3383.
[6] R. Glaser, M. Twaik, S. Geresh, J. Blumenfeld, *Tetrahedron Lett. 1977*, 4635.
[7] T. P. Dang, J. C. Poulin, H. B. Kagan, *J. Organomet. Chem. 91* (1975) 105.
[8] S. Saito, Y. Nakamura, Y. Morita, *Chem. Pharm. Bull. 33* (1985) 5284.
[9] I. Ojima, T. Kogure, N. Yoda, *J. Org. Chem. 45* (1980) 4728.
[10] H. Brunner, M. Kunz, *Chem. Ber. 119* (1986) 2868.
[11] H. Brunner, W. Pieronczyk, B. Schönhammer, K. Streng, I. Bernal, J. Korp, *Chem. Ber. 114* (1981) 1137.
[12] M. D. Fryzuk, B. Bosnich, *J. Am. Chem. Soc. 100* (1978) 5491.
[13] B. R. James, D. Mahajan, *J. Organomet. Chem. 279* (1985) 31.

Synthesis and Structure of $[NaTi(2,6\text{-}Me_2C_6H_3O)_4(py)]_2$: a Dimeric Material Containing a Novel Phenoxide Bridge**

By *Loren D. Durfee, Phillip E. Fanwick,* and *Ian P. Rothwell**

The last few years has seen a resurgence of interest in both the structure and bonding of main group element compounds.[1] In the case of the alkali metal compounds

[*] Prof. I. P. Rothwell, Dr. L. D. Durfee, Dr. P. E. Fanwick
Department of Chemistry, Purdue University
West Lafayette, Indiana 47907 (USA)

[**] This work was supported by the US National Science Foundation.

the importance of π-bonding between metal atom and organic fragment has been an area of particular interest.[2] During our studies of the sodium amalgam reduction chemistry of titanium(IV) aryloxides,[3] we have isolated an unusual double salt of sodium and titanium which consists of a dimeric unit held together via a unique sodium phenoxide linkage.

The reduction of the tetraaryloxides $Ti(OR)_4$, R = 2,6-$iPr_2C_6H_3$ or 2,6-$Me_2C_6H_3$, with Na/Hg (1 equiv.) in THF solution yields blue-green products containing both sodium and titanium. In the case of the more bulky 2,6-diisopropylphenoxide the discrete compound

$[(2,6\text{-}iPr_2C_6H_3O)_2Ti(\mu\text{-}2,6\text{-}iPr_2C_6H_3O)_2Na(thf)_2]$ **1**

was obtained and structurally characterized.[3] However, the less bulky 2,6-dimethylphenoxide substrate was found to generate a product which was more difficult to characterize. Attempts to sequester the sodium from this latter compound by treatment with pyridine failed, leading to deep-purple solids[4] which are only sparingly soluble in hydrocarbon solvents. After numerous unsuccessful attempts, we have finally been able to obtain single crystals of **2** from hot toluene solution. A single crystal X-ray diffraction analysis of **2**[5] shows the compound to consist of a pentacoordinate titanium center surrounded by four aryloxide oxygen atoms and one pyridine nitrogen atom in an approximately trigonal-bipyramidal arrangement (Fig. 1, top). Two of the aryloxide oxygen atoms, one equatorial and one axial, then bridge to the sodium atom, giving a $[Ti(\mu\text{-}OR)_2Na]$ unit similar to that in **1**.[3] However, the σ-framework of this unit does not satisfy the serious electron deficiencies of the so far only two coordinate sodium ion. The compound overcomes this problem by forming phenoxide bridges between pairs of Na,Ti units, not through oxygen atoms, but by a π-interaction between the sodium ion of one unit and the aromatic ring of one of the phenoxide groups in a second unit (Fig. 1, bottom). The distances between the sodium ion and the carbon atoms in the π-bonded ring are all similar, varying from 2.79–2.88 Å, and are slightly longer than the distances found for sodium atoms bound to carbanionic ring systems such as cyclopentadienyl anion.[1,6] The ability of phenoxide ligands to bind in this fashion to sodium atoms is of direct relevance to previous work where it has been found difficult to account for the unusual stoichiometries obtained on alkali metal reduction of titanium phenoxides.[7]

$[NaTi(2,6\text{-}Me_2C_6H_3O)_4(py)]$ **2**

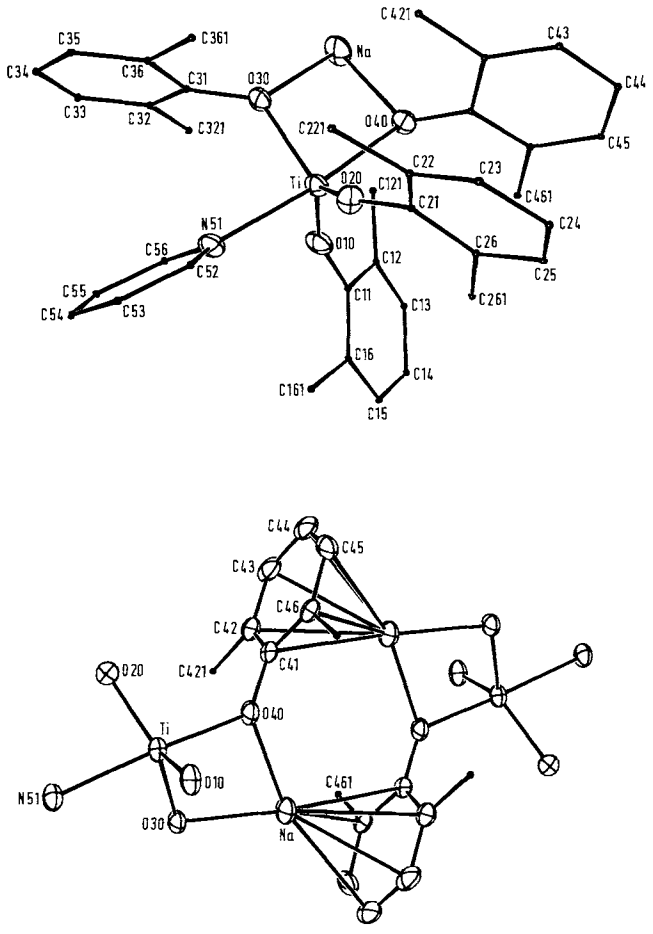

Fig. 1. Top: Structure of **2** in the crystal (ORTEP); view of the central σ-bonding framework showing the numbering scheme used; distances [pm]: Ti-O(10) 187.1(4), Ti-O(20) 190.4(4), Ti-O(30) 198.3(4), Ti-O(40) 208.0(3), Ti-N(51) 225.6(4).—Bottom: Section of the crystal structure of **2** (ORTEP); view showing the phenoxide bridges that hold the dimeric unit together. Distances [pm]: Na-O(30) 222.5(4), -O(40) 227.0(4), -C(41) 287.0(5), -C(42) 288.2(6), -C(43) 286.5(6), -C(44) 284.1(6), -C(45) 279.0(6), -C(46) 279.1(6).

Received: May 18, 1988 [Z 2765 IE]
German version: *Angew. Chem. 100* (1988) 1218

CAS Registry numbers:
2, 116302-64-8; $Ti(2,6\text{-}Me_2C_6H_3O)_4$, 49796-02-3.

[1] P. Jutzi, *Adv. Organomet. Chem. 26* (1986) 217.
[2] a) W. N. Setzer, P. von Rague Schleyer, *Adv. Organomet. Chem. 24* (1985) 353. b) G. Stucky, *Adv. Chem. Series 130* (1974), Chapter 3.
[3] L. D. Durfee, S. L. Latesky, I. P. Rothwell, J. C. Huffman, K. Folting, *Inorg. Chem. 24* (1985) 4569.
[4] Analysis calcd. for $NaTiC_{37}H_{41}NO_4$: C, 70.03; H, 6.52; N, 2.21. Found: C, 70.31; H, 6.21; N, 2.51%.
[5] Crystal data: space group $C2/c$; $a = 29.636(6)$; $b = 12.579(3)$; $c = 17.849(3)$ Å; $\beta = 93.99(2)°$; $Z = 8$; $\rho_{calcd} = 1.27$ g cm^{-3}; 2389 unique data with $I > 3\sigma(I)$ yielded $R = 0.051$, $R_w = 0.059$. Further details of the crystal structure investigation are available on request from the Fachinformationszentrum Energie, Physik, Mathematik GmbH, D-7514 Eggenstein-Leopoldshafen 2 (FRG) on quoting the depository number CSD-53302, the names of the authors, and the journal citation.
[6] a) R. D. Rogers, J. L. Atwood, M. D. Rausch, D. W. Macomber, W. P. Heist, *J. Organomet. Chem. 238* (1982) 79; b) T. Aoyagi, H. M. M. Shearer, K. Wade, G. Whitehead, *ibid. 175* (1979) 21.
[7] A. Flamini, D. J. Cole-Hamilton, G. Wilkinson, *J. Chem. Soc. Dalton Trans. 1978*, 454.

3-Lithio-2-(*o*-lithiophenyl)naphthalenedilithium—a Tetralithio Compound with σ- and π-Bonded Lithium Atoms**

By *Rainer Benken, Werner Andres,* and *Harald Günther**

In organic monolithium compounds the metal can either be σ- or π-bonded[1]—classical examples are phenyllithium[2] and naphthalenedilithium,[3] respectively—whereas organic polylithium compounds can exhibit both types of bonding.[4] We have now, for the first time, found a tetralithio compound in which a ring-metalated dianion of an aromatic π-system occurs.

[*] Prof. Dr. H. Günther, Dipl.-Chem. R. Benken, Dipl.-Chem. W. Andres Fachbereich 8, Organische Chemie II, Universität-Gesamthochschule Postfach 101240, D-5900 Siegen (FRG)

[**] This work was supported by the Fonds der Chemischen Industrie. We thank Prof. Dr. *R. Luckenbach*, Beilstein-Institut, Frankfurt, for generous help with a literature search, Prof. Dr. *A. Maerker*, Siegen, for valuable information, and Dr. *J. Opitz*, Siegen, for the mass spectrometric investigations.

Biphenylene reacts with lithium in THF to give biphenylenedilithium in good yields, which, according to its NMR spectra is a delocalized 14π (4q+2) system.[5] The analogous reaction in the case of benzo[*b*]biphenylene **1** leads to a species which according to its ^{1}H- and ^{13}C-NMR spectrum (400 and 100 MHz, respectively, −40°C, [D$_8$]THF) has lost the C_{2v} symmetry of the hydrocarbon **1**. The ^{1}H-NMR spectrum shows two ABCD systems (δ = 1.63, 3.52, 3.12, 1.69, and 7.50, 5.97, 6.46, 5.56) with the multiplicity (d, t, t, d) typical for four neighboring benzene protons and two singlets (δ = 2.24, 2.53). The ^{13}C{^{1}H}-NMR spectrum displays two signals for quaternary carbon atoms at low field (δ = 166.6, 175.4) in addition to 14 resonances between δ = 78.8 and 161.0. A comparison of the spectra rules out the new compound being the dianion $\mathbf{2}^{2\ominus}$ of the 2-phenylnaphthalene **2**;[6] trapping experiments with H_2O, however, afford the same products which are obtained on reaction of $\mathbf{2}^{2\ominus}$ with H_2O.

Chromatographic separation on silica gel doped with $AgNO_3$ furnished 1,4-dihydro-2-phenylnaphthalene[7] **3** and the previously unknown 1,4-dihydro-6-phenylnaphthalene[8] **4** in the ratio 5 : 1. Since biphenylenedilithium is converted with opening of the four-membered ring into 2,2′-dilithiobiphenyl, the formation of 3-lithio-2-(*o*-lithiophenyl)naphthalene **5** would be expected in the case of $\mathbf{1}^{2\ominus}$, which in the reaction with H_2O, however, should only furnish **2**.

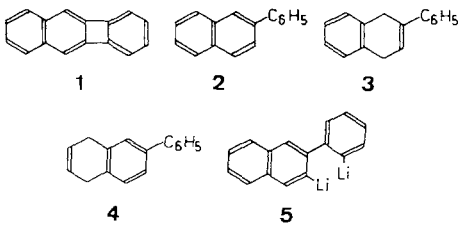

1 2 3 4 5

The experimental data, especially the high shielding for six "aromatic" protons in the ^{1}H-NMR spectrum (an ABCD system, two singlets, cf. above) are understandable if the structure **6** is assumed for the new species, which can be formed from **1** by reductive cleavage of the five-membered ring to give **5** followed by further reduction.[9] Additional findings lend support to this interpretation: 1) the chemical shifts of the strongly shielded ^{1}H and ^{13}C resonances in **6**, whose spectra were completely assigned with the help of 2D-NMR experiments of the COSY and NOESY type,[10] are very similar to those in naphthalenedilithium.[11] The downfield ^{13}C resonances (δ = 166.6, 175.4) must be those of lithiated sp^2-C atoms.[12] 3) The ^{7}Li-NMR spectrum of **6** at −100°C shows three resonances in the ratio 2 : 1 : 1 at δ = 7.26, 0.15 and −0.73,[13] which can be assigned to the σ- and π-bonded lithium

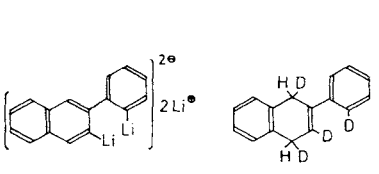

6 7

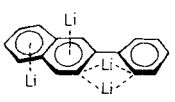

8

atoms.[14] 4) Trapping experiments with D_2O afford a [D$_4$]-1,4-dihydro-2-phenylnaphthalene, which, on the basis of its molecular mass (210.1359) and its ^{2}H-NMR spectrum with signals for two methylene-^{2}H atoms and one olefinic and one aromatic ^{2}H atom (Fig. 1) must have the structure **7**.[15]

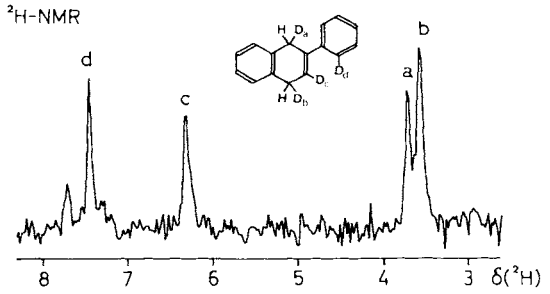

Fig. 1. 60.4-MHz ^{2}H-NMR spectrum of 1,3,4,2′[D$_4$]-1,4-dihydro-2-phenylnaphthalene **7** with ^{1}H decoupling (internal standard: tetramethylsilane). The assignment of the methylene positions a and b follows from NOE measurements for the ^{1}H-compound.

The solid-state structures found for 2,2′-dilithiobiphenyl on the one hand[16] and naphthalenedilithium on the other[3] make the structure **8** highly probable for the new Li_4-compound. Besides the ^{1}H- and ^{13}C-NMR findings, the observation that the rotation of the *ortho*-metalated phenyl ring about the C-2,C-1′ bond in **8** cannot be detected below room temperature, whereas in the dianion $\mathbf{2}^{2\ominus}$ the analogous process is first "frozen in" at −40°C on the NMR time scale, is also in agreement with this structure.[6]

Received: April 22, 1988 [Z 2718 IE]
German version: *Angew. Chem. 100* (1988) 1212

[1] a) P. von R. Schleyer, *Pure Appl. Chem. 56* (1984) 151; b) W. N. Setzer, P. von R. Schleyer, *Adv. Organomet. Chem. 24* (1985) 353.
[2] D. Thoennes, E. Weiss, *Chem. Ber. 111* (1978) 3157.
[3] J. J. Brooks, W. Rhine, G. D. Stucky, *J. Am. Chem. Soc. 94* (1972) 7346.
[4] A. Maercker, M. Theis, *Top. Curr. Chem. 138* (1987) 1.
[5] R. Benken, K. Finneiser, H. v. Puttkamer, H. Günther, B. Eliasson, U. Edlund, *Helv. Chim. Acta 69* (1986) 955, 2133.
[6] R. Benken, H. Günther, unpublished.
[7] E. J. Eisenbraun, R. G. Melton, P. W. Flanagan, M. C. Hamming, G. W. Keen, *Prep. Div. Pet. Chem. Am. Chem. Soc. 16* (1971) B43; cf. also J. J. M. Lamberts, W. H. Laarhoven, *J. Org. Chem. 48* (1983) 2202.
[8] The structure **4** follows unequivocally from the mass determination ($M^{\oplus}$ 206.1087; calcd 206.1095) and the ^{1}H-NMR spectrum with two very similar CH_2 signals (δ = 3.45, 3.47), a signal for two olefinic H atoms (δ = 5.97) and an AB system (J = 7.9 Hz) in the arene region (δ = 7.594, 7.425).
[9] This assumption is supported by the formation of 2,2′-dilithiodiphenyl from biphenylenedilithium [5] and the rapid reduction of **2** [6]. However, since **5** has not yet been trapped other modes of formation are possible for **6**.
[10] Review: R. Benn, H. Günther, *Angew. Chem. 95* (1983) 381; *Angew. Chem. Int. Ed. Engl. 22* (1983) 351.
[11] R. Benken, H. Günther, *Helv. Chim. Acta 71* (1988) 694.
[12] H.-O. Kalinowski, S. Berger, S. Braun: *^{13}C-NMR-Spektroskopie*, Thieme, Stuttgart 1984.
[13] External standard 0.1 M LiBr in THF; the signal at δ = 7.26 is distinctly broader than the high-field signals, so the chemical shift of the σ-bound lithium atoms must not be the same.
[14] R. H. Cox, H. W. Terry, Jr., L. W. Harrison, *Tetrahedron Lett. 1971*, 4815.
[15] This experiment also afforded the [D$_4$]-derivative of molecular mass 210.1359 corresponding to the formula **4**.
[16] U. Schubert, W. Neugebauer, P. von R. Schleyer, *J. Chem. Soc. Chem. Commun. 1982*, 1184.

Second Sphere Coordination Adducts of Phosphane-Transition Metal Complexes with β-Cyclodextrin and its Methylated Derivative**

By *David R. Alston, Alexandra M. Z. Slawin, J. Fraser Stoddart,* David J. Williams,* and *Ryszard Zarzycki*

The second sphere coordination[1] of transition metal complexes bearing hydrophobic ligands by cyclodextrins is a relatively unexplored field.[2] Only two such supramolecular adducts have been characterized[3] structurally in the solid state by X-ray crystallography. In both cases, the hydrophobic ligand of the complex penetrates the cavity of the cyclodextrin via the wider aperture of the receptor associated with the face bearing the secondary hydroxy groups. ^{1}H-NMR spectroscopy reveals that the hydrophobic ligand also enters the cavity in solution, though unequivocal structural information regarding the preferred face[4] at which adduct formation occurs has not been obtained. A large number of transition metal complexes bearing hydrophobic trialkylphosphane ligands find applications in catalysis.[5] In addition, some are employed in the treatment of rheumatoid arthritis.[6] Our interest[1] in the second sphere coordination of transition metal complexes has led us to investigate adduct formation between trialkylphosphaneplatinum complexes and cyclodextrins and their methylated derivatives in aqueous solution. We also describe the first example of a transition metal complex adduct with a cyclodextrin in which a crystalline adduct is formed as a result of occupation of the *narrower* primary hydroxy-group-bearing face of the receptor by the substrate.

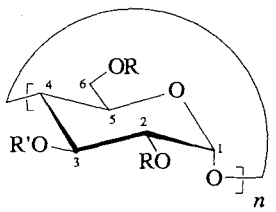

αCD: n=6; R=R'=H
βCD: n=7; R=R'=H
DMαCD: n=6; R=Me, R'=H
DMβCD: n=7; R=Me, R'=H
TMαCD: n=6; R=R'=Me

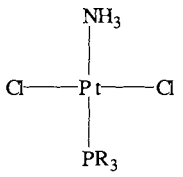

1, R=Me
2, R=Et

In the ^{1}H-NMR spectrum of a 1:1 molar mixture of β-cyclodextrin (βCD) and *trans*-[Pt(PMe$_3$)Cl$_2$(NH$_3$)] **1**, recorded in D_2O solution (5.7 mM), the signal for the H-3 protons situated *inside* the cavity of the CD is shifted to higher frequency (0.037 ppm), relative to that observed in the spectrum of the free receptor recorded in D_2O solution. Relative to the signal in the spectrum of the free transition metal complex, an analogous shift to higher frequency (0.104 ppm) was observed for the protons of the PMe$_3$ ligand in the complex **1** in the presence of 1 mol equivalent of βCD. These results indicate that, in solution, the PMe$_3$ ligand, in common with other hydrophobic first sphere ligands, enters the cavity of the cyclodextrin. Furthermore, the associated chemical shift differences vary with the concentration of the 1:1 adduct in a manner that verifies the 1:1 stoichiometry. Quantitative treatment[7] of the concentration dependence in D_2O at 22°C afforded an average value[8] for the association constant (K_a) for adduct formation of 2950 mol^{-1} kg, corresponding to a value for the free energy of adduct formation ($-\Delta G^0$) of 19.6 kJ mol^{-1}. The K_a value is ten times higher than those so far found[3] for adduct formation between αCD and other transition metal complexes.[9] Interestingly, however, the absence of ^{1}H-NMR chemical shift changes in the spectrum of a 1:1 molar mixture of **1** and αCD shows that they do not form an adduct in D_2O solution.

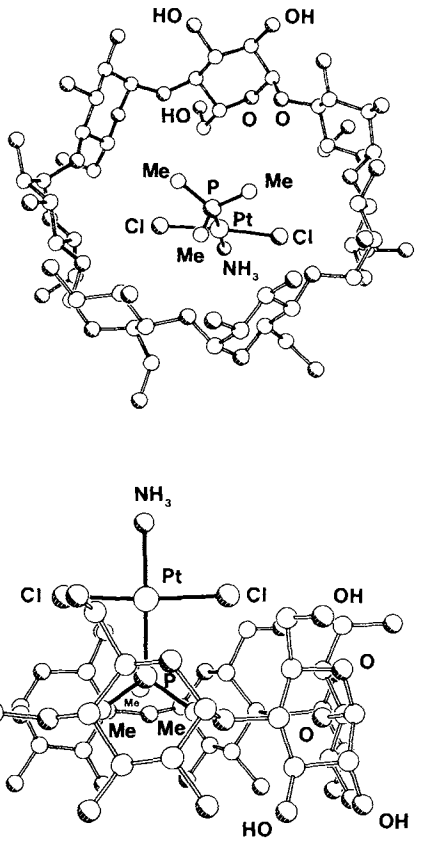

Fig. 1. Top: Structure of the adduct formed between βCD and **1** in the crystal viewed looking into the βCD face carrying the secondary hydroxy groups. Only the PMe$_3$ ligand lies in the cavity of the CD above the lower rim of primary hydroxy groups. The unresolved component of the adduct which lies within a plane parallel to the secondary hydroxy-group-bearing face, and also the peripheral water molecules, have been omitted for clarity. Bottom: In the side-on view of the adduct formed between βCD and **1** in the crystal, the degree of the penetration of the PMe$_3$ ligand of **1** into the cavity of βCD is easily discernible.—Crystal data: orthorhombic, a=19.431(7), b=24.082(12), c=32.503(11) Å, V=15209 Å^3, space group $C222_1$, Z=8, μ(Cu$_{K\alpha}$)=50 cm^{-1}, 4733 independent observed reflections with [$|F_o| \geq 3\sigma(|F_o|)$, $\theta \leq 58°$], R=0.113, R_w=0.100 [11].

Finstaking crystal-growing experiments eventually afforded[10] single crystals of the adduct of βCD and **1** suita-

[*] Dr. J. F. Stoddart, Dr. D. R. Alston [+], Dr. R. Zarzycki
Department of Chemistry, The University
Sheffield S3 7HF (UK)
Dr. D. J. Williams, A. M. Z. Slawin
Chemical Crystallography Laboratory
Department of Chemistry, Imperial College
London SW7 2AY (UK)
[+] Present address:
Smith Kline & French Research Ltd.
The Frythe, Welwyn AL6 9AR (UK)

[**] This work was supported by the Johnson Matthey Technology Centre and the Science and Engineering Research Council in the United Kingdom.

ble for X-ray crystallographic analysis.[11] The X-ray crystal structure (Fig. 1) of the 1:1 adduct indicates from refinement of the occupancy of the transition metal complex that, in 57% of the adducts, the PMe_3 ligand of **1** is inserted into and bound to (Fig. 1, bottom) the narrow primary hydroxy-group-bearing face of the βCD torus. There is evidence that, in some or all of the other 43% of adducts, **1** lies within a severely disordered surface which could be forming a lid on the wider secondary hydroxy-group-bearing face of the βCD torus. Comparison of the relative internal diameters of αCD (4.7–5.2 Å)[12] and βCD (6.0–6.4 Å)[12] with the van der Waals diameter (6.0 Å) of the PMe_3 ligand on the complex account for the inability of αCD to form an adduct with **1**.

The 2,6-per-*O*-methyl derivative of βCD, dimethyl-βCD (DMβCD) is not only soluble in organic solvents, but is also ca. 10 times more soluble in water than is the parent βCD.[13] The ^{1}H-NMR spectrum of a 1:1 mixture of DMβCD and **1** (8.6 mM) recorded in D_2O reveals shifts to higher frequencies for the signals associated with H-3 (0.062 ppm) in the receptor and the PMe_3 ligand (0.034 ppm) of the substrate, indicating that adduct formation is occurring in a manner *apparently*[4] structurally analogous to that demonstrated previously for βCD. The average K_a value[14] for adduct formation, 3160 mol^{-1} kg ($-\Delta G^0$ 19.8 kJ mol^{-1} at 22°C), determined from the concentration dependence in D_2O of the chemical shift changes for the H-3 and PMe_3 signals, shows that the strength of binding is very similar to that found with the parent cyclodextrin. Moreover, the remarkable β-selectivity towards adduct formation demonstrated by **1** in its interaction with αCD and βCD in D_2O solution is also observed with the methylated derivatives: thus, DMβCD forms an adduct in D_2O solution, whereas DMαCD does *not*.

The complex, *trans*-$[Pt(PEt_3)Cl_2(NH_3)]$ **2**, bearing a larger hydrophobic PEt_3 ligand, was also shown by ^{1}H-NMR spectroscopy to form a second sphere coordination adduct with DMβCD in D_2O solution. Once again, the average K_a value[15] for adduct formation of 3190 mol^{-1} kg ($-\Delta G^0$ 19.8 kJ mol^{-1} at 22°C), matched that observed for complex **1** with the smaller PMe_3 ligand, thus implying a similar strength of binding between DMβCD and neutral square-planar platinum(II) complexes containing either PMe_3 or PEt_3 ligands.[16, 17]

The results reported in this communication have implications for the design of drug delivery systems and water-soluble catalysts.

Received: May 2, 1988 [Z 2738 IE]
German version: *Angew. Chem. 100* (1988) 1215

[1] H. M. Colquhoun, J. F. Stoddart, D. J. Williams, *Angew. Chem. 98* (1986) 483; *Angew. Chem. Int. Ed. Engl. 25* (1986) 487; J. F. Stoddart, R. Zarzycki, *J. R. Neth. Chem. Soc.*, in press.

[2] Although numerous reports have appeared describing the second sphere coordination of transition metal complexes by cyclodextrins, in all cases the evidence presented for adduct formation is based only on analytical data and spectroscopic measurements: H. Ogino, *J. Am. Chem. Soc. 103* (1981) 1303; H. Ogino, K. Ohata, *Inorg. Chem. 23* (1984) 3312; B. Siegel, R. Breslow, *J. Am. Chem. Soc. 97* (1975) 6869; M. F. Czarniecki, R. Breslow, *ibid. 100* (1978) 7771; R. Breslow, M. F. Czarniecki, J. Emert, H. Hamaguchi, *ibid. 102* (1980) 762; G. L. Trainor, R. Breslow, *ibid. 103* (1981) 154; R. Breslow, G. L. Trainor, A. Ueno, *ibid. 105* (1983) 2739; W. J. le Noble, S. Srivastava, R. Breslow, G. L. Trainor, *ibid. 105* (1983) 2745; A. Harada, S. Takahashi, *J. Chem. Soc. Chem. Commun. 1984*, 645; *J. Inclusion Phenom. 2* (1984) 791; *Chem. Lett. 1984*, 2089; T. Matsue, U. Akiba, K. Suzufuji, T. Osa, *Denki Kagaku 53* (1985) 508; T. Matsue, D. H. Evans, T. Osa, N. Kobayashi, *J. Am. Chem. Soc. 107* (1985) 3411; A. Ueno, F. Moriwaki, T. Osa, F. Hamada, K. Murai, *Tetrahedron Lett. 26* (1985) 899; N. Kobayashi, T. Osa, *Chem. Lett. 1986*, 421; T. Matsue, T. Kato, U. Akiba, T. Osa, *ibid. 1986*, 843; Y. Maeda, N. Ogawa, Y. Takashima, *J. Chem. Soc. Dalton Trans. 1987*, 627; A. Harada, K. Saeki, S. Takahashi, *Chem. Lett. 1985*, 1157; A. Harada, M. Takeuchi, S. Takahashi, *ibid. 1986*, 1893; A. Harada, S. Takahashi, *J. Chem. Soc. Chem. Commun. 1986*, 1229; A. Ueno, F. Moriwaki, T. Osa, F. Hamada, K. Murai, *Chem. Pharm. Bull. 34* (1986) 438.

[3] D. R. Alston, A. M. Z. Slawin, J. F. Stoddart, D. J. Williams, *Angew. Chem. 97* (1985) 771; *Angew. Chem. Int. Ed. Engl. 24* (1985) 786; *J. Chem. Soc. Chem. Commun. 1985*, 1602.

[4] The difficulties associated with the elucidation of structural geometry by spectroscopic techniques are illustrated by the example of adduct formation with an organic substrate. The X-ray crystal structure of the 1:1 adduct between *p*-nitrophenol and αCD shows [K. Harata, *Bull. Chem. Soc. Jpn. 50* (1977) 1416] that the nitro group of the substrate enters the cavity of the receptor from the secondary hydroxy face. Similarly, ^{1}H-NMR spectroscopy indicates [Y. Inoue, Y. Takahashi, R. Chûjô, *Carbohydr. Res. 144* (1985) C9] that, in solution, the nitro group of *p*-nitrophenol penetrates the secondary hydroxy face of TMαCD during adduct formation. The X-ray crystal structure of this adduct, however, reveals [K. Harata, K. Uekama, M. Otagiri, F. Hirayama, *Bull. Chem. Soc. Jpn. 55* (1982) 3904] that, in the solid state, it is the *hydroxy* group that is inserted within the cavity, from the secondary hydroxy face.

[5] L. H. Pignolet (Ed.): *Homogeneous Catalysis with Metal Phosphine Complexes*, Plenum, New York 1983.

[6] B. Armer, H. Schmidbaur, *Angew. Chem. 82* (1970) 120; *Angew. Chem. Int. Ed. Engl. 9* (1970) 101; D. H. Brown, W. E. Smith, *Chem. Soc. Rev. 9* (1980) 217.

[7] D. R. Alston, T. H. Lilley, J. F. Stoddart, *J. Chem. Soc. Chem. Commun. 1985*, 1600.

[8] The K_a value afforded by use of H-3 in βCD as probe was 3200 mol^{-1} kg whilst that obtained from using the PMe_3 probe in complex **1** was 2700 mol^{-1} kg.

[9] K_a values for adduct formation between organic substrates and CDs in aqueous solution generally lie in the range ca. 10–10000 mol^{-1} L.

[10] βCD hydrate (215 mg, 0.18 mmol) and **1** (64 mg, 0.18 mmol) were dissolved in 30% aqueous isopropanol (8 mL) at 50°C. The hot solution was filtered and allowed to cool slowly (24 h) to room temperature in a sealed vial. Small crystals were formed and the solution was allowed to stand for a further 8 weeks, after which time the crystals had grown sufficiently to be amenable to X-ray crystallographic analysis.

[11] Nicolet R3m diffractometer, ω-scans, $Cu_{K\alpha}$ radiation (graphite monochromator). The crystal was coated with epoxy resin. The structure was solved by direct methods and refined anisotropically: the high value of *R* (see caption to Fig. 1) is a consequence of the disorder in the partial occupancy transition metal complex (which constitutes a not insignificant component of the total scattering), that forms the lid on the secondary hydroxy-group-bearing face of the βCD torus. The structure also contains 5.5 both ordered and disordered water molecules occupying eleven different sites of varying occupancy around the periphery of the CD ring. Further details of these structural investigations can be obtained from the Director of the Cambridge Data Centre, University Chemical Laboratory, Lensfield Road, Cambridge CB2 1EW (England). Any request should be accompanied by the full literature citation for this communication.

[12] W. Saenger in J. L. Atwood, J. E. D. Davies, D. D. MacNicol (Eds.): *Inclusion Compounds, Vol. 2*, Academic Press, London 1984, p. 231.

[13] J. Szejtli, A. Lipták, I. Jodál, P. Fügedi, P. Nánási, A. Neszmélyi, *Starch 32* (1980) 165.

[14] Using H-3 in DMβCD and the PMe_3 ligand of **1** as probes gave K_a values of 3055 and 3270 mol^{-1} kg, respectively.

[15] Using H-3 in DMβCD and CH_3 in the PEt_3 ligand of **2** as probes gave K_a values of 2270 and 4110 mol^{-1} kg, respectively.

[16] Complex **2** does not form adducts with αCD or DMαCD in D_2O solutions.

[17] It has recently been shown [P. R. Ashton, J. F. Stoddart, R. Zarzycki, *Tetrahedron Lett. 29* (1988) 2103] that adduct formation between methylated cyclodextrins and (i) neutral organic molecules, (ii) organic ammonium salts, (iii) organometallic cations, and (iv) neutral metallo-organic complexes can be probed conveniently by using fast atom bombardment mass spectrometry (FABMS). Analysis of mixtures of DMβCD with the phosphaneplatinum complexes **1** and **2** revealed primarily peaks in the FAB mass spectrum corresponding to the species [DMβCD·"$PtPR_3$"], i.e. adduct formation is occurring with the concomitant loss of one ammine and two chloride ligands. The mass spectrum of the DMβCD mixture with *trans*-$[Pt(PMe_3)_2Cl_2]$, on the other hand, revealed the presence of a peak associated with the loss of only one chloride ligand in addition to a signal arising from the 1:1 adduct [DMβCD·*trans*-$[Pt(PMe_3)_2Cl_2]$].

Induced and Non-induced Diastereoselective Intramolecular Ene Reaction of 1,6-Dienes: the Unusual Formation of *trans*-1,2-Disubstituted Cyclopentanes**

By *Lutz F. Tietze,* Uwe Beifuss, Michael Ruther, Andreas Rühlmann, Jochen Antel,* and *George M. Sheldrick*

Dedicated to Professor Heinz-Georg Wagner on the occasion of his 60th birthday

The Alder-ene reaction,[1] which for a long time was overshadowed by [4+2]-cycloadditions, has gained increasing importance in recent years.[2] By the use of modified enes[3] and enophiles[4] and activation by Lewis acids[2b] it has been possible to increase yields and selectivity considerably; thus the thermally- and Lewis-acid-induced ene reaction of 1,7-dienes bearing two electron-acceptor substituents on the enophile, e.g. **1**, yields exclusively *trans*-1,2-disubstituted cyclohexanes **2** (*trans*:*cis* > 99:1).[4] Recent STO-3G and 3-21G calculations by *Houk* et al.[5] for the reaction of propene and ethene have shown that an "envelope-like" conformation as in cyclopentane can be assumed as transition structure. It therefore follows that *trans*-disubstituted cyclohexanes are preferentially formed in intramolecular ene reactions of 1,7-dienes containing a tetramethylene chain; the cyclization of 1,6-dienes having a trimethylene chain, on the other hand, should lead via an *endo-E(ene)-syn*-orientation almost exclusively to *cis*-1,2-disubstituted cyclopentanes,[5] as has been found experimentally in a number of cases.[6] We demonstrate herein that 1,6-dienes of type **5** react highly selectively to give the *trans*-1,2-disubstituted cyclopentanes. This structural unit is found in many natural products such as prostaglandins and brefeldin. We ascribe the unexpected selectivity to the two substituents at the enophile terminus ("sp^2 geminal effect").

1 **2**

Condensation of the aldehydes **4A–C**[7] with the 1,3-dioxo compounds **3a–e** in the presence of piperidinium acetate leads, in unoptimized reactions, to the formation of the 1,6-dienes **5Aa–e**, **5Ba**, **5Ca**, and **5Cd** in 60–70% yields.[8] Varying amounts of the aldol products and the Michael adducts derived therefrom are also formed; these can be separated chromatographically. The $ZnBr_2$-catalyzed reactions of **5Aa** and **5Ab** at room temperature (1.1 mol. equiv., CH_2Cl_2, 90 min) lead almost exclusively[9a, 10] to the *trans*-1,2-disubstituted cyclopentanes **6a** and **6b** (Table 1). As expected the Lewis-acid-catalyzed reaction of **5Ad** gives predominantly the Diels–Alder adducts **14** and **15**. In addition, however, the two ene products **6d** and **7d**[9a] could also be detected. This shows, once again, that the ene reaction often displays a greater selectivity than the corresponding hetero-Diels–Alder reaction[4c] (Table 1). The amide **5Ae** does not react under the given conditions. At higher temperatures, decomposition takes place.

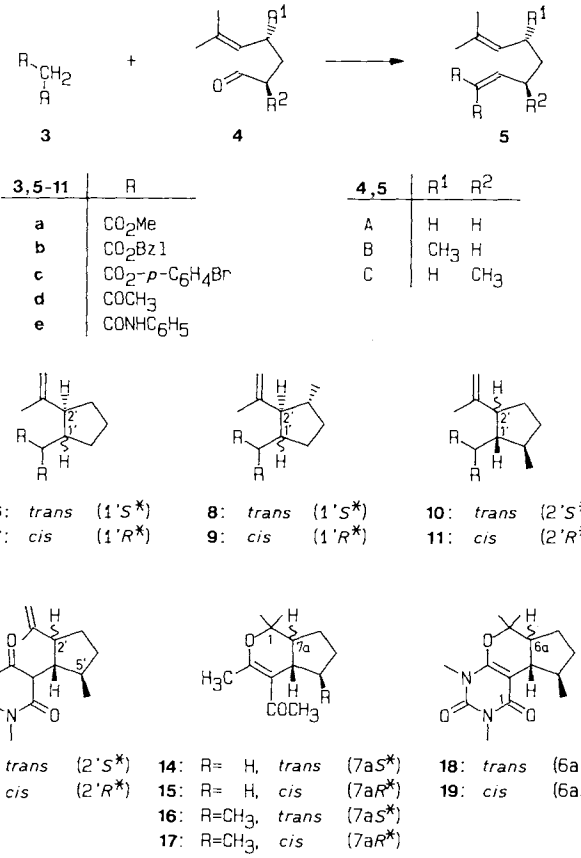

Table 1. $ZnBr_2$-catalyzed cyclization of the 1,6-dienes **5**.

Educt	Yield [%]	Products	Product ratio	*ni-de* [4a] [%]	*i-de* (*trans*) [4a] [%]	*i-de* (*cis*) [%]
5Aa	96	**6a/7a**	96.5:3.5	93.0	—	—
5Ab	89	**6b/7b**	97.5:2.5	95.0	—	—
5Ad	81	**14/15** 96:4	86.1:13.9	72.2	—	—
		6d/7d	>95:5	>90	—	—
5Ba	92	**8a/9a**	96.7:3.3	93.4	>99	>95
5Ca	91	**10a/11a**	98.2:1.8	96.4	>99	>95
5Cd	84	**16/17**	86.5:13.5	73.0	>99	>95

The asymmetric induction in the case of the ene reaction of the chiral 1,6-dienes **5Ba**[11a] and **5Ca**[11b] is especially interesting; one would expect four diastereomers to be formed. However, both the $ZnBr_2$-catalyzed cyclization of **5Ba** as well as that of **5Ca** lead only to one *trans*- and one *cis*-cyclopentane derivative in over 90% yield: **5Ba** yields **8a** and **9a** (96.7:3.3; *ni-de* = 93.4),[9a] while **5Ca** yields **10a** and **11a** (98.2:1.8; *ni-de* = 96.4)[9a] (Table 1). In both reactions the non-induced diastereoselectivity is about the same as in the reaction of the parent compound **5Aa**, whereas the induced diastereoselectivity *i-de* is >99%.

The transformation of the diketone **5Cd** is unusual. The $ZnBr_2$-catalyzed reaction leads exclusively to the two

[*] Prof. Dr. L. F. Tietze, Dr. U. Beifuss, Dipl.-Chem. M. Ruther, Dipl.-Chem. A. Rühlmann
Institut für Organische Chemie der Universität
Tammannstrasse 2, D-3400 Göttingen (FRG)
Prof. Dr. G. M. Sheldrick, Dipl.-Chem. J. Antel
Institut für Anorganische Chemie der Universität
Tammannstrasse 4, D-3400 Göttingen (FRG)

[**] Intramolecular Ene Reactions, Part 6. This work was supported by the Deutsche Forschungsgemeinschaft and the Fonds der Chemischen Industrie. We thank Dr. *R. Kummer*, BASF, for generously supplying several oxocarboxylic acid esters. — Part 5: [4e].

Diels–Alder adducts **16** and **17** in 84% yield, with the *trans*-annelated dihydropyran **16** as major product (86.5 : 13.5, Table 1), whereas in the thermal reaction (*o*-dichlorobenzene, 180 °C) the *cis*-annelated **17** predominates (**16** : **17** = 23.7 : 76.3). The *trans*-ene product **10d** is also formed thereby (**10d** : **16** + **17** = 1 : 10); the *cis*-ene product **11d** could not be detected.

The reaction of **4C** with dimethylbarbituric acid (ethylenediammonium diacetate, CCl_4/toluene = 2 : 1) proceeds as a tandem Knoevenagel-hetero-Diels–Alder[12] and -ene reaction with formation of a 4 : 1 mixture of the Diels–Alder adducts **18/19** (78.3 : 21.7; *ni-de* = 56.6; *i-de* > 98%)[9c, 9d] and the ene products **12/13** (93.7 : 6.3, *ni-de* = 87.4; *i-de* > 98%).[9b] Here also, the ene reaction is more selective than the Diels–Alder reaction. The mixture of **12** and **13** can be converted by reaction with $BF_3 \cdot OEt_2$ into **18** and **19** with retention of the diastereomeric ratio.[13]

The determination of the configuration of the ene products by NMR spectroscopy is a problem,[14] since cyclopentanes do not exist in a well-defined preferred conformation. For confirmation of the assigned structures, the *trans*-substituted cyclopentane derivative **6c** was therefore prepared by cyclization of the 1,6-diene **5Ac** and an X-ray crystal structure analysis carried out. X-ray crystal structure analyses were also carried out on the *trans*-ene product **12** and on the *cis*-Diels–Alder adduct **19**.[15]

Correlation of the ^{1}H- and ^{13}C-NMR data[16] of these compounds with the data of the other compounds enabled unequivocal assignment of all ene products except **9a**.

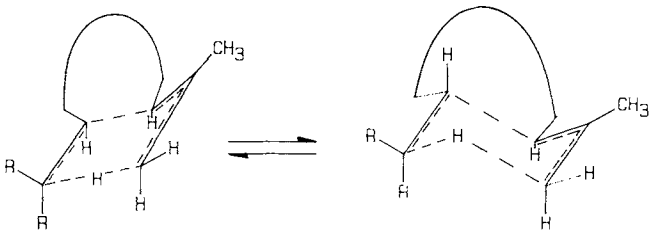

I II

We attribute the high non-induced diastereoselectivity of the intramolecular ene reaction of 1,6-dienes with two electron-acceptor substituents at the enophile terminus to the fact that the envelope transition structure **I** calculated for the basic reaction (cyclization of **5A** without substituents[5]) is destabilized due to *syn*-periplanar arrangement of the residues R with the neighboring substituents. This favors a chair-like transition state **II** with *exo-E(ene)-anti* orientation and 1,2-diequatorial arrangement of the chain. A reaction of the *Z*-ene is less likely according to experiments with labeled compounds;[6d] moreover, an *endo-Z(ene)-anti* transition structure is destabilized because of the geometry of the *Z*-ene. The high induced diastereoselectivity (*i-de* > 99%) in the formation of **8a** from **5Ba** is due to the strong steric interaction between the methyl groups on C-6 and C-8 during an attack of the enophile *syn* to the methyl group on C-6. (The (*ul-ul*-1,2)-process/the *Si(ene)-exo-E(ene)-anti* transition structure for **5Ba** is unfavorable.[17]) The same holds true for the formation of **10a** from **5Ca**; the attack of the ene *syn* to the methyl group on C-4 is destabilized by interaction of the methyl group on C-4 with an ester group. (The (*ul-ul*-1,2)-process/the *Si(ene)-exo-E(ene)-anti* transition structure for **5Ca** is in this case equally unfavorable.)

Received: April 12, 1988 [Z 2701 IE]
German version: *Angew. Chem. 100* (1988) 1200

[1] K. Alder, F. Pascher, A. Schmitz, *Ber. Dtsch. Chem. Ges. 76* (1943) 27.
[2] a) D. F. Taber: *Intramolecular Diels–Alder and Alder Ene Reactions*, Springer, Berlin 1984; b) B. B. Snider, *Acc. Chem. Res. 13* (1980) 426; c) W. Oppolzer, V. Snieckus, *Angew. Chem. 90* (1978) 506; *Angew. Chem. Int. Ed. Engl. 17* (1978) 476; d) E. C. Keung, H. Alper, *J. Chem. Educ. 49* (1972) 97; e) H. M. R. Hoffmann, *Angew. Chem. 81* (1969) 597; *Angew. Chem. Int. Ed. Engl. 8* (1969) 556; f) W. R. Roth, *Chimica 20* (1966) 229.
[3] a) J. H. Edwards, F. J. McQuillin, *J. Chem. Soc. Chem. Commun. 1977*, 838; b) H. Lehmkuhl, D. J. Reinehr, *Organomet. Chem. 25* (1970) C47; c) H. Felkin, J. D. Umpleby, E. Hagaman, E. Wenkert, *Tetrahedron Lett. 1972*, 2285; d) W. Oppolzer, P. Schneider, *ibid. 25* (1984) 3305.
[4] a) L. F. Tietze, U. Beifuss, *Angew. Chem. 97* (1985) 1067; *Angew. Chem. Int. Ed. Engl. 24* (1985) 1042; b) *Tetrahedron Lett. 27* (1986) 1767; c) *Liebigs Ann. Chem. 1988*, 321; d) *Synthesis 1988*, 359; e) L. F. Tietze, U. Beifuss, J. Antel, G. M. Sheldrick, *Angew. Chem. 100* (1988) 739; *Angew. Chem. Int. Ed. Engl. 27* (1988) 703.
[5] R. J. Loncharich, K. N. Houk, *J. Am. Chem. Soc. 109* (1987) 6947.
[6] Examples for *cis*-stereoselectivity: a) W. D. Huntsman, P. C. Lang, N. L. Madison, D. A. Uhrick, *J. Org. Chem. 27* (1962) 1983; b) W. Oppolzer, E. J. Jacobsen, *Tetrahedron Lett. 27* (1986) 1141. Exceptions: c) B. B. Snider, D. M. Roush, T. A. Killinger, *J. Am. Chem. Soc. 101* (1979) 6023; d) W. Oppolzer, S. Mirza, *Helv. Chim. Acta 67* (1984) 730.
[7] **4A** was obtained in 51% yield by Wittig reaction of isopropyl 5-oxopentanoate, reduction with $LiAlH_4$, and oxidation with DMSO and oxalyl chloride. **4B** was prepared analogously from methyl 4-formylpentanoate (yield 65%). **4C** was synthesized from citronellene by monoepoxidation and ozonolysis followed by work-up with NaI, Zn, HOAc/NaOAc (yield 37%).
[8] **5Ac** and **5Ae** were obtained in 29 and 25% yield, respectively, in unoptimized reactions.
[9] The determination of the isomeric ratios was achieved by: a) gas chromatography (Chrompack CP Sil 5 glass capillary column), standard deviation 0.1; b) analysis of the ^{13}C-NMR spectra; c) analytical HPLC (Nucleosil 7C18); d) separation by preparative HPLC (Nucleosil 5C18).
[10] Thermally induced cyclization of **5Aa** in *o*-dichlorobenzene at 180 °C and a reaction time of 5 h furnished **6a** and **7a** in a ratio of 80.5 : 19.5 (*ni-de* = 61%) in 63% yield; cf. S. K. Ghosh, T. K. Sarkar, *Tetrahedron Lett. 27* (1986) 525.
[11] The aldehydes were used in a) racemic, and b) racemic and non-racemic form. Racemization can occur in the Knoevenagel condensation of non-racemic **4Ca**.
[12] L. F. Tietze in W. Bartmann, B. M. Trost (Eds.): *Selectivity—a Goal for Synthetic Efficiency*, Verlag Chemie, Weinheim 1984, p. 299; D. L. Boger, S. M. Weinreb: *Hetero-Diels–Alder Methodology in Organic Synthesis*, Academic Press, New York 1987.
[13] In addition, the condensation products of **4A** and **4C** with malonitrile were subjected to Lewis-acid-induced cyclizations. The corresponding 7,7-dimethylbicyclo[3.2.0]heptane-6,6-dicarbonitriles were obtained as main products together with 10 and 28% respectively of the ene products (*trans* : *cis* = 89 : 11 and 87 : 13 resp.). Reaction of Meldrum's acid with the aldehyde **4C** afforded the hetero-Diels–Alder adducts (*trans* : *cis* = 81 : 19) analogous to **16** and **17**; cf. also S. Takano, S. Satoh, K. Ogasawara, *Heterocycles 23* (1985) 41; L. F. Tietze, H. Denzer, X. Holdgrün, M. Neumann, *Angew. Chem. 99* (1987) 1309; *Angew. Chem. Int. Ed. Engl. 26* (1987) 1295; S. E. Denmark, J. A. Sternberg, *J. Am. Chem. Soc. 108* (1986) 8277.
[14] K. Kondo, Y. Kondo, T. Takemoto, T. Ikenoue, *Bull. Chem. Soc. Jpn. 35* (1962) 1899.
[15] Further details of the crystal structure investigations are available on request from the Fachinformationszentrum Energie, Physik, Mathematik GmbH, D-7514 Eggenstein-Leopoldshafen 2 (FRG) on quoting the depository number CSD-53090, the names of the authors, and the journal citation.
[16] **6c**: m.p. 88–90 °C (ethanol); ^{1}H-NMR ($CDCl_3$): δ = 2.4 (m, 6H), 1.75 (s, br, 3H, CH_3), 2.3–2.9 (m, 2H), 3.82 (d, J = 7 Hz, 1H, 2-H), 4.7–4.9 (m, 2H, $=CH_2$), 6.8–7.7 (m, 8H, Ph–H). — ^{13}C-NMR ($CDCl_3$): δ = 18.91 (C-3″), 23.84, 29.71, 31.57 (C-3′, C-4′, C-5′), 41.99 (C-1′), 51.75 (C-2′), 54.95 (C-2), 112.1 (C-1″), 119.2, 119.3 (*p*-C–Ph), 122.9, 123.0 (*o*-C–Ph), 132.5, 133.5 (*m*-C–Ph), 146.0 (C-2″), 149.2, 149.3 (*ipso*-C–Ph), 166.3, 166.5 (CO).
[17] D. Seebach, V. Prelog, *Angew. Chem. 94* (1982) 696; *Angew. Chem. Int. Ed. Engl. 21* (1982) 654; V. Prelog, G. Helmchen, *ibid. 94* (1982) 614 and *21* (1982) 567.

Short, Highly Enantioselective Synthesis of a Key Intermediate for the Preparation of Leucotriene B_4 and Its 14,15-Didehydro Derivative

By *Kurt Nunn, Paul Mosset, René Grée,** and *Rolf W. Saalfrank*

Leucotriene B_4 (LTB_4) **1** is the major proinflammatory product of the 5-lipoxygenase pathway in the arachidonic cascade and as such is implicated in numerous diseases.[1] Hence, the preparation of **1** and related compounds, especially labeled derivatives, is of great interest and various elegant approaches have been reported.[2,3] The purpose of this communication is to describe a short and efficient synthesis of the enantiomerically pure polyenes **6** and **8** which are key intermediates in the preparation of LTB_4[3] and 14,15-didehydro-LTB_4.[4] This new approach, which starts from the easily accessible chiral complex (−)-**2**,[5] illustrates some of the key advantages in the use of butadiene(tricarbonyl)iron complexes in organic synthesis.

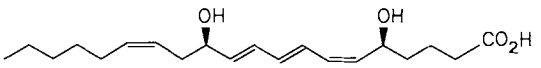

1

The reaction of (−)-**2** (of known 1*R*,4*S* absolute configuration[5b]) with allenyl silane **3** (2 equiv.)[6] in the presence of $TiCl_4$ (5 equiv.)[7] at −70°C gives the homopropargyl alcohol **4** (65% yield after chromatography). The reaction is stereospecific ($de \geq 98\%$)[8] and leads only to the ψ-*endo* derivative, with the *R* configuration at the secondary alcohol function. Noteworthy is that $Fe(CO)_3$ acts here as an efficient protecting group. Under similar conditions, the free diene corresponding to **2** gives, at best, 10% of (±)-**8**.

Semireduction of **4** occurs smoothly using Ni/P_2 catalyst[9,10] to give a quantitative yield of **5**. In agreement with preceding results,[11] decomplexation ($Ce^{4\oplus}$, MeOH, −15°C) occurs without racemization, leading to the desired compound **6**. The optical purity of **6** is ascertained by ^{1}H-NMR using $Eu(tfc)_3$.[12] Alcohol **6** is readily converted into silyl ether **7** (tBuPh$_2$SiCl, 2 equiv.; imidazole, 4 equiv.; DMF; 0°C; 15 h; 96%). The physical data of the corresponding ethyl esters obtained by transesterification of **6** and **7**[13] are in good agreement with those described earlier,[2a,3] thus confirming the *R* absolute configuration.

On the other hand, decomplexation of **4** (same conditions as for **5**, 90% yield) gives alcohol **8** which is transformed into its silyl ether **9** (same conditions as for **6**). Both compounds are very closely related to the derivatives **10** and **11** used recently for the synthesis of 14,15-didehydro-LTB_4 and labeled LTB_4.[4]

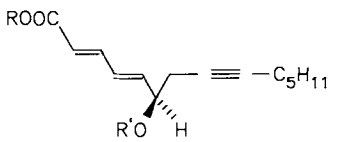

8, R = CH_3, R' = H
9, R = CH_3, R' = $SiPh_2tBu$
10, R = C_2H_5, R' = H
11, R = C_2H_5, R' = $SiMe_2tBu$

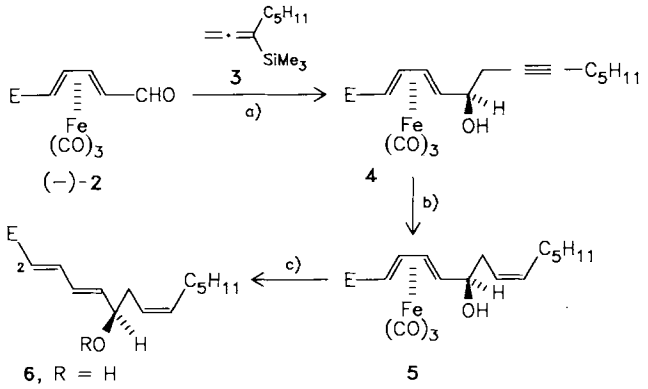

Scheme 1: E = CO_2CH_3. a) See *Experimental*; b) **4** (0.315 mmol) in EtOH (3 mL); 0.2 equiv. catalyst; 0.25 equiv. ethylenediamine; 2 atm H_2; 2 days at room temperature; c) **5** (0.54 mmol) in MeOH (5 mL); $Ce(NH_4)_2(NO_3)_6$ (3.5 equiv.), −15°C, 25 min, 91% yield.

[*] Dr. R. Grée, K. Nunn, Dr. P. Mosset
Laboratoire de Chimie Organique Biologique, CNRS UA 704,
Ecole Nationale Supérieure de Chimie de Rennes
Avenue du Gal Leclerc, F-35700 Rennes-Beaulieu (France)
Prof. Dr. R. W. Saalfrank
Institut für Organische Chemie der Universität Erlangen-Nürnberg
Henkestrasse 42, D-8520 Erlangen (FRG)

Experimental

To a cooled (−80°C) solution of (−)-**2** (361 mg, 1.29 mmol) in anhydrous dichloromethane (10 mL) was added $TiCl_4$ (0.72 mL, 5 equiv.). After 15 minutes stirring at this temperature, allene **3** (470 mg, 2.6 mmol) was added to the red solution and the reaction mixture was stirred for 130 min at −70°C. The dark red solution was poured into a vigorously stirred mixture of ether (50 mL) and 1 N aqueous bicarbonate (50 mL). The organic layer was separated and the aqueous phase extracted twice with ether. The combined organic solutions were washed with a saturated sodium chloride solution, with distilled water, and then dried ($MgSO_4$) and concentrated. The resulting orange-red oil was subjected to flash chromatography on SiO_2 (20 g). First

Table 1. Physical data for the most important products.

4: IR (film): $\tilde{\nu}$ = 3480 (w), 2070 (s), 1995 (s), 1715 (m), 1695 (m) cm^{-1}; ^{1}H NMR (300 MHz, $CDCl_3$): δ = 0.90 (pseudo t, 3H, J = 7.1 Hz), 0.97 (dd, 1H, J = 8.1, 0.9 Hz); 1.24–1.43 (m, 5H), 1.50 (pseudo tt, 2H, J = 7,7 Hz), 2.14 (d, 1H, J = 3.6 Hz), 2.17 (tt, 2H, J = 7.0, 2.3 Hz), 2.43 (ddt, 1H, J = 16.4, 7.3, 2.3 Hz), 2.50 (ddt, 1H, J = 16.4, 5.1, 2.3 Hz), 3.67 (s, 3H), 3.75 (dddd, 1H, J = 7.3, 6.2, 5.1, 3.6 Hz), 5.46 (ddd, 1H, J = 8.8, 5.0, 0.9 Hz), 5.83 (ddd, 1H, J = 8.1, 5.0, 1.0 Hz); ^{13}C NMR (22.5 MHz, $CDCl_3$): δ = 13.97 (CH_3), 18.77 (CH_2), 22.27 (CH_2), 28.67 (CH_2), 30.63 (CH_2), 31.19 (CH_2), 45.78 (CH), 51.63 (CH_3), 67.71 (CH), 71.51 (CH), 75.24 (C), 83.17 (CH), 84.30 (CH), 172.65 (C); $[\alpha]_D^{25} = -280°$ (c = 0.1, MeOH)

5: IR (film): $\tilde{\nu}$ = 3470 (w), 2065 (s), 2020 (s), 1975 (s), 1700 (m) cm^{-1}; ^{1}H NMR (300 MHz, $CDCl_3$): δ = 0.88 (pseudo t, 3H, J = 6.8 Hz), 0.97 (dd, 1H, J = 8.1, 0.9 Hz), 1.20–1.48 (m, 7H), 1.73 (d, 1H, J = 3.0 Hz), 2.05 (br. dtd, 2H, J = 7.4, 6.5, 1 Hz), 2.33 (br. dddd, 1H, J = 14, 6.4, 5, 1.2 Hz), 2.39 (br. dddd, 1H, J = 14, 8.4, 8, 1.2 Hz), 3.66 (m, 1H), 3.67 (s, 3H), 5.39 (dddt, 1H, J = 10.9, 8.4, 6.4, 1.5 Hz), 5.42 (br. dd, 1H, J = 8.8, 5.1 Hz), 5.64 (dtt, 1H, J = 10.9, 7.4, 1.2 Hz), 5.83 (ddd, 1H, J = 8.1, 5.1, 1.0 Hz); ^{13}C NMR (22.5 MHz, $CDCl_3$): δ = 14.05 (CH_3), 22.60 (CH_2), 27.51 (CH_2), 29.36 (CH_2), 31.60 (CH_2), 38.48 (CH_2), 45.78 (CH), 51.62 (CH_3), 69.29 (CH), 72.47 (CH), 83.07 (CH), 84.18 (CH), 123.98 (CH), 134.84 (CH), 172.64 (C); $[\alpha]_D^{25} = -200°$ (c = 0.1, MeOH)

6: IR (film): $\tilde{\nu}$ = 3420 (w), 1720 (s), 1645 (s), 1620 (m) cm^{-1}; ^{1}H NMR (300 MHz, $CDCl_3$): δ = 0.89 (pseudo t, 3H, J = 6.8 Hz), 1.19–1.49 (m, 6H), 1.79 (br., 1H), 2.05 (br. dtd, 2H, J = 7.3, 7.1, 1.5 Hz), 2.36 (br. t, 2H, J = 7 Hz), 3.75 (s, 3H), 4.29 (tdd, 1H, J = 6.3, 5.4, 1.3 Hz), 5.36 (dtt, 1H, J = 10.8, 7.5, 1.5 Hz), 5.61 (dtt, 1H, J = 10.8, 7.3, 1.4 Hz), 5.90 (dd, 1H, J = 15.4, 0.6 Hz), 6.14 (dd, 1H, J = 15.3, 5.4 Hz), 6.40 (dddd, 1H, J = 15.3, 11.0, 1.3, 0.6 Hz), 7.28 (dd, 1H, J = 15.4, 11.0 Hz); $[\alpha]_D^{25} = -39°$ (c = 1.21, MeOH)

8: IR (Nujol): $\tilde{\nu}$ = 3410 (w), 1715 (s), 1650 (m), 1620 (m) cm^{-1}; ^{1}H NMR (300 MHz, $CDCl_3$): δ = 0.90 (pseudo t, 3H, J = 7.1 Hz), 1.24–1.42 (m, 4H), 1.49 (pseudo tt, 2H, J = 7, 7 Hz), 2.16 (tt, 2H, J = 7.0, 2.4 Hz), 2.24 (br. d, 1H, J = 3.5 Hz), 2.43 (ddt, 1H, J = 16.4, 6.6, 2.4 Hz), 2.51 (ddt, 1H, J = 16.4, 5.4, 2.4 Hz), 3.75 (s, 3H), 4.36 (m, 1H), 5.91 (dd, 1H, J = 15.3, 0.6 Hz), 6.16 (dd, 1H, J = 15.3, 5.3 Hz), 6.44 (dddd, 1H, J = 15.3, 11.0, 1.35, 0.6 Hz), 7.29 (dd, 1H, J = 15.3, 11.0 Hz); $[\alpha]_D^{25} = -93°$ (c = 0.75, MeOH)

 © VCH Verlagsgesellschaft mbH, D-6940 Weinheim, 1988 0570-0833/88/0909-1188 $ 02.50/0 Angew. Chem. Int. Ed. Engl. 27 (1988) No. 9

elution with 10% ether/petroleum ether removed unpolar byproducts. The alcohol **4** (orange oil) was then eluted with ether/petroleum ether (1:4) (326 mg; 65% yield). Starting complex **2** (15 mg; 4%) was recovered using ether/petroleum ether (1:1).

Received: May 19, 1988 [Z 2767 IE]
German version: *Angew. Chem. 100* (1988) 1233

[1] P. Borgeat, B. Samuelsson, *J. Biol. Chem. 254* (1979) 2643; Reviews: B. Samuelsson, *Angew. Chem. 94* (1982) 881; *Angew. Chem. Int. Ed. Engl. 21* (1982) 902; *Science (Washington) 220* (1983) 568; P. Sirois, P. Borgeat, *J. Pharmacol. (Paris) 15, Suppl. 1* (1984) 53; P. J. Piper, *Trends Pharmacol. Sci. 4* (1983) 75.

[2] a) Y. Le Merrer, C. Gravier, D. Languin-Micas, J. C. Depezay, *Tetrahedron Lett. 27* (1986) 4161; b) D. Guillerm, G. Linstrumelle, *ibid. 27* (1986) 5857; c) H. Kobayashi, T. Shimazaki, F. Sato, *ibid. 28* (1987) 5849, and references cited therein.

[3] Y. Guindon, D. Delorme, C. K. Lau, R. Zamboni, *J. Org. Chem. 53* (1988) 267.

[4] Y. Leblanc, B. J. Fitzsimmons, R. Zamboni, J. Rokach, *J. Org. Chem. 53* (1988) 265.

[5] This chiral complex is obtained by resolution using fractional crystallization of diastereoisomeric oxazolidine derivatives. a) A. Monpert, J. Martelli, R. Grée, R. Carrié, *Tetrahedron Lett. 22* (1981) 1961; b) A. Monpert, D. Eng. Thesis, University of Rennes (1983).

[6] R. L. Danheiser, D. J. Carini, C. A. Kwasigroch, *J. Org. Chem. 51* (1986) 3870.

[7] Lower yields are obtained when using smaller amounts of $TiCl_4$. This is possibly due to a reaction of the Lewis acid with $Fe(CO)_3$; see for instance in the case of $AlCl_3$: K. D. Karlin, B. F. G. Johnson, J. Lewis, *J. Organomet. Chem. 160* (1978) C21.

[8] The purity of **4** has been established by ^1H and ^{13}C NMR; furthermore the ψ-*exo* isomer, which has been obtained by another route (P. Mosset, R. Grée, unpublished results) is clearly different (NMR, TLC) from **4**.

[9] C. A. Brown, V. K. Ahuja, *J. Chem. Soc. Chem. Commun. 1973*, 553.

[10] Here also, the complex has a protective role: the same reaction with **8** gives rise not only to semireduction of the triple bond but also to reduction of the electrophilic diene.

[11] R. Grée, M. Laabassi, P. Mosset, R. Carrié, *Tetrahedron Lett. 25* (1984) 3693; *ibid. 26* (1985) 2317.

[12] Racemic (±)-**6** exhibits a clear splitting of the H_2 protons in the presence of 0.3 equiv. of $Eu(tfc)_3$. This splitting is not observed in **6** under the same conditions.

[13] Ethyl ester of **6**: $[\alpha]_D^{25} = +9°$ ($c = 0.28$, $CHCl_3$), Ref. [3]: $+11.4°$ ($c = 1.31$, $CDCl_3$); ethyl ester of **7**: $[\alpha]_D^{25} = +48°$ ($c = 1.2$, $CHCl_3$); Ref. [3]: 44.8° ($c = 1.25$, $CDCl_3$); Ref. [2a]: 43° ($c = 2.2$, $CHCl_3$).

A Novel Tris(azo)macrobicyclic Molecule—Synthesis, Photochemistry, and Isomer Separation**

By *Hans-Willi Losensky, Heinz Spelthann, Albert Ehlen, Fritz Vögtle,** and *Joachim Bargon**

The reversible change of physical and chemical material properties is gaining increasing importance also in the area of host/guest chemistry[1] and the optical storage of information.[2]

We describe here for the first time the photochemically reversibly switchable azomacrocycles of type **1**–**5** and the macrobicyclic molecules **6a**, **b**, in which three azobenzene structural units are coupled in a symmetrical arrangement. The amine nitrogen atoms serve for increasing the solubility in polar or acid media.

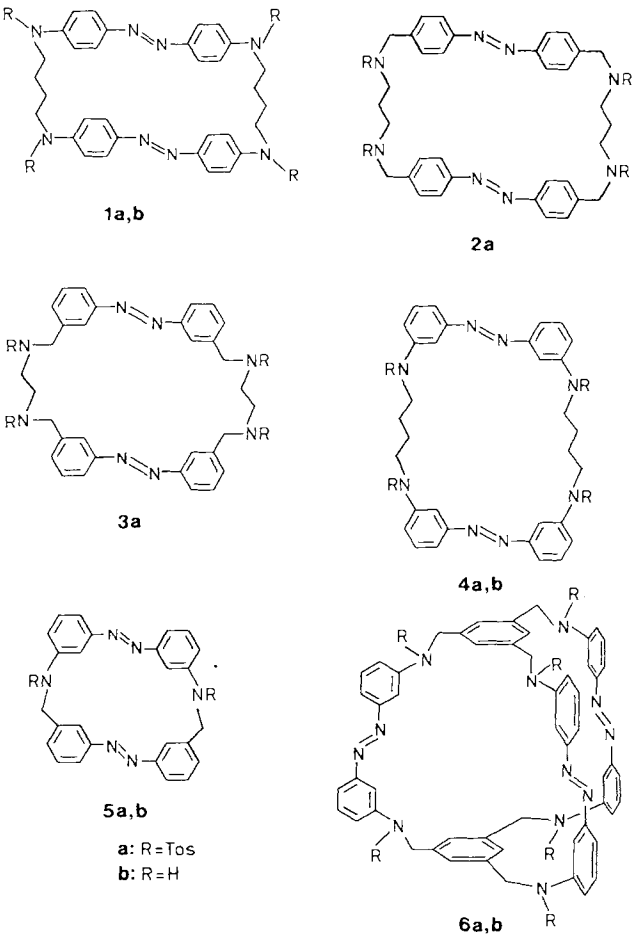

The monocycles **1a** and **4a** containing anilide units can be prepared from the corresponding bis(tosylamino)azobenzenes and 1,4-dibromobutane. The benzylamides **2a** and **3a** are accessible from bis(bromomethyl)azobenzenes and α,ω-bis(tosylamines).[3] The cyclization of 3,3′-bis(tosylamino)azobenzene with 3,3′-bis(bromomethyl)azobenzene and 1,3,5-tris(bromomethyl)benzene, respectively, finally affords the azo compounds **5a** and **6a**.[4]

The macrocycles **3a**, **4a** and **5a** derived from 3,3′-disubstituted azobenzenes precipitate, as expected, in higher yields than the corresponding 4,4′-compounds **1a** and **2a**. In the case of the macrobicyclic molecule **6a**, the use of cesium carbonate instead of potassium carbonate leads under dilution conditions to an increase in the yield of 4 to 12% (cesium effect).[5] **6a** can thus be obtained in gram amounts from readily accessible starting materials.

In the case of aromatic/aliphatic (**1a** and **4a**) or aromatic/benzylic tosylamides (**5a** and **6a**) of azo compounds the sulfuric acid hydrolysis leads to the free amines,[4] whereas in the case of benzylic/aliphatic tosylamides (**2a** and **3a**) this method fails,[6] as also the reaction with hydrobromic acid/phenol[3b] and alkaline hydrolysis[7] or alcoholysis.[8] Apart from the cyclic amine **1b** all the new azo compounds exhibit the photochemistry of azobenzene:[9] irradiation with light of wavelength $\lambda = 313$ nm and $\lambda = 436$ nm leads to two photostationary equilibria which are interswitchable.[10]

[*] Prof. Dr. F. Vögtle, Dr. H.-W. Losensky
Institut für Organische Chemie und Biochemie der Universität
Gerhard-Domagk-Strasse 1, D-5300 Bonn 1 (FRG)
Prof. Dr. J. Bargon, Dr. H. Spelthann, A. Ehlen
Institut für Physikalische Chemie der Universität
Wegelerstrasse 12, D-5300 Bonn 1 (FRG)

[**] This work was supported by the Deutsche Forschungsgemeinschaft and the Fonds der Chemischen Industrie. We thank Dipl.-Chem. *J. Heyer* (Universität Bonn) for HPLC separations, *W. Schmöller* (Max-Planck-Institut für Kohlenforschung, Mülheim a. d. Ruhr) and Dr. *M. Przybylski* (Universität Mainz) for mass spectra, Dr. *T. Uenzo* (Hitachi Research Laboratories, Tokyo) and *A. Mirza* (Universität Bonn) for helpful discussions, Prof. Dr. *H. Rau* (Universität Stuttgart-Hohenheim) for providing an experimental procedure, and Prof. Dr. *H.-J. Schneider* (Technische Universität München) for time-resolved spectroscopic measurements.

The results of the photochemical measurements enable the following generally applicable conclusions to be drawn: a) amino groups in the 4- or 4'-position (as in **1b**) reduce the stability of the (*Z*)-isomers.[11] This phenomenon could be due to an amino-azo/imino-hydrazo tautomerism which inhibits the (*E*)→(*Z*) isomerization.[12] b) The substitution of the amino hydrogen atoms by electron withdrawing sulfonyl groups (−M effect) reverses the photoisomerization-inhibiting effect of the *p*-amino groups (cf. **1a** and **1b**). c) If the *p*-amino group is "separated" from the aromatic system by insertion of a methyl group the photochemistry of the compound in question resembles that of the unsubstituted azobenzene. d) Amino groups in the 3- or 3'-position do not appear to inhibit the photoisomerization. e) In the case of 3,3'-substituted azobenzenes of the type **3**–**5**, a stronger enrichment of the (*Z*)-isomers is generally observed than in the case of the corresponding 4,4'-substituted compounds of type **1** and **2** and the macrobicyclic molecule **6b**. This can be attributed to strain effects.

The stability of the photoisomers of the cyclic amines **4b** and **6b** suffices for the isolation of *all* possible configurational isomers (*E,E*)-**4b**, (*E,Z*)-**4b** and (*Z,Z*)-**4b** or (*E,E,E*)-**6b**, (*E,E,Z*)-**6b**, (*E,Z,Z*)-**6b** and (*Z,Z,Z*)-**6b** from a solution irradiated at the equilibrium ($\lambda = 313$ nm).[13] Figure 1 shows the absorption spectra of the photoisomers of **6b**, which can be isolated by chromatography.[14] A higher dipole moment and thus smaller R_f value can be related to an increasing degree of isomerization.[15] Table 1 lists the spectroscopic data.

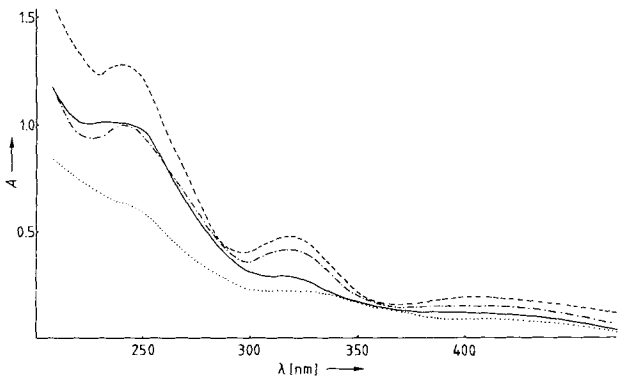

Fig. 1. UV spectra of all possible configurational isomers of the hexamine **6b**: (---) (*E,E,E*)-**6b**; (-·-·-) (*E,E,Z*)-**6b**; (——) (*E,Z,Z*)-**6b**; (·····) (*Z,Z,Z*)-**6b** [16].

Table 1. UV spectroscopic data of the configurational isomers of the macrobicyclic compound **6b** [16].

Isomers of **6b**	UV ($\log\varepsilon$)
(*E,E,E*)	209, 239, 318, 420 (4.92, 4.83, 4.42, 4.01)
(*E,E,Z*)	207, 242, 318, 420 (4.77, 4.71, 4.40, 3.87)
(*E,Z,Z*)	209, 239, 318, 432 (4.80, 4.74, 4.18, 3.81)
(*Z,Z,Z*)	212, 229, 315, 428 (4.65, 4.58, 4.11, 3.73)

The photoisomerization of the monocycle **4b** can not only be carried out in solution but also in a polymer matrix.[17] From the observation that a photoisomerization of the conformationally restricted macrobicyclic compound **6b** is possible, it can be concluded that this proceeds via an inversion mechanism.[18]

Whereas informative conclusions could hitherto only be drawn from measurements on a photostationary state,[1a] it should now be possible, as a result of the first isolation of all photoisomers of macro(bi)cyclic polyazo compounds, to study the insertion properties of (partly) isomerized azomacrocycles based on 3,3'-diaminoazobenzenes.[19]

Experimental

As example the synthesis of the hexamine **6b** is described: A suspension of 25.0 g (77 mmol) of cesium carbonate in 1 L of anhydrous dimethylformamide was treated dropwise in 7 h at room temperature with 7.80 g (15 mmol) of 3,3'-bis(tosylamino)azobenzene and 3.56 g (10 mmol) of 1,3,5-tris(bromomethyl)benzene, in each case dissolved in 250 mL of anhydrous dimethylformamide. After 2 hours' stirring the reaction mixture was evaporated to dryness under vacuum. The residue was treated with 150 mL of semiconcentrated hydrochloric acid and stirred for 12 h. The solid recovered after filtration was washed with water until neutral and then dried. The solid product mixture (ca. 10 g) was transferred to a silica gel column and eluted in the absence of light with dichloromethane/acetone (40 : 1). The fractions with R_f values of 0.35 and 0.50 were evaporated to dryness under vacuum and taken up in dichloromethane; the hexatosyl compound **6a** was filtered off as a light-yellow solid, washed with dichloromethane, and finally dried under an oil-pump vacuum: 1.08 g (12.1%), m.p. 352–354°C.

A suspension of **6a** (85 mg) in 4–5 mL of 80% (vol.-%) sulfuric acid was stirred at room temperature until a clear solution was obtained (1–2 h). This was poured onto ice (50 mL) and rendered alkaline with 5 N sodium hydroxide; the hexamine **6b** precipitated as an orange solid: 38 mg (92.7%), m.p. 350°C, decomp. above 200°C. ^{1}H-NMR and MS data were recorded. Elemental analysis and ^{1}H-NMR spectrum ($CDCl_3$) indicate inclusion of 2 moles of water per mole of **6b**.

Received: April 16, 1988;
revised: June 27, 1988 [Z 2709 IE]
German version: *Angew. Chem. 100* (1988) 1225

[1] a) S. Shinkai, O. Manabe, *Top. Curr. Chem. 121* (1984) 67; b) K. H. Neumann, F. Vögtle, *J. Chem. Soc. Chem. Commun. 1988*, 520.
[2] G. Kämpf, *Nachr. Chem. Tech. Lab. 35* (1987) 255.
[3] a) H. Stetter, E.-E. Roos, *Chem. Ber. 88* (1955) 1390; b) K. Odashima, A. Itai, Y. Ititaka, K. Koga, *J. Org. Chem. 50* (1985) 4478; c) H.-J. Schneider, R. Busch, *Chem. Ber. 119* (1986) 747.
[4] ^{1}H-NMR and MS data (except for **6a**) and correct elemental analyses (except for **1b**) have been recorded and will be published in a later review.
[5] a) L. Rossa, F. Vögtle, *Top. Curr. Chem. 113* (1983) 1; b) B. K. Vriesema, J. Buter, R. M. Kellog, *J. Org. Chem. 49* (1984) 110; c) B. Klieser, L. Rossa, F. Vögtle, *Kontakte (Merck) 1984* (1), 3; d) K. Meurer, F. Luppertz, F. Vögtle, *Chem. Ber. 118* (1985) 4433.
[6] P. Ruggli, E. Leupin, H. Dahn, *Helv. Chim. Acta 30* (1947) 1845.
[7] N. Hatanaka, N. Watanabe, M. Matsumoto, *Heterocycles 24* (1986) 1987.
[8] Y. Takata, *J. Pharm. Soc. Jpn. 71* (1951) 1474.
[9] a) J. Griffiths, *Chem. Soc. Rev. 1* (1972) 481, and references cited therein; b) H. Rau, *Angew. Chem. 85* (1973) 248; *Angew. Chem. Int. Ed. Engl. 12* (1973) 224, and references cited therein.
[10] G. Zimmerman, L.-Y. Chow, U.-J. Paik, *J. Am. Chem. Soc. 80* (1958) 3528.
[11] a) H. Rau, *Ber. Bunsenges. Phys. Chem. 75* (1971) 1343; b) H. Bisle, H. Rau, *Chem. Phys. Lett. 31* (1975) 264; c) H. Bisle, M. Römer, H. Rau, *Ber. Bunsenges. Phys. Chem. 80* (1976) 301; d) E. R. Talaty, J. C. Fargo, *J. Chem. Soc. Chem. Commun. 1967*, 65; e) N. Nishimura, T. Sueyoshi, H. Yamanaka, E. Imai, S. Yamamoto, S. Hasegawa, *Bull. Chem. Soc. Jpn. 49* (1976) 1381; f) H. Görner, H. Gruen, D. Schulte-Frohlinde, *J. Phys. Chem. 84* (1980) 3031.
[12] Time-resolved spectroscopic measurements are being carried out to clarify this problem. Cf. also G. Hallas, R. Marsden, J. D. Hepworth, D. Mason, *J. Chem. Soc. Perkin Trans. 2 1986*, 123; G. Wettermark, M. E. Langmuir, D. G. Anderson, *J. Am. Chem. Soc. 87* (1965) 476.
[13] The incomplete thermal re-isomerization of the isolated isomers of **6b** leads in each case to the maximum number of possible isomers: (*Z,Z,Z*)-**6b**: four; (*E,Z,Z*)-**6b**: three; (*E,E,Z*)-**6b**: two.
[14] Flash silica gel, dichloromethane/acetone 20 : 1, room temperature, red light.
[15] a) G. S. Hartley, R. J. W. Le Fèvre, *J. Chem. Soc. 1939*, 531; b) A. H. Cook, D. G. Jones, *ibid. 1953*, 1309; c) U. Funke, H.-F. Grützmacher, *Tetrahedron 43* (1987) 3787.
[16] The concentrations of the chromatographically isolated configurational isomers were approximated on the basis of a pseudo-isosbestic point of their UV spectra. The quoted ε values are thus lower limits.

[17] A stirred 10% solution of polycarbonate in tetrahydrofuran was treated with 5–10 μmol of **4b**. The solution was transferred to a petri dish and the solvent removed by evaporation at 55°C. The remaining film of residue was irradiated with light of wavelengths $\lambda = 313$ nm and $\lambda = 436$ nm.

[18] a) H. Rau, *J. Photochem. 26* (1984) 221; b) H. Rau, E. Lüddecke, *J. Am. Chem. Soc. 104* (1982) 1616.

[19] a) D. J. Cram, *Angew. Chem. 98* (1986) 1041; *Angew. Chem. Int. Ed. Engl. 25* (1986) 1039; b) E. Weber, F. Vögtle, *Nachr. Chem. Tech. Lab. 35* (1987) 1149; c) J.-M. Lehn, *Angew. Chem. 100* (1988) 91; *Angew. Chem. Int. Ed. Engl. 27* (1986) 89; d) F. P. Schmidchen, *Nachr. Chem. Tech. Lab. 36* (1988) 8; e) F. Diederich, *Angew. Chem. 100* (1988) 372; *Angew. Chem. Int. Ed. Engl. 27* (1988) 372.

Synthesis and Structure of 2,7-Di-*tert*-butyldicyclopenta[*a*,*e*]cyclooctene**

By *Klaus Hafner,* Georg F. Thiele,* and *Carsten Mink*

Bicyclic conjugated π-electron systems with two odd-numbered rings, such as pentalene, azulene or heptalene,[1] can be viewed as annulenes bridged by a single bond. Even when an even-numbered ring is inserted between the two odd-numbered rings, the bridging bonds in all Kekulé structures remain single bonds. The only tricyclic systems of this kind reported to date are *s*-indacene **1** and a few of its derivatives, in which the substituents have a remarkable influence on the bonding behavior.[2] Comparable with the 12 π-electron system of *s*-indacene **1** is the 14π-perimeter of the dicyclopenta[*a*,*e*]cyclooctene **2**, for which π-SCF calculations indicate that the bond localization is essentially similar to that in *s*-indacene.[3] We report here on the synthesis and molecular structure of its 2,7-di-*tert*-butyl derivative **10**.

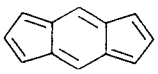

1

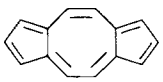

2

For construction of the tricyclic skeletal framework of **10** we chose the cyclizing condensation of a 1,2-dicyclopentadienylethane with a glyoxal equivalent. The selective attack of the glyoxal equivalent at the position adjacent to the ethano bridge, which is necessary for the cyclization, can be achieved by substitution of the cyclopentadienyl moiety with a sterically bulky *tert*-butyl group.[4] The corresponding 1,2-bis-(*tert*-butylcyclopentadienyl)ethane **4**[5] can be readily obtained from sodium *tert*-butylcyclopentadienide **3** and 1,2-dibromoethane (colorless oil, yield 61% (Scheme 1). The alkylation of **3** with 1,2-dibromoethane at low temperatures initially affords the spiro[4.2]heptadiene **5**,[6] whose cyclopropane ring is opened by nucleophilic attack of a second equivalent of **3** to give **6** on heating only in the presence of a crown ether.[7,8]

The cyclization of **4** to the eight-membered ring was accomplished by condensation of its dilithium salt **7** with glyoxal sulfate **8**[4,9] (Scheme 2). The bridged pentafulvadiene **9** (red-violet crystals, m.p. 174°C) is formed as the sole low molecular weight product in 9% yield. Unexpected difficulties were encountered with the introduction

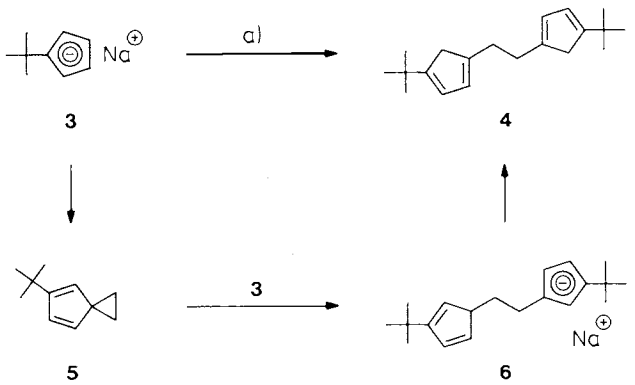

Scheme 1. a) 1,2-Dibromoethane, NaH, dibenzo[18]crown-6, bis(2-methoxyethyl) ether, −30°C to 160°C, 5 h; 2. H_2O.

of a further double bond into the eight-membered ring of **9**, since all attempts to directly dehydrogenate **9** or to functionalize the methylene groups met with no success. It was possible, however, to carry out an acid-catalyzed tautomerization of **9**, which on reaction with trifluoroacetic acid at −20°C affords a tautomeric mixture (orange-yellow oil) in up to 40% yield. According to the ^{1}H-NMR spectrum the mixture contains predominantly the 3,4-dihydro isomer **11**. The driving force behind this reaction may be the decrease of the ring strain in the eight-membered ring, which, according to inspection of models, has an almost strain-free pseudo boat conformation in **11**. In contrast to **9**, compound **11** and its tautomers can be deprotonated to the dianion **12** with lithium tetramethylpiperidide. Oxidation of **12** with molecular oxygen furnishes the completely conjugated hydrocarbon **10** in 53% yield as air-stable, reddish-brown crystals (m.p. 199°C).

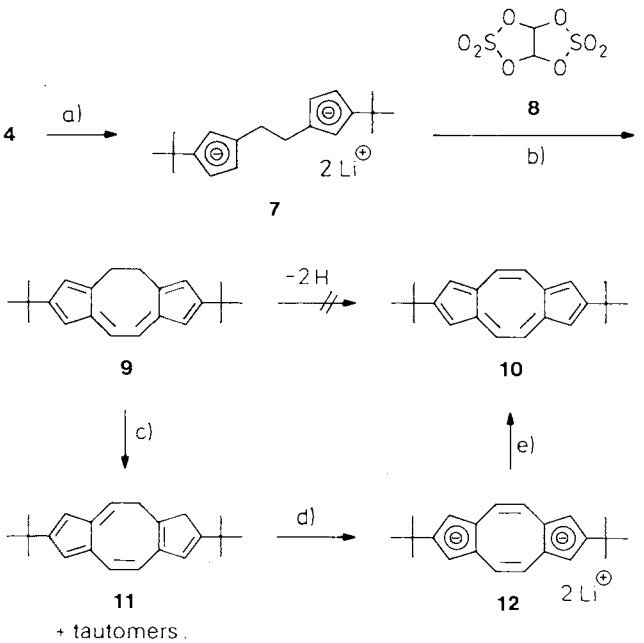

Scheme 2. a) *n*BuLi, TMEDA, *n*-hexane; b) THF, −70°C to 20°C; c) 1. CF_3COOH, CH_2Cl_2, −25°C, 30 min; 2. Et_3N; d) lithium tetramethylpiperidide, THF, −70°C to 20°C; e) O_2, THF, −70°C.

The ^{1}H-NMR spectrum of **10** shows a significant downfield shift of all signals compared to those of the dihydro compound **9**, thus indicating a noticeable diatropism. The

[*] Prof. Dr. K. Hafner, Dr. G. F. Thiele, C. Mink
Institut für Organische Chemie der Technischen Hochschule
Petersenstr. 22, D-6100 Darmstadt (FRG)

[**] This work was supported by the Deutsche Forschungsgemeinschaft, the Fonds der Chemischen Industrie, and Degussa AG, Frankfurt am Main.

presence of only three signals in the ^{1}H-NMR spectrum and of six signals in the ^{13}C-NMR spectrum (Table 1) is consistent with a molecular structure with D_{2h} symmetry

Table 1. Spectroscopic data of **4**, **9**, and **10**. ^{1}H-NMR ($CDCl_3$, 300 MHz), ^{13}C-NMR ($CDCl_3$, 75.47 MHz), UV (*n*-hexane).

4: ^{1}H-NMR: $\delta = 1.14$–1.28 (m, 18H, *t*Bu), 2.48–3.02 (m, 8H, CH_2), 5.75–6.26 (m, 4H, olefin-H); UV: $\lambda_{max}(\lg\varepsilon) = 253$ nm (3.83)

9: ^{1}H-NMR: $\delta = 1.16$ (s, 18H, *t*Bu), 2.39, 2.86 (2 br. s, 4H, CH_2), 5.65 (d, $J = 2.2$ Hz, 2H, 1/8-H), 6.15 (s, 2H, 3/6-H), 6.52 (s, 2H, 9/10-H); UV: $\lambda_{max}(\lg\varepsilon) = 228$ (3.88) sh, 262 (3.47) sh, 327 (4.17) sh, 344 (4.40) sh, 358 (4.52), 376 (4.40), 458 nm (2.78)

10: ^{1}H-NMR: $\delta = 1.33$ (s, 18H, *t*Bu), 6.84 (s, 4H, 1/3/6/8-H), 7.27 (s, 4H, 4/5/9/10-H); ^{13}C-NMR: $\delta = 30.22$ (q, $C(CH_3)_3$), 32.85 (s, $C(CH_3)_3$), 124.90 (d, C-1/3/6/8), 126.15 (d, C-4/5/9/10), 139.30 (s, C-3a/5a/8a/10a), 160.87 (s, C-2/7); UV: $\lambda_{max}(\lg\varepsilon) = 217$ (4.19), 324 (4.88) sh, 335 (5.02), 413 (3.51) sh, 425 (3.54) sh, 435 (3.59), 460 (3.53), 923 (1.99), 1015 (1.93) sh, 1064 (1.91) sh, 1375 nm (1.64) sh

and delocalized π-electron system. This is confirmed by the X-ray structure analysis,[10] which reveals a planar ring system with inversion center for **10** (Fig. 1). The maximum distance of the ring-C atoms from the mean plane is ±1.5 pm. The perimeter of the molecule, with CC bond lengths of about 140 pm, exhibits substantial bond equivalency, whereas the two bridges are noticeably longer (149 pm). Thus, the bridging bonds have predominantly single-bond character, as in azulene.[11]

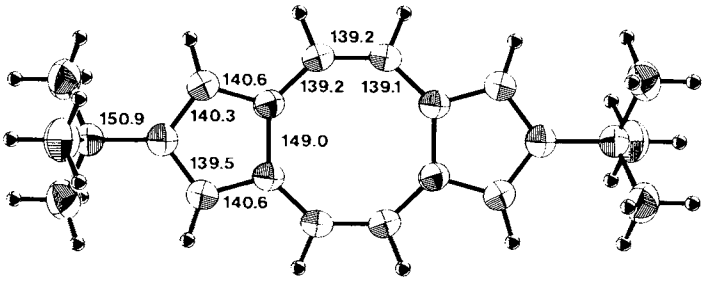

Fig. 1. Crystal structure of **10** (ORTEP, vibration ellipsoids at the 50% probability level) at room temperature with selected bond lengths [pm].

The analogy to azulene also extends to the electronic spectrum of **10**, which like that of azulene consists of three structural band systems whose extinctions decrease with increasing wavelength. Their positions compared to those of the bands of azulene, however, are strongly bathochromically shifted, so that the longest wavelength absorptions already lie in the near IR.

10 not only belongs to the few hydrocarbons with a planar eight-membered ring,[1,12] but, in addition, it is also a completely planar **14** π-electron system which has no further cyclic conjugated subunits apart from the 14 π perimeter. The molecular structure and spectroscopic properties justify the classification of **10** as a non-benzenoid aromatic hydrocarbon.

Received: April 28, 1988 [Z 2727 IE]
German version: *Angew. Chem. 100* (1988) 1213

[1] D. Lloyd: *Non-benzenoid Conjugated Carbocyclic Compounds*, Elsevier, Amsterdam 1984, and references cited therein.
[2] K. Hafner, *Angew. Chem. 75* (1963) 1041; *Angew. Chem. Int. Ed. Engl. 3* (1964) 165; *Pure Appl. Chem. Suppl. 2* (1971) 1; K. Hafner, H.-P. Krimmer, *Angew. Chem. 92* (1980) 202; *Angew. Chem. Int. Ed. Engl. 19* (1980) 199; K. Hafner, *Pure Appl. Chem. 54* (1982) 939; K. Hafner, B. Stowasser, H.-P. Krimmer, S. Fischer, M. C. Böhm, H. J. Lindner, *Angew. Chem. 98* (1986) 646; *Angew. Chem. Int. Ed. Engl. 25* (1986) 630; E. Heilbronner, Z.-Z. Yang, *ibid. 99* (1987) 369 and *26* (1987) 360; J. D. Dunitz, C. Krüger, H. Irngartinger, E. F. Maverick, Y. Wang, M. Nixdorf, *ibid. 100* (1988) 415 and *27* (1988) 387.
[3] A. Toyota, *Bull. Chem. Soc. Jpn. 48* (1975) 1152.
[4] K. Hafner, G. F. Thiele, *Tetrahedron Lett. 26* (1985) 2567.
[5] All the compounds gave correct elemental analyses.
[6] R. Y. Levina, N. N. Mezentsova, O. V. Lebeda, *Zh. Obshch. Khim. 29* (1955) 1079; B. F. Hallam, P. L. Pauson, *J. Chem. Soc. 1958*, 646; K. Alder, H.-J. Ache, F. H. Flock, *Chem. Ber. 93* (1960) 1888; C. F. Wilcox, Jr., R. R. Craig, *J. Am. Chem. Soc. 83* (1961) 3866; H. L. Lentzner, W. E. Watts, *Tetrahedron 27* (1971) 4343.
[7] T. Kauffmann, J. Ennen, H. Lhotak, A. Rensing, F. Steinseifer, A. Woltermann, *Angew. Chem. 92* (1980) 321; *Angew. Chem. Int. Ed. Engl. 19* (1980) 328.
[8] The unsubstituted 1,2-dicyclopentadienylethane can also be obtained from sodium cyclopentadienide using this method (colorless crystals, m.p. 10°C, yield 41%).
[9] H. Sauter, H. Prinzbach, *Angew. Chem. 84* (1972) 297; *Angew. Chem. Int. Ed. Engl. 11* (1972) 296; H. Sauter, B. Gallenkamp, H. Prinzbach, *Chem. Ber. 110* (1977) 1382.
[10] Crystal data for **10**: triclinic, $P\bar{1}$, $Z = 1$, $a = 955.2(4)$, $b = 866.4(4)$, $c = 621.2(3)$ pm, $\alpha = 105.39(1)°$, $\beta = 95.82(1)°$, $\gamma = 115.21(1)°$. $Mo_{K\alpha}$ radiation, 1991 independent reflections, 1741 observed ($I > 2\sigma(I)$), 141 parameters refined, $R = 0.062$, $R_w = 0.053$. Further details of the crystal structure investigation are available on request from the Fachinformationszentrum Energie, Physik, Mathematik GmbH, D-7514 Eggenstein-Leopoldshafen 2 (FRG) on quoting the depository number CSD-53 098, the names of the authors, and the journal citation. We thank Prof. Dr. *H. J. Lindner* and Dr. *H. Paulus* for the X-ray structure analysis.
[11] K.-P. Zeller in *Houben-Weyl-Müller: Methoden der organischen Chemie, Vol. 5/2c*, Thieme, Stuttgart 1985, p. 127, and references cited therein.
[12] T. Sugimoto, M. Shibata, S. Yoneda, Z. Yoshida, Y. Kai, K. Miki, N. Kasai, T. Kobayashi, *J. Am. Chem. Soc. 108* (1986) 7032; M. Oda, *Pure Appl. Chem. 58* (1986) 7.

Centrohexaindan, The First Hydrocarbon with Topologically Non-Planar Molecular Structure**

By *Dietmar Kuck** and *Andreas Schuster*

Herein we report on the synthesis of centrohexaindan **1** (hexabenzohexacyclo[5.5.2.2^{4,10}.1^{1,7}.0^{4,17}.0^{10,17}]heptadecane) and some properties of this unique hydrocarbon.

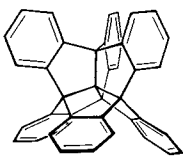

1

Like dodecahedrane **2**[1,2] among the *spherically* annelated polyquinanes, the "C_{17}-hexaquinane"[3] **3** is the most fascinating member of the *centrally* annelated so-called centropolyquinanes.[4] In contrast to **1**, however, centrohexacyclic hydrocarbons like the centrohexaquinane **3** and the corresponding hexaene **4** have not yet been synthesized, even though they are of considerable interest regarding their special ring coupling.[4–7]

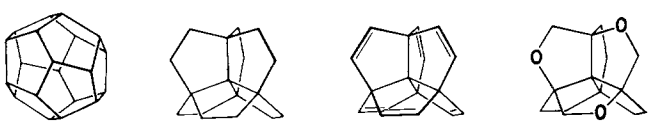

2 **3** **4** **5**

[*] Dr. D. Kuck, Dipl.-Chem. A. Schuster
Fakultät für Chemie der Universität
Universitätsstrasse 25, D-4800 Bielefeld 1 (FRG)

[**] Benzoannelated Centropolyquinanes, Part 5.—Part 4, see [13b].

The only centrohexacyclic compound known so far is the triether **5**, which was synthesized simultaneously by *Simmons* et al.[8] and *Paquette* et al.[9] Attempts to prepare **3** via a route similar to that used for the synthesis of **5** have thus far failed.[8,9] As the hexabenzo derivative of **4**, compound **1** is the first hydrocarbon with centrohexacyclic molecular structure.

The fascination of the centrohexaquinane structure of **1** lies in the annelation of six cyclopentane rings around a central C atom common to all rings.[4] The central neopentane skeleton is bridged by six *o*-phenylene groups corresponding to the six edges of a regular tetrahedron, such that the central, quaternary C atom is surrounded by four further, equivalent quaternary sp^3-C atoms[10] and therefore should exhibit ideal tetrahedral coordination.[11] Furthermore, in the ground state **1** should have prefect T_d symmetry, in analogy to the hexaene **4** calculated by *Ermer*.[6]

Centrohexaindan **1** combines a number of known lower benzoannelated centropolyquinane moieties (centropolyindans). Thus, in **1**, three 2,2'-spirobiindans are fused along the three space axes to give a three-dimensional cross, tribenzotriquinacene[12] and triptindan[13] (*sym*-tribenzo-[3.3.3]propellane) are condensed with each other fourfold degenerate, and, finally, **1** contains three fenestranes (tetrabenzo[5.5.5.5]fenestranes, "fenestrindans") **6**.[14] It is thus the first fenestrane substituted with carbon on all four bridgeheads.[15]

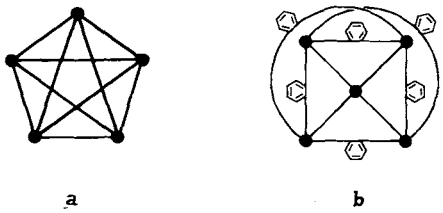

a b

Fig. 1. a) The graph K_5. b) A graph-theory representation of **1**.

The molecular structure of **1** is also of special interest from the point of view of the graph theory.[6] Like the triether **5**, compound **1** is a topologically non-planar molecule. The complete mutual coupling of the five neopentane C atoms (vertices) via the central C–C bonds and the peripheral *o*-phenylene bridges corresponds to the *complete graphs* K_5 (Fig. 1a), whose connecting lines cannot be projected into the plane without mutual intersection (Fig. 1b).

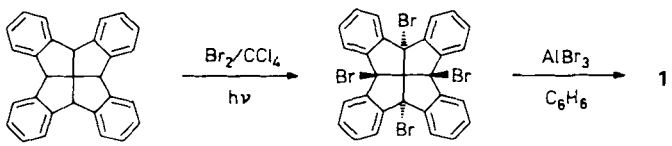

6 7

The synthesis of **1**, based on the recently reported fenestrindan **6**, which is accessible in gram amounts in nine steps from 1,3-indandione and dibenzylideneacetone,[14] is astonishingly easy. **6** can be readily functionalized with bromine at all four bridgeheads to give the tetrabromofenestrindan **7**.[16] This is most surprising, since a high torsional strain should be generated by the pairwise *syn*-oriented bromine atoms on the bridgeheads. In actual fact the double 1,3-interaction in **7** leads to a conformation with S_4 symmetry which is static on the NMR time scale (Scheme 1). Therefore, different to the case of **6**,[14] no AA'BB' system is observed in the 300-MHz ^{1}H-NMR spectrum for the four aromatic rings, but instead an ABCX system, whereby an *ortho*-proton is in each case strongly deshielded by the neighboring benzene ring.[17]

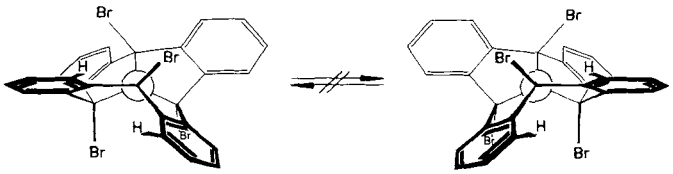

Scheme 1. Conformers of **7**.

When **7** is heated together with four equivalents of $AlBr_3$ in benzene, fourfold C–C coupling takes place with formation of the centrohexaindan **1** in 50% overall yield! During the reaction, salt-like intermediates are formed whose structural elucidation should provide interesting details about the hitherto unknown fenestrane ions with carbenium centers at the bridgeheads.

Table 1. Spectroscopic data of centrohexaindan **1**.

MS (EI, 70 eV): $m/z = 516$ ($M^{\oplus\ominus}$, 100%), 515 (12), 439 (3), 258 ($M^{2\oplus}$, 4)

IR (KBr): $\tilde{\nu} = 3070$ (m), 3020 (m), 1470 (s), 755, 751 (s), 700 cm^{-1} (m)

^{1}H-NMR (300 MHz, $CDCl_3$): $\delta = 7.27$, 7.79 (AA'BB')

^{13}C-NMR (75.8 MHz, CD_2Cl_2): $\delta = 73.5$ (s, C^{α}), 95.4 (s, C^{centro}), 124.5 (d, C^{ortho}), 129.1 (d, C^{meta}), 148.6 (C^{ipso})

UV (*n*-heptane, $c = 4 \cdot 10^{-5}$ mol·L^{-1}): $\lambda_{max}(\varepsilon) = 276.5$ (5800), 269 (4950), 263 (3000), 257 nm (s)

The spectroscopic data of **1** are unequivocal (Table 1). Although the solubility is quite high for a compound of this molecular size ($C_{41}H_{24}$) and highly symmetrical structure compared to the lower centropolyindans,[12–14] the melting point lies well above the usual limit (420 °C). As expected the mass spectrum shows no mentionable fragmentation of the molecular skeleton. The degeneracy of all six indan units of **1** manifests itself in the NMR spectra: The ^{1}H-NMR spectrum consists of only one AA'BB' system for all twelve *ortho* and *meta* H atoms; the ^{13}C-NMR spectrum shows only five signals for the total 41 C atoms. As expected, the UV spectrum of **1** resembles those of benzoannelated centrotriquinanes and centrotetraquinanes[12–14] and gives no indication of distinct electronic interactions between the six aromatic π systems.

Experimental

7: 8.0 mL of a 1 M solution of Br_2 in CCl_4 was added dropwise to a stirred suspension of 736 mg (2.0 mmol) of **6** in 50 mL of anhydrous CCl_4. After addition of 4.0 mL of the Br_2/CCl_4 solution a homogeneous solution formed, from which, on further addition of Br_2/CCl_4, the tetrabromide **7** precipitated. For completion of the reaction, the mixture was irradiated for ca. 20 min with a photolamp (500 W). After removal of the solvent by evaporation and subsequent recrystallization of the lemon-yellow residue from toluene, 865 mg of **7** (63%) were obtained in the form of colorless needles (m.p. 341 °C).

1: A solution of **7** (500 mg, 0.73 mmol) in warm anhydrous benzene (100 mL) was treated dropwise at 40 °C within 2 h with 10.0 mL of a 0.10 M solution of $AlBr_3$ in benzene. An orange-red complex first separated out, and then redissolved on completion of the addition of $AlBr_3$. The mixture was then heated under gentle reflux for 40 h. After hydrolytic work-up and recrystallization of the light-yellow crude product from 20 mL of xylene, 300 mg of **1** (80%) were obtained in the form of colorless needles.

Received: May 5, 1988 [Z 2742 IE]
German version: *Angew. Chem.* *100* (1988) 1222

[1] a) R. J. Ternansky, D. W. Balogh, L. A. Paquette, *J. Am. Chem. Soc. 104* (1982) 4503; b) L. A. Paquette, R. J. Ternansky, D. W. Balogh, G. Kentgen, *ibid. 105* (1983) 5446.
[2] a) W.-D. Fessner, Bulusu A. R. C. Murty, H. Prinzbach, *Angew. Chem. 99* (1987) 482; *Angew. Chem. Int. Ed. Engl. 26* (1987) 451; b) W.-D. Fessner, Bulusu A. R. C. Murty, J. Wörth, D. Hunkler, H. Fritz, H. Prinzbach, W. D. Roth, P. von R. Schleyer, A. B. McEwen, W. F. Maier, *ibid. 99* (1987) 484 and *26* (1987) 452, resp.
[3] L. A. Paquette, R. A. Snow, J. L. Muthard, T. Cynkowski, *J. Am. Chem. Soc. 100* (1978) 1600.
[4] P. Gund, T. M. Gund, *J. Am. Chem. Soc. 103* (1981) 4458.
[5] O. Ermer: *Aspekte von Kraftfeldrechnungen*, Wolfgang-Baur-Verlag, München 1981, Chap. 4.6.3.
[6] a) F. Harary in A. T. Balaban (Ed.): *Chemical Applications of Graph Theory*, Academic Press, London 1976, Chap. 2; b) A. T. Balaban, *ibid.*, Chap. 3; c) J. Simon in R. B. King, D. H. Rouvray (Eds.): *Graph Theory and Topology in Chemistry*, Elsevier, Amsterdam 1987, p. 43.
[7] W. Luef, R. Keese, *Helv. Chim. Acta 70* (1987) 543.
[8] a) H. E. Simmons III, J. E. Maggio, *Tetrahedron Lett. 22* (1981) 287; b) S. A. Benner, J. E. Maggio, H. E. Simmons III, *J. Am. Chem. Soc. 103* (1981) 1581.
[9] L. A. Paquette, M. Vazeux, *Tetrahedron Lett. 22* (1981) 291.
[10] For examples of the rare central coupling of five quaternary tetracoordinated but *non*-equivalent C atoms. See: a) L. F. Pelosi, W. T. Miller, *J. Am. Chem. Soc. 98* (1976) 4311; b) G. Maier, S. Pfriem, *Angew. Chem. 90* (1978) 552; *Angew. Chem. Int. Ed. Engl. 17* (1978) 520; c) J. E. Maggio, H. E. Simmons III, J. K. Kouba, *J. Am. Chem. Soc. 103* (1981) 1579.
[11] For a discussion of ideal tetrahedral coordination in hydrocarbons see: a) A. Greenberg, J. F. Liebman: *Strained Organic Molecules*, Academic Press, New York 1978, Chap. 6; b) [7].
[12] a) D. Kuck, *Angew. Chem. 96* (1984) 515; *Angew. Chem. Int. Ed. Engl. 23* (1984) 508.
[13] a) D. Kuck, B. Paisdor, H.-F. Grützmacher, *Chem. Ber. 120* (1987) 589; b) B. Paisdor, H.-F. Grützmacher, D. Kuck, *ibid. 121* (1988) 1307.
[14] D. Kuck, H. Bögge, *J. Am. Chem. Soc. 108* (1986) 8107.
[15] a) B. R. Venepalli, W. C. Agosta, *Chem. Rev. 87* (1987) 399; b) K. Krohn, *Nachr. Chem. Tech. Lab. 35* (1987) 264.
[16] **1** and **7** gave satisfactory elemental analyses.
[17] ^{1}H-NMR (300 MHz, $CDCl_3$): δ=7.46 (m, 8H), 7.50 (m, 4H), 7.95 (d, 7.3 Hz, 4H). Even at 130°C (solvent $CDCl_2CDCl_2$) no coalescence is observed in the ^{1}H-NMR spectrum of **7**.

Enantio- and Diastereoselective Synthesis of Methyl (2*R*)-2-Amino-5-oxocarboxylates from Enones and Bislactim-Ether Cuprates**

By *Ulrich Schöllkopf,* Dagmar Pettig, Edda Schulze, Michael Klinge, Ernst Egert,* Bernd Benecke*, and *Mathias Noltemeyer*

Dedicated to Professor Heinrich Nöth on the occasion of his 60th birthday

Lithiated bislactim ethers **2** react with enones to give 1,2- and 1,4-adducts.[1] In our studies on the asymmetric synthesis of non-proteinogenic amino acids according to the bislactim-ether method[2] we were interested in finding an entry to 1,4-adducts of the type **5**; we therefore decided to check whether and how the lithium compounds **2** are convertible into cuprates of bislactim ethers. Numerous alkyl and alkenyl cuprates have already been described,[3] whereas very few azaenolate-cuprates have been reported.[4] Heterocyclic azaenolate-cuprates are as yet unknown. After a number of abortive attempts with such Cu^I salts, which have already proven useful for the preparation of alkyl and alkenyl cuprates,[3] we found that the bislactim-ether cuprates **3** can be obtained by reaction of **2** with $CuBr \cdot S(CH_3)_2$ in the presence of dimethyl sulfide.

The cuprate **3a** reacts highly selectively with 2-enones **4** to give 1,4-adducts; the diastereofacial selectivity at the heterocycle is extremely high (>100:1; Table 1), i.e. one obtains almost exclusively the (2*R*,5*S*) epimers of the adducts, the precursors of the corresponding D-α-amino-δ-oxocarboxylic acids (type **14**).

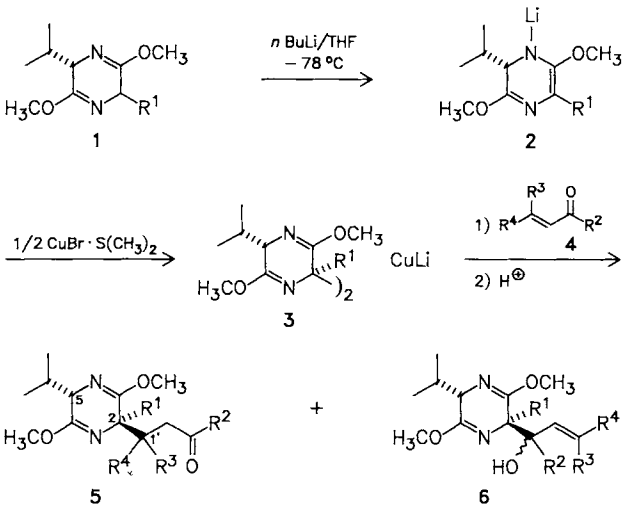

1–**3**: a, R^1 = H; b, R^1 = CH_3
5, **6**: R^1 = H

Table 1. Yields and configurations of the Michael adducts **5**, R^1 = H.

5	R^2	R^3	R^4	Yield [%]	(2*R*,1'*R*) : (2*R*,1'*S*) [a] [b]	5 : 6
a	$-(CH_2)_2-$		H	71	100 : 2	100 : ≤1
b	$-(CH_2)_3-$		H	71	100 : 6	100 : 3
c	$-(CH_2)_4-$		H	66	100 : 12	100 : ≤1
d	$-(CH_2)_2-$		CH_3	52	100 : 100	100 : 19
e	CH_3	H	Ph	62	83 : 100	100 : 6
f	CH_3	H	2-Furyl	60	100 : 64	100 : 22
g	CH_3	H	H	39	— [c] — [c]	100 : 5

[a] Determined by capillary chromatography and ^{13}C-NMR spectroscopy. [b] (2*S*)-epimers ≤1. [c] (2*R*) : (2*S*) > 100 : 1.

Simple cyclic enones such as cyclopentenone and cyclohexenone (**4a** and **4b**, resp.) react also with high enantiofacial selectivity at the double bond. Of four possible diastereomers, almost only the (2*R*,5*S*,1'*R*)-isomers **5a** and **5b** are formed, i.e. two stereocenters are created highly selectively at the same time. The (2*R*,1'*R*) configuration of **5b** was confirmed by an X-ray structure analysis. Cyclic enones with a substituent in the 3-position (e.g. **4d**) react with lesser enantiofacial selectivity. The same holds true for conformationally flexible acyclic enones with substituents in the 3-position (e.g. **4e** and **4f**).[5]

Reaction of **3a** with (−)-(*R*)-carvone **4h** leads because of favorable double stereoselection (matched case) and because of highly selective protonation at C-2', almost exclusively to (2*R*,1'*R*,2'*R*)-**5h**. The diastereomeric ratio is ca. 100:3:2:1. The structure of **5h** was confirmed by an X-ray analysis. With (+)-(*S*)-carvone (mismatched case) the diastereomers are formed in the ratio 10:5:1.5:1.5.

[*] Prof. Dr. U. Schöllkopf, Dr. D. Pettig, E. Schulze, M. Klinge
Institut für Organische Chemie der Universität
Tammannstr. 2, D-3400 Göttingen (FRG)
Dr. E. Egert, B. Benecke, M. Noltemeyer
Institut für Anorganische Chemie der Universität
Tammannstr. 4, D-3400 Göttingen (FRG)

[**] Asymmetric Synthesis via Heterocyclic Intermediates, Part 41.—Part 40: K. Schöllkopf, K.-O. Westphalen, J. Schröder, K. Horn, *Liebigs Ann. Chem. 1988*, 781.

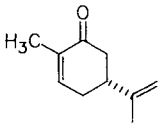

4 h

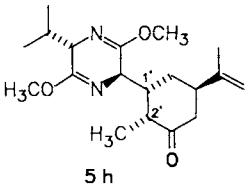

5 h

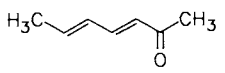

7

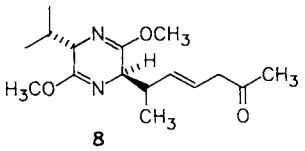

8

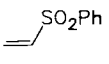

9

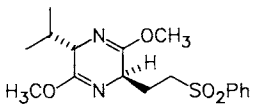

10

Since the carbonyl group is a particularly useful functional group, the compounds of type **5** (or **14**, cf. below) open up an entry to numerous non-proteinogenic amino acids that are stereoisomerically pure in the α- and partly also in the β-position (e.g. **14a** and **14b**). The cuprate **3a** reacts with the dienone **7** to give the 1,6-adduct **8** (together with ca. 10% 1,2-adduct), and again with high diastereoselectivity; only two diastereomers in the ratio 10:1 are detectable ^{13}C-NMR spectroscopically. Both have the (2*R*)-configuration, whereas the 1′-configuration is still unclear. Phenyl vinyl sulfone **9** also reacts with a high degree of diastereospecificity with **3a** (*de* > 98%) to give the "Michael adduct" **10**. Reaction of the lithium compound **2a** with **9**, on the other hand, furnishes only polymeric products.

As expected cuprates of type **3** can also be alkylated. Thus, reaction of **3a** and **3b** with ethyl 3-bromopropionate **11a** affords the alkylated products (2*R*,5*S*)-**12a** and **13a**, which are precursors of the corresponding (*R*)-glutamic acid derivatives, in satisfactory yields and with a remarkably high *de* value of ca. 98%. The lithium compounds **2a** and **2b** react with the bromopropionate **11a**,[7] not only with alkylation but also with elimination. 3-Bromopropionitrile **11b** reacts analogously with **3a** and **3b** to give **12b** and **13b** (*de* ca. 98%). Reaction of the lithium compound **2a** with acetonitrile leads to polymerization. The cuprates **3** are thus preferred over the lithium compounds **2** in the alkylation of the bislactim ethers if the alkylating agent is base-labile or if very high *de* values are aimed for.

12, R = H; **13**, R = CH_3

11, **12**, **13**: **a**, X = $CO_2CH_2CH_3$; **b**, X = CN

The hydrolysis of the adducts **5a** and **5b** (two equivalents of 0.25 N HCl, room temperature, 20 h) affords (besides L-Val-OMe) the diastereomerically and enantiomerically pure (2*R*,3*R*)-amino acid methyl esters **14**. These are thermolabile and therefore cannot be separated from the L-valine methyl ester by distillation. The separation can, however, be accomplished readily by chromatography at the stage of the *N*-Boc derivatives **15a**, **b**. In contrast, the hydrolysis of (2*R*,1′*S*)-**5f** leads as expected to the methyl (2*R*,3*S*)-3-(2′-furyl)-3,4-dihydro-5-methyl-pyrrolecarboxylate **16**, whose C=N bond is so regiostable that it can be purified by distillation.

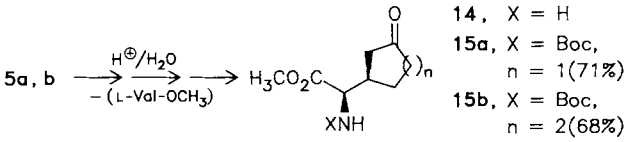

14, X = H
15a, X = Boc, n = 1 (71%)
15b, X = Boc, n = 2 (68%)

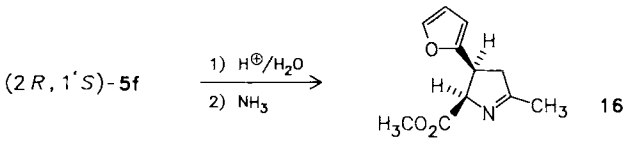

16

Experimental

5 (**8**, **10**): **1a** (1.00 g, 5.45 mmol) [8] was metalated with *n*-butyllithium in THF (10 mL) at −78 °C. The solution of **2a** was then added dropwise through a Teflon tube to a solution of CuBr·$S(CH_3)_2$ [9] (0.56 g, 2.73 mmol) and $S(CH_3)_2$ (5 mL) in THF (10 mL). After 0.5 h at −30 °C the mixture was treated with a solution of **4** (or 7, **9**) (5.45 mmol) in THF (5 mL) at −70 °C and stirred for 4–16 h at this temperature. After subsequent addition of glacial acetic acid (0.33 g, 5.45 mmol) the mixture was allowed to warm to room temperature, transferred to a column of Silica gel 60 (20 g; 0.05–0.2 mm, 70–270 mesh ASTM; 200 × 60 mm^2) and eluted with ca. 500 mL of ether. After removal of solvent the residue was distilled (Kugelrohr) or chromatographed. — **5a**: b.p. 110 °C/0.05 torr, m.p. 60–61 °C; **5b**: b.p. 150 °C/0.05 torr, m.p. 95–97 °C; **5c**: b.p. 115 °C/0.05 torr, m.p. 71–72 °C; **5d**: b.p. 110 °C/0.05 torr, R_f = 0.16, ether/pentane (1:3); **5e**: (2*R*,1′*R*)-**5e**: R_f = 0.20, (2*R*,1′*S*)-**5e**: R_f = 0.14, ethyl acetate/pentane (1:6); **5f**: (2*R*,1′*R*)-**5f**: R_f = 0.07, (2*R*,1′*S*)-**5f**: R_f = 0.04, ether/pentane (1:6); **5g**: b.p. 120 °C/0.01 torr; **5h**: b.p. 120 °C/0.05 torr, m.p. 76–77 °C; **8**: R_f = 0.05, ether/pentane (1:8); **10**: R_f = 0.15, ether/pentane (1:3).

N-Boc amino acid esters **15**: A mixture of **5a** or **5b** (3.0 mmol) and 0.25 N HCl (24 mL, 6.0 mmol) was vigorously stirred for 20 h. After removal of solvent under vacuum, the residue (hydrochlorides of the amino acid esters) was treated with $CHCl_3$ (20 mL), NaCl (1.8 h) and Boc-anhydride (1.53 g, 7.0 mmol) and then with 8 mL of a saturated $NaCO_3$ solution. The mixture was heated under reflux for 3 h, the phases separated, and the aqueous phase extracted with 2 × 20 mL of ether, dried over $MgSO_4$ and the solvent removed under vacuum. The residue was chromatographed on ca. 70 g of silica gel (Silica gel 60, 500 × 15 mm^2 column, ether/pentane (1:1). — **15a**: R_f = 0.13, m.p. 104–105 °C; **15b**: R_f = 0.18, m.p. 85–86 °C.

Correct C,H analyses were obtained for all compounds.

Received: April 20, 1988 [Z 2712 IE]
German version: *Angew. Chem. 100* (1988) 1238

[1] D. Pettig, *Diplomarbeit*, Universität Göttingen 1984.
[2] U. Schöllkopf, *Pure Appl. Chem. 55* (1983) 1799; *Chem. Scr. 25* (1985) 105; U. Schöllkopf in J. Streith, H. Prinzbach, G. Schill (Eds.): *Organic Synthesis: An Interdisciplinary Challenge*, Blackwell, Oxford 1985, p. 101.
[3] G. H. Posner, *Org. React. N. Y. 19* (1972) 1; *ibid. 22* (1975) 253; J. F. Normant, *Synthesis 1973*, 63; H. O. House, W. L. Respess, G. M. Whitesides, *J. Org. Chem. 31* (1966) 3128; *Gmelin: Handbook of Inorganic Chemistry, Cu, Organocopper Compounds, Part 2*, Springer, Berlin 1983.
[4] a) E. J. Corey, D. Enders, *Tetrahedron Lett. 1976*, 11; b) *Chem. Ber. 111* (1978) 1362; c) K. Yamamoto, M. Iijima, Y. Ogimura, *Tetrahedron Lett. 23* (1982) 3711; d) K. Yamamoto, M. Kanoh, N. Yamamoto, J. Tsuji, *ibid. 28* (1987) 6347.
[5] We attribute the high enantiofacial selectivity in the case of **4a** and **4b** to the rigid "transoid" enone arrangement. The situation is analogous to the Michael addition to acrylic acid esters [6]. In the case of "transoid" fixed 5,6-dihydropyran-2-one the enantiofacial selectivity at the double bond is > 90%; in the case of the open-chain, flexible crotonic acid methyl esters, however, it is only ca. 50%.
[6] U. Schöllkopf, D. Pettig, *Synthesis 1986*, 737.
[7] For the alkylation of **2b** see: U. Schöllkopf, K.-O. Westphalen, U. Groth, Chuanzheng Deng, *Synthesis 1981*, 969; U. Schöllkopf, U. Busse, R. Lonsky, R. Hinrichs, *Liebigs Ann. Chem. 1986*, 2150.
[8] U. Schöllkopf, U. Groth, C. Deng, *Angew. Chem. 93* (1981) 791; *Angew. Chem. Int. Ed. Engl. 20* (1981) 798; **1a** and **1b** and *ent*-**1a** and *ent*-**1b** are commercially available from Merck-Schuchardt.
[9] CuBr·$S(CH_3)_2$ is recrystallized: G. H. Posner: *An Introduction to Synthesis Using Organocopper Reagents*, Wiley, New York 1980.

Selective INADEQUATE, a Farewell to 2D-NMR?**

By *Stefan Berger**

The INADEQUATE pulse sequence,[1] especially the two-dimensional (2D) variant,[2] is one of the most important ^{13}C-NMR methods for determining the structure of organic substances.[3] When all other modern NMR methods are of no further help, decisively important information can often be obtained with 2D-INADEQUATE. Prerequisite is a sufficient concentration of ^{13}C-disubstituted molecules, since typically 128 ^{13}C-NMR spectra must be recorded for a complete data matrix. The digital resolution in ω_2 is limited in the case of 2D-methods and makes the evaluation of C,C coupling constants over more than one bond from 2D-INADEQUATE NMR spectra[4,5] difficult.

There has been no lack of attempts in recent years to make INADEQUATE more sensitive,[6-8] but none of the improvements put forward so far can be considered as of general utility. *Kessler*[9] and *Freeman*[10] have recently indicated how 2D-methods by *frequency-selective excitation* can be reduced to the recording of a few 1D-NMR spectra. Some 2D-INADEQUATE experiments of limited application have also been reported.[11-13] In continuation of our INADEQUATE studies[4,5,14,15] we present here a generally applicable frequency-selective version of INADEQUATE which makes 2D-recordings superfluous.

Figure 1 shows the pulse sequence "SELINQUATE" in which the fourth pulse of the standard INADEQUATE sequence is replaced by a frequency-selective pulse. It is therefore not a frequency-selective excitation, but a frequency-selective transfer of coherence. Only double quantum coherence of those carbon nuclei is transferred into observable magnetization for which the frequency of the frequency-selective pulse is adjusted. We have also found that the bandwidth of the frequency-selective pulse must correspond to the C,C-coupling constant. All pulse phases remain the same as described for the original experiment,[3] but the phase of the frequency-selective pulse must be correctly adjusted in relation to the phases of the non-selective pulses as well as to the receiver phase. All known variants of the 1D-INADEQUATE experiment can also be applied to the pulse sequence in Figure 1.

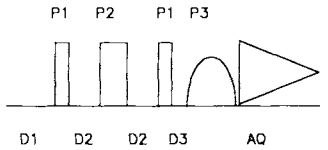

Fig. 1. Pulse sequence for SELINQUATE. D1 relaxation delay, D2 focussing delay $1/4J_{C,C}$, D3 transfer delay, P1, P2 non-selective pulses 90° and 180°, AQ acquisition time. Exact recording conditions, see [16].

The result of the pulse sequence of Figure 1 is shown in Figure 2, for the sake of simplicity in the case of *n*-propanol as example:[16] Trace (a) shows the normal ^{13}C-NMR spectrum. In traces (b-d) the frequency-selective pulse was in each case adjusted to C-3, C-2 and C-1; accordingly, in (b) only the doublet of C-2 which couples with C-3 (36.1 Hz) is observable, in (c) the doublets of C-1 and C-3 which couple with C-2 (36.1 and 34.2 Hz), and in (d) the doublet of C-2 which couples with C-1 (34.2 Hz).

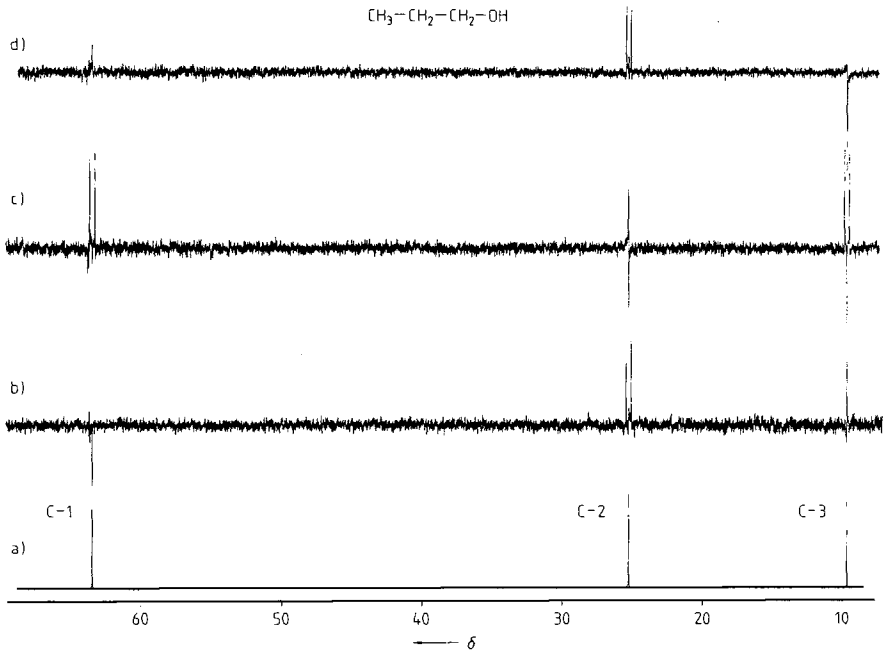

Fig. 2. ^{13}C-NMR spectra of *n*-propanol. (a) Standard ^{13}C-NMR spectrum, (b-d), Recording after pulse sequence in Fig. 1, (b) P3 adjusted to signal of C-3, (c) P3 adjusted to signal of C-2, (d) P3 adjusted to signal of C-1.

In order to obtain complete information of the coupling of all C atoms in a molecule only the recording of the ^{13}C-NMR spectra of exactly the number of differentiable carbon atoms present is necessary; moreover, this can be done with high digital resolution, so that all coupling constants can be correctly measured. The determination of

[*] Priv.-Doz. Dr. S. Berger
Fachbereich Chemie der Universität Marburg
Hans-Meerwein-Strasse, D-3550 Marburg (FRG)

[**] This work was supported by the Fonds der Chemischen Industrie.

the structure of organic compounds is thus considerably simplified,[17] and all the more so in practice, since seldom are all C,C couplings needed but only must be proven for a few C atoms.

Received: April 5, 1988;
revised: May 30, 1988 [Z 2688 IE]
German version: *Angew. Chem. 100* (1988) 1198

CAS Registry number:
1, 71-23-8.

[1] A. Bax, R. Freeman, S. P. Kempsell, *J. Am. Chem. Soc. 102* (1980) 4849.
[2] A. Bax, R. Freeman, T. A. Frenkiel, M. H. Levitt, *J. Magn. Reson. 43* (1981) 478; T. H. Mareci, R. Freeman, *ibid. 48* (1982) 158.
[3] Review: J. Buddrus, H. Bauer, *Angew. Chem. 99* (1987) 642; *Angew. Chem. Int. Ed. Engl. 26* (1987) 625.
[4] S. Berger, *Org. Magn. Reson. 22* (1984) 47.
[5] S. Berger, K. P. Zeller, *J. Org. Chem. 49* (1984) 3725.
[6] O. W. Sorensen, R. Freeman, T. A. Frenkiel, T. H. Mareci, R. Schuck, *J. Magn. Reson. 46* (1982) 180.
[7] S. W. Sparks, P. D. Ellis, *J. Magn. Reson. 62* (1985) 1.
[8] P. J. Keller, K. E. Vogele, *J. Magn. Reson. 68* (1986) 389.
[9] H. Kessler, H. Oschkinat, C. Griesinger, W. Bermel, *J. Magn. Reson. 70* (1986) 106.
[10] S. Davies, J. Friedrich, R. Freeman, *J. Magn. Reson. 75* (1987) 540.
[11] J. Brondeau, C. Millot, D. Canet, *J. Magn. Reson. 57* (1984) 319.
[12] D. Canet, J. Brondeau, J. C. Boubel, A. Retournard, *Magn. Reson. Chem. 25* (1987) 798.
[13] P. J. Hore, E. R. P. Zuiderweg, K. Nicolay, K. Dijkstra, R. Kaptein, *J. Am. Chem. Soc. 104* (1982) 4286; P. J. Hore, R. M. Scheek, A. Volbeda, R. Kaptein, *J. Magn. Reson. 50* (1982) 328.
[14] S. Berger, *J. Chem. Soc. Chem. Commun. 1984*, 1252.
[15] S. Berger, *J. Magn. Reson. 66* (1986) 555.
[16] *Experimental:* 5-mm NMR tubes with 20% solution of *n*-propanol in $CDCl_3$, 303 K. Bruker AM400 NMR spectrometer with Aspect 3000 process computer and selective irradiation unit SEU. 90° pulse P1 6.3 μs, selective 90° pulse P3 20 ms, gauss shape. Traces b, c and d in each case 512 pulse sequences, spectral width 12000 Hz, 64 K data points, D2 = 7.5 ms, D3 = 3 μs, acquisition time AQ + relaxation delay D1 = 5 s.
[17] The principle presented here has in the meantime been extended to the inverse detection of C,H correlations: S. Berger, *J. Magn. Reson.*, in press.

BOOK REVIEWS

Organic Chemistry: The Name Game. Modern Coined Terms and Their Origins. By *A. Nickon* and *E. F. Silversmith*. Pergamon Press, Oxford 1987. xii, 347 pp., bound, £ 45.00.—ISBN 0-08-035157-3; paperback, £ 18.00.—ISBN 0-08-034481-X

Named reactions are a time honored and useful feature of chemical literature and communication; the custom of *name-dropping* is at least equally old, even though it usually fails to produce the intended effect. But a *name game*?—or, more exactly, "Organic Chemistry: The Name Game", to give the recently published monograph by *Alex Nickon* and *Ernest F. Silversmith* its full title. Can the serious and sober discipline of organic chemistry be a game with words? This, and much more besides, is the theme of "The Name Game". The book, generously illustrated with excellent structural formulas, reaction schemes and other diagrams, is in the first place a collection of modern trivial names and accounts of how they originated. Developed out of a student project aimed at discovering the origins of a wide variety of expressions, the authors have based the compendium not only on an intensive study of the literature, but also on innumerable personal contacts over a period of about ten years. To limit the size of the compilation, the naming of natural products, and commercial product and brand names, are dealt with only briefly; the result is not a comprehensive index of trivial names, but instead a real book, for both serious reading and browsing. And no matter where one dips into it, fascination quickly takes hold, and one becomes absorbed in reading. To appreciate this even more fully, imagine for a moment the effect if a work of a similar kind had instead been produced in an (admittedly more comprehensive) "electronic version"!

What, then, are the origins of the names given to the many organic compounds prepared for the first time during recent years, and to newly discovered reactions? Who or what agency first coined these names, what prompted this, and what are their etymologies? Answer: the names are as varied as are the people involved in chemistry, and they reflect the personal qualities and idiosyncracies of their creators: their sense of humor (or lack of it), their vanities, their education (or its shortcomings), their knowledge of the world, or their provincialism. Nevertheless, as the authors show in the 20 chapters and six appendices of the book, it is possible to recognize certain common features and families of words and names, which together illustrate the rather childlike pleasure that chemists take in naming the objects resulting from their work. There is an abundance of names of animals; articles of apparel—especially head coverings—provide inspiration; names that clearly have their origins in children's toys, and which grown-ups (?) now have, are widespread, some of the most popular being building bricks, water-wheels and airplanes. Foodstuffs play a role to some extent. Above all, containers of every kind have a great fascination—objects into which things can be put. In due course we leave the household behind, and travel through cities and across national frontiers, even as far as the stars. In short, nothing escapes being used to form names, and inexorably there comes into being at the molecular level a more and more fully equipped micro-universe.

Furthermore, "The Name Game" shows that the number of trivial names has grown alarmingly just in recent times (and consequently the book is also very useful as a dictionary, despite the limitation on size mentioned earlier). One possible cause for this is that the standard language, i.e. the IUPAC nomenclature rules, cannot keep pace with the complexity of the structures which have been analyzed and/or synthesized. Another factor is the notorious inadequacy of this nomenclature system for describing the dynamics of chemical reactions. New developments are essential here if we are to avoid becoming completely entangled in our own special jargon. It is conceivable, for example, that for "supermolecules" (cage structures of all kinds, layered molecules) a method of nomen-

clature related to that for peptides might be used, in which the building units would be represented only by initial letters (although, of course, the problems of "branching" and "crosslinking" in the primary structures of peptides are much simpler).

Thus it can be seen that what initially at times appeared to be a collection of curiosities, even including trivia (although, just as beauty is in the eye of the beholder, so presumably the music of a name is in the ear of the listener), has now raised important and far-reaching questions. For this reason the book is also a stimulating, and often thought-provoking, contribution to the study of the language of chemistry.

The authors too must have been well aware of this aspect of the book, since some of the appendices are only meaningful in that light. Once one begins to consider the words and their meanings, one progresses very quickly from the hundredth to the thousandth. What are the origins of the expressions familiar to us? Do these words—often derived from Latin or Greek—sound better to our ears (more "euphonic") than the modern names which have been coined, sometimes making the reader or listener flinch? (on the lines of, for example, betweenanene, buckminsterfullerene—or better still, buckyball—and what if barrelene had instead been named zimmerene!). The mechanisms of (modern) word construction are by no means new. It was already common to make up composite words (acetal = acetaldehyde + alcohol; carbazole = carb + az + ole); or as an extreme example, chloramphenicol—see the book for its derivation), to use abbreviations (phthalic acid is actually (na)phthal(en)ic acid), and to make transpositions (ninhydrin from hydrindene). On the other hand, the making up of acronyms, following the modern craze for abbreviations, has recently grown to such an extent that already one can almost begin to talk in terms of a third generation of nomenclature. However, Appendix A is a mine of information on explanations and derivations of standard expressions used in organic chemistry.

It would no more be possible to translate the whole of "The Name Game" into another language than to retain its rhyming title. This is firstly because the English language, with its great differences between the spoken and written forms, lends itself much more readily to plays on words than, for example, German, and secondly because of the authors' frequent clever and imaginative use of such devices. Some nice examples are the following: "The vitamin C story began with 'ignose' and 'godnose'. Where will it end? Who knows?"; or: "Through deals made by *Alder* ..."; or: "Atrane is not something we board at a railroad station". The text abounds with puns of this sort, which, like the anecdotes, are not only intended to cause a quick smile, but are also very instructive. It is certainly true that wit or fun often lead to a much quicker and better remembered understanding of a point than does a long-winded explanation. English-speaking authors—not only when preparing textbooks or papers, but also when giving after-dinner talks (from whence, incidentally, an appreciable number of the examples in "The Name Game" seem to have originated)—use this technique more often and adeptly than we German speakers. As a general principle, when the words of one language can no longer be translated into another, this is evidence of the vitality of both words and language. One is then forced to adopt the foreign words—or remain silent.

As every competitor knows, games are not games, but are deadly earnest. In the case of the present book, whose impact depends to a large extent on correct spelling of the words, this means that it must not contain any printing or other errors. And although the authors were naturally well aware of this, some errors have nevertheless escaped their notice: *Konrad Lorenz* (in the list of Nobel prizewinners in Appendix F) is not a Dutchman, it was *Unverdorben* who isolated aniline by distillation of indigo (not Herr *Underderben*, as given in Appendix A), in *Vögtle* the umlaut has been put over the wrong letter, and so on. These are mere trifles, but the absence of an index of names must be either the final joke of the book, or a bad joke.

From time to time a plea is made for making the chemical literature more "human"—it is said to be too dry and sterile, so that one can no longer recognize the real author behind the words. It cannot be said too strongly that any such move is to be avoided. In our writing most of us are far from being great stylists, let alone literary giants, and most of our work would not gain in value by having a "humanizing" introduction included. But if now and again other books as entertaining as the all too human "Name Game" were to appear, from which one could similarly learn a surprising amount about new developments in chemistry—that would really be fine.

Henning Hopf [NB 907 IE]
Institut für Organische Chemie
der Technischen Universität Braunschweig (FRG)

The Surface Scientist's Guide to Organometallic Chemistry. By *M. R. Albert* and *J. T. Yates, Jr.* American Chemical Society, Washington, DC (USA) 1987. xiii, 214 pp., bound, $ 59.95 ($ 49.95 in USA and Canada).—ISBN 0-8412-1003-9

Since the pioneering work of *Earl Muetterties*, organometallic chemistry has received increasing attention by surface chemists and surface physicists. It is therefore not surprising that the authors of this little book have dedicated it to the memory of *Muetterties*. He showed convincingly that the structures and chemical properties of chemisorption systems can be discussed in terms of the analogous interactions between transition metal centers and their ligands.

The book by *Albert* and *Yates* clearly emphasizes the importance of organometallic chemistry for the chemistry and physics of surfaces, and addresses mainly surface chemists and surface physicists. An introduction (Chapter 1), is followed in Chapter 2 (Basic Coordination Chemistry) by a concise qualitative summary of theories of chemical bonding in coordination compounds. Chapter 3 (Overview of Coordination Ligands) is the longest chapter of the book, and occupies a central position. It begins with a description of the main methods available for preparing surface complexes and ligands on well-characterized metallic surfaces in ultra-high vacuum. This is followed by a detailed discussion of the bonding situations and reactivities for 13 different classes of ligands: lone-pair donors, diatomic ligands, substituted diatomic ligands, systems with cumulenes, heteroolefins, triatomic pseudohalogens, organic chelates, nonmetal oxyanions, aromatics, heterocycles, electron deficient ligands, molecular fragments and, lastly, atomic species. The discussion points out qualitative analogies between molecular compounds and chemisorption systems, with regard to their geometric and electronic structures and their reactivity (with particular reference to catalytic reactions). In cases where there are no comparative data for ligands and surfaces, the authors draw attention to these gaps in knowledge, as potential research top-

ics of interest to surface scientists. The chapter concludes with the comment "... that most any program of surface science research could benefit greatly by using organometallic chemistry as a reference point from which to gain understanding into the more likely results that may be expected in a given surface system and to gain insight into the results that are unique to surfaces."

Chapter 4 (Bonding Sites in Clusters and their Relationship to Surface Bonding Sites) examines to what extent the description of ligand-metal bonding in complexes and clusters, in terms of orbital symmetry and orbital overlap, can be applied to chemisorption bonding. The authors emphasize the importance of relating such models to band structure calculations.

This aspect is developed in greater detail in the concluding Chapter 5 (Application of Orbital Symmetry and Orbital Overlap to Surface Band Structure Calculations), which discusses particularly the work of *Roald Hoffman* and coworkers on the application of symmetry considerations to surface bonding, taking as examples the CO/Ni(100) and H_2/Ni(111) systems. In these studies good qualitative agreement was found between calculations on metal complexes and those on simple adsorption systems.

The book contains over 400 literature references, mainly of fairly recent publications, up to and including 1985. To help overcome the well-known language problems which arise between organometallic chemists and surface scientists, an excellent glossary is included giving expressions used by specialists in both fields. The comprehensive subject index is very useful, and the book is attractively produced and almost free of printing errors.

The book, which is the only one of its kind on this topic, is fascinating to read, and it is warmly recommended to coordination chemists as well as to surface and catalysis scientists. These latter two groups will find here a wealth of stimulating ideas. For newcomers to the field, whether their interests are experimental or theoretical, the book offers an excellent start in the field of surface chemistry and physics. Certainly one wishes the authors success with this book, which will appeal to a wide readership. It should be available in all specialist libraries, and surface scientists should have it to hand at all times.

Helmut Knözinger [NB 865 IE]
Institut für Physikalische Chemie
der Universität München (FRG)

The Chemistry of the Cyclopropyl Group. Edited by *S. Patai* and *Z. Rappoport*. Wiley, Chichester 1987. Part 1: xii, p. 1–808, bound, £ 135.00.—ISBN 0-471-90658-1; Part 2: xii, p. 809–1739, bound, £ 135.00.—ISBN 0-471-91737-0. (Two-volume set £ 250.00.—ISBN 0-471-91738-9.)

Apart from the substantial article by *D. Wendisch* (Houben-Weyl-Müller, Volume IV/3), published in 1971, the chemistry of cyclopropane and its derivatives has scarcely been described in reviews; it is treated mainly in fragmented form in chapters and books of different emphasis, and under titles that do not explicitly refer to cyclopropane. It is therefore very pleasing that *S. Patai* has added to his successful series with two volumes in collaboration with *Z. Rappoport* that are devoted entirely to the ring of three carbon atoms.

As usual, the various topics are dealt with by different authors in independent chapters. The editors' plea to the authors was that they should not compile encyclopedias, but should place the most important developments in the foreground and not repeat in detail material that had already been reviewed. This is a demand which, of course, requires a knowledge of *all* the material, in order to make a *representative* choice, and not all the authors have succeeded in this as well as could be wished. In general, the literature is reviewed up to and including 1984; in some chapters work up to the end of 1985 is taken into account.

In the first chapter, *K. B. Wiberg* gives a brief, but extremely succinct survey of structures, energies and spectra of cyclopropanes. In the next chapter *W. Runge* deals with the chirooptical properties of cyclopropane derivatives, and presents, along with other ideas, his triad theory of optical rotations. NMR and IR spectra of cyclopropanes and cyclopropenes are covered by *D. G. Morris*. Rather than confining himself to a summary of experimental results in the area of NMR chemical shifts, he struggles with the speculations on the meaning of the data by the authors concerned, without achieving lucidity. It would have been more helpful to have indicated (as in the first chapter) that chemical shifts are only very superficially understood, but that thanks to recent work by *W. Kutzelnigg* and *M. Schindler* they can now be calculated rather precisely. On pp. 105, 118, and 153, one finds molecules that can only exist in the world of *M. C. Escher*.

Chapters 4–14 are on the following topics: the chemistry of ionized cyclopropanes in the gas phase *(H. Schwarz)*, photoelectron spectroscopy *(R. E. Ballard)*, acidity and basicity of cyclopropanes *(M. A. Battiste, J. M. Coxon)*, preparation of cyclopropyl derivatives *(T. Tsuji, S. Nishida)*, organic synthesis via cyclopropanes: principles and applications *(H.-U. Reissig)*, synthesis and reactivity of electrophilic cyclopropanes *(R. Verhé, N. De Kimpe)*, conjugative and substituent properties of the cyclopropyl group *(T. T. Tidwell)*, solvolysis of cyclopropyl-substituted derivatives *(E. C. Friedrich)*, cyclopropyl radicals, anion radicals, and anions *(G. Boche, H. M. Walborsky)*, rearrangements involving the cyclopropyl group *(J. Salaün)*, and radiation chemistry and hot atom chemistry of cyclopropane and its derivatives *(Z. B. Alfassi)*.

In Chapter 15 (electrochemistry of the cyclopropyl group, *J. Y. Becker*), the work of *S. Hünig*, which was required in connection with formulas 14, 15 (p. 926) and 82 (p. 955), is absent. Chapter 16, on the biochemistry of the cyclopropyl group *(H.-W. Liu, C. T. Walsh)*, is extraordinarily interesting, and shows the importance of the chemistry of three membered carbocycles, easily labeled "exotic", for the understanding of many reactions in living systems. *B. K. Carpenter* describes the preparation and uses of isotopically labeled derivatives; *J. F. Liebman* and *A. Greenberg* treat cyclopropanes having extra strain.

Unfortunately, Chapter 19 (bicyclo[1.1.0]butanes, *S. Hoz*) falls below the expected standard. The author stresses in the introduction that the last comprehensive article on this subject dates from 1968, and that he therefore wishes to discuss it in more detail than usual. However, this aim is reached only to a very modest extent. Results from before 1968 take up disproportionate space in the text, while a number of important recent developments are missing. Thus, in discussing the addition of tetracyanoethylene to the tetramethyl derivatives of 2,3-bismethylenebicyclo[2.1.1]hexane and 3,4-bismethylenetricyclo[3.1.0.$0^{2,6}$]hexane, the original interpretation of the large difference in rate constants between the two reactions is quoted, attributing it to orbital interactions (p. 1133). More recent experiments with the parent compounds *(P. Vogel, M. Christl)*, which trace the effect almost entirely to the steric

influence of the methyl groups, are not mentioned. For the formation of the tricyclo[2.1.0.0^{2,5}]pentan-3-one system from a cyclopropen-3-carbonyldiazomethane precursor the author presents an old example (p. 1143), without referring to the synthesis of the unsubstituted compound *(G. Maier)*, though this is rectified in Chapter 21. What justification is there for citing the preparation of 1-methylbenzvalene by the method of the benzvalene synthesis, yet not mentioning the latter *(T. J. Katz) at all*? Furthermore, this reaction type *(U. Burger)* does not represent Case D in the classification of routes of formation of the bicyclobutane skeleton, but Case F, for which the author found no examples. Nor is there a single word on the fact that benzvalene is a source of dozens of bicyclobutane derivatives which are as yet inaccessible by other routes. Why does the author satisfy himself with reporting the reaction of benzvalene with diironnonacarbonyl ($Fe_2(CO)_9$, not $Fe(CO)_9$, p. 1165), but omit the studies with iron pentacarbonyl *(R. Aumann)*? Also omitted are: the remarkable formation of a 3-oxatricyclo[3.1.0.0^{2,6}]hexane from a cyclobutene derivative under acidic conditions *(M. Regitz)*, and the reactions of 2-vinylbicyclobutane derivatives, in which the σ-system takes part, and which occur either in a concerted manner or via intermediate 2-bicyclobutylcarbinyl radicals or cations. The statements on p. 1151 about the unsubstituted cyclopropylcarbinyl cation are not only superficial, but in part simply incorrect. Fortunately, this subject is described correctly in several other chapters. Equation 86 is ahead of its time, since substrates with R = Et, Bu have not yet been examined. The lack of care is evident not only in the compilation and study of sources, but also in the presentation. One finds printing errors that distort the meaning, e.g. in Equation 31, and the structural formulas for one and the same ring system vary according to how it is shown in the original articles. The two additions to the central bicyclobutane bond of the tricyclo[4.1.0.0^{2,7}]heptane system on p. 1150 are an example. The different perspectives make the stereochemical differences and similarities hard to recognize, and even harder to understand. In some places, saving space with fewer formulas would have had the added advantage of giving a more concise account. For example, Equation 77 could have been omitted in favor of Equation 81, and the contents of Equations 136 and 140 would have been more effective if placed together.

Thanks to his own reviews, *D. Ginsburg* was able to be brief with the [*m.n.*1]propellanes. His characteristic style, so full of comparisons and metaphors, makes it entertaining to read. Chapter 21 (Cyclopropenes, *B. Halton, M. G. Banwell*) is very well researched and presented, but the laurel wreath for thoroughness must be awarded to *E. Vilsmaier*, dealing with the aminocyclopropanes. He had hardly any reviews to lean on, and therefore reached a total of about 1000 references, many of them to patents. *H. H. Wasserman, D. R. Berdahl,* and *T.-J. Lu* review the chemistry of cyclopropanones in an impressive manner. Cyclopropenyl compounds *(W. E. Billups, A. W. Moorehead)* reappear once again in Chapter 24. The few new aspects introduced could easily have been included in Chapter 21. The authors promote cyclohexylcyclopropenone to the status of a natural product (p. 1547), but the significance of this compound as a model for naturally occurring cyclopropenones is correctly described in Chapter 21.

In this two volume monograph, very carefully written chapters alternate with those that do not come up to expectations. This is mainly a criticism of the authors concerned, but the editor is also at fault, since even the addresses in the list of authors (pp. v, vi) contain errors (Hokkaido is printed incorrectly several times, Ghent University is transported to Kaiserslautern, whose name is also garbled). Despite these shortcomings, the two volumes are very useful, and they should be available to every organic chemist concerned with the chemistry of three-membered carbocycles in teaching or in research.

Manfred Christl [NB 904 IE]
Institut für Organische Chemie
der Universität Würzburg (FRG)

Corrigendum

In the communication entitled "Synthesis and Conformational Behavior of Dibenzo[2.2]metaparacyclophanediene" by T. Wong, S. S. Cheung, and H. N. C. Wong (*Angew. Chem. Int. Ed. Engl. 27* (1988) 705), the following corrections should be made: p. 705, right-hand column, tenth line from bottom ... proceeds via the species $9^{[10,11]}$ ... (instead of ... proceeds via the species $9^{[1,10,11]}$ ...); p. 706, left-hand column, third line from top ... due to flipping of the *m*-phenylene ... (instead of ... due to flipping of the *p*-phenylene ...).

Registered names, trademarks, etc. used in this journal, even when not marked as such, are not to be considered unprotected by law.

© VCH Verlagsgesellschaft mbH, D-6940 Weinheim, 1988. – Printed in the Federal Republic of Germany by Zechnersche Buchdruckerei, Speyer/Rhein.

All rights reserved (including those of translation into foreign languages). No part of this issue may be be reproduced in any form – by photoprint, microfilm, or any other means – nor transmitted or translated into a machine language without written permission from the publishers. Only single copies of contributions, or parts thereof, may be made for personal use. This journal was carefully produced in all its parts. Nevertheless, authors, editors and publisher do not warrant the information contained therein to be free of errors. Readers are advised to keep in mind that statements, data, illustrations, procedural details or other items may inadvertently be inaccurate.

Valid for users in the USA: The appearance of the code at the bottom of the first page of an article in this journal (serial) indicates the copyright owner's consent that copies of the article may be made for personal or internal use, or for the personal or internal use of specific clients. This consent is given on the condition, however, that the copier pay the stated per-copy fee through the Copyright Clearance Center, Inc., for copying beyond that permitted by Sections 107 or 108 of the U.S. Copyright Law. This consent does not extend to other kinds of copying, such as copying for general distribution, for advertising or promotional purposes, for creating new collective works, or for resale. For copying from back volumes of this journal see 'Permissions to Photo-Copy: Publisher's Fee List' of the CCC.

Editorial office: Pappelallee 3, D-6940 Weinheim, Federal Republic of Germany, Telephone (06201) 602315, Telex 465516 vchwh d, Telefax (06201) 602328.

Editor: *P. Gölitz.*

Associate editors: *D. I. Loewus, A. Stimson.* **Editorial assistant:** *E. Schweikart*

Publishers: VCH Verlagsgesellschaft mbH. (Managing Directors: *Prof. Dr. Helmut Grünewald* and *Hans Dirk Köhler*), Pappelallee 3, D-6940 Weinheim, Federal Republic of Germany. Correspondence concerning advertisements should be addressed to VCH Verlagsgesellschaft mbH. (Advertising Manager *R. J. Roth*), Boschstr. 12, P.O. Box 101161, D-6940 Weinheim, Federal Republic of Germany, Telephone Weinheim (06201) 602-0, Telex 465516 vchwh d, Telefax (06201) 602 328.

ADVANCED MATERIALS

Editorial Advisors: E. M. Engler (USA), D. Haarer (FRG), N. Ogata (Japan), G. Petzow (FRG), J. M. Thomas (UK), G. Wegner (FRG)

BMFT Materials Research Program

By Dieter Kutschke*

The Importance of Materials Research

Materials research plays a pivotal role in the research efforts of the leading industrial nations such as the United States, Japan, the United Kingdom, the USSR, France, the Federal Republic of Germany, etc. This is a natural consequence of the key function of materials in any technological and economic activity. In a system of competing economies, the best possible selection and design of materials and thus the use of improved and new materials is an entrepreneurial necessity. New and improved materials are not, as a rule, just invented, but, as has been shown in the last few decades, are the result of systematic materials research. Technological progress and the further development of industrial products and processes frequently call for the existence of high-performance materials.

In 1985, in response to this challenge, the Minister for Research and Technology of the Federal Republic of Germany launched a ten year Materials Research Program, for which the Federal Government intends to make approximately DM 1.1 billion available in research grants.

Three years after its initiation a first interim review of the progress being made within the framework of this program is now arranged. A major part of the interim review is the 1988 Materials Research Symposium due to be held at Hamm/Westphalia from September 12 to 14, 1988. No fewer than 70 reviews and specialized papers, dealing with a broad range of results from basic research to applications-oriented materials development will be presented.

Aims of the Materials Research Program

In general, the program aims at a long-term improvement in the industrial efficiency and competitiveness of the Federal Republic of Germany based on the development and use of new structural and functional materials. The intention is to mobilize the scientific and technological potential of highly qualified research groups in basic and applied research institutions together with those employed in industry, so as to solve selected research and development tasks. The basic concept is that it is the original task and responsibility of industrial enterprises to conduct R & D in order to lay the foundation of their future competitiveness. The Materials Research Program has been designed above all to help advance applications-oriented basic research of a type likely to yield results which can soon be put to use in the development of new and improvement of established materials. It is essential that existing skills and capabilities be strengthened by encouraging cooperation between scientific and industrial establishments. A concerted effort is called for in several respects: firstly, concentration on a limited number of research priorities; secondly, participation of all highly qualified research institutions in the program; and thirdly, the integration of basic research and industrial development. Such a concerted effort would open up an important, as yet largely untapped potential and would at the same time offer an opportunity for the highly efficient deployment of pro-

[*] Ministerialrat Dipl.-Ing. Dieter Kutschke
Bundesministerium für Forschung und Technologie (BMFT)
Heinemannstrasse 2, D-5300 Bonn-Bad Godesberg

Contents

D. Kutschke
BMFT Materials Research Program 1201
J. W. Rabalais et al.
From Carbon Beams to Diamond Films 1203
D. Haarer, A. Blumen
Polymeric Photoconductors—New Concepts 1210
Conference Reports
Organic Materials for Nonlinear Optics 1215
European MRS Meeting in Strasbourg 1216
Research News
Ring Opening Metathesis Polymerization 1217
Book Reviews 1218
Conference Calendar 1222
Last Minute Information 1226

Editor: *P. Gölitz* **Editorial Assistant:** *L. Dominguez*

Table 1. Organization of co-operative research and development projects. Example: high-strength, fiber-reinforced ceramic-matrix composites.

Objectives	Application	Collaborators

- Improvement of crack propagation of high-strength materials ceramics by incorporating ceramic fibers and whiskers
  - increase in strength
  - increase in resistance against mechanical and thermal shock
  - improvement of high-temperature properties
- Development of parts and simple-shaped components
- Matrices: glass, glass ceramics, Al_2O_3, SiC, Si_3N_4
	Structural components for application at low and at high temperatures and this demanding improved tolerance levels	*Industry*
		Schott AG, Mainz
		Hoechst AG, Frankfurt
		Sigri GmbH, Meitingen
		Institutes
		DFVLR, Köln, Institut für Werkstoff-Forschung
		Battelle, Frankfurt
		Technische Universität Karlsruhe
		- Institut für Chemische Technik
		- Institut für Keramik im Maschinenbau

gram funds, by including industrial research to a large extent.

The program covers the following priority areas:

- high-performance ceramics
- powder metallurgy
- metallic high-temperature materials
- high-performance polymers
- composite materials

Cooperative research projects of the kind described above enjoy preferential support by the government: industrial enterprises, universities and research establishments are encouraged to pool their research facilities in order to jointly tackle, by sharing assignments and exchanging experience, R&D problems which are interrelated in terms of subject and function. Depending on the problem concerned, on the parties participating in the project, and on the particular circumstances, practical collaboration under such a cooperative research project can take different forms. The patterns of cooperation range from binding agreements on an exchange of R&D results to the execution of joint research work in one laboratory. Table 1 outlines a typical cooperative research project.

The costs of the cooperative research projects are shared by industry and the Ministry of Science and Technology (Bundesministerium für Forschung und Technologie, BMFT). In order to ensure the highest possible degree of efficiency in the cooperation between industry and its research partners (institutes), the firms are required to share in the expenditure incurred by the institutes. Generally speaking, the BMFT shoulders 50% of the total cost of the cooperative project. The participating industrial partners bear the remaining 50%, that is 50% of their own costs plus 50% of the expenditure incurred by the institutes.

In the past three years, cooperative projects incurring a total cost of DM 931 million have been started. The BMFT bears DM 497 million (Table 2).

Table 2. Priority areas and funds of the R&D activities within the BMFT Materials Research Program to date (in million marks).

Priority areas	Total R & D cost	BMFT share
High-performance ceramics	232	119
Powder metallurgy	96	59
High-temperature metallic materials	168	95
High-performance polymers	199	104
Composite materials	236	120
Total	931	497

The aim of mobilizing the scientific and technical potential has largely been realized. Closer cooperation between industry and scientific institutes at universities, the Max Planck Society, the Fraunhofer Society, the National Research Centers and the Federal Materials Testing Institute has been launched efficiently and to the mutual benefit of the private and public partners. The program is being carried out in close collaboration with the German Research Society (Deutsche Forschungsgemeinschaft, DFG), and has triggered off additional research activities. Further activities in materials research, in the form of new research programs or the foundation of new institutes, have taken place in all Federal States in the past three years. A number of EUREKA projects as well as the increased utilization of the BRITE and EURAM programs of the European Community are conducive to strengthening materials research at the European level.

Dipl.-Ing. Dieter Kutschke, born on 12 June 1930, studied engineering and chemical engineering at the Technische Hochschule Graz and Technische Hochschule Hannover from 1952–1958. Following a period of employment at Esso AG (1958–1966) he started to work in the management of the Nuclear Research Center Karlsruhe (1966–1974). He then transferred to the Federal Ministry of Research and Technology (BMFT) in 1974. Since 1985 he has been Head of the Materials Research Department.

From Carbon Beams to Diamond Films**

Ion Beam Deposition
Carbon Films
Surface Analysis

By S. R. Kasi, Y. Lifshitz, J. W. Rabalais,* and G. Lempert

1. Introduction

Diamonds have attracted mankind's attention through many centuries. The quest for synthetic artificial diamonds, as well as that of artificial gold, motivated the first experiments that led to the foundation of chemistry. Bulk diamonds were successfully produced only in 1953, however, by the ASEA group in Sweden and by the General Electric team in 1955.[1,2] A specially designed reaction vessel provided the high-temperature/high-pressure conditions needed to transform graphite, the stable carbon phase under normal conditions, to cubic diamond, the precious metastable carbon phase. Artificial bulk diamonds are now commonly used in many applications. An equally challenging goal is the deposition of diamond films on various materials, which has been the subject of intense research that started about thirty years ago and has accelerated significantly during the past few years. The interest in these films stems not from their decorative value, but from the unique set of physical properties of diamond:[1,2]

- hardest known material
- excellent electrical insulator
- best thermal conductor
- high dielectric strength
- highly transparent in the UV, visible and IR regions
- chemically inert
- resistant to oxidation and corrosion
- compatible with body tissues

Attempts to fabricate true diamond films resulted in carbon films with properties varying between those of diamond and those of graphite, within a range of many orders of magnitude.[2-7] The unique possibility of "tailoring" a combination of desired properties for a specific purpose is advantageous for a variety of applications including:[2-8]

- optical coatings suitable for hazardous environments
- protective thin films for magnetic recording materials
- heat sinks for semiconductor applications
- solid state devices
- moisture barriers
- low friction coatings for tribological applications
- hard coatings for mechanical tools
- protective coatings compatible with body tissues for medical applications

The properties of the different phases of carbon are closely related to the nature of the carbon–carbon bonds or to the electronic structure of carbon.[2,3,9] Cubic diamond has sp^3 carbon atoms and a tetrahedral structure where each carbon atom is bonded to four different carbon atoms and no "dangling bonds" exist. Graphite has sp^2 carbon atoms and a structure where each carbon atom is bonded only to three carbon atoms in a two-dimensional arrangement while the remaining p orbital forms a "dangling bond" (or a π electron band). Amorphous carbon includes a varying mixture of sp^1, sp^2, and sp^3 hybridized carbon atoms with no long range crystalline order.

Attempts to fabricate true diamond films have resulted in many deposition methods, practical processes, and films of commercial potential. Work accomplished on these topics is covered by excellent recent reviews and literature surveys.[3-5,8,10,11] Nevertheless, the understanding of the

Abbreviations

UHV	Ultra High Vacuum
RF	Radio Frequency
DC	Direct Current
IBD	Ion Beam Deposition
CVD	Chemical Vapor Deposition
TEM	Transmission Electron Microscopy
XRD	X-Ray Diffraction
SEM	Scanning Electron Microscopy
AES	Auger Electron Spectroscopy
EELS	Electron Energy Loss Spectroscopy
UPS	Ultraviolet Photoelectron Spectroscopy
XPS	X-Ray Photoelectron Spectroscopy
ILS	Ionization Loss Spectroscopy
XAES	X-Ray Induced Auger Electron Spectroscopy

[*] Prof. J. W. Rabalais, S. R. Kasi, Y. Lifshitz [+]
Department of Chemistry, University of Houston
Houston, TX 77204-5641 (USA)
G. Lempert
Soreq Nuclear Research Center
Yavne 70600 (Israel)
[+] On sabbatical leave from Soreq Nuclear Research Center, Yavne 70600 (Israel)

[**] The authors are most grateful to *T. Schaffner, W. M. Duncan, H. Y. Liu, H. L. Tsai,* and *M. W. Cowens* of Texas Instruments, Dallas, for the TEM, XRD, Raman and FTIR analysis of the samples, to *E. Rapoport*, Soreq NRC, for XRD and FTIR measurements, and to *S. Moss* and *L. Robertson*, University of Houston, for XRD analysis and helpful discussions. This material is based on work supported by the National Science Foundation under Grant No. DMR-8610597.

nature of these carbon films is still very limited. This is true of almost all aspects, such as film growth processes, deposition parameter-property relationships, film characterization and nomenclature. The major reason for this situation is the complex chemical-physical nature of the deposition techniques that have been used, where the ability for separating, controlling and studying the effects of individual deposition parameters is limited.

The present work reviews recent results of the first in-situ parametric investigations of the growth of diamond films under controlled UHV conditions.[10,12-15] These investigations were performed in the Houston facility[10,16] that uniquely combines a controlled, mass selected (carbon) ion beam system with a UHV deposition chamber and in-situ surface analysis techniques. The work has established several surface characterization methods for studying carbon films[14] and has addressed some fundamental problems involved in diamond film deposition, such as the possibility of growing diamond films on non-diamond substrates at room temperature, the evolution of the films at different stages of growth, effects of ion parameters (e.g. ion energy), substrate parameters (e.g. material, temperature) and ambient pressure. We first briefly summarize the previous work on "diamond-like" films, including deposition methods, main processes involved in carbon film deposition, and open questions in the field. Following a short description of the system and the diagnostic techniques, the use of various surface analysis methods for the characterization of the different carbon forms related to carbon film evolution is given. Next, the first conclusive proof for diamond growth and the different stages of diamond film evolution on different substrates at room temperature are presented. The results of some parametric studies including substrate material and substrate temperature effects follow. The summary gives the most important conclusions of this work and points to future applications.

2. Present Status of Research on Diamond-like Films

Since graphite is the most stable phase of carbon under ambient conditions,[1,2] simple thermal evaporation of carbon results in either graphitic or amorphous carbon films.[3-5] These films are undesirable because they have the properties of graphite, which is electrically conducting and has a high absorption coefficient in the visible and IR regions. The metastable nature of the diamond phase necessitates a combined high-pressure/high-temperature scheme for its formation.[1,2] Such a scheme is, however, impractical for routine thin film applications. Two alternative basic approaches have thus been adopted for diamond film deposition: a) The use of energetic species (10-1000 eV) that create localized high-temperature/high-pressure regions in the growing film called "thermal spikes".[3,6] These energetic species can be either carbon containing or other species (e.g. Ar). In the latter case a secondary beam of carbon containing species (either energetic or thermal) impinges on the substrate simultaneously with the energetic (Ar) species. b) Chemical reactions involving hydrocarbon-hydrogen gas mixtures, usually at elevated temperatures, resulting in the formation of diamond layers on different surfaces.[11]

Three main deposition techniques have thus been developed:

1) Ion beam deposition techniques[3,6] where different energetic particles (some of which contain carbon species) impinge on the substrate to be coated. IBD of carbon films was first introduced by *Aisenberg* and *Chabot*[6,17] in 1971 and highly developed by *Weissmantel* et al.[3]. Films produced by these methods are often called i-C (ion C) or DLC films (diamond-like C). Their properties vary between those of graphite and diamond and their exact structure is still in question.[3-5] Characterization of these films revealed a dominant amorphous nature and no rigorous proof for diamond formation was given, with the exception of studies carried out with mass selected ion beams.
2) Plasma techniques[4] where RF, DC or pulsed plasma decomposition of various hydrocarbon gases results in the deposition of carbon films on various substrates. The first work using these techniques was published in 1955,[18] but more rigorous work was started by *Holland* and *Ojha* in 1976;[19] since then these techniques have been adopted by many others.[4] These films usually contain large amounts of hydrogen (10%-70%) and are often called a-C : H films (amorphous carbon hydrogenated).[4,5] Though they may have properties that sometimes resemble those of diamond, they are definitely not diamond films.
3) CVD processes that use chemically active hydrocarbon fragments (ions and radicals) for the spontaneous growth of diamond material under rather metastable conditions.[11] These processes usually use a mixture of hydrocarbons and H_2 (ca. 99% H_2) excited by an external source (hot filament, RF or microwave plasma) to form the carbon films on hot (800-1000°C) substrates. Work on CVD processes was started by *Eversole*[20] and *Angus* et al.[21] and was further developed by *Derjaguin* et al.[22] in Russia and the Nirim group[11,23] in Japan.

Carbon films produced by the above processes have various useful properties, some close to that of diamond (e.g. hard, transparent, chemically inert, insulating films). Real cubic crystalline diamond films with crystal sizes of 1 μm and larger (identified by TEM, XRD, Raman spectroscopy and SEM) have been produced only by CVD techniques at practical (μm/h range) rates on hot (ca. 800°C) substrates.[11] Correlations between film properties and deposition parameters of specific systems have also been given.[3-5] Nevertheless, all of the systems described have a very complex nature where the different basic deposition parameters are very difficult to define and control and the

ADVANCED MATERIALS

pressure is in the range 10^{-4}–10 torr.[3–5] Many species with a complex, usually unknown, composition are involved in such deposition processes[3–5] (carbon atoms, ions and clusters, hydrocarbon ions and radicals, inert gas ions and atoms, energetic hydrogen species, impurity species due to residual gases, electrons, etc.). The energies of these species are not well defined and have wide distributions.[3–5] This results in non-reproducibility of the final product from the different deposition processes and limited understanding of the film growth mechanism. Examples of open questions, the answers for which are essential for the successful reproducible deposition of diamond films, are listed below:

a) Mechanisms of diamond formation—"Thermal spikes" are often suggested as a possible way of obtaining the temperature and pressure needed for diamond formation,[3–6] but their role is often doubted.[4] There is no direct proof for an alternative mechanism—that of preferential etching of graphitic or amorphous constituents by energetic hydrogen or argon species.[4,6] The role of hydrogen in the stabilization of carbon sp^3 bonds in the film by termination of "dangling bonds"[4,5] is only partly understood.
b) Crystal nucleus formation and crystal growth—What are the conditions needed for the nucleation of a diamond crystal and for its further growth on an existing diamond seed?
c) Carbon phases—What are the conditions necessary for the formation of the six known carbon phases in carbon films (graphite, cubic diamond, hexagonal diamond,[1,2] chaoite,[24] and two other carbon high pressure cubic phases[25,26])? Very often the identification of these phases in a given film is ambiguous.[3–5]
d) Growth mechanisms—What parameters determine amorphous–crystalline growth, crystalline size, epitaxy, adhesion to the substrate, surface morphology, etc.?
e) Bulk properties/structure/deposition parameters relationships are not well understood.
f) Characterization—There is no established correlation between different characterization techniques (e.g., Raman spectroscopy, TEM, XRD, and surface analysis methods). This correlation is essential for the characterization of thin ($< 1\ \mu m$) or microcrystalline (< 1000 Å) films where Raman measurements are misleading, XRD is not sensitive, and TEM is destructive and very often uncertain. Such thin films or small-crystalline material may be essential for future applications.

3. Mass Selected Ion Beam Deposition

Limited understanding of deposition phenomena due to the complex chemical-physical nature of many deposition systems is a general feature and not related to diamond film deposition only. Mass selected ion beam deposition has been suggested as a viable technique for fine control and separation of all the deposition parameters.[4,27] When combined with a UHV deposition chamber and in-situ diagnostics, it offers many advantages for deposition in general and for carbon/diamond film deposition in particular:[4,10]

- Ion source parameters: Selection of only one type of carbon bearing ion from various possibilities at a specific deposition stage, control of ion energy (e.g. 10–1000 eV), ion flux, and ion beam size over a wide range.
- Dual ion beam deposition of different species (e.g., carbon ions and hydrogen/argon ions) and simultaneous doping during (carbon) deposition.
- Target parameters (temperature, in-situ pre-deposition and post-deposition treatments, nature of target) are controlled with great flxibility.
- UHV environment provides pure films on atomically clean substrates and controlled admission of gases.
- In situ parametric investigation of film growth becomes feasible using surface diagnostic tools.

Several studies on diamond deposition using mass selected carbon ion beams have been performed prior to the work conducted in Houston,[28–35] the most important of which are those of *Chaikovskii* et al.,[28–30] *Freeman* et al.[31] and *Nelson* et al.[32] *Chaikovskii* et al.[28–30] deposited diamond films in UHV using a mass selected high intensity ion beam system, obtaining small crystalline (ca. 10–100 Å) diamond films on different substrates with ion energies of 30–100 eV at temperatures of 170–293 K. The true diamond nature of these films was established by ex-situ Auger analysis and by TEM. Large diamond crystalline inclusions (up to 50 μm size) were chaotically arranged in a finely dispersed small crystalline base. The effect of substrate temperature during deposition was also investigated and it was found that at 360 K the films were graphitic. This excellent work, which is, to the best of our knowledge, the only deposition under UHV conditions apart from the Houston work,[10,12–16] is unfortunately overlooked by later investigators.[3–5,31–35] *Freeman* et al.[31] found that diamond films could be deposited on existing diamond crystals at carbon ion energies of 900 eV and temperatures of ca. 700°C, using a mass selected carbon ion beam and a vacuum of ca. 10^{-6} torr. The moderate vacuum conditions, however, resulted in non-reproducibility of the films. *Nelson* et al.[32] showed that similar temperatures (ca. 700°C) were needed for the internal growth of existing diamonds using a mass selected high energy (several kV up to 100 kV) carbon beam under high vacuum conditions.

Rabalais et al.[10,16] have developed a unique facility that combines a mass selected carbon ion beam, UHV ($\leq 5 \times 10^{-10}$ torr) deposition environment, and several in-situ surface analysis tools. The Houston deposition system is a research facility; it has a much lower current density than the facility of *Chaikovskii* et al. (ca. 0.5 μA cm^{-2} compared to 1 mA cm^{-2}) in the energy region of 1–300 eV.

Nevertheless, the first and only rigorous in-situ parametric investigations of diamond film growth are being conducted in this facility,[10, 12-16] some results from which are summarized in this review. Complementary investigations of thicker films, produced by a more intense facility at Soreq NRC, Israel, at similar ion energies but poorer vacuum conditions are also being performed. The purpose of the current work is to understand the basic mechanisms involved in diamond film deposition by means of energetic species.

4. Surface Analysis Techniques for in-situ Investigation of Carbon Film Evolution

Differences in the electronic structure of diamond, graphite and amorphous carbon are reflected in the spectroscopic surface analysis features. Extensive work by *Rabalais* et al.[12-15] established the surface analysis data for diamond, graphite, and amorphous carbon as standards for further identification of the nature of deposited carbon films using Auger Electron Spectroscopy (AES), Electron Energy Loss Spectroscopy (EELS), Ultraviolet Photoelectron Spectroscopy (UPS), X-Ray Photoelectron Spectroscopy (XPS), Ionization Loss Spectroscopy (ILS), and X-Ray Induced Auger Spectroscopy (XAES). Published results were compared to those obtained in the Houston laboratory and missing data were complemented.

Figure 1 shows the surface analysis data obtained with AES, XPS, UPS and EELS for diamond, graphite, thermally evaporated amorphous carbon, and carbon films ca. 100 Å thick deposited on Ni(111) at room temperature by the Houston facility at ion energies in the range of 75–150 eV. EELS and UPS data for amorphous carbon are not presented. The features of the three different forms of carbon are different in all of these techniques, each of them being easily distinguishable. The differences lie in the lineshapes (e.g., in AES), the appearance or disappearance of peaks corresponding to π electrons (e.g., XPS, UPS and EELS), and the energy shift of corresponding loss peaks (e.g., XPS and EELS). It is therefore possible to identify the carbon form of the films deposited in the Houston facility.

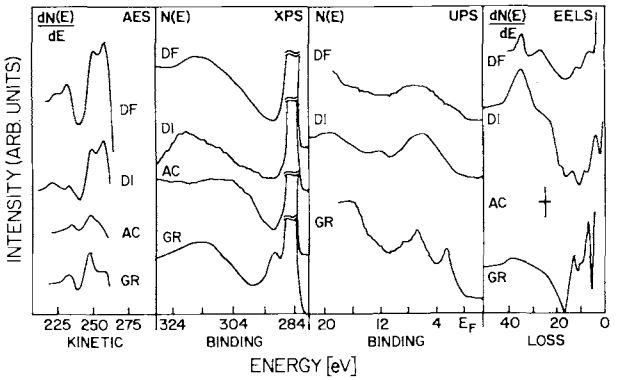

Fig. 1. Surface spectroscopic signatures of carbon in graphite (GR), amorphous carbon (AC), diamond (DI), and diamond film deposited using the Houston facility (DF), measured by AES, XPS, UPS and EELS. No information is presented for the UPS spectrum of AC. The vertical line drawn for AC in EELS indicates the energy loss position of the bulk plasmon peak. The data for GR, AC, and DI in AES, and DI in EELS are from [41] while DI in UPS is from [36].

In all four surface analysis methods, the spectra of the deposited films correspond to that of diamond and are very different from that of graphite or amorphous carbon. In the AES measurements, mild electron beam conditions are needed in order to avoid the typical electron beam damage observed for diamond surfaces.[14] Under routine experimental conditions, spectra for the electron beam damaged diamond films are measured (Fig. 2), which are

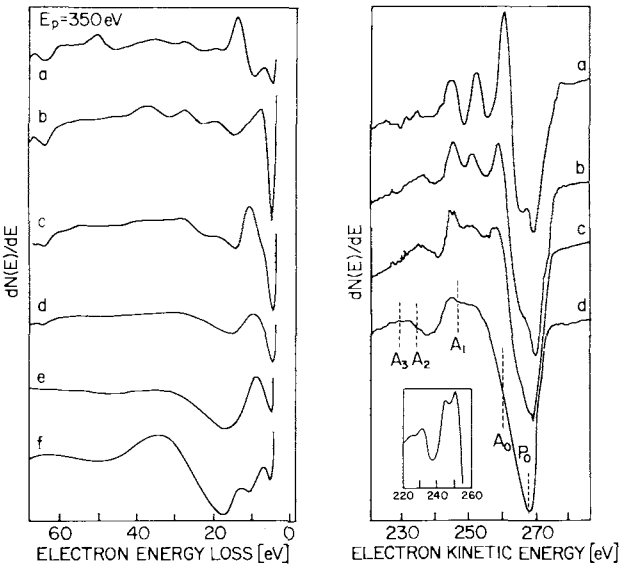

Fig. 2. Evolution of the EELS (left) and AES (right) lineshapes for 75 eV C^+ deposition on Ni(111). The doses in the EELS sequence are: a) clean Ni, b) 3×10^{15}, c) 5×10^{15}, d) 7×10^{15}, e) 9×10^{15}, and f) $>2\times10^{16}$ C^+ ions cm^{-2}. The doses in the AES are: a) 2×10^{15}, b) 6×10^{15}, c) 9×10^{15} and d) $>2\times10^{16}$ ions cm^{-2}. The inset shows an Auger electron spectrum of a diamond film subject to minimal electron beam damage.

nevertheless more similar to that of diamond than to that of graphite or amorphous carbon. The XPS spectra of the carbon films show no π electron feature at 6.7 eV from the C 1s peak and the energy of the bulk plasmon loss peak is similar to that of diamond (ca. 34 eV from the C 1s peak compared to ca. 28 eV for graphite and ca. 23 eV for amorphous carbon). The UPS spectra of the films are indicative of the typical sp^3 hybrid orbitals of diamond with no contribution in the π band region and a recession of states close to the Fermi level. The EELS spectra also exhibit the features of diamond. Additional information has also been obtained from ionization loss spectroscopy (ILS) and ellipsometry.[14]

It can thus be concluded that the short range order of the carbon films deposited at room temperature in the Houston facility is that of diamond (i.e., sp^3 hybridized

ADVANCED MATERIALS

carbon atoms). This result was reproducible on every sample tested regardless of the nature of the substrate. These films are therefore different from previously reported diamond-like carbon films (DLC's) that showed surface analysis features very different from diamond, and very similar to those of amorphous carbon.[4,5,37] The only other published data where the AES features of carbon films corresponded to diamond was that from ex-situ measurements by *Chaikovskii* et al.,[28] where the deposition conditions were very similar to those of the Houston group. In the work of the Houston group, however, several surface analysis methods were applied to establish the same result and almost all of the measurements were done in-situ. The establishment of these surface analysis data was followed by in-situ parametric investigations of the diamond film growth that are not feasible in any other existing facility.

5. Parametric Investigations of Carbon Film Growth

This section reviews results from investigations of carbon film growth that are being conducted in the Houston facility.[10,12-16]

5.1. Stages of Diamond Film Evolution

The evolution of the diamond films on atomically clean surfaces has been investigated on different materials at room temperature using the different in-situ surface analysis techniques. The three distinct stages of a) carbidic, b) graphitic, and c) diamond were observed in the film evolution on all substrates investigated. Figure 2 shows the film evolution as monitored by AES and EELS for 75 eV C^+ deposition on Ni(111). At low fluxes the impinging C^+ ions form Ni-C bonds resulting in a typical nickel carbide signature[14,38] in both the AES and EELS spectra. At higher carbon fluxes, C-C bonds begin to form and the lineshapes change accordingly. The AES and EELS nickel peak intensities start decreasing at this stage due to formation of the carbon layer. When a complete two-dimensional carbon layer is formed, the nickel lines disappear and the carbon layer gives a graphitic lineshape. This is more obvious in the EELS data since the AES lineshape at this stage still reveals some carbidic features, probably due to a contribution from the interfacial carbidic layer. At higher carbon fluxes the thicker carbon layer forms a three-dimensional short range order for which surface analysis shows the typical diamond features as discussed in the previous section.

5.2. The Role of Energy

The evolution of the carbon film was investigated by AES at different energies in the range 10–300 eV. A "phase diagram" showing the C^+ fluxes needed for the evolution of the carbidic (A), intermediate (B), and graphitic (C) stage on Ni(111) at room temperature was constructed (Fig. 3). The evolution of carbon layers is energy independent over a broad range (ca. 30–180 eV). At higher (>180 eV) or lower (<30 eV) energies, higher fluxes are required for the stabilization of the graphitic stage. The final diamond structure was not observed for energies below ca. 20 eV and is obtained only at a higher carbon flux for 300 eV. The energy threshold for diamond evolution can be interpreted in terms of the "thermal spike" theory.[3] At very low energies the ion induced "thermal spike" cannot provide the temperature-pressure conditions needed for stabilization of the diamond phase. At high energies the self-sputtering rate of carbon increases,[4,33] the net deposition rate at constant C^+ current density decreases (lower "sticking probabilities"[16]), and radiation damage may destroy the crystalline order; amorphous films are expected[33] unless the high energy deposition is performed at elevated (700–900 °C) temperatures where this damage is annealed.[31-32]

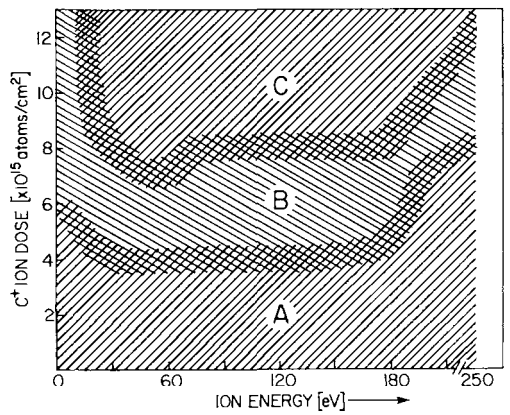

Fig. 3. Evolution of the carbon deposits monitored by AES plotted as a phase diagram of carbon ion energy and flux. Regions A, B and C correspond to deposits that have the AES lineshapes of Figure 2 (right), a, b, and c, respectively.

5.3. Substrate Structure Effects

Room temperature carbon deposition on different substrates (Ni(111), Si(100), Au, T, W, Ge and Cu) exhibited similar behavior, i.e., evolution from a carbidic through a graphitic to the final diamond stage. The carbidic stage may be important for film adhesion to the substrate. Differences in the rate of film evolution on different substrates were detected (Fig. 4), indicating the possibility of different film growth mechanisms on different substrates. The rate of the initial stages of film growth was much slower on a gold substrate than on Ni and Si, possibly due to enhanced backscattering of the C from the high Z gold substrate. The substrate material was also found to influence the temperature behavior of the films as discussed in the next section.

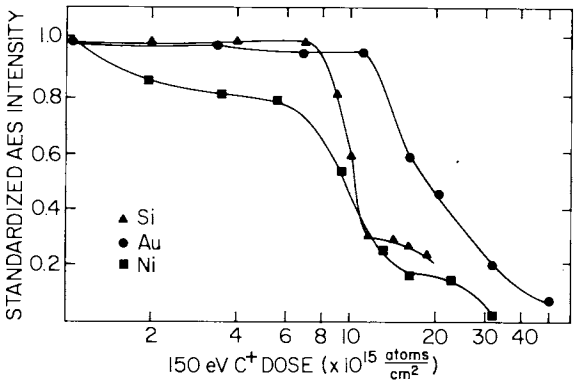

Fig. 4. Plot of the change in substrate AES peak intensity as a function of 150 eV C^+ flux. The substrate signals plotted are the Ni(61 eV), Si(92 eV), and Au(69 eV) transitions. The peak intensities are normalized to that for the clean surface.

5.4. Substrate Temperature Effects

Two kinds of temperature effects on film evolution on Ni(111) and gold were investigated, post-deposition annealing and deposition on hot substrates. The films on Ni substrates were found to be unstable under annealing. At 200°C Ni Auger lines appeared, possibly due to some Ni-C interdiffusion or film recrystallization and island formation. At temperatures exceeding 400°C carbon dissolution into the Ni associated with a graphitic transformation of the carbon was detected. This behavior is consistent with the C-Ni phase diagram.[39] Carbon ion beam deposition on the Ni substrate at 150°C resulted in graphitic films, while it was not possible to deposit carbon films on Ni at 400°C, very likely due to dissolution of C into the Ni at this temperature. Diamond films on gold were found to be much more stable under post-deposition annealing. No dissolution of the film into gold was detected, even at 875°C, although marked graphitization occurred at 650°C. Deposition of C on a gold substrate at 150°C, however, resulted in a graphitic film, similar to the results of deposition on a hot nickel substrate. This tendency to form graphitic films instead of diamond films at temperatures exceeding 100°C was also detected by *Chaikovskii* et al.[28-30] The explanation for this temperature behavior may relate to the graphite/diamond phase diagram[1,2,29] and is unclear at present.

5.5. Bulk Characterization

Bulk characterization of the diamond films is currently being performed using TEM, XRD, Raman spectroscopy, IR spectroscopy and ellipsometry. Two kinds of films are being investigated: thin (ca. 500 Å) films deposited in Houston and thick (ca. 1 μm) films deposited in Soreq NRC, Israel, under similar energy, higher current density, and poorer vacuum conditions. TEM analysis of a 500 Å diamond film deposited on Si(100) shows oriented crystals with a diameter of ca. 1000 Å. The corresponding electron diffraction pattern confirms the existence of crystals oriented with the substrate but is very complex and has not yet been resolved. The ~1 μm samples were deposited on Si(100), Si(111), Ge and Cu. They show clear interference fringes due to non-uniformity of the film thickness indicating transparency in the visible range. Ellipsometry measurements of films on Si give refractive indices that correspond to diamond. IR spectroscopy reveals very high transparency in this region as well. XRD of the carbon film on Si(111) shows a broad peak that corresponds to diamond (111) and a crystal size of ca. 50 Å. This small size may explain the absence of a sharp 1332 cm^{-1} diamond line in the Raman spectra, which are very similar to the Raman spectra of microcrystalline diamond films grown by CVD.[5] The bulk characterization of these films is still in progress; however, these preliminary results are consistent with the assumption that the films are made of a microcrystalline (20–50 Å) diamond matrix, with random inclusions of larger crystals. A similar interpretation has been given previously by *Chaikovskii*[28] and by other investigators.[3-5,40]

6. Summary and Conclusion

The most important general achievements of the work can be summarized as follows:

a) A comprehensive surface analysis procedure has been established for carbon film characterization using the AES, EELS, UPS, XPS and ILS techniques.
b) The Houston mass selected ion beam facility that combines a UHV deposition environment and in-situ surface analysis instrumentation has been established for parametric investigations of (diamond) film growth.
c) Carbon films deposited by the Houston facility have been conclusively shown, by surface analysis techniques, to have the short range diamond order. This demonstrates the feasibility of reproducible diamond film deposition using pure carbon ion beams on different substrates at room temperature (in the absence of argon or hydrogen).

In-situ parametric investigations of diamond film evolution are currently being conducted, with emphasis on film evolution, effects of ion energy, substrate temperature during deposition, post-deposition annealing, substrate features and substrate material effects, ambient pressure effects, etc. Among the most important specific results obtained are:

- The film evolution has three stages; an initial carbidic stage evolves to a final diamond structure through a graphitic stage.
- The optimal carbon ion energy range for diamond film evolution at room temperature is 30–180 eV.

ADVANCED MATERIALS

Deposition on hot (ca. 100°C and above) substrates results in graphitic films.

Substrate effects include determination of deposition rates at the initial stages and film growth modes (e.g., low deposition rates on gold) and determination of film temperature stability and the possibility of high temperature film deposition (e.g., nickel substrates are not suitable for high temperature applications unlike gold substrates).

Bulk characterization suggests that the films have the properties of diamond and that, under proper conditions, both small and large microcrystalline diamond material can be obtained.

7. Future Trends

The possibility of depositing diamond films at room temperature on different substrates has been demonstrated. These films will be useful for many applications, as mentioned in the introduction. Mass selected ion beam deposition, especially under UHV conditions, has the unique possibility of controlling and separating the different deposition parameters. These possibilities do not exist in the other deposition techniques that have a complex chemical-physical nature. Mass selected IBD can thus serve several purposes:

Parametric investigations of diamond film formation, simulating other existing deposition methods.

Development of processes with specific deposition parameters resulting in "tailored" film properties. These processes can be attempted by other deposition methods (CVD, plasma deposition, or another ion beam deposition technique) depending on economic considerations.

Actual fabrication of diamond films. Controlled, microfocused beams with in-situ flexibility of changing deposition parameters, using either dual beams for doping or successive exposures of different ions for multi-layer deposition, are most advantageous for microelectronic applications.

This review has focused specifically on diamond-film fabrication. Many arguments can, however, be extended to deposition of other materials. Mass selected ion beam deposition can therefore be applied to the development of films of a variety of materials with unique and useful properties.

Received: June 13, 1988

[1] J. E. Field (Ed.): *The Properties of Diamond,* Academic Press, London 1979.

[2] F. P. Bundy, H. M. Strong, R. H. Wentorf, Jr. in P. L. Walker, Jr., P. A. Thrower (Eds.): *Chemistry and Physics of Carbon,* Dekker, New York 1973, Vol. 10, p. 213.

[3] C. Weissmantel in K. J. Klabunde (Ed.): *Thin Films from Free Atoms and Particles,* Academic Press, Orlando, FL, USA 1985, Chapter 4.

[4] J. C. Angus, P. Koidl, S. Domitz in J. Mort, F. Jansen (Eds.): *Plasma Deposited Thin Films,* CRC Press, Boca Raton, FL, USA 1986, Chapter 4.

[5] H. Tsai, D. B. Bogi, *J. Vac. Sci. Technol. A 5* (1987) 3287.

[6] S. Aisenberg, *J. Vac. Sci. Technol. A 2* (1984) 369.

[7] J. A. Woollam, H. Chang, V. Natarajan, *Appl. Phys. Commun. 5 (4)* (1985-86) 263.

[8] J. A. Woollam, *IEEE Electro. Technol. Rev. 1986,* 54.

[9] a) J. Robertson, *Adv. Phys. 35* (1986) 317; b) J. Robertson, E. P. O'Reilley, *Phys. Rev. B35* (1987) 2946.

[10] Y. Lifshitz, S. R. Kasi, J. W. Rabalais, *Adv. Mater. Manu. Process. 3 (2)* (1988) 157.

[11] K. Kobayashi, K. Nishimura, Y. Kawate, T. Horiuchi, *Phys. Rev.,* in press.

[12] S. R. Kasi, H. Kang, J. W. Rabalais, *Phys. Rev. Lett. 59* (1987) 75.

[13] J. W. Rabalais, S. R. Kasi, *Science 239* (1988) 623.

[14] S. R. Kasi, H. Kang, J. W. Rabalais, *J. Chem. Phys. 88* (1988) 5914.

[15] Y. Lifshitz, S. R. Kasi, J. W. Rabalais, G. Lempert, E. Rapoport, *3rd Annu. SDIO/IST-ONR Diamond Technol. Initiative Symp.,* 12-14 July 1988, Crystal City, VA, USA.

[16] H. Kang, S. R. Kasi, J. W. Rabalais, *J. Chem. Phys. 88* (1988) 5882.

[17] S. Aisenberg, R. Chabot, *J. Appl. Phys. 42* (1971) 2953.

[18] H. Schmellenmeier, *J. Phys. Chem. 205* (1956) 349.

[19] L. Holland, S. M. Ojha, *Thin Solid Films 38* (1976) L17.

[20] W. G. Eversole, Can. Pat. 628567 (1961); US Pat. 3030187 and 3030188 (1962).

[21] J. C. Angus, H. A. Will, W. S. Stanko, *J. Appl. Phys. 39* (1968) 2915.

[22] B. V. Derjaguin, D. B. Fedosov, *Sci. Am. 233* (1975) No. 5, 102.

[23] M. Kamo, S. Matsumoto, Y. Sato, N. Setaka, US Pat. 4434188 (1986), Nirim, Japan.

[24] A. El-Goresy, G. Donnay, *Science 161* (1968) 363.

[25] R. B. Aust, H. G. Drickamer, *Science 140* (1963) 817.

[26] K. Fujii, N. Shohata, M. Mikami, M. Yonezawa, *Appl. Phys. Lett. 47* (1985) 370.

[27] T. Takagi, *J. Vac. Sci. Technol. A 2* (1984) 382.

[28] E. F. Chaikovskii, V. M. Puzikov, A. V. Semenov, *Sov. Phys. Crystallogr. 26* (1981) 122.

[29] E. F. Chaikovskii, G. Kh. Rozenberg, *Sov. Phys. Dokl. 29* (1984) 1043.

[30] E. F. Chaikovskii, V. M. Puzikov, A. V. Semenov, G. Kh. Rozenberg, A. Kostenko, *Arch. Nauki Mater. 7* (1986) 187.

[31] J. H. Freeman, W. Temple, G. A. Gard, *Vacuum 34* (1984) 305.

[32] R. S. Nelson, J. A. Hudson, D. J. Mazey, R. C. Piller, *Proc. R. Soc. London Ser. A 386* (1983) 211.

[33] T. Miyazawa, S. Misawa, S. Yoshida, S. Gonda, *J. Appl. Phys. 55* (1984) 188.

[34] A. Antilla, J. Koskinen, M. Bister, J. Hirvonen, *Thin Solid Films 136* (1986) 129.

[35] A. Antilla, J. Koskinen, R. Lappalainen, J. P. Hinvonen, D. Stone, C. Paszkiet, *Appl. Phys. Lett. 50* (1987) 132.

[36] B. B. Pate, *Surf. Sci. 165* (1986) 83.

[37] A. K. Green, V. Rehn, *J. Vac. Sci. Technol. A 1* (1983) 1877.

[38] J. P. Coad, J. C. Riviere, *Surf. Sci. 25* (1971) 609.

[39] a) T. Lyman (Ed.): *Metals Handbook, 8th Ed., Vol. 8, Metallograph, Structures and Phase Diagrams,* ASM, Metals Park, OH, USA 1973; b) C. J. Smithells: *Metal Reference Book,* 5th Ed., Butterworths, London 1976, p. 515.

[40] E. G. Spencer, P. H. Schmidt, D. G. Joy, F. J. Sansolone, *Appl. Phys. Lett. 29* (1976) 118.

[41] P. G. Lurie, J. M. Wilson, *Surf. Sci. 65* (1977) 476.

As of January 1989, ADVANCED MATERIALS can be subscribed to separately at the annual rate of DM 178.00. Please order through your bookseller or write to VCH Verlagsgesellschaft mbH, Pappelallee 3, D-6940 Weinheim, FRG. Customers in the UK and USA should write to VCH Publishers, Wellington Court, 8 Wellington Street, Cambridge CB1 1HW, UK and VCH Publishers, Suite 909, 220 East 23rd Street, New York, NY 10010-4606, USA, respectively.

ADVANCED MATERIALS

Polymeric Photoconductors—New Concepts**

Charge Carrier Transport
Amorphous Materials
Fractals

By Dietrich Haarer* and Alexander Blumen*

1. Introduction

The use of polymeric photoconductors in printing and copying techniques represents one of the most sophisticated applications of polymeric materials. However, there is a considerable lack of understanding of the basic electronic mechanisms involved in photoconduction. Recently, new theoretical concepts and improved experimental techniques have given new impetus to the complex problem of dispersive transport in polymeric photoconductors. On the experimental side one has succeeded in monitoring photocurrents over ten decades in time and the decay over many orders of magnitude. On the theoretical side one has been able to model not only the temporal disorder via random walks in continuous time but also the geometric disorder via fractals and the energetic disorder via ultrametric spaces. An introduction to these new concepts will be given and some topical aspects will be discussed in this article.

2. Historical Overview

The rapid growth of the electronic industry, and especially the almost exponential increase of the performance of its products, have mostly been attributed to technical advances in the field of single crystalline silicon devices. Yet, it was not until the mid-seventies and early eighties, that it became obvious that in the silicon technologies as well as in other domains of the electronic industry, sophisticated or so-called "intelligent" polymers have silently made an almost comparable progress. For instance, in the field of passive dielectric components the "natural polymer" paper (which had been widely used as dielectric medium in capacitors) was replaced by thin polymer films. In the field of "active applications"—here the word active is used to characterize "gain" or "electronic" mechanisms—the achievements are enormous, much beyond the expectation level set by research activities on organic molecular crystals, a typical field of research on organic materials in the sixties and seventies.

One of the best examples of this change is the development of photoconductive materials. This field originated with experiments on anthracene crystals where, for the first time, electron and hole mobilities were measured by the time-of-flight method.[1,2] From a historical standpoint it is interesting to note that in early work of the Göttingen school on the photoconductivity of color centers in alkali metal halide crystals similar techniques were employed half a century ago, using the modest experimental equipment of the time.[3] These investigations, however, were hampered by the lack of applications which was typical of most of the color center work in general. Even research on simple crystalline organic materials did not lead to any practical results, because nobody could think of ways to use anthracene or naphthalene crystals in technical devices, and because the quantum yields for charge carrier production were, at the normal electrical field strengths, on the order of 10^{-3} and therefore not attractive for applications.

It was several years after the discovery of the xerographic process based on the inorganic photoconductor selenium,[4] that the first patent on organic photoconductive systems was published.[5] Several key ingredients can, in hindsight, account for the success of polymeric photoconductors:

a) Polymeric systems can be easily fabricated in large area devices and can be produced perfect enough to withstand high electric fields (low pinhole densities).
b) The role of donor-acceptor interactions was discovered early as a key mechanism to enhance carrier production yields.

The first example of technical applications used the donor polymer polyvinylcarbazole (PVK) and the acceptor compound trinitrofluorenone (TNF) in low concentrations[5] or in a 1:1 stoichiometry.[6]

With the above-mentioned advantages of polymeric materials and with complex dye-matrix or dye-pigment systems replacing the donor-acceptor based polymers, the organic photoconductors were perfected between 1970 and 1980 to the extent that they are nowadays equivalent or superior to their inorganic counterparts. The yields for charge carrier production are on the order of ten percent,[7] depending on the limiting field strengths, and it is only the

[*] Prof. Dr. D. Haarer, Prof. Dr. A. Blumen
Lehrstuhl für Experimentalphysik IV und
Bayreuther Institut für Makromolekülforschung der Universität
D-8580 Bayreuth (FRG)

[**] This work was supported by grants from the Deutsche Forschungsgemeinschaft (SFB 213) and from the Fonds der Chemischen Industrie. Support of the BASF Corporation, Ludwigshafen (FRG), is also acknowledged.

ADVANCED MATERIALS

mobility aspect of the presently used systems which still favors inorganic materials like the chalcogenides.[8]

In spite of the large technical progress in photoconductive systems, many basic aspects of charge carrier generation and transport are still not well understood. In this article we focus on some recent experimental and theoretical aspects of charge carrier transport. Improved techniques to measure photocurrents over ten or more decades allow one to monitor the dispersive transport with previously unknown accuracy. Since the photocurrent can be determined over a wider time regime than most other properties (such as mechanical relaxation), photoconductors are a good model system for transport phenomena in disordered materials. New experimental data allow crucial tests for recent theories of non-Gaussian behavior.

From the theoretical viewpoint, the issue at stake in amorphous photoconductors is the dispersive transport, as contrasted to the familiar diffusive, Gaussian behavior. Diffusive motion, in its many facets, ranging from the transfer of heat (macroscopic) to Brownian motion (microscopic) is a well-understood phenomenon and may be modelled using the mathematical theory of Markov processes, in which the system keeps no memory of past events. Typical discrete examples are random walks on regular lattices—first introduced by *Bachelier* at the turn of the century for monitoring the fluctuations of the stock-market[9]—which nowadays comprise a vast mathematical literature.[10] Simple random walks on regular lattices of arbitrary dimensions lead to a time-independent diffusion coefficient, or, expressed differently, in the absence of a biasing field, to a linear increase in the mean squared displacement as a function of time.

In amorphous photoconductors the situation is different, since one encounters dispersive transport: the motion of the carriers through a sample becomes slower and slower with the passage of time, so that no diffusion constant in the usual sense can be defined. Here the diffusion coefficient may display an algebraic dependence on time:

$$D(t) \sim t^{\alpha - 1} \quad \text{with } \alpha < 1 \tag{a}$$

with a similar finding for the current $I(t)$ flowing in a biasing field. Such behavior is incompatible with the usual diffusion equation.

Progress in the advancement of theoretical models for dispersive transport was slow, due to the Gaussian character of most probability distribution functions put forward. Here we have to recall the overwhelming role of the "central limit theorem" of probability; under very general conditions, a sum of random variables will tend to form a normal (Gaussian) distribution when the number of elements in the sum increases. The position vector of a particle may be viewed as the sum of distance increments due to past events, say collisions. If energies, directions etc., are randomized after such events, most distributions will lead to regular diffusion. Hence, for a successful modeling of dispersive transport in such a framework one has to look for the (relatively rare) distributions for which the central limit theorem does *not* hold.

The basic theoretical problem which has to be solved for the understanding of the transport of light-generated charge carriers through an amorphous medium is to model the motion of individual carriers in a "hopping model", in which these charge carriers perform a specific type of random walk in the direction of the external electric field. In this random walk the probability for performing the next hopping process does not decay exponentially with *one* given decay constant but shows a much broader distribution. This is due to the fact that an amorphous material has rather irregular lattice spacings (geometrical disorder), which lead to large variations in energy levels (energetic disorder).

Mathematically the most important parameter characterizing the transport is the waiting time distribution, i.e., the distribution of waiting times between subsequent carrier jumps. Here a theoretical breakthrough occurred with the realization by *Scher, Lax* and *Montroll* that long tails in the waiting-time distributions $\psi(t)$ between the microscopic events can qualitatively describe the phenomenon of dispersive transport.[11,12] Such distributions lead to the so-called Lévy processes when

$$\psi(t) \sim t^{-1-\alpha} \quad \text{with } 0 < \alpha < 1 \tag{b}$$

so that the zeroth but not the first moment of the distribution $\psi(t)$ exists. This field was long considered to be a domain of mathematical curiosities.[13,14] The main technical point in investigating random walks in continuous time (CTRW) with such distributions was the realization that the basic CTRW framework developed ten years earlier by *Montroll* and *Weiss*[15] could easily incorporate these, less usual, $\psi(t)$ forms. However, although the theory developed[11,12] was successful in providing a scheme for a qualitative understanding of the dispersive transport, the nature of the microscopic parameters leading to $\psi(t)$ was at the time only conjectured.

Today we know that this is only one of the possible ways of obtaining algebraic time dependencies of $D(t)$, and that the key ingredient in the CTRW framework is the idea of temporal scaling, or of time fractals, as formulated by *Shlesinger*.[16] Other approaches that invoke scaling are based on geometrical and on energetic aspects: for the former we mention in this context fractals and percolation models and for the latter ultrametric (hierarchical) structures (UMS). All these concepts lead (for certain values of the parameters) to dispersive transport, as we discuss in the next Section.

3. New Experimental Data and Theoretical Aspects

We discuss charge carrier transport (mobility) by focussing on one of the historic hole-transport polymers, namely

polyvinylcarbazole (PVK).[17a] Here, recent experimental data have given rise to new questions concerning the general theoretical concept of transport in disordered media. The basic question is the nature of the disorder: Is it mainly geometric or mainly energetic or both?[17-20] Furthermore, which are the microscopic parameters that control the macroscopic mobility in polymeric materials?

PVK is prepared in 10 μm thick films in which both solvent and residual monomers have been removed.[17a] The polymer films are mounted between aluminum electrodes produced by vapor deposition (see Fig. 1). The top electrode is semi-transparent and allows illumination with laser pulses of a time duration of typically 10 ns and a wavelength of 337 nm (N_2 laser). At this wavelength the polymer absorption is characterized by the carbazole moiety; therefore the typical penetration depth of the light is less than 0.5 μm. The light pulse thus creates electron-hole pairs within a thin surface layer of less than 1/20 of the sample thickness. With the positive electrode as front electrode, one therefore observes photocurrents, where holes (positive charges) are transported through the 10μm-thick bulk PVK sample.

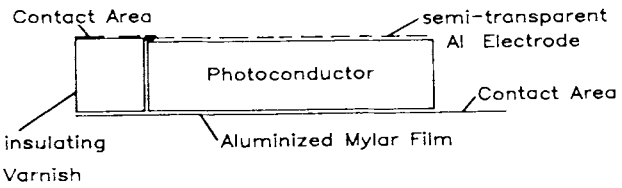

Fig. 1. Experimental arrangement for the photoconductivity measurements. The top electrode is semi-transparent aluminum. The insulating varnish prevents electrical breakthrough of the sandwich-type sample (see [17b]).

Even though the light pulse has a duration of only 10 ns and thus limits the time resolution of the experiment to the 10^{-8} s range, it triggers a photocurrent which traverses the 10μm-thick sample in roughly 10 ms and which can be experimentally monitored up to the time regime of 10 to 100 s. This wide sampling range is important for a meaningful evaluation of the experimental data.

Figures 2 and 3 show transient hole-photocurrents in PVK as a function of field and temperature taken over about nine decades in time (10 ns to 10 s) and seven or eight decades in intensity.

The gross features of the photocurrent show an initial rise time in the range of 10^{-8} s, followed by an algebraic slow decay into the 10^{-3} s time regime ($I \sim t^{\alpha-1}$, see below). At this point the first charge carriers arrive at the back electrode after having traversed the sample, and thus the slope of the photocurrent changes abruptly (to $t^{-\alpha-1}$; see below). The time at which this break in the slope occurs is called "transit time". It characterizes the macroscopic response time of the polymer sample of 10 μm thickness. For technical applications the material is some 10 μm thick and thus typical transit times are on the order of 10^{-3} to 10^{-2} s. These times are sufficiently short for technical applications in electro-photography and electroprinting.

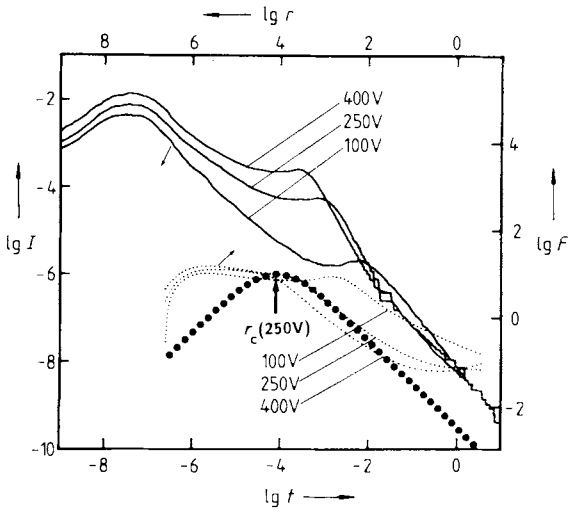

Fig. 2. Solid lines: Photocurrent of PVK (10 μm thick) at constant temperature (61.5°C) and various field strengths. Dotted lines: Analysis of rate distribution. For details see [17a].

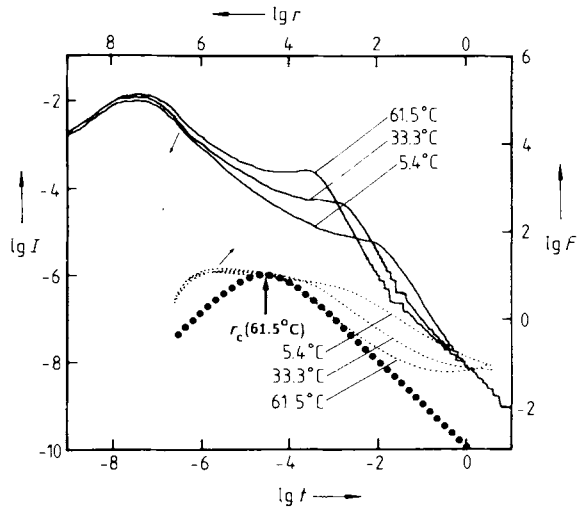

Fig. 3. Solid lines: Photocurrent of PVK (10 μm thick) at constant voltage (400 V) and various temperatures. The experimental data range over nine decades (left and lower axis). Dotted lines: Rate distributions. For details see [17a].

The difference between the data presented in Figures 2 and 3 and those published earlier (experiments on related systems) is the fact that the slope of the current (which characterizes the transport properties of the material and may be related to α) varies, as a function of time, over its full range, from 1 at short times to 0 at long times.[17a] Such a behavior can only be noticed when a sufficiently large dynamic range is monitored. If, as in many previous investigations, only four decades or less are accessible, a definite analysis to discriminate between the various microscopic processes is hardly possible.

ADVANCED MATERIALS

The analysis of the rate distribution in Figures 2 and 3[17a] is rooted in the multiple trapping (MT) formalism put forth by *Schmidlin*.[21] MT can be viewed as a phenomenological basis to characterize microscopic processes in which the main source of dispersion are energy-level fluctuations (see below). Hence, microscopic rates can be extracted from the experiment, but only when the current is monitored over many orders of magnitude in time; from measurements over nine decades one can determine rate distributions over four to five decades.[17a]

Let us remark that theoretically one usually goes the opposite way and assumes a $\psi(t)$ distribution, from which the transient currents are then calculated. This is somewhat arbitrary, but the procedure can be used to demonstrate that the current is not very sensitive to the details of the model. In fact one can show that MT and CTRW give the same result.[21–23] For a finite sample one finds[23] the following relation between the Laplace transformed current $I(u)$ and waiting-time distribution $\psi(u)$:

$$I(u) = \frac{\psi(u)}{1-\psi(u)}(1-[\psi(u)]^N) \qquad \text{(c)}$$

Nd is the thickness of the sample and d the distance between neighboring traps.

The advantage of Eq. (c) is its relatively simple structure, so that the numerical effort involved in obtaining $I(t)$ is small; only an inverse Laplace transformation is required. Our analysis[23] highlights several points, by using $\psi(t)$ forms as in Eq. (b):

1. Well inside the dispersive regime (i.e. for α around 0.5) one obtains for not-too-short times the classical Scher–Montroll behavior:[12]

$$I(t) \sim \begin{cases} t^{\alpha-1} & \text{for } t < t_T \\ t^{-\alpha-1} & \text{for } t > t_T \end{cases} \qquad \text{(d)}$$

   where t_T is the effective transit time.
2. For values of α larger than 1.0 one has, after an initial dispersive regime, Gaussian behavior.
3. The value $\alpha = 1$ is marginal; the plot of the current versus time continuously changes its slope, crossing over from dispersive to non-dispersive (Gaussian).

These findings make clear that a careful analysis of the whole current behavior is required in order to determine $\psi(t)$ from $I(t)$, since even simply structured $\psi(t)$ distributions may lead to complex $I(t)$ forms, and one cannot always rely on expressions like Eq. (d) to determine α. Moreover, up to now the microscopic mechanisms which lead to $\psi(t)$ were not discussed. The original CTRW proposition[12] was that in a chemically pure, amorphous solid the distribution of distances between the atoms gives rise to dispersive $\psi(t)$ forms, and that geometrical disorder is therefore involved. Careful computer simulations[24,25] indicate, however, that in most chemically pure solids the variation of distances can hardly lead to quite low α-values, such as $\alpha \lesssim 0.5$. The counterproposal, which leads to MT, was to invoke energetic disorder:[21,22] here the motion of the carriers is slowed down by trapping. In fact, an exponential distribution of traps[26,27] leads directly to $\psi(t)$ forms such as Eq. (b).

Due to the mathematical equivalence between CTRW and MT it is impossible to decide from a single $I(t)$ curve whether $\psi(t)$ is dominated by geometric or energetic disorder. One needs additional information. As an example, if the disorder is energetic and if the intersite transitions are thermally activated, then $\psi(t)$ will be strongly influenced by the temperature. However, the effect of temperature variation on the intersite distances is considerably smaller. As a consequence, it is very important to monitor the temperature dependence of the current. These experiments, however, are extremely difficult. On the one hand the "temperature window" in which photoconductivity experiments can be performed is rather small (typically 300 K to 400 K). At low temperatures charge carrier trapping becomes dominant and at high temperatures the polymeric materials show irreversible changes due to chemical or structural changes. On the other hand the temperature dependence of the $I(t)$ curves often does not yield a simple characteristic time exponent α (slope) if measured over a wide enough range (see Fig. 3). Here only a detailed mathematical analysis combined with measurements over more than four decades in time is sufficient to decide on the nature of the phototransport mechanism. However, measurements over such large time regimes are scarce.

The theoretical aspects of the problem are further complicated when the substrate is not chemically pure, but consists of impurity centers embedded in an inert matrix. A recent investigation used a benzotriazole derivative embedded in a polycarbonate matrix.[28] In such a situation, especially at relatively low impurity concentrations ($\lesssim 10\%$), the fluctuations in the intersite distances become very drastic. As a result, the influence of the geometric disorder may become dominant.

The prototype problem for geometric disorder in a binary mixture is percolation. In the standard model[29]—there are many variations—sites on a lattice are conducting (with probability p) or non-conducting (with probability $1-p$) and the intersite interaction is of a short-range nature (nearest neighbors only). The current flowing through the sample depends on p. For values less than a critical value p_c no current flows at all, whereas slightly above p_c one has

$$I \simeq I_0(p-p_c)^t \quad (p \gtrsim p_c) \qquad \text{(e)}$$

Here p_c depends on many details of the model (interaction range, lattice type, number of nearest neighbors), whereas t is less influenced by details, and depends mainly on the lattice dimension ($d = 2$ or 3). Note that above p_c the cur-

rent should be Gaussian (beware, however, of crossover effects near p_c). Figure 4 shows the carrier mobilities μ_T found for a mixture consisting of a charge transport component in an insulating substrate (benzotriazole in polycarbonate matrices). The experimental data seem to be consistent with the percolation picture.

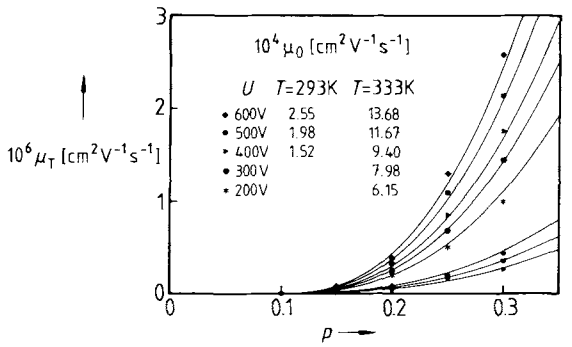

Fig. 4. The effective mobilities μ_T as a function of the benzotriazole concentration p. The μ_T data were measured at the U and T values given in the inset. All curves are fits to the percolation model, Eq. (e), with $p_c = 0.1$ and $\hat{t} = 2.5$. The resulting μ_0 values are listed in the inset.

The situation at p_c is, in the standard percolation, most interesting. Here one encounters the incipient infinite cluster on which transport is *dispersive*. This is due to the large fluctuations on connectivity at p_c, so that the incipient infinite cluster contains voids of all sizes. The structure is self-similar, or, in modern language, fractal.[14] Fractals display a subtle, lower symmetry: they are dilatationally invariant, but, in general, they lack translational symmetry.

As far as the total photocurrent is concerned, fractals can be specified by several parameters; in fact one can dispense with the stochastic intricacy of the incipient infinite cluster and model it through regular looking, deterministic fractals.[30] For diffusion on fractals one again has Eq. (a), where now α is given by:

$$\alpha = \tilde{d}/\bar{d} \tag{f}$$

$\bar{d}$ being the fractal (Hausdorff) and $\tilde{d}$ the spectral dimension of the underlying structure.[31] Use of the Einstein relation, which also holds for fractals[32,33] implies that the time dependence of the current also follows Eq. (a). In general $\tilde{d} \leqslant \bar{d}$; thus at p_c one finds $\tilde{d} \simeq 4/3$ whereas $\bar{d} = 1.9$ for $d = 2$ and $\bar{d} \simeq 2.5$ for $d = 3$.[29] Hence, the current is dispersive on percolating clusters at p_c.

It should be evident to the reader by now that the root of dispersive behavior, Eq. (a), lies in some self-similarity (scaling) of the underlying model. In the case of fractals the scaling aspect is *geometrical* (dilatation). In the CTRW model the scaling is connected to the *temporal* aspect, as expressed by Eq. (b), which is form-invariant under time-dilatation. In fact, one may use for $\psi(t)$ the Weierstrass form,[19,27] which is defined in the whole time domain:

$$\psi(t) \sim \sum_{k=1}^{\infty} (ab)^k \exp(-b^k t) \quad (a < 1,\ b < 1) \tag{g}$$

At longer times $\psi(t)$ behaves like Eq. (b), scales, and has $\alpha = \ln a / \ln b$; this prompted *Shlesinger* to call such forms time fractals.[16]

Furthermore, one may also use *energetic* self-similarity in order to obtain dispersive transport. The idea is somehow inherent in the exponential density of states, but becomes evident through model descriptions such as ultrametric spaces (UMS). Here the basic idea is to start from a Cayley tree (Bette lattice), where the tips correspond to different sites, and the energetic separation between sites is given by the length of the minimal path connecting them.[19,34] One can now show that at low temperatures the activated transport is dispersive, the parameter α being now a function of temperature, barrier-height and connectivity of the lattice.

4. Outlook

The progress that has been made recently in the theoretical description of non-Gaussian transport phenomena has created challenges for the experimentalist. It is evident that the dynamic range of most available transport data is not large enough to answer even rather basic questions such as:

- Is disorder mainly of geometric or of energetic nature?
- How well are the basic distribution functions known? (Is the trap distribution exponential, or Gaussian, or of some other type?)
- What are typical "cut-off frequencies"? Are they intrinsic or are they imposed by the nature of the experiment?

For the materials scientist the open questions are:

- What are the intrinsic limits of feasible mobilities? Can amorphous materials match the properties of crystalline materials? (Mobilities on the order of $\mu = 1$ cm^2/Vs?)
- Is the performance of polymers limited by chemical or by structural imperfections?

All of the above questions can only be dealt with if one uses modern spectroscopic tools with high time resolution. One also has to vary the materials parameters from amorphous to partially crystalline to liquid crystalline and thus utilize the flexibility offered by the wealth of organic synthetic chemistry and polymer chemistry.

Received: May 16, 1988

[1] O. H. Le Blanc, *J. Chem. Phys. 33* (1960) 626.
[2] K. G. Kepler, *Phys. Rev. 199* (1960) 1226.
[3] G. Glaser, W. Lehfeldt, *Gött. Nachr. Math. Phys. Kl. 2* (1936) 109.
[4] C. F. Carlson, US Pat. 2297691 (1942).

[5] H. Hoegl, O. Sus, W. Neugebauer, US Pat. 3037861 (1962), Hoechst AG.
[6] D. M. Shattuck, U. Vahtra, US Pat. 3484237 (1969), IBM.
[7] R. M. Schaffert: *Electrophotography*, Focal Press, London 1965.
[8] J. Mort, D. M. Pai: *Photoconductivity and Related Phenomena*, Elsevier, Amsterdam 1976.
[9] L. Bachelier, *Ann. Sci. E.N.S. III-17* (1900) 21 *("Théorie de la spéculation")*.
[10] F. Spitzer: *Principles of Random Walk*, Springer Verlag, Berlin 1976.
[11] H. Scher, M. Lax, *Phys. Rev. B 7* (1973) 4491, 4502.
[12] H. Scher, E. W. Montroll, *Phys. Rev. B 12* (1975) 2455.
[13] B. V. Gnedenko, A. N. Kolmogorov: *Limit Distributions for Sums of Independent Random Variables*, Addison-Wesley, Reading 1954.
[14] B. B. Mandelbrot: *The Fractal Geometry of Nature*, Freeman, San Francisco 1982.
[15] E. W. Montroll, G. H. Weiss, *J. Math. Phys. 6* (1965) 167.
[16] M. F. Shlesinger, *J. Stat. Phys. 36* (1984) 639.
[17] a) E. Müller-Horsche, D. Haarer, H. Scher, *Phys. Rev. B 35* (1987) 1273; b) H. Kaul, D. Haarer, *Ber. Bunsenges. Phys. Chem. 91* (1987) 845.
[18] F. C. Bos, D. M. Burland, *Phys. Rev. Lett. 58* (1987) 152.
[19] A. Blumen, J. Klafter, G. Zumofen in I. Zschokke (Ed.): *Optical Spectroscopy of Glasses*, Reidel, Dordrecht, Holland 1986, p. 199.
[20] A. Blumen, G. Zumofen, J. Klafter, *J. Lumin. 38* (1987) 320.
[21] F. W. Schmidlin, *Phys. Rev. B 16* (1977) 2362.
[22] J. Noolandi, *Phys. Rev. B 16* (1977) 4466.
[23] H. Schnörer, D. Haarer, A. Blumen, *Phys. Rev.*, in press.
[24] J. M. Marshall, *Phil. Mag. 38* (1978) 335; *43* (1980) 401.
[25] M. Silver, G. Schönherr, H. Bässler, *Phil. Mag. 43* (1981) 943; *Phys. Rev. Lett. 48* (1982) 352.
[26] T. Tiedje, A. Rose, *Solid State Commun. 37* (1980) 49.
[27] E. W. Montroll, M. F. Shlesinger in J. L. Lebowitz, E. W. Montroll (Eds.): *Nonequilibrium Phenomena II; from Stochastics to Hydrodynamics*, North-Holland, Amsterdam 1984, p. 1.
[28] H. Domes, R. Leyrer, D. Haarer, A. Blumen, *Phys. Rev. B 36* (1987) 4522.
[29] D. Stauffer: *Introduction to Percolation Theory*, Taylor and Francis, London 1985.
[30] R. Hilfer, A. Blumen, *J. Phys. A 17* (1984) L537; L783.
[31] S. Alexander, R. Orbach, *J. Phys. Lett. 43* (1982) L625.
[32] R. Hilfer, A. Blumen, *Phys. Rev. A 37* (1988) 578.
[33] I. Goldhirsch, Y. Gefen, *Phys. Rev. A 35* (1987) 1317; Y. Gefen, I. Goldhirsch, unpublished.
[34] G. Köhler, A. Blumen, *J. Phys. A 20* (1987) 5627.

Conference Reports

Organic Materials for Nonlinear Optics

The study of nonlinear optical effects in organic materials has been an active area of research for over ten years. These materials are now attracting considerable industrial interest through their potential for controlling and transforming laser radiation. The International Conference on Organic Materials for Nonlinear Optics, organized by the Royal Society of Chemistry and held at the University of Oxford, England, on 29–30 June 1988 (OMNO '88) was only one of several this year; there have already been meetings at Virginia Beach, USA, and Antibes, France, and the SPIE meeting in San Diego is yet to come. The roughly 160 delegates to OMNO '88 came from eight different countries and almost half were from industry. Its format of a single session over two days was just about right for covering the subject in depth while avoiding fatigue; the atmosphere was friendly, and the charming conference accommodation in historic Balliol College right in the center of Oxford assisted the lively evening socializing.

Fittingly, the first speaker (*J. Zyss*, CNET, France), who was among the founders of the field, spoke about the realization of one of his long-term goals, that of achieving parametric amplification in a single-crystal material. He has applied the technique as a very sensitive way of studying sub-picosecond phenomena. From his highly professional, extensively characterized and beautiful results, as well as those of *J. N. Sherwood* (Univ. of Strathclyde, UK) on crystal growth and *S. Allen*(ICI, UK) on electro-optic effects, it was apparent that second-order effects in single crystals are much better understood than any other aspect of the field. In fact, the conference heard the news that large, optical-quality crystals of 3-methyl-4-nitro-pyridine 1-oxide (POM) are now available on a commercial basis. *A. Gavezzotti* (Univ. of Milan, Italy) and *R. W. Munn* (UMIST, UK) had the design of future high-performance second-order crystalline materials in mind with their theoretical studies of molecular packing and local field effects, respectively.

Other excitement was generated by work on electro-optic effects in poled polymers. *D. R. Ulrich* (US Air Force Office of Scientific Research) gave well-reasoned arguments for his continued support of basic research in this area, and some experiments on these materials were reported by *G. R. Möhlmann* (Akzo, Netherlands) and *N. Carr* (Plessey, UK). However the most promising results were those of *J. R. Hill* (British Telecom, UK), and especially *R. Lytel* (Lockheed, USA), who appeared close to complete mastery of the technology. The electro-optic figures of merit reported are comparable with the best alternative materials, and the dispersion of dielectric constant much smaller. The major remaining task is to reduce levels of scattering.

In the area of third-order effects in conjugated polymers, there appears to have been a strategic retreat to understand the basic science. These materials, which were initially the front runners in the field, have now been faced with very effective competition from multi-quantum wells and other inorganic semiconductors materials. *P. Prasad* (SUNY, Buffalo, USA), *F. Charra* (CEN Saclay, France), *A. F. Garito* (Univ. of Pennsylvania, USA) and *D. Pugh* (Univ. of Strathclyde, UK) all attempted to understand the optical Kerr effect in terms of the interplay of molecular states, while *G. R. Meredith* (Du Pont, USA) also emphasized the contribution from cascaded second-order re-

sponse. *A. Penzkofer* (Univ. of Regensburg, FRG) reported on solution measurements of third harmonic generation. All are agreed that the effects are very fast—sub-picosecond—but *G. I. Stegeman* (Univ. of Arizona, Tucson, USA) underlined the need to consider figures of merit, which indicate that the present materials are several orders of magnitude short of usability, and require somewhat reduced attenuation and larger response. Rather than improve conjugated polymers, *K. J. McEwan* (Royal Signals & Radar Establishment, UK) tried to trade off some of the extremely high third-order response of mesogens to improve their response time and light scattering, by operating them in the isotropic phase.

Finally there were a number of talks on the general topic of Langmuir-Blodgett films. *Y. R. Shen* (Berkeley, USA) characterized the structure of monolayers on the water surface on the basis of their second harmonic generation, while *C. Bubeck* (Mainz, FRG) reported only on linear effects, mainly polarized spectroscopy, to determine the structure of deposited polymeric films. *M. C. J. Young* (Univ. of Lancaster, UK) reported some preliminary results on electro-optic response but agreed with the author of this report that optical scattering should now be the focus of applications-oriented research.

In addition to the lectures, there was a well-subscribed poster session reporting many interesting variations on the main themes discussed above, and which there is not space to review in detail here. The Proceedings of the conference are to be published by the Royal Society of Chemistry. Because of the general satisfaction all around, a further conference to be called OMNO '90 is planned in two years' time, also to be sited in Oxford.

Ian R. Peterson
Institut für Physikalische Chemie
der Universität Mainz (FRG)

European MRS Meeting in Strasbourg

Strasbourg, May 31st. No sign or poster can be seen to indicate that more than 550 highly specialized engineers and scientists from nearly all European countries and from overseas are going to meet over the next three days for an exceptional conference at the Council of Europe. Security guards routinely check the hand baggage at the entrance, a cool and impersonal climate welcomes the attendees. The atmosphere belongs to the place where European politics are handled, a place prepared for diplomatic round-table discussions rather than for the presentation of slides, transparencies and posters.

Four symposia on important aspects of materials research—high-tech ceramics, irradiation assisted processes, deep implantation and metastable alloys—were held simultaneously at the spring conference of the European Materials Research Society (E-MRS) from 31 May to 2 June 1988. "Ceramic materials research", organized by *R. Brook*, FRG, was devoted to problems of fabrication, characterization, and application of advanced ceramics and of what one could call "highly developed classical ceramics". The central topics were preparation and treatment of powders with small grain size and/or high purity (key words: "submicron powders", "zero-flaw processing"), molding processes, microstructural features caused by densification, and the resulting mechanical, thermal and electrical properties. Presentations on the mechanical testing of components, and on the statistical evaluation of flaw populations and their relevance to lifetime predictions, provoked intensive discussion; it becomes increasingly obvious that there is generally a tremendous lack of knowledge on the high-temperature behavior and on the fatigue properties of ceramics under cyclic loading. From a special session on superconductors one could form the view that the development of new compositions with higher T_c values is now stagnating, and as a result the presentations have less dramatic impact. Interest has consequently shifted to more pragmatic problems, e.g. to the preparation of well specified powders of the most promising compositions by sol-gel techniques and to the development of homogeneous microstructures with tailored grain boundaries.

The topic of the symposium on "Photon, Beam and Plasma Assisted Processing", chaired by *I. W. Boyd*, UK, and *E. F. Krimmel*, FRG, covered surface modifications of bulk materials, thin film techniques, and the preparation of high-purity powders. The compounds treated ranged from precursor materials for semiconductors and their dopants to multiply-alloyed steel. Many different deposition processes were described, and their applicability in, e.g., doping, ion beam mixing, epitaxy, recrystallization, decomposition and etching was discussed; there were also lectures on computer-assisted modeling of beam-surface interactions and characterization techniques.

Modification of semiconductors was also the most important point of interest in the session on "Deep Implant; Fundamentals and Application", directed by *G. G. Bentini*, Italy, *A. Golanski*, France, and *S. Kalbitzer*, FRG. Many lectures showed the high standard of computer simulation of ion beam interaction with matter, which can predict penetration and damage profiles in both lateral and transverse directions as a function of energy and dosage. Concerning applications, the topics were clearly governed by the interests of semiconductor research. For doping Si- or GaAs-based substrates, the trend in equipment is shifting

to large-scale MeV facilities with high current densities. Unfortunately, the topic of increasing the wear resistance of metals and ceramics by ion implantation was not addressed at all.

The symposium on "Preparation and Properties of Metastable Alloys", organized by *K. Samwer*, FRG, *M. von Allmen*, Switzerland, *J. Bottiger*, Denmark, and *B. Stritzker*, FRG, dealt with the thermodynamic aspects of metastability, the amorphization of crystals, the preparation and nucleation of undercooled liquids, the relaxation of amorphous matter, quasicrystals, ion beam modification, and the properties of metastable alloys. Although these topics seem to be rather exotic they are of high relevance not only for scientific insights but also for economic reasons; many industrial processes such as the preparation of superalloys, amorphous metals or thermodynamically impossible compounds will be able to employ such methods as powder atomization, tape casting or melt spinning to create new materials with potentially attractive properties if the basic problems of, e.g., nucleation and reaction kinetics, are understood.

Since all four symposia covered nearly every type of material from metals to ceramics, as well as all methods of preparation and characterization, all the sessions were equally attractive for the attendees. The meeting was therefore also an important opportunity to make contact with diverse groups of specialists in order to discuss new points of view and to consider unconventional strategies for solving particular problems. On the other hand, the mixing-up of related topics in four or even six parallel sessions does not permit a suitable choice of lectures without hurrying along the corridors searching out the particular room for the next session, a procedure which is even more difficult if the time schedules are not rigidly followed.

One of the advantages of this E-MRS conference was that many speakers could take part who do not normally have the opportunity to present their research in a genuinely international forum. Moreover, for many "junior scientists" Strasbourg was a very first opportunity for an international debut oral presentation before a highly expert audience; this was recognized by awards for the best presentations.

Amongst the many new competing, profit-oriented and routinely organized conferences on materials science, the merit of the annual E-MRS meeting is that it appears to be a forum specifically for European researchers—though, of course, also open to non-European attendees. The organizing committee should go on with its encouraging efforts by making further use of the charming atmosphere of the city of Strasbourg for the Fall meeting to be held on November 8–10, 1988.

R. Telle
Max-Planck-Institut für Metallforschung,
Pulvermetallurgisches Laboratorium, Stuttgart (FRG)

Research News

Ring Opening Metathesis Polymerization—Recent Developments

Ring opening metathesis polymerization (ROMP) originated in the late fifties and mid sixties when *Anderson*, *Dall'Asta* and *Natta* showed that strained cyclic olefins polymerize with breaking of the CC double bond in the presence of transition metal catalyst systems.[1] These observations initiated the growth of a whole area of research which is now known as ROMP, and led to the commercialization of new hydrocarbon polymers such as Vestenamer (Hüls), Norsorex (Chimie de France) and Metton (Hercules).

Research initially concentrated on the scope and mechanism of the polymerization. During this process a measure of control of microstructure and molecular weight was obtained. After several false starts[1] the consensus favoured a chain growth mechanism with an alternating metallo-carbene/metallacyclobutane as the chain carrying species. This hypothesis was fully confirmed by *Grubb*'s elegant work with titanacyclobutane initiators.[2] This work of *Grubbs* et al. also initiated an exciting new phase in this research area by establishing well-defined, living metathesis polymerization. *Osborn* et al.[3] and *Schrock* et al.[4] have also described such well defined initiators.

The catalyst acidity is critical in these polymerizations, both if monomers tend to undergo electrophilically induced rearrangements and if monomers contain nucleophilic heteroatoms which may coordinate to the metal center and lead to undesired side reactions or poisoning of the catalyst. Thus, these novel, fine-tuned initiators significantly widen the variety of monomers susceptible to ROMP. Some examples of the recent achievement in this area are briefly described.

The tungsten complex $[W(O\mathit{t}Bu)_2(2,6\text{-}\mathit{i}Pr_2C_6H_3N)(CH\mathit{t}Bu)]$ turned out to be specific enough to open the CC double bond of benzvalene **1**, while leaving the sensitive bicyclobutane moieties untouched.[5] The same complex opened

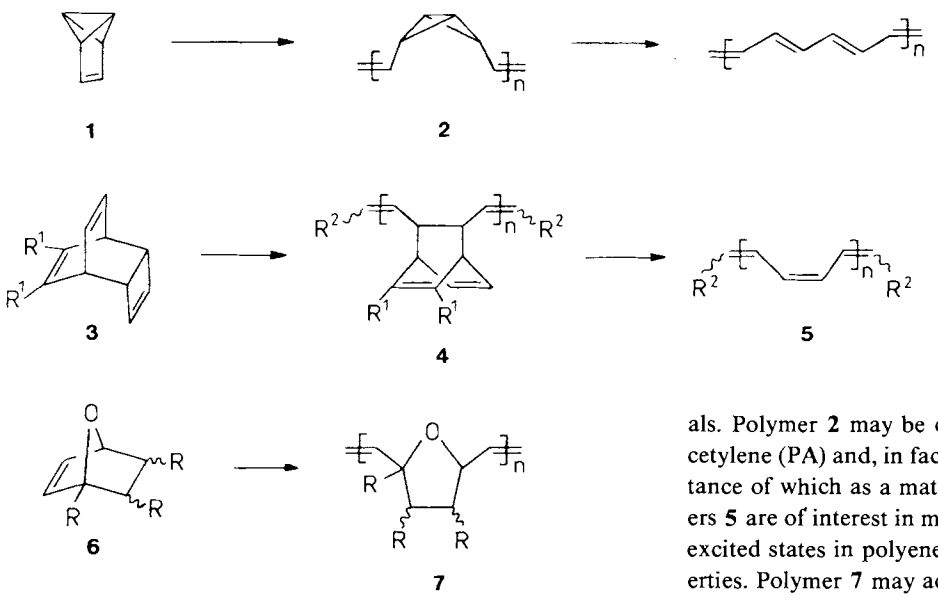

monomer **3** in a controlled manner to a set of oligomers **4**, which, after end capping and fragmentation reactions, were converted to separable polyenes **5**, with seven to fifteen double bonds.[6] Finally, a variety of substituted 7-oxanorbornenes **6** were shown to polymerize to high molecular weight compounds in the presence of $[W(OCH_2tBu)_2(CHtBu)Br_2]$, a similar tungsten catalyst. The importance of the nature of the catalyst was proven by subsequent addition of more electrophilic catalysts to polymer **7**, when complete cleavage of 1,4-epoxy units was observed.[7] These monomers may also be polymerized by ruthenium based initiators like "$RuCl_3 \cdot 3H_2O$" in the presence of water.[8]

The ROMP products **2**, **5** and **7** have entirely novel structures and are inaccessible by other methods. These polymers are not only interesting from the view-point of basic research but show remarkable properties as materials. Polymer **2** may be considered as precursor for polyacetylene (PA) and, in fact, was rearranged to PA the importance of which as a material is evident. Separated oligomers **5** are of interest in many respects, e.g. those concerning excited states in polyenes or their non-linear optical properties. Polymer **7** may act as an acyclic ionophore or as an ion permeable membrane. Thus, the new generation of ROMP catalysts has opened the way to a whole variety of novel polymers more of which might eventually gain industrial importance.

Arnulf-Dieter Schlüter
Max-Planck-Institut für Polymerforschung
Mainz (FRG)

[1] K. J. Ivin: *Olefin Metathesis*, Academic Press, London 1983.
[2] R. L. Gilliom, R. H. Grubbs, *J. Am. Chem. Soc. 108* (1986) 733.
[3] J. Kress, A. Aguero, J. A. Osborn, *J. Mol. Catal. 36* (1986) 1.
[4] C. J. Schaverien, J. C. Dewan, R. R. Schrock, *J. Am. Chem. Soc. 108* (1986) 2771.
[5] T. M. Swager, D. A. Dougherty, R. H. Grubbs, *J. Am. Chem. Soc. 110* (1988) 2973.
[6] K. Knoll, S. A. Krouse, R. R. Schrock, *J. Am. Chem. Soc. 110* (1988) 4424.
[7] B. M. Novak, R. H. Grubbs, *J. Am. Chem. Soc. 110* (1988) 960.
[8] R. H. Grubbs, paper presented at the 3rd North American Chemical Congress, Toronto, June 1988.

Book Reviews

Carbon Materials

Carbon—Electrochemical and Physicochemical Properties. By *K. Kinoshita*. Wiley, New York 1988. xiii, 533 pp., bound, £ 65.00.—ISBN 0-471-84802-6

Carbon materials have been used in electrochemistry for several decades, both in laboratory apparatus and in industrial plants. In many of the applications there is no competition whatever from other materials. The large potential range, wide variety of morphology, good corrosion resistance, high electrical and thermal conductivity and reasonable costs all contribute to carbon's benefit in electrochemical systems. Moreover, new types of materials such as pyrolytic graphite, glassy carbon and carbon fibers, have further extended the range of applications. However, many users today are not fully aware of the wide variety of carbons that can be produced by different manufacturing processes and—most importantly—neither do they know the individual physical and chemical properties of these forms. This lack of knowledge makes it difficult to

select the most appropriate form of carbon for any specific purpose. It seems that the main concern of the author *K. Kinoshita* is to bridge the gaps which exist in understanding the relevance of physicochemical properties to electrochemical specifications.

The book starts with a brief description of the manufacturing processes for carbon blacks, active carbons, graphite, glassy carbon and carbon fibers. Special emphasis is given to the commercial carbon blacks, i.e. channel blacks, oil-furnace blacks and thermal blacks.

The emphasis on carbon blacks continues in Chapter 2, which describes physical properties. Here the reader finds a thorough evaluation of the literature concerning crystallographic structure, surface area and porosity, morphology, heat treatment and electrical properties. The discussion in Chapter 3 focuses on the analysis of surface groups (chemical, spectroscopic and thermal analysis) and provides the basis for a better understanding of chemical reactivity, wettability and catalysis, the relevant properties for applications in electrochemistry. *K. Kinoshita* has succeeded in providing an excellent reference source on the physical, chemical and surface properties of carbons, most particularly carbon blacks. The description reflects the present state of knowledge, and will be of great use, not only to the electrochemist. It would have been desirable to use SI units consistently throughout the text. Data on the coefficient of thermal expansion, thermal conductivity and electrical resistivity in anisotropic graphite need to be corrected (pages 12 and 23).

Chapters 4 and 5 describe the chemical reactions as well as the characteristics and properties of carbon electrodes, thus helping the user to select specific carbon materials. In the section "nonporous structures" all the forms used in electrochemical studies are treated systematically, whereas in the section "porous structures" a distinction is made between flooded electrodes and gas-diffusion electrodes. Here again carbon black is shown to be a leading material and catalyst carrier, thus justifying the special emphasis accorded to it in the introductory chapters.

The author's approach of describing the electrochemical behavior of carbon separately (Chapter 6), rather than together with the individual applications proves to be advantageous. It allows the general aspects of electrochemical oxidation and electrocatalysis to be shown very clearly. The electrochemical reactivity of coal is also dealt with in Chapter 6.

After the efficient preparation in the preceding six chapters, the discussion devoted to the actual use of carbons in electrochemical systems is relatively short (Chapter 7, 80 pages). The reader may miss MnO_2 electrolysis as well as molten salt electrolysis yielding alkali metals and aluminum—the very applications that use by far the largest portion of carbon products. In addition, the application of carbon and graphite in chlor-alkali cells, including trials aimed at the introduction of an air-consuming cathode, appears to be treated too briefly. On the other hand the use of carbon in fuel cells, especially phosphoric acid fuel cells, and also in batteries is treated thoroughly. Within this section special attention is again devoted to carbon blacks. Reference is made to the extensive efforts undertaken to increase the life of carbon black electrodes by heat-treatment, and also by preventing the material from reaching critical potentials where corrosion occurs. It is made apparent to the reader that considerable efforts are still needed to clarify the dependence of electrochemical behavior on physical and chemical properties.

The patent literature is not considered in the text. Instead a list of recent patents concerning fuel cells, bipolar electrode separators and batteries dated after 1980 is given in the Appendix.

The motivation for writing this book arose at a workshop held in 1983 where experts from materials science and the electrochemistry of carbon came together. The author's intention has clearly been to provide a reference source for researchers and technologists interested in the electrochemistry and the electrochemical applications of carbon materials. This aim has been fully achieved. Skilful subject division, a thorough evaluation of the relevant literature and properly arranged tables all combine to make *Kinoshita*'s book an easily readable work of reference which can be highly recommended.

Graphite Fluorides. By *N. Watanabe, T. Nakajima* and *H. Touhara*. Elsevier, Amsterdam 1988. xi, 263 pp., bound, DFl 220.00.—ISBN 0-444-42885-2

The preparation and study of graphite fluorides goes back to the work of *O. Ruff, O. Bretschneider* and *F. Evert* (1934) and that of *W. Rüdorff* and *G. Rüdorff* (1947). The senior author of the book reviewed here, *N. Watanabe*, became interested in these graphite compounds while studying the "anode effect". It is undoubtedly this fact which has persuaded him to devote the first chapter of his book to the anode effect, which occurs at carbon anodes when they are used in molten fluoride electrolysis. *N. Watanabe* and his research group have worked continuously since 1961 on elucidating the chemistry of the graphite fluorides. He and his co-authors are ideally qualified to give a comprehensive account of the field.

Chapters 2 to 4 deal respectively with the preparation, the structure, and the surface properties and chemical properties of graphite fluorides. The experimental observations are described in detail with the help of numerous diagrams and tables. The interpretation of thermogravimetric data and of the X-ray, IR, NMR and X-ray photoelectron spectra is reported at considerable length, based mainly on the authors' own results. It has not been possible to avoid some repetition within the book; however this enhances its usefulness as a work of reference.

A considerable proportion of the book (about 100 pages) deals with technological applications. The outstanding properties of low surface energy, low bonding energy be-

tween the layers, and, most importantly, high electrochemical reactivity have contributed to the practical exploitation of graphite fluorides.

To bring lithium and fluorine together as reaction partners in an electrochemical primary battery is a worthwhile objective, because of the expected high cell e.m.f., but a fluorine partner in manageable form only became a possibility with the availability of $(C_xF)_n$ compounds. Using electrolytes in organic solvents it was found possible to attain a cell e.m.f. of 3.2 to 3.3 V. *Watanabe*'s laboratory carried out pioneering work on this development. The present state of knowledge on the electrode kinetics of graphite fluoride cathodes, and the effects of the crystallinity of the carbon, the method of preparation and the nature of the solvent in the cell are treated systematically in Chapter 5.

Chapter 6 describes how graphite fluorides are used to good effect in applying a fluoride film to aluminum. By using a graphite fluoride, or alternatively by simultaneous in-situ reaction of natural graphite and fluorine, films with large contact angles (125° for water) can be produced. In Chapter 7 the potential of $(CF)_n$ as a solid lubricant is evaluated by comparing it with graphite and MoS_2. It is noteworthy that metals and $(CF)_n$ can undergo co-deposition from certain electrolytic cells, e.g. from a Watts nickel cell, if surface active agents are added to force dispersion of the $(CF)_n$.

The final chapter summarizes the state of knowledge on C_xF, an intercalate of the acceptor type with ionically bound fluorine. The high cell e.m.f. observed for the combination of C_xF with lithium (3.9 to 4.2 V) is attributed to the release of active fluorine from the intercalate. However, at high current densities the increase of overpotential with current is steeper than for graphite fluorides.

The book does not make easy reading, due to the fact that it goes into considerable experimental detail. Nevertheless, it is indispensable for anyone whishing to gain a thorough knowledge of the preparation, properties and uses of graphite fluorides. For other readers it will be valuable as a work of reference, especially as it gives a full and up-to-date coverage of the literature.

Ferdinand von Sturm
Sigri GmbH, Meitingen (FRG)

Polymer Characterization

Polymer Microscopy. By *L. C. Sawyer* and *D. T. Grubb*. Chapman and Hall, London 1987. XIII, 303 pp., bound, £ 55.00.—ISBN 0-412-25710-6

The book "Polymer Microscopy" at least partially closes the gap between the large number of textbooks on electron and optical microscopy on the one hand and the problem oriented books about polymer morphology on the other. In general, a student of polymer science has a research problem which calls for the use of a variety of methods. It was always difficult to give him textbooks which would familiarize him with the possibilities and limits of microscopy applied to polymers, and would review what has already been done in his field of interest.

"Polymer microscopy" is not a textbook which enables the novice to avoid further reading of other books and review articles, but he (or she) will find out from the detailed reference list where additional information on a particular topic is available. An attempt has here been made to treat optical microscopy and scanning and transmission electron microscopy in one text. The result, however, is unbalanced to some extent. Whereas the treatment of electron microscopy takes most of the space, the field of optical microscopy on polymers is not sufficiently covered, even for a first introduction.

The main chapters which make the text worth reading in full, and which can also be used as a reference source, are those entitled "Specimen preparation methods" and "Polymer applications". The preparation chapter encompasses all the important stages that a sample can undergo on its way from the original state to the final specimen suitable for introducing into the microscope. Common sources of artefacts are also discussed, and some illustrations of them are reproduced. The applications chapter has to be seen in the light of a note in the authors' preface as follows: "Most of the applications come from work done by *Linda Sawyer* as a member of Celanese Research Company staff, and thus they come from the products and projects of interest to that company". Nevertheless, one does not get the impression that the idea for writing the book arose when someone had to tidy up the filling drawers in his office. The chapters are well organized, the index is very detailed, and a large number of references is listed up to 1984/85. But the statement that the text reflects the authors' experience and interests should certainly not be taken as detracting from the merit of having collected this material together.

A reader from an academic environment who has sometimes quite different problems regrets the omission of some guidance in the use of electron diffraction and dark field techniques for the investigation of polymers. These methods are very powerful when applied to semicrystalline samples to elucidate structural details or textures. The principles of these methods are explained and a few patterns are shown, but an unexperienced operator of an electron microscope who has read this text will not be able to use the instrument with the correct settings which are necessary for examining polymer specimens. And it is just this knowledge which one does not find in general textbooks on electron microscopy.

In the appendix a list of abbreviations for polymer names is given, but it does not help the reader to use the text as a reference book. For example, it is cumbersome to find out where abbreviations like LCP or NTP are introduced in the text.

The reproduction of photographs is of a high standard; some optical micrographs are even reproduced in color. The spelling of names, however, is incorrect in some cases. Obviously scientific publishing houses are not always able to reproduce special letters of foreign languages (e.g. as in Köhler, Poincaré, Michael-Lévy or the term Moiré pattern). This is irritating for a European reader. In spite of these remarks one can recommend the text to graduate students of polymer science as an introduction to the field, and to scientists as a reference book.

Günther Lieser
Max-Planck-Institut für Polymerforschung
Mainz (FRG)

Classical Light Scattering from Polymer Solutions. By *P. Kratochvíl*. Elsevier, Amsterdam 1987. xii, 334 pp., bound, Dfl 240.00.—ISBN 0-444-42890-9

The author deals exclusively with classical light scattering by polymer solutions, in 321 pages of text. The book treats the subject at a very elementary level, and it is presumably intended as an introductory text for students. The theoretical background of classical light scattering is treated in a way which verges on the superficial, whereas the applications and experimental details are dealt with very thoroughly. The book begins with an introduction to the physical principles of light scattering. In this it already becomes apparent that *Kratochvíl*, in his concern to present the subject in the simplest possible way, is prepared to forego a proper understanding of the physics; for example, the scattering vector is not introduced as such, but is instead referred to as "parameters for describing the angular dependence of the scattered light".

The second chapter deals in minute detail with methods of measurement and sample preparation. Here the reader benefits from the author's long experience in dealing with the everyday problems which arise in light scattering. There are also detailed descriptions of the main types of light scattering photometers, most of which are nowadays only of historical interest and are no longer marketed commercially. The currently used differential refractometers are also discussed. Surprisingly, however, *Kratochvíl* makes no mention of the existence of the modern laser light scattering photometers which have now been available for about five to eight years.

The third chapter deals with "basic light scattering techniques", such as fixed angle scattering, the dissymmetry method, and the well known Zimm method for analysis of light scattering. The only one of these which is still important nowadays is the Zimm method, which is discussed at some length; the other two methods have long since been consigned to history.

The next two chapters deal with light scattering by polymers in mixed solvents and scattering by copolymers, both of which are complex and many-faceted topics. The treatment in the book is limited to a qualitative description of the physical phenomena, but presents all necessary equations.

The book concludes by discussing the importance of light scattering for polymer characterization. It is first considered in relation to other methods such as viscometry and gel permeation chromatography, followed by a discussion of the characterization of branched structures and polyelectrolytes. The final chapter is very informative and useful since some light scattering curves for industrially important polymers such as PVC, polyethylene and polyamides are presented and discussed. The reader is (quite correctly) given the impression that the light scattering measurements as opposed to sample preparation are a relatively minor part of the work; aggregation or crystallization of the samples are usually found to interfere with their molecular characterization, and need to be minimized by choosing the most suitable experimental conditions (temperature and choice of solvent).

Considerable sections of the book are long-winded and tedious to read. The book could have been significantly reduced in length by stating the ideas more precisely and without the (superfluous) digressions into the history of light scattering. Despite this, the book will be useful for anyone wishing to begin work on classical light scattering, since no other comparable work exists.

Manfred Schmidt
Max-Planck-Institut für Polymerforschung
Mainz (FRG)

ADVANCED MATERIALS welcomes contributions from all over the world, from academia and from industry, from chemists, physicists and materials scientists, provided they are in keeping with the program outlined in the editorial published in May. Authors who are interested in writing short reviews (up to 15 pages of double-spaced manuscript together with an appropriate number of figures and/or formulas) should contact the editor. Please send all manuscripts and inquiries to:

ADVANCED MATERIALS/ANGEWANDTE CHEMIE
Postfach 1260/1280, D-6940 Weinheim, Federal Republic of Germany

Conference Calendar

October 1988

11–15 **Advanced Materials Injection Moulding and Applications**
Int. Conf.
Helsinki (Finland)
Contact: Mr. Aro/Ms. Hänninen, Eur. Adv. Mater. Inst., Reumantic 4, SF-18100 Heinola, Finland

12–14 **Ceramic Powder Processing Science,**
2nd Int. Conf.
Berchtesgaden (Fed. Rep. Germany)
Contact: Dtsch. Keram. Gesellsch., Postfach 1226, D-5340 Bad Honnef 1, FRG

12–14 **Electrochemistry and Electronics**
Basel (Switzerland)
Contact: Dr. W.-D. Luz, Metallgesellschaft AG, D-6000 Frankfurt am Main 1, FRG

12–14 **Biological and Synthetic Membranes,**
Int. Symp.
Lexington (USA)
Contact: D. Allan Butterfield, Ctr. of Membranes Sci., 12 Bradley Hall, Univ. of Kentucky, Lexington, KY 40506-0058, USA

13–14 **Laser-Materialbearbeitung,**
Eur. Conf.
Bad Nauheim (Fed. Rep. Germany)
Contact: Dtsch. Verband für Schweißtechnik e.V., Postfach 2725, D-4000 Düsseldorf 1, FRG

13–15 **Berliner Polymeren-Tage 1988**
Berlin
Contact: Bundesanstalt für Materialforschung und -prüfung (BAM), Abt. 3 - Organische Stoffe, Unter den Eichen 87, D-1000 Berlin 45, FRG

15–20 **Optics '88**
Annu. Mtg. (Part I)
Orlando (USA)
Contact: Optical Soc. of America (OSA), 1816 Jefferson Pl., NW Washington, DC 20036, USA

16–18 **Superconductors in Magnetics Commercialization,**
Workshop
San Francisco (USA)
Contact: Advantage Quest, 1110 Sunnyvale, Saratoga Rd., Suite C2, Sunnyvale, CA 94087-2515, USA

17–18 **Characterization of Polymers**
Univ. Park (USA)
Contact: J. W. Gilmer, 325 Steidle Bldg., Penn. State Univ., Univ. Park, PA 16802, USA

18–19 **Materials Futures: Strategies and Opportunities,**
US-Sweden Joint Symp.
Philadelphia (USA)
Contact: US-Sweden Joint Symp., c/o College of Eng., Univ. of Delaware, Newark, DE 19716, USA

18–20 **Industrial and Scientific Use of Lasers,**
Conf. and Exhibition
Brighton (United Kingdom)
Contact: G. Dawson, Adelphi Mill, Vollington, Macclesfield, Cheshire SK 105JB, UK

18–20 **Deutsche Keramische Gesellschaft,**
Annu. Congr.
Munich (Fed. Rep. Germany)
Contact: Dtsch. Keram. Gesellsch., Postfach 1226, D-5340 Bad Honnef 1, FRG

18–21 **Schichtsysteme für neuartige Bauelemente der Mikro-, Opto-, Bioelektronik und Optik**
Karl-Marx-Stadt (German Dem. Rep.)
Contact: Technische Univ. Karl-Marx-Stadt, Abt. Zentrale Veranstaltungen, Postfach 964, DDR-9010 Karl-Marx-Stadt, GDR

18–22 **Ceramitech '88,**
4th Int. Fair/3rd Int. Symp.
Munich (Fed. Rep. Germany)
Contact: Münchener Messe- und Ausstellungsgesellsch., Postfach 121009, D-8000 München 12, FRG

19–21 **Raw Materials for New Technologies,**
5th Int. Symp. on Mineral Resources
Hannover (Fed. Rep. Germany)
Contact: Dr. Arnt Müller, Bundesanstalt für Geowissenschaften und Rohstoffe, Postfach 510153, D-3000 Hannover 51, FRG

21–23 **Hydrogenated Amorphous Silicon Devices and Technology**
Yorktown Heights (USA)
Contact: J. Kanicki, IBM T. J. Watson Research Ctr., P.O. Box 218, Yorktown Heights, NY 10598, USA

21–24 **Functional and Fine Polymers,**
XISFFP Xian Int. Symp.
Xian (People's Rep. China)
Contact: Prof. Hua Zhao, Xian Modern Chemistry Research Inst., P.O. Box 18, Xian, People's Rep. of China

23–26 **Nonlinear Optical Materials,**
Symp. of the Am. Ceramic Soc.
San Francisco (USA)
Contact: E. M. Vogel, Bellcore, 3Z-283, 331 Newmann Springs Rd., Red Bank, NJ 07701, USA

23–26 **Combustion and Plasma Synthesis of High-Temperature Materials,**
Int. Symp.
San Francisco (USA)
Contact: Dr. J. B. Holt, Lawrence Livermore Natl. Lab., P.O. Box 808, L-369, Livermore, CA 94550, USA

23–26 **High Technology Materials Characterization**
San Francisco (USA)
Contact: W. S. Young, IBM, 5600 Cottle Rd., San Jose, CA 95193, USA

26–27 **Future Shock: Preparing for Tomorrow's Challenges in Plastics Processing,**
SPE Conf.
Indianapolis (USA)
Contact: G. Steele, Ball State Univ., PA-134, Muncie, IN 47306-1099, USA

30-1 **High-Performance Inorganic Thin Film Coatings**
Monterey (USA)
Contact: C. M. Davidson, Gorham Adv. Mater. Inst., P.O. Box 250, Gorham, ME 04038, USA

30-2 **Photopolymers,**
2nd SPE Conf. and 8th Int. Conf.
Ellenville (USA)
Contact: Maung Htoo, IBM, 10 Rabbit Trail Rd., Poughkeepsie, NY 12603, USA

31-4 **Advanced Materials**
Florida Chem. Conf.
St. Augustine (USA)
Contact: R. S. Drago, Dept. of Chem., Univ. of Florida, Gainesville, FL 32611, USA

November 1988

2-4 **Polyimides,**
SPE Conf.
Ellenville (USA)
Contact: Maung Htoo, IBM, 10 Rabbit Trail Rd., Poughkeepsie, NY 12603, USA

8-9 **Advanced Technology of Composite Materials,**
SPE Conf.
Osaka (Japan)
Contact: Toshihiko Harada, Osaka Municipal Technical Research Inst., 1-6-50 Morinomiya, Ioto-ku, Osaka 536, Japan

8-10 **European MRS**
Fall Conference
Strasbourg (France)
Contact: P. Siffert, Centre de Recherches Nucléaires, Lab. "PHASE", 23, Rue du Loess, F-67037 Strasbourg (France)

9-11 **Perspectives on the New Superconductivity**
Boston (USA)
Contact: D. Berger, Nature Publ. Co., 65 Bleecker St., New York, NY 10012, USA

10-11 **Microstructural and Microanalytic Characterization of Ceramic Materials**
Bad Nauheim (Fed. Rep. Germany)
Contact: Dtsch. Gesellsch. für Metallkunde eV., Adenauerallee 21, D-6370 Oberursel, FRG

13-15 **High T_c-Superconductors**
Monterey (USA)
Contact: C. M. Davidson, Gorham Adv. Mater. Inst., P.O. Box 250, Gorham, ME 04038, USA

15-17 **Advanced Polymer Composites for Structural Applications,**
SPE Conf.
Los Angeles (USA)
Contact: G. Yule, RTP Co., 650 Tamarack, Suite 1002, La Brea, CA 92621, USA

15-17 **Sensors and Measurement Techniques for Aeronautical Applications**
Williamsburg (USA)
Contact: Air Force Wright Aeronautical Lab., Wright-Patterson Air Force Base, OH 45433, USA

15-17 **Membrane Technology**
Int. Conf.
Sydney (Australia)
Contact: T. Fane, School of Chemical Eng., Univ. of NSW, P.O. Box 1, Kensington 2033, Australia

15-18 **Quantitative Surface Analysis,**
5th Int. Conf.
London (United Kingdom)
Contact: G. C. Smith, Division of Materials Applications, National Physical Lab., Teddington, Middlesex TW 11 OLW, UK

17-18 **Projection Plasma Spraying**
Paris (France)
Contact: IITT-International, 40 promenade Marx Dormoy, F-93460 Gournay-Sur-Marne, France

19-23 **Multiphase Macromolecular Systems,**
14th Biennial Polymer Symp.
San Diego (USA)
Contact: B. Culbertson, Ashland Chemical Co., P.O. Box 2219, Columbus, OH 43216, USA

24-25 **Intermetallic Phases**
Bad Nauheim (Fed. Rep. Germany)
Contact: Dtsch. Gesellsch. für Metallkunde eV., Adenauerallee 21, D-6370 Oberursel, FRG

27-30 **Ceramic Materials and Components for Engines,**
3rd Int. Symp.
Las Vegas (USA)
Contact: American Ceramic Soc., 757 Brooksedge Plaza Dr., Westerville, OH 43081-6136, USA

28-3 **Chemical Perspectives of Microelectronic Materials,**
MRS Fall Meeting
Boston (USA)
Contact: Materials Research Soc., 9800 McKnight Rd., Suite 327, Pittsburgh, PA 15237, USA

30 **Diffractions from Polymers**
London (United Kingdom)
Contact: Dr. M. Richardson, National Physical Lab., Teddington, Middlesex TW 11 OLW, UK

December 1988

1-4 **Water Soluble Polymers,**
Fuzhou Int. Symp.
Fuzhou (People's Rep. China)
Contact: Hu Bing-huan, Inst. of Polym. Sci., Fujian Teachers Univ., People's Rep. of China

2 **Computer Modelling of Inorganic Solid Structures**
London (United Kingdom)
Contact: Dr. A. E. Comyns, R & D Dept., Laporte Industries Ltd., Moorfield Rd., Widnes WA8 OQJ, UK

5-9 **Lasers and Applications,**
11th Int. Conf.
Lake Tahoe (USA)
Contact: Prof. H. J. Eichler, Techn. Univ. Berlin, Optisches Inst., Straße des 17. Juni 135, D-1000 Berlin 12, FRG

7 **Polymers for Life Science Applications**
London (United Kingdom)
Contact: Dr. M. D. Purbrick, Kodak. Ltd. Research Div., Headstone Drive, Harrow HA1 ATY, Middlesex, UK

7–8 **Materials Science and Eng. Towards the 21st Century,**
4th Israel Mater. Eng. Conf.
Beer-Sheva (Israel)
Contact: Peltours-Conventions, The Secretariat, 4th Israel Mater. Eng. Conf., P.O. Box 394, 61003 Tel-Aviv, Israel

7–9 **Ceramics for Environmental Protection,**
1st Int. Symp.
(ENVICERAM '88)
Köln (Fed. Rep. Germany)
Contact: G. von Landsberg, Deutscher Wirtschaftsdienst, Marienburger Straße 22, D-5000 Köln 51, FRG

12–17 **Advances in Holography and Speckle Phenomenon and their Industrial Applications,**
Int. Workshop
Madras (India)
Contact: Prof. R. S. Sirohi, Indian Inst. of Technol., Physics Dept., Madras 600036, India

14–16 **SIMCER 7/ZIRCONIA 88**
7th Int. Symp. on Ceramics
Bologna (Italy)
Contact: Centro Ceramico, Via Martelli, 26
I-43138 Bologna, Italy

January 1989

15–20 **Optics, Electro-Optics, and Laser Applications in Sci. and Eng.,**
Symp. and Exhibition
Los Angeles (USA)
Contact: Soc. of Photo-Optical Instrumentation Eng. (SPIE), P.O. Box 10, Bellingham, WA 98227, USA

31–3 **Polymer,**
17th Australian Symp.
Brisbane (Australien)
Contact: Dr. D. J. T. Hill, Chem. Dept., Univ. of Queensland, Brisbane 4067, Australia

31–3 **Sintering of Multiphase Metal and Ceramic Systems**
Int. Conf.
New Delhi (India)
Contact: G. S. Upadhyaya, Convener ICSMC '89, Dept. of Metallurgical Eng., Indian Inst. of Technol., Kanpur 208 016, India

February 1989

5–9 **Biomedical Polymers,**
Int. Symp.
Perth (Australia)
Contact: Secretary, W. A. Polymer Group, Royal Australian Chemical Inst., 125 Hay St., Perth, W. A. 6000, Australia

6–10 **Composites,**
SPI Inst. Annu. Conf.
Dallas (USA)
Contact: Composites Inst., SPI, 355 Lexington Ave., New York, NY 10017, USA

6–10 **Optical Fiber Communication,**
IEEE-LEOS-OSA Conf.
(OFC '89 and IGWO '89)
Houston (USA)
Contact: Optical Soc. of America (OSA), 1816 Jefferson Pl., NW Washington, DC 20036, USA

21–26 **Optical Fibers and their Applications,**
5th Symp.
Warsaw (Poland)
Contact: R. S. Romaniuk, IPI Warsaw Univ. of Technol., Nowowiepska 15–19, PL-00-665, Warsaw, Poland

27–3 **High-Temperature Superconducting Oxides: Processing & Related Properties,**
TMS Annu. Meeting
Las Vegas (USA)
Contact: M. Karl, The Metallurgical Soc., 420 Commonwealth Drive, Warrendale, PA 15086, USA

March 1989

2–4 **Makromolekulares Kolloquium**
Freiburg (Fed. Rep. Germany)
Contact: Prof. H. Finkelmann, Inst. für Makromolekulare Chemie der Univ., Stefan-Meier-Str. 31, D-7800 Freiburg, FRG

5–10 **Liquid Crystals,**
6th Eur. Winter Conf.
Schladming (Austria)
Contact: P. Laggner, Inst. für Röntgenfeinstrukturforschung of the Austrian Academy of Sci., Steyrergasse 17, A-8010 Graz, Austria

6–8 **Lithium Battery Technology & Applications,**
4th Int. Seminar
Deerfield Beach (USA)
Contact: S. P. Wolsky, Ansum Enterprises Inc., 950 De Soto Rd., Suite 3B, Boca Raton, FL 33432, USA

6–9 **Advanced Materials**
Denver (USA)
Contact: Dr. Fred Smith, Adv. Mater. Inst., Colorado School of Mines, 1500 Illinois, Golden, CO 80401, USA

8–9 **Molecular Chemistry of Solid-State Electronics**
London (United Kingdom)
Contact: The Royal Society, 6 Carlton House Terrace, London SW 1Y 5AG, UK

11–14 **Surface Finishing '89**
Brighton (United Kingdom)
Contact: Inst. of Metal Finishing, Exeter House, 48 Holloway Head, Birmingham B1 1NQ, UK

20–22 **Refractory Metals and Silicides**
Eur. Workshop
Houthalen (Belgium)
Contact: R. De Keersmaecker, IMBE, Kapeldreef 75, B-3030 Leuven, Belgium

20–23 **Surface Science,**
Interdisciplinary Conf.
Liverpool (United Kingdom)
Contact: P. Weightman, Liverpool Univ., Oliver Lodge Lab., Oxford St., P.O. Box 147, Liverpool L69 3BX, UK

28–31 **Aluminium-Lithium**
5th Int. Conf.
Williamsburg (USA)
Contact: Al-Li-V, School of Eng. and Applied Sci., Thornton Hall, Univ. of Virginia, Charlottesville, VA 22901, USA

29–31 **Neutron and X-Ray Scattering: Complementary Techniques**
Canterbury (United Kingdom)
Contact: Dr. R. J. Newport, Univ. of Kent, Physics Dept., Canterbury, Kent CT2 7NR, UK

30–31 **Colorado Microelectronics**
Colorado Springs (USA)
Contact: CMC '89 Conf. Secretary, Microelectronics Research Lab., Univ. of Colorado, Colorado Springs, CO 80933-7150, USA

April 1989

3–5 **Modern Practice in Stress and Vibration Analysis**
Liverpool (United Kingdom)
Contact: Inst. of Physics, Meetings Officer, 47 Belgrave Square, London SW1X8QX, UK

3–7 **Copolymerization and Copolymers in Dispersed Media**
Lyon (France)
Contact: I. Guillot/C. Pichot, Lab. des Materiaux Organiques, BP 24, F-69390 Vernaison, France

10–12 **Bayreuther Polymer Symp.,** (BPS '89)
Bayreuth (Fed. Rep. Germany)
Contact: BPS '89, Lehrstuhl Makromolekulare Chemie II, Univ. Bayreuth, Postfach 101251, D-8580 Bayreuth, FRG

11–13 **Catalysis by Well Characterized Materials**
Liverpool (United Kingdom)
Contact: Prof. R. W. Joyner, Leverhulme Ctr. for Innovative Catalysts, Univ. of Liverpool, Grove St., P.O. Box 147, Liverpool L69 3BX, UK

17–26 **Ceramics and Composite Materials,**
Spring College in Mater. Sci.
Trieste (Italy)
Contact: Int. Ctr. for Theoretical Physics, Spring College in Mater. Sci. 1989, P.O. Box 586, I-34100 Trieste, Italy

24–28 **Lasers and Electro-Optics,**
LEOS-IEEE-OSA Conf. (CLEO '89)
Baltimore (USA)
Contact: Optical Soc. of America (OSA), 1816 Jefferson Pl., NW Washington, DC 20036, USA

24–28 **MRS-Spring Mtg.**
San Diego (USA)
Contact: J. B. Ballance, MRS, 9800 McKnight Rd., Suite 327, Pittsburgh, PA 15237, USA

25–27 **Hot Isostatic Pressing of Materials: Applications and Developments**
Antwerpen (Belgium)
Contact: Hot Isostatic Pressing Conf., c/o K. VIV, Jan van Rijswijcklaan 58, B-2018 Antwerpen, Belgium

26–28 **Joining Ceramics, Glass and Metal**
3rd Int. Conf. (CGM '89)
Contact: Dtsch. Gesellsch. für Metallkunde eV., Adenauerallee 21, D-6370 Oberursel, FRG

May 1989

4–6 **Festkörper: Dynamik und Kinetik**
Siegen (Fed. Rep. Germany)
Annu. Mtg. of the Dtsch. Bunsen-Gesellsch. für Phys. Chem.
Contact: Dtsch. Bunsen-Gesellsch., Carl-Bosch-Haus, Varrentrappstr. 40/42, D-6000 Frankfurt am Main 90, FRG

9–11 **Coatings and Sensors for Acoustic and Electromagnetic-Optical Applications**
Univ. Park. (USA)
Contact: V. K. Varadan, Dept. of Eng. Sci. and Mechanics, Penn. State Univ., 227 Hammond Bldg., Univ. Park, PA 16802, USA

22–24 **Glastechnische Tagung**
Stuttgart (Fed. Rep. Germany)
Contact: Dtsch. Glastechnische Gesellsch. eV., Mendelssohnstr. 75–77, D-6000 Frankfurt am Main, FRG

22–25 **Graphite Intercalation Compounds,**
5th Int. Symp. (ISGIC-5)
Berlin
Contact: Dr. F. W. Froben, Fachbereich Physik, Freie Univ. Berlin, Arnimallee 14, D-1000 Berlin 33, FRG

29–2 **Molecular Beams**
Perugia (Italy)
Contact: V. Aquilanti, Univ. di Perugia, Dipt. di Chimica, I-06100 Perugia, Italy

June 1989

18–21 **Colloid & Surface Science,**
63rd ACS Div. of Colloid & Surface Chem. Symp.
Seattle (USA)
Contact: J. Berg, Dept. of Chemical Eng. BF-10, Univ. of Washington, Seattle, WA 98105, USA

26–28 **Molecular Design of Functional Polymers,**
IUPAC Int. Symp.
Seoul (Korea)
Contact: IUPAC Int. Symp., c/o Polymer Soc. of Korea, Rm 601, Hyecheon Bldg., 831 Yeoksam-dong, Kangnam-ku, Seoul 135-792, Korea

July 1989

10–13 **Magnetic Resonance in Polymers,**
9th Spec. Colloq. Ámpere
Prague (Czechoslovakia)
Contact: P. M. M. Secretariat, c/o. Inst. of Macromol. Chem., Czech. Acad. of Sci., 16206 Prague, Czechoslovakia

11–14 **Numerical Analysis of Semiconductor Devices and Integrated Circuits,**
6th Int. Conf.
Dublin (Ireland)
Contact: J. J. H. Miller, Nase-Code Conf., INCA, P.O. Box 2, Dún Laoghaire, Ireland

24–26 **Composite Structures,**
5th Int. Conf.
Paisley (United Kingdom)
Contact: Dr. I. H. Marshall, Dept. of Mechanical and Production Eng., Paisley College of Technol., High St., Paisley PA 12BE, UK

31–2 **Biologically-Engineered Polymers**
Cambridge (United Kingdom)
Contact: Royal Soc. of Chemistry, Burlington House, London W1V OBN, UK

August 1989

2–7 **Pure and Applied Chemistry,** 32nd IUPAC Congress Stockholm (Sweden) Contact: Stockholm Convention Bureau, P.O. Box 6911, S-10239 Stockholm, Sweden

20–24 **Imaging Systems – 150 Years of Photography,** Int. Symp. (ISIS '89) Dresden (German Dem. Rep.) Contact: Conf. Secretary, ISIS '89, Technische Univ. Dresden, Sektion Physik, Wissenschaftsbereich Photophysik, Mommsenstr. 13, DDR-8027 Dresden, GDR

28–31 **Dynamical Processes in Excited States of Solids,** 7th Int. Conf. (DPC '89) Athens (USA) Contact: DPC '89, Prof. J. E. Rives, Dept. of Physics and Astronomy, Univ. of Georgia, Athens, GA 30602, USA

28–1 **Ferroelectricity,** 7th Int. Mtg. (IMF-7) Saarbrücken (Fed. Rep. Germany) Contact: Dr. J. Albers, Univ. des Saarlandes, Fachbereich Physik, D-6600 Saarbrücken, FRG

28–1 **Sintering,** 7th World Round Table Conf. Herceg-Novi (Yugoslavia) Contact: Dr. D. P. Uskoković, Serbian Academy of Sci. and Arts, Knez-Mihailova 35, 11000 Beograd, Yugoslavia

28–1 **X-Ray Optics and Microanalysis,** 12th Int. Congr. Cracow (Poland) Contact: S. Jasienska, Academy of Mining and Metallurgy, Inst. of Metallurgy, 30-059 Cracow, Poland

Last-minute information

More Funds for German Materials Science

In collaboration with the Fonds der Chemischen Industrie, the Federal Minister for Research and Technology (BMFT) has initiated a new support program in materials science. In the next two years selected leading research groups and talented young scientists will be awarded grants-in-aid totalling some five million marks, two million marks of which will come from the BMFT, for research in materials science.

The support program will primarily concentrate on computer simulation in materials science. In the important fields organic polymers, inorganic solids and high-performance ceramics a purposefully planned support for instruments and facilities (hardware) for six specially selected research groups (see Table 1) who already have considerable experience in these fields will hopefully contribute to a prompt and effective employment of computer simulation in materials research. This should remedy a deficiency in German basic research that has occurred because of the exceptionally rapid development in this field.

Table 1. Computer simulation in materials science: research groups already funded.

group leader	location	research topic
Hk. Müller-Buschbaum	Univ. of Kiel, Inst. of Inorg. Chem.	CAMD in solid state inorganic chemistry
R. Gruehn	Univ. of Giessen, Inst. of Inorg. and Analyt. Chem.	high resolution electron microscopy with simultaneous 2D/3D reconstructions
W. Spiess	Mainz, Max Planck Inst. for Polymer Science	polymer simulation and 2D NMR spectroscopy
D. Haarer	Univ. of Bayreuth, Physics Department	dynamic processes in polymer systems: charge carriers, color centers, micelles
J. H. Wendorff	Darmstadt, Deutsches Kunststoff-Inst.	polymer liquid crystals
G. Petzow	Stuttgart, Max Planck Inst. for Metals Research	CAD of ceramic engineering materials

The funds of this support program will also be used for providing fellowships for qualified young scientists and grants for equipment to leading scientists in the fields of macromolecular chemistry, inorganic chemistry, physical chemistry and industrial chemistry. The ear-marking of part of the funds for financing subscriptions to specialized literature, participation at scientific conferences and the compilation of information addressed to scientists engaged in materials research should lead to an improved transfer of know-how among the individual researchers. The allocation of funds will be undertaken by independent advisory committees in the individual disciplines. Each of the committees will consist of academic and industrial scientists who will assess the allocation of funds exclusively according to scientific expertise.

Further information is available on request from the Fonds der Chemischen Industrie, Karlstraße 21, D-6000 Frankfurt/Main 1, Tel. 069/2556482.

ANGEWANDTE CHEMIE
International Edition in English

Volume 27 · Number 10
October 1988
Pages 1227–1388

Electron Transfer and Charge Transfer: Twin Themes in Unifying the Mechanisms of Organic and Organometallic Reactions

By Jay K. Kochi*

The broad varieties of organic and organometallic reactions merge into a common unifying mechanism by considering all nucleophiles and electrophiles as electron donors (D) and electron acceptors (A), respectively. Comparison of outer-sphere and inner-sphere electron transfers with the aid of Marcus theory provides the thermochemical basis for the generalized free energy relationship for electron transfer (FERET) in Equation (37) and its corollaries in Equations (43) and (44) that have wide predictive applicability to electrophilic aromatic substitutions, olefin additions, organometallic cleavages, etc. The FERET is based on the conversion of the weak nucleophile–electrophile interactions extant in the ubiquitous electron donor–acceptor (EDA) precursor complex [D,A] to the radical ion pair [$D^{\oplus}$, $A^{\ominus}$], for which the free energy change can be evaluated from the charge-transfer absorption spectra according to Mulliken theory. FERET analysis thus indicates that the charge-transfer ion pairs [$D^{\oplus}$, $A^{\ominus}$] are energetically equivalent to the transition states for nucleophile/electrophile transformations. The behavior of such ion pairs can be directly observed immediately following the irradiation of the charge-transfer bands of various EDA complexes with a 25-ps laser pulse. Such studies confirm the radical ion pair [$Arene^{\oplus}$, NO_2] as a viable intermediate in electrophilic aromatic nitration, as presented in the electron-transfer mechanism between arenes and the nitryl cation ($NO_2^{\oplus}$) electrophile.

1. Introduction

Despite the explosive developments in sophisticated methodologies for the syntheses, analyses, and structure elucidations of organic and organometallic compounds over the last forty years, the corresponding increase in our understanding of the dynamics of chemical reactions in solution is woefully lacking.[1] Indeed, the oft-repeated quip that "a reaction mechanism can never be proved—only proved wrong" characterizes the critical void in this important branch of chemistry. Thus the rates of chemical reactions cannot be predicted from the properties of the reactants and of the solvent. Heretofore, the limited means to correlate reaction rates have derived from empirical methods such as those based on the Hammett $\sigma\rho$, Brønsted $\alpha\beta$, and Dimroth-Reichardt E_T values, and then only under certain constrained circumstances. The problem is understandable if one considers the myriad reactions and reaction types that are possible with the wide variety of structures presently extant with organic and organometallic connotations. For example, let us examine a short list of such basic transformations as follows:

Olefin Addition:

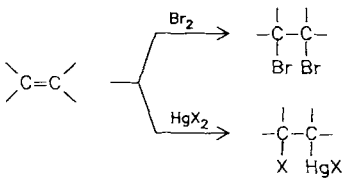

(1)

(2)

[*] Prof. J. K. Kochi
University of Houston, University Park
Department of Chemistry
4800 Calhoun Road, Houston, TX 77204-5641 (USA)

 © VCH Verlagsgesellschaft mbH, D-6940 Weinheim, 1988 0570-0833/88/1010-1227 $ 02.50/0

Aromatic Substitution:

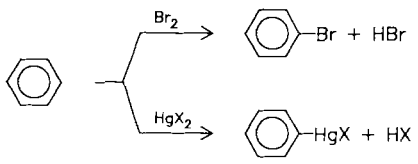

(3)

(4)

Alkylmetal Cleavage:

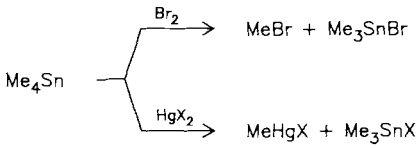

(5)

(6)

[4+2] Cycloaddition:

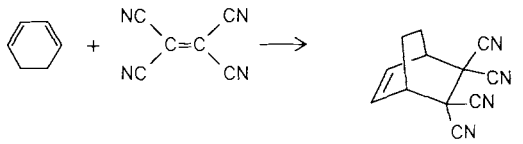

(7)

Carbonyl Addition:

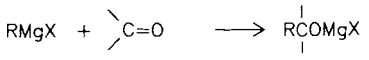

(8)

Stannane Reduction:

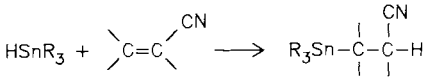

(9)

Oxidative Addition:

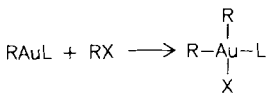

(10)

Insertion:

(11)

Carbonylation:

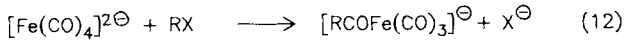

(12)

Autoxidation:
(chel = chelating ligand)

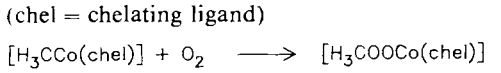

(13)

Alkylation:

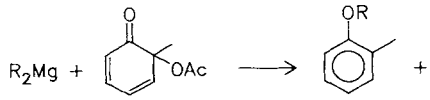

(14)

Oxygen Transfer:

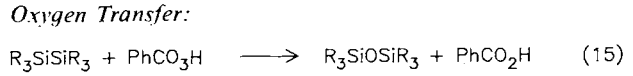

(15)

Are these reactions all unrelated? Or is there a common mechanistic thread that connects one set of reactants to another? For example, the treatment of alkenes, arenes, and alkylmetals with bromine [Eqs. (1), (3), and (5)] has been generally characterized as an electrophilic process. However, that is not generally considered to be the case in the Diels–Alder [4+2] cycloaddition [Eq. (7)], in the oxidative addition of an alkyl halide [Eq. (10)], or in the autoxidation of methylcobalamin [Eq. (13)]. How does one consider an insertion of sulfur dioxide into an alkyl–iron bond in Eq. (11), or, for that matter, the incorporation of an oxygen atom into a disilane [Eq. (15)]? Why does mercury(II) diacetate add readily to alkenes [oxymercuration, Eq. (2)], whereas under the same conditions the analogous dimethylmercury is unreactive.

A more detailed consideration of reactions (1)–(15) reveals that each pair of reactants consists of a relatively electron-rich component and an electron-poor one. Thus bromine, metal halides, tetracyanoethylene, nitric acid, carbonium ions, acrylonitrile, ketones, sulfur dioxide, alkyl halides, dioxygen, peroxy acids, etc. are all electron-poor acceptors by virtue of their relative ease of reduction and high electron affinities.[2] Conversely, alkenes, arenes, Grignard reagents, alkylmetals, dienes, stannanes, carbonylferrates, etc. are all electron-rich donors with relatively low ionization potentials.[3] On this basis mercury(II) diacetate is an electron acceptor, whereas dimethylmercury is an electron donor.[4] Indeed, the designation of various reactants as electron acceptors and electron donors can be carried over into a more traditional context by their description as electrophiles and nucleophiles, respectively.[5] As widespread as the latter notion is, however, this classification is qualitative and carries with it no mechanistic insight—certainly none of any quantitative predictive power.[6,7] Clearly a different approach is required.

Let us therefore consider the alternative classification of electron acceptors (A) and donors (D) as oxidants and reductants, respectively, since electron transfer as an oxidation–reduction process represents one of the simplest chemical transformations. Furthermore, the concept is well-established in inorganic chemistry in which two principal pathways for electron transfer have been identified.[8,9] In the *outer-sphere mechanism*, the coordination spheres [as pictorially represented by circles in Eqs. (16) and (17)] remain more or less intact as the donor–acceptor pair passes through the transition state [Eq. (16)]. As a result, the Marcus model for the outer-sphere transition state successfully provides the theoretical guide for the prediction of these electron-transfer rates.[10,11] By contrast, the interpenetration of the coordination spheres of the donor–acceptor pair in the *inner-sphere mechanism* presents the more compact transition state [Eq. (17)]. The shaded area

(16)

(17)

emphasizes the possibility of structural distortions, ligand bridging, etc., as additional contributions that are largely irrelevant in the simpler outer-sphere pathway. As a result, there is no general theoretical model of electron transfer for the more constrained inner-sphere pathway. This represents a serious deficiency since the vast majority of oxidation-reduction processes proceed via inner-sphere mechanisms.

2. Outer-Sphere and Inner-Sphere Mechanisms for Electron Transfer

Historically, the theories of electron transfer in chemical reactions have been developed largely from two quite separate and independent approaches. In the first approach, the evolution from inorganic chemistry of oxidation-reduction processes pertaining to transition-metal complexes has led to the Marcus theory,[10] as well as the intervalence transfer theory of *Hush*.[12] The other approach, tracing back to the charge-transfer theory of *Mulliken*, stems from organic substrates and deals mainly with electronic transitions.[13] *Mulliken*'s theory employs the intermolecular distance between donor and acceptor as the only nuclear parameter, and does not explicitly mention the changes in molecular structure attendant upon charge transfer. The Marcus approach, however, does not readily lend itself to the inclusion of the Franck-Condon factors for the donor and the acceptor. Experimentally, these two theoretical treatments have heretofore remained separate—the Marcus-Hush theory for inorganic redox and electrochemical systems and the Mulliken theory for organic acceptors—because they have lacked a common basis for comparative examination. Therefore, let us employ organometallic compounds, both as reducing agents and as electron donors, to provide such a common basis for comparing electron-transfer and charge-transfer interactions within a framework of steric effects.

2.1. Organometals as Electron Donors. Delineation of Polar and Steric Effects

We consider the four structurally diverse classes of organometals **I**–**IV** as electron donors, in which the configuration and coordination about the metal centers vary systematically from octahedral, square planar, and tetrahedral

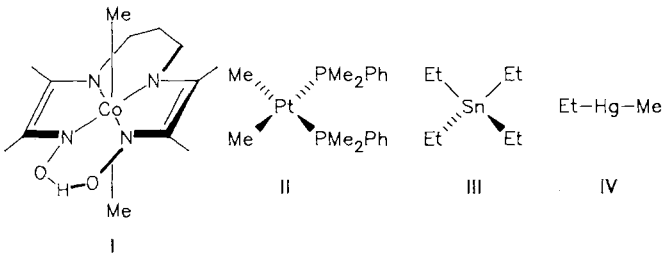

to linear, respectively. These organometal donors are especially desirable for kinetic studies since they are all sufficiently *substitution stable* in solution to allow meaningful measurements to be made. Moreover, for these neutral donors, the work term of the reactants, w_r (consisting mainly of the electrostatic energy required to bring the reactants together), is considered to be unimportant. An additional benefit derived from the use of organometal donors lies in the transient character of many of the oxidized organometal cations. As a result, the back electron transfer is minimal, and the electron-transfer process is overall *irreversible* in these systems. Since they are relatively volatile and electron-rich compounds, the photoelectron spectra of the alkylmetals **III** and **IV** are readily accessible, and the vertical ionization potentials I_D can be accurately measured. For example, the photoelectron spectra in Figure 1 illus-

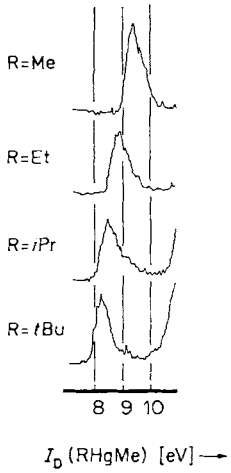

Fig. 1. He(I) photoelectron spectra of the lowest-energy bands of Me_2Hg, EtHgMe, *i*PrHgMe, and *t*BuHgMe.

trate how the lowest-energy band of a homologous series of dialkylmercurials undergoes large, systematic variations merely by branching at the α-carbon of the alkyl ligand.[14] In these alkylmetals of the main-group elements, ionization occurs from the highest occupied molecular orbital (HOMO), which has σ-bonding character; i.e., they are σ donors. Consequently, alkyl ligands exert a large dominating influence on the *ionization potentials* and the *steric properties* of alkylmetals. Both trends are illustrated in Figure 2 for the α-branched ligands (methyl, ethyl, isopropyl, and *tert*-butyl, Fig. 2a) as well as the β-branched ligands (ethyl, *n*-propyl, isobutyl, and neopentyl, Fig. 2b). Note that the steric and polar effects generally increase together in the α-branched alkyl ligands, whereas variations in the steric effect dominate in the β-branched alkyl ligands.

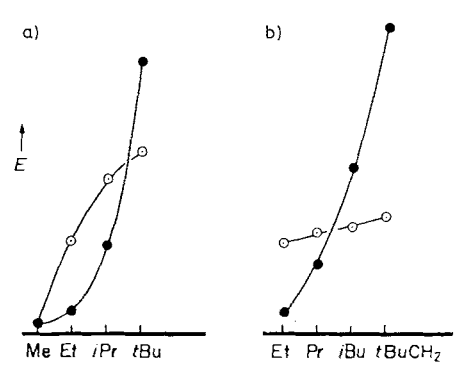

Fig. 2. Steric (●) and polar (⊙) effects of alkyl ligands with α-branching (a) and β-branching (b). Energy, *E*, in arbitrary units.

2.2. Outer-Sphere Electron Transfer from Organometal Donors

The minimal interpenetration of the coordination spheres of the reactants is inherent in any mechanistic formulation of the outer-sphere process for electron transfer [cf. Eq. (16)]. As such, steric effects provide a basic experimental criterion to establish this mechanism. Therefore, we employ the series of structurally related donors possessing the finely graded steric and polar properties described in Section 2.1 for the study of both homogeneous and heterogeneous processes for electron transfer.

2.2.1. Homogeneous Processes with Metal Oxidants

The rates of electron transfer for oxidation of the organometal donors **I**–**IV** (hereafter designated generically as RM) by a series of complexes $[ML_3]^{3\oplus}$, with $M = Fe^{III}$, Ru^{III}, Os^{III}, and L = phenanthroline or substituted phenanthroline (Scheme 1), is considered initially, since they have been previously established as outer-sphere oxidants.[15]

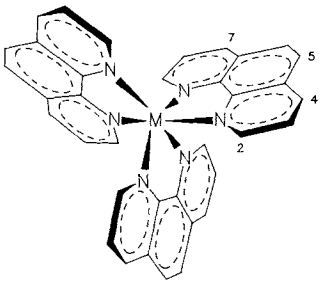

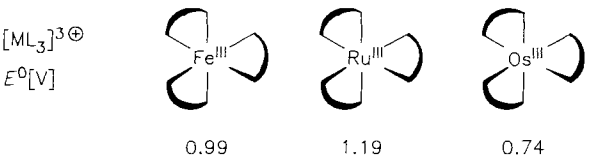

Scheme 1. Tris(phenanthroline) complexes as outer-sphere oxidants.

The iron(III) complexes $[FeL_3]^{3\oplus}$ cleave a variety of organometals in acetonitrile according to Equations (18) and (19).[16] The activation process for oxidative cleavage is represented by the electron-transfer step in Equation (18).

$$RM + [FeL_3]^{3\oplus} \xrightarrow{k_{Fe}} RM^{\oplus} + [FeL_3]^{2\oplus} \quad (18)$$

$$RM^{\oplus} \xrightarrow{fast} R^{\odot} + M^{\oplus} \longrightarrow \longrightarrow \cdots \quad (19)$$

The organometal cation $RM^{\oplus}$ is a transitory intermediate which subsequently undergoes a rapid fragmentation [Eq. (19)], rendering the electron transfer irreversible. For a particular iron(III) oxidant, the logarithm of the rate constant k_{Fe} for electron transfer is linearly correlated with the ionization potential I_D of the various alkylmetal donors (Fig. 3).[17] Similarly, for a particular alkylmetal donor, $\lg k_{Fe}$ for electron transfer varies linearly with the standard reduction potentials E^0 of the series of iron(III) complexes $[FeL_3]^{3\oplus}$, with L = substituted phenanthroline. In order to account for the foregoing kinetic behavior, we rely on the Marcus theory for outer-sphere electron transfer to provide the quantitative basis for establishing a free energy relationship, the Marcus equation (20),[10] where

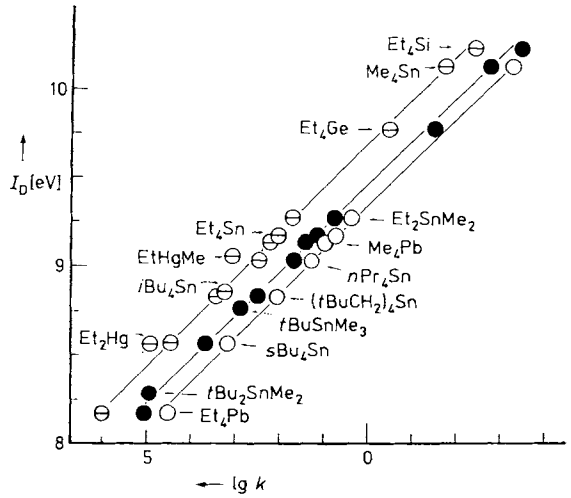

Fig. 3. Correlation of the ionization potentials of alkylmetal donors with the electron-transfer rate constant ($\lg k_{Fe}$) for $[Fe(phen)_3]^{3\oplus}$ (●), $[Fe(bpy)_3]^{3\oplus}$ (○), $[Fe(Cl\text{-}phen)_3]^{3\oplus}$ (⊖). phen = phenanthroline; bpy = bipyridine; Cl-phen = 5-chlorophenanthroline.

$$\Delta G^{\ddagger} = w_r + \Delta G_0^{\ddagger}\left[1 + \frac{\Delta G}{4\Delta G_0^{\ddagger}}\right]^2 \quad (20)$$

$\Delta G = \Delta G^0 + w_p - w_r$ and ΔG^0 is the standard free energy change accompanying electron transfer. The intrinsic barrier $\Delta G_0^{\ddagger}$ represents the activation free energy for electron transfer at $\Delta G = 0$, and w_p is the work required to separate the products. For neutral reactants such as organometals, the work term of the reactants, w_r, is considered to be nil, and the rate constants are converted to the activation free energies by $\Delta G^{\ddagger} = -RT\ln(k/Z)$, where the collision frequency Z is taken to be $3 \times 10^{10}\ M^{-1}\ s^{-1}$. In order to apply the Marcus equation to electron transfer from neutral organometals RM to the series of $[FeL_3]^{3\oplus}$ oxidants, Equation (20) can be rewritten in an alternative form [Eq. (21)],

$$\sqrt{\Delta G^{\ddagger}} = \left[\sqrt{\Delta G_0^{\ddagger}} + \frac{F}{4\sqrt{\Delta G_0^{\ddagger}}}\left(E^0_{RM} + \frac{w_p}{F}\right)\right] - \frac{F}{4\sqrt{\Delta G_0^{\ddagger}}}E^0_{Fe} \quad (21)$$

since $\Delta G^0 = F(E^0_{RM} - E^0_{Fe})$ and $w_r = 0$. E^0_{RM} and E^0_{Fe} are the standard electrode potentials of the alkylmetal and $[FeL_3]^{3\oplus}$, respectively, and F is the Faraday constant. The experimental correlation between $\sqrt{\Delta G^{\ddagger}}$ and E^0_{Fe} is linear for the various alkylmetals (Fig. 4a), and the slopes of the correlations represent $-F/(4\sqrt{\Delta G_0^{\ddagger}})$. It is important to note that the most sterically hindered alkylmetal examined, namely, tetra(neopentyl)tin, is precisely included with the other alkylmetals in the correlations shown in both Figures 3 and 4a. In other words, *alkylmetals are not distinguished from each other on the basis of their steric properties when they undergo oxidation with* $[FeL_3]^{3\oplus}$—the electron-

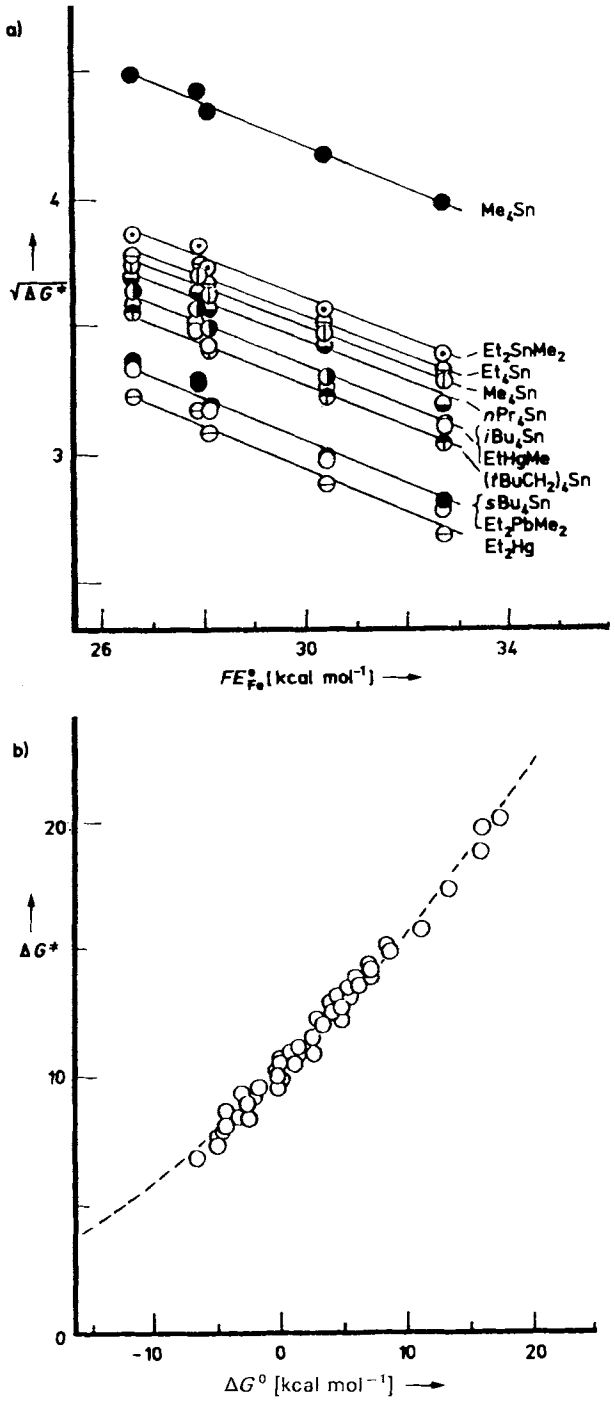

Fig. 4. Relationship of the activation free energy for electron transfer ($\Delta G^{\neq}$ [kcal mol^{-1}]) with (a) the electrode potentials of various $[FeL_3]^{3\oplus}$ according to Equation (21) and (b) the driving force according to the Marcus equation (20) (calculated for $\Delta G_0^{\neq} = 10$ kcal mol^{-1}).

donor property of the alkylmetal being the dominant factor. Such a conclusion accords with an outer-sphere mechanism for electron transfer [Eq. (18)]. The activation free energies $\Delta G^{\neq}$ obtained from the kinetics data are plotted against the driving force in Figure 4b.[17] The dashed line represents $\Delta G^{\neq}$ calculated from the Marcus equation (20) using the single value of $\Delta G_0^{\neq} = 10$ kcal mol^{-1}. Thus electron transfer from alkylmetals to $[FeL_3]^{3\oplus}$ accords well with the Marcus theory. *The absence of notable steric effects in this outer-sphere process* must be emphasized.

2.2.2. *Heterogeneous Processes at a Platinum Electrode*

The series of organometals **I**–**IV** are also readily oxidized electrochemically.[18] Thus we apply the same steric probe to the corresponding anodic process for which the analogous mechanism for electron transfer at a heterogeneous electrode [E] is represented by the electrochemical (EC) sequence shown in Equations (22) and (19).

$$RM \xrightarrow{[E]} RM^{\oplus} + e^{\ominus} \tag{22}$$

The rates of heterogeneous electron transfer in Equation (22) can be measured by two independent electrochemical methods: cyclic voltammetry (CV) and convolutive potential sweep voltammetry (CPSV). For a totally irreversible electrochemical process, the rate constant k_e for heterogeneous electron transfer at the CV peak potential E_p is given by Equation (23), where n is the number of electrons trans-

$$k_e(E_p) = 2.18[D\beta n F v/RT]^{1/2} \tag{23}$$

ferred in the rate-limiting step, v is the scan rate, β is the transfer coefficient, and the other terms have their usual significance. Equation (23) is derived from Fick's laws of diffusion together with the usual expression for the linear potential dependence of the rate constant k_e for heterogeneous electron transfer [Eq. (24)], where E^0 is the standard

$$k_e(E) = k_s \exp[(\beta n F/RT)(E - E^0)] \tag{24}$$

potential for the organometal which fixes the value of k_s. (Alternatively stated, k_s is the intrinsic rate constant for electron transfer at the equilibrium potential, i.e., $E = E^0$. It is thus related to the intrinsic barrier $\Delta G_0^{\neq}$ in Marcus theory.) The shift in the current maximum with the sweep rate accords with standard electrochemical theory,[19] and may be used with the aid of Equation (23) to determine the rate constant k_e for heterogeneous electron transfer at different values of the applied potential (driving force). The results of this analysis are shown in Figure 5 for the representative organometals **I**–**IV**.[20] The linear plots in Figure 5 correspond to the free energy relationship in Equation (24), since $\ln k_e(E) = \Delta G_e^{\neq}/RT$.

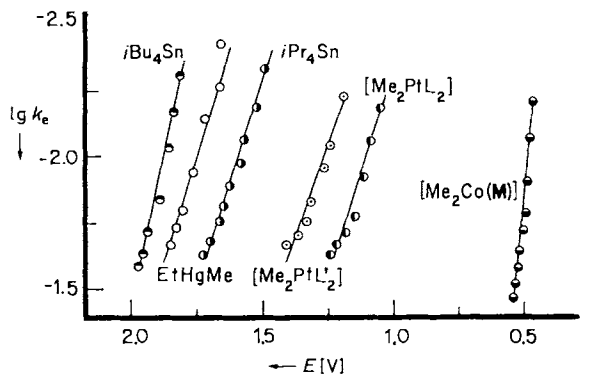

Fig. 5. Variation of the heterogeneous rate constant k_e [cm s^{-1}] with the applied potential (measured versus NaCl-SCE) for some representative organometals. **M** = macrocyclic ligand, L = PMe_2Ph; L' = $PMe_2(C_6H_4CF_3$-*p*).

2.2.3. *Comparison of Homogeneous and Heterogeneous Electron Transfers*

Let us compare the values of the rate constants k_e for the heterogeneous anodic oxidation of organometals with the rate constants k_{Fe} for the homogeneous chemical oxidation of the same organometals with $[FeL_3]^{3\oplus}$. The direct comparison of the electrochemical and chemical oxidations of organometals requires that they be evaluated at the same thermodynamic driving force; i.e., the applied electrode potential must be reasonably similar to the standard reduction potential E^0 of $[FeL_3]^{3\oplus}$. The correlation of the homogeneous and heterogeneous electron transfer, when both processes are measured under conditions of equivalent thermodynamic driving force, is presented in Figure 6.[20]

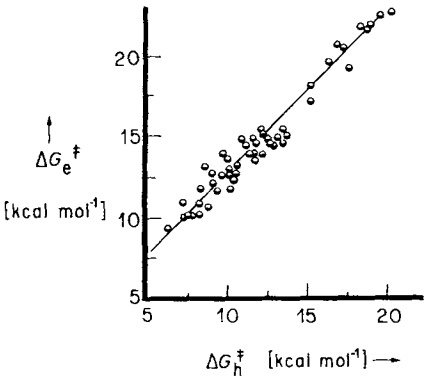

Fig. 6. Correlation of the homogeneous activation free energy $\Delta G_h^{\ddagger}$ for iron(III) oxidations and the heterogeneous activation free energy $\Delta G_e^{\ddagger}$ using the Marcus equation (20). The slope is 1.01 ± 0.03. The organometals include: $[Me_2Co(DpnH)]$, $[Me_2Co(tim)]^{\oplus}$, $[MeCo(DpnH)]^{\oplus}$, $[EtCo(DpnH)]^{\oplus}$, $[Me_2Pt(PMe_2Ph)_2]$, $[Me_2Pt\{PMe_2(C_6H_4CF_3)_2\}]$, Me_4Sn, Et_4Sn, iPr_4Sn, nBu_4Sn, iBu_4Sn, $(tBuCH_2)_4Sn$, Et_4Pb, EtHgMe, where DpnH = 2,3,9,10-tetramethyl-1,4,8,11-tetraazaundeca-1,3,8,10-tetraen-11-ol-1-olate and tim = 2,3,9,10-tetramethyl-1,4,8,11-tetraazacyclotetradeca-1,3,8,10-tetraene.

An important feature in Figure 6 is the striking absence of steric effects arising from the organometal. Thus Figure 6 establishes the essential *unity of outer-sphere mechanisms in homogeneous and heterogeneous electron transfer from organometal donors*. Furthermore, these studies emphasize the excellent behavior of *alkylmetals as prototypical donors* for the study of electron-transfer processes, particularly with regard to their easily modulated steric and polar properties.[21] Before we exploit the latter, the structural changes that accompany electron transfer from alkylmetal donors need some consideration.

2.2.4. *Structural Significance of the Intrinsic Barrier for Organometal Donors*

In Marcus theory for outer-sphere electron transfer, the intrinsic barrier represents the activation energy for electron transfer when the driving force is zero, i.e., $\Delta G^{\ddagger} = \Delta G_0^{\ddagger}$ at $\Delta G = 0$ or at the equilibrium potential E^0 [see Eq. (20), where the reorganization energy $\lambda = 4\Delta G_0^{\ddagger}$]. Some typical values of the intrinsic barriers for the organometals **I**–**IV** are listed in Table 1.[20] It is noteworthy that $\Delta G_0^{\ddagger}$ for the octahedral macrocyclic derivative $[Me_2Co(\mathbf{M})]$ **I** is significantly less than those for either the

Table 1. Effect of organometal structure on the transfer coefficient and the intrinsic barrier.

Organometal	$\Delta G^{\ddagger}$ [kcal mol^{-1}]	β [a]	$\Delta G_0^{\ddagger}$ [kcal mol^{-1}]	$\beta^2 \Delta G_0^{\ddagger}$ [kcal mol^{-1}]
$[Me_2Co(DpnH)]$ **I** [b]	7.46	0.73	2.1 [c]	1.1
sBu_4Sn **III'**	7.65	0.31	10.0	1.0
Et_4Pb **III''**	7.68	0.28	10.0	0.8
$[Me_2Pt(PMe_2Ph)_2]$ **II**	7.69	0.27	13.0	0.9
EtHgMe **IV**	7.70	0.20	22.0	0.9

[a] Measured by cyclic voltammetry at 100 mV s^{-1} [20]. [b] DpnH in legend to Figure 6. [c] When the effect of reversibility is taken into account, the value is 6.3 kcal mol^{-1} for rate-limiting electron transfer.

tetrahedral tetraalkyltin and -lead compounds **III'** and **III''**, respectively, or the square-planar dimethylplatinum(II) complex **II**. Moreover, the linear dialkylmercurials **IV** possess the highest values of the intrinsic barrier. We believe that such large differences in $\Delta G_0^{\ddagger}$ arise largely from structural changes that can occur upon the oxidation of the organometal donor. For example, the ESR spectra of $Me_4Pb^{\oplus}$ and $Me_4Sn^{\oplus}$ in Figure 7 are characterized by

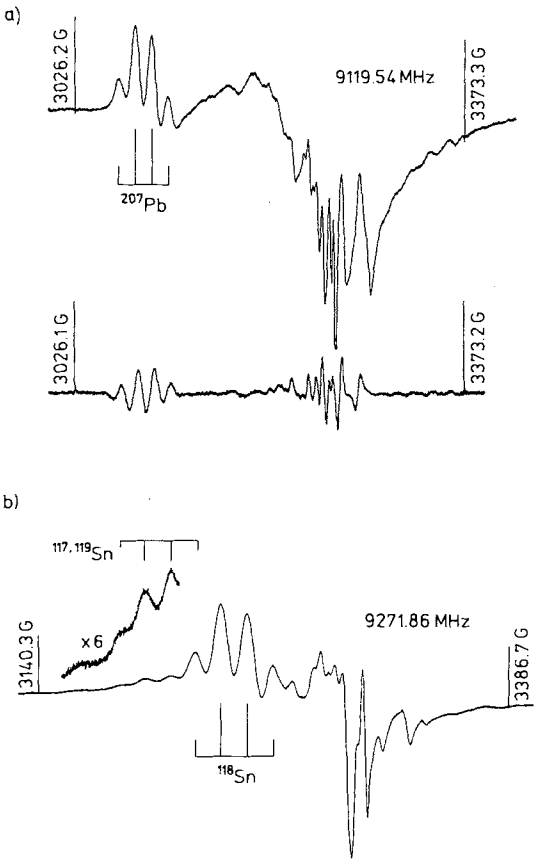

Fig. 7. a) X-band ESR spectrum of a γ-irradiated solution of 3 mol% tetramethyllead in trichlorofluoromethane at 85 K shown in first derivative (upper) and second derivative (lower). b) First-derivative ESR spectrum derived from tetramethyltin under similar conditions.

well-resolved (1:3:3:1) quartet splittings of 14.7 and 13.7 G, respectively, arising from *one unique methyl ligand*.[22] It is noteworthy that the proton hyperfine splittings from the three remaining methyl ligands are less than the spectral resolution of 2–3 G. Furthermore, in the tin

analogue, the perpendicular component of the hyperfine coupling to the naturally abundant magnetic isotopes ^{117}Sn and ^{119}Sn, with $I = 1/2$, is clearly delineated in the inset recorded at higher gain in Figure 7b. The remarkably small splitting of only 77 G is consistent with a small degree of s character in the singly occupied molecular orbital (SOMO) and indicative of a planar or near-planar metal center. Taken together, these ESR results suggest that the organometal undergoes a dramatic change in *configuration from T_d to C_{3v} symmetry attendant upon oxidation.* Judging from the similarity of the ^1H splitting and the expected larger positive g shift for the perpendicular components of $Me_4Pb^{\oplus}$, we surmise that a similar structural reorganization occurs in Me_4Pb. Accordingly, both cations are envisaged as approximating the trigonal-pyramidal structures in which the SOMO is largely localized in the dashed vertical metal-carbon bond (Scheme 2).

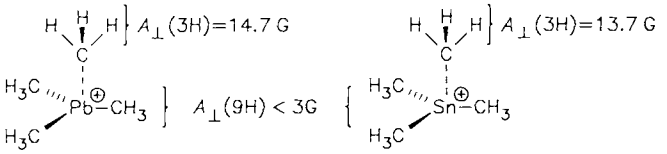

Scheme 2. Structures of $Me_4Pn^{\oplus}$ and $Me_4Sn^{\oplus}$ derived from their ESR spectra.

Although we were unable to obtain the ESR spectrum of the dimethylmercury cation, we infer by an extended reasoning (see Table 1) that this linear donor undergoes the largest structural change to a bent cation.

2.3. Inner-Sphere Electron Transfer from Organometal Donors

The series of organometal donors **I**–**IV** are also readily oxidized by the one-equivalent oxidant hexachloroiridate(IV) as well as by the organic acceptor tetracyanoethylene (TCNE).[17] In both cases, the rate-limiting step involves electron transfer [Eqs. (25) and (26)]. The stoichiom-

$$[IrCl_6]^{2\ominus} + RM \longrightarrow [IrCl_6]^{3\ominus} + RM^{\oplus} \quad (25)$$

$$TCNE + RM \longrightarrow TCNE^{\ominus} + RM^{\oplus} \quad (26)$$

etry of these reactions is essentially the same as that described for the trisphenanthroline-metal(III) oxidants in Equation (18).

2.3.1. Reactivity Patterns for $[IrCl_6]^{2\ominus}$ and TCNE as Oxidants

Although the patterns of reactivity for $[IrCl_6]^{2\ominus}$ and TCNE are similar, they are both quite distinct from the outer-sphere pattern established for $[FeL_3]^{3\oplus}$. The contrast is graphically illustrated in Figure 8 in which the second-order rate constants ($\lg k$) for each of the three oxidants are plotted against the ionization potentials of the same series of alkylmetal donors.[17] The uniquely linear correlation for $[Fe(phen)_3]^{3\oplus}$ is discussed in Section 2.2.1 for outer-sphere

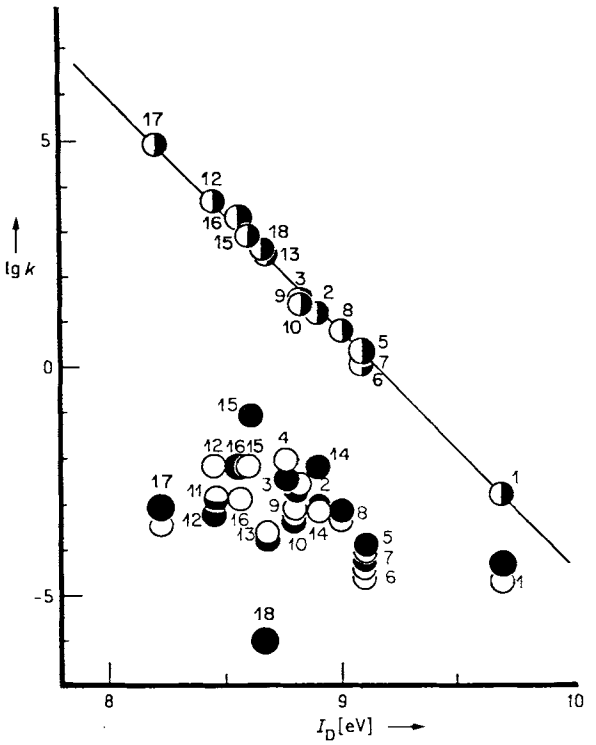

Fig. 8. Contrasting behavior of $[IrCl_6]^{2\ominus}$ (●) and TCNE (○) relative to $[Fe(phen)_3]^{3\oplus}$ (◑) in the correlation of rates of oxidation with the ionization potentials of alkylmetals: 1 = Me_4Sn, 2 = Et_4Sn, 3 = nPr_4Sn, 4 = nBu_4Sn, 5 = $EtSnMe_3$, 6 = $nPrSnMe_3$, 7 = $nBuSnMe_3$, 8 = Et_2SnMe_2, 9 = nPr_2SnMe_2, 10 = nBu_2SnMe_2, 11 = iPr_4Sn, 12 = sBu_4Sn, 13 = iBu_4Sn, 14 = $iPrSnMe_3$, 15 = $tBuSnMe_3$, 16 = iPr_2SnMe_2, 17 = tBu_2SnMe_2, 18 = $(tBuCH_2)_4Sn$ [17]. The slope of the $[Fe(phen)_3]^{3\oplus}$ correlation is $-1/2$.

oxidation. The marked deviations of all the points for $[IrCl_6]^{2\ominus}$ and TCNE from any analogous relationship is unmistakable. Furthermore, in Figure 9, the experimental values of $\Delta G^{\neq}$ for $[IrCl_6]^{2\ominus}$ and TCNE consistently fall below the solid lines representing the expected outer-sphere rates which were calculated from the Marcus equation (20) by taking into account the differences in the reorganization energies of $[IrCl_6]^{2\ominus}$ and TCNE. *With the exception of tBu_2SnMe_2 all the experimental rates are faster than the calculated values based on the Marcus outer-sphere correlation.* The magnitudes of the derivations vary from 12.5 kcal mol^{-1} for the least sterically hindered Me_4Sn to ca. 0 kcal mol^{-1} for the hindered tBu_2SnMe_2 (see Figure 2 for a qualitative expectation of steric effects). Thus among the symmetrical tetraalkyltin compounds R_4Sn, the least hindered methyl and *n*-alkyl derivatives all lie farthest from the outer-sphere correlation. Conversely, those tetraalkyltin compounds with α- and β-branched alkyl ligands consistently lie closest to the lines in Figure 9. Furthermore, the two-coordinate dialkylmercurials, which represent sterically open alkylmetals, all lie away from the outer-sphere correlation significantly beyond the tetra-*n*-alkyltin derivatives.

2.3.2. Selectivity Differences in the Oxidative Cleavage of Alkylmetals via Outer-Sphere and Inner-Sphere Pathways

The cleavage of alkyl ligands from symmetrical tetraalkyltin compounds [Eqs. (18), (25), and (26)] actually oc-

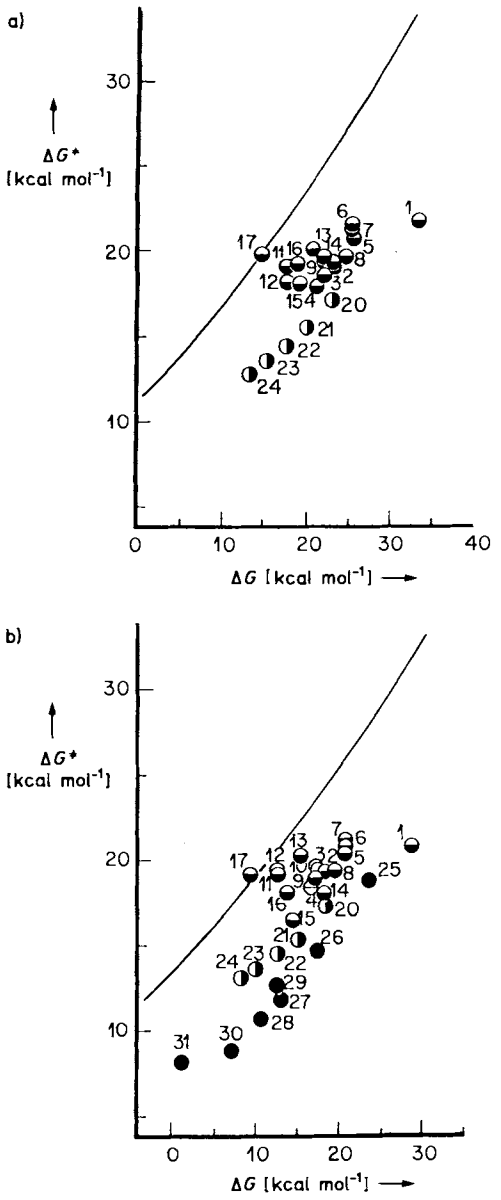

Fig. 9. Relationship between the activation free energy and the driving force for electron transfer from alkylmetals to TCNE (a) and $[IrCl_6]^{2\ominus}$ (b) according to the Marcus equation (20). Numbers 1–17 refer to alkylmetals in Figure 8: 20 = Me_4Pb, 21 = $EtPbMe_3$, 22 = Et_2PbMe_2, 23 = Et_3PbMe, 24 = Et_4Pb, 25 = Me_2Hg, 26 = EtHgMe, 27 = *i*PrHgMe, 28 = *t*BuHgMe, 29 = Et_2Hg, 30 = iPr_2Hg, 31 = tBu_2Hg. The curves are in agreement with expectations based on an outer-sphere mechanism [Eq. (20)].

curs subsequent to the rate-limiting electron transfer. If the same cation is formed as a common intermediate, it should fragment in exactly the same manner in Equation (19) for all three processes. The selectivity S(Et/Me) for the series of unsymmetrical methylethyltin compounds represents the ratio of first-order rate constants k_{ET}/k_{Me} for the intramolecular competition in Equations (27) and (28), where R = Me, Et.[17,23]

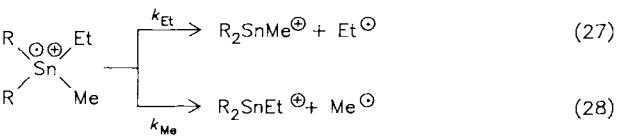

(27)

(28)

Selectivity provides the only measure available to determine the properties of the radical-cation intermediate, $R_2SnMeEt^{\odot\oplus}$. Indeed, the grouping of S(Et/Me) in Table 2 indicates that the cation derived from $[FeL_3]^{3\oplus}$ is different from those derived from $[IrCl_6]^{2\ominus}$ and TCNE. Furthermore, the similar values of S(Et/Me) for the latter accord with a related inner-sphere process.

Table 2. Selectivity studies in the oxidative cleavage of methylethyltin compounds by $[Fe(phen)_3]^{3\oplus}$, $[IrCl_6]^{2\ominus}$ and TCNE.

Alkyltin	Oxidant/Acceptor	S(Et/Me) [a]
Et_2SnMe_2	$[Fe(phen)_3](ClO_4)_3$	27±4
	$Na_2[IrCl_6]$	11±3
	TCNE	10±3
$EtSnMe_3$	$[Fe(phen)_3](ClO_4)_3$	26±4
	$Na_2[IrCl_6]$	11±3
	TCNE	11±3
Et_3SnMe	$[Fe(phen)_3](ClO_4)_3$	[b]
	$Na_2[IrCl_6]$	11±3
	TCNE	[b]

[a] Statistically corrected in $EtSnMe_3$ and Et_3SnMe. [b] Not measurable.

2.3.3. *Steric Criterion for the Inner-Sphere Mechanism with $[IrCl_6]^{2\ominus}$ and TCNE*

The measurable effects of steric perturbation on the rates of oxidation of encumbered alkylmetals by $[IrCl_6]^{2\ominus}$ and TCNE in Figure 9 are to be clearly distinguished from the corresponding outer-sphere processes identified in Figure 3, in which steric effects exert little or no influence on the rates. Such a trend for the former must reflect steric effects that perturb the inner coordination sphere of the alkylmetal donor in the transition state for electron transfer [cf. Eq. (17)]. Indeed, *we employ this conclusion as an operational definition for the inner-sphere mechanism of electron transfer.* In the context of the Marcus formulation, the lowering of the activation barrier in an inner-sphere process could arise from the reduction of the work term w_p as a result of the strong interaction in the ionic products, e.g., $[R_4Sn^{\oplus}, [IrCl_6]^{3\ominus}]$ and $[R_4Sn^{\oplus}, TCNE^{\ominus}]$. The electrostatic potential in such an ion pair is attractive and can cause the tetraalkyltin to achieve a quasi five-coordinate configuration in the precursor complex, reminiscent of a variety of trigonal-bipyramidal structures already well-known for tin(IV) derivatives (Scheme 3).

Scheme 3. Trigonal-bipyramidal structures of tin(v) ion pairs.

The extent to which steric effects adversely affect the attainment of such intimate ion-pair structures would be reflected in an increase in the work term w_p and a concomitant diminution of the inner-sphere rate. This qualitative conclusion accords with the selectivity in Table 2 and the reactivity trend in Figure 9. However, Marcus theory does not provide a quantitative basis for evaluating the variation in the work term of such ion pairs. To obtain the latter

we now turn to the Mulliken theory of charge transfer in which the energetics of ion-pair formation evolve directly and provide quantitative information on the steric effects.

2.4. Thermochemical Formulation of Electron-Transfer Rates

Before doing so, however, let us reformulate the problem in a more general thermodynamics context, in which we consider organometals as electron donors D and the oxidants $[IrCl_6]^{2\ominus}$ and TCNE as electron acceptors A.[24]

2.4.1. *Importance of the Work Term*

Electron-transfer mechanisms can be considered in the light of the standard potentials E^0 for each redox couple, i.e., E^0_{ox} for the oxidation of the donor ($D \rightarrow D^{\oplus} + e^{\ominus}$) and E^0_{red} for the reduction of the acceptor ($A + e^{\ominus} \rightarrow A^{\ominus}$). Thus the general reaction scheme for an irreversible process is represented by Equations (29),[25] in which electron transfer in the encounter complex [D,A] is rate-limiting. This scheme is particularly applicable to systems which lie in the endergonic region of the driving force (i.e., where the standard free energy change, $\Delta G^0 \gg 0$). The observed second-order rate constant k_{obs} is then given by $k_{obs} = k_{ET} K_{DA}$, where K_{DA} is the formation constant of the complex and k_{ET} is the intracomplex rate constant for electron transfer. The thermochemical cycle for an irreversible electron transfer in the highly endergonic region is schematically illustrated in Scheme 4.

$$D + A \overset{K_{DA}}{\rightleftharpoons} [D,A] \tag{29a}$$

$$[D,A] \xrightarrow{k_{ET}} [D^{\oplus}, A^{\ominus}] \tag{29b}$$

$$[D^{\oplus}, A^{\ominus}] \xrightarrow{\text{fast}} \text{products} \tag{29c}$$

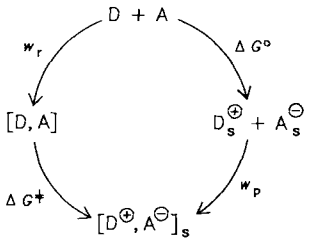

Scheme 4. Thermochemical cycle for an irreversible electron transfer.

According to the thermochemical cycle in Scheme 4, the activation free energy for electron transfer $\Delta G^{\ddagger}$ in the encounter complex is given by Equation (30), where ΔG^0 corresponds to the standard free energy change of the redox process $D + A \rightarrow D^{\oplus} + A^{\ominus}$, and the work terms w_p and w_r represent the energy required to bring together the products and reactants, respectively, to within the mean separation r_{DA} in the ion pair $[D^{\oplus}, A^{\ominus}]$. The observed second-order rate constant can be expressed in terms of the activation free energy $\Delta G^{\ddagger}$ [Eq. (30)], which leads to the free energy relationship for electron transfer [Eq. (31)], where $C_1 = \lg(kT/h)$ (k = Boltzmann constant, h = Planck constant).

$$\Delta G^{\ddagger} = \Delta G^0 + w_p - w_r \tag{30}$$

$$\lg k_{obs} = -\frac{1}{2.3RT}(\Delta G^0 + w_p) + C_1 \tag{31}$$

Since the free energy change for electron transfer ΔG^0 is obtained from the standard potentials of the donor and acceptor—i.e., $\Delta G^0 = F(E^0_{ox} + E^0_{red})$—the free energy relationship (31) may be represented by an equivalent form, Equation (32), when one is dealing with a series of electron-transfer reactions with a fixed donor. Thus Equations (31) and (32) state that the observed rate constant ($\lg k_{obs}$) for electron transfer can be expressed as the sum of the standard free energy change (ΔG^0) and the work term of the products (w_p). Previous considerations of electron transfer have tended to focus only on the magnitude of ΔG^0, without explicitly taking into account the energetics of ion-pair $[D^{\oplus}, A^{\ominus}]$ formation, i.e., the work term w_p. Such an oversimplification is perhaps understandable if one considers the experimental difficulty of directly evaluating the work terms of ion pairs by the usual procedures. The problem is severely compounded by the exceedingly short lifetimes of the transient ion pairs which must be involved in irreversible electron transfer. We now discuss how the observation of charge-transfer spectra in these systems can be used to evaluate such ion-pairing energies.

$$\lg k_{obs} = -\frac{1}{2.3RT}(FE^0_{ox} + w_p) + \text{constant} \tag{32}$$

2.4.2. *Evaluation of the Work Term from Charge-Transfer Spectra*

The intermolecular interaction leading to the precursor complex in Scheme 4 is reminiscent of the electron donor-acceptor (EDA) complexes formed between electron donors and acceptors.[26] EDA complexes are characterized by the presence of a new absorption band in the electronic spectrum. According to the Mulliken charge-transfer (CT) theory for weak EDA complexes, the absorption maximum $h\nu_{CT}$ corresponds to the vertical (Franck-Condon) transition from the neutral ground state to the polar excited state [Eq. (33)].[13] The asterisk identifies an excited ion pair with the same mean separation r_{DA} as that in the precursor or EDA complex. The thermochemical cycle for such a charge-transfer transition is schematically illustrated in Scheme 5. The vertical ionization potential of the electron donor is represented by I_D, and the electron affinity of the acceptor by E_A.

$$[D,A] \xrightarrow{h\nu_{CT}} [D^{\oplus}, A^{\ominus}]^* \tag{33}$$

The charge-transfer in Scheme 5 is akin to the adiabatic electron-transfer cycle in Scheme 4. In this case the work term w_p^* required to bring the products $D^{\oplus}$ and $A^{\ominus}$ to-

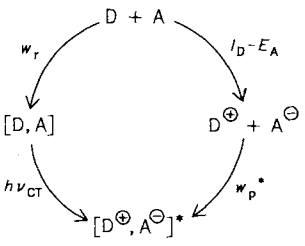

Scheme 5. Thermochemical cycle for a charge-transfer transition.

gether to the mean separation r_{DA} in the excited state is given by Equation (34), where $C_2 = E_A + w_r$; C_2 is consid-

$$w_p^* = h\nu_{CT} - I_D + C_2 \tag{34}$$

ered to be constant for a fixed acceptor.[27] In the limit of simple ion-pair interactions, the work term is largely Coulombic, i.e., $w_p^* \approx -e^2/r_{DA}$.

We can relate the work term w_p^* to that of a reference donor, w_p^{0*}, since the series of oxidations in Figure 8 involves either TCNE or $[IrCl_6]^{2\ominus}$ as the common acceptor. This comparative procedure allows the acceptor component in a given series to drop out by cancellation, and Equation (35) follows from Equation (34). In Equation

$$\Delta w_p^* = w_p^* - w_p^{0*} = \Delta h\nu_{CT} - \Delta I_D \tag{35}$$

(35), $\Delta h\nu_{CT}$ refers to the relative CT transition energy with a common acceptor, and ΔI_D is the difference in the ionization potentials of the donor and the chosen reference. Thus, by selecting a reference donor, we can express all changes in the ion-pairing energies in the CT excited state (including steric, distortional, and other effects in the D/A pair) by a single, composite energy term Δw_p^*. In so far as w_p^* is Coulombic, *the relative work term Δw_p^* measures changes in mean separation, and it is thus a reflection of steric effects*. Let us now return to the thermal electron-transfer reaction in Equation (26), for which the rate-limiting activation process has been shown to proceed from the EDA complex [Eq. (36)].[27]

$$[RM, TCNE] \xrightarrow{k} [RM^{\oplus}, TCNE^{\ominus}] \tag{36}$$

2.4.3. *Free Energy Relationship for Inner-Sphere Electron Transfer*

The variation in the driving force in Equation (36) derives from two factors: (1) the differences in the oxidation potentials of the alkylmetals and (2) the changes in the work terms in the ion pairs resulting from differences in the steric effects (i.e., mean separations r_{DA}.) The difference in the oxidation potentials is obtained from the free energy change for electron transfer (i.e., $RM \rightarrow RM^{\oplus} + e^{\ominus}$) in the outer-sphere process [see Eq. (21)]. The change in the work term is equated to Δw_p^*, determined from the CT interaction [Eq. (35)]. Thus the linear correlation in Figure 10a between the driving force and the activation free energy represents a linear free energy relationship for elec-

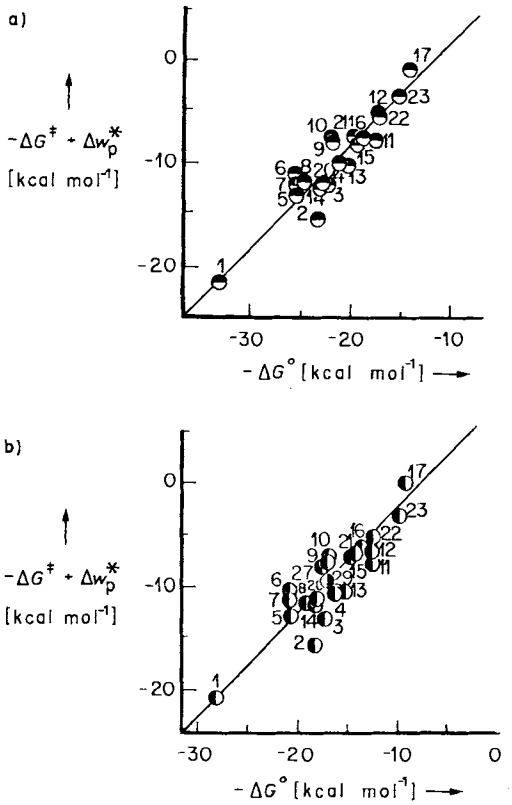

Fig. 10. Relationship between the activation free energy $\Delta G^{\ddagger}$ including the work term Δw_p^* and the driving force for electron transfer ΔG^0 to TCNE (a) and $[IrCl_6]^{2\ominus}$ (b) for alkylmetals listed in Figures 8 and 9.

tron transfer expressed as $\Delta G^{\ddagger} = \Delta G^0 + \Delta w_p^* + C_3$, where the constant C_3 represents the reference terms.[17] Furthermore, the same relationship applies to $[IrCl_6]^{2\ominus}$, as shown by the correlation in Figure 10b. (The applicability of the values of Δw_p^* obtained from TCNE to the inner-sphere oxidation with $[IrCl_6]^{2\ominus}$ is probably fortuitous. An indication of their similarity is, however, apparent from Figures 8 and 9.)

2.5. The Merging of Outer-Sphere and Inner-Sphere Mechanisms of Electron Transfer

The concepts of outer-sphere and inner-sphere electron transfer, as we have employed them, depend on the availability of various metals and alkyl ligands as highly tunable probes for steric effects. As such, we might ask how these mechanisms basically differ. One answer might focus on the properties of $RM^{\odot\oplus}$, especially with respect to selectivity in the cleavage that follows the rate-limiting electron transfer (see Table 2). Another might relate to the role of steric effects on the activation process. We suggest that both are directly related to the interaction energy in the ion pair, for which steric effects are evaluated from the CT data by means of Equation (35). According to this formulation, *outer-sphere and inner-sphere processes are largely distinguished by the magnitudes of the intermolecular separation between the donor and the acceptor in the transition states for electron transfer*. As such, there should be a continuum of activated complexes differing principally in geo-

metrical constraints, which are manifested in the context of the Marcus equation (20) by variations in the work term as well as the intrinsic barrier. In order to evaluate these contributions, let us see how they affect the free-energy correlations for outer-sphere ($[FeL_3]^{3\oplus}$) and inner-sphere (TCNE and $[IrCl_6]^{2\ominus}$) mechanisms (Fig. 4 and 10, respectively). For clarity, these correlations are redrawn and juxtaposed in Figure 11. (Note that the Brønsted slope for

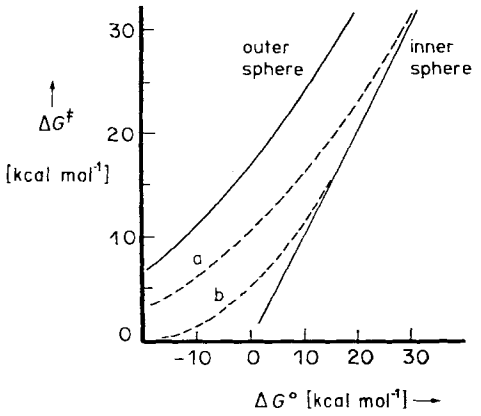

Fig. 11. The importance of the work term and the reorganization energy in the free energy correlations for outer-sphere and inner-sphere mechanisms. For details see text. The full lines correspond to the limiting cases of outer-sphere and inner-sphere mechanisms. a) Reduction of the work term w_p in the Marcus equation (20) by $\Delta w_p \approx 10$ kcal mol^{-1}; b) subsequent reduction of the intrinsic barrier by one-half.

$[FeL_3]^{3\oplus}$ is effectively one-half, whereas that for both TCNE and $[IrCl_6]^{2\ominus}$ is unity.) Initially, if the work term w_p in the Marcus equation (20) is reduced by $\Delta w_p \approx 10$ kcal mol^{-1}, the new free-energy correlation follows the dashed curve a in Figure 11. Following this, if the intrinsic barrier is reduced by one-half, curve a is transformed into b, which closely follows the inner-sphere correlation. Although the choice of $\Delta w_p \approx 10$ kcal mol^{-1} and $\Delta G_0^{\ddagger}/2$ may appear arbitrary, the procedure shows that the outer-sphere correlation can be transformed to the inner-sphere correlation by suitable reductions in the work term and intrinsic barrier. Since the experimental points in Figure 9 fall between the outer- and inner-sphere limits, it is reasonable to expect that variations in w_p and $\Delta G_0^{\ddagger}$ lead to a continuum of inner-sphere and outer-sphere mechanisms. Thus, the least hindered compound Me_4Sn and the highly hindered tBu$_2$SnMe$_2$ expectedly lie at the inner- and outer-sphere limits, respectively, as depicted for both TCNE and $[IrCl_6]^{2\ominus}$ in Figure 9.

3. Generalized Free Energy Relationships for Electron Transfer (FERET)

In Section 2 we described how the variable steric and polar properties of organometal donors provide the means to predict the electron-transfer rates of both outer-sphere and inner-sphere processes. Critical to the electron-transfer kinetics is the evaluation of the work term w_p^* of the $[D^{\oplus}, A^{\ominus}]$ ion pair from the charge-transfer absorption spectra [see Eq. (34)]. Since the charge-transfer interactions derive naturally from various electron donor-acceptor pairs, let us combine the thermodynamic cycles in Schemes 4 and 5 into the composite form shown in Scheme 6, where K is

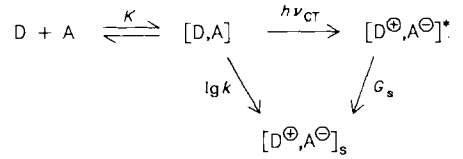

Scheme 6. Combination of the thermodynamic cycles in Schemes 4 and 5.

the formation constant of the EDA or precursor complex [D,A], and the rate of electron transfer is defined by the adiabatic rate constant k. In Scheme 6, the asterisk identifies the vertical ion pair obtained from the CT excitation; the vertical ion pair is differentiated from the adiabatic ion pair $[D^{\oplus}, A^{\ominus}]_s$ by the solvation energy G_s. Following our earlier treatment of these energy components as changes relative to a reference [see Eq. (35)], the thermodynamic cycle in Scheme 6 can be expressed as Equation (37),

$$\Delta G_r^{\ddagger} = \Delta h\nu_{CT} + \Delta G_s \tag{37}$$

where the relative rates of electron transfer (lgk/k_0) are represented by $\Delta G_r^{\ddagger}/(2.3\,RT)$ and the difference in the CT transition energies by $\Delta h\nu_{CT}$ (see Section 2.4.2). The free energy change (ΔG) for the oxidation of a donor in solution includes both the solvation term G_s for the donor cation $D^{\oplus}$ and the ionization potential (I_D) for the oxidation in the gas phase [Eq. (38)].[28] The corresponding relative

$$\Delta G = I_D + G_s \tag{38}$$

change in solvation ΔG_s for Equation (37) is evaluated independently as the difference between the gas-phase ionization potential and the oxidation potential of the donors in solution.

The validity of Scheme 6 is illustrated in Figure 12 by the excellent fit of the experimental data to the line of unit slope.[29] It must be emphasized that *this test of Equation (37) obtains from three sets of independent data.* Thus the free energy change $\Delta G_r^{\ddagger}$ is measured from the kinetics experiments, and the charge-transfer energies $\Delta h\nu_{CT}$ derive from spectral absorption measurements. The solvation change is equal to the difference between the gas-phase ionization potential I_D and the oxidation potential E_{ox}^0 in solution of the organometal donor, since the contribution from the electron acceptor cancels out in the comparative procedure for ΔG_s. For convenience the generalized free energy relationship for electron transfer in Equation (37) will be referred to hereafter by the acronym FERET.

Let us now take the charge-transfer formulation in Scheme 6 one step further and ask whether the photochemical and thermal activations of an EDA complex can actually lead to the same overall reaction. A particularly

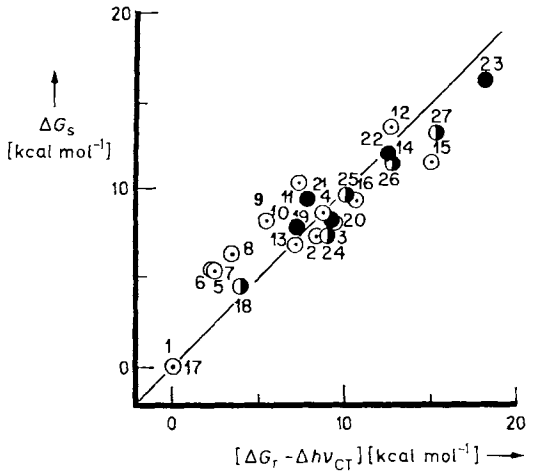

Fig. 12. FERET for the activation process for halogenolysis or insertion and the driving force for ion-pair formation as described in Equation (37): R_4Sn-I_2 (⊙), R_4Pb-TCNE (◑), and R_2Hg-TCNE (●). The dashed line drawn with unit slope represents $\Delta G_s = \Delta G_r^* - \Delta h\nu_{CT}$. 1 = Me_4Sn, 2 = Et_4Sn, 3 = nPr_4Sn, 4 = nBu_4Sn, 5 = $EtSnMe_3$, 6 = $nPrSnMe_3$, 7 = $nBuSnMe_3$, 8 = Et_2SnMe_2, 9 = nPr_2SnMe_2, 10 = nBu_2SnMe_2, 11 = iPr_2SnMe_2, 12 = tBu_2SnMe_2, 13 = Et_3SnMe, 14 = iPr_4Sn, 15 = sBu_4Sn, 16 = iBu_4Sn, 17 = Me_2Hg, 18 = EtHgMe, 19 = iPrHgMe, 20 = Et_2Hg, 21 = tBuHgMe, 22 = iPr_2Hg, 23 = tBu_2Hg, 24 = Me_4Pb, 25 = $EtPbMe_3$, 26 = Et_2PbMe_2, 27 = Et_3PbMe [29].

informative example is given by the interaction of alkylmetals with tetracyanoethylene [Eqs. (39)-(41)], in which the

$$RM + TCNE \rightleftharpoons [RM,TCNE] \quad (39)$$

$$[RM,TCNE] \xrightarrow{k} [RM^{\oplus},TCNE^{\ominus}] \quad (40)$$

$$[RM^{\oplus},TCNE^{\ominus}] \xrightarrow{\text{fast}} 1:1 \text{ adduct} \quad (41)$$

rate-limiting step for addition is given by Equation (40).[27,30] We indeed find that the *same* 1:1 adduct is produced photochemically when the CT absorption band ($\lambda_{max} = 440$ nm) is deliberately irradiated at −35°C [Eq. (42)].

$$[RM,TCNE] \xrightarrow{h\nu_{CT}} [RM^{\oplus},TCNE^{\ominus}] \longrightarrow \longrightarrow \cdots \quad (42)$$

At this low temperature, the thermal process [Eqs. (39)-(41)] is too slow to compete. Thus the observed quantum yields of unity, together with selectivities which are the same for the thermal and photochemical processes, indicate that the same ion pairs are common intermediates in Equations (40) and (42).[27] Such a direct relationship between the thermal electron transfer ($\lg k$) and the charge transfer activation ($h\nu_{CT}$) is graphically presented in Figure 13, in which ion-pairing energies of the vertical and adiabatic processes are simply represented as electrostatic terms. Thus the generalized free energy relationship in Equation (37) relates the rate of electron transfer directly to the CT transition energy of the EDA complex and the solvation energy of the ion pair.

Since the FERET correlation in Equation (37) conveys only a limited physical connotation, we replace the charge-transfer term $\Delta h\nu_{CT}$ with its equivalent in Equation (35) to obtain Equation (43).[31] The FERET in Equation (43) is a

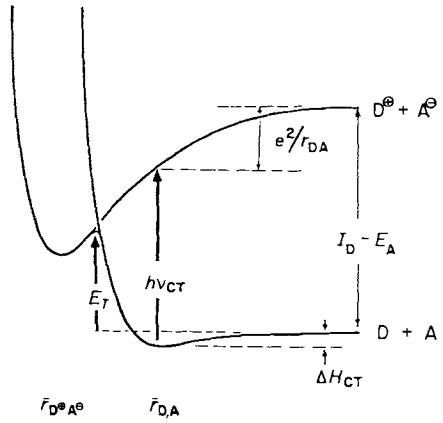

Fig. 13. The qualitative relationship between thermal (E_T) and photochemical ($h\nu_{CT}$) activation of electron transfer proceeding from the charge-transfer complex.

$$\Delta G_r^* = \Delta I_D + \Delta w_p^* + \Delta G_s \quad (43)$$

direct representation of the *electron transfer rates ($\lg k/k_0$) as a simple combination of electronic (ΔI_D), steric (Δw_p^*), and solvation terms (ΔG_s).* Alternatively, the FERET in Equation (43) can be expressed in terms of the standard free energy change ($\Delta G_r^0 = \Delta I_D + \Delta G_s$) to obtain Equation (44).

$$\Delta G_r^* = \Delta G_r^0 + \Delta w_p^* \quad (44)$$

The FERET in Equation (44) is an alternative representation of the *electron-transfer rates as a combination of the free energy change* [i.e., $\Delta G^0 = F(E_{ox}^0 + E_{red}^0)$] *and the work term of the ion pair* (Δw_p^*).

The FERET in Equation (37) together with its corollaries (43) and (44) underscores the strong energetic similarity between the CT excited state (i.e., the photochemically generated ion pair $[D^{\oplus},A^{\ominus}]^*$) and the transition state (or the adiabatic ion pair $[D^{\oplus},A^{\ominus}]_s$). The subtle balance between electronic or polar effects ΔI_D, the steric effect Δw_p, and the solvation energy ΔG_s thus determines the reactivity of electron donors, particularly with respect to solvent variation. Moreover, the prediction of electron-transfer rates derives naturally from the properties of the reactants in the gas phase (I_D,E_A) and in solution (E_{ox}^0,E_{red}^0), as well as those of the products (G_s, w_p). Most importantly, all of these energy contributions are experimentally measurable quantities.

In order to examine the applicability of this generalized free energy formulation, we now use it to resolve the critical ambiguities in some basic organic and organometallic reactions.

4. Applications of FERET to Organic and Organometallic Systems

The chemical reactions presented in Equations (1)-(7) are all examples in which EDA complexes have been actually observed as transient intermediates from the reactant donor-acceptor pairs.[5,21] Accordingly, the pertinent charge-transfer data can be applied to the generalized free energy relationships in Equations (37), (43), and (44), as described individually below.

4.1. Aromatic Substitution with Electrophiles

Halogenation and mercuration represent rather dissimilar processes for electrophilic aromatic substitution, as illustrated by the divergent trends in the relative reactivities ($\lg k/k_0$) of various arenes toward Br_2 and $Hg(O_2CCF_3)_2$ in Figure 14. Thus any mechanistic formulation of electrophilic aromatic substitution must first reconcile, in a quantitative way, such differences in arene reactivities imposed by the different electrophiles.[32] Furthermore, if the formulation is to have any generality and predictive power, it must lead to the description of the activation process for electrophilic aromatic substitution in terms of experimentally identifiable concepts. We show how the charge-transfer formulation provides physical insight into the transition state for electrophilic substitution, particularly with regard to the significance of the ρ values and the solvent effects. The CT formulation also yields a unique view into the origin of the isomeric product distributions.

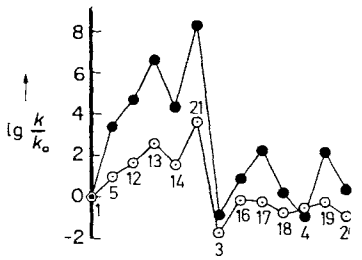

Fig. 14. Reactivities of arenes in mercuration (⊖) and bromination (●) relative to benzene(1). The following substituted benzenes were investigated. 3 = ClC_6H_5, 4 = BrC_6H_5, 5 = MeC_6H_5, 12 = *o*-$Me_2C_6H_4$, 13 = *m*-$Me_2C_6H_4$, 14 = *p*-$Me_2C_6H_4$, 16 = *o*-$ClMeC_6H_4$, 17 = *m*-$ClMeC_6H_4$, 18 = *p*-$ClMeC_6H_4$, 19 = *m*-$BrMeC_6H_4$, 20 = *p*-$BrMeC_6H_4$, 21 = 1,3,5-$Me_3C_6H_3$ [33]. $X^{\ominus} = F_3CCO_2^{\ominus}$.

4.1.1. The Charge-Transfer Correlation

The direct relationship between the relative reactivities of various arenes in electrophilic substitution and the CT transition energies is shown in Figure 15.[33] The remarkable linear correlations of the data apply equally well to mercuration, to bromination, and to chlorination. Moreover, the same relationship is applicable in solvents as diverse as dichloromethane, acetic acid, and trifluoroacetic acid. Since every line in Figure 15 is arbitrarily drawn with a slope of unity, *if all the experimental points in Figure 15 were plotted in a single figure, they would all lie on a single line.* This corresponds to the linear free energy relationship given in Equation (45), which is applicable to every electrophilic substitution process.

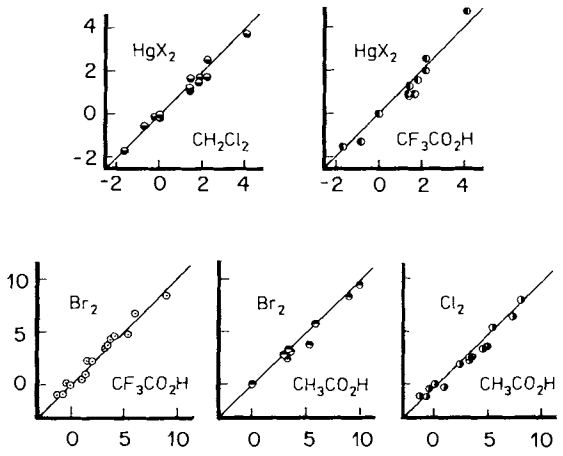

Fig. 15. The correlation of the relative reactivities of arenes with the CT transition energies in [33]. The lines are arbitrarily drawn with a slope of unity to emphasize the fit to Equation (45). Ordinate: $\lg k/k_0$. Abscissa: CT transition energies plotted as $-\Delta h\nu_{CT}/(2.3RT)$.

$$\lg \frac{k}{k_0} = -\frac{\Delta h\nu_{CT}}{2.3RT} \tag{45}$$

4.1.2. Solvent Effects

Equation (45) would represent a special case of FERET (37) for aromatic substitution if the relative solvation change ΔG_s for the donor component in Equation (37) were nil. In order to establish whether this situation actually pertains, an independent measurement of solvation changes is required. By the comparative procedure used to develop Equation (45), we need only to consider relative changes in the solvation of the aromatic cation, since the contributions from the electrophile moiety drop out by cancellation. Under these circumstances, the free energy change for solvation is represented by the difference between the gas-phase ionization potential [Eq. (46)] and the free energy change for oxidation in solution [Eq. (47)] of

$$\text{Arene} \xrightarrow{I_D} \text{Arene}^{\oplus} + e^{\ominus} \tag{46}$$

$$\text{Arene} \xrightarrow{E^0_{ox}} \text{Arene}^{\oplus}_s + e^{\ominus} \tag{47}$$

the arene, where the subscript s represents the solvated species. The correlation of the standard oxidation potentials E^0_{ox} of the aromatic hydrocarbons with the ionization potentials I_D in the gas phase is shown in Figure 16.[34] The line in the graph is described by Equation (48). The correlation coefficient of 0.975 is sufficiently high (especially since it includes 27 compounds, 12 of which are plotted in Figure 16) to ensure the validity of a linear correlation between E^0_{ox} and I_D to a confidence level of >99.9%. Thus an independent measurement of the solvation change of aromatic cations indeed accords with the prediction of the FERET in Equation (45) with $\Delta G_s \approx 0$. Thus, by taking the solvation of arene cations to be relatively constant, it follows that the vertical and adiabatic ion pairs in Scheme 6 are evaluated to be equivalent by the comparative procedure used in Equation (45).

$$E^0_{ox} = 0.71 I_D - 3.68 \tag{48}$$

It is noteworthy that the polar ion pair [Arene$^{\oplus}$, $A^{\ominus}$], when taken as a model for the transition state of electrophilic aromatic substitution, does correctly account for an otherwise inexplicable lack of sensitivity to solvent effects of the relative reactivities of various arenes, despite a strong correlation with the σ^+ parameter.[35] The *absolute* rates of electrophilic aromatic substitutions also accord with ion-pair solvation. For example, the solvation energy

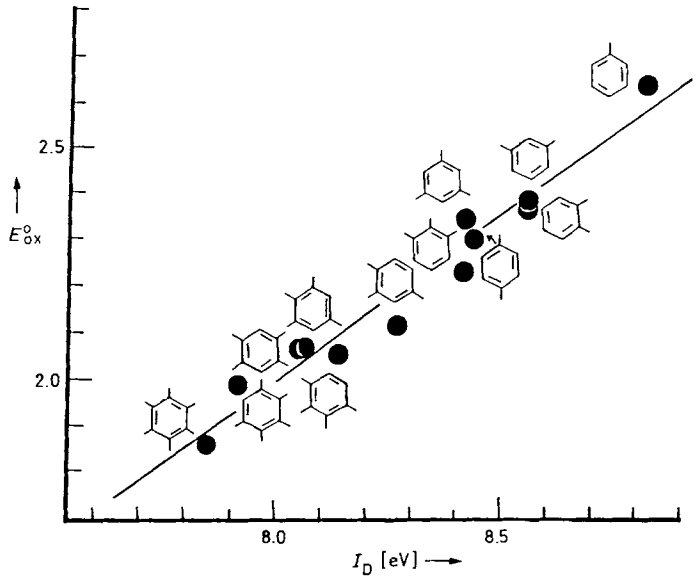

Fig. 16. Correlation of the standard oxidation potentials E^0_{ox} (in V vs. NHE) of various alkylbenzenes with the vertical ionization potentials I_D.

of aromatic cations in trifluoroacetic acid is larger than that in acetonitrile by approximately 4.6 kcal mol^{-1}, which corresponds to the difference in E^0_{ox} in these solvents. The second-order rate constant for the chlorination of benzene in trifluoroacetic acid ($k = 7 \times 10^{-3}$ M^{-1} s^{-1}) at 25°C is 1700 times larger than that in acetonitrile. This rate enhancement is equivalent to a decrease in the activation free energy of 4.4 kcal mol^{-1}, which corresponds well with the difference in solvation energy mentioned above. Although such an agreement may be fortuitous, it nonetheless underscores the importance of solvation in considering the solvent effects on the *absolute* rates of electrophilic aromatic substitution.

4.1.3. Significance of the FERET Formulation to Other Linear Free Energy Relationships

The charge-transfer formulation of electrophilic aromatic substitution leads to the conception of the transition state as an ion pair. As such, we show how the FERET formulation relates to previous linear free energy relationships which have been developed for electrophilic aromatic substitution. First, let us consider the well-known correlation [Eq. (49)] based on σ^+ substituent constants.[36]

$$\lg \frac{k}{k_0} = \rho\sigma^+ \tag{49}$$

Since the sensitivity factor ρ has been subjected to various physical interpretations, our primary task is to derive ρ from the CT data. It has been shown for a series of electrophiles and π acceptors that the CT transition energies $h\nu_{CT}$ vary linearly with the ionization potential I_D of the arene donor.[5] The relative change, as evaluated by the comparative procedure is given by Equation (50), where the slopes

$$\frac{\Delta h\nu_{CT}}{\Delta I_D} = \alpha_A \tag{50}$$

α_A are measures of the electrophile or π acceptors—varying from ca. 0.3 for $Hg(O_2CCF_3)_2$, 0.6 for 1,2,4,5-benzenetetracarbonitrile, 0.6 for Cl_2, 0.7 for Br_2 and maleic anhydride, and 0.8 for tetracyanoethylene, up to 1.0 for chloranil. The values of α_A never exceed unity. The linear free energy relationship between ΔI_D and σ^+ [Eq. (51)] has

$$\Delta I_D = -20.4\sigma^+ \tag{51}$$

been established for roughly 50 mono- and disubstituted benzenes.[33] The combination of Equations (45), (50), and (51) yields Equation (52). In other words, the electrophile-

$$\lg \frac{k}{k_0} = -16\alpha_A\sigma^+ \tag{52}$$

dependent value of ρ [Eq. (49)] is directly related to the slope of the correlation of $\Delta h\nu_{CT}$ with ΔI_D [Eq. (53)].

$$\rho = -16\alpha_A \tag{53}$$

Since $0 < \alpha_A < 1$, Equation (53) predicts that $|\rho|$ will not exceed a value of 16. Indeed, we are unaware of reports in the extant literature of $|\rho| > 16$ for any electrophilic aromatic substitution. Furthermore, the ρ values for bromination ($\rho = -12.1$) and for chlorination ($\rho = -10.0$) are readily obtained from the CT data with the aid of Equations (50) and (53). Thus, by using the values of α_A for the bromine complexes (0.7) and for the chlorine complexes (0.6), the ρ values for bromination and chlorination are $\rho = -11$ and $\rho = -9.6$, respectively. Similarly, the ρ value for mercuration (-5.7) agrees well with the calculated value of -5 based on $\alpha_A = 0.3$. Thus the absolute values of ρ, otherwise unpredictable, can be independently evaluated for various electrophiles by the use of Equation (53).

4.1.4. Variations in the Work Term

If the mean separation r_{DA} were to remain constant in a series of arenes, the relative reactivities in Equation (45) should be proportional to the differences in the ionization potentials, i.e., $\lg k/k_0 = -\Delta I_D/(2.3RT)$, since $\Delta h\nu_{CT}$ would simply be equal to ΔI_D according to Equation (35). However, a plot of the values of $\Delta I_D/(2.3RT)$ against the logarithms of the relative reactivities of arenes in bromination and mercuration shows wide scatter. The absence of any clear correlation indicates that the intrinsic donor abilities of the arenes (i.e., ΔI_D) are *alone* insufficient to account for the differences in arene reactivities in mercuration and bromination. Thus the linear correlation of $\lg k/k_0$ with $\Delta h\nu_{CT}$ in Figure 15 indicates that the work term w_p is not constant. In order to determine the effects of varying w_p, we differentiate Equation (34) to yield the slope of the correlation of $h\nu_{CT}$ and I_D [Eq. (54)]. Since the interaction

$$\alpha_A = \frac{\partial(h\nu_{CT})}{\partial I_D} = 1 + \frac{\partial w_p}{\partial I_D} \tag{54}$$

between Arene$^{\oplus}$ and A$^{\ominus}$ is attractive, the work term w_p is negative and increases with the mean separation r_{DA}. Such an increase in r_{DA} is generally accompanied by a decrease

in I_D of the substituted benzenes. As a result, the term $\partial w_p/\partial I_D$ above is negative and leads to values of α_A less than unity. Since the work term w_p in Equation (34) must also be affected by the electrophile moiety, the term $\partial w_p/\partial I_D$ is also dependent on the electrophile, as observed by the various values of α_A.[37]

4.1.5. Charge-Transfer Mechanism for Aromatic Substitution. Ion-Pair Collapse and the Isomeric Product Distribution

The various isomer distributions among meta and *para* products for the mercuration, halogenation, thallation, and nitration of monosubstituted benzenes PhZ can be separated into two groups according to whether *para* products (Z = X) or *meta* products (Z = Y) predominate. Such directive effects of the substituents X and Y have been commonly rationalized on the basis of inductive, resonance, and steric effects, the particular combination being somewhat arbitrarily chosen.[38] For example, the halogens, F, Cl, Br, and I, are classified as electron-withdrawing substituents by their values of the Hammett constants on the σ_p^0 scale and on the basis of the lower reactivity of the halobenzenes. Nevertheless, they yield predominantly *para* isomers like their more reactive counterparts, such as alkyl- and hydroxybenzenes. Such abnormalities of the halobenzenes have been troublesome to rationalize and have led to rather unsatisfactory ad hoc explanations.[39] The polar ion-pair state [Arene$^{\oplus}$, A$^{\ominus}$] as a model for the transition state avoids the ambiguous situation of reconciling reactivities and directive effects, by separating the rate-determining step from the product-forming step. Thus the rate-limiting activation process is represented by the formation of the ion pair as described in Section 3, and the product distribution is determined during the subsequent collapse of the ion pair (Scheme 7).

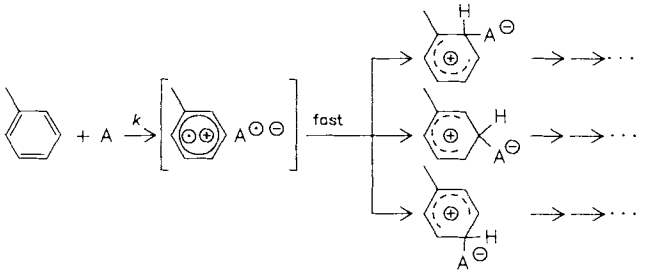

Scheme 7. Electrophilic aromatic substitution via a polar ion pair.

Indeed, the ion pair is prepared for bonding, since the unpaired electrons are located at the two centers that can be coupled to form the new bond. Under these circumstances, the most probable course for the collapse of [Arene$^{\oplus}$, A$^{\ominus}$] would be at the ring carbons of highest odd-electron spin density. In the benzene cation, the unpaired electron lies in the degenerate e_{1g} HOMOs, labeled S (for symmetric b_1) and A (for antisymmetric a_2). The spin density distributions for the odd electron in the benzene cation for these levels leads overall to a spin density of one-sixth at each carbon center. The symmetric orbital has a large spin density at the 1- and 4-positions, where the antisymmetric orbital has a node. The introduction of a substituent into benzene serves to remove the degeneracy of the symmetric and the antisymmetric orbitals—the electron-releasing substituent X leading to a raising of S and the electron-withdrawing substituent Y to a lowering of S, as in the energy level diagram shown in Figure 17. This assignment

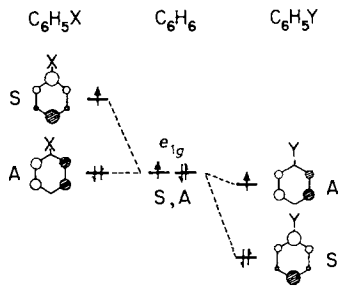

Fig. 17. Energy level diagrams for the effect of substituents on the HOMO of aromatic cations. X = electron-donating substituent, Y = electron-withdrawing substituent.

has been indeed confirmed by the analysis of the ESR spectra of various aromatic radical ions. As a result, the spin densities at the *para* and the *meta* positions of aromatic cations differ markedly, depending on whether the substituent is X or Y. In Ph–X, the HOMO is S and the increased spin density in the *para* position is at the expense of a decreased spin density in the *meta* position. In Ph–Y, the HOMO is A and the converse would apply. In order to utilize these spin densities for the prediction of the isomer distributions, we classify the substituents as either X or Y. However, the usual procedure based on some kinetic property, such as the Hammett σ constants derived from the relative reactivities ($\lg k/k_0$), is subject to changes in r_{DA} described in Section 4.1.4, and it is not an adequate criterion. Instead, we employ a more direct measure of the HOMO energy based on the ionization potential of a substituted benzene relative to benzene, as the indicator of electron release or electron withdrawal for substituents X and Y, respectively. We thus define the intrinsic electronic property of a substituent as electron-releasing or electron-withdrawing on the basis of the HOMO energy rather than the reactivity. According to this analysis, the *para*/*meta* isomer distribution would be simply predicted from the ionization potential of the monosubstituted benzene (Table 3).

Table 3. Isomer distribution for the electrophilic aromatic substitution of monosubstituted benzenes, as predicted from their ionization potentials.

Substituent	I_D	Isomer distribution
X	PhX < PhH	*para* > *ortho* ≫ *meta*
Y	PhY > PhH	*meta* > *ortho* ≫ *para*

Such a prediction is nicely borne out in Figure 18 in which the *para* and *meta* isomers obtained from a variety of electrophilic aromatic substitutions are plotted against

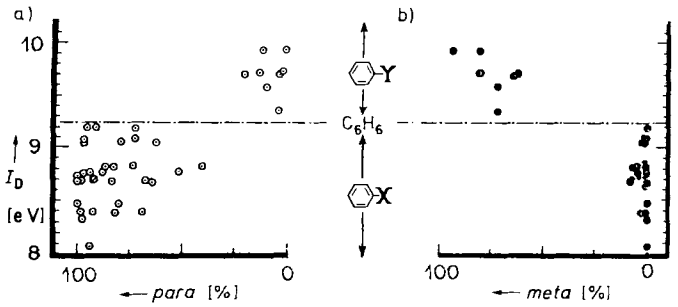

Fig. 18. The product distribution in electrophilic nitration, bromination, mercuration, and thallation among *para* isomers (a) and *meta* isomers (b) derived from monosubstituted benzenes with electron-releasing (X) and electron-withdrawing (Y) substituents, as indicated by the values of the ionization potential relative to that of benzene in [33]. Note that the halogens F, Cl, Br, and I are X substituents with $I_D = 9.18$, 9.08, 9.05, and 8.67 eV, respectively.

the ionization potential of the monosubstituted benzene. Four features in Figure 18 are noteworthy. First, the monosubstituted benzenes fall rather cleanly into one of two categories, i.e., heavily *para*- or heavily *meta*-producing with no arene yielding competitive amounts of each isomer. Second, the isomer distributions are determined solely by the ionization potential of the arene and are more or less independent of the electrophile. Third, the halogen substituents, F, Cl, Br, and I, are clearly to be included among the electron-releasing X, and no ad hoc explanation is required to account for the isomer distributions derived from the halobenzenes. Fourth and most importantly, there is an interesting *discontinuous transition* from *para*-producing aromatics to *meta*-producing aromatics, and vice versa, which occurs at benzene ($I_D = 9.23$ eV). All of these phenomena are in exact accord with the predictions listed in Table 3 and in Figure 17. Although the first three have been previously rationalized, the fourth phenomenon is not easily accounted for on the basis of conventional arguments. According to Figure 17, the discontinuity of the isomer distribution at benzene is caused by the splitting of the degenerate e_{1g} orbitals by the introduction of a substituent. It is noteworthy that such a splitting can arise from even minor perturbations, such as the mere replacement of hydrogen by deuterium. This extreme sensitivity is forcefully brought forth by the remarkable inequivalency of the proton splittings in the ESR spectrum of even the monodeuteriobenzene radical ion.[40]

4.2. Addition of Electrophiles to Olefins

The electrophilic addition to olefins has been one of the most widely studied processes in organic chemistry, the nature of the transition states and reactive intermediates being of considerable interest.[41] In particular, the bromination [Eq. (1)] and oxymercuration [Eq. (2) with X = OAc, OMe, etc.] of olefins have been examined extensively, and the generally accepted mechanisms involve similar intermediates (Scheme 8): π complexes (bromonium and mercurinium ions) and σ complexes (carbocations).

Despite such similar problems, however, there are significant differences in the reactivities of olefins in bromination compared with mercuration. For example, the rates of bromination generally increase with additional methyl substitution at the double bond whereas mercuration follows the opposite trend as illustrated in Figure 19. Clearly,

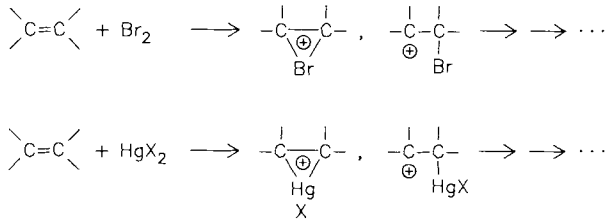

Scheme 8. Comparative mechanisms of bromination and oxymercuration of olefins.

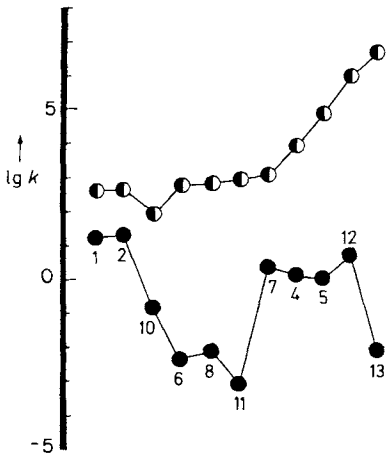

Fig. 19. Comparison of the reactivities of various olefins in oxymercuration with use of $Hg(OAc)_2$ (●) and in electrophilic bromination (◐) in methanol [42]. 1 = 1-pentene, 2 = 1-hexene, 4 = cyclohexene, 5 = cycloheptene, 6 = cyclooctene, 7 = styrene, 8 = (*Z*)-methylstyrene, 10 = 3,3-dimethyl-1-butene, 11 = (*E*)-4,4-dimethyl-2-pentene, 12 = 2-methyl-2-butene, 13 = 2,3-dimethyl-2-butene.

the reactivity patterns of the olefins are quite different for these processes—*the two generally following opposite trends*. The relative rates of bromination increase with the donor property of the olefin as measured by its ionization potential. On the other hand, the relative rates of oxymercuration show little correlation with bromination, let alone with the ionization potentials of the olefins—the most electron-rich, 2,3-dimethyl-2-butene (13 in Fig. 19), actually reacting substantially slower than the reference 1-pentene (1 in Fig. 19). Such discrepancies have been discussed in terms of differences in the rate-determining steps—that for mercuration being either the formation of π or σ complexes or the subsequent nucleophilic attack (especially by the solvent) and that for bromination being the complex formation. Generally, a combination of electronic, steric, and solvent effects has been invoked in order to understand the trends in olefin reactivity. No general mechanistic formulation has been brought forth, and the analysis of the reactive intermediates has not succeeded in explaining the significant differences in olefin reactivity between bromination and mercuration.

4.2.1. The Charge-Transfer Correlation

The relative reactivity of various olefins in electrophilic bromination, given by $\lg(k/k_0)_{Br_2}$ where k_0 refers to the reference 1-pentene, is compared directly with the relative reactivity in oxymercuration ($\lg(k/k_0)_{HgX_2}$) in Figure 20a.[42] The random, "buckshot" appearance of the plot encourages no correlation between these two electrophilic processes. However, if the work term (evaluated independently as Δw_p^* from the CT spectra according to Equation (35)) is simply included in with the relative reactivity, the remarkable transformation of the data is shown in Figure 20b. The linear correlation in Figure 20b is expressed as Equation (55). In other words, *when the work terms for the*

$$\left(\ln\frac{k}{k_0}+\frac{\Delta w_p^*}{RT}\right)_{Br_2}=\left(\ln\frac{k}{k_0}+\frac{\Delta w_p^*}{RT}\right)_{HgX_2} \qquad (55)$$

olefin-bromine and olefin-mercury(II) interactions are included, the relative reactivities of various olefins to electrophilic bromination and mercuration are identical. We interpret such an unprecedented relationship to signify that related transition states are actually involved in these apparently dissimilar processes [see Eq. (43) or (44)]. As a corollary to this conclusion, the relative reactivities in bromination and oxymercuration are expected to be the same in the absence of steric differences among olefins. Indeed, this prediction is borne out with a series of *para*-substituted styrenes that show quite similar reactivity trends in bromination and oxymercuration.[43]

4.2.2. Unity of Bromination and Oxymercuration according to FERET

The ability of the quantitative relationship in Equation (55) to successfully unify electrophilic bromination and oxymercuration is a direct consequence of FERET as generally outlined in Scheme 6. Thus the experimental correlation in Figure 20b with the work terms Δw_p^* is equivalent to the FERET with the CT energies $h\nu_{CT}$ in Equation (37), since it follows from Equation (35) that

$$[\Delta w_p^*(Br_2)-\Delta w_p^*(HgX_2)]=[\Delta h\nu_{CT}(Br_2)-\Delta h\nu_{CT}(HgX_2)]$$

for the same series of olefins with ΔI_D in common. The validity of the CT relationship depends on the ability to evaluate the work term arising from the mutual interaction of the olefin with the electrophile, be it bromine or a mercury(II) derivative. This treatment differs significantly from earlier attempts to correlate the reactivity of olefins in electrophilic additions. Although it is generally recognized that steric effects can be distinguished from polar effects in linear free-energy relationships, the approach has been largely empirical.[44] Indeed, the rate constants for bromination have been extensively analyzed in terms of Taft polar (σ^*) and steric (E_s) parameters, the relative contributions of each depending on the substitution and the topological pattern about the double bond.[45] However, in order to carry out a similar Hammett-Taft type of analysis for oxymercuration, *Pritzkow* et al.[46] were forced to employ four parameters to develop a reliable correlation. On the other hand, the direct relationship between electrophilic bromination and mercuration in Figure 20b evolves naturally from the experimental data by a purely operational approach with use of steric effects as evaluated by Equation (35).

4.3. Aromatic Substitution versus Alkene Addition

The definition of an *electrophilic reaction* forms an important pedagogical basis of organic chemistry, especially as it refers to olefin additions and aromatic substitutions.[47] It is generally recognized that alkenes are significantly more reactive than arenes in a variety of electrophilic processes. Although experimental data that allow direct quantitative comparisons between alkene and arene reactivity are scarce, there are clear indications of the problem. For example, the electrophilic chlorination of benzene ($I_D=9.23$ eV) in acetic acid proceeds slowly with a second-order rate constant of $1.54\times10^{-6}\,M^{-1}s^{-1}$, whereas the chlorination of 1-butene, which is a weaker donor ($I_D=9.63$ eV), proceeds at much faster rates even in nonpolar solvents. The electrophilic mercuration of benzene with $Hg(OAc)_2$ proceeds with a second-order rate constant of $7.5\times10^{-7}\,M^{-1}\,s^{-1}$ in acetic acid, but 1-pentene ($I_D=9.52$ eV) reacts with $Hg(OAc)_2$ in methanol more

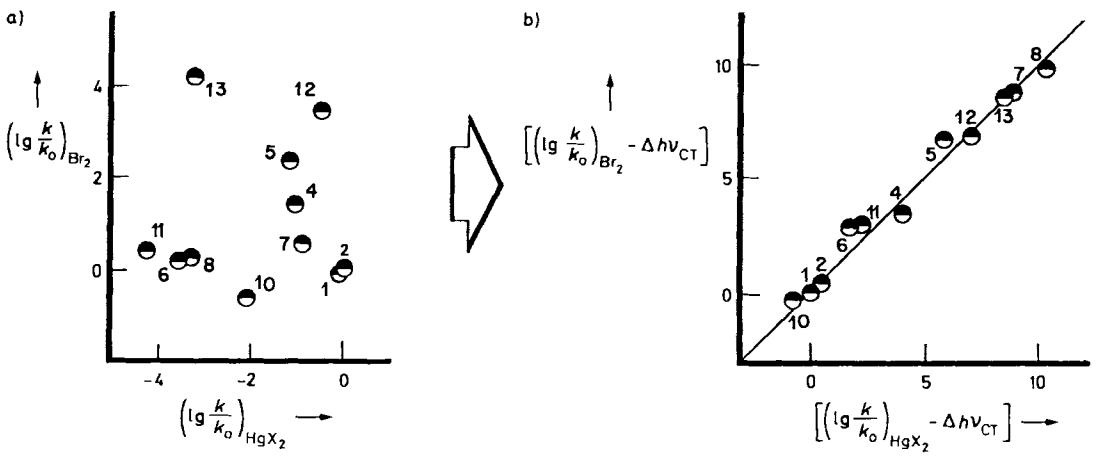

Fig. 20. Direct comparison of the relative reactivity of olefins in mercuration and bromination before (a) and after (b) inclusion of the steric effects. The line is arbitrarily drawn with a slope of unity to emphasize the fit to Equation (55). For identification of the olefins, see Figure 19 [42].

than 2×10^7 times faster than benzene. Such reactivity differences and solvent effects are difficult to assess quantitatively by the conventional mechanisms of electrophilic processes. The relative rates of various electrophilic additions and substitutions have been successfully correlated with the donor properties of substituted alkenes and arenes such as those based on the Taft σ^* constants and the Brown σ^+ constants, respectively.[32,41] Indeed, these linear free energy relationships provide considerable understanding of the influence of molecular structure on electrophilic reactivity. As successful as these empirical correlations have been for alkenes and arenes *separately*, however, no general mechanistic formulation has been brought forth to unify the concepts of electrophilic reactivity.[48] Thus no quantitative insight has been educed to relate alkene donors and arene donors with features of commonality sufficient to explain their significant differences in reactivity toward various electrophiles. Furthermore, no quantitative accounting of solvent effects in electrophilic addition and substitution is extant.

4.3.1. Charge-Transfer Correlation

Molecular bromine has served as an ideal electrophile for mechanistic studies owing to its facile reactions with both olefins and aromatic compounds. Since these reactions occur at measurable rates in a wide variety of solvents, extensive kinetic studies have been carried out on electrophilic brominations. In Figure 21a we find a direct relationship between the reactivity of alkenes and arenes in electrophilic brominations ($\lg k_{Br_2}$) and the charge-transfer transition energies ($h\nu_{CT}$) of their EDA complexes.[49] Indeed, the experimental plot shows two linear but separate correlations—the one for arenes is described by Equation (56), that for alkenes by Equation (57). The expression

$$\lg k_{Br_2} = -16 h\nu_{CT} + 55 \quad (56)$$

$$\lg k_{Br_2} = -4.1 h\nu_{CT} + 20 \quad (57)$$

for the arenes in Equation (56) merits special attention, since the slope of the correlation is remarkably close to unity when $RT\lg k_{Br_2}$ is plotted against $-\Delta h\nu_{CT}/(2.3RT)$ [cf. Eq. (45) and Fig. 15]. In other words, the reactivity of the arene in electrophilic bromination, as represented by the activation free energy $\Delta G^{\neq} = -RT\ln(k_{Br_2}/Z)$, corresponds directly to the charge-transfer transition energy in the arene–bromine complex [Eq. (58)]. However, the

$$\Delta G^{\neq} = h\nu_{CT} + \text{constant} \quad (58)$$

same does not apply to alkene bromination, as shown by the different correlation in Equation (57). Indeed, the inapplicability of Equation (58) to alkenes is reflected in the huge difference in reactivity between alkenes and arenes when they are evaluated at the same donor ability. For example, ethylene, which represents the least reactive alkene, is still more than 50 times as reactive as anisole, the most reactive arene, even after discounting the substantial difference of 32 kcal mol^{-1} in their CT donor abilities. Clearly, the CT transition energy $h\nu_{CT}$ does not provide sufficient means by itself to bridge the gap in electrophilic reactivity between alkenes and arenes. In order to understand the reactivity difference between alkenes and arenes, let us return to the FERET formulation in Scheme 6.

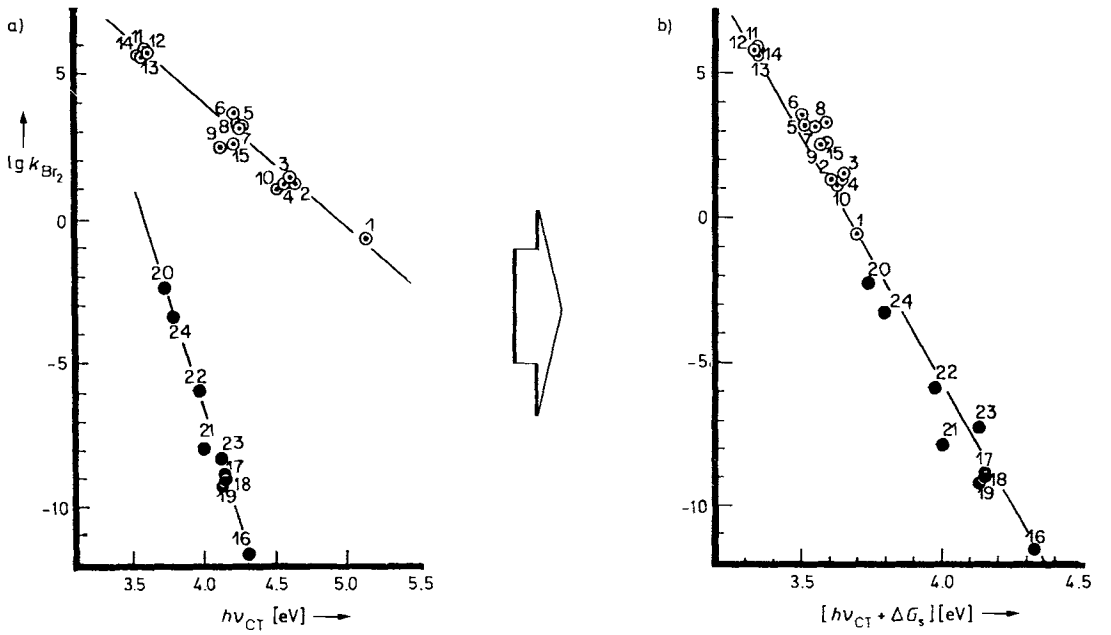

Fig. 21. a) Correlation of the logarithms of the rates k_{Br_2} [M^{-1} s^{-1}] of electrophilic bromination with the CT transition energies ($h\nu_{CT}$) of the bromine complexes of alkenes (⊙) and arenes (●): 1 = ethylene, 2 = propylene, 3 = 1-butene, 4 = 1-pentene, 5 = isobutylene, 6 = 2-methyl-1-butene, 7 = (*Z*)-2-butene, 8 = *E*-2-pentene, 9 = (*E*)-4,4-dimethyl-2-pentene, 10 = 3,3-dimethyl-1-butene, 11 = 2,3-dimethyl-2-pentene, 12 = 2,3-dimethyl-2-butene, 13 = 2,3-dimethyl-2-hexene, 14 = 2,3-dimethyl-2-heptene, 15 = cyclohexene, 16 = C_6H_6, 17 = MeC_6H_5, 18 = EtC_6H_5, 19 = $iPrC_6H_5$, 20 = $MeOC_6H_5$, 21 = *o*-$Me_2C_6H_4$, 22 = *m*-$Me_2C_6H_4$, 23 = *p*-$Me_2C_6H_4$, 24 = 1,3,5-$Me_3C_6H_3$). b) Unified correlation by FERET in Equation (60) [49]. The slope of the correlation is unity.

4.3.2. Solvation Energies of Arene Cations versus Alkene Cations

The conversion of the alkene–bromine and arene–bromine EDA complexes to their respective CT excited ion pairs $[D^{\oplus}, A^{\ominus}]^*$ occurs (Scheme 6) with minimal changes in solvation. Thus the relative donor properties of alkenes and arenes measured from the CT transitions represent essentially those in the gas phase. By contrast, the thermal activation of electrophilic brominations in solution is an adiabatic process in which the formation of the adiabatic ion pair $[D^{\oplus}, A^{\ominus}]_s$ must be accompanied by large changes in solvation. Therefore, any comparison of the reactivity of arenes and alkenes in electrophilic brominations according to this model must specifically address the question of solvation. Let us focus our attention on only the solvation change associated with the donor moiety, since the bromine acceptor is common to both systems. Indeed, for the solution process, we need consider only that energy change for the oxidation of the alkene and arene moiety, as given by the standard oxidation potentials E^0_{ox}. The latter can be measured by fast-scan cyclic voltammetry with microelectrodes [see Eq. (47)]. However, the anodic oxidation of most alkenes is irreversible even at CV scan rates of 200000 $V\,s^{-1}$ owing to the kinetic instability of their radical cations. Thus the solvation energies of the transient alkene and aromatic cations cannot be simultaneously determined by the direct method described in Equation (38). However, solvation energies can be evaluated from the free energy relationship for electron transfer such as that established for the outer-sphere oxidation of organometal donors with tris(phenanthroline)iron(III) oxidants $[FeL_3]^{3\oplus}$ [Eq. (18)]. Indeed, a detailed kinetic study of the oxidation of a series of arenes by $[FeL_3]^{3\oplus}$ establishes the outer-sphere character of the rate-limiting electron-transfer step [Eq. (59)].[50]

$$\text{ArylH} + [FeL_3]^{3\oplus} \xrightarrow{k_{Fe}} \text{ArylH}^{\oplus} + [FeL_3]^{2\oplus} \qquad (59)$$

As such, the first-order form of the Marcus free energy relationship can be used to evaluate the endergonic driving force ΔG for Equation (59). Since alkene oxidations with $[FeL_3]^{3\oplus}$ proceed in a similar manner, the difference in the driving forces for arene and alkene donors can be evaluated from the kinetics data.[49] This procedure is tantamount to the evaluation of the solvation energies of all the cations relative to that of a reference donor. We arbitrarily choose the aromatic cations as the reference, since their solvation energies are rather invariant at 2.0 eV for a series of aromatic compounds in acetonitrile (see Fig. 16). Thus the solvation energy of an alkene cation can be evaluated relative to that of an aromatic cation under isokinetic conditions, i.e., the rate at which the oxidation of an alkene is the same as that of an arene, $\Delta G^{\ddagger}(\text{Alkene}) = \Delta G^{\ddagger}(\text{Arene})$. From this we find the relative solvation energy ΔG^s_r of the alkene cation to be $\Delta G^s_r = -I_D$. The values of ΔG^s_r obtained in this manner are listed in Table 4 for the various alkenes. The relative solvation energies in acetic acid can be obtained from those evaluated in acetonitrile by using the Born model.[49] These are also listed in Table 4 together with the relative solvation energies of alkene cations in the aprotic tetrachloroethane. There is a trend for the solvation energies of transient alkene cations to vary with the substituents on the double bond. In general, the magnitude of the solvation energy is seen to decrease as the number of methyl substituents increases, approaching that of aromatic cations. Thus the solvation energies of these transient cations do reflect the degree of charge delocalization.[51]

Table 4. Solvation energies of transient alkene cations.

Alkene	I_D [eV]	ΔG^s_r [eV] MeCN	HOAc	$(ClCH_2)_2$
$H_2C{=}CH_2$	10.52	1.69	1.45	0.98
$H_2C{=}CHMe$	9.74	1.21	1.04	0.70
$H_2C{=}CHEt$	9.63	1.13	0.97	0.66
$H_2C{=}CHn\text{Pr}$	9.52	1.07	0.92	0.62
$H_2C{=}CMe_2$	9.24	0.89	0.77	0.52
$H_2C{=}C(Me)Et$	9.15	0.84	0.72	0.49
(*Z*)-MeCH=CHMe	9.12	0.82	0.71	0.48
(*E*)-MeCH=CHEt	9.04	0.77	0.66	0.45
(*E*)-MeCH=CH*t*Bu	8.91	0.73	0.48	0.42
$H_2C{=}CHt\text{Bu}$	9.45	1.03	0.89	0.60
$Me_2C{=}C(Me)Et$	8.21	0.27	0.23	0.16
$Me_2C{=}CMe_2$	8.27	0.34	0.29	0.20
$Me_2C{=}C(Me)n\text{Pr}$	8.19	0.25	0.22	0.15
$Me_2C{=}C(Me)n\text{Bu}$	8.15	0.20	0.17	0.12
cyclohexene	8.95	0.68	0.58	0.39

4.3.3. Unified View of the Transition States for Electrophilic Bromination of Alkenes and Arenes

The evaluation of the solvation energies of transient cations allows the donor abilities of alkenes and arenes in solution to be determined from the gas-phase data. Let us now make an analogous connection between the ion pairs generated photochemically by CT excitation and those formed thermally by an adiabatic electron transfer in solution, as presented in the thermochemical cycle in Scheme 6. Indeed, the extent to which the formation of the solvated ion pair in Scheme 6 is equivalent to the activation barrier $\Delta G^{\ddagger}$ for electrophilic bromination is then given by Equation (60). (Note the contribution from the solvation of the common bromine moiety is included in the constant term.[52])

$$RT\ln k_{Br_2} = h\nu_{CT} + \Delta G^s_r + \text{constant} \qquad (60)$$

The experimental fit of the rate data for electrophilic bromination to Equation (60) is shown in Figure 21b, which is a remarkable transformation of the two separate correlations for alkenes and arenes in Figure 21a. In other words, bromine addition to alkenes and bromine substitution of arenes are included in a single correlation, despite their distinctive stoichiometries and widely divergent rates. We interpret such an unprecedented interrelationship to signify that related transition states are involved in these otherwise disparate processes. The fit of the experimental data in Figure 21b to the line arbitrarily drawn with a slope of unity (i.e., $-(2.3\,RT)^{-1}$) emphasizes the 1 : 1 correspondence between the kinetic barrier $(-RT\ln(k_{Br_2}/Z))$ for electrophilic bromination and the energetics of ion-pair formation in solution. Although the precise structure of the

transition state is presently unknowable in detail, the correlation provided by Equation (60) indicates that the solvated ion pair is certainly a feasible model of the transition state for both alkene addition and aromatic substitution.[53] Indeed, it provides the common means to unify the very large differences in the reactivity of alkenes and arenes toward bromine in a quantitative way.

4.3.4. Significance of the CT Formulation to Other Linear Free Energy Relationships. Unity of Brown σ^+ and Taft σ^* Constants

The charge-transfer formulation in Scheme 6 for electrophilic bromination leads to the conception of the transition state as the solvated ion pair. In the general form, Equation (60) is applicable to both alkenes and arenes. As such, we show how this formulation unifies the two separate linear free energy relationships that have been previously developed independently for electrophilic additions to alkenes and for electrophilic aromatic substitutions. In particular, the rates of electrophilic aromatic substitution are well correlated by the Brown σ^+ aromatic substituent constants [Eq. (61)].[44] Likewise, the rates of electrophilic additions to alkenes approximate a similar free energy relationship based on the Taft σ^* aliphatic substituent constants [Eq. (62)].[55] Since the sensitivity factors ρ and ρ^* in

$$\lg \frac{k}{k_0} = \rho\sigma^+ \tag{61}$$

$$\lg \frac{k}{k_0} = \rho^*\sigma^* \tag{62}$$

Equations (61) and (62), respectively, have been subjected to various physical interpretations, our primary task is to relate ρ and ρ^* to the CT formulation in which the parameters bear definitive physical significance.

We begin by noting that the CT transition energy $h\nu_{CT}$ is linearly related to the ionization potentials of alkene and aromatic donors by a single correlation [Eq. (63)]. Likewise, the solvation term ΔG_r^s for alkenes in Table 4 is rather linear with the ionization potential [Eq. (64)], where

$$h\nu_{CT} = 0.7 I_D + \text{constant} \tag{63}$$

$$\Delta G_r^s = \alpha I_D + \text{constant} \tag{64}$$

α is the solvent-dependent slope of the relationship (e.g., $\alpha = 0.6$ for acetic acid). As mentioned earlier, the value of ΔG_r^s for the aromatic donors is constant irrespective of the solvent. Linear relationships have been well established for the substituent constants σ^* and σ^+ as a function of the ionization potential of the alkene and aromatic donors, respectively:[54]

alkenes: $\sigma^* = 1.1 I_D + \text{constant}$

arenes: $\sigma^+ = 1.1 I_D + \text{constant}$

The combinations of these equations with Equation (60) afford alternative forms of the free energy relationship:

alkenes: $\lg \frac{k}{k_0} = -15(0.7-\alpha)\sigma^*$

arenes: $\lg \frac{k}{k_0} = -11\sigma^+$

The comparison of these expressions with the original linear free energy relationships in Equations (61) and (62) leads to the important result that the sensitivity factors in electrophilic brominations are given by Equations (65) and (66) for alkenes and arenes, respectively.

$$\rho^* = -15(0.7-\alpha) \tag{65}$$

$$\rho = -11 \tag{66}$$

According to Equation (66), the relative reactivity of arenes in electrophilic substitution is solvent independent. The data available in the extant literature for glacial acetic acid and trifluoroacetic acid support this conclusion (Table 5). Furthermore, the solvent dependency of the electrophilic bromination of alkenes as predicted by Equation (65) accords with the experimental results in media as different as glacial acetic acid and tetrachloroethane. The calculated values of ρ and ρ^* in Table 5 show reasonable agreement with the experimental values. The agreement is especially noteworthy considering that the absolute magnitude of ρ and ρ^*, otherwise unpredictable, can be independently evaluated in different solvents. Since alkenes and arenes show common relationships between $h\nu_{CT}$ and I_D as well as between σ^* or σ^+ and I_D, the principal difference in their reactivities toward electrophilic bromination can be attributed to differences in the solvation of alkene and aromatic cations. The charge-transfer formulation, which we have outlined in Scheme 6 and expressed by the FERET in Equation (60), provides a direct and general method for evaluating the activation barriers of electrophilic brominations. The CT transition energy represents the energetics of ion-pair formation and serves as a model for the activation process when changes in solvation are explicitly taken into account. Thus the single correlation of the remarkable free energy relationship in Figure 21b underscores the conceptual unity of the activation process for both electrophilic addition to alkenes and electrophilic substitution of arenes. Moreover, the charge-transfer formulation of the activation process employs physical concepts amenable to direct molecular interpretation. Indeed, the notion of the solvation of ion pairs offers a general solution to solvent effects in electrophilic reactions. The question of whether the adiabatic ion pairs are actual intermediates along the reaction coordinate of electrophilic

Table 5. Comparison of the experimental and calculated values of ρ and ρ^* for electrophilic brominations in several solvents.

Donor	Solvent	ρ or ρ^*	
		exp.	calcd
Arenes	HOAc	−12.1 [a]	−11
Arenes	CF_3CO_2H	−12.3 [b]	−11
Alkenes	CH_3CO_2H	− 2.8 [b]	− 2.4
Alkenes	$Cl_2CHCHCl_2$	− 4.1 [b]	− 5.1

[a] From [32g]. [b] See [49].

brominations is, of course, not directly addressed (see Section 5). We emphasize that the charge-transfer formulation, in a more general context, relates to the electron-rich nucleophiles (such as alkenes and arenes as electron donors) and the electron-poor electrophiles (such as bromine as electron acceptors) as they were broadly envisioned by *Mulliken* in his pioneering approach to intermolecular interactions.

4.4. Halogenolysis of Alkyl-Metal Bonds

The cleavage of alkyl-metal bonds by halogens, or halogenolysis, is one of the most common reactions of organometals RM [Eq. (67)].

$$RM + X_2 \longrightarrow RX + MX \qquad (67)$$
$$X = F, Cl, Br, I$$

Such substitution reactions effected by electrophiles are basic to our understanding of a wide variety of organic syntheses via organometallic intermediates.[56] Despite extensive studies, however, there is surprisingly little quantitative information known about the structural factors important in electrophilic substitution at a carbon-metal bond. The mechanism of the electrophilic pathway is still the subject of controversy, largely revolving around the depiction of the transition state—whether it is two- or four-centered, open, cyclic, etc. Although kinetic and stereochemical probes have been extensively employed, the mechanistic difficulties have doubtlessly been exacerbated by the implicit assumption, uniformly adopted, that electrophilic processes are concerted, involving no viable intermediates. The latter is somewhat surprising in view of earlier reports of the existence of complexes between organosilanes and halogens.[57] In the cleavage of unsymmetrical alkylmetals such as tetraalkyltin Me_nSnR_{4-n} (n = 1-3) or dialkylmercury MeHgR, the selectivity S(R/Me) determines the relative rates of scission of the relevant bonds, i.e., an R-Sn bond versus a Me-Sn bond, as an intramolecular competition. Thus, iodine affords a mixture of two alkyl iodides, MeI and RI, from R_2SnMe_2 in amounts which depend upon the relative rates of cleavage [Eqs. (68) and (69)].

$$R_2SnMe_2 + I_2 \longrightarrow \begin{cases} \longrightarrow MeI + R_2SnMeI & (68) \\ \longrightarrow RI + RSnMe_2I & (69) \end{cases}$$

The selectivity, $S(R/Me) = k_R/k_{Me}$, is completely analogous to that presented for electron transfer [Eqs. (27) and (28)]. As such S(R/Me) is a measure of the intrinsic reactivity of a given alkylmetal irrespective of the substitution patterns in a series of Me_nSnR_{4-n} compounds. The solvent is known to play a large, dominating role in the iodinolysis of alkylmetals, particularly with regard to the rate and selectivity.[58] For example, the second-order rate constants for iodinolysis of tetraalkyltin compounds in acetonitrile are 10^2 to 10^3 times faster and the rate constants in tetrachloromethane 10^3 to 10^4 times slower than those obtained in dichloromethane solutions. In addition to the large sensitivity of the rates to variations in the solvent, there is a remarkable inversion in the relative rates of reactivity. For example, Et_4Sn is about ten times more reactive than Me_4Sn in dichloromethane, but the order is reversed in acetonitrile. Finally, in the iodinolysis of all tetraalkyltin compounds, there is a marked dependence of selectivity on the solvent. There are even notable reversals in selectivity with solvent polarity, e.g., $S(n\text{Bu/Me}) = 0.0040$ in acetonitrile but 1.7 in tetrachloromethane, and $S(\text{Et/Me}) = 0.11$ in acetonitrile but 6.7 in tetrachloromethane.

4.4.1. Charge-Transfer Correlation

The relative rates of iodinolysis are evaluated for various tetraalkyltins by the comparative procedure, i.e., $\Delta G_r^{\ddagger} = -2.3\,RT\lg(k/k_0)$, where k and k_0 are the rates for R_4Sn and Me_4Sn, respectively. The free-energy change ΔG_r^0 for the oxidation of a tetraalkyltin relative to Me_4Sn in solution is obtained directly from the difference in their ionization potentials in the gas phase, i.e., $\Delta G_r^0 = \alpha \Delta I_D$, where the proportionality constant α is 0.60 in acetonitrile solutions at 25 °C.[16] The accompanying change in the interaction energy ΔE of the thermal ion pair is equated to $\Delta w_p^{\ddagger}$ determined from the transition energy of the CT complex [Eq. (35)]. The striking correlation in Figure 22 with a slope of 1.0 represents a linear free energy relationship expressed as Equation (70), which is the FERET described

$$\Delta G_r^{\ddagger} = \Delta G_r^0 + \Delta w_p^{\ddagger} \qquad (70)$$

earlier in Equation (44).[54] It is important to point out that Equation (70) for alkylmetal iodinolysis obtains directly from three independent sets of experiments.

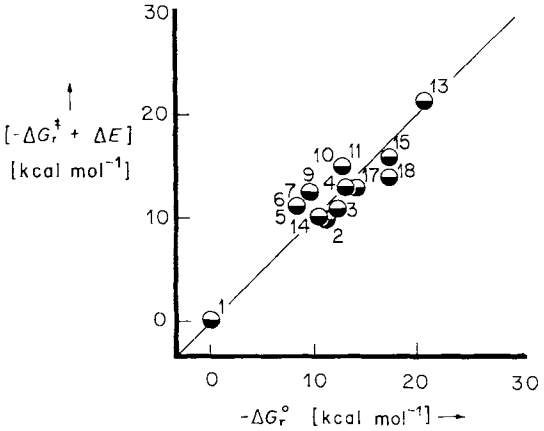

Fig. 22. The correlation of the changes in the activation free energy for iodinolysis of tetraalkyltin compounds with changes in the driving force for $[RM^{\oplus}, I_2^{\ominus}]$ formation. $\Delta E = \Delta w_p^{\ddagger}$. 1 = Me_4Sn, 2 = Et_4Sn, 3 = nPr_4Sn, 4 = nBu_4Sn, 5 = $EtSnMe_3$, 6 = $nPrSnMe_3$, 7 = $nBuSnMe_3$, 9 = Et_2SnMe_2, 10 = nPr_2SnMe_2, 11 = nBu_2SnMe_2, 13 = tBu_2SnMe_2, 14 = Et_3SnMe, 15 = iPr_4Sn, 17 = iBu_4Sn, 18 = iBu_2SnMe_2 [54].

4.4.2. FERET for the Solvent Effects in Halogenolysis

The same FERET can even be established in nonpolar solvents in which ΔG_r^0 cannot be determined. For example, the linear correlation in both Figures 23a and 23b for iodinolysis of tetraalkyltin compounds in dichloromethane and dialkylmercury compounds in tetrachloromethane, re-

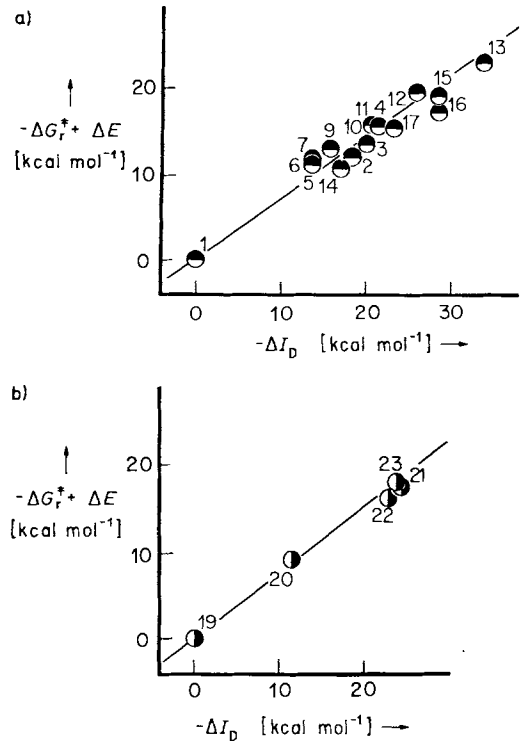

Fig. 23. Linear free energy relationships established in the iodinolysis of alkylmetals in nonpolar media. $\Delta E = \Delta w_p^{\neq}$. a) Tetraalkyltin compound in CH_2Cl_2. b) Dialkylmercury compound in CCl_4. Numbers refer to alkyltin compounds in Figure 22 (with the exception of 18) and the following alkylmercurials: 19 = Me_2Hg, 20 = EtHgMe, 21 = nPr_2Hg, 22 = nBu_2Hg, 23 = iBu_2Hg [54].

spectively, corresponds to the following linear free energy relationship:

$$\Delta G_r^{\neq} - \Delta w_p^{\neq} = \Delta G_r^0 = \alpha \Delta I_D$$

From the slopes, α is evaluated as 0.71 in dichloromethane and 0.77 in tetrachloromethane. As expected, these values are larger than $\alpha = 0.60$ in the more polar acetonitrile. Indeed, the solvent effect on the rates of iodinolysis provides an important test of FERET in dealing with the rather unusual inversion in the reactivities. Thus, the relative reactivities of various R_4Sn are obtained directly from Equation (70) [Eq. (71)].

$$-RT \ln \frac{k}{k_0} = \alpha \Delta I_D + \Delta w_p^{\neq} \qquad (71)$$

Since the variations in the relative reactivities with solvent are represented by changes in α, these are drawn in Figure 24 as a family of solid lines calculated from the FERET in Equation (71). The fit to the available experimental rate data, indicated by the shaded circles, is unmistakable.[54] In other words, a single parameter α correctly predicts the marked alteration in reactivity order of alkylmetals, which in previous treatments could only be attributed to solvent-induced changes in mechanism.[58]

4.4.3. Polarity of the Activated Complex for Halogenolysis

Since the charge-transfer formulation quantitatively accounts for the reactivities of alkylmetals in iodinolysis, we might inquire about the structural factors involved. In gen-

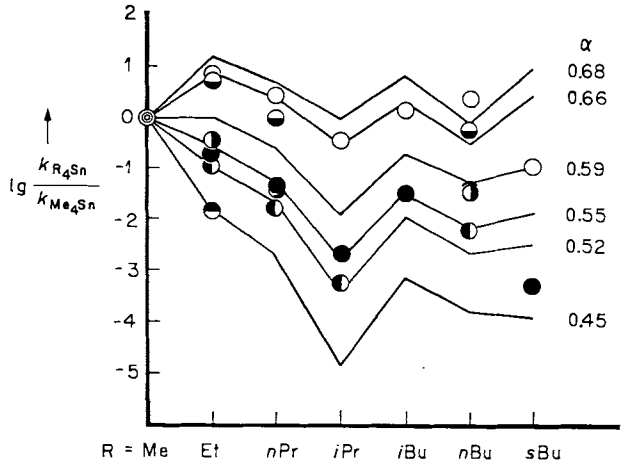

Fig. 24. Prediction of the solvent effect on the relative reactivities according to the FERET in Equation (71). The solid lines are calculated for various α in [54]. ○ = CH_2Cl_2, ◒ = PhCl, ◑ = AcOH, ● = MeCN, ◐ = MeOH, ◓ = DMF.

eral terms, $\alpha \Delta I_D$ and ΔE correspond to the electronic and steric contributions, respectively, to the activation process. The solvent effect is primarily associated with changes in the electronic effect, owing to variations in α. As the solvent increases in polarity, α decreases and steric effects become dominant—leading to $k_{Me_4Sn} > k_{Et_4Sn}$ in glacial acetic acid, acetonitrile, methanol, and dimethylformamide (Fig. 24). The reverse reactivity $k_{Me_4Sn} < k_{Et_4Sn}$ obtains in nonpolar solvents such as chlorobenzene and dichloromethane in which the electronic demand is optimized as a result of the increased values of α. The importance of solvent polarity may also be examined in another way. Thus the activation free energy, as described by the charge-transfer mechanism, relates directly to the free energy of formation of the ion pair. Consequently, the role of the solvent on the rate is largely reduced to its effect on the ion pair. Despite the lack of knowledge regarding solvent structure, we can estimate the solvation of the ion pair from a macroscopic property of the solvent.[59] Such an approach is described by the classical Kirkwood equation in which the ion pair is considered as a dipolar solute with dipole moment μ in a solvent of bulk dielectric constant ε_B. The electrostatic contribution to the chemical potential or the free energy of solvation is given by Equation (72), where $\phi(\varepsilon_B) = (\varepsilon_B - 1)/(2\varepsilon_B + 1)$ and a is the radius of the solute consid-

$$\Delta G_s = -(\mu^2/a^3)\phi(\varepsilon_B) \qquad (72)$$

ered as a sphere. In the series of alkylmetal–iodine CT complexes considered here, the reactants have no dipole moment. Accordingly, in the charge-transfer reaction, the change in the solvation term in solvents such as MeCN, EtOH, PhCl, $CHCl_3$, and Me_2CO relative to that in dichloromethane may be written as Equation (73), where $\mu^{\neq}$

$$\Delta E_s = -\Delta\Delta G_s^{\neq} = (\mu^{\neq 2}/a^3)\Delta\phi(\varepsilon_B) \qquad (73)$$

is the dipole moment in the transition state.[54] There is a more or less linear correlation of the solvation energy and the dielectric function according to Equation (73). It suggests that the slope $\mu^{\neq 2}/a^3 = 2.5$ is constant for these solvents. If, for the moment, we consider the dipolar CT so-

lute to be approximated by a sphere, then the degree of charge separation is estimated to be between 0.8 and 1. The crude model notwithstanding, this analysis of the solvent effect provides further support for the high degree of charge separation in the rate-limiting transition state for the iodinolysis of alkylmetals. These results, together with the clean linear free energy relationship in Equation (70) or its equivalent in Equation (71), provide strong evidence that the transition state for electron transfer is accurately reflected by the excited ion pair in the CT complex. As such, this conclusion forms the basis for describing the activation process for iodinolysis as electron transfer in the CT complex.

4.4.4. Selectivity and the Charge-Transfer Mechanism for Iodinolysis of Alkylmetals

The preequilibrium formation of the alkylmetal–iodine charge-transfer complex is included in the general mechanism [Eqs. (74)–(76)] for the iodinolysis of alkylmetals. The

$$RM + I_2 \overset{K_{CT}}{\rightleftharpoons} [RM, I_2] \quad (74)$$

$$[RM, I_2] \xrightarrow{k} [RM^{\oplus}, I_2^{\ominus}] \quad (75)$$

$$[RM^{\oplus}, I_2^{\ominus}] \xrightarrow{\text{fast}} RI + MI \quad (76)$$

activation process for iodinolysis is represented in Equation (75) for inner-sphere electron transfer from the alkylmetal donor to the iodine acceptor. The subsequent sequence of reactions following the CT activation process can be readily formulated on the basis of studies with other acceptors such TCNE and $[IrCl_6]^{2\ominus}$ [see Eqs. (25) and (26)].

According to Equations (74)–(76), the selectivity is determined by the cage fragmentation of the $[RM^{\oplus}, I_2^{\ominus}]$ ion pair [Eq. (76)] subsequent to the rate-limiting step. As such, an important question that evolves is: How does the nature of the ion pair affect the fragmentation pattern of the $RM^{\oplus}$ moiety leading to changes in selectivity? To answer this question, we refer to Equations (18) and (19) as well as to Equations (25) and (26), in which the selectivity was shown to decrease from 25 to 11 on going from an outer-sphere to an inner-sphere mechanism (see Table 2). Such outer-sphere and inner-sphere mechanisms are differentiated primarily by the intermolecular separation between the alkylmetal and the oxidant in the transition state for electron transfer. Extending this relationship, we consider the lower selectivities in iodinolysis to arise from selective interactions between $RM^{\oplus}$ and $I_2^{\ominus}$, which are dictated largely by steric effects. For a charge-transfer model, the alkyltin–iodine interaction can be depicted as shown in Scheme 9.[60]

The extent of the resonance interaction is given by the relationship[61] $\xi = \xi^0 V_r$ with $V_r = V_r^0 \exp(-r^*)$, where V_r is the overlap integral and r^* is the mean separation between I_2 and alkylmetal; ξ^0 and V_r^0 are constants. The extent of the resonance interaction between I_2 and the least hindered site in the alkylmetal, i.e., the Mn–Sn bond, will lead to reductions in the selectivity S(R/Me) in the following way. We first select $[IrCl_6]^{2\ominus}$ as the reference acceptor in which the resonance interaction with the alkylmetal is taken as nil, i.e., the selectivity S_0 is determined solely by the relative bond energies D_{Me} and D_R for dissociation of $Me^{\odot}$ and $R^{\odot}$ from the alkylmetal radical cation $Me_nSnR_{4-n}^{\odot\oplus}$. The selectivity for the reference system is given by $RT \ln S_0 = D_{Me} - D_R$. For iodinolysis, the selectivity can then be represented as Equation (77) if one assumes

$$RT \ln S = RT \ln S_0 - \xi \quad (77)$$

that D_{Me} is reduced to $D_{Me} - \xi$ by the resonance interaction between $MeSnR_3^{\oplus}$ and $I_2^{\ominus}$.[54] Equation (77) can be expressed in a form which emphasizes the relationship between the selectivity and mean separation [Eq. (78)]. The

$$\ln S = -A \exp(-r^*) + B \quad (78)$$

constants are $A = \xi^0 V_r^0 / RT$ and $B = \ln S_0$. Since changes in the mean separation are a measure of the steric effect, Equation (78) indicates how the selectivity may be affected by steric effects, all within the context of the charge-transfer ion pair. In other words, a strong resonance interaction in the ion pair, mediated by the mean separation, can quantitatively account for changes in selectivity with solvent variations as described above. The cleavage of an alkyl–metal bond under these circumstances is highly reminiscent of a concerted process, more commonly referred to as an electrophilic cleavage. As a result, the two concepts become largely indistinguishable at this extreme. Indeed, the charge-transfer formulation provides new meaning to the concept of electrophilic cleavage, which has heretofore been a rather generic mechanistic description.

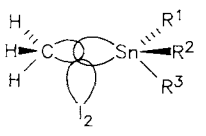

Scheme 9. Charge-transfer model of the alkyltin–iodine interaction.

4.4.5. Solvent Effect on the Relationship between Selectivity and Rate Constant for Halogenolysis

In the CT formulation, the perturbation by steric effects is included in the work term Δw_p^* [Eq. (35)]. The solvent effect may also be expressed as a perturbation in similar form, i.e., $RT \ln(k_m/k_n) = e^2(r_m^{-1} - r_n^{-1})$, where the subscripts m and n refer to different solvents.[54] Thus, the problem reduces to one of describing the solvent-induced change in the mean separation. A direct attack on this problem lies in the measurement of the CT transition energies in various solvents. Unfortunately, this route is experimentally unavailable owing to complications arising from the rapid rates of iodinolysis in all but the least polar solvents. The alternative approach derives from the strong influence of solvent on the intramolecular selectivity. To carry out this analysis, we introduce the term $\delta S = \ln(S_0/S)$, where S is the selectivity of a particular alkylmetal in iodinolysis and S_0 is that selectivity in a reference system (arbitrarily chosen as $[IrCl_6]^{2\ominus}$). The relationship between the changes in selectivity and mean separation, as

they are affected by solvent, can be represented by $\delta S_m/\delta S_n = \exp(r_n - r_m)$. The relationship between the rate constants and selectivities as they are affected by solvent is then expressed as Equation (79),[54] which correctly pre-

$$\ln \frac{k_m}{k_n} = (r_m r_n RT)^{-1} \ln \frac{\delta S_m}{\delta S_n} \tag{79}$$

dicts the inverse relationship between the rate constant and the selectivity in the iodinolysis of alkylmetals. Furthermore Equation (79) accords with the linear selectivity changes with the solvent dependence on the iodinolysis rates. The slope of the correlation is given by $(r_m r_n RT)^{-1}$, from which the mean value $\bar{r}_{mn}$, ranging from 3.7 Å for Et_2SnMe_2 to 4.1 Å for tBu_2SnMe_2, is evaluated. The relative magnitudes of $\bar{r}_{mn}$ for Et_2SnMe_2 and tBu_2SnMe_2 accord with qualitative expectations based on steric effects. More interestingly, the difference (0.40 eV) in ΔE for these alkylmetals, calculated from the differences in CT transition energies and ionization potentials according to Equation (35) is in surprisingly good agreement with the value (0.37 eV) evaluated from $\bar{r}_{mn}$.

4.5. Solvent Effects on Electrophile Behavior toward Organometals

The formulation of reaction mechanisms has been aided by the studies of solvent effects on the rates.[62] In many cases, the solvent variation is treated as a perturbation in which the lack of a smooth correlation with reactivity in a series of related compounds is often considered to be diagnostic of a change in mechanism.[63] For example, the large changes in reactivity, even inversions in the order of reactivity, when the medium for the halogenolysis of an alkylmetal is altered from a polar to a nonpolar solvent is illustrated in Figure 25.[31] As a result, the participation of different mechanisms has been proposed to account for such drastic changes. Such a conclusion is not required, however, since a complex pattern of solvent effects may be accommodated within the context of a single mechanism if

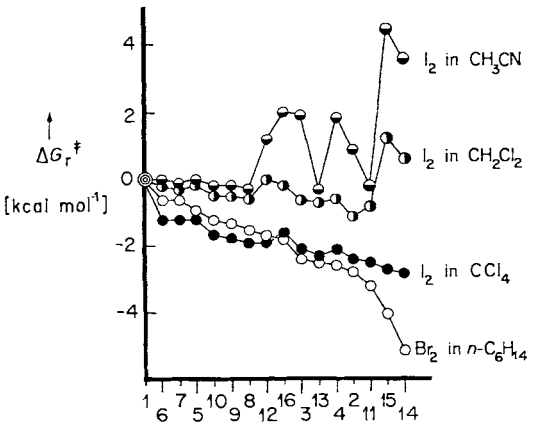

Fig. 25. The reactivity patterns in the halogenolysis of tetraalkyltin compounds in different solvents [31]. The compounds corresponding to the numbers are given in Fig. 12.

cognizance is taken of the mixing of electronic, steric, and solvation effects, as a result of solvent changes. There are several features in Figure 25 which merit special emphasis, and they may be summarized as follows: (1) Changes in reactivity resulting from structural variations in the tetraalkyltin compounds have little bearing on the solvent dependences. (2) In nonpolar solvents such as CCl_4 and hexane, the difference between brominolysis and iodinolysis is minimal. (3) The change in reactivity imposed by solvent changes can be much larger than any wrought by structural alterations of the alkyl ligands. For example, in iodinolysis the difference in the reactivity ($\Delta G^{\neq}$) of sBu_4Sn in acetonitrile and n-hexane is $RT \lg k_m/k_n = 7.2$ kcal mol^{-1}, corresponding to a rate factor of 2×10^5, whereas it is only 4.8 kcal mol^{-1} between the most reactive (sBu_4Sn) and the least reactive (Et_3SnMe) tetraalkyltin compounds in acetonitrile. (4) The change in the reactivity of alkylmetals can be as large in nonpolar solvents (hexane) as in polar solvents (acetonitrile).

4.5.1. Charge-Transfer Correlations with Solvent Variations

The free energy change for solvation ΔG_s associated with the charge-transfer process in Equation (75) is the difference between the gas-phase ionization potential I_D and the free energy change for oxidation in solution.[16] It can be evaluated directly from the FERET in Equation (37) by measuring the CT energies and halogenolysis kinetics in various solvents.[31] Indeed, the trend in ΔG_s for tetraalkyltin compounds obtained in one solvent parallels that in another, as shown by the series of striking linearities of the points in Figure 26 in which the different solvents are compared to tetrachloromethane. In other words, the solvent sensitivity of the solvation energy can be expressed simply as Equation (80), where ΔG_s^0 is taken for the reference sol-

$$\frac{\Delta G_s}{\Delta G_s^0} = \delta \tag{80}$$

vent and the δ values are the slopes in Figure 26. Since the solvation of ions is one of the least understood, but basic aspects of chemical reactions, we rely on a rather conventional model for solvation in the following analysis.

4.5.2. Solvation Energies

The modified Born equation is commonly used to estimate the free energy change associated with the solvation of simple ions.[64] As applied to the solvation energy ΔG_s of the tetraalkyltin cation, it is expressed in relative terms by Equation (81), where N is Avogadro's number, e is the

$$\Delta G_s = -\frac{N}{2} e^2 \left(1 - \frac{1}{\varepsilon}\right) \left[\frac{1}{r + r'} - \frac{1}{r_0 + r_0'}\right] \tag{81}$$

electronic charge, ε is the dielectric constant, and r and r_0 are the crystal radii of the cations $R_4Sn^{\oplus}$ and $Me_4Sn^{\oplus}$, respectively. The correction terms r' and r_0' represent the incremental changes in the corresponding radii attendant upon solvation. The solvent-induced change in ΔG_s can be

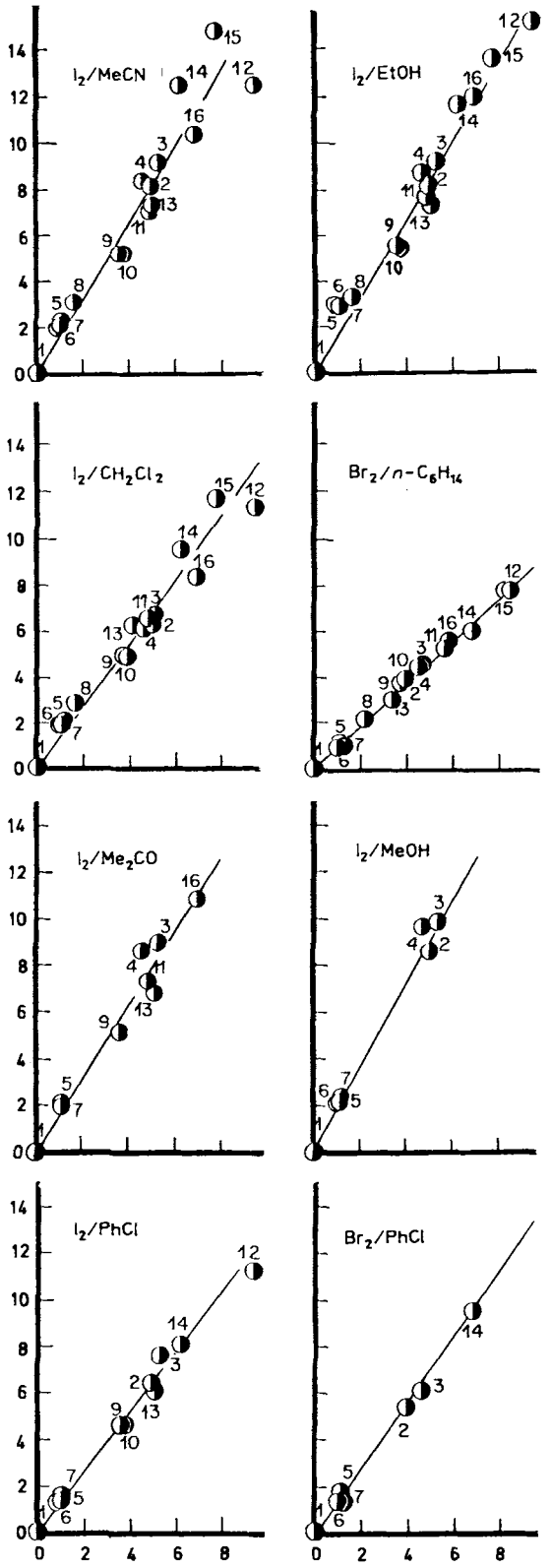

Fig. 26. Comparison of the solvation energies ($\Delta G_r^{\ddagger} - \Delta h\nu_{CT}$) [kcal mol^{-1}] obtained from the halogenolysis data for the compounds in Figure 25 according to the FERET in Equation (80) in tetrachloromethane (abscissa) with those in the solvents indicated (ordinate).

evaluated from Equation (81) relative to a reference solvent as Equation (82), where ε_0 is arbitrarily taken as the

$$\frac{\Delta G_s}{\Delta G_s^0} = \frac{1-\varepsilon^{-1}}{1-\varepsilon_0^{-1}} \qquad (82)$$

dielectric constant of tetrachloromethane. This ratio of solvation energies was represented as the slopes in Figure 26 [cf. Eq. (80)]. The reasonable agreement between the ratios calculated according to Equation (82) and the experimental ratios from Equation (80) is shown in Table 6. Although

Table 6. Comparison of the calculated ratios of the solvation energies ΔG_s in various solvents according to the Born model and the experimental values for the halogenolysis reactions given in Figure 26.

Solvent	ε	$\Delta G_s/\Delta G_s^0$ exp. I_2	Br_2	calcd
n-Hexane	1.907		0.9	0.86
CCl_4 [a]	2.238	1	1	1
PhCl	5.62	1.35	1.42	1.49
CH_2Cl_2	9.08	1.44		1.61
Me_2CO	20.74	1.60		1.72
EtOH	24.3	1.70		1.73
MeOH	32.65	1.78		1.75
MeCN	37.5	1.72		1.76

[a] Reference solvent.

neither r nor r' are known for $R_4Sn^{\oplus}$, the values of the mean separation r_{DA} in the CT complexes of tetraalkyltin and the halogen may be obtained from the Mulliken equation (34) by taking the work term to be purely Coulombic.[65] For the moment, let us assume that r_{DA} is related to $(r+r')$ by the simple additive relationship $r_{DA}+C_4=r+r'$, where C_4 is a constant, especially for the symmetrical, quasi-spherical tetraalkyltin compounds R_4Sn. Indeed, a value of $C_4=-0.75$ Å is obtained from the best fit of the Born equation (81) to the solvation energy evaluated by the FERET in Equation (37). The agreement, both in acetonitrile and in tetrachloromethane solutions, is illustrated by the fit to the line of unit slope in Figure 27. Although the choice of the Born model for solvation of $R_4Sn^{\oplus}$ may be crude, the consistency with the experimental observations based on the FERET is unmistakable.

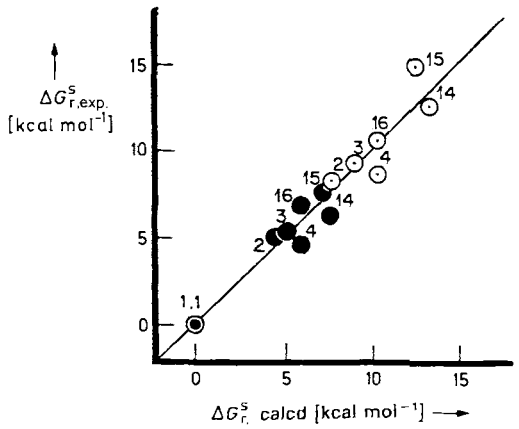

Fig. 27. Comparison of the solvation energies for symmetrical tetraalkyltin cations calculated by the Born equation (abscissa) and the experimental values obtained from Equation (80) in acetonitrile (⊙) and in tetrachloromethane (●). Note the fit to the line of unit slope. 1 = Me_4Sn, 2 = Et_4Sn, 3 = nPr_4Sn, 4 = nBu_4Sn, 14 = iPr_4Sn, 15 = sBu_4Sn, 16 = iBu_4Sn (cf. Fig. 12) [31].

4.5.3. *FERET for the Variations of Solvent and Electrophile*

The charge-transfer formulation in Equation 37 can be applied directly to the straightforward resolution of the

complex reactivity patterns which include three independent variables—namely, the changes in the donor (various alkyltin), the acceptor ($HgCl_2$, I_2, Br_2), and the solvent (CCl_4, CH_2Cl_2, CH_3OH).[66] Since the ionization potential is commonly applied to electron-transfer processes, it is plotted against the alkyltin reactivity with different acceptors for various solvents in Figure 28. No clear correlation

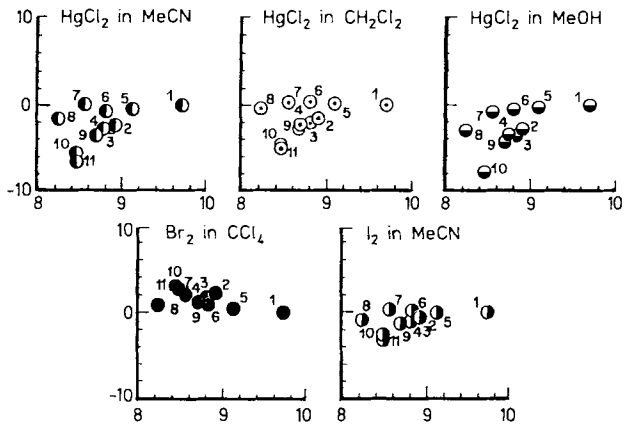

Fig. 28. Relative reactivities, as $\lg k/k_0$ (ordinate), of tetraalkyltin compounds with various electrophiles in different solvents as a function of their ionization potentials I_D [eV] (abscissa). 1 = Me_4Sn, 2 = Et_4Sn, 3 = nPr_4Sn, 4 = nBu_4Sn, 5 = $nBuSnMe_3$, 6 = nBu_2SnMe_2, 7 = iPr_2SnMe_2, 8 = tBu_2SnMe_2, 9 = iBu_4Sn, 10 = iPr_4Sn, 11 = sBu_4Sn [66].

between I_D and $\lg k/k_0$ can be discerned in any of the systems undergoing electrophilic cleavage. This is not surprising since the plot in Figure 28 is tantamount to a direct comparison of electron transfer leading to ions with that involving ion-pair formation (see Scheme 4). Figure 29 shows the new correlations of the relative reactivities after inclusion of the CT contribution by the amount $(\Delta w_p^* + \Delta G_s)$ according to the FERET in Equation (43). The striking linear correlations in Figure 29 show a remarkable transformation of the relative reactivities in Figure 28, which are severly scattered. *Indeed, if all the experimental points in Figure 29 were plotted on a single figure, they would all lie on a single line* with a slope of -16.9,

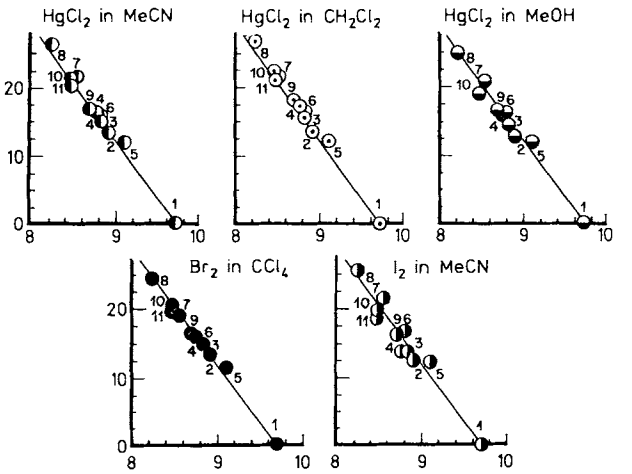

Fig. 29. Correlation of the data in Figure 28 after application of the FERET in Equation (83). Ordinate: $\lg k/k_0 + (\Delta E + \Delta G_s)/(2.3\,RT)$.

which corresponds to $-(2.3\,RT)^{-1}$ in the units used here. Since the energetics are determined from three independent measurements, namely, the ionization potential, the charge-transfer transition, and the solvation energy, these measurements are sufficient to determine completely the three variables affecting the rate of electrophilic cleavage, namely, the donor, the acceptor, and the solvent. Such a fit to the experimental data is represented by the FERET in Equation (83) [cf. Eq. (43)] as illustrated in Figure 29. This

$$-RT\ln\frac{k}{k_0} = \Delta I_D + \Delta E + \Delta G_s \qquad (83)$$

fit can hardly be fortuitous but must be taken as compelling support for the charge-transfer formulation as Equation (83). This formulation underscores the strong similarity between the CT excited state, i.e., the photochemically excited ion pair $[RM^{\oplus}, X_2^{\ominus}]^*$ and the transition state or the thermal ion pair $[RM^{\oplus}, X_2^{\ominus}]_s$ in the halogenolysis. The subtle balance between the electronic effect ΔI_D, the steric effect $\Delta E = \Delta w_p^*$, and the solvation energy ΔG_s thus determines the reactivities of alkylmetals in halogenolysis, particularly with respect to solvent variation.

4.5.4. *Charge-Transfer Mechanism for Electrophilic Cleavage of Alkylmetals by Mercury(II) Derivatives*

The preequilibrium formation of alkylmetal-mercury(II) complexes is included in the general mechanism for electrophilic cleavage [Eqs. (84)–(86)]. The activation process

$$RM + HgX_2 \overset{k_{DA}}{\rightleftharpoons} [RM,HgX_2] \qquad (84)$$

$$[RM,HgX_2] \xrightarrow{k_{ET}} [RM^{\oplus},HgX_2^{\ominus}] \qquad (85)$$

$$[RM^{\oplus},HgX_2^{\ominus}] \xrightarrow{\text{fast}} RX + RHgX \qquad (86)$$

for mercury(II) cleavages is represented in Equation (85) by the formation of the ion pair.[52] It is supported by the excellent linear correlations in Figure 29 resulting from the application of Equation (83) which directly equates the activation process for electrophilic cleavage with changes in the electronic, steric, and solvation energies for ion-pair formation. In Equations (84)–(86), the products arise subsequent to the rate-limiting electron-transfer step and are largely associated with the spontaneous fragmentation of the alkylmetal cation and recombination in the solvent cage.[67] The lability of $HgX_2^{\ominus}$ (formally a mercury(I) intermediate) accords with the facile dissociative electron capture by $HgCl_2$ to afford $Cl^{\ominus}$ and HgCl.[68]

4.6. Diels–Alder Cycloadditions with Tetracyanoethylene

Transient colors were noted in the earliest studies of the Diels–Alder reaction and ascribed to diene–dienophile complexes, then regarded as intermediates in only the vaguest sense.[69] *Andrews* and *Keefer*[70] first paid attention to the color formation and spectroscopically established the occurrence of 1 : 1 complexes between arenes and dienophiles such as maleic anhydride and benzoquinone. Transient colors have also been observed in the [2 + 2] cycloadditions of electron-rich alkenes such as aryl vinyl sulfides

and electron-poor alkenes such as tetracyanoethylene. However, the mechanistic importance of such EDA complexes has been difficult to assess quantitatively. Indeed, little or no attention has been paid to the role of EDA complexes in the majority of the mechanistic studies of either the Diels–Alder reaction or the [2+2] cycloaddition reactions. The mechanistic involvement of EDA complexes is further obscured by the kinetics dilemma as to whether they are key intermediates along the reaction pathway [Eq. (87a)] or merely innocent bystanders in an otherwise dead-end equilibrium [Eq. (87b)].

$$D + A \overset{K_{DA}}{\rightleftharpoons} [D,A] \xrightarrow{k_1} \text{adduct} \qquad (87a)$$

$$[D,A] \overset{K_{DA}}{\rightleftharpoons} D + A \xrightarrow{k_2} \text{adduct} \qquad (87b)$$

As a result, the need to accommodate EDA complexes in mechanistic considerations has generally been ignored.[71] Thus, the experimental evidence that the Diels–Alder reaction and the related [2+2] cycloadditions pass through EDA complexes has apparently had little impact on the bulk of the mechanistic output for these synthetically important reactions.[72] Since the focus heretofore has been on only the *ground-state* properties of EDA complexes in thermal cycloadditions, it is of interest to examine the role of EDA complexes from the viewpoint of their CT *excited states*.

4.6.1. The Charge-Transfer Correlation

The direct relationship between the Diels–Alder reaction of anthracene with TCNE and the transient CT absorption is illustrated in the left portion of Figure 30a, in which the second-order rate constant is plotted against the CT transition energy. The linear correlation spans a range of more than 10^6 in rates and is expressed as Equation (88),[73] with a correlation coefficient of 0.99. Such a linear relationship is strikingly akin to the FERET in Equation (56) for an electrophilic bromination that represents a distinctly *different type* of reaction. Nonetheless, the equivalence of Equations (56) and (88) establishes a common activation process for electrophilic substitution and the [4+2] cycloaddition of arene donors. Let us therefore consider the significance of the charge-transfer excited state of arene donors with various acceptors.

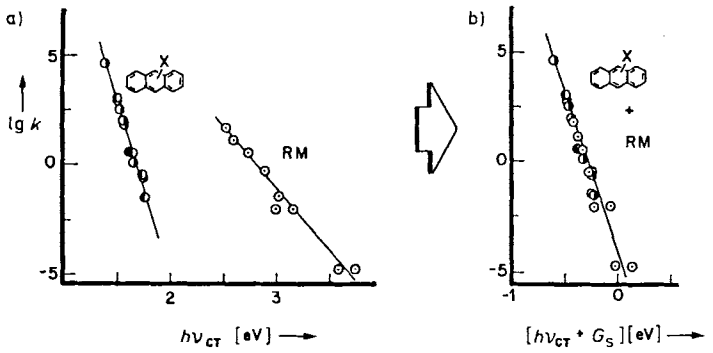

Fig. 30. a) The correlation of the logarithms of the rates ($\lg k$ [$M^{-1} s^{-1}$]) of TCNE reactions of anthracenes and alkylmetals with the charge-transfer transition energies $h\nu_{CT}$ of the EDA complexes identified in [73]. b) Unified correlation after the inclusion of solvation according to the FERET in Equation (93). X is, for example, H, 9-Me, 2-Me, 9-Et, 9-Br, 9,10-Me_2; RM = Et_nPbMe_{4-n} (n = 0–4), Me_4Sn, nBu_4Sn.

$$\lg k = -15.4 h\nu_{CT} + 26 \qquad (88)$$

4.6.2. Nature of the CT Excited State of Arene Donors

According to the Mulliken theory for weak EDA complexes of the types described for TCNE,[13] the spectral transition $h\nu_{CT}$ represents an electronic excitation from the neutral ground state to the polar excited state [Eq. (89)].

$$[\text{Arene,TCNE}] \xrightarrow{h\nu_{CT}} [\text{Arene}^{\oplus},\text{TCNE}^{\ominus}]^* \qquad (89)$$

The asterisk identifies an excited ion pair with the same mean separation r_{DA} as that in the EDA complex as described in Scheme 5. Such a Franck–Condon process can be examined directly by time-resolved picosecond spectroscopy. Thus the absorption spectra shown in Figure 31 clearly delineate the simultaneous appearance of the anthracene cation and the tetracyanoethylene anion immediately following the irradiation of the CT absorption band with a 25-ps laser pulse.[74] There is no evidence from the picosecond absorption data for either the existence of an excited state of the EDA complex or the formation of any intermediate states or species other than $Arene^{\oplus}$ and $TCNE^{\ominus}$. The electron transfer from the donor to the acceptor in the EDA complex thus effectively occurs with the absorption of a photon. Such a formulation therefore represents a direct confirmation of Mulliken theory,[13] in which excitation into the charge-transfer band of an EDA complex consisting of a relatively nonpolar ground state leads to the production of an ion pair.

4.6.3. FERET for the Diels–Alder Cycloaddition with TCNE

Based on the striking correlation shown in Figure 30a and expressed in Equation (88), we conclude that the formation of the ion pair [Eq. (89)] is tantamount to the activation process for anthracene cycloaddition to TCNE [Eq. (90)].

$$\text{Arene} + \text{TCNE} \longrightarrow [\text{Arene}^{\oplus},\text{TCNE}^{\ominus}]_s \qquad (90)$$

Taken further we suggest that the ion pair $[Arene^{\oplus},TCNE^{\ominus}]_s$ is a reasonable approximation to the transition state for the thermal Diels–Alder process. It should be noted, however, that the transition state is attained by an adiabatic process, whereas the CT excitation represents a vertical transition. As such, the CT excited ion pair in Equation (89) involves minimal changes in solvation, which occurs only in a subsequent relaxation process [Eq. (91)]. (For example, the relaxation from the Franck–Con-

$$[\text{Arene}^{\oplus},\text{TCNE}^{\ominus}]^* \xrightarrow[\text{solvent}]{\text{fast}} [\text{Arene}^{\oplus},\text{TCNE}^{\ominus}]_s \qquad (91)$$

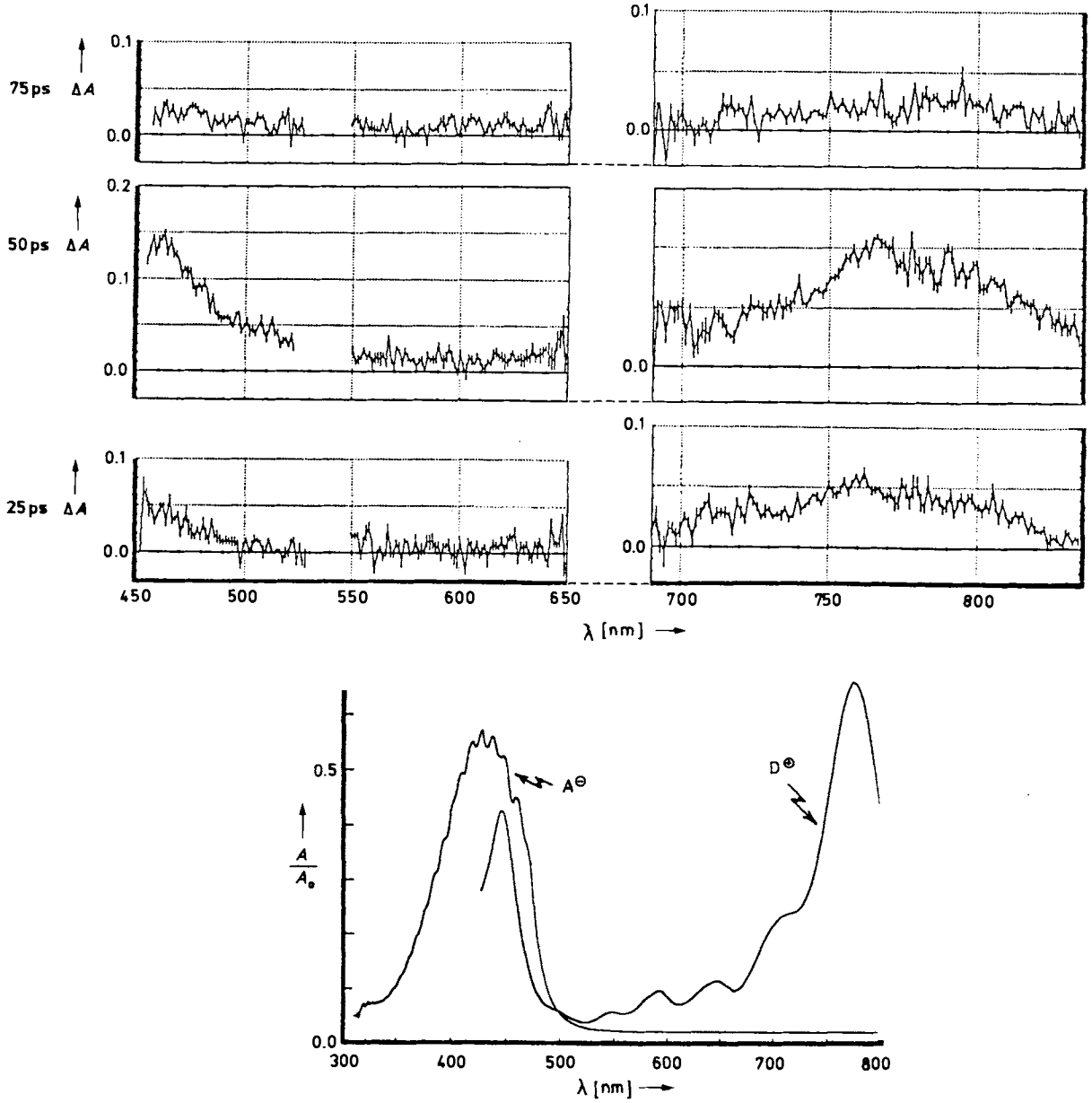

Fig. 31. Upper: Time-resolved spectra 25, 50, and 75 ps following the 532-nm, 25-ps laser pulse of the EDA complex of 9-cyanoanthracene and TCNE in CH_2Cl_2. Lower: The absorption spectra of 9-cyanoanthracene cation ($D^{\oplus}$) and tetracyanoethylene anion ($A^{\ominus}$) generated separately by spectroelectrochemical methods.

don excited state to the equilibrium fluorescent state is associated with an extraordinarily large Stokes shift of 34 kcal mol^{-1} for the toluene–benzenetetracarbonitrile EDA complex in toluene.[75]) By contrast, the formation of the polar ion pair by a thermal activation must be an adiabatic process which is accompanied by changes in solvation, as indicated by the subscript s in Equation (90). The free energy change for solvation (G_s) of anthracene cations is obtained from the gas-phase ionization potential and the reversible oxidation potential (E^0) in solution [cf. Eq. (38)]. The solvation energies are then evaluated quantitatively by use of the relationship[76] $G_s = I_D - E^0 - C$, where G_s is the free energy change in solvation relative to the neutral arene, E^0 is the standard oxidation potential of the anthracenes, and C is a constant which includes the potential of the reference electrode on the absolute scale together with the liquid junction potentials. The values of the solvation energies of the anthracene cations obtained in this manner are remarkably invariant.[77] This underscores the essential equivalence of the [Arene$^{\oplus}$,TCNE$^{\ominus}$] ion pair generated for the CT excited state [Eq. (89)] with that developed for the transition state [Eq. (90)]. Accordingly, the FERET can be expressed as Equation (92), which is equivalent to the gen-

$$\Delta G^{\neq} = h\nu_{CT} + \text{constant} \tag{92}$$

eralized free energy relationship in Equation (37) with the changes in the Arene$^{\oplus}$ solvation remaining invariant. Indeed, the extent to which the latter is true predicts that the simple FERET in Equation (92) will be applicable to all (electrophilic) aromatic reactions independent of their classification as substitution, addition, etc. As a corollary,

let us now examine the reactions of these donor–acceptor pairs in which the electrophile component is common, and solvation changes cannot be considered to be invariant.

4.6.4. *Quantitative Comparison of Anthracene Cycloaddition and Alkylmetal Insertion with TCNE as the Common Electron Acceptor*

An important test of the CT formulation for anthracene cycloaddition would be provided by demonstrating its interrelationship with the alkylmetal insertion [Eqs. (39)–(41)], particularly since the rates differ by a factor of more than 10^9. If the CT activation of the Diels–Alder reaction is valid, it must also relate directly to the activation process for alkylmetal insertion of TCNE, for which the CT interactions have already been established.[27] Such an interrelationship must be made in the teeth of the apparent diversity of the two processes shown in Figure 30a, in which the linear free energy relationship for anthracene cycloaddition differs from that for alkylmetal insertion in two important ways. First, the correlation of the alkylmetals is displaced by about 1 eV to higher energies relative to the anthracene correlation. Second, the slope of the alkylmetal correlation is quite different from the slope of the anthracene correlation, being smaller by a factor of more than 2. The correlations in Figure 30a do not specifically include solvation changes. It is clear, however, that solvation must be taken into account, since values of G_s from Equation (38)[28] in the two processes differ in significant ways. For example, G_s for the various anthracene cations is rather invariant with structure, whereas ΔG_s for the alkylmetal cations is not only structure dependent, but quite a bit larger as well.[73] If the change in solvation ΔG_s is included in the correlation, the two separate lines in Figure 30a are remarkably merged into a single line (Fig. 30b). Thus the activation processes for anthracene cycloaddition and alkylmetal insertion of TCNE are both described by a single, common relationship [Eq. (93). According to Equation

$$\Delta G^{+} = h\nu_{CT} + G_s + \text{constant} \qquad (93)$$

(93), the higher reactivity of alkylmetals relative to anthracenes derives from the larger changes in solvation during the activation process. Otherwise, there is no intrinsic difference in the activation barrier between anthracene cycloaddition and alkylmetal insertion with tetracyanoethylene.

4.6.5. *Quantitative Comparison of the Formation of Aromatic and Alkylmetal Cations in Solution*

The activation processes for anthracene cycloaddition and alkylmetal insertion with TCNE are representative of an inner-sphere mechanism for electron transfer. As such, the interaction energy w_p of the ion pairs, [Arene$^{\oplus}$,TCNE$^{\ominus}$] and [RM$^{\oplus}$,TCNE$^{\ominus}$], which is evaluated as the Coulombic work term, makes an important contribution to the activation barrier. At this juncture, the question arises as to the nature of such ion-pairs, particularly with regard to the full development of charge and the structural integrity of the component donor cation. (Note the TCNE counteranion is common to both processes.) In order to address this question, we direct our attention to the chemical oxidation of alkylmetals and aromatic compounds by the series of outer-sphere iron(III) oxidants $[FeL_3]^{3\oplus}$ with L = substituted 1,10-phenanthroline ligands [see Eqs. (18) and (59), respectively]. The second-order rate constants (k_2) of such outer-sphere electron transfers provide a means of directly comparing the energetics associated with the formation of aromatic cations, with those of alkylmetal cations, where both are formed rather free from strong counterion influences. In Figure 32a, the rate

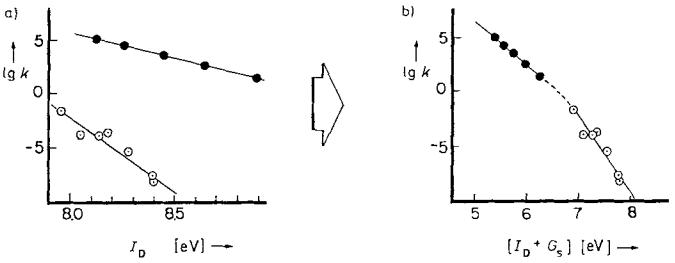

Fig. 32. Correlation of the rates of the outer-sphere oxidation with $[Fe(phen)_3]^{3\oplus}$ and the vertical ionization potentials I_D of alkylmetals (●) and aromatic compounds (⊙) before (a) and after (b) inclusion of cation solvation with the FERET in [73].

constants ($\lg k$) for the oxidations with $[Fe(phen)_3]^{3\oplus}$ are plotted against the ionization potentials of the alkylmetal and the aromatic compounds.[73] The linear correlations correspond to the relationship $\lg k = \alpha I_D + \text{constant}$, where $a = -16.9$ and -4.9 for the aromatic compounds and the alkylmetals, respectively. It is important to note that in these outer-sphere oxidations, the reactivity of a given alkylmetal is clearly more than 10^9 times greater than the reactivity of an aromatic compound with the same value of I_D. However, if the difference in cation solvation is taken into account, the reactivity of aromatic compounds follows the same trend as the alkylmetals (Fig. 32b). The resulting unity of alkylmetals and aromatic compounds in outer-sphere electron transfer can be expressed in terms of a single linear free energy relationship based on Marcus theory (compare with Section 4.3.2). At this point, however, we wish to emphasize that the dramatic effect of cation solvation in merging the outer-sphere oxidation of aromatic compounds and alkylmetals in Figure 32b is exactly the same FERET as that employed in the merging of the ion pairs in the inner-sphere mechanism in Figure 30b. Indeed, such an equality provides strong support for the CT formulation of the ion pairs [Arene$^{\oplus}$,TCNE$^{\ominus}$] and [RM$^{\oplus}$,TCNE$^{\ominus}$] as transition-state models in anthracene cycloaddition and alkylmetal insertion with tetracyanoethylene.

5. Ion Pairs [D$^{\oplus}$,A$^{\ominus}$] as Reactive Intermediates

In Section 4, we successfully demonstrated how the FERET in Equation (37) together with its corollaries (43) and (44) *quantitatively* predicts the *activation barriers* of a number of organic and organometallic reactions commonly thought of as electrophilic or nucleophilic proc-

esses. The seminal question now arises as to whether the ion pairs $[D^{\oplus}, A^{\ominus}]$ actually lie along the reaction coordinates. If so, how are such reactive intermediates related to the transition states of the electrophilic (or, equivalently, the nucleophilic) processes?

In order to address these issues let us arbitrarily select for further scrutiny only one of these processes, namely, electrophilic aromatic substitution (see Section 4.1) in which the independent evidence for the existence of the donor cation (i.e., $ArylH^{\oplus} = D^{\oplus}$)[78] facilitates its identification and the recognition of its behavior.[79] Before doing so, however, we hasten to add the caveat that the (steady-state) concentration of such a reactive intermediate is always limited in a thermal (adiabatic) process since the rate of its destruction is perforce much faster than the rate of its formation.[80] Accordingly, various indirect methods must be applied to test the viability of $[Arene^{\oplus}, A^{\ominus}]$ as a reactive intermediate in aromatic substitutions.

The traditional mechanism for aromatic substitution with an electrophile $A^{\oplus}$ is outlined in Scheme 10.[32,38]

$$ArylH + A^{\oplus} \underset{}{\overset{\text{fast}}{\rightleftharpoons}} [ArylH, A^{\oplus}] \quad \pi \text{ complex}$$

$$[ArylH, A^{\oplus}] \xrightarrow{\text{slow}} [Aryl(H)A]^{\oplus} \quad \text{Wheland intermediate}$$

$$[Aryl(H)A]^{\oplus} \xrightarrow[B]{\text{fast}} ArylA + HB^{\oplus}$$

Scheme 10. The traditional mechanism of electrophilic aromatic substitution.

Let us first reconsider one of the most important classes of aromatic substitutions, namely, nitration with $A^{\oplus} = NO_2^{\oplus}$.

5.1. Electrophilic Aromatic Nitration

The idea that charge transfer may play a key role in aromatic nitration with nitryl cations was first suggested in 1945 by *Kenner*,[81] who envisaged an initial step that "involves transference of a π-electron". Later, *Brown* postulated charge-transfer complexes as intermediates, and *Nagakura* et al. provided further theoretical support for one-electron transfer between an aromatic donor (ArylH) and an electrophile such as $NO_2^{\oplus}$.[82] Despite notable elaborations by *Pederson, Perrin, Eberson,* and others,[83] this formulation has not been widely accepted for nitration and related electrophilic aromatic substitutions.[84] As broadly conceived, the important question focuses on the activation process(es) leading up to the well-established Wheland or σ intermediate.[85] In the electron-transfer mechanism, the formation of the radical ion pair **V** is the distinctive feature (Scheme 11).

Accordingly, the properties and behavior of the intimate radical ion pair **V** are crucial to establishing its relationship with the numerous facets[86] of electrophilic aromatic nitration. For these reasons it is especially important to know whether **V** will actually lead to the appropriate Wheland intermediates, and in the amounts necessary to establish the isomer distributions commonly observed in aromatic nitrations. However, the independent proof of **V** has

$$ArylH + NO_2^{\oplus} \underset{}{\overset{\text{fast}}{\rightleftharpoons}} [ArylH, NO_2^{\oplus}] \quad \text{EDA complex}$$

$$[ArylH, NO_2^{\oplus}] \xrightarrow{\text{slow}} [ArylH^{\odot\oplus}, NO_2^{\odot}]$$

$$\mathbf{V}$$

$$\mathbf{V} \xrightarrow{\text{fast}} [Aryl(H)NO_2]^{\oplus} \quad \text{Wheland intermediate}$$

$$[Aryl(H)NO_2]^{\oplus} \xrightarrow[B]{\text{fast}} ArylNO_2 + HB^{\oplus}$$

Scheme 11. Electron-transfer mechanism of electrophilic aromatic substitution.

not been forthcoming owing to its expectedly transitory character. Thus it cannot be observed, since its rate of anihilation will always be faster than its rate of production. An alternative approach is clearly required to test the viability of the electron-transfer mechanism.

Picosecond time-resolved spectroscopy has defined the relevant photophysical and photochemical processes associated with the charge-transfer excitation of an arene complex such as anthracene with tetranitromethane (TNM).[87] As applied to benzenoid donors ArylH, the formation of the pertinent radical ion pair by charge-transfer excitation is summarized in Equations (94)–(96). All the experimental

$$ArylH + TNM \overset{K}{\rightleftharpoons} [ArylH, TNM] \quad (94)$$

$$[ArylH, TNM] \xrightarrow{h\nu_{CT}} [ArylH^{\odot\ominus}, TNM^{\odot\ominus}] \quad (95)$$

$$[ArylH^{\odot\ominus}, TNM^{\odot\ominus}] \xrightarrow{\text{fast}} [ArylH^{\odot\ominus}, NO_2^{\odot}, C(NO_2)_3^{\ominus}] \quad (96)$$

$$\mathbf{VI}$$

observations with aromatic donors and TNM indeed coincide with this formulation.[88] Thus the exposure of *p*-dimethoxybenzene (DMB) to a nitrating agent such as TNM (Fig. 33a) leads immediately to the EDA complex in Equation (94). These binary complexes are present in low steady-state concentrations owing to the limited magnitudes of K as measured by the *Benesi-Hildebrand* method.[89] Activation of the EDA complex by specific irradiation of the CT band (Fig. 33b) results in a photoinduced electron transfer [Eq. (95)] in accord with Mulliken theory.[13] The irreversible fragmentation following the electron attachment to TNM leads to the geminate triad **VI** (see Equation

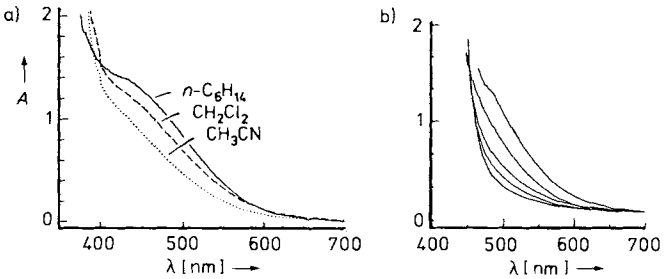

Fig. 33. a) Charge-transfer spectrum of the EDA complex of DMB and TNM in various solvents. b) Bleaching of the CT band upon constant irradiation at $\lambda > 425$ nm after (top to bottom) 0, 45, 120, 165, and 275 min.

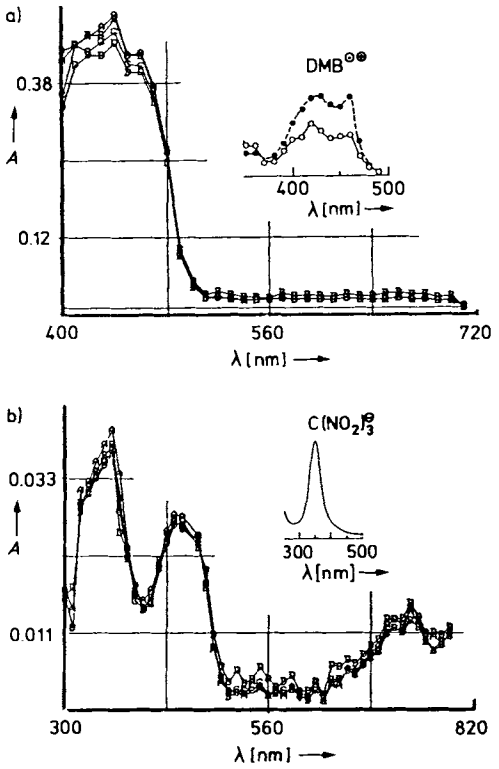

Fig. 34. Transient absorption spectra from the 25-ps laser-pulse excitation at 532 nm of the EDA complex from (a) 0.2 M DMB and 0.15 M TNM and (b) 0.1 M DMB and 0.02 M TNM in CH_2Cl_2. The insets are the absorption spectrum of (a) $DMB^{\odot\oplus}$ and (b) $C(NO_2)_3^{\ominus}$ as the tetrabutylammonium salt.

(96) and Fig. 34). The measured quantum yield of $\Phi \approx 0.5$ is similar to that ($\Phi \approx 0.7$) previously obtained for anthracene.[90] Such high quantum yields relate directly to the efficiency of geminate-triad production in Equation (96) relative to energy wastage by back electron transfer in Equation (95). Moreover, the short lifetime (<3 ps) of $TNM^{\odot\ominus}$ ensures that $ArylH^{\odot\oplus}$ and $NO_2^{\odot}$ are born as an intimate radical ion pair, initially trapped within the solvent cage, since this time scale obviates any competition from diffusional processes.[87,91] Charge-transfer excitation thus provides the experimental means to generate the intimate radical ion pair [$Aryl^{\odot\oplus}$,$NO_2^{\odot}$] **V** in sufficient concentrations and in a discrete electronic state as well as geometric configuration. In light of the fast kinetics allowed by the use of laser-flash photolytic techniques, we now focus on the pathways by which the radical ion pair collapses to nitration products.

The excellent material balance obtained in the charge-transfer nitration of DMB demands that the geminate triad **VI** proceed quantitatively to the nitration products according to Equation (97).[88]

$$\mathbf{VI} \longrightarrow ArylNO_2 + HC(NO_2)_3 \qquad (97)$$

Such a transformation must occur spontaneously with no discrimination among the reactive intermediates to accord with the absence of a deuterium kinetic isotope effect. The latter is not consistent with the collapse of **VI** as an ion pair [$ArylH^{\odot\oplus}$,$C(NO_2)_3^{\ominus}$] by proton transfer to the very weakly basic trinitromethanide. Furthermore, the presence of extra trinitromethanide (deliberately added as the tetrabutylammonium salt) exerts essentially no influence on either the course or the kinetics. Accordingly, $C(NO_2)_3^{\ominus}$ is merely an innocuous bystander insofar as the conversion of the geminate triad **VI** in Equation (97) is concerned. It follows that the disappearance of the arene radical ion must be directly related to its interaction with $NO_2^{\odot}$ [Eq. (98)].

$$\mathbf{V} \longrightarrow ArylNO_2 + H^{\oplus} \qquad (98)$$

Indeed, such radical cations have been prepared from various arenes by other experimental methods, especially electrochemical oxidation.[79] These arene radical cations are weak Brønsted acids, but they are highly susceptible to addition at the aromatic nucleus[92] [Eqs. (99) and (100)].

$$\mathbf{V} \longrightarrow Aryl(H)NO_2^{\oplus} \qquad (99)$$

$$Aryl(H)NO_2^{\oplus} \xrightarrow{k_H} ArylNO_2 + H^{\oplus} \qquad (100)$$

The σ adduct in Equation (99) is the Wheland intermediate in electrophilic nitration, which is known to show no deuterium kinetic isotope effect for k_H upon deprotonation [Eq. (100)].[93,94] The formation of the various isomeric Wheland intermediates (see Scheme 7) will occur from the collapse of the radical ion pair [Eq. (99)]. Consequently, the isomer distributions in the nitration products relate directly to the relative rates of addition to the various nuclear positions provided that the addition is irreversible and/or the adduct deprotonates rapidly. Thus the strong correlation observed between the spin densities at the various nuclear positions of $ArylH^{\odot\oplus}$ and the isomeric product distribution in aromatic nitration[33] bears directly on the mechanics of such a radical-ion-pair collapse to the Wheland intermediate.

Indeed, time-resolved spectral changes of the radical cation $ArylH^{\odot\oplus}$ provide insight as to how it is formed. Thus the relatively long lifetime of the arene radical cation from DMB is sufficient to allow diffusive separation of the radical ion pair **V** to $ArylH^{\odot\oplus}$ and $NO_2^{\odot}$ as essentially "free" species [Eq. (101)].[95] The second-order process

$$\mathbf{V} \xrightarrow{>10^{-10}\,s} ArylH^{\odot\oplus} + NO_2^{\odot} \qquad (101)$$

with the rate constant k_2 for the disappearance of $DMB^{\odot\oplus}$ in Table 7 then represents the "re"-combination of these separated species to form the Wheland intermediate [Eq. (102)].

$$ArylH^{\odot\oplus} + NO_2^{\odot} \xrightarrow{k_2} Aryl(H)NO_2^{\oplus} \qquad (102)$$

For other arenes, however, the decay pattern of the spectral transients for nitration is strikingly dependent on the stability of the radical cations as measured by the one-electron oxidation potentials E^0 [Eq. (103)].[96]

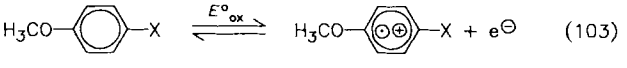

(103)

The direct comparison of E^0 in Table 7 focuses on the substantial effect of substituents [Eq. (103)] on the inherent

stability of the aromatic radical cations. The decay of the spectral transients for nitration is a reflection of the stability of the aromatic radical cation. For example, the radical cation from *p*-methylanisole decays by second-order kinetics in acetonitrile, similar to the kinetic behavior of the long-lived radical cation from DMB.[88] The large difference in the rates of diffusive combination of $Aryl^{\odot\oplus}$ with $NO_2^{\ominus}$ in Table 7 (see column 4) corresponds to their rela-

Table 7. Kinetics of electron-transfer nitration of *p*-X-anisoles.

E° [V vs. SCE] [a]	X	Kinetics order [b]	k_2 [c]
1.30	Methoxy	2	1.0×10^4
1.67	Methyl	2	2.5×10^5
2.12	Fluoro	1	1.9×10^4
2.00	Chloro	1	2.4×10^4
1.78	Bromo	1	3.7×10^4

[a] In acetonitrile containing 0.1 M Bu_4NClO_4 at 25°C according to Equation (103). [b] 2° und 1° represent second- and first-order decays, respectively. [c] In units of $A^{-1}\,s^{-1}$ for second-order and s^{-1} for first-order kinetics (A = unit of absorption).

tive stabilities as measured by $\Delta E^0 = 8.5$ kcal mol^{-1} of the parent arenes (column 1). There is a further, larger gap of $\Delta E^0 = 10.4$ kcal mol^{-1} which separates the stabilities of the radical cations of *p*-methylanisole and *p*-fluoroanisole, the least reactive haloanisole. Strikingly, every member of the family of *p*-haloanisole radical cations reacts with $NO_2^{\ominus}$ by first-order kinetics (cf. Fig. 35).[96] This decay pattern

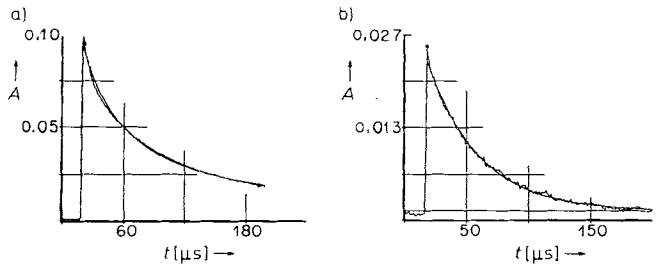

Fig. 35. Second- and first-order rate of disappearance of the radical cation from (a) *p*-methylanisole and (b) *p*-chloroanisole, respectively, as derived by CT excitation of the EDA complex from 0.2 M donor and 0.4 M TNM in acetonitrile.

strongly suggests that the CT nitration occurs by the cage collapse of the geminate radical pair $[ArylH^{\odot\oplus}, NO_2^{\ominus}]$ in Equation (104) prior to diffusive separation, except when

$$\mathbf{VI} \xrightarrow{k_{cp}} Aryl(H)NO_2^{\oplus} + C(NO_2)_3^{\ominus} \qquad (104)$$

the anisole cation is a relatively stabilized species such as those with *p*-methyl and *p*-methoxy substituents. Such a mechanism for nitration derives from polar solvents that act selectively to preferentially separate the anion from the cation and $NO_2^{\ominus}$ in the geminate triad **VI**. The σ adduct formed in Equation (104) is the Wheland intermediate in electrophilic nitration.[38] As such, it relates directly to the classical studies of *Melander*,[93] who first established the rapid, irreversible loss of a proton from the Wheland intermediate [cf. Eq. (105)].

$$Aryl(H)NO_2^{\oplus} + C(NO_2)_3^{\ominus} \xrightarrow{fast} ArylNO_2 + HC(NO_2)_3 \qquad (105)$$

The isomer distributions in CT nitration are established during radical-pair collapse according to Equation (99). Since the driving force for this process is likely to be exergonic, the transition states for the formation of the relevant aromatic σ adducts in Scheme 7 will bear a strong resemblance to the aromatic radical cation. As such, the electron density in $ArylH^{\odot\oplus}$ will be an important factor in determining the positional selectivity in the aromatic ring.[33] As a first approximation, the regiospecificity in the radical-pair collapse of **V** will be determined by the sites of highest electron spin density in $ArylH^{\odot\oplus}$. The latter are determined from ESR spectra which show that these locations in the radical cations of anisole and its derivatives are concentrated at the *ortho* and *para* positions relative to the methoxy group (Scheme 12).[79]

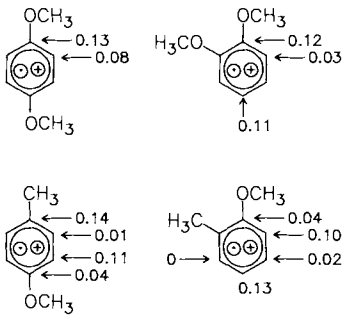

Scheme 12. Electron spin densities in the radical cations of anisole derivatives.

The isomer distributions in CT nitration are the same as those obtained by the conventional electrophilic nitrations with nitric acid.[86,96] Moreover, it is worth noting that the byproducts from CT nitration are also strongly reminiscent of the byproducts reported in electrophilic nitration. In particular, the demethylation of the methoxy group to afford nitrophenols, and the *trans*-bromination of 4-bromoanisole to afford a mixture 4-nitroanisole and 2,4-dibromoanisole are both symptomatic of radical-pair collapse at the *ipso* positions. These produce the σ adducts which are akin to the Wheland intermediates known to undergo such transformations [Eqs. (106) and (107)].

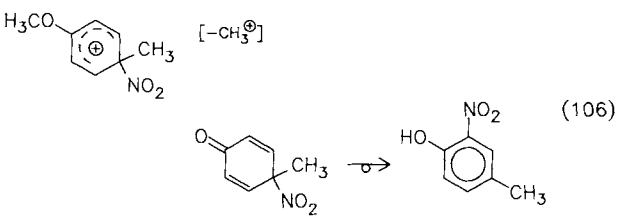

(106)

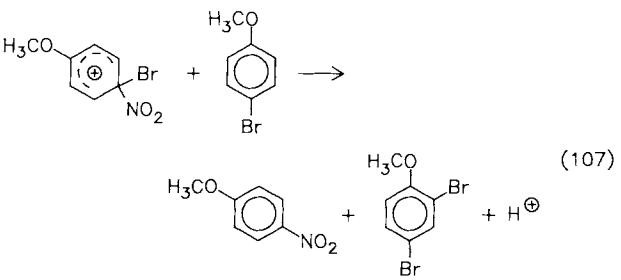

(107)

It is important to emphasize that the comparison of the behavior of various *p*-substituted anisoles shows that ion-pair collapse is strongly dependent on the stability of the radical cation, being nonexistent with the highly stabilized *p*-methoxyanisole radical cation.[88] The rates of ion-pair collapse of 4-substituted anisole cations increase in the order methyl < fluoro < chloro < bromo in line with the oxidation potentials E^0 of the parent anisole. Moreover, the rates of radical-pair collapse also increase in the same order, but with a change in the decay behavior from second-order kinetics for *p*-methylanisole to first-order kinetics for all the haloanisoles. The latter points to the importance of a geminate process for radical-pair collapse from **VI** with radical cations [see Eqs. (108)–(110)].

These studies thus underscore the strong similarity between electrophilic and charge-transfer nitration especially with regard to the spectral transients and the nitration products and byproducts. Since the latter is symptomatic of arene radical cations, the parallelism does extend to some common reactive intermediates. As such, the most *economical* formulation for electrophilic nitration would also include a pathway which is common to charge-transfer nitration, namely, via the radical ion pair **V** (Scheme 11). This mechanism differs from the conventional formulation (Scheme 10), in which the [ArylH, $NO_2^{\oplus}$] pair is directly converted into the Wheland intermediate in a single step, rather than via the radical ion pair **V**. The FERET correlation in Equation (45) has established the strong similarity in the activation barriers (i.e., energetics) for these two processes.[33] Accordingly, the problem in Scheme 11 can be considered in an alternative framework, namely, the lifetime of the radical ion pair **V**. At one extreme of a very short lifetime, the radical ion pair is tantamount to the transition state for the concerted one-step process. At the other extreme of a very long lifetime, the radical ion pair **V** is manifested by its diffusive separation. Equations (108)–(110) present this construct in a kinetics context.[85] The ef-

$$[\mathrm{ArylH},\ NO_2^{\oplus}] \underset{k_{-1}}{\overset{k_1}{\rightleftharpoons}} [\mathrm{ArylH}^{\odot\oplus},\ NO_2^{\odot}] \qquad (108)$$

$$[\mathrm{ArylH}^{\odot\oplus},\ NO_2^{\odot}] \xrightarrow{k_c} \mathrm{Aryl(H)}NO_2^{\oplus} \qquad (109)$$

$$[\mathrm{ArylH}^{\odot\oplus},\ NO_2^{\odot}] \xrightarrow{k_d} \mathrm{ArylH}^{\odot\oplus} + NO_2^{\odot} \qquad (110)$$

ficient cage collapse of the radical ion pair to the Wheland intermediate is represented by $k_c \gg k_d$. On this basis, the time scale of the "concerted" process is limited by the diffusional correlation times of $< 10^{-11}$ s. The extent to which $k_c \ll k_d$ is valid allows side reactions to compete as a result of the diffusive separation of $\mathrm{ArylH}^{\odot\oplus}$ and $NO_2^{\odot}$. The experiments with DMB clearly belong in the latter category since the evolution of nitration products takes place in the μs/ms time regime. Nonetheless, the diffusive recombination of $\mathrm{ArylH}^{\odot\oplus}$ and $NO_2^{\odot}$ pairs with the rate constant k_2 can occur in Equation (102) with very high efficiency. The competition from diffusion is represented by the cage collapse of $\mathrm{ArylH}^{\odot\oplus}$ and $NO_2^{\odot}$ in Equation (109). The radical-ion-pair formulation thus represents a unifying theme for electrophilic and charge-transfer nitration. Indeed, it can account for all the diverse experimental observations of aromatic donors with little or no ambiguity. Let us now consider a pair of aromatic substitution processes which differ primarily in the charge borne by the electrophile.

5.2. Arene Activation with Isoelectronic Mercury(II) and Thallium(III) Electrophiles

The dichotomy between the electron-transfer mechanism and the more conventional pathway for electrophilic aromatic nitration is clearly delineated in aromatic mercuration and thallation, in which the *isoelectronic* electrophiles $Hg(O_2CCF_3)_2$ and $Tl(O_2CCF_3)_2^{\oplus}$, differing only in charges, can be employed for direct comparisons. Quantitative spectrophotometric analysis has established the transient charge-transfer absorption spectra observed during mercuration and thallation to derive from the same electrophilic species as that involved in the kinetics, namely, $Hg(O_2CCF_3)_2$ and $Tl(O_2CCF_3)_2^{\oplus}$, respectively.[97] Indeed, these species form two series of arene π complexes [ArylH, $Hg(O_2CCF_3)_2$] and [ArylH, $Tl(O_2CCF_3)_2^{\oplus}$], which bear strong resemblances to each other, both in the ground state and in the CT excited state. For the mercury(II) complexes, the relevant CT transition corresponds to Equation (111), and for the thallium(III) complexes, it is given by Equation (112).

$$[\mathrm{ArylH}, Hg^{II}(O_2CCF_3)_2] \xrightarrow{h\nu_{CT}} [\mathrm{ArylH}^{\odot\ominus}, Hg^{I}(O_2CCF_3)_2^{\odot\ominus}]^* \qquad (111)$$

$$[\mathrm{ArylH}, Tl^{III}(O_2CCF_3)_2^{\oplus}] \xrightarrow{h\nu_{CT}} [\mathrm{ArylH}^{\odot\ominus}, Tl^{II}(O_2CCF_3)_2^{\odot}]^* \qquad (112)$$

Both series of π complexes share the arene cation in the form of the radical pair as the CT excited state according to expectations of Mulliken theory. The slope of 1.3 in the linear correlation of $h\nu_{CT}$ indicates that the energy of the charge-transfer excitation of the cationic π complex from $Tl(O_2CCF_3)_2^{\oplus}$ is merely ca. 30% more sensitive to changes in arene structures compared with that derived from $Hg(O_2CCF_3)_2$. Otherwise, both series of π complexes show parallel behavior in the transformation to the CT excited state. The similarity in the π complexes of $Hg(O_2CCF_3)_2$ and $Tl(O_2CCF_3)_2^{\oplus}$ with the series of sterically crowded 1,3,5-trialkylbenzenes indicates that the CT interaction is relatively long-range. The latter was confirmed by X-ray crystallography which showed a pair of long Hg–C bond distances in the η^2-bonding of the electrophilic mercury(II) to the hexamethylbenzene donor.[98] As a result, any minor difference which may exist in the steric properties of $Hg(O_2CCF_3)_2$ and $Tl(O_2CCF_3)_2^{\oplus}$ is obscured in the π complexes, both in the ground state and in the CT excited state. The kinetics studies also establish the neutral $Hg(O_2CCF_3)_2$ and the cationic $Tl(O_2CCF_3)_2^{\oplus}$ to be the principal electrophiles in mercuration and thallation, respectively. The reactivity trends in the two types of metalations can be quantitatively compared with a graded series of arenes ranging from the electron-rich pentamethylbenzene at one end to the least reactive arene, chlorobenzene, at the other extreme. The relative reactivity of an arene to elec-

trophilic metalation is represented by the activation free energy difference $\Delta G_r^{\neq} = -2.3RT\lg k/k_0$, where k represents the second-order rate constant and the subscript r refers to changes relative to that of benzene (k_0) arbitrarily chosen as the reference arene. The direct comparison between mercuration and thallation is shown in Figure 36, in which the logarithms of the ratio of second-order rate constants for mercuration are plotted against those for thallation in trifluoroacetic acid. The striking linear free energy correlations spans more than six orders of magnitude in rate with a 1 : 1 relationship, as shown by the fit of the data to the line drawn with a slope of unity. In other words, *those factors relevant to surmounting the activation barrier for mercuration are mirrored in exactly the same way during thallation* as a consequence of systematic changes in the arene donor.

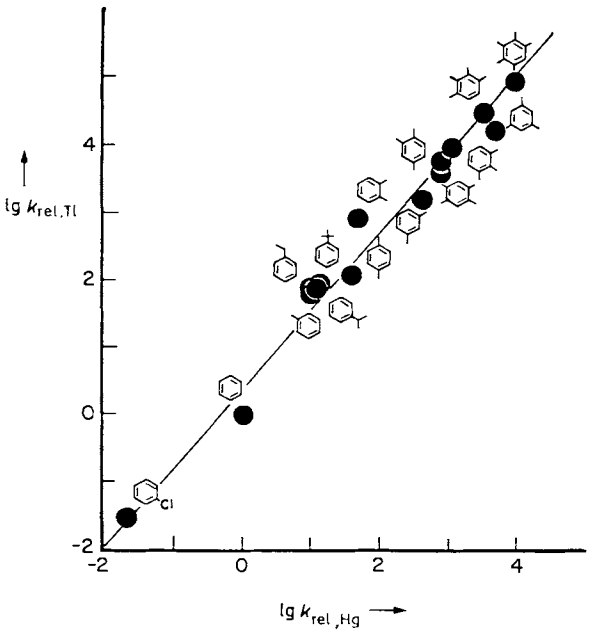

Fig. 36. Direct relationship of the relative reactivities (k_{rel}) of arenes in mercuration (abscissa) and thallation (ordinate).

The relative reactivities of arenes to metalation are represented by the activation free energy difference $\Delta G_r^{\neq}$. In the same way, the transition energy $h\nu_{CT}$ associated with the charge-transfer excitation of the π complex can be evaluated from the absorption spectrum by a similar comparative method, $\Delta h\nu_{CT} = h\nu_{CT} - h\nu_{CT}^0$, where $h\nu_{CT}^0$ is the CT transition energy of the benzene π complex.[33] The correlation of the activation barriers with the CT excitation energies shown in Figure 37 for mercury(II) clearly consists of two trends.[97] At the low end of the reactivity scale (chlorobenzene to the xylenes), a linear plot is observed for the CT transition energy with a slope of close to unity. In other words, these mercuration rates relate to the CT excited state of the π complex according to the free energy relationship described in Equation (45). On the other hand, the flat portion of the slope in Figure 37 represents the most reactive arenes (mesitylene to pentamethylbenzene) which indicates that they are all mercurated at essentially the same rate, quite independent of the donor properties as reflected in the CT transition energy of the π com-

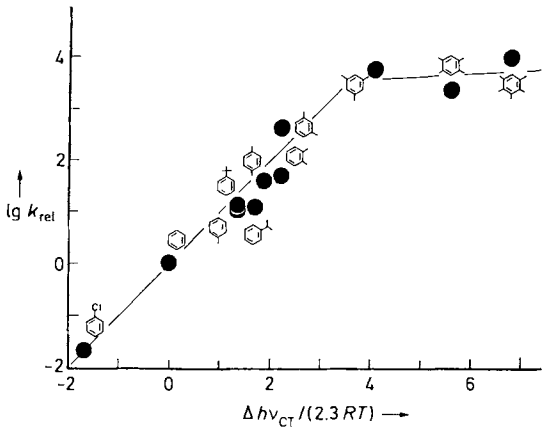

Fig. 37. Correlation of the relative reactivities (k_{rel}) of arene in mercuration with the CT transition energy according to the FERET in Equation (45). The inclined line is arbitrarily drawn with a slope of unity. $T = 25\,^{\circ}C$.

plex. This trend is also observed in the interaction of the same arenes with thallium(III). The linear free energy relationship as expressed by Equation (45) relates the activation barrier $\Delta G^{\neq}$ for aromatic substitution directly to the CT transition energy $h\nu_{CT}$ of the π complex. Since $h\nu_{CT}$ pertains to the energetics of the photoionizations in Equations (111) and (112), the correlation suggests that these arene ion pairs are reasonable approximations to the transition state for mercuration and thallation. Such a conclusion derives from the kinetics and spectral experiments with the less electron-rich arenes from chlorobenzene to the isomeric xylenes in Figure 37. Moreover, the leveling of the rates proceeding from the electron-rich arenes from mesitylene to pentamethylbenzene can be reconciled with this formulation in the following way. Consider the generalized kinetics scheme which is associated with the arene ion pair (Scheme 13).

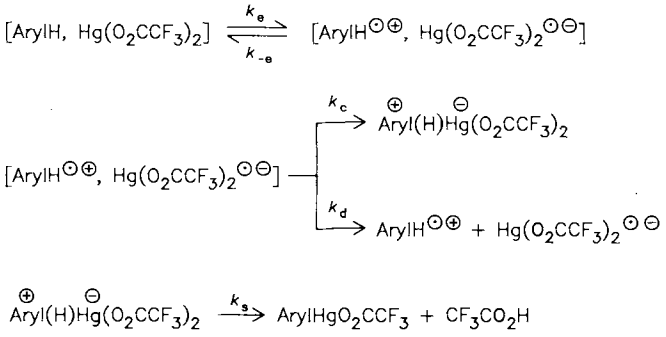

Scheme 13. Generalized scheme for arene metalation with Hg^{II} compounds.

In Scheme 13, the activation step for electrophilic substitution proceeds from the thermal conversion ($\lg k_e$) to the arene ion pair, which is to be likened to the photoactivation of the π complex in Equation (111). The substitution-product-determining process (k_s) is then dependent on the rate constants k_c and k_d for collapse to the Wheland intermediate and diffusive separation to free ions, respectively. Since the rate constant k_d is likely to be invariant for a given electrophile and a series of structurally related arenes, the rate of aromatic substitution will be strongly mediated by the value of k_c. If, for some reason, the rate of

arene-ion-pair collapse is retarded, the competition from back electron transfer (k_{-e}) will become increasingly important. Under these circumstances, the reaction rate will no longer follow the linear free energy relationship in Equation (45). Indeed, at some point, back electron transfer will dominate (i.e., $k_{-e} \gg k_c$), and it is conceivable that little or no thermal reaction will take place. The experimental variables pertaining to (1) electronic effects, (2) steric effects, (3) solvent effects, and (4) product studies can be reconciled with Scheme 13 in terms of the facility with which such an arene ion pair collapses as follows.

(1) *Electronic effects* in the collapse of the arene ion pair can be viewed as the influence of substituents on the spin density in the singly occupied orbital (SOMO) requisite to bond formation (k_c step). For example, in mesitylene the pair collapse at any of the three unsubstituted nuclear positions is unimpeded since the SOMO is degenerate (see Fig. 38b). Similarly, the SOMOs in the cations of *p*-xylene, *m*-xylene, and pseudocumene are conducive to pair collapse at the free positions owing to the available spin densities (Fig. 38a, c, and d, respectively). By contrast, the SOMOs of the cations of durene and pentamethylbenzene have nodes at the free 3- and 6-positions (Fig. 38e and f), and collapse there is not favored. Indeed, the lack of spin density at these positions of durene and pentamethylbenzene cations, respectively, accords with the observed magnitudes of the ^1H hyperfine splittings in the ESR spectra.[99] Thus the pair collapse of durene and pentamethylbenzene cations is only favored at the already substituted *ipso* positions and is probably a reversible process. Alternatively, collapse at an unsubstituted position suffers from the promotional energy of 4–7 kcal mol^{-1} from the subjacent orbital. Such a retardation of the pair collapse of durene and pentamethylbenzene cations could account for the leveling effect depicted in Figure 37 and the attendant breakdown of the linear free energy relationship. Alternatively, it is possible to consider the latter as reflecting a change in the nature of the rate-determining step (Scheme 14).

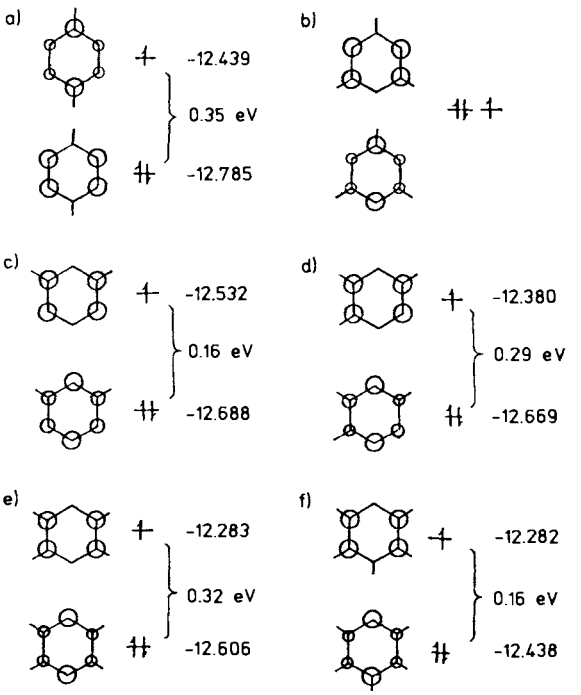

Fig. 38. The symmetries and energies of the HOMO and SOMO in the radical cations of (a) *p*-xylene, (b) mesitylene, (c) *m*-xylene, (d) pseudocumene, (e) durene, and (f) pentamethylbenzene.

$$[\mathrm{ArylH},\ Hg(O_2CCF_3)_2] \underset{k_{-\sigma}}{\overset{k_\sigma}{\rightleftharpoons}} \overset{\oplus}{\mathrm{Aryl(H)}}\overset{\ominus}{Hg}(O_2CCF_3)_2$$

$$\overset{\oplus}{\mathrm{Aryl(H)}}\overset{\ominus}{Hg}(O_2CCF_3)_2 \xrightarrow{k_s} \mathrm{ArylHgO_2CCF_3} + CF_3CO_2H$$

Scheme 14. Variation of the rate-limiting steps in arene mercuration.

If the formation of the σ complex were rate-limiting, then $k_s \gg k_{-\sigma}$. Thus the experimental rate constant is $k_{obs} = k_\sigma$, and the linear free energy relationship in Equation (45) is applicable as described above. On the other hand, if the breakup of the σ complex were rate-limiting, then $k_s \ll k_{-\sigma}$. Thus the experimental rate constant is $k_{obs} = k_s(k_\sigma/k_{-\sigma})$, and the rate of proton transfer from the σ complex is relatively slow. This situation may well lead to the observed leveling in Figure 37 as a result of compensating effects on the preequilibrium ($k_\sigma/k_{-\sigma}$) and deprotonation rate (k_s) in durene and pentamethylbenzene. However, the kinetic isotope effect for chlorobenzene is more or less the same as that for durene and pentamethylbenzene. Such an invariance of the kinetic isotope effect suggests that arene reactivity is not differentiated by the rate of proton loss from the σ adduct. We therefore conclude that a change in the rate-limiting steps in Scheme 13 is alone insufficient to account for the leveling effect in Figure 37.

(2) *Steric effects* in mercuration and thallation are manifested by the substitution rate for 1,3,5-trineopentylbenzene which is more than two orders of magnitude slower than that for mesitylene, despite their similar donor properties. Since the association constants and CT transition energies are comparable for trineopentylbenzene and mesitylene, the steric effects extant in the π complexes and in the arene ion pairs are not sufficient to account for the observed rate difference. This conclusion is also in accord with the long-range interaction observed in the X-ray structure of the crystalline complex.[98] Therefore, steric effects according to Scheme 13 arise during arene ion pair collapse (Scheme 13). In the molecular structure of the mercurated trineopentylbenzene, the heteroatom substituent occupies a position on the side opposite the aromatic ring from the pair of neighboring neopentyl groups. Thus in order for pair collapse to the σ adduct or Wheland intermediate to occur, a substantial steric barrier must be overcome to obtain a structural configuration akin to the product. Steric inhibition of aromatic substitution is even more severe in 1,3,5-tri-*tert*-butylbenzene. Although the formation of the π complex with mercury(II) and thallium(III) is comparable to that of mesitylene, the persistence of the yellow CT bands indicated that little or no thermal reaction occurred. The difficulty of attaining the σ adduct of tri-*tert*-butylbenzene is also indicated in proton exchange studies. Thus mesitylene, durene, and even pentamethylbenzene undergo efficient proton exchange in trifluoroacetic acid via an analogous intermediate.[97] Under the

same experimental conditions, no proton exchange is observed in 1,3,5-tri-*tert*-butylbenzene.

(3) *Solvent effects* in the pair collapse arise from charge stabilization by solvents with dielectric constants as different as those of trifluoroacetic acid and dichloromethane. The rates of arene mercuration are greatly increased in trifluoroacetic acid relative to those in dichloromethane—the enhancement factor being 30- to 50-fold in the second-order rate constants. However, the *relative reactivity of a series of arenes is singularly unaffected by such a change in solvent* (cf. Section 4.1.2). It is noteworthy that the arene radical ion pair, when taken as a model for the transition state of aromatic substitution, does correctly account for this otherwise inexplicable lack of solvent sensitivity on the relative reactivities of various arenes, despite the marked differences in the absolute rates. According to Scheme 13, the latter arises from the large changes in solvation which are expected to accompany the formation of the arene radical ion pair in Equation (113), since the solvation energy of the neutral precursor may be neglected in comparison with that of the ion pair.[33] However, by the comparative procedure used to develop the linear free energy relationship in Equation (45), only the relative changes in solvation of the arene cation must be considered, owing to contributions from the electrophile moiety which largely drop out by cancellation. Since the solvation energy of a series of related arene cations is relatively constant,[34] it follows for Equation (45) that the relative reactivities would be solvent independent. It is noteworthy that the latter is difficult to reconcile with reactivity changes resulting from variable transition-state structures in Scheme 10.[32]

(4) *Product studies* provide a divergent view of the arene-ion-pair collapse during mercuration and thallation. The dichotomy is most pronounced in pentamethylbenzene. Thus the treatment of pentamethylbenzene with $Hg(O_2CCF_3)_2$ affords only the nuclear substitution product pentamethylphenylmercury trifluoroacetate in high yields. No transient intermediates other than the π complex were observed in either the UV/VIS or ESR spectra. On the other hand, in the thallation of pentamethylbenzene, nuclear substitution comprised only 26%, the remainder being accounted for by side products resulting from side-chain substitution and dimer formation. Such side products are known to derive from the radical cation of pentamethylbenzene.[79] Indeed, the diversion to side products during thallation coincides with the direct observation of the arene radical cation as a transient intermediate both by UV/VIS and by ESR spectroscopy.[100] A similar dichotomy between the products of mercuration and thallation exists with durene, albeit to a lesser degree. Finally, no discrepancy is observed with mesitylene, nuclear substitution occurring exclusively in both mercuration and thallation. Such a divergence between mercuration and thallation can be reconciled by the formulation in Scheme 13 if they differ by the extent to which diffusive separation (k_d) occurs [Eq. (115)]. All factors being the same, diffusive separation of the radical pair from thallium(III) should occur more readily than that from mercury(II) owing to a significant difference in the Coulombic interactions—the arene ion being paired with the anionic $Hg^{I}(O_2CCF_3)_2^{\odot\ominus}$ in mercuration [Eq. (111)] and with the neutral $Tl^{II}(O_2CCF_3)_2^{\odot}$ in thallation [Eq. (112)]. Moreover, the same electrostatic argument provides a ready explanation for the ability of Lewis acids as additives to promote arene radical cation formation (leading to biaryls) during both mercuration and thallation of even unexceptional arenes.[101] Thus the addition of boron trifluoride (as the etherate) will foster the ionic dissociation of the uncharged $Hg(O_2CCF_3)_2$ to give the cationic $HgO_2CCF_3^{\oplus}$ and of the $Tl(O_2CCF_3)_2^{\oplus}$ monocation to give the dication $TlO_2CCF_3^{2\oplus}$. The results lead to a diminution in the Coulombic interaction in the radical pair $[ArylH^{\odot\oplus}, Hg^{I}O_2CCF_3^{\odot}]$ during mercuration and to an enhancement of the Coulombic repulsion in the radical pair $[ArylH^{\odot\oplus}, Tl^{II}O_2CCF_3^{\oplus}]$ during thallation. In both cases the increased amounts of cage escape will lead to a higher component of electron-transfer-derived products (such as biaryls). Attractive as such a simple electrostatic explanation may seem, cognizance must also be taken into account of the attendant change in the driving force for back electron transfer (k_{-e} in Scheme 13). Unfortunately, this factor cannot be evaluated at this point owing to the unavailability of the reduction potentials E^0 of these highly transient species.[102] Thus the quantitative prediction of product yields derived from Scheme 13 must await the actual measurement of these quantities. Moreover, the detailed solution of the kinetics, including the isotope effects, is likely to be even more complicated owing to rates which depend strongly on the various types of ion pairing which are likely to exist.[103] Finally, no cognizance of the spin multiplicity of the radical pairs is included in Scheme 13 and the failure to observe CIDNP during arene mercuration and thallation unfortunately leaves unanswered the question of whether singlet-triplet interconversions play a role in mediating the individual rate constants for the CT formulation.

The study of mercuration and thallation has thus provided a sharp focus on the experimental delineation of stepwise and concerted mechanisms for arene activation. The unequivocal demonstration of arene cations as key intermediates in thallation, particularly of durene and pentamethylbenzene,[97] is consistent with a stepwise (electron-transfer) mechanism for arene activation as in Scheme 13 [Eq. (113)].[104] By the same token, the singular absence of

$$[ArylH, Tl(O_2CCF_3)_2^{\oplus}] \longrightarrow [ArylH^{\odot\oplus}, Tl(O_2CCF_3)_2^{\odot}] \longrightarrow Aryl(H)Tl(O_2CCF_3)_2^{\oplus} \longrightarrow \longrightarrow \cdots \quad (113)$$

any experimental evidence for such intermediates during mercuration is directly accommodated by a concerted (electrophilic) mechanism for arene activation [Eq. (114)].

$$[ArylH, Hg(O_2CCF_3)_2] \longrightarrow Aryl^{\oplus}(H)Hg^{\ominus}(O_2CCF_3)_2 \longrightarrow \longrightarrow \cdots \quad (114)$$

The difficulty with two separate mechanisms for arene activation by mercury(II) and thallium(III) is underscored by the striking correlation in Figure 36 which shows that the *activation barriers follow identical trends*. In other words, the rate-determining processes for mercuration and thallation are similar, yet they distinctly differ in the prod-

ucts derived from the electron-rich arenes (durene and pentamethylbenzene). Such a kinetics situation commonly demands that there exists at least one intermediate which separates the activation process from the products, as in Scheme 13. This paradox can be resolved in one of two ways. *First*, the mechanistic formulation in Scheme 13 merges stepwise and concerted processes by the modulation of a pair of rate constants. According to Scheme 13, the two principal pathways are differentiated during the competition between cage collapse (k_c) and diffusive separation (k_d) of the arene ion pair. The inability to observe the arene cation (e.g., from mesitylene) could be attributed to a cage collapse to the Wheland intermediate occurring substantially faster than diffusive separation (i.e., $k_c \gg k_d$), which is tantamount to a concerted process. Likewise, the ESR observation of the arene cation would derive from a diffusive process occurring faster than collapse (i.e., $k_c \ll k_d$), which could appear as a stepwise process. Some of the structural and environmental factors which influence both rate constants have been presented in the discussion above. However, this mechanism is not without its problems since it does not as yet address the observed kinetic isotope effects in a quantitative way. *Second*, the stepwise and concerted processes for arene activation may simply represent competing pathways [Eqs. (115) and (116)],

$$[\mathrm{ArylH, Hg(O_2CCF_3)_2}] \longrightarrow [\mathrm{\overset{\oplus}{Aryl}(H)\overset{\ominus}{Hg}(O_2CCF_3)_2}]^{*} \quad (115)$$

$$[\mathrm{ArylH, Tl(O_2CCF_3)_2^{\oplus}}] \longrightarrow [\mathrm{ArylH^{\odot\oplus}, Tl(O_2CCF_3)_2^{\odot}}]^{*} \quad (116)$$

where the superscript (*) represents the activated complex. If so, those factors related to the donor properties of arenes, such as π-complex formation, CT excitation, activation barriers, are too common to both to allow any distinction between these pathways. Moreover, the common dependence on isoelectronic electrophiles, independent of charge, further obscures any difference in the transition states. This formulation thus recognizes two such dissimilar mechanisms as electron transfer and electrophilic processes in mercuration and thallation to be remarkably alike. Such kindred transition states can be theoretically accommodated within the valence bond approach to electrophile/nucleophile reactivity, as described by *Shaik* and *Pross*.[105] Crucial to the resolution of this dilemma is the understanding of the stepwise process for arene activation. Particularly germane are the microdynamics of the "intimate" arene radical ion pairs in Scheme 13, especially as they collapse or evolve to "loose" (solvent-separated) species and finally to "free" (separate) radical pairs. Indeed, the CT excitation of π complexes by a laser pulse (Section 5.1) provides access to arene radical ion pairs which can be examined directly by time-resolved spectroscopy.[87]

6. Epilogue

The merging of outer-sphere and inner-sphere mechanisms for electron transfer leads to the FERET in Equation (37) and its corollaries (43) and (44) that are applicable to a variety of organic and organometallic reactions [Eqs. (1)-(15)], otherwise referred to as electrophilic and nucleophilic processes. Critical to the FERET formulation from the thermochemical Scheme 6 is the ion pair $[D^{\oplus}, A^{\ominus}]$ as the activated complex that lies at or near the transition state for the representative electrophile/nucleophile transformations described in Section 5. Since $[D^{\oplus}, A^{\ominus}]$ arises from the weak EDA interactions inherent in the precursor complex [D, A], the evaluation of the driving force for ion-pair formation must include the work term w_p as well as the redox change $F(E^0_{ox} + E^0_{red})$. Therefore, it is important to emphasize that in any electrophile/nucleophile transformation, *the redox change is not a sufficient criterion by itself to determine whether or not electron transfer is mechanistically viable.*[106]

At one extreme of outer-sphere electron transfer at large mean separations r_{DA}, the work term w_p bears physical significance to electrostatic forces between $D^{\oplus}$ and $A^{\ominus}$, as in Marcus theory. However, at the other extreme of inner-sphere electron transfer at *very close* r_{DA}, a purely Coulombic description is no longer completely adequate (or accurate) for the interaction energy in the intimate ion pair $[D^{\oplus}, A^{\ominus}]$ (see, e.g., the treatment in Section 4.4.4). In this situation, the Mulliken treatment affords a feasible phenomenological method for the evaluation of w_p; but unfortunately it provides no physical insight into the nature and chemical properties of the ion pairs. Part of this deficiency can be made up by the examination of separate $D^{\oplus}$ and $A^{\ominus}$ which are independently generated by electron detachment from the donor and by electron attachment to the acceptor, respectively (compare, e.g., Sections 2.2.4 and 5.1).[107] Indeed, such studies have shown that significant structural changes in donors and acceptors can accompany electron transfer in a manner sufficient to allow their requisite close approach within the highly intimate ion pair. Furthermore, the radical ions $D^{\oplus}$ and $A^{\ominus}$ consistently show enhanced reactivity relative to their uncharged diamagnetic counterparts owing to the half-filled HOMO and LUMO, respectively.[108] Indeed, the spontaneous fragmentation of either $D^{\ominus}$ (e.g., $RMgX^{\oplus}$, $R_3SnH^{\oplus}$, $[CpFe(CO)_2R]^{\oplus}$, $[CH_3Co(chel)]^{\ominus}$, $R_2Mg^{\oplus}$, $R_3SiSiR_3^{\oplus}$)[109] or $A^{\ominus}$ (e.g., $Br_2^{\ominus}$, $HgX_2^{\ominus}$, $RX^{\ominus}$)[110] constitutes the single theme that unifies the diverse electrophile/nucleophile processes in Equations (1)-(15) within the common framework of charge-transfer transitions for the FERET from Scheme 6.[111] At this juncture, the contributions from additional energy terms inherent in the intimate ion pair $[D^{\oplus}, A^{\ominus}]$ with close r_{DA} cannot be experimentally evaluated. Preliminary observations of the temporal relaxation of contact ion pairs that are spontaneously generated by the laser-pulse excitation of EDA complexes encourage the further use of time-resolved spectroscopy to help to delineate this critical problem.[114] In a related context, the studies of exciplex absorptions observed in the course of diffusional quenching of excited donors and/or acceptors[115] will also doubtlessly help to delineate the properties of intimate ion pairs $[D^{\oplus}, A^{\ominus}]$ in a quantitative manner.[116]

I thank the Alexander-von-Humboldt-Stiftung for my stay at Philipps Universität Marburg with the kind hospitality of Professor Reinhard W. Hoffmann and his colleagues in Fachbereich Chemie at which this article was written. I gratefully acknowledge the numerous contributions of my

collaborators mentioned in the references and especially S. Fukuzumi, R. J. Klingler, J. M. Masnovi, and S. Sankararaman for their outstanding creative efforts. I also thank the National Science Foundation and the Robert A. Welch Foundation for financial support of this research.

Received: November 23, 1987 [A 686 IE]
German version: *Angew. Chem. 100* (1988) 1331

[1] G. C. Pimentel (Ed.): *Opportunities in Chemistry*, National Academy Press, Washington 1985, S. 86ff.

[2] a) L. G. Christophorou: *Atomic and Molecular Radiation Physics*, Wiley, New York 1971, p. 618; *Chem. Rev. 76* (1976) 409; b) R. L. DeKock, D. R. Lloyd, *Adv. Inorg. Chem. Radiochem. 16* (1974) 65; c) J. L. Franklin, P. W. Harland, *Annu. Rev. Phys. Chem. 25* (1974) 485; d) R. S. Berry, *Chem. Rev. 69* (1969) 533; e) W. A. Chupka, J. Berkowitz, *J. Chem. Phys. 55* (1971) 2724; f) G. Briegleb, *Angew. Chem. 76* (1964) 326; *Angew. Chem. Int. Ed. Engl. 3* (1964) 617.

[3] a) D. W. Turner, C. Baker, A. D. Baker, C. R. Brundle: *Molecular Photoelectron Spectroscopy*, Wiley, New York 1970; b) H. Bock, G. Wagner, J. Kroner, *Chem. Ber. 105* (1972) 3850; c) E. Haselbach, E. Heilbronner, *Helv. Chim. Acta 53* (1970) 689; d) M. J. S. Dewar, S. D. Worley, *J. Chem. Phys. 50* (1969) 654.

[4] a) S. Fukuzumi, J. K. Kochi, *J. Phys. Chem. 85* (1981) 648; b) W. A. Nugent, M. M. H. Wu, T. P. Fehlner, J. K. Kochi, *J. Chem. Soc. Chem. Commun. 1976*, 456.

[5] S. Fukuzumi, J. K. Kochi, *J. Org. Chem. 46* (1981) 4116.

[6] What usefulness lies in nucleophile/electrophile reactivity is actually based on *thinking by analogy*.

[7] For previous attempts, see a) R. G. Pearson in W. B. Chapman, J. Shorter (Eds.): *Advances in Linear Free Energy Relationships*, Plenum, New York 1972, p. 281ff; b) J. O. Edwards, *J. Am. Chem. Soc. 76* (1954) 1540; c) For qualitative approaches, see T.-L. Ho: *Hard and Soft Acid and Base Principle in Organic Chemistry*, Academic Press, New York 1977.

[8] H. Taube, *Adv. Inorg. Chem. Radiochem. 1* (1959) 1; *Angew. Chem. 96* (1984) 315; *Angew. Chem. Int. Ed. Engl. 23* (1984) 329.

[9] a) F. Basolo, R. G. Pearson: *Mechanisms of Inorganic Reactions*, Wiley, New York 1965; b) A. Haim, *Acc. Chem. Res. 8* (1975) 264.

[10] a) R. A. Marcus, B. J. Zwolinski, H. Eyring, *J. Phys. Chem. 58* (1954) 432; b) R. A. Marcus, *J. Chem. Phys. 24* (1956) 966; *ibid. 26* (1957) 867; *Discuss. Faraday Soc. 29* (1960) 21.

[11] Reviews: a) R. D. Cannon: *Electron Transfer Reactions*, Butterworths, London 1980; b) N. Sutin in G. L. Eichhorn (Ed.): *Inorganic Biochemistry, Vol. 2*, Elsevier, Amsterdam 1973, p. 611; c) W. L. Reynolds, R. W. Lumry: *Mechanisms of Electron Transfer*, Ronald Press, New York 1966; d) R. G. Wilkins: *The Study of Kinetics and Mechanism of Reactions of Transition Metal Complexes*, Allyn and Bacon, Newton, MA 1974; e) D. E. Pennington, *ACS Monogr. 174* (1978) 477.

[12] N. S. Hush, *Trans. Faraday Soc. 57* (1961) 557; *Prog. Inorg. Chem. 8* (1967) 391.

[13] a) R. S. Mulliken, *J. Am. Chem. Soc. 72* (1950) 600; b) R. S. Mulliken, W. B. Person: *Molecular Complexes, A Lecture and Reprint Volume*, Wiley-Interscience, New York 1969.

[14] T. P. Fehlner, J. Ulman, W. A. Nugent, J. K. Kochi, *Inorg. Chem. 15* (1976) 2544.

[15] See G. Dulz, N. Sutin, *Inorg. Chem. 2* (1963) 917; H. Diebler, N. Sutin, *J. Phys. Chem. 68* (1964) 174, and references cited therein.

[16] C. L. Wong, J. K. Kochi, *J. Am. Chem. Soc. 101* (1979) 5593.

[17] S. Fukuzumi, C. L. Wong, J. K. Kochi, *J. Am. Chem. Soc. 102* (1980) 2928.

[18] R. J. Klingler, J. K. Kochi, *J. Am. Chem. Soc. 102* (1980) 4790.

[19] R. S. Nicholson, I. Shain, *Anal. Chem. 36* (1964) 706.

[20] R. J. Klingler, J. K. Kochi, *J. Am. Chem. Soc. 103* (1981) 5839.

[21] Vgl. auch a) R. J. Klingler, J. K. Kochi, *J. Am. Chem. Soc. 104* (1982) 4186; b) J. K. Kochi, *Pure Appl. Chem. 52* (1980) 571; c) R. J. Klingler, S. Fukuzumi, J. K. Kochi, *ACS Symp. Ser. 211* (1983) 117.

[22] B. W. Walther, F. Williams, W. Lau, J. K. Kochi, *Organometallics 2* (1983) 688; see also M. C. R. Symons, *J. Chem. Soc. Chem. Commun. 1982*, 869.

[23] N. A. Clinton, H. C. Gardner, J. K. Kochi, *J. Organomet. Chem. 56* (1973) 227; N. A. Clinton, J. K. Kochi, *ibid. 56* (1973) 243.

[24] S. Fukuzumi, J. K. Kochi, *Bull. Chem. Soc. Jpn. 56* (1983) 969.

[25] See F. Scandola, V. Balzani, G. B. Schuster, *J. Am. Chem. Soc. 103* (1981) 2519.

[26] Cf. R. Foster: *Organic Charge-Transfer Complexes*, Academic Press, New York 1969.

[27] S. Fukuzumi, K. Mochida, J. K. Kochi, *J. Am. Chem. Soc. 101* (1979) 5961; see also H. C. Gardner, J. K. Kochi, *ibid. 98* (1976) 2460, 6150.

[28] Solvation of the neutral donor is neglected in comparison with that of its cation as discussed in footnote 48 of [49].

[29] S. Fukuzumi, J. K. Kochi, *J. Phys. Chem. 84* (1980) 2246.

[30] The formation of the 1:1 adduct in Equation (41) occurs by an initial fragmentation of $RM^{\oplus}$ and then stepwise addition to $TCNE^{\ominus}$ subsequent to the rate-limiting step in Equation (40). The process is akin to the CT-induced addition of tetranitromethane to anthracene [87].

[31] S. Fukuzumi, J. K. Kochi, *J. Phys. Chem. 84* (1980) 2254.

[32] a) R. Taylor in C. H. Bamford, C. F. H. Tipper (Eds.): *Comprehensive Chemical Kinetics, Vol. 13*, Elsevier, London 1972; b) P. B. D. de la Mare: *Electrophilic Halogenation*, Cambridge University Press, London 1976; c) G. A. Olah, *Acc. Chem. Res. 4* (1971) 240; d) P. B. D. de la Mare, *ibid. 7* (1974) 361; e) R. O. C. Norman, R. Taylor: *Electrophilic Substitution in Benzenoid Compounds*, American Elsevier, New York 1965; f) D. V. Banthorpe, *Chem. Rev. 70* (1970) 295; g) L. M. Stock, H. C. Brown, *Adv. Phys. Org. Chem. 1* (1963) 35; h) L. M. Stock: *Aromatic Substitution Reactions*, Prentice-Hall, Englewood Cliffs, NJ 1968; i) A. J. Bloodworth in C. A. McAuliffe (Ed.): *The Chemistry of Mercury*, Macmillan, Toronto 1977, p. 152; j) B. V. Smith in A. R. Butler, M. J. Perkins (Eds.): *Organic Reaction Mechanisms*, Wiley-Interscience, New York 1977, Chapter 7; k) Z. V. Todres, *Russ. Chem. Rev. (Engl. Trans) 47* (1978) 148; l) L. M. Stock, *Prog. Phys. Org. Chem. 12* (1976) 21; m) P. R. P. Skrabal, H. Zollinger, *Angew. Chem. 84* (1972) 921; *Angew. Chem. Int. Ed. Engl. 11* (1972) 874.

[33] S. Fukuzumi, J. K. Kochi, *J. Am. Chem. Soc. 103* (1981) 7240.

[34] J. O. Howell, J. M. Goncalves, C. Amatore, L. Klasinc, R. M. Wightman, J. K. Kochi, *J. Am. Chem. Soc. 106* (1984) 3968.

[35] The Hammett ρ values are singularly insensitive to the solvent polarity, despite large solvent effects on the absolute rates of electrophilic substitution. This is one factor which allows the Brown σ^+ constant to be so comprehensive. By the same token, it fails to provide information about the larger solvent effects on the absolute rates. See: C. D. Johnson, *Chem. Rev. 75* (1975) 755.

[36] Although σ^+ for many substituents is effectively constant over a wide range in the variation of ρ in various electrophilic aromatic substitution, there are substituents such as F, Cl, and Br for which there is a considerable variation in σ^+ with changes in p. See J. R. Knowles, R. O. C. Norman, G. K. Radda, *J. Chem. Soc. 1960*, 4885; H. van Bekkum, P. E. Verkade, B. M. Wepster, *Recl. Trav. Chim. Pays-Bas 78* (1959) 815. The inconsistency of σ^+ constants necessitated the introduction of multiparameter extensions to the Hammett equation.

[37] For further discussion of the changes in r_{DA} and the work term w_p in the CT interaction of various donors, the reader is referred to [24].

[38] C. K. Ingold: *Structure and Mechanism in Organic Chemistry*, 2nd ed., Cornell University Press, Ithaca, NY 1969, Chapter 6.

[39] See e.g., [32h], p. 55.

[40] J. E. Wertz, J. R. Bolton: *Electron Spin Resonance*, McGraw-Hill, New York 1972, pp. 101-102.

[41] a) F. Freeman, *Chem. Rev. 75* (1975) 439; b) G. H. Schmid, D. G. Garrat in J. Zabicky (Ed.): *Chemistry of Alkenes, Vol. 3*, Wiley-Interscience, New York 1977; c) P. B. D. de la Mare, R. Bolton: *Electrophilic Additions to Unsaturated Systems*, Elsevier, New York 1966; d) R. C. Fahey, *Top. Stereochem. 3* (1968) 237; T. G. Traylor, *Acc. Chem. Res. 2* (1969) 152; e) R. Bolton, *Compr. Chem. Kinet. 1973*, 9; f) G. A. Olah: *Carbocations and Electrophilic Reactions*, Verlag Chemie, Weinheim/Wiley, New York 1973; g) *Acc. Chem. Res. 4* (1971) 240; h) D. V. Banthorpe, *Chem. Rev. 70* (1970) 295; i) G. B. Sergeev, Yu. A. Serguchev, V. V. Smirnov, *Russ. Chem. Rev. (Engl. Transl.) 42* (1973) 697; j) P. B. D. de la Mare: *Electrophilic Halogenation*, Cambridge University Press, London 1976; k) E. Bienvenue-Goetz, J. E. Dubois, *Tetrahedron 34* (1978) 2021; l) H. R. Hudson, *Annu. Rep. Prog. Chem. Sect. B 1978*, 75; m) R. D. Bach, A. Weibel, J. Patane, L. Kevan, *J. Am. Chem. Soc. 98* (1976) 6237.

[42] S. Fukuzumi, J. K. Kochi, *J. Am. Chem. Soc. 103* (1981) 2783.

[43] a) The Hammett ρ value for the rates of mercuration of *para*-substituted styrenes is -3.2 (A. Lewis, J. Azoro, *Tetrahedron Lett. 1979*, 3627). This value compares with the corresponding ρ value of -4.2 for the rates of bromination of a similar series of *para*-substituted styrenes (J. H. Rolston, *J. Am. Chem. Soc. 91* (1969) 1483). See also: J. E. Dubois, A. Schwartz, *Tetrahedron Lett. 1964*, 2167; b) For the similarity between second-order and third-order brominations, see S. Fukuzumi, J. K. Kochi, *Int. J. Chem. Kinet. 15* (1983) 249.

[44] a) J. Shorter, *Adv. Linear Free Energy Relat. 1972*, Chapter 2; b) O. Exner, *Correl. Anal. Chem. Recent Adv. 1978*, Chapter 10; c) H. C. Brown, Y. Okamoto, *J. Am. Chem. Soc. 80* (1958) 4979; d) N. B. Chapman, J. Shorter: *Correlation Analysis in Chemistry*, Plenum, New York 1978.

[45] D. Grosjean, G. Mouvier, J. E. Dubois, *J. Org. Chem. 41* (1976) 3872.

[46] H. J. Bergmann, G. Collin, G. Just, G. Müller-Hagen, W. Pritzkow, *J. Prakt. Chem. 314* (1972) 285.

[47] a) A. Streitwieser, Jr., C. H. Heathcock: *Organic Chemistry*, Macmillan, New York 1976; *Organische Chemie*, Verlag Chemie, Weinheim 1980; b) T. H. Lowry, K. S. Richardson: *Mechanism and Theory in Organic Chemistry*, 2nd ed., Harper and Row, New York 1981.

[48] For theoretical approaches to electrophilic reactions, see: a) K. Fukui, T. Yonezawa, C. Nagata, H. Shingu, *J. Chem. Phys. 22* (1954) 1433; b)

R. D. Brown, *J. Chem. Soc. 1959*, 2232; c) S. Nagakura, J. Tanaka, *Bull. Chem. Soc. Jpn. 32* (1959) 734; d) S. Nagakura, *Tetrahedron Suppl. 19* (1963) 361; e) M. J. S. Dewar: *The Molecular Orbital Theory of Organic Chemistry*, McGraw-Hill, New York 1969; f) N. D. Epiotis, *J. Am. Chem. Soc. 95* (1973) 3188; g) H. H. Greenwood, R. McWeeny, *Adv. Phys. Org. Chem. 4* (1966) 73; h) N. D. Epiotis, S. Shaik, *J. Am. Chem. Soc. 100* (1978) 29; i) T. Takabe, T. Takenaka, K. Yamaguchi, T. Fueno, *Chem. Phys. Lett. 44* (1976) 65.

[49] S. Fukuzumi, J. K. Kochi, *J. Am. Chem. Soc. 104* (1982) 7599.

[50] a) C. J. Schlesener, C. Amatore, J. K. Kochi, *J. Am. Chem. Soc. 106* (1984) 3567; b) C. J. Schlesener, J. K. Kochi, *J. Org. Chem. 49* (1984) 3142; c) C. J. Schlesener, C. Amatore, J. K. Kochi, *J. Phys. Chem. 90* (1986) 3747.

[51] For the structural effects on some typical cation solvations, see: E. M. Arnett, H. J. Pienta, *J. Am. Chem. Soc. 102* (1980) 3329; R. Taft, J. F. Wolf, J. L. Beauchamp, G. Scorrano, E. M. Arnett, *ibid. 100* (1978) 1240, and references cited therein.

[52] a) Since the formation constants K_{DA} of these EDA complexes are small, the free energy of formation (ΔG_{DA}) of the precursor complex can be ignored in comparison with the activation barrier for the electrophilic process; b) The constant term also includes the solvation energy of aromatic cations, etc; c) For questions regarding the solvation of transition states in relation to that of stable molecular analogues, see: C. D. Ritchie, *Pure Appl. Chem. 52* (1979) 153; C. D. Ritchie, J. E. VanVerth, P. O. I. Virtanen, *J. Am. Chem. Soc. 104* (1982) 3491, and references cited therein.

[53] a) In this formulation, we do not intend to convey the notion that the configurational structure of the transition state and that of the CT excited ion pair are necessarily the same but only that the energy change in the formation of one serves as a viable model for that of the other. In more rigorous terms, Equation (60) states that alkenes and arenes are subjected to the same perturbations in electrophilic brominations as in the CT transition in the EDA complexes when changes in solvation are taken into account. It must be emphasized that the CT formulation does not require the proof that an EDA complex is (or is not) an intermediate in electrophilic brominations. For a discussion of this point, see footnotes 19 and 20 in [54]; b) The strongest kinetic evidence for the direct involvement of the EDA complex is the observation of a negative temperature coefficient; see: G. B. Sergeev, T. V. Pokolok, T. Ch'eng, *Kinet. Katal. 10* (1969) 36.

[54] S. Fukuzumi, J. K. Kochi, *J. Am. Chem. Soc. 102* (1980) 2141.

[55] a) [45]; b) R. W. Taft, Jr. in M. S. Newman (Ed.): *Steric Effects in Organic Chemistry*, Wiley, New York 1956, p. 556.

[56] a) D. S. Matteson: *Organometallic Reaction Mechanisms*, Academic Press, New York 1974; b) F. R. Jensen, B. Rickborn: *Electrophilic Substitution of Organomercuricals*, McGraw-Hill, New York 1968; c) L. G. Makarova in A. N. Nesmeyanov, K. A. Kocheshkov (Eds.): *Methods in Elemento-Organic Chemistry, Vol. 4*, North-Holland, Amsterdam 1967; d) L. G. Makarova in E. I. Becker, M. Tsutsui (Eds.): *Organometallic Reactions, Vol. 1 und Vol. 2*, Academic Press, New York 1970, 1971; e) O. A. Reutov, *Russ. Chem. Rev. (Engl. Transl.) 36* (1967) 163.

[57] a) I. Véle, J. Hetflejs, V. Vaisarová, V. Chvalovský, *Collect. Czech. Chem. Commun. 36* (1971) 4111; b) I. Velé, V. Vaisarová, V. Chvalovský, *ibid. 37* (1972) 1396.

[58] a) G. Boulé, M. Bielen, J. Nasielski, *J. Organomet. Chem. 9* (1967) 433; b) M. Gielen, J. Nasielski, *Bull. Soc. Chim. Belg. 71* (1962) 601; M. Gielen, *Acc. Chem. Res. 6* (1973) 198.

[59] See J. L. M. Abboud, R. W. Taft, *J. Phys. Chem. 83* (1979) 412; M. J. Kamlet, J. L. M. Abboud, R. W. Taft, *Prog. Phys. Org. Chem. 12* (1981) 485.

[60] For a similar conclusion based on MO calculations, see M. J. S. Dewar, P. R. Kuhn, *J. Am. Chem. Soc. 108* (1986) 551.

[61] See e.g., P. J. Trotter, *J. Am. Chem. Soc. 88* (1966) 5721.

[62] a) E. S. Amis, J. F. Hinton: *Solvent Effects on Chemical Phenomena*, Academic Press, New York 1973; b) A. J. Parker, *J. Chem. Rev. 69* (1969) 1; c) A. R. Butler, M. J. Perkins: *Organic Reaction Mechanisms*, Interscience, London 1973; d) [41c]; e) E. M. Kosower: *Physical Organic Chemistry*, Wiley, New York 1968.

[63] M. H. Abraham in C. H. Bamford, C. F. H. Tipper (Eds.): *Comprehensive Chemical Kinetics*, Elsevier, Amsterdam 1973; see also [56a, c].

[64] a) W. M. Latimer, K. S. Pitzer, C. M. Slansky, *J. Chem. Phys. 7* (1939) 108; b) R. M. Noyes, *J. Am. Chem. Soc. 84* (1962) 513; c) J. F. Coetzee, J. J. Campion, *ibid. 89* (1967) 2513; d) M. Tanaka, *Inorg. Chem. 15* (1976) 2325.

[65] Note that this procedure merely provides an operational ionic radius.

[66] S. Fukuzumi, J. K. Kochi, *J. Am. Chem. Soc. 102* (1980) 7290.

[67] For an elaboration of these processes, see [27, 28, 54].

[68] N. B. Nazhat, K.-D. Asmus, *J. Phys. Chem. 77* (1973) 614.

[69] a) P. Pfeiffer, W. Jowieff, P. Fischer, P. Monti, H. Mully, *Justus Liebigs Ann. Chem. 412* (1916) 253; b) R. Kuhn, T. Wagner-Jauregg, *Helv. Chim. Acta 13* (1930) 9; c) M. C. Kloetzel: *Organic Reactions, Vol. 4*, Wiley, New York 1948, p. 9; d) R. B. Woodward, *J. Am. Chem. Soc. 64* (1942) 3058.

[70] L. J. Andrews, R. M. Keefer, *J. Am. Chem. Soc. 75* (1953) 3776.

[71] a) J. Sauer, *Angew. Chem. 79* (1967) 76; *Angew. Chem. Int. Ed. Engl. 6* (1967) 16; b) J. Sauer, R. Sustmann, *ibid. 92* (1980) 773 and *19* (1980) 779; c) A. Wasserman: *Diels-Alder Reactions*, Elsevier, New York 1965; d) R. Huisgen, *Acc. Chem. Res. 10* (1977) 117; *Pure Appl. Chem. 52* (1980) 2283; *ibid. 53* (1981) 171.

[72] a) V. D. Kiselev, J. G. Miller, *J. Am. Chem. Soc. 97* (1975) 4036; b) M. Lofti, R. M. G. Roberts, *Tetrahedron 35* (1979) 2123, 2131; c) Y. Uosaki, M. Nakahara, M. Sasaki, J. Osugi, *Chem. Lett. 1979*, 727.

[73] S. Fukuzumi, J. K. Kochi, *Tetrahedron 38* (1982) 1035.

[74] E. F. Hilinski, J. M. Masnovi, J. K. Kochi, P. M. Rentzepis, *J. Am. Chem. Soc. 106* (1984) 8071.

[75] K. Egawa, N. Nakashima, N. Mataga, C. Yamanaka, *Chem. Phys. Lett. 8* (1971) 108; *Bull. Chem. Soc. Jpn. 44* (1971) 3287.

[76] a) M. E. Peover, *Electroanal. Chem. 2* (1967) 1; B. Case in N. S. Hush (Ed.): *Reactions of Molecules at Electrodes*, Wiley-Interscience, New York 1971, p. 125; b) R. C. Larson, R. T. Iwamoto, R. N. Adams, *Anal. Chim. Acta 25* (1961) 371.

[77] J. M. Masnovi, E. A. Seddon, J. K. Kochi, *Can. J. Chem. 62* (1984) 2552.

[78] See e.g., E. T. Kaiser, L. Kevan (Eds.): *Radical Ions*, Wiley, New York 1968.

[79] a) K. Yoshida: *Electrooxidation in Organic Chemistry*, Wiley, New York 1984; b) A. J. Bard, A. Ledwith, H. J. Shine, *Adv. Phys. Org. Chem. 14* (1976) 155.

[80] For the simplified kinetics scheme: $D + A \overset{k_1}{\underset{k_{-1}}{\rightleftharpoons}} [D^{\oplus}, A^{\ominus}] \xrightarrow{k_2}$ products, the steady-state concentration of the ion pair is proportional to the ratio $k_1/(k_2+k_{-1})$. For an endergonic electron transfer of the type described here, $k_{-1} \gg k_1$. K_{ET} for the preequilibrium step is k_1/k_{-1}.

[81] J. Kenner, *Nature (London) 156* (1945) 369.

[82] a) R. D. Brown, *J. Chem. Soc. 1959*, 2224, 2232; b) S. Nagakura, J. Tanaka, *J. Chem. Phys. 22* (1954) 563; see also [48c].

[83] a) E. B. Pederson, T. E. Petersen, K. Torsell, S.-O. Lawesson, *Tetrahedron 29* (1973) 579; b) C. L. Perrin, *J. Am. Chem. Soc. 99* (1977) 5516; c) L. Eberson, L. Jonsson, F. Radner, *Acta Chem. Scand. Ser. B 32* (1978) 749; d) L. Eberson, F. Radner, *ibid. 34* (1980) 739; e) *ibid. 39* (1985) 357; f) *ibid. 38* (1984) 861.

[84] K. Schofield: *Aromatic Nitration*, Cambridge University Press, Cambridge 1980.

[85] G. W. Wheland, *J. Am. Chem. Soc. 64* (1942) 900.

[86] a) S. R. Hartshorn, *Chem. Soc. Rev. 3* (1974) 167; b) H. Suzuki, *Synthesis 1977*, 217.

[87] J. M. Masnovi, J. K. Kochi, E. F. Hilinski, P. M. Rentzepis, *J. Am. Chem. Soc. 108* (1986) 1126; see also [74].

[88] S. Sankararaman, W. A. Haney, J. K. Kochi, *J. Am. Chem. Soc. 109* (1987) 5235.

[89] a) H. A. Benesi, J. H. Hildebrand, *J. Am. Chem. Soc. 71* (1949) 2703; b) W. B. Person, *ibid. 87* (1965) 167; c) R. Foster: *Molecular Complexes, Vol. 1*, Crane, Russak & Co., New York 1974.

[90] J. M. Masnovi, J. K. Kochi, *J. Org. Chem. 50* (1985) 5245.

[91] a) B. H. J. Bielski, A. O. Allen, *J. Phys. Chem. 71* (1967) 4544; b) S. A. Chadhuri, K. D. Asmus, *ibid. 76* (1972) 26; see also D. J. Glover, *Tetrahedron Suppl. 19* (1963) 219.

[92] a) W. D. Parker, L. Eberson, *Tetrahedron Lett. 1969*, 2839, 2843; b) [50b]; c) J. K. Kochi, R. T. Tang, T. Bernath, *J. Am. Chem. Soc. 95* (1973) 7114.

[93] L. Melander, *Arkiv Kemi 2* (1950) 211; K. Halvarson, L. Melander, *ibid. 11* (1957) 77; see also L. Melander: *Isotope Effects on Reaction Rates*, Ronald Press, New York 1960.

[94] See also a) W. M. Lauer, W. E. Noland, *J. Am. Chem. Soc. 75* (1953) 3689; b) G. A. Olah, S. J. Kuhn, S. H. Flood, *ibid. 83* (1961) 4571; c) P. C. Myhre, M. Beug, L. L. James, *ibid. 90* (1968) 2105; d) For a review, see [84].

[95] J. M. Masnovi, J. K. Kochi, *J. Am. Chem. Soc. 107* (1985) 7880.

[96] S. Sankararaman, W. A. Haney, J. K. Kochi, *J. Am. Chem. Soc. 109* (1987) 7824.

[97] a) W. Lau, J. K. Kochi, *J. Am. Chem. Soc. 108* (1986) 6720; b) *ibid. 106* (1984) 7100.

[98] W. Lau, J. C. Huffman, J. K. Kochi, *J. Am. Chem. Soc. 104* (1982) 5515.

[99] a) R. M. Dessau, S. Shih, E. I. Heiba, *J. Am. Chem. Soc. 92* (1970) 412; b) G. Vincow in [78], p. 151.

[100] a) I. H. Elson, J. K. Kochi, *J. Am. Chem. Soc. 95* (1973) 5060; b) P. D. Sullivan, E. M. Menger, A. H. Reddoch, D. H. Paskovich, *J. Phys. Chem. 82* (1978) 1158; see also [97b].

[101] A. McKillop, A. G. Turrell, D. W. Young, E. C. Taylor, *J. Am. Chem. Soc. 102* (1980) 6504.

[102] a) B. Cercek, M. Ebert, A. J. Shallow, *J. Chem. Soc. A 1966*, 612; b) D. M. Brown, F. S. Dainton, *Trans. Faraday Soc. 62* (1966) 1139; c) W. Lau, J. K. Kochi, *J. Org. Chem. 51* (1986) 1801.

[103] Cf., e.g., C. Schramm, J. I. Zink, *J. Am. Chem. Soc. 101* (1979) 4554.

[104] See a) P. J. Andrulis, M. J. S. Dewar, R. Dietz, R. L. Hunt, *J. Am. Chem. Soc. 88* (1966) 5483; [92c]; b) In the generalized formulation, each step in Equation (119) is reversible. (See Scheme 13).

[105] a) S. S. Shaik, *J. Am. Chem. Soc. 106* (1984) 1227; b) A. Pross, S. S. Shaik, *Acc. Chem. Res. 16* (1983) 363; c) A. Pross, *Adv. Phys. Org. Chem. 21* (1985) 99; *Acc. Chem. Res. 18* (1985) 212; d) S. S. Shaik, *Prog. Phys. Org. Chem. 15* (1985) 197.

[106] For an electrophile/nucleophile transformation proceeding via electron transfer as in the kinetics scheme presented in [80], the observed second-order rate constant k_{obs} is related to both the redox (pre)equilibrium (K_{ET}) and follow-up rate (k_2), i.e., $k_{obs}=K_{ET}k_2$. Accordingly, a highly endergonic electron transfer with $\Delta E^0=(E^0_{ox}+E^0_{red})\ll 0$ can be always overcome by suitably fast kinetics (k_2). See, e.g., G. S. Bodner, J. A. Gladysz, M. F. Nielsen, V. D. Parker, *J. Am. Chem. Soc. 109* (1987) 1757.

[107] By chemical redox, photoionization, electrochemistry, radiolysis, etc. See e.g., a) G. J. Jones, III, W. G. Becker, *J. Am. Chem. Soc. 105* (1983) 1276; b) H. D. Roth (Ed.): *Symp.-in-Print 28 Tetrahedron* (1986) 6097–6343; c) T. J. Richardson, F. L. Tanzella, N. Bartlett, *J. Am. Chem. Soc. 108* (1986) 4937; d) J. P. Dinnocenzo, T. E. Banach, *ibid. 108* (1986) 6063; e) R. A. Reed, R. W. Murray, *J. Phys. Chem. 90* (1986) 3829; f) H. Kunkely, A. Merz, A. Vogler, *J. Am. Chem. Soc. 105* (1983) 7241; g) H. Bock, B. Solouki in H. Sakurai (Ed.): *Organosilicon and Bioorganosilicon Chemistry*, Horwood, Chichester 1985, Chapter 5.

[108] See a) R. D. Bach, G. J. Wolber, A. Pross, *Isr. J. Chem. 23* (1983) 97; b) W. J. Bouma, D. Poppinger, L. Radon, *ibid. 23* (1983) 21; c) T. Miyasaki, K. Wakamatsu, T. Akiya, K. Kikuchi, T. Mukai, *J. Am. Chem. Soc. 109* (1987) 5270; d) H. D. Roth, *Acc. Chem. Res. 20* (1987) 343.

[109] See a) J. K. Kochi: *Organometallic Mechanisms and Catalysis*, Academic Press, New York 1978; S. Hoz, M. Livneh, D. Cohen, *J. Am. Chem. Soc. 109* (1987) 5149; c) M. J. Therein, W. Trogler, *ibid. 109* (1987) 5127; d) see also V. Caer, A. Laurent, E. Laurent, R. Tardivel, Z. Cebulska, R. Bartnik, *New J. Chem. 11* (1987) 351; e) W. Adam, M. Dorr, *J. Am. Chem. Soc. 109* (1987) 1570.

[110] See a) [109a], Chapter 7; b) C. Amatore, J. Pinson, J. M. Saveant, A. Thiebault, *J. Am. Chem. Soc. 103* (1981) 6930.

[111] This concept also includes the enhanced rates of bimolecular associative processes for radical cation such as arene cations [112], 17-electron organometallic radicals [113], etc. For the typical pathways of the stepwise reassemblage of the fragments from the CT ion pairs to the ultimate 1:1 adducts, see [29] and [90].

[112] a) L. Eberson, F. Radner, *Acc. Chem. Res. 20* (1987) 53; see also [83c]; b) R. J. Schmitt, S. E. Buttrill, Jr., D. S. Ross, *J. Am. Chem. Soc. 106* (1984) 926; c) A. Citterio, A. Gentile, F. Minisci, V. Navarrini, M. Serravalle, S. Ventura, *J. Org. Chem. 49* (1984) 4479; d) J. J. McCullough, *Chem. Rev. 87* (1987) 811.

[113] a) D. J. Kuchynka, C. Amatore, J. K. Kochi, *Inorg. Chem. 25* (1986) 4087; b) J. K. Kochi, *J. Organomet. Chem. 300* (1986) 139; c) A. Poe, *Trans. Met. Chem. 7* (1982) 65; d) M. Chanon, *Bull. Soc. Chim. Fr. 1982*, 197; e) D. Tyler, *Comments Inorg. Chem. 1986*, 215.

[114] See the kinetics behavior of the time-resolved *p*-haloanisol cations with $NO_2^{\ominus}$ in [96].

[115] a) A. Weller, H. Staerk, R. Treichel, *Faraday Discuss. Chem. Soc. 78* (1984) 271; b) A. Weller, *Z. Phys. Chem. (Wiesbaden) 133* (1982) 93; c) The absorption spectrum of the exciplex for *N,N*-diethylaniline and 1,2,4,5-benzenetetracarbonitrile is not a complete composite of the radical ions (A. Weller, Göttingen, private communication); d) N. Mataga, Y. Kanda, T. Okada, *J. Phys. Chem. 90* (1986) 3880; e) Y. Hirata, N. Mataga, *ibid. 89* (1985) 4031.

[116] For photoinduced electron transfers, see a) J. Mattay, *Angew. Chem. 99* (1987) 849; *Angew. Chem. Int. Ed. Engl. 99* (1987) 825; b) G. J. Kavarnos, N. J. Turro, *Chem. Rev. 86* (1986) 401; c) M. A. Fox, *Adv. Photochem. 13* (1986) 237; d) D. Creed, R. A. Caldwell, *Photochem. Photobiol. 41* (1985) 715; e) Y. Shirota, H. Mikawa, *J. Macromol. Sci. C16* (1977) 129; f) F. D. Lewis, *Adv. Photochem. 13* (1986) 165; g) K. Gollnick, A. Schnatterer, *Photochem. Photobiol. 43* (1986) 365.

Tumor Lectinology: At the Intersection of Carbohydrate Chemistry, Biochemistry, Cell Biology, and Oncology

By Hans-Joachim Gabius*

Dedicated to Professor Friedrich Cramer on the occasion of his 65th birthday

The scientific description of lectins, a class of sugar-binding proteins distinct from both sugar-specific enzymes and antibodies, began nearly 100 years ago. The natural ligands of lectins include the sugar moieties of cell glycoproteins, glycolipids, and proteoglycans. Lectins can selectively recognize these potential information-storing or -transferring structural elements and so contribute to regulating biological processes. Plant lectins are now a well-established means of characterizing and localizing glycoconjugate-bound sugar determinants. However, work on endogenous lectins is still confronted by many open questions, whose answers require detailed experiments using a suitable model system. Tumors offer an obvious model, particularly since they allow the possible diagnostic and therapeutic uses of lectins to be explored directly. Tumor lectinology employs a broad range of methods, from the chemical synthesis of the sugar components of neoglycoproteins, and their use to seek out cellular sugar receptors with histochemical and cell-biological techniques, to the biochemical and immunological characterization of the lectins expressed by tumor cells and the use of homology analysis to find further functional domains. The outlook for clinical applications depends on the harmonious integration of these disparate disciplines in tumor lectinology.

1. Introduction

Historically, scientific attention to lectins began nearly 100 years ago with the publication of the dissertation of *Hermann Stillmark*, a doctoral student of *Rudolf Kobert* at The University of Dorpat. His work, "Ricin, a toxic ferment from the seeds of Ricinus communis and some other Euphorbiaceae",[1] was motivated by the occurrence of poisons of unknown nature in animal feeds and documented the high toxicity of the extract from *Ricinus communis*. In addition, his preparations, which by modern standards must be considered as protein mixtures, were able to cause the agglutination of red blood cells (Fig. 1). Use of this hemagglutination as an assay soon led to the discovery of further sources for extracts, thereby showing the broad distribution of such proteins. Apart from its toxicity and capacity for hemagglutination, ricin has a third property, soon put to use by *Ehrlich*: it is a potent antigen. Using ricin, in place of bacterial toxins, he provided experimental proof of the specificity of the immune reaction.[2,3]

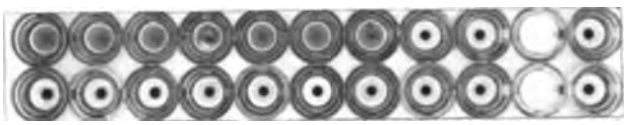

Fig. 1. Ricin-mediated hemagglutination. In the upper row, a series of increasing dilutions of ricin (1:2 to 1:612) was used. In the lower row, 0.1 M D-lactose was added to each test as a competitive inhibitor. The test at the far right in each row is a control performed without the addition of ricin; the penultimate vessels are empty.

As described in more detail elsewhere,[4,5] there followed further milestones in lectin research. In 1936, it was shown experimentally that a protein obtained from *Canavalia ensiformis* extracts causes hemagglutination by binding sugars on the erythrocytes; in 1948, certain plant proteins were found to show specificity for blood groups in hemagglutination tests.[7,8] The selectivity of different erythrocyte-agglutinating proteins obtained from plants, and so properly termed *phytohemagglutinins*, led to the introduction of the term *lectin* to distinguish between members of this class of proteins, which recognize certain molecular groups in an apparently antibody-like way, and antibodies themselves.[9] Although other terminologies were suggested, such as "receptor-specific protein",[10] these did not find general acceptance. Many of the proteins then grouped with the phytohemagglutinins were later found to be sugar-specific, and agglutinins with the same specificities were also found in other classes of organisms. In this way the foundation was laid for a more precise definition of the term *lectin*, till then used only in distinction to the term *antibody*. The definition includes sugar-binding capacity without enzymic activity together with activity in cell agglutination assays and/or precipitation of glycoconjugates. Lectins were thus specified in terms of their ligands.[11]

Compared with plant lectins, animal lectins have been investigated only recently.[12,13] The developments that have followed from the application of chemical, biochemical, and cell-biological methods will be presented in this review with particular emphasis on the possible clinical applications of endogenous lectins.

[*] Dr. H.-J. Gabius
Max-Planck-Institut für experimentelle Medizin, Abteilung Chemie
Hermann-Rein-Strasse 3, D-3400 Göttingen (FRG)

2. Can the Sugar Structures of Cell Glycoconjugates Carry Biological Information?

Sugars are generally viewed as energy-storage substances. However, as integral components of cell glycoconjugates—glycoproteins, glycolipids, and proteoglycans—they apparently perform other functions. It is attractive to suppose that the ordered arrangement of the sugar monomers in the carbohydrate part of glycoconjugates carries biological information required for the error-free performance of some recognition processes. Whereas amino acids in proteins are linked almost exclusively by peptide bonds, so that biological information can be expressed as differences between the structural units but not as differences in the types of interlinkage, sugar monomers can be linked to one another by glycosidic bonds, whose diversity opens up a great wealth of possibilities. Quite apart from the rich variety due to the location of the bond in the framework of the sugar molecule, further possibilities follow from anomerism. Even if the naturally occurring complex carbohydrate structures of glycoconjugates do not by far realize all the configurations theoretically possible (see Fig. 2), nonetheless sugar structures of relatively short sequence appear almost designed for use in information storage, as the blood groups, one example among many, conclusively demonstrate.[14–19]

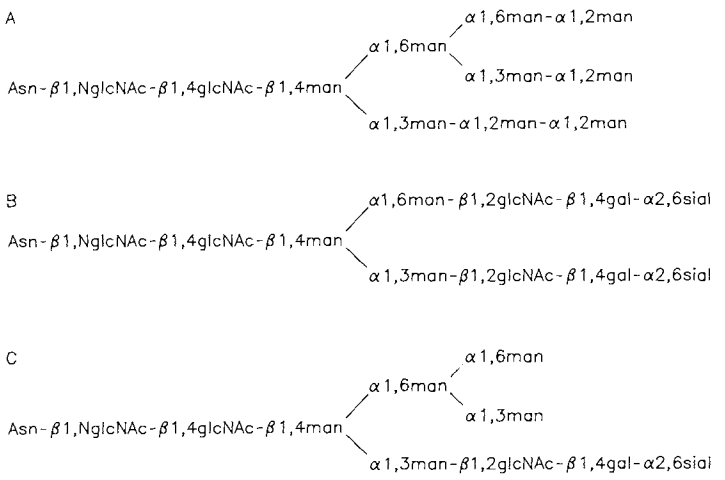

Fig. 2. Examples of the primary structure of oligosaccharides connected to the protein by *N*-glycosidic linkages via a bridging bond from *N*-acetylglucosamine to asparagine. The core part, which includes the first branching point, is identical for all three basic types. These basic types include the mannose-rich type (A), the complex type (B), and the mixed type (C), which in the peripheral parts adjacent to the core region bears elements of both the other basic types and is termed the hybrid type.

Beyond their primary structure, determined by the monomer sequence, and whose analysis has undergone significant advances in the last few years,[16–20] sugar chains can be further modified by enzymic means, such as sulfation, phosphorylation, or *O*-acetylation.[21–24] These two factors, the sequence diversity within limits set by the biosynthetic apparatus and the possibility of subsequent modifications, provide a framework underlying the immense variety of possible sugar structures. A further essential requirement for the functioning of an information-storage and -transferral device, namely, a distinct spatial organization and considerable structural rigidity, is shown to be present by conformational analysis of defined oligosaccharides and glycopeptides.[25,26] Modifications of the primary structure affect, in turn, the conformational stability. The carbohydrate part of glycoconjugates satisfies, then, the essential requirements for "coding systems" that must store and transfer information, systems that, from the moment the egg is fertilized, can cope with tasks of far-reaching importance.[27–31]

Proteins appear the most obvious partners in such recognition reactions. By definition the lectins belong to the class of proteins able to function as sugar receptors. Unlike enzymes (e.g., glycosidases or glycosyltransferases), lectins do not alter the sugar chain. The specific protein–sugar interaction between lectin and carbohydrate thus constitutes a reciprocal recognition system. Both sides of this system are open to regulation, permitting high flexibility, as shown schematically in Figure 3.

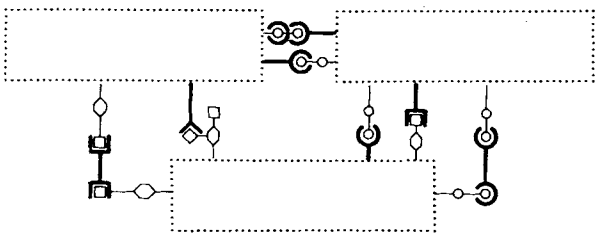

Fig. 3. Schematic illustration of a reciprocal recognition system, mediated by specific interactions between sugar ligands and cellular lectins of appropriate specificity. The lectins can also function as bridges. Large rectangles, cells; circles, mannose; squares, galactose; hexagons, *N*-acetylglucosamine; diamonds, fucose. The specific lectins, which can vary in their subspecificity, are exemplified for mannose-binding.

Although this general concept is very appealing, it should not go without remark here that carbohydrate–carbohydrate interactions have equally been documented[32,33] and that the sugar components of glycoconjugates can also serve other purposes. In glycoproteins they can influence the conformation of the protein and, by steric hindrance, protect regions of the protein surface from proteolytic degradation.[27] Glycolipids such as the sialogangliosides can modulate receptor functions by binding metal ions, without themselves (except for the sialic acid group) acting as receptors on account of their sugar structure.[34,35]

The flexibility that is required for regulatory intervention in coding systems based on sugar–protein interactions has been well documented with regard to carbohydrate structure. Apart from the availability of plant lectins as exogenous sugar receptors, the strong antigenicity of sugars was helpful in carrying out these studies.[36] Monoclonal antibodies have provided experimental means of detecting sugar epitopes and of quantifying their pattern of expression during development.[37–40] The results so obtained bear impressive witness that the pattern of sugar structures of individual glycoconjugates reflects a cell's identity during the course of differentiation. By binding to their corresponding epitopes, antibodies can spatially prevent other interactions from occurring. After the specific determi-

nants have been identified, functional studies can provide further insights into their significance.[31,41]

In a complementary approach, the sugar structures of interest can be used themselves as effectors, or they can be modified in situ. This has provided evidence for the functional significance of carbohydrate elements in such diverse processes as virus replication,[42] the regulation of cell growth in both animals and plants,[43-45] embryogenesis,[46-48] hormone distribution, and hormonally mediated signaling.[49,50] An independent approach, the use of mutant mammalian cells with genetic abnormalities in glycosylation, has provided further hints at the functional significance of the sugar part of cell glycoconjugates.[51] Taken together, these data encourage us to consider the working hypothesis to be not only attractive, but indeed plausible, namely that sugar-protein interactions involving sugar-lectin (sugar-receptor) recognition are a fundamental form of biological information transfer. However, our knowledge about the protein side of these interactions requires considerable improvement.

3. Lectins as Research Tools

Our present conception of lectins is still largely colored by the use of plant lectins as aids in biological and biochemical research. Their high selectivity for sugar structures renders them useful in studies directed at the characterization of glycoconjugates. This application presupposes that the specificity of the lectins used has been determined previously with the help of ligands of precisely defined structure, such as glycopeptides. Although there is a tendency to group together different lectins on the basis of affinity for a specific monosaccharide, exact analysis can sometimes reveal quite considerable differences in affinity within such a category.[52-54] The effort invested in gathering this further data is well repaid, because glycoconjugates of unknown fine structure can then be characterized according to their affinity as lectin ligand after gel electrophoretic separation, or they can be isolated and purified by affinity chromatography on immobilized lectins.[55-59] Work with lectins or lectin-coated carriers and cells, rather than with cell extracts, permits cell separations to be carried out, which is particularly important in hematological oncology.[58,60] The efficiency of these separations depends on such different factors as the density and mobility of the lectin ligands.[61,62]

At the level of cells and tissues lectins find application as a histological tool, with which the expression of glycoconjugate structures can be demonstrated and quantified. Examples of such applications in practical histology include the identification of certain cell types and particular functional and developmental conditions, as well as contributions to the diagnosis of tumors.[63-65]

Although plant lectins are widely used as research tools, it should not be forgotten that their presumed functions in the plant have only been roughly described.[66,67] This is true even for ricin. Just as ricin was employed in 1889, shortly after its discovery, as an antigen, on account of its potency, rather than as a sugar-binding protein, so also now, after its mechanism of toxicity has been elucidated, work with ricin centers on its application as a component of immunotoxins.[69,70] The widespread use of plant lectins as exogenous sugar receptors, however, documents their functional value and provides further support for the concept that there may be a coding system comprising endogenous lectins and their cellular ligands.

4. Neoglycoproteins as "Bloodhounds" for Endogenous Sugar Receptors

In elucidating the biological role of endogenous lectins, it is advisable to concentrate studies on established, generally accepted model systems. Those chosen should combine biological relevance with convenience in handling and a ready availability of material capable of providing satisfactory reproducibility in analysis. Tumor cells satisfy these prerequisites. In addition, the results obtained with tumor cells might be of direct clinical use. On the assumption, admittedly hypothetical but supported by the evidence presented above, that sugar-protein recognition is of significance in tumor biology, endogenous receptors for sugar structures of cell glycoconjugates are expected to provide functional markers for tumors. Such markers might serve not only as diagnostic tools or as worthwhile targets for therapeutic development in oncological practice, but they could themselves contribute to an understanding of the biological behavior of tumors.[71,72] Thus, they would provide us with more than simply a characterization of the tumor, as other types of tumor marker already do,[73] but with the further possibility of proceeding to clinically valuable judgments about such tumor properties as growth behavior, degree of differentiation, and level of malignity, as well as the capacity for metastasis.

Experimentally, appropriate reagents are used as "bloodhounds" to search for sugar-specific recognition processes involving glycoconjugates. To get some idea of the receptor capacity for sugar structures it is necessary to synthesize reagents appropriate for routine standardized use in comparative studies. A protein, chosen because it possesses no sugar component and is therefore unable itself to act as a receptor, is first conjugated synthetically with defined sugar components. The broad palette of starting substances and conjugation procedures thereby allows a wide range of precisely defined reaction products, the so-called neoglycoproteins, to be prepared.[74-76] This chemical synthesis of neoglycoproteins shows similarity to nonenzymic glycosylation of proteins, which in special cases is known to occur naturally.[77,78] Progress in the field of carbohydrate synthesis has made it possible to extend the sugar component to include even some very complex structures, thus closing the gap between the neoglycoproteins and naturally occurring—if necessary, appropriately modified—glycoconjugates.[79,80]

These neoglycoproteins open up several possibilities for the qualitative and quantitative evaluation by histochemical and cell-biological means of the pattern of sugar-specific binding capacity in comparative studies of different cell types. However, it is advisable at this stage to use the general term *sugar receptor*, because the molecular character of the individual receptors that may be involved is not

always clear. They could be endogenous lectins or, alternatively, glycosyltransferases or glycosidases, whose enzyme activity but not sugar-binding capacity is reduced in the physiological pH range. Further, some endogenous antibodies with sugar-binding specificity, as well as other proteins with sugar-binding domains, are known.[81,82] These can indeed function as lectins, but are defined operationally in terms of other functional domains, as explained in more detail in Section 6. It should also be noted that the recognition reaction responsible for detection can be influenced by the type of tissue fixation used to prepare the material and by endogenous ligands which act to inhibit the reaction.

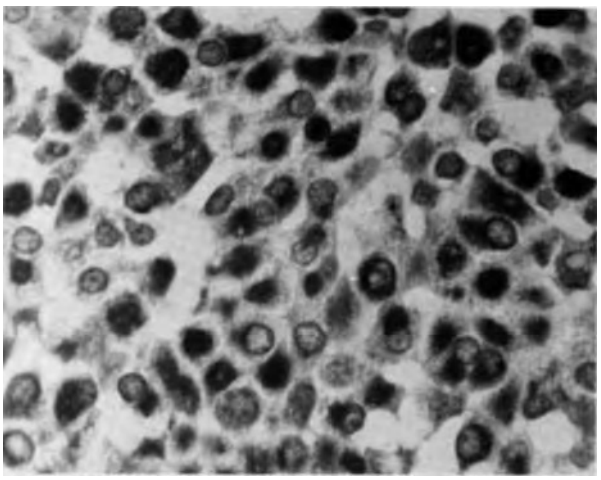

Fig. 4. Binding of labeled fucosylated albumin to cells of a poorly differentiated mucinous mammary carcinoma (magnification 600×).

For histochemistry and histopathology, appropriately labeled (e.g., "biotinylated") neoglycoproteins open the way to a more detailed analysis of endogenous sugar receptors. Biotinylation introduces a label into the carrier protein (e.g., serum albumin), thereby aiding detection. The resulting neoglycoproteins, which contain, in addition, the sugar component required for binding to the tissue section, provide complementary tools to plant lectins and sugar-specific monoclonal antibodies for use in defining a coding system based on protein-sugar interactions. The type of result obtained is exemplified in Figure 4, which shows the localization of fucose-specific receptors in a human mammary tumor of mucinous type. In control experiments, competitive inhibition with the specific sugar component prevented binding of the unmodified carrier protein, thereby proving the specificity of the interaction between the sugar part of the neoglycoprotein and the receptor in the tissue section. Comparative studies using a selection of neoglycoproteins have so far shown that analyses of this type reveal differences between normal and tumor tissues, between different types of tumor, and within a single class of tumors. This is true in particular for tumors of the breast,[83] the lung—here can be seen clearly the clinically significant differences between tumors of small-cell type and other types, and between tumor cells and inflammatory cells[84,85]—and the brain,[86,87] as shown in Table 1. Such evidence from different tumor systems shows that the use of neoglycoproteins is worth closer examination, and that their receptors are liable at least in part to dramatic regulation. A further example is provided by the course of differentiation of nonmalignant cells, for example, the different cell types during placental development (Table 2).

Table 1. Cytoplasmic binding capacity (Cp) (Σ^n) of labeled neoglycoproteins in brain tumors [a].

Receptor specificity	Neoglycoprotein	Tumor type (Σ^n Cp)														
		FA	PA	AA	DO	AO	GB	GZ	DE	ME	M	FM	AM	SM	MM	GA
β-Galactoside	lac(diaz.)-BSA	4	6	6	6	5	4	6	6	6	4	6	4	3	3	69
	lac(red.am.)-BSA	4	3	1	1	2	0	4	3	2	2	0	2	0	0	24
	gal-β-(1,3)-glcNAc-BSA	0	2	3	3	1	3	0	3	2	0	0	0	0	0	17
	Asialotransferrin	0	0	4	1	2	6	5	0	6	3	3	1	3	1	35
	Asialofetuin	6	6	4	6	6	5	6	6	6	4	4	6	6	3	68
	Asialolactoferrin	2	2	4	1	0	5	0	0	6	1	3	1	4	3	32
α-Galactoside	Melibiose-BSA	0	0	4	0	0	0	0	0	0	1	0	0	0	0	5
N-Acetylated sugars	*N*-Acetylglucosamine-BSA	2	4	6	5	3	3	4	3	5	5	3	3	2	3	51
	N-Acetylgalactosamine-BSA	0	0	4	0	0	5	0	0	3	0	0	0	2	4	18
α-Glucoside	Maltose-BSA	5	3	3	3	0	4	4	2	1	4	3	4	2	0	38
β-Glucoside	Cellobiose-BSA	0	3	1	3	3	0	0	3	2	0	0	0	0	0	15
α-Fucoside	Fucose-BSA	6	6	5	4	6	3	5	3	6	2	2	5	3	3	59
α-Mannoside	Mannose-BSA	3	4	4	5	4	4	6	3	4	6	4	6	3	3	59
Phosphorylated sugars	Mannose-6-P-BSA	3	3	6	4	4	4	5	4	6	3	6	6	3	3	60
	Galactose-6-P-BSA	2	2	5	5	2	3	3	1	5	3	2	1	0	1	35
Sugars with a carboxyl group	Sialic acid-BSA	0	0	3	0	0	3	0	0	0	0	0	0	0	0	6
	Glucuronic acid-BSA	2	2	5	1	1	4	3	0	3	4	0	0	0	1	26
β-Xyloside	Xylose-BSA	5	5	6	6	6	5	6	0	6	6	6	6	5	2	70
Total binding index	$\Sigma\Sigma^n = 43$	51	74	54	45	57	57	37	69	48	42	45	36	30		

[a] Explanations and abbreviations: $\Sigma^n = 6$ and 5, strong; $\Sigma^n = 4$ and 3, medium; $\Sigma^n = 2$ and 1, weak; $\Sigma^n = 0$, no stain; GA = summed sugar index; FA = fibrocytic astrocytoma; PA = pilocytotic astrocytoma; AA = anaplastic astrocytoma; DO = differentiated oligodendroglioma; AO = anaplastic oligodendroglioma; GB = glioblastoma; GZ = gangliocytoma; DE = differentiated ependymoma; ME = malignant ependymoma; M = meningotheliomatous meningioma; FM = fibroblastic meningioma; AM = angioblastic meningioma; SM = submalignant meningioma; MM = malignant meningioma; lac(diaz.)-BSA = lactose-bovine serum albumin (coupled by diazotization); lac(red.am.)-BSA = lactose-bovine serum albumin (coupled by reductive amination).

Table 2. The binding of labeled (neo)glycoproteins to human placenta [a, b].

Cell type \ Neoglycoprotein	lac	ASF	mel	man	fuc	mal
Decidua (8 weeks)	−/+	++	+	+++	+	−
Syncytium (8 weeks)	−/+	++++	+++	+++	++	+
Cytotrophoblast (8 weeks)	−/+	++++	+++	+++	++	+
Macrophages M [c] (8 weeks) F [d]	−	+	+	+++	+	−
	−	+	+	++	+	−
Decidua (9 months)	−/+	+	++	++	+	+
Syncytium (9 months)	−/+	++	++	+++	−	+
Cytotrophoblast (9 months)	−/+	+	−/+	+	−	−
Macrophages M (9 months) F	−/+	+++	+	+++	+	++
	−/+	+++	−/+	++	+	++

[a] All the labeled neoglycoproteins and also the β-galactoside-terminating asialofetuin were incubated with the tissue sections for 30 min at room temperature at a concentration of 10 μg mL^{-1}, except for melibiosylated albumin, which was applied for 3 h at a concentration of 100 μg mL^{-1}. [b] Abbreviations: lac = lactose, ASF = asialofetuin, mel = melibiose, man = mannose, fuc = fucose, mal = maltose. [c] M = maternal. [d] F = fetal.

To modify neoglycoproteins for use in rapid histopathological procedures, such as the surgery-associated diagnostic methods based on frozen tissue sections, the neoglycoproteins can be coupled to enzymes by means of heterobifunctional reagents in two-step procedures, thereby shortening the sequence of incubation steps prior to staining.[88] Additionally, such monoconjugates can be used to demonstrate and quantify sugar receptors. By varying the sugar component one can obtain information about the specificity of the sugar receptors involved, this feedback helping to optimize the ligand structure. "Sugar structure" is not the only variable influencing the efficiency of the neoglycoprotein; the sugar density and type of sugar–protein linkage are also important.[89–91] Taken together, these approaches provide important guidelines for research and for the subsequent biochemical purification of sugar receptors localized by histochemical procedures.

The carbohydrate portions not only of glycoproteins and glycolipids but also of proteoglycans appear to mediate important cellular functions (cell adhesion, growth control, regulation of receptor functions).[92,93] Here, too, appropriate markers can be synthesized (biotinylated polysaccharides after mild CNBr activation and aminoalkylation) to allow detection of the binding proteins involved. Standardized application of this type of marker has shown, for example, that receptors for sulfated polysaccharides are developmentally regulated[94] and are expressed differentially by different cell types.[84,94] Within a population of genetically uniform cells it is possible by use of these markers, as also by use of neoglycoproteins, to demonstrate heterogeneity both in tissue sections[83–87,94] and in tumor cells in culture.[95,96] This heterogeneity is a general phenomenon, confirmed for different parameters of tumor cells.[97a] It can be compensated for by the simultaneous application of different neoglycoproteins, whose binding specificities cover the entire cell population. This principle is decisive for precise cell characterization and for the success of therapeutic applications.

The discussion of measurements on cell populations leads us to cell-biological applications of neoglycoproteins, which include labeling by means of fluorescent dyes and the transport of chemotherapeutic agents. The latter are transported into cells via sugar-mediated binding and uptake and are released following intracellular proteolytic degradation of the carrier protein. They can then unfold their toxic activity, which can be measured at the cellular level. Their toxic effects are therefore indicative of both transport and the intracellular fate of the neoglycoprotein. Seen from another point of view, the glycosylated carrier fulfills the role of a "Trojan Horse", which smuggles the chemotherapeutic agent into the cell. The sugar component of the conjugate thus directs the fate of the conjugate, the pharmacon being exchangeable. Use of substances with a specific mode of activity—for example, amino acid analogues with aminoacyl-tRNA synthetases as target enzymes[97b]—improves further the efficiency of the conjugate. Selective uptake of neoglycoprotein–toxin conjugates via endogenous sugar receptors, the prerequisite for activity, has been demonstrated for a variety of animal and human tumor cells.[98–102] In comparison with antibodies, neoglycoproteins prove the better "Trojan Horses" in that they can be loaded synthetically with more chemotherapeutic agent, without their carrier properties being affected. It is also important for therapy that several chemotherapeutic agents applied together in this way retain their synergistic properties. For example, simultaneous application of maltosylated serum albumin complexed with *cis*-diamminedichloroplatinum(II) and lactosylated serum albumin coupled to the hemisuccinate of the phyllotoxin etoposide gave better results than those obtained by summing the results of separate applications (Table 3).

Table 3. Inhibition of [^{3}H]thymidine incorporation into human embryonic carcinoma cells by neoglyproteins conjugated to etoposide (as the hemisuccinate) or *cis*-diamminedichloroplatinum(II) (*cis*-Pt), as a model for combination therapy.

Substance	Concentration [μg mL^{-1}]	Inhibition [%]
(*cis*-Pt)-mal-BSA	1.25	1
	2.5	4
	5.0	6.5
(*cis*-Pt)-man-BSA	1.25	2
	2.5	3
	5.0	5
Etoposide-lac-BSA	7.5	8
	15	19
	30	27
(*cis*-Pt)-mal-BSA + etoposide-lac-BSA	1.25 + 7.5	28
	2.5 + 15	43
(*cis*-Pt)-man-BSA + etoposide-lac-BSA	1.25 + 7.5	22
	2.5 + 15	35

Already at this relatively low level of sugar-structure complexity, a marked increase in uptake is observed compared with use of the unmodified carrier protein.[98–102] The coupling to a carrier protein improves the pharmacokinetic properties of the therapeutic agent.[103] However,

optimizing the choice of the sugar component, which should function as a kind of postal code, should raise still further the targeting precision of the conjugate. Use of the term *therapeutic agent* signifies that, in principle, the substance brought to the target can be varied as desired. Differentiation-inducing substances such as retinoids[104] or photoactivatable dyes such as hematoporphyrin[105] can replace conventional chemotherapeutic agents. Clinical use, however, should not remain limited to local application. Therefore, the pattern of neoglycoprotein distribution in the organism, the assessment of which is now only beginning (Table 4),[106] needs to be examined more thoroughly. In this way the employment of sugars could enrich the arsenal of "drug targeting" methods presently available.[107,108] Naturally, this application is not limited to tumor cells, but can be used for any cell type and for further carrier systems such as liposomes.[109-112]

These applications show that neoglycoproteins, which were originally only conceived of as probes for sugar receptors, are also diagnostic and therapeutic tools. Furthermore, detailed molecular analysis of the receptors appears to offer much promise, especially since further functionally oriented measurements—for example, the influence of sugars on cell aggregations or on cell adhesion to sugar-coated carrier materials[113-115]—have underlined the presence of sugar receptor molecules and their functional importance.

5. Biochemical Tumor Lectinology

Conventional affinity chromatography using suitable supports and affinity ligands, whose type profoundly influences the yield of isolated lectin,[116] allows purification of endogenous lectins in relatively few steps. These analyses strengthen the conclusions drawn from the tumor-oriented application of neoglycoproteins. Moreover, the demonstrable lectin character of the isolated proteins allows us to speak of endogenous tumor lectins. The endogenous lectins isolated from different tumors display notable qualitative differences with respect to the patterns of sugar specificities, corresponding to certain components of natural glycoconjugates.[117-121] This is exemplified in Table 5 for some human tumors of differing histogenesis. An analysis of bone marrow, also shown here, indicates the differences found when tumors are compared with a mixture of nonmalignant cells. Even within a single class of tumors,

Table 4. Organ distribution of [^{125}I]neoglycoproteins in mice bearing Ehrlich tumors after 48 h [% of the injected dose per gram of tissue] [a].

Sugar \ Tissue type	Blood	Liver	Kidney	Spleen	Heart	Lung	Saliva	Muscle	Tumor
Lactose	0.061 ± 0.008	0.278 ± 0.042	0.078 ± 0.012	0.073 ± 0.010	0.030 ± 0.003	0.040 ± 0.005	0.112 ± 0.038	0.010 ± 0.001	0.025 ± 0.004
β-D-Galactose	0.047 ± 0.017	0.159 ± 0.032	0.065 ± 0.008	0.037 ± 0.006	0.018 ± 0.003	0.036 ± 0.011	0.174 ± 0.030	0.024 ± 0.008	0.037 ± 0.007
Melibiose	0.037 ± 0.005	0.218 ± 0.022	0.064 ± 0.011	0.057 ± 0.017	0.025 ± 0.009	0.031 ± 0.005	0.292 ± 0.062	0.011 ± 0.002	0.038 ± 0.012
α-D-Galactose	0.053 ± 0.012	0.320 ± 0.040	0.139 ± 0.032	0.089 ± 0.007	0.027 ± 0.009	0.113 ± 0.016	0.319 ± 0.050	0.036 ± 0.012	0.038 ± 0.004
N-Acetylglucosamine	0.043 ± 0.006	0.264 ± 0.017	0.090 ± 0.010	0.105 ± 0.019	0.082 ± 0.008	0.094 ± 0.024	0.190 ± 0.003	0.049 ± 0.001	0.058 ± 0.004
N-Acetylgalactosamine	0.053 ± 0.013	0.185 ± 0.020	0.109 ± 0.020	0.062 ± 0.012	0.067 ± 0.030	0.073 ± 0.001	0.198 ± 0.075	0.008 ± 0.002	0.036 ± 0.005
L-Fucose	0.053 ± 0.008	0.491 ± 0.083	0.147 ± 0.010	0.123 ± 0.032	0.033 ± 0.008	0.069 ± 0.012	0.268 ± 0.046	0.014 ± 0.002	0.045 ± 0.014
D-Mannose	0.074 ± 0.008	0.455 ± 0.073	0.166 ± 0.026	0.202 ± 0.020	0.043 ± 0.012	0.142 ± 0.079	0.384 ± 0.072	0.011 ± 0.002	0.056 ± 0.009
L-Rhamnose	0.064 ± 0.008	0.349 ± 0.037	0.129 ± 0.012	0.143 ± 0.037	0.042 ± 0.009	0.132 ± 0.012	0.343 ± 0.084	0.023 ± 0.005	0.043 ± 0.004
Cellobiose	0.079 ± 0.027	0.720 ± 0.199	0.140 ± 0.033	0.122 ± 0.040	0.050 ± 0.017	0.070 ± 0.043	0.181 ± 0.022	0.014 ± 0.007	0.074 ± 0.040
β-D-Glucose	0.064 ± 0.008	0.313 ± 0.060	0.154 ± 0.036	0.067 ± 0.012	0.147 ± 0.100	0.058 ± 0.013	0.313 ± 0.062	0.064 ± 0.017	0.048 ± 0.006
Mannose-6-phosphate	0.043 ± 0.010	0.548 ± 0.049	0.151 ± 0.018	0.131 ± 0.026	0.047 ± 0.004	0.052 ± 0.009	0.236 ± 0.061	0.019 ± 0.009	0.040 ± 0.006
Galactose-6-phosphate	0.047 ± 0.007	0.533 ± 0.062	0.183 ± 0.034	0.228 ± 0.029	0.021 ± 0.060	0.062 ± 0.012	0.220 ± 0.022	0.012 ± 0.003	0.050 ± 0.006
Sialic acid	0.050 ± 0.013	0.703 ± 0.101	0.203 ± 0.037	0.176 ± 0.048	0.043 ± 0.005	0.054 ± 0.006	0.215 ± 0.069	0.015 ± 0.001	0.038 ± 0.004
Glucuronic acid	0.045 ± 0.012	0.389 ± 0.049	0.127 ± 0.010	0.131 ± 0.018	0.139 ± 0.009	0.105 ± 0.063	0.254 ± 0.013	0.023 ± 0.008	0.065 ± 0.009
D-Xylose	0.045 ± 0.004	0.262 ± 0.022	0.178 ± 0.012	0.14 ± 0.016	0.348 ± 0.029	0.326 ± 0.061	0.534 ± 0.153	0.052 ± 0.015	0.14 ± 0.020
BSA	0.469 ± 0.023	0.127 ± 0.016	0.161 ± 0.023	0.086 ± 0.009	0.111 ± 0.018	0.200 ± 0.031	0.359 ± 0.067	0.053 ± 0.014	0.277 ± 0.065

[a] Each entry states the average value ± standard deviation, from four animals after injection of 7 μg per animal (≙37 kBq).

Table 5. The pattern of endogenous lectins from three types of tumor of human origin and of bone marrow. By choice of extraction and elution conditions the lectin pattern can be split into those extractable by salt (1st row, Salt), comprising soluble intra- and extracellular lectins, and those extractable by detergent (2nd row, Det.), comprising integral membrane proteins, both $Ca^{2\oplus}$-dependent (elution by EDTA) and $Ca^{2\oplus}$-independent (elution by sugar) lectins.

Tumor type	Extraction by	Elution by EDTA					Elution by sugar				
		Lactose	Asialofetuin	Melibiose	Mannose	Fucose	Lactose	Asialofetuin	Melibiose	Mannose	Fucose
		Molecular weight [a]					Molecular weight [a]				
Ewing sarcoma	Salt	31, 29	31, 29	—	31, 29	—	58, 54, 31, 29, 14	54	58, 54, 31, 29	—	—
	Det.	—	—	—	—	—	14	—	—	—	—
Embryonic carcinoma	Salt	31	31	31	31	70, 31	35, 14	—	—	—	—
	Det.	31	31	31	31	31	35, 14	—	—	68	—
Colon carcinoma	Salt	29	29	45, 43, 29, 28	31	62	64, 14	—	64	—	—
	Det.	70, 35, 29	29	—	31	70, 62	64, 35, 16, 14	—	64	—	62
Bone marrow	Salt	29	29	54, 29, 28	29	110, 54, 26	54, 29, 14	—	54, 31, 29	—	60, 54, 50, 29
	Det.	29	29	29	29	—	14	—	—	—	—

[a] The relative molecular weight is stated in thousands.

in part of similar histogenesis,[122-124] qualitative differences can be observed. This also holds for tumors of the same histogenesis but different degrees of differentiation,[125] as well as for cultured lines of tumor cells of identical genetic origin but differing in cellular morphology and growth behavior.[126]

Such data indicate that the lectin pattern of tumors has a phenomenological relation to the histogenesis and cell character, though the present state of knowledge does not permit a causal relationship to be established. Three classes of tumor lectins can be discerned: Endogenous lectins are expressed in both tumor and normal tissues. Other lectins can be found in tumors and in developing tissues but not in adult tissues, a pattern defined operationally as oncofetal expression. The third group includes the lectins which cannot yet be allocated to the other groups because we lack a full catalogue of lectin expression in different normal tissues at various stages of development.[124]

As human embryonic tissue, the placenta is an appropriate research object; its various cell types exhibit developmentally dependent regulation of the expression of sugar receptors. The changes, as visualized histochemically, are reflected clearly at the biochemical level, even when analysis is limited to the whole organ.[127] Since the growth behavior of the proliferating placenta is comparable with the invasive growth of tumors, such structural analysis provides a starting point for correlation with function.

Work with tumors is open to the objection that other, nonmalignant cells contribute to the results of analysis in spite of careful preparation of the tissue. This objection can be countered by histochemical investigations employing antibodies directed against endogenous lectins[128-130] or by studies on tumor cell lines. In using these cell lines, however, it must be borne in mind that their lectin expression may depend on culture and growth conditions.[131] Further, cell lines from primary tumors represent cell populations adapted to the culture conditions. Even if they are, for this reason, not necessarily representative of the primary tumor, they nonetheless provide an important cell-biological model system.

A clinically prominent property of tumors, organotropic metastasis, can be subjected to functional studies in such model systems.[132-134] In this connection, organotropy signifies that cells from a particular type of primary tumor colonize preferentially other particular tissues and give rise to daughter growths. Some model systems comprising cells of identical genetic origin contain subpopulations of varying metastatic capacity. In such systems the differences in the patterns of endogenous lectins can be correlated with these subpopulations.[135-137] Particular lectins have already been implicated in certain functional steps of the metastatic cascade.[138, 139] Since endogenous lectins can be involved in growth regulation,[140-142] lectin expression and the associated lectin-glycoconjugate interactions presumably also play a role in promoting tumor growth. Such interactions, however, can lead to recognition and destruction of the tumor cells by cells of the immunological defense system.[124] Clearly, therefore, normal cells, with which a tumor cell is in contact from the time of its release from the parent cell mass until it colonizes a target organ, also bear endogenous lectins capable of interaction. These can help enhance metastatic organotropy.[143, 144] The recognition of cells by means of a sugar-coding system always implies mutual recognition.

Extending this concept by viewing the tumor cell in a simplified way as a normal cell that has lost its growth control and attained parasitic character,[145] one finds similar colonization mechanisms for viruses, bacteria, and parasites.[146-148] This points the way to anti-metastatic and anti-parasitic forms of treatment based on lectins.

6. Computers as "Bloodhounds" for Lectins and Lectin Functions

The physiological significance of lectins should not be viewed as restricted simply to sugar-binding and the functions associated with it. Besides the domain which defines the protein operationally as a lectin, other active domains may also determine the overall functions of any given protein. The search for these other distinct domains is facilitated by use of computer programs. Their existence can then be confirmed by direct experiment, as exemplified by the further functional domains in the slime-mold lectin discoidin I,[149, 150] in a mannose-binding protein,[151] and in the mannose-6-phosphate receptor.[152]

Proteins that are familiar to us because of other domains and their associated properties might well be included nominally among the lectins: for example, fibronectin,[153] laminin,[154] thrombospondin,[155] or the neural cell adhesion molecule NCAM.[156] The search for sugar-binding domains in yet other proteins, followed by experimental confirmation of their functional capacity, can also be helped by use of computer programs. Homology analysis starting with known sequences from lectins furnishes the initial indication of features common to parts of the sequence of lectins and proteins hitherto defined in terms of other domains. Such common sequences have been postulated for endogenous lectins and the lymphocyte IgE receptor,[157, 158] as well as the core protein of cartilage chondroitin sulfate.[159, 160] Since saccharides exhibit inhibitory effects in proliferation assays of hematopoietic stem cells dependent on the positive action of colony-stimulating factors, a homology analysis comparing sequences of these factors with lectin sequences may be limited to those lectins that function as potent inhibitors.[161] It reveals a striking homology at the hexapeptide level (Fig. 5). However, because of the lack of structural data based on X-ray analyses of protein crystals, the sugar-binding site in endogenous lectins is not adequately defined. Moreover, it might be constructed from peptide fragments which are not consecutive in the sequence. Such results of homology analysis are therefore in no way conclusive. Further information about the nature of the sugar-binding site, such as that provided by affinity labeling with photoactive sugar ligands,[163, 164] can help focus the search for sequence homologies on the relevant structural elements. Random homology fluctuations in other regions of the sequence could in this way be filtered out. In the future, computer analysis will increasingly contribute significantly to the search for structural receptors for sugars as a prerequisite for functional analysis.

Fig. 5. Sequence homologies of the granulocyte/macrophage colony-stimulating factor (A) and the multipotential colony-stimulating factor (B) with nine lectins (left, abbreviations given below). The sequence of the colony-stimulating factor (A and B) is shown nine times. Each of the two sequences was compared (using a computer program) with the sequence (not shown) of each of the nine lectins. The partial sequences of the two factors enclosed in boxes are significantly homologous with partial sequences of the lectins. These partial sequences of the lectins may be located at various sites of the molecule. No such homologies were found for some lectins. Noteworthy is the variable distribution of the homologous regions in the two factors. Abbreviations: HBP, hepatic β-galactoside-specific sugar-binding protein from rat; GALCH, β-galactoside-specific lectin from chicken; GALHU, human β-galactoside-specific lectin; GALBO, bovine β-galactoside-specific lectin; FLYLEC, β-galactoside-specific lectin from flies; RICIN B, DISCOI, PNA, β-galactoside-specific lectin from *Ricinus communis*, from the slime-mold *Dictyostelium discoideum*, and from peanuts, respectively; MANRAT, mannose-specific lectin from rat.

7. Perspectives

Does there exist a sugar-coding system involving endogenous lectins in biological recognition? This question has opened the way for ground-breaking efforts, which are likely to have a dramatic impact on future lectinology research. The resulting complex of questions includes clarification of the exact structure of receptor–ligand pairs in this system of biological recognition at both chemical and biochemical levels, as also clarification of their cellular localization and regulation at the cell-biological level. Efforts to solve these questions in the tumor model system can proceed parallel with clinical trials using lectin-based tumor diagnosis and therapy. A deepened understanding of the emerging significance of sugar–protein (lectin) interaction for growth regulation or for immune regulation—encouraged by initial data on the stimulation of cytokine release[165]—can enrich the modes of treatment available in oncological practice. The necessity for trustful interdisciplinary collaboration is both challenge and charm in this area at the intersection of carbohydrate chemistry, biochemistry, cell biology, and oncology.

I thank U. Rust for the intelligent care and great patience with which she typed the final manuscript. I am grateful to the Dr.-Mildred-Scheel-Stiftung für Krebsforschung for their financial support of the work of my research group.

Received: February 26, 1988 [A 690 IE]
German version: *Angew. Chem. 100* (1988) 1321
Translated by Dr. *Paul Debbage*, Munich

[1] H. Stillmark in R. Kobert (Ed.): *Arbeiten des Pharmakologischen Institutes zu Dorpat, Bd. 3*, Enke, Stuttgart 1889, p. 57 ff.
[2] P. Ehrlich, *Dtsch. Med. Wochenschr. 17* (1891) 976.
[3] P. Ehrlich, *Dtsch. Med. Wochenschr. 17* (1891) 1218.
[4] a) I. E. Liener, N. Sharon, I. J. Goldstein (Eds.): *The Lectins: Properties, Functions, and Applications in Biology and Medicine*, Academic Press, New York 1986; b) J. Kocourek in [4a], p. 1 ff.
[5] N. Sharon, H. Lis, *Trends Biochem. Sci. 12* (1987) 488.
[6] J. B. Sumner, S. F. Howell, *J. Bacteriol. 32* (1936) 227.
[7] K. O. Renkonen, *Ann. Med. Exp. Fenn. 26* (1948) 66.
[8] W. C. Boyd, R. M. Reguera, *J. Immunol. 62* (1949) 333.
[9] W. C. Boyd, E. Shapleigh, *Science (Washington) 119* (1954) 419.
[10] E. R. Gold, C. F. Phelps, *Z. Immunitaetsforsch. Exp. Klin. Immunol. 143* (1972) 430.
[11] I. J. Goldstein, R. C. Hughes, M. Monsigny, T. Osawa, N. Sharon, *Nature (London) 285* (1980) 66.
[12] G. Ashwell, J. Harford, *Annu. Rev. Biochem. 51* (1982) 531.
[13] S. H. Barondes, *Science (Washington) 223* (1984) 1259.

[14] J. Montreuil, *Adv. Carbohydr. Chem. Biochem. 37* (1980) 157.
[15] S. I. Hakomori, *Annu. Rev. Biochem. 50* (1981) 733.
[16] E. G. Berger, E. Buddecke, J. P. Kamerling, A. Kobata, J. C. Paulson, J. F. G. Vliegenthart, *Experientia 38* (1982) 1129.
[17] M. W. C. Hatton, L. März, E. Regoeczi, *Trends Biochem. Sci. 8* (1983) 287.
[18] N. Sharon, *Trends Biochem. Sci. 9* (1984) 198.
[19] R. Kornfeld, S. Kornfeld, *Annu. Rev. Biochem. 54* (1985) 631.
[20] J. F. G. Vliegenthart, L. Dorland, H. van Halbeek, *Adv. Carbohydr. Chem. Biochem. 41* (1983) 209.
[21] R. Schauer, *Adv. Carbohydr. Chem. Biochem. 40* (1982) 131.
[22] K. von Figura, A. Hasilik, *Annu. Rev. Biochem. 55* (1986) 167.
[23] G. Hortin, E. D. Green, J. U. Baenzinger, A. W. Strauss, *Biochem. J. 235* (1986) 407.
[24] S. Kornfeld, *FASEB J. 1* (1987) 462.
[25] J. R. Brisson, J. P. Carver, *Can. J. Biochem. Cell Biol. 61* (1983) 1067.
[26] S. W. Homans, R. A. Dwek, T. W. Rademacher, *Biochemistry 26* (1987) 6571.
[27] K. Olden, J. B. Parent, S. L. White, *Biochim. Biophys. Acta 650* (1982) 209.
[28] J. D. Aplin, R. C. Hughes, *Biochim. Biophys. Acta 694* (1982) 375.
[29] G. M. W. Cook, *J. Cell Sci. Suppl. 4* (1986) 45.
[30] B. K. Brandley, R. L. Schnaar, *J. Leukocyte Biol. 40* (1986) 97.
[31] H. J. Gabius, *IN VIVO 1* (1987) 75.
[32] L. A. Fransson, B. Havsmark, J. K. Sheehan, *J. Biol. Chem. 256* (1981) 13039.
[33] G. N. Misevic, J. Finne, M. M. Burger, *J. Biol. Chem. 262* (1987) 5870.
[34] E. G. Bremer, S. I. Hakomori, D. F. Bowen-Pope, E. Raines, R. Ross, *J. Biol. Chem. 259* (1984) 6818.
[35] D. A. Cheresh, R. Pytela, M. D. Pierschbacher, F. G. Klier, E. Ruoslahti, R. A. Reisfeld, *J. Cell Biol. 105* (1987) 1163.
[36] T. Feizi, R. A. Childs, *Biochem. J. 245* (1987) 1.
[37] P. L. Stern, *Br. Med. Bull. 40* (1984) 218.
[38] S. I. Hakomori, *Cancer Res. 45* (1985) 2405.
[39] T. Feizi, *Nature (London) 314* (1985) 53.
[40] T. Muramatsu, *J. Cell Biochem. 36* (1988) 1.
[41] V. Künemund, F. B. Jungwala, G. Fischer, D. K. H. Chou, G. Keilhauer, M. Schachner, *J. Cell Biol. 106* (1988) 213.
[42] R. H. Yolken, R. Willoughby, S. B. Wee, R. Miskuff, S. Vonderfecht, *J. Clin. Invest. 79* (1987) 148.
[43] B. Kalvelage, G. Koch, *Eur. J. Cell Biol. 28* (1982) 238.
[44] A. G. Darvill, P. Albersheim, *Annu. Rev. Plant Physiol. 35* (1984) 243.
[45] R. J. Wieser, F. Oesch, *J. Cell Biol. 103* (1986) 361.
[46] J. M. Bird, S. J. Kimber, *Dev. Biol. 104* (1984) 449.
[47] B. A. Fenderson, U. Zahavi, S. I. Hakomori, *J. Exp. Med. 160* (1984) 1591.
[48] S. Rastan, S. J. Thorpe, P. Scudder, S. Brown, H. C. Gooi, T. Feizi, *J. Embryol. Exp. Morphol. 87* (1985) 115.
[49] G. V. Avvakumov, O. A. Strelchyonok, *Biochim. Biophys. Acta 938* (1988) 1.
[50] F. O. Calvo, R. J. Ryan, *Biochemistry 24* (1985) 1953.
[51] P. Stanley, *Trends Genet. 3* (1987) 77.
[52] H. Debray, D. Decout, G. Strecker, G. Spik, J. Montreuil, *Eur. J. Biochem. 117* (1981) 41.
[53] J. T. Gallagher, *Biosci. Rep. 4* (1984) 621.
[54] I. J. Goldstein, R. D. Poretz in [4a], p. 33ff.
[55] E. Köttgen, *Klin. Wochenschr. 55* (1977) 359.
[56] R. Lotan, G. L. Nicolson, *Biochim. Biophys. Acta 559* (1979) 329.
[57] J. P. McCoy, *BioTechniques 4* (1986) 252.
[58] H. Lis, N. Sharon, *Annu. Rev. Biochem. 55* (1986) 35.
[59] T. Osawa, T. Tsuji, *Annu. Rev. Biochem. 56* (1987) 21.
[60] H. J. Gabius, K. Vehmeyer, S. Gabius, G. A. Nagel, *Blut 56* (1988) 147.
[61] G. L. Nicolson, *Int. Rev. Cytol. 39* (1974) 89.
[62] P. L. Mann, C. M. Swartz, R. O. Kelley, *Mech. Ageing Dev. 38* (1987) 219.
[63] A. J. C. Leathem, N. J. Atkins in G. R. Bullock, P. Petrusz (Eds.): *Techniques in Immunocytochemistry, Vol. 2,* Academic Press, London 1983, p. 39ff.
[64] I. Damjanov, *Lab. Invest. 57* (1987) 5.
[65] J. Caselitz, *Curr. Top. Pathol. 77* (1988) 245.
[66] H. Rüdiger, *BioScience 34* (1984) 95.
[67] M. E. Etzler, *Annu. Rev. Plant Physiol. 36* (1985) 209.
[68] Y. Endo, K. Tsurugi, *J. Biol. Chem. 262* (1987) 8128.
[69] G. Uhlenbruck, *Naturwissenschaften 68* (1981) 606.
[70] E. S. Vitetta, R. J. Fulton, R. D. May, M. Till, J. W. Uhr, *Science (Washington) 238* (1987) 1098.
[71] H. J. Gabius, S. Gabius, K. Vehmeyer, A. Schauer, G. A. Nagel, *Onkologie 10* (1987) 184.
[72] a) H. J. Gabius, G. A. Nagel (Eds.): *Lectins and Glycoconjugates in Oncology*, Springer, Berlin 1988, in press; b) H. J. Gabius, G. A. Nagel in [72a], p. 1ff.
[73] K. Mann, R. Lamerz in H. J. Schmoll, H. D. Peters, O. Fink (Eds.): *Kompendium internistische Onkologie*, Springer, Berlin 1987, p. 473ff.
[74] W. F. Goebel, O. T. Avery, *J. Exp. Med. 50* (1929) 521.
[75] J. J. Marshall, *Trends Biochem. Sci. 3* (1978) 79.
[76] C. P. Stowell, Y. C. Lee, *Adv. Carbohydr. Chem. Biochem. 37* (1980) 225.
[77] N. Iberg, R. Flückiger, *J. Biol. Chem. 261* (1986) 13542.
[78] S. P. Wolff, R. T. Dean, *Biochem. J. 249* (1988) 618.
[79] H. Paulsen, *Chem. Soc. Rev. 13* (1984) 15.
[80] H. Kunz, *Angew. Chem. 99* (1987) 297; *Angew. Chem. Int. Ed. Engl. 26* (1987) 294.
[81] H. Towbin, G. Rosenfelder, J. Wieslander, J. L. Avila, M. Rojas, A. Szarfman, K. Esser, H. Nowack, R. Timpl, *J. Exp. Med. 166* (1987) 419.
[82] S. Kusunoki, J. E. Craft, B. Roach, J. A. Hardin, R. K. Yu, *Arch. Biochem. Biophys. 255* (1987) 226.
[83] H. J. Gabius, S. Bodanowitz, A. Schauer, *Cancer 61* (1988) 1125.
[84] K. Kayser, H. J. Gabius in [72a], p. 131ff.
[85] K. Kayser, H. J. Gabius, T. Ciesiolka, W. Ebert, S. Bach, submitted for publication.
[86] A. Bardosi, T. Dimitri, H. J. Gabius, *Acta Neuropathol. 76* (1988) 55.
[87] A. Bardosi, T. Dimitri, H. J. Gabius in [72a], p. 143.
[88] H. J. Gabius, R. Engelhardt, K. P. Hellmann, T. Hellmann, A. Ochsenfarth, *Anal. Biochem. 165* (1987) 349.
[89] M. J. Krantz, N. A. Holtzman, C. P. Stowell, Y. C. Lee, *Biochemistry 15* (1976) 3963.
[90] D. T. Connolly, R. R. Townsend, K. Kawaguchi, W. R. Bell, Y. C. Lee, *J. Biol. Chem. 257* (1982) 939.
[91] Y. C. Lee, R. R. Townsend, M. R. Hardy, J. Lönnegren, J. Arnarp, M. Haraldsson, H. Lönn, *J. Biol. Chem. 258* (1983) 199.
[92] R. Iozzo, *Lab. Invest. 53* (1985) 373.
[93] L. A. Fransson, I. Carlstedt, L. Cöster, A. Malmström, *Ciba Found. Symp. 124* (1986) 125.
[94] P. L. Debbage, W. Lange, T. Hellmann, H. J. Gabius, *J. Histochem. Cytochem.* (1988), in press.
[95] C. Kieda, M. Monsigny, *Invasion Metastasis 6* (1986) 347.
[96] H. J. Gabius, K. P. Hellmann, C. Bokemeyer, M. Andreeff, submitted for publication.
[97] a) E. N. Spremulli, D. L. Dexter, *J. Clin. Oncol. 1* (1983) 496; b) F. von der Haar, H. J. Gabius, F. Cramer, *Angew. Chem. 93* (1981) 250; *Angew. Chem. Int. Ed. Engl. 20* (1981) 217.
[98] M. Monsigny, A. C. Roche, P. Midoux, *Biol. Cell 51* (1984) 187.
[99] H. J. Gabius, K. Vehmeyer, *Naturwissenschaften 74* (1987) 37.
[100] H. J. Gabius, C. Bokemeyer, T. Hellmann, H. J. Schmoll, *J. Cancer Res. Clin. Oncol. 113* (1987) 126.
[101] H. J. Gabius, R. Engelhardt, T. Hellmann, P. Midoux, M. Monsigny, G. A. Nagel, K. Vehmeyer, *Anticancer Res. 7* (1987) 109.
[102] H. J. Gabius, *Ann. N. Y. Acad. Sci. 507* (1987) 337.
[103] B. C. F. Chu, C. C. Fan, S. B. Howell, *J. Natl. Cancer Inst. 66* (1981) 121.
[104] S. M. Lippmann, J. F. Kessler, F. L. Meyskens, *Cancer Treat. Rep. 71* (1987) 391.
[105] T. J. Dougherty, *CRC Crit. Rev. Hematol./Oncol. 2* (1984) 83.
[106] S. Kojima, H. J. Gabius, *J. Cancer Res. Clin. Oncol.*, in press.
[107] M. J. Poznansky, R. L. Juliano, *Pharmacol. Rev. 36* (1984) 277.
[108] H. Sezaki, M. Hashida, *CRC Crit. Rev. Therap. Drug Carrier Syst. 1* (1987) 1.
[109] M. R. Mauk, R. C. Gamble, J. D. Baldeschwieler, *Proc. Natl. Acad. Sci. USA 77* (1980) 4430.
[110] M. M. Ponpipom, R. L. Bugianesi, T. Y. Shen, *Can. J. Chem. 58* (1980) 214.
[111] J. L. Bodmer, R. T. Dean, *Methods Enzymol. 112* (1985) 298.
[112] A. C. Roche, P. Bailly, M. Monsigny, *Invasion Metastasis 5* (1985) 218.
[113] M. Monsigny, C. Kieda, A. C. Roche, *Biol. Cell. 47* (1983) 95.
[114] R. L. Schnaar, *Anal. Biochem. 143* (1984) 1.
[115] H. J. Gabius, R. Engelhardt, F. Cramer, *Anticancer Res. 6* (1986) 573.
[116] H. J. Gabius, R. Engelhardt, *J. Chromatogr. 391* (1987) 452.
[117] H. J. Gabius, R. Engelhardt, S. Rehm, F. Cramer, *J. Natl. Cancer Inst. 73* (1984) 1349.
[118] H. J. Gabius, R. Engelhardt, F. Cramer, R. Bätge, G. A. Nagel, *Cancer Res. 45* (1985) 253.
[119] H. J. Gabius, R. Engelhardt, D. J. Sartoris, F. Cramer, *Cancer Lett. 31* (1986) 139.
[120] H. J. Gabius, R. Engelhardt, F. Cramer, *Carbohydr. Res. 164* (1987) 33.
[121] H. J. Gabius, R. Engelhardt, *Tumour Biol. 9* (1988) 21.
[122] H. J. Gabius, R. Engelhardt, J. Casper, D. Reile, S. Schumacher, H. J. Schmoll, G. Graupner, F. Cramer, *Tumour Biol. 6* (1985) 145.
[123] H. J. Gabius, R. Engelhardt, J. Casper, H. J. Schmoll, G. A. Nagel, F. Cramer, *Tumour Biol. 6* (1985) 471.
[124] H. J. Gabius, *Cancer Invest. 5* (1987) 39.

[125] H. J. Gabius, R. Engelhardt, S. Rehm, F. Deerberg, F. Cramer, *Tumour Biol. 7* (1986) 71.
[126] H. J. Gabius, K. Vehmeyer, R. Engelhardt, G. A. Nagel, F. Cramer, *Cell Tissue Res. 241* (1985) 9.
[127] H. J. Gabius, P. L. Debbage, R. Engelhardt, R. Osmers, W. Lange, *Eur. J. Cell Biol. 44* (1987) 265.
[128] H. J. Gabius, R. Brehler, A. Schauer, F. Cramer, *Virchows Arch. B: Cell Pathol. 52* (1986) 107.
[129] H. J. Gabius, R. Engelhardt, S. Rehm, S. H. Barondes, F. Cramer, *Cancer J. 1* (1986) 19.
[130] H. J. Allen, C. Karakousis, M. S. Piver, M. Gamarra, H. Nava, B. Forsyth, B. Matecki, A. Jazayeri, D. Sucato, E. Kisailus, R. DiCioccio, *Tumour Biol. 8* (1987) 218.
[131] H. J. Gabius, K. Vehmeyer, *Biochem. Cell. Biol.*, in press.
[132] G. L. Nicolson, *Biochim. Biophys. Acta 695* (1982) 113.
[133] V. Schirrmacher, *Adv. Cancer Res. 43* (1985) 1.
[134] L. Weiss, F. W. Orr, K. V. Honn, *FASEB J. 2* (1988) 12.
[135] H. J. Gabius, K. Vehmeyer, R. Engelhardt, G. A. Nagel, F. Cramer, *Cell Tissue Res. 246* (1986) 515.
[136] A. Raz, L. Meromsky, I. Zvibel, R. Lotan, *Int. J. Cancer 39* (1987) 353.
[137] H. J. Gabius, G. Bandlow, V. Schirrmacher, G. A. Nagel, K. Vehmeyer, *Int. J. Cancer 39* (1987) 643.
[138] H. J. Gabius, R. Engelhardt, G. Graupner, F. Cramer in T. C. Bog-Hansen, E. van Driessche (Eds.): *Lectins, Vol. 5*, de Gruyter, Berlin 1986, p. 237 ff.
[139] L. Meromsky, R. Lotan, A. Raz, *Cancer Res. 46* (1986) 5270.
[140] R. Joubert, M. Caron, M. A. Deugnier, F. Rioux, M. Sensenbrenner, J. C. Bisconte, *Cell. Mol. Biol. 31* (1985) 131.
[141] S. R. Carding, S. J. Thorpe, R. Thorpe, T. Feizi, *Biochem. Biophys. Res. Commun. 127* (1985) 680.
[142] R. Lotan, D. Lotan, A. Raz, *Cancer Res. 45* (1985) 4349.
[143] G. Uhlenbruck, *Immunol. Comm. 10* (1981) 251.
[144] G. Uhlenbruck, H. J. Beuth, K. Oette, T. Schotten, H. L. Ko, K. Roszkowski, W. Roszkowski, R. Lütticken, G. Pulverer, *Dtsch. Med. Wochenschr. 111* (1986) 991.
[145] F. Ashall, *Trends Biochem. Sci. 11* (1986) 518.
[146] G. Uhlenbruck, *Funkt. Biol. Med. 2* (1983) 40.
[147] H. D. Klenk, *Forum Mikrobiol. 9* (1986) 20.
[148] N. Sharon, *FEBS Lett. 217* (1987) 145.
[149] H. J. Gabius, W. R. Springer, S. H. Barondes, *Cell 42* (1985) 449.
[150] S. H. Barondes in [4a], p. 467 ff.
[151] K. Drickamer, M. S. Dordal, L. Reynolds, *J. Biol. Chem. 261* (1986) 6878.
[152] D. O. Morgan, J. C. Edman, D. N. Standring, V. A. Fried, M. C. Smith, R. A. Roth, W. H. Rutter, *Nature (London) 329* (1987) 301.
[153] L. K. Thompson, P. M. Horowitz, K. L. Bentley, D. D. Thomas, J. F. Alderete, R. J. Klebe, *J. Biol. Chem. 261* (1986) 5209.
[154] M. Ozawa, M. Sato, T. Muramatsu, *J. Biochem. 94* (1983) 479.
[155] T. K. Gartner, *Semin. Thromb. Hemostasis 13* (1987) 281.
[156] G. J. Cole, A. Loewy, L. Glaser, *Nature (London) 320* (1986) 445.
[157] K. Ikuta, M. Takami, C. W. Kim, T. Honjo, T. Miyoshi, Y. Tagayo, T. Kawabe, J. Yodoi, *Proc. Natl. Acad. Sci. USA 84* (1987) 819.
[158] C. Lüdin, H. Hofstetter, M. Sarfati, C. A. Levy, U. Suter, D. Alaimo, E. Kilchherr, H. Frost, G. Delespesse, *EMBO J. 6* (1987) 109.
[159] K. Doege, P. Fernandez, J. R. Hassell, M. Sasaki, Y. Yamada, *J. Biol. Chem. 261* (1986) 8108.
[160] T. Krusius, K. R. Gehlsen, E. Ruoslahti, *J. Biol. Chem. 262* (1987) 13120.
[161] K. Vehmeyer, W. Brandt, G. A. Nagel, H. J. Gabius, *Life Sci.*, in press.
[162] F. A. Quiocho, *Annu. Rev. Biochem. 55* (1986) 287.
[163] R. T. Lee, Y. C. Lee, *Biochemistry 26* (1987) 6320.
[164] R. E. Kohnken, E. A. Berger, *Biochemistry 26* (1987) 8727.
[165] K. Vehmeyer, T. Hajto, H. J. Gabius in [72a], p. 207 ff.

New Transition Metal Clusters with Ligands from Main Groups Five and Six

By Dieter Fenske,* Johannes Ohmer, Johannes Hachgenei, and Kurt Merzweiler

Dedicated to Professor Hans Bock on the occasion of his 60th birthday

In both physics and chemistry, increased attention is being paid to metal clusters. One reason for this attitude is furnished by the surprising results that have been obtained from studies of the preparation, structural characterization and physical and chemical properties of the clusters. Whereas investigations of cluster reactivity are at present generally limited to three- or four-membered clusters, successful syntheses of clusters with many more metal atoms have recently been designed. These substances occupy an intermediate position between solid state chemistry and the chemistry of metal complexes. This review presents a versatile method for synthesizing metal clusters: the reaction of complexes of transition metal halides with silylated compounds such as $E(SiMe_3)_2$ (E = S, Se, Te) and $E'R(SiMe_3)_2$ (R = Ph, Me, Et; E' = P, As, Sb). Although some of the compounds thus formed have already been prepared by other routes, the method affords ready access to both small and large transition metal clusters with unusual structures and valence electron concentrations; a variety of reactions in the ligand sphere are also possible.

1. Introduction

In the widest sense, a cluster is an aggregate of molecules or atoms. Many of these clusters contain metal atom groups M_n in which the metals are chemically bonded to each other. Although it is not always easy to decide whether metal-metal bonds are present, the comparison with bonding in pure metals is often made.

Metal clusters occur in discrete molecules or in units bridged by ligands. Although "isolated" clusters, lacking the protective ligand sphere, are known, the stability of aggregates of metal atoms is generally dependent on the number and type of ligands surrounding the metal framework.[1,2] As examples, consider the many known "molecular clusters" that involve CO, Cp and halide ligands.

In order to define the concept "cluster" more precisely, such compounds, consisting of an M_n cluster and ligands bound to it, are termed "metal cluster complexes". These substances have been the subject of an extraordinarily large number of studies and have been reviewed many times.[3] This review concerns itself essentially with our research since 1984.

Our interest in cluster chemistry arose from the question whether it would be possible to synthesize polynuclear complexes with phosphino derivatives of maleic anhydride as ligands, e.g. 2,3-bis(diphenylphosphino)maleic anhydride (PP). These ligands exhibit very low redox potentials;[4] as a consequence, their reaction with transition metal complexes can lead to mononuclear complexes in which (PP) is coordinated to the metal as a radical anion.[5,6] Examples of such products are:

$[(PP)^{\ominus}Co^{\oplus}(CO)_3]$ $[(PP)^{\ominus}Mn^{\oplus}(CO)_4]$ $[(PP)_2^{\ominus}M]$, $M = Pd^{2\oplus}, Pt^{2\oplus}$

Would similar electron transfer from metal to (PP) be possible in transition metal clusters containing (PP) ligands? If so, it should be possible to prepare clusters with unusual valence electron concentrations.

There are several potential routes to such compounds. The reactions of $[(PP)MCl_2]$ (M = Pd, Pt) with $[M(PPh_3)_4]$ lead to diamagnetic or paramagnetic dinuclear complexes.[7,8] We also attempted to obtain PPh-bridged complexes by the reaction of $[(PP)MCl_2]$ (M = transition metal) with $PPh(SiMe_3)_2$.

Although it has been known for years that silylated phosphanes react with transition metal halides to form polymeric products, surprisingly few authors have pursued this reaction type.[9] In contrast, a considerable number of reactions of silylated phosphanes with halides of main group elements are known, leading to products containing bonds from phosphorus to the main group element.[10] *Schäfer* et al. were able to show that this synthetic principle could be extended to transition metal halides, and they obtained a wide variety of phosphido-transition metal complexes, four- or six-membered rings bearing P functions, and also diphosphene and diphosphorus complexes of Ni and Pt.[11-13]

Correspondingly, $[(PP)NiCl_2]$ [(PP) = 2,3-bis(diphenylphosphino)-*N*-methylmaleimide)] reacts with $E'Ph(SiMe_3)_2$ (E' = P, As), forming complexes of $(PPh)_2$ or $(AsPh)_2$.[14] The formation of $(E'Ph)_2$ units bound to Ni is promoted by the migration of the $SiMe_3$ groups to the CO of maleimide. Attempts to prepare heteroatomic clusters from these complexes and $[\{MoCp(CO)_3\}_2]$ led instead to a compound of the composition $[\{MoCp(CO)_2(PPh)\}_2]$.[15]

These results show that (PP) complexes of $NiCl_2$ can react with $PPh(SiMe_3)_2$, substituting the Cl ligands. The synthesis of polynuclear metal complexes is however not observed. We therefore decided to investigate whether PR_3 complexes of transition metal halides could react with $PR(SiMe_3)_2$ to form compounds with PR bridges.

[*] Prof. Dr. D. Fenske, Dr. J. Ohmer, Dr. J. Hachgenei, Dr. K. Merzweiler
Institut für Anorganische Chemie der Universität
Niederurseler Hang, D-6000 Frankfurt am Main 50 (FRG)

2. Clusters with E'R and E' Bridging Ligands

2.1. E' = P

Cluster compounds with ligands E'R (E' = P, As) can be prepared by various methods, e.g. the reaction of $E'RH_2$ or $E'RCl_2$ with carbonylmetals forming μ_3- or μ_4-E'R-bridged clusters.[16] We discovered a new method, the reaction of $[MCl_2(PPh_3)_2]$ (M = Co, Ni) with $PR(SiMe_3)_2$.[17] The reaction between $[CoCl_2(PPh_3)_2]$ or $[NiCl_2(PPh_3)_2]$ and $PPh(SiMe_3)_2$ in THF leads to the μ_3- or μ_4-PPh-bridged clusters **1** and **2**, respectively.[17] If $NiCl_2$, which is sparingly soluble in THF, is allowed to react with PPh_3 and $PPh(SiMe_3)_2$, a different product, the oxygen-sensitive complex **3**, is obtained; it is also formed by the reaction of **2** with an excess of $PPh(SiMe_3)_2$. Without PPh_3, the reaction of $NiCl_2$ with $PPh(SiMe_3)_2$ leads to insoluble polymeric products of unknown structure.[9] The high selectivity of the reactions is reflected in yields of **1**, **2**, and **3** of up to 90%.

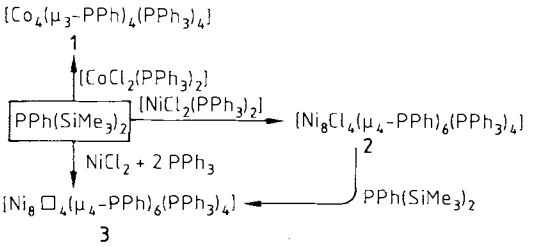

Only clusters of cobalt and nickel have so far proved accessible via the reaction between $[MCl_n(PPh_3)_m]$ and $PPh(SiMe_3)_2$. The analogous reactions with $[FeCl_3(PPh_3)_2]$, $[MCl_2(PPh_3)_2]$ (M = Cu, Hg) and $[MCl(PPh_3)]$ (M = Hg, Ag, Au) lead respectively to complexes of $Fe^{2\oplus}$ and $Cu^{\oplus}$ or metallic Hg, Ag and Au. The reactions with Rh, Pd and Pt complexes have not been explored.

It can be seen that **1** (Fig. 1) consists of a tetrahedral Co_4 cluster whose four tetrahedral faces are coordinated by μ_3-PPh ligands. Each Co atom is additionally bound to the P atom of a PPh_3 ligand. The bonding parameters observed in **1** (T_d symmetry, Co-Co 256(1) pm) are in good agreement with those in a large number of known heterocubane clusters.[18]

1, which is diamagnetic, can be reversibly oxidized to $\mathbf{1}^{\ominus}$ and $\mathbf{1}^{2\oplus}$ in THF solution.[19] Consistent with this observation, **1** is oxidized by $CHCl_3$, CCl_4 or $C_2H_4Cl_2$ to $\mathbf{1}^{\oplus}Cl^{\ominus}$. **1** also reacts with CH_3COCl at temperatures above 330 K to form the paramagnetic $\mathbf{1}^{\oplus}[CoCl_3(PPh_3)]^{\ominus}$ ($\mu_{eff} = 4.55\,\mu B$ at 300 K).

2 (Fig. 1) consists of an almost regular Ni_8 cube (Ni-Ni 259–262 pm, Ni-Ni-Ni 89.6–90.3°) whose Ni atoms are coordinated alternately by PPh_3 and Cl ligands. Each face is capped by a μ_4-PPh ligand. The structure of **2** is thus comparable with $[Ni_8(CO)_8(\mu_4\text{-}PPh)_6]$, which had already been described by *Dahl* et al.[20]

The structure of **3** (Fig. 1) is similar to that of **2**. However, the Ni_8 cube in **3** is highly distorted, with Ni-Ni-Ni bond angles between 79.2 and 100.1°; this is reflected in the differing coordination of Ni1, Ni3, Ni6, Ni7 (distorted tetrahedral coordination by the P atoms of one PPh_3 and three μ_4-PPh ligands) and Ni2, Ni4, Ni5, Ni8 (coordinated only to three P atoms of the μ_4-PPh ligands).

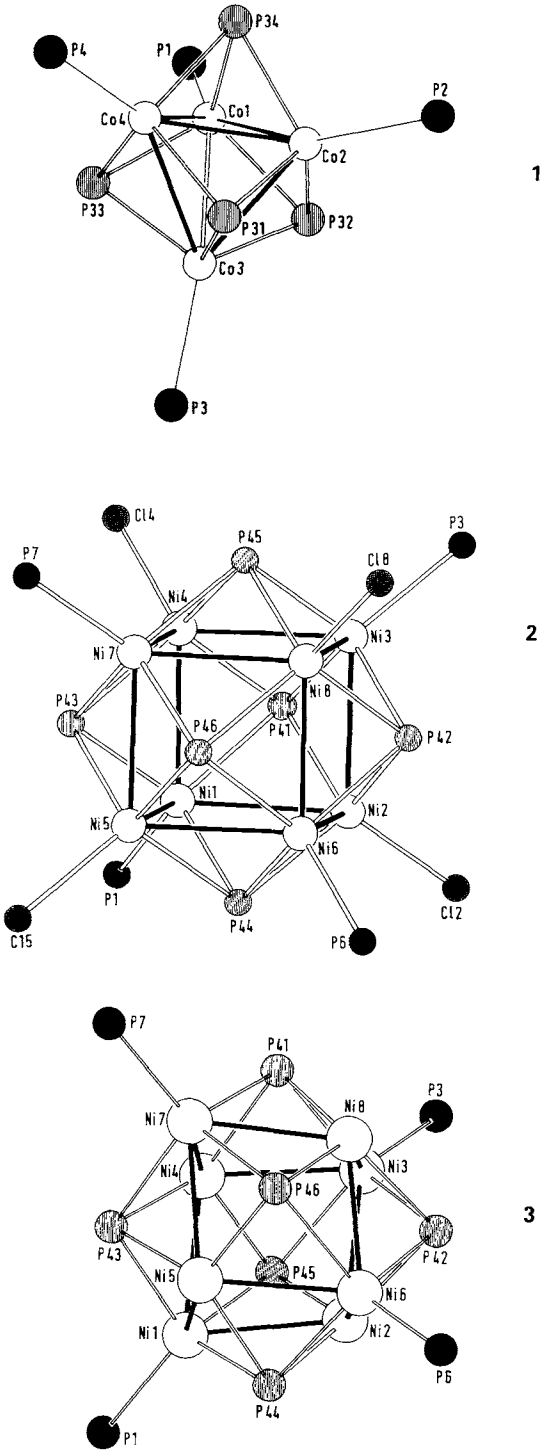

Fig. 1. Molecular structures of the clusters **1**, **2** and **3** (phenyl groups omitted). In **1**, P1–P4 and P31–P34 are the P atoms of the PPh_3 and μ_3-PPh ligands respectively. In **2** and **3**, P1–P7 and P41–P46 are the P atoms of the PPh_3 and μ_4-PPh ligands, respectively.

The usual electron counting rules indicate that Ni2, Ni4, Ni5, Ni8 are associated with 16 valence electrons, Ni1, Ni3, Ni6, Ni7 with 18. One consequence of this electron deficit may be the shortening of the face diagonals between the 16e Ni atoms to 323–325 pm and the lengthening of the distances between the 18e Ni atoms to 384–398 pm.

3 is unexpectedly stable. One reason for this may be the steric screening of the four coordinatively unsaturated Ni atoms (Ni2, Ni4, Ni5, Ni8) by six phenyl groups of the PPh_3 and PPh ligands. This crown-shaped arrangement leads to four identical free coordination sites in the molecule, with diameters restricted to 400–500 pm. Figure 2 demonstrates this for the free coordination site at Ni5 by means of a space-filling model. Further coordination of these four Ni atoms by PPh_3 ligands is no longer possible because of the steric shielding of these atoms.

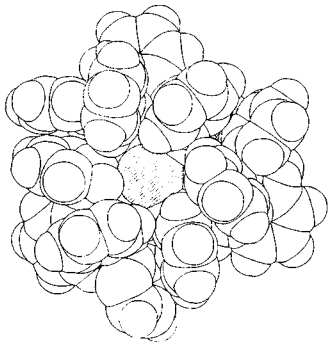

Fig. 2. Space-filling model showing a free coordination site (□) at atom Ni5 (shaded) of 3.

2.1.1. *Reactions of the Complexes 2 and 3*

Although the number of structurally characterized clusters is now immense, the study of their reactivity has mostly been limited to smaller clusters.[21] *Huttner* et al., for example, were able to show that trinuclear, μ_3-E'R-bridged carbonylmetal clusters (E' = N, P, As, Sb, Bi) are suitable for kinetic mechanistic studies.[22] The peripheral ligands of such clusters are susceptible to exchange by addition and subsequent elimination.

It is notable that the Ni_8-clusters 2 and 3 are also suitable for studies of substitution and addition reactions at the ligand periphery. The Cl ligands of 2 can be substituted, and neutral molecules can be added to the free coordination sites of 3. Scheme 1 summarizes the reactions carried out so far.

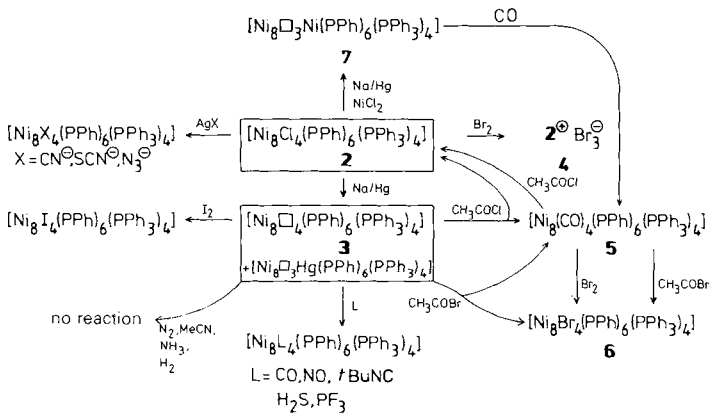

Scheme 1. Reactions leading to derivatives of the Ni_8 clusters.

The stability of the Ni_8 cluster framework is also illustrated by the reaction of 2 with concentrated methanolic solutions of bromine to form $2^{\oplus}Br_3^{\ominus}$ (4).

With sodium amalgam, 2 forms the coordinatively unsaturated 3. If the same reaction is carried out in the presence of solid $NiCl_2$, however, a "naked" nickel atom (presumably arising from reduction of $Ni^{2\oplus}$) is introduced into a free coordination site of 3, forming the Ni_9 cluster 7. Whereas all the vacant coordination sites in 3 display an identical form, the unoccupied sites of 7 have decreased in diameter. As a consequence, no further Ni atoms can be introduced.

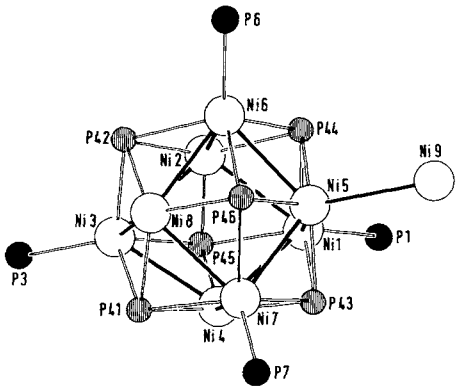

7

Fig. 3. The molecular structure of 7 (phenyl groups omitted). P41–P46 and P1–P7 represent the P atoms of the μ_4-PPh and PPh_3 ligands respectively.

The structure determination of 7 (Fig. 3) shows that the bond lengths in the Ni_8 cube are comparable to those in 3. The bond length Ni5–Ni9, 268.2 pm, lies in the range of Ni–Ni single bonds. Since Ni9 is not bound to any other ligands, only its steric screening by the six phenyl groups can be responsible for the stability of 7. The long Ni···C(Ph) contacts of 326–380 pm make interactions with the π systems improbable.

It is however possible that weak bonding interactions to three phenyl protons are involved, leading to a distorted tetrahedral coordination at Ni9 (Ni···H 247–294 pm). An NMR investigation of this hypothesis is not feasible because of the paramagnetism of 7.

By reaction of 2 with Na-amalgam we have, in the meantime, been able to isolate (besides 3) a complex which is isostructural with 7 and in which one free coordination site is occupied by an Hg atom (see Scheme 1).

Attempts to incorporate Pd, Pt and Au atoms into the free coordination site led to as yet unidentified products. The unusually large unit cells (35000–55000 $Å^3$) imply the presence of very large clusters. Other ligands (e.g. $CN^{\ominus}$, $SCN^{\ominus}$, $N_3^{\ominus}$) can be attached to the cluster by the reaction of the corresponding silver salts with 2. The alternation of PPh_3 and the newly introduced ligands is maintained, which indicates the lack of mobility of the PPh_3 groups.

The coordinatively unsaturated 3 also serves as starting material for a variety of reactions (Scheme 1). It reacts with CH_3COCl to form a mixture of 2 and 5 (Fig. 4). A possible intermediate in this reaction is an acyl complex that decomposes to form 5. 5 can also be obtained by the reaction of 7 with CO. The bromo-substituted cluster 6 is formed in the reaction of 5 with CH_3COBr.

It can further be seen from Scheme 1 that the vacant coordination sites of 3 can be occupied by ligands such as CO, *t*BuNC, H_2S, and PF_3. However, no reaction is observed with MeCN, NH_3, or H_2; no evidence for coordina-

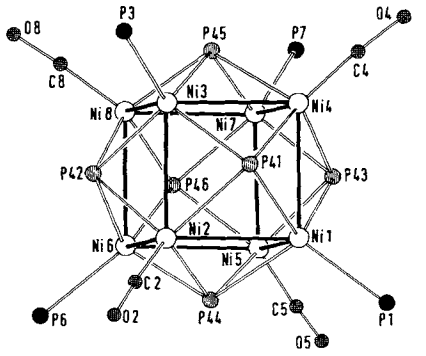

5

Fig. 4. The structure of **5** (phenyl groups omitted). P41-P46 and P1-P7 represent the P atoms of PPh and PPh_3 ligands respectively.

tion of these molecules could be found in the solid state. Finally, N_2 does not coordinate to **3**, even under a pressure of 150 bar.

2.1.2. *Structural, Spectroscopic and Magnetic Properties of Ni_8 Clusters*

A meaningful description of bonding in clusters presupposes an understanding of the relationships between structure, physical and chemical properties, and the number of valence electrons. The structural and chemical diversity of clusters has however militated against the development of a general bonding theory. There are, though, several models that can be applied with varying degrees of success; amongst these are the 18-electron rule, Wade's rules, semi-empirical MO calculations, the topological electron counting rules of *Teo* and *Mingos*, and the isolobality principle of *Hoffmann*.[23-27]

The 18-electron rule would imply a valence electron count of 120 for clusters of cubic shape; this condition is fulfilled by e.g. $[Ni_8(CO)_8(PPh)_6]$.[20] Our cluster compounds, however, often display appreciable deviations from this criterion; if PPh_3 and $Cl^{\ominus}$ are considered 2e donors and μ_4-PPh a 4e donor, **2** and **3** contain 116 and 112 valence electrons respectively.

Table 1. Valence electron count VE and Ni-Ni, Ni-P bond lengths in $[Ni_8X_4(PPh)_6(PPh_3)_4]$.

Compound	X	VE $e^{\ominus}$	for Ni-Ni bonds	Ni-Ni [pm]	Ni-P [pm] PPh_3	Ni-P [pm] PPh
3	—	112	16	251-254	221	212-216 224-228
4	Cl	115	19	256-260	222-224	220-224
2	Cl	116	20	259-262	224-225	220-222
6	Br			259-262	224-225	220-222
5	CO	120	24	265-269	226-229	218-222

Table 1 demonstrates that the Ni-Ni bond lengths are crucially influenced by the electron count. Surprisingly, the Ni-Ni bonds are shorter when fewer electrons are available for Ni-Ni bonding. The Ni-P bonds are less sensitive in this respect.

The magnetic properties of the Ni_8 clusters are also impossible to rationalize on the basis of simple assumptions. Magnetic susceptibility measurements can however provide information as to possible coupling of electrons in the cluster. *Holm* et al. carried out such measurements some years ago for clusters of the type $[Fe_4(\mu_3\text{-}S)_4(SPh)_4]^{n\ominus}$ $(n = 2, 3)$.[28]

As would be expected, **5** (120 valence electrons) is diamagnetic and **4** (115 valence electrons) paramagnetic. It is less easy to understand the paramagnetism of **3** (112 valence electrons), **2**, and **6** (each 116 valence electrons). For instance, a temperature-dependent magnetic moment is observed for **2**: $\mu_{eff}(T) = 2.37\,\mu B$ (300 K), 2.48 (200 K), 2.54 (100 K), 2.44 (25 K), 1.86 (10 K), and 0.94 (4 K). This could be rationalized if **2** contains Ni atoms in different oxidation states $(4\,Ni^0 + 4\,Ni^{\oplus})$, the magnetic properties then corresponding to an antiferromagnetic coupling of the d^9 $(Ni^{\oplus})$ centers.

Transition metal clusters undergo reversible redox processes without altering their metal framework.[29] The clusters **2** to **6** can also be reversibly oxidized and reduced. This result is consistent with the large deviations from the 18e rule that are tolerated by **2**-**6**.

The characterization of paramagnetic clusters by NMR methods is generally difficult, because very broad signals are often observed. It is thus all the more surprising that the ^{1}H-NMR spectrum of **2** displays sharp, strongly temperature-dependent resonances. The paramagnetism causes different isotropic shifts of the phenyl protons of the μ_4-PPh and PPh_3 ligands, enabling the *o*-, *m*-, and *p*-protons to be clearly distinguished. The following shifts are observed in $CDCl_3$ in the temperature range 323-213 K: PPh_3: *o*-H 3.15-0.93, *m*-H 10.60-12.75, *p*-H 3.37-1.27; PPh: *o*-H 6.82-6.01, *m*-H 6.93-7.20, *p*-H 5.59-5.22 ppm. A plot of the shifts against temperature shows that the dependence obeys Curie's law.[30]

^{31}P-NMR spectra show resonance signals only for diamagnetic derivatives. The observed chemical shifts of $\delta =$ 0-20 for PR_3 and 620-640 ppm for μ_4-PPh ligands (in THF) lie in the expected ranges.[31]

The IR spectra of the compounds **2**-**7** are almost identical, except in the range 1500-2000 cm^{-1}, and have no diagnostic value.

2.2. E′ = As; Arsenic-Bridged Clusters

Attempts to extend the above synthetic principle to the reaction of $[MCl_2(PPh_3)_2]$ and $AsPh(SiMe_3)_2$ yield no evidence for the formation of complexes with bridging AsPh ligands; the reaction of $[FeCl_2(PPh_3)_2]$ with $AsPh(SiMe_3)_2$, for instance, leads only to Fe, $(AsPh)_n$, and Me_3SiCl. The reaction between $[CoCl_2(PPh_3)_2]$ and $AsPh(SiMe_3)_2$, however, leads to (apart from a little metallic cobalt) a cluster of composition $[Co_4As_6(PPh_3)_4]$ (**8**),[32] which is paramagnetic. **8** is formed in 95% yield. A crystal structure analysis (Fig. 5) reveals a Co_4 tetrahedron whose faces are capped by three μ_3-As and one μ_3-As_3 ligand. Each Co atom is additionally coordinated by one PPh_3 group.

8 (56 valence electrons) may be derived from a heterocubane cluster $[Co_4(\mu_3\text{-}As)_4(PPh_3)_4]$ in which one μ_3-As has been replaced by a μ_3-As_3 unit. Alternatively, it can be considered as a Co_3As_3 octahedron linked through one face (Co2) with a $CoAs_3$ unit. The previously known complexes of E_3' (E′ = P, As) are generally considered to be derivatives of the tetrahedral P_4 or As_4, where As or P

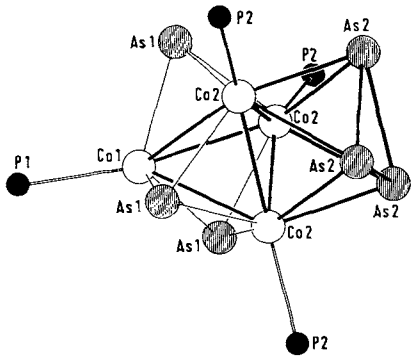

8

Fig. 5. Molecular structure of **8** (phenyl groups omitted). As2 represent the μ_3As_3 ligand, P1 and P2 the P atoms of the PPh_3 ligands, and As1 the μ_3As ligands. **8** displays a crystallographic threefold symmetry.

atoms have been replaced by isolobal transition metal fragments.[33,34]

The As–As bond length within the As_3 unit (246.3 pm) is comparable with the As–As distances in As_4, $(AsPh)_6$, and $[(triphos)CoAs_3Co(triphos)]^{2\oplus}$ and is only about 10 pm longer than the As–As distance in the As_3 complexes $[As_3Co(CO)_3]$ and $[MoCpAs_3(CO)_2]$[34,35]

The formation of **8** is surprising, because it occurs at room temperature and involves the breaking of the As–C(Ph) bond. However, examples of the instability of As–C bonds have been known for a long time.[36]

Recent results confirm that $[NiCl_2(PPh_3)_2]$ also reacts with $AsPh(SiMe_3)_2$, breaking the As–C(Ph) bonds and forming As-bridged complexes. In THF the cluster **9** can be isolated.[37]

$[Ni_9Cl_3(\mu_4\text{-}As)_6(PPh_3)_5]$ **9**

Figure 6 shows that the metal atom framework of **9** consists of an Ni_8 cube, in the center of which a further Ni atom is situated. The faces of the Ni_8 cube are capped by six μ_4-As ligands, and the Ni atoms are coordinated either by $Cl^{\ominus}$ (*Ni2*, *Ni4*, *Ni8*) or PPh_3 (Ni1, Ni3, *Ni5*, *Ni6*, Ni7).

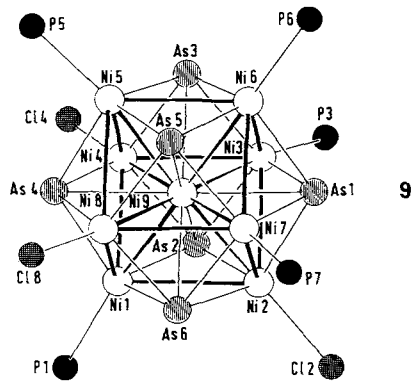

9

Fig. 6. Molecular structure of **9** (phenyl groups omitted). P1–P7 represent the P atoms of the PPh_3 ligands.

9, with 121 valence electrons, has one electron fewer than would be predicted by the 18e rule. An electron counting rule for centered metal clusters has been proposed by *Mingos*;[26a] the number of valence electrons in close-packed metal clusters should be $(12n_s + \Delta_i)$, where n_s is the number of peripheral metal atoms and Δ_i is 18 or 24 for centered cubic polyhedra. On this basis, **9** should possess 114 or 120 valence electrons.

Within the Ni_8 cube, the Ni–Ni bond lengths (277–285 pm for Ni1 to Ni8) are 40–50 pm longer than those to the central atom Ni9 (238–248 pm). In contrast, the bond lengths from the peripheral Ni atoms to the μ_4-As atoms (230–234 pm) are 30 pm shorter than the Ni9–As bonds (261–264 pm). The centered cubic cluster **9** can, like the $[Au_9(PPh_3)_8]^{\oplus}$ ion and the Rh_{14} core of the $[Rh_{14}(CO)_{25}]^{4\ominus}$ ion, be considered as a fragment of a larger centered cluster.[38,39]

Preliminary results indicate that the reaction of $[NiCl_2(PR_3)_2]$ with $AsPh(SiMe_3)_2$ can also lead to clusters with more metal atoms, formed by condensation of centered cubic clusters via common faces.

9 is interesting for another reason: analogously to **2**, it possesses three reactive Ni–Cl bonds. By breaking these bonds, it is possible to synthesize a coordinatively unsaturated complex similar to **3**. The vacant coordination sites thus formed are larger (because the μ_4-As ligands are smaller than μ_4-PPh) and thus can accommodate larger ligands.

3. S- and Se-Bridged Cluster Complexes of Cobalt and Nickel with PR_3 Ligands

The existence of the coordinatively unsaturated cluster **3** prompts the consideration whether it is possible to synthesize clusters with larger vacant coordination sites. Since these sites arise as a consequence of a steric screening of the metal atoms by peripheral ligands, several possible synthetic routes suggest themselves:

1. Substitution of PPh_3 ligands by PR_3: The reaction of $[NiCl_2(PR_3)_2]$ with $PPh(SiMe_3)_2$ leads for R = Me, Et to diphosphene complexes or clusters of unknown structure; for $R = C_4H_9$, *cyclo*-C_6H_{11}, clusters $[Ni_8\square_4(PPh)_6(PR_3)_4]$ are obtained, with properties analogous to those of **3**.

2. Substitution of PPh_3 by $E'Ph_3$ (E' = As, Sb): $[NiCl_2(E'Ph_3)_2]$ also reacts with $PPh(SiMe_3)_2$ to form clusters of the type $[Ni_8\square_4(PPh)_6(E'Ph_3)_4]$.

3. Replacement of the μ_4-PPh by μ_4-PR (R = *t*Bu, Me): The reaction of $[NiCl_2(PPh_3)_2]$ with $PR(SiMe_3)_2$ leads to complexes of unknown structure.

4. Substitution of μ_4-PPh by the less sterically demanding ligands S and Se: The compounds $E(SiMe_3)_2$ (E = S, Se, Te) react with derivatives of transition metal halides, in a manner analogous to the cleavage of the E–Si bond in $PPh(SiMe_3)_2$, to form S-, Se- and Te-substituted clusters. Although many methods are known for the synthesis of clusters with chalcogen ligands, the use of silylated chalcogenides offers easy access to transition metal clusters.[40–42]

We have so far studied the reactions of PR_3 complexes of the following metal halides with $E(SiMe_3)_2$: $MnCl_2$, $FeCl_2$, $CoCl_2$, $NiCl_2$, $PdCl_2$, $PtCl_2$, $RhCl_3$, $CuCl_2$, $HgCl_2$, "$MoCl_2$", and W_2Cl_6.

Depending on the metal and its ligands, we obtained either binary chalcogenides (Mn, Fe, Cu, Hg) or mixtures of various cluster compounds, which could be separated by fractional crystallization. Clearly, the solubility products of the chalcogenides and the stability constants of the clusters play an important role.

The IR spectra of these substances are dominated by the bands of the tertiary PR_3 ligands and are thus all practically identical. NMR spectra are difficult to obtain because of the sparing solubility and easy oxidation of the clusters in chlorinated hydrocarbons such as CH_2Cl_2 or $CHCl_3$. The information content of the spectra is anyway very limited. The identification of the products is generally dependent on crystal structure analyses.

Schemes 2 and 3 summarize the cluster products that are formed in the reactions of $E(SiMe_3)_2$ (E = S, Se) with various Co and Ni complexes. By-products such as elemental Co or Ni, CoE or NiE and EPR_3 (E = S, Se; R = *n*Bu, *t*Bu, Ph) are not shown.

The following factors exert critical influence on the nature of the products:

1. The ratio M : E : PR_3.

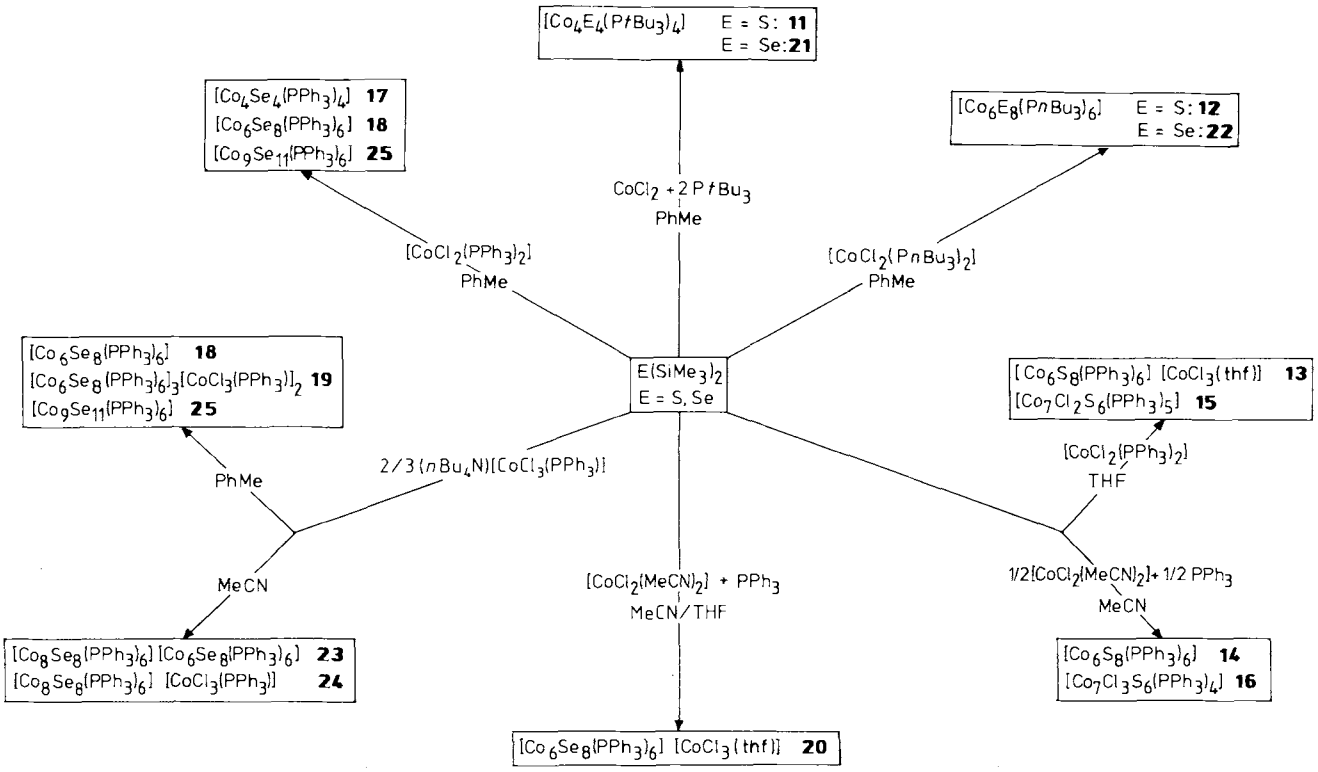

Scheme 2. Preparative reactions for chalcogen-bridged Co clusters.

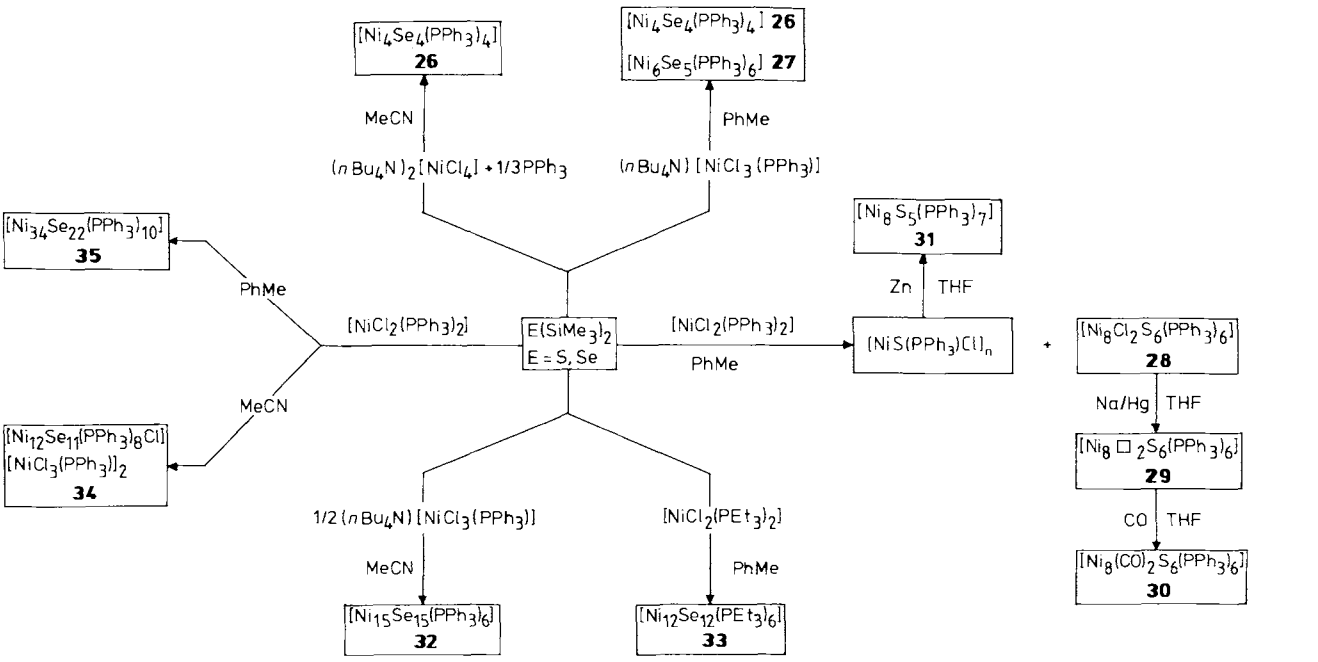

Scheme 3. Preparative reactions for chalcogen-bridged Ni clusters.

2. The solvent. The following have been used: toluene, MeCN, THF and low-melting (m.p. < 400 K) salt mixtures.

3. Conditions for crystal growth. The solubility of the products is decisively influenced by the R substituents of the PR_3 ligands. Whereas species with PPh_3-, $PtBu_3$- and $P(C_6H_{11})_3$-ligands are almost insoluble in all common solvents, the PEt_3- and $PnBu_3$-derivatives are soluble even in unpolar solvents such as heptane or ether. This initially surprising observation should enable a better control of the solubility of cluster products, and ought to make possible the spectroscopic and cyclovoltammetric studies of high molecularity clusters. It should however be stressed that mixtures of various clusters are often formed, the separation of which becomes more problematic with increasing cluster size.

The following discussion of the structures of various products is arranged according to the number of metal atoms.

3.1. M_3 and M_4 Clusters

No binuclear complexes can be isolated from the reaction between $[MCl_2(PR_3)_2]$ (M = Co, Ni) with $E(SiMe_3)_2$. The smallest cluster that we have been able to prepare so far, albeit in low yields, is the trinuclear complex $[Ni_3Cl_2S_2(PPh_3)_4]$ **10** (Fig. 7a).

In contrast, in reaction (a) with the bidentate ligand the M_3 cluster is formed in high yields. As in **10** is consists of an Ni_3 cluster in which the Ni_3 triangle (Ni-Ni 298; **10** 290–293 pm) is capped to two μ_3-Se ligands and additionally bonded to the P atoms of the bidentate phosphanes or to $Cl^{\ominus}$ and PPh_3 in **10**. $[Ni_3S_2(PEt_3)_6]^{2\oplus}$, obtained by the reaction of $[NiCl_2(PEt_3)_2]$ with H_2S, has a similar structure.[53]

$$[NiCl_2(Ph_2PCH_2CH_2PPh_2)] + Se(SiMe_3)_2 \longrightarrow [Ni_3Se_2(Ph_2PCH_2CH_2PPh_2)_3]Cl_2 \quad (a)$$

M_4E_4 heterocubane clusters (Fig. 7b) are prepared for example from $CoCl_2$, $PtBu_3$ and $E(SiMe_3)_2$ (**11** and **21**). The PPh_3-substituted compound **17**, analogous to **21**, however, is formed together with the Co_6 and Co_9 clusters **18** and **25**. The crystal structure analyses show that **11**, **17** and **21** (Fig. 7) consist of a Co_4 cluster with T_d symmetry, whose faces are capped by μ_3-S or μ_3-Se ligands. The PPh_3 ligands complete an irregular tetrahedral coordination of the metal atoms.[18,43,44]

The Co-Co bond lengths within these 60e Co_4E_4 clusters are, as would be expected, approximately equal, but they are 10–15 pm longer than in **1** (**11**: 270–272; **17**: 262–268; **21**: 264–270 pm). In contrast, in the 64e cluster **26** the four electrons in excess of the 60 electrons required by the 18e rule cause a splitting of the Ni-Ni bond lengths into four short (259–263 pm) and two long bonds (293.2, 279.1 pm). As a consequence, the Ni_4 framework is distorted towards a structure of approximately D_{2d} symmetry, as was predicted for 64e heterocubanes by *Dahl* et al.[45] Otherwise, **26** displays a structure similar to that of the Co_4 tetrahedra.

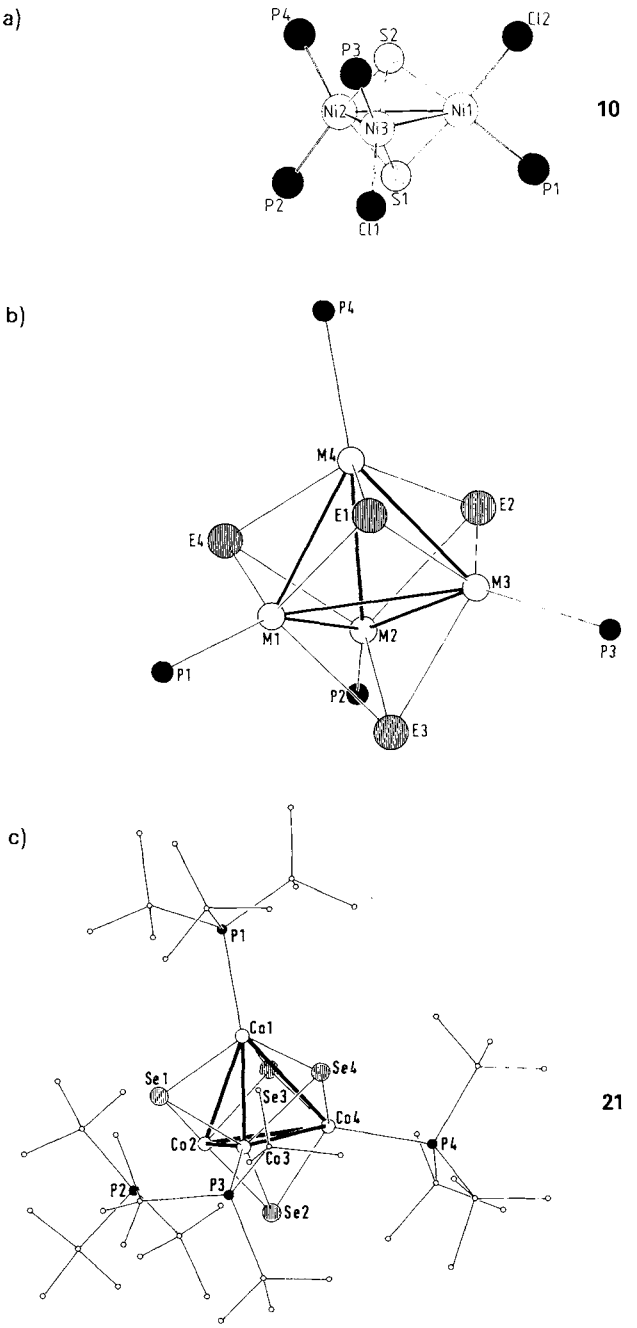

Fig. 7. a) Structure of **10** (P1–P4 are the P atoms of the PPh_3 ligands. b) Structure of the $[M_4E_4(PR_3)_4]$ framework (R groups omitted) in **11**, **17**, **21**, and **26**. c) Molecular structure of **21**.

3.2. M_6 Clusters

Not only **26** but also **27** can be isolated from the reaction of $(nBu_4N)[NiCl_3(PPh_3)]$ with $Se(SiMe_3)_2$ in toluene.[46] As can be seen from Figure 8b, **27** contains an Ni_6 prism, the faces of which are capped by two μ_3- and three μ_4-Se atoms. Each Ni atom is also coordinated by the P atom of a PPh_3 group. In the Ni_6 framework, the Ni-Ni bond lengths within the triangular faces (Ni 1,2,3 and Ni 4,5,6) are appreciably longer than those between these faces (273.0–279.8 compared to 260.2–266.3 pm). This distortion may be connected with the two electrons that the 92e cluster possesses in excess of the 90 electrons required by the 18e rule and the topological counting rules.[25]

A cluster of similar structure is the trigonal prismatic ion $[Pt_3(\mu_2\text{-}CO)_3(CO)_3]_2^{2\ominus}$,[47] although here the bonds of the Pt_3 faces (266 pm) are shorter than those between them (304 pm).

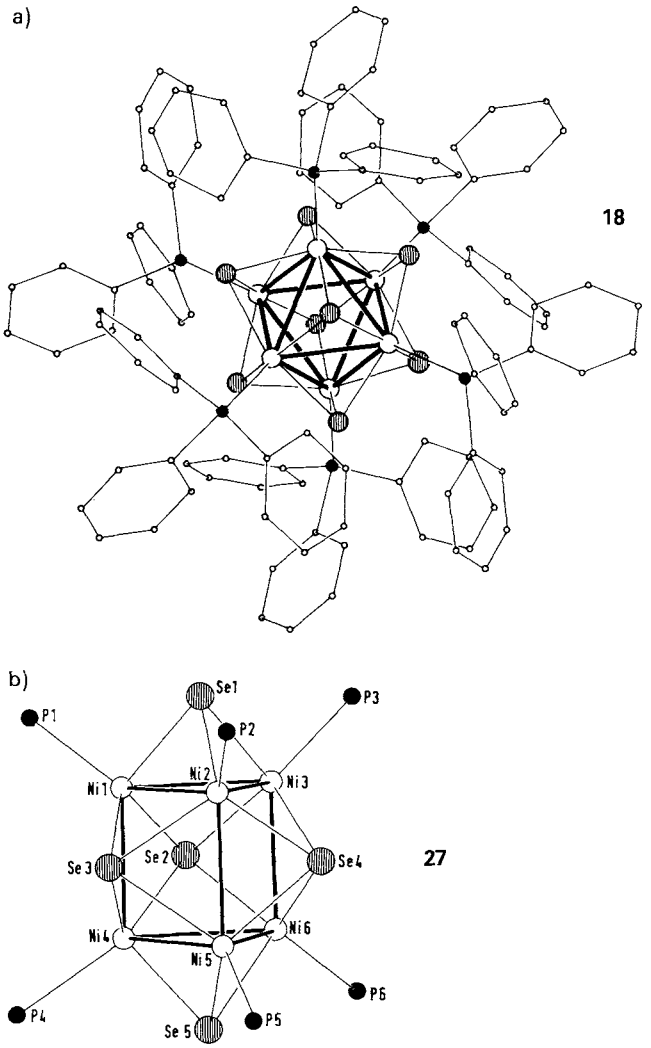

Fig. 8. a) Molecular structure of the $[Co_6E_8(PPh_3)_6]$ cluster as exemplified by **18**. b) Molecular structure of **27** (phenyl groups omitted).

We have also succeeded in preparing octahedral Co_6 clusters: the neutral compounds **12**, **14**, **18**, and **22** as well as the salts **13**, **19**, and **20**.

The basic structural principle in these compounds is illustrated in Figure 8a, using as an example **18**; an octahedron of Co atoms is capped at each triangular face by a μ_3-E ligand. The irregular tetrahedral coordination at each metal atom is completed by the P atom of a PPh_3 ligand. Table 2 compares selected bonding parameters of our Co_6 clusters[48,54] with those of the clusters $[Co_6S_8(PEt_3)_6]^{n\oplus}$ (n = 0, 1) prepared by *Cecconi* et al.[49] Four points emerge thereby:

1. All the 97e and 98e clusters possess 13 or 14 electrons more than would be expected from the 18e rule. Other electron counting rules, such as the topological rules of *Teo* et al. or *Mingos* et al.[25,26] are also unable to explain this excess of electrons. The long Co-Co distances (280–300 pm) are probably a consequence of the large number of valence electrons. Consistent with this view are the Co-Co contacts in the neutral complexes **12b**, **14**, and **18**, which are up to 10 pm longer than those in the monocations derived from them (cf., e.g., **18** and **19**). This observation implies that the one-electron oxidation of **12b**, **14**, and **18** involves the removal of the electron from an antibonding orbital. The symmetry of the clusters is unaffected by the change of valence electron number.

2. The Co-Co distances in the selenium-bridged Co octahedra **18** and **22** are appreciably longer than those in the analogous sulfur derivatives **14** and **12**. However, the nonbonding S-S or Se-Se contacts are about 50 pm less than the sum of the van der Waals' radii and could be considered weakly bonding. It is possible that the weakening of the Co-Co bonds is directly connected with the increasing interactions between the S (Se) ligands. An alternative description of all compounds in Table 2 is as cubic E_8 clusters (E = S, Se), whose E_4 faces are capped by six $Co(PPh_3)$ groups; accordingly, the Co atoms lie 42–50 pm above the E_8 cube faces. This value is clearly longer than in $[Mo_6Se_8]^{4\ominus}$ ($\pm$14.5 pm),[50] in which weak interactions between the Se ligands are also assumed to occur.

3. The PPh_3 substituted clusters display longer Co-Co bonds than the analogous derivatives with PEt_3 or $PnBu_3$ ligands.

4. The Co-E bond lengths are influenced neither by the cluster charge nor by the phosphane ligands. This implies that the bonding metal-chalcogen orbitals lie at lower energy than the Co-Co, Co-P, or E-E levels; i.e., the Co-E bonds should make an important contribution to the stability of the cluster framework.

3.3. M_7 Clusters

The reaction of $[CoCl_2(PPh_3)_2]$ or of $[CoCl_2(MeCN)_2]$ and PPh_3 with $S(SiMe_3)_2$ leads to the compounds **15** and **16**, the metal frameworks of which consist of Co_7 clusters (Fig. 9).[48]

Table 2. Averaged structural parameters for the series of isostructural clusters $[Co_6(n_3\text{-}E)_8(PR_3)_6]^{m\oplus}$ (E = S, Se; R = Et, *n*Bu, Ph; m = 0, 1).

	Co-Co [pm]	E-E [pm]	Co-E [pm]	Co-P [pm]	Co-(μ_3-E)-Co [°]	Deviation of the Co atoms from the E_4 plane [pm]
$[Co_6S_8(PEt_3)_6]^{\oplus}$	279.4	310.1	223.4	216.2	77.4	42–43
$[Co_6S_8(PEt_3)_6]$	281.7	309.5	223.3	213.8	78.2	45
$[Co_6S_8(PPh_3)_6]^{\oplus}$ in **13**	281.9	308.6	222.8	218.0	78.5	45
$[Co_6S_8(PPh_3)_6]$ **14**	287.5	308.2	223.8	216.8	80.3	49
$[Co_6S_8(PnBu_3)_6]$ **12**	281.5	309.4	223.5	213.5	78.0	45
$[Co_6Se_8(PnBu_3)_6]$ **22**	294.6	327.2	235.4	214.7	77.6	45
$[Co_6Se_8(PPh_3)_6]^{\oplus}$ in **19**	290.1	324.5	234.3	218.2	76.9	42–43
$[Co_6Se_8(PPh_3)_6]$ **18**	300.9	322.0	235.1	217.0	79.6	50

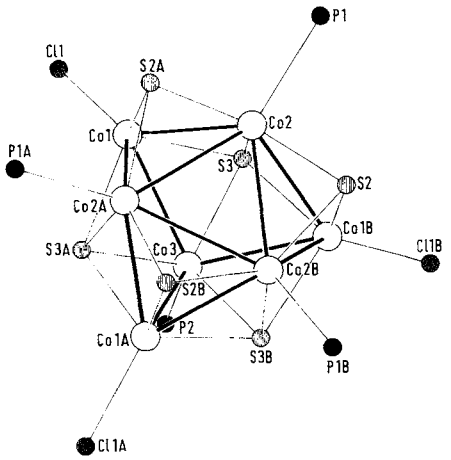

16

Fig. 9. Molecular structure of **16** (phenyl groups omitted). The threefold axis is collinear with the Co3–P2 bond.

The cluster structures central to **15** and **16** can be derived from a cube by the removal of one vertex. The resulting polyhedron is thus composed of three Co_4 and four Co_3 faces; except for the triangular face Co2–Co2A–Co2B, all faces are capped by μ_4-S or μ_3-S ligands. **15** and **16** differ in that **15** has two Cl atoms coordinated to the Co_7 cluster, **16** three; the remaining Co atoms are each bound to one PPh_3 group. There are nine short Co–Co bonds (**15**: 257.4–263.7 pm; **16**: 257.1–262.2 pm) and three longer contacts within the chalcogen-free triangular face (**15**: 289.7 pm, **16**: 283.4 pm). **16** is isostructural with $[Fe_7Cl_3S_6(PEt_3)_4]$, which was prepared by *Holm* et al., and may be considered as intermediate between prismatic and cuboctahedral geometry.[51] According to the 18e rule, the paramagnetic **15** (99e) has an electron deficit of 2 and the diamagnetic **16** (98e) of 3. This is reflected in the willingness of **15** and **16** to react with CO. With **15**, a compound of formula $[Co_7(CO)_3Cl_2S_6(PPh_3)_5]$ is formed. The CO addition presumably occurs at the triangular face not occupied by S.

3.4. M_8 Clusters

Like the μ_4-PPh-containing Ni_8 clusters **2**–**7**, (Sections 2.1 and 2.1.1) **28** contains a slightly distorted Ni_8 cube ($\bar{1}$ symmetry; Fig. 10). In contrast to **2**–**7**, however, all cube faces of **28** are capped by μ_4-S ligands, and six Ni atoms (Ni1, Ni2, Ni4, Ni1′, Ni2′, Ni4′) are each bound to a PPh_3 group. The other two Ni atoms (Ni3, Ni3′) are each bound to one Cl ligand.[48] The Ni–Ni bond lengths observed in the 118e cluster **28** (266–270 pm) lie within the range given in Table 1.

When **28** is reduced with Na/Hg in THF, **29** is formed, in which two Ni atoms (Ni3 and Ni3′) are now only bound to three μ_4-S ligands. The vacant coordination sites (□) thus formed are topologically similar to those of **3**; accordingly, **29** reacts with CO, forming **30**. The addition of larger molecules has not yet been attempted. Vacant coordination sites can also arise when **28** is treated with $AgPF_6$, and the salt $[Ni_8\square_2S_6(PPh_3)_6](PF_6)_2$ can be isolated.

The reaction of $[NiCl_2(PPh_3)_2]$ with $S(SiMe_3)_2$ in THF leads to formation of **28** and a compound $[NiSPPh_3Cl]_n$, of

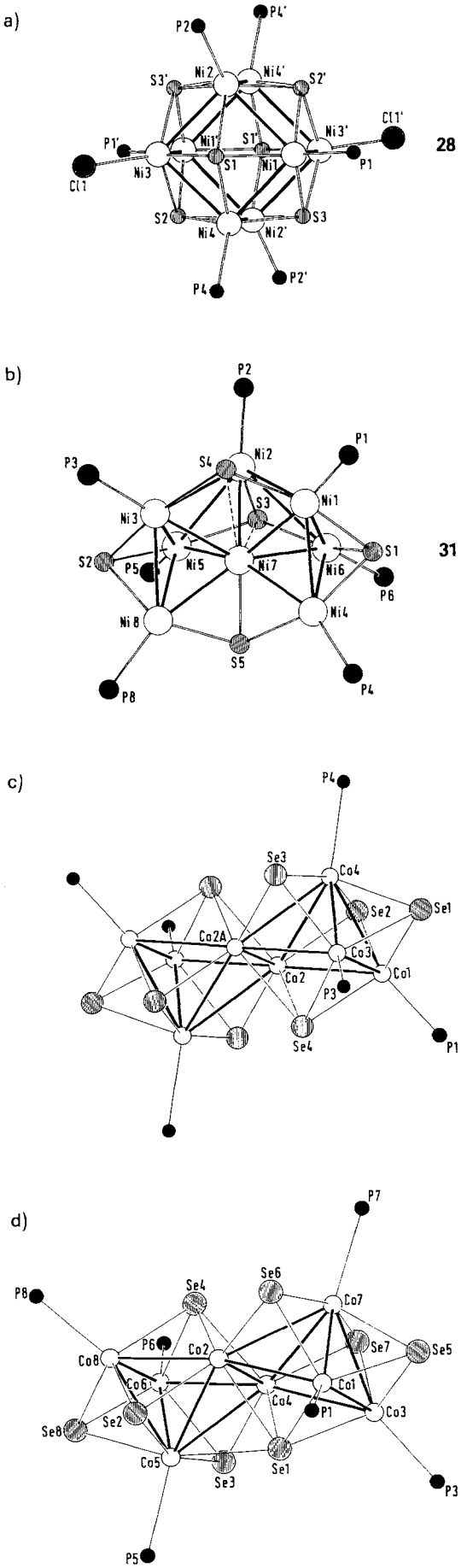

28

31

Fig. 10. Molecular structures of a) **28**, b) **31**, c) $[Co_8S_8(PPh_3)_6]^0$ in **23** and d) $[Co_8Se_8(PPh_3)_6]^{\oplus}$ in **24** (phenyl groups omitted).

unknown structure. The latter may be recrystallized from THF or acetone, but no single crystals have been obtained. If it is dehalogenated with Zn in THF, **31** is formed in 60% yield. Figure 10b shows this Ni_8 cluster, which consists of two trigonal bipyramids with a common edge. Apart from Ni7, all Ni atoms are bonded to a P atom of a PPh_3 ligand. Not all the faces of the polyhedron can be occupied by S atoms, because of the large size of the PPh_3 ligands. S1 and S2 are μ_3-ligands (Ni-S 211-217 pm); S5 can also be considered as a μ_3-ligand with unusual Ni-S-Ni bond angles (72.4-137.4°); S3 and S4 act as μ_4-ligands, if the weaker contacts to Ni7 are included, i.e. S3, S4 are μ_4 only when the S-Ni7 contacts are considered as bonds (Ni-S 213-219, but Ni7-S 258.6-268.8 pm). A description of the bonding in this 114e cluster is difficult because of the different Ni-Ni bond lengths (240-297 pm).[52,53,61]

The importance of the solvent is shown by the reaction of $(n\mathrm{Bu_4N})[CoCl_3(PPh_3)]$ with $Se(SiMe_3)_2$. In toluene, three products are obtained: **18**, discussed above (Section 3.2); a Co_9 cluster **25**, to be discussed below (Section 3.5); and the compound **19**. The crystal lattice of **19** contains both neutral and positively charged Co_6 polyhedra. The cationic and neutral species in the crystal cannot however be distinguished, because they are statistically distributed; the Co-Co distances in the Co_6 units are all equal and correspond to the average value of the metal-metal distances in the neutral **18** and in the ionic **20**.

If acetonitrile is used as solvent instead of toluene, the compounds **23** and **24** are obtained (Scheme 2). Crystals of **23** contain uncharged $[Co_8Se_8(PPh_3)_6]$ (Fig. 10c) and (octahedral) $[Co_6Se_8(PPh_3)_6]$ clusters. In contrast, **24** consists of the cations $[Co_8Se_8(PPh_3)_6]^{\oplus}$ (Fig. 10d) and the anions $[CoCl_3(PPh_3)]^{\ominus}$. Both Co_8 polyhedra consist of two square pyramids linked by a common edge and are mutually *trans*; their faces are capped by μ_3- or μ_4-Se ligands. The Co atoms of the pyramid bases (**23**: Co1, Co3, Co4; **24**: Co1, Co3, Co7, Co5, Co6, Co8) are bonded to PPh_3 ligands. Unlike the neutral **23**, the $[Co_8Se_8(PPh_3)_6]^{\oplus}$ cations of **24** do not possess an inversion center; the bases of the Co_5 square pyramids in **24** are thus no longer coplanar. This reduction of symmetry may have the following cause: the one-electron oxidation of the neutral **23** promotes the formation of an additional weak bond between Co5 and Se1 (258 pm) in **24**. The consequence is a mutual tilting of the Co_5 pyramids; the dihedral angle between the planes defined by Co1, Co2, Co3, Co4/Co2, Co4, Co6, Co8 in the cation of **24** is 12.5°. The association of this structural change with the loss of one electron in the oxidation of **23** to **24** is remarkable. However, the Co-Co bond lengths remain largely unaltered (244.2-279.5 pm in **23**, 247.3-279.4 pm in **24**), and are appreciably shorter than in **18**. This is consistent with the electron counts; in **18** the requirements of the 18e rule are exceeded by 14 electrons, whereas **23** (116e) and **24** (115e) approximately fulfill the predicted 114 valence electrons.

3.5. Clusters with Face-Sharing Co and Ni Octahedra

The condensation of octahedra via common vertices, edges or faces leads to cluster units of a type known since the end of the 1970's. Amongst these are the metal-rich subhalides of transition metals[55,56,58] and the Chevrel phases.[50,57,64] The preparation of $[Co_9Se_{11}(PPh_3)_6]$ (**25**) (Fig. 11a) makes clear that this structural principle can be extended to the more electron-rich transition metals.[44,46] All faces of the Co_9 cluster in **25** are capped by μ_3 or μ_4-Se ligands, and the Co atoms of the basal faces (Co1, Co4, Co9, Co6, Co7, Co8) are each additionally coordinated to one PPh_3 ligand. The Co-Co bond lengths are 271-298 pm; the shortest distances are found within the common triangular face (Co2, Co3, Co5). Clusters of similar structure are known in $[Ni_9S_9(PEt_3)_6]^{2\oplus}$ and $[Rh_9(CO)_{19}]^{2\ominus}$.[59,60] The condensation of two Co_6 octahedra clearly permits greater tolerance with respect to the valence electron count, because the 137e cluster **25** contains 17 valence electrons more than would be expected from the 18e rule.

The formation of **25** must proceed via smaller, reactive complexes. The two Co_8 clusters in **23** and **24** are tenable candidates for the precursors that are involved in the formation of the dioctahedral Co_9 cluster **25**; additional redox processes could cause the mutual tilting of the Co_5 pyramid bases to become so pronounced as to form a suitable cavity for the incorporation of a further Co atom.

Face-sharing metal atom octahedra are also observed in the Ni compounds **32** (Fig. 11b) and **33** (Fig. 11c) as well as in the dication of **34** (Fig. 11d) (see also Scheme 3). On the other hand, we have not yet succeeded in isolating a simple octahedral chalcogen-bridged Ni_6 cluster, although closely related compounds, e.g. $[Ni_3(\mu_2\text{-}CO)_3(CO)_3]_2^{2\ominus}$ are known.[47] Electronic factors are presumably responsible for this; a hypothetical "$[Ni_6Se_8(PPh_3)_6]$" would possess a total of 104 valence electrons. This would not only be 20 electrons more than expected from the 18e rule, but also six electrons more than in the analogous complex **18**, whose long Co···Co contacts (Table 2) already imply the occupation of antibonding orbitals.

The cluster dication of **34** consists of linked Ni_9Se_9 (Ni1-9, Se1-9) and Ni_3Se_2 (Ni10-12, Se10,11) units (Fig. 11d). These structural fragments were already known in the following complexes:[53,59,61]

$$[Ni_9S_9(PEt_3)_6]^{2\oplus} \quad [Ni_3Se_2(PEt_3)_6]^{2\ominus} \quad [Ni_3S_2Cp_3] \quad [Ni_3S_2Cl_2(PPh_3)_4] \quad (\mathbf{10})$$

The polyhedral faces of the dioctahedron in **34** are capped by μ_3-Se (Se1-3, Se7) and μ_4-Se (Se4-6) ligands. Se8 and Se9 are each bonded to three Ni atoms of the dioctahedron and also function as bridges to Ni11 and Ni10 respectively. The Ni-Ni bonds involving Ni9 are also relatively short (253-268 pm), whereas those within the cluster fragment Ni10-Ni11-Ni12 are rather long (283-311 pm). This might be related to weak Ni-Ni interactions between the atoms Ni10-12. The structural integrity of this Ni_3 triangle can therefore be ascribed primarily to the μ_4 and μ_3 ligands Se10 and Se11. The Se10-Se11 distance is very short (311 pm) and agrees well with the corresponding distance in the $[Ni_3Se_2(PEt_3)_6]^{2\oplus}$ cation.

Except for Ni4-6 and Ni9, all Ni atoms are coordinated by a P atom of a PPh_3 ligand, and Ni12 is additionally bonded to a Cl ligand. The topology of the Ni and Se atoms means that the cation of **23** must be regarded as an intermediate en route to more highly condensed clusters with *trans*-face-sharing metal atom octahedra. The Ni-Cl

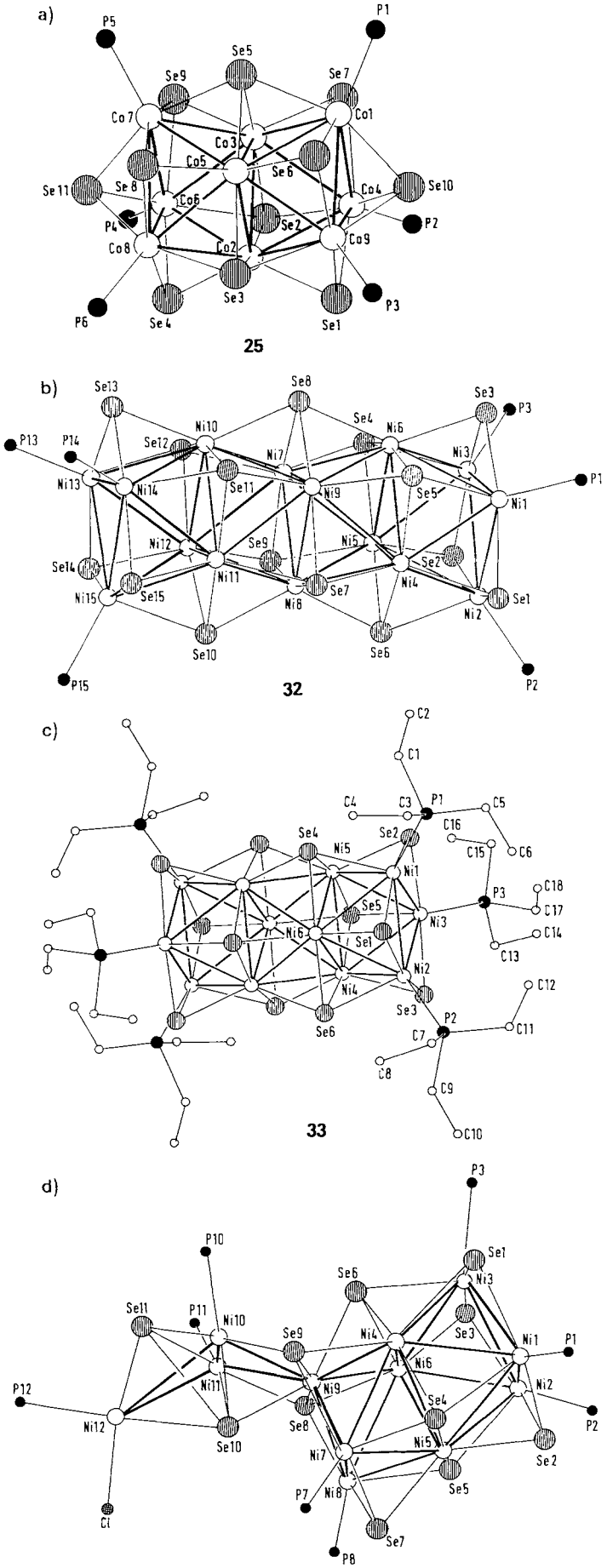

Fig. 11. Molecular structures of a) **25**, b) **32**, c) **33** and d) the dication of **34** (phenyl groups omitted in a, b and d).

bond is the reactive site of the molecule, where reaction with $Se(SiMe_3)_2$ and $[NiCl_2(PPh_3)_2]$ can promote further growth of the metal atom polyhedron.

Accordingly, **33** and **32** consist of three or four face-sharing, slightly distorted Ni_6 octahedra (Fig. 11b, c). Apart from the basal faces, all polyhedral faces of **33** and **32** are occupied by μ_3 or μ_4-Se ligands (Ni-Se: **33**, 232–244 pm; **32**, 231–249 pm). The Ni atoms of the basal faces are each bonded to a PPh_3 (**32**) or PEt_3 (**33**) group.

An alternative description of **32** and **33** is as a stacking of parallel layers (interlayer distance 216(3) pm, deviation from the plane ± 10 pm) composed of three Ni and three Se atoms. The Ni_3Se_3 planes are arranged according to an AB pattern of hexagonal close packing. (This description clearly also applies to the dioctahedra in **25** and **34**.) The Ni–Ni distances between the layers in **32**–**34** are shorter (**32**: 270–288, **33**: 272–278, **34**: 266–289 pm) than those within the Ni_3 layers (**32**: 288–301 pm, **33**: 288–297 pm, **34**: 268–313 pm). It is also observed that the Ni–Ni bonds in the outermost layers, viz. between those Ni atoms bonded to PR_3, are appreciably longer (292–301 pm) than those in the inner layers.

The structures of the Chevrel phases, such as $[Mo_{12}Se_{14}]^{2\ominus}$, $[Mo_{18}Se_{20}]^{4\ominus}$, $[Mo_{24}Se_{26}]^{6\ominus}$, or $[Mo_{30}Se_{32}]^{8\ominus}$, are governed by the same structural principle as the Ni clusters **32**–**34** and the Co compounds **18** and **25**.[57,62,63] With respect to their electron balance, however, there are considerable differences. For instance, the 222e cluster **33** and the 180e cluster **32** contain 24 and 30 electrons, respectively, more than the 18e rule would predict; in the Chevrel phases, the 18e rule is largely obeyed. Clearly, antibonding orbitals are increasingly occupied in **33** and **32**. The differences are illustrated quite distinctly by a comparison of the valence electron concentrations; whereas the Chevrel phases contain 3.33–4.33 electrons per metal atom, the Co and Ni clusters contain 6.17–6.78 or eight valence electrons per metal atom, respectively.[64]

We are certain that much larger clusters are also formed in the reactions we have described. Residues are often obtained, which from analytical results and general properties seem to possess very high molecular weights. However, the increasing insolubility makes characterization difficult. The composition of these compounds should correspond to the general formulas $[Co_{3n+3}E_{3n+5}(PR_3)_6]$ and $[Ni_{3n+3}E_{3n+3}(PR_3)_6]$ (E = S, Se; n is the number of condensed octahedra).

The valence electrons of the nickel compounds are subject to a simple counting rule: $3\times10+3\times4=42$ electrons for each Ni_3Se_3 unit plus 6×2 electrons for the terminal PPh_3 ligands.

3.6. $[Ni_{34}Se_{22}(PPh_3)_{10}]$, a Cluster with an Unusual Structure

$[Ni_{34}Se_{22}(PPh_3)_{10}]$ (**35**) crystallizes from the filtrate of the reaction of $[NiCl_2(PPh_3)_2]$ with $Se(SiMe_3)_2$. Whereas the structures of **25**, **32**, **33** and **34** can all be understood in terms of condensed octahedra, the $[Ni_{34}Se_{22}(PPh_3)_{10}]$ cluster **35** is governed by a previously unknown structural principle (Fig. 12a).[44]

The molecular structure of **35**, which possesses crystallographic $\bar{1}$ symmetry, contains a central Ni_{14} unit consisting of two staggered planar Ni_5 rings (Ni atoms shown as filled in circles in Fig. 12a) 448–456 pm apart with an Ni_4 plane (Ni9, Ni16, Ni9′, Ni16′) between them. Ni9 is disordered. The Ni_{34} polyhedron is then formally built up by adding five Ni_4 "butterfly" fragments to the pentagonal

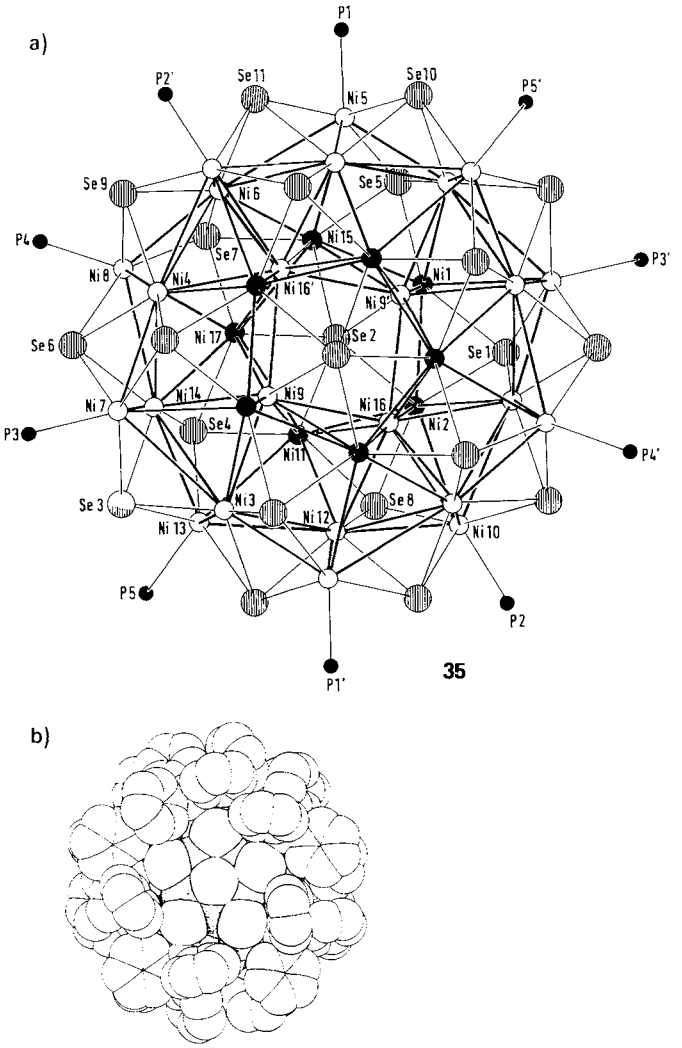

Fig. 12. a) Molecular structure of **35** (phenyl groups omitted). b) Space-filling model (H atoms omitted) of the structure of **35**. The free Ni cluster surface is the dark area.

antiprismatic Ni_{14} unit. The faces of the Ni_{34} unit are then finally capped by two μ_5-Se ligands over the Ni_5 rings and 20 μ_4-Se atoms (Ni-μ_4Se 226–246 pm, Ni-μ_5Se 236–246 pm). Additionally, ten peripheral Ni atoms (Ni5, Ni7, Ni8, Ni10, Ni13 and their symmetry equivalents) are each coordinated by one PPh_3 group. The space-filling model of **35** (Fig. 12b) demonstrates that in this way all the Ni atoms are effectively screened by the Se atoms and PPh_3 ligands.

An alternative description, which stresses the highly symmetric nature of **35**, is based on the fivefold symmetry and marked layer structure of the Ni_{34} polyhedron. The fivefold symmetry of the Ni_5 and Se_5 planes is only broken by the Ni_4 unit in the center of the cluster. This may be the reason for the disorder of Ni9 in this unit.

The cluster molecule has a diameter of about 3000 pm. The Ni–Ni distances in **35** lie in the range 236–312 pm. A description of the bonding in terms of the 18e rule is therefore impossible. **35** contains 448 valence electrons, which is in good agreement with the number predicted for M_n clusters ($n > 13$) on the basis of the Hume-Rothery rules for intermetallic phases (440–444e).[25] This shows that the properties of cluster complexes become closer to those of the metal as the number of metal atoms increases. However, it should not be forgotten that the structure of the Ni_{34} unit cannot be described in terms of principles derived from metals and intermetallic phases.

The formation of PPh_3Se is always observed in the synthesis of **35** and the compounds (except **33**) presented in Scheme 3. When large cluster molecules are formed, it may be the result of the reaction of smaller complexes with PPh_3, whereby capping μ-E ligands are extracted to form PPh_3E. The coordinatively unsaturated complexes thus generated can then react together to form metal-rich complexes.

One can only speculate about the mechanism of formation of such complex molecules. It is however a reasonable

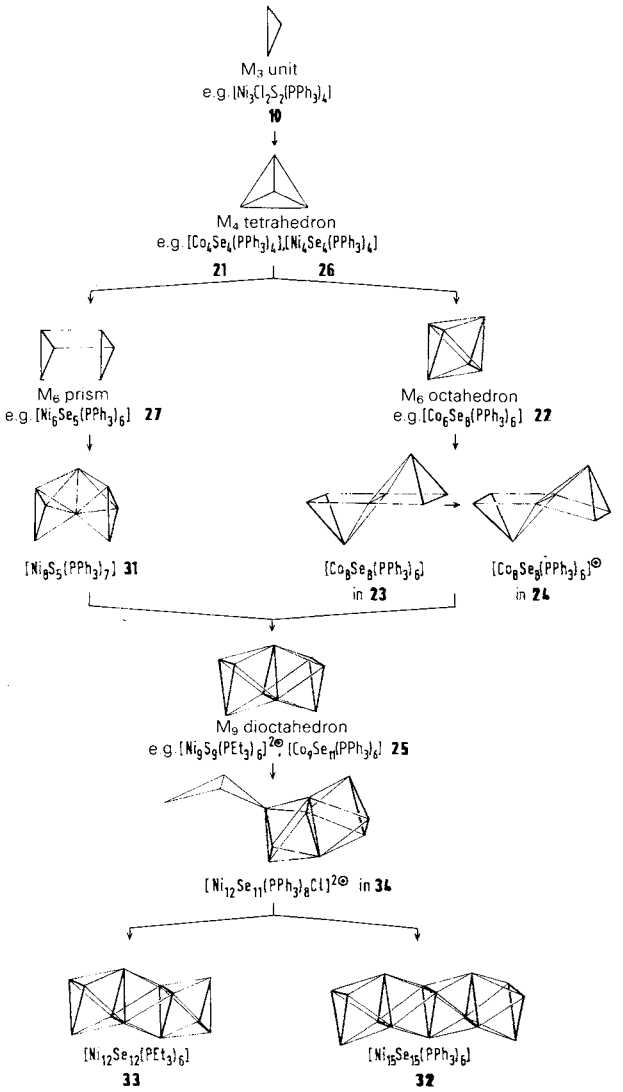

Fig. 13. Schematic representation of the metal atom frameworks of chalcogen-bridged Co and Ni clusters with terminal PR_3 ligands.

assumption that aggregation to more highly condensed compounds occurs via smaller fragments. It is not unlikely that M_3 units (M = Co, Ni) play a decisive role in our syntheses; the most direct evidence for this is the existence of **10** and of the $[Ni_3E_2(PEt_3)_6]^{2\oplus}$ cations (E = S, Se) prepared by *Cecconi* et al. It is notable that precisely such an Ni_3Se_2 unit is observed in **34**, directly linked to a "pre-condensed" group, an Ni_9 cluster (Fig. 11d) composed of three Ni_3 triangles. To demonstrate the structure-determining potential of the M_3 units, Figure 13 presents schematically the metal atom frameworks of the sulfur- and selenium-bridged Co and Ni clusters discussed here.

The starting point for this formal treatment is the M_3 unit present in **10**. The first step is the linking of this triangular unit with a fourth metal atom to form an M_4 tetrahedron (e.g. **21**, **26**). The addition of two further metal atoms leads either to a trigonal prismatic polyhedron, such as the Ni_6 prism **27**, or to an octahedron, a category to which the numerous Co_6 clusters belong. Another two-atom addition step, occurring between the two M_3 planes, leads from the Ni_6 prism to an Ni_8 polyhedron consisting of two edge-sharing trigonal bipyramids (e.g. **31**). For cobalt, this route arrives at the Co_8 clusters that are composed of two edge-sharing Co_5 square planar pyramids (e.g. **23** and **24**). The incorporation of yet another metal atom would then finally give the *trans*-face-sharing dioctahedron present in $[Ni_9S_9(PEt_3)_6]^{2\oplus}$[59] or in **25**. The stage has now been reached where three Ni_3 planes are stacked, although not exactly over each other. Further stacking processes lead via the Ni_{12} dication in **34** to the *trans*-face-sharing tri- or tetraoctahedra of **33** and **32**, respectively. The question whether the formation of **35** also proceeds via such units can probably only be answered after detailed mechanistic studies of the cluster growth.

4. Chalcogen-Bridged Transition Metal Clusters with η^5-Cyclopentadienyl, μ^3-Allyl and CO Ligands

As was shown in the preceeding chapter, tertiary phosphanes are capable of promoting the synthesis of clusters of electron-rich transition metals and simultaneously of suppressing the formation of metal pnictides or chalcogenides that is always observed in the reaction of phosphane complexes of cobalt or nickel chlorides with $E(SiMe_3)_2$ (E = PPh, AsPh, S, Se).

We have now extended the synthetic principles presented above to the preparation of polynuclear complexes with Cp, allyl, and CO ligands. Preliminary results involve the reactions of cyclopentadienyl, allyl, and CO complexes of the transition metal halides with $E(SiMe_3)_2$ (E = S, Se, Te); Me_3SiCl is eliminated and a series of novel compounds (Scheme 4) are formed, the molecular structures of which are reproduced in Figures 14–21.

4.1. Chalcogen-Bridged Clusters of Electron-Rich Transition Metals

The reaction between $[CpFe(CO)_2Br]$ and $Se(SiMe_3)_2$ produces a diamagnetic compound consisting of doubly negatively charged heterocubane clusters $[Fe_4Se_4Br_4]^{2\ominus}$ and $[Se\{Fe(CO)_2Cp\}_3]^{\oplus}$ ions. The structural parameters of the Fe_4Se_4 cage are essentially similar to those of other $[Fe_4E_4X_4]^{2\ominus}$ clusters (E = S, Se; X = Cl, SPh, Br, I) as investigated by many authors;[65,66] the Fe_4 tetrahedra display two short (276.2–278.7 pm) and four long (280.2–282.5 pm) Fe–Fe distances. The $[Se\{Fe(CO)_2Cp\}_3]^{\oplus}$ cation is isolobal with $(CH_3)_3Se^{\oplus}$; it possesses an Fe_3Se moiety shaped like a compressed pyramid, with no bonding contacts between the Fe atoms (Fe···Fe 400 pm). An identical cation was recently prepared by *Herrmann* et al.[67]

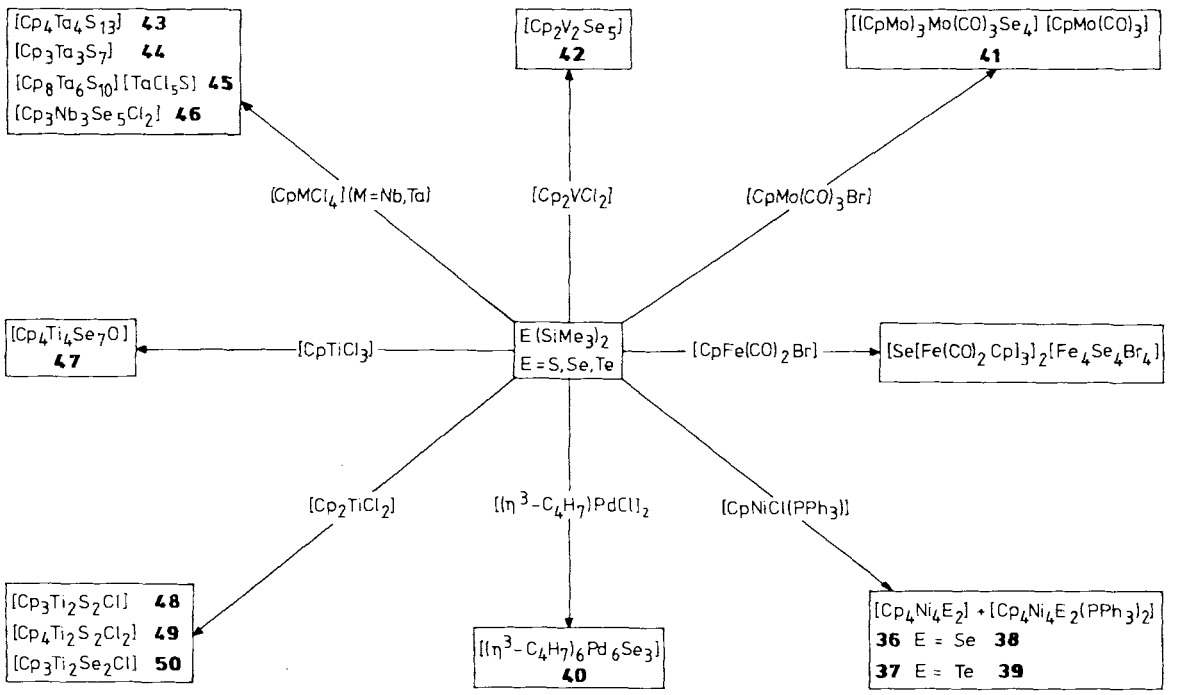

Scheme 4. Reactions of $E(SiMe_3)_2$ with Cp-, allyl-, and CO-complexes of transition metal halides.

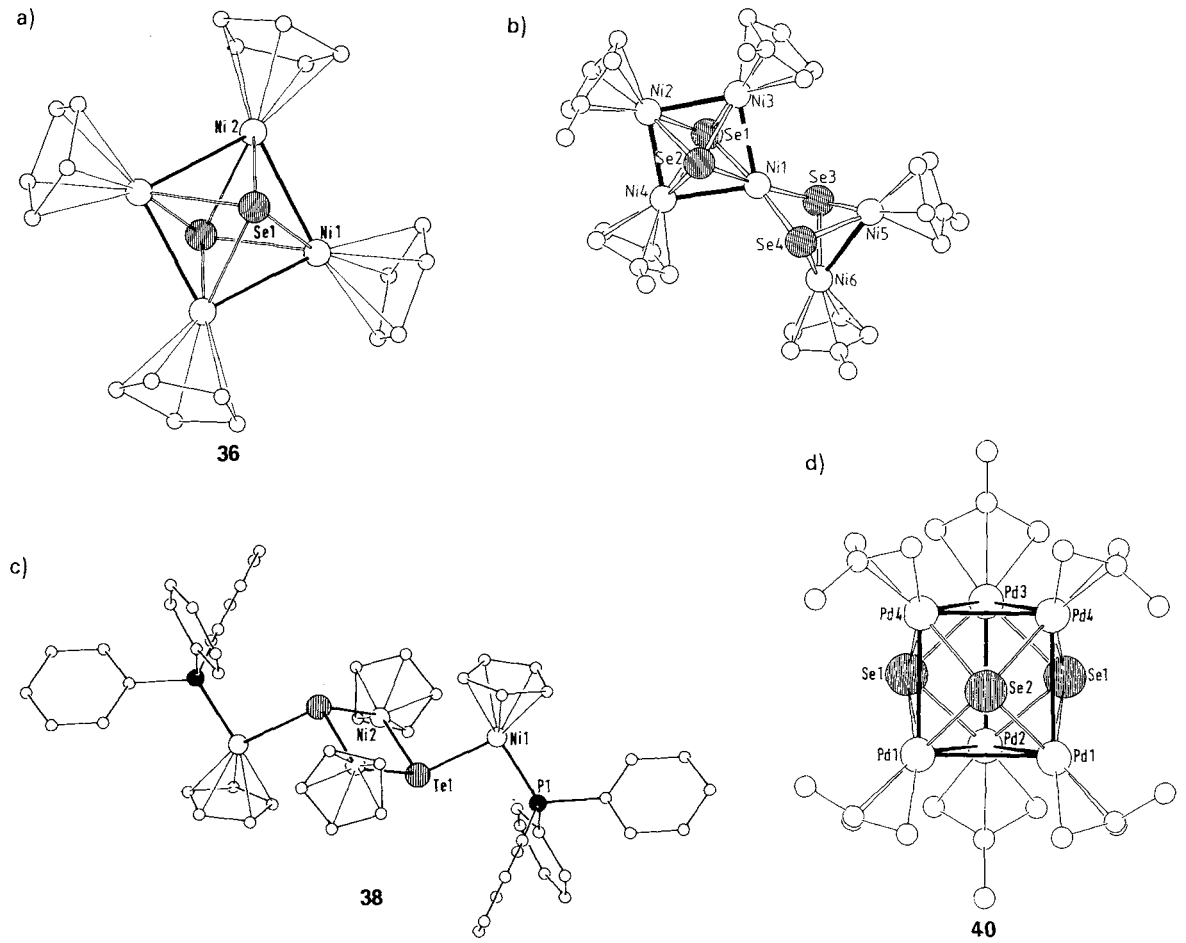

Fig. 14. Molecular structures of a) **36**, b) $[(C_5H_4Me)_5Ni_6Se_4]$, c) **38**, d) **40**, e) the cation of **41**.

Silylated chalcogens could also be used to synthesize biologically interesting complexes; this is indicated by the work of *Holm* et al.,[68] who obtained S-bridged clusters by the reaction of $[Fe_2OCl_6]^{2\ominus}$ or $[M(OEt)_5]$ (M = Nb, Ta) with $S(SiMe_3)_2$.[69,70]

As demonstrated by the synthesis of the salt **41**, a heterocubane cluster is also formed from $[CpMo(CO)_3Br]$ and $Se(SiMe_3)_2$ (Mo–Mo 294–301 pm). The cation of **41** (Fig. 14e) consists of three CpMo groups (Mo1, Mo2, Mo4), one $Mo(CO)_3$ group, and four capping Se ligands.

$E(SiMe_3)_2$ reacts with $[(\eta^3\text{-}C_3H_5)MCl]_2$ (M = Ni, Pd) to form extremely unstable, hexanuclear complexes; the S-derivatives had already been obtained by other methods.[71]

The analogous compounds with $(\eta^3\text{-}C_4H_7)$ ligands (e.g. **40**) are appreciably more stable. Analogous to the structure of $[(\eta^3\text{-}C_3H_5)_6Ni_6S_3]$, **40** contains a slightly distorted trigonal M_6 prism (Fig. 14d); the Pd_4 faces are capped by μ_4-Se ligands and the Pd atoms are each bonded to an $\eta^3\text{-}C_4H_7$ group. The Pd–Pd bond lengths within the prism are 288.4–313.2 pm, but all are considerably longer than those observed in other Pd clusters.[72]

The tetranuclear diamagnetic clusters **36** and **37** are formed in high yield from $[CpNiCl(PPh_3)]$ and $E(SiMe_3)_2$; small amounts of **38** and **39**, which are accessible from **36** and **37**, respectively, and PPh_3, are also formed. The molecular structures of **36** (Fig. 14a) and **37** consist of an almost regular Ni_4 square (crystallographic $\bar{1}$ symmetry) in which each nickel is bonded to an η^5-Cp group and two μ_4-E ligands.[73] Assuming that four Ni–Ni single bonds are present in **36** and **37**, these 68e clusters contain four electrons more than would be expected from the 18e rule. The Ni–Ni bond lengths (257 pm) lie in the expected range.[63,74] As in the Ni_3Se_2 fragment of **34**, the Se–Se contacts in **36** (303 pm) are shorter than van der Waals' contacts in selenium or $Se_8^{2\oplus}$.[75] It is possible that weak interactions between the Se ligands are responsible for this.[53,59,76]

Reaction of the unstable $[(C_5H_4Me)Ni(CO)Br]$ with $Se(SiMe_3)_2$ affords the complex $[(C_5H_4Me)_5Ni_6Se_4]$. Figure 14b shows that this complex contains an Ni_4Se_2 unit analogous to **36** (Ni–Ni 250–263 pm), which is connected by two μ_3-Se bridges to a $[(C_5H_4Me)Ni]_2$ unit (Ni–Ni 253 pm). A compound isostructural with **36** in which the μ_4-Se li-

gands are replaced by μ_4-As ligands is formed on reaction of $[CpNiCl(PPh_3)]$ with $As(SiMe_3)_3$.

The structure of **38** (Fig. 14b) can be seen as a consequence of breaking all Ni–Ni bonds of **36**. Further examples of the breaking of M–M bonds have been presented by other authors.[77] **38** and **39** contain four CpNi units linked by μ_3-E ligands, the outer Ni atoms also being coordinated by PPh_3 groups. **38** and **39** are diamagnetic; each Ni atom achieves the 18 electron configuration. Correspondingly, the Ni···Ni contacts (337–382 pm in **38**, 362–398 pm in **39**) give no indication of bonding interactions.

4.2. Clusters of Electron-Deficient Transition Metals with Cp Ligands

Organometallic derivatives of the less electron-rich transition metals have been used by several authors as precursors to polynuclear complexes. Cp-substituted transition metal halides, for example, have been allowed to react with M_2E_x (M = Li, Na; E = S, Se; x = 1,2) or elemental sulfur or selenium.[78] However, it is clear that $S(SiMe_3)_2$ or $Se(SiMe_3)_2$ could also be successfully used. Thus the reaction of $[CpCrCl_2(PnBu_3)]$ with $Se(SiMe_3)_2$ furnishes the heterocubane cluster $[Cp_4Cr_4Se_4]$.[79] $[Cp_2VCl_2]$ reacts with $Se(SiMe_3)_2$ to form the diamagnetic $[Cp_2V_2Se_5]$ (**42**); *Rauchfuss* and *Rheingold* had already reported the synthesis of this complex.[80] The structure of **42** is shown in Figure 15. There are three different Se bridges: μ_2-Se (atom Se3) with V–Se 237 pm; μ-η^1-Se_2 (atoms Se2, Se5) with V–Se 245–246, Se–Se 230.2 pm; and μ-η^2-Se_2 (atoms Se1, Se4) with V–Se 252–254, Se–Se 231 pm. Examples of such bridges are also known in other complexes.[81] Compared with $[Cp_2V_2S_5]$ (V–V 266 pm), the V–V distance in **42** (277 pm) is unusually long.[80]

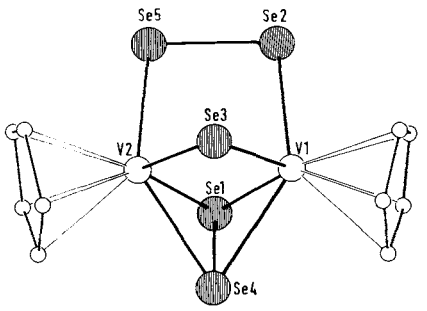

42

Fig. 15. Molecular structure of **42**.

Surprisingly, the Ta derivative analogous to **42** has not been prepared. Instead, the addition of a THF solution of $[CpTaCl_4]$ to $S(SiMe_3)_2$ leads to the formation of a crystalline mixture of **43** and **44**.[82] If however a THF solution of $S(SiMe_3)_2$ is allowed to diffuse into a THF solution of $[CpTaCl_4]$ the salt **45** can be isolated in high yield.

44 (Fig. 16b) contains a distorted Ta_3 triangle (Ta1···Ta2, Ta1···Ta3 360, Ta2···Ta3 324 pm) bonded to μ_3-S ligands S1 and S2 (S1–Ta 245–260, S2–Ta 251 pm). Ta1 and Ta3, and Ta1 and Ta2, are bridged by (μ-η^1,η^2)-S_2 groups (S–S 205–207, Ta1–S 248–255, Ta3–S4 and Ta2–S7 268 pm), and Ta2 is linked to Ta3 via a μ_2-S ligand S3

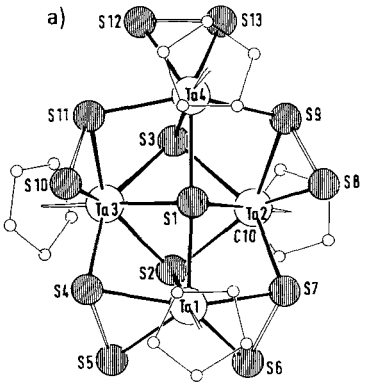

43

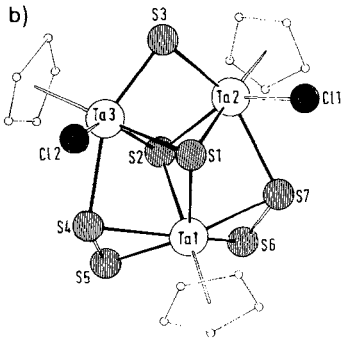

44

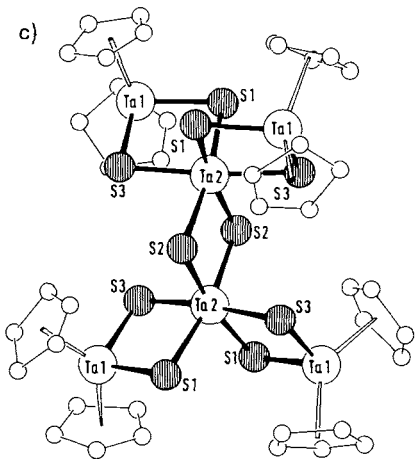

Fig. 16. Molecular structures of a) **43**, b) **44** and c) the cation of **45**.

(S3–Ta 240–242 pm). Including the Cp ligands, Ta2 and Ta3 display distorted octahedral coordination and Ta1 the coordination number 7. **44** also contains two Ta–Cl bonds, which act as reactive sites with $[CpTaCl_4]$ and $S(SiMe_3)_2$ to produce the tetranuclear $[Cp_4Ta_4S_{13}]$ (**43**). A topological comparison of **44** and **43** (Fig. 16a) indicates which reorientation of ligands is necessary in this reaction. The μ_3-S (S1, S2) and μ_2-S (S3) ligands of **44** may become the μ_4 (S1) and μ_3-S (S2, S3) ligands of **43**, and Ta4 becomes linked with Ta2 and Ta3 by two (μ-η^1,η^2)-S_2 fragments. The four Ta atoms of **43** thereby acquire a strongly distorted pentagonal bipyramidal coordination geometry. Assuming that the bridges in **43** and **44** are $S_2^{2\ominus}$ and $S^{2\ominus}$, the Ta atoms in both compounds possess the formal charge +5, consistent with their diamagnetism.

The cation of **45** (Fig. 16c) contains TaS_6 octahedra (Ta2) and tetrahedral Cp_2TaS_2 groups (Ta1) linked by μ_2-S ligands (Ta–S 235–243 pm). There are no bonding contacts between Ta atoms (Ta1···Ta2 338, Ta2···Ta2 353 pm).

We have since obtained evidence that the linking of tetrahedral Cp_2TaS_2 and octahedral TaS_6 groups can also lead to more highly condensed clusters.

The individuality of the vanadium group elements can be seen particularly clearly in the reaction of $[CpNbCl_4]$ with $Se(SiMe_3)_2$. Using toluene as solvent, complexes analogous to **43**–**45** are not obtained; instead, a brown compound **46** is formed exclusively.[82]

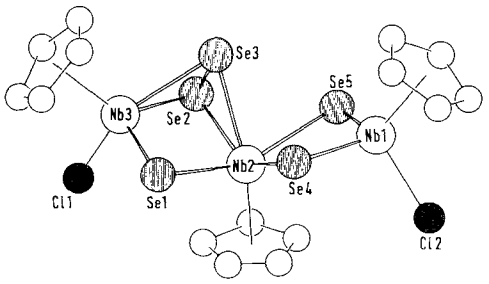

46

Fig. 17. Molecular structure of **46**.

46 (Fig. 17) contains three differently coordinated Nb atoms. Nb1 is coordinated by η^5-Cp, Se4, Se5, and Cl2 with distorted tetrahedral geometry: Nb-C(Cp) 236.6-244.2, Nb1-Se 239 pm, Nb1-Cl2 236.6 pm. Nb3 has coordination number 5, being coordinated by η^5-Cp, Se1, Se2, Se3 and Cl1: Nb3-C(Cp) 240.1-244.0, Nb3-Se1 238.3, Nb3-Se2(Se3) 261-263, Nb3-Cl1 242.9 pm. Nb2 has coordination number 6 and is coordinated by η^5-Cp and Se1-Se5, with Nb2-C(Cp) 235.0-241.8, Nb2-Se 266.5-271.7 pm. Assuming the presence of $Cp^{\ominus}$, $Se^{2\ominus}$, $Se_2^{2\ominus}$ and $Cl^{\ominus}$ ligands, **46** must be regarded as a mixed valence compound in which Nb1 and Nb3 carry the charge +4 and Nb2 +5. Correspondingly, the compound is paramagnetic, and its ESR spectrum in $C_2H_4Cl_2$ shows the expected 10-line resonance signal ($g = 2.0047$, $a_{Nb} = 11.6$ mT).

Finally, we present some results from the reactions of $E(SiMe_3)_2$ with Cp derivatives of titanium halides. The diffusion of a THF solution of $E(SiMe_3)_2$) into a THF solution of $[Cp_2TiCl_2]$ leads in good yield to the binuclear complexes **48**-**50**.[82] **48** (Fig. 18) consists of a Cp_2Ti group bridged by two μ_2-S ligands to a CpTiCl group. Both Ti atoms thereby acquire a distorted tetrahedral coordination. Just as in the isostructural $[Cp_3Ti_2Se_2Cl]$ (**50**), the Ti-E bond lengths involving Ti2 (which is bonded to Cl1) are some 20 pm shorter than those involving Ti1 (**48**: Ti2-S 223, Ti1-S 243; **50**: Ti2-Se 237, Ti1-Se 259 pm).

The structure of **49** (Fig. 18) can be derived from two Cp_2TiCl fragments bridged by an $S_2^{2\ominus}$ group (S1-S2 208.3, Ti-S 239 pm). Although both **48** and **50** possess Ti-Cl bonds, larger clusters have not yet been synthesized.

If, on the other hand, $[CpTiCl_3]$ (in THF) is allowed to react with $Se(SiMe_3)_2$, a crystalline residue is formed, from which the tetranuclear complex $[Cp_4Ti_4Se_7O]$ (**47**) is obtained in low yield by recrystallization from $C_2H_4Cl_2$.[82] **47** consists of a Ti_4 tetrahedron (Ti···Ti 311.4-346.2 pm) with a central O atom (Ti-O 195-216 pm). The Ti atoms are six-coordinate, and the Se ligands can be classified as μ_2-Se (Se1-Ti 253 pm), μ_3-Se (Ti-Se5/Se6 260-274 pm) and Se_2 bridges spanning three Ti atoms (Se3-Se4 232, Se2-Se7 234 pm) with unequal Ti-Se distances (Ti3-Se3 263, Ti3-Se4 266, Ti1-Se3 270, Ti4-Se4 268 pm). *Rauchfuss, Rheingold* et al. have recently presented the structure of $[(MeC_5H_4)_4Ti_4S_8O_2]$, which, in contrast to **47**, contains a Ti_4 cluster coordinated by four S_2 units and a μ_2-O ligand.[83] The same authors obtained the heterocubane clusters $[(RC_5H_4)_4Ti_4S_4]$ (R = Me, *i*Pr) by the reduction of $[(RC_5H_4)TiCl_3]$ with Zn and subsequent reaction with $S(SiMe_3)_2$.[83]

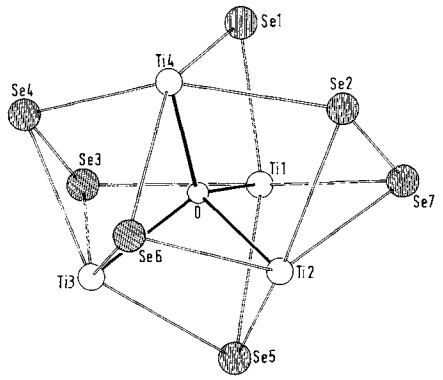

47

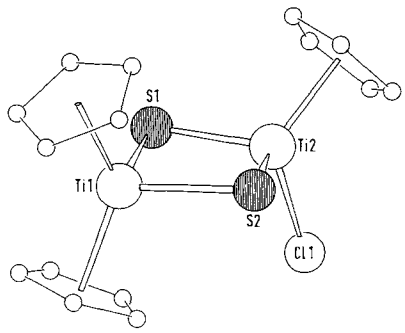

48

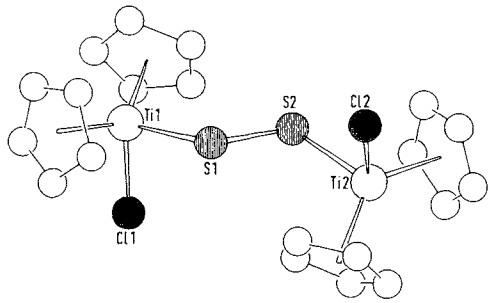

49

Fig. 18. Molecular structures of **47** (without Cp groups), **48**, and **49**.

5. Exploratory Reactions with $PMe_2(SiMe_3)$ and $SPh(SiMe_3)$

The reactions described above illustrate the synthetic potential of disilylated derivatives of elements of the fifth and sixth main groups. Predictably, however, monosilylated compounds (such as $PMe_2(SiMe_3)$ and $SPh(SiMe_3)$ also react with transition metal halides to form polynuclear complexes. For instance, the reaction between $PMe_2(SiMe_3)$ and $[Cp_2TiCl_2]$ leads in good yield to the highly oxygen-sensitive complex **51**,[84] in which Ti is coordinated by two η^5-Cp ligands (Ti-C(Cp) 237-241 pm), one Cl ligand (Ti-Cl 248.6 pm) and one $PMe_2(SiMe_3)$ ligand in a distorted tetrahedral geometry (Fig. 19). The silylphosphane forms an unusually long bond to Ti (Ti-P 263.9 pm).

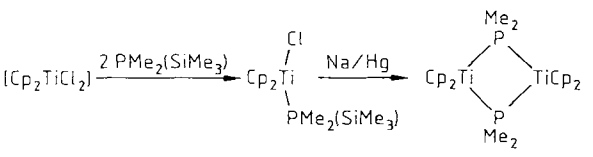

51 **52**

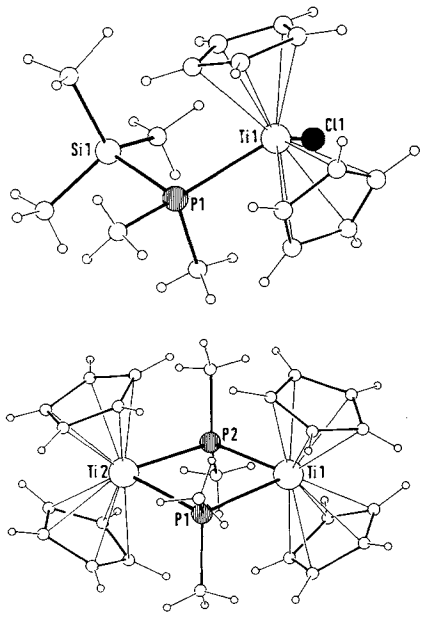

Fig. 19. Molecular structures of **51** and **52**.

This distance is markedly longer than observed in other complexes with Ti–P bonds.[85] **51**, which is paramagnetic, has 17 valence electrons. According to *Hoffmann* et al., the angle between the ligands should be determined by the d electron configuration of Ti,[86] and this is confirmed by the angle Cl1–Ti–P1, 81.2°.

In the dinuclear complex **52** (Fig. 19) each Ti is coordinated by two η^5-Cp ligands and the P atoms of the two μ_2-PMe_2 ligands. The four-membered ring Ti1, Ti2, P1, P2 is practically planar; its geometry (P1–Ti–P2 83.3°, Ti1–P–Ti2 96.1–96.8°, Ti···Ti 392 pm) corresponds well with that observed in other M_2P_2 rings lacking metal–metal bonds.[12,87] Such rings characteristically display an angle of 75–80° at the metal atom and 100–105° at the P atom. Examples are:

$[(CO)_4Mn(PH_2)]_2$: P–Mn–P 76.1°, Mn–P–Mn 103.9°
$[(diphos)Pt(PPh_2)]_2^{2\oplus}$: P–Pt–P 76.1°, Pt–P–Pt 103.9°
$[(CO)_2Rh(PtBu_2)]_2$: P–Rh–P 79.5°, Rh–P–Rh 100.5°

The 17 valence electrons of each Ti in **52** are a consequence of the two Cp ligands and the 3-electron donor PMe_2. The paramagnetism disappears at low temperatures by antiferromagnetic coupling.

Monosilylated sulfanes such as $SPh(SiMe_3)$ are also suitable for the preparation of polynuclear transition metal complexes. These complexes are however also accessible via (e.g.) the reaction of NaSPh with transition metal halides.[40,88] The reaction of $(Bu_4N)[CoCl_3(PPh_3)]$ with $SPh(SiMe_3)$ leads in practically quantitative yield to **53**.[89,90] If the neutral starting complex $[CoCl_2(PPh_3)_2]$ is used, however, then the neutral cluster **54** is formed. The

$(Bu_4N)_2[Co_4(SPh)_6Cl_4]$ **53**
$[Co_4(SPh)_6Cl_2(PPh_3)_2]$ **54**

Co atoms in **53** and **54** have the charge +2, and the complexes are thus paramagnetic. No ESR signal is observable up to a temperature of −150°C.

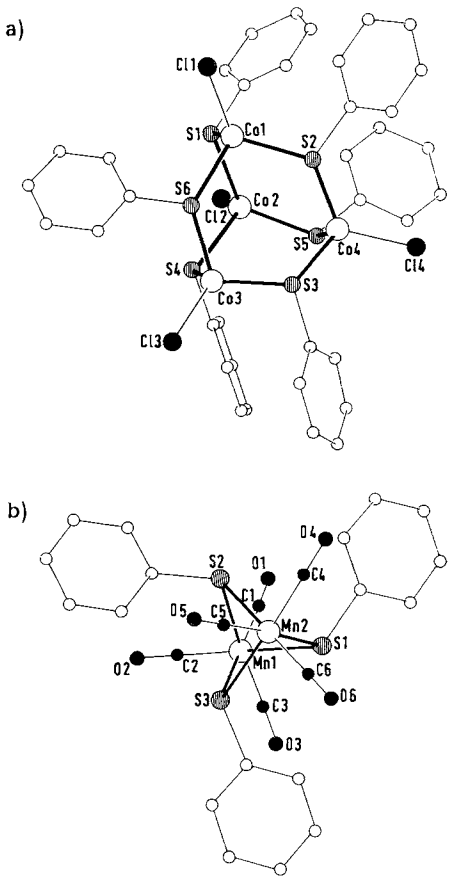

Fig. 20. Molecular structure of the anions of a) **53** and b) **55**.

The four Co atoms in the cluster anion of **53** (Fig. 20a) are linked by six μ_2-SPh bridges (Co–S 230–234 pm), forming an adamantane-like cage species in which all Co atoms display a distorted tetrahedral coordination sphere of one Cl and three SPh ligands. **53** is a representative of the commonly observed structure type $[M_4^{II}(SR)_{10-n}X_n]^{2\ominus}$ (M = Fe, Co, Cd, Zn; X = Cl, Br, SR),[91] and the Co_4 tetrahedron of **53** is slightly distorted (Co···Co 376–393 pm) in the same manner as its related species.

Attempts to substitute the Cl ligands of **53** led to a series of derivatives. However, it has not proved possible to prepare heterometallic clusters; for instance, the reaction of **53** with $NaMn(CO)_5$ leads, with exchange of the SPh ligands, to the dinuclear manganese complex **55**, the structure of which is shown in Figure 20b. The anion contains two $Mn(CO)_3$ groups bridged by three SPh ligands.[92]

$(Bu_4N)[Mn_2(SPh)_3(CO)_6]$ **55**

6. Reactions of $E(SiMe_3)_2$ (E = S, Se) with Derivatives of Main Group Halides

Silylated main group elements can serve as starting materials for the synthesis of polynuclear derivatives of those elements. An example is the reaction (b), which proceeds in good yields.

$$[Cr(CO)_5(PPh_2Cl)] + Se(SiMe_3)_2 \longrightarrow [\{Cr(CO)_5(PPh_2)\}_2Se] \qquad (b)$$

In contrast, in reaction (c) the formation of a complex iron salt, whose cation has already been described,[93] and of (as yet structurally uncharacterized) Sb–Se complexes is observed.

$$[\{FeCp(CO)_2\}_2SbCl_2][Sb_2Cl_7] + Se(SiMe_3)_2 \longrightarrow [\{FeCp(CO)_2\}_3SbCl]_2[Fe_2Cl_6] + \cdots \quad (c)$$

The reaction of $[FeCp(CO)_2BiCl_2]$ and $Se(SiMe_3)_2$ leads also to extremely insoluble products of very high molecular weight. The formation of B–Se rings is also possible, as shown in reaction (d). The B_3Se_3 complex (B–Se 193–195 pm) was generated in 80% yield (Fig. 21a).

$$[FeCp(C_5H_4BBr_2)] \cdot NEt_3 + Se(SiMe_3)_2 \longrightarrow [\{FeCp(C_5H_4B)\}_3Se_3] \quad (d)$$

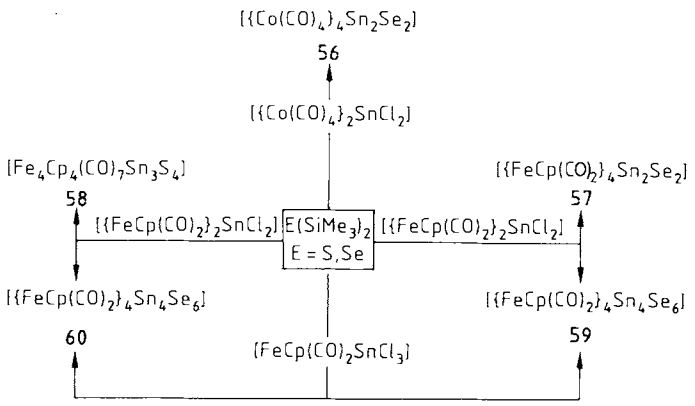

The compounds **56**–**60** have been identified by crystal structure analyses: **56** and **57** (Fig. 21) consist of an Sn_2E_2 four-membered ring in which two $Co(CO)_4$ groups (**56**) or two $FeCp(CO)_2$ groups (**57**) are bonded to the Sn atoms.

59 (Fig. 21) and **60** possess an Sn_4E_6 cage with the adamantane structure, in which the Sn atoms are each bonded to three Se atoms and one $FeCp(CO)_2$ group.[94] These compounds are formed in very small quantities (5%) upon reaction of $[\{FeCp(CO)_2\}_2SnCl_2]$ with $E(SiMe_3)_2$, but in much better yield upon reaction of $E(SiMe_3)_2$ with $[FeCp(CO)_2SnCl_3]$.

The structure of the by-product **58** is particularly interesting (Fig. 21). Like the adamantane cage in **59**, **58** also contains a corrugated Sn_3S_3 six-membered ring (E = S), in which all Sn atoms are bonded to $FeCp(CO)_2$ groups (Fe1, Fe2, Fe3). S3 functions as a μ_3-bridge between Sn2, Sn3 and the Fe atom (Fe4) of an FeCp(CO) unit that is additionally bonded to Sn1.

Considerably more complicated cage structures can also be formed [e.g. **61** in reaction (e)].

$$[NiCp(PPh_3)SnCl_3] + Se(SiMe_3)_2 \longrightarrow [Sn_6Se_9Ni_5Cp_4(PPh_3)_3] \quad (e)$$

61

A description of the molecular structure of **61** (Fig. 22) could begin with an Sn_6Se_6 ring (Sn1–Sn6, Se1–Se3, Se7–Se9) in which pairs of Sn atoms (Sn1, Sn2; Sn3, Sn6; Sn4, Sn5) are linked by additional μ_3-Se bridges (Se4–Se6).

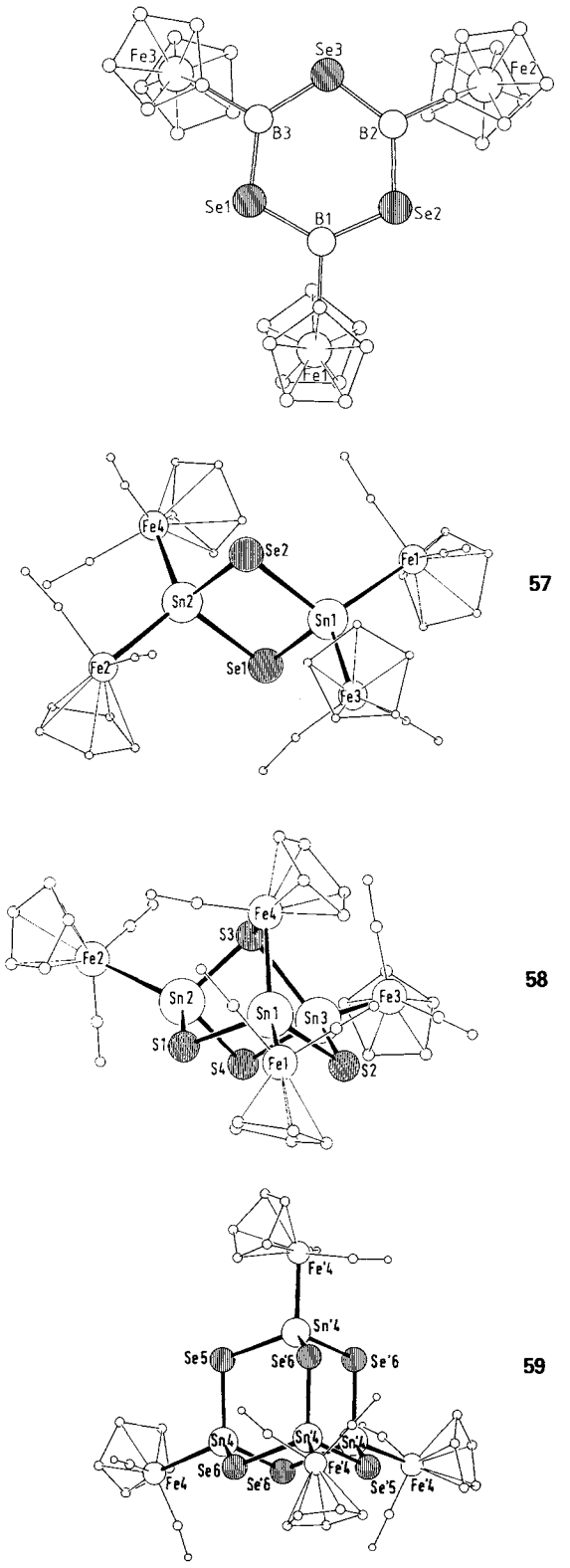

Fig. 21. Molecular structures of a) $[\{FeCp(C_5H_4B)\}_3Se_3]$, b–d) of **57**–**59**.

Se4–Se6 also function as ligands to Ni5, in the middle of the macrocycle, which is additionally bonded to a CpNi group (Ni–Ni 267.3 pm). Both Ni atoms are bridged by three Sn atoms of the twelve-membered ring (Sn1, Sn5, Sn6; Ni–Sn 249–256 pm), and the remaining Sn atoms (Sn2, Sn3, Sn4) are each bonded to the Ni atom of a terminal $CpNi(PPh_3)$ group (Ni–Sn 243–244 pm).

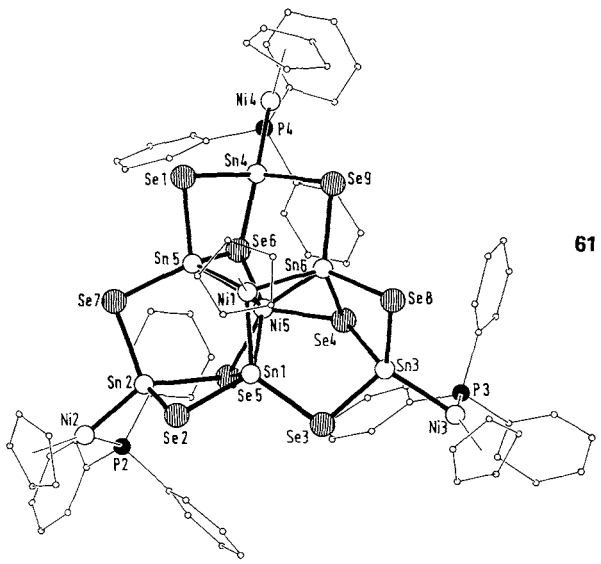

61

Fig. 22. Molecular structure of **61**.

7. Summary

The studies reported in this article demonstrate that silylated derivatives of elements of the fifth and sixth main groups can serve as starting materials for the synthesis of cluster compounds. Clearly a great deal of work remains to be done in this area. The reader will have realized that the element of chance plays an important role in many unexpected results; the deliberate synthesis of large molecular clusters will be a worthwhile goal. Such compounds, intermediates between molecular chemistry and solid state chemistry, should possess interesting physical and chemical properties.

This article presents results (some not yet published) of the following collaborators: R. Basoglu, H. Fleischer, H. Graef, K. Höffgen, A. Hollnagel, J. Magull, P. Maué, C. Persau, F. Rogel, F. Rudolpf, and L. Weisse, to whom our especial thanks are due. We are also grateful to the Institute of Crystallography at the University of Karlsruhe, where many of the structures were measured. The Fonds der Chemischen Industrie and the Deutsche Forschungsgemeinschaft provided generous financial support.

Received: March 28, 1988 [A 692 IE]
German version: *Angew. Chem. 100* (1988) 1300

[1] T. P. Martin, *Angew. Chem. 98* (1986) 197; *Angew. Chem. Int. Ed. Engl. 25* (1986) 197.

[2] G. Schmid, N. Klein, *Angew. Chem. 98* (1986) 910; *Angew. Chem. Int. Ed. Engl. 25* (1986) 922; G. Schmidt, *Struct. Bonding (Berlin) 62* (1985) 51.

[3] B. F. G. Johnson (Ed.): *Transition Metal Clusters*, Wiley, New York 1980; R. B. King, *Prog. Inorg. Chem. 15* (1972) 287; P. Chini, G. Longoni, V. G. Albano, *Adv. Organomet. Chem. 14* (1976) 285; J. D. Corbett, *Prog. Inorg. Chem. 21* (1976) 129; H. G. von Schnering, *Angew. Chem. 93* (1981) 44; *Angew. Chem. Int. Ed. Engl. 20* (1981) 33; A. Simon, *ibid. 93* (1981) 23 and *20* (1981) 1; H. Schäfer, B. Eisenmann, W. Müller, *ibid. 85* (1973) 742 and *12* (1973) 649; H. Vahrenkamp, *Struct. Bonding (Berlin) 32* (1977) 1; *Angew. Chem. 90* (1978) 403; *Angew. Chem. Int. Ed. Engl. 17* (1978) 379.

[4] H. J. Becher, D. Fenske, M. Heymann, *Z. Anorg. Allg. Chem. 475* (1981) 27.

[5] D. Fenske, *Chem. Ber. 112* (1979) 363.

[6] W. Bensmann, D. Fenske, *Angew. Chem. 91* (1979) 754; *Angew. Chem. Int. Ed. Engl. 18* (1979) 677.

[7] D. Fenske, W. Bensmann, *Z. Naturforsch. B40* (1985) 1093.

[8] W. Bensmann, D. Fenske, E. Matern, *Z. Naturforsch. B41* (1986) 575.

[9] D. Fenske, unpublished.

[10] G. Fritz, *Comments Inorg. Chem. 1* (1982) 329.

[11] H. Schäfer, *Z. Naturforsch. B33* (1978) 351; *Z. Anorg. Allg. Chem. 467* (1980) 105; *ibid. 459* (1979) 157.

[12] H. Schäfer, *Z. Naturforsch. B34* (1979) 1358; H. Schäfer, J. Zipfel, B. Migula, D. Binder, *Z. Anorg. Allg. Chem. 501* (1983) 111; B. Deppisch, H. Schäfer, D. Binder, W. Leske, *ibid. 519* (1984) 53; H. Schäfer, J. Zipfel, B. Gutekunst, U. Lemmert, *ibid. 529* (1985) 157.

[13] B. Deppisch, H. Schäfer, *Acta Crystallogr. Sect. B38* (1982) 748; *Z. Anorg. Allg. Chem. 490* (1982) 129; H. Schäfer, D. Binder, D. Fenske, *Angew. Chem. 97* (1985) 523; *Angew. Chem. Int. Ed. Engl. 24* (1985) 522.

[14] D. Fenske, K. Merzweiler, *Angew. Chem. 96* (1984) 600; *Angew. Chem. Int. Ed. Engl. 23* (1984) 635.

[15] D. Fenske, K. Merzweiler, *Angew. Chem. 98* (1986) 357; *Angew. Chem. Int. Ed. Engl. 25* (1986) 338.

[16] P. M. Treichel, W. K. Dean, W. M. Douglas, *Inorg. Chem. 11* (1972) 1609; R. C. Ryan, L. F. Dahl, *J. Am. Chem. Soc. 97* (1975) 6904; G. Huttner, K. Knoll, *Angew. Chem. 99* (1987) 765; *Angew. Chem. Int. Ed. Engl. 26* (1987) 743.

[17] D. Fenske, R. Basoglu, J. Hachgenei, F. Rogel, *Angew. Chem. 96* (1984) 160; *Angew. Chem. Int. Ed. Engl. 23* (1984) 160.

[18] Trinh-Toan, W. P. Fehlhammer, L. F. Dahl, *J. Am. Chem. Soc. 94* (1972) 3389; M. A. Neumann, Trinh-Toan, L. F. Dahl, *ibid. 94* (1972) 3383; R. S. Gall, C. T.-W. Chu, L. F. Dahl, *ibid. 96* (1974) 4019; G. Schmid, *Angew. Chem. 90* (1978) 417; *Angew. Chem. Int. Ed. Engl. 17* (1978) 392.

[19] 10^{-3} M solution in tetrahydrofuran (in $[(C_4H_9)_4N][PF_6]$ (10^{-2} mol L^{-1}) as supporting electrolyte): $\mathbf{1} \xrightarrow{0.42\,V} \mathbf{1}^{\oplus} \xrightarrow{1.09\,V} \mathbf{1}^{2\oplus}$.

[20] L. D. Lower, L. F. Dahl, *J. Am. Chem. Soc. 98* (1976) 5046.

[21] H. Vahrenkamp, *Adv. Organomet. Chem. 22* (1983) 169.

[22] G. Huttner, K. Knoll, *Angew. Chem. 99* (1987) 765; *Angew. Chem. Int. Ed. Engl. 26* (1987) 743.

[23] K. Wade, *Adv. Inorg. Chem. Radiochem. 18* (1976) 1.

[24] F. A. Cotton, T. E. Haas, *Inorg. Chem. 3* (1964) 10.

[25] B. K. Teo, *Inorg. Chem. 23* (1984) 1251; B. K. Teo, G. Longoni, F. R. K. Chung, *ibid. 23* (1984) 1257; B. K. Teo, *J. Chem. Soc. Chem. Commun. 1983*, 1362.

[26] a) D. M. P. Mingos, *J. Chem. Soc. Chem. Commun. 1985*, 1352; b) R. L. Johnston, D. M. P. Mingos, *Inorg. Chem. 25* (1986) 1661; c) D. M. P. Mingos, *Chem. Soc. Rev. 15* (1986) 31; D. M. P. Mingos, R. L. Johnston, *Struct. Bonding (Berlin) 68* (1987) 29.

[27] F. G. A. Stone, *Angew. Chem. 96* (1984) 85; *Angew. Chem. Int. Ed. Engl. 23* (1984) 89; R. Hoffmann, *ibid. 94* (1982) 725 and *22* (1982) 711.

[28] E. J. Laskowski, R. B. Frankel, W. O. Gillum, G. C. Papaefthymiou, J. Renaud, J. A. Ibers, R. H. Holm, *J. Am. Chem. Soc. 100* (1978) 5322.

[29] Trinh-Toan, B. K. Teo, J. A. Ferguson, T. J. Meyer, L. F. Dahl, *J. Am. Chem. Soc. 99* (1977) 408.

[30] F. H. Köhler, R. de Cao, K. Ackermann, J. Sedlmaier, *Z. Naturforsch. B38* (1983) 1406.

[31] a) P. S. Pregosin, R. W. Kunzin: *^{31}P and ^{13}C NMR of Transition Metal Phosphine Complexes*, Springer, Berlin 1979; b) J. Schneider, L. Zsolnai, G. Huttner, *Chem. Ber. 115* (1982) 989; c) J. Schneider, G. Huttner, *ibid. 116* (1983) 917.

[32] D. Fenske, J. Hachgenei, *Angew. Chem. 98* (1986) 165; *Angew. Chem. Int. Ed. Engl. 25* (1986) 175.

[33] C. A. Ghilardi, S. Midollini, A. Orlandini, L. Sacconi, *Inorg. Chem. 19* (1980) 301; A. Vizi-Orosz, V. Galamb, G. Palyil, L. Marko, G. Bor, G. Natile, *J. Organomet. Chem. 107* (1976) 235; review: M. Di Vaira, L. Sacconi, *Angew. Chem. 94* (1982) 338; *Angew. Chem. Int. Ed. Engl. 21* (1982) 330.

[34] K. Hedberg, E. W. Hughes, J. Wiezer, *Acta Crystallogr. 14* (1961) 369; M. DiVaira, S. Midollini, L. Sacconi, F. Zanobini, *Angew. Chem. 90* (1978) 720; *Angew. Chem. Int. Ed. Engl. 17* (1978) 676; M. DiVaira, S. Midollini, L. Sacconi, *J. Am. Chem. Soc. 101* (1979) 1757.

[35] a) A. S. Foust, M. S. Foster, L. F. Dahl, *J. Am. Chem. Soc. 91* (1969) 5631; b) I. Bernal, H. Brunner, W. Meier, H. Pfisterer, J. Wachter, M. L. Ziegler, *Angew. Chem. 96* (1984) 428; *Angew. Chem. Int. Ed. Engl. 23* (1984) 438; c) O. J. Scherer, H. Sitzmann, G. Wolmershäuser, *ibid. 96* (1984) 979 and *23* (1984) 968.

[36] A. L. Rheingold, M. J. Foley, P. J. Sullivan, *Organometallics 1* (1982) 1429; R. A. Jones, B. R. Whittlesey, *J. Am. Chem. Soc. 107* (1985) 1078.

[37] D. Fenske, J. Ohmer, K. Merzweiler, *Angew. Chem. 100* (1988) No. 11; *Angew. Chem. Int. Ed. Engl. 27* (1988) No. 11.

[38] J. G. W. van der Linden, M. L. H. Paulissen, J. E. J. Schmitz, *J. Am. Chem. Soc. 105* (1983) 1903.

[39] P. Chini, *J. Organomet. Chem. 200* (1980) 37; G. Ciani, A. Sironi, S. Martinengo, *ibid. 192* (1980) C42.

[40] H. Vahrenkamp, *Angew. Chem. 87* (1975) 363; *Angew. Chem. Int. Ed. Engl. 14* (1975) 322; F. Richter, H. Beurich, M. Müller, N. Gärtner, H. Vahrenkamp, *Chem. Ber. 116* (1983) 3774; A. Müller, E. Diemann, R. Jostes, H. Bögge, *Angew. Chem. 93* (1981) 957; *Angew. Chem. Int. Ed. Engl. 20* (1981) 934; R. H. Holm, *Chem. Soc. Rev. 10* (1981) 455; G. Henkel, W. Tremel, B. Krebs, *Angew. Chem. 95* (1983) 314; *Angew. Chem. Int. Ed. Engl. 22* (1983) 318; G. Christou, K. S. Hagen, R. H. Holm, *J. Am. Chem. Soc. 104* (1982) 1744; A. Müller, W. Jaegermann, J. H. Enmark, *Coord. Chem. Rev. 46* (1982) 245.

[41] F. Cecconi, C. A. Ghilardi, S. Midollini, *Cryst. Struct. Commun. 11* (1982) 25; G. Christou, B. Ridge, H. N. Rydou, *J. Chem. Soc. Dalton Trans. 1978, 1423; R. D. Adams, I. T. Horvath, Inorg. Chem. 23* (1984) 4718.

[42] M. Laing, P. M. Kiernau, W. P. Griffith, *J. Chem. Soc. Chem. Commun. 1977,* 221; C. E. Strouse, L. F. Dahl, *J. Am. Chem. Soc. 93* (1971) 6032.

[43] L. L. Nelson, F. Y.-K. Lo, A. D. Rae, L. F. Dahl, *J. Organomet. Chem. 225* (1982) 309; M. A. Bobrik, E. J. Laskowski, R. W. Johnson, W. O. Gillum, J. M. Berg, K. O. Hodgson, R. H. Holm, *Inorg. Chem. 17* (1978) 1402.

[44] D. Fenske, J. Ohmer, J. Hachgenei, *Angew. Chem. 97* (1985) 993; *Angew. Chem. Int. Ed. Engl. 24* (1985) 993.

[45] Trinh-Toan, B. K. Teo, J. A. Ferguson, T. J. Meyer, L. F. Dahl, *J. Am. Chem. Soc. 99* (1977) 408.

[46] D. Fenske, J. Ohmer, *Angew. Chem. 99* (1987) 155; *Angew. Chem. Int. Ed. Engl. 26* (1987) 148.

[47] J. C. Calabrese, L. F. Dahl, P. Chini, G. Longoni, S. Martinengo, *J. Am. Chem. Soc. 96* (1974) 2614.

[48] D. Fenske, J. Hachgenei, J. Ohmer, *Angew. Chem. 97* (1985) 684; *Angew. Chem. Int. Ed. Engl. 24* (1985) 706.

[49] F. Cecconi, C. A. Ghilardi, S. Midollini, *Inorg. Chim. Acta 64* (1981) L47; F. Cecconi, C. A. Ghilardi, S. Midollini, A. Orlandini, *ibid. 76* (1983) L183; F. Cecconi, C. A. Ghilardi, S. Midollini, A. Orlandini, P. Zanello, *Polyhedron 5* (1986) 2021.

[50] O. Bars, J. Guillevic, D. Grandjean, *J. Solid State Chem. 6* (1973) 6.

[51] I. Noda, B. S. Snyder, R. H. Holm, *Inorg. Chem. 25* (1986) 3851.

[52] C. A. Ghilardi, S. Midollini, L. Sacconi, *Inorg. Chim. Acta 31* (1978) L431.

[53] F. Cecconi, C. A. Ghilardi, S. Midollini, *Inorg. Chem. 22* (1983) 3802.

[54] D. Fenske, J. Ohmer, K. Merzweiler, *Z. Naturforsch. B42* (1987) 803.

[55] A. Simon, *Angew. Chem. 93* (1981) 23; *Angew. Chem. Int. Ed. Engl. 20* (1981) 1.

[56] A. Simon, *J. Solid State Chem. 57* (1985) 2.

[57] R. Chevrel, M. Sergent, B. Seeber, O. Fischer, A. Grüttner, K. Yvon, *Mater. Res. Bull. 14* (1979) 567; A. Grüttner, K. Yvon, R. Chevrel, M. Potel, M. Sergent, B. Seeber, *Acta Crystallogr. Sect. B35* (1979) 285; M. Potel, R. Chevrel, M. Sergent, M. Decourx, O. Fischer, *C. R. Hebd. Seances Acad. Sci. Ser. C288* (1979) 429.

[58] A. Simon, *Angew. Chem. 100* (1988) 163; *Angew. Chem. Int. Ed. Engl. 27* (1988) 159.

[59] C. A. Ghilardi, S. Midollini, L. Sacconi, *J. Chem. Soc. Chem. Commun. 1981,* 47.

[60] S. Martinengo, A. Fumagalli, R. Bonifichi, G. Ciani, A. Sironi, *J. Chem. Soc. Chem. Commun. 1982,* 825.

[61] H. Vahrenkamp, V. A. Uchtmann, L. F. Dahl, *J. Am. Chem. Soc. 90* (1968) 3272.

[62] R. Chevrel, M. Sergent, *Top. Curr. Phys. 32* (1982) 25.

[63] R. Chevrel, P. Gougeon, M. Potel, M. Sergent, *J. Solid State Chem. 57* (1985) 25.

[64] W. Hönle, H. G. von Schnering, A. Lipka, K. Yvon, *J. Less-Common Met. 71* (1980) 135.

[65] D. Fenske, P. Maué, K. Merzweiler, *Z. Naturforsch. B42* (1987) 928.

[66] M. A. Bobrik, K. O. Hodgson, R. H. Holm, *Inorg. Chem. 16* (1977) 1851; M. G. Kanatzidis, D. Coucouvanis, A. Kostikas, A. Simopoulos, V. Papaefthymiou, *J. Am. Chem. Soc. 107* (1985) 4925; W. Saak, S. Pohl, *Z. Naturforsch. B40* (1985) 1105; A. Müller, N. Schladerbeck, H. Bögge, *Chimia 39* (1985) 24; B. A. Averill, T. Herskovitz, R. H. Holm, J. A. Ibers, *J. Am. Chem. Soc. 95* (1973) 3523; K. S. Hagen, A. D. Watson, R. H. Holm, *Inorg. Chem. 23* (1984) 2984.

[67] C. Hecht, E. Herdtweck, J. Rohrmann, W. A. Herrmann, *J. Organomet. Chem.*, in press.

[68] Y. Do, E. D. Simhon, R. H. Holm, *Inorg. Chem. 24* (1985) 1831; *ibid. 22* (1983) 3809; J. R. Dorfman, J.-J. Girerd, E. D. Simhon, T. D. P. Stack, R. H. Holm, *ibid. 23* (1984) 4407; J. Sola, Y. Do, J. M. Berg, R. H. Holm, *J. Am. Chem. Soc. 105* (1983) 7784.

[69] D. M. Schleich, M. J. Martin, *J. Solid State Chem. 64* (1986) 359.

[70] D. Fenske, P. Maué, unpublished.

[71] B. Bogdanović, R. Goddard, P. Göttsch, C. Krüger, K. Schlichte, Y.-Hung Tsay, *Z. Naturforsch. B34* (1979) 609; D. Fenske, A. Hollnagel, K. Merzweiler, *Z. Naturforsch. B43* (1988) 634.

[72] S. Otsuka, Y. Tatsuno, M. Miki, T. Aoki, M. Matsumoto, H. Yoshioka, K. Nakatsu, *J. Chem. Soc. Chem. Commun. 1973,* 445; G. W. Bushnell, K. R. Dixon, P. M. Moroney, A. D. Rattray, CH'eng Wan, *ibid. 1977,* 709; P. M. Bailey, A. Keasey, P. M. Maitlis, *J. Chem. Soc. Dalton Trans. 1978,* 1825.

[73] D. Fenske, A. Hollnagel, K. Merzweiler, *Angew. Chem. 100* (1988) 978; *Angew. Chem. Int. Ed. Engl. 27* (1988) 965.

[74] M. S. Paquette, L. F. Dahl, *J. Am. Chem. Soc. 102* (1980) 6621; J. C. Calabrese, L. F. Dahl, A. Cavalieri, P. Chini, G. Longoni, S. Martinengo, *ibid. 96* (1974) 2616.

[75] E. H. Henninger, R. C. Buschert, L. Heaton, *J. Chem. Phys. 46* (1967) 586; R. K. McMullan, D. J. Prince, J. D. Corbett, *Inorg. Chem. 10* (1971) 1749.

[76] R. C. Ryan, L. F. Dahl, *J. Am. Chem. Soc. 97* (1975) 6904; C. H. Wei, L. F. Dahl, *Cryst. Struct. Commun. 4* (1975) 583.

[77] G. Huttner, J. Schneider, H. Müller, G. Mohr, J. von Seyerl, L. Wohlfahrt, *Angew. Chem. 91* (1979) 82; *Angew. Chem. Int. Ed. Engl. 18* (1979) 76; M. Müller, H. Vahrenkamp, *Chem. Ber. 116* (1983) 2311; [31c]; J. S. Field, R. J. Haines, D. N. Smit, K. Natarajan, O. Scheidsteger, G. Huttner, *J. Organomet. Chem. 240* (1982) C23.

[78] M. Draganjac, T. B. Rauchfuss, *Angew. Chem. 97* (1985) 745; *Angew. Chem. Int. Ed. Engl. 24* (1985) 742; C. E. Holloway, M. Melnik, *J. Organomet. Chem. 304* (1986) 41; *ibid. 303* (1986) 1, 39; C. E. Holloway, I. A. Walker, M. Melnik, *ibid. 321* (1987) 143.

[79] W. A. Herrmann, J. Rohrmann, E. Herdtweck, H. Bock, A. Veltmann, *J. Am. Chem. Soc. 108* (1986) 3135.

[80] A. L. Rheingold, C. M. Bolinger, T. B. Rauchfuss, *Acta Crystallogr. Sect. C42* (1986) 1878; J. Darkwa, J. R. Lockemeyer, P. D. W. Boyd, T. B. Rauchfuss, A. L. Rheingold, *J. Am. Chem. Soc. 110* (1988) 141; C. M. Bolinger, T. B. Rauchfuss, A. L. Rheingold, *Organometallics 1* (1982) 1551.

[81] H. Brunner, J. Wachter, E. Guggolz, M. L. Ziegler, *J. Am. Chem. Soc. 104* (1982) 1765; M. R. Du Bois, D. L. Du Bois, M. C. van Derveer, R. C. Haltiwanger, *Inorg. Chem. 20* (1981) 3064; G. J. Kubas, P. J. Vergamini, *ibid. 20* (1981) 2667; M. Herberhold, D. Reiner, B. Zimmer-Gasser, U. Schubert, *Z. Naturforsch. B35* (1980) 1281.

[82] P. Maué, D. Fenske, *Z. Naturforsch.*, in press.

[83] G. A. Zank, C. A. Jones, T. B. Rauchfuss, A. L. Rheingold, *Inorg. Chem. 25* (1986) 1886.

[84] R. Payne, J. Hachgenei, G. Fritz, D. Fenske, *Z. Naturforsch. B41* (1986) 1535.

[85] G. Fachinetti, C. Floriani, H. Stoeckli-Evans, *J. Chem. Soc. Dalton Trans. 1977,* 2297; B. H. Edwards, R. D. Rogers, D. J. Sikora, J. L. Atwood, M. D. Rausch, *J. Am. Chem. Soc. 105* (1983) 416; G. S. Girolami, G. Wilkinson, M. Thornton-Pett, M. B. Hursthouse, *J. Chem. Soc. Dalton Trans. 1984,* 2347; L. B. Kool, M. D. Rausch, H. G. Alt, M. Herberhold, U. Thewalt, B. Wolf, *Angew. Chem. 97* (1985) 425; *Angew. Chem. Int. Ed. Engl. 24* (1985) 394; D. J. Sikora, M. D. Rausch, R. D. Rogers, J. L. Atwood, *J. Am. Chem. Soc. 103* (1981) 982.

[86] J. W. Lauher, R. Hoffmann, *J. Am. Chem. Soc. 98* (1976) 1729.

[87] A. J. Carty, F. Hartstock, N. J. Taylor, *Inorg. Chem. 21* (1982) 1349; R. A. Jones, T. C. Wright, J. L. Atwood, W. E. Hunter, *Organometallics 2* (1983) 470.

[88] K. S. Hagen, R. H. Holm, *J. Am. Chem. Soc. 104* (1982) 5496; K. S. Hagen, J. G. Reynolds, R. H. Holm, *ibid. 103* (1981) 4054; G. Henkel, W. Tremel, B. Krebs, *Angew. Chem. 95* (1983) 317; *Angew. Chem. Int. Ed. Engl. 22* (1983) 319; W. Tremel, B. Krebs, G. Henkel, *ibid. 96* (1984) 604 and *23* (1984) 634.

[89] D. Fenske, J. Meyer, K. Merzweiler, *Z. Naturforsch. B42* (1987) 1207.

[90] The same, cluster anion could be prepared from NaSPh, $CoCl_2$ und Et_4NCl: W. Tremel, K. Greime, B. Krebs, G. Henkel, *Inorg. Chem.*, in press.

[91] P. J. Blower, J. R. Dilworth, *Coord. Chem. Rev. 76* (1987) 121; D. Coucouvanis, M. Kanatzidis, E. Simhon, N. C. Baenziger, *J. Am. Chem. Soc. 104* (1982) 1874; P. A. W. Dean, J. J. Vital, *Inorg. Chem. 24* (1985) 3722; I. G. Dance, A. Choy, M. L. Scudder, *J. Am. Chem. Soc. 106* (1984) 6285.

[92] J. W. McDonald, *Inorg. Chem. 24* (1985) 1734.

[93] Trinh-Toan, L. F. Dahl, *J. Am. Chem. Soc. 93* (1971) 2654.

[94] A. Haas, H. J. Kutsch, C. Krüger, *Chem. Ber. 120* (1987) 1045; A. Blecher, M. Dräger, B. Mathiasch, *Z. Naturforsch. B36* (1981) 1361; H. Berwe, A. Haas, *Chem. Ber. 120* (1987) 1175; J. C. J. Bart, J. J. Daly, *J. Chem. Soc. Dalton Trans. 1975,* 2063.

High Oxidation State Organometallic Chemistry, A Challenge—the Example of Rhenium**

By Wolfgang A. Herrmann*

Dedicated to Professor Hans Bock on the occasion of his 60th birthday

Homogeneous catalysis as the major industrial outlet of organometallic basic research has been enjoying great benefit from organotransition metal species that promote bond forming between hydrocarbon fragments. Most of the commercially important processes that serve to produce large-volume organic feedstock chemicals such as linear α-olefins (Shell Higher Olefins Process), linear aldehydes (hydroformylation), acetaldehyde (Wacker-Hoechst), acetic acid (Monsanto), adiponitrile (DuPont hydrocyanation of butadiene) operate at low-valent metal centers. It is thus hardly surprising that by far the most part of organometallic research during the past few decades has been directed towards an understanding and the improvement of these catalytic reactions as well as towards the related stoichiometric chemistry. As a matter of consequence, our present knowledge on high-valent organotransition metal compound is comparatively shallow, nor do we know much about the chemical relationship and interconvertability of high and low oxidation states within a given class of compounds. In this article I want to point out some ostensibly challenging perspectives of future organometallic research by describing a novel class of high oxidation state organorhenium compounds as well as by speculating on possible generalizations for other transition metals.

1. Introduction

When a present days' chemistry student first encounters organometallic compounds, he may be amazed about the overwhelming diversity in composition and structures, in properties and reactivity.[1,2] On the other hand, he will no longer view them as laboratory curiosities as I did when I took my first chemistry courses at Munich twenty years ago. At that very *time of excitement*[3] the recognition of metal-metal multiple bonds (*Cotton* et al.)[4,5] and metal-carbon multiple bonds (*Fischer* et al.)[6,7] was brand-new, the catalytic merit of rhodium complexes had just been uncovered (*Alderson* et al., *Osborn* and *Wilkinson* et al.),[8,9] and *Wilke* et al. were using zerovalent 'naked' nickel to tailor cyclic oligomers from butadiene.[10] Faster and more precise structure and reactivity studies of existing compounds and catalytic cycles became escorted by novel instrumental techniques. Shortly before, *Ziegler* and *Natta*[11] had received the Nobel Prize that could be considered a first public award to young organometallic chemistry in blossom. And backstage, the Wacker process of palladium-catalyzed, highly selective oxidation of ethylene to acetaldehyde was heading towards large-scale production,[12] again demonstrating the synthetic power of the metal-to-carbon bond. Acetylene which had been pioneered by *Reppe* et al. of the Badische Anilin- & Sodafabrik back in the forties,[13] was no longer the major chemical feedstock.

Many more and not less striking examples could be brought to memory[14,15] here to support the statement that the fate and future of organometallic chemistry in those days were in the hands of the low oxidation states.[16] Since organotransition metal compounds were so successful in the construction of carbon-carbon and carbon-hydrogen bonds, the field more or less merged with organic synthesis, and metal-mediated shortcuts towards sophisticated pharmaceuticals, insecticides, and fragrances is certainly an attractive research domain that greatly relies on the expertise of both organic and organometallic chemists.[17,18]

At the same time organometallic basic research moved towards organic synthesis, with all sorts of metals and metal compounds nowadays being used by 'straight' organic chemists,[17] the gap between organometallic research and the chemistry of inorganic compounds including inorganic solid state chemistry became canyon-like. This is all the more a pity in that the recent desire for 'novel materials' (e.g., ceramics, glasses, alloys, refractory materials, 'inorganic' polymers, 'electronic materials' etc.) can only come to scientific success if we understand the structures, the bonding, and the behavior of inorganic metal compounds and combine them with organometallics.[19] In doing so, we ought to open our eyes for the metals' high oxidation states and learn how to deal with them. *Roald Hoffmann* has convincingly emphasized the future impact of solid state chemistry and physics on the rest of chemistry.[20]

This proposal is nothing that would contradict even the needs of organic chemists. Who would for instance seriously claim to understand how oxidation reactions of organic compounds really work?[21] More precisely: Which reagent is best used to oxidize a specific alkyne, olefin, or alkane? Under which circumstances is an oxo group transferred upon a hydrocarbon compound to be oxidized?

[*] Prof. Dr. W. A. Herrmann
Anorganisch-chemisches Institut der Technischen Universität München
Lichtenbergstrasse 4, D-8046 Garching (FRG)

[**] Second Essay on Organometallic Chemistry. First Essay: W. A. Herrmann, *Comments Inorg. Chem.* 7 (1988) 73.

 © VCH Verlagsgesellschaft mbH, D-6940 Weinheim, 1988 0570-0833/88/1010-1297 $ 02.50/0

How does 'chromium peroxide' (CrO_5) work in oxidation, which is the active oxidant, what is the nature of the organometallic intermediates involved, and what does or do the mechanism(s) look like?[22-24] What are the pivotal mechanistic steps in the industrially so important SOHIO 'ammonoxidation' process for converting propylene into acrylonitrile in the presence of bismuth molybdate catalysts?[25] These are just two examples calling for a phalanx of organometallic chemists to tackle dozens of problems involving nothing less important than *oxidation chemistry*.

2. Organorhenium Compounds as Examples

Let us come up with a few details. I shall pick the element rhenium for the simple reason that we have found some unexpected compounds that promise useful applications in various fields of catalysis, not least in hydrocarbon oxidation. Moreover, the element rhenium—as a child of our century discovered as late as in 1925 by *Walther* and *Ida Noddack* in Germany—provides us with eleven different oxidation states, from +7 to −3. Rhenium may thus be viewed as an inorganic and organometallic 'chameleon', and Figure 1 amplifies on this picture.[26] Oxides and halides are expectedly at the higher range of the scale, while carbon monoxide extends the series towards the negative oxidation states, with dirhenium heptoxide/rhenium heptafluoride and tetracarbonylrhenate(−III) terminating at opposite ends. While the large body of carbonyl compounds has well been known to us organometallic chemists, we have hardly considered (simple?) oxides, halides, and oxohalides, nor have we thought of combining them with organic molecules. Still, even their structures are exciting. In dirhenium heptoxide (Re_2O_7), for example, we encounter both tetrahedral and octahedral coordination of the metal, with the so-called perrhenic acid merely being a hydrate of this oxide. Rhenium trioxide (ReO_3) forms a perovskite-type structure of hexacoordinate rhenium, with a counter ion being missing in the cavity of the cube; this d^1 compound shows metallic conductivity (!) resulting from delocalization of the d electrons. In Section 2.3 it will be shown how successive replacement of two methyl groups for each oxygen leads to interesting and useful 'organic' derivatives.

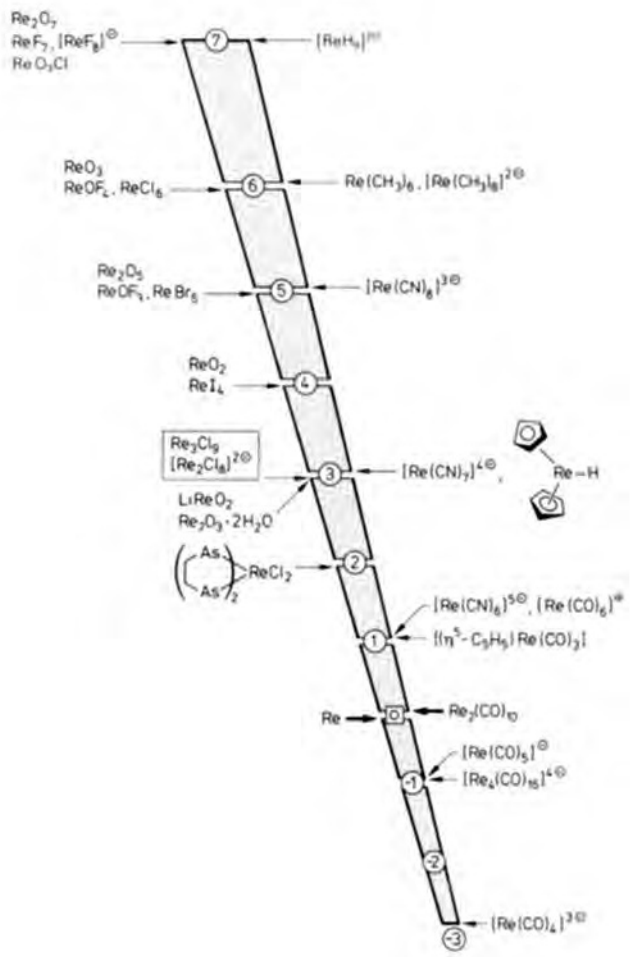

Fig. 1. Typical rhenium compounds representing oxidation states −3 to +7. The lighter homologue manganese would show up with a similar picture. A few important differences remain to be noted, however: 1. The high oxidation-state dimanganese heptoxide, Mn_2O_7, is very unstable. 2. High-valent organomanganese compounds do not exist (e.g., $[(\eta^5\text{-}C_5Me_5)MnO_3]$ and $Mn(CH_3)_6$ are unknown). 3. Manganese-manganese multiple bonds are rare (example: W. A. Herrmann, R. Serrano, J. Weichmann, *J. Organomet. Chem.* *246* (1983) C57; J. D. Korp, I. Bernal, W. A. Herrmann, R. Serrano, *Chem. Ber.* *117* (1984) 434). 4. The oxidation state +2 is the most common one in aqueous manganese chemistry, whereas only few well-defined rhenium(II) compounds have been described (e.g., $[Re_2Cl_4(PR_3)_4]$: T. J. Barder, F. A. Cotton, K. R. Dunbar, G. L. Powell, W. Schwotzer, R. A. Walton, *Inorg. Chem.* *24* (1985) 2550).

Let us come up with a few details. I shall pick the element rhenium for the simple reason that we have found some unexpected compounds that promise useful applications in various fields of catalysis, not least in hydrocarbon oxidation. Moreover, the element rhenium—as a child of our century discovered as late as in 1925 by *Walther* and *Ida Noddack* in Germany—provides us with eleven different oxidation states, from +7 to −3. Rhenium may thus be viewed as an inorganic and organometallic 'chameleon', and Figure 1 amplifies on this picture.[26] Oxides and halides are expectedly at the higher range of the scale, while carbon monoxide extends the series towards the negative oxidation states, with dirhenium heptoxide/rhenium heptafluoride and tetracarbonylrhenate(−III) terminating at opposite ends. While the large body of carbonyl compounds has well been known to us organometallic chemists, we have hardly considered (simple?) oxides, halides, and oxohalides, nor have we thought of combining them with organic molecules. Still, even their structures are exciting. In dirhenium heptoxide (Re_2O_7), for example, we encounter both tetrahedral and octahedral coordination of the metal, with the so-called perrhenic acid merely being a hydrate of this oxide. Rhenium trioxide (ReO_3) forms a perovskite-type structure of hexacoordinate rhenium, with a counter ion being missing in the cavity of the cube; this d^1 compound shows metallic conductivity (!) resulting from delocalization of the d electrons. In Section 2.3 it will be shown how successive replacement of two methyl groups for each oxygen leads to interesting and useful 'organic' derivatives.

In the intermediate oxidation state range, rhenium (like molybdenum and tungsten) forms a wealth of metal–metal multiply bonded compounds such as *Geilmann*'s old 'rhenium trichloride' which in truth is a polymer in the solid state containing Re_3Cl_9 subunits.[5a] On the other hand, even methyl groups have been attached to hexavalent rhenium; *Wilkinson* has pioneered this chemistry by synthesizing the green explosion hazard hexamethylrhenium, $Re(CH_3)_6$.[27]

2.1. Trioxo(η^5-pentamethylcyclopentadienyl)rhenium(VII)

We had to learn that hydrogen peroxide does not necessarily 'chew up' the metal-attached π-aromatic ligands[28] when we treated this reagent (or *tert*-butyl hydroperoxide) with the low-valent half-sandwich carbonyl precursor compound **1** in a boiling two-phase water/benzene system. According to Scheme 1, the yellow, thermally stable product **2** containing rhenium in its highest possible oxidation state +7 is rather formed in at least 70% yield.[29] The compound can be sublimed in a high vacuum at ca. 110°C without any deterioration, and no decomposition point under normal pressure was observed up to 250°C, showing that rhenium(VII) is perfectly compatible even with otherwise oxidizable π-aromatic hydrocarbon ligands. PE spectroscopic comparison of **1** and **2** clearly revealed this difference in metal oxidation states.[30-35] Light-induced air oxidation of **1** also generates the title compound **2**, albeit less conveniently on a preparative scale and in lower yields.[30,31]

The organorhenium oxide **2** has a conventional pyramidal structure with an entirely symmetrically bonded Cp*-

[*] General remarks: All drawings of structures have been performed using the SCHAKAL program (E. Keller: *Ein Programm für die graphische Darstellung von Molekülmodellen*, Kristallographisches Institut der Universität Freiburg (FRG), 1986).—Color code: Re violet, Cl green, S yellow, P brown, O red, C black, H orange.

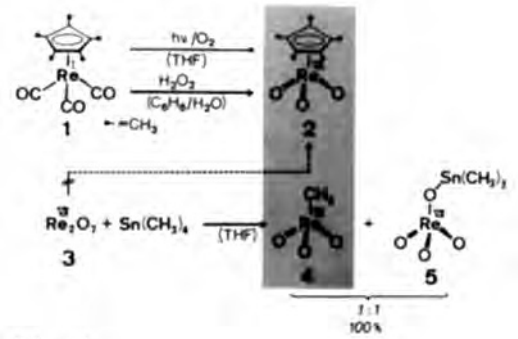

Scheme 1.

ligand (Cp* = η^5-C_5Me_5).[32] A space-filling model (Fig. 2, left)[*] tells us that the metal atom is effectively shielded from the upper side of the molecule while the three oxygen atoms take up most of the space on the opposite side. For this very reason, chemical reactions generally occur at the 'oxidic' part of the molecule (see Fig. 2b and Refs. [36–46]). An ^{17}O-NMR study comes to the result that the oxo ligands of compound **2** are relatively electron-rich (δ(O) = 646 ppm) while they are rather electron-deficient (δ(O) = 829 ppm, $CDCl_3$) in complex **4** (Section 2.2).

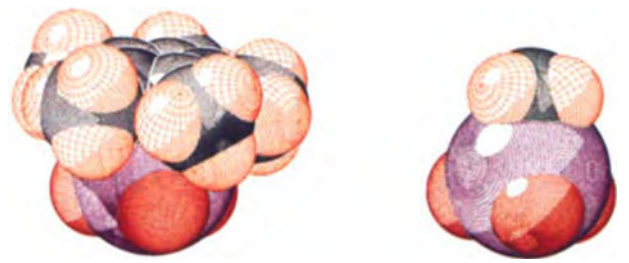

Fig. 2. Computer-generated space-filling models of the complexes [(η^5-C_5Me_5)ReO_3] **2** (left) and [CH_3ReO_3] **4** (right) correspond to an X-ray structural analysis of [(η^5-C_5Me_4Et)ReO_3] using acceptable *van der Waals* radii for rhenium (240 pm), carbon (160 pm), oxygen (140 pm), and hydrogen atoms (120 pm). For compound **4** a rhenium-methyl single bond distance of 210 pm was taken from structural data obtained for the related dinuclear derivative [$(CH_3)_4Re_2O_4$] **9a** [47].—These drawings show that the bulky π-bonded pentamethylcyclopentadienyl ligand shields the metal atom from attacking reagents on the upper side of the molecule (left) while the metal atom of compound **4** (right) is fairly exposed. It is thus understandable that compound **2** resists attachment of further ligands, whereas compound **4** forms stable adducts with such compounds (e.g., azabicyclo[2.2.2]octane, ammonia, aniline, bipyridine; see text).

2.2. Methyltrioxorhenium(VII)

We do not yet know why the parent *cyclopentadienyl* compound [(η^5-C_5H_5)ReO_3] has so far resisted all attempts at its synthesis. Neither do the oxidation reactions of Scheme 1 work in the case of [(η^5-C_5H_5)$Re(CO)_3$], nor did we succeed in making the compound from the 'right' oxidation state +7 by treating chlororheniumtrioxide (ReO_3Cl) with various cyclopentadienyl transfer reagents such as LiC_5H_5, TlC_5H_5, (C_5H_5)Sn(*n*-$C_4H_9)_3$, etc.

However, the even more interesting methyltrioxorhenium(VII), **4**, was achieved by *Kuchler* of our research group.[47] Knowing that dirhenium heptoxide and tetramethyltin are effective catalyst/cocatalyst components in olefin metathesis, even catalyzing metathesis of industrially important unsaturated carboxylic acids and nitriles under quite mild conditions,[48] he allowed these two chemicals to react in boiling tetrahydrofuran and obtained according to Scheme 1 not only colorless, completely air stable, water-soluble (!) **4** (m.p. 106 °C) but also the perrhenyl ester **5** (m.p. 213 °C, dec.); the product yields are essentially quantitative.[47] With such a simple method at hand, a whole series of high-valent organometal oxides may be opened up now, since tetramethyltin seems to be an extremely selective, non-reductive methylation reagent. No secondary reactions occur in the given example, even in the presence of a large excess of the tin reagent. *Kuchler*'s results were all the more exciting in light of the fact that compound **4** had been obtained before by *Beattie* and *Jones*[49] in small amounts by air oxidation of tetramethyloxorhenium(VI), [$(CH_3)_4ReO$], which compound in turn is difficult to make.[50a] One limitation of this synthetic strategy may, however, arise from the β-hydrogen activity of compounds [$R_2CHCH_2ReO_3$] which is evident from the reaction of Re_2O_7 with $Sn(C_2H_5)_4$ that leads to reduction of the metal with concomitant ethylene/ethane elimination.[51] Tetraphenyllead does not form the (still unknown) phenyl complex [$C_6H_5ReO_3$] with Re_2O_7 but rather the plumboxy derivative [{($C_6H_5)_3PbO$}ReO_3].[50b]

The silyl and stannyl esters [{$(CH_3)_3SiO$}ReO_3] and [{$(CH_3)_3SnO$}ReO_3], respectively, undergo reductive alkylation by aluminum alkyls to form d^1-rhenium(VI) compounds of general formulas $R_4Re_2O_4$ (e.g., **9a**) and $R_6Re_2O_3$ (e.g., **9b**; see Section 2.3).[50b,51] The latter compounds undergo oxidative cleavage with γ-picoline *N*-oxide to form the mononuclear Re^{VII} derivatives R_3ReO_2 (**9c**).[50b,51]

Replacement of the *ten*-carbon π-ligand of **2** by *one* methyl group in complex **4** must of course relieve steric crowding dramatically. Figure 2 gives a pictorial view of this issue.[50b] Evidently the metal atom is no longer buried under the surrounding ligands, so attachment of further groups at the metal should now be possible. Although investigations into the chemistry of **4** have just started, some typical reactions can already be given. Amines such as quinuclidine or 1,4-diazabicyclo[2.2.2]octane (DABCO) form stable, crystalline adducts of formulas **6a** and **6b**, respectively, demonstrating the Lewis acidity of the metal center in compound **4** (X-ray structural analysis for **6a**).[50b] These two complexes exhibit trigonal-bipyramidal geometry. Ammonia and bipyridine, however, form octahedral adducts **6c** and **6d**, respectively, the oxo ligands of

$[CH_3ReO_3]\cdot C_7H_{13}N$	$2[CH_3ReO_3]\cdot C_6H_{12}N_2$
6a	**6b**
$[CH_3ReO_3]\cdot 2NH_3$	$[CH_3ReO_3]\cdot C_{10}H_8N_2$
6c	**6d**

which are electron-rich. **4** reacts with sodium hydroxide in the presence of benzo[15]crown-5 (B15C5) according to equation (a) yielding the perrhenate **6f**, very likely via the intermediate **6e** with clean elimination of methane. **6f** has an unprecedented double-helix crystal structure.[50c]

$$[CH_3ReO_3] + NaOH \xrightarrow{B15C5} [Na(B15C5)][CH_3Re(OH)O_3] \longrightarrow [Na(B15C5)][ReO_4] + CH_4 \quad (a)$$

4 **6e** **6f**

Treatment of **4** with ^{17}O-labeled water should proceed along the same pathway: the intermediate **6g** would explain the observed rapid oxygen-exchange reaction.[50c]

$[CH_3ReO_3]\cdot x\,H_2O$ $[CH_3ReOCl_2]$

6g (x = 1, 2) **7**

Thionyl chloride converts **4** at low temperatures into a sensitive dark-red compound of the composition **7**, whose structure is still unknown.[50b] While a mixture of triphenylphosphane and chlorotrimethylsilane converts sterically crowded **2** reductively into the organorhenium(V) chloride **12** (see Scheme 4),[34b-d] the methyl compound **4** rather forms the dinuclear product **8** (Scheme 2) in which each metal atom has a total of six ligands, with the ReORe backbone being strictly linear (Fig. 3).[74]

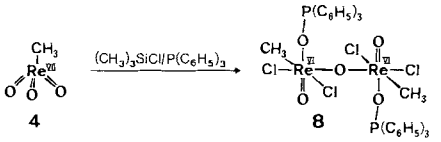

Scheme 2.

Let us speculate for a moment. Scheme 1 does not comprise any redox chemistry. Hence there is no reason to assume that analogous reactions should not be feasible in related high-valent metal oxides such as V_2O_5 (possibly yielding dimers or oligomers of net composition $[CH_3VO_2]$), Cr_2O_3 (yielding a tetramer of net composition $[(CH_3)_4Cr_4O_4]$, with a cubane-type structure like the known $[(\eta^5\text{-}C_5H_5)_4Cr_4O_4]$),[53] unless the special structural features of Re_2O_7 dictate its chemistry. With only few exceptions[53-55] our knowledge of organometallic oxides mainly suffers from a lack of synthetic strategies.

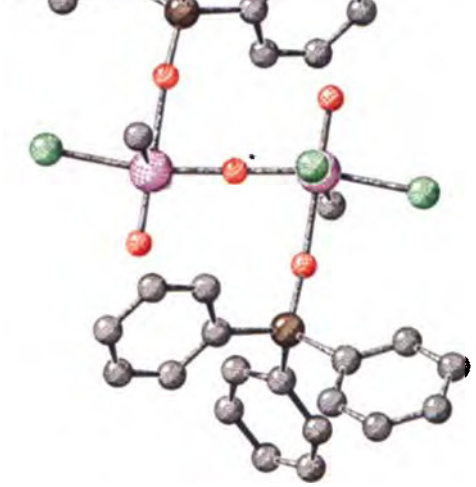

Fig. 3. Molecular structure of the dinuclear Re^{VI} complex **8**. The molecule has a center of symmetry (*) located at the central oxo bridge.

2.3. Exchange of One Oxygen for Two Methyl Groups

Dimethylzinc is generally considered by organometallic chemists to be a mild, *non-reductive* methylating reagent. This assessment does not apply, however, to its reaction with Re_2O_7 as shown in Scheme 3. In this case, the rhenium(VI) compound **9a** (Fig. 4, left; yellow, sublimable crystals; m.p. 120°C) is formed via **4**, from which it can also be made. The kinetic product **9a** is further methylated by excess dimethylzinc in a non-reductive way to the thermodynamic product **9b** (Fig. 4, right; red, sublimable needles; m.p. 88°C).[47] This last-named compound had previously only been accessible via a more tedious indirect route.[56] Only when dirheniumheptoxide **3** is treated with stoichiometric amounts of dimethylzinc (molar ratio 1/1), can the mononuclear Re^{VII} complex **4** be isolated, thus proving its intermediacy for the subsequent complexes **9a** and **9b**.[50d] This observation gives support to the expectation that phenyl and longer chain alkyl groups can be achieved in complexes of simple composition $RReO_3$ (metal-oxide substituted alkanes!) by virtue of the easily accessible organozinc compounds.

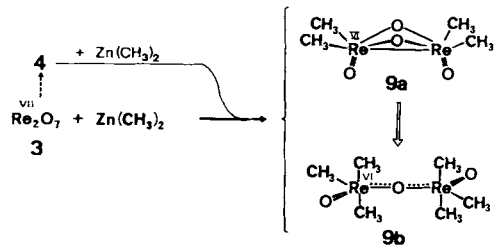

Scheme 3.

Fig. 4. Left: Molecular structure of the dinuclear Re^{VI} complex **9a**. The compound crystallizes upon vacuum sublimation in the monoclinic space group *Pn*. The hydrogen atoms have not been localized. Right: Molecular structure of the Re^{VI} complex **9b**. The diamagnetism observed for this particular organorhenium(VI) oxide is due to a 'super exchange' phenomenon typical for *linear* oxo bridges. The center of symmetry is marked with an asterix (*). The drawing was generated from the X-ray data given by *Wilkinson* et al. in Ref. [56].

If one disregards the metal-metal bond present in **9a** (259.3(< 1) pm),[47] then a strongly distorted square-pyramidal coordination geometry for rhenium is evident in the solid-state structure [two square pyramids joining the basal oxygen groups O(1) and O(2)]. Figure 5 shows how the individual dinuclear molecules are close-packed in the lattice unit cell.

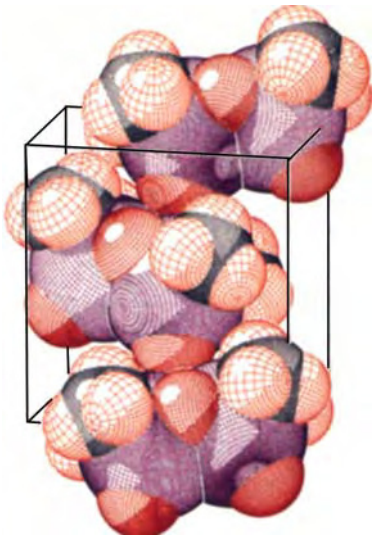

Fig. 5. Space-filling model of the unit cell of **9a**, showing that a close-packed arrangement of the individual dinuclear molecules is supported by the terminal oxo groups approaching bridging positions at neighboring molecules.

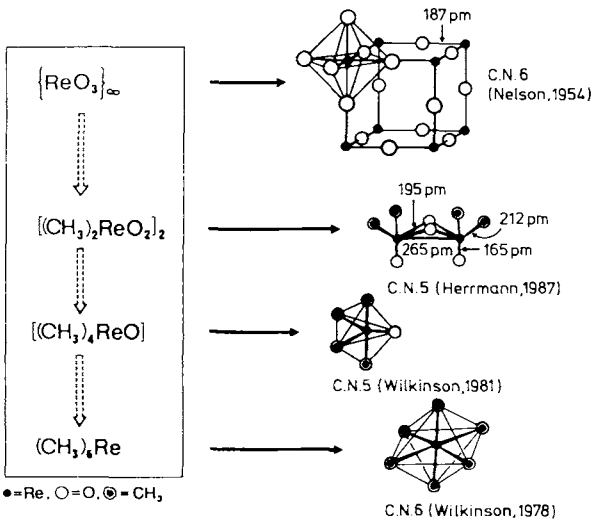

Fig. 6. From rhenium trioxide to hexamethylrhenium. In no compound of this series does the metal atom show a coordination number <5.

The novel methyl(oxo) compound **9a** can quite easily be put in the row of other, known rhenium(VI) species (Fig. 6). Rhenium trioxide is kind of a reference compound. Due to the low ligand/metal ratio of 3/1, it must have a 'polymeric' (perovskite-type) structure with several oxygen atoms joined by two metals in order to achieve an acceptable coordination number for rhenium.[26] Formal replacement of two methyl groups for one oxygen atom yields a higher ligand/metal ratio (4/1) with concomitant breakdown of the highly aggregated ReO_3 structure. This is the reason why "$(CH_3)_2ReO_2$" is just a dimer (and not paramagnetic, because of metal–metal spin pairing). Exchange of another oxygen by two more methyl groups (on paper) gives *Wilkinson*'s tetramethyl(oxo)rhenium(VI), which compound can exist as a (paramagnetic) monomer[50] since a coordination number of five has already been reached. Finally, hexamethylrhenium(VI) represents the fully methylated terminal of this series;[27] like its formal d^1-'precursor' $[(CH_3)_4ReO]$, it is paramagnetic since spin pairing is not possible.

The four compounds shown in Figure 6 form the first complete series of isovalent methyl/oxo derivatives of any transition metal. There is again no reason to assume that similar analyses will fail for other metals. Tungsten, as rhenium's uncle in the periodic table should play this game as well, e.g. $WO_3 \longrightarrow [(CH_3)_2WO_2]\,(?) \longrightarrow [(CH_3)_4WO]\,(?) \longrightarrow [(CH_3)_6W]$.[57]

When dimethylzinc reduces rhenium(VII) by one step in the reactions of Scheme 3, methyl groups appear to become oxidized at the same time since zinc is already in its highest possible oxidation state. Observation of ethane supports the idealized equation (b).

$$\underset{\mathbf{4}}{2\,[CH_3ReO_3]} + 2\,Zn(CH_3)_2 \longrightarrow \underset{\mathbf{9a}}{[(CH_3)_4Re_2O_4]} + 2\,ZnO + C_2H_6 \quad (b)$$

Reduction processes also come to the fore when higher tetraalkyltin reagents SnR_4 are subjected to high-valent rhenium compounds such as Re_2O_7 **3** (see Section 2.5).[58a] Derivatives of compound **9a** undergo symmetric cleavage when treated with alkaline metals M such as lithium, to give ionic products of the type

$$M^{\oplus}[R_2ReO_2]^{\ominus} \quad \mathbf{9c}$$

in which the d^2-Re^V anion has a distorted tetrahedral structure ($R = CH_2C(CH_3)_3$).[51a] Re^{VII} alkyl complexes of formulas $[R_2ReO_2Br(L)]$ (R = alkyl, L = pyridine) and $[R_3ReO_2]$ have been presented in further papers by *Hoffman* et al.[51b]

2.4. Functionalizations at Metal Oxide Fragments

Reductive processes govern the chemistry of $[(\eta^5\text{-}C_5Me_5)ReO_3]$ **2** no matter whether Lewis bases or Lewis acids are used as reagents. Typical examples are germanium dichloride (as 1,4-dioxane adduct $GeCl_2 \cdot C_4H_8O_2$) and alkylating agents such as AlR_3 or ZnR_2 that effect rather clean formation of the oxodichloro and oxodialkyl compounds **10** and **11**, respectively (Scheme 4a). These Re^V

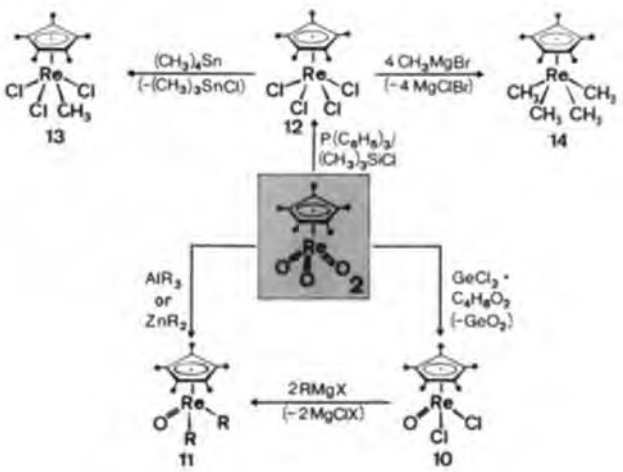

Scheme 4a.

species are once again powerful and useful synthetic intermediates for a range of other half-sandwich complexes. Thus, treatment of the oxodichloride **10** with the reagents indicated in Figure 7 yields compounds **15a–g**, most of which have (stable) rhenium–oxygen bonds. The rhena(V)-

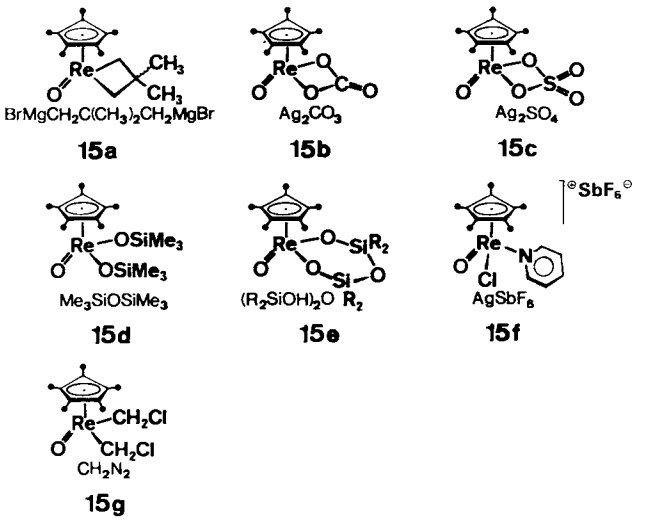

Fig. 7. Various organorhenium complexes resulting from chlorine substitution of $[(\eta^5\text{-}C_5Me_5)ReOCl_2]$ **10** by means of the reagents listed underneath the respective compounds.

cyclobutane **15a** eliminates isobutylene, while the carbonato derivative **15b** loses carbon monoxide upon gentle heating. Sulfur dioxide is (reversibly) lost from **15c** at elevated temperature. Ionic compounds of type **15f** may serve as intermediates of chiral derivatives of general composition $[(\eta^5\text{-}C_5Me_5)Re(=O)Cl(L)]^{\oplus}$. The siloxy compound **15d** as well as the stannoxy congener $[(\eta^5\text{-}C_5Me_5)ReO(OSnMe_3)_2]$ are also *directly* available from **2** and hexamethyldisilane (or the distannane, resp.) in boiling toluene [Eqn. (c)].[58b] Compound **15e** may serve as a simple model of silica-bound organorhenium catalysts.

$$[(\eta^5\text{-}C_5Me_5)ReO_3] + (Me_3Sn)_2 \longrightarrow [(\eta^5\text{-}C_5Me_5)ReO(OSnMe_3)_2] \quad (c)$$

Other Lewis base reactions of the title compound **2** are described in Section 2.10 (Scheme 14).

2.5. Alkylation or Reduction?

A nice comparison for alkylation *versus* reduction effected by tetramethyltin and its higher homologues is provided by the Re^V complex **12** (Scheme 4a) that now presents another very useful key compound in organorhenium chemistry.[34] Even when treated with an excess of *tetramethyl*stannane, the *mono*methylated product **13a** forms quantitatively while reduction of rhenium does not occur at all (Scheme 4a).[59] Successive methylation reactions of **13a** may be achieved, however, with dimethylzinc (*no* reduction again).[52,60] The fully methylated derivative **14** is a very water-, air-, light- and temperature-sensitive compound (stable only well below 0 °C).[61,62] The partially alkylated members **13b** and **13c** of this series are best synthesized *via* a detour (Scheme 4b): first, the chiral **11b**, which is an ideal precursor for complexes **11c–e** that contain different alkyl ligands,[52] is obtained *quantitatively* by hydrolysis (water/pyridine; molar ratio 1 : 2). The dimethyl derivative **11a** can be converted into **13b** by means of the oxophilic organotitanium(IV) reagent $[(\eta^5\text{-}C_5H_5)TiCl_3]$.[52] This route is all the more useful in that a selective methylation **13a** → **13b** does *not* work. Further stepwise methylation employing stoichiometric amounts of Grignard reagents lead according to Scheme 4b *via* (now isolable) trimethyl **13c** ultimately to the tetramethyl derivative **14**.[52]

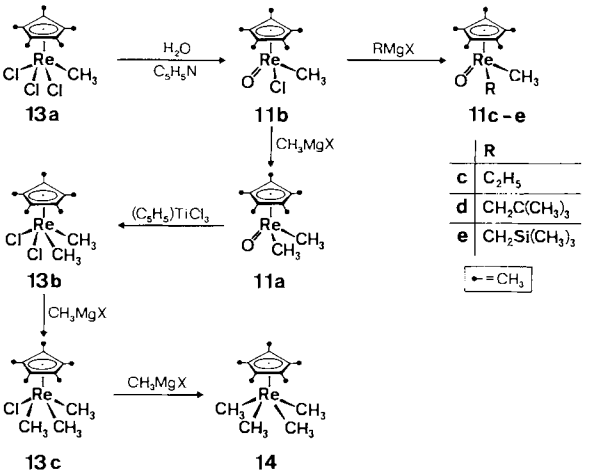

Scheme 4b.

An interesting exception is the bis(neopentyl) derivative **11a'**, which is also isolable: upon chlorination with trichloro(η^5-cyclopentadienyl)titanium(IV) cleavage of neohexane leads to formation of the paramagnetic carbyne complex **13b'** (Scheme 4c). This undergoes a reversible

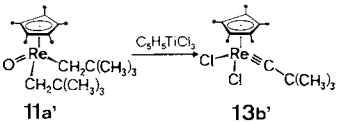

Scheme 4c.

one-electron oxidation ($E_{1/2} = 0.79$ V) and with silver hexafluoroantimonate yields the cationic, diamagnetic product $[(\eta^5\text{-}C_5Me_5)ReCl_2(\equiv C\text{–}CMe_3)]^{\oplus}[SbF_6]^{\ominus}$.[52]

All compounds of the series $[(\eta^5\text{-}C_5Me_5)ReL_4]$ are d^2-Re^V systems (L = alkyl, halogen), display singlet/triplet spin equilibria (magnetic measurements and NMR evidence),[52,59–61] and have square pyramidal crystal structures with the π-aromatic ligand always occupying the apex of the polyhedron (Fig. 8).

*Tetraethyl*stannane reacts with the tetrachloride **12** to give the dinuclear complex **16**. The ethylrhenium(V) intermediate $[(\eta^5\text{-}C_5Me_5)ReCl_3(C_2H_5)]$ (Scheme 5) is probably formed but is further *reduced* to the stable rhenium(IV) dimer of net composition $[(\eta^5\text{-}C_5Me_5)ReCl_3]$ with concomitant formation of ethylene and ethane (no hydrogen).[59] In terms of structure, the dimer **16** is related to α-$\{ReCl_4\}$ in that it also displays *two* chloro bridges between rhenium atoms. Due to the bulky five-membered ring ligand, how-

Fig. 8. All $[(\eta^5\text{-}C_5R_5)ReL_4]$ complexes have a square-pyramidal ('pianostool') geometry. The example shown here is the first homoleptic organorhenium(v) compound, tetramethyl(η^5-pentamethylcyclopentadienyl)rhenium **14**. Due to disorder phenomena, individual structural parameters cannot be given for this particular compound; average Re-C1···C4 distances 217(3) pm, average CReC angles 81(1) and 136(1)°.

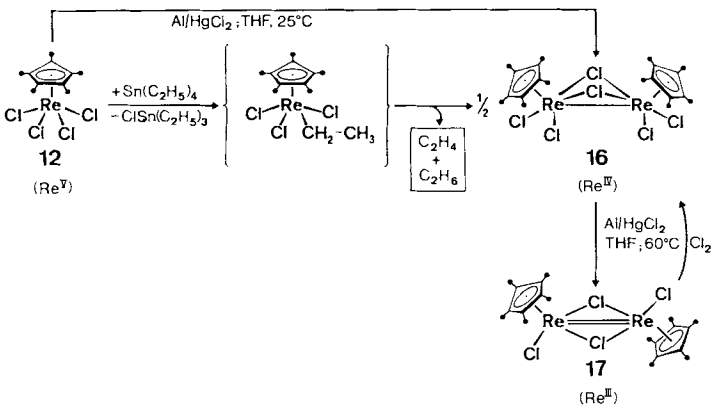

Scheme 5.

ever, the polymeric chain structure of rhenium tetrachloride[26b] is cut down to dinuclear ensembles in the 'organic' derivative **16** owing to its bulky π-aromatic ligand (Fig. 9). The compound is also available from the Re^V precursor **12** by reduction with electropositive metals, preferably powdered aluminum (Scheme 5).

Fig. 9. Molecular structure of the orgahorhenium(IV) complex **16'** $[(\eta^5\text{-}C_5Me_4Et)ReCl_3]_2$. **16'** was synthesized by reduction of $[(\eta^5\text{-}C_5Me_4Et)ReCl_4]$ **12'** with $Sn(C_2H_5)_4$ or $Al/HgCl_2$. Shown is a computer-generated space-filling model that underlines the *cis* geometry of the two five-membered ring ligands. — Re-Re' 307.4(<1) pm.

The Re_2^{III} dimer **17** obtained by further reduction of **16** (and vice versa) by means of $HgCl_2$-activated aluminum (Scheme 5) is shown in Figure 10 for the sake of comparison. From the close packing of both the bridging and the terminal chloro groups around the (formal) metal–metal double bond (250.6(<1) pm), the rather low reactivity towards neutral ligands such as alkynes becomes evident.

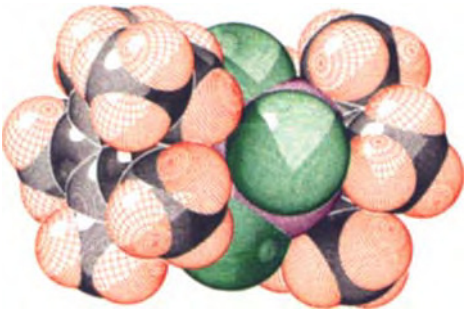

Fig. 10. Further reduction of **16'** (Fig. 9) yields the organorhenium(III) dimer $[(\eta^5\text{-}C_5Me_4Et)ReCl_2]_2$ **17'** (see also Scheme 5). The two five-membered ring ligands are parallel to each other (*trans* geometry).—Selected bond lengths [pm] and angles [°]: Re-Re' 250.6(<1), Re-Cl(terminal) 240.6(1), Re-Cl(bridge) 239.7(1) and 240.1(1); ReCl(bridge)Re' 63.0(0). The space-filling model suggests no great difference between bridging and terminal chloro ligands. A center of symmetry is located at the midpoint of the metal-metal (double) bond.

Thus, tetramethylstannane does not reduce high-valent rhenium compounds, whereas β-hydrogeno-containing tetraalkylstannanes very much do so. Consequently, these various stannanes should display distinct differences in activity when employed as cocatalysts in rhenium-containing olefin-metathesis catalysts. It is therefore difficult to understand why tetramethyl- and tetra-*n*-butylstannane are frequently used interchangeably for this purpose without too great a difference in catalyst activity and selectivity—this certainly constitutes an unsolved problem of significance.[48]

2.6. Olefin Metathesis[65]

Schrock has repeatedly pointed out that higher metal oxidation states (e.g. W^{IV}) are essential for olefin metathesis, a mechanistically interesting and commercially important process.[66] Since $Re_2O_7/Sn(CH_3)_4/Al_2O_3$ represents an effective (heterogeneous) olefin metathesis catalyst system, it appeared obvious that the methylrhenium oxide **4** would serve as a key to the understanding of this special catalyst/cocatalyst system.

As a matter of fact, **4** catalyzes both ring opening polymerization of cyclopentene and metathesis of open-chained olefins but requires aluminum trichloride and excess tetramethylstannane in order to do so.[47] The Lewis acid effect upon olefin metathesis has been emphasized by *Osborn* et al.,[67] and we believe that the Lewis acid $AlCl_3$, in our case, removes an oxygen atom of CH_3ReO_3 in order to introduce one or two more methyl groups so that the prerequisites for carbene-ligand generation via elimination of methane according to the generally assumed reaction sequence (d) are fulfilled. That this may not be a poor hypothesis is demonstrated by the fact that compound **9b** which has the higher CH_3/Re ratio of 3/1 does effect olefin metathesis, even in the absence of tetramethylstannane.[47,58a]

$$M(CH_3)_2 \longrightarrow M{=}CH_2 + CH_4 \qquad (d)$$

In the light of recent work by *Osborn* et al., it appears quite obvious that $AlCl_3$ first forms an adduct with the organometal oxide with subsequent reduction, which possibility is even more likely in that the related reaction (e) is

$$[(\eta^5\text{-}C_5Me_5)ReO_3] + Al(CH_3)_3 \longrightarrow [(\eta^5\text{-}C_5Me_5)ReO(CH_3)_2] + \cdots \quad \text{(e)}$$

2 **11a**

known.[34] We have in fact isolated a red, crystalline compound of composition $[(\eta^5\text{-}C_5Me_5)ReO(CH_3)_2]\cdot AlCl_3$ **18** at low temperature which decomposes upon warming to ca. 0 °C.[58c] By way of analogy, reductive chlorination [Eqn. (f)] of **4** with subsequent chlorine/methyl exchange by excess tetramethylstannane may not be pure fantasy. This proposal would involve oxidation state +5 at rhenium to promote olefin metathesis processes.

$$[CH_3ReO_3] + AlCl_3 \longrightarrow [CH_3ReO_2Cl_2] + \{AlOCl\} \quad \text{(f)}$$

In continuation of such considerations we have recently been able to establish a catalyst system which surpasses all previously known rhenium-containing catalysts in the *metathesis of functionalized (!) olefins*.[58a]

2.7. Oxidative Coupling of Alkynes; Model Compounds and Reality

A group at the Amsterdam Shell laboratories reported the oxidative coupling of two alkyne molecules to give furan derivatives,[68] important compounds in industry. This rather intriguing coupling reaction, in which *one* CC and *two* OC bonds are formed, also involves participation of the organorhenium(VII) oxide **2** (Scheme 6). While triphenylphosphane alone reacts with **2** with clean formation of the Re^V dimer **20** according to equation (g), the novel rhena(V)-pyrans **19** are formed as isolable compounds in the presence of alkynes, e.g. 2-butyne. These latter compounds **19** undergo double metal–carbon bond cleavage upon successive treatment with iodine.[68]

$$[(\eta^5\text{-}C_5Me_5)ReO_3] + P(C_6H_5)_3 \longrightarrow \quad \text{(g)}$$

2

$$\tfrac{1}{2}[(\eta^5\text{-}C_5Me_5)ReO_2]_2 + O{=}P(C_6H_5)_3$$

20

A further challenge for organometallic oxide chemistry is to carry out the oxidative coupling outlined in Scheme 6 as a *catalytic* reaction. A synthesis of pyrroles via participation of imido groups (NR) attached to rhenium should also be conceivable. An alkyne/alkyne/sulfur coupling reaction catalyzed by cyclopentadienylcobalt complexes has recently been described by *Bönnemann*.[69]

The attractive-looking synthesis of heterocycles mentioned in the preceeding paragraph warrants a better understanding of the largely unexplored interactions between alkynes and organorhenium fragments of intermediate oxidation states.

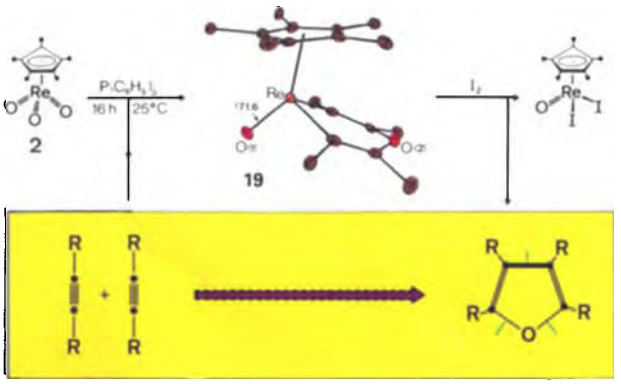

Scheme 6.

Alkynes are rarely found as ligands in organorhenium complexes, even with rhenium in low oxidation states. Probably best known are alkyne-to-vinylidene isomerizations at Re^I centers.[70] Trivalent rhenium forms several structurally simple oxidic alkyne complexes **21a**, **b**, the synthesis of which has recently been reported by *Mayer* et al. (Scheme 7).[28, 71, 72] The assignment of oxidation states is of course rather formalistic here since the alkynes seemingly act as 4e-ligands. The same problem is encountered in the case of the unprecedented Re^{II} complexes $[(RC{\equiv}CR)_4Re_2O_2]$ **21c** (characterization by means of X-ray diffraction techniques).[73]

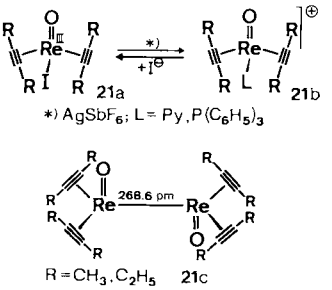

Scheme 7.

Clean reductive substitution ($Re^{7\oplus} \rightarrow Re^{5\oplus}$) of alkynes for oxo groups occurs at methyltrioxorhenium(VII) (**4**) in the presence of polymer-bound (!) triphenylphosphane as a selective reductant. A whole range of thermally rather stable π-alkyne complexes **22** has thus been prepared according to Scheme 8.[74] The occurrence of isomers in the cases of **22c** and **22e** suggests high rotational barriers between the metal and the alkyne ligands. Even the unsubstituted acetylene ligand of compound **22a** does not exhibit fast rotation on the NMR time scale up to at least 100 °C.

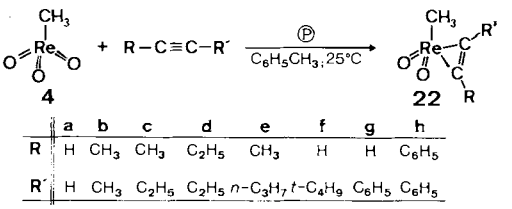

Scheme 8. Ⓟ = polymer-bound $P(C_6H_5)_3$ [74].

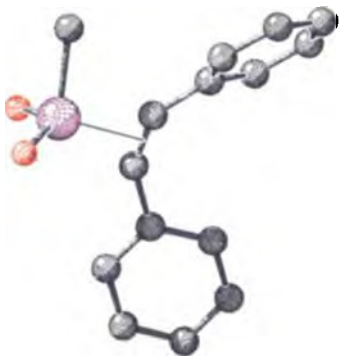

Fig. 11. Molecular structure of $[CH_3ReO_2(\eta^2\text{-}C_6H_5C{\equiv}CC_6H_5)]$ **22h**. The compound crystallizes from methylenechloride/*n*-hexane at −25°C in the monoclinic space group $P2_1/c$.—Selected bond lengths [pm] and angles [°]: Re-O 174.0(4) and 171.0(1), Re-CH_3 209.2(7), C-C(ethyne) 128.0(9); OReO 119.5(2) [74].

An X-ray structure of **22h** confirms the suggested structure (Fig. 11) which is in contrast with theoretical predictions.[99] Note that all attempts to synthesize the analogous compounds with a pentamethylcyclopentadienyl ligand in place of the methyl group have thus far failed. Thus the butyne-Re^{III} complex $[(\eta^5\text{-}C_5Me_5)ReO(\eta^2\text{-}MeC{\equiv}CMe)]$ (**33**) does not undergo oxidation to give (the hitherto unknown) Re^V derivative $[(\eta^5\text{-}C_5Me_5)ReO_2(\eta^2\text{-}MeC{\equiv}CMe)]$.[64a] Oxidation of **33** (R = Ph) with ferricinium salts cleanly furnished the dinuclear cation $[(\eta^5\text{-}C_5Me_5)_2Re_2(\mu\text{-}O)_2(tolan)_2]^{\oplus}$.[64a]

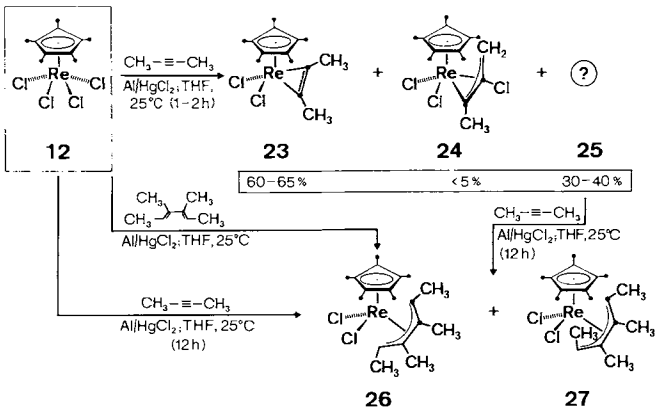

Scheme 9.

Further deoxidation of compounds **22** is only possible with polymer-bound triphenylphosphane under more drastic conditions, e.g., boiling toluene. The expected mononuclear Re^{III} derivatives $[CH_3ReO(\eta^2\text{-}RC{\equiv}CR)_2]$, however, are not formed, but rather the dinuclear Re^{IV} species of composition $[(\mu\text{-}O)\{CH_3ReO(\eta^2\text{-}RC{\equiv}CR)\}_2]$ (X-ray structural analysis for R = CH_3).[52]

The Re^{III} complex **23** (with 2-butyne as 4e-ligand) is accessible according to Scheme 9 by reduction of the parent Re^V compound **12**.[63,75] In terms of further chemical transformations, chlorine replacement at the stage of compound **23** by alkyl and oxo groups is particularly useful.[75]

The byproduct of the Re^V-reduction outlined in Scheme 9 is the Re^V-vinyl/carbene derivative **24**, whose unexpected composition and structure are shown in Figure 12 (left).[75] It derives from the C_4-alkyne by loss of a hydrogen atom, with concomitant metal-to-carbon chlorine transfer. The structure of **24** is best interpreted as an allylidene complex on geometrical grounds.[75] Finally, a third product **25** of unknown identity proved very useful for subsequent reductive carbon–carbon coupling processes. Thus, excess 2-butyne yields a mixture of two isomeric Re^{III}-1,3-diene complexes **26** and **27**, respectively (Scheme 9). The diene complex **26** can also be prepared under reductive conditions from **12** and 3,4-dimethyl-2,4-hexadiene.[76]

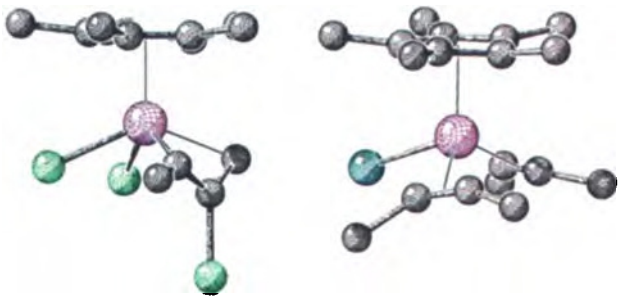

Fig. 12. Left: Molecular structure of the allylidene complex **24**. Selected bond lengths [pm] and angles [°]: Cl3-C2 178.8(3), Re-Cl1 239.1(1), Re-Cl2 241.9(1); Cl1ReCl2 82.27(3).—Right: Structure of the cationic bis(η^2-butyne) complex **29** in the crystal, Br instead of Cl (see Scheme 10).—Selected bond lengths [pm]: C≡C 136(2) and 124(2), Re-C 199(1)/201(1) and 198(2)/202(2). The crystal contains dichloromethane (1 : 1).

Chlorine/pyridine exchange at the stage of **23** to form compounds of type **28** is achieved by silver hexafluoroantimonate (Scheme 10). Likewise, a second alkyne may be introduced if one removes a chloride group from **23** by means of $AgSbF_6$ in the presence of the new alkyne to enter the molecule. The cationic bis(π-alkyne) complexes **29** (Fig. 12, right) exhibit free metal-to-alkyne rotations only at higher temperatures. Rotational barriers around 60 kJ mol^{-1} have been established by temperature-dependent NMR spectroscopy.[64b,75]

A synthetically useful acid catalysis effect is demonstrated by π-alkyne complexes of type **23** (d^4-Re^{III}); CC coupling processes that do not work in the absence of Brønsted acids take place when **23** is treated with traces of

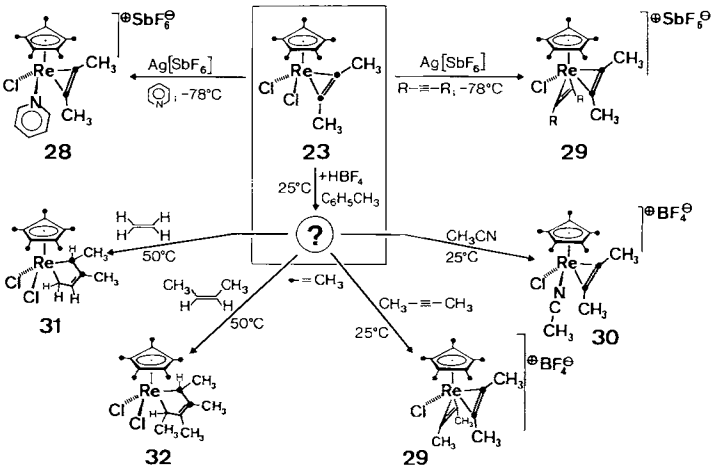

Scheme 10.

HBF_4 in the presence of ethylene or *cis*-2-butene. The 1,3-diene complexes **31** and **32** (Fig. 13, left), respectively, are thus obtained in yields around 80% (Scheme 10).[76] Stoichiometric amounts of HBF_4 suffice to achieve fast chlorine substitution in the presence of acetonitrile to give the (chiral) ionic compound **30** according to Scheme 10.[76]

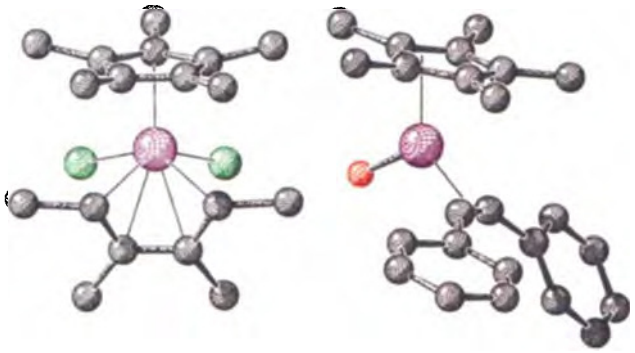

Fig. 13. Left: Structure of the 1,3-diene complex **32** in the crystal. Right: Structure of the alkyne(oxo) complex $[(\eta^5\text{-}C_5Me_5)ReO(\eta^2\text{-}C_6H_5C{\equiv}CC_6H_5)]$ **33** in the crystal.—Selected bond lengths [pm] and angles [°]: Re-O 171.0(1), C≡C 130.0(2), Re-C(alkyne) 203.0(1), 203.6(1); $C(C_6H_5)$-C-C 142.2(2) and 145.6(2).

The synthetic potential of Re^{III} alkyne complexes such as **23** (also Br and I in place of Cl, and R = alkyl, aryl) is further demonstrated by their smooth hydrolysis to give novel oxo(alkyne) derivatives **33** (**33**, R = Ph, see Fig. 13, right), and by their reaction with Grignard compounds to form **34** and **35**.[63]

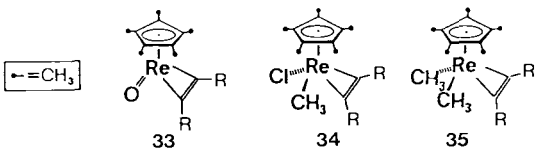

33 **34** **35**

2.8. The Search for Organorhenium Oxides that Oxidize Olefins

The formation of furans from rhena(v)-pyrans according to Scheme 6 constitutes an oxidative carbon–carbon coupling process during which the metal stays in oxidation state +5; in this reaction elemental iodine is the oxidizing agent.[68] Redox-neutral rhenium–oxygen bond cleavage occurs when five-membered metallocycles of type **36** are treated with Brønsted acids such as HBF_4 according to Scheme 11.[77]

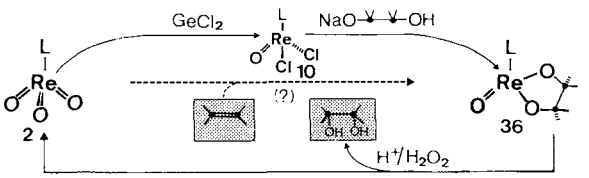

L = η^5-C_5Me_5

Scheme 11.

The metallocycles **36** may alternatively be viewed as *O,O*-glycolate complexes like those known from *Sharpless'* osmium work on the *cis* hydroxylation of olefins to 1,2-glycols.[21a,78] In spite of the fact that the osmium tetroxide used in these catalytic reactions is extremely toxic (maximum working concentration 0.002 $mg \cdot m^{-3}$!), no better replacement has been found as yet. This is a result of our rather crude general knowledge of the hydrocarbon chemistry occurring at high-valent transition metals. It may certainly be true that metals other than Os^{VIII} are inferior in oxidation power, but a 'tune up' towards the right potentials and intermediates seem possible by way of tailored auxiliary ligands. In this important area of metal-mediated oxidation chemistry, a similar development as that which occurred in low-valent coordination compounds for hydroformylation, olefin hydrogenation etc. is conceivable. Instead of the 'soft' phosphanes useful for these latter processes, the 'hard' oxo, alkoxide, and imido ligands might yield step-by-step improvements at the higher oxidation states of transition metals.

To this end, we have synthesized a number of rhenium(v) glycolates as well as their *O,N-*, *O,S-*, and *S,S* congeners.[77,79] Apart from a few exceptions, these compounds are in general thermally quite robust, but heating above the melting points effects selective oxygen–carbon bond breaking in the case of the glycolate compounds with formation of the corresponding olefins. Since $H^{\oplus}/H_2O_2$ treatment, on the other hand, cleanly gives glycols and the rhenium(VII) oxide **2** (Scheme 11), the only missing link in a catalytic cycle is direct cycloaddition of the olefins to the oxide **2**. Since activated carbon–carbon double bonds like those in ketenes undergo clean [3+2] and [2+2] cycloaddition reactions to produce compounds **37** and **38** according to Scheme 12 (X-ray characterization),[39,42] it appears just a matter of enhancing the ReO_3 core reactivity, e.g. by replacement of the C_5Me_5-ligands by more electron-withdrawing groups (e.g. CF_3), in order to reach the penultimate goal of removing the question mark from Scheme 9. This has been achieved for several derivatives of methyltrioxorhenium(VII) **4**[50b] and, at the same time, replaces the model compounds by a catalytic cycle.

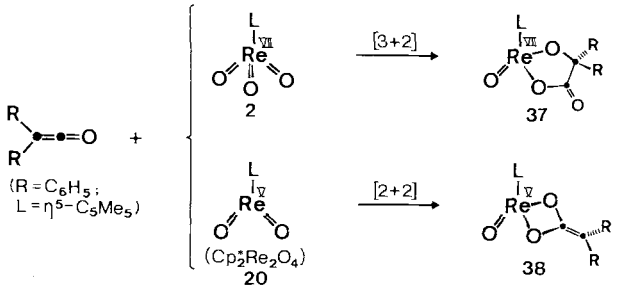

(R = C_6H_5; L = η^5-C_5Me_5)

2 **37** **20** **38**

Scheme 12.

Organometallic glycolate complexes of other metals of relevance in oxidation processes have also been synthesized. Thus, the organovanadium(v) species **39**[80,81] forms the dinuclear compound **40** having a $V_2O_3C_2$ seven-membered ring geometry (Fig. 14).[82,97]

$[(\eta^5\text{-}C_5Me_5)VOCl_2]$ **39**

$[\{(\eta^5\text{-}C_5Me_5)VO\}_2(\mu\text{-}O)(\mu\text{-}OCH_2CH_2O)]$ **40**

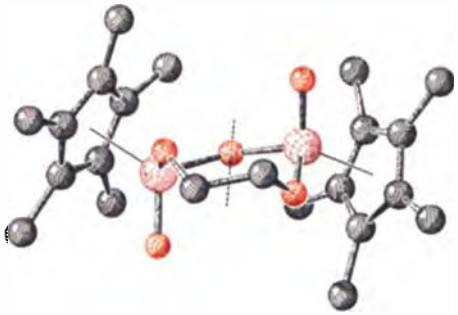

Fig. 14. Structure of the dinuclear organovanadium(v) complex **40** in the crystal. – Selected bond lengths [pm] and angles [°]: V=O 159.8(1), V-O(glycolate) 181.0(1), V-O(bridge) 177.7(1); VOV' 127.0(1).

Apart from their catalytic potential (e.g. for amine oxidation), *N,O*-metallocycles analogous to **38** provide easily accessible starting materials for the synthesis of imido complexes.[79]

Instead of glycolate ligands other anionic chelates can be attached to rhenium(v); examples are the carbonato- and sulfato complexes **15b** and **15c**, respectively (Fig. 7).[83] Rhenium-attached oxometalates of transition metals[84] (e.g. $[Cr_2O_7]^{2\ominus}$) are presently being investigated for their potential as organometallic catalysts on oxidic metal surfaces.

2.9. New Polyhydrides of Rhenium

Despite the uniqueness of our two title compounds $[(\eta^5\text{-}C_5Me_5)ReO_3]$ (**2**) and $[CH_3ReO_3]$ (**4**), it emerges from what has been outlined in the previous chapters that rhenium chemistry resembles that of molybdenum and tungsten much more than the chemistry of any other element, with the possible exception of osmium on the right and tantalum on the left.[85] Only with these three elements, molybdenum, tungsten, and rhenium is it possible to catalyze olefin metathesis at an industrially acceptable level.[66] Beyond this 'catalysis bracket', there are numerous analogous compounds, and the reader need only be reminded of the metal-metal multiple bonded compounds comprising a major, attractive part of the chemistry of these elements.[5]

Moreover, rhenium, like molybdenum and tungsten, is compatible with hydrogen and hydrido ligands (H_2 and H, resp.) across the entire range of oxidation states.[86] Let it suffice to mention only the textbook example of nonahydridorhenate(VII), $[ReH_9]^{2\ominus}$.[87] Hydrogen atoms attached to rhenium can also be found at low oxidation states such as Re^I in the examples $[HRe(CO)_5]$ or $[H_3Re_3(CO)_{12}]$ and many other complexes.[70] As a matter of fact, the redox versatility of hydridorhenium species is a great advantage of *Felkin*'s carbon-hydrogen activation catalysts of type $[L_2ReH_7]$ ($L = PR_3$)[88] while there is a demand for further improvement of catalyst activity and selectivity.[89]

The novel neutral rhenium(VII) hydride **41** – air-stable, sublimable, thermally robust up to the melting point at 192 °C! – can be prepared in 75% yield by treatment of the Re^V-complex **10** with lithium aluminum hydride in diethylether at low temperatures and subsequent reaction of the intermediate with methanol (Scheme 13).[90] The yields of

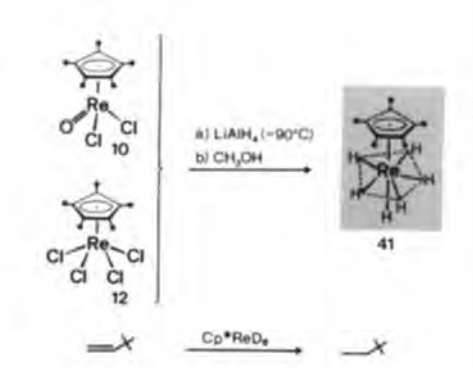

Scheme 13.

the *mononuclear* hexahydride **41** are lower when the tetrachloride **12** is used as a starting compound; in this case the dinuclear hexahydride **42** is also formed. This synthe-

$[(\eta^5\text{-}C_5Me_5)_2Re_2H_6]$ **42**

sis is mechanistically not fully understood but it is tempting to assume that the Re^V precursor compounds **10/12** are first converted into an intermediate $[(\eta^5\text{-}C_5Me_5)ReH_4]$, which subsequently undergoes formal oxidative addition of H_2 (from $LiAlH_4/CH_3OH$). The compound has a fluctional pentagonal-bipyramidal structure (temperature-dependent NMR experiments). Neohexene is hydrogenated by **41**. When $[(\eta^5\text{-}C_5Me_5)ReD_6]$ is used, a mixture of several neohexane isotopomers (Scheme 13, bottom) is observed by GC/MS.[58a]

Both thermal (> 200 °C) and light-induced elimination of hydrogen (0 °C) from **41** yield the red-colored, air-stable, dinuclear rhenium(IV) hydride **42**. According to a low-temperature X-ray diffraction study (−100 °C), two terminal and two bridging hydrogen atoms are present on each rhenium atom of **42'** (C_5EtMe_4 instead of C_5Me_5) (Fig. 15).[91]

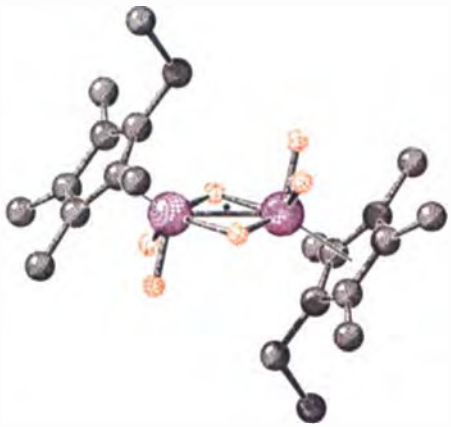

Fig. 15. Structure of the organorhenium(IV) complex bis[(μ-hydrido)dihydrido(η^5-ethyltetramethylcyclopentadienyl)rhenium](*Re≡Re*) **42'** in the crystal at −160 °C. – Re-Re distance 245.2(1) pm (triple bond).

Photolysis of **41** in the presence of trimethylphosphane, however, furnishes the derivative **43**, whereas treatment with hot carbon tetrachloride results in formation of the chloro complex **44** in a radical-type dark-reaction.[92]

trans-$[(\eta^5\text{-}C_5Me_5)Re(H)_2(PMe_3)_2]$ **43**

$[(\eta^5\text{-}C_5Me_5)Re(\mu\text{-}H)Cl_2]_2$ **44**

2.10. How Useful is the Pentamethylcyclopentadienyl Ligand Really?

The π-bonded pentamethylcyclopentadienyl ligand was fortunately retained at the metal when *Serrano* first synthesized the title compound **2** by light-induced oxidation of the parent carbonyl precursor **1**.[30] Excellent solubility of compound **2** and of essentially all derivatives in common organic solvents enabled us to quickly develop this type of high oxidation state organorhenium chemistry after we had found that purification of the compounds could be achieved by low-temperature column chromatography on silylated silica gel. The bulky ten-carbon ring ligand prevents more complicated reactions to occur but rather directs them to the ReO_3 core.

On the other hand, cleavage of the rhenium-carbon bonds of **2** is occasionally encountered. For example, deoxygenation effected by (polymer-bound[74]) triphenylphosphane cleanly yields the synthetically useful rhenium(V) compound **20** (see Scheme 14 and Section 2.7), but only if atmospheric oxygen is strictly excluded.[34] Otherwise, partial loss of the π-aromatic ring comes to the fore, with the perrhenate groups showing up in the products. The two structurally characterized compounds **45** and **46**[93] are good examples (Scheme 14).

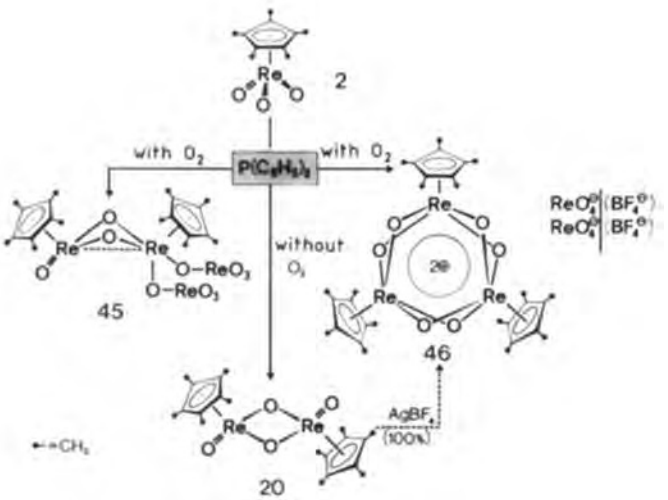

Scheme 14. In **45** we have the combination Re^{V}/Re^{VII}, in **46** $Re^{+5.66}/Re^{VII}$; **20** is a Re^{V}/Re^{V} complex.

These findings revealed that at some (mechanistically unknown) stage of the reaction atmospheric oxygen may split off the hydrocarbon π-ligand, which would therefore have to be replaced by better ones such as the more tightly bonded methyl group.[94] Now that we have achieved this goal by preparing methyltrioxorhenium(VII) (**4**) from Re_2O_7 and $Sn(CH_3)_4$, the entire range of compounds merits a firm place in catalysis research.[47] In this context, the alkyl ligand might be exploited for the generation of polymer chains that carry isolated metal oxides MO_x. Models for surface-anchored catalysts may be obtainable via *O,O*-chelation (Scheme 15).

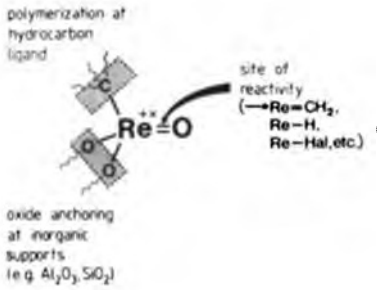

Scheme 15.

2.11. Sulfur and Selenium Instead of Oxygen?

The higher homologues of oxygen — sulfur and particularly selenium — are of great interest in organic synthesis or for medical applications.[95] The hitherto unknown sulfur and selenium congeners of compounds **2** and **4** are attractive target molecules. That oxygen is in fact prone to replacement by sulfur and selenium is evident from two reactions: (i) Treatment of $[(\eta^5\text{-}C_5Me_5)ReOCl_2]$ **10** with bis(trimethylsilyl) sulfide gives the oxygen-free compound **47** among other organorhenium sulfides from which the

$(\eta^5\text{-}C_5Me_5)_2Re_2S_4$ **47** $\quad [(\eta^5\text{-}C_5Me_5)Re(O)S_4]$ **48**

main product has so far resisted separation.[96] (ii) Four sulfur atoms are transferred from $[(\eta^5\text{-}C_5H_5)_2TiS_5]$ to the same organorhenium(V) compound **10** to form the air-stable, mononuclear complex **48** in a surprisingly clean reaction (≥90% yield). The five-membered, non-planar ReS_4 ring system thus generated is evident from Figure 16.[97]

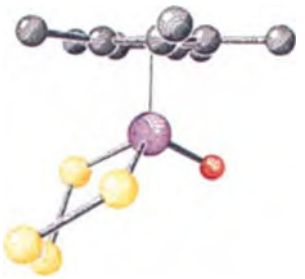

Fig. 16. Molecular structure of the ReS_4 metallacycle **48**.—Selected bond distances [pm]: Re-O 171.8(3), Re-S 226.4(1) and 224.4(2).

Due to the much higher catenation and cyclization tendency of sulfur and selenium over oxygen, this chemistry appears by far less predictable at present, but nevertheless presents another exciting challenge for skilled experimentalists.

2.12. Back to Monovalent Rhenium — A Play with Oxidation States

We now return to our starting point of monovalent rhenium. Conversely to its mode of formation, the title compound **2** can be reduced by carbon monoxide under pressure or by the oxophilic carbonylation reagent $[(\eta^5\text{-}C_5H_5)_2Ti(CO)_2]$ at normal pressure.[36] If there is only one terminal oxo group present, reductive carbonylation follows the overall equation (h).

$$[L_yM^x{=}O] + 3\,CO \longrightarrow [L_yM^{x-2}(CO)_2] + CO_2 \qquad (h)$$

Typically, the Re^V chelate complex **38** is reduced to the Re^{III} complex **49** (X-ray characterization) with concomitant isomerization of the bidentate O,C ligand (Scheme 16).[44]

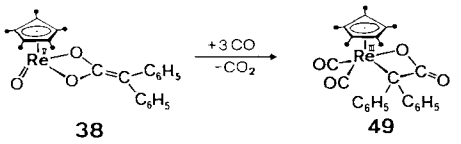

38 49

Scheme 16.

Clean redox processes also take place when the strongly reducing zirconium(III) complex **50** reacts with the organorhenium(VII) oxide **2**. The desired rhenium/zirconium oxide was unfortunately not obtained; instead, the homonuclear redox products **20** (Re^V) and **51** (Zr^{IV}; X-ray characterization) were isolated (Scheme 17).[46] The study of this type of reversible redox processes has only just begun.

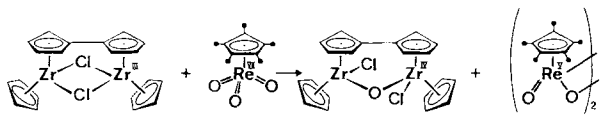

50 2 51 20

Scheme 17.

3. Pure Speculation?

Being convinced that π-aromatic ligands do in fact survive at even the highest possible oxidation states of transition metals, we may speculate about other congeners still to be discovered. If the isoelectronic principle is going to hold promise again, then benzene (or its hexamethyl derivative) should not disguise the WO_3 fragment to give (stable?) **A**. On the other hand, one should not be surprised to see a cyclobutadiene ligand in the osmium compound **B** some day (Fig. 17). At least in these two compounds, additional prerequisites for thermal stability are fulfilled: they belong to the elements of the third transition metal series that generally form more stable and less strongly oxidizing high-valent compounds than their 'lighter brothers'. Secondly, the coordination numbers are high enough to avoid kinetic lability which, for instance, would result in aggregation to dimers or oligomers. For this latter reason, the vanadium(v) compound '$[(C_5H_5)VO_2]$' announced by Russian workers[98a] turned out to be trimeric (X-ray structure of $[(\eta^5\text{-}C_5Me_5)_3V_3O_6]$[98b]).

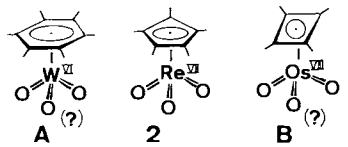

A 2 B

Fig. 17. Organometal oxides that are isoelectronic with **2**. The tungsten and osmium compounds are as yet unknown.

4. π-Acceptor versus π-Donator Ligands: Molecular Orbital Reasoning for Stability

Bursten et al. addressed the basic question of d-electron count vs. stability of high- and low-valent piano-stool complexes.[99] To this end, they subjected the structurally analogous compounds **C** and **D** of idealized C_s symmetry to Fenske-Hall molecular orbital calculations, from which the following message becomes evident (Fig. 18):

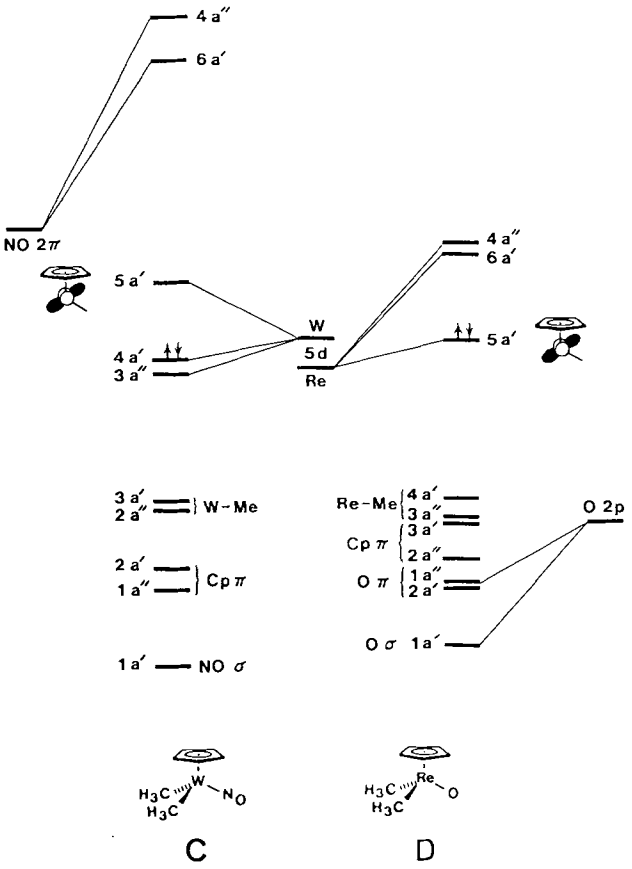

Fig. 18. Simplified molecular orbital diagram of d^4-tungsten(II) and d^2-rhenium(V) complexes **C** and **D** [99]. The neopentyl derivative $[(\eta^5\text{-}C_5H_5)W(NO)\{CH_2C(CH_3)_3\}_2]$ belonging to type **C** is a known, stable compound (P. L. Legzdins, S. J. Rettig, L. Sanchez, B. E. Bursten, M. G. Gatter, *J. Am. Chem. Soc. 107* (1985) 1411). The ring-substituted derivative $[(\eta^5\text{-}C_5Me_5)ReO(CH_3)_2]$ and a series of higher alkyl homologues have been synthesized and structurally characterized [34].

1) In the case of the nitrosyltungsten(II) complex **C** two of the metal-centered 5d orbitals are significantly stabilized as a result of an interaction (4a′ and 3a″) with the very strong π-acceptor ligand nitric oxide. By way of contrast, the 5a′ orbital remains non-bonding because the methyl ligands function only as σ-donors in the present case. The splitting of the metal 't_{2g}' orbital set amounts to 2.23 eV according to these calculations.

2) The opposite picture emerges for the rhenium(V) oxo complex **D**. Since a single oxo atom is an exceedingly good π-donator ligand (as well as a good σ-donor), it interacts with the rhenium-centered 5d orbitals to destabilize two levels by 2.36 eV (4a″ and 6a′); the nonbonding 5a′-type orbital becomes the HOMO because of the d^2 configuration of the metal atom.

Bursten et al. came to the conclusion that the stability of the 16-electron complex **C** (d^4-W^{II}) can be attributed to the nonbonding 5a′ orbital generated by the strong π-acceptor ligand NO. On the other hand, the 18-electron rule must no longer be considered in the case of high-valent organometallic complexes as in **D** (d^2-Re^V), since the d-orbital levels are generally destabilized by π-donors such as the oxo group and thus would rather remain unoccupied anyway. The entire pseudo-t_{2g} set of orbitals is destabilized when the metal atom is surrounded by *at least two oxo ligands*, with the existing compounds of type $[L_xMO_y]$ ($y \geq 2$) in fact all exhibiting d^0 configuration. However, the recently synthesized compounds of type **22** (Section 2.7) are obvious exceptions to this statement. Molecular orbital calculations of these and other catalysis-relevant transition metal oxides have already been carried out by *Goddard* et al. and *Yamaguchi* et al.[100]

5. Just at the Beginning

By no means is it of merit to make an accidental discovery. Much more important is the recognition of possible consequences that might result from serendipity. Organometallic chemistry has certainly seen many organometal oxides since *E. O. Fischer* and his group first had the cubane-type oxide $[(\eta^5\text{-}C_5H_5)_4Cr_4O_4]$ in their hands in 1960.[53a] Systematic studies have now begun in this field with the key compounds **2** and **4**. We are, as it were, just starting to learn such apparently simple things as the reaction of dirheniumheptoxide with tetramethyltin. One of the major short-term goals is to establish the relationship between redox chemistry at the metal and the reactivity of the ligands surrounding it. Any synthetic enterprise should be oriented toward new stoichiometric and catalytic hydrocarbon reactions or towards the improvement of those already known. Rhenium is certainly an ideal case for demonstrating how both low and high oxidation states are stabilized by good π-acceptor and π-donor ligands, respectively.

Further aims include the correlation of readily obtainable ^{17}O-NMR data[101] and electrochemical data with the redox processes occurring at metals attached to oxygen(s). Reduction[102] and oxidation[103] processes of great practical benefit may thus become better understood and optimized. Planned organometallic studies must be carried out in order to elucidate even simple-looking, useful reactions occurring at metal oxide structures.[104] The stage is already set for the anchorage of organometallic oxides to surfaces in order to gain more insight into the consequences of metal oxide surface effects for catalytic activity.[105] Hardly anything is known about this important issue to date; and that what is known can be quite confusing because of a lack of model substances.[106] In addition, the isomerism between dioxo- and peroxo systems $M(O)_2$ and $M(O_2)$, respectively, is of basic importance.[107]

Since this review and previous evidence[34,35,108,109] may convince us that organometallic oxides are compatible with classical "inorganic" oxides, both these areas of chemistry should converge in the near future. Suffice it to say that even bioinorganic problems also fall within the realms of high-valent organometallic oxides![110,111]

The author is greatly indebted to those co-workers who are fond of organometallic oxides. Since these scholars only happen to show up in the publications, they at least deserve being named here in appreciation of their enthusiastic, thoughtful, and skilled contributions: Dr. Tomas Cuenca, Josef K. Felixberger, Roland A. Fischer, Martina Flöel, Dr. Peter Härter, Karin A. Jung, Dr. Heinz-Josef Kneuper, Josef G. Kuchler, Dr. Ulrich Küsthardt, Jürgen Kulpe, Monika Ladwig, Dieter Marz, Dr. Babil Menjon, Dr. Jun Okuda, Dr. Rocco Paciello, Dr. Adolf Schäfer, Prof. Dr. Ricardo Serrano, Helmut Theiler, Werner Thiel, Dr. Erdmuthe Voss, Werner Wagner, and Georg Weichselbaumer. The entire research group particularly acknowledges the outstanding crystallographic performances of Dr. E. Herdtweck assisted by Pavlo Kiprof in our laboratories. Generous support comes from the Deutsche Forschungsgemeinschaft, the Fonds der Chemischen Industrie, the German Bundesministerium für Forschung und Technologie, Hoechst Aktiengesellschaft, Degussa AG, Hüls Aktiengesellschaft, BASF Aktiengesellschaft, Ruhrchemie AG, Alexander von Humboldt Foundation, Merck'sche Gesellschaft für Kunst und Wissenschaft e.V., the Spanish Ministery of Education and the Deutsche Akademische Austauschdienst. We express our gratitude for financial help that we have been receiving from these companies and institutions. Miss Juliane Geisler is greatfully acknowledged for the typescript of this article, Erich Krebs for the skilful drawings. The author had the privilege of being hosted as a 'Professeur Associé' by his colleagues Didier Astruc (Université de Bordeaux I) and Igor Tkatchenko (C.N.R.S. Toulouse), without whose generosity this essay may not have materialized. Of particular benefit were the stimulating discussions with Professor Jean-Marie Basset (C.N.R.S. Lyon-Villeurbanne) during his visit as an Humboldt Senior Awardee in our department. Freya and our five children are once again thanked for their patience.

Received: December 15, 1987 [A 691 IE]
German version: *Angew. Chem. 100* (1988) 1269
Publication delayed at author's request

[1] 14000 organometallic compounds are listed and referenced in J. Buckingham (Ed.): *Dictionary of Organometallic Compounds*, Chapman and Hall, London 1984. — This monumental series of monographs is the most comprehensive and informative one that has been published up to the present (nine volumes, 8750 pages): G. Wilkinson, F. G. A. Stone, E. W. Abel (Eds.): *Comprehensive Organometallic Chemistry*, Pergamon Press, Oxford 1984.

[2] Several readable textbooks on organometallic chemistry have recently appeared: a) A. Yamamoto: *Organotransition Metal Chemistry — Fundamental Concepts and Applications*, Wiley, New York 1986; b) C. Elschenbroich, A. Salzer: *Organometallchemie*, 2nd Edit., Teubner-Verlag, Stuttgart 1988; c) J. P. Collman, L. S. Hegedus, J. R. Norton, R. G. Finke: *Principles and Applications of Organotransition Metal Chemistry*, 2nd Edit., University Science Books, Mill Valley, CA, USA 1987; d) J. S. Thayer: *Organometallic Chemistry*, VCH Publishers, New York 1988; e) R. H. Crabtree: *The Organometallic Chemistry of the Transition Metals*, Wiley, Chichester, England 1988.

[3] Critical assessment of the present state and of the perspectives of organometallic chemistry: a) G. W. Parshall, *Organometallics 6* (1987) 687; b) W. A. Herrmann, *Kontakte (Darmstadt) 1988*, No. 1, p. 3.

[4] a) F. A. Cotton, N. F. Curtis, C. B. Harris, B. F. G. Johnson, S. J. Lippard, J. T. Mague, W. R. Robinson, J. S. Wood, *Science 145* (1964) 1305; b) F. A. Cotton, *J. Chem. Educ. 60* (1983) 713.

[5] Monographs and reviews on metal-metal bonds: a) F. A. Cotton, R. A. Walton: *Multiple Bonds between Metal Atoms*, Wiley, New York 1982; b) M. H. Chisholm (Ed.): *Reactivity of Metal-Metal Bonds (ACS Symp. Ser. Vol. 155)*, American Chemical Society, Washington D.C., USA 1981; c) M. H. Chisholm, I. P. Rothwell, *Prog. Inorg. Chem. 29* (1982) 1; d) M. H. Chisholm, *Angew. Chem. 98* (1986) 21; *Angew. Chem. Int. Ed. Engl. 25* (1986) 21; e) Bare (unsubstituted) main group element atoms as multiply bonded ligands in organotransitionmetal chemistry: W. A. Herrmann, *ibid. 98* (1986) 57 and *25* (1986) 56.

[6] E. O. Fischer, A. Maasböl, *Angew. Chem. 76* (1964) 645; *Angew. Chem. Int. Ed. Engl. 3* (1964) 580; *Chem. Ber. 100* (1967) 2445.

[7] Reviews and monographs on metal-carbon multiple bonds: a) E. O. Fischer, *Angew. Chem. 86* (1974) 651 (Nobel Lecture); *Adv. Organomet. Chem. 14* (1976) 1; b) J. E. Hahn, *Prog. Inorg. Chem. 31* (1984) 205; c) U. Schubert, H. Fischer, P. Hofmann, K. Weiss, K. H. Dötz, F. R. Kreissl: *Transition Metal Carbene Complexes*, Verlag Chemie, Weinheim 1983.

[8] a) The classical paper demonstrating the advantages of rhodium and its complexes in catalytic processes of olefins should be consulted: J. A. Osborn, F. H. Jardine, J. F. Young, G. Wilkinson, *J. Chem. Soc. A 1966*, 1711; b) Review: B. R. James, *Adv. Organomet. Chem. 17* (1979) 319; c) Asymmetric hydrogenation: J. Halpern, *Pure Appl. Chem. 55* (1983) 99; d) Mechanistic Aspects: J. Halpern, *Inorg. Chim. Acta 50* (1981) 11.

[9] The DuPont butadiene/ethylene coupling process had landmarked the catalytic power of rhodium in industrial catalysis several years before: a) T. Alderson, US-Pat. 3013066 (1961); *Chem. Abstr. 57* (1962) 11016h; cf: T. Alderson, R. V. Lindsey, jr., *J. Am. Chem. Soc. 87* (1965) 5638; b) Review: A. C. L. Su, *Adv. Organomet. Chem. 17* (1979) 269.

[10] a) G. Wilke, *J. Organomet. Chem. 200* (1980) 349; b) P. W. Jolly, G. Wilke: *The Organic Chemistry of Nickel, Vol. 1 and 2*, Academic Press, New York 1975; c) G. Wilke, *Angew. Chem. 100* (1988) 189; *Angew. Chem. Int. Ed. Engl. 27* (1988) 185.

[11] a) "Metallorganische Mischkatalysatoren": K. Ziegler, E. Holzkamp, H. Breil, H. Martin, *Angew. Chem. 67* (1955) 541; b) K. Ziegler, *ibid. 76* (1964) 545 (Nobel Lecture); *Adv. Organomet. Chem. 6* (1968) 1; c) G. Natta, *Angew. Chem. 68* (1956) 393; d) G. Natta, *ibid. 76* (1964) 553 (Nobel Lecture); e) A. Clark, *Catal. Rev. 3* (1969) 145 (Phillips Catalysts); f) H. Sinn, W. Kaminsky, *Adv. Organomet. Chem. 18* (1980) 99.

[12] a) J. Smidt, W. Hafner, J. Sedlmeier, R. Jira, R. Rüttinger, DBP 1049845 (August 6, 1959); b) W. Hafner, R. Jira, J. Sedlmeier, R. Sieber, R. Rüttinger, H. Kojer, *Angew. Chem. 71* (1959) 176; J. Smidt, R. Jira, W. Blau, D. Grimm, *Hydrocarbon Process.* (1976) No. 3, p. 97; c) Review: A. Aguilo, *Adv. Organomet. Chem. 5* (1967) 321; d) R. Jira, R. J. Laib, H. M. Bolt in: *Ullmann's* Encyclopedia of Industrial Chemistry, Vol. A 1, VCH Verlagsgesellschaft, Weinheim 1985, p. 31ff.

[13] a) W. Reppe: *Neuere Entwicklungen auf dem Gebiete der Chemie des Acetylens und Kohlenoxids*, Springer, Berlin 1949; b) Recent applications and developments: K. P. C. Vollhardt, *Pure Appl. Chem. 57* (1985) 1819; *Angew. Chem. 96* (1984) 525; *Angew. Chem. Int. Ed. Engl. 23* (1984) 539.

[14] Industrial impact of transition metal homogeneous catalysis: a) G. W. Parshall, R. E. Putscher, *J. Chem. Educ. 63* (1986) 189; b) G. W. Parshall: *Homogeneous Catalysis*, Wiley, New York 1980.

[15] For further examples cf. W. A. Herrmann, *Comments Inorg. Chem. 7* (1988) 73; *Chem. Unserer Zeit 22* (1988) 113.

[16] Leading references to the historical development of Organometallic Chemistry: a) J. S. Thayer, *Adv. Organomet. Chem. 13* (1975) 1; b) W. A. Herrmann, *J. Organomet. Chem. 250* (1983) 319.

[17] Monographs: a) E.-I. Negishi: *Organometallics in Organic Synthesis*, Wiley, New York 1980; b) S. G. Davies: *Organotransition Metal Chemistry: Applications to Organic Synthesis*, Pergamon Press, Oxford 1982; c) F. R. Hartley, S. Patai: *The Chemistry of the Metal-Carbon Bond, Vol. 1-4*, Wiley, New York 1981–1986. — For more recent individual work, the reader is referred to the proceedings of the *International Symposium on Organometallic Chemistry Directed Towards Organic Synthesis (OMCOS)*: cf. *Pure Appl. Chem. 55* (1983) No. 11; *ibid. 57* (1985) No. 12; *ibid. 59* (1987) No. 11.

[18] Recent review articles: K. H. Dötz, *Angew. Chem. 96* (1984) 573; *Angew. Chem. Int. Ed. Engl. 23* (1984) 587; B. M. Trost, *ibid. 98* (1986) 1 and *25* (1986) 1; J. K. Stille, *ibid. 98* (1986) 504 bzw. *25* (1986) 508; H. Kasuda, A. Nakamura, *ibid. 99* (1987) 745 and *26* (1987) 723; L. S. Hegedus, *ibid. 100* (1988) 1147 and *27* (1988) 1113.

[19] Metal-metal multipe bonding is featured by quite a number of simple looking inorganic compounds. For example, La_2ReO_5 and $NaNb_3O_5F$ contain multiply bonded M_2L_8 units completely analogous with $[Re_2Cl_8]^{2\ominus}$: a) K. Waltersson, *Acta Crystallogr. Sect. B 32* (1976) 1485; b) J. Köhler, A. Simon, *Angew. Chem. 98* (1986) 1011; *Angew. Chem. Int. Ed. Engl. 25* (1986) 996 and references cited therein.

[20] R. Hoffmann, *Angew. Chem. 99* (1987) 871; *Angew. Chem. Int. Ed. Engl. 26* (1987) 846.

[21] Monographs and reviews on metal-mediated oxidation processes: a) R. A. Sheldon, J. K. Kochi: *Metal-Catalyzed Oxidations of Organic Compounds*, Academic Press, New York 1981; b) B. Meunier, *Bull. Soc. Chim. Fr. 59* (1987) 759; c) H. Mimoun in G. Wilkinson, R. D. Gillard, J. A. McCleverty (Eds.): *Comprehensive Coordination Chemistry*, Pergamon Press, Oxford 1987, p. 317ff.

[22] a) G. Cainelli, G. Cardillo: *Chromium Oxidations in Organic Chemistry*, Springer, Berlin 1984; b) W. J. Mijs, R. H. de Jonge (Hrsg.): *Organic Syntheses by Oxidation with Metal Compounds*, Plenum Press, New York 1986; c) R. H. Holm, *Chem. Rev. 87* (1987) 1401.

[23] Recent examples: a) E. J. Corey, E.-P. Barrette, P. A. Magriotis, *Tetrahedron Lett. 26* (1985) 5855; b) J. Muzart, *ibid. 24* (1983) 2185; *ibid. 27* (1986) 3139; c) *Nouv. J. Chim. 8* (1984) 271; d) S. Kanemoto, K. Oshima, S. Matsubara, K. Takai, H. Nozaki, *Tetrahedron Lett. 24* (1983) 2185; e) J. Muzart, *ibid. 28* (1987) 2131, 2133.

[24] Largely unknown is also the nature of active oxidants in systems such as $Mo(CO)_6$/*t*BuOOH and MoO_5/HMPT nor have the issues of solvent effects been resolved as yet, cf. H. Mimoun, I. S. de Roch, L. Sajus, *Tetrahedron 26* (1970) 37.

[25] R. K. Grasselli, J. D. Burrington, J. F. Brazdil, *Faraday Discuss. Chem. Soc. 72* (1982) 203. – The ‚activation' (functionalization) of natural gas also occurs on oxidic sites, cf. H. Mimoun, *New J. Chem. 11* (1987) 513.

[26] For the chemistry and structures of inorganic rhenium compounds, see: a) N. N. Greenwood, A. Earnshaw: *Chemistry of the Elements*, Pergamon Press, Oxford 1984, p. 1211ff; b) A. F. Wells: *Structural Inorganic Chemistry, 5th Ed.*, Clarendon Press, Oxford 1985, p. 424.

[27] a) K. Mertis, D. H. Williamson, G. Wilkinson, *J. Chem. Soc. Dalton Trans. 1975*, 607; b) K. Mertis, L. Galyer, G. Wilkinson, *J. Organomet. Chem. 97* (1975) C65; c) P. G. Edwards, G. Wilkinson, K. M. A. Malik, M. B. Hursthouse, *J. Chem. Soc. Dalton Trans. 1980*, 2467; d) PE spectroscopy: J. C. Green, D. R. Lloyd, L. Galyer, K. Mertis, G. Wilkinson, *ibid. 1978*, 1403.

[28] R. Dagani, *Chem. Eng. News 62* (1984) No. 30, p. 28.

[29] W. A. Herrmann, E. Voss, M. Flöel, *J. Organomet. Chem. 297* (1985) C5; see also: Ref. [34b] for the synthesis procedure.

[30] Original communication: W. A. Herrmann, R. Serrano, H. Bock, *Angew. Chem. 96* (1984) 364; *Angew. Chem. Int. Ed. Engl. 23* (1984) 383; see also: *Nachr. Chem. Tech. Lab. 32* (1984) 202.

[31] W. A. Herrmann, R. Serrano, A. Schäfer, M. L. Ziegler, E. Guggolz, *J. Organomet. Chem. 272* (1984) 55.

[32] Structure: E. Herdtweck, J. Okuda, W. A. Herrmann, *Inorg. Chem. 27* (1988) 1254; see also [34b, c].

[33] This compound was independently prepared by another research group: A. H. Klahn-Oliva, D. Sutton, *Organometallics 3* (1984) 1313.

[34] Previous reviews on the chemistry of trioxo(η^5-pentamethylcyclopentadienyl)rhenium(VII): a) W. A. Herrmann, *J. Organomet. Chem. 300* (1986) 111; b) W. A. Herrmann, J. Okuda, *J. Mol. Catal. 41* (1987) 109; c) W. A. Herrmann, E. Herdtweck, M. Flöel, J. Kulpe, U. Küsthardt, J. Okuda, *Polyhedron 6* (1987) 1165; d) W. A. Herrmann in A. de Meijere, H. tom Dieck (Eds.): *Organic Synthesis with Organometallic Compounds*, Springer, Berlin 1987.

[35] Other high-valent organometallic oxides are listed in Ref. [34c]. – More recent examples: a) I. Feinstein-Jaffe, D. Gibson, S. J. Lippard, R. R. Schrock, A. Spool, *J. Am. Chem. Soc. 106* (1984) 6305 ($R_6W_2O_3$; R = neopentyl; linear W_2O_3 core structure); b) A. D. Horton, R. R. Schrock, J. H. Freudenberger, *Organometallics 6* (1987) 893 (reactions of $[Me_3SiOReO_3]$); cf. D. S. Edwards, L. V. Biondi, J. W. Ziller, M. R. Churchill, R. R. Schrock, *ibid. 2* (1983) 1505; c) S. G. Blanco, M. P. Gomez-Sal, S. Martinez-Carreras, M. Mena, P. Royo, R. Serrano, *J. Chem. Soc. Chem. Commun. 1986*, 1572 ($[(\eta^5\text{-}C_5Me_5)Ti(CH_3)O]_3$); d) B. Heyn, R. Hoffmann, *Z. Chem. 16* (1976) 195, 407 ($[mes_2MoO_2]$, mes = mesityl); e) P. Stavropoulos, P. G. Edwards, T. Behling, G. Wilkinson, M. Motevalli, M. B. Hursthouse, *J. Chem. Soc. Dalton Trans. 1987*, 169 ($[mes_2ReO_2]$); f) H. Arzoumanian, A. Baldy, R. Lai, J. Metzger, M.-L. Nkeng Peh, M. Pierrot, *J. Chem. Soc. Chem. Commun. 1985*, 1151; g) R. Lai, S. LeBot, A. Baldy, M. Pierrot, H. Arzoumanian, *ibid. 1986*, 1208; h) R. R. Schrock, I. A. Weinstock, A. D. Horton, A. H. Liu, M. H. Schofield, *J. Am. Chem. Soc. 110* (1988) 2686; i) F. M. Su, C. Cooper, S. T. Geib, A. L. Rheingold, J. M. Mayer, *ibid.* 108 (1986) 3545.

[36] W. A. Herrmann, R. Serrano, U. Küsthardt, M. L. Ziegler, E. Guggolz, T. Zahn, *Angew. Chem. 96* (1984) 498; *Angew. Chem. Int. Ed. Engl. 23* (1984) 515.

[37] W. A. Herrmann, R. Serrano, M. L. Ziegler, H. Pfisterer, B. Nuber, *Angew. Chem. 97* (1985) 50; *Angew. Chem. Int. Ed. Engl. 24* (1985) 50.

[38] W. A. Herrmann, R. Serrano, U. Küsthardt, E. Guggolz, B. Nuber, M. L. Ziegler, *J. Organomet. Chem. 287* (1985) 329.

[39] W. A. Herrmann, U. Küsthardt, M. L. Ziegler, T. Zahn, *Angew. Chem. 97* (1985) 857; *Angew. Chem. Int. Ed. Engl. 24* (1985) 860.

[40] W. A. Herrmann, U. Küsthardt, E. Herdtweck, *J. Organomet. Chem. 294* (1985) C33.

[41] W. A. Herrmann, E. Voss, U. Küsthardt, E. Herdtweck, *J. Organomet. Chem. 294* (1985) C37.

[42] U. Küsthardt, W. A. Herrmann, M. L. Ziegler, T. Zahn, B. Nuber, *J. Organomet. Chem. 311* (1986) 163.

[43] W. A. Herrmann, M. Flöel, J. Kulpe, J. K. Felixberger, E. Herdtweck, *J. Organomet. Chem.*, in press.

[44] W. A. Herrmann, U. Küsthardt, A. Schäfer, E. Herdtweck, *Angew. Chem. 98* (1986) 818; *Angew. Chem. Int. Ed. Engl. 25* (1986) 817.

[45] W. A. Herrmann, U. Küsthardt, M. Flöel, J. Kulpe, E. Herdtweck, E. Voss, *J. Organomet. Chem. 314* (1986) 151.

[46] W. A. Herrmann, T. Cuenca, U. Küsthardt, *J. Organomet. Chem. 309* (1986) C15.

[47] W. A. Herrmann, J. G. Kuchler, W. Wagner, J. K. Felixberger, E. Herdtweck, *Angew. Chem. 100* (1988) 420; *Angew. Chem. Int. Ed. Engl. 27* (1988) 394.

[48] a) R. H. A. Bosma, G. C. N. van den Aardweg, J. C. Mol, *J. Organomet. Chem. 255* (1983) 159; b) X. Xiaoding, J. C. Mol, *J. Chem. Soc. Chem. Commun. 1985*, 631 (metathesis of unsaturated carboxylic acids); c) G. C. N. van den Aardweg, R. H. A. Bosma, J. C. Mol, *ibid. 1983*, 262 (metathesis of unsaturated C_n nitriles with $n>5$); d) No sufficiently characterized organometallic compound has hitherto been obtained from catalytically active WCl_6/SnR_4 and $Re_2O_7/SnR_4/Al_2O_3$ systems; see for instance: *VIth Int. Symp. Olefin Metathesis*, Hamburg, 26.–30. August 1985; cf. *J. Mol. Catal. 36* (1986). - A compound of composition $[Cl_5WCH_3]$ has reportedly been obtained from WCl_6 and $Sn(CH_3)_4$, but was not conclusively characterized: W. Grahlert, K. Milkowski, U. Langbein, *Z. Chem. 14* (1974) 287; K. H. Thiele, W. Grahlert, *ibid. 9* (1969) 310; *Z. Anorg. Allg. Chem. 383* (1971) 144.

[49] I. R. Beattie, P. J. Jones, *Inorg. Chem. 18* (1979) 2318.

[50] a) J. G. Kuchler, *Diplomarbeit*, Technische Universität München 1987; b) W. A. Herrmann, J. G. Kuchler, E. Herdtweck, unpublished results 1987/88; c) W. A. Herrmann, G. Weichselbaumer, unpublished results 1987/88; d) W. A. Herrmann, M. Ladwig, unpublished results 1988.

[51] a) S. Cai, D. M. Hoffman, J. C. Huffman, D. A. Wierda, H.-G. Woo, *Inorg. Chem. 26* (1987) 3693; Synthesis of $[ReO(PMe_3)(CH_2SiMe_3)_3]$: S. Cai, D. M. Hoffman, D. Lappas, H.-G. Woo, *Organometallics 6* (1987) 2273; b) S. Cai, D. M. Hoffman, D. A. Wierda, *J. Chem. Soc. Chem. Commun. 1988*, 313.

[52] J. K. Felixberger, E. Herdtweck, W. A. Herrmann, unpublished results 1987/88.

[53] $[(\eta^5\text{-}C_5H_5)_4Cr_4O_4]$: a) Synthesis: E. O. Fischer, K. Ulm, H. P. Fritz, *Chem. Ber. 93* (1960) 2167; b) Improved synthesis and structure: F. Bottomley, D. E. Paez, P. S. White, *J. Am. Chem. Soc. 103* (1981) 5581; *ibid. 104* (1982) 5651.

[54] $[(\eta^5\text{-}C_5H_5)_xV_yO_z]$: a) F. Bottomley, P. S. White, *J. Chem. Soc. Chem. Commun. 1981*, 28; b) F. Bottomley, D. E. Paez, P. S. White, *J. Am. Chem. Soc. 107* (1985) 7226; c) F. Bottomley, D. F. Drummond, D. E. Paez, P. S. White, *J. Chem. Soc. Chem. Commun. 1986*, 1752; d) F. Bottomley, L. Sutin, *ibid. 1987*, 1112; e) Review: F. Bottomley, L. Sutin, *Advan. Organomet. Chem. 28* (1988) 339.

[55] $[(\eta^5\text{-}C_5H_5)_6Ti_6O_{8-n}Cl_n]^{n\oplus}$ ($n=4$, 2, 0): a) J. C. Huffman, J. G. Stone, W. C. Krusell, K. G. Caulton, *J. Am. Chem. Soc. 99* (1977) 5829; b) A. Roth, C. Floriani, A. Chiesi-Villa, C. Guastini, *ibid. 108* (1986) 6823; c) The recently reported $Ti^{4\oplus}$ compounds of composition $[(\eta^5\text{-}C_5Me_5)_4Ti_4O_6]$ resembles an adamantane-type structure: L. M. Babcock, V. W. Day, W. G. Klemperer, *J. Chem. Soc. Chem. Commun. 1987*, 858.

[56] P. Stavropoulos, P. G. Edwards, G. Wilkinson, M. Motevalli, K. M. Abdul Malik, M. B. Hursthouse, *J. Chem. Soc. Dalton Trans. 1985*, 2167.

[57] Only the (explosive) hexamethyltungsten $(CH_3)_6W$ has been reported: a) A. J. Shortland, G. Wilkinson, *J. Chem. Soc. Dalton Trans. 1973*, 872; b) L. Galyer, K. Mertis, G. Wilkinson, *J. Organomet. Chem. 85* (1975) C37, C65.

[58] a) W. A. Herrmann, W. Wagner, unpublished results 1987/88; b) W. A. Herrmann, D. Marz, unpublished results 1987/88; c) W. A. Herrmann, R. A. Paciello, unpublished results 1987/88.

[59] a) W. A. Herrmann, J. K. Felixberger, E. Herdtweck, A. Schäfer, J. Okuda, *Angew. Chem. 99* (1987) 466; *Angew. Chem. Int. Ed. Engl. 26* (1987) 466; b) J. K. Felixberger, *Diplomarbeit*, Technische Universität München 1986.

[60] J. Okuda, unpublished results 1986.

[61] M. Flöel, E. Herdtweck, W. Wagner, J. Kulpe, P. Härter, W. A. Herrmann, *Angew. Chem. 99* (1987) 787; *Angew. Chem. Int. Ed. Engl. 26* (1987) 787.

[62] Alkyl(oxo) complexes of the series $[(\eta^5\text{-}C_5Me_5)Re(=O)R_2]$ including a rhena(v)cyclobutane are also accessible by means of Grignard reagents: a) H. J. R. deBoer, B. J. J. van de Heisteeg, M. Flöel, W. A. Herrmann, O. S. Akkerman, F. Bickelhaupt, *Angew. Chem. 99* (1987) 88; *Angew. Chem. Int. Ed. Engl. 26* (1987) 73; b) W. A. Herrmann, M. Flöel, E. Herdtweck, *J. Organomet. Chem.* (1988), in press.

[63] W. A. Herrmann, R. A. Fischer, E. Herdtweck, *J. Organomet. Chem. 329* (1987) C1.

[64] a) W. A. Herrmann, R. A. Fischer, W. Amslinger, E. Herdtweck, *J. Organomet. Chem.*, in press; b) W. A. Herrmann, R. A. Fischer, J. K. Felixberger, R. A. Paciello, P. Kiprof, E. Herdtweck, *Z. Naturforsch. B 43* (1988), in press.

[65] Monographs and reviews on olefin metathesis: a) V. Dragutan, A. T. Balaban, M. Dimonie: *Olefin Metathesis and Ring-Opening Polymerization of Cyclo-Olefins*, Wiley, New York 1985; b) K. J. Ivin: *Olefin Metathesis*, Academic Press, London 1983; c) R. Streck, *Chem.-Ztg. 99* (1975) 397 (industrial applications); d) R. H. Grubbs in G. Wilkinson, F. G. A. Stone, E. W. Abel (Eds.): *Comprehensive Organometallic Chemistry, Vol. 8*, Pergamon Press, Oxford 1982, p. 499ff; e) R. H. Grubbs, *Prog. Inorg. Chem. 24* (1978) 1; f) T. J. Katz, *Adv. Organomet. Chem. 16* (1977) 283; g) B. Calderon, J. P. Lawrence, E. A. Ofstead, *ibid. 17* (1979) 449; h) N. Calderon, E. A. Ofstead, W. A. Judy, *Angew. Chem. 88* (1976) 433; *Angew. Chem. Int. Ed. Engl. 15* (1976) 401.

[66] a) R. R. Schrock, *Acc. Chem. Res. 12* (1979) 98; b) *J. Organomet. Chem. 300* (1986) 249; c) *Acc. Chem. Res. 19* (1986) 342.

[67] J. Kress, A. Aguero, J. A. Osborn, *J. Mol. Catal. 36* (1986) 1.

[68] E. J. M. deBoer, J. deWith, G. Orpen, *J. Am. Chem. Soc. 108* (1986) 8271.

[69] H. Bönnemann, W. Brijoux, *New J. Chem. 11* (1987) 549; see Fig. 27 and Ref. [24] therein.

[70] N. M. Boag, H. D. Kaesz in G. Wilkinson, F. G. A. Stone, E. W. Abel (Eds.): *Comprehensive Organometallic Chemistry, Vol. 4*, Pergamon Press, Oxford 1982, p. 161ff.

[71] J. M. Mayer, T. H. Tulip, *J. Am. Chem. Soc. 106* (1984) 3878.

[72] J. M. Mayer, D. L. Thorn, T. H. Tulip, *J. Am. Chem. Soc. 107* (1985) 7454.

[73] a) E. Valencia, B. D. Santarsiero, S. J. Geib, A. L. Rheingold, J. M. Mayer, *J. Am. Chem. Soc. 109* (1987) 6896; b) J. M. Mayer, T. H. Tulip, J. C. Calabrese, E. Valencia, *ibid. 109* (1987) 157.

[74] J. K. Felixberger, J. G. Kuchler, E. Herdtweck, R. A. Paciello, W. A. Herrmann, *Angew. Chem. 100* (1988) 975; *Angew. Chem. Int. Ed. Engl. 27* (1988) 946.

[75] W. A. Herrmann, R. A. Fischer, E. Herdtweck, *Angew. Chem. 99* (1987) 1286; *Angew. Chem. Int. Ed. Engl. 26* (1987) 1283.

[76] W. A. Herrmann, R. A. Fischer, E. Herdtweck, *Angew. Chem. 100* (1988) No. 11; *Angew. Chem. Int. Ed. Engl. 27* (1988) No. 11.

[77] W. A. Herrmann, D. Marz, E. Herdtweck, A. Schäfer, W. Wagner, H.-J. Kneuper, *Angew. Chem. 99* (1987) 462; *Angew. Chem. Int. Ed. Engl. 26* (1987) 462.

[78] Review on oxidation reactions of unsaturated hydrocarbons with osmium tetraoxide: M. Schröder, *Chem. Rev. 80* (1980) 187.

[79] W. A. Herrmann, D. Marz, unpublished results 1986/87.

[80] W. A. Herrmann, G. Weichselbaumer, H.-J. Kneuper, *J. Organomet. Chem. 319* (1987) C21.

[81] F. Bottomley, J. Darkwa, L. Sutin, P. S. White, *Organometallics 5* (1986) 2165.

[82] W. A. Herrmann, E. Herdtweck, G. Weichselbaumer, *J. Organomet. Chem.* in press.

[83] W. A. Herrmann, K. A. Jung, A. Schäfer, H.-J. Kneuper, *Angew. Chem. 99* (1987) 464; *Angew. Chem. Int. Ed. Engl. 26* (1987) 464.

[84] W. A. Herrmann, K. A. Jung, unpublished results 1987.

[85] Compounds of general formula $[(\eta^5\text{-}C_5R_5)M(CH_3)_4]$ ($M=Ta$, W, Ir) are known, too: a) R. C. Murray, L. Blum, A. H. Lin, R. R. Schrock, *Organometallics 4* (1985) 954; see also: J. M. Mayer, C. J. Curtis, J. E. Bercaw, *J. Am. Chem. Soc. 105* (1983) 2651; b) S. J. Holmes, R. R. Schrock, *Organometallics 2* (1983) 1463; c) K. Isobe, A. V. de Miguel, A. Nutton, P. M. Maitlis, *J. Chem. Soc. Dalton Trans. 1984*, 929 (first organoiridium(v) complex); d) K. Isobe, P. M. Bailey, P. M. Maitlis, *J. Chem. Soc. Chem. Commun. 1981*, 808; e) S. F. Pedersen, R. R. Schrock, M. R. Churchill, H. J. Wasserman, *J. Am. Chem. Soc. 104* (1982) 6808; f) J. Okuda, R. C. Murray, J. C. Derwan, R. R. Schrock, *ibid. 108* (1986) 1681.

[86] a) E. L. Muetterties: *Transition Metal Hydrides*, Marcel Dekker, New York 1971; b) R. Bau, *Acc. Chem. Res. 12* (1979) 176.

[87] S. C. Abrahams, A. P. Ginsberg, K. Knox, *Inorg. Chem. 3* (1964) 558.

[88] a) D. Baudry, M. Ephritikhine, H. Felkin, R. Holmes-Smith, *J. Chem. Soc. Chem. Commun. 1983*, 788; b) D. Baudry, M. Ephritikhine, H. Felkin, J. Zakrzewski, *Tetrahedron Lett. 25* (1984) 1283.

[89] Monographs and reviews on carbon-hydrogen activation: a) A. E. Shilov: *The Activation of Saturated Hydrocarbons by Transition Metal Complexes*, Reidel, Dordrecht 1984; b) R. Hoffmann, *J. Am. Chem. Soc. 106* (1984) 2006 (theoretical aspects of CH-activation); c) R. H. Crabtree, *Chem. Rev. 85* (1985) 245.

[90] W. A. Herrmann, J. Okuda, *Angew. Chem. 98* (1986) 1109; *Angew. Chem. Int. Ed. Engl. 25* (1986) 1092.

[91] W. A. Herrmann, E. Herdtweck, unpublished results 1987.

[92] W. A. Herrmann, H. Theiler, W. Wagner, E. Herdtweck, unpublished results 1987.

[93] MO theory of $[(\eta^5\text{-}C_5H_5)_3Re_3(\mu\text{-}O)_6]^{2\oplus}$: a) P. Hofmann, N. Rösch, *J. Chem. Soc. Chem. Commun. 1986*, 843; b) P. Hofmann, N. Rösch, H. R. Schmidt, *Inorg. Chem. 25* (1986) 4470.

[94] This compound withstands prolonged heating in a sealed tube at 200°C. Only traces of methane are formed under such conditions [58a].

[95] See for example: D. Medina, *5th Int. Symp. Chem. Selenium and Tellurium*, Oak Ridge, TN, USA, 24.–28. August 1987.

[96] H. Theiler, *Diplomarbeit*, Technische Universität München 1986.

[97] J. Kulpe, E. Herdtweck, G. Weichselbaumer, W. A. Herrmann, *J. Organomet. Chem. 348* (1988) 369.

[98] a) V. N. Latyaeva, V. V. Pereshein, A. N. Lineva, *Tr. Khim. Khim. Tekhnol. 1974*, 32 [*Chem. Abstr. 83* (1975) 179261z]; b) F. Bottomley, L. Sutin, *J. Chem. Soc. Chem. Commun. 1987*, 1112.

[99] B. E. Bursten, R. H. Cayton, *Organometallics 6* (1987) 2004.
[100] a) Bonding theory and reaction of CrO_2Cl_2 and $CrOCl_4$: A. Rappé, W. A. Goddard III, *J. Am. Chem. Soc. 102* (1980) 5114; *ibid. 104* (1982) 448; b) ab-initio Mo calculations for oxidic coordination compounds: K. Yamaguchi, Y. Takahara, T. Fuenco in V. H. Smith, jr. (Ed.): *Applied Quantum Chemistry*, Reidel, Dordrecht 1986, p. 155 ff.
[101] H.-J. Kneuper, P. Härter, W. A. Herrmann, *J. Organomet. Chem. 340* (1988) 353.
[102] Catalytic photoreduction of CO_2 to CO by $[Re(bpy)(CO)_3Cl]$: a) J. Hawecker, J.-M. Lehn, R. Ziessel, *J. Chem. Soc. Chem. Commun. 1983*, 536; *ibid. 1984*, 328; b) R. Ziessel in M. Aresta, G. Forti (Eds.): *Carbon Dioxide as a Source of Carbon, NATO ASI Series, Vol. 206*, Reidel, Dordrecht 1987, p. 113 ff.
[103] Enantioselective oxidations by chiral coordination compounds: a) S. Yamada, T. Mashiko, S. Terashima, *J. Am. Chem. Soc. 99* (1977) 1988; b) R. C. Michaelson, R. E. Palermo, K. B. Sharpless, *ibid. 99* (1977) 1990.
[104] Recent examples: a) T. Kauffmann, R. Abeln, S. Welke, D. Wingbermühle, *Angew. Chem. 98* (1986) 927; *Angew. Chem. Int. Ed. Engl. 25* (1986) 909; b) T. Kauffmann, M. Enk, W. Kaschube, E. Toliopoulos, D. Wingbermühle, *ibid. 98* (1986) 928 and *25* (1986) 910.
[105] a) F. J. Feher, *J. Am. Chem. Soc. 108* (1986) 3850; b) W. G. Klemperer, V. V. Mainz, R.-C. Wang, W. Shum, *Inorg. Chem. 24* (1985) 1968.
[106] J. Schwartz, *Acc. Chem. Res. 18* (1985) 302.
[107] J. W. Faller, Y. Ma, *Organometallics 7* (1988) 559; see also: P. Legzdius, E. C. Phillips, S. J. Rettig, L. Sánchez, J. Trotter, Y. C. Lee, *ibid. 7* (1988) 1877.
[108] Organometal/metal oxide combinations of defined structure are quite new; some highlights: a) C. J. Besecker, W. G. Klemperer, V. W. Day, *J. Am. Chem. Soc. 104* (1982) 6158; b) C. J. Besecker, W. G. Klemperer, *ibid. 102* (1980) 7598; c) V. W. Day, M. F. Frederick, M. R. Thompson, W. G. Klemperer, R.-S. Liu, W. Shum, *ibid. 103* (1981) 3597; d) V. W. Day, C. W. Earley, W. G. Klemperer, D. J. Maltbie, *ibid. 107* (1985) 8261; e) C. J. Besecker, V. W. Day, W. G. Klemperer, M. R. Thompson, *ibid. 106* (1984) 4125.
[109] Since writing this review numerous papers on organometallic oxides have appeared, of which the following are cited as examples: a) J. M. Huggins, D. R. Whitt, L. Lebioda, *J. Organomet. Chem. 312* (1986) C 15; b) N. Zhang, P. A. Shapley, *Inorg. Chem. 27* (1988) 976; c) J. C. Bryan, R. E. Stenkamp, T. H. Tulip, J. M. Mayer, *ibid. 26* (1987) 2283; d) J. C. Bryan, J. M. Mayer, *J. Am. Chem. Soc. 109* (1987) 7213; e) E. N. Jacobsen, M. K. Trost, R. G. Bergman, *ibid. 108* (1986) 8092; f) D. B. Morse, T. B. Rauchfuss, S. R. Wilson, *ibid. 110* (1988) 2646; g) K. G. Moloy, *Inorg. Chem. 27* (1988) 677; h) G. A. Vaughan, P. B. Rupert, G. L. Hillhouse, *J. Am. Chem. Soc. 109* (1987) 5538; i) J. F. Buzinkai, R. R. Schrock, *Organometallics 6* (1987) 1447; j) P. Jernakoff, C. de Meric de Bellefon, G. L. Geoffroy, A. L. Rheingold, S. J. Geib, *ibid. 6* (1987) 1362; k) G. Schoettel, J. Kress, J. Fischer, J. A. Osborn, *J. Chem. Soc. Chem. Commun. 1988*, 914; l) L. M. Babcock, V. W. Day, W. G. Klemperer, *ibid. 1988*, 519; m) A. van Asselt, B. J. Burger, V. C. Gibson, J. E. Bercaw, *J. Am. Chem. Soc. 108* (1986) 5347; J. W. Faller, Y. Ma, *J. Organomet. Chem. 340* (1988) 59.
[110] L. Y. Kuo, M. G. Kanatzidis, T. J. Marks, *J. Am. Chem. Soc. 109* (1987) 7209.
[111] Organomolybdate complexes relevant in enzyme chemistry: a) G. N. Schrauzer, E. L. Moorehead, J. H. Grate, L. Hughes, *J. Am. Chem. Soc. 100* (1978) 4760; b) G. N. Schrauzer, L. A. Hughes, N. Strampach, *Z. Naturforsch. B37* (1982) 380.

Laser Photochemistry at Surfaces— Laser-Induced Chemical Vapor Deposition and Related Phenomena

By Karl L. Kompa*

Dedicated to Professor Hans Bock on the occasion of his 60th birthday

The structural characterization of materials and the tailoring of their properties is an important area of chemical research. A new trend in this area is the recourse to lasers both for analytical as well as preparative purposes, exploiting the fact that lasers, by virtue of their properties (sharp energy, spatial and temporal resolution etc.), offer the most precise and selective interaction of energy and matter that we know. Furthermore, photochemical syntheses and material transformations can proceed "cold" and without causing damage to surface structures. Laser chemistry finds application in thin film deposition, in the formation of surface layers, as well as in (structuring) ablation or etching, and in the initiation and enforcing of reactions at surfaces. In the present paper an introduction to these new possibilities on the general basis of molecule-surface interactions is followed by a brief characterization of lasers suitable for such purposes. Thereafter, four examples are discussed: gas phase deposition from volatile organometallic compounds with photoelectric activation at the surface or photochemical activation of the gaseous species (e.g. by employing molecular beams). In this way (noble) metal contacts can be deposited on various substrates. Instead of surface deposition, nucleation can occur in the gaseous medium, yielding highly disperse powders, e.g. of silicon carbide. Finally, an etching reaction is discussed where the laser does not act as an energy source but as an analytical instrument to provide diagnostic and mechanistic information.

1. Introduction

A gaseous particle with a certain amount of kinetic energy as well as energy in internal degrees of freedom may approach a solid surface, whereby an attractive interaction via the surface potential occurs. The question now arises whether and to what extent energy is exchanged between the molecule and the surface. Figure 1 depicts the situation, showing three cases which can be investigated and distinguished experimentally.

The basic assumption in all three cases is that the possible energy transfer happens, if at all, in the direction from the molecule to the surface. The reverse case, in which energy flows out of the surface into the molecule will be considered later for a specific example (Section 6.1). Figure 1 shows first the case of elastic scattering proceeding without molecular relaxation. This might be caused by very weak interaction but also by a very short interaction time, too short to allow an energy adaptation (e.g. large kinetic energy of the scattering particle). The further examples given in Figure 1 (center and bottom) exhibit increasing energy transfer. One finally speaks of adsorption if the particle reaches the bottom of the surface potential and stays there long enough to be experimentally observable.

The important question of the detailed mechanisms of energy exchange, i.e. of the degrees of freedom involved in the molecule and in the solid will not be discussed here. Also not dealt with is the related question of whether or not excitation in certain degrees of freedom will hinder or further an adsorption. This has been the subject of numerous physical studies.[2] Instead, the further fate of the adsorbed particle will be discussed in some detail. The first point of interest here is the mobility of the adsorbate on the surface.

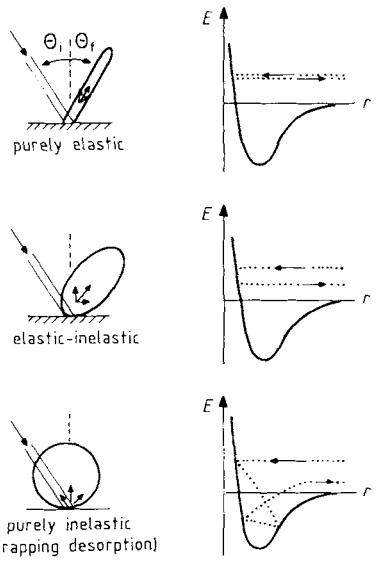

Fig. 1. Varying amounts of energy exchange in collisions of atoms or molecules with solid surfaces: Three cases with increasing interaction [1].

[*] Prof. Dr. Karl L. Kompa
Max-Planck-Institut für Quantenoptik
Ludwig-Prandtl-Str. 10, D-8046 Garching (FRG)

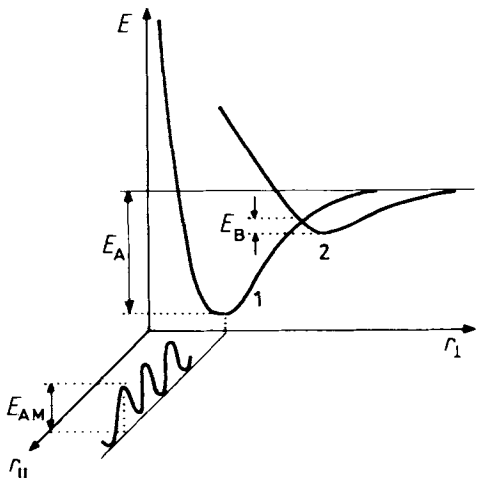

Fig. 2. Potential profile (simplified) parallel and perpendicular to the surface [3]. $r_{\parallel}$ and $r_{\perp}$: distance parallel and perpendicular to the surface, respectively.

Figure 2 shows the two different barriers which must be surmounted in the course of site changes of adsorbates on a surface. For many cases relevant to laser-CVD (laser chemical vapor deposition) such reorientations or relocations are the rule. If the deposition is continued, it can be expected, upon further energy input (radiation as well as particle impact), that the adsorbed molecule will be free to lateral diffusion and even desorption (sublimation, vaporization, photoablation). This implies that adsorption and desorption have always to be considered jointly in the study of such processes. For those interested in using laser-CVD this is a troublesome side effect, especially with regard to lateral resolution of the deposition. On the other hand, the possibility of studying the lateral motion of adsorbates without prevailing desorption is opened up by the same argument. This is then called photo-displacement spectroscopy and provides important options for studying bonding relations in adsorbates[4] (cf. Fig. 4).

Ignoring microscopic mechanisms, the sticking probability r_a (rate of adsorption) is represented by a sticking coefficient s as given in Equation (a1). This coefficient denotes the ratio of sticking particles over the sum of particles arriving at the surface [Eqn. (a3)]. Equation (a2) gives the desorption probability r_d as a function of the energy absorbed. The asterix denotes the reaction (or kinetic) order of the process.

Adsorption	$r_a = s(dn/dt)$	(a1)
Desorption	$r_d = n_s^* \exp(-E_d/RT)$	(a2)
Arrival rate at surface	$dn/dt = p(2mRT)^{-1/2}$	(a3)

The mobility of adsorbed particles will be reduced once the coverage of the surface becomes more dense; larger aggregates form which are more ponderous. In this regard it is important whether the formation of the layer starts at specified lattice sites or occurs disorderly. In the latter case island formation is possible. Special interest attaches here to the coadsorption of several components, whereby the rivalry between competitive and cooperative behavior can be observed (Fig. 3 left and right, resp.). The laws of growth of a thin layer with continuing feed from the gas phase are thus determined by the interaction of the particles impinging on the surface with the lattice of the solid and with the neighbors in the growing layer ("adsorbate interaction"). If the particle-lattice interaction dominates, a commensurable phase forms; in the other case islands are formed. If the adsorbate-adsorbate interaction dominates, vertical growth also occurs, i.e. clusters, whiskers, needles or columns appear above the surface. A homogeneous or even epitactical film formation is then excluded.

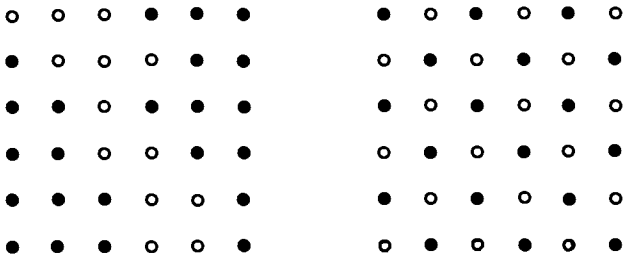

Fig. 3. Competitive (left) and cooperative (right) behavior during coadsorption of two species denoted by filled and empty circles.

Island formation and mobility of a species on a surface can also be controlling factors of the total rate of adsorbate reactions. *Ben-Shaul* et al.[5] have modeled aggregation and reaction using the Monte-Carlo simulation method (Fig. 4). One of the reactive components was assumed to be present on the surface beforehand, with lateral interaction leading to island formation. The islands grow in time and change their shape. The second reactive component can attack the islands peripherally from their boundary (although this is not beyond doubt). Hence, there is a relationship between reaction rate on the one hand, and island size and history of formation on the other, i.e. the reaction depends on the time the islands had to grow prior to arrival of the reaction partner.

In addition to the above mentioned factors, which assume the establishment of an equilibrium, in real systems other influences may be effective in inducing kinetic barriers (e.g. stabilization of thermodynamically disfavored amorphous layers).[6]

Furthermore, the influence of impurities and/or imperfect surfaces has to be taken into account. Which morphology under which conditions finally exists is thus difficult to predict, despite an understanding of the influential factors. Only experimental studies such as are described in the following sections can provide useful information in concrete cases.

As far as the desorption of a species once deposited on a surface is concerned, a simple model by *Levine* and *Zare* [see (b)] can illustrate some principal features.[7] These au-

Criterion for "cold" desorption: $\tau\nu\exp(-\xi) < 1$ (b)

(τ = duration of light pulse; ν = characteristic frequency of physisorption bond; $\xi = 2(T/T')$ = adiabaticity parameter, dependent on the characteristic times T and T' of the physisorption mode and internal mode in the free molecule)

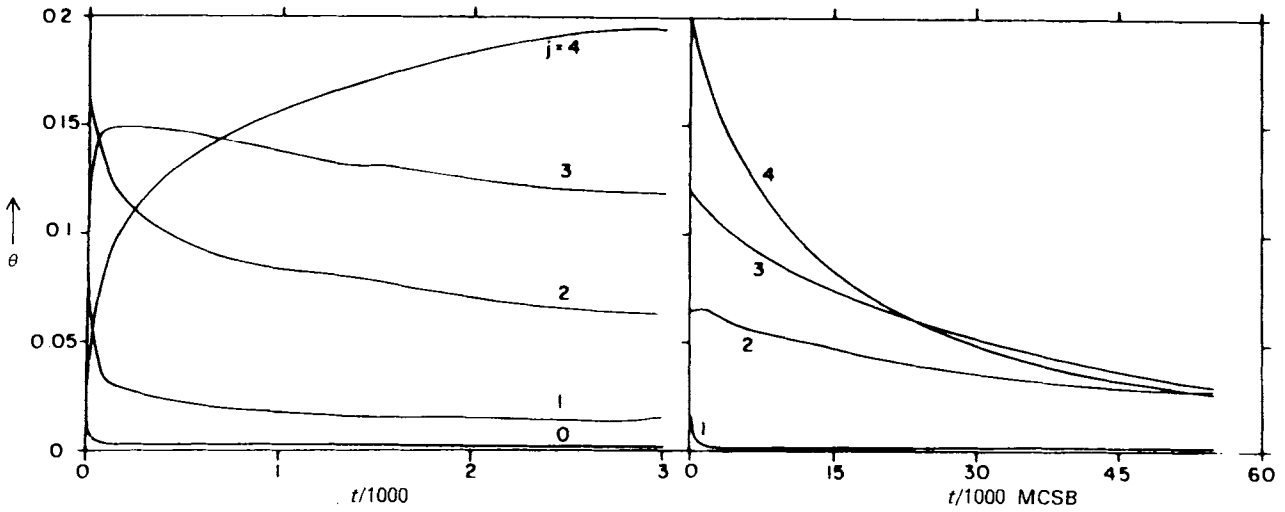

Fig. 4. Monte-Carlo simulation (MCS) of the influence of adsorbate aggregation on the kinetics of surface reactions [5]. t is given in simulation steps for species A (MCSA) and for reactions with species B (MCSB). j = 0–4 gives the number of neighbors of an atom/molecule A or B. θ is the specific coverage of the surfaces for the time of aggregation (left) and reaction (right), i.e. describes how rapid a reaction is for a given island growth.

thors have shown that the relative coupling constants, which determine the energy flow from the molecule to the surface and vice versa, the duration of the impact of laser light, and last but not least the localization of the primary energy absorption in the adsorbate or substrate are decisively important. The coupling of a molecular species to the surface by a physisorption bond is not dissimilar to the situation in a van-der-Waals-complex in the gas phase, a case for which bond-selective laser chemistry has attracted interest.[8] The important point here is that the physisorption bond acts as a bottleneck for communication between the surface and the molecule. This idea was put into quantitative terms by introducing an adiabaticity parameter ξ (exponential gap law to describe the dependence on energy mismatch), which, as shown in (b), describes the time needed to make energy flow into the physisorption bond and heat this bond sufficiently to induce bond rupture and desorption.

For the kinetics of energy transfer a balance equation (based on (b) and Fig. 5) can be derived, which describes the energy flow from the substrate into the van-der-Waals bond and from there into the adsorbed molecule with $E(t)=E_0(t)-ktf(D)$, where D denotes the energy of the bond between molecule and surface.[7] This means that the relevant rates and times decide whether a molecule will desorb internally "cold" or whether an energy-rich species before or in competition to desorption will undergo chemical changes (e.g. fragmentations). It is possible to measure the energy of the desorbing particles spectroscopically and to check the validity of this simple model.[9, 10] In the case of an energy absorption in the adsorbate rather than in the substrate (see Fig. 5) "hot" particles in particular should be desorbed, for the same reasons of blocked energy transfer to the solid. This has been confirmed experimentally—at least for some cases studied.[11]

Thus, laser flash-desorption may be used as an analytical tool to obtain a "snapshot" of the chemical nature and composition of species on a surface (unstable intermediate products, for instance, in catalytic reactions). This aspect has received special attention by *R. B. Hall* et al.[12]

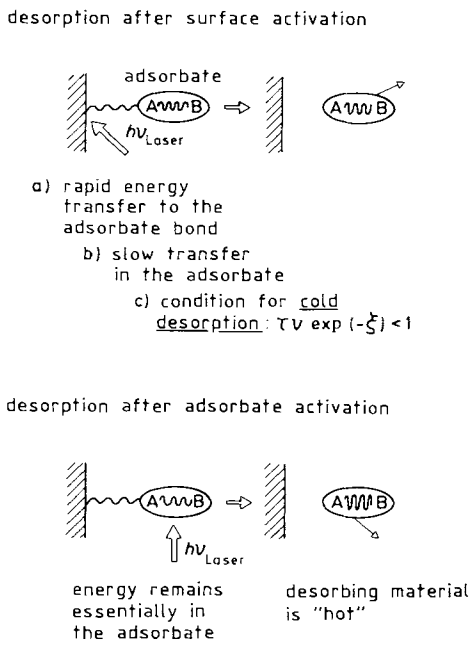

Fig. 5. Pictorial representation of laser-induced desorption without (top) and with (bottom) energy absorption in the desorbing particle [7].

It has been pointed out that the ratio of Arrhenius factor A to heating rate v and activation energy E_a determine the competing behavior of reaction and desorption. The general conclusion is that rapidly desorbing molecules will leave the surface "lukewarm" and chemically intact (examples: methanol and ethene desorption from metal surfaces[12]).

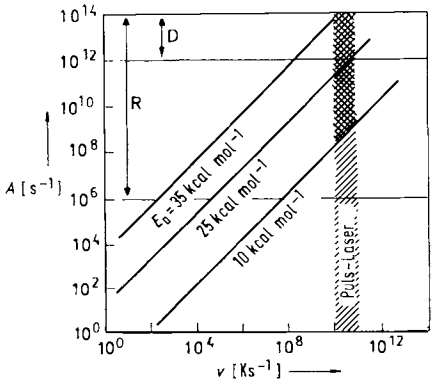

Fig. 6. Requirements for the magnitude of the pre-exponential factor A needed for a minimal yield of 1% desorption as a function of the heating rate ν. Three different activation barriers are considered. The shaded area shows the conditions under which desorption D exceeds decomposition R [12].

2. Laser-Induced Photochemical Reactions at Gas-Solid Interfaces

A deposition reaction can be activated in different ways (Fig. 7):

① By local thermal activation of the surface and transfer of energy to gaseous species adjacent to the surface.
② By photolysis in the gas phase and deposition of the products.
③ By photoelectric excitation of the solid and dissociative electron capture of gas phase particles.

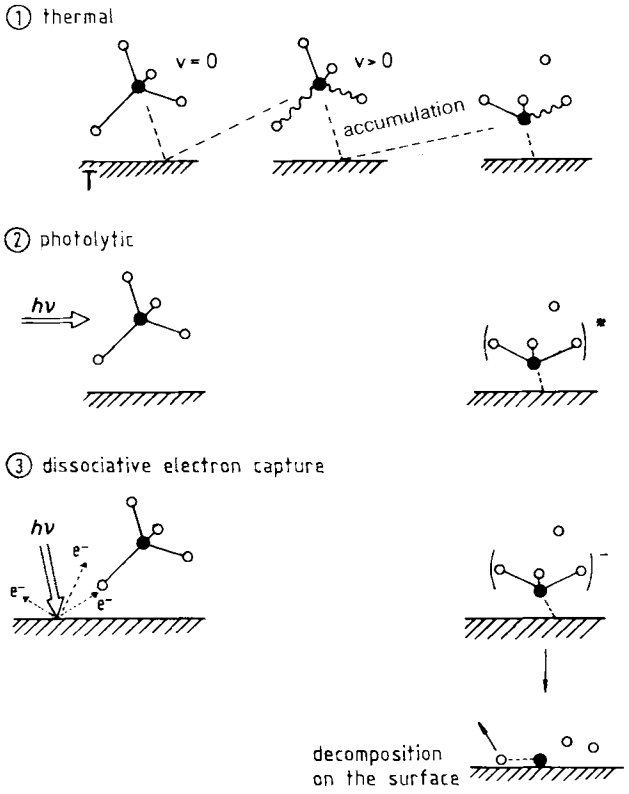

Fig. 7. Initiation of deposition by activation in the gas phase (②) or at the surface (① and ③).

In general we thus distinguish processes in the gas phase from processes that begin in the solid. Vapor phase deposition at surfaces may be initiated by sputtering, ion- or electro-plating, chemical or plasma reduction, or anodizing, whereby the generation of active species or nucleation centers may play an important role. But let us turn to a specific example, namely noble metal deposition on different substrate materials. In this case the starting materials are volatile organometallics,[13] for example tetrakis(trifluorophosphane)platinum(0). This molecule exhibits reversible photolysis in the vapor phase (Scheme 1, top).

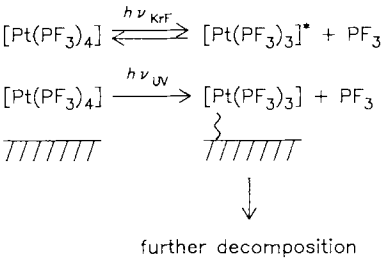

Scheme 1. Photolysis of the relatively volatile platinum compound $[Pt(PF_3)_4]$; it is reversible (top) in the gasphase, irreversible on surfaces (bottom).

In the vicinity of a surface, however, the ligand bond may be substituted by the surface bonding, in this way replacing one or several PF_3 groups (Scheme 1, bottom). This takes place particularly well if the $[Pt(PF_3)_n]$ fragment is negatively charged following photoelectric surface activation (see Scheme 2).

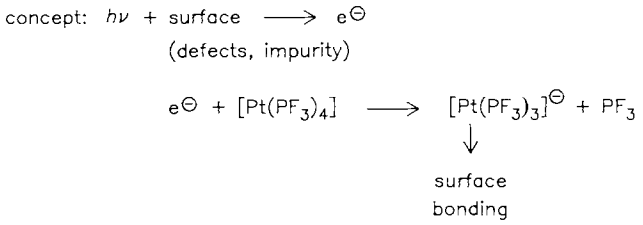

Scheme 2.

We expect first a deposition of $[Pt(PF_3)_3]$, which, presumably by dissociative chemisorption, will be converted into a pure platinum deposit. The gas column from which the local deposition is fed has a height of a few μm. By variation of the parameters a quantitative model picture of the process may be obtained. However, direct measurements of the photoeffect by UV lasers are needed (see Sections 4 and 6.4).

3. Laser Sources for Chemistry

From the extensive arsenal of lasers used in physics[14] primarily those mentioned in Figure 8 have gained importance in analytical and synthetic laser chemistry.[15]

The mode of operation of a laser can be that of an oscillator or that of an amplifier. The radiative power that is

delivered ranges (for pulsed operation) from $<10^{-6}$ W up to $>10^{12}$ W. The geometrical dimensions of the radiation path in the laser accordingly range from mm to km. Both pulsed as well as continuous operation is possible, and in the case of some lasers there are both variants. The efficiency, i.e. the ratio of emitted to absorbed (e.g. electrical) power is normally small, typically in the range $\leq 0.1\%$. There are, however, exceptions like the CO_2-laser, which can have an efficiency of $>10\%$.

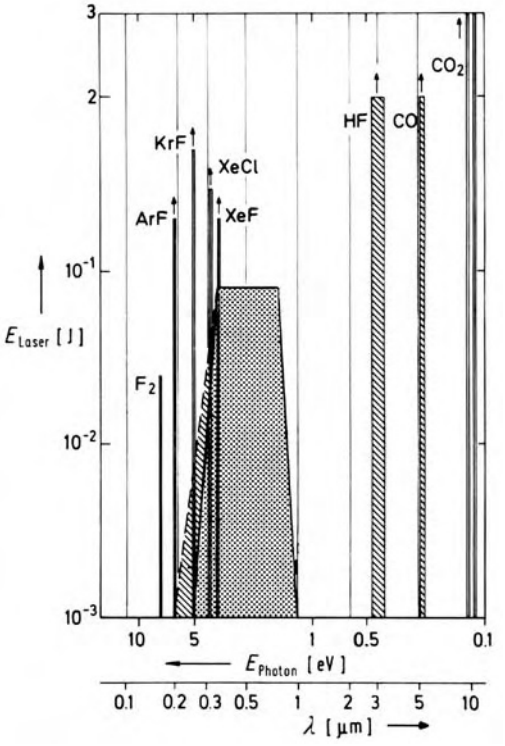

Fig. 8. Overview of the most popular types of lasers for chemistry as function of wavelength λ or photon energy E_{photon}. the cross-hatched area denotes dye lasers, the shaded area anti-Stokes-shifted or other frequency-converted dye lasers.

The photon fluxes are, in view of the many different types of laser, very different. The lasers indicated in Figure 8, which can be operated without difficulty in the power range of 100 W or above, deliver about 10^{19}–10^{21} photons per second. In molar units this amounts to 1–100 mEinstein s^{-1}. Assuming reasonable quantum yields, material conversions in the mol/min range are conceivable. For the often more important analytical applications of lasers this is irrelevant; the choice of usable laser sources here is much larger than in preparative chemistry.

The spatial coherence of laser radiation leads to ideal beam collimation—limited only by diffraction effects—and thus enables loss-free radiation transport over large distances. Here, one should not only think about laser beam transport by mirrors but also by waveguides and optical fibers. Remote laser interaction with reacting systems is in this way possible both in an analytical and a synthetic sense. If one considers for instance the use of an IR laser as a specialized heat source to bring about a reaction it should be noted that the energy can be coupled into the medium directly as radiation without being mediated through wall effects. Therefore reaction vessels are less subject to corrosion and attack.

Under certain conditions laser light is extremely monochromatic. Lasers in the visible region having frequencies of about $4\text{–}7 \times 10^{14}$ Hz have bandwidths of MHz to GHz, or relative bandwidths of up to 10^{-9}. With special stabilization measures, however, bandwidths <1 Hz have been realized. This gives a spectral purity of $\sim 10^{-15}$. As a consequence lasers can be employed as frequency and time standards.

The extreme monochromaticity, the high energy densities achievable in the focus of the beam and the possibility of generating extremely short pulses have already been mentioned above. A further brief illustration follows: Coherent radiation can be focussed to a spot size of one wavelength. With a 100 W Laser in the visible spectral region one then obtains power densities of up to 1 GW/cm^2 (for a correspondingly short time). The electrical field strength is in the MV/cm^2 to GV/cm^2 range. At such high photon densities multiphoton processes come into play—a molecule absorbs more than one photon (some times even much more) from the laser pulse. This opens up new possibilities for *nonlinear spectroscopy* and for *nonlinear photochemistry*.[16]

Depending on the frequency bandwidth[17] very short laser pulses can be generated. The record here lies at ca. 10 fs. The geometrical length of such a pulse is only 3 μm. Hence its propagation is no longer conceivable as a beam but rather as a thin film of electromagnetic energy traveling at the speed of light. Such a short pulse naturally loses its monochromaticity but exhibits a rather broad-band frequency spectrum.

A new development in the ultraviolet spectral region in the last ten years has been that of excimer lasers.[18] These have introduced a new dimension into the field of surface photochemistry since, in view of their photon energies, they not only make thermal but also electronic substrate activation possible (see Section 4). Such lasers are currently available only in the pulsed mode of operation (typical pulse durations: 10^{-8} s, repetition rates: ≥ 100 Hz, and average powers: ≥ 100 W). The more commonly used excimer lasers are listed in Figure 8.[19] There are three groups of excimer lasers, namely rare gas dimers, rare gas halides, and halogen dimers.[20] Their common feature is that the active laser materials are molecules which exist only in an excited (lasing) state and decay instantaneously once having returned to the lower (ground) state. In all technical versions of relevance here the excitation is achieved by a pulsed electrical discharge. The potential of this type of laser has not yet been fully exploited.[21]

Since a light source cannot be focussed down to spots of sizes less than their wavelength the resolution is limited to maximally 0.2 μm. This has in fact been achieved, but the field of view, as well as contrast and homogeneity of illumination are still the subject of intensive development. As has been pointed out in the preceding section, secondary changes in the deposits are frequently more limiting for a desired spatial structuring than the optical imaging parameters of the laser.

4. Photoelectrical Initiation of Vapor Phase Deposition

The possibility of initiating laser-CVD by mobilizing charges at solid surfaces has already been demonstrated in Figure 7. Of special interest here is the photoelectrical initiation of the reaction. Electron emission can be induced by elevation of temperature, by photon bombardment, and by an electric field. In the first case an increasing number of states above the fermi level is populated. The number of emitted electrons is thus proportional to the high-energy end of the Boltzmann tail, exceeding E_{vacuum}. In contrast, in the second case the emission occurs by (1) excitation via photon absorption by an electron, (2) diffusion of the electron to the surface, (3) transmission through the surface. The kinetic energy of the electron is described in terms of *Einstein*'s classical formula

$$\frac{1}{2}mv^2 = h\nu - \Phi \qquad (c)$$

A more detailed inspection shows that the work functions Φ for metals are typically, in the region of 5 eV, i.e. are accessible with the photon energies of excimer lasers. Measurements have shown that the work functions strongly depend on the adsorbate coverage and that excimer irradiation of the surface can even produce photoelectron currents which are space-charge limited. It is easy to see that the effect can be amplified by external fields and that in the limiting case even a laser-preionized plasma discharge will be obtained. This implies (Fig. 9) that the discharge remains localized and can be controlled by the path of the laser beam. In this way the spatial resolution of the deposition is more or less maintained. For comparison: If the particles to be deposited should be generated by photolysis at some distance from the surface (Fig. 7, ②) they would first have to diffuse to the surface and remain stuck there; a controlled and locally or spatially resolved formation of the deposit is then much more difficult to achieve.

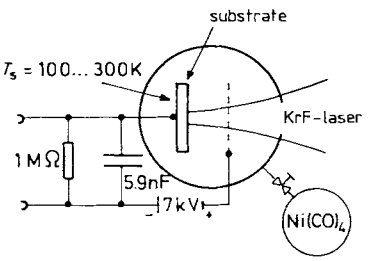

Fig. 9. Experimental scheme of photoelectrical vapor deposition, shown here for $Ni(CO)_4$. The wiring of the "diode" corresponds to one particular set of parameters discussed in [30].

For several reasons, organometallic compounds are especially suitable for such experiments with lasers: they are generally sensitive to dissociative electron capture, the range of effective electron energies ranging from mV to V. Furthermore, it is desirable that the gas-phase photolysis be reversible so that excitation in the gas remote from the surface does not lead to permanent chemical changes (see Scheme 1) and only participation of the surface leads to deposition. Besides the deposition of platinum, that of many other elements can also be realized (see Section 6.4).

5. Photochemical Deposition with Molecular Beams

Many recent papers dealing with molecule/surface interaction concern the utilization of molecular beam techniques. This type of laser-CVD is thus closely related to molecular beam epitaxy for spatially resolved materials synthesis.[22] A schematic introduction to the experimental concept is given in Figure 10. Molecular beams guarantee

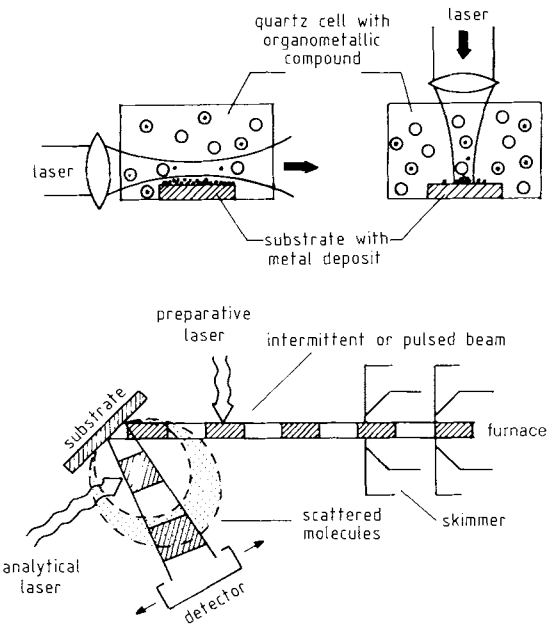

Fig. 10. Experimental setup for photochemical deposition from molecular beams (bottom) in comparison to the deposition from a static gas (top).

collision-free conditions in the gas space and thus ensure that a once excited or otherwise prepared species will not be changed due to bimolecular processes nor be withdrawn from the interaction region of the surface. One special feature compared to static gas conditions is associated with the high kinetic energy of the colliding particles which may eventually result in extremely short interaction times. Often the molecular beam is pulsed, which causes special boundary conditions for the reaction kinetics (high collision rate for a correspondingly short time).

6. Examples

The four examples discussed in the following represent a small selection from a rapidly growing and diverse field.[23] The discussion in the following sections covers a) the interaction of electronically excited carbonylnickel compounds with surfaces, b) the reactive scattering of fluorine (atomic, molecular) with copper surfaces, c) the vapor phase deposition of silicon carbide powders, and d)

the production of noble metal films for electric contacts and in particular for the metalation of non-metallic substrates. In some of these examples industrial applications are also envisaged, to which reference is made in the individual cases.

6.1. Surface Interaction of Volatile Metal Compounds

In Section 2 under item 2) the possibility of metal deposition by photolysis of suitable precursors in the gas phase and subsequent transport to the surface was addressed. As a first example the deposition of nickel from tetracarbonylnickel will be considered. The measurements were conducted under molecular beam conditions (cf. Fig. 10), which means that the beam particles undergo only a single collision with the surface. No thermal deposition is observed up to surface temperatures of >470 K; only when the beam is exposed to UV laser radiation does decomposition and formation of a nickel layer occur.

The discussion of the photochemical behavior of $Ni(CO)_4$ is based on the model by *Rösch* et al.[24] shown in Figure 11. According to this model the molecule decom-

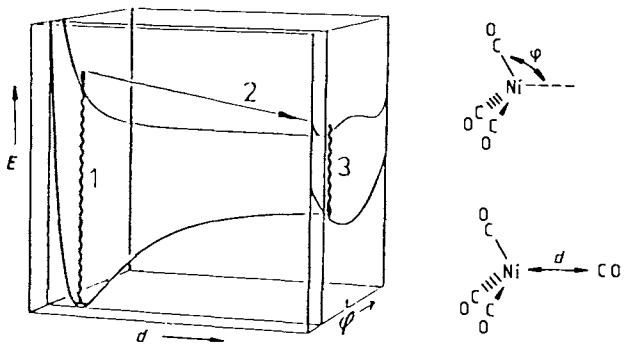

Fig. 11. Mechanism of excitation and photodissociation of $Ni(CO)_4$ showing the most important reactions [24].

poses after excitation by a XeCl laser ($\lambda = 308$ nm) in less than 10^{-10} s, losing only one of its ligands. The excess excitation energy does not lead to further bond rupture but remains in the $Ni(CO)_3$) fragment as electronic excitation. This manifests itself in a spontaneous luminescence decaying with a time constant of 15 μs. With the time of flight typically encountered in molecular beam experiments (700 m/s in the present case) and with a distance between the place of excitation and the substrate of 2.5 cm the $Ni(CO)_3$ fragments have lost most of their excitation on the way to the surface. The ground-state fragments, however, then yield a nickel film on contact with the surface which is of high quality also in a technical sense (Fig. 12).[25]

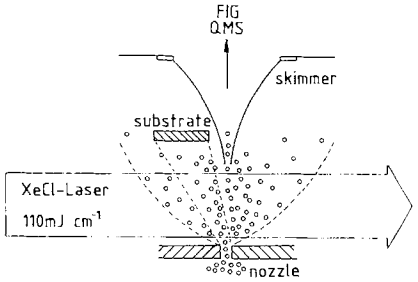

Fig. 12. Top: Schematic diagram of an apparatus for the deposition of highly pure nickel films: a pulsed $Ni(CO)_4$ molecular beam leaving the nozzle is excited with an XeCl laser. After (multistep) $Ni(CO)_4$ decomposition the nikkel atoms deposit on the substrate. The skimmer gates out the core of the molecular beam, which is thereby collimated (FIG: fast ionization gauge; QMS: quadrupole mass spectrometer). Bottom: Picture of the experiment. After emergence from the nozzle (above), the $Ni(CO)_4$ molecular beam fans out conically. Interaction with the laser pulse leads to formation of excited $Ni(CO)_3$, whose luminescence is clearly recognizable. The skimmer is faintly visible in the center.

Figure 13 again compares $Ni(CO)_4$ absorption and $Ni(CO)_3$ emission. The deposition thus proceeds as a reactive surface interaction. The removal of one ligand opens up the possibility of nickel binding to the surface. The sublimation energy set free in this process leads to dissociation of the remaining ligands. Consequently, one can speak of a surface-catalyzed deposition. The same general picture appears to be applicable in the surface decomposition of other photolysis products derived from tetrahedral or octahedral molecules.[26] A general statement about the possible dependence of the chemical nature and preconditioning of the substrate, however, cannot as yet be made on the basis of information thus far available.

It is well known that the impact of UV lasers on polyatomic molecules at elevated power densities soon leads to multiphoton excitation and ionization.[27] This possibility also has to be taken into account in the present context of UV laser photolysis of organometallic compounds. An attempt was made to clarify the question as to what extent and at what power or energy density ionic fragments form during the excitation of $Ni(CO)_4$ with excimer lasers. To this end, mass spectrometric measurements were per-

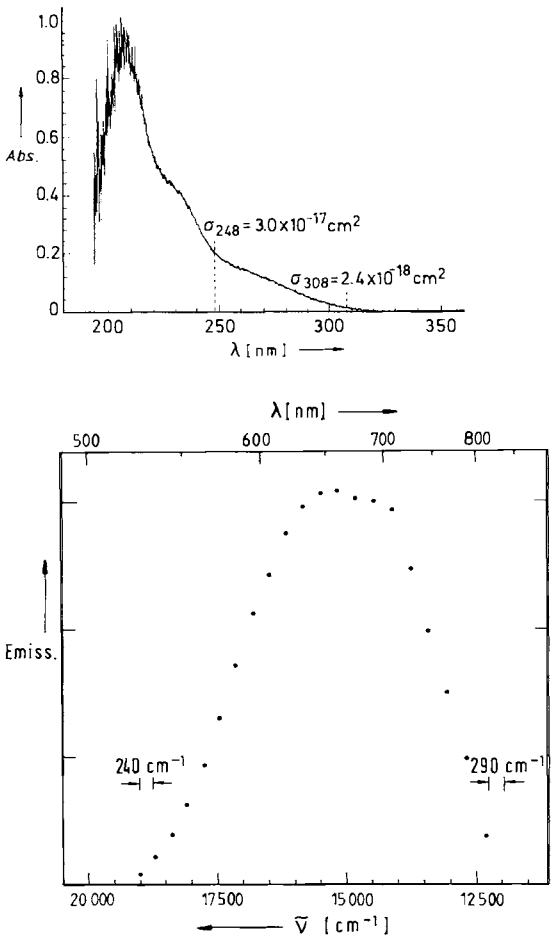

Fig. 13. Top: Absorption spectrum of $Ni(CO)_4$ at ca. 50 μbar; bottom emission spectrum of $Ni(CO)_3$ on excitation with a XeCl laser.

formed on $Ar/Ni(CO)_4$-molecular beams to determine the ion yield as function of laser energy. The experimental setup together with some results are shown in Figure 14.

By additional measurements in a static gas cell at low pressures the absolute concentration of $Ni^{\oplus}$ ions could be determined for the calibration of the molecular beam data. The complete pattern of fragment ions between molecular beam and static gas can be compared in this fashion. In the latter case, by varying the gas pressure also the electron capture cross section of neutral $Ni(CO)_4$ molecules can be measured. The corresponding values for two excimer laser wavelengths are $\sigma = 4.8 \times 10^{-14}$ cm² (XeCl) and $\sigma = 2.9 \times 10^{-14}$ cm² (KrF). From the plots of Figure 14, which are linear over the relevant range, it follows that the ions in the case of KrF laser radiation are formed in a 3rd order process and for the XeCl laser in a 4th order process. Also the corresponding effective cross sections have been derived from the measured data.

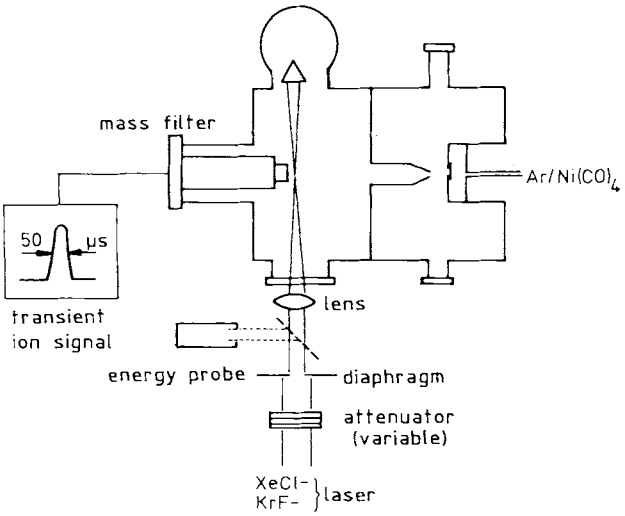

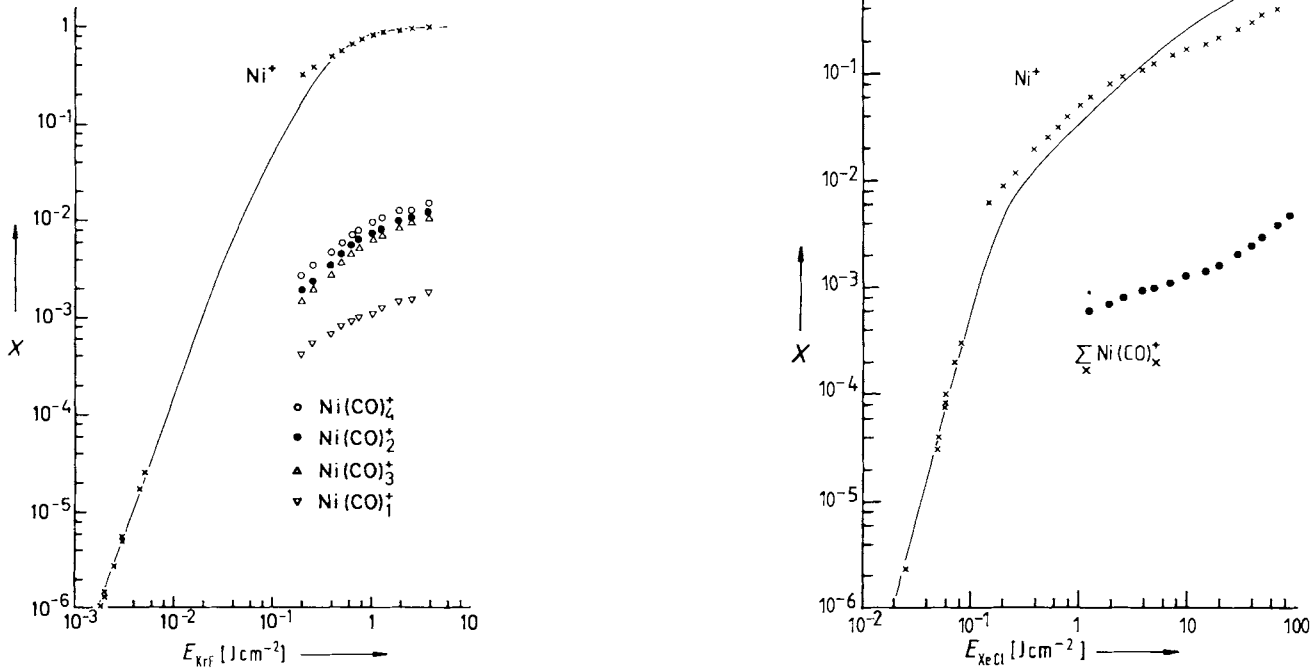

Fig. 14. Top right: Experimental arrangement for the investigation of resonance-enhanced multiphotoionization of $Ni(CO)_4$. Bottom: Comparison of calculated (unbroken curve) and mass-spectrometrically determined ion yields X on using a KrF (left) and XeCl laser (right), respectively (see also Scheme 3). E = energy flux of the KrF or XeCl laser.

All these facets of information finally yield a kinetic model based on rate equations. Without detailed discussion, the elements of this model are reproduced in Scheme 3.

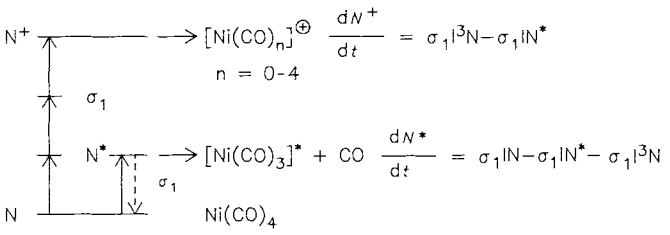

Scheme 3.

A conclusive picture is obtained if one assumes that the total excitation and ionization occurs in the mother compound and that all ionic products are formed therefrom. The $[Ni(CO)_4]^{\oplus}$ ions are then produced in a direct 3-photon process (KrF laser) and decay statistically, mainly to $Ni^{\oplus}$ and CO. The only competing channel of importance is the above mentioned process of excitation to generate $[Ni(CO)_3]^*$. This scheme resembles the situation for KrF laser photolysis. The interpretation for the corresponding behavior in the case of XeCl laser irradiation is somewhat more complicated since three competing channels have to be considered. A detailed discussion of this case is omitted here. Computational evaluation of this model yields the curves shown in Figure 14 (bottom), which are in remarkably good agreement with the experimental curves.

The special features possibly related to deposition from gas samples or molecular beams with a high degree of ionization are still subject to discussion. In this connection concepts of plasma chemistry or plasma-induced vapor phase deposition may be of interest. Attention should also be paid to a further aspect of deposition from pulsed molecular beams which is of interest both scientifically as well as with regard to industrial application. This concerns the role of clusters which are often present—depending on the experimental conditions—in molecular beams.[28,29]

In the investigations mentioned in the following section the surface where the interaction occurs was the front face of a pyroelectrical calorimeter. That is, the polyvinylidenedifluoride (PVDF) calorimeter foil was coated with a metal film (e.g. aluminum).[28,29] In this way the energy exchanged in the scattering process can be measured directly as heating or cooling of the detector. At the polymer foil a voltage is measured which is proportional to the energy content of the foil. If energy is fed into the detector foil (light, particle impact etc.) the voltage becomes more negative. The reverse is true if energy flows out of the detector. At such a metal-coated foil rare gas beams, pure and seeded with $Ni(CO)_4$, are scattered (cf. Fig. 10).

Experiments in which energy transfer to surfaces have been investigated using this same detector concept[30] generally assumed that the total amount of energy contained in the molecule is always quenched at the surface. This could not be confirmed for the systems considered here. Since the molecules are scattered at the surface they at least retain part of their kinetic energy. Moreover, it was shown that even molecules having a certain amount of internal energy often "survive". In the case of SO_2, this even included electronic excitation. In addition, not only does transfer from the molecule to the solid occur but also in the reverse direction. This means that, depending on the experimental conditions, warming or cooling of the substrate is possible. Characteristic differences exist among the rare gases as carriers, but also other parameters such as pressure in the molecular beam source and mixture ratios play a role. The calorimeter thus responds very sensitively to varying beam conditions (energy resolution better than 1 nJ).

For the beam conditions used here typically 5×10^{13} molecules or atoms in a pulse reach the detector surface and are scattered there. The average energy resolution is less than 1 meV. The time profile of the energy transfer can be determined by differentiating the signal with respect to time. The most straightforward assumption now would be that the average energy transfer for all particles is the same. This, however, as Figure 15 shows for the case of Xe, is not confirmed experimentally. Instead, the fast (early arriving) particles heat, while the slow ones cool the surface.

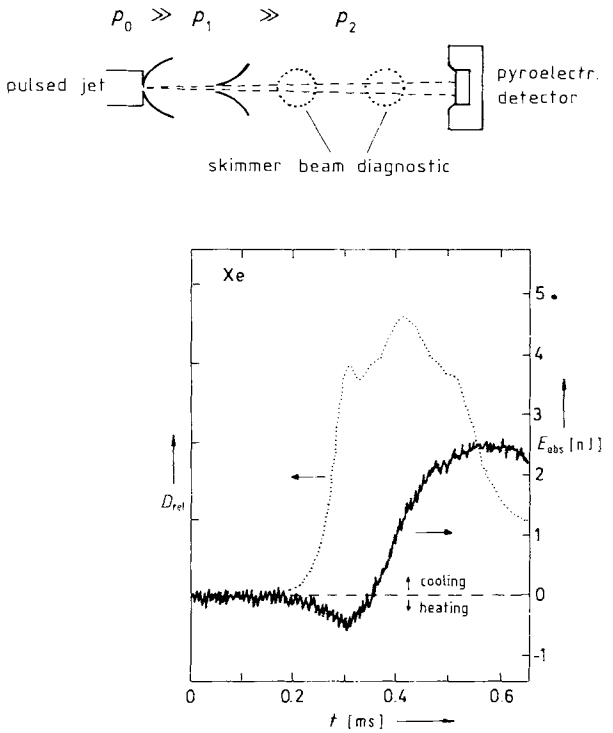

Fig. 15. Investigation of the cooling of a surface during interaction with pulsed molecular beams of specified composition. Top: Apparatus used with various detector positions. Bottom: The parts of the beam arriving early and late respectively contribute to the heating and cooling. D_{rel} = relative beam density; E_{abs} = absolute energy transfer.

The speculation that in the case of surface cooling the respective particles have a higher kinetic energy after the collision, i.e. that the energy drawn from the solid is converted into translational energy, could not be verified. Pure rare gas pulses or rare gas/carbonylnickel pulses cool the surface all the more strongly the heavier the rare gas employed. This trend qualitatively follows the tendency for cluster formation in pulsed beams. The assumption here is that the slower part of the beam contains particles of heav-

ier mass. For a more detailed discussion of the subject of film formation from cluster beams reference should be made to the literature.[31]

6.2. Interaction of Fluorine Atomic or Molecular Beams with Copper Surfaces

The laser is an ideal tool for the quantum specific investigation of molecular systems. In physical chemistry this was first exploited in the area of the dynamics and kinetics of vapor-phase processes.[32] The development now, however, extends to chemical reactions at surfaces, too. So far, there is still only a limited number of examples, concentrating primarily on the state-specific investigation of species potentially active in catalysis.[33] A general observation is that the distribution of the energy liberated in these reactions can usually be described in terms of an equilibrium which is determined by the temperature of the surface. Strong non-equilibria as are often found in elementary chemical reactions in the gas phase have so far rarely been observed. The search for non-statistical effects in (strongly exoergic) surface reactions is therefore of special interest. As examples, reactions of fluorine with metal surfaces lend themselves to study. The products formed in such "etching" reactions are volatile under the chosen temperature conditions and can be analyzed in the gas phase by the conventional techniques of laser spectroscopy. It has already been shown that laser desorption per se can be a very fast process and is expected to provide no obstacle for the detection of non-equilibrium effects [see Eqn. (a2)].[3] Dry etching reactions of metals and semiconductors are also of practical interest and may be employed in the production of electronic devices.

To gain access to an understanding of the dynamics of this class of reactions an experimental setup following basically the concept shown in Figure 10 was used. A beam of atomic or molecular fluorine is generated in a high-vacuum vessel. This is allowed to impinge onto a single-crystal copper surface whose temperature can be varied over a large range. The reaction products a few mm above the surface are then analyzed with a tunable dye laser. In this instance, CuF shows laser induced fluorescence (LIF) bands—relevant transitions $X(^1\Sigma^+)\leftarrow B(^1\Sigma^+)$ and $X(^1\Sigma^+)\leftarrow C(^1\Pi)$—which can be used to obtain information on the state of excitation of the molecule.[34]

The relevant part of the CuF excitation spectrum is shown in Figure 16. The fluorescence intensity depends linearly on the flow of gaseous fluorine and saturation effects are not observable, i.e. the concentration of fluorine on the surface is in the sub-monolayer range. The LiF spectrum of CuF exhibits a characteristic threshold behavior. A preliminary analysis of the internal product energy distribution for three surface temperatures between 800 and 900 K yields a vibrational state population which is represented by a Boltzmann distribution. The vibrational temperature, however, considerably exceeds the surface temperature. In contrast, the rotational temperature is more or less equal to the surface temperature.

The measured energy distribution poses the question as to what extent the desorbing molecules have lost or retained the "memory" of the details of their formation. A loss of memory in this case may be equivalent to a "longer" residence time on the surface. A conclusive answer to this question is not yet possible. The Arrhenius activation energy for the desorption of CuF in the temperature range 750–900 K is 135 ± 20 kJ/mol. A proof of the mechanism involved is still lacking but may well be possible on the basis of further measurements involving a kinetic energy analysis (high resolution ring laser) of the desorbing particles.

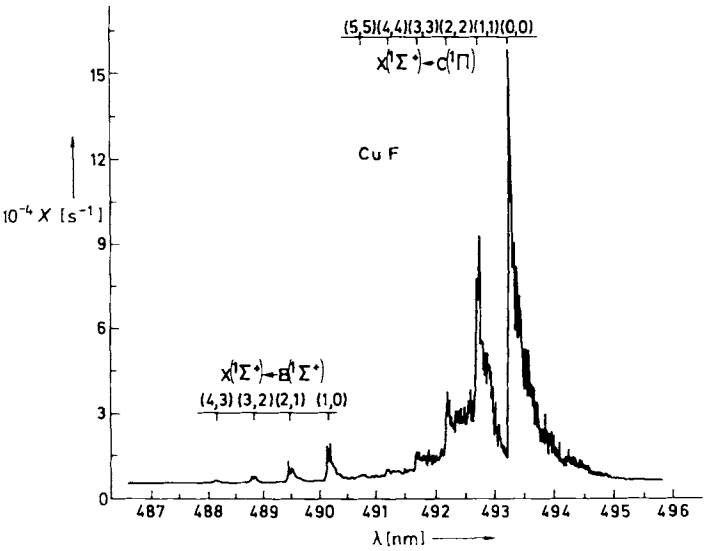

Fig. 16. Excitation spectrum of gaseous CuF formed in an etching reaction with copper at a temperature of 820 K [34]. X = count rate.

6.3. Laser Induced Powder Synthesis (Silicon Carbide)

One disadvantage of ceramic materials is their brittleness, arising from microscopic structural defects, pores, and microcracks. In contrast to metallic materials, where cracks are anealed by plastic flow, in the covalent ceramics cracks develop until rupture occurs. For high quality ceramics it is therefore necessary to avoid structural defects. To this end sinterable powders are needed which are very pure, homogeneous, of small particle size and small size distribution, and which may possibly be sintered without additives.

Powders of high purity are best produced in gas phase reaction systems since here wall effects are absent and the reagent gases can be pre-purified. It has already been demonstrated[36] that such a powder synthesis is possible by laser-induced chemical vapor deposition. In the following a special variant of this technique will be described in which the gas-phase reaction occurs in a plasma generated by gaseous breakdown in the focus of a pulsed TEA-CO_2-laser.[35] The benefit of this technique is seen in a high heating rate, the achievement of high temperatures and a well-defined reaction zone.

Other than in the case of reaction initiation by cw (= continuous wave) lasers,[36] reactions near the entrance window can be avoided without applying gas purging by choosing a wavelength of the CO_2 laser which is not (or only slightly) absorbed by the cold gas.

As first example for this type of powder synthesis silicon carbide was selected. As starting materials tetramethylsilane $Si(CH_3)_4$, hexamethyldisilane $(CH_3)_3Si\text{-}Si(CH_3)_3$ and methylsilane CH_3SiH_3 were investigated. The reagents were handled in a cyclic flow apparatus equipped with a membrane pump and a membrane filter.

The main products left in the gas phase after the reaction had occurred were methane, ethyne, ethene and propyne. The product yields amounted to 100 to 300 mg per hour. Depending on the laser pulse repetition rate (1–4 Hz) this corresponds to 3600 to 14000 laser shots with a single pulse energy of 2 J. The powders obtained still contain free carbon. According to IR spectra some $SiCH_3$, $SiCH_2Si$ groups and occasionally some SiO are also present. The $SiCH_3$ groups could be removed by heating the samples to 800–1000°C in vacuo, whereupon methane was liberated. The $SiCH_2Si$ groups remained uneffected under these conditions. This points to a reaction proceeding in two steps: After the high temperature primary reaction some (less complete) secondary product formation occurs during the cooling. Polymers are formed which are stable up to temperatures of 1000°C. Whether these polymers are favorable or disfavorable for later sintering procedures remains to be seen. Figure 17 shows an electron micrograph of a laser-produced SiC powder.

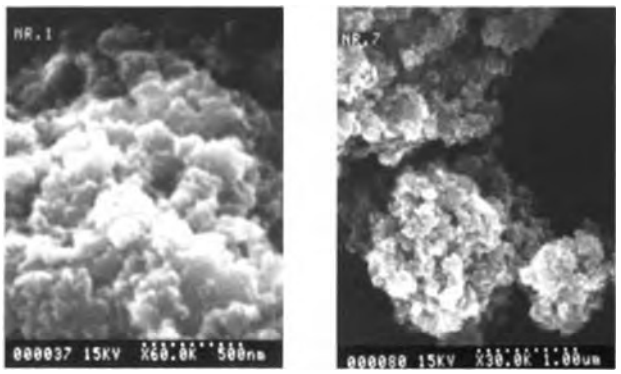

Fig. 17. Electron micrograph of SiC powder produced from hexamethyldisilane by laser radiation. Particle size: 40 to 120 nm.

To reduce the free carbon content which may be disadvantageous for later use of the powder a 0.5 nm molecular sieve was inserted into the apparatus. This fulfilled its purpose, but at the same time led to products which were pyrophoric. Since also products with Si–H bonds were now detected in the gas phase it would appear that polymers containing Si–H bonds, which react exothermally with air to give Si–O bonds, are the cause of this behavior.

At the present time experience of sintering properties is still lacking, and the question of the scaling up of the reaction still requires investigation.

6.4. Noble Metal Contacts by Laser-CVD

The photoelectric initiation of deposition processes was already introduced in Section 4. The following discussion will outline the concept in more detail and provide links to practical applications.

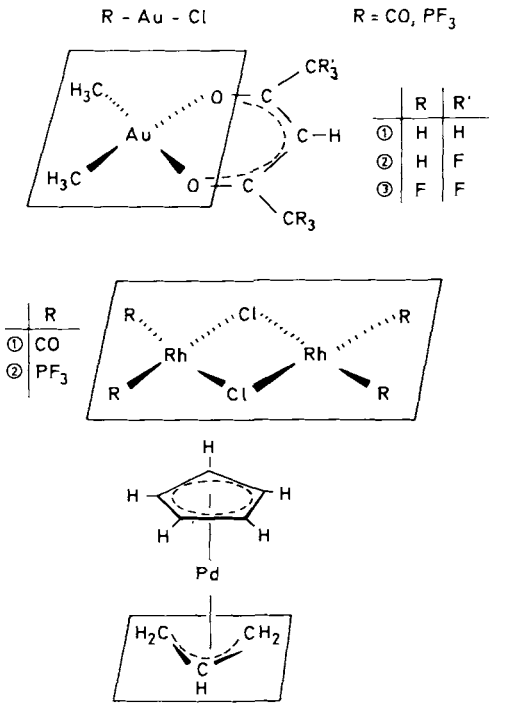

Fig. 18. Some rare metal compounds for the production of thin structured films and layers by laser-CVD [40].

Emphasis is placed here on the deposition of noble metals (gold, palladium) on metallic and non-metallic substrates. The deposition of many other elements, however, has also been investigated, e.g. that of Al, Cd, Cr, Fe, Mo, Ni, Si, W.[23] Numerous compounds such as Al_2O_3, CrMoW, CrO_x, GaAs, HgTe, HgCdTe, InP, Si_3N_4, SiC (cf. Section 6.3), SiO_2, $TiSi_2$, ZnO, and ZnSe as well as materials for high-T_c superconductors have also been deposited.[23] Nevertheless, this area of research is still at in early stage. In particular, there is a lack of data on the influence of surface defects and impurities (sometimes required to mediate sticking) and on the relationship between temperature, deposition rate and morphology of the deposit.[37]

A selection of compounds successfully used for rare metal deposition via laser activation of the surface is listed in Figure 18.[38,39,40] It could be demonstrated for some selected cases that imaging and structuring deposition is possible. For this purpose experimental setups on a pilot-plant scale have been described. These allow for quick access and interchange of samples and control of the (flowing) processing gas. Gas purging of the chamber windows helps to suppress deposits on window surfaces. So far the results obtained are still unsatisfactory as regards morphology and purity of the deposit. The limits associated with these effects may cause difficulties when thicker films (some μm) are to be fabricated. Deposition rates, process control and structural contrast, however, are basically suitable for industrial applications. Noteworthy is the possibility of forming films and ohmic contacts on ceramics and organic polymers. This can be carried out in such a way that lasers generate only the first nucleation layer on the surface, which is then strengthened by galvanic techniques.

As mentioned in Section 4 a photoelectric mechanism has been suggested for this kind of deposition. This hypothesis

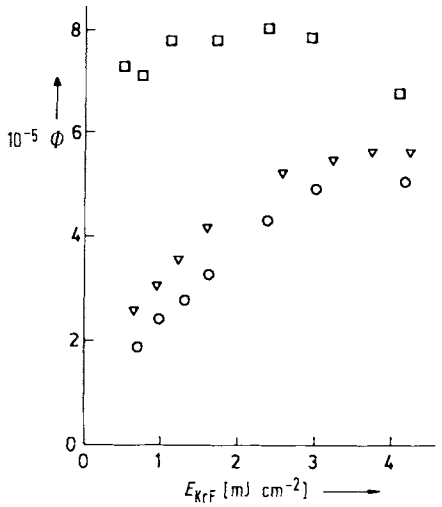

Fig. 19. Laser-induced charging and photoionization of Al with and without adsorbate coverage. Φ = quantum yield; E_{KrF} = energy density of the KrF laser. ○ clean surface. ▽ 10^{-2} mbar $Ni(CO)_4$; □ 1 mbar $Ni(CO)_4$.

could be supported by measurements of the electron yield (Fig. 19). Details of these results will not be given here, however, for lack of space. Essentially there are three different effects of the UV laser irradiation of surfaces (as a most studied example consider aluminum): 1) The quantum yield of the photoelectron emission correlates non-linearly with the energy density of the laser. 2) The quantum yield can be increased by adsorbates, e.g. $Ni(CO)_4$. 3) At higher laser energy density, ions are generated from the adsorbate.

Photo- and thermo-ionization as a general phenomenon of laser surface interaction deserves interest beyond the special case shown here. Corresponding investigations were therefore not only conducted on macroscopic surfaces but also on microscopically fine surfaces of aerosols, both in the pure form and adsorbate-covered. To achieve a desired deposition (filtration) of an aerosol from the gas phase an effective charging of the particle is necessary. To this end experiments were carried out in which for the first time aerosols were charged by pulsed laser radiation in the visible and ultraviolet spectral region.[41] Carbon aerosols (also covered with coronene adsorbates) were of primary interest, but nitrides, carbides and oxides have also been investigated.

7. Concluding Remarks

Electronic excitation, photodissociation and photoionization in the gas phase and at surfaces by pulsed UV lasers opens up new routes for the initiation, acceleration and control of gas-surface interactions. The examples discussed here are the first steps in this direction and show that lasers enable a spatially and temporally very precise impact on materials. *M. von Allmen*[6b] expressed this point in the following way: "Laser beams, in a way, might appear to be a material scientist's dream: They can deliver concentrated "pure" energy to almost any material, and they do so exactly where, when, and in the quantity desired". With laser chemical processing, material-specific factors (work functions, absorption) can be exploited and processes can be conducted under non-equilibrium conditions (photochemically, photoelectrically). Limitations emerge, but these are primarily due to a lack of availability of suitable beam handling and imaging methods.

Received: May 27, 1988 [A 693 IE]
German version: *Angew. Chem. 100* (1988) 1287

[1] General indroduction: M. C. Lin, G. Ertl, *Ann. Rev. Phys. Chem. 37* (1986) 587.
[2] J. Häger, Y. R. Shen, H. Walther, *Phys. Rev. A 31* (1985) 1962; J. Häger, H. Walther, *J. Vac. Sci. Technol. B 3* (1985) 1490.
[3] Cf. G. Ertl: "Kinetics of Chemical Processes on well-defined Surfaces" in J. R. Anderson, M. Boudart (Eds.): *Catalysis, Vol. 4*, Springer, Berlin 1983, p. 209.
[4] C. Karner, A. Mandel, F. Träger, *Appl. Phys. A 38* (1985) 19.
[5] M. Silverberg, A. Ben-Shaul, F. Rebentrost, *J. Chem. Phys. 83* (1985) 6501.
[6] a) J. Fröhlingsdorf, B. Stritzke in D. Bäuerle, K. L. Kompa, L. Laude (Eds.): *Laser Processing and Diagnostics II (Proc. E-MRS, Strassburg 1986)*, Edition Physique, Paris 1986; b) for a general introduction see also M. von Allmen: *Laser Beam Interaction with Materials*, Springer, Berlin 1987.
[7] R. N. Zare, R. D. Levine, *Chem. Phys. Lett. 136* (1987) 593.
[8] J. Jortner, R. D. Levine, *Adv. Chem. Phys. 47* (1981) 1.
[9] J. A. Barker, D. J. Auerbach, *Surf. Sci. Rep. 4* (1985) 1.
[10] See [1] and P. A. Psaras, H. D. Langford (Eds.): *Advancing Materials Research*, National Academy Press, Washington D.C. 1987.
[11] F. Engelke, J. H. Hahn, W. Henke, R. N. Zare, *Anal. Chem. 59* (1987) 909; J. H. Hahn, R. Zenobi, R. N. Zare, *J. Am. Chem. Soc.*, in press; G. Arjavalingam, T. F. Heinz, J. H. Glownia in G. R. Fleming, A. E. Siegman (Eds.): *Ultrafast Phenomena V*, Springer, Berlin 1986, p. 370.
[12] R. B. Hall, S. J. Bares: "Pulsed-Laser-Induced Desorption Studies of the Kinetics of Surface Reactions" in R. B. Hall, A. B. Ellis (Eds.): *Chemistry and Structure at Interfaces*, VCH Publishers, Deerfield Beach, FL, USA 1986.
[13] H. Schröder, K. L. Kompa, D. Masci, I. Gianninoni, *Appl. Phas. A 38* (1985) 227; D. Bäuerle: *Laser Processing and Diagnostics*, Springer, Berlin 1984.
[14] Cf., e.g., F. K. Kneubühl, M. W. Sigrist: *Laser*, Teubner, Stuttgart 1988; F. P. Schäfer, *Appl. Phys. B 46* (1988) 199.
[15] Review of lasers in chemistry: K. Kleinermanns, J. Wolfrum, *Angew. Chem. 99* (1987) 38; *Angew. Chem. Int. Ed. Engl. 26* (1987) 38.
[16] V. S. Letokhov: *Nonlinear Laser Chemistry*, Springer, Berlin 1983.
[17] S. Szatmari, B. Rasz, F. P. Schäfer, *Chem. Phys. Lett. 131* (1986) 528.
[18] C. K. Rhodes: *Excimer Lasers*, Springer, Berlin 1983.
[19] M. H. R. Hutchinson in L. F. Mollenauer, J. C. White (Eds.): *Tunable Lasers*, Springer, Berlin 1987.
[20] M. Diegelmann, K. Hohla, F. Rebentrost, K. L. Kompa, *J. Chem. Phys. 76* (1982) 1233.
[21] D. L. Huestes, G. Marowski, F. K. Tittel in [18], Kap. 6, and references cited therein.
[22] For a general survey cf. K. Ploog, *Angew. Chem. 100* (1988) 611; *Angew. Chem. Int. Ed. Engl. 27* (1988) 593.
[23] D. Bäuerle: *Chemical Processing with Lasers*, Springer, Berlin 1986, especially Table 5.1, p. 70ff.
[24] N. Rösch, M. Kotzian, H. Jörg, H. Schröder, B. Rager, S. Metev, *J. Am. Chem. Soc. 108* (1986) 4238.
[25] B. Rager, *Dissertation*, Universität München 1987.
[26] J. Krasinski, S. H. Bauer, K. L. Kompa, *Opt. Commun. 35* (1980) 363.
[27] Cf. e.g., [16] and F. Rebentrost, K. L. Kompa, A. Ben-Shaul, *Chem. Phys. Lett. 77* (1981) 394; F. Rebentrost, A. Ben-Shaul, *J. Chem. Phys. 75* (1981) 3255.
[28] A. W. Castleman, Jr., R. G. Keesee, *Acc. Chem. Res. 19* (1986) 413.
[29] A. C. Tam, H. Coufal, *Appl. Phys. Lett. 42* (1983) 33; H. Coufal, *ibid. 44* (1984) 59.
[30] a) W. Radloff, V. Stert, H. H. Ritze, *Appl. Phys. A 38* (1985) 179; V. J. Trava-Airoldi, M. E. Sbampato, A. M. dos Santos, C. C. Ghizoni, *J. Appl. Phys. 61* (1987) 2674; b) W. Roberts, *Dissertation*, Universität München 1987, and references cited therein.
[31] See e.g., T. Tagaki, *J. Vac. Sci. Technol. A 2* (1984) 382.
[32] Cf. e.g., A. Ben-Shaul, Y. Haas, K. L. Kompa, R. D. Levine: *Lasers and Chemical Change: An Introduction to Chemical Lasers and Laser-Induced Chemistry*, Springer, Berlin 1981, and references and cited therein.
[33] D. S. Y. Hsu, M. C. Lin, *J. Chem. Phys. 88* (1988) 432; F. Budde, A. Mödl, A. V. Hamza, P. M. Ferm, G. Ertl, *Surf. Sci. 192* (1987) 507; G. D. Kubiak, G. O. Sitz, R. N. Zare, *J. Chem. Phys. 81* (1984) 6397; M. Asscher, W. L. Guthrie, T. H. Lin, G. Samorjai, *J. Phys. Chem. 88* (1984) 3233.
[34] X. R. Chen, K. Wagemann, J. Wanner, *J. Vac. Sci. Technol.*, in press.
[35] M. Scholz, W. Fuss, K. L. Kompa, unpublished.
[36] J. S. Haggerty, W. R. Cannon: "Sinterable Powders from Laser-driven Reactions" in J. Steinfeld (Ed.): *Laser-Induced Chemical Processes*, Plenum, New York 1981.
[37] T. J. Chuang, *Surf. Sci. Rep. 3* (1983) 1.
[38] T. Kruck, *Angew. Chem. 79* (1967) 27; *Angew. Chem. Int. Ed. Engl. 6* (1967) 53.
[39] V. Rühe, *Diplomarbeit*, Universität München 1988.
[40] J. Ganz, H. Schröder, unpublished; Kammerer-DODUCO, Pforzheim (FRG), private communication.
[41] W. Roberts, H. Schröder, K. L. Kompa, R. Niessner, *Z. Phys. Chem.* (München), in press.

When submitting manuscripts, authors of articles intended for publication as "Communications" are requested to read the "Notice to Authors" reproduced in the January issue of the journal following the list of contents; upon request, a copy can be obtained from the editorial office.

$[Au_2Ag_4L_4]^{2\ominus}$, $[Au_2Cu_4L_4]^{2\ominus}$, $[Au_3Cu_3L_4]^{2\ominus}$, $[Cu_4L_3]^{2\ominus}$, and $[Ag_9L_6]^{3\ominus}$ (L = ethane-1,2-dithiolate)—Novel Homoleptic Complexes of the Coinage Metals, including the First Heteronuclear Metal Thiolates**

By *Gerald Henkel,* Bernt Krebs, Peter Betz, Heidrun Fietz,* and *Karlheinz Saatkamp*

Dedicated to Professor Hans Bock on the occasion of his 60th birthday

Copper reacts with simple saturated thiolates to give tetranuclear complexes of the type $[M_4(SR)_6]^{2\ominus}$ containing a central cage-like *tetrahedro*-M_4-*octahedro*-(μ-S) moiety (Fig. 1a) in which copper is surrounded by a trigonal array of sulfur atoms.[1] Surprisingly, for quite a long time it proved impossible to prepare the corresponding silver thiolates. An entry to such complexes, however, was recently accomplished by suitable choice of the ligands. The isolation and characterization of $[Ag_4L'_3]^{2\ominus}$ anions (L' = $SCH_2C_6H_4CH_2S$,[1] $SC_6H_3(Me)S$[2]) now confirms the existence of tetranuclear silver thiolates.

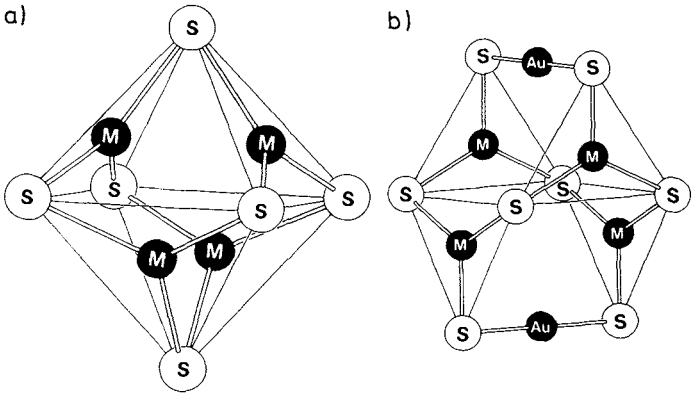

Fig. 1. The closed heavy-atom skeletons of homologous metal(I) thiolates: a) M_4S_6 cage; b) M_6S_8 cage in idealized geometries.

An interesting extension of the M_4S_6-cage occurs in the pentanuclear complex anions $[M_5(SPh)_7]^{2\ominus}$, the copper and silver variants of which are well-known.[3] Here, one metal atom is coordinated linearly by sulfur, while the other four are coordinated in a trigonal planar fashion. The resulting M_5S_7 skeleton arises from the M_4S_6 cage of the tetranuclear complex by opening of a thiolate bridge and insertion of an M–S unit.

It should be possible to extend this principle to the side of the sulfur octahedron opposite to the inserted unit and construct hexanuclear metal thiolates with the M_6S_8 cage skeleton shown in Figure 1b. A complex salt with appropriate stoichiometry, namely $[Me_4N]_2[Ag_6(SPh)_8]$ is, in fact, known;[4] however it does not contain the desired isolated hexanuclear anions, but one-dimensional infinite $[Ag_6(SPh)_8]_n^{2n\ominus}$ chains with mixed trigonal-planar and tetrahedral silver coordination.

Since chemical examples for the remarkable M_6S_8 cage were still unknown we attempted their preparation by directed cluster synthesis. It appeared meaningful to stabilize the two linear S–M–S units of the target compound by metal centers which avoid a trigonal planar coordination.

Reaction of a solution of $CuCl_2$ or $AgNO_3$ in methanol (or of CuCl in acetonitrile) with ethane-1,2-dithiolate leads initially to the formation of the homonuclear compounds **4** or **5**,[5] respectively. When the reaction solutions are subsequently allowed to react with $[Et_4N][AuBr_2]$ the desired heterohexanuclear complexes **2** and **3** or **1** are indeed formed.

We report here on the synthesis and structure of these heteronuclear (**1**–**3**) and homonuclear (**4**, **5**)[5] metal thiolates, which after addition of Ph_4PBr crystallize as complex salts **6**–**9**.

$[Au_2Ag_4(SCH_2CH_2S)_4]^{2\ominus}$ **1**
$[Au_2Cu_4(SCH_2CH_2S)_4]^{2\ominus}$ **2**
$[Au_3Cu_3(SCH_2CH_2S)_4]^{2\ominus}$ **3**
$[Cu_4(SCH_2CH_2S)_3]^{2\ominus}$ **4**
$[Ag_9(SCH_2CH_2S)_6]^{3\ominus}$ **5**
$[Ph_4P]_2[Au_2Ag_4(SCH_2CH_2S)_4]\cdot 2/3\,MeOH$ **6**
$[Ph_4P]_6[Au_2Cu_4(SCH_2CH_2S)_4]_2[Au_3Cu_3(SCH_2CH_2S)_4]\cdot 4\,MeOH$ **7**
$[Ph_4P]_2[Cu_4(SCH_2CH_2S)_3]\cdot MeOH$ **8**
$[Ph_4P]_3[Ag_9(SCH_2CH_2S)_6]\cdot 3\,MeOH$ **9**

According to the results of an X-ray structure analysis,[6] crystals of **6** consist of $Ph_4P^{\oplus}$ ions, discrete complex anions **1**, and solvate molecules (methanol). The monoclinic unit cell contains twelve anions, eight of which (**1a**) lie on general positions and four (**1b**) on twofold axes. The structures of the symmetry-independent molecules are nearly identical; the structure of **1a** is shown in Figure 2.

The hexanuclear thiolates **1** contain the M_6S_8 skeletal frameworks shown in Figure 1b (D_{2d} symmetry) in a somewhat distorted geometry. As expected gold is linearly coor-

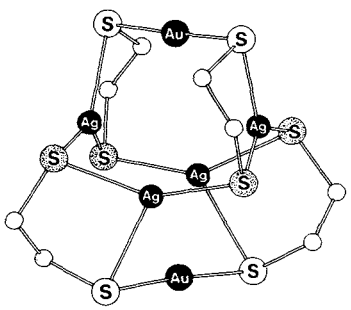

Fig. 2. Structure of the complex anion **1a** in crystals of **6** (without H atoms).

[*] Priv.-Doz. Dr. G. Henkel, Prof. Dr. B. Krebs, Dr. P. Betz, H. Fietz, Dr. K. Saatkamp
Anorganisch-chemisches Institut der Universität
Wilhelm-Klemm-Strasse 8, D-4400 Münster (FRG)

[**] This work was supported by the Bundesminister für Forschung und Technologie, the Minister für Wissenschaft und Forschung des Landes Nordrhein-Westfalen, and the Fonds der Chemischen Industrie.

dinated, whereas silver is surrounded by a trigonal planar array of sulfur atoms. The eight sulfur atoms of the four ligands form two distorted trigonal prisms sharing a common square face (dotted atoms in Fig. 2); the edges parallel to this plane contain the two gold atoms and the triangular faces of the S_8 polyhedron are completely occupied by silver atoms. This coordination leads to a central Ag_4S_4 heterocycle, which (like the complete S_8 polyhedron) is topologically related to the A_4B_4 cage of tetrasulfur tetranitride. As in the tetranuclear copper and silver thiolates, all sulfur atoms are bound to two metal atoms. The first thiolate function of each ligand bridges two silver atoms (Ag···Ag 3.170 Å), the second couples a silver atom with a gold atom (Au···Ag 2.996 Å). The angles of the Ag–S–Ag bridges (80.8°) are on average about 6.1° larger than the angles of the Au–S–Ag bridges, which exhibit a marked asymmetry (Au–S 2.293, Ag–S 2.625 Å, averaged values). The Ag–S bonds in the heterocyclic Ag_4S_4 fragments (cf. Fig. 2) are alternately short (2.416 Å) and somewhat longer (2.488 Å).

1 is stabilized by chelate rings in which the small S···S distance of the ethane-1,2-dithiolate ligand leads to very small S–Ag–S chelate angles (average 87.8°); they are on average 53.2° (!) smaller than the S–Ag–S angles in the central cyclic Ag_4S_4 fragment. The remaining S–Ag–S angles (128.3°) lie between these extremes.

Crystals of **7**[6] contain the complex anions **2** and **3** at identical lattice sites. Since the frequency of occurrence of **2** in the crystal is twice that of **3** and two anions are present in each unit cell an ordered structure can be ruled out. In principle, **2** shows all the coordination characteristics of the analogous silver compound **1**; hence Figure 2 may also be used for reference here. The Au–S bonds in **2** (average 2.286 Å) are only slightly shorter than in **1** (average 2.293 Å), whereas the expected proportional shortening (on average 0.22 Å) of all other metal–sulfur bonds is observed on going from silver to copper. This shortening is also the reason for the likewise significant widening of the S–Cu–S chelate angle to 94.4°, and in turn leads to S–Cu–S valence angles of 133.5° in the central Cu_4S_4 cycle and thus to a decrease in the ring strain (Cu···Cu 3.149 Å), but has only a very slight influence on the second group of the exocyclic S–M–S valence angles (average 130.0°, Au···Cu 2.862 Å).

The molecular structure of the gold-rich complex anion **3** is shown in Figure 3. The M_6S_8 skeleton of this compound is a variant of the cage structure shown in Figure 1b, in which a copper atom is replaced by gold. This atom is shifted from the center of the sulfur triangle into the middle of the edge belonging to the M_4S_4 ring and thereby effects the transition from the trigonal-planar coordination of the copper atom to the linear coordination of gold. At the same time the bond to the opposite sulfur atom is ruptured and the chelate ring opens.

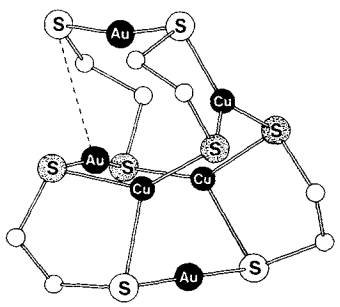

Fig. 3. Structure of the complex anion **3** in crystals of **7** (without H atoms).

The structure of **4** (point group C_3, slightly distorted) in crystals of **8**[6] is shown in Figure 4 and contains the heavy atom skeleton with copper atoms at the tetrahedral sites

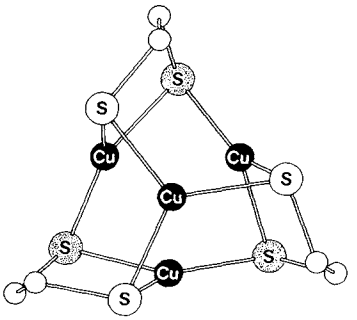

Fig. 4. Structure of the complex anion **4** in crystals of **8** (without H-atoms).

shown in Figure 1a. The coordination principle frequently found in copper–sulfur chemistry with sterically unencumbered substituents is thus observed in homoleptic ethane-1,2-dithiolate complexes, despite the short intramolecular S···S distances of the ligands. The type of ligand arrangement here is quite similar to that in the anions **10** of the related complex salts $[Ph_4P]_2 \cdot \mathbf{10} \cdot 3\,MeOH$[7a] and $[Ph_4P]_2 \cdot \mathbf{10} \cdot MeCN$.[7b] The stronger distortion of the coordination of all the copper atoms of **4** that participate in chelate rings is a direct consequence of the short "bite" (3.397 Å) of the ethane-1,2-dithiolate ligands. These copper atoms are equivalent under C_3 symmetry. Each of them shows an angle of 127.2° in their respective heterocyclic Cu_3S_3 fragment (dotted S atoms, Cu–S alternately 2.305 and 2.223 Å) besides the small valence angle of 94.9° within the chelate ring, while the third S–Cu–S valence angle (137.4°) is significantly widened. The fourth copper atom (in the center of Fig. 4) is coordinated almost regularly (valence angles 118.5(1), 119.0(1) and 121.9(1)°) by one thiolate function of all three ligands (Cu–S 2.289 Å). The average Cu–S distance is consistent with expectation (2.281 Å).

$[Cu_4(SCH_2C_6H_4CH_2S)_3]^{2\ominus}$ **10**

In contrast to the copper salts, no tetranuclear complexes are obtained in reactions of ethane-1,2-dithiolate with silver salts. Instead, and fully unexpected, the nonanuclear complex anion **5** is formed, whose structure in crystals of **9**[6] is shown in Figure 5. Here, eight silver atoms form a cubane-like metal skeleton with a further silver atom in the center. The metal cube is strongly distorted, the central silver atom being at distances of between 3.084(4) and 3.403(4) Å (mean value 3.199 Å) from its neighboring silver atoms. The six bidentate ligands are involved in chelate rings and are thus arranged such that a sulfur atom is located above the center of each edge of the silver cube. They thus define a sulfur icosahedron, which like the silver-centered cube already described is considerably distorted. The coordination of the silver atoms at the corners of the cube is distorted trigonal planar. Two opposite atoms of the cube (Ag′) are simultaneously bound to three dithiolate ligands and therefore do not participate in chelate rings. Like their trigonally coordinated neighbors

(Ag) they are unusually tolerant with regard to angle deformations. Thus, in each case one finds three different S-Ag-S valence angles (average values 101.9, 115.9 and 140.4° (Ag'), and 88.0, 130.0 and 139.7° (Ag)).

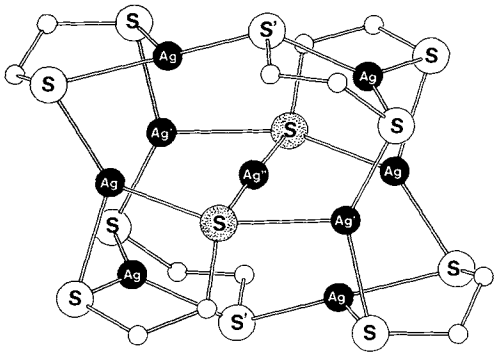

Fig. 5. Structure of the complex anion **5** in crystals of **9** (H atoms omitted).

The silver atom in the center of **5** (Ag'') is bound to two sulfur atoms (dotted atoms, S-Ag''-S 177.4(4)°), each of which additionally couples two further silver atoms at the corners of the cube. Here, we have μ_3-thiolate bridges with unusual geometry, in which the Ag-S-Ag valence angles are 76.1° if one of the silver atoms is Ag'' and on average 150.3° if the trigonal-planar coordinated silver atoms Ag and Ag' participate (for comparison: the angles of the μ_2-thiolate bridges are 114.2(4) and 119.0(3)° in the case of the atoms marked S' in Figure 5 and are on average 78.2° in the case of the other S atoms). The Ag-S distance is somewhat shorter in the case of linear coordination (average 2.478 Å) than in the trigonal-planar AgS_3 units (average 2.512 Å), in which once again the distances within the chelate rings are longer (2.546 Å) than those outside the rings (2.445 Å).

The trigonal-planar coordinated silver atoms are in part replaced by copper atoms when the methanolic solutions of the Na salts of **4** and **5** are allowed to react with each other. With a copper : silver ratio of 1 : 1, orange crystals of the composition **11** precipitate on addition of Ph_4PBr. The crystals are isotypic with crystals of **9**.

$[Ph_4P]_3[Ag_{3.9}Cu_{5.1}(SCH_2CH_2S)_6]\cdot 3\,MeOH$ **11**

The individual $[AgM_8(SCH_2CH_2S)_6]^{3\ominus}$ ions can, according to the results of an X-ray structure analysis, contain silver or copper at all metal positions at the corners of the cube. The intense wine-red colored complex salt **12** is formed at a copper : silver ratio of 5 : 2.

$[Ph_4P]_3[Ag_{2.3}Cu_{6.7}(SCH_2CH_2S)_6]\cdot 4\,MeOH$ **12**

12 crystallizes in a different lattice, presumably because of its high copper content.[7a]

The central Ag_9S_{12} fragment of the anion **5** is topologically related with the Ag_8S_{12} cage of the complex anion $[Ag_8(S_2C{=}C(CN)_2)_6]^{4\ominus}$, which contains only μ_2-sulfur atoms and no chelate rings.[8] The μ_3-S-Ag_3 unit first realized in **5** presumably owes its existence to a trigonal coordinated silver atom, which can form a long Ag-S bond of average length 2.646 Å because it is not involved in a chelate ring and therefore has two further sulfur neighbors at a distance of 2.452 Å (Ag' in Fig. 5).

Experimental

All operations were carried out under an inert gas atmosphere (N_2 or Ar) in sealed vessels. A $NaSCH_2CH_2SNa$ solution was prepared by reaction of 0.69 g (30 mmol) of sodium with 1.26 mL (15 mmol) of ethane-1,2-dithiol in 100 mL of methanol. Correct C,H analyses were obtained for the salts **6**-**9**.

6: A solution of $AgNO_3$ (0.17 g, 1 mmol) in methanol (30 mL) was treated dropwise with 10 mL of the $NaSCH_2CH_2SNa$ solution. The initially formed lemon-yellow precipitate redissolved shortly before completion of the addition. The clear reaction solution was treated dropwise with a solution of 0.24 g (0.5 mmol) of $[Et_4N][AuBr_2]$ in 20 mL of methanol and the resulting bright-yellow solution treated with 0.42 g (1 mmol) of Ph_4PBr. Within a few hours at room temperature colorless crystals separated out (yield 81%). The quality of the crystals could be improved at the expense of the yield, by using a solution of $[Et_4N][AuBr_2]$ in dimethylformamide.

7: 10 mL of the $NaSCH_2CH_2SNa$ solution was diluted to three times its volume and added dropwise to a solution of 0.10 g (1 mmol) of CuCl in 10 mL of acetonitrile. The initially formed yellow precipitate redissolved toward the end of the addition. The further steps were analogous to those for the synthesis of **6**; after a few days, **7** crystallized in the form of orange-colored crystals (42%).

8: A solution of 0.68 g (4 mmol) of $CuCl_2\cdot 2H_2O$ in 15 mL of methanol was treated dropwise with 55 mL of the $NaSCH_2CH_2SNa$ solution. The initially formed yellow precipitate redissolved on completion of the addition. Upon addition of 0.84 g (2 mmol) of Ph_4PBr, **8** crystallized in the form of orange platelets (86%).

9: A solution of 1.70 g (10 mmol) of $AgNO_3$ in methanol was treated dropwise with 67 mL of the $NaSCH_2CH_2SNa$ solution. The initially formed lemon-yellow precipitate redissolved in the course of the ensuing reaction. Upon addition of 4 mmol (1.68 g) of Ph_4PBr to the clear reaction solution, lemon-yellow needles of **9** crystallized out (95%).

Received: February 26, 1988 [Z 2635 IE]
Publication delayed at authors' request
German version: *Angew. Chem. 100* (1988) 1375

[1] G. Henkel, P. Betz, B. Krebs, *Angew. Chem. 99* (1987) 131; *Angew. Chem. Int. Ed. Engl. 26* (1987) 145, and references cited therein.
[2] K. Saatkamp, *Dissertation*, Universität Münster 1988.
[3] I. G. Dance, *Aust. J. Chem. 31* (1978) 2195.
[4] I. G. Dance, *Inorg. Chem. 20* (1981) 1487.
[5] G. Henkel, P. Betz, B. Krebs, *Proc. Int. Conf. Coord. Chem. 24* (1986) 737 (*Chim. Chron. Special Issue* (1986)).
[6] Crystal structure analyses: Syntex $P2_1$ four-circle diffractometer, $Mo_{K\alpha}$ radiation, graphite monochromator, scintillation counter, $T = 150$ K, empirical absorption corrections, EXTL and SHELXTL programs, direct methods, least squares fit.—**6**: monoclinic, space group $C2/c$, $a = 34.24(2)$, $b = 14.486(6)$, $c = 41.71(2)$ Å, $\beta = 121.13(3)°$, $V = 17709$ Å^3, $Z = 12$, $\rho_{calcd} = 2.13$ g cm^{-3}, $\mu(Mo_{K\alpha}) = 67.1$ cm^{-1}, crystal dimensions $0.30 \times 0.25 \times 0.20$ mm, ω-scan, $2\theta_{max} = 48°$, 13275 independent reflections, R (R_w) = 0.050 (0.047) for 9876 reflections with $F_0 > 3.92\sigma(F_0)$, 486 variables, phenyl rings as rigid groups with individual isotropic temperature factors for the C atoms, H atoms of the anions and cations at idealized positions ($U(H) = 1.2\,U_{eq}(C)$), all other atoms of the anions and cations refined with anisotropic, solvate molecules with isotropic temperature factors, one scaling factor.—**7**: triclinic, space group $P\bar{1}$, $a = 13.547(6)$, $b = 13.662(6)$, $c = 18.516(7)$ Å, $\alpha = 91.91(3)$, $\beta = 107.35(3)$, $\gamma = 110.74(3)°$, $V = 3022$ Å^3, $Z = 2$, $\rho_{calcd} = 1.96$ g cm^{-3}, $\mu(Mo_{K\alpha}) = 75.4$ cm^{-1}, crystal dimensions $0.27 \times 0.25 \times 0.17$ mm, $\theta - 2\theta$-scan, $2\theta_{max} = 54°$, 13274 independent reflections, R (R_w) = 0.056 (0.045) for 9266 reflections with $F_0 > 3.92\sigma(F_0)$, 706 variables, H atoms of the anions and cations at ideal positions ($U(H) = 1.2\,U_{eq}(C)$), all other atoms of the cations and of the heavy atom skeleton in the anions refined with anisotropic, solvate molecules and disordered ethylene groups of the anions with isotropic temperatures factors, one scaling factor.—**8**: triclinic, space group $P\bar{1}$, $a = 10.866(2)$, $b = 12.408(3)$, $c = 20.948(5)$ Å, $\alpha = 99.69(2)$, $\beta = 95.16(2)$, $\gamma = 108.20(2)°$, $V = 2614$ Å^3, $Z = 2$, $\rho_{calcd} = 1.58$ g cm^{-3}, $\mu(Mo_{K\alpha}) = 20.0$ cm^{-1}, crystal dimensions $0.22 \times 0.18 \times 0.17$ mm, $\theta - 2\theta$-scan, $2\theta_{max} = 52°$, 10343 independent reflections, R (R_w) = 0.044 (0.048) for 8266 reflections with $F_0 > 3.92\sigma(F_0)$, 645 variables, H atoms of the anions and cations at idealized positions ($U(H) = 1.2\,U_{eq}(C)$), all other atoms of the cations and anions refined with anisotropic, solvate molecules with isotropic temperature factors, one scaling factor.—**9**: monoclinic, space group $P2_1/n$, $a = 13.89(4)$, $b = 40.05(13)$, $c = 16.78(7)$ Å, $\beta = 93.4(3)°$, $V = 9318$ Å^3, $Z = 4$, $\rho_{calcd} = 1.89$ g cm^{-3}, $\mu(Mo_{K\alpha}) = 21.8$ cm^{-1}, crystal dimensions $0.28 \times 0.14 \times 0.12$ mm, ω-scan, $2\theta_{max} = 48°$, 14619 independent reflections, R (R_w) = 0.146 (0.138) for 10912 reflections with $F_0 > 3.92\sigma(F_0)$, 276 variables, phenyl rings as rigid groups with a common isotropic temperature factor for the C atoms (H atoms not considered), Ag atoms refined with anisotropic, methylene C atoms with a common isotropic and solvate molecules with individual isotropic temperature factors, one scaling

factor. Further details of the crystal structure investigations are available on request from the Fachinformationszentrum Energie, Physik, Mathematik GmbH, D-7514 Eggenstein-Leopoldshafen 2 (FRG), on quoting the depository number CSD-53224, the names of the authors and the journal citation.

[7] a) P. Betz, *Dissertation*, Universität Münster 1986; b) J. R. Nicholson, I. L. Abrahams, W. Clegg, C. D. Garner, *Inorg. Chem. 24* (1985) 1092.

[8] P. J. M. W. L. Birker, G. C. Verschoor, *J. Chem. Soc. Chem. Commun. 1981*, 322.

Is the Molecule BOK Quasi-Linear?**

By *Pavel Rosmus**

Dedicated to Professor Hans Bock on the occasion of his 60th birthday

Unlike the linear HCN[1] and LiNC molecules (linear cyanide, LiCN, is metastable),[2,3] the cyanides NaCN,[4,5] KCN,[6] and RbCN[7] possess triangular equilibrium structures in the gas phase. Several experimental and theoretical studies have established that the orbiting motion of $M^{\oplus}$ (M = Na, K, Rb) in the strongly polar structures $M^{\oplus}CN^{\ominus}$ is almost unhindered,[5-9] whereas higher barriers of isomerization have been found for HCN[10] and LiNC.[2] An unusual early onset of classical and quantum chaos has been reported[11-13] for the $K^{\oplus}$ vibrational modes of $K^{\oplus}CN^{\ominus}$.

Similar properties can be expected for the isoelectronic bivalent boron compounds, MBO, yet only the parent linear oxoborane, HBO, has been hitherto detected experimentally.[14,15] The BOK molecule—isoelectronic with KCN—has been investigated neither experimentally nor theoretically. Herein we report results obtained from ab initio Hartree-Fock calculations for the electronic ground-state potential energy surface of BOK.

The potential energy function $E(r,R,\Theta)$ of the electronic ground state of BOK was mapped in two dimensions. The BO distance r (orientation of the vector $\boldsymbol{r}$ from B to O) was kept fixed at the equilibrium distance of the BO radical ($r_{BO}=2.27697$ bohr,[17]) and both the distance R from K to the center of mass of BO and the angle Θ between r and R were varied. The potential energy functions in other cyanides have been represented in a similar way.[7,8,11-13] About 100 SCF total energies were calculated[16] in order to map the motion of the K atom in BOK. The SCF dissociation energy into the neutral fragments K + BO in their electronic ground states was calculated to be 212 kJ mol^{-1};[16] hence BOK is a stable species. In the entire region of the geometries considered (cf. Fig. 1) the molecule has a strongly ionic electron distribution $K^{\oplus}BO^{\ominus}$. The total SCF dipole moment at the global triangular equilibrium structure was calculated to be 11.67 debye; 13.54 debye and 13.59 debye were obtained for the minimum energy linear structures KBO and BOK, respectively. As in the cyanides,[7] the dominating part of the dipole moment originates from the charge separation in $K^{\oplus}$ and the moiety $BO^{\ominus}$. Since $K^{\oplus}BO^{\ominus}$ dissociates, within the Hartree-Fock approximation, into ionic fragments, the potential energy function of the electronic ground state will exhibit an avoided crossing with another electronic state, which will change the charge distribution and yield the neutral fragments. This crossing has not been considered in the present work.

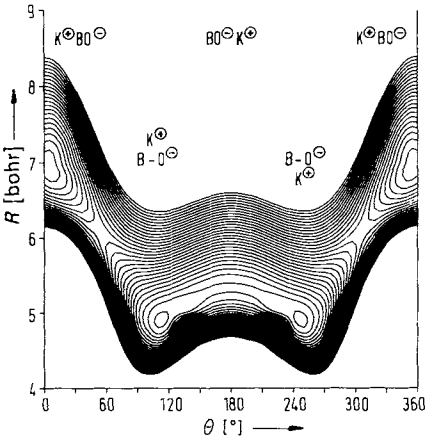

Fig. 1. Contour plot of the two-dimensional potential energy function for one orbiting period of $K^{\oplus}$ in $K^{\oplus}BO^{\ominus}$. $\Theta=0°$ for linear KBO, $\Theta=180°$ for linear BOK. The contours are plotted in 2-kJ mol^{-1} steps.

The contour plot of the potential energy surface for one orbiting period of $K^{\oplus}$ around $BO^{\ominus}$ is shown in Figure 1. The orbiting channel for $K^{\oplus}$ around $BO^{\ominus}$ can easily be recognized. The minimum energy path for $K^{\oplus}$ motion on the potential energy surface is displayed with the full line in Figure 2. This diagram shows that the linear KBO structure as calculated within the Hartree-Fock approximation represents only a local minimum separated by a barrier from the triangular global minimum with $R_{KB}=5.788$ bohr and ∢KBO 50.1° (KCN:[6] $R_{KC}=4.91\pm0.2$ bohr, ∢KCN = 76° ± 10°). Previous SCF calculations of similar quality[5,8] for KCN showed that the R_{KC} distance is reproduced to within about 6%, the KCN angle to within about 10%. It has also been shown[5] that small changes in the CN distance hardly influence either the calculated equilibrium geometry parameters or the overall picture for $K^{\oplus}$ motion around $CN^{\ominus}$. Therefore, similar accuracy for the

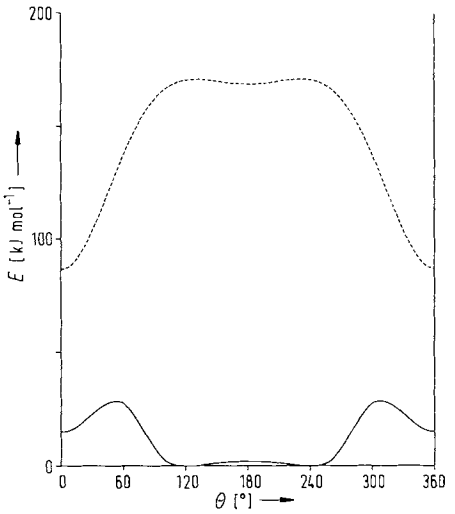

Fig. 2. The full line represents the minimum energy path of the orbiting motion of $K^{\oplus}$ on the two-dimensional potential energy function of BOK (cf. Fig. 1 and Ref. [16] for the definition of the coordinate system); the broken line corresponds to the energy path for $K^{\oplus}$ separated from the center of mass of the $BO^{\ominus}$ fragment by 9 bohr.

[*] Priv.-Doz. Dr. P. Rosmus
Fachbereich Chemie der Universität
Niederurseler Hang, D-6000 Frankfurt am Main 50 (FRG)

[**] This work was supported by the Fonds der Chemischen Industrie (Overseas Fellowship at Churchill College, University of Cambridge, Cambridge, UK).

geometric parameters and the shape of the surface can be expected for BOK. The $K^{\oplus}$ ion approaches the $BO^{\ominus}$ fragment more closely in the BOK linear structure ($R_{OK}=4.51$ bohr) than in the KBO linear structure ($R_{KB}=5.53$ bohr) (cf. Fig. 1). Similar behavior has been found for the linear KCN and KNC structures,[5] which is due to a stronger electrostatic attraction by the more electronegative atom. At a distance of 9 bohr from the center of mass of BO, the long-range interaction potential (broken line in Fig. 2) shows that at the SCF level of theory an opposite stabilization to that at short range occurs. The $K^{\oplus}$ approach is energetically more favorable for linear $K^{\oplus}BO^{\ominus}$ geometries. The barrier height between the global minimum and the KBO local minimum has been calculated to be 30 kJ mol^{-1} (KCN: 27 kJ mol^{-1},[8] 20 kJ mol^{-1}[9]). The barrier to linearity for the BOK structure relative to the global minimum has been calculated to be only about 2 kJ mol^{-1} (KCN: 7 kJ mol^{-1},[5] 8.5 kJ mol^{-1},[8] 6 kJ mol^{-1}[9]). The SCF results indicate that the barrier between the triangular equilibrium structure and the linear BOK structure is smaller than in KCN. This could mean that even the vibrational ground state of BOK lies above this barrier and the molecule is quasi-linear—with a large zero-point-energy amplitude for the $K^{\oplus}$ bending motion.

The influence of the orbiting $K^{\oplus}$ in KCN on its photoelectron spectrum has been investigated by Green's function calculations, which showed that the first three peaks in the spectrum could be broadened by up to 1.2 eV.[18] In the linear structures KBO and BOK the highest three molecular orbitals are of σ ($-\varepsilon^{SCF}=14.28$ eV (KBO), 15.67 eV (BOK)), π (11.02 eV, 12.13 eV), and σ (8.08 eV, 8.81 eV) symmetry. The π orbital splits into two components in the triangular structure, resulting in the following orbital symmetries and energies: a′($-\varepsilon^{SCF}=15.84$ eV), a′(12.35 eV), a″(12.16 eV), and a′(7.18 eV). The SCF molecular orbital energies given in parentheses suggest that the $K^{\oplus}$ orbiting in BOK will also significantly broaden the bands in its photoelectron spectrum.

The calculated energy differences and barriers between various structures are rather small. In this situation it is difficult to find a simple explanation for the structural differences. This problem has been discussed in detail in a comparison of the LiCN and KCN structures.[8] A more accurate approach including electron correlation and the calculation of the corresponding force field would require a correct treatment of the induction and dispersion forces, which would result in very extensive computations. Even for KCN only Hartree-Fock results have been reported so far. It has been suggested,[9] however, that, as in LiCN, the inclusion of electron correlation could stabilize the KCN structure relative to the KNC structure.

In summary, it has been found that the electronic ground-state potential energy function of BOK strongly resembles that of KCN, i.e., the $K^{\oplus}$ is almost freely orbiting around $BO^{\ominus}$. The molecule is probably quasi-linear and will show an early onset of classical and quantum chaos in the $K^{\oplus}$ nuclear motion. Further investigations are necessary to compute the induction and dispersion forces in this salt more accurately.

Received: February 11, 1988 [Z 2616 IE]
German version: *Angew. Chem. 100* (1988) 1376

[1] G. Herzberg: *Infrared and Raman Spectra of Polyatomic Molecules*, Van Nostrand Reinhold, New York 1966.
[2] R. Esser, J. Tennyson, P. E. S. Wormer, *Chem. Phys. Lett. 89* (1982) 223.
[3] J. J. van Vaals, W. L. Meerts, A. Dymanus, *Chem. Phys. 82* (1983) 385.
[4] J. J. van Vaals, W. L. Meerts, A. Dymanus, *Chem. Phys. 86* (1984) 147.
[5] M. L. Klein, J. D. Goddard, D. G. Bounds, *J. Chem. Phys. 75* (1981) 3909.
[6] T. Toering, J. P. Bekoy, W. L. Meerts, E. Tiemann, A. Dymanus, *J. Chem. Phys. 73* (1980) 4875.
[7] E. van Leuken, G. Broks, P. E. S. Wormer, *Chem. Phys. 110* (1986) 365.
[8] P. E. S. Wormer, J. Tennyson, *J. Chem. Phys. 75* (1981) 1245.
[9] C. J. Marsden, *J. Chem. Phys. 76* (1982) 6451.
[10] Z. Bacic, J. C. Light, *J. Chem. Phys. 86* (1987) 3065.
[11] J. Tennyson, S. C. Farantos, *Chem. Phys. Lett. 109* (1984) 160.
[12] S. C. Farantos, J. Tennyson, *J. Chem. Phys. 82* (1985) 800.
[13] S. C. Farantos, J. Tennyson, *J. Chem. Phys. 84* (1986) 6210.
[14] Y. Kawashima, Y. Endo, K. Kawaguchi, E. Hirota, *Chem. Phys. Lett. 135* (1987) 441.
[15] E. R. Lory, R. F. Porter, *J. Am. Chem. Soc. 93* (1971) 6301.
[16] Gaussian-type basis sets of the size 11 s, 7 p (B, O) [16a] and 14 s, 9 p (K) [16b] were used. For B and O only the core 4 s and 3 p, for K 4 s and 4 p functions were contracted. The basis was augmented by diffuse s functions (exponents: 0.03 (B), 0.06 (O); the last two exponents in the K basis [16b] were replaced by three s functions; exponents: 0.11, 0.035, and 0.01), diffuse p (exponents: 0.02 (B), 0.05 (O) and 0.07, 0.015 (K)), and polarization d (exponents: 0.4 (B), 0.8 (O), and 0.3354 (K)) functions. The final basis comprised 97 contracted functions. Similarly to the presentation of the cyanide potential energy functions, the origin of the coordinate system was chosen to lie at the center of mass of the BO fragment $r_{CM-O}=+0.820444$ bohr, with oxygen pointing in the positive direction of the r axis. For the global minimum on the two-dimensional surface, the total energy for BOK was calculated to be −698.789522 a.u.; for the K atom −599.156203 a.u. and for the BO fragment −99.552581 a.u.; a) S. Huzinaga: Technical Report: *Approximate Atomic Functions*, Department of Chemistry, University of Alberta 1971; b) A. J. H. Wachters, *J. Chem. Phys. 52* (1970) 1033.
[17] G. Herzberg: *Molecular Spectra and Molecular Structure, Spectra of Diatomic Molecules*, Van Nostrand Reinhold, New York 1966, p. 502.
[18] W. von Niessen, R. Combi, *J. Electron. Spectrosc. Relat. Phenom. 34* (1984) 291.

Triazatrimetallabenzenes, a New Class of Inorganic Heterocycles; Synthesis and Structure of $[Cp^*TaN(Cl)]_3$**

By *Herbert Plenio, Herbert W. Roesky,* Mathias Noltemeyer,* and *George M. Sheldrick*

Dedicated to Professor Hans Bock on the occasion of his 60th birthday

In 1983 we reported on the synthesis and structure of $(Cl_2VN_3S_2)_x$, a triaza-1,3-dithiabenzene containing a metal atom as the sixth member of the ring.[1] In 1986 we described $[Cl_3WN_3(PPh_2)_2]$, the first cyclophosphazene in which a ring phosphorus atom is replaced by a transition-metal atom in its maximum oxidation state.[2] Further members of this class of compounds were synthesized in 1987.[3] We now report the first triazatrimetallabenzene. This compound can be regarded as the trimer of a metal nitride.

Metal nitrides of the early transition metals[4] display a wide range of structures and can exist as mononitrides, dinuclear mononitrides, trinuclear dinitrides, tetramers, and linear polymers. *R. Hoffmann* et al. thus concluded that analogies exist between transition-metal nitrides, organic polyenes, and phosphazenes and that benzene-like cyclic trimers of a nitride should be particularly stable.[5]

[*] Prof. Dr. H. W. Roesky, Dipl.-Chem. H. Plenio, Dr. M. Noltemeyer, Prof. Dr. G. M. Sheldrick
Institut für Anorganische Chemie der Universität
Tammannstrasse 4, D-3400 Göttingen (FRG)

[**] This work was supported by the Deutsche Forschungsgemeinschaft and the Fonds der Chemischen Industrie.

Such a compound has now been synthesized from $[Cp^*TaCl_4]$ **1** ($Cp^* = \eta^5$-C_5Me_5) and tris(trimethylstannyl)amine **2** [Eq. (a)]. Evidence for the six-membered cyclic structure of **3** is provided by the ^1H NMR spectrum, which indicates the presence of two nonequivalent pentamethylcyclopentadienyl groups ($\delta = 2.08, 2.12$) in a ratio of 1:2. In addition to the molecular ion peak (*m/z* 1095), the mass spectrum always reveals small amounts of the tetramer $[Cp^*TaN(Cl)]_4$ (*m/z* 1460). The IR spectrum exhibits a strong absorption at 960 cm^{-1}, which we ascribe to the Ta-N valence vibration.

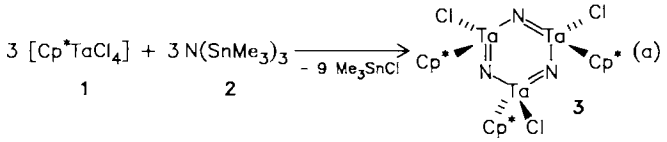

1 2 3 (a)

Crystals of **3** suitable for an X-ray structure analysis (Fig. 1)[6] were obtained by recrystallization from toluene/hexane. The six-membered $(TaN)_3$ ring, containing tetrahedrally coordinated tantalum atoms, is not completely planar in the solid state but instead exists in a kind of boat conformation, with the atoms Ta(2), N(3), Ta(3), and N(2) lying in the same plane (±0.03 pm). Ta(1) lies 13 pm and N(1) 39 pm from this plane. The molecule has a non-crystallographic mirror plane through Cl(1), Ta(1), and N(1); two Cp* rings lie below and one lies above the $(TaN)_3$ ring plane, as expected on the basis of the NMR spectrum. The Ta-N bond lengths (average 188(2) pm) are comparable to those in $[Br_5TaNTaBr_5]^{3\ominus}$ (185 pm[7]) and lie between the values for Ta=NR (175–178 pm) and $Ta-NR_2$ (195–203 pm).[8]

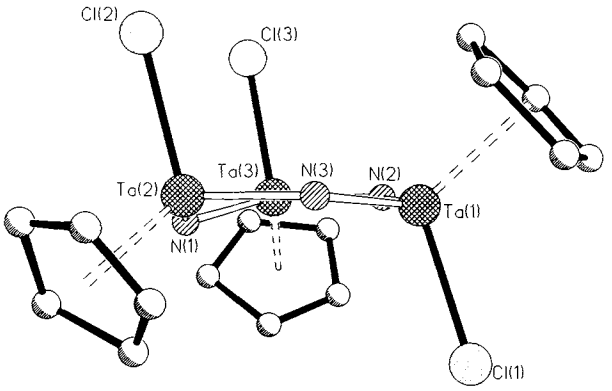

Fig. 1. Molecular structure of **3** (side view of the $(TaN)_3$ ring). Selected bond lengths [pm] and angles [°]: Ta1-N2 190(3), N2-Ta3 186(3), Ta3-N1 188(2), N1-Ta2 190(2), Ta2-N3 191(2), N3-Ta1 184(2), Ta1-Cl1 238(1), Ta2-Cl2 235(1), Ta3-Cl3 235(1), N-Ta-N (average) 109.8(10), Ta-N-Ta (average) 127.9(12), N-Ta-Cl (average) 103.6(9).

Many other triazatrimetallabenzenes should be accessible via reactions analogous to reaction (a).

Experimental Procedure

A solution of **2** (1010 mg, 2 mmol) in toluene (10 mL) was added dropwise to a stirred suspension of **1** (916 mg, 2 mmol) in dry toluene (20 mL). After stirring for 12 h at room temperature, the clear orange solution was heated at 50°C for 1 h and all volatiles were then removed under vacuum. The partly oily, partly crystalline residue was stirred with 50 mL of pentane and a crystalline solid was collected by filtration. The bright yellow product was washed several times with pentane and then dried under vacuum for 6 h. The IR, ^1H NMR, and mass spectra established its identity as **3**. Yield: 490 mg (67%).

Received: March 9, 1988 [Z 2656 IE]
Publication delayed at the authors' request
German version: *Angew. Chem. 100* (1988) 1377

CAS Registry numbers:
1, 71414-47-6; **2**, 1068-70-8; **3**, 116747-39-8.

[1] H. W. Roesky, J. Anhaus, H.-G. Schmidt, G. M. Sheldrick, M. Noltemeyer, *J. Chem. Soc. Dalton Trans. 1983*, 1207; see also J. Hanich, M. Krestel, U. Müller, K. Dehnicke, D. Rehder, *Z. Naturforsch. B39* (1984) 1686.
[2] H. W. Roesky, K. V. Katti, U. Seseke, M. Witt, E. Egert, R. Herbst, G. M. Sheldrick, *Angew. Chem. 98* (1986) 447; *Angew. Chem. Int. Ed. Engl. 25* (1986) 477.
[3] H. W. Roesky, K. V. Katti, U. Seseke, H.-G. Schmidt, E. Egert, R. Herbst, G. M. Sheldrick, *J. Chem. Soc. Dalton Trans. 1987*, 847; K. V. Katti, H. W. Roesky, M. Rietzel, *Inorg. Chem. 26* (1987) 4032.
[4] K. Dehnicke, J. Strähle, *Angew. Chem. 93* (1981) 451; *Angew. Chem. Int. Ed. Engl. 20* (1981) 413.
[5] R. A. Wheeler, R. Hoffmann, J. Strähle, *J. Am. Chem. Soc. 108* (1986) 5381.
[6] Crystal structure analysis of **3**: space group $P2_1/c$, $a = 1690.8(2)$, $b = 900.8(1)$, $c = 2316.4(3)$ pm, $\beta = 92.00(2)°$, $V = 3.5259$ nm^3, $Z = 4$, $\mu(Mo_{K\alpha}) = 9.43$ mm^{-1}. 6032 measured reflections, $2\theta_{max} = 45°$; empirical absorption correction, 3585 unique reflections with $F > 3\sigma(F)$ used in the structure solution and refinement. Ta and Cl anisotropic, N and C isotropic, H atoms not included (because of the strong thermal motion of the Cp* rings), $R = 0.086$ ($R_w = 0.082$, $w^{-1} = \sigma^2(F) + 0.0005F^2$). Further details of the crystal structure investigation may be obtained from the Fachinformationszentrum Energie, Physik, Mathematik GmbH, D-7514 Eggenstein-Leopoldshafen 2 (FRG), on quoting the depository number CSD-52976, the names of the authors, and the journal citation.
[7] K. P. Frank, J. Strähle, J. Weidlein, *Z. Naturforsch. B35* (1980) 300.
[8] M. R. Churchill, H. J. Wasserman, *Inorg. Chem. 21* (1982) 218; D. C. Bradley, M. B. Hursthouse, K. M. A. Malik, A. J. Nielson, G. B. C. Vuru, *J. Chem. Soc. Dalton Trans. 1984*, 1069; L. R. Chamberlain, I. P. Rothwell, J. C. Huffman, *J. Chem. Soc. Chem. Commun. 1986*, 1203.

π Complexes of an Amino-9-fluorenylideneborane**

By *Scott Helm* and *Heinrich Nöth**

Dedicated to Professor Hans Bock on the occasion of his 60th birthday

9-Fluorenylidene-2',2',6',6'-tetramethylpiperidinoborane **1**,[1] the first aminoorganylideneborane derivative,[2,3] is characterized by high reactivity of its BC double bond. Typical reactions are additions to the double bond to give amino-9-fluorenylborane derivatives as well as [2+2] and [2+3] cycloadditions.[1,4] However, π complexes of this system in which the benzo groups, the cyclopentadienylidene ring, or the BC double bond are bonded in an η^6, η^5, or η^2 fashion, respectively, have not been reported. This is due, among other things, to the fact that the fluorenyl moiety shows little tendency to form π complexes.[5]

We have now found that $TiCl_4$ and $TiBr_4$ react readily with **1** to give fluorenylidene-TiX_3 π complexes. Presumably, **2** is initially formed, since analogous compounds are obtained upon reaction of **1** with boron or phosphorus halides.[6]

The X-ray structure analysis of **3a** (Fig. 1)[7] does not show fully symmetrical η^5 bonding of the $TiCl_3$ fragment to the central five-membered ring, since the TiC distances to C7 and C8 are longer than those to C1, C2, and C13.

[*] Prof. Dr. H. Nöth, S. Helm, MA
Institut für Anorganische Chemie der Universität
Meiserstrasse 1, D-8000 München 2 (FRG)

[**] This work was supported by the Deutsche Forschungsgemeinschaft and the Fonds der Chemischen Industrie. We thank Dr. *W. Rattay* and *G. Linti* for help in carrying out the X-ray structure analyses. *S. Helm* thanks the DAAD for a fellowship.

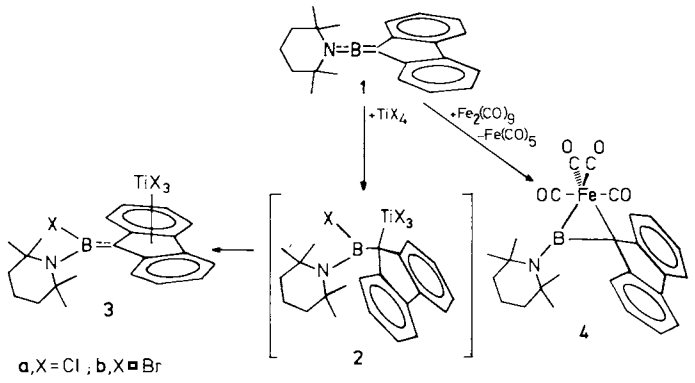

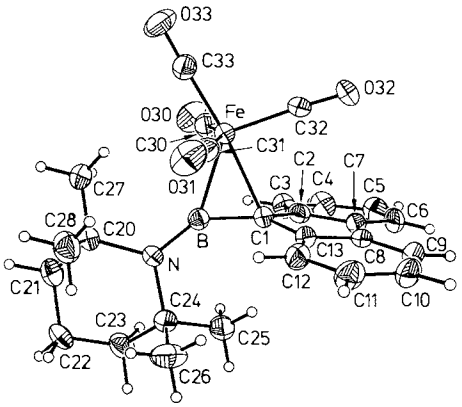

Fig. 2. Molecular structure of **4** (ORTEP). Selected bond lengths [Å] and angles [°]: Fe-B 2.125(5), Fe-C1 2.190(4), Fe-C30 1.786(5), Fe-C31 1.786(5), Fe-C32 1.820(5), Fe-C33 1.798(5), B-C1 1.518(7), B-N 1.377(6); C30-Fe-C31 151.2(2), C30-Fe-C32 104.5(2), C30-Fe-C33 85.7(2), C30-Fe-B 82.9(2), C30-Fe-C1 92.8(2), C31-Fe-C32 104.0(2), C31-Fe-B 83.4(2), C31-Fe-C1 93.4(2), C32-Fe-C33 100.2(2), C32-Fe-B 126.7(2), C32-Fe-C1 85.5(2), C33-Fe-B 133.2(2), C33-Fe-C1 174.3(2), B-Fe-C1 41.2(2), Fe-B-N 146.0(3), Fe-B-C1 71.7(2), N-B-C1 142.3, C13-C1-C2 104.3(4), Fe-C1-B 67.1(2).

However, this distortion toward η^3 coordination is still not strong enough to consider it as a purely allylic interaction of the 9-fluorenyl ligand with the $TiCl_3$ fragment.[8] The electron demand of the boron atom in **3a** is satisfied by a BN bond displaying pronounced double-bond character; this is shown in the bond lengths and in the near coplanarity of the C21-C25-N plane and the N-B-C14(C1) plane, which, in turn, forms an angle of 48.6° with the plane of the five-membered ring.

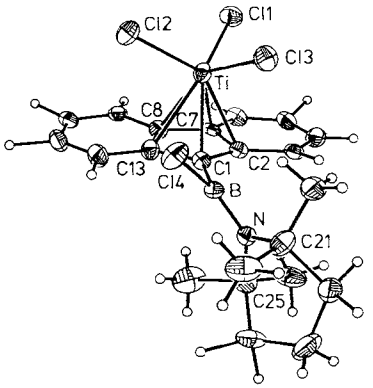

Fig. 1. Molecular structure of **3a** (ORTEP). Thermal ellipsoids at the 25% probability level. Selected bond lengths [Å] and bond angles [°]: Ti-Cl1 2.262(4), Ti-Cl2 2.213(3), Ti-Cl3 2.225(3), Ti-C1 2.27(1), Ti-C2 2.35(1), Ti-C13 2.43(1), Ti-C7 2.50(1), Ti-C8 2.52(1), B-C1 1.60(1), B-N 1.37(2), B-Cl4 1.83(1); Cl1-Ti-Cl2 101.5(1), Cl1-Ti-Cl3 98.6(1), Cl2-Ti-Cl3 104.7(1), Cl4-B-C1 110.0(8), Cl4-B-N 121.7(7), C1-B-N 128.3(9).

Reaction of **1** with nonacarbonyldiiron affords the crystalline tetracarbonyliron complex **4**, whose NMR data indicates a symmetrical molecule. The four CO groups are equivalent at room temperature on the NMR time scale; at 210 K, however, three CO groups (intensity ratio 1:1:2) become distinguishable and thus confirm the formation of a tetracarbonyliron complex. The absence of the NBC vibrational band of **1** at 1717 cm^{-1} in the IR spectrum of **4** suggests the formation of a π complex involving the BC bond. The X-ray structure analysis (Fig. 2)[9] corroborates this conclusion.

In the solid state, **4** has near C_s symmetry. The BC bond occupies an "equatorial" position in the strongly distorted trigonal-bipyramidal arrangement of the ligands around the iron atom. The bulky ligand **1** causes a reduction in the angle between the axial CO groups from 180° in $[Fe(CO)_5]$ to 151.2° in **4**. As in heterocumulene $(CO)_4Fe$ complexes,[10] which have analogous configurations, the double bond involved in the coordination is lengthened (by 0.1 Å compared with **1**), whereas the BN bond is only 0.03 Å longer (indicating that its π-bond character is only slightly changed). The C20-C24-N plane is practically parallel to the Fe-B-C1 plane (angle formed by the normals to the planes: 4.7°). Since, despite the larger covalent radius of boron, the FeB bond is shorter than the FeC bond, the boron atom apparently plays a dominating role as π acceptor and thus contributes appreciably to the stabilization of **4**. According to *Floriani* et al.,[11] the stability of heterocumulene tetracarbonyliron complexes, such as **4**, is determined by the π interaction between the C=X fragment and the metal d orbitals.

Experimental Procedure

3a, b: **1** (1.75 mg, 5.5 mmol) in toluene (10 mL) was allowed to react with an equimolar amount of TiX_4 (X = Cl, Br) in toluene (10 mL). After 1 h, the precipitated product was separated from the nearly black solution. Recrystallization from a small amount of CH_2Cl_2 at −20°C. **3a**: Yield 45%, green-black crystals, dec. >200°C; ^{11}B NMR ($CDCl_3$): δ = 38.8; ^1H NMR ($CDCl_3$): δ = 0.95, 1.67, 1.71, 1.88 (s, 3 m, 18 H; NC_9H_{18}), 7.29, 7.70, 7.74 (3 m, 8 H; $C_{13}H_8$); MS (70 eV): *m/z* 435 ([*M* − 2 Cl + 2 H], 100%). **3b**: 42%, green-black crystals, dec. >200°C; ^{11}B NMR ($CDCl_3$): δ = 39.1; ^1H NMR ($CDCl_3$): δ = 0.93, 1.54-1.76, 1.89-1.96 (s, 2 m, 18 H; NC_9H_{18}), 7.29, 7.67, 8.28 (3 m, 8 H; $C_{13}H_8$); MS (70 eV): *m/z* 394 ([*M* − $TiBr_3$], 100%).

4: Equimolar amounts of **1** and $[Fe_2(CO)_9]$ were stirred in toluene until the metal carbonyl had dissolved (16 h). The volatile components were then removed under vacuum, and the oily, reddish-brown residue was crystallized from toluene/hexane (1/3) at −20°C/−78°C. 48%, light brown crystals, m.p. 137°C. IR (hexane): $\tilde{\nu}$ = 2064, 2011, 1962, 1971 (sh) cm^{-1}; ^{11}B NMR (C_6D_6): δ = 58.5; ^1H NMR (C_6D_6): δ = 0.80, 1.33, 1.81 (s, br. m, 18 H; NC_9H_{18}), 7.15-7.74 (m, 8 H; $C_{13}H_8$); ^{13}C NMR (C_6D_6; numbering in Fig. 2): δ = 16.3 (C22), 33.2, 34.3 (C25, C26, C27, C28), 38.6, 39.2 (C21, C23), 58.7, 61.8 (C20, C24), 121.0 (C6, C9), 123.6 (C5, C10), 124.9 (C3, C12), 126.3 (C4, C11), 138.4 (C7, C8), 153.4 (C2, C13), 208.7 (CO), the signal for C1 was not observed; ^{13}C NMR (*T* = 210 K, CO region): δ = 209.4, 207.8, 206.6 (1:1:2).

Received: March 9, 1988 [Z 2654 IE]
Publication delayed at the authors' request
German version: *Angew. Chem. 100* (1988) 1378

CAS Registry numbers:
1, 96097-03-9; **3a**, 116725-85-0; **3a**·0.5 CH_2Cl_2, 116725-87-2; **3b**, 116783-47-2; **4**, 116725-86-1; $TiBr_4$, 7789-68-6; $TiCl_4$, 7550-45-0; $Fe_2(CO)_9$, 15321-51-4.

[1] B. Glaser, H. Nöth, *Angew. Chem. 97* (1985) 424; *Angew. Chem. Int. Ed. Engl. 24* (1985) 416; B. Glaser, E. Hanecker, H. Nöth, H.-U. Wagner, *Chem. Ber. 120* (1987) 659.
[2] G. Maier, J. Henkelmann, H.-P. Reisenauer, *Angew. Chem. 97* (1985) 1061; *Angew. Chem. Int. Ed. Engl. 24* (1985) 1065.
[3] R. Boese, P. Paetzold, A. Tapper, *Chem. Ber. 120* (1987) 1069.
[4] B. Glaser, H. Nöth, *Chem. Ber. 119* (1986) 3856; H. Nöth: *Boron Chem., Proc. 6th IMEBORON (Bechyne 1987)*, World Scientific, Singapore

Advertisement pages 1333-1336

1987, p. 438; B. Glaser, *Dissertation*, Universität München 1985; E. Maier, *Diplomarbeit*, Universität München 1987.
[5] E. Samuel, R. Setton, *J. Organomet. Chem. 4* (1965) 156; R. B. King, A. Efraty, *ibid. 23* (1970) 527; J. W. Johnson, P. M. Treichel, *J. Am. Chem. Soc. 99* (1977) 1427.
[6] C. Euringer, S. Helm, H. Nöth, unpublished results.
[7] X-ray structure analysis of **3a**: $C_{22}H_{26}BCl_4NTi \cdot 0.5CH_2Cl_2$, $M = 547.5$; single crystal $0.22 \times 0.30 \times 0.30$ mm^3; monoclinic, $P2_1/n$, $a = 10.672(4)$, $b = 12.079(3)$, $c = 21.179(3)$ Å, $\beta = 101.93(3)°$, $V = 2671$ Å^3, $Z = 4$, $\rho_{calcd} = 1.36$ g cm^{-3}. $\mu(Mo_{K\alpha}) = 8.33$ cm^{-1}, $2\theta = 2$–$50°$ in $hk \pm l$, 3970 measured reflections, 3295 observed reflections with $I \geq 2.5\sigma(I)$; empirical absorption correction, anisotropic refinement of the non-hydrogen atoms, H atoms of the CH_3 groups and of a CH_2 group included in the refinement with a riding model, those of the fluorenyl unit were freely refined, $U_{i,}$ fixed. The CH_2Cl_2 molecule was taken into consideration in the refinement with half occupation (without H atoms). $R = 0.103$, $R_w = 0.114$ [9b].
[8] C. Kowala, P. C. Wailes, H. Weigold, J. A. Wunderlich, *J. Chem. Soc. Chem. Commun. 1974*, 993 (they describe an η^3- and an η^5-bonded fluorenyl group at zirconium).
[9] a) X-ray structure analysis of **4** (from toluene/hexane): $C_{26}H_{26}BFeNO_4$, $M = 483.15$; single crystal: $0.22 \times 0.18 \times 0.4$ mm^3; $P2_1/c$, $a = 11.404(2)$, $b = 12.203(5)$, $c = 17.733(4)$ Å, $\beta = 101.15(2)°$, $V = 2421(1)$ Å^3, $Z = 4$, $\rho_{calcd} = 1.326$ g cm^{-3}. $\mu(Mo_{K\alpha}) = 6.51$ cm^{-1}, $(\omega - 2\theta)$ scan, $2\theta = 2$–$50°$ in $\pm hk \pm l$, 7977 measured reflections, 3188 unique reflections, internal consistence 0.0249, 2788 observed reflections with $I \geq 3\sigma(I)$; empirical and LP correction, direct methods; anisotropic refinement of the non-hydrogen atoms; H-atom positions of the fluorenylidene group freely refined; CH_3 groups included in the refinement as rigid groups, $U_{i,H}$ fixed. $R = 0.065$, $R_w = 0.077$; largest $\Delta/\sigma = 0.070$, $\rho = 0.29$ e Å^{-3}; b) Further details of the crystal structure investigation may be obtained from the Fachinformationszentrum Energie, Physik, Mathematik GmbH, D-7514 Eggenstein-Leopoldshafen 2 (FRG), on quoting the depository number CSD-53056, the names of the authors, and the journal citation.
[10] H. Le Bozec, P. H. Dixneuf, N. J. Taylor, A. J. Carty, *J. Organomet. Chem. 135* (1977) C29; E. J. Moore, D. A. Straus, J. Armantrout, B. D. Santarsiero, R. H. Grubbs, J. E. Bercaw, *J. Am. Chem. Soc. 105* (1983) 2068; S. C. H. Ho, D. A. Straus, J. Armantrout, W. P. Schaefer, R. H. Grubbs, *ibid. 106* (1984) 2210; A. D. Redhouse, W. A. Herrmann, *Angew. Chem. 88* (1976) 652; *Angew. Chem. Int. Ed. Engl. 15* (1976) 615; K. Schorpp, W. Beck, *Z. Naturforsch. B28* (1973) 738.
[11] M. Rosi, A. Sgamellotti, F. Tarantelli, C. Floriani, *Inorg. Chem. 26* (1987) 3805.

Ethylenedithione (C_2S_2): Generation and Characterization by Neutralization-Reionization Mass Spectrometry**

By *Detlev Sülzle* and *Helmut Schwarz**

Dedicated to Professor Hans Bock on the occasion of his 60th birthday

Theory leaves no doubt that ethylenedithione **1**, the dimer of carbon monosulfide, should be a "makeable" molecule, since it corresponds to the global minimum of the C_2S_2 hypersurface. Its decomposition into CS has, according to reliable ab initio calculations, a $\Delta H^{\ominus}$ of 39 kcal mol^{-1}.[1] However, beyond the presumed existence of $(CS)_2$ as transient component of the "LASER snow" (polymeric $(CS)_x$) in CS_2 vapor,[2] it has thus far been impossible to obtain unequivocal experimental evidence of the existence of **1**, despite all favorable prognoses. The reason for this is presumably linked with several factors: 1) **1** is stable with regard to unimolecular processes, but it may be very easily attacked by electrophiles, nucleophiles or even radicals. 2) Even if it were possible to find an inert medium there always remains the problem of a suitable precursor and optimal reaction conditions. Intermolecular interactions in a high vacuum, as occur, e.g., in a mass spectrometer, can essentially be ruled out. We report here how **1** can be prepared and characterized using the relatively new method of neutralization-reionization mass spectrometry (NRMS).[3]

Electron impact ionization (70 eV)[4] of 1,3,4,6-tetrathiapentalene-2,5-dione **2**[5] affords as most important fragments $C_2S_n^{\odot\oplus}$ [Eqn. (a)], including the interesting $C_2S_2^{\odot\oplus}$. This is also accessible by 70-eV ionization of **3**, the tetramethyl-substituted dithiodiamide of squaric acid [Eqn. (b)].[6]

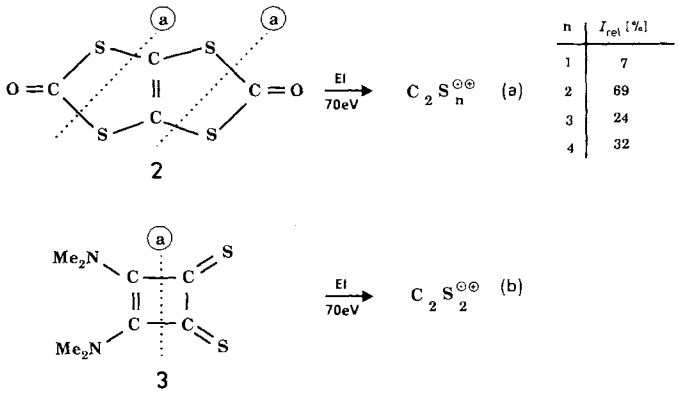

The mass selection of $C_2S_2^{\odot\oplus}$ (m/z 88) using B(1)/E (Scheme 1) in a tandem experiment,[7] followed by collisional activation[8] in the third collision chamber (collision gas helium, 80% transmission) furnished by scanning B(2)

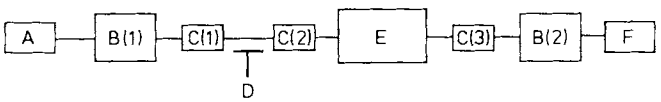

Scheme 1. Schematic diagram of the mass spectrometer setup. A = ion source, B = magnetic sector, C = collision chamber, D = deflector electrode, E = electric sector, F = ion detection.

the collisional activation (CA) mass spectrum shown in Figure 1a. Although the CA spectrum of $C_2S_2^{\odot\oplus}$ would, in principle, be consistent with the structures **4**–**7**, we presume, on the basis of the results of ab initio calculations that electron impact ionization of **2** and **3** leads via the bond ruptures indicated by ⓐ [Eqns. (a) and (b)] to the radical cation of **1**, i.e. **4**. Whereas **5** and **6** correspond neither at the UHF/3-21G/3-21G nor the UHF/6-31G*//6-31G* level to stationary points on the energy hypersurface, at the 3-21G level **7** corresponds to a transition struc-

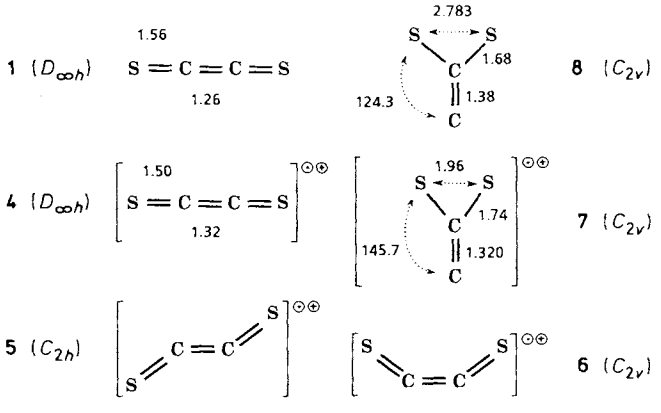

[*] Prof. Dr. H. Schwarz, Dipl.-Chem. D. Sülzle
Institut für Organische Chemie der Technischen Universität
Strasse des 17. Juni 135, D-1000 Berlin 12 (FRG)

[**] This work was supported by the Fonds der Chemischen Industrie, the Deutsche Forschungsgemeinschaft and the Gesellschaft von Freunden der Technischen Universität Berlin. We thank Dr. *K. H. Moock* (FU Berlin) for helpful discussions and *Waltraud Zummack* (TU Berlin) for her help with the synthesis of model compounds.

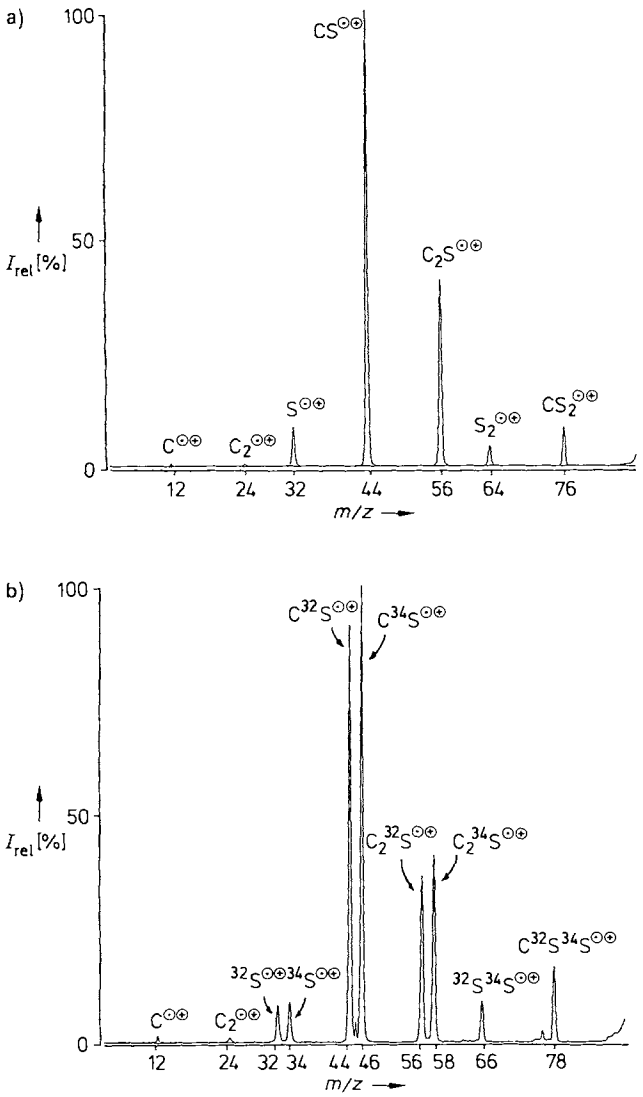

Fig. 1. CA-mass spectra a) of $C_2{}^{32}S_2^{\odot\oplus}$ (*m/z* 88), b) of $C_2{}^{32}S^{34}S^{\odot\oplus}$ (*m/z* 90).

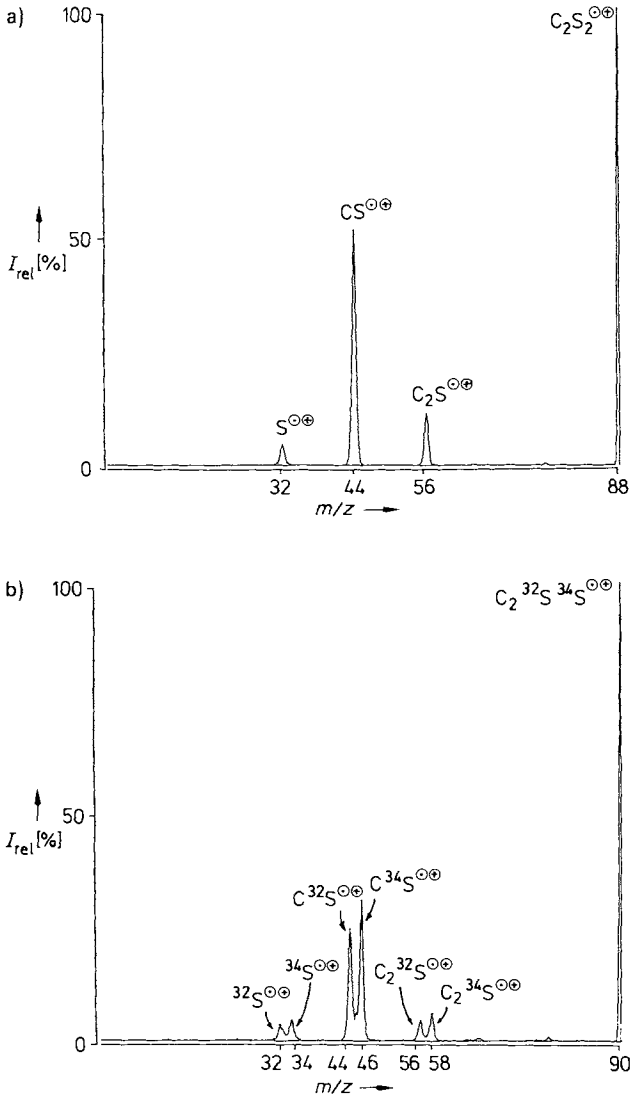

Fig. 2. NR-mass spectra (neutralization with Xe, 90% transmission *T* in the first collision chamber, reionization with O_2, 80% *T* in the second collision chamber; deflection electrode for the deflection of other ions ca. 500 V) a) of $C_2{}^{32}S_2^{\odot\oplus}$, b) of $C_2{}^{32}S^{34}S^{\odot\oplus}$.

ture for the cleavage of atomic carbon from **4**. At the distinctly better 6-31G* level, **7** corresponds to a local minimum, which, however, after taking into consideration the zero point vibration energy, lies 87.2 kcal mol^{-1} higher than the minimum calculated for **4**. Thus, **4** presumably corresponds to the global minimum on the C_2S_2 hypersurface.

Collisional activation of **4** then affords the spectrum reproduced in Figure 1a; the signal for $S_2^{\odot\oplus}$ presumably arises via the sequence $\mathbf{4} \rightarrow \mathbf{6} \rightarrow S_2^{\odot\oplus} + C_2$ or (less likely) via the intermediate $CS_2^{\odot\oplus}$. Also for the formation of this fragment, **4** would have to isomerize under the conditions of the collisional activation.

Remarkable is the isotope effect that can be gleaned from Figure 1b; according to the data ^{32}S is always preferentially cleaved as neutral particle rather than ^{34}S in the collision induced decomposition of $C_2{}^{32}S^{34}S^{\odot\oplus}$ (*m/z* 90). A convincing explanation for the strong isotope effect (up to 10%) (see also Fig. 2b) is still wanting. The signal at *m/z* 45 corresponds to the doubly charged cation $C_2{}^{32}S^{34}S^{2\oplus}$ formed by charge stripping.[9]

Can **4** not only be oxidized to the dication, but also reduced to the previously unknown neutral molecule **1**? The answer is unequivocally yes. The NMR/mass spectra (Fig. 2) not only contain very intense signals for $C_2S_2^{\odot\oplus}$ and for $C_2{}^{32}S^{34}S^{\odot\oplus}$, also the other fragments in the spectra can be readily assigned. What is the constitution of the neutral C_2S_2 thus generated, whose lifetime is at least $t \geq 0.8$ µs (determined by the time of flight from C(1) to C(2) (Scheme 1))? The neutralization is a vertical process,[3] so that if $C_2S_2^{\odot\oplus}$ is present as **4**, C_2S_2 is generated as **1**. This presumption is strengthened by the following findings: 1) The change of geometry in the transition $\mathbf{4} \rightarrow \mathbf{1}$ is, other than in the transition $\mathbf{7} \rightarrow \mathbf{8}$, relatively minor (see 6-31G* geometry parameters in the corresponding molecular structures); this could explain the unusually high fraction of $C_2S_2^{\odot\oplus}$ "survivor" signals in the NR-mass spectrum (Fig. 2a). 2) At the RHF/3-21G//3-21G level, as also at the RHF/6-31G*//6-31G* level, **1** is the most stable of all calculated C_2S_2 structures. The neutral analogues of **5** and **6** do not correspond to any stationary points, and **8** (as triplet) is around 79.4 kcal mol^{-1} less stable than the triplet state of **1** (UHF/6-31G*//6-31G* + ZPVE). Although the basis set used by us is modest in comparison to the "state-of-the-art" basis set used by *Schaefer* et al.,[1] the qualitative results lead to the same conclusions: a) the triplet state

of **1** is more stable than the singlet state; b) **1** is more stable than two monomeric CS molecules.

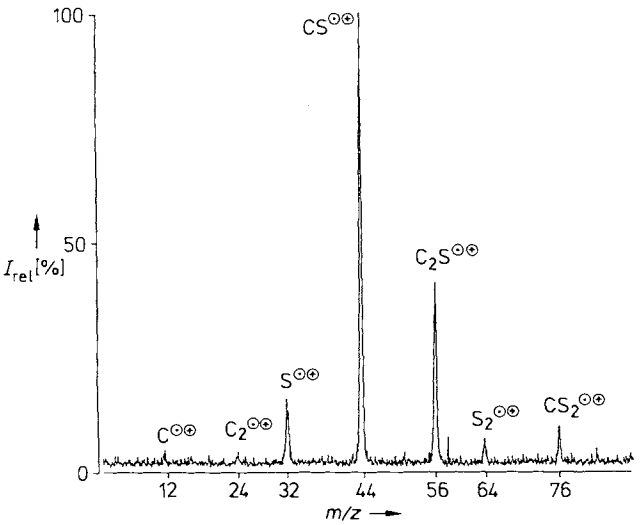

Fig. 3. CA mass spectrum of $C_2S_2^{\odot\oplus}$, generated by the sequence

$C_2S_2^{\odot\oplus} \xrightarrow[90\%\ T]{Xe} C_2S_2 \xrightarrow[80\%\ T]{O_2} C_2S_2^{\odot\oplus} \xrightarrow[80\%\ T]{He}$ products.

In view of the high yields of C_2S_2 in the neutralization step **4**→**1** we have carried out a further experiment. The ion with *m/z* 88 ($C_2S_2^{\odot\oplus}$) generated in the sequence $C_2S_2^{\odot\oplus} \rightarrow C_2S_2 \rightarrow C_2S_2^{\odot\oplus}$ was subjected, with the help of the electric sector E (Scheme 1) to a kinetic energy analysis, and the interference-free $C_2S_2^{\odot\oplus}$ beam (8 keV kinetic energy) was re-excited in the third field-free region in a collision experiment with helium (80% *T*). A CA mass spectrum thus obtained (Fig. 3) basically contains no contributions from reionized neutral particles (N), which, e.g., occur in the reaction $C_2S_2^{\odot\oplus} \rightarrow$ fragment ion + N and can lead to an uncertainty in the interpretation of ordinary NR-mass spectra. The spectrum reproduced in Figure 3 is free of these possible interferences and it is unambiguous, since it contains the characteristic fragments for **4** with the correct relative intensities (cf. Fig. 1a).

Summarizing, it can be established that *Schaefer*'s prognosis[1] "... we are convinced that C_2S_2 is a "makeable" molecule ..." has been verified by the NRMS investigations described here. Obviously other exotic molecules, e.g. the hitherto unknown dimer of carbon monoxide[1] or the only partly investigated molecules of the type $X(C)_nY$ (X, Y: free electron pairs, H_2, O, S; n = 2, 3, 4 etc.)[10] related to C_2S_2 and C_2O_2, which are of interest in astrochemistry, as well as many other transients "produced" by *Hans Bock* and his co-workers,[11] are also possibly detectable by NRMS.

Received: April 11, 1988 [Z 2698 IE]
German version: *Angew. Chem. 100* (1988) 1384
Publication delayed at authors' request

[1] G. P. Raine, H. F. Schaefer III, R. C. Haddon, *J. Am. Chem. Soc. 105* (1983) 194.
[2] a) K. Ernst, J. J. Hoffman, *Chem. Phys. Lett. 68* (1979) 40; b) N. Beverini, K. Ernst, M. Inguscio, F. Strumia, *Appl. Phys. B 26* (1981) 57; c) K. Ernst, *NATO ASI Ser. B 95* (1983) 331; d) Reviews on CS: E. K. Moltzen, K. J. Klabunde, A. Senning, *Chem. Rev. 88* (1988) 391; e) see also: R. Steudel, *Z. Anorg. Allg. Chem. 361* (1968) 180.
[3] Reviews: a) C. Wesdemiotis, F. W. McLafferty, *Chem. Rev. 87* (1987) 485; b) J. K. Terlouw, H. Schwarz, *Angew. Chem. 99* (1987) 829; *Angew. Chem. Int. Ed. Engl. 26* (1987) 805.
[4] All experiments were carried out in a commercially available VG instrument—triple-sector mass spectrometer ZAB-HF-3F (Scheme 1). For a detailed description see a) T. Weiske, *Dissertation* (D 83), Technische Universität Berlin 1985; b) J. K. Terlouw, T. Weiske, H. Schwarz, J. L. Holmes, *Org. Mass Spectrom. 21* (1986) 665.
[5] R. R. Schumaker, E. M. Engler, *J. Am. Chem. Soc. 99* (1977) 5521.
[6] H. Ehrhardt, S. Hünig, H. Pütter, *Chem. Ber. 110* (1977) 2506.
[7] F. W. McLafferty (Ed.): *Tandem Mass Spectrometry*, Wiley-Interscience, New York 1983.
[8] a) R. G. Cooks (Ed.): *Collision Spectroscopy*, Plenum, New York 1978; b) K. Levsen, H. Schwarz, *Mass Spectrom. Rev. 2* (1983) 77.
[9] For the method see a) [7]; b) T. Ast, C. J. Porter, C. J. Proctor, J. H. Beynon, *Bull. Soc. Chim. Beograd 41* (1981) 135; c) M. Rabrenovic, C. J. Proctor, T. Ast, C. O. Herbert, A. G. Brenton, J. H. Beynon, *J. Phys. Chem. 87* (1983) 3305; d) W. Koch, F. Maquin, D. Stahl, H. Schwarz, *Chimia 39* (1985) 376.
[10] a) B. P. Winnewisser, *Mol. Spectrosc. Mod. Res. 1985*, 321; b) R. D. Brown, K. G. Dyall, P. S. Elmes, P. D. Godfrey, D. McNaughton, *J. Am. Chem. Soc. 110* (1988) 789; c) H. Bock, R. Dammel, D. Jaculi, *ibid. 108* (1986) 7844; d) A. B. Raksit, D. K. Bohme, *Int. J. Mass Spectrom. Ion Processes 55* (1983) 69; e) N. W. Broten, J. M. MacLeod, L. W. Avery, W. M. Irvine, B. Hoglund, P. Friberg, A. Hjalmarson, *Astrophys. J. 276* (1984) L25; f) D. K. Bohme, *Nature (London) 319* (1986) 128; g) W. W. Duley, D. A. Williams: *Interstellar Chemistry*, Academic Press, London 1984.
[11] H. Bock, R. Dammel, *Angew. Chem. 99* (1987) 518; *Angew. Chem. Int. Ed. Engl. 26* (1987) 504, and references cited therein.

The Structures of Perchloric Acid, $HClO_4$, and Its Anhydride, Cl_2O_7

By *Arndt Simon** and *Horst Borrmann*

Dedicated to Professor Hans Bock on the occasion of his 60th birthday

Perchloric acid, or, more accurately, the aqueous solution of $HClO_4$, has been known since the beginning of the last century.[1] Numerous crystalline hydrates exist and nearly all of them have been structurally characterized.[2–9] A structure analysis of pure, anhydrous $HClO_4$ itself, however, which melts at −112 °C,[10] is still lacking. It has been concluded, from density measurements in particular, that the dissociation equilibrium

$$3\,HClO_4 \rightleftharpoons Cl_2O_7 + H_3O^{\oplus} + ClO_4^{\ominus}$$

responsible for the intrinsic conductivity of nonaqueous $HClO_4$[11,12] is shifted entirely to the right-hand side at low temperature due to the crystallization of the monohydrate $H_3O^{\oplus}ClO_4^{\ominus}$. In contrast, according to *Mascherpa*,[13] solid $HClO_4$ exists, but undergoes an allotropic phase transition at −103.5 °C and decomposes peritectically at −101.4 °C into the solid hydrate β-$HClO_4 \cdot 0.25\,H_2O$ and Cl_2O_7-rich melts.

Anhydrous $HClO_4$[14] exhibited thermal effects upon warming near −145 °C (exothermic) and −120 °C (endothermic) in DTA experiments. Both effects were accompanied by structural changes which are clearly recognizable in powder patterns recorded with the modified Guinier technique.[15] The low-temperature phases did not reappear upon cooling of the obviously stable form, which melts at −112 °C, and they were not observed with specially purified samples. The melting point of $HClO_4$ was always found to be near −112 °C.

After several attempts, a suitable single crystal of $HClO_4$ could be grown on a diffractometer by slow crystallization a few tenths of a degree below the melting point. The data were collected at −160 °C. The structure was solved in the acentric space group $Pca2_1$ and could be refined including

[*] Prof. Dr. A. Simon, H. Borrmann
Max-Planck-Institut für Festkörperforschung
Heisenbergstr. 1, D-7000 Stuttgart 80 (FRG)

the H positions without encountering any problems.[16] The four crystallographically different $HClO_4$ molecules all exhibit the same typical distortion of the tetrahedral ClO_4 unit. Three Cl-O distances have nearly equal lengths (approx. 142 pm). The fourth is 161 pm. These distances result from a rigid body refinement.[17] Compared to the results of electron diffraction on gaseous $HClO_4$,[18] the averaged single bond Cl-O distance is approx. 3 pm shorter.

The short intramolecular O-H distances of approx. 82 pm[19] already indicate that the bridges between neighboring molecules are weak. The shortest intermolecular O···H distances are 203 pm. In spite of their weakness, these bridges play an important role in the molecular arrangement. There exist rods of H-bridged molecules (Fig. 1a) which form a closest rod packing[20] (Fig. 1b). The rods are connected via very weak H-bridges ($d(O\cdots H) \geq$ 261 pm).

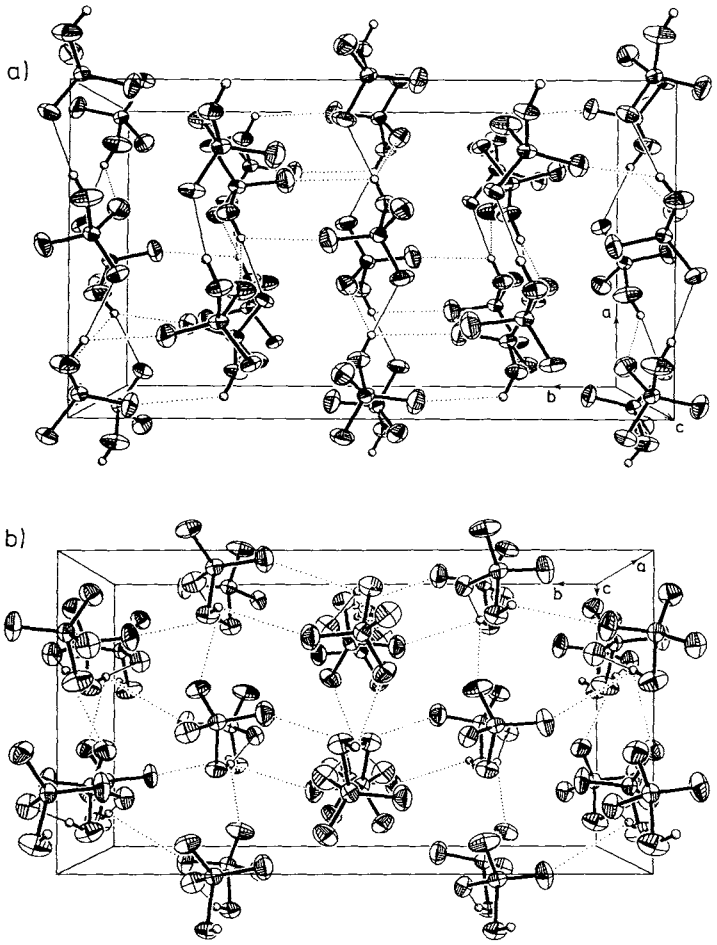

Fig. 1. Projection of the structure of $HClO_4$ onto a) (001) and b) (100). Cl and O atoms are drawn at the 70% probability level, the hydrogen atoms have an arbitrary size. The $HClO_4$ molecules are connected in chains via weak hydrogen bonding [solid lines in (a)]. The chains are arranged in a hexagonal rod packing (b) linked by weaker hydrogen bonds (dotted lines).

The structure analysis shows unambiguously that solid perchloric acid only consists of weakly interacting $HClO_4$ molecules. These are nearly identical in structure with the ClO_3F molecule (d(Cl-O) = 140.4, d(Cl-F) = 161.9 pm[21]).

The literature on the anhydride of the acid, Cl_2O_7, is also controversial about the solid state. A phase transition is said to occur at -100 °C.[22] DTA measurements on Cl_2O_7[23] showed only the effect due to melting at -92 °C. Modified Guinier diagrams, too, exhibit no sign of a phase transition. After some time of X-ray irradiation, only the strongest lines of Cl_2O_6[24] were observed with samples that slowly became yellow.

Growth of a single crystal presented similar problems as in the case of $HClO_4$. It was finally achieved with a slightly contaminated yellow sample. The structure of the compound, which crystallizes in $C2/c$, is shown as a projection along [010] in Figure 2.[25] The molecule consists of two corner-sharing ClO_4 tetrahedra and has C_2 crystallographic symmetry. The Cl-O distances corrected for librational motions of the tetrahedra are 172.3 pm for the bridging O atom and (averaged) 141.6 pm (3×) for the terminal atoms. Compared to $HClO_4$ the long "single bond" distances that involve the bridging O atom are unusual. Such long distances also occur in the Cl_2O molecule measured in the gas phase.[26]

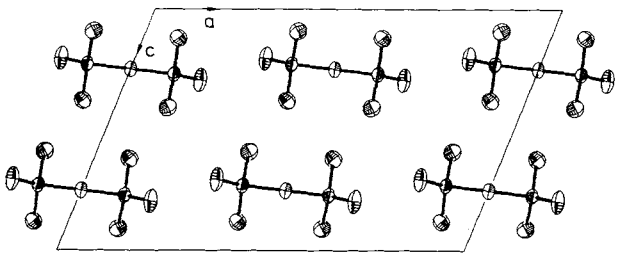

Fig. 2. The structure of Cl_2O_7 projected along [010]. The atoms are drawn at the 70% probability level.

There are significant differences between the structure of Cl_2O_7 and the recently determined structure of Mn_2O_7.[27,28] The distances with the bridging (177 pm) and terminal O atoms (159 pm) respectively do not differ to the same extent as in the structure of Mn_2O_7, and the molecules in the structure of Cl_2O_7 have nearly ideal C_{2v} symmetry. The bond angles, in particular, exhibit significant differences in both structures. The largest deviation of the angles at Mn from ideal tetrahedral is 1.8°. In contrast, in the Cl_2O_7 molecule angles between 98° and 116° occur. The Cl atom is shifted towards the plane formed by the terminal O atoms. This structural detail, as well as the large Cl-O distances for the bridging atom, possibly provides evidence of highly polar bonding in the sense of the formulation $(ClO_3^{\delta\oplus})_2O^{2\delta\ominus}$. Reference to SO_3,[29] which is isoelectronic with $ClO_3^{\oplus}$ and planar in the gas phase, might be helpful in interpreting the structure. Our arguments follow conclusions from an analysis of the distortions of tetrahedral molecules MX_4[30] in terms of ligand dissociation reaction pathways (e.g. $AlCl_4^{\ominus} \rightarrow AlCl_3 + Cl^{\ominus}$). The same kind of distortion is also obvious for $HClO_4$, which exhibits HO-Cl-O angles of between 101.1° and 106.6° without showing a bond lengthening.

In spite of the aforementioned differences the Cl_2O_7 and Mn_2O_7 structures show surprising similarities. In both, the O atoms have an approximately cubic close packed arrangement with occupied adjacent tetrahedral voids ("defect-CaF_2 structure"). Only the special choice of occupied voids is different for both compounds, and, therefore, the extent of shear deformation of the fcc arrangement differs. Whereas the monoclinic angle $\beta = 100.2°$ is near to the value of 98.1° calculated for the undistorted fcc arrange-

ment in Mn_2O_7, one finds rather large deviations ($\beta = 111.8°$ compared to 119.7°) in the case of Cl_2O_7.

Received: May 27, 1988 [Z 2783 IE]
German version: *Angew. Chem. 100* (1988) 1386

[1] F. von Stadion, *Ann. Chim. Phys. 8* (1818) 406.
[2] D. Mootz, E.-J. Oellers, M. Wiebcke, *J. Am. Chem. Soc. 109* (1987) 1200.
[3] J. Almlöf, *Chem. Scr. 3* (1973) 73.
[4] J. Almlöf, *Acta Crystallogr. Sect. B 28* (1972) 481.
[5] J. Almlöf, J.-O. Lundgren, I. Olovsson, *Acta Crystallogr. Sect. B 27* (1971) 898.
[6] I. Olovsson, *J. Chem. Phys. 49* (1968) 1063.
[7] F. S. Lee, G. B. Carpenter, *J. Phys. Chem. 63* (1959) 279.
[8] M. R. Truter, *Acta Crystallogr. 14* (1961) 318.
[9] C. E. Nordman, *Acta Crystallogr. 15* (1962) 18.
[10] H. J. van Wyk, *Z. Anorg. Allg. Chem. 48* (1906) 1.
[11] A. A. Zinov'ev, V. Ya. Rosolovskii, *Russ. J. Inorg. Chem. Engl. Transl. 3* (1958) 208.
[12] V. Ya. Rosolovskii, A. A. Zinov'ev, V. A. Prokhorov, *Russ. J. Inorg. Chem. Engl. Trans. 5* (1960) 334.
[13] G. Mascherpa, *Rev. Chim. Miner. 2* (1965) 379.
[14] $HClO_4$ was prepared (G. F. Smith, *J. Am. Chem. Soc. 75* (1953) 184) from 1 part aqueous perchloric acid (70%) and 3 parts oleum (20% SO_3). It was destilled at 35°C, 2 mbar and condensed at −80°C, yielding a yellow liquid. The immediately following rectification at 10^{-2} mbar furnished a colorless product. Very pure samples were prepared by forming the monohydrate from anhydrous and 70% aqueous acid which was decomposed in vacuum (J. B. Levy, *J. Phys. Chem. 66* (1962) 1092).
[15] A. Simon, *J. Appl. Crystallogr. 4* (1971) 138.
[16] a) *Pca2*$_1$ (No. 29); $Z = 16$; $a = 891.8(2)$, $b = 1584.2(3)$, $c = 864.4(2)$ pm, $\rho_{calcd} = 2.19$ g cm^{-3} at the temperature of the measurements, -160 ± 2°C; Syntex $P2_1$, range $3.0° < 2\theta < 68.0°$; ω-scans with 0.45 to 14.65°/min; 4980 measured symmetry independent reflections, 3562 with $F > 5\sigma(F)$, absorption correction via ψ-scans; $R = 0.036$ ($R' = 0.066$ including the unobserved reflections), $wR = 0.040$ (0.044); merit of fit 1.351; b) Program system SHELXTL-Plus (G. M. Sheldrick, Göttingen 1978). Further details of the crystal structure investigation may be obtained from the Fachinformationszentrum Energie, Physik, Mathematik GmbH, D-7514 Eggenstein-Leopoldshafen 2 (FRG), on quoting the depository number CSD-53 134, the names of the authors, and the journal citation.
[17] V. Schomaker, K. N. Trueblood, *Acta Crystallogr. Sect. B 24* (1968) 63.
[18] A. H. Clark, B. Beagley, D. W. J. Cruickshank, T. G. Hewitt, *J. Chem. Soc. A 1970*, 1613.
[19] The X-H distances determined from X-ray structure analyses are generally 15–20 pm too short; see W. C. Hamilton, J. A. Ibers: *Hydrogen Bonding in Solids*, W. A. Benjamin, New York 1968, p. 64.
[20] M. O'Keeffe, S. Andersson, *Acta Crystallogr. Sect. A 33* (1977) 914.
[21] A. H. Clark, B. Beagley, D. W. J. Cruickshank, T. G. Hewitt, *J. Chem. Soc. A 1970*, 872.
[22] A. A. Zinov'ev, V. Ya. Rosolovskii, *Russ. J. Inorg. Chem. Engl. Transl. 1* (1956) 169.
[23] Aqueous perchlorid acid (70%) was slowly added to P_4O_{10} at −196°C in an apparatus which had been pretreated with ozone for 2 h at 180°C (J. J. Manley, *J. Chem. Soc. 121* (1922) 331; G. Brauer: *Handbuch der präparativen anorganischen Chemie, 3rd Edit., Vol. 1*, F. Enke, Stuttgart 1974, p. 316). Upon warming to 50°C under vacuum in a water bath the reaction zone turned orange-red in color. A crude product of similar color collected in an attached trap and was immediately destilled at 10^{-2} mbar to yield a colorless product.
[24] K. M. Tobias, M. Jansen, *Z. Anorg. Allg. Chem. 550* (1987) 16.
[25] *C2/c* (No. 15); $Z = 4$; $a = 1369.6(4)$, $b = 461.7(1)$, $c = 872.2(3)$ pm, $\beta = 111.94(2)°$, $\rho_{calcd} = 2.38$ g/cm^3 at the temperature of the measurements, -160 ± 2°C; Syntex $P2_1$; range $3.0° < 2\theta < 70.0°$; ω-scans with 0.45 to 14.65°/min; 1132 measured symmetry independent reflections, averaged from 4506 measured reflections, 1070 with $F > 5\sigma(F)$; absorption correction via ψ-scans; $R = 0.020$ ($R' = 0.022$), $wR = 0.031$ (0.032); goodness of fit 1.702 [16b].
[26] B. Beagley, A. H. Clark, T. G. Hewitt, *J. Chem. Soc. A 1968*, 658.
[27] A. Simon, R. Dronskowski, B. Krebs, B. Hettich, *Angew. Chem. 99* (1987) 160; *Angew. Chem. Int. Ed. Engl. 26* (1987) 139.
[28] R. Dronskowski, B. Krebs, A. Simon, G. Miller, B. Hettich, *Z. Anorg. Allg. Chem. 558* (1988) 7.
[20] K. J. Palmer, *J. Am. Chem. Soc. 60* (1938) 2360.
[30] P. Murray-Rust, H. B. Bürgi, J. D. Dunitz, *Acta Crystallogr. Sect. B 34* (1978) 1793.

A New Approach to Ionic Ozonides**

By *Werner Hesse* and *Martin Jansen**

Dedicated to Professor Hans Bock on the occasion of his 60th birthday

Ionic ozonides are red, crystalline solids containing the bent molecular anion O_3^-. Only alkali-metal ozonides, which are extremely sensitive to moisture and also thermally labile, have been described so far. Their preparation is particularly difficult, since decomposition and formation reactions are both exothermic. Only recently was a solution to this preparative problem found.[1] We developed a practical procedure involving reaction of the alkali-metal hyperoxides with O_2/O_3 mixtures under controlled-temperature conditions in the sense of a self-organization, followed by extraction of the reaction products with liquid ammonia.

The preparative potential of ionic ozonides is clearly of interest to both solid-state and molecular chemistry. It has not been possible to exploit this potential, however, since, among other things, the alkali-metal salts of ionic ozonides are soluble in only a few solvents. The availability of ozonides of other cations is therefore desirable. Our experience has shown that the formation of O_3^- (from hyperoxide ions and monooxygen) is only possible for alkali-metal compounds without complications in the ozonolysis and purification of the initial products. Accordingly, we prepared the alkali-metal ozonides, which are accessible on a preparative scale, and allowed these to react with salts of the desired cation in a suitable solvent.

Our first success was the preparation of tetramethylammonium ozonide $N(CH_3)_4O_3$ from KO_3 and $N(CH_3)_4O_2$ in liquid ammonia.[2] Surprisingly, the bright red $N(CH_3)_4O_3$ is thermally more stable than all alkali-metal ozonides and does not undergo slow decomposition at room temperature as observed for the alkali-metal salts. We were unable to confirm the contradictory results obtained earlier[3] on apparently very impure samples of $N(CH_3)_4O_3$. The decomposition point (75°C) is above that of CsO_3 (53°C), the most stable ozonide previously known. In contrast to the alkali-metal ozonides, however, $N(CH_3)_4O_3$ is photochemically labile; upon exposure to sunlight, it decomposes within a few hours to give a white, not yet identified crystalline substance.

The result of the X-ray structure analysis,[4] in which all hydrogen atoms were localized and refined, is shown in Figure 1. The relationship with the CsCl structure is readily apparent. Despite this basic agreement with the structure of the alkali-metal ozonides,[1b] there is an important difference which provides an explanation for the different chemical behavior. In the alkali-metal ozonides, the O_3^- groups are arranged in such a way that the intermolecular distances are quite short (e.g., 299.2 pm for RbO_3); the terminal O atoms of each molecule, which bear most of the negative charge, are directed toward the positively polarized bridging oxygen atoms of neighboring ozonide groups. This arrangement is not observed for $N(CH_3)_4O_3$. In this case, the O_3^- dipoles are arranged in an antiferroelectric sense with the shortest intermolecular O–O distances (438.8 pm) being those between terminal oxygen atoms. These long distances, which are clearly due to the

[*] Prof. Dr. M. Jansen, Dipl.-Chem. W. Hesse
Anorganisch-chemisches Institut der Universität
Gerhard-Domagk-Strasse 1, D-5300 Bonn 1 (FRG)

[**] This work was supported by the Fonds der Chemischen Industrie.

larger effective radius of the $N(CH_3)_4^+$ ion compared with the alkali-metal ions, presumably rule out any significant intermolecular interactions.

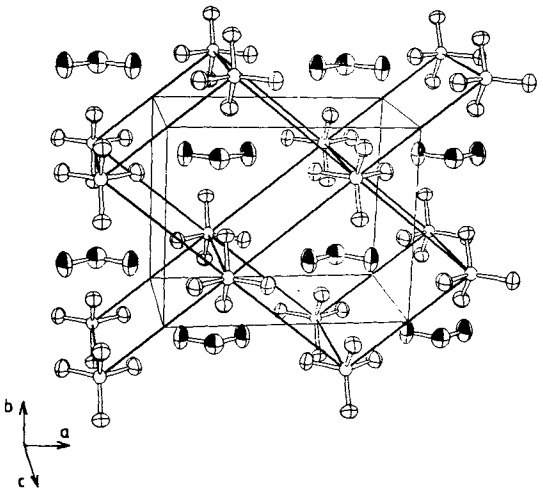

Fig. 1. Perspective drawing of the crystal structure of $N(CH_3)_4O_3$ (H atoms omitted).

The alkali-metal ozonides undergo exothermic decomposition according to the following equation:

$$AO_3 \longrightarrow AO_2 + 1/2\,O_2$$

Oxygen transport in the solid probably involves initial transfer of the oxygen atoms of the O_3^- ions to hyperoxide ions formed on the surfaces. It is easy to imagine how the larger intermolecular O–O distances in the case of $N(CH_3)_4O_3$ make this reaction more difficult and thus may explain its unexpected high thermal stability. This interpretation is supported by the fact that $N(CH_3)_4O_3$ decomposes by a mechanism different from that for the alkali-metal ozonides. MS and DTA/TG investigations indicate that the first step is an oxidative attack on the cation, resulting in exothermic formation of the white crystalline substance mentioned above, which, above ca. 100 °C, decomposes into gaseous products, identified by mass spectrometry as $N(CH_3)_3$, CO, O_2, H_2O, $(CH_3)_2O$, CH_3OH, and C_3H_7NO (possibly DMF).

The synthesis and structural elucidation of $N(CH_3)_4O_3$ demonstrate, for the first time, the stability of the O_3^- ion in the presence of cations other than alkali-metal ions. The surprisingly high stability, which is mainly determined by the intermolecular O–O distances, points the way toward the synthesis of even more stable ozonides.

Received: May 30, 1988 [Z 2787 IE]
German version: *Angew. Chem. 100* (1988) 1387

[1] a) W. Schnick, M. Jansen, *Angew. Chem. 97* (1985) 48; *Angew. Chem. Int. Ed. Engl. 24* (1985) 54; *Z. Anorg. Allg. Chem. 532* (1986) 37; M. Jansen, W. Hesse, *ibid. 560* (1988) 47; H. Lueken, M. Deussen, M. Jansen, W. Hesse, W. Schnick, *ibid. 553* (1987) 179; b) W. Schnick, M. Jansen, *Rev. Chim. Miner. 24* (1987) 446.

[2] KO_3 and $N(CH_3)_4O_2$ (1 mol each) were each placed, with exclusion of moisture, in one leg of an H tube containing a frit. Subsequently, 15 mL of liquid ammonia was condensed onto each substance. Mixture of the red KO_3 solution and the colorless $N(CH_3)_4O_2$ solution resulted in the formation of a cloudy solution owing to precipitation of KO_2. The red $N(CH_3)_4O_3$ solution thereby obtained was decanted through the frit of the H tube to separate it from the poorly soluble KO_2. Slow evaporation of the ammonia yielded red, transparent crystals of $N(CH_3)_4O_3$ in nearly quantitative yield.

[3] I. J. Solomon, A. J. Kacmarek, J. M. McDonough, K. Hattori, *J. Am. Chem. Soc. 82* (1960) 5640.

[4] $N(CH_3)_4O_3$: *Pmmn*, $a = 850.96(25)$, $b = 689.95(32)$, $c = 544.39(16)$ pm (-90 °C), $V = 319.63 \times 10^6$ pm^3, $Z = 2$; Enraf-Nonius CAD4 diffractometer, $Mo_{K\alpha}$ radiation, graphite monochromator, 1336 measured reflections with $1° < \theta < 26°$, 175 unique reflections with $F > 4\sigma(F)$, anisotropic refinement (H atoms isotropic). $R = 0.047$ for 38 free parameters. $R_w = 0.033$, $w = 2.79/(\sigma^2(F))$. Selected distances [pm] and angles [°] (standard deviations in parentheses): N1-C1 150.0(5), N1-C2 150.7(5), O1-O2 128.6(4), O2-O2′ 222.2(4), O2-O2′ intermolecular 438.8(3); C2-N1-C1 109.5(1), C1-N1-C1 110.3(5), C2-N1-C2 108.4(4), O2-O1-O2′ 119.5(5). Further details of the crystal structure investigation may be obtained from the Fachinformationszentrum Energie, Physik, Mathematik GmbH, D-7514 Eggenstein-Leopoldshafen 2 (FRG), on quoting the depository number CSD-53225, the names of the authors, and the journal citation.

3- and 3,6-Silylated 2-Pyridinethiols: New Hindered Bidentate Ligands and Their Novel Silver and Copper Clusters**

By *Eric Block,* Michael Gernon, Hyunkyu Kang,* and *Jon Zubieta**

Dedicated to Professor Hans Bock on the occasion of his 60th birthday

Thiolate ligands are of great current interest in tailor-making models for enzyme active sites, new conducting materials, and structurally unusual metal complexes.[1] We have demonstrated that the range of available thiolate ligands can be substantially increased through attachment of single or multiple silyl functions to methanethiol, ethane-1,2-dithiol, and thiophenol, affording new structures such as **1**–**5**.[2] To this list we now add 3- and 3,6-

$(Me_3Si)_3C\text{-}SH$ $Me_3SiCH(SH)CH(SH)SiMe_3$ $HSCH_2SiMe_2CH_2SH$

1 **2** **3**

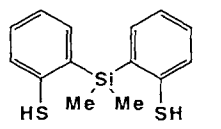

4

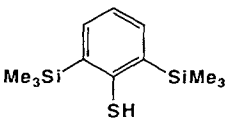

5

silylated 2-pyridinethiols **6** and **7**, respectively, which can be directedly prepared from the parent compound and which afford novel clusters with Cu^I and Ag^I. Although a characteristic feature of the chemistry of Cu^I and Ag^I with thiolate ligands is the occurrence of polymeric materials and large clusters,[1] the introduction of bulky substituents onto the thiolate unit modifies the tendency of thiolates to bridge the metal sites and allows the isolation of mononuclear or low oligomeric complexes.[3,4,5] The substituted 2-pyridinethiolate ligand presents both a bulky substituent to sterically impede the aggregation process and an addi-

[*] Prof. E. Block, Prof. J. Zubieta, M. Gernon, H. Kang
Department of Chemistry
State University of New York at Albany
Albany, New York 12222 (USA)

[**] This work was supported by the National Institutes of Health, the National Science Foundation, the Petroleum Research Fund, administered by the American Chemical Society, the Herman Frasch Foundation, and the Société Nationale Elf Aquitaine.

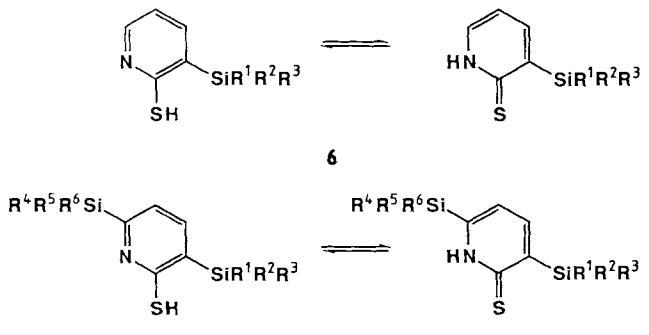

6

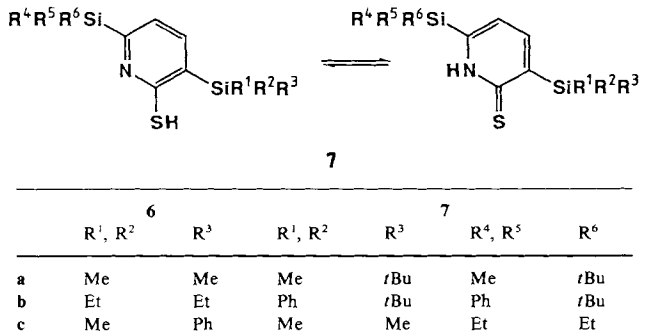

7

	6		7			
	R^1, R^2	R^3	R^1, R^2	R^3	R^4, R^5	R^6
a	Me	Me	Me	*t*Bu	Me	*t*Bu
b	Et	Et	Ph	*t*Bu	Ph	*t*Bu
c	Me	Ph	Me	Me	Et	Et

tional ligating functionality, the pyridine nitrogen, which should dramatically affect the coordination geometry. The choice of R_3Si as the bulky substituent offers the additional advantage of control of size through variation of R. The complexes **8** and **9**, whose preparation and structure

$[Cu_6(SC_5H_3NSiMe_3)_6]$ **8** $[Ag_6(SC_5H_3NSiMe_3)_6]$ **9**

we report, represent unique examples of MS_2N coordination and novel examples of hexanuclear thiolate clusters for these metals. Significantly, in the absence of the bulky silyl substituent, 2-pyridinethiol itself affords only polymeric materials in reactions with Cu^I and Ag^I under conditions affording clusters with **6a**.

By the one-pot reaction of 2-pyridinethiol with lithium diisopropylamide (LDA) and addition of chlorotrimethylsilane, followed by sublimation or recrystallization of the product from benzene, **6a** can be conveniently prepared on a large scale in 55% yield.[6] Similar sequences afford **6b** (45%) and **6c** (36%); surprisingly, use of the same conditions with the more hindered *tert*-butylchlorodimethylsilane and *tert*-butylchlorodiphenylsilane gives bis-silylated compounds **7a** (52%) and **7b** (37%).[6] Treatment of **6a** with LDA followed by chlorotriethylsilane gave bis-silylated compound **7c** (28%).[6] The ^{13}C NMR data for **6**–**7**[6] is consistent with a significant structural contribution from the thioamide form. Deuteration studies are more in keeping with *S*-silylation of 2-pyridinethiol followed by C-3 deprotonation[7a] and an Si–S to Si–C shift[7b] rather than direct formation of a dilithio species.[4]

Reactions of the ligand **6a** with Cu^I or Ag^I precursors yield isomorphous structures **8** and **9**.[8] The hexanuclear complexes, as illustrated in Figure 1 for **8**, possess $2/m$ symmetry with pseudo threefold axes passing through the centroids of the two M_3S_3 rings of both structures. The overall geometry of this type of cluster is best described as a molecular paddlewheel, a structure reminiscent of the cyclophanes.[9] The central cylinder of the paddlewheel consists of the two M_3S_3 heterocyclic rings, with the $-C_5H_3N(SiMe_3)$ fragments of the ligands providing the six paddles. The M_3S_3 units are distinctly crown-shaped rather than planar and are staggered with respect to each other.

The six substituted pyridinethiolate ligands bridge the two M_3S_3 rings, alternating such that three thiolate donors

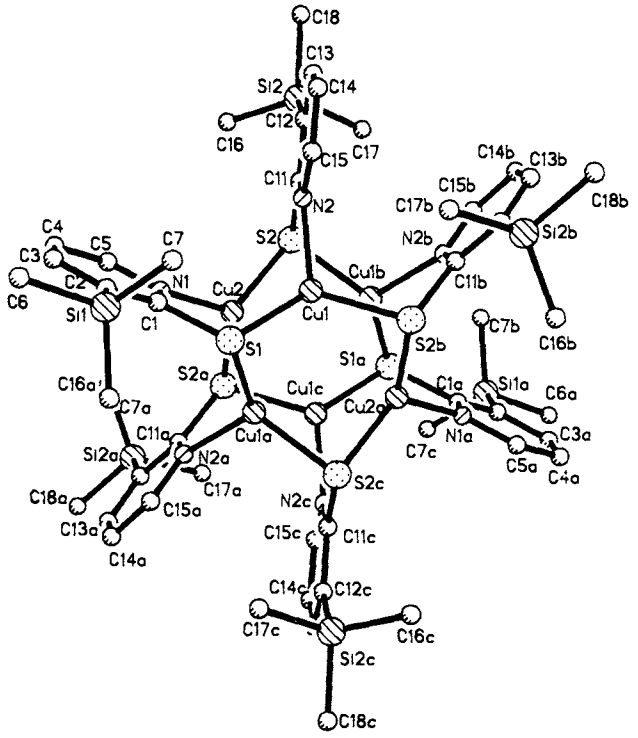

Fig. 1. ORTEP view of the structure of $[Cu_6(SC_5H_3NSiMe_3)_6]$ **8** viewed parallel to the pseudo-threefold axis passing through the centroids of the Cu_3S_3 rings. Relevant bond lengths [Å] and angles [°]: Cu1-S1 2.236(2), Cu1-S2b 2.254(2), Cu1-N2 2.041(5), Cu2-S2 2.245(2), Cu2-N1 2.019(9), Cu1-Cu2 3.139(1); S1-Cu1-N2 119.2(2), S1-Cu1-S2b 119.2(2), S2b-Cu1-N2 112.1(2), S2-Cu2-N1 119.2(1), S2-Cu2-S2a 113.3(1), Cu1-S1-Cu1a 82.6(1), Cu2-S2-Cu1b 88.5(1). Relevant bond lengths [Å] and angles [°] for the isostructural silver complex **9** (not shown): Ag1-S1 2.479(2), Ag1-S2b 2.479(2), Ag1-N2 2.312(9), Ag2-S2 2.474(2), Ag2-N1 2.300(6), Ag1-Ag2 3.323(1); S1-Ag1-N2 117.0(2), S2-Ag2-N1 118.6(2); S2-Ag2-S1b 124.8(2); Ag1-S1-Ag1a 83.9(1), Ag2-S2-Ag2a 77.4(1).

and three pyridine donors are presented to each ring. The thiolate sulfur atoms bridge adjacent metal sites within an M_3S_3 ring, while a pyridine nitrogen completes the pseudo trigonal-planar geometry about each metal site. The distortions from idealized trigonal-planar geometry are primarily a consequence of the inequivalence of the donor groups in the MS_2N coordination sites, with no significant metal-metal interactions (Cu1···Cu2, 3.139(1) Å; Ag1···Ag2, 3.323(1) Å).

While analogous structures for anionic Cu^I and Ag^I structures of the types $[M(SR)_2]^{\ominus}$,[3] $[M_5(SR)_6]^{\ominus}$,[10–12] and $[M_5(SR)_7]^{2\ominus}$[13] have been described, neutral homoleptic complexes of Cu^I and Ag^I do not present analogous structural types,[4,5] a feature which appears to be a consequence of the pronounced tendency of Ag^I centers to participate in secondary interactions with thiolate donors, resulting in higher oligomers.[5] The substituted pyridinethiolate ligand has been designed specifically to preclude secondary interactions at the metal sites and to favor small molecular cages. The bulky $-SiMe_3$ substituent prevents close approach of additional [M(SR)] units required in the formation of large oligomers or polymeric materials, while the presence of the additional ligand functionality, the pyridine nitrogen, serves to satisfy the coordination requirements of the metal atoms, obviating the need for secondary interactions.

The structural consequences of the sterically constraining Me_3Si substituent are dramatically illustrated by a

comparison of compounds **8** and **9** with the materials isolated from reactions of Cu^I and Ag^I with the parent 2-pyridinethiolate. Although 2-pyridinethiol has been demonstrated to form a variety of molecular complexes with transition-metal cations,[14, 15] under conditions similar to those employed for the syntheses of **8** and **9**, polymeric materials are formed exclusively with Cu^I and Ag^I. The isolation of the molecular clusters **8** and **9** is thus attributed to the introduction of the steric constraints associated with the Me_3Si substituent.

Experimental Procedure

6a: A solution of 2-pyridinethiol (2.2 g, 20 mmol) in dry THF (30 mL) was added slowly under argon to a stirred THF (100 mL) solution of LDA at 0°C prepared from iPr_2NH (6.1 g, 60 mmol) and nBuLi (25 mL of 2.5 M solution; 62 mmol). The solution was stirred at 0°C for 2 h, quenched with Me_3SiCl (8.7 g, 80 mmol), and stirred for a further 6 h at room temperature. The reaction was quenched with water (5 mL) and then concentrated in vacuo. The organic residue was taken up in CH_2Cl_2 (200 mL), the organic phase was washed two times with water (100 mL), the solvent was removed under vacuum, and the yellow solid was washed with hexane and then recrystallized from benzene. Yield 2.0 g (55%); m.p. 194–195°C (after sublimation at 110°C/0.5 torr).

9: Addition of a solution of $AgNO_3$ (0.170 g, 1 mmol) in acetonitrile (10 mL) to a solution of **6a** (0.183 g, 1 mmol) in acetonitrile (10 mL), followed by triethylamine (0.101 g, 1 mmol), led to immediate formation of a white precipitate. After stirring for 15 h, the resultant solution was concentrated giving a white solid. The solid was dissolved in CH_2Cl_2 (7 mL) and filtered to remove impurities, and the filtrate was slowly diluted with acetonitrile (7 mL). After several days, pale yellow crystals were collected and recrystallized from CH_2Cl_2/CH_3OH. Yield 0.152 g (52%); dec. >200°C.

8: A procedure similar to that described above using $[Cu(CH_3CN)_4]PF_6$ in CH_3OH, followed by recrystallization from CH_2Cl_2/CH_3OH (3:1, v/v), afforded **8** as orange, block-shaped crystals. Yield 75%; dec. >190°C.

Received: May 4, 1988 [Z 2741 IE]
German version: *Angew. Chem. 100* (1988) 1389

[1] a) I. G. Dance, *Polyhedron 5* (1986) 1037; b) P. G. Blower, J. R. Dilworth, *Coord. Chem. Rev. 76* (1987) 121.

[2] E. Block, M. Aslam, *Tetrahedron 44* (1988) 281, and references cited therein.

[3] S. A. Koch, R. Fikar, M. Miller, T. O'Sullivan, *Inorg. Chem. 24* (1984) 122.

[4] B. K. Koo, E. Block, S. Liu, J. Zubieta, *Polyhedron 7* (1988) 1397; E. Block, V. Eswarakrishnan, M. Gernon, G. Ofori-Okai, C. Saha, K. Tang, J. Zubieta, *J. Am. Chem. Soc.*, in press; E. Block, M. Gernon, H. Kang, S. Liu, J. Zubieta, *J. Chem. Soc. Chem. Commun. 1988*, 1031.

[5] K. Tang, M. Aslam, E. Block, T. Nicholson, J. Zubieta, *Inorg. Chem. 27* (1987) 1488.

[6] **6a**: 55%; GC-MS: m/z 183 ($M^{\oplus}$, 14%), 168 ($M^{\oplus}-15$, 100%); ^1H NMR ($CDCl_3$): $\delta=17.59$ (d, 1H, $J=7.2$ Hz), 7.56 (d, 1H, $J=6.4$ Hz), 6.76 (t, 1H, $J=6.6$ Hz), 0.42 (s, 9H); ^{13}C NMR ($CDCl_3$): $\delta=181.00$ (C), 144.55 (CH), 144.10 (C), 137.13 (CH), 113.57 (CH), −1.31 (CH_3); IR (KBr): $\tilde{\nu}=2850$ (br), 1600, 1570, 1320, 1240, 1140, 1040, 850, 750 cm^{-1}. **6b**: 45%; m.p. 135–136°C (sublimed 130°C/0.1 torr); GC-MS: m/z 225 ($M^{\oplus}$, 3%), 196 (10%), 168 (33%), 140 (37%); ^1H NMR ($CDCl_3$): $\delta=7.56$–7.52 (m, 2H), 6.74 (t, 1H, $J\cong6.6$ Hz), 1.07–0.92 (m, 15H); ^{13}C NMR ($CDCl_3$): $\delta=81.35$ (C), 145.80 (CH), 141.71 (C), 137.02 (CH), 113.31 (CH), 7.54, 2.67; IR (KBr): $\tilde{\nu}=2900$ (br), 1570, 1300, 1150, 1010, 730 cm^{-1}. **6c**: 36%; m.p. 161–162°C (sublimed at 150°C/0.1 torr); GC-MS: m/z 245 ($M^{\oplus}$, 21%), 230 (70%), 196 (39%), 168 ($M^{\oplus}-77$, 100%), 167 ($M^{\oplus}-78$, 96%), 152 (39%); ^1H NMR ($CDCl_3$): $\delta=7.61$–7.58 (m, 2H), 7.46 (dd, 1H, $J\cong6.5$, 2.1 Hz), 7.38–7.35 (m, 3H), 7.32 (dd, 1H, $J=7.6$, 2.1 Hz), 6.61 (t, 1H, $J=6.6$ Hz), 0.74 (s, 6H); ^{13}C NMR ($CDCl_3$): $\delta=181.09$ (C), 146.00 (CH), 142.54 (C), 137.57 (C), 137.46 (CH), 134.42 (CH), 129.11 (CH), 127.84 (CH), 113.40 (CH), −2.79 (CH_3); IR (KBr): $\tilde{\nu}=2850$, 1605, 1580, 1430, 1305, 1150 cm^{-1}. **7a**: 52%; m.p. 174–175°C (sublimed at 165°C/0.1 mm); GC-MS: m/z 339 ($M^{\oplus}$, 4%), 282 (100%), 224 (57%), 210 (21%), 73 (38%), 57 (42%); ^1H NMR ($CDCl_3$): $\delta=10.4$ (br s, 1H), 7.46 (d, 1H, $J=6.8$ Hz), 6.72 (d, 1H, $J=6.8$ Hz), 1.00 (s, 9H), 0.95 (s, 9H), 0.41 (s, 6H), 0.33 (s, 6H); ^{13}C NMR ($CDCl_3$): $\delta=184.58$ (C), 152.52 (C), 143.94 (CH), 142.69 (C), 119.84 (CH), 27.90 (CH_3), 26.24 (CH_3), 18.32 (C), 16.87 (C), −3.80 (CH_3), −7.16 (CH_3); IR (KBr): $\tilde{\nu}=2950$, 1570, 1550, 1470, 1290 cm^{-1}. **7b**: 37%; m.p. 193–194°C; CI-MS: m/z 587 ($M^{\oplus}$); ^1H NMR ($CDCl_3$): $\delta=10.4$ (br s, 1H), 7.60–7.30 (m, 21H), 6.85 (d, 1H, $J=6.7$ Hz), 1.33 (s, 9H), 1.22 (s, 9H); ^{13}C NMR ($CDCl_3$): $\delta=185.34$ (C), 150.45 (C), 146.83 (CH), 141.33 (C), 137.17 (CH), 136.11 (CH), 134.96 (C), 130.81 (CH), 129.71 (C), 128.94 (CH), 128.70 (CH), 127.56 (CH), 121.25 (CH), 30.65 (CH_3), 28.34 (CH_3), 19.08 (C), 18.84 (C); IR (KBr): $\tilde{\nu}=3325$, 2950, 1540, 1430, 1295, 1150, 1140, 1110, 740, 700 cm^{-1}. **7c**: 28%; m.p. 126–127°C (sublimed at 120°C/0.1 mm); GC-MS: m/z 297 ($M^{\oplus}$, 34%), 282 ($M^{\oplus}-15$, 100%), 252 (42%), 224 (27%), 196 (38%), 73 (26%), 59 (33%); ^1H NMR ($CDCl_3$): $\delta=10.7$ (br. s, 1H), 7.44 (d, 1H, $J=6.5$ Hz), 6.75 (dd, 1H, $J=6.5$, 2.5 Hz), 1.00 (t, 9H, $J=7.4$ Hz), 0.86 (q, 6H, $J=7.4$ Hz), 0.40 (s, 9H); ^{13}C NMR ($CDCl_3$): $\delta=183.98$ (C), 152.40 (C), 144.10 (C), 142.35 (CH), 120.32 (CH), 7.04 (CH_3), 2.32 (CH_2), −1.39 (CH_3); IR (KBr): $\tilde{\nu}=3120$, 3000, 2850, 2800, 1580, 1560, 1300, 1250, 1160, 875, 860, 740 cm^{-1}. **8**: ^1H NMR (CD_2Cl_2): $\delta=7.63$ (d, 1H), 7.25 (d, 1H), 6.47 (t, 1H), 0.43 (s, 9H). **9**: ^1H NMR (CD_2Cl_2): $\delta=7.55$ (d, 1H), 7.20 (d, 1H), 6.45 (t, 1H), 0.46 (s, 9H). Satisfactory elemental analyses were obtained for all new compounds.

[7] a) D. L. Comins, D. H. LaMunyon, *Tetrahedron Lett. 29* (1988) 773; b) A. Wright, R. West, *J. Am. Chem. Soc. 96* (1974) 3222.

[8] **8**·CH_2Cl_2: monoclinic, space group $A2/m$, $a=10.968(2)$, $b=20.123(4)$, $c=16.779(3)$ Å, $\beta=96.45(1)°$, $V=3679.9(12)$ Å^3, $Z=2$, $\rho_{calcd}=1.33$ g cm^{-3}; structure solution and refinement based upon 1787 reflections with $F_0\geq6\sigma(F_0)$ ($Mo_{K\alpha}$, $\lambda=0.71073$ Å), $R=0.0530$, $R_w=0.0583$ (192 variables). Cu2 and Cu2a and the associated ligand groups occupy the crystallographic mirror plane; the twofold axis normal to this plane and passing between the Cu_3S_3 rings generates other symmetry related positions. **9**·CH_2Cl_2: isomorphous with **8**, space group $C2/m$, $a=17.201(3)$, $b=20.611(3)$, $c=10.977(2)$ Å, $\beta=95.46(1)°$, $V=3873.8(13)$ Å^3, $Z=2$, $\rho_{calcd}=1.49$ g cm^{-3}; structure solution and refinement based upon 2260 reflections with $F_0\geq6\sigma(F_0)$ ($Mo_{K\alpha}$, $\lambda=0.71073$ Å), $R=0.0561$, $R_w=0.0654$ (189 variables). Both structures present a CH_2Cl_2 molecule of crystallization disordered about a mirror plane. Structural data were collected on a Nicolet R3m/V diffractometer at 23°C, using a graphite monochromator. All non-hydrogen atoms were refined anisotropically for both **8** and **9**.

[9] P. M. Keehn in P. M. Keehn, S. M. Rosenfeld (Eds.): *Cyclophanes, Vol. I*, Academic Press, New York 1983, pp. 69–239.

[10] G. A. Bowmaker, L.-C. Tan, *Aust. J. Chem. 32* (1979) 1443.

[11] I. G. Dance, *J. Chem. Soc. Chem. Commun. 1976*, 68.

[12] G. A. Bowmaker, G. R. Clark, J. K. Seadon, I. G. Dance, *Polyhedron 3* (1984) 535.

[13] I. G. Dance, *Aust. J. Chem. 31* (1978) 2195.

[14] S. G. Rosenfield, H. P. Buends, L. Gilmini, D. W. Stephen, P. K. Mascharak, *Inorg. Chem. 26* (1987) 2792.

[15] A. J. Deeming, K. I. Hardcastle, M. N. Meah, P. A. Bates, H. M. Dawes, M. B. Hursthouse, *J. Chem. Soc. Dalton Trans. 1988*, 227; A. J. Deeming, M. N. Meah, P. A. Bates, M. B. Hursthouse, *ibid. 1988*, 235, and references cited therein.

Reactions of Pentacarbonyl(trichloromethyl isocyanide)chromium**

By *Gerhard Beck* and *Wolf P. Fehlhammer**

Dedicated to Professor Hans Bock on the occasion of his 60th birthday

We have recently shown that the radical alkylation of cyano complexes opens up a surprisingly simple and efficient route to the synthesis of complex-stabilized α-haloalkyl isocyanides [Eq. (a), $CHCl_2R$ as solvent; R = H,

$$[Cr(CN)(CO)_5]^{\ominus} + ArylN_2^{\oplus} + CHCl_2R \longrightarrow [(OC)_5CrCNCCl_2R] + ArylH + N_2 \quad (a)$$

Cl].[1] The chemistry of pentacarbonyl(trichloromethyl isocyanide)chromium **1** (Scheme 1) has now revealed a surprising and unusual isocyanide reactivity together with a high mobility of the α-chloro atoms. Although it is possible, in some cases, to limit the reaction to the trichlorome-

[*] Prof. Dr. W. P. Fehlhammer, Dr. G. Beck
Institut für Anorganische und Analytische Chemie
der Freien Universität
Fabeckstrasse 34–36, D-1000 Berlin 33

[**] Metal Complexes of Functional Isocyanides, Part 17. This work was supported by the Deutsche Forschungsgemeinschaft and the Fonds der Chemischen Industrie.—Part 16: W. P. Fehlhammer, A. Völkl, U. Plaia, G. Beck, *Chem. Ber. 120* (1987) 2031.

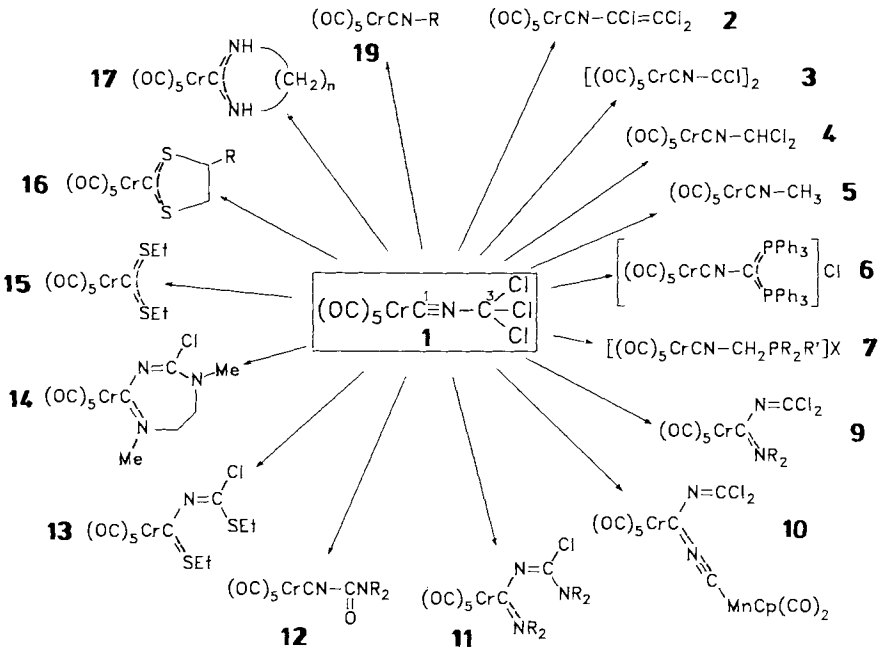

Scheme 1. Products and reaction conditions **2**, **3**: Zn-Hg.—**4**, **5**: cf. text.—**6**: PPh_3 in excess, MeCN.—**7** (R, R′ = Ph, Et; R = Me, R′ = Ph; X = Cl, PF_6): PR_2R', MeCN, H_2O.—**9** (R = Et, 2R = $(CH_2)_4$, $(CH_2)_5$): HNR_2.—**10**: $Na[Mn(CN)(Cp)(CO)_2]$.—**11** (2R = $(CH_2)_4$, $(CH_2)_5$): HNR_2 in excess.—**12** (R as for **9**): 1. HNR_2 in excess, 2. dioxane-H_2O.—**13**, **15**: HSEt in excess, NEt_3.—**14**: $MeHN(CH_2)_2NHMe$.—**16** (R = H, Me): $HSCH_2CHRSH$, NEt_3.—**17** (n = 2, 3): $H_2N(CH_2)_nNH_2$ in excess.—**19** (R = e.g., adamantyl, $CH_2CH{=}CH_2$, CH(Me)Et, $CH_2CH_2NCCr(CO)_5$): RNH_2 in excess.

thyl group of **1** and thereby obtain new functional isocyanides (cf. point 1), most reactions occur at the two electrophilic centers (C^1, C^3) jointly; i.e., the trichloromethyl isocyanide ligand reacts like a masked azaalleniumylidene or even like a dichlorocarbene equivalent, affording a broad variety of carbene, heterocycle, and isocyanide complexes (Scheme 1).

1. Reductions of **1** proceed relatively unspecifically but the isocyano function remains intact. Reaction with zinc in aprotic medium leads to a product mixture from which the alkenyl isocyanide complexes **2** and **3** were isolated along with other products.[2,3] Similar CC coupling products are formed upon reaction of **1** with iron carbonyl. On the other hand, the main product of the reaction with cobalt carbonyl is the isocyanomethylidyne-bridged tetranuclear cluster $[(OC)_5CrCN{-}C[Co(CO)_3]_3]$ ("permetalated methyl isocyanide").[4] The replacement of Cl by H dominates in protic solvents; with PPh_3 in ethanol, this process can be stopped at the stage of the dichloromethyl isocyanide **4**; with zinc in glacial acetic acid, complete reduction to the methyl isocyanide complex **5** occurs.

Even slight changes in the reaction conditions lead to the formation of organophosphorus ligands (**6**, **7**) with interesting possible uses in synthesis: for example, **7**, which is also accessible via a different route,[5] opens up a simple approach to the synthesis of alkenyl isocyanides and diverse triphenylphosphonio-substituted five-membered heterocycles.[5,6]

2. In contrast to reducing agents or organometallic bases and phosphanes (cf. point 1), N and S nucleophiles attack the isocyanide carbon atom and simultaneously cause the departure of a chloride ion from the trichloromethyl group. Examples of such products, which are best explained as arising from one of the two isomeric forms **8** (azaallenium chloride **a** or chlorocarbene **b**) of the trichloromethyl isocyanide starting complex **1**, are the molecules **9** and **10**. The analogy between **1** and complexes of the allenylidene type $[L_nM{=}C^1{=}C^2{=}C^3R_2']$ becomes even more obvious from the identical preferences of the corresponding electrophilic centers C^1 (for O and N nucleophiles) and C^3 (for P nucleophiles).[7]

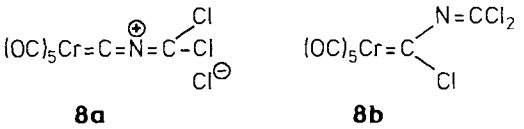

8a **8b**

An X-ray structure analysis (Fig. 1)[8] has been carried out for the deep dark-green heterobinuclear complex **10** prepared from **1** and $[Mn(CN)(Cp)(CO)_2]^{\ominus}$. It reveals the presence of a novel isocyanocarbene bridging ligand which

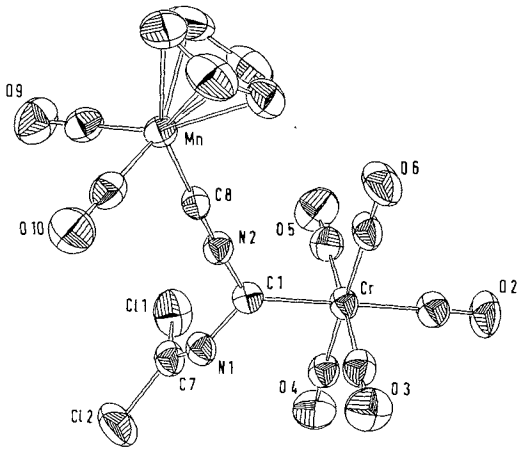

Fig. 1. Molecular structure of **10**, space group $P\bar{1}$, $a = 8.949(1)$, $b = 11.122(2)$, $c = 11.763(2)$ Å, $\alpha = 109.68(1)$, $\beta = 102.33(1)$, $\gamma = 110.22(1)°$, $V = 959.6$ Å^3, $Z = 2$, 3246 measured reflections, 2902 observed ($I > 2\sigma(I)$), 273 refined parameters, $R = 0.031$, residual electron density < 0.40 e Å^{-3}. Important bond lengths [Å] and bond angles [°]: Cr-C1 2.012(4), C1-N1 1.397(3), N1-C7 1.232(4), C1-N2 1.332(4), N2-C8 1.196(4), Mn-C8 1.796(3); C1-N1-C7 127.9(3), C1-N2-C8 172.9(4) [8].

contains both a linear and a bent CNC unit sharing the carbene carbon atom. Both forms are under current discussion in connection with the bonding in 2-azaallenium compounds[9] and imino-substituted carbene complexes.[10] Interestingly, the isocyano function, which is known for its ability to stabilize carbanions, is also most effective in carbene (carbenium) stabilization in **10**, thus confirming predictions on this matter made on the basis of MO theory.[11] On the other hand, the contribution of the dichloroisocyanide substituent to the stabilization remains small, despite its nearly perpendicular orientation with respect to the carbene plane—the N2-C1-N1-C7 torsion angle is 82.0°—which would be ideal for an $n_\pi(N1)$-$p_\pi(C1)$ bond.

3. When amine or thiol is used in excess, a second molecule of the nucleophile is incorporated into the azomethyne part of the polyfunctional ligand. In this way, the complexes **11**, **13**, and **14** are obtained. Under hydrolytic conditions, however, carbamoyl isocyanide complexes **12** can also be formed. The X-ray structure analysis of **14** (Fig. 2)[8] shows that its seven-membered ring is folded along C7–C9, a conformation also observed for metal-free triazepane derivatives.[12] In contrast to **10**, however, the again very different $C_{carbene}$–N distances are due to the constrained coplanar arrangement of the N2-C1-N1-C7 unit in the ring, which rules out an interaction of the lone pair on N1 with the $C_{carbene}$ p_z orbital.

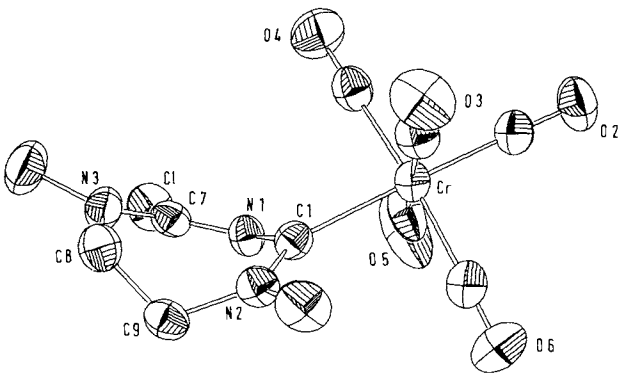

Fig. 2. Molecular structure of **14**. Yellow rhombs from chloroform (−25°C); crystal dimensions, 0.35 × 0.20 × 0.30 mm³; triclinic, space group $P\bar{1}$, $a = 8.079(4)$, $b = 9.845(5)$, $c = 10.495(4)$ Å, $\alpha = 92.32(3)$, $\beta = 110.21(3)$, $\gamma = 105.24(4)°$, $V = 749.9$ Å³, $Z = 2$, 2839 measured reflections, 2429 observed ($I > 2\sigma(I)$), 230 refined parameters, $R = 0.032$, residual electron density < 0.39 e Å^{-3}, H positions isotropically refined. Selected bond distances [Å] and bond angles [°]: Cr-C1 2.114(3), C1-N1 1.389(3), C1-N2 1.329(4), N1-C7 1.275(3), N2-C9 1.467(4); Cr-C1-N1 113.1(2), Cr-C1-N2 131.0(1).

4. Reactions with $EtSH/NEt_3$, dithiols, or primary diamines result in a further degradation of the complex-bound trichloromethyl isocyanide: in the molecules **15**–**17**, only the isocyanide carbon atom is left, i.e., $CNCCl_3$ reacts like dichlorocarbene, which as such is not available in a pentacarbonylchromium complex. In the reaction giving the dithiocarbene complex **16**, 1,3-dithiolane imine **18**

18

was isolated. Thus, at least in this case, information regarding the fate of the leaving group "$NCCl_3$" was obtained. The following reaction sequence, alternating between the electrophilic centers C^1 and C^3, thus emerges:

- "Carbene addition" of the nucleophile NuH followed by HCl elimination
- Cl/Nu substitution(s) on the dichloromethylene group
- Nucleophilic addition at C^1 once again and elimination of a carbonic acid derivative $HN{=}C(Nu)_2$

As in the synthesis of **10**, however, redox steps may be involved before or during certain stages of this reaction sequence.

5. Complex **1** also acts as a dichlorocarbene equivalent toward primary amines, effecting the spontaneous formation in high yields of a wide variety of isocyanide complexes **19**, including those containing sterically demanding, functional, chiral, or divalent isocyanide ligands (see caption to Scheme 1). We reported earlier[13] on similar interconversions of nonfunctional isocyanides, whereby an auxiliary agent ($COCl_2$) was required. It is remarkable that these complex-based isocyanide syntheses ($[L_nMC{\equiv}N{-}R] \rightarrow [L_nMC{\equiv}N{-}R']$ do not imply substitutions at the isocyanide nitrogen atom; instead, the CN triple bond is successively broken with ensuing bond formation to the newly entering amino nitrogen atom.

Experimental Procedure

7 (R = R' = Ph): First water (0.07 mL) and then triphenylphosphane (2.40 g, 9.16 mmol) were added to a vigorously stirred solution of **1** (1.00 g, 2.97 mmol) in a mixture of diethyl ether (40 mL) and acetonitrile (15 mL). Within a few minutes, small bright yellow crystals began to separate from the yellow-red solution thus formed. The crystals were collected by filtration after 1–2 h and dried under vacuum. Yield after recrystallization from dichloromethane/diethyl ether: 710 mg (45%) **7** (dec. at 170°C).

9 (2 R = $(CH_2)_4$): **1** (800 mg, 2.39 mmol) was dissolved in 30 mL of diethyl ether and the resulting solution was treated with pyrrolidine (339 mg, 4.76 mmol), resulting in the immediate formation of a white precipitate. After 24 h, the precipitate was collected and washed with a small amount of ether and all volatiles were removed under vacuum. The residue was dissolved in petroleum ether and purified by column chromatography ($l = 20$ cm, $d = 2$ cm; Merck, 0.063–0.200 mm). Elution with petroleum ether/diethyl ether (40 : 1 v/v) gave **9** as a pale yellow band; the eluate was concentrated until the onset of crystallization. At −25°C, 647 mg (73%) of bright yellow needles (m.p. 77–78°C) was obtained.

10: A solution of **1** (760 mg, 2.26 mmol) in a mixture of 20 mL of dichloromethane and 10 mL of acetonitrile was treated with $Na[Mn(CN)(Cp)(CO)_2]$ (500 mg, 2.22 mmol); the color of the reaction solution turned from yellow to red-violet. The solvent was removed, the residue was extracted with a small amount of diethyl ether, and the ether phase was chromatographed on silica gel (15 × 22-cm column). The blue fraction thereby obtained was subjected to thin layer chromatography (silica gel/petroleum ether) to remove small amounts of $[(OC)_5CrCN]_2CCl_2$ and **3**. Concentration and cooling of the petroleum ether solution to −78°C yielded **10** as green leaflets and black needles (m.p. 98–100°C).

19: In a typical experiment, **1** (650 mg, 1.93 mmol) was dissolved in 20 mL of ether and treated with an excess of primary amine; the solution was then stirred for 18 h at room temperature. The solvent was removed, the residue was extracted three times with 20 mL of petroleum ether, and the concentrated petroleum ether phases were chromatographed on silica gel (15 × 2-cm column, petroleum ether). The colorless product fraction was detected by IR spectroscopy and, after removal of the eluent, the product was sublimed (cold finger: −5°C) or purified by recrystallization from petroleum ether. Yield 50–90%.

Received: February 23, 1988 [Z 2631 IE]
Publication delayed at the authors' request
German version: *Angew. Chem. 100* (1988) 1391

[1] W. P. Fehlhammer, F. Degel, G. Beck, *Chem. Ber. 120* (1987) 461.
[2] Presumably, **2** is formed from the initially formed CC coupling product $[(OC)_5CrCNCHCl{-}CCl_2NCCr(CO)_5]$ by elimination of $[Cr(CO)_5CNH]$.
[3] All new compounds were characterized by their spectra (^1H, ^{13}C, ^{31}P NMR, IR, MS) and elemental analyses. For example: **3**, bright yellow leaflets (12%), m.p. 174°C (dec.). IR (Nujol): $\tilde{\nu} = 2119$, 2059, 1999, 1953 (CN, CO), 837 cm^{-1} (CCl); Raman (solid): $\tilde{\nu} = 1592$ cm^{-1} (C=C); MS (80 eV): m/z 530 ($M^{\oplus}$, 54%), 474 ($[M^{\oplus} - 2CO]$, 3) and all CO-loss fragments to 250 ($[Cr_2C_4N_2Cl_2]^{\oplus}$, 50).—**6**: colorless crystals (50%), m.p. 195°C; $^{13}C\{^1H\}$ NMR (CD_2Cl_2): $\delta = 216.7$ (*trans*-CO), 213.8 (*cis*-CO),

162.7 (CN), 134.4 (s; phenyl-C4), 133.3, 129.8, 120.4 (each AXX', J(CP+CP')=11, 13 and 93 Hz; phenyl-C_2, -C_3, -C_1), 31.6 (t, J(CP)=130 Hz; CP_2); $^{31}P\{^1H\}$ NMR (CD_2Cl_2, 85% H_3PO_4 ext.): δ=24.8; IR (KBr): $\tilde{\nu}$=2112, 2047, 1939 cm^{-1} (CN, CO).—**11** (2R = $(CH_2)_4$): colorless needles (71%), m.p. 95°C; ^1H NMR ($CDCl_3$): δ=3.98, 3.49 (2m, 2H and 6H; NCH_2), 1.97 (complex signal, 8H; $CH_2(CH_2)_2CH_2$); $^{13}C\{^1H\}$ NMR ($CDCl_3$): δ=240.4 (C(carbene)), 223.0 (*trans*-CO), 218.0 (*cis*-CO), 126.1 (N=CCl), 55.0, 50.6, 49.3 (NCH_2), 25.2, 24.6, 23.2 ($CH_2(CH_2)_2CH_2$); IR (KBr): $\tilde{\nu}$=2053, 1956, 1916, 1889 (CO), 1678 cm^{-1} (C=N); MS (80 eV): m/z 405 ($M^{\oplus}$, 9%), 265 ([$M^{\oplus}$ − 5 CO], 100).—**16** (R = H): red platelets (50%), m.p. 100°C; ^1H NMR ($CDCl_3$): δ=3.66 (s; CH_2); $^{13}C\{^1H\}$ NMR ($CDCl_3$): δ=315.5 (C(carbene)), 224.8 (*trans*-CO), 215.5 (*cis*-CO), 46.4 (CH_2); IR (*n*-hexane): $\tilde{\nu}$=2062, 1990, 1957 cm^{-1} (CO); MS (80 eV): m/z 296 ($M^{\oplus}$, 30%), 156 ([$M^{\oplus}$ − 5 CO], 100).

[4] W. P. Fehlhammer, F. Degel, H. Stolzenberg, *Angew. Chem. 93* (1981) 184; *Angew. Chem. Int. Ed. Engl. 20* (1981) 214.

[5] G. Zinner, W. P. Fehlhammer, *Angew. Chem. 97* (1985) 990; *Angew. Chem. Int. Ed. Engl. 24* (1985) 979.

[6] a) G. Zinner, *Dissertation*, Freie Universität Berlin 1988; b) W. P. Fehlhammer, G. Zinner, M. Bakola-Christianopoulou, *J. Organomet. Chem. 331* (1987) 193.

[7] M. I. Bruce, A. G. Swincer, *Adv. Organomet. Chem. 22* (1983) 59.

[8] STOE four-circle diffractometer, $Mo_{K\alpha}$ radiation, $4° \leq 2\theta \leq 50°$; ω-scan, structure solution by direct methods. Programs used: X-Ray, Multan-77, ORTEP. Further details of the crystal structure investigation may be obtained from the Fachinformationszentrum Energie, Physik, Mathematik GmbH, D-7514 Eggenstein-Leopoldshafen 2 (FRG), on quoting the depository number CSD-53291, the names of the authors, and the journal citation.

[9] a) M. Al-Talib, I. Jibril, E.-U. Würthwein, J. C. Jochims, G. Huttner, *Chem. Ber. 117* (1984) 3365; b) R. Kupfer, E.-U. Würthwein, M. Nagel, R. Allmann, *ibid. 118* (1985) 643.

[10] H. Fischer, F. Seitz, J. Riede, *Chem. Ber. 119* (1986) 2080.

[11] J. B. Moffat, *Tetrahedron Lett. 22* (1981) 1001; *J. Am. Chem. Soc. 104* (1982) 3949; *Int. J. Quantum Chem. 19* (1981) 771.

[12] M. Dobler, W. Retter, *Cryst. Struct. Commun. 7* (1978) 321.

[13] W. P. Fehlhammer, A. Mayr, G. Christian, *J. Organomet. Chem. 209* (1981) 57.

Tentacled Iron Sandwiches**

By *Françoise Moulines** and *Didier Astruc**

Dedicated to Professor Hans Bock on the occasion of his 60th birthday

The synthesis of hexasubstituted benzene derivatives has attracted attention for more than 50 years.[1-4a] Friedel-Crafts reactions were first employed, followed by the reaction of hexakis(bromomethyl)benzene or hexakis(thiomethyl)benzene[1] and the transition-metal-catalyzed trimerization of alkynes.[2] Now, we report a method providing the first hexafunctionalization of a transition-metal-arene complex in one step, and we illustrate the possibilities of chain design in a series of "tentacled" sandwich molecules containing a reversible redox center.

Hexaalkylation of $[Fe^{II}Cp(C_6Me_6)]PF_6$ **1** is known to proceed with *t*BuOK and CH_3I, giving $[Fe^{II}Cp(C_6Et_6)]PF_6$,[4a,b] but extension to higher RX fails when the alkyl chain bears β-hydrogens because dehydrohalogenation is faster than alkylation.[4c] We find that the reaction of the readily available complex **1** with *t*BuOK and allyl bromide in THF yields the hexabutenylbenzene complex **2** quantitatively (Scheme 1, 4-mmol scale).[5] Recrystallization from acetone/pentane (1/3) after chromatography on silica with CH_2Cl_2 gives yellow crystals of **2** in 75% yield. Spectroscopic and electrochemical data for **2** are given in Table 1. The Fe^{II} center[6] of **2** can be reduced with complete chemical and electrochemical reversibility

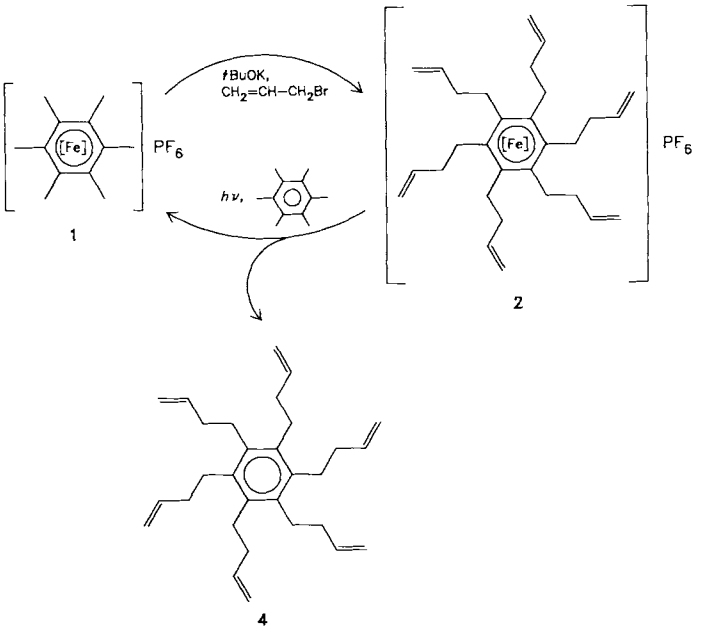

Scheme 1. [Fe] = $(\eta^5\text{-}C_5H_5)Fe^{\oplus}$.

Table 1. Spectroscopic and electrochemical data [a] of the new compounds. Correct elemental analyses were obtained for **2**–**7**.

2: ^1H NMR (CD_3CN): δ=5.8-6.1 (6H; CH=CH_2), 5.1-5.28 (12H; CH=CH_2) [b], 4.65 (5H; C_5H_5), 2.9-3 (12H; ArylCH_2), 2.35-2.45 (12H; ArylCH_2–CH_2–) [c].—^{13}C NMR (22.63 MHz, CD_3COCD_3): δ=137.7 (CH=CH_2), 116.03 (CH=CH_2), 103.9 (C_6R_6), 79.2 (C_5H_5), 35.7, 30.5 (ArylCH_2–CH_2). E^0 = −1.42 V [d]

3, mixture of stereoisomers: ^1H NMR (CD_3CN): δ=4.88, 4.87, 4.85, 4.80 (5H; C_5H_5), 4.54 (br., 6H; CHBr), 4.05, 3.9 (br., 12H; CH_2Br), 3.15-2.94 (br., 12H; ArylCH_2), 2.44, 2.25 (br., 12H; ArylCH_2–CH_2).—^{13}C NMR (22.63 MHz, $CDCl_3$): δ=103.1-103.6 (C_6R_6), 79.74, 79.58 (C_5H_5), 62.34, 52.72 (CHBr), 38.75, 37.94 (ArylCH_2–CH_2), 29.80 (CH_2Br)

4: ^1H NMR ($CDCl_3$): δ=5.89-5.98 (6H; CH=CH_2), 5.01-5.17 (12H; CH=CH_2) [c], 2.63-2.71 (12H; ArylCH_2), 2.24-2.29 (12H; ArylCH_2–CH_2) [c].—^{13}C NMR (50.3 MHz, $CDCl_3$) [e]: δ=138.4 (CH=CH_2), 136.8 (C_6R_6), 114.78 (CH=CH_2), 35.9 (ArylCH_2–CH_2), 29.7 (ArylCH_2)

5: ^1H NMR ($CDCl_3$, based on comparison with $[CH_3(CH_2)_7Si(CH_3)]_2O$): δ=4.55 (s, 5H; C_5H_5), 2.75 (br., 12H; ArylCH_2), 1.58 (br., 24H; ArylCH_2–$(CH_2)_2$), 1.27 (br., 72H; $(CH_2)_6$), 0.88 (t, 18H; CH_2–CH_3), 0.56 (br., 24H; CH_2–SiCH_2), 0.01 (36H; CH_3–Si–CH_3).—^{29}Si NMR ($CDCl_3$): δ=2.85.—^{13}C NMR (50.2 MHz, $CDCl_3$) [e]: δ=103.45 (C_6R_6), 77.9 (C_5H_5), 33.99, 32.33, 29.66, 29.59, 29.14, 22.95 ((CH_2)$_6$), 36.02, 25.22 (ArylCH_2–$(CH_2)_2$), 30.75 (ArylCH_2), 15.56, 15.50 (CH_2–Si–CH_2), 14.37 (CH_2–CH_3), 3.11 (CH_3–Si–CH_3). E^0 = −1.34 V [d]

6: ^1H NMR (CD_3COCD_3): δ=4.85 (5H; C_5H_5), 3.9 (br., 6H; OH), 3.63 (br., 12H; CH_2OH), 2.97 (br., 12H; ArylCH_2), 1.76 (br., 24H; ArylCH_2–$(CH_2)_2$.—^{13}C NMR (50.3 MHz, CD_3COCD_3) [e]: δ=104.43 (C_6H_6), 78.53 (C_5H_5), 61.49 (CH_2–OH), 30.94 (ArylCH_2), 33.77 (ArylCH_2–CH_2–CH_2), 28.84 (ArylCH_2–CH_2). E^0 = −1.475 V [f], −1.72 V [d]

7: ^{13}C NMR (22.63 MHz, $CDCl_3$): δ=166.8 (O–CO), 133.5)*p*-C of CO–C_6H_5), 133.2 (*i*-C), 129.8 (*m*-C), 128.8 (*o*-C), 102.75-103.75 (C_6R_6), 78.5 (C_5H_5), 64.4 (CH_2–O), 30.9, 29.7, 28.6 (Aryl$(CH_2)_3$). E^0 = −1.45 V [d]

8: ^{13}C NMR (50.3 MHz, $CDCl_3$) [e]: δ=173.8 (O–CO), 103.5 (C_6R_6), 81.5 (C_5H_5), 64.1 (CH_2–O), 36.6 (CO–CH_2), 33.2, 29.7, 28.13 (Aryl$(CH_2)_3$), 18.7 (CO–CH_2–CH_2), 14.0 (CH_3).—[g]

9: ^1H NMR (CD_3COCD_3): δ=3.4-3.7 (br., 18H; CH_2–OH), 2.5-2.8 (br., 12H; ArylCH_2), 1.1-1.9 (br., 24H; ArylCH_2–$(CH_2)_2$).—^{13}C NMR (22.63 MHz, CD_3OD): δ=137.7 (C_6R_6), 62.7 (CH_2OH), 34.24, 30.47, 29.23 (Aryl$(CH_2)_3$)

[a] 200-MHz ^1H NMR, $^{13}C\{^1H\}$ NMR, and 39.73-MHz $^{29}Si\{^1H\}$ NMR spectra with Me_4Si as standard; cyclic voltammetry vs. SCE, reversible. For **2**, **3**, and **9**, ^{13}C off resonance spectra were also recorded. [b] The ABX pattern of the terminal double bond appears by spin decoupling on the protons of the CH_2 group in β position. [c] Spin decoupling. [d] Hg or Pt cathode, dimethylformamide, 0.1 M $nBu_4N^{\oplus}BF_4^{\ominus}$. [e] INEPT and selective spin decoupling. [f] Hg cathode, aqueous 1 M LiOH. [g] The ^{13}C NMR spectra and elemental analyses indicate slight decomplexation.

[*] Ing. F. Moulines, Prof. D. Astruc
Laboratoire de Chimie Organique et Organométallique
Université de Bordeaux I
351 Cours de la Libération, F-33405 Talence Cedex (France)

[**] We thank *M. Petraud* and *B. Barbe* (CESAMO) for NMR assistance, *M.-H. Desbois* for helpful experiments, and the CNRS (ATP grant No. 959.278).

to Fe^{I} at $E^{0} = -1.42$ vs. SCE; the Fe^{I} state can also be generated using Na/Hg in THF (ESR at 77 K: $g_x = 2.0087$, $g_y = 2.0414$, $g_z = 1.8475$). On the other hand, **2** is extremely robust toward oxidation. Thus, reaction with Br_2 does not lead to decomplexation, but rather results in addition of Br_2 to the six double bonds, giving the golden hexakis(3,4-dibromobutylbenzene)(cyclopentadienyl)iron(II) complex **3** in quantitative yield as a mixture of fourteen stereoisomers (Scheme 2). Decomplexation of the hexasubstituted arene ligands is easily achieved by simply using visible-light photolysis in the presence of C_6Me_6 in CH_2Cl_2 (regenerating **1**, Scheme 1) or of dppe in CH_3CN (forming $[Fe^{II}Cp(dppe)(CH_3CN)]PF_6$[7]). In this way, the new arene **4** is obtained from **2** (white crystals, m.p. 47–48 °C, 94%).

Regiospecific hydrosilylation of **2** is effected in THF with $CH_3(CH_2)_7SiMe_2H$ using $H_2[PtCl_6]$[8] (0.1 M in 2-propanol) and provides the hexasilylated iron(II) complex **5** as a yellow resin (97% on a 1-mmol scale after chromatography on silica using CH_2Cl_2 and CH_3CN); **5** shows a single peak ($\delta = 2.85$) in the ^{29}Si NMR spectrum. Regiospecific hydroboration[9] is obtained using 9-borabicyclononane or, still better, disiamylborane (0.5 M in THF). After alkaline hydrogen peroxide oxidation, the hexol complex **6** is obtained as a yellow powder in 87% yield. Compound **6** exhibits sugarlike behavior; it is extremely hygroscopic and insoluble in nonaqueous solvents in the anhydrous state. Acylation of **6** in neat RCOCl (R = Ph or *n*Pr) at 20 °C for 72 h gives the hexaesters **7** and **8** (35 and 70% yield, respectively, after chromatography). Compounds **7** and **8** show broad ^{13}C NMR signals, specifically in the alkyl-chain region, as a result of very short relaxation times typical of structural organizations found in discotic

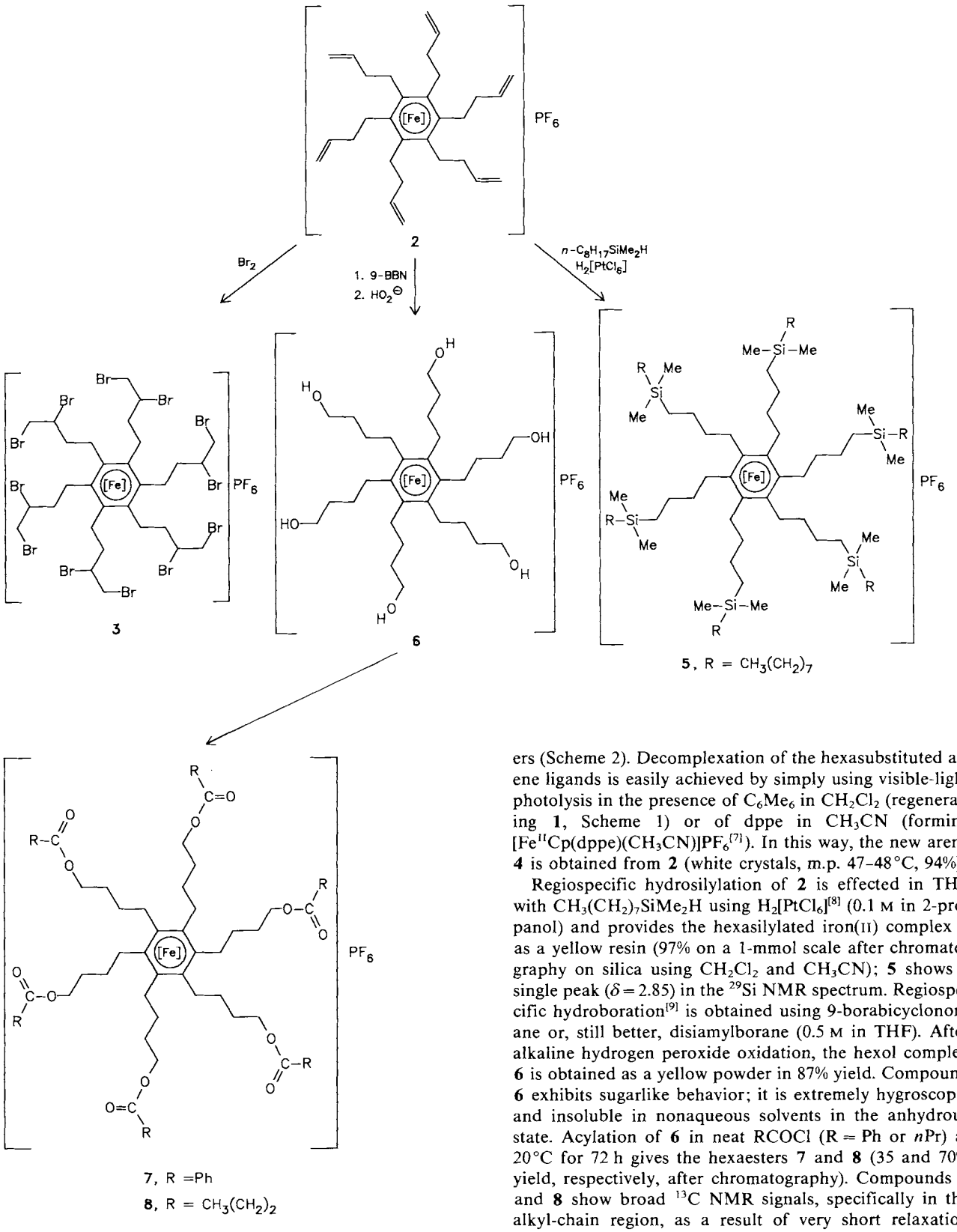

Scheme 2. [Fe] = $(\eta^5\text{-}C_5H_5)Fe^{\oplus}$.

liquid crystals.[10] Decomplexation of **6** can be effected as indicated above for **2** to provide the hexol $C_6[(CH_2)_3CH_2OH]_6$, **9** (white crystals, m.p. 115–120°C, 76% yield), which is hygroscopic and insoluble in nonaqueous solvents.

Received: March 14, 1988 [Z 2661 IE]
Publication delayed at the authors' request
German version: *Angew. Chem. 100* (1988) 1394

[1] a) H. J. Backer, *Recl. Trav. Chim. Pays-Bas 54* (1935) 833, 905; *ibid. 55* (1936) 17; b) E. Weber, *Angew. Chem. 95* (1983) 632; *Angew. Chem. Int. Ed. Engl. 22* (1983) 616; *Angew. Chem. Suppl. 1983*, 840; c) F. Vögtle, E. Weber, *ibid. 91* (1979) 813 and *18* (1979) 753; d) A. D. U. Hardy, D. D. MacNicol, S. Swanson, D. R. Wilson, *J. Chem. Soc. Perkin Trans. 2 1980*, 999, 1011.

[2] a) C. W. Bird: *Transition Metal Intermediates in Organic Synthesis*, Logos Press, Academic Press, New York 1967, p. 1; b) P. W. Jolly, G. Wilke in G. Wilkinson (Ed.): *Comprehensive Organometallic Chemistry, Vol. 8*, Pergamon Press, New York 1982, p. 649; c) K. P. C. Vollhardt, *Angew. Chem. 96* (1984) 525; *Angew. Chem. Int. Ed. Engl. 23* (1984) 539; d) U. Rosenthal, W. Schulz, *J. Prakt. Chem. 328* (1986) 335.

[3] See also the dendrimers: D. A. Tomalia, M. Hall, D. M. Hedstrand, *J. Am. Chem. Soc. 109* (1987) 1601.

[4] a) J. R. Hamon, J. Y. Saillard, A. Le Beuze, M. McGlinchey, D. Astruc, *J. Am. Chem. Soc. 104* (1982) 7549; b) the reaction proceeds by a set of deprotonation-alkylation sequences. c) This is, for instance, the case with iodoethane or 1,2-diiodoethane. Complex **1** is recovered unreacted.

[5] The volume of THF is minimal (15 mL per mmol); the reaction mixture is heated 3 h at 60°C, then 20 h at 40°C to achieve complete reaction.

[6] N. Connelly, W. E. Geiger, *Adv. Organomet. Chem. 23* (1984) 1.

[7] T. P. Gill, K. R. Mann, *Inorg. Chem. 19* (1980) 3007.

[8] J. L. Speier, J. A. Webster, G. H. Barnes, *J. Am. Chem. Soc. 79* (1957) 974.

[9] H. C. Brown: *Organic Syntheses via Boranes*, Wiley, New York 1975, p. 29 and 52 (disiamylborane), 32 and 56 (9-BBN).

[10] G. R. Luckhurst in G. W. Grey, P. A. Windsor (Eds.): *Liquid Crystals and Plastic Crystals, Vol. 2*, Ellis Horwood, Chichester 1974, p. 144.

Phosphane-Stabilized Cu^I and Ag^I Silanes

By *Alan H. Cowley,* Tammy M. Elkins, Richard A. Jones,** and *Christine M. Nunn*

Dedicated to Professor Hans Bock on the occasion of his 60th birthday

Amides,[1] phosphides,[2] and alkyls[3] of Cu^I have been prepared and found to be tetrameric in the solid state. Interestingly, the corresponding Cu^I silanes have not been reported. Silyl cuprates of the general type $[(R_3Si)_2Cu]Li$ are, of course, well known[4] and find increasing utility as organic reagents. However, such compounds are prepared in situ and structural information is unavailable. To the best of our knowledge, no compounds are known with Ag–Si bonds.[5]

Our first attempts to synthesize Cu^I silanes were not successful. Thus, the reaction of $(Me_3Si)_3SiLi$ or Ph_3SiLi with CuCl in THF solution did not result in tractable products. However, treatment of a THF solution of CuCl with one equivalent of Ph_3SiLi and three equivalents of Me_3P resulted, after recrystallization from toluene, in yellow crystals corresponding to the composition **1**. The ^{31}P NMR chemical shift for **1** ($\delta = -43.4$) is indicative of coordinated Me_3P ligands and the ^{29}Si NMR chemical shift ($\delta = -21.5$) seems reasonable for a Ph_3Si–metal moiety.[6]

$[Ph_3SiCu(PMe_3)_3]$ **1**

[*] Prof. A. H. Cowley, Prof. R. A. Jones, T. M. Elkins, Dr. C. M. Nunn
Department of Chemistry, The University of Texas at Austin
Austin, TX 78712 (USA)

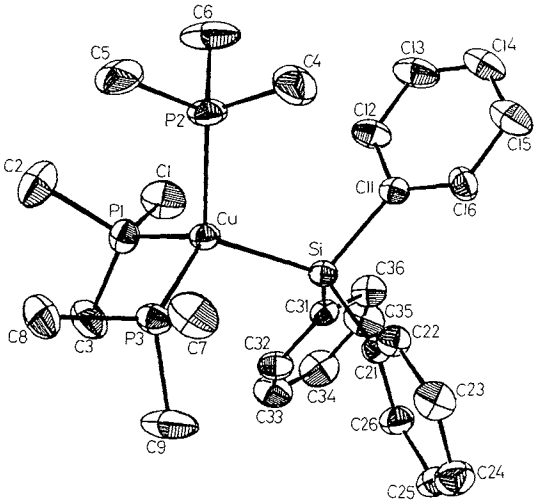

Fig. 1. Structure of **1** in the crystal. Selected bond lengths [Å] and angles [°]: Cu-Si 2.340(2), Cu-P1 2.278(3), Cu-P2 2.278(2), Cu-P3 2.273(2); P1-Cu-P2 107.0(1), P1-Cu-P3 108.11, P1-Cu-Si 112.09(7), P2-Cu-P3 105.70(8), P2-Cu-Si 111.38(8), P3-Cu-Si 112.17(8), Cu-Si-C11 113.6(2), Cu-Si-C21 114.9(2), Cu-Si-C31 117.5(3), C11-Si-C21 104.1(3), C11-Si-C31 102.8(3), C21-Si-C31 102.2(3).

An X-ray analysis[7] showed that, in the solid state, **1** (Fig. 1) consists of individual molecules with no short intermolecular contacts. The geometry around Cu is approximately tetrahedral and comprises three Me_3P ligands and a Ph_3Si group. The geometry at Si is also approximately tetrahedral. We are not aware of any previous measurement of a Cu–Si bond length, which in **1** (2.340(2) Å) is somewhat longer than the sum of the covalent radii (2.28 Å). This may be due, at least in part, to steric interactions, because the Cu–P distances are at the high end of the range established for this linkage. Moreover, the P–Cu–P and C–Si–C angles are smaller than the remainder of the bond angles at Cu and Si. It would be interesting to compare the structure of **1** with that of the isoelectronic complex $[(Me_3P)_3NiPPh_3]$.[8] Unfortunately, however, the structure of the latter has not been determined. The coordination of three Me_3P ligands in **1** provides an 18-electron configuration at Cu and avoids the formation of (presumably weak) Cu–Si–Cu three-center, two-electron bonds.

$[Ph_3SiAg(PMe_3)_3]$ **2**

A similar procedure was employed for the preparation of the analogous silver compound **2**. Unfortunately, crystals of **2** were not suitable for X-ray diffraction study. However, the ^{31}P ($\delta = -48.2$) and ^{29}Si ($\delta = -21.5$) NMR chemical shifts for **2** are very similar to those for **1**. Moreover, the ^{13}C and ^1H NMR data (see *Experimental Procedure*) are in accord with the proposed formula. Finally, the EI mass spectrum (70 eV) of **2** exhibits peaks corresponding to $(Me_3P)_3Ag$ and Ph_3Si fragments.

Experimental Procedure

1: THF solutions of Ph_3SiLi (7.02 mmol) and Me_3P (21.06 mmol) were added simultaneously to a solution of CuCl (0.7 g, 7.07 mmol) in THF (40 mL) at −78°C. The reaction mixture became yellow-brown and a small amount of black precipitate formed. After stirring the reaction mixture for 1 h at 0°C, it was warmed to 25°C and the solvent and volatiles were removed in vacuo. The resulting residue was dissolved in toluene, filtered, concentrated, and allowed to stand at −20°C. Yellow, crystalline **1** formed in 65% yield. ^1H NMR (300 MHz, C_6D_6, TMS ext.): $\delta = 0.74$ (s, 27H; Me), 7.1, 7.2, 7.7 (each br. m, 15H; C_6H_5).—$^{13}C\{^1H\}$ NMR (75.5 MHz, C_6D_6, TMS ext.): $\delta = 18.5$

(br.; Me), 125.4, 126.8, 136.6 (each s, C_6H_5).—$^{31}P\{^1H\}$ NMR (121.5 MHz, C_6D_6, 85% H_3PO_4 ext.): $\delta = -43.4$ (br. s).—^{29}Si NMR (59.6 MHz, C_6D_6, TMS ext.): $\delta = -21.5$ (s). A similar method to the foregoing was used for the preparation of yellow, crystalline **2** in 70% yield. ^1H NMR (300 MHz, C_6D_6, TMS ext.): $\delta = 0.84$ (d, 27 H, $^2J(PH) = 6.0$; Me), 7.1, 7.2, 7.9 (each m, 15 H; C_6H_5).—$^{13}C\{^1H\}$ NMR (75.5 MHz, C_6D_6, TMS ext.): $\delta = 15.7$ (d, $^1J(PC) = 5.3$ Hz; Me), 126.8, 127.1, 136.9 (each s, C_6H_5).—$^{31}P\{^1H\}$ NMR (121.5 MHz, C_6D_6, 85% H_3PO_4 ext.): $\delta = -48.2$ (br. s).—^{29}Si NMR (59.6 MHz, C_6D_6, TMS ext.): $\delta = -21.5$ (*m*). Silver-phosphorus and silver-silicon couplings were not resolved.

Received: April 28, 1988 [Z 2726 IE]
German version: *Angew. Chem. 100* (1988) 1396

[1] H. Hope, P. P. Power, *Inorg. Chem. 23* (1984) 936.
[2] A. H. Cowley, D. M. Giolando, R. A. Jones, C. M. Nunn, J. M. Power, *J. Chem. Soc. Dalton Trans. 1988*, 208.
[3] J. A. J. Jarvis, R. Pearce, M. F. Lappert, *J. Chem. Soc. Dalton Trans. 1977*, 999.
[4] See, for example, I. Fleming, T. W. Newton, F. Roessler, *J. Chem. Soc. Perkin Trans. 1 1981*, 2527; H.-M. Chen, J. P. Oliver, *J. Organomet. Chem. 316* (1986) 255, and references cited therein.
[5] B. J. Aylett, *Adv. Inorg. Chem. Radiochem. 25* (1982) 1.
[6] H. Marsmann in P. Diehl, E. Fluck, R. Kosfeld (Eds.): *NMR 17. Basic Principles and Progress*, Springer, Berlin 1981.
[7] **1**: monoclinic, space group *Cc* (No. 9), $Z = 4$; $a = 17.211(4)$, $b = 9.686(2)$, $c = 19.298(6)$, $\beta = 105.31(2)$, $V = 3102.8$ Å^3; $\rho_{calcd} = 1.180$ g/cm^3, $3° \leq 2\theta \leq 50°$ ($Mo_{K\alpha}$, $\lambda = 0.71069$ Å, $\mu = 9.08$ cm^{-1}), 5454 unique reflections collected, of which 4107 ($I > 3.0\sigma(I)$) were used to solve (direct methods) and refine (full matrix-least squares) the structure of **1**. $R = 0.0518$, $R_w = 0.0599$. Further details of the crystal structure investigation can be obtained from the Fachinformationszentrum Energie, Physik, Mathematik GmbH, D-7514 Eggenstein-Leopoldshafen 2, by quoting depository number CSD-53355, the names of the authors, and the journal citation.
[8] H.-F. Klein, H. H. Karsch, *Chem. Ber. 105* (1972) 2628.

First Direct Evidence for Nitrile Imine–Diazo Isomerization. Synthesis of Relatively Stable *N*-Silylated Nitrile Imines**

By *Michel Granier, Antoine Baceiredo,* and *Guy Bertrand**

Dedicated to Professor Hans Bock on the occasion of his 60th birthday

Transient nitrile imines, first prepared by *Huisgen* et al.,[1] have been widely used in organic synthesis. Depending on the nature of the carbon and nitrogen substituents, it has been shown by matrix spectroscopy that these 1-3 dipolar species could undergo rearrangements into carbodiimides or azines,[2] fragmentations into nitriles and nitrenes[2a] or intramolecular cyclization.[3] The possible existence of a diazomethane–nitrile imine equilibrium was reported in the sixties,[4] but was later considered to be highly controversial.[5] Nitrile imine–diazo rearrangements have been postulated[6] to explain the nature of the products obtained in the thermolysis of potential nitrile imine precursors; however, the nitrile imines have never been observed and apart from one case[6a] the resulting diazo derivatives were also not stable under the experimental conditions used. Here we wish to report the synthesis of relatively stable *N*-silylated nitrile imines and several examples of nitrile imine–diazo isomerization.

[*] Dr. G. Bertrand, M. Granier, Dr. A. Baceiredo
Laboratoire des Organométalliques, U.A. 477
Université Paul Sabatier
118, route de Narbonne, F-31062 Toulouse Cédex (France)

[**] We thank Drs. *I. Tkatchenko, Y. Dartiguenave* and *M. Dartiguenave* (Laboratoire de Chimie de Coordination du CNRS, Toulouse) for providing us with laboratory facilities after the destruction, on March 25, 1987, of the chemistry building at the Université Paul Sabatier.—In our previous paper on nitrile *oxides* (G. Sicard, A. Baceiredo, G. Groco, G. Bertrand, *Angew. Chem. 100* (1988) 289; *Angew. Chem. Int. Ed. Engl. 27* (1988) 301, an important literature reference should be added: H. Dahn, B. Favre, J.-P. Leresche, *Helv. Chim. Acta 56* (1973) 457.

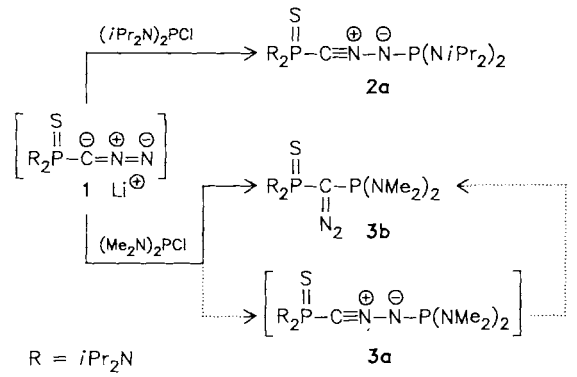

Recently, we prepared the first stable nitrile imine **2a** (m.p. 100 °C)[7] by reaction of the lithium salt of diazomethylthiophosphonic bis(diisopropylamide) **1** with chlorobis(diisopropyl)aminophosphane. In contrast, when the chlorobis(dimethylamino)phosphane was used, the diazo derivative **3b** was obtained in 87% yield and all attempts to trap the possible intermediate **3a**, even at −78 °C, failed (Table 1).

Table 1. ^{31}P-NMR and IR spectroscopic data for the nitrile imines (**a** series) and diazomethanes (**b** series). The ^{31}P-NMR spectra were recorded at 32.438 MHz in THF or $CDCl_3$, the IR spectra in THF or $CDCl_3$.

	^{31}P NMR [a] δ (J [Hz])	IR $\tilde{\nu}$ [cm^{-1}]
2a	35.4, 99.9 (5.25)	2040 (br., s)
2b	74.5, 72.8 (140.10)	2028
3b	63.4, 106.0 (104.94)	2035
4b	57.6	2080
7a	32.5	2010 (br., s)
7b	65.8	2050
8a	31.1	2120 (br., s)
8b	59.5	2100

These results might indicate that N or C substitution occurs at the diazo moiety, depending on the steric hindrance of the chlorophosphane. However, when a chloroform solution of nitrile imine **2a** is heated at 55 °C for 6 hours the phosphino(thiophosphinoyl)diazomethane **2b** is obtained in almost quantitative yield. Moreover, although **2a** is not very sensitive to water, filtration on silica gel affords diazomethylthiophosphonic bis(diisopropylamide) **4b** (82% yield) and the phosphane oxide **5** (89% yield). It is reasonable to postulate a phosphorus–nitrogen bond hydrolysis of **2a**, leading to nitrile imine **4a** and the hydroxyphosphane **6**, followed by subsequent isomerization to **4b** and **5**.

As reported by *Bock* et al.[8] and *Wentrup* et al.,[2c] *N*-silyl substituents prevent most intramolecular isomerizations.

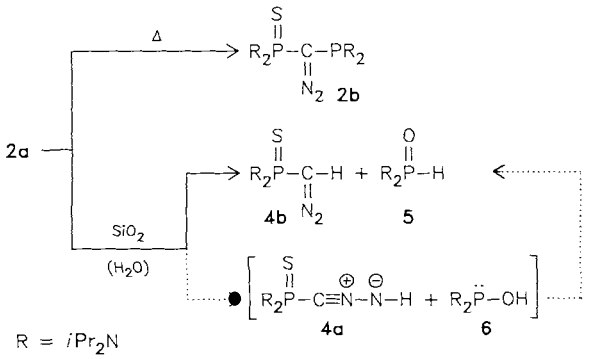

We have therefore investigated the reaction of the lithium salt **1** with chlorotrimethylsilane and chlorotriphenylsilane.[9] After workup, we obtained the diazo derivatives **7b** (90% yield) and **8b** (82% yield), respectively. However, when the reactions were monitored by spectroscopy, the *N*-silylated nitrile imines **7a** and **8a** were characterized at $-40°C$. Compared with the spectroscopic data for the diazo derivatives (**2b**, **3b**, **4b**, **7b**, **8b**), nitrile imines (**2a**, **7a**, **8a**) show a ^{31}P-NMR chemical shift at high field and an extremely broad IR absorption (see Table 1). **7a** is only stable in solution below 0°C, but **8a** is still observable after a few hours, at room temperature. The nitrile imines **7a** and **8a** react with methylacrylate to give the expected [2+3] adducts **9** and **10**, respectively, in good yield.[10,11] With methanol the diazo compound **4b** is obtained in 92% yield along with quantitative amounts of methoxytrimethyl- and methoxytriphenylsilane. This last reaction is analogous to that observed upon filtration of **2a** over silica gel, and probably involves the primary formation of nitrile imine **4a**.

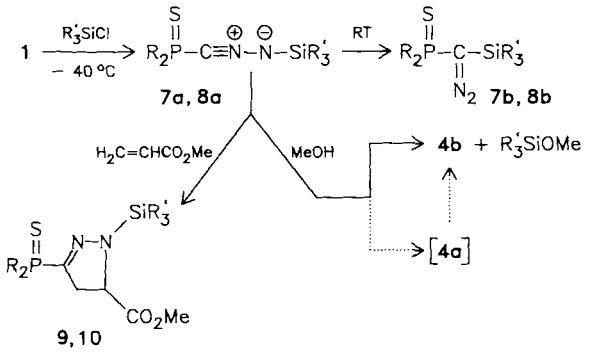

7, **9**: R = iPr_2N, R' = Me
8, **10**: R = iPr_2N, R' = Ph

These results as a whole strongly suggest that, in contrast to what is generally admitted, nitrile imines (**a** series) are the kinetic products of the electrophilic attack of diazolithium salts such as **1**, whereas the isomeric diazo derivatives (**b** series) are the thermodynamic products. The stability of nitrile imines is strongly dependent on the steric hindrance of the nitrogen substituent.

Received: April 29, 1988 [Z 2733 IE]
German version: *Angew. Chem. 100* (1988) 1397

[1] a) R. Huisgen, M. Seidel, J. Sauer, J. W. McFarland, H. Wallbillich, *J. Org. Chem. 24* (1959) 892; b) R. Huisgen, M. Seidel, G. Wallbillich, H. Knupfer, *Tetrahedron 17* (1962) 3.

[2] a) H. Toubro, A. Holm, *J. Am. Chem. Soc. 102* (1980) 2093; b) H. Meier, W. Heinzelmann, H. Heimgartner, *Chimia 34* (1980) 504, 506; c) C. Wentrup, S. Fischer, A. Maquestiau, R. Flammang, *Angew. Chem. 97* (1985) 74; *Angew. Chem. Int. Ed. Engl. 24* (1985) 56; d) S. Fischer, C. Wentrup, *J. Chem. Soc. Chem. Commun. 1980*, 502.

[3] See, e.g.: a) L. Garanti, A. Vigevani, G. Zecchi, *Tetrahedron Lett. 1976*, 1527; b) L. Garanti, A. Sala, G. Zecchi, *J. Org. Chem. 42* (1977) 1389; c) H. Meier, H. Heimgartner, *Helv. Chim. Acta 60* (1977) 3035; d) G. Schmitt, B. Laude, *Tetrahedron Lett. 1978*, 3727; e) C. Wentrup, A. Damerius, W. Reichen, *J. Org. Chem. 43* (1978) 2037.

[4] a) I. M. Mills, H. W. Thompson, *Trans. Faraday Soc. 50* (1954) 1270; b) J. F. Ogilvie, *J. Mol. Struct. 3* (1969) 513.

[5] S. Patai: *The Chemistry of Diazonium and Diazo Groups*, Wiley, New York 1978.

[6] a) C. Wentrup, *Helv. Chim. Acta 61* (1978) 1755; b) R. Gleiter, W. Rettig, C. Wentrup, *ibid. 57* (1974) 2111; c) A. Padwa, T. Caruso, S. Nahm, A. Rodriguez, *J. Am. Chem. Soc. 104* (1982) 2865.

[7] G. Sicard, A. Baceiredo, G. Bertrand, *J. Am. Chem. Soc. 110* (1988) 2663.

[8] H. Bock, R. Dammel, S. Fisher, C. Wentrup, *Tetrahedron Lett. 28* (1987) 617.

[9] *Experimental:* A solution of diazomethylthiophosphonic bis(diisopropylamide) (0.81 g, 2.6 mmol) in THF (30 mL) was treated dropwise at $-78°C$ with a stoichiometric amount of BuLi in hexane. After stirring for 30 minutes at $-78°C$, the chlorophosphane or chlorosilane (2.6 mmol) in THF (20 mL) was added to the mixture. The reaction was monitored by NMR and IR spectroscopy in order to characterize the nitrile imines (**a** series). After warming up to room temperature, the solution was stirred for 6 hours, the solvent removed by evaporation, and the yellow residue recrystallized from cold pentane, affording the diazo derivatives (**b** series) in analytically pure form.

[10] On attempting to purify **9** by column chromatography (silica gel, hexane/ether 1:1) the desilylated product was isolated [11].

[11] Selected spectroscopic data: **9**: ^{31}P NMR: $\delta = 55.0$; ^{29}Si NMR: $\delta = 17.97$.—de(trimethylsilyl)-**9**: 74% yield; ^{31}P-NMR: $\delta = 53.3$; ^{13}C NMR: $\delta = 41.25$ (d, J(PC) = 24.9 Hz, CH_2), 52.7 (s, OMe), 59.7 (d, J(PC) = 4.5 Hz, $CHCO_2Me$), 152.5 (d, J(PC) = 144.9 Hz, C=N), 173.6 (s, CO); ^{1}H-NMR: $\delta = 3.29$ (dd, J(HH) = 11.8, 17.8 Hz, 1 H, CH_2), 3.56 (dd, J(HH) = 4.0, 17.8 Hz, 1 H, CH_2), 3.71 (s, 3 H, OMe), 4.23 (dd, J(HH) = 4.0, 11.8 Hz, 1 H, $CHCO_2Me$), 6.67 (s, 1 H, NH).—**10**: 89% yield; ^{31}P-NMR: $\delta = 55.8$; ^{29}Si NMR: $\delta = -15.44$; ^{13}C NMR: $\delta = 43.0$ (d, J(PC) = 25.6 Hz, CH_2), 51.7 (s, OMe), 61.2 d, J(PC) = 4.5 Hz, $CHCO_2Me$), 148.4 (d, J(PC) = 149.5 Hz, C=N), 173.4 (s, CO); ^{1}H NMR: $\delta = 3.28$ (s, 3 H, *OMe*), 3.33 (*dd*, J(HH) = 6.7, 17.9 Hz, 1 H, CH_2), 3.61 (dd, J(HH) = 13.5, 17.9 Hz, 1 H, CH_2), 4.41 (dd, J(HH) = 6.7, 13.5 Hz, 1 H, $CHCO_2Me$).

Reactivity of (*R*)-2-*tert*-Butyldihydrooxazole Derivatives Prepared from Serine and Threonine: Novel, Versatile Chiral Building Blocks

By *Dieter Seebach** and *Gerhard Stucky*

Dedicated to Professor Hans Bock on the occasion of his 60th birthday

Two years ago we reported on the preparation of methyl (*R*)-2-*tert*-butyldihydrooxazole-3-carboxylate **1** from (*S*)-serine, using electrolytic decarboxylation as a key step.[1] The heterocycle **1**, and its methyl derivative **2**, prepared from (*S*)-threonine, are readily available on a 100-g scale,[2] so that their reactivity and use as chiral building blocks could be studied. A preliminary account of some surprising results of this investigation is given here.

Both olefinic carbon atoms of **1** can be caused to react with electrophiles. Lithiation at C-4 (→ **3**)[3] and addition of methyl chlorocarbonate or acetone give products **4** and **5**, respectively, while direct Vilsmeier formylation and Friedel–Crafts acetylation occur on C-5 (see compounds **6**–**10**). Hydrogenation of the double bond in the products thus obtained, **4**, **7**, and **8**, is highly stereoselective, with formation of the *cis*-disubstituted heterocycles **11**, **12**, and **13**, respectively. These results show (1) that the cyclic *N,O*-acetal **1** is quite stable under both nucleophilic and elec-

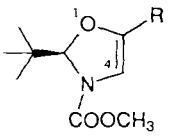

1, R = H
2, R = CH_3

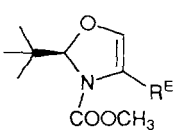

3, R^E = Li
4, R^E = $COOCH_3$
5, R^E = $C(OH)(CH_3)_2$

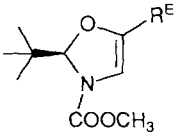

6, R^E = CHO
7, R^E = $CH(OCH_3)_2$
8, R^E = $CH(OCH_2)_2$
9, R^E = $COCH_3$
10, R^E = $CH=CH_2$

[*] Prof. Dr. D. Seebach, Dipl.-Chem. G. Stucky
Laboratorium für organische Chemie der
Eidgenössischen Technischen Hochschule
ETH-Zentrum, Universitätstrasse 16, CH-8092 Zürich (Switzerland)

trophilic conditions, (2) that the iminium ion **A** is more stable than the oxonium ion **B**,[4] and (3) that attack of nucleophiles and of catalytically activated hydrogen occurs from the face *trans* to the *tert*-butyl group.[1,5]

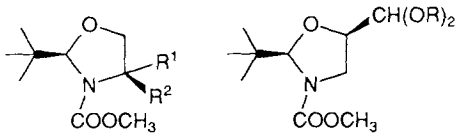

11, $R^1 = H$, $R^2 = COOCH_3$ **12**, $R = CH_3$ **13**, $R = CH_2$

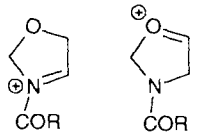

A **B**

Strong diastereofacial bias is also observed in cycloadditions to the double bond of **1**. Thus, reaction with tetracyanoethylene or osmium tetroxide or cyclopropanation (via the Simmons–Smith or Makosza reactions or by Cu^{II}-induced decomposition of ethyl diazoacetate) gave bicyclic products **14**–**19** with the *tert*-butyl group on the *exo* face (bromine/lithium exchange with the dibromocarbene adduct **18** was *endo*-selective and furnished the products **20**–**23** with electrophiles). Also, Lewis acid-catalyzed cycloaddition of 4-methyl-2-oxo-3-pentenonitrile[6] to **1** and Diels–Alder reaction of the diene **10** with maleic anhydride[7] gave the bicyclic and tricyclic products **24** and **25**, respectively, in a single diastereomeric form. Subsequent reactions such as the catalytic hydrogenation of the double bond in **25** (→**26**) and the acid-catalyzed ring opening of the oxaspiropentane derivative **23** (→**27**) were highly selective. Some of the reactions that we carried out with the 5-methyl derivative **2** are evident from the product structures **28**–**31**.

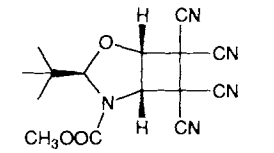

14

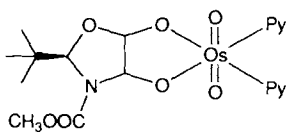

15

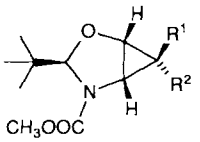

16, $R^1 = R^2 = H$
17, $R^1 = R^2 = Cl$
18, $R^1 = R^2 = Br$
19, $R^1 = H$, $R^2 = COOH$
20, $R^1 = Br$, $R^2 = H$
21, $R^1 = Br$, $R^2 = C(OH)(CH_2)_5$
22, $R^1 — R^2 = OC(CH_2)_5$
23, $R^1 — R^2 = OCH(C_6H_5)$

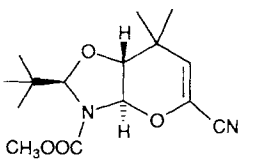

24

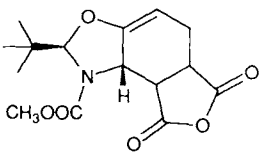

25

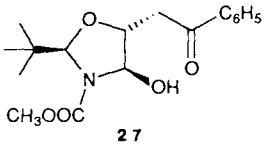

27

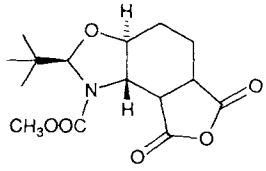

26

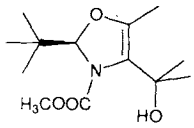

28

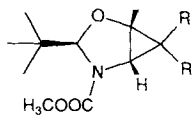

29, (R = H)
30, (R = Br)

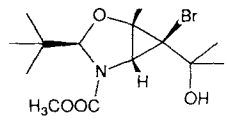

31

Table 1. Data of the products **4**–**31** and comments on the corresponding reactions. The yields given are those of recrystallized products. The specific rotations were measured in chloroform with a concentration of ca. 1. When the ratio of diastereoisomers (*d.r.*) is not given, the isomer illustrated in the text was formed in >50:1 ratio (high-field NMR, crude product).—TEBACl = benzyltriethylammonium chloride, LDA = lithium diisopropylamide.

Starting material	Conditions and comments	Product	Yield [%]	M.p. [°C]	$[\alpha]_D$
1	BuLi, then $ClCOOCH_3$	**4**	42	70.8–71.6	+ 65.4
1	BuLi, then acetone	**5**	30	—	+219.1
1	$DMF/POCl_3$, $NaOAc/H_2O$	**6**	75	—	+163.0
6	$HC(OCH_3)_3$/Dowex $50W \times 8\,H^{\oplus}$	**7**	53	—	+248.6
6	$HO(CH_2)_2OH$/ ΔC_6H_6/TsOH	**8**	71	—	+325.5
1	$CH_3COCl/SnCl_4$/ CH_2Cl_2	**9**	25	53.2–54.4	+ 79.7
6	$(C_6H_5)_3P^{\oplus}CH_3Br^{\ominus}$/ BuLi/ether	**10**	50	—	+463.2
4	30 atm H_2/Pd-C	**11**	87	57.9–58.6	− 24.3
7	50 atm H_2/Pd-C/ *d.r.* 20:1	**12**	98	—	+ 71.6
8	50 atm H_2/Pd-C/ *d.r.* 12:1	**13**	97	51.6–52.8	+ 66.4
1	$(NC)_2C{=}C(CN)_2$/ CH_2Cl_2	**14**	94	189–192	+ 90.6 [c]
1	OsO_4/benzene/pyridine	**15**	75	174 dec.	—
1	$Zn(C_2H_5)_2/CH_2I_2$/ ether	**16**	83	—	+168.9
1	$CHCl_3$/NaOH/ TEBACl	**17**	71	68.3–68.7	+127.0
1	$CHBr_3$/NaOH/ TEBACl	**18**	50	73–74	+105.6
1	$N_2CHCOOEt$/ Cu^{II}/KOH [a]	**19**	44	142.8–144.6	+ 91.5
18	BuLi/THF/−100°C/ then H_2O	**20**	80	—	+ 69.8
18	BuLi/−100°C/cyclohexanone	**21**	58	107.4–108.0	+ 79.6
21	*t*BuOK in THF	**22**	70	87.4–88.4	+113.2
18	BuLi/THF/−100°C/ C_6H_5CHO/then *t*BuOK in THF [b]	**23**	21	112–113	[d]
1	$(CH_3)_2C{=}CHCOCN$/ $TiCl_4$/−30°C	**24**	65	—	+239.6
10	maleic anhydride/ benzene/RT	**25**	93	158	+231.0
25	30 atm H_2/Pd-C/ ethyl acetate	**26**	71	126.4–127.6	+153.1
23	2% $HClO_4$/THF/ RT/*d.r.* 4:1	**27**	60	115.8–116.8	+ 28.3
2	LDA/THF/ −78°C/acetone	**28**	39	—	+164.1
2	$Zn(C_2H_5/CH_2I_2$/ ether	**29**	52	—	+143.2
2	$CHBr_3$/NaOH/ TEBACl	**30**	59	72.8–74.2	+ 45.1
30	BuLi/THF/−100°C/ acetone	**31**	10	122 dec.	+129.9

[a] Two isomers (7:3), epimeric at the α-CO position, readily separated by chromatography. [b] Mixture of diastereoisomers. [c] Solvent acetonitrile. [d] The crude product was directly used for the next step.

Table 1 contains the yields, melting points, and specific rotations of the products obtained from the dihydrooxazoles **1** and **2**, along with some information about the reaction conditions. All compounds were fully characterized by IR, NMR, and MS spectra and by elemental analyses. The configurational assignments rest upon NOE measurements. The surprising structure of the solvolysis product **27** was determined by X-ray diffraction.[8] Centers whose absolute configuration has not been determined with certainty so far are not specified.

Received: May 9, 1988;
supplemented: June 6, 1988 [Z 2752 IE]
German version: *Angew. Chem. 100* (1988) 1398

[1] P. Renaud, D. Seebach, *Angew. Chem. 98* (1986) 836; *Angew. Chem. Int. Ed. Engl. 25* (1986) 843.
[2] D. Seebach, G. Stucky, P. Renaud, *Chimia 42* (1988) 176.
[3] a) For a review on amine-d^1 reagents see D. Seebach, D. Enders, *Angew. Chem. 87* (1975) 1; *Angew. Chem. Int. Ed. Engl. 14* (1975) 15; b) for a review on heteroatom-directed metalations see P. Beak, A. I. Meyers, *Acc. Chem. Res. 19* (1986) 356.
[4] Reviews on acyliminium ions: a) W. N. Speckamp, H. Hiemstra, *Tetrahedron 41* (1985) 4367; b) T. Shono: *Electroorganic Chemistry as a New Tool in Organic Synthesis*, Springer, Berlin 1984. Ab initio calculations (R = H) indicate that **A** is ca. 11 kcal mol^{-1} more stable than **B** (T. K. Ha, B. Lamatsch, unpublished work, ETH Zürich 1987).
[5] This is not a trivial issue; there are several cases known in which five- and six-membered cyclic enolates and iminium ions react from the seemingly more hindered face: a) D. Seebach, R. Imwinkelried, T. Weber in R. Scheffold (Ed.): *Modern Synthetic Methods*, Springer, Berlin 1986; b) D. Seebach, J. Zimmermann, *Helv. Chim. Acta 71* (1988) 1143; c) A. I. Meyers, B. A. Lefker, *J. Org. Chem. 51* (1986) 1541.
[6] R. A. John, V. Schmid, H. Wyler, *Helv. Chim. Acta 70* (1987) 600, and references cited therein.
[7] Cf. T. Shono, Y. Matsumura, K. Tsubata, Y. Sugihara, S. Yamane, T. Kanazawa, T. Aoki, *J. Am. Chem. Soc. 104* (1982) 6697.
[8] We thank *P. Seiler* of our laboratory for carrying out the X-ray analysis. Details will be described in a forthcoming full paper.

A New Cubane Cluster with the $[MoFe_3S_4]^0$ Core and Possible Relevance to the Fe_3-Centers in Ferredoxins. The Synthesis, Structure and Properties of the $[Fe_3S_4(SEt)_3Mo(CO)_3]^{3\ominus}$ Anion**

By *Dimitri Coucouvanis,* Saleem Al-Ahmad, Athanasios Salifoglou, W. Richard Dunham,* and *Richard H. Sands*

Dedicated to Professor Hans Bock on the occasion of his 60th birthday

Interest in the coordination chemistry of Fe/S and Fe/Mo/S clusters derives mainly from the importance of such clusters in biomolecules like the non-heme iron proteins (ferredoxins) and the nitrogenases. The former are essential for many biological electron transfer processes and the latter are involved in the catalytic reduction of small substrate molecules (N_2, H_2, C_2H_2, etc.).

The heterometallic clusters with cubane structure $[MoFe_3S_4]^{3\oplus}$ cores and have been obtained by solvolysis of the doubly-bridged double-cubane **2**.[2] The latter are formed in reactions of the clusters **3**[3] with 3,6-disubstituted catecholate ligands (R_2'cat).

[*] Prof. Dr. D. Coucouvanis, S. Al-Ahmad, A. Salifoglou, W. R. Dunham, R. H. Sands
Department of Chemistry, The University of Michigan
Ann Arbor, MI 48109-1055 (USA)

[**] This research was supported by a grant from the National Institutes of Health (GM-26671).

$[MoFe_3S_4(SR)_3(R_2'cat)L]^{2\ominus}$ **1**
L = CH_3CN, DMF, DMSO

$[MoFe_3S_4(\mu_2\text{-}SR)(SR)_2(R_2'cat)]_2^{4\ominus}$ **2**

$[Mo_2Fe_7S_8(\mu_2\text{-}SR)_6(SR)_6]^{3\ominus}$ **3**

On the basis of ^{57}Fe Mössbauer isomer shift data, the clusters **1** are described[4] as formally containing $Fe^{+2.67}$ and Mo^{+3} ions. These clusters display magnetic ground states[1] ($S = 3/2$), and Mo K-edge EXAFS[5] similar to those reported for nitrogenase;[6,7] however, they are deficient in Fe content and do not qualify as stoichiometric structural analogues for the Fe/Mo/S active site. For the latter, both spectroscopic results[6] and chemical analyses[8] suggest an Fe/Mo ratio of at least 6:1. In our search for Fe/Mo/S clusters as possible structural analogues for the center in nitrogenase we have shown that a new type of Fe/Mo/S clusters (**4**) can be obtained[9] by coordination of $Mo(CO)_3$ fragments to the hexagonal faces of the $(Fe_6S_6L_6')^{n\ominus}$ prismanes.[10]

$[(Fe_6S_6L_6')(Mo(CO)_3)_2]^{n\ominus}$ **4**

These clusters, that show the same deficiency in Fe content as the $MoFe_3$ cubanes, also can be obtained (L' = Cl) by the condensation of three $[Fe_2S_2(Cl)_4]^{2\ominus}$ dimers[9e] in the presence of **5**.[11]

$[Mo(CO)_3(CH_3CN)_3]$ **5**

This reaction, which may be taking place on $Mo(CO)_3$ "template" units, prompted us to investigate the possible rearrangement of the known $[Fe_3S_4(SEt)_4]^{3\ominus}$ linear trimers **6**[12] in the presence of "$Mo(CO)_3$". The reaction of **6** (as Et_4N-salt) with **5**[11] in CH_3CN, in a 1:1 molar ratio, proceeds readily [Eqn. (a)] and the crystalline product **7**[13] is isolated in 62% yield after recrystallization from CH_3CN/ether.

$$\underset{\mathbf{6}}{[Fe_3S_4(SEt)_4]^{3\ominus}} + \mathbf{5} \longrightarrow \underset{\mathbf{7}}{[Fe_3S_4(SEt)_3Mo(CO)_3]^{3\ominus}} + 1/2\,EtSSEt \quad (a)$$

Cyclovoltammetric measurements of **7** (Pt electrode, CH_2Cl_2, vs. SCE) show two one-electron reversible waves at -0.36 V and -0.89 V that correspond to the $7^{2\ominus}/7^{3\ominus}$ and $7^{3\ominus}/7^{4\ominus}$ redox couples. The Mössbauer spectra of **7** ($T = 120$ K, vs. Fe) can be deconvoluted into two quadrupole doublets with a 2:1 intensity ratio. The isomer shift (IS) and quadrupole splitting are 0.37(2) and 0.76 mm s^{-1}, respectively, for the higher intensity doublet, and 0.46(2) and 0.95 mm s^{-1}, respectively, for the lower intensity doublet. The 2:1 site ratio, which corresponds to crystallographically imposed C_s symmetry, has already been observed previously[4] in clusters with $[MoFe_3S_4]^{3\oplus}$ cores. For FeS_4 tetrahedral units the IS values for Fe^{III} and Fe^{II} are 0.25 and 0.70 mm s^{-1}, respectively, and the change in isomer shift that accompanies an Fe valence change of 1 is ca. 0.45 mm s^{-1}. Furthermore, for a cluster with n electronically equivalent Fe atoms, a change in oxidation level of 1 would correspond roughly to a change in IS values of $1/n(0.45)$.[9e] Under these empirical rules, the average IS value of 0.40 mm s^{-1} for **7** would indicate that the Fe atoms are in a +2.67 formal oxidation state. The similarity in the Fe formal oxidation levels in the $[MoFe_3S_4]^0$ core of

7 and in the $[MoFe_3S_4]^{3\oplus}$ cores reported previously suggests that, while the latter probably contains Mo^{III}, the former contains zerovalent Mo. The C–O stretching vibrations in 7 observed at 1750 and 1864 cm^{-1} are also consistent with the presence of Mo^0 and indicate the rather poor π-accepting properties of the $[Fe_3S_4(SR)_3]^{3\ominus}$ "ligand".

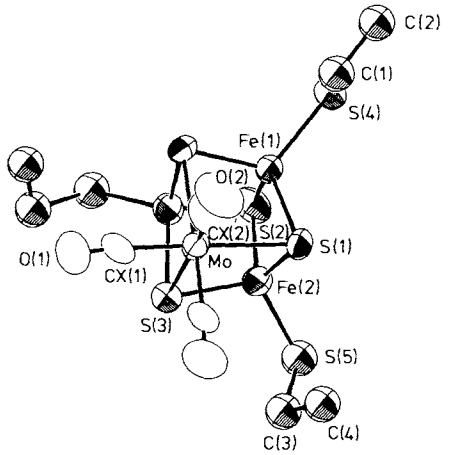

Fig. 1. Structure and atomic labeling of 7 [14]. Thermal ellipsoids as drawn by ORTEP represent the 40% probability surfaces. The thermal ellipsoids for the S(5) and C atoms of the SEt terminal ligands have been drawn smaller for clarity.

The structure of 7 has been determined[14] and the anion (Fig. 1), contains the same basic $[MoFe_3S_4]$ structural unit previously found in other similar cubane clusters.[1] A closer examination of the crystallographic data (Table 1), reveals some rather unusual structural features. In comparison to the $[MoFe_3S_4]^{3\oplus}$ cores in the clusters reported by *Holm* et al.,[1] the $[MoFe_3S_4]^0$ core in 7 has undergone a trigonal elongation that is a consequence of weak $Mo(CO)_3$–Fe_3S_4 bonding interactions that are apparent in the rather long Mo–S bonds and Mo–Fe distances in 7. The Mo–S bonds of ca. 2.63 Å are longer than the weak Mo–S bonds in the adducts **4** (L′ = Cl)[9] (ca. 2.57 Å for n = 3 and ca. 2.61 Å for n = 4). Similarly, the Mo–Fe distances in 7 (ca. 3.25 Å) are significantly longer than those in the adducts **4** (L′ = Cl): ca. 2.93 Å for n = 3 and ca. 2.99 Å for n = 4. The Mo–S and Mo–Fe bonds in 7 are too long and do not resemble those determined by EXAFS for either the Fe/Mo/S site in nitrogenase[7] or for the $[MoFe_3S_4]^{3\oplus}$ cores.[5]

We suggest that 7 can best be described as a weak complex of the $Mo(CO)_3$ unit and the $[Fe_3S_4(SR)_3]^{3\ominus}$ cluster. The latter could be considered as the first synthetic analog of one of the proposed[15] models for the reduced form of the Fe_3S_4 center in *A. vinelandii*. The $[CoFe_3S_4]$[16a] and $[ZnFe_3S_4]$[16b] cubane derivatives of the Fe_3S_4 center in *D. Gigas* ferredoxin II (Fd II) are obtained by the addition of $Co^{2\oplus}$ or $Zn^{2\oplus}$ to dithionite-reduced Fd II. The "oxidized" form of the $[CoFe_3S_4]$ derivative formally contains $[Co^{II}\,Fe^{II}Fe_2^{III}]$, shows Mössbauer parameters similar to those found for 7, and is characterized by a $S = 1/2$ ground state.

Solutions of pure 7 in CH_3CN are EPR silent at temperatures as low as 9 K. In contrast, partially oxidized solutions of 7 show an EPR spectrum characteristic of a $S = 3/2$ ground state, with signals at $g = 5.8$, 3.16 and 1.98. Preliminary analysis of the spectrum indicates $D > 0$ and an E/D ratio of 0.18. At present we are pursuing the synthesis and characterization of this oxidation product as well as of other derivatives of 7.

Table 1. Selected bond lengths [Å] and angles [°] in 7 and **1** (R = Et, R′ = Cl, L = CH_3CN).

	7		$[MoFe_3S_4(SEt)_3(Cl_4cat)(CN)]^{3\ominus}$ [a]
	Bond lengths [b]		
Mo-Fe(1)	3.272(4)	[3.274(5)]	
Mo-Fe(2)	3.225(4)	[3.220(4)]	2.741(11)[c]
Mo-S(1)	2.638(5)	[2.651(6)]	
Mo-S(3)	2.623(8)	[2.611(8)]	2.376(12) [c]
Fe(1)-Fe(2)	2.742(4)	[2.736(5)]	
Fe(2)-Fe(2′)	2.739(4)	[2.723(6)]	2.708(11) [c]
Fe(1)-S(2)	2.289(9)	[2.301(10)]	
Fe(2)-S(2)	2.298(7)	[2.304(8)]	2.280(9) [d]
Fe-S[e]	2.268(7)	[2.261(11)]	2.272(8)
Fe(1)-S(4)	2.301(8)	[2.294(10)]	
Fe(2)-S(5)	2.283(6)	[2.293(7)]	2.26(1) [f]
Mo-CX(1)	1.94(2)	[1.92(2)]	
Mo-CS(2)	1.91(4)	[1.89(4)]	
CS(1)-O(1)	1.16(2)	[1.19(2)]	
CX(2)-O(2)	1.19(3)	[1.22(4)]	
	Bond angles [b]		
S(1)-Mo-S(3)	88.0(2)	[87.9(2)]	
S(1)-Mo-S(1′)	86.4(2)	[86.5(2)]	102.5(15) [c]
Fe(2)-S(2)-Fe(2′)	73.0(3)	[72.2(5)]	
Fe(1)-S(2)-Fe(2)	73.4(2)	[72.9(3)]	72.9(5) [g]
Fe-S-Fe [h]	74.3(3)	[74.4(3)]	73.2(6)

[a] From Ref. [1a]. [b] The values in brackets represent results of a structure determination on a second data set obtained from an independently grown new crystal [14]. [c] The average values ofchemically equivalent bond lengths are given. For definition of the standard deviations in parenthesis see Ref. [1a]. [d] Bonds with the μ-S ligand diagonally across from the Mo atom. [e] Mean value of all other Fe–S bonds. [f] Mean value of the Fe–S bonds with the SEt ligands. [g] Angles with the μ-S ligand diagonally across from the Mo atom. [h] Mean value of all other Fe–S angles.

Received: May 9, 1988 [Z 2753 IE]
German version: *Angew. Chem. 100* (1988) 1404

[1] a) R. E. Palermo, R. Singh, J. K. Bashkin, R. H. Holm, *J. Am. Chem. Soc. 106* (1984) 2600; b) R. H. Holm, W. H. Armstrong, G. Christou, P. K. Mascharak, Y. Mizobe, R. E. Palermo, T. Yamamura: *Proc. 2nd Int. Kyoto Conf. New Aspects Organic Chem.*, Kodansha, Tokyo 1983, pp. 79–99.

[2] W. H. Armstrong, P. K. Mascharak, R. H. Holm, *J. Am. Chem. Soc. 104* (1982) 4373.

[3] P. K. Mascharak, W. H. Armstrong, Y. Mizobe, R. H. Holm, *J. Am. Chem. Soc. 105* (1983) 475.

[4] M. J. Carney, J. A. Kovacs, Y. P. Zhang, G. C. Papaefthymiou, K. Spartalian, R. B. Frankel, R. H. Holm, *Inorg. Chem. 26* (1987) 719.

[5] S. D. Conradson, B. K. Burgess, W. E. Newton, K. O. Hodgson, J. W. McDonald, J. F. Rubinson, S. F. Gheller, L. E. Mortenson, M. W. W. Adams, P. K. Mascharak, W. A. Armstrong, R. H. Holm, *J. Am. Chem. Soc. 107* (1985) 7935; EXAFS is an abbreviation for *E*xtended *X*-ray *A*bsorption *F*ine *S*tructure.

[6] a) J. Rawlings, V. K. Shah, J. R. Chisnell, W. J. Brill, R. Zimmerman, E. Munck, W. H. Orme-Johnson, *J. Biol. Chem. 253* (1978) 1001; b) B. M. Hoffman, J. E. Roberts, W. H. Orme-Johnson, *J. Am. Chem. Soc. 104* (1982) 860.

[7] S. P. Cramer, K. O. Hodgson, W. O. Gillum, L. E. Mortenson, *J. Am. Chem. Soc. 100* (1978) 3398.

[8] a) B. K. Burgess, D. B. Jacogs, E. I. Stiefel, *Biochim. Biophys. Acta 614* (1980) 196; b) W. E. Newton, B. K. Burgess, E. I. Stiefel in W. E. Newton, S. Otsuka (Eds.): *Molybdenum Chemistry of Biological Significance*, Plenum, New York 1980, p. 191; c) B. K. Burgess, W. E. Newton in A. Mueller, W. E. Newtons (Eds.): *Nitrogen Fixation*, Plenum, New York 1983, p. 83; d) M. J. Nelson, M. A. Levy, W. H. Orme-Johnson, *Proc. Natl. Acad. Sci. USA 80* (1983) 147; e) W. H. Orme-Johnson, D. A. Wink, P. A. Mclean, G. S. Harris, A. E. True, B. Hoffman, E. Munck, V. Papaefthymiou, *Recl. Trav. Chim. Pays-Bas 106* (1987) 299.

[9] a) D. Coucouvanis, M. G. Kanatzidis, *J. Am. Chem. Soc. 107* (1985) 5005; b) M. G. Kanatzidis, D. Coucouvanis, *J. Am. Chem. Soc. 108* (1986) 337; c) A. Salifoglou, M. G. Kanatzidis, D. Coucouvanis, *J.*

Chem. Soc. Chem. Commun. 1986, 559; d) D. Coucouvanis, A. Salifoglou, M. G. Kanatzidis, A. Simopoulos, A. Kostikas, *J. Am. Chem. Soc. 109* (1987) 3807; e) D. Coucouvanis, A. Salifoglou, M. G. Kanatzidis, W. R. Dunham, A. Simopoulos, A. Kostikas, unpublished.

[10] a) M. G. Kanatzidis, W. R. Dunham, W. R. Hagen, D. Coucouvanis, *J. Chem. Soc. Chem. Commun. 1984*, 356; b) W. Saak, G. Henkel, S. Pohl, *Angew. Chem. 96* (1984) 153; *Angew. Chem. Int. Ed. Engl. 23* (1984) 150; c) D. Coucouvanis, M. G. Kanatzidis, W. R. Dunham, W. R. Hagen, *J. Am. Chem. Soc. 106* (1984) 7998; d) M. G. Kanatzidis, W. R. Hagen, W. R. Dunham, R. K. Lester, D. Coucouvanis, *ibid. 107* (1985) 953; e) M. G. Kanatzidis, A. Salifoglou, D. Coucouvanis, *ibid. 107* (1985) 3358; f) M. G. Kanatzidis, A. Salifoglou, D. Coucouvanis, *Inorg. Chem. 25* (1986) 2460; g) D. Coucouvanis, M. G. Kanatzidis, A. Salifoglou, W. R. Dunham, A. Simopoulos, J. R. Sams, V. Papaefthymiou, A. Kostikas, C. E. Strouse, *J. Am. Chem. Soc. 109* (1987) 6863.

[11] B. L. Ross, J. G. Grasselli, W. M. Ritchey, H. D. Kaesz, *Inorg. Chem. 2* (1963) 1023.

[12] K. S. Hagen, R. H. Holm, *J. Am. Chem. Soc. 104* (1982) 5496.

[13] Analysis: Calcd for $(Et_4N)_3 \cdot 7 \cdot CH_3CN$: C 38.50, H 7.22, N 5.13, S 20.56, Fe 15.35, Mo 8.79. Found: C 38.06, H 6.80, N 4.63, S 19.73, Fe 15.16, Mo 8.57.

[14] Crystal structure analysis of $(Et_4N)_3 \cdot 7 \cdot CH_3CN$ (the values in brackets represent results of a structure determination on a second data set obtained from an independently grown new crystal): $a = 16.557(5)$ [16.563(4)], $b = 18.915(6)$ [18.879(6)], $c = 17.110(6)$ [17.108(5)] Å, $\alpha = \beta = \gamma = 90°$; space group, *Pbcm*, $Z = 4$, $\rho_{calcd} = 1.35$ g cm^{-3}, $\rho_{obsd} = 1.40$ g cm^{-3}, $\mu = 12.9$ cm^{-1}, $2\theta_{max} = 40°$ ($Mo_{K\alpha}$, $\lambda = 0.71069$ Å); 2620 unique reflections; used in refinement with $F_0^2 > 3\sigma(F_0^2)$: 1290 [1376]; parameters 198. Final $R = 0.0699$ [0.0733], $R_w = 0.0647$ [0.0689]. The low number of observed reflections for both data sets is due to the fact that crystals of high crystallographic quality could not be isolated. This problem, coupled with positional disorders encountered with two of the three $[Et_4N]^{\oplus}$ cations, accounts for the rather high temperature factors obtained for some of the carbon atoms. Further details of the crystal structure investigation are available on request from the Fachinformationszentrum Energie, Physik, Mathematik GmbH, D-7514 Eggenstein-Leopoldshafen 2 (FRG), on quoting the depository number CSD-53196, the names of the authors, and the journal citation.

[15] H. Beinert, A. J. Thompson, *Arch. Biochem. Biophys. 222* (1983) 333.

[16] a) I. Moura, J. J. G. Moura, E. Munck, V. Papaefthymiou, J. LeGall, *J. Am. Chem. Soc. 108* (1986) 349; b) K. K. Surerus, E. Munck, I. Moura, J. J. G. Moura, J. LeGall, *J. Am. Chem. Soc. 109* (1987) 3805.

Convenient Routes to Di-*tert*-butylsilanediyl: Chemical, Thermal and Photochemical Generation**

By *Philip Boudjouk,** *Upasiri Samaraweera, Ratnasabapathy Sooriyakumaran, Jerzy Chrusciel,** and *Kevin R. Anderson*

Dedicated to Professor Hans Bock on the occasion of his 60th birthday

Although the chemistry of the silanediyls is well developed and of continuing interest,[1] there are few convenient methods for generating these species on a preparative scale. We had need for a variety of methods for making di-*tert*-butylsilanediyl (**2**) and in this communication we report three convenient routes for generating this intermediate, possibly in a complexed form like **8**, in high yields.[2]

2 has been proposed as a product of the photolyses of hexa-*tert*-butylcyclotrisilane[3] and di-*tert*-butylsilyldiazide.[4] We have found [Eqn. (a)] that when di-*tert*-butyldichlorosilane (**1a**) and lithium in THF in the presence of excess of triethylsilane, were irradiated with ultrasonic waves using an ultrasonic cleaning bath, the di-*tert*-butylsilanediyl insertion product 1,1,1-triethyl-2,2-di-*tert*-butyldisilane (**3**) was isolated in 60% yield.[5] The same product was obtained in comparable yields from **1b** and **1c**. This is the first example of a metal-promoted α-elimination of dihalosilanes on a preparative scale.

$$t\mathrm{Bu_2SiX_2} + \mathrm{Li} \xrightarrow{)))} [t\mathrm{Bu_2Si:}] \xrightarrow{\mathrm{Et_3SiH}} \mathrm{Et_3Si{-}SiH}t\mathrm{Bu_2} \qquad \text{(a)}$$

1a, X = Cl; **1b**, X = Br; **1c**, X = I — **2** — **3**

We have investigated the reactions of **1a** and lithium with other trapping agents and in the absence of a quenching agent. With *trans*-butene for example, 1,1-di-*tert*-butyl-*trans*-2,3-dimethylsilirane (**4**), was isolated in 65–70% yield. None of the *cis* isomer was detected by gas chromatography. When *cis*-butene was used as a trap, 1,1-di-*tert*-butyl-*cis*-2,3-dimethylsilirane was also isolated in 65–70% yield.[6] A small amount (<5%) of **4** was detected along with **5** but was understood to arise from the presence of 2–5% *trans*-butene in our samples of *cis*-butene.

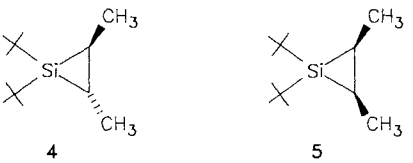

4 **5**

The siliranes **4** and **5** (Table 1) are rare examples of isolable siliranes with hydrogen substituents on the ring carbon atoms. They are surprisingly stable, surviving distillation (65 °C/4 torr) and exposure to dry methanol. They are, however, very reactive towards water and oxygen. Upon thermolysis (200 °C, benzene, sealed tube) both siliranes produce di-*tert*-butylsilanediyl **2** and only one butene. The silanediyl produced in this fashion can also be trapped with Et_3SiH to give **3** in 72–84% yields.

$$\mathbf{4}\ (\mathbf{5}) \xrightarrow[C_6H_6]{200\,^\circ C} \mathbf{2} \xrightarrow{\mathrm{Et_3SiH}} \mathbf{3} + \textit{trans}\text{-butene}\ (\textit{cis}\text{-butene}) \qquad \text{(b)}$$

Table 1. Characteristic data of the compounds **4**–**7**. 90-MHz ^{1}H-NMR, 90-MHz ^{13}C-NMR and 90-MHz (**7**), 400-MHz (**4**, **5**), and 300-MHz (**6**) ^{29}Si-NMR spectra in C_6D_6 ($CDCl_3$ for **7**) with TMS as standard.

4: ^{1}H NMR: $\delta = 1.63$ (d, $J = 6$ Hz, 6H, CH_3), 1.23 (s, 18H, *t*Bu), 0.80 (m, 2H, CH); ^{13}C NMR: $\delta = 16.66$ (CCH_3), 17.4 (CCH_3), 19.7 ($C(CH_3)_3$), 30.9 ($C(CH_3)_3$); ^{29}Si NMR (benzene-d^6): $\delta = -43.92$; MS: 198 ($M^{\oplus}$, 4%), 141 ($M^{\oplus} - t$Bu, 15%). Elemental analysis was obtained on the methanol addition product.

5: ^{1}H NMR: $\delta = 1.55$ (d, $J = 6$ Hz, 6H, CCH_3), 1.23 (m, 2H, CH), 1.3, 1.13 (each s, each 9H, *t*Bu). ^{13}C NMR: $\delta = 10.02$ (CCH_3), 10.22 (CCH_3), 18.51, 20.7 ($C(CH_3)_3$), 29.91, 31.47 ($C(CH_3)_3$).—^{29}Si NMR: $\delta = -53.21$; MS: *m/z* 198 ($M^{\oplus}$, 4%), 141 ([$M^{\oplus} - t$Bu], 13)

6: ^{1}H NMR: $\delta = 1.13$ (s, 18H, *t*Bu), 0.36 (s, 18H, $SiMe_3$).—^{13}C NMR: $\delta = 184.9$ (C=C), 31.1 ($C(CH_3)_3$), 28.0 ($C(CH_3)_3$), 0.22 ($SiMe_3$).—59.6-MHz ^{29}Si NMR: $\delta = -12.78$ ($SiMe_3$), −86.16 ($SitBu_2$).—MS: *m/z* 312 ($M^{\oplus}$, 64%), 297 ([$M^{\oplus} - 15$], 11), 255 ([$M^{\oplus} - t$Bu], 76); correct C,H analysis was obtained on the methanol addition product

7: ^{1}H NMR: $\delta = 1.33$ (s, 18H, $C(CH_3)_3SiH$), 1.40 (s, 36H, tBu_2Si), 4.00 (s, 2H, SiH).—17.9-MHz ^{29}Si NMR: $\delta = -35.77$ (Si(H)*t*Bu), 31.15 (tBu_2Si).—MS: *m/z* 456 ($M^{\oplus}$), 400 ($M^{\oplus} - 56$); correct C,H analysis for $C_{24}H_{56}Si_4$

[*] Prof. Dr. P. Boudjouk, U. Samaraweera, Dr. R. Sooriyakumaran, K. R. Anderson
Department of Chemistry, North Dakota State University
Fargo, ND 58105 (USA)
Dr. J. Chrusciel
Technical University, Institute of Polymers
PL-90-924 Lodz (Poland)

[**] This work was supported by the United States Air Force of Scientific Research (Grant No. 84-0008). *J. C.* was visiting research fellow in Fargo. The authors thank Prof. *N. Woolsey* for the ^{29}Si-NMR spectra of **6** and Prof. H. Sakurai for the ^{29}Si-NMR spectra of **7**.

These reactions are characteristic of a singlet silanediyl.[7] All silanediyls for which there is experimental[8] or theoretical[9] data indicate a singlet ground state although large groups on silicon should lead to a more nearly linear geometry and close the gap between the singlet and triplet states.[9]

When **4** or **5** is photolyzed (Rayonet, 254 nm, hexane) in methanol, di-*tert*-butylmethoxysilane is obtained in approximately 70% yield from silanediyl insertion into the O–H bond of methanol [Eq. (c)]. With triethylsilane as

$$\mathbf{4}\ (\mathbf{5}) \xrightarrow[MeOH]{h\nu} t\mathrm{Bu_2Si(H)OMe} \qquad \text{(c)}$$

trapping agent, **3** is isolated in 72–84% yield after photolysis. In the presence of a three-fold excess of bis(trimethylsilyl)acetylene, **2** gave, as expected,[6] the silirene **6** (Table 1) which was isolated in 90% yield.

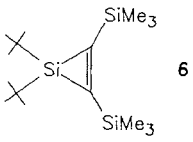

6

4 and **5** are the only alkylsiliranes known to be photochemically active, attributable perhaps to additional strain put on the molecule by the steric interaction between the *tert*-butyl groups on silicon and the methyl groups on the carbon atoms.

We have also examined the products of the reaction of lithium with **1a**, **1b** and **1c** in the absence of a trapping agent. To our surprise, we found that the dichloro derivative **1a** forms different products from those obtained from **1b** and **1c**. From **1a** we obtained tetra-*tert*-butyldisilane (65%) as did *Masamune*[10] and *Watanabe*,[11] but were also able to isolate for the first time the novel ring compound, *trans*-1,1,2,3,3,4-hexa-*tert*-butylcyclotetrasilane (Table 1) in 15% yield. **1b**, on the other hand, gave good yields (> 50%) of pure hexa-*tert*-butylcyclotrisilane, similar to that reported for **1c**.[3]

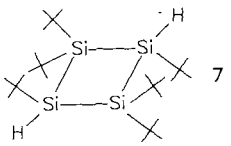

7

From these preliminary studies it is apparent that dihalosilanes are convenient sources of silanediyls, that the silanediyls produced from the three dihalides **1a–c** differ in their chemistry, and that free silanediyls are, at least in one or two of the three examples, probably not involved. More likely "silylenoid" species with structures like **8** are produced in which the halogen, X, plays an important role in the structure, and therefore the reactivity, of the intermediate.

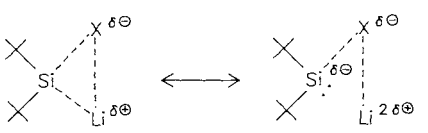

8

Moreover, these results suggest that other highly hindered dihalosilanes may react with lithium to produce silanediyls in synthetically useful quantities.

Experimental

A dispersion of 0.1 g (14.3 mmol) of lithium (30% in mineral oil) and 1% sodium was washed with hexane to remove the mineral oil and treated in a flask under N_2 with anhydrous THF (5 mL), triethylsilane (3.65 g, 31.5 mmol) and di-*tert*-butyldichlorosilane (**1a**) (1.5 g, 7.1 mmol). After irradiating the reaction mixture with ultrasonic waves (Bransonic model 220, 55 kHz, 150 W) for 6 h, the THF was removed by evaporation and replaced by hexane. The hexane soluble fraction was separated from the lithium chloride by filtration and 1,1,1-triethyl-2,2-di-*tert*-butyldisilane (**3**) was isolated by preparative GC in 60% yield.

Received: May 16, 1988 [Z 2759 IE]
German version: *Angew. Chem. 100* (1988) 1406

[1] P. P. Gaspar in M. Jones, R. A. Moss, Jr. (Eds.): *Reactive Intermediates, Vol. 3*, Wiley Interscience, New York 1985.
[2] Presented in part at the VIIIth Int. Symp. Organomet. Chem. (St. Louis, June 7–12, 1987), Mo. Abstract No. PAB-13.
[3] A. Schäfer, M. Weidenbruch, K. Peters, H. G. von Schnering, *Angew. Chem. 96* (1984) 511; *Angew. Chem. Int. Ed. Engl. 23* (1984) 302; see also Al Schäfer, M. Weidenbruch, W. Saak, S. Pohl, *ibid. 99* (1987) 806 and *26* (1987) 776.
[4] K. M. Welsh, J. Michl, R. West, *J. Am. Chem. Soc.*, in press.
[5] K. R. Anderson, *M. S. Thesis*, North Dakota State University, Fargo, ND, USA 1984. For a review of synthetic applications of ultrasonic waves in heterogeneous systems see, P. Boudjouk, *ACS Symp. Ser. 333* (1987) 209.
[6] The chemistry and properties of siliranes and silirenes have been investigated: D. Seyferth, D. C. Annarelli, S. C. Vick, *J. Organomet. Chem. 272* (1984) 123, and references cited therein.
[7] V. Torterelli, M. Jones, Jr., S.-H. Wu, Z.-H. Li, *Organometallics 2* (1983) 759.
[8] A. Kasden, E. Herbst, W. C. Lineberger, *J. Chem. Phys. 62* (1975) 541, and references cited therein.
[9] M. S. Gordon, *Chem. Phys. Lett. 114* (1985) 348, and references cited therein.
[10] S. Masamune, S. Murakami, H. Tobita, *Organometallics 2* (1983) 1464.
[11] H. Watanabe, T. Muroaka, M. Kageyama, K. Yoshizumi, Y. Nagai, *Organometallics 3* (1984) 141.

The Microwave Spectrum and Structure of the Ethylene–Sulfur Dioxide Complex**

By *Marabeth S. LaBarge, Kurt W. Hillig II*, and *Robert L. Kuczkowski**

Dedicated to Professor Hans Bock on the occasion of his 60th birthday

Ethylene and SO_2 each form complexes with a variety of species. However, there is not much information about the complex formed between them although it has been observed by mass spectrometry.[1,2] We were interested in the structure of the ethylene–SO_2 dimer in part because it might model the early stages of the classic cycloaddition reaction between ethylene and ozone. This report describes the assignment of the microwave spectrum of this complex. The structure which is deduced indicates that the SO_2 plane sits over the C_2H_4 plane, suggestive of an interaction between the π systems. The data do not discriminate between structures which place the oxygens versus the sulfur closer to the carbon atoms. While the former would resemble a precursor to 1,3-dioxa-2-thiocyclopentane, the latter would resemble a precursor to thiirane dioxide. The complex also shows evidence of tunneling between two equivalent forms.

[*] Prof. Dr. R. L. Kuczkowski, K. W. Hillig II, M. S. LaBarge
Department of Chemistry, The University of Michigan
Ann Arbor, MI 48109 (USA)

[**] This work was supported by the National Science Foundation (Grant CHE-8614340).

The spectrum was observed with a Fourier transform microwave spectrometer.[3] The complex was formed when a mixture of 1% ethylene, 1% SO_2 and 98% neon (or argon) at total pressures of 1–2 atm expanded through a supersonic nozzle; both C_2H_4 and SO_2 were necessary to observe the spectrum. The spectrometer was equipped with Stark plates to examine transitions in an applied electric field to aid in the assignment of quantum numbers; combination differences were also helpful in some assignments.

Fifty-six transitions were assigned; selected transitions are given in Table 1. The spectrum was characterized by

Table 1. Selected rotational transitions of the C_2H_4–SO_2 complex [a].

J'	K'_p	K'_o	v'	J''	K''_p	K''_o	v''	ν(MHz)	o-c
1	1	0	1	0	0	0	0	8680.110	−0.173
1	1	0	0	0	0	0	1	8653.911	0.111
3	1	2	1	2	0	2	0	16890.173	0.184
3	1	2	0	2	0	2	1	16864.198	−0.207
4	0	4	1	3	1	2	0	8511.810	0.111
4	0	4	0	3	1	2	1	8487.551	−0.063
2	2	0	1	2	1	2	0	14998.963	−0.002
2	2	0	0	2	1	2	1	15061.264	−0.006
4	2	2	1	4	1	4	0	16520.810	0.081
4	2	2	0	4	1	4	1	16581.117	−0.118
2	2	1	1	2	1	1	0	13925.001	−0.009
2	2	1	0	2	1	1	1	13987.692	0.026
7	2	6	1	7	1	6	0	9829.805	0.084
7	2	6	0	7	1	6	1	9891.021	−0.117
2	0	2	0	1	0	1	0	7307.476	−0.032
2	0	2	1	1	0	1	1	7307.264	0.040
4	0	4	0	3	0	3	0	14464.251	0.103
4	0	4	1	3	0	3	1	14463.109	−0.095
2	1	1	0	1	1	0	0	7677.424	−0.098
2	1	1	1	1	1	0	1	7677.424	0.106
4	1	3	0	3	1	2	0	15313.382	−0.096
4	1	3	1	3	1	2	1	15313.254	0.160

[a] J is the rotational quantum number, K_p and K_o are the quantum numbers in the prolate and oblate limit, respectively, v is the vibrational quantum number (o-c is observed minus calculated frequencies).

doublets of unequal intensity. The μ_a transitions had splittings of 0–2 MHz, while the μ_c transitions were split by 20–63 MHz. The intensity variations and splittings indicate a tunneling motion in which the μ_c component changes its direction; the vibrational selection rule is $\Delta v=0$ for μ_a transitions and ± 1 for μ_c lines. The presence of such splitting precludes an equilibrium structure with C_2 or C_{2v} symmetry but is consistent with C_s symmetry and dipole components along the a and c inertial axes.

All of the transitions were simultaneously fit to rotational and quartic centrifugal distortion constants and an energy difference for two states, using the formalism of *Pickett*.[4] The derived constants are given in Table 2. While the frequency fit is not within experimental error (0.124 MHz rms), addition of the remaining quartic or sextic distortion terms or a P_{ac} term to account for a vibration-rotation interaction arising from the tunneling motion did not improve the fit.

An average structure for the complex can be estimated from the moments of inertia of the lower energy state. Assuming that the structures of ethylene and SO_2 do not change in the complex, the model shown in Figure 1 depends on the distance between the centers of mass of the moieties (R_{cm}) and two angles, $\theta+90°$ and $\phi+90°$, describing the angle that the ethylene and SO_2 planes make with the line between their centers of mass. For this model,

Table 2. Spectroscopic constants of the C_2H_4–SO_2 complex [a].

		$v=0$	$v=1$–$v=0$
A	[MHz]	6670.9565(27) [b]	−22.3538(18)
B	[MHz]	2007.5165(6)	− 0.1050(5)
C	[MHz]	1655.8947(5)	− 0.0144(4)
E	[MHz]		24.4456(30)
D_J	[kHz]	5.401(15)	− 1.001(4)
D_{JK}	[kHz]	177.395(69)	−23.460(87)
D_K	[kHz]	−153.86(57)	0.0 [c]
d_1	[kHz]	1.253(4)	0.0 [c]
d_2	[kHz]	0.839(5)	0.0 [c]

[a] Watson S reduction, I^r representation [9]. [b] In parenthesis, one standard deviation in the last figures given. [c] Constrained in the fit.

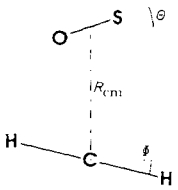

Fig. 1. Projection of Et-SO_2 onto the symmetry plane showing the definitions of R_{cm}, θ and ϕ.

the structures of ethylene and SO_2[5] predict a value for the out-of-plane moment of inertia arising from the b coordinates ($P_{bb}=1/2(I_a+I_c-I_b)$) of 65.9066 amu·Å^2 which agrees well with the observed value of 64.6073 amu·Å^2. The discrepancy is typical for weakly bonded complexes and arises from their large-amplitude motions.

The data are relatively insensitive to the sign of θ or ϕ; hence four structures are compatible with the data as shown in Figure 2. Values of $R_{cm}=3.509$ Å, $\theta=\pm 26.6°$

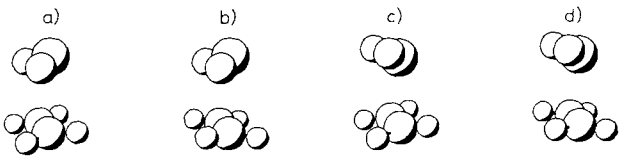

Fig. 2. Views of four conformations compatable with the rotational constants. a) $+\theta$, $-\phi$; b) $+\theta$, $+\phi$; c) $-\theta$, $-\phi$; d) $-\theta$, $+\phi$.

and $\phi=\pm 6.8°$ (taken with the same sign) give (in MHz) $A=6669$, $B=2007$, $C=1645$ while with opposite signs $A=6671$, $B=2007$, $C=1644$. Preliminary measurements of the dipole moment components ($\mu_c>\mu_a$; $\mu_b=0$) are also compatible with the orientation of the SO_2 obtained from the inertial moments. In all of the structures the C_2H_4 and SO_2 planes are more or less parallel. While this is suggestive of a HOMO–LUMO interaction, it has been pointed out that electrostatic interactions may also account for the orientational preference, even when the interaction is as large as 9 kcal as in $NMe_3 \cdot SO_2$.[6,7] The interaction between ethylene and SO_2 is probably much weaker; a dissociation energy of 426 cm^{-1} is obtained from the D_J distortion constant using the standard approximations for weak complexes.[8] It is not difficult to envisage several possible tunneling motions which could give equivalent forms and change the direction of μ_c, such as an internal rotation or flipping of the SO_2 from one side of the a axis to the other along with a concerted motion of the ethylene.[10] Since the

energy difference between the states is only 24.45 MHz, the barrier hindering the tunneling is appreciable.

At this point it is difficult to estimate how closely the average structural parameters may be to the equilibrium values. Isotopic data will be necessary to further refine the structural model, distinguish between the possible structures in Figure 2 and shed more light on the tunneling motion. The possibility of tunneling to equivalent forms by more than one pathway with different barriers also cannot be excluded without further study.

Received: May 19, 1988 [Z 2768 IE]
German version: *Angew. Chem. 100* (1988) 1407

CAS Registry number:
$H_2C{=}CH_2{\cdot}SO_2$, 84508-07-6.

[1] J. S. Muenter, R. L. DeLeon, A. Yokozeki, *Faraday Discuss. Chem. Soc. 73* (1982) 63.
[2] R. L. DeLeon, J. S. Muenter, *Atmos. Environ. 18* (1984) 995.
[3] K. W. Hillig II, J. Matos, A. Scioly, R. L. Kuczkowski, *Chem. Phys. Lett. 133* (1987) 359.
[4] H. Pickett, *J. Chem. Phys. 59* (1972) 1715.
[5] M. D. Harmony, V. W. Laurie, R. L. Kuczkowski, R. H. Schwendman, D. A. Ramsay, F. J. Lovas, W. J. Lafferty, A. G. Maki, *J. Phys. Chem. Ref. Data 8* (1979) 619.
[6] P. Kollman, *Acc. Chem. Res. 10* (1977) 365.
[7] M. S. LaBarge, J. Matos, K. W. Hillig II, R. L. Kuczkowski, *J. Am. Chem. Soc. 109* (1987) 7222.
[8] M. R. Keenan, E. J. Campbell, T. J. Balle, L. W. Buxton, T. K. Minton, P. D. Soper, W. H. Flygare, *J. Chem. Phys. 72* (1980) 3070.
[9] J. K. G. Watson in J. R. Durig (Ed.): *Vibrational Spectra and Structure*, Elsevier, Amsterdam 1977, pp. 1–88.
[10] Note added in proof (Sept. 22, 1988). Another assignment has been found which does not reguire a change in v and which fits to 0–10 kHz (o-c, Table 1). Since the reassignment involves only vibrational quantum numbers, the rotational constants and structural conclusions are essentially unchanged. With this assignment, the doublets arise from an internal motion where μ_c does not change direction, for example, rotation of ethylene about the C–C bond.

Solubilization of Elemental Sulfur in Water by Cationic and Anionic Surfactants**

By *Ralf Steudel** and *Gabriele Holdt*

Elemental sulfur belongs to the particularly hydrophobic substances that are neither wetted nor dissolved by water. The solubility of α-S_8 in water is 5 μg L^{-1} at 20°C[1] and is thus practically negligible. The dissolution of larger amounts of sulfur in aqueous media has so far only been accomplished by chemical reactions, e.g. oxidation or nucleophilic degradation with sulfides. We have now found that the solubility of α-S_8 in H_2O is increased by a factor of at least 5000 when neutral surfactants are present which do not alter the S_8 molecule chemically. The following amphiphilic surfactants[2] have been investigated regarding their suitability for the solubilization of sulfur:

1: "SDS", sodium dodecylsulfate [$C_{12}H_{25}SO_4Na$]
2: "Tergitol 7", sodium [4-ethyl-1-(3-ethylpentyl)octyl]sulfate [$C_{17}H_{35}SO_4Na$]
3: "CTAB", hexadecyl(trimethyl)ammonium bromide [$C_{16}H_{33}(CH_3)_3NBr$]

[*] Prof. Dr. R. Steudel, G. Holdt
Institut für Anorganische und Analytische Chemie der Technischen Universität, Sekr. C 2
Strasse des 17. Juni 135, D-1000 Berlin 12

[**] Sulfur compounds, Part 119. This work was supported by the Deutsche Forschungsgemeinschaft and the Fonds der Chemischen Industrie. We thank Prof. Dr. *J.-G. Kuenen* (Delft) for drawing our attention to Refs. [12] and [13]. – Part 118: D. M. Giolando, M. Papavassilion, J. Pickardt, T. B. Rauchfuss, R. Steudel, *Inorg. Chem. 27* (1988) 2596.

A mixture of excess cyclooctasulfur (α-S_8, recrystallized from CS_2; 1 mg mL^{-1}, particle size 160–200 μm), water (10–50 mL), and a known amount of surfactant was stirred for a known period of time in a flask fitted with a magnetic stirrer. Small samples (ca. 1 mL) were withdrawn from the mixture with a syringe, forced through a filter of 0.45 μm pore width,[3] and quantitatively analyzed for S_8 by high-pressure liquid chromatography using an octadecylsilane separating column.[4] Blank runs without surfactant gave no S_8 peak, since the limit of detection of our apparatus lies at ca. 0.1 μg mL^{-1}. Figure 1 shows the increase in S_8

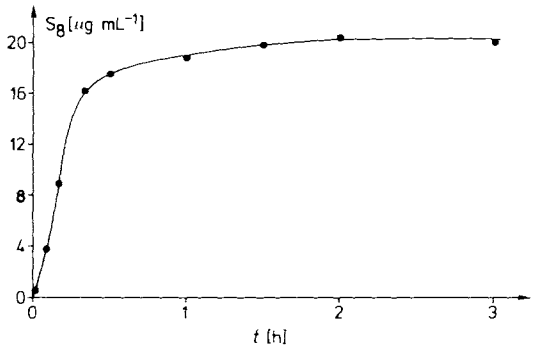

Fig. 1. Increase of S_8 concentration with time in an aqueous solution of SDS at 22°C (50 mg of **1** per mL) after mixing the components at $t = 0$.

concentration with time for the case of SDS **1** at 22°C and a surfactant concentration of 50 mg mL^{-1}. The saturation concentration reached after 90 min is 20 μg mL^{-1} S_8, i.e. 4000 times more than in pure water. With 10 mg of **1** per mL, a saturation concentration of 2.8 μg of S_8 per mL was achieved. In a completely analogous way the S_8-saturation value was also achieved within 90 minutes on using **2** or **3** (in each case 10 mg mL^{-1}); at 22°C, the values are 7.5 μg mL^{-1} in the case of **2** and 8.2 μg mL^{-1} in the case of **3**.[6] Thus, referred to the same amount of surfactant, **3** dissolves the most S_8. A saturated solution of **3** gave an S_8 concentration of 26.5 μg mL^{-1} (22°C) after 60 min—that is 5300 times the solubility in pure water.

Figure 2 shows the dependence of the S_8-saturation concentration on the surfactant concentration at 22°C. For all three surfactants investigated, similar and, in a certain range, linear functions were obtained. In the case of **1** the best fitted straight line cuts the abscissa at about 3.9 mg mL^{-1} (0.014 mol L^{-1}), i.e. a marked solubilization first

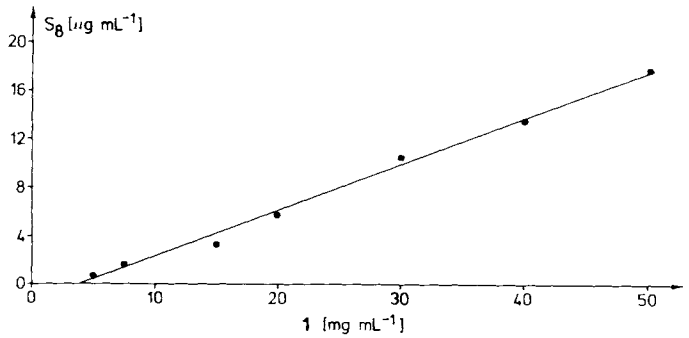

Fig. 2. S_8 saturation concentration in aqueous SDS **1** at 22°C as a function of the surfactant concentration. The best fitted straight line has the form $y = 0.38x + 3.9$ (correlation coefficient: 0.994).

takes place above this concentration, which is in good agreement with the critical concentration of **1** for micelle formation at room temperature (0.011 mol L^{-1}[7]). However, small S_8 concentrations (0.5 ± 0.2 μg mL^{-1}) were still measured with only 1 or 2 mg of **1** per mL. The absorption spectrum of an S_8-solution in aqueous Tergitol 7 **2** is very similar to the spectra of equally concentrated S_8-solutions in methanol/water (80/20 v/v)[8] and in cyclohexane; the extinctions in the range 235–300 nm for S_8 in **2** lie between those in CH_3OH/H_2O and C_6H_{12} (see Fig. 3).

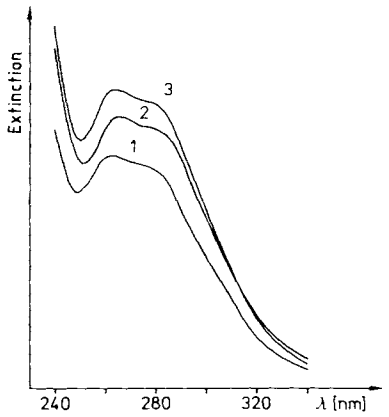

Fig. 3. UV absorption spectra of S_8 in methanol/water (80/20 v/v; 16.0 mg mL^{-1}; curve 1), in aqueous Tergitol 7 **2** (16.7 mg S_8/mL; curve 2), and in cyclohexane (17.1 mg S_8/mL; curve 3). All three spectra were measured with reference cuvettes containing the pure solvent.

As expected, the S_8-saturation concentration at constant surfactant concentration increases with increasing temperature, particularly in the range 40–60°C (see Fig. 4).

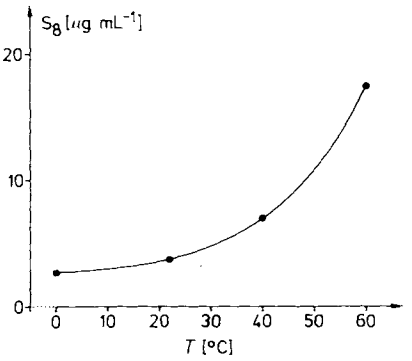

Fig. 4. Temperature-dependence of the S_8 saturation concentration in an aqueous solution of Tergitol 7 (10 mg of **2**/mL).

Above a critical concentration in water, **1**, **2** and **3** form spherical or rod-shaped micelles, the average number of particles per micelle being ca. 55 in the case of **1**.[8] The apolar hydrocarbon residues, which behave like a liquid solvent and can intercalate S_8 molecules are located in the interior of the micelle.[9] The longer the hydrocarbon chains the higher the saturation concentration, because the length of the hydrocarbon chains determines the volume of the apolar part of the micelles. The number and size of the micelles increases with increasing surfactant concentration and, accordingly, the S_8-saturation concentration increases linearly. If one assumes a micelle size of 55 anions in the case of **1** then the S_8 concentration of 0.77 μg mL^{-1} at a surfactant concentration of 5 mg mL^{-1} corresponds to ca. one molecule of S_8 in 100 micelles or to 5500 molecules of **1**. This number can be regarded as the lower limit, since those portions of the surfactant that are bound at the phase boundaries or are dissolved as monomers have been neglected in the calculation. The solubility of α-S_8 in comparable hydrocarbons such as *n*-heptane is one S_8 molecule to 700 heptane molecules at 25°C.

Exploratory experiments show that other allotopes of sulfur (e.g. S_6) can also be dissolved in aqueous surfactant solutions, although in this case a slow conversion into the more stable S_8 is observed. It can be expected that other apolar molecular compounds (e.g. white phosphorus P_4, cyclic selenium sulfides Se_xS_y, diorganosulfanes R_2S_n, sulfur–nitrogen compounds such as S_4N_4, etc.) can be dissolved in the same way in aqueous phases, so that chemical reactions of these substances in water should be accelerated considerably by surfactants.

Our findings now explain how it is possible that certain sulfur bacteria enzymatically oxidize elemental sulfur despite its insolubility at 20–25°C. These include, e.g. *Thiobacillus ferrooxidans* and *Thiobacillus thiooxidans*, which play a decisive role in bacterial ore leaching processes.[11] These organisms grow directly on sulfur particles suspended in the culture medium, from which S_8 is thereby apparently extracted, so that, on the one hand, the bacterium secretes various surfactants (e.g. hydroxy fatty acids, phosphatidylinositol, ornithine derivatives[12]), and, on the other hand, the S_8 molecules dissolves in the hydrophobic regions of the outer bacterial membranes, which resemble the surfactant micelles.[13] Probably S_8 is transported into the interior of the cell in this way, where the chemical degradation—oxidation to sulfate—takes place.

Received: May 13, 1988;
revised: June 21, 1988 [Z 2758 IE]
German version: *Angew. Chem. 100* (1988) 1409

CAS Registry numbers:
1, 151-21-3; **2**, 3282-85-7; **3**, 57-09-0; **S**, 7704-34-7.

[1] J. Boulegue, *Phosphorus Sulfur 5* (1978) 127; S_8 is colloidally dissolved in hydrophilic sulfur sols, where polythionate micelles or vesicles function as solvent (see R. Steudel, T. Göbel, G. Holdt, *Z. Naturforsch. B Anorg. Chem. Org. Chem. 43* (1988) 203).
[2] **1**: Merck, content 99%; **2**: Fluka, aqueous solution (25%); **3**: Fluka, content ca. 98%.
[3] Higher S_8 values were obtained on using other filters (e.g. folded paper filters or glass frits (G4).
[4] Eluent: methanol (1 mL min^{-1}), column: Radial-Pak 10C18 (Waters), UV detector (254 nm), S_8 retention time: ca. 5 min; for further experimental details, including the calibration of the chromatographic system, see [5].
[5] R. Strauss, R. Steudel, *Fresenius Z. Anal. Chem. 326* (1987) 543.
[6] A very small portion of the sulfur (< 1%) is present in these surfactant solutions as S_7 and S_6.
[7] R. Steudel, D. Jensen, P. Winchen, P. Hugo, *Ber. Bunsenges. Phys. Chem. 92* (1988) 118.
[8] H. G. Hauthal (Ed.): *Alkansulfonate*, VEB Deutscher Verlag für die Grundstoffindustrie, Leipzig 1985, p. 87, 118–119.
[9] Probably water-soluble cyclophanes [10] can also intercalate S_8 and other hydrophobic inorganic molecules in their hydrophobic cavities in a similar way.
[10] F. Diederich, *Angew. Chem. 100* (1988) 372; *Angew. Chem. Int. Ed. Engl. 27* (1988) 362.
[11] S. A. Waksman, I. S. Joffe, *J. Bacteriol. 7* (1922) 239; K. Bosecker, *Forum Mikrobiol. 2* (1980) 98; K. Bosecker in P. Präve, U. Faust, W. Sittig, D. A. Sukatsch (Eds.): *Handbuch der Biotechnologie, 2. Aufl.*, Oldenbourg-Verlag, München 1984, p. 535.
[12] J. L. Beebe, W. W. Umbreit, *J. Bacteriol. 108* (1971) 612; H. W. Knoche, J. M. Shively, *J. Biol. Chem. 247* (1972) 170; C. Dees, J. M. Shively, *J. Bacteriol. 149* (1982) 798.
[13] T. A. Pivovarova, G. I. Karavaiko, *Mikrobiologiya 44* (1975) 269; L. A. Gromova, G. I. Karavaiko, A. V. Sevtsov, N. A. Pereverzev, *ibid. 52* (1983) 455.

1,4-Diphosphabutatrienes

By *Gottfried Märkl** and *Peter Kreitmeier*

Whereas cumulenes **1** up to the decanonaenes (n = 8) are known[1] (although their stability decreases with increasing n) azacumulenes **2** and diazacumulenes **3** are only represented, to the best of our knowledge, by ketenimines and carbodiimides, respectively (i.e., the parent compounds with n = 1).[2] For the higher α,ω-diazacumulenes **3**, n = 2, 3, an MO study on possible mechanisms of

$R_2C{=}C{=}_nCR_2$ **1** n = 1–8

$R'N{=}C{=}_nCR_2$ **2** n = 1 $RN{=}C{=}_nNR$ **3** n = 1

$R'P{=}C{=}_nCR_2$ **4** n = 1,2 $R'P{=}C{=}_nPR'$ **5** n = 1

isomerization has been carried out.[3] In the series of phosphacumulenes **4**, so far it has been possible to prepare a number of axially chiral phosphaallenes **4**, n = 1,[4,5] as well as the first *E*/*Z*-isomeric phosphabutatrienes **4**, n = 2.[6]

The only diphosphacumulene, the axially chiral "parent compound" diphosphaallene **5**, n = 1 (R' = 2,4,6-tri-*tert*-butylphenyl) is known through the work of *Karsch* et al.,[7] *Appel* et al.,[4b] and *Yoshifuji* et al.[8] *Yoshifuji* et al. succeeded in carrying out the chromatographic separation of the two optical antipodes.[9]

Herein we report on the synthesis of the 1,4-diphosphabutatriene **12**, a compound of type **5**, n = 2. It is the next higher homologue of diphosphaallene **5**, n = 1 and, accordingly, the first *E*/*Z*-isomeric α,ω-diphosphacumulene. The synthetic route is shown in Scheme 1.

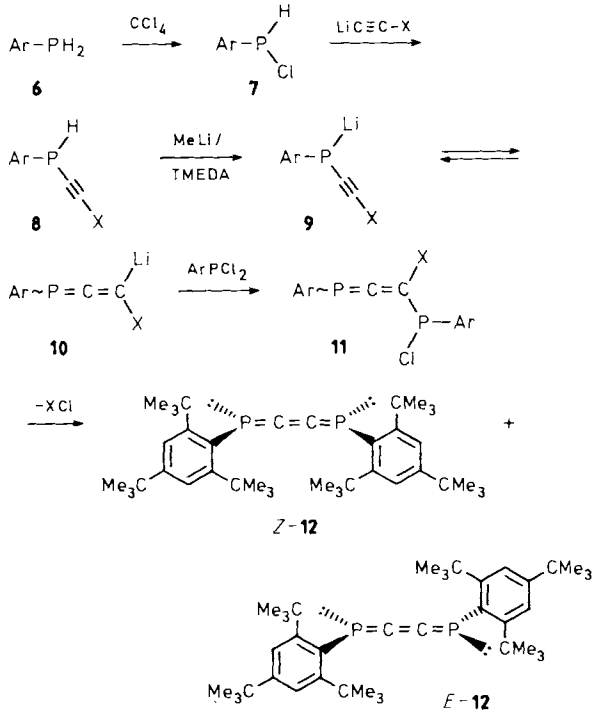

Scheme 1. Ar = 2,4,6-tri-*tert*-butylphenyl; X = trimethylsilyl.

[*] Prof. Dr. G. Märkl, Dipl.-Chem. P. Kreitmeier
Institut für Organische Chemie der Universität
Universitätsstrasse 31, D-8400 Regensburg (FRG)

The monochlorophosphane **7**,[10] accessible by chlorination of 2,4,6-tri-*tert*-butylphenylphosphane **6**[11] with tetrachloromethane, was first converted into the alkynylphosphane **8** (cf. Table 1).[12]

The lithium phosphide **9**, expected to be formed upon metalation of **8** with MeLi in tetramethylethylenediamine in THF (−60 to +25 °C), appears to exist in metallotropic equilibrium with the lithiated allene **10**. Reaction of **9**/**10** with trimethylchlorosilane results in formation of the bis(trimethylsilyl)phosphaallene **15** (yield 70%, cf. Table 1), whose structure was confirmed by independent synthesis from the silylphosphane **13** and bis(trimethylsilyl)ketene **14** (yield 40%). Complete shift of the equilibrium **9** ⇄ **10** toward **10** is presumably possible because direct substitution at phosphorus does not occur for steric reasons.

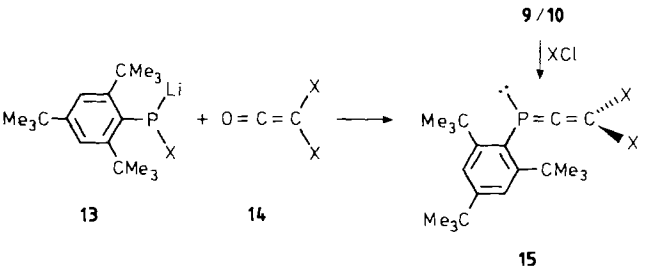

Reaction of **9**/**10** with 2,4,6-tri-*tert*-butyldichlorophosphane[13] in THF at −78 to +25 °C results initially in formation of the coupling product **11**, which can be isolated as a pale yellow solid but is impure owing to the partial loss of Me_3SiCl. Complete elimination of Me_3SiCl from **11** was achieved by treatment with KF/18-crown-6 in refluxing toluene. The desired 1,4-diphosphabutatriene **12** separates from the cooled solution as a yellow, finely crystalline solid which is only sparingly soluble in conventional solvents.

Table 1. Selected physical and spectroscopic data for **8**, **12**, and **15**.

8 [13]: Yield 42%; m.p. 91–93 °C (from EtOH); ^{1}H NMR ($CDCl_3$): $\delta = 0.20$ (s, $Si(CH_3)_3$), 1.44 (s, *p*-$C(CH_3)_3$), 1.76 (s, *o*-$C(CH_3)_3$), 5.81 (d, $J(P/H) = 247.4$ Hz, P–H), 7.55 (d, $J(P/H) = 2.9$ Hz, aryl-H); IR (KBr): $\tilde{\nu} = 2400$ (P–H), 2100 cm^{-1} (C≡C)

12: Yellow to orange, finely crystalline powder, yield 44%; m.p. 224–226 °C (dec.) (from toluene or tetrachloroethylene); ^{1}H NMR ($CDCl_3$, 250 MHz): *E*-**12**: $\delta = 1.34$ (s, *p*-$C(CH_3)_3$), 1.57 (s, *o*-$C(CH_3)_3$), 7.43 (s, aryl-H); *Z*-**12**: $\delta = 1.28$ (s, *p*-$C(CH_3)_3$), 1.55 (s, *o*-$C(CH_3)_3$), 7.29 (s, aryl-H); ^{31}P NMR ($CDCl_3/CHCl_3$, 101.257 Hz, 305 K): *E*-**12**: $\delta = 180.6$ (78%); *Z*-**12**: $\delta = 170.0$ (22%); (*n*-hexane): $\lambda_{max} = 213$ ($\varepsilon = 19700$), 244 (29700), 311 (3600), 387 (14700), 465 sh nm (1850); MS (70 eV): *m*/*z* 576 ($M^{\oplus\ominus}$, 70%), 520 ($[M - C_4H_8]^{\oplus\ominus}$, 10), 464 ($[520 - C_4H_8]^{\oplus\ominus}$, 10), 346 ($[Ar{-}P{=}C{=}C{-}P{-}Me]^{\oplus\ominus}$, 4), 288 ($[M/2]^{\oplus\ominus}$, 25), 575 ($[M - H]$, 69), 519 ($[575 - C_4H_8]$, 12), 463 ($[519 - C_4H_8]$, 11), 345 ($[Ar{-}P{=}C{=}C{-}P{=}CH_2]^{\oplus\ominus}$, 14), 315 ($[345 - 2CH_3]^{\oplus\ominus}$, 17), 301 ($[315 - CH_2]$, 20), 57 ($[C_4H_9]^{\oplus\ominus}$, 100)

15: Yellow, highly viscous oil; ^{1}H NMR ($CDCl_3$): $\delta = 0.22$ (s, $Si(CH_3)_3$), 1.79 (s, *o*-$C(CH_3)_3$), 1.46 (s, *p*-$C(CH_3)_3$), 7.47 (d, $J(P/H) = 2$ Hz, aryl-H); ^{31}P NMR ($CDCl_3$): $\delta = 3.84$; IR (neat): $\tilde{\nu} = 1650$, 1685 cm^{-1}; MS (70 eV): *m*/*z* 446 ($M^{\oplus\ominus}$, 11%), 276 ($[aryl\text{-}P]^{\oplus\ominus}$, 12), 261 ($[276 - {}^{\ominus}CH_3]^{\oplus}$, 10)

The formation of **12** (cf. Table 1) is essentially the result of a Wittig-Peterson-like condensation. The metallotropic rearrangement **9** → **10** suggests a novel principle for the synthesis of α,ω-diphosphacumulenes.

The ^{1}H NMR data reveal that **12** is present as an *E*/*Z*-isomeric mixture; we have assigned the *E* configuration to the main component (78%). The isomeric distribu-

 © VCH Verlagsgesellschaft mbH, D-6940 Weinheim, 1988 0570-0833/88/1010-1360 $ 02.50/0

tion is supported by the ^{31}P NMR spectrum: The δ values agree with that for the diphosphaallene **5**, n = 1 (δ = 141.6), and an upfield shift on going from the *E* isomer to the *Z* isomer was also found, for example, in the case of bis(2,4,6-tri-*tert*-butylphenyl)diphosphene (*E* isomer, δ = 492; *Z* isomer, δ = 368).[14]

Received: February 29, 1988;
revised: June 3, 1988 [Z 2638 IE]
German version: *Angew. Chem. 100* (1988) 1411

[1] See, e.g., *Methoden Org. Chem. Houben-Weyl 5th ed. 2a.*
[2] F. Kutzer, K. Douraghi-Zadeh, *Chem. Rev. 67* (1967) 107.
[3] M. S. Gordon, H. Fischer, *J. Am. Chem. Soc. 90* (1968) 2471.
[4] a) M. Yoshifuji, K. Toyota, K. Shibayama, N. Inamoto, *Tetrahedron Lett. 25* (1984) 1809; b) R. Appel, P. Fölling, B. Josten, M. Siray, V. Winkhaus, F. Knoch, *Angew. Chem. 96* (1984) 620; *Angew. Chem. Int. Ed. Engl. 23* (1984) 619.
[5] G. Märkl, S. Reithinger, *Tetrahedron Lett. 29* (1988) 463.
[6] G. Märkl, H. Sejpka, S. Dietl, B. Nuber, M. L. Ziegler, *Angew. Chem. 98* (1986) 1020; *Angew. Chem. Int. Ed. Engl. 25* (1986) 1003.
[7] H. H. Karsch, F. H. Köhler, H.-U. Reisacher, *Tetrahedron Lett. 25* (1984) 3687; H. H. Karsch, H.-U. Reisacher, G. Müller, *Angew. Chem. 96* (1984) 619; *Angew. Chem. Int. Ed. Engl. 23* (1984) 618.
[8] M. Yoshifuji, K. Toyota, N. Inamoto, *J. Chem. Soc. Chem. Commun. 1984*, 689.
[9] M. Yoshifuji, K. Toyota, T. Niitsu, N. Inamoto, Y. Okamoto, R. Aburatani, *J. Chem. Soc. Chem. Commun. 1986*, 1550.
[10] J. Escudie, personal communication.
[11] K. Issleib, H. Schmidt, C. Wirkner, *Z. Anorg. Allg. Chem. 488* (1982) 75.
[12] S. Reithinger, *Diplomarbeit*, Universität Regensburg 1987.
[13] M. Yoshifuji, J. Shima, N. Inamoto, *J. Am. Chem. Soc. 103* (1981) 4587.
[14] A.-M. Caminade, M. Verrier, C. Ades, N. Paillous, M. Hoenig, *J. Chem. Soc. Chem. Commun. 1984*, 875.

Novel Layer Structure of Sodium Calix[4]arenesulfonate Complexes—a Class of Organic Clay Mimics?**

By *Anthony W. Coleman, Simon G. Bott, S. David Morley, C. Mitchell Means, Kerry D. Robinson, Hongming Zhang,* and *Jerry L. Atwood**

Calixarenes[1] **1** have been studied primarily for their use as enzyme mimics since they have the ability to bind both organic and inorganic substrates.[2,3] Recently, water-

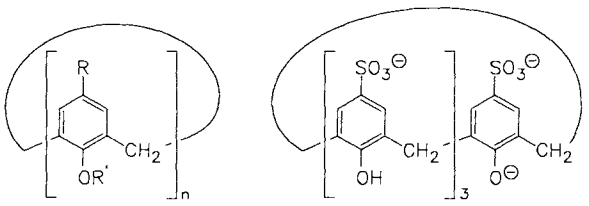

1 2

soluble calixarenes **1**, R = CO_2H, NO_2, SO_3H, have been prepared and successfully applied in areas of transport and selective complexation, although little is known of their structure.[4] To better understand the properties of these compounds, we prepared the sodium salt of calix[4]arenesulfonate **2** and obtained single crystals from an aqueous solution.[5] X-ray structural analysis revealed that, in the solid state, the calixarene sulfonate ion combines with sodium ions and water molecules in the ratio 1 : 5 : 12 to produce the highly ordered arrangement **2** · 5 $Na^{\oplus}$ · 12 H_2O (Fig. 1a). While at first glance this appears highly reminiscent of a bioorganic bilayer membrane,[6] the similarity to a clay is, in fact, far more compelling.

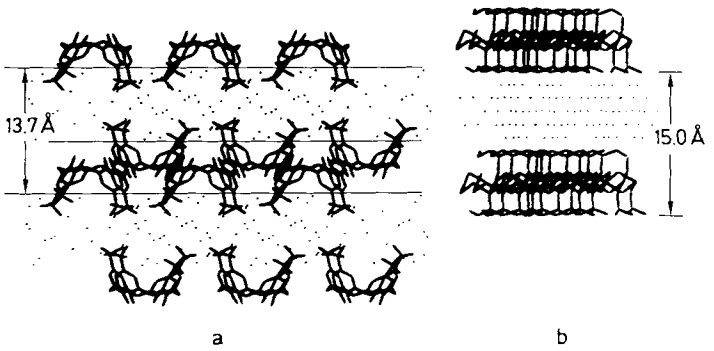

Fig. 1. a) Bilayer structure of **2** · 5 $Na^{\oplus}$ · 12 H_2O in the crystal; b) layer structure of hydrated sodium vermiculite.

The structure may be divided into organic and inorganic layers. The organic layer is formed by interlocking calixarenes in an up-down fashion, a sodium ion and a water molecule interacting simultaneously with the phenolic oxygen atoms of one calixarene and the sulfonate oxygen atoms of others. To accommodate this cation, the superacidic proton[7] of each calixarene has been removed; the resultant negatively charged oxygen atom forms a strong electrostatic bond with the sodium ion. The inorganic layer is comprised of the remaining four sodium ions and eleven water molecules. These exist in a vast hydrogen-bonded array which includes the sulfonate head groups of the calixarenes.

Upon recrystallization of sodium calix[4]arenesulfonate from acetone/water, thin plates are obtained. These tend to aggregate in sheets, but may easily be cleaved in a manner resembling micas. The X-ray structure[8] shows this to be the calix[4]arenesulfonate ion associated with five sodium ions, eight water molecules, and one acetone molecule. As with the parent compounds, **2** · 5 $Na^{\oplus}$ · 8 H_2O · Me_2CO consists of bilayers of calixarenesulfonates intercalating layers of water molecules and sodium ions. The acetone molecule, however, is a guest within the cavity of the calixarene anion,[9] with the polar carbonyl group projecting into the inorganic layer (Fig. 2).

To compare the overall layer structure with that of a clay of 2 : 1 layer type, Figure 1a shows the parent water systems, and Figure 1b the structure of hydrated sodium vermiculite.[10] The similarity is striking. Both consist of layers of covalent material with hydrated cations between. If one

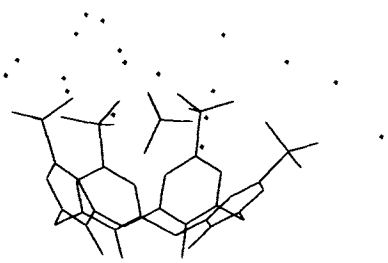

Fig. 2. Inclusion of the acetone molecule in the calixarene cavity in the calix[4]arenesulfonate complex **2** · 5 $Na^{\oplus}$ · 8 H_2O · Me_2CO. The carbonyl oxygen atom is positioned so that it projects into the polar layer.

[*] Prof. J. L. Atwood, Dr. A. W. Coleman, Dr. S. G. Bott, S. D. Morley, Dr. C. M. Means, K. D. Robinson, Dr. H. Zhang
Department of Chemistry, University of Alabama
Tuscaloosa, AL 35487 (USA)

[**] This work was supported by the U. S. National Science Foundation.

considers the sulfonate groups as part of the hydrated layer, the comparisons of Figure 1 are close. The hydrated layers are 8.3, 8.4, and 9.4 Å in the calixarene/water parent system ($2 \cdot 5\,Na^{\oplus} \cdot 12\,H_2O$), the calixarene/acetone structure ($2 \cdot 5\,Na^{\oplus} \cdot 8\,H_2O \cdot Me_2CO$), and the sodium vermiculite clay,[10] respectively. The sum of the distances between the two layers in the title calixarene materials is near 13.7 Å. This may be compared with 15.0 Å in sodium vermiculite and 14.4–15.6 Å in smectite.[11]

As with the clays, the sodium ions are exchangeable. Structural verification has been obtained for $K^{\oplus}$, $Rb^{\oplus}$, $Cs^{\oplus}$,[12] and $NH_4^{\oplus}$ analogues.[13] With the $NH_4^{\oplus}$ derivative, the displacement of water by the ammonium cations is seen, a feature also observed for clays.[14]

In conclusion, we have shown that the sodium calix[4]arenesulfonate complexes with water or water/acetone closely mimic the structural behavior of clays. However, they possess the advantage of a secondary size- and polarity-selective cavity formed by the cone of the calixarene coupled with an ease of chemical modification of the organic calixarene fragment.

Received: April 12, 1988;
revised: July 7, 1988 [Z 2700 IE]
German version: *Angew. Chem. 100* (1988) 1412

[1] C. D. Gutsche, *Top. Curr. Chem. 123* (1985) 1.
[2] S. G. Bott, A. W. Coleman, J. L. Atwood, *J. Am. Chem. Soc. 108* (1986) 1709.
[3] S. G. Bott, A. W. Coleman, J. L. Atwood, *J. Chem. Soc. Chem. Commun. 1986*, 610.
[4] S. Shinkai, *Pure Appl. Chem. 58* (1986) 1523.
[5] $2 \cdot 5\,Na^{\oplus} \cdot 12\,H_2O$: Synthesis was accomplished by reaction of the calix[4]arene **1**, R = H, R′ = H, with H_2SO_4 at 60°C for 3 h. This was followed by neutralization with $BaCO_3$ and addition of Na_2CO_3 to pH 9. Large, colorless crystals of $2 \cdot 5\,Na^{\oplus} \cdot 12\,H_2O$ were obtained by slow evaporation of the solution. The compound crystallized in the triclinic space group $P\bar{1}$ with $a = 10.998(6)$, $b = 13.582(5)$, $c = 14.472(5)$ Å, $\alpha = 74.01(3)$, $\beta = 89.09(4)$, $\gamma = 86.50(4)°$, $Z = 2$. Refinement based on 4727 observed reflections led to a conventional R value of 0.050 [15].
[6] S. J. Singer, G. L. Nichelson, *Science (Washington) 175* (1972) 720.
[7] S. Shinkai, T. Mori, T. Tsubaki, T. Sone, O. Manobe, *Chem. Lett. 1986*, 1351.
[8] $2 \cdot 5\,Na^{\oplus} \cdot 8\,H_2O \cdot Me_2CO$: Colorless crystals of the compound were prepared by recrystallization of $2 \cdot 5\,Na^{\oplus} \cdot 12\,H_2O$ from an acetone/water solution. The compound belongs to the monoclinic space group $P2_1/n$ with $a = 11.05(4)$, $b = 14.157(4)$, $c = 27.162(7)$ Å, $\beta = 97.47(3)°$, $Z = 4$. Refinement based on 4724 observed reflections led to $R = 0.054$ [15].
[9] The acetone molecules are, in fact, complexed in aqueous solution by the calixarenes **2**, as shown by ^1H NMR studies. In the ratio 2 : 1 **2** : acetone, the acetone methyl resonance is found as a broad singlet at $\delta = 0.7$–0.8. This demonstrates that the methyl groups are well shielded in the vicinity of the aromatic rings. In the ratio 1 : 1, the signal is found at $\delta = 1.0$, and in the ratio 1 : 4 the chemical shift of $\delta = 1.8$ is near the uncomplexed value of $\delta = 2.05$ for **2**. The NMR experiments were performed at 19°C in D_2O on a Nicolet NT 200.
[10] P. G. Slade, R. A. Stone, E. W. Radoslovich, *Clays Clay Miner. 33* (1985) 51.
[11] S. W. Bailey in G. W. Brindley, G. Brown (Eds.): *Crystal Structures of Clay Minerals and their Identification*, Monograph 5 of the Mineralogical Society, London 1980, pp. 1–123.
[12] J. L. Atwood, A. W. Coleman, S. G. Bott, *J. Inclusion Phenom.*, in press.
[13] S. G. Bott, A. W. Coleman, J. L. Atwood, *J. Am. Chem. Soc. 110* (1988) 610.
[14] B. Mason, L. G. Berry: *Elements of Mineralogy*, Freeman, San Francisco 1968.
[15] Further details of the crystal structure investigations can be obtained from the Director of the Cambridge Crystallographic Data Centre, Lensfield Road, Cambridge CB2 1EW (England), by quoting the full literature citation.

A Photolytic Entry into Oxepane Systems**

By *K. C. Nicolaou,* C.-K. Hwang,* and *D. A. Nugiel*

The oxepane ring skeleton is becoming an increasingly common structural feature of natural products, particularly those of marine origin.[1] As part of our program directed toward the total synthesis of brevetoxin B **1**,[2] and in an effort to develop general and mild methods for the construction of oxepanes,[3] we designed the strategy shown in Scheme 1 as a potential route to these systems that may be applicable to the above target. According to this strategy, the dithionoester **2** was expected to generate

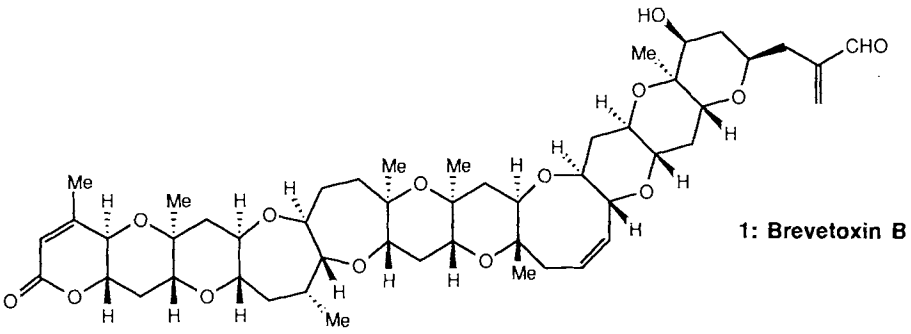

1: Brevetoxin B

the 1,2-dithietane system **3** via diradical formation under photolytic conditions.[4] Expulsion of disulfur under the reaction conditions should then lead to the didehydrooxe-

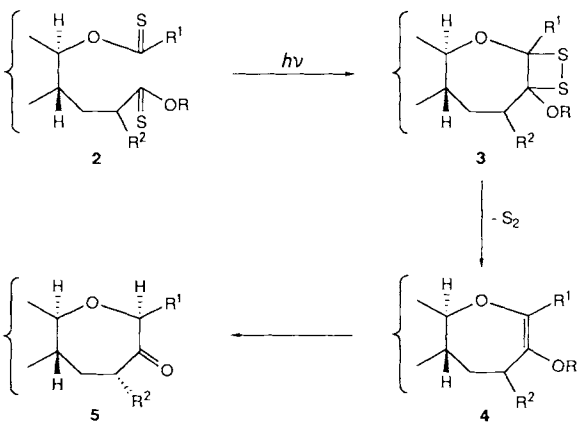

Scheme 1. General strategy for the synthesis of oxepanes by photolytic cyclization of dithionoesters.

[*] Prof. K. C. Nicolaou, Dr. C.-K. Hwang, D. A. Nugiel
Department of Chemistry, University of Pennsylvania
Philadelphia, PA 19104 (USA)

[**] This work was supported by the National Institutes of Health, the National Science Foundation, and Merck Sharp & Dohme (USA).

Table 1. Synthesis of didehydrooxepanes **4** and oxepanes **5** from dithionoesters **2**.

Entry	2	4	Yield [%] [a]	5	Yield [%]
	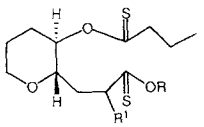	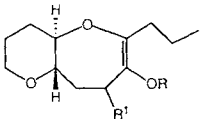		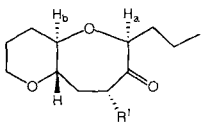	
1	**2a** : R = $CH_2CH_2SiMe_3$, R^1 = Me	**4a** : R = $CH_2CH_2SiMe_3$, R^1 = Me	66	**5a** : R^1 = Me	95
2	**2b** : R = CH_2CCl_3, R^1 = Me	**4b** : R = CH_2CCl_3, R^1 = Me	63		81
3	**2c** : R = R^1 = Me	**4c** : R = R^1 = Me	63		80
4	**2d** : R = Me, R^1 = H	**4d** : R = Me, R^1 = H	60	**5b** : R^1 = H	85
5	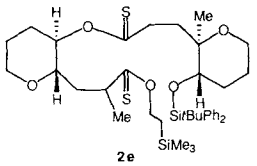 **2e**	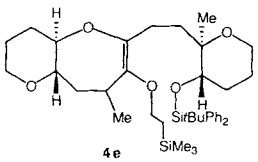 **4e**	62	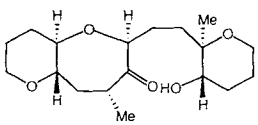 **5c**	94
6	**2f** : R = Me, R^1 = $CH_2CH_2CH_3$, R^2 = Me	**4f** : R = Me, R^1 = $CH_2CH_2CH_3$, R^2 = Me	75	**5d** : R^1 = $CH_2CH_2CH_3$, R^2 = Me	75
7	**2g** : R = $CH_2CH_2SiMe_3$, R^1 = $(CH_2)_4OCH_2Ph$, R^2 = H	**4g** : R = $CH_2CH_2SiMe_3$, R^1 = $(CH_2)_4OCH_2Ph$, R^2 = H	72	**5e** : R^1 = $(CH_2)_4OCH_2Ph$, R^2 = H	95
8	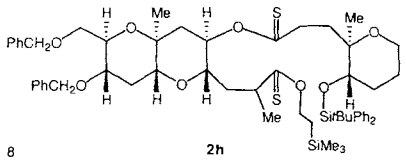 **2h**	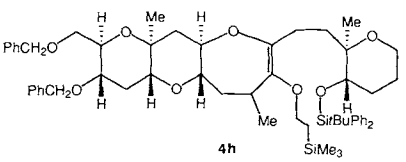 **4h**	72	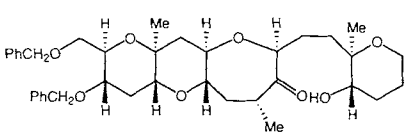 **5f**	88

[a] Based on consumed starting material **2**. Recovered starting material: **2a**, 42%; **2b**, 43%; **2c**, 43%; **2d**, 44%; **2e**, 50%; **2f**, 35%; **2g**, 37%; **2h**, 37%.

pane **4**, which may be regioselectively hydrolyzed to afford the highly functionalized oxepane intermediate **5**.

As Table 1 shows, this idea turned out to be successful, providing a facile entry into a variety of didehydrooxepanes and oxepanes of the type present in brevetoxin B **1**. Thus, the dithionoester **2a**[5] (Table 1, entry 1, mixture of methyl epimers), upon photolysis in toluene solution (Hanovia UV lamp, 70°C, 2 h), produced didehydrooxepane **4a**[6] (mixture of methyl epimers, ca. 1 : 1, 66% yield based on 42% recovered **2a**), presumably via the corresponding 1,2-dithietane **3**.[4] Regioselective enol ether rupture and tautomerization in **4a** was induced by fluoride treatment (nBu$_4$NF, THF, 45°C, 8 h), leading to oxepane ketone **5a** as a single isomer[7] (95%). The indicated structure was tentatively assigned on the basis of NOE studies, molecular modeling, and MM2 calculations.[8] Apparently, under the reaction conditions (basic), epimerization leads to the thermodynamically most stable product. The regioselective conversion **4** → **5** was also possible with other groups R such as CH_2CCl_3 (Table 1, entry 2, removed with Zn/AcOH) or Me (Table 1, entry 3, removed with aqueous HCl). In both cases, however, an epimeric mixture of **5a** (ca. 1 : 1) was obtained which was converted by basic treatment (NaH, THF, 12 h, 95%) into the same isomer as that obtained from **4a**.

A number of comments regarding the present photoinduced cyclization **2** → **3** are in order. (1) From studies with acyclic precursors, it appears that preexisting rings in the substrates **2** are necessary for the success of this reaction. (2) Photolysis at elevated temperatures leads to cleaner reactions and higher yields as compared with lower temperatures, suggesting that thermal energy may be necessary to achieve the proper conformation for coupling to take place. (3) Several of the presumed 1,2-dithietanes **3**[4a] were detected by thin layer chromatography (yellow coloration); their isolation is currently being pursued. The potential application of this procedure to the total synthesis of brevetoxin B **1** is also in progress.

Experimental Procedure

4a: The dithionoester **2a** (390 mg, 1.0 mmol) in anhydrous toluene (200 mL) was photolyzed (Hanovia UV lamp, 450 W) at 70°C for 2 h. The solvent was removed under reduced pressure and the residue was flash chromatographed (silica, 10% ether in petroleum ether) to afford **4a** (104 mg, 66% based on consumed starting material) and recovered starting material (**2a**, 163 mg, 42%). **4a**: oil, R_F = 0.33 (silica, 10% ether in petroleum ether); IR (neat), $\tilde{\nu}_{max}$ = 1660 cm^{-1}; ^{1}H NMR (500 MHz, $CDCl_3$), δ = 3.85 (m, 1H, CH_2–O,

equatorial), 3.60 (m, 2H, C*H*–O), 3.30 (m, 1H, C*H*–O), 3.15 (m, 1H, CH_2–O, axial), 3.02 (m, 1H, C*H*–O), 2.75, 2.52 (2 × m, 2 × 0.5H, C*H*), 2.30–1.40 (m, 10H, CH_2), 1.25, 1.12 (2 × d, J = 7.4 Hz, 2 × 1.5H, CH–CH_3), 1.0 (m, 3H, CH_2–CH_3), 0.88 (m, 2H, CH_2–SiMe_3), 0.0 (s, 9H, SiMe_3); HRMS, calcd for $C_{18}H_{34}O_3Si$ ($M^{\oplus}$) 326.2285, found 326.2284.

5a: The didehydrooxepane system **4a** (326 mg, 1.0 mmol) in anhydrous THF (5 mL) was treated under argon with nBu$_4$NF (1.0 M solution in THF, 1.2 mL, 1.2 mmol) at ambient temperature and then stirred at 45°C for 8 h. Removal of the solvent, followed by flash column chromatography (silica, 20% ether in petroleum ether) gave **5a** (215 mg, 95%). **5a**: oil, R_F = 0.30 (silica, 20% in petroleum ether); IR (neat), $\tilde{\nu}_{max}$ = 2940, 2880, 1720 (s, ketone), 1475, 1160, 1000, 955 cm^{-1}; ^{1}H NMR (500 MHz, [D$_6$]benzene), δ = 3.90 (dd, J = 9.4, 3.6 Hz, 1H, C*H*–O), 3.70 (m, 1H, C*H*–O, equatorial), 3.25 (m, 1H, C*H*–O), 3.20 (m, 1H, CH_2–O, axial), 3.01 (m, 1H, C*H*), 2.80 (m, 1H, C*H*–O), 2.05–1.45 (m, 10H, CH_2), 1.22 (d, J = 7.4 Hz, 3H, CH–CH_3), 1.05 (t, J = 7.3 Hz, 3H, CH_2–CH_3); ^{13}C NMR (125 MHz, CDCl$_3$), δ = 217.60 (C=O), 86.95, 80.82, 80.47, 67.52, 38.79, 37.72, 35.17, 30.92, 25.66, 12.65, 16.33, 13.68; HRMS, calcd for $C_{13}H_{22}O_3$ ($M^{\oplus}$) 226.1569, found 226.1567.

Received: June 7, 1988 [Z 2808 IE]
German version: *Angew. Chem. 100* (1988) 1413

[1] For some recent and excellent reviews, see: D. J. Faulkner, *Nat. Prod. Rep. 3* (1986) 1; *1* (1984) 251.

[2] Y. Y. Lin, M. Risk, M. S. Ray, J. Clardy, J. Golik, J. C. James, K. Nakanishi, *J. Am. Chem. Soc. 103* (1981) 6773.

[3] For some examples of oxepane synthesis, see: a) K. C. Nicolaou, D. G. McGarry, P. K. Somers, C. A. Veale, G. T. Furst, *J. Am. Chem. Soc. 109* (1987) 2504; b) L. Coppi, A. Ricci, M. Taddei, *J. Org. Chem. 53* (1988) 911; c) R. Whitby, C. Yeates, P. Kocienski, G. Costello, *J. Chem. Soc. Chem. Commun. 1987*, 429; d) W. T. Brady, Y. F. Giang, L. Weng, M. M. Dad, *J. Org. Chem. 52* (1987) 2216; e) L. E. Overman, T. A. Blumenkopf, A. Castaneda, A. S. Thompson, *J. Am. Chem. Soc. 108* (1986) 3516; f) L. E. Overman, A. Castaneda, T. A. Blumenkopf, *ibid. 108* (1986) 1303; g) P. A. Bartlett, P. C. Ting, *J. Org. Chem. 51* (1986) 2230; h) A. P. Kozikowski, A. K. Ghosh, *ibid. 50* (1985) 3017; i) C. N. Barry, S. A. Evans, Jr., *ibid. 46* (1981) 3361; j) K. C. Nicolaou, D. A. Claremon, W. E. Barnette, *J. Am. Chem. Soc. 102* (1980) 6611; k) W. H. Rastetter, *ibid. 98* (1976) 6350.

[4] For precedents for such couplings, see: a) K. C. Nicolaou, C.-K. Hwang, M. E. Duggan, P. J. Carroll, *J. Am. Chem. Soc. 109* (1987) 3801; b) R. Jahn, V. Schmidt, *Chem. Ber. 108* (1975) 630; c) N. Ishibe, M. Odani, K. Teramura, *J. Chem. Soc. Chem. Commun. 1970*, 371.

[5] This and the other dithionoesters shown in Table 1 were synthesized by thionation of the corresponding diesters using the Lawesson reagent.

[6] All new compounds exhibited satisfactory spectral and exact mass data.

[7] Selected properties of compounds **5**. **5b**: R_F = 0.30 (silica, 30% ether in petroleum ether); IR (neat), $\tilde{\nu}_{max}$ 1718 cm^{-1} (C=O); ^{1}H NMR (500 MHz, CDCl$_3$), δ = 3.83 (m, 1H, C*H*–O, equatorial), 3.79 (dd, J = 9.6, 3.4 Hz, 1H, C*H*–O), 3.30 (m, 2H, C*H*–O, CH_2–O), 2.90 (m, 2H, C*H*–O, CH_2–C(O)), 2.35–1.50 (m, 11H, CH_2), 0.90 (t, J = 7.3 Hz, 3H, CH_2–CH_3). **5c**: R_F = 0.30 (silica, ether); IR (neat), $\tilde{\nu}_{max}$ = 1715 cm^{-1} (C=O); ^{1}H NMR (500 MHz, CDCl$_3$), δ = 3.84 (dd, J = 9.2, 3.5 Hz, 1H, C*H*–O), 3.80 (m, 1H, CH_2–O, equatorial), 3.55 (m, 2H, C*H*–O, CH_2–O), 3.42 (dd, J = 8.0, 3.2 Hz, 1H, C*H*–O), 3.05 (m, 1H, C*H*), 2.85 (m, 1H, C*H*–O), 2.10–1.30 (m, 14H, CH_2), 1.15 (s, 3H, CH_3), 1.05 (d, J = 7.5 Hz, 3H, CHCH_3), 3.32 (m, 2H, CH_2–O). **5d**: R_F = 0.5 (silica, 30% EtOAc in benzene); IR (neat), $\tilde{\nu}_{max}$ = 1712 cm^{-1} (C=O); ^{1}H NMR (250 MHz, CDCl$_3$), δ = 3.82 (m, 2H, CH_2–O, C*H*–O), 3.60–3.00 (m, 7H, CH_2–O, C*H*–O, C*H*), 3.48, 3.42 (s, 3H each, OCH_3), 2.35–1.50 (m, 10H, CH_2), 1.20 (s, 3H, CH_3), 1.05 (d, J = 7.4 Hz, 3H, CHCH_3), 0.90 (t, J = 7.3 Hz, 3H, CH_2–CH_3). **5e**: R_F = 0.25 (silica, 60% ether in petroleum ether); IR (neat), $\tilde{\nu}_{max}$ = 1725 cm^{-1} (C=O); ^{1}H NMR (500 MHz, CDCl$_3$), δ = 7.50–7.20 (m, 5H, aromatic), 4.50 (s, 2H, benzylic), 3.75 (dd, J = 9.4, 3.7 Hz, 1H, C*H*–O), 3.55–2.70 (m, 9H, C*H*–O, CH_2–O), 3.40, 3.35 (s, 3H each, OCH_3), 2.35–1.40 (m, 14H, CH_2), 1.15 (s, 3H, CH_3). **5f**: R_F = 0.60 (silica, ether); IR (neat), $\tilde{\nu}_{max}$ = 1716 cm^{-1} (C=O); ^{1}H NMR (500 MHz, CDCl$_3$), δ = 4.62, 4.52 (d, J = 11.5 Hz, 1H each, benzylic), 4.54, 4.38 (d, J = 12.0 Hz, 2H, benzylic), 3.80 (m, 1H, C*H*–O), 3.70–3.00 (m, 11H, C*H*–O, CH_2–O, C*H*), 2.30–1.50 (m, 14H, CH_2), 1.15 (s, 3H, CH_3), 1.09 (s, 3H, CH_3), 1.05 (d, J = 7.3 Hz, 3H, CH–CH_3); ^{13}C NMR (125 MHz, CDCl$_3$), δ = 216.96, 138.04, 137.92, 128.37, 128.37, 128.30, 128.30, 128.27, 127.77, 127.77, 127.73, 127.73, 127.47, 87.73, 81.40, 77.97, 77.74, 75.97, 73.38, 73.11, 72.56, 72.36, 71.6, 71.03, 69.66, 60.54, 44.62, 38.54, 37.96, 34.06, 30.22, 29.66, 27.64, 26.51, 24.08, 16.36, 15.27.

[8] Irradiation of H$_a$ (structure **5a**, Table 1) produced a 17% NOE indicating a *syn* relationship for H$_a$ and H$_b$. Molecular models of **5a** suggest a pseudoequatorial position for the Me group as depicted in **5a** (rather than the opposite stereochemistry which forces the Me into a pseudoaxial orientation); MM2 calculations (MacroModel) of the energies give 40.05 kJ mol^{-1} for **5a** and 42.99 kJ mol^{-1} for its epimer, also pointing to the assigned stereochemistry.

$Cs_2Bi_{10}Ca_6Cl_{12}O_{16}$: A New Type of Catalyst for Selective Oxidation Derived from Bismuth Oxychloride**

By *Kenneth D. M. Harris, Wataru Ueda, John M. Thomas,** and *Gallienus W. Smith*

When a 1:1:1:2 mixture of Bi_2O_3, BiOCl, CsCl and $CaCl_2$ is heated for 12 h in an open alumina or platinum container at 1073 K a new type of compound is formed. The predominant crystalline product contains single crystals suitable for structural analysis using conventional X-ray diffractometric techniques. This product (idealized formula $Cs_2Bi_{10}Ca_6Cl_{12}O_{16}$) possesses attractive properties as a catalyst for the selective oxidation of methane in O_2 ($CH_4:O_2 = 2:1$, partial pressure of CH_4 20 kPa, total flow rate 50 mL m^{-1} with N_2 as diluent up to atmospheric pressure in the temperature range 873 to 1023 K).

A typical run at 994 K results in 21.3 and 46.3 percent conversion of CH_4 and O_2 respectively, and the following product selectivities: C_2H_4, 39.5; C_2H_6, 11.6; C_3 and C_4 compounds, 3.5 and 3.9, respectively; CO, 7.6; CO_2, 25.0%; with $C_2H_4/C_2H_6 = 3.4$. Further details of the catalytic performance of this and of related materials will be given elsewhere.[1]

As with other[1] complex layered oxyhalides derived from or related to the Sillen structure[2] (for example, $NaBi_3O_4Cl_2$ and $Ca_{1.25}Bi_{1.5}O_2Cl_3$), the mechanism of catalytic selective oxidation is unclear, but likely to involve[3–5] methyl radicals.

The structure[6] of $Cs_2Bi_{10}Ca_6Cl_{12}O_{16}$ is quite novel (Fig. 1, Table 1) and exhibits interesting features including the presence of a layer which is itself structurally similar to that in CsCl with the alkali cation, as expected, in eightfold coordination. Within this layer, however, there are two types of Cs site (designated Cs1 and Cs2), both of which are only partially occupied, with fractional occupancies of 0.78 and 0.21 respectively. This layer is flanked on either side by layers of modified BiOCl with $Bi^{3\oplus}$ and $Ca^{2\oplus}$ ions occupying the same sites (subsequently designated M sites). In the crystal structure refinement, the ratio of $Bi^{3\oplus}$ and $Ca^{2\oplus}$ on these sites has been allowed to vary subject to the constraint that the total occupancy on each M site is unity.[7] The fact that the fractional occupancies of $Bi^{3\oplus}$ and $Ca^{2\oplus}$ are not 0.625 (10/16) and 0.375 (6/16) respectively for each of the M sites indicates that the $Bi^{3\oplus}$ and $Ca^{2\oplus}$ cations, whilst capable of occupying the same type of site, are not distributed at random in the modified BiOCl layers. (We note, in passing, that a tendency for non-random, supermesh arrangements involving $Bi^{3\oplus}$ and $Ca^{2\oplus}$ cations within layers of the warm superconducting compounds[8–10] of Bi/Ca/Sr/Cu/O (suggested formulas[11,12] $Bi_2Sr_{2-x}CaCu_2O_8$ and $Bi_{2+x}Ca_{1-x}Sr_2Cu_2O_{8+x}$)

[*] Prof. Dr. J. M. Thomas, K. D. M. Harris [+], Dr. W. Ueda [+ +]
Davy Faraday Research Laboratory, The Royal Institution
21, Albemarle Street, London W1X 4BS (UK)

[+] Also at Department of Physical Chemistry,
University of Cambridge
Lensfield Road, Cambridge CB2 1EP (UK)

[+ +] Permanent address: Tokyo Institute of Technology
4259 Nagatsuta, Midori-ku, Yokohama 227 (Japan)

Dr. G. W. Smith
1, West Farm Avenue
Ashtead, Surrey KT21 2LD (UK)

[**] This work was supported by the Science and Engineering Research Council, The Ramsay Memorial Trust (who awarded a Japanese Ramsay Fellowship to W. U.) and by BP (through a studentship to K. D. M. H.).

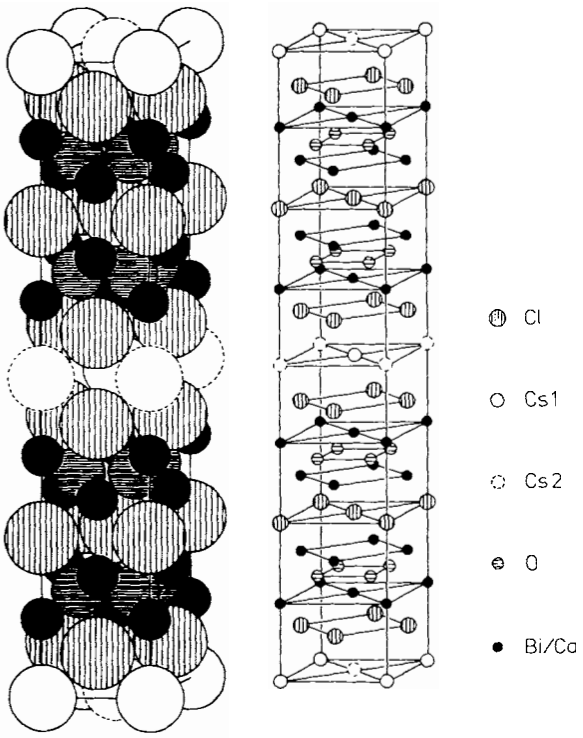

Fig. 1. Two representations of the stacking of the constituent ions in the structure of the oxidation catalyst $Cs_2Bi_{10}Ca_6Cl_{12}O_{16}$. (In b, conventional ionic radii are represented.) In the layers of modified BiOCl which are integral parts of this novel structure the $Bi^{3\oplus}$ and $Ca^{2\oplus}$ cations share the same sites but not completely at random (see text). Note also the existence of two different types of Cs site within the CsCl layers. In both of these sites the Cs is in eight-fold coordination.

Table 1. Fractional coordinates and site occupancies in $Cs_2Bi_{10}Ca_6Cl_{12}O_{16}$ (with estimated standard deviations in parentheses).

	x/a	*y/b*	*z/c*	Site occupancy	Sites [a]	Wyckoff notation
Cs1	0	0	0	0.78(1)	2	*a*
Cs2	1/2	1/2	0	0.211(8)	2	*b*
Cl1	1/2	0	0.0722(1)	1	8	*g*
M1	0	0	0.1222(1)	0.70(1) (Bi) **0.30(1) (Ca)**	4	*e*
M2	1/2	1/2	0.1187(1)	**0.206(6) (Bi)** **0.794(6) (Ca)**	4	*e*
O	0.2484(9)	0.2484(9)	0.1574(2)	1	16	*m*
M3	1/2	0	0.1907(0)	0.80(1) (Bi) **0.20(1) (Ca)**	8	*g*
Cl2	0	0	0.2499(5)	1	4	*e*

[a] Number of sites in the unit cell.

has recently been postulated by *Zhou* et al.[12] Indeed, from the magnitude of the thermal parameter quoted by *Subramanian* et al.[10] for the $Bi^{3\oplus}$ site in their 'warm' superconductor one may suspect that, in that material also, both $Bi^{3\oplus}$ and $Ca^{2\oplus}$ may tend to occupy this site.)

The new structure reported here (for $Cs_2Bi_{10}Ca_6Cl_{12}O_{16}$) is corroborated by other evidence.[13] It is not far removed, architecturally, from the rich variety of discrete structures in the so-called 'Bipox' series[14] formed from unit-cell-level intergrowths[15] of Aurivillius phases[16] and Sillen phases.

Received: May 30, 1988 [Z 2791 IE]
German version: *Angew. Chem. 100* (1988) 1415

[1] a) W. Ueda, J. M. Thomas, *9th Int. Congr. on Catalysis*, Calgary, June 1988, Paper 123; b) W. Ueda, J. M. Thomas, *J. Chem. Soc. Chem. Commun 1988*, 1148.

[2] L. G. Sillen, *Z. Anorg. Allg. Chem. 242* (1939) 41; 246 (1941) 115.

[3] J. M. Thomas, W. J. Thomas: *Introduction to the Principles of Heterogeneous Catalysis*, Academic Press, London 1967, p. 383.

[4] T. Ito, J. H. Lunsford, *Nature (London) 314* (1985) 721; J. M. Thomas, *ibid. 314* (1985) 669.

[5] K. D. Campbell, H. Zhang, J. H. Lunsford, *J. Phys. Chem. 92* (1988) 750.

[6] Crystal structure of $Cs_{1.98}Bi_{10.02}Ca_{5.98}Cl_{12}O_{16}$: tetragonal, space group *I4/mmm*, $a = 547.71(9)$, $c = 3286.2(7)$ pm, $\rho_{calcd} = 5.53$ g cm^{-3}, $\mu = 463.19$ cm^{-1}, $F(000) = 1393.98$. Data collection at room temperature on a CAD4 diffractometer, $Mo_{K\alpha}$ radiation ($\lambda = 71.069$ pm); $1.5° < \theta < 36°$, $h = -9$, $k = 0$ to 9, $l = 0$ to 54. Numerical absorption correction applied after indexing crystal faces and using the crystal size ($0.18 \times 0.18 \times 0.01$ mm^3) which minimized R_{merge} (0.038) for the merging of equivalent reflections. (For comparison, $R_{merge} = 0.282$ with no absorption correction.) Total of 760 unique reflections measured, of which 531 (satisfying $|F| > 3\sigma(F)$) were used in refinement. Scattering factors for neutral atoms were assumed. Anisotropic thermal parameters were used finally for all atoms. $R = 0.0419$, $R_w = 0.0354$ using weight $1.6917/[\sigma^2(F) + 0.0002F^2]$. Salient data (with fractional coordinates *x/a*, *y/b*, *z/c*; and occupancies) are given in Table 1.

[7] In a given refinement job, the occupancies of the two types of Cs site and the relative $Bi^{3\oplus}/Ca^{2\oplus}$ occupancies on the M sites were refined with the thermal parameters for all of these sites fixed, while, in the following refinement job, the occupancies were fixed at these new values and the thermal parameters allowed to refine. This iterative procedure was continued until constancy of both occupancies and thermal parameters produced from successive pairs of refinement jobs was obtained for all of the Cs and M sites (see K. D. M. Harris, *Ph. D. Thesis* (1988), University of Cambridge, for further details).

[8] C. Michel, B. Raveai, *Z. Phys. B68* (1987) 421.

[9] A. H. Maeda, Y. Tanaka, N. Fukutomi, T. Asamo, *Jap. J. Appl. Phys. 27* (1988) 2.

[10] M. A. Subramanian, C. C. Torardi, J. C. Calabrese, J. Gopalakrishnan, K. J. Morrissey, T. R. Askew, R. B. Flippen, U. Chowdhry, A. W. Sleight, *Science (Washington, DC) 239* (1988) 1015.

[11] A. K. Cheetham, A. M. Chippindale, S. J. Hibble, *Nature (London) 333* (1988) 21.

[12] W. Zhou, D. A. Jefferson, private communication; see also E. A. Hewat, P. Bordet, J. J. Capponi, C. Chaillout, J. L. Hodlan, M. Marezio, *Nature (London) 333* (1988) 53.

[13] Briefly, the validity of the refined occupancies of Cs, Bi and Ca is supported by the three following facts. First, crystal structure refinements starting from different initial sets of occupancies produce, in all cases, the values given in Table 1, within the quoted standard deviations. Second, from the stoichiometry that follows from these occupancies (i.e. $Cs_{1.98}Bi_{10.02}Ca_{5.98}Cl_{12}O_{16}$) the net charge is 0.00, indicating that, within errors, this stoichiometry satisfies the requirement of electro-neutrality. Refinements in which the total occupancy of individual M sites are fixed at values less than unity (e.g. 0.95 or 0.90), while the $Bi^{3\oplus}/Ca^{2\oplus}$ ratio for these sites is allowed to refine, lead to stoichiometries for which the net charge is distinctly non-zero, thus vindicating our assumption that the total occupancy of each of the M sites is unity. Third, the bond valence sum (S) for the oxygen site in the structure, when computed using the parameters R_i^{Ca}, N_{Ca}, R_i^{Bi}, N_{Bi} (compiled by I. D. Brown, K. K. Wu, *Acta Crystallogr. Sect. B32* (1976) 1957) yields a value of $S = 2.04$ (theoretical value 2.00). Here

$$S = \sum_{\text{M sites}} \left(f_{Ca} \left(\frac{R_{M-O}}{R_i^{Ca}} \right)^{-N_{Ca}} + f_{Bi} \left(\frac{R_{M-O}}{R_i^{Bi}} \right)^{-N_{Bi}} \right)$$

where f_{Ca} and f_{Bi} are the fractional occupancies of $Ca^{2\oplus}$ and $Bi^{3\oplus}$ on the M site and R_{M-O} is the M–O interatomic distance.

[14] J. F. Ackerman, *Mater. Res. Bull. 17* (1982) 883.

[15] C. N. R. Rao, J. M. Thomas, *Accnts. Chem. Res. 18* (1985) 113.

[16] B. Aurivillius, *Ark. Kemi 1* (1950) 463, 499.

Solid-Phase Synthesis of *O*-Glycopeptide Sequences

By *Hans Paulsen,* Gunnar Merz,* and *Udo Weichert*

Glycoproteins are of great interest owing to their numerous biological functions on cell surfaces and as enzymes, serum proteins, and mucins.[1] Glycopeptides, containing a

[*] Prof. Dr. H. Paulsen, Dipl.-Chem. G. Merz, Dipl.-Chem. U. Weichert
Institut für Organische Chemie der Universität
Martin-Luther-King-Platz 6, D-2000 Hamburg 13 (FRG)

peptide moiety and a carbohydrate moiety, are desired for elucidating the functions of glycoproteins. The synthesis of such *O*-glycopeptides has so far been carried out stepwise using the standard methods of peptide coupling.[2,3] The question therefore arose whether solid-phase synthesis, developed initially for peptides,[4] might offer a quicker and simpler approach to the preparation of *O*-glycopeptides. Herein we report on several examples of this approach.

Only some of the standard methods and protecting groups of peptide chemistry are applicable to the synthesis of *O*-glycopeptides. This is due to the acid lability of the glycosidic bond between 2-acetamido-2-deoxy-D-galactose and the hydroxyl group of L-serine or L-threonine and to the facile cleavage of this bond via β-elimination under alkaline conditions. Solid-phase syntheses that involve cleavage of the peptide from the resin with HF are therefore not useful.[5] A resin bearing allyl groups, only recently described by *Kunz* et al.,[6] appears applicable since Pd-catalyzed cleavage is used. A study of the methods commonly employed in peptide chemistry revealed that a carrier resin developed by *Wang*[7] is most promising. The solid phase is a polystyrene resin containing *p*-alkoxybenzyl alcohol groups as shown in **2**. The synthesized peptides can be cleaved from this resin under mild acid conditions.

The synthetic procedure involves several steps (Scheme 1). In the first step, the symmetrical anhydride of an Fmoc-amino acid **1**[8] (3 mole equiv.) is esterified with the hydroxyl group of the anchor in **2** under mild catalysis with 4-dimethylaminopyridine[9] (0.06 mole equiv.) to give **4**. 4-Alkoxybenzyl alcohol resin (Bachem, capacity 0.45 mmol g^{-1}) was employed and, under these conditions, underwent 50% esterification. The unreacted OH groups of the resin were subsequently acetylated by reaction with acetic anhydride. An important carbohydrate-containing building block is the L-threonine glycoside **3**.[10] It contains the protecting group combination Fmoc/O*t*Bu, which has proven advantageous for solid-phase synthesis.[11]

Cleavage of Fmoc in **4** and O*t*Bu in **3** and conversion of the product obtained from **3** to the *N*-hydroxybenzotriazole ester (6 mole equiv.) is followed by coupling to give **5** (reaction time 1.5 h). After deprotection of the *N*-terminus of **5** by cleavage of the Fmoc group with morpholine, further amino acids can be joined to give **6**. All coupling steps of the amino acids (6 mole equiv.) are carried out with DCC/HOBT in dimethylformamide (reaction time 1 h in each case). If a Boc-amino acid is chosen in the final step, treatment of the resin with aqueous trifluoroacetic acid (95%) results in simultaneous cleavage of both the glycopeptide from the resin and the Boc group from the *N*-terminus, thereby affording **7**. No glycoside cleavage was observed over a reaction time of 1.5 h. To accomplish complete deprotection, the acetyl groups of the carbohydrate moiety are removed with $NaOCH_3$ in methanol maintained at exactly pH 8.5. A β-elimination or racemization does not usually occur under these conditions.

The application of the above procedure is exemplified by the synthesis of the hexapeptides **9** and **10**. For **9**

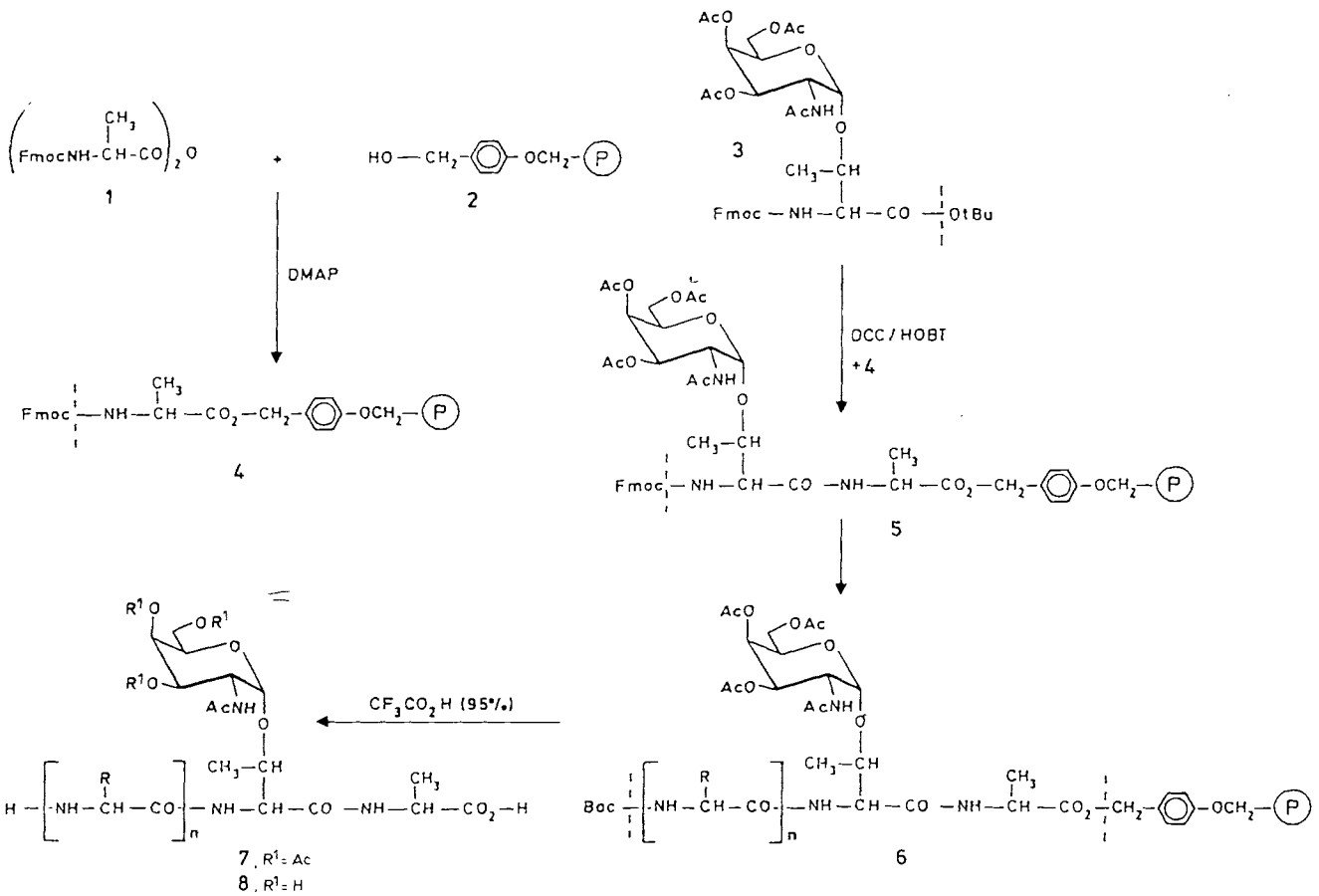

Scheme 1. Solid-phase synthesis of *O*-glycopeptide sequences. DMAP = 4-dimethylaminopyridine, DCC = dicyclohexylcarbodiimide, HOBT = 1-hydroxybenzotriazole, Fmoc = 9-fluorenylmethoxycarbonyl, Boc = *tert*-Butyloxycarbonyl, Ⓟ = polymer.

(Scheme 2), L-alanine is first coupled to the carrier. Cleavage of the Fmoc group is followed by coupling with the glycosylated L-threonine building block. The other amino acids are then added sequentially. Completion of the reaction steps is checked using the Kaiser test.[12] After cleavage of the glycopeptide from the resin, the product is purified first on Sephadex LH20 and, after further deprotection of the sugar moiety, on Sephadex G10. With 0.25 g of resin it is possible to obtain 20 mg of hexapeptide **9** (55% based on the first amino acid to be coupled) in pure form. The sequence **9** is a partial structure of the ovine submaxillary mucin.[13]

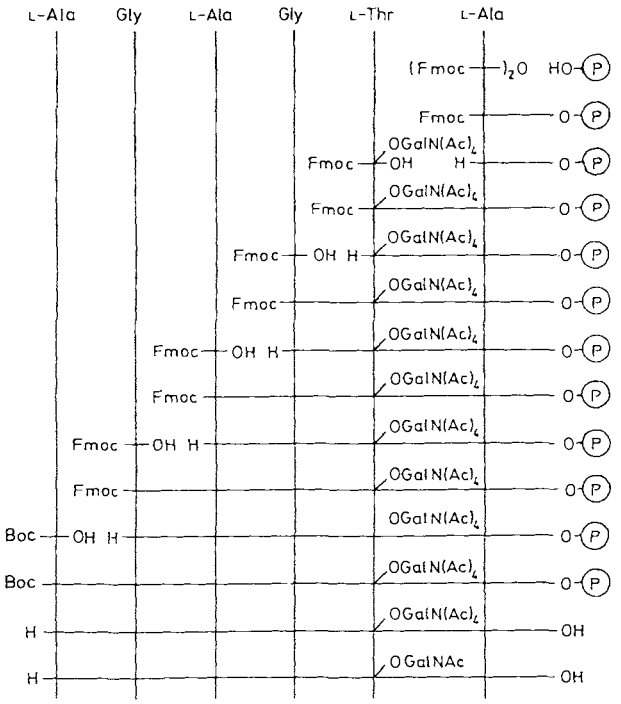

9

Scheme 2. Solid-phase synthesis of the glycopeptide **9**, a partial structure of ovine submaxillary mucin.

The reaction steps for the synthesis of **10**, which contains two carbohydrate chains (Scheme 3), are analogous to those for **9**. Only an additional glycosylated L-threonine building block is introduced. The cleavage from the carrier and the deprotection present no difficulties. With 0.25 g of resin, it is possible to obtain 25 mg of hexapeptide **10** (48% based on the first amino acid to be coupled). The hexapeptides **9** and **10** were checked for purity using ^{1}H NMR spectroscopy, including 2D techniques. Side products or racemization of the amino acids could not be detected. The sequence **10** is a partial structure of porcine glycophorin.[14]

The procedure described here affords glycopeptides in considerably shorter time than the corresponding syntheses in solution and can be extended further. The building block **3** may also be suitable for use in an automated peptide synthesis.

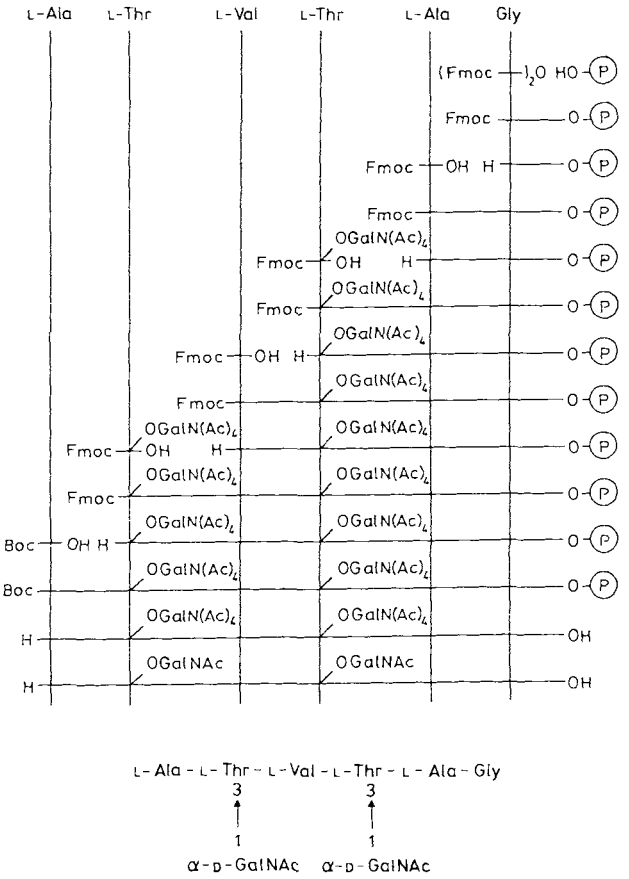

10

Scheme 3. Solid-phase synthesis of the glycopeptide **10**, a partial structure of porcine glycophorin.

Received: May 19, 1988 [Z 2769 IE]
German version: *Angew. Chem. 100* (1988) 1425

CAS Registry numbers:
1, 70626-39-0; **9**, 116747-53-6; **10**, 116747-63-8; Fmoc-Gly, 29022-11-5; Fmoc-L-Ala, 35661-39-3; Fmoc-L-Val, 68858-20-8; Boc-L-Ala, 15761-38-3; $(Fmoc\text{-}Gly)_2O$, 70626-38-9; Fmoc-L-Thr(OGalN(Ac)$_4$), 116783-35-8; (L-Ala-Gly-)$_2$L-Thr(OGalN(Ac)$_4$)-L-Ala, 116747-52-5; L-Ala-L-Thr(OGalN(Ac)$_4$)-L-Val-L-Thr(OGalN(Ac)$_4$)-L-Ala-Gly, 116747-62-7.

[1] J. Montreuil, *Adv. Carbohydr. Chem. Biochem. 37* (1980) 157.
[2] H. Kunz, *Angew. Chem. 99* (1987) 297; *Angew. Chem. Int. Ed. Engl. 26* (1987) 294.
[3] H. Paulsen, M. Schultz, *Liebigs Ann. Chem. 1986*, 1435; *Carbohydr. Res. 159* (1987) 37; B. Ferrari, A. Pavia, *Tetrahedron 41* (1985) 1939; V. V. Bencomo, P. Sinaÿ, *Carbohydr. Res. 116* (1983) C9.
[4] R. B. Merrifield, *J. Am. Chem. Soc. 85* (1963) 2149.
[5] S. Lavielle, N. C. Ling, R. C. Guillemin, *Carbohydr. Res. 89* (1981) 221.
[6] H. Kunz, B. Dombo, *Angew. Chem. 100* (1988) 732; *Angew. Chem. Int. Ed. Engl. 27* (1988) 711.
[7] S. S. Wang, *J. Am. Chem. Soc. 95* (1973) 1328.
[8] L. A. Carpino, G. Y. Han, *J. Am. Chem. Soc. 92* (1970) 5748.
[9] W. Steglich, G. Höfle, *Angew. Chem. 81* (1969) 1001; *Angew. Chem. Int. Ed. Engl. 8* (1969) 981.
[10] K. Adermann, H. Paulsen, unpublished results.
[11] E. Atherton, M. Caviezel, H. Fox, D. Harkiss, H. Over, R. C. Sheppard, *J. Chem. Soc. Perkin Trans. 1 1983*, 65.
[12] E. Kaiser, E. L. Colescott, C. D. Bossingler, P. I. Cook, *Anal. Biochem. 34* (1970) 595.
[13] H. D. Hill, M. Schwyzer, H. M. Steinman, R. L. Hill, *J. Biol. Chem. 252* (1977) 3799.
[14] K. Honma, M. Tomita, A. Hamada, *J. Biochem. 88* (1980) 1679.

Does a 1,1′-Diazaferrocene Exist?**

By *Norbert Kuhn,* Eva-Maria Horn, Roland Boese,* and *Norbert Augart*

Although the formal replacement of CH groups by phosphorus atoms in ferrocene[1] recently culminated in the synthesis of "FeP_{10}",[1e] diazaferrocenes and their nitrogen-richer analogues have been considered for 20 years to be unstable.[2] The recently demonstrated stabilization of nitrogen-containing metallocenes by permethylation of the heterocyclic ring[3] prompted us to attempt the synthesis of $[(\eta^5\text{-}C_4Me_4N)_2Fe]$.

The complex **1**, accessible by reaction of $FeCl_2$ with C_4Me_4NLi in tetrahydrofuran [Eq. (a)], contains *N*-coordinated pyrrolyl ligands, as shown by the δ values for the ring C atoms in the ^{13}C NMR spectrum ($\delta = 119.81$, 113.05). Compound **1** is stable in the solid state under argon as well as in THF and toluene at $-40\,^\circ C$. At room temperature, however, it decomposes in solution within a few hours with liberation of THF; the desired 1,1′-diazaferrocene **2** could *not* be detected. The decomposition of **1**

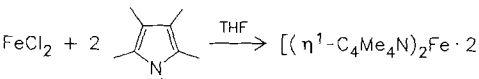

(a)

1

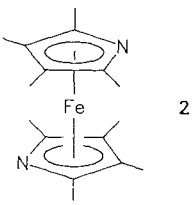

2

is appreciably accelerated by traces of water [Eq. (b)]. The stable adduct **3** is formed as the reaction product in useful yields.[4]

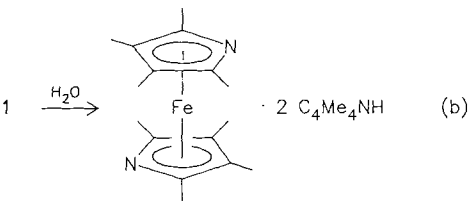

(b)

3

Complex **3** is present in the crystal as a centrosymmetric molecule (Fig. 1).[5] The η^5-pyrrole ligands, which lie in parallel planes, are arranged in a stacked fashion and the nitrogen atoms are situated in *anti* positions. Further, the η^5-pyrrole ligands are each linked through hydrogen bonds to an additional tetramethylpyrrole molecule, whose plane is nearly perpendicular (81.2°) to that of the ligand. All C_4N rings are planar within the limits of experimental error. The line joining the geometric centers of the η^5-pyrrole ligands forms an angle of 1.6° with the normal from the coordination center Fe to the average plane of the ligands, the projection of the coordination center being displaced slightly toward the nitrogen atom. The distance between the ring center and the iron atom, 1.651 Å, is in the expected range.

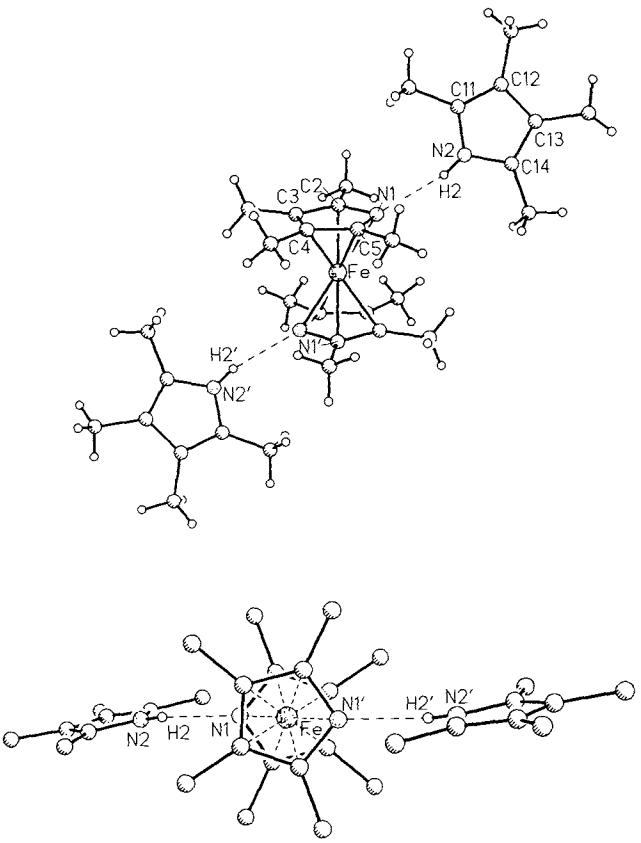

Fig. 1. Two views of the molecular structure of **3**. Selected bond lengths [Å] and bond angles [°]: Fe-N1 2.015(2), Fe-C2 2.023(3), Fe-C3 2.064(3), Fe-C4 2.066(3), Fe-C5 2.019(3), N1-C2 1.395(3), C2-C3 1.414(4), C3-C4 1.413(4), C4-C5 1.407(4), N1-C5 1.390(3), N2-C11 1.371(3), C11-C12 1.355(3), C12-C13 1.425(3), C13-C14 1.352(4), N2-C14 1.365(3), H2-N2 0.806, H2-N1 2.224, Fe-C_4N(center) 1.651; N1-C2-C3 109.8(2), C2-C3-C4 107.0(2), C3-C4-C5 106.6(2), C4-C5-N1 110.5(2), C2-N1-C5 106.2(2), N2-C11-C12 107.4(2), C11-C12-C13 107.5(2), C12-C13-C14 107.5(2), C13-C14-N2 107.7(2), C11-N2-C14 109.8(2), N1-H2-N2 163.1, C_4N(center)-N1-H2 152.7, interplanar angle [C(2-5)N1]-[C(11-14)N2] 81.2.

In the η^5-coordinated pyrrole rings, the CN and the neighboring CC bonds are ca. 0.03 and 0.06 Å longer, respectively, than those in the rings that are not directly bonded to the coordination center, whereas the CC bond opposite the nitrogen atom is slightly shorter. Also clearly revealed is the reduction of the angle at the nitrogen atom of the η^5 ligand (106.2(2), compared with 109.8(2)°), which is accompanied by an enlargement of ca. 3° in the angles at the carbon atoms neighboring the nitrogen atoms.

The hydrogen atom of the unsymmetrical hydrogen bond lies closer to the more strongly basic nitrogen atom N2 (H2-N2 0.806, H2-N1 2.224 Å); the NHN angle (163.1°) is that expected for this type of compound.[6]

[*] Prof. Dr. N. Kuhn, Dipl.-Chem. E.-M. Horn
Fachbereich 6 der Universität-Gesamthochschule
Lotharstrasse 1, D-4100 Duisburg 1 (FRG)
Dr. R. Boese, Dipl.-Chem. N. Augart
Institut für Anorganische Chemie der Universität-Gesamthochschule
Universitätsstrasse 5-7, D-4300 Essen 1 (FRG)

[**] Heterocycles as Ligands, Part 3. This work was supported by the Deutsche Forschungsgemeinschaft and the Fonds der Chemischen Industrie. We thank Prof. *P. Sartori* for assistance. Part 2: [9].

In solution, the ^{13}C NMR shifts of the ring atoms ($\delta = 120.56$, 113.76, 99.29, and 84.36) of **3** indicate the presence of η^5- and η^1-coordinated pyrroles. The hydrogen bonds are so stable that the η^1-pyrrole ligands cannot be exchanged at room temperature by addition of tetramethylpyrrole in excess.

The *anti* positions of the ring heteroatoms in **3** contrast to the structures of known 1,1'-diphospha- and 1,1'-diarsaferrocenes.[1b, 7] Apparently, the reduction of the charge density at the nitrogen atoms that accompanies formation of the hydrogen bonds contributes appreciably to the stability of the 1,1'-diazaferrocene system in **3**[8] and points to a possible approach for the stabilization of nitrogen-richer metallocenes.

Experimental Procedure

1: Anhydrous $FeCl_2$ (1.57 g, 12.4 mmol) and C_4Me_4NLi (2.58 g, 20 mmol), prepared from C_4Me_4NH and *n*BuLi, were stirred in 30 mL of THF for 10 min. The residue remaining after removal of the solvent under vacuum was extracted at -40°C with 20 mL of toluene. After addition of 20 mL of *n*-pentane, **1** crystallized at -78°C as an ocher-colored solid. Yield: 2.13 g (48%).—^1H NMR (60 MHz, [D$_8$]toluene, -40°C, TMS int.): $\delta = 3.50$ (m, 8H; OCH_2), 1.97 (s, 12H; C(2,5)-CH_3), 1.93 (s, 12H; C(3,4)-CH_3), 1.43 (m, 8H; CCH_2).—$^{13}C\{^1H\}$ NMR (75.43 MHz, [D$_8$]toluene, -40°C, TMS int.): $\delta = 119.81$ (C2,5), 113.05 (C3,4), 68.42 (OCH_2), 26.26 (CCH_2), 11.33 (C2,5-CH_3), 9.73 (C3,4-CH_3).—MS (70 eV): *m/z* 300 ([$M^{\oplus} - 2C_4H_8O$], fragment of highest mass).

3: **1** (2.50 g, 5.60 mmol) was dissolved in dichloromethane (30 mL) and treated with 0.2 mL of water. Complex **3** precipitated from the filtrate after 10 min and was crystallized from dichloromethane at -78°C as an orange-yellow, stable solid. Yield: 9.09 mg (59.4% based on C_4Me_4NH).—^1H NMR (60 MHz, [D$_8$]toluene, TMS int.): $\delta = 2.05$ (s, 12H; C2,5-CH_3), 1.95 (br. s, 24H; C11,12,13,14-CH_3), 1.57 (s, 12H; C3,4-CH_3), NH not observed.—$^{13}C\{^1H\}$ NMR (75.43 MHz, [D$_8$]toluene, TMS int.): $\delta = 120.56$ (C11,14), 113.76 (C12,13), 99.29 (C2,5), 84.36 (C3,4), 12.62 (C11,14-CH_3), 10.98 (C2,5-CH_3), 9.21 (C3,4-CH_3), 8.77 (C12,13-CH_3).—MS (70 eV): *m/z* 300 ([$M^{\oplus} - 2C_4Me_4NH$], fragment of highest mass).

Received: May 24, 1988;
revised: June 29, 1988 [Z 2775 IE]
German version: *Angew. Chem. 100* (1988) 1433

[1] a) F. Mathey, A. Mitschler, R. Weiss, *J. Am. Chem. Soc. 99* (1977) 3537; b) G. de Lauzon, B. Deschamps, J. Fischer, F. Mathey, A. Mitschler, *ibid. 102* (1980) 994; c) R. Bartsch, P. B. Hitchcock, J. F. Nixon, *J. Chem. Soc. Chem. Commun. 1987*, 1146; d) O. J. Scherer, T. Brück, *Angew. Chem. 99* (1987) 59; *Angew. Chem. Int. Ed. Engl. 26* (1987) 59; e) M. Baudler, S. Akpapoglou, D. Ouzounis, F. Wasgestian, B. Meinigke, H. Budzikiewicz, H. Münster, *ibid. 100* (1988) 288 and *27* (1988) 280.

[2] F. Seel, V. Sperber, *J. Organomet. Chem. 14* (1968) 405.

[3] N. Kuhn, E.-M. Horn, E. Zauder, D. Bläser, R. Boese, *Angew. Chem. 100* (1988) 572; *Angew. Chem. Int. Ed. Engl. 27* (1988) 579.

[4] The course of this reaction is still unclear; evidence against the involvement of **2** as an intermediate is provided by the fact that **3** cannot be detected after addition of tetramethylpyrrole to solutions of **1**. Complex **3** is also not accessible by reaction of $[Fe(H_2O)_6](BF_4)_2$ with C_4Me_4NLi.

[5] **3**: monoclinic, $P2_1/n$, $a = 8.1538(17)$, $b = 8.9063(19)$, $c = 21.817(5)$ Å, $\beta = 93.350(19)°$, $V = 1581.7(6)$ Å^3, $Z = 2$, $\rho_{calcd} = 1.49$ g cm^{-3}, $Mo_{K\alpha}$ radiation, scan range $3° \leq 2\theta \leq 50°$, 2780 unique reflections, 2309 observed ($F_0 \geq 4\sigma(F_0)$), $R = 0.039$, $R_w = 0.049$, $w^{-1} = (\sigma^2(F_0) + 0.00391 \times F_0^2)$. Number of refinement parameters 205, maximum residual electron density 0.23 e Å^{-3}. Further details of the crystal structure investigation are available on request from the Fachinformationszentrum Energie, Physik, Mathematik GmbH, D-7514 Eggenstein-Leopoldshafen 2 (FRG), on quoting the depository number CSD-51183, the names of the authors, and the full journal citation.

[6] Cf. I. Olovsson, P.-G. Jönsson: *The Hydrogen Bond*, Schuster-Zundel-Sandorfy, Amsterdam 1976.

[7] P. L. Chiche, J. Galy, G. Thiollet, F. Mathey, *Acta Crystallogr. Sect. B 36* (1980) 1344.

[8] This is in accordance with the argument presented in [2]. Additional stabilization in this case is provided by the blocking of the lone pair on the nitrogen atom; worthy of note, however, is the fact that a stability maximum is attained in the series of azaferrocenes $[(C_5H_5)Fe(C_4Me_4N)]$ despite the highest nitrogen basicity: N. Kuhn, E. Zauder, unpublished.

[9] N. Kuhn, E.-M. Horn, E. Zauder, *Inorg. Chim. Acta 149* (1988) 163.

Tricyclo[3.1.0.0^{2,6}]hexanedione (the Valene of *o*-Benzoquinone), Bicyclo[2.1.1]hexane-2,3-dione, and Valenes of a Quinoxaline, of Phenazine, and of a Benzophenazine**

By *Manfred Christl** and *Arno Kraft*

α-Diketones are of interest to photochemists[1] and, along with triketones, to spectroscopists and theoretical chemists[2] as well. Further, their importance as precursors of hetero-[3] and carbocyclic[4] compounds is growing. The starting materials for the preparation of α-diketones include 1,2-diols, which can be oxidized by various reagents.[5] However, each case usually requires a search for a suitable oxidizing agent and the optimal conditions. Recently, the oxidations described by *Corey* and *Kim*,[6] *Pfitzner* and *Moffatt*,[7] and *Swern*[8] have been employed for this purpose.

Some time ago we prepared the *cis*-diol **1** from benzvalene and converted it into the cyclobutyl thioether **2**.[9a] The desulfurization of **2** to give bicyclo[2.1.1]hexane-*cis*-2,3-diol **3** has now been achieved in 70% yield.[9b]

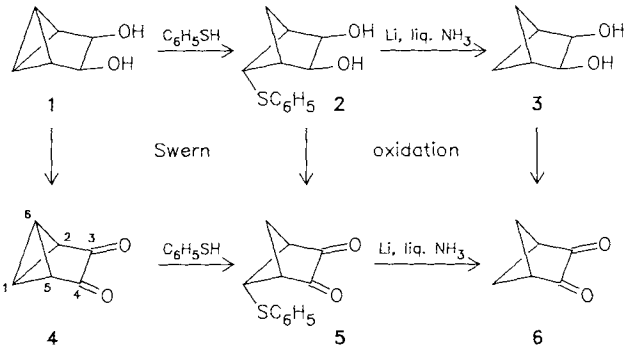

The successful application of the Corey–Kim oxidation to a substrate[6] structurally related to **1** encouraged us to subject **1** to these conditions. Although the desired product, tricyclo[3.1.0.0^{2,6}]hexanedione **4** (16%)[11] was indeed obtained, 4-(methylthiomethoxy)tricyclo[3.1.0.0^{2,6}]hexan-3-one[11] was also formed. Swern oxidation gave pure **4** in only 41% yield (see *Experimental Procedure*). Similarly, bicyclo[2.1.1]hexane-2,3-dione **6** (45%)[12] and its 5-phenylthio derivative **5** (59%)[11] were obtained from **3** and **2**, respectively.

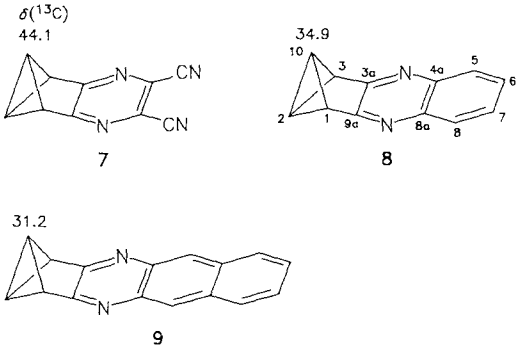

[*] Prof. Dr. M. Christl, Dipl.-Chem. A. Kraft
Institut für Organische Chemie der Universität
Am Hubland, D-8700 Würzburg (FRG)

[**] This work was supported by the Fonds der Chemischen Industrie and the Deutsche Forschungsgemeinschaft.

As expected,[3] treatment of **4** with the primary 1,2-diamines diaminomaleodinitrile, *o*-phenylenediamine, and 2,3-diaminonaphthalene gave the valenes **7** (50%, m.p. 209–210 °C),[11] **8** (95%, m.p. 122–125 °C),[11,13] and **9** (24%, m.p. 209–211 °C)[11] of quinoxaline-2,3-dicarbonitrile, phenazine, and benzo[*b*]phenazine, respectively. We also prepared analogues of **8** from **5** and **6**.

Whereas the ^{13}C NMR chemical shift of the bicyclobutane bridgehead carbon atoms ($\delta = 10.0$) of **4** is found in the normal region, the annelation of the pyrazine ring in **7**, a quinoxaline unit in **8**, and a benzoquinoxaline system in **9** to the tricyclo[3.1.0.0^{2,6}]hexane framework leads, as expected,[14] to considerable deshielding. The chemical shift values written above the formulas of **7**–**9** show an interesting tendency—namely, the deshielding decreases with increasing size of the aromatic system; on going from **7** to **9**, $\Delta\delta = 12.9$ ppm.

Experimental Procedure

4: Dimethyl sulfoxide (910 mg, 11.7 mmol) was added under N_2 over 3 min to a mixture of oxalyl chloride (1.27 g, 10.0 mmol) and dichloromethane (36 mL) cooled to −70 °C. The resulting, stirred solution was treated within 5 min with **1** (500 mg, 4.46 mmol) in dichloromethane (9 mL) and then stirred for 40 min at −70 °C. Subsequently, triethylamine (2.70 g, 26.7 mmol) was added to the milky mixture at this temperature. The mixture was stirred for an additional 5 min and then allowed to warm to 20 °C, affording a colorless precipitate in a yellow to dirty green solution. Silica gel (3.0 g, 0.063–0.2 mm) was added, the resulting suspension was stirred for 5 min, and the dichloromethane was then carefully removed at 20 torr. The brown residue was placed on a column already containing 5.0 g of silica gel. After elution with *tert*-butyl methyl ether (ca. 180 mL) until the column and the eluate were nearly colorless, the eluate was concentrated at 20 torr and dissolved in 3 mL of dry dichloromethane. Compound **4** was precipitated by addition of 4 mL of petroleum ether. Yield 179 mg (41%) yellow crystals, dec. 145–155 °C (in a sealed tube). IR (KBr): $\tilde{\nu} = 3140, 3125, 3080, 1755\ cm^{-1}$. UV ($CH_3CN$): $\lambda_{max}(\varepsilon) = 431$ nm (28). ^1H NMR ($CDCl_3$): $\delta = 3.13$ (t, $J_{1,2} = 2.2$ Hz; 2-H), 3.83 (t; 1-H), the assignments were made by means of the ^{13}C satellites: $J_{C\text{-}1,1\text{-}H} = 240$, $J_{1,6} = 4.5$, $J_{C\text{-}2,2\text{-}H} = 181$, $J_{2,5} = 3.7$ Hz. ^{13}C NMR ($CDCl_3$): $\delta = 10.0$ (dd, $J_{C\text{-}1,6\text{-}H} = 3$ Hz; C-1), 43.3 (dd, $J_{C\text{-}2,5\text{-}H} = 7$ Hz; C-2), 198.5 (t, $J_{C\text{-}3,1\text{-}H} = 5$ Hz; C-3).

5: The oxidation of **2** was effected according to the procedure described for **4** but with tetrahydrofuran instead of dichloromethane as solvent. The workup was not carried out by adsorption on silica gel but rather by hydrolysis with 2 N HCl and subsequent extraction with ether. Yield after dissolution in dichloromethane and precipitation with petroleum ether: 59%, m.p. 98–101 °C.

6: The oxidation of **3** was effected according to the procedure described for **4**. The workup was not carried out by adsorption on silica gel but rather by concentration of the reaction mixture in vacuo followed by treatment of the residue with ether, filtration of the ether suspension to remove the precipitate ($HEt_3N^{\oplus}Cl^{\ominus}$), concentration of the filtrate in vacuo until the onset of crystallization, and driving the crystallization to completion by addition of petroleum ether. Strict exclusion of moisture is necessary. Yield: 45%. For physical data, see [12].

Received: April 21, 1988 [Z 2715 IE]
German version: *Angew. Chem. 100* (1988) 1427

[1] M. B. Rubin, *Top. Curr. Chem. 129* (1985) 1.
[2] H.-D. Martin, M. Kummer, G. Martin, J. Bartsch, D. Brück, A. Heinrichs, B. Mayer, S. Röver, A. Steigel, D. Mootz, B. Middelhauve, D. Scheutzow, *Chem. Ber. 120* (1987) 1133.
[3] For example, pyrazine: A. E. A. Porter in A. R. Katritzky, C. W. Rees, A. J. Boulton, A. McKillop (Eds.): *Comprehensive Heterocyclic Chemistry, Vol. 3*, Pergamon, Oxford 1984, p. 157.
[4] For example, the Weiss reaction: H.-U. Reissig, *Nachr. Chem. Tech. Lab. 34* (1986) 162.
[5] E. Schaumann in *Houben-Weyl, Methoden der organischen Chemie, 4. Aufl., Bd. VI/1b*, Thieme, Stuttgart 1984, p. 892.
[6] R. A. Russell, P. A. Harrison, R. N. Warrener, *Aust. J. Chem. 37* (1984) 1035.
[7] R. Schobert, *Synthesis 1987*, 741.
[8] R. E. Ireland, D. W. Norbeck, *J. Org. Chem. 50* (1985) 2198; C. M. Amon, M. G. Banwell, G. L. Gravatt, *ibid. 52* (1987) 4851.
[9] a) M. Christl, H. Leininger, P. Kemmer, *Chem. Ber. 117* (1984) 2963. In procedure b) for the synthesis of **1**, $(C_2H_5)_4N^{\oplus}Cl^{\ominus}$ should be replaced by $(C_2H_5)_4N^{\oplus}OH^{\ominus}$. b) Thus, **3** is accessible in 10% overall yield in four steps from cyclopentadiene; in the earlier synthesis from acrolein and allyl chloride,[10] the product was obtained in only 3% overall yield in a six-step synthesis. This comparison highlights the importance of the bicyclobutane route for the preparation of cyclobutanes.
[10] W. Trautmann, H. Musso, *Chem. Ber. 114* (1981) 982.
[11] Elemental analyses, NMR, IR, UV, and MS data are in agreement with the structures of the new compounds.
[12] The transformation of cyclopentadiene to **6** is thus possible in five steps in 5% overall yield. In the only earlier route to **6**, a nine-step synthesis from pentaerythritol gave the product in 11% overall yield: P. Hofmann, E. Beck, unpublished work, presented at the Chemiedozenten-Tagung 1987 in Göttingen; E. Beck, *Dissertation*, Technische Universität München 1985. We thank Prof. *P. Hofmann* for providing us with these results.
[13] **8**, ^1H NMR ($CDCl_3$): $\delta = 2.98$ (t, $J_{1,2} = 1.8$ Hz; 1-H), 4.38 (t; 2-H), 1-H and 2-H were assigned on by means of the ^{13}C satellites: $J_{C\text{-}1,1\text{-}H} = 177$, $J_{1,3} = 4.8$, $J_{C\text{-}2,2\text{-}H} = 226$, $J_{2,10} = 7.0$ Hz; 7.53 and 7.84 (AA'XX' spectrum, 5-H, 6-H). ^{13}C NMR ($CDCl_3$): $\delta = 34.9$ (dd, $J_{C\text{-}2,10\text{-}H} = 5$ Hz; C-2), 36.7 (ddt, $J_{C\text{-}1,3\text{-}H} = 9$, $J_{C\text{-}1,2\text{-}H} = 3$ Hz; C-1), 127.8 and 128.0 (each dm, $^1J_{C,H} = 161$ Hz; C-5, C-6), 139.3 (≈t, $J = 7$ Hz; C-4a), 163.7 (t, $J = 5$ Hz; C-3a).
[14] M. Christl, S. Freund, *Chem. Ber. 118* (1985) 979.

A Monomeric Diboryldilithiomethane with a 1,3-Diborataallene Structure**

By *Monika Pilz, Jürgen Allwohn, Ralf Hunold, Werner Massa,* and *Armin Berndt**

Dedicated to Professor Heinrich Nöth on the occasion of his 60th birthday

Boryllithioalkenes[1] are boron-stabilized[2] carbanions having the borataalkene structure **1**.[3] We have now prepared the first diboryldilithiomethane **2b** and present here data establishing its 1,3-diborataallene structure **2**.[4]

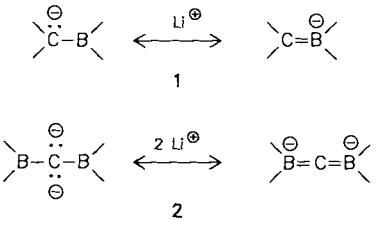

When we attempted to prepare the 1,3-diborataallene **2a** by addition of *tert*-butyllithium to **3**,[5] we obtained instead the 1,3-diborataallene **2b**, which contains a second *tert*-butyl group in place of the $CH(SiMe_3)_2$ group. The dilithium

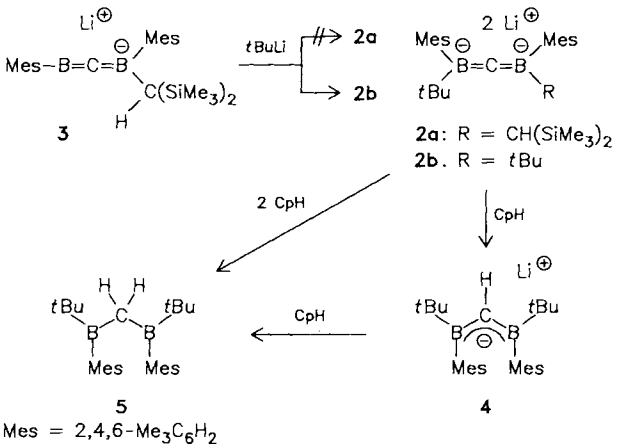

[*] Prof. Dr. A. Berndt, Priv.-Doz. Dr. W. Massa, M. Pilz, J. Allwohn, Dr. R. Hunold
Fachbereich Chemie der Universität
Hans-Meerwein-Strasse, D-3550 Marburg (FRG)

[**] This work was supported by the Deutsche Forschungsgemeinschaft and the Fonds der Chemischen Industrie.

salt **2b** crystallizes with two ether molecules from a pentane solution of the complex reaction mixture as yellow cubes (yield: 50%).

Upon treatment with one equivalent of cyclopentadiene (CpH), **2b** is transformed into the monoprotonated form **4**, which can be protonated with a further equivalent of CpH to give **5**. Compound **5** is also accessible directly by treatment of **2b** with CpH in excess. Thus, **2b** reacts like a dilithiomethane.

Table 1. Selected physical and spectroscopic data for **2b**, **4**, and **5**. Spectra in [D$_8$]THF (**2b**, **4**) and $CDCl_3$ (**5**).

2b: yellow crystals, m.p. 148°C (dec.), yield 50%. ^{1}H NMR: $\delta = 0.80$ (s, 18H, $C(CH_3)_3$), 2.07, 2.21 (each s, each 6H, *o*-CH_3), 2.50 (s, 6H, *p*-CH_3), 6.63 (s, 4H, *m*-H); ^{13}C NMR (−40°C): $\delta = 21.2$ (2C, *p*-CH_3), 25.1, 26.1 (each 2C, *o*-CH_3), 34.5 (6C, $C(CH_3)_3$), 127.9, 128.0 (each 2C, *m*-C), 134.2 (2C, *p*-C), 140.8, 142.6 (each 2C, *o*-C), 149.2 (br., 2C, *i*-C), 180.2 (br., 1C, CB_2); ^{11}B NMR: $\delta = 32$ ($\nu_{1/2} = 595$ Hz)

4: ^{1}H NMR: $\delta = 0.75$ (s, 18H, $C(CH_3)_3$), 1.88 (s, 18H, *o*- and *p*-CH_3), 4.56 (s, 1H, CHB_2), 5.92 (s, 4H, *m*-H); ^{13}C NMR (−40°C): $\delta = 21.6$ (q, 2C, *p*-CH_3), 25.0 (q, 4C, *o*-CH_3), 33.0 (q, 6C, $C(CH_3)_3$), 99.7 (d, 1C, CHB_2, $^1J_{C-D} = 107.3$ Hz), 125.0 (d, 4C, *m*-C), 129.5 (s, 2C, *p*-C), 136.2 (s, 4C, *o*-C), 154.4 (s, 2C, *i*-C); ^{11}B NMR: $\delta = 61$ ($\nu_{1/2} = 1071$ Hz)

5: colorless crystals, m.p. 57°C, yield: quantitative (NMR spectroscopy). ^{1}H NMR: $\delta = 1.09$ (s, 18H, $C(CH_3)_3$), 1.84 (s, 12H, *o*-CH_3), 2.31 (s, 6H, *p*-CH_3), 2.54 (s, 2H, CH_2B_2), 6.65 (s, 4H, *m*-H); ^{13}C NMR: $\delta = 21.1$ (q, 2C, *p*-CH_3), 22.6 (q, 4C, *o*-CH_3), 28.6 (q, 6C, $C(CH_3)_3$), 29.6 (br. s, 2C, $C(CH_3)_3$), 36.6 (br. t, 1C, CH_2B_2, $^1J_{C-H} = 99.3$ Hz), 127.1 (d, 4C, *m*-C), 134.8 (s, 4C, *o*-C), 135.6 (s, 2C, *p*-C), 144.0 (br. s, 2C, *i*-C); ^{11}B NMR: $\delta = 88$ ($\nu_{1/2} = 952$ Hz)

The structures of **2b**, **4**, and **5** were established from the ^{1}H, ^{13}C, and ^{11}B NMR spectra (Table 1); the structure of **2b** was corroborated by an X-ray structure analysis. In **2b**, the C atom bonded to two boron atoms is strongly deshielded ($\delta(^{13}C) = 180$) compared with the corresponding atoms in **3** (127) and **4** (100). The boron atoms ($\delta(^{11}B) = 32$) are appreciably shielded (**3**, 41 and 54; **4**, 61). Shielding of the terminal atoms and deshielding of the central atom are characteristic properties of allenes.[6] In tetra-*tert*-butylallene, the chemical shift of the central C atom is $\delta = 199.2$.[7] The (linear) chirality of **2b** is revealed by the different chemical shifts of the diastereotopic *ortho*- and *meta*-C atoms and *ortho*-methyl groups in the ^{13}C and ^{1}H NMR spectra.

The X-ray structure analysis[8] of **2b** (Fig. 1) reveals a slightly deformed 1,3-diborataallene structure with a C_2 axis through the central C atom C1. The B-C1-B′ bond angle is 168°, with the boron atoms displaced away from the center of gravity of the lithium ions. The planes B, C11, C21 and B′, C11′, C21′ form an angle of 83°. The mesityl ring is twisted by 88° with respect to the plane C1, B, C21. The B-Cl distance (145 pm) is shorter than the corresponding distance in **3** (149 pm), which has only partial BC double-bond character,[5] and similar in length to that in **1** (144 pm).[3] The lithium ions, each coordinated by one ether molecule, exhibit short distances to C1 (204 pm; in **3**, 209 pm); in addition, each displays a short distance to one boron atom (239 pm; in **3**, 249 pm). The distance to the other boron atom (272 pm) is significantly longer, whereas the distance (234 pm) to the *ipso*-C atom of the mesityl group (C11) corresponds to that in **3** (235 pm). The larger negative charge in the dianion **2b** compared with the monoanion **3** is responsible, owing to stronger attraction of the lithium ions, for the shorter distances. The tendency of the lithium ions to coordinate the *ipso*-C atom of the mesityl groups—C1, B, C11, Li lie practically in the same plane—presumably leads to the Li, C1, Li′ angle of 120° and to the deviation from orthogonality of the planes

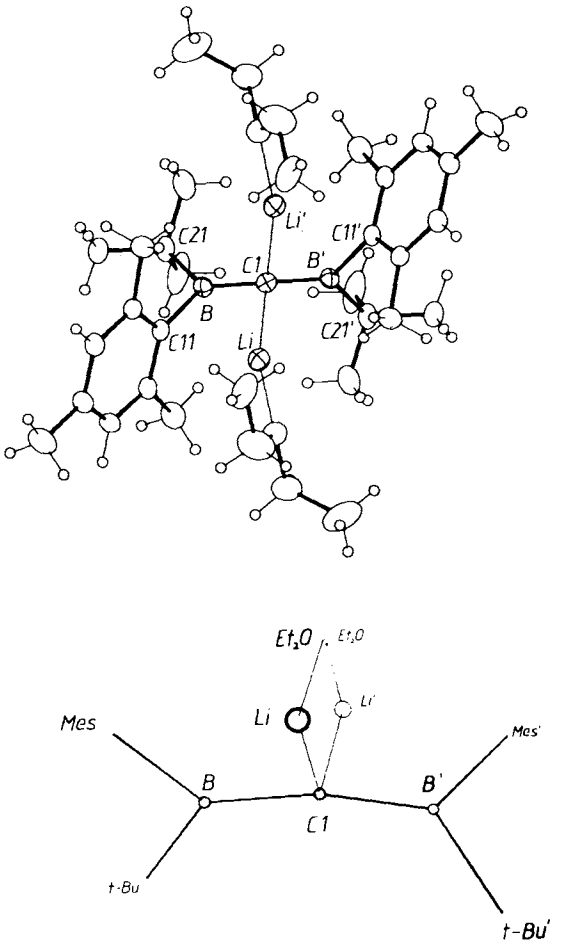

Fig. 1. Top: ORTEP drawing of the molecular structure of **2b** · 2 Et_2O, projection along the C_2 axis. Thermal ellipsoids at the 30% probability level. Bottom: Geometry of the CB_2Li_2 framework, projection roughly perpendicular to the C_2 axis. Important distances [pm] and angles [°]: C1-B 145.0(5), C1-Li 204.0(8), Li-B 239.0(8), Li-B′ 272.3(9), Li-C11 233.5(8), B-C11 164.5(6), B-C21 166.0(6); B-C1-B′ 168.4(4), Li-C1-Li′ 120.1(3), B-C1-Li 84.6(2), B-C1-Li′ 101.2(2), C1-B-C11 124.2(3), C1-B-C21 123.1(3), C11-B-C21 112.7(3).

Li, C1, Li′ and B, C1, B′, reflected in the angles B-C1-Li (84.6°) and B-C1-Li′ (101.2°). The planarity of the mesityl rings is not influenced by the coordination.

The dilithiomethane derivatives characterized so far are aggregated;[9] **2b** is the first derivative with a monomeric structure.

Received: May 13, 1988 [Z 2757 IE]
German version: *Angew. Chem. 100* (1988) 1421

CAS Registry numbers:
2b, 116724-56-2; **3**, 116724-55-1; **4**, 116724-57-3; **5**, 116724-58-4; CpH, 542-92-7.

[1] J. W. Wilson, *J. Organomet. Chem. 186* (1980) 297; A. Pelter, B. Singaram, L. Williams, J. W. Wilson, *Tetrahedron Lett. 24* (1983) 623, and references cited therein.
[2] A. Pross, D. J. DeFrees, B. A. Levi, S. K. Pollack, L. Radom, W. J. Hehre, *J. Org. Chem. 46* (1981) 1693.
[3] M. M. Olmstead, P. P. Power, K. J. Weese, *J. Am. Chem. Soc. 109* (1987) 2541.
[4] Diborylamides isoelectronic to **2** were recently described by *Nöth* et al. and by *Power* et al.: H. Nöth, H. Prigge, *Chem. Ber. 120* (1987) 907; R. A. Bartlett, H. Chen, H. V. R. Dias, M. M. Olmstead, P. P. Power, *J. Am. Chem. Soc. 110* (1988) 446.
[5] R. Hunold, J. Allwohn, G. Baum, W. Massa, A. Berndt, *Angew. Chem. 100* (1988) 961; *Angew. Chem. Int. Ed. Engl. 27* (1988) 961.
[6] W. Runge, J. Firl, *Ber. Bunsenges. Phys. Chem. 79* (1975) 913, and references cited therein.
[7] R. Bolze, H. Eierdanz, K. Schlüter, W. Massa, W. Grahn, A. Berndt, *Angew. Chem. 94* (1982) 927; *Angew. Chem. Int. Ed. Engl. 21* (1982) 924.

[8] **2b** · $2Et_2O$: X-ray structure analysis: $C_{35}H_{60}B_2Li_2O_2$, space group *Pbcn*, $Z=4$, $a=1441.4(3)$, $b=1467.3(3)$, $c=1687.6(2)$ pm; 1934 unique reflections with $F_0>3\sigma(F_0)$ measured at $-90°C$ on a four-circle diffractometer (CAD4, Enraf-Nonius) with $Cu_{K\alpha}$ radiation; no absorption correction ($\mu=3.7\ cm^{-1}$), H atoms included at calculated positions using a riding model and refined in groups using isotropic temperature factors. Anisotropic temperature factors were used for all other atoms. 190 parameters, $R=0.0730$, $wR=0.0658$ ($w=1/\sigma^2(F_0)$). The moderate residuals are presumably due to the strong thermal motions or disorder of the ether molecules and the methyl groups. Further details of the crystal structure investigation may be obtained from the Fachinformationszentrum Energie, Physik, Mathematik GmbH, D-7514 Eggenstein-Leopoldshafen 2 (FRG), on quoting the depository number CSD-53 158, the names of the authors, and the journal citation.

[9] A. J. Gais, J. Vollhardt, H. Günther, D. Moskau, H. J. Lindner, S. Braun, *J. Am. Chem. Soc. 110* (1988) 978, and references cited therein.

Catalytic Syntheses of Functionalized Nitrogen Heterocycles from Cyanogen**

By *Jörg Sundermeyer* and *Herbert W. Roesky**

Dedicated to Professor Wolfgang Sundermeyer on the occasion of his 60th birthday

A number of reports on novel heterocycle syntheses starting from cyanogen have appeared in this journal in recent years.[1] Using the catalyst systems HCl/Adogen® and $HBr/NBu_4^{\oplus}Br^{\ominus}$, we have now surprisingly found a simple route leading directly to the synthesis of halogenated aromatic heterocycles in good yields starting from cyanogen and oxalyl chloride or bromide.

In the presence of catalytic amounts of HCl and a quaternary ammonium chloride, cyanogen reacts with oxalyl chloride at 70–120 °C to give the tricyclic compound **1** [Eq. (a)]. Carbon dioxide and phosgene, along with small amounts of CO, are formed as gaseous reaction products.

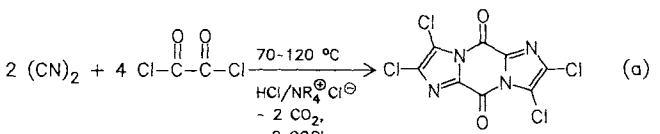

(a)

1

Compound **1** can be regarded as an unusual head-to-tail 1,3 dimer of the ketene **2**, which has not yet been isolated in condensed phase. Indeed, $1/2\,M^{\oplus}$ is observed as the base peak in the EI mass spectrum. The ^{13}C NMR spectrum of **1** shows four signals. A reaction behavior deviating from that expected for ketene dimers[2] and the $\nu_{C=O}$ absorption at 1745 cm^{-1} in the IR spectrum corroborate the central dilactam structure. Compound **1** is cleaved by ammonia and by primary and secondary amines in an exothermic reaction, and by alcohols and water upon warming in a base-catalyzed reaction, to give in near quantitative yield two equivalents of the 4,5-dichloroimidazole-2-carboxylic acid derivatives **3a**,**c**–**e**, which are not otherwise accessible via a simple route. Compound **3a** can be decarboxylated to give **3b**. Characteristic data for these imidazoles are presented in Table 1.

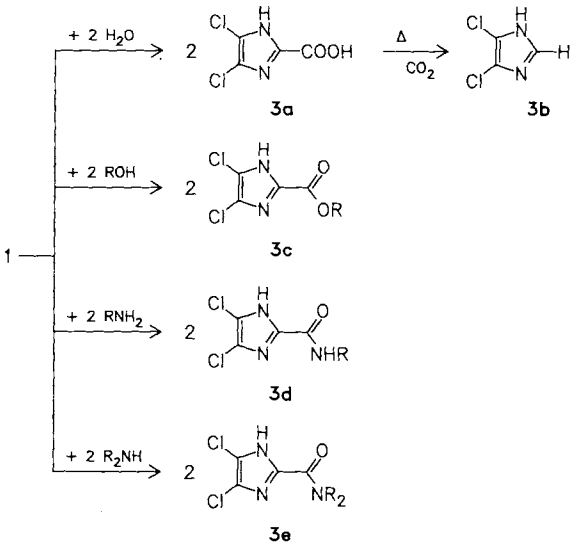

Table 1. Characteristic data for imidazoles **3a**–**e**.

3a: m.p. 160 °C (dec.); yield: 91%.—FI-MS: *m/z* 180 ($M^{\oplus\ominus}$, 50%), 136 ($[M^{\oplus\ominus}-CO_2]$, 100).—IR (Nujol): $\tilde{\nu}=2650$–3400 (ν(NH assoc.) + ν(OH)), 1600–1700 cm^{-1} (br)

3b: m.p. 179 °C; yield: 60%.—EI-MS: *m/z* 136 ($M^{\oplus\ominus}$, 100%), 109 ($[M^{\oplus\ominus}-HCN]$, 95).—IR (Nujol): $\tilde{\nu}=2500$–$3100\ cm^{-1}$ (ν(NH assoc.)).—^1H NMR ([D6]acetone, 25 °C): $\delta=12.2$ (br; NH), 7.82 (s, 1 H)

3c (R = CH_2CF_3): m.p. 187 °C; yield: 78%.—EI-MS: *m/z* 262 ($M^{\oplus\ominus}$, 24%), 162 ($[M^{\oplus\ominus}-F_3CCH_2OH]$, 100).—IR (Nujol): $\tilde{\nu}=1740$ (ν(C=O), vs), 1160–1200 cm^{-1} (ν(C–F), vs).—^1H NMR ([D6]acetone, 25 °C): $\delta=13$ (br, NH), 4.93 (q, 2 H, $^3J_{CF}=8.7$ Hz).—^{19}F NMR ([D6]acetone, 25 °C): $\delta=-73.22$ (t, $^3J_{CF}=8.7$ Hz)

3d (R = C_6H_5): m.p. 246 °C; yield: 92%.—EI-MS: *m/z* 255 ($M^{\oplus\ominus}$, 20%), 163 ($[M^{\oplus\ominus}-C_6H_5NH]$, 10).—IR (Nujol): $\tilde{\nu}=1660\ cm^{-1}$ (ν(C=O), vs)

3e (R_2 = $CH_2CH_2OCH_2CH_2$): m.p. 218 °C, yield: 93%.—EI-MS: *m/z* 249 ($M^{\oplus\ominus}$, 10%), 163 ($[M^{\oplus\ominus}-NC_4H_8O]$, 20).—IR (Nujol): $\tilde{\nu}=1610\ cm^{-1}$ (ν(C=O), br, vs)

Remarkably, the reaction of cyanogen with oxalyl bromide under analogous catalytic conditions affords the tetrabromopyrazine **4** and carbon dioxide in over 70% yield [Eq. (b)].

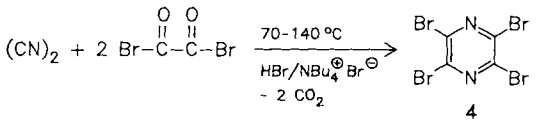

(b)

4

Compound **4** exhibits a broad bactericidal activity.[3] Since the bromine atoms can undergo facile nucleophilic substitution, **4** is also of interest as a central building block in the synthesis of antitumor agents[4a] as well as of heterocycles with high electron affinity.[4b] Chloroimidazoles of type **3**, as well as the tetrabromopyrazine **4** and its derivatives, can only be prepared in poor yields, if at all, by halogenation[5] of the parent structures synthesized via classical routes.

Presumably, in both reactions (a) and (b), cyanogen first reacts with the catalyst to establish an equilibrium with the oxalimidic halide **5**, which is unstable as a free species. Compound **5** then undergoes partially irreversible reactions (*N*-acylation, ring closure, *O*-acylation, decarboxyla-

[*] Prof. Dr. H. W. Roesky, Dipl.-Chem. J. Sundermeyer
Institut für Anorganische Chemie der Universität
Tammannstrasse 4, D-3400 Göttingen (FRG)

[**] This work was supported by the Deutsche Forschungsgemeinschaft and the Fonds der Chemischen Industrie.

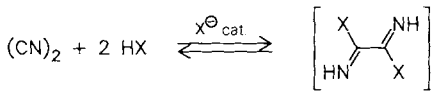

5, X = Cl, Br

tion) with oxalyl halide to give functionalized heteroarenes, the catalyst being re-formed.

Experimental Procedure

1: Anhydrous Adogen® 464 (9 g; Aldrich) and oxalyl chloride (125 mL) were dissolved in dichloromethane (220 mL) contained in a 500-mL Monel cylinder, and cyanogen (26 g) and HCl (3 g) were then condensed into the solution. This mixture was stirred for 3 d, the temperature being increased stepwise from 70 to 120°C. The autoclave was then opened and the precipitated crude product, obtained as gold-yellow crystalline platelets, was separated from soluble impurities by filtration and subsequent washing with THF. Yield 48.5 g (60% based on $(CN)_2$). Traces of $(CN)_x$ give the product a greenish-yellow color. Loss-free purification was carried out by sublimation at 300°C/10^{-1} mbar; m.p. >270°C. Compound **1** is poorly soluble in the conventional solvents.—IR (Nujol): $\tilde{\nu}$ = 1745 cm^{-1} (ν(C=O), vs).—EI-MS: *m/z* 326 ($M^{\odot\ominus}$, 24%), 162 ($1/2\,M^{\odot\ominus}$, 100), 134 ([$1/2\,M^{\odot\ominus}$ − CO], 17); FI-MS: *m/z* 326 ($M^{\odot\ominus}$), correct isotopic pattern for $C_8N_4O_2Cl_4$.—^{13}C NMR ([D$_6$]dimethyl sulfoxide, 50°C): δ = 145.9, 135.5, 131.9, 116.8.

4: Tetrabutylammonium bromide (5 g) and oxalyl bromide (53 mL) were dissolved in dichloromethane (150 mL) contained in a 300-mL Monel cylinder, and cyanogen (8 g) and HBr gas (8 g) were then condensed into the solution. This mixture was stirred for 3 d, the temperature being increased stepwise from 70 to 140°C. The autoclave was then opened and the brown reaction solution was evaporated to dryness under vacuum. Compound **4** was sublimed at 100–130°C/10^{-1} mbar from the residue remaining after evaporation. Yield: ca. 45 g white crystals (73% based on cyanogen). If necessary, **4** can be purified further by recrystallization from CH_2Cl_2/hexane or by column filtration (40 g of product on 80 g of SiO_2 (0.060–0.200 mm), elution with $CHCl_3$), m.p. 150–151°C.—IR (Nujol): $\tilde{\nu}$ = 1348 (m), 1270 (vs), 1195 (w), 1140 (s), 1035 (s), 515 (m), 468 cm^{-1} (m).—EI-MS: *m/z* 396 ($M^{\odot\oplus}$, 100%), 315 ([$M^{\odot\ominus}$ − Br], 50).—^{13}C NMR ($CDCl_3$, 25°C): δ = 139.6.

Received: May 6, 1988 [Z 2747 IE]
German version: *Angew. Chem. 100* (1988) 1417

[1] H. W. Roesky, N. Amin, G. Remmers, A. Gieren, U. Riemann, B. Dederer, *Angew. Chem. 91* (1979) 243; *Angew. Chem. Int. Ed. Engl. 18* (1979) 223; D. Günther, D. Bosse, *ibid. 92* (1980) 138 and *19* (1980) 138; H. W. Roesky, K. Keller, J. W. Bats, *ibid. 95* (1983) 904 and *22* (1983) 881; *Angew. Chem. Suppl. 1983*, 1323.

[2] *Houben-Weyl-Müller: Methoden der Organischen Chemie, Bd. VII/4*, Thieme, Stuttgart 1968, p. 264ff.

[3] A. H. Gulbenk, US-Pat. 3471496 (1966), Dow Chemical Co.; *Chem. Abstr. 71* (1969) P 124489b.

[4] a) Y. C. Tong, *J. Heterocycl. Chem. 12* (1975) 1127; b) Y. Yamashita, K. Saito, T. Suzuki, C. Kabuto, T. Mukai, T. Miyashi, *Angew. Chem. 100* (1988) 428; *Angew. Chem. Int. Ed. Engl. 27* (1988) 434.

[5] a) K. H. Büchel, H. Erdmann, *Chem. Ber. 109* (1976) 1625; b) J. J. Baldwin, P. K. Lumma, F. C. Novello, G. S. Ponticello, J. M. Spragne, D. E. Duggan, *J. Med. Chem. 20* (1977) 1189; c) A. W. Lutz, S. DeLorenzo, *J. Heterocycl. Chem. 4* (1967) 399.

Metal-free Carbanion Salts as Initiators for the Anionic Polymerization of Acrylic and Methacrylic Acid Esters**

By *Manfred T. Reetz,* Thomas Knauf, Ulrich Minet,* and *Carsten Bingel*

The polymerization of alkyl acrylates at room temperature with quantitative formation of living polyacrylates having a narrow molecular weight distribution has only recently been made possible.[1] Reaction of alkylthiosilanes as initiators with acrylic acid esters in the presence of catalytic amounts of ZnI_2 results in a group transfer polymerization[2] with formation of polymers having M_w/M_n values (ratio of weight average molecular weight to the number average molecular weight) of < 1.3. A second and in principle quite different method uses tetrabutylammonium thiolates $Bn_4N^{\oplus}RS^{\ominus}$ as initiators.[3] This metal-free anionic polymerization requires no catalysts, but has the disadvantage that the initiators are highly nucleophilic and therefore relatively unstable, and that only oligomers with molecular weights of less than ca. 2000 can be obtained.[4] We report here on a method which overcomes both these problems.

The initiators in this new method are the resonance-stabilized, metal-free ammonium methanides[5] **2**, **5** and **8**, which are accessible either by deprotonation of the corresponding C–H acidic precursors **1**, **4** and **7**, respectively, with $Bu_4N^{\oplus}OH^{\ominus}$ or by reaction of the sodium salts **3**, **6** and **9**, respectively, with $Bu_4N^{\oplus}Cl^{\ominus}$.

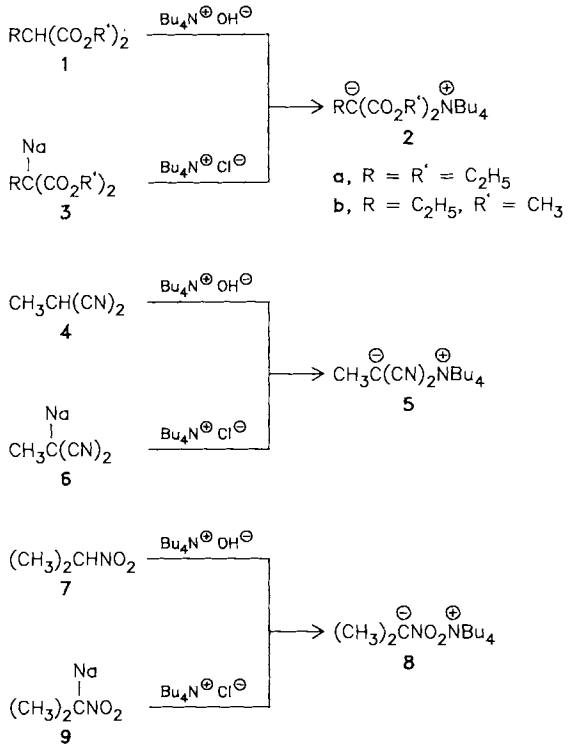

These carbanion salts are either colorless oils (**2b**) or white crystals (**2a**, **5**, **8**) and have been characterized by NMR and IR spectroscopy.[6] They are storable for months in a refrigerator, but can also be handled at room temperature without problems. When acrylic acid butyl ester **10** is added dropwise to solutions of **2**, **5** or **8** in THF or toluene at room temperature, a spontaneous exothermic reaction takes place with formation of the polyacrylate **13** (>95% conversion after acidic workup of **12**).

Table 1 clearly demonstrates that the molecular weight distribution is influenced by the solvent, the initiator, and the monomer/initiator ratio (reflected in M_n (calcd)). Low, i.e. good M_w/M_n values (≤ 1.3) are achieved in particular with the malonates **2** (e.g. Nos. 1, 3, 6, 8, 10), whereas the nitromethanide **8** affords larger M_w/M_n values (≈ 2–3). Significantly, a polymer with a molecular weight of ca. 20000 and relatively narrow molecular weight distribution

[*] Prof. Dr. M. T. Reetz, Dr. T. Knauf, Dipl.-Chem. U. Minet, C. Bingel
Fachbereich Chemie der Universität
Hans-Meerwein-Strasse, D-3550 Marburg (FRG)

[**] This work was supported by the Fonds der Chemischen Industrie and Bayer AG.

Table 1. Polymerization of butyl acrylate **10** with metal-free carbanions at room temperature [a].

No.	Initiator	Solvent	M_n (calcd) [b] [kg mol^{-1}]	M_n (exp) [kg mol^{-1}]	M_w/M_n [c]
1	**2a**	THF	1.15	0.90	1.16
2	**2a**	THF	5.32	3.13	1.36
3	**2a**	THF	10.44	7.42	1.25
4	**2b**	THF	1.44	1.51	1.50
5	**2b**	toluene	1.44	0.64	1.37
6	**2b**	THF	5.29	5.86	1.30
7	**2b**	toluene	5.29	6.82	1.36
8	**2b**	toluene	10.41	10.92	1.30
9	**2b**	THF	20.67	17.43	1.38
10	**2b**	toluene	20.67	20.39	1.30
11	**5**	THF	1.36	0.61	1.14
12	**5**	toluene	1.36	0.71	1.61
13	**5**	THF	5.21	2.59	1.43
14	**5**	toluene	5.21	4.21	1.34
15	**8**	THF	1.37	0.85	2.71
16	**8**	toluene	1.37	1.25	2.18

[a] The temperature rises 10–25 °C during the polymerization. [b] Calculated from the ratio [monomer]/[initiator]. [c] The breadth of a molecular weight distribution can be characterized by M_w/M_n. The M_n values were determined gel-chromatographically using a standard calibration. The calibration samples were supplied by Bayer AG.

($M_w/M_n = 1.3$; No. 10) can be prepared; this is not possible with ammonium thiolates as initiators.[3]

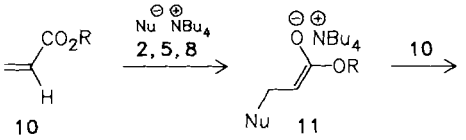

R = n-C_4H_9

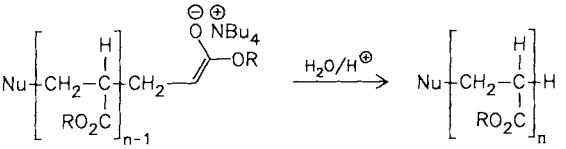

Dianions of the type **14** also initiate the polymerization of acrylic acid butyl ester (→ **15**: e.g. M_n(calcd) = 1717, M_n(exp) = 1624, $M_w/M_n = 1.1$; THF/room temperature).

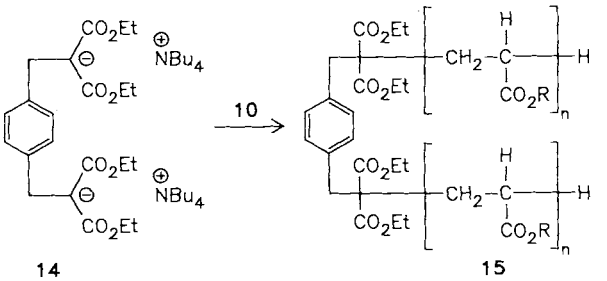

Not only acrylic acid methyl and ethyl esters, but also the less reactive methacrylic acid butyl ester can be polymerized in the same way. Surprisingly, the nitro-stabilized carbanion **8** proved to be optimal in the polymerization of methacrylates (e.g. M_n(calcd) = 2090, M_n(exp) = 2050; $M_w/M_n = 1.17$; THF/room temperature).

Why can α-activated olefins such as acrylic acid alkyl esters (and even the very reactive methyl ester) be smoothly polymerized with **2**, **5** and **8** at room temperature, while such classical initiators as bulky organolithium compounds generally lead to moderate yields and high M_w/M_n values, even at low temperatures?[7] Perhaps this has to do with the fact that the typical side reactions and chain-terminating reactions like the intramolecular Claisen condensation require a metal ion for the activation of the ester function and expulsion of the alkoxide, so that this back-biting reaction[7] cannot compete in the same way in the case of the metal-free system. Relevant is the observation that polymers with a wider molecular weight distribution ($M_w/M_n > 3$) are obtained in poor yields on using the sodium or potassium salts instead of the ammonium salts **2**, **5** and **8**. In contrast to the group transfer polymerization, in which covalently bonded silyl groups migrate along the growing chain,[1,2] in the metal-free polymerization electrostatic forces between the anionic chain terminal and the ammonium counterion are expected to play an important role. Mechanistic and theoretical investigations relating to this hypothesis are presently under way.[8]

Received: May 16, 1988 [Z 2761 IE]
German version: *Angew. Chem. 100* (1988) 1422

[1] M. T. Reetz, R. Ostarek, K.-E. Piejko, D. Arlt, B. Bömer, *Angew. Chem. 98* (1986) 1116; *Angew. Chem. Int. Ed. Engl. 25* (1986) 1108.
[2] O. W. Webster, W. R. Hertler, D. Y. Sogah, W. B. Farnham, T. V. Rajan-Babu, *J. Am. Chem. Soc. 105* (1983) 5706; W. R. Hertler, D. Y. Sogah, O. W. Webster, B. M. Trost, *Macromolecules 17* (1984) 1417.
[3] M. T. Reetz, R. Ostarek, *J. Chem. Soc. Chem. Commun. 1988*, 213.
[4] This is due to the fact that the thiolate ions are eliminated during the chain growth and can then initiate a new chain.
[5] Carbanions with ammonium counterions are mentioned in the literature, but have seldom been characterized. See, e.g.: W. Schlenk, J. Holtz, *Chem. Ber. 49* (1916) 603; G. Wittig, M. Heintzeller, M. W. Wetterling, *Justus Liebigs Ann. Chem. 557* (1947) 201; I. N. Roshkov, I. L. Knunyants, *Dokl. Akad. Nauk SSSR 199* (1971) 614; A. Brändström, U. Junggren, *Acta Chem. Scand. 25* (1971) 1469.
[6] Spectroscopic data of the salt **2a**: ^{13}C-NMR ([D$_8$]THF): $\delta = 14.2$, 15.9, 17.2, 20.6, 24.9, 26.4, 56.5, 58.9, 75.8, 170.9; as expected, in the IR spectrum (THF) the carbonyl vibration is split (1740 and 1680 cm^{-1}).
[7] See, e.g.: W. K. Busfield, J. M. Methven, *Polymer 14* (1973) 137; Y. K. Han, J. M. Park, S. K. Choi, *J. Polym. Sci. Polym. Chem. Ed. 20* (1982) 1549; W. Fowells, C. Schuerch, F. A. Bovey, F. P. Hood, *J. Am. Chem. Soc. 89* (1967) 1396.
[8] Preliminary investigations on the tacticity of poly(ethyl acrylate) of molecular mass 4000 indicate a predominantly atactic product; solvent effects have not yet been investigated.

5-Isopropyliden-1,2-oxathiole 2-Oxide by Photoisomerization of 2,2-Dimethyl-3(2*H*)-thiophenone 1-Oxide

By *Ronald Kowalewski* and *Paul Margaretha**

3(2*H*)-Thiophenones **1** are cyclic enones. Upon excitation with light, **1a** forms tricyclic dimers[1] and **1b** undergoes intramolecular [2 + 2] cycloaddition to give thiatricyclooctanones.[2] We now report that the sulfoxides **2**, which are readily accessible by oxidation of the cyclic γ-ketovinyl sulfides **1**,[3] behave completely differently in light-induced reactions.

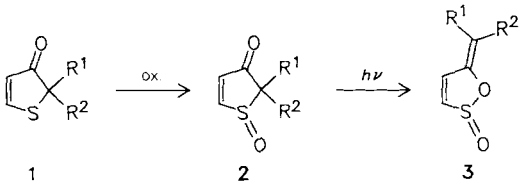

a: $R^1 = R^2 = CH_3$
b: $R^1 = COOCH_3$, $R^2 = CH_2CH{=}CH_2$

[*] Prof. Dr. P. Margaretha, Dipl.-Chem. R. Kowalewski
Institut für Organische Chemie der Universität
Martin-Luther-King-Platz 6, D-2000 Hamburg 13 (FRG)

Thus, irradiation ($\lambda = 350$ nm) of **2a** in CH_3CN or CH_2Cl_2—even in the presence of an alkene, e.g. isobutene—leads selectively to 5-isopropylidene-1,2-oxathiole 2-oxide **3a** which can be isolated in 90% yield by chromatography.[4] In an analogous way, **2b** isomerizes exclusively (NMR) to **3b**, which, however, could not be isolated since it partially decomposes, both on SiO_2 as well as on Al_2O_3. Above 50 °C, re-isomerization to **2a** is observed in the case of **3a**, whereas the diene ester **3b** polymerizes. The compounds **3** were characterized by ^{1}H-NMR, ^{13}C-NMR, IR and mass spectroscopy.[5] The alternative structure of a 1,2-oxathiin-5(6*H*)-one can be ruled out by the absence of carbonyl absorptions.

In principle, in the photoisomerization of **2b** two diastereomeric esters can be formed. The selective formation of **3b**, which on the basis of the downfield shift[6] of H-4 ($\delta = 8.15$) can be assigned the depicted *E* configuration, could be attributed to destabilizing dipole-dipole interactions between the ester-O and ring-O atoms in the *Z* isomer.

In analogy to the photo-Fries rearrangement[7] of non-enolizable 1,3-diketones to enol lactones,[8] the formation of the diradical **4** by α-cleavage of the $\geqslant$C–S bond[9] can be assumed as reaction mechanism for the isomerization **2** → **3**. From the values determined for the quantum yields ($\Phi = 0.6$–0.7) it follows that **4** preferentially cyclizes to **3** and that the recombination to give **2** plays only a subordinate role.

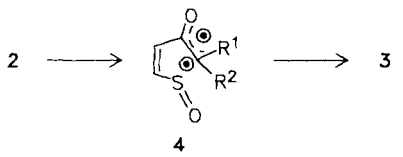

The 1,2-oxathioles are a class of heterocycles that have rarely been studied.[10] Whereas the unsubstituted 5*H*-1,2-oxathiole 2-oxide,[11] 4-bromo-5-alkyl derivatives,[12] and the 3,4-diphenyl compound[13] have been prepared, 5-alkylidene-1,2-oxathiole 2-oxides such as **3** were hitherto unknown. These *S*- and *O*-functionalized *s-trans*-1,3-dienes **3** are now readily accessible and could prove to be interesting intermediates for organic synthesis.

Received: May 30, 1988 [Z 2789 IE]
German version: *Angew. Chem. 100* (1988) 1437

[1] E. Anklam, R. Ghaffari-Tabrizi, H. Hombrecher, S. Lau, P. Margaretha, *Helv. Chim. Acta 67* (1984) 1402.
[2] E. Anklam, S. Lau, P. Margaretha, *Helv. Chim. Acta 68* (1985) 1129.
[3] Oxidation of **1a**, **1b** with *m*-chloroperbenzoic acid in CH_2Cl_2. **2a**: 62% yield; m.p. 97 °C, from Et_2O; ^{1}H NMR ($CDCl_3$): $\delta = 8.08$, 6.75 (AB, $J = 6.4$ Hz), 1.55, 1.43 (s, CH_3). **2b**: 60% yield; m.p. 89 °C from Et_2O; ^{1}H NMR ($CDCl_3$): $\delta = 8.10$, 6.90 (AB, $J = 6.4$ Hz), as well as ester and allyl protons.
[4] Procedure: **3a**: A solution of 1.44 g (10^{-2} mol) of **2a** in 20 mL of CH_3CN was irradiated for 6 h under argon in a Rayonet RPR-100 photoreactor fitted with 350-nm lamps. After removal of the solvent under vacuum and chromatography (SiO_2, CH_2Cl_2/MeOH 97/3), 1.30 g (90%) of **3a** (m.p. 57 °C) were obtained.
[5] Spectroscopic data: **3a**: ^{1}H NMR ($CDCl_3$): $\delta = 7.25$, 6.75 (AB, $J = 6.2$ Hz, H-4, H-3), 1.96, 1.94 (s, CH_3); ^{13}C NMR ($CDCl_3$): $\delta = 152$ (s), 135 (d), 128 (d), 120 (s), 20 (q), 18 (q); MS: *m/z* 144 ($M^{\oplus}$, 50%), 86 (C_3H_2OS, 100%); IR: $\tilde{\nu} = 1140$ cm^{-1}.—**3b**: ^{1}H NMR ($CDCl_3$): $\delta = 8.15$, 7.13 (AB, $J = 6.3$ Hz, H-4, H-3), 5.82 (m, 1H), 5.10 (m, 2H), 3.81 (s, OCH_3), 3.30 (dt, $J = 6.2$, 1.4 Hz, 2H); ^{13}C NMR ($CDCl_3$): $\delta = 166$ (s), 163 (s), 142 (d), 134 (d), 131 (d), 116 (t), 114 (s), 52 (q), 31 (t); MS: *m/z* 214 ($M^{\oplus}$, 33%), 102 ($C_3H_2O_2S$, 100%); IR: $\tilde{\nu} = 1142$ cm^{-1}.
[6] O. Wallquist, M. Rey, A. Dreiding, *Helv. Chim. Acta 66* (1983) 1876.
[7] D. Bellus, *Adv. Photochem. 8* (1971) 109.
[8] J. Rigaudy, P. Derible, *Bull. Soc. Chim. Fr. 1965*, 1307.
[9] J. D. Coyle, *Chem. Soc. Rev. 4* (1975) 523.
[10] A. J. Elliott in A. Katritzky, C. Rees (Eds.): *Comprehensive Heterocyclic Chemistry, Vol. 6*, Pergamon, Oxford 1984, p. 749.
[11] By thermolysis of 1,2-dihydrothiete 1,1-dioxide: J. F. King, P. de Mayo, C. L. McIntosh, K. Piers, D. J. H. Smith, *Can. J. Chem. 48* (1970) 3704.
[12] From allenesulfonates and bromine: S. Braverman, Y. Duar, *J. Am. Chem. Soc. 105* (1983) 1061.
[13] From vinyl Grignard compounds and SO_2: E. Thoumaseau, B. Josseaume, F. Tiffon, J. G. Duboudin, *Heterocycles 19* (1982) 2247.

The *p*-Nitrocinnamyloxycarbonyl (Noc) Moiety—an Acid-stable Amino-protecting Group Removable under Neutral Conditions for Peptide and Glycopeptide Synthesis**

By *Horst Kunz** and *Joachim März*

On attempting to synthesize glycopeptides[1] one is always confronted with a lack of protecting groups which, on the one hand, are reliably stable for handling, and, on the other, can be removed again under almost neutral conditions. Aside from the classical benzylic[2] and the two-step protecting groups,[3] the allyl esters[4] and allyloxycarbonyl protecting groups[5] fulfill these requirements the best. They can be removed from the blocked functions by palladium(0)-catalyzed allyl transfer under practically neutral conditions. Even the sensitive *O*-glycosyl-serine and *O*-glycosyl-threonine bonds remain intact.[4]

We have now modified the principle of the allyl-protecting moiety in the *p*-nitrocinnamyloxycarbonyl (Noc) protecting group such that acid-stability and tendency to crystallize are increased and a strong UV absorption ($\lambda_{max} = 310$ nm) is observed. At the same time the cleavability under neutral conditions remains unaltered. Neither the cinnamyl esters[6] nor the cinnamyloxycarbonyl group[7] fulfill these conditions because they are already attacked upon cleavage of the *tert*-butyl ester and carbamate with HCl in ether. For the preparation of a reagent for intro-

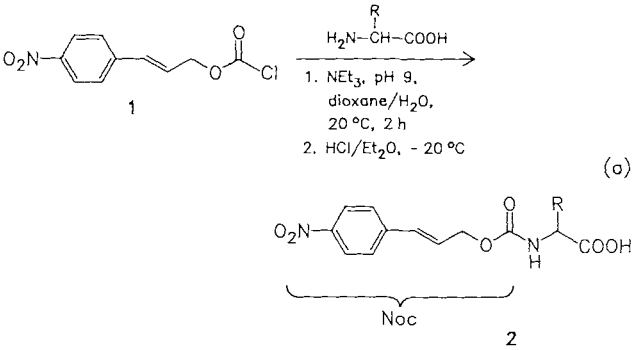

Table 1. *p*-Nitrocinnamyloxycarbonyl (Noc) amino acids **2** prepared according to Equation (a).

Compound	Amino acid	Yield [%]	M.p. [°C]	$[\alpha]_D^{22}$ ($c = 1$, $CHCl_3$)
2a	Ile	95	83	+21.0
2b	Ser	98	76	+15.2 [a]
2c	Phe	85	68	+26.8
2d	Ala	81	93-95	+ 2.3
2e	Leu	64	86	− 3.68
2f	Val	61	72	+ 8.1
2g	Asp(OH)-O*t*Bu	72	oil	+14.8

[a] $c = 1$, acetone.

[*] Prof. Dr. H. Kunz, Dipl.-Chem. J. März
Institut für Organische Chemie der Universität
Johann-Joachim-Becher-Weg 18-20, D-6500 Mainz (FRG)

[**] This work was supported by the Deutsche Forschungsgemeinschaft and the Fonds der Chemischen Industrie.

ducing the Noc group, *p*-nitrocinnamaldehyde[8] was prepared from *p*-nitrobenzaldehyde and acetaldehyde and then reduced with sodium tetrahydroborate to cinnamyl alcohol, which on reaction with phosgene furnished the *p*-nitrocinnamyl chloroformate **1**. This reacts, either as such or after conversion into the analogous *N*-hydroxysuccinimide-active ester at pH 9 (under pH-stat conditions) with amino acid salts to give, as a rule, crystalline *p*-nitrocinnamyloxycarbonyl(Noc) amino acids **2** in high yields [Eqn. (a); Table 1].

Owing to the stability of the Noc-protecting group, the Noc amino acids **2** can smoothly react with amino acid *tert*-butyl or allyl esters[9] both in the presence of ethyl-2-ethoxy-1,2-dihydroquinoline-1-carboxylate (EEDQ) [method B in Eqn. (b)][10] as well as according to the modified carbodiimide method [method A in Eqn. (b), DCC = dicyclohexylcarbodiimide, HOBt = 1-hydroxybenzotriazole][11] to give the Noc dipeptide esters **3** (Table 2).

$$\underset{\mathbf{2}}{\text{Noc–Xaa–OH}} + \text{H–Xaa'–OR} \xrightarrow[\text{B: EEDQ, } CHCl_3,\ 20\,^\circ C,\ 8\,h]{\text{A: DCC/HOBt, } 20\,^\circ C,\ 8\,h} \underset{\mathbf{3}}{\text{Noc–Xaa–Xaa'–OR}} \quad \text{(b)}$$

Table 2. Noc dipeptide esters **3** prepared according to Equation (b).

Compound	Xaa-Xaa'	OR	Method	Yield [%]	M.p. [°C]
3a	Ile-Phe	O*t*Bu	A	93	86–89
3a	Ile-Phe	O*t*Bu	B	84	104–105
3b	Ser-Phe	O*t*Bu	B	96	54
3c	Phe-Phe	O*t*Bu	B	92	98–99
3d	Ala-Phe	O*t*Bu	B	92	65–67
3e	Val-Phe	O*t*Bu	B	97	70–72
3f	Phe-Val	OAllyl	B	93	134
3g	Phe-Ala	OAllyl	B	91	148

A comparison of the samples of **3a** prepared according to methods A and B showed that pure compounds are more easily obtained according to the EEDQ method. Therefore, the other Noc dipeptide esters **3** were prepared by this method.

Due to the acid stability of the Noc group, the *tert*-butyl esters **3a–e** can be removed with trifluoroacetic acid selectively and quantitatively within 30 min to give **4** [Eqn. (c)].

$$\underset{\mathbf{3}}{\text{Noc–Xaa–Xaa'–O}t\text{Bu}} \xrightarrow[1\,h,\ 20\,^\circ C]{CF_3COOH} \underset{\mathbf{4}}{\text{Noc–Xaa–Xaa'–OH}} \quad \text{(c)}$$

3a: 70%
3d: 90%
3e: 90%

The Noc group can be cleaved quantitatively and selectively from the compounds **3** under neutral conditions by palladium(0)-catalyzed allyl group transfer [Eq. (d)]. The reaction times are noticeably longer than in the case of the unsubstituted allyloxycarbonyl (Aloc) protecting group[5] (up to 8 hours).[12] Therefore, dimedone[5] is less suited as allyl acceptor, because it reacts further with the liberated amino components to give the enaminoketone[13] (Dche-protecting group). The practically non-carbonyl-active CH acid *N,N'*-dimethylbarbituric acid[14] (DMBS, $pK_s = 4.7$) proved to be a much more suitable allyl acceptor; its 5-(*p*-nitrocinnamyl) derivative is easy to separate from the liberated dipeptide esters **5**.

$$3 \xrightarrow[THF,\ 8\,h,\ 20\,^\circ C]{[Pd(PPh_3)_4]/DMBS} \underset{\mathbf{5}}{\text{H–Xaa–Xaa'–O}t\text{Bu}} \quad \text{(d)}$$

3a: 96%
3d: 91%
3e: 84%

Most advantageous is that the new protecting group Noc is stable towards the rhodium(I)-catalyzed isomerization and hydrolysis by which the allyl ester is selectively removed [Eqn. (e)].[9]

$$\underset{\mathbf{3f}}{\text{Noc–Phe–Val–OAllyl}} \xrightarrow[EtOH/H_2O,\ 1\,h,\ 70\,^\circ C]{[(Ph_3P)_3RhCl]} \underset{87\%}{\text{Noc–Phe–Val–OH}} \quad \text{(e)}$$

Thus, the Noc moiety is a valuable protecting group which can be removed under neutral conditions and which is even partially orthogonally stable to the protection by the unsubstituted allyl group. Its suitability in the synthesis of glycopeptides is demonstrated by the reaction sequence in Scheme 1.

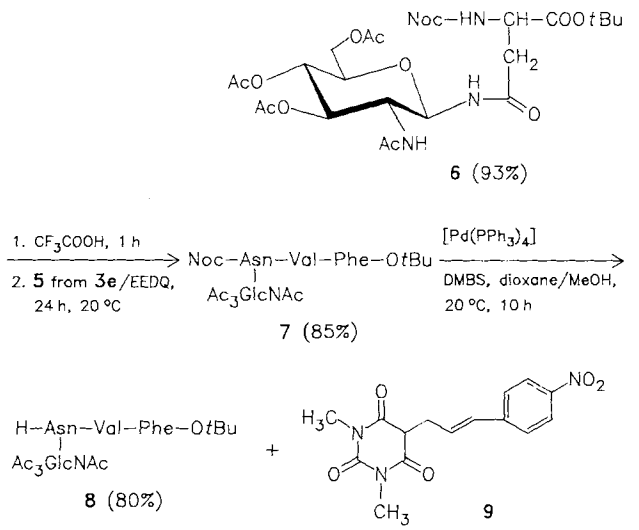

Scheme 1. Use of the Noc protecting group in peptide synthesis.

The stability of the Noc group towards acids and its completely selective removal under neutral conditions are clearly demonstrated in the synthesis of **8**. The CH acid **9** ($\lambda_{max} = 277$ nm in trifluoroacetic acid), like free DMBS, can easily be separated from the *N*-deblocked glycopeptide **8**.

General procedure for 5

A solution of 1 mmol of Noc-dipeptide *tert-butyl ester* **3a–e** in 30 mL of acid-free THF (or dioxane/methanol) was treated with 0.78 mmol of *N,N'*-dimethylbarbituric acid (DMBS), 0.26 g (0.1 mmol ≙ 10 mol-%) of tetrakis(triphenylphosphane)palladium(0) and 0.26 g (1 mmol) of triphenylphosphane and the resulting mixture stirred in the dark. The *N,N'*-dimethyl-5-(*p*-nitrocinnamyl)barbituric acid **9** which precipitated was filtered off and the solvent was then removed from the filtrate by distillation in vacuo. The resulting residue was taken up in 80 mL of $CHCl_3$ and extracted four times with 0.5 N Na_2CO_3 solution. The $CHCl_3$ solution was extracted five times with 0.5 N HCl and the combined aqueous solutions were extracted once with $CHCl_3$. The aqueous phase was brought to pH 10–11 with Na_2CO_3 and extracted with 50 mL of $CHCl_3$. After drying of the $CHCl_3$ solution with $MgSO_4$ and removal of the solvent by distillation in vacuo the remaining oils were treated at −20 °C with HCl-saturated ether and immediately evaporated to dryness in vacuo. The hydrochlorides of the peptide esters **5** were recrystallized from ethyl acetate/petroleum ether or $CHCl_3$/petroleum ether.

In this way we obtained, e.g. L-valyl-L-phenylalanine *tert*-butyl ester as the hydrochloride: m.p. 173–176°C; $[\alpha]_D^{22}$ of the free ester = +3.1 (c = 1, $CHCl_3$).

Received: May 20, 1988 [Z 2771 IE]
German version: *Angew. Chem. 100* (1988) 1424

[1] H. Kunz, *Angew. Chem. 99* (1987) 297; *Angew. Chem. Int. Ed. engl. 26* (1987) 294.
[2] M. Bergmann, L. Zervas, *Chem. Ber. 65* (1932) 1192.
[3] See, e.g.: H. Kunz, S. Birnbach, *Angew. Chem. 98* (1986) 354; *Angew. Chem. Int. Ed. Engl. 25* (1986) 360.
[4] H. Kunz, H. Waldmann, *Angew. Chem. 96* (1984) 49; *Angew. Chem. Int. Ed. Engl. 23* (1984) 71.
[5] H. Kunz, C. Unverzagt, *Angew. Chem. 96* (1984) 426; *Angew. Chem. Int. Ed. Engl. 23* (1984) 436.
[6] D. Hennen, *Diplomarbeit*, Universität Mainz 1985.
[7] M. Kinoshita, K. Inomata, T. Kameda, H. Kotake, *Chem. Lett. 1985*, 515.
[8] a) S. G. Waley, *J. Chem. Soc. 1948*, 2008; b) G. Carrera, R. Ettore, F. Fava, G. Rolland, E. Testa, A. Vecchi, *J. Am. Chem. Soc. 76* (1954) 4391; c) H. B. W. Kortenaar, B. G. Van Dijk, J. M. Peeters, B. J. Raaben, N. M. Adams, G. I. Tesser, *Int. J. Pept. Protein Res. 27* (1986) 398.
[9] H. Waldmann, H. Kunz, *Liebigs Ann. Chem. 1983*, 1712.
[10] B. Belleau, G. Malek, *J. Am. Chem. Soc. 90* (1968) 1651.
[11] W. König, R. Geiger, *Chem. Ber. 103* (1970) 788.
[12] K. Okasada, T. Chiba, Y. Nakamura, T. Yamamoto, A. Yamamoto, *J. Chem. Soc. Chem. Commun. 1986*, 1589.
[13] B. Halpern, L. B. James, *Aust. J. Chem. 17* (1964) 1282.
[14] J. W. Clark-Lewis, M. J. Thompson, *J. Chem. Soc. 1959*, 1628.

A Donor Cage with Bent Tetrathiafulvalene Moiety**

By *Jorg Röhrich, Peter Wolf, Volker Enkelmann,* and *Klaus Müllen**

Upon reaction with suitable acceptors, tetrathiafulvalene (TTF) can form crystalline charge transfer (CT) complexes displaying high electrical conductivity.[1–3] Particularly attractive from the electronic point of view are derivatives with two or more phane-like[4] or chain-like[5–8] coupled TTF units, with or without conjugation. We have searched for a route to oligomeric TTF systems which can furnish chain- and/or cage-like molecules and enables the introduction of solubility-improving substituents. The readily accessible title compounds **1b,c** contain a strained donor cage with an unusually bent TTF unit.

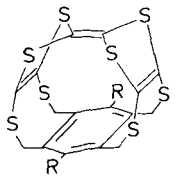

1
b: R = OPr
c: R = OHex

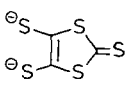

2

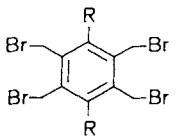

3
a: R = H
b: R = OPr
c: R = OHex

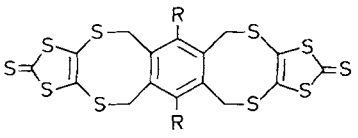

4
a: R = H
b: R = OPr
c: R = OHex

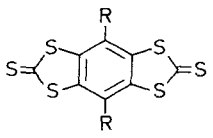

5

Reaction of the 1,3-dithiole-2-thione-4,5-dithiolate **2** (as tetraethylammonium salt of the zincate)[9] with the tetrafunctional electrophilic tetrabromodurene **3a** in tetrahydrofuran (THF) provided the dithione **4a** in 65% yield. This compound is a further potential polyfulvalene precursor like the dithione **5** recently described by us,[10,11] but it is unsuitable for further reactions because of its sparing solubility. Therefore, starting from duroquinone,[12] we synthesized the dialkoxytetrabromides **3b** and **3c**,[13] which react with **2** to give the significantly more soluble dithiones **4b** and **4c**, respectively.[13]

The intramolecular coupling of **4b** or **4c** in boiling xylene in the presence of triethyl phosphite leads to formation of the macrocycles **1b** or **1c** respectively, which contain a TTF unit. There is no evidence of linear oligomers being formed; the formation of **1** does not necessitate high dilution. Characteristic in the NMR spectra of **1b,c** are the resonances of only four sp^2-hybridized C atoms and the absorption of an AB spin systems, which can be ascribed to the eight-membered ring methylene protons.[13]

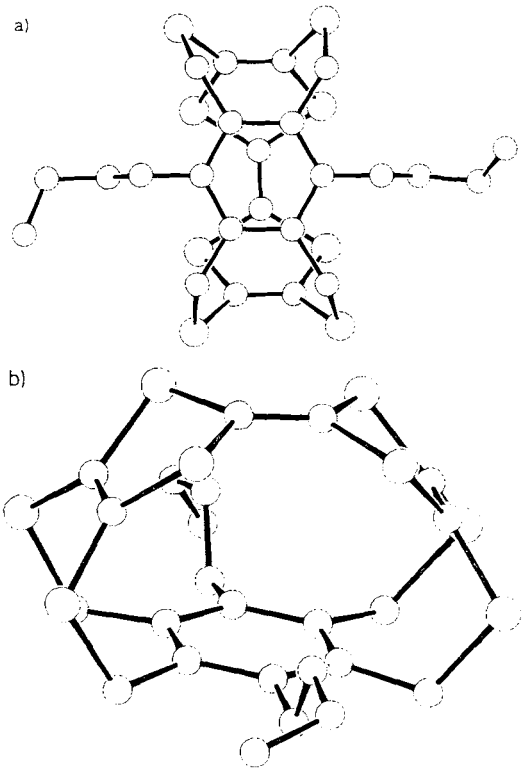

Fig. 1. Molecular structure of **1b** [14, 15]. a) Projection onto the plane of the benzene ring. b) Side view of the molecule.

The result of a crystal structure analysis is shown in Figure 1. As the view onto the plane of the benzene ring shows, the basic skeleton of the compound has approximately ideal *mm*2 (C_{2v}) symmetry, i.e. the fulvalenic double bond is located centrally above the benzene ring at a transannular distance of 391 pm. Due to the high ring strain the TTF skeleton deviates considerably from planarity. The planes defined by the sulfur atoms and the outer double bonds are inclined at angles of 49.5° and 47.6° to the central double bond. Within the accuracy of the structure analysis (0.6 pm) the benzene ring is planar, but in contrast to normal cyclophane structures the bonds to the

[*] Prof. Dr. K. Müllen, Dipl.-Chem. J. Röhrich, Dipl.-Chem. P. Wolf
Institut für Organische Chemie der Universität
J.-J.-Becher-Weg 18-20, D-6500 Mainz 1 (FRG)
Dr. V. Enkelmann
Max-Planck-Institut für Polymerforschung
Postfach 3148, D-6500 Mainz 1 (FRG)

[**] This work was supported by the Bundesminister für Forschung und Technologie.

bridgehead atoms are bent outwards, i.e. away from the TTF system. The distance of these atoms from the plane of the benzene ring is 1-2 pm.

Compound **1** contains a TTF moiety which is coupled via four-S-CH_2 groups to a benzene ring, and thus can be compared with the well-known donor bis(ethylenedithio)-TTF.[16] **6a** can serve as a linear model compound for **1**,[17] but its sparing solubility impairs a spectroscopic characterization. We therefore synthesized the thione **7** from 4-bromo-3,6-dibutoxy-*o*-xylene dibromide and the dithiolate **2**. Coupling of **7** in the presence of triethyl phosphite furnishes the spectroscopically fully characterizable fulvalene **6b** as a *cis/trans* mixture.[13]

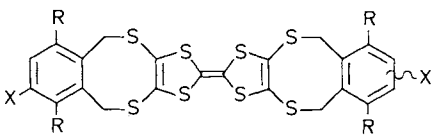

6

a: R=H; X=H
b: R=OBu; X=Br

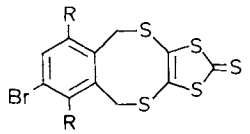

7, R=OBu

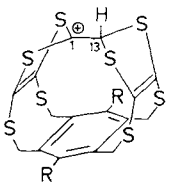

8, R=OPr

A comparison of **1b,c** and **6b** reveals marked differences in the physical properties:

- the ^{13}C resonance of the fulvalenic centers in the cage compound **1c** ($\delta = 134.5$) is shifted noticeably downfield compared to that in the "linear" species **6b** ($\delta = 112.0$);
- the electrochemical oxidation of **6b** with cyclovoltammetric monitoring (dichloromethane, tetraethylammonium perchlorate, SCE) shows two reversible one-electron transfers at 0.52 V and 0.96 V. Under the same conditions, an electron is irreversibly removed from **1b** at 1.09 V; the secondary product can be oxidized reversibly ($E_{1/2} = 0.55$ V);
- the longest wavelength band in the absorption spectrum of **6b** ($\lambda = 303$ nm) is shifted hypsochromically compared to that of **1b** ($\lambda = 311$ nm); however, the band in the cyclic compound **1b** is less intense [**6b**: $\varepsilon = 22730$ L mol^{-1} cm^{-1}, **1b**: $\varepsilon = 8600$ L mol^{-1} cm^{-1}].

To determine the consequences of the unusual structure of **1b,c** on the reactivity we treated **1b** with gaseous hydrogen chloride and monitored the reaction ^1H- and ^{13}C-NMR spectroscopically. Protonation of the fulvalenic double bond takes place, accompanied by a change in color from yellow to red. The resulting cation **8** is stable at 0°C and displays a dynamic effect due to migration of the added proton to the neighboring C atom [$\delta(^{13}C) = 220.8$ (C-1), 60.0 (C-13); $\delta(^1H) = 4.45$ and 4.54 (two AB systems for the SCH_2 protons)].

Following the recently reported acid-catalyzed *cis/trans* isomerization of unsymmetrically substituted TTF compounds,[18] this now provides an example of the spectroscopic detection of a protonated intermediate. The protonation is reversible: neutralization of a four-days-old solution of **8** in chloroform with gaseous ammonia led to quantitative recovery of the intact cyclic compound **1b**.

The red coloration observed on protonation of **1** also occurs with other acceptors such as copper(II) triflate, dichlorocyano-*p*-benzoquinone or iodine. The ^1H-NMR and FAB-MS spectra of the copper complex furnish proof of the intact constitution of **1**; the absorption spectrum shows a characteristic long wavelength band at $\lambda = 533$ nm. This band can also be observed in a solution of **8** in dichloromethane and possibly corresponds to an intramolecular CT transition from the electron-rich benzene system to the dithiolylium fragment; it does not occur on protonation of the linear analogue **6b**.

The synthesis of **1** described here also offers the possibility of changing the size of the molecular cage with tetrafunctional electrophiles other than tetrabromodurene.

Received: July 11, 1988 [Z 2855 IE]
German version: *Angew. Chem. 100* (1988) 1429

[1] F. Wudl, *Acc. Chem. Res. 17* (1984) 227, and references cited therein.
[2] L. Alcácer (Ed.): *The Physics and Chemistry of Low Dimensional Solids*, Reidel, Dordrecht 1980.
[3] W. E. Hatfield (Ed.): *Molecular Metals*, Plenum, New York 1979.
[4] J. Ippen, C. Tao-pen, B. Starker, D. Schweitzer, H. A. Staab, *Angew. Chem. 92* (1980) 51; *Angew. Chem. Int. Ed. Engl. 19* (1980) 67.
[5] R. R. Schumaker, E. M. Engler, *J. Am. Chem. Soc. 99* (1977) 5519.
[6] M. L. Kaplan, R. C. Haddon, F. Wudl, *J. Chem. Soc. Chem. Commun. 1977*, 388.
[7] V. Y. Lee, R. R. Schumaker, *Abstracts, ACS/CSJ Chemical Congress*, Honolulu, Hawai, April 1979, Orgu 424.
[8] E. Nishikawa, H. Tatemitsu, Y. Sakata, S. Misumi, *Chem. Lett. 12* (1986) 2131.
[9] G. Steinmecke, H. J. Sieler, R. Kirmse, E. Hoyer, *Phosphorus Sulfur 7* (1979) 49.
[10] P. Wolf, K. Müllen, M. Przybylski, *Chimia 40* (1986) 200.
[11] P. Wolf, H. Naarmann, K. Müllen, *Angew. Chem. 100* (1988) 290; *Angew. Chem. Int. Ed. Engl. 27* (1988) 288.
[12] A. A. Bothner-By, *J. Am. Chem. Soc. 75* (1953) 728; F. von Werder, T. Moll, *Hoppe-Seyler's Z. Physiol. Chem. 254* (1938) 39.
[13] All the new compounds gave correct elemental analyses.—**1c**: 38% (after filtration over silica gel and recrystallization from ethyl acetate); yellow needles, m.p. 205°C (decomp.); ^1H-NMR (200 MHz, $CDCl_3$): $\delta = 4.53$ (t, OCH_2), 4.35 and 4.22 (AB system, SCH_2), 1.91 (OCH_2CH_2), 1.62-1.30 (m, CH_2), 0.92 (t, CH_3); ^{13}C-NMR (50 MHz, $CDCl_3$): $\delta = 152.8$, 136.6, 134.5, 130.8, 75.3, 31.8, 31.7, 30.5, 25.6, 22.7, 14.1.—**3b**: 78% (from 1,4-dihexyloxy-2,3,5,6-tetramethylbenzene); m.p. 89°C; ^1H-NMR (90 MHz, $CDCl_3$): $\delta = 4.75$ (s, CH_2Br), 4.12 (t, OCH_2), 1.25-2.00 (m, CH_2), 0.92 (t, CH_3).—**4b**: 58% (after crystallization from xylene, orange microcrystals); m.p. 238°C; ^1H-NMR (90 MHz, $CDCl_3$): $\delta = 4.60$ (t, OCH_2), 4.35 (s, SCH_2), 1.20-2.00 (m, CH_2), 0.92 (t, CH_3).—**6a**: yellow powder, m.p. 116°C; ^1H-NMR (200 MHz, $CDCl_3$): $\delta = 7.01$ (s, H_{arom}), 4.39 and 4.38 (s, SCH_2), 3.94 and 3.92 (t, OCH_2), 1.94-1.26 (m, CH_2), 1.00 and 0.98 (t, CH_3).—**6b**: pink solid, m.p. 206°C (decomp.); ^1H-NMR (200 MHz, $CDCl_3$): $\delta = 6.99$ (s, H_{arom}), 4.29 and 4.26 (s, SCH_2), 3.95 and 3.93 (t, OCH_2), 1.94-1.66 (m, CH_2), 1.66-1.40 (m, CH_2), 1.00 and 0.97 (t, CH_3); ^{13}C-NMR (50 MHz, $CDCl_3$): $\delta = 153.0$, 147.9, 133.2, 131.1, 128.1, 124.5, 117.0, 116.4, 112.0, 74.9, 68.9, 32.4-31.3, 19.3, 19.2, 14.0, 13.8.
[14] Crystallographic data: Enraf-Nonius CAD-4 diffractometer, $Cu_{K\alpha}$ radiation, $\lambda = 1.5405$ Å, graphite monochromator, monoclinic, space group $P2_1/n$, $a = 11.3921(10)$, $b = 14.666(11)$, $c = 17.746(2)$ Å, $\beta = 71.537(8)°$, $\rho_{calcd} = 1.64$ g cm^{-1}, $Z = 4$, $T = 140$ K, $\mu(Cu_{K\alpha}) = 87.1$ cm^{-1}. 4546 reflections, 2841 observed [$I > 3\sigma(I)$]. Empirical absorption correction; anisotropic temperature factors for Cl [15], S, O and C excepting the terminal C atoms of the side groups, which like the H atoms were refined with isotropic temperature factors. $R = 0.051$, $R_w = 0.053$, $w = 1$, for 455 parameters. Further details of the crystal structure investigation are available on request from the Fachinformationszentrum Energie, Physik, Mathematik GmbH, D-7514 Eggenstein-Leopoldshafen 2 (FRG), on quoting the depository number CSD-53228, the names of the authors, and the journal citation.
[15] All bond lengths and angles have ordinary values with exception of the bonds to the terminal C atoms of the propyl moiety. This is due to a disorder which is associated with high temperature factors and a larger uncertainty of the coordinates. In each case two positions are found for the terminal CH_3 groups; in the refinement these were taken into account with a population parameter of 50%. For clarity, only one of the two orientations is shown in Figure 1. In each case the conformation of the side chains deviates considerably from an all-*trans* conformation.

After recrystallization from chloroform, the crystals of **1b** contain one molecule of $CHCl_3$ per cage molecule, which they slowly lose at room temperature. The structure analysis was therefore carried out at 140 K.
[16] S. S. P. Parkin, E. M. Engler, R. R. Schumaker, R. Lagier, V. A. Lee, J. C. Scott, R. L. Greene, *Phys. Rev. Lett. 50* (1983) 270.
[17] L. M. Gol'denberg, R. N. Lyubovskaya, *Khim. Geterotsikl. Soedin. 6* (1986) 855.
[18] A. Souizi, A. Robert, P. Batail, L. Ouahab, *J. Org. Chem. 52* (1987) 1610.

Paraformaldehyde as Possible Chirality Amplifier**

By *Christian R. Noe,* Max Knollmüller,* and *Peter Ettmayer*

Not long ago it was reported that the space probe "Giotto" had, on encountering the vapor trail of Halleys comet, discovered a short-chain polyoxymethylene, possibly deposited on silicates or graphite, as the first polymer in the universe.[1] It is well-known[2] that polyoxymethylene has a helical conformation; therefore there should be levorotatory and dextrorotatory enantiomers of such helices.

For some time we have been concerned with the role of stereoelectronic effects of the anomeric type in the chiral recognition and especially in the amplification (perpetuation) of chirality in evolution.[3] Since the helicity of polyoxymethylene is attributed to such stereoelectronic effects[4] it appeared interesting to us to carry out experiments on asymmetric induction with the help of such structures. The fundamental requirement for a role of paraformaldehyde in chirality transfer, for example from silicates to organic molecules, would be an unambiguously predictable direction of the asymmetric induction, independent of the number of oxymethylene groups.

For the preparation of model chiral oligooxymethylene compounds we used the model terpenoid carbohydrate **1**, to which we added formaldehyde and, subsequently, hydroxyacetonitrile under acid conditions at $-20°C$. The compounds **2a-d**[5] could be readily isolated from the resulting nitrile mixture by flash chromatography and then characterized and converted by reaction with phenylmagnesium bromide into the arylketones **3a-d**.

The nucleophilic methylation of prochiral carbonyl groups in **3** was chosen as model reaction for the asymmetric induction. Besides methylmagnesium iodide, also methyllithium and, in two cases, methylmagnesium iodide with zinc chloride were used for the methylation so as to be able to relativize the chelating effect on the ratio of the diastereomeric pairs (**4a-d/5a-d**). The addition to the ketone **3a** was accomplished with moderate selectivity, and the ratio of the diastereomers (**4a/5a**) could easily be determined ^{1}H-NMR analytically (see Tables 1 and 2); the absolute configuration of the end products could be determined by characterization of the cleaved tertiary alcohol.[7]

Since the induction in this case is effected by an acetalic center and therefore fundamentally stereoelectronic effects[8] should play a role, it could be expected that the direction of the induction is maintained upon introduction of oxymethylene groups.

Table 1. Selected ^{1}H-NMR data for the differentiation of the diastereomeric pairs (**4a-d/5a-d**). δ values referred to TMS, J in [Hz], $CDCl_3$, 20°C.

Diastereomer	AB, $J=10$; 2H, O-CH_2-C* δ_A/δ_B	t; 1H, O-CH-O	d, $J=6$; 1H, 7aH	s; 3H, CH_3-C*
4a	3.82/3.72 [a]	5.08	3.62	1.44
5a	3.71/3.61 [a]	5.08	3.62	1.52
4b	3.75/3.69 [a]	5.24	3.93	1.52
5b	3.83/3.65 [a]	5.15	3.93	1.50
4c	3.78/3.71 [b]	5.33	3.89	1.52
5c	3.85/3.67 [b]	5.33	3.89	1.52
4d	3.79/3.68 [b]	5.32	3.89	1.50
5d	3.81/3.67 [b]	5.32	3.89	1.50

[a] NMR spectra: Jeol FX90Q, 90 MHz. [b] NMR spectra: Bruker Spectrospin, 250 MHz.

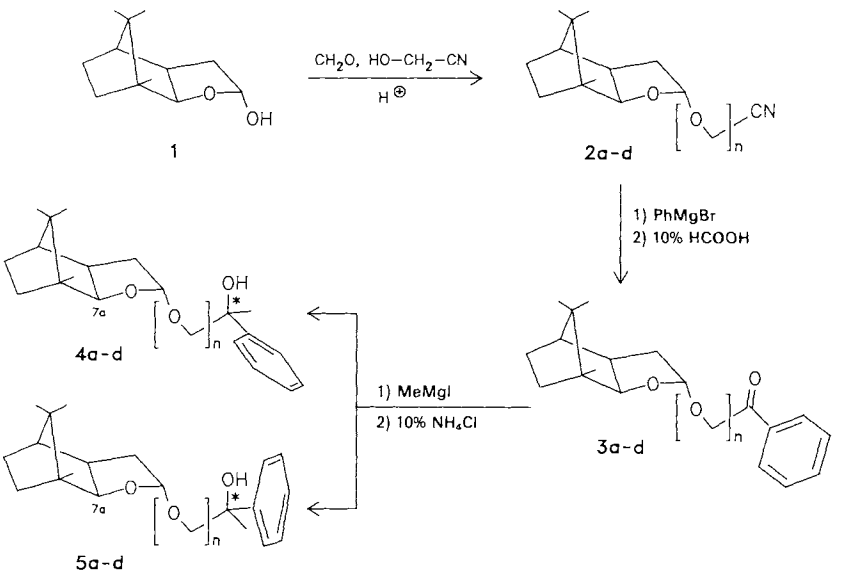

2-5: **a**, n = 1; **b**, n = 2; **c**, n = 3; **d**, n = 4

All the alcohols (**4b-d/5b-d**) obtained by nucleophilic methylation of the ketones **3b-d** showed, analogously to the diastereomeric pair (**4a/5a**), significant differences in the positions of the AB signal of the O-CH_2-C*- group in the ^{1}H-NMR spectrum. The absolute configuration of (**4b-d/5b-d**) could be elucidated by conversion (cleavage

[*] Univ.-Doz. Dr. C. R. Noe, Prof. Dr. M. Knollmüller, Dipl.-Ing. P. Ettmayer
Institut für Organische Chemie der Technischen Universität
Getreidemarkt 9, A-1060 Wien (Austria)

[**] We thank Dr. *G. Schulze* of Sandoz-Forschungsinstitut (Vienna) for recording the 250-MHz ^{1}H-NMR spectra and Loba Feinchemie (Fischamend) for supplying the fine chemicals.

Table 2. Experimental data for the nucleophilic methylation.

Ketone	Nucleophile	T [°C]	Diastereomere	Selectivity	Yield [%]	Config. 4 and 8
3a	MeMgI	−40	**4a** : **5a**	3.3 : 1	95	*S*
3a	$MeMgI/ZnCl_2$	−40	**4a** : **5a**	5.0 : 1	81	*S*
ea	MeLi	−40	**4a** : **5a**	2.5 : 1	96	*S*
3b	MeLi	−60	**4b** : **5b**	1.8 : 1	92	*S*
3b	MeMgI	−40	**4b** : **5b**	3.1 : 1	81	*S*
3b	MeMgI/ZnCl	−40	**4b** : **5b**	3.6 : 1	61	*S*
3c	MeLi	−80	**4c** : **5c**	1.5 : 1	80	*S*
3c	MeMgI	−80	**4c** : **5c**	1.5 : 1	80	*S*
3d	MeLi	−80	**4d** : **5d**	1.2 : 1	90	*S*
3d	MeMgI	−40	**4d** : **5d**	2.0 : 1	95	*S*
7c	MeMgI	−40	**8c** : **9c**	1.1 : 1	95	*S*
7d	MeMgI	−40	**8d** : **9d**	1.03 : 1	95	—

of formaldehyde under acidic conditions and reacetalization) into (**4a**/**5a**).

The experiments showed that the diastereofacial selectivity of the organometal addition decreased with increasing chain length, but always had the same direction (Fig. 1).

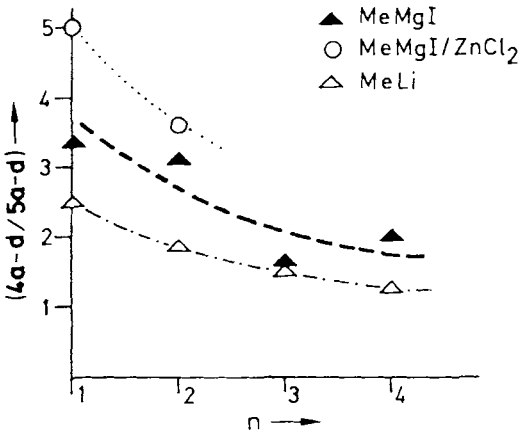

Fig. 1. Selectivity (diastereomeric ratio (**4a-d**/**5a-d**)) as a function of the number *n* of the OCH_2 members.

The shielding of the *Si* side of the prochiral carbonyl group is thus independent of the number of $O-CH_2$ units. This is consistent with the assumption illustrated in Figure 2 of a stabilized helix conformation with equal participation of all lone electron pairs and an antiperiplanar orientation of the terminal C–CO bond to that free electron pair of the neighboring acetalic oxygen which is still not involved in the anomeric interaction.

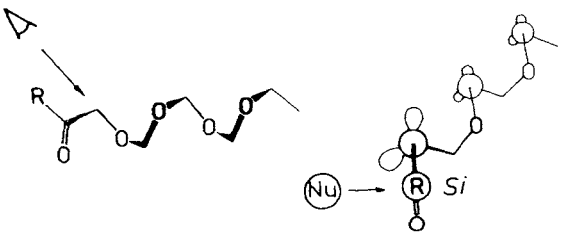

Fig. 2. Shielding of the *Si* side of the carbonyl group in **3** by the left-handed helix. R = phenyl.

The synperiplanar position of the oxygen of the carbonyl group to the acetalic oxygen corresponds to the arrangement observed in a similar compound[9] (X-ray structure analysis) and is also that conformation which is determinative in the reactions of α-alkoxycarbonyl compounds in *Cram*'s cyclic model[10] (Fig. 3).

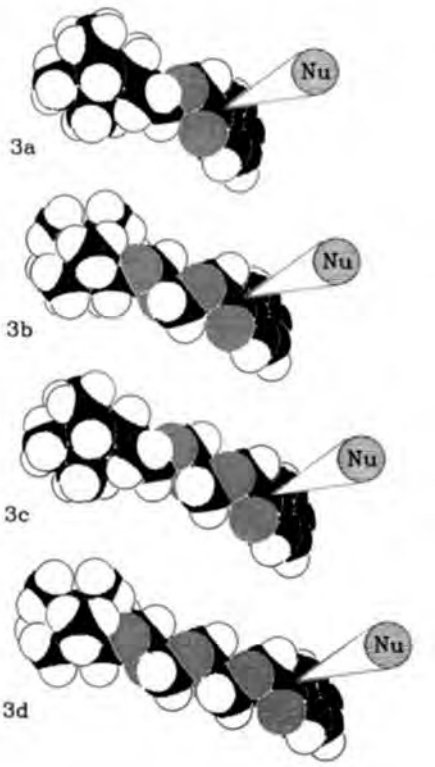

Fig. 3. Nucleophilic attack at the helix in **3**. The oxygen atoms are shaded.

In order to exclude coincidental influences and to guarantee that the ensuing inductions are clearly attributable to the oligooxymethylene groups, the non-terminal oxygen atoms of the oxymethylene chain in the compounds **3c** and **3d** were formally replaced by CH_2 groups. The corresponding compounds **7c** and **7d** were synthesized from **6c** and **6d**, respectively,[11] and allowed to react with methylmagnesium iodide as described in the experimental section.

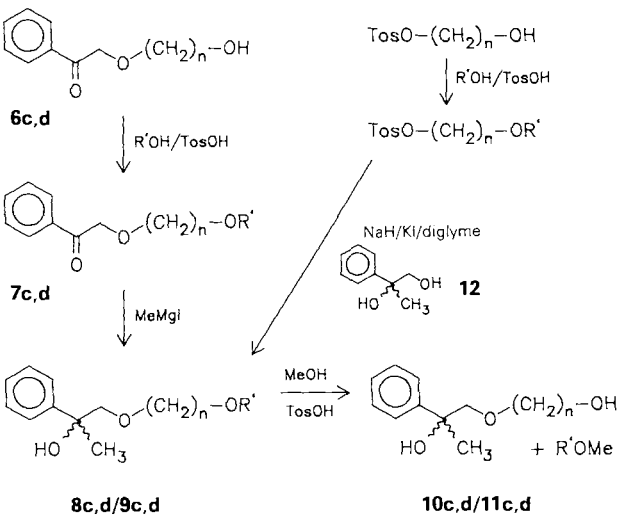

R'OH ≡ 1

6-**11**: **c**, n = 3; **d**, n = 5

Whereas the diastereomeric pair (**4d**/**5d**) was still clearly distinguishable in the ^{1}H-NMR spectrum (see Table 1), in the case of (**8d**/**9d**) a nuclear resonance spectroscopic assignment was no longer possible. The selectivity achieved was less than 1.5% *ee*, as shown by a comparison of the specific rotations of the liberated alcohols (**10d**/**11d**) and the reference compound (**10d**/**11d**)[12] prepared from the enriched 2-phenylpropanediol **12** ($S:R = 3.3:1 \triangleq 54\%$ *ee*). The ratio of (**8c**/**9c**) determined by 250-MHz ^{1}H-NMR[13] (1.1 : 1 ≙ 5.0% *de*) was also significantly lower than that of the corresponding oxymethylene diastereomers (**4c**/**5c**).[14]

With the experiments presented here it could be shown that an asymmetric induction with predictable direction (even with slightly decreasing selectivity with increasing chain length) is possible via an oxymethylene structure. If one considers the reaction from the formal aspect of a 1,*n*-asymmetric induction then the ratio 2 : 1 (≙ 33% *de*) found experimentally for (**4d**/**5d**) is so far the highest value known to us for a 1,10-asymmetric induction. From the point of view of a naturally related system of chiral compounds,[3] based on stereoelectronic effects, the direction of the reaction effected by a left helix corresponds fundamentally to that which is induced by an acetal group of the B family (configuration like α-L-glucose or β-D-glucose). Consequently, there is also a correlation of α-D-glucose (acetalic center of the A-type) with a dextrorotatory oxymethylene helix.

The actual occurrence of oxymethylene structures in the presence of silicates under potentially prebiotic conditions together with the predictable specificity of the enantiomerically pure helix make it seem possible that optically active paraformaldehyde has played a role in the amplification (perpetuity) of chirality in the course of chemical evolution.

Experimental

The compounds **2** to **5** (in each case **b**, **c**, **d**) were characterized ^{1}H-NMR and ^{13}C-NMR spectroscopically and by elemental analyses. For data and experimental details not mentioned in this communication see: P. Ettmayer, *Diplomarbeit*, Technische Universität Wien 1987. The compounds **6** to **11** (each **c** and **d** were characterized ^{1}H- and ^{13}C-NMR spectroscopically.

Reaction with methylmagnesium iodide: A 0.705 M solution of MeMgI (5.4 mL, 3.82 mmol) was diluted with 5 mL of ether, cooled, and treated with 0.636 mmol of ketone **3** in 10 mL of anhydrous ether. After 20 min the mixture was diluted with 10 mL of petroleum ether and extracted with 20 mL of 10% NH_4Cl solution. The organic phase was washed once with $NaHCO_3$, dried, and evaporated to dryness.

Reaction with methylmagnesium iodide and zinc chloride: A solution of ketone **3** (0.636 mmol) in anhydrous ether (10 mL) was cooled to 0°C and treated with a solution of $ZnCl_2$ (150 mg, 1.1 mmol) in anhydrous ether (10 mL). After 15 min the cloudy solution was added in bulk to a solution of 5.4 mL (3.82 mmol) of a 0.705 M MeMgI solution and 5 mL of anhydrous ether cooled to −40°C. After 20 min the heterogeneous reaction solution was diluted with 30 mL of petroleum ether and extracted with 20 mL of 10% NH_4Cl solution. The organic phase was washed once with saturated $NaHCO_3$ solution, dried, and evaporated to dryness.

Reaction with methyllithium: The reaction was carried out in ether analogously to the reaction with methylmagnesium iodide.

Received: May 9, 1988;
revised: July 18, 1988 [Z 2751 IE]
German version: *Angew. Chem. 100* (1988) 1431

[1] W. F. Huebner, *Science (Washington, D.C.) 237* (1987) 626, 628.
[2] A. Novak, E. Whalley, *Trans. Faraday Soc. 55* (1959) 1484; R. M. Minyaev, Yu. A. Zhdanov, I. I. Zakharov, V. I. Minkin, *Vysokomol. Soedin. Ser. B 16* (1974) 190.
[3] C. R. Noe, M. Knollmüller, G. Göstl, B. Oberhauser, H. Völlenkle, *Angew. Chem. 99* (1987) 467; *Angew. Chem. Int. Ed. Engl. 26* (1987) 442; E. Wagner, *Dissertation*, Technische Universität Wien 1987.
[4] a) A. J. Kirby: *The Anomeric Effect and Related Stereoelectronic Effects on Oxygen*, Springer, Berlin 1983; b) P. Deslongchamps: *Stereoelectronic Effects in Organic Chemistry (Org. Chem. Ser. Vol. 1)*, Pergamon, Oxford 1983, and references cited therein.
[5] 35.8% **2a**, 19.0% **2b**, 6.9% **2c**, 4.3% **2d**, and 11.5% **1a** were obtained. For further experimental data and ^{13}C-NMR and ^{1}H-NMR spectra of **2a** see Ref. [3].
[6] **3a** could be obtained in 70% **3b** in 72%, **3c** in 66%, and **3d** in 66% yield. According to 90-MHz ^{1}H-NMR and 22.5-MHz ^{13}C-NMR all the products are pure compounds at room temperature.
[7] a) The absolute configuration of (**4a**/**5a**) could be determined via the specific rotation of the alcohol described in the literature [7b], which was obtained from (**4a**/**5a**) by methanolysis (cleavage of the protecting group **1a** under acid conditions in methanol; b) see E. L. Eliel, J. P. Freeman, *J. Am. Chem. Soc. 74* (1952) 23.
[8] We assume that one of the free electron pairs on the acetal oxygen is stabilized exo-anomerically with the σ* orbital of the C-O bond in the ring and that the aryl ketone is so arranged that a further anomeric stabilization by n-σ* interaction of the second electron pair on the oxygen with the σ* orbital of the C-CO-aryl bonding is possible. We obtained evidence for this conformation by an X-ray structure analysis of compound **2a**.
[9] [2*R*-[2α(*R**),3aα,4α,7α,7aα]]-2-[(Octrahydro-7,8,8-trimethyl-4,7-methanobenzofuran-2-yl)oxy]-1-phenylbutan-1-one.
[10] M. T. Reetz, *Angew. Chem. 96* (1984) 542; *Angew. Chem. Int. Ed. Engl. 23* (1984) 556.
[11] The compounds **6c** and **6e** were synthesized analogously to the procedure given in the literature: D. J. Pasto, K. Garves, M. P. Serve, *J. Org. Chem. 32* (1967) 774.
[12] $[\alpha]_{365}^{20} = 18.5$ ($c = 3.5$, ether) based on 100% *ee*.
[13] Selected ^{1}H-NMR data for diffraction of the diastereomeric pairs **8c**/**9c**: **8c**, $\delta = 3.979$ (d, $J = 7.3$ Hz, 1H, 7aH), **9c**, $\delta = 3.968$ (d, $J = 7.3$ Hz; 1H, 7aH) (NMR spectra: Bruker Spectrospin, 250 MHz, $CDCl_3$, 20°C, referred to TMS).
[14] The specific rotation, $[\alpha]_{436}^{20} = -1.4$ ($c = 2.6$, ether) based on 100% *ee*, was too low for an informative comparison.

Solid State Structure of a Lithium Triorganostannate

By *Michael Veith*,* *Cornelius Ruloff*, *Volker Huch*, and *Fritz Töllner*

Dedicated to Professor Hans Bock on the occasion of his 60th birthday

Lithium triorganostannates have been used for several years for the transfer of triorganostannyl groups to electrophilic centers.[1,2] Although there is no lack of methods for their synthesis,[3] all attempts to determine their structures directly have thus far failed because the compounds were neither isolable nor crystallizable. Especially regarding mechanistic problems there are controversial discussions as to whether, e.g., the lithium atom is bound to the tin atom or an ion pair is present,[3] or when these different structures must be reckoned with. In continuation of our studies in the area of metal alkoxystannates,[4] we have now succeeded in preparing lithium tris(α-furyl)stannate **1** as the first compound of this kind in crystalline form and in investigating it by X-ray structure analysis.

For the synthesis of **1** we used α-furyllithium[5] and tin(II) chloride. The colorless crystalline platelets of **1** obtained as precipitate formally contain three dioxane molecules per lithium atom.

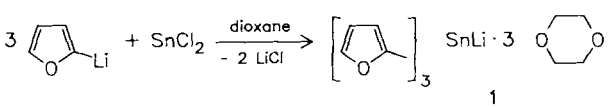

1

The dioxane molecules are bound with different strengths. Two of these molecules can be cleaved from the

[*] Prof. Dr. M. Veith, Dipl.-Chem. C. Ruloff, Dr. V. Huch, Dr. F. Töllner
Institut für Anorganische Chemie der Universität
D-6600 Saarbrücken (FRG)

compound (elemental analysis of the remaining product) under reduced pressure and at slightly elevated temperature (10^{-3} torr, 50°C). The chemical shifts and the coupling constants of the hydrogen atoms of the furyl moiety of **1** and the characteristics of the unit cell of **1** are collected in Table 1.

Table 1. Some ^{1}H-NMR, crystal, and structural parameters of **1**.

$C_{48}H_{66}Li_2O_{18}Sn_2$, $M_r = 1182.29$ g mol^{-1}

^{1}H NMR (furyl region only, [D$_3$]acetonitrile):
$\delta = 6.25$ (dd, $J(H_b,H_c) = 1.6$ Hz, 1H, $-O-CH=CH-CH=$),
6.33 (d, $J(H_a,H_b) = 2.9$ Hz, 1H, $-O-CH=CH-CH=$),
7.71 (d, $J(H_a,H_c) = 0.5$ Hz, 1H, $-O-CH=CH-CH=$)

Triclinic space group: $P\bar{1}$, $a = 1089(1)$, $b = 1372(1)$, $c = 1974(3)$ pm, $\alpha = 102.5(1)$, $\beta = 104.6(1)$, $\gamma = 91.25(8)°$, $V = 2775 \times 10^6$ pm^3, $Z = 2$, 7037 reflections in the range $3° < 2\theta < 50°$, 2603 classified as "not observed" ($F_0 < 4\sigma(F_0)$), 445 parameters. $R = 0.073$, $R_w = 0.084$

Figure 1 shows a drawing of the centrosymmetric anion of **1** based on the results of the X-ray structure analysis.[6] It follows therefrom that compound **1** is not to be formulated as a simple tris(furyl)lithium stannate, but as an ion

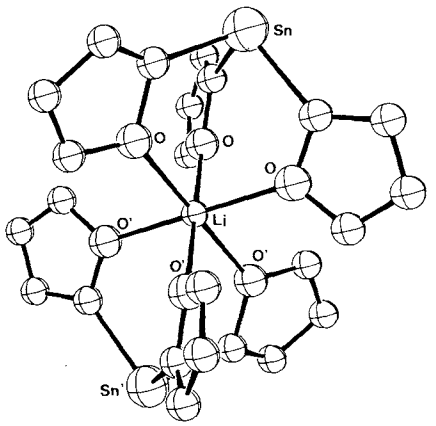

Fig. 1. Structure of the anion $[(Sn(furyl)_3Li(furyl)_3Sn]^{\ominus}$ of **1**. The unmarked atoms are C atoms. The following Li-O distances are found in the cation $[Li(dioxane)_4]^{\oplus}$: 186(3), 193(3), 193(3) and 194(3) pm. Some averaged bond lengths [pm] and angles [°] in the anion: Sn-C 218.8(9), Li-O_{eq} 209.6(9), Li-O_{ax} 229(1), C_α-C_β 136(1), C_β-C_γ 141(1), C_γ-C_δ 131(1), C_α-O 141(1), C_δ-O 138(1); C-Sn-C 96(2), O-Li-O 87-93.

pair consisting of a lithium ion coordinated by four dioxane units and a complex anion. The anion is formally formed by reaction of a lithium ion with two tris(furyl)stannate ions. Two crystallographically independent but structurally very similar anions are located with their inversion centers at the positions 0,0,0 and 0,0,0.5 of the unit cell, while the cation assumes a general position. Two further dioxane molecules are accommodated in the crystal without interacting with metal atoms; hence, the following general formula can be given for the crystalline compound **1**:

$[Li(dioxane)_4]^{\oplus}[Sn(furyl)_3Li(furyl)_3Sn]^{\ominus} \cdot 2\,dioxane$ **1**

The tin atoms have the typical pyramidal geometry for threefold coordinated tin(II) atoms,[7] with C-Sn-C angles of approximately 90°. The lithium atom in the cation $[Li(dioxane)_4]^{\oplus}$ has almost ideal tetrahedral coordination, whereas in the anion it is coordinated by a distorted octahedral array of oxygen atoms from the furyl groups. Four "equatorial" Li-O distances (mean value 209.6(9) pm) can easily be differentiated from the "two axial" distances (229(1) pm), so that the coordination geometry around the lithium atom can also be described as square planar with additional axial interaction. We attribute the observed distortion about the lithium atom in the anion of **1** not to electronic but to steric effects: on the one hand, lithium atoms normally strive for tetrahedral coordination (with an expected Li-O value of 190-195 pm)[8] and, on the other, the mutual distance of the oxygen atoms is predetermined by the specific geometry in the tris(furyl)stannate ions. The only possible alternative would appear to be the compromise found in the given structure.

Experimental

A suspension of $SnCl_2$ (1.26 g, 6.6 mol) in Et_2O (40 mL) was treated rapidly at −50°C with a solution of furyllithium (20 mmol) [5] in Et_2O (50 mL). After warming to room temperature the mixture was stirred for 8 h and filtered (to remove LiCl). After separation of volatile components by condensation there remained pale yellow crystals, which were recrystallized from 30 mL of dioxane; **1** forms colorless platelets. Yield: 1.76 g (45%).

Received: May 16, 1988 [Z 2762 IE]
German version: *Angew. Chem. 100* (1988) 1418

[1] M. Pereyre, J. P. Quintard, *Pure Appl. Chem. 53* (1981) 2401.
[2] A. S. Alnajjar, G. F. Smith, H. G. Kuivila, *J. Org. Chem. 49* (1984) 1271.
[3] M. Pereyre, J. P. Quintard, A. Rahm: *Tin in Organic Synthesis*, Butterworth, London 1987.
[4] M. Veith, R. Rösler, *Z. Naturforsch. B41* (1986) 1071.
[5] V. Ramanathan, R. Levine, *J. Org. Chem. 27* (1962) 1216.
[6] Further details of the crystal structure investigation are available on request from the Fachinformationszentrum Energie, Physik, Mathematik GmbH, D-7514 Eggenstein-Leopoldshafen 2 (FRG) on quoting the depository number CSD-53 159, the names of the authors, and the journal citation.
[7] M. Veith, O. Recktenwald, *Top. Curr. Chem. 104* (1982) 1.
[8] P. Hubberstey, *Coord. Chem. Rev. 66* (1985) 1.

A Novel Entry to the PC-Double Bond: the "Phospha-Wittig" Reaction

By *Angela Marinetti* and *François Mathey**

The archetypal Wittig and Wittig-Horner olefinations of carbonyl compounds have less popular equivalents in nitrogen chemistry[1] [Eqn. (a)]. We therefore wondered

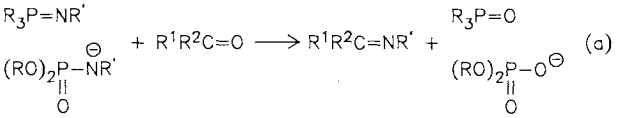

(a)

whether it would be possible to extend this kind of chemistry [Eqn. (a)] to phosphorus. In practice, this meant that it was necessary to have a ready and general access to phosphorus species such as **1** or **2**.

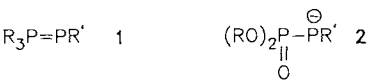

[*] Prof. Dr. F. Mathey, Dr. A. Marinetti
Laboratoire de Chimie du Phosphore et des Métaux de Transition
DCPH, Ecole Polytechnique
F-91128 Palaiseau Cedex (France)

 © VCH Verlagsgesellschaft mbH, D-6940 Weinheim, 1988

Some phosphoranylidenephosphanes (**1**) are known[2] but they appear to be stable only with very specific sets of substituents. On the other hand, to our knowledge, no anion such as **2** has been reported in the literature so far.[3] It was therefore clear to us that it was necessary to provide some extra stabilization to the dicoordinate phosphorus in order to facilitate the synthesis of **1** and **2**. Thus, we focused our work on the synthesis of the P^{II}-complexed species **3** and **4**. This was all the more tempting since we

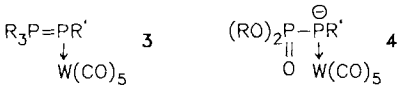

knew that P-$W(CO)_5$ complexation had a strong stabilizing effect upon the P=C double bond,[4] which was the ultimate target of our program.

After some disappointing experiments, we discovered that it was indeed possible to prepare secondary phosphorylphosphane complexes such as **7** from the appropriate phosphirane complexes **5**[5] [Eqn. (b)].

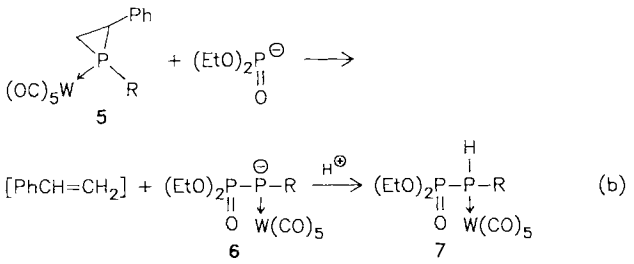

[PhCH=CH_2] + $(EtO)_2P(O)-P^{\ominus}-R$ (**6**) $\xrightarrow{H^{\oplus}}$ $(EtO)_2P(O)-PH-R$ (**7**) (b)

a, R = Ph; b, R = Me

These stable phosphorylphosphane complexes **7** furnish the corresponding anions **6** again upon reaction with *n*BuLi or basic tertiary amines (1,4-diazabicyclo[2.2.2]octane (DBO)) in THF. These anions easily react with aldehydes and ketones to give the expected phosphaalkene complexes **8** [Eqn. (c)], which are either isolated or trapped with various reagents.

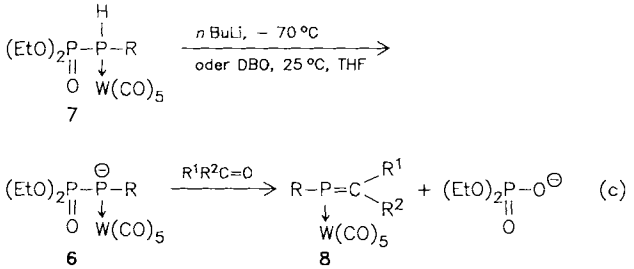

7 $\xrightarrow[\text{oder DBO, 25 °C, THF}]{n\text{BuLi, } -70\,°C}$ **6** $\xrightarrow{R^1R^2C=O}$ $R-P(W(CO)_5)=C(R^1)(R^2)$ (**8**) + $(EtO)_2P(O)-O^{\ominus}$ (c)

Some examples will illustrate the various possibilities that are offered by this scheme (important spectroscopic data of the products are listed in Table 1).

The reaction of **7a** with DBO and acetone or cyclopentanone gives the stable phosphaalkene complexes **9** and **10** [Eqns. (d) and (e)]. These complexes were purified by chromatography on silica gel with pentane.

The corresponding phosphaalkene complexes formed with aldehydes tend to be unstable; the P=C double bond was therefore allowed to react in situ with methanol or conjugated dienes [Eqns. (f)–(h)]. The phosphaalkene complex **11** was characterized in situ by ^{31}P-NMR spectroscopy. As expected, on replacing the phenyl substituent (**7a**) by a methyl substituent (**7b**), the stability of the phosphaalkene complexes decreases. Nevertheless, we were able to monitor the clean and almost quantitative formation of **15**

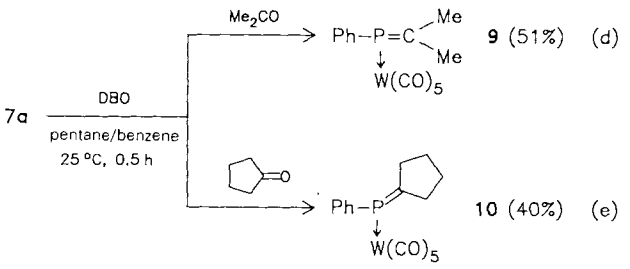

Table 1. Most important spectroscopic data of compounds **9**–**14**, **16** and **17** [a].

9: ^{31}P NMR (pentane): $\delta = 176$ ($^1J(^{31}P\text{-}^{183}W) = 261$); ^{1}H NMR ($C_6D_6$): $\delta = 1.55$ (d, ^3J(H-P) = 24.5, Me), 1.93 (d, ^3J(H-P) = 30.8, Me); ^{13}C NMR (C_6D_6): $\delta = 26.11$ (Me), 26.41 (d, ^2J(C-P) = 7.5, Me), 138.25 (d, ^1J(C-P) = 24.6, *i*-C), 184.60 (d, ^1J(C-P) = 43.8, P=C), 195.61 (d, ^2J(C-P) = 10, *cis*-CO), 199.72 (d, ^2J(C-P) = 28.2, *trans*-CO); MS: *m/z* 474 ($M^{\oplus}$, 36%), 334 ([$M^{\oplus} - 5$CO], 87), 332 (100); IR (pentane): $\tilde{\nu}$(CO) = 2075, 1955 cm^{-1}

10: ^{31}P NMR (pentane): $\delta = 156$ ($^1J(^{31}P\text{-}^{183}W) = 259$); ^{1}H NMR ($C_6D_6$): $\delta = 1.22$ (m, β-CH_2), 1.35 (m, β-CH_2), 2.17 (m, ^3J(H-P) = 25.4, α-CH_2), 2.65 (m, ^3J(H-P) = 26.6, α-CH_2); ^{13}C NMR (C_6D_6): $\delta = 27.08$ (d, ^3J(C-P) = 12, β-CH_2), 27.45 (d, ^3J(C-P) = 8.4, β-CH_2), 37.99 (d, ^2J(C-P) = 15.7, α-CH_2), 39.83 (d, ^2J(C-P) = 10.5, α-CH_2), 138.61 (d, ^1J(C-P) = 24.6, aryl *i*-C), 195.66 (d, ^2J(C-P) = 9.6, *cis*-CO), 196.18 (d, ^1J(C-P) = 43.8, P=C), 199.69 (d, ^2J(C-P) = 28.2, *trans*-CO); MS: *m/z* 500 ($M^{\oplus}$, 19%), 360 ([$M^{\oplus} - 5$CO], 58), 358 (100); IR (decalin): $\tilde{\nu}$(CO) = 2070, 1948 cm^{-1}, correct C,H analyses

11 (both isomers): ^{31}P NMR (THF): $\delta = 185.6$ ($^1J(^{31}P\text{-}^{183}W) = 259$), 190.6

12: ^{31}P NMR (hexane): $\delta = 129.8$ ($^1J(^{31}P\text{-}^{183}W) = 275.9$); ^{1}H NMR ($C_6D_6$): $\delta = 0.77$ (d, ^3J(H-H) = 6.3, Me), 1.86–2.07 (m, CH–CH_2), 2.96 (d, ^3J(H-P) = 12.7, OMe); ^{13}C NMR (C_6D_6): $\delta = 23.83$ (d, ^3J(C-P) = 5.5, Me), 24.80 (d, ^3J(C-P) = 10, Me), 25.79 (s, CH_2), 45.06 (d, ^2J(C-P) = 22.6, CH), 54.22 (d, ^2J(C-P) = 5.5, OMe), 139.19 (d, ^1J(C-P) = 38.2, aryl *i*-C), 197.07 (d, ^2J(C-P) = 8, *cis*-CO), 199.65 (d, ^2J(C-P) = 24.2, *trans*-CO); MS: *m/z* 520 ($M^{\oplus}$, 80%), 436 ($6M^{\oplus} - 3$CO], 100), 380 ([$M^{\oplus} - 5$CO], 66); IR (decalin): $\tilde{\nu}$(CO) = 2070, 1952, 1942 cm^{-1}

13: minor isomer; ^{31}P NMR (hexane): $\delta = 22.3$.—Main isomer: ^{31}P NMR (hexane): $\delta = 15.4$ ($^1J(^{31}P\text{-}^{183}W) = 243.4$); ^{1}H NMR ($C_6D_6$): $\delta = 0.62$ (d, ^3J(H-H) = 6.5, Me), 1.22 (d, ^3J(H-H) = 6.2, Me), 1.3–1.6 (m, 3H), 2.43 (m, ^3J(H-P) = 9.7, ^3J(H-H) = 9.7, 3.5, 1H, CH_2-bridge), 2.6 (m, ^2J(H-P) = 17.2, PCH), 3.24 (m, ^3J(H-P) = 12.5, CH bridgehead), 5.44 (m, $^3J(H_A\text{-}H_B) = 5.7$, ^2J(H-P) = 5.7, ^3J(H-H) = 3.3, C*H* bridgehead), 5.60 (^3J(H-H) = 2.8, ^3J(H-P) ≈ 0, *HC*=C); MS: *m/z* 555 ([$M^{\oplus}$ + H], 64%), 471 ([$M^{\oplus}$ + H − 3CO], 66), 415 ([$M^{\oplus}$ + H − 5CO], 100); IR (decalin): $\tilde{\nu}$(CO) = 2060, 1935 cm^{-1}

14: ^{31}P NMR (hexane): $\delta = -4.9$ ($^1J(^{31}P\text{-}^{183}W) = 245$); ^{1}H-NMR ($C_6D_6$): $\delta = 1.28$ (s, Me), 1.56 (s, Me), 2.0 (m, 2H, CH_2), 4.55 (*AB*, $^2J(H_A\text{-}H_B) = 17.5$, 1H, PCH_2), 2.73 (*AB*, ^{2}J(H-P) = 8.9, 1H, PCH_2), 2.89 (dt, ^2J(H-P) = 10.8, ^3J(H-H) = 6.0, aryl-CH); ^{13}C NMR (C_6D_6): $\delta = 19.90$ (s, Me), 21.45 (d, ^3J(C-P) = 7.0, Me), 32.42 (d, ^1J(C-P) = 24.7, PCH_2), 36.47 (s, CH_2), 42.88 (d, ^1J(C-P) = 19.1, aryl CH), 196.90 (d, ^2J(C-P) = 7.0, *cis*-CO), 198.93 (d, ^2J(C-P) = 22.6, *trans*-CO); MS: *m/z* 638 ($M^{\oplus}$, 19%), 554 ([$M^{\oplus} - 3$CO], 100); IR (decalin): $\tilde{\nu}$(CO) = 2070, 1950, 1940 cm^{-1}

16: ^{31}P NMR (hexane): $\delta = 137.6$ ($^1J(^{31}P\text{-}^{183}W) = 270.9$); ^{1}H NMR ($C_6D_6$): $\delta = 0.77$ (dd, ^3J(H-P) = 17.5, ^3J(H-H) = 7.1, Me), 0.89 (dd, ^3J(H-P) = 16.8, ^3J(H-H) = 7.0, Me), 1.30 (d, ^2J(H-P) = 5.1, PMe), 1.62 (m, CH), 2.96 (d, ^3J(H-P) = 12.1, OMe); ^{13}C NMR (C_6D_6): $\delta = 15.96$ (d, ^2J(C-P) = 5.0, Me), 16.44 (d, ^2J(C-P) = 2.5, Me), 19.34 (d, ^1J(C-P) = 21.6, PMe), 34.02 (d, ^1J(C-P) = 27.7, CH), 53.25 (d, ^2J(C-P) = 6.0, OMe), 197.18 (d, ^2J(C-P) = 8.1, *cis*-CO); 199.44 (d, ^2J(C-P) = 23.1, *trans*-CO); MS: *m/z* 444 ($M^{\oplus}$, 36%), 358 (100%); IR (decalin): $\tilde{\nu}$(CO) = 2070, 1950, 1940 cm^{-1}

17: ^{31}P NMR (C_6D_6): $\delta = 127.45$ ($^1J(^{31}P\text{-}^{183}W) = 275.9$); ^{1}H-NMR ($C_6D_6$): $\delta = 1.29$ (d, ^2J(H-P) = 4.0, PMe), 2.96 (d, ^3J(H-P) = 12.6, OMe), 3.95 (d, ^2J(H-P) = 1.8, PCH); ^{13}C NMR (C_6D_6): $\delta = 22.84$ (d, ^1J(C-P) = 21.9, PMe), 54.18 (s, CH), 61.80 (d, ^2J(C-P) = 21.8, OMe); MS: *m/z* 568 ($M^{\oplus}$, 19%), 484 ([$M^{\oplus} - 3$CO], 42), 401 ([$M^{\oplus}$ − $CHPh_2$], 100); IR (decalin): $\tilde{\nu}$(CO) = 2075, 1955, 1940 cm^{-1}

[a] 200.132-MHz ^{1}H-, 50.323-MHz ^{13}C-, 32.435-MHz ^{31}P-NMR: δ positive for downfield shifts from external 85% H_3PO_4, *J* in Hz; MS: EI, 70 eV, ^{184}W.

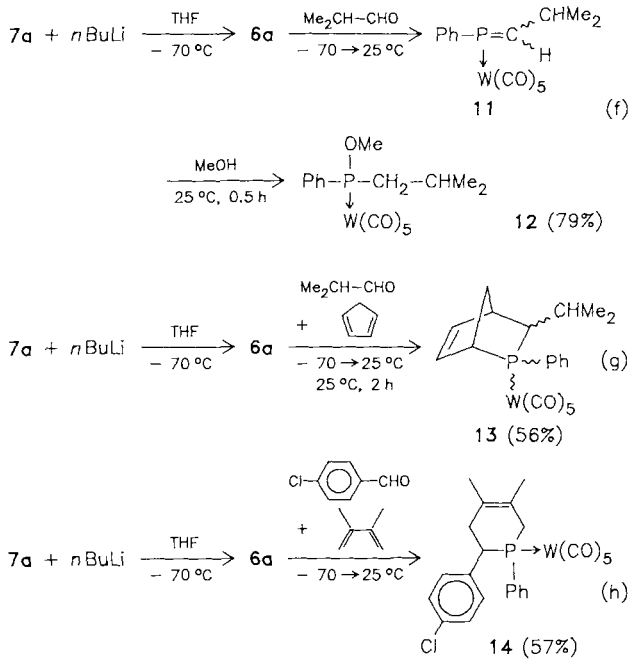

from **6b** and acetone by ^{31}P-NMR spectroscopy, but only the methanolysis product **16** was isolated [Eqn. (i)]. The phosphide **6b** appears to be more reactive than **6a**. In-

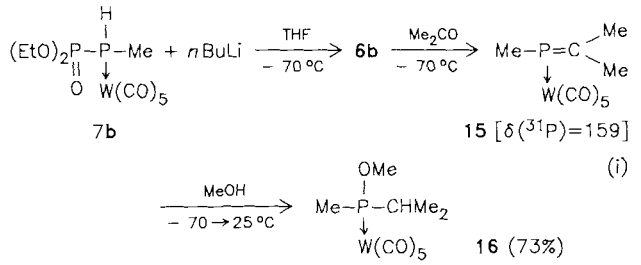

deed, **6b** reacts with benzophenone whereas **6a** does not [Eqn. (j)].

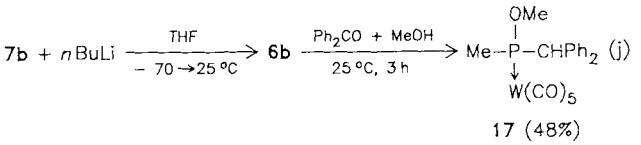

On the basis of this first series of examples, it is quite clear that the scope of the "phospha-Wittig" reaction is extremely wide.[6] From stable reagents such as **7** and carbonyl compounds, it is possible to prepare in a one pot reaction under mild conditions either PC single bonds, PC double bonds, or PC heterocycles.[7] Various synthetic applications of this scheme are currently under active investigation.

Experimental

9 and **10**: Complex **7a** (0.57 g, 1 mmol), the appropriate carbonyl compound (8 mmol) and DBO (0.12 g, 1 mmol) were stirred in benzene/pentane (1:2) for 0.5 h at room temperature. The reaction mixture was then directly chromatographed, as fast as possible, on a silica gel column with pentane as eluent. The final product was crystallized from pentane. **9**: yellow solid, m.p. 60°C; **10**: yellow solid, m.p. 81°C.

Trapping reactions: A solution of **7a** (or **7b**) (1 mmol) in THF was cooled to −78°C. *n*BuLi (0.7 mL, 1.6 M solution in hexane) was then added. After a few minutes, an excess of the trapping reagent (MeOH, 2,3-dimethylbutadiene or cyclopentadiene) and the carbonyl compound (1 mmol in the case of aldehydes, about 5 mmol for ketones) were added. The reaction mixture was then allowed to warm to room temperature. Reactions (f), (h) and (i) are very fast. Reactions (g) and (j) need a longer reaction time (2–3 h at room temperature). After hydrolysis, evaporation of the solvent and extraction with ether, the final product was purified by chromatography on silica gel with hexane as eluent.

Received: June 20, 1988 [Z 2819 IE]
German version: *Angew. Chem. 100* (1988) 1435

[1] See for example W. S. Wadsworth, Jr., W. D. Emmons, *J. Am. Chem. Soc. 84* (1962) 1316; *J. Org. Chem. 29* (1964) 2816.

[2] A. B. Burg, W. Mahler, *J. Am. Chem. Soc. 83* (1961) 2388; A. B. Burg, *J. Inorg. Nucl. Chem. 33* (1971) 1575; F. Zurmühlen, M. Regitz, *Angew. Chem. 99* (1987) 65; *Angew. Chem. Int. Ed. Engl. 26* (1987) 83.

[3] Somewhat related diphosphoryl phosphides $[(RO)_2P(O)]_2P^{\ominus}$ are known but are of no use for our purpose: D. Weber, G. Heckmann, E. Fluck, *Z. Naturforsch. B 31* (1976) 81; D. Weber, K. Peters, H. G. von Schnering, E. Fluck, *Z. Naturforsch. B 38* (1983) 208.

[4] See for example B. Deschamps, F. Mathey, *J. Chem. Soc. Chem. Commun. 1985*, 1010; N. H. Tran Huy, L. Ricard, F. Mathey, *Organometallics 7* (1988) 1791.

[5] This synthesis is described elsewhere: A. Marinetti, F. Mathey, *Tetrahedron*, in press.

[6] For this reason, the "phospha-Wittig" reaction compares favorably with the other available syntheses of PC double bonds (B. Weber, M. Regitz in: *Houben-Weyl-Müller, Methoden der organischen Chemie, Vol. E1 (Phosphor-Verbindungen)*, Thieme, Stuttgart 1982, pp. 28–51).

[7] Decomplexation of the phosphorus species thus obtained is easily achieved: A. Marinetti, F. Mathey, J. Fischer, A. Mitschler, *J. Chem. Soc. Chem. Commun. 1984*, 45; A. Marinetti, J. Fischer, F. Mathey, *J. Am. Chem. Soc. 107* (1985) 5001.

An Introduction to Chemisorption and Catalysis by Metals. By *R. P. H. Gasser*. Oxford Science Publishers, Clarendon Press, Oxford 1987. xii, 260 pp., paperback, £ 12.95.—ISBN 0-19-855271-8

To write an introduction to chemisorption and catalysis by metals at the present time is no easy task, in view of the rapid developments occurring in this field. The author of this book avoids these difficulties by confining himself to an account of long-accepted facts, well established methods, and only one example of a heterogeneously catalyzed reaction. He deliberately excludes any discussion of the theory of the bonding of molecules to the surface.

The book begins with a brief description of the interaction between the adsorbate and the surface and the thermodynamics of adsorption (isotherms, isobars and heats of adsorption), such as one finds in other books of a similar kind. The reader is then prepared for the chapters which follow by a useful account of the primary processes that occur during collision (elastic and inelastic processes, energy exchange). A longer chapter is devoted to the kinetics of adsorption and desorption, including especially a discussion of sticking probability and of temperature programmed thermal desorption.

Next a short introduction to the structure of metals and surfaces, the real and reciprocal lattices, the use of the Ewald sphere, and the behavior of electrons in metals leads into an essentially qualitative treatment of low energy electron diffraction. Under the heading "Electron emission" is given a 31-page account of ultraviolet photoelectron spectroscopy (UPS), X-ray photoelectron spectroscopy (XPS), Auger electron spectroscopy (AES), field electron microscopy and field ion microscopy. This chapter certainly does not do justice to the present-day importance of these techniques. For example, in the treatment of UPS we find no mention of the important information that can be obtained by using polarized radiation or by measuring the angular dependence. Similarly the ways in which XPS and AES can be used are only briefly touched on. The most recent developments in field emission are not included.

The treatment of chemisorption concludes with a very brief section on modification of work functions, infrared spectroscopy and high resolution electron energy loss spectroscopy (HREELS).

Heterogeneous catalysis is introduced by referring to the theory of the transition state, and discussing selectivity and the relationship between strength of chemisorption bonding and catalytic activity; rate equations are derived for reactions involving the Langmuir-Hinshelwood and the Eley-Rideal mechanisms. The principles are illustrated by reference to the *ortho-para* interconversion in hydrogen and to hydrogen-deuterium exchange.

In a concluding chapter, as an example of the application of the methods described in the previous chapters, the catalytic oxidation of carbon monoxide on palladium and platinum is discussed with reference to model reactions under high vacuum conditions.

Anyone working in the area of adsorption and catalysis will find few new ideas in this book. New techniques which have been developed in the last few years, such as those which have become possible by using synchrotron radiation, inverse photoemission, tunneling microscopy, ion scattering and many others are not mentioned. The bibliography consists mainly of references to monographs and review articles; it covers publications up to 1981, and is thus not very up-to-date. However, the readership aimed at by the author is not the expert one mentioned above. The book originated from an introductory lecture course, and is intended for students who have mastered the fundamentals of physical chemistry and now wish to study special topics, in this case that of adsorption as the primary step in heterogeneous catalysis. These readers will find the book useful. As a textbook to accompany a course such as that mentioned it is an appropriate choice, being clearly presented, adequately illustrated, and concentrating on the essentials.

Gerd Wedler [NB 913 IE]
Institut für Physikalische und Theoretische Chemie
der Universität Erlangen-Nürnberg (FRG)

Chemicals from Coal: New Processes (Series: Critical Reports on Applied Chemistry, Vol. 14). Edited by *K. R. Payne*. Wiley, New York 1987. 114 pp., bound, $ 50.30.—ISBN 0-471-91325-1

The book "Chemicals from Coal: New Developments" appeared in 1985 as Volume 9 in the series "Critical Reports on Applied Chemistry". That first 122-page volume, edited by *K. R. Payne*, contained three articles: *J. Schulze* (Technische Universität Berlin) and *H. Gaensslen* (Lurgi GmbH) discussed the economics of coal conversion processes, and in the two following articles *J. O. H. Newman* and *G. O. Davies* of the National Coal Board (Great Britain) reported on possibilities and recent advances in obtaining chemical feedstocks from coal by pyrolysis or direct liquefaction. The same editor (but a different publisher) has now produced the book under review here, as Volume 14 of the series, under the very similar title "Chemicals from Coal: New Processes". In this volume the discussion of chemical feedstocks from coal is taken further, with five articles on coal gasification, synthesis gas chemistry, Fischer-Tropsch syntheses and the production of acetylene from calcium carbide.

In the first chapter, "Syngas via coal gasification", *B. Cornils*, formerly of Ruhrchemie and now with Hoechst, reviews the present state of the art in coal gasification technology. Starting from the thermodynamic and kinetic relationships, and the existing first-generation gasification processes (the Lurgi, Winkler, and Koppers-Totzek gasifiers), the discussion proceeds to the modern second-generation processes, some of which are still at the development stage. The process engineering principles of fixed bed, fluidized bed and entrained bed gasification processes, as well as the differences between the many new developments which are competing with each other, are clearly explained. As a possible third-generation process, the allothermal fluidized bed gasification using process heat from a high temperature nuclear reactor is discussed. This chapter is a concise but successful review of the topic by a competent author who was for some years involved in the advanced development of the Texaco gasification process.

In the second chapter, "Chemicals from coal via the carbide route", *F.-W. Kampmann* and *W. Portz* of Knapsack/

Hoechst describe the production of acetylene via calcium carbide. Only the manufacture of the carbide is described in detail. The reader learns that since 1962 the production of carbide has greatly declined throughout the world; regrettably, though, he is not told about alternative routes to acetylene, such as by partial combustion of hydrocarbons, by the Hüls process in which hydrocarbons undergo conversion in a plasma arc torch, or by similar attempts to produce acetylene in the plasma directly from coal.

Chapter 3, "Catalysis in the conversion of synthesis gas to chemicals", by *I. Wender*, and Chapter 5, "Syngas chemistry to chemical feedstock: New frontiers", by *B. Cornils*, are the most informative ones for the chemist interested in C_1 chemistry. The two chapters overlap to some extent in the topics covered, but on the other hand they complement each other through their different viewpoints and in the literature cited. *Wender*, formerly at the Pittsburgh Energy Technology Center and now an emeritus professor at the University of Pittsburgh, generally discusses methods of catalyzing reactions of carbon monoxide and C_1 compounds. Accordingly the conversion of methanol using zeolites, and the acid catalyzed Koch-Haaf synthesis of carboxylic acids from carbon monoxide, olefins and water, are addressed as well as the many different catalytic reactions using heterogeneous and homogeneous transition metal catalyst systems. Some of the reaction schemes given here for catalytic cycles do not quite correspond to the presentations found in modern textbooks of organometallic chemistry, but this does not detract from the value of the information collected together in the review. *Cornils* limits his discussion to recent developments in C_1 chemistry, such as the production of C_2 to C_4 olefins using modified Fischer-Tropsch syntheses, the dehydration of methanol using zeolites, and methods for directly synthesizing carboxylic acids, acetaldehyde, ethanol or ethylene glycol from synthesis gas. As alternatives to such direct manufacturing routes from synthesis gas, multistage processes via methanol, acetic acid, formaldehyde or oxalic acid esters as intermediates are also discussed. Further possibilities for using C_1 compounds as building blocks in synthetic routes to methyl methacrylate, vinyl acetate, styrene, heterocyclic compounds, urethanes, acrylonitrile and long chain unbranched fatty acids are also indicated.

In Chapter 4, "The Fischer-Tropsch synthesis as a source of raw materials for the chemical industry", *M. E. Dry* describes the South African plants in Sasolburg and Secunda which operate the Fischer-Tropsch synthesis. Compared with other similar articles by the same author, this review emphasizes the different spectrum of products obtained from the two variants of the Sasol process using fixed bed reactors and circulating fluid bed reactors, and the downstream industrial processing of the mixture of products obtained.

New processes for making chemicals from coal were promised in the title of the book. The reader learns something of these in Chapters 1, 3 and especially 5, but little in Chapters 2 and 4. Apart from a very few exceptions, the literature cited does not extend beyond 1984; as is unfortunately so often the case, this appears to be due to the long delay between the completion of the manuscript and the publication of the book.

For chemists and chemical engineers who wish to familiarize themselves with synthesis gas and C_1 chemistry, the book is quite useful. So long as oil and natural gas continue to be cheaply available in sufficient quantities, processes based on coal will scarcely be economic. However, the present situation in energy markets cannot blind one to the fact that eventually it will become necessary to make greater use of coal. The route via coal gasification and synthesis gas chemistry which is discussed here as a way of producing chemical feedstocks appears very promising.

Finally, a comment on the short preface by the editor: This reviewer, who happens to work in the laboratories where *Franz Fischer* did his research, was surprised by the following sentence: "The Fischer-Tropsch process was originally developed in Germany by BASF before the First World War, and was improved over the years until, by the advent of World War II, it became an important source of chemicals and fuel for the Third Reich." The 1913 BASF patent D.R.P. 293787, which first described the formation of saturated and unsaturated hydrocarbons and of oxygen-containing compounds from synthesis gas at high pressure, was certainly one of the starting points which in 1922 prompted *Fischer* and *Tropsch* at the Kaiser-Wilhelm-Institut in Mülheim to carry out their work on "Synthol", a mixture consisting mainly of oxygen-containing compounds. *Franz Fischer* himself confirmed this fact in a controversy with *Alwin Mittasch* (*Angew. Chem. 40* (1927) 164 and 166). Systematic investigation of the reaction conditions led in 1925 to a hydrocarbon synthesis carried out without increased pressure and at lower temperatures, which was patented (D.R.P. 484337 and others) and given the name Fischer-Tropsch synthesis. The history of the discovery is described by *Otto Roelen*, one of the research team involved at the time, in a paper presented and published in 1977 (*Erdöl, Kohle, Erdgas, Petrochem. 31* (1977) 524).

Matthias W. Haenel [NB 876 IE]
Max-Planck-Institut für Kohlenforschung,
Mülheim a. d. Ruhr (FRG)

Multinuclear NMR. Edited by *J. Mason*. Plenum Press, New York 1987. 639 pp., bound, $ 115.00.—ISBN 0-306-42153-4

The publication of this book has been eagerly anticipated for some time in specialist circles, particularly in view of the many new and important directions of research which NMR spectroscopy has helped to stimulate in nearly every area of chemistry and in interdisciplinary fields. The 23 chapters of the book have been written by twelve authors, and the editor is herself a co-author in five of the chapters.

An explanation of the arrangement of the book's contents and the scope of the different topics treated (Chapter 1) is followed by a concise account of the fundamentals of the various NMR parameters (Chapter 2). Chapters 3–5 contain detailed discussions in turn of the chemical shift (δ), spin-spin coupling constants (^nJ), and relaxation processes. Chapters 1–5 take up about a quarter of the book. Much of what they contain is, necessarily, familiar ground, but they also bring out many aspects, especially concerning δ and J, which could otherwise only be discovered more laboriously from theoretical treatments, and might therefore remain unknown to the preparative chemist. As the title indicates, the book then continues, from Chapter 6 onwards, by dealing with the NMR parameters for the different nuclides, starting with ^1H, ^2H, and ^3H, and continuing through to the magnetically active isotopes of Cu, Ag, Au, Zn, Cd, and Hg (Chapter 21). The arrangement of the subject matter follows the groups of the Periodic System. Some important nuclides (e.g. ^1H, ^{11}B, ^{13}C, ^{19}F, ^{31}P) are only dealt with briefly, the main emphasis being on inor-

ganic and organometallic applications. These chapters vary greatly in their usefulness, as can be seen from the critical appraisal of individual chapters which follows.

Chapter 8 (^{11}B-NMR) concentrates on polyboranes, giving a clear and systematic presentation of the complex NMR spectroscopic properties of these compounds. By contrast, in Chapter 10 (^{13}C NMR), an attempt has been made to summarize an enormous quantity of data. A purely graphical presentation may be helpful for some purposes but it precludes access to detailed information. In the case of coupling constants only a few actual values are given, though unfortunately marred by an error which has been pointed out several times before: $^1J(^{13}C,^{11}B)$ in $[BMe_4]^{\ominus}$ is 39.4 Hz, not 22.0 Hz. Insufficient space (28 pages) has been given in Chapter 11 to the important nuclides ^{29}Si, (^{77}Ge), ^{119}Sn and ^{207}Pb. An error from earlier work remains uncorrected here: $\delta(^{119}Sn)$ in $Sn(C{\equiv}CH)_4$ is -356.3, not -279. Chapter 12 (^{14}N and ^{15}N NMR) is a pleasure to read. Here some important relationships between NMR parameters and structure are brought out, attention is given to the growing importance of NMR spectroscopy of solids, and reference is made to numerous recently published papers. On the other hand, in Chapter 13 the reader is in places not very well served, e.g. when ^{31}P chemical shifts are under discussion. The treatment of $\delta(^{31}P)$ values for phosphorus atoms with coordination numbers 1 and 2 is very vague. Here the reader would be well advised to refer instead to the excellent Chapter 3 (or even Chapter 14) for interpretation purposes. More confusion is added when the compound $[t\text{Bu}-P\{Cr(CO)_5\}_2]$ is assigned to the group in which phosphorus has the coordination number 2. Compound classes which have already been covered in detail in earlier review articles are given a lot of space. In Chapter 14 (^{17}O NMR) scant reference is made to boron–oxygen compounds, for which a large number of ^{17}O chemical shifts were reported in the period 1980–83 alone. In Chapter 16 ^{19}F NMR spectroscopy, in keeping with its relative importance, and in view of the existence of various review articles, some of which are now quite old, is discussed very briefly. The help which the experimental chemist is given towards interpreting his data is rather limited. For example, it is stated that in compounds with the general formula XF_n the shielding of the ^{19}F nucleus decreases with increasing n, and that this behavior is not unlike that of the ^{31}P shielding in PCl_3, $[PCl_4]^{\oplus}$, PCl_5, and $[PCl_6]^{\ominus}$ (even though the shielding increases in this case!). Chapters 19–21 (110 pages) on the NMR spectroscopy of transition metal nuclides are satisfyingly comprehensive in the information which they give. There is currently an upsurge of interest in this topic, and the data presented here will be of considerable value in helping future research. The interpretation of NMR parameters for these nuclides is very complex. It is therefore quite appropriate in view of the present state of research that in these chapters most of the pages are occupied by data and graphs.

In each chapter the arrangement of the material essentially follows a constant pattern, treating in turn chemical shifts, coupling constants and relaxation behavior. For newcomers to the field especially, this makes it easier to begin using NMR data to obtain information, and this is especially helpful when one is concerned with the less common nuclides. The structure of the book as a whole is similar to that of the work which paved the way in this field (*R. K. Harris* and *B. E. Mann* (Editors): *NMR and the Periodic Table*, Academic Press, London 1978). In this context the striking resemblance between several chapters in the two books is not solely due to the fact that parts of them have been written by the same authors. Most of the chapters include references to the applications of NMR spectroscopy of solids (sometimes under the heading "Miscellaneous"), but the great upsurge which is occurring in the development of this technique is not conveyed to the reader. The large quantity of NMR data from measurements in solution is for the most part clearly presented (in the form of tables and graphs). The last two chapters (22 and 23) have been included so as to complete the broad coverage of the book; they deal briefly with NMR spectroscopy in inorganic biochemistry, and with biomedical aspects. The effort which has been made to soften the otherwise rather abrupt conclusion of the book by including references to the literature in these two areas makes a favorable impression.

To cover multinuclear NMR in a single book was a formidable undertaking. The problem of condensing as much material as possible into a small space (for which even 639 pages is insufficient!), while maintaining the required standards of quality, topicality and breadth of coverage, has no perfect solution. Nevertheless, there are grounds for criticism when the literature coverage in the majority of the chapters extends only up to mid-1983. The cosmetic remedy of fitting in individual more recent references afterwards cannot hide this defect. If one regards this book as an attempt to organize the ever faster growing avalanche of NMR data into manageable channels, then despite certain reservations one must on balance give it a positive vote. The NMR literature market cannot at present offer any other comparable work. In view of these comments, the book is definitely a worthwhile purchase as a work of reference for chemists in academic departments and industry, whether or not NMR spectroscopy applications are in the foreground of their interests. For both undergraduate and graduate students too, this book could fill a troublesome gap, provided that the high price is not prohibitive.

Bernd Wrackmeyer [NB 884 IE]
Laboratorium für Anorganische Chemie
der Universität Bayreuth (FRG)

Inductively Coupled Plasmas in Analytical Atomic Spectrometry. Edited by *A. Montaser* and *D. W. Golightly*. VCH Verlagsgesellschaft, Weinheim/VCH Publishers, New York 1987. xxiii, 660 pp., bound, DM 220.00.— ISBN 3-527-26529-5/0-89573-334-X

Inductively coupled high frequency plasmas (ICPs), which were first used in the early sixties as radiation sources for emission spectrometry, by *Greenfield* in Great Britain and by *Fassel* in the United States, have developed to become the basis of a powerful analytical method for multielement determinations. ICP emission spectrometers are now available from more than fifteen manufacturers throughout the world. ICPs are also used as atom reservoirs for fluorescence spectrometry, and as ion sources for mass spectrometry, and systems for these types of measurements are also commercially available. ICP spectrometry is now used as a routine method in many analytical laboratories, together with other elemental analysis methods such as atomic absorption spectrometry (AAS), X-ray spectrometry, and electrochemical and chromatographic techniques. Its fields of application include biology and medicine, the analysis of ores, minerals, soils and ceramics, environmental analysis, and checking the purity of chemicals and of metals. This book, which is the second comprehensive treatment of ICP to appear within a short time, follow-

ing the two-volume work by *Boumans* on ICP atomic emission spectrometry, therefore meets a considerable need on the part of analysts. The editors *Montaser* and *Golightly*, by bringing together a group of eminent authors in this field, have produced an account of the fundamentals of ICP as a technique of optical emission spectrometry (OES). The book also deals with the use of ICPs as ion sources for mass spectrometry and as atom reservoirs for atomic fluorescence work.

In the introductory chapter (15 pages) a brief account is given of the important advantages which the introduction of ICP, compared with other types of electrically generated plasmas, has brought to the analysis of liquids. The chapters which follow are arranged in four parts. The first part (304 pages) deals with ICPs as radiation sources for optical emission spectrometry. This begins with a chapter on basic plasma spectroscopy rather than on analytical plasma spectrometry. Next a chapter on emission spectrometers deals with the construction and performance criteria of modern sequential and simultaneous spectrometers, together with trends for their future development. A further chapter discusses elementary aspects of high frequency generators for ICP spectrometry, and gives characteristic data on plasma torches and nebulizers. The chapter on the analytical capabilities of ICP deals with optimization techniques such as simplex procedures, the relationship between operating conditions and analytical performance. Limits of detection, quantitative analysis, and calibration in ICP-OES are treated thoroughly. The problems of choosing suitable spectral lines and of spectral interferences, which are very important in analytical practice, are clearly and concisely treated in one chapter. In a further chapter, using analytical results on actinides as an example, it is impressively demonstrated that optical ICP atomic spectrometry using high resolution spectrometers is very effective even with difficult matrices. In another chapter on the spectroscopic properties of the inductively coupled plasma, the reader is given a clear understanding and a good review of this aspect of the literature on ICP, which also is of importance to analytical chemists.

The second part (75 pages), deals with the analytical capabilities of ICPs in fields other than optical emission spectrometry. The first chapter of this section gives an account of the principles of atomic fluorescence spectrometry and the most recent results from ICP atomic fluorescence. The chapter on ICP mass spectrometry too gives an indication of future developments, and provides an insight into a technique which is now being used more and more for multielement determinations in the sub-μg/mL range of concentrations.

The third part (101 pages), on sample introduction, gives a clear description in three chapters of the various methods for generating aerosols from liquid and solid samples, and for introducing gases into the ICP. Two further chapters report on important developments such as ICPs with a gas consumption of less than 2 L/min, and ICPs which operate with gas mixtures and with gases other than argon; the development of ICPs of medium power (0.6–1 kW) and medium gas requirement ($\leq$8 L/min), which are now available from several manufacturers, is briefly touched on.

In the final part (29 pages) the analytical capabilities of ICP spectrometry are described. The reader is referred to important published work in various areas of application. Also in this part the performance of ICP spectrometry is compared with that of other atomic spectrometry techniques, such as AAS, DCP (directly coupled plasma) and X-ray spectrometry, and problem-orientated developments of ICP-related techniques are described; these topics are treated in a clear, but quite brief manner. An appendix, which is especially useful for users of the technique, lists data on prominent ICP emission lines, as published by *Winge*, *Peterson* and *Fassel*.

The information which this book on ICP spectrometry contains will certainly be greatly welcomed by the circle of analytical chemists, built up during the past fifteen years, who now use the technique. It also provides research scientists engaged in further development of ICP with a good review of the current state of the art and useful literature references. Because of its presentation and the amount of detailed information included, the book is a standard work on this important elemental analysis technique.

J. A. C. Broekaert [NB 890 IE]
Institut für Spektrochemie,
Dortmund (FRG)

Registered names, trademarks, etc. used in this journal, even when not marked as such, are not to be considered unprotected by law.

© VCH Verlagsgesellschaft mbH, D-6940 Weinheim, 1988. – Printed in the Federal Republic of Germany by Zechnersche Buchdruckerei, Speyer/Rhein.

All rights reserved (including those of translation into foreign languages). No part of this issue may be be reproduced in any form – by photoprint, microfilm, or any other means – nor transmitted or translated into a machine language without written permission from the publishers. Only single copies of contributions, or parts thereof, may be made for personal use. This journal was carefully produced in all its parts. Nevertheless, authors, editors and publisher do not warrant the information contained therein to be free of errors. Readers are advised to keep in mind that statements, data, illustrations, procedural details or other items may inadvertently be inaccurate.

Valid for users in the USA: The appearance of the code at the bottom of the first page of an article in this journal (serial) indicates the copyright owner's consent that copies of the article may be made for personal or internal use, or for the personal or internal use of specific clients. This consent is given on the condition, however, that the copier pay the stated per-copy fee through the Copyright Clearance Center, Inc., for copying beyond that permitted by Sections 107 or 108 of the U.S. Copyright Law. This consent does not extend to other kinds of copying, such as copying for general distribution, for advertising or promotional purposes, for creating new collective works, or for resale. For copying from back volumes of this journal see 'Permissions to Photo-Copy: Publisher's Fee List' of the CCC.

Editorial office: Pappelallee 3, D-6940 Weinheim, Federal Republic of Germany, Telephone (06201) 60 23 15, Telex 465516 vchwh d, Telefax (06201) 602328.

Editor: *P. Gölitz.*

Associate editors: *D. I. Loewus, A. Stimson.* **Editorial assistant:** *E. Schweikart*

Publishers: VCH Verlagsgesellschaft mbH. (Managing Directors: *Prof. Dr. Helmut Grünewald* and *Hans Dirk Köhler*), Pappelallee 3, D-6940 Weinheim, Federal Republic of Germany. Correspondence concerning advertisements should be addressed to VCH Verlagsgesellschaft mbH. (Advertising Manager *R. J. Roth*), Boschstr. 12, P.O. Box 101161, D-6940 Weinheim, Federal Republic of Germany, Telephone Weinheim (06201) 602-0, Telex 465516 vchwh d, Telefax (06201) 602 328.

ADVANCED MATERIALS

Editorial Advisors: E. M. Engler (USA), D. Haarer (FRG), N. Ogata (Japan), G. Petzow (FRG), J. M. Thomas (UK), G. Wegner (FRG)

Intelligent Materials—A New Frontier

Functional Ceramics
Ceramic Sensors
Sensor Tuning

By Hiroaki Yanagida*

1. The Need for Intelligent Materials

The incentive for materials R&D is to achieve improvements in either manufacture or performance, or to introduce novel functions. Until very recently only the first two of these have been recognized as important. Improved manufacturing methods have led to large scale production systems. Iron and plastics are examples of progress in this direction. Research on engineering ceramics has been aimed at improving performance, in particular to give improved durability under severe conditions. There is another direction for R&D in materials, namely the introduction of novel functions. Various specialized functions have been discovered. Nonlinear electrical and/or optical behavior, various types of transducers, chemically interesting properties, etc. give rise to many types of novel devices, using what are described as functional materials.

Materials with excellent performance *and* novel functions are ideal candidates for future technology. One such class of materials is that of functional ceramics. Various functional ceramics have already been developed or are still undergoing development. Some of these have the special properties mentioned above. It may be said that no electronic devices can be constructed without ceramic components. Various novel devices have been developed using functional ceramics. These might be described in a sense as keys to the development of an advanced technological society.[1]

The ultimate functions may be those with "intelligence". There are potential demands for so-called intelligent materials. Although computers with integrated circuits are normally used to control operations or to make judgements, neither these nor any other devices containing electrical connections can be introduced into hazardous environments. Some operations or judgements therefore need to be carried out within materials which satisfy the required safety conditions. Even under non-hazardous conditions, where computers are used for complicated functions the result is often a tangle of electrical leads, a situation which has been referred to by medical electronics scientists as the "spaghetti syndrome".[2] Here again it is an advantage if some of the intelligent judgements can be made within materials. Thus there is a need for intelligent materials.

Examples of what is meant by the term intelligent are concepts such as self-recovery, self-adjustment or control, self-diagnosis, stand-by capability for detecting nonlinear onset, ability to be externally tuned, etc. These concepts seem to be realized only in living organisms, which, however, cannot survive in hostile environments, and in some senses, therefore, intelligent materials must perform better than living organisms, by being able to withstand very hos-

[*] Prof. H. Yanagida
Department of Industrial Chemistry, Faculty of Engineering
University of Tokyo
7-3-1 Hongo, Bunkyo-ku, Tokyo (Japan)

Contents

H. Yanagida
Intelligent Materials – A New Frontier 1389
R. Schöllhorn
From Electronic/Ionic Conductors to Superconductors: Control of Materials Properties 1392
Conference Reports
Better High-Tech Ceramics by Improved Processing 1401
Advanced Concepts for Ceramic Toughening 1403
Polymer Crystals 1405
Research News
NMR Imaging of Materials 1406
Book Reviews 1407
Conference Calendar 1412

Editor: *P. Gölitz* Editorial Assistant: *L. Dominguez*

tile environments. Nevertheless, to achieve intelligence in materials one must learn from living organisms which are not necessarily ideally adapted, since in the modern technological age hostile conditions of previously unknown kinds are encountered. To carry out work in environments which human beings could not tolerate, robots with capabilities exceeding those of living organisms, and able to withstand such severe conditions, must be used. Living organisms lack some important sensing mechanisms, e.g. the ability to detect insufficient oxygen pressures or the presence of so toxic a gas as carbon monoxide. With the help of intelligent materials, living organisms can survive under severe conditions.

2. Functions Required from Intelligent Materials

Some of the functions that may be demanded of intelligent materials have already been mentioned above. The meanings of these functions will be explained in this section.

2.1. Self-recovery

Most materials inevitably degenerate continuously until they are no longer usable. Living organisms, on the other hand, frequently recover their original function and performance through a self-recovery mechanism. They may recover through resting, for example. A disadvantage arising from the lack of a self-recovery mechanism is seen in the case of the humidity sensor consisting of a porous ceramic semiconductor. The conductivity of the porous material usually increases with adsorption of water vapor under humid conditions, and decreases with removal of adsorbed water molecules under dry conditions. Removal is, however, very slow at room temperature. A large hysteresis loop is observed in the humidity-conductivity characteristic. A measured conductivity value will not necessarily indicate the humidity level existing at the time of the reading. In order that the water molecule adsorption sites should remain fully active one must frequently carry out a so-called cleaning operation to remove the adsorbed water molecules at high temperature. During such cleaning treatments the sensor cannot supply any information about humidity.

A few years ago we constructed a new type of ceramic humidity sensor.[3] This uses point contacts between a p-type semiconductor (copper oxide or nickel oxide) and an n-type semiconductor (zinc oxide). The voltage-current characteristic changes with humidity as shown in Figure 1. The mechanism of this device has been analyzed as follows.[3c] The amount of water adsorption in the vicinity of the hetero contacts changes with humidity, as is also found for porous humidity sensors of the usual type with homo phase contacts. Electron holes are injected from the p-type semiconductor electrode into the adsorbed water molecules, giving rise to protons in the adsorbed water phase. The positive charge is liberated at the surface of the n-type semiconductor electrode. As a consequence of this process the adsorbed water is electrolyzed. During measurements the cleaning process is always working, since the cleaning or self-recovery treatment is itself the working mechanism.

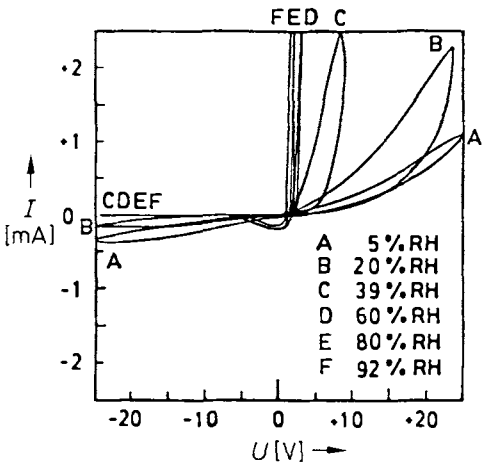

Fig. 1. Humidity dependent voltage-current characteristic changes of an intelligent humidity sensor made of hetero-contacts between copper oxide and zinc oxide [5]. RH = relative humidity.

The change from the usual porous ceramic humidity sensors to the p/n contact type discussed here is from single phase contacts to two different phase contacts. The morphology appears to be very similar in the two cases. However, the working mechanism is significantly different. Both are typical examples of two-dimensional structures,[4] as shown in Figure 2. However, the p/n contact type has greater potential than the former type, at least as far as intelligence is concerned. Table 1 gives a comparison between the usual porous type ceramic humidity sensor and the p/n contact type.

Fig. 2. Difference in structure and working mechanism between single phase contact type (left) and two phase contact type humidity sensors (right). Left is a porous zinc oxide humidity sensor and right a p/n hetero-contact type humidity sensor.

2.2. Self-adjustment or Control

The types of control systems that have been proposed are many and varied. Most of them use feedback logic with conventional electric circuits. There are, however, some self-control devices without feedback circuits, although they may still be primitive from an intelligence standpoint.

ADVANCED MATERIALS

Table 1. Comparison of two types of ceramic humidity sensors.

	porous zinc oxide humidity sensor	CuO/ZnO contact humidity sensor
structure [4]	open interface between identical materials	open interface between different materials
measurement	conductivity change	*U/I* characteristic
mechanism	protonic conduction	electrolysis of adsorbed water
hysteresis	causes problems	none, no problems
cleaning	necessary	not needed (working mechanism itself gives cleaning)
self-recovery	ineffective (frequent cleaning treatments needed)	effective

The temperature of heating elements may be roughly controlled if the resistance increases with temperature, as occurs in silicon carbide heating elements above 1000°C. The most typical self-control mechanism is seen in perovskite type ceramic (PTC) heating elements; semiconductor PTCs are well known and used in practical applications. They have very low resistivity below the transition temperature, and can be used for heating elements in this range. Above the transition temperature the resistivity begins to increase dramatically. The change in resistivity can be used to measure the temperature. The resistivity reaches a very high value, so that only a very small current passes. This constitutes a switch which does not rely on a change in contact behavior. Through the intrinsic properties of the material, the element performs simultaneously the functions of heater, temperature monitor and switch. Here again the origin of the intelligent character lies in a type of two-dimensional structure:[4] a closed interface between identical materials, with the phenomenon occurring across the interface.

2.3. Self-diagnosis

The reason why we try to improve the performance of materials is that we hope to use the materials for as long as possible. We also try to establish methods whereby the life of the materials in a particular application can be predicted. However, in a significant proportion of samples the lifetime is shorter than that predicted. We therefore need to periodically check the condition of the materials during use. One method of monitoring which can be used is to observe acoustic emission from the materials. However, it is not practicable to install acoustic emission apparatus in every application. When living organisms go wrong, they signal to others that they are in difficulties, and help from others may then relieve their problems. Although they may not have the self-recovery mechanism within themselves, they can receive help by telling others of the difficulty occurring in them. If materials could be made with such a self-diagnostic mechanism, we could take action to avert disasters caused by failures of materials. We could also avoid unnecessarily sacrificing materials through replacing them prematurely lest they should fail.

2.4. Stand-by Capability

Machines are sometimes criticized because their response is slower than that of living organisms. For example, the motion of robots is slower than that of humans. Machines are also said to be incapable of releasing stored energy as rapidly as living organisms. A flea can jump very high very quickly. Rockets, on the other hand, take off very slowly. Most machines cannot release a very high concentration of energy within a very short time. The difference is in the stand-by mechanism. There are, nevertheless, some cases where devices have an effective stand-by mechanism. Consider the mechanism of amplification in transistors. Between source and sink a large bias is applied. Unless the barrier height is reduced no significant current flows from source to sink. The barrier (or gate) works as a trigger. The humidity sensor of the p/n contact type, which was discussed earlier from the standpoint of self-recovery, may also be analyzed in terms of its stand-by capability. Under dry conditions only a very small current flows through the contacts, although there is a bias across the p/n contact, whereas in humid conditions the current increases with the adsorption of water molecules. The sensor behaves like a hungry animal waiting for food.

If materials can be equipped with a stand-by mechanism in which they wait for nonlinear onset triggered by certain signals, they become interesting candidates for use as intelligent materials.

2.5. Ability to be Externally Tuned

Sometimes we need to change the behavior or characteristics of materials from outside. We may call this "tuning" the device. This avoids having to employ a large number of different components. The most convenient form of control signal is to change an applied voltage. Various ceramic capacitors exist whose capacitance varies with the applied voltage. The optical transmission of ferroelectric ceramic films made of PLZT (lead lanthanum zirconate and titanate) can be altered by changing the applied voltage, which is known as the Kerr or Pockels effect. The p/n contact humidity sensor also works as a very selective carbon monoxide gas sensor.[5] The selectivity towards carbon monoxide arises from selective adsorption of carbon monoxide at the copper oxide surface. The capacitance of the p/n contact increases when carbon monoxide is introduced into the ambient atmosphere (nitrogen and oxygen). The sensitivity changes with the bias applied across the p/n contact as shown in Figure 3. The maximum sensitivity is obtained when the CuO side is positively biased at about 0.5 V. This effect constitutes a tuming. The chemical

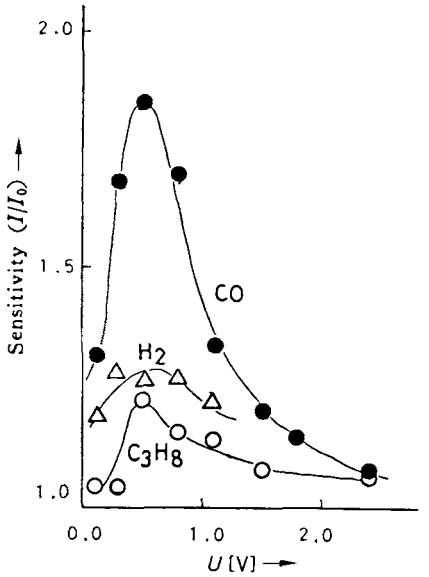

Fig. 3. Tuning of the sensitivity to carbon monoxide by bias in the CuO/ZnO contact type gas sensor [5]. ●: with CO, △: with H_2, ○: with C_3H_8; gas concentrations: 8000 ppm; temperature: 260°C.

reaction between carbon monoxide adsorbed on the positively charged copper oxide surface and oxygen adsorbed on the negatively charged zinc oxide surface, giving rise to carbon dioxide, is enhanced when the bias is greater than 0.5 V. If this explanation is correct, we have here an electric field controlling a chemical reaction.

A difficulty in applying control voltages is the need to connect leads. If the tuning is achieved by optical or magnetic means, the materials can be regarded as being more intelligent.

3. Conclusion

Intelligent materials can be developed through learning about the mechanisms in living organisms. However, we require materials that can be used in environments not tolerated by living organisms. Intelligent materials perform better than living organisms from the durability standpoint. Key functions for intelligent materials are self-recovery, self-adjustment or control, self-diagnosis, stand-by capability, and ability to be externally tuned. Some examples of intelligent materials have been discussed here. One example in which we can see self-recovery and stand-by capabilities, and ability to externally tune the behavior, is the p/n (CuO/ZnO) contact structure. Research and development on intelligent materials has only just begun. It is one of the most challenging frontiers of materials science.

Received: August 1, 1988

[1] H. Yanagida: "*Industrial and Cultural Revolution through High-Tech Ceramics*" in *Advanced Ceramic Materials, Vol. 2*, American Ceramic Society, Chicago, IL, USA 1987, p. 31.
[2] T. Furukawa, Medical Electronics Laboratory, University of Tokyo, personal communication.
[3] a) NiO/ZnO hetero-contact type: H. Yanagida, K. Kawakami, *Yogyo Kyokaishi 87* (1979) 112; b) CuO/ZnO prototype: H. Yanagida, Y. Toyoshima, M. Miyayama, K. Koumoto, *Jpn. J. Appl. Phys. 22* (1983) 1933; c) CuO/ZnO modified type: H. Yanagida, Y. Nakamura, M. Ikejiri, M. Miyayama, K. Koumoto, *Nippon Kagaku Kaishi 1985*, 1154.
[4] H. Yanagida, *Kagaku to Kogyo (Tokyo) 39* (1986) 831.
[5] Y. Nakamura, T. Tsurutani, M. Miyayama, O. Okada, K. Koumoto, H. Yanagida, *Nippon Kagaku Kaishi 1987*, 477.

From Electronic/Ionic Conductors to Superconductors: Control of Materials Properties

High T_c Perovskites
Electron/Ion Transfer
Topotactic Reactions

By Robert Schöllhorn*

1. Introduction

Modern materials science may be defined in analytical terms as the effort to understand the macroscopic properties of solids by considering their structure on the microscopic (atomic) level. The term "structure" comprises here the geometrical/crystallographic aspects, the total of electronic interactions between the atoms which constitute the material, and the lattice dynamics. In synthetic terms one major approach in materials science is the aim of "tailoring" materials with a given set of particular properties on the basis of analytical knowledge in order to meet optimally and economically the needs of specific applications. The thermal synthesis of solid compounds is usually related to a substantial structural reorganization at high temperatures. However, the properties of the products are not

[*] Prof. Dr. R. Schöllhorn
Institut für Anorganische und
Analytische Chemie der Technischen Universität
Strasse des 17. Juni 135, D-1000 Berlin 12

ADVANCED MATERIALS

determined solely by thermodynamics, but are frequently strongly dominated by kinetic phenomena leading to non-equilibrium states. One interesting alternative route for preparing new materials that makes use of the consequences of kinetics is low temperature synthesis, which exploits the fact that metastable intermediate states can be stabilized at lower temperatures. A particular case here is the synthesis of solids at or close to ambient temperature; under specific conditions such reactions can be carried out as reversible processes. One most attractive aspect of these "topotactic" reactions is the fact that they can be used for the *modification and control of physical properties* of solid materials by isothermal chemical reactions at ambient temperature. We shall briefly outline here the principles of this concept, and illustrate through a few selected examples the potential and the problems encountered.

2. Concepts

In terms of charge carrier transport properties, solid materials can be classified by a simple scheme in three groups: 1) electronic conductors, 2) ionic conductors, and 3) mixed electronic/ionic conductors, the latter being able to transport electrons as well as ions simultaneously. A large number of solids [H] (binary or multinary phases) which have electronic conductivity together with an appropriate band structure for the uptake of additional electrons and a system of interconnected vacant lattice sites may react with mobile ions A^+ according to the following scheme:[1-3]

$$\underset{\text{electronic conductor}}{[H]} + x e^- + x A^+ \rightleftharpoons \underset{\text{electronic/ionic conductor}}{A^+[H]^{x-}} \qquad (1)$$

This electron/ion transfer process can be performed by chemical or electrochemical techniques. The electrons are taken up into the upper band level (conductivity band) of the host matrix [H] (Fig. 1), while the guest ions A^+ fill up the vacant sites in [H]. Reactions of this type are usually reversible and proceed at or close to ambient temperature while retaining the structure of the rigid matrix [H] (topotactic process). In terms of composition, inorganic host materials are mainly binary or multinary compounds of non-metals with redox-active transition metals, e.g. oxides (WO_3, MoO_2, V_2O_5 etc.), chalcogenides (TiS_2, Mo_6S_8, $NiPSe_3$ etc.) or halides ($RuCl_3$, $RuBr_3$, FeOCl etc.). Similarly a large number of organic conducting polymers (e.g. polyacetylene, polypyrrole, polyaniline etc.) have been found to undergo electron/ion transfer reactions. Non-crystalline inorganic materials with electronic conductivity, such as amorphous MoS_3, TiS_2 and V_2O_5 have also been shown to be able to act as host lattices for these reversible topotactic processes.

The structural dimensionality of the host compounds may range from three-dimensional to one-dimensional (Fig. 2), and strongly affects the reactivity in geometrical terms. Framework hosts with vacant "lattice channels" can accept only atomic guest ions (metal ions, protons) up to a critical diameter determined by the geometry of the channel system. Layered host lattices are flexible and can easily adapt to the geometry of the guest species; they may also

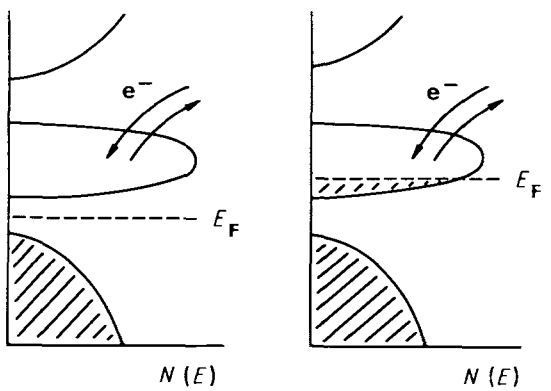

Fig. 1. Electron/ion transfer scheme for semiconducting (left) and metallic (right) materials (E_F = Fermi energy, $N(E)$ = density of states.

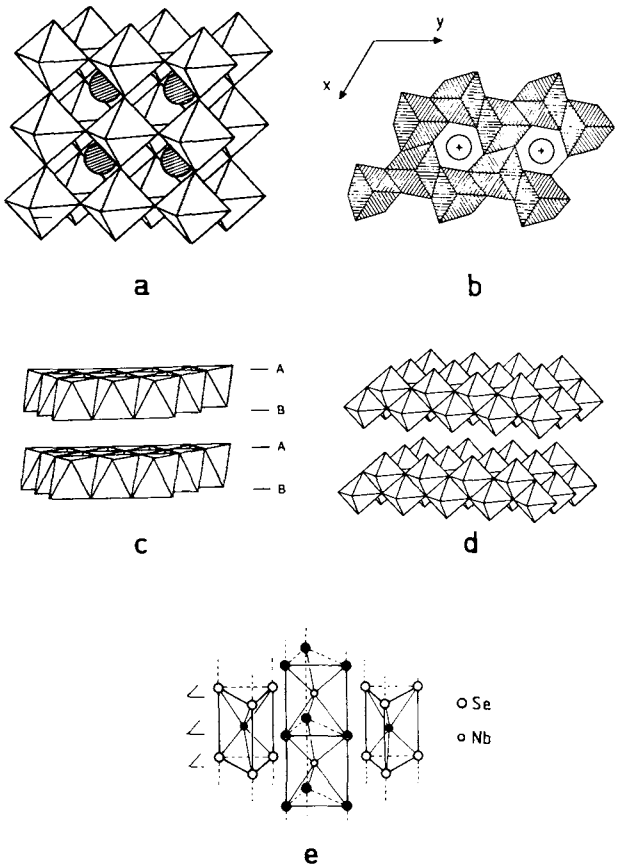

Fig. 2. Host lattices with different structural dimensionality. Framework structures: a) WO_3, b) Nb_3S_4; layered structures: c) TiS_2, d) MoO_3; chain structure: e) $NbSe_3$ (spheres in a) and b) indicate guest positions on lattice sites) [19].

intercalate organic and organometallic ions with or without neutral solvate molecules. The tremendous variety of the latter phases represents an interesting area in which molecular chemistry and solid state chemistry are closely associated. Reactions of layered host systems exhibit a number of structural peculiarities such as "staging" (partial occupation of the van der Waals gaps between the layers in an ordered sequence), "stacking" (different layer order sequence perpendicular to the basal planes), order/disorder transitions of guest or host sublattice, incommensurate phases, cooperative exchange reactions and hysteresis. Similar phenomena are observed for one-dimensional host lattices.

Reaction (1) describes the electron/ion transfer process for an "empty" conductor host lattice. Many ternary phases $A_xM_yX_z$ (M = transition metal, X = non-metal) with electronic conductivity are known, however, which are characterized by a rigid lattice framework (M_yX_z) and cations A^+ selectively mobile at ambient temperature. Many of these phases have an appropriate band structure that allows the following (reversible) electron/ion transfer process:

$$A_x^+[M_yX_z]^{x-} \rightleftharpoons M_yX_z + xA^+ + xe^- \quad (2)$$

A few examples may illustrate the reaction principles outlined above. Niobium disulfide is a metal with a layered structure related to that of the CdI_2 type, which may intercalate Li^+ ions, for example, according to equation (3). For $x = 1$ the lithium ions occupy all octahedral

$$xLi^+ + xe^- + NbS_2 \rightleftharpoons Li_x^+[NbS_2]^{x-} \quad (3)$$

sites in the van der Waals gap between the NbS_2 layer units which themselves have a negative excess charge $[NbS_2]^{1-}$ (macroanions). The intercalation of solvated ions or molecular ions (Cp_2Co^+ = cobaltocenium ion) is similarly illustrated by equations (4) and (5). An example for

$$xNa^+ + yH_2O + xe^- + NbS_2 \rightleftharpoons Na_x^+(H_2O)_y[NbS_2]^{x-} \quad (4)$$

$$xCp_2Co^+ + xe^- + NbS_2 \rightleftharpoons (Cp_2Co^+)_x[NbS_2]^{x-} \quad (5)$$

$$Cu^+[Ti_2S_4]^- \rightleftharpoons Cu^+ + e^- + Ti_2S_4 \quad (6)$$

the deintercalation of a ternary phase with a selectively mobile cation species (Cu^+) is the reaction of the metallic copper chalcogen spinel $CuTi_2S_4$ [equation (6)] that leads to the formation of $Ti_2S_4 = TiS_2$, i.e. a new modification of titanium disulfide with cubic structure (Table 1).

The reactions considered above represent electron/cation transfer processes. Only a few host lattices able to undergo the symmetrical reaction of electron/anion transfer

Table 1. Metastable binary transition metal chalcogenides prepared from ternary phases via electron/ion transfer reactions. A^+ = mobile lattice ion, D = structural dimensionality of the product.

Ternary Phase	A^{n+}	Binary Phase	D	Ref.
$Fe_2Mo_6S_8$	Fe^{2+}	Mo_6S_8	3	[5]
$K_xTi_3S_4$	K^+	Ti_3S_4	3	[6]
$CuTi_2S_4$	Cu^+	c-TiS_2	3	[7, 8]
Na_xWS_2	Na^+	o-WS_2	2	[9]
$LiVS_2$	Li^+	VS_2	2	[10]
$KCrSe_2$	K^+	$CrSe_2$	2	[11]
$TlMo_6Se_6$	Tl^+	Mo_6Se_6	1	[12]

[equation (7), [H] = host lattice] have been found so far. Examples are graphite and conducting polymers, which are

$$[H] + xA^- \rightleftharpoons (A^-)_x[H]^{x+} + xe^- \quad (7)$$

redox amphoteric systems accessible to electron/cation as well as to electron/anion transfer. Layer charge sign transition $[H]^- \rightarrow [H]^+$ and electron/anion transfer reactions have been reported recently, however, for a series of layered transition metal hydroxide oxide phases,[4] and we shall discuss below in more detail an example of an electron/oxide ion transfer.

3. Control Functions and Potential Application

The primary chemical properties of solids that can be controlled by electron/ion transfer processes are changes in composition (type of guest species), stoichiometry (concentration of guest species), redox state, and structure. Since these reactions are performed at low temperatures the influence of kinetics becomes dominant. For this reason the reaction products are frequently metastable new phases that cannot be prepared by conventional thermal synthesis techniques. Table 1 presents a few examples of binary chalcogenides which have been obtained from ternary compounds by electrochemical or chemical oxidation. None of these phases can be synthesized from the elements with the stoichiometry or structure indicated. The (reversible) structural changes within the host matrix elements are always rather small (0.01–0.1 Å); for low dimensional host lattices with flexible matrix units (layers, chains) the geometrical separation between these units can, however, be controlled between ca. 6 and 60 Å, e.g. by intercalation of large or anisometric guest species. Lattice defect concentration and order/disorder transitions in the guest or host sublattice can be strongly influenced by the kinetics of the reaction. In layered solvated compounds significant changes in the interlayer spacing can be controlled by minor changes in the equilibrium electrolyte concentration, due to structure induced selectivity resulting from cooperative transitions.[2–4]

One most important aspect is the possibility of inducing and controlling changes in the *physical* properties of a given solid by reversible chemical reactions at ambient temperature. These changes concern in particular the elec-

ADVANCED MATERIALS

tronic properties (i.e. electronic transport, metal/semiconductor and metal/superconductor transitions, charge density waves, magnetic ordering phenomena), optical properties and ionic transport. Mechanical properties can similarly be strongly affected: the layered chalcogenide NbS_2 is a highly elastic compound with lubricant properties, whereas after intercalation even of small amounts of copper (Cu_xNbS_2) a brittle material results.

In terms of applications, electron/ion transfer reactions are of interest from various aspects. As already discussed above, they provide a wide base for the low temperature synthesis of new materials. A quite obvious application in energy storage is their use as reversible electrodes, e.g. in high energy density secondary batteries with aprotic electrolytes.[13] Galvanic cells for this purpose have been designed not only with inorganic materials but also with conducting organic polymers.[14] Changes in optical properties with the redox state have been used for the construction of passive display systems, with the advantage that the information stored is retained in the absence of an external voltage.[15] Recently a rear mirror with dimmer function for automobiles has been developed with a thin film galvanic cell around the reflector plane[16] (Fig. 3). Mixed conductor materials with redox properties can be used as sensor systems (e.g. ion-sensitive field effect transistors) and in microelectronic devices.[17] Further applications relate to the use of electronic/ionic conductors in heterogeneous catalysis, electrocatalysis, in photoelectrochemical systems[18] and for the controlled release and uptake of reagents by host solids.

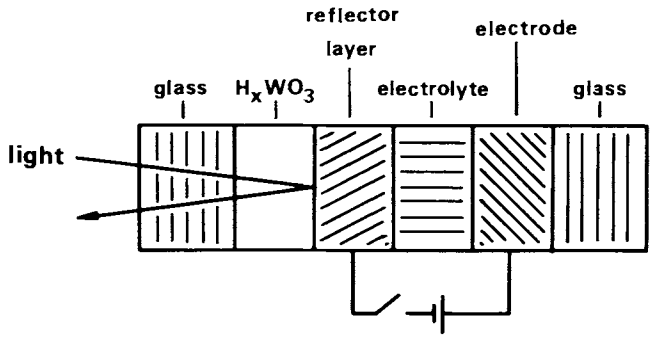

Fig. 3. Scheme of the design of a rear mirror for automobiles (cross section) with dimmer function based on the reversible formation of H_xWO_3 (see section 4) [19].

A major requirement in setting out to exploit the potential of electron/ion transfer reactions for the control of the physical properties of solid materials is the understanding of the reaction mechanism and the changes in structure and bonding with the redox state. We shall discuss in the following a few examples of systems which have recently been studied in more detail; for simplicity we will restrict the scope to atomic species as the guest ions.

4. Electron/Proton Transfer: Mechanism, Kinetics, Anisotropic Dynamics

The intercalation of hydrogen via electron/proton transfer into electronically conducting solids with the formation of hydrogen bronzes is a well known phenomenon.[1,2] These systems can be used as battery electrodes, for passive displays, for hydrogen storage, and as heterogeneous catalysts. An instructive example for the reversible changes in composition, structure and physical properties is the reaction of tungsten trioxide WO_3 (ReO_3 type framework structure, Fig. 2a):

change in stoichiometry:	$WO_3 + xH^+ + xe^- \rightleftharpoons H_x[WO_3]$
change in structure:	monoclinic $\rightleftharpoons$ tetragonal
change in electronic transport:	semiconductor $\rightleftharpoons$ metal
change in optical properties:	yellow transparent $\rightleftharpoons$ blue metallic

Similar reactions are observed for the layered binary molybdenum oxide MoO_3 (Fig. 2d). Five different phases have been identified for H_xMoO_3: I, blue orthorhombic, $0.25 \leqslant x \leqslant 0.4$; II, blue monoclinic, $0.6 \leqslant x \leqslant 0.8$; III, blue monoclinic, $0.95 \leqslant x \leqslant 1.05$; IV, red monoclinic, $1.55 \leqslant x \leqslant 1.72$ and V, green monoclinic, $x = 2.0$. The H_xMoO_3 system displays a characteristic strong kinetic influence: 1) IV and V are metastable phases with potentials lying below the equilibrium potential of H_2/H^+, 2) the reaction cycle exhibits strong hysteresis, phases II and III appear only in the oxidation cycle, which has been explained by the large changes in unit cell volume;[19] 3) the complete transformation of $H_{0.25}MoO_3$ (lower limit of phase I) back to MoO_3 is not possible at equilibrium potentials due to an electron transport threshold. MoO_3 is a wide gap semiconductor (insulator), which at first sight is in conflict with the requirement of electronic conductivity for host lattices as stated above. However, upon reduction the first phase $H_{0.2}MoO_3$ formed at the triphase boundary electronic lead/electrolyte/MoO_3 is a metal, and is thus able to transport electrons. On the way back (anodic oxidation) in the two phase region from $H_{0.2}MoO_3$ to MoO_3, the latter forms a thin layer (metal/insulator transition) blocking the electron transport across the phase boundary. Similar characteristic kinetic phenomena are frequently found in electron/ion transfer reactions of other systems.[2,19]

A further characteristic is the observation of anisotropy effects in low-dimensional host lattices, not only with respect to electronic transport but also regarding the dynamics of the mobile guest species. It is surprising to find that this applies also to proton mobility, since protons are the smallest mobile ions, and could be expected to show iso-

tropic motion independent of the host lattice dimensionality. An interesting example that has been thoroughly studied by solid state ^{1}H-NMR is provided by the layered H_xMoO_3 phases. At low hydrogen concentration ($x \approx 0.25$) hydrogen shows quasi-one-dimensional mobility between the zigzag chains of edge sharing MoO_6 octahedra that constitute the MoO_3 layer units. At intermediate hydrogen concentration ($x \approx 1$) a quasi-two-dimensional motion in the *a/c* layer planes is observed, while at high concentration ($x = 2$) three-dimensional mobility appears. The motional dimensionality of hydrogen can thus be controlled via the redox state and the corresponding stoichiometry.[20]

Early use was made of hydrogen bronzes for galvanic cells, although the reaction mechanisms were established only later. The nickel/hydroxide electrode in the Ni/Cd and Ni/Fe battery is basically an electron/proton transfer process [equation (8)]. The accessible range is $0.2 \leqslant x \leqslant 1.4$;

$$H_2NiO_2 \rightleftharpoons H_{2-x}NiO_2 + xe^- + xH^+ \quad (8)$$

the lower limit corresponding to $Ni(OH)_2$ cannot be reached in electrochemical systems for kinetic reasons, since nickel(II) hydroxide is an insulator (electron transport threshold, see above). Equation (8) represents a simplified version of the overall process; investigations on the solid state chemistry of layered hydroxide oxides have shown that the real process is far more complex.[4,21]

The first discharge region of the MnO_2 electrode in the Leclanché cell [equation (9)] is reversible and corresponds

$$MnO_2 + xH^+ + xe^- \rightleftharpoons H_xMnO_2 \quad (9)$$

to the insertion of protons into the vacant lattice channels of the rutile structure of MnO_2; however, further reduction leads to irreversible lattice transformations. Replacement of H^+ by Li^+ and the use of aprotic electrolytes have led to the development of secondary batteries (reversible cells) of the Leclanché type with higher energy density.

Topotactic electron/proton transfer reactions have also been found to occur in molecular solids, e.g. planar transition metal complexes with columnar structures and cluster halides.[22] In the latter phases long-range electron/proton transfer across insulator barriers occurs, as in certain organized biological cell components; the mechanism of this process is not yet understood.

5. Stoichiometry: Electronic and Geometrical Thresholds

An important point in the control of stoichiometry is the question of the upper intercalation limit, which can be governed either by electronic (band structure) or by steric factors. We will briefly demonstrate these aspects by using the molybdenum cluster chalcogenide Mo_6S_8 as an example.[23,24] The structure of Mo_6S_8 can be described as consisting of sulfur cubes surrounding Mo_6 octahedra. These units are interconnected via Mo-S bonding to a framework which contains "channels" of vacant sites along the rhombohedral axes. The simple valence electron counting scheme shows that the Mo_6 clusters have a deficit of four electrons in terms of metal-metal two-electron cluster bonds. This is in agreement with band structure calculations. We can now predict easily that the maximum number of electrons that can be taken up into the valence band is four [equation (10)], corresponding to an intercalation limit of four monovalent or two bivalent guest ions. This prediction on electronic grounds has turned out to be valid for all cations with small ionic radii.

$$Mo_6S_8 + 4e^- \rightleftharpoons [Mo_6S_8]^{4-} \quad (10)$$

A steric threshold appears for guest ion radii > 0.9 Å: $Cd_1Mo_6S_8$ can be obtained easily, while $Cd_2Mo_6S_8$ does not form, although the system is not saturated in electronic terms. Physical properties change significantly with stoichiometry as is shown, e.g., by the electronic transport characteristics of the lithium system:

Mo_6S_8	$Li_1Mo_6S_8$	$Li_3Mo_6S_8$	$Li_4Mo_6S_8$
metal	superconductor	metal	semiconductor

After a transfer of $4e^-$ the band is filled and the compound becomes a semiconductor.

In spite of this simple and consistent scheme, detailed investigations revealed that these transitions can be more complex. ^{7}Li-NMR studies have recently shown that in the lithium system $Li_xMo_6S_8$ at $x = 3$ partial charge transfer is observed, which has been explained by the formation of Li_3^{2+} guest ion clusters with one-electron three-center bonding; after a transfer of four electrons and transition to the semiconductor state, however, normal NMR shift values and quantitative charge transfer are found.[24]

6. Control of Isothermal Magnetic Phase Transitions: Critical Valence States

An interesting specific example of the modification of electronic properties of solids by electron/ion transfer reactions is the possibility of isothermal control of magnetic ordering states which has been observed recently for copper chromium chalcogen spinels $CuCr_2X_4$ (X = S, Se, Te).[25] The structure of these phases can be described schematically by a cubic close-packed anion lattice with Cr ions on octahedral lattice sites and Cu ions on tetrahedral sites. In terms of electron transport properties these phases are metals; the copper ions are mobile at ambient temperature. These spinels are able to intercalate additional copper ions according to equation (11). As shown in Figure 4, this reaction corresponds, e.g. for the selenide, to a one phase region with $x_{max} = 1$ (i.e. $Cu_2Cr_2Se_4$) and a contin-

ADVANCED MATERIALS

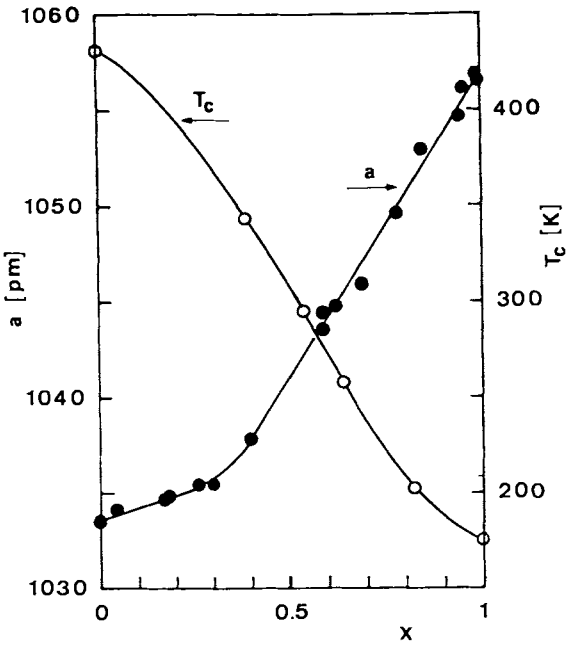

Fig. 4. $Cu_{1+x}Cr_2Se_4$: change of the cubic lattice parameter a (300 K) and Curie temperature T_c with the stoichiometry [25].

uous change in lattice parameters. $CuCr_2Se_4$ is a ferromagnetic metal at 300 K with a rather high Curie temperature T_C. Figure 4 shows the change in T_C with increasing copper content. Reaction (11) corresponds to the 300 K isotherm in Figure 4: it can be seen that at a critical value x_c an isothermal phase transition [equation (12)] from the spin-ordered magnetic state to the disordered system is observed. The reaction is reversible and represents the first example of the control of isothermal magnetic order-disorder transitions by chemical reactions at ambient temperature. In principle, this process can be used to design chemically operated magnetic switches or magnetic sensor systems indicating the redox state of a chemical reaction.

$$\underset{\substack{x=0\\ \text{ferromagnetic}\\ \text{metal}}}{CuCr_2Se_4} + x\,Cu^+ + x\,e^- \rightleftharpoons \underset{\substack{x=1\\ \text{paramagnetic}\\ \text{semiconductor}}}{Cu_{1+x}Cr_2Se_4} \qquad (11)$$

$$\text{ferromagnetic ordered state} \underset{x<x_c}{\overset{x>x_c}{\rightleftharpoons}} \text{paramagnetic state} \qquad (12)$$

In order to discuss the correlation between redox state, magnetic behavior and chemical bonding, we come back to equation (6) which concerns the reaction of the spinel $CuTi_2S_4$[7] that is obviously at variance with the chromium system. The titanium spinel can be oxidized to c-TiS_2, which is easy to understand in terms of the ionic formula [equation (13)].

$$Cu^+[Ti^{3+}Ti^{4+}(S^{2-})_4]^- \rightleftharpoons [(Ti^{4+})_2(S^{2-})_4] + Cu^+ + e^- \qquad (13)$$

Ti^{3+} is oxidized to Ti^{4+}. The formula is based on the well established fact that Cu ions in chalcogenides are invariably monovalent;[26] the metallic properties of $CuTi_2S_4$ are explained by cation mixed valence states with identical lattice positions. The equivalent reaction of the chromium spinels which should lead to cubic CrS_2 [equation (14)] is

$$Cu^+[Cr^{3+}Cr^{4+}(S^{2-})_4]^- \rightleftharpoons [(Cr^{4+})_2(S^{2-})_4] + Cu^+ + e^- \qquad (14)$$

not accessible, however. Instead, the chromium spinels may be reduced [equation (11)] with the uptake of one additional electron. Earlier polarized neutron diffraction studies[27] and recent XPS/UPS investigations[28] have now provided experimental evidence for the presence of holes in the anion p band of the copper chromium spinels $CuCr_2X_4$ and for the exclusive presence of chromium(III) in the reduced and oxidized state. The correct description of $CuCr_2Se_4$ by formal valence states is thus given by

$$Cu^+[(Cr^{3+})_2(Se^{2-})_3(Se^{\bullet-})]^-$$

This description explains the metallic properties of $CuCr_2Se_4$ by anion mixed valence. The ferromagnetic properties have been discussed in the original bonding model given above [equation (14)][29] in terms of super-exchange via excited anion states; however, this cannot easily explain the high Curie temperature. The revised model explains the strong spin coupling by super-exchange $Cr^{3+}/Se^{\bullet-}/Cr^{3+}$ via a high concentration of delocalized ground state anion holes in the valence band. The reaction mechanisms of the titanium and chromium spinels are thus quite different in terms of bonding changes. The oxidation of $CuTi_2S_4$ to c-TiS_2 is related to a conventional oxidation state change of the transition metal ions [equation (15)].

$$Ti^{3+}/Ti^{4+} \rightleftharpoons Ti^{4+}/Ti^{4+} + e^- \qquad (15)$$

The reduction of the chromium spinels is correlated with a new electron transfer mechanism via host lattice anion redox reactions equivalent to the annihilation and generation of anion p band holes:[30]

$$\underset{\text{anion mixed valence; ferromagnetic metal}}{Cu^+[(Cr^{3+})_2(X^{2-})_3(X^{\bullet-})_1]^-} \quad \begin{matrix}+x\,e^- + x\,Cu^+ \\ \text{hole generation process} \uparrow \\ \downarrow \text{hole annihilation process} \end{matrix} \quad \underset{\text{integral valence; paramagnetic semiconductor}}{(Cu^+)_2[(Cr^{3+})_2(X^{2-})_4]^{2-}}$$

The behavior of the chromium spinel phases has been rationalized recently in terms of a "critical valence state" (CVS) model.[28,30] The latter is defined for an internal redox couple M^{n+}/X^{m-} in a solid as the critical redox state, where the electron affinities E_A of the metal ion M^{n+} and the anion X^{m-} become equivalent

$$E_A(M^{n+}) \triangleq E_A(X^{m-})$$

The limiting states are given by equation (16); for low valent M^{n+} the left side is favored, with the upper band being

$$M^{n+}/X^{m-} \longleftrightarrow CVS \longleftrightarrow M^{(n-1)+}/X^{(m-1)-} \quad (16)$$

dominated by cation states, while the anion retains a closed valence shell. For high-valent M^{n+} the metal ion becomes reduced to a lower valency by electron transfer from X^{m-} (right side). The upper band is now dominated by anion states with p band holes. In chemical terms the anion loses its closed valence shell and becomes a "radical". As in molecular chemistry, where radical ions are known to tend to dimerize so as to for complete the valence shell, anion holes are frequently "dimerized" also in the solid state. Well-known examples are pyrites MS_2 with S_2^{2-} ions. In some cases, however, delocalized hole systems with metallic properties occur, e.g. $CuS=(Cu^+)_3(S_2^{2-})S^{\cdot-}$, where localized hole dimers S_2^{2-} coexist with delocalized $S^{\cdot-}$ in different lattice planes.

For the copper chromium chalcogen spinels the equilibrium is clearly above the critical valence state on the right side of equation (17). The fundamental difference in reac-

$$Cr^{4+}/X^{2-} \rightleftharpoons Cr^{3+}/X^{\cdot-} \quad (17)$$

tivity and reaction mechanism between the titanium spinel and the chromium spinels can thus be rationalized in terms of the model outlined above. An important aspect is that one can now make predictions of the reactivity of related phases.[30] To illustrate this we shall consider here only the case of a simple system. The pyrite FeS_2 is a semiconductor with a rock salt type lattice; Fe is located on the cation positions in a distorted octahedral environment, while the anisometric anions display statistical orientation so that the overall symmetry is cubic. In FeS_2 iron is above the critical valence state, i.e. $Fe^{2+}/S^{\cdot-}$. The anion holes are dimerized, resulting in $^{-}S-S^{-}$ units which explains the semiconducting properties. It should thus be possible to generate decocalized holes by electron/anion transfer, e.g. by intercalation of Li^+ ions according to equation (18) and to simultaneously achieve a semiconductor/metal transition.

$$Fe^{2+}S_2^{2-} + xLi^+ + xe^- \rightleftharpoons (Li^+)_x[Fe^{2+}(S_2^{2-})_{1-x}(S^{2-})_xS^{\cdot-}]^{x-} \quad (18)$$

7. Control of the Transition Temperature of Defect Perovskite Superconductors

The concept of controlling physical properties of materials by intercalation reactions led at a relatively early stage to studies on the modification of the critical temperature T_c of superconducting phases.[1,31-33] It has been possible to verify this concept with a variety of systems; examples that have been studied in more detail are layered transition metal dichalcogenides (e.g. NbS_2, TaS_2, $NbSe_2$) and molybdenum cluster chalcogenides Mo_6X_8 (X = S, Se). The results show that T_c can be either increased or decreased

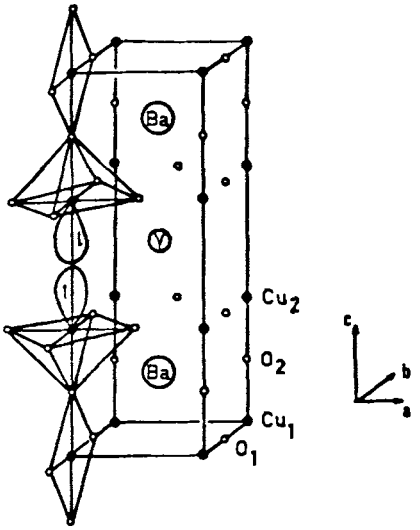

Fig. 5. Structure of the high temperature superconductor $YBa_2Cu_3O_7$ (schematic).

depending upon the band structure of the host lattice. The accessible temperature range extends from ca. 0.8 K to ca. 12 K. The recent rapid development in the area of high temperature superconductors[34] has provided a series of new materials, whose properties are of major interest also in terms of the aspects under discussion here. We shall take the quaternary copper oxide $YBa_2Cu_3O_7$ as an example for the consideration of chemical reactivity, stoichiometry, reaction mechanism, and corresponding changes in superconducting behavior.

$YBa_2Cu_3O_7$ has a defect perovskite type structure[35] (Fig. 5) with copper ions in tetragonal pyramidal (sheets in the *a*/*b* planes) and in square planar (chains in *b*/*c* planes) coordination. The simple ionic formula may be described by

$$Y^{3+}(Ba^{2+})_2(Cu^{2+})_2(Cu^{3+})_1O_7$$

Obviously a part of the copper ions is present in the unusual valence state Cu^{III}. Interatomic distances based on refined structural data suggest that Cu^{III} is primarily located in chain positions along the *b* axis, while Cu^{II} occupies positions in the *a*/*b* plane.

Investigations on the synthesis conditions revealed a significant influence of oxygen partial pressure and annealing temperature on the superconducting properties of $YBa_2Cu_3O_7$. Similar observations were made earlier on several ternary perovskite systems which show temperature and $p(O_2)$ dependent changes in oxygen stoichiometry correlated with high defect concentrations.[36] Detailed studies have shown that $YBa_2Cu_3O_7$ may react according to equation (19) with a rather broad nonstoichiometric range ($0 \leq x \leq 0.9$).[37-39] This reaction is clearly a topotactic process which is fully reversible in the range indicated. $YBa_2Cu_3O_7$ is a metal at ambient temperature, but transforms into an electronic/ionic conductor at a rather low

ADVANCED MATERIALS

temperature (ca. 300°C), where the oxygen ions become selectively mobile. Reaction (19) can similarly be performed in a galvanic cell; the oxygen intercalation and deintercalation thus correspond to an electron/anion transfer process [equation (20)]. The oxygen ions are selectively removed from the copper/oxygen chains in the basal planes of the unit cell.

$$YBa_2Cu_3O_7 \rightleftharpoons YBaCu_3O_{7-x} + x/2\,O_2 \quad (19)$$

$$YBa_2Cu_3O_7 + 2xe^- \rightleftharpoons YBa_2Cu_3O_{7-x} + xO^{2-} \quad (20)$$

The reaction discussed in equation (20) can be used to control the superconducting transition temperature of $YBa_2Cu_3O_{7-x}$ as is shown in Figure 6, which illustrates the

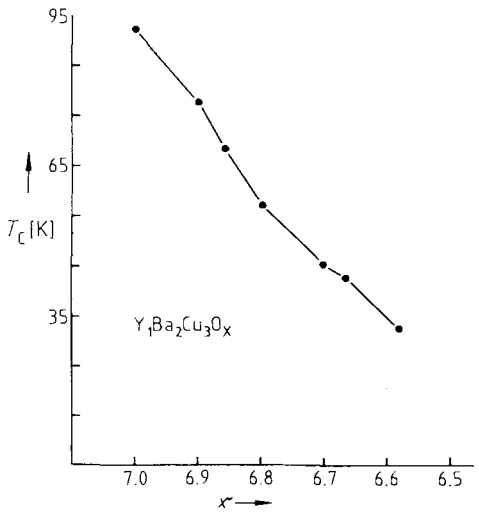

Fig. 6. Change of the superconducting transition temperature T_c of $YBa_2Cu_3O_x$ with the stoichiometry [39].

correlation between oxygen stoichiometry and T_c. By topotactic oxygen intercalation/deintercalation the transition temperature can be varied continuously between 93 K and 30 K. From $x=0$ to $x=0.5$ the lattice parameters a and b vary simultaneously with the oxygen loss such that a transition from orthorhombic to tetragonal is attained at $x=0.5$. This structural transformation is accompanied by an electronic metal/semiconductor transition: at $y=0.5$ the oxide displays semiconductor properties. In terms of chemical bonding this effect can be explained by the correlated valency changes [equation (21)]. For $x=0$ the metallic properties are related to the mixed valence system Cu^{2+}/Cu^{3+}, while at $x=0.5$ all Cu ions are bivalent, which results in semiconductor behavior.

$$\underset{\text{mixed valence metal superconductor (93 K)}}{Y^{3+}(Ba^{2+})_2(Cu^{2+})_2(Cu^{3+})O_7} \rightleftharpoons \underset{\text{integral valence semiconductor}}{Y^{3+}(Ba^{2+})_2(Cu^{2+})_3O_{6.5}} + 1/4\,O_2 \quad (21)$$

One most interesting aspect of the $YBa_2Cu_3O_{7-x}$ system is the observation that the oxygen anions become mobile at an exceptionally low temperature, which is quite unusual for a ceramic oxide with high lattice energy. In order to explain this behavior a model has been proposed recently that suggests a critical valence state situation:[30,38,39]

$$Cu^{3+}/O^{2-} \rightleftharpoons Cu^{2+}/O^{\bullet-} \quad (22)$$

i.e. the simultaneous presence of Cu^{3+} as well as $O^{\bullet-}$ (anion holes). This implies that the electron affinities of Cu^{3+} and O^{2-} are approximately equivalent; the upper band level must exhibit considerable anionic character. This model can explain the high oxygen mobility in terms of the lower activation energy of site change for a monovalent anion (Fig. 7), and the reduced effective size of $O^{\bullet-}$. As in the case of the chromium chalcogen spinels (see Section 6) the appearance of anion 2p band holes may result in strong super-exchange coupling between the Cu ions close to the Y planes inducing antiferromagnetic order (Fig. 5), which in turn would explain the absence of local magnetic moments in $YBa_2Cu_3O_7$.

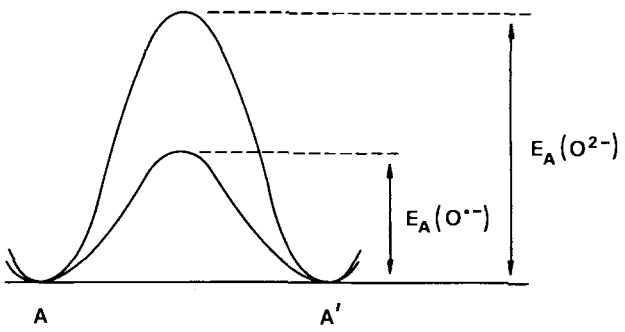

Fig. 7. Scheme of difference in activation energy E_A for site change between regular lattice sites A,A' for bivalent and monovalent oxygen anions.

With respect to the bonding situation, several other models have recently been proposed, some of them rejecting the presence of Cu^{III};[40-42] a decision in this controversial situation must await further experimental evidence.

8. Conclusions

The few examples presented in the foregoing focussed on the demonstration of the attractive potential for controlling major functional properties of solid materials by reversible chemical reactions at low temperature under isothermal conditions. One obviously critical point with respect to these systems is the level of understanding of the correlation between chemical reactivity, geometrical structure and chemical bonding, which in turn is a prerequisite for undertaking a systematic search for new systems. As

shown in the preceding sections, even seemingly simple reactions may turn out to be rather complex at various levels of description. At the same time there is an evident trend in advanced materials—when specific requirements have to be met—towards an increasing degree of complexity in terms of stoichiometry. An illustrative example is the development of superconductor materials, where high transition temperatures are one particular objective for application purposes. The first superconductors were elements with an upper T_c limit of ca. 10 K under normal pressure. The investigation of binary and ternary alloys increased T_c to as high as 23 K. Ternary compound superconductors attained ca. 40 K, and only polynary phases containing four or more different elements were found to yield transition temperatures above the boiling point of liquid nitrogen. Obviously a large number of different atomic species is required for optimal "tuning" of these phases with respect to the property desired.

It is hard to see at present how materials science, as defined in the introductory paragraph of this article, can keep pace with the progress made via the predominantly empirical traditional approach. It is apparent that both lines will coexist in the near future; what we can expect from modern materials science is the development of firm qualitative guide lines indicating more economic routes to the tailoring of solids with defined functional properties.

One additional note should be made concerning bonding concepts in inorganic solid state chemistry. In the last decade major trends in studies on metal/non-metal systems M_nX_m have been the concentration on compounds with high n/m ratio, i.e. cluster phases with metal-metal bonding, and on compounds with low n/m ratio exhibiting anion homonuclear bonding. The example of the critical valence state discussed above demonstrates that, also in the intermediate n/m range of "classical" compounds, interesting bonding situations may arise which may be correlated with specific solid state properties.

Received: August 8, 1988

[1] R. Schöllhorn, *Angew. Chem. 92* (1980) 1015; *Angew. Chem. Int. Ed. Engl. 19* (1980) 983.
[2] R. Schöllhorn in J. L. Atwood, J. E. D. Davies, D. D. MacNicol (Eds.): *Inclusion Compounds, Vol. I*, Academic Press, New York 1984, p. 249.
[3] R. Schöllhorn in M. S. Whittingham, A. J. Jacobson (Eds.): *Intercalation Chemistry*, Academic Press, New York 1982, p. 315.
[4] R. Schöllhorn, B. Otto, *J. Chem. Soc. Chem. Commun. 1987*, 1559; *1986*, 1222.
[5] R. Chevrel, M. Sergent, J. Prigent, *Mater. Res. Bull. 2* (1974) 1487.
[6] R. Schöllhorn, W. Schramm, D. Fenske, *Angew. Chem. 92* (1980) 477; *Angew. Chem. Int. Ed. Engl. 19* (1980) 492.
[7] R. Schöllhorn, A. Payer, *Angew. Chem. 97* (1985) 57; *Angew. Chem. Int. Ed. Engl. 24* (1985) 67.
[8] S. Sinha, D. W. Murphy, *Solid State Ionics 20* (1986) 81.
[9] R. Schöllhorn, U. Bethel, W. Paulus, *Rev. Chim. Miner. 21* (1984) 545.
[10] D. W. Murphy, C. Cros, F. J. Di Salvo, J. V. Waszak, *Inorg. Chem. 16* (1977) 3027.
[11] C. F. van Bruggen, R. J. Haange, G. A. Wiegers, D. K. G. de Boer, *Physica B99* (1980) 166.
[12] M. Potel, *Thesis*, Université de Rennes 1981; J. M. Tarascon, *Solid State Ionics 18/19* (1986) 802.
[13] M. S. Whittingham, A. J. Jacobson (Eds.): *Intercalation Chemistry*, Academic Press, New York 1982; D. W. Murphy, J. Broadhead, B. C. H. Steele (Eds.): *Materials for Advanced Batteries*, Plenum Press, New York 1980.
[14] B. J. Feldman, P. Burgmayer, R. W. Murray, *J. Am. Chem. Soc. 107* (1985) 872; B. Scrosati, P. Prosperi, S. Panero, M. Mastragostino, A. Corradini, *J. Power Sources 19* (1987) 27; E. M. Arnett, *Tetrahedron Lett. 29* (1988) 1507.
[15] B. Reichman, A. J. Bard, *J. Electrochem. Soc. 126* (1979) 2133; B. W. Fanghnan, R. S. Crandall in J. F. Pankove (Ed.): *Display Devices (Top. Appl. Phys. 40* (1980) 181); T. Kobayashi, H. Yoneyama, H. Tamura, *J. Electroanal. Chem. 177* (1984) 281.
[16] F. G. K. Baucke, *Schott Informationen 1* (1983) 11; F. G. K. Baucke, B. Metz, J. Zauner, *Phys. Unserer Zeit 18* (1987) 21.
[17] G. P. Kittlesen, H. S. White, M. S. Wrighton, *J. Am. Chem. Soc. 106* (1984) 7339; E. W. Paul, J. J. Ricco, M. S. Wrighton, *J. Phys. Chem. 89* (1985) 1441.
[18] H. Tributsch, *Solid State Ionics 9/10* (1983) 41.
[19] R. Schöllhorn in R. Setton (Ed.): *Chemical Reactions in Organic and Inorganic Constrained Systems*, Reidel, Dordrecht 1986, p. 323.
[20] C. Ritter, W. Müller-Warmuth, R. Schöllhorn, *J. Chem. Phys. 83* (1985) 6130.
[21] H. Bode, K. Dehmelt, J. Witte, *Z. Anorg. Allgem. Chem. 366* (1969) 1.
[22] R. Schöllhorn, K. Wagner, H. Jonke, *Angew. Chem. 93* (1981) 122; *Angew. Chem. Int. Ed. Engl. 20* (1981) 109.
[23] J. M. Tarascon, F. J. Di Salvo, D. W. Murphy, G. W. Hull, E. A. Rietman, J. V. Waszczak, *J. Solid State Chem. 54* (1985) 204; J. M. Tarascon, G. W. Hull, P. Marsch, L. Ter Haar, *J. Solid State Chem. 66* (1987) 204.
[24] E. Gocke, R. Schöllhorn, G. Aselmann, W. Müller-Warmuth, *Inorg. Chem. 26* (1987) 1805.
[25] R. Schöllhorn, A. Payer, *Angew. Chem. 89* (1986) 895; *Angew. Chem. Int. Ed. Engl. 25* (1986) 905.
[26] J. C. W. Folmer, F. Jellinek, *J. Less Common Met. 76* (1980) 153.
[27] O. Yamashita, Y. Yamaguchi, I. Nakatani, H. Watanabe, K. Matsumoto, *J. Phys. Soc. Jpn. 46* (1979) 1145.
[28] R. Schlögl, H. Eickenbusch, R. Schöllhorn, unpublished.
[29] F. K. Lotgering, R. P. van Stapele, *Solid State Commun. 5* (1967) 143; *J. Appl. Phys. 39* (1968) 417; J. B. Goodenough, *Solid State Commun. 5* (1967) 577.
[30] R. Schöllhorn, *Solid State Ionics*, in press.
[31] F. R. Gamble, T. H. Geballe in N. B. Hannay (Ed.): *Treatise on Solid State Chemistry, Vol. 3*, Plenum Press, New York 1976, p. 89.
[32] G. V. Subba Rao, M. W. Shafer in F. Lévy (Ed.): *Intercalated Layered Materials*, Reidel, Dordrecht 1979, p. 99.
[33] A. Lerf, F. Sernetz, W. Biberacher, R. Schöllhorn, *Mater. Res. Bull. 14* (1979) 797; R. Schöllhorn, M. Kümpers, A. Lerf, E. Umlauf, W. Schmidt, *ibid. 14* (1979) 1039.
[34] J. G. Bednorz, K. A. Müller, *Angew. Chem. 100* (1988) 757; *Angew. Chem. Int. Ed. Engl. 27* (1988) 728.
[35] R. J. Cava, B. Batlogg, R. B. van Dover, D. W. Murphy, S. A. Sunshine, T. Siegrist, J. P. Remeika, E. A. Rietman, S. Zahurak, G. P. Espinos, *Phys. Rev. Lett. 58* (1987) 1676.
[36] A. Reller, *Ber. Bunsenges. Phys. Chem. 90* (1986) 742.
[37] P. K. Gallagher, H. M. O'Bryan, S. A. Sunchine, D. W. Murphy, *Mater. Res. Bull. 22* (1987) 995.
[38] H. Eickenbusch, W. Paulus, R. Schöllhorn, R. Schlögl, *Mater. Res. Bull. 22* (1987) 1505.
[39] H. Eickenbusch, W. Paulus, E. Gocke, J. F. March, H. Koch, R. Schöllhorn, *Angew. Chem. 99* (1987) 1201; *Angew. Chem. Int. Ed. Engl. 26* (1987) 1188.
[40] C. N. R. Rao, P. Ganguly, J. Gopalakrishnan, D. D. Sarma, *Mater. Res. Bull. 22* (1987) 1159.
[41] B. K. Chakraverty, D. Feinberg, H. Zheng, M. Avignon, *Solid State Commun. 64* (1987) 1147.
[42] J. B. Goodenough, *Mater. Res. Bull. 23* (1988) 401.

Conference Reports

Better High-Tech Ceramics by Improved Processing

The 90th Annual Meeting of the American Ceramic Society from 2–6 May in Cincinnati was, with more than 4000 participants, once again the most exciting congress event of the year for the ceramic community. The general trend towards obtaining better high-tech ceramics by improved processing resulted in a noticeable emphasis on processing steps such as powder production methods, powder handling, and on forming and sintering. In this report some special aspects illustrating the general trends will be discussed.

Powder Synthesis

The sessions on powder synthesis showed the efforts being made to produce powders of higher purity and smaller, controlled particle size. *G. M. Crosbie* et al. (Ford Motor Company, Dearborn, Michigan) reported on the synthesis of Si_3N_4 powder of outstanding purity by the reaction of $SiCl_4$ with liquid NH_3 at 0°C. The intermediate reaction product was described as "$Si(NH)_2$" which reacted further to Si_3N_4 at elevated temperatures. An optimized method to obtain a homogeneous distribution of yttria in a Si_3N_4 powder matrix yielding homogeneous densification and microstructural development was described by *A. K. Garg* and *A. L. C. DeJonghe* (University of California, Berkeley). The beneficial effect of Y_2O_3 additions to Si_3N_4 itself is well known. The additive forms a liquid phase at temperatures between 1500 and 1800°C, which results in the benefits of fast densification and satisfactory microstructural development of Si_3N_4. In the work described, a better distribution of the additive was obtained when yttrium hydroxycarbonate was precipitated from a liquid suspension on to the Si_3N_4 matrix powder and transformed into Y_2O_3 during calcining. A number of speakers described other methods which are particularly suitable for the synthesis of highly pure, monosized submicron powders, namely sol-gel technique, hydrothermal synthesis and emulsion techniques. All of them expected an enhanced sinterability and improved mechanical and physical properties due to the high purity and narrow size distribution of powders produced by these methods.

An entire session was devoted to AlN, which has a considerable potential for technical applications where its outstandingly high thermal conductivity can be used. A new method of AlN powder production was proposed by *L. D. Silverman* (Engelhard Corporation, Edison, NJ). An Al_2O_3 sol is embedded in a polymer matrix and heated in nitrogen. During heating the pyrolysis of the polymer matrix provides free carbon, which reacts at still higher temperatures with Al_2O_3 in a carbothermic reaction. In the presence of nitrogen the reacting Al_2O_3 forms AlN.

Interesting possibilities for controlled texture formation in ceramics were reported, which also have implications with regard to the anisotropy of critical currents in the new ceramic superconductors. Precursor powders consisting of faceted cubic MgO particles were converted into textured MgO ceramics by cold pressing and sintering. The existence of texture was established by a new application of EPR spectroscopy showing that after sintering the MgO (111) cubic axes are preferentially oriented along the cold pressing direction. EPR spectroscopy seems to be an important new tool for studying texturing effects in a wide range of ceramics.

Nanocrystalline Ceramics

Nanocrystalline solid bulks of strongly covalent ceramics such as SiC, Si_3N_4 and BN were synthesized and consolidated by *G. D. Soraru* et al. (University of California, Los Angeles) by the pyrolysis of organometallic polymers. The initially amorphous powders transformed into the nanocrystalline solid bulks during tempering. No information was available at the conference on the properties of these nanocrystalline materials.

Forming

D. J. Rhee and *I. A. Aksay* (University of Washington, Seattle) presented an improved understanding of the debindering of injection molded ceramic parts, which is one of the potential future methods for producing high-tech ceramics with complex shapes. Debindering in ceramic–polymer composites not only determines the properties of the residual matrix, but also the required debindering time has a decisive influence on the economic viability of the method.

Sintering and Hot Isostatic Pressing

During the Annual Meeting the three day symposium "Sintering of Advanced Ceramics" effectively summarized the present knowledge in this field. A book containing the papers presented orally or as posters will be published

soon by the American Ceramic Society. The symposium was also intended to honor Professor *Robert L. Coble* (Massachusetts Institute of Technology), who has made outstanding contributions to the field of ceramic materials development (LUCALOX). In the mid-1970's, *R. L. Coble* had stimulated a series of questions about an ideal approach to powder processing, from which the proposal for optimized programs for sintering single phase ceramics evolved. *K. Bowen* (Massachusetts Institute of Technology) summarized some of the experimental results that were subsequently obtained and concluded that the sintering programs have been a necessary stage in structuring the problem of improving the sintering process. This improves the reliability of ceramics, which is essential for the broader application of structural ceramic components. *A. G. Evans* (University of California, Santa Barbara) explained how reliability enhancement may be achieved by combining control of defects with high toughness microstructures, a problem which includes topics such as defects caused by differential densification and grain growth in the presence of pores and second phases. In electronic ceramics the reliability of the products is considerably affected by impurities which influence processing and the final properties. *P. Morris* (Bellcore, Red Bank, NJ) pointed out that most of the present ceramic materials typically contain at least several thousand ppm of impurities, due to chemical inhomogeneities present in the powdered starting materials or introduced during processing.

Impurity and Additive Control

Unintentional impurities or intentional additives were shown to result in complex chemical reactions, often involving liquid phases, which frequently cause discontinuous grain growth (see Fig. 1). A quite surprising effect of the particle size distribution on liquid phase sintering of alumina was found in the case of three alumina powders with equivalent purity levels but varying particle size distributions, which were sintered using a calcium-magnesium-aluminum silicate glass additive. Although the samples sintered to essentially identical densities, radical differences in the fired microstructure were observed. Alumina powders having a bimodal particle size distribution were observed to have the most uniform fired microstructure. Questions regarding the role of a liquid phase (often a glass) in sintering of technologically important ceramics, and also on tungsten when cofired with ceramics in multilayer ceramic packages were generally thought to be of considerable practical importance. Controlled use of impurities and additives can improve the production of, for example, electronic ceramic-metal composites. Tungsten, for example, is commonly used to form conductors in ceramic multilayer packages. During cofiring in hydrogen, densification of the tungsten was shown to be promoted by a silicate liquid that forms either in the ceramic body (typically 90% alumina) or from glass forming components added to the tungsten screen printing paste. In lead perovskite systems a controlled small change in the cation stoichiometry can lead to a substantial reduction of the sintering temperature. This is thought to be due to the formation of a liquid phase during sintering, which would be detrimental to the electronic properties if allowed to remain in the material. However, as some components of the liquid phase have relatively high vapor pressures, the liquid phase can be removed by the evaporation process. Thus, a single perovskite phase is obtained by liquid phase sintering at low temperatures.

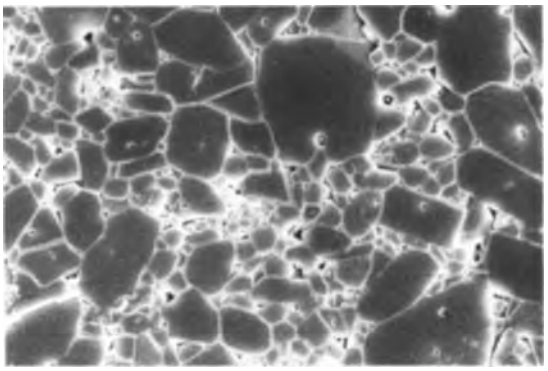

Fig. 1. Uncontrolled abnormal grain growth during sintering of MgO-doped alumina due to the presence of a small amount of liquid phase.

A considerable number of presentations dealt with sintering and hot isostatic pressing of nanoscale powders of Si_3N_4 and Si_3N_4/AlN, obtained by pyrolysis of organometallic precursors in ammonia, or described the effects of sintering aids on densification and microstructural development of SiC, Si_3N_4 and oxide ceramics. Major emphasis was put on the advantages of rare earth oxides which are increasingly used as sintering aids in high performance ceramics. The chemical stability of these oxides should theoretically result in very little oxidation reaction with the host material. In addition, the eutectic mixtures of rare earth oxides with silica have unusually high melting points, which provide a decreased tendency towards uncontrolled grain growth.

High Temperature Creep

Special sessions treated sintering and creep of two phase materials as a subject of growing importance with regard to understanding ceramic processing and improving the reliability of ceramic materials at elevated temperatures. Again, trace amounts of a second phase at grain boundaries were shown to have disastrous effects on component lifetime, since cavities that form during creep tend to propagate as cracks. The viscosity and Poisson's ratio of sintering glass/ceramic and metal pastes used in multilayer substrates can be used to predict stresses and strains produced by differential strain during sintering of composites. Meth-

ods of measuring and avoiding these strains were described by a number of authors, emphasizing the enormous amount of recent research activity in the USA in the field of ceramic composites.

The Long Road of Materials Research

A most illuminating example of the subtle and complex chemical and physical problems involved in research on existing and emerging advanced materials was presented by *M. P. Harmer* (Lehigh University, Bethlehem, PA) when he gave the keynote lecture on the perennial topic "Alumina". He commented: "Twenty-seven years have elapsed since *R. L. Coble* reported that small additions of magnesia promote the sintering of alumina to full density—the LUCALOX invention. A steady succession of papers have subsequently appeared concerning the role of the additive, and a considerable amount of controversy has surrounded this topic until today. After critically reviewing what progress has been made over that twenty-seven year period in understanding the role of MgO in the sintering of alumina, I have to conclude that, although we have come a long way in understanding the phenomenology of this classic additive effect, much still remains to be done to understand the detailed mechanisms involved at the atomic level".

Many of the talks at the 90th Annual Meeting of the American Ceramic Society suggested that *Harmer*'s statement is equally applicable to most of the other major topics of current research on the processing of advanced ceramics.

Wolfgang A. Kaysser
Max-Planck-Institut für Metallforschung
Pulvermetallurgisches Laboratorium, Stuttgart (FRG)

Advanced Concepts for Ceramic Toughening

A workshop on Advanced Concepts for Ceramic Toughening was held on 14–17 April 1988 at Schloss Weitenburg, FRG. The objective of the workshop was to clarify current understanding of toughening mechanisms in ceramics and to identify future patterns of work needed for the development of materials with the mechanical properties required for applications.

The meeting was divided into four sections concerned respectively with the theory of toughening mechanisms, with the role of interfaces in toughened microstructures, with the requirements of processing and with the transfer of these concepts into industrial practice. An additional discussion session was devoted to the significance of toughness for the acceptability of ceramics.

It was recognized that different sectors of the subject were at very different levels of development. Thus, work on transformation toughening had been brought to a level of maturity where significant issues remained but where the basic understanding was now sound. In contrast, work on fiber and whisker reinforcement was at a very preliminary level in terms of the understanding of the desired interface structure between the reinforcing phase and the matrix. There was in particular concern that high temperature events in toughened microstructures had received little attention and were not well understood.

Toughness and Microstructure

The majority of contributions in this session were concerned with transformation toughening and this subject was also emphasized in the discussion. The common opinion expressed in the summary was that the understanding of transformation toughening is already very high; we have a good understanding of the microstructural contributions (grain size, grain shape, glassy phase, inclusions, etc.) to the toughness. In general it is possible to tailor a microstructure towards a desired toughness.

In selecting particular items from the session, ceria-stabilized tetragonal zirconia (Ce-TZP) is seen as a new material in the group of transformation toughened zirconias. The strongly nonlinear crack diffraction curve will be a subject for many investigations in the future. The origin for the curve is the unusual transformation zone which reaches far ahead of the crack tip and whose shape and elongation are not yet understood. The crystallographic origin of this shape is probably the related transformation tensor, which is not known and which has to be investigated. The scatter of the mechanical properties, especially that of the K_{Ic} values, is dramatic and reaches from just 5 MPa m^{-1} to over 30 MPa m^{-1}. There is strong evidence for a microcrack mechanism in this material; however, the microscopic proof for this is still missing. For this material, the fracture mechanical description using only a K_{Ic} value is no longer valid and has to be replaced by a set of R-curves.

Interfaces

Compared to transformation toughening, the understanding of the role of interfaces is pretty weak. The audience agreed that experiments on the characterization of interfaces in model systems and, of course, in practical systems are missing. For most materials the fracture energies

for the interfaces are not known; thus the effect of inclusions on crack propagation cannot be predicted theoretically. In particular the characterization of interfaces at the high temperatures encountered in many applications has not been investigated and is surely a subject for the future.

Basically, a similar judgement can be made for reinforcement with ductile particles. It is already known that a certain degree of debonding at the interface between the ductile particles and the brittle matrix is wanted in order to allow an extended deformation of the particle. However, numbers such as the required percentage of debonded surface, the optimal inclusion size, the preferred level of ductility, etc. are not known and have to be measured in the future. For the technical application of ductile particle reinforcement, long term properties such as corrosion, wear, oxidation behavior, etc. have to be taken into account.

Acceptability of Ceramics

The measurements on fatigue, i.e. the degradation of strength under cyclic load, were the most exciting and impressive news in the discussion session. The fact that toughening and resistance to fatigue are contradictory targets has not been recognized until now; microstructural optimization and design have been directed only to the improvement of the K_{Ic} value. For the future, of course, microstructural design has to consider long term properties. The description of materials behavior in terms of fracture mechanics is losing its dominating importance, i.e., consideration of long crack behavior will be one part of the truth which must be supplemented by the mechanics of short cracks. Hence, fatigue, subcritical crack growth, and creep will recieve more attention.

Brittle materials have been described by one K_{Ic} value and non-linear materials by just one R curve. However, R curve measurements with different starting crack length have shown that the slope of the R curve depends on the length of the initial crack. A complete description of the materials properties thus requires the knowledge of a whole set of R curves. Materials designed with contact shielding (crack surface interactions behind the crack tip) will be very difficult to describe and many measurements must be done in the future.

Processing

The discussion of the processing session was relatively short. The wet chemistry processing routes for single phase powders are standard techniques now and will be optimized in the future. Whisker and fiber reinforced systems will require hot isostatic pressing or hot pressing for densification. However, when these materials are densified at a certain temperature they will not be able to carry load in this same temperature range (creep, oxidation etc.). Consequently, non-sintering processing routes are being developed such as gas phase infiltration, liquid phase infiltration, displacement reactions and melt-oxidation. Undoubtedly these preparation techniques will attract more attention in the future.

Applications

This session was planned to link the basic scientific aspects with industrial applications. It is obvious that there is a need in industry for more damage tolerant materials, and industry therefore welcomes the newly developed ceramics. But it has to be stated that toughness and high K_{Ic} values are not the only properties required of a material. The relationship between different properties, and the response of the behavior of a material to various microstructural modifications have to be studied. A conflicting relationship between toughness and fatigue is already visible. This is not an unusual situation in the development of materials: in metallic systems, an understanding of the properties-microstructure relationship has been a prerequisite in applying these materials safely in well designed constructions. In the future one has to study the effects of preparation conditions on the microstructures and the correlation between microstructures and properties, with toughness being one important parameter. These studies will be done in the area of basic science with feedback, however, from the applications side.

The meeting was encouraging in that it demonstrated the progress that could be made with a topic such as transformation toughening when the resources of the materials community were focussed on its solution. The meeting raised matters of real concern in respect to the possible fatigue penalty which could ensue from the use of toughening mechanisms, and in particular with respect to the absence of identified toughening mechanisms suitable for high temperature applications. The two topics were seen as a suitable basis for future research programs which could then be reported at a subsequent workshop.

H. Schubert and *R. Brook*
Max-Planck-Institut für Metallforschung
Pulvermetallurgisches Laboratorium, Stuttgart (FRG)

ADVANCED MATERIALS welcomes contributions from all over the world, from academia and from industry, from chemists, physicists and materials scientists, provided they are in keeping with the program outlined in the editorial published in May. Authors who are interested in writing short reviews (up to 15 pages of double-spaced manuscript together with an appropriate number of figures and/or formulas) should contact the editor. Please write to:
ADVANCED MATERIALS/ANGEWANDTE CHEMIE
Postfach 101161, D-6940 Weinheim, Federal Republic of Germany

ADVANCED MATERIALS

Polymer Crystals

Forty scientists from Europe, the United States and Japan were invited to Gargnano, Italy (Europhysics Conference on Advanced Topics in Polymer Science, June 19–24, 1988) to lecture on the progress achieved in topics concerning polymer morphology and kinetics in recent years. The opening session was overshadowed by the announcement of Dr. *David Sadler*'s death. Professor *Keller* (Bristol, UK) gave a memorial address, in which he paid tribute to Dr. *Sadler*'s work in many different fields of polymer science and biophysics.

Subsequently theoretical aspects of polymer crystallization were presented. These indicated the diversity of models still under discussion, ranging from tight folding (*J. D. Hoffman*, Midland, USA) via bundles (*G. Allegra*, Milan, Italy) to rough surface growth (*J. Point*, Mons, Belgium). The question of sharp folding and adjacent re-entry was also discussed, both theoretically (*E. Passaglia*, Gaithersburg, USA) and experimentally (*G. Wegner*, Mainz, FRG; *G. Ungar*, Zagreb, Yugoslavia) for *n*-alkanes. Although similar experimental techniques were used, the interpretations differed, suggesting regular fold surfaces and integer long spacings (*G. Ungar*) or, alternatively, a lack of sharp folds (*G. Wegner*).

Diversity was again demonstrated on the second day of the conference regarding the multitude of morphologies observed in polymers. A critical examination of the variety of growth habits exhibited by polymer crystals grown from dilute solution (*F. Khoury*, Gaithersburg, USA) and their crystal surface structure (*B. Lotz*, Strasbourg, France), as well as by those grown from the melt (*D. C. Bassett*, Reading, UK), provided a basis which should allow an evaluation of the different models proposed for crystal growth, as well as helping to correlate polymer morphology with mechanical properties. In this connection, two lectures presented evidence for the existence of a transition region between the crystalline and amorphous regions, both theoretically and on the basis of dielectric relaxation measurements (*D. Yoon*, San Jose, USA), as well as by thermal analysis (*B. Wunderlich*, Troy, USA).

In view of the complex morphologies observed in homopolymers, it was not surprising to find a large variety of differing observations for polymer blends in which at least one component is a crystallizable polymer. Depending on the compatibility of the components, the non-crystallizable component is generally rejected into the interlamellar regions, forming a homogeneous solution with that part of the crystallizable component which is not incorporated into the lamellae (*E. Martuscelli*, Naples, Italy), and thus strongly influencing the tensile and impact properties of the blend. Small angle X-ray and neutron scattering experiments indicated that there is a third phase near the crystal surface where crystalline order is dissipated (transition region), and from which the non-crystallizable component is excluded (*T. Russel*, San Jose, USA).

In the section on advances in experimental techniques, progress was reported particularly in vibrational spectroscopy, synchrotron radiation and high resolution electron microscopy. Synchrotron scattering was used as a technique for studying the early stages of crystallization (*A. Keller*) and crystallization kinetics (*H. Zachmann*, Hamburg, FRG). In contrast to the later stages in crystallization, where the crystal thickness is known to increase logarithmically with time, the initial process was shown to involve thickening in discrete steps (*A. Keller*). Direct imaging using high resolution electron microscopy was demonstrated to be a highly powerful technique for providing information at the molecular level in single crystals of poly(*p*-xylylene) (*E. Thomas*, Amherst, USA), in polymeric liquid crystals (*I. G. Voigt-Martin*, Mainz, FRG) and in polymeric whiskers (*H. Chanzy*, Saint Martin d'Heres, France). In all these cases a comparable stage of sophistication had been achieved with regard to information acquisition as well as image analysis. Various techniques were discussed for correctly taking account of the phases and amplitudes, thus avoiding misinterpretation of defect structures.

The final day of the conference was reserved for advances in processing and properties. This involved morphological engineering, particularly the creation of highly oriented, high modulus fibres (*A. Keller*), and processing techniques which have been developed to improve polymer properties (*J. M. Magill*, Pittsburg, USA).

From the lectures, as well as from the 42 posters that were also presented, it became clear that our understanding of polymer crystals has grown enormously in recent years.

I. G. Voigt-Martin
Universität Mainz (FRG)

As of January 1989, ADVANCED MATERIALS can be subscribed to separately at the annual rate of DM 178.00. Please order through your bookseller or write to VCH Verlagsgesellschaft mbH, Postfach 101161, D-6940 Weinheim, FRG. Customers in the UK and USA should write to VCH Publishers, Wellington Court, 8 Wellington Street, Cambridge CB1 1HW, UK and VCH Publishers, Suite 909, 220 East 23rd Street, New York, NY 10010-4606, USA, respectively.

Research News

NMR Imaging of Materials

In the past ten years NMR imaging has developed into a valuable diagnostic tool for clinical applications, because images of arbitrary cross-sections of living objects are obtained in a non-invasive fashion free of radiation hazards.[1] During the same period various efforts have been undertaken to apply NMR imaging to materials. However, for two reasons the results turned out to be of limited significance for practical applications: 1) The NMR signals of nuclei in solids are several orders of magnitude broader than those in liquids, which limits the achievable spatial resolution. Instead of a few Hertz linewidth encountered in medical applications, the resonances of solid materials are several Kilohertz wide. Because of the slow molecular mobility in solids, the anisotropy of the chemical shift and the dipole-dipole interactions of the nuclear spins are not averaged to their isotropic values as in liquids. 2) There seem to be few arguments against dissecting a dead object for analysis.

To circumvent the linewidth restriction, much attention focussed on the imaging of highly mobile species in solids, such as liquids diffused into solids, or on narrow solid-state resonances. Some representative applications are investigations of the pore size and binder distribution in green-state ceramics,[2] the distribution of liquids in polymers,[3] the oil and water contents of sand and rock,[4] and stress induced crystallization of polyisoprene rubber.[5]

To answer these questions, non-invasiveness is not a prerequisite, but for the investigation of properties dependent on the shape or function of the sample it is. Such properties are for instance nonequilibrium distributions of heat or strain, transport phenomena, and the progress and extent of chemical reactions. A few such questions have been addressed employing basically liquid state imaging techniques, for example the temperature distribution in a KBr sample,[6] the cross-linking of polyesters as a function of the flow rate of the resin, changes in viscosity, differential cross-linking before gelation, and catalyst concentration,[7] and the growth and mineralization of bones.[8]

In materials science, however, liquid-state NMR techniques are inadequate for handling the large linewidths, and special solid-state imaging techniques need to be developed. Recently two new significant approaches to solid-state imaging have been demonstrated, which rely upon line-narrowing techniques known in high resolution solid-state NMR spectroscopy.[9] 1) By homonuclear multi-pulse decoupling dipolar broadened lines can be narrowed up to a factor of 400.[10] An application of the technique is shown in Figure 1, which displays the images of a neoprene rubber annulus around a cylindrical tube of adamantane.[11] In Figure a) both, cylinder and annulus are seen. By exploiting differences of relaxation times of these two materials in the rotating frame, the rubber (b) and the adamantane (c) signals can be discriminated. The spatial resolution is about 0.25 mm. 2) Higher resolution, even in truly rigid samples, can be achieved by spinning the sample at the magic angle of 54.7° relative to the magnetic field with speeds of 3 kHz and more. If the magnetic field gradients needed for spatial resolution are rotated with the sample, basically all known imaging methods can be adapted.[12] The sample size, however, is restricted to cylinders smaller than about 12 mm in length and 6 mm in diameter. With such methods, the ultimate spatial resolution in solids is not so much restricted by the linewidth anymore, but rather by the number of nuclei producing the

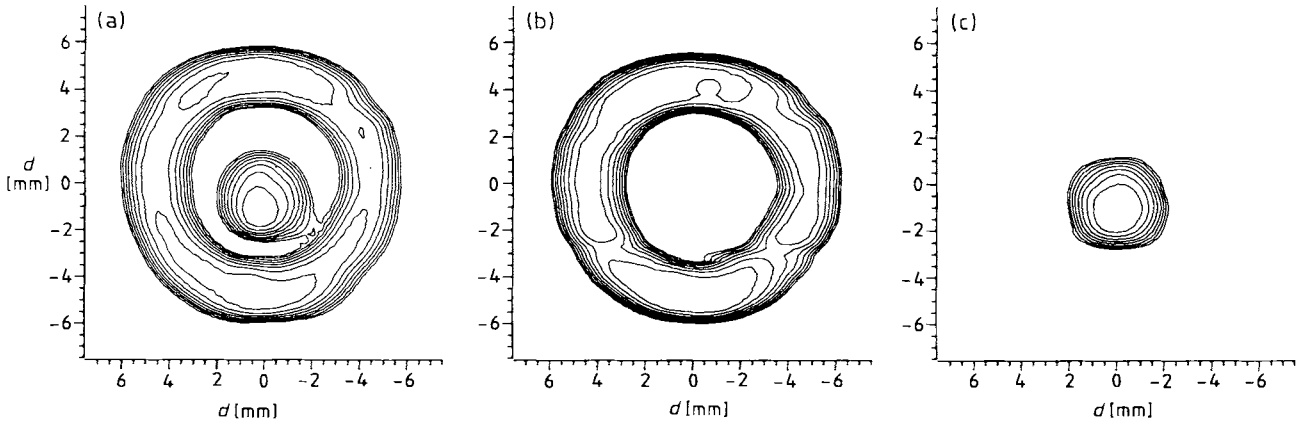

Fig. 1. Solid-state ^1H NMR image of an adamantane cylinder in a neoprene rubber annulus (a). The different molecular mobility in the two materials is exploited via the relaxation time in the rotating frame to discriminate the rubber signal (b) from the adamantane signal (c). (Adapted from ref. 11.)

signal. A practicable value is 100 μm. Thus microscopic resolution is not achievable, but other properties of solid materials varying on a macroscopic scale now seem to become amenable to investigation. Examples are the material's response to nonlinear mechanical wear, crazing, locally controlled polymerization, crystallization, and self-organization of molecular segments as well as strain, heat conductivity, convection and diffusion in composite materials.

Bernhard Blümich
Max-Planck-Institut für Polymerforschung
Mainz (FRG)

[1] F. W. Wehrli, D. Shaw, J. B. Kneeland (Eds.): *Biomedical Magnetic Resonance Imaging; Principles, Methodology and Applications*, VCH Publishers, New York 1988; P. Mansfield, P. G. Morris (Eds.): *Adv. Magn. Reson. Suppl. 2*, Academic Press, New York 1982; P. G. Morris: *Nuclear Magnetic Resonance Imaging in Medicine and Biology*, Clarendon Press, Oxford 1986; K. Roth: *NMR-Tomographie und -Spektroskopie in der Medizin*, Springer, Berlin 1984.
[2] W. A. Ellingson, J. L. Ackerman, L. Garrido, J. D. Weyand, R. A. diMilia, *Ceram. Eng. Sci. Proc. 8* (1987) 503; L. Garrido, J. L. Ackerman, W. A. Ellingson, J. D. Weyand, *Proc. Conf. Comp. Adv. Ceram.*, 18–20 January 1988, Cocoa Beach, FL, USA.
[3] W. P. Rothwell, D. R. Holecek, J. A. Kershaw, *J. Polym. Sci. Polym. Lett. Ed. 22* (1984) 241.
[4] S. Blackband, P. Mansfield, J. R. Barnes, A. D. H. Clague, S. A. Rice, *SPE Form. Eval. 1* (1986) 31; L. D. Hall, V. Rajanayagam, C. Hall, *J. Magn. Reson. 68* (1986) 185.
[5] J. L. Ackermann, application note, Doty Scientific Instruments, Inc., Columbia, SC, USA, 1988.
[6] B. H. Suits, D. White, *J. Appl. Phys. 60* (1986) 3772.
[7] P. O. Frickland, *Int. SAMPE Tech. Conf. 18* (1986) 876.
[8] J. L. Ackerman, D. P. Raleigh, R. G. Griffin, M. J. Glimcher, *Soc. Magn. Reson. Med., 6th Annu. Meet.*, New York 1987.
[9] U. Haeberlen: *Adv. Magn. Reson. Suppl. 1*, Academic Press, New York 1976; M. Mehring: *Principles of High Resolution NMR in Solids*, Springer, Berlin 1983; B. C. Gerstein, C. Dybowski, *Transient Techniques in NMR of Solids*, Academic Press, New York 1985.
[10] P. Mansfield, P. K. Grannell, *Phys. Rev. 12* (1975) 3618.
[11] J. B. Miller, A. N. Garroway in D. O. Thompson, D. E. Chimenti (Eds.): *Review of Progress in Quantitative Nondestructive Evaluation*, Plenum Press, New York 1988, p. 287.
[12] R. A. Wind, C. S. Yannoni, US-Pat. 4301410 (17 November 1981), IBM; D. G. Cory, J. W. M. van Os, W. S. Veeman, *J. Magn. Reson. 76* (1988) 543; D. G. Cory, A. M. Reichwein, J. W. M. van Os, W. S. Veeman, *Chem. Phys. Lett. 143* (1988) 467; S. Matsui, K. Sekihara, H. Shiono, H. Kohno, *J. Magn. Reson. 77* (1988) 182.

Book Reviews

Corrosion of Materials

DECHEMA Corrosion Handbook: Corrosive Agents and their Interaction with Materials, Volume 1. Edited by *D. Behrens*. VCH, Weinheim 1987, 333 pp., bound, DM 775.00.—ISBN 3-527-26652-6

Materials scientists have developed a huge number of technically important materials based on metals, inorganic and organic compounds and composites, suitable for applications which are sometimes very specific. One criterium for choosing a material for a given technical use is its corrosion behavior. However, the prediction of corrosion properties is a rather difficult task due to the complex nature of corrosion processes, involving in a typical case a metallic substrate, a corrosive medium, the hydrodynamic properties of the medium, and the geometric properties of the construction itself. Therefore, a *Corrosion Handbook* collecting together the vast literature and knowledge in this area is highly welcome.

The DECHEMA Corrosion Handbook—a series of at least twelve volumes is planned—is a completely new English edition of the DECHEMA-Werkstoff-Tabelle. The chapters are arranged according to the aggressive media, but instead of being arranged alphabetically these are treated in an apparently random order. Each chapter, which reviews the data concerning one medium, is divided into metallic materials, non-metallic inorganic materials, organic materials and materials with special properties. In this first volume metallic materials predominate. At the beginning of each chapter all materials are classified in a table according to their corrosion properties in the given medium; following this table a detailed description of their corrosion behavior is given. Owing to the very different technical applications for the different materials in the given medium, the ratings in the table may be misleading, if the detailed description is not taken into account. For example, in the chapter "Chlorine" the material gold is classified from resistant to unsuitable due to the fact that on the one hand the contact resistance of Au contacts is high in chlorine atmospheres, whereas on the other hand Au has only limited resistance to high temperature corrosion. In the same table high alloy cast iron is classified as fairly resistant, yet in the detailed description it is stated that not much literature is available about the corrosion of this material in chlorine atmospheres, and therefore the rating is based only on very specific applications.

It is therefore essential for the user of this handbook to read and understand the detailed description and not to rely on the ratings in the well presented tables by themselves. In order to understand the data presented in the different chapters, the reader needs to have a sound background in corrosion science, as the handbook offers only very limited background information concerning the basic mechanisms of corrosion processes. As some interested users might not have this background in electrochemistry or physical chemistry of solids, the reviewer would have liked the first chapter "General remarks and instructions for use" to contain much more information than the one page can offer to the reader. In this chapter only corrosion rates are classified, by which the different materials are evaluated. There is a lengthy explanation of how to convert

rates given in g/m^2d into mm/y (with some mistakes: the symbols < and > are mixed up, the comparison of light and heavy metals is wrong), yet no information is provided concerning the different types of corrosion (general corrosion, and localized corrosion such as pitting corrosion, grain-boundary attack, crevice corrosion etc.), nor on standards used in corrosion (ASTM, DIN), typical corrosion tests, etc. Nothing is said in this chapter concerning the basic mechanisms of corrosion, e.g. the extent to which metallic corrosion is governed by anodic and cathodic reactions and the resulting electrode potentials, how the corrosion rate is calculated using polarization curves, and how corrosion can be accelerated or retarded by an external polarization or by galvanic elements (see e.g. cathodic protection potential). This is important, since in later chapters numerous electrochemical data are presented and—to give only one example—many different reference systems are used for the potential scale (potentials quoted without any reference!, potentials vs. NHE, vs. SHE, vs. H, vs. SCE etc.), which might be quite confusing for some readers. In order to avoid dangerous mistakes, it would be very helpful if this handbook had contained a chapter in which the user could find this basic information which is necessary to understand the different figures and tables. At least some textbooks or standards on corrosion should be cited, so as to provide the missing background. The same comment applies to high temperature corrosion. In later chapters different time laws are mentioned (e.g. the parabolic law), which are sometimes explained and sometimes not, and again this will provide information only to those readers who have a thorough knowledge of the corrosion field.

The next two short chapters are concerned with acetates and aluminum chloride as corrosive media. The introduction to the chapter dealing with acetates is rather long, and contains information concerning the chemistry and preparation of acetates which belongs more appropriately to a chemistry textbook. The rest of both chapters is clearly written and easy to understand, but does not contain as many diagrams as the longer chapters which follow.

The fourth chapter discusses the corrosion behavior of different materials in contact with chlorine and chlorinated water. In general, this chapter is a well written and adequately illustrated summary, including both the wet corrosion of materials in chlorine-containing electrolytes and in chlorine atmospheres, and high temperature corrosion in different chlorine-containing gases. The information is illustrated by numerous figures and tables. Considering the very different corrosion conditions (wet corrosion, atmospheric corrosion, high temperature corrosion), the distinction between these conditions could be more clear. Again, this chapter is presumably addressed to corrosion scientists with a sound background of knowledge in the field; other readers will find that the diagrams and tables are not easy to understand. Some topics in this chapter are discussed in detail (e.g. the high temperature corrosion of Ni), but there are some mistakes and ambiguous diagrams. Some examples: in Table 1 rate constants are given in cm^2/h (?); Figure 4 shows rate constants for the chlorination of Ag in mol/cm s; page 40 cites 50 K instead of 50 bar; in Table 11 the duration of the experiment is given without any unit (s?, h?) and a "theoretical rate" is mentioned, which seems to be an experimental one; in Table 21 the activity of O_2 is given in the wrong order, and Figure 52 shows a potential axis in V without mentioning any reference electrode. In the part of this chapter devoted to Ti the importance of the passivity of Ti to its corrosion resistance in Cl_2-containing media is emphasized, but the electrochemical basis of the effect of alloying Pd to Ti (acceleration of the cathodic reaction and therefore passivation) is not very clearly explained. This is one example, representative of many other instances in this handbook, of a situation where a large number of empirical facts regarding the corrosion of materials would be made much easier to understand if they were also discussed from a fundamental standpoint.

Whereas the chapter "Chlorine" is mainly concerned with high temperature and atmospheric corrosion, the fifth chapter "Fluorides" deals predominantly with the corrosion behavior in wet media and melts. The introduction is well written, short and precise. In general the same is true for the rest of this chapter, the text again being illustrated by a number of diagrams. Two reservations should be mentioned: the reference electrode for the potentials which are quoted is indicated by three different subscripts: V_H, V_{SHE}, and V_{NHE} (all three meaning the same), whereas V_{SCE} refers to a different standard. A number of the figures (e.g. 12, 20, 28) show a potential axis in "Volt" without mentioning any reference. Since there is no uniform reference system in this first volume of the Corrosion Handbook, these figures are useless, as the reader does not know to which reference the potentials refer. The second reservation refers to some statements such as "the corrosion of steel is reduced by the exclusion of oxygen" (page 114), or "the corrosion is promoted by oxygen" (page 124), which are trivial if one considers the O_2-reduction as the cathodic part of the corrosion process.

The sixth chapter deals with the corrosion properties of materials in KOH. Like the others, this chapter contains much valuable information with many illustrations. The reservations are the same as the ones mentioned above: potentials are frequently given without any reference (Figs. 1, 2, 4, 13, 22, 26, 38), and some electrochemical information is not very precise (distinction between increasing voltage and increasing anodic polarization?, page 165; negative protection potential $= -1$ V vs. which reference?, page 168). The part dealing with iron contains only a little information about the stress corrosion cracking of this material in KOH electrolytes and on the range of potentials in which the material is susceptible to this localized attack.

The last two chapters deal with steam and sulfonic acid as aggressive media. In general, both chapters are well written. The chapter "Steam" in particular contains a good introduction, and the detailed description of the corrosion behavior of the different materials is clearly arranged. The part dealing with iron discusses high temperature oxidation in depth, and contains a description of the parabolic rate law, which is missing from the chapter "Chlorine", where also parabolic rate constants are discussed. It would be much better to summarize this fundamental theory in an introductory chapter than to distribute the information over the different chapters of the handbook.

Altogether the DECHEMA Corrosion Handbook is a very valuable reference book for all engineers working in the area of corrosion, provided that the reader has a thorough knowledge of this area and is thus able to critically evaluate the information in the figures, tables and text of individual chapters. The organization of the Handbook is clear, and it is rather easy for the user to find the desired information. In addition to this, the large number of literature references cited in the Handbook (about 400 for most chapters, citations up to 1980) offers even more information to users who have to solve special corrosion problems.

Martin Stratmann
Max-Planck-Institut für Eisenforschung
Düsseldorf (FRG)

Miscellanea

Photophysics of Polymers. Edited by *Charles E. Hoyle* and *John M. Torkelson*. American Chemical Society, Washington, D.C., USA 1987. 531 pp., $ 119.95.—ISBN 0-8412-1439-5

This clearly structured and nicely presented book stems from a symposium of the Division of Polymer Chemistry of the American Chemical Society which took place in Anaheim, CA, in September 1986. The book is designed to provide scientists engaged in basic and applied polymer research with a comprehensible text on polymer photophysics. The philosophy of the book is that photophysical phenomena allow one to gain an accurate picture of the properties of polymers, both in solution and in solid phases. Based on the historical development as well as on current practice, the book is divided into six main sections: 1) Overviews, 2) Polymer Dynamics and Complexation, 3) Excimer Photophysics, 4) Energy Migration, 5) Luminescent Polymerization Probes, 6) Photophysics of Silicon-Based Polymers.

On the whole, the book is a timely and most welcome addition to the literature in a field which has recently seen a strong increase of interest. In fact several works on related subjects have been published over the last few years: the monographs by *J. Guillet:* "Polymer Photophysics and Photochemistry; an Introduction to the Study of Photoprocesses in Macromolecules" (Cambridge Univ. Press, 1985) and *J. F. Rabek:* "Mechanisms of Photophysical Processes and Photochemical Reactions in Polymers; Theory and Applications" (Wiley, New York 1987) as well as the multi-author volumes: "Polymer Photophysics, Luminescence, Energy Migration and Molecular Motion in Synthetic Polymers" (edited by *D. Phillips*, Chapman and Hall, London 1985), "Photophysical and Photochemical Tools in Polymer Science: Conformation, Dynamics, Morphology" (edited by *M. A. Winnik*, NATO ASI-Series C, Vol. 182, D. Reidel, Dordrecht, Netherlands 1986) and "New Trends in the Photochemistry of Polymers" (edited by *N. S. Allen* and *J. F. Rabek*, Elsevier, London 1986). In my opinion the new book edited by *Hoyle* and *Torkelson* is extremely valuable, since it stands at the forefront of this dynamic field which offers many possibilities for future developments. The presentation is—unusually for a multi-author book!—balanced; most of the active research groups in the field are well represented. Of course, one cannot expect a book with some eighty contributors to present a unified viewpoint; however, one gets a good snapshot of the situation. Furthermore, even the camera-ready printing does not impair the presentation too much.

The individual contributions stress the application of photophysical methods to polymers, and it is indeed gratifying for a physicist to see such devoted use of physical methods in chemistry research. While most groups have realized the importance of time-resolved measurements (the contributions by the groups of *M. D. Fayer, H. F. Kauffmann* and *S. E. Webber* highlight this trend), an intimate connection between theory and experiment is—in general—still lacking. Several contributors have, in my opinion, not always been cautious in interpreting their data, and one sometimes gets the feeling that the method is over emphasized; in many cases I would welcome a comparison of photophysical results with data obtained by other physicochemical methods.

In summary, the editors have achieved their goal of providing a picture of the state-of-the-art situation in the photophysics of polymers. I view the book as a valuable addition to the library of scientists actively involved in polymer research.

Alexander Blumen
Experimentalphysik IV
Universität Bayreuth (FRG)

Physics at Surfaces. By *A. Zangwill.* Cambridge University Press, Cambridge 1988. xiii, 454 pp., hardcover £ 40.00.—ISBN 0-521-32147-6

Physics at Surfaces is an excellent introductory book for students or other researchers interested in surface processes. It is certainly the best source of general information about the concepts and techniques of surface physics/chemistry, painting a broad-brush picture of the current state of the field and covering a broad range of topics. Characteristics of both metal and semiconductor surfaces, clean and adsorbate-covered are described. Topics such as the thermodynamics and electronic structure of surfaces, and adsorption/desorption phenomena are discussed. Several emerging, albeit not understood areas, such as metal organic chemical vapor deposition (MOCVD) and energy transfer at or near surfaces are also introduced.

There is rather comprehensive coverage of the myriad of techniques used in surface science so that the reader is exposed to the spectroscopic methods currently available and their typical applications. Necessarily, the discussion of the large number of topics is somewhat superficial. A student who would actually use one or more methods would most certainly need to read more broadly. While the bibliography serves as a good starting point for more in-depth reading, it is not comprehensive because of the large number of topics discussed in the book. Only selected examples are referenced on a given topic, e.g. the study of activated adsorption using molecular beam techniques. Therefore, if the reader or instructor of a course wishes to go beyond the text, an independent review of the literature will be necessary in many cases.

The text is also a useful overview of the developments in the field of surface chemistry for experienced researchers in surface physics and related fields. Results of experiments performed over the past two decades are synthesized into a general framework. The overview serves as a conceptual basis for the vast research encompassed in the area of surface physics and induces one to cast current work within this framework.

Overall, *Physics at Surfaces* is an excellent introduction to the emerging and developing field of surface science from which both students and experienced researchers will benefit.

Cynthia M. Friend
Department of Chemistry
Harvard University (USA)

Metallic Superlattices—Artificially Structured Materials. Edited by *T. Shinjo* and *T. Takada*. Elsevier, Amsterdam 1987. xii, 271 pp., bound, DFl 240.00.—ISBN 0-444-42863-1

Advances in ultrahigh-vacuum deposition techniques have made possible the sequential monolayer-by-monolayer deposition of artificially layered materials including semiconductors, metals, etc. This volume 49 of the series "Studies in Physics and Theoretical Chemistry" is a collection of review papers on artificially layered metal structures presented by several principal investigators. The majority of the authors (five out of eight) are university professors in Japan, so that the book has a somewhat eastern asian flavor, although the research activities in this field are equally spread all over the industrialized world. However, with the recent rapid growth of activity on artificially layered materials and the concomitant dramatic increase in the number of published papers, finding a book that can serve as a comprehensible text for an introductory course is particularly important. This book addresses that purpose very well, and it is to be highly recommended for that use, as well as to the individual reader seeking an introduction to one of the special topics discussed in five of the chapters.

The book consists of seven chapters: 1. Overview of metallic superlattices (*T. Shinjo*), 2. X-ray diffraction studies on metallic superlattices (*Y. Fujii*), 3. Neutron diffraction studies on metallic superlattices (*Y. Endoh, C. F. Majkrzak*), 4. Mössbauer spectroscopic studies on superlattices (*T. Shinjo*), 5. NMR studies on superlattices (*H. Yasuoka*), 6. Superconductivity in superlattices (*V. Matijasevic, M. R. Beasley*), 7. Theories on metallic superlattices (*K. Terakura*). Much credit must be given to the editors for providing an extensive list of element combinations used in layered metallic structures and a comprehensive bibliography in the appendix.

In the areas covered this fine book is close to being a state-of-the art summary of current research.

Klaus Ploog
Max-Planck-Institut für Festkörperforschung
Stuttgart (FRG)

High-Resolution Solid-State NMR of Silicates and Zeolites. By *G. Engelhardt* and *D. Michel*. John Wiley & Sons, Chichester 1987. xiv, 485 pp., hardcover £ 55.00.—ISBN 0-471-91597-1

For many years solid-state NMR spectroscopy was regarded merely as a tool for specialists in the shadow of the more important magnetic resonance applications to the liquid state. This changed after novel sophisticated high-resolution techniques such as magic angle spinning (MAS) and multi-pulse experiments were developed for solid materials. Nowadays multinuclear high-resolution solid-state NMR spectroscopy is attracting increasing interest in chemistry, materials science and many other domains. The new book by *G. Engelhardt* and *D. Michel* gives a survey of one of the most important applications, i.e. that to silicates, aluminosilicates, zeolites and silicate sorbents. It is an excellent introduction to high-resolution solid-state NMR spectroscopy in general, and gives an overview of current research activities in silicate and zeolite science in particular.

The text is organized in seven chapters beginning with a short introduction to the historical background. Chapter 2 treats the basic principles of high-resolution NMR of solids. The nuclear spin interactions affecting the spectral features are described in the irreducible tensor notation, and the most important experimental techniques (MAS, cross-polarization, dipolar decoupling, multi-pulse methods) are briefly discussed. The peculiarity of adsorbed molecules is emphasized. Since detailed information about the structure of species containing silicon has been obtained from studies of the liquid state, the third chapter of the book is completely devoted to ^{29}Si NMR of silicate solutions.

The next two chapters deal with general aspects and applications of ^{29}Si and ^{27}Al NMR studies of silicates, aluminosilicates and zeolites. Experimental methods, general features of the spectra, spectral parameters and correlations with structure are discussed in Chapter 4, whereas Chapter 5 summarizes the large amount of data that have already been accumulated from studies on natural and synthetic silicate and aluminosilicate materials and zeolites. In addition to crystalline materials and especially zeolites, other materials included are glasses, layer silicates, silica polymorphs and tectoaluminosilicates.

Chapter 6 focusses on NMR studies of nuclei other than ^{29}Si and ^{27}Al in zeolites and non-zeolitic silicates. The topics covered are ^{11}B NMR studies of borosilicates and borozeolites, ^{17}O resonances of framework oxygen, NMR of charge-compensating cations, and ^{13}C and ^{1}H studies of zeolites. The final chapter is devoted to high-resolution NMR of adsorbed molecules. Adsorption on zeolites, silica surfaces, silicates and aluminosilicates, and diamagnetic and paramagnetic adsorption sites are considered. Most work discussed in this chapter deals with ^{1}H, ^{13}C, ^{15}N, and ^{129}Xe resonances.

The book as a whole is well organized and gives useful information for anyone who is interested in the wide range of applications to silicates, zeolites, and all kinds of adsorbed systems. But it is equally important for NMR spectroscopists who are already engaged in studying crystals and glasses and plan to extend their activity to new techniques and materials. Particular emphasis is given to all types of chemical information obtainable from the spectra, but the treatment is by no means confined to a purely descriptive presentation. A real advantage of this monograph is that it is readily comprehensible to chemists, while at the same time including the necessary physical background. Zeolite and silicate scientists will appreciate the wealth of literature references given in connection with the various NMR applications. Without hesitation this book may be recommended as an excellent approach to high-resolution solid-state NMR spectroscopy. It should not be considered as an alternative to *Colin Fyfe*'s "Solid-State NMR for Chemists", but as a useful supplement with emphasis on inorganic silicates and a more physico-chemical style of description.

Werner Müller-Warmuth
Institut für Physikalische Chemie
der Universität Münster (FRG)

Inorganic Thermochromism. By *K. Sone* and *Y. Fukuda*. Springer, Berlin 1987. xi, 134 pp., bound, DM 168.00.—ISBN 3-540-17662-4

The color change of chemical species with temperature is a widespread phenomenon and can be traced back to a variety of causes. The book of *Sone* and *Fukuda* concentrates mainly on the thermochromism of transition metal complexes in solution which results from changes in the crystal field. The introductory chapter defines the subject and gives some instructive examples, including the red to violet to green color change of Cr^{3+} doped α-Al_2O_3 with increasing temperature. Chapter B considers chromotropic phenomena, mainly of cobalt(II)chloro complexes, which result from the tetrahedral–octahedral interconversion and from ligand exchange reactions in various protic and aprotic solvents (including an analysis of inert salt effects). The color shift from the blue tetrahedral $CoCl_4^{2-}$ to the pink octahedral $Co(OH_2)_6^{2+}$ complex is a well known example of this category.

Chapter C concentrates on nickel(II) chelates in solution. An analysis of the spectral changes which accompany the conversion of paramagnetic octahedral, square pyramidal and tetrahedral to diamagnetic square-planar complexes is given. Interconversions of this type which depend on the donor properties of the solvent are extensively discussed. Geometrical changes of this kind may also occur within monomer-polymer equilibria. Finally isomerization reactions (nitro–nitrito) are mentioned. The next chapter is devoted to the thermochromism of copper(II) complexes. They are geometrically extremely variable as a consequence of the Jahn-Teller effect of the d^9 configurated central ion, and change their coordination sphere rather continuously from elongated octahedral or square pyramidal to square-planar—in line with corresponding color shifts.

Chapter E comprises miscellaneous chromotropic phenomena of other transition metal complexes in solution. Thermochromism may be observed, for example, in octahedral Fe^{II} or Fe^{III} complexes if the ligand strength is very near to the critical value of the ligand field parameter, which determines the transition from the high-spin to the low-spin configuration. Equally interesting is the color change which accompanies the addition of a second axial ligand to square-pyramidal $[O{V^{IV}}(acac)_2]$ complexes. The last chapter outlines the thermochromism of transition metal complexes in the solid state. After considering irreversible reactions caused by thermal dehydration, desammination and isomerization, a few examples of reversible thermochromism are presented. In particular, the compressed tetrahedral–square-planar interconversion of $Cu^{II}L_4$ complexes, which often occurs continuously with temperature, is discussed and compared with the discontinuous (but also reversible) change from a tetrahedral to an octahedral coordination in the case of Ni^{II} complexes. Finally, the fluorescence thermochromism of certain copper^{I} complexes is mentioned, and a short section describes the application of thermochromic compounds as color indicators for temperature changes.

The book under review is the first attempt to give a rather thorough description of the exciting world of thermochromism and related chromotropic phenomena in inorganic chemistry. It is easy and enjoyable to read, and will certainly be extremely informative for scientists and graduate students who are involved in the spectroscopy of transition metal complexes and compounds in solution or in the solid state. Because the authors have themselves been engated for many years in the solution chemistry of transition metal complexes, the main emphasis is laid upon this subject; the equally fascinating thermochromism of solid compounds is unfortunately not very extensively treated. Although the authors state in the preface that this was not their intention, the book would have fulfilled its purpose even more effectively if there had been a higher degree of sophistication in the discussion of the physical basis of the thermochromic properties, and an even stronger emphasis on the correlation of these properties with the electronic structures of the transition metal ions involved. However, this is a book with many merits, which can be warmly recommended to all chemists who are interested in and fascinated by color phenomena in inorganic chemistry.

Dirk Reinen
Fachbereich Chemie
der Universität Marburg (FRG)

Conference Calendar

November 1988

8-10 **European MRS**
Fall Conference
Strasbourg (France)
Contact: P. Siffert, Centre de Recherches Nucléaires, Lab. "PHASE", 23, Rue du Loess, F-67037 Strasbourg (France)

9-11 **Perspectives on the New Superconductivity**
Boston (USA)
Contact: D. Berger, Nature Publ. Co., 65 Bleecker St., New York, NY 10012, USA

10-11 **Microstructural and Microanalytic Characterization of Ceramic Materials**
Bad Nauheim (Fed. Rep. Germany)
Contact: Dtsch. Gesellsch. für Metallkunde eV., Adenauerallee 21, D-6370 Oberursel, FRG

13-15 **High T_c-Superconductors**
Monterey (USA)
Contact: C. M. Davidson, Gorham Adv. Mater. Inst., P.O. Box 250, Gorham, ME 04038, USA

15-17 **Advanced Polymer Composites for Structural Applications,**
SPE Conf.
Los Angeles (USA)
Contact: G. Yule, RTP Co., 650 Tamarack, Suite 1002, La Brea, CA 92621, USA

15-17 **Sensors and Measurement Techniques for Aeronautical Applications**
Williamsburg (USA)
Contact: Air Force Wright Aeronautical Lab., Wright-Patterson Air Force Base, OH 45433, USA

15-17 **Membrane Technology**
Int. Conf.
Sydney (Australia)
Contact: T. Fane, School of Chemical Eng., Univ. of NSW, P.O. Box 1, Kensington 2033, Australia

15-18 **Quantitative Surface Analysis,**
5th Int. Conf.
London (United Kingdom)
Contact: G. C. Smith, Division of Materials Applications, National Physical Lab., Teddington, Middlesex TW 11 OLW, UK

17-18 **Projection Plasma Spraying**
Paris (France)
Contact: IITT-International, 40 promenade Marx Dormoy, F-93460 Gournay-Sur-Marne, France

19-23 **Multiphase Macromolecular Systems,**
14th Biennial Polymer Symp.
San Diego (USA)
Contact: B. Culbertson, Ashland Chemical Co., P.O. Box 2219, Columbus, OH 43216, USA

21-23 **Hydrogenated Amorphous Silicon Derices and Technology**
Yorktown Heights (USA)
Contact: J. Kanicki, IBM T.J. Watson Research Ctr., P.O. Box 218, Yorktown Heights, NY 10598, USA

24-25 **Intermetallic Phases**
Bad Nauheim (Fed. Rep. Germany)
Contact: Dtsch. Gesellsch. für Metallkunde eV., Adenauerallee 21, D-6370 Oberursel, FRG

27-30 **Ceramic Materials and Components for Engines,**
3rd Int. Symp.
Las Vegas (USA)
Contact: American Ceramic Soc., 757 Brooksedge Plaza Dr., Westerville, OH 43081-6136, USA

28-3 **Chemical Perspectives of Microelectronic Materials,**
MRS Fall Meeting
Boston (USA)
Contact: Materials Research Soc., 9800 McKnight Rd., Suite 327, Pittsburgh, PA 15237, USA

30 **Diffractions from Polymers**
London (United Kingdom)
Contact: Dr. M. Richardson, National Physical Lab., Teddington, Middlesex TW 11 OLW, UK

30-1 **Plastics on the Road '88,**
Biennial Int. Conf.
London (United Kingdom)
Contact: Miss D. Varley, Plastics and Rubber Inst., 11 Hobart Place, London SW1W OHL, UK

December 1988

1-4 **Water Soluble Polymers,**
Fuzhou Int. Symp.
Fuzhou (People's Rep. China)
Contact: Hu Bing-huan, Inst. of Polym. Sci., Fujian Teachers Univ., People's Rep. of China

2 **Computer Modelling of Inorganic Solid Structures**
London (United Kingdom)
Contact: Dr. A. E. Comyns, R & D Dept., Laporte Industries Ltd., Moorfield Rd., Widnes WA8 OQJ, UK

5-9 **Lasers and Applications,**
11th Int. Conf.
Lake Tahoe (USA)
Contact: Prof. H. J. Eichler, Techn. Univ. Berlin, Optisches Inst., Straße des 17. Juni 135, D-1000 Berlin 12, FRG

7 **Polymers for Life Science Applications**
London (United Kingdom)
Contact: Dr. M. D. Purbrick, Kodak. Ltd. Research Div., Headstone Drive, Harrow, Middlesex HA1 ATY, UK

7-8 **Materials Science and Eng. Towards the 21st Century,**
4th Israel Mater. Eng. Conf.
Beer-Sheva (Israel)
Contact: Peltours-Conventions, The Secretariat, 4th Israel Mater. Eng. Conf., P.O. Box 394, 61003 Tel-Aviv, Israel

7-9 **Ceramics for Environmental Protection,**
1st Int. Symp.
(ENVICERAM '88)

Köln (Fed. Rep. Germany)
Contact: G. von Landsberg, Deutscher Wirtschaftsdienst, Marienburger Straße 22, D-5000 Köln 51, FRG

12–17 **Advances in Holography and Speckle Phenomenon and their Industrial Applications,**
Int. Workshop
Madras (India)
Contact: Prof. R. S. Sirohi, Indian Inst. of Technol., Physics Dept., Madras 600036, India

14–16 **SIMCER 7/ZIRCONIA 88**
7th Int. Symp. on Ceramics
Bologna (Italy)
Contact: Centro Ceramico, Via Martelli, 26, I-43138 Bologna, Italy

January 1989

15–20 **Optics, Electro-Optics, and Laser Applications in Sci. and Eng.,**
Symp. and Exhibition
Los Angeles (USA)
Contact: Soc. of Photo-Optical Instrumentation Eng. (SPIE), P.O. Box 10, Bellingham, WA 98227, USA

31–3 **Polymer,**
17th Australian Symp.
Brisbane (Australien)
Contact: Dr. D. J. T. Hill, Chem. Dept., Univ. of Queensland, Brisbane 4067, Australia

31–3 **Sintering of Multiphase Metal and Ceramic Systems**
Int. Conf.
New Delhi (India)
Contact: G. S. Upadhyaya, Convener ICSMC '89, Dept. of Metallurgical Eng., Indian Inst. of Technol., Kanpur 208 016, India

February 1989

5–9 **Biomedical Polymers,**
Int. Symp.
Perth (Australia)
Contact: Secretary, W. A. Polymer Group, Royal Australian Chemical Inst., 125 Hay St., Perth, W. A. 6000, Australia

6–10 **Composites,**
SPI Inst. Annu. Conf.
Dallas (USA)
Contact: Composites Inst., SPI, 355 Lexington Ave., New York, NY 10017, USA

6–10 **Optical Fiber Communication,**
IEEE-LEOS-OSA Conf.
(OFC '89 and IGWO '89)
Houston (USA)
Contact: Optical Soc. of America (OSA), 1816 Jefferson Pl., NW Washington, DC 20036, USA

7–9 **Physics and Chemistry of Semiconductor Interfaces (PCSI-6)**
Bozeman (USA)
Contact: G. J. Lapeyre, Physics Dept., Montana State Univ., Bozeman, MT 59717, USA

21–26 **Optical Fibers and their Applications,**
5th Symp.
Warsaw (Poland)
Contact: R. S. Romaniuk, IPI Warsaw Univ. of Technol., Nowowiepska 15–19, PL-00-665, Warsaw, Poland

27–3 **High-Temperature Superconducting Oxides: Processing & Related Properties,**
TMS Annu. Meeting
Las Vegas (USA)
Contact: M. Karl, The Metallurgical Soc., 420 Commonwealth Drive, Warrendale, PA 15086, USA

March 1989

1–3 **Technical Ceramics,**
2nd Int. Congr. and Exhibition (Techkeram 2)
Wiesbaden (Fed. Rep. of Germany)
Contact: Demat Exposition Managing, P.O. Box 110611, D-6000 Frankfurt, FRG

2–4 **Makromolekulares Kolloquium**
Freiburg (Fed. Rep. Germany)
Contact: Prof. H. Finkelmann, Inst. für Makromol. Chemie der Univ., Stefan-Meier-Str. 31, D-7800 Freiburg, FRG

5–10 **Liquid Crystals,**
6th Eur. Winter Conf.
Schladming (Austria)
Contact: P. Laggner, Inst. für Röntgenfeinstrukturforschung of the Austrian Academy of Sci., Steyrergasse 17, A-8010 Graz, Austria

6–8 **Lithium Battery Technology & Applications,**
4th Int. Seminar
Deerfield Beach (USA)
Contact: S. P. Wolsky, Ansum Enterprises Inc., 950 De Soto Rd., Suite 3B, Boca Raton, FL 33432, USA

6–9 **Condensed Matter Division**
9th Gen. Conf.
Nice (France)
Contact: Dr. F. Raymond CNRS-Bât. 3, Rue Albert Einstein, F-06560 Valbonne, France

6–9 **Advanced Materials**
MRS Industry-Univ. Conf.
Denver (USA)
Contact: Dr. Fred Smith, Adv. Mater. Inst., Colorado School of Mines, 1500 Illinois, Golden, CO 80401, USA

8–9 **Molecular Chemistry of Solid-State Electronics**
London (United Kingdom)
Contact: The Royal Society, 6 Carlton House Terrace, London SW 1Y 5AG, UK

11–14 **Surface Finishing '89**
Brighton (United Kingdom)
Contact: Inst. of Metal Finishing, Exeter House, 48 Holloway Head, Birmingham B1 1NQ, UK

20–22 **Refractory Metals and Silicides**
Eur. Workshop
Houthalen (Belgium)
Contact: R. De Keersmaecker, IMBE, Kapeldreef 75, B-3030 Leuven, Belgium

20–23 **Surface Science,**
Interdisciplinary Conf.
Liverpool (United Kingdom)
Contact: P. Weightman, Liverpool Univ., Oliver Lodge Lab., Oxford St., P.O. Box 147, Liverpool L69 3BX, UK

28–31 **Aluminum-Lithium**
5th Int. Conf.
Williamsburg (USA)
Contact: Al-Li-V, School of Eng. and Applied Sci., Thornton Hall, Univ. of Virginia,

Charlottesville, VA 22901, USA

29-31 **Neutron and X-Ray Scattering: Complementary Techniques**
Canterbury (United Kingdom)
Contact: Dr. R. J. Newport, Univ. of Kent, Physics Dept., Canterbury, Kent CT2 7NR, UK

30-31 **Colorado Microelectronics**
Colorado Springs (USA)
Contact: CMC '89 Conf. Secretary, Microelectronics Research Lab., Univ. of Colorado, Colorado Springs, CO 80933-7150, USA

30-10 **Frontiers of Laser Spectroscopy of Gases,**
NATO Adv. Study Inst.
Vimelro (Portugal)
Contact: J. M. Hollas, Dept. of Chemistry, Univ. of Reading, Reading RG6 2AD, UK

30-14 **High-T_c Superconductors,**
Exp. Workshop
Miramare (Italy)
Contact: Int. Ctr. for Theoretical Physics, P.O. Box 586, I-34100 Trieste, Italy

April 1989

3-5 **Modern Practice in Stress and Vibration Analysis**
Liverpool (United Kingdom)
Contact: Meetings Officer, Inst. of Physics, 47 Belgrave Square, London SW1X 8QX, UK

3-6 **Low Energy Ion Beams,**
5th Conf.
Guildford (United Kingdom)
Contact: Meeting Office, Inst. of Physics, 47 Belgrave Sq., London SWIX 8QX, UK

3-7 **Copolymerization and Copolymers in Dispersed Media**
Lyon (France)
Contact: I. Guillot/C. Pichot, Lab. des Materiaux Organiques, BP 24, F-69390 Vernaison, France

6-7 **Modeling in Crystal Growth from the Melt,**
NATO Workshop
Parma (Italy)
Contact: G. Müller, Inst. für Werkstoffwissenschaften 6, Martensstraße 7, D-8520 Erlangen, FRG

10-12 **Bayreuther Polymer Symp.,** (BPS '89)
Bayreuth (Fed. Rep. Germany)
Contact: BPS '89, Lehrstuhl Makromolekulare Chemie II, Univ. Bayreuth, Postfach 101251, D-8580 Bayreuth, FRG

11-13 **Catalysis by Well Characterized Materials**
Liverpool (United Kingdom)
Contact: Prof. R. W. Joyner, Leverhulme Ctr. for Innovative Catalysts, Univ. of Liverpool, Grove St., P.O. Box 147, Liverpool L69 3BX, UK

17-26 **Ceramics and Composite Materials,**
Spring College in Mater. Sci.
Trieste (Italy)
Contact: Int. Ctr. for Theoretical Physics, Spring College in Mater. Sci. 1989, P.O. Box 586, I-34100 Trieste, Italy

18-19 **Industrial Water-Soluble and Water-Swellable Polymers**
Manchester (United Kingdom)
Contact: The Registar (Mid-Career Training), UMIST, P.O. Box 88, Manchester M60 1QD, UK

23-28 **Nondestructive Testing,**
12th World Conf. (WCNDT '89)
Amsterdam (Netherlands)
Contact: B. de Jong, RAI Organisatie Bureau Amsterdam bv, Europaplein 12, 1078 GZ Amsterdam, Netherlands

24-28 **Lasers and Electro-Optics,**
LEOS-IEEE-OSA Conf. (CLEO '89)
Baltimore (USA)
Contact: Optical Soc. of America (OSA), 1816 Jefferson Pl., NW Washington, DC 20036, USA

24-28 **MRS-Spring Mtg.**
San Diego (USA)
Contact: J. B. Ballance, MRS, 9800 McKnight Rd., Suite 327, Pittsburgh, PA 15237, USA

25-27 **Hot Isostatic Pressing of Materials**
Antwerpen (Belgium)
Contact: Hot Isostatic Pressing Conf., c/o K. VIV, Jan van Rijswijcklaan 58, B-2018 Antwerpen, Belgium

26-28 **Joining Ceramics, Glass and Metal**
3rd Int. Conf. (CGM '89)
Contact: Dtsch. Gesellsch. für Metallkunde eV., Adenauerallee 21, D-6370 Oberursel, FRG

May 1989

4-6 **Festkörper: Dynamik und Kinetik**
Siegen (Fed. Rep. Germany)
Annu. Mtg. Dtsch. Bunsen-Gesellsch. für Phys. Chem.
Contact: Dtsch. Bunsen-Gesellsch., Carl-Bosch-Haus, Varrentrappstr. 40/42, D-6000 Frankfurt am Main 90, FRG

9-11 **Coatings and Sensors for Acoustic and Electromagnetic-Optical Applications**
Univ. Park. (USA)
Contact: V. K. Varadan, Dept. of Eng. Sci. and Mechanics, Penn. State Univ., 227 Hammond Bldg., Univ. Park, PA 16802, USA

16-19 **Deutsche Gesellsch. für Metallkunde, Annual Meeting**
Karlsruhe (Fed. Rep. Germany)
Contact: Dtsch. Gesellsch. für Metallkunde, e.V., Adenauerallee 21, D-6370 Oberursel, FRG

22-24 **Glastechnische Tagung**
Stuttgart (Fed. Rep. Germany)
Contact: Dtsch. Glastechnische Gesellsch. eV., Mendelssohnstr. 75-77, D-6000 Frankfurt am Main, FRG

22-25 **Graphite Intercalation Compounds,**
5th Int. Symp. (ISGIC-5)
Berlin
Contact: Dr. F. W. Froben, Fachbereich Physik, Freie Univ. Berlin, Arnimallee 14, D-1000 Berlin 33, FRG

29-2 **Molecular Beams**
Perugia (Italy)
Contact: V. Aquilanti, Univ. di Perugia, Dipt. di Chimica, I-06100 Perugia, Italy

31-2 **Applied Surface Analysis,**
11th Symp.
Cleveland (USA)
Contact: J. Grant, Research Inst., 300 College Park, Dayton, OH 45469-0001, USA

June 1989

18-21 **Colloid & Surface Science,**
63rd ACS Div. of Colloid & Surface Chem. Symp.
Seattle (USA)
Contact: J. Berg, Dept. of Chemical Eng. BF-10, Univ. of Washington, Seattle, WA 98105, USA

26-28 **Molecular Design of Functional Polymers,**
IUPAC Int. Symp.
Seoul (Korea)
Contact: IUPAC Int. Symp., c/o Polymer Soc. of Korea, Rm 601, Hyecheon Bldg., 831 Yeoksam-dong, Kangnam-ku, Seoul 135-792, Korea

27-28 **Polymer Latex III**
London (United Kingdom)
Contact: Miss M. Peacock, Plastics and Rubber Inst., 11 Hobart Place, London SW1W OHL, UK

July 1989

3-6 **Conduction and Breakdown in Solid Dielectries**
3rd Int. Conf. (ICSD '89)
Trondheim (Norway)
Contact: Prof. Sletbak, ICSD '89, The Norwegian Inst. of Technol., Sem Sælands V 13, N-7034 Trondheim, Norway

4-7 **Nonlinear and Electro-optics**
Int. Conf.
Cambridge (United Kingdom)
Contact: The Meeting Officer, The Inst. of Physics, 47 Belgrave Square, London SW1X 8QX, UK

10-12 **Applied Organometallic Chemistry: an Entry to the New Technology**
The Pines Resort (Australia)
Contact: Dr. A. F. Masters, School of Chemistry, Univ. of Sydney, Sydney, N. S. W. 2006, Australia

10-13 **Magnetic Resonance in Polymers,**
9th Spec. Colloq. Ámpere
Prague (Czechoslovakia)
Contact: P. M. M. Secretariat, c/o. Inst. of Macromol. Chem., Czech. Acad. of Sci., 16206 Prague, Czechoslovakia

11-14 **Numerical Analysis of Semiconductor Devices and Integrated Circuits,**
6th Int. Conf.
Dublin (Ireland)
Contact: J. J. H. Miller, Nase-Code Conf., INCA, P.O. Box 2, Dún Laoghaire, Ireland

18-20 **Polymer Chemistry: Aspects of Radical Polymerization**
Lancaster (United Kingdom)
Contact: Dr. J. R. Ebdon, Dept. of Chemistry, Univ. of Lancaster, Lancaster LA1 4YA, UK

24-26 **Composite Structures,**
5th Int. Conf.
Paisley (United Kingdom)
Contact: Dr. I. H. Marshall, Dept. of Mechanical and Production Eng., Paisley College of Technol., High St., Paisley PA 12BE, UK

31-2 **Biologically-Engineered Polymers**
Cambridge (United Kingdom)
Contact: Royal Soc. of Chemistry, Burlington House, London W1V OBN, UK

August 1989

2-7 **Pure and Applied Chemistry,**
32nd IUPAC Congress
Stockholm (Sweden)
Contact: Stockholm Convention Bureau, P.O. Box 6911, S-10239 Stockholm, Sweden

20-24 **Imaging Systems - 150 Years of Photography,**
Int. Symp. (ISIS '89)
Dresden (German Dem. Rep.)
Contact: Conf. Secretary, ISIS '89, Technische Univ. Dresden, Sektion Physik, Wissenschaftsbereich Photophysik, Mommsenstr. 13, DDR-8027 Dresden, GDR

28-31 **Dynamical Processes in Excited States of Solids,**
7th Int. Conf. (DPC '89)
Athens (USA)
Contact: DPC '89, Prof. J. E. Rives, Dept. of Physics and Astronomy, Univ. of Georgia, Athens, GA 30602, USA

28-1 **Ferroelectricity,**
7th Int. Mtg. (IMF-7)
Saarbrücken (Fed. Rep. Germany)
Contact: Dr. J. Albers, Univ. des Saarlandes, Fachbereich Physik, D-6600 Saarbrücken, FRG

28-1 **Sintering,**
7th World Round Table Conf.
Herceg-Novi (Yugoslavia)
Contact: Dr. D. P. Uskoković, Serbian Academy of Sci. and Arts, Knez-Mihailova 35, 11000 Beograd, Yugoslavia

28-1 **X-Ray Optics and Microanalysis,**
12th Int. Congr.
Cracow (Poland)
Contact: S. Jasienska, Academy of Mining and Metallurgy, Inst. of Metallurgy, 30-059 Cracow, Poland

28-2 **Photochemistry for High Technology,**
Int. Summer School
Leuna-Merseburg (German Dem. Rep.)
Contact: Prof. H.-J. Timpe, Sektion Chemie, Technische Hochschule für Chemie, Leuna-Merseburg, Gensaerstr., DDR-42 Merseburg, GDR

September 1989

4-8 **Macromolecules 89,**
Oxford (United Kingdom)
Contact: Prof. R. Epton, School of Appl. Sciences, The Polytechnic, Wulfruna St., Wolverhampton WV1 1SB, UK

5-8 **Optical, Electrical and Acoustic Properties**
Kent (United Kingdom)
Contact: M. D. Shuttleworth, Plastics and Rubber Inst., 11 Hobart Pl., London SW1W OHL, UK

11-13 **Charge Transfer in Polymeric Systems,**
RSC, Faraday Div.
Contact: Dr. J. F. Gibson, Royal Soc. of Chemistry, Burlington House, Piccadilly, London W1V OBN, UK

13-15 **Microscopy,**
150th Anniversary Commemorative Mtg.
Oxford (United Kingdom)
Contact: Microscopical Soc., 37-38 St. Clements, Oxford OX4 1AJ, UK

20-22 **Structural Adhesives in Engineering**
SAE II '89
Bristol (United Kingdom)
Contact: J. Herriot, SAE II '89, Butterworth Scientific Ltd., PO Box 63, Westbury House, Bury St., Guildford, Surrey GU2 5BH, UK

21-22 **Fire Retardant Polymers**
Torino (Italy)
Contact: Prof. L. Costa, Dipt. di Chim. dell'Università di Torino, Via P. Giuria, 7, 10125 Torino, Italy

27-29 **New Polymers**
1st Materials Symp.
Regensburg (Fed. Rep. Germany)
Contact: OTTI-Fortbildung, Martin-Luther-Straße 10, D-8400 Regensburg, FRG

October 1989

11-13 **Werkstoffe für die Elektrochemie**
Stuttgart (Fed. Rep. Germany)
Contact: Prof. F. von Sturm, Jahnstr. 26, D-8901 Biberbach, FRG

11-13 **Surface Technology Forum**
SURTEC '89
Berlin
Contact: AMK Berlin, M 3/Surtec, Messedamm 22, D-1000 Berlin 19, FRG

16-19 **High-Tech-Coating,**
Congr. and Exhibition
Wiesbaden (Fed. Rep. Germany)
Contact: Demat Exposition Managing, P.O. Box 110611, D-6000 Frankfurt, FRG

November 1989

5-8 **Solid State Ionics,**
7th Int. Conf.
Hakone (Japan)
Contact: Dr. Y. Saito, Res. Lab. of Engineering Materials, Tokyo Inst. of Technol., 4259 Nagatsuta-cho, Midori-ku, Yokohama 227, Japan

23-24 **Eucomat '89**
Eur. Conf. on Materials
Aachen (Fed. Rep. Germany)
Contact: Dtsch. Gesellsch. für Metallkunde eV., Adenauerallee 21, D-6370 Oberursel, FRG

December 1989

12-15 **Pacific Polymer**
Hawaii (USA)
Contact: J. C. Vogl, Pacific Polym. Federation, Polytechnic Univ., 333 Jay St., Brooklyn, NY 11201, USA

ADVANCED MATERIALS

is a successful new special section of ANGEWANDTE CHEMIE. In order to strengthen it further, we offer the position of an

Associate Editor

You have an advanced degree in materials science, chemistry or physics and, perhaps, some editing experience; English is your mother tongue. You feel challenged by using the full range of your knowledge for aquiring articles, writing short news items and carefully editing texts on the varied aspects of materials research and engineering. You like to talk to scientists and you are comfortable working with tight schedules.

VCH is a major international scientific publisher with subsidiaries in Basel (Switzerland), Cambridge (United Kingdom), and New York (USA). The editorial office of ADVANCED MATERIALS/ANGEWANDTE CHEMIE is in Weinheim, a pleasant small town near Heidelberg in the southwest of Germany. A competitive salary and excellent benefits are guaranteed.

Please apply in writing and send full career details to:

VCH Verlagsgesellschaft, Personalabteilung, Postfach 101161, D-6940 Weinheim (West Germany)

ANGEWANDTE CHEMIE
International Edition in English
Volume 27 · Number 11
November 1988
Pages 1417–1592

Synthesis of the Heaviest Chemical Elements—Results and Perspectives**

By Günter Herrmann*

Dedicated to Professor Christoph Schmelzer on the occasion of his 80th birthday

All 17 artificially produced elements heavier than uranium were discovered by nuclear-chemical synthesis. The three heaviest ones—elements 107, 108 and 109—were synthesized at the heavy-ion accelerator UNILAC in Darmstadt by nuclear fusion from the heaviest stable nuclei, lead-208 and bismuth-209, and the most neutron-rich stable isotopes of chromium and iron: element 107 from bismuth-209 (atomic number $Z=83$) and chromium-54 ($Z=24$), element 108 from lead-208 ($Z=82$) and iron-58 ($Z=26$), and element 109 from bismuth-209 and iron-58. The first isotopes detected were those with mass numbers 262 ($Z=107$), 265 ($Z=108$) and 266 ($Z=109$); these nuclei are short-lived α-emitters with half-lives of 8.2 ms, 1.8 ms and 3.4 ms, respectively. The yields of these reactions are extremely small; only three atoms of element 109 have ever been observed. Experiments to synthesize element 110 have given ambiguous results. All attempts to detect the "superheavy" elements with proton numbers near $Z=114$ and neutron numbers near $N=184$ have thus far failed. These elements have been predicted theoretically, and many attempts to synthesize them have been made, e.g. at UNILAC by fusion of calcium-48 ($Z=20$) with curium-248 ($Z=96$), or by transference of protons in the collision of two very heavy nuclei such as uranium-238 ($Z=92$). Surprisingly, the heaviest known nuclei are far more stable toward spontaneous fission into two fragments than was expected, but their synthesis is strongly hindered—much more than was initially anticipated. It is this hindrance rather than the decreasing nuclear stability which seems to presently limit the extent of the periodic table: even heavier elements should be able to exist, but no way has yet been found to produce them.

1. Some Historical Remarks

Some fifty years ago the newly introduced methods of nuclear chemical-element synthesis opened up, for the first time, a way to produce new elements beyond the heaviest then known, uranium (atomic number $Z=92$). *Fermi* and his co-workers transformed numerous elements into radioactive isotopes by adding a neutron. Via subsequent β-decay—emission of an electron from the nucleus—these isotopes transform into elements with the next higher atomic number. In the case of uranium, for example, one expected the formation of element 93, i.e. capture of a neutron by uranium-238, and β-decay of the newly formed uranium-239, as follows:

$$^{238}_{92}U + {}^{1}_{0}n \longrightarrow {}^{239}_{92}U \xrightarrow{\beta^-} {}^{239}93$$

[*] Prof. Dr. G. Herrmann
Institut für Kernchemie der Universität,
Fritz-Strassmann-Weg 2, D-6500 Mainz, and
Gesellschaft für Schwerionenforschung,
Planckstr. 1, D-6100 Darmstadt (FRG)

[**] After a paper presented at the 20th Biannual GdCh Meeting in Heidelberg on September 17, 1985.

According to the periodic table as it was understood at that time (see Fig. 1), element 93 was said to correspond to eka-rhenium in the 7th group of transition elements. And indeed, after irradiating uranium with neutrons several β-emitters were found. The difficult radiochemical analysis of this mixture, performed by *Hahn, Meitner* and *Strassmann,*[1] indicated that three chains of transuranic elements had been produced. One of them even reached as far as eka-platinum ($Z=96$). However, not all of the new β^--emitters fitted into this scheme. In 1938, during a rigorous examination of such discrepancies, *Hahn* and *Strassmann*[2] arrived at a completely unexpected conclusion, which is commemorated this year: after capture of a neutron, uranium fissions into two fragments, and the activities originally ascribed to transuranic elements rather belong to medium-heavy, known elements.[3]

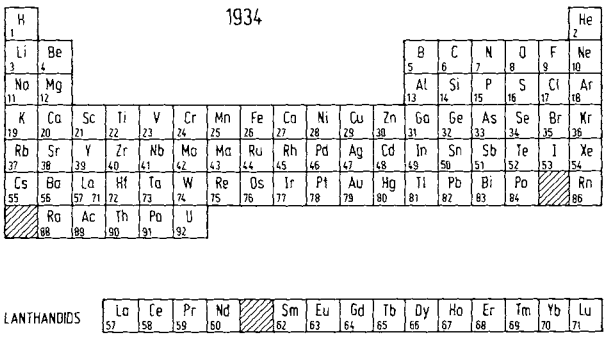

Fig. 1. The periodic table of the elements in 1934. Missing elements at that time are shown as dashed boxes. The present symbols for the elements are used, except for masurium (43).

We will not dwell further on the events that led to the abandonment of the idea of transuranics in favor of nuclear fission,[4–6] nor shall we describe how *McMillan* and *Abelson*[7] eventually found element 93, neptunium, among the irradiation products of uranium with neutrons. It was identified as a β^--emitter with a half-life of 2.3 d but with chemical properties completely different from what was expected. Instead of eka-rhenium, an element closely related to uranium had been found. Nor shall we describe in much detail how, step by step, further elements were synthesized and identified.[8–10] From 1944 onwards this was pursued systematically according to the concept of 14 actinoid elements, formulated by *Seaborg*.[11] The basis of the idea is that an inner electron shell is being filled (5f subshell[12]) as in the case of the 14 lanthanoid elements (4f subshell). Today the elements thorium to uranium are placed in the rows under the main part of the periodic table (Fig. 2); this arrangement emphasizes the similarities between lanthanoid and actinoid elements.

What we shall do is to start again with eka-rhenium, which has the atomic number 107 in today's periodic table, i.e. with the element with which studies on the synthesis of new elements started at the heavy-ion-accelerator UNILAC (UNIversal Linear ACcelerator) designed by *Schmelzer*.[13] We shall report on the elements 107, 108, 109 and 110, and on the search for "superheavy" elements near 114. And we shall also look at the possibilities of extending the periodic system beyond today's limits: what can we

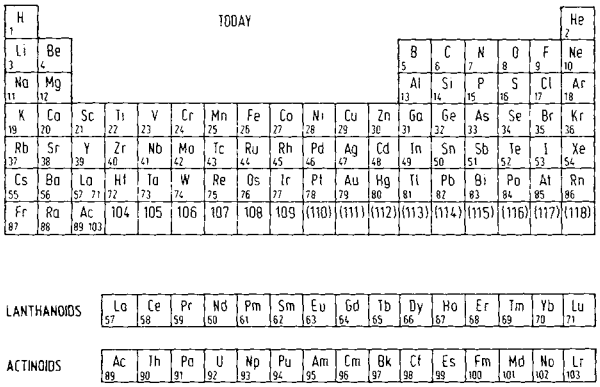

Fig. 2. The periodic table of the elements today. The atomic numbers of unknown elements are given in brackets.

expect with regard to the stability of even heavier atomic nuclei and the possibilities of their production?

2. Stability of the Heaviest Atomic Nuclei

A first impression of the stability of the heaviest nuclei can be obtained from Figure 3.[14] Starting with uranium, the half-lives of the longest-lived isotopes are shown as a function of their atomic number. The half-lives are shown separately for the two decay modes which are important here; α-decay (emission of helium-4 nuclei) and spontaneous fission into two fragments. Despite some fluctuations, the trend is obvious: for both decay modes the half-lives decrease exponentially with increasing atomic number, the respective slopes being different, however. For the lighter elements α-decay is by far the faster process. The

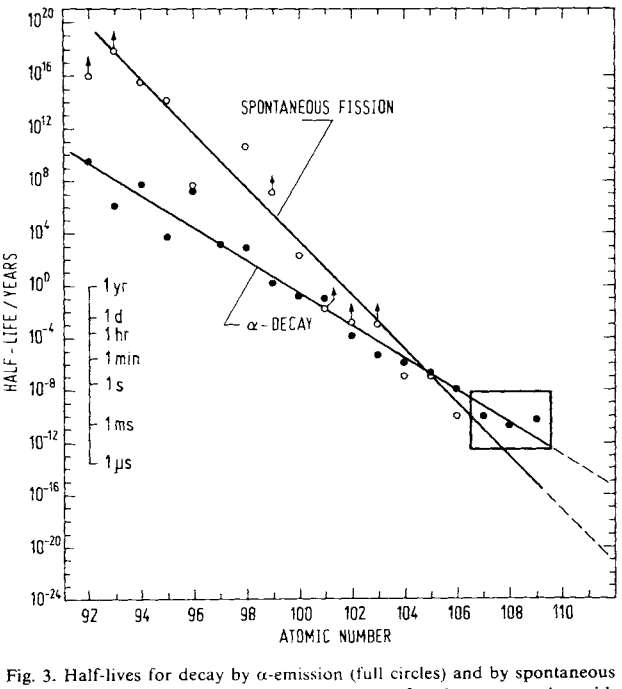

Fig. 3. Half-lives for decay by α-emission (full circles) and by spontaneous fission (open circles) versus the atomic number for elements starting with uranium [14]. The values for the most long-lived isotope for each element are given. The new elements reported on here are contained in a rectangle.

heavier the elements become, the stronger is the competition by spontaneous fission. If we ignore the elements 107 to 109, and just look at the situation as it was ten years ago, spontaneous fission would be expected to become the dominating decay mode near element 106. Close to element 115 the life-time of the nuclei would be as small as the period of their zero-point vibrations. This would be the end of the periodic table, because nuclear stability would cease to exist. This consequence was already noted in the first theoretical interpretations of nuclear fission[15, 16] based on the liquid-drop model of atomic nuclei.

Even today the liquid-drop model is still a strong conceptual basis for describing nuclear stability, or, in other words, for describing the binding energy of nuclei. The binding energy is the difference between the actual mass of a nucleus and the total mass of its constituents, the neutrons and protons. This is the amount of energy that would be released if the respective number of protons and neutrons were united to form a nucleus. The upper part of Figure 4 shows the various contributions to the binding energy within the framework of the liquid-drop model. For better comparison of the relative stability the energy is given in terms of binding energy per nucleon.

"surface energy" diminishes the binding energy, especially for light nuclei. In this case the binding energy decreases to about 8 MeV per nucleon. The binding energy decreases to this value also in the case of heavier nuclei, albeit for a different reason, namely because of the coulomb repulsion between the protons. The nuclear force increases only linearly with the proton number Z, whereas the "coulomb energy" increases quadratically. This effect is diluted for heavy nuclei because they contain up to 1.5 times more neutrons than protons which reduces the charge density. On the other hand, an increasing difference between the neutron and proton numbers results in a loss of binding energy ("asymmetry energy") due to a quantum mechanical effect. Thus, there is also a limit on the neutron excess. The binding energy per nucleon is finally the sum of all these contributions and has a maximum near the mass number 50. The region of most stable nuclei is near iron and nickel. This result is very important for the formation of the chemical elements in the cosmos by nuclear processes inside stars.

If one compares the experimental binding energies with the values calculated from the liquid-drop model, striking deviations are found for certain proton and neutron num-

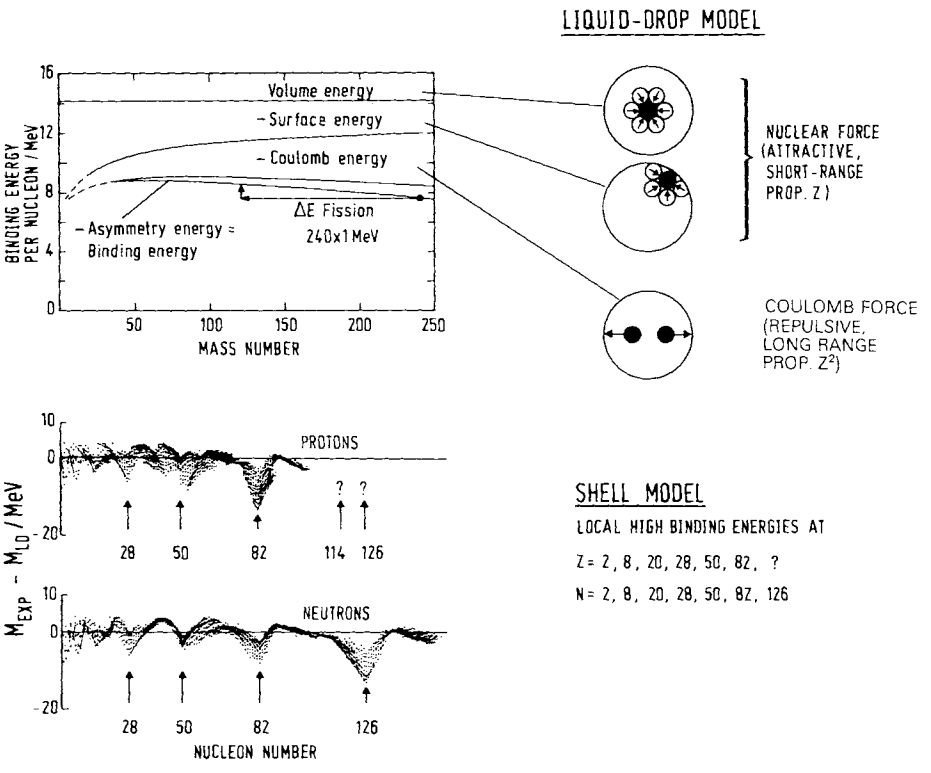

Fig. 4. Binding energy of nuclei according to the liquid-drop model of atomic nuclei and the influence of the shell structure. Top: the different components of the liquid-drop model in the binding energy per nucleon are shown as a function of mass number (after [17]). Starting with a constant volume energy, the surface, coulomb, and asymmetry energies are successively subtracted. Bottom: the difference between experimental nuclear masses and theoretical values obtained from the liquid-drop model are shown. Large differences occur at the "magic" proton and neutron numbers where nuclear shells are filled and strongly bound nuclei are found [18].

According to the liquid-drop model there are two large counteracting forces inside nuclei; the short-range, attractive nuclear force between the nucleons, and the long-range, repulsive coulomb force which acts only between protons. Each nucleon inside the nucleus interacts with the same number of nucleons via the nuclear force, and therefore adds a constant contribution to the binding energy. This "volume energy" is a constant of about 14 MeV per nucleon. The nucleons at the surface, however, have fewer neighbors, and contribute less to the binding energy; this

bers: the nuclei in certain vicinities are more stable than expected. The lower part of Figure 4 shows such a comparison on the basis of nuclear masses. This local stability is a consequence of nuclei being quantum-mechanical. Nuclei must also be viewed as an ensemble of nucleons with individual orbital and intrinsic angular momenta, as becomes evident in their nuclear spin. This recognition leads to a completely different kind of nuclear model, the shell model, in which certain nuclear properties are attributed to the motion of individual nucleons in a mean potential pro-

vided by all the other nucleons. The resulting nuclear energy levels can only be occupied by limited numbers of nucleons, as is also the case in electron shells, and when energetically favorable levels are exactly filled one obtains a gain in binding energy, the shell energy. For protons as well as for neutrons the nuclear shells contain the same "magic" numbers of nucleons: 2, 8, 20, 28, 50 and 82. In the case of neutrons there is an additional, experimentally verified, shell at neutron number 126; whether there is a corresponding proton shell will be discussed below. It can arise that both a proton and a neutron shell is filled for some nuclei; these doubly magic nuclei are characterized by an extremely high stability. One example is lead-208 with 82 protons and 126 neutrons.

The liquid-drop model demonstrates that the heaviest nuclei are unstable toward nuclear fission; *Meitner* and *Frisch*[19] realized this fact shortly after the discovery of nuclear fission. The binding energy per nucleon for a nucleus with 240 nucleons is about 1 MeV ($=1\times10^6$ eV) smaller than that for a nucleus with just 120 nucleons (see upper part of Fig. 4). This means that if nuclei in the uranium region undergo fission into two fragments of the same size approximately $2\times120\times1=240$ MeV of energy should be released, quite close to the observed value of 207 MeV.[20]

The liquid-drop model also explains why, in spite of this enormous energy release, such heavy nuclei still exist instead of promptly undergoing fission. The model assumes nuclei to be spherical objects in order to minimize the loss of binding energy at the surface. During the lead-up to fission, nuclei must elongate. This requires some energy input because the surface tension counteracts the elongation. Only beyond a certain deformation does the repulsive coulomb force start to dominate over the attractive nuclear force; then the way to fission is free. The activation energy for fission, i.e. the fission barrier, is around 6 MeV in the uranium region. This energy is quite small if compared to the total binding energy of about 1900 MeV or even the energy release from fission of about 200 MeV. The influence of the fission barrier is, however, very strong; uranium-238, e.g., has a half-life of 8×10^{15} years against spontaneous fission, i.e. fission without some external energy input. Spontaneous fission is a tunneling process through the fission barrier, analogous to the tunneling of α-particles through the coulomb barrier. According to the liquid-drop model, the fission barriers decrease as the nuclear charge increases and eventually disappear near element 110.[21] Very heavy nuclei are somewhat elongated instead of being spherical and their barriers are more complicated than expected on the basis of the liquid-drop model, but this does not change the general trend just outlined.

The shell structure of nuclei, however, might cause a drastic change in this trend. Closed nuclear shells stabilize shapes of high symmetry, such as the spherical one, against deformation. As a result, fission barriers appear even in cases where none should be expected from the liquid-drop model. *Myers* and *Swiatecki*[21] were the first to show that these shell-induced barriers can be even higher than the liquid-drop barriers in the uranium region.

The problem is now to find the next shell closure for protons. First it was assumed that in analogy to the neutron shell 126 element 126 should be "magic". This was too far away from the heaviest known elements to seriously consider a synthesis. The situation changed dramatically when, in 1967, *Meldner* showed[22] that such an analogy is not valid. The next proton shell is expected to be closed at element 114 and the next neutron shell for neutron number 184.[21,22] It seemed that a synthesis might be feasible for elements near 114. Moreover, very high fission barriers were expected,[23] and, in turn, extremely long half-lives. Thus, it was speculated that such "superheavy" elements could exist even in nature. This triggered off the publication of a multitude of theoretical papers on the nuclear properties, electronic structure, and chemical properties of these elements, and, of course, the search for such elements in nature and the first attempts at their synthesis. A review published in 1975[25] cited no less than 329 publications. More recent reviews can be found in Refs. [26, 27] and reviews of the heaviest elements recently synthesized in Refs. [28–31]. The somewhat exotic and exaggered name "superheavy elements" was adopted in the course of earlier speculations[24] about the existence of even much heavier nuclei.

Let us now have look at the nuclear landscape shown in Figure 5.[32] In the plane we find the two coordinates atomic number Z and neutron number N which define the location of each atomic nucleus. The third, vertical coordinate is the stability, measured in terms of binding energy per nucleon. In order to clarify the global trend, only nuclei with a half-life of more than one second are shown. If all nuclei were shown, the "beaches" would extend a little more into the "sea of instability", and the small "waterway" between the lead-mountain and the uranium-island would disappear.

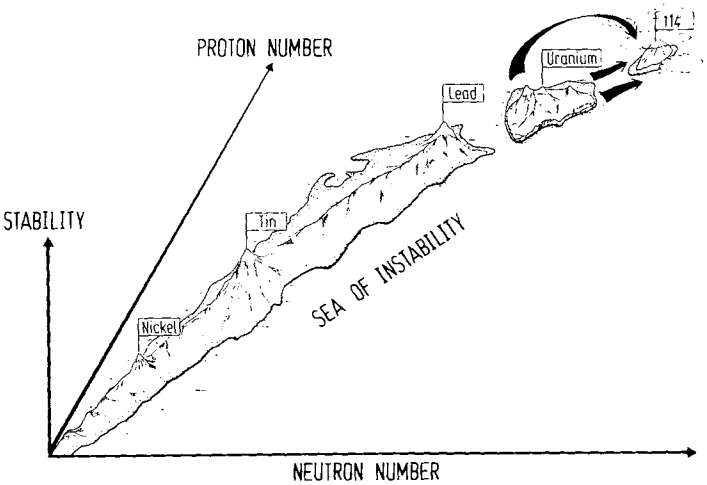

Fig. 5. The nuclear landscape. The nuclear stability measured by the binding energy per nucleon is shown as a function of neutron number N and proton number Z. Only nuclei with a half-live of more than one second are included [32].

The nuclear world of Figure 5 looks like an elongated mountain ridge slightly bent towards the neutron axis reflecting the liquid-drop character of nuclei. On top of this we have the shell effects which create mountains and valleys, the doubly magic nuclei being the highest peaks. The island of superheavy nuclei remains hidden behind the

clouds, as we shall discuss later. It should be noted, however, that this landscape would be a lot poorer if the delicate balance between nuclear and coulomb forces were to deviate a little, a few percent, in one direction or the other. The build-up of complex nuclei from hydrogen by nuclear reactions inside stars would have already terminated at very light nuclei, at deuterium or helium-2.[33]

3. Synthesis of the Heaviest Elements

There are two ways of approaching the synthesis of new elements; they are represented by arrows in Figure 5. One might gain a new piece of land, element by element, or one might try to jump to the island of superheavy elements in one big step. In either case the yield is expected to be very small, and therefore the synthesis has to start with elements which can still be obtained in weighable amounts. It turns out that einsteinium ($Z=99$) is the heaviest potential target material; the isotope einsteinium-254 with 276 d half-life can be produced in microgram quantities. The reaction partner must always be a heavy ion, in order to provide a reasonable number of protons in one step.

One should choose the reaction partners such that the sum of their proton numbers equals the proton number of the element to be synthesized. If one succeeds in fusing the two nuclei the task is, in principle, accomplished. This concept has been a great success in the synthesis of the heaviest elements. Starting with element 102, all the new elements were first made by this method.[9, 10, 29, 31]

Such a fusion of two nuclei is shown in Figure 6 for the example of element 107. Chromium-54, the projectile nucleus, is delivered by an accelerator, and bismuth-209 serves as target nucleus. The comparatively small projectile collides with the larger target nucleus, and forms an excited, rotating collision-complex. After some time the projectile is swallowed by the target, the reaction partners lose their previous identities and an excited "compound nucleus" (107)-263 is formed. The energy released is distributed statistically over all the nucleons. It is removed by prompt emission of one or more neutrons, and by further deexcitation via γ-rays. The final nucleus, here (107)-262, has the desired proton number and a neutron number which is one unit lower than that in the compound nucleus. This evaporation residue is now in its ground state and its further transformation proceeds on a much longer time scale via radioactive decay.

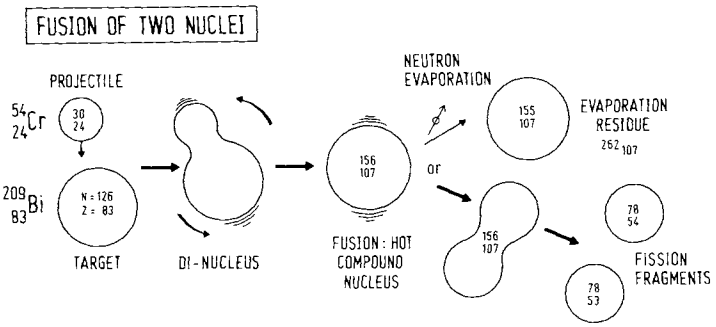

Fig. 6. Scheme of the synthesis of heavy nuclei by nuclear fusion, for the case of element 107 by fusion of bismuth-209 with chromium-54.

This sequence of events, however, occurs very rarely. It is much more likely, about 100 times on average, that the fragile compound nucleus undergoes fission decay rather than that a neutron evaporates. Suppose four evaporation steps are needed for deexcitation, then the survival probability of the evaporation residue reduces down to $1:10^8$. This explains why such compound nuclei should be produced in a cold state with as little excitation energy as possible. On the other hand, the projectile needs a certain minimum kinetic energy in order to establish contact with the target nucleus. This minimum energy is, of course, given by the coulomb repulsion between the two reaction partners. Part of it will be needed to counteract the loss of binding energy, but there always remains some excitation energy, the amount of which strongly depends on the system.

It should be noted that the proton number of the detected reaction product does not necessarily equal the total proton number of the two partners. The fusion reaction can either be incomplete or the primary fusion products may evaporate protons or decay radioactively. An unambiguous experimental identification of the proton number of the reaction products is clearly necessary.

After some early abortive attempts to synthesize superheavy elements via fusion reactions the search was made for other possible synthetic routes. Such an alternative was provided by the UNILAC, because it was the first machine capable of accelerating all elements up to uranium with kinetic energies high enough to induce nuclear reactions with any element up to uranium.

Thus, it became possible to transfer many nucleons during the collision of two very heavy nuclei like uranium-238 (see Fig. 7). Because the coulomb repulsion between the

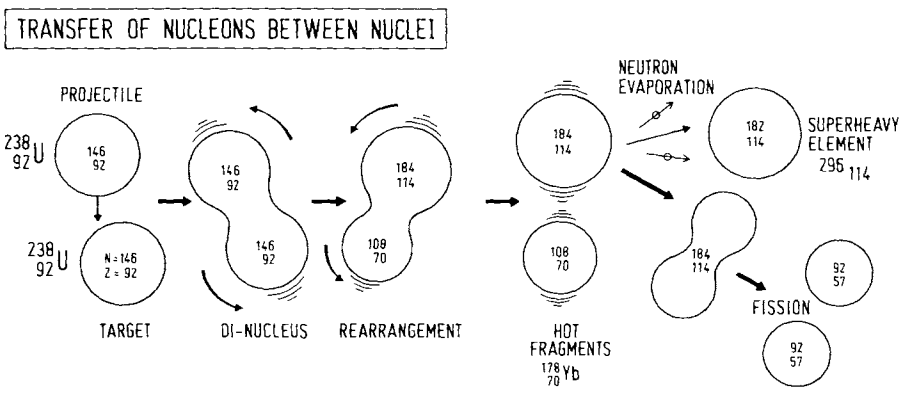

Fig. 7. Scheme of the synthesis of heavy nuclei by nucleon transfer during the collision of heavy nuclei, in this case two uranium-238 nuclei.

reaction partners is very high, the nuclei only touch each other, forming a dinucleus rather than a compound nucleus. The rotating dinucleus separates again after about 10^{-20} s, usually into nuclei similar to the initial ones. Occasionally it may happen that a large number of nucleons diffuse in one direction within the dinucleus, or, in other words, one half of the dinucleus grows at the expense of the other. In extreme cases (transfer of 22 protons within the uranium-uranium dinucleus) this could result in the formation of a superheavy nucleus, the remaining half shrinking down to a light nucleus (ytterbium in this case). Such complementary light nuclei indeed emerge from the reaction, indicating that a large nucleon transfer has taken place. But again most of the newly formed superheavy nuclei undergo prompt fission, because diffusion of nucleons also heats up the product nuclei. It is important to note that the excitation energy of the superheavy nuclei is broadly distributed, in contrast to the case of fusion reactions where it is well defined. One may hope, therefore, to obtain a sufficiently large number of nuclei with low excitation energy.

4. Separation and Detection of Heaviest Nuclei

Irrespective of how the synthesis of the heaviest elements proceeds, they are always formed in extremely small amounts. The number of detected atoms, N, is given by:

$$N = \sigma N_t N_p \varepsilon$$

where σ is the production cross section for the nucleus formed, N_t the number of target atoms per cm^2, N_p the dose of projectile nuclei, and ε the efficiency of the detection method. As an example, let us take values of $N_t = 2 \times 10^{18}$ atoms/cm^2 (i.e. 1 mg/cm^2 target thickness), $\varepsilon = 0.2$, and a dose of 1×10^{18} projectiles per day (or 1×10^{13} per s) which is typical for the UNILAC. If the cross section is of the order of $\sigma = 1 \times 10^{-35}$ cm^2, then each day only four atoms would be detected. The example cross section implies that a surviving heavy nucleus is produced in about 1 out of 10^{11} nuclear collisions.

This ratio cannot be greatly improved as the cross sections are well defined physical quantities. Larger amounts of target material do not help, because the reactions take place only in a very small depth zone of the target. Neither can the projectile dose be increased very much because the targets are subject to radiation and temperature damage, and also because the neutron-rich nuclei needed as projectiles are available only in very limited amounts. One therefore has to accept the small number of atoms produced. To make things worse, they have to be isolated from a huge surplus of target and projectile atoms and from radioactive products of concurrent nuclear reactions. Present day experimental techniques have reached such a high standard that the production of a few atoms per day is already sufficient for the detection of new elements.

An additional experimental problem is the life-time of the nuclei to be detected. For element 107 and those immediately after it is of the order of milliseconds. This is too short for chemical separations, even though the field of fast chemical separation techniques is quite advanced.[34] Only with physical methods may one hope to be successful. For the superheavy elements with their supposedly much longer half-lives, chemical separation techniques might again be applicable.

The following concept emerged for the experiments to be carried out at UNILAC: in order to proceed step by step to heavier elements, *Armbruster, Münzenberg* et al. built a physical separation apparatus at the Gesellschaft für Schwerionenforschung (GSI), namely the velocity filter SHIP.[35] The search for superheavy elements was initiated using simple techniques, and then continued also with the use of chemical methods.[36] The latter were mainly worked out and applied by a group of nuclear chemists from the University of Mainz and from GSI.

4.1. Physical Methods

The velocity filter SHIP is shown schematically in Figure 8. The apparatus, 11 m long, separates the slow evaporation residues flying out of the target from the faster projectiles and also to a large extent from products of competing reactions. The targets are mounted on a rotating wheel in order to minimize the heat deposited by the beam spot. After leaving the target the beams of projectiles and products are focussed by magnetic lenses and are separated from each other during traversal of a number of electric and magnetic fields. The reaction products are again focussed and implanted in solid-state detectors. One of the decay modes of the new elements is α-decay which serves to connect them genetically with known nuclei.

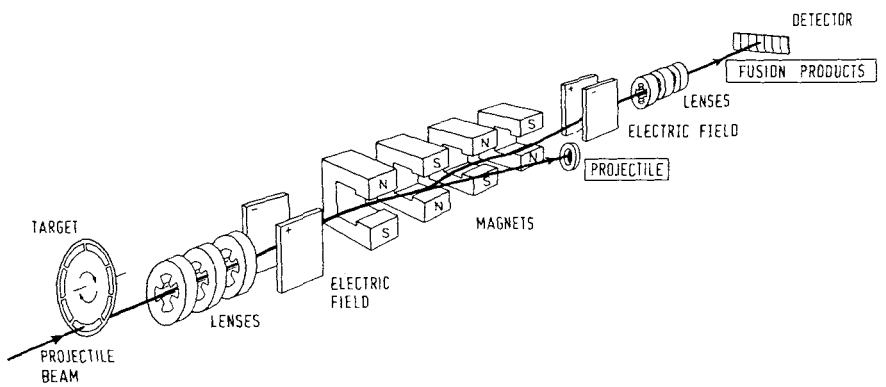

Fig. 8. Schematic diagram of the velocity filter SHIP that separates fusion products from the projectile beam by a combination of electric and magnetic fields (after [30]).

Figure 9 outlines this procedure. In collisions of bismuth-209 with chromium-54 one finds nuclei with a half-life of 4.7 ms that emit an α-particle of 10.38 MeV energy, leading to three known α-emitters—(105)-258, lawrencium-254 and mendelevium-250. Since the first α-emitting nucleus must have 2 protons and 4 nucleons more than (105)-258, the nucleus in question can only be element 107 with mass number 262. This technique was brought to such a high standard by the SHIP group[37] that even very small numbers of nuclei can be detected. This is achieved with a solid-state detector following the velocity filter that measures the arrival time and position of an incoming atom. Taking the arrival as the time reference, the decay mode—α-decay or spontaneous fission—the energy, and the time of the subsequent decay processes are registered. This decay must, of course, occur at the place where the atom initially hit the detector. All this information gives the decay history of the primary atom (this will be explained in another example in Section 5). The minimum half-life required is of the order of microseconds, corresponding to the time-of-flight through the apparatus.

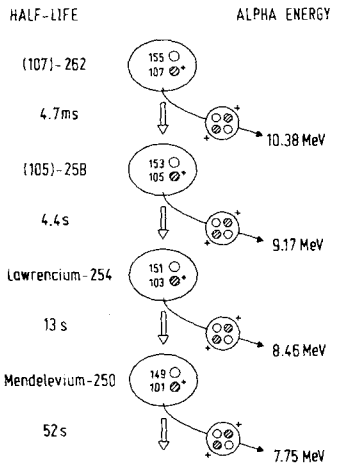

Fig. 9. Detection scheme for a new element, e.g. element 107, via its α-decay leading to a chain of known radioactive nuclei.

Another possible way[38] to identify new elements via subsequent α-decay chains is, instead of detecting the short-lived daughter-nuclei just described, to detect a long-lived member late in the decay chain after chemical isolation. It is necessary, however, to ensure that this member of the chain cannot be formed in any other way than that which would involve the synthesis of the new element.

The method of using spontaneous fission as the characteristic decay mode of new elements is applied by the group of *Flerov* and *Oganessian*, who work at the heavy ion cyclotron of the Joint Institute for Nuclear Research in Dubna. They use a very simple technique[39] which is outlined schematically in Figure 10. It covers half-lives down to milliseconds. The target material, e.g. bismuth metal, is attached to the surface of a rotating, cooled drum. The beam hits the target material along a tangent. The drum is surrounded by a fixed ring of mica foils. If a new isotope is formed in the target and decays by spontaneous fission, then its fragments are emitted from the rotating drum and hit the mica. This damages the solid, and after the experiment these damaged areas can be enlarged by chemical etching to form tracks. Once the rotational velocity of the drum is chosen properly, the number of tracks along the mica will decrease continuously. From this decrease one can calculate the isotope's half-life for spontaneous fission, as is shown at the bottom of Figure 10.

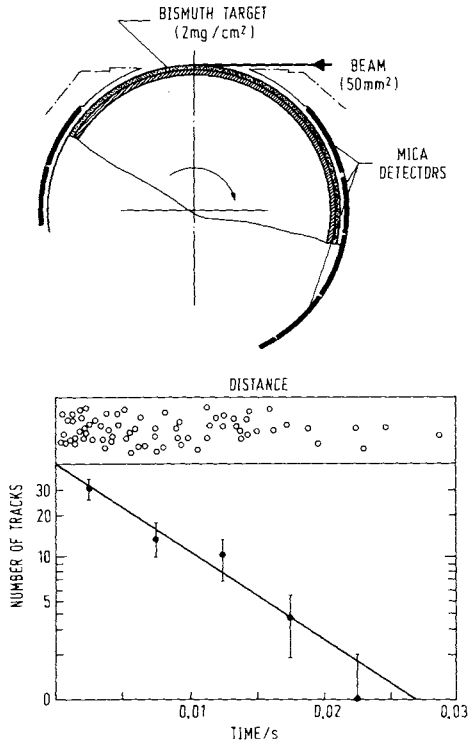

Fig. 10. Top: Apparatus for the detection of short-lived spontaneous-fission isotopes with a rotating drum and mica detectors [40]. Bottom: Positions of the etched fission-fragment tracks on a sheet of mica, and the resulting decay curve for the nuclide (104)-256 with 8 ms half-life produced on bombardment of lead-208 with titanium-50 [39].

This procedure, however, does not allow a direct identification of the nuclear charge and mass numbers. Each fission fragment, wherever it may come from, produces the same kind of track. One cannot rule out a priori the production of spontaneously fissioning actinoid isotopes by transfer reactions which occur along with the desired fusion reaction.[41] Thus, in order to unambiguously identify an element, additional information is needed. The Dubna group relies mainly on some characteristics of the nuclear reaction used for production. If one compares the results from several projectile-target combinations, where only one of them can lead to the sought after new element (whereas all the others have fewer protons) the new activity must only appear with the proper combination. Also, for each reaction in question, the production rate depends in a characteristic way on the projectile energy. And, finally, one can make use of differences in the spatial distribution; fusion products leave the target in a cone which is narrower than that for products from transfer reactions.

There is controversy[42,43] as to which criteria need to be fulfilled in order to identify a new element by spontaneous

fission. This is the reason for the ongoing debate[31,44] about the priority of the discovery of some of the heaviest elements, especially the elements 104 and 105.

When searching for the island of superheavy elements, the problem of element identification is especially critical because one can no longer expect α-decay chains leading to known nuclei. In the world of Figure 5, each chain will sooner or later end in the sea of instability, viz. the region of spontaneous fission, without ever reaching beaches of known territory. It is quite likely, however, that the fission of superheavy nuclei will result in unusually high fragment energies and a large number of neutrons.[45] Such unusual events of spontaneous fission might be the first hints of superheavy nuclei. But again one needs additional proofs, e.g. the requirement that the spontaneously fissioning nuclei behave chemically like superheavy elements.

4.2. Chemical Methods

Which chemical properties can be expected for the heaviest elements and which ones can be used for their separation? If one naively extends the periodic table, as in Figure 2, then element 112 is placed below mercury and element 114 below lead. And indeed, quantum-mechanical calculations justify this continuation.[46] The predicted electronic structures of the atomic ground states of the related elements are very similar. For element 112 one expects the valence electrons to be in the $7s^2$ state, in analogy to $6s^2$ for mercury, and for element 114 in the $7s^27p_{1/2}^2$ state, in analogy to $6s^26p_{1/2}^2$ for lead. The same is true for the neighboring elements. For element 118 the $7p_{3/2}$ state would be filled, and the next noble gas configuration reached. Based on this kind of reasoning many chemical and physical properties of superheavy elements and their respective compounds were extrapolated by using systematic trends.[47] As an example, Figure 11 shows the extrapolation of the evaporation enthalpies[48] indicating, for example, that element 114 should be fairly volatile.

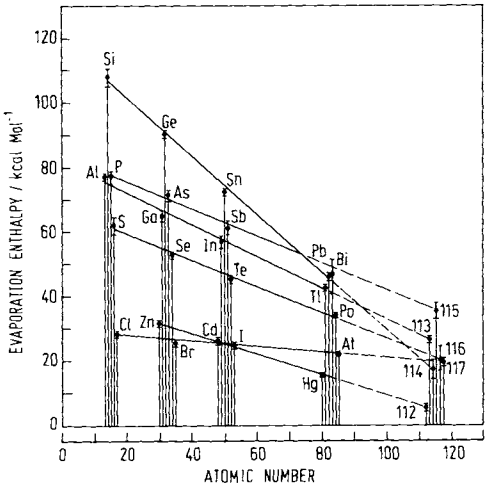

Fig. 11. Extrapolation of evaporation enthalpies for the elements 112 to 117 [48].

On the other hand, the chemical properties of these elements might deviate from such systematic trends.[49] Due to their high orbital velocity, the outermost electrons experience a relativistic mass increase and, in turn, a stronger binding. Therefore, the $7s^2$ subshell in element 112 and the $7p_{1/2}^2$ subshell in element 114 could be stabilized like complete electron shells. These elements would then be chemically inert and highly volatile, perhaps even gaseous at room temperature. For the neighboring elements low oxidation states would dominate. Relativistic effects could thus become obvious in the test tube. Because of the small production rates and the short half-lives there are as yet few studies of the chemistry of the heaviest elements which extend to element 105. The information thus far available has been collected in several review articles.[50-52] In those and in very recent studies of elements 103[53-56] and 105,[57] large relativistic effects have not yet been observed.

The validity of extrapolating macroscopic properties cannot be taken for granted in experiments with only a few atoms of superheavy elements. The chemical behavior at such low concentrations could well be different from that of macroscopic amounts. Even amounts that are usually considered very small are still huge in comparison to those dealt with here: 1 pg (10^{-12} g) of lead still contains 3×10^9 atoms! The chemistry at lowest concentrations has long been an attractive area of research in radiochemistry.[58] Recent theoretical[59] and empirical[60,61] studies have shown that even for very small amounts one can expect normal behavior. Of course, some macroscopic properties like the melting point and density cannot be determined with a few atoms.

The methods used to chemically separate superheavy elements should not be very specific at first. On the contrary, since the region of highest nuclear stability can only be estimated, it is advisible to separate as many superheavy elements as possible in one experiment.[26] If spontaneous fission is used as the method of detection, one only needs to remove any actinoid element contamination because these elements also decay by spontaneous fission. Lighter homologues of superheavy elements, such as mercury or lead, are no problem in this respect. If this kind of group-separation should give any indication of the presence of superheavy elements, then more specific separation methods would have to be employed in a subsequent experiment.

Three types of group separations are shown in Figure 12. Extrapolations of evaporation enthalpies, like those in Figure 11, indicate that the elements 112 to 118 should be volatile at temperatures around 1000 °C;[48,47] this is the

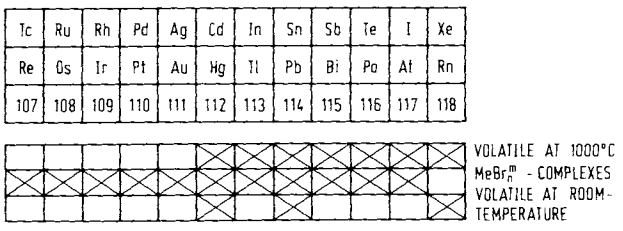

Fig. 12. Detection scheme for superheavy elements with three different chemical separations. Elements which should be volatile at 1000 °C are indicated by crosses in the upper line, in the middle line those which should form negatively charged bromide complexes with hydrobromic acid are indicated, and in the lower line those which might already be volatile at room temperature. To facilitate comparison, a section of the periodic system is also depicted.

group of "lead-like" superheavy elements. For the non-volatile "platinum-like" elements 107 to 111 one can apply a separation based on ion-exchange which makes use of the expected formation of negatively charged bromide complexes;[62] this separation should also include the elements 112 to 117. Finally, the elements 112 and 114 together with 118 might be "radon-like", i.e. volatile at room temperature.[49]

If one is searching for long-lived superheavy nuclei, it is possible to combine several different "off-line" separation techniques.[63] In this case, either the targets or metal foils used to collect reaction products emitted from the target are chemically processed after the irradiation. The different chemical fractions are finally measured with extremely sensitive detectors for spontaneous fission events.

A schematic diagram of such a detector[64] is shown in Figure 13. It detects the two fission fragments, records their respective kinetic energies, and the number of neutrons emitted from the fragments. It will clearly identify events with high kinetic energy and neutron number. Thin samples are placed between two solid-state detectors in order to observe the fission fragments that are emitted in opposite directions. Six samples can be measured simultaneously in different solid-state detectors. The neutrons are first slowed down in paraffin, and are then detected in a ring of 30 helium-3 filled counters. To give an impression of the size of the detector, the length and the diameter of the paraffin cylinder are 130 and 65 cm, respectively. In order to suppress the cosmic-ray background, shielding counters are put above and below the detector. In addition the whole system is placed underground. If the detector is operated to register only events which consist of both fission fragments and neutrons, the background is less than one event per month.

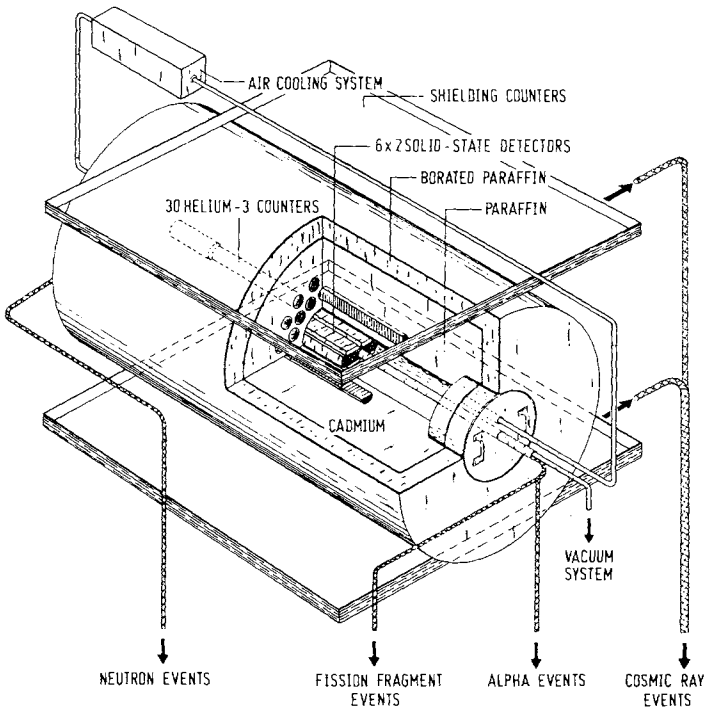

Fig. 13. Schematic drawing of a highly sensitive detection system for superheavy nuclei by simultaneous observation of fission fragments with solid-state detectors and of fission neutrons with helium-3 counters [64].

For an "on-line"chemical process the transport of the reaction products, the chemical separation and the subsequent measurement all take place continuously during the irradiation. The main features are depicted in Figure 14 for

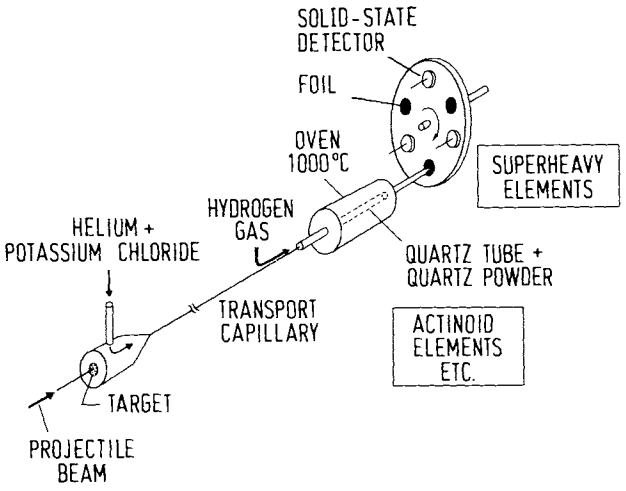

Fig. 14. Chemical on-line separation and subsequent measurement with a wheel system of lead-like superheavy elements by volatilization at 1000°C [36] (after [65]).

the example of lead-like elements.[36] The beam of projectiles hits a thin target and kicks the reaction products into a chamber where they are slowed down in helium. The helium gas contains minute amounts of small potassium chloride particles. The reaction products become attached to these aerosols and are transported at high velocity through a capillary to the separation and detection device, usually many meters away in a low background area. During the transport, hydrogen is added to serve as a reducing agent. Lead-like elements are thus stabilized in elemental form. The stream of gas passes a tube filled with quartz powder at a temperature of 1000°C where less-volatile species, especially the undesired actinoid elements, are adsorbed. Any volatile superheavy elements, however, pass through the tube and are deposited on thin cooled metal foils. These foils are mounted on a rotating wheel that positions the foils successively between pairs of solid-state detectors to detect fission fragments and α-particles. The efficiency of the method is continuously monitored by measuring short-lived α-emitters of homologous elements such as polonium and lead that are formed in side reactions. This technique is able to detect nuclei with half-lives down to a few seconds.

The platinum-like elements, after being attached to aerosols, are also transported with the gas stream. The aerosols are then dissolved in hydrobromic acid and transferred to a cation exchange column. The actinoids are adsorbed as cationic species whereas the negatively charged bromide complexes of the superheavy elements and their homologues pass through the column. Solid samples are prepared subsequently by evaporating the eluates.[36] All essential steps are computer-controlled, e.g. the switching on and off of the sampling processes, the preparation and addition of different solutions for elution, and the conditioning of the columns for the next separation. One column is

used for a separation, while at the same time another one undergoes conditioning.[66] In this way the discontinuous column chromatography becomes "quasi on-line". The limit of detectable half-lives is of the order of several minutes.

Radon-like elements are transported by a gas stream without aerosols and are fed through a column filled with quartz powder at 1000°C to filter out less volatile components. The volatile elements are condensed on the surface of a cooled solar cell which is facing a solid-state detector. Spontaneous fission events are registered by simultaneously detecting fragments in both detectors.[67] It is again possible to cover half-lives down to the order of seconds.

5. The Heaviest Elements

All elements at the end of the periodic table up to element 106 were first produced from heavy actinoid nuclei by fusion with light projectiles; e.g. element 106 by fusion of californium-249 and oxygen-18.[68] The compound nucleus is highly excited, as evidenced by the emission of four neutrons:

$$^{249}_{98}\mathrm{Cf} + {}^{18}_{8}\mathrm{O} \longrightarrow {}^{263}106 + 4\,{}^{1}_{0}\mathrm{n}$$

Usually a shorthand notation is used for nuclear reactions where the projectile and ejecta are written in parentheses:

$$^{249}_{98}\mathrm{Cf}({}^{18}_{8}\mathrm{O}, 4\mathrm{n})\,{}^{263}106$$

This large excitation energy dramatically reduces the survival probability of the evaporation residues, as was already explained in Section 3. For the synthesis of even heavier elements a technique suggested by *Oganessian*[69,70] turned out to be essential. He proposed the use of target nuclei with closed nuclear shells, such as lead-208 or bismuth-209. A large fraction of the energy deposited by the projectile has to be used for breaking the shells, preventing it from being turned into excitation energy. This cold fusion was demonstrated for the first time in reactions such as

$$^{208}_{82}\mathrm{Pb}({}^{40}_{18}\mathrm{Ar}, 2\mathrm{n})\,{}^{246}_{100}\mathrm{Fm}$$

which led to previously known nuclei.[69-72] Sometimes it is even possible to keep the excitation energy of the compound nucleus so low that it is insufficient to evaporate a neutron, and only γ-rays are emitted instead:[38]

$$^{208}_{82}\mathrm{Pb}({}^{50}_{22}\mathrm{Ti}, \gamma)\,{}^{258}104$$

The SHIP group has systematically investigated cold fusion in the region of known heavy nuclei.[28,73] These studies led also to a characterization of the decay chains to be genetically connected to the new elements produced later. It became clear, however, that very neutron-rich projectiles like chromium-54, iron-58 and nickel-64 are needed for the synthesis of new elements. These isotopes have natural abundances of only a few percent or even less. They therefore have to be enriched by electromagnetic isotope separators, a costly process.

5.1. Element 107

The first synthesis of a new element at UNILAC was accomplished in 1981, when *Münzenberg* et al.[74] obtained element 107 by fusion of bismuth-209 and chromium-54, as outlined schematically in Figure 6. A previously unknown α-emitter of 4.7 ms half-life and 10.38 MeV α-energy could be connected to the decay chain shown in Figure 9. The reaction is thus

$$^{209}_{83}\mathrm{Bi}({}^{54}_{24}\mathrm{Cr}, \mathrm{n})\,{}^{262}107$$

Within three days of beam time a total of five correlated decay chains were found, all starting with this new α-emitter. One of these chains, together with the lifetimes τ of the individual nuclei in the intermediate steps, is shown in Figure 15. The lifetimes may differ from the average values; however, the width of this deviation is well defined by statistical laws. The resulting errors in the average lifetimes will, of course, be large if only a few nuclei are observed. From the lifetime of 12.6 ms of the initial nucleus (107)-262 in Figure 15 one formally obtains a half-life

$$T_{1/2} = (\ln 2)\,\tau = 0.693 \times 12.6 = 8.7 \text{ ms}.$$

This agrees well with the mean half-life of 8.2 ± 2.2 ms resulting from later experiments.[75,76] Figure 15 shows a case in which mendelevium-250 decayed via electron capture into the α-emitter 30-min fermium-250, and not by α-decay as indicated in the scheme of Figure 9. Up to now 14 decay chains of this isotope have been observed (Table 1).

Table 1. The heaviest elements discovered at the heavy-ion accelerator UNILAC.

Atomic number Z	Mass number	Half-life	α-Decay energy [MeV]	Synthesis reaction	Number of atoms observed	Time of discovery	Ref. for discovery
107	262	8.2 ± 2.2 ms	10.38, 10.24	$^{209}_{83}\mathrm{Bi}(^{54}_{24}\mathrm{Cr}, \mathrm{n})$	14	February 1981	[74]
		106 ± 30 ms	10.01, 9.91, 9.74		15		
	261	$9.0^{+4.4}_{-2.3}$ ms	10.39, 10.10, 10.03	$^{209}_{83}\mathrm{Bi}(^{54}_{24}\mathrm{Cr}, 2\mathrm{n})$	9		
108	265	$1.8^{+2.2}_{-0.7}$ ms	10.36	$^{208}_{82}\mathrm{Pb}(^{58}_{26}\mathrm{Fe}, \mathrm{n})$	3	March 1984	[83]
	264	76^{+364}_{-36} µs	11.0 [a]	$^{207}_{82}\mathrm{Pb}(^{58}_{26}\mathrm{Fe}, \mathrm{n})$	1		
109	266	$3.4^{+6.1}_{-1.3}$ ms	11.10	$^{209}_{83}\mathrm{Bi}(^{58}_{26}\mathrm{Fe}, \mathrm{n})$	3	August 1982	[87]

[a] The α-decay energy was estimated from the measured half-life using the known relationship between these quantities.

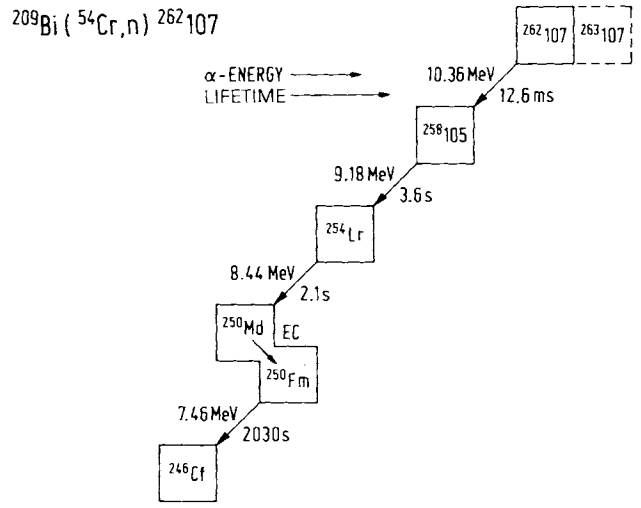

Fig. 15. The first detection of element 107: one of the observed α-decay chains from the irradiation of bismuth-209 with chromium-54 [74]. EC = electron capture.

During later experiments at SHIP[75,76] an additional group of α-decays of element 107 was discovered in 15 correlated decay chains; such a group had already been suspected to occur in this reaction.[74] The decay chain also belongs to mass number 262, but starts with a half-life of 106 ± 30 ms and a complex α-energy spectrum (see Table 1). This phenomenon is called nuclear isomerism, i.e. there are two nuclei of the same mass number but with different binding energy and decay properties. The 8-ms activity is the metastable isomeric state, and the 106-ms activity is the ground state of (107)-262.

The existence of these nuclei with mass number 262 was confirmed in Dubna[38] by detecting 1.5-d californium-246, the nucleus at the end of the decay chain in Figure 15. Californium was chemically isolated after bombardment of bismuth-209 with chromium-54. The lower part of Figure 16 shows the α-spectrum of the californium fraction. The presence of californium-246 is statistically quite well determined.

A second isotope of element 107 with mass number 261 was produced at UNILAC with the same projectile-target combination at somewhat higher projectile energy. Three decay chains were observed,[75] and could be connected via α-decay with the known nucleus 1.4-s (105)-257 and its respective decay chain.[77] The reaction is

$$^{209}_{83}\mathrm{Bi}(^{54}_{24}\mathrm{Cr},2n)^{261}107$$

The nuclide has a half-life of $9.0^{+4.4}_{-2.3}$ ms,[76] and a complex α-energy spectrum (see Table 1). No spontaneous fission events have been observed along with the nine α-decay events known up to now.[76] *Oganessian* et al.[78] claim to have detected this isotope as early as 1976 in the same reaction via spontaneous fission, but with a half-life of 1 to 2 ms. In the meantime the half-life of the spontaneous fission activity has been corrected to $2.8^{+2.1}_{-1.1}$ ms,[79] still considerably shorter than the value found at UNILAC. For this spontaneously fissioning nuclide the Dubna group calculated a production cross section of about 1×10^{-34} cm^2.[78] The SHIP group, on the other hand, concludes that because spontaneous fission has not been observed in their experiments, the production cross section must be at least ten times lower.[76] Thus, the existence of this fission activity has not been confirmed by the SHIP group.

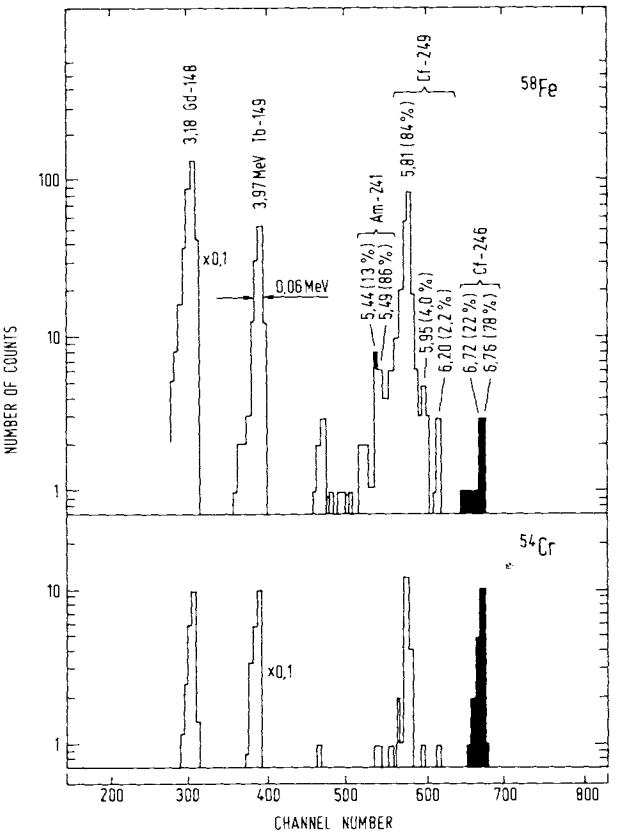

Fig. 16. Indirect evidence for the formation of elements 107 (bottom) and 109 (top) in a chemically isolated californium fraction after the irradiation of bismuth-209 with chromium-54 (107) and iron-58 (109), respectively. The heavy elements were identified via 1.5-d californium-246 produced late in the α-decay chains. The characteristic α-peak of californium-246 is shown in black. The remaining peaks are α-emitters used for calibration (after [38]).

Table 1 summarizes our present knowledge about the isotopes of element 107, including results of the most recent experiment carried out by the SHIP group.[76] A total number of 38 atoms has been observed, 13 of which were correlated with the decay products lawrencium-253 and -254 ($Z = 103$). The most recent summary by the Dubna group[31] no longer contains the isotope with mass 260 which was included earlier.[80] A search for neutron-rich isotopes of element 107 such as (107)-266, which might have half-lives of the order of minutes,[81] was carried out during the bombardment of einsteinium-254 with oxygen-16, albeit without success.[82]

To summarize: element 107 was first identified unambiguously by the SHIP group.[74] They succeeded in detecting the α-decay of isotope 262 into previously known nuclei. The earlier assignment of a 1–2 ms spontaneous fission activity to the isotope 261 by the Dubna group[78] seems less justified.

5.2. Element 108

Münzenberg et al.[83,84] have been able to detect three atoms of the isotope 265 of element 108, again via α-decay chains, two of which are depicted in Figure 17. The reaction for the synthesis is

$^{208}_{82}Pb(^{58}_{26}Fe,n)^{265}108$

The half-life of (108)-265 is 1.8 ms with an α-decay energy of 10.36 MeV (see Table 1). Figure 17 again demonstrates the statistical fluctuations of the measured lifetimes as compared to the mean values. It also shows that if the α-particles are sometimes emitted towards the surface of the detector (i.e. "escape"), only a fraction of their energy is detected. This fraction is around 1 MeV, and it is not specific at all. The observation of an α-decay and the lifetime are, however, still unambiguous. The existence of the nucleus (108)-265 was confirmed in the same reaction by the radiochemical detection of a long-lived end product of the decay chain, the 20-d einsteinium-253.[38]

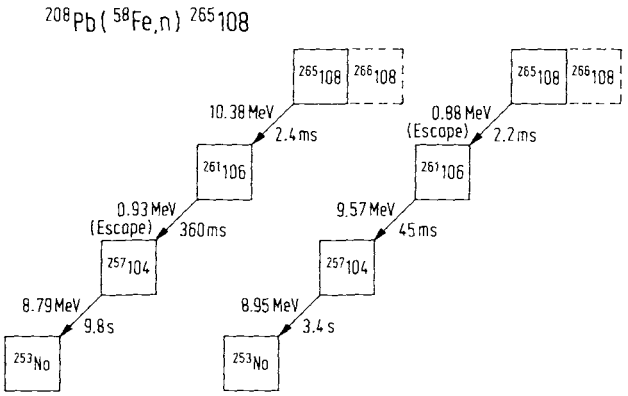

Fig. 17. Discovery of element 108: α-decay chains of two nuclei of the isotope 265 formed by fusion of lead-208 with iron-58 (after [83]).

Taking the reaction of lead-208 with iron-58 as an example, we shall describe what the original data look like when they are obtained during the detection of new elements with SHIP. Figure 18a shows the complete α-spectrum measured in a detector at the end of SHIP, without any selection criteria. The spectra in (b)–(e) have been subjected to boundary conditions: the α-decay must first be correlated in space and time with the implantation of a heavy nucleus (b); this nucleus must have a mass between 235 and 295 (c), and successive α-decays must originate from it (d, e). The first generation of α-decays is shown in (d), the second and third in (e). The heaviest nuclei searched for become recognizable in part (b), constitute the only remaining events in (c), and are identified unambiguously in (d) and (e) as members of a decay chain starting with the new element (d).

A second isotope of element 108 with mass 264 and half-life 0.08 ms (Table 1) was produced at UNILAC by fusion of lead-207 with iron-58;[85,84] we shall discuss it in Section 7. There is some evidence for a third isotope of mass 263, but the half-life is still unknown.[86]

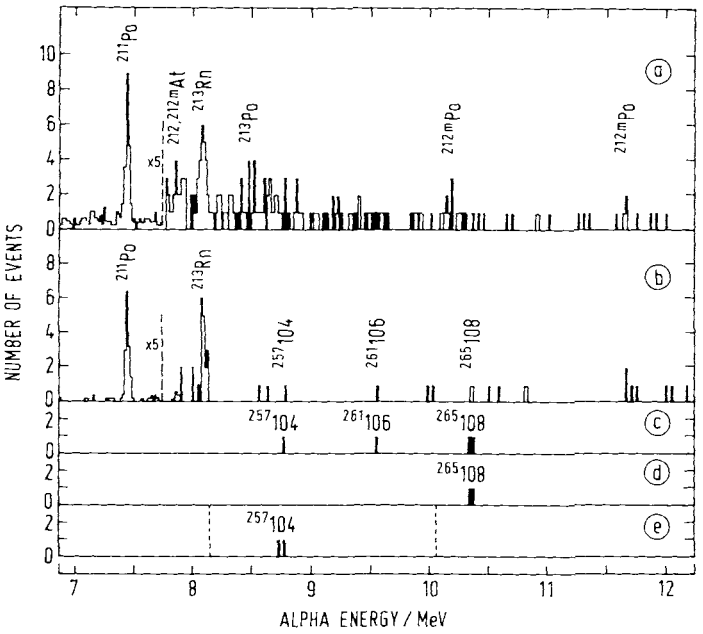

Fig. 18. α-Spectra observed from products of the bombardment of lead-208 with iron-58: (a) spectra taken between the beam pulses of the UNILAC; (b) α-decays that are connected with the implantation of a heavy nucleus; (c) α-decays connected with nuclei of mass 235 to 295; (d, e) correlated α-decays starting with the new element (d) and its known decay products (e) (after [84]).

5.3. Element 109

The periodic table presently ends at element 109. In 1982, during a ten day long bombardment of bismuth-209 with iron-58, *Münzenberg* et al.[87] succeeded in detecting one single decay chain, depicted in Figure 19. It connects a new α-emitter with a decay chain already known from the synthesis of element 107. Thus, the synthesis was carried out via the reaction

$^{209}_{83}Bi(^{58}_{26}Fe,n)^{266}109$

This nucleus decayed with a lifetime of 5.0 ms corresponding to a half-life of $3.5^{+16.6}_{-1.6}$ ms, and with 11.10 MeV α-energy into the isotope 262 of element 107. The following nuclide (105)-258 did not decay via α-emission but rather by electron capture (EC), which occurs with 33% probability; the resulting isotope (104)-258 decayed via

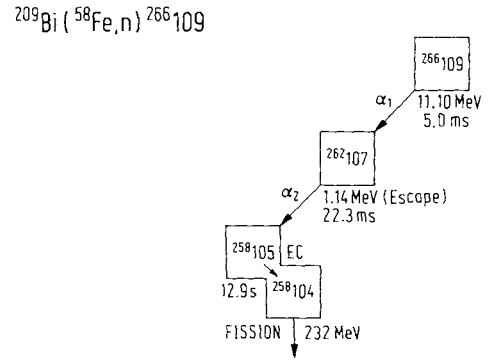

Fig. 19. Discovery of element 109. A single α-decay chain of mass number 266 was observed in the irradiation of bismuth-209 with iron-58 (after [88]).

spontaneous fission. In a very careful analysis of this single event *Münzenberg* et al.[88] were able to demonstrate that it is significant. The analysis involved additional information, for example the approximate mass number calculated from the time-of-flight, the systematics of α-decay energies, and possible side reactions. In a second experiment performed in February 1988 the SHIP group found a second atom of element 109 with almost the same lifetime which was correlated with the following successive nuclei:[89]

$$^{266}109 \xrightarrow{\alpha} {}^{262}107 \xrightarrow{\alpha} {}^{258}105 \xrightarrow{\alpha} {}^{254}_{103}\mathrm{Lr} \xrightarrow{EC} {}^{254}104 \xrightarrow{\alpha} {}^{250}_{102}\mathrm{No}.$$

In addition, a third decay chain of (109)-266 was observed in which the first member was not, however, detected.

This discovery is corroborated by *Oganessian* et al.,[38] who radiochemically detected a long-lived end product of the α-decay chain, the 1.5-d californium-246 which was already observed in the production of element 107. The α-spectrum of the chemically isolated californium fraction is shown in the upper part of Figure 16. The peak at 6.75 MeV, characteristic of the californium isotope, contains seven events.

5.4. Attempts to Synthesize Element 110

It seemed natural to extend this successful concept one step further, to element 110, and to try to fuse lead-208 with nickel-64:

$$^{208}_{82}\mathrm{Pb}(^{62}_{28}\mathrm{Ni}, 1\text{-}2n)^{271,270}110$$

The search for this element with SHIP in an experiment lasting 11 days, again using the α-correlation technique as detection method, remained unsuccessful; no event was observed with a cross-section limit of 5×10^{-36} cm^2.[90,91] Nor has it been possible in Dubna to fuse bismuth-209 and cobalt-59 to form element 110 or to fuse bismuth-209 and nickel-64 to form element 111. In these experiments it was again intended to identify the new elements by long-lived members of possible decay chains.[38]

The difficulties encountered in these experiments become obvious from Figure 20. The production cross-section of the heaviest nuclei by cold fusion is seen to decrease rapidly with increasing atomic number by about a factor of three per element step. For element 110 a value between 10^{-35} and 10^{-36} cm^2 is extrapolated that is just at the limit of present experimental techniques. It is still not completely hopeless to discover element 110 in the way just described, but a beam time of the order of two months would be required.

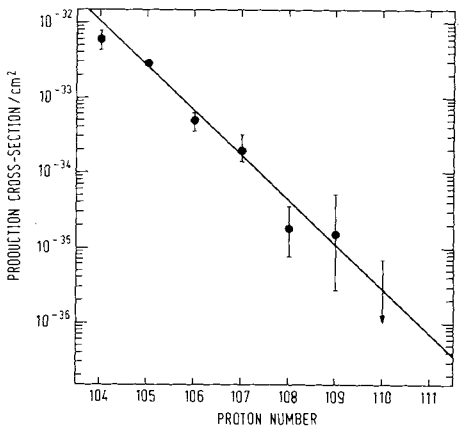

Fig. 20. Production cross sections of the heaviest elements by cold fusion versus the proton number (after [91]).

From systematic studies of the fusion of heavy nuclei[28,73] and from theoretical work[92,93] one realizes that the fusion process becomes increasingly difficult with increasing mass and charge of the nuclei involved. It is no longer sufficient for fusion to establish some contact between the nuclei at the coulomb barrier. Rather, the contact has to be strong enough for the attractive nuclear force to dominate over the coulomb force. This requires a higher projectile energy or an "extra push" that increases the excitation energy of the compound nucleus and, as a result, drastically diminishes its survival probability against spontaneous fission.

This hindrance is less severe when a small projectile nucleus and a larger target nucleus are used than in the case of cold fusion with lead or bismuth targets. The smaller projectile nucleus is more likely to be absorbed by the much larger target nucleus. The disadvantage, however, is that since one no longer starts with shell-stabilized target nuclei the excitation energy of the compound nucleus is higher, even if fusion takes place at the coulomb barrier. Nevertheless, according to this concept suggested by *Flerov*,[40] element 110 might be more likely to survive than if the synthesis had started with lead. However, the systematic trend of production cross sections for "warm fusion" speaks against this possibility.[73]

Among many possible combinations one may choose argon-40 as the projectile and a uranium isotope as target, e.g.:

$$^{235}_{92}\mathrm{U}(^{40}_{18}\mathrm{Ar}, 3n)^{272}110$$

As in the case of the other heaviest elements one still remains in an area where some local stability is expected; more will be said about this in Section 7. None the less, the search[90,94] for characteristic decay chains of element 110 with SHIP in the above reaction remained unsuccessful down to a cross-section limit of 8×10^{-36} cm^2. Negative results were also obtained in radiochemical experiments[95] in the case of reactions of argon-40 with uranium-233, -235, and -238.

In contrast *Oganessian* et al.[96,97] found a spontaneously fissioning isotope of about 8 ms half-life in irradiations of thorium-232 with calcium-44, and of uranium-236 with argon-40. Both reactions lead to the same compound nucleus of element 110 with mass number 276. In the argon plus uranium reaction 16 fission tracks were found, corresponding to a production cross-section of 1×10^{-35} cm^2. The observed activity might be due to the well known spontaneous fission isomer of americium-242 ($Z=95$) with 14 ms half-life, because the close neighbor, the 0.8-ms spontaneous fission isomer of americium-240, is known to be produced with a large cross section. *Oganessian* et al.[97] believe, however, that the americium-242 isomer can be excluded on grounds of additional experiments, and they

"are inclined" to ascribe the observed activity to the decay of a nucleus of element 110. It remains an open question as to whether this can be corroborated.

5.5. The Names

No names have yet been suggested for the new elements 107, 108, and 109. Some reluctance is prevalent, because there have been controversies about the discovery of some transactinoid elements resulting in different names in the East and West, kurchatovium and rutherfordium for element 104, and nielsbohrium and hahnium for element 105. It is desirable at first to come to an agreement on how to judge the results of such experiments at the limits of technology. In order at least to come to temporarily agreed names and element symbols, e.g. for registrary purposes and literature searches, the International Union of Pure and Applied Chemistry decided some years ago to name future elements according to their atomic number.[98] With unabashed optimism a nomenclature was developed for elements up to 999.[98,99] Element 107 is called unnilseptium, with symbol Uns, element 108 unniloctium (Uno), element 109 unnilennium (Une), and element 110 ununnilium (Uun). One may very well question the usefulness of such a scheme. As far as can be seen at the moment it will only be necessary to find names for a few more elements anyway, and discussions about the priority of discoveries cannot be avoided either.

6. Superheavy Elements

When trying to synthesize superheavy elements by fusion, even the choice of the reaction system is a problem. This is obvious from Figure 21, which shows schematically the upper end of the chart of nuclides. The heaviest known nuclei are found in the lower left-hand corner, marked by squares, while the island of superheavy elements is represented in the upper right-hand corner by the hatched area. The island results from theoretical estimates of the half-lives of all competing decay modes, viz. α-decay, β-decay, and spontaneous fission. Rather than showing all its details, we indicate the island by a contour line which connects all nuclei with a one microsecond half-life. This is about the shortest detectable half-life. Depending on how the theoretical calculations are carried out, different landscapes will be obtained. The results of two such studies are shown in Figure 21; one predicts a broad beach extending to the west,[100] the other a steep cliff in just the same area.[101] Both calculations expect the longest half-life, i.e. 10^9 years[100] or 10^5 years,[101] respectively, for element 110 with neutron number 184, and not for the magic atomic number 114. The reason is that α-decay should be dominant near $Z = 114$, and is not reduced as much by shell closures as spontaneous fission.

Figure 21 shows that with respect to the proton number the heaviest known nuclei are already up to the island, but the neutron number is still far away from it. Superheavy nuclei are predicted to be extremely neutron-rich and even fusion of the most neutron-rich projectile and target nuclei barely reaches the north-western shore of the island. This is indicated by parachutes in Figure 21 which stand for the compound nuclei resulting from fusion of the neutron-rich calcium-48 and the neutron-rich nuclei plutonium-244, curium-248, and einsteinium-254.

One can, of course, quite optimistically rely on a shallow western shore which can be reached by projectile-target combinations more readily available. A large number of such syntheses had already been performed before the construction of the UNILAC was completed. A review published in 1979[102] quotes 16 different combinations, and by 1982 the number had increased to 22.[26] The list includes systems ranging from calcium-48 plus thorium-232 with the compound nucleus (110)-280 up to krypton-84 plus uranium-238 with the compound nucleus (128)-322. None of these fusion experiments has been successful, even though positive results have been reported from time to time. None of the positive results could ever be confirmed. Therefore, when heavy projectiles became available at UNILAC, another type of reaction was preferred: nucleon transfer between very heavy nuclei. We shall discuss these experiments later, and instead concentrate on the most recent attempts at synthesis via fusion.

6.1. Attempted Synthesis by Nuclear Fusion

Among the three combinations depicted in Figure 21, the reaction of calcium-48 with curium-248 seems to be the

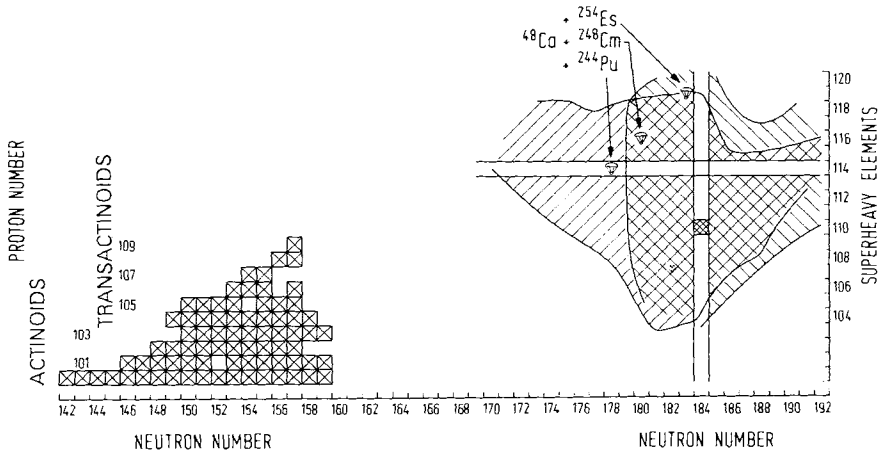

Fig. 21. Upper end of the present chart of nuclides and two predicted versions of the island of superheavy elements [100, 101], enclosed in contour lines corresponding to a half-life of 1 μs (see text).

most promising one. This results in a compound nucleus with 116 protons and 180 neutrons, not far from the closed proton and neutron shells. With plutonium-244 one would reach the proton shell 114 exactly, and with einsteinium-254 one would get closer to the neutron shell 184, but the other nuclear shell in both cases would be further away. Curium-248, with a 3.4×10^5 years half-life, is produced in milligram quantities from lighter actinoids by neutron capture in the high-flux reactor at Oak Ridge. Calcium-48, a stable isotope with 0.19% abundance in natural calcium, is produced in nearly pure form by electromagnetic isotope separators. As early as 1977/78 scientists from the Lawrence Berkeley Laboratory and the Lawrence Livermore Laboratory[103-106] as well as from the Joint Institute for Nuclear Research[107] tried to produce superheavy elements with this reaction at the respective heavy-ion accelerators at Berkeley and Dubna. However, the experiments were not successful.

In these experiments it had been assumed that an "extra-push", i.e. some additional projectile energy, is needed in order to fuse these two nuclei. A number of later experimental and theoretical studies raised doubts as to whether an "extra push" was really necessary. Therefore, it was decided to try again to fuse these nuclei, this time under very gentle conditions close to the coulomb barrier. Even in this case, 20 MeV of excitation energy remains in the compound nucleus. This is quite a large value considering the fragility of these nuclei. This new series of experiments were carried out in collaboration by scientists from GSI Darmstadt, the Lawrence Berkeley Laboratory, the University of Mainz, the Los Alamos National Laboratory, and the Universities of Berne and Göttingen using the heavy ion accelerators at Darmstadt and Berkeley. Making use of the whole repertoire of physical and chemical separation and detection methods, they intended to cover a region of half-lives as large as possible with highest sensitivity.[108]

This search for superheavy elements, probably the most elaborate one, also ended without clear evidence of their existence. The quantity used to describe such negative results is the upper limit of the production cross-section of the sought after nuclei that is compatible with the negative result. Its value depends on the half-life; neither the very short-lived nuclei can be detected (because they already decay before being separated) nor the very long-lived ones (because they do not decay in appreciable amounts during the limited time of measurement). Between these extremes the detection limit is independent of the half-life. Thus the production cross-section limits, depicted as a function of the half-life, have a trapezoidal shape, as in Figure 22. For the sake of clarity the cross-section limits are replaced in Figure 22 by an equivalent quantity, viz. the probability for superheavy nuclei to be formed in a collision between the reaction partners. This probability is at most $1:10^{10}$ for 14 orders of magnitude in half-life. Even lower values result for half-lives of the order of weeks and months. The formation of superheavy nuclei is excluded in the hatched area, i.e. for half-lives ranging from several microseconds to several years at most a few nuclei per day could have been produced.

A more correct description of the results is given in Figure 23, which shows the regions of half-lives in which different methods are sensitive. Very short-lived nuclei would have been detected by the velocity filter SHIP at GSI (curve 2), and the gas-filled fragment-separator SASSY at Berkeley (1). Chemical on-line methods were sensitive to lead- and radon-like (3, 4) as well as platinum-like (5) elements with medium half-lives. Off-line separations in combination with highly sensitive detector arrays were used to search for long-lived nuclei in the radon (6), platinum (7), and lead fractions (8).

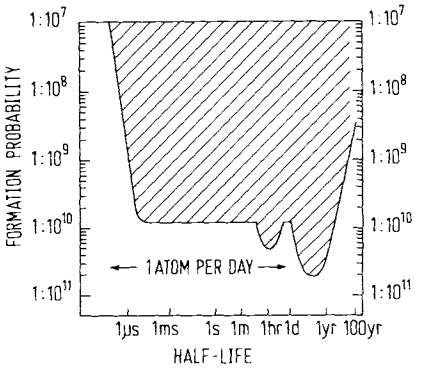

Fig. 22. Results from a search for superheavy elements in the reaction of calcium-48 with curium-248. As a function of the half-life the upper limit for the formation probability per collision is depicted which is still compatible with a negative result; the hatched area is ruled out by the experiments. The diagram is actually made up from several parts shown individually in Figure 23 (from [65]).

Another reaction indicated in Figure 21 was recently carried out in Berkeley, the fusion of calcium-48 with einsteinium-254.[109] The experiments were again negative with a cross-section limit of 3×10^{-31} cm^2 for half-lives ranging from one day to several months. Future experiments with better sensitivity are feasible if the current pro-

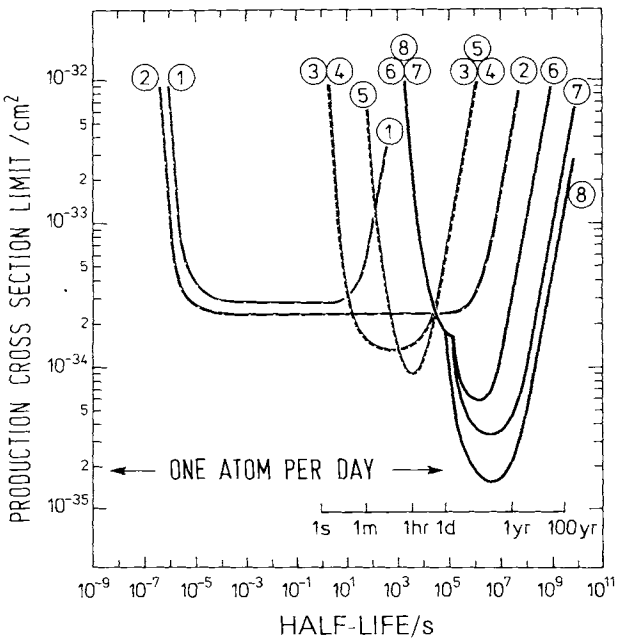

Fig. 23. Results from a search for superheavy elements in the reaction of calcium-48 with curium-248. The upper limits of production cross-sections determined with different separation techniques are shown as a function of the half-life. The results were obtained with fragment separators (curves 1 and 2), chemical on-line (3-5) and chemical off-line separations sensitive to lead- (3, 8), platinum- (5, 7), and radon-like (4, 6) elements (after [108]).

duction rate of einsteinium-254 of several micrograms per year is increased by one order of magnitude. Such an increase has been proposed[110] for a number of scientific reasons.

6.2. Attempts to Synthesize by Nucleon Transfer

The typical spectrum of products resulting from a fusion reaction is quite well known, in contrast to products from nucleon transfer between heavy nuclei. Questions of whether a broad or a narrow spectrum of product nuclei is formed and whether the excitation energy of these nuclei is distributed sharply or not have to be verified experimentally and interpreted by theoretical models.[111]

The first reaction to be studied at UNILAC was that of xenon-136 with uranium-238. In this reaction the Dubna group had observed a spontaneous fission activity with 150 d half-life[112, 113] which they attributed to a superheavy element.[113] This activity could not be found at UNILAC.[114]

A more attractive case, of course, was the reaction between two uranium-238 nuclei, the study of which was only possible with the UNILAC. The question was, what would happen in reactions between the heaviest naturally occurring nuclei. The first radiochemical studies[115] of the uranium-uranium reaction were encouraging; nuclei beyond uranium being formed. The respective yields, however, decrease strongly with increasing atomic number because the nuclei tend to be more and more fissile. On the other hand, the occurrence of complementary nuclei near element 70 indicated (see Fig. 7) that the proton transfer in the collision complex is large enough to produce superheavy elements with the appreciable cross section of 10^{-28} cm^2. It remained open, however, whether their survival probability was sufficiently large.

During the first experiments to detect superheavy elements in the uranium-uranium reaction the reaction products were measured without separation from other products. They were either implanted in solid-state detectors[116, 117] or transported to the detector system by a carrier gas[118–120] or by a wheel.[121, 122] In these cases the detection threshold was limited by the background of α- and spontaneous fission decay of the actinoids. More sensitive measurements were performed with radiochemical off-line methods[121] that separated the actinoids. These experiments were complemented by on-line measurements of radon-like products.[67] All these attempts had negative results. The respective cross-section limits are depicted in Figure 24.

Two different ideas prompted further experiments. The reaction of uranium-238 as projectile and curium-248 as target was studied[123] because transfer towards superheavy nuclei should be more favorable when starting with a heavier target. This was shown in the build-up of heavy actinoids.[124] The reaction between uranium-238 and lead-208 was also studied[125] because the structural properties of the reaction partners might favor the transfer. These experiments were unsuccessful, too. The cross-section limit for the uranium-curium reaction was 4×10^{-35} cm^2 for lead-, platinum-, and radon-like elements with half-lives between several days and years, and 1×10^{-33} cm^2 for radon-like elements with half-lives of several minutes to hours. For the uranium-lead reaction the corresponding limits are 1×10^{-33} cm^2 for half-lives of milliseconds to days and one order of magnitude lower for half-lives of some hours to years.

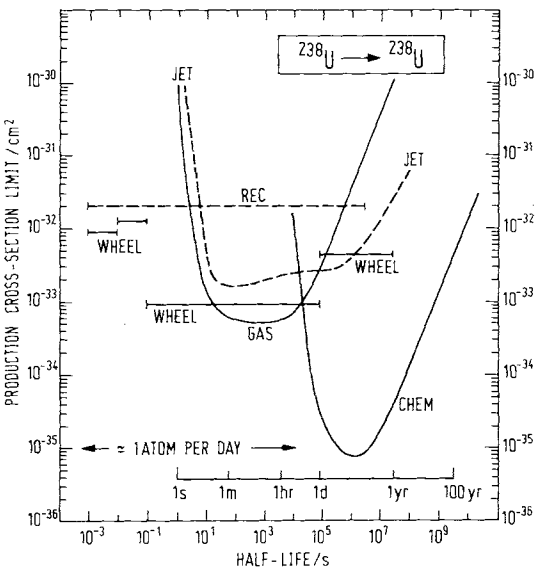

Fig. 24. Results from a search for superheavy elements in the reaction of uranium-238 with uranium-238. Upper limits of the production cross-sections as a function of half-life, measured after implantation of the unseparated reaction products into solid-state detectors ("rec") [116, 117], after transport of the products by a gas jet ("jet") [118–120] or a wheel ("wheel") [121] to the detectors, after chemical on-line separation of radon-like elements ("gas") [67], and after off-line separation of lead-, platinum-, and radon-like elements ("chem") [121] (after [67]).

7. Perspectives

The nuclei at the end of the periodic table decay differently from what would be expected from Figure 3. Spontaneous fission does not tend to dominate in the rectangular, new region; α-decay remains the dominant decay process. This is even true for nuclei with even numbers of protons and neutrons. In this case spontaneous fission competes most favorably with α-decay, whereas for odd numbers of protons or neutrons the unpaired nucleon slows down spontaneous fission by orders of magnitude more than α-decay. Such α-emitters with even proton and neutron numbers, like the heaviest one, the isotope 264 of element 108,[84, 85] are especially informative, because their most energetic α-transition ends in the ground state of the resulting daughter nucleus. From the decay energies one can therefore calculate the binding energies of the successively decaying nuclei of a whole decay chain, and derive the corresponding nuclear masses. These masses allow the calculation of the shell energies from which one can deduce the fission barriers shown in Figure 25.[84, 30] These barriers have the unexpectedly large values of 6 to 7 MeV over the whole range from element 92 to 108, whereas the liquid-drop model predicts their continuous decrease to vanishingly small values. More recent theoretical calculations are able to reproduce the barrier heights deduced from experiment, as is obvious in Figure 25. These barriers are caused

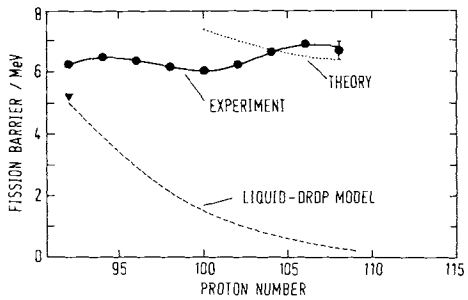

Fig. 25. Fission barriers of heavy nuclei with $N-Z=48$ as a function of proton number. Dots: values obtained from experimentally determined nuclear masses. Dotted line: calculated theoretical values. Dashed line: barrier heights expected from the liquid-drop model (after [30]).

by shell effects in non-spherical, slightly elongated nuclei.[127, 128]

The heaviest known nuclei are only able to exist because of the strong stabilization against fission, which corresponds to 18 orders of magnitude in half-life for element 108.[73] If the attribute "superheavy" means that an element exists only by virtue of the stabilizing effect of nuclear shells and not the requirement to be spherical, as is expected for element 114, then the superheavy elements have already been found; *Armbruster* has stressed this point.[28, 73] The idea that superheavy, shell-stabilized nuclei do not necessarily have to be spherical but might be deformed was already formulated by *Bohr* in 1974;[129] shell closures would then occur for different nucleon numbers, in regions more easily accessible to experiments.

The nuclear landscape, as it should look according to the most recent theoretical studies,[81, 126–128, 130] is shown in Figure 26. The "microscopic" contribution to the binding energy is represented by contour lines. The numbers in the figure give these values in MeV for the respective contour lines. This contribution is due to the nuclear structure and causes the stabilization. The heaviest known nuclei are again shown as squared boxes near the lower left-hand corner. Nuclei above the dashed line cannot exist because they promptly emit a proton. Nuclei above the dotted line should not exist according to the liquid-drop model, because they do not have any fission barriers. Nuclei that may exist due to shell stabilization fall between these two lines. Taking into account that for detection the lifetime has to be longer than microseconds, the barrier height has

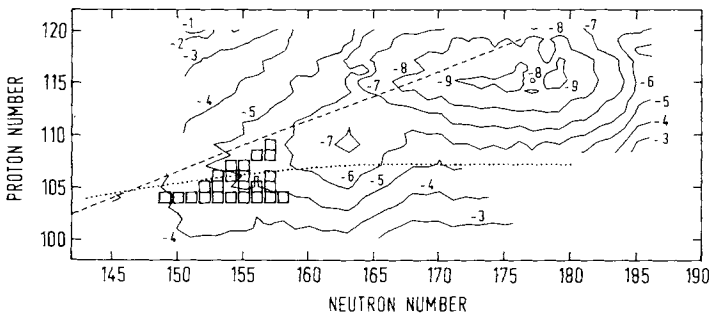

Fig. 26. Predicted shell correction energies of heavy and superheavy nuclei [130]. Nuclei with the same shell correction (given in MeV) are connected by contour lines. Known nuclei are marked as squares. Above the dashed line prompt emission of protons is expected. The dotted curve indicates the limit for spontaneous fission from the liquid-drop model. No nuclei should exist above this line according to this model (after [30]).

to be at least 4 MeV.[73] Thus, the elements 107 to 109 reported here owe their existence only to these shell-induced fission barriers.

The landscape looks much different now than in Figure 21. It has been changed by the experimental results of recent years and the refined theoretical calculations that they stimulated. The center of the island of spherical nuclei is located around the region of largest microscopic corrections of more than 8 MeV. The elements 114 to 116 are still at the center, but now with the lower neutron numbers of 171 to 179. From the center a ridge develops towards the south-west, exactly in the direction of the heaviest known nuclei. It includes a little peak around element 109 and neutron number 163.[130, 126, 128] In this local region half-lives of, e.g., 40 ms for (110)-272, an α-emitter, are estimated,[127] or even of some hours for the spontaneous-fission isotope (106)-268.[81] However, it is possible that, due to a special kind of fission, spontaneous fission is more dominant in this region. This special fission process is observed in the region of element 100, fermium,[131, 132] and might be present also for heavier nuclei.[133] It occurs faster than usual fission and involves a compact form of the fissioning nucleus rather than the usual elongated one. Similarly, the resulting fragments are spherical rather than deformed.

The fusion of calcium-48 with curium-248 results in a compound nucleus of 116 protons and 180 neutrons, which, after some neutrons have evaporated, is quite close to the center of the newly determined island of spherical superheavy nuclei. From there, α-decay chains should start with half-lives of milliseconds to minutes,[127] which eventually reach the area of spontaneous fission near element 110.[81] The fact that these decay chains could not be found, even though the prediction about the island's location is more favorable now, most likely means that fusion is already strongly hindered. Some recent theoretical[93] and experimental[134] studies point in that direction, too.

It should be possible to reach the region of local stability near neutron number 163 by fusion of easily accessible nuclei. One might use, for example, the reactions of argon-40 with uranium isotopes. As already discussed in Section 5.4, results of such experiments are still ambiguous.

The stability of the heaviest nuclei is still a topic with open problems but it does not seem to be a major obstacle to further extension of the periodic table. The syntheses are much more of a problem. The general trend of an increasing hindrance to fusion with increasing masses of the nuclei involved is well established. For the individual case, however, the situation is less transparent, in spite of the systematic experiments carried out at UNILAC[28, 73] and theoretical studies.[92, 93] First of all, the onset of hindrance depends on the nuclear charge and mass numbers of projectile and target, reflecting the opposing effects of attractive and repulsive forces. A second complication comes from the nuclear structure of the reaction partners. Its influence is not easy to predict for the systems of interest here. What has been learned from lighter systems that are quite easy to study does not necessarily apply to these heavy systems.

The over all situation is represented in Figure 27 (after *Armbruster*).[28] The proton numbers of target Z_T and pro-

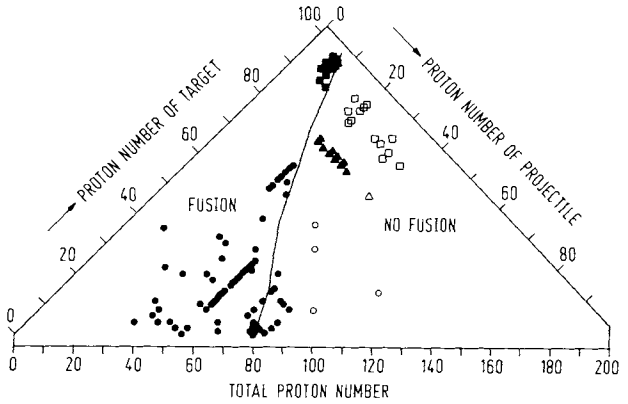

Fig. 27. Fusion reactions for different target-projectile combinations, after [28, 30]. The proton numbers of target and projectile are given on the tilted axes, the sum of both, i.e. the proton number of the compound nucleus, on the bottom axis. Full symbols: fusion was observed via evaporation residues. Empty symbols: fusion was not observed. With combinations to the right of the solid line (calculated from a macroscopic model [93]) an "extra push" should be needed.

jectile Z_p are given on the skewed axes and the sum of both, the proton number of the compound nucleus, is shown on the horizontal axis. Each projectile-target combination is represented by a full symbol if fusion has been detected via evaporation residues and by an empty symbol if none has been observed. Reactions with lead as target are shown as triangles, those with actinoids as squares. Let us take the compound nucleus thorium, $Z_p + Z_T = 90$, as an example. In the vertical direction one finds the different target-projectile combinations: the ones between nuclei of about the same size with Z_p and Z_T from 40 to 50 are in the lower part, the more asymmetric combinations with Z_p and Z_T around 20 and 70 in the upper part. Up to about thorium it seems that any combination of nuclei results in fusion. Beyond it, for example for fermium ($Z = 100$), only asymmetric systems are successful, either with lead or with actinoids as a target (see upper corner in Fig. 27). Fusion finally ends around element 109.

The prediction of the "extra push" model for the limits of fusion is shown by the theoretically derived solid line.[93] It describes the general situation but certainly not the details. Syntheses starting with lead or bismuth (triangles in Fig. 27) work much better than expected. The closed shells are helpful for two reasons: the resulting compound nuclei have a very low excitation energy and the extra push is obviously reduced or not needed at all.[73] It is necessary to shed more light on the remaining mysteries of the fusion hindrance in order to clarify whether it can be circumvented for the purpose of producing even heavier elements, the stability of which may well be high.

Recently, an aspect of cosmic dimensions was added to the speculations about superheavy elements. Figure 28 shows the chart of nuclides as viewed by some elementary particle theorists.[135, 136] The lower left-hand corner shows a conventional chart of nuclides, somewhat mutilated at its upper end. In the upper right one sees an island of stability, the neutron stars, with mass and "atomic" numbers around 10^{57} and 10^{55}, respectively. "Nuclides" with even higher masses are unstable against gravitational collapse leading to black holes. In the middle region one finds the

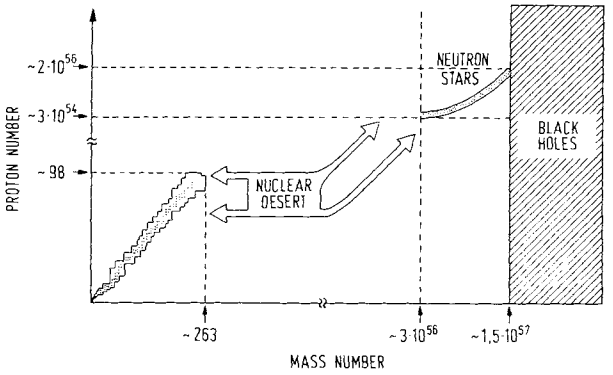

Fig. 28. All-inclusive chart of the nuclides, hopefully incomplete in the nuclear desert region [135].

nuclear desert. It might, however, not be completely empty. Conventional nuclei consist of protons and neutrons. These are, in turn, made up of three quarks each. The proton contains two "up" quarks with charge + 2/3 and one "down" quark with − 1/3. The neutron contains one "up" and two "down" quarks. More massive quarks probably existed only in the very early times of our universe. It is still possible, however, that the "strange" quark, either during these early times or after having been produced later in the course of some high energy processes, formed larger aggregates together with the "up" and "down" quarks. These multi-quark aggregates might constitute the true ground state of nuclear matter,[137, 135] and thus might still be present today. They are candiates for being part of the "dark matter" which fills the universe.[137, 135] The radii of these lumps of "strange" matter may be between 10^{-15} and 10^{3} m.[135, 137] Different methods can be used to search for these lumps in natural samples.[135, 137] At UNILAC this is done by backscattering of very heavy ions like uranium.[138, 139] Superheavy elements as messengers of strange matter—what a perspective!

To arrive at the results and ideas presented here many scientists worked together in friendship and competition. Their names can be found in the references. Christoph Schmelzer contributed to all these subjects, not only by the design and the construction of the UNILAC, but also by his steady encouragement of the "Nuclear Alchemists". Thanks are due to Helmut Ahrens, Peter Armbruster, Hans-Otto Denschlag, Heinz Gäggeler, Jens Volker Kratz, Klaus Lützenkirchen, Gottfried Münzenberg, Matthias Schädel and Norbert Trautmann for their critical reading of the manuscript.

Received: December 2, 1987 [A 694 IE]
German version: *Angew. Chem. 100* (1988) 1471
Translated by Dr. *Klaus Lützenkirchen*, Darmstadt (FRG)

[1] O. Hahn, L. Meitner, F. Strassmann, *Ber. Dtsch. Chem. Ges. 70* (1937) 1374; *Naturwissenschaften 26* (1938) 475.
[2] O. Hahn, F. Strassmann, *Naturwissenschaften 27* (1939) 11, 89.
[3] H. Menke, G. Herrmann, *Radiochim. Acta 16* (1971) 119.
[4] O. Hahn: *Vom Radiothor zur Uranspaltung - eine wissenschaftliche Selbstbiographie*, Vieweg, Braunschweig 1962.
[5] G. Herrmann, *Radiochim. Acta 3* (1964) 169; *U. K. Atomic Energy Research Establishment Harwell report AERE-Transl. 1036* (1965).
[6] F. Krafft: *Im Schatten der Sensation - Leben und Wirken von Fritz Strassmann*, Verlag Chemie, Weinheim 1981.
[7] E. McMillan, P. H. Abelson, *Phys. Rev. 57* (1940) 1185.
[8] C. Keller: *The Chemistry of the Transuranium Elements*, Verlag Chemie, Weinheim 1971.

[9] G. T. Seaborg (Ed.): *Transuranium Elements - Products of Modern Alchemy*, Dowden, Hutchinson & Ross, Stroudsburg 1978.
[10] J. J. Katz, G. T. Seaborg, L. R. Morss (Eds.): *The Chemistry of the Actinide Elements*, 2nd edit., Chapman and Hall, London 1986.
[11] G. T. Seaborg, *Chem. Eng. News 23* (1945) 2190.
[12] M. S. Fred in [10], p. 1196.
[13] N. Angert, C. Schmelzer, *Kerntechnik 19* (1977) 57.
[14] After G. T. Seaborg, *Phys. Scr. A 10* (1974) 5, updated.
[15] E. Feenberg, *Phys. Rev. 55* (1939) 504.
[16] N. Bohr, J. A. Wheeler, *Phys. Rev. 56* (1939) 426.
[17] U. Schindewolf: *Physikalische Kernchemie*, Vieweg, Braunschweig 1959, p. 27.
[18] After W. D. Myers (1971), from J. O. Rasmussen in J. Cerny (Ed.): *Nuclear Spectroscopy and Reactions, Vol. D*, Academic Press, New York 1975, p. 106.
[19] L. Meitner, O. R. Frisch, *Nature (London) 143* (1939) 239.
[20] R. A. Knief: *Nuclear Energy Technology*, McGraw-Hill, New York 1981, p. 45.
[21] W. D. Myers, W. J. Swiatecki, *Nucl. Phys. 81* (1966) 1.
[22] H. Meldner, *Ark. Fys. 36* (1967) 593.
[23] S. G. Nilsson, S. G. Thompson, C. F. Tsang, *Phys. Lett. B 28* (1969) 458.
[24] F. G. Werner, J. A. Wheeler, *Phys. Rev. 109* (1958) 126.
[25] G. Herrmann in A. G. Maddock (Ed.): *Radiochemistry (Int. Rev. Sci. Inorg. Chem. Ser. Two, Vol. 8)*, Butterworths, London 1975, p. 221.
[26] J. V. Kratz, *Radiochim. Acta 32* (1983) 25.
[27] a) G. N. Flerov, G. M. Ter-Akopian, *Rep. Prog. Phys. 46* (1983) 1817; b) G. N. Flerov, G. M. Ter-Akopian in [27c], p. 333; c) D. A. Bromley (Ed.): *Treatise on Heavy-Ion Science, Vol. 4*, Plenum, New York 1985.
[28] a) P. Armbruster, *Annu. Rev. Nucl. Part. Sci. 35* (1985) 135; b) P. Armbruster, G. Münzenberg, *Spektrum Wiss. 1988*, No. 9, p. 42 and *Sci. American*, in press; c) P. Armbruster, *Phys. Bl. 44* (1988) 359.
[29] G. T. Seaborg, W. D. Loveland in [27c], p. 255.
[30] G. Münzenberg, *Rep. Prog. Phys. 51* (1988) 57.
[31] G. N. Flerov, G. M. Ter-Akopian, *Jt. Inst. Nucl. Res. Dubna USSR Prepr. (Ob'edin. Inst. Yad. Issled. Dubna USSR Prepr.) JINR E7-87-167* (1987).
[32] After G. N. Flerov, private communication 1975.
[33] P. Brix, *Jahrb. Heidelberger Akad. Wiss. 1986*, Heidelberg 1987, p. 105.
[34] G. Herrmann, N. Trautmann, *Annu. Rev. Nucl. Part. Sci. 32* (1982) 117.
[35] G. Münzenberg, W. Faust, S. Hofmann, P. Armbruster, K. Güttner, H. Ewald, *Nucl. Instrum. Methods 161* (1979) 65.
[36] K. Sümmerer, W. Brüchle, M. Brügger, H. Gäggeler, M. Schädel, D. Schardt, G. Wirth, C. Frink, N. Greulich, G. Herrmann, N. Hildebrand, U. Hickmann, J. V. Kratz, P. Peuser, N. Trautmann, A. Ghiorso, K. E. Gregorich, D. Lee, K. J. Moody, G. T. Seaborg, R. B. Welch, P. Wilmarth, E. K. Hulet, A. D. Dougan, R. J. Dougan, J. H. Landrum, R. W. Lougheed, J. F. Wild, W. R. Daniels, M. Fowler, D. C. Hoffman, R. L. Hahn, R. C. Ferguson, D. O'Kelley, H. R. von Gunten, H. Dornhöfer, *Contrib. XXII. Int. Meeting on Nuclear Physics*, Bormio, Jan. 1984; *Gesellschaft für Schwerionenforschung Darmstadt, preprint GSI-84-17* (1984).
[37] S. Hofmann, G. Münzenberg, F. P. Hessberger, H. J. Schött, *Nucl. Instrum. Methods Phys. Res. 223* (1984) 312.
[38] Yu. Ts. Oganessian, M. Hussonnois, A. G. Demin, Yu. P. Kharitonov, H. Bruchertseifer, O. Constantinescu, Yu. S. Korotkin, S. P. Tretyakova, V. K. Utyonkov, I. V. Shirokovsky, J. Estevez, *Radiochim. Acta 37* (1984) 113.
[39] Yu. Ts. Oganessian, A. G. Demin, A. S. Iljinov, S. P. Tretyakova, A. A. Pleve, Yu. E. Penionzhkevich, M. P. Ivanov, Yu. P. Tretyakov, *Nucl. Phys. A 239* (1975) 157.
[40] G. N. Flerov, *Proc. Int. Conf. Nucl. Phys. Florence 1983*, 365.
[41] V. E. Viola, A. C. Mignerey, H. Breuer, K. L. Wolf, B. G. Glagola, W. W. Wilcke, W. U. Schröder, J. R. Huizenga, J. R. Birkelund, D. Hilscher, *Phys. Rev. C 22* (1980) 122.
[42] G. N. Flerov, I. Zvara, *Jt. Inst. Nucl. Res. Dubna USSR Rep. (Ob'edin. Inst. Yad. Issled. Dubna USSR Prepr.) JINR D7-6013* (1971).
[43] B. G. Harvey, G. Herrmann, R. W. Hoff, D. C. Hoffman, E. K. Hyde, J. J. Katz, O. L. Keller, M. Lefort, G. T. Seaborg, *Science (Washington) 193* (1976) 1271.
[44] E. K. Hyde, D. C. Hoffman, O. L. Keller, *Radiochim. Acta 42* (1987) 57.
[45] H. W. Schmitt, U. Mosel, *Nucl. Phys. A 186* (1972) 1.
[46] B. Fricke, *Struct. Bonding (Berlin) 21* (1975) 89.
[47] O. L. Keller, G. T. Seaborg, *Annu. Rev. Nucl. Sci. 27* (1977) 139.
[48] B. Eichler, *Kernenergie 19* (1976) 307.
[49] K. S. Pitzer, *J. Chem. Phys. 63* (1975) 1032.
[50] E. K. Hulet, *Radiochim. Acta 32* (1983) 7.
[51] O. L. Keller, *Radiochim. Acta 37* (1984) 169.
[52] R. J. Silva in [10], p. 1085.
[53] B. Eichler, S. Hübener, H. W. Gäggeler, D. T. Jost, *Inorg. Chim. Acta 146* (1988) 261.
[54] D. T. Jost, H. W. Gäggeler, C. Vogel, M. Schädel, E. Jäger, B. Eichler, K. E. Gregorich, D. C. Hoffman, *Inorg. Chim. Acta 146* (1988) 255.
[55] U. W. Scherer, J. V. Kratz, M. Schädel, W. Brüchle, K. E. Gregorich, R. A. Henderson, D. Lee, M. Nurmia, D. C. Hoffman, *Inorg. Chim. Acta 146* (1988) 249.
[56] W. Brüchle, M. Schädel, U. W. Scherer, J. V. Kratz, K. E. Gregorich, D. Lee, M. Nurmia, R. Chasteler, H. Hall, R. A. Henderson, D. C. Hoffman, *Inorg. Chim. Acta 146* (1988) 267.
[57] K. E. Gregorich, R. A. Henderson, D. M. Lee, M. J. Nurmia, R. M. Chasteler, H. L. Hall, D. A. Bennett, C. M. Gannett, R. B. Chadwick, J. D. Leyba, D. C. Hoffman, G. Herrmann, *Radiochim. Acta 43* (1988) 223.
[58] O. Hahn: *Applied Radiochemistry*, Cornell University Press, Ithaca 1936.
[59] R. J. Borg, G. J. Dienes, *J. Inorg. Nucl. Chem. 43* (1981) 1129.
[60] F.-J. Reischmann, N. Trautmann, G. Herrmann, *Radiochim. Acta 36* (1984) 139.
[61] F.-J. Reischmann, B. Rumler, N. Trautmann, G. Herrmann, *Radiochim. Acta 39* (1986) 185.
[62] J. V. Kratz, J. O. Liljenzin, G. T. Seaborg, *Inorg. Nucl. Chem. Lett. 10* (1974) 951.
[63] G. Herrmann, *Pure Appl. Chem. 53* (1981) 949.
[64] P. Peuser, U. Tharun, H. J. Keim, N. Trautmann, G. Herrmann, G. Wirth, *Nucl. Instrum. Methods Phys. Res. A 239* (1985) 529.
[65] G. Herrmann, *Umschau 84* (1984) 640.
[66] M. Schädel, W. Brüchle, B. Haefner, *Nucl. Instrum. Methods Phys. Res. A 264* (1988) 308.
[67] N. Hildebrand, C. Frink, N. Greulich, U. Hickmann, J. V. Kratz, N. Trautmann, G. Herrmann, M. Brügger, H. Gäggeler, K. Sümmerer, G. Wirth, *Nucl. Instrum. Methods Phys. Res. A 260* (1987) 407.
[68] A. Ghiorso, J. M. Nitschke, J. R. Alonso, C. T. Alonso, M. Nurmia, G. T. Seaborg, E. K. Hulet, R. W. Lougheed, *Phys. Rev. Lett. 33* (1974) 1490.
[69] Yu. Ts. Oganessian, *Lect. Notes Phys. 33* (1974) 221.
[70] Yu. Ts. Oganessian, Yu. A. Lazarev in [27c], p. 1.
[71] Yu. Ts. Oganessian, A. S. Iljinov, A. G. Demin, S. P. Tretyakova, *Nucl. Phys. A 239* (1975) 353.
[72] H. Gäggeler, A. S. Iljinov, G. S. Popeko, W. Seidel, G. M. Ter-Akopian, S. P. Tretyakova, *Z. Phys. A 289* (1979) 415.
[73] P. Armbruster, *Proc. Int. Sch. Phys. Enrico Fermi, Course "Trends in Nuclear Physics"*, Varenna, June/July 1987, in press; *Gesellschaft für Schwerionenforschung Darmstadt, Preprint GSI-87-59* (1987).
[74] G. Münzenberg, S. Hofmann, F. P. Hessberger, W. Reisdorf, K. H. Schmidt, J. H. R. Schneider, P. Armbruster, C. C. Sahm, B. Thuma, *Z. Phys. A 300* (1981) 107.
[75] G. Münzenberg, S. Hofmann, F. P. Hessberger, K.-H. Schmidt, G. Berthes, H. Folger, H. Geissel, J. G. Keller, P. Lemmertz, M. Montoya, K. Poppensieker, A. B. Quint, H.-J. Schött, I. Zychor, P. Armbruster, M. E. Leino, U. Gollerthan, *Gesellschaft für Schwerionenforschung Darmstadt, Sci. Rep. 1985, GSI 86-1* (1986) 31.
[76] G. Münzenberg, S. Hofmann, F. P. Hessberger, D. Ackermann, H. Folger, V. Ninov, K. Poppensieker, A. B. Quint, W. Reisdorf, K.-H. Schmidt, H.-J. Schött, K. Sümmerer, P. Armbruster, W. Morawek, U. Gollerthan, E. Hanelt, J. Fujita, T. Schwab, M. E. Leino, *Gesellschaft für Schwerionenforschung Darmstadt, Sci. Rep. 1987, GSI 88-1* (1988) 13.
[77] F. P. Hessberger, G. Münzenberg, S. Hofmann, Y. K. Agarwal, K. Poppensieker, W. Reisdorf, K.-H. Schmidt, J. R. H. Schneider, W. F. W. Schneider, H.-J. Schött, P. Armbruster, B. Thuma, C.-C. Sahm, D. Vermeulen, *Z. Phys. A 322* (1985) 557.
[78] Yu. Ts. Oganessian, A. G. Demin, N. A. Danilov, G. N. Flerov, M. P. Ivanov, A. S. Iljinov, N. N. Kolesnikov, B. N. Markov, V. M. Plotko, S. P. Tretyakova, *Nucl. Phys. A 273* (1976) 505.
[79] Yu. Ts. Oganessian, unpublished, quoted in [31].
[80] Yu. Ts. Oganessian, *Proc. Int. Sch.-Sem. Heavy-Ion Phys.*, Alushta, April 1983; *Jt. Inst. Nucl. Res. Dubna USSR Rep. (Ob'edin. Inst. Yad. Issled. Dubna USSR Prepr.) JINR D7-83-644* (1983) 55.
[81] K. Böning, Z. Patyk, A. Sobiczewski, S. Cwiok, *Z. Phys. A 325* (1986) 479.
[82] M. Schädel, W. Brüchle, E. Jäger, K. Sümmerer, E. K. Hulet, J. F. Wild, R. W. Lougheed, R. J. Dougan, K. J. Moody, *Gesellschaft für Schwerionenforschung Darmstadt, Sci. Rep. 1986, GSI 87-1* (1987) 15.
[83] G. Münzenberg, P. Armbruster, H. Folger, F. P. Hessberger, S. Hofmann, J. Keller, K. Poppensieker, W. Reisdorf, K.-H. Schmidt, H.-J. Schött, M. E. Leino, R. Hingmann, *Z. Phys. A 317* (1984) 235.
[84] G. Münzenberg, P. Armbruster, G. Berthes, H. Folger, F. P. Hessberger, S. Hofmann, J. Keller, K. Poppensieker, A. B. Quint, W. Reisdorf, K.-H. Schmidt, H.-J. Schött, K. Sümmerer, I. Zychor, M. E. Leino, R. Hingmann, U. Gollerthan, E. Hanelt, *Z. Phys. A 328* (1987) 49.
[85] G. Münzenberg, P. Armbruster, G. Berthes, H. Folger, F. P. Hessberger, S. Hofmann, K. Poppensieker, W. Reisdorf, A. B. Quint, K.-H.

Schmidt, H.-J. Schött, K. Sümmerer, I. Zychor, M. E. Leino, U. Gollerthan, E. Hanelt, *Z. Phys. A 324* (1986) 489.
[86] Yu. Ts. Oganessian, A. G. Demin, M. Hussonnois, S. P. Tretyakova, Yu. P. Kharitonov, V. K. Utyonkov, I. V. Shirokovsky, O. Constantinescu, H. Bruchertseifer, Yu. S. Korotkin, *Z. Phys. A 319* (1984) 215.
[87] G. Münzenberg, P. Armbruster, F. P. Hessberger, S. Hofmann, K. Poppensieker, W. Reisdorf, J. R. H. Schneider, W. F. W. Schneider, K.-H. Schmidt, C.-C. Sahm, D. Vermeulen, *Z. Phys. A 309* (1982) 89.
[88] G. Münzenberg, W. Reisdorf, S. Hofmann, Y. K. Agarwal, F. P. Hessberger, K. Poppensieker, J. R. H. Schneider, W. F. W. Schneider, K.-H. Schmidt, H.-J. Schött, P. Armbruster, C.-C. Sahm, D. Vermeulen, *Z. Phys. A 315* (1984) 145.
[89] G. Münzenberg, S. Hofmann, F. P. Hessberger, H. Folger, V. Ninov, K. Poppensieker, A. B. Quint, W. Reisdorf, H.-J. Schött, K. Sümmerer, P. Armbruster, M. E. Leino, D. Ackermann, U. Gollerthan, E. Hanelt, W. Morawek, J. Fujita, T. Schwab, A. Türler, *Z. Phys. A 330* (1988) 435.
[90] G. Münzenberg, *Proc. Int. Sch.-Sem. Heavy-Ion Phys.*, Dubna, Sept. 1986; *Jt. Inst. Nucl. Res. Dubna USSR Rep. (Ob'edin. Inst. Yad. Issled. Dubna USSR Prepr.) JINR D7-87-68* (1987) 127.
[91] G. Münzenberg, F. P. Hessberger, P. Armbruster, S. Hofmann, K.-H. Schmidt, G. Berthes, H. Folger, H. Geissel, J. G. Keller, P. Lemmertz, M. Montoya, K. Poppensieker, A. B. Quint, H.-J. Schött, I. Zychor, M. E. Leino, U. Gollerthan, *Gesellschaft für Schwerionenforschung Darmstadt, Sci. Rep. 1985, GSI 86-1* (1986) 29.
[92] S. Bjørnholm, W. J. Swiatecki, *Nucl. Phys. A 391* (1982) 471.
[93] J. P. Blocki, H. Feldmeier, W. J. Swiatecki, *Nucl. Phys. A 459* (1986) 145.
[94] G. Münzenberg, P. Armbruster, G. Berthes, H. Folger, F. P. Hessberger, S. Hofmann, K. Poppensieker, A. B. Quint, W. Reisdorf, K.-H. Schmidt, H.-J. Schött, K. Sümmerer, I. Zychor, M. Leino, U. Gollerthan, E. Hanelt, *Gesellschaft für Schwerionenforschung Darmstadt, Sci. Rep. 1986, GSI 87-1* (1987) 14.
[95] K. Sümmerer, W. Brüchle, E. Jäger, K. J. Moody, M. Schädel, G. Wirth, U. W. Scherer, C. Frink, G. Herrmann, J. V. Kratz, N. Trautmann, H. Gäggeler, *Gesellschaft für Schwerionenforschung Darmstadt, Sci. Rep. 1985, GSI 86-1* (1986) 30.
[96] Yu. Ts. Oganessian in N. Angert, P. Kienle (Eds.): *Proc. Symp. 10 Years of Uranium Beam at the Unilac*, Darmstadt, April 1986; *Gesellschaft für Schwerionenforschung, Darmstadt, Sci. Rep. GSI 86-19* (1986) 201.
[97] Yu. Ts. Oganessian, Yu. V. Lobanov, M. Hussonnois, Yu. P. Kharitonov, B. Gorski, O. Constantinescu, A. G. Popeko, H. Bruchertseifer, R. N. Sagaidak, S. P. Tretyakova, G. V. Buklanov, A. V. Rykhlyuk, G. G. Gulbekyan, A. A. Pleve, G. N. Ivanov, V. M. Plotko, *Proc. Int. Sch. Phys. Enrico Fermi, Course "Trends in Nuclear Physics"*, Varenna, June/July 1987, in press; *Jt. Inst. Nucl. Res. Dubna USSR Prepr. (Ob'edin. Inst. Yad. Issled. Dubna USSR Prepr.) JINR D7-87-392* (1987).
[98] D. M. P. Mingos (Ed.): *Appendices on Provisional Nomenclature, Symbols, Terminology, and Conventions - Number 55*, International Union of Pure and Applied Chemistry, Oxford 1976.
[99] W. C. Fernelius, K. Loening, R. M. Adams, *J. Chem. Educ. 52* (1975) 583.
[100] E. O. Fiset, J. R. Nix, *Nucl. Phys. A 193* (1972) 647.
[101] J. Randrup, S. E. Larsson, P. Möller, A. Sobiczewski, A. Lukasiak, *Phys. Scr. A 10* (1974) 60.
[102] G. T. Seaborg, W. Loveland, D. J. Morrissey, *Science (Washington) 203* (1979) 711.
[103] E. K. Hulet, R. W. Lougheed, J. F. Wild, J. H. Landrum, P. C. Stevenson, A. Ghiorso, J. M. Nitschke, R. J. Otto, D. J. Morrissey, P. A. Baisden, B. F. Gavin, D. Lee, R. J. Silva, M. M. Fowler, G. T. Seaborg, *Phys. Rev. Lett. 39* (1977) 385.
[104] J. D. Illige, E. K. Hulet, J. M. Nitschke, R. J. Dougan, R. W. Lougheed, A. Ghiorso, J. H. Landrum, *Phys. Lett. B 78* (1978) 209.
[105] R. J. Otto, D. J. Morrissey, D. Lee, A. Ghiorso, J. M. Nitschke, G. T. Seaborg, M. M. Fowler, R. J. Silva, *J. Inorg. Nucl. Chem. 40* (1978) 589.
[106] A. Ghiorso, J. M. Nitschke, M. J. Nurmia, R. E. Leber, L. P. Somerville, S. Yashita, *Lawrence Berkeley Lab. Rep. LBL 6575* (1977) 242.
[107] Yu. Ts. Oganessian, H. Bruchertseifer, G. V. Buklanov, V. I. Cherpigin, Choy Val Sek, B. Eichler, K. A. Gavrilov, H. Gäggeler, Yu. S. Korotkin, O. A. Orlova, T. Reetz, W. Seidel, G. M. Ter-Akopyan, S. P. Tretyakova, I. Zvara, *Nucl. Phys. A 294* (1978) 213.
[108] P. Armbruster, Y. K. Agarwal, W. Brüchle, M. Brügger, J. P. Dufour, H. Gäggeler, F. P. Hessberger, S. Hofmann, P. Lemmertz, G. Münzenberg, K. Poppensieker, W. Reisdorf, M. Schädel, K.-H. Schmidt, J. H. R. Schneider, W. F. W. Schneider, K. Sümmerer, D. Vermeulen, G. Wirth, A. Ghiorso, K. E. Gregorich, D. Lee, M. Leino, K. J. Moody, G. T. Seaborg, R. B. Welch, P. Wilmarth, S. Yashita, C. Frink, N. Greulich, G. Herrmann, U. Hickmann, N. Hildebrand, J. V. Kratz, N. Trautmann, M. M. Fowler, D. C. Hoffman, W. R. Daniels, H. R. von Gunten, H. Dornhöfer, *Phys. Rev. Lett. 54* (1985) 406.
[109] R. W. Lougheed, J. H. Landrum, E. K. Hulet, J. F. Wild, R. J. Dougan, A. D. Dougan, H. Gäggeler, M. Schädel, K. J. Moody, K. E. Gregorich, G. T. Seaborg, *Phys. Rev. C 32* (1985) 1760.
[110] A. Ghiorso, D. C. Hoffman, E. K. Hulet, O. L. Keller, G. T. Seaborg, *Lawrence Berkeley Lab. Rep. PUB 5118* (1986).
[111] H. Freiesleben, J. V. Kratz, *Phys. Rep. 106* (1984) 1.
[112] G. N. Flerov, Yu. Ts. Oganessian, *Proc. Moscow Symp. Chem. Transuranium Elements, J. Inorg. Nucl. Chem. Suppl. 1976*, 131.
[113] G. N. Flerov, *Proc. Int. Conf. React. Complex Nucl. (Nashville) 1974*, 459.
[114] H. Gäggeler, W. Brüchle, H. Ahrens, H. Folger, G. Franz, J. V. Kratz, M. Schädel, I. Warnecke, G. Wirth, N. Trautmann, G. Herrmann, N. Kaffrell, P. Peuser, G. Tittel, M. Weber, M. Zendel, *Z. Phys. A 286* (1978) 419.
[115] M. Schädel, J. V. Kratz, H. Ahrens, W. Brüchle, G. Franz, H. Gäggeler, I. Warnecke, G. Wirth, G. Herrmann, N. Trautmann, M. Weis, *Phys. Rev. Lett. 41* (1978) 469.
[116] K. D. Hildenbrand, H. Freiesleben, F. Pühlhofer, W. F. W. Schneider, R. Bock, D. von Harrach, H. J. Specht, *Phys. Rev. Lett. 39* (1977) 1065.
[117] H. Freiesleben, K. D. Hildenbrand, F. Pühlhofer, W. F. W. Schneider, R. Bock, D. von Harrach, H. J. Specht, *Z. Phys. A 292* (1979) 171.
[118] D. C. Aumann, H. Faleschini, L. Friedmann, D. Weismann, *Phys. Lett. 82B* (1979) 361.
[119] H. Jungclas, D. Hirdes, R. Brandt, P. Lemmertz, E. Georg, H. Wollnik, *Phys. Lett. B 79* (1978) 58.
[120] D. Hirdes, H. Jungclas, R. Brandt, P. Lemmertz, R. Fass, H. Wollnik, *Gesellschaft für Schwerionenforschung Darmstadt, Annu. Rep. 1978*, GSI 79-11 (1979) 71.
[121] H. Gäggeler, N. Trautmann, W. Brüchle, G. Herrmann, J. V. Kratz, P. Peuser, M. Schädel, G. Tittel, G. Wirth, H. Ahrens, H. Folger, G. Franz, K. Sümmerer, M. Zendel, *Phys. Rev. Lett. 45* (1980) 1824.
[122] H. Gäggeler, W. Brüchle, J. V. Kratz, M. Schädel, K. Sümmerer, W. Weber, G. Wirth, G. Herrmann, *Nucl. Instrum. Methods Phys. Res. 188* (1981) 367.
[123] J. V. Kratz, W. Brüchle, H. Folger, H. Gäggeler, M. Schädel, K. Sümmerer, G. Wirth, N. Greulich, G. Herrmann, U. Hickmann, P. Peuser, N. Trautmann, E. K. Hulet, R. W. Lougheed, J. M. Nitschke, R. L. Ferguson, R. L. Hahn, *Phys. Rev. C 33* (1986) 504.
[124] M. Schädel, W. Brüchle, H. Gäggeler, J. V. Kratz, K. Sümmerer, G. Wirth, G. Herrmann, R. Stakemann, G. Tittel, N. Trautmann, J. M. Nitschke, E. K. Hulet, R. W. Lougheed, R. L. Hahn, R. L. Ferguson, *Phys. Rev. Lett. 48* (1982) 852.
[125] T. Lund, D. Hirdes, H. Jungclas, D. Molzahn, P. Vater, R. Brandt, P. Lemmertz, R. Fass, H. Wollnik, H. Gäggeler, *Z. Phys. A 303* (1981) 115.
[126] A. Sobiczewski, Z. Patyk, S. Cwiok, *Phys. Lett. B 186* (1987) 6.
[127] P. Möller, G. A. Leander, J. R. Nix, *Z. Phys. A 323* (1986) 41.
[128] S. Cwiok, V. V. Pashkevich, J. Dudek, W. Nazarewicz, *Nucl. Phys. A 410* (1983) 254.
[129] A. Bohr, discussion remark in *Phys. Scr. A 10* (1974) 52.
[130] P. Möller, J. R. Nix, *Atom. Nucl. Data Tables*, in press.
[131] J. P. Balagna, G. P. Ford, D. C. Hoffman, J. D. Knight, *Phys. Rev. Lett. 26* (1971) 145.
[132] E. K. Hulet, J. F. Wild, R. J. Dougan, R. W. Lougheed, J. H. Landrum, A. D. Dougan, M. Schädel, R. L. Hahn, P. A. Baisden, C. M. Henderson, R. J. Dupzyk, K. Sümmerer, G. R. Bethune, *Phys. Rev. Lett. 56* (1986) 313.
[133] P. Möller, J. R. Nix, W. J. Swiatecki, *Nucl. Phys. A 469* (1987) 1.
[134] H. Gäggeler, W. Brüchle, M. Brügger, M. Schädel, K. Sümmerer, G. Wirth, J. V. Kratz, M. Lerch, Th. Blaich, G. Herrmann, N. Hildebrand, N. Trautmann, D. Lee, K. J. Moody, K. E. Gregorich, R. B. Welch, G. T. Seaborg, D. C. Hoffman, W. R. Daniels, M. M. Fowler, H. R. von Gunten, *Phys. Rev. C 33* (1986) 1983.
[135] A. De Rújula, *Nucl. Phys. A 434* (1985) 605c.
[136] A. De Rújula, S. L. Glashow, *Nature (London) 312* (1984) 734.
[137] E. Witten, *Phys. Rev. D 30* (1984) 272.
[138] K. Lützenkirchen, S. Polikanov, G. Herrmann, M. Overbeck, N. Trautmann, A. Breskin, R. Chechik, Z. Fraenkel, *Gesellschaft für Schwerionenforschung Darmstadt, Sci. Rep. 1986, GSI 87-1* (1987) 16.
[139] M. Brügger, K. Lützenkirchen, S. Polikanov, G. Herrmann, M. Overbeck, N. Trautmann, A. Breskin, R. Chechik, Z. Fraenkel, U. Smilansky, *Nature (London)*, in press.

Donor-Acceptor-Substituted Cyclic π-Electron Systems—Probes for Theories and Building Blocks for New Materials

By Rudolf Gompper* and Hans-Ulrich Wagner

Donor and acceptor substituents stabilize (4n)π-electron systems and destabilize those with (4n+2)π electrons. The same is true for the transition states of pericyclic reactions, which explains the appearance of dipolar intermediates in symmetry-allowed cycloadditions and sigmatropic rearrangements. Donor-acceptor-substituted semibullvalenes undergo rapid Cope rearrangement, as do tetraazabarbaralanes. In contrast, tetraazasemibullvalenes cannot be isolated, since the isomeric tetrazocines always result. The usefulness of the donor-acceptor concept in preparative chemistry is demonstrated by numerous stable cyclic (4n)π-electron systems, like donor-acceptor-substituted cyclobutadienes, tetraaminobenzene, and *p*-benzoquinone dications, benzodiazepinyl anions, and donor-acceptor-substituted cyclopentadienyl cations and their heteroatom-containing analogues. The new compounds are of interest in the fields of organic metals and ferromagnets, nonlinear optics, and dyestuffs, among others.

1. Introduction

The special properties of cyclic π-electron systems, well known to everybody from time immemorial, have always been attracting to chemists. For the chemist it is also routine to include donor and acceptor effects in planning syntheses. The concepts of aromaticity and donor-acceptor effect can be traced back to *Kekulé*'s benzene formula (1865)[1] and beyond and to *Witt*'s theory of chromophores and auxochromic groups (1876).[2,3] Though these ideas have been used successfully for over 100 years, their heuristic power and interpretative potential remain unexhausted. As regards the donor-acceptor concept, there are so many examples that only a few can be mentioned here: capto-dative-substituted radicals[4] (merostabilization:[5] the concept of capto-dative stabilization has been disputed[5c]), the use of donor-acceptor molecules in nonlinear optics (NLO),[6-9] TICT compounds (TICT=twisted intramolecular charge transfer),[10] and the allopolarization principle that describes the regioselectivity of ambident ions.[11]

The continuing topicality of aromaticity is to some extent surprising, since even today aromaticity has no generally applicable or accepted definition.[12-14] Indeed, quite a few chemists are extremely skeptical of the usefulness of this concept. *Heilbronner*,[15] for example, has stated that "aromaticity is not an observable property ... and it is not even a concept which, in my experience, has proved very useful". *Binsch*[16] gave an instructive article the title "Aromaticity—an Exercise in Chemical Futility".

Nevertheless, there has been an unbroken chain of remarkable results up to the present day. Clearly, an intuitive grasp of the phenomenon of "aromaticity" is very fruitful for the chemist. From a theoretical point of view, aromaticity is a complex phenomenon, and its usefulness as a concept can only be maintained by applying aromaticity criteria to precisely defined areas.[17-19] In spite of the skepticism towards aromaticity, new "aromaticities" have constantly been put forward (homoaromaticity,[20,21] bicycloaromaticity,[22] Y-aromaticity,[23-25] "4n+2 interstitial electron rule",[19] "in-plane aromaticity",[26,27] "trefoil aromaticity"[28,29]) and the transition states of pericyclic reactions have also been included.[30-32] On the other hand, questions as fundamental as the D_{6h} symmetry of benzene[33] and the driving force of double-bond delocalization in the "aromatic" sextet[34-40] are still open or, at least, the classical answers have been called into question (if the symmetrical hexagonal structure of benzene is driven by the σ framework alone, the π system favoring a localized structure, the π-electron delocalization energy can no longer be a criterion for the empirical resonance energy[40]). Significantly, VB theory is once again gaining importance in this field.[41-44]

In view of the many studies on the theoretical background of aromaticity on one hand and the great significance of substituents for the course of aromatic substitutions on the other, it is amazing that the influence of substituents on aromaticity has not been systematically studied. Substituents have only been discussed in connection with the stabilization of heterocycles (topological charge stabilization[45,46]) and of a few special π systems (tetra-*tert*-butylcyclobutadiene,[47] tri-*tert*-butylazete,[48] pentalenes[49,50] such as 1,3-bis(dimethylamino)-2-azapentalene,[51] and 4,8-bis(dimethylamino)- or 1,3,5,7-tetra-*tert*-butyl-*s*-indacene[52,53]) and with distortion (Mills-Nixon effect[54]) or bending of the benzene ring.[55,56a] It is obvious that any unsymmetrical distortion of annulenes will lead to a loss of frontier orbital degeneracy. The principal distinction between the orbital schemes of aromatic and antiaromatic compounds on one hand and polyenes on the other disappears, and the question arises which "character" substituted polyenes possess. Particularly strong substituent effects are to be expected with acceptor groups (A) like NO_2, CN, COR, SO_2R, with donor groups (Do) like NR_2, SR, OR, and with combinations of A and Do. The following discussion will pursue this question and, on the basis

[*] Prof. Dr. R. Gompper, Dr. H.-U. Wagner
Institut für Organische Chemie der Universität
Karlstrasse 23, D-8000 München 2 (FRG)

of synthesized compounds, will explain the usefulness of the concepts arising from it.

1.1. Donor-Acceptor-Substituted Polyenes

The dramatic influence exerted by donor-acceptor groups on the properties of cyclopolyenes can best be demonstrated with cyclobutadiene **1**.[56b] Although it is rectangular[57-63] (valence tautomerism[64]) and therefore no longer fully antiaromatic, **1** is extremely unstable and can only be detected in a matrix below −196 °C. Diethyl 2,4-bis(diethylamino)cyclobutadiene-1,3-dicarboxylate **2**,[65-70] by contrast, forms yellow crystals (m.p. 56 °C), has four equal-length ring C–C bonds corresponding to a low tendency towards second-order bond fixation ("λ_{max}" = 1.24; see below), and only dimerizes above 120 °C to a red cyclooctatetraene. (1,3-Bis(diethylamino)-2,4-bis(phenylthio)cyclobutadiene[71] and tris(dimethylamino)azete[72] can also be synthesized.)

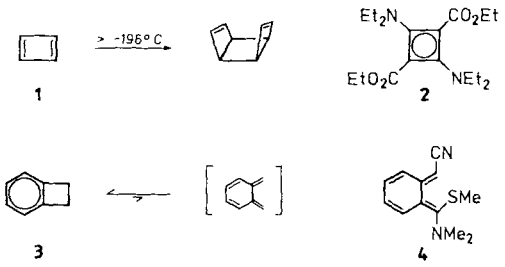

Only on heating to > 150 °C do cyclobutabenzenes **3** (cf. Refs. [73, 74]) show noticeable valence tautomerization to *o*-quinodimethanes, which can be trapped with dienophiles. The aromaticity of the annelated benzene ring hence hinders ring opening of the cyclobutene system. Donor-acceptor-substituted *o*-quinodimethanes[75] like **4**, however, show no tendency at all to dimerize or polymerize, nor any tendency to rearrange into cyclobutabenzenes.

Clearly, donor-acceptor groups reduce both the antiaromatic destabilization of **1** and the aromatic stabilization of the benzene system in **3**. Therefore, (4n+2)π cyclopolyenes are generally made more weakly aromatic by donor-acceptor substituents, while (4n)π cyclopolyenes become more weakly antiaromatic and may even become "aromatic". As explained above, the classification of cyclopolyenes as aromatic, nonaromatic, and antiaromatic depends on what criteria are used; it must be "defined"[15] each time what "aromaticity" means. As a basis, the Hückel rule (antiaromaticity[76]) is used almost exclusively and, in addition, despite their problematic nature, the following criteria:

Resonance energy (Hückel,[77] DRE,[13,79-81] TRE,[82] PMO[78b,c])
NMR data (diatropism, paratropism)[83-85] (problems with homotropylium cations[86])
Bond alternation,[53,87,88] bond order[89,90]
HOMO-LUMO gap[91-93] (LUMO vs. $E^{red.}_{1/2}$, cf. Ref. [94])

How do the above experiments with cyclobutadienes and cyclobutabenzenes relate to these criteria? Predictions from resonance energy are frequently problematic, particularly with polycyclic compounds (see pentalenes, Section 2.4). More dependable results can generally be obtained from the HOMO-LUMO gap. Cyclopolyenes with (4n+2)π electrons have larger HOMO-LUMO gaps than the corresponding polyenes; in cyclopolyenes with (4n)π electrons, degenerate frontier orbitals (SOMOs) are present (cf. Ref. [91]). How do donor-acceptor substituents affect the HOMO-LUMO gap in these π-electron systems? From Figure 1 it can be seen that donor and acceptor groups reduce the HOMO-LUMO gap of 2β in benzene to 1β in a 1,4-A_2-2,5-Do_2-benzene, which, according to this model, is therefore more weakly aromatic than benzene. The corresponding substituents increase the HOMO-LUMO gap of cyclobutadiene from 0β to the same value as for the substituted benzene, 1β. Resonance energies give a similar picture. A 1,3-A_2-2,4-Do_2-cyclobutadiene is therefore just as "aromatic" as an analogously substituted benzene derivative. The values in Figure 1 support the experimental results, and the following rule may be defined: *Donor-acceptor substituents destabilize (4n+2)π-electron systems and can stabilize (4n)π-electron systems to such an extent that they acquire aromatic properties.*

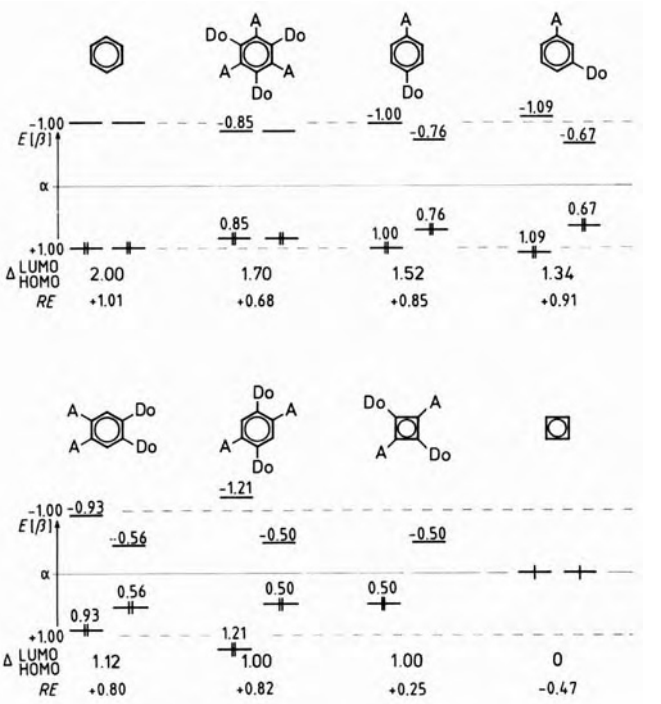

Fig. 1. HOMO-LUMO gaps [β] and resonance energies *RE* [β] of donor-acceptor-substituted benzene and cyclobutadiene derivatives (HMO)

$RE = E_\pi(\text{ring}) - E_\pi(\text{polyene})$
$\alpha_x = \alpha_c + h_x\beta_{cc}$, $h_A = -1.5$, $h_{D_o} = +1.5$

The same conclusion is reached if the relative HOMO-LUMO gaps $\Delta\Delta E$ are considered,[95] i.e., the difference in energy between the HOMO-LUMO gaps of the cyclopolyenes on one hand and the corresponding polyenes on the other (Figs. 2 and 3). The numerical value of $\Delta\Delta E$ is diminished by donor substituents in cations and by acceptor substituents in anions (Fig. 2), leading to a weakening of the aromaticity of 2π and 6π systems ($\Delta\Delta E$ positive) and to a weakening of the antiaromaticity of 4π systems

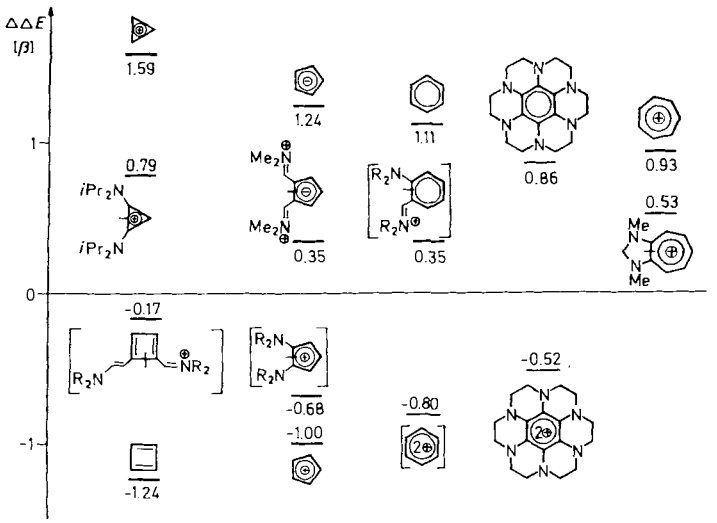

Fig. 2. Influence of donor or acceptor groups on the relative HOMO-LUMO gap $\Delta\Delta E$ [β] (HMO) of cyclic π systems.

$\Delta\Delta E = \Delta E_{\text{HOMO-LUMO(ring)}} - \Delta E_{\text{HOMO-LUMO(polyene)}}$

($\Delta\Delta E$ negative). However, when $\Delta\Delta E$ is used instead of $\Delta E_{\text{HOMO-LUMO(ring)}}$, the (4n)$\pi$ systems still remain in the antiaromatic region. This is also true of systems with donor *and* acceptor substituents (Fig. 3). With an identical acceptor group, the numerical value of $\Delta\Delta E$ falls with donors

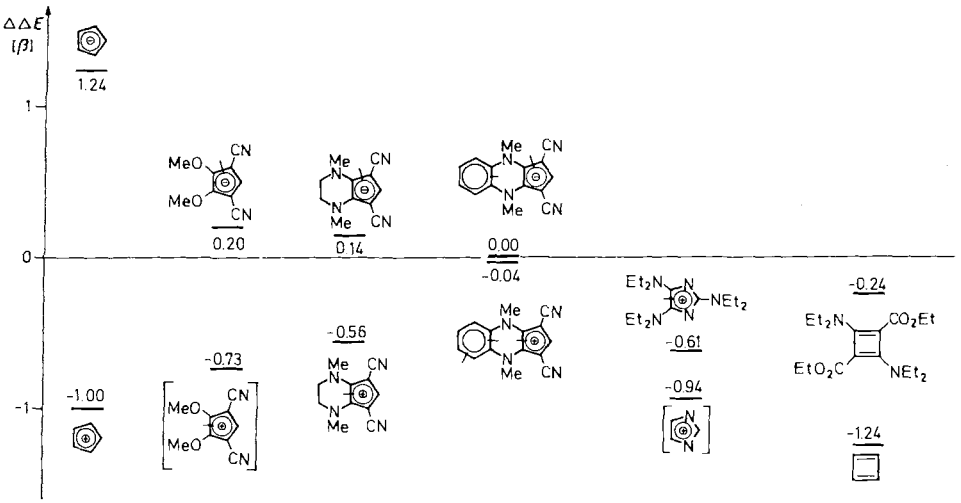

Fig. 3. Influence of donor *and* acceptor groups on the relative HOMO-LUMO gap $\Delta\Delta E$ [β] (HMO) of cyclic π systems.

$\Delta\Delta E = \Delta E_{\text{HOMO-LUMO(ring)}} - \Delta E_{\text{HOMO-LUMO(polyene)}}$

of increasing strength. It is remarkable that the cyclopentadienyl cation is stabilized to the same extent by two amino and two cyano groups ($\Delta\Delta E = -1.00 \Rightarrow -0.56$) as by two amino groups ($\Delta\Delta E = -1.00 \Rightarrow -0.68$). The benzoannelated diamino(dicyano)cyclopentadiene system, for example, demonstrates particularly clearly how the charcteristics of these opposing π-electron systems converge under the influence of donor-acceptor substituents. The 6π anion is destabilized, the 4π anion is stabilized.

1.2. Transition States

Donor-acceptor substituents should influence the transition states of pericyclic reactions just as they do the ground states of cyclopolyenes. In reactions which, according to the Woodward-Hoffmann rules,[30] are symmetry-forbidden as one-step processes[96] (antiaromatic transition states),[31,32] *this symmetry-prohibition can be circumvented by using polar reactants in two-step reactions involving 1,4-dipolar intermediates.*[97] It should be possible for such two-step reactions to take place in one step, however, if substitution with sufficiently strong donor and acceptor groups gives the transition states aromatic character and thereby reduces the activation energies. (Interpretation by configuration interaction;[98] the possibility of SET processes in [2+2][99-101] and [4+2] cycloadditions[102-107] can be only briefly mentioned here.) In polar [2+2] cycloadditions, for example, **2** would be the model for the transition state. On the other hand, symmetry-allowed one-step reactions should be slower under the influence of donor-acceptor groups, and two-step reactions with dipolar intermediates should gain in significance. The transition state for the Cope rearrangement of a 2-acceptor-5-donor-substituted 2,5-hexadiene, for example, is comparable with a 1-A-4-Do-benzene, which is more weakly aromatic than benzene (see Fig. 1).

The donor-acceptor effect can be illustrated in pericyclic reactions with numerous examples (reaction rates, isolation and trapping of dipolar intermediates). Several of these will now be discussed.

1.2.1 Electrocyclic Reactions

Reaction of **2** with methanol yields butadiene **6** rather than cyclobutene **5**,[108a] apparently because **5** is unstable as a result of donor-acceptor substitution (see also Ref.

[109]). The reaction of **2** with acetylenes, via the 1,4-dipole **7**, does not afford the Do-A-substituted Dewar benzenes **8**, but the benzene derivatives **9**,[108b] even at low temperature. The symmetry-forbidden rearrangement of **8** to **9** is hence greatly accelerated by Do-A substituents.

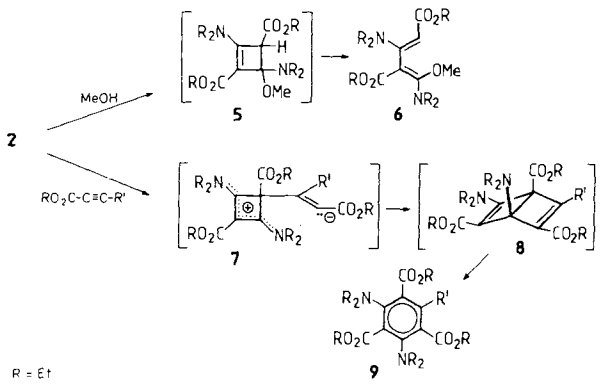

1.2.2. [2+1] Cycloadditions; Stable Non-Kekulé Systems

Singlet carbenes add to olefins stereospecifically.[110] However, if electron-poor allenes like tetraethyl allenetetracarboxylate are reacted with nucleophilic carbenes, the products are not cyclopropanes, but stable, crystalline 1,3-dipoles **10–12**.[111] An analogous compound **13** is obtained if the electron-rich tetrakis(dimethylamino)allene is combined with diazomalonic ester.[112] Compounds **10–13** can also be viewed as stable trimethylenemethanes; if trimethylenemethanes, as 4π-electron systems, are classified as antiaromatic, the stabilization of destabilized π systems is seen again. Finally, combination of electron-poor and electron-rich allenes gives the crystalline tetramethyleneethane derivative **14**.[113] Compounds **10–14** are of interest because, among other things, they are stable examples of non-Kekulé systems.

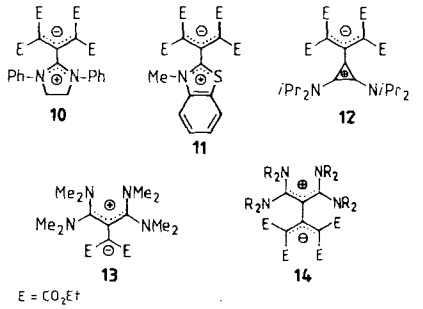

1.2.3. [4+2] Cycloadditions

The mechanism of the Diels-Alder reaction still arouses discussion.[114] Reactions of oppositely polarized components take place very quickly, and dipolar intermediates can be detected. The reaction of cyclohexenylmethylenemalonodinitrile with 1-(1-cyclohexenyl)pyrrolidine at room temperature gives the colorless Diels-Alder cycloadduct **15b**, but at −40 °C the crystalline, yellow, 1,6-dipole **15a** is obtained, which is converted into **15b** on warming.

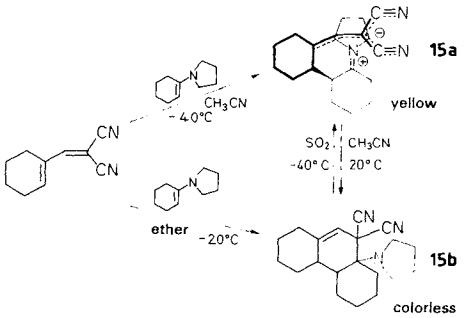

In liquid sulfur dioxide, even at −40 °C, **15b** is transformed into **15a**.[66,115] (Two-step polar Diels-Alder reactions have also been observed with other dienes[116] and heterodienes.[117–121])

1.2.4 [3,3]-Sigmatropic Rearrangements (the Semibullvalene Problem; Tetrazocines; Tetraazabarbaralanes)

Just as with the Diels-Alder reaction, the question of the concertedness of the Cope rearrangement of "normal" 1,5-hexadienes still remains open.[122] Cope and hetero-Cope rearrangements of 2-donor-5-acceptor-substituted 1,5-(hetero)dienes like **16** and **19**, for example, proceed extremely rapidly, and 1,4-dipoles (**17**, **20**) can be detected.[123–129] Dipole **17**, which is in equilibrium with **16**, eventually affords **18** by prototropism, and **20** can be trapped with benzaldehyde or acrylonitrile to give the tricyclic compound **21**.[123] (Two-step [2,3]-sigmatropic rearrangements are also known.[130,131]) The formation of 1,4-dipoles could be caused by a slowing of the one-step Cope rearrangement

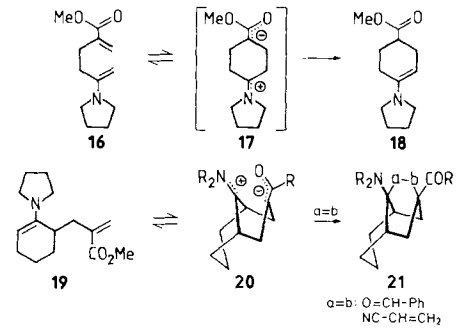

(higher activation energy due to the weaker aromaticity of the transition state) and an acceleration of the two-step reaction (stabilization of the transition state leading to the 1,4-dipole).

Cope rearrangement of semibullvalenes proceeds extremely rapidly.[132] According to *Dewar* et al.[133] and *Hoffmann* et al.[134] 1,5-didonor-2,4,6,8-tetraacceptor-substituted semibullvalenes **22** could have a bishomoaromatic ground state **23**. Till now, such systems have been sought in vain (**24a**,[135] **24b**,[136,137] **25a**,[138] **25b**,[139]). There could be two reasons for this. Either the rearrangement of the donor-acceptor-substituted semibullvalenes studied so far does not go through a bishomoaromatic ground state or it is not stabilized sufficiently for the reasons outlined above. Possibly, the substituents used (Do, CH_3; A, 4 CO_2R, 2 CN, 2 ring N) were not "strong" enough.

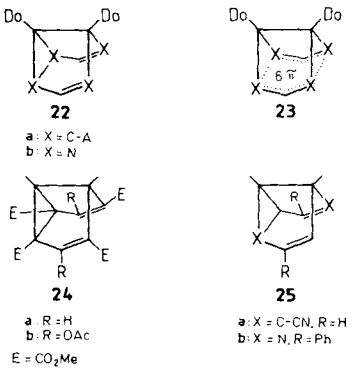

Since synthesis of semibullvalene-2,4,6,8-tetracarbonitriles[140] has not yet been possible, we have attempted to produce the electronically equivalent 2,4,6,8-tetraazasemibullvalenes **22b**. Oxidation of the bisimidates **26** of the glycouril series does not, however, lead to tetraazasemibullvalenes **29**, but to the tetrazocines **28**.[141] Either the tetraazasemibullvalenes **29** and the bishomoarenes **30** are both destabilized relative to the "nonaromatic" tetrazocines (the X-ray crystal structure shows a boat form, as for cyclooctatetraene) and rearrange rapidly to **28** (path b), or a fragmentation of **27** occurs (path a). 1,5-Dimethyl-3,7-diphenyl-2,6-diazasemibullvalene also rearranges to 2,6-dimethyl-4,8-diphenyl-1,5-diazocine, though only at 90 °C.[142]

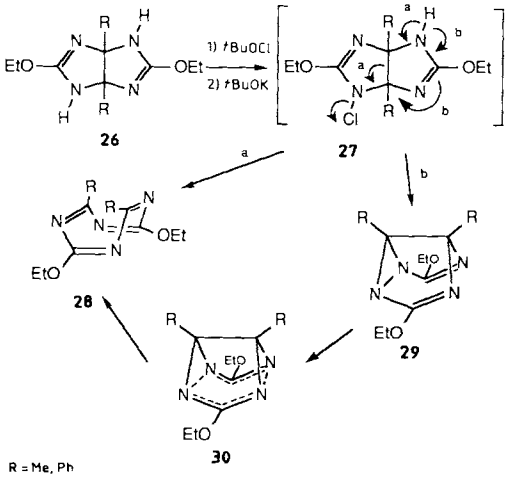

To prevent conversion to tetrazocines, 3a,6a-bridged-glycourils such as **31** were synthesized (cf. cyclooctatetraenes containing $(CH_2)_n$ bridges between the 1,3-,[143a] 1,4-,[143b] and 1,5-positions[143c]) and transformed into **32**, which were then oxidized. However, tetrazocines[144] were produced here too[143] (e.g., **34** and **33**, prepared from an analogue of **31**). This is all the more astonishing since, although **33** is a derivative of bicyclo[3.3.3]undec-1-ene and is therefore counted as a member of the "isolable" bridgehead olefins,[145,146] it is the only "anti-Bredt" bridgehead imine isolated to date, apart from 2-azabicyclo[3.3.1]non-1-ene[147] (cf. Ref. [148]). The synthesis of 1,5-bridged cyclooctatetraenes with five, six, or ten methylene groups in

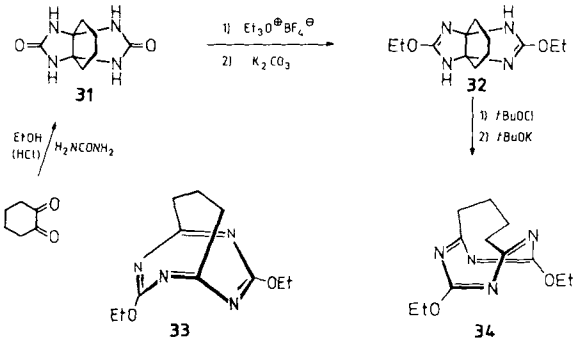

the bridge[143c] was only possible on heating the corresponding semibullvalenes to 500–521 °C.

If **29** (and **30**) are inherently unstable, then the 2,4,6,8-tetraazabarbaralanes ought also to be so, at least in part. 2,6-Diphenylbarbaralanes and 2,6-barbaralanedicarbonitriles have localized double bonds and undergo faster Cope rearrangement than the parent compound.[149–151] (Substituents at C-3,7 have a moderate rate effect;[152–154] in the crystal, though not in solution, a 9-phosphoniobarbaralane is nearest to a bishomaromatic state.[155]) The tetraazabarbaralanes **36** can be synthesized from **35** by the same procedure as **28, 33,** and **34**.[158] Compound **35** itself is available from the corresponding urea derivative.[156,157]

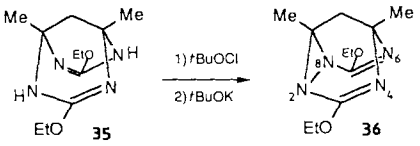

The X-ray crystal structure of **36** shows a large difference between the N2–N8 (158 pm) and N4–N6 (236 pm) distances, in accord with the given formula. However, the N2–N8 distance is significantly greater than the N–N distance in diaziridines[159–161] (145.3–150.6 pm), and is comparable with that in highly substituted 1,2-bis(*p*-bromo-α,α-dimethylbenzyl)diaziridinone[162] (160.1 pm). The NMR spectra establish that **36** in solution also has a localized structure, for which the Cope rearrangement becomes fast between 25 and −60 °C. A variable-temperature NMR study showed that **36** rearranges more slowly (!) ($\Delta G^{\ddagger}_{210} = 38.9$ kJ mol^{-1}) than barbaralane ($\Delta G^{\ddagger}_{200} = 31.5$ kJ mol^{-1}).[153] This can be rationalized by assuming a bishomoaromatic transition state in the rearrangement of **36**, resembling 3,6-diethoxy-1,2,4,5-tetrazine and therefore, according to Figure 1, being less aromatic than a benzene-like transition state. In the rearrangement of 2,6-barbaralanedicarbonitrile, however, the transition state may have a diallyl structure (cf. Ref. [153]).

2. Novel Donor-Acceptor-Substituted Aromatic Compounds

Of all compounds synthesized recently by us and other groups, the ones that will be presented are primarily

those examples of 8π- and 4π-electron systems which demonstrate the stabilization and double-bond delocalization effects of donor-acceptor substituents on one hand, and particular characteristics of the substances on the other (color, oxidizability or reducibility, electrical conductivity).

2.1. Ten π Electrons in an Eight-Membered Ring

Cyclooctatetraene (8π, nonplanar) can be reduced to its aromatic dianion (10π, planar);[163-165] azocines[166,167] and diazocines[142] behave similarly. Surprisingly, however, tetrazocines **28** do not afford the monocyclic dianions **38**, but the bicyclic dianions **37**, which can also be obtained from **26** with strong base.[144] This appears to contradict the observed ring-opening of the dianionic bicyclo[3.3.0]octadienediide.[168] In fact, when the energies of dianionic (diaza/tetraaza)bicyclo[3.3.0]octadienediides are compared with those of (diaza/tetraaza)cyclooctatetraenediides, using calculated heats of formation (Table 1), the monocyclic dianions are found to be more favored. In donor-acceptor-substituted systems, however, the balance swings to the side of the bicyclic dianions. While **37** can be viewed as a bishomoantiaromatic[22] 8π-electron system, it is doubtful whether homoaromaticity plays any role at all in carbanions.[169] The formation of **37** rather than **38** demonstrates particularly clearly how a (4n)π system can be stabilized at the expense of a (4n+2)π system by donor-acceptor groups.

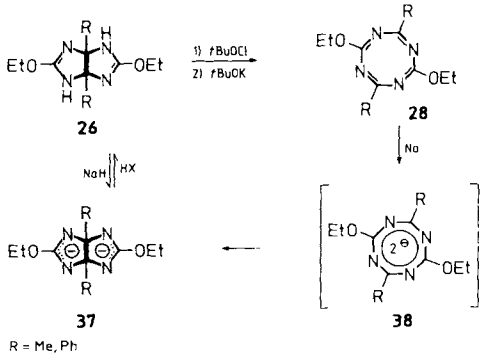

26 **28** **37** **38**

Table 1. Heats of formation [kcal mol^{-1}] of bicyclic and isomeric monocyclic dianions (MNDO).

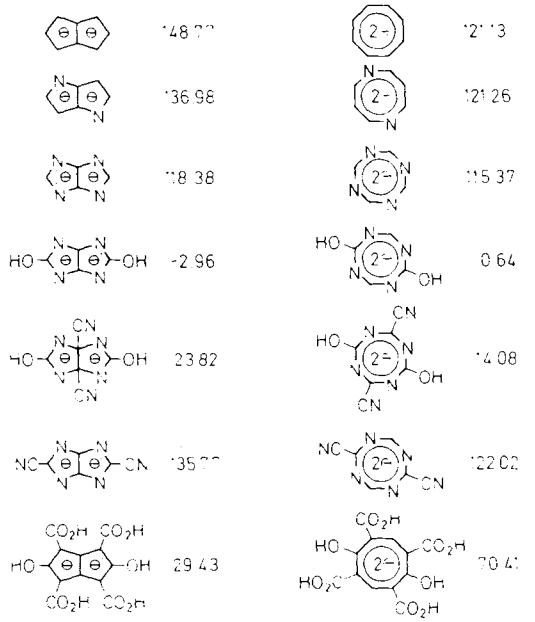

2.2. Six π Electrons in a Seven-Membered Ring (Azatropylium Ions)

Like benzene and pyridine, the tropylium ion and the azatropylium ion are a pair of Hückel-aromatic 6π-electron systems. However, while for pyridine and benzene the effect of aza-substitution on the calculated heats of formation is negligible ($\Delta\Delta H_f = -0.1$ kcal mol^{-1}) (MNDO),

$\Delta H_f^0 = H_f(\text{PhCH=NPh}) - H_f(\text{PhCH=CHPh}) = 7.6$ kcal mol^{-1}
$\Delta\Delta H_f = H_f(\text{AzaAr}) - H_f(\text{Ar}) - 7.6$

the azatropylium ion proves to be significantly less stable than the tropylium ion ($\Delta\Delta H_f = 10.7$ kcal mol^{-1}). In view of its "aromatic" electron sextet, it is nonetheless surprising that it has not yet been possible to synthesize any azatropylium salts. An attempt to oxidize 2-amino-3*H*-azepines **39** to 2-aminoazatropylium salts **42** with trityl tetrafluoroborate, where the destabilizing influence of the ring N atom ought to be (over)compensated for by the donor group, led to salts **43** of 2-azanorcaradienes **47**, the first salts of this type[170] (3-azanorcaradienes, see Ref. [171]). Obviously, this occurs by initial electrophilic addition to give **40**, followed by deprotonation (→**41**), reprotonation (→**44**), and electrocyclization to yield **43**. Treating **43** with alkali gives **47**, which suffers ring-opening to **46**, and on warming affords the 6-substituted 2-amino-3*H*-azepines **45**. The more electron-rich 2-dialkylamino-6-methylthio-3*H*-azepines cannot be dehydrogenated to azatropylium salts either.[170]

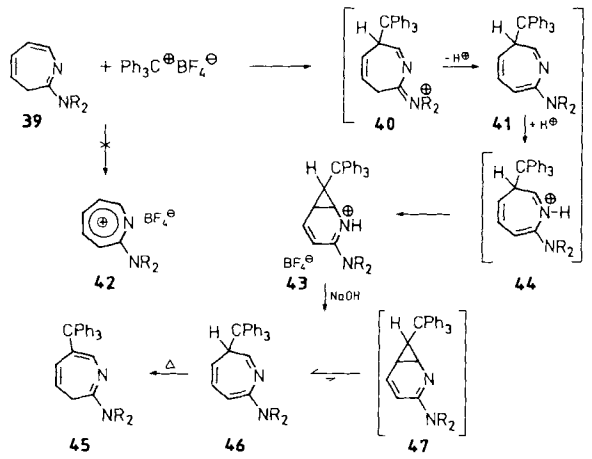

39 **40** **41** **42** **43** **44** **45** **46** **47**

The first derivatives of azatropylium salts have now been synthesized[174] via aminodibenzoazatropones **48** from morphanthridinediones.[172,173] The electronic differences between the tropones and **48** can be seen in the fact

that unlike tropones, **48** are not *O*-alkylated, but can be *N*-alkylated to form **51**. Compound **48** can only be converted into the red salt **50** with trimethylsilyl triflate; this is then transformed in situ into the stable orange salt **49**.

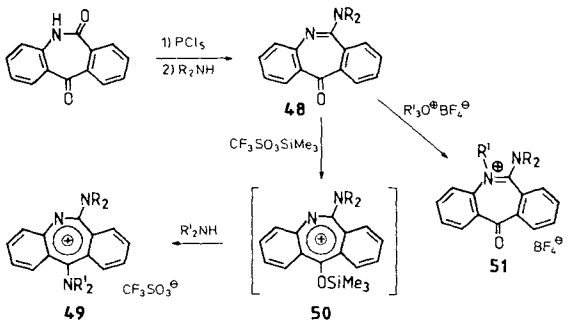

Only by severely changing the azatropylium system by annelation of two benzene rings is it possible to obtain stable derivatives. Just as for the compound types mentioned above, the Hückel rule is no help here. As yet, benzodiazepinium ions of type **52** have not been obtained

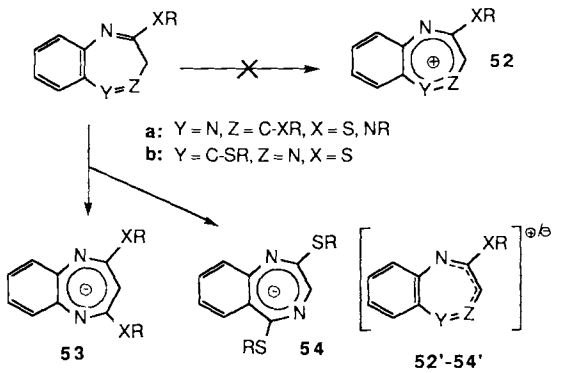

either,[175,176] though, as 6(10)π-electron systems combined with donor substituents (SR, NR_2), they ought to be sufficiently stabilized. The low tendency to form **52** is probably connected with the high contribution of resonance structure **52'**, and is illustrated by the observation that on reaction of **55** it is not the seven-membered ring but the five-

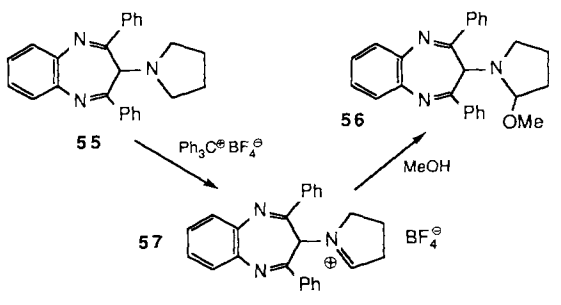

membered ring that is dehydrogenated to give **57**, which yields **56**.[175] The reaction of silver tetrafluoroborate and 2,4-diphenyl-3-bromo-1,5-benzodiazepine, which gives the red salt **59**,[175] might involve the benzodiazepinium ion **58** as an intermediate, but other mechanisms are also conceivable. Salt **59** can be deprotonated to give the yellow *N,C*-bis(benzodiazepine) **61**, which on heating affords the *C,C* dimer **60**.

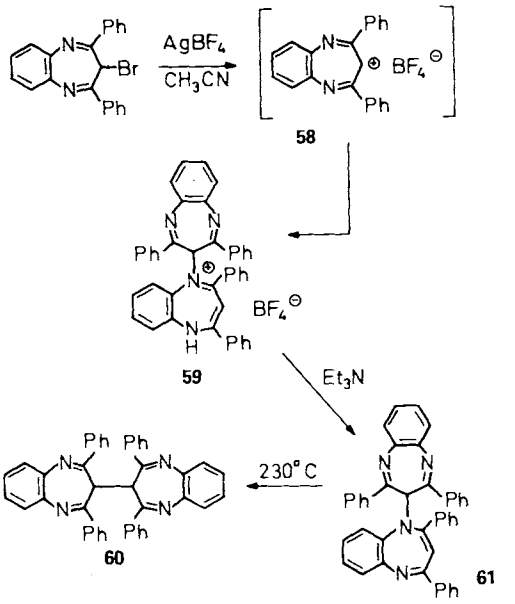

2.3. Eight π Electrons in a Seven-Membered Ring

While azepinium and benzodiazepinium ions have not yet been detected, 8π-[176] and 12π-electron anions[174,175,177] have been produced for the two classes of compounds, respectively (cf. carbon analogues[178-182]). The anions **53**[175,177] and **54**[174] are easy to synthesize and undergo numerous reactions. In solution, the lithium salts of **54**, R = alkyl, and **53**, RX = alkylthio, are purple and red, respectively, and therefore probably have strongly ionic character. Compounds **53**, RX = dialkylamino, with lithium as counterion, are colorless and are therefore likely to be covalent species. Compounds **53** and **54**, whose stabilities can be ascribed to resonance structures **53'** and **54'**, react at C-3 with electrophiles to form novel sesquifulvalenes and heptafulvalenes, among other products (Scheme 1).

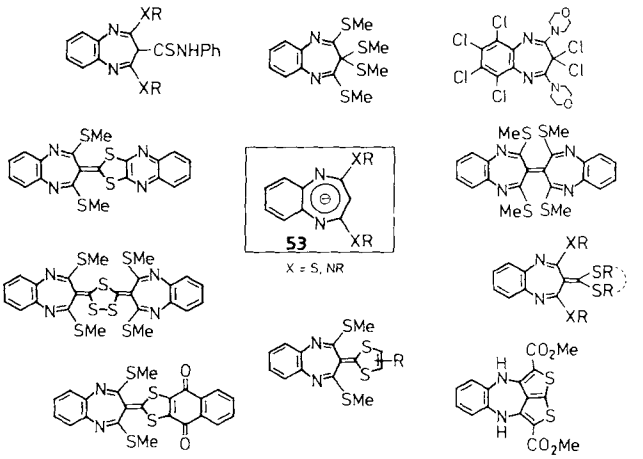

Scheme 1. Reactions of 1,5-benzodiazepinyl anions **53** with electrophiles.

2.4 Eight π Electrons in a 5/5-Ring System ((2,5-Diaza)pentalenes) and Twelve π Electrons in a 5/6/5-Ring System (2,6-Diaza-*s*-indacenes)

2.4.1. *Donor-Substituted 2,5-Diazapentalenes*

As planar analogues of the nonplanar cyclooctatetraene, pentalenes are usually classified as antiaromatic.[78c, 183–187] However, use of sterically demanding groups makes it possible to obtain stable pentalenes like **62** and to prove that these are compounds showing bond alternation, which undergo rapid valence tautomerization.[51, 188] With aza- and diazapentalenes,[82, 187] the destabilizing effect can become smaller.[49, 50] The diazapentalene **64**, described as "electronically pure",[189] (cf. Ref. [190]) is clearly a localized system and therefore actually nonaromatic[189] (incidentally, alkyl substituents are in no way electronically "pure", i.e., without influence, as is shown, for example, by the orientation effect in aromatic electrophilic substitution, by Hammett constants, and by the structural discussion on *s*-indacene,[52, 53] where *tert*-butyl groups are not treated differently from amino groups). Bond localization also seems

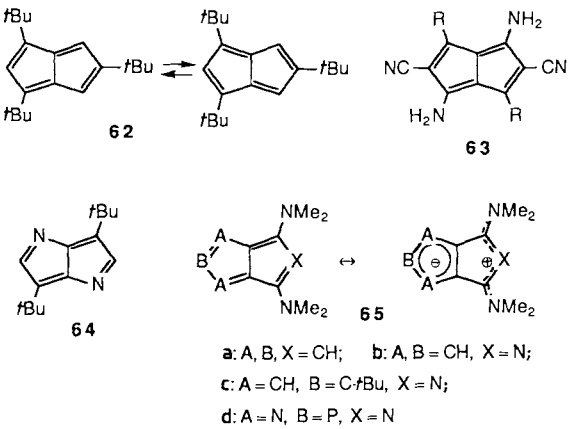

dominant in **65b,c**,[51] while **65a**[51] and **65d**[191] are best characterized by dipolar resonance structures. The bond localization in **62** agrees with the bond-localization parameter "λ_{max}" calculated according to *Binsch* and *Heilbronner*'s method[53, 87, 88] (see Table 2), while that of **64** agrees with the calculated bond orders; by calculation, **65a–c** should show approximately the same bonding situation. 1,3,4,6-Tetraamino-, 2,5-diaza-, and especially 1,3,4,6-tetraamino-2,5-diazapentalene have "λ_{max}" values which fall below the critical value. This, and the larger HOMO–LUMO gap, leads one to expect 1,3,4,6-Do_4-2,5-A_2-substituted pentalenes to be aromatically stabilized and to show a delocalized π-bond system (cf. also Refs. [49, 50]). At this point the interesting Do-A-substituted pentalene derivatives **63**, R = alkyl or phenyl,[192] should also be mentioned.

The reaction of succinamide with the amidoacetals **66** is, along with the reaction of succinic acid and aromatic nitriles[193] (cf. also Ref. [194]), a simple method of producing diones such as **70**,[195] which are of great interest, not least as pigments.[193] With **66b** one obtains the colorless compound **69**[196] in high yield. In contrast to the red **70**, compound **69** does not exist in the enamine form. Compound **67b**, which can be detected as an intermediate, can also be synthesized from tetramethylguanidine and succinyl dichloride and converted into **69** by treatment with sodium hydride in dimethylformamide.

Table 2. Calculated substituent effects on double-bond delocalization in (aza)pentalenes ($\lambda_{crit} \approx 1.7$). Numbers on the bonds, π bond order; numbers in parentheses, π charge; numbers in square brackets, "λ_{max}".

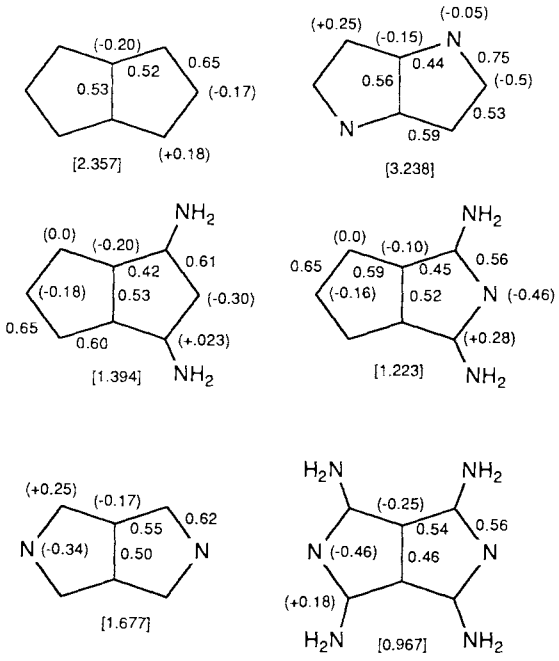

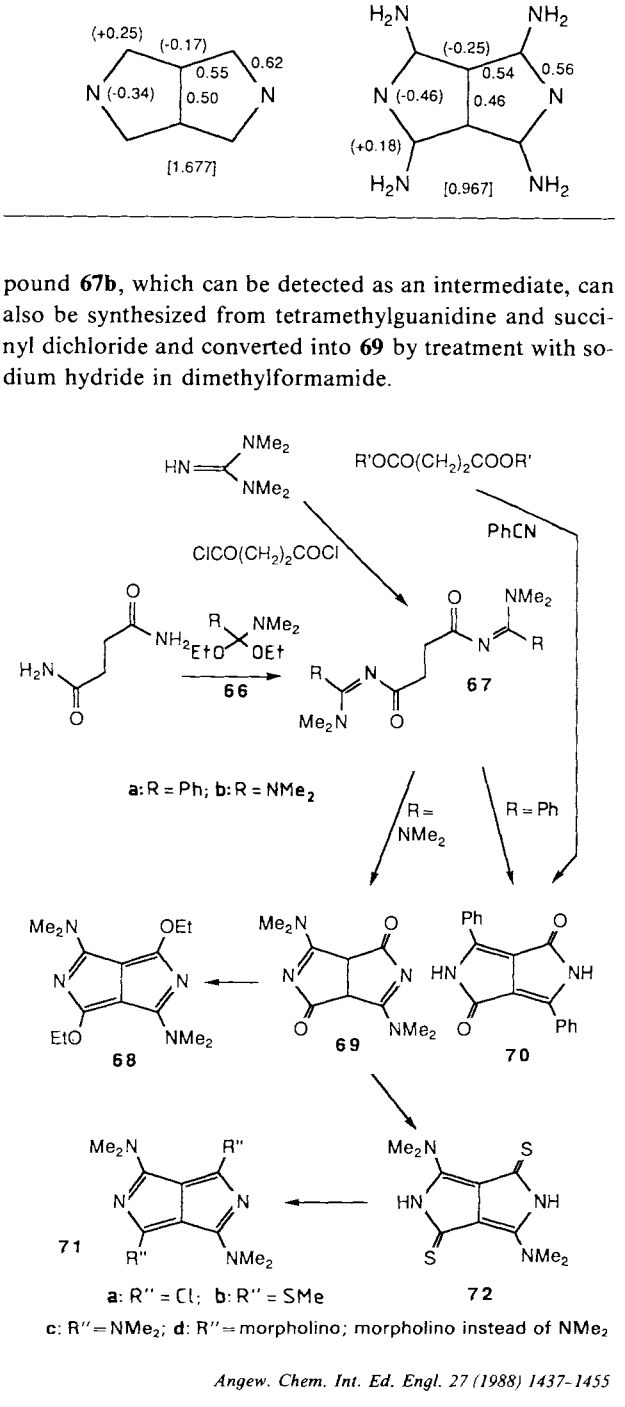

From **70** and the dithione derived from it,[195,197a] one can synthesize bis(trimethylsiloxy)- and bis(alkylthio)-2,5-diazapentalenes, respectively.[175] Compound **69** is the starting material for 1,3,4,6-tetradonor-2,5-diazapentalenes. Using triethyloxonium tetrafluoroborate one obtains **68**; with Lawesson's reagent **72** is obtained; **72** gives **71b**, which yields **71c** upon treatment with dimethylamine at 140 °C. Phosphorus oxychloride gives **71a**, from which **71d** can be obtained. The high thermal stability of these crystalline compounds dramatically demonstrates the effectiveness of the donor-acceptor effect (cf. Table 2). The 1,3,4,6-tetraamino-2,5-diazapentalenes **71c,d** are especially interesting from a theoretical point of view. They allow an investigation of the question of whether **71** has a localized (C_{2v} symmetry) or delocalized structure (D_{2h} symmetry).

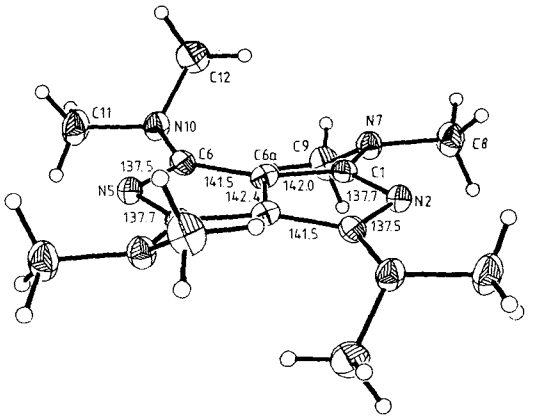

Fig. 4. Crystal structure of **71c** (ORTEP).

X-ray analysis of **71c** (Fig. 4) reveals double-bond delocalization, as required by theory (as to the question of equilibrium structure, stabilized transition state or disorder in the crystal, cf. Ref. [197b]). Compounds **71c,d** must therefore be described as "aromatic Hückel antiarenes", since they show neither strong first-order bond fixation nor strong second-order bond fixation.[87,88] (If the expression "electronic purity"[189] is adopted, then the "electronically impure" Hückel antiarenes **71c,d** represent delocalized cyclopolyenes, i.e., arenes, while the "electronically pure" Hückel antiarenes **63** and **64** are localized cyclopolyenes and therefore nonaromatic compounds.)

Compounds **68** and **71** provide examples of reversible multistep redox systems (formation of radical anions and radical cations (cf., e.g., **73**), dianions and dications (cf., e.g., **74**)). The salt **74a**, X = BF_4, can be obtained as reddish-purple crystals on a preparative scale by reaction of **71d** with trityl tetrafluoroborate in dichloromethane; **73a**, X = BF_4, which is bluish-purple in acetonitrile solution, arises by combination of **71d** and **74a**, X = BF_4.

With **74**, dications of pentalene have been isolated and characterized for the first time. Though the synthesis of a hexachloropentalenediylium bis(hexachloroantimonate) has been reported,[198] its structure was not proved. Dications of dibenzopentalene have been generated in solution and characterized by NMR spectroscopy,[199] and the radical cation of 1,3,5-tri-*tert*-butylpentalene, stable up to −77 °C, has also only been obtained in solution.[200,201]

The use of tetradonor-substituted diazapentalenes now makes possible the synthesis of an entire series of stable, crystalline pentalene dication salts. The Wiberg bond index[202] for C3a-C6a in **74** is 1.852, which corresponds almost to a CC double bond, as in the given formula (π charges: C-1, +0.35; C-3a, +0.09; N-2, −0.46). The 6π system formed by oxidation of **71c,d** is therefore converted from a delocalized into a localized structure by first-order bond fixation.

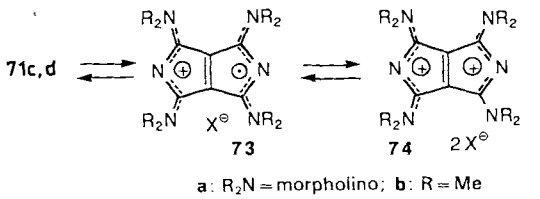

a: R_2N = morpholino; b: R = Me

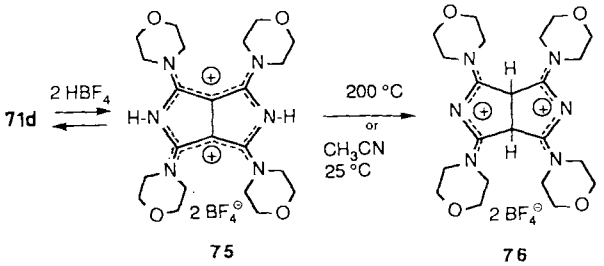

Tetradonor-substituted-2,5-diazapentalenes are quite strong bases (pK_a1, pK_a2 (in 50% EtOH): **71c**, 6.40, 10.35; **71d**, 4.28, 8.63). It is interesting to note that **71c** is as basic as 1,8-bis(dimethylamino)naphthalene (pK_a = 10.40 (in H_2O, pK_a = 12.34[203,204])), but 1,3-bis(dimethylamino)-2-azapentalene **65b**[205,206] is a markedly weaker base (pK_a = 6.82). Protonation of **71c,d** does not take place on the dialkylamino groups as in "proton sponge", though, but on the ring N atoms. Reaction of tetrafluoroboric acid etherate with **71d** in dichloromethane leads to the yellow NH salt **75**, which decomposes to the colorless CH salt **76** either thermally or on standing in acetonitrile solution.

2.4.2. *1,3,5,7-Tetraamino-2,6-diaza-s-indacenes*

In **76**, two azaallylium or azavinamidinium units are connected by a CC single bond, while in **74** it is a CC double bond that links the two. The analogous yellow dicationic salt **79**,[207] which has a benzene ring as the linking unit, is obtained by reaction of the hexachloro compound **77**, which is available from pyromellitimide, with diethyl(trimethylsilyl)amine. (A structure corresponding to **79** has been calculated for the dication of *s*-indacene.[208a]) Like **74**, though at a more negative potential, **79** can be reversibly electrochemically reduced to **78** via a stable radical cation. If the reduction is carried out with sodium in liquid ammonia, then **78** can be isolated as air-sensitive violet crystals. X-ray analysis (Fig. 5) shows that **78** has a delocalized structure corresponding to **78'**, though, like **71c** it belongs to the Hückel antiarenes. The predictions arising from "λ_{max}" and *RE* (*s*-indacene, 1.57,[53,88] 1.145; 2,6-diaza-*s*-indacene, 1.36, 1.341; 1,3,5,7-tetraamino-*s*-indacene, 1.18, 1.151; 1,3,5,7-tetraamino-2,6-diaza-*s*-inda-

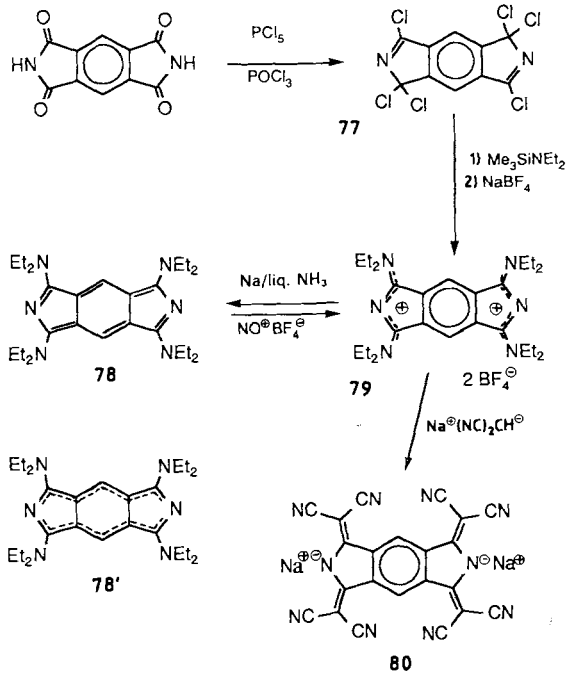

cene, 1.22, 1.367) of increasing delocalization and stabilization of *s*-indacene by donor and acceptor groups are therefore fulfilled. These had already proved to be correct with the compounds synthesized by *Hafner* et al. (4,8-bis(dimethylamino)-*s*-indacene,[51,53] 1,3,5,7-tetra-*tert*-butyl-*s*-indacene[52,53]). Hexamethyl 4,8-dihydroxy-*s*-indacene-1,2,3,5,6,7-hexacarboxylate[208b] is also a stable compound. Compound **79** is the phenyl analogue of **74** and **78'** is the quinodimethane homologue of **71c,d**.

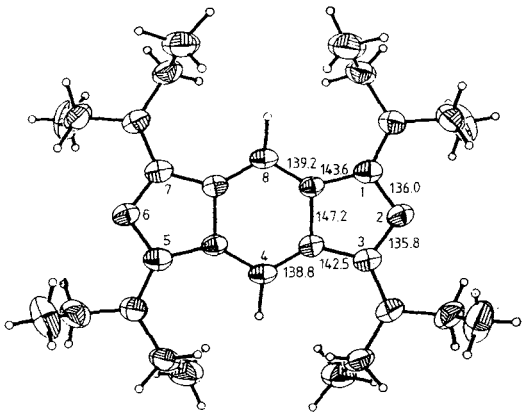

Fig. 5. Crystal structure of **78** (ORTEP).

Compounds **76** and **79** readily react with nucleophiles. The formation of the dianionic salt **80** is remarkable; it reacts with **79** to form a red dicationic dianionic salt containing a small proportion of radical ions. Compounds **79** and **78** combine to form a radical cation (λ_{max}(THF) = 795, 875 nm).

It is worth noting that the transformation of **78'** (λ_{max}(benzene) = 614 nm) to **79** (λ_{max}(CH_2Cl_2) = 440 nm) is associated with a strong hypsochromic shift, while that of **71d** (λ_{max}(C_6H_6) = 483 nm) to **74a** (λ_{max}(CH_3CN) = 520 nm) shows a bathochromic shift.

2.4.3. Derivatives of Dibenzopentalenes

In contrast to pentalenes, dibenzo[*a,e*]pentalene[209] and its 1,9-dimethyl[210] and 1,9-dichloro derivatives[211] are thermally stable. Dications and dianions of dibenzo[*a,e*]pentalene can be obtained[199,212] from the parent compound by oxidation and reduction, respectively, or by metalation of 1,9-dihydrobenzo[*a,e*]pentalene **80**, X = H_2.[211] The ability of the dibenzopentalene system to form both a stable 14π dication and a stable 18π dianion is reflected in the properties of the electron-rich dihydrobenzopentalene derivatives **81a**, and the corresponding electron-poor compounds **81b**, X = N–CN,[213] $C(CN)_2$.[214] From **81b**, X = $C(CN)_2$, and **81a**, X = 2-(3-methylbenzthiazolylidene), for example, a complex is formed that has high electrical conductivity (σ = 0.74 S cm^{-1}, as a powder). By the same routes used for **81** the "phenylogous" dibenzopentalene derivatives **82** can be synthesized,[213,218] from 6,12-dihydroindene[1,2-*b*]fluorene[215] or the corresponding dione.[216,217] Compounds **81** and **82** can both be reversibly oxidized or reduced via radical cations/anions to give the dications/dianions **83** and **84**, respectively. De-

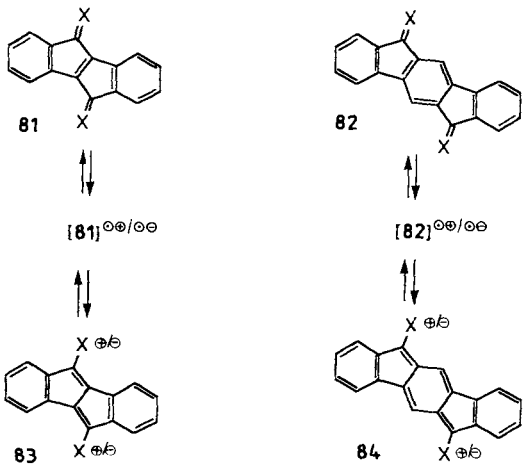

pending on the oxidant, one obtains, for example, colored crystalline bis(tetracyano-*p*-quinodimethides) or bis(tetrafluoroborates) of **83a** and **84a**.

2.5. Four π Electrons in a Six-Membered Ring (Benzene and Quinone Dications)

The benzene dication, the simplest Hückel antiaromatic[219–221] carbodication, has to date only been detected by mass spectrometry.[222] Naturally, with increasing donor strength, substituted benzene derivatives are more easily oxidized.[223,224] The hexachlorobenzene dication can be detected spectroscopically at 77 K[225] (the hexamethyl benzene dication has a pentagonal-pyramidal structure[226,227]). As materials for ferromagnets,[228–231] these unstable compounds are of as little use as the colorless quinone diiminium salts.[232] A system with a triplet ground state is required,[228–231] or one in which the triplet state is easily accessible from the singlet ground state.[231]

The hexaaminobenzene derivative **85a**[224] and the hexaaminotriphenylene derivative **86a**[233,234] can be easily oxidized to the stable dications **85b** ($RE = +0.14\beta$!) and **86b**, respectively. These have a triplet ground state in solution and are therefore a priori of special interest as materials for organic ferromagnets.

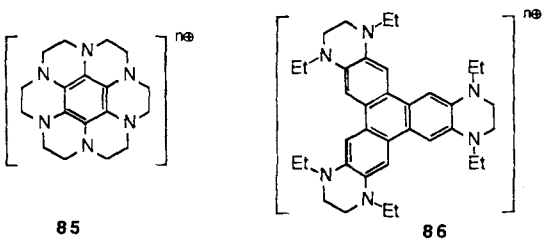

85 **86**

a: n = 0; **b**: n = 2

Tetraaminohydroquinone derivatives **89** are structurally very similar to the hexaaminobenzene derivative **85a**. They are obtained by reductive acetylation (**89**, R = Ac) of decahydro-1,4,6,9-tetramethylpyrazino[2,3-*g*]quinoxaline-5,10-dione **88**, or by reaction of tetramethoxy-*p*-benzoquinone **87** and dimethylethylenediamine (**89**, R = Me).[235,236] They are converted into the blue benzene dicationic salts **91** with silver or nitrosyl tetrafluoroborate ($\lambda_{max}(CH_3CN) = 631$ and 680 nm, respectively). Interestingly, the donor effect of four amino groups is sufficient to cause "umpolung" of the *p*-benzoquinone system; both **88** and **89** can be oxidized to the violet dicationic salt **90** ($\lambda_{max}(CF_3COOH) = 588$ nm), either electrochemically, at very similar potentials, or with silver tetrafluoroborate (the product of oxidation of tetrakis(dimethylamino)-*p*-benzoquinone is reported to be a radical cation[237]). The mesomeric structures **90a** and **90b** emphasize the benzenedicationic nature of **90** and its relationship to **91**.

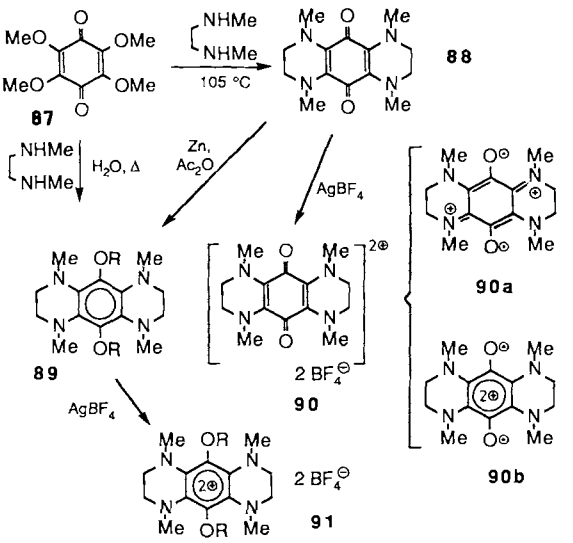

Further derivatives of tetraaminobenzene dications can be synthesized from pyrazino[2,3-*g*]quinoxalines such as **92** and quinoxalino[2,3-*b*]phenazines such as **94**. By alkylation of **92**[238] one arrives at the green, orange-yellow-fluorescing dicationic salt **93**[236] ($\lambda_{max}(CF_3COOH) = 572$ nm), whose long-wavelength absorption maximum is bathochromically shifted relative to that of **91**. Methylation of **94**[239] with trimethyloxonium tetrafluoroborate in nitromethane affords the green dicationic salt **95**[236] ($\lambda_{max}(CH_3CN) = 639$ nm; salts of this type have been reported in a patent,[240] without synthetic details; a bis(*N*-methylsulfate) of **94**, Me instead of Ph, is also known[241]). The salt **95** is reduced by naphthalenesodium to a radical cation, which can be isolated as a green-black tetrafluoroborate ($\lambda_{max}(CH_3CN) \approx 900$ nm). The radical cation is also formed when the electronic spectrum of **95** is recorded in DMF ($\lambda_{max} = 910$ nm).

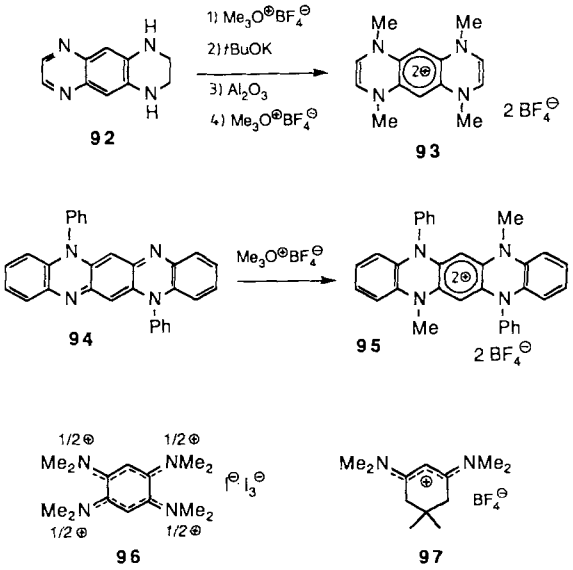

92 **93** **94** **95** **96** **97**

The dicationic salt **96** is produced from 1,2,4,5-tetrakis(dimethylamino)benzene and iodine.[242] X-ray structural analysis shows that in **96** the two vinamidinium units are linked by what are almost single bonds, possibly because of steric hindrance. In **91**, **93**, and **95** a similar distortion of the central ring is either impossible or only possible to a reduced extent, because of the additional rings. However, the length of the CC bonds in the central ring does not appear to have a great influence on the electronic state of the dications, since the chemical shifts of the vinamidinium proton signals in **96** ($\delta = 5.85$) and **93** ($\delta = 5.96$) are not significantly different from those in **97** ($\delta = 5.484$).[243] Only in **95** ($\delta = 6.32$) does one see a stronger downfield shift, in agreement with the calculated charge density (HMO charge densities: **95**, −0.141; **93**, −0.159; **97**, −0.163). In their color, too, **91**, **93**, **95**, and **96** (blue to green) do not differ fundamentally from one another.

2.6. Four π Electrons in a Five-Membered Ring ((Aza)cyclopentadienyl Cations)

Initially, cyclopentadienyl cations were only obtained in solution; the cyclopentadienyl cation and its pentachloro derivative have triplet ground states,[228] while the pentaphenyl and pentakis(*p*-methoxyphenyl) derivatives[228,244] have singlet ground states and a low-lying triplet state. One way of generating cyclopentadienylium salts, which are also of interest in the production of organic ferromagnets, among other things,[228-231] is shown by the donor-acceptor

effect (cf. Figs. 1 and 2). The HMO charge densities point in the same direction (Fig. 6). In the framework of this model one sees no destabilization of the π system on moving from the allyl cation to the 2-azaallyl cation, because of the greater electronegativity of the N atom; in the 2-azavinamidinium cation the N atom has a stabilizing effect (cf. electron-gas model[245-247]). Because of the positive charge on all the ring atoms of the cyclopropenylium and tropylium ions, an N atom in these positions destabilizes the π-electron system. With the corresponding diamino derivatives this effect is smaller or not present at all. While the azacyclopentadienyl cation is, naturally, destabilized relative to the cyclopentadienyl cation, with the diaminoazacyclopentadienyl cation one observes a dramatic stabilization. It should be stressed that as yet the "aromatic" azacyclopropenylium and azatropylium salts could not be synthesized (cf. Section 2.2), but that the "antiaromatic" (aza)cyclopentadienylium salts have been prepared!

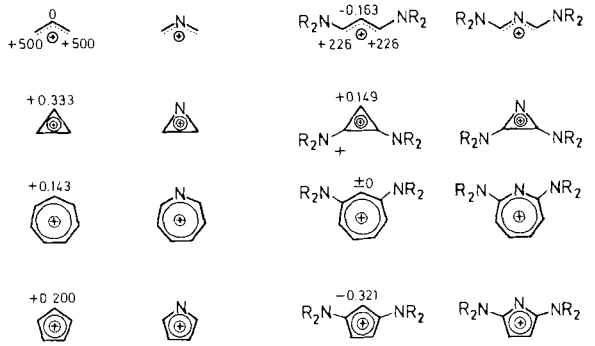

Fig. 6. HMO charge densities of systems with allylic cation structure.

The relationship between color and structure in the compounds synthesized to date is given in Figure 7. The long-wavelength absorption maxima are hypsochromically shifted proportionally to the increases in the HOMO-LUMO gap of the parent compounds.

The compounds presented in Figure 7, and related ones, can basically all be synthesized by (1) substitution or (2) dehydrogenation processes.

(1) Reaction of **101a**,[248] **100b**,[249] or **101b**,[250] with dialkyl(trimethylsilyl)amines gives the red azacyclopentadienylium salts **99**,[251] the benzo analogues **102b**,[252] and the yellow 1,3-diazacyclopentadienylium salt **103**.[252] Like **98** and **102a**[254] (accessible from **100a**[253]), these are stable, crystalline compounds. (Anilino and amino derivatives of type **102** are also known,[255-257] as are several other indenylium salts;[258-261] cf. also solvolyses with indenylium cation intermediates.[262,263])

A variant of this method is to synthesize enaminoketone **105b** from **105a**[264] or by other routes,[265] and from it to obtain thioketone **105c**[266] (2-phenyl derivatives[267,268]). By alkylation of **105b,c** one arrives at **104**, and from this one eventually obtains **102a**[266] (DMAP = 4-dimethylaminopyridine).

(2) The 1,3-diazacyclopentadienylium salt **107**, the phenyl analogue of **103** and structurally related to **98**, has been synthesized by dehydrogenation of imidazole **106**.[269] By

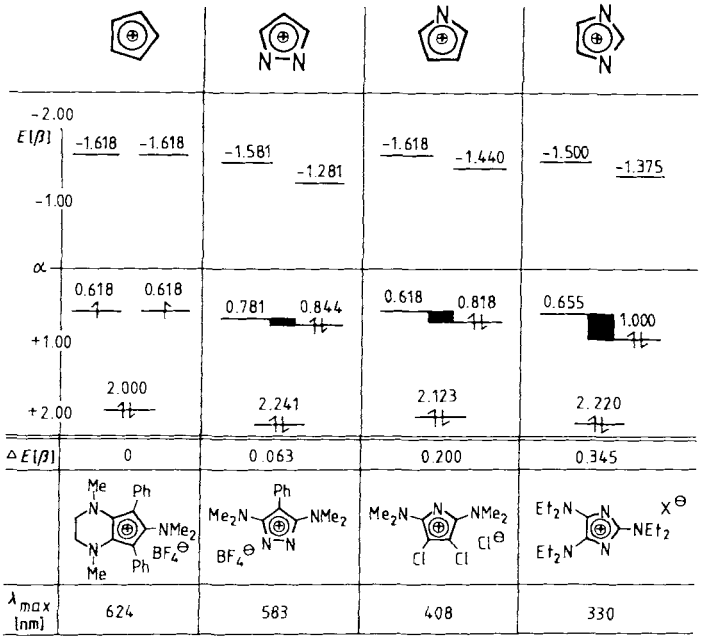

Fig. 7. HOMO-LUMO gaps (HMO) of (aza)cyclopentadienyl cations, and long-wavelength absorption maxima of several typcial (aza)cyclopentadienylium salts.

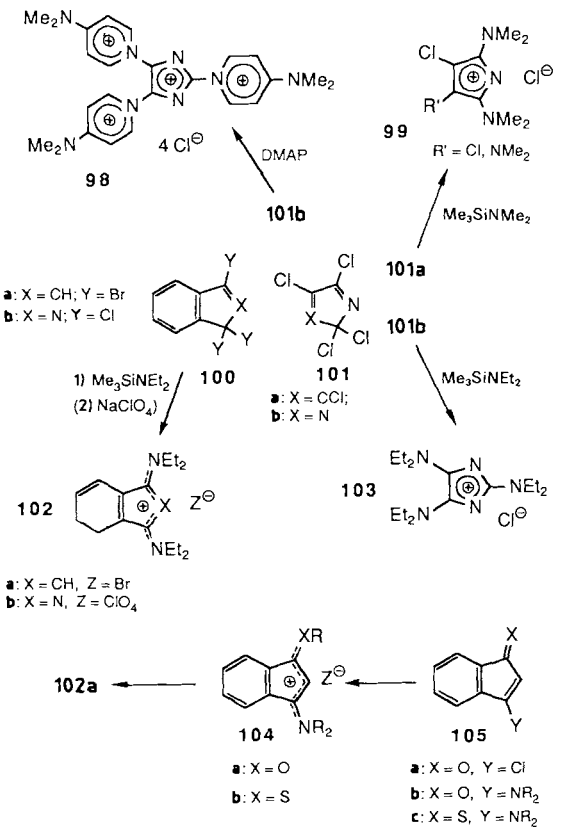

the same principle, it has been possible to obtain 1,2-diazacyclopentadienylium salts **110** by dehydrogenation of **108** or **109**[270] (as to the parent compound, cf. Ref. [271]). The difference in color between the colorless 6π system **109** and the blue 4π system **110** is striking.

These two routes can be used for the synthesis of numerous thermally stable, crystalline cyclopentadienylium salts.

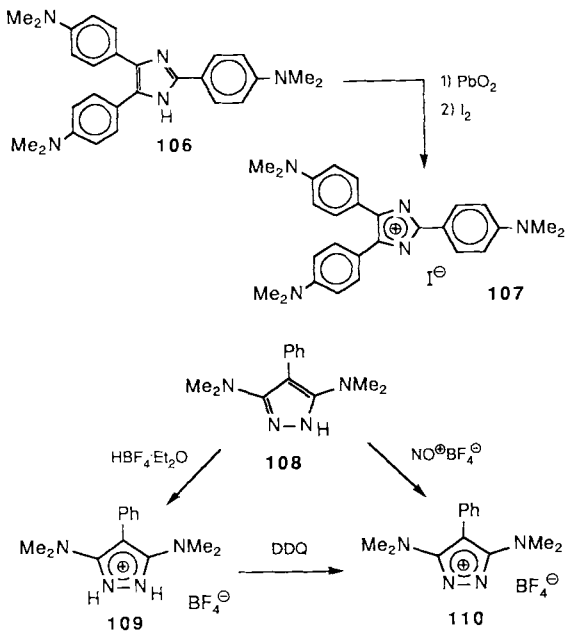

For example, condensation of diphenylcyclopentanetrione with *N,N'*-dimethylethylenediamine yields the stable, red diaminocyclopentanedienone **111**. Whereas protonation of this leads to **113**, reacting it with triethyloxonium tetrafluoroborate gives the green ethoxydiaminocyclopentadienyl salt **112** in quantitative yield ($\lambda_{max}(Ac_2O) = 735$ nm).

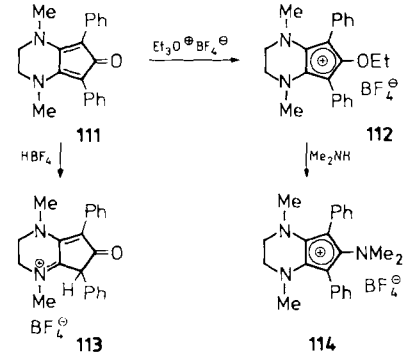

Further reaction with secondary amines affords crystalline blue triaminocyclopentadienylium salts like **114** ($\lambda_{max}(CHCl_3) = 624$ nm).[271] By the same principle, one can obtain cyclopentadienylium salts **115–118**.[272] The dependence of the long-wavelength absorption maxima on substituents agrees with MO calculations.

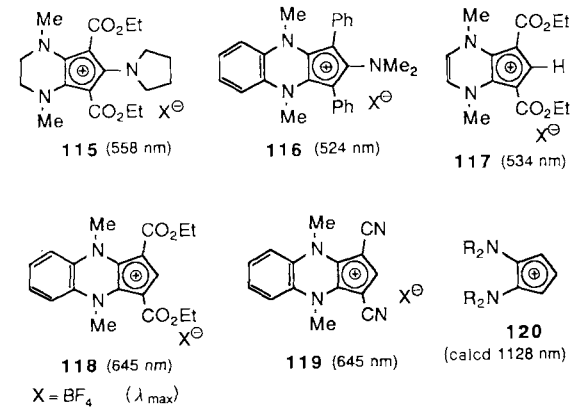

Analogously to the synthesis of **111**, the donor-acceptor-substituted cyclopentadiene **121** is obtained by condensation of dioxocyclopentanedicarbonitrile with *N,N'*-dimethylethylenediamine.[95,273] If one assumes that the effects of the donor and acceptor groups cancel each other out, then the compound ought to behave almost like a normal cyclopentadiene. This is indeed the case, permitting formation of the yellow **122** and the synthesis of numerous fulvenes and fulvalenes,[95,273] whose UV/VIS spectra display a bathochromic shift of 60–100 nm relative to those of the corresponding non-Do-A-substituted compounds. The peculiarity of **121**, however, is that it can be easily converted not only into the salt **122** of a 6π-electron anion, but also to the stable, crystalline, deep-green salt **123** of a 4π-electron cation;[95,273] **119** is another compound of this type.[95] The fact that **122** and **123** are both stable, despite belonging to different π-electron categories, shows the consequence of the donor–acceptor effect particularly graphically. In contrast to the cyclopentadienyl cation ($RE = -0.23\beta$), the cation of **123** has a positive resonance energy ($RE = +0.11\beta$ (HMO)).

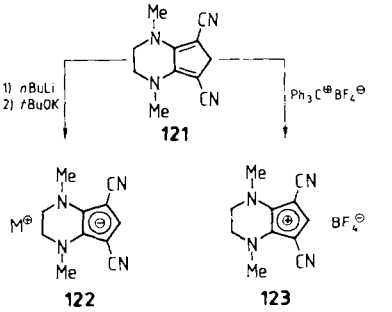

The UV/VIS spectra of all donor-acceptor-substituted cyclopentadienediylium salts show very long-wavelength absorption maxima, with medium extinction coefficients ($\log \varepsilon \approx 3$). So far **123** is the record holder, with $\lambda_{max} = 810$ nm, and thereby comes very close to the value calculated for the as yet unknown **120**.[274–277]

Cyclopentadienylium salts **117–119**, **122**, and **123** are most suitable for examining the question of the ring-current effect in stable anti-Hückel systems with positive *RE*. Figure 9 reveals that the donor-acceptor-substituted anions **122**, **124**, **125**, and **127**, the aminocyclopentadiene imine **126** and the cation **119** all fall on regression line for aromatic compounds ($\delta(^1H) = 10.4 q_{N\mu} + 7.59$; $r = 0.988$), produced by plotting $\delta(^1H)$ values against calculated charge densities. (For a detailed discussion of other regressions,[278–284] see Ref. [95].) They can therefore be classified as arenes.

In contrast to this, and above all to the position of **119**, one finds a large upfield shift with cation **123**. From the difference in the net π charge at C-6 between **122** and **123**, a charge-induced shift $\Delta\delta_q = 3.45$ ppm can be calculated, which is significantly larger than that found ($\Delta\delta = 2.10$ ppm). Though the paratropic shift for **123** ($\Delta\delta_p = \Delta\delta_q - \Delta\delta = 1.35$ ppm) is smaller than that for the benzocycloheptenyl anion ($\Delta\delta_p = 3.7$–6.8 pm, relative to the corresponding cation[285]), it is comparable to that observed for tri-*tert*-butylcyclobutadiene ($\Delta\delta_p = 1.04$ ppm, relative to cyclopentadiene[286]) and for **63**, R = alkyl or phenyl ($\Delta\delta_p = 1.10$–1.64 ppm, relative to 1,2-dihydropentalene).[287] According to NMR criteria (paratropism) and

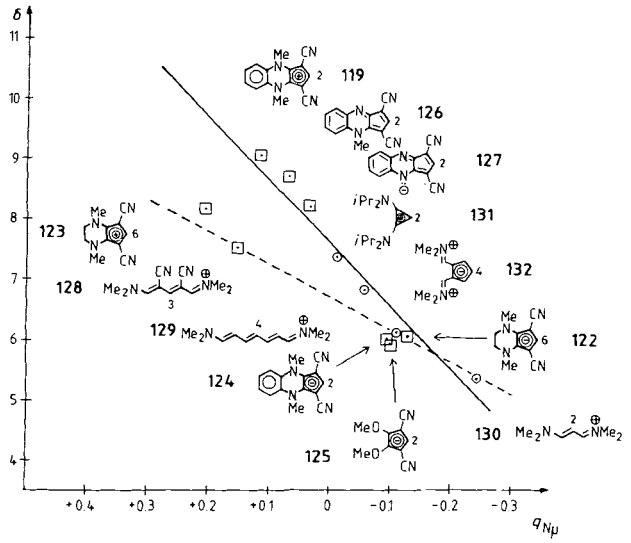

Fig. 8. Chemical shifts $\delta(^1H)$ of the protons in the five-membered ring of donor-acceptor-substituted cyclopentadiene derivatives and related cyanine systems, relative to the calculated net π charges $q_{N\mu}$(PPP). Solid line, aromatic systems; broken line, cyanine systems. ⊡ and ⊙ mean systems with Do or A and systems with Do and A, respectively.

$\Delta\Delta E_{\text{HOMO-LUMO}}$ (cf. Fig. 3), **123** is classified, then, as antiaromatic (cf. Refs. [288, 289]). According to *RE*, however, it is aromatic (cf. the difference between absolute and relative antiaromaticity.[78b])

In addition to the regression line for aromatic systems, Figure 8 shows that for cyanines ($\delta(^1H) = 5.36q_{N\mu} + 6.69$; cf. also Ref. [290]). The open-chain compound **129** ($(\lambda_{max}(CH_3CN) = 389$ nm),[95] a model compound for **123**, fits in here. Accordingly, **123** can also be viewed as a cyanine salt without a ring-current effect, though in view of the positions of the open-chain cyanines **129** and **130**, and of the cyclic **131**[291] and **132**,[292,293] this appears problematic. The enormous color difference between **123** and **128** ($\Delta\lambda_{max}(CH_3CN) = 421$ nm) must also be taken into account. It is also informative that the cyanine salts **131** and **132** fit in best as (4n+2)π systems and are therefore quite distinct from the (4n)π system **123**.

The great stability of **123** is proved in the reversible formation of dication **136**[95] from the fulvalene **133**[273] (cyclic voltammetry; 10^{-3} M, 0.1 M $KPtF_6$ in acetonitrile). It is noteworthy that in the oxidation the stable radical cation **135** appears first, while on reduction only dianion **134** can be detected.

Although **135** has not yet been successfully isolated, the related dicationic salt **140**[95] has been made

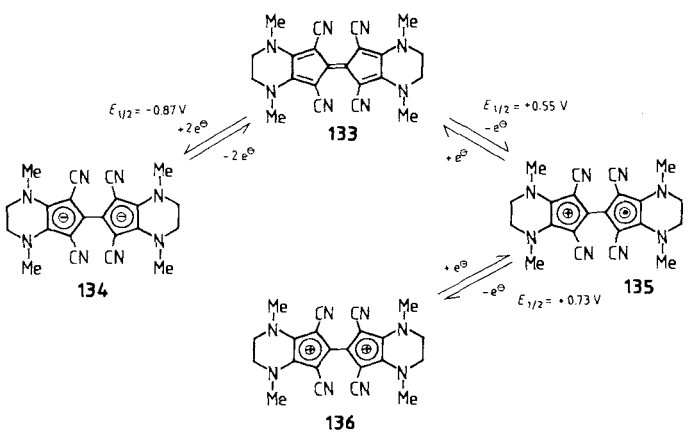

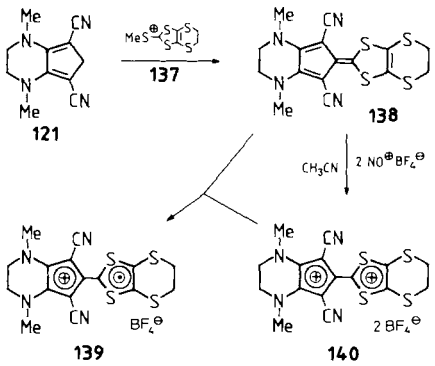

($\lambda_{max}(H_2SO_4) = 724$ nm). The salt **140** is obtained by oxidation of fulvalene **138** ($\lambda_{max}(DMF) = 500$ nm), synthesized from **121** and **137**. If one combines **138** and **140**, the radical cation salt **139** is formed ($\lambda_{max}(CF_3COOH) = 819$ nm).

3. Applications and Prospects

Above, all, this review has aimed to show that antiaromatic compounds and antiaromatic transition states can be stabilized by donor-acceptor groups. Knowledge of the properties of donor-acceptor-substituted cyclic π-electron systems naturally does not allow statements to be made about the properties of the parent compounds. Indeed, the very aim of donor-acceptor substitution is to obtain compounds that do *not* have the same characteristics as the parent compounds. This means that in the main the novel π systems have properties that are not determined by the outer-shell π electrons in the classical sense of "(4n)π = unstable, (4n+2)π = stable". Typically, donor-acceptor substitution causes a benzene-like delocalization of the ring electrons of (4n)π systems, while that of (4n+2)π systems brings about a localization to a certain extent (cf. crystal structures of *p*-nitroaniline,[294] *N,N*-dimethyl-*p*-nitroaniline,[295] *p*-nitrophenol,[296] and other benzene derivatives (cf. Ref. [297])). We therefore suggest extending the traditional classification of cyclic π systems as aromatic and antiaromatic with the class of "aromatic (4n)π systems":

Aromatic systems ("stable")
(4n+2)π electrons
$RE > 0$
diatropic
$\Delta E_{\text{HOMO-LUMO}} > 0$
$\Delta\Delta E = \Delta E_{\text{HOMO-LUMO(ring)}} - \Delta E_{\text{HOMO-LUMO(polyene)}} > 0$
weak bond fixation
Antiaromatic systems ("unstable")
(4N)π electrons
$RE < 0$
paratropic
$\Delta E_{\text{HOMO-LUMO}} = 0$
$\Delta\Delta E = \Delta E_{\text{HOMO-LUMO(ring)}} - \Delta E_{\text{HOMO LUMO(polyene)}} < 0$
strong bond fixation (⇒ nonaromatic system)
Aromatic (4n)π systems ("stable")
(4n)π electrons
$RE > 0$
paratropic
$\Delta E_{\text{HOMO-LUMO}} > 0$
$\Delta\Delta E = \Delta E_{\text{HOMO-LUMO(ring)}} - \Delta E_{\text{HOMO LUMO(polyene)}} > 0$
weak bond fixation

Scheme 2. Proposed classification of cyclic π systems.

One can, of course, have different opinions on whether a (4n)π system that satisfies significant criteria for aromaticity (low tendency towards bond fixation, relatively large HOMO-LUMO gap) should be termed "aromatic". (*Heilbronner*:[15] "'Aromaticity', if to be used at all, should be a purely structural concept. We should define certain molecules as 'aromatic', depending on the formal aspects of their structure." *Binsch*:[88] "A conjugated π-electron system is called aromatic if it shows neither strong first-order nor second-order double-bond fixation. ... Whether [this criterion] is an important one or not will have to be decided by the experimentalist."). However, since the aromaticity criteria presented at the beginning are routinely used with the traditional π systems, including the substituted ones, donor-acceptor-substituted cyclic π systems should not be made an exception.

By use of the donor-acceptor effect, classes of compounds whose members could previously only be generated at very low temperature or as very strongly hindered derivatives have become accessible, and indeed relatively easily so. Where can one generally make use of these Do-A-substituted cyclic π systems? With the change in HOMO-LUMO gap by donor-acceptor substitution there is a possibility of constructing new chromophores (cf. Refs. [3, 247]). Since the novel species are commonly electron-rich or electron-poor π systems, they have the ability to become radical cations or anions, dications or dianions. With this, new substances can be synthesized that, among other things, are suitable in the field of "organic metals" and related areas of application (cf. Ref. [298]). In this respect one should recall that the electrical conductivity of organic donor-acceptor complexes has been traced back to a "migration of aromaticity" within molecular stacks.[299] Despite its not being generally accepted,[300,301] this model offers the synthetic chemist some guidelines.

Many of the compounds described are disc-shaped and carry substituents that could be provided with long-chain alkyl groups. Liquid-crystalline (discotic) mesophases (cf. Ref. [302]) and monolayers should therefore also form.

The above discussions were limited to aromatic and antiaromatic systems. If the above question as to the character of substituted cyclopolyenes is to be fully answered, then nonaromatic systems (fulvenes, fulvalenes, quinones, quinone methides, quinodimethanes) and all those compounds whose aromaticity can be seen only in polar resonance structures (cyclopropenone, tropone, etc.; (pseudo)oxohydrocarbons, radialenes) must be considered. *p*-Quinodimethanes **141**,[303-305] for example, have a strongly polar character, and, as has been demonstrated with materials based on **141a**, they are therefore predestined for nonlinear optics.[306] Quinone methides like **142** (synthesized from **123**),[307] are also of interest in this area.

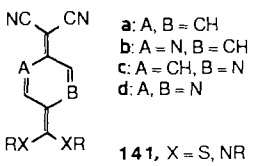

a: A, B = CH
b: A = N, B = CH
c: A = CH, B = N
d: A, B = N

141, X = S, NR

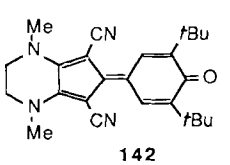

142

Acceptor and donor groups should make it possible to synthesize several cyclic π systems which until now have been unknown or have only been detected as reactive intermediates—e.g., the cyclopropenyl anion derivatives **143** and **144**, the azacyclopropenylium salts **145** (cf. attempted syntheses[308,309]), and the azatropylium salts **146**.

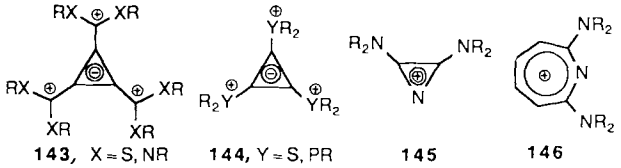

143, X = S, NR **144**, Y = S, PR **145** **146**

Antiaromatic compounds, which till recently have been a curiosity, are now gaining increasingly more interest in the search for organic ferromagnets.[228-231] In this area non-Kekulé systems like trimethylenemethane[310] and tetramethyleneethane[311,312] also have a role to play, because of their triplet ground state. One possibility for stabilizing trimethylenemethane with donor and acceptor groups has been outlined in **10**–**13**. Another could be the oxidation of Y-aromatic dianions of type **147a** ($n=2^{\ominus}$)[15-17,313,314] or **147d** ($n=2^{\ominus}$), if it were possible to suppress ring closure to methylenecyclopropanes.[266,315] This could especially be the case with **147c** ($n=2^{\ominus}$) or **147d** ($n=2^{\ominus}$). But even the reduction of Y-shaped dications of type **147b,c** ($n=2^{\oplus}$) (cf. Ref. [316]) could lead to (stable?) trimethylenemethanes **147** ($n=2^{\odot}$). A closer investigation of **147** ($n=2^{\oplus}$) would also be of interest because of the fact that no (Y-aromatic) stabilization has been found for the parent compound or for the alkyl and phenyl derivatives.[317] Trihydroxy derivatives have, however, been detected,[317] and the salts of **149**,[318] **150**,[319] and **151**[320] are stable compounds (cyclic voltammetry of derivatives of **151** reveals two reversible reduction waves).

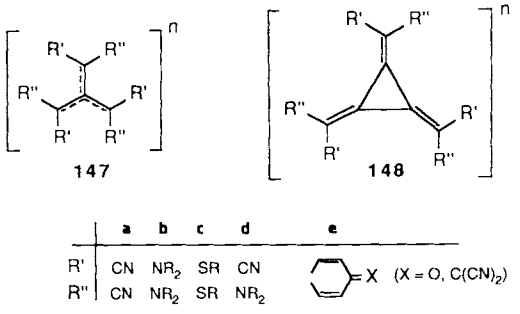

	a	b	c	d	e
R'	CN	NR_2	SR	CN	=X (X = O, $C(CN)_2$)
R"	CN	NR_2	SR	NR_2	

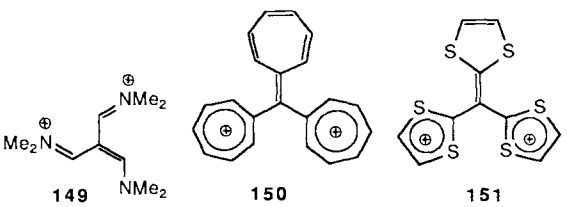

149 **150** **151**

The [3]radialenes **148** are also synthetic targets with respect to organic metals and ferromagnets. Compound **148a** ($n=2^{\ominus}$)[321] is known (heteroderivatives, cf. Refs. [322-327]) and can be oxidized to the diamagnetic(!)[328] **148a** ($n=1^{\odot\ominus}$). Compound **148e** (X = O, $n=0,2^{\ominus}$)[329,330] is also known. Compound **148e**

($X=C(CN)_2$) would, of course, be interesting as a tetracyanoquinodimethane (TCNQ) analogue; so too would the [3]radiaalenes **148b,c** (n=0) as electron-rich systems, and compounds **148d** as "neutral" systems.

Compounds like **152** and **154** are further precursors of trimethylenemethane.[300,331] The neighboring CS double bonds are reminiscent of the bonding in 1,6,6a-λ^4-trithiapentalenes **156**[332] and in **157**,[333,334] which can be viewed as a "sulfur-coated" [6]radialene or benzene. Compound **152** can be seen as a precursor of **153** ($n=2^{\odot}$),[300] which, as a trimethylenemethane derivative, should have a triplet ground state and therefore must be considered in the production of "ferromagnetic organic metals" (FOM).[230] Radical anions **153** ($n=1^{\odot\oplus}/1^{\odot\ominus}$) and dications or dianions **153** ($n=2^{\oplus}/2^{\ominus}$) would also be interesting.[300] Though it has not yet been possible to synthesize **152**, the closely related salts **155** have been made.[335]

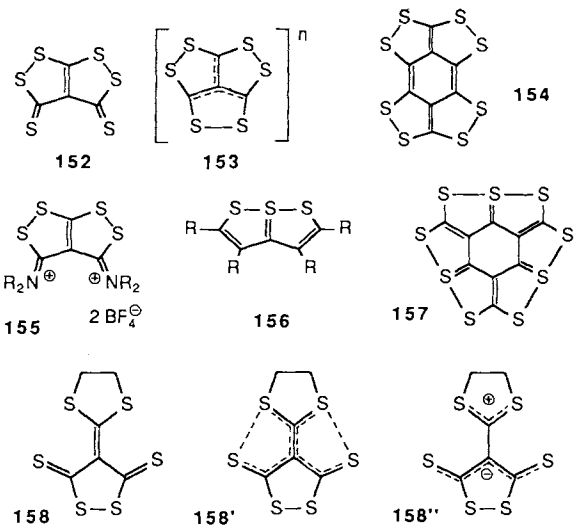

An interesting variant of structure type **153** is compound **158**. Based on the nonbonded S-S distances it can be regarded, in accordance with formula **158'**, as a "trimethylenemethane imbedded in a pseudo-1,2-dithiolo[5,4-*c*]-[1,2]dithiole, (4n+2) π-electron, milieu" or as "heteroaromatic trimethylenemethane".[336] However, the dipolar structure **158"** has to be considered as well.

Acepentalene, which is structurally related to **153**, has also not yet been synthesized.[337,338] The unfavorable electronic structure of the parent compound (two SOMOs) would no longer be present in **159** and **160** and, therefore, such compounds may be synthesizable.

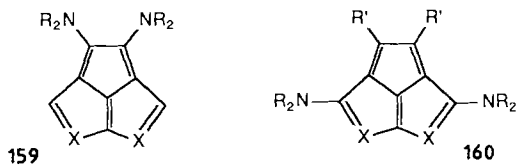

X = CR, N, C-CN, C-CR=$NR_2^{\oplus}$; R' = R, CN

By varying the donor and acceptor groups, donor-acceptor-substituted cyclic π systems can be synthesized whose electron donating/accepting properties are suitable for the application concerned. It does not need to be mentioned that such substituent effects have always been used with success in the past, and it is not only in this respect that the boundary between classical aromatic chemistry and the Do-A π systems described here is a fluid one.

This article has had to omit discussion of many workers results which have contributed significantly to progress in this area. We express our thanks both to them and to those workers mentioned in the references for their commitment. The Deutsche Forschungsgemeinschaft and the Fonds der Chemischen Industrie earn special thanks for their generous support of this research over many years.

Received: March 4, 1988 [A 697 IE]
German version: *Angew. Chem. 100* (1988) 1492
Translated by Dr. *Michael Kertesz*, Cambridge, UK.

[1] A. Kekulé, *Bull. Soc. Chim. Fr. 3* (1865) 98.
[2] O. N. Witt, *Ber. Dtsch. Chem. Ges. 9* (1876) 522.
[3] J. Griffiths, *Rev. Prog. Color. Relat. Top. 11* (1981) 37.
[4] H. G. Viehe, R. Merényi, L. Stella, Z. Janousek, *Angew. Chem. 91* (1979) 982; *Angew. Chem. Int. Ed. Engl. 18* (1979) 917; H. G. Viehe, Z. Janousek, R. Merényi, *Acc. Chem. Res. 18* (1985) 148.
[5] a) R. Baldock, P. Hudson, A. R. Katritzky, F. Soti, *Heterocycles 1973*, 67; b) A. R. Katritzky, M. C. Zerner, M. M. Karelson, *J. Am. Chem. Soc. 108* (1986) 7213; c) H. Birkhofer, J. Hädrich, H.-D. Beckhaus, C. Rüchardt, *Angew. Chem. 99* (1987) 592; *Angew. Chem. Int. Ed. Engl. 26* (1987) 573; d) C. J. Rhodes, E. Roduner, *Tetrahedron Lett. 29* (1988) 1437.
[6] D. S. Chemla, J. Zyss (Hrsg.): *Non-linear Optical Properties of Organic Molecules and Crystals, Vol. 1*, Academic Press, New York 1987.
[7] D. Williams, *Angew. Chem. 96* (1984) 637; *Angew. Chem. Int. Ed. Engl. 23* (1984) 690.
[8] H. E. Katz, K. D. Singer, J. E. Sohn, C. W. Dirk, L. A. King, H. M. Gordon, *J. Am. Chem. Soc. 109* (1987) 6561.
[9] Vgl. J.-M. Lehn, *Angew. Chem. 100* (1988) 91; *Angew. Chem. Int. Ed. Engl. 27* (1988) 89.
[10] W. Rettig, *Angew. Chem. 98* (1986) 969; *Angew. Chem. Int. Ed. Engl. 25* (1986) 971.
[11] R. Gompper, H.-U. Wagner, *Angew. Chem. 88* (1976) 389; *Angew. Chem. Int. Ed. Engl. 15* (1976) 321.
[12] G. Maier, *Chem. Unserer Zeit 9* (1975) 131.
[13] L. J. Schaad, B. A. Hess, Jr., *Pure Appl. Chem. 54* (1982) 1097.
[14] P. J. Garratt in J. F. Stoddart (Hrsg.): *Comprehensive Organic Chemistry*, Pergamon Press, Oxford 1979, S. 215.
[15] Siehe E. D. Bergmann, I. Agranat in E. D. Bergmann, B. Pullmann (Hrsg.): *Aromaticity, Pseudo-Aromaticity, Anti-Aromaticity*, The Jerusalem Symposia on Quantum Chemistry and Biochemistry III, Israel Academy of Sciences and Humanities, Jerusalem 1971.
[16] G. Binsch, *Naturwissenschaften 60* (1973) 369.
[17] A. Balaban, *Pure Appl. Chem. 52* (1980) 1409.
[18] M. N. Glukhovtsev, B. Y. Simkin, V. I. Minkin, *Russ. Chem. Rev. Engl. Trans. 54* (1985) 54.
[19] E. D. Jemmis, P. von R. Schleyer, *J. Am. Chem. Soc. 104* (1982) 4781.
[20] S. Winstein, *Q. Rev. Chem. Soc. 23* (1969) 141.
[21] a) L. A. Paquette, *Angew. Chem. 90* (1978) 114; *Angew. Chem. Int. Ed. Engl. 17* (1978) 106; b) R. C. Haddon, *Acc. Chem. Res. 21* (1988) 243.
[22] M. J. Goldstein, R. Hoffmann, *J. Am. Chem. Soc. 93* (1971) 6193.
[23] P. J. Gund, *J. Chem. Educ. 49* (1972) 100.
[24] I. Agranat, A. Skancke, *J. Am. Chem. Soc. 107* (1985) 867.
[25] J. Klein, *Tetrahedron 39* (1983) 2733.
[26] J. Chandrasekhar, E. D. Jemmis, P. von R. Schleyer, *Tetrahedron Lett. 1979*, 3707.
[27] A. B. McEwen, P. von R. Schleyer, *J. Org. Chem. 51* (1986) 4357.
[28] T. Fukunaga, H. E. Simmons, J. J. Wendoloski, M. D. Gordon, *J. Am. Chem. Soc. 105* (1983) 2729.
[29] R. W. Alder, J. C. Petts, *Tetrahedron Lett. 26* (1985) 1585.
[30] R. B. Woodward, R. Hoffmann: *Die Erhaltung der Orbitalsymmetrie*, Verlag Chemie, Weinheim 1970; *The Conservation of Orbital Symmetry*, Academic Press, New York 1971.
[31] M. G. Evans, E. Warhust, *Trans. Faraday Soc. 34* (1938) 614; *35* (1939) 824.
[32] M. J. S. Dewar: *Aromaticity*, Special Publication of The Chemical Society No. 21, London 1967, S. 177; *Angew. Chem. 83* (1971) 859; *Angew. Chem. Int. Ed. Engl. 10* (1971) 761.

[33] a) O. Ermer, *Angew. Chem. 99* (1987) 791; *Angew. Chem. Int. Ed. Engl. 26* (1987) 782; b) R. Janoschek, *ibid. 99* (1987) 1332 bzw. *26* (1987) 1298.
[34] N. D. Epiotis, *Nouv. J. Chim. 8* (1984) 11; *Lect. Notes Chem. 34* (1983) 358; *Pure Appl. Chem. 55* (1983) 229.
[35] S. S. Shaik, R. Bar, *Nouv. J. Chim. 8* (1984) 411.
[36] S. S. Shaik, P. C. Hiberty, *J. Am. Chem. Soc. 107* (1985) 3089.
[37] P. C. Hiberty, S. S. Shaik, J.-M. Lefour, G. Ohanessian, *J. Org. Chem. 50* (1985) 4657.
[38] N. C. Baird, *J. Org. Chem. 51* (1986) 3907.
[39] a) P. C. Hiberty, S. S. Shaik, G. Ohanessian, J.-M. Lefour, *J. Org. Chem. 51* (1986) 3908; b) S. S. Shaik, P. C. Hiberty, J.-M. Lefour, G. Ohanessian, *J. Am. Chem. Soc. 109* (1987) 363.
[40] M. Kataoka, T. Nakajima, *J. Org. Chem. 52* (1987) 2323.
[41] D. J. Klein, *Pure Appl. Chem. 55* (1983) 299.
[42] S. Kuwajima, *J. Am. Chem. Soc. 106* (1984) 6496.
[43] A. F. Voter, W. A. Goddard III, *J. Am. Chem. Soc. 108* (1986) 2830.
[44] a) D. L. Cooper, J. Gerratt, M. Raimondi, *Nature (London) 323* (1986) 699; b) J. Gerratt, *Chem. Br. 1987*, 327.
[45] B. M. Gimarc, *J. Am. Chem. Soc. 105* (1983) 1979.
[46] J. K. Burdett, E. Canadell, T. Hughbanks, *J. Am. Chem. Soc. 108* (1986) 3971.
[47] a) G. Maier, S. Pfriem, U. Schäfer, R. Matusch, *Angew. Chem. 90* (1978) 552; *Angew. Chem. Int. Ed. Engl. 17* (1978) 520; b) H. Irngartinger, N. Riegler, K.-D. Malsch, K.-A. Schneider, G. Maier, *ibid. 92* (1980) 214 bzw. *19* (1980) 211; c) H. Irngartinger, M. Nixdorf, *ibid. 95* (1983) 415 bzw. *22* (1983) 403; d) G. Maier, *ibid. 100* (1988) 317 bzw. *27* (1988) 309.
[48] U.-J. Vogelbacher, M. Regitz, R. Mynott, *Angew. Chem. 98* (1986) 835; *Angew. Chem. Int. Ed. Engl. 25* (1986) 842.
[49] B. A. Hess, Jr., L. J. Schaad, C. W. Holyoke, Jr., *Tetrahedron 31* (1975) 295.
[50] M. Kataoka, T. Ohmae, T. Nakajima, *J. Org. Chem. 51* (1986) 358.
[51] K. Hafner, *Nachr. Chem. Tech. Lab. 28* (1980) 222; *Pure Appl. Chem. 54* (1982) 939.
[52] K. Hafner, B. Stowasser, H.-P. Krimmer, S. Fischer, M. C. Böhm, H. J. Lindner, *Angew. Chem. 98* (1986) 646; *Angew. Chem. Int. Ed. Engl. 25* (1986) 630.
[53] E. Heilbronner, Z. Yang, *Angew. Chem. 99* (1987) 369; *Angew. Chem. Int. Ed. Engl. 26* (1987) 360.
[54] a) W. H. Mills, I. G. Nixon, *J. Chem. Soc. 1930*, 2510; b) G. M. Q. Badger, *Q. Rev. Chem. Soc. 5* (1951) 147; c) P. C. Hiberty, G. Ohanessian, F. Delbecq, *J. Am. Chem. Soc. 107* (1985) 3095; d) Y. Apeloig, D. Arad, *ibid. 108* (1986) 3241.
[55] a) H. Hopf, *Chem. Unserer Zeit 10* (1976) 114; J. Kleinschroth, H. Hopf, *Angew. Chem. 94* (1982) 485; *Angew. Chem. Int. Ed. Engl. 21* (1982) 169; b) K.-L. Noble, H. Hopf, L. Ernst, *Chem. Ber. 117* (1984) 455, 474.
[56] a) J. Liebe, C. Wolff, C. Krieger, J. Weiss, W. Tochtermann, *Chem. Ber. 118* (1985) 4144; b) J. D. Roberts, *Spec. Publ. Chem. Soc. London 12* (1958) 111; R. Hoffmann, *Chem. Commun. 1969*, 240.
[57] G. Maier, *Angew. Chem. 86* (1974) 491; *Angew. Chem. Int. Ed. Engl. 13* (1974) 425.
[58] T. Bally, S. Masamune, *Tetrahedron 36* (1980) 343.
[59] D. W. Whitman, B. K. Carpenter, *J. Am. Chem. Soc. 102* (1980) 4272.
[60] H. Kollmar, V. Staemmler, *J. Am. Chem. Soc. 100* (1978) 4304.
[61] J. Kreile, N. Münzel, A. Schweig, H. Specht, *Chem. Phys. Lett. 124* (1986) 140.
[62] M.-J. Huang, M. Wolfsberg, *J. Am. Chem. Soc. 106* (1984) 4039.
[63] M. J. S. Dewar, K. M. Merz, Jr., J. S. P. Stewart, *J. Am. Chem. Soc. 106* (1984) 4040.
[64] G. Maier, H.-O. Kalinowski, K. Euler, *Angew. Chem. 94* (1982) 706; *Angew. Chem. Int. Ed. Engl. 21* (1982) 693.
[65] R. Gompper, G. Seybold, *Angew. Chem. 80* (1968) 804; *Angew. Chem. Int. Ed. Engl. 7* (1968) 824.
[66] H. J. Lindner, B. von Gross, *Chem. Ber. 107* (1974) 598.
[67] R. Gompper, J. Kroner, G. Seybold, H.-U. Wagner, *Tetrahedron 32* (1976) 629.
[68] R. Gompper, G. Seybold in T. Nozoe, R. Breslow, K. Hafner, S. Ito, I. Murata (Hrsg.): *Topics in Nonbenzenoid Aromatic Chemistry, Vol. II*, Hirokawa, Tokyo 1977, S. 29.
[69] M. Neuenschwander, A. Niederhauser, *Helv. Chim. Acta 53* (1970) 519.
[70] V. Bonačić-Koutecký, J. Koutecký, J. Michl, *Angew. Chem. 99* (1987) 216; *Angew. Chem. Int. Ed. Engl. 26* (1987) 170.
[71] R. Gompper, S. Mensch, G. Seybold, *Angew. Chem. 87* (1975) 711; *Angew. Chem. Int. Ed. Engl. 14* (1975) 704.
[72] G. Seybold, U. Jersak, R. Gompper, *Angew. Chem. 85* (1973) 918; *Angew. Chem. Int. Ed. Engl. 12* (1973) 847.
[73] R. P. Thummel, *Acc. Chem. Res. 13* (1980) 70.
[74] J. J. McCullough, *Acc. Chem. Res. 13* (1980) 270.
[75] R. Gompper, E. Kutter, H. Kast, *Angew. Chem. 79* (1967) 147; *Angew. Chem. Int. Ed. Engl. 6* (1967) 171.
[76] a) R. Breslow, *Acc. Chem. Res. 6* (1973) 393; b) N. L. Bauld, T. L. Welsher, J. Cessac, R. L. Holloway, *J. Am. Chem. Soc. 100* (1978) 6920; c) B. L. Podlogar, W. A. Glauser, W. R. Rodriguez, D. J. Raber, *J. Org. Chem. 53* (1988) 2128.
[77] M. Kataoka, T. Nakajima, *J. Org. Chem. 52* (1987) 2323.
[78] a) M. J. S. Dewar: *The Molecular Orbital Theory of Organic Chemistry*, McGraw-Hill, New York 1969; b) M. J. S. Dewar, R. C. Dougherty: *The PMO Theory of Organic Chemistry*, Plenum, New York 1975, S. 89–119; c) K. A. Durkin, R. F. Langler, *J. Phys. Chem. 91* (1987) 2422.
[79] N. C. Baird, *J. Chem. Educ. 48* (1971) 509.
[80] B. A. Hess, Jr., L. J. Schaad, *J. Am. Chem. Soc. 105* (1983) 7500.
[81] W. R. Roth, *Nachr. Chem. Tech. Lab. 31* (1983) 964.
[82] a) I. Gutman, M. Milun, N. Trinajstić, *J. Am. Chem. Soc. 99* (1977) 1692; b) M. Randić, N. Trinajstić, *ibid. 109* (1987) 6823.
[83] Vgl. K.-U. Klabunde, K. Müllen, H. Vogler, *Tetrahedron 43* (1987) 1183.
[84] S. Kuwajima, Z. G. Goos, *J. Am. Chem. Soc. 109* (1987) 107.
[85] K. Müllen, *Chem. Rev. 84* (1984) 603.
[86] R. F. Childs, R. Faggiani, C. J. L. Lock, M. Mahendran, *J. Am. Chem. Soc. 108* (1986) 3613.
[87] a) G. Binsch, E. Heilbronner, J. N. Murrell, *Mol. Phys. 1* (1966) 305; b) G. Binsch, E. Heilbronner, *Tetrahedron 24* (1968) 1215.
[88] G. Binsch, I. Tamir, *J. Am. Chem. Soc. 91* (1969) 2450.
[89] K. Jug, *J. Org. Chem. 48* (1983) 1344.
[90] C. W. Bird, *Tetrahedron 41* (1985) 1409.
[91] U. Norinder, O. Wennerström, *Tetrahedron 41* (1985) 713.
[92] O. Wennerström, U. Norinder, *Acta Chem. Scand. Ser. B40* (1986) 328.
[93] A. Minsky, A. Y. Meyer, M. Rabinovitz, *Tetrahedron 41* (1985) 785.
[94] A. J. Fry, P. C. Fox, *Tetrahedron 42* (1986) 5255.
[95] T. Geßner, *Dissertation*, Universität München 1986.
[96] J. E. Baldwin, A. H. Andrist, R. K. Pinschmidt, Jr., *Acc. Chem. Res. 5* (1972) 402.
[97] R. Gompper, *Angew. Chem. 81* (1969) 348; *Angew. Chem. Int. Ed. Engl. 8* (1969) 312.
[98] N. D. Epiotis, *Angew. Chem. 86* (1974) 825; *Angew. Chem. Int. Ed. Engl. 13* (1974) 751.
[99] J.-P. Fleury, *Helv. Chim. Acta 60* (1977) 2576.
[100] T. Tsuji, S. Nishida, *Acc. Chem. Res. 17* (1984) 56.
[101] T. Mukai, K. Sato, Y. Yamashita, *J. Am. Chem. Soc. 103* (1981) 670.
[102] V. D. Kiselev, J. G. Miller, *J. Am. Chem. Soc. 97* (1975) 4036.
[103] M. Lofti, R. M. G. Roberts, *Tetrahedron 35* (1979) 2131.
[104] Y. Uosaki, M. Nakahara, M. Sasaki, J. Osugi, *Chem. Lett. 1979*, 727.
[105] M. Dern, H.-G. Korth, G. Kopp, R. Sustmann, *Angew. Chem. 97* (1985) 324; *Angew. Chem. Int. Ed. Engl. 24* (1985) 337.
[106] S. Fukuzumi, J. K. Kochi, *Tetrahedron 38* (1982) 1035.
[107] E. F. Hilinski, J. M. Masnovi, J. K. Kochi, P. M. Rentzepis, *J. Am. Chem. Soc. 106* (1984) 8071.
[108] a) R. Gompper, G. Seybold, *Angew. Chem. 83* (1971) 44; *Angew. Chem. Int. Ed. Engl. 10* (1971) 67; b) *ibid. 83* (1971) 45 bzw. *10* (1971) 68.
[109] R. Breslow, D. Kivelevich, M. J. Mitchell, W. Fabian, K. Wendel, *J. Am. Chem. Soc. 87* (1965) 5132.
[110] W. Kirmse: *Carbene, Carbenoide und Carbenanaloga*, Verlag Chemie, Weinheim 1969, S. 49, 51.
[111] R. Gompper, U. Wolf, *Liebigs Ann. Chem. 1979*, 1406.
[112] J. Schelble, *Dissertation*, Universität München 1981.
[113] R. Gompper, J. Schelble, C. S. Schneider, *Tetrahedron Lett. 1978*, 3897.
[114] M. J. S. Dewar, S. Olivella, J. J. P. Stewart, *J. Am. Chem. Soc. 108* (1986) 5771.
[115] G. Hultzsch, *Dissertation*, Universität München 1970.
[116] M. Heuschmann, *Chem. Ber. 121* (1988) 39.
[117] G. Desimono, G. Tacconi, *Chem. Rev. 75* (1975) 651.
[118] P. Righetti, G. Tacconi, A. C. C. Piccolini, M. T. Pesenti, G. Desimoni, R. Oberti, *J. Chem. Soc. Perkin Trans. 1 1979*, 863.
[119] G. Tacconi, M. Leoni, P. Righetti, G. Desimoni, R. Oberti, *J. Chem. Soc. Perkin Trans. 1 1979*, 2687.
[120] J. Bitter, J. Leitich, H. Partale, O. E. Polansky, W. Riemer, U. Ritter-Thomas, B. Schlamann, B. Stilkerieg, *Chem. Ber. 113* (1980) 1020.
[121] A. B. Padias, S. T. Hedrick, H. K. Hall, Jr., *J. Org. Chem. 48* (1983) 3787; H. K. Hall, Jr., A. B. Padias, *ibid. 52* (1987) 4536.
[122] M. J. S. Dewar, C. Jie, *J. Am. Chem. Soc. 109* (1987) 5893.
[123] R. Gompper, W.-R. Ulrich, *Angew. Chem. 88* (1976) 298; *Angew. Chem. Int. Ed. Engl. 15* (1976) 299.
[124] R. Gompper, W.-R. Ulrich, *Angew. Chem. 88* (1976) 300; *Angew. Chem. Int. Ed. Engl. 15* (1976) 301.
[125] R. Gompper, B. Kohl, *Tetrahedron Lett. 21* (1980) 907.
[126] R. Gompper, B. Kohl, *Tetrahedron Lett. 21* (1980) 917.

[127] R. Gompper, B. Kohl, *Angew. Chem. 94* (1982) 202; *Angew. Chem. Int. Ed. Engl. 21* (1982) 198.
[128] H. Stetter, H. G. Thomas, *Chem. Ber. 101* (1968) 1115.
[129] M. J. Strauss, *Acc. Chem. Res. 7* (1974) 181.
[130] R. Gompper, B. Kohl, *Angew. Chem. 94* (1982) 202; *Angew. Chem. Int. Ed. Engl. 21* (1982) 198; *Angew. Chem. Suppl. 1982,* 398.
[131] R. Gompper, B. Kohl, *Angew. Chem. 94* (1982) 203; *Angew. Chem. Int. Ed. Engl. 21* (1982) 199; *Angew. Chem. Suppl. 1982,* 405.
[132] C. Schnieders, K. Müllen, *Tetrahedron Lett. 25* (1984) 749.
[133] M. J. S. Dewar, D. H. Lo, *J. Am. Chem. Soc. 93* (1971) 7201; M. J. S. Dewar, Z. Náhlovská, B. D. Náhlovsky, *Chem. Commun. 1971,* 1377; M. J. S. Dewar, C. Lie, *Tetrahedron 44* (1988) 1351.
[134] R. Hoffmann, W. D. Stohrer, *J. Am. Chem. Soc. 93* (1971) 6941.
[135] L. S. Miller, K. Grohmann, J. J. Dannenberg, L. Todaro, *J. Am. Chem. Soc. 103* (1981) 6249.
[136] R. Gompper, M.-L. Schwarzensteiner, *Angew. Chem. 94* (1982) 447; *Angew. Chem. Int. Ed. Engl. 21* (1982) 438.
[137] R. Gompper, M.-L. Schwarzensteiner, H.-U. Wagner, *Tetrahedron Lett. 26* (1985) 611.
[138] H. Quast, J. Christ, E.-M. Peters, H. G. von Schnering, *Chem. Ber. 118* (1985) 1154; H. Quast, J. Christ, *Angew. Chem. 96* (1984) 606; *Angew. Chem. Int. Ed. Engl. 23* (1984) 631.
[139] C. Schnieders, H.-J. Altenbach, K. Müllen, *Angew. Chem. 94* (1982) 638; *Angew. Chem. Int. Ed. Engl. 21* (1982) 637.
[140] L. S. Miller, K. Grohmann, J. J. Dannenberg, *J. Am. Chem. Soc. 105* (1983) 6862.
[141] R. Gompper, M.-L. Schwarzensteiner, *Angew. Chem. 95* (1983) 553; *Angew. Chem. Int. Ed. Engl. 22* (1983) 543; *Angew. Chem. Suppl. 1983,* 817.
[142] C. Schnieders, W. Huber, J. Lex, K. Müllen, *Angew. Chem. 97* (1985) 579; *Angew. Chem. Int. Ed. Engl. 24* (1985) 576.
[143] a) T.-Z. Wang, L. A. Paquette, *Tetrahedron Lett. 29* (1988) 41; b) L. A. Paquette, M. P. Trova, *ibid. 27* (1986) 1895; c) *ibid. 28* (1987) 2795, 4354.
[144] R. Gompper, H. Nöth, W. Rattay, M.-L. Schwarzensteiner, P. Spes, H.-U. Wagner, *Angew. Chem. 99* (1987) 1071; *Angew. Chem. Int. Ed. Engl. 26* (1987) 1039.
[145] W. F. Maier, P. von R. Schleyer, *J. Am. Chem. Soc. 103* (1981) 1891.
[146] G. Szeimies in R. A. Abramovitch (Hrsg.): *Reactive Intermediates,* Plenum, New York 1983, S. 329-359.
[147] M. Toda, Y. Hirata, S. Yamamura, *Chem. Commun. 1970,* 1597; *Tetrahedron 28* (1972) 1477.
[148] J. G. Radziszewski, J. W. Downing, M. Jawdosiuk, P. Kovacic, J. Michl, *J. Am. Chem. Soc. 107* (1985) 594.
[149] L. M. Jackman, G. Ibar, A. J. Freyer, Y. Görlach, H. Quast, *Chem. Ber. 117* (1984) 1671.
[150] H. Quast, Y. Görlach, J. Stawitz, E.-M. Peters, K. Peters, H. G. von Schnering, *Chem. Ber. 117* (1984) 2745.
[151] H. Quast, E. Geissler, A. Mayer, L. M. Jackman, K. L. Colson, *Tetrahedron 42* (1986) 1805.
[152] H. Kessler, W. Ott, *J. Am. Chem. Soc. 98* (1976) 5015.
[153] H. Günther, J. Runsick, H. Schmickler, P. Schmitt, *J. Org. Chem. 50* (1985) 289.
[154] A. Busch, H. M. R. Hoffmann, *Tetrahedron Lett. 1976,* 2379.
[155] S. A. Weissman, S. G. Baxter, A. M. Arif, A. H. Cowley, *J. Am. Chem. Soc. 108* (1986) 529.
[156] H. Petersen, *Synthesis 1973,* 243.
[157] P. H. Boyle, E. O'Brien, *Proc. R. Ir. Acad. Sect. B 83* (1983) 13.
[158] R. Gompper, H. Nöth, P. Spes, *Tetrahedron Lett. 29* (1988) 3639.
[159] G. V. Shustov, A. B. Zolotoi, N. L. Zaichenko, O. A. Dyachenko, L. O. Atovmyan, R. G. Kostyanovskii, *Tetrahedron 40* (1984) 2151.
[160] O. A. Dyachenko, L. O. Atovmyan, S. M. Aldoshin, A. E. Polyakov, R. G. Kostyanovskii, *J. Chem. Soc. Chem. Commun. 1976,* 50.
[161] A. Nabeya, Y. Tamura, T. Kodama, Y. Iwakura, *J. Org. Chem. 38* (1973) 3758.
[162] P. E. McGann, J. T. Groves, F. D. Greene, G. M. Stack, R. J. Majeste, L. M. Trefonas, *J. Org. Chem. 43* (1978) 922.
[163] T. J. Katz, *J. Am. Chem. Soc. 82* (1960) 3784.
[164] G. Schröder: *Cyclooctatetraen*, Verlag Chemie, Weinheim 1965, S. 22-26.
[165] S. Z. Goldberg, K. N. Raymond, C. A. Harmon, D. H. Templeton, *J. Am. Chem. Soc. 96* (1974) 1348.
[166] L. A. Paquette, J. F. Hansen, T. Kakihana, *J. Am. Chem. Soc. 93* (1971) 168; L. A. Paquette, T. Kakihana, J. F. Hansen, *Tetrahedron Lett. 1970,* 529.
[167] L. A. Paquette, *Angew. Chem. 83* (1971) 11; *Angew. Chem. Int. Ed. Engl. 10* (1971) 11.
[168] D. Wilhelm, T. Clark, P. von R. Schleyer, A. G. Davies, *J. Chem. Soc. Chem. Commun. 1984,* 558.
[169] R. Lindh, B. O. Roos, G. Jonsäll, P. Ahlberg, *J. Am. Chem. Soc. 108* (1986) 6554.
[170] S. Bátori, R. Gompper, J. Maier, H.-U. Wagner, *Tetrahedron 44* (1988), im Druck.
[171] U. Göckel, W. Hartmannsgruber, A. Steigel, J. Sauer, *Tetrahedron Lett. 21* (1980) 599.
[172] M. M. Coombs, *J. Chem. Soc. 1958,* 4200.
[173] E. J. Moriconi, I. A. Maniscalco, *J. Org. Chem. 37* (1972) 208.
[174] G. Glas, *Dissertation,* Universität München 1987.
[175] S. Bátori, R. Gompper, unveröffentlichte Ergebnisse.
[176] J. W. Streef, H. C. van der Plas, *Tetrahedron Lett. 1979,* 2287.
[177] J. Maier, *Dissertation,* Universität München 1985.
[178] a) H. J. Dauben, Jr., M. R. Rifi, *J. Am. Chem. Soc. 85* (1963) 3041; b) W. von E. Doering, P. P. Gaspar, *ibid. 85* (1963) 3043; c) R. Breslow, W. Chu, *ibid. 95* (1973) 411.
[179] S. W. Staley, A. W. Orvedal, *J. Am. Chem. Soc. 96* (1974) 1618.
[180] K. N. Rapp, T. Burgemeister, J. Daub, *Tetrahedron Lett. 1978,* 2685.
[181] G. Kaupp, H.-W. Grüter, E. Teufel, *Chem. Ber. 115* (1982) 3208.
[182] F. G. Klärner, S. Yaslak, M. Wette, *Chem. Ber. 110* (1977) 107.
[183] S. W. Staley, A. W. Orvedal, *J. Am. Chem. Soc. 95* (1973) 382.
[184] L. J. Schaad, B. A. Hess, Jr., *J. Am. Chem. Soc. 94* (1972) 3068.
[185] W. C. Herndon, M. L. Ellzey, Jr., *J. Am. Chem. Soc. 96* (1974) 6631.
[186] M. Randić, *J. Am. Chem. Soc. 99* (1977) 444.
[187] T. Nakajima, *Fortschr. Chem. Forsch. 32* (1972) 1.
[188] B. Kitschke, H. J. Lindner, *Tetrahedron Lett. 1977,* 2511.
[189] S. Tanaka, K. Satake, A. Kiyomine, T. Kumagai, T. Mukai, *Angew. Chem. 100* (1988) 1134; *Angew. Chem. Int. Ed. Engl. 27* (1988) 1061.
[190] T. Mukai, A. Konno, T. Kumagai, K. Satake, *Chem. Lett. 1985,* 1809.
[191] K. Karaghiosoff, W. S. Sheldrick, A. Schmidpeter, *Chem. Ber. 119* (1986) 3213.
[192] K. Hartke, K. Matusch, *Angew. Chem. 84* (1972) 61; *Angew. Chem. Int. Ed. Engl. 11* (1972) 50; *Chem. Ber. 105* (1972) 2584.
[193] L. Cassar, A. Iqbal, A. C. Rochat, Eur. Pat.-Anm. 133 156 (1984), Ciba-Geigy.
[194] D. G. Farnum, G. Mehta, G. I. Moore, F. P. Siegal, *Tetrahedron Lett. 1974,* 2549.
[195] F. Closs, R. Gompper, *Angew. Chem. 99* (1987) 564; *Angew. Chem. Int. Ed. Engl. 26* (1987) 552.
[196] F. Closs, R. Gompper, H. Nöth, H.-U. Wagner, *Angew. Chem. 100* (1988) 875; *Angew. Chem. Int. Ed. Engl. 27* (1988) 842.
[197] a) A. C. Rochat, A. Iqbal, R. Jeanneret, J. Miziguchi, Eur. Pat. Anm. 0187620 (1985), Ciba-Geigy; b) J. D. Dunitz, C. Krüger, H. Irngartinger, E. F. Maverick, Y. Wang, M. Nixdorf, *Angew. Chem. 100* (1988) 415; *Angew. Chem. Int. Ed. Engl. 27* (1988) 387.
[198] K. Kusuda, N. Osaka, *J. Chem. Soc. Chem. Commun. 1972,* 508.
[199] I. Willner, J. Y. Becker, M. Rabinovitz, *J. Am. Chem. Soc. 101* (1979) 395.
[200] R. W. Johnson, *J. Am. Chem. Soc. 99* (1977) 1461.
[201] P. Fürderer, F. Gerson, K. Hafner, *Helv. Chim. Acta 61* (1978) 2974.
[202] M. A. Natiello, H. R. Reale, J. A. Medrano, *J. Comput. Chem. 6* (1985) 108.
[203] R. W. Alder, P. S. Bowman, W. R. S. Steele, D. R. Winterman, *Chem. Commun. 1968,* 723.
[204] F. Hibbert, *J. Chem. Soc. Chem. Commun. 1973,* 463.
[205] H.-J. Gais, K. Hafner, *Tetrahedron Lett. 1974,* 771.
[206] K. Hafner, H.-G. Kläs, M. C. Böhm, *Tetrahedron Lett. 21* (1980) 41.
[207] F. Closs, R. Gompper, U. Nagel, H.-U. Wagner, *Angew. Chem. 99* (1987) 1068; *Angew. Chem. Int. Ed. Engl. 26* (1987) 1037.
[208] a) C. Glidewell, D. Lloyd, *Tetrahedron 40* (1984) 4455; b) E. LeGoff, R. B. LaCount, *Tetrahedron Lett. 1964,* 1161.
[209] C. T. Blood, R. P. Linstead, *J. Chem. Soc. 1952,* 2263.
[210] K. Brand, F. Schlager, *Ber. Dtsch. Chem. Ges. 56* (1923) 2541.
[211] K. Brand, W. Gabel, H. Ott, *Ber. Dtsch. Chem. Ges. 69* (1936) 2504.
[212] M. Rabinovitz, I. Willner, A. Minsky, *Acc. Chem. Res. 16* (1983) 298.
[213] W. Frank, R. Gompper, *Tetrahedron Lett. 28* (1987) 3083.
[214] E. LeGoff, R. B. LaCount, *J. Org. Chem. 23* (1968) 2529.
[215] L. Chardonnens, L. Salamin, *Helv. Chim. Acta 51* (1968) 1095.
[216] W. Deuschel, *Helv. Chim. Acta 34* (1951) 2403.
[217] F. Ebel, W. Deuschel, *Chem. Ber. 89* (1956) 2794.
[218] W. Frank, R. Gompper, unveröffentlichte Ergebnisse.
[219] B. A. Hess, Jr., L. J. Schaad, *Pure Appl. Chem. 52* (1980) 1471.
[220] W. D. Hobey, *J. Org. Chem. 37* (1972) 1137.
[221] J.-i. Aihara, *Bull. Chem. Soc. Jpn. 49* (1976) 1427.
[222] J. R. Appling, G. W. Burdick, M. J. Hayward, L. E. Abbey, T. F. Moran, *J. Phys. Chem. 89* (1985) 13.
[223] N. L. Weinberg, H. R. Weinberg, *Chem. Rev. 68* (1968) 449.
[224] R. Breslow, P. Maslak, J. S. Thomaides, *J. Am. Chem. Soc. 106* (1984) 6453.
[225] E. Wasserman, R. S. Hutton, V. J. Kuck, E. A. Chandross, *J. Am. Chem. Soc. 96* (1974) 1965.
[226] H. Hogeveen, P. W. Kwant, *Tetrahedron Lett. 1973,* 1665, 3747; *J. Am. Chem. Soc. 96* (1974) 2208.
[227] M. J. S. Dewar, M. K. Holloway, *J. Am. Chem. Soc. 106* (1984) 6619.
[228] R. Breslow, *Pure Appl. Chem. 54* (1982) 927.
[229] T. J. LePage, R. Breslow, *J. Am. Chem. Soc. 109* (1987) 6412.

[230] E. Dormann, M. J. Nowak, K. A. Williams, R. O. Angus, Jr., F. Wudl, *J. Am. Chem. Soc. 109* (1987) 2594.
[231] J. S. Miller, A. J. Epstein, *J. Am. Chem. Soc. 109* (1987) 3850.
[232] S. Hünig, W. Daum, *Chem. Ber. 88* (1955) 1238; S. Hünig, P. Richters, *ibid. 91* (1958) 442.
[233] R. Breslow, B. Jaun, R. Klutz, C.-Z. Xia, *Tetrahedron 38* (1982) 863.
[234] R. Breslow, *Mol. Cryst. Liq. Cryst. 125* (1985) 261.
[235] R. Gompper, R. Binder, H.-U. Wagner, *Tetrahedron Lett. 27* (1986) 691.
[236] R. Binder, *Dissertation*, Universität München 1986.
[237] H. Bock, P. Hänel, W. Kaim, U. Lechner-Knoblauch, *Tetrahedron Lett. 26* (1985) 5115.
[238] J. Harley-Mason, A. H. Laird, *Tetrahedron 7* (1959) 70.
[239] O. Fischer, E. Hepp, *Ber. Dtsch. Chem. Ges. 28* (1895) 293.
[240] K. Koga, K. Abe, Jpn. Kokai Tokkyo Koho 7513413 (February 12, 1975), Sumitomo Chemical Co.; *Chem. Abstr. 89* (1978) 26020u.
[241] H. Wahl, M.-T. Le Bries, D. Berkovitch, *Bull. Soc. Chim. Fr. 1973*, 1289.
[242] K. Elbl, C. Krieger, H. A. Staab, *Angew. Chem. 98* (1986) 1024; *Angew. Chem. Int. Ed. Engl. 25* (1986) 1023.
[243] E. Kottmair, *Dissertation*, Universität München 1982.
[244] W. Broser, H. Kurreck, P. Siegle, *Chem. Ber. 100* (1967) 788.
[245] H. Kuhn, *Angew. Chem. 71* (1959) 93.
[246] S. Hünig, H. Quast in W. Foerst (Hrsg.): *Optische Anregung organischer Systeme*, Verlag Chemie, Weinheim 1966, S. 184.
[247] J. Fabian, H. Hartmann: *Light Absorption of Organic Colorants*, Springer, Berlin 1980.
[248] P. H. Daniels, J. L. Wong, J. L. Atwood, L. G. Canada, R. D. Rogers, *J. Org. Chem. 45* (1980) 435.
[249] Br. Pat. 704595 (1954), Bayer AG; *Chem. Abstr. 49* (1955) 7001d; H. Vollmann, F. Baumann, B. Bienert, US Pat. 2701252 (1955), Bayer AG; *Chem. Abstr. 49* (1955) 10374b.
[250] K. H. Büchel, H. Erdmann, *Chem. Ber. 109* (1976) 1625.
[251] R. Gompper, M. Junius, *Tetrahedron Lett. 21* (1980) 2883.
[252] R. Gompper, K. Bichlmayer, *Angew. Chem. 91* (1979) 170; *Angew. Chem. Int. Ed. Engl. 18* (1979) 156.
[253] F. Straus, L. Kollek, W. Heyn, *Ber. Dtsch. Chem. Ges. 63* (1930) 1868.
[254] M. Junius, *Dissertation*, Universität München 1981.
[255] P. F. Clark, J. A. Elvidge, R. P. Linstead, *J. Chem. Soc. 1953*, 3593.
[256] W. Wislicenius, H. Pfannenstiel, *Ber. Dtsch. Chem. Ges. 50* (1917) 185.
[257] J. Freimanis, G. Vanags, *Latv. PSR Zinat. Akad. Vestis Kim. Ser. 31* (1961) 1945; *Chem. Abstr. 55* (1961) 27229c.
[258] K. Bodendorf, R. Mayer, *Chem. Ber. 98* (1965) 3565.
[259] J. Freimanis, V. Nakele, G. Vanags, *Izv. Akad. Nauk Latv. SSR Ser. Khim. 1965*, 561; *Chem. Abstr. 64* (1966) 15807d.
[260] V. Usov, V. Nakele, J. Freimanis, *Zh. Org. Khim. 6* (1970) 384; *Chem. Abstr. 72* (1970) 111132a.
[261] V. M. Karpov, V. E. Platonov, G. G. Yakobson, *Tetrahedron 34* (1978) 3215; *Izv. Akad. Nauk SSSR Ser. Khim. 1978*, 2655; *Chem. Abstr. 90* (1979) 86461u.
[262] E. C. Friedrich, T. M. Tam, *J. Org. Chem. 47* (1982) 315.
[263] E. C. Friedrich, G. De Lucca, *J. Org. Chem. 48* (1983) 4563.
[264] H. Möhrle, H. J. Novak, *Chem.-Ztg. 106* (1982) 19.
[265] J. Freimanis, G. Vanags, *Zh. Obshch. Khim. 34* (1964) 445; *Chem. Abstr. 60* (1964) 13118f.
[266] R. Mertz, *Dissertation*, Universität München 1983.
[267] N. A. Korchevin, V. A. Usov, M. G. Voronkov, N. M. Borodina, *Zh. Org. Khim. 22* (1986) 1276.
[268] K. A. Petriashvili, V. A. Usov, L. E. Protasova, V. A. Shagun, V. F. Sidorkin, M. G. Voronkov, *Zh. Org. Khim. 22* (1986) 575.
[269] H. Baumgärtel, H. Zimmermann, *Chem. Ber. 99* (1966) 843.
[270] R. Gompper, R. Guggenberger, R. Zentgraf, *Angew. Chem. 97* (1985) 998; *Angew. Chem. Int. Ed. Engl. 24* (1985) 984.
[271] D. Pasto, J. P. Freeman, M. K. Fields, *J. Org. Chem. 52* (1987) 4058.
[272] a) R. Gompper, H. Glöckner, *Angew. Chem. 96* (1984) 48; *Angew. Chem. Int. Ed. Engl. 23* (1984) 53; b) H. Glöckner, *Dissertation*, Universität München 1986.
[273] R. Gompper, T. Geßner, *Angew. Chem. 97* (1985) 996; *Angew. Chem. Int. Ed. Engl. 24* (1985) 982.
[274] J. Fabian, A. Mehlhorn, F. Dietz, N. Tyutyulkov, *Monatsh. Chem. 115* (1984) 21.
[275] N. Tyutyulkov, B. Kurtev, Y. Stavanovsky, F. Dietz, J. Fabian, A. Mehlhorn, G. Olbrich, O. E. Polansky, *J. Mol. Struct. 114* (1984) 279.
[276] J. Fabian, *J. Prakt. Chem. 323* (1981) 551.
[277] A. Mehlhorn, J. Fabian, N. Tyutyulkov, G. Olbrich, F. Dietz, *J. Prakt. Chem. 328* (1986) 603.
[278] G. Fraenkel, R. E. Carter, A. McLachlan, J. H. Richards, *J. Am. Chem. Soc. 82* (1960) 5846.
[279] H. Spiesecke, W. G. Schneider, *Tetrahedron Lett. 1961*, 468.
[280] J. I. Musher, *J. Chem. Phys. 37* (1962) 34.
[281] T. Schaefer, W. G. Schneider, *Can. J. Chem. 41* (1963) 966.
[282] D. G. Farnum, *Adv. Phys. Org. Chem. 11* (1975) 123.
[283] H. Vogler, *Z. Naturforsch. B Anorg. Chem. Org. Chem. 40* (1985) 1415.
[284] H. Günther: *NMR-Spektroskopie, 2nd ed.*, Thieme, Stuttgart 1983, p. 70.
[285] S. W. Staley, A. W. Orvedal, *J. Am. Chem. Soc. 95* (1973) 3382, 3384.
[286] S. Masamune, N. Nakamura, M. Suda, H. Ona, *J. Am. Chem. Soc. 95* (1973) 8481.
[287] K. Hafner, H. U. Süss, *Angew. Chem. 85* (1973) 626; *Angew. Chem. Int. Ed. Engl. 12* (1973) 575.
[288] J. A. Pople, K. G. Untch, *J. Am. Chem. Soc. 88* (1966) 4811.
[289] H. Vogler, *J. Chem. Soc. Perkin Trans. 2 1985*, 2033.
[290] R. Radeglia, E. Gey, K.-D. Nolte, S. Dähne, *J. Prakt. Chem. 312* (1970) 877.
[291] R. Weiss, C. Priesner, *Angew. Chem. 90* (1978) 484; *Angew. Chem. Int. Ed. Engl. 17* (1978) 445.
[292] K. Hafner, K. H. Völpel, G. Ploss, C. König, *Liebigs Ann. Chem. 661* (1963) 52.
[293] K. Hafner, persönliche Mitteilung 1986.
[294] M. Colapietro, A. Domenicano, C. Marciante, G. Portalone, *Z. Naturforsch. B Anorg. Chem. Org. Chem. 37* (1982) 1309.
[295] T. C. Mar, J. Trotter, *Acta Crystallogr. 18* (1965) 68.
[296] P. Coppens, G. M. J. Schmidt, *Acta Crystallogr. 18* (1965) 654.
[297] C. W. Bock, M. Trachtman, P. George, *J. Comput. Chem. 6* (1985) 592.
[298] D. O. Cowan, F. M. Wlygul, *Chem. Eng. News 64* (1986) No. 29, p. 28.
[299] J. H. Perlstein, *Angew. Chem. 89* (1977) 534; *Angew. Chem. Int. Ed. Engl. 16* (1977) 519.
[300] F. Wudl, *Pure Appl. Chem. 54* (1982) 1051.
[301] F. Wudl, *Acc. Chem. Res. 17* (1984) 227.
[302] H. Ringsdorf, B. Schlarb, J. Venzmer, *Angew. Chem. 100* (1988) 117; *Angew. Chem. Int. Ed. Engl. 27* (1988) 113.
[303] R. Gompper, H.-U. Wagner, E. Kutter, *Chem. Ber. 101* (1968) 4123.
[304] H.-U. Wagner, R. Gompper, *Angew. Chem. 81* (1969) 1004; *Angew. Chem. Int. Ed. Engl. 8* (1969) 986.
[305] W. Breitschaft, *Dissertation*, Universität München 1984.
[306] J. M. Noonan, Eastman Kodak Co., Rochester, NY, persönliche Mitteilung 1986.
[307] R. Gompper, G. Nilz, unveröffentlichte Ergebnisse.
[308] T. C. Gallagher, R. C. Storr, *Tetrahedron Lett. 22* (1981) 2905.
[309] L. Ghosez, F. Notté, C. Bernard-Henriet, R. Maurin, *Heterocycles 15* (1981) 1179.
[310] P. M. Lahti, A. R. Rossi, J. A. Berson, *J. Am. Chem. Soc. 107* (1985) 2273.
[311] P. Dowd, W. Chang, Y. H. Paik, *J. Am. Chem. Soc. 108* (1986) 7416; *109* (1987) 5284.
[312] P. Du, W. T. Borden, *J. Am. Chem. Soc. 109* (1987) 930.
[313] W. J. Middleton, E. L. Little, D. D. Coffman, V. A. Engelhardt, *J. Am. Chem. Soc. 80* (1958) 2795.
[314] R. Gompper, U. Wolf, *Liebigs Ann. Chem. 1979*, 1388.
[315] R. B. Bates, W. A. Beavers, M. G. Greene, J. H. Klein, *J. Am. Chem. Soc. 96* (1974) 5640.
[316] R. Schwesinger, M. Mißfeldt, K. Peters, H. G. von Schnering, *Angew. Chem. 99* (1987) 1210; *Angew. Chem. Int. Ed. Engl. 26* (1987) 1165.
[317] K. Schötz, T. Clark, H. Schaller, P. von R. Schleyer, *J. Org. Chem. 49* (1984) 733.
[318] C. Jutz, H. Amschler, *Chem. Ber. 97* (1964) 3331.
[319] K. Mizumoto, H. Kawai, K. Okada, M. Oda, *Angew. Chem. 98* (1986) 930; *Angew. Chem. Int. Ed. Engl. 25* (1986) 930.
[320] R. Gompper, A. Hohenester, unveröffentlichte Ergebnisse.
[321] a) T. Fukunaga, *J. Am. Chem. Soc. 98* (1976) 610; b) T. Fukunaga, M. D. Gordon, P. J. Krusic, *ibid. 98* (1976) 611.
[322] R. West: *Oxocarbons*, Academic Press, New York 1980.
[323] F. Serratosa, *Acc. Chem. Res. 16* (1983) 170.
[324] A. H. Schmidt, *Chem. Unserer Zeit 16* (1982) 57.
[325] G. Seitz, *Nachr. Chem. Tech. Lab. 28* (1980) 804.
[326] G. Baum, F.-J. Kaiser, W. Massa, G. Seitz, *Angew. Chem. 99* (1987) 1199; *Angew. Chem. Int. Ed. Engl. 26* (1987) 1163.
[327] J.-i. Aihara, *J. Am. Chem. Soc. 103* (1981) 1633.
[328] S. C. Abrahams, H. E. Bair, F. J. DiSalvo, P. Marsh, L. A. Deuring, *Phys. Rev. B Condens. Matter 1984*, 1258.
[329] R. West, D. C. Zecher, S. K. Koster, D. Eggerding, *J. Org. Chem. 40* (1975) 2295.
[330] D. E. Wellman, R. West, *J. Am. Chem. Soc. 106* (1984) 355.
[331] G. Calzaferri, R. Gleiter, *J. Chem. Soc. Perkin Trans. 2 1975*, 559.
[332] N. Lozac'h, *Adv. Heterocycl. Chem. 13* (1971) 161.
[333] J. P. Brown, T. B. Gay, *J. Chem. Soc. Perkin Trans. 1 1974*, 866.
[334] L. K. Hansen, A. Hordvik, *J. Chem. Soc. Chem. Commun. 1974*, 800.
[335] W. Breimaier, R. Gompper, unveröffentlichte Versuche.
[336] F. Wudl, G. Srdanov, B. Rosenau, D. Wellman, K. Williams, S. D. Cox, *J. Am. Chem. Soc. 110* (1988) 1316.
[337] H. Butenschön, A. de Meijere, *Helv. Chim. Acta 68* (1985) 1658; *Chem. Ber. 118* (1985) 2557.
[338] L. A. Paquette, J. D. Kramer, *J. Org. Chem. 49* (1984) 1445.

Ketenimine Complexes from Carbene Complexes and Isocyanides: Versatile Building Blocks for Carbocycles and N-Heterocycles

New Synthetic Methods (74)

By Rudolf Aumann*

Dedicated to Professor Ernst Otto Fischer on the occasion of his 70th birthday

Ketenimine complexes are readily available in great variety by reaction of isocyanides with carbene complexes. They have proven to be useful building blocks in new synthetic approaches to carbocyclic and *N*-heterocyclic four-, five-, and six-membered rings. The reactions involve new metal-induced bond formation patterns of the ketenimine ligands, which can be influenced across a wide range by varying the following five parameters: the metal, the ligands, and the three substituents on the N=C=C unit.

1. Introduction

The potential of classical synthetic methods involving typically "organic" reactivity patterns and selectivities can be considerably extended by including metal complexes as "non-classical" building blocks. Almost any functional group can be bonded to metal residues, thereby changing its reactivity completely. In this article this will be exemplified by the ketenimines:[**] we shall see how the reactivity[1] of these compounds is altered on complexation and how

Table 1. Coordination of N=C=C units to one-, two-, and four-electron acceptors in mono- and binuclear complexes.

Coordination type		L_nM	R^1	R, R	Ref.
Mononuclear complexes					
type A $\eta^2(C=N)$	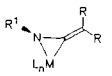	$[V(C_5H_5)_2]$	Ph	Me Me	[4]
		$[Fe(CO)_2\{P(OMe)_3\}_2]$	*p*-tolyl	Ph Ph	[5]
		$[Ni(CN\,tBu)_2]$	*t*Bu	CN CN	[6]
		$[U(C_5H_5)_3]$	*cyclo*-C_6H_{11}	$=CH-PPh_2Me$	[7]
type B $\eta^2(C=C)$	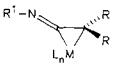	$[Fe(CO)_3]$	*cyclo*-C_6H_{11}	$C(CO_2Me)=CH_2$ OMe	[8]
		$[Fe(CO)_2(C_5H_5)]^{\oplus}$	H	H H	[9]
		$[OsCl(PPh_3)_2NO]$	*p*-tolyl	H H	[10]
type C $\eta^1(N)$	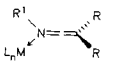	$[Cr(CO)_5]$	*cyclo*-C_6H_{11}	Me	[11]
type D $\sigma(N)$ (1-aza-allenyl)	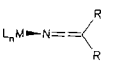	$[SnEt_3]$		Et CN	[12]
		$[Fe(CO)_2(C_5H_5)]$		$C(CN)_2CH_2Ph$ CN	[13]
		$[Ir(tcne)CO(PPh_3)_2]$ [a]		$CH(CN)_2$ CN	[14]
type E $\sigma(C)$ (3-aza-allenyl)	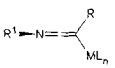	$[Mn(CO)_2(C_5H_5)]^{\oplus}$	*t*Bu	Ph	[15]
		$[Re(CO)_2(C_5H_5)]^{\oplus}$	*t*Bu	Me	[16]
type F $\sigma(O)$	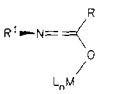	$[Th(C_5Me_5)_2Cl]$	*p*-tolyl	CH_2tBu	[17]
Binuclear complexes					
type G $\mu,\eta^3(C=C=N)$ (1-azaallyl)	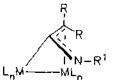	$[Fe(CO)_3]$	Ph	Ph Ph	[18]
type H $\mu,\eta^2(C=C=N)$	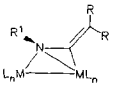	$[Mo(CO)_2(C_5H_5)]$	*p*-tolyl	Ph Ph	[5]

[a] tcne = tetracyanoethylene.

[*] Prof. Dr. R. Aumann
Organisch-chemisches Institut der Universität
Orléansring 23, D-4400 Münster (FRG)

[**] According to IUPAC rules ketenimines should be called 1-alkenylideneamines; however, the term "ketenimines" continues to be used in Chemical Abstracts.

ketenimine complexes can be used as versatile synthetic building blocks.

The preparative usefulness of new reagents highly depends on their ready availability. In the present case carbene complexes[2] and isocyanides[3] form a broad base of starting materials for the generation of ketenimine complexes. We shall commence by discussing different bonding modes in these compounds.

2. Classification of Ketenimine Complexes

At least eight types of complex can be derived from ketenimines: their characteristic features are collected in Table 1. The complexation with *two-electron* acceptors L_nM can occur laterally (side-on) via the C=N or C=C π bonds or terminally (end-on) via the nitrogen lone pair (types A–C). Electron-rich metal residues and electron-withdrawing substituents on the ketenimine appear to favor the coordination via π bonds (types A and B); in such cases the ligand is considerably bent. The CN bond in complexes of type A has the length of a single bond, and the ν(N=C=C) band in the IR spectrum undergoes a bathochromic shift (Table 2). Electron-poor metal residues can be coordinated via the nitrogen lone pair (type C): in such cases the N=C=C skeleton remains almost linear, and the interatomic distances are scarcely changed from those in the free ketenimine. However, there is a great change in reactivity on complexation of the ketenimine to give complexes of type C (see Sections 4–7). Bonding between the N=C=C unit and *one-electron* acceptors L_nM (types D–F) can occur via nitrogen, via the terminal carbon, or via a side chain, and the properties of these σ complexes differ considerably from those of the π complexes. The π,σ complexes of type G are of particular interest: in these the originally orthogonal π system of the ligand is "decoupled", so that one π-allyl bond and one σ bond to a *four-electron* acceptor can be formed. In complexes of type H, also π,σ complexes, the C=C bond remains free.

Table 2. Some structural and IR-spectroscopic parameters for ketenimine complexes of type A (see Table 1; the complexes listed therein are denoted here only by giving the metal).

M	∢ N–C–C [°]	d(C–N) [pm]	d(C–C) [pm]	$\tilde{\nu}$(NCC) [cm^{-1}] [a]
V [4]	140.5(8)	137.1(9)	132.0(9)	1670
Fe [5]	137.6(15)	134.4(21)	138.3(23)	
Ni [6]	144.2(4)	124.5(4)	138.6(5)	1710
U [7]	122.(2)	139.(4)	133.(3)	

[a] In free ketenimines at ca. 2050–2000 cm^{-1}.

It may be dangerous to draw conclusions as to the reactivity of complexes merely on the basis of their structures, since this would completely disregard the transition states of the reactions. Nevertheless, one can predict to a first approximation that all the various types of complexes (A–H) will react differently from each other. The reactivity of a given substrate can be modified gradually and over a wide range by complexing it in different ways. The reactions of ketenimine complexes show no similarity with those of free ketenimines; the complexation causes complete "umpolung".

3. Preparation of Ketenimine Complexes

Ketenimine complexes with different substitution patterns and their *N*- or *C*-metalated or *N*-alkylated derivatives can be most efficiently prepared by C=C coupling reactions within the ligand sphere of transition metals: e.g., by reacting carbene[11,19] or carbyne[15,16] complexes with isocyanides or by treating isocyanide complexes with carbene sources (e.g., diazoalkanes).[6] Other methods of preparation include electrophilically induced σ/π rearrangements of α-cyanoalkyl ligands,[9] insertions of cyanoolefins into M–H or M–C bonds,[12–14] oxidative addition of α-chloroenamines (or suitable precursors thereof)[20] to carbonyl metalates, and the introduction of tricyanomethanide ligands.[21] In only a few cases have ketenimine complexes been prepared directly by complexation of free ketenimines.[5,18]

3.1. Addition of Isocyanides to Carbene Complexes

Carbene complexes **1** add one equivalent of an isocyanide **2** to give ketenimine complexes **3** via a 1,2-insertion of the N≡C bond into the M=C bond[11,19] [Eq. (1)].

$$[L_nM{=}CXR] + R^1{-}\overset{\oplus}{N}{\equiv}\overset{\ominus}{C}: \rightarrow [L_nM(R^1N{=}C{=}CXR)] \qquad (1)$$

1 **2** **3**

X = O-alkyl,[11,19] S-alkyl,[26] $N{=}CR_2$,[27] PR_3[7]

R, R^1 = alkyl, aryl, alkenyl, akynyl

M = Cr,[11] Mo,[22] W,[23] Mn,[24] Fe,[25] Os,[10] Th,[17] U[7]

L = CO, PR_3, η^5-$CH_3C_5H_4$, η^5-C_5H_5

Of particular interest for synthetic applications are functionalized ketenimine complexes **3**: these are obtainable in great variety from heterocarbene complexes **1**[7,11,19,26,27] and are generally reacted further in situ.

The insertion of isocyanides into M=C bonds is not metal-specific: complexes **3** with M = V,[4] Cr,[11c] Fe,[5,8] Ni,[6] Os,[10] Th,[17] and U[7] have been characterized crystallographically.

The coupling of isocyanides with carbene ligands probably occurs in several steps via ylide complexes **4**[28] and/or (with charge neutralization) via metallacyclopropanes **5** [Eq. (2)].[29]

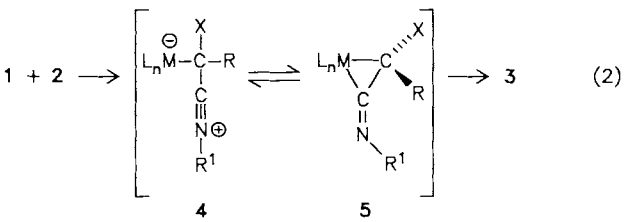

(2)

The isocyanide undergoes addition to the carbene carbon directly, instead of first coordinating to the metal atom. This is suggested by the observation that chromium complexes **7**, with carbene and isocyanide ligands in a *cis* arrangement, are stable under the reaction conditions.[27,30] Complexes **7** can be prepared[27] from **6** via the standard procedure[11a] [Eq. (3)] and, when heated under CO, give

neither ketenimine complexes nor products derived therefrom.[31]

$$[(R^1\text{–NC})Cr(CO)_5] \xrightarrow[2.\ [Et_3O]BF_4]{1.\ C_6H_5Li} [cis\text{-}(CO)_4Cr(R^1\text{–NC})\{C(OEt)C_6H_5\}] \quad (3)$$

(6) (7)

$R^1 = CH_3$, *cyclo*-C_6H_{11}

The reaction sequence shown in Equation (2) for *chromium* is not general: thus, in the case of *nickel* [Eq. (4)], the coupling of carbene and isocyanide ligands to give ketenimine ligands occurs readily[6] when the external carbene source diazomalodinitrile **10** is allowed to react with the isocyanide complex **9**. Complex **11** was detected as an intermediate in this reaction.[32]

$$[(R^1\text{–NC})_4Ni] + N_2C(CN)_2 \rightarrow [(R^1\text{–NC})_3Ni\{N_2C(CN)_2\}] \rightarrow [(R^1\text{–NC})_2Ni\{R^1\text{–N=C=C(CN)}_2\}] \quad (4)$$

9 **10** **11** **12**

$R^1 = t\text{-}C_4H_9$

On the other hand, it is possible to construct *palladium* ketenimine complexes catalytically from isocyanides **2**, allyl bromides **13**, and triethylamine [Eq. (5)].[33] The catalysis involves the *N*-substituted alkenimidoyl complexes **15** as intermediates (**15**, $R = CH_3$, H, has been isolated[33,34]), probably formed by insertion of R^1–NC into a Pd-C σ bond; however, coupling via Pd=C bonds cannot be excluded.

$$R^1\text{–NC} + BrCH_2\text{–CH=CHR} + Et_3N \xrightarrow{[PdCl_4]^{2\ominus}} R^1\text{–N=C=CH–CH=CHR} + [Et_3NH]Br \quad (5)$$

2 **13** **14**

$R^1 = cyclo\text{-}C_6H_{11}$, C_6H_5, $p\text{-}NO_2\text{–}C_6H_4$

$[(R^1\text{–NC})ClM\text{–}C(=NR)CH_2\text{–CH=CHR}]$ **15**, M = Pd

Coupling reactions of (metal-free) carbenes (dichloro-, diphenyl-, dimethoxycarbonylcarbene) with isocyanides to give ketenimines are also known.[35]

3.2. Addition of Isocyanides to Metal Carbyne Complexes

Isocyanides undergo insertion not only into M–C[3b] and M=C bonds (see Section 3.1) but also into M≡C bonds: for example, the carbyne complex **16** adds R^1–NC to give the keteniminyl complex **17**[15,16] [Eq. (6)].

$$[L_nM{\equiv}C(C_6H_5)]X + R^1\text{–NC} \longrightarrow \left[\begin{array}{l} H_5C_6 \\ L_nM \end{array}\!\!>\!\!=\!\!=\!\!N\text{–}R^1\right]^{\oplus} X^{\ominus} \quad (6)$$

16 **2** **17**

$L_nM = [Mn(CO)_2(C_5H_5)]$, $X = BCl_4^{\ominus}$, $R^1 = t\text{-}C_4H_9$

Complexes of type **17** generally undergo further isocyanide insertions into the (M–C) σ bond: thus, **18** adds a total of four molecules of **2** to give the η^3-1,5-diazapentatrienyl complex **19**[36] [Eq. (7)], two molecules being inserted into the M≡C bond.

$$[\,|P(OMe)_3|_2L_nM{\equiv}CCH_2t\text{Bu}] + 4\ R^1\text{–NC} \longrightarrow \longrightarrow$$

18 **2**

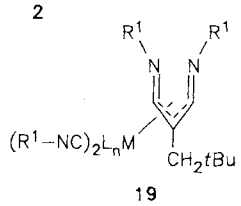

(7)

19

L_nM = $[Mo(C_5H_5)]$, $[W(C_5H_5)]$; R^1 = 2,6-xylyl

3.3. Electrophilically Induced σ,π Rearrangements

Protonation of the cyanomethyl complex **20** leads, via σ,π rearrangement, to a cationic complex **21**[9] of the simplest ketenimine [Eq. (8)]; while the free ketenimine is not stable,[37] the π complex **21** bearing the electron-rich $[Fe(CO)_2(C_5H_5)]$ residue is stable.[38a,b]

$$[L_nM\text{–}CH_2\text{–}C{\equiv}N] + H^{\oplus} \rightarrow [L_nM(H_2C{=}C{=}NH)]^{\oplus} \quad (8)$$

20 **21**

$L_nM = [Fe(CO)_2(C_5H_5)]$

3.4. Complexation of Ketenimines

The formation of ketenimine complexes by direct complexation of ketenimines is problematic, since both ketenimines and ketenimine complexes are very prone to undergo condensation reactions, so that unwanted secondary reactions often occur. The few exceptions known include the complexation of **23a,b** with vanadocene **22** to give mononuclear **24** [Eq. (9)][4] and of **23c** with (photochemically generated) coordinatively unsaturated **25** to give binuclear **26** [Eq. (10)].[4]

$$L_nM + R^1N{=}C{=}CR_2 \rightarrow [L_nM(R^1N{=}C{=}CR_2)] \quad (9)$$

22 **23a,b** **24a**, 91%; **b**, 87%

$L_nM = [V(C_5H_5)_2]$; $R^1 = C_6H_5$

$$(L_nM)_2 + \textbf{23c} \rightarrow [(L_nM)_2(R^1N{=}C{=}CR_2)] \quad (10)$$

25 **26**

$L_nM = [Mo(CO)_2(C_5H_5)]$

a, $R = C_6H_5$; **b**, $R = CH_3$; **c**, $R = p\text{-}CH_3\text{–}C_6H_4$

In contrast to neutral metal residues, metal carbonylates cleanly form adducts **28**, which subsequently isomerize to stable metallaazetidinones **29**[39] [Eq. (11)].

Metal carbonyls react much less cleanly with **23** than do the carbonylates: thus, $[Fe_2(CO)_9]$ gives binuclear azaallyl complexes **30**[18] as well as imidazolidinones **31**[18b] formed by coupling of two ketenimine units with cyclocar-

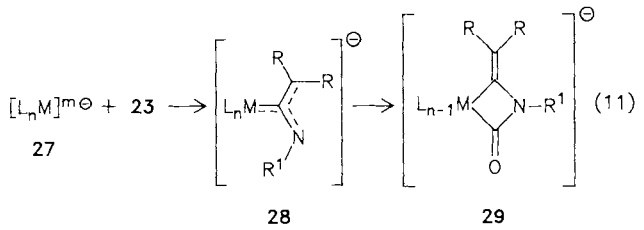

$[L_nM]^{m\ominus}$ = $[Cr(CO)_5]^{2\ominus}$, $[Re(CO)_5]^{\ominus}$

bonylation [Eq. (12)]. Compound **23a** also gave a ferraindene **32**, while **23b** yielded the azaferrole **33**, which is structurally related to **31**.

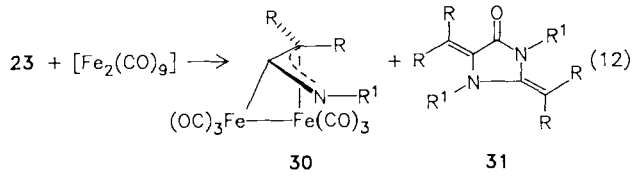

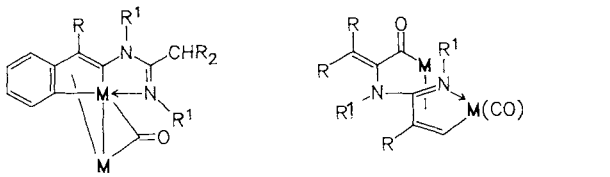

32, M = $[Fe(CO)_2]$
R = R^1 = C_6H_5

33, M = $[Fe(CO)_2]$
R = CH_3; R^1 = C_6H_5

Complexes **32** and **33** are apparently formed by intra- or intermolecular transfer of hydrogen atoms with the participation of M–H bonds. In this connection, 1,4-additions of metal hydrides **34** to cyanoethylene are of interest; these lead to 1-azaallenyl complexes **35** [Eq. (13)].

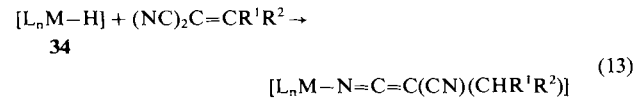

L_nM	R^1	R^2	Ref.
$[Ir(CO)_2(PPh_3)_2]$	CN	CN	[14]
$[Fe(CO)_2(C_5H_5)]$	CN	CN	[13]
$[Sn(n\text{-}C_4H_9)_3]$	H	CH_3	[12]

The ketenimine **23b** undergoes a novel type of addition to the M=C bond of **36** (Table 3) to give the π, σ complex

Table 3. L_nM groups in **36a–e** and the compounds obtained therefrom.

a	b	c	d	e
$[Fe(CO)_4]$	$[W(CO)_5]$	$[Mo(CO)_5]$	$[Cr(CO)_5]$	$[Mn(CO)_2(CH_3C_5H_4)]$

37[40] [Eq. (14)]. This reaction has a parallel in the addition of allenes to carbene complexes to give trimethylenemethane complexes.[41]

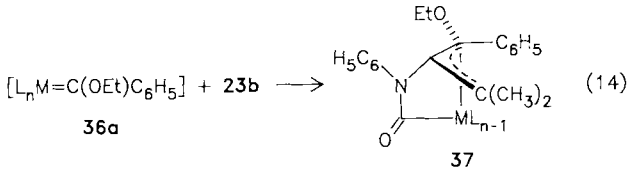

4. Simple Addition and Isomerization Reactions of Ketenimines

The typical reactivity patterns[1] of metal-free ketenimines are completely changed on complexation. The reactivities of ketenimine complexes can be varied across a wide range by means of five parameters (R, R^1, X, M, L). We shall first discuss some typical transformations at the N=C=C skeleton of chromium, molybdenum, tungsten, manganese, and iron complexes and shall then proceed to reactions also involving substituents R, R^1, and X. These "basic reactions", **A** and **B**, are listed in Scheme 1. Either the metal residue L_nM undergoes a shift to the central carbon atom (formation of an aminocarbene unit, Sections 4.1.1–4.1.3 and 4.2.1) or the coordination at nitrogen is preserved (Sections 4.2.2, 4.3, and 4.4).

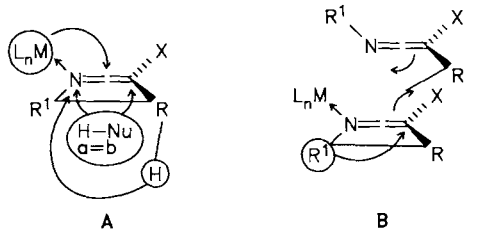

Scheme 1. Principal conversions of ketenimine complexes involving either 1,2-shift of the metal residue (**A**) or retention of coordination via nitrogen (**B**).

4.1. 1,3-Additions to the N=C=C Skeleton

4.1.1. Additions of Protic Nucleophiles

In contrast to metal-free ketenimines, ketenimine complexes **3** react like 1,3-dipoles, the metal undergoing a shift to the central carbon of the N=C=C unit: the products are aminocarbene complexes **38**. The "reactivity umpolung" of ketenimine ligands by the metal residue permits addition of protic nucleophiles to the terminal carbon atom [Eq. (15)][25,26,31] of the ketenimine ligand. In contrast, me-

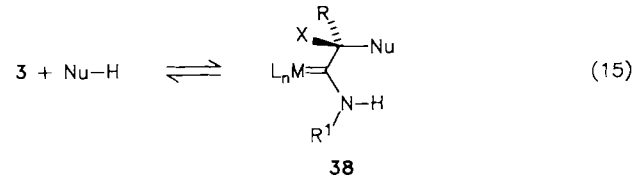

Nu–H = R'O–H, R'S–H, R'_2N–H
L_nM = $[Cr(CO)_5]$, $[Mo(CO)_5]$, $[W(CO)_5]$, $[Mn(CO)_2(CH_3C_5H_4)]$, $[Fe(CO)_4]$

tal-free ketenimines add protic nucleophiles to the central carbon atom; for example, **39** gives amides **40** on treatment with water [Eq. (16)]. Ketenimine complexes **3**, on

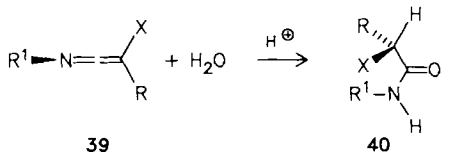

(16)

39 40

$R = C_6H_5$, CH_3, $CH{=}CH{-}C_6H_5$; $R^1 = cyclo\text{-}C_6H_{11}$; X = OEt

the other hand, give aminocarbene or acylaminocarbene complexes **41** or **42** [Eq. (17)].

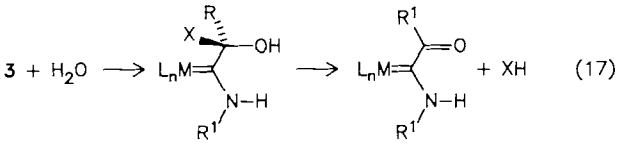

(17)

41 42

$L_nM = [Cr(CO)_5]$, $[Mo(CO)_5]$, $[W(CO)_5]$, $[Mn(CO)_2(CH_3C_5H_4)]$, $[Fe(CO)_4]$

The addition of nucleophiles Nu-H to **3** is reversible: thus, in the case of bulky substrates (e.g., $t\text{-}C_4H_9SH$) the ketenimine complexes are re-formed when the aminocarbene complexes are heated.[42] The isomerization reaction of aminocarbene complexes via a 1,2-N/C hydrogen shift to give aldimine complexes competes with this reverse reaction;[42] for example, the condensation product **43** from **3** and aniline undergoes thermal rearrangement to **44** [Eq. (18)], the rearrangement being catalyzed by bases such as $t\text{-}C_4H_9OK$ in THF. The net reaction **3**→→→**44** corresponds to a metal-induced 1,2-addition of Nu-H to the C=C bond of the ketenimine ligand (followed by loss of XH) and thus exhibits the reverse regiochemistry to that observed in corresponding additions to metal-free **39** [Eq. (16)].

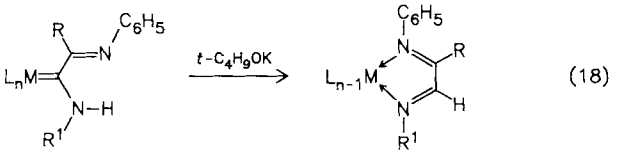

(18)

43 44

$L_nM = [W(CO)_5]$, $R = C_6H_5$, $R^1 = cyclo\text{-}C_6H_{11}$

Since ketenimine complexes can be formed by addition of isocyanides to carbene complexes on the one hand and undergo conversion to (amino)carbene complexes via addition of Nu-H on the other, it should be possible to build up carbon chains in a stepwise manner by applying this principle.

4.1.2. [3+2] Cycloadditions

The 1,3-dipolar properties of **3** make possible [3+2] cycloadditions of polarized double bonds, e.g., of aldehydes or isocyanates, to give oxazolidine or imidazolidine complexes **45a** or **45b**, respectively [Eq. (19)]. These conversions can be readily carried out under mild conditions as three-component reactions without isolation of the intermediate ketenimine complexes;[23,31,43] however, the addition is greatly slowed by the presence of bulky substituents. Oxidative decomposition of **45b** ($R' = cyclo\text{-}C_6H_{11}$) with $KMnO_4/Fe(NO_3)_3$ yielded the previously inaccessible 5-ethoxyhydantoins **46b**.

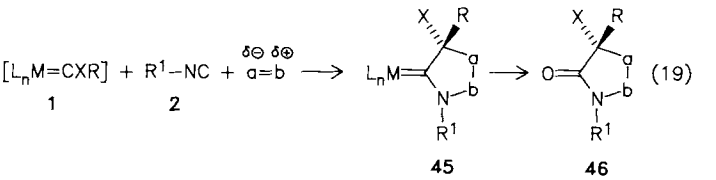

(19)

1 2 45 46

$L_nM = [W(CO)_5]$[23, 43], $[Mn(CO)_2(CH_3C_5H_4)]$[31]

$R = CH_3$, C_6H_5; X = OEt

$R^1 =$ $cyclo\text{-}C_6H_{11}$, CH_3, $CH_2C_6H_5$

a=b: **a**, O=CHR';[31, 43] **b**, R'N=CO;[23] **c**, R'N=CNR';[31, 42] **d**, S=CS;[31] **e**, S=CNR'[31]

4.1.3. [3+1] Cycloadditions

The tendency of ketenimine complexes to form aminocarbene complexes permits [3+1] cycloadditions of **3** with isocyanides (see Sections 5.2 and 5.3) or vinylidene ligands (see Section 6.1) to give four-membered heterocyclic rings.

4.2. Isomerizations

Ketenimine complexes are thermally labile and may isomerize under certain conditions to aminocarbene or nitrile complexes.

4.2.1. Ketenimine/Aminocarbene Rearrangements

C-Alkylketenimine complexes **47** rearrange readily via 1,4-C/N hydrogen shifts to give the alkenylaminocarbene complexes **48**[11a] [Eq. (20)]. The reaction can be induced

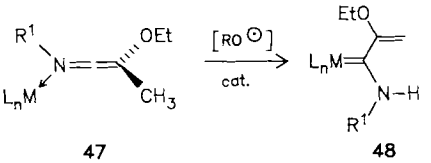

(20)

47 48

$L_nM = [Cr(CO)_5]$, $[W(CO)_5]$

by air or traces of peroxide and is weakly exothermic. The 1,4-C/N shift of the allylic hydrogen probably occurs via a chain mechanism (e.g., via a radical cation).

4.2.2. Ketenimine/Nitrile Rearrangements

The isomerization of ketenimines to nitriles via a 1,3-N/C shift of R^1 from nitrogen to the terminal carbon of the N=C=C unit can be favored or hindered by complexation, depending on L_nM. Thus NH ketenimines ($R^1 = H$) are unstable in the free form, but can be stabilized in the iron complex **21** (Section 3.3).[9] However, *N*-allyl, **49**,[44] and *N*-benzylketenimine complexes, **53**,[31] of Cr, Mo, and W isomerize even at 0 °C to nitrile complexes **51** and **55**,

respectively [Eqs. (21) and (22)]. The rearrangement takes place within the ligand sphere and is probably favored by a metal-induced bending of the N=C=C unit. Complex **53e** (M = Mn; see also Table 3) is stable for several hours at 80 °C and isomerizes at a measurable rate only above 100 °C,[31] while **53c** (M = Mo) isomerizes rapidly even at 0 °C. The N/C shift of the allyl group exhibits the regiochemistry of a [3,3] shift (as shown by deuterium labeling). Since the nitrile ligands of **51** (and **55**) can be readily substituted by pyridine, thermolabile chiral olefins **52** can be obtained in this sequence [Eq. (21)].

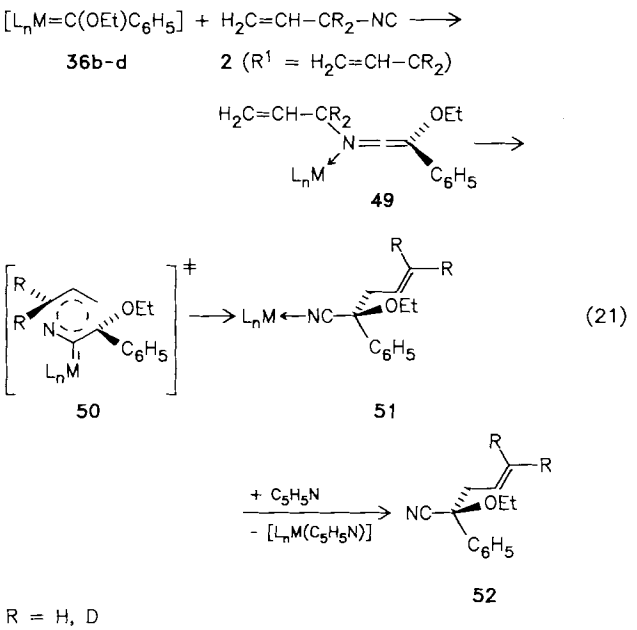

(21)

If **36** (Table 3) is allowed to react with benzyl isocyanide **2**, $R^1 = CH_2C_6H_5$, at 20 °C in the presence of methanol, a mixture of the isomerization and addition products **55** and **54** is obtained [Eq. (22)]. Isomerization dominates in the case of the molybdenum complex **53c**, while for the tungsten (**53b**), manganese (**53e**), and iron (**53a**) complexes

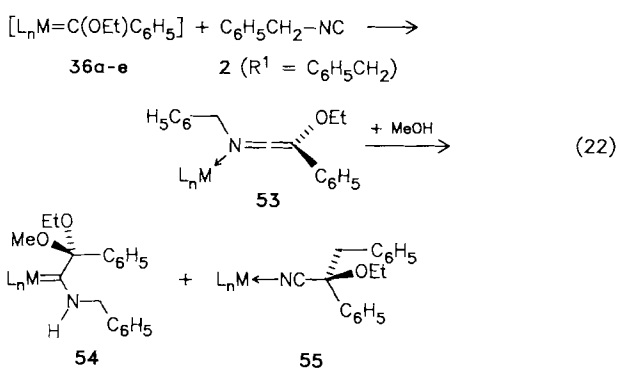

(22)

a	> 95	:	1
b	> 95	:	1
c	1	:	10
d	1	:	3
e	> 95	:	3

practically only addition to **54** is observed. This change in reactivity has a parallel in a change of the coordination mode of the ketenimine ligands in **53**. The chromium complex **53d** is coordinated via the lone pair on nitrogen. The manganese complexes **53e** exist in solution[24] as η^2(C=C) complexes of type B (Table 1)].[31]

4.3. [2+2] Dimerization of Ketenimine Ligands

Ketenimine complexes **3** (M = Cr, Mo, W) dimerize on warming, possibly via an intermediate **56**, to give $[M(CO)_6]$ and 1,2-bis(imino)cyclobutane complexes **57** [Eq. (23)].

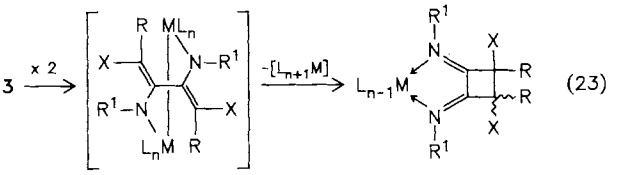

(23)

L_nM = $[Cr(CO)_5]$, $[Mo(CO)_5]$, $[W(CO)_5]$; X = OCH_3
R: a, CH_3; b, C_6H_5; c, $C_{10}H_7$; d, C_4H_4S
R^1 = CH_3, *cyclo*-C_6H_{11}, t-C_4H_9

The dimerization of the ketenimine ligands leads solely to symmetrical [2+2] adducts.[45] The carbocyclic four-membered ring in **57** is formed from four C_1 units (carbenes, isocyanides) via a template-induced coupling. Treatment of **57** with hydroxylamine leads to bis(hydroximino)cyclobutanes.[45]

4.4. Template-Directed Expansion of Four-Membered to Six-Membered Rings

1,2-Bis(imino)cyclobutane complexes **57** with R = aryl are thermally labile and isomerize on warming to bis(imino)tetrahydronaphthalene complexes **58**;[45b] the four-membered ring undergoes an expansion to a six-membered ring in which the aryl group participates [Eq. (24)]. The

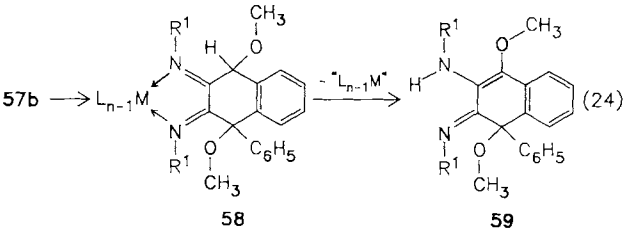

(24)

isomerization occurs within the ligand sphere of the metal complex and is stereoselective, the chirality transfer being ca. 80%.

Complexes **58** decompose above 100 °C to dihydronaphthalenes **59**; the latter are available directly from carbene complexes and isocyanides without isolation of intermediates in a one-pot procedure.[45] Complex **58** adsorbed on silica is rapidly oxidized by air to give the ketone complex **60** and other products [Eq. (25)].[22]

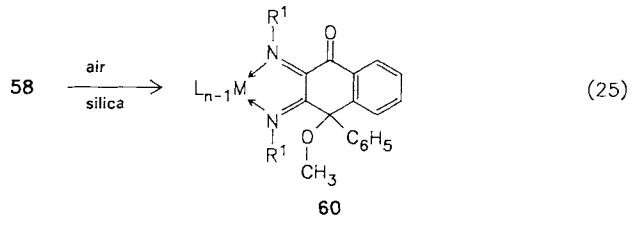

(25)

5. Addition of Isocyanides to Ketenimine Complexes

Both carbene complexes **1** and ketenimine complexes **3** add to isocyanides **2**, and the relative rates of the addition processes determine whether 1:1, 1:2, 1:3, or 1:4 adducts between **1** and **2** are formed. An analysis of the many possibilities leads to the identification of the following six basic reaction patterns (Scheme 2):

① addition of isocyanides to the metal with displacement of ketenimine ligands
② [3+1] cycloaddition of isocyanides to the ketenimine ligand from the side opposite to the metal
③ [2+2] cycloaddition of isocyanides to the C=C bonds of ketenimine ligands from the metal side
④ [2+1+1] cycloaddition of two isocyanide molecules to N=C bonds of ketenimine ligands
⑤ [4+1] cycloaddition of isocyanides to *C*-aryl-substituted ketenimine ligands with *ortho*-substitution at the aryl residue
⑥ [4+1] cycloaddition of isocyanide to *N*-aryl-substituted ketenimine ligands with *ortho*-substitution at the aryl residue

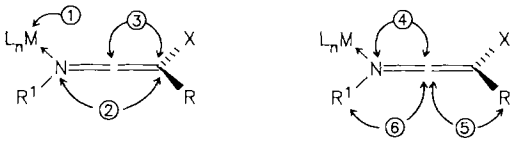

Scheme 2. Addition of isocyanides to ketenimine complexes.

5.1. Addition of Isocyanides to the Metal

Ketenimines **39** can be displaced from **3** by isocyanides: this is true in particular for bulky ketenimines (R^1 = *cyclo*-C_6H_{11}, *t*-C_4H_9), for which reactions involving addition to the ligand (see Sections 5.2–5.5) to give nonlinear C–N–R^1 bonds become difficult for steric reasons.[11b,24,31] Instead of isocyanides, other aprotic nucleophiles (**61**) may be used [Eq. (26)]: for example, ketenimine **39** is obtained simply and readily by treating carbene complex **1** with isocyanide **2** in the aprotic nucleophilic solvent acetonitrile.

$$[L_nM(R^1N{=}C{=}CXR)] + Nu \rightarrow [L_nM(Nu)] + R^1N{=}C{=}CXR \quad (26)$$
3 **61** **39**

R^1 = *cyclo*-C_6H_{11}, *t*-C_4H_9; X = OEt
L_nM = [Cr(CO)$_5$], [Mo(CO)$_5$], [W(CO)$_5$], [Mn($CH_3C_5H_4$)(CO)$_2$]
Nu = $P(C_6H_5)_3$, C_5H_5N, CH_3CN, *cyclo*-$C_6H_{11}NC$, *t*-C_4H_9NC

5.2. [3+1] and [2+2] Cycloadditions

The construction of four-membered *N*-heterocycles from isocyanides[46] and carbene complexes is also of interest for synthetic purposes. This reaction occurs in a particularly uniform manner with carbene complexes of iron:[25] thus, **36a** (Table 3) adds two equivalents of **2** even in the cold to give 4-iminoazetidinylidene complexes **63a** [Eq. (27), Table 4]. Compound **36e** similarly gives the manganese complex **63e**. Since in the case of **36e** the isocyanide reacts more slowly with the intermediate ketenimine complex **62** than in the case of **36a**, **62e** can be isolated. It is thus possible to incorporate two *different* isocyanides into the four-membered ring of **63**. However, this reaction is limited by the fact that bulky isocyanides cause a ligand displacement in the ketenimine complex **62e**; in addition, an unwanted side reaction to give **65** [Eq. (28)] is observed. In the case of the tungsten complex **36b**, four-membered rings (**63b**) are formed only in low yields, with the exception of the addition of alkenyl isocyanides.[47]

$$[L_nM{=}C(OEt)C_6H_5] + R^1{-}NC \rightarrow [L_nM\{R^1N{=}C{=}C(OEt)C_6H_5\}]$$
36a,b,e **2** **62a,b,e**

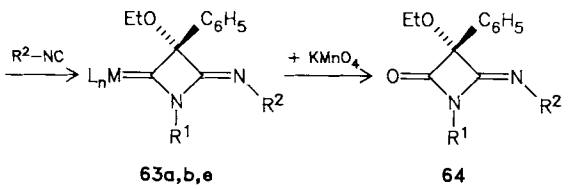

(27)

Table 4. Yields of **63** in reactions (27). See also Table 3.

63	R^1, R^2	Yield [%]	R^1, R^2	Yield [%]
a	*cyclo*-C_6H_{11}	77	CH_3	94
	C_6H_5	76	$CH_2C_6H_5$	80
b	$CH{=}CH_2$	20	$CH{=}CHCH_3$	31
e	CH_3	30	C_6H_5	67

β-Lactams **64** can be obtained by oxidative decomposition of **63** in the two-phase system ether/water: practically no side reactions are observed.[24]

The reaction of **36** with **2** is influenced by the reaction conditions as well as by the nature of the reaction partners: thus, on careful warming of the reaction mixture, the manganese complex **36e** and methyl or phenyl isocyanide preferably form 4-iminoazetidinylidene complexes **63e**, while rapid warming gives the 3-iminoazetidinylidene complex **65** as the main product [Eq. (28)].[24] Thermal isomerization of **63e** to **65** (via metathesis) can be excluded, as shown by control experiments: thus, the two complexes are formed in competition. If **63b** and **65** are

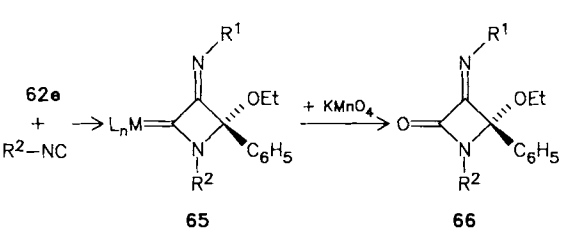

(28)

R^1, R^2 = CH_3, C_6H_5

each constructed from two different isocyanides R^1–NC and R^2–NC, it can be shown that R^2–NC has attacked the ketenimine ligand from the side opposite to the metal in one case and from the metal side in the other.

The processes leading to **63** and **65** can be regarded as [3+1] and [2+2] cycloadditions, respectively (**C** and **B**). We assume that in the formation of **65** the ketenimine ligand is first substituted by isocyanide; this is followed by addition of the electron-rich double bond of the ketenimine to the isocyanide ligand. An alternative possibility would be a [3+2] cycloaddition to give **E**, followed by ring contraction with elimination of L_nM.

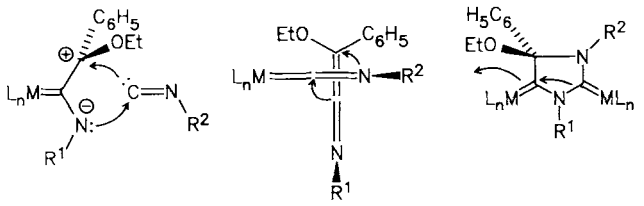

C D E

5.3. [2+1+1] Cycloaddition of Two Isocyanides

A further possibility for the synthesis of azetidines from carbene complexes and isocyanides is shown in Equation (29). The reaction of **36d** with four equivalents of *p*-nitrophenyl isocyanide **2**, R^1=*p*-NO_2–C_6H_4, gives the 2,3-bis(imino)azetidine **67** in metal-free form via [2+1+1] cycloaddition of **2** to an intermediate ketenimine complex. The acid hydrolysis of **67** occurs cleanly to give a 3-butenamide **68**; the C_4 skeleton of this molecule is built up from one carbene and three isoycanide carbons.[48]

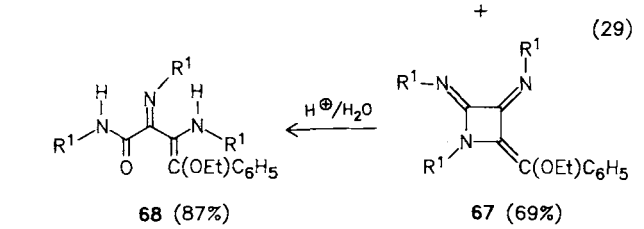

$[L_nM{=}C(OEt)C_6H_5]$ + 4 R^1–NC ⟶ $[L_nM(R^1{-}NC)]$

36d 2 (R^1 = *p*-NO_2–C_6H_4)

+

68 (87%) **67** (69%) (29)

5.4. [4+1] Cycloadditions to Give Indanes

Ketenimine complexes of Cr, Mo, and W react differently with isocyanides than do those of Mn or Fe, substituents on the N=C=C skeleton often being involved in the reactions. Arylcarbene complexes of Cr, Mo, and W add two equivalents of methyl or benzyl isocyanide via a cyclization involving *ortho* attack at the *C*-aryl residue to give deep blue 1,2-bis(imino)indane complexes **69** [Eq. (30)]. The reaction takes place in a stepwise manner via a *C*-arylketenimine complex **62** (from **36** and R^1–NC). This complex adds R^2–NC in the sense of a [4+1] cycloaddition involving the annelation of a carbocyclic five-membered ring to the aryl residue.[22]

The five-membered ring annelation to arenes occurs in a regiospecific manner; 1- and 2-naphthyl- or 1- and 2-thienylcarbene complexes give only the angularly annelated isomers.[22]

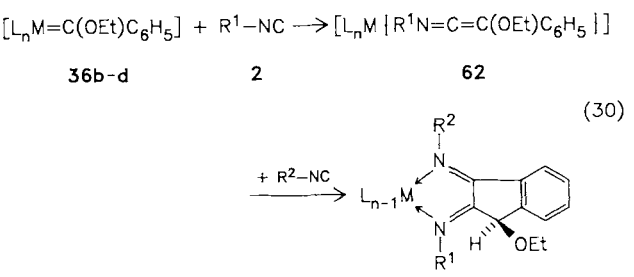

$[L_nM{=}C(OEt)C_6H_5]$ + R^1–NC ⟶ $[L_nM\{R^1N{=}C{=}C(OEt)C_6H_5\}]$

36b-d **2** **62**

+ R^2–NC ⟶ $L_{n-1}M$ **69** (30)

R^1, R^2 = CH_3, $CH_2C_6H_5$

5.5. [4+1] Cycloadditions to Give Indoles

Not only *C*-aryl- but also *N*-arylketenimine complexes of Cr, Mo, and W form [4+1] cycloadducts with further isocyanide. Since *N*-aryl groups are considerably more reactive than *C*-aryl groups, the reaction products are indoles rather than indanes. The reaction is regiospecific and can be varied in a number of ways.[43,48] In contrast to the synthesis of bis(imino)indane complexes, the preparation of indoles requires three equivalents of isocyanide: the second equivalent is required for the construction of the indole ring from the ketenimine complex, the third for its displacement from the metal. With three equivalents of aryl isocyanide, **36** forms 2-alkylidene-3*H*-indoles, which dimerize to pyrazinodiindoles **70** [Eq. (31)].

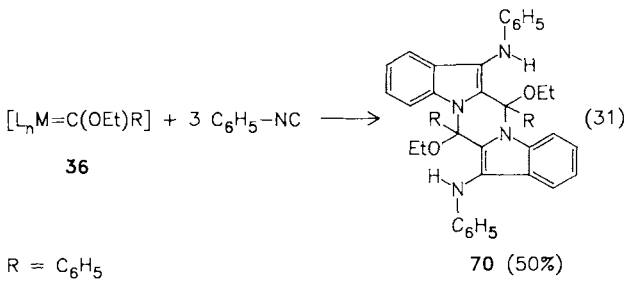

$[L_nM{=}C(OEt)R]$ + 3 C_6H_5–NC ⟶

36

R = C_6H_5 **70** (50%) (31)

The indole synthesis [Eq. (31)] is capable of considerable variation: thus, in the presence of water, **36b-d** react with aryl isocyanides in a three-component reaction to give 3-amino-2-aroylindoles **71**, which are obtained only with difficulty by other routes [Eq. (32), Table 5].[48]

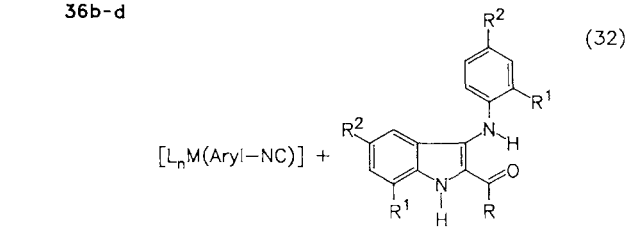

$[L_nM{=}C(OEt)C_6H_5]$ + 3 Aryl–NC + H_2O ⟶

36b-d

$[L_nM(Aryl{-}NC)]$ + **71** (32)

Aryl = 2,4-$R^1R^2C_6H_3$

Table 5. Yields of **71**, R = C_6H_5, in reaction (32) for various aryl residues 2,4-$R^1R^2C_6H_3$. Complex **36d** was employed.

R_1	R^2	Yield of **71** [%]
H	H	72
H	CH_3	59
H	NO_2	—
H	OCH_3	58
OCH_3	H	66

The indole synthesis is possible only when electron-rich aryl isocyanides are used. Electron-poor aryl isocyanides form azetidines (see Section 5.4), since in this case the *ortho* attack at the aromatic ring required for the formation of the indole is unfavored.

6. Addition of Alkynes to Ketenimine Complexes

Three-component reactions of carbene complexes with isocyanides and alkynes afford a great variety of products: as examples we shall consider reactions with 1-alkynes and ynamines.

6.1. 1-Alkynes

Complex **62b** and 1-alkynes **72** (R = C_6H_5, $Si(CH_3)_3$, CH_2OCH_3, OC_2H_5) give the azetidinylidene complexes **73** and **74** [Eq. (33), Table 6]. In **73** the C_2 unit of the alkyne residue is on the same side as the metal, in **74** on the side opposite to the metal.[49] This suggests that these products are formed from vinylidene units via [2+2] or [3+1] cycloadditions, just as in the case of the corresponding four-membered ring ligands built up from isostructural isocyanides [cf. Eqs. (27) and (28)]; the vinylidene complexes are formed by isomerization of 1-alkyne complexes.

The reactions of 1-alkynes with ketenimine complexes can, as expected, be influenced by the metal. The tungsten complex **62b** forms only four-membered ring heterocycles

$[L_nM\{R^1N{=}C{=}C(OEt)C_6H_5\}]$ + HC≡C–R ⟶

62b **72**

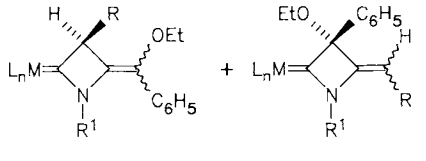

(33)

73 **74**

R^1 = *cyclo*-C_6H_{11}

Table 6. Yields of **73** and **74** in reactions (33).

R	Yield of **73** [%]	[(*E*):(*Z*)]	Yield of **74** [%]
C_6H_5	28	[1:12]	—
$Si(CH_3)_3$	[a]		[a]
CH_2OCH_3	18	[1:2]	—
H	13	[2:3]	10

[a] Not isolated.

via [2+2] and [3+1] cycloadditions [Eq. (33)], while the electron-rich manganese complex **62e** yields five-membered ring heterocycles **76** via [3+2] cycloadditions[31] [Eq. (34)], presumably with **75** as an intermediate.

$[L_nM\{R^1N{=}C{=}C(OEt)C_6H_5\}]$ + HC≡C–CH_2OCH_3 ⟶

62e **72** (R = CH_2OCH_3)

(34)

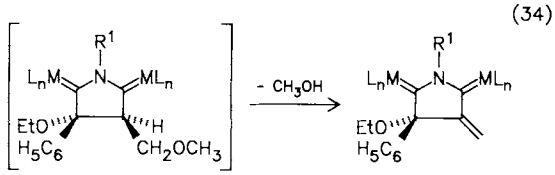

75 **76**

R^1 = CH_3

6.2. Ynamines

The addition of an electron-rich ynamine **77** to **62b,d** unexpectedly yields 2,3-dihydroazete complexes **78** [Eq. (35)].[50] In this case the four-membered ring is built up from three(!) atoms of the isocyanide used to synthesize **62** and a carbene carbon of the starting material **36**. An α-H in R^1 is transferred to the C=C unit of **77**. In addition, "normal" [2+2] cycloaddition products are formed: these are hydrolyzed to azetidinones **79** during chromatographic workup.

$[L_nM\{R^1N{=}C{=}C(OEt)C_6H_5\}]$ + H_3C–C≡C–$N(C_2H_5)_2$ ⟶

62b,d **77**

(35)

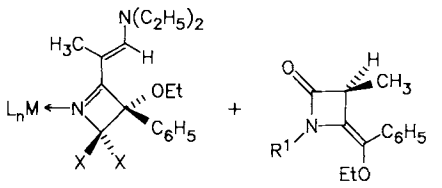

78 **79**

L_nM	R^1	X, X
$[Cr(CO)_5]$	CH_3	H, H
$[W(CO)_5]$	*cyclo*-C_6H_{11}	$(CH_2)_5$

7. Cyclizations with *N*- and *C*-Alkenylketenimine Complexes and Synthesis of *C*-Alkylidenaminoketenimine Complexes

Since ketenimine complexes can be formed from **1** and **2** under very mild, neutral conditions, our procedure is also suitable for the synthesis of thermolabile and reactive compounds such as *N*-alkenylketenimine complexes **100** [Eq. (43)] or *C*-alkenylketenimine complexes **86** [Eq. (38)] as well as *C*-alkylidenaminoketenimine complexes **102** [Eq. (44)].

The carbene complexes **82**[51] and **85**[52] required as starting materials can be prepared in a particularly simple manner by a base-catalyzed condensation[53] of the (CH-

acid) methylcarbene complex **80** with aldehydes **81** in the presence of chlorotrimethylsilane [Eq. (36), yield 50–70%] or of the aminocarbene complex **83** with acid chlorides **84**[59] [Eq. (37), yield 70–90%].

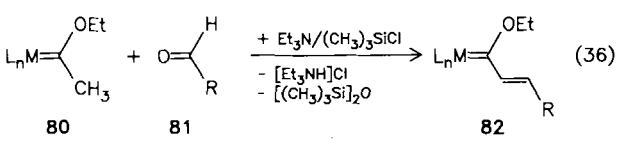

(36)

80 **81** **82**

L_nM = $[Cr(CO)_5]$

R = C_6H_5, *trans*-CH=CH–C_6H_5, *o*-$(CH_3)_3SiO$–C_6H_4, *o*-HO–C_6H_4, 2-thienyl, 2-furyl, 2-pyrrolyl

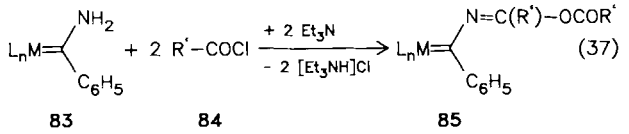

(37)

83 **84** **85**

L_nM = $[Cr(CO)_5]$; R' = C_6H_5, $C(CH_3)_3$

7.1. Pyrroles and δ-Carbolines

C-Alkenylketenimine complexes **86** of Cr, Mo, W (R^1 = alkyl,[54] alkenyl,[31] aryl[11c]) are well suited for cyclizations owing to their many double bonds. These reactions can occur both inter- and intramolecularly.

Thus, the *N*-cyclohexyl-substituted Cr complex **86** (L_nM = $[Cr(CO)_5]$) isomerizes spontaneously at 25 °C to the dihydropyrrolylidene complex **87** [Eq. (38)], the metal resi-

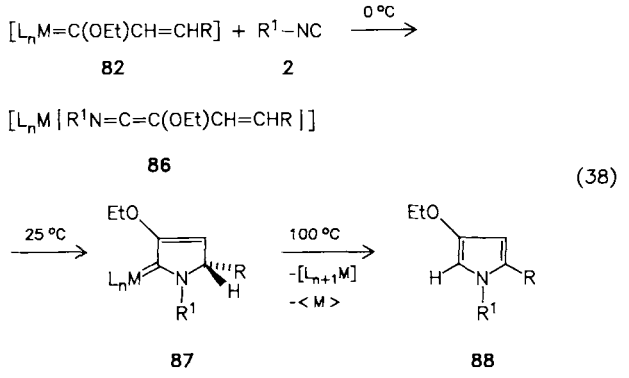

(38)

82 **2**

86

87 **88**

R = C_6H_5, *trans*-CH=CH–C_6H_5; R^1 = *cyclo*-C_6H_{11}

due undergoing a shift from nitrogen to the neighboring carbon. Complex **87** decomposes on warming via a hydrogen shift and elimination of the metal residue to give the ethoxypyrrole **88**; the latter can also be obtained directly without the isolation of organometallic intermediates by warming a 1:1 mixture of **82** and cyclohexyl isocyanide to 100 °C.[54]

Multiple cyclizations to partially hydrogenated δ-carbolinones **90**[11c] were observed when **82** was treated with three equivalents of an aryl isocyanide [Eq. (39)]. Organometallic intermediates of type **89** were isolated during a pyrrole synthesis which occurred in an analogous manner

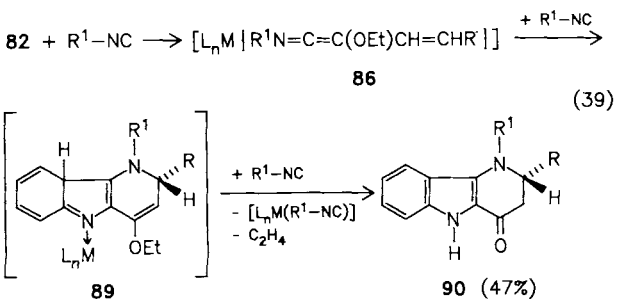

(39)

86 **89** **90** (47%)

R = C_6H_5, $CH{=}CHC_6H_5$; R^1 = C_6H_5

(see Section 7.4). The synthesis of δ-carbolines [Eq. (40)] starting from the particularly reactive thienylcarbene complex **91** leads spontaneously to the tetracyclic molecule **92**.[11c]

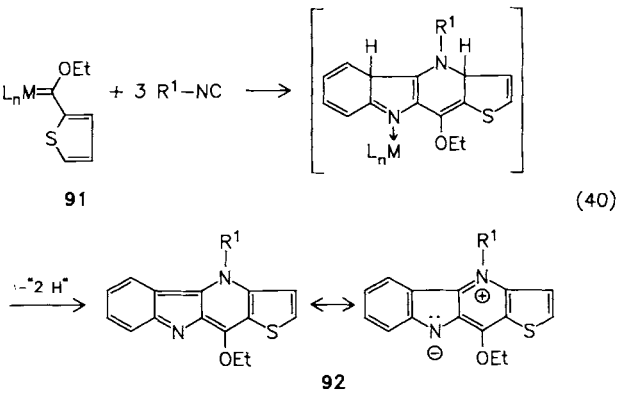

(40)

91 **92**

L_nM = $[Mo(CO)_5]$, R^1 = C_6H_5

7.2. [4+2] Cycloadditions with *C*-Alkenylketenimines

The reactions of **86** are strongly influenced not only by the metal residue L_nM but also by R^1, i.e., by the isocyanide used in the preparation of the complex. In the series M = Cr, Mo, W the intramolecular cyclization of the *N*-cyclohexyl-substituted Cr complex to give **87** is a borderline case. Since, in principle, competing reactions are possible which are influenced in a subtle manner by the spatial requirements of the substituents on nitrogen, the cyclization to the pyrrolylidene complex of type **87** "loses out" for both primary and tertiary isocyanides, with different results in each case. Only in the case of the ketenimine complex which is derived from (secondary) cyclohexyl isocyanide are the subsequent intermolecular reactions with isocyanides so slow (cf. Section 7.3) that time is available for the cyclization.

The bonding of the ketenimine ligand to the metal becomes weaker as the size of R^1 increases; i.e., it can be more easily replaced by other ligands. Therefore, the complete reaction of carbene complexes with tertiary isocyanides generally requires two equivalents of isocyanide. In this way it is possible to obtain ketenimines in a preparatively simple manner, to isolate them, or, as illustrated in reaction (41), to capture them with a third component: thus, the three-component reaction of **82** with two equivalents of *tert*-butyl isocyanide in the presence of maleic anhydride (MA) gives the adduct **94**. The latter is rapidly

oxidized in solution in the presence of air and light to the aminoethoxyphthalic anhydride **95** [Eq. (41)].[54,55]

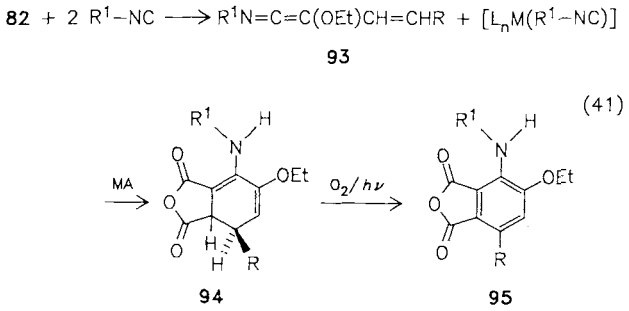

(41)

R = C_6H_5, R^1 = t-C_4H_9

7.3. [4 + 1] Cycloadditions with *C*-Alkenylketenimine Complexes

Alkenylcarbene complexes **82** of Cr, Mo, and W react with methyl isocyanide or primary isocyanides in a 2:1 ratio. In contrast to the reactions of bulky isocyanides, the second isocyanide is here added to the intermediate ketenimine ligand [Eq. (42)].[54,56]

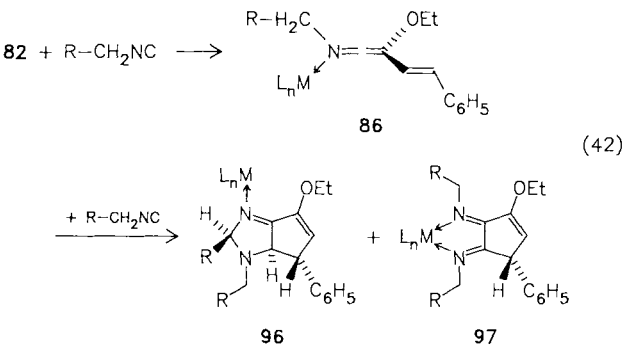

(42)

Table 7. Yields and product distributions in reactions (42). L_nM = [Cr(CO)$_5$].

R	Yield [%]	**96:97**
H	42	1:2
C_6H_5	46	> 10:1
CH_2=CH	10 [cf. Eq. (21)]	> 50:1

Complexes **96** and **97** (Table 7) are formed by [4 + 1] cycloaddition of the isocyanide to **86** from the side opposite to the metal and from the metal side, respectively, in multistep processes and, in the first case, additionally via insertion into an α-CH bond (see Section 6.2[57,58]).

7.4. [4 + 1] and [3 + 1] Cycloadditions with *N*-Alkenylketenimine Complexes

Carbene complexes **36** of Cr, Mo, and W add alkenyl isocyanides **99** to give *N*-alkenylketenimine complexes **100**, from which it is possible by means of competing reactions with further **99** to prepare the 1-azafulvene complexes **101** via [4 + 1] cycloaddition or the 2-azetidinylidene complexes **63** via [3 + 1] cycloaddition [Eq. (43), Table 8]. Complexes **101** are hydrolyzed to 3-amino-2-benzoylpyrroles [cf. Eq. (32)] and give a pyrrolopyridine on thermolysis.[47]

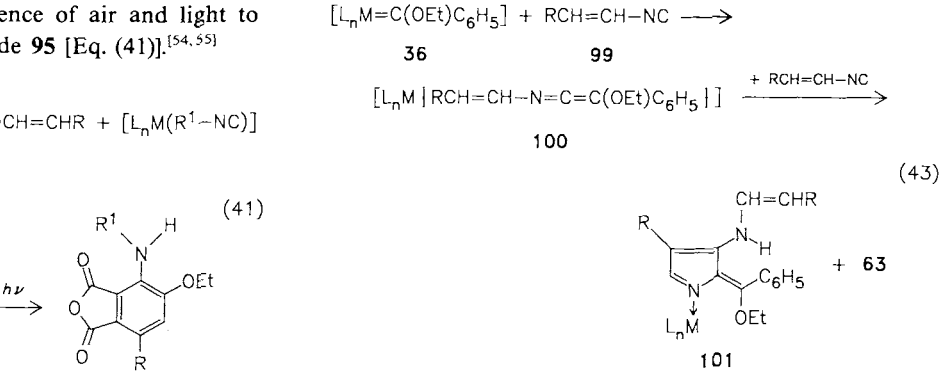

(43)

Table 8. Yields and product distributions in reactions (43). L_nM = [W(CO)$_5$] (**36b**).

R	Yield [%]	**101:63b**
H	80	3:1
CH_3 [a]	93	2:1

[a] *cis*-**99** : *trans*-**99** = 10:1.

7.5. *C*-Alkylidenamino and *C*-Mercaptoketenimines

Not only alkoxy- but also mercapto- and aminocarbene complexes can be cleanly converted into ketenimine complexes by means of our procedure. The aminocarbene complex **85** (R' = C_6H_5) gives the alkylidenamino-substituted ketenimine **102**[27] with two equivalents of cyclohexyl isocyanide [Eq. (44)], while the mercaptocarbene

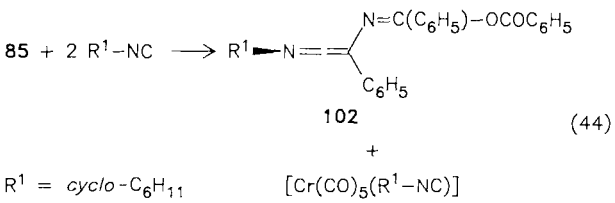

(44)

complexes **103** give ketenimine complexes **104** which are coordinated via sulfur[26] [Eq. (45)].

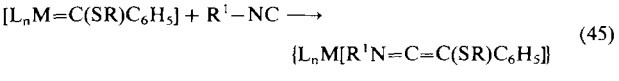

(45)

L_nM = [W(CO)$_5$]; R, R^1 = *cyclo*-C_6H_{11}, t-C_4H_9

8. Future Prospects

The use of metal complexes in organic synthesis offers a vast potential for novel "umpolung" reactions and possibilities for "nonclassical" construction of synthetic building blocks via template reactions. Our knowledge of procedures for the preparation of ketenimine complexes from carbene complexes, together with an extrapolation of previously analyzed reaction patterns of these compounds, opens numerous possibilities for their application in synthesis which—as a further advantage—involve only relatively simple procedures; we have taken care to adjust our

procedures to fit the capabilities of a conventionally equipped synthetic laboratory.

It would appear to be of importance to carry out systematic studies involving various metals and ligands and asymmetric syntheses via induced chirality, as well as to transfer the results obtained for stoichiometric reactions to catalytic processes.

Our work has been supported by the Deutsche Forschungsgemeinschaft, the Stiftung Volkswagenwerk and the Fonds der Chemischen Industrie. The development of the synthetic procedures described here required careful sorties into virtually unexplored territory. Exact predictions on the basis of known reactions were hardly possible: instead, our reactions were discovered on the basis of critical and creative analytical-strategic reflections and discussion at the laboratory bench and were then developed into synthetic procedures. I thank my co-workers whose names are mentioned in the list of references for their efforts and their enthusiasm for their research topics.

Received: January 28, 1988 [A 698 IE]
German version: *Angew. Chem. 100* (1988) 1512
Translated by Prof. Dr. *T. N. Mitchell*, Dortmund.

[1] G. R. Krow, *Angew. Chem. 83* (1971) 455; *Angew. Chem. Int. Ed. Engl. 10* (1971) 435; M. W. Barker, W. E. McHenry in S. Patai (Ed.): *The Chemistry of Ketenes, Allenes and Related Compounds, Vol. 2*, Wiley, New York 1980, pp. 701-720; N. P. Gambaryan, *Russ. Chem. Rev. Engl. Transl. 45* (1976) 630; D. Borrmann in Houben-Weyl (Ed.): *Methoden der Organischen Chemie, Bd. VII/4*, Thieme, Stuttgart 1968, p. 323-339; A. Dondoni, *Heterocycles 14* (1980) 1547; L. Ghosez, M. L. O'Donnell in P. Marchand, R. E. Lehr (Eds.): *Pericyclic Reactions, Vol. 2*, Academic Press, New York 1977, p. 79.

[2] E. O. Fischer, *Rev. Pure Appl. Chem. 30* (1972) 353; K. H. Dötz, H. Fischer, P. Hofmann, F. R. Kreissl, U. Schubert, K. Weiss: *Transition Metal Carbene Complexes*, Verlag Chemie, Weinheim 1983; K. H. Dötz, *Angew. Chem. 96* (1984) 573; *Angew. Chem. Int. Ed. Engl. 23* (1984) 587; H. Fischer in S. Patai (Ed.): *The Chemistry of Metal-Carbon Bonds*, Wiley, New York 1982, pp. 181-224; P. L. Pauson in Houben-Weyl (Ed.): *Methoden der Organischen Chemie, Bd. E18*, Thieme, Stuttgart 1987, p. 282ff.

[3] a) I. Ugi (Ed.): *Isonitrile Chemistry*, Academic Press, New York 1971; C. Grundmann in Houben-Weyl (Ed.): *Methoden der Organischen Chemie, Bd. 5*, Thieme, Stuttgart 1985, p. 1611-1658; H. M. Walborsky, M. P. Periasamy in S. Patai, Z. Rappoport (Ed.): *The Chemistry of Triple-Bonded Functional Groups, Vol. 2EC*, Wiley, New York 1983, pp. 835-887; b) E. Singleton, H. E. Oosthuizen, *Adv. Organomet. Chem. 22* (1983) 209.

[4] U. Behrens, T. Sielisch, *J. Organomet. Chem. 310* (1986) 179.

[5] T. Sielisch, *Dissertation*, Hamburg 1986 (U. Behrens, personal communication.

[6] D. J. Yarrow, J. A. Ibers, Y. Tatsuno, S. Otsuka, *J. Am. Chem. Soc. 95* (1973) 8590.

[7] R. E. Cramer, K. Panchanatheswaran, J. W. Gilje, *Angew. Chem. 96* (1984) 888; *Angew. Chem. Int. Ed. Engl. 23* (1984) 912.

[8] T. Mitsudo, H. Watanabe, Y. Komiya, Y. Watanabe, Y. Takaegami, K. Nakatsu, K. Kinoshita, Y. Miyagawa, *J. Organomet. Chem. 190* (1980) C39.

[9] J. K. P. Ariyaratne, M. L. H. Green, *J. Chem. Soc. 1963*, 2976; P. M. Treichel, D. W. Firsich, T. H. Lemmon, *J. Organomet. Chem. 202* (1980) C77.

[10] W. R. Roper, A. H. Wright, cited in W. R. Roper, M. A. Gallop, *Adv. Organomet. Chem. 25* (1986) 168.

[11] a) R. Aumann, E. O. Fischer, *Chem. Ber. 101* (1968) 954; b) C. G. Kreiter, R. Aumann, *ibid. 111* (1978) 1223; c) R. Aumann, H. Heinen, C. Krüger, Y.-H. Tsay, *ibid. 119* (1986) 3141.

[12] W. P. Neumann, R. Sommer, E. Müller, *Angew. Chem. 78* (1966) 545; *Angew. Chem. Int. Ed. Engl. 5* (1966) 514.

[13] S. R. Su, J. A. Hanna, A. Wojcicki, *J. Organomet. Chem. 21* (1970) P21.

[14] J. S. Ricci, J. A. Ibers, M. S. Fraser, W. H. Baddley, *J. Am. Chem. Soc. 92* (1970) 3489.

[15] E. O. Fischer, W. Schambeck, F. R. Kreissl, *J. Organomet. Chem. 169* (1979) C27.

[16] E. O. Fischer, W. Schambeck, *J. Organomet. Chem. 201* (1980) 311.

[17] K. G. Moloy, P. J. Fagan, J. M. Manriquez, T. S. Marks, *J. Am. Chem. Soc. 108* (1986) 56.

[18] a) K. Ogawa, A. Torii, H. Kobayashi-Tamura, T. Watanabe, T. Yoshida, S. Otsuka, *J. Chem. Soc. Chem. Commun. 1971*, 991; b) U. Behrens, T. Sielisch, *J. Organomet. Chem. 322* (1987) 203; *ibid. 327* (1987) 85; c) S. Otsuka, A. Nakamura, T. Yoshida, *ibid. 70* (1967) 339.

[19] R. Aumann in H. tom Dieck, A. de Meijere (Eds.): *Organometallics in Organic Synthesis*, Springer, Berlin 1987, pp. 69-84.

[20] R. B. King, K. C. Hodges, *J. Am. Chem. Soc. 97* (1975) 2702; R. B. King, M. S. Saran, *Inorg. Chem. 14* (1975) 1018; R. B. King, S. P. Diefenbach, *ibid. 18* (1979) 69.

[21] W. Beck, W. Hieber, G. Neumair, *Z. Anorg. Allg. Chem. 344* (1966) 285; W. Beck, R. E. Nitzschmann, H. S. Smedal, *J. Organomet. Chem. 8* (1967) 547.

[22] R. Aumann, H. Heinen, *Chem. Ber. 118* (1985) 4186.

[23] R. Aumann, E. Kuckert, *Chem. Ber. 119* (1986) 156.

[24] R. Aumann, H. Heinen, *Chem. Ber. 121* (1988) 1085.

[25] R. Aumann, H. Heinen, *Chem. Ber. 120* (1987) 1297.

[26] R. Aumann, J. Schröder, H. Heinen, unpublished.

[27] R. Aumann, S. Althaus, unpublished.

[28] Analogously prepared phosphorus ylide complexes [H. Fischer, E. O. Fischer, C. G. Kreiter, H. Werner, *Chem. Ber. 107* (1974) 2459] and nitrogen ylide complexes [F. R. Kreissl, E. O. Fischer, C. G. Kreiter, K. Weiss, *Angew. Chem. 85* (1973) 617; *Angew. Chem. Int. Ed. Engl. 12* (1973) 563] are unknown.

[29] J. P. Collman, L. S. Hegedus: *Principles and Applications of Organotransition Metal Chemistry*, University Science Books, Mill Valley, CA, USA 1980.

[30] M. P. Guy, J. T. Guy, D. W. Bennett, *Organometallics 5* (1986) 1696.

[31] R. Aumann, H. Heinen, *Chem. Ber. 121* (1988) in press.

[32] S. Otsuka, A. Nakamura, T. Koyama, Y. Tatsuno, *Justus Liebigs Ann. Chem. 1975*, 626.

[33] T. Kajimoto, H. Takahashi, J. Tsuji, *J. Organomet. Chem. 23* (1970) 275; T. Boschi, B. Crociani, *Inorg. Chim. Acta 5* (1971) 477.

[34] G. Carturan, A. Scrivanti, U. Belluco, *Inorg. Chim. Acta 21* (1977) 103.

[35] A. Halleux, *Angew. Chem. 76* (1964) 899; *Angew. Chem. Int. Ed. Engl. 3* (1964) 752; J. H. Boyer, W. Beverung, *J. Chem. Soc. Chem. Commun. 1969*, 1377; J. A. Green, L. A. Singer, *Tetrahedron Lett. 1969*, 5093; E. Ciganek, *J. Org. Chem. 35* (1970) 862; N. Obata, H. Mizuno, T. Koitabashi, T. Takizawa, *Bull. Chem. Soc. Jpn. 48* (1975) 2287.

[36] D. S. Gill, P. K. Baker, M. Green, K. E. Paddick, M. Murray, A. J. Welch, *Chem. Commun. 1972*, 458.

[37] E.-U. Würthwein, *J. Org. Chem. 49* (1984) 2971; L. L. Lohr, Jr., M. Hanamura, K. Morokuma, *J. Am. Chem. Soc. 105* (1983) 5541.

[38] a) J. Hillis, J. N. Francis, M. Ori, M. Tsutsui, *J. Am. Chem. Soc. 96* (1974) 4800; F. A. Cotton, J. N. Francis, B. A. Frenz, M. Tsutsui, *ibid. 95* (1973) 2483; b) R. Aumann, H. Wörmann, *Chem. Ber. 112* (1979) 1233.

[39] W. P. Fehlhammer, P. Hirschmann, A. Völkl, *J. Organomet. Chem. 294* (1985) 251; W. P. Fehlhammer, P. Hirschmann, A. Mayr, *ibid. 224* (1982) 153; W. P. Fehlhammer, P. Hirschmann, H. Stolzenberg, *ibid. 224* (1982) 165.

[40] R. Aumann, H. Heinen, J. Uphoff, U. Schönfelder, unpublished.

[41] R. Aumann, J. Uphoff, *Angew. Chem. 99* (1987) 361; *Angew. Chem. Int. Ed. Engl. 26* (1987) 357.

[42] R. Aumann, E. Kuckert, unpublished.

[43] R. Aumann, E. Kuckert, H. Heinen, *Angew. Chem. 97* (1985) 960; *Angew. Chem. Int. Ed. Engl. 24* (1985) 978.

[44] R. Aumann, E. Kuckert, H. Heinen, *Chem. Ber. 120* (1987) 1293.

[45] a) R. Aumann, H. Heinen, C. Krüger, *Angew. Chem. 97* (1985) 960; *Angew. Chem. Int. Ed. Engl. 24* (1985) 978; b) R. Aumann, H. Heinen, *Chem. Ber. 118* (1985) 952.

[46] D. Moderhack, *Synthesis 12* (1985) 1083.

[47] R. Aumann, E. Kuckert, C. Krüger, K. Angermund, *Angew. Chem. 99* (1987) 587; *Angew. Chem. Int. Ed. Engl. 26* (1987) 563.

[48] R. Aumann, H. Heinen, *Chem. Ber. 119* (1986) 2289.

[49] R. Aumann, E. Kuckert, *Chem. Ber. 120* (1987) 1939.

[50] R. Aumann, E. Kuckert, C. Krüger, R. Goddard, K. Angermund, *Chem. Ber. 121* (1988) in press.

[51] C. P. Casey, W. R. Brunsvold, *J. Organomet. Chem. 77* (1974) 345; W. D. Wulff, S. R. Gilbertson, *J. Am. Chem. Soc. 107* (1985) 503.

[52] H. Fischer, U. Schubert, R. Märkl, *Chem. Ber. 114* (1981) 3412; H. Fischer, S. Zeuner, *J. Organomet. Chem. 327* (1987) 63.

[53] R. Aumann, H. Heinen, *Chem. Ber. 120* (1987) 537.

[54] R. Aumann, H. Heinen, *Chem. Ber. 119* (1986) 3801.

[55] G. Barbaro, A. Battaglia, P. Giorgianni, *J. Org. Chem. 52* (1987) 3289.

[56] R. Aumann, H. Heinen, C. Krüger, *Chem. Ber. 120* (1987) 1287.

[57] T. Saegusa, Y. Ito, H. Kinoshita, S. Tomita, *J. Org. Chem. 36* (1971) 3316.

[58] Y. Yamamoto, K. Aoki, H. Yamazaki, *J. Am. Chem. Soc. 96* (1974) 2647.

[59] R. Aumann, S. Althaus, C. Krüger, P. Betz, *Chem. Ber.*, in press.

High-Resolution Solid-State ^{13}C-NMR Spectroscopy of Polymers

New Analytical Methods (37)

By Rüdiger Voelkel*

Dedicated to Professor Helmut Dörfel on the occasion of his 60th birthday

Until a few years ago, solid-state nuclear resonance yielded spectra containing broad lines only. Meanwhile, CP/MAS-NMR spectroscopy has provided a method which gives narrow nuclear resonance lines from a solid-state specimen as well. Using this technique, it is now possible to produce spectra of "rare" nuclei (^{13}C, ^{29}Si, ^{15}N etc.) which are resolved in terms of chemical structure. The analytical capabilities of NMR spectroscopy can be applied to the solid state: it may be that it is necessary to identify compounds in the solid state because, for example, a solvent would alter the coordination sphere, or that it is desired to monitor chemical reactions in the solid state, for example the baking of an enamel. Where a substance in the solid state is concerned, high-resolution ^{13}C-NMR spectroscopy provides not only information about the chemical structure, but also about the solid state itself. To mention just a few examples, information on the conformation, crystal structure and molecular dynamics, as well as molecular miscibility is given. This opens up a broad spectrum of applications, from a statement concerning the crystal modification of an active substance in ready-to-use pharmaceutical preparations, e.g. tablets, to the question of whether two polymers are miscible with one another at a molecular level.

1. Introduction

Since the introduction of the CP/MAS (*c*ross *p*olarization, *m*agic *a*ngle *s*pinning) ^{13}C-NMR experiment in its present form[1] as a combination of dipolar decoupling,[2] sample rotation at the magic angle[3] and cross polarization,[4] a number of articles[5] and monographs[6] presenting an introduction to the method have been published, as well as articles providing an overview of individual areas of application, e.g. polymers,[7] carbohydrates[8] and biopolymers.[9]

CP/MAS-NMR spectroscopy opens up the possibility of obtaining, even from a substance in the solid state, ^{13}C-NMR spectra, the signals of which can be correlated with chemical structures. The resolution of individual signals can be useful in two ways on the one hand, solid-state NMR spectroscopy can be used in direct analogy with solution NMR spectroscopy as an analytical tool for the investigation of compounds which have low solubility or are insoluble. On the other hand, it is also possible to make a number of statements regarding the physics of the solid substance. In both cases, the correlation of individual signals with chemical structural elements is an indispensible prerequisite. Accordingly, Section 2 deals initially with the question of the line width, and, in connection with the generation of the signals, quantifiability is also discussed. In Section 3, relating to analytical applications, consideration is given only to insoluble polymers. Attention centers on reaction resins, which otherwise are analytically accessible only with difficulty on account of their cross-linked nature. They are however of great technical importance, for example as matrix materials in composites.

In the second part (Sections 4 and 5) a number of physical applications are presented, which are less familiar to chemists accustomed to NMR spectroscopy in solution. One of the strengths of solid-state NMR spectroscopy is that it provides information on questions of conformation, crystal modification, molecular dynamics, and molecular adjacency. An understanding of the physical behavior of the sample is essential in order to take advantage of the unique possibilities offered by solid-state NMR spectroscopy: for example, selectivity with respect to certain components is also useful in the case of analytical applications.

The present article is limited to the one-dimensional methods which have already become well-established in practice. Very promising additional possibilities offered by two-dimensional NMR experiments will be dealt with separately by *B. Blumich* and *H. W. Spiess*.[10]

2. Line Width, Quantifiability

When reference is made to "magic angle spinning" NMR spectroscopy, what is almost always meant is the combination of *c*ross *p*olarization (CP), the actual rotation of the sample at the magic angle of 54.7° (MAS) and dipolar decoupling (DD) of the ^{1}H nuclei from the observed ^{13}C nucleus. With rigid solid substances only the combination of all three experimental "tricks" makes it possible and practicable to record spectra of rare nuclei (most commonly ^{13}C) resolved in terms of chemical structure.

Magic angle spinning, however, imposes the most stringent requirements on the experimental procedure, and makes the most striking contribution to the narrowing of the lines. The effect of MAS can be seen particularly well in the case of pure polyacetylene with only one chemical environment of the ^{13}C nuclei (Fig. 1). When the sample is

[*] Dr. R. Voelkel
Plastics Laboratory
BASF Aktiengesellschaft
D-6700 Ludwigshafen (FRG)

 © VCH Verlagsgesellschaft mbH, D-6940 Weinheim, 1988 0570-0833/88/1111-1468 $ 02.50/0

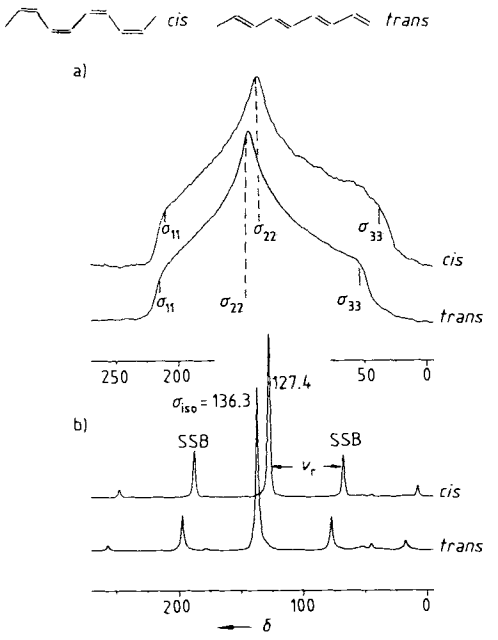

Fig. 1. Solid-state ^{13}C-NMR spectra of *cis*- and *trans*-polyacetylene. a) Stationary powder sample. The spectrum scans the entire range of the chemical shift. b) With sample rotation (ν_r = 4500 Hz) at the magic angle. A narrow line is obtained at the isotropic value of the chemical shift, and spinning sidebands (SSB) are spaced at intervals of ν_r (all spectra cross polarized with 3 ms, dipolar decoupled with ν_{1H} = 50 kHz, each 20000 recordings at intervals of 2 s).

stationary, a powder spectrum is measured, which sweeps over the entire range of the chemical shift. The principal values σ_{ii} of the chemical shift tensor can be obtained by matching of the theoretical spectrum.[6a, 11a] However, if the sample were rotated at speeds of rotation which are large in relation to the width of the powder spectrum (in Hz), the result obtained would be only one sharp line at the isotropic value of the chemical shift, the position of which is different for the *cis* and *trans* isomers of polyacetylene.

When the sample is rotated more slowly, spinning sidebands (SSB) occur, in addition to the isotropic signal, at a spacing corresponding to the frequency of rotation (in Fig. 1, 4500 Hz). The chemical shift tensor can be reconstructed from the intensity of these sidebands.[11b,c] If the recording is synchronized stepwise with the rotor position in a two-dimensional measurement, the sideband intensity gives the orientation distribution of anisotropic samples.[10, 12] In the event of interfering superpositions of the spinning sidebands with other signals, it is possible to suppress the sidebands by appropriate sequences of pulses.[13] When such suppression is applied, the signal intensities are often distorted to a great extent. Except in the case of extremely broad signals, for example when examining coal or charged, electrically conductive polymers, another measurement at a different speed of rotation frequently proves to be more advantageous.

With regard to the use of MAS-^{13}C-NMR spectroscopy as an analytical tool, especially for compounds which have low solubility or are insoluble, two questions are of prime importance: the question of the attainable resolution, i.e. the line widths which can be obtained in comparison with the range of the chemical shift (^{13}C: approximately 200 ppm), and the question of the quantifiability of the spectra.

2.1. Line Width

In solid-state NMR spectra the line widths are usually 10–100 times greater than those of solution NMR spectra. The attainable line width of 10–100 Hz at 7T for rigid, crystalline solid substances is determined, on the one hand, by susceptibility variations and by dipolar interactions which are not entirely averaged out. On the other hand, effects which are typical of solid substances frequently limit the resolution which can be attained.[14] Errors in the setting of the magic angle play virtually no part, provided that adjustment is carried out using KBr[15] and double-bearing rotors are used.

When several molecules are situated at non-equivalent positions within a crystal, or if the symmetry of the crystal is less than that of the molecule, molecular positions which are equivalent to one another in solution can lead to several signals in the solid state. In the case of small differences in shift, a broadening of the signal may result[16] (Fig. 2). Similarly, the freezing-in of conformations in the solid substance leads to the non-equivalence of signals. Such a conformational effect on the solid-state spectrum has been described both in the case of peptides[17] and also in the case of synthetic polymers.[18, 44]

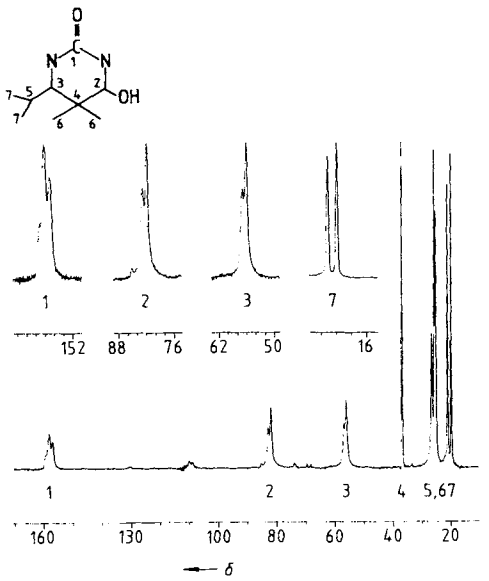

Fig. 2. Effect of the crystal structure on the solid-state NMR spectrum (for the example of a urea derivative). Two molecules in non-equivalent positions lead to a doubling of the signals (each 1000 recordings at intervals of 6 s, CP 2 ms, $\nu_{1H} = \nu_{1C}$ = 50 kHz, ν_r = 3650 Hz).

Conformation and, to a lesser extent, packing, are variables which contribute to the determination of the line position. This frequently results in complications when interpreting the solid-state NMR spectra of crystalline samples with respect to chemical structures; on the other hand, the influence of conformation and packing enables the spectroscopist to distinguish various modifications of chemi-

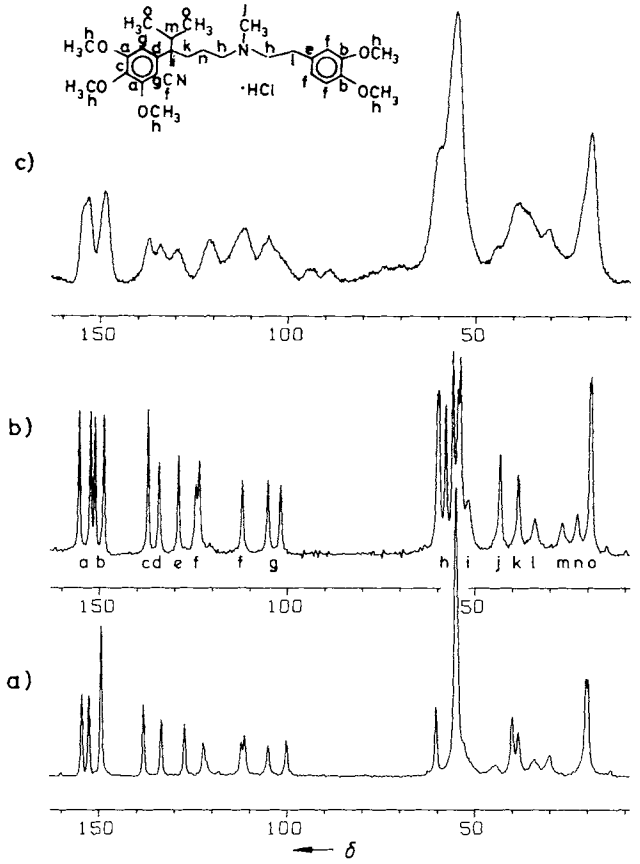

Fig. 3. Effect of crystal modification and crystallinity on the solid-state NMR spectrum of an amine hydrochloride. a) Crystallization from 2-propanol/diisopropyl ether. b) Recrystallized from ethyl acetate. Attention is drawn to the non-equivalence within the positions a, b, g and h and the modification effect (compare (a) with (b)). c) Amorphous sample (quenched from the melt). Conformational and packing disorder leads to broad signals ((a) and (b) each 2000 recordings plus 3000 recordings added with inverted 1st order SSB [13a], in order to suppress the sidebands, $\nu_r = 4500$ Hz, CP 2 ms, $\nu_{1H} = \nu_{1C} = 50$ kHz; c) 4000 recordings at intervals of 2 s, CP 2 ms, without SSB suppression).

cally identical compounds (Fig. 3). Under conditions of increasing temperature, e.g. by interconversion of conformers[19] or tautomerism,[20] there may be a dynamic exchange between signals which are distinguishable in the solid-state NMR spectrum. Whenever the atoms undergoing exchange with one another differ in chemical shift by a few ppm at the most, slow dynamic processes with a lifetime in the region of 10^{-4} s can be investigated by line shape analysis.

Below the glass-transition temperature the conformational and packing disorder leads to relatively broad lines for amorphous samples. Line widths between 100 and 500 Hz (Fig. 3c) are typical at 75 MHz (^{13}C). Accordingly, differing tacticities in polymers can only be measured in the solid state if they result in differing conformations in the crystal[21] or if the formation of hydrogen bonds is restricted to a specific tacticity.[22]

In the case of elastomers having a glass-transition point below room temperature, the modulation of the C-H dipole coupling due to motion plays a part in determining the line width.[14,20,23] Indeed, if the frequency of the jump process and that of the decoupling field (usually $\omega_{1H}/2\pi \simeq 50$ kHz) are comparable, the suppression of the dipolar coupling becomes inefficient; the natural line width of ^{13}C-NMR signals (T_2) due to relaxation via the C-H dipolar interaction then limits the resolution attainable.[24] Figure 4 shows an appropriate example: in this case, a spin-lock frequency in the median kHz range was employed. The maximum line width is therefore to be expected at approximately 30 K above the glass-transition temperature (in the case of poly(butyl acrylate) $T_G = -46$ °C) (cf. Section 5.3). The agreement between the decoupling frequency ω_{1H} and the jump frequency of the motion leads to line broadening. There is also a broadening due to modulation of the resonance frequency on account of the anisotropy of the chemical shift, if the mobility is comparable with the rotor frequency (in most cases, approximately 4000 Hz).[14a]

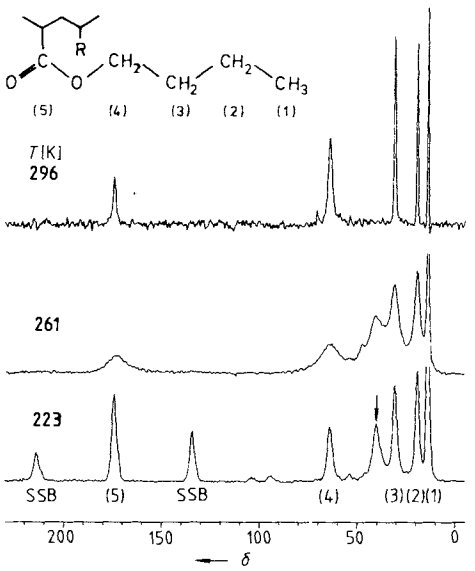

Fig. 4. Effect of the molecular dynamics on the CP/MAS-NMR spectrum of polybutyl acrylate. If the frequency of the molecular dynamics is comparable with the strength of the decoupling field ($\omega_{1H}/(2\pi) = 50$ kHz), a line broadening results ($T = 261$ K). In contrast to $T = 296$ K, there are spinning sidebands at $T = 223$ K. Attention is drawn to the absence of the signal from the chain (arrow in the spectrum at $T = 223$ K, $\delta \approx 40$) at $T = 296$ K.

When measurements are taken far above the glass transition, which is the case with rubbers even at room temperature, the dipolar interaction is to a large extent averaged out by the high molecular mobility, so that very narrow lines are measured even without dipolar decoupling.[6c,24,25] On account of the small line widths of rubbers, it is possible to determine the microstructure of elastomers and elastomeric copolymers even in the solid state. Even the scalar ^{13}C-^{1}H coupling was resolved in a two-dimensional experiment in the case of polyisoprene.[26]

2.2. Quantifiability

The ^{13}C-NMR signal in solid-state NMR spectroscopy is enhanced by cross polarization,[4] a transfer of magnetization from ^{1}H to ^{13}C in a double resonance experiment. In order to achieve the transfer of magnetization, a Hartmann-Hahn contact is at present almost always used, i.e., the simultaneous application of two radio-frequency fields

in resonance with ^{13}C and ^{1}H respectively with the same frequency of the nuclei in the rotating coordinate system. Other cross polarization techniques[4b, 27] are not considered in the text which follows. The reason for using cross polarization for enhancing the ^{13}C signal resides, on the one hand, in the ratio of the gyromagnetic ratios $\gamma_H/\gamma_C \simeq 4$. Additionally the maximum permissible repetition rate with cross polarization is determined by the very much faster relaxation of the ^{1}H and not by the ^{13}C; in favorable circumstances it is possible to achieve an enhancement factor of up to 20 in the signal-to-noise ratio. This is why cross polarization is frequently a necessary prerequisite for the practical feasibility of MAS-^{13}C-NMR spectroscopy. Among polymers, the elastomers are an exception—measurements are made far above the glass-transition temperature and excitation takes place directly by a 90° pulse with the resonant frequency of the ^{13}C nuclei.

Signal enhancement by cross polarization implies that the signal intensities are influenced by the kinetics of this transfer of magnetization[6a, 28] and are not a priori quantitative. Figure 5 shows the growth of the magnetization for

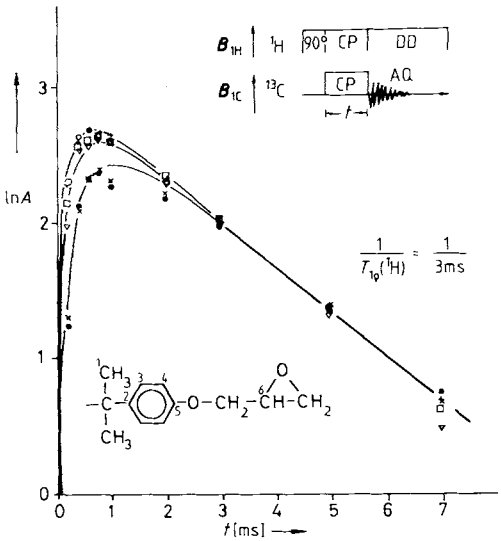

Fig. 5. Rise of the ^{13}C-NMR signal during cross polarization, for the example of an epoxy resin of bisphenol-A diglycidyl ether and diaminodiphenylmethane (0.172 epoxide units/bisphenol-A unit). The individual positions in the molecule have an individual time of build-up (cf. Table 1). In the case of long contact times, the signal amplitude declines with the common time constant $T_{1\rho}(^{1}H)$ (4000 recordings in each instance, at intervals of 2 s, $\nu_r = 3850$ Hz, $\nu_{1C} = \nu_{1H} = 50$ kHz). AQ = acquisition time of the FID, □ C1, ● C2, + C3, ○ C4, × C5, ▽ C6.

the various positions in a hardened epoxy resin. The mechanism which couples the ^{13}C nuclei to the ^{1}H "reservoir" is the dipole-dipole interaction. On account of its $1/r^6$ dependence upon the spacing r between ^{13}C and ^{1}H, the signal build-up for the various resonance lines takes place at differing speeds: quaternary C nuclei without ^{1}H nuclei within bonding distance cross-polarize in the Hartmann-Hahn contact[4] more slowly than H-substituted C nuclei. Where methyl groups are present, the dipolar interaction is reduced by the rotation about the ternary axis, so that a CH_3 group behaves in a similar way to a CH group (cf. Fig. 5). In the case of single-phase systems with adequate dipole-dipole interaction between the protons the signal intensity $M(t)$ passes through a maximum and then falls off exponentially with increasing contact time t. The time constant $T_{1\rho}(^{1}H)$ of the decay is common to all C atoms [Eq. (a)-(d)].[6a, 7b, 28]

$$M(t) = M_0 \lambda^{-1} \left\{1 - \exp\left(-\frac{\lambda t}{T_{CH}}\right)\right\} \exp\left(-\frac{t}{T_{1\rho}(^{1}H)}\right) \quad (a)$$

$$M(t) = M_0 \lambda^{-1} f(t) \quad (b)$$

where

$$\lambda = 1 + \frac{T_{CH}}{T_{1\rho}(^{13}C)} - \frac{T_{CH}}{T_{1\rho}(^{1}H)} \quad (c)$$

and

$$f(t) = \exp\left(-\frac{t}{T_{1\rho}(^{1}H)}\right) - \exp\left[-t\left(\frac{1}{T_{CH}} + \frac{1}{T_{1\rho}(^{13}C)}\right)\right] \quad (d)$$

In order to treat the protons as a spin reservoir with a single spin temperature, the derivation of equation (a) is based on a strong homonuclear H-H dipole interaction, i.e. a short proton relaxation time $T_2(^{1}H)$. Equation (a) describes the rise of the ^{13}C magnetization with a time constant $\lambda^{-1} T_{CH}$, during the contact of the ^{13}C nuclei with the ^{1}H reservoir which in the "locked" condition is cold with regard to the spin temperature. Superimposed on the rise of the ^{13}C magnetization, there is a contrary process: the "heating" of the proton reservoir, i.e. reduction of the proton magnetization, due to the relaxation of the protons in the rotating coordinate system with the time constant $T_{1\rho}(^{1}H)$. As a result of the reduction of the proton magnetization during the double resonance experiment, the maximum ^{13}C magnetization attainable in the cross polarization experiment also falls to $M_0 \lambda^{-1} \exp(-t/T_{1\rho}(^{1}H))$. For large radio-frequency field strengths, $M_0 = \gamma_H/\gamma_C M_{eq}$, i.e. the theoretically attainable ^{13}C magnetization M_0 amounts to approximately four times the equilibrium magnetization M_{eq} in the external field B_0. As already mentioned, an even more significant gain in the signal-to-noise ratio is observed in cross polarization, because the repetition rate of the experiment is not determined by the longitudinal relaxation of the ^{13}C nuclei but by the very much more rapid relaxation of the protons.

In the quantitative evaluation of the spectra,[7b] magnetizations of the various positions in the molecule which are generated with a fixed contact time t are compared. The scaling of M_0 is different for the individual positions; the relaxation time in the rotating coordinate system, $T_{1\rho}(^{13}C)$, and the cross polarization constant T_{CH} are both individual quantities for the various positions in the molecule [see equations (a) and (c)]. $T_{1\rho}(^{1}H)$ is determined from the gradient $1/T_{1\rho}(^{1}H)$ of the straight line at long contact times in a logarithmic plot of the signal amplitudes, assuming $T_{1\rho}(^{1}H) \gg T_{CH}$ (Fig. 5). The initial part of the curve is analyzed according to equation (d) in order to obtain $1/T_{CH} + 1/T_{1\rho}(^{13}C)$ (Table 1). $T_{1\rho}(^{13}C)$ can be measured in a separate experiment (cf. Section 5.2). $T_{1\rho}(^{1}H)$, T_{CH} and $T_{1\rho}(^{13}C)$ are used to compute the scaling factors λ [Eq. (c)] and $f(t)$ [Eq. (d)]; finally, $\lambda/f(t)$ gives the factor by which the measured intensity according to equation (b) must be multiplied in order to guarantee a "correct" count of the spins (Table 2).

Table 1. Dynamics of the cross polarization in the case of an epoxy resin [cf. Fig. 5 and Eq. (a)-(d)]. The time constant for the transfer of magnetization, T_{CH}, can be determined from the rise of the signal amplitudes A at the commencement of the C-H contact in Figure 5 (time constant in column (2)). $T_{1\rho}(^{13}C)$ must be obtained from a separate experiment. $T_{1\rho}(^{1}H)$ is obtained from the graph in Figure 5 for long contact times. The scaling λ for the various signals is computed from T_{CH}, $T_{1\rho}(^{13}C)$ and $T_{1\rho}(^{1}H)$ in accordance with equation (c).

C nucleus	$\frac{1}{T_{CH}}+\frac{1}{T_{1\rho}(^{13}C)}$ [a] $[ms^{-1}]$	$\frac{1}{T_{1\rho}(^{13}C)}$ [b] $[ms^{-1}]$	$\frac{1}{T_{CH}}$ $[ms^{-1}]$	$\frac{T_{CH}}{T_{1\rho}(^{13}C)}$	$\frac{T_{CH}}{T_{1\rho}(^{1}H)}$ [c]	λ
C1	3.18	0.19	2.99	0.064	0.111	0.953
C2, C5	1.80	0.10	1.70	0.059	0.196	0.863
C3, C4	3.71	0.35	3.36	0.100	0.099	1.001
C6	2.85	0.28	2.57	0.110	0.130	0.980

[a] With $\nu_{1C}=\nu_{1H}=62.5$ kHz, $\nu_r=3850$ Hz. [b] With $\nu_{1C}=30$ kHz (separate measurement). [c] $T_{1\rho}(^{1}H)=3$ ms.

Table 2. Falsification of the signal intensities by cross polarization. The magnetization M_0 corresponding to a true "spin counting" is falsified by a factor of $f(t)/\lambda$ on account of the cross polarization dynamics [Eq. (b)]. The smaller the difference in $f((t)/\lambda$ for the individual positions in the molecule, the better is the reproduction of the quantitative conditions in the spectrum. $f(t)$ was computed for two contact times t ($t=1$ ms and $t=2$ ms respectively) using equation (d) and the experimental times derived from Table 1. λ was taken from Table 1. The values in column 7 and the renormalized values (column 8) show that quantitativity is satisfied to an accuracy of $\pm 5\%$ for $t=2$ ms ($0.95 \le f(t)/\lambda < 1.05$).

C nucleus (Fig. 5)	λ [a]	$t=1$ ms			$t=2$ ms		
		$f(t)$ [b]	$\frac{f(t)}{\lambda}$	$\left(\frac{f(t)}{\lambda}\right)_{norm}$ [c]	$f(t)$ [b]	$\frac{f(t)}{\lambda}$	$\left(\frac{f(t)}{\lambda}\right)_{norm}$ [c]
C1	0.953	0.68	0.71	1.00	0.512	0.54	1.00
C2, C5	0.863	0.55	0.64	0.89	0.486	0.56	1.05
C3, C4	1.001	0.69	0.69	0.97	0.513	0.51	0.95
C6	0.980	0.66	0.67	0.94	0.510	0.52	0.97

[a] From Table 1. [b] Calculated according to equation (d) with the values from Table 1 for $t=1$ and 2 ms. [c] For easier comparison scaled to $f(t)/\lambda=1$ for CH_3 (C1).

As $T_{CH}/T_{1\rho}(^{13}C) \le 0.1$ and $T_{CH} \gg T_{1\rho}(^{1}H)$, the scaling factor λ differs for the individual positions in the epoxy resin only to a slight extent (cf. Table 1, $0.85 < \lambda \approx 1.0$). If the value of T_{CH} is short in comparison with $T_{1\rho}(^{13}C)$ and $T_{1\rho}(^{1}H)$, at least approximately quantitative cross polarization spectra are recorded, even without measurement of the cross polarization dynamics, as already described in the literature.[7b] However, it is necessary to ensure adequately long contact times, $t > 3T_{CH}$. The second term in $f(t)$ [Eq. (d)], which is dependent upon the C position, then approximates to the value zero and thus $f(t)$ becomes almost unitary (Table 2, $t=2$ ms $0.48 \le f(t) \le 0.52$). As the value of $T_{1\rho}(^{1}H)$ is unitary, too, as a result of spin diffusion, the first term in equation (d) is a constant for all positions in the molecule.

The condition of a contact time t which is long in comparison with the cross polarization constant T_{CH}, $t \ge 3T_{CH}$, clearly means that, for the sake of quantifiability, a measurement on the rising branch of the ^{13}C magnetization should be avoided (cf. Fig. 5). The price which is paid is a deterioration in the signal-to-noise ratio (cf. $f(t)/\lambda$ in Table 2 for $t=1$ and 2 ms; the magnetization of CH_3 (C1), for example falls from $0.71M_0$ to $0.54M_0$, i.e. to 2/3). On the other hand, the distortion of the signal intensities $f(t)/\lambda$ as compared with the true intensity ratios is very small at $t=2$ ms (Table 2, column 8, $\pm 5\%$).

To be able to evaluate quantitatively, measurements close to the $T_{1\rho}$ minima should be avoided. It is also true that the line widths increase close to $[T_{1\rho}(^{13}C)]_{min}$ (cf. Sections 2.1 and 5.3) and that close to $[T_{1\rho}(^{1}H)]_{min}$ the signal amplitudes decline strongly [Eq. (a)].

To sum up, then, sufficiently long contact times (≥ 2 ms) give spectra of homogeneous samples which are, as a rule, at least approximately quantitative, even without laborious normalization. It is not necessary to measure the cross polarization dynamics or to use calibration samples. An exception is systems which are strongly heterogeneous in terms of dynamics, e.g. polymeric glasses modified for high impact strength. In this case a quantitative comparison of the rubber and matrix signals is not permissible. The problem of quantifiability of partially crystalline samples has been investigated in detail with polyethylene as a model compound.[29]

3. Reaction Plastics

The application of high-resolution solid-state ^{13}C-NMR spectroscopy to insoluble polymer networks[7h] is, in particular, of industrial interest, since such cross-linked polymers participate in a multiplicity of processes which are important at the industrial level. Examples are, to mention just a few, the baking of enamels, controlled thermal decomposition in the production of carbon fibers, adhesion and coating processes, and especially the curing of resins.

Investigations, in addition to those on resins based on furfuryl alcohol[30] and polydiacetylene[31] as well as end-capped polyimides,[32] have principally been carried out on methacrylate-based resins,[33] urea/formaldehyde condensates[43] as well as phenolic[35] and epoxy resins.[7b, 19, 36]

In the case of the dimethacrylates, the investigations were aimed at the determination of the residual double

bonds[33c,d] and at the part played by the melamine/formaldehyde adduct, which is added in most cases. The hardening[33a,b] is essentially determined by the reaction of the hydroxymethyl groups of the melamine/formaldehyde. The extent to which it is possible to make statements concerning the number of hydroxymethyl radicals by means of solid-state NMR spectroscopy is shown by Figure 6. A

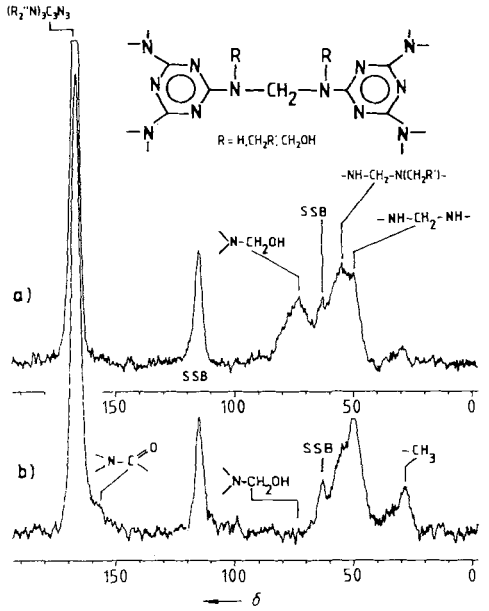

Fig. 6. Heat treatment of a melamine/formaldehyde condensate. a) After 2 h at 200 °C, a large number of hydroxymethyl groups is still present ($\delta \approx 70$). b) After 24 h at 240 °C, no CH_2OH groups can be detected any longer, but there are signs of degradation (CH_3 and $>N-CO-$); 1000 recordings in each instance, waiting time 2 s, $\nu_r = 3900$ Hz).

pure melamine/formaldehyde condensate (a foam) was used. At the end of the foaming process, there are initially considerable proportions of $N-CH_2OH$ functions, which can, however, be virtually entirely eliminated by subsequent tempering. A similar behavior is shown by urea/formaldehyde condensates.[34] It is important that tempering should not be excessive, since this would not only lead to oxidative decomposition, but also to the formation of methyl groups because of undesired reactions (Fig. 6). Both effects have also been observed in the case of phenolic resins, in spite of the different starting materials used.[35a] In order to monitor the hardening of phenolic resins and the formation of methylene bridges from the hydroxymethyl radicals, the contact time for the transfer of magnetization from ^1H to ^{13}C was varied. With the aid of model substances, suitable conditions of measurement for a quantitative determination of the ratio of methylene bridges to aromatic rings were found[35b] (cf. Section 2.2 with regard to quantitative evaluation).

Even at a very early stage, epoxy resins were investigated in detail using MAS-NMR spectroscopy;[36a,7b] such resins have great technological importance as matrix resins for composite materials consisting of polymer and carbon fibers embedded therein for strengthening. The epoxy resins are made from two components, which may be, for example, a bifunctional resin (diepoxide) and a diamine as tetrafunctional hardener. The network structure present in the finished articles (and thus also the mechanical properties) is critically dependent upon the final conversion obtained during curing. In the MAS-^{13}C-NMR spectrum (Fig. 7) measured for the cured resin, the individual signals can be correlated with the different chemical structures.[36b] The possibilities described in the literature with regard to solid-state NMR spectroscopy in the investigation of epoxy resins have recently been reviewed.[36c]

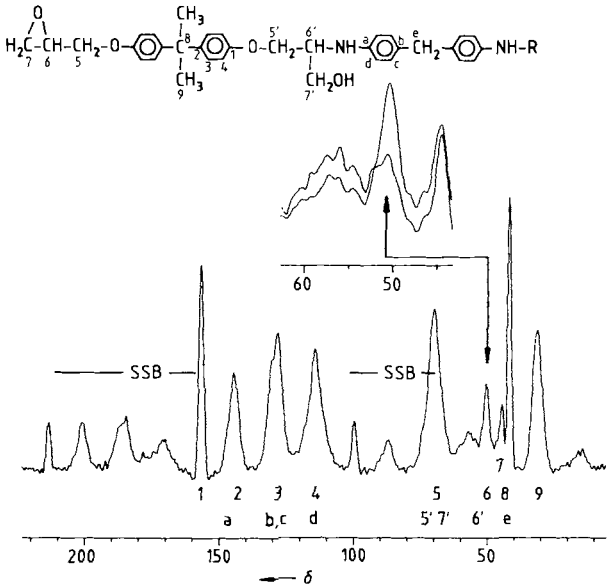

Fig. 7. Solid-state ^{13}C-NMR spectrum of an epoxy resin based on the diglycidyl ether of bisphenol-A (DGEBA), cured with 4,4'-diaminodiphenylmethane (DDM). By evaluating the epoxide signal (arrow, signal 6, $\delta = 53.7$) the epoxide content can be measured to an accuracy of approximately ± 0.04 epoxide units/bisphenol-A unit and the curing conversion can be determined. The figure shows the spectrum of the starting mixture containing 0.64 epoxide units/bisphenol-A unit and a partially cured sample containing 0.42 epoxide units/bisphenol-A unit. The signals 1 or 9 are suitable for internal standardization. They are not affected by superposition of DDM (4000 recordings in each instance, 2 s, $\nu_r = 4300$ Hz, CP 2 ms).

In epoxy resins too, the line width of the signals is essentially based on an inhomogeneous broadening, which arises as a result of a distribution of the values of the isotropic chemical shift on account of the differing conformations.[7b] In the case of the aromatic carbons *ortho* to the ether bond in bisphenol-A, at a low temperature a signal doubling was resolved. At room temperature and above, these two signals coalesce as a result of "chemical" exchange of the two *ortho* carbons by 180° ring flips. The correlation time of this movement was determined from investigations of the line shape and compared with mechanical relaxation data.[19]

Particular importance is ascribed to the question of the quantifiability of the spectra when it is desired to measure the curing conversion by means of NMR spectroscopy. One possibility consists in investigating the dynamics of the cross polarization[7b] and thus arriving at scaling factors for the areas of the individual signals (including sidebands) (cf. Section 2.2). Because of the necessity to evaluate areas, this process is, however, relatively inaccurate.

A more reliable and simpler method is the evaluation of the signal amplitudes of the solid-state NMR spectra of model substances (e.g. oligomers of the diglycidyl ether of bisphenol-A). If the model substances are soluble, it is possible to determine the epoxide content in solution and to plot calibration curves of the signal amplitude against the epoxide content. For this purpose, the signal of the central carbon (C6) in the glycidyl radical ($\delta = 53.7$, Fig. 7) is, for example, normalized internally with reference to another signal of bisphenol-A, e.g. to that of C9 ($\delta = 35.2$).

For a predetermined measurement condition, the residual epoxide content and thus an upper limit for the conversion can be determined by means of such a calibration line from the signal amplitude of the epoxide. Residual epoxide contents of up to approximately 1 epoxide/20 bisphenol-A are measurable and can be correlated with the curing conditions.

If cross-linkable thermoplastic materials are employed as matrix materials, it is possible to utilize the advantage of the thermoplastic processability and storage stability, without having to accept the sensitivity of non-crosslinking thermoplastic materials, for example, to solvents. Figure 8 shows the spectrum of such a cross-linking thermoplastic material based on aromatic thioether ether sulfones. After tempering at 350 °C, the homopolymer shows only a relatively small shift in peak intensity from $\delta > 130$ to $\delta < 125$, which is in accord with a partial neutralization of the pure *para*-substitution of the aromatic compounds by opening and reforming the thioether linkages. On the other hand, under the same temperature conditions a copolymer with bisphenol-A units (Fig. 8b) shows a drastic change of the spectrum (Fig. 8a). After 24 h at 350 °C, the spectrum still consists of the starting material spectrum only to the extent of a proportion of 50% in terms of area. In 12 h, the signals of the central propylidene unit in bisphenol-A ($\delta = 29$ and 41.6) fall to 60% of the initial intensity; after 24 h only 25% is still present, which demonstrates the direct participation of the comonomer in the cross-linking. In the case of a thermal cross-linking under the very drastic conditions chosen here, a multiplicity of in some cases very similar structures are produced. Accordingly, the difference spectrum between product and starting material (Fig. 8c) also shows only broad ^{13}C-NMR signals. However, this is not a weakness of MAS-NMR spectroscopy caused by the method itself, but a consequence of the fact that an unspecific reaction cannot generate a specific spectrum.

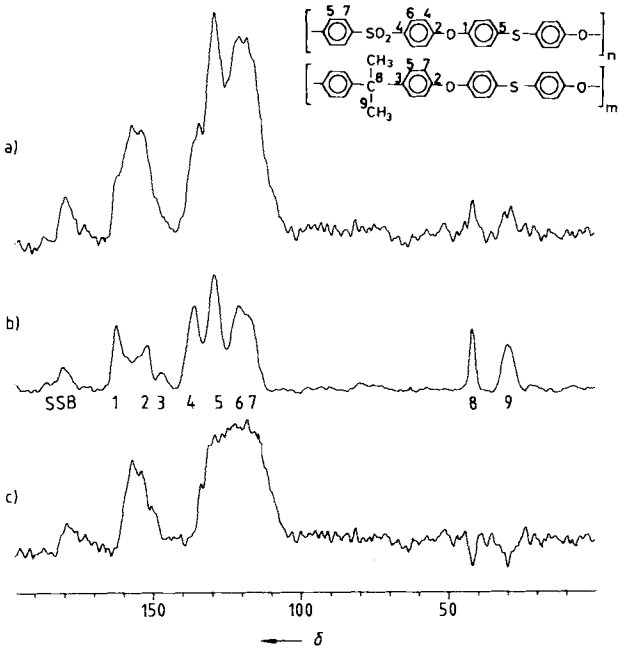

Fig. 8. Solid-state ^{13}C-NMR spectra of a cross-linking thermoplastic material consisting of a copolymer of poly(thioether ether) and poly(thioether ether sulfone). a) Spectrum after 24 h at 350 °C. b) Educt spectrum. c) Difference spectrum a–b. The spectrum a consists only to the extent of 50% of the educt signals. The signals (8 and 9) of the propylidene unit in bisphenol-A are reduced to 25%, which demonstrates participation of this unit in the cross-linking mechanism. The newly formed structures are non-unitary, as is evident from the difference spectrum showing poor resolution (at the bottom in the figure). (The sidebands have been eliminated mathematically.)

4. Physical Influences

A number of physical properties of the solid substance either influence the line position and line shape or determine the relaxation behavior of the nuclei (Table 3).

Table 3. Physical effects in CP/MAS-NMR spectra and their possible applications for the characterization of solid substances.

Effect on	by	Information on
Line position	conformation, packing	crystal structure, polymorphism, partial crystallinity
	coordination	catalysis
	chemical exchange	molecular dynamics, tautomerism, conformational transformations
Relaxation	spin dynamics, spin diffusion	amorphous components, high-impact modifier, block copolymers and graft content from relaxation time-selective spectra
	adjacency	polymer blends, plasticizers, antioxidants, heterogeneous systems
	molecular dynamics	block copolymers, additives, polymer mixtures, glass transitions, mechanical properties

It is precisely the physical influence on the spectra which broadens the range of application of CP/MAS-NMR spectroscopy considerably beyond the purely analytical application: as a result of the conformational effect on the *line position*, it is possible to obtain information concerning the conformation in the solid substance, and modifications and crystalline or amorphous components also become indirectly distinguishable (sections 4.1 and 4.2).

The combination of high resolution with *relaxation time measurements* gives, on account of the resolution of signals of individual positions of a molecule, very detailed information, at the local, molecular level, concerning the dynamics (Section 5) and the molecular adjacency relationships which are present (Section 4.4). However, the relaxation behavior may also be utilized with advantage for analytical applications, in order to achieve selectivity of the spectrum with respect to specified components in the case of heterogenous samples. Depending upon the selection of the experimental parameters, a determination is made in

terms of crystalline or amorphous material (Section 4.2), or in terms of the elastomer component or matrix (Section 4.3).

4.1. Conformation, Modification, Amorphous Components

The conformation plays an important part with regard to the line position in solid-state NMR spectra: two methylene signals are observed at a spacing of 8.7 ppm ($\delta = 39.6$ and 48.3 respectively) as a result of conformational nonequivalence in syndiotactic polypropylene[21] as a consequence of a γ-*gauche* effect.[37,38] In one half of the methylene groups, two γ-carbon atoms are present in the *gauche* (*g*) conformation, while in the other half both γ-carbons occupy the *trans* conformation. The conformation of isotactic polypropylene is distinct, in turn, from that of the syndiotactic polymer and gives a methylene signal at $\delta = 44.5$.[21,39] This is, besides polyvinyl alcohol,[22] one of the few examples where differing tacticities can be discerned in the solid-state NMR spectrum.

The methylene groups of the α- and γ-modifications of polypivolactone should be mentioned as a further example of a signal doubling as a result of conformational nonequivalence.[40]

Very much more frequent than the creation of two different conformations of otherwise equivalent positions of a molecule in the same crystal is the formation of differing conformations in polymorphism.

The modifications can then be detected because of the conformational effect on the chemical shift (see Fig. 3). Examples from the field of polymers are polybutylene terephthalate with a *gtg* conformation in the α form and *ttt* conformation in the β form,[41] α- and γ-polypivolactone (2_1 helix) in comparison with β-polypivolactone (planar zig-zag conformation)[40] and peptides (α-helix vs. γ-sheet).[17b,42] In the case of isotactic poly(1-butene), the various modifications differ only in the dihedral angle of the *gt* conformation, which is, however, sufficient for their identification by means of NMR spectroscopy.[39,43]

While in the above-cited cases the conformation and thus an *intra*molecular effect is responsible for the ability of NMR spectroscopy to distinguish the modifications, in other cases the conformations are the same and the modifications vary only in the nature of the packing of the polymer chains in the crystal. However, the *inter*molecular effect of the packing leads only to small differences in the signal position: $\Delta\delta = 0.8$ ppm between the α- and the β-modification of isotactic polypropylene[39] and 1.4 ppm between orthorhombic and monoclinic polyethylene.[29b]

In α-olefins of greater chain length (e.g. poly[(*S*)-3,7-dimethyl-1-octene]), the side chain is in rapid movement even in the solid state, and the carbon atoms of the side chain from C5 onwards are conformationally disordered.[44] Thus, the situation is very similar to that in the case of partially crystalline polymers, where the conformation, packing and mobility of the crystalline component differ from those of the amorphous component, which has appropriate consequences for the NMR spectrum: in addition to a sharper signal from the crystalline regions, there is a broader signal, frequently shifted in its position, from the chains in the amorphous region. This was first observed in polyethylene;[45] there have meanwhile been further examples, e.g. polyethylene terephthalate,[46] *trans*-polybutadiene,[47] polymethylene oxide[48] and polyethylene oxide.[14a,49]

In polyethylene (see Fig. 9a), the signal of the amorphous regions is shifted by 2.3 ppm upfield.[18b,45,50] The reason for this is the proportion of *gauche* conformations, which can be estimated from this difference in shift at approximately 1/3. By using cycloalkanes as model substances,[18a,51] an attempt was made to obtain information on the conformation of the folds contained in the amorphous covering layers of polyethylene single crystals.[18b] In this case, the problem resides principally in the low proportion by mass of the folds in the entire sample and thus the poor signal-to-noise ratio of the corresponding signals. On the other hand, with regard to solution-crystallized *trans*-polybutadiene it is known that, in spite of the restriction due to the adjacent re-entry of the chains, the folds of the chains adopt the same conformation as in entirely amorphous samples.[47]

4.2. Partial Crystallinity

In order to separate the signals from the crystalline and amorphous component respectively, use is frequently made of the very much shorter longitudinal relaxation time $T_1(^{13}C)$ of the amorphous regions.[52] In the case of direct ^{13}C-NMR signal generation using 90° pulses, short waiting times preferentially emphasize the signal originating from the amorphous regions (cf. Figs. 9a and 9b). The physical cause of the shorter $T_1^{am}(^{13}C)$ is the higher spectral density in the MHz range due to fluctuating fields on account of the higher molecular mobility. Since the transport of mag-

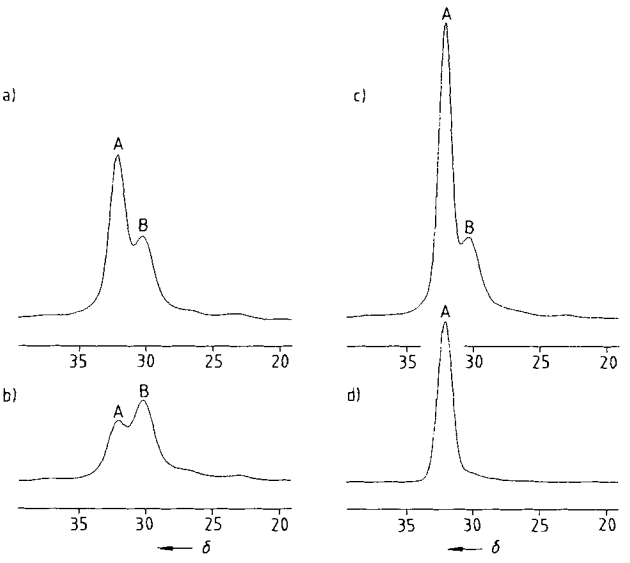

Fig. 9. Effect of conditions of measurement on the spectrum of polyethylene [56]. The conformational difference between the crystalline (all-*trans*) and the amorphous modification (*trans/gauche*) leads to the separated signals A and B ($\Delta\delta = 2.3$ ppm). a) 90° excitation, 800 s waiting time reproduces the correct intensities. b) 90° excitation, 4 s waiting time gives preference to the amorphous signal. c) CP contact (1 ms) gives preference to the crystalline signal. d) "Spin locking" of the protons (20 ms) before cross-polarization gives only the signal of the crystalline components. Scaling to the same amplitudes of B (a–c) and A (a, d).

netization through spin diffusion for ^{13}C nuclei at natural abundance is very slow as a result of the high degree of isotopic dilution, the $T_1^{am}(^{13}C)$ is determined by the high-frequency components of the local molecular dynamics: along the side chain of an ethylene-1-octene copolymer, the value of $T_1(^{13}C)$ rises on account of the increasing mobility.[53] Thus, in the stricter sense, $T_1(^{13}C)$ is not a phase property. Nevertheless, in appropriate systems a selectivity of the spectrum with respect to mobile (= amorphous) and rigid (= crystalline) components can be achieved as a result of the very much more rapid relaxation of the ^{13}C nuclei in the mobile component.

Whilst the mobile components are preferentially recorded in a rapidly repeated 90° pulse experiment, conversely in the case of polarization transfer from ^1H to ^{13}C with short contact times the signal of the crystalline component (cf. Figs. 9a and 9c) is maintained at an intensified level. The increased molecular mobility in the amorphous substance partially averages out the dipole-dipole interaction necessary for the transfer of magnetization from ^1H to ^{13}C, and leads to slower transfer rates $1/T_{CH}$ for the mobile (amorphous) components. Both in the case of selection via the more rapid longitudinal relaxation $T_1^{am}(^{13}C)$ of the mobile components and also in the case of selection of the rigid components via a short cross polarization contact (shorter T_{CH} in the rigid component), use is made of the molecular dynamics in order to make the distinction. The same applies to $T_{1\rho}(^{13}C)$, the relaxation time of the ^{13}C nuclei in the rotating coordinate system, which is likewise a quantity that is local at the molecular level and is determined by the dynamics in the median kHz range (cf. Section 5.2). Nevertheless, in rigid systems, $T_{1\rho}(^{13}C)$ is shortened by spin-spin processes, so that $T_{1\rho}^{am}(^{13}C) \gg T_{1\rho}^{cryst}(^{13}C)$ is applicable.[52a,54]

In cases where the association of rigid with crystalline and mobile with amorphous does not apply, the relaxation behavior of the protons must be used for selection. Spin diffusion between the protons leads to a volume averaging of the polarization state (cf. Section 4.4). Thus, for example, the question of the distribution of the ethyl branches over the two phases of semi-crystalline polyethylene was investigated by a $T_{1\rho}(^1H)$-NMR experiment[52a,56,57] preceding the cross-polarization as pre-contact delay[55] (Fig. 9d). Since ethyl side chains within the crystalline regions are certainly to be regarded as mobile, on account of their defect property in comparison with the crystallized main chain of the polyethylene, in this case a selection by means of the local molecular mobility, i.e. the relaxation of the ^{13}C nuclei, would lead to erroneous results.

4.3. Elastomer Components

The very much more rapid longitudinal relaxation of rubber components in a sample consisting of several components frequently permits the spectrum of the elastomer components to be selectively recorded without special preparation of the samples, by means of 90 degree ^{13}C pulses.

In order to achieve decoupling of the residual dipolar interaction between ^1H and ^{13}C, it is sufficient to provide a "low power decoupling" (LPD) similar to that employed in NMR of solutions, since the dipolar interaction is to a large extent averaged out just by the high molecular mobility and the sample rotation at the magic angle.[50]

In this way, investigations were carried out not only on the homopolymers[58] but also, for example, on a polypropylene grafted with butadiene, in order to determine quantitatively the proportion of grafts.[59] Even in the case of segmented copolymers consisting of poly(tetramethylene terephthalate) hard segments and poly(tetramethyleneoxy-terephthalate) soft segments

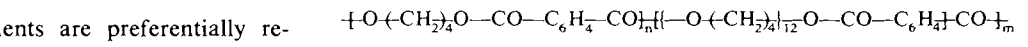

(Hytrel®)

only the soft phase is recorded at 90° ^{13}C excitation and low power decoupling.[60] The same applies to poly(acrylonitrile-butadiene-styrene) block copolymers (ABS), in which case the spectrum is selectively measured for the butadiene blocks, for which the glass transition temperature is far below room temperature.[61] In the case of polybutadiene, the resolution is so good that a sequence analysis of the microstructure is possible as far as triads. In the case of ABS, cross polarization and dipolar decoupling give, as a complement to the 90°-LPD measurement, the spectrum of the styrene-acrylonitrile blocks. In analogous terms, Figure 10 shows two spectra of a poly(styrene-butadiene-isoprene) block copolymer.

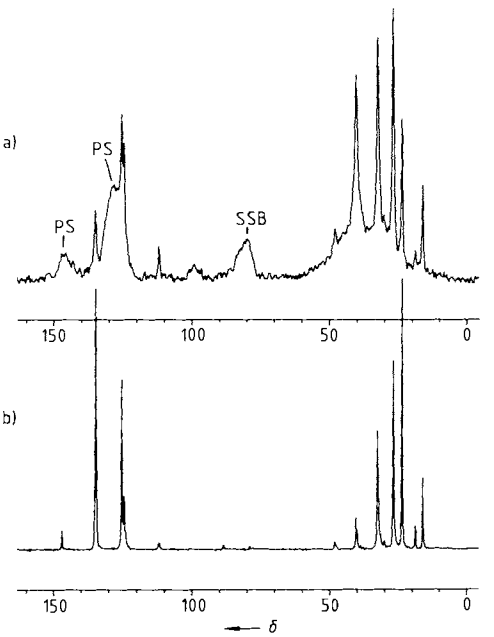

Fig. 10. Solid-state ^{13}C-NMR spectra of a poly(styrene-butadiene-isoprene) rubber. a) CP 2 ms gives the polystyrene signal PS (17%) (20000 recordings FIDs broadened by 30 Hz with exponential multiplication). b) Polyisoprene component, measured with 90°-τ-180°-τ-AQ, $\tau = 2.9$ ms (6000 recordings, waiting time 0.1 s, low power decoupling (LPD), inverse gating).

Figure 11 also follows the idea of the selective recording of the soft phase by a 90°-LPD experiment, in this case with the investigation of an unsaturated polyester resin (UP resin) which is toughened by rubber particles. The detection of a rubber in such a matrix, which is also frequently filled

with glass fibers, confronts other techniques with particular problems: the matrix is insoluble and double bonds are invariably present in a UP resin on account of incomplete conversion.

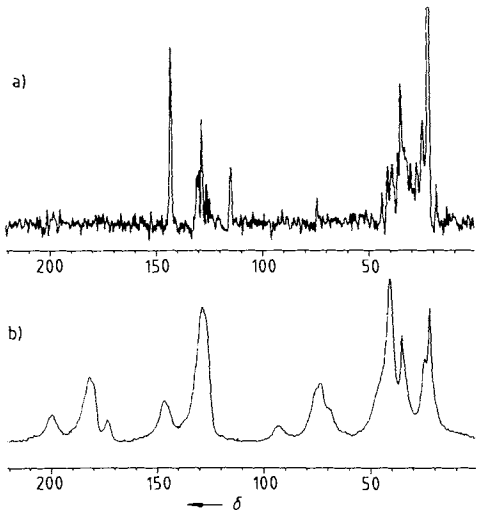

Fig. 11. Detection of 5% rubber (poly(styrene-butadiene) with 20% styrene) in a matrix consisting of unsaturated polyester (adipic acid/neopentyl glycol/maleic acid/styrene). a) Rubber signal (90000 recordings as in Fig. 10b, $\tau = 2.5$ ms, waiting time 0.5 s). Attention is drawn to the high 1,2 linkage content (signals at $\delta = 142.7$ an 114.6). Only CH_3 groups of the matrix ($\delta = 21.8$) are included in the recording. b) Matrix signals (CP 1 ms, 4000 recordings, dipolar (DD) decoupled with $\nu_{1H} = 50$ kHz).

MAS-NMR not only detects the rubber (in the present case 5% by weight), but also permits statements concerning the chemical structure of the rubber employed (a polybutadiene with a considerable proportion of 1,2 linkages).

If the proportions of the soft phase amount to a few percent only, rapid 90° excitation and low power decoupling are frequently not sufficient to suppress the matrix signal entirely. Accordingly, in the examples given (Figs. 10 and 11), use was additionally made of the fact that under the condition of weak decoupling the signals of the soft phase are very much narrower (longer T_2) than those of the hard phase: a 180° pulse of the ^{13}C nuclei within the longer free induction decay of the rubber component refocuses only the signals of the rubber, whereas the broad signals from the matrix are already irreversibly relaxed. Thus, even in the case of difficult samples, what is obtained is the rubber signal without the broad matrix and blank signal background (Fig. 11).

Rubbers are usually measured by direct 90° excitation of the ^{13}C nuclei, since cross polarization is based on dipole–dipole interaction and is therefore of low effectiveness, on account of the high molecular mobility. Nevertheless, cross polarization represents an alternative of interest even for pure elastomers: by variation of the mismatch of the Hartmann-Hahn condition ($\gamma_C \boldsymbol{B}_{1C} \neq \gamma_H \boldsymbol{B}_{1H}$) or alteration of the speed of rotation of the rotor, statements can be made on the degree of cross-linking of the rubber.[62]

4.4. Molecular Neighborhood: Blends

While the ^{13}C relaxation times $T_1(^{13}C)$, $T_{1\rho}(^{13}C)$ and T_{CH} are quantities which are individual to each position in the molecule, in the $T_{1\rho}$ of the *protons* there is a volume property averaged over a distance of approximately 2 nm.[63] The cause of this spatial averaging of $T_{1\rho}(^1H)$ is the small mean distance between the ^1H nuclei, since ^1H is an abundant nucleus, in contrast to the "rare" nucleus ^{13}C. As a result of the spatial closeness of the protons to one another, an exchange of spin energy of the individual protons within the transverse relaxation time $T_2(^1H)$ takes place, i.e. in rigid systems within less than 0.1 ms.

The residual ^1H magnetization at the end of the spin-lock time in the $T_{1\rho}(^1H)$-NMR experiment is not measured directly. Instead, a polarization transfer $^1H \rightarrow {}^{13}C$ is undertaken and the ^1H magnetization is detected indirectly via the ^{13}C-NMR signal (Fig. 12).

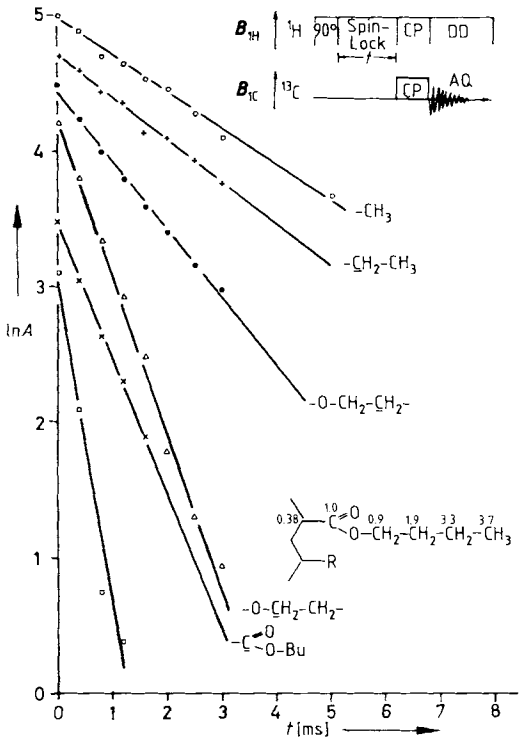

Fig. 12. Indirect measurement of $T_{1\rho}(^1H)$ of the protons of solid polybutyl acrylate via the ^{13}C-NMR spectrum (298 K). The proton magnetization is "locked" after 90° excitation for a variable time t in the radio-frequency field, and the remaining magnetization is detected by cross polarization with a fixed contact time. At room temperature, the T_2 of the protons is too long to produce a common $T_{1\rho}(^1H)$ by spin diffusion; individual values of $T_{1\rho}(^1H)$ [ms] in the formula (10240 recordings in each instance, CP 1 ms, ordinates arbitrarily shifted, $\nu_C = 3000$ Hz, $\nu_{1H} = 50$ kHz, D_2(contact time, already given as CP 1 ms) = 1 ms). □ measured values for skeleton C atoms.

This process appears at first sight to be awkward and of little advantage, since the experiment becomes more complicated on account of the indirect detection of the ^1H magnetization. Moreover, there is a loss by a factor exceeding 1000 in the signal-to-noise ratio. However, the benefit of the indirect detection of the $T_{1\rho}$ of the protons via ^{13}C resides in that this process combines the high resolution of the MAS-^{13}C-NMR spectrum with a volume property, namely $T_{1\rho}(^1H)$. In view of the fact that the remaining ^1H magnetization is detected at the end of a specified ^1H spin-lock time via the signal amplitude of a ^{13}C-NMR signal, which is to be correlated with a quite specific

chemical structure, the $T_{1\rho}(^1H)$ can be interrogated in the environment of this structure.[64] If, for example, a blend of two polymers A and B is present, which differ in their solid-state ^{13}C-NMR spectra, the $T_{1\rho}(^1H)$ can be separately determined in the environment of molecules of type A and B respectively by evaluation of the signals from A and B respectively. If there is molecular miscibility of A with B in the sense of a spacing of less than 2 nm, what is expected is a common $T_{1\rho}^{AB}(^1H)$, or otherwise, depending upon the $T_{1\rho}(^1H)$ of the homopolymers, two separate $T_{1\rho}^{A}(^1H)$ and $T_{1\rho}^{B}(^1H)$ values. This process was employed in the first instance with blends of polystyrene and polyphenylene oxide[65] and later with polystyrene/polyvinyl methyl ether[66] and polyvinylidene fluoride/polymethyl methacrylate.[67]

Two different measurement processes are possible for the measurement of $T_{1\rho}(^1H)$ via ^{13}C.[55,65b] The more frequently employed pulse program varies the length of the CP contact and determines the $T_{1\rho}(^1H)$ from the ^{13}C-NMR signal amplitudes for long contact times[65b] (cf. Fig. 5). The advantage is that it is possible to determine the magnetization transfer rate $1/T_{CH}$ with short contact times by the same measurement program. However, the evaluation presupposes $T_{CH} < T_{1\rho}(^{13}C) \ll T_{1\rho}(^1H)$ and moreover the beginning of the $T_{1\rho}(^1H)$ curve is absent. During the spin lock time the ^1H and the ^{13}C nuclei are irradiated simultaneously, so that the sample head has to cope with a relatively high power. As an alternative to the $T_{1\rho}(^1H)$ measurement via variable length of the contact time, it is possible in the first instance to carry out the ^1H spin-lock experiment, and only at the end of the ^1H spin-lock time to cross-polarize with a fixed contact time as usual.[55] The latter process (Fig. 12) was used, which avoids the disadvantages mentioned above and is more reliable in terms of evaluation. Last but not least this procedure permits the selective recording of a specified phase by means of a suitable contact time in the case of heterogeneous systems.

A system which is of interest for such investigations with regard to molecular miscibility comprises dispersions, made into films, obtained by emulsion copolymerization. This may be, for example, a butyl acrylate/acrylic acid copolymer, which was produced by emulsion polymerization. Such films from emulsions are spatially heterogeneous with one phase predominantly containing the hydrophobic building block (in this case the butyl acrylate), and other regions which principally consist of a polymer of the hydrophilic monomer (in this case, acrylic acid). The question of how sharp the separation is, i.e. to what extent, for example, the acrylic acid is also present in the phase rich in butyl acrylate, can be investigated by such $T_{1\rho}(^1H)$ measurements. What is important is to select the correct temperature for the measurement: in the case of elastomers such as, for example, polybutyl acrylate ($T_G = -46\,^\circ C$), at room temperature the proton line width under MAS conditions amounts to only approximately 150 Hz. The proton-proton dipolar interaction is averaged out by the molecular mobility to such an extent that an individual $T_{1\rho}(^1H)$ is measured for the protons at each position in the butyl radical of the polybutyl acrylate homopolymer (see values [ms] quoted in the structural formula in Fig. 12). As is expected, the ^1H line width increases rapidly with decreasing measurement temperature. At $-25\,^\circ C$ it reaches approximately 13 kHz, and thus leads to a common $T_{1\rho}(^1H)$ (Fig. 13). When acrylic acid is incorporated as co-

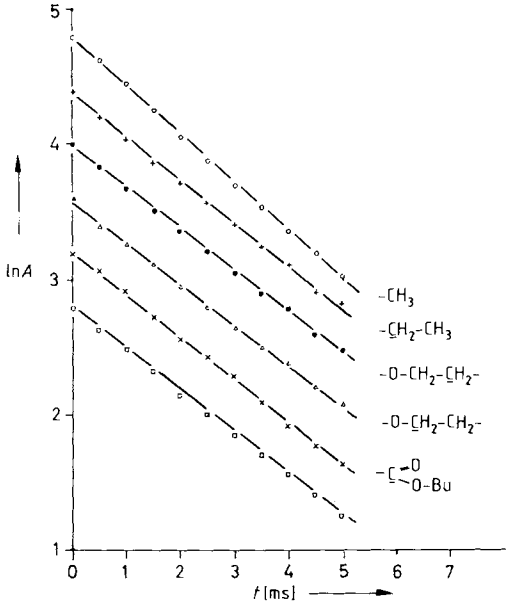

Fig. 13. $T_{1\rho}(^1H)$ via ^{13}C in a dispersion made into a film (emulsion copolymer consisting of 85% butyl acrylate (BA) and 15% acrylic acid (AA)). At 248 K, spin diffusion leads to a unitary $T_{1\rho}(^1H)$ for all protons (768 recordings in each instance, otherwise conditions as in Fig. 12). □ measured values for skeleton C atoms.

monomer into the phase rich in polybutyl acrylate, the glass transition temperature should rise in comparison with the homopolymer consisting of polybutyl acrylate. This is why a temperature of $-25\,^\circ C$ satisfies the requirements with regard to adequate spin diffusion for the copolymer as well. Therefore $T_{1\rho}(^1H)$ is a volume property. The evaluation of the signal amplitudes as a function of the proton spin lock time is, in fact, purely exponential and gives a unitary $T_{1\rho}(^1H)$ for all signals. This $T_{1\rho}(^1H)$ is between the values for the homopolymers polybutyl acrylate and polyacrylic acid respectively, and shows that acrylic acid and butyl acrylate in the phase rich in butyl acrylate are present alongside one another at a spacing of less than 10 Å (Fig. 14).

On the other hand, a non-exponential decline of the signal amplitude in the $T_{1\rho}(^1H)$-NMR experiment cannot be taken as unambiguous evidence leading to the opposite conclusion as to a multiphase system.[68]

In addition to the $T_{1\rho}(^1H)$ measurement via ^{13}C, there are certain other CP/MAS NMR techniques for detecting molecular adjacency. These include the intermolecular magnetization transfer from a molecule containing ^1H to a deuterium-containing polymer. However, this presupposes the availability of a corresponding deuterium-containing polymer, and is accordingly a process which is not suitable for the investigation of commercial products. But it can certainly answer questions concerning the fundamental understanding of, for example, the functioning of block copolymers as compatibility promotors in blends. Thus, the formation of a mixture of the styrene block from a

poly(styrene-butadiene) block copolymer with the surrounding styrene matrix was demonstrated,[69] but also block copolymers of polyether/polyester segments[70] and the miscibility of polystyrene with polymethyl methacrylate or polyvinyl methyl ether[71] were investigated. Furthermore, the compatibility of low-molecular-weight additives with the polymer matrix and selective interactions of these additives with functional groups of the polymer are detectable by intermolecular cross polarization, as has been demonstrated for a photoconductive compound in a polycarbonate matrix[72] and a plasticizer in PMMA.[70]

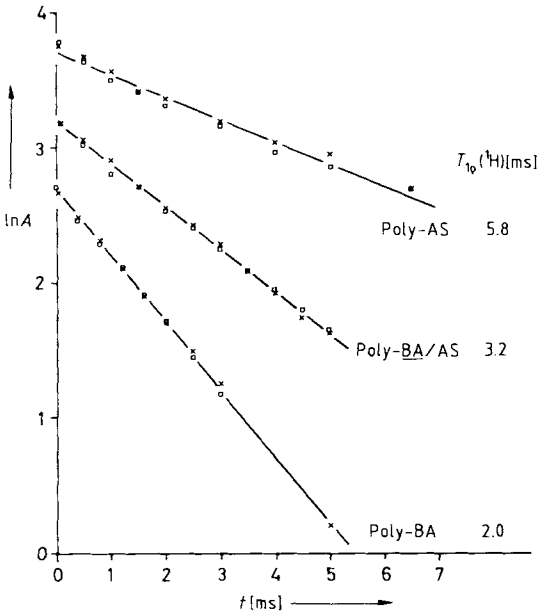

Fig. 14. $T_{1\rho}(^1H)$ via ^{13}C of polyacrylates for the detection of molecular adjacency. The emulsion copolymer, made into a film, consisting of BA/AA (85/15% by weight) shows a $T_{1\rho}(^1H)$ between the corresponding values for the homopolymers (P-BA/AA: 3.2 ms, P-BA: 2.0 ms, P-AA: 5.8 ms). The phase rich in butyl acrylate contains polymerized acrylic acid at the molecular level (presumably as comonomer) (conditions of measurement as in Fig. 13). × –COO–, □ skeleton C atoms.

Instead of using the $1/r^3$ dependence of the C–H dipolar interaction upon the C–H spacing r for the detection of adjacency by intermolecular cross polarization, it is possible to use the dipolar interaction with a nucleus, e.g. ^{19}F, which, in contrast to ^1H, is not decoupled, in order to demonstrate adjacency: this is true of suitable systems, as has been proved for a number of polyvinylidene(PVF_2) blends. In the event of miscibility, the adjacency of ^{19}F nuclei broadens the ^{13}C-NMR signal of the admixed components at ^{13}C–^{19}F spacings of ca. 0.1 nm, in such a manner that the ^{13}C nuclei adjacent to the ^{19}F nuclei are no longer recorded in the MAS-NMR experiment and a reduction of the signal intensities results, as has been shown for PVF_2/PMMA and other PVF_2 blends.[67a,73]

Finally, in order to demonstrate adjacency, it is possible to use the homonuclear dipole–dipole interaction and to measure directly the residual protons in an (almost) deuterated matrix. If a ^1H-containing polymer is admixed, only isolated ^1H nuclei are measured as sharp lines, and their intensity evaluated.[74] Whilst here, as a result of the deuteration, ^1H becomes the "rare" nucleus, ^{13}C can conversely also be abundant, as a result of ^{13}C enrichment, so that intermolecular spin diffusion from the ^{13}C-labeled molecule (e.g. a plasticizer) to the unlabeled neighbor (the polymer) becomes possible.[75] If both components are ^{13}C-labeled, as in the case of a polyethylene terephthalate/polycarbonate mixture,[76] it is finally possible for spin diffusion between the ^{13}C nuclei to be used for the investigation of blends in the same way as in the case of ^1H multipulse MAS-NMR experiments.[77]

5. Molecular Dynamics

Relaxation time measurements under CP/MAS conditions give individual ^{13}C-relaxation times for the positions in the molecule which are resolved in the spectrum.[64] This gives rise to the hope that it will be possible to investigate the molecular dynamics of the pertinent group in this way.

5.1. Longitudinal Relaxation Time $T_1(^{13}C)$

Measurements[78] of the longitudinal relaxation time $T_1(^{13}C)$ are used to detect motions with a spectral density in the region of the Larmor frequency, i.e. in the MHz range. In the case of polymers in the glassy state, by reason of this high frequency, it is frequently a methyl group which determines the relaxation behavior, in the event that such a group is present: the dipole field which is generated by the protons of the rapidly rotating methyl group contributes most strongly to the fluctuations in the range of high frequencies at the location of the neighboring ^{13}C nuclei, although the effectiveness of the dipole field for the relaxation decreases strongly with the distance r ($\sim 1/r^6$). In polymethyl methacrylate, the α-CH_3 group, for which room temperature is above the T_1 minimum,[79a] determines the T_1 behavior of the polymer chain as well.[79b] The mobility of the polymer chain does not contribute to the spectral density in the MHz range, so that, even when the glass point is exceeded, the effects on the T_1 value of the carbon atoms in the chain are small.[79c] For the same reason, plasticizer effects in the case of PMMA[79b] are not detectable via $T_1(^{13}C)$, in contrast to polycarbonate.[80] However, in the case of PMMA,[81a] just as in the case of polyethylene oxide,[81b] T_1 can be employed for the selective recording of the amorphous component (see Section 4.2).

When elastomers are analyzed, individual $T_1(^{13}C)$ relaxation times can also be measured using a stationary sample. The position of the $T_1(^{13}C)$ minimum in the case of a stationary measurement but with variable temperature is dependent upon the content of 1,2 linkages, in the case of polybutadiene. If it is borne in mind that the T_1 minimum occurs at correlation times which correspond to the Larmor frequency, then good agreement is found between the temperature of the T_1 minimum and the glass point of the samples.[82] Stationary investigations were likewise carried out above the glass point on polyterephthalic acid esters and polysuccinic acid esters respectively.[83]

5.2. Relaxation in the Rotating Coordinate System, $T_{1\rho}(^{13}C)$

A matter of particular interest for the investigation of polymers is the relaxation time in the rotating coordinate system, $T_{1\rho}(^{13}C)$[64] (Fig. 15). The amplitude of the radio-

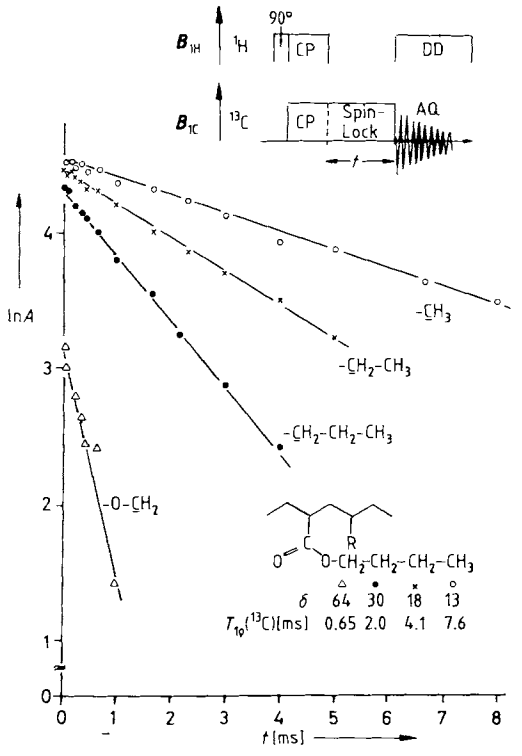

Fig. 15. $T_{1\rho}^{*}(^{13}C)$ of polybutyl acrylate at 283 K. The usual generation of the signal via a CP contact is followed by a "spin locking" of the ^{13}C nuclei for a variable time t. The plot of the signal amplitudes as a function of t gives, as a reciprocal of the gradients of the straight lines, individual relaxation times $T_{1\rho}(^{13}C)$ for the various positions in the molecule (768 recordings in each instance, CP 0.75 ms, $\nu_r = 3000$ Hz, $\nu_{1C} = 25$ kHz.

frequency field which is applied during the relaxation and which is parallel to the magnetization determines the frequency $\nu_{1C} = \omega_{1C}/(2\pi)$ of the spins within the rotating coordinate system. Molecular motions having a spectral component at this frequency are of crucial importance for the relaxation. In the case of the conventional radio-frequency field strengths, this is 25 kHz–75 kHz. Now, the median kHz range is of particular interest in the case of polymers, since the mechanical properties are also governed by the molecular dynamics in this frequency range.

The interpretation of $T_{1\rho}(^{13}C)$ data, however, is complicated by the fact that the relaxation in the rotating coordinate system is caused by the fluctuating dipole fields of the protons.

This fluctuation can arise on account of changes of the C–H bond vector $\boldsymbol{r}$, e.g. a change of direction in the case of the rotational diffusion of a methine group. This phenomenon (i.e. the change of $\boldsymbol{r}$) is referred to as spin-lattice relaxation, and it is possible to draw conclusions as to the molecular dynamics from $T_{1\rho}(^{13}C)$. However, the measured $T_{1\rho}^{*}(^{13}C)$ [Eq. (e)] consists of two possible components, the spin-lattice $T_{1\rho}(^{13}C)$ just mentioned and a possible spin-spin contribution T_{CH}^{D}.[14b,28,54,64]

$$\frac{1}{T_{1\rho}^{*}(^{13}C)} = \frac{1}{T_{1\rho}(^{13}C)} + \frac{1}{T_{CH}^{D}} \qquad \text{(e)}$$

It is indeed possible for fluctuating dipole fields to be generated not only by molecular dynamics but also by a change of the spin state of the proton adjacent to the ^{13}C nucleus. In this case, the dipole field at the location of the ^{13}C nucleus changes, without a change of the space coordinates of the molecule being associated with this. Thus, relaxation due to such spin-spin processes does not give any information on the molecular dynamics. Before measured $T_{1\rho}^{*}(^{13}C)$ values can be interpreted in terms of molecular dynamics, it must be certain that the spin-spin relaxation time $T_{CH}^{D} \gg T_{1\rho}(^{13}C)$, i.e. the spin-lattice relaxation $T_{1\rho}(^{13}C)$ determines the measured $T_{1\rho}^{*}$.[84a] T_{CH}^{D} can be measured separately.[28,84b] It becomes evident that the condition $T_{CH}^{D} \gg T_{1\rho}(^{13}C)$ in the case of amorphous polymers is also satisfied in the glassy state, as is the case for plastic crystals at room temperature. In amorphous polymers, the measured $T_{1\rho}^{*}(^{13}C)$ is predominantly ($\approx 80\%$) determined by spin-lattice processes, and may thus be interpreted in terms of molecular dynamics.[54b] Polystyrene, polymethyl methacrylate and polyphenylene oxide, as well as polyethylene terephthalate and polycarbonate, may serve as examples.[28,54b,64,84b] However, when rigid polymers with strongly coupled protons are analyzed, and particularly when crystalline samples are used, spin-spin relaxation is predominant, as for example in the case of polyethylene[54a] and polyoxymethylene.[28] Besides the homopolymers, investigations were also carried out on poly(ether-ester) block copolymers[85] and anti-plasticizer effects on polycarbonate.[86] Measurements on polypropylene with variable measurement temperatures[87] do indeed indicate spin-lattice processes determining the relaxation at a low temperature, in which connection, however, the movement of the CH_3 groups contributes to relaxation. For this reason, statements concerning the dynamics of the main chain were not possible. Relaxation due to the rotation of the CH_3 groups is likewise found in PMMA.[88] Furthermore, a cured epoxy resin was investigated over a broad temperature range, and the relaxation was at least predominantly ascribed to spin-lattice processes.[89] Apparently a very broad correlation time distribution is present, since $T_{1\rho}(^{13}C)$ hardly varied at all with the temperature.

Figure 16 shows an example with a marked $T_{1\rho}(^{13}C)$ minimum, as is expected for spin-lattice-determined $T_{1\rho}(^{13}C)$. On account of the measurement frequency of 25 kHz, the minimum is situated approximately 30 K above the glass point ($T_G = -46\,^{\circ}C$). In the case of copolymerization of the butyl acrylate with acrylic acid, the position of the minimum is shifted by approximately 10 K (Fig. 17); a value of 9 K was measured by differential scanning calorimetry.

With an adequate radio-frequency field strength a clear dominance on the part of spin-lattice processes can be expected, particularly in the vicinity of the $T_{1\rho}^{*}$ minimum. This dominance also extends into the temperature range above the minimum provided that the rotational diffusion is not excessively anisotropic.[54a] This likewise applies below the minimum, at least for the quaternary carbons which are less strongly coupled to ^1H and for methyl

groups, both of which show an appropriately marked $T^*_{1\rho}(^{13}C)$ minimum (Fig. 16). At the minimum, the correlation time τ of the motion causing the minimum can be inferred from $\omega_{1C}\tau = 1$. The depth of the minimum is determined by the magnitude of the second moment, modulated by the variation of the C–H dipolar interaction.[14b, 54a] Accordingly, the expectation for all CH_2 groups is the same $[T^*_{1\rho}(^{13}C)]_{min}$ and that for quaternary C is a longer $[T^*_{1\rho}(^{13}C)]_{min}$, as, in fact, is verified (Fig. 16). The large

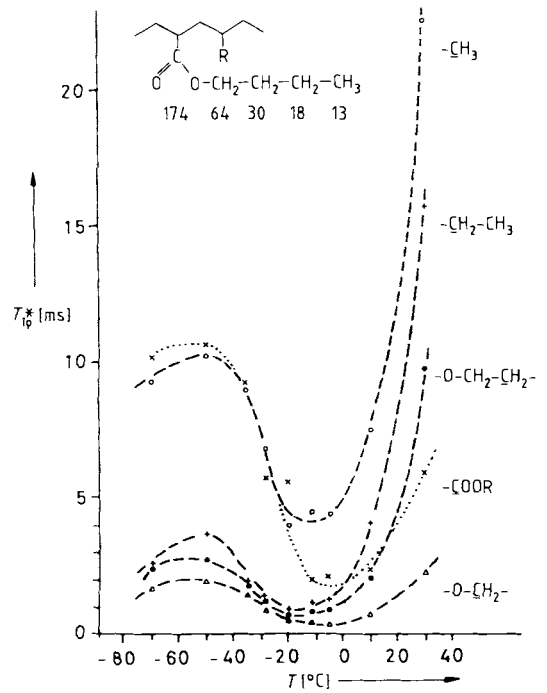

Fig. 16. $T^*_{1\rho}(^{13}C)$ of polybutyl acrylate as a function of temperature. At the minimum, the correlation time $\tau = 1/(2\pi\nu_{1C})$ of the motion ($\tau = 6.4$ µs) is obtained from the "spin lock" frequency ν_{1C}. As a result of the frequency of $\nu_{1C} = 25$ kHz, the position of the minimum is shifted by approximately 30 K above the glass-transition temperature. $\nu_r = 3000$ Hz.

long $T^*_{1\rho}(^{13}C)$ of the CH_3 groups at the minimum is due to the rotation which is still present about the ternary axis, and corresponds to the finding that the cross-polarization behavior of CH_3 groups is also rather similar to that of CH groups (cf. Fig. 5 and the $1/T_{CH}$ value in Table 1).

In the copolymer of butyl acrylate with 10% by weight of acrylic acid, all butyl positions have a minimum of the same depth as in the homopolymer. On the other hand, the position of the minimum is shifted by 10 K towards a higher temperature. An exception with regard to the magnitude of $[T^*_{1\rho}(^{13}C)]_{min}$ is the C nucleus of the carboxy group, whose $[T^*_{1\rho}(^{13}C)]_{min}$ rises from approximately 2 ms (homopolymer) to 3.2 ms in the copolymer (Fig. 17). A broader distribution of the correlation times can be ruled out as a possible reason, since the shape of the $T^*_{1\rho}(^{13}C)$/temperature curve is, in the case of the copolymer, the same as in the case of the homopolymer. There remains a greater anisotropy of the motion as a possible cause, presumably on account of hydrogen bonds between the ester and acid radicals.

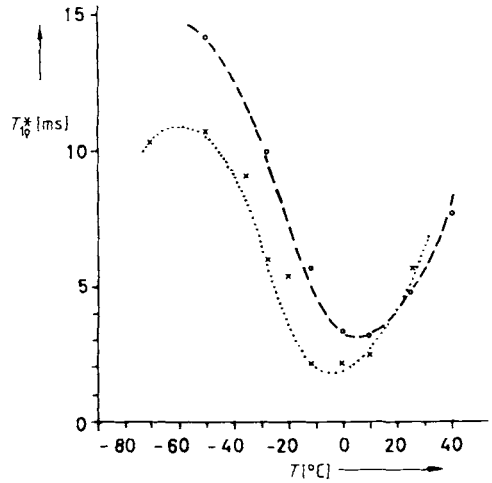

Fig. 17. $T^*_{1\rho}(^{13}C)$ of the BA-carboxy group of the BA-homopolymer (×) and of a copolymer (○) consisting of BA/AA (85/15% by weight). In the copolymer, the position of the minimum is shifted by approximately 10 K, corresponding to the rise in the glass transition temperature. The greater $T^*_{1\rho}(^{13}C)$ at the minimum in the case of the copolymer is presumably due to a higher degree of anisotropy of the carboxy group motion due to hydrogen bonds.

5.3. Transverse Relaxation $T_2(^{13}C)$

The transverse relaxation rate $[T_2(^{13}C)]^{-1}$ is affected by the spectral density at the frequency ω_{1H} of the protons in the rotating coordinate system under the influence of the decoupling field. If no other effects determine the line width $\Delta\nu_C$ of the ^{13}C-NMR signal, then $\Delta\nu_C \sim 1/T_2(^{13}C)$ is applicable, and $\Delta\nu_C$ passes through a maximum when the stochastic dynamics possesses the same frequency as the coherent decoupling. In the event of equality of frequency, the latter becomes inefficient.[23] In CP/MAS-NMR spectroscopy, the Hartmann-Hahn condition[4a] $\omega_{1C} = \omega_{1H}$ is usually satisfied for the purpose of cross polarization, and the angular frequency in the radio-frequency field is equal for ^1H and ^{13}C (Section 2.2). In the $T_{1\rho}(^{13}C)$-NMR experiment, the spectral density is detected at ω_{1C} (cf. Section 5.2). $T_2(^{13}C)$ (or the line width $\Delta\nu_C$ of the ^{13}C-NMR signal) is determined by the spectral density at ω_{1H}. Thus, for $\omega_{1C} = \omega_{1H}$ in CP/MAS-NMR experiments, both $T_{1\rho}(^{13}C)$ and also $T_2(^{13}C)$ are affected by the same spectral density.[20] Accordingly, the line width of the ^{13}C-NMR signal should pass through a maximum at the $T_{1\rho}(^{13}C)$ minimum, if the molecular dynamics determine the two quantities. This is in fact the case for polybutyl acrylate (compare Fig. 16 with Fig. 4).

As the measurement of relaxation times only permits statements on the spectral density at the measurement frequency no information on the geometry of the movement can be obtained for isotropic samples. If, for example, we add a plasticizer to polystyrene,[90] no distinction can be made as to whether the reduction of the $T_{1\rho}(^{13}C)$ is based on a change in the frequency of the motion or its amplitude. Only processes which utilize the anisotropy of a magnetic interaction permit statements on the geometry of the motion. They include the two-dimensional methods[10] of the "dipolar rotational spin-echo"[91] and of the "chemical exchange"[92] under MAS conditions. The "dipolar rotational spin-echo" experiment is based on the dipolar inter-

action of a C–H pair, in which connection the homonuclear interaction of the protons with one another must be suppressed by multiple-pulse sequences. Investigations were carried out principally on polycarbonate[91b] and polystyrene.[91c] The selectivity with respect to a specified position in the molecule is achieved, in the case of the "dipolar rotational spin-echo", by MAS-NMR spectroscopy via the chemical shift. In contrast to this, for the evaluation of powder spectra of stationary samples[93] it is necessary to have ^{13}C-labeled substances, i.e. the selectivity is obtained by a preparative route, as in the case of deuteron-NMR spectroscopy.

In two-dimensional exchange spectroscopy[92] information on jump angles and correlation times is obtained from the anisotropy of the chemical shift. The possibilities offered by this process regarding the investigation of slow motions[10] with correlation times τ_c in the range $T_1 > \tau_c > 1$ ms have been demonstrated with reference to the example of polyoxymethylene.[92b]

6. Summary and Outlook

The recording of solid-state ^{13}C-CP/MAS-NMR spectra is now no longer a problem; however, when measurement at variable temperature is concerned, this statement is only partly true. If we have sufficient prior knowledge of the sample, the chemical structures in the compounds which exhibit low solubility or are insoluble are accessible by means of this technique. When dealing with partially crystalline samples, familiarity with the particular solid-state effects on the spectrum is required. Where soluble compounds are concerned and where chemical analysis only is involved, recourse will also be had in future to NMR spectroscopy in solution, since the line widths achievable in solution are smaller by more than an order of magnitude.

Quite apart from the analytical application in the case of insoluble samples, the strength of solid-state CP/MAS NMR spectroscopy becomes clear in two areas: it becomes evident in the techniques for correlating chemical shifts (= chemical structure) with the relaxation behavior (= dynamics, adjacency). By this means, it is possible to make very detailed statements on the dynamics of individual positions in the molecule. A second strength resides in the possible selectivity which in the case of heterogeneous samples can be achieved by utilizing the relaxation behavior. Simply by selecting the measurement conditions, i.e. without sample preparation, it is possible to investigate selectively the chemical structure, molecular dynamics and possibly the orientation of a specified component of the sample. It is precisely this selectivity which is of great advantage in connection with the frequently very complex composition of industrial products.

By way of analogy with NMR spectroscopy in solution, future development gives rise to the expectation of a diversification from ^{13}C nuclei to other nuclei; even at the present time, ^{29}Si is playing an important part in certain areas of research, and there is increasing interest in ^{15}N. In specific cases outside the field of pure analysis, solid-state ^{1}H-NMR spectra could also be used to an increasing extent. Both the recording of ^{15}N-NMR spectra and also increasing utilization of variable temperature measurements, relaxation time measurements and a greater range of 2-D NMR experiments in the solid state will result in an increasing measurement time requirement for solid-state NMR spectroscopy.

Two-dimensional solid-state NMR spectroscopy[10] is still at the start of its development. In this instance, additional information is to be expected in the future concerning molecular structure, e.g. bond lengths, concerning molecular dynamics, such as the nature and time scale of motions, and concerning molecular order.

Received: February 13, 1988 [A 695 IE]
German version: *Angew. Chem. 100* (1988) 1525

[1] J. Schaefer, E. O. Stejskal, R. Buchdahl, *Macromolecules 8* (1975) 291.
[2] a) F. Bloch, *Phys. Rev. 111* (1958) 841; b) L. R. Sarles, R. M. Cotts, *ibid. 111* (1958) 853.
[3] E. R. Andrew, *Prog. Nucl. Magn. Reson. Spectrosc. 8* (1971) 1.
[4] a) S. R. Hartmann, E. L. Hahn, *Phys. Rev. 128* (1962) 2042; b) A. Pines, M. G. Gibby, J. S. Waugh, *J. Chem. Phys. 59* (1973) 569.
[5] a) J. Schaefer, E. O. Stejskal, *Top. Carbon-13 NMR Spectrosc. 3* (1979) 283; b) B. C. Gerstein, *ibid. 4* (1984) 123; c) C. S. Yannoni, *Acc. Chem. Res. 15* (1982) 201; d) D. J. O'Donnell, *ACS Symp. Ser. 247* (1984) 21.
[6] a) M. Mehring: *Principles of High Resolution NMR in Solids*, Springer, Berlin 1983; b) C. A. Fyfe: *Solid State NMR for Chemists*, CFC Press, Guelph, Canada 1983; c) R. A. Komoroski (Ed): *High Resolution NMR Spectroscopy of Synthetic Polymers in Bulk*, VCH Publishers, Deerfield Beach, FL, USA 1986.
[7] a) J. R. Lyerla, *Contemp. Top. Polym. Sci. 3* (1979) 143; b) A. N. Garroway, W. B. Moniz, H. A. Resing, *ACS Symp. Ser. 103* (1979) 67; c) L. W. Jelinski, J. J. Dumais, F. C. Schilling, F. A. Bovey, *Pure Appl. Chem. 54* (1982) 345; d) E. O. Stejskal, J. Schaefer, M. D. Sefcik, G. S. Jocob, R. A. McKay, *ibid. 54* (1982) 461; e) H. A. Resing, A. N. Garroway, D. C. Weber, J. Ferraris, O. Slotfeldt-Ellingsen, *ibid. 54* (1982) 595; f) D. E. Axelson, K. E. Russel, *Prog. Polym. Sci. 11* (1985) 221; g) J. Schaefer, E. O. Stejskal, M. D. Sefcik, R. A. McKay, *Philos. Trans. R. Soc. London A 299* (1981) 593; h) D. R. Bauer, *Prog. Org. Coat. 14* (1986) 45.
[8] J. J. Lindberg, B. Hortling, *Adv. Polym. Sci. 66* (1985) 1.
[9] S. J. Opella, J. G. Hexem, M. H. Frey, T. A. Cross, *Philos. Trans. R. Soc. London A 299* (1981) 665.
[10] B. Blümich, H. W. Spiess, *Angew. Chem. 100* (1988) Nr. 12; *Angew. Chem. Int. Ed. Engl. 27* (1988) Nr. 12.
[11] a) M. Mehring, H. Weber, W. Müller, G. Wegner, *Solid State Commun. 45* (1983) 1079; b) M. M. Maricq, J. S. Waugh, *J. Chem. Phys. 70* (1979) 330; c) J. Herzfeld, A. E. Berger, *ibid. 73* (1980) 6021.
[12] a) G. S. Harbison, H. W. Spiess, *Chem. Phys. Lett. 124* (1986) 128; b) G. S. Harbison, V.-D. Vogt, H. W. Spiess, *J. Chem. Phys. 86* (1986) 1206.
[13] a) W. T. Dixon, *J. Chem. Phys. 77* (1982) 1800; b) M. A. Hemminga, P. A. De Jager, K. P. Datema, J. Breg, *J. Magn. Reson. 50* (1982) 508; c) D. P. Raleigh, E. T. Olejniczak, S. Vega, R. G. Griffin, *ibid. 72* (1987) 238.
[14] a) D. L. Van Der Hart, W. L. Earl, A. N. Garroway, *J. Magn. Reson. 44* (1981) 361; b) A. N. Garroway, D. L. Van Der Hart, W. L. Earl, *Philos. Trans. R. Soc. London A 299* (1981) 609.
[15] J. S. Frye, G. E. Maciel, *J. Magn. Reson. 48* (1982) 125.
[16] G. E. Balimann, C. J. Groombridge, R. K. Harris, K. J. Packer, B. J. Say, S. F. Tanner, *Philos. Trans. R. Soc. London A 299* (1981) 643.
[17] a) H. R. Kricheldorf, D. Müller, *Colloid Polym. Sci. 262* (1984) 856; b) A. Shoji, T. Ozaki, H. Saito, R. Tabeta, I. Ando, *Macromolecules 17* (1984) 1472.
[18] a) H.-J. Cantow, D. Emeis, W. Gronski, A. Hasenhindl, D. Lausberg, M. Möller, Y. Shahab, *Makromol. Chem. Suppl. 7* (1984) 63; b) I. Ando, T. Sorita, T. Yamanobe, T. Komoto, H. Sato, K. Deguchi, M. Imanari, *Polymer 26* (1985) 1864.
[19] A. N. Garroway, W. M. Ritchey, W. B. Moniz, *Macromolecules 15* (1982) 1051.
[20] F. Lauprêtre, L. Monnerie, J. Virlet, *Macromolecules 17* (1984) 1397.
[21] A. Bunn, M. E. A. Cudby, R. K. Harris, K. J. Packer, B. J. Say, *J. Chem. Soc. Chem. Commun. 1981*, 15.
[22] T. Terao, S. Maeda, A. Saika, *Macromolecules 16* (1983) 1535.
[23] W. P. Rothwell, J. S. Waugh, *J. Chem. Phys. 74* (1981) 2721.
[24] R. A. Komoroski, *J. Polym. Sci. Polym. Phys. Ed. 21* (1983) 2551.
[25] J. J. Dechter, R. A. Komoroski, D. E. Axelson, L. Mandelkern, *J. Polym. Sci. Polym. Phys. Ed. 19* (1981) 631.
[26] A. P. M. Kentgens, W. S. Veeman, J. van Bree, *Macromolecules 20* (1987) 1234.
[27] a) A. Bax, N. M. Szeverenyi, G. E. Maciel, *J. Magn. Reson. 50* (1982) 227; b) P. Caravatti, G. Bodenhausen, R. R. Ernst, *Chem. Phys. Lett. 89* (1982) 363.

[28] E. O. Stejskal, J. Schaefer, T. R. Steger, *Faraday Symp. Chem. Soc. 13* (1979) 56.
[29] a) B. Schröter, A. Posern, *Macromol. Chem. Rapid Commun. 3* (1982) 623; b) D. L. Van der Hart, F. Khoury, *Polymer 25* (1984) 1589.
[30] I. S. Chuang, G. E. Maciel, G. E. Myers, *Macromolecules 17* (1984) 1087.
[31] J. R. Havens, M. Thakur, J. B. Lando, J. L. Koenig, *Macromolecules 17* (1984) 1071.
[32] a) M. D. Sefcik, E. O. Stejskal, R. A. McKay, J. Schaefer, *Macromolecules 12* (1979) 423; b) A. C. Wong, A. N. Garroway, W. M. Ritchey, *ibid. 14* (1981) 832.
[33] a) A. D. English, D. B. Chase, H. J. Spinelli, *Macromolecules 16* (1983) 1422; b) D. R. Bauer, R. A. Dickie, J. L. Koenig, *J. Polym. Sci. Polym. Phys. Ed. 22* (1984) 2009; c) P. E. Allen, G. P. Simon, D. R. G. Williams, E. H. Williams, *Eur. Polym. J. 22* (1986) 549; d) R. G. Earnshaw, C. A. Price, J. H. O'Donnell, A. K. Wittaker, *J. Appl. Polym. Sci. 32* (1986) 5337.
[34] a) G. E. Maciel, N. M. Szeverenyi, T. A. Early, G. E. Myers, *Macromolecules 16* (1983) 598; b) F. S. Chuang, B. L. Hawkins, G. E. Maciel, G. E. Myers, *ibid. 18* (1985) 1482.
[35] a) C. Fyfe, M. McKinnon, A. Rudin, W. Tchir, *Macromolecules 16* (1983) 1216; b) S. So, A. Rudin, *J. Polym. Sci. Polym. Lett. Ed. 23* (1985) 403; c) G. E. Hatfield, G. E. Maciel, *Macromolecules 20* (1987) 608.
[36] a) H. A. Resing, W. B. Moniz, *Macromolecules 8* (1975) 560; b) M.-F. Grenier-Loustalot, P. Grenier, *Eur. Polym. J. 22* (1986) 457; c) E. Metzel, J. L. Koenig, *Adv. Polym. Sci. 75* (1986) 73.
[37] D. M. Grant, E. G. Paul, *J. Am. Chem. Soc. 86* (1964) 2984.
[38] A. E. Tonelli, *J. Am. Chem. Soc. 102* (1980) 7635.
[39] A. Bunn, M. E. A. Cudby, R. K. Harris, K. J. Packer, B. J. Say, *Polymer 23* (1982) 694.
[40] R. P. Veregin, C. A. Fyfe, R. H. Maressault, *Macromolecules 19* (1986) 2379.
[41] M.-F. Grenier-Loustalot, G. Bocelli, *Eur. Polym. J. 20* (1984) 957.
[42] H. R. Kricheldorf, D. Müller, *Macromolecules 16* (1983) 615.
[43] L. A. Belfiore, F. C. Schilling, A. E. Tonelli, A. J. Lovinger, F. A. Bovey, *Macromolecules 17* (1984) 2561.
[44] M. C. Sacchi, I. Tritto, P. Locatelli, L. Zetta, D. R. Ferro, H. Förster, *Macromolecules 19* (1986) 1634.
[45] W. L. Earl, D. L. Van Der Hart, *Macromolecules 12* (1979) 762.
[46] M. D. Sefcik, J. Schaefer, E. O. Stejskal, R. A. McKay, *Macromolecules 13* (1980) 1132.
[47] F. C. Schilling, F. A. Bovey, A. E. Tonelli, S. Tseng, A. E. Woodward, *Macromolecules 17* (1984) 728.
[48] A. L. Cholli, W. M. Ritchey, J. L. Koenig, *Spectrosc. Lett. 16* (1983) 21.
[49] a) W. W. Fleming, C. A. Fyfe, R. D. Kendrick, J. R. Lyerla, H. Vanni, C. S. Yannoni, *ACS Symp. Ser. 142* (1980) 193; b) J. J. Dechter, *J. Polym. Sci. Polym. Lett. Ed. 23* (1985) 261.
[50] R. Kitamaru, F. Horii, K. Marayama, *Polym. Bull. 7* (1982) 583.
[51] M. Möller, W. Gronski, H.-J. Cantow, H. Höcker, *J. Am. Chem. Soc. 106* (1984) 5093.
[52] a) W. S. Veeman, E. M. Menger, H. H. C. de Moor, *Proc. I.U.P.A.C. Macromol. Symp. 28th, 1982,* 2; b) F. C. Schilling, F. A. Bovery, A. E. Tonelli, *Polym. Mater. Sci. Eng. 50* (1984) 256.
[53] D. C. McFaddin, K. E. Russell, E. C. Kelusky, *Polym. Commun. 27* (1986) 204.
[54] a) D. L. Van Der Hart, A. N. Garroway, *J. Chem. Phys. 71* (1979) 2773; b) J. Schaefer, E. O. Stejskal, T. R. Steger, M. D. Sefcik, R. A. McKay, *Macromolecules 13* (1980) 1121.
[55] R. S. Aujla, R. K. Harris, K. J. Packer, M. Parameswaran, B. J. Say, A. Bunn, M. E. A. Cudby, *Polym. Bull. 8* (1982) 253.
[56] a) D. L. Van Der Hart, E. Perez, *Macromolecules 19* (1986) 1902; b) E. Perez, D. L. Van Der Hart, B. Crist, P. R. Howard, *ibid. 20* (1987) 78.
[57] F. Lauprêtre, L. Monnerie, L. Barthelemy, J. P. Vairon, A. Sauzeau, D. Roussel, *Polym. Bull. 15* (1986) 159.
[58] a) R. A. Komoroski, *Rubber Chem. Technol. 56* (1983) 959; b) D. J. Patterson, J. L. Koenig, J. R. Shelton, *ibid. 56* (1983) 971.
[59] P. F. Barron, F. Horii, K. Murayama, *Polym. 24* (1983) 1252.
[60] a) L. W. Jelinski, F. C. Schilling, F. A. Bovey, *Macromolecules 14* (1981) 581; b) F. A. Bovey, *Pure Appl. Chem. 54* (1982) 559.
[61] L. W. Jelinski, J. J. Dumais, P. T. Watnick, S. V. Bass, L. Shephard, *J. Polym. Sci. Polym. Chem. Ed. 20* (1982) 3285.
[62] S. A. Curran, A. R. Padwa, *Macromolecules 20* (1987) 625.
[63] V. J. McBrierty, D. C. Douglas, *Macromol. Rev. 16* (1981) 295.
[64] J. Schaefer, E. O. Stejskal, R. Buchdahl, *Macromolecules 10* (1977) 384.
[65] a) J. Schaefer, M. D. Sefcik, E. O. Stejskal, R. A. McKay, *Polym. Prepr. Am. Chem. Soc. Div. Polym. Chem. 20* (1979) 247; b) E. O. Stejskal, J. Schaefer, M. D. Sefcik, R. A. McKay, *Macromolecules 14* (1981) 275.
[66] S. Kaplan, *Polym. Prepr. Am. Chem. Soc. Div. Polym. Chem. 25* (1984) 356.
[67] a) T. S. Lin, T. C. Ward, *Polym. Prepr. Am. Chem. Soc. Div. Polym. Chem. 24* (1983) 136; b) P. Tekely, F. Lauprêtre, L. Monnerie, *Polymer 26* (1985) 1081.
[68] a) J. I. Kaplan, A. N. Garroway, *J. Magn. Reson. 49* (1982) 464; b) N. Zumbulyadis, *ibid. 53* (1983) 486.
[69] J. Schaefer, M. D. Sefcik, E. O. Stejskal, R. A. McKay, *Macromolecules 14* (1981) 188.
[70] a) L. A. Belfiore, *Polym. Mater. Eng. 51* (1984) 223; b) *Polymer 27* (1986) 80.
[71] G. C. Gobbi, R. Silvestri, T. P. Russell, J. R. Lyerla, W. W. Fleming, T. Nishi, *J. Polym. Sci. Polym. Lett. Ed. C25* (1987) 61.
[72] J. M. Hewitt, P. M. Henrichs, M. Scozzafava, R. Scaringe, M. Linder, L. J. Sorriero, *Macromolecules 17* (1984) 2566.
[73] T. C. Ward, T. S. Lin, *Adv. Chem. Ser. 206* (1984) 59.
[74] D. L. Van Der Hart, W. F. Manders, R. S. Stein, W. Herman, *Macromolecules 20* (1987) 1724.
[75] A. K. Roy, P. T. Inglefield, J. H. Shibata, A. A. Jones, *Macromolecules 20* (1987) 1434.
[76] M. Linder, P. M. Henrichs, J. M. Hewitt, D. J. Massa, *J. Chem. Phys. 82* (1985) 1585.
[77] a) P. Caravatti, P. Neuenschwander, R. R. Ernst, *Macromolecules 18* (1985) 119; b) *ibid. 19* (1986) 1889.
[78] D. A. Torchia, *J. Magn. Reson. 30* (1978) 613.
[79] a) B. Gabrys, F. Horii, R. Kitamaru, *Macromolecules 20* (1987) 175; b) H. T. Edzes, W. S. Veeman, *Polym. Bull. 5* (1981) 255; c) H. T. Edzes, A. H. Montree, W. S. Veeman, E. de Boer, *Proc. I.U.P.A.C. Macromol. Symp. 28th 1982,* 13.
[80] M. K. Gupta, J. A. Ripmeester, D. J. Carlsson, D. M. Wiles, *J. Polym. Sci. Polym. Lett. Ed. 21* (1983) 211.
[81] a) W. S. Veeman, E. M. Menger, *Bull. Magn. Reson. 2* (1981) 77; b) W. S. Veeman, E. M. Menger, W. Ritchey, E. de Boer, *Macromolecules 12* (1979) 924.
[82] S. Ni, L. Shen, F. Yu, B. Quian, *Polym. Commun. 27* (1986) 318.
[83] F. Horii, A. Hirai, K. Murayama, R. Kitamaru, T. Suzuki, *Macromolecules 16* (1983) 273.
[84] a) J. Schaefer, M. D. Sefcik, E. O. Stejskal, R. A. McKay, *Macromolecules 17* (1984) 1118; b) *ibid. 14* (1981) 280.
[85] L. W. Jelinski, J. J. Dumais, P. I. Watnick, A. K. Engel, M. D. Sefcik, *Macromolecules 16* (1983) 409.
[86] T. R. Steger, J. Schaefer, E. O. Stejskal, R. A. McKay, *Macromolecules 13* (1980) 1127.
[87] a) J. R. Lyerla, C. S. Yannoni, C. A. Fyfe, *Acc. Chem. Res. 15* (1982) 208; b) W. W. Fleming, J. R. Lyerla, C. S. Yannoni, *ACS Symp. Ser. 247* (1984) 83.
[88] M. Wobst, *Acta Polym. 36* (1985) 492.
[89] A. N. Garroway, W. B. Moniz, H. A. Resing, *Faraday Symp. Chem. Soc. 13* (1979) 63.
[90] L. A. Belfiore, S. L. Cooper, *Polym. 25* (1984) 645.
[91] a) J. Schaefer, R. A. McKay, E. O. Stejskal, W. T. Dixon, *J. Magn. Reson. 52* (1983) 123; b) J. Schaefer, E. O. Stejskal, R. A. McKay, W. T. Dixon, *Macromolecules 17* (1984) 1479; c) J. Schaefer, M. D. Sefcik, E. O. Stejskal, R. A. McKay, W. T. Dixon, R. E. Cais, *ibid. 17* (1984) 1107.
[92] a) A. F. De Jong, A. P. M. Kentgens, W. S. Veeman, *Chem. Phys. Lett. 109* (1984) 337; b) A. P. M. Kentgens, A. F. De Jong, E. de Boer, W. S. Veeman, *Macromolecules 18* (1985) 1045.
[93] A. K. Roy, A. A. Jones, P. T. Inglefield, *Macromolecules 19* (1986) 1356.

Phosphaalkynes—Syntheses, Reactions, Coordination Behavior**

New Synthetic Methods (73)

By Manfred Regitz* and Paul Binger

Organophosphorus compounds have been applied in two ways in chemical synthesis. They can either be used as a reagent in a step of the synthesis (for example, in the Wittig reaction) or they can be incorporated directly into the target molecule. This second application, in particular, has expanded greatly in the last few years with the preparation of low-coordination phosphorus compounds. These include the phosphaalkynes, which are of great interest to organic and inorganic chemists. Phosphaalkynes have been employed in the synthesis of heterocyclic compounds, phosphaarenes and their valence isomers, and polycyclic compounds. Further applications have been the use of phosphaalkynes as new ligand systems in complex chemistry and their cyclooligomerization with organometallic reagents. While the chemical properties of phosphaalkynes have little in common with those of nitriles, they are in many ways very similar to those of the isoelectronic acetylenes.

1. Introduction

Whoever believed that the development of organophosphorus chemistry was temporarily coming to a close with the synthesis of classical compounds, such as derivatives of phosphoric acid in the widest sense or phosphane oxides, has had to reconsider that opinion. The barrier presented by the double bond rule[1]—generally valid until the 1960s—which states that stable (p-p) π multiple bonds should not be formed between, for example, phosphorus and elements of the first period, can now be regarded as finally breached. The synthesis of the first compounds of trivalent phosphorus containing PC double bonds, such as the phosphamethinecyanine cations[2] and the phosphabenzenes (λ^3-phosphinines)[3], paved the way for the comprehensive chemistry of low-coordinate phosphorus compounds that we know today.[4]

In the last fifteen years it has proved possible to produce and trap derivatives of five-valent tricoordinate phosphorus (**1**)[5] and also to stabilize them sufficiently by the incorporation of bulky groups to be able to isolate them.[6] Milestones in this development are compounds with $\lambda^3\sigma^2$ phosphorus (**2**),[7] which in the case of $Z = CR_2$ (phosphaalkenes) are also to be regarded as forming a bridge to organic chemistry.

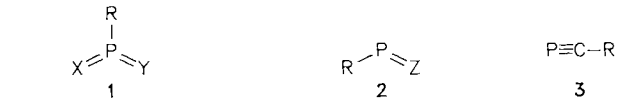

Finally, at the beginning of this decade, the first stable phosphaalkynes (alkylidynephosphanes) **3** were isolated.[8,9] These compounds, which were soon recognized as valuable materials for synthesis, are the central theme of this review. Interestingly, the parent compound of this series, phosphaacetylene **4**, was prepared as long ago as 1961 by *Gier*[10] from phosphane in a rotating arc struck between graphite electrodes; the product was quenched in a cold trap, purified by rapid gas chromatography, and finally characterized by IR spectroscopy.

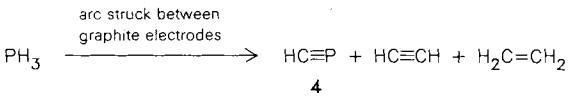

Naturally, attempts have also been made to prepare and isolate phosphaalkynes with $\lambda^5\sigma^3$ phosphorus (**6a**). Such compounds can also be described as ylids **6b** and they can even be regarded as phosphinocarbenes **6c**. They are apparently only short-lived and have not been isolated. An ab initio study has demonstrated the importance of the contribution of the zwitterionic canonical structure **6b**.[11] This structure also provides the best explanation for the known trapping reactions. *Appel* et al.[12] have postulated that a species of type **6** is an intermediate in the conversion of methylenephosphoranes to methylenephosphanes.

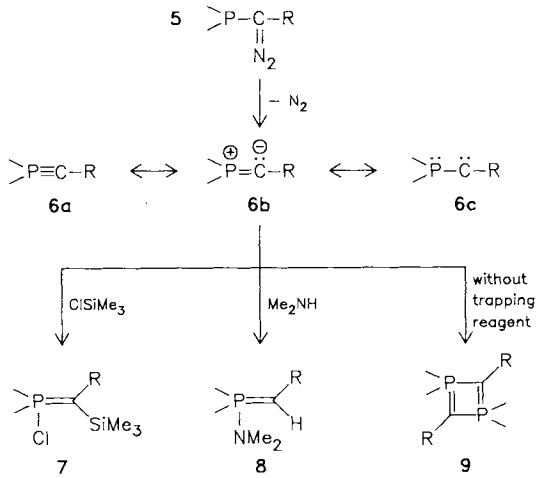

[*] Prof. Dr. M. Regitz
Fachbereich Chemie der Universität
Erwin-Schrödinger-Strasse, D-6750 Kaiserslautern (FRG)
Prof. Dr. P. Binger
Max-Planck-Institut für Kohlenforschung
Kaiser-Wilhelm-Platz 1, D-4330 Mülheim a. d. Ruhr (FRG)

[**] Phosphorus Compounds with Unusual Coordination, Part 30. Part 29: [119].

The photolytic or thermal elimination of N_2 from phosphinodiazoalkanes **5**[13,14] results in the formation of short-lived intermediates which can be trapped[15] by 1,2 addition by, for example, chlorotrimethylsilane (→ **7**)[13] or dimethylamine (→ **8**).[13] A further indication of the zwitterionic character of **6** is found in the dimerization of **5** to give $1\lambda^5,3\lambda^5$-diphosphete derivatives **9**,[14,16] which is not accompanied by any of the olefin formation that is characteristic of carbenes. If the residue R in **6** is a phosphoryl group, a P→P oxygen shift takes place before the dimerization to **9** occurs.[14] The O-shift has also been found in other phosphinocarbenes with PO or CO groups.[17]

2. Synthesis

β-Elimination is the method of choice for preparing phosphaalkynes.[18] In the case of the rather unstable phosphaacetylene **4** and simple substituted phosphaalkynes, only flash pyrolysis is successful.

2.1. Short-Lived Phosphaalkynes

Nowadays the historical procedure of *Gier*[10] to prepare HC≡P **4** has been superseded by flash pyrolysis of dichloro(methyl)phosphane at 900–1100°C. The hydrogen chloride produced at the same time has to be removed by basic adsorption materials[19–22] because it interferes with trapping reactions and also reverses the process of formation. Although the latter problem does not arise when **4** is prepared by the elimination of isobutylene from **3d**,[22] this advantage is outweighed by the low yield (ca. 10% conversion to **3d**, as opposed to ca. 30% from $MePCl_2$) and by the effort required to synthesize **3d**.

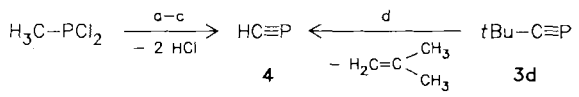

a) 1000°C/0.02 torr, KOH at −78°C [19]. b) 900°C/10^{-3} torr, 1,3,5-tricyclohexyl(hexahydro)-*s*-triazine at 20°C [21]. c) 1100°C/4×10^{-5} torr, KOH/K_2CO_3 at −78°C [22]. d) 950°C/5×10^{-4} mbar.

Phosphaacetylene **4** can be stored as a colorless solid at < −124°C; above this temperature it "polymerizes". The monomer and fresh "polymer" are pyrophoric in air.[10] An NMR sample dissolved in toluene is unchanged after two weeks at −70°C. When the sample is warmed up, one of the products is white phosphorus.[22] Under reduced pressure **4** can even be kept at room temperature.[23] It has been shown that HC≡P is also found in space.[24,25] The physical properties of phosphaacetylene **4** have been investigated thoroughly. Selected physical data for **4** are collected in Table 1.

HC≡N has a much smaller carbon-heteroatom bond length (1.155 Å) than **4**. On the other hand, it has a much larger dipole moment ($\mu = 2.957$ D),[29] which is oriented in the opposite direction to that of HC≡P because of the different charge distribution.[30] The ionization potential of phosphaacetylene is lower than that of hydrogen cyanide but its π/n separation is much larger.[31]

In analogy to **4**, 1-phospha-1-propyne (ethylidynephosphane, **3a**) is obtained from dichloroethylphosphane.[21,32,33] The phosphaalkyne can be separated from the HCl gas either by trapping the former in a cold trap or by reacting the latter with a base.[21,33] If it is intended to use the phosphaalkyne in a synthesis, it is best to add triethylamine directly to the pyrolysis mixture and to filter off the ammonium salt formed with a G1 frit.[33] Some physical data for **3a** are given in Table 1.

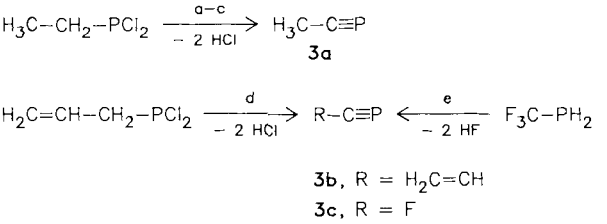

a) 900°C/0.03 torr, **3a** is trapped in a cold trap at −120°C [32]. b) 750°C/10^{-3} torr, 1,3,5-tricyclohexyl(hexahydro)-*s*-triazine at 20°C [21]. c) 500–700°C (temperature gradient in the oven)/10^{-4} torr, triethylamine [33]. d) 1000°C/0.03–0.06 torr [35]. e) 0.03 torr, KOH [39, 40].

Vinylphosphaacetylene (2-propenylidynephosphane), **3b** has been produced by an analogous HCl elimination and characterized by microwave spectroscopy.[35,37,38]

In contrast to the previous cases, the elimination of hydrogen fluoride from trifluoromethylphosphane initiated by potassium hydroxide (here the groups to be eliminated have the opposite orientation to the examples already discussed) proceeds even at room temperature. It has been proved that 2,2-difluoro-1-phosphaethene is an intermediate, which, on longer contact with the base, is completely converted into **3c**.[39,40] The product was identified by photoelectron spectroscopy (the first three ionization potentials are 10.57, 13.55, and 17.63 eV)[39] as well as by IR (CP stretch, 1671 cm^{-1})[41,42] and microwave spectroscopy.[43]

Table 1. Some physical properties of HC≡P **4** and Me–C≡P **3a**.

	HC≡P	Ref.	Me–C≡P	Ref.
CP-bond length	1.5421(5) Å	[26]	1.5438(4) Å	[34]
dipole moment	0.39 D	[26]	1.499 D	[34]
1st ionization potential (π MO)	10.79 eV	[27]	9.89 eV	[35]
2nd ionization potential (n_σ MO)	12.86 eV	[27]	12.19 eV	[35]
IR stretch	1278.3 cm^{-1}	[10, 28]	1558.7 cm^{-1}	[36]
NMR(CD_2Cl_2, −80°C, δ) ^1H	2.90	[21, 22] [a]	2.20	[21] [c]
^{13}C	158.0	[21] [b]	170.8	[21] [d]
^{31}P	−32	[21, 22] [a]	−60	[21] [c]

[a] $^2J(P,H) = 44.0$ Hz. [b] $^1J(P,C) = 56.0$ Hz. [c] $^3J(P,H) = 15.0$ Hz. [d] $^1J(P,C) = 49.0$ Hz.

Finally, phosphaalkynes are now known containing acetylene and nitrile groups so placed that they can conjugate with the phosphaalkyne group. They are obtained by copyrolysis or by substitution.

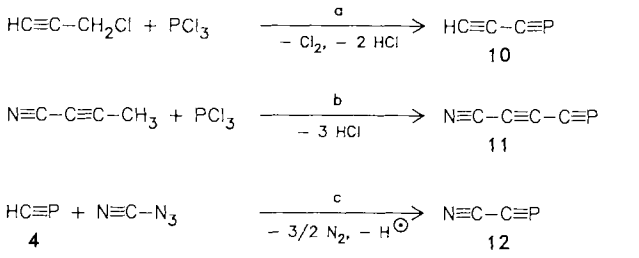

a) 1100°C/0.03–0.06 torr. b) 1100°C/0.08 torr. c) 700°C.

For example, the flash pyrolysis of propargyl chloride and phosphorus trichloride produces 1-phospha-1,3-butadiyne **10** ($\mu = 0.745$ D).[38,44] The heteropolyyne **11** ($\mu = 4.3$–4.5 D)[45] can be prepared similarly. Lastly, the hydrogen of HC≡P **4** can be replaced by cyanide radicals by passing **4** and cyanazide together through a pyrolysis oven: the product **12** ($\mu = 3.44$ D) has been identified by microwave spectroscopy.[46]

2.2. Kinetically Stable Phosphaalkynes

tert-Butylphosphaacetylene **3d** has played a decisive role in the synthesis of kinetically stable phosphaalkynes. Its reactivity has been investigated more thoroughly than that of any other compound with a PC triple bond. The synthesis published by *Becker* et al. in 1981[8,47] (**13c** → **15c** → **16c** → **3d**) was later generalized (see Table 2), above all by significant developments in the step in which hexamethyldisiloxane is eliminated (**16** → **3**) to form the phosphaalkyne.[48,49]

The starting material for the phosphaalkyne synthesis is the silyl phosphane **14**,[50] which can be readily obtained from white phosphorus, sodium/potassium alloy, and chlorotrimethylsilane. Compound **14** has often been replaced successfully by the more reactive lithium bis(trimethylsilyl)phosphide·2THF (**14**, Li instead of a $SiMe_3$ group).[51] The acyl phosphides **15** formed in the first step by reaction of acyl chlorides **13** with **14** can be detected,[52,53] but they generally rearrange rapidly by a 1,3-

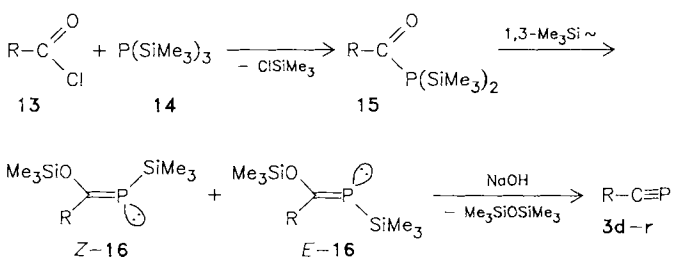

shift of a trimethylsilyl group to the oxygen atom of the acyl group to form the phosphaalkenes **16**, the *Z* isomer of which usually predominates.[52,53] The configuration of **16** apparently has no influence upon the subsequent elimination step (→ **3d**–**r**). However, it has proved to be decisive for the general application of this elimination step in synthesis that it should take place at high temperature without solvent and that the phosphaalkyne together with the silyl ether should be removed rapidly from the reaction vessel.[48,49,54] Information relating to specific examples is either given below or is to be found in the footnotes to Table 2.

Phosphaalkynes having tertiary substituents, such as **3d**–**j**, have an unusually high thermal stability. Those with secondary substituents or a neopentyl residue, such as **3k**–**p**, also survive the temperatures of the elimination steps, but the yields clearly suffer. At room temperature they tend to "oligomerize". Substitution with a phenyl group[58] (see below) produces a rather unstable phosphaalkyne. Methyl (→ **3r**)[55] or *tert*-butyl (→ **3q**)[57] substituents in the 2-, 4-, and 6-positions of the phenyl ring improve the kinetic stability decisively.

It was reported recently that the elimination step **16a** → **3d** can also be carried out with the aid of diiron nonacarbonyl;[59] it is immaterial whether one starts with the *Z*- or the *E*-phosphaalkene. These isomers can be prepared selectively when **13d** is reacted with lithium bis(trimethylsilyl)phosphide·2THF either at +20°C (→ *Z*-**16d**) or at −78°C (→ *E*-**16d**).[59] The elimination step **16** → **3** can also be carried out with tetrabutyl ammonium fluoride,[53] as was shown for the preparation of **3i**. Finally, one can do without additives entirely, as in the preparation of **3j**[56] and **3q**.[57]

Phosphaalkynes have been well characterized by their ^{31}P and ^{13}C chemical shifts and their $^{1}J_{P,C}$ coupling constants (see Table 2). Aromatic substituents (**3q**,**r**) cause a marked shift of the phosphorus resonance to lower field. The structure of **3d** in the gas phase has been studied in detail by electron diffraction and by microwave spectroscopy (P≡C = 1.536(2) Å)[60] and the ionization potentials have been determined (first IP = 9.7 eV, second IP = 11.45 eV) and compared with those of other phosphaalkynes.[31,61]

The stabilities of the precursor and of the product limit the extent to which this method of synthesizing phosphaalkynes can be applied. A further limitation is shown by the attempt to prepare the bis(phosphaalkyne) **18**.

Thus, when dimethylmalonyl dichloride is treated with two equivalents of lithium bis(trimethylsilyl)phosphide,[51] the bis(phosphaalkyne) **18** is not formed. Instead, an intramolecular [2 + 2] cycloaddition occurs to afford 2,3-diphosphabicyclo[2.1.0]pentane **19**.[62]

The elimination of chlorotrimethylsilane from suitably substituted phosphaalkenes **20** by flash pyrolysis can also be used to form PC triple bonds. Phenylphosphaacetylene **3s**[58,63] and trimethylsilylphosphaacetylene **3t**[9] have been prepared in this way.

Their half-lives (**3s**, $\tau/2$ (0°C) = 7 min; **3t**, $\tau/2$ (20°C) = 50 min) indicate that their stabilities lie between those of the short-lived phosphaalkynes on the one hand and the kinetically stabilized ones on the other.

Finally, a variant should be mentioned which permits acyl chlorides to be converted into phosphaalkynes using lithium phosphide (DME complex).[64] The primary prod-

Table 2. Kinetically stabilized phosphaalkynes **3d–r** prepared by the elimination of hexamethyldisiloxane from phosphaalkenes **16d–r**. NMR data (C_6D_6, J in Hz). DEG = diethylene glycol; DME = 1,2-dimethoxyethane.

Phosphaalkyne		Reaction conditions		Yield [%]	$\delta(^{31}P)$	$\delta(^{13}C)$ ($^1J(C,P)$)	Ref.
3d	tBu–C≡P	DEG	NaOH, 20°C	76	−69.2	184.8 (38.5)	[8]
3e	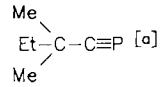 [a]	— —	NaOH, 160°C NaOH, 150–200°C	96 80	−62.0	183.8 (37.6)	[49, 54] [55]
3f	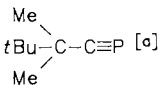 [a]	—	NaOH, 150–200°C	83	−57.7	184.4 (37.5)	[55]
3g	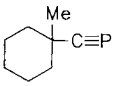	—	NaOH, 120–160°C	76	−57.0	184.9 (37.2)	[48]
3h	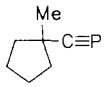	—	NaOH, 120–160°C	66	−66.0	184.9 (37.9)	[48]
3i	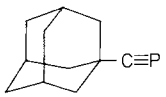	DME —	NaOH, 20°C, nBu$_4$N$^{\oplus}$F$^{\ominus}$ on silica gel, 90°C	83	−66.9	184.7 (39.0)	[53]
3j	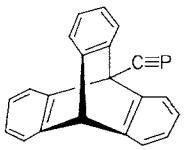	DME	−85°C	12–18	−17.5	164.6 [b] (46.5)	[56]
3k	Me_2CH–C≡P [c]	—	NaOH, 120–160°C	63	−64.3	183.4 (41.3)	[48]
3l	tBu–CH_2–C≡P [d]	—	NaOH, 120–160°C	75	−51.4	173.7 (45.5)	[48]
3m	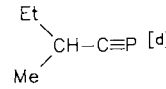 [d]	—	NaOH, 160–200°C	41	−59.3	—	[55]
3n	Et_2CH–C≡P [d]	—	NaOH, 160–200°C	49	−53.9	179.4 (41.3)	[55]
3o	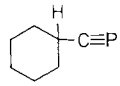	—	NaOH, 160–200°C	28	−60.9	179.7 (41.3)	[55]
3p	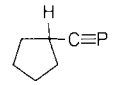	—	NaOH, 160–200°C	29	−62.9	179.9 (41.6)	[55]
3q	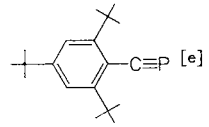 [e]	DME	−85°C	10–15	+34.4 [b]	168.7 [b] (53.2)	[57]
3r	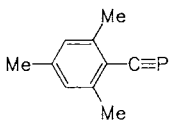	—	NaOH, 140°C	43	+ 2.5	163.7 (46.0)	[55]

[a] Stable at 20°C, but the complete removal of hexamethylsiloxane has not yet been achieved. This is of no significance for further reactions. [b] Measured in $CDCl_3$. [c] Stored at −30°C. [d] Mixed with hexamethyldisiloxane; stored at −30°C. [e] The modest yield is partly the result of the competing formation of a 2,3-diphospha-1,3-butadiene.

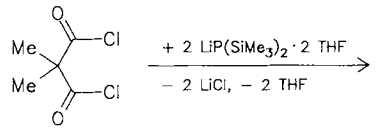

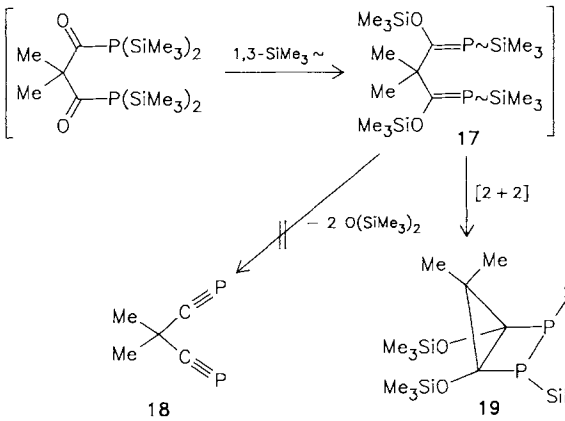

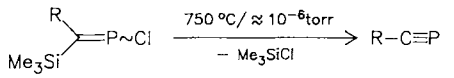

20a: R = Ph **3s**: R = Ph
20b: R = Me_3Si **3t**: R = Me_3Si

3s: ^{31}P NMR (solvent not reported), $\delta = -32$; ^{13}C NMR (CD_2Cl_2), $\delta = 164.9$ ($^1J(P,C) = 48.3$ Hz) [59]. **3t**: ^{31}P NMR (solvent not reported), $\delta = 96$; ^{13}C NMR (solvent not reported), $\delta = 201.4$ ($^1J(P,C) = 13.9$ Hz) [9].

ucts of the reaction are the dimeric "lithium monoacylphosphides" **21**, which afford the phosphaalkenes **22** upon silylation. The reaction sequence is completed by lithiation and the spontaneous elimination of lithium triethylsilanolate (**22** → **23** → **3**).[65]

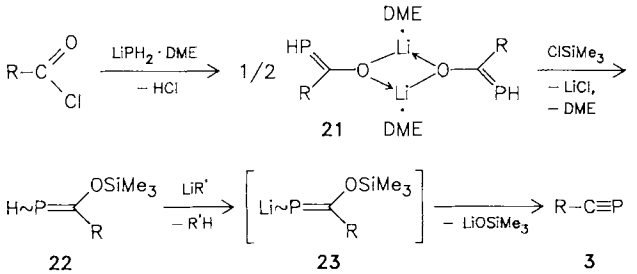

Although the experimental details of this reaction sequence have not been reported and its versatility is unknown, it is difficult to see any advantage it may have over the corresponding reaction of acyl chlorides **13** with tris(trimethylsilyl)phosphane **14**.

3. Reactions

3.1. 1,2 Additions

The 1,2 addition of HCl to the triple bond of a phosphaalkyne is as old as the discovery of phosphaacetylene **4** itself.[10] Dichloro(methyl)phosphane is produced, reflecting the Pauling electronegativities of carbon (2.5) and phosphorus (2.1)[66] and the charge distribution in phosphaacetylene.[67] HCl has been found to add to 1-phospha-1-propyne **3a** in the same orientation.[32] In the case of 2-phenyl-1-phosphaacetylene **3s** it is assumed that first a stereospecific *cis* addition of hydrogen chloride occurs, followed by addition of a second equivalent in the same orientation to form benzyldichlorophosphane.[58] A similar sequence is also known for the silylated phosphaalkyne **3t**.[9]

The addition of halogens to **3d** has been investigated. First, a mixture of *cis/trans*-1,2-dihalophosphaalkenes is produced, followed by saturation of the double bond. Finally, the PC bond is cleaved by a third equivalent of the halogen.[47,68]

The 1,2 addition of boron tribromide and tin tetrabromide to **3d** is also known. The product is a mixture of *E/Z*-isomeric phosphaalkenes, in which the phosphorus atom is halogen-substituted and the boron or tin residue is bonded to carbon.[68]

3.2. [2+1] Cycloaddition

Attempts to add carbenes such as dichloro-, chloro(phenyl)-, or diphenylcarbene to the phosphaacetylene **3d** have not yet succeeded. The Simmons-Smith reaction has also produced no concrete results.[69] However, when the silanediyl (silylane) **25** is produced photolytically from the cyclotrisilane **24** in the presence of the phosphaacetylenes **3d** or **3i**, the phosphasilirenes **26a** or **26b**, respectively, are isolated without difficulty.[70]

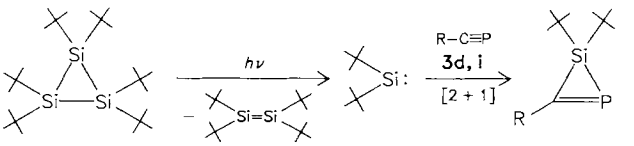

24 **25** **26a**, R = *t*Bu; **26b**, R = Ad

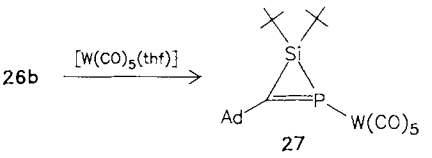

27

26a: ^{31}P NMR (C_6D_6), $\delta = 274.0$. **26b**: ^{31}P NMR (C_6D_6), $\delta = 272.6$. Ad = 1-adamantyl.

When $[W(CO)_5 \cdot (thf)]$ reacts with **26b**, the tungsten complex **27** is obtained, the crystal structure of which reveals that the PC bond distance is 1.686 Å,[70] a typical value for phosphaalkenes.

3.3. [3+2] Cycloadditions

Chemists have only relatively recently become interested in phospholes with further heteroatoms in the ring.[71,72] These compounds are playing a significant role in the development of the chemistry of compounds of low-coordinate phosphorus. Like alkynes, phosphaalkynes have a marked potential for undergoing cycloaddition reactions[49,73,74] and, in view of the variety of 1,3-dipoles avail-

able, they widen the scope of the phosphole synthesis enormously.

3.3.1. 1H-1,2,4-Diazaphospholes

Detailed investigations have been carried out on cycloaddition reactions of **3d** with diazomethane **28a** itself and with its alkyl-, aryl-, acyl-, phosphoryl-, and silyl-substituted derivatives **28b–i**. All these reactions proceed regioselectively in the first stage to give 3*H*-1,2,4-diazaphospholes **29a–i**. The orientation of the dipole is in agreement with the electronegativities of carbon and phosphorus[66] and with the calculated charge distribution in unsubstituted phosphaacetylene **4**.[67] Steric influences do not oppose the mode of reaction favored by electronic factors. Only **29f** can be detected in the NMR spectrum; this compound, like the other primary products, rapidly undergoes an H-shift to form an aromatic ring (**31a–h**). In the case of **29i** the silyl shift is more rapid, giving an *N*-silylated diazaphosphole (**31i**: Me_3Si instead of H, R = H). Regioisomers of type **30** are not present within the limits of detection of ^{31}P NMR spectroscopy.[54,73,74]

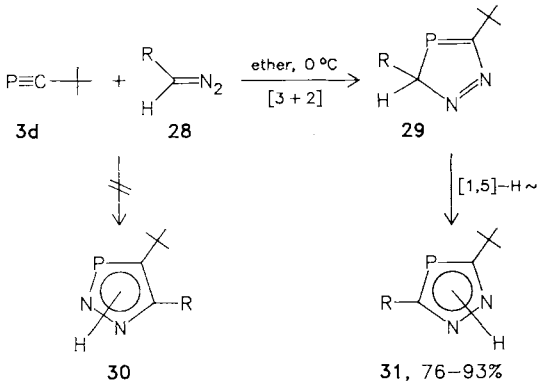

3d 28 29

30 31, 76–93%

a, R = H; b, R = Me; c, R = Ph; d, R = *t*Bu; e, R = CO_2*t*Bu
f, R = CO_2Me; g, R = PhCO; h, R = Ph_2PO; i, R = Me_3Si

31: ^{31}P NMR ($CDCl_3$), δ = 67.6–110.8.

The kinetically stabilized phosphaalkynes **3e,f**,[55] **3g, h**,[48] and **3i**[53] react in a similar fashion with diazomethane **28a**. It should be pointed out that the short-lived parent compound HC≡P **4** can also be converted in this way into 1,2,4-diazaphosphole.[22] Its reaction with **28e** is the only cycloaddition of this type known which does not proceed regiospecifically (**31e** : **30e** (H instead of *t*Bu) = 6 : 1).[22] 1-Phosphapropyne **3a**, the stability of which is similar to that of **4**, adds diazo compounds with the usual orientation of the dipole.[33]

α-Diazoketones **32a–c**, which, unlike **28**, have no diazomethyl hydrogen, react with **3d** to give mixtures of *N*-acylated 1,2,4-diazaphospholes, **34a–c**/**36a–c** in which the isomers **34** dominate (≥85%). They can be separated from the other components.[54]

The reaction **3d** + **32a–c** has been monitored by ^{31}P NMR spectroscopy. The 4*H*-1,2,4-diazaphosphole isomers **35a–c** were thereby detected as intermediates (δ = 37.0–54.8) preceding the acyl shift to the ring nitrogen atom (→ **34**, **36**). The rapid [1,5]-sigmatropic shift (to phosphorus in the first instance) precludes any chance of the primary products **33a–c** being detected.[54] Phosphoryl-substituted diazo compounds (**32**, R^2PO instead of R^2CO) react in the same way with **3d**;[54] sigmatropic phosphoryl shifts are known in pyrazoles.[75,76]

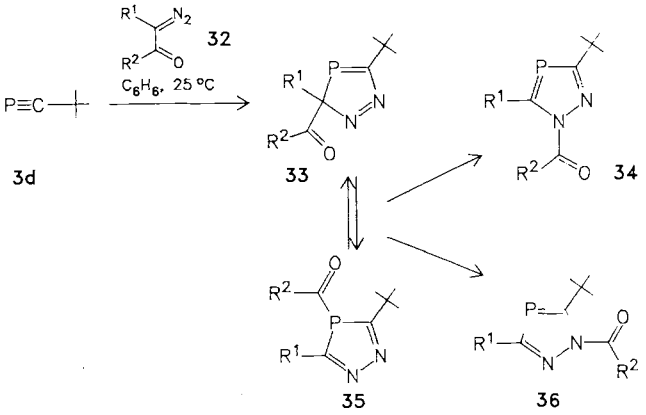

3d 33 34 35 36

a, $R^1 = R^2$ = Me; b, R^1 = Me, R^2 = Ph; c, $R^1 = R^2$ = Ph

The vast range of applications of this synthetic principle can be recognized from the formation of the annelated *N*-acyl-1,2,4-diazaphospholes **37**, **39**, and **41** from **3d** and the cyclic α-diazoketones **36**, **38**, and **40**, respectively (all reactions carried out in benzene at 25 °C).[54,73]

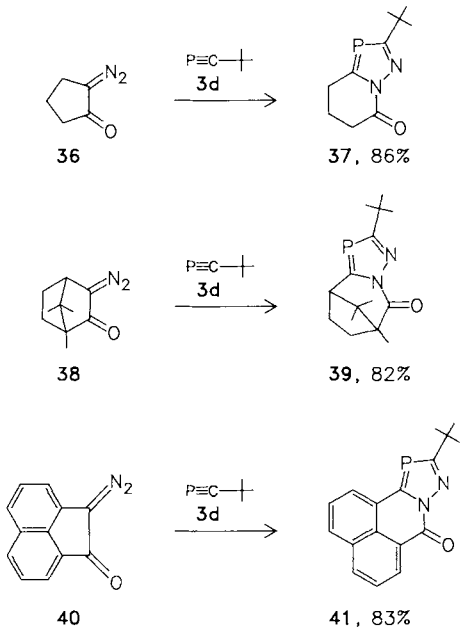

36 37, 86%

38 39, 82%

40 41, 83%

37: ^{31}P NMR (C_6D_6), δ = 95.9. **38**: ^{31}P NMR ($CDCl_3$), δ = 90.5. **41**: ^{31}P NMR ($CDCl_3$), δ = 98.2.

In analogy to **33**, the spirocyclic compounds are formed first, followed by the kinetically determined acyl shift to the phosphorus atom, after which the thermodynamically stable isomers are finally produced.[54]

Cycloaddition reactions of bis[diazo(trimethylsilyl)-methyl]phosphanes **42**[77] and tris[diazo(trimethylsilyl)-methyl]phosphane **45**[77] with the phosphaalkyne **3d** are the starting point of a highly promising synthesis of complicated molecules with numerous heteroatoms. Thus, **42**—easily prepared from dichloro(phenyl)phosphane and two

equivalents of diazo(trimethylsilyl)methyllithium—adds smoothly to **3d** in the usual orientation with subsequent trimethylsilyl shift to afford bis(1,2,4-diazaphospholyl)phosphane **43**.

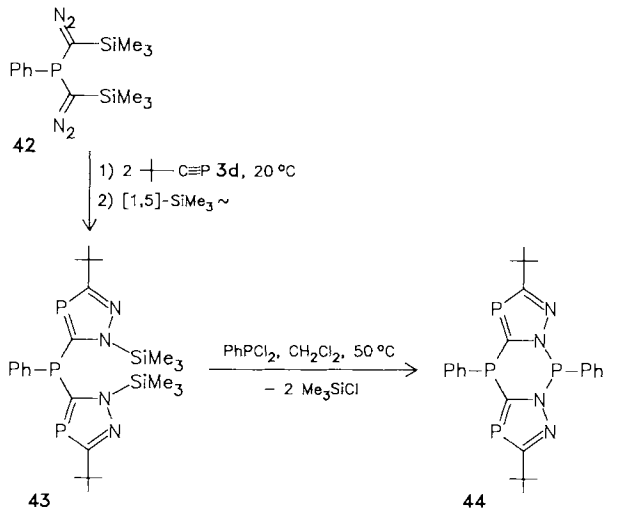

Condensation with additional dichloro(phenyl)phosphane and elimination of chlorotrimethylsilane gives **44**.[77] Analogous reactions with tetrachlorosilane result in the formation of a spirocyclic silicon compound.[77]

The rather unstable compound **45**, which is obtained from phosphorus trichloride and diazo(trimethylsilyl)methyllithium, adds **3d** in a molar ratio of 1 : 3 and undergoes the usual silyl shift to yield tris(1,2,4-diazaphospholyl)phosphane **46**. Cyclocondensation with the trichlorides of phosphorus, arsenic, or antimony, or with trichloro(methyl)silane or -germane in ether or CH_2Cl_2 provides an easy route to the heteroatom-substituted barrelenes **47a–e**.[77]

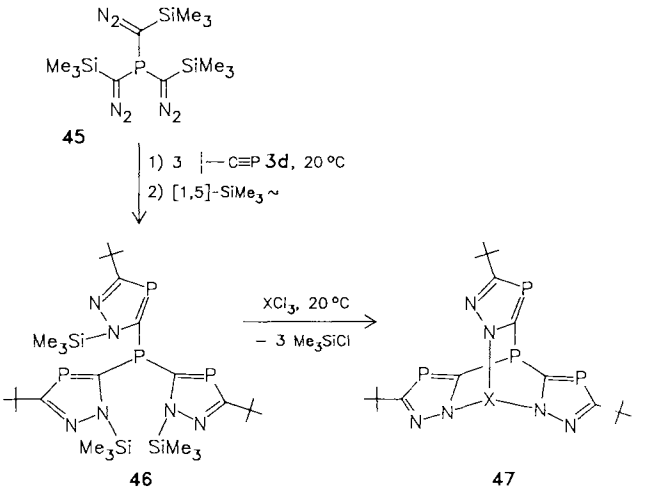

a, X = P; b, X = As; c, X = Sb; d, X = MeSi; e, X = MeGe

3.3.2. 3H-1,2,4-Diazaphospholes

The previous section showed that the 3*H*-1,2,4-diazaphospholes obtained as the primary products of reaction between diazo compounds and phosphaalkynes become aromatic by rapid sigmatropic shifts of hydrogen as well as acyl, phosphoryl, or silyl groups. The potential access to the chemistry of phosphavinylcarbenes by photochemical elimination of N_2 is thereby lost unless the shift of the substituent is prevented, for example, by cycloaddition of dialkyl-substituted diazo compounds.[78]

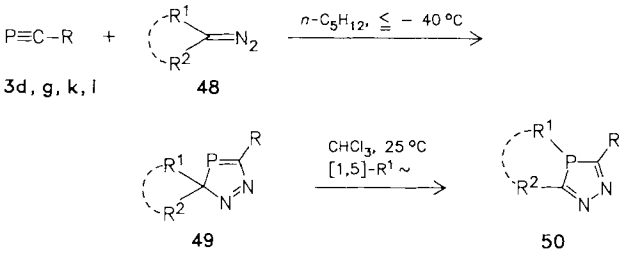

	a	b	c	d	e	f	g	h
R	*t*Bu	*t*Bu	*t*Bu	*t*Bu	*t*Bu		*i*Pr	CH_2-*t*Bu
R^1	*t*Bu	*t*Bu	*i*Pr			*t*Bu	*t*Bu	*t*Bu
R^2	*t*Bu	Me	*i*Pr			*t*Bu	*t*Bu	*t*Bu

This approach allows the 3*H*-1,2,4-diazaphospholes **49a–c** and **49e–h** (yields 92–100%; ^{31}P NMR, $\delta = 263$–304) to be obtained as colorless to pale yellow oils when **3d**, **g**, **k**, **l** are treated with diazo compounds of type **48** at low temperature.[49,69,79–81] The cycloadduct **49d** cannot be prepared in this way since even at −40 °C a sigmatropic alkyl migration occurs, giving the 4*H*-1,2,4-diazaphosphole **50d**.[80] All other 3*H*-diazaphospholes **49** also undergo the same R^1 shift (→ **50**) on standing in chloroform at 25 °C (yield 82–100%; ^{31}P NMR ($CDCl_3$), $\delta = 38$–58).[69,79–81] That this rearrangement is promoted by all the substituents being bulky can be concluded indirectly from the fact that **49b** does not rearrange even when distilled.[79] 4*H*-1,2,4-Diazaphospholes such as **50a,f,g** with a *tert*-butyl group in the 4-position lose the *tert*-butyl group R^1 as isobutylene on heating, forming heterocycles of type **31**.[79,80]

Therefore, to convert 3*H*-1,2,4-diazaphospholes **49** into phosphavinylcarbenes, one can irradiate **49e**, for example, at −40 °C, upon which ring opening to the diazo isomer **51** first occurs,[82] followed by the elimination of nitrogen to afford the desired carbene **52**. At this point different reactions can occur: CH insertion gives the phosphacyclopen-

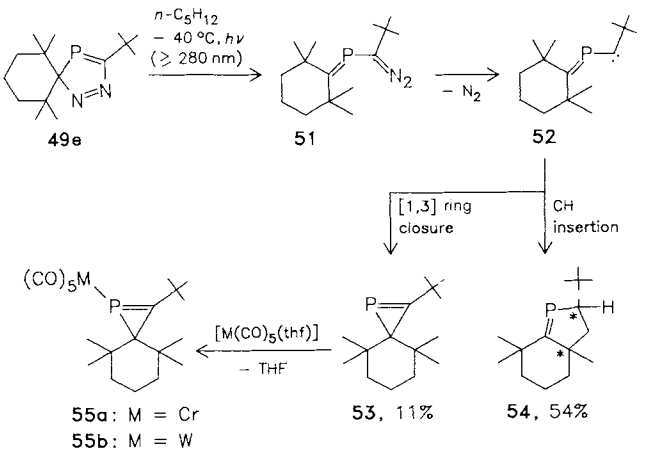

tene **54** and 1,3 ring closure forms the 2*H*-phosphirene **53**, the first phosphacyclopropene with a PC double bond.[81]

To remove any last doubts about the constitution of **53**—the phosphorus resonance at $\delta = 71.7$ ($CDCl_3$) lies to rather high field (compare, for example, the phosphasilirenes **26a** and **26b**)—the metal complexes **55a** and **55b** were prepared and the structure of the tungsten derivative **55b** was confirmed by X-ray crystallography. The P=C bond length is 1.634(4) Å, shorter than the corresponding bonds in the tungsten complex **27**[70] or in open-chain phosphaalkenes bound in metal complexes.[83,84]

The photolysis of other 3*H*-1,2,4-diazaphospholes such as **49a**[79] and **49f-h**[80] affords the phosphaalkenes corresponding to **54** in high yield (63–81%; ^{31}P ($CDCl_3$), $\delta = 250$–263). However, when **49b** is irradiated the rearrangement proceeds differently. While the carbene is formed as before (→**56**), the CH insertion occurs at the methyl and not at the *tert*-butyl group. The first isolable product is the 2-phospha-1,3-butadiene **57**, which results from the electrocyclic ring opening of the insertion product **58**.[85] The same sequence of reactions can be achieved with **49c**.[69]

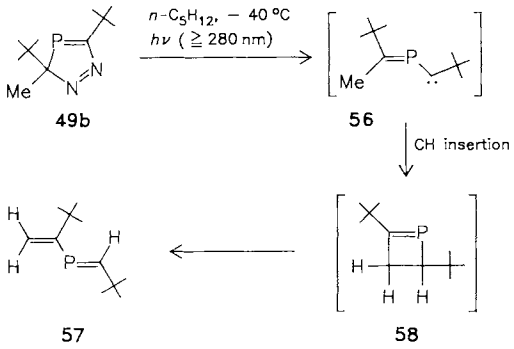

3.3.3. 3*H*-1,2,3,4-Triazaphospholes

3*H*-1,2,3,4-Triazaphospholes were first prepared in 1984 by the 1,3-dipolar cycloaddition of azides to phosphaalkynes.[73,74] Thus, **59a-i** add regiospecifically to **3d** in the same orientation as the isoelectronic diazo compounds (see Sections 3.3.1 and 3.3.2) to afford the 3*H*-1,2,3,4-triazaphospholes **60a-i**.[85] These compounds show no tendency towards a substituent shift of the type found for **60**→**61**. This is observed only when **3d** is treated with trimethylsilyl azide **59j** or hydroazoic acid, which produces **61j** or **61k**, respectively.[85]

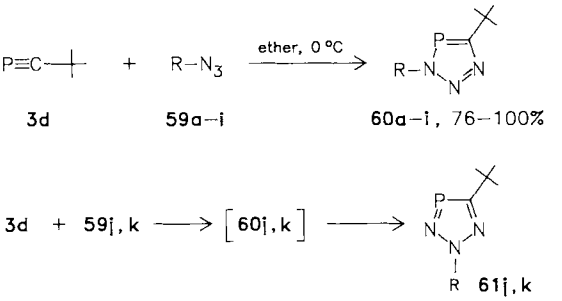

a, R = Me; **b**, R = *t*Bu; **c**, R = Ph; **d**, R = 4-EtO_2C-C_6H_4; **e**, R = 1-naphthyl; **f**, R = $CH{=}CH_2$; **g**, R = CO_2Me; **h**, R = CH_2CN; **i**, R = CH_2SiMe_3; **j**, R = $SiMe_3$; **k**, R = H

60a-i: ^{31}P NMR ($CDCl_3$; **60d**, **e**, C_6D_6), $\delta = 161.8$–180.7.

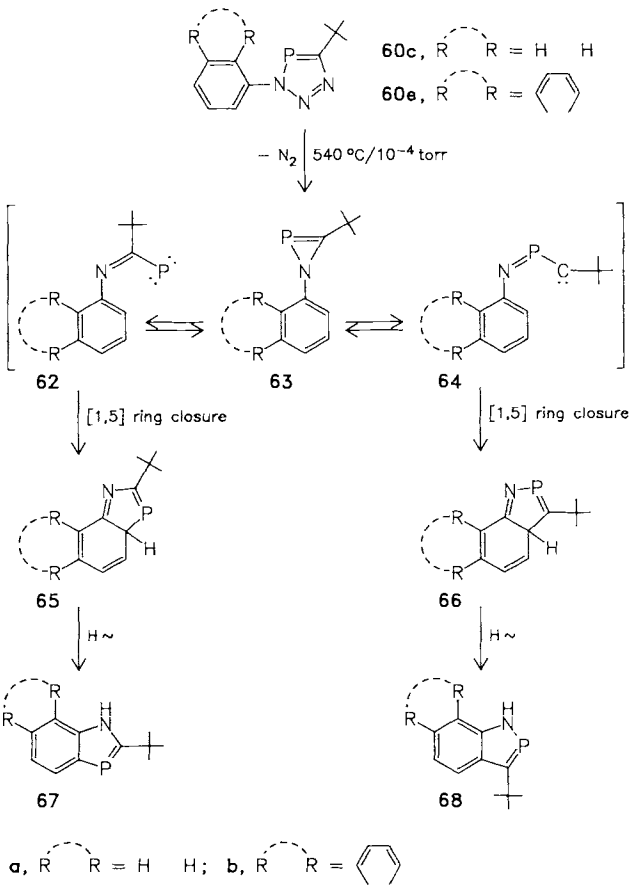

^{31}P NMR ($CDCl_3$): **67a**, $\delta = 66.3$; **67b**, $\delta = 74.4$; **68a**, $\delta = 210.3$; **68b**, $\delta = 180.1$.

Azide additions are not limited to **3d**: adducts of methyl azide of type **60** are known for the parent compound **4**,[22] as well as for the phosphaalkynes **3e,f**,[55] **3g,h**,[48] **3i**,[53] **3k,l**,[48] **3m-p**,[55] and **3r**.[55]

The 3*H*-1,2,3,4-triazaphospholes have an extraordinary thermal stability and lose nitrogen only during flash pyrolysis. Model reactions with **60c** and **60e** give mixtures of isomers of benzoannelated azaphospholes **67a/68a** (95%, 1:4) and **67b/68b** (99%, 1:3).[85]

This result can be interpreted as arising from competing phosphanediyl and carbene reactions, where the azaphosphirenes can react in two different ways (**60**→**63**⇄**62** or **64**). A [1,5] electrocyclization[86] of the intermediate with the electron-deficient (six-electron) phosphorus atom (**62**→**65**, **64**→**66**) and subsequent H-shift gives the products **67** and **68**.[85] Analogous reaction sequences are known for styryl-[87] and aryliminocarbenes.[88]

3.3.4. 1,2,4-Oxazaphospholes

Intuitively one would expect that 1,2,5-oxazaphospholes **71** would be formed when nitrile oxides **69** undergo addi-

tion with phosphaalkynes, if only because of the proverbial oxygen affinity of phosphorus. The process **3d** + **69** actually proceeds specifically in the opposite sense, affording **70**.[73,89] No doubt this is more favorable on steric grounds. Other phosphaalkynes, such as **3e**,**f**,[55] **3g**,**h**,[48] **3i**,[53] **3k**,**l**,[48] and **3r**,[55] show the same orientation when [3+2] cycloadditions occur with nitrile oxides.

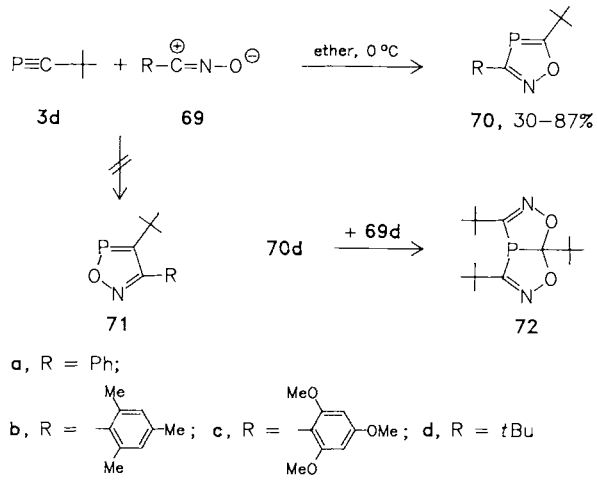

70a–c: ^{31}P NMR ($CDCl_3$; **70a**, C_6D_6), δ = 66.8–81.9.

Despite the steric bulk of its substituents, the PC double bond of **70d** is so reactive that it takes up a further mole of the dipole **69d** to give the heterobicyclic compound **72**.[89] A corresponding reaction of **3d** with 4-chlorophenylnitrile oxide is also known.[74] The trapping reaction of HC≡P **4** with **69a** also is a 1:2 addition.[22]

3.3.5. 1,2,4-Thiazaphospholes

Phenylnitrile sulfide **74**, produced by thermal cycloelimination of carbon dioxide from the oxathiazolone **73**,[90] adds to **3d** in the same orientation as nitrile oxides and affords the thiazaphosphole **75**.[89] To our knowledge, compounds of this type were previously unknown.

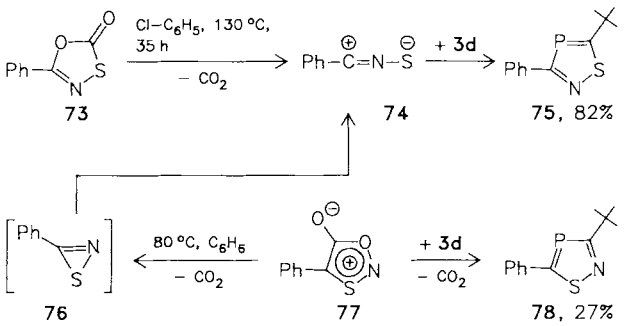

Surprisingly, **75** is also produced when the mesoionic oxathiazolylium-5-olate **77**[91] is heated with **3d** in benzene, although the yield is only 3%. The major product of the cycloaddition, which is accompanied by CO_2 elimination, is the isomer **78**.[92] A possible interpretation of the formation of the unusual thiazaphosphole **75** is that, to a small extent, **77** forms the thiazirine **76**, which, in turn, is transformed into the nitrile sulfide **74**; this then adds **3d** in the normal way.

3.3.6. N-Substituted 1,2,4- and 1,2,3-Diazaphospholes

Nitrilimine dipoles such as **79a** and **79b** do not react regiospecifically with **3d**. In both cases, the product ratios **80a** : **81a** and **80b** : **81b** determined by ^{31}P NMR spectroscopy are 98 : 2. The difference between the chemical shifts (^{31}P NMR ($CDCl_3$): **80a**,**b**, δ = 86.7, 91.9; **81a**,**b**, δ = 224.4, 218.5) is so large that the compounds can be assigned unambiguously.[89] Although **81a** and **81b** can be enriched by fractional crystallization, they cannot be obtained pure. In the reaction **3d** + **79c**, no regioisomer **81c** could be found by ^{31}P NMR spectroscopy.[89]

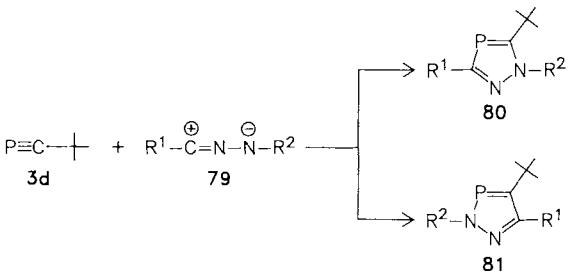

	R^1	R^2	**80** : **81**	Yield **80** + **81** [%]
a	Ph	Me	90 : 2	85
b	Me	Ph	98 : 2	55
c	Ph	Ph	100 : 0	72

Diazaphospholes closely related structurally to **80**, differing only in that the *N*-substituent is on the other nitrogen atom, can be obtained by the reaction of **3d** with sydnones **82a–e**. Primary products of the type **83** could not be detected; the products **85a–e** were isolated directly.[92] Only in the reaction **3d** + **82a** is a mixture of regioisomers formed (**85a**/**84a** in the ratio 87 : 13, determined by ^{31}P NMR spectroscopy). Attempts to separate the isomers by MPLC led to decomposition of **84a**.[92]

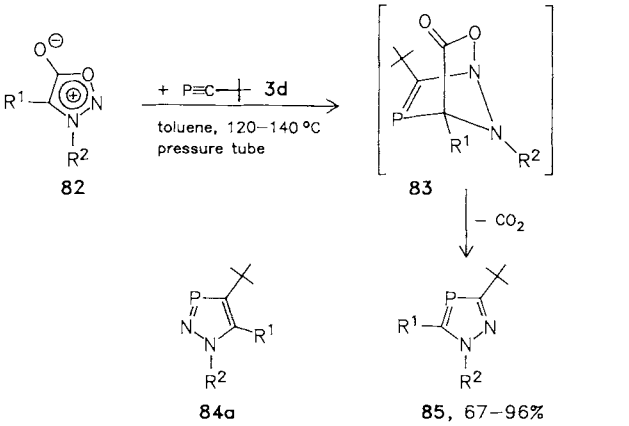

a, R^1 = H, R^2 = Me; **b**, R^1 = H, R^2 = Ph; **c**, R^1 = R^2 = Me; **d**, R^1 = Me, R^2 = Ph; **e**, R^1 = Ph, R^2 = Me

As a general principle, diazaphospholes of type **85** can also be obtained by lithiation of 1*H*-diazaphospholes **31** and subsequent alkylation.[54]

3.3.7. 1,3-Aza- and 1,3-Thiaphospholes

The munchnone **86** is much more reactive towards **3d** than the sydnones **82**. The product is the 1,3-azaphosphole **87**;[92] the first representatives of this type of compound have only recently been prepared.[93,94] Phosphaacetylene **4** also reacts smoothly with **86** to give 1-methyl-2,5-diphenyl-1,3-azaphosphole (**87**, H instead of *t*Bu): the addition reaction and CO_2 elimination take place as the ice bath warms up.[22]

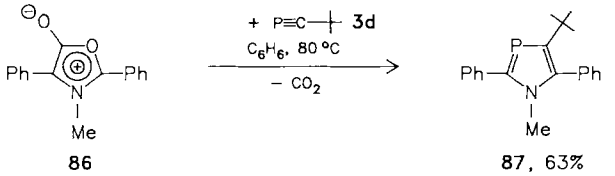

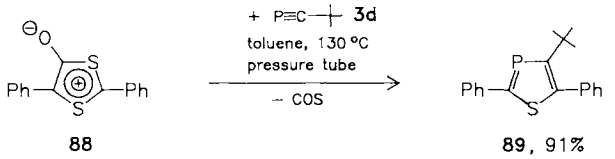

87: ^{31}P NMR ($CDCl_3$), $\delta = 96.6$. **89**: ^{31}P NMR ($CDCl_3$), $\delta = 220.6$.

One can obtain a derivative of the previously little known 1,3-thiaphosphole system when **3d** is treated with the 1,3-dithiolylium-4-olate **88** under more drastic conditions.[95] The phosphorus resonance of the product, **89**, is found at remarkably low field.[92]

3.3.8. Dihydro-1,2,4- and Dihydro-1,2,5-oxazaphospholes

In comparison with the reaction **3d** + **79** → **80** + **81**, a further loss of regiospecificity is found when the nitrone **90** reacts with **3d**. After workup by chromatography, the dihydrooxazaphospholes **91** and **94** are obtained in the ratio ≈ 2 : 1.[79]

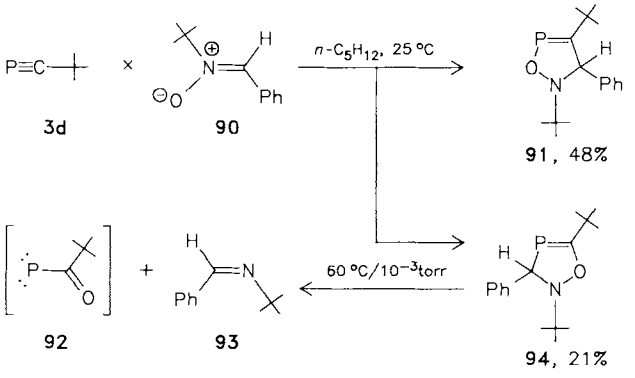

91: ^{31}P NMR ($CDCl_3$), $\delta = 260.1$. **94**: ^{31}P NMR ($CDCl_3$), $\delta = 130.2$.

A first attempt to separate the mixture of regioisomers by distillation in a kugelrohr apparatus caused decomposition of **94** by [3 + 2] cycloreversion—although not the reverse of its reaction of formation. The Schiff base **93** was identified unambiguously, but the fate of the pivaloyl phosphanediyl (phosphinidene) **92** is uncertain.[79]

3.4. [4 + 2] Cycloadditions

Most of the phosphaalkenes that have been synthesized are open-chained.[4a,7b] However, Diels–Alder reactions with phosphaalkynes open up numerous possibilities of exploring the chemistry of mono- and polycyclic compounds with a PC double bond. Compounds of these kinds were previously unknown.

3.4.1. The Valence Isomers of Phosphinines

Phosphinines (phosphabenzenes) are a class of heteroarenes that have been investigated thoroughly.[96] There have been no reports on their valence isomers such as Dewar-phosphinines, phosphaprismanes, or phosphabenzvalenes. In just the same way that the pair of reactants "cyclobutadiene/acetylene" has allowed access to the chemistry of the valence isomers of benzene,[97] the problem of the synthesis of valence-isomeric phosphabenzenes can be solved by using phosphaalkynes and the same cyclic 1,3-dienes.[49]

1- and 2-Dewar-Phosphinines: When the kinetically stabilized cyclobutadienes **95a** and **95b** are treated with the phosphaalkynes **3d,g,i,k,l**, the reaction is regioselective (only the reaction **95a** + **3i** is regiospecific), affording the 2-Dewar-phosphinines **96** (≥ 85%) and **97** (≤ 15%) (Table 3).[98]

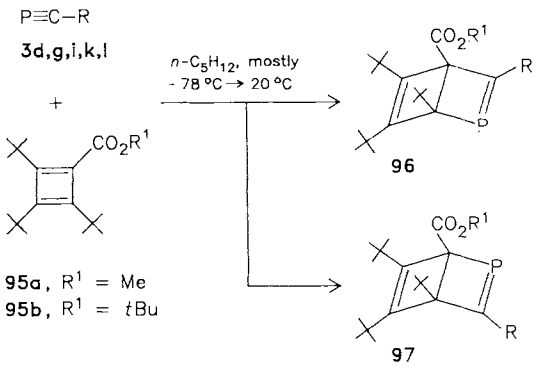

Table 3. Regioisomeric 2-Dewar-phosphinines **96**, **97** prepared from phosphaalkynes **3** and cyclobutadienes **95**. ^{31}P NMR (C_6D_6).

	R [a]	R^1	**96** : **97**	$\delta(^{31}P)$
3d + **95a** → **96a**	*t*Bu	Me	96 : 4	315
3g + **95a** → **96b**	C_7H_{13}	Me	98 : 2	315
3i + **95a** → **96c**	Ad	Me	100 : 0	314
3k + **95a** → **96d**	*i*Pr	Me	97 : 3	312
3l + **95a** → **96e**	CH_2–*t*Bu	Me	93 : 7	314
3d + **95b** → **96f**	*t*Bu	*t*Bu	85 : 15	316
3g + **95b** → **96g**	C_7H_{13}	*t*Bu	85 : 15	316
3i + **95b** → **96h**	Ad	*t*Bu	85 : 15	317

[a] C_7H_{13} = 1-methylcyclohexyl; Ad = 1-adamantyl.

The reaction is therefore mainly kinetically controlled (→ **96**), as can also be recognized in the appreciable increase in the proportion of **97** formed in going from **95a** to

95b.[98] X-ray crystallographic data are available for **96c** (length of the PC double bond: 1.68(1) Å).[98] Typical of all phosphabicyclic compounds of type **96** is the narrow range of their ^{31}P resonances ($\delta = 312$–317); the phosphorus signals of the isomers **97** are found at higher field ($\delta = 285$–300).[98]

Unsubstituted bicyclobutadiene—liberated from its corresponding iron tricarbonyl complex by oxidation[99]—also adds **3d**, but the bicyclic primary product isomerizes spontaneously to the 2-*tert*-butylphosphinine **113d**.[79] Similarly, the recently prepared azete **98**[100] undergoes a Diels–Alder reaction with **3d** and **3l**: this reaction also proceeds under kinetic control and affords the Dewar isomers of the 1,3-azaphosphinines **99a** and **99b**.[101, 102]

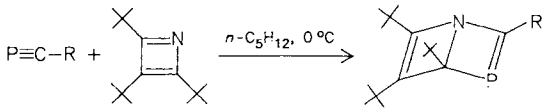

3d,l **98** **99a**, R = *t*Bu; **99b**, R = CH_2–*t*Bu

When the 2-Dewar-phosphinines **96a,c,d** are heated they isomerize to the 1-phosphabicyclic compounds **100a–c**.[79, 103–105] The change from $\lambda^3\sigma^2$ phosphorus to $\lambda^3\sigma^3$ phosphorus is accompanied by a striking shift of the ^{31}P resonance to higher field (**96**, see Table 3; **100** ($CDCl_3$), $\delta = -19$ to -25). One can reasonably assume that the 1-isomers **100** are thermodynamically more stable than the 2-isomers **96**. The intermediates in the isomerization are probably λ^3-phosphinines, at least as far as the process **96a** → **100a** is concerned. Evidence for this comes from the isomerization of the 1-Dewar-phosphinine **100a** (≥ 280 nm, $CHCl_3$, 25 °C): it isomerizes on irradiation to the heteroarene **101**, which as expected reverts to **100a** on heating to 160 °C.[103]

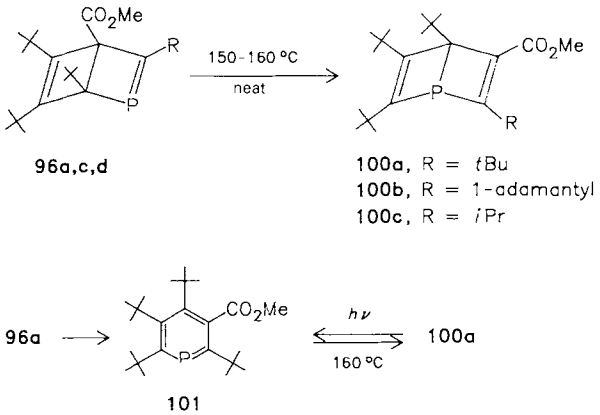

This electrocyclic reaction is at first glance surprising. The explanation is certainly of steric nature: as a result of the accumulation of bulky groups, **101** is no longer planar. Its crystal structure shows that it has a twisted boat conformation with angles at the bow and the stern of 33.7 and 17.9, respectively.[106] The phosphinine **101** has the most distorted structure in a 6π system yet known, except for fused-ring and bridging systems.

Phosphaprismane and Phosphabenzvalene: When the 2-Dewar-phosphinines **96a,c–e** are irradiated in pentane or $CDCl_3$, they undergo relatively fast intramolecular [2+2] cycloadditions to afford the phosphaprismanes **102a–d**.[79, 103–105] This is followed by the photochemical isomerization to the phosphabenzvalenes **105** and **106**: thus, as soon as the concentration of phosphaprismane has peaked, the photolysis must be stopped and the products worked up. This limits the yields that can be achieved (see Table 4).

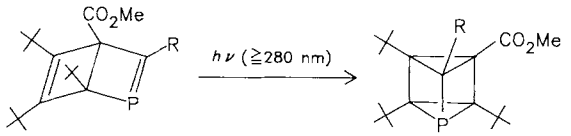

96a, c–e **102a–d**

Table 4. Phosphaprismanes **102** prepared from 2-Dewar-phosphinines **96**. ^{31}P NMR ($CDCl_3$).

	R [a]	*t* [b]	Yield [%]	$\delta(^{31}P)$	Ref.
96a → **102a**	*t*Bu	4 h	40	−130.2	[103]
96c → **102b**	Ad	30 min	59	−133.0	[104]
96d → **102c**	*i*Pr	45 min	63	−128.4	[79]
96e → **102d**	CH_2–*t*Bu	45 min	70	−101.3	[105]

[a] Ad = 1-adamantyl. [b] Reaction time.

The incorporation of the $\lambda^3\sigma^2$ phosphorus into the phosphirane ring of the tetracyclic compound **102** is associated with an enormous high-field shift of the ^{31}P resonance (compare the values in Tables 3 and 4).

When the 2-Dewar-phosphinine **96a** (or the phosphaprismane **102a**) is subjected to extended photolysis, a further isomerization takes place, yielding the phosphabenzvalenes **105** and **106**. Compound **106** is thermally stable and can be isolated. However, even at room temperature, **105** rearranges to the phosphinine **101**.[103]

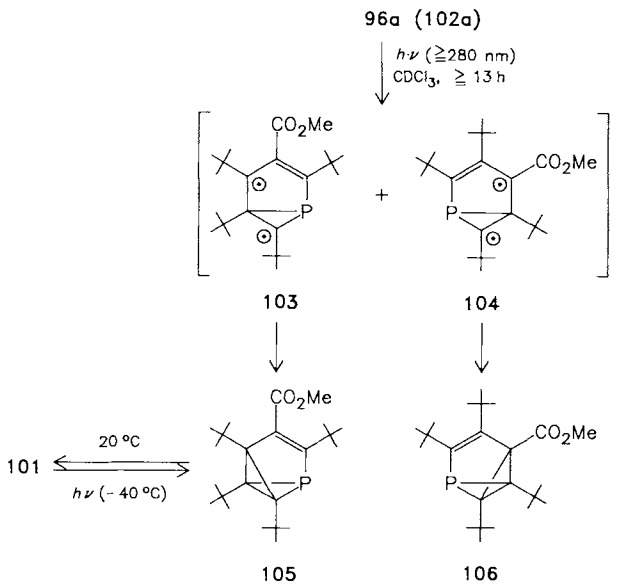

105: ^{31}P NMR ($CDCl_3$), $\delta = -89.8$. **106**: ^{31}P NMR ($CDCl_3$), $\delta = -83.3$.

That this reaction pathway is correct emerges partly from the photochemical retroisomerization of the phosphabenzene **101** to phosphabenzvalene **105** at −40 °C and partly from the reversal of the isomerization at room temperature. Furthermore, it is completely consistent with the

detection by ^{31}P NMR spectroscopy of the phosphabenzvalene **105** (together with **106**) when **96a** is photolyzed at low temperature.[103] The biradicals **103** and **104** are presumed intermediates in the phosphaprismane/phosphabenzvalene isomerization.[103] Stable phosphabenzvalenes corresponding to **106** are also formed during the extended photolysis of **96d** and **96e**.[79]

Oxidation Reactions of Valence Isomers of Phosphinine: When the stable phosphabenzvalene **106** is heated with sulfur, the bicyclic phosphane sulfide **107** is formed, the structure of which has been confirmed by X-ray crystallography.[103] The assumption that the isomerization **106** → **108** precedes the oxidation is inconsistent with the fact that this step only occurs at much higher temperature (160°C as opposed to 120°C). Thus, the formation of **107** by oxidation of **108** with sulfur allows no conclusions to be drawn regarding the mechanism. It seems more plausible that **106** is first oxidized to the corresponding sulfide, which, in turn, gives the bicyclic compound **107**.[79]

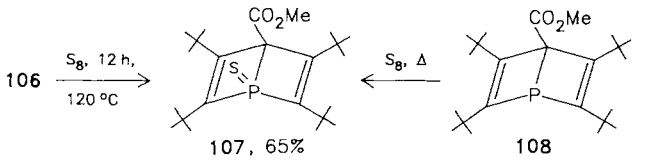

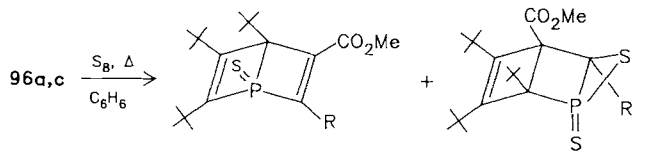

109a: R = *t*Bu, 10%
109b: R = 1-Ad, 9%

110a, R = *t*Bu, 66%
110b, R = 1-Ad, 79%

107: ^{31}P NMR ($CDCl_3$), $\delta = 39.3$.

The oxidation of the 2-Dewar-phosphinines **96a** and **96c** with sulfur is more complicated; various products are formed. The 1-Dewar-phosphinine sulfides **109a** and **109b** are side products, while the main reaction is the incorporation of two equivalents of sulfur without rearrangement of the skeleton, giving the thiaphosphirane sulfides **110a** and **110b**.[104] There are no difficulties in interpreting the mechanism of the latter reaction. The structure of **110b** has been confirmed by X-ray crystallography.[104, 107]

The conversion of **96** to **109** is most easily understood if one assumes that a phosphinine sulfide (**101**, P=S instead of P) is first formed, which then undergoes an electrocyclic ring closure.[104]

3.4.2. New Phosphinines

Phosphinines with $\lambda^3\sigma^2$ phosphorus are mostly synthesized from pyrylium salts and one PH_3 equivalent.[96] New and versatile synthetic possibilities are opened up by the Diels–Alder reaction of phosphaalkynes with cyclic 1,3-dienes that have an easily eliminated group connecting C-1 and C-4.[49] Although all the reactions require rather high temperatures, the phosphaalkyne **3d** survives them without problem.

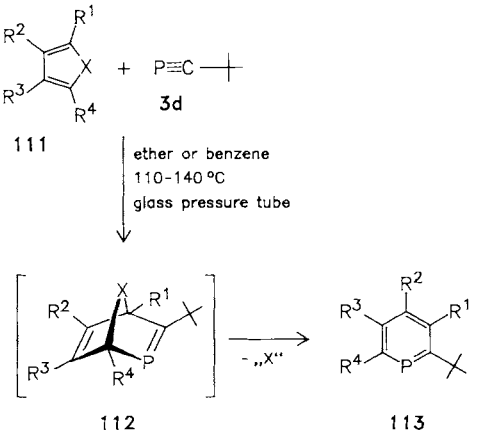

	a	b	c	d	e	f
R^1	Ph	Pr	H	H	Ph	H
R^2	Ph	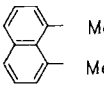	Me	H	H	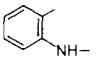
R^3	Ph		Me	H	Ph	
R^4	Ph	Pr	H	H	H	Et
X						
Yield [%]	92	93	61	91	48	54
δ (^{31}P)($CDCl_3$)	202	266	187	202	187	187

Suitable reactants include cyclopentadienones (**111a,b**; CO elimination) and the phosphole sulfide **111c** (Ph–P(=S) elimination)[108] as well as a α-pyrones (**111d–f**; elimination of CO_2). In all cases the yields of phosphinines (**113a**,[109] **113b**,[110] **113c,d**,[109] **113e,f**[110]) are good to very good. The bicyclic intermediates **112a–f** cannot, of course, be detected under these drastic reaction conditions.

Highly reactive phosphaacetylene **4** reacts with **111a**, even as the cooling bath warms up, to give 2,3,4,5-tetraphenyl-λ^3-phosphinine.[111] The Diels–Alder route can also be used to prepare 1,3λ^3-azaphosphinines from **3d** or **3i** and 2-trifluoromethyl-1,3-oxazin-6-one.[112]

3.4.3. Polycyclic Phosphorus Compounds

Bi-, tri-, and tetracyclic compounds containing three-valent two- or three-coordinate phosphorus can also be obtained by cycloaddition processes involving phosphaalkynes. It is important that, in contrast to **111**, the 1,3-dienes employed should have no easily eliminated "X" group.

Bicyclic Compounds: Apart from the reactions of cyclobutadienes such as **95a,b**, [4+2] cycloadditions with homologous cycloalka-1,3-dienes offer good chances of preparing 2-phosphabicyclic compounds with methano or ethano bridges. The 2-phosphabicyclo[2.2.2]octa-2,5-dienes **115a** and **115b**, prepared from **114** and the phosphaalkynes **3d**[109] and **3e**,[113] are thermally so stable that they can be purified by distillation. On the other hand, the 2-phosphabicycloheptadiene **116**, prepared from cyclopentadiene and **3d**, can only be handled in solution (ether, 20°C); attempts to isolate it led to its oligomerization.

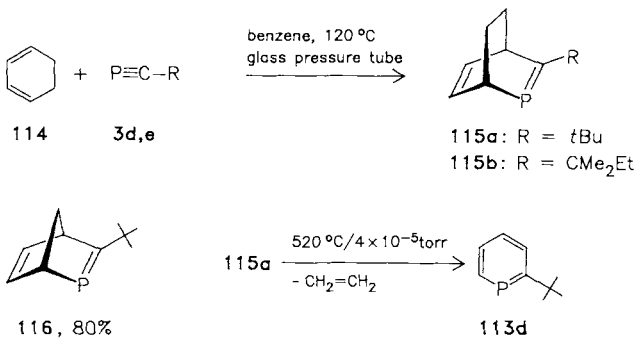

115a: ^{31}P NMR ($CDCl_3$), $\delta = 226$. **115b**: ^{31}P NMR (C_6D_6), $\delta = 232$. **116**: ^{31}P NMR (C_6D_6), $\delta = 246$.

Flash pyrolysis of **115a** causes it to undergo a retro-Diels-Alder reaction. However, this is not the reverse of the reaction of formation, but involves the elimination of ethylene and the formation of the phosphabenzene **113d**.[109]

Phosphabarrelenes with $\lambda^3\sigma^3$ phosphorus are quite well known,[114] but those with a phosphaalkene unit still unknown. Attempts to synthesize a compound of this class by [4+2] cycloaddition of hexafluoro-2-butyne to 3-methyl-2-phosphanaphthalene failed, because the benzobarrelene, which is presumably formed initially, decomposed to 2,3-bis(trifluoromethyl)naphthalene and the phosphaalkyne **3a**.[115]

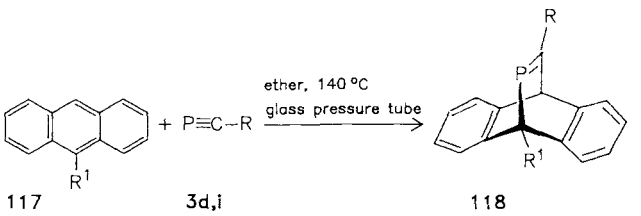

	R^1	R	Yield [%]	$\delta(^{31}P)$ ($CDCl_3$)
a	H	*t*-Bu	91	230
b	H	1-Ad	65	234
c	Me	*t*-Bu	87	246
d	Ph	*t*-Bu	28	235

In contrast, no difficulties are encountered in the Diels-Alder reaction of anthracene and its 9-substituted derivatives **117** with the phosphaalkynes **3d** and **3i**; this reaction gives the barrelenes **118a–d** containing low-coordinate phosphorus.[116]

Tricyclic Compounds: The result of the reaction of the phosphaalkyne **3d** with acyclic 1,3-dienes **119a–d** is unexpected in that tricyclooctenes **122a–d** containing one diphosphirane unit are formed, irrespective of the ratio of the reactants. The dienophile and the diene react in the ratio 2:1. The structure of the products is based upon the X-ray analysis of **122a**. The high-field chemical shifts of both phosphorus nuclei in the ^{31}P NMR spectra of **122** reflect the conversion of the phosphorus from $\lambda^3\sigma^1$ to $\lambda^3\sigma^3$.[117]

The mechanism of the formation of the tricyclic compound can be understood as involving an initial Diels-Alder reaction **119** + **3d** → **120** followed by the ene reaction **120** + **3d** → **121**, which has not previously been observed

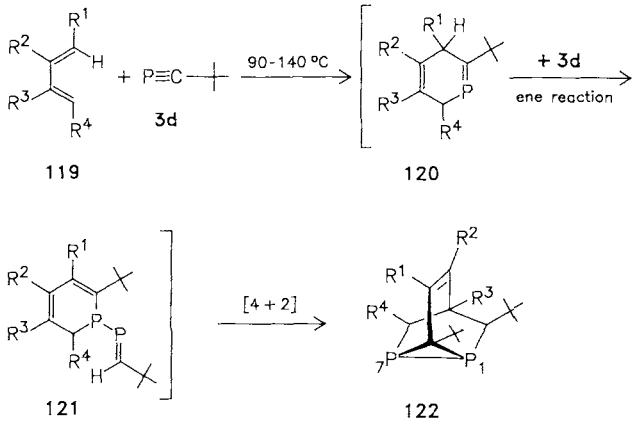

	R^1	R^2	R^3	R^4	Yield [%]	$\delta(^{31}P)$ P-1 / P-7
a	H	H	H	H	90	−190 / −195 [a]
b	H	H	Me	H	85	−166 / −202 [a]
c	H	Me	Me	H	86	−166 / −211 [b]
d	H	H	H	Me	66	−174 / −176 [b]

[a] In C_6D_6. [b] In $CDCl_3$.

for phosphaalkynes (see Section 3.5). Finally, the intramolecular [4+2] cycloaddition **121** → **122** takes place. The first step is not regiospecific: with 1,3-butadienes **119b** and **119d**, in addition to the major products **122b** and **122d**, respectively, side products are obtained in which the order of the substituents R^1 to R^4 is reversed. On the other hand, the subsequent ene reaction always proceeds with the formation of a PP bond.[117]

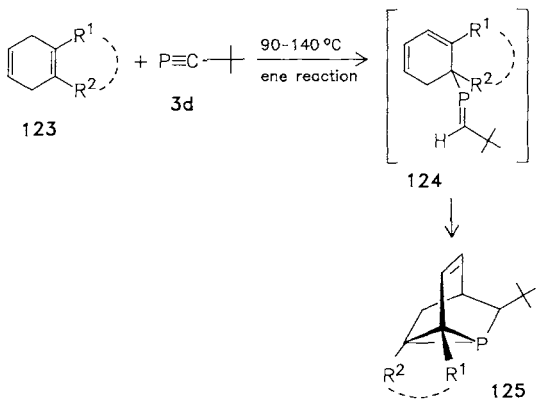

	R^1	R^2	Yield [%]	$\delta(^{31}P)$ ($CDCl_3$)
a	H	H	90	−234
b	CH_2–CH=CH–CH_2		33	−197
c	Me	Me	60	−192
d	CH_2–CH_2–CH_2		46	−205

These conclusions on the sequence of reactions are confirmed by the reaction of the cyclohexa-1,4-dienes **123a–d** with **3d** under similar conditions to yield the phosphatricyclooctenes **125a–d**, although in this case, too, the product of the ene reaction (**124**) cannot be detected directly. However, as seen from the composition of the products formed, the ene reaction must be highly specific.[117]

Tetracyclic Compounds (Homo-Diels-Alder Reaction): Homo-Diels-Alder reactions in the chemistry of carbon compounds are, by comparison with the Diels-Alder reac-

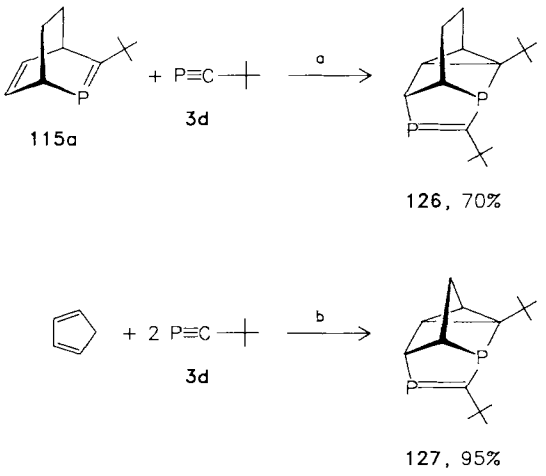

a) C_6H_6, 140°C/5 bar. b) Ether, 180°C/5 bar. **126**: ^{31}P NMR (C_6D_6), $\delta = -16, 316$. **127**: ^{31}P NMR (C_6D_6), $\delta = 5, 322$.

tion itself, a rarity.[118] However, they expand enormously the methods available for preparing phosphorus-containing tetracyclic compounds.

Thus, when the phosphaalkyne **3d** is heated with **115a**, it adds regiospecifically to form the tetracyclic compound **126**. Three- and two-coordinate phosphorus can be identified unambiguously from the high- and low-field chemical shifts in the ^{31}P NMR spectrum.[119] This diphosphatetracyclodecene **126** has ultimately been built up from cyclohexa-1,3-diene **114** and two equivalents of **3d**. A corresponding sequence of reactions has been achieved with cyclopentadiene and **3d**, leading to the formation of **127**.[119]

3.5. The Ene Reaction

Ene reactions with phosphaalkynes have previously been postulated to provide a plausible explanation of the reaction of **119** with **3d** (molar ratio 1:2) to give **122** and of **123** with **3d** to give **125**.[117] This suggested that this type of reaction should be attempted with phosphaalkynes directly.

This has been achieved with 2,3-dimethyl-2-butene and **3d** and leads to the formation of the kinetically stabilized phosphaalkene **128**.[117] This addition reaction can also be carried out with isobutene and **3d**. Indeed, it occurs not once but twice, first on **3d** and then on the phosphaalkene

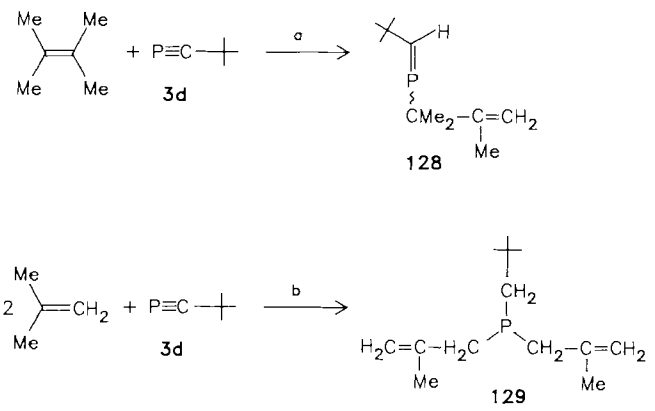

a) C_6H_6, 130°C, pressure vessel. b) 120°C, pressure tube.

formed as an intermediate, yielding the phosphane **129**.[117]

A particularly fascinating reaction is observed between 1,2,3,4,5-pentamethylcyclopentadiene and the phosphaalkynes **3d** and **3i**, where the Diels–Alder reaction is completely suppressed in favor of the ene products **130a** and **130b**, respectively.[119] The room temperature ^1H NMR

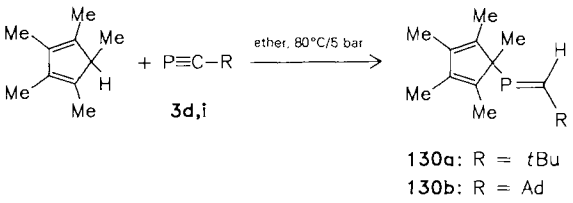

spectrum of **130a** shows only one resonance for the 15 methyl hydrogen atoms, which can only be interpreted as meaning that the phosphaalkene unit undergoes a rapid degenerate [1,5]-sigmatropic shift. On cooling the sample, the coalescence temperature is reached at ca. −40°C, and at −70°C three signals are observed, as expected for a nonfluctuating system **130a** ($\delta = 1.27$, 1.77, and 1.85, ratio 3:6:6).[119]

3.6. Synthetic Equivalents of Phosphaalkynes

Phosphaalkynes in cycloaddition processes can be replaced by their phosphaalkene precursors. Thus, the nitrile oxides **69a–c** add to the phosphaalkene **16d** in ether or pentane at 25°C to give the corresponding dihydro-1,2,4-oxazaphospholes **131**, which then eliminate hexamethyldisiloxane either spontaneously (**131a,b**) or catalyzed by sodium hydroxide (**131c**) to aromatize to **70a–c**.[120] Compounds **70a–c** can also be prepared directly from **3d** and the same dipoles (see Section 3.3.4). 1*H*-1,2,4-Diazaphos-

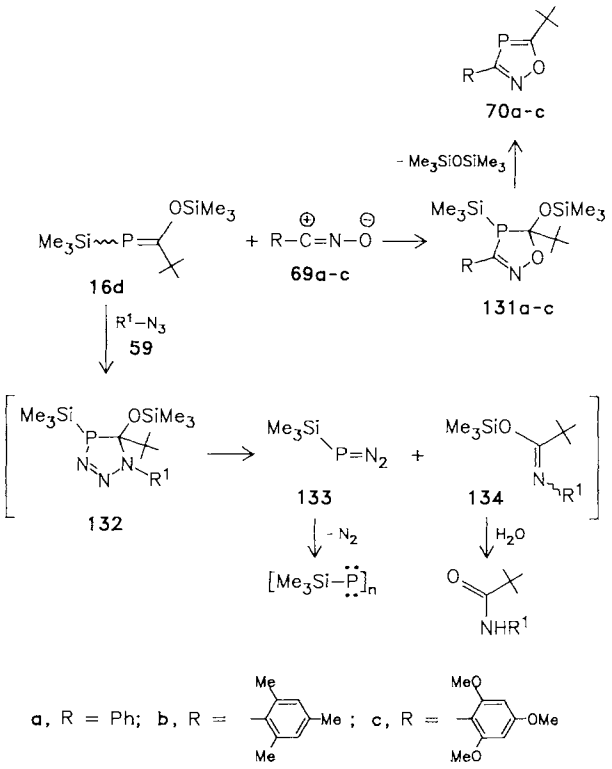

pholes with phenyl or trimethylsilyl substituents in the 5-position can be prepared similarly by the reaction of the phosphaalkenes **20a** and **20b** with diazomethyl compounds. In this case the elimination of chlorotrimethylsilane is responsible for the formation of the heteroarenes.[22, 121, 122]

Limitations to this method become obvious when the orientations of the dipoles of the phosphaalkene and phosphaalkyne are no longer identical. For example, reaction of **16d** with azides **59** (at −15 to +25°C in ether) does not give 3*H*-1,2,3,4-triazaphosphole **60**, since the orientation of the dipole is reversed in the primary step (see Section 3.3.3). The regioisomeric adducts **132** undergo rapid cycloreversion to the phosphazide **133** (which is thermally unstable and decomposes) and the imidoesters **134** (which hydrolyze during the workup).[120]

Phosphaalkenes with groups that can be eliminated are also used for the synthesis of phosphinines. Thus, the phosphinine **135** is obtained from **20a** and pyrone in the presence of potassium fluoride and 18-crown-6 at very high temperature.[123] When **20b** reacts with 2,3-dimethyl-1,3-butadiene in *o*-dichlorobenzene at room temperature, the first product is the usual Diels–Alder adduct. To effect its aromatization to **136**, however, similarly drastic conditions are required as for the reaction just discussed.[122]

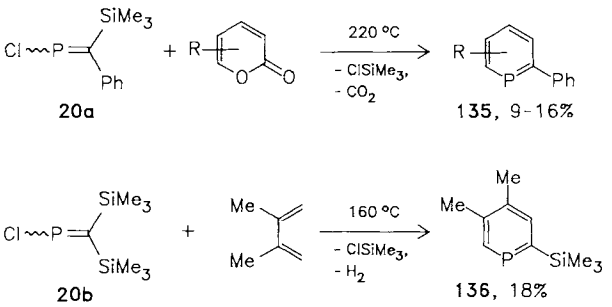

In the synthesis of the first phosphaazulene **137**, the phosphaalkene **20a** was taken as the equivalent of Ph–C≡P **3s**. The decisive step is an [8+2] cycloaddition with methoxyheptafulvene, which is followed by the elimination of chloromethylsilane and hydrogen to afford **137**.[124] For both the cycloadditions with **20a** it cannot be excluded a priori that the products are formed in part or entirely from the phosphaalkyne **3s** that has formed in the reaction mixture (see Section 2.2). Both reactions also require the addition of [18]crown-6.

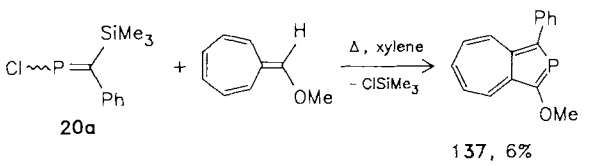

3.7. Metal Complexes

The reactions discussed above show that phosphaalkynes are much more closely related to acetylenes than to nitriles. Their photoelectron spectroscopic properties[31, 61] suggest that they should be good ligands in metal complexes.[61] In principle, they could act as two-, four-, or six-electron donors. Side-on, end-on, and bridging coordination are conceivable and all have been realized. In practice, the thermally stable *t*BuC≡P **3d** has nearly always been chosen as the ligand.

3.7.1. Side-on Coordination

Mononuclear complexes with η^2-bonded phosphaalkynes have been prepared with platinum, titanium, and zirconium as the central metal. Thus, the complexes **138**, **139**, and **141** can be prepared from **3d** and ethenebis(triphenylphosphane)platinum,[125] [Pt(diphos)$_2$],[126] and the complex **140**, respectively.[127] Replacement of a phosphane ligand in the corresponding bis(trimethylphosphane) compounds by **3d** affords the titanium and zirconium complexes **142a** and **142b**.[128]

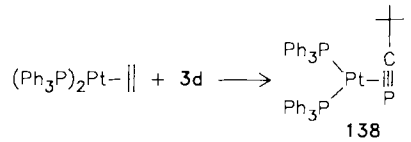

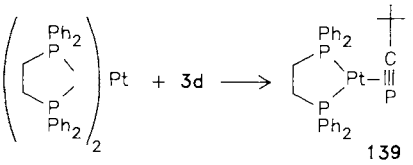

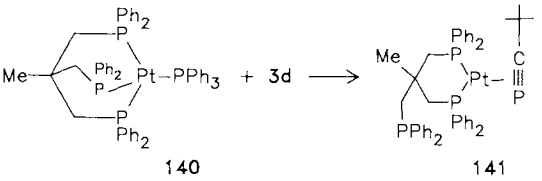

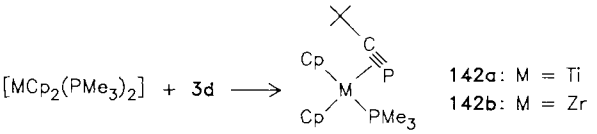

The side-on coordination of the phosphaalkyne in complexes **138**[125] and **142a**[129] has been confirmed by X-ray crystallography. Characteristic of both compounds is the lengthening of the PC bond from 1.54 Å in **3d** when not coordinated to 1.672 Å (**138**) and 1.636 Å (**142a**) when complexed.

3.7.2. End-on Coordination

Until recently, end-on coordination of phosphaalkynes by the nonbonding electron pair on the phosphorus atom was unknown. Apparently, this mode of bonding is found only when η^2-bonding cannot occur for steric reasons.

The only known examples are the compounds **144a–c**, where the end-on-bound N_2 ligands in the dinitrogen complexes **143a** and **143b** have been replaced by the phosphaalkynes **3d** and **3i** to form 2:1 complexes.[130] A mixed complex has also been synthesized by exchange of just one dinitrogen ligand (**143**, M = Mo, R′ = C_6H_4–Cl(4), *t*Bu–C≡P instead of one N≡N).[130]

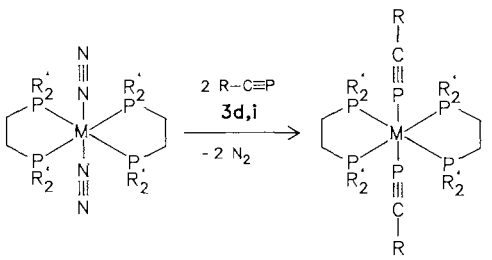

143a: M = Mo, R' = Et
143b: M = W, R' = Ph

144a: M = Mo, R = *t*Bu, R' = Et
144b: M = Mo, R = 1-Ad, R' = Et
144c: M = W, R = *t*Bu, R' = Ph

The crystal structure of **144b** is characterized by a linear chain of seven atoms, C-C-P-Mo-P-C-C, which includes the two phosphaalkyne ligands in *trans* positions. The PC bond length of 1.520 Å in **144b** is shorter than in "free" **3d** and in the side-on complexes **138** and **142a** (see Section 3.7.1).

3.7.3. Bridging Coordination

Several dinuclear metal carbonyl complexes that form tetrahedral bimetallic complexes with η^2,η^2-coordinated alkynes[131] behave in an analogous fashion with the phosphaalkyne **3d**. The dinuclear complexes **145**,[125,132] **146**,[133] and **147**,[132,134] all of which have a tetrahedrane skeleton, were thereby obtained.

The crystal structure of **147** reveals that the PC bond length is not typical of a single bond (≈1.82–1.87 Å); the bond distance of 1.719 Å falls more in the range expected for a double bond.[134] In the complexes **145**, **146**, and **147** the phosphorus atom can coordinate to a second metal complex fragment using its nonbonding electron pair. Thus, treatment of the dimolybdenum complex **147** with $[Fe_2(CO)_9]$ leads to the formation of compound **148**,[135] in which the phosphaalkyne acts as a six-electron donor. Similar displacement reactions can be carried out such that moieties with tungsten,[132] platinum, or palladium[136] as the central atom can be coordinated to the phosphorus atom of **147**. The coordination number of the phosphorus atom in the dicobalt complex **145** can be increased in the same way.[132,137]

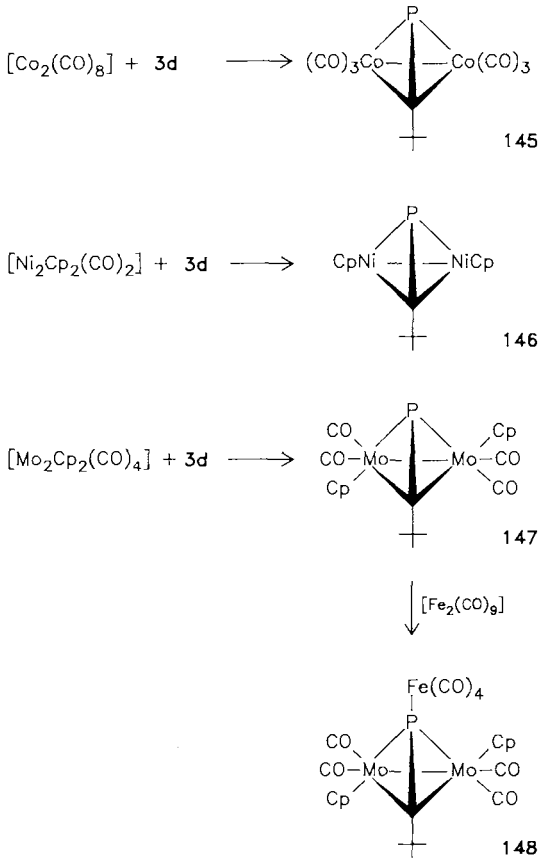

145

146

147

148

Instead of a phosphaalkyne as a four-electron donor, one can take its synthetic equivalents to prepare dicobalt complexes that have a tetrahedrane structure. Thus, the reaction of $[Co_2(CO)_4]$ with dichloro(dichloromethyl)phosphanes ($RCCl_2-PCl_2$, R = Me, Ph, $SiMe_3$) proceeds with dehalogenation to give complexes of the type **145** (R instead of *t*Bu) in rather low yields.[137]

In contrast to $[Mo_2Cp_2(CO)_4]$, the initial reaction of hexa-*tert*-butoxyditungsten (which also has a metal–metal triple bond) with **3d** is a metathesis to afford the intermediate **149**.

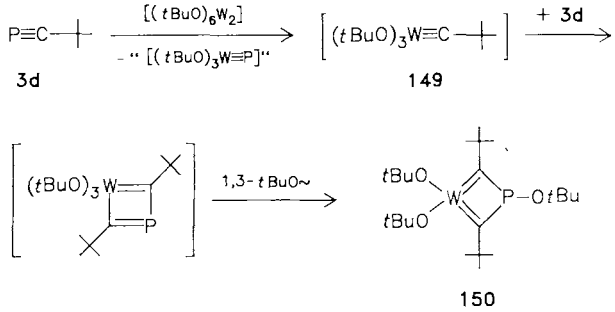

3d **149** **150**

Cycloaddition of the phosphaalkyne **3d** to the tungsten–carbon triple bond is held to account for the formation of a further intermediate with antiaromatic character. This gives the stable final product **150** by a 1,3 shift of a *tert*-butoxy residue from tungsten to phosphorus.[47,68]

When the CO-bridged metal complex $[RhMCp^*_2(CO)_2]$ (M = Rh, Co) is treated with the phosphaalkyne **3d**, the

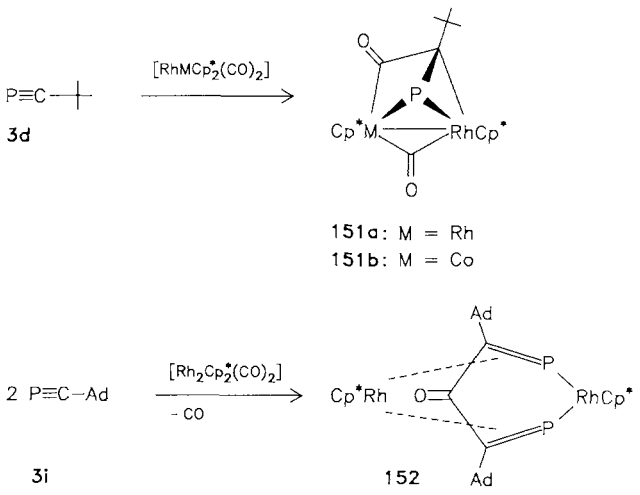

3d

151a: M = Rh
151b: M = Co

3i **152**

$Cp^* = (\eta^5\text{-}C_5Me_5)$

products are not, as might have been expected, complexes with a tetrahedrane structure. Instead, the compounds **151a**[134] and **151b**[138] are formed. As with the corresponding reactions of alkynes,[139] the addition of the phosphorus atom of the phosphaalkyne to the Rh–Rh or Rh–Co double bond is accompanied by insertion of the phosphaalkyne carbon into one of the Rh–CO bonds. The second carbonyl group remains as a bridging ligand.

If an excess of the phosphaalkyne **3i** reacts with $[Rh_2Cp^*_2(CO)_4]$, then, in addition to **151a** (Ad instead of *t*Bu), the complex **152** is formed, which contains the previously unknown ligand unit P=CR–C(=O)–CR=P. According to the crystal structure analysis, the P–C distance is 1.783 Å.[138] In this case, too, the formation of this complex has its parallel in the chemistry of alkynes.[140]

Metal complexes with bridging phosphaalkyne ligands can also be obtained from the side-on complexes mentioned at the beginning of this section. An example is the trinuclear cluster compound **153** formed from **139** and $[Fe_2(CO)_9]$.[126] The X-ray crystallographic study of **153** shows that each metal atom is bound to all the others.[126]

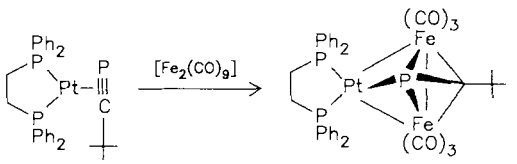

139 153

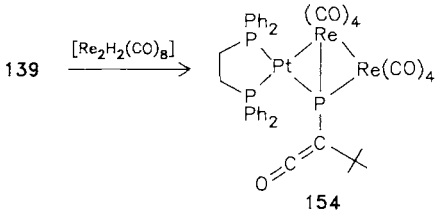

154

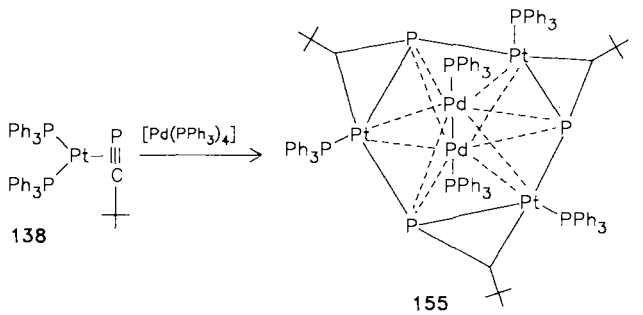

138 155

A new and unusual result is obtained when **139** is treated with $[Re_2H_2(CO)_8]$: the phosphanediyl complex **154** is formed in a low yield (10%).[141] The critical step in incorporating the originally η^2-coordinated phosphaalkyne into the phosphanediyl ligand in the product, in which it is bound to all three metal atoms, is the coupling of CO with the carbon atom of the phosphaalkyne.

Finally, the cluster compound **155**, prepared from **138** and $[Pd(PPh_3)_4]$, should be mentioned: this compound contains five metal atoms.[142] Both palladium atoms take up axial sites (bond length: 2.679 Å), while the platinum atoms are found in equatorial positions. The three phosphaalkyne units each bridge two platinum atoms; they are η^2-coordinated to one of these platinum atoms, the other forming a σ bond with the nonbonding electron pair of the phosphorus.

3.7.4. Cycloaddition in the Coordination Sphere of Metal Atoms

In the previous sections it was shown that in metal complexes phosphaalkynes can act as two-, four-, or six-electron ligands. However, until recently it was not known whether they can be cyclooligomerized in the coordination sphere of suitable metals. This has now been achieved, once again most notably with the phosphaacetylene **3d**, which undergoes di- and trimerization to give new ligand systems.

Complexes of Cyclic Dimers: The cyclodimerization of the phosphaalkyne **3d** was achieved by drawing upon experience gained in the cyclooligomerization of acetylenes with $[CoCp(C_2H_4)_2]$.[143] The reaction, carried out in ether/pentane at $-30°C$, is regiospecific and affords η^5-cyclopentadienyl(η^4-1,3-diphosphacyclobutadiene)cobalt **156a** (67%).[144–146] If the relative amount of $[CoCp(C_2H_4)_2]$ is increased significantly, then **156a** reacts further to produce the di- and trinuclear complexes **157** and **158**, respectively. The cobalt ligands σ-bound to phosphorus can be removed again by adding **3d** to produce **156a**.[145, 146]

$[RhCp(C_2H_4)_2]$ can also be used to cyclodimerize **3d** (→ **156b**), but the yield is unconvincing.[144] The formation of compounds containing two and three rhodium complex fragments (**157** and **158**, Rh instead of Co) is not observed. However, **156b** can be converted with $[RhCl(C_2H_4)_2]_2$ into the hexarhodium complex **159** by a similar substitution process.[147]

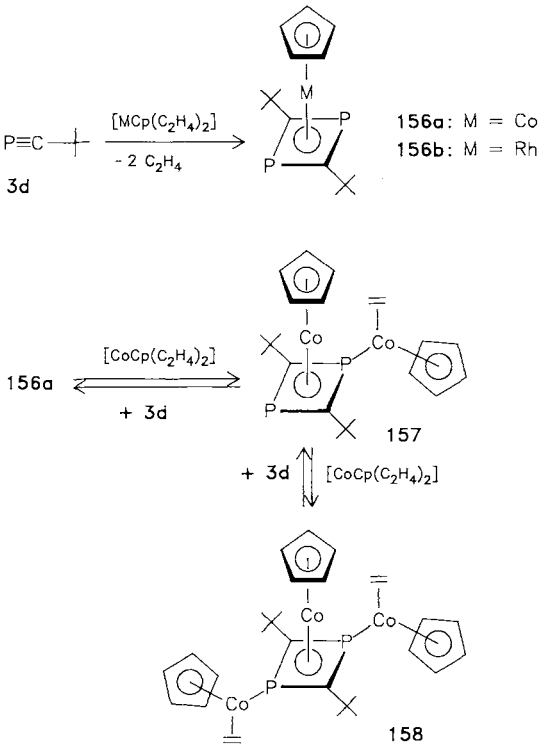

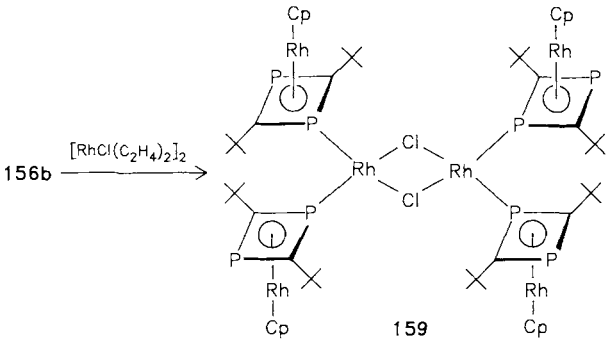

Cyclodimerization with the bis(ethene)pentamethylcyclopentadienyl complexes of cobalt, rhodium, and iridium[144] appears to have no advantages over the reaction **3d** → **156a**.

Whereas the indenyl complex $[CoInd(C_2H_4)_2]$ reacts with **3d** and **3k** to form the expected 1,3-diphosphacyclobutadiene complexes of type **156** in the normal way,[145,146] the corresponding reaction with $[RhInd(C_2H_4)_2]$ is unusual.

Although in this case, too, the dimer complex **160** is formed, a second product, a dinuclear complex with the structure **161**, is isolated.[148] According to the X-ray crystallographic analysis, the six-membered ring is somewhat distorted. The *t*Bu–C fragments that have apparently been "lost" turn up as di-*tert*-butylacetylene. It is presumed that steric interactions prevent further $MInd(C_2H_4)_2$ ligands from binding to η^4-diphosphacyclobutadiene(η^5-indenyl)cobalt and -rhodium complexes in the same way as in **157** and **158**.[146]

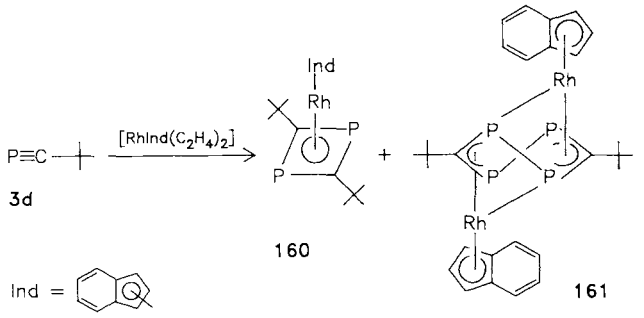

The tricarbonyliron complexes have a special significance in the chemistry of cyclobutadienes because the antiarene can be liberated from them in various ways.[149] The corresponding iron complex of 2,4-di-*tert*-butyl-1,3-diphosphacyclobutadiene (**162**, 65%) is obtained by the cyclodimerization of **3d** with diiron nonacarbonyl at 100°C or with tricarbonylbis(cyclooctene)iron at only −30°C.[150]

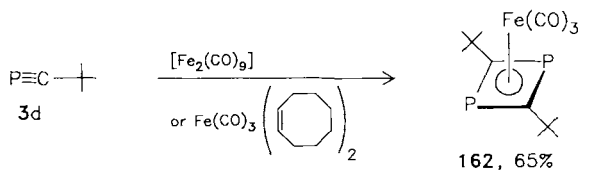

By contrast, the reaction of **3d** with bis(ethene)(toluene)iron and 1-methylnaphthalene(toluene)iron is somewhat more complicated.[151] In both cases the major product is the 1,3-diphosphacyclobutadieneiron complex **163**, but, in addition, a mixture of the two new sandwich complexes **164** and **165** is formed.[152] Although the presence of di- and triphosphacyclopentadienyl ligands in these two complexes must mean that **3d** has been cleaved in a metathetical reaction, no mechanistic studies have yet been carried out on this reaction.[153] It should be mentioned that the 3,5-di-*tert*-butyl-1,2,4-triphosphacyclopentadienide ligand in **165** can be isolated as the lithium salt (with three moles of coordinated 1,2-dimethoxyethane) if the phosphaalkyne precursor **16d**, used to prepare **3d**, is treated with $LiP(SiMe_3)_2 \cdot 2THF$.[47,68]

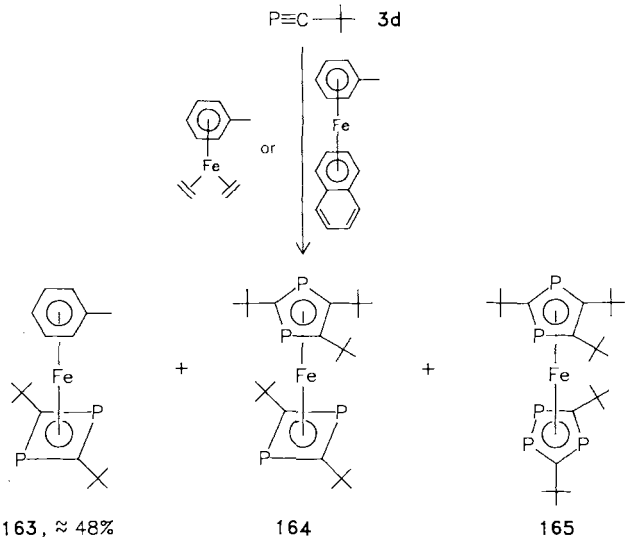

Attempts to codimerize **3d** and 2-butyne using $[CoInd(C_2H_4)_2]$ failed because the triple bond systems react independently of one another: the phosphaalkyne dimerizes to the 1,3-diphosphacyclobutadiene complexes of type **156**, while the alkyne trimerizes to hexamethylbenzene, probably via η^6-hexamethylbenzene(η^5-indenyl)cobalt.[146]

On the other hand, the codimerization experiment with the sterically demanding bis(trimethylsilyl)acetylene (which apparently cannot trimerize because it is too bulky), $[CoCp(C_2H_4)_2]$, and **3d** succeeded. In addition to the desired phosphacyclobutadiene complex **167**, the "pure"

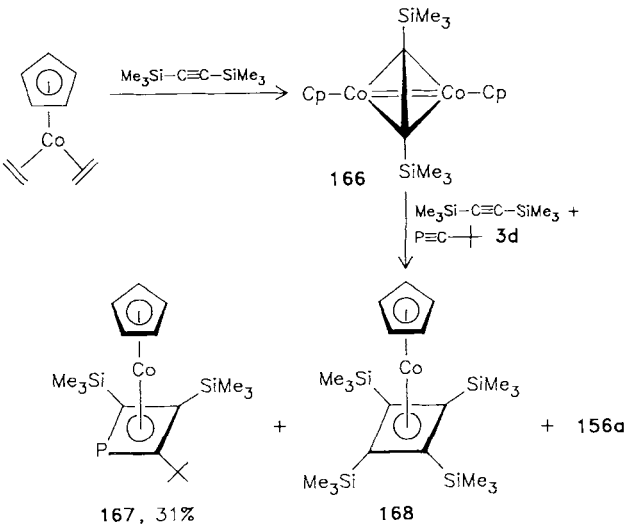

dimer complexes **168** and **156a** are formed.[154] One must assume that the dinuclear cobalt complex **166** is formed first[143,155] and that this then reacts with the molecules containing triple bonds to form the products.

Some of the spectroscopic and structural properties of the 1,3-diphosphacyclobutadiene complexes are illustrated by the data for **156a** and **160** (Co instead of Rh). The crystal structure analysis of **160** (Co instead of Rh) shows that the bonding relationships correspond to those of metal cyclobutadiene complexes.[149] The delocalization of the electrons in the four-membered ring can be seen from the equidistant PC bond distances (1.797 Å)[146] (see also Ref. [144]). The signals in the ^{31}P NMR spectrum are observed at $\delta = 38.1$ and 38.0, respectively.[146] The ions $M^{\oplus} - P_2$ and $M^{\oplus} - t\text{Bu}-\text{C}\equiv\text{C}-t\text{Bu}$ are particularly prominent following fragmentation induced by electron collision.[146] It is not clear whether they are formed after **156a** and **160** (Co instead of Rh) isomerize to tetrahedrane-like compounds or complexes similar to **170**.

A completely new type of phosphaalkyne dimerization is encountered when $[ZrCp_2Cl_2]$ is treated with **3d** in the presence of magnesium or butyllithium. Presumably, it starts with the coordinatively unsaturated zirconocene Cp_2Zr. The product is the 1,3-diphosphabicyclo[1.1.0]butane complex **170** (53 and 26% yields, respectively).[156] The corresponding hafnium compound is obtained under similar conditions in only a low yield (7%).[128]

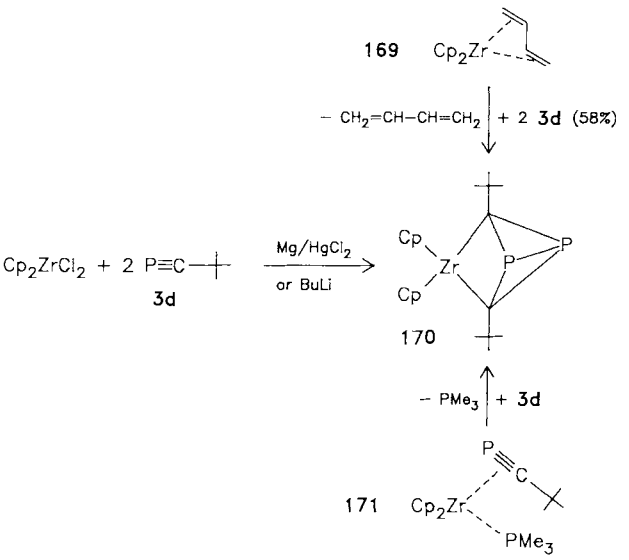

Complex **170** can also be prepared from the complexes **169** and **171**, which contain the Cp_2Zr^{II} fragment, by displacement of the ligands and incorporation of two equivalents of **3d**.[156,128] The crystal structure indicates that the PP bond is relatively short (2.147 Å) and that there is no interaction between Zr and the phosphorus atoms (2.906 and 2.909 Å. respectively).[156] Interestingly, there are no parallels here with the chemistry of the alkynes, which form metallacyclopentadienes, not bicyclic dimeric complexes.[157]

Complexes of Cyclic Trimers: It is well known that the preferred reaction of alkynes on transition-metal centers is the trimerization to benzene derivatives.[158] Since the chemistry of alkynes, including complex chemistry, is with few exceptions, astoundingly similar to that of phosphaalkynes, it would seem quite possible to trimerize the heteroalkynes to 1,3,5-triphosphabenzenes. However, this was not achieved, as one might have expected, on the classical catalysts involving Co^{I}, Ni^{0}, or Ni^{II} and Pd^{0} compounds, but on derivatives of metals of the vanadium and chromium groups.

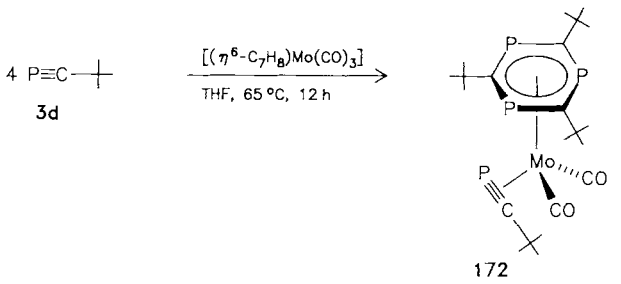

When tricarbonyl(η^6-cycloheptatrienyl)molybdenum is heated with **3d** in tetrahydrofuran, the heteroarene complex **172** is formed.[159] The structure has been assigned on the basis of high-resolution mass spectroscopy and ^{31}P NMR spectroscopy ($\delta = +25.2$, -228.2, intensity ratio 3 : 1).

At the same time, **3d** was successfully cyclotrimerized in the coordination sphere of vanadium.[160] The primary product of the reaction with the arene complex **173**[161] at room temperature is the 14-electron trimer complex **174**, the structure of which has been confirmed by X-ray crystallography.[160] However, only one signal is observed for P-1 and P-3 in the ^{31}P NMR spectrum at room temperature ($\delta = -58.2$ at 20°C). On cooling the sample, this signal splits into two resonances ($\delta = +140.4$ and -234.4 at -100°C) and the chemical shift of P-2 remains constant ($\delta = -130.9$). A valence isomerization **174A** ⇄ **174B** must therefore be taking place.

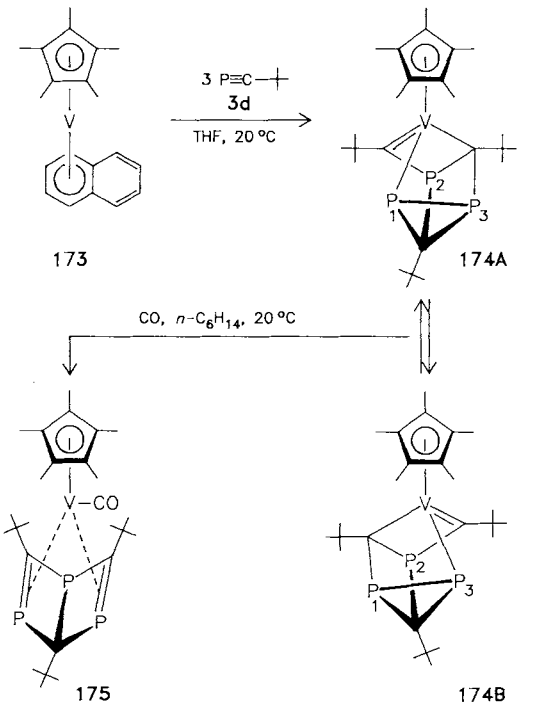

Treatment of **174** with carbon monoxide results in binding of CO to vanadium and rearrangement of the trimer skeleton. The product, **175**, is the first example of a complex containing a Dewar 1,3,5-triphosphabenzene bound to a metal (crystal structure).[160]

3.7.5. *Further Aspects*

It has already been mentioned that the halides of the main-group elements undergo 1,2-addition on the PC triple bond (see Section 3.1). The same is basically true of the reaction of germanium tetrachloride and phosphorus tribromide with **3d**, but in both cases the phosphaalkenes formed initially (**176** and **178**, respectively) undergo further reactions.[47,68]

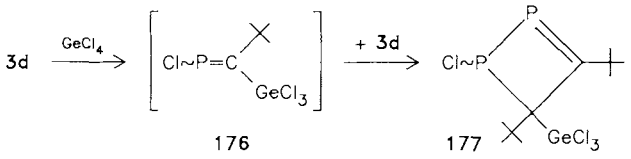

176 177

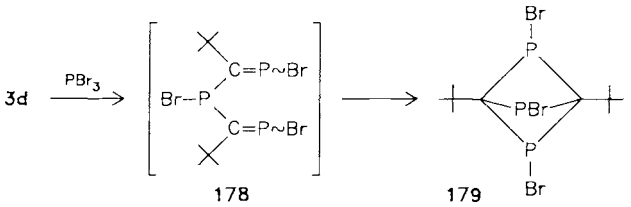

178 179

A further equivalent of **3d** adds to **176** in a [2+2] process to form the substituted 1,2-diphospha-2-cyclobutene **177**.[68] It appears certain that **177** does not undergo the electrocyclic ring-opening reaction to form the vinyldiphosphene for energetic reasons. The 1,4-bis(phosphaalkenyl)phosphane **178** isomerizes with conversion of the $\lambda^3\sigma^2$ phosphorus to $\lambda^3\sigma^3$, yielding the triphosphabicyclo[1.1.1]pentane **179**.[47,68] Tungsten hexachloride and molybdenum pentachloride react with **3d** in an unusual manner in that the PC triple bond of the phosphaalkyne is cleaved with the formation of the ("phosphorus-free") di-*tert*-butylacetylene complexes of tetravalent tungsten[47,68,162] and trivalent molybdenum,[47,68,163] in which the remaining available coordination sites are occupied by the solvent (Cl_3PO).

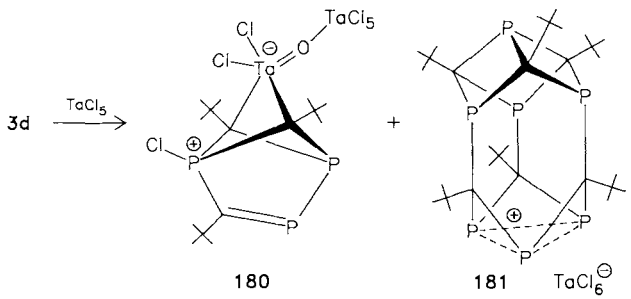

180 181

On the other hand, the reaction of **3d** with tantalum pentachloride takes a completely different course. The major product is the chlorophosphonium oxotantalate **180**, the zwitterionic structure of which incorporates three *t*BuCP units.[47,68] Its structure and that of the side product **181** have been confirmed by X-ray analysis. The latter contains six phosphaalkyne molecules and has triphosphatrishomocyclopropenylium character.[47,68]

4. Prospects

There can be no doubt that entry into the chemistry of the phosphaalkynes has been achieved. The behavior of the heteroalkyne in 1,2 additions, 1,3-dipolar additions, and Diels–Alder reactions, as well as its fixation to metal centers, is now known in outline. However, by comparison with the synthetic potential of the acetylenes, many questions remain unanswered. While almost all the reactions that have been carried out to date have involved kinetically stabilized phosphaalkynes (i.e., those with bulky substituents), in the future greater attention will have to be paid to the more short-lived members of this class of compounds. The introduction of donor and acceptor substituents, which has been neglected, will allow conclusions to be reached on the mechanisms of the reactions. The behavior of phosphaalkynes as ligands awaits a more thorough investigation. The same can be said of their oligomerization, which promises more unexpected results. There is almost nothing known about the $\lambda^5\sigma^3$-phosphaalkynes mentioned in the introduction. One does not need to be a prophet to predict surprises in this particular field.

5. Addendum

The rapid rate of development in the chemistry of phosphaalkynes is reflected in the appearence of important results during the period between the submission of the manuscript of this review and the preparation of the galley proofs. This justifies an update.

5.1. Synthesis

A new synthesis of λ^3-phosphaalkynes has been reported, starting with phosphino-diazo compounds, which, as discussed in Section 1, are also suitable for preparing λ^5-phosphaalkynes (**5**→**6**). A necessary condition for the preparation of phosphaalkynes of type **3** is that the phosphorus atom should have substituents that can be eliminated.

When lithiated diazomethyl compounds are subjected to electrophilic diazoalkane substitution[164] with di-*tert*-bu-

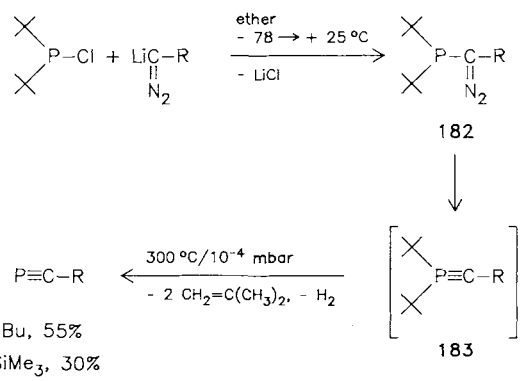

3d: R = *t*Bu, 55%
3t: R = $SiMe_3$, 30%

tyl(chloro)phosphane, the thermally rather stable (diazomethyl)phosphane **182** is formed.[165] The flash pyrolysis of this compound was originally carried out with the intention of isolating kinetically stabilized λ^5-phosphaalkynes **183**. This failed since even at moderate temperatures abstraction of isobutylene and hydrogen occurs to afford the λ^3-phosphaalkynes **3d** and **3t**.[165]

5.2. 1,2 Additions

Although the addition reactions of hydrogen halides, boron tribromide, and tin tetrabromide to phosphaalkynes (see Section 3.1) reveal the polarization of the PC triple bond, they are of no preparative value. A 1,2 addition of more promise as regards synthetic application is the reaction of **3q** with methyllithium, the result of which is dependent upon the ratio of the reactants.

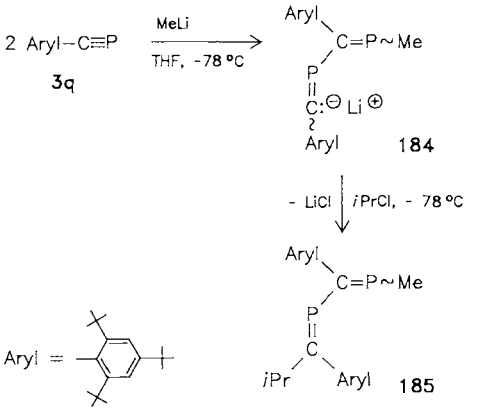

After hydrolysis, the 1:1 reaction yields, as expected, 2,4,6-tri-*tert*-butylbenzylidene(methyl)phosphane (i.e., a phosphaalkene).[166] On the other hand, when the same reaction is carried out in the ratio 2:1, the methyllithium adduct formed initially reacts with the "excess" **3q** to afford the lithium derivative **184**. This can be alkylated with isopropyl chloride to give the 1,3-diphospha-1,3-diene **185**.[166]

5.3. [2+1], [2+2], and [2+3] Cycloaddition

The potential of cycloaddition reactions of phosphaalkynes towards electron-deficient species has recently been expanded most significantly. The germanediyl (germylene) $Ge[CH(SiMe_3)_2]_2$ adds smoothly to **3d**, analogously to the previously known reaction of the Si analogues (see Section 3.2), to afford the corresponding phosphagermirene (**26a**, $Ge[CH(SiMe_3)_2]_2$ instead of $SitBu_2$, 80%). The P–C bond distance has been determined by X-ray crystallography to be 1.661(11) Å.[167]

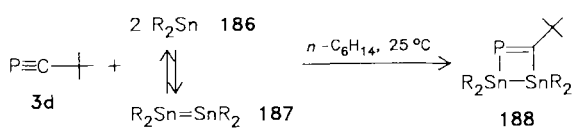

R = $CH(SiMe_3)_2$

It might be anticipated that **3d** would react analogously with the stannanediyl (stannylidene) **186**, which is presumably in equilibrium with the corresponding distannene **187**, at least in solution.[168] However, instead of a [2+1] cycloaddition, a [2+2] cycloaddition occurs, forming the phosphadistannacyclobutene **188**.[169] The P=C bond distance [1.697(15) Å] is in agreement with the suggested structure.[169]

The addition of carbenes to phosphaalkynes **3** opens up completely new perspectives. While diazo compounds are unsuitable as precursors for the carbenes because they undergo rapid 1,3-dipolar cycloaddition with the triple bond (see Sections 3.3.1 and 3.3.2), the cycloisomeric diazirines serve the purpose.

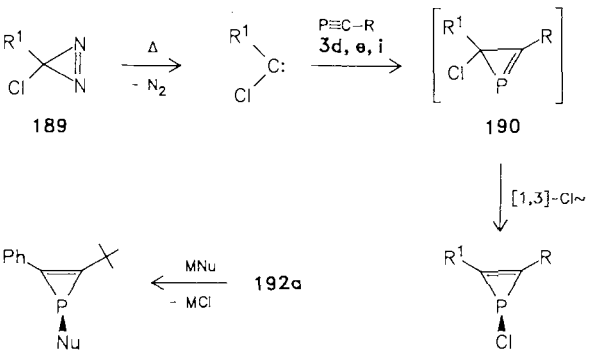

191a: Nu = N_3
191b: Nu = $C(=N_2)SiMe_3$

192a: R = *t*Bu, R^1 = Ph, 63%
192b: R = CMe_2Et, R^1 = OPh, 26%
192c: R = 1-Ad, R^1 = Ph, 24%

If one warms the chlorine-substituted diazirines **189** in an excess of **3d**, **3e**, or **3i**, the carbenes formed in the initial reaction undergo [2+1] cycloaddition to yield the 2*H*-phosphirenes **190**, which, however, cannot be isolated. Instead one obtains the 1*H* isomers **192a–c**, which are formed by a [1,3] chlorine shift and which are obviously more stable than the isomers with a PC double bond.[170] Presumably the chlorine substituent does not lie in the plane of the three-membered ring, since possible aromatic character would then be lost.[171]

Nucleophilic exchange of halogen allows numerous variations on the substitution at phosphorus to be achieved. Thus, **192a** can be converted into the 1-azido-1*H*-phosphirene **191a** by treating it with trimethylsilyl azide in $CDCl_3$ at room temperature. With lithiated diazo(trimethylsilyl)methane (ether, −78 °C) one obtains **191b** just as smoothly.[170]

The cycloaddition of $[Ph-C^{\ominus}=N-CH^{\ominus}-p-C_6H_4-NO_2]$, a nitrilylidene, to the phosphaalkynes **3d,e,i** has now been achieved. The reaction is regiospecific and involves a [1,5] H-shift to the ring nitrogen atom: it is a useful complement to the synthesis of the 1,3-azaphosphole from **3d** and the munchnone **86** (see Section 3.3.7). Finally, the unusual 1,5-substituent shift in 3*H*-1,2,4-diazaphospholes (see Section 3.3.2) from the sp^3-hybridized carbon atom to the neighboring phosphorus atom has been confirmed by X-ray crystallographic analysis of **50** ($R^1 = R^2 = Ph$, R = *t*Bu).[173]

5.4. [4+2] Cycloaddition

1,3-Azaphosphinines are readily obtained from 1,3-oxazinylium(3-azapyrylium) salts by O/P exchange with tris(trimethylsilyl)phosphane **14**,[174] but very little is known about their classical valence isomers, which can be prepared starting from the Dewar isomer **99a**[175] (see Section 3.4.1).

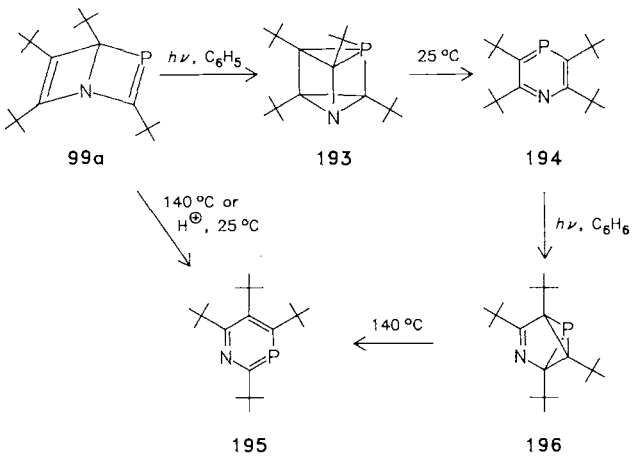

Photolysis of **99a** leads first to azaphosphaprismane **193**, which is thermally considerably less stable than aza-[176] and phosphaprismane[103] and isomerizes to the 1,4-azaphosphinine **194** even at room temperature. Photochemical excitation of **194** leads to the first azaphosphabenzvalene **196**, which is thermally very stable indeed.[175] Only on heating to 140°C does it isomerize further to the heteroarene and this proceeds not by re-forming **194** but by producing the 1,3-azaphosphinine **195**. The latter can also be prepared directly from the Dewar isomer **99a** by heating it or by carrying out the acid-catalyzed isomerization at room temperature.[175]

The 1,3,5-triphosphabenzene **198** with two λ^5,σ^4-phosphorus atoms and one λ^3,σ^2-phosphorus atom is formed directly from **3d** and the $1\lambda^5,3\lambda^4$-diphosphete **197**,[177] but the Dewar isomer that must have been formed initially in the reaction cannot be detected.

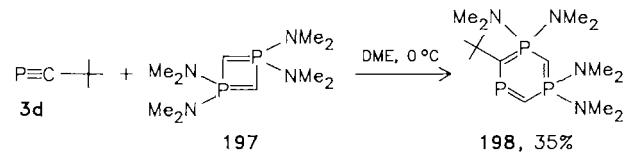

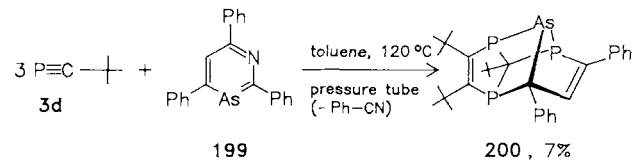

The formation of the triphosphaarsatetracyclodecadiene **200** by the reaction of the 1,3-azarsinine **199** with **3d** in the molar ratio 1:3 also occurs with an initial [4+2] cycloaddition step at the 1,4 positions of the heteroarene. This is followed by the cycloelimination of benzonitrile[178] to form the 1,3-phosphaarsinine which then gives the final product (→ **200**).[178]

5.5. The Ene Reaction

The ene reaction of the phosphaalkyne **3d** is the decisive factor in the formation of the diphospha- and monophosphatricyclooctenes **122** and **125** (see Section 3.4.3). Their direct preparation with pentamethylcyclopentadiene (→ **130**; Section 3.5) suggests that 2-methylphosphinine should also be a suitable enophile. The reaction with **3d** provides experimental confirmation of this: the products of the ene reaction formed first (**201**) subsequently undergo an intramolecular Diels–Alder reaction to give the diphosphatricyclooctenes **202a–c**.[113]

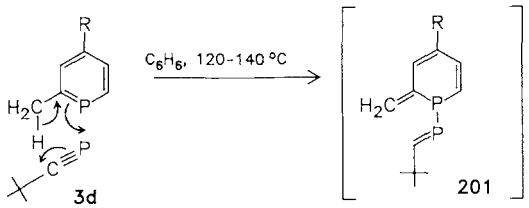

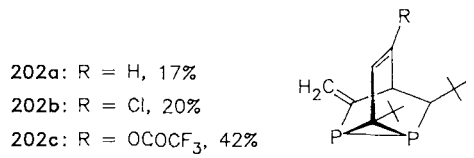

Finally, the formation of the azatriphosphatetracyclodecadiene **204** from the 1,3-azaphosphinine **203** and **3d** in a molar ratios of 1:2 should be mentioned.[179] Once again, the decisive step in the formation of the diphosphirane unit is an ene reaction. In this way the second equivalent of **3d** is incorporated into the molecule to afford **204**.[179]

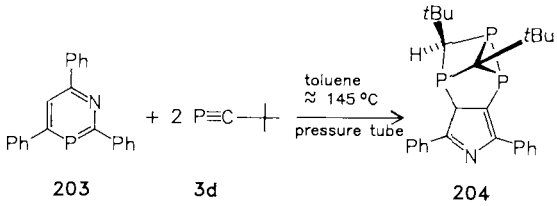

5.6. Metal Complexes

The structure of the third product of the reaction of **3d** with [RhInd(C_2H_2)] (the others are **160** and **161**; see Section 3.7.4)[148] has been established by X-ray crystallography to be the unusual trinuclear complex **205** incorporating four phosphaalkyne units.[128]

A further way of forming rhodium-complexes of 1,3-diphosphacyclobutadiene (see Section 3.7.4) begins with the treatment of **3d** with dimeric bis(ethylene)rhodium chloride in the presence of trimethylphosphane. The product is the first diphospharhodacyclopentadiene **206** to have been isolated and characterized by X-ray crystallography.[180] At room temperature it isomerizes slowly to **207**, in which the four-membered ring has considerable η^1,η^3 character.[180]

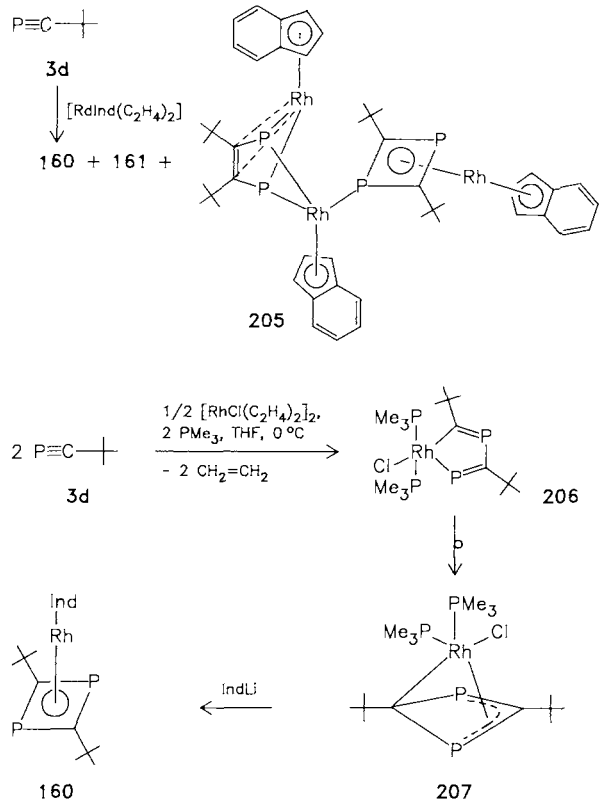

Reaction of **207** with indenyllithium leads to the formation of the 1,3-diphosphacyclobutadiene complex **160** described earlier.[180] This result supports the assumption that 2,4-diphosphametallacyclopentadienes are generally the intermediates in the cyclodimerization of phosphaalkynes.

1-Phospha-3-metallacyclopentadienes of type **209** and **211** with titanium and zirconium as the ring metal atom can be readily prepared by two methods.

The first method is to heat the diphenylmetallocenes **210** (M = Ti or Zr) with **3d**, which affords the derivatives **209** in good yields.[181] It is reasonable to suppose that the attack of the phosphaalkyne is preceded by the formation of the dehydrobenzene complex **208**.

The second method is to treat the complexes **142a,b**, which have side-on-coordinated **3d**, with alkynes. With

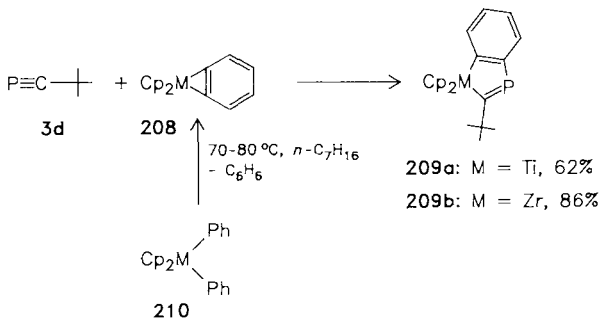

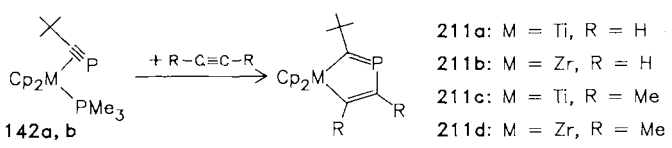

acetylene itself the displacement of the trimethylphosphane ligand and the formation of the ring (→ **211a,b**) occurs at 0 °C, while with 2-butyne the products (→ **211c,d**) are formed only after warming to 60 °C.[128]

The cyclotrimerization reaction between two molecules of **3d** and the complex-bound carbon monoxide in $[(\eta^5\text{-}C_5H_5)_2Ti(CO)_2]$ was reported recently. The product is a diphosphatricyclo[2.1.0.0^{2,5}]pentane (**170**, O=C instead of Cp_2Zr).[182]

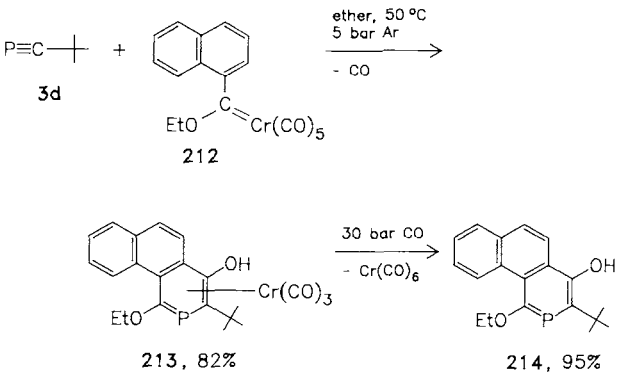

Another example of the similarity in the behavior of alkynes and phosphaalkynes is found in the annelation of carbene ligands. When the chromium carbene complex **212** reacts with **3d**, the functionalized phosphaphenanthrene complex **213** is isolated in high yield.[183]

The metal-free heteroarene **214** can be liberated by treating **213** with carbon monoxide.[183]

The results of our own work cited here came from research generously supported by the Deutsche Forschungsgemeinschaft, the Stiftung Volkswagenwerk, the Fonds der Chemischen Industrie, and the State of Rheinland-Pfalz. We would also like to express our thanks to our co-workers whose work has been reviewed here. Their enthusiasm has contributed greatly to the development of phosphaalkyne chemistry.

Received: January 25, 1988 [A 696 IE]
German version: *Angew. Chem. 100* (1988) 1541
Translated by Dr. *R. Mynott*, Mülheim a. d. Ruhr

[1] K. S. Pitzer, *J. Am. Chem. Soc. 70* (1948) 2140; R. S. Mulliken, *ibid. 72* (1950) 4493.
[2] K. Dimroth, P. Hoffmann, *Angew. Chem. 76* (1964) 433; *Angew. Chem. Int. Ed. Engl. 3* (1964) 384.
[3] G. Märkl, *Angew. Chem. 78* (1966) 907; *Angew. Chem. Int. Ed. Engl. 5* (1966) 846.
[4] For the historical development, see also a) R. Appel, F. Knoll, I. Ruppert, *Angew. Chem. 93* (1981) 771; *Angew. Chem. Int. Ed. Engl. 20* (1981) 731; b) J. I. G. Cadogan, P. K. G. Hodgson, *Phosphorus Sulfur 30* (1987) 3.
[5] Reviews: a) M. Regitz, G. Maas, *Top. Curr. Chem. 97* (1981) 71; b) F. H. Westheimer, *Chem. Rev. 81* (1981) 313.
[6] Reviews: a) M. Regitz in *Houben-Weyl: Methoden der Organischen Chemie, Bd. E1*, Thieme, Stuttgart 1982, p. 583; b) H. Germa, J. Navech, *Phosphorus Sulfur 26* (1986) 327.
[7] Reviews: a) E. Niecke, O. J. Scherer, *Nachr. Chem. Tech. 23* (1975) 395 (iminophosphanes); b) B. Weber, M. Regitz in *Houben-Weyl: Methoden der Organischen Chemie, Bd. E1*, Thieme, Stuttgart 1982, p. 27 (methylenphosphanes, see also [4a]), p. 51 (oxo- and thioxophosphanes), p. 56 (iminophosphanes); c) A. Cowley, *Polyhedron 3* (1984) 389 (diphosphenes).
[8] G. Becker, G. Gresser, W. Uhl, *Z. Naturforsch. B Anorg. Chem. Org. Chem. 36* (1981) 16.
[9] R. Appel, A. Westerhaus, *Tetrahedron Lett. 22* (1981) 2159.

[10] T. E. Gier, *J. Am. Chem. Soc. 83* (1961) 1769.
[11] M. T. Nguyen, M. A. McGinn, A. F. Hegarty, *Inorg. Chem. 25* (1986) 2185.
[12] R. Appel, J. Peters, R. Schmitz, *Z. Anorg. Allg. Chem. 475* (1981) 18.
[13] A. Baceiredo, G. Bertrand, G. Sicard, *J. Am. Chem. Soc. 107* (1985) 4781.
[14] H. Keller, G. Maas, M. Regitz, *Tetrahedron Lett. 27* (1986) 1903.
[15] Phosphinonitrenes react similarly: G. Sicard, A. Baceiredo, G. Bertrand, J.-P. Majoral, *Angew. Chem. 96* (1984) 450; *Angew. Chem. Int. Ed. Engl. 23* (1984) 459; J.-P. Majoral, G. Bertrand, A. Baceiredo, E. O. Mavarez, *Phosphorus Sulfur 27* (1986) 75.
[16] J. Svara, E. Fluck, H. Riffel, *Z. Naturforsch. B Anorg. Chem. Org. Chem. 40* (1985) 1258.
[17] A. Baceiredo, A. Igau, G. Bertrand, M. J. Menu, Y. Dartiguenave, J. J. Bonnet, *J. Am. Chem. Soc. 108* (1986) 7868.
[18] Short reviews: a) [4a]; b) M. Regitz in *Houben-Weyl: Methoden der Organischen Chemie, Bd. E1*, Thieme, Stuttgart 1982, p. 28; c) G. Becker, W. Becker, O. Mundt, *Phosphorus Sulfur 14* (1983) 267.
[19] T. A. Cooper, H. W. Kroto, J. F. Nixon, O. Ohashi, *J. Chem. Soc. Chem. Commun. 1980*, 333.
[20] For the first mention of the elimination of HCl from dichloromethylphosphane, see M. J. Hopkinson, H. W. Kroto, J. F. Nixon, N. P. C. Simmons, *J. Chem. Soc. Chem. Commun. 1976*, 513.
[21] B. Pellerin, J.-M. Denis, J. Perrocheau, R. Carrié, *Tetrahedron Lett. 27* (1986) 723.
[22] E. P. O. Fuchs, M. Hermesdorf, W. Schnurr, W. Rösch, H. Heydt, M. Regitz, *J. Organomet. Chem. 338* (1987) 329.
[23] K. K. Lehmann, S. C. Ross, L. L. Lohr, *J. Chem. Phys. 82* (1985) 4460.
[24] E. Lellouch, J. L. Destombes, *Astron. Astrophys. 152* (1985) 405.
[25] J. A. Kaye, D. F. Strobel, *Icarus 59* (1984) 314.
[26] J. K. Tyler, *J. Chem. Phys. 40* (1964) 1170.
[27] D. C. Frost, S. T. Lee, C. A. McDowell, *Chem. Phys. Lett. 23* (1973) 472.
[28] J.-M. Garneau, A. Cabona, *J. Mol. Spectrosc. 79* (1980) 502.
[29] S.-N. Ghosh, R. Trambarulo, W. Gordy, *J. Chem. Phys. 21* (1953) 308.
[30] J. B. Robert, H. Marsmann, J. Obsar, J. R. van Wazer, *J. Am. Chem. Soc. 93* (1971) 3320.
[31] J. C. T. R. Burckett-St. Laurent, M. A. King, H. W. Kroto, J. F. Nixon, R. J. Suffolk, *J. Chem. Soc. Dalton Trans. 1983*, 755.
[32] M. J. Hopkinson, H. W. Kroto, J. F. Nixon, N. P. C. Simmons, *Chem. Phys. Lett. 42* (1976) 460.
[33] M. Hermesdorf, *Dissertation*, Universität Kaiserslautern 1988; M. Hermesdorf, H. Heydt, M. Regitz, *Phosphorus Sulfur 29* (1989), in press.
[34] H. W. Kroto, J. F. Nixon, N. P. C. Simmons, *J. Mol. Spectrosc. 77* (1979) 270 (comparison with Me–C≡N).
[35] N. P. C. Westwood, H. W. Kroto, J. F. Nixon, N. P. C. Simmons, *J. Chem. Soc. Dalton Trans. 1979*, 1405.
[36] K. Ohno, Y. Yamamoto, H. Matsuura, H. Murata, *Chem. Lett. 1984*, 413.
[37] K. Ohno, H. W. Kroto, J. F. Nixon, *J. Mol. Spectrosc. 90* (1981) 507.
[38] J. C. T. R. Burckett-St. Laurent, T. A. Cooper, H. W. Kroto, J. F. Nixon, O. Ohashi, K. Ohno, *J. Mol. Struct. 79* (1982) 215.
[39] H. W. Kroto, J. F. Nixon, N. P. C. Simmons, N. P. C. Westwood, *J. Am. Chem. Soc. 100* (1978) 446.
[40] H. Eshtiagh-Hosseini, H. W. Kroto, J. F. Nixon, *J. Chem. Soc. Chem. Commun. 1979*, 653.
[41] K. Ohno, H. Matsuura, H. W. Kroto, H. Murata, *Chem. Lett. 1982*, 981.
[42] K. Ohno, H. Matsuura, D. McNaughton, H. W. Kroto, *J. Mol. Spectrosc. 111* (1985) 415.
[43] H. W. Kroto, J. F. Nixon, N. P. C. Simmons, *J. Mol. Spectrosc. 82* (1980) 185.
[44] H. W. Kroto, J. F. Nixon, K. Ohno, *J. Mol. Spectrosc. 90* (1981) 512.
[45] M. C. Durrant, H. W. Kroto, D. McNaughton, J. F. Nixon, *J. Mol. Spectrosc. 109* (1985) 8.
[46] T. A. Cooper, H. W. Kroto, J. F. Nixon, O. Ohashi, *J. Chem. Soc. Chem. Commun. 1980*, 333.
[47] G. Becker, W. Becker, R. Knebl, H. Schmidt, U. Weeber, M. Westerhausen, *Nova Acta Leopold. (neue Folge) 59* (1985) 55.
[48] W. Rösch, U. Vogelbacher, T. Allspach, M. Regitz, *J. Organomet. Chem. 306* (1986) 39.
[49] M. Regitz, W. Rösch, T. Allspach, U. Annen, K. Blatter, J. Fink, M. Hermesdorf, H. Heydt, U. Vogelbacher, O. Wagner, *Phosphorus Sulfur 30* (1987) 479.
[50] G. Becker, W. Hölderich, *Chem. Ber. 108* (1975) 2484.
[51] G. Fritz, W. Hölderich, *Z. Anorg. Allg. Chem. 422* (1976) 104; the compound contains 2 molecules of tetrahydrofuran of crystallization.
[52] G. Becker, *Z. Anorg. Allg. Chem. 430* (1977) 66; R = *t*Bu, ^{31}P NMR: $\delta = -107.0$.
[53] T. Allspach, M. Regitz, G. Becker, W. Becker, *Synthesis 1986*, 31; R = 1-Ad, ^{31}P NMR: $\delta = 110.6$.
[54] W. Rösch, U. Hees, M. Regitz, *Chem. Ber. 120* (1987) 1645.
[55] T. Allspach, *Dissertation*, Universität Kaiserslautern 1986.
[56] G. Märkl, H. Sejpka, *Tetrahedron Lett. 26* (1985) 5507.
[57] G. Märkl, H. Sejpka, *Tetrahedron Lett. 27* (1986) 171.
[58] R. Appel, G. Maier, H.-P. Reisenauer, A. Westerhaus, *Angew. Chem. 93* (1981) 215; *Angew. Chem. Int. Ed. Engl. 20* (1981) 197.
[59] A. R. Barron, A. H. Cowley, S. W. Hall, *J. Chem. Soc. Chem. Commun. 1987*, 980.
[60] H. Oberhammer, G. Becker, G. Gresser, *J. Mol. Struct. 75* (1981) 283.
[61] B. Solouki, H. Bock, R. Appel, A. Westerhaus, G. Becker, G. Uhl, *Chem. Ber. 115* (1982) 3747.
[62] M. Regitz, T. Allspach, *Chem. Ber. 120* (1987) 1269.
[63] J. C. T. R. Burckett-St. Laurent, H. W. Kroto, J. F. Nixon, K. Ohno, *J. Mol. Spectrosc. 92* (1982) 158.
[64] H. Schäfer, G. Fritz, W. Hölderich, *Z. Anorg. Allg. Chem. 428* (1977) 222.
[65] See [48], where it is cited as G. Becker, M. Westerhausen, unpublished.
[66] O.-A. Neumüller: *Römpps Chemie-Lexikon, 8. Aufl., Bd. 2*, Franckh, Stuttgart 1981, p. 1097.
[67] J. B. Robert, H. Marsmann, J. Absar, J. R. van Wazer, *J. Am. Chem. Soc. 93* (1971) 3320.
[68] G. Becker, W. Becker, R. Knebel, H. Schmidt, M. Mildenbrand, M. Westerhausen, *Phosphorus Sulfur 30* (1987) 349.
[69] O. Wagner, M. Regitz, unpublished.
[70] A. Schäfer, M. Weidenbruch, W. Saak, S. Pohl, *Angew. Chem. 99* (1987) 806; *Angew. Chem. Int. Ed. Engl. 26* (1987) 776.
[71] Review: A. Schmidpeter, K. Karaghiosoff, *Nachr. Chem. Tech. Lab. 33* (1985) 793.
[72] See also particularly S. Kerschel, B. Wrackmeyer, A. Willhalm, A. Schmidpeter, *J. Organomet. Chem. 319* (1987) 49, and the previous publications in this series.
[73] W. Rösch, M. Regitz, *Angew. Chem. 96* (1984) 898; *Angew. Chem. Int. Ed. Engl. 23* (1984) 900.
[74] Y. Y. C. Yeng Lam Ko, R. Carrié, A. Münch, G. Becker, *J. Chem. Soc. Chem. Commun. 1984*, 1634.
[75] U. Felcht, M. Regitz, *Angew. Chem. 88* (1976) 377; *Angew. Chem. Int. Ed. Engl. 15* (1976) 378.
[76] U. Felcht, M. Regitz, *Chem. Ber. 109* (1976) 3675.
[77] H. Keller, M. Regitz, *Tetrahedron Lett. 29* (1988) 925.
[78] M. Regitz, H. Heydt in A. Padwa (Ed.): *1,3-Dipolar Cycloaddition Chemistry, Vol. 1*, Wiley, New York 1984, p. 393.
[79] W. Rösch, *Dissertation*, Universität Kaiserslautern 1986.
[80] O. Wagner, *Diplomarbeit*, Universität Kaiserslautern 1986.
[81] O. Wagner, G. Maas, M. Regitz, *Angew. Chem. 99* (1987) 1328; *Angew. Chem. Int. Ed. Engl. 26* (1987) 1257.
[82] Irradiation of **49b** affords the diazoisomer as a red oil [IR (neat): $\tilde{\nu} = 2030$ cm^{-1} (C=N$_2$)] [69].
[83] T. C. Klebach, R. Lourens, F. Bickelhaupt, C. H. Stam, A. van Herk, *J. Organomet. Chem. 210* (1981) 211.
[84] R. Appel, C. Casser, M. Immenkeppel, F. Knoch, *Angew. Chem. 96* (1984) 905; *Angew. Chem. Int. Ed. Engl. 23* (1984) 895.
[85] W. Rösch, T. Facklam, M. Regitz, *Tetrahedron 43* (1987) 3247.
[86] Review: R. Huisgen, *Angew. Chem. 92* (1980) 979; *Angew. Chem. Int. Ed. Engl. 19* (1980) 947.
[87] W. Welter, A. Hartmann, M. Regitz, *Chem. Ber. 111* (1978) 3068.
[88] G. Mitchel, C. W. Rees, *J. Chem. Soc. Perkin Trans. 1 1987*, 413.
[89] W. Rösch, M. Regitz, *Synthesis 1987*, 689.
[90] J. E. Franz, L. L. Black, *Tetrahedron Lett. 1970*, 1381.
[91] H. Gotthardt, *Chem. Ber. 105* (1972) 188.
[92] W. Rösch, H. Richter, M. Regitz, *Chem. Ber. 120* (1987) 1809.
[93] H. Heinicke, *Tetrahedron Lett. 27* (1986) 5699.
[94] G. Märkl, G. Dorfmeister, *Tetrahedron Lett. 27* (1986) 4419.
[95] K. Issleib, R. Vollmer, *Tetrahedron Lett. 21* (1980) 3483.
[96] Review: G. Märkl in *Houben-Weyl: Methoden der Organischen Chemie, Bd. E1*, Thieme, Stuttgart 1982, p. 72.
[97] H. Wingert, M. Regitz, *Chem. Ber. 119* (1986) 244; G. Maier, J. Bauer, U. Huber-Patz, R. Jahn, D. Kallfaß, H. Rodewald, H. Irngartinger, *ibid. 119* (1986) 1111; H. Wingert, M. Regitz, *Z. Naturforsch. B Anorg. Chem. Org. Chem. 41* (1986) 1306; H. Wingert, G. Maas, M. Regitz, *Tetrahedron 42* (1986) 5341.
[98] J. Fink, W. Rösch, U.-J. Vogelbacher, M. Regitz, *Angew. Chem. 98* (1986) 265; *Angew. Chem. Int. Ed. Engl. 25* (1986) 280.
[99] G. F. Emerson, L. Watts, R. Pettit, *J. Am. Chem. Soc. 87* (1965) 131; L. Watts, J. D. Fitzpatrick, R. Pettit, *ibid. 87* (1965) 3253.
[100] U.-J. Vogelbacher, M. Regitz, R. Mynott, *Angew. Chem. 98* (1986) 835; *Angew. Chem. Int. Ed. Engl. 25* (1986) 842.
[101] U.-J. Vogelbacher, M. Ledermann, T. Schach, G. Michels, U. Hees, M. Regitz, *Angew. Chem. 100* (1988) 304; *Angew. Chem. Int. Ed. Engl. 27* (1988) 272.
[102] U.-J. Vogelbacher, *Dissertation*, Universität Kaiserslautern 1986.
[103] K. Blatter, W. Rösch, U.-J. Vogelbacher, J. Fink, M. Regitz, *Angew. Chem. 99* (1987) 67; *Angew. Chem. Int. Ed. Engl. 26* (1987) 85.
[104] J. Schneider, *Diplomarbeit*, Universität Kaiserslautern 1987.
[105] K. Blatter, *Diplomarbeit*, Universität Kaiserslautern 1987.

[106] G. Maas, J. Fink, H. Wingert, K. Blatter, M. Regitz, *Chem. Ber. 120* (1987) 819.

[107] See also: M. Caira, R. H. Neilson, W. H. Watson, P. Wisian-Neilson, Ze-Min Xie, *J. Chem. Soc. Chem. Commun. 1984*, 698.

[108] Phenyl(thioxo)phosphane formed by cycloelimination can be trapped: R. Hussong, H. Heydt, M. Regitz, *Phosphorus Sulfur 25* (1985) 201 (addition of alcohols); *Z. Naturforsch. B Anorg. Chem. Org. Chem. 41* (1986) 915 ([4 + 1] cycloaddition); R. Hussong, H. Heydt, G. Maas, M. Regitz, *Chem. Ber. 120* (1987) 1263 (trapping reaction with hexacarbonylbis(cyclopentadienyl)dimolybdenum).

[109] W. Rösch, M. Regitz, *Z. Naturforsch. B Anorg. Chem. Org. Chem. 41* (1986) 931.

[110] U. Annen, *Diplomarbeit*, Universität Kaiserslautern 1986.

[111] E. P. O. Fuchs, H. Heydt, M. Regitz, unpublished results, Universität Kaiserslautern 1986.

[112] R. Appel, M. Große-Bley, H. Souady, W. Steglich, *Phosphorus Sulfur 30* (1987) 757.

[113] U. Annen, M. Regitz, unpublished.

[114] G. Märkl, F. Lieb, *Angew. Chem. 80* (1968) 702; *Angew. Chem. Int. Ed. Engl. 7* (1968) 733; A. J. Ashe, M. D. Gordon, *J. Am. Chem. Soc. 94* (1972) 7596; G. Märkl, K. H. Heier, *Tetrahedron Lett. 1974*, 4369; G. Märkl, F. Lieb, C. Martin, *ibid. 1971*, 1249.

[115] T. C. Klebach, L. A. M. Turkenburg, F. Bickelhaupt, *Tetrahedron Lett. 1978*, 1099.

[116] U. Annen, M. Regitz, *Tetrahedron Lett. 28* (1987) 5141.

[117] E. P. O. Fuchs, W. Rösch, M. Regitz, *Angew. Chem. 99* (1987) 1058; *Angew. Chem. Int. Ed. Engl. 26* (1987) 1011.

[118] Review: M. Wollweber in *Houben-Weyl: Methoden der Organischen Chemie, Bd. V/1c*, Thieme, Stuttgart 1970, p. 1125.

[119] U. Annen, M. Regitz, *Tetrahedron Lett. 29* (1988) 1681.

[120] F. Zurmühlen, W. Rösch, M. Regitz, *Z. Naturforsch. B Anorg. Chem. Org. Chem. 40* (1985) 1077.

[121] G. Märkl, J. Trötsch, *Angew. Chem. 96* (1984) 899; *Angew. Chem. Int. Ed. Engl. 23* (1984) 901.

[122] Y. Y. C. Yeng Lam Ko, R. Carrié, *J. Chem. Soc. Chem. Commun. 1984*, 1640.

[123] G. Märkl, G. Yu Jin, E. Silbereisen, *Angew. Chem. 94* (1982) 383; *Angew. Chem. Int. Ed. Engl. 21* (1982) 370; *Angew. Chem. Suppl. 1982*, 881.

[124] G. Märkl, E. Seidl, I. Trötsch, *Angew. Chem. 95* (1983) 891; *Angew. Chem. Int. Ed. Engl. 22* (1983) 879.

[125] J. C. T. R. Burckett-St. Laurent, P. B. Hitchcock, H. W. Kroto, J. F. Nixon, *J. Chem. Soc. Chem. Commun. 1981*, 1141.

[126] S. I. Al-Reayes, P. B. Hitchcock, M. F. Meidine, J. F. Nixon, *J. Chem. Soc. Chem. Commun. 1984*, 1080.

[127] S. I. Al-Reayes, S. I. Klein, H. W. Kroto, M. F. Meidine, J. F. Nixon, *J. Chem. Soc. Chem. Commun. 1983*, 930.

[128] P. Binger, B. Biedenbach, unpublished results, MPI für Kohlenforschung, Mülheim a. d. Ruhr 1987; B. Biedenbach, *Dissertation*, Universität Kaiserslautern 1988.

[129] C. Krüger, K. Angermund, unpublished results, MPI für Kohlenforschung, Mülheim a. d. Ruhr 1987.

[130] P. B. Hitchcock, M. J. Maah, J. F. Nixon, J. A. Zora, G. Heffery Leigh, M. Abu Bakar, *Angew. Chem. 99* (1987) 497; *Angew. Chem. Int. Ed. Engl. 26* (1987) 474.

[131] a) G. Wilkinson, F. G. A. Stone, E. W. Abel (Eds.): *Comprehensive Organometallic Chemistry*, Pergamon, Oxford 1982; b) Co: R. D. W. Kemmit, D. R. Russell in [131a], *Vol. 5*, p. 239; c) Ni: W. P. Jolly in [131a], *Vol. 6*, p. 135; d) Mo: R. Davis, L. A. P. Kane-Maguise in [131a], *Vol. 3*, p. 1176.

[132] J. C. T. R. Burckett-St. Laurent, P. B. Hitchcock, H. W. Kroto, M. F. Meidine, J. F. Nixon, *J. Organomet. Chem. 238* (1982) C82.

[133] R. Bartsch, J. F. Nixon, N. Sarjudeen, *J. Organomet. Chem. 294* (1985) 267.

[134] G. Becker, W. A. Herrmann, W. Kalcher, G. W. Kriechbaum, C. Pahl, C. T. Wagner, M. L. Ziegler, *Angew. Chem. 95* (1983) 417; *Angew. Chem. Int. Ed. Engl. 22* (1983) 413; *Angew. Chem. Suppl. 1983*, 501.

[135] P. B. Hitchcock, M. F. Meidine, J. F. Nixon, *J. Organomet. Chem. 333* (1987) 337.

[136] M. F. Meidine, C. J. Meir, S. Morton, J. F. Nixon, *J. Organomet. Chem. 297* (1985) 255.

[137] D. Seyferth, J. S. Merola, R. S. Henderson, *Organometallics 1* (1982) 859.

[138] P. B. Hitchcock, M. J. Maah, J. F. Nixon, *J. Chem. Soc. Chem. Commun. 1987*, 658.

[139] See the review by W. A. Herrmann, *J. Organomet. Chem. 250* (1983) 319, and references cited therein.

[140] R. S. Dickson: *Organometal Chemistry of Rhodium and Iridium*, Academic Press, New York 1983, p. 265ff.

[141] S. I. Al-Reayes, P. B. Hitchcock, J. F. Nixon, *J. Chem. Soc. Chem. Commun. 1987*, 928.

[142] S. I. Al-Reayes, P. B. Hitchcock, J. F. Nixon, D. M. P. Mingos, *J. Chem. Soc. Chem. Commun. 1985*, 365.

[143] K. Jonas, *Angew. Chem. 97* (1985) 292; *Angew. Chem. Int. Ed. Engl. 24* (1985) 295.

[144] P. B. Hitchcock, M. J. Maah, J. F. Nixon, *J. Chem. Soc. Chem. Commun. 1986*, 737.

[145] P. Binger, R. Milczarek, R. Mynott, M. Regitz, W. Rösch, *Angew. Chem. 98* (1986) 645; *Angew. Chem. Int. Ed. Engl. 25* (1986) 644.

[146] P. Binger, R. Milczarek, R. Mynott, Yi-Huang Tsai, E. Raabe, C. Krüger, M. Regitz, *Chem. Ber. 121* (1988) 637.

[147] P. B. Hitchcock, M. J. Maah, J. F. Nixon, C. Woodward, *J. Chem. Soc. Chem. Commun. 1987*, 844.

[148] See [128]; a third product with the formula $[Rh_3Ind_3P_4C_4(tBu)_4]$ has been isolated, but its structure has not yet been determined.

[149] Review: A. Efraty, *Chem. Rev. 77* (1977) 691.

[150] P. Binger, R. Schneider, M. Regitz, unpublished.

[151] For the corresponding alkyne trimerization, see U. Zenneck, W. Frank, *Angew. Chem. 98* (1986) 806; *Angew. Chem. Int. Ed. Engl. 25* (1986) 831.

[152] M. Driess, D. Hu, H. Pritzkow, H. Schäufele, U. Zenneck, M. Regitz, W. Rösch, *J. Organomet. Chem. 334* (1987) C35.

[153] For further ferrocenes with wholly or partially substituted cyclopentadienyl groups, see O. J. Scherer, T. Brück, *Angew. Chem. 99* (1987) 59; *Angew. Chem. Int. Ed. Engl. 26* (1987) 59; R. Bartsch, P. B. Hitchcock, J. F. Nixon, *J. Chem. Soc. Chem. Commun. 1987*, 1146.

[154] P. Binger, R. Milczarek, R. Mynott, M. Regitz, *J. Organomet. Chem. 323* (1987) C35.

[155] B. Eaton, J. M. O'Connor, K. P. C. Vollhardt, *Organometallics 5* (1986) 394.

[156] P. Binger, B. Biedenbach, C. Krüger, M. Regitz, *Angew. Chem. 99* (1987) 798; *Angew. Chem. Int. Ed. Engl. 26* (1987) 764.

[157] S. Thanedar, M. F. Farona, *J. Organomet. Chem. 235* (1982) 65; V. Skibbe, G. Erker, *ibid. 241* (1983) 15; M. B. Sabade, M. F. Farona, *ibid. 310* (1986) 311.

[158] G. W. Parshall: *Homogeneous Catalysis*, Wiley, London 1980, p. 165. In this context see also the formal cyclotrimerization of P_2: O. J. Scherer, H. Sitzmann, G. Wolmershäuser, *Angew. Chem. 97* (1985) 358; *Angew. Chem. Int. Ed. Engl. 24* (1985) 351.

[159] A. R. Barron, A. H. Cowley, *Angew. Chem. 99* (1987) 956; *Angew. Chem. Int. Ed. Engl. 26* (1987) 907.

[160] R. Milczarek, W. Rüsseler, P. Binger, K. Jonas, K. Angermund, C. Krüger, M. Regitz, *Angew. Chem. 99* (1987) 957; *Angew. Chem. Int. Ed. Engl. 26* (1987) 907.

[161] K. Jonas, W. Rüsseler, C. Krüger, E. Raabe, *Angew. Chem. 98* (1986) 902; *Angew. Chem. Int. Ed. Engl. 25* (1986) 908.

[162] G. Uhl, E. Hey, G. Becker, F. Weller, K. Dehnicke, *Z. Anorg. Allg. Chem. 497* (1983) 213.

[163] E. Hey, F. Weller, B. Simon, G. Becker, K. Dehnicke, *Z. Anorg. Allg. Chem. 501* (1983) 61.

[164] Review: M. Regitz, G. Maas: *Diazo Compounds—Properties and Synthesis*, Academic Press, Orlando 1986, p. 436ff.

[165] T. Facklam, M. Regitz, unpublished.

[166] A. M. Arif, A. R. Barron, A. H. Cowley, S. W. Hall, *J. Chem. Soc. Chem. Commun. 1988*, 171. This paper describes the crystal structure of **3q**: P≡C = 1.516(13) Å.

[167] A. H. Cowley, S. W. Hall, C. M. Nunn, J. M. Power, *J. Chem. Soc. Chem. Commun. 1988*, 753.

[168] P. J. Davidson, D. H. Harris, M. F. Lappert, *J. Chem. Soc. Dalton Trans. 1976*, 2268; D. E. Goldberg, P. B. Hitchcock, M. F. Lappert, K. M. Thomas, T. Fjelberg, A. Haaland, B. E. R. Schilling, *ibid. 1986*, 2387; K. W. Zilm, G. A. Lawless, R. M. Merill, J. M. Millar, G. G. Webb, *J. Am. Chem. Soc. 109* (1987) 7236.

[169] A. H. Cowley, S. W. Hall, C. M. Nunn, J. M. Power, *Angew. Chem. 100* (1988) 874; *Angew. Chem. Int. Ed. Engl. 27* (1988) 838.

[170] O. Wagner, M. Ehle, M. Regitz, *Angew. Chem. 101* (1989), in press; *Angew. Chem. Int. Ed. Engl. 28* (1989), in press.

[171] Compare with triphenyl-1*H*-phosphirene: A. Marinetti, F. Mathey, J. Fischer, A. Mitschler, *J. Chem. Soc. Chem. Commun. 1984*, 45.

[172] B. Burkhart, M. Regitz, unpublished.

[173] A. H. Cowley, S. W. Hall, R. A. Jones, C. M. Nunn, *J. Chem. Soc. Chem. Commun. 1988*, 867.

[174] G. Märkl, G. Dorfmeister, *Tetrahedron Lett. 28* (1987) 1093.

[175] S. Haber, U. Hees, M. Regitz, *Tetrahedron Lett. 30* (1989), in press.

[176] U. Hees, U.-J. Vogelbacher, G. Michels, M. Regitz, *Tetrahedron 45* (1989), in press.

[177] E. Fluck, G. Becker, B. Neumüller, R. Knebl, G. Heckmann, H. Riffel, *Angew. Chem. 98* (1986) 1018; *Angew. Chem. Int. Ed. Engl. 25* (1986) 1002.

[178] G. Märkl, S. Dietl, M. L. Ziegler, B. Nuber, *Angew. Chem. 100* (1988) 720; *Angew. Chem. Int. Ed. Engl. 27* (1988) 709.

[179] G. Märkl, S. Dietl, M. L. Ziegler, B. Nuber, *Angew. Chem. 100* (1988) 426; *Angew. Chem. Int. Ed. Engl. 27* (1988) 389.

[180] P. Binger, B. Biedenbach, R. Mynott, C. Krüger, P. Betz, M. Regitz, *Angew. Chem. 100* (1988) 1219; *Angew. Chem. Int. Ed. Engl. 27* (1988) 1157.

[181] P. Binger, B. Biedenbach, R. Mynott, M. Regitz, *Chem. Ber. 121* (1988) 1455.

[182] A. R. Baron, A. H. Cowley, S. W. Hall, C. M. Nunn, *Angew. Chem. 100* (1988) 873; *Angew. Chem. Int. Ed. Engl. 27* (1988) 837.

[183] K. H. Dötz, A. Tiriliomis, K. Harms, M. Regitz, U. Annen, *Angew. Chem. 100* (1988) 725; *Angew. Chem. Int. Ed. Engl. 27* (1988) 713.

When submitting manuscripts, authors of articles intended for publication as "Communications" are requested to read the "Notice to Authors" reproduced in the January issue of the journal following the list of contents; upon request, a copy can be obtained from the editorial office.

Acid-Catalyzed Alkyne/Alkene Coupling at Re^{III} Centers**

By *Wolfgang A. Herrmann,* Roland A. Fischer,* and *Eberhardt Herdtweck*

Dedicated to Professor Ernst Otto Fischer on the occasion of his 70th birthday

Whereas the oligomerizations of ethylene and acetylene provide model examples for the effectiveness of organotransition metal catalysts in the chemical industry,[1] the CC coupling of alkenes and alkynes in stoichiometric or catalytic cocyclizations has gained importance only in preparative organic chemistry.[2] The majority of the previously known coupling reactions of these classes of compounds at metal centers preferentially yield metallacyclopentenes, but seldom the tautomeric 1,3-dienes.[3] We report here on a model organometallic system for the synthetic reaction depicted in Scheme 1, which, at the same time, demonstrates differences in reactivity of the analogous d^2-Ta^{III} and d^4-Re^{III} complexes.

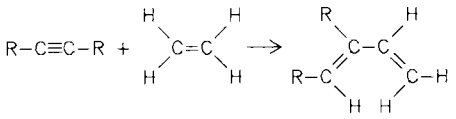

Scheme 1.

Starting from the organorhenium(v) complex **1**, π-alkyne derivatives such as the 2-butyne complex **2**,[4] are accessible via reductive routes in accordance with Scheme 2. Like its Ta^{III} analogues $[(\eta^5\text{-}C_5Me_5)Ta(\eta^2\text{-}RCCR)Cl_2]$, **2** is inert towards ethylene or excess alkyne even under drastic conditions. Only the Ta^{III} complex of unsubstituted acetylene, $[(\eta^5\text{-}C_5Me_5)Ta(\eta^2\text{-}HCCH)Cl_2]$, adds ethylene in toluene solution, and only then at 80°C, forming the corresponding metallacyclopentene $[(\eta^5\text{-}C_5Me_5)Ta(CH{=}CH{-}CH_2CH_2)Cl_2]$.[5]

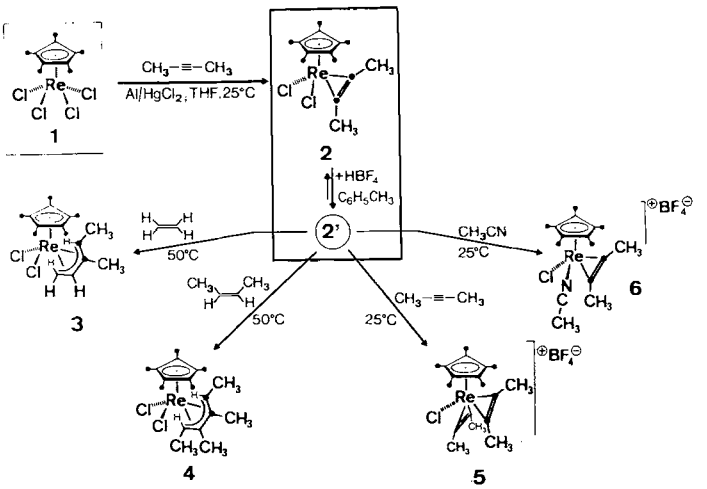

Scheme 2.

When, however, the light-yellow solution of **2** in toluene is treated with a catalytic amount of tetrafluoroboric acid, and ethylene is then fed into the mixture, a color change to wine-red is observed within minutes. Chromatographic work-up of the crude product affords the red, air-stable compound **3** in 80% yield whose analytical and spectroscopic data are consistent with a Re^{III} complex of (*E*)-3-methyl-1,3-pentadiene.[6]

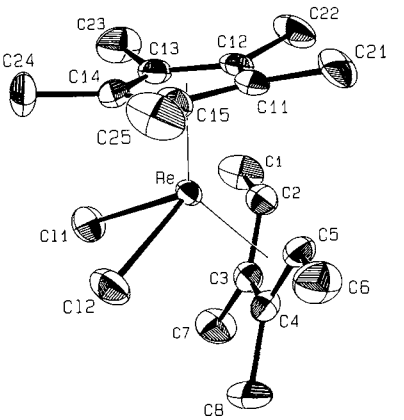

Fig. 1. Molecular structure (ORTEP) of the (*E,E*)-3,4-dimethyl-2,4-hexadiene complex **4** in the crystal. The thermal ellipsoids correspond to the 50% probability level. Selected bond lengths [pm] and angles [°]: Re-Cl1 244.1(1), Re-Cl2 243.8(1), Re-C2 222.0(3), Re-C3 236.4(3), Re-C4 235.5(3), Re-C5 222.1(3), C2-C3 143.8(4), C3-C4 139.6(4), C4-C5 144.0(4); Cl1-Re-Cl2 79.83(3). The dihedral angle between the Re-C2-C5 and C1-C8 planes is 95.8(1)°. Further details of the crystal structure investigations are available on request from the Fachinformationszentrum Energie, Physik, Mathematik GmbH, D-7514 Eggenstein-Leopoldshafen 2 (FRG) on quoting the depository number CSD-52936, the names of the authors, and the full journal citation.

Apparently the methyl-substituted butadiene ligand is formed from ethylene and the 2-butyne attached to the metal of **2** by CC coupling with H-migration. **3** can also be prepared by reductive dehalogenation of the Re^V compound **1** with $HgCl_2$-activated Al-granules in the presence of *cis/trans*-3-methyl-1,3-pentadiene. Although the constitution of **3** could be confirmed by a single crystal X-ray

[*] Prof. Dr. W. A. Herrmann, R. A. Fischer, Dr. E. Herdtweck
Anorganisch-chemisches Institut der Technischen Universität München
Lichtenbergstrasse 4, D-8046 Garching (FRG)

[**] Multiple Bonds between Main Group Elements and Transition Metals, Part 56. This work was supported by the Deutsche Forschungsgemeinschaft and the Fonds der Chemischen Industrie.—Part 55: J. K. Felixberger, J. G. Kuchler, E. Herdtweck, R. A. Paciello, W. A. Herrmann, *Angew. Chem. 100* (1988) 975; *Angew. Chem. Int. Ed. Engl. 27* (1988) 946.

structure analysis, because of a disorder of the chiral molecule in the crystal the analogous symmetrical derivative **4** was synthesized and characterized by its structural chemistry (Fig. 1).[6, 7]

The atoms C2–C5 of the 1,3-diene ligand lie, as also their methyl substituents, in one plane; the distances between them are almost identical, with a mean value of 142.5(4) pm. C2 and C5 are noticeably closer to the metal (220.0(3) and 222.1(3) pm, respectively) than C3 and C4 (236.4(3) and 235.5(3) pm, respectively). **4** cannot be described as a metalla-3-cyclopentene; the compound rather corresponds to a η^4-*s-cis*-1,3-diene complex.[8] The different Re–C distances, which lead to an unsymmetrical diene coordination, are presumably a result of steric interactions of the butadiene ligand with the $[(\eta^5\text{-}C_5Me_5)ReCl_2]$ fragment. This would also explain the preferred *supine* position of the ligand over the prone arrangement.[8] Moreover, no configurational stability can be observed NMR spectroscopically in solution. The selectivity with which exclusively (*E,E*)-3,4-dimethyl-2,4-hexadiene is formed at the Re[11] center, is certainly also governed by the steric demand of the pentamethylcyclopentadienyl ligand, which should determine the preferred position of the methyl groups on the atoms C2 and C5.

As expected, if an unsymmetrical olefin such as propene instead of ethylene is used as reaction partner, a ca. 1:1 mixture of two positional isomers is obtained with the CH_3 group originating from the propene molecule appearing either on C4 or on C5.

In the presence of equimolar amounts of acid, **2** also reacts with alkynes or nitriles at room temperature in toluene solution. CC coupling to form metallacyclopentadiene derivatives, however, does not occur. Rather, the complex salts **5** and **6**, respectively, whose formation does not occur without addition of acid, are obtained in quantitative yield according to Scheme 2. When **2** is allowed to react in a competition experiment with excess 2-butyne and ethylene in the presence of traces of acid, formation of the 1,3-diene does not occur. Rather, some **5**, the amount of which corresponds to the acid used, is obtained along with unchanged **2**.

The assumption of a protonation of the alkyne complex **2** appears to be meaningful for the action of the activating acid. A novel example for this is provided by the protonation of the Rh^I complex $[(\eta^5\text{-}C_5H_5)Rh(\eta^2\text{-}RCCR)(PiPr_3)]$; migration of a proton from the metal atom to the alkyne ligand results in σ-vinyl intermediates, which are amenable to further reactions.[9] However, no NMR spectroscopic evidence could be obtained for an H atom attached to metal or to vinyl ligands upon reaction of mineral acids with **2**.

Although the mechanisms of the reactions depicted in Scheme 2 have not been clarified and the reactive intermediate **2'**, in particular, has not yet been identified, the *intramolecular* character of the formation of the butadiene from free olefin and acetylene fixed to metal can be considered as established. Labeling experiments indicated, for example, that no deuterium is incorporated in the 1,3-diene complex on using deuterated acids in [D8]toluene. As expected, completely substituted olefins, e.g. 2,3-dimethyl-2-butene, do not react with **2**, whereas 2-methyl-2-butene, with one less methyl group, leads to complexes of type **3** and **4**. It can be concluded therefore that the H-migration with formation of the 1,3-diene system provides the driving force behind the described coupling reaction.[3] Since such an H-migration is not possible when acetonitrile and 2-butyne are used as reaction partners with **2**, this also explains the other type of reaction course to **5** and **6**, respectively.

Experimental

4: A solution of **2** (200 mg, 0.5 mmol) in toluene (50 mL) was heated to 50 °C and treated with a catalytic amount of HBF_4 in diethyl ether. A vigorous stream of dry *cis*-2-butene was then fed through the yellow solution. Within 5 min a color change to wine red was observed. After ca. 15 min the solvent was removed under vacuum. The red residue was chromatographed at 15 °C on a column charged with silylated silica gel/*n*-hexane (30 cm × 1 cm). **4** was then eluted as a red zone with methylene chloride/*n*-hexane (10:3). Recrystallization from *n*-hexane/methylene chloride (1:1) afforded 190 mg (75%) of analytically pure **4** as red, thin, transparent crystalline platelets. Decomp. 226 °C. **3** can be synthesized analogously from **2**.

5: A solution of **2** (200 mg, 0.5 mmol) in toluene (50 mL) was treated with 0.1 mL of 2-butyne. 0.1 mL of an HBF_4 solution in diethyl ether (c = 7.2 mmol/mL) was then added to the reaction solution with vigorous stirring. Yellow droplets immediately separated out. The mixture was stirred for a further 30 min and all volatiles then removed under vacuum. The residue was repeatedly washed with diethyl ether and recrystallized several times from *n*-hexane/methylene chloride (1:2). Yield 235 mg (85%) of analytical pure **5** as orange-yellow needles. Decomp. 188 °C.

Received: February 22, 1988 [Z 2630 IE]
German version: *Angew. Chem. 100* (1988) 1566
Publication delayed at authors' request

[1] a) Recent review: G. Wilke, *Angew. Chem. 100* (1988) 190; *Angew. Chem. Int. Ed. Engl. 27* (1988) 185; b) S. Otsuka, A. Nakamura, *Adv. Organomet. Chem. 14* (1976) 246; c) M. J. Winter in F. D. Hartley (Ed.): *Chemistry of the Metal-Carbon Bond, Vol. 3*, Wiley, New York 1985, S. 259; d) A. Yamamoto: *Organotransition Metal Chemistry—Fundamental Concepts and Applications*, Wiley, New York 1986; e) J. P. Collman, L. S. Hegedus, J. R. Norton, R. G. Finke: *Principles and Applications of Organotransition Metal Chemistry, 2nd Ed.*, University Science Books, Mill Valley, CA (USA) 1987.

[2] Recent examples: a) S. L. Buchwald, B. T. Watson, *J. Am. Chem. Soc. 109* (1987) 2544; b) E. Negishi, S. J. Holmes, J. M. Tour, J. A. Miller, *ibid. 107* (1985) 2568; c) K. Tamao, K. Kobayashi, Y. Ito, *ibid. 110* (1988) 1286; d) K. P. C. Vollhardt, *Angew. Chem. 96* (1984) 525; *Angew. Chem. Int. Ed. Engl. 23* (1984) 523.

[3] a) B. M. Trost, J. M. Tour, *J. Am. Chem. Soc. 109* (1987) 5268; b) B. M. Trost, M. Lautens, *ibid. 107* (1985) 1781; c) S. R. Allen, M. Green, G. Moran, A. G. Orpen, G. E. Taylor, *J. Chem. Soc. Dalton Trans. 1984*, 441.

[4] W. A. Herrmann, R. A. Fischer, E. Herdtweck, *J. Organomet. Chem. 329* (1987) C1.—Review: W. A. Herrmann, *Angew. Chem. 100* (1988) 1269; *Angew. Chem. Int. Ed. Engl. 27* (1988) 1297.

[5] G. Smith, R. R. Schrock, M. R. Churchill, W. J. Youngs, *Inorg. Chem. 20* (1981) 387.

[6] *Spektroscopic data*: **3**: IR (KBr; extract): $\tilde{\nu}$ = 2960, 2955, 2923, 1491, 1459, 1375, 1103, 1032, 340 cm^{-1}; EI-MS (70 eV): m/z 474 ($M^{\oplus}$ w.r.t. ^{187}Re, ^{35}Cl, 8%), 392 ([$M^{\oplus}-C_6H_{10}$], 49), 356 ([$M^{\oplus}-C_6H_{10}-HCl$], 100); ^1H-NMR (400 MHz, $CDCl_3$, 20 °C): δ = 5.77 (td, 1H, $^4J_{trans}(H,H)$ = 1.2, $^3J_{cis}(H,H)$ = 7.5, $^3J_{trans}(H,H)$ = 7.2 Hz; =C–H), 3.57 (dd, 1H, $^2J(H,H)$ = 1.4, $^3J(H,H)$ = 7.5 Hz; =CH_2), 2.26 (s, 3H; =C(CH_3)), 1.87 (q, 1H, $^3J(H,H)$ = 6.1, $^4J_{trans}(H,H)$ = 1.2 Hz; =C(CH_3)H), 1.73 (s, 15H; $C_5(CH_3)_5$), 1.40 (d, 1H, $^3J_{trans}(H,H)$ = 7.2, $^2J(H,H)$ = 1.4 Hz; =CH_2), 1.34 (d, 3H, $^3J(H,H)$ = 6.1 Hz; =C(H)CH_3); ^{13}C-NMR (98.5 MHz, $CDCl_3$, 20 °C): δ = 135.8 (s; =C(CH_3)–CH=), 120.7 (d, $^1J(C,H)$ = 173 Hz; =C(CH_3)–CH=), 98.9 (s; $C_5(CH_3)_5$), 50.7 (d, $^1J(C,H)$ = 163 Hz; =C(CH_3)H), 45.6 (t, $^1J(C,H)$ = 157 Hz; =CH_2), 19.5 (q, $^1J(C,H)$ = 129 Hz; C(H)(CH_3)=C(CH_3)–), 13.5 (q, $^1J(C,H)$ = 127 Hz; C(H)(CH_3)=C(CH_3)–), 9.8 (q, $^1J(C,H)$ = 129 Hz; $C_5(CH_3)_5$).
4: IR (KBr; extract): $\tilde{\nu}$ = 2998, 2969, 2946, 2920, 2869, 1493, 1482, 1381, 1357, 1046, 1025, 340 cm^{-1}; EI-MS (70 eV): m/z 502 ($M^{\oplus}$ w.r.t. ^{187}Re, ^{35}Cl, 17%), 392 ([$M^{\oplus}-C_8H_{14}$], 56), 356 ([$M^{\oplus}-C_8H_{14}-HCl$], 100); ^1H-NMR (270 MHz, $CDCl_3$, 20 °C): δ = 2.03 (s, 6H; =C(CH_3)–), 1.93 (d, 2H, $^3J(H,H)$ = 5.9 Hz; =C(CH_3)H), 1.72 (s, 15H; $C_5(CH_3)_5$), 1.41 (d, 6H, $^3J(H,H)$ = 5.9 Hz; =C(CH_3)H); ^{13}C NMR (68 MHz, $CDCl_3$, 30 °C): δ = 128.3 (s; =C(CH_3)–), 98.1 (s; $C_5(CH_3)_5$), 53.7 (d, $^1J(C,H)$ = 144 Hz; =C(CH_3)H), 15.9 (qd, $^1J(C,H)$ = 129, $^2J(C,H)$ = 2.5 Hz; =C(CH_3)H), 15.1 (q, $^1J(C,H)$ = 127 Hz; =C(CH_3)–), 9.2 (q, $^1J(C,H)$ = 129 Hz; $C_5(CH_3)_5$).
5: IR (KBr; extract): $\tilde{\nu}$ = 2966, 2917, 1771, 1385, 1145, 1085, 1035;—FD-MS (CH_2Cl_2): m/z 465 ($M^{\oplus}$, w.r.t. ^{187}Re, ^{35}Cl); ^1H-NMR (270 MHz, CD_2Cl_2, −30 °C): δ = 3.21 (s, 6H; $CH_3C{\equiv}$), 2.72 (s, 6H; $CH_3C{\equiv}$), 1.90 (s, 15H; $C_5(CH_3)_5$); $^{13}C\{^1H\}$ NMR (68 MHz, $CDCl_3$, −30 °C): δ = 179.5, 167.3 (C≡C), 110.5 ($C_5(CH_3)_5$), 18.1, 15.2 (CH_3–C≡), 10.9 ($C_5(CH_3)_5$.

[7] **3**: Reddish-brown platelets from *n*-hexane/methylene chloride, monoclinic $P2_1/n$ (No. 14); a = 832.3(2), b = 1418.9(3), c = 1464.0(7) pm, β = 106.74(3)°; refinement terminated at R_w = 0.069 and unsatisfactorily

refineable butadiene ligands, enantiomeric molecules at equivalent lattice sites.—**4**: satin-red, trigonal platelets; monoclinic, $P2_1/c$ (No. 14); $a = 859.4(1)$, $b = 2745.4(4)$, $c = 855.5(1)$ pm, $\beta = 117.73(1)°$; $V = 1787 \times 10^6$ pm^3, $Z = 4$; $M_r = 502.5$; $T = 24°C$; $\rho_{exp.} = 1.868$ g cm^{-3}; $F_{000} = 984$; CAD4 (Enraf-Nonius), graphite monochromator, $\lambda = 0.7107$ Å ($Mo_{K\alpha}$), measuring range: $2° \le e\theta \le 25°$, $t(max) = 60$ s, $h(-10/10)$, $k(0/32)$, $l(-10/10)$; 6368 measured reflections, 161 resolved, 3112 independent reflections, 2903 with $I > 0.5\sigma(I)$ used for the refinement; solution of structure by Patterson methods; 190 parameters, full matrix least squares refinement; all non-hydrogen atoms anisotropic, H atoms calculated at ideal positions and incorporated in the structure factor calculation, numerical absorption correction, $\mu = 71.9$ cm^{-1}, six faces, crystals dimensions $0.42 \times 0.05 \times 0.42$ cm^3, transmission factors 0.1975 to 0.7425; $R = \Sigma(||F_o| - |F_c||)/\Sigma|F_o| = 0.023$; $R_w = [\Sigma w(|F_o| - |F_c|)^2/\Sigma w F_o^2]^{1/2} = 0.023$; $GOF = [\Sigma w(|F_o| - |F_c|)^2/(NO - NV)]^{1/2} = 2.639$ ($w = 1/\sigma^2[F_o]$); $\Delta e_o/$ Å$^3 = 0.87$; shift/err = 0.00.

[8] Review: H. Yasuda, A. Nakamura, *Angew. Chem. 99* (1987) 745; *Angew. Chem. Int. Ed. Engl. 26* (1987) 723.—Electronic factors do not suffice for the observed conformational stability.

[9] J. Wolf, H. Werner, *Organometallics 6* (1987) 1164, and references cited therein.

Diastereospecific Gas/Solid Additions with Cholesterol Derivatives**

By *Gerd Kaupp** and *Christine Seep*

Gas/solid additions are very simple, mild, and economical procedures. They often allow the selective synthesis of highly reactive compounds;[1] however, pronounced stereoselectivities have only seldom been observed.[1,2] We have now found that cholesterol and some of its esters exhibit gas/solid reactivity and undergo diastereospecific additions even as crystalline powders.

Owing to its cholesteric liquid-crystalline phase, cholesteryl oleate **1** has found wide application.[3] When crystalline **1** (**1**$_s$) is allowed to react at -30 to $-20°C$ for 10 h with gaseous hydrogen bromide in excess, the HBr adds regio- and diastereospecifically to give **2** (100%, m.p. 58–59 °C, $[\alpha]_D^{20} = +0.7$, $\tilde{\nu}_{CBr} = 669$ cm^{-1}), without the crystal melting.

Crystalline cholesteryl acetate **3**$_s$ reacts more slowly with gaseous HBr (1 bar, $-30°C$, 6 d). The known 5α-bromide **4**[4] (100%, $[\alpha]_D^{20} = +2.3$, $\tilde{\nu}_{CBr} = 669$ cm^{-1}) is obtained regio- and diastereospecifically. These reactions are very easy to carry out. In solution (e.g., dichloromethane), both reactions yield, in addition to **2** and **4**, respectively, an appreciable amount of side products, even if every attempt is made to exclude water.

Surprisingly, the gases HCl and HI (1 bar, -30 to $+25°C$) do not react at all with **1**$_s$ or **3**$_s$—apart from changes in the color of the crystal to pale yellow or to reddish brown—and cholesteryl stearate is not even attacked by the especially effective HBr. These findings show that, instead of the reaction enthalpies, specific crystal effects are presumably the crucial criterion in determining the gas/solid reactivity. This is even true when the gases can penetrate into the crystal, as shown by the change in color without chemical reaction.[5]

The gas/solid addition of bromine to cholesterol **5** (1 : 1 ratio of the reactants, 25 °C, 2 h) also proceeds quantitatively and diastereospecifically to give the thermodynamically less favored 5α,6β-dibromide **6a**[4,6] ($[\alpha]_D^{20} = -52$, $\tilde{\nu}_{CBr} = 566$, 591, 616 cm^{-1}). Thus, without stabilization by acetic acid of crystallization, this compound is now accessible in a form that can be stored for weeks at room temperature. It is a welcome starting material for mild and economical gas/solid reactions with reactive gases such as NH_3, CH_3NH_2, HI, and CH_3SH.[7]

The reaction of chlorine gas with **5**$_s$ (1 : 1 to 2 : 1, <0.2 bar, $-50°C$, 5 h) exhibits little regioselectivity but is diastereospecific with respect to the proportion of addition at the 5,6-positions, which maintains the steroid framework. Thus, only the 5α,6β-dichloride **6b**[4] can be isolated (after preparative thin layer chromatography: 34%, $[\alpha]_D^{20} = -32$, $\tilde{\nu}_{CCl} = 656$ cm^{-1}).[8] At higher temperatures (above $-30°C$), the reaction becomes appreciably slower owing to partial melting, since this protects the crystal from further contact with the gas. In this case, the gas/solid technique appears to offer little advantage over conventional chlorination.

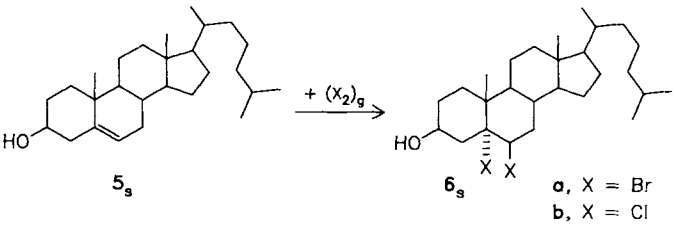

The configurations of the products **2**, **4**, **6a**, and **6b** are supported[9] by the optical rotations (see Ref. [4] and references cited therein) and by characteristic CCl(CBr) vibrational frequencies.[4,10]

The products **2**, **4**, and **6**, easily and economically obtained by the gas/solid technique under mild conditions, are interesting intermediates for further reactions in solution.

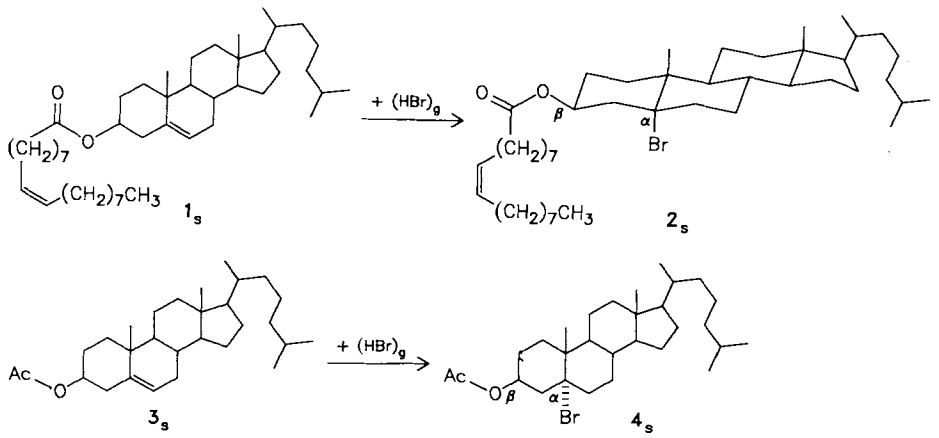

[*] Prof. Dr. G. Kaupp, C. Seep
Fachbereich Chemie - Organische Chemie I - der Universität
Postfach 2503, D-2900 Oldenburg (FRG)

[**] This work was supported by the Deutsche Forschungsgemeinschaft and the Fonds der Chemischen Industrie.

Experimental Procedure

Commercially available **5** (Aldrich or Fluka) contains water of crystallization (^{1}H NMR detection) and is purified by sublimation in vacuo (5×10^{-4} torr, bath temperature 140 °C). The X-ray powder diagrams before and after sublimation are nearly identical. However, the FT-IR difference spectra show weak new bands in the fingerprint region ($\tilde{\nu}$ = 1262, 1100, 1027, and 806 cm^{-1}) for the sublimed cholesterol. The cholesteryl esters **1** (m.p. 44.5 °C) and **3** (m.p. 116.5 °C) (Aldrich) did not require further purification. $[\alpha]_D^{20}$ values in $CHCl_3$; IR spectra in KBr.

A 500-mL round-bottom flask containing 1.0–3.0 g of powdered **1**, **3**, or **5** was evacuated (5×10^{-4} torr). At the temperature given in the text, the gas was passed through a vacuum line fitted with a pressure relief valve or the reaction vessel was connected via a vacuum line with a reservoir containing the calculated amount of gas, the reaction assembly being protected from sunlight. After the required reaction time, the excess gas was pumped off. The crystals were mixed and a representative sample was taken for ^{1}H NMR analysis. The finely crystalline products can be reacted further without initial purification. They can be recrystallized from CH_3OH or CCl_4.

Received: May 24, 1988 [Z 2774 IE]
German version: *Angew. Chem. 100* (1988) 1568

CAS Registry numbers:
1, 303-43-5; **2**, 117021-04-2; **3**, 604-35-3; **4**, 1857-88-5; **5**, 57-88-5; **6a**, 1857-80-3; **6b**, 1857-79-0.

[1] G. Kaupp, D. Matthies, *Chem. Ber. 119* (1986) 2387; *ibid. 120* (1987) 1897; review: *Mol. Cryst. Liq. Cryst. 161* (1988) 119.
[2] P. C. Chenchaiah, H. L. Holland, B. Munoz, M. F. Richardson, *J. Chem. Soc. Perkin Trans. 2 1986*, 1775.
[3] See, for example, L. M. Blinov: *Electro-Optical and Magneto-Optical Properties of Liquid Crystals*, Wiley, New York 1983; H. Kelker, R. Hatz: *Handbook of Liquid Crystals*, Verlag Chemie, Weinheim 1980.
[4] C. W. Shoppee, M. E. H. Howden, R. Lack, *J. Chem. Soc. 1960*, 4874.
[5] This is shown even more clearly when **5**, is treated with gaseous HCl (at −20 to +25 °C, yellow-green, later brown-orange) or HI (at −20 to +25 °C, beige, later red-brown; after pumping off the gas, colorless; after exposure to air, initially dark green, then anthracite-colored). In neither case does a chemical reaction take place (^{1}H NMR in $CDCl_3$).
[6] In syntheses carried out in solution, this isomer has to be protected from mutarotation to the 5β,6α isomer by crystallization with 1 mole equivalent of acetic acid: *Org. Synth. Collect. Vol. 4* (1965) 195 (cf. D. H. R. Barton, E. Miller, *J. Am. Chem. Soc. 72* (1950) 1066). The optical rotation in [4] is given as $[\alpha]_D^{20} = -44$. In solution the value slowly decreases owing to mutarotation.
[7] These reagents, available as gases, react in the usual manner with crystals of **6a**.
[8] Further 5,6-dichlorides of **5** cannot be detected, even before chromatographic purification, although the 5α,6α isomer is known to be stable (no mutarotation) [S. P. J. Maas, J. G. De Heus, *Recl. Trav. Chim. Pays-Bas 77* (1958) 531; [10]] and, in the case of the dibromide, the 5β,6α form is more stable than **6a**. In the reactions competing with 5,6-addition, the steroid framework undergoes rearrangement according to the ^{1}H NMR spectrum. The exact constitution of the rearrangement products, however, could not yet be determined.
[9] Further data supporting the constitution and purity were provided by elemental analyses, mass spectroscopy, and ^{1}H NMR spectroscopy at high field strengths (300 MHz).
[10] D. H. R. Barton, J. E. Page, C. W. Shoppee, *J. Chem. Soc. 1956*, 331.

$[Ni_9(\mu_4\text{-}As)_6(PPh_3)_5Cl_3]$, a Cubic Body-centered Ni_9-Cluster**

By *Dieter Fenske,* Kurt Merzweiler,* and *Johannes Ohmer*

Dedicated to Professor Ernst Otto Fischer on the occasion of his 70th birthday

Phosphane complexes of electron-rich transition-metal halides react with $E(SiMe_3)_2$ (E = S, Se, Te) and $RP(SiMe_3)_2$ (R = Ph, Me, Et) with formation of Me_3SiCl and mixtures of metal-rich clusters. For example, reaction

$[Co_4(PPh_4)(PPh_3)_4]$ **1** $[Ni_8(PPh)_6(PPh_3)_4]$ **2**

$[Ni_8(PPh)_6Cl_4(PPh_3)_4]$ **3**

of $[MCl_2(PPh_3)_2]$ (M = Co, Ni) with $PhP(SiMe_3)_2$ affords the clusters **1–3** in very high yields.

The clusters contain Co_4-tetrahedra or distorted cubic Ni_8-polyhedra whose faces are capped by PPh ligands.[1]

The analogous reaction of $[CoCl_2(PPh_3)_2]$ with $PhAs(SiMe_3)_2$, on the other hand, leads to formation of the complex $[Co_4(\mu_3\text{-}As)_3(\mu_3,\eta^3\text{-}As_3)(PPh_3)_4]$ **4**, via a redox reaction in which all As–C bonds of $PhAs(SiMe_3)_2$ are cleaved.[2]

We have now investigated the reaction of $[NiCl_2(PPh_3)_2]$ with $PhAs(SiMe_3)_2$ [Eq. (a)]. A rapid dissolution of the normally sparingly soluble $[NiCl_2(PPh_3)_2]$ is observed in THF; a crystalline mixture of various clusters and small amounts of metallic nickel separate out from the brown solution.[3] Crystals of **5** and **6** (yield: 50% referred to Ni) are obtained on treatment of the precipitate with $1,2\text{-}C_2H_4Cl_2$ and subsequent covering of the solution with hexane.

$$[NiCl_2(PPh_3)_2] \xrightarrow{PhAs(SiMe_3)_2} [Ni_9(\mu_4\text{-}As)_6(PPh_3)_5Cl_3] + [Ni_9(\mu_4\text{-}As)_6(PPh_3)_6Cl_2] \quad \text{(a)}$$

5 **6**

Derivatives of **5** are obtained in an analogous way from $[NiCl_2(PR_3)_2]$ ($R = C_2H_5$, C_6H_{11}). The IR spectra of **5** and **6** are almost identical with the spectrum of $[NiCl_2(PPh_3)_2]$ above $\tilde{\nu}$ = 400 cm^{-1}, and the recording of NMR spectra is problematic owing to the sparing solubility and paramagnetic behavior of **5**. According to crystal structure analyses **5** and **6** contain the same cluster skeleton.[4] However, an accurate determination of the structure of **6** is not possible because of a disorder of the PPh_3 ligands and the co-crystallizing $C_2H_4Cl_2$ molecules. **5** (Fig. 1) contains a cubic Ni_8 cluster (Ni1–Ni8), with a further Ni atom (Ni9) located in its center. The distances between the Ni atoms of the cube

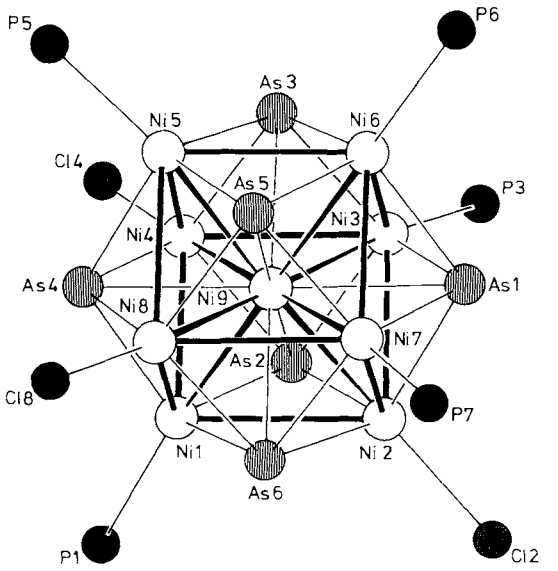

Fig. 1. Molecular structure of **5** (without phenyl groups) in the crystal. Important bond lengths [pm] and angles [°] (±0.1°): Ni-Ni (in the Ni_8 cube) 276.9–284.6(5), Ni-Ni9 238.2–248.4(6), Ni(1–8)-As 229.8–235.0(5), Ni9-As 261.0–264.1(6), Ni-Cl 216.5–218.1(7), Ni-P 217.7–222.9(9); Ni-Ni-Ni (in the Ni_8 cube) 87.0–92.4, Ni-Ni9-Ni 69.8–71.2, 108.6–110.2, 178.4–179.7, Ni-As-Ni 72.6–75.1, 115.9–119.1, Ni(1–8)-As-Ni9 57.0–59.6.

[*] Prof. Dr. D. Fenske, Dr. K. Merzweiler, Dr. J. Ohmer
Institut für Anorganische Chemie der Universität
Niederurseler Hang, D-6000 Frankfurt am Main 50 (FRG)

[**] This work was supported by the Deutsche Forschungsgemeinschaft and the Fonds der Chemischen Industrie.

(277–285 pm) are about 40 pm longer than the distances to the central Ni9 (238–248 pm).

The bonds from Ni9 to the Ni atoms bound to $Cl^{\ominus}$ (Ni2, Ni4, Ni8) are significantly longer (245–248 pm) than the other Ni–Ni bonds (238–242 pm). The distances in the Ni_8 cube of **5** also differ markedly from the values (251–269 pm) found for Ni_8 clusters without an interstitial Ni atom.[1,5] Ni1–Ni8 are coordinated in a distorted tetrahedral fashion to three μ_4-As ligands and one $Cl^{\ominus}$ ligand (Ni2, Ni4, Ni8) or to three μ_4-As ligands and the P atom of a PPh_3 group (Ni1, Ni3, Ni5, Ni6, Ni7). The Ni(1–8)–As bonds (230–235 pm) are only about 30 pm shorter than the distance between Ni9 and the μ_4-As bridges (261–264 pm).

If the μ_4-As ligands are regarded as 3e donors and PPh_3 and $Cl^{\ominus}$ as 2e donors, then **5** and **6** contain 121 and 122 valence electrons, respectively, in remarkable agreement with the number of valence electrons (122) expected according to the 18-electron rule, although this provides no conclusive evidence for the Ni–Ni two-center bonds in the Ni_9 skeleton. An electron counting rule was developed by *Mingos*[6] for clusters with interstitial metal atoms; the number of valence electrons in closest packed metal clusters should be $12n_s + \Delta i$ (n_s = number of metal atoms at the cluster surface, Δi = electron number dependent upon cluster type and central atom). For cubic body centered metal clusters of Au, Rh, and Pt, Δi is 18 or 24. Assuming similar bonding situations in the Ni_9 clusters, **5** and **6** should contain either 114 or 120 valence electrons. The actual number of valence electrons in **5** and **6** show that this rule does not always apply. Other authors have already reported on compounds which contain a section of the cubic body-centered metal structure; examples are $[Rh_{14}(CO)_{25}]^{4\ominus}$, $[Rh_{14}(CO)_{26}]^{2\ominus}$, and $[Au_9(PPh_3)_8]^{n\oplus}$[7,8] ($n = 1, 3$).

Received: April 15, 1988;
revised: May 16, 1988 [Z 2704 IE]
German version: *Angew. Chem. 100* (1988) 1572

CAS Registry numbers:
5, 115792-21-7; **6**, 115887-22-4; $[NiCl_2(PPh_3)_2]$, 14264-16-5; $[NiCl_2(P(C_2H_5)_3)_2]$, 17523-24-9; $[NiCl_2(P(C_6H_{11})_2)_2]$, 19999-87-2; $[Ni_9(\mu_4\text{-}As)_6(P(C_2H_5)_3)_5Cl_3]$, 115792-19-3; $[Ni_9(\mu_4\text{-}As)_6(P(C_6H_{11})_3)_5Cl_3]$, 115792-20-6; $PhAs(SiMe_3)_2$, 38003-96-2.

[1] D. Fenske, *Nachr. Chem. Tech. Lab. 34* (1986) 432; D. Fenske, R. Basoglu, J. Hachgenei, F. Rogel, *Angew. Chem. 96* (1984) 160; *Angew. Chem. Int. Ed. Engl. 23* (1984) 160; D. Fenske, J. Hachgenei, F. Rogel, *ibid. 96* (1984) 959 and *23* (1984) 982.

[2] D. Fenske, J. Hachgenei, *Angew. Chem. 98* (1986) 165; *Angew. Chem. Int. Ed. Engl. 25* (1986) 175.

[3] Procedure: A suspension of $[NiCl_2(PPh_3)_2]$ (8 g, 12.2 mmol) in THF (100 mL) was treated with a solution of $PhAs(SiMe_3)_2$ (5.5 g, 18.5 mmol) in THF (20 mL). After 4 d, 2.5 g of a fine crystalline precipitate were recovered by filtration. Treatment of the precipitate with 100 mL of $C_2H_4Cl_2$ led to dissolution of about 1.6 g of **5** + **6**. After covering with a layer of hexane, black crystals of **5** and **6** separated at the interface.

[4] Siemens AED II, ω-scan (profile analysis), empirical absorption correction, Patterson methods, Ni, As, P, Cl refined anisotropically. **5** crystallizes with four molecules $C_2H_4Cl_2$ per formula unit: space group $P\bar{1}$, lattice constants (210 K): $a = 1440.7(6)$, $b = 1616.6(8)$, $c = 2473.1(10)$ pm, $\alpha = 99.63(4)$, $\beta = 96.96(4)$, $\gamma = 109.72(4)°$; $Z = 2$, $\mu(Mo_{K\alpha}) = 41.1$ cm^{-1}; $2\theta \leq 48°$, 15700 reflections, 8174 with $I > 2\sigma(I)$. Ph refined as rigid group (C–C: 139.5 pm), $R_1 = 0.083$, $R_2 = 0.079$. **6** crystallizes with 16 molecules of $C_2H_4Cl_2$ and two molecules of THF per formula unit; space group C_m; lattice constants (180 K): $a = 2361.8(12)$, $b = 2262.9(11)$, $c = 1611.9(8)$ pm, $\beta = 94.50(4)°$; $Z = 2$, $\mu(Mo_{K\alpha}) = 41.1$ cm^{-1}; $2\theta \leq 52°$, 8878 reflections, 3876 with $I > 2\sigma(I)$. Owing to a disorder of the PPh_3 groups and the $C_2H_4Cl_2$ molecules only the structure of the cluster could be refined; $R_1 = 0.14$, $R_2 = 0.13$. Further details of the crystal structure investigations are available on request from the Fachinformationszentrum Energie, Physik, Mathematik GmbH, D-7514 Eggenstein-Leopoldshafen 2 (FRG), on quoting the depository number CSD-53110, the names of the authors and the journal citation.

[5] L. D. Lower, L. F. Dahl, *J. Am. Chem. Soc. 98* (1976) 5046; D. Fenske, J. Hachgenei, J. Ohmer, *Angew. Chem. 97* (1985) 684; *Angew. Chem. Int. Ed. Engl. 24* (1985) 706.

[6] D. M. P. Mingos, *J. Chem. Soc. Chem. Commun. 1985*, 1352; *Chem. Soc. Rev. 15* (1986) 31.

[7] J. G. M. van der Linden, M. L. H. Paulissen, J. E. J. Schmitz, *J. Am. Chem. Soc. 105* (1983) 1903.

[8] G. Ciani, A. Sironi, S. Martinengo, *J. Organomet. Chem. 192* (1980) C42; S. Martinengo, G. Ciani, A. Sironi, *J. Chem. Soc. Chem. Commun. 1980*, 1140; P. Chini, *J. Organomet. Chem. 200* (1980) 37.

Organobimetallic Mg–Pd Complexes as Intermediates in the Formation of Amorphous $MgPdC_xH_y$ from $Mg(C_2H_5)_2$ and $[Pd(\eta^3\text{-}C_3H_5)_2]$**

By *Borislav Bogdanović*,* *Sara C. Huckett*, *Ursula Wilczok*, and *Anna Rufińska*

Intermetallic compounds are usually prepared by metallurgical methods,[1] although metal-organic chemical vapor deposition has become increasingly important.[2] We recently described[3] the synthesis of amorphous Mg-based intermetallic compounds and their hydrides and carbides under mild conditions ($T \leq 25°C$) in organic solvents from catalytically prepared magnesium hydride[4] or from magnesium alkyls and bis(allyl)metal compounds. We report here the formation of amorphous $MgPdC_xH_y$ **3** ($x = 0.4$–0.8, $y = 0.4$–2.3) from $Mg(C_2H_5)_2$ **1** and $[Pd(\eta^3\text{-}C_3H_5)_2]$ **2** and the identification of intermediate organobimetallic complexes.

The reaction of **1** with **2** (molar ratio 2:1, 25°C) proceeds as shown in Equation (a) (neglecting the C and H in **3**).

$$\underset{\mathbf{1}}{\tfrac{3}{2}Mg(C_2H_5)_2} + \underset{\mathbf{2}}{[Pd(\eta^3\text{-}C_3H_5)_2]} \xrightarrow{THF} \underset{\mathbf{3}}{MgPdC_xH_y} + 2\,H_2C{=}CH_2 + H_2C{=}CHCH_3 + C_2H_6 + \underset{\mathbf{4}}{\tfrac{1}{2}Mg(\eta^1\text{-}C_3H_5)_2} \quad (a)$$

No reflections were observed in the X-ray powder pattern of the black, pyrophoric **3** (crystalline MgPd[5] and $Mg_{0.9}Pd_{1.1}$[5b,6] are known); the same result was obtained even after annealing **3** (650°C, 72 h). Further, **3** does not react with H_2 (20–400°C, normal H_2 pressure), suggesting that substantial amounts of free, finely divided Mg or Pd are not present in the sample.[7] Therefore, **3** is probably a new amorphous Mg–Pd carbide which, in contrast to the analogous amorphous $MgNiC_xH_y$[3a] ($x = 1.2$–1.8, $y = 2.3$–3.4), does not transform into crystalline intermetallic compounds and carbides upon annealing. A more detailed description of the properties of **3** will be presented elsewhere.[8] Efforts are currently being made to learn more about the structure of **3**.

[*] Prof. Dr. B. Bogdanović, Dr. S. C. Huckett, U. Wilczok, Dr. A. Rufińska [†]
Max-Planck-Institut für Kohlenforschung
Kaiser-Wilhelm-Platz 1, D-4330 Mülheim a. d. Ruhr (FRG)

[†] ^1H NMR spectroscopy.

[**] This work was supported by the North Atlantic Treaty Organization under a Grant awarded to *S. C. H.* (1987). We gratefully acknowledge Dr. *R. Mynott*, *B. Gabor*, and *S. Zöcklein* for obtaining and interpreting the ^{13}C NMR data, as well as *R. Ettl* and *G. Schroth* for their contributions in obtaining and analyzing the ^1H NMR data.

To elucidate the pathway(s) leading to the formation of **3**, the reaction [Eq. (a)] was begun at −78 °C in [D_8]THF. After 2 h this led to precipitation of a white solid which redissolved upon warming to −55 °C. ^{1}H NMR spectra were obtained at several temperatures (Fig. 1).[9] The spectrum at −60 °C shows that **5** is formed via transfer of an ethyl group from **1** to **2** and an $\eta^3 \rightarrow \eta^1$ rearrangement of the Pd-allyl group [see Eq. (b)]. The ^{1}H NMR shift differences for H16 and H18[10] are small and an overlap of the peaks for H15 and H17 is observed, but the ^{13}C NMR spectrum[11] clearly shows the distinction between Mg-ethyl groups in **5**[11] and **1**.[12] Precedence for the formation of $MgR^{\oplus}$ ions from MgR_2[13] exists. The ^{13}C NMR chemical shifts and coupling constants for the Pd ligands in **5** are also consistent with the proposed structure. Similar shifts are found for the analogous $[(\eta^3\text{-}C_3H_5)(\eta^1\text{-}C_3H_5)NiCH_3]Li(thf)_4$[14] and $[(\eta^3\text{-}C_3H_5)(\eta^1\text{-}C_3H_5)PdCH_3]Li(thf)_4$.[15]

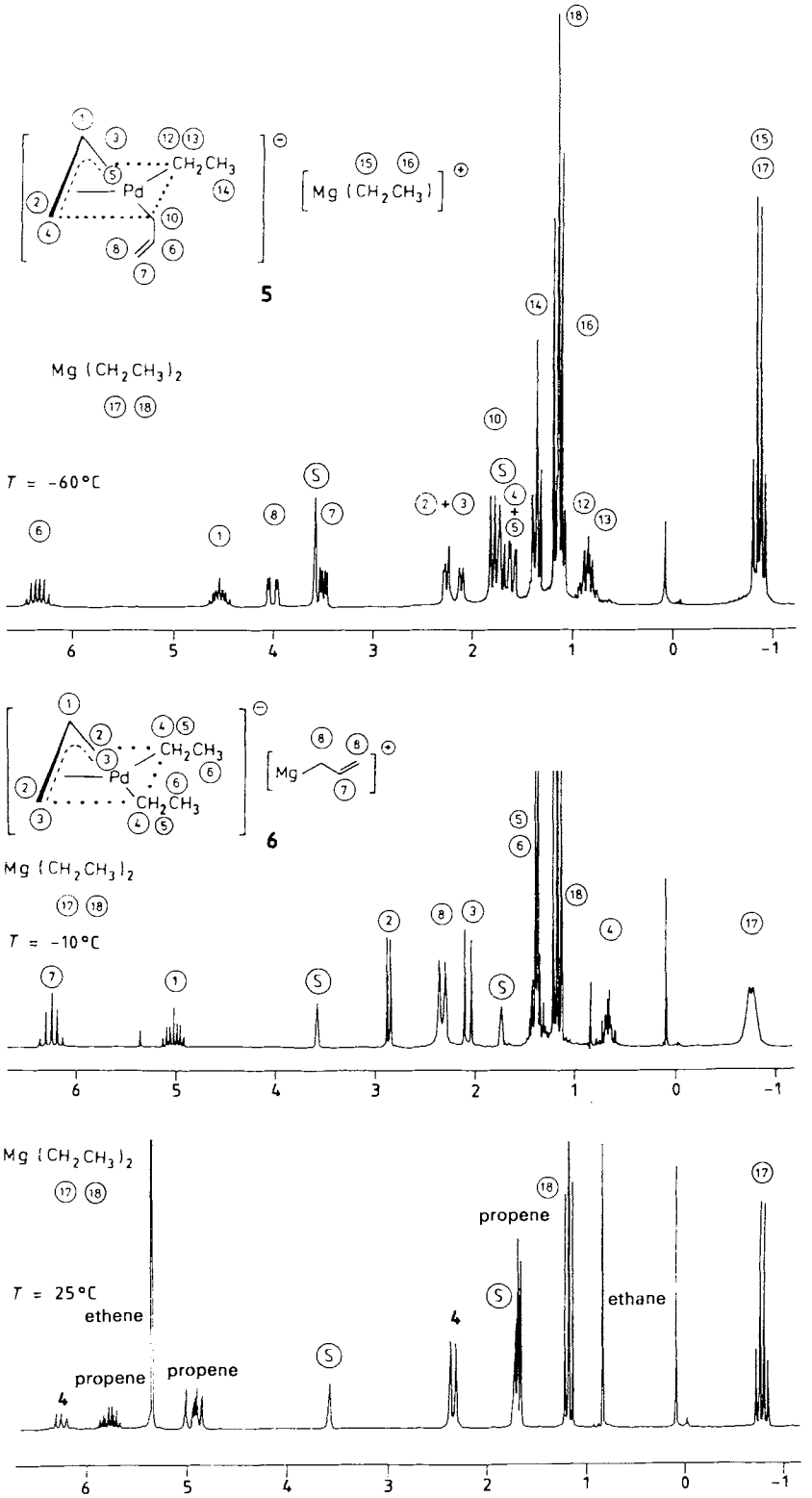

Fig. 1. Variable-temperature ^{1}H NMR spectra of the reaction mixture of **1** and **2** in [D_8]THF (S).

At $-10\,^{\circ}C$ resonances corresponding to **6** are observed as a result of transfer of a second ethyl group to Pd and an allyl group to Mg [Eq. (b)]. The ^1H NMR (η^1-C_3H_5) reso-

$$\mathbf{1} + \mathbf{2} \xrightleftharpoons{-60\,^{\circ}C} \underset{\mathbf{5}}{[(\eta^3\text{-}C_3H_5)(\eta^1\text{-}C_3H_5)(C_2H_5)Pd]^{\ominus}Mg(C_2H_5)^{\oplus}} \xrightleftharpoons{-10\,^{\circ}C} \underset{\mathbf{6}}{[(\eta^3\text{-}C_3H_5)(C_2H_5)_2Pd]^{\ominus}Mg(\eta^1\text{-}C_3H_5)^{\oplus}} \quad (b)$$

nances for **6** are similar to those for **4**[16] but also to those reported for $[CpCo(\eta^3\text{-}C_3H_5)Mg(\eta^1\text{-}C_3H_5)(thf)_2]$.[17] However, the broadness of the terminal ^{13}C NMR resonances[11] precludes definitive assignments for the Mg-allyl ligand in **6**. At 25 °C the only signals in the ^1H NMR spectrum (Fig. 1) are those of **4**,[16] ethene, propene, ethane, and excess **1**.

Intermediates **5** and **6** are shown in Figure 1 and Equation (b) as ionic; however, the presence of a bridging alkyl group or a covalent Pd–Mg bond cannot be ruled out on the basis of the NMR data. Of the known Mg–transition-metal complexes,[10, 17, 18] the following have been shown to contain Mg–transition-metal bonds by X-ray structure determination:

$[Cp(diphos)FeMgBr]\cdot 3\,THF$,[18e] $diphos = (Ph_2P{-}CH_2{-})_2$
$[Cp(C_2H_4)(C_6H_5)CoMgBr](tmeda)$
$[Cp(\eta^3\text{-}C_3H_5)CoMgBr]\cdot 2\,THF$[17]
$[(tmeda)MgCH_3(\mu\text{-}CH_3)Ni(C_2H_4)_2]$[10, 18k]

The stoichiometry of reaction (a) requires, however, that prior to the decomposition of **6** the exchange of an allyl and ethyl group between **6** and excess **1** to produce a third intermediate, presumably **7** [Eq. (c)], should occur. The

$$\mathbf{6} + \tfrac{1}{2}\,\mathbf{1} \longrightarrow \underset{\mathbf{7}}{[(\eta^3\text{-}C_3H_5)(C_2H_5)_2Pd]^{\ominus}Mg(C_2H_5)^{\oplus}} + \tfrac{1}{2}\,\mathbf{4} \quad (c)$$

broadening of the Mg–ethyl resonances observed in both the ^1H and ^{13}C NMR spectra at $-10\,^{\circ}C$ could support this proposal.

Decomposition of **7** via β-hydrogen and reductive[19] elimination [Eq. (d)] would produce **3**, ethene, propene,

$$\mathbf{7} \longrightarrow \mathbf{3} + 2\,H_2C{=}CH_2 + H_2C{=}CHCH_3 + C_2H_6 \quad (d)$$

and ethane in the molar ratio 1 : 2 : 1 : 1 as was experimentally observed. Examples of reductive elimination of hydrocarbons from binuclear organometallic compounds to produce transition-metal complexes have been reported.[20]

Further information concerning intermediates **5** and **6**, and their modes of decomposition was obtained by reacting **1** and **2** (molar ratio 1 : 1, $-78\,^{\circ}C$, THF) and isolating the resulting white solid. The extremely air- and temperature-sensitive solid was shown, on the basis of Mg and Pd elemental analysis, to be a 1 : 1 complex of **1** and **2** with 6 moles of THF per mole of complex (i.e., **5** or **6**). Once isolated, the complex is no longer soluble at $-60\,^{\circ}C$; therefore, a stirred suspension of the solid in $[D_8]$THF was warmed to $-25\,^{\circ}C$, and ^1H NMR spectra were recorded at -30, -10, and 25 °C. At $-30\,^{\circ}C$ broad resonances were observed; however, at $-10\,^{\circ}C$ the resonances corresponding to **6** were present, suggesting that **5** was initially present and was converted into **6** by increasing the temperature of the solution. In contrast to spectra obtained with an excess of **1** present, resonances corresponding to **2** were observed in the spectra at -30 and $-10\,^{\circ}C$. At 25 °C only signals corresponding to ethene, propene, and ethane were observed.

The decomposition of **6** would be expected to produce ethene and propene [Eq. (e)] but not ethane, as observed in

$$\mathbf{6} \longrightarrow \mathbf{3} + 2\,H_2C{=}CH_2 + 2\,H_2C{=}CHCH_3 \quad (e)$$

the ^1H NMR spectrum. However, larger-scale reactions of 1 : 1 molar ratios of **1** and **2** under various conditions (Table 1) were consistent with this observation. Production of ethane can be explained by assuming that the decomposition takes place partially as shown in Equation (f).

$$\mathbf{6} \longrightarrow \tfrac{2}{3}\,\mathbf{3} + \tfrac{4}{3}\,H_2C{=}CH_2 + \tfrac{2}{3}\,H_2C{=}CHCH_3 + \tfrac{2}{3}\,C_2H_6 + \tfrac{1}{3}\,\mathbf{4} + \tfrac{1}{3}\,\mathbf{2} \quad (f)$$

Table 1. Yields of gaseous products [a] and **3** from reaction of **1** and **2**.

Experiment	Yields [%] $H_2C{=}CH_2$	$H_2C{=}CHCH_3$	C_2H_6	**3**
1 [b]	1.8	1.6	0.40	84.2
2 [c]	1.9	1.4	0.55	89.9
3 [d]	1.8	1.6	0.40	86.0

[a] mol gas/mol Mg. [b] Isolated $\mathbf{5}\cdot 6\,THF$ decomposed by warming from -78 to 25 °C in THF. [c] **1** and **2** (molar ratio 1 : 1) reacted at $-78\,^{\circ}C$ to form the white solid which was then decomposed in situ by warming to 25 °C. [d] Reaction of **1** and **2** (molar ratio 1 : 1) at 25 °C.

The yields of the gases and **3** (Table 1) are in agreement with those calculated for simultaneous decomposition via Equations (e) and (f) to the extent of approximately 60 and 40%, respectively. The decomposition of **6** via Equation (f) probably occurs, owing to the reversibility of Equation (b), by reaction of **6** with small amounts of **1** to produce **7**, which can subsequently decompose as shown in Equation (d). The presence of **1** and **2** in the ^1H NMR spectrum of the isolated **5** supports this proposed pathway. The partial decomposition of **6** via Equation (f) in the absence of excess **1** suggests that reductive elimination of ethane from **6** is more favorable than that of propene. This parallels the decreasing order of reactivity towards reductive elimination from $[(Ph_3P)_2Pt(H)R]$ complexes (R): Ph > C_2H_5 > CH_3 > $CH_2{=}CHCH_2$.[21]

These results are, to our knowledge, the first observations of discrete organobimetallic complexes which undergo reductive elimination to produce intermetallic compounds or intermetallic carbides as reaction products.

Experimental Procedure

All manipulations were performed in air- and water-free solvents under Ar. All ^1H and ^{13}C NMR spectra were referenced to $[D_8]$THF.

3: **2** (5.68 g, 30.2 mmol) in THF (40 mL) was added dropwise to a stirred solution of **1** (5.51 g, 66.8 mmol) in THF (30 mL) over 45 min. The gases evolved from the reaction were collected in a gas buret and quantitatively analyzed by mass spectrometry. After 18 h the THF and remaining gaseous products were removed in vacuo (0.1 mbar) into -78 and $-196\,^{\circ}C$ traps, respectively. The GC analysis of the THF from the $-78\,^{\circ}C$ trap showed that it only contained trace amounts of propene (<0.05%). The $-196\,^{\circ}C$ trap gases were also subjected to MS analysis. THF was added to the black residue remaining in the reaction flask and the solution stirred for 12 h. The resulting black solid was collected by filtration, washed with THF and pen-

tane, and dried under high vacuum. Yield: 3.91 g (93.1%). Elemental analysis: Pd 76.29%, Mg 17.58%, C 4.93%, H 1.11% ($PdMg_{1.01}C_{0.57}H_{1.54}$).

5: **1** (0.71 g, 8.61 mmol) and **2** (1.65 g, 8.60 mmol) were dissolved in THF (20 mL) in separate flasks; the solutions were cooled to −78°C and then combined. After stirring for 24 h, the resulting white solid was filtered at −78°C, washed with THF and pentane, and dried under high vacuum at −78°C. Elemental analyses: calculated for **5**·6THF, Pd 15.12%, Mg 3.45%, C 58.02%, H 9.76%; found, Pd 14.69%, Mg 3.54%, C 48.11%, H 8.38%. Low-temperature elemental analysis performed by Dornis & Kolbe, Mülheim a. d. Ruhr (FRG). Intermediate **5** used for the decomposition experiment (Table 1) was prepared analogously.

Received: May 24, 1988;
revised: Aug. 8, 1988 [Z 2773 IE]
German version: *Angew. Chem. 100* (1988) 1569

CAS Registry numbers:
1, 557-18-6; **2**, 12240-87-8; **3** (x = 0.57), 117120-67-9; **3** (x = 0.4–0.8), 117120-67-9; **4**, 6928-75-2; **5**, 117098-45-0; **6**, 117098-47-2; **7**, 117098-48-3; $H_2C{=}CH_2$, 74-85-1; $H_2C{=}CHCH_3$, 115-07-1; C_2H_6, 74-84-0.

[1] a) H. Buchner: *Energiespeicherung in Metallhydriden*, Springer, Berlin 1982; b) E. Amberger, U. Siefken, *J. Less-Common Met. 75* (1980) 273.
[2] P. D. Dapkus, *Annu. Rev. Mater. Sci. 12* (1982) 243.
[3] a) B. Bogdanović, K.-H. Claus, S. Gürtzen, B. Spliethoff, U. Wilczok, *J. Less-Common Met. 131* (1987) 163; b) B. Bogdanović, U. Wilczok (Studiengesellschaft Kohle mbG), Offenlegungsschrift DE 3613532.
[4] B. Bogdanović, *Angew. Chem. 97* (1985) 253; *Angew. Chem. Int. Ed. Engl. 25* (1985) 262.
[5] a) Cubic MgPd (CsCl type): S. N. Sharma, A. Weiss, *J. Less-Common Met. 104* (1984) L5; b) P. I. Kripjakevič, E. I. Gladysevskij, *Kristallografiya 5* (1960) 577.
[6] Tetragonal $Mg_{0.9}Pd_{1.1}$(AuCu type): L. Westin, *Acta Chem. Scand. 22* (1968) 2574; *Chem. Commun. Univ. Stockholm No. 5* (1972) 1.
[7] Both metallic Pd and Mg, in a finely divided active form, react with H_2 under these conditions: U. Wilczok, unpublished results.
[8] B. Bogdanović, S. C. Huckett, B. Spliethoff, U. Wilczok, *Z. Phys. Chem.* (Munich), in press.
[9] A solution of **1** (0.066 g, 0.80 mmol) in [D$_8$]THF (1.9 mL), which had been cooled to −78°C for 45 min, was cannulated into a flask containing **2** (0.067 g, 0.36 mmol, also at −78°C) stirred for 2 h, and then warmed to −55°C; a portion of the resulting solution was transferred to an NMR tube, which was then sealed under Ar. ^{1}H NMR (200 MHz, [D$_8$]THF): $T = -60$°C: $\delta = 6.34$ (ddt, $^3J_{6,7} = 9.6$, $^3J_{6,8} = 16.6$, $^3J_{6,10} = 9.2$ Hz; H6), 4.53 (m, $^3J_{1,2/3} = 7.6$, 7.2, $^3J_{1,4/5} = 12.6$, 13.0 Hz; H1), 3.99 (dd, $^2J_{7,8} = 3.6$ Hz; H8), 3.49 (dd; H7), 2.15, 2.11 (each d; H2, H3), 1.80 (d; H10), 1.65, 1.59 (each d; H4, H5), 1.36 (t; H14), 1.14 (t; H18), 1.11 (t; H16), 0.88 (m; H12), 0.79 (m; H13), −0.86 (q; H15, H17); $T = -30$°C: broadening of peaks in the $\delta = 6.2$, 1.8, 0.9, and −0.9 regions. $T = -10$°C: $\delta = 6.24$ (quint, $^3J_{7,8} = 11.3$ Hz; H7), 5.03 (tt, $^3J_{1,2} = 7.5$, $^3J_{1,3} = 13.3$ Hz; H1), 2.87 (d; H2), 2.32 (d; H8), 2.05 (d; H3), 1.4 (m; H5, H6), 1.16 (t; H18), 0.66 (m; H4), −0.76 (br.; H17); 25°C: $\delta = 6.26$ (quint.; Mg(η^3-CH_2CHCH_2)$_2$ **4**), 5.76 (m; CH_3CHCH_2), 5.35 (s; CH_2CH_2), 4.98 (m; *Z*-H from CH_3CHCH_2), 4.88 (m; *E*-H from CH_3CHCH_2), 2.34 (d; Mg(η^1-CH_2CHCH_2)$_2$ **4**), 1.67 (m; CH_3CHCH_2), 1.18 (t; H18), 0.84 (s; C_2H_6), −0.78 (q; H17).
[10] W. Kaschube, *Dissertation*, Universität Bochum 1987.
[11] ^{13}C NMR (75.5 MHz, [D$_8$]THF): **5** ($T = -80$°C): $\delta = 153.2$ (d, $J_{CH} = 142 \pm 2$ Hz; Pd(η^1-CH_2CHCH_2), 113.5 (d, $J_{CH} = 146 \pm 2$ Hz; Pd(η^3-CH_2CHCH_2), 91.4 (t, $J_{CH} = 151 \pm 1$ Hz; Pd(η^1-CH_2CHCH_2), 49.7, 46.3 (each $J_{CH} = 154$, 153 ± 2 Hz; Pd(η^3-CH_2CHCH_2), 24.2 (t; Pd(η^1-CH_2CHCH_2)), 23.2 (q, $J_{CH} = 122 \pm 2$ Hz; Pd(CH_2CH_3), 15.5 (q, $J_{CH} = 120 \pm 1$ Hz; Mg(CH_2CH_3), 8.8 (t, $J_{CH} = 123 \pm 2$ Hz; Pd(CH_2CH_3), 2.4 (t, $J_{CH} = 102 \pm 1$ Hz; Mg(CH_2CH_3)). **6** ($T = -10$°C): $\delta = 149.7$ (d, $J_{CH} = 138 \pm 2$ Hz; Mg(η^1-CH_2CHCH_2), 119.9 (d, $J_{CH} = 150 \pm 2$ Hz; Pd(η^3-CH_2CHCH_2)), 56.7 (t, $J_{CH} = 155 \pm 2$ Hz; Pd(η^3-CH_2CHCH_2), 18.7 (q, $J_{CH} = 125 \pm 1$ Hz; Pd(CH_2CH_3)), 2.4 (t, $J_{CH} = 122 \pm 2$ Hz; Pd(CH_2CH_3)$_2$). The terminal carbon resonances of the Mg(η^1-C_3H_5) group are evidently too broad to be observed owing to an exchange process which was also evidenced by broadening of the corresponding ^{1}H NMR resonances.
[12] Mg(CH_2CH_3)$_2$: ^{13}C NMR (75.5 MHz, [D$_8$]THF, $T = -80$°C): $\delta = 15.2$ ($J_{CH} = 120 \pm 1$ Hz; CH_3), −1.3 ($J_{CH} = 106 \pm 1$ Hz; CH_2).
[13] a) A. D. Pajerski, M. Parvez, H. G. Richey, Jr., *J. Am. Chem. Soc. 110* (1988) 2660; b) E. P. Squiller, R. R. Whittle, H. G. Richey, Jr., *ibid. 107* (1985) 432; c) P. Sobota, M. Novak, *J. Organomet. Chem. 340* (1988) 1.
[14] S. Holle, P. W. Jolly, R. Mynott, S. Salz, *Z. Naturforsch. B37* (1982) 675.
[15] ^{13}C NMR (25.2 MHz, [D$_8$]THF, $T = -50$°C): $\delta = 153.5$ (Pd(η^1-CH_2CHCH_3)), 112.0 (Pd(η^3-CH_2CHCH_2)), 91.5 (Pd(η^1-CH_2CHCH_2)), 51.6, 44.0 (Pd(η^3-CH_2CHCH_2)), 22.6 (Pd(η^1-CH_2CHCH_2)), −12.0 ($PdCH_3$) (S. Holle, P. W. Jolly, R. Mynott, unpublished results).
[16] H. E. Zieger, J. D. Roberts, *J. Org. Chem. 34* (1969) 1976.
[17] K. Jonas, G. Koeppe, C. Krüger, *Angew. Chem. 98* (1986) 901; *Angew. Chem. Int. Ed. Engl. 25* (1986) 923.
[18] a) R. J. Cross, F. Glocking, *J. Organomet. Chem. 3* (1969) 253; b) G. B. McVicker, R. S. Matyas, *J. Chem. Soc. Chem. Commun. 1972*, 972; c) H. Felkin, P. J. Knowles, *J. Organomet. Chem. 37* (1972) C14; d) S. W. Ulmer, P. M. Skarstad, J. M. Burlitch, R. E. Hughes, *J. Am. Chem. Soc. 95* (1973) 4469; e) H. Felkin, P. J. Knowles, B. Meunier, A. Mitschler, L. Ricard, R. Weiss, *J. Chem. Soc. Chem. Commun. 1974*, 44; f) S. Kato, M. Wakamatsu, M. Mizuta, *J. Organomet. Chem. 78* (1974) 405; g) G. B. McVicker, *Inorg. Chem. 14* (1974) 2087; h) M. L. H. Green, T. Luong-thi, G. A. Moser, I. Packer, F. Pettit, D. M. Roe, *J. Chem. Soc. Dalton Trans. 1976*, 1988; i) H. Felkin, P. J. Knowles, B. Meunier, *J. Organomet. Chem. 146* (1978) 151; j) H. Schenkluhn, *Dissertation*, Universität Bochum 1971; k) G. Wilke, *Angew. Chem. 100* (1988) 189; *Angew. Chem. Int. Ed. Engl. 27* (1988) 185.
[19] a) P. W. Jolly in G. W. Wilkinson, F. G. A. Stone, E. W. Abel (Eds.): *Comprehensive Organometallic Chemistry, Vol. 6*, Pergamon, Oxford 1982, p. 81; b) K. Fischer, K. Jonas, P. Misbach, R. Stabba, G. Wilke, *Angew. Chem. 85* (1973) 1002; *Angew. Chem. Int. Ed. Engl. 12* (1973) 943.
[20] a) M. J. Chetcui, M. H. Chisholm, K. Folting, D. A. Haitko, J. C. Huffman, *J. Am. Chem. Soc. 104* (1982) 2138; b) K. M. Motyl, J. R. Norton, C. K. Schauer, O. P. Anderson, *ibid. 104* (1982) 7325.
[21] L. Abis, A. Sen, J. Halpern, *J. Am. Chem. Soc. 100* (1978) 2915.

Host-Guest Bonding of Oxoanions to Guanidinium Anchor Groups**

By *Gerhard Müller, Jürgen Riede,* and *Franz Peter Schmidtchen**

Our concept for the construction of synthetic, selective host molecules by linear coupling of recognition functions[1,2] requires, inter alia, the most specific anchor groups possible for the anionic substructures of the guest. This suggests adaptation of the recognition principle of many biogenic hosts which preferentially utilize the interaction between the guanidinium function of arginyl side chains and carboxylate or phosphate groups[3] (Scheme 1a). On the basis of this bonding pattern of the natural receptors, for which theoretical calculations also confirm a high stability,[4] we designed the abiotic binding groups shown in Scheme 1b for oxoanions, for these should essentially fulfill the following requirements: by the binding of the guanidine structure in an essentially strain-free bicyclic compound, host-guest complexation should lead, as in the case of the natural prototypes, not only to a topologically unmistakable complex structure but, at the same time, orientation and spacing of the guest should be defined within narrow limits by the host without having to resort to molecular inclusion in a macrocyclic host. The substituents on the α,α′-C atoms should provide for the covalent coupling of further bonding groups and be utilizable for the anchoring of the host to a solid support; the stereogenicity of these ring positions should force the guest into a fixed dissymmetric environment. The combined effect of several bonding functions ought to make the desired enantioselective recognition of the substrate possible. We present here

[*] Prof. Dr. F. P. Schmidtchen
Organisch-chemisches Institut der
Technischen Universität München
Lichtenbergstrasse 4, D-8046 Garching (FRG)
Dr. G. Müller, J. Riede
Anorganisch-chemisches Institut der
Technischen Universität München
Lichtenbergstrasse 4, D-8046 Garching (FRG)

[**] This work was supported by the Deutsche Forschungsgemeinschaft and the Fonds der Chemischen Industrie. The results of this communication were delivered in part in a lecture at the 193rd ACS Meeting in Denver, CO (USA), Spring 1987.

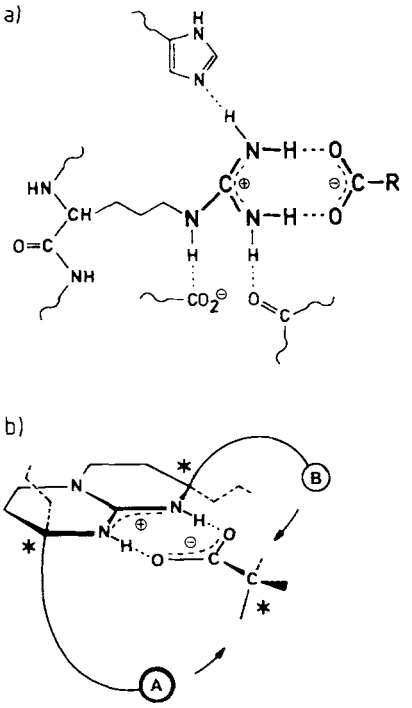

Scheme 1.

NMR spectroscopic and crystallographic proof that the symmetrically substituted guanidinium salts **1**–**3** fulfill the premise of this concept, the binding of oxoanions analogously to that found in natural products (Scheme 1b).

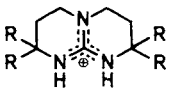

1, R = CH_3
2, R = CH_2-CH=CH_2
3, R = CH_2-CH_2-CH_2-OH

The construction of the characteristic hydrogen-bonding pattern in the course of the host-guest complexation with anions ought to be easily observed if the host does not already contain this structural element. Therefore, the readily crystallizable tetraphenylborates of **1** and **2**[5] and of the hydroxypropyl derivative accessible from **2** by hydroboration and oxidation were suitable for investigations with the aid of NMR spectroscopy. The salts are readily soluble in dipolar solvents (acetonitrile, nitromethane) and their NMR signals do not show any concentration dependence. Even the addition of tetrabutylammonium perchlorate ($TBAClO_4$) has no influence on the signal positions. If, however, a solution of **2** · BPh_4 in CD_3CN is titrated with TBA·*p*-nitrobenzoate in the same solvent, significant shifts of all resonances are observed in the ^{1}H-NMR spectrum (Fig. 1). Especially drastic is the down-field shift of the NH signal ($\Delta\delta > 5$ ppm). Apart from slight changes in the region of the strongly coupled olefinic protons no new signals appear in the spectrum. This picture is to be expected for a host-guest system in which host and complex show the same symmetry elements on time average and rapid guest exchange leads to concentration-weighted signal positions. The shape of the titration curve shows a distinct 1 : 1 stoichiometry of the host-guest interaction, but only a lower limit for the complex stability ($K_{diss} < 10^{-4}$ M) can be estimated under these conditions. Even the ^{1}H-resonances of the *p*-nitrobenzoate are shifted a small amount ($\Delta\delta < 0.03$ ppm) to higher field, whereby the four-line AB system degenerates into almost a singlet. Like the proton signals, the ^{13}C- (see Fig. 1) and ^{15}N-resonances[6] of the bicyclic guanidinium ion **2** are also shifted. Especially striking is that large shifts are observed only for the signals of the molecular hemispheres which are constitutively or spatially in the neighborhood of the guanidinium NH. The host-guest complexation must therefore occur at this substructure of the host, although we have not succeeded in demonstrating a homonuclear intermolecular nuclear Overhauser effect between **2** and *p*-nitrobenzoate.

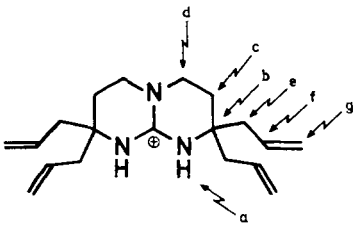

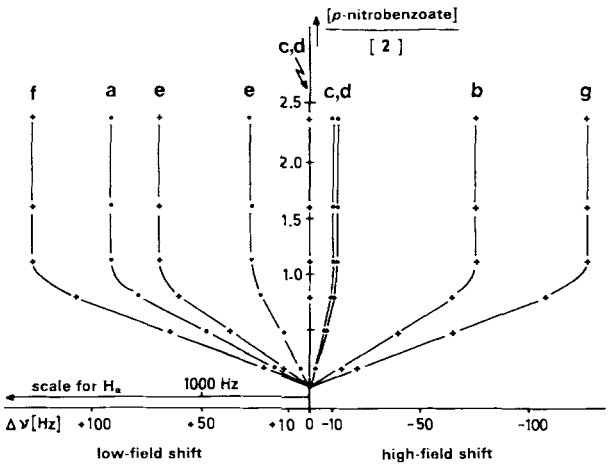

Fig. 1. NMR titration (360 MHz ^{1}H = ●; 90 MHz ^{13}C = +) of **2** · BPh_4 (0.05 M) with TBA·*p*-nitrobenzoate in CD_3CN.

In a similar way as for the described carboxylate, NMR signal shifts are also found with $H_2PO_4^\ominus$ or $Cl^\ominus$ as guest anions. Since qualitatively the same effects are observed, the site of binding of the guest is undoubtedly the same in all cases. Even the hydroxy functions in the side chains of **3** do not decisively alter the mode of binding of an oxoanion to the guanidinium fragment. Only the distinctly smaller overall shift of the NH signal, in particular, gives an indication that additional hydrogen bridges of the carboxylate to the side chains weaken the interaction between the guanidinium fragment and the anion.

In the weaker solvating solvent $CDCl_3$ the free rotation of the allyl substituents of **2** · BPh_4 is hindered, so that the methylene protons show an ABX coupling pattern. Addition of *p*-nitrobenzoate simplifies this to an A_2X system, thus confirming the large flexibility of the host in the host-guest complex. Moreover, even more pronounced line shifts are observed in the ^{1}H-NMR spectrum in this solvent, and also a small hypsochromic shift of the long wavelength UV absorption bands of the guest now accompanies the host-guest bonding. According to *Benesi* and *Hildebrand* the dissociation constant of the host-guest complex can be determined as $K_{diss} = 7 \times 10^{-6}$ M. This extraordinary stability of the ion-pairing between two monovalent ions likewise indicates a special complex structure.

Direct observation of the host-guest configuration was made possible by the determination of the crystal structure of **3**·acetate.[7] It confirms the symmetric bonding pattern of the acetate ions via two H-bridges to both N-atoms of the guanidinium counterion (Fig. 2). The guanidinium fragment is, to a very good approximation coplanar with the acetate ion and the H-bridge system; this can be regarded as an indication of considerable stability of the observed host-guest interaction. The short N2...O01 distance (2.850(5) Å) also indicates that the H-bridges are strong. Moreover, there is a further connection between host and guest via two of the side chains of **3** by two further H-bridges O1-HO1...O01'' (O1...O01'' 2.733(5) Å) to acetate O-atoms. Particularly remarkable is the fact that, at least in the crystal, this connection is not intramolecular but links the cation-anion pair **3**·acetate into polymer strands (Fig. 2).

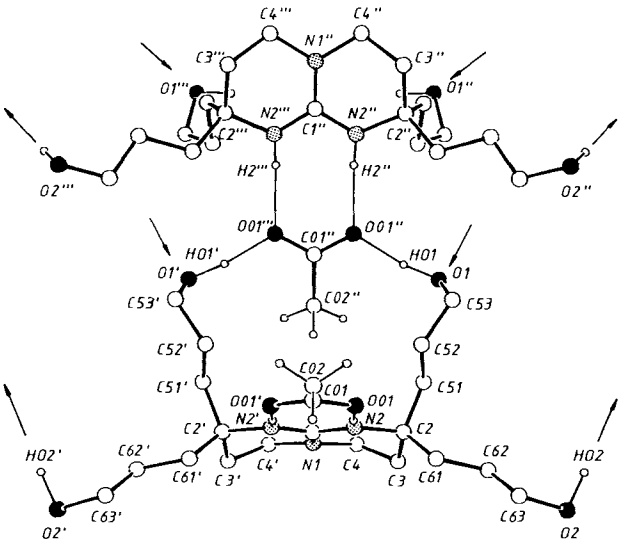

Fig. 2. Section of the crystal structure of **3**·acetate (ORTEP, atoms with arbitrary radii, only N- and O-bonded H atoms are shown). The molecular moiety **3**·acetate has crystallographic mirror symmetry, the mirror plane contains the atoms N1, C1, C01 and C02. The illustrated strands (**3**·acetate)$_x$ are generated by a crystallographic glide plane (a) and connected with one another by four H-bridges per **3**·acetate (O2-HO2...O1*/O2*-HO2*...O1; indicated by arrows) via inversion centers.—Important bond lengths [Å] and angles [°]: N1-C1 1.333(7), N2-C1 1.338(5), C01-C02 1.497(8), C01-O01 1.258(4); N1-C1-N2 121.4(3), N2-C1-N2' 117.2(5), C02-C01-O01 118.5(3), O01-C01-O01' 123.1(6). H-bridges: N2-H2···O01 0.88(4)/1.97(4), O1-HO1···O01'' (−0.5+x,y,2.5−z) 1.08/1.66, O2-HO2···O1* (−x,1−y,2−z) 1.20/1.70.

Since these H-bridges are shorter they must be even stronger than those between acetate ion and guanidinium fragment, which is consistent with the NMR observations. The two remaining side chains surprisingly do not participate in the host-guest interaction, but couple the strands together by H-bonding with the hydroxy O-atoms O1* of neighboring guanidinium ions **3**, so that all NH- and OH-functions participate in H-bonding in the crystal.

Received: May 30, 1988 [Z 2790 IE]
German version: *Angew. Chem. 100* (1988) 1574

CAS Registry numbers:
2$^{\oplus}$·*p*-$NO_2C_6H_4CO_2^{\ominus}$, 117161-61-2; **3**$^{\oplus}$·$AcO^{\ominus}$, 117161-62-3.

[1] a) F. P. Schmidtchen, *J. Am. Chem. Soc. 108* (1986) 8249; b) *Nachr. Chem. Tech. Lab. 8* (1988) 10.
[2] For other concepts on the design of synthetic host-guest molecules see D. J. Cram, *Angew. Chem. 100* (1988) 1041; *Angew. Chem. Int. Ed. Engl. 27* (1988) 1009 (Nobel lecture); F. Diederich, *Angew. Chem. 100* (1988) 372; *Angew. Chem. Int. Ed. Engl. 27* (1988) 362; J. Rebek, Jr., *Science Washington 235* (1987) 1478.
[3] a) J. F. Riordan, *Mol. Cell. Biochem. 26* (1979) 71; b) K. W. Hart, A. R. Clarke, D. B. Wigley, A. D. B. Waldman, W. N. Chia, D. A. Barstow, T. Atkinson, J. B. Jones, J. J. Holbrook, *Biochem. Biophys. Acta 914* (1987) 294.
[4] a) R. D. Gandour, *Bioorg. Chem. 10* (1981) 169; b) A. M. Sapse, C. S. Russel, *THEOCHEM. 30* (1986) 43.
[5] F. P. Schmidtchen, *Chem. Ber. 113* (1980) 2175.
[6] The ^{15}N-NMR spectra were measured by polarization transfer experiments (DEPT; $J(NH)=90$ Hz; $\theta=90°$ with ^{1}H-decoupling). Only the protonated guanidinium N-atoms are observed. The signal shifts $\Delta\delta$ due to complex formation are ≤ 3 ppm in CD_3CN.
[7] Crystal structure data of **3**·acetate: $C_{21}H_{41}O_6N_3$, $M_r=431.58$, orthorhombic, space group *Pnma* (No. 62), $a=12.415(2)$, $b=24.464(3)$, $c=7.474(1)$ Å, $V=2270.0$ Å^3, $Z=4$, $\rho_{calcd}=1.263$ g cm^{-3}, $\mu(Mo_{K\alpha})=0.9$ cm^{-1}, $F(000)=944$, $T=-35$°C, Syntex $P2_1$ diffractometer, $Mo_{K\alpha}$ radiation, $\lambda=0.71069$ Å, graphite monochromator. 3411 measured reflections (*hkl*: ±13, +26, +8), 1615 independent and 1211 "observed" with $F_0 \geq 4.0\sigma(F_0)$ (ω scan, $\Delta\omega=0.9°$, $(\sin\theta/\lambda)_{max}=0.594$ Å^{-1}). Solution by direct methods (MULTAN-87), $R(R_w)=0.066$ (0.059), $w=1/\sigma^2(F_0)$ (anisotropic, H2 isotropic, all other H-atoms constant in observed positions with $U_{iso}=0.05$ Å^2, SHELX-76). $\Delta\rho_{fin}$(max/min) = 0.33/−0.30 e Å^{-3}. Further details of the crystal structure investigation are available on request from the Fachinformationszentrum Energie, Physik, Mathematik GmbH, D-7514 Eggenstein-Leopoldshafen 2 (FRG), on quoting the depository number CSD-53 239, the names of the authors, and the journal citation.

Methoxyallenes as Components in Diels–Alder Reactions with Inverse Electron Demand: Synthesis of 6*H*-1,2-Oxazines**

By *Reinhold Zimmer* and *Hans-Ulrich Reissig**

During the last few years acceptor-substituted allenes have been used for various pericyclic reactions.[1] In contrast, electron-rich allenes, some of which are much more readily accessible, have hardly been employed at all. Herein we report on Diels–Alder reactions with inverse electron demand[2] involving various methoxyallenes.

The nitrosoalkenes **2**, generated in situ from α-halo oximes **1** and sodium carbonate (Scheme 1),[3] add smoothly to methoxyallene **3**[4] (five equivalents). Of the four conceivable regioisomeric cycloadducts, only the heterocycles **4** containing an *exo*-methylene group at C-5 are formed, as

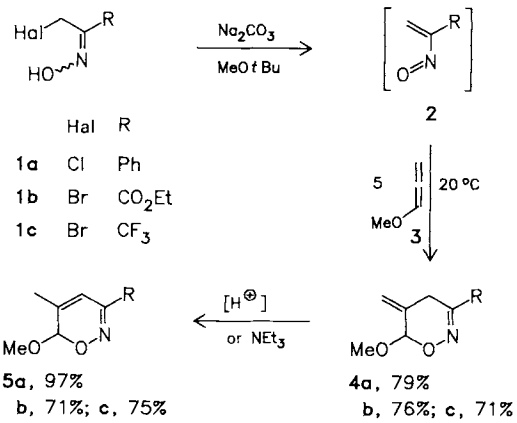

Scheme 1. Synthesis of 6*H*-1,2-oxazines **4** and **5**. The yields given are based on **1** or **4**, respectively.

[*] Prof. Dr. H.-U. Reissig, Dipl.-Ing. R. Zimmer
Institut für Organische Chemie der Technischen Hochschule
Petersenstrasse 22, D-6100 Darmstadt (FRG)

[**] This work was supported by the Deutsche Forschungsgemeinschaft, the Fonds der Chemischen Industrie, and the Karl-Winnacker-Stiftung (Hoechst AG).

expected in view of the electronic properties of the reaction partners.[5] Conjugation of the exocyclic double bond may be achieved by treatment with bases or, more quickly, under acid catalysis. The 6*H*-1,2-oxazines **5** are thereby obtained in good yields.

Since **3** can be easily substituted at C-1 by deprotonation and subsequent reaction with electrophiles,[6] it is also possible to synthesize 1,2-oxazine derivatives containing two substituents in the 6-position. Whereas the addition of **2** to 1-alkylated methoxyallenes affords only moderate yields (e.g., 30% yield of 1-methyl-1-methoxyallene and **2a**), the sterically encumbered hydroxylated allenes **6** and **7** give the functionalized heterocycles **8** and **9**, respectively, with reasonable efficiency. A moderate diastereoselectivity (60:40) was found in the cycloaddition of **2a** to **7** to give **9**. The products **8** and **9** can also be transformed into the conjugated systems **5** by treatment with base.

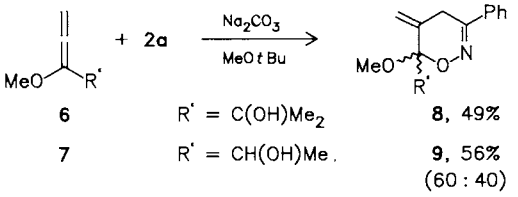

1,2-Oxazines are compounds of little explored but readily apparent synthetic potential.[7] We therefore investigated transformations of the heterocycles **5**. Oxidation of **5a** with pyridinium chlorochromate (PCC) affords the 1,2-oxazin-6-one **10**;[8] treatment with $BF_3 \cdot OEt_2$/allyltrimethylsilane results in C–C bond formation to give **11**. This reaction, like the reduction with triethylsilane in the presence of the Lewis acid $BF_3 \cdot OEt_2$ to give **12**, probably proceeds via the intermediacy of an azapyrylium ion.[9] Reaction of **5a** with aluminum amalgam[7a] gives the pyrrole derivative **13**.[10] These reactions point to the diverse possible reactions of 6*H*-1,2-oxazines. Table 1 contains relevant physical data of characteristic compounds.

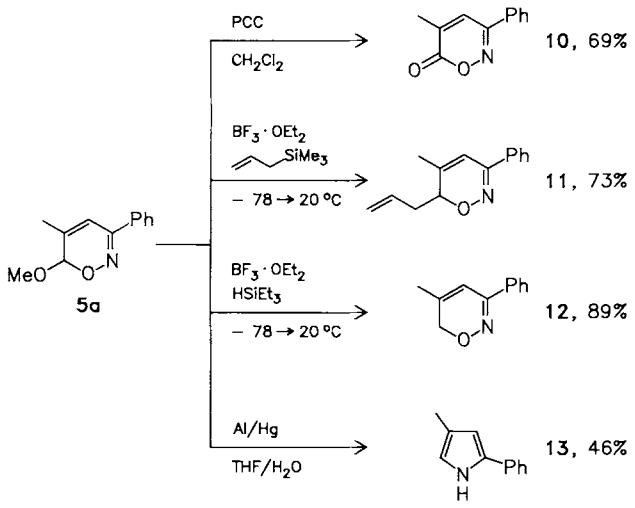

Table 1. Physical data of characteristic compounds [a].

4a: b.p. 90°C/0.06 torr; ^{1}H NMR: δ = 7.76–7.68, 7.45–7.35 (2m, 2H, 3H; Ph), 5.22, 5.12 (2d, ^4J = 2.5 Hz, each 1H; =CH_2), 5.21 (s, 1H; 6-H), 3.51 (s, 3H; OMe), 3.50, 3.19 (td, d, AB part of a ABXY system, ^4J = 2.5, $^2J_{AB}$ = 19.5 Hz, 2H, 4-H); ^{13}C NMR: δ = 156.2 (s; C-3), 135.2, 134.9 (2s; C-5, *ipso*-C), 129.9, 128.5, 125.5 (3d;Ph), 112.3 (t; =CH_2), 99.6 (d; C-6), 55.3 (q; OMe), 19.2 (t; C-4)

5a: b.p. 95°C/0.06 torr; ^{1}H NMR: δ = 7.78–7.67, 7.48–7.32 (2m, 2H, 3H; Ph), 6.32 (q, ^4J = 1.5 Hz, 1H; 4-H), 5.31 (s, 1H; 6-H), 3.53 (s, 3H; OMe), 2.05 (d, ^4J = 1.5 Hz, 3H; 5-Me); ^{13}C NMR: δ = 154.1 (s; C-3), 137.5, 134.1 (2s; C-5, *ipso*-C), 129.5, 128.6, 126.2 (3d; Ph), 111.9 (d; C-4), 97.1 (d; C-6), 55.9 (q; OMe), 19.3 (q; 5-Me)

12: m.p. 31.5–33°C; ^{1}H NMR: δ = 7.7–7.6, 7.4–7.3 (2m, 2H, 3H; Ph), 6.18 (br. s, 1H; 4-H), 4.38 (s, 2H; 6-H), 1.96 (s, 3H; 5-Me); ^{13}C NMR: δ = 156.8 (s; C-3), 141.4 (s; C-5), 134.0, 129.8, 128.6, 126.0 (s. 3d; Ph), 110.9 (d; C-4), 66.5 (t; C-6), 19.6 (q; 5-Me)

[a] All compounds gave satisfactory elemental analyses and appropriate spectra. 300 MHz ^{1}H NMR and 75.5 MHz ^{13}C NMR spectra in $CDCl_3$ with TMS as standard.

Received: June 14, 1988 [Z 2813 IE]
German version: *Angew. Chem. 100* (1988) 1576

CAS Registry numbers:
1a, 21572-32-7; **1b**, 73472-94-3; **1c**, 117341-57-8; **3**, 13169-00-1; **4a**, 117341-58-9; **4b**, 117341-59-0; **4c**, 117341-60-3; **5a**, 117341-61-4; **5b**, 117341-62-5; **5c**, 117341-63-6; **6**, 22141-88-4; **7**, 22141-90-8; **8**, 117369-63-8; **9** (isomer 1), 117341-64-7; **9** (isomer 2), 117341-65-8; **10**, 113549-23-8; **11**, 117341-67-0; **12**, 117341-66-9; **13**, 20055-04-3; allyltrimethylsilane, 762-72-1.

[1] a) A. Bosum, S. Blechert, *Angew. Chem. 100* (1988) 596; *Angew. Chem. Int. Ed. Engl. 27* (1988) 558; b) S. E. Denmark, M. A. Harmata, K. S. White, *J. Org. Chem. 52* (1987) 4031; c) A. Padwa, S. P. Craig, U. Chiacchio, D. N. Kline, *ibid. 53* (1988) 2231; d) G. Himbert, D. Fink, K. Diehl, *Chem. Ber. 121* (1988) 431, and earlier work of these groups and references cited therein.

[2] a) Recent reviews: D. L. Boger, *Tetrahedron 39* (1983) 2869; D. L. Boger, S. N. Weinreb: *Hetero Diels-Alder Methodology in Organic Synthesis*, Academic Press, New York 1987; b) for the incompletely described reaction of allene with a 1,2,4,5-tetrazine, see R. A. Carboni, R. V. Lindsey, Jr., *J. Am. Chem. Soc. 81* (1959) 4342; c) recently, the intramolecular cycloaddition of a molecule with an allene and with a 1,2-diazine unit was reported: D. L. Boger, S. M. Sakya, *J. Org. Chem. 53* (1988) 1445; Note added in proof (October 5, 1988): A hetero-Diels–Alder reaction with inverse electron demand using **3** under high-pressure conditions was very recently published: D. L. Boger, K. D. Robarge, *ibid. 53* (1988) 3373.

[3] Review: T. L. Gilchrist, *Chem. Soc. Rev. 12* (1983) 53.

[4] S. Hoff, L. Brandsma, J. F. Arens, *Recl. Trav. Chim. Pays-Bas 87* (1968) 916; F. J. Weiberth, S. S. Hall, *J. Org. Chem. 50* (1985) 5308.

[5] MO coefficients of methoxyallene: M. Yoshida, Y. Hidaka, Y. Nawata, J. M. Rudzinski, E. Osawa, K. Kanematsu, *J. Am. Chem. Soc. 110* (1988) 1232.

[6] S. Hoff, L. Brandsma, J. F. Arens, *Recl. Trav. Chim. Pays-Bas 87* (1968) 1179.

[7] See a) E. J. Chrystal, T. L. Gilchrist, W. Stretch, *J. Chem. Res. (S) 1987*, 180; *J. Chem. Res. (M) 1987*, 1563 and earlier work of this group; b) C. Hippeli, H.-U. Reissig, *Synthesis 1987*, 77; see also transformations of the related isoxazolines: V. Jäger, I. Müller, R. Schohe, M. Frey, R. Ehrler, B. Häfele, D. Schröder, *Lect. Heterocycl. Chem. 8* (1985) 79, and references cited therein.

[8] A. Padwa, U. Chiacchio, D. N. Kline, J. Perumattam, *J. Org. Chem. 53* (1988) 2238.

[9] For the formation of azapyrylium salts, see Q. B. Broxterman, H. Hogeveen, R. F. Kingma, F. van Bolhuis, *J. Am. Chem. Soc. 107* (1985) 5722, and references cited therein.

[10] T. W. Thompson, *Chem. Commun. 1968*, 533.

Tetrakis[bis(trimethylsilyl)ethyne]diiron**

By *Hartmut Schäufele, Hans Pritzkow*, and *Ulrich Zenneck**

Dedicated to Professor Heinrich Nöth on the occasion of his 60th birthday

The existence of homoleptic transition-metal alkyne clusters is, to the best of our knowledge, only clearly supported by one example so far, tris[bis(trimethylsi-

[*] Dr. U. Zenneck, Dipl.-Chem. H. Schäufele, Dr. H. Pritzkow
Anorganisch-chemisches Institut der Universität
Im Neuenheimer Feld 270, D-6900 Heidelberg (FRG)

[**] Reactive π-Complexes of the Electron-rich Transition Metals, Part 7. This work was supported by the Stiftung Volkswagenwerk. Part 6: [1].

lyl)ethyne]diplatinum,[2] which, according to its spectra, has a dimetallatetrahedrane structure. Since such clusters are of considerable importance as intermediates in the catalytic and stoichiometric reactions of alkynes with transition metals, there has been no lack of attempts to synthesize further complexes of this type. Among other methods, metal-atom chemistry has been employed[3] and, especially in the case of iron, has afforded unexpected results. Thus, the cocondensation of iron atoms with butyne-2 yielded decamethylferrocene[4] and the corresponding reaction with bis(trimethylsilyl)ethyne gave a product of variable composition ($[Fe\{(SiMe_3)_2C_2\}_x]$, $x = 1.8$–4.0).[5]

The reaction of the reactive iron complexes **1** and **2**, readily accessible by a metal-atom reaction, with alkynes results in catalytic cyclotrimerization. This is not the case, however, for bis(trimethylsilyl)ethyne **3**.[1] When a mixture consisting of **3** and either **1** or **2** is allowed to stand *with-*

$[Fe(\eta^2\text{-}C_2H_4)_2(\eta^6\text{-PhMe})]$ **1**[6]
$[Fe(\eta^4\text{-1-Me-}C_{10}H_7)(\eta^6\text{-PhMe})]$ **2**[7]

out agitation at room temperature for several days, **4** (tetrakis[bis(trimethylsilyl)ethyne]diiron) crystallizes as large, analytically pure, lustrous black crystals, containing, as the sole impurity, 0.1 to maximally 0.3% of metallic iron.

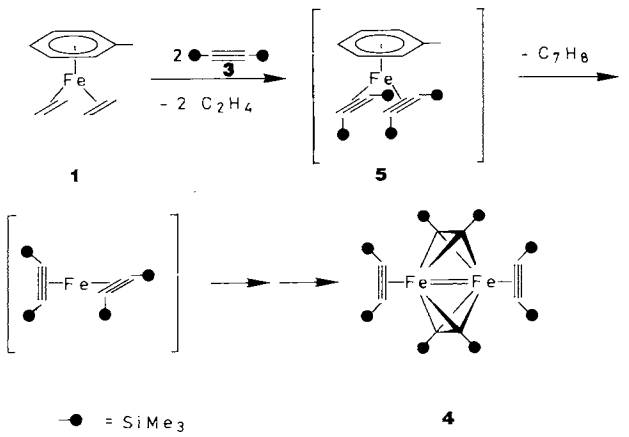

The yield lies between 70 and 98%, independent of which of the reaction components is used in excess. Compound **4** is only sparingly soluble in the conventional polar and nonpolar solvents at room temperature and, as a solid, only slightly air-sensitive. To remove the traces of metallic iron, **4** is dissolved in a large volume of toluene at 80 °C, the solution is stirred in the presence of pieces of ferrite, and the suspension is then filtered. Compound **4** crystallizes from the filtrate at 20 °C. The ^1H NMR spectrum of **4** shows two singlets at $\delta = 0.3$ and -0.2 in a ratio of 1 : 1. The low solubility of **4** prevented the recording of a ^{13}C NMR spectrum.

The nearly quantitative formation of **4** by reaction of **1** or **2** with **3** is easily explained if the bis(alkyne)-(toluene)iron **5** is assumed as an intermediate.

Normally, compounds of type **5** rearrange to ferrols,[1] a reaction pathway that is blocked in the case of **3** as alkyne ligand owing to the large substituents. If, instead, the toluene ligand is lost, a bis(alkyne)iron is formed which formally dimerizes via at least one further intermediate. The existence of a further intermediate is shown by a trapping experiment with trimethyl phosphite, which, at -20 to 0 °C, affords the paramagnetic binuclear complex **6** in good yields; the structure of **6** has not yet been established. Neither **5** nor **4** can be considered as a direct precursor of **6**, since **5** reacts with trimethyl phosphite to

$[Fe_2\{(Me_3Si)_2C_2\}_3\{P(OMe)_3\}_2]$ **6**[1]

give tris(trimethylphosphite)(bis(trimethylsilyl)ethyne)-iron[1] and **4** reacts with trimethyl phosphite only above 80 °C and then to afford only low yields of **6**. In contrast to many other binuclear complexes containing metal-metal multiple bonds,[8] **4** has so far proved to be quite resistant to reaction.

Complex **4** was characterized by a crystal structure analysis[9] (Fig. 1). The cluster framework can be described as two edge-sharing tetrahedra in which the iron atoms define

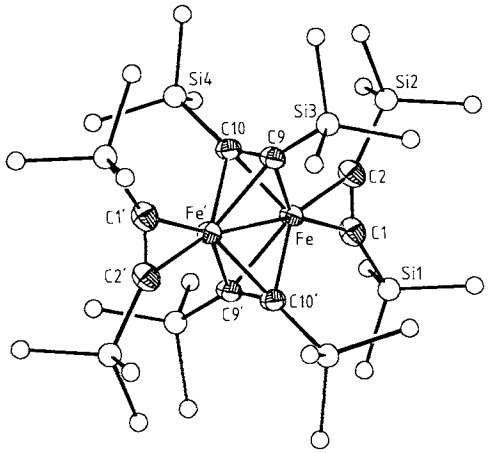

Fig. 1. Molecular structure of **4**. Selected bond lengths [Å] and angles [°]: Fe-Fe' 2..465(1), Fe-C1 and Fe-C2 1.972(2), Fe-C9 2.078(2), Fe-C9' 2.079(2), Fe-C10 2.076(2), Fe-C10' 2.082(2), C1-C2 1.288(3), C9-C10 1.314(3); C1-C2-Si2 141.8(2), C2-C1-Si1 141.4(2), C9-C10-Si4 149.8(1), C10-C9-Si3 149.6(1).

the shared edge. Accordingly, the bridging carbon atoms C9, C10, C9', and C10' define a rectangle lying perpendicular to the edge Fe-Fe'. The axes C1-C2 and C1'-C2' of the terminal alkyne ligands lie perpendicular to the axes C9-C10 and C9'-C10'. The Fe-Fe' distance lies in the range expected for localized single bonds;[10] however, the presence of a single bond is contradicted by the diamagnetism of the cluster, which has 32 valence electrons if one assumes that the terminal $(Me_3Si)_2C_2$ provide four π-electrons.

In terms of structure and electron count, **4** is closely related to the clusters $[(\mu\text{-}t\text{Bu}_2C_2)_2Fe_2(CO)_4]$[11] and [(μ-3,3,6,6-$Me_4$-1-thiacyclohept-4-yne)$_2Fe_2(CO)_4$].[12] In those two cases, the short Fe-Fe distance (2.215 and 2.225 Å, respectively), corresponds to a double bond. Owing to its diamagnetism, **4** should also have a double bond which, compared with those in carbonyl clusters, is lengthened by about 10%. Its length is similar to that determined for μ-hexamethylbenzenebis(cyclopentadienyliron) (2.424 Å).[13]

Comparison of the results presented here with the little information available on the cocondensation product formed between iron atoms and **3**[5] indicates that, in that case, too, a large part of the product consists of **4**, which, owing to its sparing solubility, could not be separated from the side products. The contrasting high selectivity and high yields of the reaction of **1** or **2** with **3** documents the value of multistep syntheses based on an effective cocondensation reaction. Complex **4** was formed here in a total of three reaction steps:

① iron atoms + toluene ⟶ bis(toluene)iron

② bis(toluene)iron + ethene ⟶ **1**[6]

or

② bis(toluene)iron + 1-methylnaphthalene ⟶ **2**

③ **1** (**2**) + **3** ⟶ **4**

The yields via the three steps are 30–50% based on the iron vaporized.

Received: February 1, 1988;
revised: July 20, 1988 [Z 2601 IE]
German version: *Angew. Chem. 100* (1988) 1577

CAS Registry numbers:
1, 100190-46-3; **2**, 117310-53-9; **3**, 14630-40-1; **4**, 117310-54-0.

[1] A. Funhoff, H. Schäufele, U. Zenneck, *J. Organomet. Chem. 345* (1988) 331.
[2] N. M. Boag, M. Green, J. A. K. Howard, F. G. A. Stone, H. Wadepohl, *J. Chem. Soc. Dalton Trans. 1981*, 862.
[3] R. W. Zoellner, K. J. Klabunde, *Chem. Rev. 84* (1984) 545.
[4] L. H. Simons, J. J. Lagowski, *J. Organomet. Chem. 249* (1983) 195.
[5] See Ref. 65 in [3].
[6] U. Zenneck, W. Frank, *Angew. Chem. 98* (1986) 806; *Angew. Chem. Int. Ed. Engl. 25* (1986) 831.
[7] H. Schäufele, D. Hu, H. Pritzkow, U. Zenneck, *Organometallics*, in press.
[8] W. A. Herrmann, *Adv. Metallorg. Chem. 20* (1982) 159.
[9] Crystal structure analysis of **4**: space group $P2_1/n$; $a = 10.286(3)$, $b = 12.649(4)$, $c = 19.017(7)$ Å; $\beta = 104.80(3)°$; $V = 2392$ Å^3; $Z = 2$; 4155 unique reflections ($I \geq 2\sigma(I)$); four-circle diffractometer, $Mo_{K\alpha}$, ω scan ($3° \leq 2\theta \leq 60°$); empirical absorption correction; 262 parameters (Fe, Si, C anisotropic, CH_3 as rigid group (C-H = 0.95 Å), H with individual isotropic temperature factors; $R = 0.036$, $R_w = 0.034$ ($w = \sigma_F^{-2}$); no appreciable residual electron density; $\rho_{calcd} = 1.10$, $\rho_{exp.} = 1.10$ g cm^{-3}. Further details of the crystal structure investigation may be obtained from the Fachinformationszentrum Energie, Physik, Mathematik GmbH, D-7514 Eggenstein-Leopoldshafen 2 (FRG), on quoting the depository number CSD-52967, the names of the authors, and the journal citation.
[10] W. P. Fehlhammer, H. Stolzenberg in G. Wilkinson, F. G. A. Stone, E. W. Abel (Eds.): *Comprehensive Organometallic Chemistry, Vol. 4*, Pergamon Press, Oxford 1982, p. 513 ff.
[11] K. Nicholas, L. S. Bray, R. E. Davis, R. Pettit, *Chem. Commun. 1971*, 608.
[12] H.-J. Schmitt, M. L. Ziegler, *Z. Naturforsch. B28* (1973) 508.
[13] K. Jonas, G. Koepe, L. Schieferstein, R. Mynott, C. Krüger, Y.-H. Tsay, *Angew. Chem. 95* (1983) 637; *Angew. Chem. Int. Ed. Engl. 22* (1983) 620; *Angew. Chem. Suppl. 1983*, 920.

Partially Reversible Intercalation of Ferrocene in a Zeolite-like Host Lattice Consisting of $Fe(CN)_6$ and Me_3Sn Units**

By *Peter Brandt, Abdul K. Brimah,* and *R. Dieter Fischer**

Dedicated to Professor Ernst Otto Fischer on the occasion of his 70th birthday

While the existence of highly symmetric 3D networks of the general type

$[M(\mu\text{-}CN\text{-}A\text{-}NC)_3]_\infty$ **1**

1, composed of exclusively linear $\dashv M-C\equiv N\rightarrow A\leftarrow N\equiv C\vdash_\infty$ chains ("super Prussian blue" analogues), has not been established with certainty,[1] 3D coordination polymers of a similar composition but with chains bent at the N atom have been known for some time (e.g., M = Co and A = Ag, H[2]).

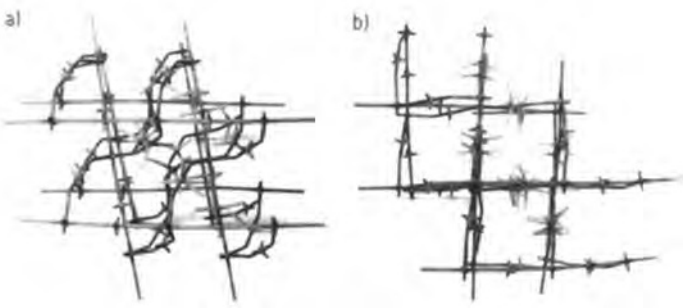

Fig. 1. Minit model (section) of the lattice structure of **1a**. a) View in the direction of "closest" packing. b) View in the direction of parallel channels.

Interestingly, in the recently described compound **1a**, M = Co, A = Me_3Sn, up to one-third of the $\dashv Co-C\equiv N\rightarrow Sn\leftarrow N\equiv C\vdash_\infty$ chains are linear.[1] Although the structure of **1a** (Fig. 1) cannot give rise to a density as low as that of its hypothetical isomer composed of exclusively linear chains, the lattice of **1a** displays strictly parallel channels extending in one direction with nearly square cross sections (Fig. 1b). Their maximum size is ca. 6.8×6.8 Å^2 since the positions of the methyl groups are not rigidly fixed, and the inclusion of, e.g., ferrocene molecules (ca. 4.4×3.3 Å^2[3]) may therefore be expected.

Actually, simple grinding of the orange-yellow, slightly wetted (H_2O) **1b**, M = Fe,[4] with ferrocene (Cp_2Fe) results in quantitative formation of the deep blue and, like **1**, paramagnetic[5] ferrocenium intercalate **2**[6] [Eq. (a)].

$$[(Me_3Sn)_3Fe^{III}(CN)_6]_\infty + Cp_2Fe^{II} \longrightarrow [Cp_2Fe^{III}(Me_3Sn)_3Fe^{II}(CN)_6]_\infty \quad \text{(a)}$$

1b → **2**

The likewise rapid formation of blue **2** from the starting materials spatially separated by a **1a** pellet[7,8] demonstrates a high diffusion rate of the guest species in **1a**, too,[9] in accordance with the earlier X-ray analysis.

In addition to some vibrational bands diagnostic of the ferrocenium ion, the ν_{CN} absorptions characteristic of distorted $[Fe^{II}(CN)_6]$ octahedra and the $(\nu_{SnC})_{as}$ band, the IR spectrum[10] of **2** shows, e.g., the medium-intense $\delta_{Fe^{II}C}$ band at 600 cm^{-1}[18] which is absent in the spectra of **1a** and **1b**. The ^{57}Fe Mössbauer spectrum[11] displays the singlets of the newly formed $[Fe^{II}(CN)_6]^{4\ominus}$ unit and of the $[Cp_2Fe^{III}]^{\oplus}$ ion, while the doublet of the $[Fe^{III}(CN)_6]^{3\ominus}$ unit of **1b** is absent.

The spectroscopic data confirm that the solid-state reaction of Cp_2Fe with **1b** is—in contrast to that with, e.g., tetracyanoethylene[12]—a genuine redox reaction. At moderately high temperatures (80–160 °C) under high vacuum, it is, nevertheless, possible to sublime off about half of the incorporated Cp_2Fe. In the IR spectrum of the black powder (**3**) of empirical formula $Fe_{0.4}(Me_3Sn)_3Fe(CN)_6$ remaining after exhaustive sublimation,[13] all $[Cp_2Fe^{III}]^{\oplus}$ bands are absent, while the other absorption regions in the spectrum of **3** do not differ notably from those of **2**.[10]

Apart from a singlet due to the presumably diamagnetic $[Fe^{II}(CN)_6]^{4\ominus}$ structural unit, the ^{57}Fe Mössbauer spectrum of **3**[11] shows a new, broad doublet, which, owing to its isomeric shift and the relatively high paramagnetism of **3**[5] (based on the concentration of incorporated iron), may be

[*] Prof. Dr. R. D. Fischer, Dipl.-Chem. P. Brandt, Dipl.-Chem. A. K. Brimah
Institut für Anorganische und Angewandte Chemie der Universität
Martin-Luther-King-Platz 6, D-2000 Hamburg 13 (FRG)

[**] This work was supported by the Fonds der Chemischen Industrie and the Deutsche Forschungsgemeinschaft.

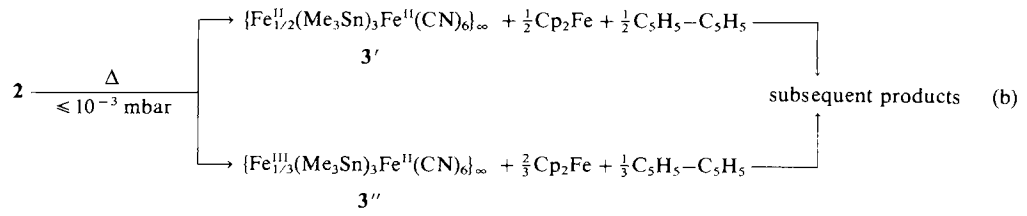

best ascribed to high-spin Fe^{II} ions. The elemental analysis and the black "color" of **3**, as well as an optimal calculated fit of the Mössbauer spectrum, do not rule out that **3** is an intercalate of both Fe^{II} and Fe^{III} (**3′**/**3″**) ions [Eq. (b)].

The X-ray powder patterns of microcrystalline **2** and **3** are very similar; however they differ markedly from those of compounds **1a** and **1b**.

Whereas many examples of an intercalation of metallocenes in inorganic layer-structure compounds are known,[14] little information is available on the inclusion of Cp_2Fe into "classical zeolites.[15] A major goal of such experiments is to obtain, after replacement of the organic ligands in the intercalated complex, iron/zeolite intercalates that are likely to exhibit optimal catalytic activity. The readily accessible iron-ion intercalate **3** described here, as well as analogous products containing other metal ions,[16] could be an interesting alternative to metal-ion intercalates based on zeolites or $AlPO_4$.[17]

Received: June 27, 1988 [Z 2830 IE]
German version: *Angew. Chem. 100* (1988) 1578

CAS Registry numbers:
1a, 98104-58-6; **1b**, 117341-33-0; **2**, 117341-34-1; **3**, 1173-41-2; 4, 102-54-5.

[1] K. Yünlü, N. Höck, R. D. Fischer, *Angew. Chem. 97* (1985) 863; *Angew. Chem. Int. Ed. Engl. 24* (1985) 879.
[2] A. Ludi, H. U. Güdel, *Helv. Chim. Acta 51* (1968) 1762; H. U. Güdel, A. Ludi, P. Fischer, W. Hälg, *J. Chem. Phys. 53* (1970) 1917.
[3] Cf. M. Rosenblum: *Chemistry of the Iron Group Metallocenes, Vol. 1*, Wiley, New York 1965.
[4] Cf. footnote 7 in [1]; analogues of **1b**, "$(R_3Sn)_3Fe(CN)_6$" with R = CH_3, have also been described by *Uson* et al.: R. Uson, J. Fornies, M. A. Uson, E. Lalinde, *J. Organomet. Chem. 185* (1980) 359.
[5] Effective magnetic moment μ_{eff} (corr.) of **1b**, 2.18; **2**, 3.65; **3**, 3.56 μ_B (susceptometer after *D. F. Evans*, Johnson Matthey).
[6] *Experimental Procedure* for **2**: **1b** (500 mg, 0.71 mmol), wetted with 5–10 drops of distilled water, was thoroughly ground with Cp_2Fe (400 mg, 2.15 mmol) under N_2 atmosphere by means of a pestle-like glass rod. The initially orange mixture very rapidly adopted a greenish color, which, after ca. 5 min, turned blue. After the mixture was uniformly blue, the solid-state reaction was ended and the product washed with 100 mL of toluene in portions. Elemental analyses (after short drying at room temperature under high vacuum): calculated for $C_{25}H_{37}N_6Fe_2Sn_3$, C 33.76, H 4.19, N 9.45, Fe 12.56, Sn 40.03%; found, C 31.00, H 4.14, N 9.45, Fe 12.75, Sn 39.90%. Suspension of **1b** in concentrated solutions of Cp_2Fe (in toluene, CH_2Cl_2, THF, etc.) did not lead to **2**.
[7] Thickness: ca. 1.0–1.5 mm. The formation of **2** did not take place in control experiments with pellets prepared from KBr, Teflon, and zeolite.
[8] By gentle warming, Cp_2Fe was caused to undergo rapid diffusion through a **1a** pellet.
[9] Finely powdered samples of **1a** and **1b** gave practically identical Debye-Scherrer powder photographs.
[10] IR $\tilde{\nu}$ [cm^{-1}] for **2**: $\nu[Cp_2Fe^{III}]^{\oplus}$ bands = 3108 w, 1415 vw, 885 m; ν(CN) = 2080 s, 2058 sh, 2043 vs; $[\nu(SnC)]_{as}$ = 553 s; $\delta(Fe^{II}C$(host framework)) = 600 m [18]; for **3**, ν(CN) = 2080 vs, 2058 sh, 2043 vs; $[\nu(SnC)]_{as}$ = 553 s; $\delta(Fe^{II}C$(host framework)) = 600 m.
[11] IS/QS (in mm s^{-1}; standard, α-Fe): $K_3[Fe(CN)_6]$, 0.12/0.26; **1b**, −0.40/0.30; **2**, −0.10/0, 0.40/0; **3**, −0.02/0, 0.86/1.95. Elscint-Promeda spectrometer with ^{57}Co/Rh source. We thank *G. Haack, C. Meyer.* and Prof. Dr. *K. Nagorny*, Hamburg, for the measurements.
[12] Cf. E. Adman, M. Rosenblum, S. Sullivan, T. N. Margulis, *J. Am. Chem. Soc. 89* (1967) 4540.
[13] *Experimental Procedure* for **3**: **2** (ca. 200 mg) was placed in a Schlenk tube fitted with a cold finger and heated for 3 d under high vacuum (1st day, 80°C; 2nd day, 120°C; 3rd day, 160°C). Elemental analysis of the black residue: calculated for $C_{15}H_{27}N_6Fe_{1.4}Sn_3$, C 24.83, H 3.75, N 11.58, Fe 10.77%; found, C 26.40, H 3.68, N 11.50, Fe 10.55%.
[14] Cf. T. R. Halbert, J. Scanlon, *Mat. Res. Bull. 14* (1979) 415; T. R. Halbert, D. C. Johnston, L. E. McCandlish, A. H. Thompson, J. S. Scanlon, *Physica B+C (Amsterdam) 99* (1980) 128; H. Schäfer-Stahl, R. Abele, *Angew. Chem. 92* (1980) 493; *Angew. Chem. Int. Ed. Engl. 19* (1980) 477.
[15] A. Mahay, G. Lemay, A. Adnot, I. M. Szöghy, S. Kaliaguine, *J. Catal. 103* (1987) 480.
[16] P. Brandt, R. D. Fischer, unpublished results.
[17] Cf. A. Tißler, U. Müller, K. K. Unger, *Nachr. Chem. Tech. Lab. 36* (1988) 624.
[18] W. P. Griffith, G. T. Turner, *J. Chem. Soc. A 1970*, 858.

Structure of a Chiral Lithium Azaenolate: Monomeric, Intramolecular Chelated Lithio-2-acetylnaphthalene-SAMP-hydrazone**

By *Dieter Enders,* Gerhard Bachstädter, Kenneth A. M. Kremer, Michael Marsch, Klaus Harms,* and *Gernot Boche**

In the form of metalated alkylideneamines, oximes, oxime ethers, hydrazones and their heterocyclic analogues, "1-azaallyl anions" (metalloenamines, alkylideneamine anions, azaenolates) **1** have gained increasing importance in synthetic chemistry over the past 15 years.[1] In particular, the fact that practically complete asymmetric inductions can be achieved with chiral azaallylmetal reagents **1**[1–3] has prompted numerous experimental[1–3] and theoretical[4] investigations of the structure of these compounds and their selective reactions with electrophiles. Thereby, η^1-N_a-, η^1-N_b-, η^1-C-, and η^3- and η^4-structures have been discussed (Scheme 1).

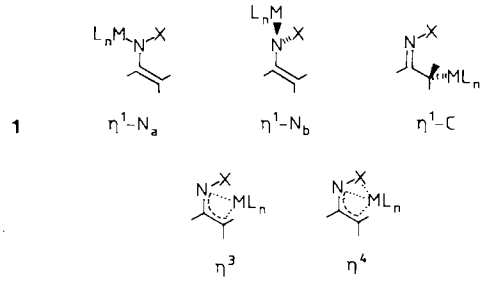

Scheme 1. Possible structures of 1-azaallyl anions 1.

Although it has recently been possible to gain insights into the bonding behavior of some 1-azaallylmetal com-

[*] Prof. Dr. D. Enders, Dipl.-Chem. G. Bachstädter, Dr. K. A. M. Kremer [+]
Institut für Organische Chemie der Technischen Hochschule
Professor-Pirlet-Strasse 1, D-5100 Aachen (FRG)
Prof. Dr. G. Boche, M. Marsch, Dr. K. Harms
Fachbereich Chemie der Universität
Hans-Meerwein-Strasse, D-3550 Marburg (FRG)
[+] Alexander-von-Humboldt Scholarship, 1982–1984.

[**] This work was supported by the Fonds der Chemischen Industrie and the Deutsche Forschungsgemeinschaft. We thank Degussa AG and BASF AG for gifts of chemicals.

pounds by X-ray structure analyses,[5-12] of more particular importance are X-ray structure investigations on synthetically useful chiral azaenolates.[1-3] In the following communication we report on the crystal structure of an enantiomerically pure lithium azaenolate. Deprotonation of 2-acetylnaphthalene-SAMP-hydrazone (*S*)-**2** with lithium

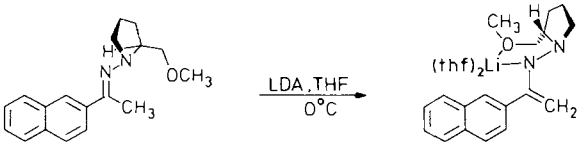

(*S*)-**2** (*S*)-**3**

diisopropylamide (LDA) in tetrahydrofuran at 0°C affords the lithio-SAMP-hydrazone (*S*)-**3**, which crystallizes in the form of ruby-red crystals as monomeric, intramolecularly chelated (*S*)-**3** · 2 THF[13,14] (Fig. 1).[15]

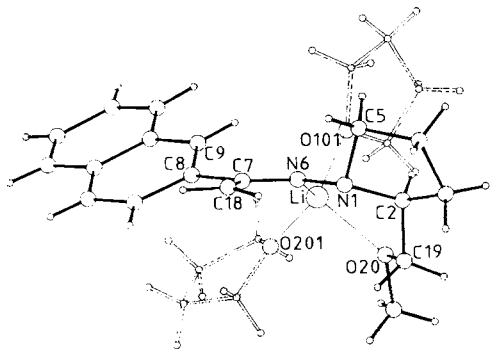

Fig. 1. Crystal structure of (*S*)-**3** · 2 THF [18]. Important bond lengths [pm] and angles [°]: C18-C7 137.2(2), C7-N6 136.9(2), N6-N1 145.0(2), N6-Li 195.8(3), O20-Li 200.4(3), O201-Li 198.2(3), O101-Li 198.9(3), C7-C8 149.4(3),; C18-C7-N6 129.0(2), C7-N6-N1 110.0(1), N1-N6-Li 118.8(1), C7-N6-Li 127.6(1), C18-C7-N6-Li 157.73(0.31), C18-C7-N6-N1 −0.52(0.41), C7-N6-N1-C5 −87.85(0.27), C7-N6-N1-C2 163.64(0.22), C18-C7-C8-C9 149.60(0.29).

(*S*)-**3** · 2 THF contains an almost planar N1-N6-C7-C18 array (torsion angle −0.52(0.41)°), in which, in analogy to enamine structures,[19] the N–N bond is synperiplanar to the CC "double bond" (C7-C18) (C18-C7-N6 129.0(2); C7-N6-N1 110.0(1)°). The C7–C18 bond (137.2(2) pm) is somewhat longer than the CC double bond in enamines (134 pm[19]), whereas the N6–C7 bond (136.9(2) pm) is somewhat shorter than the CN bond in enamines (138–142 pm[19]).

The sum of the angles at N6 is 356.4°, indicating only a slight pyramidalization and thus a relatively high sp^2 character at N6.[20] Accordingly, a favorable overlapping of the lone pair on N6 with the π electrons of the CC "double bond" and thus a pronounced delocalization in the azaallyl moiety is possible, consistent with the results of earlier NMR spectroscopic measurements.[21] It can be concluded from the C18–C7–C8–C9 torsion angle of 149.60(0.29)° that the naphthyl moiety on C7 is inclined at an angle of ca. 30° to the azaallyl plane.

As can be seen from the schematic side view of (*S*)-**3** · 2 THF (Fig. 2), the N6–Li axis is inclined downwards at an angle of 17.5(4)° relative to the azaallyl plane due to the intramolecular chelation by the methoxy group (the lithium atom lies 59(4) pm below the azaallyl plane). At the same time the pyrrolidine ring is bent upwards from the azaallyl plane (C7–N6–N1–C5 −81.85(0.27)°). The structure of (*S*)-**3** · 2 THF in the crystal shows the hitherto postulated intramolecular methoxy-chelation of the lithium ion and the (*Z*)-configuration at C7–N6 (*syn* effect).[22] The structure in solution could be similar, since according to cryoscopic measurements in tetrahydrofuran—i.e. under the standard conditions of asymmetric induction—and according to ^{1}H-NMR spectroscopic investigations (*S*)-**3** · 2 THF is likewise present as monomer.[14,23] Moreover, the "puckered" η^1-N_a structure with "lone pair"(N6)–π(CC) overlapping found here (see Scheme 1 and Figs. 1 and 2), as also the η^1-N_b structure (σ(NLi)–π(CC) overlapping[2]) postulated for lithiated oxazolines, is consistent with the proposed metallo-retentive S_E2'-front mechanism for asymmetric electrophilic substitutions at chiral azaenolates.[2,23-25]

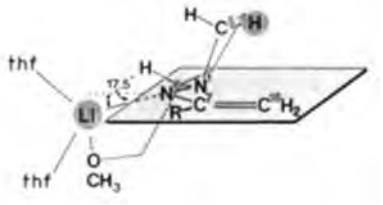

Fig. 2. "Side view" of (*S*)-**3** · 2 THF (schematic). R = 2-naphthyl.

Received: June 24, 1988 [Z 2821 IE]
German version: *Angew. Chem. 100* (1988) 1580

CAS Registry numbers:
(*S*)-**2**, 95682-82-9; (*S*)-**3**, 117201-59-9; (*S*)-**3**(unsolvated) · Li, 117146-27-7.

[1] Reviews: a) P. W. Hickmott, *Tetrahedron 38* (1982) 1975; b) D. Enders in H. Nozaki (Ed.): *Current Trends in Organic Synthesis*, Pergamon, Oxford 1983, p. 151; c) J. K. Whitesell, M. A. Whitesell, *Synthesis 1983*, 517; d) J. D. Morrison (Ed.): *Asymmetric Synthesis*, Academic Press, Orlando, FL, USA; e) D. E. Bergbreiter, M. Newcomb in [1d], *Vol. 2* (1983), p. 243; f) R. R. Fraser in E. Buncel, T. Durst (Eds.): *Comprehensive Carbanion Chemistry, Part B*, Elsevier, Amsterdam 1984, p. 65; g) D. Enders in [1d], *Vol. 3* (1984), p. 275.

[2] K. A. Kutomski, A. I. Meyers in [1d], *Vol. 3* (1984), p. 213, and references cited therein.

[3] K. Tomioka, K. Koga in [1d], *Vol. 2* (1983), p. 201, and references cited therein.

[4] a) K. N. Houk, R. W. Strozier, N. G. Rondan, R. R. Fraser, N. Chuaqui-Offermanns, *J. Am. Chem. Soc. 102* (1980) 1426, and references cited therein; b) R. Glaser, A. Streitwieser, Jr., *ibid. 109* (1987) 1258.

[5] D. Seebach, W. Bauer, J. Hansen, T. Laube, W. B. Schweizer, J. D. Dunitz, *J. Chem. Soc. Chem. Commun. 1984*, 853.

[6] a) D. B. Collum, D. Kahne, S. A. Gut, R. T. DePue, F. Mohamadi, R. A. Wanat, J. Clardy, G. Van Duyne, *J. Am. Chem. Soc. 106* (1984) 4865; b) R. A. Wanat, D. B. Collum, G. Van Duyne, J. Clardy, R. T. DePue, *ibid. 108* (1986) 3415; c) N. Kallman, D. B. Collum, *ibid. 109* (1987) 7466 (in this work the structure investigations on azaenolates are excellently reviewed).

[7] H. Dietrich, W. Mahdi, R. Knorr, *J. Am. Chem. Soc. 108* (1986) 2462.

[8] a) D. Colgan, R. I.Papasergio, C. L. Raston, A. H. White, *J. Chem. Soc. Chem. Commun. 1984*, 1708; b) R. I. Papasergio, C. L. Raston, A. H. White, *ibid. 1983*, 1419.

[9] a) T. Fjeldberg, P. B. Hitchcock, M. F. Lappert, A. J. Thorne, *J. Chem. Soc. Chem. Commun. 1984*, 822; b) B. Cetinkaya, P. B. Hitchcock, M. F. Lappert, M. C. Misra, A. J. Thorne, *ibid. 1984*, 148.

[10] R. A. Bartlett, H. V. Rasika Dias, H. Hope, B. D. Murray, M. M. Olmstead, P. P. Power, *J. Am. Chem. Soc. 108* (1986) 6921.

[11] P. von R. Schleyer, R. Hacker, H. Dietrich, W. Mahdi, *J. Chem. Soc. Chem. Commun. 1985*, 622.

[12] D. Barr, W. Clegg, R. E. Mulvey, R. Snaith, *J. Chem. Soc. Chem. Commun. 1984*, 469, 700.

[13] As alternative to the earlier procedure, which led to crystals that were unsuitable (twinning) for an X-ray structure analysis [14], the following method was used: An LDA solution, prepared from 2.5 mL of THF, 0.2 g (1.9 mmol) of diisopropylamine and 1.4 mL (2.2 mmol) of *n*-butyllithium (1.6 M in *n*-hexane) was treated dropwise under argon at 0°C with a solution of (*S*)-**2** [m.p. 62.63°C, $[\alpha]_D^{25} = +1041$ ($c = 1$, $CHCl_3$) (0.51 g, 1.8 mmol)]. The blood-red solution was stirred for 4 h at 0°C and than allowed to stand for 1 h at −78°C. Finally, the reaction product was crystallized out overnight at −18°C.

[14] a) W. Bauer, D. Seebach, *Helv. Chim. Acta 67* (1984) 1972; b) D. Enders, K. A. M. Kremer, unpublished results from 1983; c) D. Seebach, T. Laube, J. Hansen, K. A. M. Kremer, unpublished results from 1983/1984; d) J. Hansen, *Dissertation* (No. 7863), ETH, Zürich 1985.

[15] X-ray structure analysis: $C_{18}H_{21}N_2OLi \cdot 2(C_4H_8O)$, $M = 432.55$, monoclinic, space group $P2_1$, $a = 7.894(1)$, $b = 16.227(2)$, $c = 9.707(2)$ Å, $\beta = 101.01°$, $Z = 2$, $\rho_{calcd} = 1.18$ g cm^{-3}. Data collection on an Enraf-Nonius CAD4 diffractometer with graphite monochromator, $Cu_{K\alpha}$ radiation, $T = -90°C$, ω scans, 2739 measured reflections. Solution by direct methods [16], refinement [17] to $R = 0.036$, $R_w = 0.037$ for 2357 independent reflections with $I > 3\sigma(I)$, all non-hydrogen atoms anisotropic, hydrogen atoms apart from those on C19 "riding" with an isotropic temperature factor ($B(H) = 1.3 \times B_{equ}(C)$), H19 and H19a free with a fixed isotropic temperature factor, 400 parameters. The absolute configuration of **3** · 2 THF followed from the known configuration of the starting compound. Further details of the crystal structure investigation are available on request from the Fachinformationszentrum Energie, Physik, Mathematik GmbH, D-7514 Eggenstein-Leopoldshafen 2 (FRG) on quoting the depository number CSD-53 195, the names of the authors, and the journal citation.

[16] G. M. Sheldrick (Universität Göttingen), *SHELXS-86*, 1986.

[17] SDP/VAX, Enraf-Nonius & B. A. Frenz & Associates, Delft, NL 1978.

[18] E. Keller (Universität Freiburg), *SCHAKAL-86*, 1986.

[19] K. L. Brown, L. Damm, J. D. Dunitz, A. Eschenmoser, R. Hobi, C. Kratky, *Helv. Chim. Acta 61* (1978) 3108.

[20] For comparison: The sum of the angles at pyramidally surrounded N1 is 326.8°.

[21] a) H. Ahlbrecht, E. O. Düber, D. Enders, H. Eichenauer, P. Weuster, *Tetrahedron Lett. 1978*, 3691; b) K. G. Davenport, H. Eichenauer, D. Enders, M. Newcomb, D. E. Bergbreiter, *J. Am. Chem. Soc. 101* (1979) 5654.

[22] D. Enders, H. Eichenauer, *Angew. Chem. 88* (1976) 579; *Angew. Chem. Int. Ed. Engl. 15* (1976) 549.

[23] D. Enders, *Chem. Scr. 25* (1985) 139.

[24] J. K. Whitesell, M. A. Whitesell, *J. Org. Chem. 42* (1977) 377.

[25] As in the case of chiral oxazolines [2], a previously undiscussed, cooperative effect must also be taken into consideration in lithiated SAMP- and RAMP-hydrazones, namely the steric hindrance of an electrophilic attack at C18 from above by the C5 methylene group of the pyrrolidine ring (see Fig. 2). Accordingly, a sterically more demanding hydrazine auxiliary in this molecular region (two methyl groups on C5) shows, in preliminary experiments, an even more pronounced diastereofacial selectivity: D. Enders, G. Bachstädter, unpublished work.

On the Structure of the Cation $N_2H_7^{\oplus}$ with an N–H···N Hydrogen Bond in the Monoammonia Adduct of Ammonium Iodide**

By *Hans Joachim Berthold,* Wolfgang Preibsch,* and *Elke Vonholdt*

The cation $N_2H_7^{\oplus}$, which has the structure $[H_3N{-}H\cdots NH_3]^{\oplus}$, has only been detected so far in the gas phase by mass spectrometry and IR spectroscopy.[1-5] The energy of the hydrogen bond is ca. 104 kJ mol^{-1}.[1,2] By X-ray studies of powders and single crystals of $NH_4I \cdot NH_3$, we found that the unit cell of this compound contains the cation $N_2H_7^{\oplus}$. This afforded us the opportunity to investigate, for the first time, the structure of the cation in the solid state and to compare the results with those of calculations on the interaction $NH_4^{\oplus}\cdots NH_3$.

Owing to the great importance of the hydrogen bond in every field of chemistry and to the significance of the mechanism of proton transfer in biological processes for systems containing hydrogen bonds, interactions of the type $H_3O^{\ominus}\cdots H_2O$, $NH_4^{\oplus}\cdots NH_3$, $NH_4^{\oplus}\cdots H_2O$, etc. have been the subject of intensive theoretical investigation in recent years. The focus of interest in these studies has been on the bonding energy in the cationic complexes, the equilibrium distance (O–O, N–N, N–O, etc.), and the shape of the potential curve in both the equilibrium state and the transition state.[6-16]

The structure of the cation $H_5O_2^{\oplus}$ in crystalline compounds has been known for a long time—$[H_2O{-}H\cdots OH_2]^{\oplus}$[17-25]—so that the results of calculations carried out on this cation can be checked in detail. By contrast, reliable structural data for the cation $N_2H_7^{\oplus}$ are still lacking. The N–N equilibrium distances determined for the cation in the gas phase were calculated to be 250 to 296 pm, depending on the parameters and assumptions used in the ab initio calculations. Correspondingly large are the variations in the bonding energies (93–151 kJ mol^{-1}) as well as in the potential barriers in the equilibrium state (15–65 kJ mol^{-1}) and in the transition state for the transfer of the proton to the second minimum (6–31 kJ mol^{-1}). The proton transfer is associated with a contraction of the cation; all calculations were in close agreement as to the N–N distance in the transition state (258–259 pm).[7,11,13]

Assuming C_{3v} symmetry and a staggered conformation of the two NH_3 groups (all HNH angles 109.5°), *Scheiner* and *Harding*[13] calculated for the equilibrium distance (273.1 pm) a bonding energy of 130 kJ mol^{-1} and a potential barrier between the two minima (for fixed N positions) of 15.9 kJ mol^{-1}. In the transition state the barrier amounts to only 8.8 kJ mol^{-1}. The structural data are presented in Figure 1.

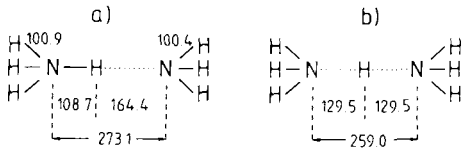

Fig. 1. Calculated distances [pm] in the $N_2H_7^{\oplus}$ cation according to *Scheiner* and *Harding* [13]. a) Equilibrium state. b) Transition state.

We have now been able to show that, owing to the interaction $NH_4^{\oplus}\cdots NH_3$, the cation $N_2H_7^{\oplus}$ is present in the crystalline monoammonia adduct of ammonium iodide $NH_4I \cdot NH_3$.

$NH_4I \cdot NH_3$ can be prepared according to the procedure of *Lindenberg*[26] by treatment of NH_4I at 298 K with gaseous NH_3 ($p = 195$ torr). *Lindenberg* determined a tetragonal unit cell ($Z = 4$) by powder diffractometry, but a structure determination was not carried out.[27,28]

X-ray investigations of powders of $NH_4I \cdot NH_3$—prepared at NH_3 pressures of between 350 and 450 torr—showed that the compound crystallizes in the cubic space group $Pm3m$ ($Z = 1$) at 298 K. Preliminary intensity calculations indicated the existence of the cation $N_2H_7^{\oplus}$ in the crystal.[29] The single-crystal X-ray structure analysis, carried out recently, confirmed these earlier results.

By using the refined positional parameters for nitrogen, one obtains an N–N distance of 269(5) pm. This value is somewhat smaller than the distance (273.1 pm) calculated by *Scheiner* and *Harding*[13] and clearly indicates a strong interaction between the $NH_4^{\oplus}$ ion and the NH_3 molecule in $NH_4I \cdot NH_3$. The assumption of the formation of the cation $N_2H_7^{\oplus}$ containing a hydrogen bond thus appears to be justified.

[*] Prof. Dr. H. J. Berthold, Dr. W. Preibsch, Dipl.-Chem. E. Vonholdt
Institut für Anorganische Chemie und Sonderforschungsbereich 173 der Universität
Callinstrasse 9, D-3000 Hannover 1 (FRG)

[**] This work was supported by the Deutsche Forschungsgemeinschaft and the Fonds der Chemischen Industrie. We thank Dr. *R. Wartchow* and Dipl.-Chem. *P. M. Kaese* for their assistance.

The cubic symmetry of the structure is the consequence of orientational disorder of the cation, whose center of gravity lies in ½½½ on a time average and whose N–H···N axis in the various unit cells points statistically in the direction of one of the three cubic crystallographic axes. Further, there is a positional disorder of the terminal H atoms around the threefold axes of $NH_4^{\oplus}$ and NH_3.

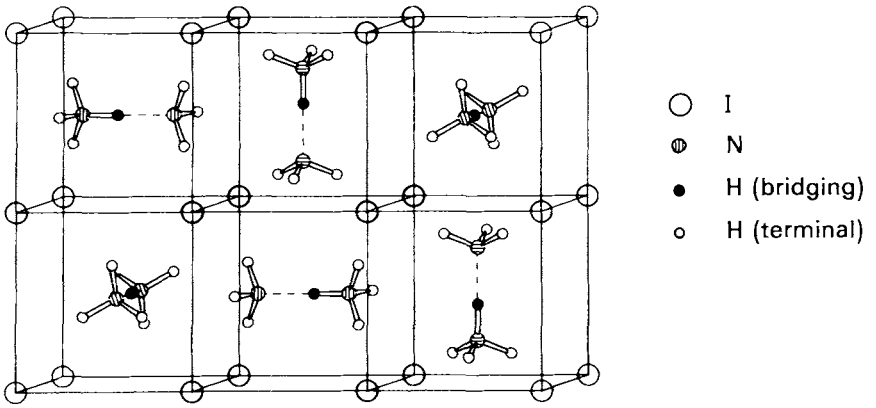

Fig. 2. Section of the structure of $NH_4I \cdot NH_3$ (298 K) containing six unit cells, assuming an arbitrarily specified transient order; cf. text.

Figure 2 shows a section of the structure of $NH_4I \cdot NH_3$ at 298 K assuming an arbitrary transient order. It shows the three orientations of the cation that are adopted statistically. The fact that the H atoms in the hydrogen bond can occupy two different positions has been taken into consideration for the six cations shown. Owing to the low potential barrier for proton transfer, exchange between the two minima is almost unhindered.[7]

Upon cooling $NH_4I \cdot NH_3$, three new phases appear, which are characterized by increasing order. In the tetragonal phase (ca. 203–230 K), the cation displays only a two-dimensional orientational disorder in the *xy* plane. In the orthorhombic phase (ca. 143–203 K), the cations are presumably ordered in the *xy* plane. Below ca. 143 K, a phase with a complex diffraction diagram appears which could not be indexed. We assume that, in this phase, the terminal H atoms occupy ordered equilibrium positions. The deuterated compound $ND_4I \cdot ND_3$ has the same cubic structure as $NH_4I \cdot NH_3$ at 298 K. However, upon cooling, direct transformation to the orthorhombic phase occurs at ca. 237 K and an unknown phase is formed at ca. 147 K. Further details on the structure of the cation—particularly in the phase that is stable at very low temperatures—should be provided by neutron diffraction studies, which are in progress.

Investigations of $NH_4I \cdot NH_3$ and $ND_4I \cdot ND_3$ in the various phases (including partially deuterated samples) by laser Raman spectroscopy, as well as by neutron scattering experiments on the two compounds at 5–298 K, have confirmed the strong interaction $NH_4^{\oplus} \cdots NH_3$ and $ND_4^{\oplus} \cdots ND_3$.

Experimental Procedure

$NH_4I \cdot NH_3$: Cubic phase: $a = 512.9(3)$ pm (298 K), space group *Pm3m*, $Z = 1$. Three-dimensional intensity data were obtained by measurement of a single crystal of $NH_4I \cdot NH_3$ contained in a capillary by means of a four-circle diffractometer (Stoe Siemens AED2) with $Mo_{K\alpha}$ radiation (graphite monochromator): 2051 reflections, $2\theta(\max) = 51°$). After data reduction, 44 unique reflections were available for the least-squares refinement (program: SHELX 76). Iodine occupies the position 1a (000); the two nitrogen atoms are distributed statistically at the positions 6*f* (x 1/2 1/2, occupation factor 1/3, $x = 0.238(5)$). $R = 1.9\%$, $R_w = 1.7\%$, and $R_G = 1.9\%$, N–N distance 269(5) pm; tetragonal phase: $a = 525(1)$, $c = 485(1)$ pm (220 K), space group *P4/mmm*, $Z = 1$; orthorhombic phase: $a = 751(1)$, $b = 743(1)$, $c = 479(1)$ pm (202 K), $Z = 2$ (C-centered).

$ND_4I \cdot ND_3$: Cubic phase: $a = 513.3(7)$ pm (298 K), space group *Pm3m*, $Z = 1$; orthorhombic phase: $a = 759(1)$, $b = 745(1)$, $c = 478(1)$ pm (233 K), $Z = 2$ (C-centered).

Received: August 4, 1988 [Z 2905 IE]
German version: *Angew. Chem. 100* (1988) 1581

[1] R. Yamdagni, P. Kebarle, *J. Am. Chem. Soc. 95* (1973) 3504.
[2] J. D. Payzant, A. J. Cunningham, P. Kebarle, R. D. Gillard, *Can. J. Chem. 51* (1973) 3242.
[3] S. T. Ceyer, P. W. Tiedemann, B. H. Mahan, Y. T. Lee, *J. Chem. Phys. 70* (1979) 14.
[4] H. A. Schwarz, *J. Chem. Phys. 72* (1980) 284.
[5] A. J. Illies, M. F. Jarrold, L. M. Bass, M. T. Bowers, *J. Am. Chem. Soc. 105* (1983) 5775.
[6] P. A. Kollman, L. C. Allen, *Chem. Rev. 72* (1972) 283.
[7] P. Merlet, S. D. Peyerimhoff, R. J. Buenker, *J. Am. Chem. Soc. 94* (1972) 8301.
[8] P. Schuster, *Z. Chem. 13* (1973) 41.
[9] N. C. Baird, *Int. J. Quantum Chem. Quantum Biol. Symp. 1* (1974) 49.
[10] A. Pullman, A.-M. Armbruster, *Chem. Phys. Lett. 36* (1975) 558.
[11] J. J. Delpuech, G. Serratrice, A. Strich, A. Veillard, *Mol. Phys. 29* (1975) 849; *J. Chem. Soc. Chem. Commun. 1972*, 817.
[12] L. P. Tan, J. W. Linnett, *J. Chem. Soc. Chem. Commun. 1976*, 364.
[13] S. Scheiner, L. B. Harding, *J. Am. Chem. Soc. 103* (1981) 2169.
[14] S. Scheiner, *Int. J. Quantum Chem. Quantum Biol. Symp. 8* (1981) 221.
[15] S. Scheiner, *J. Phys. Chem. 86* (1982) 376.
[16] S. Scheiner, *J. Chem. Phys. 77* (1982) 4039.
[17] J. O. Lundgren, I. Olovsson, *Acta Crystallogr. 23* (1967) 966.
[18] J. O. Lundgren, I. Olovsson, *Acta Crystallogr. 23* (1967) 971.
[19] J. M. Williams, *Inorg. Nucl. Chem. Lett. 3* (1967) 297.
[20] I. Olovsson, *J. Chem. Phys. 49* (1968) 1063.
[21] R. D. Gillard, G. Wilkinson, *J. Chem. Soc. 1964*, 1640.
[22] A. C. Pavia, P. A. Giguere, *J. Chem. Phys. 52* (1970) 3551.
[23] G. J. Kearley, A. N. Fitch, B. E. F. Fender, *J. Mol. Struct. 125* (1984) 229.
[24] H. Henke, *Z. Kristallogr. 172* (1985) 263.
[25] G. J. Kearley, H. A. Pressman, R. C. T. Slade, *J. Chem. Soc. Chem. Commun. 1986*, 1801.
[26] W. Lindenberg, *Z. Anorg. Allg. Chem. 318* (1962) 1.
[27] W. Lindenberg, *Z. Anorg. Allg. Chem. 322* (1963) 81.
[28] W. Lindenberg, W. Ilgner, G. Simon, *Z. Naturforch. B 19* (1964) 273.
[29] W. Preibsch, *Dissertation*, Universität Hannover 1978.

Selective Photochemical Dehydrogenation of Saturated Hydrocarbons with Quantum Yields Approaching Unity**

By *Roman F. Renneke* and *Craig L. Hill**

The development of systems for the effective and selective catalytic functionalization of alkanes continues to be a topic of intense research interest. The activation and/or functionalization of alkanes by organometallic complexes,[1] metalloporphyrin-based systems,[2] electrophilic species,[3] the Gif and Gif-Orsay systems,[4] photosensitized Hg vapor,[5] and polyoxometalates[6, 7] continue to evolve rapidly. Our group recently developed both thermal[6] and photochemical[7] systems for the selective functionalization of unactivated hydrocarbons based on early-transition-metal polyoxometalate derivatives, for these complexes are not only thermodynamically resistant to oxidative degradation, but also soluble, experimentally tractable, and amenable to extensive synthetic modification. The initial research on polyoxometalate-based photochemical alkane functionalization involved primarily an in-depth examination of the reactions of α-$H_3PW_{12}O_{40}$ and related polyoxotungstate compounds of T_d symmetry [Eq. (a)].

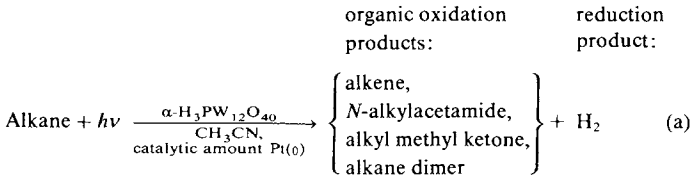

(a)

These systems exhibit moderate to high selectivities with respect to production of organic products, operate best with mid UV light, and use only 10% of the incident radiation for the formation of the products shown in Equation (a); greater than 90% is lost in radiationless processes. Three processes sum to the net reaction in Equation (a): absorption of light by polyoxometalate, P [Eq. (b)]; oxidation of the alkane by the polyoxometalate excited state, P*, with production of reduced polyoxometalate, P_r [Eq. (c)]; and a thermal reoxidation of P_r by H_2 evolution [Eq. (d)].[7]

$$P + h\nu \longrightarrow P^* \quad (b)$$

$$P^* + \text{alkane} \longrightarrow P_r + \text{alkene and other products} + 2H^{\oplus} \quad (c)$$

$$P_r + 2H^{\oplus} \longrightarrow P + H_2 \quad (d)$$

We report here the remarkable effect of acid on the catalytic photochemical functionalization of alkanes by polyoxometalates and the development of a new system based on two types of oxidatively resistant species, decatungstate and strong mineral acids, that utilizes near UV and visible light ($\lambda > 360$ nm) and results in the selective dehydrogenation of alkanes with quantum yields approaching unity.

Table 1 summarizes the results from several alkane photochemical dehydrogenation reactions by representative polyoxometalates present in free acid ($H^{\oplus}$), $NH_4^{\oplus}$, or n-$Bu_4N^{\oplus}$($Q^{\oplus}$) forms. The quantum yields are specifically defined here as the number of electrons in the reduced polyoxometalate product divided by the number of photons absorbed by that polyoxometalate. All reactions were run using 3.3 mM polyoxometalate and 0.45 M alkane substrate in acetronitrile contained in quartz cuvettes under an Ar atmosphere at 25°C. The light for all reactions was from a 1000-W Xe lamp filtered through infrared and UV/VIS cut-off filters ($\lambda > 360$ nm) for determination of organic products, or filtered through a 320-nm interference filter (peak width at half height = 9.6 nm, transmission maximum at 320 nm = 21%) for determination of the quantum yields. All measurements of the quantum yields were conducted under optically dense conditions (> 99% of the incident light was absorbed by the systems). The cyclooctane and cyclohexane reactions with decatungstate, both in the presence and absence of acid, showed product distributions that were independent of the light intensity and the wavelength of irradiation; a 320-nm interference filter and 295-, 320-, 360-, and 395-nm cut-off filters were all used in the latter experiments. For the acidified decatungstate reactions, irradiation even at the tail end of the absorption envelope (395-nm cut-off filter) results in the reasonably fast functionalization of alkanes. This light, although substantially lower in energy and hence potentially more selective than that often used in photochemical reactions (e.g., Hg light/quartz vessel; $\lambda > 190$ nm), is nevertheless adequate to produce the excited states of polyoxometalates that are kinetically competent to oxidize even saturated hydrocarbons! None of the acids at the concentrations given in Table 1 produced any detectable decomposition of $[W_{10}O_{32}]^{4\ominus}$ over the time period of the experiments (5–30 min), although some of these acids in higher concentrations produced appreciable decomposition of the complex

Table 1. Quantum yields for production of the reduced polyoxometalate in homogeneous photooxidation of alkanes by polyoxometalates [a].

Reaction	System [b]	Alkane	Φ [c]
(1)	α-$H_3PW_{12}O_{40}$/no acid	cyclooctane	0.08
(2)	α-$H_3PW_{12}O_{40}$/TFA	cyclooctane	0.12
(3)	α-$H_3PW_{12}O_{40}$/H_2SO_4(0.82 M)	cyclooctane	0.12
(4)	α-$Q_3PW_{12}O_{40}$/no acid	cyclooctane	0.02
(5)	α-$Q_3PW_{12}O_{40}$/TFA	cyclooctane	0.02
(6)	α-$Q_3PW_{12}O_{40}$/H_2SO_4 (0.82 M)	cyclooctane	0.10
(7)	α-$H_3PMo_{12}O_{40}$/no acid	cyclooctane	0.01
(8)	α-$H_3PMo_{12}O_{40}$/TFA	cyclooctane	0.02
(9)	α-$Q_3PMo_{12}O_{40}$/no acid	cyclooctane	0.002
(10)	α-$Q_3PMo_{12}O_{40}$/TFA	cyclooctane	0.004
(11)	$(NH_4)_6P_2W_{18}O_{62}$/no acid	cyclooctane	0.01
(12)	$(NH_4)_6P_2W_{18}O_{62}$/TFA	cyclooctane	0.03
(13)	$Q_2W_6O_{19}$/no acid	cyclooctane	0.01
(14)	$Q_2W_6O_{19}$/TFA	cyclooctane	0.06
(15)	$Q_4W_{10}O_{32}$/no acid	cyclooctane	0.14
(16)	$Q_4W_{10}O_{32}$/TFA	cyclooctane	1.0
(17)	$Q_4W_{10}O_{32}$/H_3PO_4 (0.82 M) [d]	cyclooctane	0.8
(18)	$Q_4W_{10}O_{32}$/HCl (0.026 M)	cyclooctane	1.0
(19)	$Q_4W_{10}O_{32}$/H_2SO_4 (0.82 M)	cyclooctane	1.0
(20)	$Q_4W_{10}O_{32}$/CF_3SO_3H (0.026 M)	cyclooctane	1.1
(21)	$Q_4W_{10}O_{32}$/$HClO_4$ (0.026 M) [d]	cyclooctane	1.1
(22)	$Q_4W_{10}O_{32}$/no acid	cyclohexane	0.02
(23)	$Q_4W_{10}O_{32}$/TFA	cyclohexane	0.53
(24)	$Q_4W_{10}O_{32}$/no acid	n-octane	0.03
(25)	$Q_4W_{10}O_{32}$/TFA	n-octane	0.45
(26)	$Q_4W_{10}O_{32}$/no acid	2,2-dimethylbutane	0.01
(27)	$Q_4W_{10}O_{32}$/TFA	2,2-dimethylbutane	0.29
(28)	$Q_4W_{10}O_{32}$/no acid	2,3-dimethylbutane	0.03
(29)	$Q_4W_{10}O_{32}$/TFA	2,3-dimethylbutane	0.49

[a] Reaction conditions given in text. [b] Q in all cases is tetra-n-butylammonium cation; TFA = trifluoroacetic acid; acid concentrations given in parenthesis after name of acid; [TFA] = 0.82 M in all TFA-containing reactions. [c] Quantum yields defined in text. [d] H_3PO_4 and $HClO_4$ were 85% and 70% aqueous solutions, respectively.

[*] Prof. Craig L. Hill, R. F. Renneke
Department of Chemistry, Emory University
Atlanta, GA 30322 (USA)

[**] This work was supported by the National Science Foundation (CHE-8715322) and ARCO Chemical Company.

after several hours. Although the presence of trifluoroacetic acid (TFA) increased the ability of $[W_{10}O_{32}]^{4\ominus}$ to oxidize both $nBu_4N^{\oplus}$ and the acetonitrile solvent in alkane-free control reactions, no products resulting from the photooxidation of either of these species were observed in the presence of alkane (0.45 M), for any of the reactions in Table 1, with the exception of reactions 26 and 27 involving 2,2-dimethylbutane.

The presence of the strong acids greatly accelerates the rates for the photoredox process [Eq. (c)]. The rates of photoreduced polyoxotungstate reoxidation [Eq. (d)] are negligible compared to the rate of photochemical polyoxotungstate reduction both in the presence and absence of acids. The acid-containing reactions in Table 1, along with the nonacidified reactions, then, are effectively stoichiometric based on the complex. Addition of the hydrogen-evolution catalyst RuO_2, however, causes reaction (d) to proceed rapidly and the overall photochemical dehydrogenation reactions become catalytic, proceeding at rates of over 15 turnovers of $[W_{10}O_{32}]^{4\ominus}$ per hour (conditions: 3.3 mM $[W_{10}O_{32}]^{4\ominus}$, cyclooctane substrate, 320-nm cut-filter). Additional alkane oxidation products are formed in some cases.

The data in Table 1 indicate that both polytungstates and polymolybdates of several different structures present in different salt forms are all active for the photochemical dehydrogenation of alkanes. The data in Table 1 and gas-chromatographic analyses of the organic product distributions of the reactions indicate that the presence of the moderate to strong acids TFA, H_3PO_4, HCl, H_2SO_4, CF_3SO_3H, and $HClO_4$ increases the rate of formation of alkane oxidation products and the selectivity for production of alkenes at the expense of the other products shown in Equation (a). In most of the acid-containing reactions, the alkene (or isomeric alkenes) are the only detectable alkane oxidation products, although in some cases, additional unidentified oxidation products are formed in low yields. For most of the cyclooctane reactions in Table 1, cyclooctane oxidation products represent at least 80% of the total oxidation products based on the concentration of P_r. For the optimally effective and stable $Q_4W_{10}O_{32}$/TFA system, the ratio of detected alkane oxidation products to P_r is 0.55 for the cyclohexane and 0.82 for the cyclooctane reactions. For most of the other alkanes, this ratio lies between these values. Also for this system, *cis*-cyclooctene, cyclohexene, the isomeric *n*-octenes, and 2,3-dimethyl-2-butene are the only detectable alkane oxidation products resulting from reaction of cyclooctane, cyclohexane, *n*-octane, and 2,3-dimethylbutane, respectively [reactions 16, 23, 25, and 29 in Table 1; see also Eq. (e)].

$$[HW_{10}O_{32}]^{3\ominus} + h\nu + \text{alkane} \longrightarrow [HW_{10}O_{32}]^{5\ominus} + 2\,H^{\oplus} + \text{alkene} \quad \text{(e)}$$

The $Q_4W_{10}O_{32}$/strong acid systems display quantum yields for the photoreduction of this polyoxotungstate complex by cyclooctane on the order of 1 (reactions 16 and 18–21). These are the highest quantum yields, by a good margin, for any polyoxometalate-based photochemical process. Since Equation (e) is endothermic in the dark (80–125 kJ mol^{-1}), depending on the alkane used, $Q_4W_{10}O_{32}$/acid/acetonitrile/alkane also represent truly efficient homogeneous systems for the conversion of light into chemical energy.

Absorption spectra, redox titrations, and quantum yields as a function of [acid]/$[Q_4W_{10}O_{32}]$ ratio establish that, for Equation (e) the form of the reduced $[W_{10}O_{32}]^{n\ominus}$ moiety is the monoprotonated two-electron reduced species, $[HW_{10}O_{32}]^{5\ominus}$.[8] The rate of production of $[HW_{10}O_{32}]^{5\ominus}$ is first order in light intensity and first order in both alkane and $H^{\oplus}$ at low concentrations of these species, but tends toward zero order in both at higher concentrations of each. Optically dense conditions render the rate effectively independent of the concentration of the catalyst, $[W_{10}O_{32}]^{4\ominus}$, because all incident light is being absorbed by the complex. Both the protonated and deprotonated forms of $[W_{10}O_{32}]^{4\ominus}$ are capable of photooxidizing alkane.

Received: May 17, 1988;
revised version: September 16, 1988 [Z 2764 IE]
German version: *Angew. Chem. 100* (1988) 1583

CAS Registry numbers:
2-$H_3PW_{12}O_{40}$, 1343-93-7; 2-$Q_3PW_{12}O_{40}$, 53749-37-4; 2-$H_3PMo_{12}O_{40}$, 12026-57-2; 2-$Q_3PMo_{12}O_{40}$, 53749-36-3; $(NH_4)_6P_2W_{18}O_{62}$, 117184-97-1; $Q_2W_6O_{19}$, 12329-10-1; $Q_4W_{10}O_{32}$, 68109-03-5; F_3CCO_2H, 76-05-1; H_2SO_4, 7664-93-9; F_3CSO_3H, 1493-13-6; $Me_2C{=}CMe_2$, 563-79-1; H_3PO_4, 7664-38-2; HCl, 7647-01-0; $HClO_4$, 7601-90-3; *t*-BuEt, 75-83-2; *n*-octene, 25377-83-7; cyclooctane, 292-64-8; cyclohexane, 110-82-7; (*Z*)-cyclooctene, 931-87-3; cyclohexene, 110-83-8.

[1] Recent reviews: a) R. H. Crabtree, *Chem. Rev. 85* (1985) 245; b) I. P. Rothwell, *Polyhedron 4* (1985) 177; c) M. Ephritikhine, *Nouv. J. Chim. 10* (1986) 9.
[2] Reviews on metalloporphyrin-catalyzed oxygenation: a) B. Meunier, *Bull. Soc. Chim. Fr. 1986*, 578; b) D. Mansuy, *Pure Appl. Chem. 59* (1987) 759.
[3] Review: G. Olah, *Acc. Chem. Res. 11* (1987) 422.
[4] D. H. R. Barton, J. Bovin, P. Le Coupanec, *J. Chem. Soc. Chem. Commun. 1987*, 1379, and references cited therein.
[5] S. H. Brown, R. H. Crabtree, *J. Chem. Soc. Chem. Commun. 1987*, 970.
[6] a) C. L. Hill, R. B. Brown, Jr., *J. Am. Chem. Soc. 108* (1986) 536; b) M. Faraj, C. L. Hill, *J. Chem. Soc. Chem. Commun. 1987*, 1487; C. L. Hill, R. F. Renneke, M. K. Faraj, R. B. Brown, Jr. in W. Ando (ed.): *The Role of Oxygen in Chemistry and Biochemistry*, Elsevier, New York 1988, p. 185.
[7] a) R. F. Renneke, C. L. Hill, *J. Am. Chem. Soc. 108* (1986) 3528; b) R. F. Renneke, C. L. Hill, *New J. Chem. 11* (1987) 763; c) R. F. Renneke, C. L. Hill, *J. Am. Chem. Soc. 110* (1988) 5461.
[8] a) T. Yamase, T. Usami, *J. Chem. Soc. Dalton Trans. 1988*, 183; b) A. Chemseddine, C. Sanchez, J. P. Launay, M. Fournier, *Inorg. Chem. 23* (1984) 2609.

Slow Tautomerization in a Rhenium–Oxo–Hydroxide Complex**

By *Torsten K. G. Erikson* and *James M. Mayer**

Metal–oxo ("yl") groups play a critical role in a variety of metal-mediated transformations, from stoichiometric reactions to heterogeneous catalysis and enzymatic processes.[1] The reactivity of the metal–oxygen multiple bond ranges from very low (e.g., the vanadyl ion $VO^{2\oplus}$[2]) to exceptionally high (cf. the "ferryl" unit believed to be the active site in cytochrome P-450 enzymes[3]). Despite much interest in the chemistry of metal–oxo species, few elementary steps involving metal–oxo groups have been examined in detail. We describe here our studies of one of the simplest reactions of a metal–oxo group, degenerate proton transfer between oxo and hydroxide ligands. We have prepared the rhenium–oxo–hydroxide complex **3** and observed that proton transfer from the hydroxide to the oxo ligand occurs very slowly, requiring more than 24 h at ambient temperatures to reach equilibrium.

The rhenium–oxo–hydroxide complex **3** is formed quantitatively (by NMR) on reaction of the ethoxide or

[*] Prof. J. M. Mayer, T. K. G. Erikson
Department of Chemistry, University of Washington
Seattle, WA 98195 (USA)

[**] Low-Valent Metal–Oxo Compounds, Part 6. This work was supported by Research Corporation, Chevron Research Co., the National Science Foundation, and the Petroleum Research Fund. Part 5: [4].

methylamide derivatives (**1**, **2**)[4] with one equivalent of water [Eq. (a)].

$$[Re(O)X(MeC{\equiv}CMe)_2] + H_2O \longrightarrow [Re(O)(OH)(MeC{\equiv}CMe)_2] + HX \quad (a)$$

1, X = OEt
2, X = NHMe

3

This type of ligand exchange reaction occurs readily in this system: for instance, the ethoxide in **1** is displaced by alcohols, ammonia, acetic acid, or H_2S.[4] Complex **3** reacts with acetic acid to give the rhenium acetate complex $[Re(O)(O_2CCH_3)(MeC{\equiv}CMe)_2]$[5] and water; with phenol an equilibrium mixture of **3** and $[Re(O)OPh(MeC{\equiv}CMe)_2]$ is observed.[4] Preparation of **3** from **2** is particularly useful because the methylamine byproduct evaporates readily, leaving a pure benzene solution of **3**. Although **3** is readily generated in solution, it has not been isolated because of its high solubility (even in pentane at $-80\,^{\circ}C$) and because concentration of solutions of **3** results in condensation to form the μ-oxo complex **4**.[6]

$[\{Re(O)(MeC{\equiv}CMe)_2\}_2(\mu\text{-}O)]$ **4**

The NMR, IR, and mass spectra of **3**[7] are very similar to those of analogous alkoxide,[4] halide,[5] and alkyl[8] derivatives. Therefore, these compounds undoubtedly have the pseudo-tetrahedral structure established by X-ray crystal structure analysis for the phenoxide, iodide, and ethyl derivatives. The assignments of the Re≡O and Re–OH stretching frequencies at 971 and 587 cm^{-1} is supported by their shift on ^{18}O labeling to 920 and 558 cm^{-1} ($\tilde{\nu}_{Re\text{-}OD} = 573\ cm^{-1}$). The sharp O–H stretch at 3607 cm^{-1} (O-D, 2660 cm^{-1}) in the solution IR spectrum indicates that **3** is not hydrogen-bonded in benzene solution. Complex **3** is not deprotonated by dimethylamine or by "proton sponge" (1,8-bis(dimethylamino)naphthalene) in benzene solution; reaction of **3** with stronger bases such as LiO*t*Bu or MeLi results in rapid decomposition.

Addition of one equivalent of $H_2{}^{18}O$ to solutions of **1** or **2** yields the oxo–hydroxide complex **3′** with the ^{18}O label predominantly in the hydroxide position (Scheme 1). The

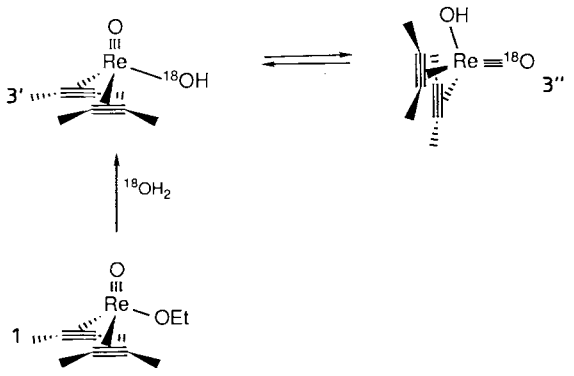

Scheme 1.

position of the ^{18}O is easily monitored by IR spectroscopy. Over 1.5 d at ambient temperatures in a solution IR cell (NaCl windows) the label gradually becomes evenly distributed between the oxo and hydroxide positions. The IR spectra suggest a first-order approach to equilibrium, with a half-life of roughly 11 h, although precise kinetic studies were hampered by a lack of reproducibility and by catalysis of the reaction by stirring in a Pyrex flask. The observed rate does not appear to depend on whether **3** was formed from **1** or from **2** and is not strongly affected by the presence or absence of stoichiometric ethanol or methylamine, or catalytic amounts of benzoic acid or "proton sponge". However, addition of even trace quantities of trifluoromethanesulfonic acid results in complete equilibration of the ^{18}O label before an initial spectrum can be taken. The acid catalysis probably occurs via protonation of the oxo ligand of **2** to give a symmetrical bis-hydroxide complex; trifluoromethanesulfonic acid has been shown to protonate the oxo ligand of the related ethyl complex $[Re(O)Et(MeC{\equiv}CMe)_2]$.[8]

The observation of slow tautomerization in **3** is surprising, because the reaction is essentially a proton transfer between oxygen bases. Proton transfer among oxygens is usually fast because the addition of a proton to an oxygen lone pair does not cause a substantial change in structure.[9] For example, the tautomerization of carboxylic acids, which are formally analogous to **3**, is very facile. In **3**, however, transfer of the proton from the hydroxide to the oxo group is accompanied by a large change in structure and bonding because it involves the rhenium–oxygen multiple bond, which is quite different from an organic carbonyl group.

The rhenium–oxo bond in **3** is best described as a triple bond, following the theoretical study of the iodide derivative[5] (compare $\tilde{\nu}(Re{\equiv}O) = 971$, 975 cm^{-1} for $[Re(O)X(MeC{\equiv}CMe)_2]$, X = OH, I). The rhenium–oxygen bonding causes the acetylene ligands to lie perpendicular to the Re≡O bond, with a sizable barrier to acetylene rotation.[5] Tautomerization of **3** therefore requires movement of the acetylene ligands (see **3″** in Scheme 1); this movement is probably in large part responsible for the significant activation barrier to and hence the slow rate of proton transfer. The substantial change in rhenium–oxygen bond lengths on proton transfer (ca. 0.25 Å based on Re≡O 1.712(13), Re–OPh 1.966(14) Å in the structure of the phenoxide complex[4]) should also be contribute to the barrier.

Slow proton transfer between oxygen or nitrogen atoms has been observed in other systems[10] where a π-bonding orbital is the proton-accepting site: for instance, reactions involving the vanadyl oxo group[11] or proton transfer among imido, amido, and amine ligands in a tungsten complex.[12] In sum, tautomerization of **3** is slow because the proton transfers not to an oxygen lone pair but to a rhenium–oxygen π-bonding orbital, so proton motion is coupled to dramatic changes in bonding and structure.

Received: June 9, 1988 [Z 2809 IE]
German version: *Angew. Chem. 100* (1988) 1585

CAS Registry numbers:
1, 115017-37-3; **1** X = NH_2, 115017-46-4; **1** X = SH, 115017-48-6; **2**, 115017-47-5; **3**, 115017-53-3; **3′**, 117098-42-7; **3″**, 117098-43-8; **4**, 117098-41-6; $H_2{}^{18}O$, 14314-42-2; dimethylamine, 124-40-3; 1,8-bis(dimethylamino)naphthalene, 20734-58-1.

[1] R. A. Sheldon, J. K. Kochi: *Metal-Catalyzed Oxidations of Organic Compounds*, Academic Press, New York 1981.
[2] F. A. Cotton, G. Wilkinson: *Advanced Inorganic Chemistry* 4th ed., Wiley, New York 1980.
[3] P. R. Ortiz de Montellano (Ed.): *Cytochrome P-450: Structure, Mechanism, and Biochemistry*, Plenum, New York 1986.
[4] T. K. G. Erikson, J. C. Bryan, J. M. Mayer, *Organometallics 7* (1988) 1930.
[5] J. M. Mayer, D. L. Thorn, T. H. Tulip, *J. Am. Chem. Soc. 107* (1985) 7454.
[6] IR (nujol): $\tilde{\nu}$ = 1789 w (C≡C), 1779 w (C≡C), 1156 s, 1040, 958 s (907, $Re^{18}O$), 946 vs (896, $Re^{18}O$), 799 vs (756, $Re^{18}O$), 621 cm^{-1}.

^{1}H NMR (C_6D_6): δ = 2.53, 1.99 (2 q, $^5J_{HH}$ = 1 Hz) $CH_3C{\equiv}CCH_3$. ^{13}C NMR ($CDCl_3$): δ = 157.4, 144.9 (2 s, $MeC{\equiv}C'Me$), 17.5, 7.2 (2 q, $^2J_{HH}$ = 129 Hz, $CH_3C{\equiv}CC'H_3$). MS: *m/z* 584 ($M^{\oplus}$ − MeCCMe), 530 ($M^{\oplus}$ − 2 MeCCMe). Complex **4** has not been isolated in pure form because of its facile decomposition in solution.

[7] ^{1}H NMR (C_6D_6): δ = 4.66 (s, O*H*), 2.39, 2.26 (2q, $^5J_{HH}$ = 1 Hz, $CH_3C{\equiv}CCH_3$). ^{13}C{^{1}H} NMR (C_6D_6): δ = 152.2, 141.2 ($MeC{\equiv}C'Me$), 16.3, 7.3 ($CH_3C{\equiv}CC'H_3$). MS: *m/z* 328 ($M^{\oplus}$), 274 ($M^{\oplus}$ − MeCCMe, base peak).

[8] E. Spaltenstein, T. K. G. Erikson, S. C. Critchlow, J. M. Mayer, *J. Am. Chem. Soc.*, in press.

[9] A. J. Kresge, *Acc. Chem. Res. 8* (1975) 354; M. Liler, *Adv. Phys. Org. Chem. 11* (1975) 267; R. F. Jordan, J. R. Norton, *J. Am. Chem. Soc. 104* (1982) 1255; R. G. Pearson, P. C. Ford, *Comments Inorg. Chem. 1* (1982) 279.

[10] Amido and hydrosulfido complexes [Re(O)(EH)($MeC{\equiv}CMe)_2$] (E = NH, NMe, S [4]) analogous to **3** do not rearrange to give imido- or sulfido-hydroxide tautomers over weeks at 70°C (C_6D_6) or upon addition of 0.1 equivalent of trifluoromethanesulfonic acid. This is probably due to the imido and sulfido complexes being thermodynamically unfavorable with respect to their oxo tautomers.

[11] M. D. Johnson, R. K. Murmann, *Inorg. Chem. 22* (1983) 1068; S. P. Harmalker, M. T. Pope, *J. Inorg. Biochem. 28* (1986) 85.

[12] D. M.-T. Chan, W. C. Fultz, W. A. Nugent, D. C. Roe, T. H. Tulip, *J. Am. Chem. Soc. 107* (1985) 251.

Linear Twofold Coordination of Arsenic in $[Cp'(CO)_2Mn{=}As{=}Mn(CO)_2Cp']^{\oplus}$**

By *Albert Strube, Gottfried Huttner,** and *Laszlo Zsolnai*

Dedicated to Professor Ernst Otto Fischer on the occasion of his 70th birthday

Linear μ_2-coordination in the case of the heavier elements of the fourth[1] and sixth[2] main groups was first demonstrated a few years ago by *E. Weiss* et al.[1a] and *L. Sacconi* et al.[2a] Corresponding examples for the fifth main group have so far never been described. Herein we report on the dimanganese complex **2** (Cp′ = η^5-MeC_5H_4), the first compound of a new, unusual class of substances.

An entry to complexes of this kind appeared to be opened up with the availability of $[(L_nM)_2EHal]$[3] (E = P,[4] As,[5] Sb,[6] Bi[7]); however, all attempts to cleave halogen from such potential precursors with $AlCl_3$,[8] $BHal_3$,[9] $TlPF_6$[10] or $AgPF_6$[11], with formation of $[(L_nM)_2E]^{\oplus}$, were unsuccessful. We have now found a reagent, namely $CF_3SO_3SiMe_3$, which reacts smoothly with **1** to give **2** [Eq. (a)].

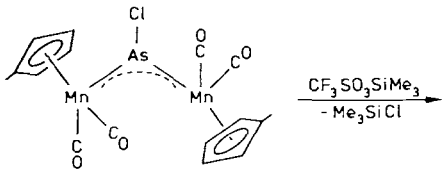

1

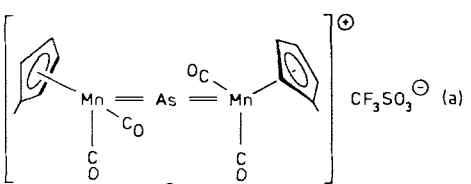

(a)

2

[*] Prof. Dr. G. Huttner, Dipl.-Chem. A. Strube, Dr. L. Zsolnai
Anorganisch-chemisches Institut der Universität
Im Neuenheimer Feld 270, D-6900 Heidelberg (FRG)

[**] This work was supported by the Fonds der Chemischen Industrie and the Deutsche Forschungsgemeinschaft.

2 is a dark-brown, crystalline solid, which is sensitive to hydrolysis but can be stored for weeks under inert gas at 20°C; its brown CH_2Cl_2 solution, however, reacts with trace amounts of moisture.

The $\tilde{\nu}_{CO}$ bands of **2** are shifted about 40 cm^{-1} to larger wave numbers compared to those of **1** [IR (CH_2Cl_2): $\tilde{\nu}$ [cm^{-1}] for **2**: 2037 s, 2006 vs, 1983 s, 1951 m; for **1**: 1994 s, 1951 vs, 1928 s, 1912 sh] thus indicating the positive charge of the organometal ion.

The ^{1}H-NMR signals of **2** are correspondingly shifted downfield relative to those of **1** [^{1}H-NMR ($CDCl_3$, 293 K): δ for **2**: 1.97 (s, 6H), 4.93 (m, 4H), 5.32 (m, 4H); for **1**: 1.89 (s, 6H), 4.60 (m, 4H), 4.94 (m, 4H)].

It follows from the electronic spectra that the bonds in **1** and **2** must be described in terms of different Mn–As–Mn π-systems:[12,13] the wavelength for the ππ* transition in the case of **2** is considerably shorter than in the case of **1** [UV (CH_2Cl_2): λ [nm] (ε [L mol^{-1} cm^{-1}][14]) for **2**: 380 (13000); for **1**: 512 (14000)]. An X-ray structure analysis of **2** was rendered difficult by the disorder of the $CF_3SO_3^{\ominus}$ ion; the linear arrangement of the Mn–As–Mn unit in **2** was, however, established beyond all doubt. Better results were obtained in the case of **3** (Cp* = η^5-Me_5C_5)[15] (Fig. 1).

$[Cp^*(CO)_2Mn{=}As{=}Mn(CO)_2Cp^*]BF_4$ **3**

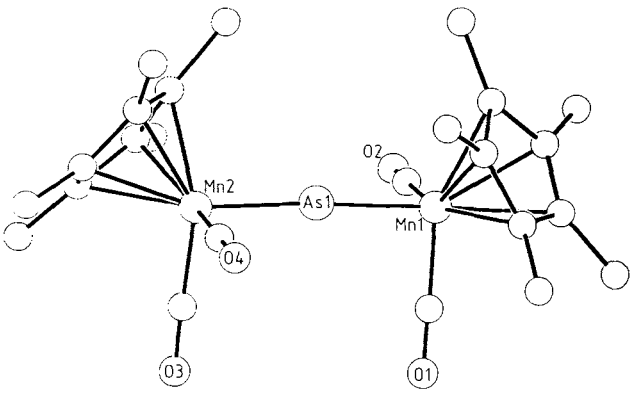

Fig. 1. Crystal structure of **3**: d_{MnAs} = 214.2(2), 215.1(2) pm; MnAsMn = 176.3(1)°; torsion angle Z1Mn1Mn2Z2 = 88.5° (Z1, Z2: midpoints of Cp*).

The cations in **2** and **3** are isoelectronic with the compounds with linear coordinated elements of the fourth[1] and sixth[2] main groups. Thus, the Mn–As distances are very short (Fig. 1), distinctly shorter than the Mn–As bonds in arsanediyl complexes,[3,12] which are shortened in any case by π-interaction (cf. $[Cp(CO)_2Mn]_2AsCl$, d_{MnAs} = 222.3 pm[9]). The {$L(CO)_2Mn$} fragments (L = Cp′, Cp*) in **2** and **3** are twisted through about 90° referred to the Mn–As–Mn axis, as is required for formulation of the cations as allene analogues.[13]

Experimental

All experiments were carried out under argon with anhydrous solvents. ^{1}H-NMR: Bruker AC200; IR: Perkin-Elmer 983G; UV/VIS: Perkin-Elmer Lambda 9; m.p. not corrected.

1 was prepared by a method analogous to that for $[(\eta^5\text{-}C_5H_5)(CO)_2Mn]_2AsCl$ [9].

2: A stirred solution of **1** (180 mg, 0.37 mmol) in CH_2Cl_2 (17 mL) was treated at 20°C with 0.23 mL (283 mg, 1.27 mmol) of $CF_3SO_3SiMe_3$ (the deep-red solution turned pale red within 1 min). After three hours' stirring, all volatile components were removed under high vacuum at 20°C. The oily, brown residue became solid after repeated washing with *n*-pentane and drying in a

high vacuum. Crystallization at −80°C from 6 mL of CH_2Cl_2/Et_2O (3/1) gave analytically pure crystals of **2** (m.p. 73°C); yield: 155 mg (69% referred to **1**); correct C,H,F,S analysis for $C_{17}H_{14}AsF_3Mn_2O_7S$.

3: ^{1}H-NMR ($CDCl_3$, 293 K): $\delta = 2.01$ (s, 30H); correct C,H,F analysis for $C_{24}H_{30}AsBF_4Mn_2O_4$.

Received: June 27, 1988 [Z 2824 IE]
German version: *Angew. Chem. 100* (1988) 1586

CAS Registry numbers:
1, 82948-98-9; **2**, 117310-56-2; **3**, 117310-58-4; $CF_3SO_3SiMe_3$, 27607-77-8.

[1] a) W. Gäde, E. Weiss, *J. Organomet. Chem. 213* (1981) 451; b) J. D. Korp, I. Bernal, R. Hörlein, R. Serrano, W. A. Herrmann, *Chem. Ber. 118* (1985) 340; c) W. A. Herrmann, H. J. Kneuper, E. Herdtweck, *Angew. Chem. 97* (1985) 1060; *Angew. Chem. Int. Ed. Engl. 24* (1985) 1062; d) C. Zybill, D. L. Wilkinson, G. Müller, *ibid. 100* (1988) 574 and *27* (1988) 583.

[2] [a] C. Mealli, S. Midollini, L. Sacconi, *Inorg. Chem. 17* (1978) 632; b) T. J. Greenhough, B. W. S. Kolthammer, P. Legzdins, J. Trotter, *ibid. 18* (1979) 3543; c) C. Potvin, J.-M. Manoli, J.-M. Brégeault, *Inorg. Chim. Acta 72* (1983) 103; d) J. Schiemann, P. Hübener, E. Weiss, *Angew. Chem. 95* (1983) 1021; *Angew. Chem. Int. Ed. Engl. 22* (1983) 980; e) D. L. Lichtenberger, J. L. Hubbard, *Inorg. Chem. 23* (1984) 2718; f) W. A. Herrmann, J. Rohrmann, A. Schäfer, *J. Organomet. Chem. 265* (1984) C1; g) S. Lincoln, S.-L. Soong, S. A. Koch, M. Sato, J. H. Enemark, *Inorg. Chem. 24* (1985) 1355; h) N. Albrecht, P. Hübener, U. Behrens, E. Weiss, *Chem. Ber. 118* (1985) 4059.

[3] G. Huttner, K. Evertz, *Acc. Chem. Res. 19* (1986) 406; G. Huttner, *Pure Appl. Chem. 58* (1986) 585.

[4] H. Lang, L. Zsolnai, G. Huttner, *Z. Naturforsch. B40* (1985) 500.

[5] J. von Seyerl, U. Moering, A. Wagner, A. Frank, G. Huttner, *Angew. Chem. 90* (1978) 912; *Angew. Chem. Int. Ed. Engl. 17* (1978) 844.

[6] U. Weber, L. Zsolnai, G. Huttner, *J. Organomet. Chem. 260* (1984) 281.

[7] J. von Seyerl, G. Huttner, *J. Organomet. Chem. 195* (1980) 207.

[8] Dehalogenation of $[(CO)_5Cr]_2AsCl$ with $AlCl_3$ furnished a compound, which, on the basis of IR spectroscopic data, is ascribed a cationic structure. The crystals obtained by diffusion experiments, however, were not suitable for an X-ray structure analysis.

[9] J. von Seyerl, B. Sigwarth, H.-G. Schmid, G. Mohr, A. Frank, M. Marsili, G. Huttner, *Chem. Ber. 114* (1981) 1392.

[10] G. Huttner, A. Strube, unpublished.

[11] A. Strube, *Diplomarbeit*, Universität Heidelberg 1987.

[12] G. Huttner, J. von Seyerl, M. Marsili, H.-G. Schmid, *Angew. Chem. 87* (1975) 455; *Angew. Chem. Int. Ed. Engl. 14* (1975) 434.

[13] See also N. M. Kostić, R. F. Fenske, *J. Organomet. Chem. 233* (1982) 337.

[14] The ε values quoted are only lower limits because of the instability of the compounds.

[15] X-ray structure analysis of **3**: $a = 1325.8(9)$, $b = 1458.7(8)$, $c = 1562.1(9)$ pm, $\beta = 113.17(4)°$, space group $P2_1/c$, $Z = 4$. The $BF_4^\ominus$ tetrahedron showed a rotational disorder which could be modeled by a rigid $BF_4^\ominus$ tetrahedron with appropriate temperature factors. Solution and refinement of the structure [Program system SHELX 76 and SHELX 86 (G. Sheldrick, Universität Göttingen)] led to $R_1 = 0.091$, $R_2 = 0.074$. Further details of the crystal structure investigation are available on request from the Fachinformationszentrum Energie, Physik, Mathematik GmbH, D-7514 Eggenstein-Leopoldshafen 2 (FRG), on quoting the depository number CSD-53 186, the names of the authors, and the journal citation.

A Morphology-Selective Copper Organosol**

By *Andrew C. Curtis, Daniel G. Duff, Peter P. Edwards,* David A. Jefferson, Brian F. G. Johnson,* Angus I. Kirkland,* and *Andrew S. Wallace*

There is continuing interest in colloidal metal particles, especially those which are important in commercial catalytic processes. However, while it has recently been demonstrated[1,2] that conventional chemical routes provide samples which are just as suitable for structural studies as those prepared by vacuum evaporation[3] or impregnation/reduction[4] methods, total control over particle morphology in both routes has proved difficult to achieve. In this communication we wish to report the preparation of a polymer-protected copper organosol in which a high percentage of the particles exhibit a single well-defined morphology within a relatively narrow particle-size range.

A solution of copper(II) acetate in acetonitrile was reduced with hydrazine hydrate under an inert atmosphere at 80°C under reflux, in the presence of poly(vinyl-2-pyrrolidone) as a stabilizing agent, to yield a deep red copper sol. This sol, which exhibited no appreciable Tyndall effect, was subsequently transferred to a controlled-argon-atmosphere glove box for all further manipulations. Under these conditions the sol was indefinitely stable against aggregation. A typical optical spectrum of this copper sol is illustrated in Figure 1 (curve I). The peak maximum at 575 nm was in good agreement with that predicted by the theory of *Mie*,[5] and the extinction coefficient at the peak maximum, $\varepsilon_{max} = 2803$ mol^{-1} dm^3 cm^{-1}, was more than an order of magnitude larger than that of the original copper(II) acetate solution ($\varepsilon_{max} = 111$ mol^{-1} dm^3 cm^{-1} at ca. 668 nm). If the sols prepared as described above were subject to limited air exposure, they were observed to become progressively paler. The peak in the optical spectrum, however, remained at 575 nm, although the extinction coefficient decreased as shown by curves II to VII in Figure 1.

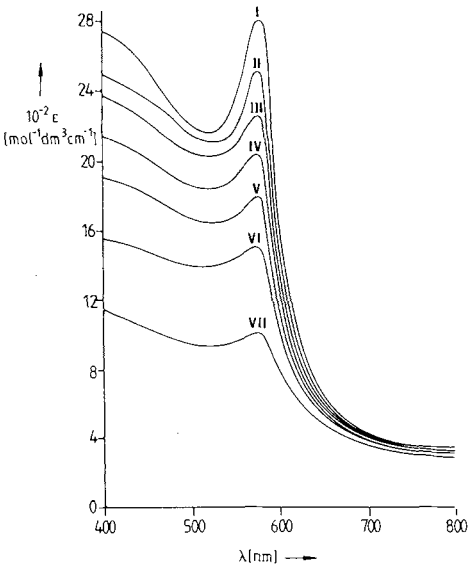

Fig. 1. The optical spectrum of the sol with a peak maximum at $\lambda_{max} = 575$ nm (curve I) together with the changes in optical spectra on limited oxidation (curves II to VII).

Low-resolution transmission electron microscopy (TEM) indicated large numbers of particles with approximately hexagonal outlines, referred to hereafter as "hexagons". Among these particles, the majority exhibited almost perfect hexagonal outlines, although a significant minority possessed an approximately truncated trigonal outline. These "hexagons" were generally of low contrast with no internal features visible (Fig. 2), and if the specimen was tilted with respect to the electron beam, the hexagonal outline of these particles was observed to foreshorten (Fig.

[*] Dr. P. P. Edwards, Dr. A. C. Curtis, Dr. D. G. Duff, Dr. D. A. Jefferson, Dr. B. F. G. Johnson, Dr. A. I. Kirkland, Dr. A. S. Wallace
University Chemical Laboratory
Lensfield Road, Cambridge CB2 1EW (England)

[**] We thank the Science and Engineering Research Council (SERC), British Alcan *(A. I. K.)*, ICI *(A. C. C.)*, and Johnson Matthey *(D. G. D.)* for financial support.

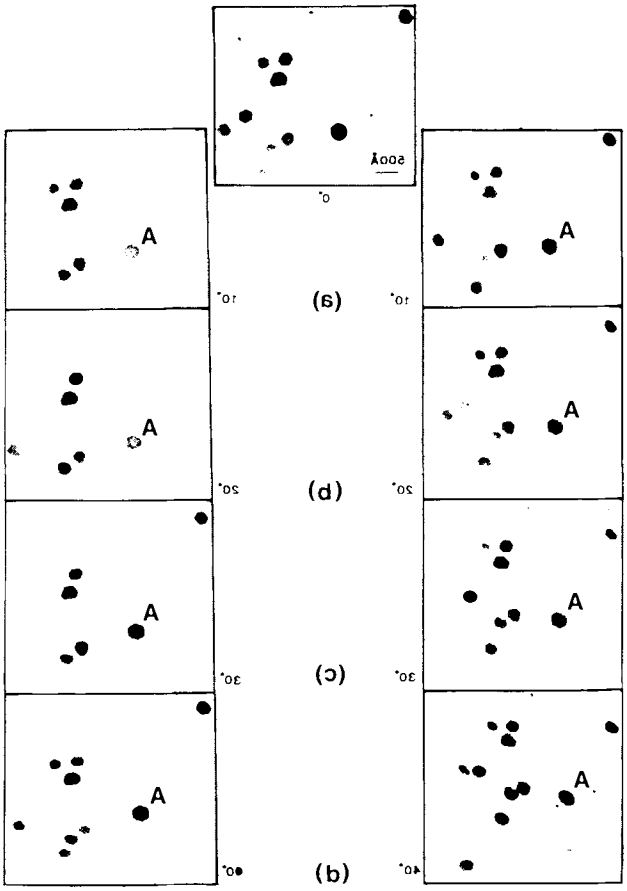

Fig. 2. Typical low-magnification TEMs of the sol recorded at different specimen tilts. The outline of the particle marked A clearly foreshortens as the specimen tilt is increased. a) ±10°. b) ±20°. c) ±30°. d) ±40°.

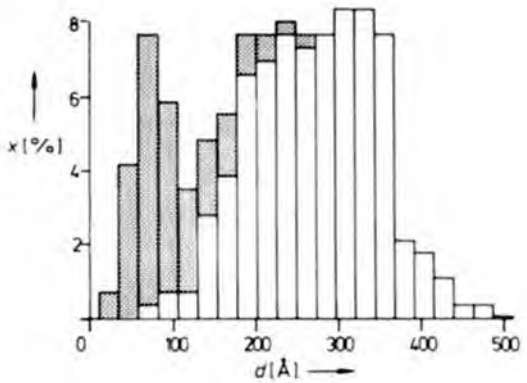

Fig. 3. The measured size distribution for the sol, with the unshaded areas representing the "hexagons" and the shaded areas the elliptical particles. For the whole system the mean particle diameter is 226 Å and $C_v = 45\%$.

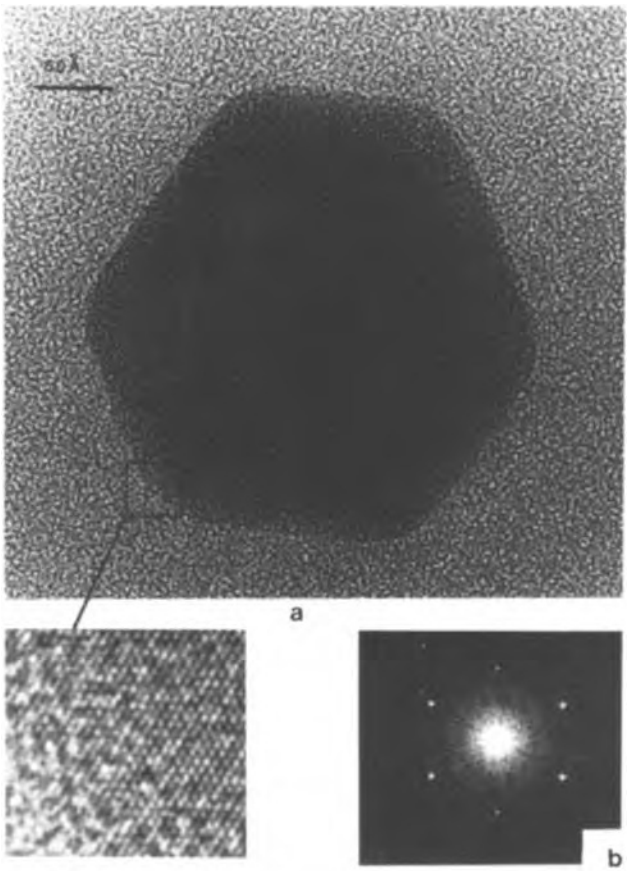

Fig. 4. a) A high-resolution image of a platelet in a ⟨111⟩ orientation showing two sets of {110} fringes across the entire platelet. b) Optical diffractogram from the image of Fig. 4a.

2a–d). This suggested a platelike morphology, with the effect being clearly illustrated for the particle marked A in Figure 2, the outline of which becomes noticeably narrower as the specimen tilt is increased. Measurement of diffraction contrast images recorded at differing amounts of specimen tilt gives an average aspect ratio of 0.2 for the "hexagons" subject to the errors in the measurement[6, 7] imposed by variations in objective-lens defocus, specimen height, and residual astigmatism with the degree of tilt. The remaining particles in the system were observed to be approximately elliptical in projection, and many of these exhibited striped diffraction contrast indicative of parallel twinning.[2]

Detailed analysis of the low-resolution micrographs (Fig. 2a) showed that the "hexagons", with a mean edge-to-edge diameter of 270 Å and a coefficient of variation C_v of 28% ($C_v = \sigma/d \times 100$, where σ is the standard deviation of the measured diameters and d is the mean particle diameter), represented ca. 75% of the particles present. The elliptical particles, with an equivalent circle diameter of ca. 100 Å and a C_v of 50% accounted for the remainder (Fig. 3).

High-resolution examination showed that, if suitably oriented, particles displayed faint fringes across the entire plane of the platelets (Fig. 4a), these having a spacing of 2.56 Å and an interplanar angle of 60°. Optical diffractometry (Fig. 4b) from recorded images confirmed that such particles were in ⟨111⟩ orientations and that the fringes corresponded to formally forbidden {110} diffraction maxima. These can arise in one of three ways: (1) as a result of the particle possessing a number of close-packed layers which is not a multiple of three, therefore breaking the systematic absence condition of the bulk metal; (2) as a result of non-zero Laue zone effects[8, 9] due to the extreme thinness of the crystals; (3) because of twins/stacking faults parallel to the platelet surface. The latter can be expected to reinforce the effects of the first two factors. In the light of recent studies of gold and silver platelets, where stacking faults have been observed directly using the profile imaging tech-

nique,[8, 10] it would appear likely that similar features are present in the copper platelets. Whereas some platelets in ⟨110⟩ orientations can inevitably be found in partially aggregated gold and silver sols, similar studies in the case of the copper "hexagons" have as yet proved impossible as a result of difficulties encountered in attempting to aggregate this sol. Neither solvent evaporation nor addition of a miscible "non-solvent" for the polymer (e.g., diethyl ether) succeeded in providing suitably aggregated samples, the latter process causing the solution to become turbid. TEM of this solution revealed a large proportion of particles to be well separated with some clumps of particles embedded in a dense polymer matrix. Even within these groups the particle surfaces were never in contact, and although some of the hexagons contained therein were possibly in ⟨110⟩ orientations, the polymer rendered them unsuitable for high-resolution examination as a result of extensive carbon contamination arising from polymer degradation.

Platelets of copper in colloidal solution have not previously been reported. However, flat platelets of colloidal gold are well known from sols formed under slow-growth conditions.[11, 12] Although their formation has been attributed to growth via raftlike aggregation of nuclei,[13] they are conventionally thought to arise from selective growth on non-{111} faces on a nucleus without radial twins. This has been explained in terms of the Kossel–Stranski theory of face-selective development of crystals,[14] possibly reinforced by proton adsorption on {111} surfaces inhibiting growth in the normal direction.[15] In gold sols platelets are usually accompanied by numbers of large decahedral and icosahedral MTPs (multiply twinned particles).[1, 11] These develop under slow-growth conditions from small MTPs into near-perfect decahedral and icosahedral forms enclosed by {111} faces with little or no Wulff-faceting,[16] by analogy with platelet formation. Their absence in this sol suggests that the nuclei are of standard close-packed form. In previously reported copper sols prepared in methanol[2] MTPs, although present, were considerably less frequent than in typical gold and silver colloids. Indeed, EXAFS of very small copper clusters in argon[17] shows fcc-based cubeoctahedral structures for clusters containing as few as 13 atoms, whereas icosahedra and icosahedral MTPs are calculated to be the minimum energy forms for very small particles.[18–20] The slower rate of growth in the present sol relative to the sols in methanol may be due to the formation of a stable copper(I) intermediate, probably the colorless tetrakis(acetonitrile) copper(I) complex[21] in this case. The formation of this stable intermediate is probably the cause of the smaller number of nuclei (and hence the larger particles) and the kinetically controlled growth forms exhibited by these sols. Another possibility is that a face-selective reaction involving the cross-linking of the polymer by acetonitrile may hinder the diffusion of reagents to the {111} planes.

As previously mentioned, evaporation of the solvent under an inert atmosphere by heating did not induce particle aggregation and an associated color change from red to green, in contrast to unprotected copper organosols,[2] and the sol, even if dried completely, could always be redispersed. If the sol was heated after drying for 30 minutes, however, a red film formed which was insoluble in methanol, ethanol, 1-propanol, 2-propanol, tetrahydrofuran, water, and acetonitrile.

TEM of the insoluble film revealed the presence of both circular and rounded hexagonal particles, most of which exhibited no diffraction or strain contrast. A typical micrograph of this film is shown in Figure 5a, from which it has been possible to measure the size distribution illustrated in Figure 5b, corresponding to an overall mean particle size of 231 Å with a C_v of 45%. Comparison of the size distributions of Figure 3 and 5b clearly indicates that the rounded particles showing no internal diffraction or strain contrast are derived from the "hexagons" in the sol.

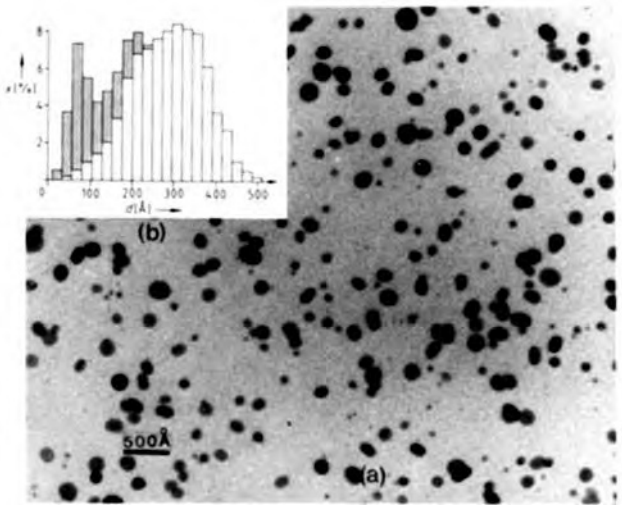

Fig. 5. a) Low-resolution TEM of the insoluble red film clearly indicating the absence of any interparticle contact. b) Measured size distribution of the particles in this film with the unshaded areas representing the "hexagons" (mean particle diameter = 248 Å, $C_v = 32\%$) and the shaded areas the eliptical particles (mean particle diameter = 97 Å, $C_v = 49\%$).

If the solvent was similarly removed via evaporation under vacuum, a red solid was again formed which was redispersible in all the solvents in which the previously described heat-treated film was insoluble. TEM indicated no particle aggregation even when this solid was redispersed in any of these solvents and repeatedly dried under vacuum. If, however, the system redispersed in these various other solvents was heat-treated as before, an insoluble red film again resulted.

The formation of this intractable red film after heating and removal of the solvent is attributed to cross-linking of the loops and tails of the polymer surrounding the copper particles. A similar reaction indeed occurs in the absence of copper particles. The resistance of the sol to particle aggregation and interparticle contact can be explained by cross-linking of the polymer at the metal surface, possibly catalyzed by the metal. This would be expected to result in highly effective steric stabilization which can account for the redispersible nature of the red solids, as well as the inability of the miscible non-solvents to induce interparticle contact. The precise nature of the cross-linking reaction is uncertain, although it should be noted that the presence of acetonitrile appears essential to this and hence towards the high degree of stabilization against aggregation.

Experimental Procedure

Copper(II) acetate monohydrate (25.5 mg, 0.128 mmol) and poly(vinyl-2-pyrrolidone) (average molecular weight = 40000; 158 mg, 1.423 mmol monomer units) were dissolved in freshly distilled, deoxygenated acetonitrile (100 mL). This solution was heated at 80 °C under reflux in a nitrogen atmosphere; on addition of a solution of hydrazine hydrate in deoxygenated acetonitrile, a deep red sol of zero-valent copper particles formed via a colorless intermediate which persisted for a period of ca. 2 min. Initial characterization of the copper sol by optical spectroscopy was performed using a Pye Unicam SP8800 UV/VIS spectrophotometer with the sol contained in 1-cm stoppered quartz cells.

Low-resolution transmission electron microscopy (TEM) of these samples was performed using a JEOL JEM-200CX electron microscope operating at 200 kV and fitted with a standard double-tilt side-entry goniometer allowing specimen tilts of ±45° about two orthogonal axes with respect to the incident electron beam. Subsequent high-resolution electron-microscopic (HREM) examination was carried out using our modified JEOL JEM-200CX electron microscope [22], thus permitting structural characterization at an interpretable point resolution of 1.95 Å. For such high-resolution studies care was taken to correct illumination-system misalignments and objective-lens astigmatism prior to recording micrographs at electron-optical magnifications of either ca. 450000× or ca. 690000×.

Received: May 10, 1988 [Z 2754 IE]
German version: *Angew. Chem. 100* (1988) 1588

[1] A. C. Curtis, D. G. Duff, P. P. Edwards, D. A. Jefferson, B. F. G. Johnson, A. I. Kirkland, D. E. Logan, *Angew. Chem. 99* (1987) 688; *Angew. Chem. Int. Ed. Engl. 26* (1987) 676.
[2] A. C. Curtis, D. G. Duff, P. P. Edwards, D. A. Jefferson, B. F. G. Johnson, A. I. Kirkland, A. S. Wallace, *J. Phys. Chem. 92* (1988) 2270.
[3] L. D. Marks, D. J. Smith, *J. Microsc. (Oxford) 130* (1983) 249.
[4] L. A. Freeman, A. Howie, M. M. J. Treacy, *J. Microsc. Oxford 111* (1977) 165.
[5] G. Mie, *Ann. Phys. (Leipzig) 25* (1908) 377.
[6] P. L. Flynn, S. E. Wanke, P. S. Turner, *J. Catal. 33* (1974) 233.
[7] M. M. J. Treacy, A. Howie, *J. Catal. 63* (1980) 265.
[8] D. Chearns, *Philos. Mag. 30* (1974) 549.
[9] N. Tanaka, J. M. Cowley, *Mater. Res. Soc. Symp. Proc. 41* (1985) 155.
[10] A. C. Curtis, D. G. Duff, P. P. Edwards, D. A. Jefferson, B. F. G. Johnson, A. I. Kirkland, manuscript in preparation.
[11] J. Turkevich, P. C. Stevens, J. Hillier, *Discuss. Faraday Soc. 11* (1951) 55.
[12] Y.-S. Chiang, J. Turkevich, *J. Colloid Sci. 18* (1963) 772.
[13] J. Turkevich, *Gold Bull. 18* (1985) 86.
[14] B. Brüche, *Kolloid-Z. 170* (1960) 97.
[15] R. H. Morriss, W. O. Milligan, *J. Electron Micros. 8* (1960) 17.
[16] L. D. Marks, *Philos. Mag. A 49* (1984) 81.
[17] P. A. Montano, G. K. Shenoy, E. E. Alp, W. Schulze, J. Urban, *Phys. Rev. Lett. 56* (1986) 2076.
[18] M. R. Hoare, P. Pal, *J. Cryst. Growth 17* (1972) 77.
[19] S. Ino, *J. Phys. Soc. Jpn. 27* (1969) 941.
[20] A. Howie, L. D. Marks, *Philos. Mag. A 49* (1984) 95.
[21] G. J. Kubas, *Inorg. Synth. 19* (1979) 90.
[22] D. A. Jefferson, R. D. Brydson, A. Harriman, G. R. Millward, J. M. Thomas, K. Tsuno, *Nature London 323* (1986) 428.

Generation and Characterization of Sulfurous Acid (H_2SO_3) and of Its Radical Cation as Stable Species in the Gas Phase**

By *Detlev Sülzle, Marjon Verhoeven, Johan K. Terlouw,* and *Helmut Schwarz**

Dedicated to Professor Geo Dijkstra on the occasion of his 65th birthday

Sulfurous acid, H_2SO_3, has in common with carbonic acid **1** and carbamic acid **2** (X = NH_2), that general textbook knowledge takes it to be nonexistent in the free state.[1] Recently we were able to show[2] that this instability is determined only by the environment and is not an inherent property of the molecules: This we achieved by generating the molecules **1** and **2** by thermolysis of ammonium hydrogen carbonate and ammonium carbamate, respectively [Eqn. (a)] and showing them to be stable in the gas phase. **1** and **2** could be oxidized by electron impact ionization (70 eV) to the likewise stable radical cations $\mathbf{1}^{\oplus\odot}$ and $\mathbf{2}^{\oplus\odot}$, respectively, whose neutralization was accomplished under the conditions of neutralization reionization mass spectrometry (NRMS).[3] The obvious route to sulfurous acid, namely via removal of NH_3 from ammonium hydrogen sulfite by thermolysis, is thwarted by the fact that anhydrous NH_4HSO_3 is unknown. (Drying of $MHSO_3$ salts (M = metal) usually produces disulfites.[1a,b])

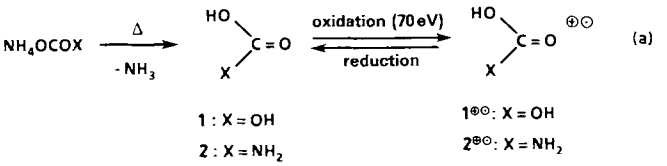

On the other hand, both the radical cation of sulfurous acid $\mathbf{5}^{\oplus\odot}$ and the neutral molecule **5** are easily generated in the gas phase by dissociative ionization (70 eV) of diethyl sulfite **3** or ethanesulfonic acid **4** [Eqn. (b)]. Reduction of $\mathbf{5}^{\oplus\odot}$ in an NRMS experiment affords sulfurous acid **5**. The experimental finding is substantiated by ab initio calculations (HF/6-31G*//6-31G*).

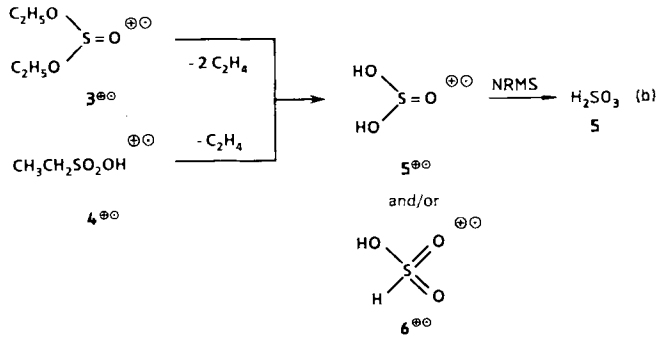

First, however, it has to be established whether the $(H_2,S,O_3)^{\oplus\odot}$ ions *m/z* 82, generated from **3** or **4**, exist in the form $\mathbf{5}^{\oplus\odot}$ or $\mathbf{6}^{\oplus\odot}$. Both upon unimolecular as well as collision-induced decomposition, the mass selected *m/z* 82 ions (MSMS-experiment) overwhelmingly split off $OH^{\odot}$ (*m/z* 82→*m/z* 65). This can be considered indicative of the presence of $\mathbf{5}^{\oplus\odot}$, as simple thermochemical considerations based on literature data compellingly lead to the conclusion that the reaction $\mathbf{5}^{\oplus\odot} \rightarrow HOSO^{\oplus} + OH^{\odot}$ is the favored fragmentation over all conceivable decomposition processes of $\mathbf{5}^{\oplus\odot}$. For $\mathbf{6}^{\oplus\odot}$ the situation is less clear; since not all thermochemical data (e.g. ΔH_f^0 of $HSO_2^{\oplus}$) are reliably known it cannot be established in the case of $\mathbf{6}^{\oplus\odot}$ whether the loss of $OH^{\odot}$ is favored or whether other modes of dissociation such as the loss of H_2O are more important.

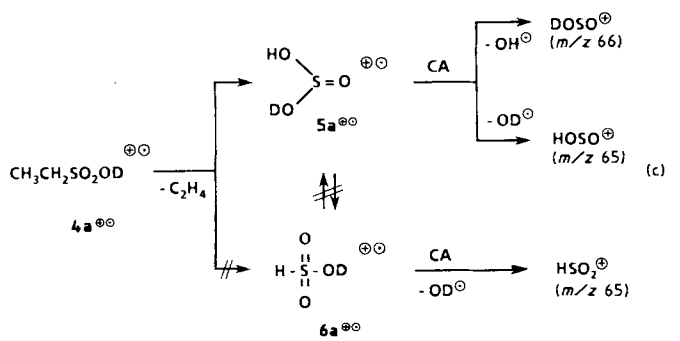

[*] Prof. Dr. H. Schwarz, D. Sülzle
Institut für Organische Chemie der Technischen Universität
Strasse des 17. Juni 135, D-1000 Berlin 12
Dr. J. K. Terlouw, M. Verhoeven
Analytical Chemistry Laboratory, University of Utrecht
Croesestraat 77A, NL-3522 AD Utrecht (The Netherlands)

[**] This work was supported by the Deutsche Forschungsgemeinschaft, the Fonds der Chemischen Industrie and the Fondsgesellschaft von Freunden der Technischen Universität Berlin e.V.

The following experiment provides a clear decision in favor of $5^{\oplus\odot}$ [Eqn. (c)]: if **4a** generates the isotopomer $\mathbf{5a}^{\oplus\odot}$ loss of both $OH^{\odot}$ *and* $OD^{\odot}$ will be observed in MSMS-experiments; should $\mathbf{6a}^{\oplus\odot}$ be generated, then (provided the isomers are separated by considerable barriers) elimination of $OD^{\odot}$ would occur exclusively. The assumption of a barrier preventing the rapid equilibration $\mathbf{5a}^{\oplus\odot} \rightleftharpoons \mathbf{6a}^{\oplus}$ is justified: ab initio MO calculations[4] (UHF 6-31G*//6-31G*+ZPVE) indicate that $5^{\oplus\odot}$ is 37.3 kcal/mol more stable than $6^{\oplus\odot}$ but that the barrier against the conversion $6^{\oplus\odot} \rightarrow 5^{\oplus\odot}$ is 44.5 kcal/mol.

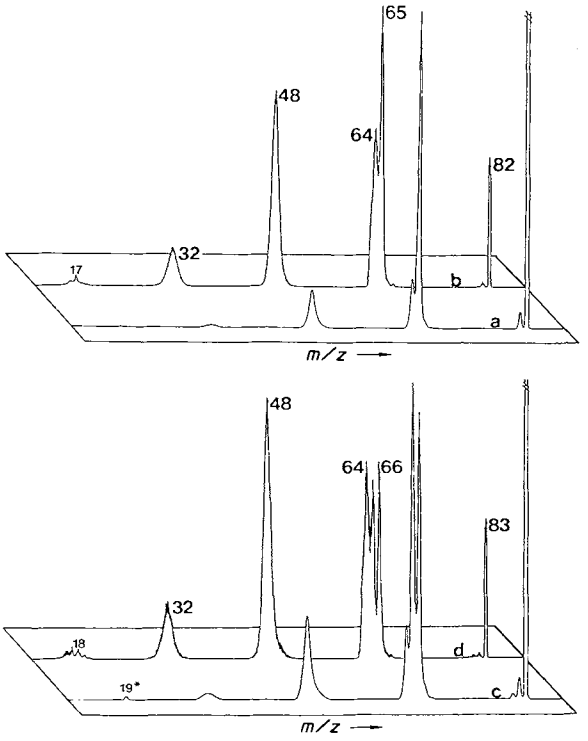

Fig. 1. CA and NR mass spectra (Xe/O_2) of $H_2SO_3^{\oplus\odot}$ (precursor **4**) and $HDSO_3^{\oplus\odot}$ (precursor **4a**). a) CA of $H_2SO_3^{\oplus\odot}$. b) NR of $H_2SO_3^{\oplus\odot}$. c) CA of $HDSO_3^{\oplus\odot}$. d) NR of $HDSO_3^{\oplus\odot}$. The spectra were recorded on VG-Instruments mass spectrometers of types ZAB-2F (Utrecht), and ZAB-HF-3F (Berlin) under the conditions given in Refs. [2, 3b].

The experimental result (Fig. 1c) is unambiguous. Under collisional activation (CA) conditions both *m/z* 65 (loss of $OD^{\odot}$) and *m/z* 66 (loss of $OH^{\odot}$) occur, so the dissociative ionization of **4a** generates the radical cation of sulfurous acid $\mathbf{5a}^{\oplus\odot}$.[5] Since the ions $H_2SO_3^{\oplus\odot}$ generated from **3** and from **4** are identical in all mass spectrometric properties it must be concluded that the double elimination of ethylene from diethyl sulfite **3** also leads to $5^{\oplus\odot}$ and not to $6^{\oplus\odot}$.[6]

In the neutralization-reionization experiments carried out on $5^{\oplus\odot}$ and $\mathbf{5a}^{\oplus\odot}$ the spectra given in Figures 1b and 1d, respectively, are obtained; they do not require any detailed interpretation. The "survivor" signals at *m/z* 82 and *m/z* 83 tell us that neutrals with lifetimes of $t > 10^{-5}$ s are generated upon neutralization of $5^{\oplus\odot}$ and $\mathbf{5a}^{\oplus\odot}$.[7] The isotope effect mentioned in Ref. [5] also favors the loss of $OH^{\odot}$ over that of $OD^{\odot}$ in the NRMS experiment. That, once again, the neutral molecule **6** does not come into consideration is clear not only from the competitive loss of $OH^{\odot}/OD^{\odot}$ but also from MO calculations (RHF/6-31G*//6-31G*+ZPVE). According to these calculations **6** is 16.8 kcal/mol less stable than sulfurous acid **5**, and the transition structure TS **5/6** is 88.0 kcal/mol more energetic than **5**.

Summary: Sulfurous acid **5** and its radical cation $5^{\oplus\odot}$ are stable in the gas phase. The "nonexistence" of H_2SO_3 in solution does not reflect an intrinsic instability but, as also in the cases of carbonic acid and carbamic acid, is the result of bimolecular reactions.

Received: July 27, 1988 [Z 2890 IE]
German version: *Angew. Chem. 100* (1988) 1591

[1] a) N. N. Greenwood, A. Earnshaw: *Chemistry of the Elements*, Pergamon Press, Oxford 1985; b) R. Steudel: *Chemie der Nichtmetalle*, de Gruyter, Berlin 1974; c) S. Hauptmann: *Organische Chemie*, Verlag H. Deutsch und Thun, Frankfurt/Main 1985; d) *Gmelin Handbuch der Anorganischen Chemie: Kohlenstoff, Teil C3*, Verlag Chemie, Weinheim 1973; e) D. C. Frasco, *J. Chem. Phys. 41* (1964) 2134; f) A. Müller, B. Krebs: *Studies in Organic Chemistry, Sulfur*, Elsevier, Amsterdam 1984.

[2] a) J. K. Terlouw, C. B. Lebrilla, H. Schwarz, *Angew. Chem. 99* (1987) 352; *Angew. Chem. Int. Ed. Engl. 26* (1987) 354; b) K. J. van den Berg, C. B. Lebrilla, J. K. Terlouw, H. Schwarz, *Chimia 41* (1987) 122.

[3] a) C. Wesdemiotis, F. W. McLafferty, *Chem. Rev. 87* (1987) 485; b) J. K. Terlouw, H. Schwarz, *Angew. Chem. 99* (1987) 829; *Angew. Chem. Int. Ed. Engl. 26* (1987) 805.

[4] Stationary products were considered to indicate unambiguously minima or transition structures (TS). Geometrical data are available upon request. The $\langle S^2 \rangle$ values, whose deviation from the expected value $\langle S^2 \rangle = 0.75$ may be considered a measure for UHF calculations, are 0.76 for $5^{\oplus\odot}$, 0.76 for $6^{\oplus\odot}$ and 0.84 for the transition structure TS $5^{\oplus\odot}/6^{\oplus\odot}$.

[5] The ratio of the signals for *m/z* 65 to *m/z* 66 is not a straightforward indication for the isotope effect in the elimination of $OD^{\odot}$ and $OH^{\odot}$. The reasons for this are: 1) The deuterium substitution in **4a** amounts at most to 50%, and 2) *m/z* 83 is not isotopically pure but is a mixture of $\mathbf{5a}^{\oplus\odot}$ (H, D, S, O_3)$^{\oplus\odot}$ and $(H_3,S,O_3)^{\oplus}$. $H_3SO_3^{\oplus}$ results from the loss of C_2H_4 from protonated **4**. Semiquantitative corrections indicate that 30 to 40% of the signal at *m/z* 65 can be traced back to an elimination of H_2O from $H_3SO_3^{\oplus}$. If this is taken into consideration then an isotope effect $k_{OH}/k_{OD} = 1.4$ is obtained for the decomposition of $\mathbf{5a}^{\oplus\odot}$.

[6] It remains to be seen whether the hydrogen transfers involved in the reaction $3^{\oplus\odot} \rightarrow 5^{\oplus\odot} + 2C_2H_4$ occur via a four-centered or a six-centered mechanism. This could only be resolved by a double isotope labeling experiment. This aspect, however interesting in itself, has no bearing upon the question of the generation of $5^{\oplus\odot}$ or $6^{\oplus\odot}$.

[7] It must be pointed out that neutralization of $H_3SO_3^{\oplus}$ does not generate detectable amounts of $H_3SO_3^{\oplus}$ with a lifetime of $t > 10^{-5}$ s. The question whether this is the result of an inherent instability of $H_3SO_3^{\oplus}$ or, more probably, whether $H_3SO_3^{\oplus}$ has a short half-life when generated in a highly excited state upon vertical neutralization remains open. Here, the only fact of importance is that the *m/z* 83 signal in Figure 1d is not due to $H_3SO_3^{\oplus}$.

The SF_5-Unit as Steric Protecting Group; Synthesis and Structure of $F_5S-C{\equiv}SF_3$**

By *Rolf Gerhardt, Thomas Grelbig, Jürgen Buschmann, Peter Luger,* and *Konrad Seppelt**

Surprisingly, the bonding angle at the central carbon atom of $F_3C-C{\equiv}SF_3$[1a] is 171.5(2.0)° in the solid state,[1b] and, in the gaseous state, it is even smaller: 155.0(3.0)°.[2] Ab initio calculations[2–4] with inclusion of configurational interaction showed that the molecule tolerates bending to 140° without any mentionable resistance, and that the energy minimum possibly does not lie at 180°.[2] In view of this unusual behavior it appeared worthwhile synthesizing

[*] Prof. Dr. K. Seppelt, Dipl.-Chem. R. Gerhardt, T. Grelbig
Institut für Anorganische und Analytische Chemie
der Freien Universität
Fabeckstrasse 34-36, D-1000 Berlin 33
Prof. Dr. P. Luger, Dr. J. Buschmann
Institut für Kristallographie der Freien Universität
Takustrasse 6, D-1000 Berlin 33

[**] This work was supported by the Deutsche Forschungsgemeinschaft and the Fonds der Chemischen Industrie.

at least one further compound containing a sulfur-carbon triple bond in order to establish whether the non-linearity of $F_3C-C\equiv SF_3$ is a special case or not.[5] However, the necessity for steric and presumably also electronic stabilization of the sulfur-carbon triple bond drastically limits the number of possible stable compounds of the type $R-C\equiv SF_3$. Herein we describe the synthesis of $F_5S-C\equiv SF_3$ and its crystal structure analysis at $-168\,^{\circ}C$.

Since the $C\equiv SF_3$-group was meant to be formed in a final step from a CH_2-SF_5-group, the synthesis required a compound bearing two SF_5 groups on one carbon atom. This could be obtained by twofold addition of SF_5Cl to 1,1-difluoroethene (Scheme 1). The addition of SF_5Cl—corresponding to the radical mechanism—is regiospecific both times.[6, 7]

$$H_2C{=}CF_2 + SF_5Cl \xrightarrow{h\nu} F_5S{-}CH_2{-}CF_2Cl\ [8] \xrightarrow[-HCl]{KOH}$$
$$F_5S{-}CH{=}CF_2\ [8] \xrightarrow{SF_5Cl,\ h\nu} (SF_5)_2CH{-}CF_2Cl \xrightarrow[-HCl]{KOH}$$
$$(SF_5)_2C{=}CF_2 \xrightarrow[-HF]{H_2O} (SF_5)_2CH{-}COF \xrightarrow[-HF]{H_2O}$$
$$(SF_5)_2CH{-}COOH \xrightarrow[-CO_2]{} F_5S{-}CH_2{-}SF_5 \xrightarrow[-2HF]{KOH,\ 80^{\circ}} F_5S{-}C\equiv SF_3$$

Scheme 1. Synthesis of $F_5S-C\equiv SF_3$.

The intermediate product $(SF_5)_2CH-CF_2Cl$ is present in the form of two conformers, even above room temperature. This is undoubtedly a result of hindrance of rotation by the two rigid, square-pyramidal SF_5 groups. The energy profile of the rotation about the C–C bond can be derived from the temperature-dependence of the NMR spectra (Fig. 1).

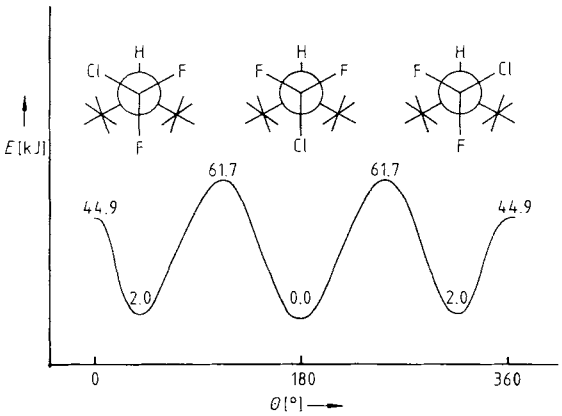

Fig. 1. Energy profile of the rotation about the C–C bond in $(SF_5)_2CH-CF_2Cl$. The energies were calculated according to known methods from the temperature-dependent ^{19}F-NMR spectra [9].

In certain cases hydrolyses of 1,1-difluoroethenes are known;[10] acid fluoride and acid can then be isolated as intermediates. The decisive step of the synthesis according to Scheme 1 is the double elimination of HF from $F_5S-CH_2-SF_5$ to give $F_5S-C\equiv SF_3$. $F_4S{=}C{=}SF_4$ is (unfortunately) not observed. Pentafluorothiomethylidine sulfur trifluoride is a colorless liquid, which is already volatile at $-78\,^{\circ}C$ in vacuo; it decomposes slowly above this temperature, and rapidly at room temperature, to give as yet unknown compounds. The existence of the compound was confirmed by the usual physical methods, especially ^{19}F-NMR spectroscopy. Noteworthy here is that the resonance of the four equatorial F atoms of the SF_5 group appear at lower field than the resonance of the axial F atom. This phenomenon was hitherto observed in F_5S-C compounds only in the case of acetylenes $F_5S-C\equiv C-X$. It is explained in terms of the opposing influence on axial and equatorial fluorine atoms by the anisotropic cylindrical triple bond.[11]

Investigation of the crystal structure of the compound, which melts at $-130\,^{\circ}C$, revealed an arrangement of the molecule on a threefold crystallographic axis with resulting disorder of the SF_5 group (Fig. 2).[12] Nevertheless, the molecule is clearly recognizable. An extremely short S–C distance of 139.2(4) pm is observed for the triple bond, which contrasts with the C–S single bond length of 168.2(4) pm in the same molecule.

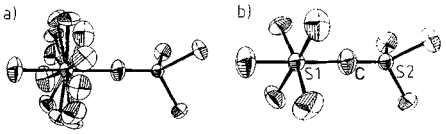

Fig. 2. Crystal structure of $F_5S-C\equiv SF_3$ at $-168\,^{\circ}C$. a) Threefold rotational symmetric disordered model. Vibration ellipsoids at the 20% probability level. b) One molecule; ellipsoids at the 30% probability level. Bond lengths [pm] and angles [°]: S1-C 168.2(4), S2-C 139.2(4), S2-F 153.4(3); S1-C1-S2 180, F-S1-F 93.5(1), C-S2-F 122.7(2).

In complete constrast to $F_3C-C\equiv SF_3$, $F_5S-C\equiv SF_3$ is linear. The exact 180° angle at the carbon atom is prescribed by the crystal symmetry. A deviation from linearity would give rise to a threefold disorder of the carbon atom and of the axial fluorine atom. A quantitative evaluation of the thermal parameters of both atoms shows that their mean vibration amplitudes ($\bar{u} = \sqrt{u}$) are only 8 and 11 pm greater than those of the sulfur atoms, respectively. This gives deviations from linearity of, at the most, 3–4°.

Unfortunately, the disorder of the SF_5 moiety limits the quality of the crystal structure determination to such an extent that it is not suitable for accurate statements about the electron density distribution—despite accurate intensity measurements, a five- to six-fold redundancy in determination for the measured data, and a very good R value. Nevertheless, in a density difference chart, an expanded disk-like electron-density plateau is seen perpendicular to the bond direction. Its maximum is located not quite centrally between C and S but somewhat nearer to the C atom. Exact details are not recognizable.

The question of whether the linearity is caused by the SF_5 groups, or is a result of the packing forces in the lattice, remains unanswered. An answer is not furthcoming by vapor phase structure investigations (electron diffraction, microwave spectroscopy, matrix IR spectroscopy). This is very difficult because of the size of the molecule.

Experimental

$(SF_5)_2CH-CF_2Cl$: A mixture of 0.2 mol of $F_5S-CH{=}CF_2$, 0.23 mol of SF_5Cl and 400 g of $C_2F_4Cl_2$ was irradiated at $-30\,^{\circ}C$ with a Hg high-pressure lamp for 2 d. After spinning band distillation $(SF_5)_2CH-CF_2Cl$ was obtained as a colorless liquid in 30% yield, b.p. 56°C/130 mbar.—^1H-NMR ($-80\,^{\circ}C$): $\delta = 5.7$. ^{19}F-NMR ($-80\,^{\circ}C$): $\delta = 80$–82 (SF), -35.4 (CF_2 of the symmetric conformer), -34.1 and -51.2 ($^2J_{FF} = 200.0$ Hz, CF_2 of the asymmetric conformer): IR (gas): strong bands at $\tilde{\nu} = 1281, 1173, 1149, 1113, 1042, 976, 932, 876, 857, 818, 769, 684, 615, 592\ cm^{-1}$; MS: m/z 317 ($[M-Cl]^{\oplus}$, 21% referred to $SF_3^{\oplus}$ = 100%) and numerous lighter fragments.

$(SF_5)_2C{=}CF_2$: $(SF_5)_2CH-CF_2Cl$ (30 mmol) was allowed to react with an excess of KOH pellets at room temperature. All compounds volatile in vacuum were distilled with a spinning band column. $(SF_5)_2C{=}CF_2$ was obtained as a colorless liquid in 80% yield, b.p. 88°C.—^{19}F-NMR: $\delta = 72.3$ (SF_{ax}), 74.9 (SF_{eq}), -54.8 (CF_2); IR (gas): strong bands at $\tilde{\nu} = 1706, 1667, 1337, 956, 928, 879, 857, 804, 696, 621, 595\ cm^{-1}$; MS: m/z 316 ($M^{\oplus}$, 18% referred to $SF_3^{\oplus}$ = 100%) and numerous lighter fragments.

$F_5S-CH_2-SF_5$: A solution of $(SF_5)_2C{=}CF_2$ in an excess of water/tetraglyme (bis(2-(2-methoxylethoxy)ethyl)ether) was stirred for several days in a closed

system at room temperature. After vacuum distillation for quick separation of tetraglyme and most of the water the volatiles were distilled on a spinning band column. $F_5S-CH_2-SF_5$ was obtained in 70% yield as a colorless liquid, b.p. 67°C.—^{1}H-NMR: $\delta = 5.5$; ^{19}F-NMR: $\delta = 73.4$ (SF_{ax}), 69.2 (SF_{eq}); IR (gas): strong bands at $\tilde{\nu} = 934$, 863, 752, 655, 598 cm^{-1}; MS: m/z 249 ($[M-F]^{\oplus}$, 11% referred to $SF_5^{\oplus} = 100\%$) and lighter fragments.

$F_5S-C\equiv SF_3$: $F_5S-CH_2-SF_5$ was passed, in amounts of 1-3 g, through a glass tube filled with KOH at 80°C. The reaction products were frozen out with liquid nitrogen. NMR mointoring revealed completion of the reaction. $F_5S-C=SF_5$ was obtained as colorless gas in ca. 30% yield, m.p. −130°C, b.p. above room temperature (extrapolated).—^{19}F-NMR: AB_4C_3 spectrum, $\delta_A = 75.9$, $\delta_B = 96.9$, $\delta_C = 61.3$, $J_{AB} = 154$, $J_{BC} = 22$ Hz; IR (gas): strong bands at $\tilde{\nu} = 1717$ ($\nu_{C=S}$), 1150, 926, 897, 784, 692, 610, 564 cm^{-1}; MS: m/z 227.9306 ($M^{\oplus}$); calcd. for $CS_2F_8^{\oplus}$: 227.9314.

Received: June 3, 1988 [Z 2880 IE]
German version: *Angew. Chem. 100* (1988) 1592

CAS Registry numbers:
SF_5Cl, 13780-57-9; $CF_2=CHSF_5$, 58636-78-5; $(SF_5)_2CHCF_2Cl$, 109735-72-0; $(SF_5)_2C=CF_2$, 117146-24-4; $(SF_5)_2CH_2$, 117146-25-5; $F_5SC\equiv SF_3$, 117146-26-6.

[1] B. Pötter, K. Seppelt, A. Simon, E.-M. Peters, B. Hettich, *J. Am. Chem. Soc. 107* (1985) 980.
[2] D. Christen, H. G. Mack, C. J. Marsden, H. Oberhammer, G. Schatte, K. Seppelt, H. Willner, *J. Am. Chem. Soc. 109* (1987) 4009.
[3] J. Boggs, *Inorg. Chem. 23* (1984) 3577.
[4] D. E. Dixon, B. E. Smart, *J. Am. Chem. Soc. 108* (1986) 2688.
[5] Linearity seems to be a structural principle in heteroacetylenes of the type R–C≡P: according to spectroscopic and electron diffraction measurements F–C≡P and *t*Bu–C≡P are linear: H. W. Kroto, J. F. Nixon, N. P. C. Simmons, *J. Mol. Spectrosc. 82* (1980) 185; H. Oberhammer, G. Becker, G. Gresser, *J. Mol. Struct. 75* (1983) 283; in the crystal, 2,4,6-tBu$_3$C$_6$H$_2$–C≡P shows a bond angle of 177(1)°: A. M. Arif, A. R. Barron, A. H. Cowley, S. W. Hall, *J. Chem. Soc. Chem. Commun. 1988*, 171.
[6] T. Grelbig, T. Krügerke, K. Seppelt, *Z. Anorg. Allg. Chem. 544* (1987) 74.
[7] H. W. Sidebottom, J. M. Tedder, J. C. Walton, *Trans. Faraday Soc. 65* (1969) 2103.
[8] R. A. DeMarco, W. B. Fox, *J. Fluorine Chem. 12* (1978) 37.
[9] H. Shanan-Atidi, K. H. Bar-Eli, *J. Phys. Chem. 74* (1970) 961.
[10] Thus, $(CF_3)_2CH-COOH$ is formed on hydrolysis of $(CF_3)_2C=CF_2$: Y. A. Cheburkov, I. L. Knunyants, M. P. Krasuskaya, USSR-Pat. 129653 (1960); *Chem. Abstr. 55* (1961) P4364g.
[11] J. A. M. Cannich, M. M. Ludvig, W. W. Paudler, G. L. Gard, J. M. Shreeve, *Inorg. Chem. 24* (1985) 3668.
[12] Crystals grown, as described by P. Luger, J. Buschmann, *J. Am. Chem. Soc. 102* (1984) 7118, directly on a Siemens four-circle diffractometer; measurement of the diffraction intensities at −168°C. Space group $P2_13$ (No. 198), cubic, $a = 857(1)$ pm, $Z = 4$. 1964 reflections ($4° \le \theta \le 60°$), 360 independent reflections, 7 reflections $I < 2\sigma(I)$, $R = 0.024$, $R_w = 0.022$. Corresponding to the infinite cylindrical shape of the crystal the reflection intensities were corrected as a function of θ and χ. Further details of the crystal structure investigation are available on request from the Fachinformationszentrum Energie, Physik, Mathematik GmbH, D-7514 Eggenstein-Leopoldshafen 2, on quoting the depository number CSD-53347, the names of the authors, and the journal citation.

α-Methylene-β-lactone, a Novel Heterocyclic Ring System via Deoxygenation of α-Methylene-β-peroxylactones with Triphenylphosphane**

By *Waldemar Adam,* Ludwig Hasemann,* and *Frank Prechtl*

Aldolketene dimers, 4-methyleneoxetan-2-ones **1**, belong to a well established heterocyclic ring system that is readily accessible by dimerization of aldehydic ketenes.[1] Surprisingly, however, no examples of the isomeric 3-methyleneoxetan-2-ones **2** have thus far been reported. This is especially puzzling in view of the high degree of functionality contained in this as yet unknown heterocyclic ring system, which should lend itself to diversified synthetic utilization.

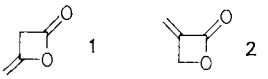

For example, besides the usual electrophilic sites of the carbonyl and oxetane carbon atoms contained in β-lactones, Michael-type additions of nucleophiles and radicals at the methylene carbon atom are feasible and offer attractive possibilities for preparative purposes. Moreover, the carboxy-activated exomethylene double bond should serve as reactive dienophile, while the α,β-unsaturated carbonyl moiety promises potential as heterodiene for [4+2] cycloadditions. Finally, on thermolysis the 4-methyleneoxetan-2-ones **1** suffer retrocleavage to aldoketenes, while in the case of 3-methyleneoxetan-2-ones **2** decarboxylation to allenes is expected; thus, such α-methylene-β-lactones could represent allene equivalents.

We have already shown that trivalent phosphorus nucleophiles are effective reagents for the deoxygenation of cyclic peroxides. Thus, the β-peroxy lactones **3** afford the β-lactones **4**[2] and the malonyl peroxides **5** the anhydrides **6**[3] on treatment with triphenylphosphane. It was, therefore, anticipated that the recently discovered α-methylene-β-peroxylactones **8**[4] should constitute convenient precursors for the desired α-methylene-β-lactones **9** under these reaction conditions. That this is indeed the case is demonstrated by reaction (a), which now provides a convenient entry to the versatile 3-methyleneoxetan-2-ones **9**.

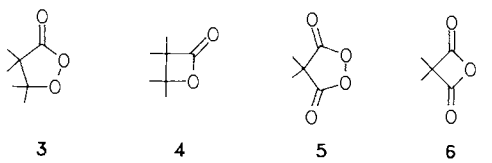

3 4 5 6

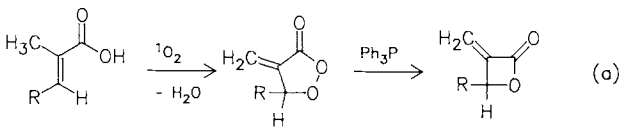

7 8 9

a, R = Me; b, R = Et; c, R = *i*Pr

The methacrylic acid derivatives **7a–c** were prepared by Wittig-Horner reaction of α-bromopropionic acid with the corresponding aldehydes.[5] The photosensitized oxygenation of **7** was carried out in chloroform at −5 to 0°C with tetraphenylporphine as sensitizer, and afforded the hydroperoxy acrylic acids as ene products essentially quantitatively. These were cyclized with catalytic amounts of concentrated sulfuric acid to the α-methylene-β-peroxylactones **8a–c** in 70, 57 and 50% yields, respectively. Satisfactory elemental analyses, appropriate spectral data (IR, ^{1}H- and ^{13}C-NMR, MS), and peroxide tests support the structure assignments for the peroxides **8**, of which the methyl derivative **8a** was already known.[4]

The oxygen extrusion from **8** was achieved with equimolar amounts of triphenylphosphane in chloroform at

[*] Prof. Dr. W. Adam, Dipl.-Chem. L. Hasemann, F. Prechtl
Institut für Organische Chemie der Universität
Am Hubland, D-8700 Würzburg (FRG)

[**] This work was supported by the Deutsche Forschungsgemeinschaft (SFB 172, Molekulare Mechanismen kanzerogener Primärveränderungen) the Fritz-Thyssen Stiftung, the Sander-Stiftung, and the Fonds der Chemischen Industrie.

$-40\,^{\circ}C$. Slow warm-up to room temperature, column chromatographic work-up (silica gel flash chromatography, elution with a 10:1:1 mixture of dichloromethane, petroleum ether (30–50 °C) and diethyl ether), and Kugelrohr distillation (bath temperature 45 °C at 0.1 torr) afforded the α-methylene-β-lactones **9a–c** in 27, 48 and 40% yields, respectively, as pale yellow liquids with a pungent odor. Satisfactory elemental composition (**9a** exact mass by mass spectrometry and **9b**, **c** combustion analyses) and appropriate spectral data (IR; ^{1}H- and ^{13}C-NMR, MS) substantiate the proposed 3-methyleneoxetan-2-one structures for **9**. Significant in this context is that the position of the IR absorption of the exo −C=C− bond in **8** and **9** remained essentially constant at $\tilde{\nu}=1700$–$1710\ cm^{-1}$, while the carbonyl stretching frequency underwent the expected hypsochromic shift from $\tilde{\nu}=1790$–$1795\ cm^{-1}$ in **8** to $\tilde{\nu}=1820$–$1825\ cm^{-1}$ in **9**.

As anticipated, preliminary results of reactions with **9** reveal that the α-methylene-β-lactones are highly reactive. For example, **9a** reacts as dienophile nearly quantitatively with cyclopentadiene, yielding a diastereomeric mixture of [4+2]-cycloadducts. At elevated temperatures (ca. 60 °C), this highly activated heterocyclic ring system readily polymerizes. The chemistry of these potentially useful building blocks should be of general interest. In view of the high genotoxicity of the analogous α-methylene-γ-butyrolactones, which are naturally occurring biologically active compounds,[6] the potential carcinogenic behavior of this novel class of heterocyclics should be checked.

Received: July 18, 1988 [Z 2865 IE]
German version: *Angew. Chem. 100* (1988) 1594

CAS Registry numbers:
7a, 13201-46-2; **7b**, 3142-72-1; **7c**, 66634-97-7; **8a**, 99268-56-1; **8b**, 117203-14-2; **8c**, 117203-15-3; **9a**, 117203-16-4; **9b**, 117203-17-5; **9c**, 117203-18-6.

[1] Y. Etienne, N. Fischer in A. Weissberger (Ed.): *The Chemistry of Heterocyclic Compounds, Vol. 19 Part II*, Wiley, New York 1964, p. 729–884.
[2] W. Adam, N. Narita, Y. Nishizawa, *J. Am. Chem. Soc. 106* (1984) 1843.
[3] W. Adam, J. W. Diehl, *J. Chem. Soc. Chem. Commun. 1972*, 797.
[4] W. Adam, A. Griesbeck, *Angew. Chem. 97* (1985) 1071; *Angew. Chem. Int. Ed. Engl. 24* (1985) 1070.
[5] D. R. Britelle, *J. Org. Chem. 46* (1981) 2514.
[6] H. M. R. Hoffmann, J. Rabe, *Angew. Chem. 97* (1985) 96; *Angew. Chem. Int. Ed. Engl. 24* (1985) 94.

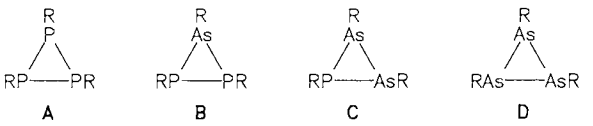

$$K(R^1)E^1\text{–}E^1(R^1)K + Cl_2E^2R^2 \longrightarrow \underset{R^1E^1\text{—}E^1R^1}{\overset{R^2}{\overset{E^2}{\triangle}}} + 2\ KCl \qquad (a)$$

R^1, R^2 = *t*Bu; E^1, E^2 = P, As

Herein we report on an alternative route to diphosphaarsiranes **B** and phosphadiarsiranes **C** and on the X-ray structure analysis of the substituted diphosphaarsirane **4**. Contrary to other findings,[6] 2,4,6-tBu$_3$C$_6$H$_2$AsCl$_2$ **2**, the required reactant, is readily formed from 2,4,6-tBu$_3$C$_6$H$_2$Li and $AsCl_3$ in THF/hexane.

The bis(trimethylsilyl)phosphidoiron complex **1**[7] reacts with **2** in THF at 0 °C [Eq. (b)] to give the red-violet diphosphaarsirane **4** (10% yield), which can be separated from the orange phosphadiarsirane **5** (5% yield) and the diphosphadiarsetane **6** (27% yield) by fractional crystallization. Further, the presence of the P=As complex **3** in the reaction solution can be shown by ^{31}P NMR spectroscopy ($\delta=765.7$, s); it could not be isolated, however.

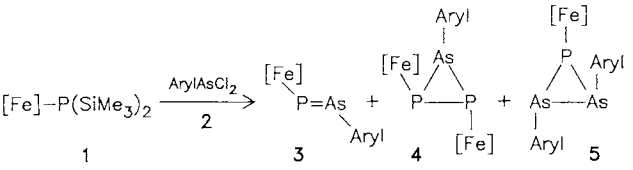

(b)

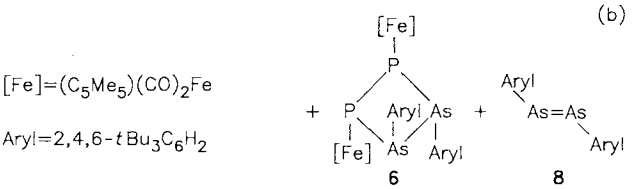

$$[((Z)\text{-}C_8H_{14})Cr(CO)_5] + \mathbf{3} \longrightarrow \underset{(CO)_5Cr}{\overset{[Fe]}{\overset{}{\triangle}}}P{=}As\text{—}Aryl + (Z)\text{-}C_8H_{14} \qquad (c)$$

7

Synthesis and Molecular Structure of the Diphosphaarsirane [{[(η^5-C$_5$Me$_5$)(CO)$_2$Fe]P}$_2$AsC$_6$H$_2$*t*Bu$_3$]**

By *Lothar Weber,* Dagmar Bungardt, Uwe Sonnenberg,* and *Roland Boese*

The study of small rings is currently a focus of interest in inorganic chemistry.[1] In the last few years, for example, *Baudler* et al. have explored the ring systems **A**–**D**.[2–5] In general, the compounds were synthesized by cyclocondensation [Eq. (a)].

On the other hand, treatment of the reaction solution with [((*Z*)-C_8H_{14})Cr(CO)$_5$][8] in excess prior to workup allows complex **7** to be isolated in 32% yield [Eq. (c)]. Since **6** is formed here in 31% yield, it is probably not produced by dimerization of **3**. In these experiments it was also possible to isolate chromatographically the previously unknown diarsene **8** (2% yield).

The constitutions and configurations of **4**–**8** were established from the elemental analyses and the spectroscopic data. Doublets at $\delta=6.4$ and 40.6 ($^1J(PP)=227$ Hz) in the ^{31}P NMR spectrum of **4** as well as two ^{1}H NMR signals for the protons of the C_5Me_5 ligands are in agreement only with the relative *trans* orientation of the substituents on the P atoms and rule out more highly symmetric structures.

The ^{31}P NMR spectra of the heterocycles **5** and **6** show singlets at $\delta=24.3$ and 87.7, respectively, whereas the ^{31}P NMR resonance of **7** ($\delta=616.3$) is markedly shifted upfield relative to **3** ($\Delta\delta(^{31}P)=-149.4$ ppm). The ν(CO) region in the IR spectrum of **7** features seven sharp bands, which, with respect to position and

[*] Prof. Dr. L. Weber [+], Dipl.-Chem. D. Bungardt, U. Sonnenberg, Dr. R. Boese
Institut für Anorganische Chemie der Universität
Universitätsstrasse 5-7, D-4300 Essen 1 (FRG)
[+] Present address:
Fakultät für Chemie der Universität
Postfach 8640, D-4800 Bielefeld (FRG)

[**] This work was supported by the Fonds der Chemischen Industrie, the Deutsche Forschungsgemeinschaft, and BASF AG, Ludwigshafen (FRG).

intensity, are identical with those observed for the complex $[\{(C_5Me_5)(CO)_2Fe\}P\{Cr(CO)_5\}=PAryl]$[9] and the complex $[\{(C_5Me_5)CO)_2Fe\}As\{Cr(CO)_5\}=PAryl]$,[10] thus indicating a similar σ-donor/π-acceptor relationship of the ligands $[\{(C_5Me_5)(CO)_2Fe\}E^1=E^2Aryl]$ (E^1, E^2 = P, As) toward the $Cr(CO)_5$ group. In the mass spectra (EI) of **4** and **5**, the peaks with the largest *m/z* value correspond to the molecular ions, whereas the molecular ion peak of **6** was not observed under comparable conditions. In the FD mass spectrum of **6**, the molecular ion of **3** produces the peak of greatest intensity. An additional signal at *m/z* = 918 (37%) is assigned to **5**. The facile fragmentation of **6** to **3** and **5** is possibly due to the very bulky substituents.

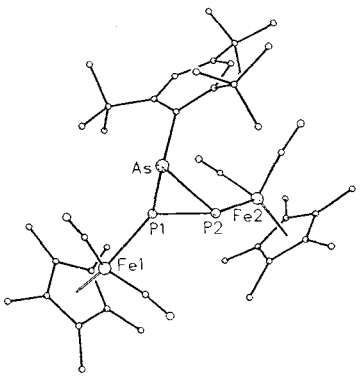

Fig. 1. Molecular structure of **4**. Selected bond lengths [Å] and angles [°]: As-P1 2.316(1), As-P2 2.350(2), P1-P2 2.207(2), As-C 2.010(6), Fe1-P1 2.373(2), Fe2-P2 2.326(2); P1-As-P2 56.5(1), As-P1-P2 62.5(1), As-P2-P1 61.0(1), P1-As-C 105.8(1), P2-As-C 104.5(2), As-P1-Fe1 110.5(1), P2-P1-Fe1 117.1(1), As-P2-Fe2 124.6(1), P1-P2-Fe2 105.3(1).

The X-ray structure analysis of **4** is of particular importance[11] since there is little available structural information on molecules containing As–P bonds[12] and such data are fully lacking for As–P three-membered rings. The basic framework of the molecule consists of an AsP_2 triangle in which the As–P2 bond (2.350(2) Å), with the substituents in *cis* orientation, is slightly lengthened compared with the As–P1 bond (2.316(1) Å). The P–P bond lengths (2.207(2) Å) correspond to the normal value.[13] As expected, the endocyclic angle at the As atom (56.5(1)°) is smaller than those at the phosphorus centers (61.0(1)° and 62.5(1)°).

The $[(\eta^5\text{-}C_5Me_5)(CO)_2Fe]$ groups on P1 and P2 are oriented in a *trans* fashion. The steric bulk of the substituents on the AsP_2 framework results in markedly increased exocyclic bond angles at P1 (110.5°, 117.1°) and P2 (124.6°, 105.3°).

Experimental procedure

NMR spectra recorded in C_6D_6 at 22°C; ^1H NMR, 200 MHz; IR spectra recorded in cyclopentane.

2: A 2.5 M solution of *n*-butyllithium in hexane (23 mL) was added dropwise to a solution of 1-bromo-2,4,6-tri-*tert*-butylbenzene (18.1 g, 55.6 mmol) in THF (250 mL). After stirring for 1 h at −50°C, the reaction mixture was cooled to −70°C and treated dropwise with $AsCl_3$ (4.7 mL, 55.6 mmol). The green reaction solution was evaporated to dryness (−30°C) and the residue was dissolved in *n*-pentane (150 mL), the resulting solution filtered, and the filtrate concentrated until the onset of crystallization. Colorless crystalline needles formed at −28°C and were recrystallized from *n*-pentane. Yield 5.3 g (24%) **2**. ^1H NMR: δ = 1.15 (s, 9H, *p*-*t*Bu), 1.51 (s, 18H, *o*-*t*Bu), 7.44 (s, 2H, aryl). EI-MS: *m/z* 390 ($M^{\oplus}$).

4–**6**: A solution of **1** (1.40 g, 3.30 mmol) [7] in THF (30 mL) at 0°C was treated with **2** (1.29 g, 3.30 mmol), resulting in a spontaneous change in color from red-brown to dark green. The reaction mixture was stirred for an additional 5 min at 20°C and then evaporated to dryness. The solution of the residue in 20 mL of ether afforded red-violet crystals of **4** at −28°C (0.14 g, 10%). ^1H NMR: δ = 1.39 (s, 9H, *p*-*t*Bu), 1.53 (s, 15H, C_5Me_5), 1.67 (s, 15H, C_5Me_5), 1.98 (s, 18H, *o*-*t*Bu), 7.35 (s, 2H, aryl). $^{31}P\{^1H\}$ NMR (AB spectrum): δ_A = 6.4 (P1), δ_B = 40.6 (P2), *J*(AB) = 227 Hz. IR (CO): $\tilde{\nu}$ = 1994 (m), 1988 (s), 1948 (s), 1945 (s) cm^{-1}. EI-MS: *m/z* 876 ($M^{\oplus}$). On concentration of the mother liquor to ca. 15 mL, 0.07 g (5%) of **5**, m.p. 157°C (dec.), was obtained. ^1H NMR: δ = 1.36 (s, 18H, *p*-*t*Bu), 1.58 (s, 15H, C_5Me_5), 1.65 (s, 36H, *o*-*t*Bu), 7.26 (s, 4H, aryl). $^{31}P\{^1H\}$ NMR: δ = 24.2 (s); IR (CO): $\tilde{\nu}$ = 1992 (vs), 1980 (w), 1949 (vs), 1939 (w) cm^{-1}. EI-MS: *m/z* 917 ($M^{\oplus}$). The green mother liquor was concentrated to ca. 5 mL and allowed to stand overnight at −28°C, thereby affording 0.54 g (27%) of dark green crystals of **6**, m.p. 133°C (dec.). ^1H NMR: δ = 1.36 (s, 18H, *p*-*t*Bu), 2.10 (s, 18H, *o*-*t*Bu), 7.36 (AB spectrum, J_{AB} = 2 Hz, 2H, aryl), 7.55 (AB spectrum, J_{AB} = 2 Hz, 2H, aryl). $^{31}P\{^1H\}$ NMR: δ = 87.7 (s); IR (CO): $\tilde{\nu}$ = 1983 (vs), 1947 (s), 1931 (m) cm^{-1}. FD-MS: *m/z* 598 ($[(\eta^5\text{-}C_5Me_5)(CO)_2Fe\text{–}P{=}As\text{–}Aryl]^{\oplus}$, 100%).

7: After a reaction time of 5 min, the solution of **1** (3.14 g, 7.40 mmol) and **2** (2.90 g, 7.40 mmol) in THF (50 mL) was treated with 80 mL of a photochemically freshly prepared solution of $[((Z)\text{-}C_8H_{14})Cr(CO)_5]$ (10.00 mmol) in hexane. After stirring for 1 h at 20°C, the reaction solution was evaporated to dryness and the solid residue was chromatographed (Al_2O_3 Woelm TSC); column, *d* = 5 cm, *l* = 25 cm). Elution with petroleum ether gave an orange zone containing 0.05 g of **8** (2%). Subsequent elution with a mixture of petroleum ether and ether (5 : 1) gave a dark green zone, from which 1.36 g (31%) of **6** could be isolated. A red fraction followed which contained 1.88 g (32%) of red **7**, m.p. 184°C (dec.). ^1H NMR: δ = 1.38 (s, 9H, *p*-*t*Bu), 1.47 (s, 15H, C_5Me_5), 1.71 (s, 18H, *o*-*t*Bu), 7.65 (s, 2H, aryl). $^{31}P\{^1H\}$ NMR: δ = 616.3 (s). IR: $\tilde{\nu}$ = 2061 (s), 1986 (w), 1946 (vs), 1938 (s), 1925 (s) [Cr(CO)], 2018 (s), 1973 (s) cm^{-1} [Fe(CO)]. EI-MS: *m/z* 790 ($M^{\oplus}$).—**8**: m.p. 173°C; ^1H NMR: δ = 1.34 (s, 18H, *p*-*t*Bu), 1.50 (s, 36H, *o*-*t*Bu), 7.64 (s, 4H, aryl). EI-MS: *m/z* 640 ($M^{\oplus}$).

Received: May 31, 1988 [Z 2795 IE]
German version: *Angew. Chem. 100* (1988) 1595

CAS Registry numbers:
1, 9601-32-0; **2**, 117184-75-7; **3**, 117184-70-0; **4**, 117184-71-1; **5**, 117184-72-2; **6**, 117184-73-3; **7**, 117184-74-4; **8**, 117184-76-6; $[(Z)\text{-}C_8H_{14}]Cr(CO)_5$, 92889-73-1; $(Z)\text{-}C_8H_{14}$, 931-87-3.

[1] Reviews: a) M. Baudler, *Pure Appl. Chem. 52* (1980) 755; *Angew. Chem. 94* (1982) 520; *Angew. Chem. Int. Ed. Engl. 21* (1982) 492; *Z. Chem. 24* (1984) 352; b) H. W. Roesky, M. Witt, *Rev. Inorg. Chem. 4* (1982) 45.
[2] a) M. Baudler, J. Hahn, H. Dietsch, G. Fürstenberg, *Z. Naturforsch. B 31* (1976) 1305; b) M. Baudler, B. Makowka, *Z. Anorg. Allg. Chem. 528* (1985) 7.
[3] M. Baudler, S. Klautke, *Z. Naturforsch. B 36* (1981) 527.
[4] M. Baudler, D. Habermann, *Angew. Chem. 91* (1979) 939; *Angew. Chem. Int. Ed. Engl. 18* (1979) 877.
[5] M. Baudler, P. Bachmann, *Angew. Chem. 93* (1981) 112; *Angew. Chem. Int. Ed. Engl. 20* (1981) 123.
[6] A. H. Cowley, J. G. Lasch, N. C. Norman, M. Pakulski, *J. Am. Chem. Soc. 105* (1983) 5506.
[7] L. Weber, K. Reizig, R. Boese, *Chem. Ber. 118* (1985) 1193.
[8] F.-W. Grevels, V. Skibbe, *J. Chem. Soc. Chem. Commun. 1984*, 681.
[9] L. Weber, G. Meine, R. Boese, D. Bläser, *Chem. Ber. 121* (1988) 853.
[10] L. Weber, D. Bungardt, R. Boese, *Chem. Ber. 121* (1988) 1535.
[11] **4**: monoclinic, *Pn*, *a* = 11.182(1), *b* = 16.134(2), *c* = 13.017(1) Å, β = 114.73(1)°, *V* = 2133.0(4) Å^3, *Z* = 2, ρ_{calcd} = 1.365 g cm^{-3}, $Mo_{K\alpha}$ radiation, scan range $3° \le 2\theta \le 55°$, 5042 unique reflections, 4854 observed reflections ($F_o \ge 4\sigma(F_o)$), 228 refined parameters, R = 0.051, R_w = 0.056, $w^{-1} = \sigma^2(F_o) + 0.00152 \cdot F_o^2$.
[12] a) L. Weber, D. Bungardt, R. Boese, D. Bläser, *Chem. Ber. 121* (1988) 1033; b) M. Baudler, Y. Aktalay, T. Heinlein, K.-F. Tebbe, *Z. Naturforsch. B 37* (1982) 299; c) W. S. Sheldrick, *Acta Crystallogr. 4, Sect. B 31* (1975) 1789.
[13] K.-F. Tebbe, *Z. Anorg. Allg. Chem. 468* (1980) 202, and references cited therein.

Carbon as Leaving Group—Stereochemistry of Nucleophilic Substitution

By *Wolfgang Kirmse** and *Klaus Zander*

Dedicated to Professor Günther Snatzke on the occasion of his 60th birthday

Grob's cationic fragmentation[1] can be regarded as the reverse of electrophilic addition to alkenes or—referred to

[*] Prof. Dr. W. Kirmse, Dr. K. Zander
Fakultät für Chemie der Universität
Postfach 102148, D-4630 Bochum 1 (FRG)

C-3—as nucleophilic substitution. Whereas an antiperiplanar arrangement of the C-X and C-2-C-3 bonds is known to be a prerequisite for many fragmentations,[1] the stereochemistry at C-3 has, to our knowledge, not yet been investigated. Frequently, the fragmentation is supported by donor substituents (NR_2, OR) on C-3; it then leads to planar, resonance-stabilized fragment ions (route a in Scheme 1). Our studies are concerned with bicyclic educts whose fragmentation is promoted by the release of ring strain.

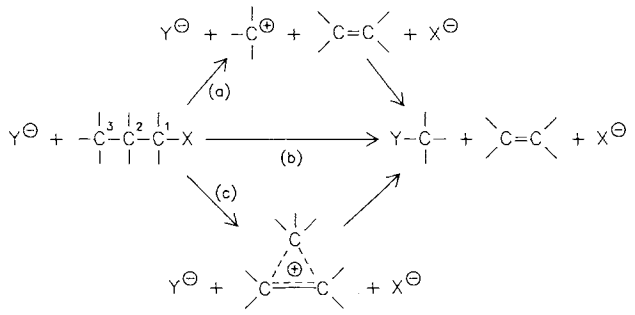

Scheme 1.

In the bicyclo[2.2.1]heptane[2-4] and bicyclo[3.1.1]heptane series,[5] fragmentation takes place only with a peralkylated carbon atom as electrofugal group and with *endo*(*trans*) position of X. Suitably labeled starting compounds for our studies were obtainable from the known lactones **1**[6] and **2**[7] by stepwise reduction[8] with $LiAlD_4$ (Scheme 2). The diazonium ions **5** and **6**, (*exo,endo* mixtures, only the *endo*-diazonium ions fragment[2-5]) were generated from the tosylhydrazones **3b/4b** of the ketones **3a/4a**, respectively, by irradiation in aqueous sodium hydroxide. The ring-opening product **7** (9% from **3b**, 15% from **4b**) shows separate signals in its ^{1}H-NMR spectrum (400 MHz) for the diastereotopic methyl groups ($\delta = 1.12$ and 1.13), the intensities of which give the amounts of **7a** and **7b**, respectively. For the determination of the configuration, **7** was converted by epoxidation and base-induced ring-closure into **8**, whose methyl groups ($\delta = 1.10$ and 1.28) can be assigned by NOE measurements. **3b** preferentially affords **7a**, **4b** preferentially **7b**; both starting compounds chiefly react with inversion (Table 1).

The increased ring strain of the bicyclo[2.1.1]hexane skeleton facilitates fragmentations also with a secondary carbon atom as electrofugal group.[9] Reduction of the racemic ketone **9**[9,10] with fermenting yeast yielded the alcohols **10a** ($ee = 98\%$)[11] and **11a** ($ee = 66\%$) in the ratio 1.2 : 1 (Scheme 3). Reoxidation of **10a** and **11a** afforded enantiomeric ketones; the (1*R*,4*R*,5*R*)-configuration was assigned to the dextrorotatory ketone **9a** on the grounds of its positive circular dichroism.[12] Irradiations of the tosylhydrazone **9b** in aqueous sodium hydroxide and solvolysis of the brosylates **10b** and **11b** in acetone/water (3 : 2, 110 °C, 18 h) furnished product mixtures from which the ring-opening product **15** was separated; its configuration was determined by ring expansion (1. dibromocarbene; 2. hydrogenation) to the known (+)-(*S*)-**17**.[13] The configuration of the brosylate not only influences the yield of **15**

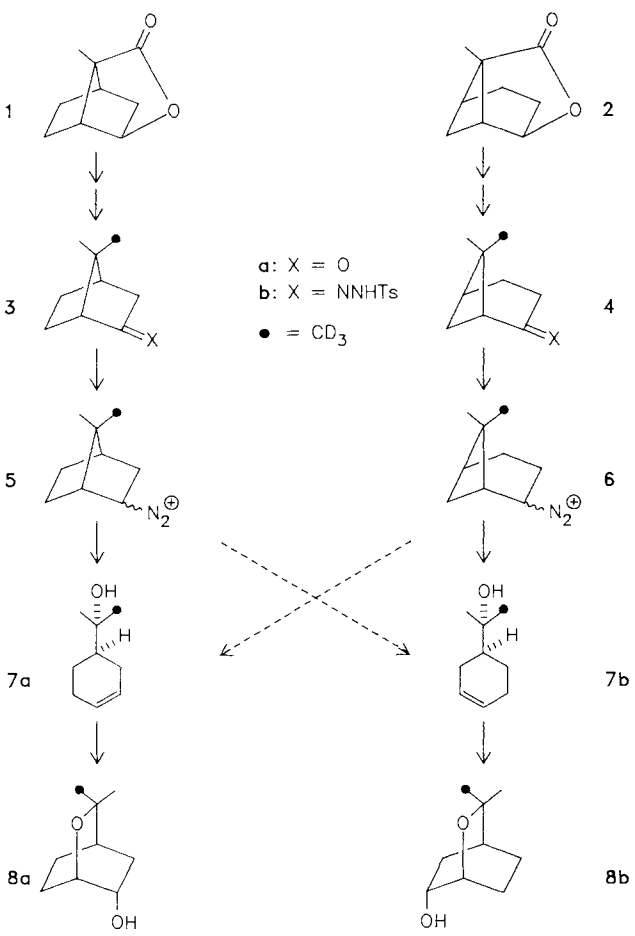

Scheme 2.

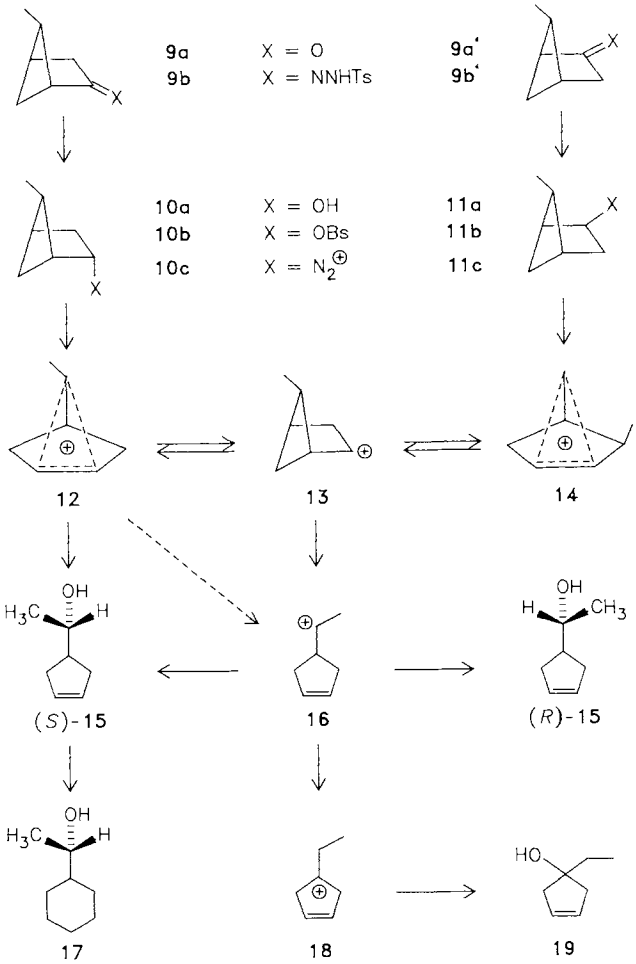

Scheme 3.

Table 1. Stereochemistry of the fragmentations.

Starting compound	Product	Inversion : Retention
3b	**7**	81 : 19
4b	**7**	75 : 25
9b	**15**	88 : 12
10b	**15**	93 : 7
11b	**15**	79 : 21

(**10b**: 36%, **11b**: 9%), but also its enantiomeric purity (Table 1).[11] A 1:1 mixture of the epimeric diazonium ions (**10c**, *ent*-**11c**) is expected from the tosylhydrazone **9b**; the results (18% **15**) lie between those for **10b** and **11b**. **15** is always formed with pronounced inversion (Table 1).

The substitution reactions of the methylbicyclo-[2.1.1]hexane derivatives indicate the participation of bridged (e.g. **12** and **14**) and open carbocations (e.g. **13**).[9] The transformation **14** ⇄ **12** via **13** is probably the reason for the (inefficient) fragmentation of **11b**, despite the "wrong" position of the OBs group. The ring-opening with inversion to (*S*)-**15** can be ascribed to the bridged ion (π-complex) **12**, whereas racemic **15** is formed from **16**. Evidence for the occurrence of **16** is provided by the H-shift **16** → **18**, which leads to the tertiary alcohol **19**. The amount of **19** formed in the fragmentation reactions is, however, markedly smaller than in the direct generation of **16**. That **12** can be formed directly from **10b** but only indirectly (via **13**) from **11b** would explain the differences in yield and enantiomeric purity of **15** from the two processes.

The ring opening **5/6** → **7** can be formulated in an analogous way, whereby a 7-bridged norbornyl cation[14] is formed instead of **12**. The predominant but incomplete inversion indicates that the fragmentations investigated here are limiting cases of nucleophilic substitution. Such borderline cases (e.g. solvolyses of secondary alkylsulfonates) have been explained in terms of a competition between or "blending" of the mechanistic extremes (e.g. S_N1/S_N2).[15] In our opinion the observed stereoselectivity is best explained in terms of a competition of the fragmentation routes (a) and (c) in Scheme 1.[16]

Received: June 3, 1988 [2798 IE]
German version: *Angew. Chem. 100* (1988) 1596

CAS Registry numbers:
3b, 117408-44-3; **4b**, 117408-45-4; **7a**, 117408-49-8; **7b**, 117408-50-1; **8a**, 117408-53-4; **8b**, 117468-01-6; **9b**, 117408-46-5; **10b**, 117408-47-6; **11b**, 117408-48-7; (*R*)-**15**, 117408-52-3; (*S*)-**15**, 117408-51-2.

[1] Summary reviews: C. A. Grob, P. W. Schiess, *Angew. Chem. 79* (1967) 1; *Angew. Chem. Int. Ed. Engl. 6* (1967) 1; C. A. Grob, *ibid. 81* (1969) 543 and *8* (1969) 535; K. B. Becker, C. A. Grob in S. Patai (Ed.): *The Chemistry of Double-Bonded Functional Groups, Part 2*, Wiley, New York 1977, Chapter 8.
[2] W. Hückel, F. Nerdel, *Justus Liebigs Ann. Chem. 528* (1937) 57; W. Hückel, P. Rieckmann, *ibid. 625* (1959) 1; W. Hückel, H. J. Kern, *ibid. 728* (1969) 49.
[3] D. V. Banthorpe, D. G. Morris, C. A. Bunton, *J. Chem. Soc. B 1971*, 687.
[4] W. Kirmse, G. Arend, *Chem. Ber. 105* (1972) 2738; W. Kirmse, S. Brandt, *ibid. 117* (1984) 2510.
[5] H. Indyk, D. Whittaker, *J. Chem. Soc. Perkin Trans. 2 1974*, 646.
[6] R. M. Moriarty, C. C. Chien, T. B. Adams, *J. Org. Chem. 44* (1979) 2206.
[7] T. W. Gibson, W. F. Erman, *J. Am. Chem. Soc. 91* (1969) 4771.
[8] In both cases the reduction led first to the diol. The CD_2OH group of the diol from **1** could be selectively tosylated; renewed reduction of the tosylate generated the methyl group. In tosylation experiments the diol from **2** yielded the cyclic ether (**2**, CD_2 instead of C=O), which was cleaved reductively with LiAlD $(OtBu)_3/BEt_3$; cf. H. C. Brown, S. Krishnamurthy, *J. Am. Chem. Soc. 94* (1972) 1750.
[9] W. Kirmse, K. H. Kampmann, V. Zellmer, *Chem. Ber. 120* (1987) 1301.
[10] T. W. Gibson, W. F. Erman, *J. Org. Chem. 37* (1972) 1148; W. R. Roth, A. Friedrich, *Tetrahedron Lett. 1969*, 2607.
[11] The enantiomeric purity (*ee*) of the alcohols **10a**, **11a**, and **17** was determined by gas chromatography of their camphanates.
[12] G. Snatzke, U. Wagner, unpublished.
[13] K. Freudenberg, P. J. Todd, R. Seidler, *Justus Liebigs Ann. Chem. 501* (1933) 199.
[14] Review: W. Kirmse, *Acc. Chem. Res. 19* (1986) 36.
[15] Discussion and literature: J. March, *Advanced Organic Chemistry*, 3rd Edit., Wiley, New York 1985, p. 265; G. W. Klumpp: *Reaktivität in der Organischen Chemie*, Thieme, Stuttgart 1978, p. 443.
[16] We consider a participation of the completely concerted route (b) in Scheme 1 as unlikely. The contribution of (b) should increase with increasing ring strain (**5/6**) and with poorer leaving groups (**10b/10c**) and should increase the stereoselectivity. This was not observed.

Synthesis and Structure of [*cyclo*-C_3H_4–$SO_2Ph]_2Ti[OCH(CH_3)_2]_2$, a *C*-Titanated "α-Sulfonyl Carbanion"**

By *Hans-Joachim Gais,* Jürgen Vollhardt, Hans J. Lindner,* and *Helmut Paulus*

The titanation of heteroatom- or resonance-stabilized "carbanions" is a valuable instrument for control of selectivity.[1,2] However, little is known on the structures[3] of the titanium compounds formed.[1,2,4] Our investigations on the reactivity of titanated sulfones[2b] led us, therefore, to investigate their structure.[5]

Herein we report on the synthesis, crystal structure analysis, and characterization by NMR spectroscopy of the titanium compound **2**, which was generated from (phenylsulfonyl)cyclopropyllithium **1** and chlorotriisopropoxytitanium by Li–Ti exchange and crystallized from *n*-hexane. Crystalline **2** is stable at room temperature if protected from air and moisture.

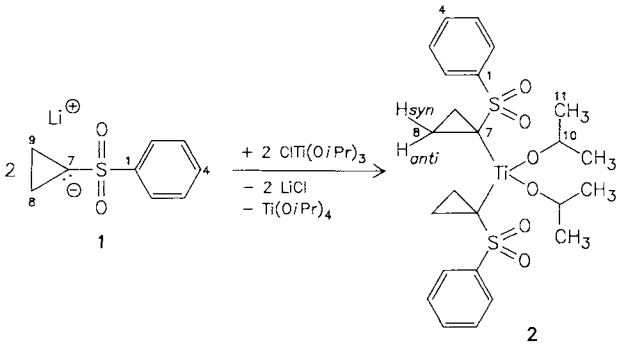

1 2

According to the crystal structure analysis,[6] **2** is a true diorganotitanium compound containing two enantiomeric (phenylsulfonyl)cyclopropyl moieties and displaying normal Ti–C distances (average value 2.177 Å) and short Ti–O*i*Pr bonds (average value 1.763 Å) (Fig. 1). Noteworthy is the observation that one O atom of each sulfonyl group is coordinated to the Ti atom, thereby extending the coordination number of the metal atom to 6. Evidence for the existence of the two O–S–C–Ti chelate rings and thus for

[*] Prof. Dr. H.-J. Gais, Dipl.-Ing. J. Vollhardt
Institut für Organische Chemie und Biochemie der Universität
Albertstrasse 21, D-7800 Freiburg (FRG)
Prof. Dr. H. J. Lindner
Institut für Organische Chemie der Technischen Hochschule
Petersenstrasse 22, D-6100 Darmstadt (FRG)
Dr. H. Paulus
Institut für Physikalische Chemie der Technischen Hochschule
Petersenstrasse 21, D-6100 Darmstadt (FRG)

[**] This work was supported by the Deutsche Forschungsgemeinschaft. We thank Prof. Dr. *G. Boche* for communication of unpublished results.

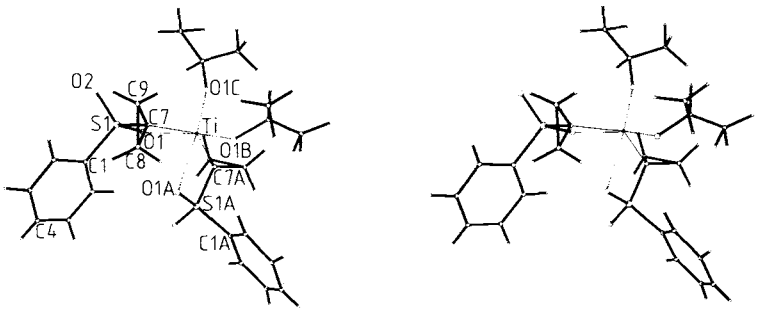

Fig. 1. Stereoview of the molecular structure of **2**. Selected distances [Å] and angles [°]: Ti-C7 2.181(3), Ti-C7A 2.174(4), C7-S1 1.725(4), C7A-S1A 1.719(4), C1-S1 1.779(4), C1A-S1A 1.759(4), S1-O1 1.476(2), S1-O2 1.445(3), C7-C8 1.503(5), C7-C9 1.497(6), C8-C9 1.466(6), Ti-O1B 1.771(3), Ti-O1C 1.755(2), Ti-O1 2.315(3), Ti-O1A 2.243(2); O1B-Ti-O1C 102.6(1), C7-Ti-C7A 139.7(1), Ti-C7-S1 95.9(2), Ti-C7A-S1A 95.0(2), Ti-C7-C8 124.7(3), Ti-C7-C9 135.3(3), C7-Ti-O1-S1 3.2, C7A-Ti-O1A-S1A 3.8, O1-S1-C7-C8 −133.8, O1-S1-C7-C9 156.6, O2-S1-C7-C8 101.2, O2-S1-C7-C9 31.6.

the binding of the titanium atom via a C *and* an O atom to the deprotonated sulfone is provided by the Ti-O1/O1A distances (average value 2.279 Å), the dihedral angles C-Ti-O-S (average value 3.5°), the conformation around C7-S1, the bond angles Ti-C-S (average value 95.4°), and the distortion of the tetrahedral coordination geometry at the Ti atom. The greater length of the S1-O1 bond compared with the S1-O2 bond also fits this description. For dilithiosulfones,[7] lithiosulfoximines,[8] and a phenylsulfonyl-substituted Sb ylide,[9] similar chelate rings were found in the crystal. The bond between the "carbanionic" C atom and the sulfonyl group in **2**, 1.722 Å (average value), is significantly longer than that (1.676(7) Å) in **3**,[10a] which, remarkably in contrast to other alkali-metal sulfones,[10b,c] exhibits a C-Li bond and a Li-C-S-O chelate ring in the crystal; **2** also does not have the C_α-S conformation of **3** required for an $n_C-\sigma^*_{SPh}$ interaction.[10b]

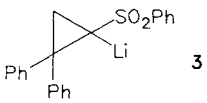

3

Table 1. ^1H and ^{13}C NMR data of **1** and **2** [a].

1: ^1H NMR (60 MHz, [D$_8$]THF, 25°C, 0.2 M, [D$_7$H]THF: δ(β-H) = 1.72): δ = 0.42 (d, ^2J(C7,8/9-H) = 2.0 Hz; 8-H, 9-H), 7.2 (m; 2-H, 6-H), 7.5 (m; 3-H, 4-H, 5-H); 400 MHz: δ = 0.43 (br. s; 8-H, 9-H), 7.33 (m; 3-H, 4-H, 5-H), 7.63 (m; 2-H, 6-H). ^{13}C NMR (100 MHz, [D$_8$]THF, 25°C, 0.2 M, [D$_8$]THF: δ(β-C) = 25.2): δ = 7.6 (s, ^{1+2}J(C7,C8/9) ≤ 1.4 Hz; C8, C9) [b], 28.5 (br. s, C7), 129.0, 128.1 (C2, C6, C3, C5), 130.2 (C4), 139.8 (br. s; C1) [c]

2: ^1H NMR (400 MHz, [D$_6$]benzene, 25°C, 0.3 M, [D$_5$H]benzene: δ = 7.16): δ = 1.24 (d, J = 6 Hz; 11-H), 1.27 (m; 8-H$_{anti}$, 9-H$_{anti}$) [d], 1.58 (m; 8-H$_{syn}$, 9-H$_{syn}$) [d], 4.86 (sept., J = 6 Hz; 10-H), 6.98 (m; 3-H, 4-H, 5-H), 8.25 (m; 2-H, 6-H). ^1H NMR (400 MHz, [D$_8$]THF, 25°C, 0.3 M, [D$_7$H]THF: δ(β-H) = 1.72): δ = 1.06 (m; 8-H$_{syn}$, 9-H$_{syn}$) [d], 1.29 (d, J = 6 Hz; 11-H), 1.43 (m; 8-H$_{anti}$, 9-H$_{anti}$) [d], 4.90 (sept., J = 6 Hz; 10-H), 7.50 (m; 3-H, 5-H), 7.60 (m; 4-H), 8.07 (m; 2-H, 6-H). ^{13}C-NMR (20 MHz, [D$_6$]benzene, 25°C, 0.3 M, [D$_6$]benzene: δ = 128.0): δ = 16.9 (C8, C9), 26.0 (C11), 52.4 (C7), 80.4 (C10), 128.63, 128.69 (C2, C6, C3, C5), 132.7 (C4), 140.5 (C1)

[a] *cyclo*-$C_3H_5SO_2Ph$: ^1H NMR (250 MHz, $CDCl_3$, TMS): δ = 1.04 (m, 8-H$_{anti}$, 9-H$_{anti}$), 1.36 (m, 8-H$_{syn}$, 9-H$_{syn}$), 2.48 (tt, J = 7.8, 4.3 Hz; 7-H), 7.57 (m; 3-H, 5-H), 7.65 (m; 4-H), 7.91 (m; 2-H, 6-H). ^{13}C NMR (100 MHz, $CDCl_3$, TMS): δ = 6.0 (C8, C9), 32.9 (C7), 127.6 (C2, C6), 129.3 (C3, C5), 133.4 (C4), 140.8 (C1). [b] For (1-trimethylsilylcyclopropyl)phenylsulfone and cyclopropylphenylsulfone, on the other hand, ^{1+2}J(C7,8/9) = 6.0 and 10.5 Hz, respectively. [c] Measured for [^{13}C,^{6}Li]-**1**. [d] AA'XX' system.

The ^1H and ^{13}C NMR spectroscopic data of **2** (Table 1) show that it, too, exists in solution as an organotitanium compound. Evidence is provided by the chemical shift of δ = 52.4 for the cyclopropyl C atom bearing the Ti atom and the diastereotopism of the cyclopropyl H atoms 8-H$_{syn}$/9-H$_{syn}$ and 8-H$_{anti}$/9-H$_{anti}$ manifested by the signals at δ = 1.06 and 1.43. In the ^{13}C NMR spectrum of the lithiosulfone **1**, on the other hand, the signal of the "carbanionic" C atom is found at δ = 28.5; no ^1J(^{13}C,^{6}Li) coupling is apparent down to −110°C and, owing to rapid (on the NMR time scale) inversion of this C atom and rotation of the SO_2Ph group,[11] only a broad signal at δ = 0.43 is found for the four cyclopropyl H atoms in the 400-MHz ^1H NMR spectrum (Table 1). The downfield shift of the signal for C7 upon exchange of lithium for titanium with formation of a C-Ti bond (**1** → **2**) is in agreement with expectations.[1a,4,12]

The lithium and titanium species **1** and **2**, respectively, differ markedly in their reactivity. Whereas **1** reacts rapidly with methyl iodide at −35°C in THF to give (1-methylcyclopropyl)phenylsulfone[14] (97%), **2** is not methylated under these conditions. Workup of **2** with CF_3COOD affords a C7-deuterated cyclopropylphenylsulfone. We made similar findings with other titanated sulfones.[2b] The existence of a titanium species **2** in solution with O-Ti bonds, but no C-Ti bonds, would be in poor agreement with the available spectroscopic and chemical findings.

Experimental Procedure

Cyclopropylphenylsulfone (632 mg, 3.47 mmol) was dissolved in 15 mL of water- and oxygen-free ether and treated at −80°C with 2.1 mL of a 1.67 M solution of *n*BuLi in *n*-hexane. The resulting suspension of **1** [15] was warmed to room temperature (RT) and then added dropwise to a solution of $ClTi(OiPr)_3$ (905 mg, 3.47 mmol) in 10 mL of water- and oxygen-free ether at −50°C. Upon warming to RT, dissolution takes place followed a short time later by precipitation of LiCl. After 1 h at RT, the reaction solution was filtered, the solvent was removed, and the residue was dissolved in 25 mL of water- and oxygen-free *n*-hexane by warming to 60°C. The hot solution was filtered and the filtrate cooled to 6°C, affording, after 5 h, **2** (630 mg, 69%) as colorless crystals.

Received: June 24, 1988 [Z 2822 IE]
German version: *Angew. Chem. 100* (1988) 1598

[1] a) M. T. Reetz, *Struct. React. 24* (1986) 1, and references cited therein; b) B. Weidmann, D. Seebach, *Angew. Chem. 95* (1983) 12; *Angew. Chem. Int. Ed. Engl. 22* (1983) 31.

[2] a) L. Widler, T. Weber, D. Seebach, *Chem. Ber. 118* (1985) 1329; b) J. Vollhardt, H.-J. Gais, K. L. Lukas, *Angew. Chem. 97* (1985) 607, 695; *Angew. Chem. Int. Ed. Engl. 24* (1985) 610, 696; c) M. T. Reetz, M. von Itzstein, *J. Organomet. Chem. 334* (1987) 85.

[3] Crystal structure investigations: a) benzyl Ti compound: J. W. Bassi, G. Allegra, R. Scordamaglia, G. Chioccola, *J. Am. Chem. Soc. 93* (1971) 3787; D. J. Brauer, H. H. Bürger, K. Wiegel, *J. Organomet. Chem. 150* (1978) 215; b) allyl Ti compound: R. B. Helmholdt, F. Jellinek, H. A. Martin, A. Vos, *Recl. Trav. Chim. Pays-Bas 86* (1967) 1263; c) P-ylide Ti compounds: W. Scharf, D. Neugebauer, U. Schubert, H. Schmidbaur, *Angew. Chem. 90* (1978) 628; *Angew. Chem. Int. Ed. Engl. 17* (1978) 601; H. Schmidbaur, R. Pichl, G. Müller, *ibid. 98* (1986) 572 and *25* (1986) 574; H. J. R. de Boer, O. S. Akkerman, F. Bickelhaupt, G. Erker, P. Czisch, R. Mynott, J. M. Wallis, C. Krüger, *ibid. 98* (1986) 641 and *25* (1986) 639.

[4] a) M. Bottrill, P. D. Gavens, J. W. Kelland, J. McMeeking in G. Wilkinson, F. G. A. Stone, E. W. Abel (Eds.): *Comprehensive Organometallic Chemistry, Vol. 3*, Pergamon, Oxford 1982, pp. 271-433; b) *Gmelin Handbuch: Titan-Organische Verbindungen, Bd. 1-4*, Springer, Berlin 1977-1984.

[5] Crystal structure investigations of sulfones with transition-metal elements on the α-C atom: a) palladium: L. Benchekroun, P. Herpin, M. Julia, L. Saussine, *J. Organomet. Chem. 128* (1977) 275; b) platinum: K. W. Chiu, J. Fawcett, W. Henderson, R. D. W. Kemmitt, D. R. Russell, *J. Chem. Soc. Dalton Trans. 1987*, 733; c) gold: G. Boche (Marburg), personal communication.

[6] Crystal structure data of **2**: $C_{24}H_{32}O_6S_2Ti$, $M_r = 528.5$, monoclinic, $P2_1/c$, $a = 9.483(1)$, $b = 9.704(1)$, $c = 29.831(4)$ Å, $\beta = 101.59(1)°$, $V = 2689.16$ Å^3, $\rho_{calcd} = 1.305$ g cm^{-3} for $Z = 4$, $\mu(Mo_{K\alpha}) = 4.65$ cm^{-1}, intensities measured at room temperature, STOE four-circle diffractometer, $Mo_{K\alpha}$ radiation, 4724 reflections measured, 3525 unique and 3037 observed with $|F_{hkl}| \geq 2\sigma(F)$, empirical absorption correction: $T_{min} = 0.661$, $T_{max} = 0.861$. Structure determination by direct methods (SHELX 86). Least-squares refinement, H positions assigned geometrically, then (except for CH_3 groups) refined. $R = 0.048$, $R_w = 0.049$ (SHELX 76). Further details of the crystal structure investigation may be obtained from the Fachinformationszentrum Energie, Physik, Mathematik GmbH, D-7514 Eggenstein-Leopoldshafen 2 (FRG), on quoting the depository number CSD-53371, the names of the authors, and the journal citation.

[7] H.-J. Gais, J. Vollhardt, H. Günther, D. Moskau, H. J. Lindner, S. Braun, *J. Am. Chem. Soc. 110* (1988) 978.

[8] a) H.-J. Gais, I. Erdelmeier, H. J. Lindner, J. Vollhardt, *Angew. Chem. 98* (1986) 914; *Angew. Chem. Int. Ed. Engl. 2* (1986) 938; b) H.-J. Gais, U. Dingerdissen, C. Krüger, K. Angermund, *J. Am. Chem. Soc. 109* (1987) 3775.

[9] G. Ferguson, C. Glidewell, D. Lloyd, S. Metcalfe, B. L. Ruhl, *J. Chem. Res. 1987*, 32.

[10] a) W. Hollstein, K. Harms, M. Marsch, G. Boche, *Angew. Chem. 100* (1988) 868; *Angew. Chem. Int. Ed. Engl. 27* (1988) 846; b) H.-J. Gais, J. Vollhardt, G. Hellmann, H. Paulus, H. J. Lindner, *Tetrahedron Lett. 29* (1988) 1259, and references cited therein; c) H.-J. Gais, J. Vollhardt, C. Krüger, *Angew. Chem. 100* (1988) 1108; *Angew. Chem. Int. Ed. Engl. 27* (1988) 1092.

[11] G. Boche, H. M. Walborsky in Z. Rappoport (Ed.): *The Chemistry of the Cyclopropyl Group, Vol. 1*, Wiley, New York 1987, p. 701, and references cited therein.

[12] Cf. ^{13}C NMR data (partial): a) $(PhSO_2CH_2)_2Ti(OiPr)_2$ [prepared from 2 equiv. of $LiCH_2SO_2Ph$ (100% ^{13}C-labeled at C7) and 1 equiv. of $Cl_2Ti(OiPr)_2$ at −30°C in THF] [20 MHz, [D$_8$]THF, −30°C, [D$_8$]THF: $\delta(\beta\text{-C}) = 25.3$]: $\delta = 59.4$ (^1J(C7,7-H) = 134 Hz, C7); b) $LiCH_2SO_2Ph$ [20 MHz, [D$_8$]THF, 25°C]: $\delta = 35.4$ (^1J(C7,7-H) = 139 Hz, C7) [13]; c) CH_3SO_2Ph (20 MHz, [D$_8$]THF): $\delta = 44.4$ (^1J(C7,7-H) = 138 Hz, C7).

[13] G. Chassaing, A. Marquet, *Tetrahedron 34* (1978) 1399.

[14] Y.-H. Chang, H. W. Pinnick, *J. Org. Chem. 43* (1978) 373.

[15] H. E. Zimmerman, B. S. Thyagarajan, *J. Am. Chem. Soc. 82* (1960) 2505.

Use of the CH Acidity of 2,4,4-Trimethyl-4,5-dihydrooxazole to Synthesize Triauriomethanes and Novel Gold Clusters**

By *Franz Scherbaum, Brigitte Huber, Gerhard Müller,* and *Hubert Schmidbaur**

Gold forms numerous organometallic compounds, those with discrete Au–C σ bonds dominating by far. However, π complexes of this element are rare and usually of low stability.[1] In this respect, gold shows similarities to the organometallic chemistry of the neighboring elements mercury and thallium.[2] A unique feature of organometallic compounds of gold, on the other hand, is the existence of surprisingly strong bonding interactions between two-coordinate gold atoms with a d^{10} electron configuration. In the case of *intra*molecular bonding forces between polynuclear compounds, for example, certain conformations are favored.[3] For mononuclear gold complexes or polynuclear analogues having an unfavorable relative arrangement of the metal atoms, *inter*molecular interactions occur.[4] These as yet poorly understood phenomena, which are at least in part due to relativistic effects, should become particularly pronounced when many gold atoms are bonded to one common center. For this reason, we have attempted, inter alia,[5] to synthesize polyauriomethanes whose structures and properties could provide further insight into the nature and consequences of secondary Au···Au interactions.

Polyauriomethanes are formed particularly readily from substrates containing CH-acidic groups.[6] For instance, the only *tri*auriomethane so far known is derived from ylide-forming phosphonium salts.[7] Accordingly, we have now succeeded in generating a triauriomethane derivative by exploiting the CH acidity of 2-methyl-4,5-dihydrooxazoles.[8] However, the new product, generated in a very unusual way (Scheme 1), exhibited a surprisingly high acceptor strength for further Au^I ions, which led to the formation of a novel cluster containing exclusively metal atoms in the oxidation state +I.

The synthesis starts from 2,4,4-trimethyl-4,5-dihydrooxazole **1**: Trilithiation followed by derivatization with chlorotrimethylsilane gives the open-chain, triply silylated ketenimine **2** (Scheme 1). Without further purification, **2** can react with four equivalents of triphenylphosphanegold(I) chloride in hexamethylphosphoric triamide (HMPT) at 20°C in the presence of cesium fluoride to give the yellow-orange gold cluster **3** in nearly quantitative yield. The analytical and spectroscopic data of the product corresponded in no way to those expected for **4**. In solution, however, **3** decomposes to **4**, thereby indicating that **4** is a component of **3**.

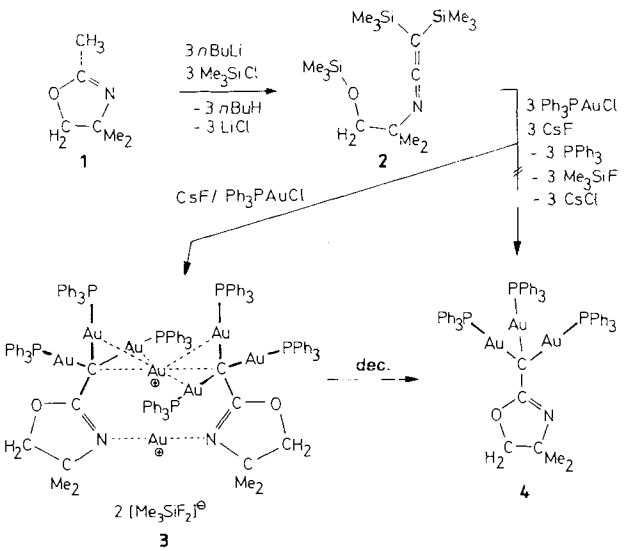

Scheme 1.

The X-ray structure analysis[9] of **3** allowed not only the elucidation of the structure of the cluster cation, but also revealed the presence of the likewise unexpected trimethyldifluorosilicate anions. Although this anionic species has been described,[10] it is difficult to characterize spectroscopically owing to rapid exchange processes.

The cation possesses a crystallographic twofold axis (through the gold atoms Au4 and Au5, Fig. 1). The central

[*] Prof. Dr. H. Schmidbaur, Dipl.-Chem. F. Scherbaum, Dipl.-Chem. B. Huber, Dr. G. Müller
Anorganisch-chemisches Institut der Technischen Universität München
Lichtenbergstrasse 4, D-8046 Garching (FRG)

[**] This work was supported by the Deutsche Forschungsgemeinschaft (Leibniz program), the Fonds der Chemischen Industrie, and Degussa AG. We thank *J. Riede* for measurement of the crystallographic data set and Finnigan MAT for an FAB-MS measurement.

C atom of each moiety (C1, C1′) was originally the methyl C atom of the dihydrooxazole (in position 2). The heterocycle, which is opened in going to **2**, is once again closed in the course of the polyauration. Apparently, the molecules **4**, thereby formed, efficiently bind further Au^I ions. In this process, the formation of a bridge (N3-Au4-N3′) involving the two N atoms of the dihydrooxazole rings and an Au^I ion is less surprising than the unprecedented binding of an Au^I ion, Au5, to the triangles defined by C1-Au1-Au3 and C1′-Au1′-Au3′. The $RC(AuL)_3$ molecule thus proves to be "aurophilic".[12]

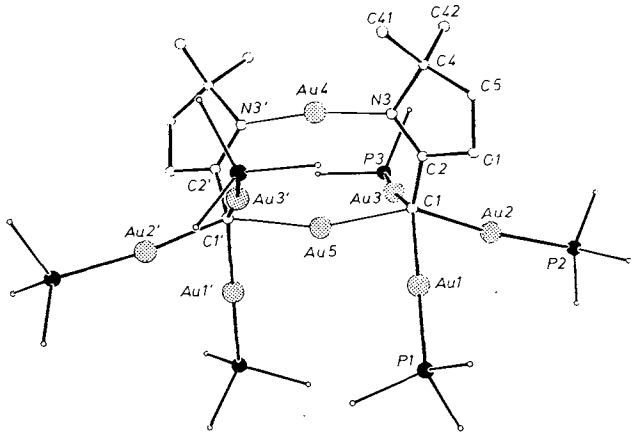

Fig. 1. Molecular structure of the dicationic gold cluster **3** (ORTEP, arbitrary radii). A twofold axis through Au4 and Au5 lies in the plane of the paper. Only the C_{ipso} atoms of the phenyl groups are shown. Selected bond lengths [Å] and angles [°]: C1-Au1 2.12(1), C1-Au2 2.16(1), C1-Au3 2.12(1), C1-Au5 2.22(1), N3-Au4 1.99(1), Au1-P1 2.265(5), Au2-P2 2.273(5), Au3-P3 2.259(4), C1-C2 1.50(2); C2-C1-Au1 117.7(9), C2-C1-Au2 106.8(9), C2-C1-Au3 111.2(8), C2-C1-Au5 109.6(9), Au1-C1-Au2 83.3(4), Au2-C1-Au3 83.1(5), Au3-C1-Au5 80.2(4), Au5-C1-Au1 83.6(4), C1-Au5-C1′ 161.9(6), N3-Au4-N3′ 170.3(7).

The carbon atom C1 (C1′) in **3** is bonded to C2 (C2′) and, in addition, to four gold atoms, which form a four-sided polygon of roughly equal edge length: Au1-Au2 2.839(1), Au2-Au3 2.839(1), Au3-Au5 2.799(1), Au5-Au1 2.893(1) Å. Thus, the pentacoordinated atoms C1 and C1′ have a tetragonal-pyramidal environment; Au5 is the common corner of the two pyramids. The planes through the gold atoms Au1, Au2, Au3, Au5, and Au1′, Au2′, Au3′, Au5 form an angle of 73.2°. The Au4–Au5 distance (2.811(1) Å) is also short; thus, all eight Au atoms are components of a single cluster. C1, C2, N3, Au4, N3′, C2′, C1′, and Au5 thereby form a slightly twisted eight-membered ring system (angle formed by the planes Au4,N3,C2,C1,Au5/Au4,N3′,C2′,C1′,Au5 = 17.5°) having a transannular Au···Au contact distance, as is typical of many binuclear gold(I) complexes.[11]

The gold atoms Au1–Au3 bear phosphorus atoms lying on the line defined by the C1–Au bonds; the ^{31}P NMR spectra show that, even in solution, these phosphorus atoms are not equivalent. The ABC spin system can be simulated. In agreement with the C_2 symmetry, the H atoms on C5, as well as the methyl groups on C4, are diastereotopic (^1H and ^{13}C NMR). The phenyl groups give rise to three sets of ^{13}C NMR signals. These findings prove that the double Au^I bridging of the two moieties **4** to give **3** is also occurs in solution and is not affected by solvation.

In the crystal, the counterions $[(CH_3)_3SiF_2]^{\ominus}$ display a nearly trigonal-bipyramidal structure with the fluorine atoms in axial positions. In solution, only singlets are observed in the ^1H, ^{13}C, and ^{19}F NMR spectra owing to rapid $F^{\ominus}$ exchange. The crystals of **3** contain, in addition, CH_2Cl_2 and (strongly disordered) diethyl ether molecules. Both are also revealed upon dissolution by NMR spectroscopy.

It is remarkable that formation of **3** occurs in the presence of the triphenylphosphane released from Ph_3PAuCl. Therefore, binding of the phosphane ligand is suppressed not only by the N atoms of the dihydrooxazole but also by the σ framework of the triauriomethane **4**, which also functions, unexpectedly, as a donor. This phenomenon demonstrates the high formation tendency of the cluster.

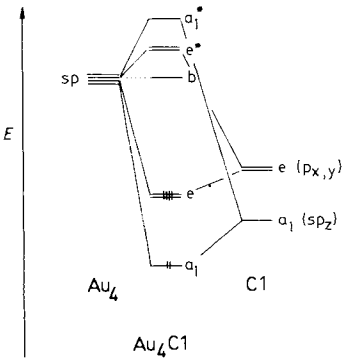

Fig. 2. MO scheme describing the bonding in the tetragonal pyramids around the atoms C1 and C1′ in **3** (idealized point group C_{4v}; only one sp hybrid orbital of each gold atom and the orbitals p_x and p_y of C1 are shown).

The MO description of the bonding in the $C2C1Au_4$ structural unit offers no difficulties. On the contrary, it is amazing that, in the point group C_{4v} according to the scheme shown in Figure 2, the linear combination of the frontier orbitals of the atoms involved gives rise to exactly three binding cluster orbitals, which can be filled with the six available electrons. Here, the four Au atoms, as well as the C1 atom, were assumed to be sp hybridized, which corresponds well to the actual geometry in the two tetragonal pyramids in **3**.

Experimental Procedure

2: **1** (8.73 g, 77.2 mmol) was dissolved in diethyl ether (75 mL) and treated at −55 °C with a solution of *n*-butyllithium (77.4 mmol) in *n*-hexane. The solution was stirred for 30 min, Me_3SiCl (8.4 g, 77.3 mmol) was then added, and the resulting mixture was stirred for 2 h at −45 to −20 °C. The same silylation procedure was repeated with two more equivalents of the same reagents. The reaction was allowed to proceed for 10 h at −20 to +10 °C; 100 mL of hydrochloric acid was then added at 0 °C (pH = 2), the two-phase mixture was separated, and the aqueous phase was extracted with 2 × 50 mL of ether. Drying of the combined organic extracts over sodium carbonate and removal of all volatiles in vacuo afforded **2** as a colorless oil. IR (neat): $\tilde{\nu}$ = 2002 cm^{-1} (C=C=N). ^1H NMR (C_6D_6): δ = 0.08 (s, 9H; $SiMe_3$), 0.19 (s, 18H; $SiMe_3$), 1.23 (s, 6H; CMe_2), 3.38 (s, 2H; CH_2). ^{13}C NMR (C_6D_6): δ = −0.46 (Me_3SiO), 1.29 (s; Me_3SiC), 25.61 (s; Me_2C), 59.39 (s; CMe_2), 71.39 (s; CO), 169.18 (s; C=N). The ^1H-coupled spectrum gave the expected multiplicities. ^{29}Si NMR (C_6D_6): δ = −1.83 (s, 1Si; SiO), 17.86 (s, 2Si; Si_2C).

3: CsF (2.5 g, 16.5 mmol, excess) was added to a solution of Ph_3PAuCl (1.50 g, 3.03 mmol) in 40 mL of HMPT. Compound **2** (0.25 g, 0.76 mmol) in 20 mL of HMPT was added to the resulting suspension with stirring. The reaction mixture was stirred for 3 d at 22 °C under nitrogen in the dark; it was then filtered and the filtrate was diluted with 60 mL of benzene. Addition of 300 mL of pentane resulted in precipitation of a yellow product, which was collected by filtration, crystallized from CH_2Cl_2/Et_2O, washed with pentane, and dried in vacuo. Yield 1.31 g (96.2%) **3**, dec. 134–136 °C. ^1H NMR (CD_3CN): δ = 0.27, 1.31 (s, each 3H; Me_2C), 3.68, 4.22 (each 1H, AB, $J(HH)$ = 8.79 Hz; CH_2), 6.8–7.8 (m, 45H; Ph), −0.18 (s; Me_3Si), 1.08, 3.37 (t and q, J = 6.95 Hz; Et_2O). ^{13}C NMR (CD_3CN): δ = 27.88, 29.89 (s; Me_2C), 66.11, 81.33, 187.10 (s, C6, C5, and C4); C3 is not observed owing to overlap of other signals; three sets of Ph resonances; Me_3Si, broadened by

exchange. ^{31}P NMR (CD_3CN): $\delta = 28.50, 28.55, 29.97$ (ABC, $J(PP) = 4.4$ Hz). FAB MS: m/z 1684.7 for the dication of **3**.

Received: July 1, 1988 [Z 2839 IE]
German version: *Angew. Chem. 100* (1988) 1600

[1] H. Schmidbaur, *Gmelin Handbuch der Anorganischen Chemie, Organogold Compounds*, Springer, Berlin 1980.
[2] G. Wilkinson, F. G. A. Stone, E. W. Abel (Eds.): *Comprehensive Organometallic Chemistry, Vol. 1, 2*, Pergamon, Oxford 1984.
[3] H. Schmidbaur, W. Graf, G. Müller, *Angew. Chem. 100* (1988) 439; *Angew. Chem. Int. Ed. Engl. 27* (1988) 417; *Helv. Chim. Acta 69* (1986) 1748.
[4] H. Schmidbaur, A. Schier, G. Reber, G. Müller, *Inorg. Chim. Acta 147* (1988) 143, and references cited therein.
[5] H. Schmidbaur, O. Gasser, *Angew. Chem. 88* (1976) 542; *Angew. Chem. Int. Ed. Engl. 15* (1976) 502.
[6] H. Schmidbaur, F. Scherbaum, B. Huber, G. Müller, *Angew. Chem. 100* (1988) 441; *Angew. Chem. Int. Ed. Engl. 27* (1988) 419.
[7] Cf. [6], but also P. G. Jones, *Gold Bull. 14* (1981) 102, 159; *ibid. 16* (1983) 114.
[8] A. I. Meyers, E. D. Mihelich, *Angew. Chem. 88* (1976) 321; *Angew. Chem. Int. Ed. Engl. 15* (1976) 270; A. I. Meyers, D. L. Temple, R. L. Nolen, E. D. Mihelich, *J. Org. Chem. 39* (1974) 2778; A. I. Meyers, E. D. Mihelich, R. L. Nolen, *ibid. 39* (1974) 2783.
[9] Crystal structure data of **3**: $[C_{50}H_{58}Au_8N_2O_2P_6][C_3H_9SiF_2]_2 \cdot 2CH_2Cl_2 \cdot 2(C_2H_5)_2O$, $M_r = 3910.26$, monoclinic, space group $C2/c$, $a = 22.301(3)$, $b = 20.286(2)$, $c = 28.504(3)$ Å, $\beta = 98.03(1)°$; $V = 12768.7$ Å^3, $Z = 4$, $\rho_{calcd} = 2.034$ g cm^{-3}, $\mu(Mo_{K\alpha}) = 93.63$ cm^{-1}, $F(000) \geq 7455$, $T = -30°C$. 10012 unique reflections, 7570 "observed" with $F_0 = 4.0\sigma(F_0)$, $[(\sin\theta/\lambda)_{max} = 0.572$, hkl region: +25, +23, +32, $Mo_{K\alpha}$ radiation, $\lambda = 0.71069$ Å, graphite monochromator, Syntex $P2_1$]. Solution by automated Patterson methods (SHELXS-86). R (R_w) = 0.064 (0.055), $w = 1/\sigma^2(F_0)$; (Au, P, CCl_2 anisotropic, remaining atoms isotropic, $[Me_3SiF_2]^{\ominus}$ with idealized trigonal-bipyramidal geometry; only the O atom of disordered diethyl ether could be refined). $\Delta\rho_{fin} = +1.97/-1.65$ e·Å^{-3}. Further details of the crystal structure investigation may be obtained from the Fachinformationszentrum Energie, Physik, Mathematik GmbH, D-7514 Eggenstein-Leopoldshafen 2 (FRG), on quoting the depository number CSD-53401, the names of the authors, and the journal citation.
[10] R. Noyori, I. Nishida, J. Sakata, *Tetrahedron Lett. 22* (1981) 3993; *J. Am. Chem. Soc. 105* (1983) 1598.
[11] H. Schmidbaur, T. Pollok, R. Herr, F. E. Wagner, R. Bau, J. Riede, G. Müller, *Organometallics 5* (1986) 566.
[12] F. Scherbaum, A. Grohmann, B. Huber, C. Krüger, H. Schmidbaur, *Angew. Chem. 100* (1988) 1602; *Angew. Chem. Int. Ed. Engl. 27* (1988) 1544.

"Aurophilicity" as a Consequence of Relativistic Effects: The Hexakis(triphenylphosphaneaurio)methane Dication $[(Ph_3PAu)_6C]^{2\oplus}$**

By *Franz Scherbaum, Andreas Grohmann, Brigitte Huber, Carl Krüger,* and *Hubert Schmidbaur**

Recent work on polyauriomethanes[1-3] has revealed that the highly aurated compounds containing two or more gold atoms on one and the same carbon atom readily bond further gold(I) units $LAu^{\oplus}$ (L = R_3P), a property termed aurophilicity. The coordination number of the polyauriated C atoms is thereby increased beyond 4, so that, for example, tetragonal-pyramidal structures with close Au···Au contacts are formed. Based on local C_{4v} symmetry, a simple MO scheme for the cations $[RC(AuL)_4]^{\oplus}$ shows full occupation of the bonding orbitals, which well explains, at least qualitatively, the unexpected formation tendency of such systems.[2] The resulting bonds, directed toward the C atom, are complemented by contributions from Au···Au interactions, which, owing to relativistic effects, can be ascribed in part to the d^{10} systems.[4] Our investigation of this novel phenomenon has led us to seek synthetic routes to the first *tetraauriomethane*, which, because of its presumably still greater aurophilicity, would make it possible to prepare even more highly coordinated auriomethanes.

In analogy to relevant work on related mercuriomethanes,[5,6] we selected tetrakis(dimethoxyboryl)methane as our starting material.[5] This readily accessible precursor reacts with Ph_3PAuCl in tetrahydrofuran in the presence of CsF in excess within one day at room temperature to give a yellow-red suspension. After filtration and addition of benzene to the filtrate, a stable, colorless, crystalline substance can be isolated in high yields. The product is insoluble in diethyl ether, pentane, and benzene, but dissolves in di- and trichloromethane as well as in hexamethylphosphoric triamide to afford dilute solutions. Both the solid and the solutions are hardly sensitive toward air, but they are very hygroscopic.[7]

$\{^1H\}^{31}P$ NMR spectra of such solutions (CD_2Cl_2, $-60°C$) display a single signal, the position of which is largely temperature independent ($\delta = 27.73$). The $\{^1H\}^{13}C$ NMR spectrum displays one set of signals, indicating that the phenyl groups are equivalent. The resonances of C_{ipso}, C_{ortho}, and C_{meta} can be interpreted by simulation as $AA'A''X$ spin systems (A = P, X = C). C_{para} appears as a singlet. A slight temperature dependence (-60 to $+30°C$) does not lead to significant changes, but only affects the signal width and resolution. Further, a weak-intensity quartet is found ($\delta = 49.1$, $J(CF) = 4.4$ Hz), which can be assigned to the anion $[F_3BOCH_3]^{\ominus}$.[8] This corresponds to a quartet in the ^{11}B NMR spectrum ($\delta = -17.8$, $J(BF) = 14.2$ Hz) and to a broad singlet ($\delta = 3.20$) in the ^1H NMR spectrum. Two ^1H NMR multiplets at $\delta = 6.75$–7.10 and 7.10–7.52 can once again be assigned to the equivalent phenyl groups.

The substance is diamagnetic. In the mass spectrometric ionization (FAB), the heaviest ions detected are $[(Ph_3PAu)_6C]^{2\oplus}$ and the *mono*cation (m/z 1383.9 and 2767.8, respectively), which, together with the spectroscopic data and the values of the elemental analysis, support the formulation shown in Equation (a) for the reaction course:

$$C[B(OCH_3)_2]_4 + 6\,Ph_3PAuCl + 6\,CsF \longrightarrow 6\,CsCl + 2\,B(OCH_3)_3 + [(Ph_3PAu)_6C]^{2\oplus}[CH_3OBF_3]_2^{\ominus} \quad (a)$$

Despite much effort, it was not possible to detect the presumed carbon atom in the center of the proposed gold cluster by NMR spectroscopy. The X-ray structure analysis,[9] however, removed any doubts as to the structure. The investigation revealed the presence of an only slightly distorted octahedron of gold atoms, the crystallographic inversion center of which is occupied by a carbon atom (Fig. 1). A Ph_3P ligand is attached to each of the gold atoms, so that the Au(I) centers are each bonded classically (sp hybrids) in a linear fashion to one phosphorus atom and to the central carbon atom. The Au–P distances (average value 2.271 Å) are in good agreement with the values ex-

[*] Prof. Dr. H. Schmidbaur, Dipl.-Chem. F. Scherbaum, A. Grohmann, Dipl.-Chem. B. Huber, Prof. Dr. C. Krüger [+]
Anorganisch-chemisches Institut der Technischen Universität München
Lichtenbergstrasse 4, D-8046 Garching (FRG)
[+] Guest professor from the Max-Planck-Institut für Kohlenforschung, Mülheim a. d. Ruhr (FRG)

[**] This work was supported by the Deutsche Forschungsgemeinschaft (Leibniz program), the Fonds der Chemischen Industrie, and Degussa AG, Hanau. We thank *J. Riede* for measurement of the crystallographic data set and Finnigan MAT for the FAB-MS measurements.

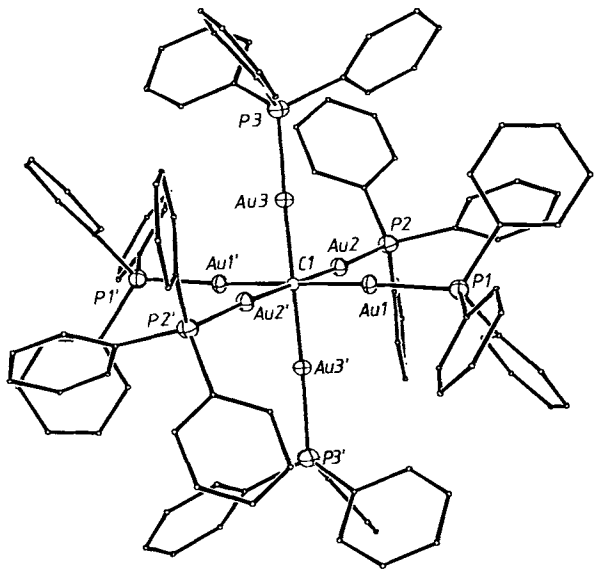

Fig. 1. Structure of the dication $[(Ph_3PAu)_6C]^{2\oplus}$. The central C atom occupies a crystallographic inversion center. Selected distances [Å] and angles [°]: Au1-C1 2.122(1), Au2-C1 2.123(1), Au3-C1 2.129(1), Au1-P1 2.273(2), Au2-P2 2.269(2), Au3-P3 2.274(3), Au1-Au1' 4.243(1), Au2-Au2' 4.244(1), Au3-Au3' 4.257(1), Au1-Au2 2.910(1), Au1-Au2' 3.090(1), Au1-Au3 3.037(1), Au1-Au3' 2.974(1), Au2-Au3 2.960(1), Au2-Au3' 3.053(1); P1-Au1-C1 172.4(1), P2-Au2-C1 175.1(1), P3-Au3-C1 175.7(1).

pected from the coordination chemistry of univalent, two-coordinate gold.[10]

The bonding between the central atom of the cluster and the six metal atoms can be described (not taking into consideration, initially, the closed-shell d^{10} states) by a simple MO diagram (Fig. 2; cf. also Ref. [11]). The scheme shows that, for the local symmetry O_h, four strongly bonding states (a_{1g} and t_{1u}) result from the six σ orbitals of the Au atoms (simplified: sp hybrids) and the s and p orbitals of the C atom. These four orbitals can just be fully occupied by the eight available electrons (diamagnetic singlet ground state). An e_g state remains as the LUMO. The gap between t_{1u} and e_g is so large that the compound does not absorb in the visible region. The six medium-length Au–C

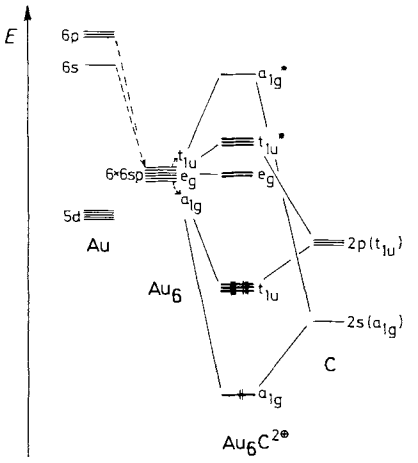

Fig. 2. MO diagram of the Au_6C framework in the cation $[(Ph_3PAu)_6C]^{2\oplus}$ not taking into consideration the d/s/p(Au,C) interactions: local symmetry O_h; s and p orbitals of the central C atom (right); the six sp hybrid orbitals of the metal atoms (left) are appreciably lowered by relativistic s contraction and almost attain the level of the d^{10} states. The six P atoms are bonded via electron-pair bonds formed from the other six sp(Au) hybrid orbitals, which leads to the radial arrangement of the C1–Au–P bonds (see Fig. 1).

bonds (2.124 Å) can be assigned a formal bond order of 2/3.[10] The reduction in energy due to overlap of the C and Au orbitals is improved considerably by the lowering of the energy levels of these orbitals by relativistic contraction.[12]

The average value (3.003 Å) of the Au···Au contacts along the edges of the octahedron lies in the range of those usually found for numerous polynuclear gold complexes.[13] The lowering in energy resulting here mainly from d^{10}–d^{10} interactions was recently estimated from a binuclear model to be ca. 6–8 kcal mol^{-1}, the first such experimental determination.[14] Even if this amount must be reduced in the cluster owing to polycoordination of each metal atom (four nearest Au neighbors), the twelve edges of the cluster give rise to a considerable lowering in energy upon aggregation, which explains quite well the aurophilicity of the tetraauriomethanes $C(AuL)_4$ toward $LAu^{\oplus}$.

In the long series of reported clusters containing low-valent gold atoms (having an average oxidation state between 0 and +I), there is one example[15] in which six gold atoms form an octahedron, which, however, is supposedly *not occupied at the center:* namely, $[\{(p\text{-}MeC_6H_4)_3PAu\}_6][B(C_6H_5)_4]_2$. This cluster is of interest because the synthesis, carried out only once and affording a minimal yield, could not be repeated[16, 17] and because its geometry could not be fitted into the overall scheme of noble-metal clusters: For $(LAu)_6^{2\oplus}$ aggregates, the structure is predicted to be an edge-sharing double tetrahedron, which, in other cases, was indeed found.[18] An analysis of the X-ray data of the tolylphosphane complex mentioned above showed that its dication not only has nearly the same crystal dimensions as the title compound but also exhibits appreciable residual electron density at the center of the octahedron. This finding indicates that the structure of this compound most probably is also a C-centered octahedron, the formation of which is presumably due to C-contributing impurities. Thus, the chemistry of *homo*atomic gold clusters, which are still only accessible by somewhat alchemistic methods, would have one less "exception". At the same time, a new class of carbido clusters is emerging; these compounds may be prepared directly in high yield by exploiting what is known about the aurophilicity of polyauriomethanes. Following a suggestion made by *King*,[19] they have already been given a name, at least for *metal*-centered coinage-metal clusters, namely, "porcupine compounds", which is a good choice indeed (see Fig. 1).

Finally, it should be noted that ab initio calculations for $(CLi_6)^{2\oplus}$ gave a "local" energy minimum for O_h symmetry but no absolute thermodynamic stability. The binding of $Li^{\oplus}$ to $(CLi_5)^{\oplus}$ is thus endothermic,[20] and mass spectrometric studies have only shown $(CLi_5)^{\oplus}$.[20, 21] The molecule CLi_6, on the other hand, was shown to exhibit "global" stability.[22]

Received: August 1, 1988 [Z 2896 IE]
German version: *Angew. Chem. 100* (1988) 1602

[1] H. Schmidbaur, F. Scherbaum, B. Huber, G. Müller, *Angew. Chem. 100* (1988) 441; *Angew. Chem. Int. Ed. Engl. 27* (1988) 419.
[2] F. Scherbaum, B. Huber, G. Müller, H. Schmidbaur, *Angew. Chem. 100* (1988) 1600; *Angew. Chem. Int. Ed. Engl. 27* (1988) 1542.
[3] E. I. Smyslova, E. G. Perevalova, V. P. Dyadchenko, K. I. Grandberg, Y. L. Slovokhotov, Y. T. Struchkov, *J. Organomet. Chem. 215* (1981) 269.
[4] H. Schmidbaur, *Gold 100, Vol. 3*, S. 83, SAMM, Johannesburg 1986.
[5] R. B. Castle, D. S. Matteson, *J. Organomet. Chem. 20* (1969) 19; D. S. Matteson, G. P. Allies, *ibid. 54* (1973) 35; D. S. Matteson, R. B. Castle, *J. Am. Chem. Soc. 92* (1970) 231.
[6] K. P. Jensen, D. Breitinger, W. Kress, *Z. Naturforsch. B36* (1981) 188; D. Breitinger, G. Pietrowski, G. Liehr, R. Sendelbeck, *ibid. 38* (1983)

357; W. Kress, D. Breitinger, R. Sendelbeck, *J. Organomet. Chem. 246* (1983) 1; D. Breitinger, K. Geibel, W. Kress, R. Sendelbeck, *ibid. 191* (1980) 7.

[7] *Experimental Procedure:* The reaction mixture consisting of Ph_3PAuCl (1.96 g, 3.96 mmol), CsF (6.0 g, 39.5 mmol), and $C[B(OMe)_2]_4$ (0.30 g, 0.99 mmol) in 45 mL of HMPT was stirred for 24 h at 20°C and then filtered. Benzene (200 mL) was added to the filtrate and the resulting precipitate was recrystallized three times from benzene/CH_2Cl_2. Yield 1.32 g (67%). Colorless crystals, dec. above 140°C. ^{13}C NMR (CD_2Cl_2, 0°C): $\delta = 129.71$ ($AA'A''$, $N = 56.24$ Hz; C_{ipso}), 133.91 ($N = 13.69$, C_{ortho}), 129.50 ($N = 11.25$; C_{meta}), 132.06 (s; C_{para}).

[8] V. N. Plakhotnik, V. V. Evsikov, *Dokl. Akad. Nauk SSSR 228* (1976) 1112.

[9] Crystal structure data: Syntex $P2_1$, $Mo_{K\alpha}$ radiation, $\lambda = 0.71069$ Å, graphite monochromator, $T = -45$°C; monoclinic, space group $P2_1/c$, $a = 12.287(2)$, $b = 15.746(2)$, $c = 26.169(3)$ Å, $\beta = 96.52(1)$°, $V = 5030.2$ Å^3, $\rho_{calcd} = 1.957$ g cm^{-3}, $Z = 2$, $\mu(Mo_{K\alpha}) = 88.441$ cm^{-1}, 8597 measured reflections, of which 7828 were unique ($R_{int} = 0.03$), and 6444 "observed" with $I \geq 2.0\sigma(I)$ (ω scan, $\Delta\omega = 0.7$°, $(\sin\theta/\lambda)_{max} = 0.572$, $+h$, $+k$, $\pm l$); measurement data corrected for Lp and absorption effects (empirical) as well as for instability during the data collection. Solution by Patterson methods (SHELXS-86); $R = 0.038$, $R_w = 0.036$, $w = 1/\sigma^2(F_o)$. 595 parameters, $\Delta\rho$(max/min) $+2.60/-1.06$ e Å^{-3} (GFMLX). An analogous refinement omitting the interstitial carbon atom C1 converged to only $R = 0.041$ ($R_w = 0.040$). Further details of the crystal structure investigation may be obtained from the Fachinformationszentrum Energie, Physik, Mathematik GmbH, D-7514 Eggenstein-Leopoldshafen 2 (FRG), on quoting the depository number CSD-53402, the names of the authors, and the journal citation.

[10] H. Schmidbaur, *Gmelin Handbuch der Anorganischen Chemie, Organogold Compounds*, Springer, Berlin 1980.

[11] D. M. P. Mingos, *J. Chem. Soc. Dalton Trans. 1976*, 1163.

[12] P. Pyykkö, J.-P. Desclaux, *Acc. Chem. Res. 12* (1979) 276.

[13] H. Schmidbaur, A. Schier, G. Reber, G. Müller, *Inorg. Chim. Acta 147* (1988) 143; H. Schmidbaur, T. Pollok, R. Herr, F. E. Wagner, R. Bau, J. Riede, G. Müller, *Organometallics 5* (1986) 566.

[14] H. Schmidbaur, W. Graf, G. Müller, *Angew. Chem. 100* (1988) 439; *Angew. Chem. Int. Ed. Engl. 27* (1988) 417.

[15] P. L. Bellon, M. Manassero, M. Sansoni, *J. Chem. Soc. Dalton Trans. 1973*, 2423; P. L. Bellon, M. Manassero, L. Naldini, M. Sansoni, *J. Chem. Soc. Chem. Commun. 1972*, 1035.

[16] C. E. Briant, K. P. Hall, D. M. P. Mingos, *J. Organomet. Chem. 254* (1983) C18.

[17] J. J. Steggerda, J. J. Bour, J. W. A. van der Velden, *Recl. Trav. Chim. Pays-Bas 101* (1982) 164.

[18] D. G. Evans, D. M. P. Mingos, *J. Organomet. Chem. 232* (1982) 171; C. E. Briant, K. P. Hall, D. M. P. Mingos, A. C. Wheeler, *J. Chem. Soc. Dalton Trans. 1986*, 687.

[19] R. B. King, *Prog. Inorg. Chem. 15* (1971) 287.

[20] E. D. Jemmis, J. Chandrasekhar, E.-U. Würthwein, P. von R. Schleyer, J. W. Chinn, Jr., F. J. Landro, R. J. Lagow, B. Luke, J. A. Pople, *J. Am. Chem. Soc. 104* (1982) 4275.

[21] J. W. Chinn, Jr., R. J. Lagow, *J. Am. Chem. Soc. 106* (1984) 3694.

[22] P. von R. Schleyer, E.-U. Würthwein, E. Kaufmann, T. Clark, *J. Am. Chem. Soc. 105* (1983) 5930; J. P. Ritchie, S. M. Bachrach, *ibid. 109* (1987) 5909.

Iodine-Induced Stereoselective Carbocyclizations: A New Method for the Synthesis of Cyclohexane and Cyclohexene Derivatives**

By *José Barluenga,* José M. González, Pedro J. Campos,* and *Gregorio Asensio*

Intramolecular cyclization of unsaturated systems is of theoretical and synthetic interest and has attracted considerable attention,[1] especially those processes dealing with biomimetic reactions of polyenes.[2] Different electrophiles have been tested for C–C bond formation in reactions leading to ring closure.[1–3] Reactions involving bromine-containing reagents, and following biosynthetic pathways,[4] have been presented.[5] Nevertheless, little attention has been paid to iodine-induced carbocyclizations and only a few examples of limited application are known.[6] The current importance of carbocyclizations stimulated us to search for a methodology based on iodine electrophiles.

Recently, we described the preparation of $I(py)_2BF_4$ **1** and its reactivity towards olefins in the presence of several nucleophiles, including aromatic compounds.[7] We now report a diastereoselective and high-yield intramolecular reaction for six-membered-ring construction initiated by **1**. Simple protonation of **1** takes place in dry dichloromethane at −90°C, using HBF_4 or CF_3SO_3H to neutralize the pyridine; the addition of the appropriate arene–olefin or olefin–olefin system to the **1**/acid solution readily promotes C–C bond formation (see Table 1).[8]

The excellent yields of isolated products and the diastereoselectivity obtained in these reactions, as well as the purity of the crude reaction mixture, are noteworthy. These features, along with the low reaction temperature and the known versatility of the iodine atom in functional group exchange, are relevant advantages of this reaction, in comparison with other carbocyclizations promoted by electrophiles. This iodine-promoted carbocyclization could be initiated by interaction of the iodine cation with a C–C double or triple bond. The regio- and stereochemistry found can be explained by assuming a chairlike transition state for the reaction, in agreement with the Stork–Eschenmoser postulate[1] (see Scheme 1).

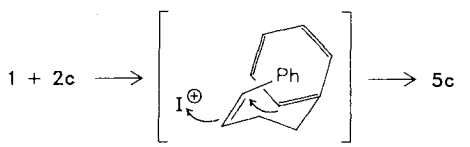

Scheme 1.

All attempts to carry out iodine-induced carbocyclization of allylbenzene were unsuccessful and led to the exclusive formation of a fluorinated product **9** (see Scheme 2),[9] irrespectively of the reaction temperature (−90°C to 20°C).

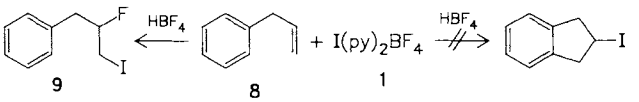

Scheme 2.

Baldwin's rules for ring closure[10] account for the striking control observed in these carbocyclizations. According to these rules, the favored reactions leading to six-membered rings can be characterized as 6-*exo-trig*, 6-*endo-trig*, or 6-*endo-dig* ring closures. On the other hand, ring construction from allylbenzene should involve a 5-*endo-trig* closure, and hence would be a disfavored process.

This is the first general intramolecular iodine-induced carbocyclization reaction. The availability of the unsaturated starting materials and the suitability of the resulting products as synthetic building blocks are also noteworthy. In fact, **7b** is a highly versatile synthon, which allows a simple entry into C4-functionalized cyclohexenes by io-

[*] Prof. J. Barluenga, Dr. M. González, Dr. P. J. Campos
Departamento de Química Organometálica, Facultad de Química
Universidad de Oviedo, E-33071 Oviedo (Spain)
Prof. G. Asensio
Departamento de Química Orgánica, Facultad de Farmacia
Universidad de Valencia, E-46010 Valencia (Spain)

[**] This work was supported in part by the Comisión Asesora de Investigación Científica y Técnica (CAICYT). *J. M. G.* thanks the Ministerio de Educación y Ciencia for a fellowship (Plan FPI).

Table 1. Intramolecular carbocyclization induced by $I(py)_2BF_4$ **1**/HBF_4.

Starting material	Cyclization product [a]	Yield [%] [b]
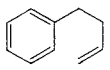 **2a**	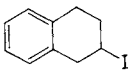 **5a**	80
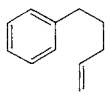 **2a**	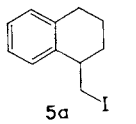 **5a**	92
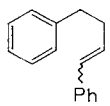 (**2c** + **2d**)[c]	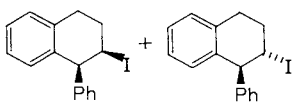 **5c** **5d**	75[d]
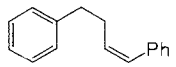 **2c**[e]	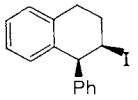 **5c**[f]	86
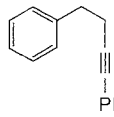 **3a**	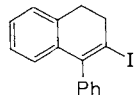 **6a**	91[g]
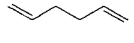 **4a**	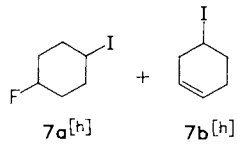 **7a**[h] **7b**[h]	85
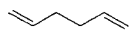 **4a**	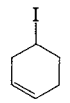 **7b**	70[i]
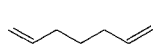 **4b**	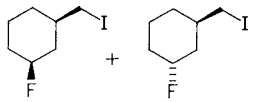 **7c**[j] **7'c**[j]	86

[a] All products were unequivocally characterized on the basis of their spectroscopic and mass spectral data and gave satisfactory microanalyses. [b] Yield based on isolated product. [c] (*Z*):(*E*) mixture (**2c** : **2d**) = 22 : 78 (GC). [d] **5c** : **5d** ratio = 23 : 77 (determined from the crude mixture of products by GC). [e] Prepared from **3a** by treatment with diisobutylaluminum hydride and further hydrolysis (72%). [f] A single diastereoisomer is formed. Its stereochemistry was assigned from the 300-MHz ^{1}H NMR coupling constants. [g] Reaction temperature: −60°C. [h] **7a** : **7b** ratio = 5 : 1 (by GC). Compound **7a** is obtained as a mixture of diastereoisomers in a 90 : 10 ratio. A *trans* stereochemistry can be tentatively assigned to the major product from the 300-MHz ^{1}H NMR coupling constant. [i] With CF_3SO_3H, −60°C. [j] As a 1 : 1 mixture of **7c** : **7'c** (by ^{13}C NMR).

dine exchange. The strategy reported here should be an alternative to the Diels–Alder reaction and the Birch reduction for the synthesis of cyclohexane and cyclohexene derivatives.

Received: June 1, 1988;
revised: August 3, 1988 [Z 2796 IE]
German version: *Angew. Chem. 100* (1988) 1604

[1] P. A. Bartlett in J. D. Morrison (Ed.): *Asymmetric Synthesis, Vol. 3*, Academic Press, Orlando, FL, USA 1984, Chapter 5, p. 341.
[2] E. E. van Tamelen, *Acc. Chem. Res. 8* (1975) 152; W. S. Johnson, *Angew. Chem. 88* (1976) 33; *Angew. Chem. Int. Ed. Engl. 15* (1976) 9.
[3] J. K. Sutherland, *Chem. Soc. Rev. 9* (1980) 265.
[4] W. Fenical, *Science Washington 215* (1982) 923.
[5] Y. Yamaguchi, T. Uyehara, T. Kato, *Tetrahedron Lett. 26* (1985) 343; J. D. Martin, C. Pérez, J. L. Ravelo, *J. Am. Chem. Soc. 108* (1986) 7801.
[6] H. J. Günther, V. Jäger, P. S. Skell, *Tetrahedron Lett. 1977*, 2539; S. Uemura, S. Fukuzawa, A. Toshimitsu, M. Okano, H. Tezuka, S. Sawada, *J. Org. Chem. 48* (1983) 270.
[7] J. Barluenga, J. M. González, P. J. Campos, G. Asensio, *Angew. Chem. 97* (1985) 341; *Angew. Chem. Int. Ed. Engl. 24* (1985) 319.
[8] *Typical Experimental Procedure:* To a Schlenk tube containing a solution of **1** (8×10^{-2} M) in dry dichloromethane under argon was added at −90°C the acid (2 : 1 referring to **1**) and then a precooled 1 M solution of the unsaturated starting material in dichloromethane (1 : 1 referring to **1**). The temperature was kept at −90°C for 30 min and then allowed to rise (except for **4a** carbocyclization, which was quenched in water at −90°C). When the temperature was near −60°C, quenching of the solution in water and standard workup afforded crude reaction products in ca. 90% yield (GC). Purification (recrystallization or column chromatography) gave pure products.
[9] Only the Markownikoff regioisomer **9** (by GC and ^{13}C NMR analyses) was fund to be present in yields of 69%–91% after quenching in water.
[10] J. E. Baldwin, *J. Chem. Soc. Chem. Commun. 1976*, 734.

Cyclobis(paraquat-*p*-phenylene). A Tetracationic Multipurpose Receptor

By *Barbara Odell, Mark V. Reddington, Alexandra M. Z. Slawin, Neil Spencer, J. Fraser Stoddart,** and *David J. Williams*

Recently, we reported[1] on cyclophane-like molecular receptors, such as bisparaphenylene-34-crown-10 **1**, which contains π-electron-rich hydroquinone units for face-to-face complexation (Fig. 1) with paraquat **2**, a π-electron-deficient dication. These observations led us to propose that it might be possible to reverse constitutionally the roles of the receptor and the substrate and so bind a π-electron-rich diphenol ether, such as 1,4-dimethoxybenzene **3a**, inside a tetracationic molecular receptor (Fig. 1). Such a receptor is the tetracation cyclobis(paraquat-*p*-phenylene) **4** which incorporates two π-electron-deficient paraquat residues connected in a phane-like manner by means of two *para*-phenylene groups.[2] Here, we describe (i) the synthesis of **4** as its tetrakis(hexafluorophosphate) **4** · 4 PF_6, (ii) its X-ray structural characterization as the acetonitrile solvate **4** · 4 PF_6 · 3 MeCN, (iii) the UV and ^{1}H-NMR spectroscopic evidence for 1 : 1 complex formation (a) between **4** · 4 PF_6 and 1,2-, 1,3-, and 1,4-dimethoxybenzene **3a/3b/3c** in acetonitrile (CD_3CN) and (b) between **4** · 4 Cl and 1,4-dihydroxybenzene **6** in water (D_2O),[3] and (iv) the results of molecular and semiempirical quantum mechanical calculations on **4** and on **4** · 2 MeCN.

[*] Dr. J. F. Stoddart, Dr. N. Spencer, M. V. Reddington
Department of Chemistry, The University
Sheffield S3 7HF (UK)
Dr. D. J. Williams, A. M. Z. Slawin
Chemical Crystallographic Laboratory
Department of Chemistry, Imperial College
London SW7 2AY (UK)
Dr. B. Odell
Analytical Chemistry Division, Sittingbourne Research Centre
Shell Research Limited, Sittingbourne
Kent ME9 8AG (UK)

[**] This work was supported by the Agricultural and Food, and Science and Engineering Research Councils in the United Kingdom

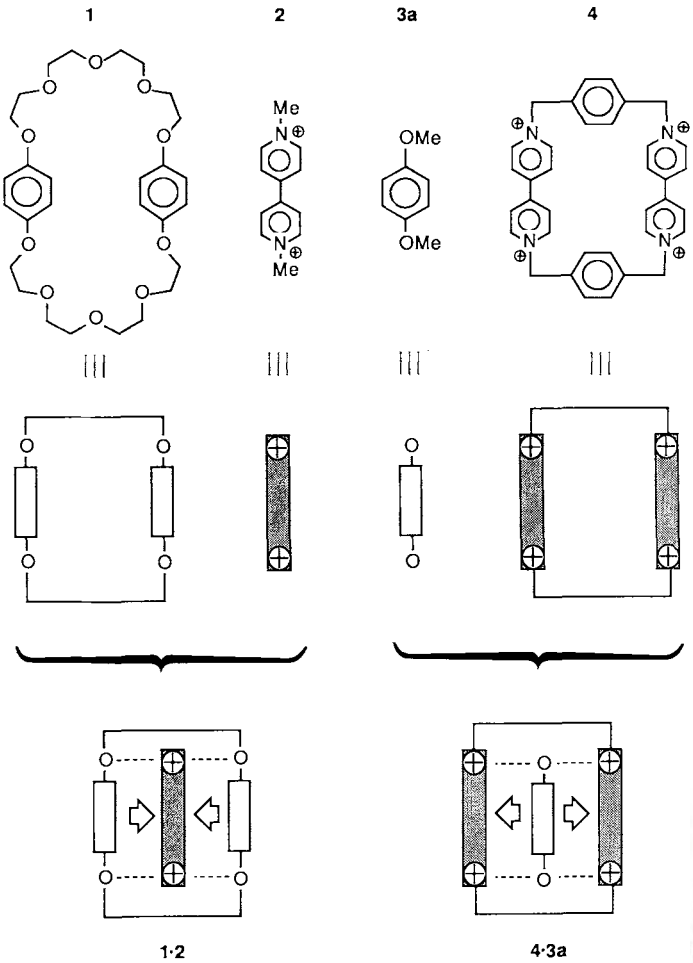

Fig. 1. Schematic representation of the basis for the proposal that the cyclobis(paraquat-*p*-phenylene) **4** should act as a tetracationic receptor for 1,4-dimethoxybenzene **3a**.

The procedure (cf. Ref. [2]) employed for the preparation of $4 \cdot 4PF_6$ starting from the bis(pyridinium) salt **5** and 1,4-bis(bromomethyl)benzene is outlined in Scheme 1. $4 \cdot 4PF_6$ is soluble in MeCN and $MeNO_2$, sparingly soluble in Me_2CO, and insoluble in Et_2O, $CHCl_3$, MeOH, and H_2O. Exchanging the counterion to afford (Scheme 1) the tetrachloride $4 \cdot 4Cl$ confers aqueous solubility (cf. Refs. [1] and [2]) upon the tetracation **4** but renders it insoluble in Me_2CO, MeCN, and $MeNO_2$. Thus, simply by altering the nature of the counterion the receptor properties of **4** can be investigated in *both aqueous and non-aqueous media*, as well as in the solid state.

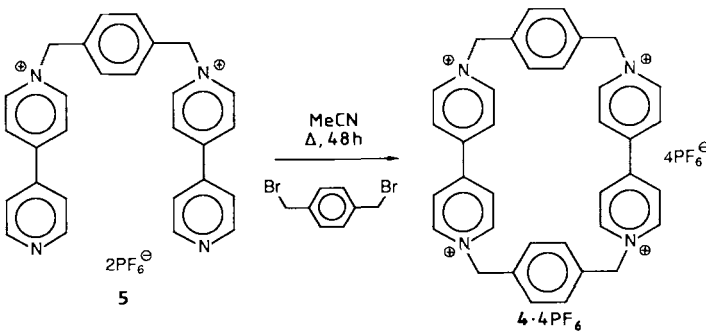

Scheme 1.

An X-ray structural analysis[4] of $4 \cdot 4PF_6 \cdot 3MeCN$[5] shows (Fig. 2, top) that **4** adopts a rigid centrosymmetric rectangular box-like conformation with the two paraquat units forming the longer sides and the two *para*-xylylene residues, the shorter ones. There is a 19° twist angle between the two pyridinium rings of each paraquat unit: in addition, there are deformations of both the paraquat and *para*-xylylene components producing a bowing of the sides of the cyclophane. Thus, the strain within the molecule is relieved by out-of-plane bending of the six aromatic rings and is distributed throughout the macrocycle with the maximum deviations associated with the exocyclic C-CH_2 bonds emanating from the *para*-phenylene residues: these bonds subtend an angle of 14° with respect to each other whilst the two $N^{\oplus}$-CH_2 bonds associated with the paraquat units subtend an angle of 23°. There is also a concomitant reduction in the macrocyclic valence angles at C7 and C14 [108.3(7)° and 108.5(7)°, respectively, instead of ca. 111°]. The overall dimensions of the macrocycle are 10.3 Å between the centroids of the two *para*-phenylene rings and 6.8 Å between C1 and C18.[6] Inspection of the space-filling representation (Fig. 2, bottom) shows there to be a significant free pathway through the center of the macrocycle. Furthermore, each macrocyclic ring is stacked almost directly above its neighbor in adjacent unit cells in the crys-

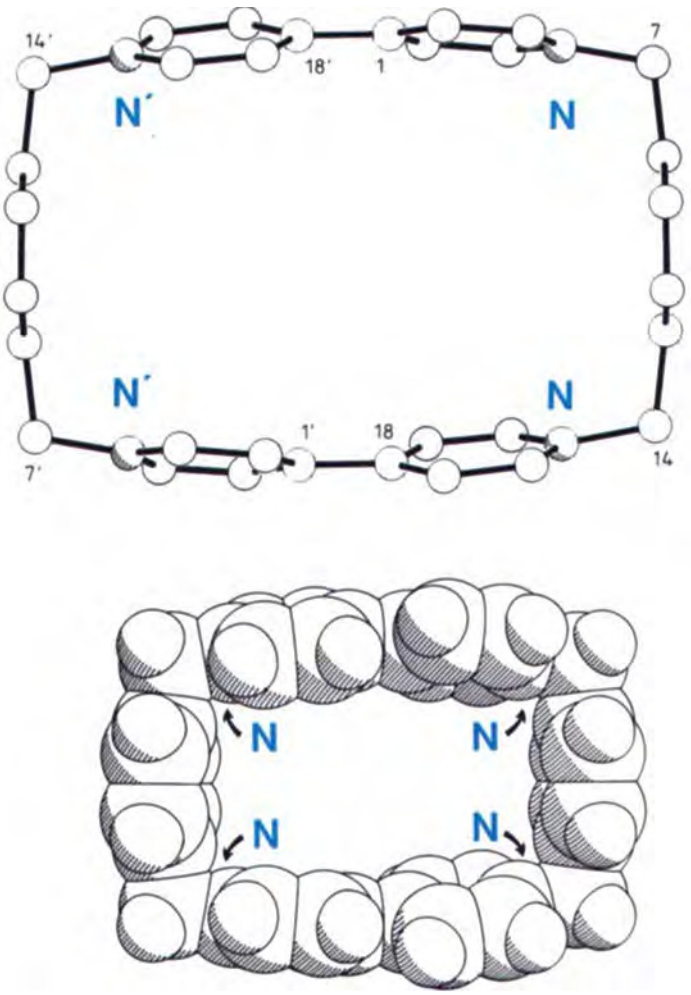

Fig. 2. Top: Structure of **4** in the crystal. Crystal data for $4 \cdot 4PF_6 \cdot 3MeCN$: monoclinic, $a = 10.805(1)$, $b = 19.819(2)$, $c = 14.027(2)$ Å, $\beta = 109.36(1)°$, $V = 2834$ Å^3, space group $P2_1/n$, $Z = 2$ (the molecule is disposed about a center of symmetry), $\rho = 1.43$ g cm^{-3}, $\mu(Cu_{K\alpha}) = 23$ cm^{-1}, 2027 independent observed reflections with $[|F_o| > 3\sigma(|F_o|)$, $\theta \leq 50°]$, $R = 0.100$, $R_w = 0.087$. Bottom: Space-filling representation of the structure of **4**.

tallographic *a* direction: the small off-set is a result of the unit cell β angle. The region between unit-cell translated tetracations is occupied by four $PF_6^{\ominus}$ counterions and two MeCN molecules arranged in the form of a torus. The gross structure (Fig. 3) has continuous parallel open channels bounded by alternatively-charged entities. Measurements of the dimensions of the free pathways within these channels show these to be large enough to accommodate a wide range of different substrates. In this case, in the solid state, part of this void is filled by a MeCN molecule in two centrosymmetrically-related partial occupancy sites.

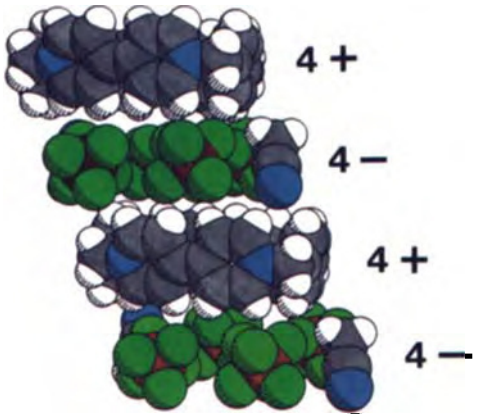

Fig. 3. Space-filling representation of alternately-charged entities of $4 \cdot 4PF_6 \cdot 3MeCN$ in the solid state (H = white, C = gray, N = blue, P = brown, F = green).

A significant result of semiempirical quantum mechanical calculations, based on the X-ray coordinates of **4** and using AM1[6] in conjunction with the program VSSPOT[7] (VSS approximation), which treats the charge distribution as having arisen from ZDO-type valence quantum mechanical calculations and approximates the nuclear charge attraction integrals in terms of spherically-symmetric functions, is to highlight (Fig. 4) the existence of regions of relatively more positive electrostatic potential lining the interior of the two paraquat components of the cyclophane. This anisotropic distribution of molecular electrostatic potential, associated with the paraquat residues, may be a consequence of the bowing distortions in the tetracation as a whole.

Addition of equimolar proportions of any of the isomeric dimethoxybenzenes, **3a**, **3b**, or **3c**, to $4 \cdot 4PF_6$ in CD_3CN results instantaneously in the formation of red or orange colored solutions (cf. Table 1),[8] suggesting that the π-electron-rich aromatic ethers are entering the cavity of **4** and experiencing stabilizing charge transfer interactions with the π-electron-deficient bipyridinium rings of **4**. This proposal is supported by ^{1}H-NMR spectroscopic studies on the 1:1 complexes (0.01–0.03 M) in CD_3CN solution: although, relative to spectra recorded for the free receptor and the substrates, the chemical shift changes ($\Delta\delta$) experienced by protons in the receptor are small ($\Delta\delta < 0.1$ ppm), those observed[9] for protons in **3a**, **3b**, and **3c** are appreciable ($\Delta\delta = -0.10$ to -0.91 ppm). When 0.5 molar equivalents of **3a** was added to a 0.01 M solution of $4 \cdot 4Cl$ in D_2O, the $\Delta\delta$ values were even more dramatic (-0.47 to -2.99 ppm for the methoxyl and aromatic protons, respectively, in **3a**) and, in this case, the chemical shift changes observed[10] for some of the protons in **4** were not insignificant. By employing (Table 1) the charge transfer band as a quantitative spectroscopic probe and subjecting the data to

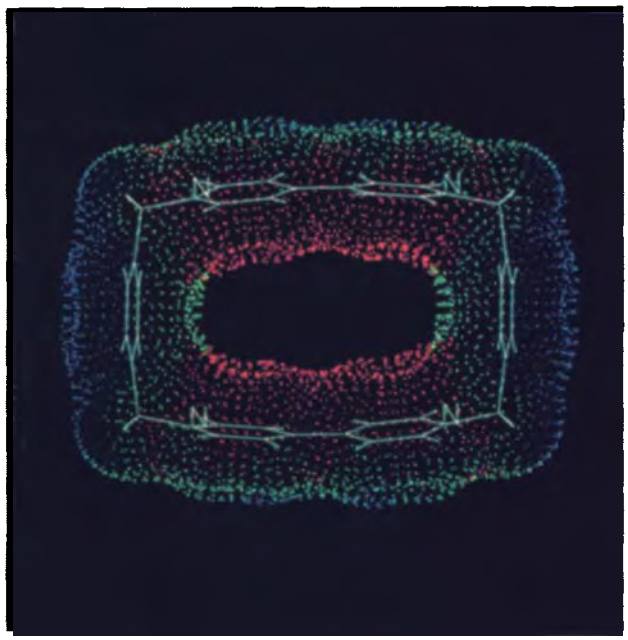

Fig. 4. The molecular electrostatic potential for **4** computed on a Connolly (QCPE Program No. 429) surface (red = positive, green = neutral, blue = negative).

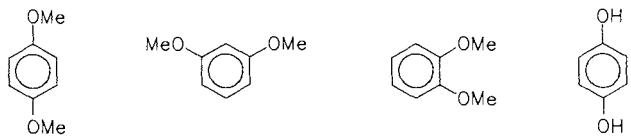

3a 3b 3c 6

a modified[11] Benesi-Hildebrand treatment[12] using experimental procedures recommended[13] for weak complex formation, 1:1 stoichiometries were established in MeCN solution for $4 \cdot 4PF_6 \cdot$ **3a**, $4 \cdot 4PF_6 \cdot$ **3b**, and $4 \cdot 4PF_6 \cdot$ **3c** with K_a values of 17.0, 8.0, and 8.1 M^{-1}, respectively. When the ^{1}H-NMR spectrum of $4 \cdot 4Cl \cdot$ **6** is recorded in D_2O, $\Delta\delta$ values of appreciable magnitude were noted[10] for some of the protons in **4**, whereas all the protons in **6** underwent rapid H/D exchange.[14]

Although many cyclophane hosts have been described[15] in the literature during the last decade, the new cyclobis(paraquat-*p*-phenylene) **4** offers novel design features of both a steric and electronic nature which give it considerable promise as a tetracationic multipurpose receptor.

Table 1. UV/VIS Spectroscopic data for complexes formed between the dimethoxybenzenes **3** and $4 \cdot PF_6$ in MeCN at 25°C [a].

Substrate	CT band λ_{max} (nm)	CT band $\varepsilon_{\lambda max}$ [b]	Substrate concentration [b] [M]	K_a [c] [M^{-1}]	$-\Delta G^0$ [kcal mol^{-1}]
3a	478	631	0.023–0.230	17.0 ± 0.5	1.68 ± 0.01
3b	484	392	0.023–0.450	8.0 ± 0.3	1.23 ± 0.02
3c	462	1025	0.034–0.454	8.1 ± 0.2	1.24 ± 0.01

[a] MeCN was distilled from P_2O_5 and then degassed. [b] The receptor concentration was held constant at 2.27×10^{-3} M and the substrate concentrations were varied accordingly to ensure that UV/VIS absorption data were obtained in those regions of the 'saturation curve' where errors are minimal, see ref. [11]. Since the UV/VIS spectrum of $4 \cdot 4PF_6$ in MeCN changes slowly with time, the substrates were added immediately after the spectrum for the receptor had been recorded, recognizing the need to correct for a very weak absorption ($\varepsilon_{\lambda max} \cong 30$) for the receptor in the 460–500 nm region. [c] The K_a values were obtained from the 'non-reciprocal format' modification described in Ref. [9] for expressing a Benesi-Hildebrand plot (see Ref. [10]) as well as establishing the 1:1 stoichiometry of the complex.

Experimental

4·4 PF_6: 1,4-Bis(bromoethyl)benzene (520 mg, 1.96 mmol) and **5** (1.20 g, 1.98 mmol) were dissolved in dry MeCN (300 mL) and the solution was heated under reflux for 24 h. A further quantity (200 mg, 0.76 mmol) of the dibromide was added to the reaction mixture and heating was continued for another 24 h. The yellow precipitate which formed was filtered off, dried, and subjected to chromatography [SiO_2 : MeOH/H_2O/satd. aq. NH_4Cl (6 : 3 : 1)] to afford a solid residue containing **4** as its tetrahalide after evaporation of the solvents under vacuum. This crude product was dissolved in the minimum volume of H_2O and a concentrated aqueous solution of NH_4PF_6 was added until no further precipitation was observed. The precipitate was filtered off, washed (H_2O), and recrystallized from Me_2CO/H_2O to give **4**·4 PF_6 (271 mg, 12%, assuming the salt is not solvated) as white needle-like crystals, decomp. >275 °C (It should be noted that these crystals become bluish-green on standing in the open laboratory during a few hours.)—FAB-MS: m/z = 955 ($[M-PF_6]^{\oplus}$); ^{1}H-NMR (CD_3CN): δ = 5.74 (s), 7.52 (s), 8.16 (d), 8.86 (d) with all signals having equal intensities (8H); ^{13}C-NMR (CD_3CN): δ = 65.7, 128.3, 131.4, 137.0, 146.2, 150.4.

4·4Cl: The pure tetrachloride **4**·4Cl was isolated as a precipitate from a solution of **4**·4 PF_6 in $MeNO_2$ after addition of an excess of Et_4NCl dissolved in $MeNO_2$ and careful washing of the precipitate with $MeNO_2$.

Received: June 16, 1988 [Z 2815 IE]
German version: *Angew. Chem. 100* (1988) 1605

CAS Registry numbers:
3a·(**4**·4 $PF_6^{\ominus}$), 117271-79-1; **3b**·(**4**·4 $PF_6^{\ominus}$), 117308-57-3; **3c**·(**4**·4 $PF_6^{\ominus}$), 117308-56-2; **4**·4 $PF_6^{\ominus}$, 117271-77-9; **4**·4 $Cl^{\ominus}$, 117271-78-0; (**4**·4 $PF_6^{\ominus}$)·3MeCN, 117271-81-5; (**4**·4 $PF_6^{\ominus}$)·2 $MeNO_2$·H_2O, 117271-80-4; **5**, 108861-20-7; 1,4-$(BrCH_2)_2C_6H_4$, 623-24-5.

[1] H. M. Colquhoun, J. F. Stoddart, D. J. Williams, *New Sci. 1 May 1986*, p. 44; B. L. Allwood, N. Spencer, H. Shahriari-Zavareh, J. F. Stoddart, D. J. Williams, *J. Chem. Soc. Chem. Commun. 1987*, 1064; P. R. Ashton, A. M. Z. Slawin, N. Spencer, J. F. Stoddart, D. J. Williams, *ibid. 1987*, 1066; A. M. Z. Slawin, N. Spencer, J. F. Stoddart, D. J. Williams, *ibid. 1987*, 1074; P. R. Ashton, E. J. T. Chrystal, J. P. Mathias, K. P. Parry, A. M. Z. Slawin, N. Spencer, J. F. Stoddart, D. J. Williams, *Tetrahedron Lett. 28* (1987) 6367; J. F. Stoddart, *Pure Appl. Chem. 60* (1988) 467.

[2] The systematic name for the tetracation cyclobis(paraquat-*p*-phenylene) is 5,12,19,26-tetraazoniaheptacyclo[24.2.2.2^{2,5}.2^{7,10}.2^{12,15}.2^{16,19}.2^{21,24}]tetraconta-1(28),2,4,7,9,12,14,16,18,21,23,26,29,31,33,35,37,39-octadecaene. The syntheses of the constitutionally isomeric derivatives containing (a) two *ortho*-, (b) two *meta*-, and (c) one *ortho*- and one *meta*-phenylene ring(s) have already been reported (W. Geuder, S. Hünig, A. Suchy, *Angew. Chem. 95* (1983) 501; *Angew. Chem. Int. Ed. Engl. 22* (1983) 489; *Tetrahedron 42* (1986) 1665. Although these tetracations were characterized as their tetrabromides and tetrakis(hexafluorophosphates), there is no report in these publications of them forming inclusion complexes. However, after our communication had been submitted for publication, we received from Professor *Hünig* a copy of a communication (M. Buhner, W. Geuder, W.-K. Gries, S. Hünig, M. Koch, T. Poll, *Angew. Chem. 100* (1988) 1611; *Angew. Chem. Int. Ed. Engl. 27* (1988) 1553) in which the ability of a number of different tetracationic macrocycles (containing two paraquat units connected in a phane-like manner by means of bridges incorporating different aromatic residues) to form inclusion complexes with a range of neutral guests is described.

[3] Interestingly, it proved impossible to dissolve more than 0.5 molar equivalents of 1,4-dimethoxybenzene (**3c**) in a 0.01 M solution of **4**·4Cl in D_2O.

[4] Nicolet R3m diffractometer, ω-scans, $Cu_{K\alpha}$ radiation (graphite monochromator). The structure was solved by direct methods and refined anisotropically. Further details of the crystal structure investigation can be obtained from the Cambridge Crystallographic Data Centre, University Chemical Laboratory, Lensfield Road, Cambridge CB2 1EW (England). Any request should be accompanied by the full literature citation for this communication.

[5] Single crystals, suitable for X-ray crystallography, were grown by vapor diffusion of iPr_2O into a solution of **4**·4 PF_6 (3 mg) in MeCN (1.5 mL). Change of the crystallization solvent from MeCN to $MeNO_2$ results in exchange of the acetonitrile molecules in the interleaving tori by nitromethane molecules without any noticeable perturbation of the extended channel structure. Crystal data for **4**·4 PF_6·2 $MeNO_2$·H_2O: monoclinic, a = 10.478(2), b = 20.152(4), c = 13.757(3) Å, β = 106.45(2)°, V = 2786 Å^3, space group $P2_1/n$, Z = 2 (the molecule is disposed about a center of symmetry), ρ = 1.48 g cm^{-3}, $\mu(Cu_{K\alpha})$ = 24 cm^{-1}, 2847 independent observed reflections [($|F_o| > 3\sigma|F_o|$), $\theta \leq 55°$], R = 0.089, R_w = 0.091. The H_2O molecule lies within the channels in two centrosymmetrically-related partial occupancy sites.

[6] Force field calculations using AMBER (P. A. Kollman, S. J. Weiner, D. T. Nguyen, D. A. Case, *J. Comput. Chem. 1* (1986) 230) and semiempirical quantum mechanical calculations, using AM1 (QCPE Program No. 506) (M. J. S. Dewar, E. G. Zoebisch, E. F. Healy, J. J. P. Stewart, *J. Am. Chem. Soc. 107* (1985) 3902) to encompass the residual charges required for modeling electrostatic interactions, predict a gross conformation for **4** that is in close accord (cyclophane dimensions, 10.3 × 7.2 Å, cf. 10.3 × 6.8 Å) with that observed by X-ray crystallography. Furthermore, these studies have demonstrated that there are two regions within the cyclophane that constitute favorable binding sites for MeCN molecules in accord, once again, with the X-ray structural observations.

[7] C. Giessner-Prettre, A. Pullman, *Theor. Chim. Acta (Berlin) 25* (1972) 83 (QCPE Program No. 249).

[8] Whilst the complexes formed by **3a** and **3c** afford deep-red solutions in MeCN and exhibit strong charge transfer bands at λ_{max} = 478 and 462 nm respectively, the complex formed by **3b** in MeCN is associated with a weak charge transfer band at λ_{max} = 484 nm and is orange in color.

[9] $\Delta\delta$ Values [ppm] in CD_3CN for substrate protons: in **4**·4 PF_6·**3a**, $\Delta\delta$ = −0.64 (H-2/3), −0.10 (OMe); in **4**·4 PF_6·**3b**, $\Delta\delta$ = −0.91 (H-2), −0.57 (H-4/6), −0.77 (H-5), −0.12 (OMe); in **4**·4 PF_6·**3c**, $\Delta\delta$ = −0.54 (H-3/6), −0.25 (H-4/5), −0.13 (OMe).

[10] $\Delta\delta$ Values [ppm] in D_2O for receptor protons: in **4**·4Cl·0.5 **3a**, $\Delta\delta$ = +0.14 (C_6H_4), +0.01 (CH_2), +0.03 (H-α), −0.10 (H-β); in **4**·4Cl·**6**, $\Delta\delta$ = +0.20 (C_6H_4), 0.01 (CH_2), +0.04 (H-α), −0.15 (H-β).

[11] R. Foster, D. L. Hammick, A. A. Wardley, *J. Chem. Soc. 1953*, 3817; R. Foster: *Organic Charge-Transfer Complexes*, Academic Press, London 1969, p. 125.

[12] H. A. Benesi, J. H. Hildebrand, *J. Am. Chem. Soc. 71* (1949) 2703.

[13] W. B. Person, *J. Am. Chem. Soc. 87* (1965) 167; D. A. Deranleau, *ibid. 91* (1969) 4044.

[14] In the absence of **4**·4Cl, the singlet resonance (δ = 6.72) for the aromatic ring protons of hydroquinone **6** can be detected in the ^{1}H-NMR spectrum recorded in D_2O. The catalysis of H/D exchange by **4**·4Cl is presently under investigation. The observation recalls the enhanced H/D exchange of the aromatic ring protons vicinal to the hydroxyl groups in 2,6- and 2,7-dihydroxynaphthalene when these two diols are dissolved in D_2O/DCl containing either a large macrobicyclic hexamine incorporating two triphenylethane bridgeheads (J. Franke, F. Vögtle, *Angew. Chem. 97* (1985) 224; *Angew. Chem. Int. Ed. Engl. 24* (1985) 219) or macrocyclic hexamides with side-arms containing pyridine units (F. Vögtle, W. M. Muller, *Angew. Chem. 96* (1984) 711; *Angew. Chem. Int. Ed. Engl. 23* (1984) 712).

[15] F. Diederich, *Angew. Chem. 100* (1988) 372; *Angew. Chem. Int. Ed. Engl. 27* (1988) 362 and references cited therein.

Isostructural, Alternately-Charged Receptor Stacks. The Inclusion Complexes of Hydroquinone and Catechol Dimethyl Ethers with Cyclobis(paraquat-*p*-phenylene)**

By *Peter R. Ashton, Barbara Odell, Mark V. Reddington, Alexandra M. Z. Slawin, J. Fraser Stoddart,** and *David J. Williams*

Spectroscopic studies in solution[1] have provided evidence for the formation of 1 : 1 complexes between the cyclobis(paraquat-*p*-phenylene) tetracation **4**[2] and the constitutionally isomeric dimethoxybenzenes **3a**, **3b**, and **3c**. Here, we describe solid state structures of the 1 : 1 complexes formed between **4**·4 PF_6·2MeCN and (a) hydro-

[*] Dr. J. F. Stoddart, P. R. Ashton, M. V. Reddington
Department of Chemistry, The University
Sheffield S3 7HF (UK)
Dr. D. J. Williams, A. M. Z. Slawin
Chemical Crystallography Laboratory
Department of Chemistry, Imperial College
London SW7 2AY (UK)
Dr. B. Odell
Analytical Chemistry Division, Sittingbourne Research Centre
Shell Research Limited, Sittingbourne
Kent ME9 8AG (UK)

[**] This work was supported by the Agricultural and Food, and Science and Engineering Research Councils in the United Kingdom.

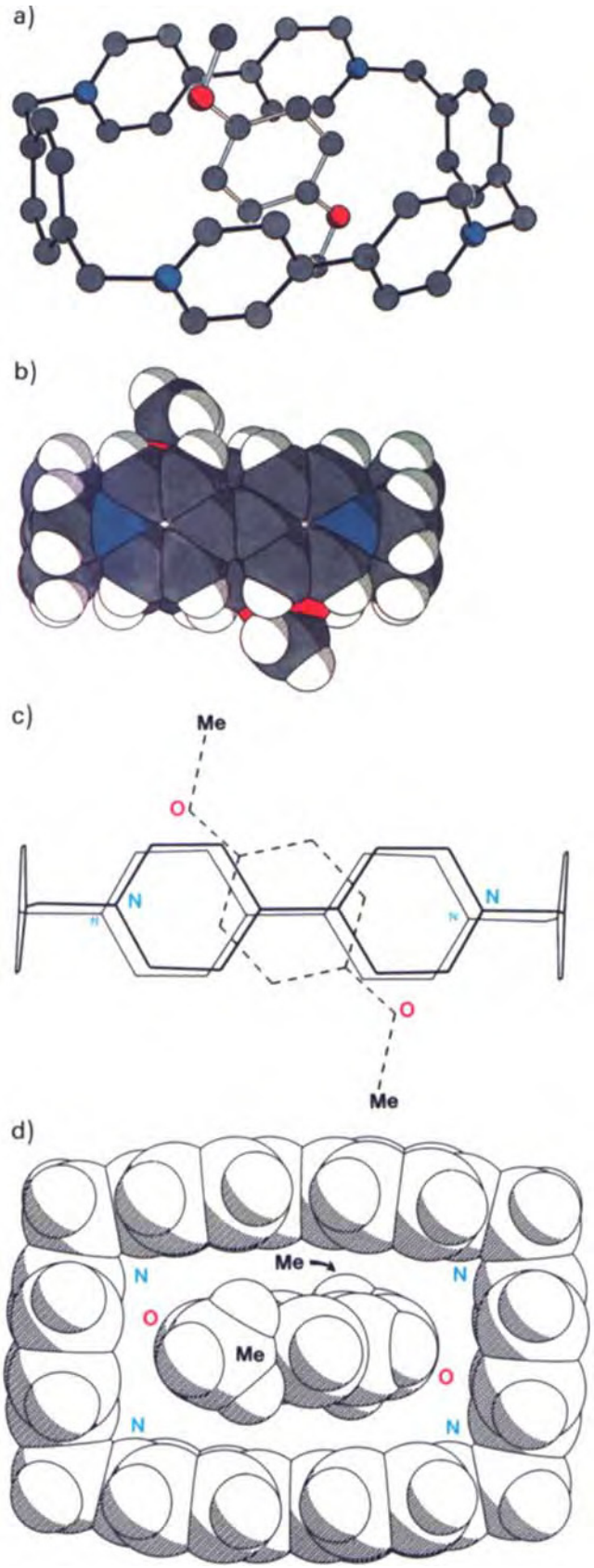

Fig. 1. a) Structure of **4**·**3a** in the crystal. Crystal data: monoclinic, $a = 10.948(4)$, $b = 19.869(8)$, $c = 13.886(6)$ Å, $\beta = 110.55(3)°$, $V = 2828$ Å^3, space group $P2_1/n$, $Z = 2$ (the molecule is disposed about a center of symmetry, $\rho = 1.45$ g cm^{-3}, $\mu(Cu_{K\alpha}) = 23$ cm^{-1}, 2935 independent observed reflections with ($|F_o| > 3\sigma(|F_o|$, $2\theta \leq 116°$), $R = 0.101$, $R_w = 0.110$. b/c) Space-filling and skeletal representation of **4**·**3a** viewed normal to the plane of **3a** showing the degree of envelopment of **3a** by **4**. d) Space-filling representation of **4**·**3a** viewed perpendicular to the mean plane of the cyclophane (H = white, C = gray, N = blue).

quinone dimethyl ether **3a** and (b) catechol dimethyl ether **3c**.

A striking feature of both complexes is the distinctive red color of the crystals: this indicates the retention, in the solid state, of the charge transfer (CT) interaction observed[1] in solution. Preliminary X-ray measurements showed that both complexes have the same space group, and virtually identical unit cell dimensions to those observed[1] for **4**·4 PF_6·3 MeCN.

The X-ray structure analysis[3] of **4**·4 PF_6·2 MeCN·**3a** shows (Fig. 1a) that the neutral hydroquinone dimethyl ether molecule is inserted through the center of the centrosymmetric tetracationic macrocyclic receptor **4** with the methyl groups of the methoxy substituents protruding above and below the rims of **4** (Fig. 1b/c). The gross structure of the **4**·4 PF_6·2 MeCN receptor is essentially the same as that observed previously[1] in the absence of **3a**. The overall dimensions of the rigid macrocyclic ring of **4** are virtually unchanged on complexation with **3a**. Likewise, the degree of bowing of the sides of the cyclophane is the same with the C–CH_2 bonds emanating from the *para*-phenylene units subtending an angle of 13° and the $N^{\oplus}$–CH_2 bonds associated with the paraquat units subtending an angle of 24°. The only significant change in the conformation of **4** on complexation with **3a** is a noticeable reduction (Fig. 1d) in the twist angle between the two pyridinium rings from 19° to 4°. This demonstrates the ability of **4** to flex so as to accommodate the π-electron-rich substrate **3a** within its π-electron-deficient cavity: this stereoelectronically-induced fit[4] does not, however, perturb the overall channel structure of the alternately-charged receptor stack. The relative arrangements of the four interleaving $PF_6^{\ominus}$ ions and two MeCN molecules is unchanged (Fig. 2) from that observed previously.[1] These are sandwiched in fixed positions between the upper and lower rims of adjacently-stacked tetracations, indicating a strong degree of stabilizing pole-pole and pole-dipole interactions.

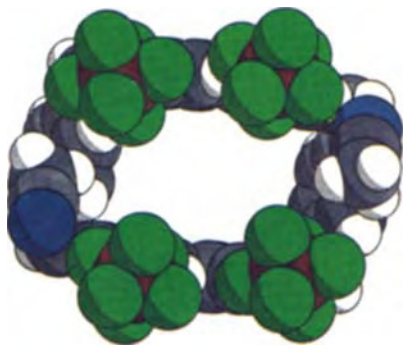

Fig. 2. Space-filling representation of part of the continuous stacked channel structure formed by **4** with the toroidal arrangement of the four $PF_6^{\ominus}$ ions and two MeCN molecules uppermost (H = white, C = gray, N = blue, P = brown, F = green).

The X-ray structural analysis[3] of **4**·4 PF_6·2 MeCN·**3c** shows (Fig. 3) that the neutral catechol dimethyl ether molecule is also included within the cavity of the tetracationic receptor **4**. However, unlike **3a**, which was positioned at about the center of symmetry within **4**, **3c** is disordered about this point.[5] As a consequence the catechol rings protrude significantly above and below the rims of **4**, though the external oxygen atoms of the methoxyl groups

Fig. 3. Skeletal representation of **4**·**3c** viewed approximately normal to the mean plane of **3c** showing the disordered arrangement of **3c** about the center of symmetry within **4** and the degree of protrusion of **3c** above and below the torus of **4**. One molecule of **3c** is highlighted in red and the other in blue. Crystal data: monoclinic, $a = 11.076(3)$, $b = 19.805(9)$, $c = 13.962(5)$ Å, $\beta = 111.57(2)°$, $V = 2848$ Å^3, space group $P2_1/n$, $Z = 2$ (the molecule is disposed about a center of symmetry), $\rho = 1.44$ g cm^{-3}, $\mu(Cu_{K\alpha}) = 23$ cm^{-1}, 3281 independent observed reflections with ($|F_o| > 3\sigma(|F_o|)$, $2\theta \leq 116°$), $R = 0.097$, $R_w = 0.110$.

occupy positions similar to those of the hydroquinone dimethyl ether in **4**·**3a** (Fig. 1c). A fortuitous consequence of this disordered arrangement[4] is an indication of the potential ability of **4** to complex with 1,5-dimethoxynaphthalene and related substrates.

Molecular mechanics geometry calculations using the AMBER force field,[6] together with atomic charges obtained using the AM1 SCF-MO procedure,[7] result in (Fig. 4) a predicted geometry of complexation for **4**·**3a** that is

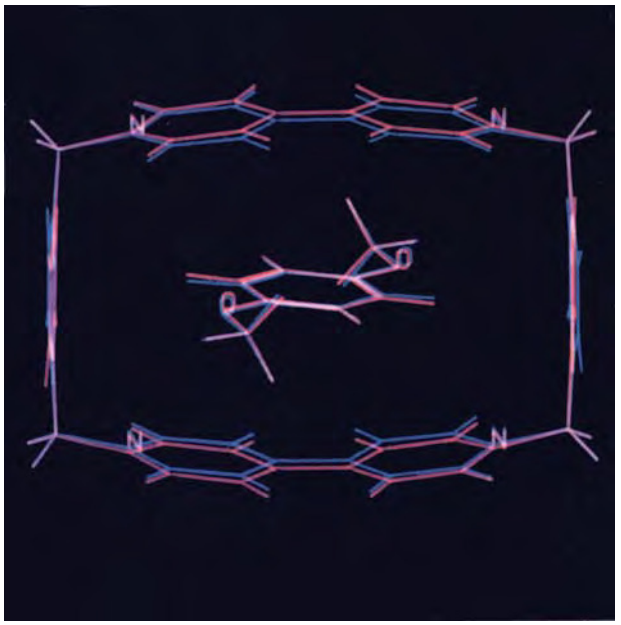

Fig. 4. Comparison of the calculated structure (red) of **4a**·**3a** with that (blue) obtained by X-ray crystallography.

almost identical with that observed in the X-ray crystal structure.

The majority of the cyclophane hosts already described[8] in the literature are just as likely to form clathrates in which the substrate molecules are accommodated between host molecules in the crystal lattice as they are to form complexes of the cavity inclusion type. By contrast, **4**·4 PF_6·2 MeCN appears, possibly as a result of the unique steric characteristics and electronic properties of **4**, to offer the exciting reality of an inexpensive synthetic receptor which is probably quite versatile in its substrate acceptance. Another fascinating feature of **4** is its propensity to form a channel structure in the crystalline state in which the rigid tetracations form an alternating charged stack cemented together electrostatically with *four* $PF_6^{\ominus}$ counterions and also *two* neutral MeCN molecules, irrespective of the nature of the substrate occupying the preorganized cavity of **4**. This type of crystal packing is characteristic of many of the inclusion complexes formed by the cyclodextrins[9] where intermolecular hydrogen bonding can stabilize stacks of these rigid naturally-occurring receptor molecules. Like the cyclodextrins, **4**·4 PF_6·2 MeCN can form inclusion complexes with a wide variety of substrates, some (e.g. **3c**) of which can diffuse out of and into the polar molecular chimneys of the receptor, producing the anticipated color changes under appropriate conditions[10] of temperature and pressure. The tantalizing prospect of a new class of inclusion compounds possessing 'zeolitic' characteristics and comprised of organic and inorganic ions and capable of including neutral organic molecules looms over the horizon.[11] The weak complexation exhibited by **4** in solution has important implications for its potential use in catalysis.

Experimental

4·4 PF_6·2 MeCN·**3a** and **4**·4 PF_6·2 MeCN·**3c**: In separate experiments, equimolar amounts (1 mg) of **3a** or **3c** were added to solutions of **4**·4 PF_6 (9 mg) in MeCN (0.7 mL). Crystals, suitable for X-ray crystallography, of **4**·4 PF_6·2 MeCN·**3a** and **4**·4 PF_6·2 MeCN·**3c**, were obtained from the deep-red solutions by vapor diffusion with iPr_2O. An attempt to determine the melting point of **4**·4 PF_6·2 MeCN·**3a** resulted in the following sequence of events: (i) during 5 min, the transparent crystals darkened and became opaque over the temperature range 87–92 °C, and then (ii) after raising the temperature for a further 10 min to 145 °C, the crystals gradually began to lose their color until (iii) this decoloration was complete after the temperature had been increased to 173 °C during 15 min before finally (iv) the crystals decomposed at > 275 °C. An attempt to determine the melting-point of **4**·4 PF_6·2 MeCN·**3c** resulted in the following sequence of events: (i) the transparent crystals darkened and became opaque at ca. 90 °C, and then (ii) over the temperature range 90–110 °C, the crystals gradually lost their red color during 8 min and became white before finally (iii) the crystals behaved in a manner reminiscent [1] of **4**·4 PF_6, i.e. they decomposed > 275 °C. In a separate experiment, **4**·4 PF_6·2 MeCN·**3c** (9 mg) was subjected to gradual heating under high vacuum (0.03 torr): at ca. 100 °C, the red color disappeared and subsequent ^{1}H-NMR spectroscopic analysis revealed only the presence of **4**·4 PF_6. When fresh clear crystals (14 mg) of **4**·4 PF_6 were immersed in **3c** for several days they gradually assumed a deep-red color: isolation after 14 days, followed by ^{1}H-NMR spectroscopy showed that **4**·4 PF_6 and **3c** were present in the ratio 1 : 1.

Received: June 16, 1988 [Z 2816 IE]
German version: *Angew. Chem. 100* (1988) 1608

CAS Registry numbers:
3a·**4**, 117409-26-4; **3a**·(**4** PF_6)·2 MeCN, 117409-22-0; **3b**·(**4** PF_6)·2 MeCN, 117409-24-2; **3c**·**4**, 117409-25-3.

[1] B. Odell, M. V. Reddington, A. M. Z. Slawin, N. Spencer, J. F. Stoddart, D. J. Williams, *Angew. Chem. 100* (1988) 1605; *Angew. Chem. Int. Ed. Engl. 27* (1988) 1547.
[2] The compound numbers are the same as those employed in the previous communication [1] where the structural formulas are also given.

[3] Nicolet R3m diffractometer, ω-scans, $Cu_{K\alpha}$ radiation (graphite monochromator). The structures were solved by direct methods and refined anisotropically. Further details of the crystal structure investigations can be obtained from the Cambridge Crystallographic Data Centre, University Chemical Laboratory, Lensfield Road, Cambridge CB2 1EW (England). Any request should be accompanied by the full literature citation for this communication.

[4] The principal intermolecular binding interactions in both **4**·**3a** and **4**·**3c** are (i) dispersion forces, including charge transfers (B. L. Allwood, N. Spencer, H. Shahriari-Zavareh, J. F. Stoddart, D. J. Williams, *J. Chem. Soc. Chem. Commun. 1987*, 1064; J. F. Stoddart, *Pure Appl. Chem. 60* (1988) 467), which involve the two paraquat units which are each separated by ca. 3.45 Å from the central parallelly-aligned dimethoxybenzene molecules (e.g. Fig. 1d) and (ii) electrostatic 'T-type' edge-to-face interactions (R. O. Gould, A. M. Gray, P. Taylor, M. D. Walkinshaw, *J. Am. Chem. Soc. 107* (1985) 5921; S. K. Burley, G. A. Petsko, *Science (Washington, DC) 229* (1985) 23; *J. Am. Chem. Soc. 108* (1986) 7995; A. M. Z. Slawin, N. Spencer, J. F. Stoddart, D. J. Williams, *J. Chem. Soc. Chem. Commun. 1987*, 1070; G. J. Moody, R. K. Owusu, A. M. Z. Slawin, N. Spencer, J. F. Stoddart, J. D. R. Thomas, D. J. Williams, *Angew. Chem. 99* (1987) 939; *Angew. Chem. Int. Ed. Engl. 26* (1987) 890) involving the *para*-phenylene units and the orthogonally-aligned dimethoxybenzene molecules (Figs. 1c and 3) with centroid-centroid distances of 5.1 and 4.8 Å for **4**·**3a** and **4**·**3c**, respectively.

[5] The degree of deformation of **4** in **4**·**3c** is the same as that observed in **4**·**3a**. The stacking of the tetracations **4** and the associated anions and MeCN molecules is also unchanged.

[6] P. A. Kollman, S. J. Weiner, D. T. Nguyen, D. A. Case, *J. Comp. Chem. 1* (1986) 230.

[7] QCPE Program No. 506. See also M. J. S. Dewar, E. G. Zoebisch, E. F. Healy, J. J. P. Stewart, *J. Am. Chem. Soc. 107* (1985) 3902.

[8] F. Diederich, *Angew. Chem. 100* (1988) 372; *Angew. Chem. Int. Ed. Engl. 27* (1988) 362 and references therein.

[9] W. Saenger, *Angew. Chem. 92* (1980) 343; *Angew. Chem. Int. Ed. Engl. 19* (1980) 344; W. Saenger in J. L. Atwood, J. E. D. Davies, D. D. MacNicol (Eds.): *Inclusion Compounds*, Vol. 2, Acacemic Press, London 1984, p. 231.

[10] The conditions under which catechol dimethyl ether (**3c**) will diffuse out of **4**·4 PF_6·2 MeCN·**3c** and into **4**·4 PF_6·2 MeCN are described in the *Experimental* section. The ease of diffusion of **3c** relative to that of hydroquinol dimethyl ether (**3a**) reflects (i) the observed disorder of **3c** in **4**·4 PF_6·2 MeCN·**3c** in the solid state and (ii) the relatively low K_a value (8.1 M^{-1}) for 1:1 complex formation between **3c** and **4**·4 PF_6 in MeCN solution. It is also interesting that, even although FABMS has proved to be a highly successful technique for the detection of noncovalently bonded complexes (i) between crown ethers and metal cations (R. A. W. Johnstone, M. E. Rose, *J. Chem. Soc. Chem. Commun. 1983*, 1286; R. A. W. Johnstone, I. A. S. Lewis, M. E. Rose, *Tetrahedron 39* (1983) 1597; P. D. Beer, *J. Chem. Soc. Chem. Commun. 1985*, 1115; D. W. Anderson, P. R. Ashton, R. M. Black, D. A. Leigh, A. M. Z. Slawin, J. F. Stoddart, D. J. Williams, *J. Chem. Soc. Chem. Commun. 1988*, 904), organic (B. L. Allwood, N. Spencer, H. Shahriari-Zavareh, J. F. Stoddart, D. J. Williams, *J. Chem. Soc. Chem. Commun. 1987*, 1064; P. R. Ashton, A. M. Z. Slawin, N. Spencer, J. F. Stoddart, D. J. Williams, *J. Chem. Soc. Chem. Commun. 1987*, 1066), and metalloorganic substrates (B. L. Allwood, H. M. Colquhoun, S. M. Doughty, F. H. Kohnke, A. M. Z. Slawin, J. F. Stoddart, D. J. Williams, R. Zarzycki, *J. Chem. Soc. Chem. Commun. 1987*, 1054; D. R. Alston, A. M. Z. Slawin, J. F. Stoddart, R. Zarzycki, *Angew. Chem. 99* (1987) 698; *Angew. Chem. Int. Ed. Engl. 26* (1987) 693), and (ii) between methylated cyclodextrins (P. R. Ashton, J. F. Stoddart, R. Zarzycki, *Tetrahedron Lett. 29* (1988) 2103) and organic ammonium salts, organometallic cations, and neutral metalloorganic complexes, all attempts, using a variety of different conditions, to obtain evidence for complex formation between either **3a** or **3c** and **4**·4 PF_6 were fruitless. When samples were run from a sulpholane-3-nitrobenzyl alcohol (3:1 v/v) matrix on a stainless steel probe, using a primary atom beam Xe^0 (8 keV) on a Kratos MS80RF mass spectrometer coupled to a DS55 data system, only evidence for the parent receptor $[M-PF_6]^{\oplus}$ ion at m/z 955 [1] was obtained. Considering that, with crown ethers K_a values (in organic solvents) of 10^3–10^7 M^{-1}, and with methylated cyclodextrins K_a values (in water) of ca. 10^3 have been measured for 1:1 complexes, it is hardly surprising that, in the case of **3a**·**4** and **3c**·**4**, where K_a values (in acetonitrile) of ca. 10 have been obtained, detection of complexed positive ions by FABMS is not revealed: this observation is entirely consistent with very weak complexation and lends support to the view that the technique is a reliable one for at least the semiquantitative evaluation of complexation strengths.

[11] In exhibiting clathration and inclusion simultaneously, the solid state structures of **4**·4 PF_6·2 MeCN·**3a** and **4**·4 PF_6·2 MeCN·**3c** have analogies with the recently reported [S. G. Bott, A. W. Coleman, J. L. Atwood, *J. Am. Chem. Soc. 110* (1988) 610] crystal structure of $[NH_4]_6$-[calix[4]arylsulfonate][$MeOSO_3$]·$(H_2O)_2$.

A Novel Type of Cationic Host Molecules with π-Acceptor Properties**

By *Manfred Bühner, Wolfram Geuder, Willi-Kurt Gries, Siegfried Hünig,* Michael Koch,* and *Thomas Poll*

Dedicated to Professor Friedrich Cramer on the occasion of his 65th birthday

The positive charges of macrocyclic onium host compounds have been used for two purposes: for the bonding of anions in host molecules[1,2] and to make macrocyclic compounds water-soluble; they can then take up lipophilic guests (such as chloroform, durene, naphthalene derivatives and polynuclear arenes as well as even cycloaliphatics like *trans*-1,4-cyclohexanediol and adamantanol) in their hydrophilic cavity in aqueous solution.[3,4]

Since most cationic host molecules are tailored for a multisided clasping of the guest,[1-3] the complex stability in the case of suitable host-guest complementarity is mainly determined by van der Waals, electrostatic, and hydrohobic interactions.[4] Aromatic guest molecules can, in addition, be more tightly bound by electron donor-acceptor (EDA) effects (polarization and electrostatic interactions). The weak donor properties of the alkyl-substituted benzene and/or anisole units of the known host compounds with passable topology do not suffice, however, to form charge transfer (CT) complexes even with strong acceptor guests.[3] Only when dibenzo[30–34]crown ethers are used as host for 2,2′- and 4,4′-bipyridinium ions are complexes with CT stabilization formed.[5] Bipyridinium ions are such strong π-acceptors that CT-complexes are even formed from **5** (with Me instead of $PhCH_2$ however) and hydroquinone,[6] *p*-phenylenediamine[7] or polynuclear arenes.[7]

Reversing the roles of host and guest we now present as host molecules the tetracations **1** and **2** in which two 4,4′-bipyridinium and 1,2-bis(4-pyridinium)ethene moieties, respectively, are so parallely arranged that they can embrace flat guest molecules in a sandwich-like fashion. **1** and **2** should form CT as well EDA complexes with π-donor guest compounds.

The following variations of the hosts have been examined:

1) π-System: different lengths (**1**, **2**).
2) Bridges X: a) same length but different flexibilities (**b**/**c**, *vide infra*); b) different lengths (**b**,**c** compared to **d**).

As reference substances we used the tetracationic cyclophanes **1a** and **2a**, the singly bridged derivatives **3a**[8]–**3d** and **4a**–**4d**, as well as the dicationic systems **5** and **6**.

The new onium compounds were synthesized according to a previously used scheme.[8-10] The dibromides **7a**–**7d** were first allowed to react with 4,4′-bipyridine and 1,2-bis(4-pyridinio)ethene, respectively, in acetonitrile to give the salts **8** and **9** (35–96%), which, upon reaction with further **7a**–**7d** in nitromethane furnished **1** and **2** respective-

[*] Prof. Dr. S. Hünig, Dr. W. Geuder, Dr. W.-K. Gries, Dipl.-Chem. M. Koch
Institut für Organische Chemie der Universität
Am Hubland, D-8700 Würzburg (FRG)
Dr. M. Bühner, Dr. T. Poll
Physiologisch-chemisches Institut der Universität
Am Hubland, D-8700 Würzburg (FRG)

[**] This work was supported by the Stiftung Volkswagenwerk, the Fonds der Chemischen Industrie, and BASF AG, Ludwigshafen (FRG).

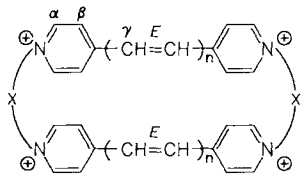

1, n = 0; 2, n = 1

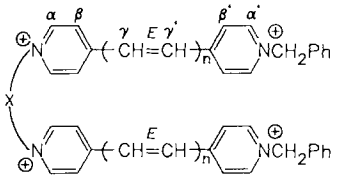

3, n = 0; 4, n = 1

X =

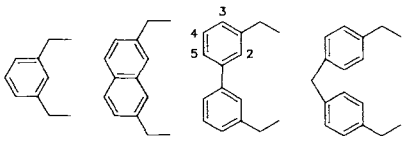

a b c d

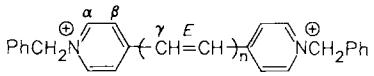

5, n = 0; 6, n = 1

ly, or with benzyl bromide **3** and **4**, respectively, in almost quantitative yields. The required dilution conditions are determined by the low solubility of the intermediary trications **8** and **9**. Nevertheless, polymers must be separated

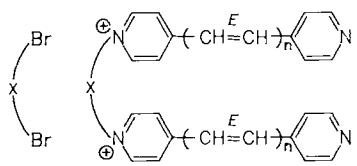

7a-d 8, n = 0; 9, n = 1

chromatographically. The synthesis of **1** and **2** frequently succeeds in a single-pot process from the bases and **7**. The yield increases thereby in the case of **1d** from 3-5% to 16% if phenanthrene is present in excess. This appears to be the first template effect of a hydrocarbon.[11]

The cations **1**-**6** have been isolated and characterized as PF_6-salts which are sparingly soluble in water.[12] Treatment of their solutions with tetrabutylammonium chloride leads to separation of the corresponding chlorides,[8] which we employed as the most readily soluble salts in water and methanol for the present studies.

The formation of complexes and especially of host-guest compounds of the cations **1**-**6** was tested as follows:

1. Detection of complex formation: Since all cations **1**-**6** are firmly retained on silica gel, the complex formation can be compared by thin-layer chromatography with a large number of UV-detectable arenes. The strength of the host-guest bond can thus be measured by the percentage lowering of the R_f value, referred to as the selectivity S.[13] According to Table 1 structurally very different pyridinium derivatives and almost all donors form adducts which are also identifiable by their typical CT absorptions (pale yellow to orange). Whereas the open-chain di- and tetracations **6** and **4d** hardly differ in their bonding ability, in the case of the cyclic tetracation **2a** with a small cavity the acceptor strength is frequently diminished. On the other hand, **2b**-**2d** and **1d**, as cyclophane hosts, bind some donors very strongly. **2b** and **2c** apparently have the most

Table 1. Thin-layer chromatographically determined selectivities $S=(1-R_f)/R_f^0\times 100$ (%) of various quaternary salts towards the donors **10**-**19** (silica gel, $MeOH/H_2O = 9:1$, $c = 1.7\times10^{-3}$ mol L^{-1}; **6**: $c = 6.7\times10^{-3}$ mol L^{-1}).

Donor		**6**	**4d**	**2a**	**2b**	**2c**	**2d**	**1d**
10	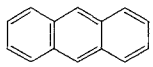	4	6	0	16	19	10	10
11	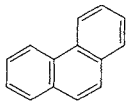	6	7	1	15	20	11	15
12	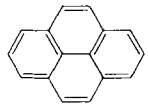	4	9	4	24	26	13	18
13	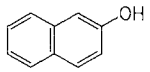	0	2	2	6	5	4	4
14	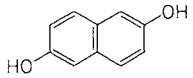	2	5	6	28	24	7	7
15	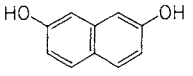	2	6	7	31	28	7	7
16	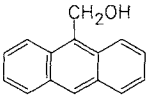	6	10	4	15	24	20	11
17	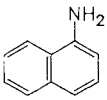	1	4	3	6	5	3	5
18	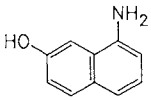	5	9	9	52	25	16	10
19	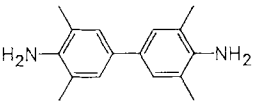	1	5	3	7	4	23	4

favorable dimensions for the majority of donors (**10**-**12**, **14**-**16**, **18**) whereas **2d** has too wide a bridge for some donors (**10**-**12**, **14**, **15**, **18**) and **1d** too short a π-acceptor system for some others (**16**, **18**, **19**). The large cavity of **2d** is of advantage only in the case of the particularly expanded donor **19**. Remarkable is the minimal binding of the monosubstituted naphthalenes **13** and **17** compared to the disubstituted derivatives **14**, **15**, and **18**.

2. Stoichiometry of the complex: By variation of the concentration ratio in CD_3OD/D_2O (3:1) of 2,7-dihydroxynaphthalene **15** as donor and the cationic acceptors **5**, **6** (reference compound), **3a**, **3d** (open-chain) and **2b**-**2d** (cyclic), the stoichiometry of the complex can be determined (Job's method[14]) from the change of the chemical shift of ^{1}H-NMR signals and from the change in extinction of the CT bands (**2b**-**2d** + **15**: $\lambda_{max} = 420$ nm). In all cases a 1:1 ratio is found. This suggests the accommodation of **15** in the cavity of **2b**-**2d** and a scissor-like clasping of the donor by **3a** and **3d**. An analogous behavior is assumed

for a tetracation in which the bipyridinium ions of **3d** are replaced by 2,7-diazapyrenium moieties.[15]

3. Association constants: Evaluation of ^{1}H-NMR titrations with **15** according to *Benesi* and *Hildebrand*[16] or *Scatchard*[17] gives the following association constants K (L mol^{-1}): **5**: 1.5±0.1; **6**: 2.1±0.3; **3a**: 2.3±0.6; **3d**: 2.7±0.5; **1d**: 3.5±1.2; **2d**: 13±3.3 (CD_3OD/D_2O 3:1; RT). From UV titrations the following were calculated: **6**: 9.1±0.1; **2b**: 95±5.8; **2c**: 46±4.9; **2d**: 20±0.1 (CH_3OH/H_2O 3:1; RT). In the case of the NMR and UV spectroscopically determined values, those for the cationic cyclophanes **2b**–**2d** are outstanding. As is often observed, the association constants in organic solvents are relatively small with narrow margins of variation.[2,3]

To find out the effects of water, the association constants for the systems **2b**–**2d**/anthracene **10**, phenanthrene **11** and pyrene **12** were estimated by solid/liquid extraction.[18] With $K = 10^5$–10^6 L mol^{-1}[19] they reach stabilities that have previously been achieved only with tetracationic hosts bearing outward directing ionic centers.[3]

4. Transport reactions in a triple-compartment stirrer system:[20] The tetracations transport arenes dissolved in hexane through water to a second hexane phase at different rates. From a comparison of solutions with tetracations and a carrier-free solution of the same ionic strength ($PhCH_2NEt_3Cl$) transport rates can be calculated as described previously,[21] the relative values of which (referred to **2a**) are listed in Table 2. The π-interactions between the arenes and the reference system **6**, the cyclic tetracation with too small a cavity (**2a**), and the open-chain cation **4d** suffice no longer for complexation. Obviously the accommodation in the cavities of **1d** or **2b**–**2d** is necessary for the transport of the hydrocarbons. The bond strength increases in the series anthracene, phenanthrene, pyrene, and decreases markedly for perylene, which is obviously too large for all cavities. Expansion of the cavity by the diphenylmethane bridges in **2d** has a destabilizing effect on all host-guest complexes, an effect which should have importance for the synthesis of intercalation compounds for nucleic acids.[15,22]

Table 2. Acceleration factors F, referred to **2a**, for the transport of arenes by carriers dissolved in water between two hexane phases (triple compartment system [20], 20°C, cf. text).

Arene	Carrier						
	1d	**2a**	**2b**	**2c**	**2d**	**4d**	**6**
Anthracene **10**	2	1	13	17	2	0.5	0.1
Phenanthrene **11**	6	1	16	39	3	—	—
Pyrene **12**	9	1	41	63	10	1.5	—
Perylene	1	1	4	3	3	0.6	0.4

5. Structure of the complex: Using **12** as example it can be shown that the required complementarity of the cavity of the host molecule is achievable in two ways: When solutions of **1b**, **2c** and **1d** in D_2O are treated with pyrene, only the ^{1}H-NMR spectrum of the solution of **1b** remains unchanged after brief sonication, whereas in the case of **2c** and **1d** the signals of the pyrene are observed. Since the bridges **b** and **c** keep the pyridinium units at the same distance of ca. 750 pm[23] the acceptor unit (including CH_2 groups) in **1b** must be too short (1020 pm); extension by a vinyl group to ca. 1230 pm provides an adequately sized cavity. This can, however, also be realized if the shorter acceptor system **1** is retained and a maximum cavity length of 1810 pm is provided by the longer bridge **d** (1020 pm) which is bent in the middle.

Upon accommodation of pyrene **12** the solutions of **2c** and **1d** become yellowish. This is due to a broadening of the long-wavelength absorption bands of **2c** (λ_{max} = 313, 322, 340 (sh) nm) and **1d** (λ_{max} = 256 nm) out to the visible range. In **1d**·pyrene, the typical pyrene absorption bands are not masked by those of the host. They are shifted, as in other host-guest complexes,[3] to longer wavelengths (324 nm and 341 nm). Also in these complexes the donor strength of the pyrene does not suffice for a CT interaction.

The opposing influence of the π-systems manifests itself ^{1}H-NMR spectroscopically in characteristic $\Delta\delta$ values (Table 3). The sandwich-like inclusion of pyrene **12** leads, in contrast to the stronger spherical inclusion,[3,24] to the signal of the apical H^2-atoms experiencing the largest upfield shift. Also the stronger influence of the pyridinium H-atoms in **2c** compared to those in **1d** is plausible.

Simulation of the energies (with optimized geometry) of pyrene **12** (49 kJ mol^{-1}), **1b** (179), **1d** (190), **2c** (234) and of their host-guest complexes with the aid of MM2 force field calculations[23] gives the following overall picture, which, however, takes neither EDA- and hydrophobic interactions nor entropic effects into account: For the host **1b**, which does not accomodate **12** in the cavity, the equilibrium host + guest ⇄ host·guest (382) in the case of longitudinal incorporation of the guest is completely on the lefthand side ($\Delta H = +154$ kJ mol^{-1}).

In the cases of lateral insertion of **12** in **1b**, ΔH is calculated to be -60 kJ mol^{-1}; however the overlapping of the π systems is then substantially smaller, so that the hydrophobic interactions cannot be fully exploited. In contrast, the complexes **1d**·**12** ($\Delta H = -58$ kJ mol^{-1}) and **2c**·**12** ($\Delta H = -77$ kJ mol^{-1} are already strongly favored according to the interactions taken into account by the MM2 program.

The models of the host-guest compounds **2c**·**12** and **1d**·**12** (Fig. 1) generated according to the calculations also clearly indicate that a smaller complexation constant can

Table 3. ^{1}H-NMR shifts $\Delta\delta$ of host and guest protons upon formation of the complexes **1d**·pyrene and **2c**·pyrene in D_2O [a]. Ar = aryl.

	Host: **1d**					Guest: pyrene **12** [b]		
	Ar–CH_2–Ar	Ar–CH_2–Py$^\oplus$	Ar–H	β-Py$^\oplus$	α-Py$^\oplus$	H^1	H^2	H^4
$\Delta\delta$	−0.06	+0.12	−0.09	+0.88	+0.24	+1.37	+1.73	+0.94

	Host: **2c**						Guest: pyrene **12** [b]		
	biphenylene			HC=	β-Py$^\oplus$	α-Py$^\oplus$	H^1	H^2	H^4
$\Delta\delta$	−0.01	−0.12	+0.64	−0.04	−0.07	+0.18	+1.57	— [c]	+0.79

[a] 200 MHz, $c_{host} = 1.4 \times 10^{-2}$ mol L^{-1} (**1d**); 3.4×10^{-4} mol L^{-1} (**2c**). After 15 minutes ultrasonic treatment with excess pyrene, the filtered solution was measured. +$\Delta\delta$ = high-field shift **2c** and **1d** are present at least up to 0.1 mol L^{-1} as molecular dispersion (^{1}H-NMR). [b] Comparative value in [D_4]methanol (δ = 3.5): δ = 8.38 (d, $J_{1,2}$ = 7.3 Hz; 1-H), 8.19 (t, $J_{1,2}$ = 1.3 Hz; 2-H), 8.27 (s; 4-H). [c] Signals cannot be assigned with certainty.

be expected in the second case. The structure of the host molecules remains virtually unchanged during the adduct formation.

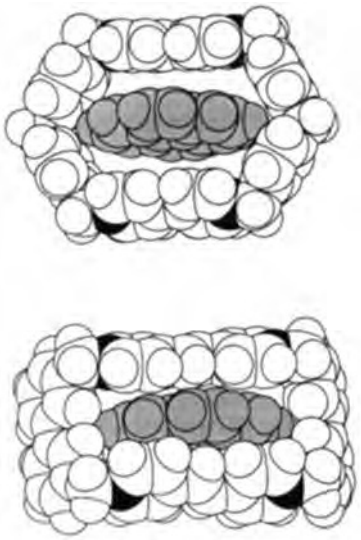

Fig. 1. Top: Space-filling model (SCHAKAL program) according to the optimized geometries [23] of the host-guest molecule **2c**·pyrene. Bottom: Space-filling model (SCHAKAL program) according to the optimized geometries [23] of the host-guest molecule **1d**·pyrene.

The examples given here show that arenes are bound by cationic hosts when these are stabilized in the sandwich-like structure of the host-guest complex by strong EDA and/or CT interactions and the otherwise usual factors. It is then unnecessary for the host cavity to be completely enveloped and the charge centers to lie on the periphery.[2,3] As reported in the preceding communications, *J. F. Stoddart* et al. have synthesized a tetracation of type **1** with two *p*-xylylene bridges by the method described here and have characterized host-guest compounds containing dimethoxybenzenes.[25]

Received: July 15, 1988 [Z 2863 IE]
German version: *Angew. Chem. 100* (1988) 1611

[1] Review: F. P. Schmidtchen, *Nachr. Chem. Tech. Lab. 36* (1988) 8.
[2] Review: F. Vögtle, H.-G. Löhr, J. Franke, D. Worsch, *Angew. Chem. 97* (1985) 721; *Angew. Chem. Int. Ed. Engl. 24* (1985) 727.
[3] Review: F. Diederich, *Angew. Chem. 100* (1988) 372; *Angew. Chem. Int. Ed. Engl. 27* (1988) 362.
[4] C. Tanford, *Science Washington 200* (1978) 1012.
[5] J. F. Stoddart, *Pure Appl. Chem. 60* (1988) 467, and earlier publications.
[6] A. Ledwith, H. J. Woods, *J. Chem. Soc. Chem. Commun. 1970*, 1422.
[7] B. G. White, *Trans. Faraday Soc. 65* (1969) 2000.
[8] W. Geuder, S. Hünig, A. Suchy, *Tetrahedron 42* (1986) 1665; *Angew. Chem. 95* (1983) 501; *Angew. Chem. Int. Ed. Engl. 22* (1983) 489.
[9] W. Geuder, *Dissertation*, Universität Würzburg 1985.
[10] W.-K. Gries, *Dissertation*, Universität Würzburg 1987.
[11] Whether the increase in yield described by K. Saigo, R.-J. Lin, M. Kubo, A. Youda, M. Hasegawa (*J. Am. Chem. Soc. 108* (1988) 1996) is to be considered as a template effect must remain open, since the macrocycle formed only binds benzene in the lattice in the crystalline state.
[12] IR, UV, ^{1}H- and ^{13}C-NMR spectra as well as elemental analyses are consistent with the given structures.
[13] H.-J. Schneider, W. Müller, D. Güttes, *Angew. Chem. 96* (1984) 909; *Angew. Chem. Int. Ed. Engl. 23* (1984) 910.
[14] P. Job, *Ann. Chim. Paris 9* (1928) 113; E. Asmus, *Z. Anal. Chem. 183* (1961) 321, 401.
[15] A. J. Blacker, J. Jazwinski, J.-M. Lehn, *Helv. Chim. Acta 70* (1987) 1.
[16] H. A. Benesi, J. H. Hildebrand, *J. Am. Chem. Soc. 71* (1949) 2703.
[17] G. Scatchard, *Ann. N. Y. Acad. Sci. 51* (1949) 660.
[18] F. Diederich, K. Dick, *J. Am. Chem. Soc. 106* (1984) 8024.
[19] A discussion of the individual values is not possible because of the inaccuracy of the method. Cf. M. A. Petti, T. J. Shepodd, D. A. Dougherty, *Tetrahedron Lett. 27* (1986) 807.
[20] A slightly modified version of the apparatus originally developed for enantiomeric separations was used: V. Prelog, M. Dumic, *Helv. Chim. Acta 69* (1986) 5.
[21] A. Xenakis, C. Tondre, *J. Phys. Chem. 87* (1983) 4737.
[22] A. J. Blacker, J. Jazwinski, J.-M. Lehn, F. X. Wilhelm, *J. Chem. Soc. Chem. Commun. 1986*, 1035.
[23] MM2 program: N. L. Allinger, *J. Am. Chem. Soc. 99* (1977) 8127. The distances are referred to the atomic centers.
[24] F. Vögtle, W. M. Müller, U. Werner, H. W. Losensky, *Angew. Chem. 99* (1987) 930; *Angew. Chem. Int. Ed. Engl. 26* (1987) 901.
[25] J. F. Stoddart, N. Spencer, M. V. Reddington, D. J. Williams, A. M. Z. Slawin, B. Odell, *Angew. Chem. 100* (1988) 1605; *Angew. Chem. Int. Ed. Engl. 27* (1988) 1547; J. F. Stoddart, P. R. Ashton, M. V. Reddington, D. J. Williams, A. M. Z. Slawin, B. Odell, *ibid. 100* (1988) 1608 and *27* (1988) 1550.

Gas Chromatographic Separation of Enantiomeric Olefins**

By *Jens Ehlers, Wilfried A. König,* Sabine Lutz, Gerhard Wenz,* and *Heindirk tom Dieck**

Dedicated to Professor Hans Bock on the occasion of his 60th birthday

The enantiomeric excess in catalytic reactions of olefinic substrates is often very difficult to determine, because mixtures of substances can form and the optical rotations of many compounds are not known. Since, in addition, the synthesis of diastereomers frequently poses problems, the enantioselectivity in some cases cannot be determined at all or only with great difficulty.

We were able to show that optically active 1,4-diaza-1,3-dienes (dad = $R^1N{=}CR'{-}CR''{=}NR^2$) in catalytically active fragments "(dad)Fe" catalyze the enantioselective coupling of dienes to give cyclodimers.[1] The reaction of ethene with 1,3-dienes and norbornadiene may also be achieved under mild conditions. For example, (*Z*)-3-methyl-1,4-hexadiene **1** is obtained by reaction of (*E*)-1,3-pentadiene and ethene. Similary, norbornadiene gives *endo*-3-vinylnortricyclane **2**, which has also been obtained with cobalt catalysts.[2] By using chiral dad cocatalysts, op-

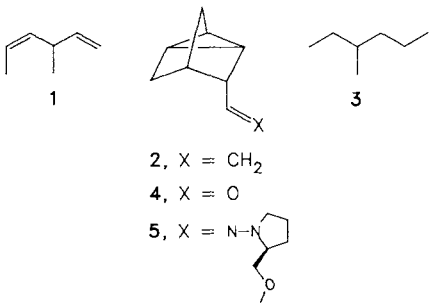

[*] Prof. Dr. H. tom Dieck, Dipl.-Chem. J. Ehlers
Institut für Anorganische und Angewandte Chemie der Universität
Martin-Luther-King-Platz 6, D-2000 Hamburg 13 (FRG)
Prof. Dr. W. A. König, Dipl.-Chem. S. Lutz
Institut für Organische Chemie der Universität
Martin-Luther-King-Platz 6, D-2000 Hamburg 13 (FRG)
Dr. G. Wenz
Max-Planck-Institut für Polymerforschung
Jakob-Welder-Weg 11, D-6500 Mainz (FRG)

[**] Diazadienes as Controlling Ligands in Homogeneous Catalysis, Part 16. Part 15: H. tom Dieck, M. Mallien, R. Diercks, *J. Mol. Cat.*, in press. Part 14: M. Mallien, E. T. K. Haupt, H. tom Dieck, *Angew. Chem. 100* (1988) 1091; *Angew. Chem. Int. Ed. Engl. 27* (1988) 1062.

tically active products are obtained. The enantiomeric excess and the configuration of the major isomer were determined for **1** by hydrogenation and comparison of the optical rotation with that of independently synthesized, optically pure 3-methylhexane **3**—a relatively involved procedure.[3,4] In the case of **2**, the vinyl group was transformed into an aldehyde function (**4**) by oxidation with *m*-chloroperbenzoic acid and cleavage with periodic acid, and the aldehyde was then converted into the aldehyde-SAMP hydrazone **5**.[5] The *ee* value of **5** could be determined from the OCH_3 signal in the ^1H NMR spectrum.

König et al. recently introduced new α- and β-cyclodextrin phases as chiral stationary phases for capillary gas chromatography[6] to separate a variety of enantiomers at temperatures up to at least 210°C. The enantiomeric separation of the aldehyde **4** was achieved on heptakis(2,3,6-tri-*O*-*n*-pentyl)-β-cyclodextrin as a stationary phase.

Surprisingly, it was also possible to separate easily the olefins **1** (Fig. 1) and **2** into their enantiomers. The results (Table 1) are in good agreement with the enantiomeric excesses determined by chemical methods. There have only been scattered reports on the chromatographic separation of chiral olefins.[7]

Table 1. Enantiomeric yields and absolute configuration of the major isomer of catalysis products separated by gas chromatography.

Product	*ee* [%] (configuration)	$[\alpha s]_D^{20}$ [a] (c [g mL^{-1}])	Controlling ligand [b]
1	37 (*S*)	−34.8 (0.1)	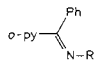
2	20 (?)	−12.6 (neat)	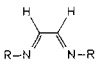
6	31 (*S*)	−12.0 (0.8)	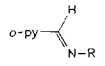
7	34 (?)	[c]	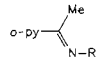

[a] **1** in CH_2Cl_2, **6** in Et_2O. [b] *o*-py = 2-pyridyl; R = (1*R*,2*S*,5*R*)-menthyl. [c] Not determined.

In further experiments, we were able to show that 3,5-dimethyl-1,4-hexadiene **6**,[4] obtained from ethene and 2-methyl-1,3-pentadiene on an optically active catalyst, could be resolved into enantiomers on this phase (Fig. 1). Finally, two products of the iron-catalyzed addition of isoprene to norbornadiene (**7** and **8**) were investigated. The *exo* adduct **7** is separated (Table 1), the 1,6 *endo* adduct is

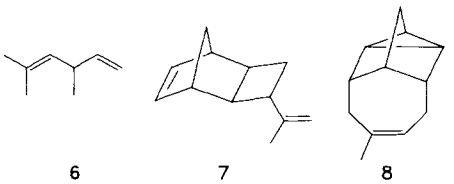

6 7 8

not. The latter finding might be due to the spherical shape of the molecule or the absence of a sterically easily accessible double bond.

The possibility of separating many chiral olefins by gas chromatography will undoubtedly encourage the optimization of enantioselective homogeneously catalyzed reactions.

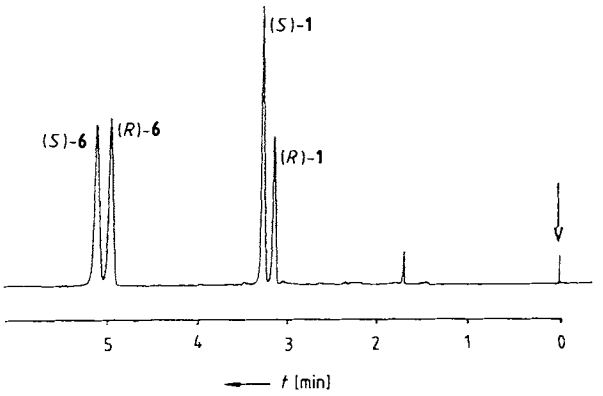

Fig. 1. Gas-chromatographic separation of the chiral olefins **1** and **6** (42-m perpentyl-β-CD column, 25°C, 1 bar H_2, head-space injection).

Experimental Procedure

1 was obtained from (*E*)-1,3-pentadiene and ethene in excess (carried out in a glass ampoule, 50 bar counter pressure in an autoclave) in the presence of 1 mol% of "(dad)Fe" [1] at room temperature. ^1H NMR (360 MHz, $CDCl_3$): $\delta = 5.75$ (dddd), 5.43 (dq), 5.22 (ddq), 4.97 (ddd), 4.89 (ddd), 3.45 (ddq), 1.61 (dd), 1.05 (d). Hydrogenation of **1** on Pd/C gave 3-methylhexane **3**. Optically pure (*R*)-(−)-3-methylhexane was obtained from (*S*)-(−)-citronellol by a similar procedure to that in [3]: it was transformed into the olefin by tosylation and $LiAlH_4$ reduction. (*S*)-4-Methylhexanal, obtained by oxidation of this olefin with *m*-chloroperbenzoic acid and cleavage with periodic acid, was reduced to (*R*)-(−)-**3** by Wolff-Kishner reduction: $[\alpha]_D^{20} = -6.8$ ($c = 0.1$ in Et_2O) [4]. From the gas-chromatographic separation and the *ee* value of **1**, we calculated a value of +6.5 for (*S*)-(+)-**3** ($c = 0.1$ in CH_2Cl_2).

2: Synthesized from norbornadiene and ethene in analogy to **1**. ^{13}C NMR (90.5 MHz, $CDCl_3$): $\delta = 139.33$, 114.46, 48.28, 34.29, 34.17, 29.13, 14.19, 11.28, 9.54. MS (70 eV): *m/z* 120 (23%, $M^{\oplus}$), 105 (80), 92 (100), 91 (96), 79 (89), 77 (49), 66 (68).

4: IR: $\tilde{\nu} = 1760$ cm^{-1} (C=O); ^1H NMR (360 MHz, $CDCl_3$): $\delta = 9.64$ ($^3J = 2.3$ Hz, CHO). MS (70 eV): *m/z* 122 (25%, $M^{\oplus}$), 93 (57), 91 (97), 79 (25), 78 (74), 77 (100), 66 (38). Isothermal gas-chromatographic separation at 50°C (in CH_2Cl_2).

5: Synthesis from **4** following the procedure in [5]. ^1H NMR (360 MHz, $CDCl_3$): $\delta = 3.394$, 3.390 (OCH_3). MS (70 eV): *m/z* 234 (3%, $M^{\oplus}$), 189 (100), 118 (21), 93 (16), 91 (32), 77 (20), 70 (30). *ee* from the NMR spectrum 20%.

6: Synthesis from 2-methyl-1,3-pentadiene in analogy to **1**. ^{13}C NMR (90.5 MHz, $CDCl_3$): $\delta = 149.4$, 130.9, 128.6, 111.7, 36.5, 25.7, 20.6, 17.8. ^1H NMR (360 MHz, $CDCl_3$): $\delta = 5.76$ (ddd), 4.96 (dqq), 4.95 (dd), 4.88 (dd), 3.04 (ddq), 1.69 (d), 1.62 (d), 1.03 (d). MS (70 eV): *m/z* 110 (36%, $M^{\oplus}$), 95 (100), 67 (64), 55 (37), 53 (14), 41 (37), 39 (29). Synthesis of **7** and **8** from norbornadiene and isoprene; purification by preparative GC and separation of isodimers.

7: ^{13}C NMR (90.5 MHz, $CDCl_3$): $\delta = 148.8$, 135.8, 135.0, 107.4, 44.4, 44.1, 42.3, 40.6, 40.4, 33.3, 24.9, 20.5. MS (70 eV): *m/z* 160 (5%, $M^{\oplus}$), 94 (58), 93 (46), 92 (52), 91 (83), 79 (100), 66 (65), 39 (30). Temperature-programmed gas-chromatographic separation: $T_0 = 50$°C, *T* increase 2°/min, in CH_2Cl_2, retention times ca. 26 and 26.2 min.

8: ^{13}C NMR (90.5 MHz, $CDCl_3$): $\delta = 134.9$, 121.4, 41.2, 40.9, 40.6, 35.4, 29.7, 27.5, 13.7, 10.6. MS (70 eV): *m/z* 160 (16%, $M^{\oplus}$), 94 (30), 91 (52), 81 (23), 80 (100), 79 (71), 77 (29), 39 (29).

Received: July 1, 1988 [Z 2840 IE]
German version: *Angew. Chem. 100* (1988) 1614

CAS Registry numbers:
(±)-**1**, 117310-08-4; (*S*)-**1**, 117406-02-7; (±)-**2**, 117310-11-9; (±)-**6**, 117310-09-5; (*S*)-**6**, 117406-03-8; (±)-**7**, 117310-10-8; (±)-**8**, 117310-12-0; heptakis(2,3,6-tri-*o*-*n*-pentyl)-β-cyclodextrin, 117340-78-0.

[1] H. tom Dieck, J. Dietrich, *Angew. Chem. 97* (1985) 795; *Angew. Chem. Int. Ed. Engl. 24* (1985) 781; *Chem. Ber. 117* (1984) 694.
[2] J. E. Lyons, H. K. Myers, A. Schneider, *J. Chem. Soc. Chem. Commun. 1978*, 638.
[3] K. Mori, T. Suguro, M. Uchida, *Tetrahedron 34* (1978) 3119.
[4] In P. A. Levene, R. E. Marker, *J. Biol. Chem. 91* (1931) 761, a value of $[\alpha]_D^{22} = 3.67$ was given for (*S*)-(+)-**3** and adjusted to 9.9 by a presumably false comparison. For (*S*)-(+)-2,4-dimethylhexane, the hydrogenation

product of **6**, a value of $[\alpha]_D^{22} = 21.3$ (homogeneous) was given. By means of a chiral catalysis, gas-chromatographic *ee* determination, and hydrogenation, the *R/S* sequence shown in Figure 1 can be assigned to **6**. $[\alpha]_D^{20}$ of the hydrogenation product was determined to be +19.5 ($c = 0.15$ in CH_2Cl_2).

[5] D. Enders, H. Kipphardt, *Nachr. Chem. Tech. Lab. 33* (1985) 882.

[6] W. A. König, S. Lutz, G. Wenz, *Angew. Chem. 100* (1988) 989; *Angew. Chem. Int. Ed. Engl. 27* (1988) 979; W. A. König, S. Lutz, G. Wenz, E. von der Bey, *J. High Resolut. Chromatogr. Chromatogr. Commun. 11* (1988) 506; W. A. König, S. Lutz, C. Colberg, N. Schmidt, G. Wenz, E. von der Bey, A. Mosandl, C. Günther, A. Kustermann, *ibid. 11* (1988), in press.

[7] Gas-chromatographic separation on a chiral Rh complex: V. Schurig, *Angew. Chem. 89* (1977) 113; *Angew. Chem. Int. Ed. Engl. 16* (1977) 110; gas-chromatographic separation of e.g. α-pinene on methylated cyclodextrin phases: T. Koscielski, D. Sybilska, S. Belniak, J. Jurczak, *Chromatographia 21* (1986) 413; V. Schurig, H.-P. Novotny, *J. Chromatogr. 441* (1988) 155; liquid chromatographic separation on Pt complexes: M. Goldmann, Z. Kustanovich, A. Tishbee, E. Gil-Av, *Vth Int. Symp. Column Liquid Chromatogr.* (Avignon, May 1981); J. Köhler, G. Schomburg, *Chromatographia 14* (1981) 559; *J. Chromatogr. 255* (1983) 311.

Reaction of Tropone with a Homopyrrole. The Result of a Computer-Assisted Search for Unique Chemical Reactions**

By *Dietmar Forstmeyer, Johannes Bauer, Eric Fontain, Rainer Herges, Rudolf Herrmann,* and *Ivar Ugi**

Dedicated to Professor Heinrich Nöth on the occasion of his 60th birthday

The computer-assisted discovery of novel molecules and reactions is especially challenging with regard to the use of computers in chemistry. The computer program IGOR (Interactive Generation of Organic Reactions) first described by *Bauer* and *Ugi* in 1982[1] is based on the theory of ***B/E*** and ***R*** matrices (the matrices ***B*** and ***E*** describe the chemical constitution of starting materials and products, respectively; the matrix ***R*** corresponds to the electron shift scheme of the reaction)[2] and can generate any desired molecules and chemical reactions with a reaction generator.[3,4] From the theory of the ***B/E*** and ***R*** matrices a hierarchical classification of chemical reactions can also be derived,[5] which enables the degree of novelty of a unique reaction to be determined.[6,7] In the search for reactions with a high degree of novelty the irreducible matrix $\boldsymbol{R}^{C}_{10,10}$ of the resonance of $10\pi_e$-arenes was incorporated into IGOR2, a modified PC-adaptable FORTRAN 77 version of IGOR.

$$\boldsymbol{R}^{C}_{10,10} = \begin{pmatrix} 0 & -1 & 0 & 0 & 0 & 0 & 0 & 0 & 0 & 1 \\ -1 & 0 & 1 & 0 & 0 & 0 & 0 & 0 & 0 & 0 \\ 0 & 1 & 0 & -1 & 0 & 0 & 0 & 0 & 0 & 0 \\ 0 & 0 & -1 & 0 & 1 & 0 & 0 & 0 & 0 & 0 \\ 0 & 0 & 0 & 1 & 0 & -1 & 0 & 0 & 0 & 0 \\ 0 & 0 & 0 & 0 & -1 & 0 & 1 & 0 & 0 & 0 \\ 0 & 0 & 0 & 0 & 0 & 1 & 0 & -1 & 0 & 0 \\ 0 & 0 & 0 & 0 & 0 & 0 & -1 & 0 & 1 & 0 \\ 0 & 0 & 0 & 0 & 0 & 0 & 0 & 1 & 0 & -1 \\ 1 & 0 & 0 & 0 & 0 & 0 & 0 & 0 & -1 & 0 \end{pmatrix}$$

[*] Prof. Dr. I. Ugi, Dipl.-Chem. D. Forstmeyer, Dr. J. Bauer, Dr. E. Fontain, Dr. R. Herrmann
Institut für Organische Chemie der
Technischen Universität München
Lichtenbergstrasse 4, D-8046 Garching (FRG)
Dr. R. Herges
Institut für Organische Chemie der Universität
Erlangen-Nürnberg
Henkestrasse 4, D-8520 Erlangen (FRG)

[**] This work was supported by the Deutsche Forschungsgemeinschaft and the Fonds der Chemischen Industrie.

One of the results (***B***, ***E***) of the IGOR 2 analysis of ***R***, the reaction **1** + **2** → **3**, corresponds to the unique basic reaction[3] **4** + **5** → **6**.

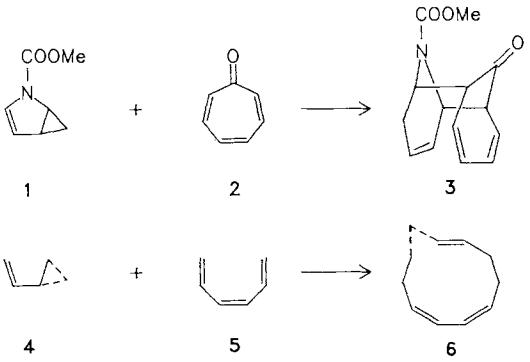

The homopyrrole **1** was already found to be a suitable homodiene component in cycloadditions.[8,9] Tropone **2** was chosen as triene component. On attempting to obtain **3** by reaction of **1** with **2**, however, **7** was formed (as racemate), as follows from the NMR data (Table 1) and the X-ray structure analysis.[10] All C atoms of the cage molecule **7** are constitutionally non-equivalent.[11]

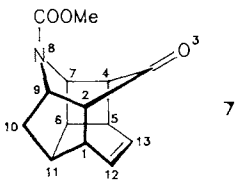

7

Table 1. NMR spectroscopic and mass spectrometric data of **7**.

^{1}H NMR [a] ($CDCl_3$, 360 MHz, TMS): δ = 1.92 (s, 2H; H^{10}), 2.18 (m, 1H; H^{11}), 2.95 (m, 1H; H^1), 3.05 (m, 1H; H^6), 3.15 (m, 1H; H^5), 3.23 (m, 1H; H^2), 3.45 (m, 1H; H^4), 3.65 (s, 3H; OCH_3), 4.77 (m, 1H; H^7), 4.88 (m, 1H; H^9), 6.15 (t, 1H, $J_{13,12}$ = 7.9 Hz; H13), 6.31 (t, 1H, $J_{12,13}$ = 7.9 Hz; H12)
^{13}C NMR ($CDCl_3$, 90.56 MHz, TMS): δ = 29.56 (1C), 36.29 (1C), 38.48 (2C), 45.47 (1C), 48.18 (1C), 52.48 (1C), 56.44 (1C), 57.17 (1C), 59.51 (1C), 130.86 (1C), 132.91 (1C), 153.39 (1C), 207.40 (1C)
MS (70 eV): *m/z* 246 (100%, $M^{\oplus}$), 214 (5), 154 (3), 138 (3), 107 (1), 80 (1)

[a] Assignment of signals by means of NOE difference measurements.

When **1** and **2** as starting compounds and **7** as product are fed into the recently implemented program RAIN,[3,12] a reaction network is obtained which contains two further reaction pathways besides that of **1** + **2** → **3** → **7**, namely: **1** + **2** → **8** → **7** and **1** + **2** → **9** → **7**. The first step in the formation of **7**, however, is probably an *endo*-[4 + 6]-addition of the homodiene **1** to the triene **2** to give **3**, since the reactions via **8** and **9** include steps that are forbidden under thermal conditions.[13]

The reason for the relatively high reactivity of **1** as homodiene (compared to other vinylcyclopropane systems) can be deduced from an analysis of the frontier orbitals

(Fig. 1). For vinylcyclopropanes, **1** has an energetically high-lying "Walsh orbital" in the three-membered ring, which, together with the π-system of the double bond has suitable symmetry for interaction with the LUMO of **2**.[14] The *endo*-addition is preferred over the *exo*-addition, presumably on steric grounds (hindrance by the methoxycarbonyl group in **1**).

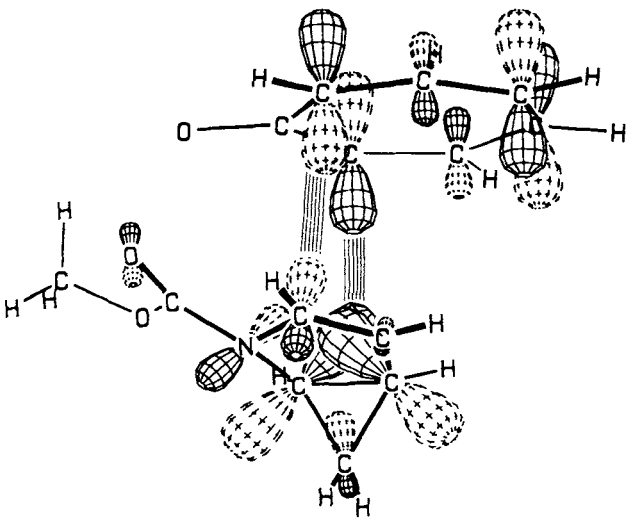

Fig. 1. Interaction of the LUMO of tropone with the second highest occupied MO of homopyrrole.

According to *Houk* and *Woodward*,[15] 2,5-dimethyl-3,4-diphenylcyclopentadione and tropone form a [4+6]-cycloadduct. The product is present in the *exo*-configuration; at elevated temperatures it rearranges by intramolecular Diels–Alder reaction into a cage compound. The structure of the hypothetical [4+6]-adduct **3** was calculated using the semiempirical method AM1.[16] The molecular geometry obtained after optimization of all parameters (Fig. 2) shows that the diene unit and the double bond of **3** are fixed by the molecular skeleton in an arrangement that is favorable for the subsequent Diels–Alder reaction leading to **7**.

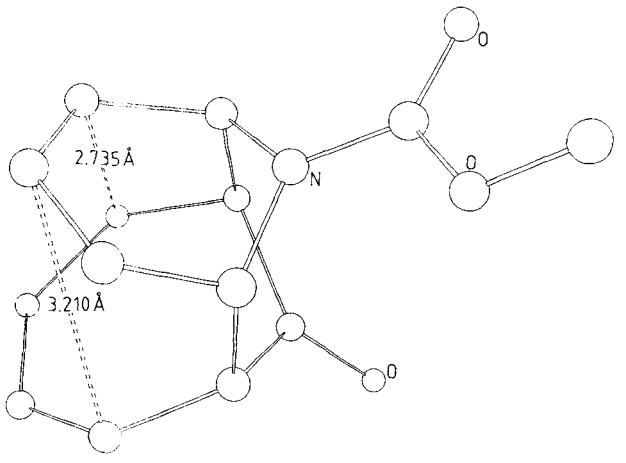

Fig. 2. The structure of the [4+6]-adduct **3** calculated by AM1.

Experimental

7: *N*-methoxycarbonyl-1-aza[3.1.0]bicyclohex-3-ene **1** (0.66 g, 4.7 mmol) was treated with 0.5 g (4.7 mmol) of **2** at 180°C in the absence of solvent. The reaction product was recrystallized from toluene. Yield: 92%; m.p. 173–174°C.

Received: June 27, 1988 [Z 2831 IE]
German version: *Angew. Chem. 100* (1988) 1618

CAS Registry numbers:
1, 31709-40-7; **2**, 539-80-0; **7**, 117409-34-4.

[1] J. Bauer, I. Ugi, *J. Chem. Res. Synop. 1982*, 298; *J. Chem. Res. Miniprint 1982*, 3101, 3201; see also J. Bauer, *Dissertation*, Technische Universität München 1981.
[2] J. Dugundji, I. Ugi, *Top. Curr. Chem. 39* (1973) 19; see also V. Kvasnička, M. Kratochvil, J. Koča, *Collect. Czech. Chem. Commun. 48* (1983) 2284; V. Kvasnička, *ibid. 48* (1983) 2097, 2118; I. Ugi, *J. Indian Chem. Soc. 62* (1985) 864; J. Brandt, I. Ugi (Eds.): *Proc. 8th ICCCRE (Int. Conf. Comput. Chem. Res. Educ.)*, Hüthig, Stuttgart, in press.
[3] I. Ugi, E. Fontain, J. Bauer, *Anal. Chim. Acta 210* (1988) 123.
[4] J. Bauer, E. Fontain, I. Ugi, *Tetrahedron Comput. Methodol. 1* (1988) No. 2, in press.
[5] J. Brandt, J. Bauer, E. M. Frank, A. von Scholley, *Chem. Scr. 18* (1981) 53; J. Brandt, A. von Scholley, *Comput. Chem. 7* (1983) 51; J. Brandt, A. von Scholley-Pfab, H. Schönmann, M. Wochner, *Vortrag ACHEMA 1988*.
[6] J. Bauer, R. Herges, E. Fontain, I. Ugi, *Chimia 39* (1985) 43.
[7] R. Herges, *Tetrahedron Comput. Methodol. 1* (1988) 15.
[8] F. W. Fowler, *Angew. Chem. 83* (1971) 148; *Angew. Chem. Int. Ed. Engl. 10* (1971) 135.
[9] For analogous reactions with homofuran and homothiophene see R. Herges, I. Ugi, *Angew. Chem. 97* (1985) 596; *Angew. Chem. Int. Ed. Engl. 24* (1985) 594; *Chem. Ber. 119* (1986) 829.
[10] A. Gieren, T. Hübner, unpublished.
[11] W. Schubert, I. Ugi, *J. Am. Chem. Soc. 100* (1978) 37; *Chimia 33* (1979) 183; I. Ugi, J. Dugundji, R. Kopp, D. Marquarding: *Perspectives in Theoretical Stereochemistry (Lecture Note Ser. 36)*, Springer, Berlin 1984, Chapter 8.
[12] E. Fontain, J. Bauer, I. Ugi, *Chem. Lett. 1987*, 37; *Z. Naturforsch. B 42* (1987) 889.
[13] R. Hoffmann, R. B. Woodward, *J. Am. Chem. Soc. 87* (1965) 4388.
[14] The molecular orbitals were calculated with MNDO as described by M. J. S. Dewar, W. Thiel, *J. Am. Chem. Soc. 99* (1977) 4899.
[15] K. N. Houk, R. B. Woodward, *J. Am. Chem. Soc. 92* (1970) 4145.
[16] M. J. S. Dewar, E. G. Zoebisch, E. F. Healy, J. J. P. Stewart, *J. Am. Chem. Soc. 107* (1985) 3902.

First Structure Analysis and Photoelectron Spectroscopic Investigation of an Azete and an Azete–Cobalt Complex**

By *Martin Ledermann, Manfred Regitz,* Klaus Angermund, Paul Binger, Carl Krüger, Richard Mynott, Rolf Gleiter,* and *Isabella Hyla-Kryspin*

Dedicated to Professor Robert Carrié on the occasion of his 60th birthday

In contrast to cyclobutadienes,[1] no crystal structure investigations of azetes (azacyclobutadienes) have hitherto been described in the literature. The synthesis of **3**,[2] the first kinetically stabilized azete, provided us with the chance of studying the influence of the ring nitrogen atom on the structure of the molecule. However, because of a phase transformation at −75°C, the crystal structure anal-

[*] Prof. Dr. M. Regitz, Dipl.-Chem. M. Ledermann
Fachbereich Chemie der Universität
Erwin-Schrödinger-Strasse, D-6750 Kaiserslautern (FRG)
Dr. K. Angermund, Prof. Dr. P. Binger,
Prof. Dr. C. Krüger, Dr. R. Mynott
Max-Planck-Institut für Kohlenforschung
Kaiser-Wilhelm-Platz 1, D-4330 Mülheim a. d. Ruhr (FRG)
Prof. Dr. R. Gleiter, Dr. I. Hyla-Krypsin
Organisch-chemisches Institut der Universität
Im Neuenheimer Feld 270, D-6900 Heidelberg (FRG)

[**] Antiaromatics, Part 25. This work was supported by the Deutsche Forschungsgemeinschaft, the Fonds der Chemischen Industrie, and the Stiftung Volkswagenwerk.—Part 24: U. Hees, U.-J. Vogelbacher, G. Michels, M. Regitz, *Tetrahedron 44* (1988), in press.

ysis of **3** (m.p. 37°C) could only be carried out above this temperature and the results were unsatisfactory due to disorder effects in the region of the methyl groups. In order to acquire accurate information about the azete structures we have now prepared and investigated the unequally substituted antiaromatic heterocycle **2** and the cobalt complex **5**.

The novel azete **2** is formed in analogy to the synthesis of **3** by thermolysis of the cyclopropenyl azide **1**[3] in a pressure Schlenk tube in the form of extremely oxygen-sensitive, reddish-brown crystals (80%, m.p. 59°C, from pentane at −78°C). The ring expansion is highly selective; there is no NMR evidence for the formation of the isomeric 2,4-di-*tert*-butyl-3-mesitylazete.

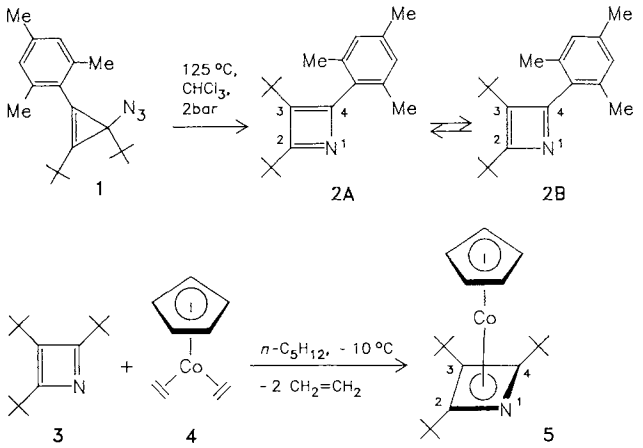

The complex **5** is obtained as light-brown crystals (79%, m.p. 117°C, from pentane at −78°C)[5] on reaction of **3**[2] with cyclopentadienylbis(ethylene)cobalt **4**;[4] **5** is the first metal complex of an azete.[6]

The crystal structure analysis of the azete **2** (Fig. 1, top) clearly shows that the antiaromatic compound crystallizes as the valence isomer **2A**. The four-membered ring has a planar, distorted rectangular structure with long C2–C3 and N–C1 single bonds (1.59(1) and 1.58(1) Å, resp.);[7] the lengths of the C1–C2 and N–C3 double bonds, on the other hand, are normal. Steric interaction of the mesityl moiety with the neighboring *t*Bu group leads to an interplanar angle of 70° between the two rings, so that a π-interaction with the four-membered ring is almost impossible (see also the photoelectron (PE) spectrum). The bulky ring substituents are responsible for the, in part relatively large, widening of the exocyclic angles C2–C1–C4, C3–C2–C13, and C2–C3–C17.

On comparing these findings with the structural data of kinetically stabilized cyclobutadienes,[1] one finds several parallels to the methyl tri-*tert*-butylcyclobutadienecarboxylates with regard to four-membered ring geometry, the angle of the plane of the substituent relative to the ring, and the steric effects on the exocyclic bond angles.[9] This close relationship also manifests itself on comparing the first band in the He(I)-PE spectrum of this cyclobutadiene with that of **3**.[10]

The ^{13}C-NMR spectrum of **2** measured at 40°C (75.5 MHz, [D$_8$]toluene) shows three sharp singlet signals for the four-membered ring (δ = 200.9, 141.2, 151.2).[11] These largely temperature-independent resonances[12] can be assigned to the carbon atoms C2, C3, and C4 of the valence isomer **2A**, which is also present in the crystalline state. A valence isomer equilibrium **2A** ⇄ **2B** is thus, other than in the case of **3**,[2] not detectable; the isomer **2B** participates at best to the extent of 5%. The signals were assigned with the help of a 2D-^{13}C,^{1}H-correlated spectrum (optimized for long-range couplings $^{n}J_{(C,H)}$), on the basis of estimations of the chemical shifts and by a comparison of the signal position of the azomethine carbon atom C-2 with the signals in the low-temperature spectrum of **3**.

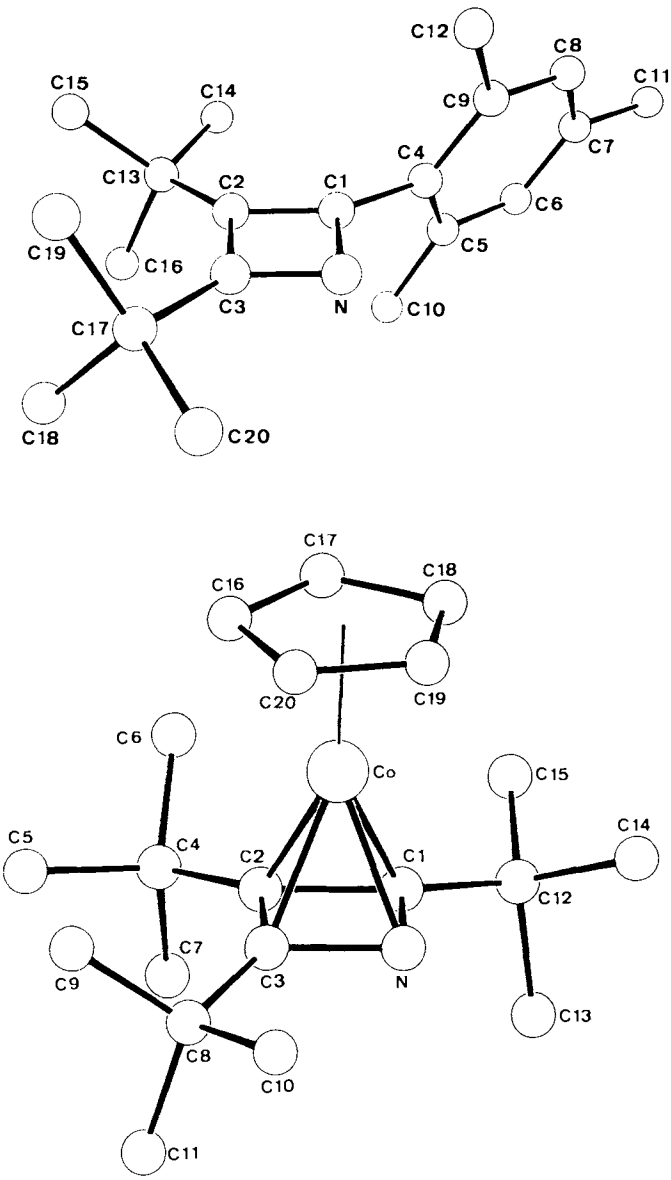

Fig. 1. Top: Molecular structure of **2**. $C_{20}H_{29}N$: $P2_1/c$, a = 14.256(3), b = 8.222(1), c = 16.078(4) Å, β = 93.06(2)°, T = 20°C, Z = 4, ρ_{calcd} = 1.00 g cm^{-3}, $\mu(Mo_{K\alpha})$ = 0.53 cm^{-1}. Enraf-Nonius diffractometer CAD-4; 4686 measured reflections, averaged to 424, 1043 observed ($I \geq 2\sigma(I)$): R = 0.076, R_w = 0.071 ($w = 1/\sigma^2(F_0)$) for 190 parameters [8]. Selected bond lengths [Å] and angles [°]: N-C1 1.58(1), N-C3 1.28(1), C1-C2 1.35(1), C2-C3 1.59(1), C1-C4 1.48(1), C2-C13 1.49(1), C3-C17 1.48(1); C1-N-C3 87.4(6), N-C1-C2 92.6(6), C1-C2-C3 84.9(6), C2-C3-N 95.1(6), N-C1-C4 124.3(7), C2-C1-C4 143.1(8), C1-C2-C13 134.5(7), C3-C2-C13 140.6(7), C2-C3-C17 137.7(7), N-C3-C17 127.3(8).—Bottom: Molecular structure of **5**. $C_{20}H_{32}CoN$; *Pbca*, a = 14.179(5), b = 16.82(1), c = 15.939(6) Å, T = −162°C, Z = 8, ρ_{calcd} = 1.21 g cm^{-3}, $\mu(Mo_{K\alpha})$ = 8.98 cm^{-1}. Enraf-Nonius diffractometer CAD-4; 25564 measured reflections, averaged to 11622 (R_{ave} = 0.06), 4516 observed ($I \geq 2\sigma(I)$): R = 0.046, R_w = 0.040 ($w = 1/\sigma^2(F_0)$) for 327 parameters [8]. Selected bond lengths [Å] and angles [°]: N-Co 1.958(2), C2-Co 2.027(2), C3-Co 1.958(2), C1-Co 1.960(2), N-C3 1.433(2), N-C1 1.424(3), C2-C3 1.462(3), C2-C1 1.478(3), N-C3-C2 92.8(2), N-C1-C2 92.5(2), C3-C2-C1 85.8(2), C3-N-C1 88.9(1).

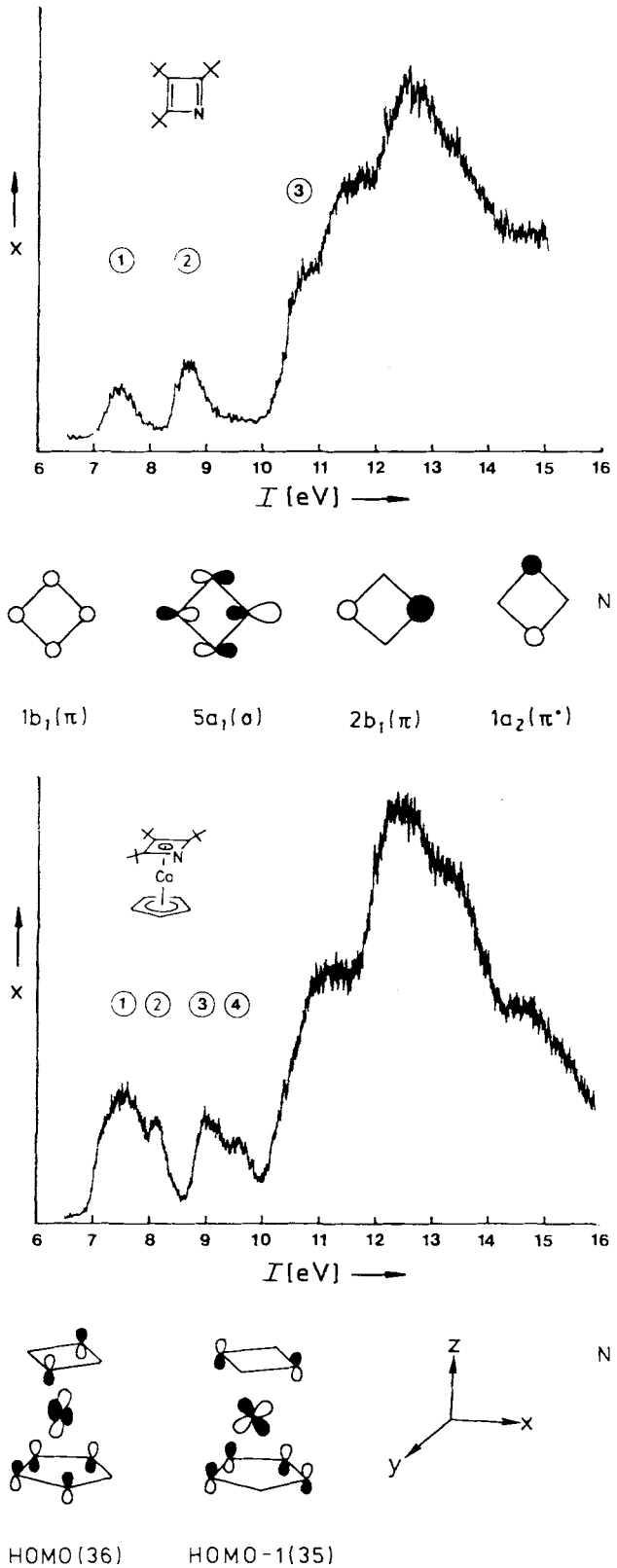

Fig. 2. PE spectra of **3** (top) and **5** (bottom). x = count rate. The MOs associated with the bands are given below the two spectra.

The comparison of the PE spectra of **2** and **3** shows that the position and shape of the bands involving the outer valence electrons are very similar.[10] This is best explained in terms of the interaction between the mesityl and azete moieties being very weak. The PE spectrum of **3** (Fig. 2, top) shows two bands in the outer valency range (① and ②), which we assign to the ionization from the two MOs $2b_1(\pi)$ and $5a_1(\sigma)$ (see below). The ionization energy for $1b_1(\pi)$ is, according to the PE spectrum, 10.7 eV (band ③). Comparison of the PE ionization energies with the results of MO calculations (semiempirical and ab initio methods[13]) confirms this.

Table 1. Orbital sequence of **5**, Me instead of *t*Bu, calculated according to the INDO method.

MO	ε_i [eV]	% Co	% L	% Cp	MO type
36	− 8.74	8	37	55	Cp(π), L($1a_2$), dxz, dyz
35	− 9.02	3	51	46	L($2b_1$), Cp(π), dxz, dyz
34	−10.70	40	45	15	L($1b_1$), dz^2, dxz, dyz
33	−11.25	47	35	18	d_{z^2}, dxz, dyz, L($1b_1$), Cp(π)
32	−11.40	34	26	40	Co(π), dxz, dyz
31	−11.62	22	61	17	L($5a_1$), dxz, dxy, dyz, dz^2
30	−11.96	88	8	4	dx^2-y^2
29	−12.10	80	13	7	dxy

The crystal structure analysis of the cobalt complex **5** (Fig. 1, bottom) reveals that the bond lengths in the planar four-membered ring become much more similar as a result of electron delocalization (1.478(3)) and 1.462(3) Å for C–C and 1.424(3) and 1.433(2) Å for N–C). The distances of N, Cl, and C3 to the metal atom are almost equal, only the C2–Co distance is somewhat longer. The coplanarity of the two rings (interplanar angle: 2°) indicates an analogous situation in the case of the Co–C cyclopentadiene distances. The bonds of the quaternary *t*Bu–C atoms C4, C8 and C12 to the azete C atoms are bent out of the plane of the four-membered ring away from the Co atom by 9°, 10° and 11°, respectively.[14]

According to INDO calculations[15] the two highest occupied MOs of the cyclopentadienyl(trimethylazete) cobalt complex (**5**, Me instead of *t*Bu) can be described as linear combinations of the $1a_2(\pi^*)$ and $2b_1(\pi)$ of the azete with the CpCo fragment (see Fig. 2, bottom and Table 1). As a result of this interaction the electron density in the four-membered ring of **5** is increased compared to **3**. This explains why the bond lengths in the ring in **5** are found to approach one another. In the PE spectrum of **5** (Fig. 2, bottom), the ionizations from the two HOMOs are superposed by other bands which we ascribe to ionizations from MOs that are strongly localized at the metal.[16]

Received: July 27, 1988 [Z 2889 IE]
German version: *Angew. Chem. 100* (1988) 1616

CAS Registry numbers:
1, 117270-99-2; **2**, 117271-00-8; **3**, 103794-87-2; **4**, 69393-67-5; **5**, 117308-54-0; di-*tert*-butylcyclopropenone, 19985-79-6; mesityllithium, 5806-59-7.

[1] Review: H. Irngartinger, M. Nixdorf, N. H. Riegler, A. Krebs, H. Kimling, J. Pocklington, G. Maier, K.-D. Malsch, K. A. Schneider, *Chem. Ber. 121* (1988) 673.

[2] U.-J. Vogelbacher, M. Regitz, R. Mynott, *Angew. Chem. 98* (1986) 835; *Angew. Chem. Int. Ed. Engl. 25* (1986) 842.

[3] The azide was obtained as colorless crystals (m.p. 88°C) by reaction of di-*tert*-butylcyclopropenone with mesityllithium in ether at 0°C and subsequent reaction with hydrazoic acid. *IR* (KBr): $\tilde{\nu}$ = 2100 cm^{-1} (N_3); ^1H NMR (90 MHz, $CDCl_3$): δ = 0.92, 1.23 (each s, slightly broadened, each 9 H, *t*Bu); 2.29, 2.41 (each s, 3 H and 6 H resp., mesityl-Me), 6.90 (s, arene-H).

[4] K. Jonas, E. Defense, D. Habermann, *Angew. Chem. 95* (1983) 729; *Angew. Chem. Int. Ed. Engl. 22* (1983) 716.

[5] **5**: ^1H NMR (200 MHz, [D_8]toluene): δ = 1.18, 1.23 (each s, 9 and 18 H, *t*Bu), 4.95 (s, 5 H, cyclopentadienyl-H); ^{13}C NMR (75.5 MHz, C_6D_6, 40°C): δ = 29.9 [s, $C(CH_3)_3$-3], 30.5 [q, $^1J(C,H)$ = 125 Hz, $C(CH_3)_3$-2,4], 32.1 [q, $^1J(C,H)$ = 126 Hz, $C(CH_3)_3$-3], 32.5 [s, $C(CH_3)_3$-2,4], 80.0 [d, $^1J(C,H)$ = 175 Hz, C_5H_5], 89.9 (s, C-3), 104.2 (s, C-2/C-4); MS (70 eV): *m/z* = 345 ($M^{\oplus}$, 17%).

[6] Review of cyclobutadiene-metal complexes: A. Efraty, *Chem. Rev. 77* (1977) 691.

[7] The standard value for $C(sp^2)$-$C(sp^2)$ single bonds is 1.47–1.48 Å: D. R. Lide, *Tetrahedron 17* (1962) 125.
[8] Further details of the crystal structure investigation are available on request from the Fachinformationszentrum Energie, Physik, Mathematik GmbH, D-7514 Eggenstein-Leopoldshafen 2 (FRG), on quoting the depository number CSD-53306, the names of the authors, and the journal citation.
[9] L. T. J. Delbaere, M. N. G. James, N. Nakamura, S. Masamune, *J. Am. Chem. Soc. 97* (1975) 1973.
[10] Ionization energies [eV] and assignments **2**: 7.6 (π_2, azete), 8.4 (π_1, π_2, aryl), 8.9 ($5a_1$, azete), 10.6 (π_1, azete); **3**: 7.5 [$2b_1$, (π)], 8.7 [$5a_1$, (σ)], 10.7 [$1b_1$ (π)]; methyltri-*tert*-butylcyclobutadienecarboxylate (**3**, C–CO_2Me instead of N): 7.1 (π_2, cyclobutadiene), 8.8 (σ), 9.5 (n, ester).
[11] Further resonances: δ=20.5, 21.2 (mesityl-CH_3-2,6,4), 26.0, 28.5 ($C(CH_3)_3$-2,3), 31.8, 36.7 ($C(CH_3)_3$-2,3), 128.1, 130.3, 136.8, 137.8 (arene-C). Measurements at higher temperature are problematic, since the azete dimerizes via the CN double bond; a colorless powder (m.p. 198 °C (decomp.) is obtained.
[12] At −110 °C they appear—only slightly shifted—at δ=202.2, 140.9, and 150.0.
[13] We thank Prof. *P. von R. Schleyer* for a 3-21G-21G and 6-31G* calculation on unsubstituted azete.
[14] See also D. M. P. Mingos, *Adv. Organomet. Chem. 15* (1977) 33.
[15] M. C. Böhm, R. Gleiter, *Theor. Chim. Acta 59* (1981) 127.
[16] Ionization energies [eV] and assignment (No. of the MOs in Table 1) of the bands ①–④ in the PE spectrum of **5**: ① 7.5 (29, 30, 34); ② 8.1 (36); ③ 8.9 (35); ④ 9.5 (33).

4-Iodo-1,3,5,7-tetramethyl-1,3,5,7-tetraaza-4λ⁵-phosphaspiro[3.3]heptane-2,6-dione: Synthesis and Crystal Structure of the First Iodophosphorane**

By *Johannes Breker, Peter G. Jones, Dietmar Stalke,* and *Reinhard Schmutzler**

Dedicated to Professor Ernst Otto Fischer on the occassion of his 70th birthday

The earlier described iodine-phosphorus compounds containing phosphorus in the oxidation state 5 have been shown by electrical conductivity measurements[1,2] to be phosphonium iodides with tetracoordinated phosphorus. A report on a stable iodophosphorane formed by oxidation of triethyl phosphite with iodine[3] has meanwhile been retracted.[4] The crystal structure analysis[5] of a 1:1 adduct obtained on reaction of tri-*tert*-butylphosphane with iodine revealed a linear arrangement of the P–I–I structural unit with tetracoordinated phosphorus. This geometry represents a structural alternative to the earlier postulated[2,6] undissociated precursor R_3PI_2 of phosphonium iodides $R_3PI^{\oplus}I^{\ominus}$. Here we describe the synthesis of the first λ^5P iodophosphorane. The postulated pentacoordination of the P atom was confirmed by an X-ray structure analysis.

The phosphorane **1**, whose Cl atom has already been exchanged for other substituents,[7,8] is a readily accessible compound containing a pentacoordinated P atom. Indeed, the synthesis of the iodophosphorane **2** from **1** was accomplished by Cl/I exchange with $ISiMe_3$[9] in benzene.

Crystals of **2**[10] (correct elemental analysis), which are pale yellow at −30 °C, are pale brown at room temperature. The ^{31}P NMR signal of the iodophosphorane **2** (δ = −119.1) is markedly shifted upfield compared with that of **1**; this is in agreement with the findings reported

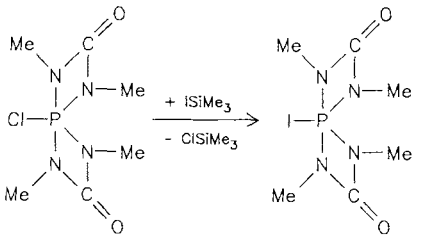

for iodo- and chlorophosphanes.[11] Because of the rapid exchange of the axial and equatorial positions on the NMR time scale at room temperature (pseudorotation), only one doublet is observed for the ^{1}H and ^{13}C resonances of the methyl groups. The positions of the signals in the ^{1}H and ^{13}C NMR spectra are similar to those for the chloro derivative **1**.[7]

The structure of **2** was determined by X-ray structure analysis.[12] The molecule (Fig. 1, Table 1) displays the distorted trigonal-bipyramidal geometry typical of related phosphoranes.[7] As expected, the axial bonds P-N2 (176(1) pm) and P-N4 (175(1) pm) are longer than the equatorial

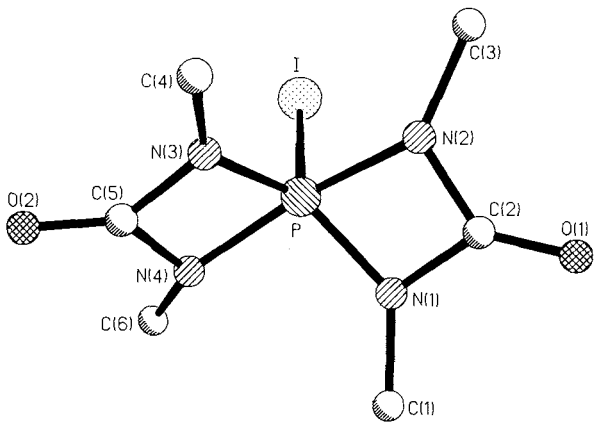

Fig. 1. Molecular structure of **2** (H atoms omitted) [12].

Table 1. Bond lengths [pm] and angles [°] of **2**.

Bond lengths			
I-P	245.8(3)	P-N1	167.0(8)
P-N2	176.0(9)	P-N3	167.6(9)
P-N4	175.3(10)	N1-C1	143.9(15)
N1-C2	139.9(15)	N2-C2	139.7(14)
N2-C3	143.9(18)	N3-C4	141.4(15)
N3-C5	141.6(15)	N4-C5	139.6(15)
N4-C6	142.1(16)	O1-C2	121.0(12)
O2-C5	118.6(15)		
Bond angles			
I-P-N1	114.7(4)	I-P-N2	96.9(3)
N1-P-N2	75.4(4)	I-P-N3	112.3(3)
N1-P-N3	133.0(4)	N2-P-N3	98.5(5)
I-P-N4	96.8(3)	N1-P-N4	99.1(5)
N2-P-N4	166.3(5)	N3-P-N4	75.9(5)
P-N1-C1	136.1(7)	P-N1-C2	95.5(7)
C1-N1-C2	128.0(8)	P-N2-C2	91.6(7)
P-N2-C3	136.4(7)	C2-N2-C3	123.7(10)
P-N3-C4	137.6(8)	P-N3-C5	94.6(7)
C4-N3-C5	127.6(10)	P-N4-C5	92.0(7)
P-N4-C6	138.8(9)	C5-N4-C6	124.0(9)
N1-C2-N2	97.2(8)	N1-C2-O1	130.0(11)
N2-C2-O1	132.8(12)	N3-C5-N4	97.3(9)
N3-C5-O2	130.6(11)	N4-C5-O2	132.1(12)

[*] Prof. Dr. R. Schmutzler, Dr. J. Breker
Institut für Anorganische und Analytische Chemie
der Technischen Universität
Hagenring 30, D-3300 Braunschweig (FRG)
Prof. Dr. P. G. Jones, Dr. D. Stalke
Institut für Anorganische Chemie der Universität
Tammannstrasse 4, D-3400 Göttingen (FRG)

[**] This work was supported by the Fonds der Chemischen Industrie.

bonds P-N1 (167(1) pm) and P-N3 (168(1) pm). To the best of our knowledge, there is no reference value against which to compare the P–I bond length (245.8(3) pm).

The decision whether the P atom is coordinated in a trigonal-bipyramidal (in the ideal case, D_{3h}) or square-pyramidal (C_{4v}) fashion can be made on the basis of the following considerations: (1) The sum of the squared deviations (relative to the ideal values) of all angles at the P atom[13] is $\Sigma\Delta^2(D_{3h}) = 1105$ and $\Sigma\Delta^2(C_{4v}) = 1387$, respectively, and thus does not permit a clear distinction. (2) However, the four-membered rings have N–P–N angles that must deviate considerably from the ideal value of 90°. (3) The P–N bond lengths can be unambiguously distinguished as axial (long) and equatorial (short). The P coordination should therefore be classified as trigonal-bipyramidal. The dihedral angle between axial and equatorial planes (defined by P, I, N2, N4 and P, I, N1, N3, respectively) is 77°.

The synthesis of the F and Br analogues of **1**, as well as of a pseudohalogen derivative (CN), was also accomplished, along with the corresponding structure determinations.[14]

Experimental Procedure

1 (6.22 g, 26 mmol) was dissolved in benzene (60 mL) in a Schlenk tube protected from light, and iodotrimethylsilane (15.4 g, 78.2 mmol) was added to the stirred solution at 0°C. After complete conversion of **1** (4 d), the brown solution was removed by pipette from the dark brown solid residue. The benzene was removed in vacuo and the resulting residue was dissolved in 30 mL of toluene. Insoluble solid matter was filtered off and the solution was kept at 0°C. The solution was subsequently separated by pipette from a reddish oil that had formed. Addition of 30 mL of methylcyclohexane to this solution at 0°C resulted in the formation of brown crystals, which were freed of an accompanying red oil by washing with methylcyclohexane. The crude product was stirred with copper powder in 20 mL of toluene to form a suspension, which, after 15 min, was filtered. Compound **2** crystallized from the filtrate within a few days at −30°C. The crystals were dried at 10^{-2} torr. Yield 2.0 g (23%), decomposition > 50°C.

Received: June 6, 1988 [Z 2804 IE]
German version: *Angew. Chem. 100* (1988) 1620

CAS Registry numbers:
1, 77507-70-1; **2**, 117068-57-2; $ISiMe_3$, 16029-98-4.

[1] K. Issleib, W. Seidel, *Z. Anorg. Allg. Chem. 288* (1959) 201.
[2] A. D. Beveridge, G. S. Harris, F. Inglis, *J. Chem. Soc. A 1966*, 520.
[3] D. Cooper, S. Trippett, *Tetrahedron Lett. 1979*, 1725.
[4] A. Skowronska, M. Pakulski, J. Michalski, D. Cooper, S. Trippett, *Tetrahedron Lett. 1980*, 321.
[5] W.-W. du Mont, M. Bätcher, S. Pohl, W. Saak, *Angew. Chem. 88* (1987) 945; *Angew. Chem. Int. Ed. Engl. 26* (1987) 91.
[6] L. Horner, H. Winkler, *Tetrahedron Lett. 1964*, 455.
[7] D. Schomburg, U. Wermuth, R. Schmutzler, *Chem. Ber. 120* (1987) 1713.
[8] H.-M. Schiebel, R. Schmutzler, D. Schomburg, U. Wermuth, *Z. Naturforsch. B38* (1983) 702.
[9] V. D. Romanenko, V. I. Tovstenko, L. N. Markovskii, *Synthesis 1980*, 823.
[10] Spectroscopic data of **2**: ^1H NMR ($CDCl_3$): $\delta = 2.70$ (d, $^3J_{HP} = 16.75$ Hz; H_3C-N); $^{31}P\{^1H\}$ NMR (CH_2Cl_2): $\delta = -119.1$ (s); ^{13}C NMR ($CDCl_3$): $\delta = 27.46$ (d, $^2J_{CP} = 3.08$ Hz; H_3C-N), 154.52 (d, $^2J_{CP} = 12.37$ Hz; C=O); IR (CH_2Cl_2): $\tilde{\nu}$(C=O) = 1770 cm^{-1}; MS (70 eV): *m/z* 203 (100%, $(dmh)_2P$), 146 (64, (dmh)PNMe), 127 (3, I), 117 (2, $(dmh)P$), 70 (7, $(MeN)_2C$), 69 (7, $(MeN)_2C-H$), 60 (58, MeNP); (dmh) ≙ $MeN-C(=O)-NMe$.
[11] V. Mark, C. H. Dungan, M. M. Crutchfield, J. R. van Wazer, *Top. Phosphorus Chem. 5* (1967) 227.
[12] Crystal data: $C_6H_{12}IN_4O_2P$ (330.066), $P2_1/c$, $a = 1063.1(4)$, $b = 1269.1(6)$, $c = 901.6(3)$ pm, $\beta = 105.87(3)°$, $V = 1.170$ nm^3, $Z = 4$, $\rho_{calcd} = 1.87$ Mg m^{-3}; $Mo_{K\alpha}$ radiation, $\mu = 2.8$ mm^{-1}, $2\Theta_{max} = 50°$, $R = 0.073$, $R_w = 0.065$ for 1340 reflections with $F > 4\sigma(F)$. All measurements were carried out at −85°C. Further details of the crystal structure investigation may be obtained from the Fachinformationszentrum Energie, Physik, Mathematik GmbH, D-7514 Eggenstein-Leopoldshafen 2 (FRG), on quoting the deposition number CSD-53246, the names of the authors, and the journal citation.
[13] W. S. Sheldrick, *Top. Curr. Chem. 73* (1978) 1.
[14] J. Breker, P. G. Jones, D. Schomburg, R. Schmutzler, unpublished.

Coordination of H_2 and O_2 to $[OsHCl(CO)(PiPr_3)_2]$: A Catalytically Active $M(\eta^2\text{-}H_2)$ Complex**

By *Miguel A. Esteruelas, Eduardo Sola, Luis A. Oro,* Uwe Meyer,* and *Helmut Werner**

Dedicated to Professor Ernst Otto Fischer on the occasion of his 70th birthday

The binding of small (diatomic) molecules to transition-metal centers is regarded as the key step in many homogeneously catalyzed processes.[1] Numerous examples of the coordination of O_2 to the central atom of metal complexes[2] are known, and compounds of the type $[(M(O_2)L_n]$ are not only of interest as intermediates in catalytic oxidations but also have long attracted attention as O_2 reservoirs.[3] However, the isolation and structural characterization of the first $M(H_2)$ complex containing side-on-bonded H_2 ligands was only accomplished a few years ago.[4] To the best of our knowledge, up to now no compound has been described which coordinates H_2 as well as O_2 without the subsequent occurrence of spontaneous reduction or oxidation with cleavage of the E_2 bond.

Two years ago we reported[5] that complex **1**, containing presumably square-pyramidally pentacoordinated os-

$[OsHCl(CO)(PiPr_3)_2]$ **1**

mium, is formed in nearly quantitative yield (96%) upon reaction of osmium trichloride with triisopropylphosphane in methanol. At room temperature, it adds Lewis bases L that are not too bulky, such as CO, PMe_3, $P(OMe)_3$, $H_2C{=}CHX$ (X = CN, COMe, CO_2Me) to form octahedral compounds $[OsHCl(CO)L(PiPr_3)_2]$.[5] Alkynes (C_2H_2, PhC_2H) undergo insertion into the Os–H bond.[6] In the presence of $NaBH_4$ or KOH, moreover, **1** is catalytically active and promotes hydrogen transfer from 2-propanol to ketones (acetophenone, cyclohexanone) and to phenylacetylene.[7]

In continuation of the catalytic studies, we have now found that, under normal conditions (25°C, 1 bar) in benzene, **1** also reacts with H_2 and O_2. In both cases, the initially red benzene solution rapidly turns colorless. In addition to the well-resolved hydride signal at $\delta = -7.90$ (**1**, δ(in C_6D_6) = −31.92 (t, $J(PH) = 14$ Hz; [OsH])),[5] the ^1H NMR spectrum of **2**,[8] recorded under H_2 atmosphere, exhibits a relatively broad resonance at $\delta = -1.30$ ($\omega_{1/2} = 13$ Hz), which is characteristic of η^2-bonded H_2 ligands.[4b,9,10] Integration of the two signals gives an intensity ratio of 1:2. The IR spectrum of a benzene solution of **2** shows a strong absorption for the CO stretching vibration at 1913 cm^{-1}, which, as expected, is shifted by ca. 25 cm^{-1} to higher wavenumbers compared with that of **1**. Upon removal of the H_2 atmosphere, **2** is slowly transformed back into the starting complex **1**—this reaction is very fast under vacuum.

[*] Prof. Dr. L. A. Oro, Dr. M. A. Esteruelas, Dipl.-Chem. E. Sola
Departamento de Química Inorgánica
Instituto de Ciencia de Materiales de Aragón
Universidad de Zaragoza—C.S.I.C.
E-50009 Zaragoza (Spain)
Prof. Dr. H. Werner, Dipl.-Chem. U. Meyer
Institut für Anorganische Chemie der Universität
Am Hubland, D-8700 Würzburg (FRG)

[**] This work was supported by the Deutscher Akademischer Austauschdienst (DAAD) as part of the scientific exchange between the Federal Republic of Germany and Spain (Acción Integrada) and by Degussa AG.

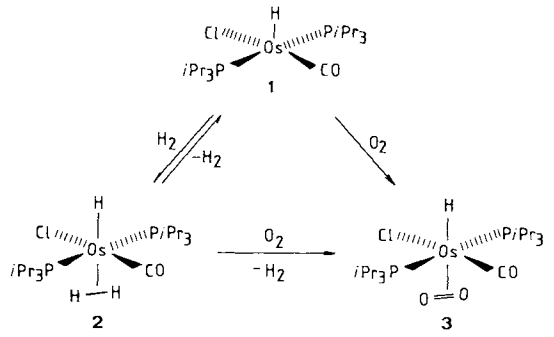

Even *traces* of oxygen result in displacement of H_2 from **2** to give **3**, which is also formed upon stirring a suspension of **1** in 2-propanol exposed to air or under oxygen atmosphere.[11] The dioxygen ligand is very strongly bound, a fact reflected not only in the stability of **3** under high vacuum but also in the spectroscopic data (e.g., lowering of the O–O stretching absorption to 862 cm^{-1}). The *trans* position of the O_2 relative to the hydride ligand, a very good σ donor, is probably responsible for this strong binding.[2] An η^2-O_2 complex of osmium(0) was first described by *Roper* et al.[12] and one of osmium(II) having a composition similar to that of **3** was first synthesized by *Moers* et al.[13]

At room temperature, **2** does not rearrange to the isomeric trishydridoosmium(IV) compound **4**.[14] Only upon

$[OsH_3Cl(CO)(PiPr_3)_2]$ **4**

warming to about 40°C does exchange of the hydrido and H_2 ligands of **2** occur, along with re-formation of **1**. This process is revealed in the broadening of the corresponding signals in the ^1H NMR spectrum. Theoretical studies have indicated[15] that the presence of good donor ligands at an electron-rich metal center promotes charge transfer (i.e., backbonding) from M to the σ^* orbital of H_2 and thus favors cleavage of the H_2 molecule with the formation of two M–H bonds. We assume that the CO and Cl ligands in **2** largely compensate for the electron donation from the phosphane ligands, so that, at room temperature, detectable formation of $[OsH_3Cl(CO)(PiPr_3)_2]$ does not occur. Transformation of the $Os(\eta^2\text{-}H_2)$ unit to an OsH_2 unit might also be suppressed by steric hindrance due to the bulky $PiPr_3$ groups.[16]

Complex **2** is also a catalyst—or, more likely, a catalytic precursor. Whereas **1** does not react with styrene, cyclohexene, cyclohexa-1,4-diene, or benzylideneacetone under the conditions given in Table 1, addition of the respective substrate to a solution of **2** results, in part, in very rapid reaction. The rate v depends on the solvent (for styrene, $v[C_6H_6] < v[1,2\text{-}C_2H_4Cl_2] < v[i\text{PrOH}]$) and on the olefin (in *i*PrOH, benzylideneacetone < cyclohexene < styrene). Phenylacetylene is selectively reduced to styrene, and benzylideneacetone to benzylacetone; for cyclohexa-1,4-diene and diphenylacetylene (preferential formation of (*Z*)-stilbene), on the other hand, the selectivity is rather low. Kinetic investigations indicate[17] that a trishydrido(alkene)osmium or trishydrido(alkyne)osmium complex, respectively, occurs as intermediate, which, via an insertion reaction, gives an alkyl or vinyl species. In contrast to **2**, the Kubas compounds $[M(\eta^2\text{-}H_2)(CO)_3(PR_3)_2]$ (M = Mo, W; $PR_3 = PiPr_3$, $P(cyclo\text{-}C_6H_{11})_3$, $PiPr(cyclo\text{-}C_6H_{11})_2$) are inactive in the catalytic hydrogenation of ethylene,[16] which might be due to a kinetic barrier to formation of the intermediate $[MH_2(C_2H_4)(CO)_{4-n}(PR_3)_n]$ (n = 1, 2).

Table 1. Catalytic hydrogenations with **2** [a].

Substrate Su [b]	Solvent	t [min]	mol SuH_2 / mol **2**	Product SuH_2 [c]
Styrene	C_6H_6	120	56.0	Ethylbenzene
Styrene	$1,2\text{-}C_2H_4Cl_2$	120	80.0	Ethylbenzene
Styrene	*i*PrOH	5	100.0	Ethylbenzene
Cyclohexene	$1,2\text{-}C_2H_4Cl_2$	15	51.0	Cyclohexane
Cyclohexene	*i*PrOH	15	68.0	Cyclohexane
Cyclohexa-1,4-diene	*i*PrOH	5	42.0	Cyclohexane
			50.0	Cyclohexene
			6.5	Cyclohexa-1,3-diene
		120	57.0	Benzylacetone
Benzylideneacetone	C_6H_6		1.0	4-Phenylbutan-2-ol
		120	81.0	Benzylacetone
Benzylideneacetone	*i*PrOH		1.5	4-Phenylbutan-2-ol

[a] Generated in situ by stirring a 55×10^{-3} M solution of **1** for 30 min under H_2 (1 bar). [b] Reaction conditions: $\mathbf{2} = 2.5 \times 10^{-3}$ M, [Su]/**2** = 100, $T = 60$°C, $p(H_2) = 1$ bar. [c] Gas-chromatographic product analysis.

Received: May 6, 1988 [Z 2746 IE]
Publication delayed at authors' request
German version: *Angew. Chem. 100* (1988) 1621

[1] a) G. Henrici-Olivé, S. Olivé: *Coordination and Catalysis*, Verlag Chemie, Weinheim 1977; b) G. W. Parshall: *Homogeneous Catalysis*, Wiley, New York 1980; c) J. P. Collman, L. S. Hegedus, J. R. Norton, R. G. Finke: *Principles and Applications of Organotransition Metal Chemistry, Part II, 2nd Ed.*, University Science Books, Mill Valley, CA, USA 1987.

[2] a) G. Henrici-Olivé, S. Olivé, *Angew. Chem. 86* (1974) 1; *Angew. Chem. Int. Ed. Engl. 13* (1974) 29; b) L. Vaska, *Acc. Chem. Res. 9* (1976) 175; c) M. H. Gubelmann, A. F. Williams, *Struct. Bonding (Berlin) 55* (1983) 1.

[3] a) G. McLendon, A. E. Martell, *Coord. Chem. Rev. 19* (1976) 1; b) E. C. Niederhoffer, J. H. Timmons, A. E. Martell, *Chem. Rev. 84* (1984) 137.

[4] a) G. J. Kubas, R. R. Ryan, B. I. Swanson, P. J. Vergamini, H. J. Wasserman, *J. Am. Chem. Soc. 106* (1984) 451; b) most recent review: G. J. Kubas, *Acc. Chem. Res. 21* (1988) 120.

[5] M. A. Esteruelas, H. Werner, *J. Organomet. Chem. 303* (1986) 221.

[6] H. Werner, M. A. Esteruelas, H. Otto, *Organometallics 5* (1986) 2295.

[7] M. A. Esteruelas, E. Sola, L. A. Oro, H. Werner, U. Meyer, *J. Mol. Catal. 45* (1988) 1.

[8] ^1H NMR (80 MHz, C_6H_6, H_2) of **2**: $\delta = 2.55$ (m; PCH), 1.27 (dvt, $J(HH) = 7.6$, $N = 13.6$ Hz; CH_3), −1.30 (br. s; $Os(\eta\text{-}H_2)$), −7.90 (t, $J(PH) = 18.6$ Hz; OsH). An attempt to demonstrate η^2 coordination by determination of the relaxation time T_1 [9] failed owing to the lability of **2** under the conditions of measurement.

[9] R. H. Crabtree, M. Lavin, L. Bonneviot, *J. Am. Chem. Soc. 108* (1986) 4032.

[10] a) R. H. Morris, J. F. Sawyer, M. Shiralian, J. D. Zubkowski, *J. Am. Chem. Soc. 107* (1985) 5581; b) M. Bautista, K. A. Earl, R. H. Morris, A. Sella, *ibid. 109* (1987) 3780.

[11] *Experimental procedure* for **3**: O_2 was admitted to a suspension of **1** (100 mg, 0.18 mmol) in 2-propanol (10 mL) until a colorless precipitate formed (ca. 2 min). The precipitate was filtered off, washed with a small amount of hexane, and dried under high vacuum. Yield 93%. M.p. 122°C (dec.). Correct elemental analysis. IR (Nujol): $\tilde{\nu}(OsH) = 2095$ (w), $\tilde{\nu}(CO) = 1947$ (vs), $\tilde{\nu}(O_2) = 862$ (s) cm^{-1}; ^1H NMR (90 MHz, $CDCl_3$): $\delta = 2.90$ (m; PCH), 1.42 (dvt, $J(HH) = 6.0$, $N = 14.0$ Hz; CH_3), −2.40 (t, $J(PH) = 30.0$ Hz; OsH); ^{31}P-NMR (90 MHz, $CDCl_3$): $\delta = 25.50$ (s, off-resonance experiment d).

[12] B. E. Cavit, K. R. Grundy, W. R. Roper, *J. Chem. Soc. Chem. Commun. 1972*, 60.

[13] F. G. Moers, R. W. M. ten Hoedt, J. P. Langhout, *J. Inorg. Nucl. Chem. 36* (1974) 2279.

[14] The related tetrahydridoosmium(IV) complex $[OsH_4(CO)(PiPr_3)_2]$ is known: H. Werner, M. A. Esteruelas, U. Meyer, B. Wrackmeyer, *Chem. Ber. 120* (1987) 11.

[15] a) J. Y. Saillard, R. Hoffmann, *J. Am. Chem. Soc. 106* (1984) 2006; b) Y. Jean, O. Eisenstein, F. Volatron, B. Maouche, F. Sefta, *ibid. 108* (1986) 6587; c) P. J. Hay, *ibid. 109* (1987) 705; d) J. K. Burdett, M. R. Pourian, *Organometallics 6* (1987) 1684.

[16] See G. J. Kubas, C. J. Unkefer, B. I. Swanson, E. Fukushima, *J. Am. Chem. Soc. 108* (1986) 7000.

[17] A. Andriollo, M. A. Esteruelas, U. Meyer, L. A. Oro, R. A. Sánchez-Delgado, E. Sola, C. Valero, H. Werner, manuscript in preparation.

The Art of Scientific Writing. From Student Reports to Professional Publications in Chemistry and Related Fields. By *H. F. Ebel, C. Bliefert,* and *W. E. Russey.* VCH Verlagsgesellschaft, Weinheim/VCH Publishers, New York 1987. xix, 493 pp., hard cover, DM 98.00.—ISBN 3-527-26469-8; 0-89573-495-8; paperback, DM 48.00.—ISBN 3-527-26677-1; 0-89573-645-4

American English has become the international language of science in the last 40 years. Scientists who desire international recognition must publish in English. The book under consideration, a substantially expanded translation of an German forerunner, makes due recognition of this development.

"The Art of Scientific Writing" is best characterized as a handbook or guide, designed to help the scientist with all aspects of writing and publishing. Although the book mainly addresses chemists, other scientists would also find it quite useful, unless they expect to find information specific to their own field.

An important aspect of the book is that it is itself designed to serve as an example of the techniques and guidelines presented. As a result, for example, it is extensively cross referenced and indexed. However, the too frequent use of substantive footnotes often hinders the easy flow of the text. One of the book's strongest points is its superb documentation.

The work is divided into two parts, followed by 11 appendixes, a section for references and further reading, and an index. Part 1 describes all forms of scientific writing. The first two chapters (56 pages), on laboratory notebooks, laboratory reports, research reports, and theses, are written for students, except for the short discussion of grant reports and proposals. The rest of the book chiefly addresses the needs of professional chemists. This presents a problem. As the authors themselves point out (p. 122), fundamentally different approaches are required for a student textbook or for a book whose "reader is expected to be a busy specialist". Indeed, the first two chapters have the character of a college textbook (unfortunately, not a very good one), whereas the rest of the book has the quality of a well-written monograph. Chapters 3 and 4 (91 pages) contain a highly informative description of the different types of journals and books, and of the process involved in their publication. These chapters and much of the rest of the book are written by authors with extensive knowledge and experience in publishing.

Part 2 covers the technical aspects of preparing scientific publications. Chapter 5 (17 pages) deals with the production of the manuscript and its transformation into the finished product. The use and advantages of word processors are discussed, as well as such technical questions as paper, format, and proofreading. Chapter 6 (31 pages), a description of chemical nomenclature, is something of an enigma. Although I found the treatment interesting, and obviously written by an expert, it is much too brief to teach the reader this incredibly difficult subject. In a shortened form this chapter could serve as an appendix, but I would much prefer that it be expanded and made into a book of its own. Chapter 7 (29 pages) is also a digression, this time into the subject of quantities, units, and numbers. It would certainly make a good addition to a modern general chemistry textbook. The reader seeking comprehensive information on this subject should consult the IUPAC "Green Book" (*Quantities, Units and Symbols in Physical Chemistry,* Blackwell, Oxford 1988) or "The ACS Style Guide" (edited by *Janet S. Dodd,* American Chemical Society, Washington 1986). Chapters 8 to 10 (62 pages) return to the technical aspects of the publishing process, providing a detailed treatment of equations, formulas, figures, and tables. My only criticism here is that in the coverage of stencils only those products of VCH Publishers are described. Chapter 11 (44 pages), after briefly discussing personal literature card files (or databases), gives a thorough treatment of literature citation.

The appendixes (104 pages) range from short chapters (oral presentations, English grammar and style, copyrights and publishing agreements, an overview of the chemical literature, preparation of an index, ISSN and ISBN) to supplementary tables (journal abbreviations, other common abbreviations, proofreader's marks, recommended citation forms, and quantities, units, and constants).

A discussion of "The Art of Scientific Writing" would not be complete without a comparison with the most authoritative book for chemists on this subject, namely "The ACS Style Guide" mentioned earlier. In short, the two books are more complementary than competitive. Almost half of the "Style Guide" is devoted to grammar, style, and usage. "The Art of Scientific Writing", on the other hand, contains a detailed description of the publishing process, both for books and journals. The "Style Guide" presents guidelines specific to ACS publications, whereas the present book attempts to address the needs of authors internationally, and largely succeeds.

This book will be of service to chemists and especially to chemistry editors and should also be in every technical library.

Joe P. Richmond [NB 925 IE]
Editorial Office of "Synthesis"
Georg Thieme Verlag, Stuttgart (FRG)

Experimental Design: A Chemometric Approach. By *S. N. Deming* and *S. L. Morgan.* Elsevier, Amsterdam 1987. xiii, 275 pp., bound, HFl 225.00.—ISBN 0-444-42734-1

Good planning is half the battle! It is beyond question that scientific curiosity and researchers' intuition have led to many important discoveries. However, it is also indisputable that rationally planned experiments are essential in a scientific investigation with specific objectives.

What does the term "experimental design" mean? The best interpretation is that it is the art of planning an investigation. *Stanley N. Deming* and *Stephen L. Morgan* teach this skill in what is, it must be said at the outset, on the whole a very good book—good because it is so different from other books on this theme. It succeeds in the aim of providing a simple introduction to planning scientific experiments and dealing with the problems which arise. Mathematical statistics does not occupy a central position in the book, but is instead developed naturally alongside the main theme, where it is essential to understanding the treatment and carrying it forward.

The two introductory chapters pose the questions: what is a system? how is the system under investigation influenced by the input variables and conditions? what are

the responses which result as the output from the system, and how can the relationship between the input variables and the resulting output be described? Following a short account of the basic concepts of statistics (Chapter 3), the next four chapters deal in turn with developing a model (Chapter 4. One experiment), linear regression analysis (Chapter 5. Two experiments), testing hypotheses (Chapter 6), and the variance-covariance matrix (Chapter 7). The chapters which follow lead into the central theme of the book, the statistical design of experiments. Taking the case of three experiments as an example, linear models and second order models are treated (Chapter 8), then the analysis of variance (Chapter 9), followed by an example in which the pH dependence of the activity of an enzyme is determined from a series of ten experiments (Chapter 10). Chapter 11 discusses for the first time cases in which a system is influenced by several factors, and introduces standard experimental schemes (e.g. 2^n factorial schemes). Following Chapter 12, which deals with randomized block schemes, we suddenly reach the end of the book. Did the authors tire of their task? Or did they feel that, in a book which is based on courses given to college and university students, the reader should not be expected to go further than the classes to which they lectured? Special experimental schemes, such as the Latin square, the Greek-Latin square and the Youden square are explained briefly in the exercises of Chapter 12; other methods, such as simplex procedures or Plackett-Burman designs are only mentioned, with an invitation to the reader to look these up in the literature and critically evaluate them.

In marked contrast to the quality of the text (and indeed of the price), the publishers show a noticeable lack of care. Perhaps only a pedant would be troubled by the fact that from p. 150 onwards the sub-headings suddenly become larger. The description of a minimum as a maximum in Fig. 2.6 is also not a very serious matter. However, the fact that under the initial letter L in the key-word index one finds only entries with the letter M cannot be allowed to pass. The publishers have not even considered it necessary to insert a page listing corrections. If one is looking for the key-word "Latin square", for example, there are several possibilities: look in the contents list (nothing there), look under "Square design" (nothing), thumb through the pages of the book (a hit on p. 250), or look under "Experimental designs, Latin square" (hit).

This book is recommended as an introduction to the statistical design of experiments. Readers who already have some knowledge of this field should follow the advice of the authors and consult other monographs.

Hugo Kubinyi [NB 896 IE]
BASF, Ludwigshafen (FRG)

Variety in Coordination Modes of Ligands in Metal Complexes. By *S. Kawaguchi*. Springer, Berlin 1988. ix, 123 pp., bound, DM 128.00.—ISBN 3-540-18305-1

Nearly all ligands can occur in metal complexes in several different bonding situations. To write a comprehensive monograph on this subject is a scarcely manageable task. Even the book reviewed here is not such a work, despite the hopes raised by its title. The author has selected a few examples and discussed them in order of the number of atoms in the ligands, under the headings: Monoatomic Ligands (H), Diatomic Ligands (CO, N_2), Triatomic Ligands ($SCN^{\ominus}$) and Polyatomic Ligands (β-diketones). Whether or not this choice of examples is representative or rational is an open question; however, the reader of a monograph is entitled to expect that he will be offered a balanced overview of the topic covered. Regrettably that is not the case here.

The book begins with a short introduction to the classification of ligands (with an incorrect formula for EDTA even on the first page), and the phenomenon of linkage isomerism. Here it already becomes apparent that the author has not thought sufficiently about which group of readers he is aiming at: a commonplace statement such as "When a ligand connects two or more metal atoms, it is called a bridging ligand" is given equal weight alongside a detailed discussion on the formation of $[Co(NH_3)_5ONO]^{2\oplus}$. The second chapter (Monoatomic Ligands), which is devoted to the hydrido ligand, gives a similarly inconsistent impression. A discussion of the possible types of bonding (terminal or bridging) is followed by sections on synthesis and characterization. The information given here is anything but complete. Although some M–H vibrational frequencies and ^1H NMR data are included, the treatment of ^{31}P NMR spectroscopy is limited to the laconic comment "... also helpful". In discussing structures the author, for some obscure reason, limits himself to trigonal-prismatic, octahedral and pentagonal-bipyramidal examples, leaving the reader unaware of the existence of square-planar, trigonal-bipyramidal and many other types of structures. The sections on hydrogen-bridged complexes contain essentially nothing more than a mention of the structures. There follows a chapter on the reactions of hydrido-complexes, beginning with a list of Brønsted acidities and a discussion of some typical reactions. The chapter concludes with an excursion into homogeneous catalytic hydrogenation using rhodium complexes (who would expect this in a book with the above title?); here, though, one learns nothing more than can be found in the standard textbooks. For example, there is a section on "Asymmetric Hydrogenation" which consists of only ten lines of text, three formulas and five literature references.

The third chapter (Diatomic Ligands) likewise contains less than is promised. After listing the types of bonding for carbon monoxide, the chapter continues by describing only structures in which the oxygen atom of the CO group is coordinated to a metal. This is apparently intended as an introduction to the section on "CO Cleavage and Reduction", which, in a mere two pages, contains only a somewhat naive description of the Fischer-Tropsch synthesis and of CO reduction at $[Fe_4(CO)_{13}]^{2\ominus}$; it therefore cannot in any way claim to be a full account of the topic. The section on N_2 complexes appears to be rather more complete, although here there is less material to be covered.

The fourth chapter (Triatomic Ligands) begins with a discussion of the structures of $SCN^{\ominus}$-bridged complexes. A page and a half is devoted to the IR spectroscopy of these compounds; other spectroscopic methods receive only a bare mention and no literature references. The discussion of terminal thiocyanate complexes (with N or S bonding) allows the author to digress into the HSAB concept, which is probably already quite familiar to the average reader of such a monograph.

The final chapter (Polyatomic Ligands), which stands out impressively from the preceding parts of the book in the standard of treatment and information content, is essentially a reprint of an article by the author on this topic, which appeared in *Coordination Chemistry Reviews*. Here the reader learns that in addition to the usual β-dionate chelates there exist many other types of complexes which contain a β-diketone, as the neutral molecule, as monoden-

tate ligands (O or C bonded), as bridging ligands, as allyl-type η^3-ligands, or in a wide variety of ways as dianions. The structures, spectroscopic properties and reactions are discussed in detail, and published work up to 1985 is covered, with occasional references to more recent papers.

On balance, this book contains much less than its all-embracing title suggests. Half of the costly space (DM 1.00 per page!) is taken up by information which one can find equally well or better in standard textbooks. The claim to completeness is only justified in the case of the overview of β-diketone complexes, but that is already available in every well stocked library.

Wolfdieter A. Schenk [NB 917 IE]
Institut für Anorganische Chemie
der Universität Würzburg (FRG)

Two-Dimensional NMR Spectroscopy. (Methods in Stereochemical Analysis. Vol. 9.) Edited by *W. R. Croasmun* and *R. M. K. Carlson*. VCH Verlagsgesellschaft, Weinheim/VCH Publishers, New York 1987. 511 pp., bound, DM 210.00.—ISBN 3-527-26528-7/0-89573-308-0

During the last decade nuclear magnetic resonance (NMR) has become one of the main spectroscopic tools in research laboratories for structural analysis of biological and chemical compounds. Several factors have contributed to the increase in popularity of NMR. The construction of high-field NMR magnets and the use of modern computers in NMR spectrometers were a prerequisite. However, the major advances came from the development of the two-dimensional (2D) NMR method by *Ernst* and coworkers, and the sequencial assignment strategy for proteins by *Wüthrich* and coworkers. The rapid growth of the NMR field has led to impressive scientific results, published initially in scientific journals. In addition, in the past two years a number of good books on various subjects and at various levels have been published. For expert NMR spectroscopists, for example, there appeared the texts of *Ernst* et al. ("Principles of Nuclear Magnetic Resonance in One and Two Dimensions", Clarendon 1987) and *Wüthrich* ("NMR of Proteins and Nucleic Acids", Wiley-Interscience 1986), while for students a number of suitable NMR textbooks have been published in England (*R. K. Harris* and *A. E. Derome*, or *J. K. M. Sanders* and *B. K. Hunter*). Any new book explaining 2D NMR techniques faces the difficult task of having to compete with these publications.

Croasmun and *Carlson*, researchers at two large industrial laboratories, have edited a new volume of the "Methods in Stereochemical Analysis" series, which is devoted entirely to 2D NMR and contains contributions from various authors. The book is aimed at chemists and biochemists who are not NMR spectroscopists, but who may want to apply 2D NMR to their field of interest. However, it is doubtful whether this volume is really attractive for readers other than researchers who already use NMR techniques. It is certainly not recommended as a general introduction to 2D NMR, for which purpose the books mentioned previously are much more suitable. Nevertheless, the volume contains a number of reviews which are certainly worthwhile reading. *Horst Kessler*'s group have reviewed their extensive 2D NMR studies of the cyclic peptide Cyclosporin A, and compare various experimental techniques for assigning the resonances and extracting *J*-coupling parameters from 2D spectra. In another fine chapter, *David Kearns* describes the internal motions in DNA and their effects on the relaxation parameters as measured by NMR, and summarizes his 2D NMR studies of simple-sequence DNAs such as poly(dA-dT)·poly(dA-dT). *Janusz Dubrowski* reviews the application of 2D NMR in the structural analysis of oligosaccharides, and demonstrates the usefulness of NMR in this area. Furthermore, the book contains three chapters on the use of 2D techniques in studies of natural products. *William Croasmun* and *Robert Carlson* have written a chapter on steroid structure analysis by 2D NMR, *Gary Martin* has done the same for coal-derived heterocyclics, terpenoids and alkaloids, while *Peter Rinaldi* compares the characterization of an intermediate in the organic synthesis of spatol using several different high- and low-field 2D NMR experiments.

However, the outstanding chapter, and also the longest (more than 150 pages), on the experimental aspects of 2D NMR, is written by *William Hull*. This chapter gives a clear treatise on good 2D practice, and an insight into many 2D pulse sequences and their phase cycles. It is by virtue of this chapter that I would recommend keeping the book beside your 2D NMR spectrometer (even if it isn't a Bruker). Unfortunately, the book is dated, which is not very harmful for the last mentioned contribution, but more so for the other chapters on research topics, since NMR has developed very rapidly in the last few years. Most references do not extend beyond 1985 or the start of 1986, and it is rather unfortunate that the publisher was unable to bring it out at the end of 1986 or early 1987. In general, the book is rather specialized; it will probably find its way into major university libraries or research institutes.

Rolf Boelens [NB 900 IE]
Department of Organic Chemistry
University of Utrecht (Netherlands)

Silicon Reagents in Organic Synthesis. (Series: Best Synthetic Methods.) By *E. Colvin*. Academic Press, New York 1988. xxii, 147 pp., bound, £ 27.00.—ISBN 0-12-182560-4

A report on the new series "Best Synthetic Methods" has already appeared.[*] The fourth volume has now been published; this is quite a slim one with 140 pages of text, dealing with silicon as a key element in organic syntheses. The author, *E. Colvin*, has already set standards in this field several years ago with his excellent monograph "Silicon in Organic Synthesis" (Butterworth, London 1981).

The present volume follows the well proven division of the subject that was used in the previous work. A general introduction to the chemistry of silicon compounds is followed by representative examples of the various compound classes and types of reactions (e.g., vinylsilanes, allylsilanes, silyl anions, silyl enol ethers, the Peterson olefination, etc.). The lists of relevant review articles and the inclusion of information about suppliers of organosilicon intermediates are very useful features; however, both of these are treated from an English-speaking viewpoint, so that, for example, the Houben-Weyl volume on silicon is missing from the list of publications.

The treatment of individual compound classes includes, in addition to detailed schemes showing syntheses and reactivity, very useful experimental details for carrying out many of the typical transformations; each chapter ends with a list of literature references. The last chapter con-

[*] See *Angew. Chem. Int. Ed. Engl. 26* (1987) 593.

tains a list of those compounds and syntheses for which more detailed experimental information can be found in other compilations (e.g., "Organic Syntheses"). However, it would have been more sensible to incorporate this information into the appropriate earlier chapters.

The question is, who are the readers most likely to benefit from this comparatively inexpensive little book? It is true that, in thumbing through the book, one picks up the occasional stimulus or new idea, but beginners will certainly gain a better understanding from the older monographs. On the other hand, those already experienced in this field will already have their own compilations of experimental methods, and therefore the main feature of this series—the more or less detailed descriptions of syntheses—will scarcely be a useful additional resource for this group either. An element-oriented methods collection of this type is really of little help in searching out the *best method* for a problem in synthesis. "*Best Synthetic Procedures*" would perhaps be a less misleading title for the whole series.

Hans-Ulrich Reissig [NB 918 IE]
Institut für Organische Chemie
der Technischen Hochschule Darmstadt (FRG)

Mechanisms of Photophysical Processes and Photochemical Reactions in Polymers. By *J. F. Rabek*. Wiley, Chichester 1987. xix, 756 pp., bound, £ 99.00.—ISBN 0-471-91180-1

In a total of 750 pages this book covers the most important findings of photochemistry and photophysics in polymer systems up to 1984 inclusive, and according to its author it is suitable both for polymer scientists and for advanced students who have some familiarity with or interest in this field.

The contents are arranged systematically, beginning with an introductory summary of the most important basic facts and concepts of photophysics, followed by an account of the relationships that are specific to energy transfer and excimer and/or exciplex formation in polymers, and of luminescence methods in polymer analysis. The remaining three-quarters of the book deals with various aspects of photochemistry in relation to polymers, together with a brief section on photochromic polymers. The individual topics covered are photoinitiation and photopolymerization (ca. 185 pages), polymer photodegradation and light stabilizers for polymers (ca. 170 pages), and the more applications-orientated topics of photoresists, photopolymer-coated printing plates, and the use of polymers in solar energy utilization (altogether ca. 90 pages).

Those chapters that deal with photochemical topics, making up more than half of the book, give an excellent up-to-date survey of current knowledge in this field. All the chapters and sections that are concerned more with photophysical aspects are, in comparison, too brief to cover these topics adequately, and consequently do not really justify the book's title; here, and also in the treatment of photochromicity, the importance of some of the key research contributions is not sufficiently brought out, and in some cases they are not referred to at all, or are cited incorrectly.

The book assumes that the reader has, in addition to a sound basic knowledge of the chemistry and physics of polymers, a grounding in the essentials of photochemistry and photophysics, and it is consequently not really suitable for those without a minimum of previous knowledge. Taken as a whole, however, the book is to be recommended, especially for the wealth of literature references which it contains, and for the generally good treatment of this field of importance to polymer science and technology.

Claus D. Eisenbach, Karl Fischer [NB 919 IE]
Institut für Makromolekulare Chemie
der Universität Bayreuth (FRG)

Registered names, trademarks, etc. used in this journal, even when not marked as such, are not to be considered unprotected by law.

© VCH Verlagsgesellschaft mbH, D-6940 Weinheim, 1988. - Printed in the Federal Republic of Germany by Zechnersche Buchdruckerei, Speyer/Rhein.

All rights reserved (including those of translation into foreign languages). No part of this issue may be be reproduced in any form - by photoprint, microfilm, or any other means - nor transmitted or translated into a machine language without written permission from the publishers. Only single copies of contributions, or parts thereof, may be made for personal use. This journal was carefully produced in all its parts. Nevertheless, authors, editors and publisher do not warrant the information contained therein to be free of errors. Readers are advised to keep in mind that statements, data, illustrations, procedural details or other items may inadvertently be inaccurate.

Valid for users in the USA: The appearance of the code at the bottom of the first page of an article in this journal (serial) indicates the copyright owner's consent that copies of the article may be made for personal or internal use, or for the personal or internal use of specific clients. This consent is given on the condition, however, that the copier pay the stated per-copy fee through the Copyright Clearance Center, Inc., for copying beyond that permitted by Sections 107 or 108 of the U.S. Copyright Law. This consent does not extend to other kinds of copying, such as copying for general distribution, for advertising or promotional purposes, for creating new collective works, or for resale. For copying from back volumes of this journal see 'Permissions to Photo-Copy: Publisher's Fee List' of the CCC.

Editorial office: Pappelallee 3, D-6940 Weinheim, Federal Republic of Germany, Telephone (06201) 602315, Telex 465516 vchwh d, Telefax (06201) 602328.

Editor: *P. Gölitz.*

Associate editors: *D. I. Loewus, A. Stimson.* **Editorial assistant:** *E. Schweikart*

Publishers: VCH Verlagsgesellschaft mbH. (Managing Director: *Hans Dirk Köhler*), Pappelallee 3, D-6940 Weinheim, Federal Republic of Germany.
Correspondence concerning advertisements should be addressed to VCH Verlagsgesellschaft mbH. (Advertising Manager *R. J. Roth*), Boschstr. 12, P.O. Box 101161, D-6940 Weinheim, Federal Republic of Germany, Telephone Weinheim (06201) 602-0, Telex 465516 vchwh d, Telefax (06201) 602 328.

ADVANCED MATERIALS

Editorial Advisors: E. M. Engler (USA), D. Haarer (FRG), N. Ogata (Japan), G. Petzow (FRG), J. M. Thomas (UK), G. Wegner (FRG)

Materials Federations—The State of Play

Editorial Essay

By Robert W. Cahn*

In May of this year, the Federation of Materials Institutes (of the United Kingdom) gave the press the news of its impending creation. The Institute of Ceramics, the Institute of Metals and the Plastics and Rubber Institute announced the formation, on June 1, of the new Federation.

The beginnings of the new federation lie two years in the past: the Institute of Ceramics and the Plastics and Rubber Institute, both British professional bodies, federated in November 1986. This decision represented, in the words of one of the senior officers concerned, 'a natural meeting of minds.' Earlier this year the Institute of Metals, London, decided to join the new federation, and soon afterwards the creation of the new body was announced to the world. What lies behind this innocuous news item?

A dignified contest has been in progress for many years between the drive to mark the emergence of the new superdiscipline of Materials Science and Engineering (MSE) by the creation of corresponding professional institutes, and the equally strong urge to strengthen the existing sectional bodies in the traditional fields of metallurgy, ceramics and polymers, as well as the newer fields of electronic materials, composites, solid-state chemistry, and others.

Probably the earliest manifestation of the MSE lobby's activity was the formation, in 1963, of the (British) Materials Science Club. The initiative stemmed from the late Mr. *Leslie Holliday* of the Institute of Chemical Engineers and several colleagues in the same Institute. At its apogee, this Club had several hundred members: it was always administered from within one of the British industrial companies to which its members belonged, first Shell and subsequently other bodies in the chemical engineering field—it never reached the dignity of a fulltime secretariat—and it held frequent meetings focused on industrial applications of various fields of MSE. The Club never sought to appropriate the other functions of a professional body and in particular it never tried to arrogate to itself the role of a professional qualifying body. This role may seem surprising to some readers outside the U.K. ... but in that country, the right to put letters such as F.I.M., F.R.I.C. or F.I.P.—or 'Chartered Engineer' or 'Chartered Physicist'—after one's name has always been highly prized and has

[*] Prof. R. W. Cahn
University of Cambridge
Department of Materials Science and Metallurgy
Pembroke Street, Cambridge CB2 3QZ (England)

Contents

R. W. Cahn
Materials Federations—The State of Play 1569
Z. Yoshida, T. Sugimoto
New Donors for Molecular Organic (Super)Conductors and Ferromagnets 1573
Research News
S. Stiltz
Beryllium Crystals for Neutron Monochromators 1578
R. Eidenschink
Liquid Crystals in Variable Friction Devices 1579
Conference Reports
H. Stegemeyer
Liquid Crystals Centenary 1580
J. Rühe, T. A. Ezquerra
Synthetic Metals—Coming of Age But Still Controversial 1583
N. Ogata
Surface and Colloid Science 1584
Conference Calendar 1586

Editor: *P. Gölitz* **Editorial Assistant:** *L. Dominguez*

always enhanced the holder's chance of securing a good post in industry—though it rarely influenced academic appointment committees! Some four years ago, the Materials Science Club, which had fallen on hard times, applied to amalgamate with the Metals Society, itself soon to become part of the Institute of Metals, and thereupon became one of its 'activity groups'. Existing members who were not metallurgists—the majority—were invited to join the Institute of Metals on favorable terms, but few accepted this offer, and the Materials Science Club, having fulfilled what was expected of it, is now to all intents and purposes dead.

The history of this pioneering Club illustrates a tendency which, rightly or wrongly, worries many materials scientists and engineers (let us call them MSEists) who are not primarily metallurgists. They have for some years perceived the large national metallurgical bodies as being engaged in a ruthless takeover campaign for the world's MSEists. Where Britain is concerned, the evidence for this worry is not strong: The Materials Science Club takeover, though it seemed innocuous enough, perturbed some; and the Institute's research journals, which had been entitled *Metal Science* and *Metals Technology*, were conflated to form *Materials Science and Technology*. The Institute of Metals sought to persuade ceramists, composite and polymer people to publish in its revamped periodical; when they did (as one eminent polymer specialist declared to the writer) they might receive no requests at all for reprints, which of course served as clear evidence that their papers had been read by few of those at whom they had been directed. The Institute of Metals certainly made it clear to the world that it wished to broaden its field of activities, after long years when much of its membership fiercely resisted any such broadening. The Institute may be forgiven if it feels aggrieved that, when at length it has reacted positively to this long-standing pressure, it has encountered a strongly negative reaction from some of its sister institutions! This is certainly unfortunate ... but, as we shall see below, this is probably a defensive response to the buccaneering activities of one of the American metallurgical societies.

Another body which has been in existence for some years in Britain is the Materials Forum, which owes its existence to the initiative of the (British) Institution of Mechanical Engineers and, more specifically, to the advocacy of a distinguished mechanical engineer, *Sir Hugh Ford*. The Materials Forum is intended to be a materials users' representative body. This body seeks to cover a wider range of engineering materials, and also to play a political (lobbying) role. By no means all British MSEists would accord the Metals Forum such a central position, and indeed would consider its claims as yet further evidence of metallurgical hubris!

America is another matter altogether. There are two major metallurgical bodies in the U.S.: The Metallurgical Society (TMS) of the American Institute of Mining, Metallurgical and Petroleum Engineers, and the American Society for Metals. The former has always maintained a decent reticence vis-à-vis its sister societies, but the ASM has recently gone unashamedly on the warpath. It has rechristened itself 'ASM International ... a Society for Materials', it has opened an ASM-Europe office, has created ASM 'chapters' in Benelux and Finland and has sought to create similar chapters (in some cases involving attempted takeovers of existing bodies) in countries such as India. This activity (which in the business world would be called an attempt at hostile takeovers) has not gone unnoticed and in this writer's view may have played a significant role in promoting the federation initiatives such as that between the ceramics and polymer bodies in Britain two years ago. Following that particular initiative, the Institute of Metals felt bound to become involved, which showed an impressive capacity for taking a long-term view.

The ASM action, and the subsequent actions in Europe, were no doubt partly a response to the runaway success of the (American) Materials Research Society, formed in the early seventies by a group of industrial materials physicists and, to a lesser extent, chemists who were frustrated by the lack of interest of the American Physical Society and American Chemical Society, at that time, in their concerns. The MRS, which now has more than 6000 members, has excited considerable suspicion and even hostility among some metallurgists in America and is perceived as a threat to the viability of the metallurgical societies by some of their members. While a European clone has recently started operations—the E-MRS or European Materials

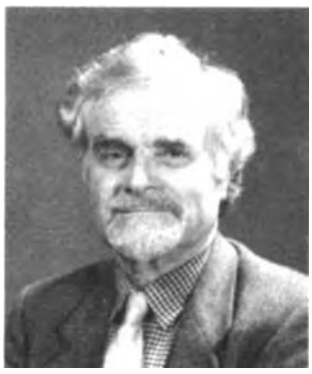

Prof. Robert W. Cahn was for many years Professor of Materials Science at the University of Sussex, UK, following that with a shorter period as Professor of Physical Metallurgy at the University of Paris-Sud. He is now retired, and attached to the Department of Materials Science and Metallurgy at Cambridge University, in the capacity of Senior Associate, and continuing to do research. His researches have been in various aspects of physical metallurgy, including ordered alloys, recrystallization of deformed metals, twinning and rapid solidification. He has been active for many years as an editor and correspondent: jointly with others, he created the Journal of Nuclear Materials and the Journal of Materials Science, has edited three editions of a text on Physical Metallurgy, has for 16 years edited a monograph series for the Cambridge University Press, has been materials science correspondent for 'Nature' for 20 years, is a principal editor of the new Journal of Materials Research and has embarked on a new editing venture, a series of 18 texts in MSE, for the publishers of 'Advanced Materials'.

ADVANCED MATERIALS

Research Society—it is at far too early a stage to be a serious threat to existing European bodies, but nevertheless the evidence is that it is already viewed with alarm.

Even before the Federation of Materials Institutes—to give it its formal name—began operations in Britain, other defensive initiatives had been seen in Europe. About five years ago, the various national polymer societies of Europe formed a European Polymer Federation, and last year, under the presidency of a distinguished Dutch ceramist, Dr. *R. Metselaar*, the ceramics societies of Europe formed the European Ceramic Society (in fact, though not in name, a federation) which is soon to hold its first international conference. This ceramics initiative apparently owed much to the discreet support offered by the American Ceramic Society, which wished to see a strong Europe-wide activity in ceramics (perhaps to counter what it may have perceived as metallurgical presumption!) Until this year the metallurgical bodies of Europe had not yet federated in any shape or form, although for some years their administrators have met regularly to prevent timetable conflicts with respect to their various national conferences. Indeed, such efforts to avoid timetable conflicts constitute one of the more basic objectives of European federations. However, as this editorial is being revised for press, an invitation is being circulated to a conference, entitled Euromat '89 and sponsored by a Federation of European Materials Societies! On closer examination, their brandnew Federation consists of the national metallurgical bodies of Britain, France and Germany, with the Swiss Society of Materials Technology for seasoning. The administrative seat is in Germany, so the initiative presumably stemmed from the Deutsche Gesellschaft für Metallkunde. Once again, metallurgical hubris has prevailed ... the latest Federation claim to represent all materials, not just metals!

Inaugural party, or ... wearing many hats

Reverting to the recently formed (British) Federation of Materials Institutes, this body is now taking active steps to enlarge its scope. Negotiations with the recently formed British Composites Society are at an advanced stage; there have been preliminary contacts with the Institute of Textiles and with other bodies. The Federation is strongly placed financially. Its administrative headquarters will soon move to the premises of the Plastics and Rubber Institute in London, and *Sir Geoffrey Ford*, the recently retired Secretary of the Institute of Metals, has already taken over as Secretary of the new Federation. The Chairman is *Sir John Collyear*, an industrialist who was Chairman of a Committee which, in 1985, was charged by the British Government with formulating a "Programme for the Wider Application of New and Improved Materials and Processes". (Their excellent report, like so many others in the materials field, led to no action whatsoever.) The Council will include, inter alios, the Presidents of the constituent societies. The aims of the new Federation are announced as being to "coordinate the activities of professional bodies and learned societies involved in the science, engineering and applications of materials in order to provide unbroken coverage of the entire field; improve services to members, to industry, and to the whole materials community; and to promote a wider understanding of engineered materials." The only possible response to that is: Amen!

Even more to the point is the following forthright assertion: "The three founding societies ... see as their ultimate aim the formation of a single Institute of Materials in the UK." This is undoubtedly difficult to achieve; the Institute of Metals will be the first to concede this, in view of its long years of effort directed, successfully in the end, to its mergers, first with the Iron and Steel Institute and then with the Institution of Metallurgists (which last was largely a professional qualifying body). One should not forget the trauma suffered by the Institute of Physics in London, many years ago, when it engineered its merger with the Physical Society; a very eminent physicist was reported as saying, in a moment of exasperation, that he supposed his Nobel Prize had really been awarded for his role in forcing through the merger!—Nevertheless, for the first time the objective of creating a materials institute in a European country has been announced, not unrealistically by a single existing body but rather by a federation of several such bodies: one can only hope that the creation of the metallurgically biased Federation of European Materials Societies will not interfere with the objective of eventually creating a British Institute of Materials.

An interesting question is the future relation between the international discipline-based European federations such

as those in the ceramics and polymer fields (and possibly a future metallurgical one), and the trans-disciplinary single-nation federation represented by the new body. It seems that no initiatives have yet been seen in other European countries to establish trans-disciplinary federations or societies in these countries. Perhaps we face a competition between single-nation trans-disciplinary bodies and international single-disciplinary bodies. One possibility, idealistic no doubt, is that the projected British Institute of Materials will actually come into existence and act as a template for a large European Institute of the same kind. That will certainly work better than the Federation of European Materials (i.e. Metals) Societies! A genuine European Materials Institute is certainly quite some years ahead and—who knows?—by then the European Materials Research Society, at present still a fairly modest enterprise, may have taken off as successfully as its American progenitor.

There have been suggestions in the foregoing that metallurgical bodies fear the MRS and that non-metallurgical bodies fear the metallurgists—perhaps more than they fear the MRS. The fear, so far as can be assessed, seems to be that the existing, traditional functions of the many bodies involved—the organizing and publishing of conferences, the holding of short discussion meetings, the publication of learned periodicals and news-filled house journals, the pleasant activity of formal dinners and (possibly the most important psychologically) the behind-the-scenes influencing of ministers and prime-ministerial science advisers—that all these varied activities are at risk from predators of one kind or another. The response of the ASM has been to undertake preemptive strikes across the world, and this is really rather odd, taking into consideration the fact that bodies such as the ASM have no shareholders to clamor for more profits. It is hard to see what benefit is achieved, for such a society, in growing beyond a certain size and income. Indeed, the MRS, ASM and AIME alike have all grown to a size which makes their meetings somewhat uncomfortable as social occasions. The most curious aspect of the situation, perhaps, is that the MRS has to be regarded, for the present, as a sleeping giant so far as political influence goes. It is so busy running and publishing specialized symposia, publishing one of the best house journals in the business and getting its new learned periodical off the ground, that it has not found time or inclination to lobby members of Congress for funds and to bend the ears of the President's Science Advisor or of the beleaguered minions of the National Science Foundation. That may change, of course—voices are beginning to be raised inside the MRS in favor of a higher political profile—but for the moment there are many smaller bodies which are far more active politically, for weal or woe. So perhaps the widespread apprehension is premature. There exists, in fact, a primarily politically oriented body, the Federation of Materials Societies (of the U.S.A.), founded in 1972. It is run from a small office in Washington, and unites twelve societies (in metallurgy, ceramics, engineering and chemistry ... i.e. polymers, electronics and crystal growth; The Materials Research Society is not a member). It organizes impressive, biennial conferences devoted primarily to policy issues, and through these seeks to influence the Administration and Congress. The Executive Director is an expert in public relations. The participants in the conferences are mostly research directors and other policy makers. The technical papers are surveys, not research reports. One wonders whether one of the European federations will go this way ... targeted on the Brussels bureaucrats!

One other consideration warrants careful thought. As stated, the Institute of Metals has sought to broaden the scope of its technical journal, and encountered some difficulty in doing so. Presumably, its partners in the new British Federation will now press it to leave ceramics to the ceramists, polymers to the polymer scientists and composites to the compositeers. If and when the Federation is replaced by a (national) Institute of Materials, that will be the time to go for a broad materials journal. But, in the view of the writer (who is an editor of long and varied experience) this will only work if the old journals close down and an entirely new journal, under entirely new management, starts up. Journals are like the Old Man of Siam:

There was an old man of Siam
Who said: "I perceive that I am
A creature that moves
In predestinate grooves,
Not a car, not a bus, but a tram."

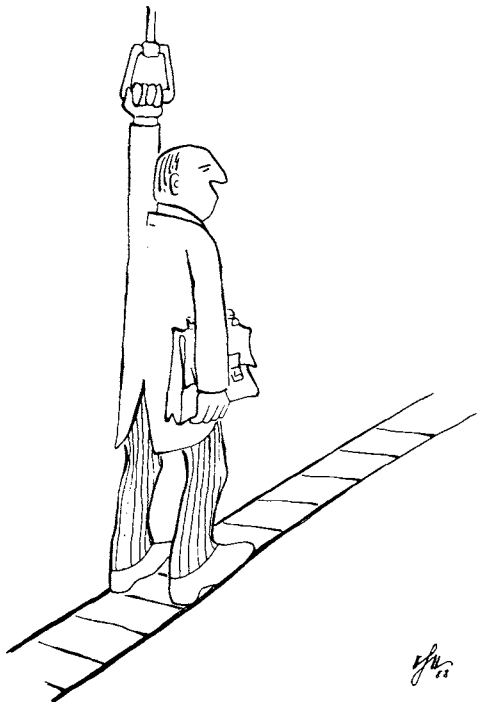

"... not a car, not a bus, but a tram"

Within a year or two of the creation of a new journal, its scope and readership become set in stone (or grooves), and therafter extensions of either, however sincerely sought, become ever more difficult. The MRS started its new journal after the Society had become established in the eye of the technical public, and was thus able to aim immediately at a wide scope and readership; even so, it has had difficulties to overcome ... a tendency by readers to suspect the new journal of electronic favoritism, and problems in extending readership across the Atlantic. It has scored with a striking innovation, however: it may well be the first learned periodical (as distinct from house journal) to be distributed free to all members who pay their modest membership subscriptions. There is undoubtedly much to learn, on this side of the Atlantic, from the MRS's new *Journal of Materials Research*.

For better or worse, Europe has embarked on a new route marked with much promise and numerous difficulties: it will be next to impossible to stop at a halfway point, and we may all expect to witness a rapid succession of mergers, federations and recreations. Good luck ... bonne chance ... zum Wohle!

New Donors for Molecular Organic (Super)Conductors and Ferromagnets**

Organic Metals
Organic Ferromagnets
Charge-Transfer Complexes
1,3-Dithiol-2-ylidene Donors

By Zen-ichi Yoshida* and Toyonari Sugimoto

1. Introduction

Synthetic chemistry has in the past been directed towards "structural" synthesis, in which compounds of known structure (e.g. natural products) or structure designed new systems (e.g. novel π systems) are the synthetic targets. This sort of chemistry will continue to be important in the future. However, "functional" synthesis, directed towards synthesizing organic compounds with novel functions, has recently started to emerge as a very important new field of chemistry, which will make valuable contributions to creating new advanced materials. Since we have already succeeded in creating an excellent new molecular energy storage system ("DONAC") based on our concept, in this review we shall discuss experiments aimed at synthesizing organic compounds with interesting electrical or magnetic properties.

The discovery in the early 1970's that single crystals of a tetrathiafulvalene-tetracyanoquinodimethane (TTF-TCNQ) charge-transfer (CT) complex showed metal-like electrical conductivity[1] marked an epoch in a new area of chemistry and physics. The energetic investigations that followed led in 1980 to another big discovery, that of the first organic superconductor, $(TMTSF)_2PF_6$, where TMTSF is tetramethyltetraselenafulvalene. This has a critical temperature T_c of 0.9 K under a pressure of 12 kbar.[2] Looking back on the brilliant history of organic conducting materials, one recognizes that two organic molecules originally synthesized for their structural interest as novel π-electron systems, TTF[3] and TCNQ,[4] played a crucial role in this new scientific field. From this viewpoint it can be said that organic and organometallic syntheses, which have yielded a number of promising organic molecules used to prepare interesting and useful organic materials, provide a springboard for new developments in this field.[5] However, the electrical, magnetic and optical properties of organic solids arise from special types of interactions between several organic constituents in ways that are as yet little understood. Therefore, in addition to the preparation of organic compounds that show promise as such constituent molecules, there is an urgent need to develop guiding concepts regarding the problem of crystal growth, to bring a deeper understanding of the properties of organic solids.

[*] Prof. Dr. Z. Yoshida, Dr. T. Sugimoto
Department of Synthetic Chemistry, Kyoto University
Yoshida, Kyoto 606 (Japan)

[**] The authors thank the Grants-in-Aid for Scientific Research on Priority Areas, New Functionality Materials—Design, Preparation and Control, the Ministry of Education, Science and Culture, Japan (Grant No. 62604004) for financial support. Discussions with Prof. *N. Kasai*, Dr. *Y. Kai*, Dr. *T. Kobayashi*, Dr. *H. Anzai*, Dr. *J. Yamauchi* and *Y. Misaki* are highly appreciated.

At present the usual course is to synthesize suitable organic compounds and investigate the properties of organic solids made up of these constituents, in the hope of discovering improved or novel effects. With many different systems under investigation it is likely that now and again someone will be lucky enough to make a new discovery. Our research on the design of new 1,3-dithiol-2-ylidene electron donors, with the aim of preparing molecular organic conductors and ferromagnetic materials, must be viewed in this context.

2. New 1,3-Dithiol-2-ylidene Electron Donors

In the early 1970's metallic conductivity was observed for two organic solids, consisting of the chloride salt of TTF[6] and the CT complex formed by TTF with TCNQ.[2] This discovery not only destroyed the belief hitherto held that "all organic compounds are electrically insulating", but also encouraged chemists to synthesize other such "organic metals", and hopefully even "organic superconductors", with physical properties that had previously been observed only in some metals and alloys. The electron donors so far used to prepare organic metals and superconductors are virtually limited to TTF and its chalcogen (Se and Te) analogs, TSF and TTeF. It appears that if high-T_c organic superconductors are ultimately to be achieved, new donors with skeletal structures different from that of TTF will be needed. Based on this view, research has begun on synthesizing new types of donors, in the belief that this will lead to the preparation of organic conductors and superconductors with properties superior to those hitherto obtained. The donors synthesized for this purpose are ethanediylidene-2,2'-bis(1,3-dithiole) **1**,[7] 2-butene-1,4-diylidene-2,2'-bis(1,3-dithiole) **2**,[8] ethenediylidene-2,2'-bis(1,3-dithiole) **3**,[9] butatrienediylidene-2,2'-bis(1,3-dithiole) **4**,[9] and [3]-,[10] [4]-,[11] [5]-,[12] and [6]-radialenes[13] substituted with 1,3-dithiole **5**–**8**. Among the compounds **1**–**4**, which have structures containing two or four sp^2 or sp carbon atoms between two 1,3-dithioles, **1** and **2** and their alkyl- and aryl-substituted derivatives were readily synthesized, but **3** and **4** could not be isolated owing to their extreme instability. In addition, two derivatives of **1** substituted with two or four selenium atoms in place of the corresponding sulfur atoms (ethanediylidene-2-(1,3-dithiole)-2'-(1,3-diselenole) **9**[14] and ethanediylidene-2,2'-bis(1,3-diselenole) **10**[14]) were prepared by the same method as for **1**. These new donors apparently have a one-dimensional arrangement of two 1,3-dithiol-2-ylidene moieties which differs from that in TTF. On the other hand, **5**–**8** have a two-dimensional arrangement of three, four, five, and six of the same moieties, respectively, if it is assumed that their molecular structures are completely planar. The X-ray structure analyses indicated instead a three-dimensional arrangement for **6**, **7** and **8**. A high degree of planarity is expected for **5**, but unfortunately this compound has not yet been prepared. Instead, [3]-radialene substituted with a sterically bulky, but still electron-donating, thioxanthenyl group in place of the 1,3-dithiole group **11** was prepared. In spite of considerable efforts, single crystals suitable for X-ray structure analysis have not yet been obtained.

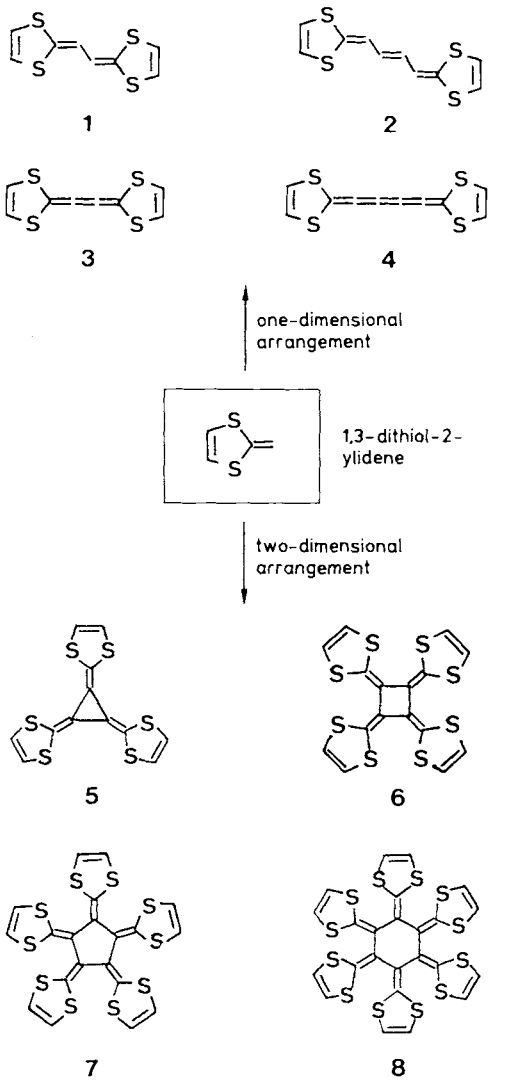

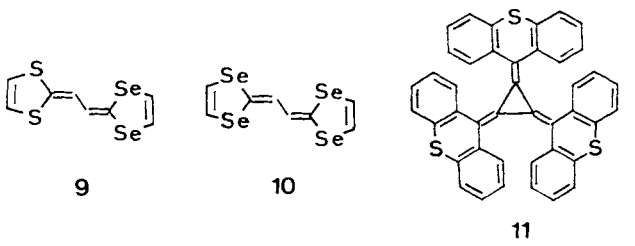

3. Redox Behavior

Data on redox potentials, especially the first (E_1) and second (E_2) values for donors, is very important in designing organic materials with interesting and useful physical

ADVANCED MATERIALS

Table 1. Redox potentials E_1–E_4 of new 1,3-dithiol-2-ylidene donors [a].

Donor	E_1	E_2	E_3	E_4
1	+0.20 [g]	+0.36 [g]		
9	+0.26 [g]	+0.40 [g]		
10	+0.33 [g]	+0.47 [g]		
2 [b]	+0.23 [g]			
3 [c]	(+0.07) [g, j]	(+0.31) [g, j]		
4 [c]	(−0.12) [g, j]	(+0.25) [g, j]		
11	+0.67 [h]	+0.80 [h]		
6	+0.19 [h]		(+0.98) [h, j]	(+1.30) [h, j]
7 [d]		+0.36 [i]		
8 [d, e]	+0.43 [i]	(+0.65) [i, j]		
8 [d, f]	+0.82 [i]			

[a] V vs. Ag/AgCl. [b] 2-Cyclohexen-1,4-diylidene-2,2′-bis(1,3-dithiole) was used. [c] The BF_4 salts of the corresponding dications were used. [d] The benzo derivatives were used. [e] Twisted-boat form. [f] Chair form. [g] Solvent: CH_3CN. [h] Solvent: CH_2Cl_2. [i] Solvent: PhCN. [j] Parentheses indicate that the redox reaction is irreversible.

properties such as electrical conductivity and ferromagnetism. Table 1 summarizes the redox potentials of the new donors. Except for **8**, where the central six-membered ring is in the chair form, and **11** the other donors have either smaller or similar E_1 values compared with that for TTF ($E_1 = +0.34$ V and $E_2 = +0.71$ V vs. Ag/AgCl in CH_2Cl_2). However, results from cyclic voltammetry indicate that **3**, **4** and **8** (twisted-boat form of the central six-membered ring) are undesirable donors by reason of extreme instability of the neutral species and radical cations for **3** and **4**, and of the dication for **8**. Eventually, the remaining six new 1,3-dithiol-2-ylidene systems might meet our expectations as promising donors. Brief information is given on the redox behavior of each donor. As is observed for TTF, two consecutive one-electron redox processes also occur for **1**, **9**, **10** and **11**. It should be noted that the second redox process can proceed at a lower potential than that of TTF, indicating that in the radical cation and dication states of these donors the on-site Coulomb repulsion is greatly reduced. For **2** and **6** the first and second one-electron redox processes occur simultaneously, although the subsequent electrochemically irreversible third and fourth ones are observed for the latter donor. Very interestingly, **7** exhibits only one redox process involving four-electron migration in one step. These unique types of redox behavior can reasonably be interpreted by considering that their conformations change so drastically as to increase the conjugation of the whole π electron system, as the oxidation proceeds. From consideration of the redox potentials these new donors show great promise for the preparation of organic conductors, and also of organic ferromagnets. However, the design of these new donors is lacking in another important respect, i.e. the stacking of the donor molecules. All the new donors have conformations that are far from planar, as is shown by their X-ray structure analyses and by spectroscopy. It is hoped that the donors can adopt molecular conformations sufficiently planar to allow close stacking in the form of CT complexes and radical cation salts.

4. New Organic Metals

The six new electron donor compounds that have been successfully prepared were used to investigate the formation of CT complexes with familiar acceptors, and of radical cation salts. All the donors gave CT complexes with TCNQ, tetrafluoro-substituted TCNQ, and 2,3-dicyano-5,6-dichloro-*p*-benzoquinone (DDQ). Comparatively high electrical conductivities (3×10^{-2} to 8×10^{-1} S cm^{-1}) in the form of compressed pellets at room temperature were observed for **1**·TCNQ, $\mathbf{9}_2(TCNQ)_3$, $\mathbf{10}_2(TCNQ)_3$, **2**·TCNQ, and **6**·$(TCNQ)_2$.[15] Attempts were made to obtain their CT complexes as single crystals, but this was successful only for **1**·TCNQ. The electrical conductivity of a **1**·TCNQ single crystal at 300 K was 16 S cm^{-1}, and the value gradually increased as the temperature was reduced from 300 to 200 K, reaching a maximum of 23 S cm^{-1}. This change of electrical conductivity with temperature implies that the crystals have metallic properties in this temperature range. However, at 200 K a metal-to-insulator phase transition occurred, and below this temperature semiconductor type behavior was observed. Thus, the **1**·TCNQ single crystal does not behave as a metal at low temperatures, much less as a superconductor.

Radical cation salts were prepared from the donor compounds using electrochemical crystallization. Here again single crystals were not easily obtained. Only the PF_6 and ClO_4 salts of the radical cation of a tetrabenzo-substituted derivative of **6** were obtained as single crystals of very small size.[16] The electrical conductivity at room temperature was ca. 1 S cm^{-1}, and unfortunately showed a temperature dependence characteristic of a semiconductor. Judging from the results obtained so far on the new 1,3-dithiol-2-ylidene donors, it appears that the nonplanar conformations of the new donors have an undesirable effect on the stacking of donor molecules in the CT complexes and radical cation salts. This situation was not unexpected from the outset. However, this difficult problem might be solved by introducing a suitable substituent group so as to give stronger intermolecular interaction, and/or by urgent synthesis of the planar molecule **5**, which appeared most promising in our first donor design considerations.

5. Molecular Organic Ferromagnets

In contrast to the considerable developments that have occurred in organic materials with electrical conductivity, and especially superconductivity, ferromagnetism, another very important and useful physical property, has not yet been achieved in organic materials. Ferromagnetism is a special state of complete spin alignment throughout the bulk. Several theoretical models have already been proposed for achieving a linear-chain ferromagnetic coupling in an organic solid. The most attractive of these are two models proposed by *McConnell*, based respectively on Heitler–London spin exchange between positive spin den-

sity on one radical and negative spin density on another,[17] and on configurational mixing of a virtual triplet excited state with the ground state for a chain of alternating radical cation donors and radical anion acceptors,[18] and a ferromagnetic superexchange model proposed by *Soos*.[19] Very recently, *Miller* et al. have developed an extended *McConnell* model leading to the spin alignment throughout the bulk that is necessary for bulk ferromagnetism.[20]

Guided by the theoretical background, current experimental programs are very actively concentrated in two directions, starting from polymeric systems and molecular solids respectively. For the latter types of organic ferromagnets with which we are concerned, particularly those based on CT solids, the second McConnell model can serve as a reliable initial guide. To give ferromagnetic behavior the donor or acceptor component needs to occupy at least one pair of degenerate highest occupied (HO) or lowest unoccupied (LU) molecular orbitals (MOs). This situation appears very often in d and f orbitals of transition metals, but very rarely in organic molecules, except for the case where there is an odd-fold axis of symmetry. *Breslow*[21] and *Miller* et al.[20] are continuing their efforts to prepare organic ferromagnets based on a mixed stack of CT complexes of a donor and an acceptor as above. On the other hand, *Torrance* et al.[22] and *Wudl* et al.[23] are investigating the possibility of organic ferromagnets in a stack of either all donors or all acceptors, as commonly found in electrically conducting radical ion salts.

Until now all the attempts have been limited to the CT complexes and radical cation salts of organic donors with C_3 or higher symmetry. Such donors are hexaazatritetralin **12**,[24] hexakis(alkylthio)benzenes **13**, **14** and **15**,[25] tris(ethyleneoxythio)benzene **16**,[25] tris(ethyleneaminothio)benzene **17**,[26] tris(ethyleneoxyamino)benzene **18**,[26] and hexaazaoctadecahydro-coronene **19**,[26] as shown below. Of these, the last donor is very attractive by virtue of its high symmetry and very low redox potentials (−0.771 V, −0.285 V, +0.178 V and +0.556 V vs. Ag/0.01 M $AgNO_3$, CH_3CN, 25 °C). Detailed investigations have been carried out on **12** and **19**. Unfortunately their CT complexes and radical cation salts, whose magnetic susceptibilities were examined as a function of temperature, were antiferromagnetic, not ferromagnetic. The dications of their donors generated in solution are ground state triplets, and the CT complex and radical cation salts have 1:1 stoichiometry of donor and acceptor components. These facts appear to fulfil the requirements of *McConnell*'s second model. However the actual situation turns out to be otherwise. A possible reason is that the molecular symmetry of the donor is reduced by Jahn-Teller distortion in the solid environment.

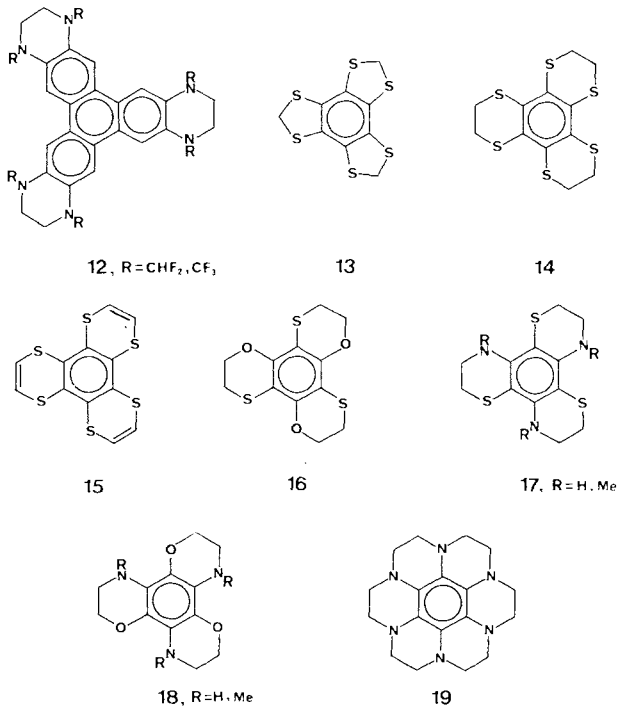

Our group is currently investigating the preparation of molecular organic ferromagnets by using electron-donating odd-numbered [n]-radialenes, which have a pair of degenerate HOMOs of comparatively high energy, assuming that the molecular symmetry is C_n or higher. With this assumption the radialenes are a pentabenzosubstituted derivative of **7** (**20**) and **11**. Compound **11** did not form a

20

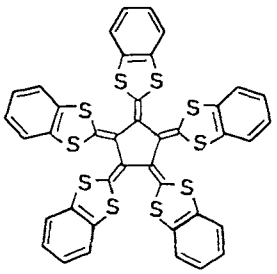

CT complex with any of the usual acceptors. This might be due to the high first redox potential and large steric hindrance of this donor. In addition, the dication generated chemically or electrochemically in solution was not a ground-state triplet, but a thermally accessible triplet.[10] On the other hand, **20** formed CT complexes with comparatively strong acceptors such as DDQ.[12b] We have investigated the magnetic properties of the CT complex of **20** with DDQ, whose composition was **20**:DDQ = 1:2, in contrast to the 1:1 ionic CT pair expected theoretically for the CT ferromagnet. The temperature change of the paramagnetic susceptibility of the **20**·$(DDQ)_2$ solid followed a Curie-Weiss law, and the Weiss constant was ca. −2 K. In the EPR spectrum at room temperature (298 K) the half-field (triplet state) resonance signal also appeared. The temperature change of the signal intensity in the range 298 to 4.5 K followed a Curie law, indicating involvement of a ground-state triplet in the solid. Both these results lead to the conclusion that $\mathbf{20}^{2\oplus}$ is a ground-state triplet which undergoes a weak antiferromagnetic interaction with two

ADVANCED MATERIALS

$DDQ^{\odot\ominus}$ radical ions in the CT solid. In contrast to the difficulty in achieving linear-chain ferromagnetic coupling in a purely molecular organic solid, a ferromagnetic organometallic molecular CT solid, decamethylferrocenium tetracyanoethylide, was very recently prepared.[27] Also for CT complexes of decamethylferrocene with DDQ,[28] and with hexacyanobutadiene,[29] linear-chain ferromagnetic coupling was observed, although a bulk ferromagnetic material was not achieved. In these complexes two spins which occupy a pair of degenerate HOMOs (d orbitals of the iron atom) are forced into a parallel orientation by their strong exchange interaction. This lowest excited state, formed via virtual CT between the ferrocene radical cation and the tetracyanoethylene radical anion, induces the triplet to be the ground state by admixing each other, resulting in stabilization of ferromagnetic coupling for this complex. In a pure organic donor with s and p orbitals such a lowest excited triplet state can arise only accidentally or from intrinsic π-orbital degeneracies, which are easily broken by Jahn-Teller distortion.

6. Prospects

The pace of research on organic conductors and superconductors has lost some of its impetus since the discovery of high-T_c ceramic superconductors. Nevertheless, it must be emphasized that research on organic (super)conductors needs to be actively pursued with the aim of preparing organic superconductors with higher T_c and elucidating the detailed mechanisms of superconductivity. Research on organic ferromagnetic materials is still in its infancy. Further development of these two research topics, especially on molecular organic (super)conductors and ferromagnets, depends ultimately on the synthesis of reliable organic donors, as this short review makes clear. To the best of our belief, the 1,3-dithiol-2-ylidene systems are still promising as donors for the preparation of the two types of organic materials, despite the fact that the six donor compounds investigated have not yet led to either organic superconductors or ferromagnetic materials. With regard to organic superconductors we are now investigating two new donors, a bis(ethylenedithio)-substituted derivative of **1** (**21**), and a tetramethyl-substituted derivative of **10** (**22**), which are the ethanediylidene analogs of the well-known bis-

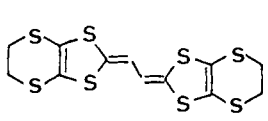

21

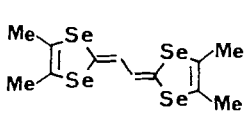

22

23

(ethylenedithio)-TTF and TMTSF, many of whose radical cation salts are superconductors. With regard to organic ferromagnets, **5** and its benzo-substituted derivative are the prospective donor compounds whose preparation is now our most urgent objective. These resemble hexa(dimethylamino)trimethylenecyclopropane **23**, which has been proposed by *Miller* et al. as a most promising donor. Also, the 1:1 CT complexes of **20** with appropriate acceptors might exhibit favorable magnetic properties, if $\mathbf{20}^{2\oplus}$ retains its ground state triplet in the complexes, as is the case in the $\mathbf{20}\cdot(DDQ)_2$ complex. We believe there is a good prospect that a new organic superconductor and/or a first purely organic ferromagnet will emerge from these newly designed 1,3-dithiol-2-ylidene donors.

Received: September 13, 1988

[1] J. Ferraris, D. O. Cowan, V. V. Walatka, J. H. Perlstein, *J. Am. Chem. Soc. 94* (1973) 948.
[2] K. Bechgaard, C. S. Jacobsen, K. Mortensen, H. J. Pedersen, N. Thorup, *Phys. Rev. 33* (1980) 1119.
[3] F. Wudl, D. Wobschall, E. Hufnagel, *Chem. Commun. 1970*, 1453.
[4] D. S. Acker, W. R. Hertler, *J. Am. Chem. Soc. 84* (1962) 3370.
[5] D. O. Cowan, F. M. Wlygul, *Chem. Eng. News 64* (1986) No. 29, p. 28.
[6] F. Wudl, D. Wobschall, E. Hufnagel, *J. Am. Chem. Soc. 94* (1972) 670.
[7] Z. Yoshida, T. Kawase, H. Awaji, I. Sugimoto, T. Sugimoto, S. Yoneda, *Tetrahedron Lett. 24* (1983) 3469.
[8] Z. Yoshida, T. Kawase, H. Awaji, S. Yoneda, *Tetrahedron Lett. 24* (1983) 3473.
[9] H. Awaji, T. Sugimoto, Z. Yoshida, *J. Phys. Org. Chem. 1* (1988) 47.
[10] T. Sugimoto, Y. Misaki, T. Kajita, T. Nagatomi, Z. Yoshida, J. Yamauchi, *Angew. Chem. 100* (1988) 1129; *Angew. Chem. Int. Ed. Engl. 27* (1988) 1078.
[11] T. Sugimoto, H. Awaji, Y. Misaki, Z. Yoshida, Y. Kai, H. Nakagawa, N. Kasai, *J. Am. Chem. Soc. 107* (1985) 5729.
[12] a) T. Sugimoto, Y. Misaki, Y. Arai, Y. Yamamoto, Z. Yoshida, Y. Kai, N. Kasai, *J. Am. Chem. Soc. 110* (1988) 628; b) T. Sugimoto, Y. Misaki, H. Hastakeyama, H. Oka, Z. Yoshida, J. Yamauchi, unpublished.
[13] T. Sugimoto, Y. Misaki, T. Kajita, Z. Yoshida, Y. Kai, N. Kasai, *J. Am. Chem. Soc. 109* (1987) 4106.
[14] Z. Yoshida, H. Awaji, T. Sugimoto, *Tetrahedron Lett. 25* (1984) 4227.
[15] a) T. Sugimoto, H. Awaji, I. Sugimoto, Y. Misaki, Z. Yoshida, *Synth. Metals 19* (1987) 569; b) T. Sugimoto, H. Awaji, I. Sugimoto, Y. Misaki, T. Kawase, S. Yoneda, Z. Yoshida, T. Kobayashi, H. Anzai, unpublished.
[16] K. Kikuchi, T. Ikemoto, T. Sugimoto, Y. Misaki, Z. Yoshida, unpublished.
[17] H. M. McConnell, *J. Chem. Phys. 39* (1963) 1910.
[18] H. M. McConnell, *Proc. R. A. Welch Found. Chem. Res. 11* (1967) 144.
[19] T. P. Radhakishnan, Z. G. Soos, H. Endres, L. J. Azevedo, *J. Chem. Phys. 85* (1986) 1126.
[20] a) J. S. Miller, A. J. Epstein, J. Am. Chem. Soc. 109 (1987) 3850; b) J. S. Miller, A. J. Epstein, W. M. Reiff, *Chem. Rev. 88* (1988) 201; c) *Science (Washington) 240* (1988) 40; d) *Acc. Chem. Res. 21* (1988) 114.
[21] R. Breslow, *Pure Appl. Chem. 54* (1982) 927.
[22] J. B. Torrance, S. Oostra, A. Nazzal, *Synth. Metals 19* (1986) 709.
[23] E. Dormann, M. J. Nowak, K. A. Williams, R. O. Angus, Jr., F. Wudl, *J. Am. Chem. Soc. 109* (1987) 2594.
[24] T. J. LePage, R. Breslow, *J. Am. Chem. Soc. 109* (1987) 6412.
[25] J. P. Morand, L. Brzezinski, R. Lapouyade, *Mol. Cryst. Liq. Cryst. 156* (1988) 237.
[26] a) R. Breslow, P. Maslak, J. Thomaides, *J. Am. Chem. Soc. 106* (1984) 6453; b) J. Thomaides, P. Maslak, R. Breslow, *ibid. 110* (1988) 3970.
[27] a) J. S. Miller, P. J. Krusic, A. J. Epstein, J. H. Zhang, W. Miller, J. C. Calabrese, R. W. Bigelow, A. J. Epstein, J. H. Zhang, W. M. Reiff, *J. Chem. Soc. Chem. Commun. 1986*, 1026; c) J. S. Miller, J. C. Calabrese, H. Rommelmann, S. R. Chittapeddi, J. H. Zhang, W. M. Reiff, A. J. Epstein, *J. Am. Chem. Soc. 109* (1987) 769.
[28] J. S. Miller, P. J. Krusic, D. A. Dixon, W. M. Reiff, J. H. Zhang, E. Anderson, A. J. Epstein, *J. Am. Chem. Soc. 108* (1986) 4459.
[29] J. S. Miller, J. H. Zhang, W. M. Reiff, *J. Am. Chem. Soc. 109* (1987) 4584.

ADVANCED MATERIALS

Research News

Beryllium Crystals for Neutron Monochromators

Since the introduction of neutron diffraction for the investigation of condensed systems, beryllium has been known as the most efficient material for thermal neutron monochromators. Additionally, a great demand has grown in recent years for beryllium single crystals as X-ray monochromators. Compared to the common neutron monochromator materials such as copper, silicon and niobium, beryllium crystals yield a distinctly higher intensity of the monochromated neutron beam. In most cases high reflectivity of the monochromator is not demanded for a distinct wavelength only, but for a small wavelength range. Therefore, the monochromator crystals should have a uniform distribution of dislocations, the so-called mosaic spread, throughout the bulk.

For a long time no single crystals of a sufficient size and with the desired mosaic spread were available because of difficulties in crystal growth.[1] Using a double ellipsoid mirror furnace, developed at the Crystallographic Institute of the University of Freiburg,[2] *Jönsson* succeeded in growing a small crystal by crucible-free zone melting.[3] Encouraged by this success, several neutron scattering laboratories joined the collaborative team formed by the Institute Laue-Langevin, Grenoble, and the Max Planck Institute for Metals Research, Stuttgart, in 1984.[4] In 1987 the Rheinisch-Westfälische Technische Hochschule Aachen also joined in this project.

A double and a triple ellipsoid mirror furnace were constructed, using designs developed in the universities of Freiburg and Stuttgart.[2,5] The growth conditions, described and discussed in deteil recently,[4], were steadily improved. In particular it became necessary to incorporate a complex purification process to radically reduce the high beryllium oxide content which interferes with crystal growth.

At present, crystals of 15 to 17 mm in diameter and 50 to 70 mm in length can be grown. Their quality is checked by Laue transmission photographs, by X-ray, γ-ray and neutron diffraction, and by neutron topography. Figure 1 shows a typical series of neutron rocking curves for different crystal lengths. Plastic deformation techniques are now being studied in order to obtain the desired mosaic spread of 15′ to 30′. The construction of the first beryllium monochromator, using some thirty beryllium crystals, will soon be achieved.

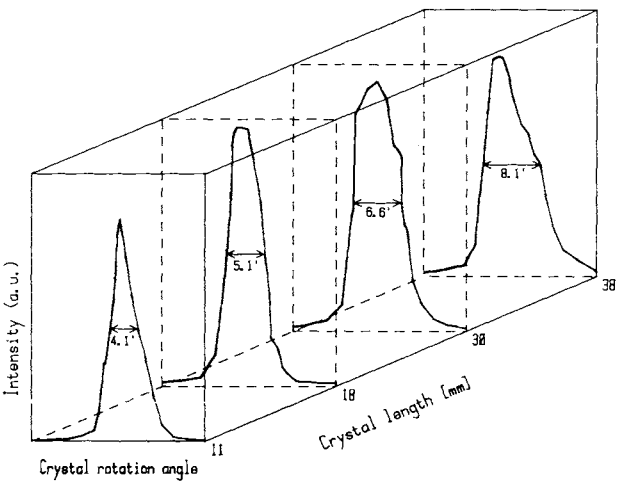

Fig. 1. Neutron rocking curves for different crystal lengths.

Sibylle Stiltz
Max-Planck-Institut für Metallforschung
Pulvermetallurgisches Laboratorium, Stuttgart (FRG)

[1] S. Jönsson, *J. Cryst. Growth 63* (1983) 116.
[2] A. Eyer, R. Nitsche, H. Zimmermann, *J. Cryst. Growth 47* (1979) 219.
[3] S. Jönsson, *Deutsche Gemeinschaft für Luft- und Raumfahrt, Report 82-02*, Bonn 1982, p. 83.
[4] S. Stiltz, A. K. Freund, *J. Cryst. Growth 88* (1988) 321.
[5] S. Stiltz, S. Jönsson, *Metall 38* (1984) 748.

As of January 1989, ADVANCED MATERIALS can be subscribed to separately at the annual rate of DM 178.00. Please order through your bookseller or write to VCH Verlagsgesellschaft mbH, Postfach 101161, D-6940 Weinheim, FRG. Customers in Switzerland, in the UK and in the USA should write to VCH Verlags AG, Hardstrasse 10, Postfach, CH-4020 Basel, Switzerland, VCH Publishers, Wellington Court, 8 Wellington Street, Cambridge CB1 1HW, UK, and VCH Publishers, Suite 909, 220 East 23rd Street, New York, NY 10010-4606, USA, respectively.

ADVANCED MATERIALS

Liquid Crystals in Variable Friction Devices

Although the first thermotropic liquid crystalline compound was discovered in 1888 by *Reinitzer*, it was not until almost 80 years later that the phenomenon of an ordered fluid found its first application in electrooptical displays. The ability to switch the orientation of molecules between transparent electrodes is nowadays exploited for displays in wrist watches, pocket calculators, data screens and pocket TV's.[1] The anisotropic physical properties of liquid crystalline materials depend on chemical structure and molecular order. Compounds with rod-shaped molecules can form nematic, different types of smectic (A to I), and also cholesteric including the so-called blue phases, depending on the detailed intermolecular interactions. In the course of the rapid developments in the physics and chemistry of liquid crystals in the last 20 years, it appears to have been overlooked that transitions between such phases, or between the isotropic phase and a liquid crystalline phase, have an enormous potential in mechanical engineering applications. These transitions can be brought about by changes of temperature or pressure. At the Hannover Messe Industrie 1988, a water-cooled brake was presented which exploited the drastic change in effective viscosity which accompanies the transition at 29 °C from a nematic to a smectic B phase[2] in *trans,trans*-4-methoxy-4′-pentylbicyclohexane.[3] The rate of conversion of mechanical to thermal energy in such a brake depends on the appropriate heat-transfer coefficients, the thermal conductivities of the materials involved, and the temperature of the coolant.

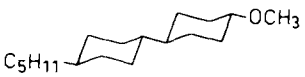

At the 12th International Liquid Crystals Confererence held in Freiburg, 15–19 August 1988, some measurements of the change of torque in such a device as it changes its function from a plain bearing to an effective brake were reported.[4] Figure 1 shows schematically a lubricated bearing of given clearance tempered with water. The axle is rotated by a motor with constant speed. The torque M in Nm is the momentum of friction transmitted from the axle to the bearing. Figure 2 gives its dependence on the reciproke temperature for compound **1** as lubricant in the region of mixed friction.

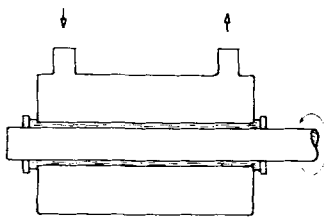

Fig. 1. Scheme of a lubricated axle rotating in a tempered bearing; the form of the lubrication layer corresponds to fully hydrodynamic conditions [5].

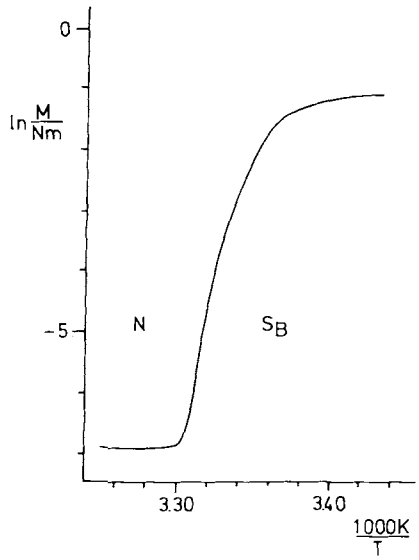

Fig. 2. Plot of the friction moment M transmitted by an axle rotating with constant speed with **1** as lubricant vs. $1/T$; N = nematic, S_B = smectic B phase.

The application of this principle in clutches, valves and hydraulic devices, as well as in bearings in which the effective viscosity of the lubricant can be adjusted to the rotating speed of the axle using two or more Stribeck curves,[5] was also suggested. In this way, "intelligent lubricants" should make it possible to construct bearings with less abrasion and less energy loss. The fast and reversible transition between phases of quite different effective viscosity also suggests new ways of designing mechanical components.

The basis for the understanding of friction in bearings under pure hydrodynamic conditions is given by the Reynold's differential equation. Although this has not been completely solved, the behavior is adequately understood for the case of isotropic lubricants, also including the case of mixed friction.[5] The description of friction in ordered fluids, taking into account the coefficients in the viscosity tensor (5 independent coefficients for the nematic phase, and many more for a smectic phase depending on its symmetry) is a formidable task. The measurements reported demonstrate that the orientation at the surfaces of the materials making up the device has a great influence on the frictional torque.

The phase transition is most easily brought about by changes of temperature. The use of Peltier elements seems to be of particular interest for low power devices. For many types of devices it would be useful to have high viscosities at high temperatures and low viscosities at low temperatures, i.e. the opposite of the usual situation. Leaving aside the possibility in principle of using liquid crystals with re-entrant phases,[6] there is no solution to this problem under isobaric conditions. In these cases phase transitions induced by changes of pressure are a possibility. At constant temperature the more highly ordered phase appears at higher pressure.[7] Thus, changes in effective viscosity can be expected at pressures much lower than those used with transmission fluids and oils, e.g. in gear-transmissions.[8] Unfortunately, kinetic data on transitions between the isotropic phase and a smectic phase, or between a nematic phase and a smectic phase, are not yet available. From isobaric microscopic observations it can be estimated that in compounds such as 4,4'-dialkylbiphenyls the molecular rearrangement will take place within a small fraction of a second at room temperature.

To be applicable in engineering many tribological conditions must be fulfilled. Obviously the compounds tested so far wet metals very well. There are many compounds of low molecular weight that are apparently resistant to hydrolysis and oxidation by air at not too high temperatures. A lucky circumstance is the fact that many stable and relatively easily synthesized compounds have an S_B phase, a highly ordered phase within the smectic layers. The occurrence of such a phase was undesirable in compounds synthesized for electrooptical displays. One can predict that, because of the low molecular weight, the resistance to molecular cleavage by shear forces should be good. The role of cavitation forces in highly stressed layers needs to be investigated by long-term tests. The point to be careful about seems to be the presence of organic impurities in the friction layer, which can cause a shift of the transition temperature.

R. Eidenschink
Nematel, Mainz (FRG)

[1] G. W. Gray (Ed.): *Thermotropic Liquid Crystals*, Wiley, New York 1987; R. Eidenschink, *Chemie Unserer Zeit 18* (1984) 168.
[2] *Chem. Rundsch. 1988*, No. 17, p. 9.
[3] R. Eidenschink, G. W. Gray, K. J. Toyne, A. E. F. Wächtler, *Mol. Cryst. Liq. Cryst. Lett. 5* (1988) 177.
[4] R. Eidenschink in: *Proc. 12th Int. Liquid Cryst. Conf.*, to be published in *Liq. Cryst.*
[5] G. Vogelpohl, *Zeitschr. VDI 96* (1954) 261.
[6] P. E. Cladis, *Phys. Rev. Lett. 35* (1975) 48; L. Longa, W. H. de Jeu, *Phys. Rev. A 26* (1982) 1632.
[7] G. M. Schneider,A. Bartelt, J. Friedrich, H. Reisig, A. Rothert, *Physica 139 & 140 B* (1986) 616.
[8] O. Dittrich in: *Das Öl als Konstruktionselement, VDI Berichte 680*, VDI Verlag, Düsseldorf 1988, pp. 201-219.

Conference Reports

Liquid Crystals Centenary

The 12th International Liquid Crystals Conference, held in Freiburg, FRG, on 15-19 August 1988, was attended by over 700 scientists from 31 countries; it is especially noteworthy that these included delegates from the German Democratic Republic and other eastern block countries. The conference, which was sponsored this time by the Deutsche Bunsen-Gesellschaft für Physikalische Chemie, is one of a series that began in 1965 in Kent, Ohio, USA; it is held bienially, the preceding one having been in Berkeley, California. One of the reasons for holding this year's conference in the Federal Republic of Germany is that the discovery of liquid crystals by *Friedrich Reinitzer* took place there 100 years ago. German scientists in Karlsruhe, Freiburg and Halle/Saale became closely involved in further studies of this fourth state of aggregation of matter, whose existence did not at first go unchallenged.

The scientific program of the conference included eight plenary lectures (45 min), 17 invited lectures (30 min), 58 short contributions (15 min), and 420 poster presentations. Apart from the plenary lectures, the meeting was divided into two parallel sessions covering the following main topics:

1. Synthesis and molecular properties (SY)
2. Polymer liquid crystals (PO)
3. Lyotropic liquid crystals (LY)
4. Chiral liquid crystals, blue phases (CH)
5. Ferroelectric liquid crystals (FE)
6. Applications (AP)
7. Surfaces and interfaces (SU)
8. Phase structure and transitions (PH)
9. Molecular dynamics and molecular theory (DY)
10. Instabilities, defects and fluctuations (IN)
11. Nonlinear optics in liquid crystals (NO)

During the course of the twelve conferences held since 1965 the number of scientific contributions has grown in an approximately linear fashion (Fig. 1). The Scientific

ADVANCED MATERIALS

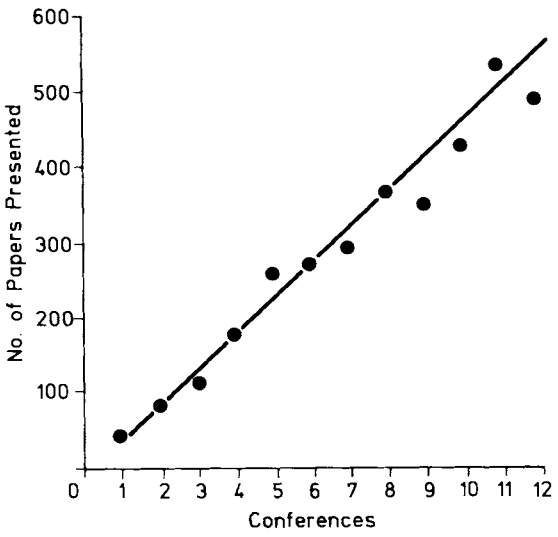

Fig. 1. Total number of papers presented at the International Liquid Crystals Conferences.

Committee of the Freiburg conference applied exacting standards to the papers submitted, and found it necessary to reject about 100 papers to maintain the required high level of scientific quality.

The 100th anniversary of the discovery of liquid crystals was acknowledged in a *historical session* with additional plenary lectures on the history of liquid crystals by *H. Kelker* (Frankfurt) and *H. Sackmann* (Halle/Saale), and in an exhibition entitled "100 Years of Liquid Crystal Research", prepared by *H. Kelker, G. Baur* and *M. Schadt*.

The conference's principal organizers were *G. Meier* of the Fraunhofer-Institut IAF, Freiburg (Conference Chairman), *H. Stegemeyer* of the University of Paderborn (Chairman of the Scientific Committee), *G. Baur* of the Fraunhofer-Institut IAF, Freiburg (Chairman of the Organizing Committee), and *H. Kelker* of the University of Frankfurt/Main (Treasurer).

Session SY was concerned with the synthesis of new types of liquid crystalline materials, and the relationship between molecular structure and physical chemical behavior. The main objective of these investigations is to develop materials with greater "intelligence" for applications in liquid crystal display devices, an area in which there are increasingly stringent demands from applications engineers with regard to switching by electric fields, image resolution, and information storage density. The contributions here emphasized the special importance not only of substances which contain polar and chiral groups and form ferroelectric liquid crystalline phases, but also of classical nematogenic compounds with high multiplexing capability.

Session PO was devoted to the chemistry of *polymer liquid crystals*. The number of groups working in this field and the volume of publications continue to grow, and closer contacts between these groups and those working on low molecular weight liquid crystals proved again very fruitful scientifically at this conference. The upward trend in research on polymer liquid crystals is clearly seen from the large increase in the numbers of papers on this topic over the last five conferences (Fig. 2, ×). While polymers

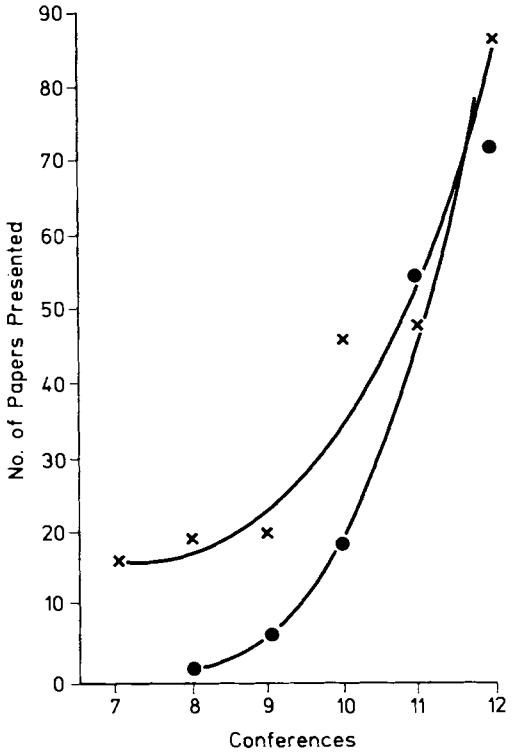

Fig. 2. Number of papers presented on polymer liquid crystals (×) and ferroelectric liquid crystals (●).

with main chain liquid crystalline behavior have for some time had an established place in applications, e.g. in the manufacture of high tensile strength fibers, the prospect of a technical breakthrough for liquid crystalline side chain polymers is only just emerging. The results reported at the conference suggest that we may expect this to occur in the area of thin films made from high molecular weight liquid crystals frozen in a glassy phase, and having special optical and dielectric properties; these could be used as ultra-high density data storage media. Another area where significant progress can be seen is the development of ferroelectric liquid crystalline polymers.

In *Session LY* the Scientific Committe aimed to direct special attention to *lyotropic liquid crystals* as an area with potential for further development. Liquid crystals of this type, which occur especially in aqueous solutions of surface active substances, have been studied with regard to their structures and their relationship to classical liquid crystals. As lyotropic liquid crystals have an important role in biological systems such as membranes and cell tissues, there is increasing research activity on this topic, which deserves a greater input of resources than in the past.

Nearly all the papers in *Session CH* were concerned with the *blue phases* observed in some *cholesterogenic liquid crystals*, perhaps still at present no more than a scientific

curiosity, but now attracting increasing attention, both experimentally and theoretically. Studies are in progress aimed at discovering how nature, starting from disordered systems of optically active molecules, builds up highly ordered cubic lattice structures in phases of extremely high chirality, with the result that one even observes liquid single crystals; studies have been made of the distortion of such single crystals in applied electric fields. These studies have led to the discovery of a number of distinct blue phases that are only stable in the presence of an electric field, and whose structures are in some cases still a subject of controversy.

Session FE was of particular importance, being devoted to the highly topical theme of *ferroelectric liquid crystals*. From the materials standpoint the preparation of these types of liquid crystals had already been covered in Session SY, and this session was therefore concerned mainly with physical processes in an applied electric field. In an electric field these ferroelectric systems can be switched between two stable states, and by suitably immobilizing these on surfaces in thin cells (up to 2 μm) they can be preserved after the field is removed. The switching times in these processes are extremely short, resulting in switching that is several orders of magnitude faster than can be achieved using nematic phases. It may therefore be possible to use these materials to make faster optical information storage devices, which accounts for the enormous interest shown by applications engineers. Because of this overwhelming interest in applications, the physics of dynamic field effects in ferroelectric liquid crystals has unfortunately been rather neglected. The conference illustrated that much basic research still remains to be done in order to elucidate, for example, the detailed mechanism of switching between the bistable states, and how molecular structural features such as chirality and polarity influence the spontaneous polarization. This area of ferroelectric materials is now clearly emerging as an important direction in liquid crystal research, as is evident from Figure 2 (●) which also shows the growth in the numbers of scientific contributions on this theme over the last five conferences.

In *Session AP, applications* were the theme. Improvements in the LC display devices which have now been in common use for some years are aimed at increasing the information storage density,and improving switching times and multiplexing capability. Important developments here are supertwist cells and active matrix displays. Developments in LCD technology now in progress in Japan, making it possible to produce TV screens with a higher information density, were especially impressive.

The papers in *Session SU* dealt with surface and interface effects in liquid crystals. The binding of liquid crystal molecules on surfaces prepared by vapor plating with inorganic materials or coating with amphiphilic monolayers was described. These techniques, and orientation effects on liquid crystals near to interfaces, also attracted much attention from applications engineers, since such processes are very important in the formation of ultrathin LCD films. Liquid crystal structures at free surfaces were also discussed, including the use of nonlinear optical effects to investigate these systems. The theoretical treatment of smectic layer structures consisting of only a few molecular layers requires an entirely new approach in contrast to the bulk behavior.

Session PH was mainly concerned with theories of *phase transitions* between polymorphic liquid crystal phases, and with experimental testing of such theories. The discussions included insights into the detailed topology of smectic layer structures (e.g. sub-types of the classical S_A phase); multicritical behavior and new types of phase structures were also discussed.

In *Session DY* the *dynamic behavior* of liquid crystals was discussed. An interesting aspect of this was the flow properties of liquid crystals, which one needs to know in order to understand the reorientation processes that occur during switching in a field. Molecular dynamics in monomeric, and more especially polymeric, liquid crystals have also been intensively studied; by using nuclear spin methods it has been possible to study the dynamic behavior of individual molecular segments. This has led to a deeper understanding of motional and relaxation processes in the different liquid crystal phases, the earlier considerations based on rigid rod-like molecules having been shown to be insufficiently detailed for this.

The papers in *Session IN* were again of predominantly theoretical interest, being concerned with *instabilities, defects and fluctuations* in liquid crystals. In this case, however, the results based on considerations of electrohydrodynamic instabilities have also turned out to have practical implications, since it is only thus that a deeper understanding of some of the long familiar processes involved in the switching of liquid crystals is now emerging.

Session NO was arranged by the Scientific Committee to allow a discussion of problems in *nonlinear optics* of liquid crystals. This was the smallest of the sessions, with only seven poster contributions, though by no means least in importance. It became evident that more efforts of research groups should be directed to this field. First of all, a number of problems related to the materials must be solved. Nevertheless, the possibility of using liquid crystalline components in integrated optics where nonlinear optical effects are important is now beginning to emerge.

In summary one can conclude from the results reported at this conference that polymeric liquid crystals, lyotropic systems and ferroelectrics are especially important topics for future research, with corresponding implications for applications technology, in some cases with a direct bearing on applications. The conference papers will be published in *Liquid Crystals* 5 early in 1989.

Horst Stegemeyer
Institut für Physikalische Chemie
der Universität-Gesamthochschule Paderborn (FRG)

ADVANCED MATERIALS

Synthetic Metals—Coming of Age But Still Controversial

The "International Conference on Science and Technology of Synthetic Metals" (ICSM '88) was held from 26 June to 2 July 1988 in Santa Fe, New Mexico, USA. It was attended by more than 550 physicists, chemists and materials scientists, more than half of whom came from Europe and Japan. There were over 700 contributions—lectures and posters—in four parallel sessions. The conference, organized by *M. Aldissi* from the Los Alamos National Laboratory, was primarily concerned with experimental and theoretical aspects of low dimensional conductors. Since the discovery of the first conducting polymer, more than ten years ago, there has been a growing interest in organic conducting materials. The main purpose of these investigations is the synthesis and study of new materials which combine the electrical properties of semiconductors or metals with the mechanical properties of polymers or other compounds. These have, in addition, the advantage that their properties can be tuned through molecular engineering, leading to well defined chemical structures.

The program of the conference covered the following areas: conducting crystals, conducting polymers, organic and high-T_c superconductors, organic ferromagnets, and materials with nonlinear optical properties. In contrast to the latest three ISCM meetings in Les Arcs (1982), Abano Terme (1984) and Kyoto (1986), the interest was focused on applications of conducting polymers. More than fifty presentations dealt with applications and many participants came from industry; however, only one or two products have been introduced to the market.

The meeting started with three plenary lectures: *V. J. Emery* (Brookheaven National Lab., Upton, USA) talked about the relationship between organic and high-T_c superconductors, and made a critical comparison of the mechanisms of superconductivity in both materials. It was hoped that the knowledge gained recently in the high-T_c ceramics field would help to improve organic superconductors as well. *K. Bechgaard* (Copenhagen, Denmark) reported on new molecular metals based on various heterocyclic donors. *H. Shirakawa* (Univ. of Tsukuba, Japan) chose as his topic polyacetylene with high conductivity (up to 22000 S cm^{-1}), high density and good mechanical strength. He stressed the importance of synthesizing polyacetylene films with very long conjugated segments and highly oriented polymer chains free of chemical defects. This can be achieved by a special treatment of the catalyst such as ageing and solvent evaporation prior to the polymerization process. Unfortunately, the chemical stability toward autoxidation could not be improved.

Three different types of polymers dominated the conducting polymers sessions: polyacetylene, polyaniline and substituted conducting polymers, especially substituted polyheterocycles (polypyrroles and polythiophenes) and poly-*p*-phenylenevinylenes. Substituents improve the solubility and processability of these materials. Nevertheless, a more accurate characterization of the polymers with respect to structural details, molecular weights etc. was not achieved.

Of particular interest in this area were talks dealing with composites or blends of conducting polymers and insulating matrix polymers. Such materials combine the intrinsic conductivity of the polyconjugated system and the mechanical properties of the matrix polymer.

M. F. Rubner (MIT, Cambridge, USA), *S. Tripathy* (Lowell Univ., USA) and *T. A. Skotheim* (Brookhaven National Lab., Upton, USA) presented results on conducting thin films of substituted polypyrroles and polythiophenes, which were made using the Langmuir-Blodgett technique. Such conducting thin films are of interest for developing molecular electronics.

Another polymer which received particular attention was polyaniline. Despite the fact that the conduction mechanism and the exact structure of this polymer are still a matter of controversy, as a large number of contributions proved, the first example of a commercial application of a conducting polymer in energy storage was reported by *T. Nakayima* (Bridgestone Corp., Tokyo, Japan). He described a rechargeable battery, developed in a joint project by Bridgestone and Seiko, which consisted of a polyaniline cathode and a lithium/aluminium alloy anode. Such a battery is used as a back-up power source for integrated circuit memories, or as an energy store for clocks with solar cells. That conducting polymers are promising materials for energy storage was also demonstrated in the subsequent talks by *M. Mizumoto* (Hitachi Ltd, Hitachi-she, Japan), *E. M. Genies* (Centre d'etudes Nucleaires, Grenoble, France) and *L. W. Shacklette* (Allied Signal Inc., Morristown, USA).

Polyacetylene again attracted a lot of interest, particularly because its conductivity has been improved significantly; the value of about 10^5 S cm^{-1} that has recently been reported by *Naarmann* et al. (BASF, Ludwigshafen, FRG) is almost equal to that of copper. Several other authors reported conductivity values of more than 10^4 S cm^{-1} in oxidized and highly oriented samples of polyacetylene [*T. Schimmel* (Univ. of Bayreuth, FRG), *M. Galtier* (Univ. of Montpellier, France); *Y. W. Park* (Seoul National Univ., Korea) and *J. Chiang* (UC Santa Barbara, USA)]. The improvement in the conductivity is achieved by a further development of the Shirakawa technique of acetylene polymerization using different solvent and polymerization conditions. This procedure probably leads to a more uniform catalyst with a smaller number of different

reactive species. Nevertheless, a complete understanding of the structural parameters and nature of the charge carriers and their mobility is still lacking.

An increasing number of contributions—compared with the Kyoto meeting two years ago—dealt with the possibility of using polymers with conjugated backbones in semiconductor devices [*F. Garnier* (Lab. Photochimie Solaire, Thiais, France), *R. H. Friend* (Cavendish Laboratory, Cambridge, UK) and *H. Koezuda* (Mitsubishi Electric Corp., Japan)]. The idea of an all-plastic electronic device constructed from semiconducting polymers is challenging. In these presentations it was shown that such devices work in principle, but up to now either the charge carrier mobility and/or the long term stability of the device is not sufficient compared to conventional inorganic semiconductors.

Next to polymers, the synthesis, structure and theory of superconducting low molecular weight crystals were covered in many contributions. The most promising candidates as organic superconductors are various BEDT-TTF radical salts; the onset of superconductivity has been measured at about 10 K at ambient pressure! Although this temperature is not very high compared to the values of the new high-T_c ceramics, the steady increase in the transition temperature and the more detailed knowledge of the structure encourage further investigations of these new organic materials.

A variety of social events such as receptions and excursions to places of interest near Santa Fe provided a relaxing diversion from the intense scientific program (up to 13 hours per day). The large number of lectures and poster presentations made it difficult to attend contributions in different fields. The shortness of the lectures (15 or 25 minutes plus five minutes for discussion) led to the situation that in some cases the results of one research project were reported in different lectures and poster presentations. It would be better to restrict the number of oral contributions in order to keep track of the progress made in the different fields. For reasons of clarity a combination of longer plenary lectures and short communications would be preferred.

The contributions to the ICSM '88 will be published in "Synthetic Metals" before the end of this year. The next ICSM meeting will be held in 1990 in Tübingen (FRG) and will be organized by *M. Hanack* (Univ. Tübingen, FRG) and *S. Roth* (Max Planck Institute for Solid State Research, Stuttgart, FRG).

Jürgen Rühe and *Tiberio A. Ezquerra*
Max-Planck-Institut für Polymerforschung
Mainz (FRG)

Surface and Colloid Science

The 6th International Conference on Surface and Colloid Science (6-ICSCS) was held on June 5–10, 1988 in Hakone, Japan, organized by the Division of Colloid and Surface Chemistry of the Chemical Society of Japan. Surface and colloid science has made rapid progress in recent years, due to the development of completely new experimental techniques and the industrial needs arising from the introduction of advanced technologies. Studies of amphiphilic substances are being pursued alongside research on organized molecular assemblies in solutions and at interfaces. Rapid progress is being made in investigating solid surfaces using the experimental techniques of high-vacuum physics, leading to many new results related to catalysis and chemical and photochemical reactions at surfaces. Biosurfaces and biocolloids are important research topics in the context of the recent upsurge in biological science. The preparation of fine particles and of concentrated dispersions are important topics in relation both to new industrial applications and to pure research, e.g. the direct measurement of interparticle forces.

Nearly 800 participants from 25 countries throughout the world came together for the 6-ICSCS, and 530 papers and poster presentations made up the five sessions: 1) Organized Molecular Assemblies in Solution, 2) Organized Molecular Assemblies at Interfaces, 3) Solid Surfaces and Catalysis, 4) Biomembranes and Biocolloids, and 5) Fine particles and Dispersed Systems. In addition to exchanging information on fundamental aspects of surface and colloid science and their applications to advanced materials, participants were able to enjoy the beautiful scenery of Mt. Fuji.

Six plenary lectures were presented on the mornings of Monday and Wednesday. In the first of these, *E. Matijević* (Potsdam, NY, USA) discussed "Colloidal Science of Ceramic Powders", pointing out that the properties and processing of ceramic materials are strongly influenced by the nature of the powders from which they are made. With the help of many beautiful electron micrographs he showed that a large number of dispersions can now be obtained with uniform particles, ranging in size from several μm to several nm, in a variety of shapes including spheres, rods, ellipsoids, cubes, platelets, discs, etc.

K. Shinoda (Yokohama, Japan) lectured on "Conceptual Advances in Organized Solutions: a Milestone in the Physical Chemistry of Biological Organization", and described the ideal organized solution.

J. M. Thomas (London, England) gave a lecture entitled "Colloidal Metals: Past, Present and Future", starting from the beautifully colored colloidal gold prepared by *Michael Faraday* in 1856, and incorporating some material from his Christmas Lecture last winter. He reviewed newly developed technologies that can be used to determine the structure of metal colloids, and presented a variety of new results on the structure of colloidal metals, alloys, oxides, etc., and their application to catalysts.

G. A. Somorjai (Berkeley, CA, USA) lectured on "The Molecular Surface Science of Organic Monolayers", focussing on studies of alkanes and arenes adsorbed on flat metal surfaces of low Miller index as models for catalyst surfaces. The studies employed a combination of new surface science techniques including surface crystallography by low energy electron diffraction (LEED), high resolution electron energy loss spectroscopy (HREELS), and scanning tunneling microscopy (STM), as well as second harmonic and sum frequency generation using non-linear laser optics, and scanning atomic force microscopy (AFM).

Other plenary lectures were on "Measurements and Relation between the Static and Dynamic Interaction between Surfaces Separated by Thin Liquid and Polymer Films", by *J. N. Israelachvili* (Santa Barbara, CA, USA) and "Forces between Colloidal Particles and Phase Equilibria", by *H. Wennerström* (Lund, Sweden).

42 invited lectures were also presented. Of these, eight were described as invited general lectures, presenting selected topics from the latest Japanese technology. They were "Mass Spectrometric Analysis of Gas Molecule Adsorption on Solids", by *T. Kurabayashi* et al. (Tohoku University, Sendai), "Advanced Conducting and Superconducting Organic Materials", by *H. Inokuchi* (Institute of Molecular Science, Okazaki), "Chemical and Physical Properties of Oxide Superconductors", by *K. Kitazawa* et al. (University of Tokyo), "Preparation of Monodisperse Particles of Precious Metals and their Applications for Electronics", by *Y. Zeniya* et al. (Tanaka Matthey K. K., Kanagawa), "Preparation of Stable Ultrafine Emulsions", by *H. Nakajima* (Shisheido Co., Yokohama), "New Applications of Polystyrene Sulfonate Dispersant for Coal-Water Mixture and other Uses", by *K. Ohbu* et al. (Lion Corp., Tokyo), "Properties and Applications of Amino-acid-based Surfactants", by *M. Takehara* (Ajinomoto Co., Kawasaki), and "Principles of Production and Stability Assurances of Liposomes", by *S. Hirota* et al. (Daiichi Seiyaku Co., Tokyo).

The success of the conference confirmed the importance of continuous exchange of information. The next international conference is to be held in France in 1991. In association with 6-ICSCS, five pre- and post-conference symposia were held in Japan. These were the Kyushu Symposium on Surfactant Solutions and Interfaces (June 2–3), the Tsukuba Pre-conference Congress on Dispersed Systems and Biocolloids (June 3–4), Fuji Post-conference Symposium on Current Problems and Possibilities for the Future of Organized Molecular Assemblies at Interfaces (June 10–12), Symposium on Solid Surface Phenomena (June 11), and International Symposium on Adsorption (June 13–15). They were also very successful.

Naoya Ogata
Department of Chemistry
Sophia University, Tokyo (Japan)

Call for Short Communications · Call for Short Communications · Call for Short Communications

ADVANCED MATERIALS from now on welcomes short communications from all over the world, from academia and from industry, from chemists, physicists and materials scientists, provided they are in keeping with the program outlined in the editorial published in May. Authors who are interested in submitting short communications (up to six pages of double-spaced manuscript together with an appropriate number of figures and/or formulas) should prepare their manuscripts in accordance with the "Notice to Authors" of Angewandte Chemie reproduced in the January issue of the journal following the list of contents; upon request, a copy can be obtained from the editorial office:
ADVANCED MATERIALS/ANGEWANDTE CHEMIE
Postfach 101161
D-6940 Weinheim
Federal Republic of Germany

Call for Short Communications · Call for Short Communications · Call for Short Communications

Conference Calendar

December 1988

7 **Polymers for Life Science Applications**
London (United Kingdom)
Contact: Dr. M. D. Purbrick, Kodak. Ltd. Research Div., Headstone Drive, Harrow, Middlesex HA1 ATY, UK

7-8 **Materials Science and Eng. Towards the 21st Century,**
4th Israel Mater. Eng. Conf.
Beer-Sheva (Israel)
Contact: Peltours-Conventions, The Secretariat, 4th Israel Mater. Eng. Conf., P.O. Box 394, 61003 Tel-Aviv, Israel

7-9 **Ceramics for Environmental Protection,**
1st Int. Symp.
(ENVICERAM '88)
Köln (Fed. Rep. Germany)
Contact: G. von Landsberg, Deutscher Wirtschaftsdienst, Marienburger Straße 22, D-5000 Köln 51, FRG

8-16 **Semiconductor Materials,**
Int. Conf.
New Delhi (India)
Contact: Prof. P. C. Mathur, Univ. of New Delhi, Dept. of Physics, Delhi 110007, India

11-14 **Electron Devices,**
Int. Mtg.
San Francisco (USA)
Contact: M. Widekehr, c/o Courtesy Assoc. Inc., 655 15th St. NW, Suite 3000, Washington, DC 20005, USA

12-17 **Advances in Holography and Speckle Phenomenon and their Industrial Applications,**
Int. Workshop
Madras (India)
Contact: Prof. R. S. Sirohi, Indian Inst. of Technol., Physics Dept., Madras 600036, India

14-16 **SIMCER 7/ZIRCONIA 88**
7th Int. Symp. on Ceramics
Bologna (Italy)
Contact: Centro Ceramico, Via Martelli, 26, I-43138 Bologna, Italy

15-16 **Amorphous and Crystalline Silicon Carbide and Related Materials,**
Int. Conf.
Santa Clara (USA)
Contact: Prof. M. Rahman, Dept. of Electrical Eng. and Computer Sci., Univ. of Santa Clara, Santa Clara, CA 95050, USA

19-21 **Biosensors,**
Winter Mtg.
London (United Kingdom)
Contact: Prof. D. Chapman, Royal Free Hospital, School of Medicine, Rowland Hill St., London NW3, UK

20-22 **Solid State Physics,**
Annu. Conf.
Nottingham (United Kingdom)
Contact: Inst. of Physics, 47 Belgrave Sq., London SW1X 8QX, UK

January 1989

2-7 **Solid State Physics,**
2nd Int. Symp.
Kandy (Sri Lanka)
Contact: The Coordinator, Conf. Div., Inst. of Fundamental Studies, Hantana Rd., Kandy, Sri Lanka

11-13 **Superconductivity Applications,**
2nd. Annu. Int. Convention (SC '89)
San Francisco (USA)
Contact: Superconductor Applications Assoc., 24781 Camino Villa Ave., El Toro, CA 92630, USA

15-18 **Composites and Advanced Ceramics,**
13th Annu. Conf.
Cocoa Beach (USA)
Contact: The American Ceramic Soc., 757 Brooksedge Plaza Dr., Westerville, OH 43081-6136, USA

15-20 **Optics, Electro-Optics, and Laser Applications in Sci. and Eng.,**
Symp. and Exhibition
Los Angeles (USA)
Contact: Soc. of Photo-Optical Instrumentation Eng. (SPIE), P.O. Box 10, Bellingham, WA 98227, USA

23-24 **Commercial Applications of Superconductivity,**
2nd Annu. Cambridge Conf.
Boston (USA)
Contact: World Tech. Press, 1 Kendall Sq., Suite 2200, Cambridge, MA 02139, USA

31-3 **Polymer,**
17th Australian Symp.
Brisbane (Australien)
Contact: Dr. D. J. T. Hill, Chem. Dept., Univ. of Queensland, Brisbane 4067, Australia

31-3 **Sintering of Multiphase Metal and Ceramic Systems**
Int. Conf.
New Delhi (India)
Contact: G. S. Upadhyaya, Convener ICSMC '89, Dept. of Metallurgical Eng., Indian Inst. of Technol., Kanpur 208 016, India

February 1989

2-4 **Nonlinear Guided Wave Phenomena: Physics and Applications,**
Top. Mtg.
Houston (USA)
Contact: Optical Soc. of America (OSA), 1816 Jefferson Pl. NW, Washington, DC 20036, USA

5-9 **Biomedical Polymers,**
Int. Symp.
Perth (Australia)
Contact: Secretary, W. A. Polymer Group, Royal Australian Chemical Inst., 125 Hay St., Perth, W. A. 6000, Australia

6-10 **Composites,**
SPI Inst. Annu. Conf.
Dallas (USA)
Contact: Composites Inst., SPI, 355 Lexington Ave., New York, NY 10017, USA

6–9 **Optical Fiber Communication,**
IEEE-LEOS-OSA Conf.
(OFC '89 and IGWO '89)
Houston (USA)
Contact: Optical Soc. of America (OSA), 1816 Jefferson Pl., NW Washington, DC 20036, USA

7–9 **Physics and Chemistry of Semiconductor Interfaces (PCSI-6)**
Bozeman (USA)
Contact: G. J. Lapeyre, Physics Dept., Montana State Univ., Bozeman, MT 59717, USA

12–15 **High-Resolution Optical Fourier Transform Spectrometry and Noninvasive Assessment of Visual Systems,**
Top. Mtgs.
Santa Fe (USA)
Contact: Optical Soc. of America (OSA), 1816 Jefferson Pl. NW, Washington, DC 20036, USA

19–22 **Adhesion,**
12th. Annu. Mtg.
Hilton Head Island (USA)
Contact: D. Hunston, NBS, Polym. Div., Gaithersburg, MD 20899, USA

21–24 **Recent Advances in Drug Delivery**
Salt Lake City (USA)
Contact: K. Knutson, Univ. of Utath, Dept. of Pharmaceutics, CCCD, 421 Wakara Way, Suite 318, Salt Lake City, UT 84108, USA

21–26 **Optical Fibers and their Applications,**
5th Symp.
Warsaw (Poland)
Contact: R. S. Romaniuk, IPI Warsaw Univ. of Technol., Nowowiepska 15–19, PL-00-665, Warsaw, Poland

26–3 **Microlithography,**
Symp. and Exhibition (Micro '89)
Santa Clara (USA)
Contact: Soc. of Photo-Optical Instrumentation Eng. (SPIE), P.O. Box 10, Bellingham, WA 98227, USA

27–1 **Microphysics of Surfaces, Beams and Adsorbates,**
3rd Top. Mtg.
Salt Lake City (USA)
Contact: R. B. Hall, Exxon Research & Eng., Rt. 22E, Annandale, NJ 08801, USA

27–3 **Superconductivity,**
Gordon Conf.
West Coast (USA)
Contact: A. Sleight, E. I. Du Pont de Nemours, Experimental Station 356/301, Wilmington, DE 19898, USA

27–3 **High-Temperature Superconducting Oxides: Processing & Related Properties,**
TMS Annu. Mtg.
Las Vegas (USA)
Contact: M. Karl, The Metallurgical Soc., 420 Commonwealth Drive, Warrendale, PA 15086, USA

March 1989

1–3 **Technical Ceramics,**
2nd Int. Congr. and Exhibition (Techkeram 2)
Wiesbaden (Fed. Rep. Germany)
Contact: Demat Exposition Managing, P.O. Box 110611, D-6000 Frankfurt, FRG

5–10 **Liquid Crystals,**
6th Eur. Winter Conf.
Schladming (Austria)
Contact: P. Laggner, Inst. für Röntgenfeinstrukturforschung of the Austrian Academy of Sci., Steyrergasse 17, A-8010 Graz, Austria

6–8 **Lithium Battery Technology & Applications,**
4th Int. Seminar
Deerfield Beach (USA)
Contact: S. P. Wolsky, Ansum Enterprises Inc., 950 De Soto Rd., Suite 3B, Boca Raton, FL 33432, USA

6–9 **Condensed Matter Division**
9th Gen. Conf.
Nice (France)
Contact: Dr. F. Raymond CNRS-Bât. 3, rue Albert Einstein, F-06560 Valbonne, France

6–9 **Advanced Materials**
MRS Industry-Univ. Conf.
Denver (USA)
Contact: Dr. Fred Smith, Adv. Mater. Inst., Colorado School of Mines, 1500 Illinois, Golden, CO 80401, USA

6–10 **Quantum Wells for Optics and Optoelectronics; Picosecond Electronics and Optoelectronics,**
Top. Mtg.
Salt Lake City (USA)
Contact: Optical Soc. of America (OSA), 1816 Jefferson Pl. NW, Washington, DC 20036, USA

8–9 **Molecular Chemistry of Solid-State Electronics**
London (United Kingdom)
Contact: The Royal Society, 6 Carlton House Terrace, London SW 1Y 5AG, UK

9–11 **Makromolekulares Kolloquium**
Freiburg (Fed. Rep. Germany)
Contact: Prof. H. Finkelmann, Inst. für Makromol. Chemie der Univ., Stefan-Meier-Str. 31, D-7800 Freiburg, FRG

11–14 **Surface Finishing '89**
Brighton (United Kingdom)
Contact: Inst. of Metal Finishing, Exeter House, 48 Holloway Head, Birmingham B1 1NQ, UK

12–14 **High-Tech-Materials and Finishing**
Berlin
Contact: Technik + Kommunikation-Verlag GmbH, Ritterfelddamm 82 h + i, D-1000 Berlin 22

12–25 **Diffusion in Materials,**
NATO Adv. Study Inst.
Aussois (France)
Contact: A. L. Laskar, Phys. and Astron. Dept., Clemson Univ., Clemson, SC 29631, USA

13–14 **Regio Macro II**
Basel (Switzerland)
Contact: Prof. M. Mutter, Inst. für Org. Chem., Univ. Basel, St. Johanns-Ring 19, CH-4056 Basel, Switzerland

15–17 **Intelligent Materials,**
Int. Workshop
Ibaraki (Japan)
Contact: T. Kurino, The Soc. of Nontraditional Technol., Toranomon Kotohira-Kaikan Bldg. 3F, 1-2-8 Toranomon, Minato-ku, Tokyo 105, Japan

20-22 **Mechanical Properties of Materials at High Rates of Strain,** 4th Int. Conf.
Oxford (United Kingdom)
Contact: J. Harding, Eng. Sci. Dept., Univ. of Oxford, Parks Rd., Oxford OX1 3PJ, UK

20-22 **Refractory Metals and Silicides**
Eur. Workshop
Houthalen (Belgium)
Contact: R. De Keersmaecker, IMBE, Kapeldreef 75, B-3030 Leuven, Belgium

20-23 **Surface Science,**
Interdisciplinary Conf.
Liverpool (United Kingdom)
Contact: P. Weightman, Liverpool Univ., Oliver Lodge Lab., Oxford St., P.O. Box 147, Liverpool L69 3BX, UK

28-31 **Aluminum-Lithium**
5th Int. Conf.
Williamsburg (USA)
Contact: Al-Li-V, School of Eng. and Applied Sci., Thornton Hall, Univ. of Virginia, Charlottesville, VA 22901, USA

29-31 **Neutron and X-Ray Scattering: Complementary Techniques**
Canterbury (United Kingdom)
Contact: Dr. R. J. Newport, Univ. of Kent, Physics Dept., Canterbury, Kent CT2 7NR, UK

30-31 **Colorado Microelectronics**
Colorado Springs (USA)
Contact: CMC '89 Conf. Secretary, Microelectronics Research Lab., Univ. of Colorado, Colorado Springs, CO 80933-7150, USA

30-10 **Frontiers of Laser Spectroscopy of Gases,**
NATO Adv. Study Inst.
Vimelro (Portugal)
Contact: J. M. Hollas, Dept. of Chemistry, Univ. of Reading, Reading RG6 2AD, UK

30-14 **High-T_c Superconductors,**
Exp. Workshop
Miramare (Italy)
Contact: Int. Ctr. for Theoretical Physics, P.O. Box 586, I-34100 Trieste, Italy

April 1989

1-6 **Superconductivity,**
2nd World Congr.
Houston (USA)
Contact: R. D. Kane, World Congr. on Superconductivity, P.O. Box 27805, Houston, TX 77227-7805, USA

3-5 **Modern Practice in Stress and Vibration Analysis**
Liverpool (United Kingdom)
Contact: Meetings Officer, Inst. of Physics, 47 Belgrave Sq., London SW1X 8QX, UK

3-6 **Low Energy Ion Beams,**
5th Conf.
Guildford (United Kingdom)
Contact: Meeting Officer, Inst. of Physics, 47 Belgrave Sq., London SWIX 8QX, UK

3-7 **Copolymerization and Copolymers in Dispersed Media**
Lyon (France)
Contact: I. Guillot/C. Pichot, Lab. des Materiaux Organiques, BP 24, F-69390 Vernaison, France

3-7 **High Temperature Materials '89**
Gaithersburg (USA)
Contact: J. W. Hastie, National Bureau of Standards, Gaithersburg, MD 20899, USA

6-7 **Modeling in Crystal Growth from the Melt,**
NATO Workshop
Parma (Italy)
Contact: G. Müller, Inst. für Werkstoffwissenschaften 6, Martensstraße 7, D-8520 Erlangen, FRG

10-12 **Bayreuther Polymer Symp.,** (BPS '89)
Bayreuth (Fed. Rep. Germany)
Contact: BPS '89, Lehrstuhl Makromolekulare Chemie II, Univ. Bayreuth, Postfach 101251, D-8580 Bayreuth, FRG

10-13 **Microscopy of Semiconducting Materials,**
MRS 6th Oxford Conf.
Oxford (United Kingdom)
Contact: Administrator, Royal Microscopy Soc., 37/38 St. Clements, Oxford OX4 1AJ, UK

11-13 **Catalysis by Well Characterized Materials**
Liverpool (United Kingdom)
Contact: Prof. R. W. Joyner, Leverhulme Ctr. for Innovative Catalysts, Univ. of Liverpool, Grove St., P.O. Box 147, Liverpool L69 3BX, UK

17-26 **Ceramics and Composite Materials,**
Spring College in Mater. Sci.
Trieste (Italy)
Contact: Int. Ctr. for Theoretical Physics, Spring College in Mater. Sci. 1989, P.O. Box 586, I-34100 Trieste, Italy

18-19 **Industrial Water-Soluble and Water-Swellable Polymers**
Manchester (United Kingdom)
Contact: The Registar (Mid-Career Training), UMIST, P.O. Box 88, Manchester M60 1QD, UK

23-28 **Nondestructive Testing,**
12th World Conf.
(WCNDT '89)
Amsterdam (Netherlands)
Contact: B. de Jong, RAI Organisatie Bureau Amsterdam bv, Europaplein 12, 1078 GZ Amsterdam, Netherlands

23-27 **American Ceramic Society,**
91st Annu. Mtg. and Expo.
Indianapolis (USA)
Contact: Dr. K. M. Nair, Electronics Dept., E.I. du Pont de Nemours Co., Inc., 3181 Buffalo Ave., Niagara Falls, NY 14302, USA

24-28 **Optical Science and Engineering,**
2nd Int. Congr.
Paris (France)
Contact: Soc. of Photo-Optical Instrumentation Eng. (SPIE), P.O. Box 10, Bellingham, WA 98227, USA

24-28 **Lasers and Electro-Optics,**
LEOS-IEEE-OSA Conf.
(CLEO '89)
Baltimore (USA)
Contact: Optical Soc. of America (OSA), 1816 Jefferson Pl., NW Washington, DC 20036, USA

24–28 **MRS-Spring Mtg.**
San Diego (USA)
Contact: J. B. Ballance, MRS, 9800 McKnight Rd., Suite 327, Pittsburgh, PA 15237, USA

25–27 **Hot Isostatic Pressing of Materials**
Antwerpen (Belgium)
Contact: Hot Isostatic Pressing Conf., c/o K. VIV, Jan van Rijswijcklaan 58, B-2018 Antwerpen, Belgium

26–28 **Joining Ceramics, Glass and Metal**
3rd Int. Conf. (CGM '89)
Contact: Dtsch. Gesellsch. für Metallkunde eV., Adenauerallee 21, D-6370 Oberursel, FRG

May 1989

1–3 **Tunable Solid State Lasers,**
Top. Mtg.
North Falmouth (USA)
Contact: Optical Soc. of America (OSA), 1816 Jefferson Pl. NW, Washington, DC 20036, USA

1–5 **Scanning Microscopy,**
Salt Lake City (USA)
Contact: O. Johari, Scanning Microscopy Int., P.O. Box 66507, Chicago, IL 60666, USA

4–6 **Festkörper: Dynamik und Kinetik**
Siegen (Fed. Rep. Germany)
Annu. Mtg. Dtsch. Bunsen-Gesellsch. für Phys. Chem.
Contact: Dtsch. Bunsen-Gesellsch., Carl-Bosch-Haus, Varrentrappstr. 40/42, D-6000 Frankfurt am Main 90, FRG

7–12 **High-T_c Superconductor Technologies**
175th Mtg. Electrochem. Soc.
Los Angeles (USA)
Contact: S. Raider, IBM T. J. Watson Research Ctr., P.O. Box 218, York Town Heights, NY 10598, USA

9–11 **Coatings and Sensors for Acoustic and Electromagnetic-Optical Applications**
Univ. Park. (USA)
Contact: V. K. Varadan, Dept. of Eng. Sci. and Mechanics, Penn. State Univ., 227 Hammond Bldg., Univ. Park, PA 16802, USA

10–11 **Polyimides**
Montpellier (France)
Contact: Prof. M. Abadie, LEMD/MAO-USTL, F-34060 Montpellier Cedex 1, France

16–19 **Deutsche Gesellsch. für Metallkunde,**
Ann. Mtg.
Karlsruhe (Fed. Rep. Germany)
Contact: Dtsch. Gesellsch. für Metallkunde e.V., Adenauerallee 21, D-6370 Oberursel, FRG

22–24 **Werkstoffanalytik,**
Wien (Austria)
Contact: Prof. Dr. M. Grasserbauer, Inst. für Analytische Chem. der Tech. Univ. Wien, Getreidemarkt 9, A-1060 Wien, Austria

22–24 **Glastechnische Tagung**
Stuttgart (Fed. Rep. Germany)
Contact: Dtsch. Glastechnische Gesellsch. eV., Mendelssohnstr. 75–77, D-6000 Frankfurt am Main, FRG

22–25 **Graphite Intercalation Compounds,**
5th Int. Symp. (ISGIC-5)
Berlin
Contact: Dr. F. W. Froben, Fachbereich Physik, Freie Univ. Berlin, Arnimallee 14, D-1000 Berlin 33

24–26 **Advances in the Stabilization and Controlled Degradation of Polymers,**
11th Int. Conf.
Luzern (Switzerland)
Contact: Dr. A. V. Patsis, Inst. in Materials Sci, State Univ. of New York, New Paltz, NY 12561, USA

29–31 **Crosslinked Polymers,**
3rd Int. Conf.
Luzern (Switzerland)
Contact: Dr. A. V. Patsis, Inst. in Materials Sci, State Univ. of New York, New Paltz, NY 12561, USA

29–2 **Molecular Beams**
Perugia (Italy)
Contact: V. Aquilanti, Univ. di Perugia, Dipt. di Chimica, I-06100 Perugia, Italy

31–2 **Applied Surface Analysis,**
11th Symp.
Cleveland (USA)
Contact: J. Grant, Research Inst., 300 College Park, Dayton, OH 45469-0001, USA

June 1989

6–9 **Chemistry of Functional Dyes,**
Int. Symp. (ESTech '89)
Osaka (Japan)
Contact: Prof. T. Kitao, General Secretary of the Symp., Kinki Chem. Soc., Japan 1-8-4, Utsubo honmachi, Nishi-ku, Osaka 550, Japan

12–14 **Rubber,**
Int. Conf. 90 IRC Exhibition Paris (France)
Contact: Soc. de Chimie Industrielle, 28, rue Saint-Dominique, F-75007 Paris, France

12–15 **Narrow-Gap Semiconductors and Related Materials,**
Int. Conf.
Ogunquit (USA)
Contact: D. G. Seiler, Phys. Dept., Univ. of North Texas, P.O. Box 5368, Denton, TX 76203, USA

18–21 **Colloid & Surface Science,**
63rd ACS Div. of Colloid & Surface Chem. Symp.
Seattle (USA)
Contact: J. Berg, Dept. of Chemical Eng. BF-10, Univ. of Washington, Seattle, WA 98105, USA

19–21 **SAMPE-Electronics,**
3rd Int. Conf.
Los Angeles (USA)
Contact: M. Smith, Business Director, SAMPE, P.O. Box 2459, Covina, CA 91722, USA

21–23 **Chemically Modified Surfaces,**
Midland (USA)
Contact: W. T. Collins, Dow Corning Corp., Mail Stop C41C00, Midland, MI 48686, USA

25-30 **Solid State Sensors and Actuators (Transducers -5)/ Eurosensors III**
Montreux (Switzerland)
Contact: COMST S.A., P.O. Box 415, CH-1001 Lausanne 1, Switzerland

26-28 **Molecular Design of Functional Polymers,**
IUPAC Int. Symp.
Seoul (Korea)
Contact: IUPAC Int. Symp., c/o Polymer Soc. of Korea, Rm 601, Hyecheon Bldg., 831 Yeoksam-dong, Kangnam-ku, Seoul 135-792, Korea

26-30 **Solid State Chemistry,**
2nd Int. Symp.
Pardubice (Czechoslovakia)
Contact: Dr. L. Koudelka, Inst. of Chem. Technol., Leninovo nam., 565, CS-53210 Pardubice, Czechoslovakia

27-28 **Polymer Latex III**
London (United Kingdom)
Contact: Miss M. Peacock, Plastics and Rubber Inst., 11 Hobart Place, London SW1W OHL, UK

28-30 **Oxide Surfaces**
Midland (USA)
Contact: W. T. Collins, Mail Stop C41C00, Dow Corning Corp., Midland, MI 48686-0994, USA

July 1989

2-7 **Solid State Organic Materials,**
9th Int. Conf.
Como (Italy)
Contact: Centro di Cultura Scientifica, "A. Volta", Villa Olmo, Via Cantoni 1, I-22100 Como, Italy

3-6 **Conduction and Breakdown in Solid Dielectrics**
3rd Int. Conf. (ICSD '89)
Trondheim (Norway)
Contact: Prof. Sletbak, ICSD '89, The Norwegian Inst. of Technol., Sem Sælands V 13, N-7034 Trondheim, Norway

4-7 **Nonlinear and Electro-optics**
Int. Conf.
Cambridge (United Kingdom)
Contact: The Meetings Officer, The Inst. of Physics, 47 Belgrave Square, London SW1X 8QX, UK

9-14 **Zeolites,**
8th Int. Conf.
Amsterdam (Netherlands)
Contact: M. Laboushere, 792 Keizersgracht, 1017 EC, Amsterdam, Netherlands

10-12 **Applied Organometallic Chemistry: an Entry to the New Technology**
The Pines Resort (Australia)
Contact: Dr. A. F. Masters, School of Chemistry, Univ. of Sydney, Sydney, N. S. W. 2006, Australia

10-13 **Magnetic Resonance in Polymers,**
9th Spec. Colloq. Ámpere
Prague (Czechoslovakia)
Contact: P. M. M. Secretariat, c/o. Inst. of Macromol. Chem., Czech. Acad. of Sci., 16206 Prague, Czechoslovakia

10-14 **Electron Spectroscopy,**
4th Int. Conf.
Honolulu (USA)
Contact: G. E. McGuire, Microelectronics Ctr. of North Carolina, P.O. Box 12889, Research Triangle Park, NC 27709, USA

10-14 **Organic Coatings Science and Technology,**
15th Int. Conf.
Athens (Greece)
Contact: Dr. A. V. Patsis, Inst. in Materials Sci, State Univ. of New York, New Paltz, NY 12561, USA

11-14 **Numerical Analysis of Semiconductor Devices and Integrated Circuits,**
6th Int. Conf.
Dublin (Ireland)
Contact: J. J. H. Miller, Nase-Code Conf., INCA, P.O. Box 2, Dún Laoghaire, Ireland

16-21 **Catalysis,**
Eur. Conf.
Berlin
Contact: Prof. G. Ertl, Fritz-Haber-Inst. der Max-Planck-Gesellsch., Faradayweg 4-6, D-1000 Berlin

17-20 **Polymer Blends**
Prague (Czechoslovakia)
Contact: P. M. M. Secretariat, c/o. Inst. of Macromol. Chem., Czech. Acad. of Sci., 16206 Prague, Czechoslovakia

18-20 **Polymer Chemistry: Aspects of Radical Polymerization**
Lancaster (United Kingdom)
Contact: Dr. J. R. Ebdon, Dept. of Chemistry, Univ. of Lancaster, Lancaster LA1 4YA, UK

23-28 **Materials and Mechanisms of Superconductivity: High-Temperature Superconductors,**
Int. Conf. (HTSC-M^{2}S)
Stanford (USA)
Contact: Dr. T. H. Geballe, Dept. of Applied Phys., Stanford Univ., Stanford, CA 94305, USA

24-26 **Composite Structures,**
5th Int. Conf.
Paisley (United Kingdom)
Contact: Dr. I. H. Marshall, Dept. of Mechanical and Production Eng., Paisley College of Technol., High St., Paisley PA 12BE, UK

31-2 **Biologically-Engineered Polymers**
Cambridge (United Kingdom)
Contact: Royal Soc. of Chemistry, Burlington House, London W1V OBN, UK

August 1989

2-7 **Pure and Applied Chemistry,**
32nd IUPAC Congr.
Stockholm (Sweden)
Contact: Stockholm Convention Bureau, P.O. Box 6911, S-10239 Stockholm, Sweden

13-26 **High-T_C Superconductors,**
Nato Adv. Study Inst.
Bad Windsheim (Fed. Rep. Germany)
Contact: R. Kossowsky, Applied Res. Lab., Pennsylvania State Univ., P.O. Box 30, State College, PA 16804, USA

14-17 **Shock Compression of Condensed Matter,**
APS Top. Conf.
Albuquerque (USA)
Contact: A. Roach, MS-P 915, Los Alamos Nat. Lab., Los Alamos, NM 87545, USA

20–24 **Imaging Systems – 150 Years of Photography,**
Int. Symp. (ISIS '89)
Dresden (German Dem. Rep.)
Contact: Conf. Secretary, ISIS '89, Technische Univ. Dresden, Sektion Physik, Wissenschaftsbereich Photophysik, Mommsenstr. 13, DDR-8027 Dresden, GDR

20–25 **Crystal Growth: Progress in Science and Technology,**
9th Int. Conf.
Sendai (Japan)
Contact: Prof. T. Nishinaga, Inter Group Corp., Akasaka Yamakatsu Bldg., 8-5-32, Akasaka Minato-ku, Tokyo 107, Japan

21–26 **Photochemistry,**
Int. Conf.
Beijin (People's Rep. China)
Contact: Prof. S. Wu, Inst. of Photographic Chem., Academia Sinica, Beijing, People's Rep. China

28–31 **Dynamical Processes in Excited States of Solids,**
7th Int. Conf. (DPC '89)
Athens (USA)
Contact: DPC '89, Prof. J. E. Rives, Dept. of Physics and Astronomy, Univ. of Georgia, Athens, GA 30602, USA

28–1 **Ferroelectricity,**
7th Int. Mtg. (IMF-7)
Saarbrücken (Fed. Rep. Germany)
Contact: Dr. J. Albers, Univ. des Saarlandes, Fachbereich Physik, D-6600 Saarbrücken, FRG

28–1 **Sintering,**
7th World Round Table Conf.
Herceg-Novi (Yugoslavia)
Contact: Dr. D. P. Uskoković, Serbian Academy of Sci. and Arts, Knez-Mihailova 35, 11000 Beograd, Yugoslavia

28–1 **X-Ray Optics and Microanalysis,**
12th Int. Congr.
Cracow (Poland)
Contact: S. Jasienska, Academy of Mining and Metallurgy, Inst. of Metallurgy, 30-059 Cracow, Poland

28–2 **Photochemistry for High Technology,**
Int. Summer School
Leuna-Merseburg (German Dem. Rep.)
Contact: Prof. H.-J. Timpe, Sektion Chemie, Technische Hochschule für Chemie, Leuna-Merseburg, Gensaerstr., DDR-42 Merseburg, GDR

29–2 **Innovation and Perspectives in Solid Phase Synthesis,**
Int. Symp.
Oxford (United Kingdom)
Contact: R. Epton, School of Appl. Sci., Wolverhampton Polytech., Wolverhampton WV1 1SB, UK

September 1989

4–8 **Macromolecules 89,**
Oxford (United Kingdom)
Contact: Prof. R. Epton, School of Appl. Sciences, The Polytechnic, Wulfruna St., Wolverhampton WV1 1SB, UK

4–8 **Olefin Metathesis and Polymerization,**
8th Int. Symp.
Bayreuth (Fed. Rep. Germany)
Contact: Office ISOM 8, Lab. für Anorg. Chem., Univ. Bayreuth, Postfach 101251, D-8580 Bayreuth, FRG

5–7 **Interfacial Phenomena in Composite Materials,**
Int. Conf.
Sheffield (United Kingdom)
Contact: J. Herriot, Conf. Organizer, Butterworth Scientific Ltd., P.O. Box 63, Westbury House, Bury St., Guildford, Surrey GU2 5BH, UK

5–8 **Optical, Electrical and Acoustic Properties**
Kent (United Kingdom)
Contact: M. D. Shuttleworth, Plastics and Rubber Inst., 11 Hobart Pl., London SW1W OHL, UK

6–9 **Magnetic Materials and Applications '89**
Rimini (Italy)
Contact: I. Pareti, Local Chairman EMMA '89, Istituto Maspec CNR, Via Chiavari 18/A, 43100 Parma, Italy

10–14 **Optical Communications,**
15th Eur. Conf.
Gothenburg (Sweden)
Contact: P. A. Andrekson, Dept. of Optoelectronics, Chalmers Univ. of Technol., S-41296 Gothenburg, Sweden

11–13 **Charge Transfer in Polymeric Systems,**
RSC, Faraday Div.
Contact: Dr. J. F. Gibson, Royal Soc. of Chemistry, Burlington House, Piccadilly, London W1V OBN, UK

13–15 **Microscopy,**
150th Anniversary Commemorative Mtg.
Oxford (United Kingdom)
Contact: Microscopical Soc., 37–38 St. Clements, Oxford OX4 1AJ, UK

20–22 **Structural Adhesives in Engineering**
SAE II '89
Bristol (United Kingdom)
Contact: J. Herriot, SAE II '89, Butterworth Scientific Ltd., PO Box 63, Westbury House, Bury St., Guildford, Surrey GU2 5BH, UK

21–22 **Fire Retardant Polymers**
Torino (Italy)
Contact: Prof. L. Costa, Dipt. di Chim. dell'Università di Torino, Via P. Giuria, 7, 10125 Torino, Italy

25–29 **Vacuum (IVC-11)/Solid Surfaces (CSS-7),**
11th. Int. Conf./7th. Int. Conf.
Cologne (Fed. Rep. Germany)
Contact: D. A. Benninghoven, Physikalisches Inst. der Univ. Münster, Wilhelm-Klemm-Str. 10, D-4000 Münster, FRG

26–28 **Optical Memory,**
Int. Symp. (ISOM '89)
Kobe (Japan)
Contact: ISOM '89 Secretariat, Business Ctr. for Academic Soc. Japan, 3-23-1 Hongo, Bunkyo-ku, Tokyo 113, Japan

27–29 **New Polymers**
1st Materials Symp.
Regensburg (Fed. Rep. Germany)
Contact: OTTI-Fortbildung, Martin-Luther-Straße 10, D-8400 Regensburg, FRG

October 1989

1-5 **The Metallurgical Society,**
Fall Mtg.
Indianapolis (USA)
Contact: Mtgs. Dept., TMS, 420 Commonwealth Dr., Warrendale, PA 15086, USA

2-4 **Electron and Optical Beam Testing of Integrated Circuits,**
2nd Eur. Conf.
Duisburg (Fed. Rep. Germany)
Contact: E. Kubalek, Werkstoffe der Elektronik, Univ. Duisburg, Kommandanten-Str. 60, D-4100 Duisburg 1, FRG

11-13 **Werkstoffe für die Elektrochemie**
Stuttgart (Fed. Rep. Germany)
Contact: Prof. F. von Sturm, Jahnstr. 26, D-8901 Biberbach, FRG

11-13 **Surface Technology Forum**
SURTEC '89
Berlin
Contact: AMK Berlin, M 3/Surtec, Messedamm 22, D-1000 Berlin 19

15-18 **Unconventional Photoactive Solids,**
4th Int. Conf.
San Jose (USA)
Contact: Dr. C. G. Willson, IBM Almaden Research Ctr., 650 Harry Road, San Jose, CA 95120, USA

16-19 **High-Tech-Coating,**
Congr. and Exhibition
Wiesbaden (Fed. Rep. Germany)
Contact: Demat Exposition Managing, P.O. Box 110611, D-6000 Frankfurt, FRG

24-29 **Applications of Surface and Interface Analysis,**
Eur. Conf. (ECASIA '89)
Antibes (France)
Contact: J. Fauvet, Soc. Français du Vide, 19, rue du Renard, F-75004 Paris, France

November 1989

5-8 **Solid State Ionics,**
7th Int. Conf.
Hakone (Japan)
Contact: Dr. Y. Saito, Res. Lab. of Engineering Materials, Tokyo Inst. of Technol., 4259 Nagatsuta-cho, Midori-ku, Yokohama 227, Japan

14-15 **Polypropylene**
Madrid (Spain)
Contact: D. Varley, PRI, 11 Hobart Pl., London SW1W OHL, UK

22-24 **Euromat '89**
Eur. Conf. on Materials
Aachen (Fed. Rep. Germany)
Contact: Dtsch. Gesellsch. für Metallkunde eV., Adenauerallee 21, D-6370 Oberursel, FRG

27-2 **MRS Fall Meeting**
Boston (USA)
Contact: A. Wagner, Materials Research Soc. (MRS), 9800 McKnight Rd., Suite 327, Pittsburgh, PA 15237, USA

December 1989

12-15 **Pacific Polymer**
Hawaii (USA)
Contact: J. C. Vogl, Pacific Polym. Federation, Polytechnic Univ., 333 Jay St., Brooklyn, NY 11201, USA

Call for Short Communications: See page 1645! Call for Short Communications: See page 1585!

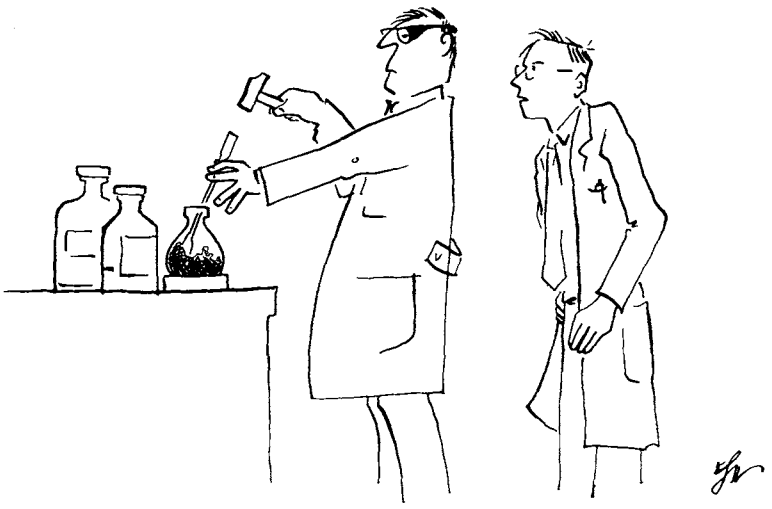

... doesn't melt, won't dissolve, just can't be broken down — let's send it to ADVANCED MATERIALS!

ANGEWANDTE CHEMIE
International Edition in English
Volume 27 · Number 12
December 1988
Pages 1593–1764

Under the Surface of the Chemical Article**

By Roald Hoffmann*

You open an issue of a modern chemical periodical, say the important German *Angewandte Chemie*[1] or the *Journal of the American Chemical Society*, and what do you see? Riches upon riches: reports of new discoveries, marvelous molecules, unmakeable, unthinkable yesterday—made today, reproducibly, with ease. The chemist reads of the incredible properties of novel high-temperature superconductors, organic ferromagnets, and supercritical solvents. New techniques of measurement, quickly equipped with acronyms—EXAFS, INEPT, COCONOESY—allow you to puzzle out the structure of what you make more expeditiously. Information just *flows*. No matter if it's in German, if it's in English. It's chemistry—communicated, exciting, alive.

Let's, however, take another perspective. To the pages of the same journal turns a humanist, a perceptive, intelligent observer who has grappled with *Shakespeare, Pushkin, Joyce*, and *Paul Celan*. I have in mind a person who is interested in what is being written, and also in how and why it is written. My observer notes in the journal short articles, a page to ten pages in length. She notes an abundance of references, trappings familiar to literary scholars, but perhaps in greater density (number of references per line text) than in scholarly texts in the humanities. She sees a large proportion of the printed page devoted to drawings. Often these seem to be pictures of molecules, yet they are curiously iconic, lacking complete atom designations. The chemist's representations are not isometric projections, nor real perspective drawings, yet they are partially three-dimensional.

My curious observer reads the text, perhaps defocusing from the jargon, perhaps penetrating it with the help of a chemist friend. She notes a ritual form. The first sentences often begin: "The structure, bonding and spectroscopy of molecules of type X have been subjects of intense interest.[a-z]" There is general use of the third person and a passive voice. She finds few overtly expressed personal motivations, and few accounts of historical development. Here and there in the neutered language she glimpses stated claims of achievement or priority—"a novel metabolite", "the first synthesis", "a general strategy", "parameter-free calculations". On studying many papers she finds a mind-deadening similarity. Nevertheless, easy to spot in some of the articles, she also sees style—a distinctive, connected scientific/written/graphic way of looking at the chemical universe.

I want to take a look, now not hiding behind this observer, at the language of my science, as it is expressed in the essential written record, the chemical journal article. I will argue that much more goes on in that article than one imagines at first sight; that what goes on is a kind of dialectical struggle between what a chemist imagines should be said (the paradigm, the normative) and what he or she must say to convince others of his or her argument or achievement. That struggle endows the most innocent-looking article with a lot of suppressed tension. To reveal that tension, I will claim, is not at all a sign of weakness or

[*] Prof. R. Hoffmann
Department of Chemistry, Cornell University
Ithaca, NY 14853 (USA)

[**] This article is derived from the text of a lecture I presented at the Chemiedozententagung in Mainz on March 14, 1988. At a special session of that meeting the 100th anniversary of *Angewandte Chemie* was celebrated.

irrationality, but a recognition of the deep humanity of the creative act in science.

The Scientific Article: A Brief History

There was chemistry before the chemical journal. It was described in books, in pamphlets or broadsides, in letters to secretaries of scientific societies. These societies, for instance the Royal Society in London, chartered in 1662, played a critical role in the dissemination of scientific knowledge. Periodicals published by these societies helped to develop the particular combination of careful measurement and mathematization that shaped the successful new science of the time.[2]

The scientific articles of the period are a curious mixture of personal observation and discussion, with motivation, method, and history often given firsthand. Polemics abound. Cogent arguments for the beginning of a codification of the style of the scientific article in France and England in the 17th century have been given by *Shapin*,[3a] *Dear*,[3b] and *Holmes*.[3c] I think the form of the chemical article rigidified finally in the 1830s and 1840s and that Germany was the scene of the hardening. The formative struggle was between the founders of modern German chemistry—people such as *Justus von Liebig*—and the *Naturphilosophen*. In that particular period the latter group might be represented by *Goethe*'s followers, but their like was present elsewhere in Europe even earlier, in the eighteenth century. The Natural Philosophers had well-formed notions, all-embracing theories, of how Nature should behave, but did not deign to get their hands dirty to find out what Nature actually did. Or they tried to fit Nature to their peculiar philosophical or poetic framework, not caring about what our senses and their extension, our instruments, said. The early 19th century scientific article evolved to counter the pernicious influence of the Natural Philosophers. The ideal report of scientific investigation should deal with the facts (often labeled explicitly or implicitly as truth; more on this later). The facts had to be believable independent of the identity of the person presenting them. It followed that they should be presented unemotionally (so in the third person) and with no prejudgment of structure or causality (therefore the agentless or passive voice).

The fruits of this model reportage were immense. An emphasis on experimental facts stressed the reproducible.

211. Fr. Goldmann: Ueber Derivate des Anthranols.

(Vorgetragen vom Hrn. Professor Liebermann.)

In einer früheren Mittheilung[1]) habe ich über die Einwirkung von Brom auf Anthranol berichtet und ein dabei entstehendes Dibromsubstitutionsproduct als analog dem Anthrachinondichlorid von Thörner und Zincke bezeichnet. Die Bildung des Anthrachinondichlorides war hiernach bei der Einwirkung von Chlor auf Anthranol zu erwarten.

Anthrachinondichlorid, Dichloranthron, $C_6H_4\langle{}^{CO}_{CCl_2}\rangle C_6H_4$

In eine kalte concentrirte Lösung von Anthranol in Chloroform wurde während etwa 20 Minuten trockenes Chlorgas geleitet, wobei die Lösung auf Zimmertemperatur erhalten wurde. Nach beendeter Reaction, bei der reichliche Chlorwasserstoffentwicklung stattfand, wurde das Chloroform auf dem Wasserbade verjagt, der Rückstand mit heissem Ligroïn ausgezogen und das in Lösung gegangene Product aus einer heissen Mischung von Benzol und Ligroïn umkrystallisirt.

Die Substanz wird so in Form von wasserklaren dünnen Prismen erhalten. Dieselben schmelzen bei 132–134°.

Die Verbindung ist in Benzol, Schwefelkohlenstoff, Chloroform sehr leicht, in kaltem Ligroïn oder Aether ziemlich schwer löslich. Aus der Schwefelkohlenstofflösung erhält man die Substanz beim Verdunsten in schönen wasserklaren Krystallen.

	Gefunden		Ber. für $C_{14}H_8OCl_2$
C	64.62	—	64.12 pCt.
H	3.25	—	3.05 »
Cl	—	26.96	26.72 »

Durch Kochen mit Eisessig oder Alkohol wird die Verbindung vollständig in Anthrachinon übergeführt. Die Chloratome müssen daher in der Mittelkohlenstoffgruppe sich befinden. Die Verbindung ist hiernach und nach ihren Eigenschaften mit dem Anthrachinondichlorid, welches Thörner und Zincke[2]) bei der Einwirkung von Chlor auf o-Tolylphenylketon erhielten, indentisch.

[1]) Diese Berichte XX, 2436.
[2]) Diese Berichte X, 1480.

Aus dem Anthranol entsteht sie nach der Gleichung:

$$C_6H_4\langle{}^{C(OH)}_{CH}\rangle C_6H_4 + 2Cl_2 = C_6H_4\langle{}^{CO}_{CCl_2}\rangle C_6H_4 + 2HCl.$$

Hr. Privatdozent Dr. A. Fock hatte die Güte, mir über die Krystallform des aus Schwefelkohlenstoff auskrystallisirten Anthrachinondichlorides Folgendes mitzutheilen:

Die Krystalle sind monosymmetrisch:

$$a : b : c = 0.7973 : 1 : 0.6262.$$
$$\beta = 72^\circ 48'.$$

Beobachtete Formen:

$$m = \infty P (110),\ c = 0 P (001),\ p = -P (111).$$

Die Krystalle bilden schwach gelblich gefärbte dünne Prismen, die Basis tritt nur an einzelnen Individuen und zwar ganz untergeordnet auf.

	Beob.	Berechnet
$m : m = 110 : \bar{1}10$	$= 74^\circ 36'$	—
$m : c = 110 : 001$	$= 76^\circ 24'$	—
$p : c = 111 : 001$	$= 37^\circ 54'$	—
$p : p = 111 : \bar{1}11$	$= 45^\circ 30'$	$45^\circ 2'$
$p : m = 111 : 110$	$= 38^\circ 38'$	$38^\circ 30'$
$p : m = 111 : \bar{1}10$	$=$ —	$71^\circ 25'$

Spaltbarkeit nicht beobachtet.

Auch das analoge Anthrachinondibromid hat Hr. Dr. Fock zu messen die Güte gehabt, wobei er folgende Resultate erhielt:

Die Krystalle sind monosymmetrisch:

$$a : b : c = 1.5009 : 1 : 1.4708.$$
$$\beta = 70^\circ 43'.$$

Beobachtete Formen:

$$c = 0 P (001),\ p = -P (111),\ o = +P (\bar{1}11),$$
$$q = {}^1/_2 \breve{P}\infty (012),\ w = +2\breve{P}2 (\bar{1}21).$$

Schwach gelblich gefärbte Krystalle von 1—4 mm Grösse und recht verschiedenartiger Ausbildung. Meistens herrschen die Flächen der vorderen Pyramide p und der Basis vor, während die übrigen nur ganz untergeordnet ausgebildet sind. Bisweilen sind die Flächen der Pyramide w grösser ausgebildet und zwar theilweise nur einseitig, so dass die Krystalle eine ganz verzerrte Ausbildung erhalten.

Fig. 1. The first two pages of a typical article from 1888 [4].

The conciseness of the German language seemed ideally suited to the developing paradigm. Cadres of chemists were trained. The development of the dyestuff industry that followed in England and Germany is a particularly well studied manifestation of the industrial application of the new, organized chemistry.

The scientific article acquired in this period a canonical or ritual form. In Figure 1, I reproduce part of a typical article of that period.[4,5] Note most of the features of a modern article—references, experimental part, discussion, diagrams. All that's lacking is the acknowledgment thanking the Deutsche Forschungsgemeinschaft or the National Science Foundation.

In Figure 2, a contemporary article, we approach the present. This particular contribution, an important one by *O. J. Scherer* and *T. Brück*[6] reports a remarkable ferrocene-type system in which one cyclopentadienyl ring has been replaced by P_5. The work is novel and significant, but I want to focus on the mode of presentation rather than the content. How does this article differ from one published a hundred years ago? The dominant language has changed, for interesting geopolitical reasons, to English.[7] Yet it seems to me that there is not much change in the construction or tone of the chemical article. Oh, marvelous, totally new things are reported. Measurements that took a lifetime are made in a millisecond. Molecules unthinkable a cen-

[(η^5-P_5)Fe(η^5-C_5Me_5)], a Pentaphosphaferrocene Derivative**

By *Otto J. Scherer** and *Thomas Brück*

After having demonstrated that *cyclo*-P_5 could be stabilized as bridging ligand in the mixed-valence triple-decker complex **1**,[1] we then attempted to realize the classical

[(η^5-C_5Me_5)Cr(μ,η^5-P_5)Cr(η^5-C_5Me_5)]

1

sandwich coordination of this ligand (cyclo-$P_5^\ominus$ as 6π electron donor). Success was achieved upon cothermolysis of **2** with white phosphorus.

Pentamethylpentaphosphaferrocene **3** forms sublimable, green crystals which can be handled in the presence of air and which begin to melt (with partial sublimation and slight decomposition) at 270°C when heated in a sealed tube. **3** is very soluble in dichloromethane, readily soluble in benzene and toluene, and moderately soluble in pentane.

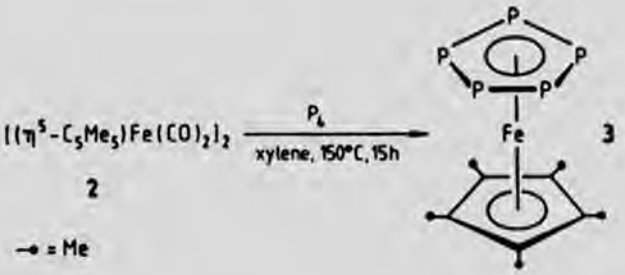

In the ^{1}H-NMR spectrum (200 MHz, 293 K, C_6D_6, TMS int.) of **3** a sharp singlet is observed at $\delta = 1.08$ which is shifted 0.6 ppm upfield compared to that of decamethylferrocene [(η^5-C_5Me_5)$_2$Fe] **4**.[3] In comparison to the ^{13}C{^{1}H}-NMR signals of **4**,[2,3] those of **3**[2] are shifted slightly downfield. The ^{31}P{^{1}H}-NMR signal shows a continuous downfield shift within the series triple-decker **1** ($\delta = -290.5$[1]), monophosphaferrocene [(η^5-C_5H_5)Fe(η^5-PC_4H_4)] **5** ($\delta = -67.5$[4]), **3** (81.01 MHz, C_6D_6, 85% H_3PO_4 ext., $\delta = 153.0$ (s)), and Li(P_5) ($\delta = 470$[5]). In the mass spectrum,[2] the most intense peak is the molecular peak of **3**, followed by the peak for $M^\oplus - P_2$. So far, all attempts to prepare a single crystal suitable enough for an X-ray structure analysis have failed, both by sublimation as well as recrystallization. *cyclo*-$P_5^\ominus$ is probably formed from $P_3^\ominus$ and P_2.[6]

Experimental

A mixture of **2** [7] (980 mg, 2.3 mmol) and P_4 (1500 mg, 12.1 mmol) in xylene (80 mL) was stirred under reflux for 15 h and the insoluble material removed by filtration on a D3 frit and extracted three times with 80 mL each of CH_2Cl_2 (393 mg of residue after drying under high vacuum). The solvent was removed from the combined extracts under oil-pump vacuum. After three extractions with 50 mL each of pentane there remained 726 mg of a brown solid whose composition could not be unequivocally established. After removal of the solvent from the green extracts (oil-pump vacuum), the residue remaining behind was sublimed. At 60°C/0.01 torr, excess phosphorus was removed; between 90° and 110°C, green needles sublimed on the wall of the glass vessel. Recrystallization from pentane furnished 175 mg of **3** (yield 11%). Correct elemental analysis.

Received: October 20, 1986;
supplemented: November 7, 1986 [Z 1957 IE]
German version: *Angew. Chem.* 99 (1987) 59

[*] Prof. Dr. O. J. Scherer, Dipl.-Chem. T. Brück
Fachbereich Chemie der Universität
Erwin-Schrödinger-Strasse, D-6750 Kaiserslautern (FRG)

[**] This work was supported by the Fonds der Chemischen Industrie.

[1] O. J. Scherer, J. Schwalb, G. Wolmershäuser, W. Kaim, R. Gross, *Angew. Chem.* 98 (1986) 349; *Angew. Chem. Int. Ed. Engl.* 25 (1986) 363.
[2] ^{13}C{^{1}H}-NMR (50.28 MHz, C_6D_6, TMS intern) **3**: $\delta = 90.6$ (s; C_5Me_5), 10.6 (s; CH_3); **4**: $\delta = 78.5$ (s; C_5Me_5), 9.8 (s; CH_3). EI-MS (70 eV) of **3**: *m/z* 346 ($M^\oplus$, $I_{rel.} = 100\%$), 284 ($M^\oplus - P_2$, 91%), P_4 (19.8%), P_3 (7.9%), P_2 (53%), P (7.8%) and further, weak intensity lines.
[3] Cf. : J. L. Robbins, N. Edelstein, B. Spencer, J. C. Smart, *J. Am. Chem. Soc.* 104 (1982) 1882.
[4] F. Mathey, *Struct. Bonding (Berlin)* 55 (1983) 153.
[5] M. Baudler, *Phosphorus Sulfur*, in press; M. Baudler, D. Düster, D. Ouzounis, *Z. Anorg. Allg. Chem.*, in press.
[6] Cf. also the theoretical studies on $N_5^\ominus$ and its complex stabilization. M. T. Nguyen, M. Sana, G. Leroy, J. Elguero, *Can. J. Chem.* 61 (1983) 1435; M. T. Nguyen, M. A. McGinn, A. F. Hegarty, J. Elguero, *Polyhedron* 4 (1985) 1721.
[7] D. Catheline, D. Astruc, *Organometallics* 3 (1984) 1094, and references cited therein.

Fig. 2. A contemporary article [6].

tury ago are easily made, in a flash revealing their identity to knowledgeable us. All communicated, with better graphics and computer typesetting, in a flashier journal, printed probably on poorer paper. But essentially in the same form. Is that good, is that bad?

Well, I think both. The periodical-article system of transmitting knowledge has worked remarkably well for two centuries or more. But I think there are real dangers (to which I will return) implicit in its current canonical form. My primary concern is what is really going on in the writing and reading of a scientific article, which is much more than just communication of facts. To set the stage for a discussion of the journal article, I need to say something about what I think science, chemistry in particular, is.

A Personal View of Chemistry

No one else's than my own, and others will see it in a different way:[8]

1. Science is the acquisition of knowledge about the world

That sense is clear in the etymology of the English word, or in the German *Wissenschaft* or *Naturwissenschaft*. Note that "truth" doesn't enter explicitly into that etymology. To be sure, reproducibility, verifiability, reliability, which are essential to any scientific enterprise, depend on *honest* measurement. Scientists would like to think that they acquire truth (morally and ethically valued) and not just knowledge (quite neutral; recall the tree of knowledge of good and evil in Genesis). But I would warn my colleagues that to purvey to the world at large the image of scientists as seekers of truth, rather than reliable knowledge,[9] is dangerous. It makes us out as priests, with the attendant hazards. I suspect much of the exaggerated interest of the public in the rare cases of fraud in science bears some similarity to the prurient interest of the world at large in the moral failings of priests and ministers. I think we gain knowledge, and do that as truthfully as possible.

2. Science is part discovery, part creation

I take discovery in the sense of revealing some perhaps obscured laws of nature, creation in the sense of making new things. In describing their work most scientists will stress the discovery metaphor, while most artists will emphasize creation. Well, I think much of what we do in science is creation. Especially so in chemisty. The synthesis of molecules not present on earth before is clear evidence of this. Synthesis is a marvelous congeries of discovery and creation that brings chemistry close to the arts—and to engineering.[10]

3. Science is done by human beings and their tools

Which means that it is done by fallible human beings. The driving forces for acquiring knowledge are, to be sure, curiosity and altruism, rational motives. But creation is just as surely rooted in the irrational, in the dark, murky waters of the psyche, where fears, power, sex, childhood traumas swim in all their hidden, mysterious movements. And spur us on. To follow *Pushkin*'s *Mozart and Salieri* or its modern reincarnation in *Peter Shaffer*'s play *Amadeus* and the movie based on it: Angelic music (read chemistry) is brought into this world by such crass vessels. Not only do character and deep-down motivations not matter—their "unsavory" side may well be the driving force of the creative act.

4. Science proceeds in part by the rules

The modern model of the scientific method, associated in this century perhaps with the name of *Karl Popper*, begins with measurable, reproducible observations. One then forms alternative hypotheses or models, explaining these observations. Finally, with the aid of further experiments or reliable theory, the hypotheses are culled, eliminated one by one, until the one most likely to be right remains. Sometimes it works this way,[11] though rather interestingly this happens mostly with everyday and not ground-breaking science. But does the model apply to a modern synthesis of an unnatural molecule, for instance dodecahedrane, a beautiful $C_{20}H_{20}$ molecule shaped like its name? Or the development of the technique of nuclear magnetic resonance, equally useful to chemists seeking the arrangement of atoms in space and to a physician looking for a brain tumor?

5. Science depends on argument

"Argument" has several meanings—it could be taken as a simple process of reasoning, a statement of fact; the word also may mean disagreement, the confrontation of opposites. I would argue that both senses are essential to science: dispassionate logical reasoning *and* impassioned conviction that one (model, theory, measurement) is right and another is wrong. I feel that scientific creativity is rooted in the inner tension, within one and the same person, of knowing that he or she is right and knowing that

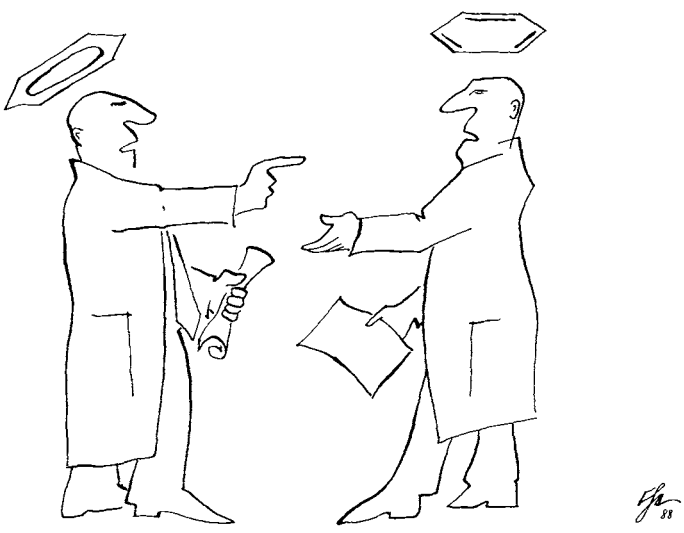

that conviction has to be proven to others' satisfaction. By a journal article.

6. *As a system, science works*

Individual scientists struggle to acquire knowledge, and in their struggle they are driven by many complex motivations. Because researchers are human, they are subject not only to inaccuracy, but sometimes prejudice. Remarkably, the error and prejudice of individual chemists does not matter to the progress of chemistry. Chemistry as a science, the collective activity of the half-million people in the world who are chemists, advances despite mistakes by individual chemists.[12] The science has self-correcting features in abundance: the most important one is that the more interesting the observation or theory, the more likely it is to be checked by someone else. Often for entirely the "wrong" reasons—driven by plain disbelief arising from the conviction that the initial observation must be wrong. It doesn't matter why an individual chemist repeats a critical synthesis, or tries an alternative theory. Chemistry progresses.

And yet, that a chemist *try* to prove someone else's mechanism wrong, or to make a molecule first, does matter. For without the human impulse nothing would get accomplished. It's a curious creation, this science of ours—an incredibly sturdy, exciting, and useful system of knowledge built by imperfect people, and depending for progress on their imperfection.

7. *Chemistry is the science of molecules*

Need I say more? There are limitations to the definition, but molecules, from diatomics to carbonic anhydrase and $YBa_2Cu_3O_{7-x}$ are our business. They're also big business—there are 10^{11} kilograms of sulfuric acid made per year around the world, and more pounds of ammonia than there are human beings.

8. *Chemistry is not reducible to physics*

Reductionism is something we've been saddled with for two centures. By the term I mean the setting up of a hierarchical ordering of the sciences: social sciences, biology, chemistry, physics, and a corollary definition of understanding in one science as a reduction to the next, deeper level.[13] My feeling is that scientists buy this as an ideology, but it does not represent the reality of productive work in any science, and the idea is dangerous. I'll come back to the dangers later. What I think happens in reality is that from every activity of human beings there evolves a set of objects, questions and concepts. We might call these categories. Understanding may be defined vertically, in a reductionist way, but also horizontally, in terms of the concepts and questions of that science. Most of the useful concepts of chemistry (for the chemist: aromaticity, the concept of a functional group, steric effects, and strain) are imprecise. When reduced to physics they tend to disappear.[14] But with them marvelous chemistry has been—is—wrought.

What Really Goes on in a Chemical Paper

One could proceed and list other points of view on science and chemistry, but for me these suffice to begin a discussion of the chemical article and what transpires in it.

On the face of it the article purports to be a communication of facts, perhaps a discussion, always dispassionate and rational, of alternative mechanisms or theories, and a more or less convincing choice between them. Or the demonstration of a new measurement technique, a new theory. And, remarkably, the article works. An experimental procedure detailed in *Angewandte Chemie* in German or English can be reproduced (actually how easily it can be reproduced is another story[15]) by someone with a rudimentary knowledge of either language, working in Okazaki or Krasnoyarsk. This underlying feature of potential or real reproducibility is to me the ultimate proof that science is reliable knowledge.[16]

But in so many ways there is more than meets the eye in the scientific article. I see in it the following themes, many of which are also described and analyzed in a much deeper way in a remarkable forthcoming book by *David Locke, Science as Writing*.[17]

Art

The chemical article is an artistic creation. Let me expand on what might be viewed as a radical exaggeration. What is art? Many things to many people. One aspect of art is aesthetic, another that it engenders an emotional response. In still another attempt to frame an elusive definition of that life-enhancing human activity, I will say that art is the seeking of the essence of some aspect of nature or of some emotion, by a human being. Art is constructed, human and patently unnatural.

What is written in a scientific periodical is not a true and faithful representation (if such a thing were possible) of what transpired. It is not a laboratory notebook, and one knows that that notebook in turn is only a partially reliable guide to what took place. It is a more or less (one wishes more) carefully constructed, man- or woman-made *text*. Most of the obstacles that were in the way of the synthesis or the building of the spectrometer have been excised from the text. Those that remain serve the rhetorical purpose (no weaker just because it's suppressed) of making us think better of the author. The obstacles that are overcome highlight the success story.

The chemical article is a man-made, constructed abstraction of a chemical activity. If one is lucky, it creates an emotional or aesthetic response in its readers.

Is there something to be ashamed of in acknowledging that our communications are not perfect mirrors, but in substantial part literary texts? I don't think so. In fact, I think that there is something exquisitely beautiful about our texts. These "messages that abandon", to paraphrase *Jacques Derrida*,[18] indeed leave us, are flown to careful readers in every country in the world. There they are read, in their original language, and understood; there they give pleasure *and*, at the same time, they can be turned into

chemical reactions, real new things. It would be incredible, were it not happening thousands of times each day.

History

One of the oft cited distinguishing features of science, relative to the arts, is the more overt sense of chronology in science. It is made explicit in the copious use of references. But is it real history, or a prettified version?

A leading chemical style guide of my time admonished: "... one approach which is to be avoided is narration of the whole chronology of work on a problem. The full story of a research may include an initial wrong guess, a false clue, a misinterpretation of directions, a fortuitous circumstance; such details possibly may have entertainment value in a talk on the research, but they are probably out of place in a formal paper. A paper should present, as directly as possible, the objective of the work, the results, and the conclusions; the chance happenings along the way are of little consequence in the permanent record."[19]

I am in favor of conciseness, an economy of statement. But the advice of this style guide, if followed, leads to real crimes against the humanity of the scientist. In order to present a sanitized, paradigmatic account of a chemical study, one suppresses many of the truly creative acts. Among these are the "fortuitous circumstance"—all of the elements of serendipity, of creative intuition at work.[20]

Taken in another way, the above prescription for good scientific style demonstrates very clearly that the chemical article is *not* a true representation of what transpired or was learned, but a constructed text.

Language

Scientists think that what they say is not influenced by the language they use, meaning both the national language (German, French, Chinese) and the words within that language. They think that the words employed, providing they're well-defined, are just representations of an underlying material reality which they, the scientists, have discovered or mathematicized. Because the words are faithful representations of that reality they should be perfectly translatable, into any language.

That position *is* defensible—as soon as the synthesis of the new high-temperature superconductor $YBa_2Cu_3O_{7-x}$ was described, it *was* reproduced, in a hundred laboratories around the globe.

But the real situation is more complex. In another sense words are all we have. And the words we have, in any language, are ill-defined, ambiguous. A dictionary is a deeply circular device—just try and see how quickly a chain of definitions closes upon itself. Reasoning and argument, so essential to communication in science, proceed in words. The more contentious the argument, the simpler and more charged the words.[21]

How does a chemist get out of this? Perhaps by realizing what some of our colleagues in linguistics and literary criticism learned over the last century.[22] The word is a sign, a piece of code. It signifies something, to be sure, but what it signifies must be decoded or interpreted by the reader. If two readers have different decoding mechanisms, then they will get different readings, different meanings. The reason that chemistry works around the world, so that BASF can build a plant in Germany or Brazil and expect it to work, is that chemists have in their education been taught the same set of signs.

I think this accounts in part for what *Carl Friedrich von Weizsäcker* noted in a perceptive article on "The Language of Physics":[23] If one examines a physics (read chemistry) research lecture in detail one finds it to be full of imprecise statements, incomplete sentences, halts, etc. The seminar is usually given extemporaneously, without notes, whereas humanists most often read a text verbatim. The language of physics or chemistry lectures is often imprecise. Yet chemists understand those presentations (well, at least some do). The reason is that the science lecturer invokes a code, a shared set of common knowledge. He or she doesn't have to complete a sentence—most everyone knows what is meant halfway through that sentence.

Graphics

The semiotics of chemistry is most apparent in the structures of molecules that grace most every page of a chemical journal, that identify at a glance a paper as chemical.[24,25] The given, just over a century old, is that the structure of a molecule matters. It's not only what the atomic constituents are. It's also how the component atoms are connected up, how they are arranged in three-dimensional space, and how easily they move from their preferred equilibrium positions. The structure of a molecule, by which I mean the disposition in space of nuclei and electrons, both the static equilibrium structure and its dynamics, determines every physical, chemical, and ultimately biological property of the molecule.

It is crucial for chemists to communicate three-dimensional structural information to each other. The media for that communication are two-dimensional—a sheet of paper, a screen. So one immediately encounters the problem of representation.

Actually that problem is already there. What is a ball-and-stick model of a molecule? Is that reality? Of course not. The model is just one representation of the equilibrium positions of the nuclei, with some further assumptions about bonding. An instructive videotape from the laboratory of *F. P. Brooks, Jr.* at the University of North Carolina is entitled "What Does a Protein Look Like?" It shows 40 different representations (recalling to my mind the woodcut suite of *Hokusai* entitled "36 Views of Mt. Fuji") of one and the same enzyme, superoxide dismutase—a "ball-and-stick" model, a "space-filling" model, the electrostatic field experienced by a probe charge near the molecule, and so on.[26]

Let me return to the communication problem. Chemists are impelled to communicate three-dimensional information in two dimensions. But they're not *talented* at that. Young people are not selected or select themselves to be chemists on the basis of their artistic ability.

So people are required to do what they're not talented at. That's one definition of life! Chemists cope, by the expedient of inventing a code for communicating three-di-

mensional structure. *And* they train people in that code. The various elements of that code are known to chemists as Fischer or Newman projections, or as the wedge-dash representation. A molecule of ethane, C_2H_6, is represented in two possible geometries, **1** and **2**.

1 **2**

Note another piece of code: carbon is that vertex of the graph which has four lines to it, but it's not labeled C. There are hydrogens at the ends of the lines. They're also not labeled. The notation is simple: a solid line is in the plane of the paper, a wedge in front, a dashed line in back. Saying that may be enough to make these structures rise from the page for some people, but the neural networks that control representation are effectively etched in, for life, when one handles (in human hands, not in a computer) a ball-and-stick model of the molecule while looking at this picture.

It's fascinating to see the chemical structures floating on the page of every journal and to realize that from such minimal information people can actually *see* molecules in their mind's eyes. The clues to three-dimensionality are minimal. The molecules do float, and you're usually discouraged from putting in a reference set of planes to help you see them (**3** vs. **4**).

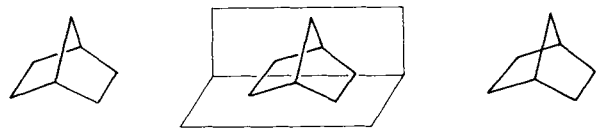

3 **4** **5**

Some chemists rely so much on the code that they don't draw **3** but **5**. What's the difference? One line "crossed" instead of "broken". What a trivial clue to three-dimensional reconstruction, that one part of a molecule is behind another one, is given in **3**, absent in **5**! The person who draws **5** is making many assumptions about his audience. I bet he or she hardly thinks about that.

The policies of journals, their economic limitations, and the available technology put constraints not only on what is printed but also on how we *think* about molecules. Take norbornane, C_7H_{12}, molecule **3**. Until about 1950 no journal in the world was prepared to typeset this structure as **3**. Instead you saw it in the journal as **6**. Now everyone

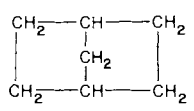

6

knew, since 1874, that carbon was tetrahedral, meaning that the four bonds to it were formed along the four directions radiating out from the center of a tetrahedron to its vertices. You can see this geometry in the two carbon atoms of structures **1** and **2**. Molecular models were available or could be relatively easily built. Yet I suspect that the image or icon of norbornane that a typical chemist had in his mind around 1925 was **6** and not **3**. He was conditioned by what he saw in a journal or textbook—an image. He was moved to act, in synthesizing a derivative of this molecule, for instance, by that unrealistic image.

Maybe it's not that different from the way we approach romance in our lives, equipped with a piecewise reliable set of images from novels and movies.

Style

Every manual of scientific writing I've seen exhorts you to use an impersonal, agentless, superrational style. Please give us the facts, gentlemen, and just the facts! Still style rears its head.

My papers are recognizable in a journal just by the proportion of the space given to graphical material, or the way I "line" my orbitals. *R. B. Woodward*'s papers were recognizable in the (constructed) elegance of their scientific storyline, and in the matching elegance, the cadence of his words. I can read a paper by *Jack Dunitz*, by *Rolf Huisgen*, *Rudolf Hoppe*, or *Bill Doering* and hear their voices in these papers just as surely as I hear the voice of *A. R. Ammons*, a great American poet, or of *Bertolt Brecht*, a German one, when I see their work on a printed page.

It is in the nature of creative human beings to have a style. Why should I write my theory the way *Bill Goddard*, a theorist I admire, does, anymore than you expect *Karlheinz Stockhausen* and *Pierre Boulez* to write piano pieces that sound alike?

Dialectical Struggles

A nice, even-toned, scientific article may hide strong emotional undercurrents, rhetorical maneuvering, and claims of power. One has already been mentioned—the desire to convince, to scream "I'm right, all of you are wrong", clashing with the established rules of civility supposedly governing scholarly behavior. Where this balance is struck depends on the individual.

Another dialogue that is unvoiced is between experiment and theory. There is nothing special about the love-hate relationship between experimentalists and theorists in chemisty. You can substitute "writer" and "critic" and talk about literature, or find the analogous characteristics in economics. The lines of the relationship are easily caricatured—experimentalists think theorists are unrealistic, build castles in the sky. Yet they need the frameworks of understanding that theorists provide. Theorists may distrust experiments, wish that people would do that missing experiment, but where would the theorists be without any contact with reality?

An amusing manifestation of the feelings about this issue is to be found in the occasionally extended quasi-theoretical discussion sections of experimental papers. These

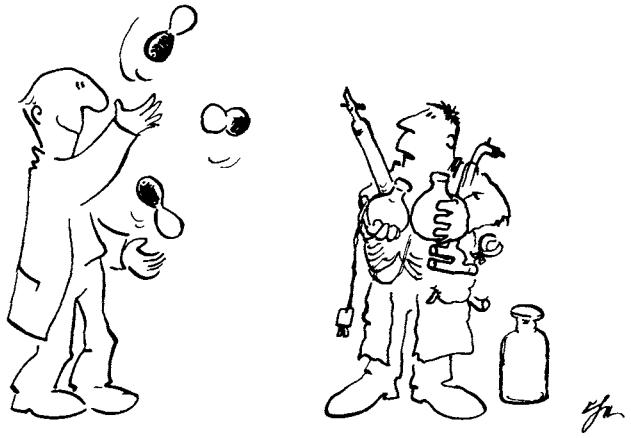

sections in part contain a true search for understanding, but in part what goes on in them is an attempt to use the accepted reductionist ideal (with its exaggerated hailing of the more mathematical)—so as to impress one's colleagues. On the other side, I often put more references to experimental work in my theoretical papers than I should, because I'm trying to "buy credibility time" from my experimental audience. If I show experimental chemists that I know of their work, perhaps they'll give me a little time, listen to my wild speculations.

Another struggle, related, is between pure and applied chemistry. It's interesting to reflect that this separation also may have had its roots in Germany in the mid-nineteenth century; it seems to this observer that in the other chemical power of that time, Britain, the distinction was less congealed. Quite typical in a pure chemical paper is a reaching out after some justification in terms of industrial use. But at the same time there is a falling back, an unwillingness to deal with the often unruly, tremendously complicated world of, say, industrial catalysis. And in industrial settings there is a reaching after academic credentials (quite typical, for instance, of the leaders of chemical industry in Germany).

The Id Will Out

I use the subject word in the psychoanalytical sense, referring to the complex of instinctive desires and terrors that inhabit the collective unconscious. On one hand, these irrational impulses, sex and aggression figuring most prominently, are our dark side. On the other hand, they provide the motive force for creative activity.[27]

The irrational seems to be effectively suppressed in the written scientific word. But of course scientists are human, no matter how much they might pretend in their articles that they are not. Their inner illogical forces push out. Where? If you don't allow them in the light of day, on the printed page, then they will creep out or explode in the night, where things are hidden, and no one can see how nasty you are. I refer, of course, to the anonymous refereeing process, and the incredible irrational responses unleashed in it by perfectly good and otherwise rational scientists. You have to let go sometime ...

I actually think that what saves the chemical article from dullness is that its language comes under stress. We are trying to communicate things that perhaps cannot be expressed in words but require other signs—structures, equations, graphs. And we are trying hard to eliminate emotion from what we say. Which is impossible. So the words we use occasionally become supercharged with the tension of everything that's *not* being said.

. . .

So, many things go on in a scientific article. I will spare you the charts that I've seen hanging in many laboratories, that translate shop-worn phrases into what they really mean. Like "A regime of slow cooling over a period of four weeks produced a 90% yield of black crystals of...", meaning "I went on vacation and forgot to wash out the flask. When I came back ..." And so on.

I want to return to the complexity of deciding what is truth in the scientific process. In a recent article, *Harald Weinrich*[28] describes the classic paper of *Watson* and *Crick* on the structure of DNA in *Nature* in 1953. It is succinct, beautifully reasoned, elegant. *David Locke,* in his book, analyzes the rhetorical structure and the use of irony in the same paper.[17] I think most readers were immediately convinced that the Watson and Crick model was the truth, that this was the way it had to be. And so it is (with some minor variation on hydrogen-bonding schemes in unusual forms of DNA). The Watson and Crick model was and is right. One needs little more.

But then in 1968 *Watson* writes a book, *The Double Helix,* in which he tells the story of how it really happened. Of course, it's a self-centered story, and not kind or fair to *Rosalind Franklin* and others. *Watson*'s story is much like one of the four views of an event in *Akira Kurosawa*'s masterful film *Rashomon.* It needs other views, which some historians have provided. But there is no question that *Watson*'s account is vibrant, full of life. It tells us how he saw the truth, and I think it's a great book.

So (and here I follow *Weinrich*) what *is* the truth: Is it the 1953 paper of *Watson* and *Crick*, or is it the 1968 book by *Watson*? Does the latter diminish the former? It bears reflection.

What Is to Be Done?

I have tried to deconstruct, to borrow some language from critical theory, the scientific article, ossified in its present form for over a hundred years. I think I could have done this better with a specific text before me, but then I would have run the danger of libel suits or loss of friendship. And it is in the nature of human beings to be unable to criticize, truly, deeply, their own work. So I can't do it to myself. But I'm sure every chemist knows some superb example of what I allude to, especially in the work of one of his less favorite scientists.

The deconstruction is done by me not with malice, but with care. I love this molecular science. I love its richness, and the underlying simplicity, but most of all the rich, life-giving variety and connection of all of chemistry. Let me give you an example in Figure 3. I see C_2 in a carbon arc and in the tail of Halley's Comet.[29a] I see it in acetylene, ethylene, and ethane. I see it in the lovely molecular complexes of *P. Wolczanski,*[29b] *M. I. Bruce,*[29c] and *G. Lon-*

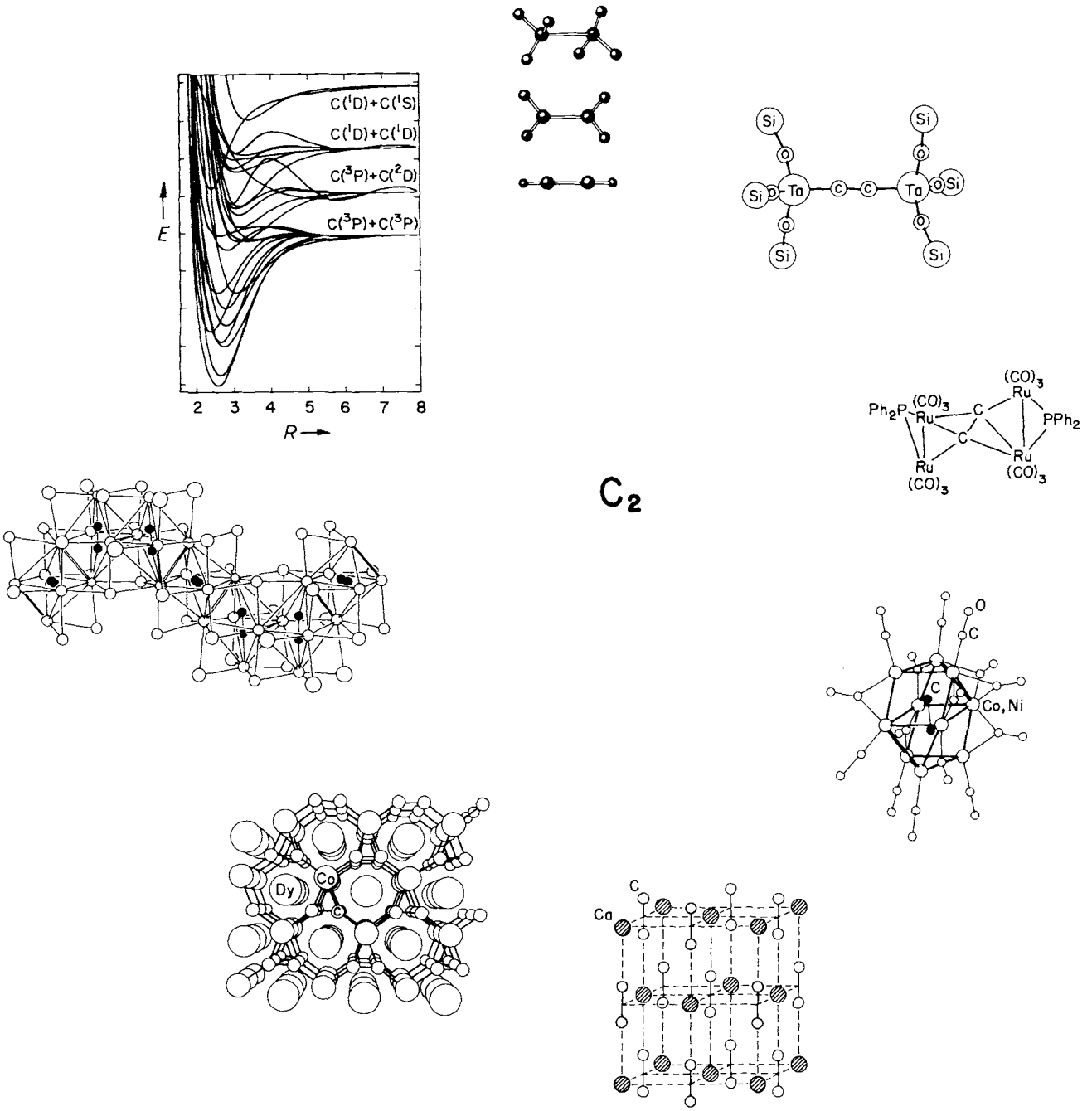

Fig. 3. Some of the ways in which C_2 finds its way in this world. Clockwise from 10:30: a) some calculated potential energy curves for diatomic C_2 [29a]; b) ethane, ethylene, acetylene; c) a dinuclear tantalum complex of C_2 [29b]; d) Ru_4C_2 cluster [29c]; e) C_2 inside a Co_3Ni_7 cluster [29d]; f) calcium carbide; g) $DyCoC_2$ [29e]; h) $Gd_{12}C_6I_{17}$ [29f].

goni[29d] and their co-workers, shown in Figure 3. I see it in CaC_2, in *W. Jeitschko*'s[29e] and *A. Simon*'s[29f] and their co-workers' rare-earth carbides. It's staggering!

I know that that richness was created by human beings. So I'm unhappy to see their humanity suppressed in the way they express themselves in print. I also think that there are some real dangers in the present intellectual stance of scientists and in their ritual mode of communication.

Here are the dangers as I perceive them. Acceptance of a facile reductionist philosophy, a vertical mode of understanding appropriated as the *only* mode of understanding, creates a gap between us and our friends in the arts and humanities. They know very well that there isn't only one way of "understanding" or dealing with the death of a parent, or a political election, or a woodcut by *Ernst Ludwig Kirchner*. The world out there is refractory to reduction, and if we insist that it must be reducible, all that we do is to put ourselves into a nice box. The box is the small class of problems that are susceptible to a reductionist understanding.

A second danger, more specific to the scientific article, is that by dehumanizing our mode of communication, by removing emotion, motivation, the occasionally irrational, we may have in fact done much more than chase away the

Natural Philosophers. That we've accomplished, to be sure. But 150 years down the line what we have created is a mechanical, ritualized product that 3×10^5 times per year propagates the notion that scientists are dry and insensitive, that they respond only to wriggles in a spectrum. The public at large types us by the nature of our product. How can it do otherwise when we do not make a sufficient effort to explain to the public what it is that we really do in our jargon-barricaded world?

What is to be done? I would argue for a general humanization of the publication process. Let's relax those strictures, editorial or self-imposed, on portraying in words, in a primary scientific paper, motivation, whether personal and scientific, emotion, historicity, even some of the irrational. So what if it takes a little more space? We *can* keep up with the chemical literature, and tell the mass of hack work from what is truly innovative, without much trouble as it is. The humanizing words will not mislead; they may actually encourage us to read more carefully the substance of what is said. I would plead for a valuation and teaching of style, in the written and spoken language of one's own country, as well as in English. I think chemistry has much to gain from reviving the personal, the emotional, the stylistic core of the struggle to discover and create the molecular world.

Received: March 13, 1988 [A 701 IE]
German version: *Angew. Chem. 100* (1988) 1653
Cartoons: *Constance Heller*

[1] *Angewandte Chemie* has been very important to me personally, and it is a pleasure for me to dedicate this lecture to the past and present editorial staffs of one of the world's greatest journals.

[2] E. Garfield: *Essays of an Information Scientist*, ISI Press, Philadelphia 1981, pp. 394–400 and references therein.

[3] a) S. Shapin, *Social Stud. Sci. 14* (1984) 487; b) P. Dear, *Isis 76* (1985) 145; c) F. L. Holmes in P. Dear (Ed.): *The Paper Laboratory*, University of Pennsylvania Press, Philadelphia, in press.

[4] F. Goldmann, *Ber. Dtsch. Chem. Ges. 21* (1888) 1176.

[5] For a discussion of the evolution of science writing see B. Coleman, *New York Times Book Review*, September 27, 1987, p. 1; also R. Wallsgrove, *New Sci. 116* (1987) No. 24, p. 55.

[6] O. J. Scherer, T. Brück, *Angew. Chem. 99* (1987) 59; *Angew. Chem. Int. Ed. Engl. 26* (1987) 59.

[7] The version shown here is in English. Angewandte Chemie is unique in printing (since 1963) the same article in English and German versions.

[8] For a demonstration of the range of attitudes about what science is, see the discussion in the pages of *Nature (330* (1987) 308, 689; *331* (1988) 129, 558; following an article by *T. Theocharis* and *M. Psimopoulos* (*Nature 329* (1987) 595).

[9] The phrase is used after J. Ziman: *Reliable Knowledge*, Cambridge University Press, Cambridge, England 1978. I disagree with some points in this book, but there is no better, nor more humanistic, description of what science is and should be than this small volume.

[10] M. Berthellot: *Chimie Organique Fondée sur la Synthèse, Tome 2*, Mallet-Bachelier, Paris 1860. See also J.-P. Malrieu, *L'Actualité Chimique 1987*, No. 3, p. IX; A. F. Bochkov, V. A. Smit: *Organicheskii Sintez* (Organic Synthesis), Nauka, Moscow 1987; and an essay "*In Praise of Synthesis*" by R. Hoffmann, to be published.

[11] For different views of the way science works see a) P. Feyerabend: *Against Method*, NLB, London 1975; *Wider den Methodenzwang*, Suhrkamp, Frankfurt am Main 1976; b) B. Latour, S. Woolgar: *Laboratory Life*, Princeton University Press, Princeton 1986; c) K. Knorr-Cetina: *Die Fabrikation von Erkenntnis*, Suhrkamp, Frankfurt am Main 1984.

[12] I was reminded of the importance of the individual-system distinction through a conversation with *Barry Carpenter*. I'm grateful to him for a discussion of the points raised in this essay, as well as to another colleague, *Bruce Ganem*, for his comments.

[13] Several types of reductionism must be distinguished. See the interesting debate between *S. Weinberg* (*Nature 330* (1987) 443; *331* (1988) 475) and *E. Mayr* (*Nature 331* (1988) 475 and references therein).

[14] See, inter alia, K. Mislow, P. Bickart, *Israel J. Chem. 15* (1976/77) 1; D. W. Theobald, *Chem. Soc. Rev. 5* (1976) 203.

[15] *R. G. Bergman*, in an unpublished lecture on "Values in Science", cites some fascinating raw data on this question, coming from the experience of the journals *Organic Synthesis* and *Inorganic Synthesis*.

[16] *Latour* and *Woolgar* ([11b], p. 183) are rather scornful of the kind of marveling at verification and reproducibility of scientific facts that I engage in here. I think they've gotten caught in the consistently questioning and skeptical ideology of their otherwise incisive anthropological investigation of how scientific facts are constructed. They should take a look at the systematic, worldwide, industrial production of pharmaceuticals, just to take one example of a reproducible experimental activity.

[17] D. Locke: *Science as Writing*, to be published.

[18] J. Derrida in his essay "Signature Event Context" in *Marges de la Philosophie*, Editions Minuit, Paris 1972, pp. 365–393; translation (by A. Bass): *Margins of Philosophy*, University of Chicago Press, Chicago 1982, pp. 307–330.

[19] L. F. Fieser, M. Fieser: *Style Guide for Chemists*, Reinhold, New York 1960, pp. 51–52.

[20] P. B. Medawar, *Saturday Review*, August 1, 1964, p. 42, also argues that the standard format of the scientific article misrepresents the thought processes that go into discovery.

[21] See R. Hoffmann, *Am. Sci. 75* (1987) 619; *76* (1988) 182.

[22] For an introduction to modern literary theories see T. Eagleton: *Literary Theory*, University of Minnesota Press, Minneapolis 1983.

[23] C. F. von Weizsäcker: *Die Einheit der Natur*, dtv, Munich 1974, pp. 61–83.

[24] For a description of the geometrical and topological information processing that goes on in organic chemistry, see also N. J. Turro, *Angew. Chem. 98* (1986) 872; *Angew. Chem. Int. Ed. Engl. 25* (1986) 882.

[25] *Pierre Laszlo* has written an illuminating article on technical illustration ("The Pictures of Science") that is relevant to my discussion. A French version of this article ("Science en images") has been accepted for publication in *ECALE*, No. 2, published by Ecole Cantonale d'Art, Lausanne.

[26] M. Pique, J. S. Richardson, F. P. Brooks, Jr., *Invited Videotape, 1982 SIGGRAPH Conference*. I am grateful to *J. S. Lipscomb* for showing this videotape to me.

[27] *P. B. Medawar* says, along the same lines, that "scientists should not be ashamed to admit ... that hypotheses appear in their minds along uncharted by-ways of thought ..." (see [20]).

[28] H. Weinrich, *Merkur 39* (1985) No. 436, p. 469. I'm grateful to *P. Gölitz* for bringing this paper to my attention.

[29] a) The C_2 potential energy curves are drawn after *P. P. Fougere* and *R. K. Nesbet* (*J. Chem. Phys. 44* (1966) 285; b) $[\{(t\mathrm{Bu_3SiO})_3\mathrm{Ta}\}_2\mathrm{C_2}]$: R. E. LaPointe, P. T. Wolczanski, J. F. Mitchell, *J. Am. Chem. Soc. 108* (1986) 6382; c) $[\mathrm{Ru_4C_2(PPh_2)_2(CO)_{12}}]$: M. I. Bruce, M. R. Snow, E. R. T. Tiekink, M. L. Williams, *J. Chem. Soc. Chem. Commun. 1986*, 701; d) $[\mathrm{Co_3Ni_7C_2(CO)_{15}}]^{3\ominus}$: G. Longoni, A. Ceriotti, R. Della Pergola, M. Manassero, M. Perego, G. Piro, M. Sansoni, *Phil. Trans. R. Soc. London, Ser. A 308* (1982) 47; e) $DyCoC_2$: W. Jeitschko, M. H. Gerss, *J. Less. Common Met. 116* (1986) 147; f) $Gd_{12}C_6I_7$: A. Simon, E. Warkentin, *Z. Anorg. Allg. Chem. 497* (1983) 79.

The Chemistry of Amino Imino Boranes

By Heinrich Nöth*

Dicoordinated boron compounds can no longer be considered as "exotic" species in boron chemistry: this is proved by the extensive chemistry of bis(dialkylamino)boron(1+) ions, alkylidene boranes, and imino boranes. The latter are characterized by high reactivity and chemical versatility. A special position is taken by amino imino boranes, whose chemistry is reported here. The presence of an amino group enhances the reactivity of imino boranes on the one hand and increases their kinetic stability on the other. New types of diamino boranes accessible via amino imino boranes often undergo intramolecular ring closure. These heterocycles are well suited to generate new types of cations of boron. Cycloaddition reactions using amino imino boranes open up a new heterocyclic chemistry of boron. The chemistry of *N*-functional amino imino boranes, which is still its infancy, shows much promise.

1. Introduction

Among the elements of the second period, boron is unique in attaining coordination numbers greater than 4. Many metal borides,[1] but particularly polyboranes, carboranes, and metallaboranes,[2] display this topology, which is explained in terms of multicenter bonding by theories of chemical bonding.[3] This exceptional position, however, should not blind one to the fact that boron is tricoordinate in most of its compounds, corresponding to its three valence electrons, or tetracoordinate due to the four valence orbitals with which a boron atom can contribute to bonding.

Will it be possible to realize even lower coordination numbers? A first answer to this question is provided by gas-phase studies: several physical methods have allowed the detection of boroxanes X–B=O,[4] borthianes X–B=S,[5] and borselenanes X–B=Se.[6] These linear, highly reactive molecules have been prepared so far only in the gas phase. The latter two types of molecules contradict *Goubeau*'s rules for systems containing multiple bonds;[7] these boron compounds polymerize or decompose in the condensed phase. To prevent polymerization, their kinetic stabilization is necessary. It is impossible to predict, however, whether this can be achieved by steric effects alone or only with electronic assistance. As has been demonstrated in recent years by the rapidly developing chemistry of dicoordinated boron compounds, both concepts for stabilization are valid.

Of the classes of compounds known so far, the boroxanes,[4,8] the imino boranes,[9] the bis(dialkylamino)boron(1+) ions,[10] and the alkylidene boranes,[11] *Paetzold* et al. have investigated diorgano imino boranes R–B≡N–R′ particularly extensively. These compounds not only are isoelectronic with diorgano acetylenes but also exhibit similar chemical behavior. It is well known that introduction of an amino group enhances and modifies the reactivity of the CC triple bond of alkynes.[12] This status report asks the question whether this holds also for amino imino boranes, which are isoelectronic with ynamines.[12]

2. Synthesis

Among possible synthetic strategies for amino imino boranes, elimination reactions play an important role. Such reactions can be divided into four general categories:

a) thermal elimination of stable molecules from suitable borane precursors,
b) thermally induced ring-opening of cyclic systems,
c) rearrangement reactions,
d) chemically induced elimination reactions.

2.1. Thermally Induced Elimination

Paetzold et al.[9] have developed the vacuum gas-phase pyrolysis of (trimethylsilylamino)boron halides [Eq. (1)] into an effective method of generating imino boranes R–B≡N–R′.[*] This process can also be used in the synthesis of amino imino boranes, as shown in Equation (2). *tert*-Butylimino(2,2,6,6-tetramethylpiperidino)borane **1a** — the first amino imino borane to be isolated and fully characterized — was obtained in high yield via this pathway as a

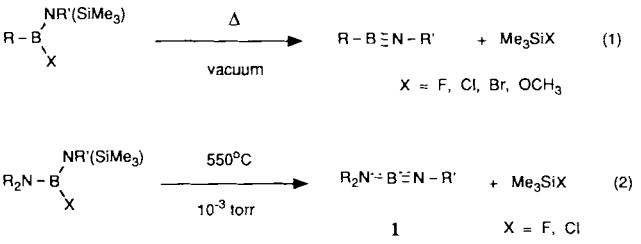

colorless liquid.[13,14] Further examples are listed in Table 1. The limits of this method have certainly not been fully explored. It remains to be tested, for example, whether the

[*] Prof. Dr. H. Nöth
Institut für Anorganische Chemie der Universität
Meiserstrasse 1, D-8000 München 2 (FRG)

[*] Formal charges in valence formulas are not indicated here, nor will they be used in this work. This is in accord with the notation suggested by *Paetzold* [9].

species $Me_2N{=}B{\equiv}N{-}tBu$, an electronically stabilized compound, can be isolated and characterized.

2.2. Thermal Ring-Opening of Cyclic Systems

The conceivable thermal decomposition of borazines (1,3,5,2,4,6-triazatriborinanes) and 1,3,2,4-diazadiboretidines into their monomeric imino borane units via gas-phase pyrolysis according to Equation (3) has not yet been achieved. However, that this possibility represents a realistic synthetic pathway for amino imino boranes can be seen from the recently discovered thermal decomposition (ca. 100°C) of the azaphosphaboriridine **2**.[8] The three-membered heterocycle thus serves as a source of the amino imino borane **1a**. However, since **2** was synthesized from **1a** in two steps, the reaction represented in Equation (4) would only be of preparative interest if precursors of type **2** become more readily accessible by a different route.

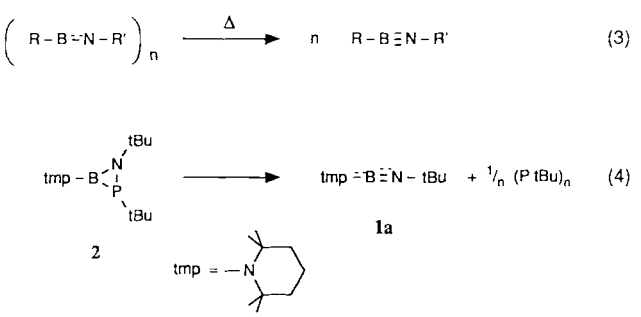

2.3. Rearrangement Reactions

Imino boranes $R{-}B{\equiv}N{-}R'$ result from the pyrolysis of azido diorgano boranes. The intermediate is assumed to be a boryl-substituted nitrene $RR'B\ddot{N}$, which then rearranges to the imino borane.[9] The decomposition of the amino azido borane **3** at 400°C does not allow detection of either the nitrene **4** or the amino imino borane **5**, since the rearrangement of **4** to **5** and the dimerization of **5** to the corresponding diazadiboretidine **6** occur extremely rapidly.[15] Apparently, owing to their relatively low steric bulk, the alkyl substituents R (butyl, isopropyl) do not protect the amino imino borane **5** effectively from undergoing dimerization; even the derivative **1b** (see Table 1; **1b** ≡ **5**, R = *t*Bu) dimerizes, albeit slowly, to yield **6**.[16]

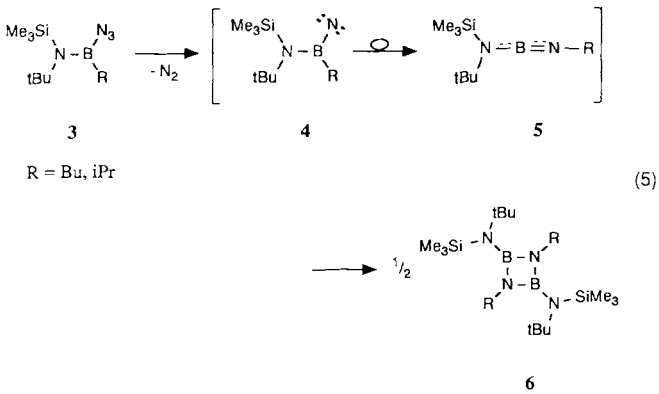

2.4. Dehydrohalogenation Reactions

In principle, amino boranes $RB(NR'E)X$ and diamino boranes $R_2NB(NR'E)X$ should be suitable starting materials for the synthesis of amino imino boranes if the elimination of EX can occur at a relatively low temperature. This requires the presence of weak NE bonds (E = electrophilic group) and relatively weak BX bonds (X = nucleophilic group). On the other hand, a strong EX bond will favor the elimination thermodynamically. These are difficult requirements to meet; however, in the diamino borane $tmpB[NtBu(SiPh_2Cl)]Cl$ they are partially fulfilled.[19] For EX = HF, HCl (and, in exceptional cases, HBr) strong bases Do make the dehydrohalogenation from diamino halo boranes $R_2NB(NHR')X$ possible, as shown in Equation (6). The competing substitution reaction (7) and/or addition reaction (8) must be suppressed. Neutral bases such as trimethylamine, pyridine, DBU, and 1,8-bis(dimethylamino)naphthalene are not suitable for dehydrohalogenation of $tmpB(NHtBu)X$ (X = F, Cl, Br). However, strong anionic bases $Do^{\ominus}$ well serve this purpose since these give rise to weakly protic compounds DoH (e.g., hydrocarbons, amines). These latter substances must, of course, be inert towards the amino imino boranes.

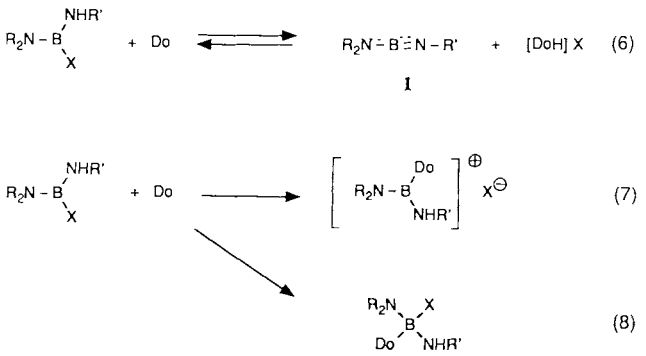

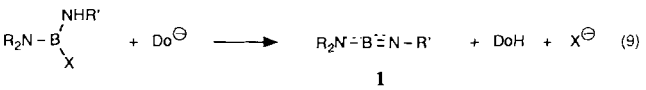

Whereas *n*-butyllithium mostly leads to substitution of the halogen atom, *tert*-butyllithium reacts at least partly via dehydrohalogenation.[16,20] With triphenylmethylpotassium, the elimination occurs at temperatures as low as −50°C; however, separation problems prevent the general application of this method.[16] The best reagents for the dehydrohalogenation according to Equation (9) are bulky alkali-metal amides MNR_2.[16,20,21] Of the compounds lithium tetramethylpiperidide, lithium *tert*-butyl(isopropyl)amide; lithium or sodium bis(trimethylsilyl)amide, and lithium *tert*-butyl(trimethylsilyl)amide, the latter has proved to be the most useful: it is a strong base (base 1 in

Table 1) and the amine (DoH) formed in the course of reaction (9) is relatively volatile. Furthermore, the steric bulk of the resulting amine prohibits further reaction with the amino imino borane formed. All compounds **1** in Table 1, except for **1c** and **1d**, were synthesized according to Equation (9). From Table 1 it should be clear that only amino imino boranes containing bulky substituents, that is, kinetically stabilized derivatives, can be synthesized according to this method.

Table 1. Amino imino boranes **1**, their ^{11}B chemical shifts, and their ^{11}B≡N stretching frequencies. Method of synthesis: **1a**, according to Section 2.1, 2.2, or 2.4; **1b** according to Section 2.1 or 2.4; **1c** and **1d** according to Section 2.1; **1e** to **1y** according to Section 2.4 [a].

$R_2N{=}B{\cong}N{-}R'$ **1**

1	R_2N	R′	Base [b]	$\delta(^{11}B)$	$\nu(^{11}BN)$ [cm^{-1}]	Ref.
1a	tmp	*t*Bu	1, 2	5.2	1990	[14, 21]
1b	$Me_3Si(tBu)N$	*t*Bu	2	4.1	1980	[15, 16]
1c	iPr_2N	*t*Bu	—	3.3	1985	[17]
1d	tmp	$SiMe_3$	—	17.4	1922	[14]
1e	tmp	*i*Pr	1, 2, 3, 4	4.8	—	[16]
1f	tBu_2N	*t*Bu	1, 2	5.2	1990	[16]
1g	tmp	Ar^1	1	12.1	1985	[16]
1h	tmp	Ar^2	1	12.0	1982	[14]
1i	tmp	Ar^3	3	12.9	1987	[14]
1k	Bzl(*t*Bu)N	Ar^1	3	4.8	—	[16]
1l	tmp	R^2	1	5.1	—	[20]
1m	tmp	$SiiPr_3$	1	16.8	1922	[20]
1n	tmp	$NiPr_2$	1	−0.5	—	[20]
1o	tmp	tmp	1, 2	−0.7	2000	[20]
1p	tmp	$PtBu_2$	1	16.6	1935	[20]
1q	tmp	$AstBu_2$	1	17.5	1910	[20]
1r	tmp	$B(NMeCH_2)_2$	1	15.0	1970	[20]
1s	$(Me_3Si)_2N$	*t*Bu	1	4.4	—	[20]
1t	$Me_3Si(tBu)N$	$SiMe_3$	1	17.3	—	[20]
1u	$Me_3Si(tBu)N$	Ar^1	1	12.2	1985	[20]
1v	$(Me_3Si)_2N$	Ar^1	1	11.7	—	[20]
1w	$Me_3Si(tBu)N$	R^1	1	5.1	1990	[20]
1x	$(Me_3Si)_2N$	R^1	1	4.5	1995	[20]
1y	*t*Bu(*i*Pr)N	*t*Bu	1	6.7	1990	[20]

[a] Abbreviations: tmp = 2,2,6,6-tetramethylpiperidino; Bzl = benzyl; Ar^1 = 2,6-diisopropylphenyl; Ar^2 = mesityl; Ar^3 = 2,4,6-tri-*tert*-butylphenyl; R^1 = CMe_2CH_2tBu. [b] 1 = LiN*t*Bu(SiMe$_3$), 2 = Litmp, 3 = *t*BuLi, 4 = Ph_3CK.

3. Physical and Structural Characterization

Paetzold and co-workers, using both physical and theoretical methods, have thoroughly studied diorgano imino boranes R−B≡N−R′, and they have established the triple-bond character of the BN bond.[9] The data on amino imino boranes **1**, summarized in Table 1, allow one to study substituent effects.

3.1. Infrared Spectra

The ^{11}BN absorption in H−B≡N−H is found at 2009 cm^{-1},[22] that of *t*Bu−B≡N−*t*Bu at 1785 cm^{-1}.[23] This shift to longer wavelength is caused by coupling of $\nu(^{11}BN)$ with the ^{11}BC and NC stretching vibration.[23] The ^{11}BN force constants of the two molecules (13.14 and 12.79 Nm^{-1}, respectively) do not differ significantly.

In all amino imino boranes a prominent band is found in the region between 2000 and 1900 cm^{-1}, accompanied by a less intense, higher frequency band; these bands are assignable to $\nu(^{11}BN)$ and $\nu(^{10}BN)$, respectively. It is readily seen from the data in Table 1 that the imino substituents R have a much stronger influence on the position of this band than the amino substituents R. This band, assignable to the B≡N stretching vibration, is observed at 1990 cm^{-1} for both **1a** and **1f**, that is, closer to the frequency (2009 cm^{-1}) characteristic of H−B≡N−H (for comparison, the band for *t*Bu−B≡N−*t*Bu is found at 1785 cm^{-1}). This arises from the coupling of $\nu(B(NR_2))$ with $\nu(B{\equiv}N)$. The introduction of a Me_3Si group (**1d**) in place of a *t*Bu group (**1a**) shifts the frequency of the observed band by only 68 cm^{-1}. This allows the cautious conclusion that altering the substituent on the amino nitrogen has only a small effect on the position of the B≡N band, in contrast to substitution at the imino nitrogen.

In Figure 1 the observed ^{11}B≡N frequencies are plotted versus calculated bond indices *P*(BN), obtained by the CNDO method for $H_2N{=}B{\cong}N{-}R'$ as model compound.[20] The almost linear relation implies that $\nu(^{11}B{\equiv}N)$—and therefore the strength of the BN bond—is primarily influenced by the inductive effect of the imino substituents.

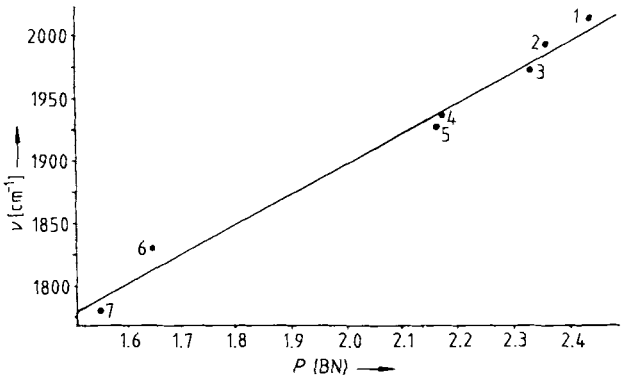

Fig. 1. Correlation of the $\nu(B{\equiv}N)$ frequency of the amino imino boranes **1** with the calculated bond indices *P*(BN) for $H_2N{=}B{\cong}N{-}R'$ as model compound. The linear dependence excludes any significant π-bonding effects involving the imino substituent. In No. 3 the influence of the $B(NH_2)_2$ group (calculated) or of the diazaborolidinyl group (found) must also be mostly inductive in nature as a result of the electronic saturation of the boron atom via π-interaction with the NH_2 groups or N ring atoms, respectively. Bzl = benzyl.

1: $tmp{=}B{\cong}N{-}tmp$ / $H_2N{=}B{\cong}N{-}NMe_2$
1o

2: $tmp{=}B{\cong}N{-}tBu$ / $H_2N{=}B{\cong}N{-}Me$
1a

3: $tmp{=}B{\cong}N{-}B(tBuNCH_2)_2$ / $H_2N{-}B{\equiv}N{-}B(NH_2)_2$

4: $tmp{=}B{\cong}N{-}PtBu_2$ / $H_2N{-}B{\equiv}N{-}PMe_2$
1p

5: $tmp{=}B{\cong}N{-}SiiPr_3$ / $H_2N{-}B{\equiv}N{-}SiMe_3$
1m

6: $(tBuBzlN)_2B^{\oplus}$ / $Me_2N{=}B{=}NMe_2^{\oplus}$

7: $tBuBzlN{=}B{=}N(SiMe_3)_2^{\oplus}$ / $H_2N{=}B{=}N(SiH_3)_2^{\oplus}$

3.2. ^{11}B Nuclear Magnetic Resonance Spectra

The ^{11}B chemical shifts of the amino imino boranes **1** show the same tendencies as the $^{11}B{\equiv}N$ stretching frequencies. $\delta(^{11}B)$ is only slightly influenced by solvents ($\Delta\delta = \pm 1$ ppm), not even by pyridine; this finding provides a clear indication that the boron center in **1** is both electronically and sterically shielded.

Since the magnetic shielding of the ^{11}B nucleus in boron compounds increases with increasing coordination number,[24] the observed strong shielding in the amino imino boranes comes at first as a surprise. However, the same also holds true for acetylenic C atoms. Since the paramagnetic term of the shielding plays a significant role in the shielding of alkyne ^{13}C nuclei, it is understandable that the correlation found for the borane derivatives between $\delta(^{11}B)$ and π-electron density[25a,b] cannot be true for either the imino boranes[9] or the amino imino boranes. The empirical correlation between $\delta(^{11}B)$ and $\delta(^{13}C)$ values for isoelectronic systems with tricoordinate boron and carbon[25c] can surprisingly also be used satisfactorily to estimate $\delta(^{13}C)$ and $\delta(^{11}B)$ of alkynes and imino boranes, respectively. As indicated in Figure 2, a linear correlation

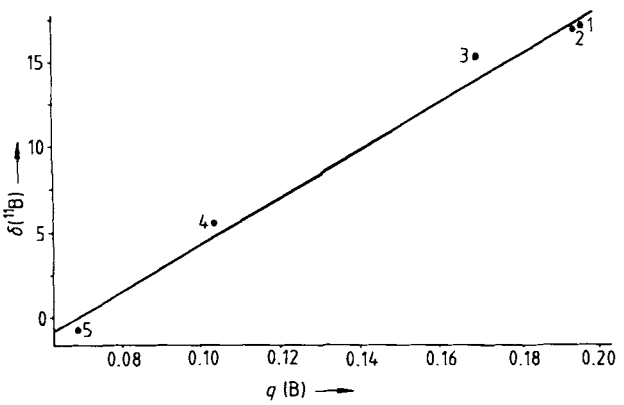

Fig. 2. Correlation of $\delta(^{11}B)$ values of amino imino boranes with calculated net charges q(B) at the boron atoms. Since $\delta(^{11}B)$ and $\delta(^{13}C)$ of comparable imino boranes and acetylenes are related via $\delta(^{11}B) = 0.393\,\delta(^{13}C) - 30.73$ [25c], the screening constants of both nuclei are influenced analogously.

1: tmp–B=N–Si*i*Pr$_3$ / H_2N–B=N–SiH_3
1m

2: tmp–B=N–P*t*Bu$_2$ / H_2N–B=N–PH_2
1p

3: tmp–B=N–B(*t*BuNCH_2)$_2$ / H_2N–B=N–BH_2

4: tmp–B=N–*t*Bu / H_2N–B=N–H
1a

5: tmp–B=N–tmp / H_2N–B=N–NH_2
1o

also exists between $\delta(^{11}B)$ values of the amino imino boranes studied and the net charge q(B) at the boron atoms.

3.3. Theoretical Studies

According to ab initio calculations, the parent imino borane, H–B≡N–H, possesses the symmetry of the point group $C_{\infty v}$[26,27] and a calculated BN bond length of 127 pm[24] or 123 pm.[27] For the dimethyl derivative, Me–B≡N–Me, the point group C_{3v} and a BN bond length of 119 pm have been determined by MNDO/1 calculations.[28] By analogy to the corresponding acetylenes, the HOMO of the imino borane is a degenerate BN π orbital; however, in contrast to acetylenes, imino boranes possess dipole moments due to the differing electronegativities of boron and nitrogen. Therefore, the atomic dipoles of the HB and HN bonds or the CB and CN bonds no longer compensate. However, the calculated dipole moments are small: 0.86 D for H–B≡N–H[27] and 0.14 D for Me–B≡N–Me.[28]

Answers to the questions how substituents at the B atom influence bonding in imino boranes (cf. entry 1 in Table 2) and what effects the substituents have on the net charge at the boron atom can be found in Table 2, which contains data obtained from STO-3G calculations.[14,29] According to these results, a fluorine substituent increases the positive charge at the boron atom and, at the same time, slightly weakens the B≡N bond (entry 2). In the parent (entry 3) amino imino borane, H_2N–B=N–H, a relatively large partial charge is also found at the boron atom, whereas the introduction of a methyl group at the boron atom significantly decreases this charge (entry 4). A methyl group at the imino nitrogen is electron-donating (cf. entries 1 and 7), whereas the BH_2 group (entry 5) and even more so the BF_2 group (entry 6) reduce the electron density at the boron atom. The reason for this is less an inductive effect than a BN π interaction with the substituent. In contrast, an *N*-bonded amino group enhances the charge density at the boron atom.

Table 2. BN bond lengths d, π-bond orders $p_{\mu\nu}$, and net charges q(B) at the boron atom for several B- and N-substituted imino boranes calculated according to STO-3G. The π-bond order is defined as $p_{\mu\nu} = \sum_i n_i C_{\mu i} C_{\nu i} S_{\mu\nu}$, where C are the orbital coefficients and S represents the overlap matrix of the atoms μ and ν [29]. n is the number of electrons [29].

Entry		d(BN) [pm]	$p_{\mu\nu}$	q(B)
1	H–B≡N–H	119.6	0.759	0.291
2	F–B≡N–H	119.9	0.744	0.478
3	H_2N–B=N–H	120.1	0.746	0.454
4	Me–B≡N–H	119.7	0.757	0.362
5	H–B≡N–BH_2	121.7	0.719	0.321
6	H–B≡N–BF_2	121.3	0.729	0.315
7	H–B≡N–Me	119.7	0.754	0.267
8	H_2N–B=N–Me	120.3	0.741	0.437

As an estimate of the reactivity towards nucleophiles and electrophiles, one can use the HOMO-LUMO separation. Values for a series of typical BN compounds are given in Figure 3. As can be seen, bis(amino)boron cations can be labeled as strong electrophiles, whereas amino imino boranes should possess nucleophilic character.[14] As will be demonstrated below, amino imino boranes can indeed be described as electron-rich systems.

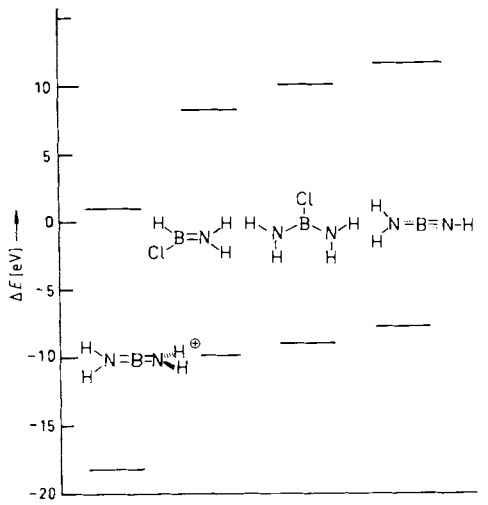

Fig. 3. HOMO-LUMO separations ΔE for a series of typical BN compounds. Included in the formulas are the calculated BN bond orders. All HOMOs and LUMOs are π type; the N atoms of the amino group are sp^2-hybridized. For the cation, the data are valid for a molecule possessing D_{2d} symmetry.

3.4. Direct Structural Information

The high BN bond order of imino boranes, which was inferred from the vibrational spectra and theoretical studies, has been verified by results of X-ray crystal structure determinations. The BN bond length for the compound *t*Bu–B≡N–*t*Bu, found to be 125.8 pm,[27] cannot be used as a relative measure for the BN triple bond lengths because of disorder phenomena. A better experimental standard is provided by $(Me_3Si)_3Si$–B≡N–*t*Bu, for which a BN bond length of 122.1 pm was determined.[30] What influence does an amino group have on the imino group? 2,2,6,6-Tetramethylpiperidino[(2,4,6-tri-*tert*-butylphenyl)imino]borane **1i** crystallizes orthorhombically with two molecules per asymmetric unit cell. The average B≡N distance is 125 pm, the average BN distance to the tmp group 138 pm. The latter distance corresponds to the BN bond length found in monoamino boranes. In spite of the numerical agreement, this value cannot represent the same degree of multiple bonding, since the boron atom in monoamino boranes is tricoordinate whereas in amino imino boranes the boron atom is only dicoordinate. Since the covalent radius of a boron atom is 7 pm larger than that of a carbon atom but that of nitrogen is 5 pm smaller, BN compounds should have somewhat longer BN bonds than the CC distance in comparable isosteric analogues. The BN lengths observed are, however, almost always longer than those of the carbon analogues, a result of the polarity of the BN bond. It must be added, however, that it is difficult to justify the choice of a standard bond length for a BN single bond. Should one choose the BN bond length in H_3B–NH_3 or that found in the cubic form of boron nitride? The latter choice makes more sense.

Amino imino boranes **1** can be described with the use of resonance structures (**A**–**C**), whereby the boron atom in structures **A** and **B** possesses a formal negative charge. The simplest representation for amino imino boranes is the one that has been used in this work, R_2N=B≡N–R′.

$$R_2\ddot{N}\text{–}B{\equiv}N\text{–}R' \longleftrightarrow R_2N{=}B{=}\ddot{N}\text{–}R' \longleftrightarrow R_2\ddot{N}\text{–}B{=}\ddot{N}\text{–}R'$$

A **B** **C**

1

4. Reactions of Amino Imino Boranes

The chemistry of amino imino boranes should reflect the unsaturated character of the BN triple bond; in this respect, it should be similar to that of imino boranes R–B≡N–R′.[9] Thus, addition and insertion reactions as well as cycloaddition reactions are to be expected. Furthermore, the amino group opens up additional reaction possibilities.

4.1. Addition Reactions at the Imino Nitrogen

The simplest imaginable reaction of amino imino boranes is coordination via the imino nitrogen in a simple Lewis acid–base reaction. Particularly well suited are transition-metal carbonyl fragments as Lewis acids. $Cr(CO)_6$ and $W(CO)_6$ react with **1a** to give the pentacarbonyl complexes **7**.[33] The X-ray crystal structure of the chromium complex confirms the allene-like structure. It contains two BN bonds of different length (129.5(6) pm to the NC(Cr) group, 136.8(6) pm to the NC_2 group).

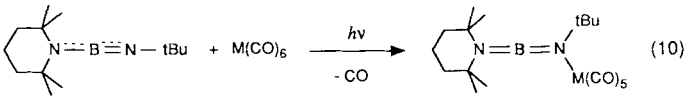

(10)

1a **7**

It is also possible to isolate 1 : 1 adducts **8** when suitable Lewis-acidic metal halides are used—e.g., $AlCl_3$, $AlBr_3$, $GaCl_3$,[34] HgI_2,[35] or $PdCl_2$[36] (see also Section 4.5.1). $PdCl_2$ adds two molecules of **1a** to form **9**. The amino imino borane units in **9** are almost perpendicular to the $PdCl_2N_2$ plane. The two BN bond lengths are 132 and 135 pm and are thus somewhat more balanced than in **7**.

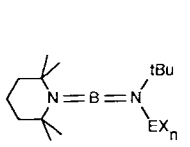

8

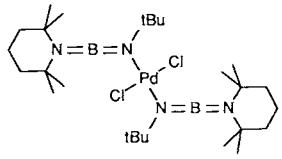

9

The addition of carbenium ions at the imino nitrogen of **1a** has not yet been successful. In contrast, the addition of the trimethylsilyl cation is known. The reaction of trimethylsilyl iodide or triflate with **1a** leads cleanly to the boron(1+) salts **10**. The weak nucleophilicity of the anion is important for the stability of the product; however, the steric bulk of the Me_3Si group also plays a role: methyl triflate reacts with **1a** forming the diaminoboryl triflate **11**[37] as the insertion product.

These reactions are typical of amino imino boranes, owing to the stabilization of the diaminoboron(1+) stage, the formation of which is not possible using imino boranes

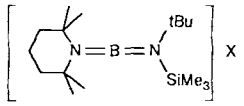

10

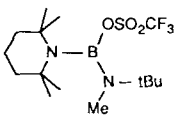

11

R–B≡N–R′. Analogous reactions involving amino alkynes are unknown to our knowledge.[12]

4.2. Reactions with Protic Compounds

The polar imino borane group in amino imino boranes **1** undergoes a rapid and straightforward reaction with protic compounds HY with insertion into the HY bond according to Equation (11). However, carrying out the reaction under

(11)

1

controlled reaction conditions or stoichiometry is usually required since an excess of the reagent results in most cases in cleavage of BN bonds.

4.2.1. Reactions with Acids

Hydrogen chloride[38] and trifluoromethanesulfonic acid[37] react with amino imino boranes in a 1:1 molar ratio according to Equation (11) to give the corresponding diamino(chloro)- or diamino(trifluoromethylsulfonyloxy)boranes. Compound **1b** reacts similarly with HCl.[15] An excess of HY results in cleavage of BN bonds, partly in ways which are difficult to define. Analogous reactions have been found for carboxylic acids, which react with **1a** in the first reaction step to yield monomeric acyloxy(*tert*-butylamino)tetramethylpiperidinoboranes **12**. Excess carboxylic acid leads eventually to the tetracarboxylatoborates **13**.[39]

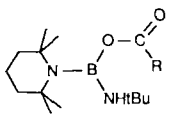

12

R = CH_3, CF_3

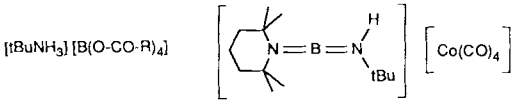

13 14

Mechanistically, all of these reactions proceed via the *tert*-butylamino(tetramethylpiperidino)boron(1+) ion, as shown by the reaction of tetracarbonylhydridocobalt[36] with **1a** in a 1:1 ratio to give the thermally unstable salt **14**. The weakly nucleophilic, bulky cobaltate ion fails to attack the boron center of the cation to form the corresponding insertion product.

4.2.2. Reactions with Alcohols, Thiols, Amines, and Phosphanes

In contrast to the undefined nature of the hydrolysis products of amino imino boranes, **1a** reacts as a model system with alcohols in a rapid reaction to yield the alkoxy(diamino)boranes **15**.[39] Failure of this reaction has only been found in the case of extremely bulky alcohols such as 2,4,6-tri-*tert*-butylphenol. Compound **16** can be prepared from **1b** and isopropyl alcohol.[15]

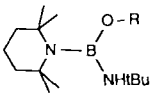

15

R = Me, iPr, tBu, Ph, 2,4,6-$tBu_3C_6H_2$

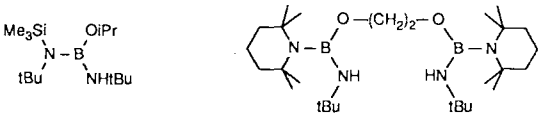

16 17

Whereas alkoxy(dimethylamino)boranes decompose during distillation into $B(OR)_3$ and $B(NMe_2)_3$,[40] the compounds **15** and **16** remain stable. The same holds true for the product **17**, which is obtained from the reaction between **1a** and glycol.[41]

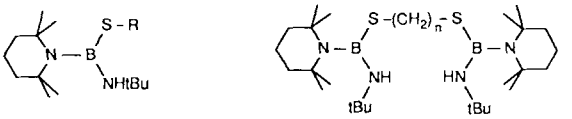

18 19

R = tBu, Ph n = 2, 3

Hydrogen sulfide is rapidly taken up by **1a**; however, the suspected reaction product **18**, R = H, characterized by a ^{11}B NMR signal at $\delta = 37.7$ decomposes very rapidly.[42] In contrast to this behavior, thiols[39,41] and α,ω-dithiols yield stable, distillable compounds **18** and **19**. Thus, in these cases, the equilibrium for the reaction (12)

(12)

lies far to the right. This is in marked contrast to the boranes with R = Me, Et.[43]

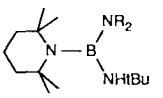

20

NR_2 = NH_2, NH iPr, NH tBu, NHPh, NMe_2, pyrrolidino, 1-pyrrolyl, 1-imidazolyl, NH-NMe_2, NMe-NHMe

21 22

By addition of ammonia, amines, or hydrazines to **1a**,[39] the triamino boranes **20** become accessible, which contain three different amino groups. Compound **1b** behaves similarly.[15] In addition, no ligand exchange reactions occur, a consequence of the "steric overloading" of the molecules. For the same reason, the pyrazolylborane derivative **22**[39] fails to dimerize. Compound **21** is formed by addition of $Me_3SiNHiPr$ to **1a**.[19]

Diethylamine, bis(trimethylsilyl)amine, *tert*-butyl(trimethylsilyl)amine, and 2,2,6,6-tetramethylpiperidine fail to react with **1a** for steric reasons. This is the essential prerequisite for the success of dehydrohalogenation reactions [Eq. (9)], in which the anions of these amines have been used successfully.

That the rate of amination of **1a** is more dependent on the steric bulk and less on the basicity (or the nucleophilicity) of the amines involved is indicated by the qualitatively determined series $NH_3 > NH_2R > NHR_2$. Compared with aniline (100% reaction in 30 min), phenylphosphane reacts only very slowly with **1a** (50% reaction in 24 h) to give tmp–B(PHPh)–NH*t*Bu.[42]

All reactions of **1a** with protic compounds occur regiospecifically with protonation of the imino nitrogen atom only. Mechanistically, the reactions of **1a** with amines could proceed via an attack of the nitrogen atom at the boron center. However, since $\delta(^{11}B)$ of **1a** is not significantly influenced by pyridine, such a reaction path seems

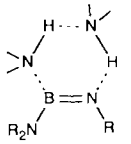

23

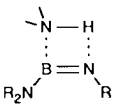

24

highly unlikely. The latent electrophilic nature of the boron atom in amino imino boranes is increased significantly, however, upon protonation of the imino nitrogen. The protonation step could be induced by hydrogen bonding between the amino imino borane and the amine or the alcohol. *Paetzold*[9] has suggested a cyclic transition state **23**. However, the alternative **24** cannot be excluded.

4.2.3. Reactions with Carboxylic Acid Amides

N-Methylacetamide reacts rapidly and quantitatively with **1a** to give the *N*-acyl-substituted triamino boranes **25**. The formation of the *O*-isomer is ruled out by the NMR spectra (^1H, ^{11}B, ^{13}C, ^{14}N).[44] 2-Pyrrolidone behaves analogously as a cyclic carboxylic acid amide, affording **26**.[45] Both **25** and **26** correspond to the *N*-methylacetamido borane **27** described by *Meller* et al.[46]

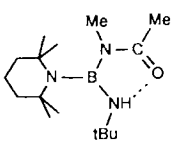

25

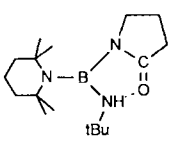

26

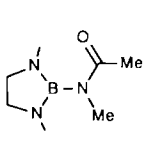

27

The question whether the acetamides react with **1a** in their amide or their imide form remains open.[44] The BO bond would be thermodynamically more favorable; evidently, the resonance-stabilized form of the acid amide determines the course of the reaction.

4.2.4. Reactions with Amino Acids and Their Derivatives

Compound **1a** is extremely well suited to borate amino acids under very mild conditions.[47] In this way **1a** dramatically differs from the isoelectronic ynamines, which cause the condensation of amino acids.[12]

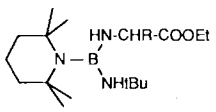

28

R = H, Me, $CHMe_2$, CH_2CHMe_2

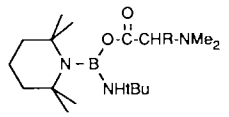

29

R = H, Me, $CHMe_2$, CH_2CHMe_2

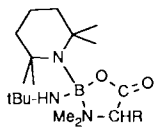

30

Amino acid esters behave like amines in the presence of **1a**: triamino boranes of type **28** are obtained in yields of up to 85%. NMR spectra indicate an *anti* conformation of the HNCH group, which is probably sterically induced. *O*-Borylated amino acid derivatives **29** are obtained from the *N,N*-dimethylamino acids. ^{11}B nuclear resonance data rule out the possibility that ring closure to **30** has occurred.[47] Furthermore, no formation of borates of the type $[B(OCO{-}CHR{-}NMe_2)_4]^{\ominus}$ is observed, in marked contrast to the reaction of **1a** with carboxylic acids. This is presumably due to the heterogeneous reaction conditions used for the synthesis of **29**; i.e., **1a** is always present in excess. Compound **1a** fails to differentiate between the two carboxylic acid functions of *N,N*-dimethyl-L-aspartic acid. A single reaction product **31** is obtained.

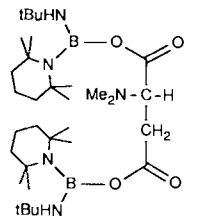

31

Based on these results, one could expect that in free amino acids both the carboxylic acid and the amino function would react with **1a**. In fact, however, there is a competition between such a double borylation to yield **33** and an amine elimination which leads to **34** [Eq. (13)]. The monoboration product **32** could serve as a common intermediate in these reactions.[47]

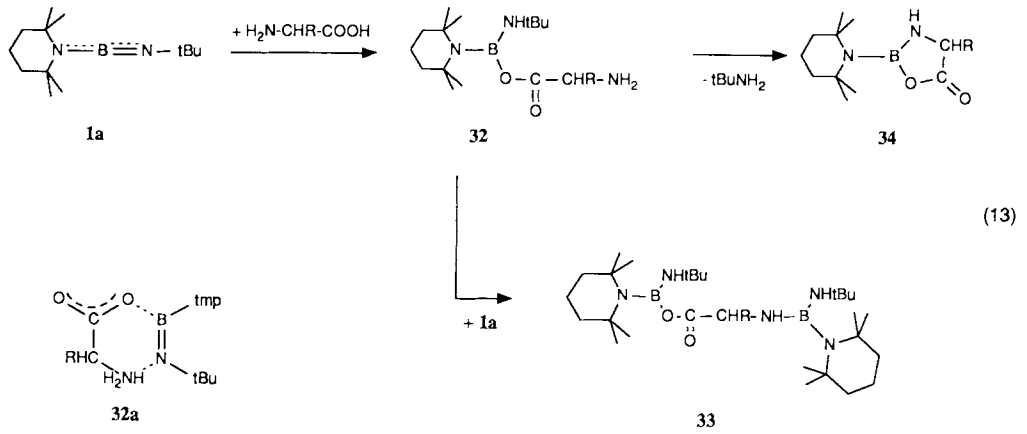

(13)

Table 3. Product distribution [mol %] between the borylation products **33** and **34** formed by reaction of amino acids with **1a**.

Amino acid	33	34
Glycine	100	–
L-Alanine	50	50
L-Valine	20	80
L-Leucine	35	65
L-Isoleucine	5	95
L-Phenylalanine	20	80

The product distribution **33/34** is controlled by the steric demand of the organic group R, as the data in Table 3 indicate. This is best seen by comparing the results for L-leucine and L-isoleucine.

We postulate that the formation of **32** results from proton transfer from the zwitterionic structure of the amino acid to the imino nitrogen, as shown in **32a**. Attack of the carboxylate moiety at the boron atom leads to **32**. Increasing bulkiness of the amino group hinders the second boration step to **33**. This allows the intramolecular condensation to the oxazaborolidinone derivative **34**, whose almost planar five-membered ring structure has been confirmed by an X-ray analysis.[47]

4.3. Boration Reactions

Lewis-acidic boron compounds correspond in many ways to protic acids. For instance, alkynes not only add hydrogen halides[12] but also borane derivatives. The boration of acetylenes proceeds stereospecifically, yielding *cis*-alkenylboranes.[48] No stereospecific boration of the B≡N bond has so far been detected owing to the smaller rotational barrier of the B=N bond present in amino boranes as compared with the C=C bond in alkenes, but this reaction allows an easy synthesis of new, even *B*-functionalized, diborylamines, as shown by *Paetzold*.[9] Using amino imino boranes, one obtains diborylamines, the isoelectronic analogues of butadiene—a formalism which is valid structurally only in part.[49]

4.3.1. Hydroboration Reactions

The use of diorgano boranes (or their dimers) instead of diborane allows a better control of the regiospecificity of the hydroboration of unsaturated CC systems.[48] This problem is invalid with amino imino boranes because the mode of addition and therefore the regiospecificity is predetermined by the polarity of the BN bond. The relative inertness of the BC bond is the prerequisite for the regiospecific hydroboration of amino imino boranes by diorgano boranes (or their dimers) according to Equation (14). Compound **1a** reacts with dicyclohexyl- and disiamylborane and with 9-borabicyclo[3.3.1]nonane at ambient temperature to yield amino-substituted diborylamines of type **35**.[50] The rate of reaction with these hydrides increases in this sequence of compounds approximately in the ratio 1 : 12 : 48. This is surprising insofar as the sterically least hindered diorgano borane, namely, dicyclohexylborane, hydroborates *most slowly*.

(14)

This gradation in reactivity is, however, easily explained by taking the equilibrium (15) into account; i.e., the hydroboration rate is determined by the equilibrium concentration of the monomeric diorgano borane. The higher the value of ν(BHB), the stronger is the hydrogen bond, the smaller the equilibrium concentration of the monomer, and the slower the hydroboration. This corresponds to the experimental facts for the three dimeric diorgano boranes investigated.[50] It becomes clear under this presumption why dithexyldiborane **36** hydroborates the amino imino borane **1a** according to Equation (16) very slowly to give **37**. Only one of the two hydridic hydrogens of the RBH_2 units in dithexyldiborane is used in the hydroboration of **1a**.[50]

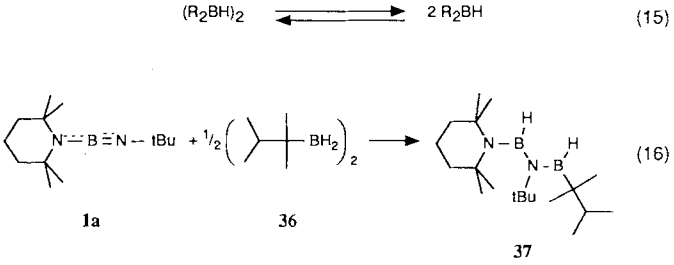

(15)

(16)

In contrast to the examples cited above, a more complex pattern of reactivity during the hydroboration of **1a** is ob-

served with either diborane or $BH_3 \cdot THF$.[50,51] Under carefully controlled reaction conditions, **38** is the principal product. The coordinatively unsaturated $N-BH_2$ group first formed is saturated by coordination to the N atom of the tmp group. Compound **38**, however, is not very stable thermally. Thus, its $tmpBH_2$ component is trapped by "BH_3" as the μ-aminodiborane derivative **39**. In addition, **40** is produced, along with the borazine $(HBNtBu)_3$.[14,51]

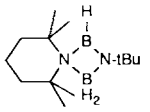

38

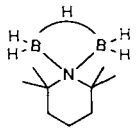

39

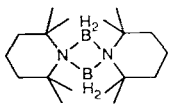

40

Use of $H_3B \cdot SMe_2$ reduces the concentration of free BH_3 to such an extent that **38** becomes the main product (>80%); i.e., the relatively small amount of rapidly accessible BH_3 results in suppression of subsequent and side reactions.[50]

4.3.2. *Haloboration Reactions*

The boron trihalides BF_3,[14] BCl_3, and BBr_3[21] haloborate **1a** according to Equation (17) to give compounds **41**. Instead of BBr_3, the adduct $BBr_3 \cdot SMe_2$ can also be used.[50] The bonding between the two tetracoordinated ring atoms in **41** is weak as shown by the long BN bond

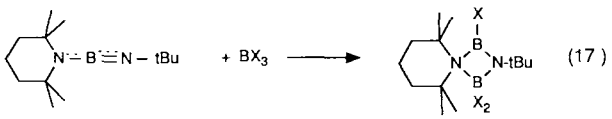

1a **41**

X = F, Cl, Br, (17)

(172(1) pm) of the bromine derivative.[21] By means of $AlBr_3$, a bromide ion may be removed from **41** (X = Br) to produce the salt **42**. A single ^{11}B NMR signal at $\delta = 36.8$ shows the chemical equivalence of the two boron atoms.[52] When $^{10}BBr_3$ is used for the bromoboration of **1a**, the intensities of the two boron NMR signals of **41** (X = Br) in both the ^{11}B NMR spectrum and the ^{10}B NMR spectrum are equal. This corresponds to an equilibrium (18). Whether the bromine migration occurs by a dissociative step or via a Br-bridge across a folded four-membered ring has not yet been definitely established. MNDO calculations favor the intramolecular process.[50]

In contrast to **1a**, a fluoroboration product **43** is obtained in the reaction of **1g** with BF_3. It contains only tricoordinated boron atoms ($\delta(^{11}B) = 26.7, 18.7$).[44] This result is intelligible by assuming a *cis* attack of BF_3 and a sterically determined high rotational barrier at the central BN bond.

From **1a** and methylboron dichloride, the compound type **44** forms exclusively;[52] this finding was corroborated by an X-ray structure analysis.[14] In contrast, phenylboron dichloride and dibromide yield mixtures of the isomers **44** and **45** (R = Ph, X = Cl, Br).[51] It seems, therefore, that

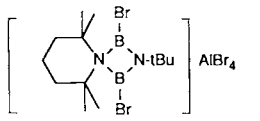

42

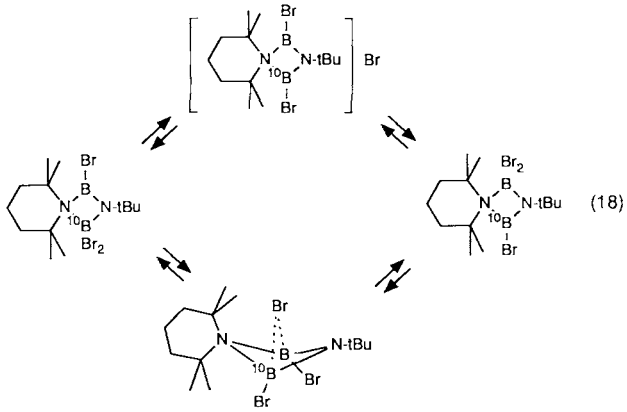

(18)

organoboration is faster than the haloboration. By using $^{10}MeBBr_2$ it has been shown[50] that haloboration occurs exclusively, because the methyl group remains at the ^{10}B atom. Therefore, in **45** (R = Me, X = Br) a bromine atom must migrate until it is finally held tightly by the more acidic BBr group. However, in boiling hexane the methyl group becomes mobile.

That two isomers appear for R = Ph and X = Cl (**44** : **45** = 3 : 1) can be explained by the stronger Lewis-acidic character of the $PhBN_2$ group as compared with the $MeBN_2$ group. Practically only a single isomer **45** ($\delta(^{11}B) = 31.0, 8.5$) results if $PhBBr_2$ is employed. In the case of $tBuBBr_2$, the bulky *t*Bu group prohibits an intramolecular saturation of the bromoboration product **46** ($\delta(^{11}B) = 38.7, 26.0$).[50]

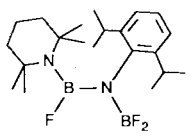

43

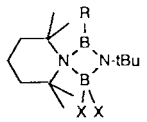

44

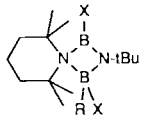

45

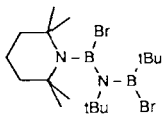

46

Imino boranes R−B≡N−R′ are chloroborated by dialkylboron chlorides R''_2BCl (R″ = *i*Pr, *n*Bu, *t*Bu) to yield diborylamines of type $R''_2B-NR'(Cl)$.[9] The amino group present in amino imino boranes opens up an additional reaction channel. According to Equation (19), the expected chloroboration product is formed with **1b** at low temperature: However, the chloroboration product easily decomposes with elimination of Me_3SiCl, forming the diazadi-

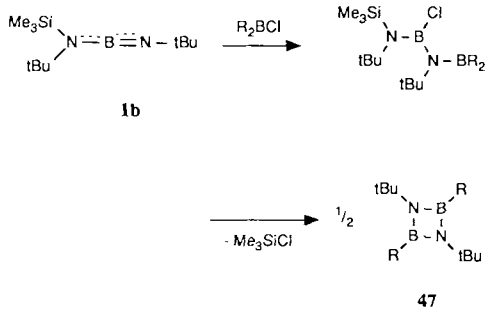

1b

47

(19)

boretidine **47**, whose structure was established by X-ray analysis, as the final product.[15]

In contrast, salts of type **48** arise from **1a** and diorgano boron halides. In solution, **48** (R = Et, X = Cl) exists in equilibrium with the "simple" chloroboration product tmp–BCl–N*t*Bu–BEt_2.[50] Following the arguments put forward by *Eisch* et al.,[53] derived from results obtained by studying the boration of alkynes, we have to regard the chloroboration products of amino imino boranes as the kinetically controlled reaction products, whereas the organoboration products (or their cyclic isomers **48**) would be the thermodynamically controlled compounds.

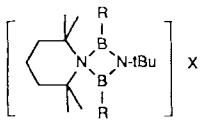

48

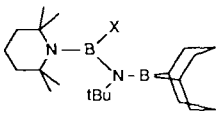

49

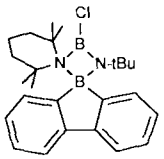

50

If one suppresses the migration of organo groups from diorgano boron halides by incorporating the boron atom into a ring system (e.g., by reaction of **1a** with 9-borabicyclo[3.3.1]non-9-yl chloride, bromide, or triflate, then the diborylamines **49** are obtained. On the other hand, 9-chloro-9-borafluorene furnishes the spirocyclic compound **50**,[50] because the boron atom in the planar five-membered ring is more acidic.

4.3.3. Alkoxy- and Alkylthioboration

Trimethyl borate, $B(OMe)_3$, reacts with **1a** readily to yield the methoxyboration product **51**. Only one methoxy group is transferred. Compound **51** distills undecomposed. $B(OPh)_3$ behaves similarly. With 2-methoxy and 2-butoxy-1,3,2-benzodioxaborole, **1a** undergoes alkoxyboration to give **52** exclusively, and 2-methylthio-1,3,2-dithiaborolane reacts, also regiospecifically, to give **53**.[50]

Still more interesting is the reaction of $B(OMe)_3$ with **1b**. Smooth methoxyboration at −40 °C according to Equation (20) is followed by elimination of Me_3SiOMe. Instead

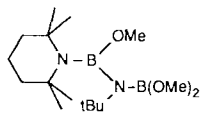

51

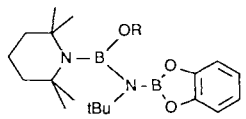

52

R = Me, Bu

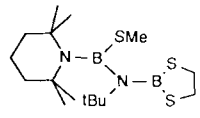

53

of a diazadiboretidine, its dimer, the crystalline tetraazatetraborocane **54**, is thereby formed.[20]

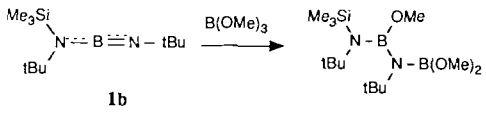

1b

(20)

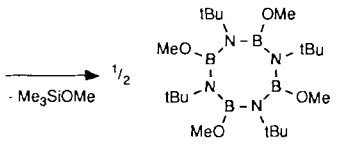

54

4.3.4. Aminoboration

Tris(dimethylamino)borane does not react with **1a**, even under reflux conditions. It does not attack at the imino nitrogen atom for electronic and steric reasons. The same holds for $MeB(NMe_2)_2$ and Ph_2BNEt_2. However, 9-dimethylamino-9-borafluorene aminoborates **1a** to yield **55**, because the planar 9-borafluorenyl group is sterically less demanding than the Ph_2B group. That steric requirements are responsible in addition to Lewis acidity—the two factors naturally go together—for a successful aminoboration is demonstrated by the smooth reaction of **1a** with Ph_2B–NHEt to yield **56**, whose structure was established by X-ray methods.[50] Thus, the amino boranes are more reactive towards amino imino boranes **1** than towards imino boranes R–B≡N–R′,[9] since the latter are only aminoborated by the more acidic hydroxyamino boranes R'_2B–N($SiMe_3$)$OSiMe_3$.[9,54]

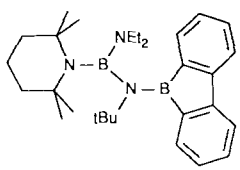

55

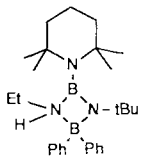

56

4.3.5. *Organoboration Reactions*

Whereas the organoboration of imino boranes $R-B{\equiv}N-R'$ by trialkyl boranes BR_3'' leads to pentaorganodiborylamines $RR''B-NR'-BR_2''$, amino-substituted diborylamines of type **57** are formed when amino imino boranes such as **1a** are employed. The rate of the organoboration is primarily controlled by the steric requirement of the organo groups R'': the relative rates for R'' = Me, Ph, Bu, *i*Pr are approximately 1 : 16 : 24 : 336.[50]

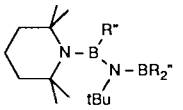

57

R = Me, Bu, iPr, Ph

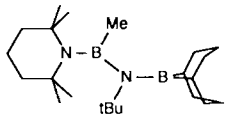

58

The organoboration of **1a** with 9-methyl-9-borabicyclo[3.3.1]nonane furnishes the methylboration product **58** exclusively; i.e., the insertion of **1a** into a BC bond of the ring is suppressed. Compounds **1b,c** readily react with BEt_3 in a similar fashion.[15,17]

4.3.6. *Competing Boration Reactions*

As shown in Section 4.3.5, an organo group bound to boron is not inert towards the attack of an imino borane. However, in most cases the imino borane undergoes insertion into the more polar BX bond.[55] By studying boration reactions with mixed boranes RBX_2 or BX_2Y, useful information regarding the relative migratory aptitude of the substituents R and X or Y and X are obtained.

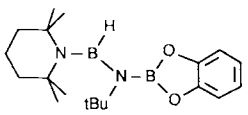

59

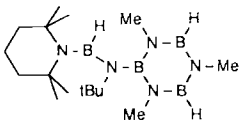

60

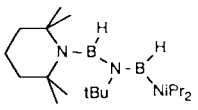

61

Benzodioxaborole serves as a selective hydroboration reagent. It hydroborates **1a** specifically to produce **59**.[56] This is true also for bis(dimethylamino)borane and 1,3-dimethyl-1,3,2-diazaborolidine as well as for 1,3,5-trimethylborazine, which yields **60**.[50] Of the three BN compounds cited, $(Me_2N)_2BH$ reacts most slowly whereas the other two species hydroborate **1a** even at ambient temperature. This underlines again the influence of the acidity of the borane on the reaction rate.

Compound **61** is formed from **1a** and monomeric iPr_2NBH_2.[20] The amino imino borane **1a** is therefore much more reactive than alkynes, which react at the BH bond of alkoxy or amino boranes only at elevated temperature and pressure.[57] Regarding the migratory aptitude one finds H > OR and H > NR_2.

The reaction of diethoxyboron chloride with **1a** proceeds even at −50 °C. It leads to a mixture of isomers consisting of the ethoxy- and chloroboration products.[50] However, a specific chloroboration is achieved in the reaction of **1a** with 2-chloro-1,3,2-benzodioxaborolane.[50] Only chloroboration is observed when 2-chloro-1,3,2-dithiaborolane reacts with **1a**, in spite of the presence of the labile BS bond. The reaction of **1a** with tribromoborthiine **62** deviates from this simple reaction scheme: the product is the 1,3,2,4-thiazadiboretidine derivative **63**, whose formation can be imagined to occur via an intermediate product [Eq. (21)], which, in turn, bromoborates **1a** to give **63**.[58]

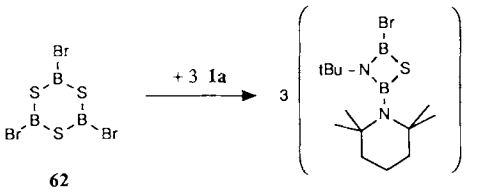

62

(21)

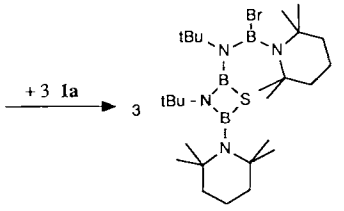

63

Diamino boron halides and amino boron dihalides react with **1a** with haloboration only. Compound types **64** and **65** are formed with $(Me_2N)_2BCl$, $(Me_2N)_2BBr$, and 2-chloro-1,3-dimethyl-1,3,2-diazaborolidine (not shown),[50] and with Me_2NBCl_2, Me_2NBBr_2, Et_2NBCl_2,[50] Et_2NBBr_2,[58] iPr_2NBCl_2,[50] iPr_2NBBr_2,[58] and $tmpBCl_2$,[18] respectively. $tmpBF_2$ will not react with **1a** to give a fluoroboration product.[50] Provided that the R_2N group is small ($R_2N = Me_2N$, X = Cl, Br), then **66** is observed in solution besides **65**.[50] Structure **66** will probably dominate for these compounds in the solid state, whereas they are present as type **65** in solution.

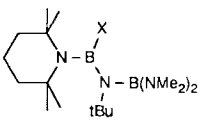

64

X = Cl, Br

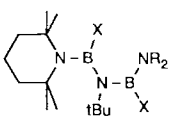

65

X = Cl, Br

$R_2N = Et_2N$, iPr_2N, tmp

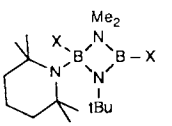

66

The haloboration products **65** react with alkali metals to yield azadiboriridines **67**.[58-60] These heterocycles, in turn, readily undergo oxidative ring expansion[58] with sulfur or selenium to give **68** [Eq. (22)].

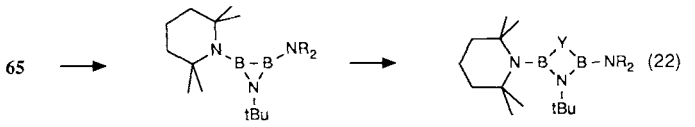

67 **68** Y = S, Se

Of the two boron–halogen bonds in dichloro- and dibromo(dimethylamino)diborane $B_2(NMe_2)X_2$, only one is involved in the haloboration of **1a**. Both products **69** show no tendency to undergo an intramolecular BN coordination. This holds also for the chloroboration product **70**, which was also characterized by an X-ray structure analysis.[58]

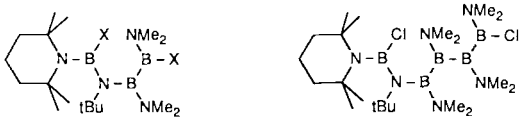

69 X = Cl, Br **70**

The rate of chloroboration of **1a** decreases as the steric shielding at the boron–halogen group increases:

$B_2(NMe_2)_2Br_2 < B_2(NMe_2)_2Cl_2$ and
$B_2(NMe_2)_2X_2 < B_4(NMe_2)_4X_2$ (X = Br, Cl).[58]

*t*Bu(Me$_2$N)BB(NMe$_2$)Cl is inert towards **1a**.

The instability of simple alkoxy amino boranes and alkylthio amino boranes excludes an investigation of the relative migration of the RO/R$_2$N and RS/R$_2$N groups, respectively. Instead, one has to investigate stable ring systems. 2-Dimethylamino-1,3,2-dioxa- and 2-dimethylamino-1,3,2-dithiaborolanes act as specific aminoboration reagents toward **1a**.[50] Of these two compounds, the more acidic and more electrophilic sulfur species reacts substantially faster.

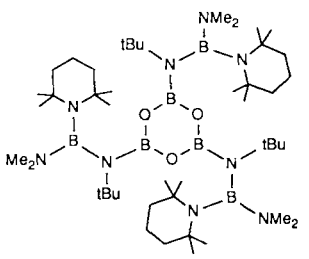

71

Tris(dimethylamino)boroxine also proved to be an aminoboration reagent. Irrespective of the molar ratio, the boroxine **71** is obtained by reaction with **1a**.[19] Tris(dimethylamino)borthiine is attacked by **1a** not at the BN bonds but rather at the ring BS bonds. Ring degradation leads to the thiazadiboretidine **72** according to Equation (23); i.e., the six-membered borthiine ring will be broken down by

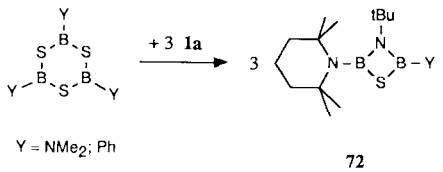

Y = NMe$_2$; Ph **72** (23)

loss of X–B=S fragments. The exact course of this borthiine degradation is still unknown. Possibly, insertion of **1a** into the ring of the borthiine with ring expansion to an eight-membered ring occurs; **72** then cleaves off with formation of **73**. The latter reacts with **1a** with thioboration, giving **74**.[58] Its further reaction to **72** is shown in Equation (25). It should also be mentioned, however, that **1a** inserts into the BN bond of the cluster compound **75** to give **76**,[58] indicating that in this case the BN bond is more reactive than the BS bond. The reactivity pattern of the system **75** differs, however, owing to the sulfonium character of its sulfur atoms, from the aminoborthiine $(R_2NBS)_3$

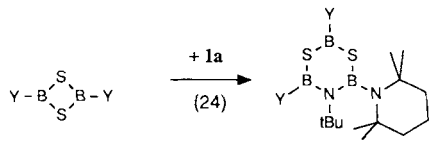

73 Y = NMe$_2$, NEt$_2$ **74** (24)

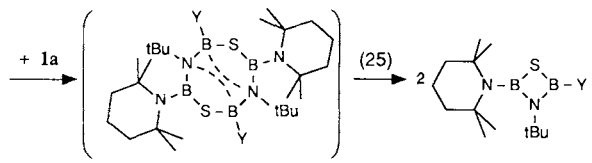

72 (25)

discussed above. While exocyclic BN bonds are more reactive than ring BO bonds in the case of amino boroxines, the same does not hold generally for systems with exocyclic BN and endocyclic BS bonds.

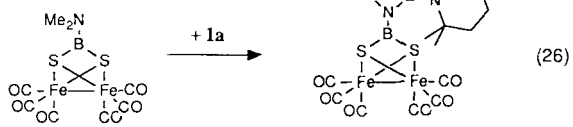

75 **76** (26)

One may state as a rule, however, that the BO, BS, and BN bonds of 1,3,2-dioxaborolanes, 1,3,2-dithiaborolanes, and 1,3,2-diazaborolidines are inert against an attack of **1a** because both the 2-methyl and 2-phenyl derivatives of these heteroycles react with **1a** exclusively by organoboration.[50] Therefore, the insertion of the B≡N unit into BY ring bonds to produce seven-membered rings is not realized.

4.4. Hydrometalation Reactions

Hydroboration is a special case of hydrometalation.[61] Since alkenes and alkynes are readily hydroaluminated by diisobutylalane, it is not surprising that the B≡N bond of the amino imino borane **1a** is also reduced by this reagent. The oily compound **77**, containing a tetracoordinated Al atom ($\delta(^{27}Al) = 109$),[50] is formed regiospecifically.

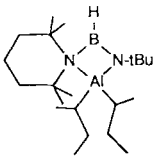

77

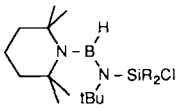

78

R = Me, Cl

Whereas in most cases the hydrosilylation of alkenes or alkynes requires a catalyst, the hydrosilylation of **1a** needs only a sufficiently acidic Si center. Me_3SiH does not add to **1a** either in the presence of a radical initiator or of a hydrosilylation catalyst. However, reactions with Me_2SiHCl and $SiHCl_3$ to give **78** occur even at ambient temperature without a catalyst. The possible chlorosilylation (see Section 4.5.2), which could compete with the hydrosilylation, does not occur. Chlorosilylation is thermodynamically favored by 55 kJ mol^{-1} over hydrosilylation;[36] even statistically, the chlorosilylation should be dominant at least in the case of $SiHCl_3$. Since a strong Lewis acidity of the silane is a prerequisite for the success of the reaction, one can conclude that hydrogen transfer occurs anionically. Under this assumption, the better polarizability of the hydrogen atom explains the kinetically controlled formation of **78**. Accordingly, the hydrometalation of amino imino boranes should occur more readily the more polar the hydrogen-metal bond. Me_3GeH will not react with **1a**; however, Me_3SnH and Bu_3SnH yield the hydrostannation products (SnR_3 instead of SiR_2Cl) analogous to **78**; these are thermally labile liquids which destannylate during distillation.

Compound **1a** is also hydrometalated by transition-metal hydrides such as Cp_2TiH,[36] Cp_2ZrH_2, and Cp_2ZrHCl.[56] Compound **79** is a hydride-bridged species according to its X-ray structure. Spectroscopic data (^{11}B NMR, IR) prove the presence of a double hydride bridge for **80**. The hydride bridge in **79** is exceptional insofar as a tricoordinated boron atom is involved. Such a hydrido bridge is only weakly indicated (d(B–H) = 137(3) pm) in

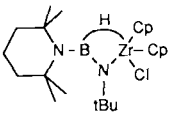

79

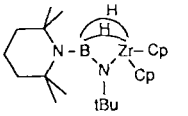

80

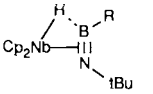

81

R = N(SiMe$_3$) tBu, tBu

compounds **81**, which are formed by reaction of Cp_2NbH_3 with **1b** or tBu–B≡N–tBu whereby elemental hydrogen is lost. The most remarkable structural part of **81** is the side-on coordination of the imino borane unit.[62]

4.5. Halometalation Reactions

Covalent element halides EX_n react readily with amino imino boranes. Depending on their Lewis acidity, the polarity of the element halogen bond, the steric bulk of the amino imino borane fragment, and the halogen atom, as well as the Lewis-acidic character of the resulting $N-EX_{n-1}$ group, the reaction (27) stops at one of the stages **82**–**85**.[63] For these reactions **1a** and **1g** were used as model compounds.

4.5.1. Adduct Formation and Equilibria

The Lewis acidity of the attacking element halides determines the position of the equilibrium (27a). Me_3SiCl, Me_3SiBr,[14] Ph_3SiCl,[19] Me_3GeCl, Me_2GeBr_2,[36] Me_3SnCl, Me_3SnBr,[14] $CpTiCl_3$, Cp_2TiCl_2, Cp_2ZrCl_2, and Ph_3PAuCl[36] do not react with **1a**. Analogously, **1g** is not attacked by Me_3SiCl, Me_3SiBr, Me_3SiN_3, Me_3SiCN, $EtSiCl_3$,[19] $HgBr_2$, HgI_2, CuCl, $RhCl_3$, VCl_3, or $MnCl_2$.[64] However, **1g**, *like* **1a**, adds $AlCl_3$, $AlBr_3$, and $GaCl_3$[64] to produce compounds of type **82**, and this is also true for AsI_3, SbI_3, and $BiCl_3$.[65] This type is also formed by the action of **1a** on $SnCl_2$, Me_2SnCl_2, Me_2SnBr_2, $SnBr_4$,[36] AsI_3, $SbBr_3$, SbI_3, $BiCl_3$,[65] $TiBr_4$, $ZrCl_4$, and $PdCl_2 \cdot 2\,PhCN$.[36] The Lewis acids $SnCl_2$, Me_2SnCl_2, and Me_2SnBr_2 are only loosely coordinated to **1a**, as reflected in the solution equilibrium (27a). This can be shown by a decreased intensity of the characteristic IR band of **1a** at 990 cm^{-1} or by molecular weight determinations. Thus, **1a** · Me_2SnCl_2 in benzene at 0°C is dissociated to the

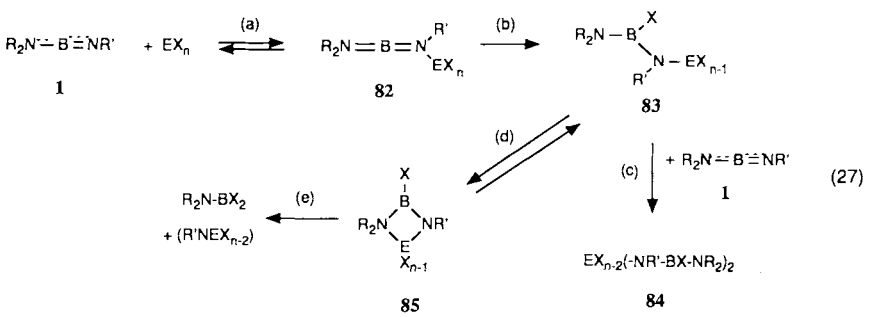

(27)

extent of 61% in a 0.001 M solution. Adduct **1a** · Me_2SnBr_2 in toluene at −78 °C is present as a stable adduct of type **82** according to ^1H and ^{13}C NMR spectra, and the $^2J(^{119}Sn^1H)$ coupling constant of 81 Hz indicates pentacoordinated Sn.[66] At 57 °C, however, the complex is totally dissociated into its components.

Compound **1g** is sterically more demanding than **1a**. This explains why the former will not react with HgI_2 and $HgBr_2$, in contrast to **1a**, nor with TiI_4 or $TiCl_3$.[44]

4.5.2. Insertion Reactions

If less polar covalent element halides are employed, halometalation to give compounds of type **83** dominates. Borylamino-substituted element halides **83** are thereby formed, mostly in a straightforward manner. These compounds are of high potential precursors in the synthesis of heterocycles which cannot be obtained by other routes.

Borylamino-substituted silanes of type **83** result from **1a** and SiF_4, $SiCl_4$, $MeSiCl_3$,[36] Me_2SiCl_2, $EtSiCl_3$, Me_2SiCl_2, Ph_2SiCl_2, Si_2Cl_6,[19] and $SiBr_4$.[36] Double insertion to give the compound type **84** occurs only with SiF_4.[36] However, Si_2Cl_6 also reacts with a second mole of **1a**, the second $SiCl_3$ group being converted into an $SiCl_2NtBu-BCl(tmp)$ group.

Compound **1g** is also subject to halosilylation. Insertions to produce the compound type **83** occur with $SiCl_4$, $SiBr_4$, $PhSiCl_3$, Ph_2SiCl_2, and Si_2Cl_6.[50,64] Double insertion into the SiCl bonds of these chlorosilanes has not been achieved.

The structure of the insertion product **1g** · Ph_2SiCl_2 was established by X-ray methods. In solution this compound dissociates in part into Ph_2SiCl_2 and **1g**.[19] This chlorosilane elimination occurs at the lowest temperature so far observed. If this compound and similar material were made available by a different route in high yield, then one would have excellent sources for amino imino boranes at hand.

Chlorosilylation has also been observed for **1c**, with Me_2SiCl_2 and $EtMeSiCl_2$, as well as for **1b** with $SiCl_4$ and Me_2SiCl_2. The latter products eliminate Me_3SiCl in chloroform solution with condensation to diazasilaboretidines **86**.[67]

Halogermylation and halostannylation, respectively, of **1a** and **1g** to the compound type **83** is achieved with $GeCl_4$ or $MeSnCl_3$.[36,64] The same holds for **1b** and $GeCl_4$, Me_2GeCl_2, and $SnCl_4$. The products are stable in $CHCl_3$ solution, in contrast to the chlorosilylation products. However, they decompose on heating.[67]

Borylamino-substituted phosphorus(III), arsenic(III), antimony(III), and sulfur compounds are formed in the reactions of **1a,b,g** with PCl_3, PBr_3, AsF_3, $AsCl_3$, $AsBr_3$, SbF_3, $SbCl_3$, SCl_2, and S_2Cl_2.[41,65,67] Many of these are not very stable. Thus, $tmp-BF-NtBu-AsF_2$ decomposes readily at ambient temperature according to Equation (27d) into $tmpBF_2$ and the diazadiarsetidine $(tBuNAsF)_2$.[65] Although the structures of these insertion products **84** are uniquely established by their NMR spectra in solution, some of them may represent more likely the compound type **85** in the solid state. Proof for this statement is provided by the X-ray structures of $tmp-NtBu-ECl_2$ (E = As, Sb).[65] The coordinative EN bond is more pronounced for the antimony compound due to the stronger acceptor strength of the antimony moiety.

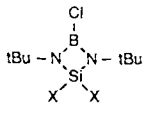

86

X = Cl, Me

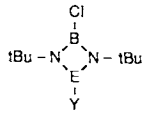

87

E = P, As, Sb
Y = Cl, Et, tBu, Ph

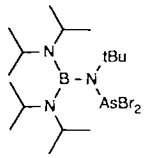

88

The product of type **83** obtained at −30 °C from **1b** and $AsCl_3$ is unstable at ambient temperature and decomposes with elimination of Me_3SiCl.[67] Reactions of **1b** with PCl_3, $AsCl_3$, or $SbCl_3$ in $CHCl_3$ lead directly to the four-membered heterocycles **87** instead of compounds of type **83**.[67]

The chemospecific insertion of the B≡N bond of **1a,c,g** into the element halogen bond of $MePCl_2$,[44,67] iPr_2PCl,[20,68] $PhPCl_2$,[44] $MeAsCl_2$,[67] and $tBuAsCl_2$[44] to give diamino boranes **83** can be understood in terms of the low chemical reactivity of the respective element carbon bonds. This chemoselectivity remains, astonishingly, in the reactions of **1a,g** with $(MeO)_2PCl$ or with 2-fluoro-1,3,2-benzodioxaarsolane and -stibolane.[44] While the products formed from **1a** and Me_2NPCl_2 are unaccounted for,[44] chloroarsenation occurs exclusively in the reaction of iPr_2NAsCl_2 with **1b**. However, the primary insertion product **88** rearranges subsequently.[67] $EtPCl_2$, $tBuPCl_2$, and Et_2NPCl_2 do not give interceptable chlorophosphorylation products; only the heterocycles **87**[67] can be isolated.

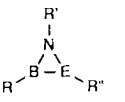

89

E	P	Si	Si	P
R''	*i*Pr	Me_2	MeEt	N*i*Pr

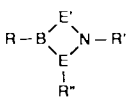

90

E	PPh	AsPh	PPh	AsPh
E'	$SiMe_2$	$SiMe_2$	B(N*i*Pr$_2$)	B(N*i*Pr$_2$)

Many of the insertion compounds **83** mentioned can be dehalogenated to produce the three-membered heterocycles **89** or, via nucleophilic substitution reactions, the four-membered heterocycles **90**. From this point of view these compounds are valuable synthons.[67,68]

4.5.3. Intramolecular Stabilization

Halotitanation of the B≡N bond of **1g** is observed when $TiCl_4$, $TiBr_4$, and Me_2NTiCl_3 are used.[19] TiF_4 reacts very slowly in boiling hexane beyond the stage **83** with elimination of $tmpBF_2$.[19,64] In contrast, the insertion product of $TiCl_4$ and **1a** stabilizes itself as a compound of type **85**. The same is true for the products obtained from **1a** and $SnCl_4$, $NbCl_5$, $TaCl_5$, and $PdCl_2 \cdot 2\,PhCN$.[36]

The ^{13}C NMR spectra of compounds **85** are characterized by a substantial low-field shift ($\Delta\delta$ = 10–20 ppm) of

the C atoms bound to the nitrogen atom of the tmp group. In the case of the tin compounds, the ^{119}Sn resonance lies in the range for pentacoordinated tin.[66] Finally, this mode of bonding is proved by an X-ray structure determination of the centrosymmetric insertion product **91**.[36,63]

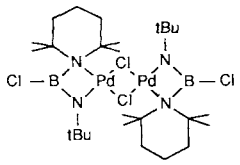

91

The intramolecular stabilization requires acidic metal centers and substituents offering little steric hindrance, as provided by chlorides and the amino imino borane **1a**. It is conceivable that the compound type **85** cannot form in reactions of silicon, phosphorus, and arsenic halides with imino boranes R–B≡N–R′, reactions recently investigated extensively by *Paetzold* et al.[67]

4.6. Aminometalation and Alkoxymetalation Reactions

The acceptor character of the central atom E decreases in the series E–Hal, E–OR, E–NR_2 due to the decreasing bond polarity as well as the increasing steric shielding. For that reason the insertion of **1a**, for example, into the element nitrogen bond of a covalent amide should be more difficult than insertion into an element-halide bond. Since, except for Me_3SiI, trimethylsilyl halides will not react with **1a**, it is surprising to find that Me_3SiOMe adds readily at ambient temperature to give **92**. It is conceivable that the greater nucleophilicity of the MeO group as compared with the halogen plays a decisive role.[19]

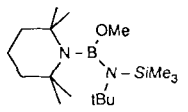

92

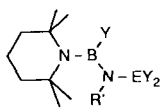

93

E	As	As	Sb	Sb
Y	OMe	NMe_2	OMe	NMe_2

$P(OMe)_3$, $P(NMe_2)_3$, and $Sb(SMe)_3$ do not react with **1a**, in contrast to $As(OMe)_3$, $Sb(OMe)_3$, $As(NMe_2)_3$, and $Sb(NMe_2)_3$.[44] Borylated amides **93** of arsenic and antimony are obtained. Compound **1g** behaves analogously. In this case, however, an aminoarsenation with $As(NMe_2)_3$ is also possible.[44] The enhanced electrophilicity of phosphorus, arsenic, and antimony in 1,3,2-dioxaphospholane, -arsolane, and -stibolane derivatives allows reactions according to Equation (28) to occur. The same holds for the corresponding benzodioxa compounds. In each case it is the exocyclic bond that will be broken. However, in the case of the 2-halo and 2-methyl derivatives of dioxaphospholane and benzodioxaphosphole, the PO ring bond is more reactive, resulting in a ring expansion to the seven-membered heterocycles **94** and **95**.[44] Arbusov rearrangement to **96** is not observed, either on heating or in the presence of carbenium ions.[44] This reaction cannot compete with the ring contraction to the 1,3,2-dioxaborolane **97** [Eq. (29)].[44]

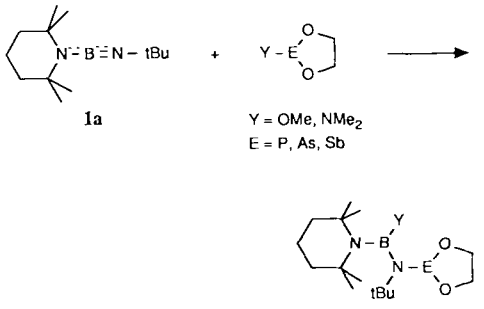

1a Y = OMe, NMe_2; E = P, As, Sb (28)

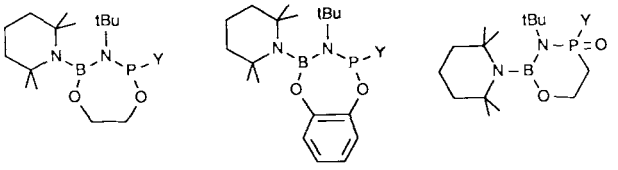

94 Y = Me, F, Cl, Br **95** **96**

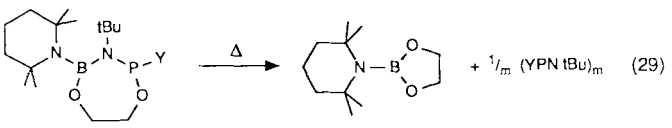

94 **97** (29)

In reactions of **1a** with 2-chloro-1,3,2-dibenzodioxarsole and -stibole, only benzoannelated compounds of type **97** are observed besides AsN and SbN heterocycles.[44] The formation of the benzodioxaborole is explained by an intramolecular ring contraction of the seven-membered rings of type **95**. Finally, it is worth mentioning that **1a** is aminostannylated by Me_3SnNEt_2.[20]

4.7. Azidation Reactions

Boryl azides, R_2BN_3, and trimethylsilyl azide react with imino boranes by azidation of the boron atom. A [2+3] cycloadduct is formed as a byproduct.[69] The latter is not observed at all in the reaction of Bu_2BN_3 or Me_3SiN_3 with **1b**[15] or of Me_3SiN_3 with either **1a** or **1g**.[19,36,69]

4.8. Organometalation Reactions

The organoboration of amino imino boranes is matched by organoalumination, -gallation, and -indation according to Equation (30). These reactions are successful in hexane

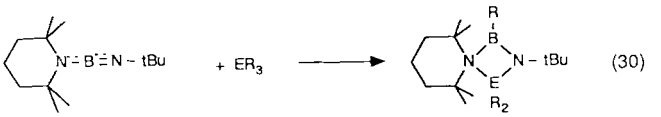

1a E = Al, Ga, In; R = Me, Et, Ph; Me, Et, Ph; Ph **98** (30)

solution by using either the associated compounds $(ER_3)_n$ or the ether adduct $AlEt_3 \cdot OEt_2$.[50] An acid-base product can be expected in the first step of the reaction. However, only the compounds **98**, having a cyclic structure as evidenced by ^{13}C and ^{27}Al (for E = Al) NMR spectra, are observed.

$SnMe_4$ will not methylstannylate **1a**.[50] This failure is due to the low Lewis acidity of this organometallic compound.

4.9. Cycloaddition Reactions

Contrary to alkynes and ynamines,[12] no high activation energy or enhancement by a catalyst is generally necessary for the oligomerization of imino boranes in spite of the fact that some compounds act catalytically.[9] The reason lies in the polarity of the BN bond. Depending on the steric bulk of the organo groups R and R′ of imino boranes R−B≡N−R′, these stabilize themselves by undergoing transformation to the cyclodimeric diazadiboretidines, the cyclotrimeric borazines, or "Dewar-borazines", to the cyclotetrameric tetraza-2,4,6,8,1,3,5,7-tetraborocanes, or to polymeric imino boranes, as has been shown by *Paetzold*[9] in fundamental studies.

4.9.1. Dimerization of Amino Imino Boranes

The oligomerization of amino imino boranes **1** has been limited so far to a monotonous dimerization to diazadiboretidines **99** as shown in Equation (31);[14,17,20,21] imino boranes R−B≡N−R′ behave differently. The X-ray structure analysis of the two diazadiboretidines **99a**[38] and **99f**[19] shows that these possess a planar, slightly diamond-shaped B_2N_2 four-membered ring (cf. Ref. [9]). The BNC_2 planes of the planar-coordinated amino nitrogens are oriented almost perpendicular to the ring B_2N_2 plane (for the substituents of **1** and **99** see Table 1).

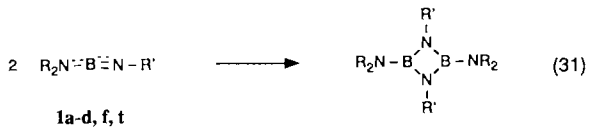

(31)

The rate of dimerization of the amino imino boranes is sterically controlled. While pure, liquid **1a** remains monomeric for only a few hours,[21] the likewise liquid **1m** remains monomeric even after several months.[19] While the initiation of the dimerization of **1h** requires about 100°C, it is suppressed for **1i**.[14] However, **1d** dimerizes within a few minutes.[20] Dimerization is detectable in liquid **1f** only after two days,[16] whereas it is spontaneous for **1c**.[17] This is convincing evidence that amino imino boranes are kinetically stabilized by bulky substituents.

Total energies, calculated for molecules with optimized geometries, show that the diazadiboretidine model molecules gain substantially in stability ($E_{stab.}$) as compared to the amino imino borane precursors (cf. Table 4).[14] Accordingly, the amino imino boranes possess a higher thermodynamic tendency to dimerize than the imino boranes R−B≡N−R′.

Table 4. Gain in stability, $E_{stab.} = E_{total,\,dimer} - 2E_{total,\,monomer}$ [kJ mol^{-1}], of some model amino imino boranes (type **1**) by dimerization to diazadiboretidines (type **99**).

H−B≡N−H −386	F−B≡N−H −499	H_2N−B≡N−H −495
Me−B≡N−H −300	H−B≡N−Me −245	H−B≡N−NH_2 −286

According to STO-3G calculations, the dimerization of imino boranes is a thermally allowed one-step process,[14,20] which is forbidden for the isoelectronic carbon counterparts.[70] A nonconcerted two-step process of the dimerization of imino boranes can be excluded on the basis of MNDO calculations.[14,20] The following activation energies E_A [kJ mol^{-1}] for the dimerization of amino imino boranes have been obtained from calculated potential plots: H−B≡N−H 96.3, Me−B≡N−Me 146.5, Me−B≡N−SiH_3 134, H_2N−B≡N−Me 121.[20]

The second-order rate for the dimerization of **1a**, as demanded by Equation (31), is observed experimentally. The rate depends slightly on the solvent. Thus, the dimerization rate for **1a** at 20°C is about twice as fast in toluene as in CCl_4.[71]

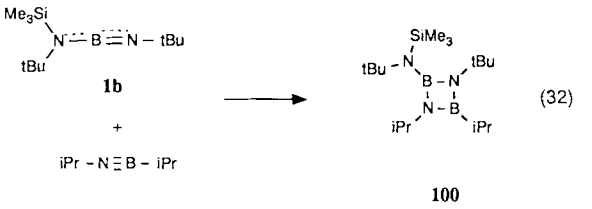

(32)

Codimerization of **1b** succeeds with the reactive imino borane *i*Pr−B≡N−*i*Pr; i.e., the cycloaddition of two different imino boranes is achieved according to Equation (32) to give the asymmetrically substituted diazadiboretidine **100**.[15]

4.9.2. [2+1] Cycloaddition Reactions

[2+1] cycloaddition reactions of amino imino boranes should make three-membered ring systems available. However, diphenylcarbene, generated from diphenyldiazomethane, did not react with **1a**. Since methylene, prepared from diazomethane, also did not react with **1a** to produce an azaboriridine, but instead yielded only polymethylene, the reason for the failure of the reaction with diphenylcarbene cannot be steric in nature.[36]

Dodecamethylcyclohexasilane yields dimethylsilanediyl photochemically,[72] which reacts, in turn, with **1a**. However, the separation of the various reaction products has not yet been possible.[36] On the other hand, dimethylgermanediyl, generated from 7-germanorbornadienes according to *Neumann* et al.,[73] does not react with **1a**.[36]

4.9.3. [2+2] Cycloaddition Reactions

With Olefins and Alkynes: It is well known that concerted [2+2] cycloaddition reactions of carbon systems are thermally forbidden but photochemically allowed.[70] This

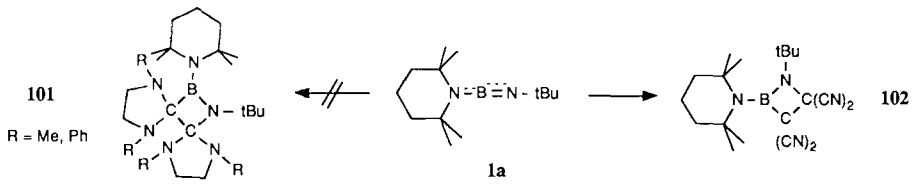

does not apply strictly for the isoelectronic BN bonding systems due to their lower symmetry. However, the polarity of the BN bond may favor multistep reactions.

Electron-rich 2,2'-biimidazolidinylidene derivatives do not react with **1a** at 70°C to produce **101**, in contrast to the electron-deficient tetracyanoethylene, which cycloadds within a few minutes to give the 1,2-azaboretidine **102**. Its four-membered ring is planar according to its X-ray structure,[36] in contrast to isoelectronic cyclobutenes. Not only the ring CC bond (159 pm) but also the ring BC bond (171 pm) of **102** is longer than standard single bond distances. The ring BN bond length (141 pm) indicates double-bond character.

Nonactivated alkynes such as acetylene and diphenylacetylene, but also methoxyacetylene, produce no [2+2] cycloadducts with **1a**. However, they accelerate its dimerization slightly.[36] Reaction with dihydrobenzene, generated from 1-bromo-2-fluorobenzene and magnesium,[74] leads to no defined product.[36] Also, hexafluorobutyne does not undergo cycloaddition with **1a**, in contrast to dimethyl acetylenedicarboxylate which prefers, however, a different reaction path (see Section 4.9.6).

With Carbonyl Compounds: Paetzold et al. (cf. Ref. [9]) observed that imino boranes R–B≡N–R′ react with aldehydes and ketones to produce oxazaboretidines, whereas ketones having an enolizable proton provide access to aminovinyloxy boranes RB(NHR′)OCR″=CR‴₂. This reaction mode [see Eq. (33)] holds also for the amino imino

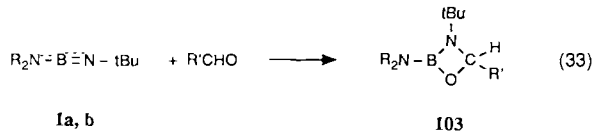

1a → **103**: R_2N = tmp, R′ = H
1b → **103**: R_2N = *t*Bu(Me₃Si)N,
R′ = Ph, MeCH=CH, CH_2=CMe

borane **1b**, which reacts with aldehydes to afford high yields of the heterocycles **103**.[15] Crotonaldehyde and 2-methylacrylaldehyde, therefore, do not react as 1,4-dipolar systems. Formaldehyde cleanly furnishes in its reaction with **1a** the distillable [2+2] cycloadduct.[36]

Benzophenone is unreactive towards **1a**, and acetone only reacts at 57°C to generate, via its enolic form, tmp–B(NH*t*Bu)OC(Me)=CH_2.[36] Phosgene reacts readily even at low temperature according to Equation (34). However, distillative workup produces tmpBCl_2, which most likely is formed via the product **104**.[36] Therefore, the chlorine transfer dominates the cycloaddition in this case, presumably because the RN–C(O)Cl group is well stabilized by resonance.

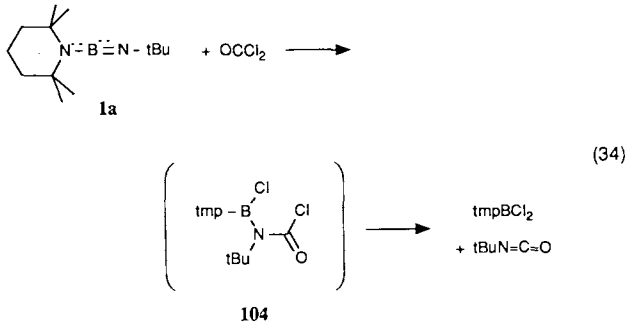

With Iminoalkenes: As shown in Section 4.2.2, amino boranes react rapidly with NH functional groups. In order to observe [2+2] cycloaddition with imino alkenes, which are well known from imino borane chemistry,[9] a reaction with HN=CR_2 compounds, as well as with imine–enamine tautomeric azomethines, is therefore prohibited. In analogy to benzophenone, MeN=CPh_2 and **1a** do not react to give a diazaborolidine.[36]

With Iminophosphanes: The [2+2] cycloaddition of *t*Bu–B≡N–*t*Bu with the amino imino phosphane $(Me_3Si)_2N$–P=N–$SiMe_3$ proceeds regioselectively to give the 1,3,2,4-diazaphosphaboretidine **105**.[75] Reaction of *t*Bu–N=P–*t*Bu with *t*Bu–B≡N–*t*Bu occurs, however, approximately in a molar ratio of 1.5 : 1. The heterocycle **106** is thereby formed as the oxidation product and the diazadiphosphaborolidine **107** as the reduction product.[76]

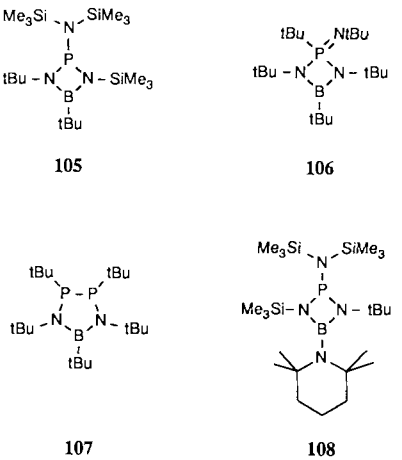

The cycloaddition of **1a** with $(Me_3Si)_2N$–P=N–$SiMe_3$ proceeds rapidly and regiospecifically yielding the heterocycle **108**, whose ^{11}B and ^{31}P atoms are very well shielded in comparison with those of 1,3,2,4-diazadiboretidines and 1,3,2,4-diazadiphosphetidines, indicating transannular interactions.[36]

With Allenes: The heterocumulenes CO_2, COS, CS_2, and CSe_2 cycloadd to **1a**, rapidly producing the four-mem-

bered rings **109**. It is interesting to note that COS yields exclusively the 1,3,2-thiazaborolidin-4-one (**109**, X = O, Y = S); i.e., the thermodynamically preferred C=O bond remains intact. On heating, the heterocycles **109** decompose with cycloreversion according to Equation (35), producing the diboretanes **110**.[77]

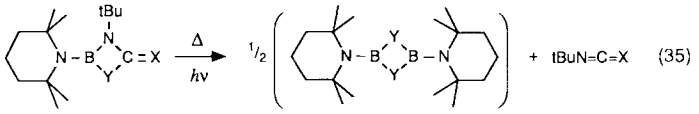

109 **110** (35)

[2+2] cycloadducts of **1a** with MeN=C=O, *t*BuN=C=O, and dicyclohexylcarbodiimide extend the range of new four-membered heterocycles of boron.[36] When phenyl isothiocyanate and **1a** are allowed to react, a 7:3 mixture of isomers consisting of **111** and **112** results.[36] In contrast, $Ph_3P{=}C{=}PPh_3$ proved to be unreactive.[36]

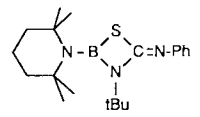

111

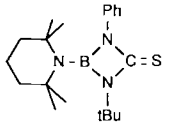

112

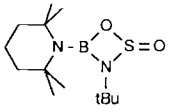

113

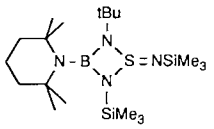

114

In addition, SO_2[41] and $S(NSiMe_3)_2$,[20] bent heteroallenes, react quickly with **1a** to give the two cycloadducts **113** and **114**. The former decomposes at about 200°C into $(tmpBO)_2$ and $(tmpBO)_3$.[41] A cycloaddition between **1a** and $S(NtBu)_2$ is prevented on steric grounds.[41]

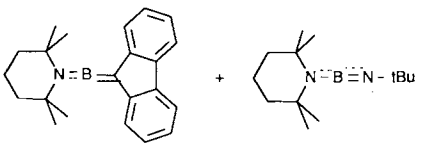

115 **1a**

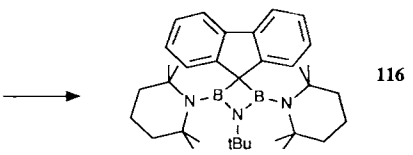

116

The amino alkylidene borane **115** counts also as a heteroallene. Its cycloaddition with **1a** makes the nonplanar 1,2,4-azadiboretidine **116** available, as also shown by X-ray crystallography. The nonplanarity of the ring indicates strong 1,3-transannular interactions.[78]

4.9.4. [2+3] Cycloaddition Reactions

In contrast to Me_3SiN_3, which azidosilylates **1a** and **1b**—explainable by nucleophilic attack of the imino nitrogen on the silicon atom—phenyl azide reacts as a 1,3 dipole with **1b**,**c**, producing the dihydrotetrazaboroles

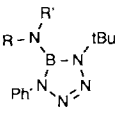

117

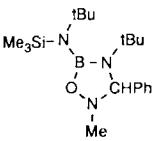

118

117.[15,17] *N*-Methylbenzylideneamine *N*-oxide analogously leads to the 1,2,4,5-oxadiazaborolidine **118**.[15]

4.9.5. [4+2] Cycloaddition Reactions

The imino borane $C_6F_5{-}B{\equiv}N{-}tBu$ reacts as a dienophile with cyclopentadiene to give a Diels–Alder adduct.[79] Compound **1b** should yield, in analogy, the compound **119**.[15] However, no such adduct has been obtained from **1a**; instead, a mixture of isomers **120/121** is formed, whereby the structural assignment required ^{11}B-decoupled ^{13}C NMR spectra.[36] That cyclopentadiene acts only as a protic species towards amino imino boranes has been established meanwhile also for the product obtained from this diene and **1b**,**c**.[17]

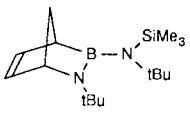

119

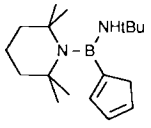

120

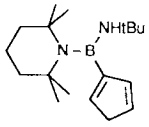

121

No [4+2] cycloaddition takes place between **1a** and 1,1-dimethyl-2,3,4,5-tetraphenylgermole or -stannole or between **1a** and 2,5-dimethylfuran.[36]

4.9.6. Reactions with Dimethyl Acetylenedicarboxylate

Alkynes R–C≡C–H are in most cases too weakly acidic to react with amino imino boranes with CH insertion. Also, their CC triple bond is not reactive towards these compounds. Methyl propiolate provides an exception: it protonates **1a** to give $tmpB(NHtBu){-}C{\equiv}C{-}C(O)OMe$. In contrast, dimethyl acetylenedicarboxylate reacts with **1a** in a 2:1 molar ratio. The NMR data of the product could be interpreted in terms of an azaborabenzene **122**.[63] However, an X-ray structure analysis definitely showed a bicyclic structure **123**.[36] Therefore, the amino imino borane attacks with its imino nitrogen atom at one of the alkyne carbon atoms. A second molecule of the ester adds in a more rapid second step to the 1,3-dipolar intermediate **124** to produce **123**.

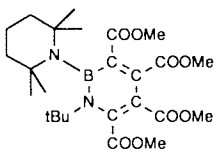

122

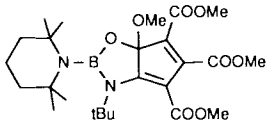

123

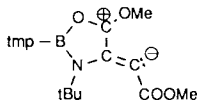

124

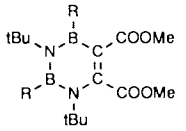

125

R = Me, Et

An analogous reaction is unknown for imino boranes R–B≡N–*t*Bu, but their dimers add dimethyl acetylenedicarboxylate in a molar ratio of 1 : 1 to give a diazadiborabenzene derivative **125** which is not planar.[80]

4.10. Reactions with Organotransition-Metal Compounds

The imino borane *t*Bu–B≡N–*t*Bu[81] and the amino imino borane **1a**[82] add to electron-deficient carbene complexes of titanium by [2+2] cycloaddition, giving the metallacycles **126**. In contrast to the hafnium complex, compounds **126** are not susceptible to cycloreversion, thereby opening up an elegant route to alkylidene boranes $R_2N-B=CR_2$.[83]

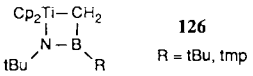

126

R = tBu, tmp

In contrast, the electron-rich Fischer carbene complex [$(CO)_5Cr=C(OMe)Me$] reacts with **1a** approximately in a molar ratio of 4 : 1. The products **127**–**129** are formed in this process, and a vinylidene complex [$(CO)_5Cr=C=CH_2$] is discussed as an intermediate. Some of the postulated reaction steps have been verified by deuterium labeling.[82]

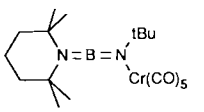

127

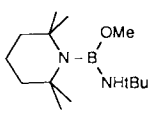

128

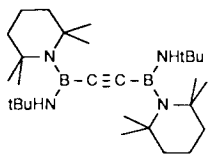

129

How enormous a variability can be unraveled by studying the chemistry of amino imino boranes with organometallic compounds is convincingly demonstrated by the reaction of **1b** with dehydrobenzene complexes: azaborametallaindanes **130** result with **1b**. The titanium compound shows an almost planar five-membered ring.[84] Alkynes interact in a similar fashion with the dehydrobenzene complex.[85]

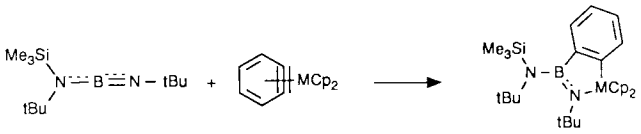

1b

130

M = Ti, Zr

4.11. Reactions with Strong Bases

The steric and electronic shielding of the boron atom in amino imino boranes prevents proton-inactive neutral bases, such as ether, tetrahydrofuran, or pyridine, from adding to **1a**. However, **1b** reacts readily with strong anionic bases such as MeLi, BuLi, and *t*BuLi to yield *N*-lithio bis(amino) boranes *t*Bu(Me_3Si)NBR(NLi*t*Bu), whose Li atom can be complexed by tetramethylethylenediamine without opening the original NLi bond.[87] Analogous reactions have been observed between **1a** and Grignard compounds. We are dealing again, in principle, with insertion reactions (i.e., an organolithiation of the imino borane bond). It remains at present an open question whether the carbanion attacks the boron atom or the lithium atom the imino nitrogen.

However, the reaction of RLi with an amino imino borane does not always follow the path just outlined, because *t*BuLi cleaves the tmp group of **1a**. The diazadiboretidine (*t*Bu–N=B–*t*Bu)$_2$ results,[14] an indication that either the reaction conditions or the steric crowding will influence the course of the reaction.

4.12. Reactions at the Imino Substituent

N-functionalized imino boranes open up new reaction channels similar to *B*-functionalization. The chemistry of *N*-functional amino imino boranes has not yet been well investigated except for the di-*tert*-butylphosphane derivative **1p**. As a phosphane derivative, **1p** readily adds sulfur or selenium at its P atom to give the compounds **131**. The oxidation of the phosphorus atom influences the shielding at the boron nucleus only slightly. $\delta(^{31}P)$ is now found in the region typical of the $R_2NP(S)tBu$ group. The position of the $\nu(B\equiv N)$ band reveals that the oxidation brings about a weakening of the BN triple bond, because there is a shift by 55 cm^{-1} to longer wavelengths for X = S and by 95 cm^{-1} for X = Se.[20]

Methyl iodide transforms **1p** ($\nu(B\equiv N) = 1935$ cm^{-1}) into the phosphonium salt **132**, whose $\nu(B\equiv N)$ band lies at 1870 cm^{-1}, a 65-cm^{-1} shift to longer wavelength as compared with the starting material.

Of the various reaction possibilities which are available for a metal carbonyl fragment—side-on coordination of the BN triple bond, addition to the imino nitrogen, dimerization and complexation, and *P*-coordination—only the latter occurs for $Cr(CO)_5$, $W(CO)_5$, and $MeCpMn(CO)_2$ (cf. **133** and **134**).[20] Thus, the P atom dominates as the

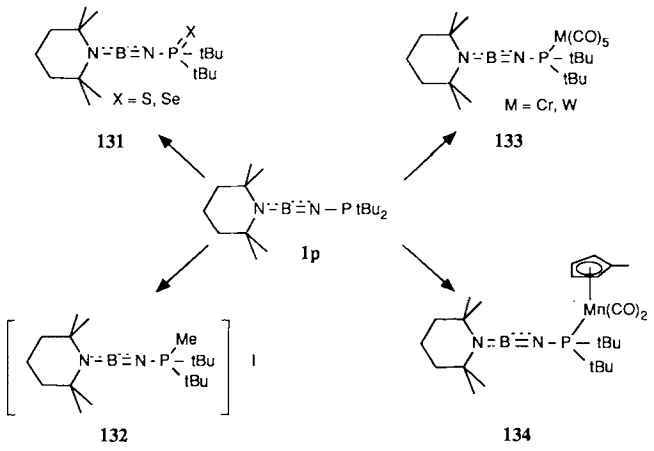

coordination center over the imino nitrogen, thereby demonstrating the validity of the HSAB concept. Addition of the metal carbonyl fragment causes $\nu(B{\equiv}N)$ to shift by 5–25 cm^{-1} to longer wavelengths and consequently changes the amino imino borane bonding system much less than the methylation to the salt **132**.

According to MNDO/CNDO calculation (see Table 5) on the model compound $H_2N{-}B{\equiv}N{-}PMe_2$, neither the addition of sulfur to phosphorus nor the phosphonium salt formation influences the BN bond order of the $H_2N{-}B$ group significantly, but the salt formation weakens the BN triple bond considerably and strengthens the PN bond. The net positive charge at the boron is increased. Consequently, **133** and **134** should be attacked electrophilically at the boron atom.

Table 5. Calculated bond enthalpies ΔH [kJ mol^{-1}], dipole moments μ [D], total bond orders P, net charges q at the B atom and imino N atom, and HOMO-LUMO energy differences ΔE [eV] for three phosphorus-containing amino imino boranes $H_2N{-}B{\equiv}N{-}X$.

X	ΔH	μ	P		q		ΔE
PMe_2	−239.9	1.68 [a]	1.18	B–NH_2	0.006	B	10.65
		3.22 [b]	2.25	B≡N	−0.46	N	
			1.28	P–N			
$PMe_3^{\oplus}$	+492.8	—	1.31	B–NH_2	0.22	B	8.70
		17.1 [b]	1.99	B≡N	−0.58	N	
			1.49	P–N			
$P(S)Me_2$	−107.2	4.86 [a]	1.19	B–NH_2	0.08	B	7.72
		2.29 [b]	2.19	B≡N	−0.50	N	
			1.27	P–N			

[a] MNDO. [b] CNDO.

5. Concluding Remarks

The developing chemistry of imino boranes in general[9] and of the amino imino boranes in particular has not only substantiated former speculations that they may appear as intermediates in the synthesis of boron heterocycles, especially borazines.[87] As unsaturated systems, even the kinetically stabilized members exhibit high reactivity and a versatile chemisty which allows access to new classes of compounds. In addition, it emerges that they will be suitable for the boration of biochemically interesting molecules, which, in turn, may be useful for the development of new reagents and compounds for neutron therapy.[88]

Amino imino boranes **1** enhance the chemical versatility of imino boranes considerably due to allene-type intermediates and new coordination possibilities. The amino group may adopt the function of a protecting group if it is possible to remove it from the reaction product, thus generating new reactive centers. This function will not be fulfilled by the 2,2,6,6-tetramethylpiperidino group; the $Me_3Si(t\text{Bu})N$ group is a much better candidate in this respect. The Me_2N group would possibly be ideal, but it will most likely not augment the kinetic stabilization of amino imino boranes.

From the point of view of a preparative chemist, the amino- and the imino-functional amino imino boranes should become particularly attractive in the near future, especially with regard to the synthesis of small rings and for chemical vapor deposition (CVD) processes.

The present report contains many results so far available only in the form of doctoral theses. It is hoped that these will become more readily accessible in the near future. The following co-workers have contributed to the development of the field in our laboratories: G. Geisberger, P. Kölle, D. Männig, Ch. K. Narula, K. Neukirchinger, E. Salzbrenner, M. Schwartz, B. Stoeber, E. Striedl, W. Rattay, and S. Weber. I would like to express my sincere thanks for their engagement, interest, and careful work and for many inspiring discussions. Also, I wish to thank my colleague, Prof. Dr. P. Paetzold, Technische Universität Aachen, for helpful cooperation. Without additional financial support we would not have been able to investigate the chemistry of amino imino boranes so comprehensively: we therefore thank the Deutsche Forschungsgemeinschaft, the Fonds der Chemischen Industrie, BASF Aktiengesellschaft and, last but not least, Chemetall GmbH for supporting our research.

Received: August 29, 1988 [A 699 IE]
German version: *Angew. Chem. 100* (1988) 1664

[1] V. I. Matkovich (Ed.): *Boron and Refractory Borides*, Springer, Berlin 1977.
[2] E. L. Muetterties: *The Chemistry of Boron and its Compounds*, Wiley-Interscience, New York 1967; R. N. Grimes: *Carboranes*, Academic Press, New York 1970; *Metal Interactions with Boron Clusters*, Plenum, New York 1982; S. Heřmánek (Ed.): *Boron Chemistry*, World Scientific, Singapore 1987.
[3] W. N. Lipscomb: *Boron Hydrides*, Benjamin, New York 1963; K. Wade: *Electron Deficient Compounds*, Nelson & Sons, London 1971.
[4] K. Kawaguchi, Y. Endo, E. Hirota, *J. Mol. Spectrosc. 93* (1982) 38; D. C. Frost, C. Kirby, W. M. Lau, A. McDowell, W. P. C. Westwood, *J. Mol. Struct. 100* (1983) 87.
[5] R. W. Kirk, P. L. Timms, *Chem. Commun. 1967*, 18; E. F. Pearson, R. V. McCormick, *J. Chem. Phys. 58* (1973) 1619; E. F. Pearson, C. L. Norris, W. H. Flygare, *ibid. 60* (1974) 1761; H. W. Kroto, R. J. Suffolk, N. P. C. Westwood, *Chem. Phys. Lett. 22* (1973) 495; C. Kirby, H. W. Kroto, M. J. Taylor, *J. Chem. Soc. Chem. Commun. 1978*, 10; C. Kirby, H. W. Kroto, *J. Mol. Spectrosc. 83* (1980) 1.
[6] C. Kirby, H. W. Kroto, *J. Mol. Spectrosc. 83* (1980) 130; T. A. Cooper, M. A. King, C. Kirby, H. W. Kroto, R. J. Suffolk, *J. Chem. Soc. Chem. Commun. 1981*, 354.
[7] J. Goubeau, *Angew. Chem. 69* (1957) 77.
[8] M. Groteklaes, P. Paetzold, *Chem. Ber. 121* (1988) 809.
[9] P. Paetzold, *Adv. Inorg. Chem. 31* (1987) 123.
[10] P. Kölle, H. Nöth, *Chem. Rev. 85* (1985) 399.
[11] J. Henkelmann, G. Maier, H. P. Reisenauer, *Angew. Chem. 97* (1985) 1061; *Angew. Chem. Int. Ed. Engl. 24* (1985) 1065; B. Glaser, E. Hanecker, H. Nöth, H. Wagner, *Chem. Ber. 120* (1987) 659; B. Glaser, H. Nöth, *Angew. Chem. 97* (1985) 424; *Angew. Chem. Int. Ed. Engl. 24* (1985) 416; A. Berndt, H. Klusik, *ibid. 95* (1983) 895 and *22* (1983) 877; R. Boese, P. Paetzold, A. Tanner, *Chem. Ber. 120* (1987) 1069.

[12] G. Viehe: *The Chemistry of Acetylenes*, Marcel Dekker, New York 1969.
[13] Investigations carried out with *P. Paetzold*.
[14] S. Weber, *Dissertation*, Universität München 1984.
[15] P. Paetzold, E. Schröder, G. Schmid, R. Boese, *Chem. Ber. 118* (1985) 3205.
[16] P. Kölle, *Diplomarbeit*, Universität München 1984.
[17] K. H. von Bonn, T. von Bennigsen-Mackiewicz, J. Kiesgen, C. von Plotho, P. Paetzold, *Z. Naturforsch. B 43* (1988) 61.
[18] P. Kölle, H. Nöth, *Chem. Ber.*, in press.
[19] B. Stöber, unpublished results, 1987–1988.
[20] P. Kölle, *Dissertation*, Universität München 1987.
[21] H. Nöth, S. Weber, *Z. Naturforsch. B 38* (1983) 1460.
[22] E. R. Lory, R. F. Porter, *J. Am. Chem. Soc. 95* (1973) 1766.
[23] P. Klaeboe, D. Bougeard, B. Schrader, P. Paetzold, *Spectrochim. Acta A 41* (1985) 53.
[24] G. R. Eaton, W. N. Lipscomb: *NMR-Studies of Boron Hydrides and Related Compounds*, Benjamin, New York 1969.
[25] a) J. Kroner, D. Nölle, H. Nöth, *Z. Naturforsch. B 28* (1973) 413; b) F. A. Davies, M. J. S. Dewar, R. Jones, *J. Am. Chem. Soc. 50* (1968) 706; c) H. Nöth, B. Wrackmeyer, *Chem. Ber. 107* (1974) 3089.
[26] D. R. Armstrong, D. T. Clark, *Theor. Chim. Acta 24* (1972) 30.
[27] C. Baird, R. K. Datta, *Inorg. Chem. 11* (1972) 17.
[28] P. Paetzold, C. von Plotho, G. Schmid, R. Boese, B. Schrader, D. Bougeard, K. Pfeiffer, R. Gleiter, W. Schäfer, *Chem. Ber. 117* (1984) 1989.
[29] W. J. Hehre, W. A. Lathan, M. D. Newton, R. Ditchfield, J. A. Pople, *Program 236, Quantum Chemistry Program Exchange*, Indiana University, Bloomington, IN; W. J. Hehre, R. F. Stewart, J. A. Pople, *J. Chem. Phys. 51* (1969) 2657; P. C. Harikaran, J. A. Pople, *Theor. Chim. Acta 28* (1973) 213.
[30] M. Haase, U. Klingebiel, *Chem. Ber. 119* (1986) 1117.
[31] This problem has been discussed recently also by *P. Paetzold* (see [9]). He recommends the following bond lengths: $\geqslant$B–N$\leqslant$ 158 pm, $>$B=N$<$ 141 pm, –B≡N– 126 pm.
[32] The notion "addition" is used for the formation of Lewis acid-base adducts; i.e., the boron atom remains dicoordinated. In insertion reactions both the boron and the nitrogen atoms of the imino borane become tricoordinated.
[33] H. Nöth, U. Wietelmann, *Chem. Ber. 120* (1987) 859.
[34] H. Nöth, S. Weber, *Chem. Ber. 118* (1985) 2554.
[35] A. Brandl, H. Nöth, *Chem. Ber. 121* (1988) 1371.
[36] U. Wietelmann, *Dissertation*, Universität München 1986.
[37] H. Nöth, S. Weber, *Chem. Ber. 118* (1985) 2144.
[38] H. Nöth, M. Schwartz, S. Weber, *Chem. Ber. 118* (1985) 4716.
[39] A. Brandl, H. Nöth, *Chem. Ber. 118* (1985) 3759.
[40] I. Kronawitter, H. Nöth, *Chem. Ber. 105* (1972) 2423.
[41] E. Striedl, *Diplomarbeit*, Universität München 1988.
[42] A. Brandl, *Diplomarbeit*, Universität München 1984.
[43] K. Niedenzu, R. B. Read, S. S. Seelig, *Synth. React. Inorg. Met. Org. Chem. 10* (1980) 373.
[44] A. Brandl, *Dissertation*, Universität München 1987.
[45] K. Neukirchinger, *Dissertation*, Universität München 1986.
[46] A. Meller, W. Maringgele, *Chem. Ber. 111* (1978) 538.
[47] G. Geisberger, *Diplomarbeit*, Universität München 1987.
[48] H. C. Brown: *Organic Synthesis via Boranes*, Wiley, New York 1975.
[49] D. Männig, H. Nöth, H. Prigge, A.-M. Rotsch, J. W. Wilson, *J. Organomet. Chem. 310* (1986) 1.
[50] M. Schwartz, *Dissertation*, Universität München 1987.
[51] D. Männig, H. Nöth, M. Schwartz, S. Weber, U. Wietelmann, *Angew. Chem. 97* (1985) 979; *Angew. Chem. Int. Ed. Engl. 24* (1985) 998.
[52] H. Nöth, S. Weber, *Angew. Chem. 96* (1984) 998; *Angew. Chem. Int. Ed. Engl. 23* (1984) 984.
[53] J. J. Eisch, L. J. Gonsior, *J. Organomet. Chem. 8* (1967) 53.
[54] P. Paetzold, T. von Bennigsen-Mackiewicz, *Chem. Ber. 114* (1981) 298.
[55] A decision whether kinetic or thermodynamic product control prevails is difficult to make because, although BX bonds are opened in boration reactions, a new BX bond is formed; however, the strength of the BN bond decreases in the order monoamino, diamino, triamino boranes [56]. The observed effect should be larger in amino boranes with very bulky substituents than in the thermochemically investigated series of dimethylamino chloro boranes.
[56] H. A. Skinner, N. B. Smith, *J. Chem. Soc. 1954*, 2324.
[57] R. Köster, H. Bellut, S. Hattari, L. Weber, *Justus Liebigs Ann. Chem. 720* (1968) 32.
[58] W. Rattay, *Dissertation*, Universität München 1987.
[59] F. Dirschl, H. Nöth, W. Wagner, *J. Chem. Soc. Chem. Commun. 1984*, 1533.
[60] F. Dirschl, E. Hanecker, H. Nöth, W. Rattay, W. Wagner, *Z. Naturforsch. B 41* (1986) 32.
[61] F. O. Stark, J. R. Falender, A. Wright in G. Wilkinson, F. G. A. Stone, E. W. Abel (Eds.): *Comprehensive Organometallic Chemistry, Vol. 2*, Pergamon, Oxford 1982, p. 330.
[62] E. Bulak, G. E. Herberich, I. Manners, H. Mayer, P. Paetzold, *Angew. Chem. 100* (1988) 964; *Angew. Chem. Int. Ed. Engl. 27* (1988) 958.
[63] H. Nöth, *Nova Acta Leopold. N. F. 264* (1985) 277.
[64] B. Stöber, *Diplomarbeit*, Universität München 1986.
[65] A. Brandl, H. Nöth, *Chem. Ber. 121* (1988) 1321.
[66] V. S. Petrosyan, N. S. Yashina, V. I. Bakhmutor, A. B. Permin, O. A. Reutov, *J. Organomet. Chem. 72* (1974) 71; A. G. Davies, P. G. Harrison, J. D. Kennedy, T. N. Mitchell, R. J. Puddephat, W. McFarlane, *J. Chem. Soc. C 1969*, 1136.
[67] K. H. von Bonn, P. Schreyer, P. Paetzold, R. Boese, *Chem. Ber. 121* (1988) 1045.
[68] P. Kölle, H. Nöth, *Phosphorus Sulfur 30* (1987) 475.
[69] P. Paetzold, C. von Plotho, *Chem. Ber. 115* (1982) 2819; H.-U. Meier, P. Paetzold, E. Schröder, *ibid. 117* (1984) 1954.
[70] R. B. Woodward, R. Hoffmann: *Die Erhaltung der Orbitalsymmetrie*, Verlag Chemie, Weinheim 1970; *The Conservation of Orbital Symmetry*, Academic Press, New York 1970.
[71] E. Salzbrenner, *Diplomarbeit*, Universität München 1987.
[72] P. F. Gaspar, *React. Intermed. 1* (1978) 229; *2* (1981) 335.
[73] W. P. Neumann, M. Schriever, *Tetrahedron Lett. 21* (1980) 3273.
[74] G. Wittig, L. Pohmer, *Chem. Ber. 89* (1952) 1334.
[75] P. Paetzold, C. von Plotho, E. Niecke, R. Rüger, *Chem. Ber. 117* (1984) 1089.
[76] D. Gudat, E. Niecke, M. Nieger, P. Paetzold, *Chem. Ber. 121* (1988) 565.
[77] D. Männig, C. K. Narula, H. Nöth, U. Wietelmann, *Chem. Ber. 118* (1985) 3748.
[78] B. Glaser, E. P. Mayer, H. Nöth, W. Rattay, U. Wietelmann, *Z. Naturforsch. B 43* (1988) 449.
[79] P. Paetzold, A. Richter, T. Thijssen, S. Würtenberg, *Chem. Ber. 112* (1979) 3811.
[80] P. Schreyer, P. Paetzold, R. Boese, *Chem. Ber. 121* (1988) 195.
[81] P. Paetzold, K. Delpy, R. P. Hughes, W. A. Herrmann, *Chem. Ber. 118* (1985) 1724.
[82] H. Nöth, U. Wietelmann, *Chem. Ber. 120* (1987) 863.
[83] P. Paetzold, personal communication.
[84] B. Heßner, I. Manners, P. Paetzold, *Chem. Ber. 120* (1987) 1065.
[85] H. Massai, K. Sonogashina, N. Hagihara, *Bull. Chem. Soc. Jpn. 41* (1968) 750; J. Mattia, M. B. Humphrey, R. D. Rogers, J. L. Atwood, M. D. Rausch, *Inorg. Chem. 17* (1978) 3257.
[86] P. Paetzold, C. Pelzer, R. Boese, *Chem. Ber. 121* (1988) 51.
[87] E. Wiberg, *Naturwissenschaften 35* (1948) 182, 212.
[88] H. Soloway in S. Heřmánek (Ed.): *Boron Chemistry*, World Scientific, Singapore 1987.

Structure and Reactivity of Lithium Enolates. From Pinacolone to Selective *C*-Alkylations of Peptides. Difficulties and Opportunities Afforded by Complex Structures

By Dieter Seebach*

The chemistry of lithium enolates is used to demonstrate that complex structures held together by noncovalent bonds ("supramolecules") may dramatically influence the result of seemingly simple standard reactions of organic synthesis. Detailed structural data have been obtained by crystallographic investigations of numerous Li enolates and analogous derivatives. The most remarkable features of these structures are aggregation to give dimers, tetramers, and higher oligomers, complexation of the metal centers by solvent molecules and chelating ligands, and hydrogen-bond formation of weak acids such as secondary amines with the anionoid part of the enolates. The presence in nonpolar solvents of the same supramolecules has been established by NMR-spectroscopic, by osmometric, and by calorimetric measurements. The structures and the order of magnitude of the interactions have also been reproduced by ab-initio calculations. Most importantly, supramolecules may be product-forming species in synthetic reactions of Li enolates. A knowledge of the complex structures of Li enolates also improves our understanding of their reactivity. Thus, simple procedures have been developed to avoid complications caused by secondary amines, formed concomitantly with Li enolates by the common methods. Mixtures of achiral Li enolates and chiral Li amides can give rise to enantioselective reactions. Solubilization by LiX is observed, especially of multiply lithiated compounds. This effect is exploited for alkylations of N-methylglycine (sarcosine) CH_2 groups in open-chain oligopeptides. Thus, the cyclic undecapeptide cyclosporine, a potent immunosuppressant, is converted into a THF-soluble hexalithio derivative (without epimerization of stereogenic centers) and alkylated by a variety of electrophiles in the presence of either excess lithiumdiisopropyl amide or of up to 30 equivalents of lithium chloride. Depending on the nature of the LiX additive, a new stereogenic center of (*R*) or (*S*) configuration is created in the peptide chain by this process. A structure-activity correlation in the series of cyclosporine derivatives thus available is discussed.

Nowadays, the molecular program of
chemistry has arrived at its successful termination.
H. Primas, ETH Zürich (1982)

1. Introduction—from α-Carbonyl Carbanions to Metal Enolates

Carbon-carbon bond formation in α-carbonyl positions is one of the most important processes for elaboration of carbon skeletons ("backbone of organic synthesis"). From the very beginning,[1] the variety of reactions of this type carried out under alkaline conditions was described as involving enolates which were drawn with the negative charge on carbon, pragmatically so, because that is where they react (Scheme 1). This notation continued to be used, especially in teaching, even when these reactions were no longer carried out in aqueous or other protic media, where solvent-separated "free" ions occur, and even though one realized that the negative charge is located on the more electronegative oxygen atom. The decisive role of the metal was appreciated when silyl enol ethers ("silyl enolates") were discovered for synthetic purposes[2]—they can be activated[3,4] by transmetalation or by treatment with fluoride ion, and they combine with electrophiles in reactions mediated by Lewis acids—and when the correlation between the configuration of the Li, B, Mg, and Sn[11] enolate double bond and the steric course of aldol additions[5-7] and other reactions[8] was disclosed.[9,10] Most of these reactions are

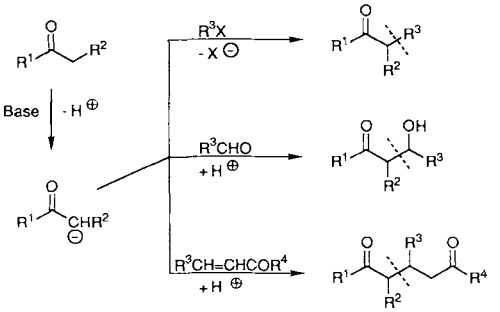

Scheme 1. Three classical reactions of carbonyl compounds: α-alkylation, aldol addition, and Michael addition.

[*] Prof. Dr. D. Seebach
Laboratorium für Organische Chemie der
Eidgenössischen Technischen Hochschule
ETH-Zentrum, Universitätstrasse 16, CH-8092 Zürich (Switzerland)

performed in nonpolar solvents (hydrocarbons, chlorohydrocarbons, open-chain or cyclic ethers, amines),[11] preferably at low temperatures, i.e., under conditions disfavoring the formation of ions, the separation of charges.[12-14]

While the important role of the metal in aldol additions quickly became part of synthetic planning, another property of the polar alkali and alkaline-earth enolates remained the "esoteric science" of only a few specialists: *the aggregation to higher-order structures.* It was known that potassium *tert*-butoxide is tetrameric in the solid state and in the gas phase[15] and that alkali enolates, even of β-diketones, form dimeric aggregates in the crystalline state.[16-18] It was concluded from ebullioscopic measurements[19] and from NMR spectra[20,21] that Li and Na enolates and phenolates are dimeric or tetrameric[22] in nonpolar solvents.[11] It is especially in the footnotes of early synthetic papers where one finds speculative suggestions that such enolate aggregates may be influential in product formation. In contrast, it has been well known for almost 30 years that aggregates of organolithium compounds with carbon–lithium bonds *may be* the product-forming species.[23,24] References are found in a classical monograph on the structure and reactivity of alkali and alkaline-earth metal derivatives[25] and in more recent books[26-36] and review articles (general,[37-41] NMR spectroscopy,[42-46] crystal structure analysis[47-53]).

In this article we describe results of the past decade which not only increased our knowledge of Li enolates[53] but also enlarged the scope of these most important reagents and their nitrogen analogues, which are widely applied in research laboratories as well as in industrial development and production of drugs, pesticides, and fine chemicals. The choice of examples to be discussed is necessarily influenced by the personal experiences of the author and his collaborators: by making structural investigations on synthetically relevant reagents we try to reduce frustration originating from the fact that part of our group keeps discovering highly selective transformations which we do not understand at all.[54-57] Thus, the route of the sorcerer's apprentice is described, as indicated by the sequence of formulae in Scheme 2.

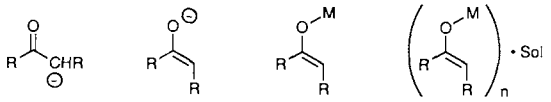

Scheme 2. From the deprotonated carbonyl derivative, via the metal enolate (M = metal), to aggregates, solvated and complexed by additives ("supramolecules" [58]). Sol = solvent molecules (ligands) in the coordination sphere of the metal.

2. The Complex World of Li Enolates—in Crystals and in Solution

Today's standard method of doing enolate reactions involves deprotonation of carbonyl compounds by lithium amide bases, for instance, lithium diisopropylamide (LDA),[59] tetramethylpiperidide (LTMP),[60] or hexamethyldisilazanide (LHMDS)[61] in THF, possibly in the presence of a cosolvent[8,62-65] or of a complexing agent.[26,52,66] The enolate solution thus obtained is combined with an electrophile. For CC bond formation this is usually an alkyl halide (Scheme 3) or a carbonyl compound (aldehyde/ketone,[67] Scheme 4). During these procedures, mixtures of the species shown inside the boxes of Schemes 3 and 4 are present. Since the first crystal structure analyses of ketone Li enolate aggregates[68] in 1981, numerous aggregates and complexes between these species have been isolated as single crystals suitable for X-ray analysis and/or have been

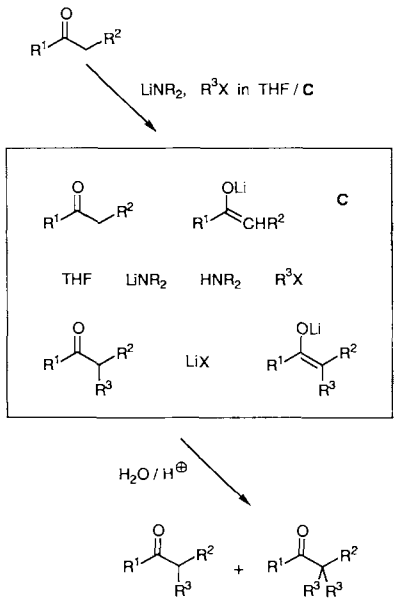

Scheme 3. Components which may coexist in a reaction mixture under the normal alkylation conditions of carbonyl compounds. **C** should be taken to represent an additive [cosolvent, complexing agent, e.g., hexamethylphosphoric triamide (HMPT) [62], "*N,N'*-dimethylpropyleneurea" (1,3-dimethyltetrahydropyrimidin-2(1*H*)-one, DMPU) [63], *N,N,N',N'*-tetramethylethylenediamine (TMEDA) [26], *N,N,N'*-trimethylethylenediamine (TriMEDA) [66], pentamethyldiethylenetriamine (PMDET) [26], dimethoxyethane (DME)].

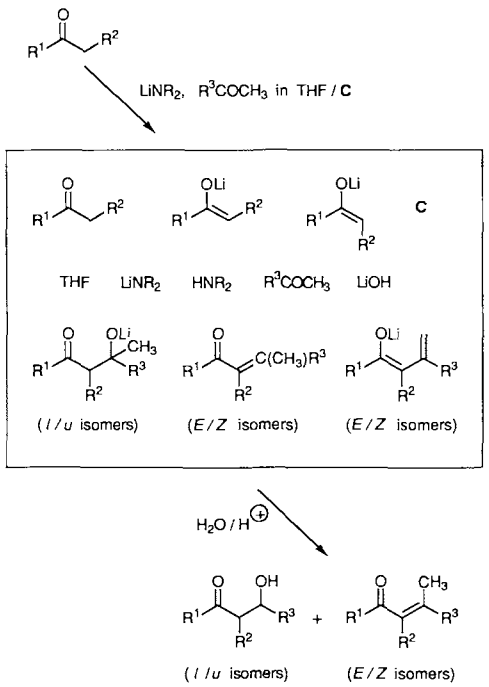

Scheme 4. Components that may occur in an aldol reaction performed with an enolate generated by R_2NLi. **C** is an additive (see caption to Scheme 3).

detected in solution. Thermochemical data were collected and force-field calculations, as well as quantum-mechanical "investigations", were performed. This will form the subject of the following sections, before we turn to the question of whether these complex structures are involved in product-forming steps.[69]

2.1. Li enolates and "Ingredients" in the Crystalline State

... la virtùe della geometria esser il più potente strumento d'ogni altro per acuir l'ingegnio e disporlo al perfettamente discorrere e specolare.[*]
Galileo Galilei

All crystalline Li enolates for which an X-ray structure analysis has been successfully performed so far are dimeric, tetrameric, or hexameric aggregates, the degree of aggregation depending less upon the particular enolate structure than upon solvent and added complexing or chelating agents (Figs. 1–12). Dimers tend to be favored in the presence of ethylenediamines and tetramers with ethers such as THF; a hexamer was crystallized from a non-donor hydrocarbon solvent. Lithium enolates of pinacolone (3,3-dimethyl-2-butanone, Figs. 1–3) and its derivatives (Figs. 7, 8, 10) prevail among the structures solved, for obvious reasons (high stability, only one enolate possible).

Lithium enolates of esters are unstable even in the crystalline state, due to their decomposition to ketenes and alkoxides.[72,73] Special techniques are required for the generation and isolation of suitable single crystals at low temperatures[51,67c,87] (Figs. 4 and 13). Amide enolates are much more stable (Figs. 5 and 6, compare the leaving groups $LiNR_2$ and LiOR). Again, dimeric and tetrameric aggregates are present in the crystals of these Li enolates containing additional heteroatoms. Other components of the mixtures present during generation and during reactions of Li enolates with electrophiles have been crystallized and successfully subjected to X-ray crystal structure analysis in recent years. Oligomeric aggregates of Li amides (Fig. 9, dimer), of an aldolate (Fig. 7, tetramer), and of a dienolate (Fig. 8, dimer) were found, the Li atoms of which are solvated by the oxygens of ethers (Figs. 2, 6, 9) or carbonyl compounds (Fig. 7, 8, 11), by the oxygens of HMPT (Fig. 12), or by the nitrogens of secondary or tertiary amines (Figs. 3–5). The formation of aggregates, $[(LiX)_n]$, is not limited to identical components; mixed aggregates $[(LiX)_n(LiY)_m]$ may also be formed from different components, for instance, the complex skeleton assembled from LDA and a siloxy-substituted Li enolate (Fig. 10).

Since lithium is *usually* tetracoordinated, it is possible—with due care—to deduce the degree of aggregation of Li enolates, alkoxides, phenolates,[90] and their nitrogen analogues from the stoichiometric composition of isolated samples. In order to achieve tetracoordination, one, two, or three "external" ligand atoms are present per lithium in a tetramer, dimer, or monomer, respectively. The ratios given in Table 1 confirm that aggregation of LiX in the crystalline state is a general phenomenon, also by this criterion. Furthermore, inspection of Table 1 reveals that lithiated nitriles (Li ketene imines) and iminoesters (Li enamides) are also aggregated, which was confirmed by crystal structure analysis:[98] see Table 2 and Figures 14 and 15, showing a lithio "bis-lactim ether" (reagent for enantioselective amino acid synthesis[99,100]) and the HMPT-solvated lithio malononitrile, respectively.

The structures of sodium, magnesium, aluminum, and zinc enolates (Figs. 16–19) exemplify the fact that aggregation is by no means a peculiarity of Li derivatives, but is a general phenomenon in polar metal enolates.[115]

Many a crystallographer and inorganic chemist does not quite share the excitement of us organic chemists about the structures described here; these colleagues live with the fact that aggregates and clusters are "ubiquitous all over the periodic table".[115] For synthetic organic chemists[116]

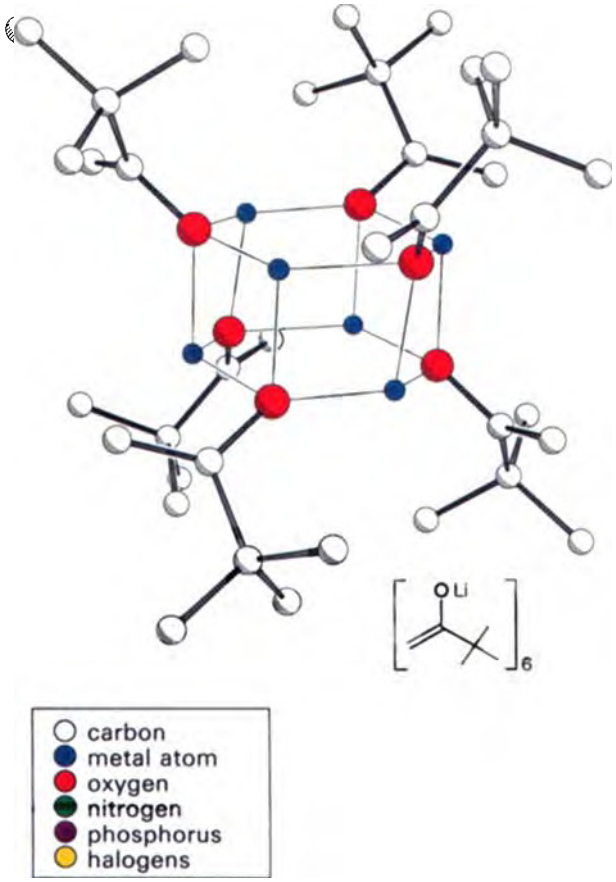

Fig. 1. Hexameric lithium enolate derived from pinacolone (enolate generated with LDA in heptane) [70, 71]. The crystal does not contain any solvent. The Li atoms are only threefold coordinated. Three square units of dimers are assembled in a hexagonal prism. A threefold axis runs perpendicularly to the hexagonal basis plane. The coordinates are stored in the *Cambridge Structural Database (CSD)* under the code CUYVOH. Here, and in all other illustrated structures (Figs. 1–12, 14–20, 23, 25, as well as the structures in [115]), the atoms are color-coded according to the key shown above. Other, non-carbon atoms are signified by their chemical symbol. The first coordination sphere of the metals is represented throughout by thin connection lines—for clarity, the neutral ligands or solvent molecules are not drawn to the same scale—while the anionic ligands are emphasized by bolder connection lines and larger spheres for the atoms.

[*] ... whoever has a grasp of geometry is capable of understanding this world.

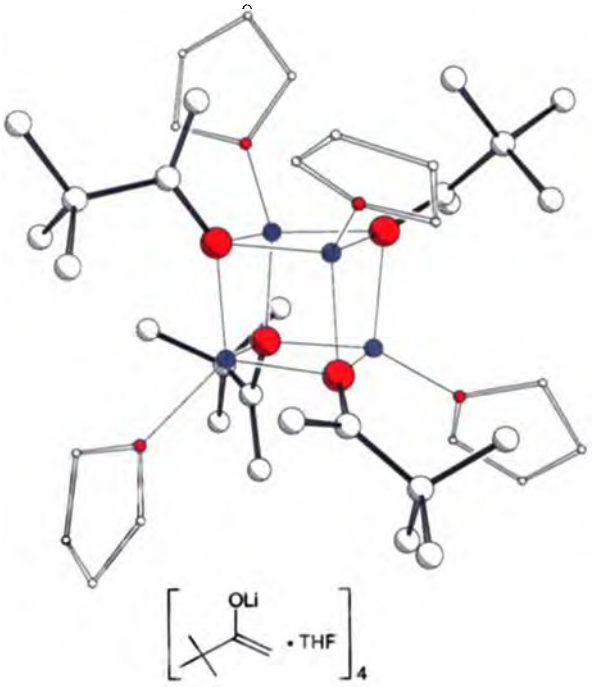

Fig. 2. Tetrameric Li enolate of pinacolone, crystallized from tetrahydrofuran. An almost perfect cube of four Li and four O atoms is surrounded by a "shell" of organic units—the enolate carbon skeleton and the THF molecules. The Li atoms are each surrounded by three enolate oxygens and one THF oxygen, so that a distorted tetrahedral coordination sphere results [68] (*CSD*: BEDYOY). The structure of the analogously arranged cyclopentanone-derived Li enolate is described in the same publication [68]; the corresponding coordinates are deposited under the *CSD* code BEDYUE.

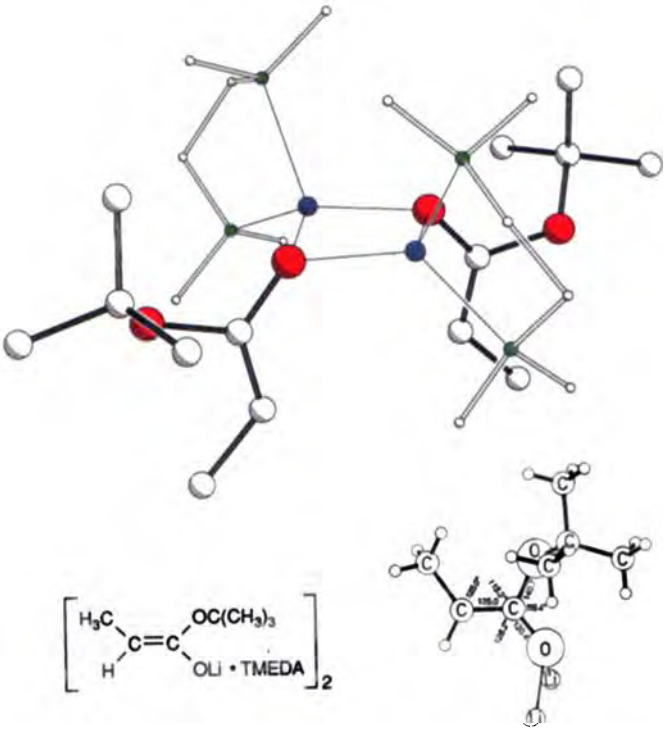

Fig. 4. Dimeric lithium (*Z*)-enolate of *tert*-butyl propionate, crystallized in the presence of TMEDA. The two enolate units are *cis* to each other on the LiOLiO four-membered ring through the center of which runs a C_2 axis of the dimeric aggregate. Even in the crystal, the ester enolate is unstable above −30°C. Its decomposition to a ketene [72, 73] and lithium *tert*-butoxide is perhaps indicated by the different C-O bond lengths (141 vs. 130 pm) and C=C−O bond angles (ca. 115 vs. 128°) at the trigonal O-substituted center of the double bond [73]. The *tert*-butyl group stands nearly perpendicular to the enolate plane (*CSD*: DEDXEP).

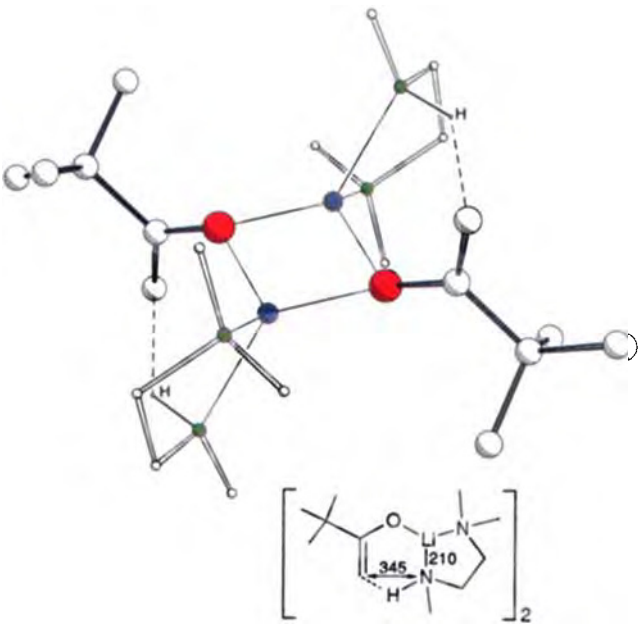

Fig. 3. Dimeric Li enolate of pinacolone crystallized in the presence of TriMEDA [66]. The nitrogens of the bidentate chelate ligand and two enolate oxygen atoms form a pseudo-tetrahedral arrangement around the Li atom. The distance between the NH hydrogen of the secondary amino group and the terminal C atom of the enolate double bond amounts to ca. 260 pm. The plane in which the atoms H···C=C lie forms an angle of ca. 60°C with that of the double bond. In the center of the LiOLiO quadrangle, there is a center of symmetry (*CSD*: DETRAV) [66], i.e., the enolate units are *trans* to each other (like the TriMEDA complex in Fig. 5 and the dienolate in Fig. 8, but unlike the dimers "solvated" with TMEDA or THF in Figs. 4 and 6).

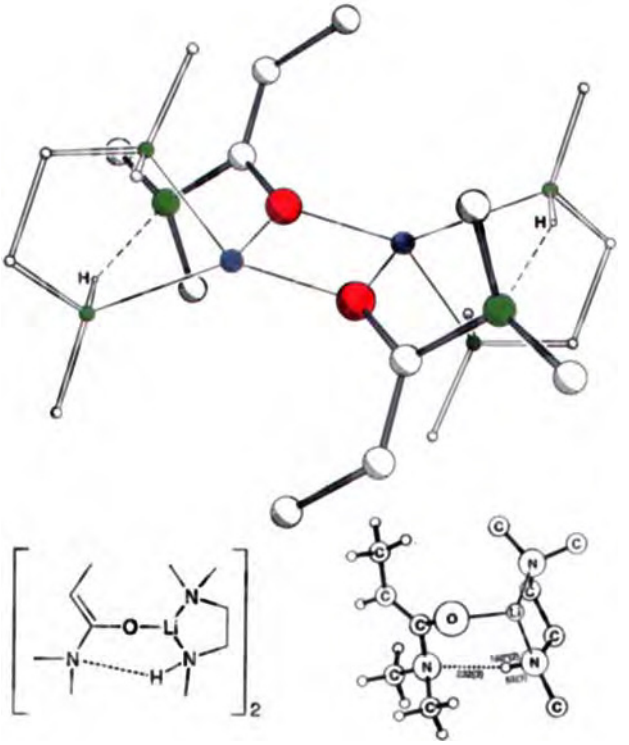

Fig. 5. *N,N*-Dimethylpropionamide lithium (*Z*)-enolate dimer, crystallized with TriMEDA. The center of the LiOLiO quadrangle is a center of inversion in the aggregate. The dimethylamino group of the enolate is like that in enamines [74], but much more strongly pyramidalized; the H atom of the secondary amino group lies in the direction of the virtual electron pair on this enamine nitrogen (lengths of hydrogen bonds, see [75, 76]) (*CSD*: DETPUN) [66].

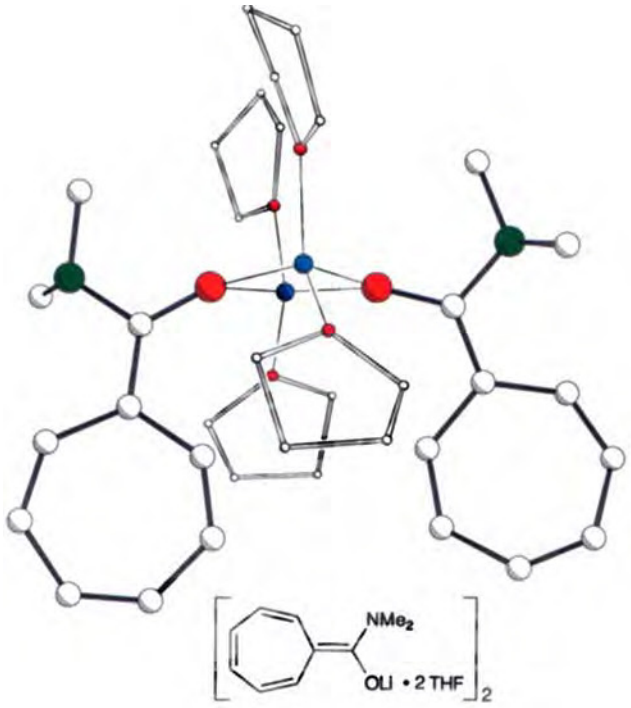

Fig. 6. Dimeric lithium enolate of *N,N*-dimethylcycloheptatrienecarboxamide, crystallized from THF [77]. As in the dimeric Li enolates of esters (Fig. 4), the enolate units are *cis* to each other at the LiOLiO quadrangle (with a C_2 axis through the ring center). THF molecules occupy quasi-axial and quasi-equatorial positions at the Li atoms of the folded four-membered ring (puckering angle between OLiO planes 68.6°, between the LiOLi planes 47.3°). The extended π systems do not participate in the complexation of the Li atoms. The Me_2N groups are turned out of the π plane, and the nitrogen is pyramidal (Δ = 36.5 pm) as in the propionamide enolate of Fig. 5.

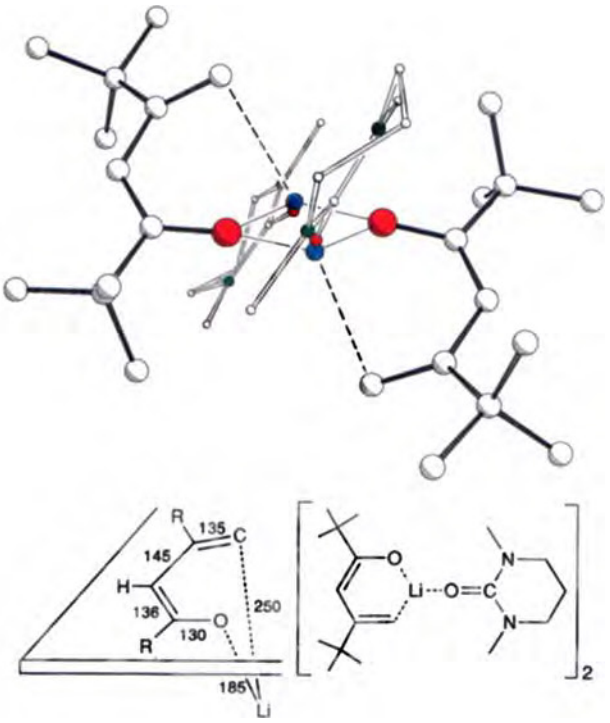

Fig. 8. Dimeric lithium (*Z*)-dienolate of 2,2,5,6,6-pentamethylhept-4-en-3-one (the product of aldol condensation between two pinacolone molecules), crystallized in the presence of DMPU [79]. The carbonyl oxygens of the cyclic urea and the terminal C atom of the dienolate (LiC bond distance 250 pm; cf. that in trityllithium, 223 pm [80]), as well as two oxygen atoms of the LiOLiO ring, surround the Li atom in the centrosymmetric dimeric aggregate (*CSD*: DIXWIQ).

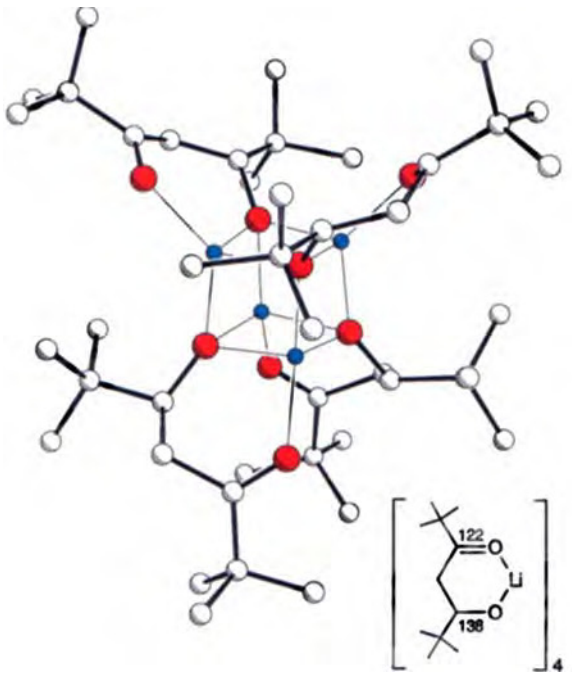

Fig. 7. Tetrameric aggregate of the Li aldolate from pinacolone and pivalaldehyde [78]. The negatively charged alkoxide oxygens and four Li atoms form a distorted cube (LiO distances 191–195 pm). The carbonyl oxygens of the aldolates are bonded to the Li atoms from outside (LiO distance 197 pm), as in other cases with the oxygen atoms of the solvent or nitrogen atoms of the ethylenediamine unit. In this arrangement, four "external" six-membered rings are formed, fused to alternating edges of the cube. The tetramer crystallized from pentane (*CSD*: DEWBIQ).

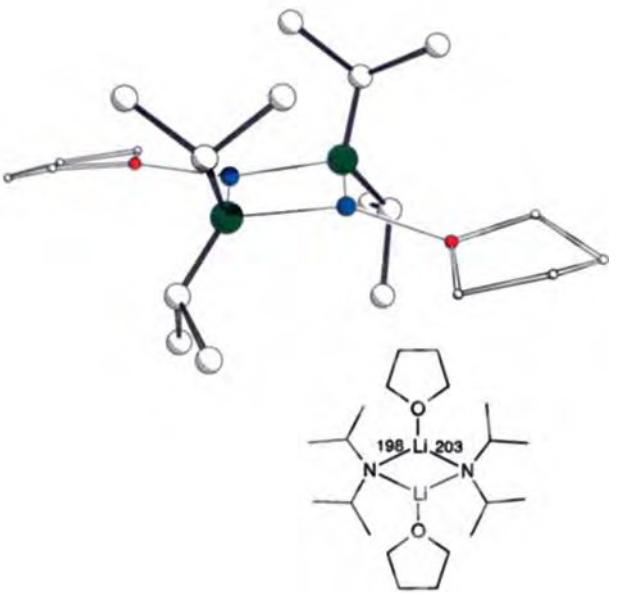

Fig. 9. Dimeric lithium diisopropylamide, obtained from THF [$(LDA)_2 \cdot (THF)_2$] [81]. The methyl groups of the isopropyl units point inwards, i.e., towards the LiNLiN four-membered ring. The Li atoms are each threefold coordinated as in other lithium amides (steric hindrance?). Additional $LiNR_2$ structures (monomer, four-membered ring dimer, six-membered ring trimer, and eight-membered ring tetramer) are shown in a review article on Li structures [47]; among these are also found lithium tetramethylpiperidide and hexamethyldisilazanide. (For more recent structure determinations of lithium anilide derivatives, see [82–84].)

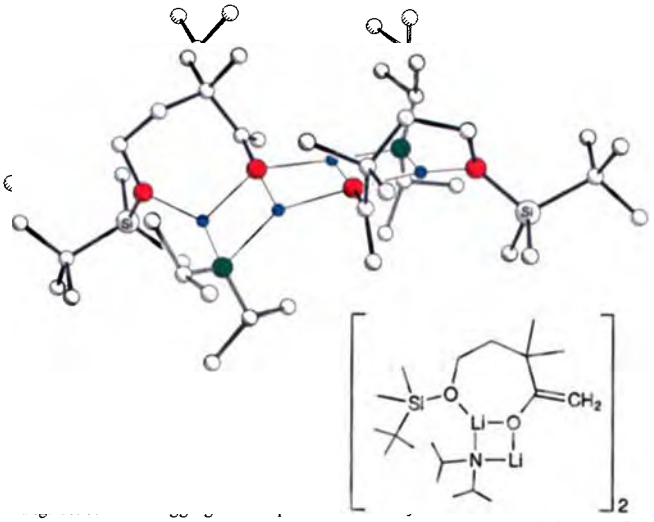

(from a methyl ketone, 5-(*tert*-butyldimethylsiloxy-3,3-dimethylpentan-2-one) and LDA. Three LiXLiY four-membered rings are fused to form a step-like structure. The siloxy oxygen serves as an "external" ligand to Li [85].

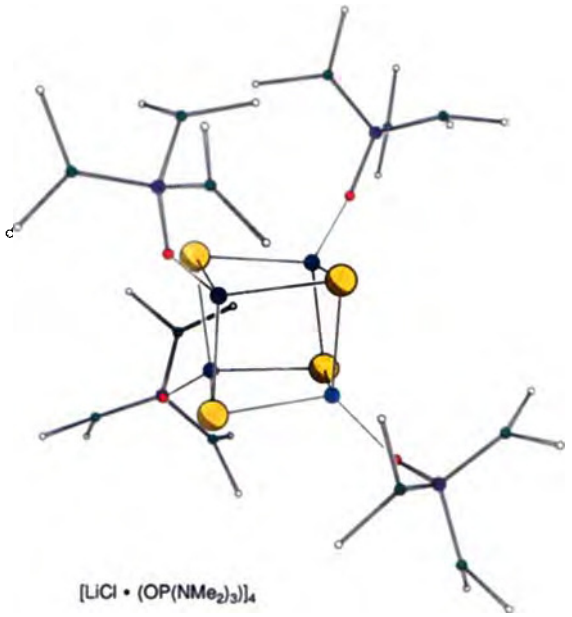

Fig. 12. Lithium chloride tetramer with four HMPT molecules, which are bonded to lithium via oxygen (from an "utterly fortuitous in situ preparation in high yield" involving $LiNCBu_2$, HMPT, $AlCl_3$ (1:1:0.3) in hexane/ether) [86] (*CSD*: CAWSIC). (For additional crystal structures with HMPT as "solvating ligand", see the review in [47], cf. also Fig. 15.)

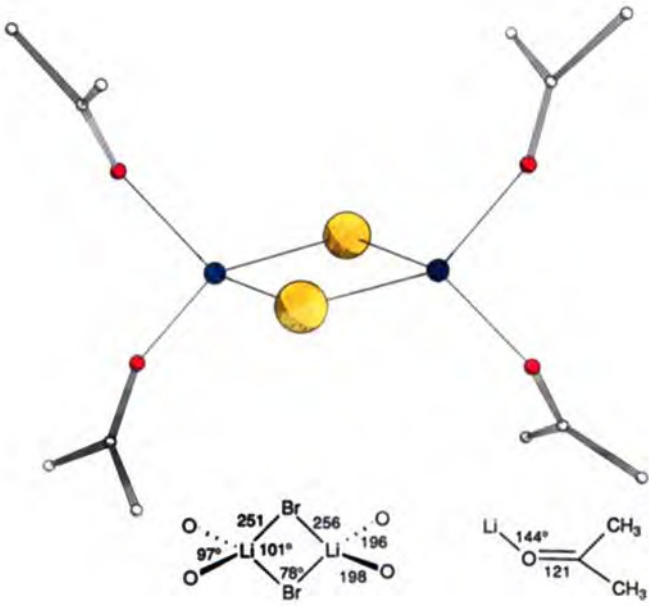

lithium atoms form a rhombus with acute angles at the bromine atoms. As in the case of protonated carbonyl compounds, the bond angle at oxygen is less than 180° in this complex between a ketone and LiBr (*CSD*: DECXEO 01). (See also the other adducts involving alkali-metal derivatives and carbonyl compounds in Figs. 7, 8, and 16 and in Tables 1, 2, 4, and 7 as well as the discussions in [79] and in Sections 2.3, 3, and 4.)

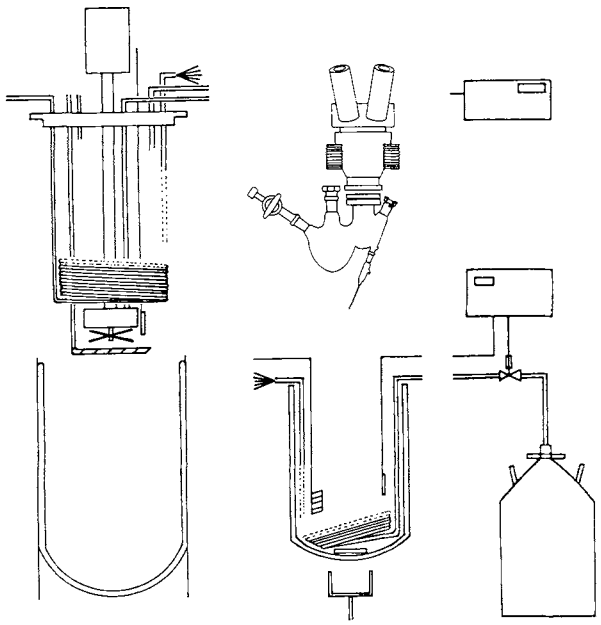

Fig. 13. Apparatus for the preparation of single crystals at low temperatures under inert atmosphere following the procedure in [67c, 73]. In this way, crystals of the ester enolates [73] (Fig. 4) and of a very unstable lithiated allyl thioether [87] were obtained; cf. also the X-ray structure analyses of aliphatic carbocation derivatives [88, 89] and the review article cited above [51].

these structures are of enormous importance for the following reasons: (1) With an accuracy provided only by X-ray crystal structure analysis, we finally have structural parameters of the reactive intermediates used in the most important CC bond-forming synthetic methods. (2) Applications of the structure-reactivity correlation principle[117–124] lead to conclusions about mechanistic details of the reactions of these species, and these conclusions become more and more reliable with an increasing number of structures. (3) The less stable these species are, the more their structures hint at their reactivity; reaction trajectories can be read from distortions of the molecules as they occur in the crystalline state.[73,87–89] (4) Finally, knowing the rich complexity of the reagents involved, we can use these structures to reconsider and discuss in a more systematic way the jumble of excellent preparative results, useful recipes, and procedures.

Before doing so, the results of structural investigations of Li enolates in solution will be briefly discussed.

Table 1. Composition of crystalline samples of Li enolates and nitrogen analogues. The samples were obtained in the course of attempted preparations of single crystals for X-ray structure analysis. The solvent content was determined, after drying the crystals under high vacuum, by addition of excess CD_3COOD in an NMR tube and integration of appropriate signals in the resulting spectra [91-94]; for further examples see [66].

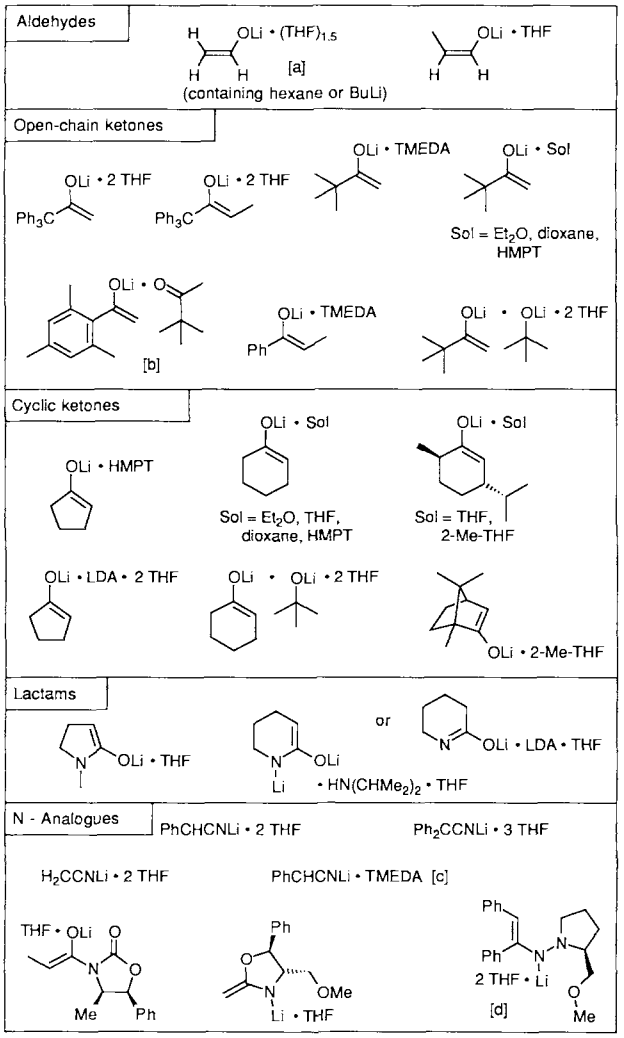

[a] Beautiful looking crystals separated from THF to which BuLi/hexane had been added [95]. Unfortunately, the crystals are not suitable for X-ray crystal structure analysis. [b] Compare with the Na enolate solvated by pinacolone (Fig. 16). [c] In the meantime, the dimeric Li phenylacetonitrile-TMEDA complex solvated by one molecule of benzene per aggregate unit was isolated and successfully subjected to X-ray crystal structure analysis [96]. [d] For the crystal structure of the Li enehydrazide of the hydrazone obtained from 2-naphthyl methyl ketone and *N*-aminoprolinol methyl ether, see [97] (monomeric, with two THF oxygens and the oxygen of the prolinol ether unit surrounding the Li atom).

Table 2. Schematic representation of some crystal structures of N-analogues of Li enolates. The PLUTO plots of two further structures of this type are shown in Figures 14 and 15 (see also a review article [47] covering the literature up to the beginning of 1984).

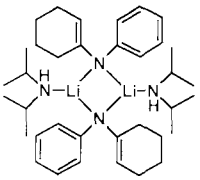	Li enamide of the product formed from cyclohexanone and aniline [102]
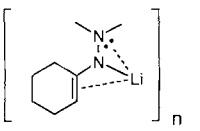	Polymeric Li enehydrazide of the product formed from 1,1-dimethylhydrazine and cyclohexanone [102]
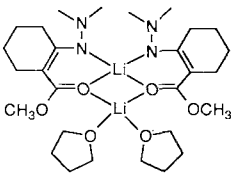	Dimeric Li enehydrazide of the product formed from 1,1-dimethylhydrazine and 1-oxocyclohexanecarboxylate. The compound contains two "very different" Li atoms [101a] (cf. Fig. 14)
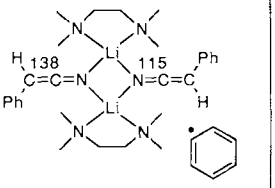	Dimeric Li ketenimide formed from phenylacetonitrile and TMEDA. A molecule of "crystal benzene"[96, 98] is present (for "simple" Li imides see [103-105])
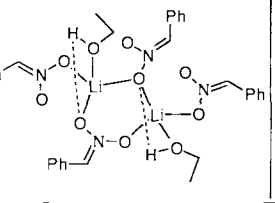	Section of the polymeric structure of the Li nitronate of phenylnitromethane $[PhCH{=}NO_2Li \cdot EtOH]_n$ [106]

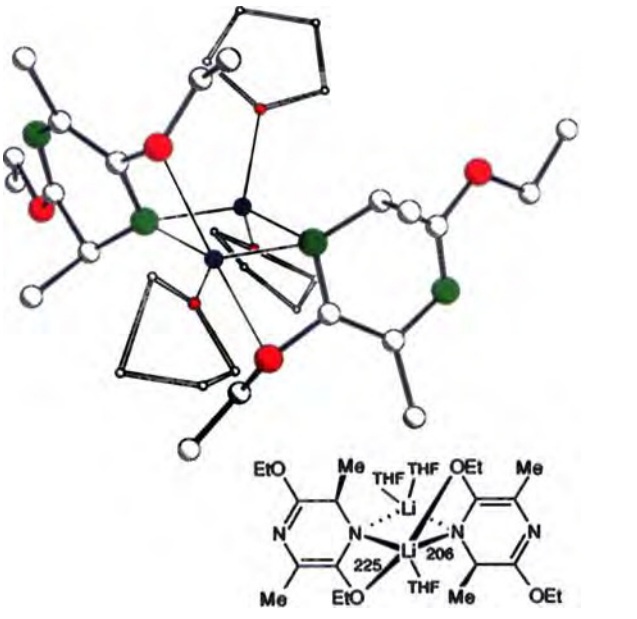

Fig. 14. Dimeric aggregate of the lithium bis-lactim ether derived from alanine [107] (*CSD*: CIFBOI). The two lithium atoms have very different environments; if the Li-Li neighborhood is not included, one Li atom is fivefold coordinated, the other fourfold. In this way, the diastereotopic faces of the dihydropyrazine ring are differentiated more strongly than by the methyl group at the stereogenic center (cf. the structure of the lithiated oxocyclohexanecarboxylic acid derivative in Table 2).

2.2. Li Enolate Structures in Solution—Not Simple Either!

2.2.1. Osmometric Measurements—Colligative Properties

From effects which ideally depend upon the number of particles per volume, the average molecular weight can be calculated, in the present case the degree of aggregation of Li enolates in solution. Ebullioscopy, vapor pressure osmometry, differential vapor pressure barometry, and cryoscopy applied to enolate solutions thus led to aggregation numbers between 1.0 and 4.0 (in certain cases several hundred), depending upon the type of enolate, the solvent,

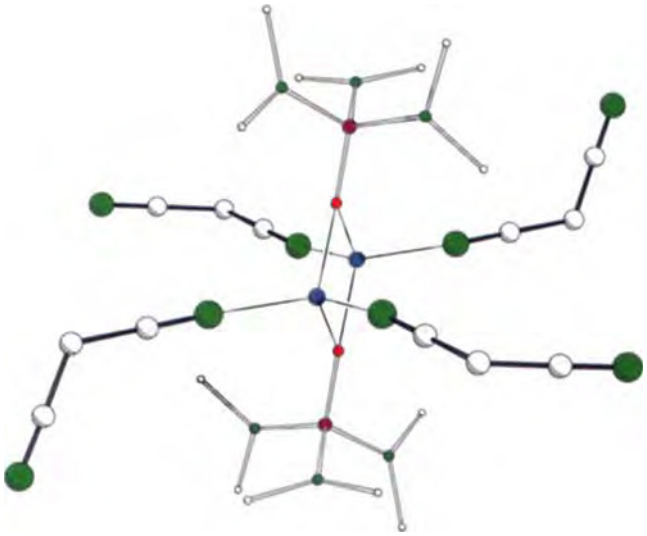

Fig. 15. Section of the polymeric structure of lithiated malononitrile $[LiCH(CN)_2 \cdot HMPT]_n$, which crystallized from a mixture of HMPT, hexane, and THF [108]. It is striking that the LiXLiX four-membered ring is not built up from the heteroatoms of the counterion (here the nitrogen) with the Li atoms, as usual, but from the oxygens of the HMPT. The nitrogen atoms of the dicyanomethanide lie "outside" of the aggregate. In the LiCl structure of Fig. 12, the HMPT oxygens are "outside". (Compare the structures in Fig. 12 and in Fig. 15 with a possible interpretation [69] of the HMPT effect on enolate reactions given in 1981, when there was no structural information about HMPT complexes. See also Scheme 9.)

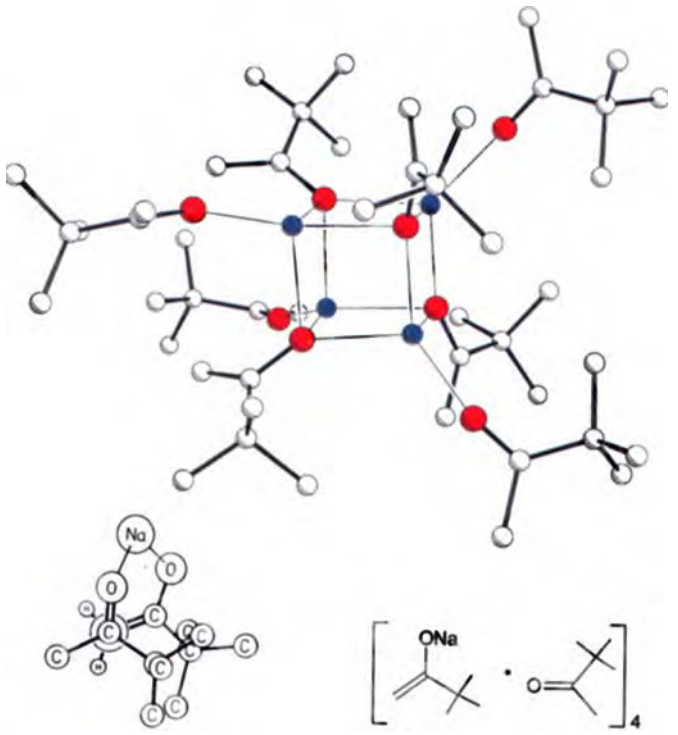

Fig. 16. Tetrameric sodium enolate of pinacolone, with pinacolone as "solvate molecule" (*CSD*: DIPSAW) [71]. A section shows that the planes of the π systems of the enolate and the ketone (bound together by the sodium) are more or less parallel, as they would have to be in a reaction between the electrophilic carbonyl carbon and the nucleophilic enolate one (separation distance 380 pm). The structure of the hexameric pinacolone K enolate solvated with THF, $[t\mathrm{BuC(OK)CH_2} \cdot \mathrm{THF}]_6$, is described in the same publication (*CSD*: DIPSEA). A complete collection of the structures of Na, K, Rb, and Cs organometallic compounds was published in 1987 [48].

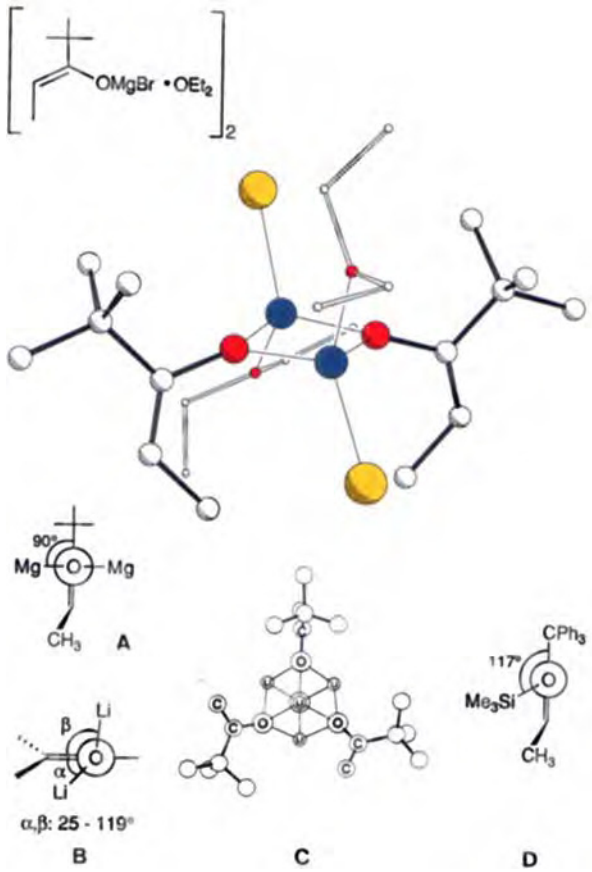

Fig. 17. Dimeric bromomagnesium (*Z*)-enolate of *tert*-butyl ethyl ketone (2,2-dimethylpentan-3-one), crystallized from diethyl ether (*CSD*: DILPUJ) [109]. The plane of the MgOMgO four-membered ring and that containing the enolate double bond are more or less perpendicular to each other (A). In the Li enolate dimers, the Li atoms lie outside the plane of the double bonds (Figs. 3-6) with very different LiOC=C torsion angles (B). In the tetramer (Fig. 2), however, a lithium atom does lie in the plane of the enolate (C). In a crystalline silyl enol ether (*CSD*: DIWXOW), the Si-O bond forms an angle of 117° with the plane of the enolate double bond [110a] (D).

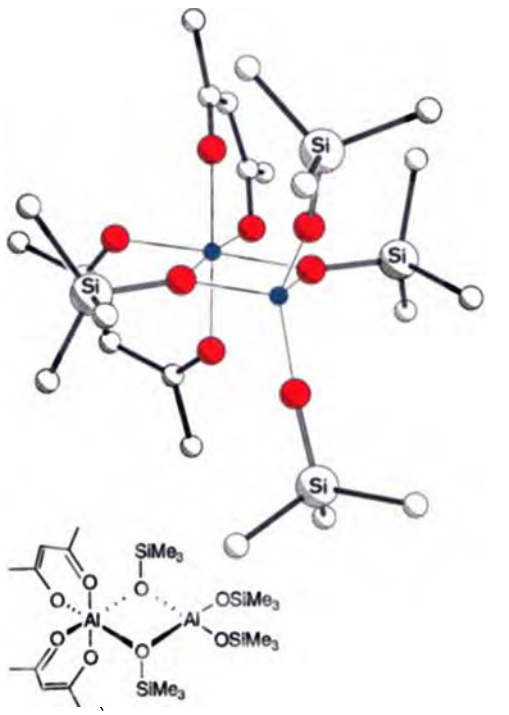

Fig. 18. Crystal structure of $[Al(OSiMe_3)_2(acac)]_2$, with two very different aluminum atoms (*CSD*: CIRMOF) [111]. In the opinion of the authors, the unexpectedly complex structure of these kinds of Al derivatives has to be borne in mind when considering their application as catalysts and as precursors of ceramic materials!

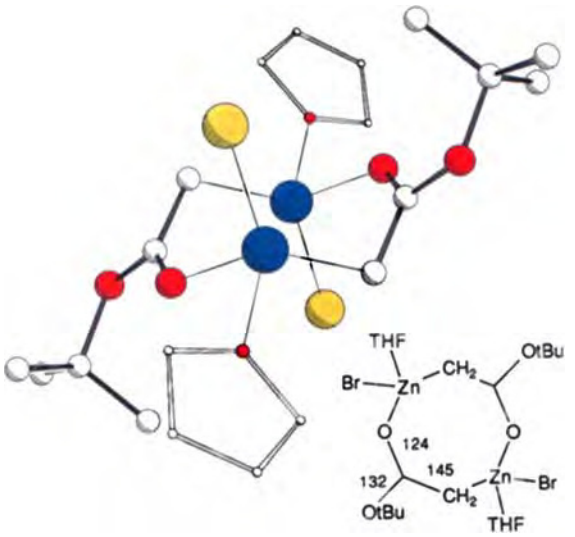

Fig. 19. Crystal structure of a Reformatsky reagent, $[BrZnCH_2COO(tBu)\cdot THF]_2$, crystallized from THF (*CSD*: BUDKAM) [112]. Two each of Zn, CH_2, C(O-*t*Bu), and O form an eight-membered ring. Each Zn bears a Br and a THF as substituents. In contrast to the alkali and Mg enolates, where the metal atoms are always bound to oxygens, the Zn atom here is simultaneously attached to the CH_2 group of one unit and the CO group of the other (see also the C-C and C-O bond lengths of the eight-membered ring). A discussion on the structures of cyclopropane and aziridine carboxylic ester enolates in which α-metallocarbonyl derivatives may also be present instead of the usual metal enolates can be found in [113, 114]. It is noteworthy that the Zn is σ-coordinated to oxygen, but π-coordinated to carbon (torsion angle Zn-O-C-O 164°, Zn-C-C-O −83°, respectively).

and the temperature.[22, 25, 27, 30, 94, 125, 126] Since many Li enolate reactions are preferentially carried out at dry-ice temperature in THF, the melting-point depressions measured[94] in this solvent (m.p. −107 °C) are especially "realistic". Of the numerous measurements only one will be referred to here: the Li enolate of cyclopentanone, which crystallizes as a tetramer from THF (see Fig. 2[68]), gives an aggregation number of 2.6–2.8 in THF solution at −107 °C, corresponding to a tetramer/dimer mixture of ca. 1:2. Vapor pressure measurements at higher temperature indicate that Li phenolates are largely tetrameric in ether solvents[127] (with polar organometallic compounds the entropy term may be such that larger aggregates—fewer solvent molecules bonded per Li—prevail at higher temperature and smaller ones at lower temperature[42c]).

2.2.2. *NMR Spectroscopy—More Detail*

By definition (*W. Wundt* and *W. Ostwald*) it is not possible to obtain information about the structure of aggregates in solution from colligative effects. Today's method of choice for studying solution structures is NMR spectroscopy. With the modern techniques (2D, 3D[128–131]) proximity between *nonbonded nuclei* (nuclear Overhauser effects) is detected, relaxation times are measured, quadrupole resonance spectra are obtained, dynamic processes are studied at very low temperatures, and the sensitivity is increased by isotopic labeling (^6Li, ^{13}C, ^{15}N, ^{17}O). All of this has provided a vast amount of detailed information about the species present in solution and the equilibria between them.[132] With *C*-metalated, "true" organolithium compounds the direct $^6Li,^{13}C$ coupling is the most valuable source of information about bonding between these two nuclei, about aggregation and the lifetime of aggregates (the multiplicity of the ^{13}C signals reveals the number of Li atoms bonded to the observed carbon[133]). Corresponding $^6Li,^{15}N$ coupling was used most recently for the determination of $LiNR_2$ aggregation in weakly polar solvents.[101b, 132b, 132c, 134, 135] There are no reports about Li,O coupling in enolates and phenolates; the investigation of Li enolates in solution by NMR spectroscopy is more difficult. So far, we owe the measurements in this area essentially to a single research group.[21, 22, 127, 136–140] From elaborate studies, especially of isobutyrophenone Li enolate and of Li phenolates, rather stable representatives of this type of species, many structural details have been deduced. Not only was the equilibrium between dimeric and tetrameric aggregates discovered, but also the presence of mixed aggregates between Li enolates or phenolates and LiBr, LiCl, and $LiClO_4$ in solution (all of this work has been carefully described; for an early review article on structure and reactivity of Li enolates see Ref. [22]). From hitherto unpublished ^1H and ^{13}C NMR measurements of the Li (*Z*)-enolate of propiophenone in THF, the following conclusions were drawn:[141] (1) There is an equilibrium between dimers and tetramers. (2) The dimer, but not the tetramer, forms a mixed aggregate with LDA. (3) Complexes between the Li enolate and diisopropylamine are formed; most likely these are more stable with the tetramer than with the dimer. (4) Addition of HMPT does not destroy the dimeric and tetrameric aggregates. (5) Mixed aggregates are formed upon addition of LiCl to the Li enolate solution. Also from NMR measurements, it is known that the parent compound, the Li enolate of acetaldehyde, is tetrameric in THF solution[142] (cf. Table 1 and Section 3), and that dimeric aggregates and mixed aggregates with LiBr exist in solutions of lithium amides.[101b, 102b, 132b, 132c, 143]

2.2.3. *ate Complexes—Also of Li Enolates?*

In the early fifties, *Wittig* interpreted the fact that organolithium compounds self-associate as arising from the formation of "autocomplexes"[144a] ("triple ions"). He ranked the dimeric phenyllithium in ether as $[Ph_2Li]Li$ in a series with the complexes $[Ph_3Be]Li$ and $[Ph_4B]Li$. Subsequently, such species were called *ate* complexes,[144b] by analogy with *onium* salts (cf. $[Me_4N]Cl$). When the first X-ray crystal structure analyses of Li,C and Li,O compounds appeared, it was realized that ate complexes form especially in those cases in which different metal cations or different anions are involved. In both the crystal[145, 146] (Fig. 20) and in solution[21] organolithium compounds with lithium halides were shown to be present as mixed aggregates rather than ate complexes, the formation of the latter being accompanied by charge separation.[150] Under these circumstances it is questionable whether ate complexes are present in solutions of Li enolates under the usual conditions, i.e., in nonpolar solvents and at low temperatures. Indeed, the only Li enolates for which ate complex-type structures have been detected are derived from β-dicarbonyl compounds (e.g., acetylacetone, acetoacetic esters; see the examples in Refs. [22, 47]). Some recent examples of Li ate complexes are collected in Table 3; cryptands and HMPT seem to favor their formation.

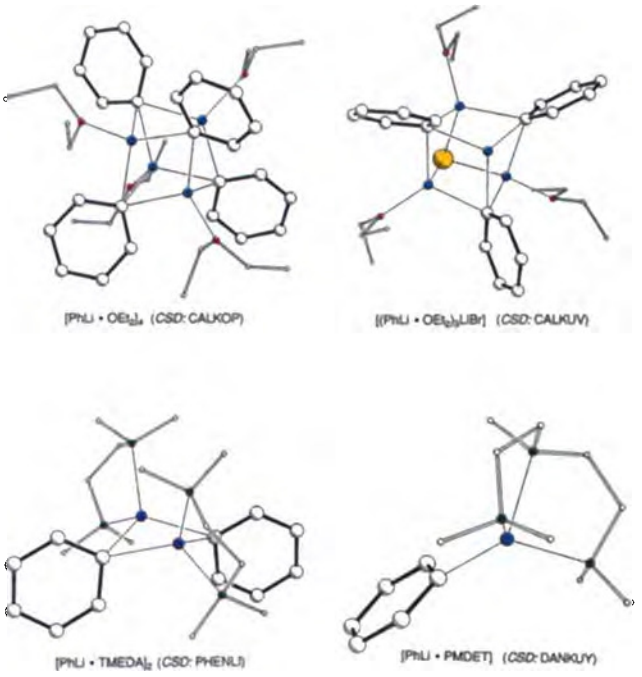

Fig. 20. Four different forms of phenyllithium in the crystalline state. From ether, a tetrameric aggregate crystallizes; in its center there are two "intertwined" tetrahedra, a larger one of four carbons and a smaller one of four lithiums [145]. In the presence of LiBr, a mixed tetrameric aggregate of three PhLi and one LiBr was crystallized from ether; three of the four Li atoms are complexed by ether oxygens, the fourth one, diagonally across the cube from the bromide, is not [145]. With TMEDA, a dimeric aggregate crystallizes [147], with PMDET a monomer was isolated [148] (for recent papers on PhLi structures in solution see Ref. [42a, 94, 149]). Until now, the "de-aggregation" of Li derivatives by addition of the tridentate PMDET has hardly been used by preparative organic chemists as a simple means of avoiding complications caused by aggregation.

Table 3. Some Li ate complexes detected in the solid state and in solution. In the examples chosen, oxygen-, nitrogen-, or carbon-centered anionic ligands are present.

Li ate complex ("triple ion")	*Method*	*Ref.*
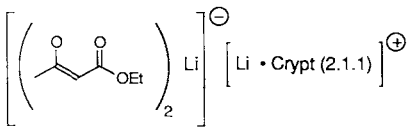	NMR	[151]
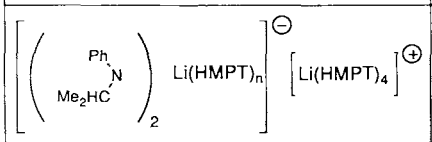	NMR	[135]
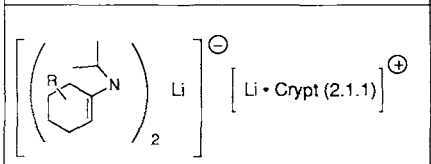	NMR	[102b]
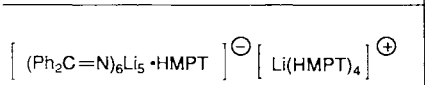	X - ray crystal structure	[103]
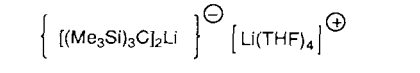 (C-Li-C linear, C,Li: 216-220 pm)	X - ray crystal structure	[152]
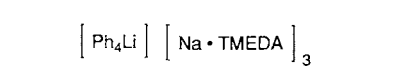	X - ray crystal structure	[153]

There are mixtures of bases (see Scheme 5) which exhibit properties drastically different from those of the components. It is not clear at this point[158] whether this is due to ate complexes or to dimeric, tetrameric, or even higher-order aggregates.

NaOR / NaR "complexes" [154]

$NaNH_2$ / NaOR "complex bases" [155]

KO*t*Bu / LiBu "super bases" [156,157]

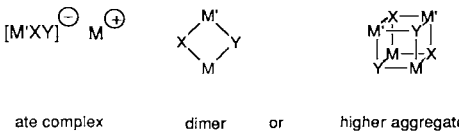

Scheme 5. Mixtures of bases may cause rate enhancements of deprotonations or eliminations in THF by several orders of magnitude as compared to the individual components.

2.3. Thermodynamic Data

Some thermodynamic data relevant to our discussion are listed in Tables 4–6. Again, many more measurements have been performed with Li,C than with Li,O derivatives.[22–53, 150] The most simple model for explaining the formation of aggregates may be to assume that it is caused by charge attraction. Lithium may be considered a small sphere of high positive charge density. In a Li enolate dimer each Li is "neutralized" by two counterions (and vice versa), and in a tetramer, by three (cf. the Madelung energy stabilization in an ionic crystal lattice). The large solvation energy of $Li^{\oplus}$ (interestingly, it is 7 kcal mol^{-1} more with NH_3 than with H_2O) is a consequence of the high charge density, and so is the exothermicity of LiX dimerization—the first step in formation of an ionic inorganic crystal lattice (Table 4).

The heats of deprotonation of carbonyl compounds by Li amides and of formation of an aldolate from Li enolate and aldehyde were measured only very recently (Table 5). The latter reaction is exothermic by 18 kcal mol^{-1} in THF and by 30 kcal mol^{-1} in cyclohexane (the calculated average bond energy change is $\Delta mBE = -19.4$ kcal mol^{-1}, i.e., the difference between a CC double and two CC single bonds).

The contributions of charge neutralization and complexation of the Li atoms by oxygens is clearly evident from these calorimetric measurements. Some of the reactions are so highly exothermic that their transition states should be more similar to the starting material than to the product (cf. the more selective deprotonations by LHMDS with the smaller heat of reaction!).

Some properties of Li enolates, such as the equilibrium ratios between regioisomers and between *E*/*Z* isomers (cf.

Table 4. Enthalpies of solvation, dimerization, and complexation of $Li^{\oplus}$ and LiX, respectively.

Gas-phase solvation enthalpies ΔH_{sol} (kcal mol^{-1}) of the lithium cation with water [159] and with ammonia [160]

$Li^{\oplus} + n\,H_2X \longrightarrow [Li{\bullet}(H_2O)_n]^{\oplus}$ or $[Li{\bullet}(NH_3)_n]^{\oplus}$

n	1	2	3	4	5	6
$\Delta H_{sol}^{H_2O}$	-34	-60	-81	-97	-111	-123
$\Delta H_{sol}^{NH_3}$	-39	-72	-93	-109	-121	-130

Gas-phase dimerization enthalpies ΔH_{dim} (kcal mol^{-1}) of lithium halides [161]

$2\,LiX \longrightarrow$

X	F	Cl	Br	I
ΔH_{dim}	-60	-49	-48	-43

Complexation of LiX with amides

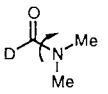

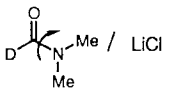

Rotation barrier [162]			
E_a	21.6	25.0	kcal mol^{-1}
$\Delta G^{\neq}$	21.2	21.8	kcal mol^{-1}
$\Delta S^{\neq}$	-1.0	+5.8	cal K^{-1} mol^{-1}

Equilibrium constant [163]

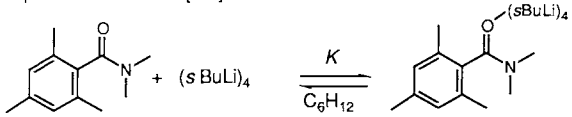

$K = 300 \pm 50$ (25°C)

Table 5. Calorimetric determination of the different steps of the aldol reaction of Li enolates at 25 °C by *Arnett* et al. [164]. All the ΔH values are given in kcal mol^{-1} (compare with the structures in Figs. 3, 5, 7, 8, 11, and 16). ΔH_{dep}, enthalpy of deprotonation; ΔH_{comp}, enthalpy of complexation; ΔH_{ald}, enthalpy of aldol addition.

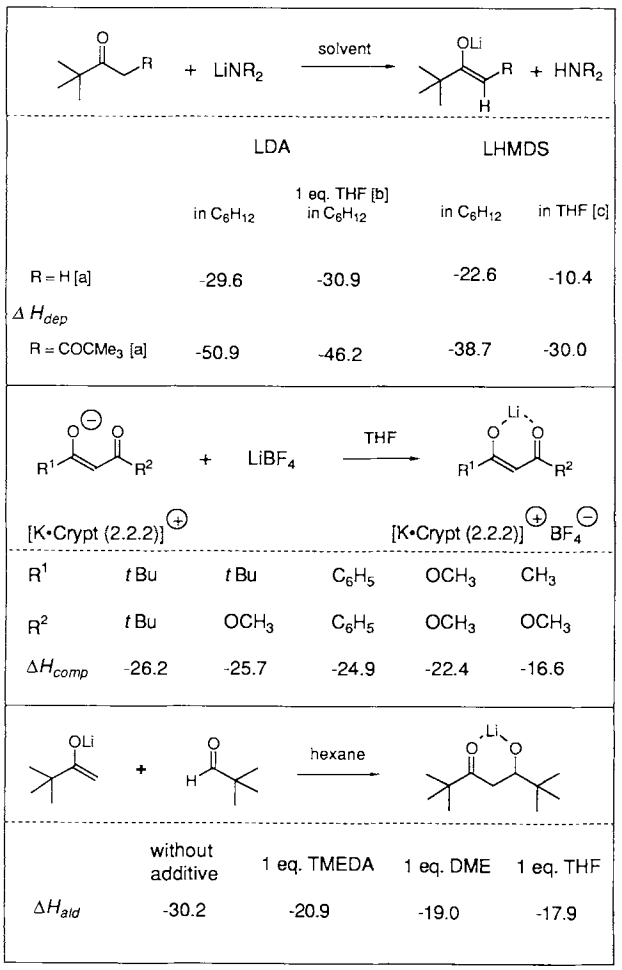

	LDA		LHMDS	
	in C_6H_{12}	1 eq. THF [b] in C_6H_{12}	in C_6H_{12}	in THF [c]
ΔH_{dep} R = H [a]	-29.6	-30.9	-22.6	-10.4
ΔH_{dep} R = $COCMe_3$ [a]	-50.9	-46.2	-38.7	-30.0

R^1	*t*Bu	*t*Bu	C_6H_5	OCH_3	CH_3
R^2	*t*Bu	OCH_3	C_6H_5	OCH_3	OCH_3
ΔH_{comp}	-26.2	-25.7	-24.9	-22.4	-16.6

	without additive	1 eq. TMEDA	1 eq. DME	1 eq. THF
ΔH_{ald}	-30.2	-20.9	-19.0	-17.9

[a] pK_a (DMSO scale [165]) of pinacolone, 27.7; of dipivaloylmethane, 15.4. [b] Other ketones and 1,3-dicarbonyl compounds give similar values under the same conditions: cyclohexanone, −34.9; dimethyl malonate, −52.5 kcal mol^{-1}. [c] Under these conditions, enthalpies for the deprotonation (ΔH_{dep} of phenylethanol [$PhCH(OH)CH_3$] and of ephedrine derivatives [$PhCH(OH)CH(CH_3)NR_2$] are between −18.7 and −20.6 kcal mol^{-1}, thus, there is no indication of (OLi···N) chelation (see, however, Refs. [166–169]).

the correlation between enolate and product configuration in aldol and other addition reactions[5–10, 72a, 173, 174]), are collected in Table 6.

3. Computational Studies of Formation and Reactions of Li Enolates—Contributions from Force-Field Calculations and Quantum Mechanics

In view of the availability of more and more powerful (super) computers, and of ab-initio[175] and force-field programs with an increasing number of improved parameters,[176] it is not surprising to see that almost all of the renowned research groups in this area of theoretical chemistry have contributed calculations of ground-state and transition-state geometries of Li and other polar metal enolates and of their reactions. It is impossible to do justice to this work in these pages and it is hoped that the accompanying Tables 7 and 8 and Figure 21 may suffice for the presentation of some of the results.

The examples in Table 7 and Figure 21 show that very large supramolecular structures have become subject to computational studies. These confirm the decisive role of solvation in the structures of polar Li derivatives; reasonable results, i.e., compatibility with experimental parameters, are frequently not obtained unless Li is given a solvent shell or is "removed" from an intramolecular chelating heteroatom by fixing the geometry otherwise (see the Li dienolate and the dioxanone Li enolate in entries 4 and 5, respectively, of Table 7). Table 8 contains the results of modeling, MNDO, and ab-initio calculations of reaction coordinates involving enolates. The layman certainly has cause to marvel at the ability of theory to reach conclusions about the structures of extremely complex arrangements of atoms, including those of higher periods such as zinc.

With the calculations, we have gone on to the gas phase in which minimum-energy structures may deviate from those in solution even more noticeably than in the crystalline state. It is evident that computations have become so

Table 6. Rotational barriers in Li enolates and relative stabilities of isomeric Li enolates as determined by equilibrium studies under various conditions.

Rotational barriers	Determined by NMR spectroscopy
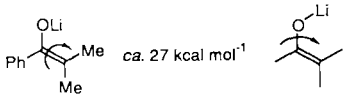	*ca.* 27 kcal mol^{-1} 1.6 kcal mol^{-1} [136,142]
Equilibria	Ph_3CLi as base / excess ketone DME as solvent at room temperature [2, 170,171]
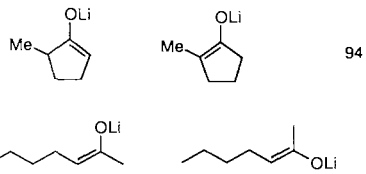	94 : 6
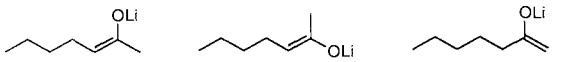	65 : 22 : 13
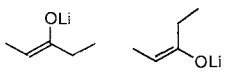	$LiNR_2$ in THF at 0°C various secondary amines with / without addition of HMPT / TMEDA [64]
84 : 16 bis 94 : 6	
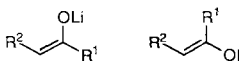	Equilibrations with cat. PhHgCl at 25°C in THF [172]

Z		*E*			
R^1	Me	Me	*t* Bu	H	H
R^2	Me	*t* Bu	Me	Me	*t* Bu
Z/E	82 : 18	20 : 80	99.8 : 0.2	65 : 35	3.5 : 96.5

Table 7. Calculations on complexation and aggregation of LiX derivatives and on the structures of Li enolates.

Calculated structure, remarks, and references to the experimental results	Method (basis set)	Ref.
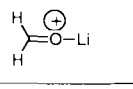 Linear structure most stable (cf. Figs. 7, 8, 11,16)	3 - 21G 6 - 31G*	[177a]
4 LiX ⟶ $(LiX)_4$ X F OH NH_2 ΔH - 188 - 190 - 167 kcal mol^{-1} 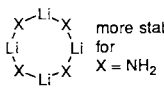 more stable for X = NH_2 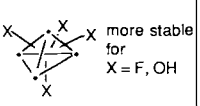 more stable for X = F, OH (see references in Fig. 9) (cf. Figs. 1 - 12 and Table 4)	6 - 31G + sp + d // 3 -21G	[177b]
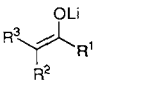 Force-field parameters for Li enolates [a]	MM2	[172]
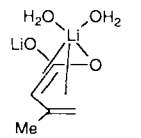 Calculation and comparison with NMR data (cf. Fig. 8) [b]	STO - 3G	[178] [179]
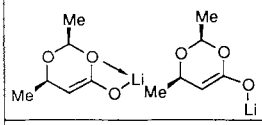 Pyramidalization and reactivity (cf. Figs. 4 and 17)	3 -21G	[182]
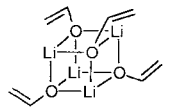 Modeling and ab initio calculation (cf. also Figs. 2 and 21)	Modeling 3 - 21G	[183] [184]

[a] From isomerization equilibria and crystal structure data. [b] Compare also with 3-21+G, 4-31G and 6-31+G* calculations of lithiated acetaldoxime [180], of *E/Z*-isomeric enamide, enehydrazide, and oximate anions [181], and of lithiated thioallyl ethers [87].

powerful that solvent molecules can also be included. It is to be expected that discrepancies between calculated and observed values will eventually vanish. So far, theory has reproduced experimental results in this area. As far as I know, there is no instance of an organometallic reaction mechanism being put forward solely on the basis of calculation which was not first proposed, prior to calculation, on grounds of structural investigations in the solid or liquid phase,[199] or on the basis of preparative results, or of chemical intuition.

4. Reactions of Li Enolates—Supramolecules as Product-Forming Species

The behavior and properties of any organized system arise not only from its parts but also from the manner in which they are arranged.[200]

The fact that Li enolates are found to be more or less aggregated in solution and crystals does not, of course, tell us anything about the actual reactive species, at this point. As with Li,C derivatives,[24,25] it is not at all easy to furnish proof for the participation of aggregates in product-forming steps. Elaborate kinetic measurements of fast reactions of air-sensitive compounds at low temperature are necessary. NMR spectroscopy is the method of choice, and it was used early on, in a masterly manner,[21,137,138,201] to demonstrate that Li enolate aggregates *may* be directly involved in reactions, rather than being the pre-equilibrium precursors of monomeric reactants: the degree of aggregation and the presence of Li salts were clearly correlated with ratios of isomeric products formed (e.g., *C*- vs. *O*-alkylation of Li enolates[21,137,138]), the conclusion being that "ion-pair aggregates are the true reactants".[137] Dimeric aggregates turn out to be more reactive than tetrameric ones, according to these measurements.[138]

A new dimension of mechanistic details was made accessible by a new NMR technique, the method of rapid injection (RINMR):[202,203] reactants are quickly mixed in an NMR tube—also possible at very low temperatures—and the first spectrum can be taken after a few milliseconds.[204-206] This allows one to see different species, as well as transient ones, disappearing and appearing in the reaction mixture. Thereby, it was found[141] that the reac-

Table 8. Calculations on various nucleophilic additions to carbonyl groups, including the aldol addition of Li enolates and the Reformatsky reaction.

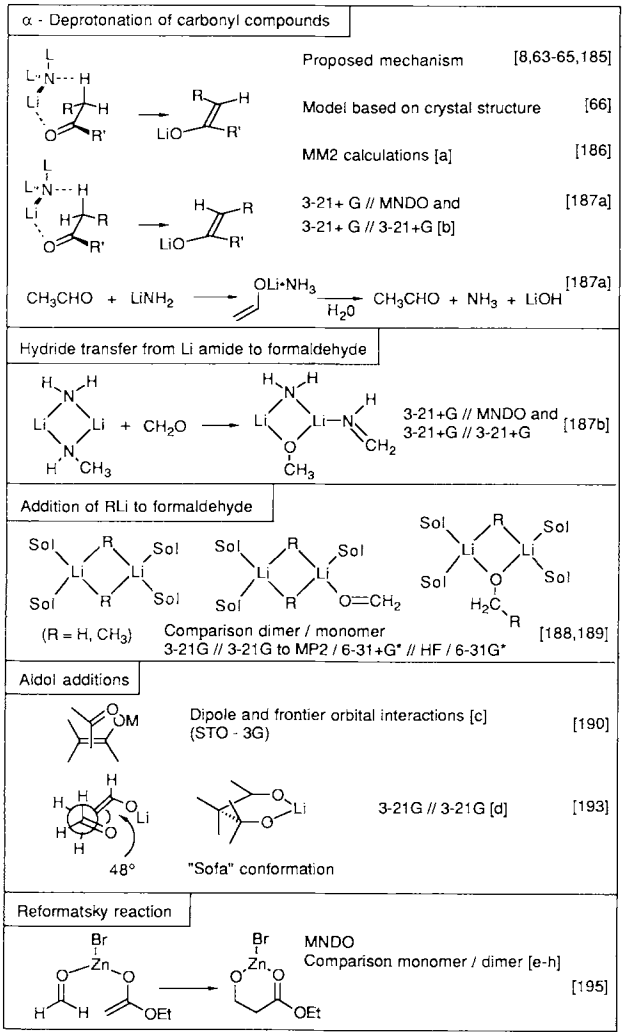

[a] Calculations without consideration of experimental results. [b] The protonation of the enolate-ammonia complex was also calculated (cf. the discussion in Section 3.1 (R_2NH effect)). [c] Compare the model of "unsuccessful cycloaddition" [191], earlier comments on the significance of HOMO-LUMO interaction [192], the chelate model [5, 12], and the general topological rules for coupling of trigonal centers following the Bürgi–Dunitz trajectory,[13,14] see also: D. Seebach, V. Prelog, *Angew. Chem. 94* (1982) 696-702; *Angew. Chem. Int. Ed. Engl. 21* (1982) 654-660. [d] For MNDO calculations of the aldol addition of *E*/*Z*-isomeric boron enolates to aldehydes, see Ref. [194]. [e] According to this calculation, reactions starting from the dimeric Reformatsky reagent, as present in the crystal (Fig. 19), have an activation energy at least 15 kcal mol^{-1} higher than those with the monomeric reagent. [f] According to the calculation, a reaction starting from the α-Zn-ester (*C*-metalated enolate), a formal [3,1]-sigmatropic rearrangement, has a higher activation barrier (by ca. 15 kcal mol^{-1}). [g] A general comparison of aldol addition and other reactions of metal derivatives in nonpolar solvents with pericyclic processes (Woodward-Hoffmann type) is certainly apparent [102c, 195]. The present example would have to be called a [3,3]-sigmatropic rearrangement [196], a metallo-oxa-Claisen, or a metallo-dioxa-Cope reaction [197]. However, considering the involvement of strongly polar (ionic?) bonds and, more importantly, the presence of an element of the higher periods (Zn), this comparison should be regarded as a formalism. [h] According to the formalism proposed by *Baldwin* [198], a metal-atom-involving aldol addition between the two trigonal carbon atoms of the carbonyl and the enolate double bond may be regarded as an "allowed bis-(*6-endo-trig*) process". On the other hand, the 1,3-shift mentioned in footnote [f] would be a "forbidden (*4-endo-trig*) process"!

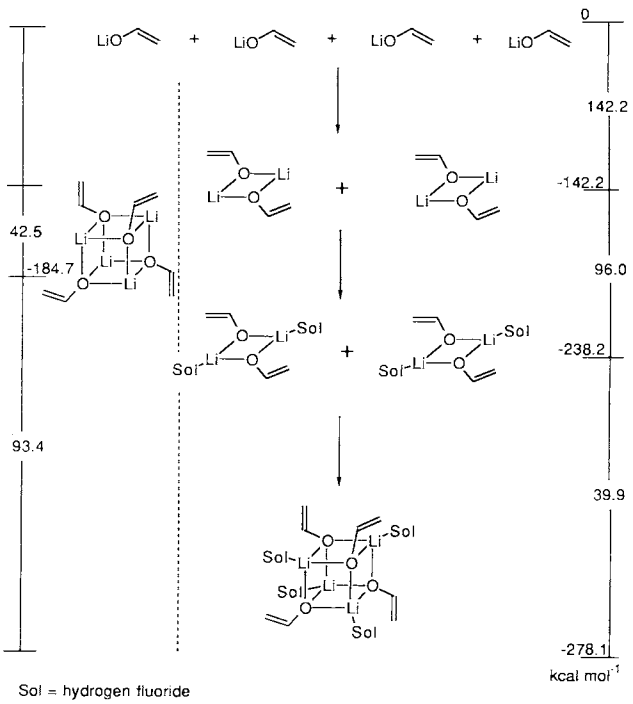

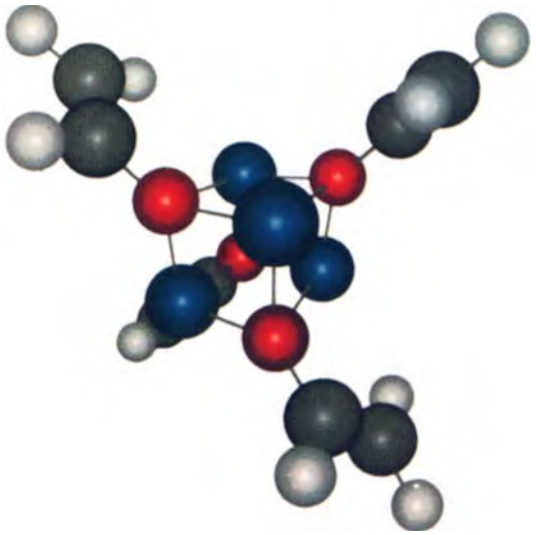

Fig. 21. Calculated (ab-initio 3-21G) aggregation and solvation enthalpies of the Li enolates of acetaldehyde (cf. Table 1) with HF as solvent molecule (Sol) [184]. According to this calculation, 33.5 kcal mol^{-1} of energy is liberated upon complexation of two additional solvent molecules to the dimer $[(EnOLi)_2Sol_2 \rightarrow (EnOLi_2) \cdot Sol_4]$ (En = CH_2=CH); therefore, without consideration of the entropy effect [42c], the difference in the stability between the dimer and the tetramer would be 27 kcal mol^{-1}, the latter being more stable. In THF, this difference is found to be significantly smaller: one often observes both species coexisting (see also Section 2.2). The color picture of the tetramer was generated from the calculated coordinates with the program *MacModel* [184].

tion of a dimeric Li enolate aggregate with an added aldehyde is much faster than its regeneration from the equilibrium with the tetrameric aggregate. The higher reactivity of the dimer may be attributed to less steric hindrance and more negative charge density, the enolate moiety being "neutralized" by two, rather than three, Li counterions; a monomeric Li enolate would be expected to be even more reactive,[207] and an ate complex should exhibit further increased reactivity (enolate "neutralized" by only 1/2 Li!).[208,209]

It is much easier for the chemist dealing with synthetic and preparative aspects of Li enolate reactions to demonstrate that complex structures rather than a simple reagent

molecule *must* be responsible for an observed result. On the other hand, he or she has very little choice but to speculate exactly which species did it! Little fantasy is required to imagine what a wealth of complications can be caused by aggregations and complexations in processes as fundamental as deprotonation of a carbonyl compound (Scheme 6), aldol addition (Scheme 7), alkylation in the α-position of a carbonyl group (Scheme 8), with (Scheme 9) or without addition of a polar aprotic cosolvent.[216] An almost confusing situation results[217] in which a great variety of structurally different Li enolates of different reactivity may arise in the course of a simple transformation such as the reaction of an enolate with an electrophile[218]—a nightmare for the synthetic chemist, just like the one a crystallographer may experience, who, by pushing the wrong button, generates the chaos shown in Figure 22 instead of a beautiful three-dimensional representation of a structure. After all, it is surprising how well we fared with the simple model, how forgiving the Li enolates are! In the following sections I will describe results to show not only how we might reduce but also how we might exploit the complexity we gained. Once again, it must be emphasized

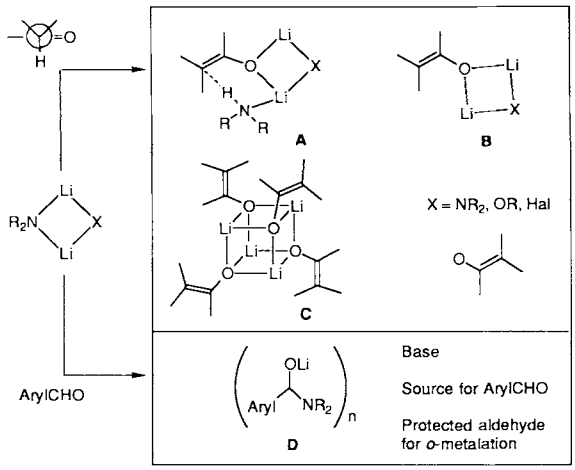

Scheme 6. Reaction of a carbonyl compound with LDA or with an LDA/Li halide or Li alkoxide mixture (cf. the structures in Figs. 2-4, 9, 10). **A**: Dimeric Li enolate or mixed aggregate complexed with a secondary amine. **B**: Pure or mixed aggregate from two LiX units. **C**: Tetrameric aggregate. **D**: Adducts of Li amides with nonenolizable, aromatic aldehydes [210-212].

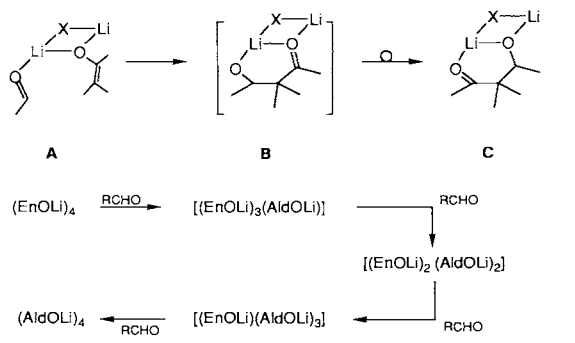

Scheme 7. Possible reactions of Li enolate aggregates with an aldehyde (cf. structures in Figs. 2, 7, 16). In the process of C-C bond formation, complex **A** is converted, through adduct **B** with the negative oxygen in an "outer position", into the aldolate **C**. The reaction of a Li enolate tetramer $(EnOLi)_4$ may take place over four steps to give the aldolate tetramer! (Cf. the structure in Fig. 7.)

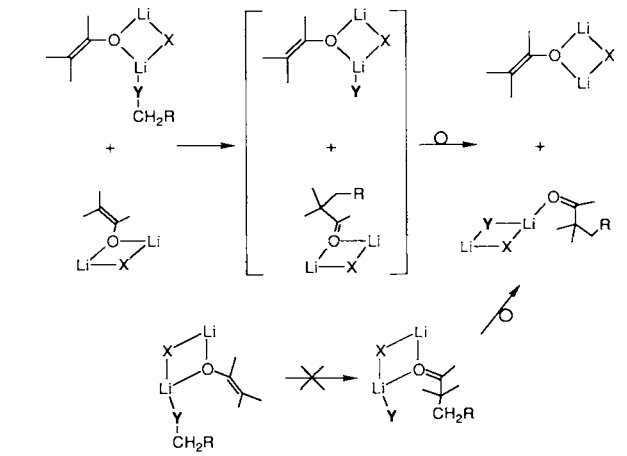

Scheme 8. Formulation of a reaction between two Li enolate aggregates and an alkyl halide to give an α-alkylated ketone and Li halide (cf. the structures in Figs. 11, 20). Because the alkylation of Li enolates occurs with inversion at the alkylating C atom [213], it should not be able to take place in an "intrasupramolecular" ("intraaggregate") fashion (linear S_N2 transition state!) [214].

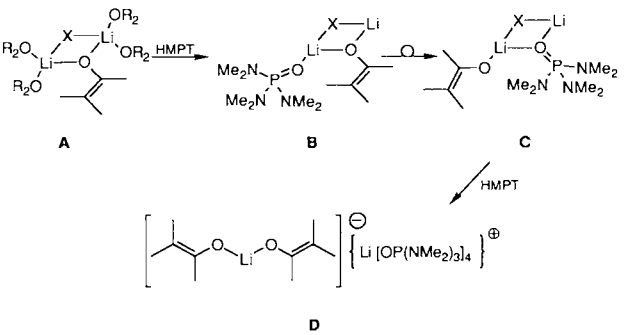

Scheme 9. Structures that may be formed from a Li enolate by addition of HMPT with enhancement or alteration of reactivity as compared to nonpolar solvent systems. The enolate unit in **A** (enolate inside, cf. Figs. 3-6) can attain increased charge density through complexation of the Li with an HMPT oxygen (**B**), the enolate O atom being still "neutralized" by two $Li^{\oplus}$ (cf. the tetrameric LiCl with HMPT complexation in Fig. 12). Through reorganization, the HMPT oxygen may become part of the aggregate nucleus (**C**), the enolate oxygen outside being "neutralized" only by one $Li^{\oplus}$, which should increase the nucleophilicity/basicity (cf. Fig. 15). In the ate complex **D** (cf. Table 3), the enolate would be even more activated. Very much the same effects are observed with the nonmutagenic cyclic urea DMPU as with HMPT (see Fig. 8 and Ref. [63]) [215].

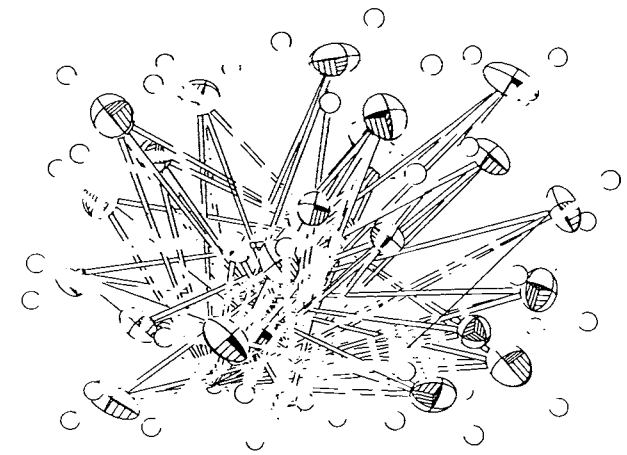

Fig. 22. Unsuccessful ORTEP plot, due to erroneous data input, of the structure of the TriMEDA-complexed amide enolate shown in Fig. 5.

that other polar organometallic compounds behave similarly, so that the discussion of Li enolates will lead to quite general conclusions.[219,220]

4.1. The Effect of Secondary Amines

It has been known since the beginning of the LDA era[59,221] that the secondary amine concomitantly generated with the Li enolate from a carbonyl compound and LDA *may* have an effect upon the reactivity of the enolate.[67b,222-224] In many reactions with electrophiles the amine-free Li enolate solution gives better results; examples for the generation of amine-free solutions are given in Scheme 10—note that some of these methods are "pre-LDA"!

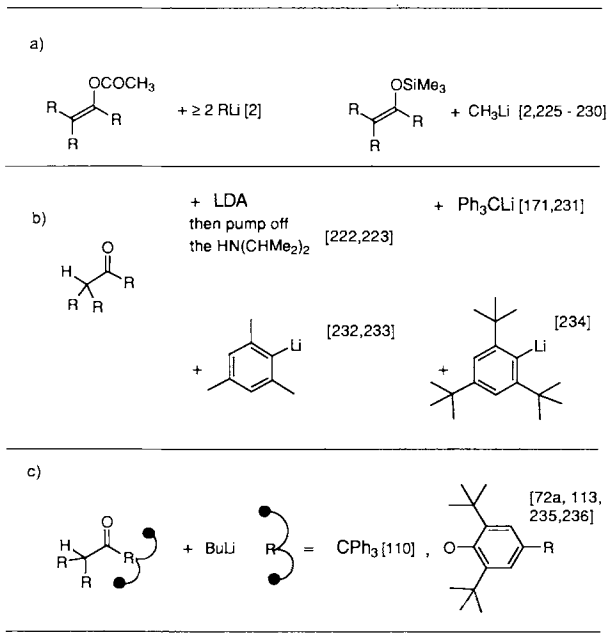

Scheme 10. Generation of amine-free Li enolate solutions. a) From enol esters and silyl enol ethers. b) From carbonyl derivatives and LDA (pumping off the secondary amine formed), or with sterically hindered, and therefore regioselective, organolithium compounds (with formation of a hydrocarbon). c) From a compound having a sterically hindered, but electronically effective [237] carbonyl group, with butyllithium [238].

Recently, a number of cases have come to light in which totally unexpected results were obtained with Li enolate reactions in the presence of secondary amines, mostly diisopropylamine: Addition of deuterating or alkylating reagents (DX and RX, respectively) does not furnish the desired α-deuterio or α-alkyl carbonyl compound, but a more or less completely α-protonated product, i.e., starting material, and it was shown that the proton stems from the secondary amine.[239] The expected products are often isolated in high yields if butyllithium is added prior to the electrophiles. The amine as a proton source for much too weak bases was observed especially with substrates having more than one acidic proton (effect of the "hidden proton").[240] The general effect is pictured in Scheme 11, which also contains some examples from the recent literature. Obviously, the complexes that we have discovered in crystals[66] (Figs. 3, 5) are also present in solution, and are much more stable than anticipated. Under quenching conditions the "intra-supramolecular" proton transfer from the diisopropylamine to the Li enolate, which are linked together by Li-N complexation and hydrogen bonding,[247,248] competes successfully with the expected intermolecular attack of the electrophile.[249] Formally, huge isotope effects occur in such deuterolysis experiments

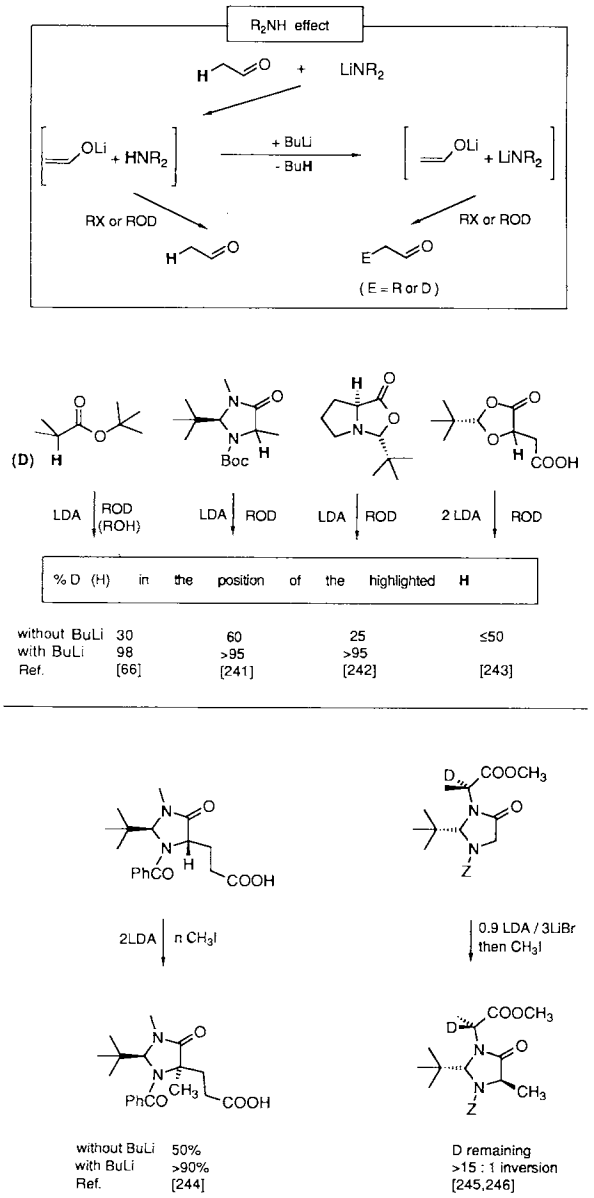

Scheme 11. Reactions of Li enolate-diisopropylamine complexes (in THF). *Top:* In the enolate-amine complex, a (partial) reprotonation occurs under the influence of the electrophile; by removal of the amine with BuLi, the yield of the desired product may be improved. *Middle:* Examples of deuterolyses; only after removal of the NH proton is a good deuterium incorporation achieved; a control experiment with the deuterated precursor and hydrolysis gives a complementary result (D replaced by H only after treatment of the enolate-DNR_2 with BuLi). *Bottom:* Examples for methylation of LDA-generated enolates with iodomethane. *Left:* Only after removal of the R_2NH proton is a high yield of the α-methylglutamic acid derivative obtained. *Right:* The deuterated imidazolidinone derived from glycylalanine is epimerized and alkylated, without loss or scrambling of deuterium over the two α-carbonyl positions, by treatment with LDA/LiBr (LDA alone does not cause a clean conversion, see Section 4.3) and CH_3I (with acetic acid instead of CH_3I as an electrophile, the starting material is recovered without loss of the D and without epimerization!).

when the Li enolate/amine solution in THF is added dropwise to a many thousandfold excess of perdeuteroacetic acid. The "internal return" of the originally removed proton is reminiscent of an effect termed *conducted-tour mechanism* coined many years ago by *Cram* to characterize the stereochemical course of certain ion-pair reactions,[250-252] and of proton-transfer mechanisms[253,254] discussed for active sites of enzymes (cf. serine proteases[255]).

Treatment of an LDA-generated enolate with BuLi is, of course, a drastic cure for removal of the villainous NH proton. Since an LDA/enolate mixture is formed, the product will be exposed to the base LDA; furthermore, an enolate results which may have quite different properties as compared to the original one, due to the presence of LDA (see Section 4.2). This is why the methods collected in Scheme 10 for the generation of amine- and amide-free Li enolate solutions should be kept in mind. To avoid many a complication, the use of sterically more hindered Li amides such as lithium *tert*-butyl(1,1,3,3-tetramethylbutyl)amide (also called LOBA ≡ *l*ithium-*tert*-*o*ctyl-*tert*-*b*utyl-*a*mide[65]) or of the less basic, but also less highly aggregated, disilazanides[256] (LHMDS, KHMDS; cf. the heats of deprotonation in Table 5), producing the poorer complexing $HN(SiMe_3)_2$ in the deprotonation step, is recommended.

The complexes of Li enolates and secondary amines dealt with here are probably also involved in some of the processes discussed in the following section, when achiral enolates are generated by chiral Li amides.

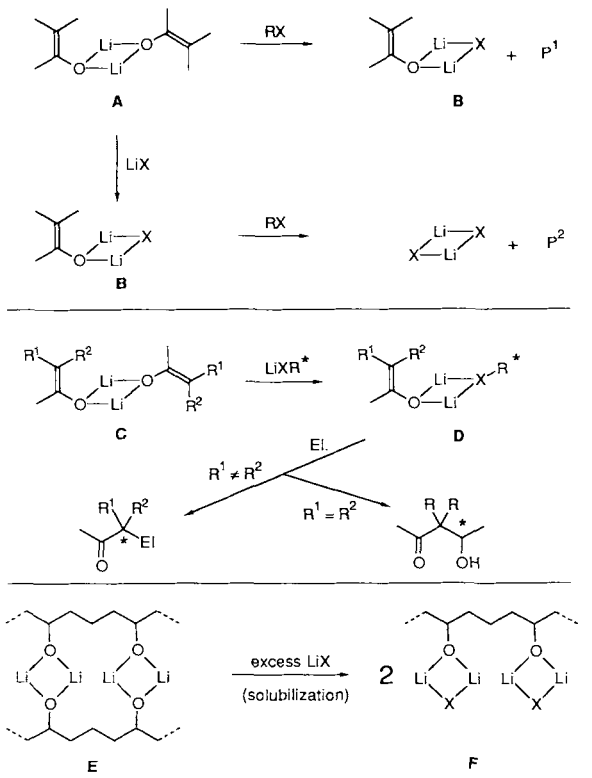

Scheme 12. Addition of LiX to an enolate solution could lead to formation of a mixed aggregate (**A** → **B**), and therefore change the product ratio P^1/P^2. A chiral additive puts an achiral enolate in a chiral environment (**C** → **D**), which may lead to the formation of enantiomerically enriched products. The LiX addition can have a solubilizing effect with a polylithiated derivative (**E** → **F**).

4.2. The LiX Effect in Li Enolate Reactions

Gedanken ohne Inhalt sind leer,
Anschauungen ohne Begriffe sind blind.[*]
Immanuel Kant

If the result of Li enolate reactions, carried out under the usual conditions in nonpolar solvents and at low temperatures, does depend upon the complex processes indicated in Schemes 6-8, then we not only need to worry about the secondary amine being a component of the mixture (Section 4.1); the formation of mixed aggregates may cause the following additional phenomena:

(1) The properties of Li amides used for deprotonations might be influenced by LiX additives, especially with more complex substrates.

(2) An enolate may exhibit different reactivity at the beginning ("pure" aggregate) and at the end ("mixed" aggregate with the LiX formed) of a reaction.

(3) The mode of addition and large excesses of one reactant in small-scale runs may strongly influence the results.

(4) LiX additives that are not part of the stoichiometric equation may decisively change the properties of an enolate.

In the three parts of Scheme 12 these effects are exemplified. *Firstly*, a Li enolate dimer may be converted into a mixed dimer by addition of LiX, which is formed in alkylations by alkyl halides or sulfonates. Assuming that the dimeric enolate gives rise to one product, the mixed aggregate of Li enolate and LiX another one; in the absence of interaggregate exchange, this would lead to formation of the two products in a 1 : 1 ratio. On the other hand, addition of excess LiX could convert all of the "pure" into the "mixed" aggregate so that a single product would be formed. *Secondly*, addition of a chiral Li derivative LiXR* to the dimer of an achiral Li enolate should give a chiral mixed aggregate, the enolate component of which has diastereotopic faces or, depending upon the substitution pattern of its double bond, can differentiate enantiotopic faces of a reactant. *Thirdly* (bottom part of Scheme 12), a polylithiated, self-aggregated compound (insoluble) may be converted into a mixed aggregate with added LiX and thus be solubilized (a kind of cross-linking is disrupted).

Of course, the LiX effect as sketched here is oversimplified, perhaps in a single-minded way: especially when added in large amounts, Li halides, thiolates, alkoxides, enolates, and amides will also change the medium itself,[257] rendering it more polar ("salt effect").[150] In addition, formation of ionized species[258] (ate complexes, ion pairs) will be more likely even at low temperatures. Still, the concept of mixed-aggregate formation turned out to be extremely fruitful in the course of our own work, some of which will be outlined in the following sections.

[*] Thoughts without content are empty, intuitions without concepts blind. *Critique of Pure Reason*. Edited and translated by W. Schwarz, Scientia Verlag, Aalen 1982, p. 29.

4.3. Achiral Enolates for the Preparation of Enantiomerically Enriched Products—Making a Virtue of Necessity

In Section 4.1, methods of avoiding the problems caused by the complexation of Li enolates with secondary amines were discussed. Here, we turn our attention to potentially very useful transformations which depend on the complexation between Li enolate and Li amide. For an enantioselective reaction, instead of coupling an enolate with a chiral auxiliary covalently, which requires a cleavage later on, the components are joined through a complexation, an interaction which is simply broken during aqueous workup! Just like in a chiral solvent,[259, 260] two achiral reactants, such as an enolate and an aldehyde, may thus be coupled to give enantiomerically enriched products (Scheme 12, middle). This procedure is fundamentally different from the use of a chiral Li amide[261] for enantioselective deprotonations or of a chiral acid for protonations[262, 263] (Scheme 13). A number of examples are collected in Table 9. As can be seen, metals other than Li can be employed. Chiral alkoxides are less effective than amides. Usually a Li enolate/$LiNR^*_2$ ratio of 1:3 gives rise to the highest enantiomer excesses.[278] Most of the chiral Li amides used are prepared from 1-phenylethyl amine or from amino acids and are thus readily available. Since there is very little structural information (Fig. 10) about complexes of Li amides with Li enolates, all attempts toward interpretations of these results are highly speculative, and we refrain from reproducing them here.

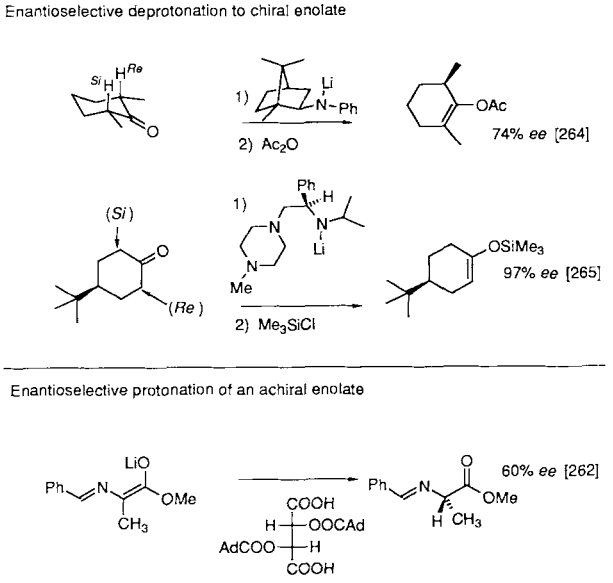

Scheme 13. Enantioselective protonations/deprotonations involving Li enolates. The chiral reagent (base or acid) selectively attacks enantiotopic groups or faces [266–268]. (With the protonations, the R_2NH effect discussed in Section 4.1 may be involved as well; with the deprotonations, the LiX effect may be operative—carefully excluded only in one case [264, 269].)

5. Alkylations of Sarcosine Units in Peptides—from Expectation to Surprise

What we learned about structure and reactivity of Li enolates was found to be successfully applicable to a seemingly unrelated project. For several years now, our group has been engaged in the development of new methods for the preparation of nonproteinogenic amino acids.[56, 100] These are required for incorporation into peptides whose biological properties are to be modified.[279] Normally, a separate synthesis is necessary for every peptide analogue [Scheme 14, route (a)]. A method by which a glycine unit in a given oligopeptide could be converted into other amino acid moieties by direct *C*-alkylation would not only be much more efficient; it would no doubt provide valuable information about the influence of chirality centers of neighboring amino acid units on the formation of a new stereogenic center in an open-chain peptide[280] [Scheme 14, route (b)].

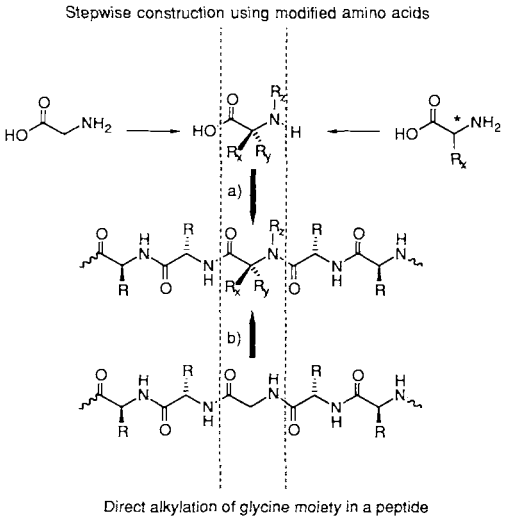

Scheme 14. Synthesis of modified peptides. a) By stepwise construction from the appropriately modified amino acid building blocks. b) Elaboration of an amino acid by introduction of side chains; many analogous derivatives could thus be obtained from a common precursor peptide.

The notion of generating an enolate in a peptide chain seems to be absurd:

Firstly, there is an acidic amide NH hydrogen ($pK_a < 20$) per amino acid unit to be removed before the CH_2 group of a glycine moiety can be deprotonated (there are even more acidic hydrogens in side-chain functionalized amino acids).

Secondly, strongly basic conditions are bound to be applied for such a CH deprotonation under which epimerizations of stereogenic centers might occur (in an n-oligopeptide a maximum of 2^n different diastereoisomers could be formed!).

Thirdly, it is usually necessary to generate Li enolates in an aprotic medium at low temperatures, conditions in which an oligopeptide itself, and even more so a polylithiated one, might be expected to have little solubility.

At the outset of our investigations in this area, we did not entertain such reflections; rather, a gifted young chemist[281] did a bold and careful experiment with an already rather large oligopeptide. For reasons of systematization, let us start with the simple cases, reversing the order of events.

Table 9. Enantioselective aldol additions, Michael additions to a nitroolefin, carboxylation, and alkylation of achiral enolates in the presence of chiral lithium alkoxides or amides. The examples 1–12 and 16 are taken from our own work [53, 91–93, 270–273], whereas we owe the results in entries 13 [274], 14 [275], and 15 [276] to research done by others. Enolate solutions free of amine were obtained either by addition of BuLi to enolates generated with $LiNR_2^1$ or by use of the silyl enol ether/methyllithium procedure. The configurations shown and the enantiomer ratios given were determined by NMR spectroscopy or with chiral HPLC columns [277].

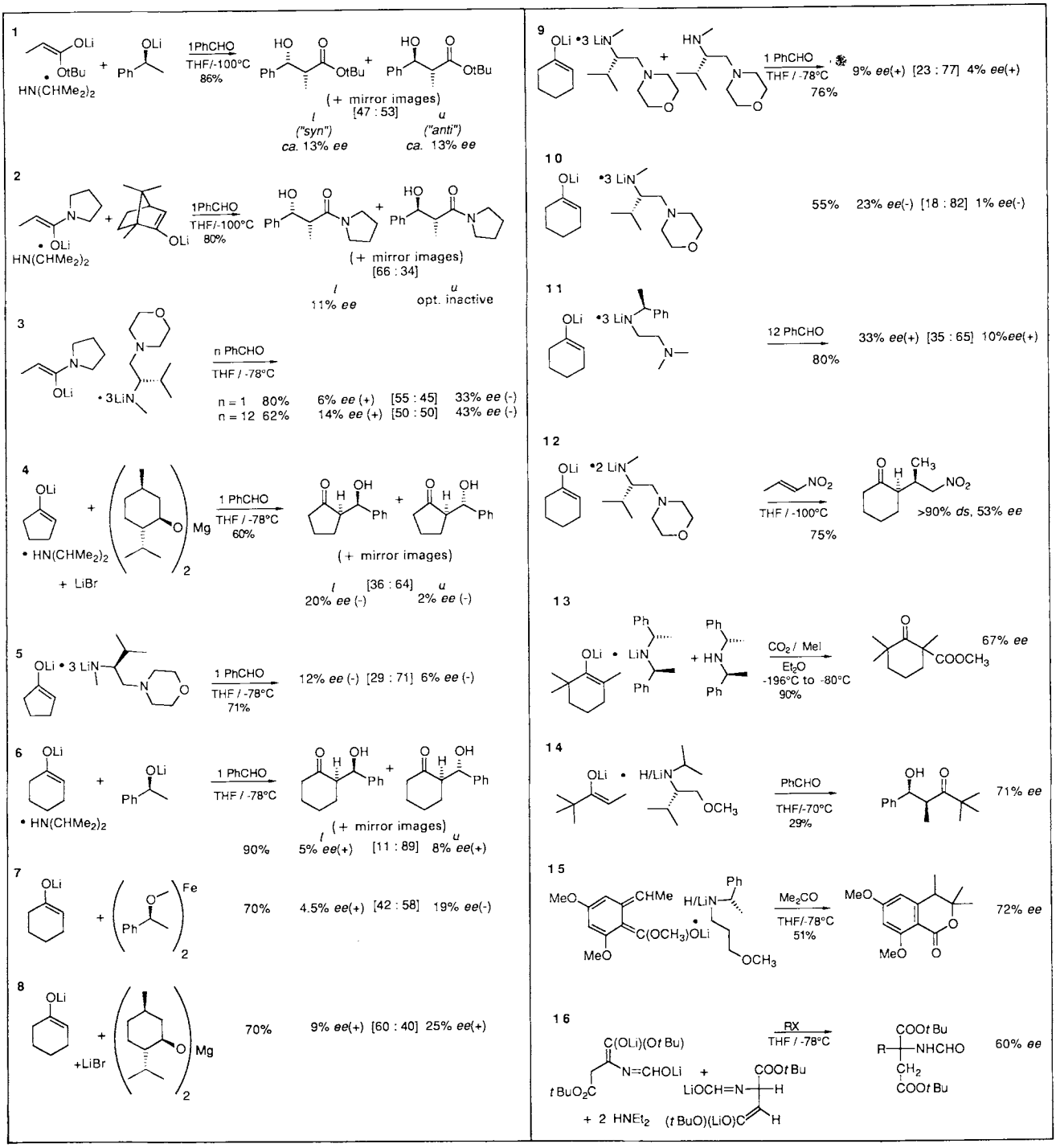

Two nonpeptide examples pictured in Scheme 15 may be used to demonstrate the LiX effect. The (*R*)-*N*-benzoyl-3-aminobutyrate shown in the upper part of Scheme 15 can be alkylated through a dilithium derivative in the 2-position.[41i, 282] At dry-ice temperature the reaction mixture in THF is heterogeneous; warming is necessary to complete the reaction with iodomethane. In contrast, the reaction takes place in homogeneous solution if LiCl[285] is added, with greatly improved result! Other Li salts such as LiBr, $LiClO_4$, $LiOSO_2R$ have similar effects (cf. the lower part[283] of Scheme 15).

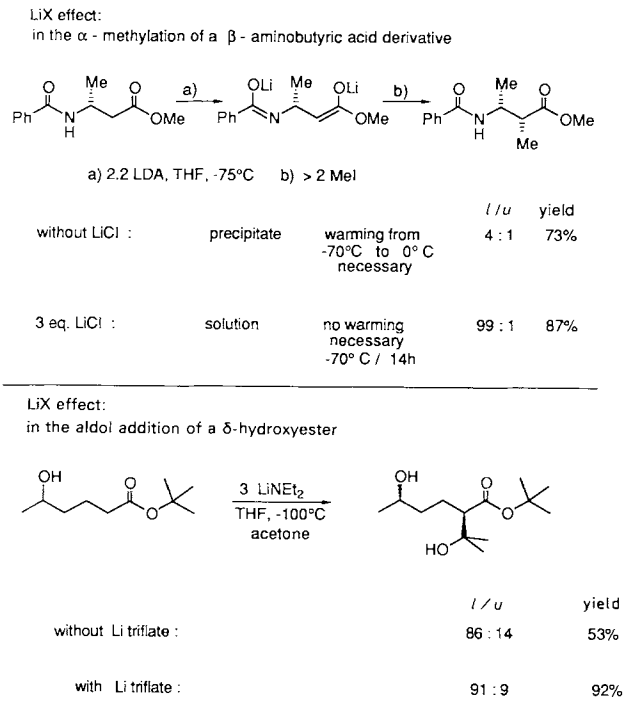

Scheme 15. LiX effect on the generation and behavior of two dilithium derivatives [41i, 282, 283]. In the case of the *N*-benzoyl β-amino acid ester the reagent to be alkylated is rendered soluble by addition of LiCl [41i]. In both cases, yields and stereoselectivities are increased. (C=C and C=N configurations here, in Schemes 16-21, and in Fig. 24 are drawn arbitrarily! [284].)

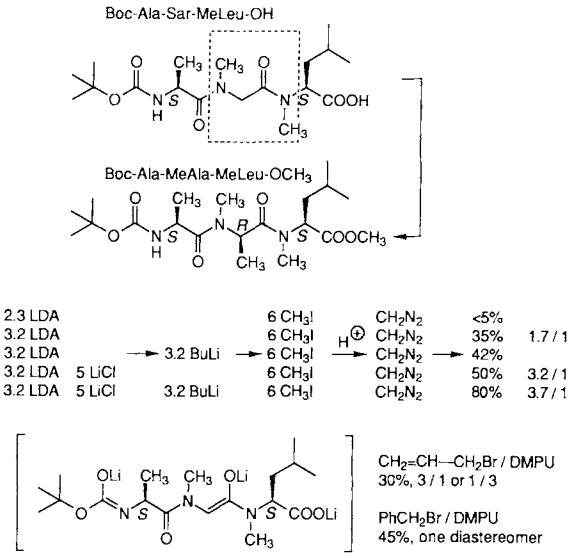

Scheme 16. Diastereoselective alkylations of the sarcosine unit in a Boc-protected tripeptide [286]. For the allylation and benzylation reactions, the cosolvent DMPU [63] had to be added to afford the yields shown.

5.1. Open-Chain Tri-, Tetra-, and Hexapeptides

For *C*-alkylations of open-chain peptides we first chose those containing (1) a sarcosine (*N*-methylglycine) substructure (shown in Scheme 16, sarcosine = *N*-methylglycine), (2) a Boc-protected amino end group (Boc = *tert*-butoxycarbonyl), and (3) a nonprotected carboxylic acid end group. Upon mixing of such peptides with the prerequisite number of equivalents of LDA, a more or less dense precipitate is formed. An enolate at the methylglycine (sarcosine) component of the tripeptide shown in Scheme 16 must arise when slightly more than three equivalents of LDA is added, because subsequent addition of iodomethane furnishes a new tripeptide with *N*-methylalanine at the former sarcosine position.

Removal of the diisopropylamine with butyllithium (cf. Section 4.1) led to marginal improvement of the yield, but addition of LiCl *and* BuLi (after LDA deprotonation) led to the isolation of the new peptide in 80% yield. More importantly, the reaction is diastereoselective (*R*-MeAla/*S*-MeAla almost 4 : 1), and it occurs without epimerization at the two stereogenic centers which were present in the starting material! The configuration was proved by comparison with authentic samples.[286-288]

Likewise, with the hexapeptide depicted in Scheme 17, containing four acidic OH and NH hydrogens besides a sarcosine CH_2 group, a precipitate is formed upon addition of the stoichiometric amount of LDA. Twice the calculated amount of LDA[289] or LiCl[285] causes the solid to dissolve.[290] A homogeneous, nonviscous, slightly yellow THF solution results, readily stirred at dry-ice temperature, and typical of polylithiated compounds under these conditions. Methylation again produces, in yields ranging from 30 to 67%, a new *N*-methylalanine unit in the peptide chain, the yield increasing in the presence of LiCl and with diisopropylamine deprotonation by BuLi.[285] Again, the reaction is diastereoselective, with the *R* configuration at the newly created stereogenic center prevailing (by comparison with authentic samples[288]). The hexalithio hexapeptide that ought to give rise to the observed product is shown at the bottom of Scheme 17.

Inspection of the *formulae* in Schemes 16 and 17 reveals that the peptides used have two characteristic features in common: (1) adjacent to each and every stereogenic center a deprotonation has occurred, rendering a certain protection from further deprotonation, i.e., from epimerization (see Scheme 18); (2) the peptides employed carry aliphatic side chains and are thus lipophilic, which should increase the solubility of their Li derivatives in the nonpolar THF. Had these properties been found to be essential for successful application of the above alkylation procedure, the method would be rather limited. The following two examples show that this is not the case.

The Boc-protected alanyl-glycyl-glycyl-glycine was selected as an example of an especially hydrophilic oligopeptide which, in fact, can hardly be retrieved from water. This also led to the discovery of a quite different LiX effect. As evident from the data in Scheme 19, the peptide, which itself is very insoluble in THF at room temperature, and LiCl form an extremely soluble complex. Furthermore, addition of five equivalents of LDA neither causes precipitation nor decomposition; hydrolysis leads to recovery of the peptide in optically active form. The possibility of carrying out reactions with the solutions thus obtained is currently being investigated. While the great solubility of peptide-LiCl complexes in an organic solvent is very surprising, the fact that anhydrous crystalline adducts

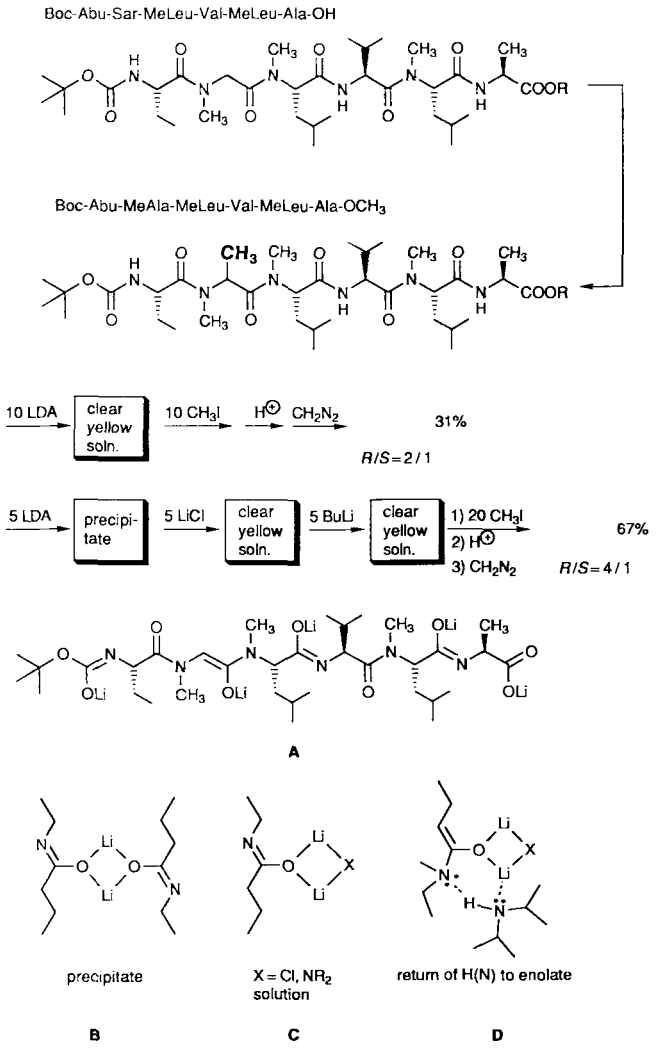

Scheme 17. Fivefold deprotonation of a Boc-protected hexapeptide (consisting of three *N*-methyl and three normal amino acid building blocks) by LDA and diastereoselective methylation at a sarcosine unit [285]. The yields shown were recorded after simple column chromatography and refer to the sum of the two epimers [2-(*R*-MeAla) and 2-(*S*-MeAla)]; the configurations at the other stereogenic centers are the same as in the starting material. **A**, pentalithium derivative; **B**, aggregates of **A**, poorly soluble; **C**, solubilization with LDA or LiCl, probably by formation of mixed aggregates (cf. Figs. 10, 20); **D**, complexation with diisopropylamine results in "reprotonation", i.e., lower yields without subsequent BuLi "treatment" (cf. Fig. 5 and Section 4.1).

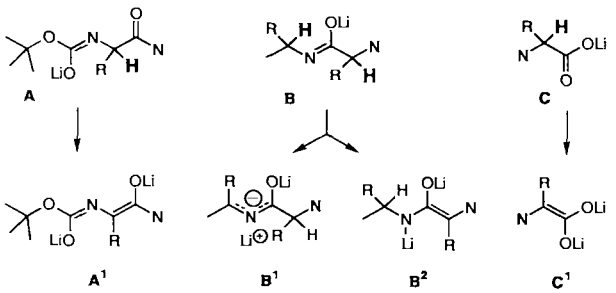

Scheme 18. Deprotonation of the carboxylic acid, carbamate, and amide groups of Boc-peptides, as applied to the reactions shown in Schemes 16 and 17, results in protection of the adjacent stereogenic center from epimerization. The highlighted hydrogens are less acidic in these structures than those in which a neighboring anionoid group is absent. The generation of doubly lithiated systems $\mathbf{A}^1$, $\mathbf{B}^1$, $\mathbf{B}^2$, and $\mathbf{C}^1$ from the respective precursors **A**, **B**, and **C** is indeed possible, as shown with simple molecules [126, 248, 291–293], but demands harsher conditions. (Protection of carbonyl groups against metal hydride reduction, and against addition of MeLi, by directed Li enolate formation in di- and tricarbonyl compounds has been well known for a long time [294, 295].

of Li salts with peptides may separate from aqueous solutions has been known since the beginning of this century (*Pfeiffer*'s "Neutralsalzverbindungen der Polypeptide und Eiweisskörper"[298]).[299] Furthermore, the solubilization in water of a protein antigen by addition of LiBr is described in a patent.[300] Some amide, peptide, and urea complexes of Li salts have been subjected to X-ray crystal structure analysis;[301] one such structure is shown in Figure 23.[303]

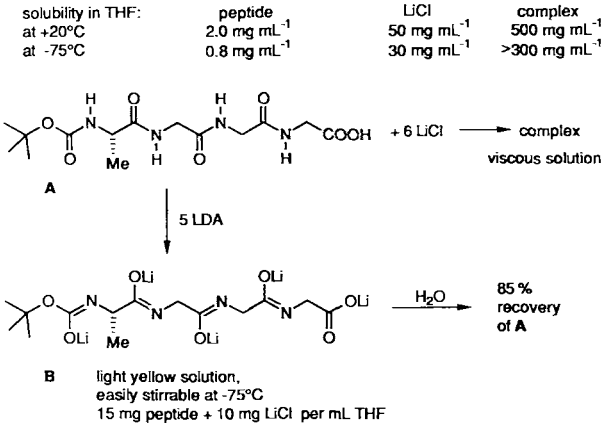

Scheme 19. Enormous increase in the solubility of a 1:6 mixture of Boc-Ala-Gly-Gly-Gly-OH and anhydrous LiCl in THF compared to that of the components. After removal of the solvent (5 h/10^{-3} torr/20°C), a solid residue is left which contains peptide, LiCl, and THF in the ratio 1:6:2.5. Adding five equivalents of LDA to the mixture of **A** and LiCl, at −75°C, produces a clear solution which probably contains the pentalithio derivative **B** [296, 297].

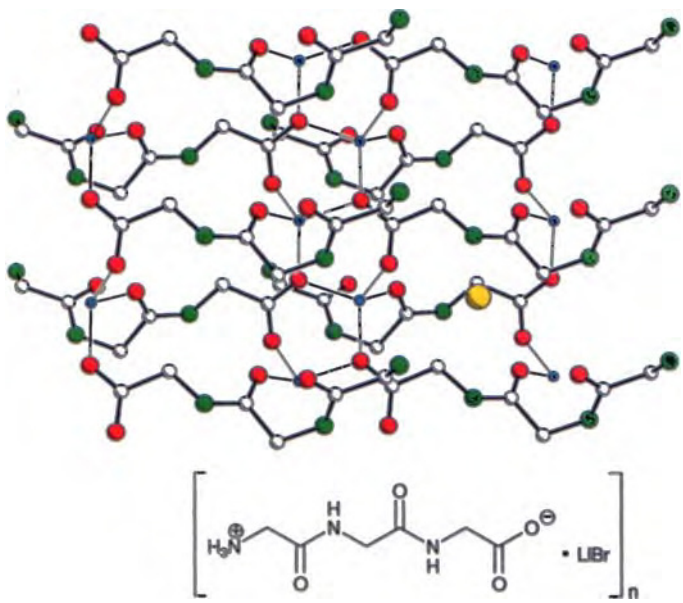

Fig. 23. Crystal structure of the LiBr complex of glycyl-glycyl-glycine [302] (section of the polymeric arrangement; *CSD*: GLYLIB). Cf. the LiX complexes with amides in Table 4, and the structures in Figs. 8, 11, and 16. The "addition ability" of Li salts toward amino acids decreases in the following series: Li > Na > K and I > Br > Cl (after *Pfeiffer*) [299].

5.2. Cyclosporine A

Nescire quaedam magna pars est sapientiae[304][*]

So far, the largest peptide in which we have been able to alkylate a sarcosine unit is cyclosporine A (CyA)[305,306] and some of its analogues.[307-311] CyA contains a series of amino acid moieties which are not protected against epimerization in the way indicated in Scheme 18. CyA is a novel immunosuppressive drug,[312] the discovery and use of which is as important as skilled surgery for the recent rapid developments in organ transplantations. CyA is a cyclic undecapeptide containing seven *N*-methyl amino acids (Fig. 24), four of which are adjacent to each other

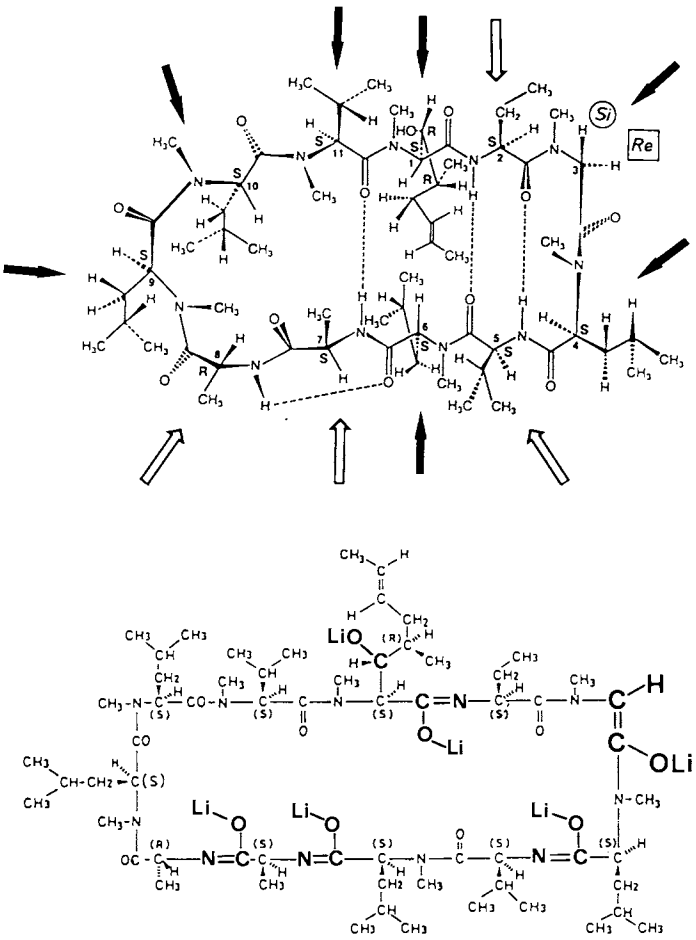

Fig. 24. Cyclosporine A (top) and the hexalithio derivative (bottom). The seven *N*-methyl amino acid building blocks are indicated by solid arrows, the four normal ones by open arrows. The conformation of CyA is identical in the crystal [306] and in solution [130a, 313], except for the orientation of the side chains of amino acids No. 1 and No. 11. There is no structural information available for the Li derivative (*E/Z* configuration at CC and CN double bonds is drawn arbitrarily). The Li derivative exists in THF solution in the presence of diisopropylamine, or LDA, or of LiCl, or mixtures of all three. The yellow solution (≥ 20 g L^{-1}), generated at -75°C, can be warmed up to $+20$°C without decomposition, at least for a short period of time.

(Nos. 9, 10, 11, 1). The amino acid No. 3 is sarcosine, which is followed by another *N*-methyl amino acid, MeLeu. CyA is highly lipophilic and insoluble in water due to the aliphatic side chains and the presence of transannular hydrogen bonds between opposite NH and CO groups in the pleated-sheet-type part of the molecule. In organic solvents CyA exhibits extremely high solubility (>600 mg mL^{-1} in THF at room temperature and >300 mg mL^{-1} at -75°C), and with LiCl a complex is formed, as evidenced gravimetrically or NMR spectroscopically[314] (cf. the LiBr complex of the cyclic decapeptide antamanide in Fig. 25).

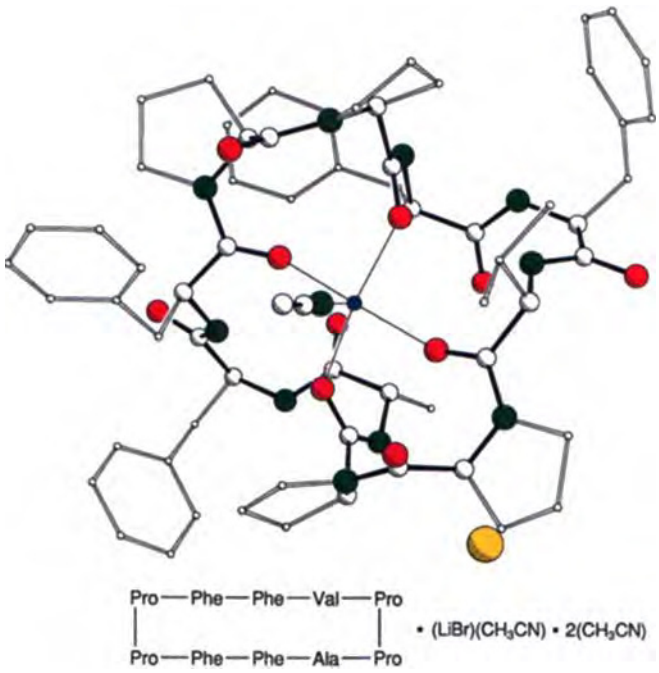

Fig. 25. LiBr complex of antamanide, *cyclo*(Val-Pro-Pro-Ala-Phe-Phe-Pro-Pro-Phe-Phe), crystallized from acetonitrile (*CSD*: ANTAML 10) [315]. The four carbonyl oxygens bound to Li form the base of a nearly square pyramid, with the acetonitrile nitrogen at the apex. The cyclic decapeptide originates from the green death cup mushroom *(Amanita phalloides)* [316]. There are two additional molecules of CH_3CN per cyclic peptide in the crystal.

When treated with the required number of equivalents of LDA (≥ 6) in THF, CyA is deprotonated at the sarcosine unit to give a Li enolate without destruction of the peptide ring. Reactions with electrophiles give derivatives with substituents in the former sarcosine position.[281, 285, 286, 289, 314, 317] With CyA and LDA alone a precipitate or a viscous mixture, which may solidify as a gel, results at -78°C. If an amount of LDA exceeding the six equivalents required (for removal of one OH, one CH_2, and four NH protons) is added (up to 15 equivalents), a clear, yellow, readily stirred solution is obtained, quenching of which with water leads to the recovery of more than 90% CyA. Epimerizations are observed only to a very small extent, and they do indeed occur mainly at the amino acids Nos. 9, 10, and 11, those lacking the protection discussed above. Simple column chromatography readily frees CyA from the impurities thus generated. With electrophiles other than water, products of substitution of the diastereotopic *Re* hydrogen ($\leq 90\%$ *ds*) in the sarcosine unit (Sar^3)

[*] Not knowing is the essence of wisdom.

are formed in yields ranging from 10 to 50%, with a large amount of unreacted CyA being recovered. Some of the substituents that were introduced into CyA by this procedure are indicated in Scheme 20.

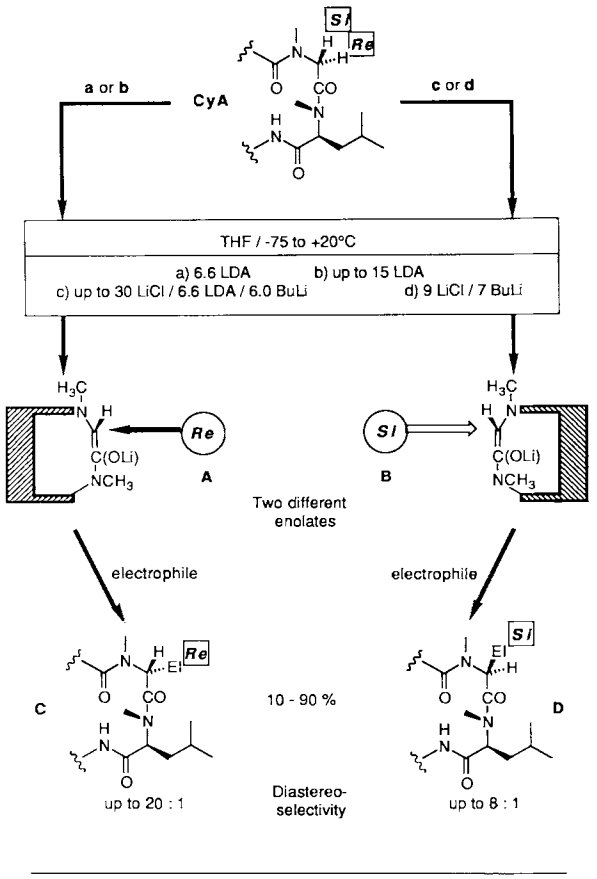

El = D, CH_3, $CH_2CH{=}CH_2$, $CH_2COO(t\,Bu)$, CH_2OH, $CH(OH)Ph$, $COOCH_3$, F, SCH_3

Scheme 20. Alkylation of CyA on the sarcosine unit via the Li enolate shown in Fig. 24 [317]. Depending on the conditions of deprotonation either an enolate **A** is generated that is preferentially attacked from the *Re* side, or an enolate **B** with *Si* selectivity (see the products **C** and **D**, respectively) [318]. The highest yields were recorded under "amine-free, LiCl conditions" [c and d], and the best selectivities under the "LDA conditions" [a and b]. CD_3CO_2D, MeI, alkyl bromides, aldehydes, CO_2/CH_2N_2, $FClO_3$, and disulfides were used in excess as electrophiles. The products **C** and **D** can be separated by flash chromatography and isolated in pure form.

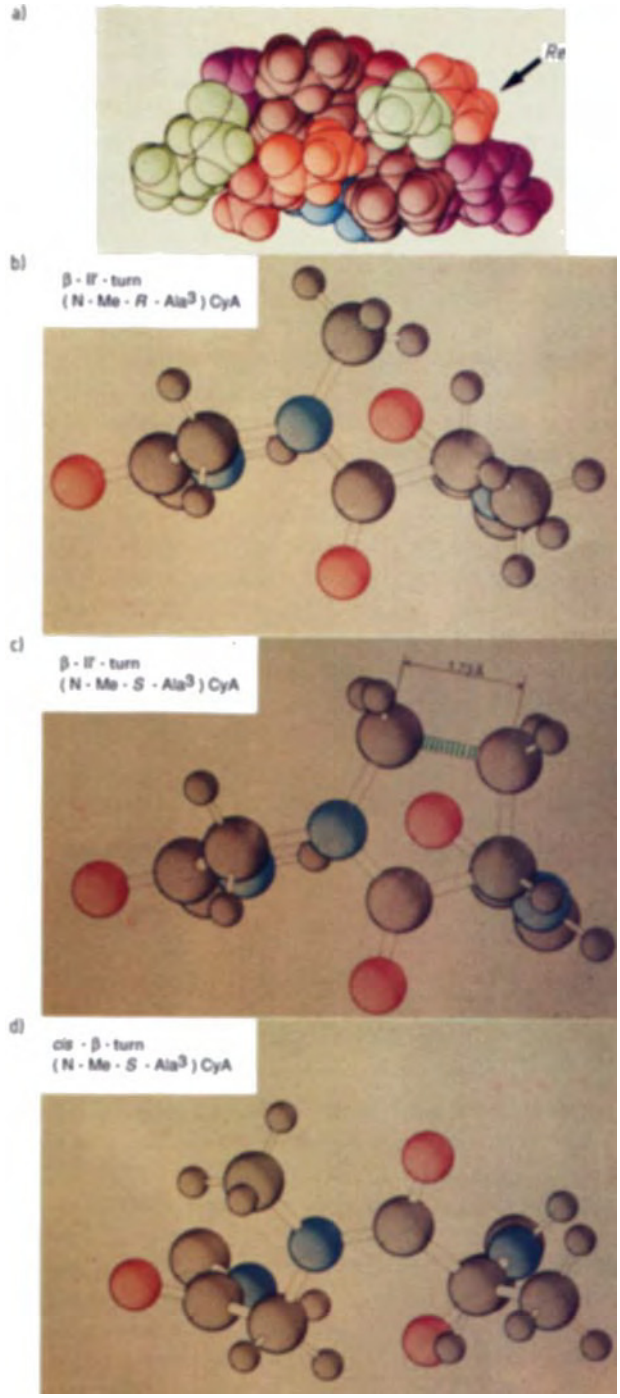

Fig. 26. Space-filling model of CyA generated with the data of the structure analysis, and ball-and-stick model of the partial structure around the β-turn at which the stereoselective alkylation through a Li enolate occurs (Fig. 24, Scheme 20). a) Overview, in which the *Re* hydrogen on sarcosine is emphasized; the *Si* hydrogen and the neighboring NCH_3 group are quasi-1,3-diaxial to each other as viewed by the reader. b) H(*Re*) substituted by CH_3, no steric hindrance [the NMR spectra of CyA and (*N*-Me-(*R*)-Ala^3)CyA are superimposable over wide regions]. c) H(*Si*) substituted by CH_3, strong penetration of van der Waals radii of the two CH_3 groups in maintaining the β-II'-turn. d) Equatorial (*Si*)-CH_3 group in a *cis* β-turn, with formation of a *cisoid* peptide bond [the NMR spectra of the (*R*) and (*S*) derivatives differ greatly].

We were overjoyed that the products derived from replacement of the diastereotopic *Si* hydrogen can also be obtained selectively; yields of over 90% may be obtained if the deprotonation of CyA by LDA is carried out in the presence of large amounts of LiCl (up to 30 equivalents), and if the diisopropylamine is removed by BuLi addition. We do not know whether the enolates generated under the two different sets of conditions are configurationally different (*E*/*Z* on C=N and/or C=C) or whether they differ only by different LiX effects exerted by LDA and LiCl. At any rate, the *Re* face of the enolate double bond must be hindered in one case, the *Si* face in the other, by the arrangement of the macrocyclic ring (see Scheme 20).

The pure products are readily isolated by medium-pressure chromatography on SiO_2. Miraculously, CyA ($M_r = 1202$) and the two diastereomeric products of methylation [N-Me-(*R*)-Ala^3)CyA and (N-Me-(*S*)-Ala^3)CyA,

$M_r = 1216$] clearly separate on a simple analytical silica gel thin-layer plate![319] (The structural assignment of the two methyl derivatives was arrived at by comparison of the NMR spectra with those of authentic samples.[287,288])

Cleavages of the CyA peptide backbone or alkylations of amino acids other than the sarcosine occur only to a very small extent. Upon treatment of CyA with BuLi in the presence of LiCl (Scheme 20, d) appreciable amounts of a butyl ketone may be isolated, if desired, which results from attack at the carbonyl group of amino acid No. 9 (an "unprotected" site!).

The biological activity of the products thus available follows a simple rule: derivatives with substituents in the *Re* position still have immunosuppressive properties comparable to CyA, those substituted in the *Si* position do not. The reason for this is obvious from modeling as shown in Figure 26; the *Re* hydrogen of the sarcosine in CyA occupies a quasi-equatorial position, the *Si* hydrogen a quasi-axial one; introduction of a substituent into the latter position imposes such severe steric hindrance by van der Waals overlap with the NCH_3 group of the adjacent amino acid that the peptide chain must adopt a different conformation, causing the shape of the entire molecule to change.

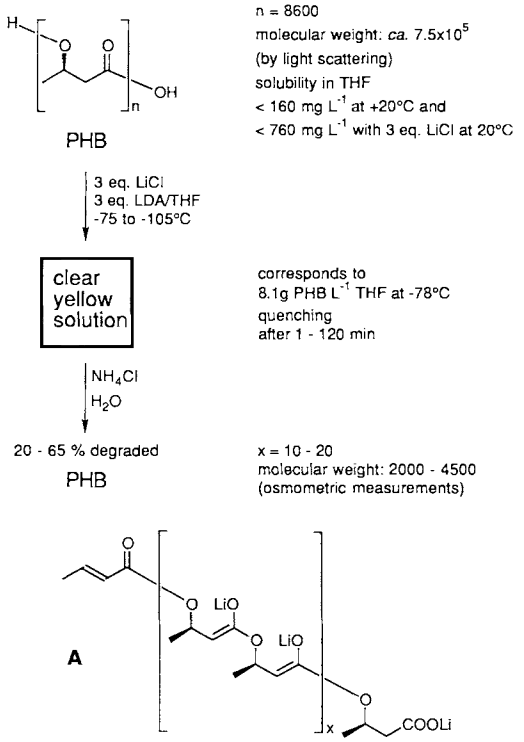

Scheme 21. Deprotonating solubilization and partial degradation of poly-[(*R*)-3-hydroxybutyrate], PHB, with LDA/LiCl in THF at low temperature. The solubilities described for PHB in THF are upper limits, which have been extrapolated from experiments in volumes of much less than 1 L. The upper limit of the solubility accessible by addition of LDA/LiCl was not investigated. The enolate could also decompose by α-elimination [72] (lithium oxybutyrate end group) instead of β-elimination (crotonate terminal group). There is no indication of a direct attack by LDA on the ester carbonyl groups of the polymer (aminolysis, resulting in formation of carboxamide end groups).

6. Outlook—on to Even More Complex Systems

An experiment is in progress
but it is uncertain
if we are in control
or just observers
Roald Hoffmann[320]

Encouraged by the solubilization of polylithiated organic compounds, such as peptides, by addition of inorganic Li salts, we also investigated other systems. We found, for instance, that when a suspension of the biopolymer PHB (polyhydroxybutyrate, $M_r = 7.5 \times 10^5$), which itself is totally insoluble both in water and THF, was treated with excess LDA in the presence of LiCl at low temperature, a clear, slightly yellow THF solution was obtained. Subsequent quenching with water leads to recovery of up to 65% of a polymer of lower molecular weight (Scheme 21).[321,322] The fact that decomposition of the polyester polyenolate does not take place all the way to the monomer (Li crotonate), but that an unexpectedly long-lived species containing ca. 30 units persists, suggests the answer must have something to do with the structure of this species—which we do not know.[323]

Our excursion into the world of Li enolate aggregate structures and the quest for proof of their involvement in product-forming steps did not only furnish important new knowledge, but led us continuously back to the laboratory. There, we have arrived at systems of a complexity with which we could not have hoped to cope at the outset; they exhibit reactivities which we observe with pleasure and with excitement, but which we again do not understand.

Lesson: Even the synthetic organic chemist must consider very complex structures, supramolecules in *Lehn*'s terminology, in his everyday work. I have nothing to add to the statement of *Lord Todd*:[324]

> Apart from consideration of the hydrogen bond, we organic chemists have really paid little attention to linkages other than the purely covalent. I believe that it will be the duty of organic chemists in the future to study the weak non-bonding interactions which are of enormous importance in the large natural macromolecules. Such studies will lead to a new blossoming of organic chemistry in the future.
>
> *Lord Alexander R. Todd*

My sincere thanks go to the co-workers who have contributed to the work described here; their names are given in the list of references. Collaboration with them was and still is a source of great pleasure for me. I thank my colleague Jack Dunitz for many enlightening discussions. The preparation of this review article would not have been possible without the help and dedication of Silvia Sigrist (typing), Albert K. Beck (list of references), Bernd Lamatsch and Thomas Maetzke (figures), Gerhard Stucky and Geo Adam (schemes and tables), Ulf Misslitz (corrections), Hans-Jörg Gründler (application of the programs WORD® and ChemDraw®), and Edward Dziadulewicz, Robert Fitzi, and Soo Y. Ko (parts of the English version).

Received: September 14, 1988 [A 702 IE]
German version: *Angew. Chem. 100* (1988) 1685

[1] Articles on this topic worth reading: A. Lapworth, *J. Chem. Soc. 79* (1901) 1265; *ibid. 121* (1922) 416 (reactivity and alternating polarity); R. Robinson in H. Grossmann (Ed.): *Sammlung chemischer und chemisch-technischer Vorträge, Neue Folge, Heft 14*, F. Enke Verlag, Stuttgart 1932; C. K. Ingold, *Chem. Rev. 15* (1934) 225-274 (electronic theory of organic reactions); C. R. Hauser, D. S. Breslow, *J. Am. Chem. Soc. 62* (1940) 2389; H. B. Watson, *Trans. Faraday Soc. 37* (1941) 707; V. Franzen, *Chem.-Ztg. 80* (1956) 446 (aldol additions and condensations); Sir Robert Robinson, *Memoirs of a Minor Prophet (70 Years of Organic Chemistry)*, Elsevier, Amsterdam 1976; D. Seebach, *Angew.* Chem. 91 (1979) 259-278; *Angew. Chem. Int. Ed. Engl. 18* (1979) 239-258 (reactivity umpolung—also of carbonyl compounds).

[2] H. O. House: *Modern Synthetic Reactions, 2nd ed.*, W. A. Benjamin, Menlo Park 1972.

[3] T. Mukaiyama, *Org. React. 28* (1982) 203-331.

[4] R. Noyori, I. Nishida, J. Sakata, *J. Am. Chem. Soc. 105* (1983) 1598; I. Kuwajima, E. Nakamura, *Acc. Chem. Res. 18* (1985) 181.

[5] a) P. Fellmann, J.-E. Dubois, *Tetrahedron 34* (1978) 1349; b) C. H. Heathcock: *The Aldol Addition Reaction* in J. D. Morrison (Ed.): *Asymmetric Synthesis, Vol. 3*, Academic Press, Orlando, FL 1984, pp. 111-212.

[6] D. A. Evans: Stereoselective Alkylation Reactions of Chiral Metal Enolates in J. D. Morrison (Ed.): *Asymmetric Synthesis, Vol. 3*, Academic Press, Orlando, FL 1984, pp. 1-110.

[7] Double Asymmetric Synthesis and a New Strategy for Stereochemical Control in Organic Synthesis: S. Masamune, W. Choy, J. S. Petersen, L. R. Sita, *Angew. Chem. 97* (1985) 1-31; *Angew. Chem. Int. Ed. Engl. 24* (1985) 1-30.

[8] R. E. Ireland, R. H. Mueller, A. K. Willard, *J. Am. Chem. Soc. 98* (1976) 2868.

[9] T. Mukaiyama, K. Inomata, *Bull. Chem. Soc. Jpn. 44* (1971) 3215; T. Mukaiyama, T. Inoue, *Chem. Lett. 1976*, 559.

[10] E. Shimada, K. Inomata, T. Mukaiyama, *Chem. Lett. 1974*, 689.

[11] The effect of polar cosolvents like hexamethylphosphoric triamide (HMPT) or *N,N'*-dimethylpropyleneurea (DMPU), of chelating additives, or of crown ethers or cryptands will be discussed further below; see Schemes 3, 5, 9, Table 3, Figs. 12, 15, and Section 2.2.3.

[12] H. E. Zimmerman, M. D. Traxler, *J. Am. Chem. Soc. 79* (1957) 1920.

[13] D. Seebach, J. Goliński, *Helv. Chim. Acta 64* (1981) 1413.

[14] M. A. Brook, D. Seebach, *Can. J. Chem. 65* (1987) 836.

[15] E. Weiss, H. Alsdorf, H. Kühr, H.-F. Grützmacher, *Chem. Ber. 101* (1968) 3777.

[16] F. A. Schröder, H. P. Weber, *Acta Crystallogr. B31* (1975) 1745.

[17] D. Bright, G. H. W. Milburn, M. R. Truter, *J. Chem. Soc. A1971*, 1582.

[18] D. E. Fenton, C. Nave, M. R. Truter, *J. Chem. Soc. Dalton Trans. 1973*, 2188.

[19] H. D. Zook, T. J. Russo, *J. Am. Chem. Soc. 82* (1960) 1258; H. D. Zook, W. L. Gumby, *ibid. 82* (1960) 1386.

[20] H. O. House, M. Gall, H. D. Olmstead, *J. Org. Chem. 36* (1971) 2361.

[21] L. M. Jackman, N. Szeverenyi, *J. Am. Chem. Soc. 99* (1977) 4954.

[22] Review article: *Structure and Reactivity of Alkali Metal Enolates:* L. M. Jackman, B. C. Lange, *Tetrahedron 33* (1977) 2737-2769.

[23] Reaction of benzoyl chloride with ethyllithium (hexamer) in benzene: R. West, W. Glaze, *J. Chem. Phys. 34* (1961) 685.

[24] Reaction of ethylene with *tert*-butyllithium (tetramer) in diethyl ether/hexane: P. D. Bartlett, C. V. Goebel, W. P. Weber, *J. Am. Chem. Soc. 91* (1969) 7425.

[25] M. Schlosser: *Struktur und Reaktivität polarer Organometalle*, Springer, Berlin 1973.

[26] A. W. Langer (Ed.): *Polyamine-Chelated Alkali Metal Compounds, Adv. Chem. Ser. 130* (1974) ACS, Washington DC (USA).

[27] B. J. Wakefield: *The Chemistry of Organolithium Compounds*, Pergamon Press, Oxford 1974.

[28] *Organolithium Compounds in Organic Synthesis.* Recent developments: D. Seebach, K.-H. Geiss: *J. Organomet. Chem. Libr. 1* (1976) 1-92.

[29] J. C. Stowell: *Carbanions in Organic Synthesis*, Wiley, New York 1979.

[30] B. J. Wakefield in D. H. R. Barton, W. D. Ollis (Eds.): *Comprehensive Organic Chemistry, Vol. 3*, Pergamon Press, Oxford 1979, Part 15, pp. 943-1012.

[31] M. E. O'Neill, K. Wade, J. L. Wardell, N. A. Bell, W. E. Lindsell in G. Wilkinson, F. G. A. Stone, E. W. Abel (Eds.): *Comprehensive Organometallic Chemistry, Vol. 1*, Pergamon Press, Oxford 1982, pp. 1-252; B. J. Wakefield, *ibid. Vol. 7*, pp. 1-110.

[32] R. B. Bates, C. A. Ogle: *Carbanion Chemistry*, Springer, Berlin 1983.

[33] R. O. Bach (Ed.): *Lithium-Current Applications in Science, Medicine and Technology*, Wiley, New York 1985.

[34] Symposium on Advances in Carbanion Chemistry, Division of Petroleum Chemistry, ACS Meeting, Chicago (September 1985): *Prepr. Div. Pet. Chem. Am. Chem. Soc. 30* (1985) No. 4.

[35] L. Brandsma, H. Verkruijsse: *Preparative Polar Organometallic Chemistry—1*, Springer, Berlin 1987.

[36] C. Elschenbroich, A. Salzer: *Organometallchemie*, Teubner, Stuttgart 1986.

[37] Heteroatom-Facilitated Lithiations: H. W. Gschwend, H. R. Rodriguez, *Org. React. 26* (1979) 1-360.

[38] Lithium Halocarbenoids—Carbanions of High Synthetic Versatility: H. Siegel, *Top. Curr. Chem. 106* (1982) 55-78.

[39] Stereo- and Regiocontrol by Complex Induced Proximity Effects: Reactions of Organolithium Compounds: P. Beak, A. I. Meyers, *Acc. Chem. Res. 19* (1986) 356-363.

[40] Oxygen- and Nitrogen-assisted Lithiation and Carbolithiation of Non-aromatic Compounds; Properties of Non-aromatic Organolithium Compounds Capable of Intramolecular Coordination to Oxygen and Nitrogen: G. W. Klumpp, *Recl. Trav. Chim. Pays-Bas 105* (1986) 1-21.

[41] Some review articles on polylithiated compounds: a) T. M. Harris, C. M. Harris, *Org. React. 17* (1969) 155-211; b) E. M. Kaiser, J. D. Petty, P. L. A. Knutson, *Synthesis 1977*, 509-550; c) D. Seebach, E.W. Colvin, F. Lehr, T. Weller, *Chimia 33* (1979) 1-18; d) D. Seebach, M. Pohmakotr, *Tetrahedron 37* (1981) 4047-4058; e) P. von R. Schleyer, *Pure Appl. Chem. 56* (1984) 151-162; f) B. Bogdanović, *Angew. Chem. 97* (1985) 253-264; *Angew. Chem. Int. Ed. Engl. 24* (1985) 262-273; g) A. Maercker, M. Theis, *Top. Curr. Chem. 128* (1987) 1-61; h) K. Müllen, *Angew. Chem. 99* (1987) 192-205; *Angew. Chem. Int. Ed. Engl. 26* (1987) 204-217; i) D. Seebach, H. Estermann, *Helv. Chim. Acta 71* (1988), in press.

[42] a) Low-Temperature ^{13}C NMR Spectroscopy of Organolithium Derivatives.—$^{13}C,^{6}Li$-Coupling, a Powerful Structural Information: D. Seebach, R. Hässig, J. Gabriel, *Helv. Chim. Acta 66* (1983) 308-337; b) Low Temperature ^{13}C-NMR Spectra of ^{6}Li- and ^{13}C-Labelled Sulfur- and Selenium-Substituted Organolithium Derivatives: D. Seebach, J. Gabriel, R. Hässig, *ibid. 67* (1984) 1083-1099; c) J. Heinzer, J. F. M. Oth, D. Seebach, *ibid. 68* (1985) 1848-1862.

[43] The Structure and Dynamic Behaviour of Organolithium Compounds in Solution, ^{13}C, ^{6}Li, and ^{7}Li-NMR: G. Fraenkel, H. Hsu, B. M. Su, see [33], Chapter 19, pp. 273-290.

[44] High-Resolution Metal-NMR Spectroscopy of Organometallic Compounds: R. Benn, H. Rufińska, *Angew. Chem. 98* (1986) 851-871; *Angew. Chem. Int. Ed. Engl. 25* (1986) 861-881.

[45] Aggregation States and Exchange Properties of Alkyllithium Compounds in Hydrocarbon Solvent from ^{13}C-^{6}Li Coupling: R. D. Thomas, R. M. Jensen, T. C. Young, *Organometallics 6* (1987) 565.

[46] Modern NMR Spectroscopy of Organolithium Compounds: H. Günther, D. Moskau, P. Bast, D. Schmalz, *Angew. Chem. 99* (1987) 1242-1250; *Angew. Chem. Int. Ed. Engl. 26* (1987) 1212-1220.

[47] X-Ray Structural Analyses of Organolithium Compounds: W. N. Setzer, P. von R. Schleyer, *Adv. Organomet. Chem. 24* (1985) 353-451.

[48] Sodium, Potassium, Rubidium and Cesium—X-Ray Structural Analysis of Their Organoalkali Compounds: C. Schade, P. von R. Schleyer, *Adv. Organomet. Chem. 27* (1987) 169-278.

[49] High-Resolution X-ray Crystallography—an Experimental Method for the Description of Chemical Bonds: K. Angermund, K. H. Claus, R. Goddard, C. Krüger, *Angew. Chem. 97* (1985) 241-252; *Angew. Chem. Int. Ed. Engl. 24* (1985) 237-247.

[50] Unsaturated Molecules Containing Main Group Metals: M. Veith, *Angew. Chem. 99* (1987) 1-14; *Angew. Chem. Int. Ed. Engl. 26* (1987) 1-14.

[51] Low-Temperature X-ray Structure Techniques for the Characterization of Thermolabile Molecules: M. Veith, W. Frank, *Chem. Rev. 88* (1988) 81-92.

[52] Free Inorganic, Organic, and Organometallic Ions by Treatment of Their Lithium Salts with 12-Crown-4: P. P. Power, *Acc. Chem. Res. 21* (1988) 147-153.

[53] A preliminary report on our work, which received only little attention, appeared in a conference volume; Crystal Structures and Stereoselective Reactions of Organic Lithium Derivatives: D. Seebach, *Proc. Robert A. Welch Found. Conf. Chem. Res. 27: Stereospecificity in Chemistry and Biochemistry* (November 7-9, 1983), Houston, TX 1984, pp. 93-145.

[54] Review article: B. Weidmann, D. Seebach, *Angew. Chem. 95* (1983) 12-26; *Angew. Chem. Int. Ed. Engl. 22* (1983) 31-45.

[55] D. Seebach, B. Weidmann, L. Widler in R. Scheffold (Ed.): *Modern Synthetic Methods, Vol. 3*, Salle + Sauerländer, Aarau/Wiley, New York 1983, pp. 217-353.

[56] D. Seebach, R. Imwinkelried, T. Weber in R. Scheffold (Ed.): *Modern Synthetic Methods, Vol. 4*, Springer, Berlin 1986, pp. 125-259.

[57] D. Seebach, S. Roggo, J. Zimmermann in W. Bartmann, K. B. Sharpless (Eds.): *Stereochemistry of Organic and Bioorganic Transformations, Workshop Conferences Hoechst, Vol. 17*, VCH Verlagsgesellschaft, Weinheim 1987, pp. 85-126.

[58] Review article, Nobel lecture: J.-M. Lehn, *Angew. Chem. 100* (1988) 91-116; *Angew. Chem. Int. Ed. Engl. 27* (1988) 89-112.

[59] G. Wittig, H. Reiff, *Angew. Chem. 80* (1968) 8; *Angew. Chem. Int. Ed. Engl. 7* (1968) 7; G. Wittig, A. Hesse, *Org. Synth. 50* (1970) 66.

[60] R. A. Olofson, C. M. Dougherty, *J. Am. Chem. Soc. 95* (1973) 581, 582.

[61] M. W. Rathke, *J. Am. Chem. Soc. 92* (1970) 3222.

[62] H. Normant, *Angew. Chem. 79* (1967) 1029–1050; *Angew. Chem. Int. Ed. Engl. 6* (1967) 1046–1067.

[63] Replacement of the mutagenic phosphoric amide HMPT by DMPU and other cosolvents (see also Scheme 3): T. Mukhopadhyay, D. Seebach, *Helv. Chim. Acta 65* (1982) 385; D. Seebach, *Chem. Br. 21* (1985) 632.

[64] Z. A. Fataftah, I. E. Kopka, M. W. Rathke, *J. Am. Chem. Soc. 102* (1980) 3959.

[65] E. J. Corey, A. W. Gross, *Tetrahedron Lett. 25* (1984) 495.

[66] T. Laube, J. D. Dunitz, D. Seebach, *Helv. Chim. Acta 68* (1985) 1373.

[67] Special precautions have to be taken in synthesizing 1,3-dicarbonyl compounds via lithium enolates to avoid double addition. a) A well-known method especially applied to synthesizing methyl ketones is the use of Li carboxylates as acylating agents. Review article: M. J. Jorgenson, *Org. React. 18* (1970) 1–97. b) The acylation succeeds directly with acid chlorides by (inverse) addition of Li enolates at very low temperatures, even with 3-nitropropanoyl and 4-nitrobutanoyl chloride: D. Seebach, T. Weller, G. Protschuk, A. K. Beck, M. S. Hoekstra, *Helv. Chim. Acta 64* (1981) 716. c) Review article on "Synthese bei Temperaturen unter −80°C": D. Seebach, A. Hidber, *Chimia 37* (1983) 449–462. d) A trick that avoids complications is the reaction of the enolate with acyl cyanides, which at first results in cyanohydrin derivatives: S. Hünig, R. Schaller, *Angew. Chem. 94* (1982) 1–15; *Angew. Chem. Int. Ed. Engl. 21* (1982) 36–49 (review). L. N. Mander, S. P. Sethi, *Tetrahedron Lett. 24* (1983) 5425.

[68] R. Amstutz, W. B. Schweizer, D. Seebach, J. D. Dunitz, *Helv. Chim. Acta 64* (1981) 2617.

[69] D. Seebach, R. Amstutz, J. D. Dunitz, *Helv. Chim. Acta 64* (1981) 2622.

[70] P. G. Williard, G. B. Carpenter, *J. Am. Chem. Soc. 107* (1985) 3345.

[71] P. G. Williard, G. B. Carpenter, *J. Am. Chem. Soc. 108* (1986) 462.

[72] a) R. Häner, T. Laube, D. Seebach, *J. Am. Chem. Soc. 107* (1985) 5396; b) H. R. Seikaly, T. T. Tidwell, *Tetrahedron 42* (1986) 2587–2613 (review); c) C. Fehr, J. Galindo, *J. Org. Chem. 53* (1988) 1828.

[73] D. Seebach, R. Amstutz, T. Laube, W. B. Schweizer, J. D. Dunitz, *J. Am. Chem. Soc. 107* (1985) 5403. The structures of the *tert*-butyl 2-methylpropionate lithium enolate (dimer with TMEDA; *CSD*: DEDXIT) and of the tetrameric methyl 3,3-dimethylbutyrate lithium (*Z*)-enolate solvated by four THF molecules (*CSD*: DEDXOZ) are described in the same paper. It is striking that in all dimeric ester and amide enolates with THF and TMEDA as ligands to Li, the two enolate units are on the same side of the OLiOLi quadrangle, as if it were a bisected cube in which the enolates are necessarily *cis* to each other.

[74] a) L. Ghosez, J. Marchand-Brynaert in H. Böhme, H. G. Viehe (Eds.): *Iminium Salts in Organic Chemistry, Part 1*, Wiley, New York 1976, pp. 421–532, especially pp. 465–467; b) K. L. Brown, L. Damm, J. D. Dunitz, A. Eschenmoser, R. Hobi, C. Kratky, *Helv. Chim. Acta 61* (1978) 3108; c) A. Kümin, E. Maverick, P. Seiler, N. Vanier, L. Damm, R. Hobi, J. D. Dunitz, A. Eschenmoser, *ibid. 63* (1980) 1158; d) S. J. Blarer, W. B. Schweizer, D. Seebach, *ibid. 65* (1982) 1637; e) Latest comprehensive review on the structure of enamines: A. G. Cook (Ed.): *Enamines*, 2nd ed., Marcel Dekker, New York 1988, Chapter 1, pp. 1–101.

[75] Hydrogen Bond Geometry in Organic Crystals: R. Taylor, O. Kennard, *Acc. Chem. Res. 17* (1984) 320–326.

[76] W. Saenger: *Principles of Nucleic Acid Structure*, Springer, Berlin 1984.

[77] W. Bauer, T. Laube, D. Seebach, *Chem. Ber. 118* (1985) 764.

[78] P. G. Williard, J. M. Salvino, *Tetrahedron Lett. 26* (1985) 3931.

[79] R. Amstutz, J. D. Dunitz, T. Laube, W. B. Schweizer, D. Seebach, *Chem. Ber. 119* (1986) 434.

[80] J. J. Brooks, G. D. Stucky, *J. Am. Chem. Soc. 94* (1972) 7333.

[81] P. G. Williard, *J. Am. Chem. Soc. 110* (1988), in press. I thank Professor *Williard* for sending us the manuscript and the coordinates prior to publication of the structure of $[(LDA)_2(THF)_2]$.

[82] T. Fjeldberg, P. B. Hitchcock, M. F. Lappert, A. J. Thorne, *J. Chem. Soc. Chem. Commun. 1984*, 822.

[83] R. Hacker, E. Kaufmann, P. von R. Schleyer, W. Mahdi, H. Dietrich, *Chem. Ber. 120* (1987) 1533.

[84] D. Barr, W. Clegg, R. E. Mulvey, R. Snaith, D. S. Wright, *J. Chem. Soc. Chem. Commun. 1987*, 716.

[85] P. G. Williard, M. J. Hintze, *J. Am. Chem. Soc. 109* (1987) 5539. I thank Professor *Williard* for transmitting the coordinates of this structure prior to their entry in the Cambridge Structural Data Base.

[86] D. Barr, W. Clegg, R. E. Mulvey, R. Snaith, *J. Chem. Soc. Chem. Commun. 1984*, 79.

[87] Isolation of a lithiated allyl thioether, unstable above −30°C: D. Seebach, T. Maetzke, R. K. Haynes, M. N. Paddon-Row, S. S. Wong, *Helv. Chim. Acta 71* (1988) 299.

[88] T. Laube, *Angew. Chem. 98* (1986) 368; *Angew. Chem. Int. Ed. Engl. 25* (1986) 349.

[89] T. Laube, *Angew. Chem. 99* (1987) 580; *Angew. Chem. Int. Ed. Engl. 26* (1987) 560.

[90] Examples of crystal structure analyses of Li-phenolate aggregates can be found in the following two papers: a) B. Cetinkaya, I. Gümrükcü, M. F. Lappert, J. L. Atwood, R. Shakir, *J. Am. Chem. Soc. 102* (1980) 2086; b) J. C. Huffman, R. L. Geerts, K. G. Caulton, *J. Crystallogr. Spectrosc. Res. 14* (1984) 541.

[91] R. Amstutz: *Struktur und Reaktivität von Lithiumorganischen Verbindungen, Dissertation Nr. 7210*, ETH Zürich 1982.

[92] T. Laube: *Beiträge zu Struktur und Reaktivität von Ester- und Amid-Lithiumenolaten. Dissertation Nr. 7649*, ETH Zürich 1984.

[93] J. Hansen: *Beiträge zu Struktur und Reaktivität aggregierter Lithiumorganischer Verbindungen, Dissertation Nr. 7863*, ETH Zürich 1985.

[94] W. Bauer, D. Seebach, *Helv. Chim. Acta 67* (1984) 1972.

[95] R. B. Bates, L. M. Kroposki, D. E. Potter, *J. Org. Chem. 37* (1972) 560.

[96] G. Boche, M. Marsch, K. Harms, *Angew. Chem. 98* (1986) 373; *Angew. Chem. Int. Ed. Engl. 25* (1986) 373.

[97] D. Enders, G. Bachstädter, K. A. M. Kremer, M. Marsch, K. Harms, G. Boche, *Angew. Chem. 100* (1988) 1580; *Angew. Chem. Int. Ed. Engl. 27* (1988) 1522.

[98] Review articles on the structures of lithiated nitriles, nitroalkanes, sulfides, sulfoxides, and sulfones (with emphasis on the work of *G. Boche* and *H.-J. Gais*): G. Boche, *Angew. Chem. 101* (1989) and *Angew. Chem. Int. Ed. Engl. 28* (1989), in press.

[99] U. Schöllkopf, *Top. Curr. Chem. 109* (1983) 65–84.

[100] Tetrahedron Symposia-in-Print Number *33* on the methods to synthesize α-amino acids with CC bond formation at the stereogenic center: *Tetrahedron 44* (1988) 5253–5614.

[101] a) X-ray structure analysis: R. A. Wanat, D. B. Collum, G. Van Duyne, J. Clardy, R. T. De Pue, *J. Am. Chem. Soc. 108* (1986) 3415; b) ^{6}Li, ^{13}C, ^{15}N NMR investigation of the same compound: N. Kallman, D. B. Collum, *ibid. 109* (1987) 7466.

[102] a) X-ray structure analysis: D. B. Collum, D. Kahne, S. A. Gut, R. T. De Pue, F. Mohamadi, R. A. Wanat, J. Clardy, G. Van Duyne, *J. Am. Chem. Soc. 106* (1984) 4865; b) ^{6}Li,^{23}Na NMR of the alkali-metal derivatives: A. S. Galiano-Roth, D. B. Collum, *ibid. 110* (1988) 3546; c) Kinetic measurements: R. A. Wanat, D. B. Collum, *ibid. 107* (1985) 2078.

[103] D. Barr, W. Clegg, R. E. Mulvey, R. Snaith, *J. Chem. Soc. Chem. Commun. 1984*, 226.

[104] D. Barr, W. Clegg, R. E. Mulvey, R. Snaith, *J. Chem. Soc. Chem. Commun. 1984*, 285.

[105] D. Barr, W. Clegg, R. E. Mulvey, R. Snaith, K. Wade, *J. Chem. Soc. Chem. Commun. 1986*, 295.

[106] G. Klebe, K. H. Böhn, M. Marsch, G. Boche, *Angew. Chem. 99* (1987) 62; *Angew. Chem. Int. Ed. Engl. 26* (1987) 78.

[107] D. Seebach, W. Bauer, J. Hansen, T. Laube, W. B. Schweizer, J. D. Dunitz, *J. Chem. Soc. Chem. Commun. 1984*, 853.

[108] K. Jens, J. Kopf, N. P. Lorenzen, E. Weiss, *Chem. Ber. 121* (1988) 1201.

[109] P. G. Williard, J. M. Salvino, *J. Chem. Soc. Chem. Commun. 1986*, 153.

[110] a) D. Seebach, M. Ertas, R. Locher, W. B. Schweizer, *Helv. Chim. Acta 68* (1985) 264; b) M. Ertas, D. Seebach, *ibid. 68* (1985) 961.

[111] J. H. Wengrovius, M. F. Garbauskas, E. A. Williams, R. C. Going, P. E. Donahue, J. F. Smith, *J. Am. Chem. Soc. 108* (1986) 982; M. F. Garbauskas, J. H. Wengrovius, R. C. Going, J. S. Kasper, *Acta Crystallogr. Sect. C 40* (1984) 1536.

[112] J. Dekker, J. Boersma, G. J. M. van der Kerk, *J. Chem. Soc. Chem. Commun. 1983*, 553; J. Dekker, P. H. M. Budzelaar, J. Boersma, G. J. M. van der Kerk, A. L. Spek, *Organometallics 3* (1984) 1403.

[113] R. Häner, T. Maetzke, D. Seebach, *Helv. Chim. Acta 69* (1986) 1655.

[114] R. Häner, B. Olano, D. Seebach, *Helv. Chim. Acta 70* (1987) 1676.

[115] Some structures, in part also important in biology, with $(metal)_2X_2$ four-membered ring units of Si, Sn, and transition metals are: the step-like arrangement in **A** and the distorted cube in the solvent-free **B**, the distorted cube in **C** (only those C atoms of the butyl and cyclohexyl groups which are coordinated to the metal are drawn), the dimer of a dimethyl titanate in **D**, the dimer of the general formula **E**, a model for the (FeS)$_x$ units in the oxo-transferases with iron (**F**) or molybdenum (**G**) in the active site. **A**, **B**: M. Veith, F. Goffing, V. Huch, *Chem. Ber. 121* (1988) 943, see also [50]; **C**: K. C. K. Swamy, R. O. Day, R. R. Holmes, *J. Am. Chem. Soc. 109* (1987) 5546 (We thank Professor *R. O. Day* (University of Massachusetts, Amherst, MA) for transmitting the coordinates of structure **C** to us prior to publication); **D** (*CSD*: MPTIDM): A. Yoshino, Y. Shuto, Y. Iitaka, *Acta Crystallogr. Ser. B 26* (1970) 744; **E** (*CSD*: XLDTSF), **F**: R. H. Holm, *Acc. Chem. Res. 10* (1977) 427–434; **G** (*CSD*: CESXIH): T. Shibahara, H. Kuroya, K. Matsumoto, S. Ooi, *J. Am. Chem. Soc. 106* (1984) 789. Further examples see [50] and the review article "*Clusters of Valence Electron Poor Metals—Structure, Bonding, and Properties*": A. Simon, *Angew. Chem. 100* (1988) 163–188; *Angew. Chem. Int. Ed. Engl. 27* (1988) 159–183.

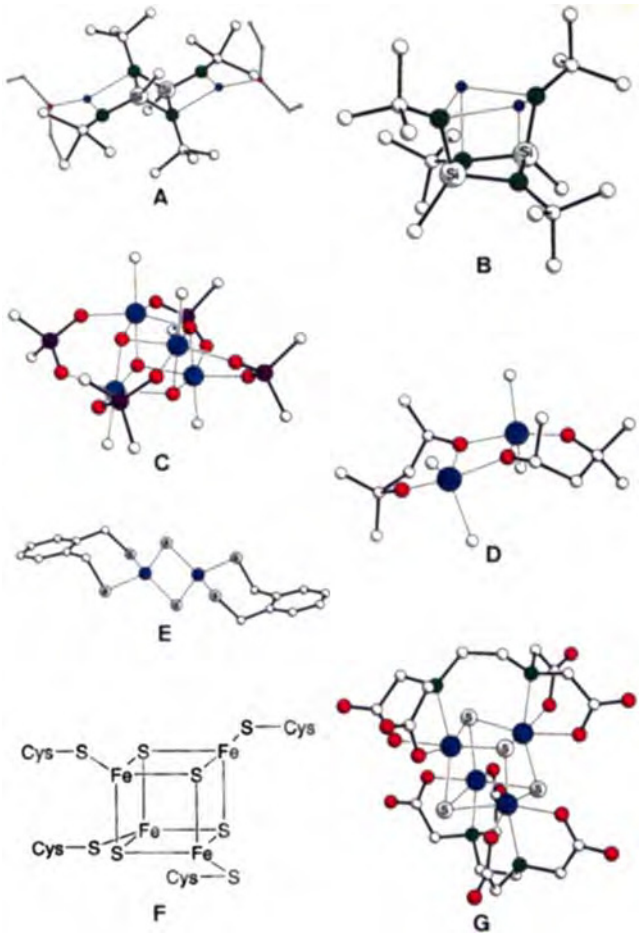

$[(t\mathrm{BuN})_2(\mathrm{CH_3Si})\mathrm{Li}]_2 \cdot 2\mathrm{OEt_2}$ **A**
$[(t\mathrm{BuN})_2(\mathrm{CH_3Si})\mathrm{Li}]_2$ **B**
$[\mathrm{BuSn(O)O_2P(C_6H_{11})_2}]_4$ **C**
$[\mathrm{Me_2TiOC(Me_2)CH_2CH(Me)O}]_2$ **D**
$[(\mathrm{R,S})_2\mathrm{FeS}]_2$ **E**
For **F**, **G**, see text

[116] It might be appropriate at this point to mention that, in the discussion of structures, we draw formulae and use a language not according to the usual conventions in organic chemistry but rather according to those in crystallography. A line between two atoms thereby does not correspond to an electron pair but indicates that their distance is smaller than the sum of the van der Waals' radii. Here, we do not observe the octet rule; otherwise we would have to add a ⊕ charge to all the oxygens of the THF molecules bound to Li. We also speak of an X atom not of a $Li^{\oplus}$ cation or an $RO^{\ominus}$ anion! (See also the remarks in the caption of Fig. 1.)

[117] H.-B. Bürgi, *Angew. Chem. 87* (1975) 461–496; *Angew. Chem. Int. Ed. Engl. 14* (1975) 460–473.

[118] J. D. Dunitz: *X-Ray Analysis and the Structure of Organic Molecules*, Cornell University Press, Ithaca 1979, Chapter 7, pp. 301–390.

[119] H.-B. Bürgi, J. D. Dunitz, *Acc. Chem. Res. 16* (1983) 153–161.

[120] P. G. Jones, A. J. Kirby, *J. Am. Chem. Soc. 106* (1984) 6207.

[121] H.-B. Bürgi, J. D. Dunitz, *J. Am. Chem. Soc. 109* (1987) 2924; H.-B. Bürgi, K. C. Dubler-Steudle, *ibid. 110* (1988), in press.

[122] H.-B. Bürgi, K. C. Dubler-Steudle, *J. Am. Chem. Soc. 110* (1988) 4953; H.-B. Bürgi, J. D. Dunitz, *Acta Crystallogr. Ser. B44* (1988) 445.

[123] See also the discussion about protonation/deprotonation in our paper about TriMEDA-Li enolate complexes [66].

[124] Application of the structure-reactivity correlation to reactions of α,β-unsaturated carbonyl compounds (D. Seebach, J. Zimmermann, U. Gysel, R. Ziegler, T.-K. Ha, *J. Am. Chem. Soc. 110* (1988) 4763) and to the addition to carbonyl groups (T. Laube, H. U. Stilz, *ibid. 109* (1987) 5876).

[125] J. L. Wardell in G. Wilkinson, F. G. A. Stone, E. W. Abel (Eds.): *Comprehensive Organometallic Chemistry, Vol. 1*, Pergamon Press, Oxford 1982, Chapter 2, pp. 43–120.

[126] As to doubly lithiated carboxylic acids $R_2C{=}C(OLi)_2$ in THF, degrees of aggregation of 65–250 have been measured ("colloidal" solutions): P. E. Pfeffer, L. S. Silbert, *J. Org. Chem. 36* (1971) 3290.

[127] L. M. Jackman, C. W. DeBrosse, *J. Am. Chem. Soc. 105* (1983) 4177.

[128] a) Two-Dimensional NMR Spectroscopy: A Powerful Tool for the Investigation of Molecular Structure and Dynamics: R. R. Ernst, *Chimia 41* (1987) 323–340; b) K. Wüthrich: *NMR of Proteins and Nucleic Acids*, Wiley-Interscience, New York 1986.

[129] W. R. Croasmun, R. M. K. Carlson (Eds.): *Two Dimensional NMR Spectroscopy*, VCH Verlagsgesellschaft, Weinheim 1987.

[130] a) Conformation and Biological Activity of Cyclic Peptides: H. Kessler, *Angew. Chem. 94* (1982) 509–520; *Angew. Chem. Int. Ed. Engl. 21 (1982) 512–523; b) Two-Dimensional NMR Spectroscopy: Background and Overview of the Experiments: H. Kessler, M. Gehrke, C. Griesinger, Angew. Chem. 100* (1988) 507–554; *Angew. Chem. Int. Ed. Engl. 27* (1988) 490–536.

[131] 3D NMR techniques: C. Griesinger, O. W. Sørensen, R. R. Ernst, *J. Magn. Reson. 73* (1987) 474; *J. Am. Chem. Soc. 109* (1987) 7227; H. Oschkinat, C. Griesinger, P. J. Kraulis, O. W. Sørensen, R. R. Ernst, A. M. Gronenborn, G. M. Clore, *Nature (London) 332* (1988) 374.

[132] See the general reviews mentioned above [34, 42–46] and special papers [101b, 102b] as well as: a) W. Bauer, G. Müller, R. Pi, P. von R. Schleyer, *Angew. Chem. 98* (1986) 1130; *Angew. Chem. Int. Ed. Engl. 25* (1986) 1103 (^{6}Li,^{1}H-2D HOESY); b) A. S. Galiano-Roth, E. M. Michaelides, D. B. Collum, *J. Am. Chem. Soc. 110* (1988) 2658 (^{6}Li,^{13}C,^{15}N NMR of lithium cyclohexylisopropylamide); c) J. S. DePue, D. B. Collum, *ibid. 110* (1988) 5524. d) J. S. DePue, D. B. Collum, *ibid. 110* (1988) 5518.

[133] a) As the following details of the ^{13}C NMR spectra (A^1 and A^2) show, the content of dimeric aggregate increases by cooling a solution of butyllithium (THF), and dynamic processes that "smear out" the ^{6}Li, ^{13}C coupling at −70°C are frozen out at −90°C, so that the coupling of two ^{6}Li($I=1$) with the neighboring ^{13}C atom can be recognized from the quintet splitting [42a, c]. b) Mixed aggregates $(R^1Li \cdot n\,R^2Li)_m$ are formed by addition of Bu^6Li to a solution of ^{6}Li,^{13}C-labeled lithium phenylacetylide: the pure acetylide dimer (B^1) first equilibrates with the mixed dimer (B^2) and, after addition of 6 equiv. of BuLi, only the mixed tetramer (B^3) is present: R. Hässig, D. Seebach, *Helv. Chim. Acta 66* (1983) 2269.

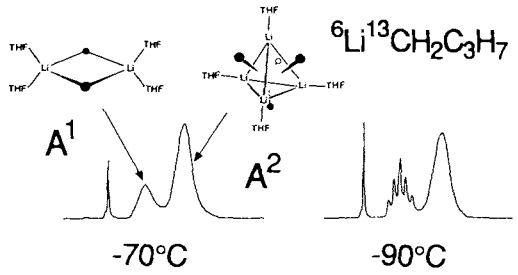

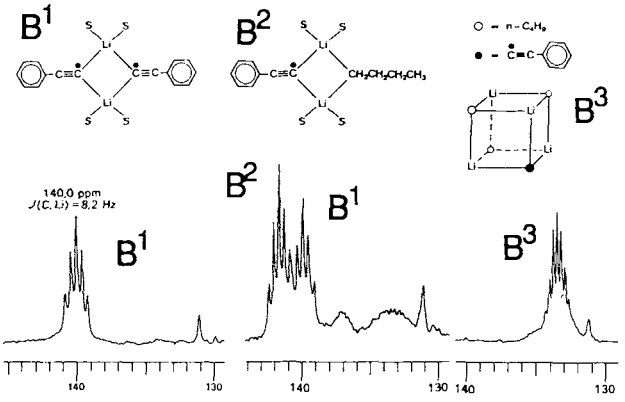

[134] L. M. Jackman, L. M. Scarmoutzos, *J. Am. Chem. Soc. 109* (1987) 5348.

[135] L. M. Jackman, L. M. Scarmoutzos, W. Porter, *J. Am. Chem. Soc. 109* (1987) 6524.

[136] L. M. Jackman, R. C. Haddon, *J. Am. Chem. Soc. 95* (1973) 3687.

[137] L. M. Jackman, B. C. Lange, *J. Am. Chem. Soc. 103* (1981) 4494.

[138] L. M. Jackman, T. S. Dunne, *J. Am. Chem. Soc. 107* (1985) 2805.

[139] L. M. Jackman, L. M. Scarmoutzos, C. W. De Brosse, *J. Am. Chem. Soc. 109* (1987) 5355.

[140] L. M. Jackman, B. D. Smith, *J. Am. Chem. Soc. 110* (1988) 3829.

[141] R. R. Hunma, R. Cloux, A. Haider, University of Lausanne, unpublished work. I thank the aforementioned colleagues as well as Professor *H. Dahn* for sharing his results prior to publication.
[142] J. Q. Wen, J. B. Grutzner, *J. Org. Chem. 51* (1986) 4220.
[143] This footnote must be sufficient for the remark that the N-analogues of the Li enolates also form aggregates, mixed aggregates, and all the complex arrangements in solution, as has been shown especially by *Collum* and his group [101, 102, 132]. Higher alkali metals can also be present within complex structures in solution (see also the discussion about ate complexes in Section 2.2.3). In the pK_a determination of cesium ion pair acidities in THF (Streitwieser scale) aggregation effects also occur: M. J. Kaufman, A. Streitwieser, Jr., *J. Am. Chem. Soc. 109* (1987) 6092.
[144] a) G. Wittig, F. J. Meyer, G. Lange, *Justus Liebigs Ann. Chem. 571* (1951) 167; G. Wittig, R. Ludwig, R. Polster, *Chem. Ber. 88* (1955) 294; b) Reviews: G. Wittig, *Angew. Chem. 70* (1958) 65–71; *Q. Rev. Chem. Soc. 20* (1966) 191–210; W. Tochtermann, *Angew. Chem. 78* (1966) 355–375; *Angew. Chem. Int. Ed. Engl. 5* (1966) 351–371.
[145] H. Hope, P. P. Power, *J. Am. Chem. Soc. 105* (1983) 5320.
[146] H. Schmidbaur, A. Schier, U. Schubert, *Chem. Ber. 116* (1983) 1938 (X-ray structure of $[Li_2(cyclopropyl)Br\cdot(OEt_2)_2]_2$, a tetrameric aggregate of 2 LiBr and 2 cyclopropyllithium).
[147] D. Thoennes, E. Weiss, *Chem. Ber. 111* (1978) 3157.
[148] U. Schümann, J. Kopf, E. Weiss, *Angew. Chem. 97* (1985) 222; *Angew. Chem. Int. Ed. Engl. 24* (1985) 215.
[149] L. M. Jackman, L. M. Scarmoutzos, *J. Am. Chem. Soc. 106* (1984) 4627.
[150] M. Szwarc (Ed.): *Ions and Ion Pairs in Organic Reactions, Vol. 1 and 2,* Wiley, New York 1972 and 1974, respectively.
[151] C. Cambillau, M. Ourevitch, *J. Chem. Soc. Chem. Commun. 1981,* 996.
[152] C. Eaborn, P. B. Hitchcock, J. D. Smith, A. C. Sullivan, *J. Chem. Soc. Chem. Commun. 1983,* 827.
[153] U. Schümann, E. Weiss, *Angew. Chem. 100* (1988) 573; *Angew. Chem. Int. Ed. Engl. 27* (1988) 584.
[154] A. A. Morton, C. E. Claff, Jr., F. W. Collins, *J. Org. Chem. 20* (1955) 428.
[155] Reviews on "complex bases": P. Caubère, *Acc. Chem. Res. 7* (1974) 301–308; *Top. Curr. Chem. 73* (1978) 49–124; *Angew. Chem. 95* (1983) 597–611; *Angew. Chem. Int. Ed. Engl. 22* (1983) 599–613; *Pure Appl. Chem. 57* (1985) 1875–1882. Two recent papers about interesting applications of complex mixtures of $NaH/NaOR/MX_n$ (with or without Me_3SiCl): A. Feghouli, Y. Fort, R. Vanderesse, P. Caubère, *Tetrahedron Lett. 29* (1988) 1379, 1383.
[156] L. Lochmann, J. Pospíšil, J. Vodňanský, J. Trekoval, D. Lím, *Collect. Czech. Chem. Commun. 30* (1965) 2187; L. Lochmann, J. Pošpišil, D. Lim, *Tetrahedron Lett. 1966,* 257.
[157] M. Schlosser, *J. Organomet. Chem. 8* (1967) 9; M. Schlosser, J. Hartmann, M. Stähle, J. Kramar, A. Walde, A. Mordini, *Chimia 40* (1986) 306.
[158] More and more structural information about the cuprates (copper ate complexes, Gilman reagents) has been made available in recent times. Reference to the X-ray structures by *Hope* and *Power* as well as by *van Koten* and NMR investigations by *Lipshutz* and *Bertz* are compiled in a recently published communication: S. H. Bertz, G. Dabbagh, *J. Am. Chem. Soc. 110* (1988) 3668.—Enantioselective cuprates: E. J. Corey, R. Naef, F. J. Hannon, *ibid. 108* (1986) 7114; R. K. Dieter, M. Tokles, *ibid. 109* (1987) 2040; K. Yamamoto, M. Kanoh, N. Yamamoto, J. Tsuji, *Tetrahedron Lett. 28* (1987) 6347.—A comprehensive review about structures of organocopper reagents is also found in: *Gmelin, Handbook of Inorganic Chemistry,* 8th edition, Part 1-4, Springer, Berlin 1983–1987.
[159] P. Kebarle, *Annu. Rev. Phys. Chem. 28* (1977) 445.
[160] A. W. Castleman, Jr., P. M. Holland, D. M. Lindsay, K. I. Peterson, *J. Am. Chem. Soc. 100* (1978) 6039.
[161] V. G. Solomonik, K. S. Krasnov, *Russ. J. Phys. Chem. (Engl. Transl.) 53* (1979) 161, and references cited therein.
[162] K. G. Rao, E. D. Becker, C. N. R. Rao, *J. Chem. Soc. Chem. Commun. 1977,* 350. Rotation barrier of dimethylacetamide: M. Feigel, *ibid. 1980,* 456.
[163] From IR-spectroscopic "stop-flow" measurements: M. Al-Aseer, P. Beak, D. Hay, D. J. Kempf, S. Mills, S. G. Smith, *J. Am. Chem. Soc. 105* (1983) 2080.
[164] E. M. Arnett, F. J. Fisher, M. A. Nichols, *22nd Reaction Mechanism Conference, Pittsburgh, June 12–16, 1988* (Poster Session I, 1); also reported at the ACS Fall Meeting in Los Angeles, September 1988. See also earlier work of this group: E. M. Arnett, S. G. Maroldo, S. L. Schilling, J. A. Harrelson, *J. Am. Chem. Soc. 106* (1984) 6759, and references cited therein. I thank Professor *Arnett* (Duke University, Durham, NC) for a detailed summary of his lectures prior to publication.
[165] F. G. Bordwell, *Pure Appl. Chem. 49* (1977) 963–968; a more recent paper on acidity in DMSO: F. G. Bordwell, D. J. Algrim, *J. Am. Chem. Soc. 110* (1988) 2964.
[166] Chelation in the reaction of α-alkoxy ketones with Grignard reagents: S. V. Frye, E. L. Eliel, R. Cloux, *J. Am. Chem. Soc. 109* (1987) 1862.
[167] P. J. A. Geurink, G. W. Klumpp, *J. Am. Chem. Soc. 108* (1986) 538; G. W. Klumpp, M. J. Sinnige, *Tetrahedron Lett. 27* (1986) 2247.
[168] P. Beak, B. Siegel, *J. Am. Chem. Soc. 96* (1974) 6803.
[169] The "cyclic model" of *Cram*'s rule, today called "chelation control" was formulated 30 years ago: a) D. J. Cram, K. R. Kopecky, *J. Am. Chem. Soc. 81* (1959) 2748. b) M. T. Reetz, *Angew. Chem. 96* (1984) 542–555; *Angew. Chem. Int. Ed. Engl. 23* (1984) 556–569 ("Chelation or Non-Chelation Control in Addition Reactions of Chiral α- and β-Alkoxy Carbonyl Compounds").
[170] H. O. House, V. Kramar, *J. Org. Chem. 28* (1963) 3362.
[171] H. O. House, B. M. Trost, *J. Org. Chem. 30* (1965) 1341.
[172] G. W. Spears, C. E. Caufield, W. C. Still, *J. Org. Chem. 52* (1987) 1226.
[173] R. Häner, T. Laube, D. Seebach, *Chimia 38* (1984) 255.
[174] R. Häner, W. B. Schweizer, P. Seiler, D. Seebach, *Chimia 40* (1986) 97.
[175] W. J. Hehre, L. Radom, P. von R. Schleyer, J. A. Pople: *Ab Initio Molecular Orbital Theory,* Wiley, New York 1986; R. D. Amos, J. E. Rice: *The Cambridge Analytical Derivatives Package,* Issue 4.0, Cambridge 1987.
[176] N. L. Allinger, *J. Am. Chem. Soc. 99* (1977) 8127; U. Burkert, N. L. Allinger: *Molecular Mechanics, ACS Monogr. 177* (1982); W. C. Still, *MacroModel,* Columbia University, New York 1986.
[177] a) J. E. Del Bene, M. J. Frisch, K. Raghavachari, J. A. Pople, P. von R. Schleyer, *J. Phys. Chem. 87* (1983) 73; b) A.-M. Sapse, K. Raghavachari, P. von R. Schleyer, E. Kaufmann, *J. Am. Chem. Soc. 107* (1985) 6483.
[178] a) See also the interesting dienolate of cyclogeraniol and the discussion of possible structures, which might explain the reactivity: C. Fehr, J. Galindo, *J. Org. Chem. 53* (1988) 1823 and [72]; b) C. Fehr, J. Galindo, *J. Am. Chem. Soc.* (1988), in press (*I* thank Dr. *Fehr* for sending us the manuscript).
[179] A. Bongini, M. Orena, S. Sandri, *J. Chem. Soc. Chem. Commun. 1986,* 50.
[180] R. Glaser, A. Streitwieser, Jr., *J. Am. Chem. Soc. 109* (1987) 1258.
[181] K. N. Houk, R. W. Strozier, N. G. Rondan, R. R. Fraser, N. Chuaqui-Offermanns, *J. Am. Chem. Soc. 102* (1980) 1426.
[182] J. Zimmermann, D. Seebach, T.-K. Ha, *Helv. Chim. Acta 71* (1988) 1143.
[183] J. H. Horner, M. Vera, J. B. Grutzner, *J. Org. Chem. 51* (1986) 4212.
[184] S. D. Kahn, lectures and poster: *The Third Chemical Congress of North America,* Toronto, June 5–11, 1988; *22nd Reaction Mechanism Conference,* Pittsburgh, June 12–16, 1988. I thank Professor *Kahn* (School of Chemical Sciences, University of Illinois at Urbana-Champaign, Urbana) for sending us a manuscript and for permission to cite the data prior to publication and to reproduce here the color picture generated by the program *MacModel* and printed out with a Tektronix 4693 D.
[185] A. S. Narula, *Tetrahedron Lett. 22* (1981) 4119.
[186] D. W. Moreland, W. G. Dauben, *J. Am. Chem. Soc. 107* (1985) 2264.
[187] a) M. L. McKee, *J. Am. Chem. Soc. 109* (1987) 559. b) M. L. McKee, *ibid. 107* (1985) 7284.
[188] E. Kaufmann, P. von R. Schleyer, K. N. Houk, Y.-D. Wu, *J. Am. Chem. Soc. 107* (1985) 5560. Similar calculations concerning the addition of LiH and $LiCH_3$ to ethylene and acetylene: K. N. Houk, N. G. Rondan, P. von R. Schleyer, E. Kaufmann, T. Clark, *ibid. 107* (1985) 2821.
[189] S. M. Bachrach, A. Streitwieser, Jr., *J. Am. Chem. Soc. 108* (1986) 3946; correction: *ibid. 109* (1987) 5888.
[190] N.-T. Anh, B.-T. Thanh, *Nouv. J. Chim. 10* (1986) 681.
[191] J. Mulzer, G. Brüntrup, J. Finke, M. Zippel, *J. Am. Chem. Soc. 101* (1979) 7723.
[192] G. Kyriakakou, A. Loupy, J. Seyden-Penne, *J. Chem. Res. Synop. 1978,* 8.
[193] Y. Li, M. N. Paddon-Row, K. N. Houk, *J. Am. Chem. Soc. 110* (1988) 3684.
[194] C. Gennari, R. Todeschini, M. G. Beretta, G. Favini, C. Scolastico, *J. Org. Chem. 51* (1986) 612.
[195] M. J. S. Dewar, K. M. Merz, Jr., *J. Am. Chem. Soc. 109* (1987) 6553.
[196] R. B. Woodward, R. Hoffmann, *Angew. Chem. 81* (1969) 797–869; *Angew. Chem. Int. Ed. Engl. 8* (1969) 781–853.
[197] W. von E. Doering, W. R. Roth, *Tetrahedron 18* (1962) 67–74; *Angew. Chem. 75* (1963) 27–35; *Angew. Chem. Int. Ed. Engl. 2* (1963) 115–122.
[198] J. E. Baldwin, *J. Chem. Soc. Chem. Commun. 1976,* 734.
[199] Complex structures are present not only according to the calculations mentioned in Section 3 [15, 25] but also in the gaseous state; see the dimer $[LiN(SiMe_3)_2]_2$, discovered by electron diffraction in the gas phase [82], or the mass spectroscopically identified oligomers of polylithiated alkanes [41g] and: L. A. Shimp, J. A. Morrison, J. A. Gurak, J. W. Chinn, Jr., R. J. Lagow, *J. Am. Chem. Soc. 103* (1981) 5951; J. A. Gurak, J. W. Chinn, Jr., R. J. Lagow, *ibid. 104* (1982) 2637; F. J. Landro, J. A. Gurak, J. W. Chinn, Jr., R. M. Newman, R. J. Lagow, *ibid. 104*

(1982) 7345; H. Kawa, B. C. Manley, R. J. Lagow, *ibid. 107* (1985) 5313.

[200] R. E. Dickerson, I. Geis: *Chemistry, Matter and the Universe*, 3rd Printing, Benjamin, Menlo Park CA, 1979, p. 458.

[201] Accordingly, "dramatic induction periods" in reactions of Li derivatives with alkyl halides have been reported; the generated lithium halide acted as an "accelerator" [102b, 132d].

[202] J. F. McGarrity, J. Prodolliet, T. Smyth, *Org. Magn. Resonance 17* (1981) 59.

[203] J. F. McGarrity, J. Prodolliet, *J. Org. Chem. 49* (1984) 4465.

[204] J. F. McGarrity, C. A. Ogle, *J. Am. Chem. Soc. 107* (1985) 1805.

[205] J. F. McGarrity, C. A. Ogle, Z. Brich, H.-R. Loosli, *J. Am. Chem. Soc. 107* (1985) 1810.

[206] By this method the rate of equilibration [204, 205] between dimeric and tetrameric BuLi in THF (cf. [42a,c, 133]) was measured at -60 to $-85\,^{\circ}C$ as well as that of the reaction of butyllithium with oxygen [204], with cyclopentadiene, and with benzaldehyde [205]. Most important findings: no indication of monomeric BuLi down to concentrations of 10^{-4} M; $(BuLi)_2$ as well as the mixed aggregate $[Bu_2(BuO)_2Li_4]$ react about ten times faster with PhCHO than does $(BuLi)_4$; the alkoxide $PhCH(OLi)C_4H_9$, formed from BuLi and PhCHO, adds to benzaldehyde to give the alkoxide of a hemiacetal (cf. Scheme 6 and references cited there). See also the RINMR measurement of the addition of Grignard compounds to alkoxy ketones [166].

[207] In the case of Li enehydrazide it was concluded from kinetic measurements of the alkylation that the monomeric species forms product, not the aggregate, though the latter is the predominant species in solution [102c].

[208] See Schemes 5 and 9, Table 3, and Section 2.2.3.

[209] A "free" anion (not neutralized by *any* Li) must of course be even more reactive. A "fairly free" carbanion was recently proposed as the product-forming species from results obtained for Sn/Mg exchange processes in the reaction of Me_3Sn-substituted aryl bromides: H. J. R. de Boer, O. S. Akkerman, F. Bickelhaupt, *Angew. Chem. 100* (1988) 735; *Angew. Chem. Int. Ed. Engl. 27* (1988) 687.

[210] a) $LiNR_2$ adducts to aromatic aldehydes for *ortho*-metalations: U. Michael, S. Gronowitz, *Acta Chem. Scand. 22* (1968) 1353; D. L. Comins, J. D. Brown, *Tetrahedron Lett. 22* (1981) 4213; D. L. Comins, J. D. Brown, N. B. Mantlo, *ibid. 23* (1982) 3979; b) $LiNR_2$ adducts to aromatic aldehydes for aminative alkylations and reductive aminative coupling with low-valent titanium: D. Seebach, M. Schiess, *Helv. Chim. Acta 65* (1982) 2598; D. Seebach, A. K. Beck, M. Schiess, L. Widler, A. Wonnacott, *Pure Appl. Chem. 55* (1983) 1807–1822; D. Seebach, C. Betschart, M. Schiess, *Helv. Chim. Acta 67* (1984) 1593; C. Betschart, D. Seebach, *ibid. 70* (1987) 2215.

[211] $LiNR_2$ and LiOR adducts [*t*BuOCH(OLi)R] to nonenolizable aldehydes as bases and precursors for the in-situ liberation of an aldehyde: D. Seebach, T. Weber, *Tetrahedron Lett. 24* (1983) 3315; *Helv. Chim. Acta 67* (1984) 1650.

[212] Sulfur analogues [ArylCH(SLi)SR]: D. Seebach, K.-H. Geiss, *Angew. Chem. 86* (1974) 202; *Angew. Chem. Int. Ed. Engl. 13* (1974) 202; K.-H. Geiss, D. Seebach, B. Seuring, *Chem. Ber. 110* (1977) 1833.

[213] L. M. Jackman, B. C. Lange, *J. Org. Chem. 48* (1983) 4789.

[214] L. Tenud, S. Farooq, J. Seibl, A. Eschenmoser, *Helv. Chim. Acta 53* (1970) 2059.

[215] See also the amide complexes in Table 4, urea and amide complexes of Li in crystals [47], and the discussion about LiX effects on peptides in Section 5.

[216] Most of the reaction paths via aggregates shown in Schemes 6–9 had been proposed by us already in 1981 and 1983 [53, 69]; only the complexity, not the principle, is changed if the reaction is formulated for tetrameric aggregates instead of dimeric ones as done here.

[217] The scenario is even extended if one considers that single-electron transfers (SET) become more probable with increasing degree of aggregation of polar organometallic compounds; a supramolecule can more likely donate an electron (as in the present case), or accept one, than one of its components, because the resulting charge deficiency is distributed over a larger area (higher lying HOMO, lower LUMO). Accordingly, for example, it was recently proved that the tendency of single-electron transfer to occur from a Li amide strongly increases with its degree of aggregation (P. Renaud, M. A. Fox, *J. Am. Chem. Soc. 110* (1988) 5702). An SET mechanism with participation of the aggregate (Fig. 14) was also proposed [56] to explain the reversal of stereoselectivity of reactions of the Li enamides of diketopiperazine-bislactim ethers when going from "normal" electrophiles [99] to C_2Cl_6 (U. Schöllkopf, H.-J. Neubauer, M. Hauptreif, *Angew. Chem. 97* (1985) 1065; *Angew. Chem. Int. Ed. Engl. 24* (1985) 1066).

[218] In the case of participation of aggregates in product-forming steps, different results are possible depending on the use of the respective enolates as racemic mixtures (which can form diastereomeric aggregates) or of enantiomerically pure reagents! Compare the nonlinear dependence of the product *ee* values in numerous enantioselective reactions on the enantiomeric purity of the reagents used. Several examples can be found in the following references: [53]; A. Horeau, *Tetrahedron Lett. 1969*, 3121; C. Agami, C. Puchot, H. Sevestre, *ibid. 27* (1986) 1501; C. Puchot, O. Samuel, E. Dunach, S. Zhao, C. Agami, H. B. Kagan, *J. Am. Chem. Soc. 108* (1986) 2353; Review on *Kinetic Resolution*, H. B. Kagan, J. C. Fiaud, *Top. Stereochem. 18* (1988) 249.

[219] Two "aggregate effects" may prove this. a) In the reaction of *gem*-dibromocyclopropane with an excess of butyllithium and subsequent addition of an excess of electrophile, products of double substitution

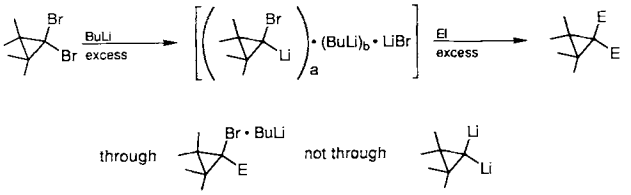

are formed which originally was seen as proof for the occurrence of *gem*-dilithiocyclopropanes. These species, however, could not be detected by NMR spectroscopy of ^{6}Li- and ^{13}C-labeled samples. It turns out that a mixture of bromolithium carbenoid and BuLi is present instead. The added electrophiles react faster with the carbenoid than with BuLi, and "interaggregate" Br/Li exchange leads to the observed result. See flow chart (R. Dammann, *Dissertation Nr. 6277*, ETH Zürich 1978). b) In the reaction of phenylacetonitrile with 2 BuLi (see structure

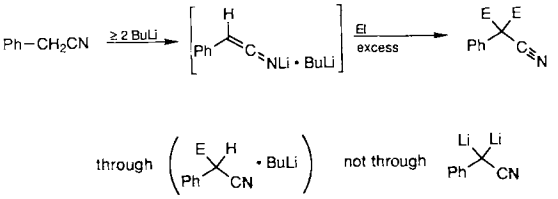

in Table 2) it is not a dilithium derivative that is responsible for the formation of double substituted products, but a fast "interaggregative" proton transfer during addition of electrophile (P. J. Crowley, M. R. Leach, O. Meth-Cohn, B. J. Wakefield, *Tetrahedron Lett. 27* (1986) 2909). c) Cf. also the discussion in: P. Beak, T. J. Musick, C. Chen, *J. Am. Chem. Soc. 110* (1988) 3538.

[220] Representations from publications by *Schlosser* show what has been concluded from kinetic measurements of the HCl elimination with potassium alkoxides: "Alcoholate Clusters ("Aggregates") and Their Role in Alkyne-Forming Elimination Reaction." M. Schlosser, T. D. An, *Angew. Chem. 93* (1981) 1114; *Angew. Chem. Int. Ed. Engl. 20* (1981) 1039; M. Schlosser, C. Tarchini, T. D. An, R. Ruzziconi, P. J. Bauer, *ibid. 93* (1981) 1116 and *20* (1981) 1041, respectively.

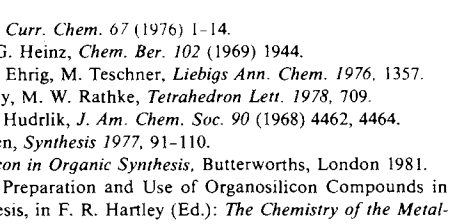

[221] G. Wittig, *Top. Curr. Chem. 67* (1976) 1–14.

[222] M. Schlosser, G. Heinz, *Chem. Ber. 102* (1969) 1944.

[223] D. Seebach, V. Ehrig, M. Teschner, *Liebigs Ann. Chem. 1976*, 1357.

[224] R. P. Woodbury, M. W. Rathke, *Tetrahedron Lett. 1978*, 709.

[225] G. Stork, P. F. Hudrlik, *J. Am. Chem. Soc. 90* (1968) 4462, 4464.

[226] J. K. Rasmussen, *Synthesis 1977*, 91–110.

[227] E. Colvin: *Silicon in Organic Synthesis*, Butterworths, London 1981.

[228] E. W. Colvin: Preparation and Use of Organosilicon Compounds in Organic Synthesis, in F. R. Hartley (Ed.): *The Chemistry of the Metal-Carbon Bond, Vol. 4*, Wiley, New York 1987, Chapter 6, pp. 539–621.

[229] E. W. Colvin: *Silicon Reagents in Organic Synthesis*, Academic Press, London 1988.

[230] W. P. Weber: *Silicon Reagents for Organic Synthesis*, Springer, Berlin 1983.

[231] P. J. Reider, R. S. E. Conn, P. Davis, V. J. Grenda, A. J. Zambito, E. J. J. Grabowski, *J. Org. Chem. 52* (1987) 3326.

[232] A. K. Beck, M. S. Hoekstra, D. Seebach, *Tetrahedron Lett. 1977*, 1187.

[233] D. Seebach, T. Weller, G. Protschuk, A. K. Beck, M. S. Hoekstra, *Helv. Chim. Acta 64* (1981) 716.

[234] M. Yoshifuji, T. Nakamura, N. Inamoto, *Tetrahedron Lett. 28* (1987) 6325.

[235] C. H. Heathcock, M. C. Pirrung, S. D. Young, J. P. Hagen, E. T. Jarvi, U. Badertscher, H.-P. Märki, S. H. Montgomery, *J. Am. Chem. Soc. 106* (1984) 8161, and earlier papers of the same group cited therein.

[236] R. Häner, D. Seebach, *Chimia 39* (1985) 356; D. Seebach, R. Häner, T. Vettiger, *Helv. Chim. Acta 70* (1987) 1507.
[237] T. Hassel, D. Seebach, *Helv. Chim. Acta 61* (1978) 2237, and earlier papers of our group cited therein.
[238] P. Beak, D. B. Reitz, *Chem. Rev. 78* (1978) 275–316; P. Beak, W. J. Zajdel, D. B. Reitz, *ibid. 84* (1984) 471–523.
[239] In this case alkylated diisopropylamine can be formed under conditions, under which pure diisopropylamine would not be alkylated (−80°C, in THF); thus, one must conclude that the amine is activated by the Li enolate for the alkylation to the tertiary amine! (See [244].)
[240] a) The effect of the "hidden proton" has been observed in substrates with several acidic sites also in the absence of secondary amines; see, e.g., the results of protonation of Schiff bases of penicillamine benzyl esters: R. A. Firestone, N. Schelechow, D. B. R. Johnston, B. G. Christensen, *Tetrahedron Lett. 1972*, 375; R. A. Firestone, N. S. Maciejewicz, R. W. Ratcliffe, B. G. Christensen, *J. Org. Chem. 39* (1974) 437; R. A. Firestone, B. G. Christensen, *J. Chem. Soc. Chem. Commun. 1976*, 288. b) Doubly deprotonated species—bis(enolates)—can be more stable than the corresponding simply deprotonated ones; see the following newer papers and the references cited therein: K. G. Bilyard, P. J. Garratt, R. Hunter, E. Lete, *J. Org. Chem. 47* (1982) 4731; K. Furuta, A. Misumi, A. Mori, N. Ikeda, H. Yamamoto, *Tetrahedron Lett. 25* (1984) 669. Solvation and chelation (see Tables 4,5) can invert the normal order of acidity: S. M. Bachrach, *J. Am. Chem. Soc. 108* (1986) 6406. But also here, as a warning, we must point to the intraaggregate effects mentioned in [219].
[241] E. Dziadulewicz, postdoctoral fellow, ETH Zürich 1987/88, hitherto unpublished results.
[242] D. Seebach, M. Boes, R. Naef, W. B. Schweizer, *J. Am. Chem. Soc. 105* (1983) 5390.
[243] P. Strazewski, C. Tamm, *Helv. Chim. Acta 69* (1986) 1041; P. Strazewski, *Dissertation*, Universität Basel 1986.
[244] J. D. Aebi, D. Seebach, *Helv. Chim. Acta 68* (1985) 1507.
[245] R. Polt, D. Seebach, *Helv. Chim. Acta 70* (1987) 1930; *J. Am. Chem. Soc. 111* (1989), in press.
[246] Cf. the protonations and alkylations of Schiff base enolates formed from amino acids and hydroxypinanone; under otherwise identical conditions, the epimeric precursors give rise to two enolates, **A** and **B**, that behave very differently (both should have the (*E*) configuration of the enolate double bond!); A. El Achqar, M.-L. Roumestant, P. Viallefont, *Tetrahedron Lett. 29* (1988) 2441.

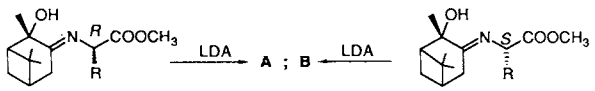

[247] Cf. the cooperative hydrogen bonds [76] in many biologically important structures in which, for example, three hydrogen bonds are arranged in a cyclic array, **A**, with the complexes **B** and **C** (Figs. 3, 5, Table 2). Here, as there, the bond strength is greater than anticipated from simple O···HO, N···HN or πC···HN hydrogen bonds. Much stronger are hydrogen bonds between ions, and between ions and neutral molecules, see [250, 251, 252c].

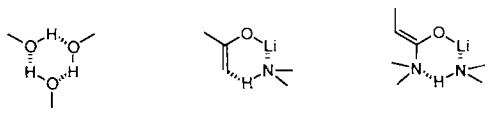

[248] The effect of the complexation of Li carboxylate (or the [RR'C=CO_2Li]Li derivative) with the secondary amine and the return of the proton in attempted deuterations of doubly metalated toluic acids as well as aliphatic or alicyclic carboxylic acids was already discussed at the beginning of the 1970s: P. L. Creger, *J. Am. Chem. Soc. 92* (1970) 1396; P. E. Pfeffer, L. S. Silbert, J. M. Chirinko, Jr., *J. Org. Chem. 37* (1972) 451.
[249] Reports on the observation of such effects in carbonyl additions, which occur much faster than nucleophilic substitutions, are not known to us. The enolate **A** generated with LDA, e.g., adds smoothly to acetaldehyde to give the expected product **B** (84%), while with CH_3I a 3:1 product **C**, R = CH_3, is generated in ca. 50% yield, which was attributed to the existence of tetrameric aggregates [183].

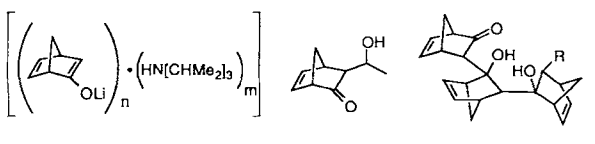

[250] D. J. Cram: *Fundamentals of Carbanion Chemistry*, Academic Press, New York 1965. In spite of the protic medium, the rate of racemization ($k_{rac.}$) is greater than that of the D/H exchange ($k_{exch.}$) via an ion pair. The formulae show the "conducted tour mechanism" (*Cram*), $k_{rac.}:k_{exch.} = 20:1$. Cf. also: A.-M. Weidler, G. Bergson, *Act. Chem. Scand. 18* (1964) 1487; K. Bott, *Tetrahedron Lett. 1965*, 4569.

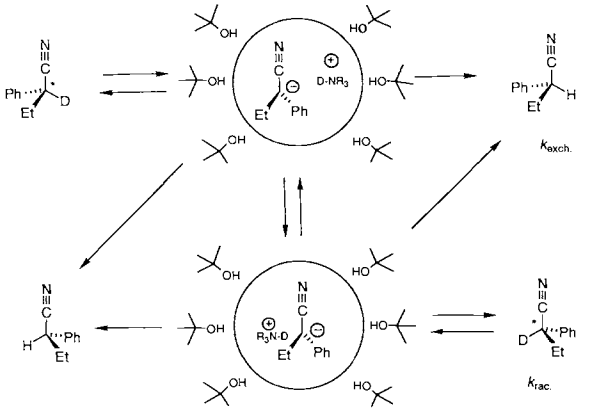

[251] There are very strong hydrogen bonds formed between ammonium or oxonium ions and π systems: C. A. Deakyne, M. Meot-Ner (Mautner), *J. Am. Chem. Soc. 107* (1985) 474 (measurements and ab-initio calcula-

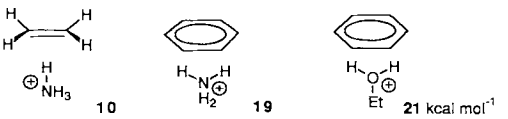

tions), cf. also [257]. Hydrogen bonds between an amine NH and the fluorenyl carbanion: S. Buchholz, K. Harms, M. Marsch, W. Massa, G. Boche, *Angew. Chem. 101* (1989) No. 1; *Angew. Chem. Int. Ed. Engl. 28* (1989) No. 1. Intramolecular hydrogen bonds between an OH group and an indenyl carbanion: P. Ahlberg, B. Johnsson, I. McEwen, M. Rönnqvist, *J. Chem. Soc. Chem. Commun. 1986*, 1500.
[252] Recent reviews on hydrogen bonds see [75, 76] and: a) A. C. Legon, D. J. Millen, *Acc. Chem. Res. 20* (1987) 39; b) E. B. Wilson, Z. Smith, *ibid. 20* (1987) 257; c) H. A. Staab, T. Saupe, *Angew. Chem. 100* (1988) 895–909; *Angew. Chem. Int. Ed. Engl. 27* (1988) 865–879.
[253] C. F. Bernasconi, D. E. Fairchild, C. J. Murray, *J. Am. Chem. Soc. 109* (1987) 3409, and earlier papers of this group cited therein.
[254] Theoretical Studies of Proton Transfers: S. Scheiner, *Acc. Chem. Res. 18* (1985) 174–180.
[255] S. Sprang, T. Standing, R. J. Fletterick, R. M. Stroud, J. Finer-Moore, N.-H. Xuong, R. Hamlin, W. J. Rutter, C. S. Craik, *Science (Washington, DC) 237* (1987) 905; C. S. Craik, S. Roczniak, C. Largman, W. J. Rutter, *ibid. 237* (1987) 909.
[256] See [47, 61, 82], Table 5, and papers about basicity [LDA (pK_a 35.7)/$LiN(SiMe_3)_2$ (pK_a 29.5)] and about aggregation in solution: B. Y. Kimura, T. L. Brown, *J. Organomet. Chem. 26* (1971) 57; R. R. Fraser, T. S. Mansour, *J. Org. Chem. 49* (1984) 3442.
[257] Effect of $LiClO_4$ on the Diels-Alder reaction: R. Braun, J. Sauer, *Chem. Ber. 119* (1986) 1269. In the presence of $LiClO_4$ the equilibrium constant of the deprotonation of tropolone with pyridine in Et_2O is raised by a factor of 12500; this finding was related to ion pairs and aggregates of the Li salt: Y. Pocker, J. C. Ciula, *J. Am. Chem. Soc. 110* (1988) 2904. Influence of $LiClO_4$ on the *C*- vs. *O*-alkylation of Li enolates, see [138]; on the addition of MeLi to ketones: E. C. Ashby, S. A. Noding, *J. Org. Chem. 44* (1979) 4371; on the S_N2 reaction of MeLi with vinyloxiranes: J. C. Saddler, P. L. Fuchs, *J. Am. Chem. Soc. 103* (1981) 2112.
[258] Mixtures of LiBr and a tertiary amine can be applied for the α-alkylation of special base-labile and/or polymerization-prone carbonyl compounds. In these cases "complexes" such as **A** and **B** are proposed as the reactive species (cf. the data in [251]). **A**: O. Tsuge, S. Kanemasa, M. Yoshioka, *J. Org. Chem. 53* (1988) 1384. **B**: M. A. Blanchette, W.

Choy, J. Davis, A. P. Essenfeld, S. Masamune, W. R. Roush, T. Sakai, *Tetrahedron Lett. 25* (1984) 2183; M. W. Rathke, M. Nowak, *J. Org.*

Chem. 50 (1985) 2624; T. Rosen, C. H. Heathcock, *J. Am. Chem. Soc. 107* (1985) 3731. Cf. also an enantioselective version: T. Yamashita, H. Mitsui, H. Watanabe, N. Nakamura, *Bull. Chem. Soc. Jpn. 55* (1982) 961.

[259] D. Seebach, H. Dörr, B. Bastani, V. Ehrig, *Angew. Chem. 81* (1969) 1002; *Angew. Chem. Int. Ed. Engl. 8* (1969) 982; D. Seebach, H.-O. Kalinowski, B. Bastani, G. Crass, H. Daum, H. Dörr, N. P. DuPreez, V. Ehrig, W. Langer, C. Nüssler, H.-A. Oei, M. Schmidt, *Helv. Chim. Acta 60* (1977) 301; D. Seebach, W. Langer, *ibid. 62* (1979) 1701.

[260] Cf. also chiral ethylenediamine derivatives of proline (with and without alkoxide group) for the enantioselective addition of Li compounds and of tin enolates to aldehydes (in part very high *ee*), see references cited in T. Mukaiyama: *Organic Synthetic Reactions*, Tokyo Kagaku Dojin, Tokyo 1987 (ISBN 4-8079-0286-5), Chapter 11.3 and 13.2, respectively. (An English translation of this book published in Japanese, is being prepared. Its title will be *Challenges in Synthetic Organic Chemistry*.) Chiral binaphthyl-substituted ethylenediamine for enantioselective addition of alkyllithium to aldehydes: J.-P. Mazaleyrat, D. J. Cram, *J. Am. Chem. Soc. 103* (1981) 4585.

[261] J. K. Whitesell, S. W. Felman, *J. Org. Chem. 45* (1980) 755.

[262] L. Duhamel, J.-C. Plaquevent, *J. Am. Chem. Soc. 100* (1978) 7415. Review: L. Duhamel, P. Duhamel, J.-C. Launay, J.-C. Plaquevent, *Bull. Soc. Chim. Fr. 1984*, II 421–430.

[263] H. Hogeveen, L. Zwart, *Tetrahedron Lett. 23* (1982) 105.

[264] N. S. Simpkins, *J. Chem. Soc. Chem. Commun. 1986*, 88.

[265] R. Shirai, M. Tanaka, K. Koga, *J. Am. Chem. Soc. 108* (1986) 543.

[266] Further enantioselective protonations of achiral enolates and N-analogues with chiral acids or in the presence of chiral amines/Li amides: [178b, 262, 263] and L. Duhamel, S. Fouquay, J.-C. Plaquevent, *Tetrahedron Lett. 27* (1986) 4975; U. Gerlach, S. Hünig, *Angew. Chem. 99* (1987) 1323; *Angew. Chem. Int. Ed. Engl. 26* (1987) 1283; *Tetrahedron Lett. 28* (1987) 5805.

[267] Diastereoselective protonations: H. E. Zimmerman, *Acc. Chem. Res. 20* (1987) 263–268; ... of nitronates: D. Seebach, A. K. Beck, T. Mukhopadhyay, E. Thomas, *Helv. Chim. Acta 65* (1982) 1101; T. M. Williams, R. Crumbie, H. S. Mosher, *J. Org. Chem. 50* (1985) 91; M. Eyer, D. Seebach, *J. Am. Chem. Soc. 107* (1985) 3601; U. Brändli, M. Eyer, D. Seebach, *Chem. Ber. 119* (1986) 575.

[268] Further enantiooselective deprotonations have been performed, e.g., with the bases **A**–**C** (see also Table 9 and N. S. Simpkins, lecture held at the Society of Chemical Industry Symposium "Chirality Recognition in Synthesis", London, March 17, 1988). For **A**, see [261, 263, 264] and

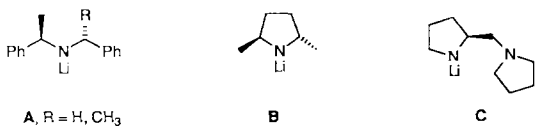

A, R = H, CH_3 **B** **C**

J. A. Marshall, J. Lebreton, *Tetrahedron Lett. 28* (1987) 3323; *J. Am. Chem. Soc. 110* (1988) 2925; L. Duhamel, A. Ravard, J.-C. Plaquevent, D. Davoust, *Tetrahedron Lett. 28* (1987) 5517; For **B** see [26]; For **C**, see M. Asami, *Chem. Lett. 1984*, 829; *Tetrahedron Lett. 26* (1985) 5803; M. Asami, H.Kirihara, *Chem. Lett. 1987*, 389; S. K. Hendrie, J. Leonhard, *Tetrahedron 43* (1987) 3289.

[269] When the precursor of the achiral enolate is a mixture of enantiomers and a chiral base is used for the deprotonation, a kinetic resolution may be responsible for the optical activity of the product; this has to be considered especially in cases of yields below 50%, see for example: M. B. Eleveld, H. Hogeveen, *Tetrahedron Lett. 27* (1986) 631, and review article cited in [218].

[270] M. Simpson, *Diplomarbeit*, ETH Zürich 1982.

[271] T. Mukhopadhyay, Postdoctoral fellow at the ETH Zürich 1981–1982.

[272] D. Wasmuth, *Dissertation Nr. 7033*, ETH Zürich 1982.

[273] D. Seebach, D. Wasmuth, *Angew. Chem. 93* (1981) 1007; *Angew. Chem. Int. Ed. Engl. 20* (1981) 971.

[274] H. Hogeveen, W. M. P. B. Menge, *Tetrahedron Lett. 27* (1986) 2767.

[275] A. Ando, T. Shioiri, *J. Chem. Soc. Chem. Commun. 1987*, 1620; cf. also *ibid. 1987*, 656.

[276] A. C. Regan, J. Staunton, *J. Chem. Soc. Chem. Commun. 1983*, 764; cf. also T. A. Carpenter, G. E. Evans, F. J. Leeper, J. Staunton, M. R. Wilkinson, *J. Chem. Soc. Perkin Trans. I 1984*, 1043; A. C. Regan, J. Staunton, *J. Chem. Soc. Chem. Commun. 1987*, 520. It is not clear from these papers if and which excess of $LiNR_2$ has been used. Cf. also the complexes of Li toluic acid dianion derivatives and diisopropylamine [248].

[277] With the aldol-type products (Nos. 1–11), chiral shift reagent [Eu(dmc)$_3$] and the Mosher method or Pirkle columns [93] were used. With the nitroketone (No. 12), Eu(tfc)$_3$ was used, the product being compared with that of an authentic racemic sample [173] by NMR [93].

[278] It has not been investigated to what extent the adducts **D** shown in Scheme 6 are involved in the aldol additions to benzaldehyde (Nos. 1–11 from Table 9), which proceed most selectively by using a large excess of aldehyde (Nos. 3, 11).

[279] a) A. F. Spatola in B. Weinstein (Ed.): *Chemistry and Biochemistry of Amino Acids, Peptides, and Proteins, Vol. 7*, Marcel Dekker, New York 1983, pp. 267–357.—See also the articles by *Benner, Fersht*, and *Kaiser* in: S. A. Benner (Ed.): *Redesigning the Molecules of Life*, Springer-Verlag, Berlin 1988. b) M. Mutter, *Trends Biochem. Sci. 13* (1988) 260. I thank Professor *Mutter* for kindly allowing us to reproduce the following cartoon (drawn by the graphic division of the journal *Trends in Biochemical Sciences* ("TIBS") after a draft of Prof. *Mutter*).

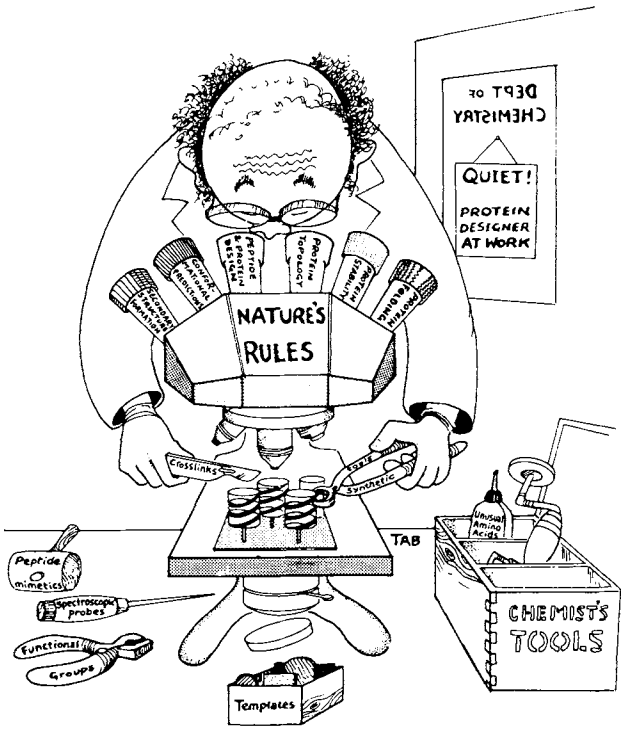

[280] Cf. the path via the cyclic dipeptide derivatives, Scheme 11 (bottom right) and [245].

[281] R. Naef, ETH Zürich 1983, hitherto unpublished results.

[282] D. Seebach, H. Estermann, *Tetrahedron Lett. 28* (1987) 3103.

[283] K. Narasaka, Y. Ukaji, K. Watanabe, *Chem. Lett. 1986*, 1755.

[284] The configuration of the CC and CN double bond of the enolate drawn in Scheme 15 is, as with all deprotonated peptides in this section (Schemes 15–19 and 24), chosen arbitrarily (or better, by the "technique of illustration"). There are no structural investigations of such species known to us. There is probably no doubt about the position of the Li at the more electronegative heteroatom oxygen (**A**–**C** vs. **D**). Of the four possible geometric isomers of the butyric acid derivative, **A** seems to be especially "attractive". Besides the *Z* isomer **B**, the *E* isomer **C** may be also considered for the lithiated peptides. See also entry 16 in Table 9.

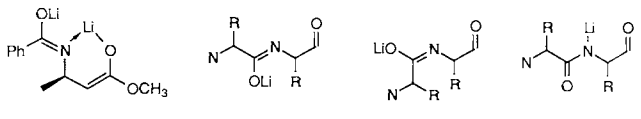

A (*E*,*E*) **B** (*Z*) **C** (*E*) **D**

[285] The first experiments on solubilization and alkylation of polylithiated open-chain peptides in the presence of LiCl have been performed in our laboratory by *S. Shoda* (Postdoctoral fellow at the ETH Zürich 1984–1986).

[286] H. Gründler, Part of the projected *Ph. D. thesis*, ETH Zürich.

[287] a) R. M. Wenger, *Helv. Chim. Acta 67* (1984) 502; b) *Angew. Chem. 97* (1985) 88–96; *Angew. Chem. Int. Ed. Engl. 24* (1985) 77–85; *Progr. Chem. Org. Nat. Prod. 50* (1986) 123–168; *Prog. Allergy 38* (1986) 46–64; R. M. Wenger, T. G. Payne, M. H. Schreier, *Prog. Clin. Biochem. Med. 3* (1986) 157–191.

[288] I sincerely thank Dr. *R. M. Wenger* of Sandoz AG, Basel, for the temporary acceptance of co-workers of my group into his laboratory, for

numerous discussions about oligopeptides and about cyclosporine, and for authentic samples and help in the identification of our products. Dr. *Wenger* has also kindly provided us with the color prints of Fig. 26.

[289] The solubilizing effect of an excess of LDA on polylithiated peptides was first observed in our laboratory by *C. W. Murtiashaw* (Postdoctoral fellow at the ETH Zürich 1983–1984).

[290] Probably other highly aggregated lithium derivatives can also be solubilized in this way, e.g., the geminal enediolates $R_2C{=}C(OLi)_2$, derived from carboxylic acids, for which "polymerization degrees" of up to 250 in THF were reported [126].

[291] A. P. Krapcho, E. A. Dundulis, *Tetrahedron Lett. 1976*, 2205.

[292] D. A. Evans, P. J. Sidebottom, *J. Chem. Soc. Chem. Commun. 1978*, 753.

[293] A general discussion of 4-atom 6-electron and of 6-atom 8-electron π systems is found in [41c, d] and in: R. Schlecker, D. Seebach, *Helv. Chim. Acta 60* (1977) 1459.

[294] D. H. R. Barton, R. H. Hesse, M. M. Pechet, C. Wiltshire, *J. Chem. Soc. Chem. Commun. 1972*, 1017.

[295] D. J. Goldsmith, A. J. Lewis, W. C. Still, Jr., *Tetrahedron Lett. 1973*, 4807.

[296] A. Thaler, *Diplomarbeit*, ETH Zürich 1987.

[297] D. Seebach, A. K. Beck, A. Thaler, *Helv. Chim. Acta 71* (1988), in press.

[298] a) P. Pfeiffer, J. von Modelski, *Hoppe Seyler's Z. Physiol. Chem. 81* (1912) 331; *85* (1913) 1; b) P. Pfeiffer, *ibid. 133* (1924) 22.

[299] One can imagine that the complexation of Li with peptides is linked to the application of Li salts in the long-term treatment of depressions; the mechanism is unknown to date, see [33] and: F. N. Johnson: *The History of Lithium Therapy* and *The Psychopharmacology of Lithium*, Macmillan Press, London 1984.

[300] T. H. Haskell, S. Hanessian, US Patent 3405218 (Oct. 8, 1968); *Chem. Abstr. 68* (1968) 89875p.

[301] See [47] and references [113, 122, 123, 135] therein.

[302] R. Meulemans, P. Piret, M. van Meerssche, *Acta Crystallogr. Sect. B27* (1971) 1187.

[303] The solubilization of proteins in aqueous/organic solvent mixtures is an important method in protein chemistry. Review: P. Douzou, C. Balny, *Adv. Protein Chem. 32* (1978) 77–189.

[304] P. T. d'Holbach (pseudonym: J. B. Mirabaud): *Système de la nature ou des lois du monde physique et du monde moral* (First edition 1770, London).

[305] Cyclosporine A (CyA): A. Rüegger, M. Kuhn, H. Lichti, H.-R. Loosli, R. Huguenin, C. Quiquerez, A. von Wartburg, *Helv. Chim. Acta 59* (1976) 1075.

[306] X-ray structure of a derivative of CyA: T. J. Petcher, H.-P. Weber, A. Rüegger, *Helv. Chim. Acta 59* (1976) 1480.

[307] CyC: R. Traber, M. Kuhn, A. Rüegger, H. Lichti, H.-R. Loosli, A. von Wartburg, *Helv. Chim. Acta 60* (1977) 1247.

[308] CyB,D,E: R. Traber, M. Kuhn, H.-R. Loosli, W. Pache, A. von Wartburg, *Helv. Chim. Acta 60* (1977) 1568.

[309] CyE,F,G,H,I: R. Traber, H.-R. Loosli, H. Hofmann, M. Kuhn, A. von Wartburg, *Helv. Chim. Acta 65* (1982) 1655.

[310] CyK-Z: R. Traber, H. Hofmann, H.-R. Loosli, M. Ponelle, A. von Wartburg, *Helv. Chim. Acta 70* (1987) 13.

[311] For the total synthesis of CyA and of analogues, see [287] and D. H. Rich, M. K. Dhaon, B. Dunlap, S. P. F. Miller, *J. Med. Chem. 29* (1986) 978; R. D. Tung, M. K. Dhaon, D. H. Rich, *J. Org. Chem. 51* (1986) 3350; I. J. Galpin, A. K. A. Mohammed, A. Patel, *Tetrahedron Lett. 28* (1987) 6517.

[312] J. F. Borel in D. J. G. White (Ed.): *Cyclosporine*, Elsevier, Amsterdam 1982, pp. 5–17.

[313] H. Kessler, H.-R. Loosli, H. Oschkinat, *Helv. Chim. Acta 68* (1985) 661; H.-R. Loosli, H. Kessler, H. Oschkinat, H.-P. Weber, T. J. Petcher, A. Widmer, *ibid. 68* (1985) 682.

[314] A. Thaler, part of the projected *Dissertation*, ETH Zürich.

[315] I. L. Karle, *J. Am. Chem. Soc. 96* (1974) 4000.

[316] More alkali-metal complexes of cyclic peptides are collected in the following monograph: M. Dobler: *Ionophores and Their Structures*, Wiley, New York 1981.

[317] D. Seebach, P. Bollinger, C. Gerber, H. Gründler, S. Y. Ko, M. Krieger, H.-R. Loosli, C. W. Murtiashaw, R. Naef, S. Shoda, A. Thaler, R. M. Wenger, *Helv. Chim. Acta*, in preparation; hitherto unpublished experiments, ETH Zürich and Sandoz AG, Basel.

[318] With all other El groups shown, except $COOCH_3$, the new amino acid has *R* configuration in **C**, and *S* configuration in **D**. By the change of the CIP order of priority, the afore mentioned assignment is inverted with the aminomalonic acid moiety ($El = COOCH_3$), a demonstration that the pro-*R*/pro-*S* specification is not constitutionally invariant! In the products with El = F and $El = SCH_3$ the newly introduced substituents have highest priority, so that **C** is *R* and **D** *S*. Generally, substitution of the C^{Re} ligand on a tetrahedral center $XABC_2$ by a new group D (→ XABCD) will lead to *R*-specification in exactly 50% of all cases, depending upon whether D is No. 1, 2, 3, or 4 in the priority sequence!

[319] R_f values with 10% MeOH in Et_2O: (*R*)-Ala^3 0.56, (*S*)-Ala^3 0.51, CyA 0.47.

[320] Taken from the poem "Flag of Poland" in *The Metamict State*, Poems by Roald Hoffmann, University Presses of Florida 1987.

[321] U. Brändli, *Dissertation No. 8680*, ETH Zürich 1988.

[322] D. Müller, *Diplomarbeit*, ETH Zürich 1988.

[323] a) There are indications, that LiCl formed in situ increases the solubility of polybenzamides in an aprotic solvent (e.g., DMF) ("solubility mediator"): F. Schultze-Gebhart in B. von Falkai (Ed.): *Synthesefasern*, Verlag Chemie, Weinheim 1981, Chapter II, p. 452; Z. A. Rogowin: *Chemiefasern*, Thieme Verlag, Stuttgart 1982, Chapter 30, p. 375. b) The solubilization and reaction of polyamides with electrophiles by deprotonation of the amide groups with NaH in the aprotic polar solvent DMSO has recently come into use to modify the properties of polymers: M. Takayanagi, T. Katayose, *J. Polym. Sci. Polym. Chem. Ed. 19* (1981) 1133; D. R. Moore, L. J. Mathias, *J. Appl. Polym. Sci. 32* (1986) 6299; M. Takayanagi, S. Ueta, W.-Y. Lei, K. Koga, *Polym. J. 19* (1987) 467. c) The effect of the deprotonation, and solubilization with LiX, is reminiscent of the xanthate-method in the production of artificial silk from cellulose: M.-L. Kehren, A. Reichle: *Cellulose-Chemiefasern* in *Ullmanns Enzyklopädie der technischen Chemie, 4th ed., Vol. 9*, Verlag Chemie, Weinheim 1975, pp. 213–226.

[324] Taken from a speech given in Frankfurt, see [130a].

Two-Dimensional Solid-State NMR Spectroscopy: New Possibilities for the Investigation of the Structure and Dynamics of Solid Polymers

New Analytical Methods (38)

By Bernhard Blümich and Hans Wolfgang Spiess*

Dedicated to Professor Dr. Helmut Dörfel on the occasion of his 60th birthday

NMR spectroscopy is an effective method not only for examining liquid samples but also for characterizing molecular structure, order and dynamics in amorphous and ordered solids. Recent developments in the area of solid-state NMR spectroscopy span from model-dependent studies of conventional one-dimensional spectra to the more definitive two-dimensional (2D) spectra which provide more specific information. For example, with 2D-NMR spectroscopy it is possible to determine the orientational distribution functions of molecular segments in drawn polymers and to distinguish different mechanisms of complex molecular motions. Following an introduction to basic NMR spectroscopy, an overview of the current state-of-the-art of 2D methods in solid-state NMR spectroscopy is presented and demonstrated with selected examples.

1. Introduction

Polymeric materials are valued not only for their light weight and low production costs, but also for their diversity of physical properties. For these reasons polymers are increasingly replacing conventional materials and constitute essential components of new technologies. The exceptional mechanical, electrical, optical and transport properties of polymers are ultimately determined by the structure and organization of the macromolecules.

A classical example of the relationship between molecular organization and macroscopic properties is the partial crystallinity of polymers such as polyethylene.[1] In the crystalline regions the polymer chains are highly ordered and immobile. These regions give the plastic material its mechanical strength. In the amorphous layers, however, the polymer chains are mainly disordered and mobile. These regions allow plastic deformation of the material.

The precise characterization of molecular order and dynamics is consequently an important prerequisite for understanding the macroscopic properties of polymer materials. The achievement of this goal is very important but also very difficult, since the macromolecules of synthetic polymers possess an enormous number of internal degrees of freedom. Therefore, there are numerous possible molecular motions with characteristic times of about 10^{-11} s to minutes.[1a] Solid polymers often occur in the glassy state. Even in this amorphous state, however, it is possible to establish molecular order in the polymers by controlled deformation, macroscopic orientation of the polymer chains or preferential packing of the macromolecules.[1b] Solid-state NMR spectroscopy[2-6] offers new possibilities for polymer characterization and has repeatedly proven itself useful in recent years in this area.[7-16]

The main advantage of NMR spectroscopy is its high selectivity. For instance, the individual functional groups of a macromolecule can be distinguished in a ^{13}C-NMR spectrum because of their different chemical shifts. However, the necessary spectral resolution in solids can only be achieved by mechanically rotating the sample at the "magic" angle of 54.7° relative to the magnetic field (MAS: *M*agic *A*ngle *S*pinning).[17,18] In addition, the sensitivity of ^{13}C-NMR spectroscopy can be significantly increased by means of cross polarization (CP: *C*ross *P*olarization).[19]

The signal intensities observed in a CP/MAS-^{13}C-NMR spectrum depend on various spin relaxation times.[3,4] These reflect the mobility of the respective functional groups in the solid state. On the basis of these differences, one can successfully examine molecular structure and dynamics with relatively simple 1D-NMR methods, as described in a review article by *R. Voelkel*.[20]

Selectivity can also be achieved by isotope labeling, whereby the ^{2}H-NMR spectroscopy of selectively deuterated solids has become a standard procedure.[13-16] Exploiting the differences in relaxation time and using suitable pulse sequences, molecular motions can be investigated in the entire range of interest (10^{-11} to ca. 100 s) by using relatively simple 1D-NMR methods. The orientational distribution functions of macromolecules in partially ordered polymers can likewise be exactly assessed.

One-dimensional solid-state NMR spectroscopy already provides highly selective information and is therefore used on a routine basis nowadays. Nonetheless, this method often fails to sufficiently characterize molecular structure, order and dynamics in solid polymers, because the data analysis is based on model concepts and different models cannot always be unequivocally differentiated. It is not surprising then, that 2D-NMR spectroscopy, which has proven most effective for elucidating the structure of biomolecules in solution, is now being used to gain this information.[21,22]

The present article is therefore concerned with 2D solid-state NMR spectroscopy. Although this procedure is more complicated than 1D-NMR, considerably more informa-

[*] Prof. Dr. H. W. Spiess, Priv. Doz. Dr. B. Blümich
Max-Planck-Institut für Polymerforschung
Postfach 3148, D-6500 Mainz (FRG)

tion can be acquired by its application. For example, a 2D spectrum allows one to either correlate various molecular properties or molecular states at different times,[23-28] or to separate different molecular properties.[29-33] The following section (Section 2) covers the basics of solid-state NMR spectroscopy which are necessary for understanding these new techniques. Section 3 then presents a systematic overview of 2D-NMR methods for the investigation of solids. Sections 4 and 5, respectively, cover molecular motion and molecular order, which are especially relevant for an understanding of solid polymers. These sections provide a more detailed account of new 2D-NMR experiments. In this way, we not only hope to provide detailed information to those readers who are already acquainted with modern NMR spectroscopy, but also to show the layman the potential of these new methods.

2. Basic Solid-State NMR Spectroscopy

Molecules are less mobile in the solid state than in the liquid state. Therefore, a number of anisotropic (orientation dependent) interactions occur in the solid state, whereas in the liquid state these interactions are averaged by fast molecular motions.[2-6] The three most important interactions are listed as follows:

1) The *magnetic dipole-dipole coupling* of two nuclei: One hereby distinguishes between the homonuclear dipole-dipole coupling of like nuclei (e.g. ^{1}H) and the heteronuclear dipole-dipole coupling of different nuclei (e.g. ^{1}H and ^{13}C). In the case of ^{1}H, each nucleus couples with many other nuclei which causes wide structureless bands in the spectrum.
2) The *electric quadrupole coupling* of nuclei with a spin $I > 1/2$; such nuclei possess a quadrupole moment which couples to the electric field gradient at the site of the nucleus.
3) The *magnetic shielding* of the nucleus by the surrounding electrons is also anisotropic. In liquids, the time average of this interaction is seen as the chemical shift, while dipole-dipole and quadrupole coupling are averaged to zero by the molecular motion.

The quadrupole coupling generally dominates in solids for nuclei with a spin $I > 1/2$. Although the quadrupole coupling is small for ^{2}H, in hydrocarbons it leads to spectra typically having a line width of 250 kHz. The homonuclear dipole-dipole coupling between ^{1}H results in line widths up to 100 kHz, whereas the heteronuclear dipole-dipole coupling between ^{1}H and ^{13}C yields line widths up to 50 kHz. These values are independent of the Larmor frequency, while the frequency shifts due to the anisotropy of the magnetic shielding are proportional to the static magnetic field $\boldsymbol{B}_0$ and are therefore proportional to the Larmor frequency. At an anisotropy of the chemical shift of 200 ppm, a typical value for hydrocarbons with π-bonds,[3,4,34] the ^{13}C-NMR spectrum has a line width of 15 kHz at a field strength of 7 T.

Because of the anisotropy of the interactions, in solids the NMR frequency depends on the orientation of the molecules in the magnetic field. Consequently, for many years narrow signals which shift in a characteristic way on rotating the sample were observed only with single crystals. However, powders can also furnish spectra with narrow signals if the orientation-dependent terms of the nuclear interactions are eliminated during the measurement by:

1) *Heteronuclear decoupling*[2,3,35,36] especially of ^{1}H and ^{13}C through irradiation at the ^{1}H resonance frequency;
2) *Rotation of the sample at the magic angle*;[3,4-6,17]
3) *Homonuclear decoupling*,[2,3,37,38] in particular of ^{1}H-^{1}H by pulsed irradiation at the ^{1}H resonance frequency (multi-pulse methods for selective averaging).

2.1. Orientation Dependence of the NMR Frequency

The orientation-dependent nuclear-spin interactions introduced here are described by second-rank tensors. The angular dependence of the NMR frequency is then given by the following equation:[2-4]

$$\Omega = \Omega_0 + \tfrac{1}{2}\Delta(3\cos^2\theta - 1 - \eta\sin^2\theta\cos 2\phi). \quad (1)$$

Ω_0 denotes the Larmor frequency including the part of the isotropic chemical shift, Δ is the coupling constant, and the asymmetry parameter $0 \le \eta \le 1$ represents the deviation from axial symmetry around the principal Z axis of the coupling tensor; the polar coordinates θ and ϕ describe the orientation of the magnetic field $\boldsymbol{B}_0$ in the principal axes system of the tensor. The principal axes system for the generally dominating intramolecular contributions is determined by the local symmetry of the molecule in the vicinity of the nucleus under study. Some especially significant examples for ^{13}C- and ^{2}H-NMR spectroscopy are illustrated in Figure 1. The NMR spectrum for a particular molecular orientation is shown in the middle. The powder spectrum, obtained as a superposition of the spectra for all orientations, is displayed on the right-hand side.

The anisotropic interactions are partially or totally averaged in the presence of fast molecular motions with correlation times $\tau_c \ll \Delta^{-1}$. Nevertheless, the tensorial character of the coupling is maintained and is characterized by $\bar{\Delta}$ and $\bar{\eta}$.[4] Equation (2) then applies for the resonance frequency:

$$\Omega = \Omega_0 + \tfrac{1}{2}\bar{\Delta}(3\cos^2\theta' - 1 - \bar{\eta}\sin^2\theta'\cos 2\phi), \quad (2)$$

whereby θ' and ϕ' represent the polar angles of $\boldsymbol{B}_0$ in the principal axes system of the averaged tensor. Hereby, deviations of the axial symmetry can occur. This means that $\bar{\eta} \neq 0$, although $\eta = 0$.[13] For motions with cubic symmetry, such as tetrahedral jumps which occur in crystalline hexamethylenetetramine,[39] and consequently also for isotropic reorientations, the anisotropic coupling vanishes, so that $\bar{\Delta} = 0$.

2.2. Rotation at the Magic Angle: MAS

If a sample is rotated with angular velocity $\Omega_R > \Delta$ (Fig. 2) about an axis which is inclined at an angle of Φ with respect to the magnetic field $\boldsymbol{B}_0$, then the orientation-de-

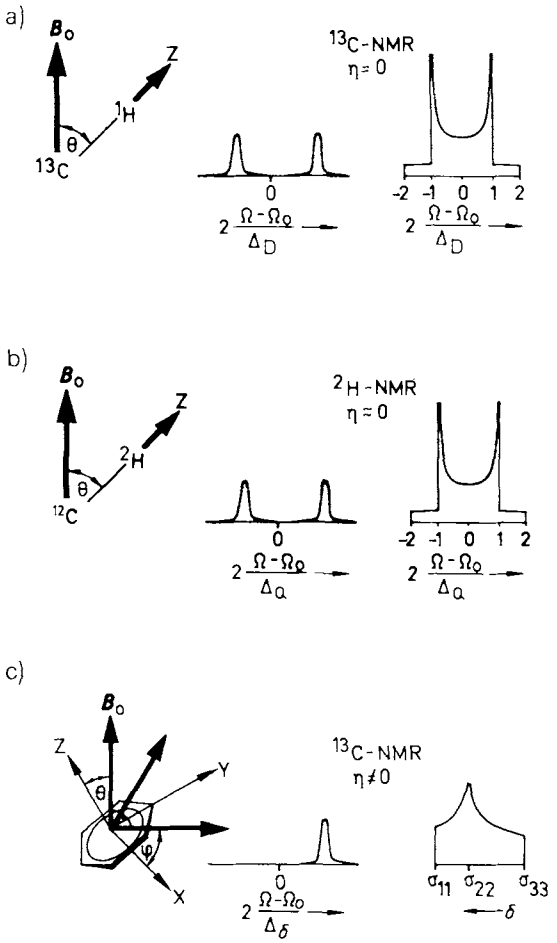

Fig. 1. Anisotropic interactions in the solid state which make the NMR frequency dependent on the molecular orientation: a) dipole-dipole coupling between ^{1}H and ^{13}C. Because the total spin amounts to $I=1$, the ^{13}C-NMR spectrum is made up of two signals, the separation of which is dependent on the orientational angle θ. b) Quadrupole coupling of the ^{2}H nucleus with the electrical field gradient of the C-^{2}H bond. Because the ^{2}H nucleus possesses a spin $I=1$, the NMR spectrum looks similar to that of the dipole-dipole coupling between ^{1}H and ^{13}C. c) Anisotropic magnetic shielding of the ^{13}C nuclei. Because ^{13}C has a spin of 1/2, only one NMR signal is observed.

pendent nuclear-spin interactions are scaled by a factor of $\frac{1}{2}(3\cos^2\Phi-1)$.[3,17] For the magic angle of $\Phi=54.7°$, the anisotropic interaction averages to zero. This applies, however, only under the condition, that the rotation frequency Ω_R is considerably larger than the coupling constant Δ. This prerequisite can still be met for the anisotropy of the magnetic shielding at rotation frequencies of up to 20 kHz which can be currently attained. Therefore, MAS-^{13}C-NMR spectroscopy together with high-power proton decoupling has become a routine method for measuring highly resolved spectra of solids[36] as shown in Figure 2d with dimethyl sulfone as an example.

By rapid MAS, the wide solid-state resonances are narrowed to small lines (see Figs. 2c and 2d). One simultaneously gains signal intensity thereby shortening the measurement time from hours to minutes. Such MAS-NMR spectra are comparable to NMR spectra of liquids, even though they exhibit lower resolution.[20] However, because the information about the anisotropic coupling is lost, the carrier of information regarding molecular order and dynamics is lost as well (see Sections 4 and 5).

On the other hand, for slower sample rotations ($\Omega_R<\Delta$), one observes rotational sidebands separated by multiples of Ω_R from the center line at the isotropic chemical shift (Fig. 2e). The sideband spectrum covers the same frequency range as the spectrum of the static sample (Fig. 2c), so that information about the anisotropic coupling is basically retained.[40,41] Sideband spectra of ^{13}C nuclei with different isotropic chemical shifts are shifted accordingly and therefore can be resolved.

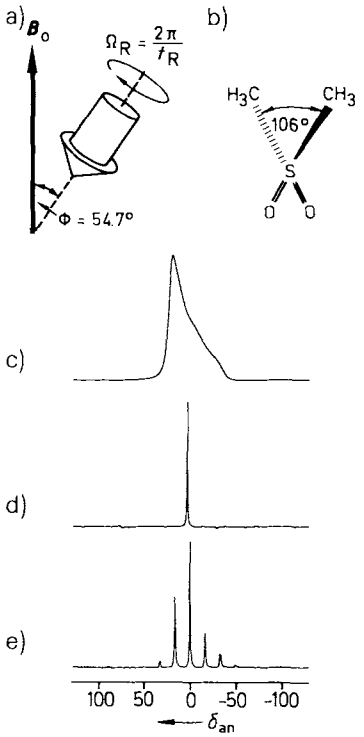

Fig. 2. Sample geometry during rotation at the magic angle a) and proton decoupled ^{13}C-NMR spectra of dimethyl sulfone b) at room temperature, c) static sample, d) fast sample rotation at $\Omega_R=5000$ Hz and e) slow sample rotation at 1000 Hz.

If rotational sidebands are unwanted, they can be suppressed by means of the so-called TOSS method (TOSS: *T*otal *S*uppression of *S*idebands) (Fig. 3).[42-46] Application of 180° pulses causes the sidebands to cancel during the detection period. The TOSS method demonstrates that averaging processes are possible not only by manipulating the sample in the spacial dimension (rotation at the magic angle), but also by manipulating the sample in the spin di-

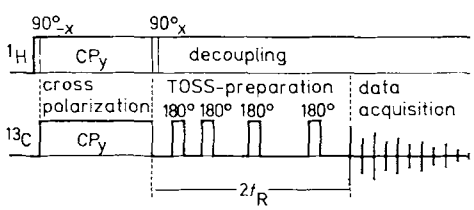

Fig. 3. Excitation scheme for TOSS and cross polarization. By means of cross polarization, transverse magnetization is transferred from the protons to the ^{13}C nuclei (see Figure 4 and caption). In order to prevent cross-polarization effects during the TOSS pulses, the transverse proton magnetization is rotated back to the z-direction by a 90° pulse at the beginning of the TOSS preparation period [47].

mension (rotation of the nuclear moments by radio-frequency pulses, selective averaging). The TOSS procedure, however, is problematic for analytical applications,[20] because the intensities of the center lines deviate from their theoretical values. As was recently shown, the TOSS method can, nonetheless, be used to detect ultra-slow molecular motions.[48]

2.3. Cross Polarization

With pulse spectroscopy the signal-to-noise ratio depends on the spin-lattice relaxation time[4] and on the degree of nuclear magnetization which can be achieved. Both of these parameters are unfavorable for ^{13}C nuclei, because the relaxation times are longer than those of ^{1}H nuclei, and the natural abundance of ^{13}C amounts to only 1%. However, by using the cross polarization technique illustrated in Figure 4, these disadvantages can be circumvented by transferring magnetization from ^{1}H to ^{13}C.[18,49,50]

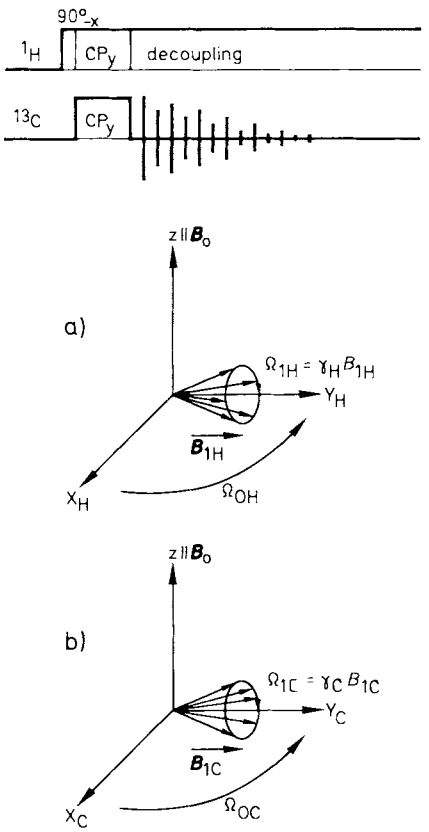

Fig. 4. Cross polarization: Transfer of magnetization from ^{1}H to ^{13}C. ^{1}H- and ^{13}C-nuclear spins precess around their respective transverse magnetic fields. For details see text.

Transverse ^{1}H-magnetization is generated by a 90° pulse. After the pulse, the phase of the ^{1}H transmitter is shifted by 90°, causing the magnetic field $\boldsymbol{B}_{1H}$ of the ^{1}H transmitter to lie parallel to the transverse ^{1}H magnetization. Therefore, in the coordinate system, which rotates with the Larmor frequency Ω_{0H}, the ^{1}H nuclear spins precess with a frequency $\gamma_H B_{1H} = \Omega_{1H}$ (Figure 4a) around the $\boldsymbol{B}_{1H}$ field. During this period, the carbon spins are likewise irradiated with a radio-frequency magnetic field $\boldsymbol{B}_{1C}$. The amplitude is selected in such a way as to fulfill the Hartmann-Hahn condition (Fig. 4b),[19] so that $\gamma_C B_{1C} = \Omega_{1C} = \Omega_{1H} = \gamma_H B_{1H}$. In the coordinate system, which rotates with the Larmor frequency Ω_{0C}, the ^{13}C spins then precess around the $\boldsymbol{B}_{1C}$ field with the same frequency as the ^{1}H spins do around the $\boldsymbol{B}_{1H}$ field. Because of the ^{1}H-^{13}C dipole-dipole interaction, the magnetization of the highly polarized ^{1}H nuclei can then be transferred to the unpolarized ^{13}C nuclei.[19] As a result of this cross polarization, the ^{13}C nuclei can be polarized by a factor of up to 4 higher than by their spin-lattice relaxation. Furthermore, the repetition rate of the cross polarization is now determined by the spin-lattice relaxation of ^{1}H, which is typically shorter than that of ^{13}C.

In practice, all the phases of the radio frequency fields are cyclically varied to reduce the degradation of the ^{13}C-NMR signal by relaxation effects and pulse distortions. The phase cycle for the cross-polarization sequence is compiled in Table 1 for one phase of the ^{1}H-cross-polarization field (Y). It is extended to the other phases by means of cyclic permutation.

Table 1. Phase cycle for cross polarization.

90° (^{1}H)	CP (^{1}H)	CP (^{13}C)	Receiver
X	Y	X	X
X	Y	Y	Y
X	Y	−X	−X
X	Y	−Y	−Y
−X	Y	X	−X
−X	Y	Y	−Y
−X	Y	−X	X
−X	Y	−Y	Y

To simplify complicated sideband spectra, the cross-polarization technique can be varied, so that either protonated or unprotonated carbons alone are polarized.[51,52] This type of selectivity is reached on the basis of variations in the dipole-dipole coupling between ^{1}H and ^{13}C in different functional groups such as $-CH_3$, $=CH_2$, $\equiv CH$ and $-COO^{\ominus}$. Some polarization schemes are summarized in Figure 5. In Figure 5a the cross-polarization time (1–5 ms) is selected such that all ^{13}C positions are polarized. At shorter cross-polarization times (50 μs, Fig. 5b), only protonated nuclei with strong dipole-dipole couplings are polarized. The process according to Figure 5c leads to the complementary spectrum: first all C atoms are polarized. Thereafter, the proton decoupling is turned off for a period of $t_d \approx 100$ μs (gated decoupling). Because of the dipole-dipole coupling, the transverse magnetization of the protonated C atoms is destroyed faster during t_d than that of the unprotonated C atoms, the signals of which therefore dominate during the detection period. To avoid phase errors, the data acquisition starts only after the resulting ^{13}C magnetization has been refocussed by a 180° pulse to the beginning of a rotor period $t_R = 2\pi/\Omega_R$.[32]

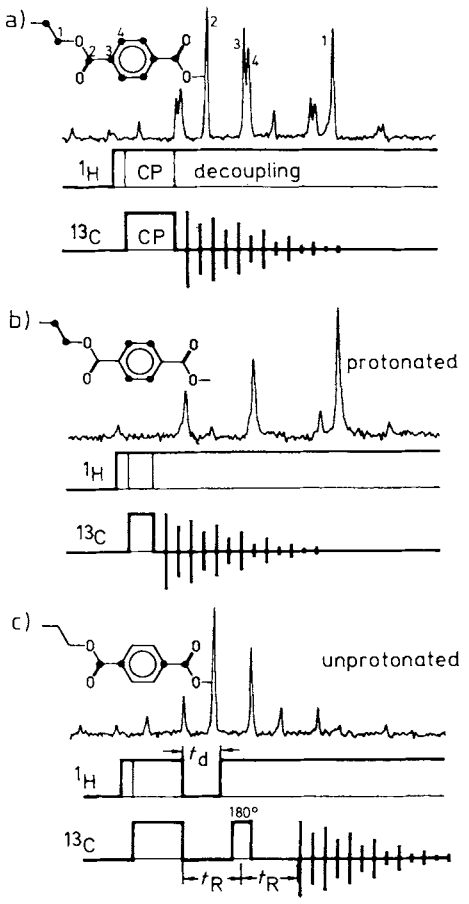

Fig. 5. The selectivity of different cross polarization schemes is illustrated on polyethylene terephthalate at room temperature at a sample rotation frequency of $\Omega_R/2\pi = 4090$ Hz. a) Polarization of protonated and unprotonated ^{13}C nuclei. b) Polarization of protonated ^{13}C nuclei. c) Polarization of unprotonated ^{13}C nuclei.

3. Review of Two-Dimensional Solid-State NMR Spectroscopy

3.1. Basics

The time scheme of two-dimensional, solid-state NMR spectroscopy (Fig. 6) is identical with that of high-resolution 2D-NMR spectroscopy of liquids.[21-24] The nuclear spin system is first brought into a well-defined initial state during the *preparation period*. During this time, spin-lattice relaxation typically occurs followed by a 90° pulse or cross polarization (Section 2.3). During the following *evolution period* t_1, the spin system develops under the influence of various nuclear spin interactions (Section 2.1). In conventional 1D-NMR spectroscopy, the nuclear signal is recorded during the time t_1, and the spectrum is produced after Fourier transformation. In 2D-NMR spectroscopy, however, the state of the spin system after a certain time t_1 is generally altered abruptly by at least one further radio-frequency pulse. The resonance signal is then recorded during a subsequent *detection period* (t_2). Afterwards, the entire experiment is repeated with an incremented evolution time t_1, whereby the initial state of the nuclear spin system during the detection period at $t_2 = 0$ changes accordingly. The 2D-NMR spectrum is produced by two successive Fourier transformations after t_2 and t_1.

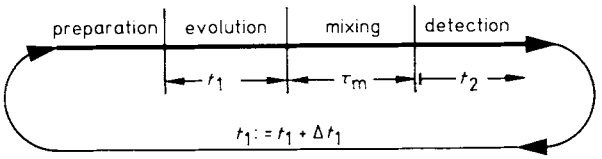

Fig. 6. Timing diagram of two-dimensional-NMR spectroscopy. During the detection period t_2 transverse magnetization is measured, the history of which is determined by the preparation period and the evolution period t_1 and by the fixed mixing time τ_m, respectively. Data acquisition is repeated after incrementing the evolution period.

As explained in Section 2, the interactions which influence a nuclear spin during the preparation period, the evolution time t_1 or the detection time t_2, can be manipulated in many ways such as by homo- or heteronuclear decoupling, through MAS or by polarization transfer. Finally, a fixed mixing period of duration τ_m can be introduced between the evolution and detection times (Fig. 6), during which the nuclear magnetization is mixed between different resonances. This occurs, for example, during chemical reactions and chemical exchange. In solids, the nuclear spin interactions are also anisotropic, so all feasible molecular orientations must be considered. Correlations, which associate different interactions with particular nuclear positions or which indicate the exchange of molecular groups or orientations due to dynamic processes, are marked by cross peaks. In all, there are a large number of 2D-NMR methods which can be utilized for the study of molecular structure, order, and dynamics. In Section 3.2 a systematic overview of the various types of solid-state 2D-NMR spectroscopy is presented.

3.2. The State-of-the-Art

In order to simplify the summary of the numerous 2D-NMR techniques, the various methods are compiled in two tables. Table 2 concerns static samples, whereas Table 3 deals with rotating samples, i.e. MAS-NMR spectroscopy. The rows and columns a–j contain the nuclear spin interactions which determine the NMR frequencies on both axes of the 2D-NMR spectra and take effect during the evolution time t_1 and the detection time t_2. The isotopic chemical shift is given by δ_{iso}, whereas J denotes the indirect hetero- or homonuclear spin-spin coupling,[2-6] R the relaxation effects, δ_{an} the anisotropy of the magnetic shielding (chemical shift), D_{II} the homonuclear dipole-dipole coupling, D_{IS} the heteronuclear dipole-dipole coupling, Q the quadrupole coupling, and ϕ the sample orientation at the beginning of data collection. The upper triangle refers to crystals and ordered samples, and the lower triangle to amorphous and powdered samples.

The entries S, D, O specify the suitability of the particular method for studying molecular structure (S), molecular dynamics (D) or molecular order (O).

All experiments having a mixing time are labeled with D. These include exchange experiments as well as spin-diffusion experiments, whereby the latter essentially yield information about structure. The term "exchange" denotes frequency exchange caused by either chemical reactions or

Table 2. 2D solid-state NMR methods for static samples (see text).

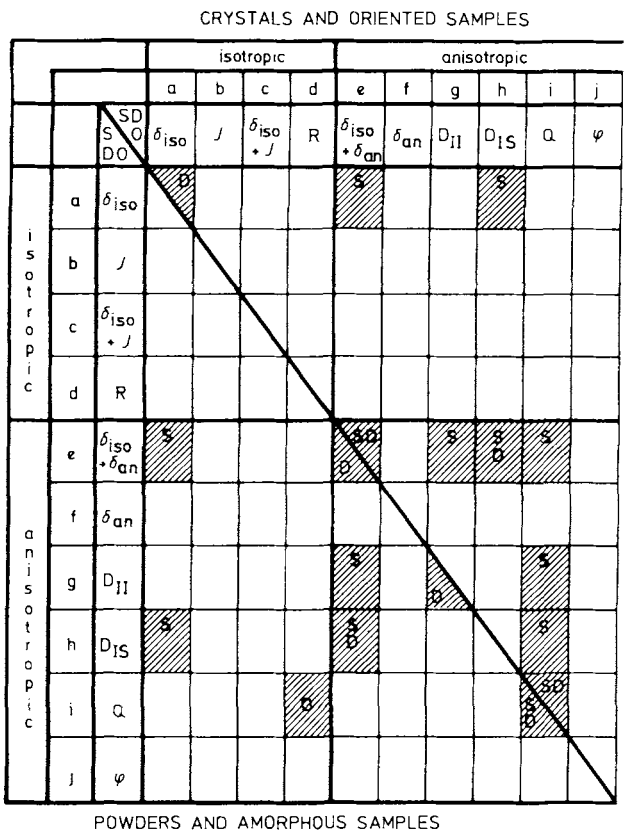

References

Crystals and ordered samples

aeS [54]
ahS [55]
eeS [56, 57]
egS [58]
ehS [59–63]
eiS [64]
giS [65]
hiS [65, 66]
iiS [55, 67, 68]
aaD [69]
eeD [59, 70]
ehD [71]
iiD [72]

Powders and amorphous samples

eaS [73]
geS [74]
haS [55]
heS [75–77]
iiS [78–84]
eeD [85–90]
ggD [78]
heD [77]
idD [91]
iiD [24–28]

Table 3. 2D solid-state NMR methods for rotating samples (see text).

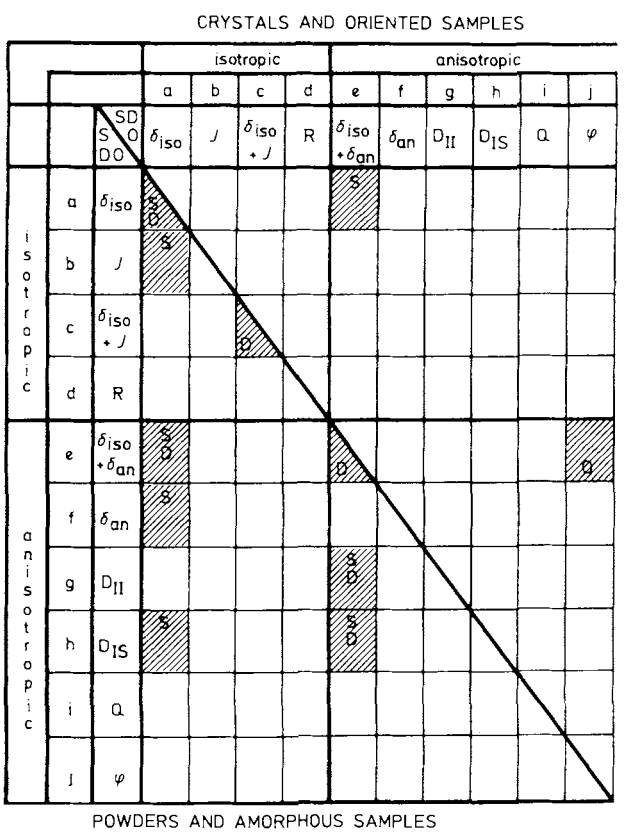

References

Crystals and ordered samples

aeS [92]
ejO [30–33, 41]

Powders and amorphous samples

aaS [93–96]
baS [97–99]
eaS [100–103]
faS [104]
geS [105]
haS [106, 107]
heS [41, 108–111]
aaD [95, 96, 112–118]
ccD [119]
eaD [120]
eeD [121, 122]
geD [123]
heD [124]

molecular reorientation. The correlation of different, isotropic chemical shifts is sufficient for detecting chemical exchange. However, in order to detect molecular reorientation, an isotropic interaction must be present. Many of the correlation experiments denoted with S can in principle also be applied for examining molecular dynamics. A particular method is labeled with D only in cases in which such applications have been experimentally demonstrated.

Rows and columns of the tables are marked with small letters (a–j) which refer to the corresponding literature references. Two examples are presented to demonstrate how the tables should be used. The 2D-^{2}H-exchange experiment for detecting ultra-slow molecular motions described later in Section 4 is found in Table 2 in the lower triangle under the heading iiD, since a static isotropic sample is measured, the quadrupole coupling is detected during the evolution and detection times, and because molecular dynamics are investigated. The MAS method used to determine molecular order and which is described further in Section 5 is accordingly found in Table 3 under ejO, since the sample rotates and is ordered. Furthermore, one frequency axis corresponds to the magnetic shielding (chemical shift), and the other corresponds to the mechanical sample rotation.

The particular techniques applied during the various experiments are not specified in the tables, for this would be beyond the scope of this article. For NMR specialists, however, the relevant publications are cited: multi-pulse methods for homonuclear decoupling,[2, 53, 56, 60–63, 69, 71, 93, 94, 97–99, 107, 110, 111, 118, 119, 124] and for scaling of the chemical shift[97, 103, 106, 125] multiquantum NMR spectroscopy,[54, 65, 126] switching of the spinning axis,[92, 101, 102, 107, 127] discrete sample reorientations,[57, 73] rotor synchronization of the excitation sequence,[30–33, 41, 101, 104, 107, 108, 121, 122, 124] dynamic nuclear polarization,[74] overtone excitation and

detection,[55] and the reduction of the effective magnetic field by nutation in the B_1 field,[55,67,80–83] switching of the B_0 field,[79] or by zero-field NMR spectroscopy.[78,84,128]

On the diagonals of Tables 2 and 3, the 2D-NMR methods appear, in which an interaction is correlated with itself. The other experiments correlate various interactions with each other which, with the exception of the sample orientation ϕ, correspond to local fields that influence the NMR frequency. As proposed by *J. S. Waugh*, such experiments are named "separated local field" (SLF) experiments,[61] although this name is frequently used only to signify the correlation of the heteronuclear dipole-dipole coupling with the anisotropic chemical shift.

For a number of 2D solid-state NMR experiments, the information about the anisotropy of the nuclear spin interactions is deliberately dispensed with by selecting samples with extremely high molecular mobility, or by examining highly-ordered samples or crystals. In other cases, the respective information is discarded by averaging the anisotropy by means of multi-pulse or MAS techniques. With regard to their informational value, these methods are comparable with the 2D-NMR techniques known in the high-resolution NMR spectroscopy of liquids. They are found in Tables 2 and 3 in the rows and columns labeled a–d.

On the other hand, all 2D-NMR experiments based on the anisotropy of nuclear spin interactions are typical solid-state methods. For example, these include the SLF experiments, which can be used to study the relation of the a priori unknown principal axes system of a ^{13}C chemical shift tensor with the C–H bond axes, from which information about structure and dynamics can be obtained.[76] Other typical solid-state techniques involve experiments with a mixing time for longitudinal magnetization components, by which the molecular reorientations can be followed (see Section 4).[25]

The methodological development of 2D solid-state NMR spectroscopy is in no way complete. This is demonstrated by the fact that many of the fields in Tables 2 and 3 are still open. There are several reasons for this. For example, solid-state NMR signals are currently still too broad for resolving the *J*-coupling between light nuclei such as ^1H, ^{13}C, ^{15}N etc.; MAS-NMR spectroscopy of quadrupolar nuclei will only be extensively used when the rotation velocity can be raised to 100 kHz.[129] Moreover, it has only recently been recognized that MAS-NMR spectroscopy of partially ordered samples can yield useful structural information.[30]

In order not only to demonstrate the effectiveness of 2D solid-state NMR spectroscopy but also to show how complex these methods can be, a few representative experiments are briefly introduced in Sections 3.3–3.7.

3.3. Correlation of Dipole-Dipole Coupling and Chemical Shift

In such a correlation one frequency axis of the spectrum depicts the local field of the homo- or heteronuclear dipole-dipole coupling D_{11} or D_{1S}. The other axis denotes the isotropic[55,106,107] (δ_{iso}) or isotropic and anisotropic chemical shift ($\delta_{iso}+\delta_{an}$), via which the local dipolar spectra can be assigned to the corresponding chemical structure (see Tables 2 and 3).

This has been the subject of numerous studies, most of which, however, deal with heteronuclear dipole-dipole coupling; very few concern homonuclear dipole-dipole coupling.[58,74,123,195] Crystals[55,58–60,62,63,71] and highly ordered samples[61] were examined without sample rotation, because the necessary resolution of the chemical shift is already achieved by the molecular orientation. For disordered static samples isotope labeling is necessary.[74,75,76]

To illustrate dipolar SLF-NMR spectroscopy, Figure 7[61] shows the ^{13}C-NMR spectrum of highly-ordered polyethylene and the corresponding excitation sequence. During the evolution period homonuclear decoupling is applied to the protons by a multi-pulse sequence, so that only the heteronuclear coupling between the protons and ^{13}C is effective. The orientation of the dipolar coupling tensors can be determined from the dipolar splitting measured in the 2D-NMR spectrum for different molecular orientations. Furthermore, the position of the chemical shift tensor can be ascertained from the form of the spectrum. Consequently, with this method one obtains precise informa-

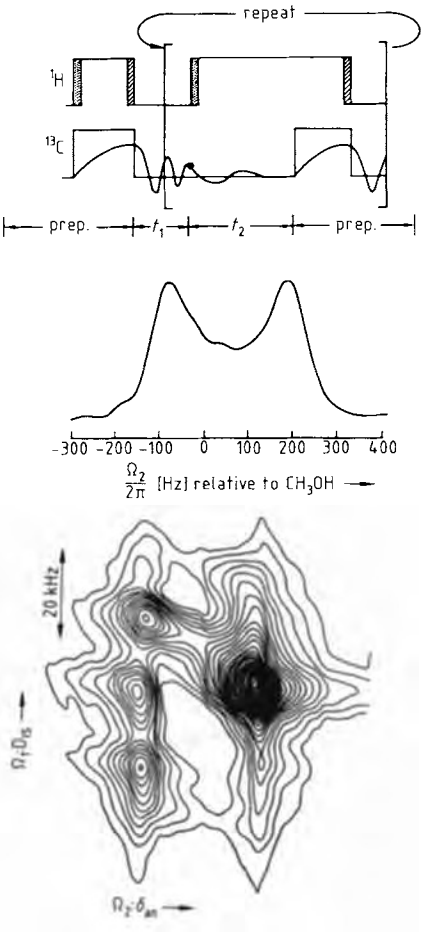

Fig. 7. Excitation sequence (above), 1D-^{13}C spectrum (middle) and 2D SLF-^{13}C-NMR spectrum (below) of highly oriented polyethylene with the draw direction perpendicular to the magnetic field. The hatched pulses are $\pi/2$ pulses phase-shifted by 90° to lock the proton magnetization during cross polarization and decoupling. The protons were homonuclearly decoupled during the evolution period t_1. The axes of the 2D-NMR spectrum denote the anisotropic chemical shift δ_{an} of the ^{13}C nuclei (horizontal) and the heteronuclear dipole-dipole coupling D_{1S} (vertical).

tion about bond angles and orientations of the various structural elements which can be distinguished on the chemical shift axis.

Besides obtaining detailed information about molecular structure, one can also examine molecular motion via a line shape analysis.[6] However, there are only a few experimental examples of this, because complicated model-dependent simulations are necessary to quantitatively analyze dipolar line shapes.[77, 107, 124] For instance the powder ^{13}C-NMR spectra of calcium formate, measured as a function of the dipolar coupling between ^{13}C and ^{1}H, cannot be explained without the assumption of molecular motion.[77] More exact and less model-dependent information about molecular dynamics can be expected from methods which correlate the local fields after a mixing time through an exchange of magnetization components (see Section 4).[71]

For disordered samples MAS must be applied in order to increase resolution (see Section 2.2).[41, 105–111, 123, 124] To exemplify this, Figure 8 depicts the excitation sequence

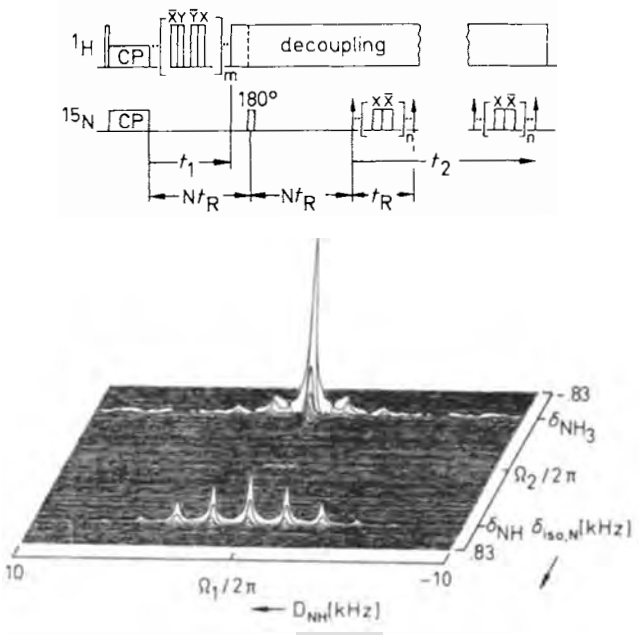

Fig. 8. Pulse sequence of the dipolar SLF-^{15}N-NMR spectrum of Gly-Gly·HCl·H_2O. Evolution time and detection time were synchronized with the rotor period. During the detection period the chemical shift was scaled by 50%.

and the SLF-^{15}N-NMR spectrum of the dipeptide Gly-Gly·HCl·H_2O.[106] During the evolution period, the protons are subject to homonuclear decoupling, and ^{15}N nuclear magnetization is subsequently focused with a 180° pulse at the beginning of a rotor period t_R (see also Fig. 5c). During t_1 the homonuclear dipole-dipole coupling dominates. Afterwards, the nitrogen is completely decoupled from the protons until data acquisition begins at the echo maximum at $t_1 = 0$. The echo is therefore modulated by the heteronuclear dipole-dipole coupling. In order to avoid rotational sidebands, only one data point per rotor period is recorded during the detection period. Because the spectral width is then limited by the rotor frequency, the chemical shift is scaled by a multi-pulse sequence.[125]

In the spectrum shown in Figure 8 the rotational sideband spectra of the dipole-dipole coupling between ^{15}N and ^{1}H nuclei, which are separated from each other on the vertical axis by the isotropic chemical shifts of the ^{15}NH- and the $^{15}NH_3$ resonances, appear parallel to the horizontal axis. In this way the strength of the dipole-dipole coupling tensors can be determined in polycrystalline and amorphous materials. Consequently, the N-H- (or C-H-) bond lengths can be determined. If the strength of the dipole-dipole coupling is known, then information about the molecular dynamics can be derived from the signal shape, as *Schaefer* et al. demonstrated in a related experiment on polystyrene and polycarbonate.[124]

For unprotonated C atoms, the dipole-dipole coupling to the nearest ^{1}H nuclei is often so weak that no dipolar rotational sidebands occur. The SASS (*S*witching-*A*ngle *S*ample *S*pinning) technique is suitable for examining such weak local fields.[107] During the evolution period, the rotor axis is inclined to the magnetic field at an angle different from the magic angle.[127] Between the evolution period and detection period, the rotor axis is turned back to the magic angle. A narrower powder spectrum is obtained in this way and is correlated with the high-resolution chemical shift.[101] By means of such spectra, for example, the bond lengths and angles of such enclosure compounds as the clathrates of β-quinone–methanol and of urea and *trans*-4-octene were determined.[107]

3.4. Heteronuclear Correlation Spectroscopy

Solid-state techniques have been developed which deliver information similar to two-dimensional methods in the high-resolution NMR spectroscopy of liquids. An example of this is the heteronuclear correlation experiment,[56, 93, 94] in which the chemical shifts of an abundant nucleus, e.g. ^{1}H, are correlated with the shifts of rare nuclei such as ^{13}C coupled to ^{1}H. Because of the higher resolution that is often associated with the rare nucleus, the spectrum of the abundant nucleus can then be more easily assigned to the chemical structure.

This is demonstrated in Figure 9 by the heteronuclear correlation spectrum of threonine and the corresponding excitation sequence.[93] The axes of the spectrum show the isotropic chemical shifts of ^{13}C and ^{1}H, while the signals indicate which nuclei are coupled by the heteronuclear dipole-dipole interaction. The homonuclear dipole-dipole interaction of the protons is suppressed during the evolution period by a multi-pulse sequence (BLEW-12,[130]) such that the cross peaks only occur between neighboring heteronuclei. At the same time ^{13}C and ^{1}H are heteronuclearly decoupled by another multi-pulse sequence (WALTZ-8[131]). During the detection period, the ^{13}C nuclei are decoupled from the protons by strong continuous irradiation of the protons. In this way, each type of nucleus becomes isolated from the other during the evolution and detection periods. Sample rotation at the magic angle reduces the anisotropic contributions of the nuclear spin interactions, so that finally only isotropic chemical shifts are correlated with each other.

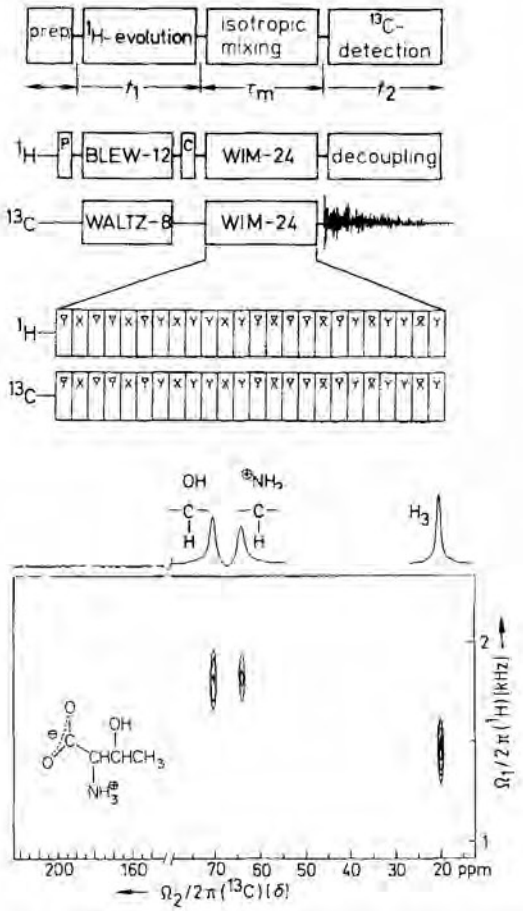

Fig. 9. Excitation sequence and resulting heteronuclear correlation spectrum for threonine with sample rotation at the magic angle. BLEW-12 [130] and WALTZ-8 [131] are multi-pulse sequences for homo- and heteronuclear decoupling. The WIM-24 pulse sequence (WIM, *W*indowless *I*sotropic *M*ixing) causes an isotropic magnetization transfer from ^{1}H to ^{13}C.

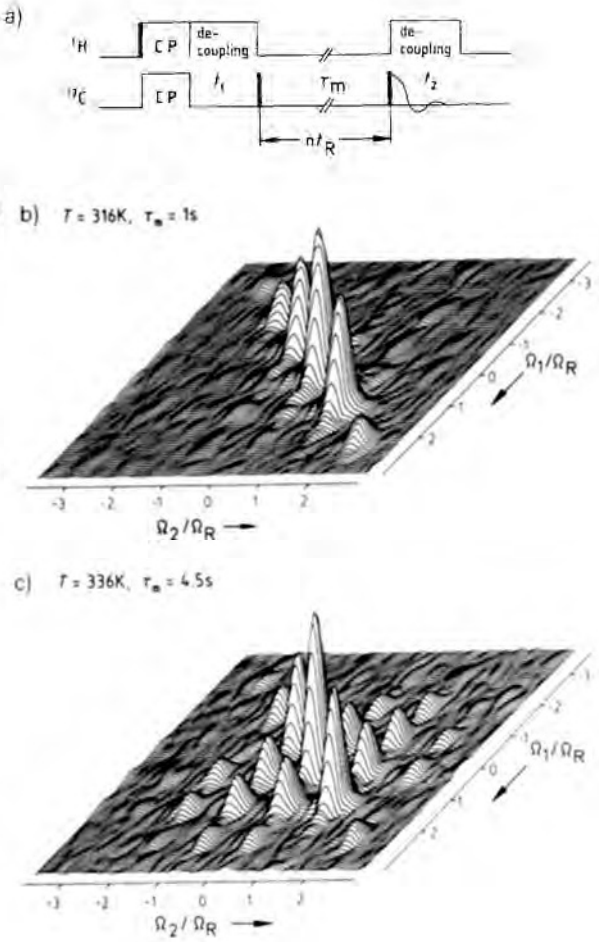

Fig. 10. a) Excitation sequence for 2D-MAS-exchange spectroscopy. The mixing period τ_m amounts to an integral multiple of the rotor period t_R. b) and c) ^{13}C-exchange spectra of the crystalline fraction of polyoxymethylene. b) No exchange; measurement time 13 h. c) Cross signals caused by molecular reorientation; measurement time 37 h.

3.5. MAS-^{13}C-NMR Spectroscopy for the Investigation of Molecular Reorientation in Powdered and Amorphous Samples

MAS-^{13}C-NMR spectroscopy is increasingly becoming an important method for studying molecular reorientational processes, since the sensitivity of the MAS method is higher than that of static methods and the samples need not be isotopically labeled. Nevertheless, because of the typical asymmetric chemical shift tensors, the resulting exchange spectra cannot be as directly interpreted as can the ^{2}H-exchange spectra described in Section 4, where the coupling tensors are approximately axially asymmetric.[24–28]

Figure 10 depicts the pulse sequence and exchange spectra of the crystalline parts of polyoxymethylene at different mixing times.[122] A diagonal spectrum is obtained at short mixing times (Fig. 10b). At long mixing times, the rotation of the polymer chain in the solid state leads to off-diagonal cross peaks (Fig. 10c). In order to rule out artifacts, the mixing time τ_m must be a multiple of the rotor period.[122] By analyzing the pattern of the cross peaks, the geometry of the dynamic process can be ascertained. The spectra in Figure 10 are explained by a rotation of the helix by $\pm 200°$ together with a translation. By varying the mixing time, the correlation time of the process can be determined; by varying the temperature, the activation energy, in this case 80 kcal/mol, can also be determined.[122]

3.6. Spin Diffusion for the Characterization of Polymer Mixtures

In the exchange experiment,[23] not only chemical exchange and molecular reorientation can be detected in solids, but also spin diffusion can be measured at longer mixing times.[69, 70, 72, 87–89, 95, 116–118] Spin diffusion can be understood as an energy-conserving flip-flop process between two dipolar coupled nuclear spins. Because the dipole-dipole coupling in the MAS method with typical rotor frequencies under 10 kHz cannot be completely averaged, spin diffusion occurs also during MAS-NMR of disordered materials. Grain boundaries and the walls between domains differing in composition hinder the spin diffusion. As a result, the heterogeneity of polymer mixtures and other amorphous materials can be determined by 2D-diffusion spectroscopy.[88, 95, 96, 118]

In order to observe diffusion between ^{13}C nuclear spins, the sample must be enriched in ^{13}C. Otherwise spin diffu-

sion would be very weak, because of the low natural abundance of the nuclei.[69,89,90,95] Although the spin diffusion of protons is strong, the resolution necessary to differentiate the various proton chemical shifts can be attained only with extensive experimental effort, that is with homonuclear decoupling and rotation at the magic angle.

Figure 11 depicts the pulse sequence and experimental spectra of ^{1}H-spin-diffusion measurements for two different mixtures of polystyrene and poly(vinyl methyl ether).[118] In the 1D-^{1}H-NMR spectrum (Fig. 11b), the signals of the aromatic hydrogen positions of polystyrene are clearly separated from those of the OCH_3 and OCH groups of poly(vinyl methyl ether). The mixture precipitated from chloroform shows no cross peaks between the signals of the aromatic and the OCH_3 and OCH protons (Fig. 11c). The mixture precipitated from toluene, on the other hand, additionally yields the corresponding cross peaks. These indicate spin diffusion between the components of the mixture and prove that the macromolecules in the material precipitated from toluene are intimately mixed on the molecular level, whereas those in the material precipitated from chloroform are not.

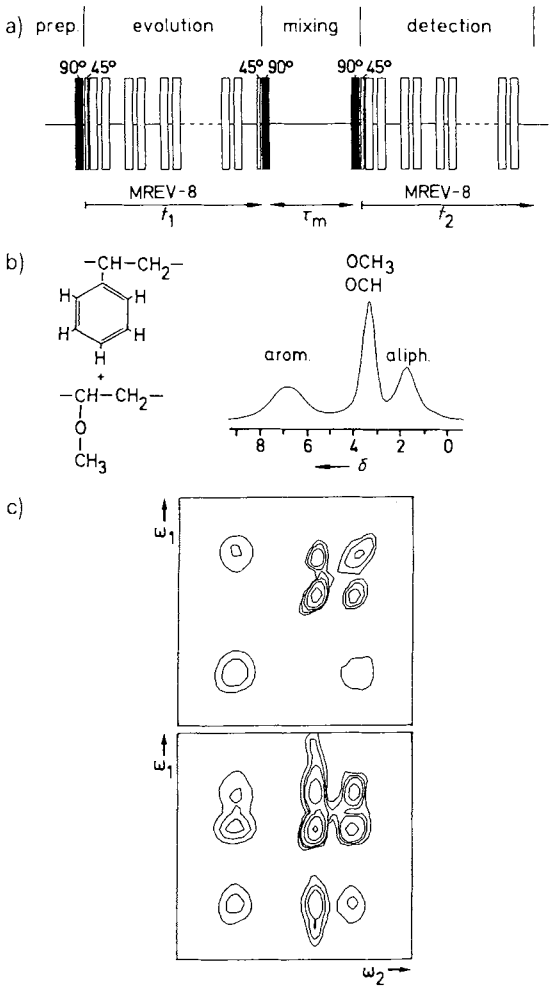

Fig. 11. a) Pulse sequence for 2D-spin diffusion experiments. b)–d) Spectra of polymer mixtures of polystyrene and poly(vinyl methyl ether). Spectral resolution is obtained through homonuclear multiple-pulse decoupling during the evolution and detection periods combined with MAS. Cross peaks between both components were only observed for the mixture precipitated from toluene (d) and not for the mixture precipitated from chloroform (c).

3.7. Variation of the Effective Magnetic Field

In the case of powder samples the NMR spectra of nuclei with quadrupole moments are generally difficult to observe with pulse methods because of their width. For non-integral spins, a 2D nutation experiment was devised which incorporates high resolution and high sensitivity.[55,67,80–83,132] The nuclear spins precess around the B_1 field during the evolution period, and the free induction decay in the B_0 field occurs during the detection period. In the resulting 2D-NMR spectrum, the spectrum of the nuclei in the low B_1 field is correlated with that in the high B_0 field. The low field yields high resolution due to the reduced angular dependence of the anisotropic nuclear-spin interactions. The high field, on the other hand, raises the sensitivity of detection. Related techniques are 2D Zeeman quadrupole-resonance spectroscopy[65] and zero-field NMR spectroscopy.[78,84,128,133,134] With the latter method, evolution occurs in the magnetic field-free space, and the detection takes place in the high magnetic field B_0. Because no preferred orientation exists for the spins in the absence of a magnetic field, sharp signals are observed for powders and amorphous samples. In zero-field NMR spectroscopy, the sample is either moved in and out of the B_0 magnetic field, or the magnetic field itself is cycled.[134] With two-dimensional zero-field NMR spectroscopy,[74,84] one hopes to be able to determine internuclear distances in powders and amorphous materials by means of the dipole-dipole coupling, similar to 2D-NOE-NMR spectroscopy in the liquid phase,[21,135] which forms the basis for the determination of the structure of proteins in solution.

4. Molecular Motion: 2D-Exchange Spectroscopy

With 2D-exchange spectroscopy, changes in the resonance frequency can be detected with high accuracy if they occur during a mixing period which is longer than the evolution period and shorter than the longitudinal relaxation time T_1. Consequently, this method is especially suitable for the detection of very slow dynamic processes in the range of 10^{-3} to ca. 100 s.

For anisotropic coupling with axial symmetry, e.g. ^{2}H quadrupole coupling (Fig. 1), one obtains in powder spectra exchange signal patterns with extremely simple geometry which supply immediate information about the type and rate of the dynamic process. 2D-^{2}H-exchange spectroscopy therefore makes possible the model-free determination of the angle at which a selectively deuterated group rotates during the mixing period τ_m.[25] This is presently not possible with any other method. Therefore, a more detailed account of this method will be presented here.

The study of molecular reorientation processes by the ^{2}H-alignment procedure has already established itself as one initial step toward 2D solid-state spectroscopy.[13,14] In this experiment the echo stimulated by three radio-frequency pulses analogous to the time scheme of 2D-NMR spectroscopy (Fig. 6) is observed. The echo senses a quadrupolar state of order of the ^{2}H nuclear spin which is termed "alignment".[16] In the case of molecular reorienta-

tion during the mixing period τ_m, the observed spins precess during t_2 with a different frequency than during t_1 after the first pulse. As a consequence of this, the echo amplitude is reduced.

Nevertheless, one cannot immediately deduce the motion from the resulting spectra obtained through Fourier transformation of the echo decay. Information is lacking about which molecular orientations during t_1 have been transformed into which orientations during t_2. Equation (1) denotes the various molecular orientations θ in the frequency dimension of the NMR spectrum. In order to study the molecular reorientation from an angle θ_1 at a time t_1 to an angle θ_2 at a time t_2, the NMR spectrum measured at t_1 must be correlated to the NMR spectrum measured at t_2. This is exactly the information which is delivered by the corresponding 2D-NMR spectrum,[28] which therefore represents a two-time distribution function.[28]

4.1. Experimental Aspects

2D-^{2}H exchange spectroscopy, which is especially informative regarding the measurement of very slow molecular motions, will be used to illustrate how 2D-NMR experiments are performed.[27] In the corresponding excitation sequence (see Fig. 6), the various time periods are separated by radio-frequency pulses. The magnetization decays between the pulses in free precession (Fig. 12). The initial

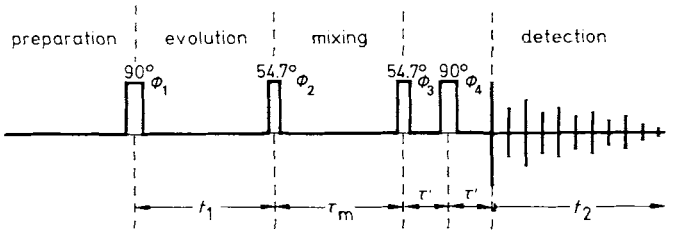

Fig. 12. Pulse sequence for 2D-^{2}H-exchange-NMR spectroscopy. The pulse lengths are selected such that the same heights result for the stimulated and the alignment echo in the absence of longitudinal relaxation processes, despite different spin states during the mixing time τ_m [27]. τ' = refocusing time.

pulse produces transverse magnetization. During the subsequent evolution period t_1, each magnetization component builds up a particular phase which is determined by its precession frequency. The second pulse induces longitudinal magnetization and spin alignment, the amplitudes of which correspond to the real part (cosine) or the imaginary part (sine) of the preceding transverse magnetization. The remaining transverse magnetization decays to zero during the mixing period, and the quadrupole coupling of the nuclear spin can alter by molecular reorientation. After the third pulse, the generally much more slowly relaxing longitudinal magnetization and the spin alignment are again transformed into measurable transverse magnetization. With regard to molecular reorientation during the mixing period, the precession frequencies of the affected magnetization components have changed, allowing the various frequencies in the evolution and detection periods to be correlated with each other.

In order to circumvent the dead time of the receiver, data is first collected after refocussing by a fourth pulse.[136] In order to obtain 2D-NMR spectra in absorption the sine and the cosine components of the transverse magnetization, which precesses during the evolution period, have to be measured.[137, 138] This is achieved in two separate experiments. The alignment echo of a nucleus with spin $I=1$ is formed from the sine component, whereas the stimulated echo is formed from the cosine component. On the assumption that the carrier frequency lies exactly in the middle of the ^{2}H-NMR spectrum and disregarding relaxation, one measures the following signals [(3a) and (3b)]:

$$\text{stimulated echo: } \langle \mathrm{cis}(\Omega_1 t_1) \cdot \cos(\Omega_2 t_2) \rangle \tag{3a}$$

$$\text{alignment echo: } \langle \sin(\Omega_1 t_1) \cdot \sin(\Omega_2 t_2) \rangle \tag{3b}$$

The symbols Ω_1 and Ω_2 denote the resonance frequencies of a nucleus in the evolution and in the detection phases, respectively, and the symbol $\langle \cdots \rangle$ denotes the summation over all magnetization components. With regard to the orientation dependence of the resonance frequencies [Eq. (1)], Equations (3a) and (3b) define two correlation functions of the different molecular orientations θ_1 and θ_2, whereby, however, only even powers of the angles are correlated with each other.

Both functions are measured with the pulse sequence shown in Figure 12 but with different phases. The respective minimal phase cycles necessary to eliminate artifacts are listed in Table 4. The complete phase cycle results whenever the phases ϕ_1 and ϕ_3 in Table 4 are varied independently of each other. The total measurement time typically amounts to one day.

Table 4. Phase cycles for the cosine and the sine correlation function. For the definition of ϕ_1–ϕ_4 see Figure 18.

Cosine: Stimulated echo					*Sine: Alignment echo*				
ϕ_1	ϕ_2	ϕ_3	ϕ_4	Receiver	ϕ_1	ϕ_2	ϕ_3	ϕ_4	Receiver
+Y	+Y	+Y	+X	+X	+Y	+X	+X	+X	+X
+Y	+Y	+Y	−X	+X	+Y	+X	+X	−X	+X
+Y	−Y	+Y	+X	−X	+Y	−X	+X	+X	−X
+Y	−Y	+Y	−X	−X	+Y	−X	+X	−X	−X

The matrices of the time data and the resulting 2D-NMR spectrum should be symmetrical to the main diagonal, because of the equivalence of the evolution period and the detection period. Pulse width effects, however, generally lead to asymmetrical measured data. Consequently, the two-dimensional time function must be interpolated to symmetrical time values before the 2D-Fourier transformation. Since the required interpolation routines are currently lacking in commercial spectrometer software, the data is processed on an external computer.[27]

In ^{13}C-exchange spectroscopy, experiment and data processing are conducted accordingly. As opposed to the ^{2}H nucleus with $I=1$, ^{13}C has a spin $I=1/2$, so that only one spectroscopic transition is observed. Therefore, no alignment state exists, and the sine and cosine correlation

functions are both measured with the stimulated echo [Eqs. (3c) and (3d)].

$$\langle \cos(\Omega_1 t_1) \cdot \exp\{i\Omega_2 t_2\} \rangle \tag{3c}$$

$$\langle \sin(\Omega_1 t_1) \cdot \exp\{i\Omega_2 t_2\} \rangle \tag{3d}$$

Pulse sequence and phase cycle correspond to Figure 12 and Table 4; however, the 54.7° pulses are replaced by 90° pulses, and the fourth pulse is a 180° pulse. In order to increase the ^{13}C nuclear polarization, the initial pulse is replaced by a cross-polarization sequence.

4.2. Theory

Instead of isolated cross peaks as seen in the 2D-exchange spectra of liquids and crystals, the exchange signals in the 2D-NMR spectra of powders are broad spectra which can stretch over the entire frequency range of the powder spectrum. However, they contain singularities. For a molecular jump reorientation of a particular angle θ_s which, for example, can be fixed by the molecular geometry, these singularities yield defined geometrical patterns. The patterns for aliphatic deuterons with an asymmetry parameter $\eta \approx 0$ appear as straight lines parallel to the frequency axes (thick lines in Fig. 13) and as one ellipse for

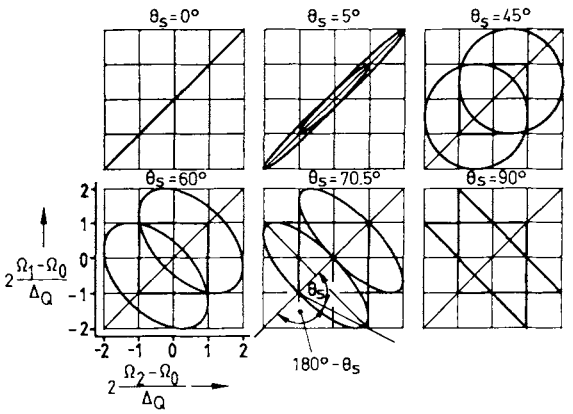

Fig. 13. Exchange singularities for ^2H powder spectra with an axially symmetrical, quadrupole coupling tensor at various molecular reorientational angles θ_s. For the case $\theta_s = 70.5°$, the jump angle is marked for illustration.

each spectroscopic transition.[25] For extrapolation of the lines: $-1 \leq 2(\Omega_{1,2} - \Omega_0)/\Delta \leq 3\sin^2\theta_s - 1$. The ellipses are characterized for all initial orientations θ of the magnetization components by the Equations (4). These are parameter representations of two spheres which are centered at the coordinates $\Omega_{1,2} - \Omega_0 = \pm\frac{1}{2}\Delta$. The molecular reorientation angle θ_s appears as the phase difference $2\theta_s$ in the coordinates of the singularities, the patterns of which in this way resemble Lissajous figures.

$$\Omega_1 - \Omega_0 = \pm\tfrac{1}{2}\Delta(3\cos^2\theta - 1) = \pm\tfrac{1}{4}\Delta(1 + 3\cos 2\theta) \tag{4a}$$

$$\Omega_2 - \Omega_0 = \pm\tfrac{1}{2}\Delta(3\cos^2(\theta \pm \theta_s) - 1) = \pm\tfrac{1}{4}\Delta(1 + 3\cos 2(\theta \pm \theta_s)) \tag{4b}$$

The ratio of the half-axes b and a of an ellipse yields the reorientation angle θ_s according to Equation (5). Since the magnitude of the tangent function appears in Equation (5), the jump angles θ_s and $180° - \theta_s$ lead to identical ellipses.

$$b/a = |\tan(\theta_s)|. \tag{5}$$

Whenever more than one jump angle is involved in a motional mechanism, the corresponding number of ellipses is observed in the ^2H-exchange spectrum. The exchange spectra of diffuse motions can be understood as superimpositions of the spectra for an infinite number of jump angles.[28] Consequently, no more sharp contours appear in the 2D-exchange spectrum. For an isotropic rotational diffusion, Figure 14 shows calculated exchange spectra for different ratios of mixing time τ_m and correlation time τ_c. For each spectrum the angular distribution of a particular molecular orientation is also depicted according to the solution obtained from the isotropic rotational diffusion equation. If the mixing time is $\tau_m = 0$, no reorientation can occur. The angular distribution is sharp, and the exchange spectrum incorporates the conventional 1D-^2H NMR spectrum along the diagonal. The angular distribution as well as the signal along the diagonal of the exchange spectrum "flow apart" with increasing mixing time. In the final state ($\tau_m/\tau_c = 10$), an isotropic angular distribution is obtained, and the 2D-NMR spectrum extends over the entire frequency range. The only singularities now ob-

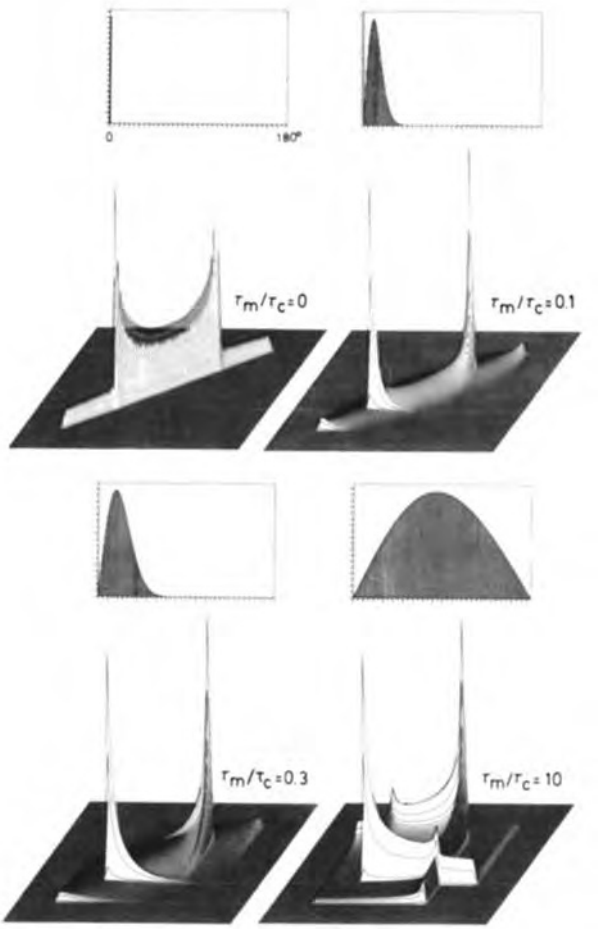

Fig. 14. Calculated ^2H-exchange spectra for isotropic rotational diffusion with correlation time τ_c and different mixing times τ_m in the 2D-NMR experiment. The form of the 2D-NMR spectrum directly reflects the evolution of the angular distribution of a given molecular orientation (plotted above the spectra).

served are sharp ridges parallel to the frequency axes. They stem from the 1D singularities of the diagonal spectrum and exhibit the form of a 1D powder spectrum for a single transition. These singularities also occur during jump reorientation, and can serve as an indication of molecular motion whenever the quality of the measured data is poor. Apparent cross peaks at the cross-over points of these exchange singularities are observed as a result of a superposition of the signals.

4.3. Applications

Figure 15 shows the 2D-^{2}H-exchange spectrum of dimethyl sulfone at 310 K[25] as an example of molecular reorientation through discrete jumps. The mixing time was 3 ms and therefore was longer than the correlation time $\tau_c \approx 1$ ms of the motion. The evolution and detection periods were each scanned in 256 steps at intervals of 1 μs. The refocussing time τ' amounted to 25 μs. At the measurement temperature, the methyl groups rotate so rapidly about their respective C_3 axes that in the case of the methyl deuterons an axially symmetric quadrupole coupling tensor results with its principal axis lying along the S–C bond axis. From the geometry of the elliptical exchange singularities, one can directly read off the jump angle as 106°. The negative signals on the subdiagonal can be explained by different relaxation of longitudinal magnetization and alignment states during the mixing time.

Whereas the jump angle can be directly ascertained from the geometry of the ellipse with a goniometer (see Fig. 13), a numerical analysis of the signal form is necessary for motional processes involving diffusion. As an example, Figure 16 exhibits the experimental and the calcu-

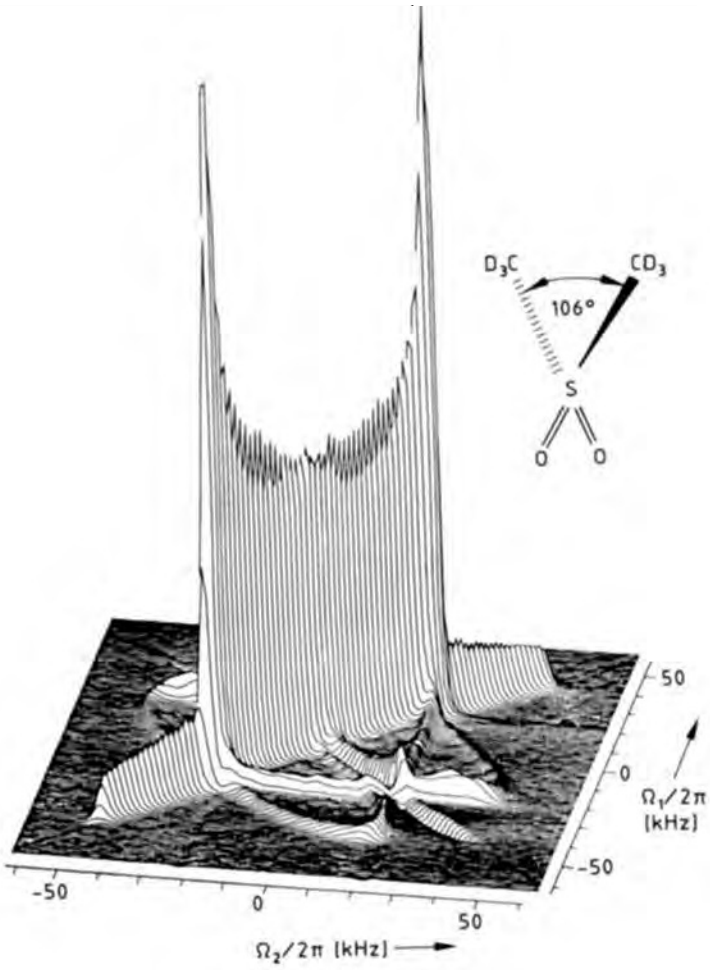

Fig. 15. ^{2}H-exchange spectrum of dimethyl sulfone.

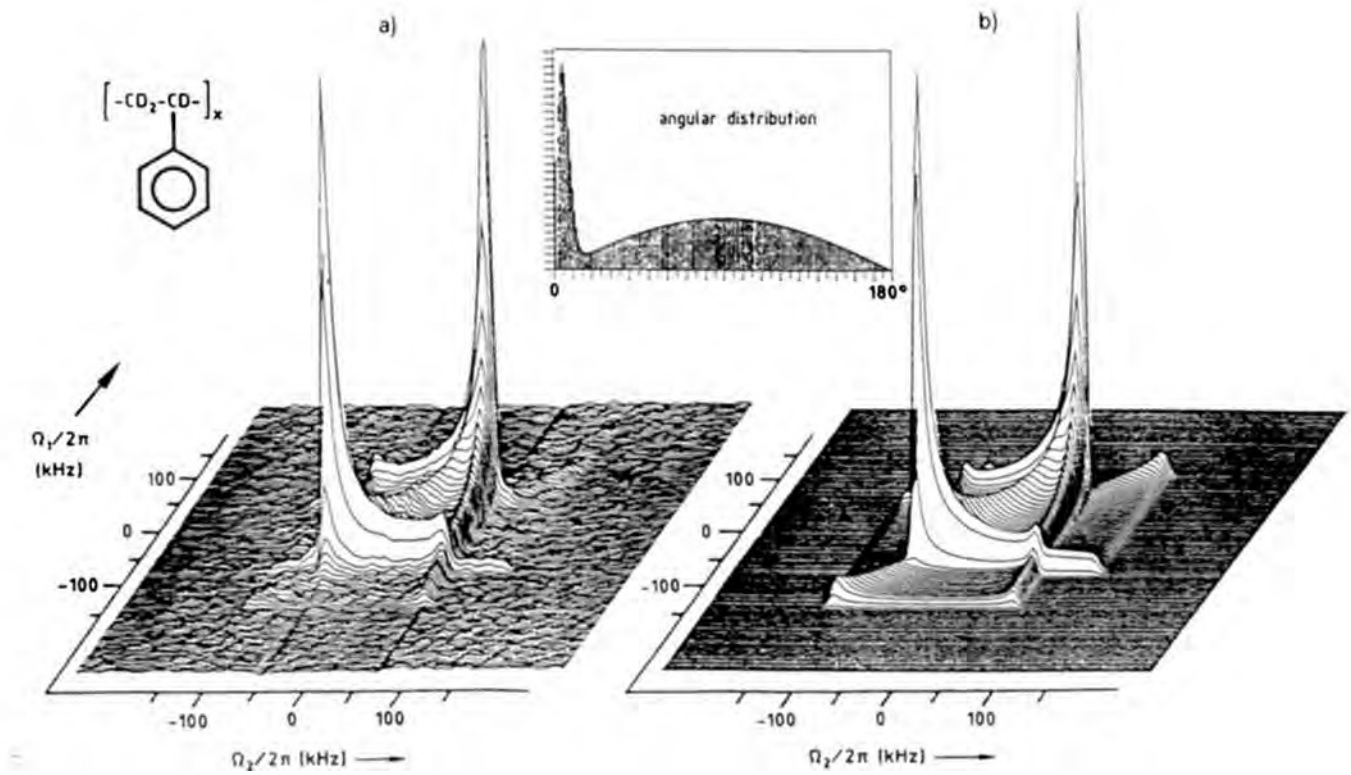

Fig. 16. ^{2}H-exchange spectra of chain-deuterated polystyrene. The analysis (b) of the experimental data (a) points towards a faster and a slower diffusive motion of the chain.

lated spectrum of the chain motion of polystyrene.[28] The experimental spectrum (Fig. 16a) was measured at about 25 °C above the glass transition temperature with a mixing time of 12 ms. The broadened signal nearby the diagonal indicates diffusive chain motion (cf. Fig. 15). The spectrum could be simulated by assuming both a rapid and a slow rotational diffusion process (Fig. 16b).

Both examples demonstrate that reorientational jumps at well-defined angles can be clearly differentiated from rotational diffusion in 2D-^{2}H exchange spectra. From the exchange spectra of aliphatic deuterons, the jump angle can be determined directly without model assumptions from the excentricity of the elliptical exchange singularities [Eq. (5)].

For an asymmetric coupling tensor such as the anisotropic magnetic shielding in ^{13}C-NMR spectroscopy, the geometrical form of the exchange singularities is affected by the asymmetry parameter η.[76,85] ^{13}C-exchange spectroscopy was recently used in an experiment to detect the previously suggested collective motion of phenyl and carbonate groups in bisphenol-A polycarbonate.[90,140] No exchange could be detected at room temperature in a sample enriched with up to 99% ^{13}C at the carbonate group even with a mixing time of $\tau_m = 10$ ms. Noticeable changes of the signal form first resulted at a mixing time of $\tau_m = 2$ s. The experimental spectrum in Figure 17 shows a line broadening which infers a diffusive process.[90] The comparably long mixing time and the temperature independence of the exchange process can be explained by spin diffusion. In fact, the 2D spectrum can be simulated by merely considering spin diffusion (Fig. 17b).[90,141] A significant reorientation of the polymer chain cannot therefore occur, even within a mixing period of 2 s.

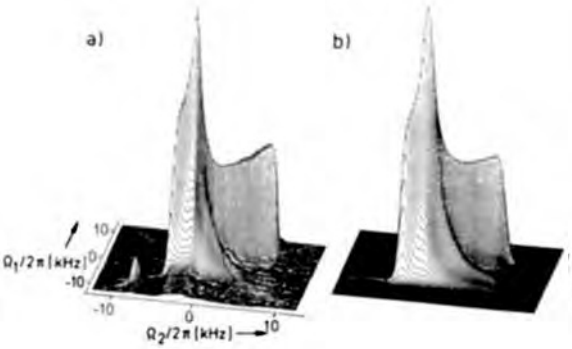

Fig. 17. a) 2D-^{13}C-exchange spectrum of bisphenol-A polycarbonate. $\tau_m = 2$ s, $T = 298$ K. b) The calculated spectrum for spin diffusion and a correlation time of $\tau_c = \tau_m$.

5. Molecular Order: MAS-NMR Spectroscopy with Rotor Synchronization

There are various methods for determining the degree of molecular order. Birefringence or IR dichroism measurements only yield the second moment of the orientational distribution function without differentiation of molecular structural elements. The complete orientational distribution can be obtained, however, from X-ray and neutron-scattering data as well from solid-state NMR spectroscopy.[142,143] Moreover, the selectivity of NMR spectroscopy makes it possible to ascertain the orientational distribution of several functional groups of the monomer unit. Consequently, for partially ordered polymers the chain alignment as well as the respective conformation can be studied in the ordered state. MAS-^{13}C-NMR spectroscopy is especially useful here, because it is applicable for practically all synthetic polymers and biopolymers. The 2D-NMR method described below for determining molecular order is therefore well suited for routine applications.[30,31]

A macroscopically oriented sample is packed in a rotor in such a way that its preferential ordering axis is not parallel to the rotor axis. Liquid crystalline polymers can often be magnetically oriented in the rotor and then cooled down below the glass transition temperature for the measurement. Fibers are glued parallel together into layers which are stacked in the rotor. In order to balance the rotor, remaining empty spaces are filled with a mixture of KBr and talcum which has approximately the same density as the sample.

Because of the dependence of the resonance frequency on orientation [Eq. (1)], the MAS-^{13}C-NMR spectrum of an oriented sample depends on the rotor position at the beginning of the measurement.[41] The degree of orientation of the sample is probed by conducting several measurements for different rotor phases.[30,31] Figure 18 shows the

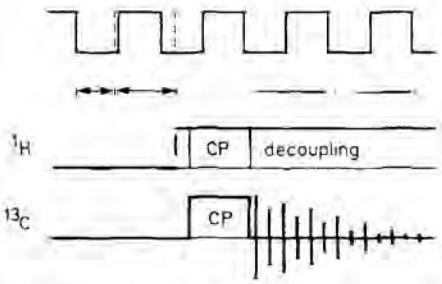

Fig. 18. Timing diagram of rotor-synchronized 2D MAS-NMR spectroscopy for the investigation of molecular order.

course of the measurement with time.[30] The rotor position is determined from the signal which is produced in commercial spectrometers to count the rotor frequency. By means of the pulse program software, the negative slope of the rotor signal is probed to trigger the beginning of the measurement. A fixed time delay t_0, which sets the phase in the Ω_1-direction, is followed by the evolution period t_1, which is varied from experiment to experiment in 16 equidistant steps within one rotor period. Cross polarization and detection of the ^{13}C-NMR signal subsequently occur after the evolution period.

The sidebands in the Ω_1 direction are denoted by $\pm$M, those in the Ω_2 dimension by $\pm$N. The intensities I of the sidebands obey a simple symmetry relationship (6) described below which can be employed to control the measurement results.[31]

$$I_{M,N} = I_{-M,N-M} \qquad (6)$$

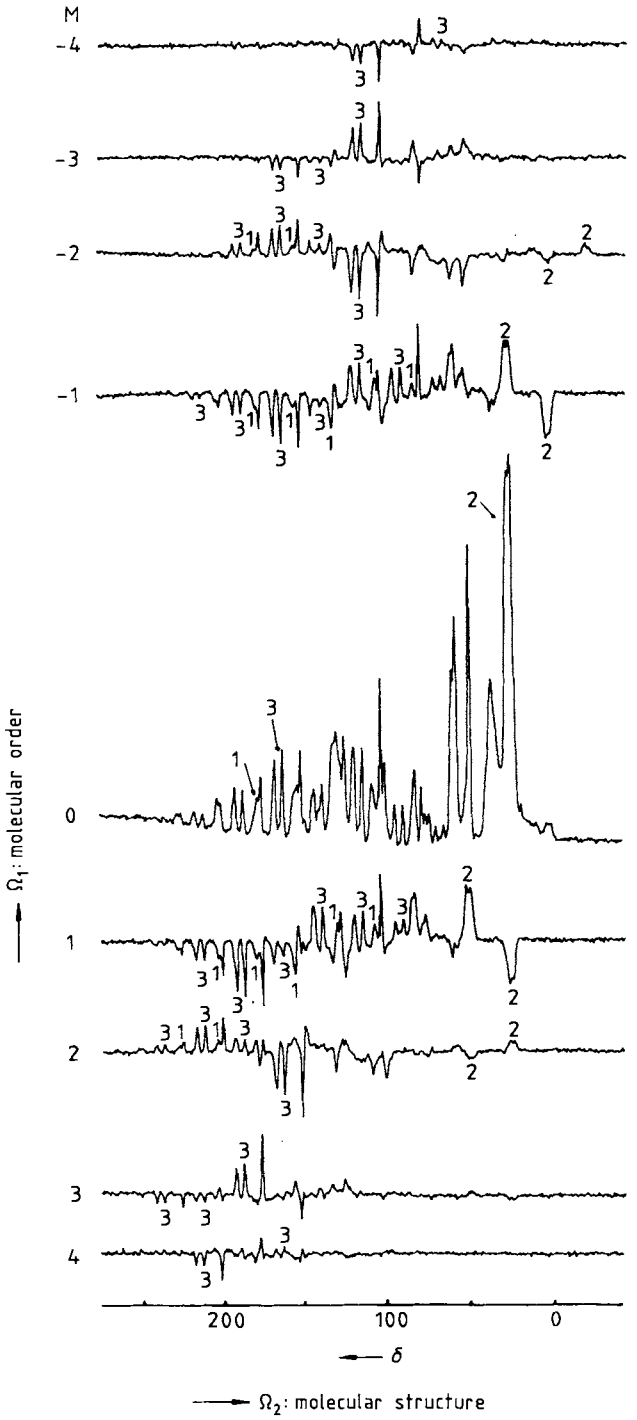

Fig. 19. 2D MAS-^{13}C-NMR spectrum of a liquid-crystalline polyacrylate (molecular structure in Fig. 20). The signals of the carbon atom of the acrylic group (**1**), the spacer (**2**) and the mesogenic group **3** are marked. Only the isotropic chemical shifts are identified in the spectrum with M = 0.

Figure 19[32] shows the significant lines of the 2D MAS-^{13}C-NMR spectrum of a liquid crystalline polyacrylate in the frozen smectic phase. **1** denotes the signals of the acrylic carbon close to the chain, **2** the signals of the spacer, and **3** the signals of the mesogenic groups (see Fig. 20 regarding the molecular structure).[32] The spectrum in the row labeled by M = 0 is the center band spectrum which is also observed when the sample is macroscopically disordered. But the rows labeled by $M \neq 0$ contain signals only if the sample is macroscopically ordered. The higher the degree of order, the higher is the value of M for which significant signals in the corresponding sideband spectrum are still observed. The orientational distributions for all magnetically distinguishable structural elements can be gained from the sideband intensities. In general the following applies: in the calculation of the sideband spectrum of the order $\pm M$, at least the Mth moment of the orientational distribution function[142-147] is required,[31] whereby, however, odd moments, are inaccessible. Thus, according to Figure 14, at least the fourth moment is still significant in the orientational distribution function of the mesogenic group **3** (see the following section).

5.2. Determination of the Orientational Distribution from 2D MAS-NMR Spectra

The analysis of MAS sideband spectra requires appropriate numerical resources.[40] This holds true especially for 2D-MAS sideband spectra. The basics of the method developed for the analysis[31] will therefore be outlined in the following.

For simplification, only uniaxially ordered samples which can be characterized by a one-dimensional orientational distribution are considered. The orientational distribution function is expanded into a series of Legendre polynomials $P_l(\cos\beta)$ [Eq. (7)],[143,144] where the P_{l00} are the moments of the orientational distribution function and β is the angle between the molecular axis and the direction of order of the sample. The P_{l00} are defined by the averages $\langle P_l \rangle$ of the Legendre polynomials [Eq. (8)]. The average over P_2 is *Saupe*'s order parameter S,[145] [Eq. (9)]. In Eq. (9), $\langle \cdots \rangle$ signifies the average over the orientational distribution function.

$$P(\beta) = \sum_{l=0}^{\infty} P_{l00} P_l(\cos\beta), \tag{7}$$

$$\langle P_l \rangle = \langle P_l(\cos\beta) \rangle = \frac{8\pi^2}{2l+1} P_{l00} \tag{8}$$

$$\langle P_2 \rangle = S = \tfrac{1}{2}\langle 3\cos^2\beta - 1 \rangle, \tag{9}$$

Corresponding to the series expansion of the orientational distribution function, the 2D MAS-NMR spectrum $S(\Omega_1,\Omega_2)$ is expanded into a series of 2D subspectra $S_l(\Omega_1,\Omega_2)$, from which the moments of the distribution function P_{l00} [Eq. (8)] are directly obtained via Equation (10),

$$S(\Omega_1,\Omega_2) = \sum_{l=0}^{\infty} \langle P_l \rangle S_l(\Omega_1,\Omega_2). \tag{10}$$

The subspectra $S_l(\Omega_1,\Omega_2)$ must be calculated once for each respective ^{13}C position. The subsequent data fitting for determination of $\langle P_l \rangle$ is no longer numerically complicated.[31] The method can be extended in a straightforward fashion for studying macroscopically or microscopically biaxial samples.[31,141]

5.3. Applications

The 2D MAS-^{13}C-NMR experiment was first tested on highly oriented polyethylene[30] and has since been applied to various other oriented polymers. For example, the degree of order S as the function of the draw ratio was measured on drawn polycarbonate. The result correlates well with X-ray data,[147] showing, that this NMR method is suitable for ascertaining small degrees of order ($\langle P_2 \rangle < 0.2$). Furthermore, microscopic biaxiality could be determined for commercial polyethylene terephthalate fibers.[31]

Application of the technique to liquid-crystalline polymers frozen in the mesophase is particularly interesting, because orientational distributions of various widths can be observed for different structural elements. Figure 20 shows the result of an evaluation of the sideband spectra of the liquid-crystalline side-chain polymer displayed in Figure 19.[32] The respective, orientational distribution functions for the carbon atoms **1** (acryl group), **2** (spacer) and **3** (mesogenic group) were calculated by means of the subspectral analysis. The C atoms of the polymer chain do not show any preferential orientation. The acrylic carboxyl group, however, shows a noticeable orientation of the side chain. The orientation increases at the spacer, but no order gradient for its different CH_2 groups was observed. The highest order was found for the mesogenic group. Consideration of the 8th moment of the orientational distribution function for the mesogenic group carbon was necessary in the analysis of the measured sideband spectra in Figure 19.

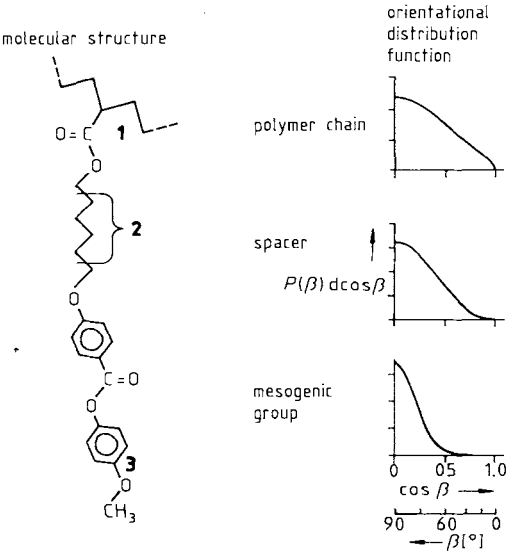

Fig. 20. Orientational distribution functions of different structural elements of polyacrylate. For the definition of $P(\beta)$ see Equation (7).

This example shows, that even complicated spectra can be handled with the 2D MAS-^{13}C-NMR method. Such spectra can also be simplified with the pulse sequences depicted in Figure 5, with which the signals of the protonated or the unprotonated ^{13}C nuclei can be suppressed. Other than in the case of ^{2}H-NMR spectroscopy, isotope labeling is not necessary. The measurement itself only takes 16 times longer than the measurement of a conventional solid-state ^{13}C-NMR spectrum, because generally only 16 rows are necessary in the additional dimension due to the limited number of possible sidebands. These properties therefore make this method especially interesting for applications with commercial products.

6. Summary and Outlook

Solid-state NMR spectroscopy differs considerably from the high-resolution NMR spectroscopy of liquids. The difference results from the numerous orientation-dependent spin interactions which affect the NMR spectrum of solids. The intensity of the interactions and the resulting width of the spectra necessitate more powerful equipment and more complicated experimental procedures. Consequently, only the simple, one-dimensional MAS technique is currently employed on a routine basis.

For studying solid polymers ^{2}H-NMR spectroscopy[13, 14] and MAS-^{13}C-NMR spectroscopy[6-12] are especially relevant. ^{2}H-NMR spectroscopy has proven useful through the quantitative evaluation of results with respect to models of molecular motion, time scales of dynamic processes and orientational distribution functions. Unlike ^{2}H-NMR spectroscopy MAS-^{13}C-NMR spectroscopy does not require isotope labeling. Because of the broad range of chemical shifts, various structural elements can be assessed with only one measurement. The anisotropic magnetic shielding (chemical shift) as well as the dipole-dipole coupling to the protons can be used as a source of information about molecular order and molecular dynamics. The sensitivity of ^{13}C-NMR spectroscopy is considerably increased by the MAS method, since the spectral intensity is focussed in narrow rotational sidebands and is no longer distributed over a wide powder spectrum.

With 2D-NMR spectroscopy one obtains information about chemical structure, molecular motion and molecular order in solids. The study of the chemical structure of polymers is especially interesting whenever the respective materials are insoluble, for the molecular structures of dissolved substances can be determined quite easily. The questions about molecular order and type and rate of molecular motion are particularly relevant. 2D solid-state NMR spectroscopy is more effective in obtaining answers to these questions than the experimentally more simple 1D-NMR methods. Whereas there are currently many 2D-NMR methods available for studying dynamical processes, there is only one such technique[30-33] for examining molecular order, and that is based on the rotor synchronized acquisition of MAS-^{13}C-NMR spectra.

The presently known 2D-NMR methods correlate molecular structure and dynamics or structure and order. Multi-dimensional techniques which correlate the molecular order with molecular motion are still lacking. The TOSS experiment combined with a mixing period, however, is a start in this direction.[48]

For practical purposes 2D-NMR methods are particularly interesting which allow: 1) simple sample preparation, 2) uncomplicated experimentation, and 3) the quantification of measurements. Consequently, ^{13}C-NMR spectroscopy takes the lead with regard to applications to or-

ganic solids. The number of high frequency pulses can be used as a criterium for the straightforwardness of an experiment. In this respect, the exchange experiment and the 2D-MAS experiment with rotor synchronization are simple experiments. Quantitative, largely model-independent data can likewise be obtained from the corresponding 2D-NMR spectra. Although the spin-diffusion experiment for examining the compatibility of macromolecules in polymer mixtures provides highly interesting information for the polymer chemist, it demands multi-pulse excitation as well as sample rotation at the magic angle.[118] Currently, only a few laboratories have access to these techniques.

The previously cited 2D-NMR methods make it possible to correlate various molecular parameters with one another. On the other hand, 2D-NMR spectroscopy also allows one to correlate the NMR spectrum directly with macroscopic properties of the sample. In this respect, totally new possibilities are emerging to probe the fundamental questions about the relationship between molecular structure and material properties of polymers. For example, if the sample is stressed during the mixing period by a jump in temperature,[149] voltage, pressure, mechanical rotation or electrical fields, its relaxation into the new state of molecular equilibrium can be traced with NMR on a molecular scale. This has recently been demonstrated in an experiment focussing on the rotational viscosity of liquid-crystalline polymers.[150]

A number of colleagues in the NMR group at the Max-Planck-Institut für Polymerforschung were considerably involved in the 2D-NMR research work cited in Sections 4 and 5. We would especially like to thank Dr. C. Boeffel, Dr. G. Harbison, Mr. S. Kaufmann, Dr. C. Schmidt and Mr. S. Wefing. We are likewise grateful to the Deutsche Forschungsgemeinschaft and the Fonds der Chemischen Industrie for their continuing support of our work.

Received: November 27, 1987;
revised: April 28, 1988 [A 700 IE]
German version: *Angew. Chem. 100* (1988) 1716

[1] a) J. D. Ferry: *Viscoelastic Properties of Polymers*, 3rd edit., Wiley, New York 1980; N. G. McCrum, B. E. Read, G. Williams: *Anelastic and Dielectric Effects in Polymeric Solids*, Wiley, New York 1967; b) I. M. Ward: *Structure and Properties of Oriented Polymers*, Applied Science, London 1975; *Mechanical Properties of Solid Polymers*, Wiley, New York 1971.
[2] U. Haeberlen: *High Resolution NMR in Solids: Selective Averaging (Adv. Magn. Reson. Suppl. 1)*, Academic Press, New York 1976.
[3] M. Mehring: *High Resolution NMR in Solids*, 2nd edit., Springer, Berlin 1983.
[4] H. W. Spiess, *NMR Basic Principles and Progress 15* (1978) 55.
[5] C. A. Fyfe: *Solid State NMR for Chemists*, CFC Press, Guelph, Ontario, Canada 1983.
[6] B. C. Gerstein, C. Dybowski: *Transient Techniques in NMR of Solids*, Academic Press, New York 1985.
[7] J. Schaefer, E. O. Stejskal, *Top. Carbon-13 NMR Spectrosc. 3* (1979) 283.
[8] V. J. Mc Brierty, D. C. Douglass, *Macromol. Rev. 16* (1981) 295.
[9] D. E. Axelson, K. E. Russel, *Prog. Polym. Sci. 11* (1985) 221.
[10] M. Möller, *Adv. Polym. Sci. 66* (1985) 59.
[11] F. A. Bovey, L. W. Jelinski, *J. Phys. Chem. 89* (1985) 571.
[12] R. A. Komorowski: *High Resolution NMR Spectroscopy of Synthetic Polymers in Bulk*, VCH Publishers, New York 1986.
[13] H. W. Spiess, *Colloid Polym. Sci. 261* (1984) 193.
[14] H. W. Spiess, *Adv. Polym. Sci. 66* (1985) 23; L. W. Jelinski, *Adv. Mater. Sci. 15* (1985) 359; K. Müller, P. Meier, G. Kothe, *Progr. NMR Spectrosc. 17* (1985) 211.
[15] R. Hentschel, J. W. Spiess, *J. Magn. Reson. 35* (1979) 157; H. W. Spiess, H. Sillescu, *ibid. 42* (1981) 381.
[16] H. W. Spiess, *J. Chem. Phys. 72* (1980) 6755; M. Lausch, H. W. Spiess, *J. Magn. Reson. 54* (1983) 466.
[17] E. R. Andrew, R. G. Eades, *Proc. R. Soc. London A 216* (1953) 398; I. Lowe, *Phys. Rev. Lett. 2* (1959) 285; E. R. Andrew, *Prog. NMR Spectrosc. 8* (1971) 1.
[18] C. S. Yannoni, *Acc. Chem. Res. 15* (1982) 201; B. C. Gerstein, *Adv. Colloid Interface Sci. 23* (1985) 45.
[19] S. R. Hartmann, E. L. Hahn, *Phys. Rev. 128* (1962) 2042.
[20] R. Voelkel, *Angew. Chem. 100* (1988) 1525; *Angew. Chem. Int. Ed. Engl. 27* (1988) 1468.
[21] R. R. Ernst, G. Bodenhausen, A. Wokaun: *Principles of Nuclear Magnetic Resonance in One and Two Dimensions*, University Press, Oxford 1987.
[22] H. Kessler, M. Gehrke, C. Griesinger, *Angew. Chem. 100* (1988) 507; *Angew. Chem. Int. Ed. Engl. 27* (1988) 490.
[23] W. P. Aue, E. Bartholdi, R. R. Ernst, *J. Chem. Phys. 64* (1976) 2229.
[24] J. Jeener, B. Meier, P. Bachmann, R. R. Ernst, *J. Chem. Phys. 71* (1979) 4546; B. H. Meier, R. R. Ernst, *J. Am. Chem. Soc. 101* (1979) 6441.
[25] C. Schmidt, S. Wefing, B. Blümich, H. W. Spiess, *Chem. Phys. Lett. 130* (1986) 84.
[26] C. Schmidt, B. Blümich, S. Wefing, S. Kaufmann, H. W. Spiess, *Ber. Bunsenges. Phys. Chem. 91* (1987) 1141.
[27] C. Schmidt, B. Blümich, H. W. Spiess, *J. Magn. Reson. 79* (1988) 269.
[28] S. Wefing, H. W. Spiess, *J. Chem. Phys. 89* (1988) 1219; S. Wefing, S. Kaufmann, H. W. Spiess, *ibid. 89* (1988) 1234.
[29] W. P. Aue, J. Karhan, R. R. Ernst, *J. Chem. Phys. 64* (1976) 4226.
[30] G. S. Harbison, H. W. Spiess, *Chem. Phys. Lett. 124* (1986) 128.
[31] G. S. Harbison, V.-D. Vogt, H. W. Spiess, *J. Chem. Phys. 86* (1987) 1206.
[32] B. Blümich, C. Böffel, G. S. Harbison, Y. Yang, H. W. Spiess, *Ber. Bunsenges. Phys. Chem. 91* (1987) 1100.
[33] C. Böffel, H. W. Spiess in C. B. McArdle (Ed.): *Side Chain Liquid Crystal Polymers*, Blackie & Son, Glasgow 1988, Chapter 8.
[34] W. S. Veeman, *Prog. NMR Spectrosc. 16* (1984) 193.
[35] L. R. Sarles, R. M. Cotts, *Phys. Rev. 111* (1958) 853.
[36] J. Schaefer, E. O. Stejskal, J. Buchdahl, *Macromolecules 10* (1977) 384.
[37] J. S. Waugh, L. M. Huber, U. Haeberlen, *Phys. Rev. Lett. 20* (1968) 180.
[38] U. Haeberlen, *Magn. Reson. Rev. 10* (1985) 81.
[39] U. Pschorn, H. W. Spiess, *J. Magn. Reson. 39* (1980) 217.
[40] J. Herzfeld, A. E. Berger, *J. Chem. Phys. 73* (1980) 6021.
[41] M. Maricq, J. S. Waugh, *Chem. Phys. Lett. 47* (1977) 327; J. S. Waugh, M. M. Maricq, R. Cantor, *J. Magn. Reson. 29* (1978) 183; M. M. Maricq, J. S. Waugh, *J. Chem. Phys. 70* (1979) 3300.
[42] W. T. Dixon, *J. Magn. Reson. 44* (1981) 220.
[43] W. T. Dixon, *J. Chem. Phys. 77* (1982) 1800.
[44] Y. Yarim-Agaev, P. N. Tutunjian, J. S. Waugh, *J. Magn. Reson. 47* (1982) 51.
[45] E. T. Olejniczak, S. Vega, R. G. Griffin, *J. Chem. Phys. 81* (1984) 4804; E. T. Olejniczak, J. E. Roberts, S. Vega, R. G. Griffin, *J. Magn. Reson. 56* (1984) 156.
[46] D. P. Raleigh, E. T. Olejniczak, S. Vega, R. G. Griffin, *J. Magn. Reson. 72* (1987) 238.
[47] P. DuBois Murphy, *J. Magn. Reson. 49* (1982) 368.
[48] Y. Yang, M. Schuster, B. Blümich, H. W. Spiess, *Chem. Phys. Lett. 139* (1987) 239.
[49] A. Pines, M. G. Gibby, J. S. Waugh, *J. Chem. Phys. 56* (1972) 1776; *ibid. 59* (1973) 569; *Chem. Phys. Lett. 15* (1972) 373; A. Pines, J. S. Waugh, *J. Magn. Reson. 8* (1972) 354.
[50] M. H. Levitt, D. Suter, R. R. Ernst, *J. Chem. Phys. 84* (1986) 4243.
[51] M. Alla, E. Lippmaa, *Chem. Phys. Lett. 37* (1976) 260.
[52] S. J. Opella, M. H. Frey, *J. Am. Chem. Soc. 101* (1979) 5854.
[53] M. G. Munowitz, R. G. Griffin, *J. Chem. Phys. 76* (1982) 2848.
[54] E. M. Menger, S. Vega, R. G. Griffin, *J. Magn. Reson. 56* (1984) 338.
[55] R. Tycko, S. J. Opella, *J. Chem. Phys. 86* (1987) 1761.
[56] P. Caravatti, G. Bodenhausen, R. R. Ernst, *Chem. Phys. Lett. 89* (1982) 363.
[57] C. M. Carter, D. W. Alderman, D. M. Grant, *J. Magn. Reson. 73* (1987) 114; *ibid. 65* (1985) 183.
[58] N. Schuff, U. Haeberlen, *J. Magn. Reson. 52* (1983) 267.
[59] A. Naito, P. B. Barker, C. A. McDowell, *J. Chem. Phys. 81* (1984) 1583.
[60] J. S. Waugh, *Proc. Natl. Acad. Sci. USA 73* (1976) 1394; R. K. Hester, J. L. Ackerman, B. L. Neff, J. S. Waugh, *Phys. Rev. Lett. 36* (1976) 1081.
[61] S. J. Opella, J. S. Waugh, *J. Chem. Phys. 66* (1977) 4919.
[62] E. F. Rybacyewski, B. L. Neff, J. S. Waugh, J. S. Sherfinski, *J. Chem. Phys. 67* (1977) 1231.
[63] T. A. Cross, P. Tsang, J. S. Opella, *Biochemistry 22* (1983) 721.
[64] V. W. Miner, P. M. Tyrell, J. H. Prestegard, *J. Magn. Reson. 55* (1983) 438.

[65] R. Ramachandran, A. C. Kunwar, H. S. Gutowsky, E. Oldfield, *J. Magn. Reson. 60* (1984) 352.
[66] G. Bodenhausen, R. E. Stark, D. J. Ruben, R. G. Griffin, *Chem. Phys. Lett. 67* (1979) 425.
[67] A. Trokiner, P. P. Man, H. Theveneau, P. Papon, *Solid State Commun. 55* (1985) 929.
[68] H. Schlemmer, U. Haeberlen, *J. Magn. Reson. 70* (1986) 436.
[69] P. M. Henrichs, M. Linder, J. M. Hewitt, *J. Chem. Phys. 85* (1986) 7077.
[70] T. A. Cross, M. H. Frey, S. J. Opella, *J. Am. Chem. Soc. 105* (1983) 7471.
[71] K. Takegoshi, C. A. McDowell, *J. Chem. Phys. 86* (1987) 6077.
[72] D. Suter, R. R. Ernst, *Phys. Rev. B 5* (1982) 6038.
[73] A. Bax, N. M. Szeverenyi, G. E. Maciel, *J. Magn. Reson. 52* (1983) 147.
[74] M. J. Duijvestijn, A. Manenshijn, J. Smidt, R. A. Wind, *J. Magn. Reson. 64* (1985) 461.
[75] R. K. Hester, J. L. Ackerman, V. R. Cross, J. S. Waugh, *Phys. Rev. Lett. 16* (1975) 993; R. K. Hester, J. L. Ackerman, V. R. Cross, J. S. Waugh, *J. Chem. Phys. 63* (1975) 3603.
[76] M. Lindner, A. Höhener, R. R. Ernst, *J. Chem. Phys. 73* (1980) 4959.
[77] M. E. Stoll, A. J. Vega, R. W. Vaughan, *J. Chem. Phys. 65* (1976) 4093.
[78] A. M. Thayer, A. Pines, *Acc. Chem. Res. 20* (1987) 47.
[79] R. Ramachandran, E. Oldfield, *J. Chem. Phys. 80* (1984) 674.
[80] P. P. Man, H. Thevenau, P. Papon, *J. Magn. Reson. 64* (1985) 271.
[81] F. M. M. Geurts, A. P. M. Kentgens, W. S. Veeman, *Chem. Phys. Lett. 120* (1985) 206.
[82] P. P. Man, *J. Magn. Reson. 67* (1986) 78.
[83] A. P. M. Kentgens, J. J. M. Lemmens, F. M. M. Geurts, W. S. Veeman, *J. Magn. Reson. 71* (1987) 62.
[84] A. M. Thayer, J. M. Milar, A. Pines, *Chem. Phys. Lett. 129* (1986) 55.
[85] H. T. Edzes, J. P. C. Bernards, *J. Am. Chem. Soc. 106* (1984) 1515.
[86] E. Rössler, *Chem. Phys. Lett. 128* (1986) 330.
[87] P. Caravatti, J. A. Deli, G. Bodenhausen, R. R. Ernst, *J. Am. Chem. Soc. 104* (1982) 5506.
[88] C. E. Bronniman, N. M. Szeverenyi, G. E. Maciel, *J. Chem. Phys. 79* (1983) 3694.
[89] P. M. Henrichs, M. Linder, *J. Magn. Reson. 58* (1984) 458.
[90] D. R. Theimer, *Diplomarbeit*, Universität Mainz 1987.
[91] L. Müller, S. I. Chan, *J. Chem. Phys. 78* (1983) 4341.
[92] G. E. Maciel, N. Szeverenyi, M. Sardashti, *J. Magn. Reson. 64* (1985) 365.
[93] P. Caravatti, L. Braunschweiler, R. R. Ernst, *Chem. Phys. Lett. 100* (1983) 305.
[94] J. E. Roberts, S. Vega, R. G. Griffin, *J. Am. Chem. Soc. 106* (1984) 2506.
[95] M. Linder, P. M. Henrichs, J. M. Hewitt, D. J. Massa, *J. Chem. Phys. 82* (1985) 1585.
[96] N. J. Clayden, *J. Magn. Reson. 68* (1986) 360.
[97] C. L. Mayne, R. J. Pugmire, D. L. Grant, *J. Magn. Reson. 56* (1984) 151.
[98] H. Miura, T. Terao, A. Saika, *J. Magn. Reson. 68* (1986) 593.
[99] A. P. M. Kentgens, W. S. Veeman, J. van Bree, *Macromolecules 20* (1987) 1234.
[100] W. P. Aue, D. J. Ruben, R. G. Griffin, *J. Magn. Reson. 43* (1981) 427.
[101] A. Bax, N. Szeverenyi, G. E. Maciel, *J. Magn. Reson. 55* (1983) 494.
[102] T. Terao, T. Fujii, T. Ondera, A. Saika, *Chem. Phys. Lett. 107* (1984) 145.
[103] W. P. Aue, D. J. Ruben, R. G. Griffin, *J. Chem. Phys. 80* (1984) 1729.
[104] A. Bax, N. M. Szeverenyi, G. E. Maciel, *J. Magn. Reson. 51* (1983) 400.
[105] N. Zumbulyadis, *Phys. Rev. B 33* (1986) 6495.
[106] M. G. Munowitz, W. P. Aue, R. G. Griffin, *J. Chem. Phys. 77* (1982) 1686.
[107] T. Terao, H. Miura, A. Saika, *J. Chem. Phys. 85* (1986) 3816.
[108] M. G. Munowitz, R. G. Griffin, G. Bodenhausen, T. H. Huang, *J. Am. Chem. Soc. 103* (1981) 2533; M. G. Munowitz, R. G. Griffin, *J. Chem. Phys. 78* (1983) 613.
[109] A. Bax, T. A. Early, G. E. Maciel, *J. Magn. Reson. 52* (1983) 35.
[110] M. G. Munowitz, T. H. Huang, C. M. Dobson, R. G. Griffin, *J. Magn. Reson. 57* (1984) 56.
[111] J. Herzfeld, J. E. Roberts, R. G. Griffin, *J. Chem. Phys. 86* (1987) 597.
[112] N. M. Szeverenyi, M. J. Sullivan, G. E. Maciel, *J. Magn. Reson. 47* (1982) 462.
[113] N. M. Szeverenyi, A. Bax, G. E. Maciel, *J. Am. Chem. Soc. 105* (1983) 2579.
[114] M. H. Frey, S. J. Opella, *J. Am. Chem. Soc. 106* (1984) 4942.
[115] B. H. Meier, C. B. Storm, W. L. Earl, *J. Am. Chem. Soc. 108* (1986) 6072.
[116] N. Zumbulyadis, P. M. Roberts, W. T. Ferrar, *J. Magn. Reson. 72* (1987) 388.
[117] K. M. Morden, S. J. Opella, *J. Magn. Reson. 70* (1986) 476.
[118] P. Caravatti, P. Neuenschwander, R. R. Ernst, *Macromolecules 18* (1985) 119.
[119] K. Takegoshi, C. A. McDowell, *J. Chem. Phys. 84* (1986) 2084.
[120] G. S. Harbison, D. P. Raleigh, J. Herzfeld, R. G. Griffin, *J. Magn. Reson. 64* (1985) 284.
[121] A. F. de Jong, A. P. M. Kentgens, W. S. Veeman, *Chem. Phys. Lett. 109* (1984) 337; A. P. M. Kentgens, A. F. de Jong, E. de Boer, W. S. Veeman, *Macromolecules 18* (1985) 1045.
[122] A. P. M. Kentgens, E. de Boer, W. S. Veeman, *J. Chem. Phys. 87* (1987) 6859.
[123] J. Schaefer, M. D. Sefcik, E. O. Stejskal, R. A. McKay, *Macromolecules 14* (1981) 280.
[124] J. Schaefer, R. A. McKay, E. O. Stejskal, W. T. Dixon, *J. Magn. Reson. 52* (1983) 123; J. Schaefer, E. O. Stejskal, R. A. McKay, *ibid. 57* (1984) 85; J. Schaefer, E. O. Stejskal, R. A. McKay, W. T. Dixon, *Macromolecules 17* (1984) 1479; J. Schaefer, M. D. Sefcik, E. O. Stejskal, R. A. McKay, W. T. Dixon, R. E. Cais, *ibid. 17* (1984) 1107.
[125] W. P. Aue, D. J. Ruben, R. G. Griffin, *J. Magn. Reson. 46* (1982) 354.
[126] Y.-S. Yen, A. Pines, *J. Chem. Phys. 78* (1983) 3579; J. Baum, M. Munowitz, A. N. Garroway, A. Pines, *ibid. 83* (1985) 2015; S. Emid, *Physica B+C (Amsterdam) 128* (1985) 79.
[127] E. M. Menger, D. P. Raleigh, R. G. Griffin, *J. Magn. Reson. 63* (1985) 579.
[128] D. P. Weitekamp, A. Bielecki, D. Zax, A. Pines, *Phys. Rev. Lett. 50* (1983) 1807; D. B. Zax, A. Bielecki, K. W. Zilm, A. Pines, *Chem. Phys. Lett. 106* (1984) 550; J. W. Hennel, A. Bierczynski, S. F. Sagnowski, M. Stachurowa, *Z. Phys. B 56* (1984) 133; *ibid. 60* (1985) 49; J. M. Miller, A. M. Thayer, A. Bielecki, D. B. Zax, A. Pines, *J. Chem. Phys. 83* (1985) 934; D. B. Zax, A. Bielecki, K. W. Zilm, A. Pines, D. P. Weitekamp, *ibid. 83* (1985) 4877; R. Kreis, D. Suter, R. R. Ernst, *Chem. Phys. Lett. 118* (1985) 120; P. Jonson, M. Luzar, A. Pines, M. Mehring, *J. Chem. Phys. 85* (1986) 4873.
[129] R. A. Wind, S. F. Dec, G. E. Maciel, *28th Experimental NMR Conference* (Asilomar, CA, USA) 1987.
[130] D. P. Burum, M. Lindner, R. R. Ernst, *J. Magn. Reson. 44* (1981) 173.
[131] A. J. Shaka, J. Keeler, T. Frenkiel, R. Freeman, *J. Magn. Reson. 52* (1983) 335.
[132] A. Samoson, E. Lippmaa, *Chem. Phys. Lett. 100* (1983) 205; *Phys. Rev. B 28* (1983) 6567.
[133] A. Bielecki, D. B. Zax, K. W. Zilm, A. Pines, *Rev. Sci. Instrum. 57* (1986) 393.
[134] F. Noack, *Prog. NMR Spectrosc. 18* (1986) 171; G. Schauer, W. Nusser, M. Blanz, R. Kimmich, *J. Phys. E 20* (1987) 43.
[135] A. Kumar, R. R. Ernst, K. Wüthrich, *Biochem. Biophys. Res. Commun. 95* (1980) 1.
[136] K. R. Jeffrey, *Bull. Magn. Reson. 3* (1981) 60.
[137] D. Marion, K. Wüthrich, *Biochem. Biophys. Res. Commun. 113* (1983) 967; K. Nagayama, *J. Magn. Reson. 66* (1986) 240; J. Keeler, D. Neuhaus, *ibid. 63* (1985) 454.
[138] D. J. States, R. A. Haberkorn, D. J. Ruben, *J. Magn. Reson. 48* (1982) 286.
[139] A. A. Jones, *Macromolecules 18* (1985) 902.
[140] P. M. Henrichs, M. Linder, J. M. Hewitt, D. Massa, H. V. Isaacson, *Macromolecules 17* (1984) 2412.
[141] D. Suter, R. R. Ernst, *Phys. Rev. B 25* (1982) 6038.
[142] I. M. Ward (Ed.): *Structure and Properties of Oriented Polymers*, Applied Science, London 1975.
[143] H. W. Spiess in I. M. Ward (Ed.): *Developments in Oriented Polymers 1*, Applied Science, New York 1982.
[144] R. Hentschel, H. Sillescu, H.W. Spiess, *Polymer 22* (1981) 1516.
[145] W. Maier, A. Saupe, *Z. Naturforsch. A 13* (1958) 564; *ibid. 14* (1959) 882; *ibid. 15* (1960) 287.
[146] V. J. McBrierty, *J. Chem. Phys. 61* (1974) 872.
[147] M. Pietralla, H. R. Schubach, M. Dettenmaier, B. Heise, *Prog. Colloid Polym. Sci. 71* (1985) 125.
[148] A. Hagemeyer, Y. Yang, B. Blümich, H. W. Spiess, *Chem. Phys. Lett. 150* (1988) 1.
[149] T. Gullion, M. S. Conradi, *Phys. Rev. B 30* (1984) 1133.
[150] B. Blümich, C. Böffel, R. Bost, Y. Yang, H. W. Spiess, *8th Colloq. Ampère Liq. Cryst. Polym.* (Lisbon, Portugal) 1987.

Uniform Heterogeneous Catalysts: The Role of Solid-State Chemistry in their Development and Design**

By John M. Thomas*

Heterogeneous catalysts are generally assumed to be multiphasic and multicomponent; many of them are, and this is one of the reasons why disentangling the factors that govern their mode of action is so difficult. But there is a large class of heterogeneous catalysts where the solid is monophasic and where the activity may be envisaged as being dispersed in a spatially uniform fashion throughout its bulk. This is true both of zeolites and many other microporous catalysts on the one hand, and of certain mixed metal oxides, where the non-stoichiometry is inextricably mingled with the catalysis, on the other. By recognizing this broad classification numerous operational advantages follow: the performance of existing catalysts and the design of those yet to be prepared can be placed on a rational footing; moreover, the myriad techniques of solid-state chemistry and physics, often regarded as inapplicable to the subtle and special problems of surface chemistry, are seen to be of direct relevance as probes for the structure and properties of proven uniform heterogeneous catalysts as well as for the synthesis and development of new ones. This review, which draws analogies with and lessons from the chemistry of enzyme catalysts, focuses largely on the catalytic conversions of hydrocarbons over zeolites, clays, microporous $AlPO_4$ and a wide range of metal oxides.

1. Setting the Scene: What is a Uniform Heterogeneous Catalyst?

Every chemist knows that there is a large class of heterogeneous catalyst the function of which is to accelerate chemical conversion at *the exterior surface* of the solid. As an undergraduate, the chemist learns that, in the catalytic synthesis of ammonia from H_2 and N_2, for example, or in the Fischer-Tropsch conversion of mixtures of H_2 and CO to hydrocarbons and alcohols, the seat of reaction is the surface of metallic iron and the surface of metallic cobalt respectively. And these surfaces, on the atomic scale, are thought to look like the enlarged view of a precious opal, shown in Figure 1. Many other familiar catalytic reactions fall into this category (Table 1); and it follows that the detailed chemistry of the exterior surfaces holds the key to the deeper understanding of the intricacies of this class of catalyst. It is far less widely appreciated that there is an equally large class of heterogeneous catalysts where all, or nearly all, *atoms in the bulk* of the solid either participate directly or are implicated indirectly in the crucial catalytic act. Prominent examples are the zeolites,[1-6] certain clays[7-12] and pillared clays.[13-17] A large number of oxides,[18-24] including those listed in Table 1, also falls into this category.

In zeolites, and other related microporous solids[25-29] such as those derived from crystalline low density $AlPO_4$ and metal-substituted (in the framework) variants of $AlPO_4$ and $(Si_xAl_yP_z)O_2$, all bulk atoms are, at one and the same time, surface atoms in that they are accessible to gaseous reactants capable of entering the apertures (3 to 8 Å) of their cages and channels. Likewise, in layered aluminosilicate (clay) catalysts, the active sites are situated in ac-

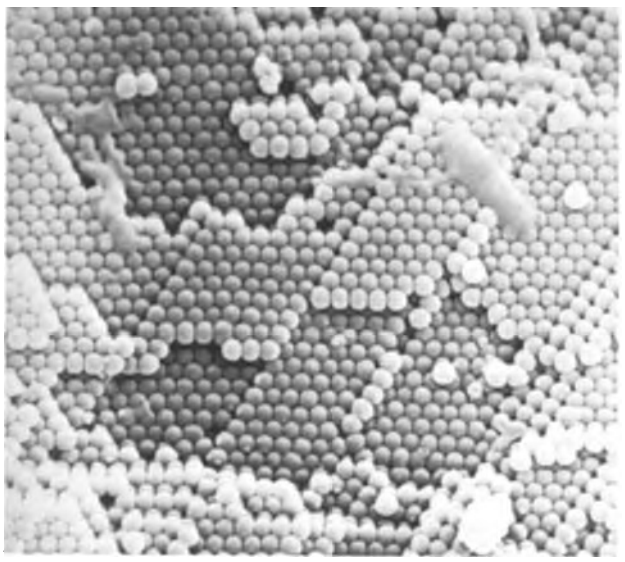

Fig. 1. The surface of a metallic catalyst, when suitably enlarged, is thought to look like this surface of an opal examined by scanning electron microscopy. Picture each spherical particle of silica to be an atom; and note the monatomic steps (terraces), the kinks in the steps and the tendency for some atoms to exist individually, as pairs or as two-dimensional clusters of twelve or more bound to the underlying structure. Antiphase boundaries, vacancies and even impurity (rogue) species are also present. The SiO_2 particles have a diameter of 5000 Å. Micrograph taken by *J. V. Sanders*.

[*] Prof. Dr. J. M. Thomas
Davy Faraday Research Laboratory
The Royal Institution of Great Britain
21 Albemarle Street, London W1X 4BS (UK)

[**] Based, in part, on the Hund-Klemm Lecture given at the Max Planck Institute for Solid State Research, Stuttgart (20 May 1987), and on seminars given at the Institute of Fundamental Chemistry, Kyoto (14 June, 1988), the Fritz Haber Institute of the Max-Planck-Gesellschaft, Berlin (12 March 1987), and the University of California, Berkeley (19 April 1988).

Table 1. Two classes of heterogeneous catalysts.

Composition of Catalyst	Reaction Catalyzed	Whether Already Commercial (C) or Demonstrated on Laboratory Scale (L)
Category 1: Spatially non-uniform distribution of active sites, often of different kinds and consisting of multiple phases		
Cobalt and other transition-metals on a variety of supports (Fischer-Tropsch Reaction)	$CO + H_2 \longrightarrow \begin{cases} C_nH_{2n+2} \\ C_nH_{2n} \\ C_nH_{2n+1}OH \end{cases}$	C
Copper on ZnO/Al_2O_3 (ICI Methanol Synthesis)	$CO + 2H_2 \longrightarrow CH_3OH$	C
Nickel on Al_2O_3 (methanation reaction)	$CO + H_2 \longrightarrow CH_4$	C
Iron with traces of Al, Si, K (Haber Process)	$N_2 + 3H_2 \longrightarrow 2NH_3$	C
Rhodium (and platinum and palladium) on cerium oxide and cordierite (Auto exhaust catalyst)	$CO + NO \longrightarrow CO_2 + N_2$ $C_xH_y + O_2 \longrightarrow CO_2 + H_2O$ $CO + O_2 \longrightarrow CO_2$	C
Palladium on Al_2O_3	$CH_4 \xrightarrow{[O]} CH_3OH$	C
Silver powder	$CH_3OH \xrightarrow{[O]} HCHO$	C
Silver on Al_2O_3 + chloride	$C_2H_4 \xrightarrow{[O]} H_2\overbrace{C-O-C}H_2$	C
Tungsten oxide on silica (Olefin Metathesis)	$R^1R^2C=CH_2 + R^3R^4C=CH_2 \longrightarrow C_2H_4 + R^1R^2C=CR^3R^4$	C
Category 2: Spatially uniform distribution of structurally equivalent active sites in a monophasic solid		
Zeolite ZSM-5 ($H^\oplus$ form) (Ethyl benzene formation) (Mobil-Badger process)	$C_6H_6 + C_2H_4 \longrightarrow C_6H_5C_2H_5$	C
ZSM-23 or theta-1 (Zeolites in $H^\oplus$ form)	Alkylation of Benzene	L
SAPO-5 (or 11) (Silicon aluminum phosphate)	Methanol to olefin conversion	L
ZSM-5 ($H^\oplus$ form)	Methanol to petrol (gasoline) conversion	C
$La^{3\oplus}$ exchanged zeolite Y	Cracking and Hydrocracking of gas oil	C
Zeolite rho (or ZSM-5) ($H^\oplus$ forms)	$NH_3 + CH_3OH \longrightarrow HN(CH_3)_2$	L
Zeolite ZSM-5 ($H^\oplus$ form) Xylene isomerization and toluene disproportionation	Synthesis of *para*-xylene	C
$Al^{3\oplus}$-exchanged montmorillonite and pillared clay	Production of *tert*-butylmethyl ether from MeOH and 2-methylpropene	L
Ti-silicalite	Synthesis of hydroquinone from phenol and H_2O_2	C
Ti-silicalite	Synthesis of propene oxide from propene and H_2O_2	L
Bi_2MoO_6 (or $Bi_2Mo_2O_9$ or $Bi_2Mo_3O_{12}$)	Selective oxidation of propene to acrolein Selective ammoxidation of propene to acrylonitrile	C
$Ba_2Bi_{2-x}La_xO_{6-y}$	Selective oxidation of propene to 1,5 hexene and benzene	L

cessible, interlamellar regions. And in pillared clays the active (acid) sites drape the walls of the pillar, the initial function of which is to enhance the utility of the catalyst by, inter alia, enlarging the separation of the layers and keeping them apart.

Those ternary oxides that are efficient selective oxidation catalysts of hydrocarbons such as propylene—and the bismuth molybdenum oxides as well as the calcium manganates[24] and other perovskites[30] are in this class—entail *sacrificial loss of oxygen*. Experiments[22] using isotopically labelled reactants or solid catalysts reveal beyond doubt that structural oxygen is released from the catalyst, thereby converting it—at least temporarily—to a non-stoichiometric oxide. The gaseous oxygen present as one of the reactants is then taken up by the catalyst, thus making good its anion deficiency. The cycle repeats itself for as long as the catalyst is active. The idea that this was how certain selective oxidation catalysts worked was first clearly enunciated in 1954 by *Mars* and *van Krevelen*.[18]

It is to be noted that, both for the zeolites and pillared clays on the one hand, and the oxide catalysts capable of sacrificial loss of structural oxygen on the other, *the bulk of the solid is of central importance in the catalysis*. Moreover, as we shall show below, in the zeolitic catalysts the special (active) sites situated within the bulk (and at the surface) of the solid are distributed in a spatially uniform fash-

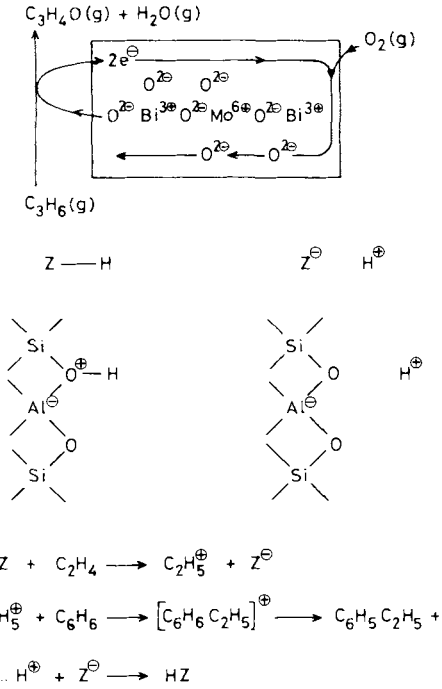

Fig. 2. Top: Certain oxides (e.g. Bi_2MoO_9, $Bi_2Mo_2O_9$, $Bi_2Mo_3O_{12}$) release their structural oxygen to the hydrocarbon that is being selectively oxidized (e.g. propene to acrolein). But they can also assimilate oxygen from the gas phase. They are, effectively, flexible carriers of oxygen. Bottom: Zeolites in their protonic form (see Section 2), represented HZ, likewise may be regarded as carriers of protons. The proton assimilated by ethene in reaction 1 is jettisoned in 2 at the instant preceding catalytic formation of ethyl benzene in a ZSM-5 (or other) zeolite catalyst.

ion.[31] All these active sites are accessible to the reactants. In the sacrificial oxide catalyst, again we see that the bulk atoms are crucial, in that *all* the oxygen ions participate in the turmoil of events—loss, gain and migration (Fig. 2)—involved in the overall catalysis. It follows, therefore, that, since *any* oxygen ion in the solid can, through migration, appear at the surface and be removed by the oxidizable hydrocarbon, these oxide catalysts may also be legitimately termed uniform; there is, again, a spatial uniformity in the arrangement of the species within the solid implicated in the catalysis.

We can now appreciate the essential differences between metal, alloy and other examples of heterogeneous catalysis belonging to category 1 in Table 1 on the one hand, and those that belong to category 2 on the other. Category 1 catalysts have reactions restricted to their exterior surface and there is a substantial body of experimental evidence that only a small fraction of that exterior surface is involved in the catalytic act. Such surfaces are catalytically non-uniform. In category 2 catalysts, however, the chemical conversions entail participation of atoms uniformly distributed within the bulk of the solid.

1.1. Pointers from Enzyme Catalysis and Organometallic Chemistry

It is relevant to cite here the kinship that exists between category 2 catalysts, as defined above, and biological (enzyme) catalysts. Ever since the classic work of *Phillips*[33] in this laboratory on the mode of action of lysozyme, it has been recognized that enzymes generally have active sites which consist of pockets, or clefts, the lining of which contain the key set of amino acids, in the right sequence and conformation, required to 'process' the substrate (i.e. the reactant species). Each molecule of an enzyme is itself a massive entity possessing a well-defined, three-dimensional structure. In a crystal or quasi-crystalline assembly of an enzyme the active sites are arranged in a spatially uniform fashion.[34] It is precisely because this is so that, with the aid of X-ray crystallography, we know so much, and in considerable atomic detail, about the nature of the active center in many enzymes. The very uniformity of the enzyme lends itself to the elucidation of its three-dimensional structure by X-ray diffractometry (and, more recently, by NMR spectroscopy). Nowadays, with site-selective mutagenesis, the constituent amino acids of the lining of the active center can be delicately modified.[35] X-ray techniques then reveal the subtle changes wrought upon the active site and the catalytic consequences—changes in activity and selectivity—can be assessed by standard tests of the performance of the enzyme. The key point here is that, because the catalyst is structurally uniform, the three-dimensional structure deduced from X-ray crystallography immediately clarifies mechanistic and other features associated with the catalytic action (Fig. 3).

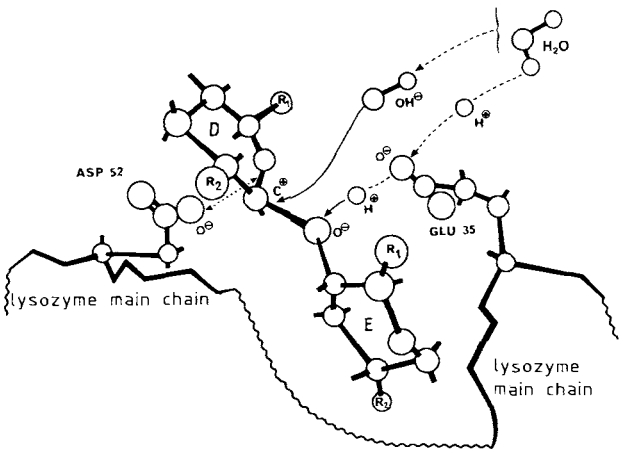

Fig. 3. Outline of the mechanism of the catalysis of a polysaccharide hydrolysis by lysozyme. This was deduced from the classic X-ray study of *Phillips* [33].

As a result of the enormous progress achieved recently in two-dimensional crystallography[37,38] (based mainly on low-energy electron diffraction, LEED) it might be thought that our knowledge of the mode of action of category 1 catalysts is now comparable to that of the mode of action of enzymes. After all, there have been dramatic steps forward taken in arriving at the nature of the structures formed at metal surfaces known to be active catalysts. A brief selection of some of the two-dimensional metal-organic structures that have come to light recently[39] is shown in Figure 4. Almost all of these structures have their analogues in the three-dimensional solid states of organometallic compounds.[39] Despite this remarkable insight into the atomic structure of the two-dimensional entities formed at the exterior surfaces of metal and alloy catalysts,

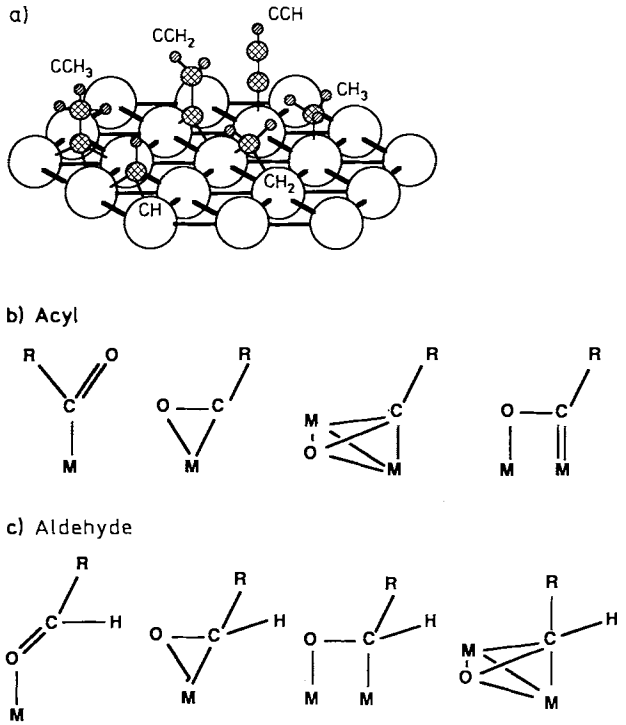

Fig. 4. A selection of some of the structures adapted by small hydrocarbon fragments and other molecules adsorbed at the surfaces of metal catalysts.

comparatively little has been gained so far as enhancing our knowledge of the mode of operation of heterogeneous catalysts in category 1 is concerned. And the reason for this state of affairs is because, as *Somorjai* et al.,[37] *Yates* et al.[40] and others[39] have shown, these surface structures (or the chemisorbed phase) are simply spectator species—they are not crucially involved in the key catalytic act. To know the structure of the predominant surface phase is of little value if that phase plays only a secondary or no role—other than rendering the surface more non-uniform—in catalytic events. So, even though recent progress in surface science has brought us to the stage where we can characterize the structural details of two-dimensional phases and learn that they mirror the bonding patterns that abound in the rich diversity of organometallic compounds, this is not enough to bring us to the ultimate frontier for category 1 catalysts. Only a mere fraction of the surface—and possibly[37] also a small fraction of the sub-surface atoms—is thought to be involved in the catalysis. It is the structure of transitory complexes formed at these sites that is crucial; and present day surface techniques are not yet good enough to determine such structures.[41]

The situation is different for category 2 catalysts, which, from now on, we shall call uniform heterogeneous catalysts. Here, because bulk structure is a quintessential, determinative feature of the catalytic act, a knowledge of that structure permits both an atomic interpretation of the catalysis and, at the same time, points the way to the design of new catalysts. This is precisely what has already been achieved in the realm of enzymatic reactions, as may be gleaned from the recent work of *Fersht, Blow* and others.[35] Analogues of enzymes, built up, for example, from cyclodextrins have been shown by *Bender, Breslow, Lehn* and *Tabushi* and their coworkers to be capable of mimicking the catalytic performance of enzymes. These catalysts are however homogeneous and lie outside the scope of this review.[36]

Although it is a salutary situation that a knowledge of the three-dimensional bulk structure of uniform heterogeneous catalysts holds the key to deeper understanding of their mode of action and for the design of superior ones, it must be emphasized that seldom is it possible to prepare single crystals of the numerous individual solid catalysts that fall into this category suitable for conventional X-ray study. (This situation often plagues the enzyme and protein crystallographer who spends much time in endeavoring to grow good quality crystals.) In the vast majority of cases these uniform, inorganic catalysts are polycrystalline phases which may or may not be catalytically active. Fortunately, several techniques,[4,42] used singly or in combination, have been developed to cope with the determination of the structure of materials in polycrystalline states (Table 2). Some of these techniques have recently been adapted to cope with structure determination under in situ conditions. Since enzymatic reactions take place around room temperature, X-ray and other techniques can be reasonably modified to work under in situ, generally in vitro, conditions. Heterogeneous reactions with uniform catalysts, however, almost invariably take place at elevated temperatures and often under high pressure. Devising suitable in situ techniques for structure determination is, therefore, no mean task. But encouraging progress has been made. Even so, just as with homogeneous gas-phase reactions probing transition states at the femtosecond level is inordinately difficult. About the only prospect currently in sight for the temporal resolution of surface processes utilizes sum-frequency generation.[43]

Table 2. Techniques used singly or in combination for structural elucidation of poylcrystalline catalysts [a].

High resolution electron microscopy
Electron, X-ray and neutron diffraction
Rietveld powder profile analysis
High-resolution, multinuclear, solid-state NMR spectroscopy
Extended X-ray absorption fine structure (EXAFS)
Differential anomalous X-ray diffraction

[a] Some of these, along with other techniques like neutron-inelastic scattering or diffuse reflectance infra-red (Fourier-transform) spectroscopic techniques, may be used under in situ conditions.

2. Uniform Zeolitic Catalysts

By virtue of their structure, crystallinity and variable stoichiometry, zeolitic catalysts have sharply defined pore-size distributions, high and adjustable acidity (see below), very high surface areas (typically 600 $m^2 g^{-1}$), the majority of which (ca. 90%) is, depending upon crystal size, internal and accessible through apertures of well-defined dimensions. They also have good thermal stability (e.g. they can survive heat treatments in air up to 1000°C, the precise temperature being dependent upon the composition of the zeolitic framework).

Catalytic activity in zeolites may be of at least two distinct kinds: the one based on their Brønsted acidity[1-6] (which serves, for example, to generate carbocations in intrazeolitic cavities and channels); the other on transition-metal cations,[6,44-47] which, in the microenvironment of the interior of the zeolite, can facilitate various kinds of redox reactions. We concentrate here on the first of these. (There are other catalytic uses to which zeolites are put. For example, finely-divided platinum group metals may be dispersed in zero-valent state more or less uniformly throughout the interior of the zeolite, thereby making it a bifunctional catalyst, in which 'acid' reactions proceed at one set of uniformly distributed sites and hydrogenation-dehydrogenation as well as bond-shift reactions proceed at the distributed metal particles.[47] We shall not pursue further discussions of these bifunctional catalysts, partly because, upon continued use, there is a tendency for the dispersed metals to aggregate and become non-uniformly distributed).

One of the root causes of the Brønsted acidity of a zeolite which confers upon it its catalytic activity is the mere existence of a heteroatom (Al, Ga, B, Fe etc.) in a silica framework.[3] The situation that exists in the zeolitic catalyst known as ZSM-5 is summarized in Figure 5.[48] The hydrogen atom bonded to the oxygen adjacent to the tetrahedrally incorporated aluminum (or gallium, etc.) has a propensity to free itself as a proton, thereby leaving a macroanionic framework. Evidence from IR spectroscopy substantiates this picture, and corroborative evidence comes from high-resolution solid-state ^{27}Al NMR spectroscopy[3,49] and other probes which monitor the concentration of tetrahedrally-coordinated aluminum. The catalytic activity of a range of ZSM-5 samples containing different quantities of a particular heteroatom in the silica framework of ZSM-5 is shown in Figure 5a left. The first-order rate coefficient for the cracking of *n*-hexane is known to be a good measure of the (Brønsted) catalytic activity of the solid. *Haag* et al.[3] have in particular shown that the catalytic activity per Al atom in the unit-cell remains constant over large concentrations of this, uniformly distributed "active site". The microporosity, viewed (Fig. 5b) in projection along the [010] axis, is clearly apparent.

Another source of detachable protons that make zeolites such good Brønsted acid catalysts is a strongly polarizing cation which can be inserted into certain intrazeolitic cavities. Thus, uniformly distributed (by cation-exchange) ions such as $La^{3\oplus}$ or $Ca^{2\oplus}$ will, because they facilitate hydrolysis, yield more-or-less free protons [Equation (a)]. At low temperatures the liberated proton would be expected to attach itself to a framework oxygen as symbolized in Figure 5c, whereas at elevated temperatures it would be quasi-free.

$$La(OH_2)^{3\oplus} + \text{Zeolite} \longrightarrow La(OH)^{2\oplus} + \text{Zeolite-H}^{\oplus} \qquad \text{(a)}$$

Acid catalysis by zeolites, as well as being used for the cracking and isomerization of hydrocarbons is also the basis of several useful syntheses like the production, on an industrial scale, of ethylbenzene (Figures 2 and 6). Such are the dimensions of the pores of ZSM-5 that shape-selectivity (see Figure 6 bottom) is conferred upon the catalytic

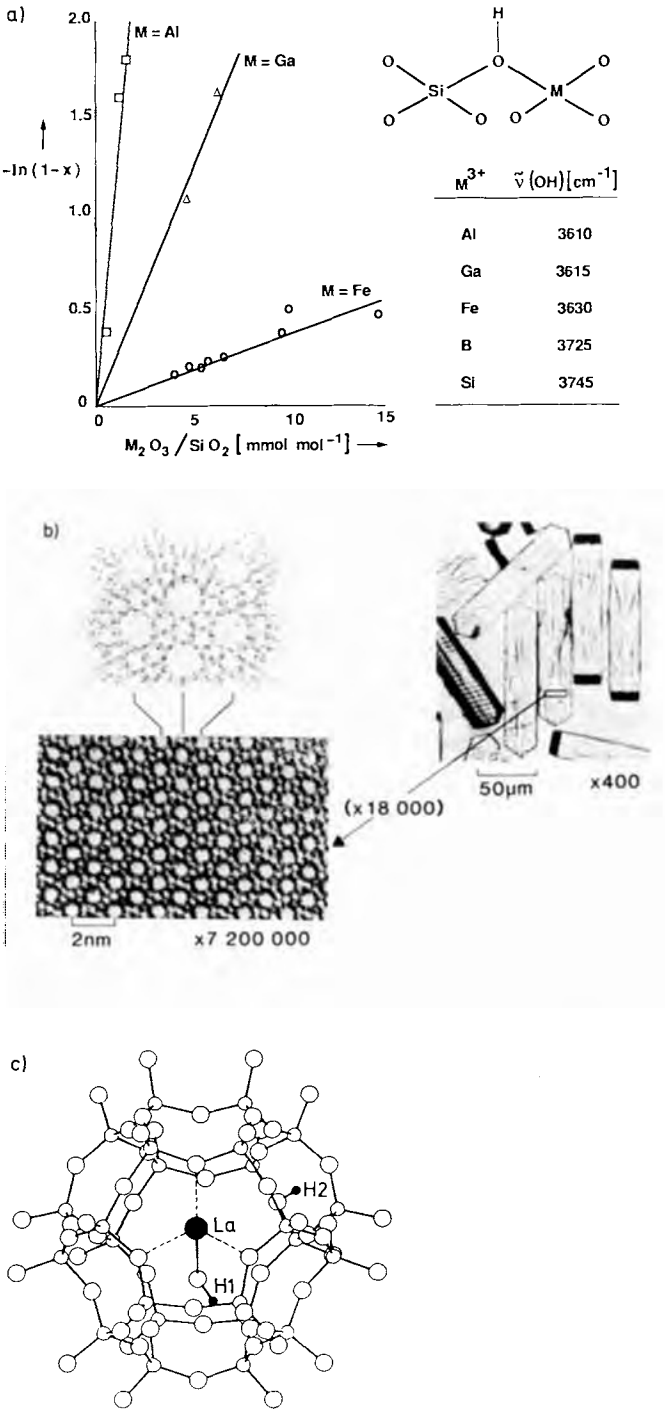

Fig. 5. a) Pentasils, of which ZSM-5 is the archetype, are good catalysts for the thermal cracking of *n*-hexane. There is a correlation between catalytic activity and the acidity of the OH group attached to heteroatom M [48]. b) Structure of ZSM-5 viewed in projection along the straight channels of diameter ca. 5.5 Å. The electron micrograph (bottom left) is taken of the area shown in the optical micrograph (top right). c) The catalytically active site in $La^{3\oplus}$-exchanged zeolite Y consists of a proton (H2) which, although bound to the framework oxygen at 5 K, is mobile at higher temperatures.

action of this uniform heterogeneous catalyst, thereby leading to the highly efficient generation of mono-ethylbenzene from benzene and ethene. This is the essence of the Mobil-Badger process. It has many advantages in comparison with the traditional Friedel-Crafts process previously preferred for the production of ethylbenzene, espe-

cially in regard to the high selectivity for the mono substituted product.

Redox catalysis on an industrial scale entailing the conversion of phenol to hydroquinone and of propylene to propylene oxide also uses a uniform heterogeneous catalyst of the ZSM-5 type.[50] To be sure, the framework is predominantly SiO_2 but some $Ti^{4\oplus}$ ions are incorporated; and these are thought to be the active sites. The mechanism of the conversion has not been fully clarified, but $>Ti=O$ linkages, embedded uniformly in the framework are implicated.[50]

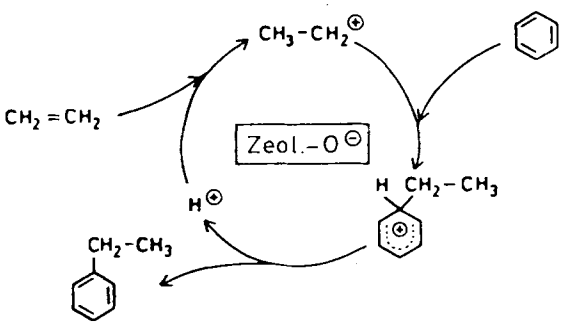

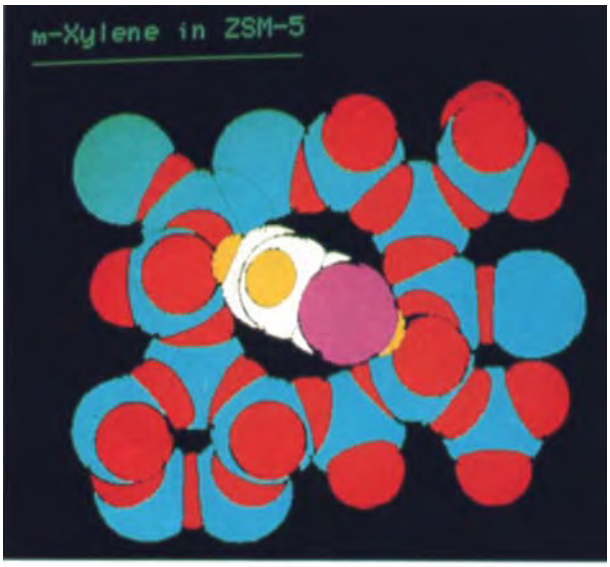

Fig. 6. Top: Mechanism of the proton catalyzed alkylation of arenes. Ethene and benzene yield ethyl benzene over ZSM-5. It is easier for *para*-xylene (bottom), more difficult for *meta*-xylene (middle), to diffuse through a ZSM-5 catalyst.

The kinship between zeolitic and enzymatic catalysts is underlined when one recognizes the importance of shape-selectivity in the chemistry of zeolites. Not only are certain reactants favored—because they possess the requisite dimensions to gain access into the internal area of the zeolite (where the majority of the active sites reside)—but certain products are also preferentially released from within the interior of the catalyst according to their ability to diffuse out. Diffusivities of enzymes and zeolites are directly governed by molecular size and shape. Table 1 shows those reactions where shape-selective catalysis is at work.

The application of various characterizing techniques, including some of those enumerated in Table 2, leads to the conclusion that the active sites—the locus of detachable protons—are uniformly distributed throughout the bulk. One especially powerful method of structural elucidation of polycrystalline zeolitic catalysts is the so-called Rietveld powder profile method.[51,52] This is a refinement procedure, in which a model structure can be tested, and quantitative values of bond lengths and bond angles determined, from profile analysis of the diffractogram (either X-ray or neutron). Using deuterated $La^{3\oplus}$-exchanged zeolite Y catalysts, such as those employed for the cracking of hydrocarbons, the nature of the active site in the catalyst was determined by *Eddy, Cheetham* and *Thomas*.[53] At temperatures below ca. 20 K the location of loosely bound protons attached to framework oxygens could be determined. At higher temperatures (above 300 K), in line with expectation, the proton is mobile and migrates rather freely over the framework; the proton associated with the OH group anchored to the $La^{3\ominus}$ could also be readily located (Fig. 5c).

One expects that, in due course, with the development of in situ structural techniques for the study of zeolitic catalysts, progress comparable to that already achieved by the molecular biologists in elucidating metal catalyzed reactions might be accomplished. Take, for example, the work of *Brown* et al.[54] They examined by single-crystal X-ray studies the manner in which Pb^{II} ions catalytically depolymerize RNA. Using yeast tRNA they showed that site-specific cleavage can be brought about by the action of Pb^{II}. Since single-crystals of yeast tRNA soaked in Pb^{II} acetate (at pH 5.0) and containing the complex formed between the catalyst and the reactant yield good X-ray data, it was possible, by difference Fourier analysis, to deduce the structure of the Pb^{II}-tRNA reaction center (Fig. 7). These workers also observed, again by difference Fourier analysis, sugar-phosphate strand scission between the residues labelled 17 and 18 in crystals of the yeast tRNA soaked in dilute Pb^{II} solutions at pH 7.4 where the catalysis is marked. At pH 5.0 the catalysis is essentially zero. *Brown* et al.,[54] therefore, succeeded in arriving, just as *Phillips* did with lysozyme,[33] at a picture of the reactants and products of the cleavage reaction, and this, in turn, led to their proposed mechanism.

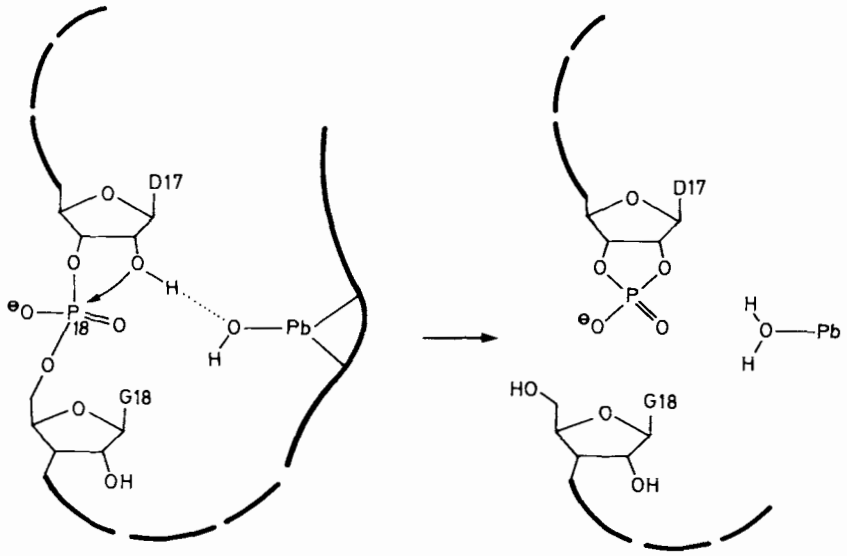

Fig. 7. X-ray diffraction studies yield the mechanistic outlines of the Pb^{II}-catalyzed cleavage of the sugar-phosphate backbone in tRNA.

In the uniform heterogeneous catalysis prominently displayed by zeolites it is unlikely that much success will come from single-crystal X-ray studies since zeolitic catalysts tend to be microcrystalline. But Rietveld powder methods may provide the necessary routes.

2.1. Designing New Zeolitic Catalysts

Very many (some seventy) distinct zeolitic structure-types are known, and numerous recipes are available for the hydrothermal or other more or less demanding syntheses of monophasic, microcrystalline catalysts. Ease of preparation of a zeolitic catalyst, mundane as it may seem as one of the attributes of this class of solid, is as important a factor as any in determining the widespread use of zeolites in industrial catalysis. Faujasite, for example, is a very rare mineral: it occurs in only a few geological locations, and in minute amounts, but its synthetic analogues, zeolites X and Y (Fig. 8) are very easily prepared from solutions of silicates and aluminates. To convert an as-prepared faujasitic zeolite into its acid form capable of exerting its influence as a Brønsted catalyst involves either cation substitution, in which $Ca^{2\oplus}$, $Mg^{2\oplus}$ or $La^{3\oplus}$ ions (capable of causing hydrolysis of bound water) are introduced into the intrazeolitic cavities, or the preparation of the $NH_4^{\oplus}$ exchanged form followed by heating (to drive off the ammonia). Alternatively the synthesis can be effected in the presence of $La^{3\oplus}$ or other polarizing ions. In each case uniform heterogeneous catalysts, in the sense defined earlier, are produced.

The framework composition of some zeolites, especially faujasitic ones, can be changed from the extremes of low-silica to high-silica contents (i.e. from Si/Al ratios of 1.0, which is the lower ratio for zeolite X, through to 1.5 to 3.0 (zeolite Y) and beyond to well above 100). This may be accomplished in several ways. One procedure involves treatment with gaseous $SiCl_4$, another with solutions of $(NH_4)_2SiF_6$. Moreover, after the Si/Al ratio has been greatly increased by such treatment, it is possible[55] to re-aluminate in a rather delicate fashion so as to favor one particular framework environment for the aluminum re-inserted into the framework. This strategem promises a route to fine-tune catalytic performance for a given structural type of zeolite. High resolution solid-state ^{29}Si MAS-NMR spectroscopy[49] is an invaluable tool for monitoring the framework composition, especially the loss and preferential gain of Si (Fig. 9).

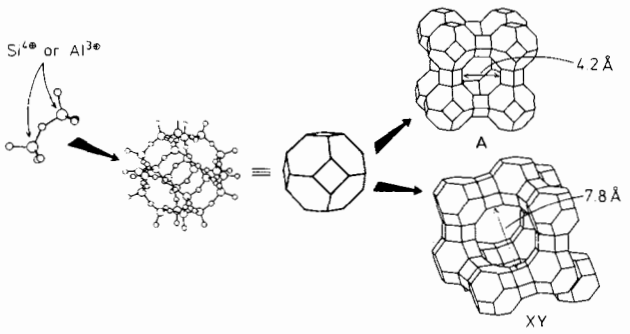

Fig. 8. Schematic illustration of how the structures of zeolites X, Y and A are built up from corner-sharing tetrahedron TO_4 (T = Si and Al).

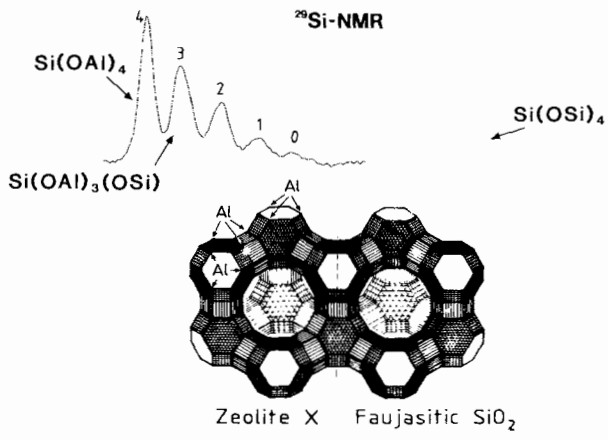

Fig. 9. Crystalline faujasitic silica (right) may be prepared from zeolite X or Y (left) by treatment with $SiCl_4$. The ^{29}Si MAS-NMR spectrum of the product shows one peak corresponding to one type of silicon site in the monophasic silica.

In the numerous zeolitic solids that are known there are several well-defined so-called secondary building units (Fig. 10).[56] Faujasitic zeolites are built up of a combination of β-cages (i.e. truncated octahedra which are synonymous with the tetradecahedron) and double six rings (D6R). The β-cages are arranged as in the diamond lattice.

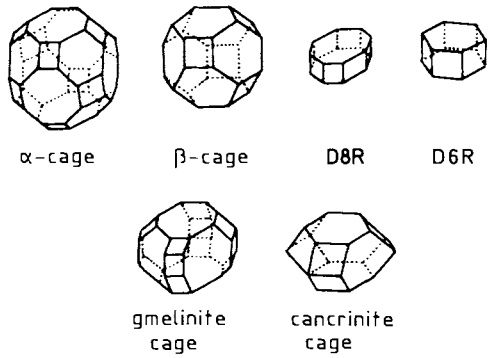

Fig. 10. A selection, presented as polyhedral analogues (compare Fig. 8), of the so-called secondary building units from which many of the more common zeolites are constituted. (D8R and D6R refer to double-eight and double-six rings, respectively.)

But just as lonsdaleite (a rare mineral and polymorph of carbon) is a variant of diamond where ABAB rather than ABCABC stacking exists so also is it possible to conceive of similar polymorphic forms of faujasite in the world of zeolitic catalysts. Indeed, knowing the ease with which irregular as well as regular stacking sequences occur in zeolitic solids,[32,57,58] the distinction between polymorphism and polytopism tends to vanish. In this connection, it is noteworthy that high-resolution electron microscopy (HREM) has brought to light hitherto unsuspected subtleties and patterns in the internal structure of zeolites.[58,59] And, significantly, HREM has led to the discovery of two new zeolitic frameworks closely related to faujasite. Thus two related[60] frameworks tend to intergrow (as many closely related solids do[32]) and the resulting solid is a well-known catalyst and sorbent, zeolite beta.

HREM has recently brought to light another[61] novel zeolitic structure termed ECR-1. It has been shown by a combination of solid-state structure-probing techniques to be a recurrent intergrowth of strips of two naturally occuring minerals, mordenite and mazzite (see Fig. 11). It has recently been realized[62] on the basis of both computed energy and other principles of the stacking of layers that other variants of this solid, labelled DF-1 and shown in Figure 12, are possible. It is not yet clear whether ECR-1, which has been isolated and characterized, and DF-1, which at present is known only as a theoretically possible structure, have any potential as catalysts.

Intergrowths, of a more or less random nature, depending upon the precise conditions of preparation of the catalyst, can occur[57,63] in the so-called pentasil zeolites of which ZSM-5, shown in Figure 5, and a closely-related analogue, ZSM-11 are prominent members (Fig. 13). Such intergrowths lead to quite significant catalytic consequences. We shall illustrate this point by recalling the Mobil synthesis of petrol (gasoline) from methanol using a

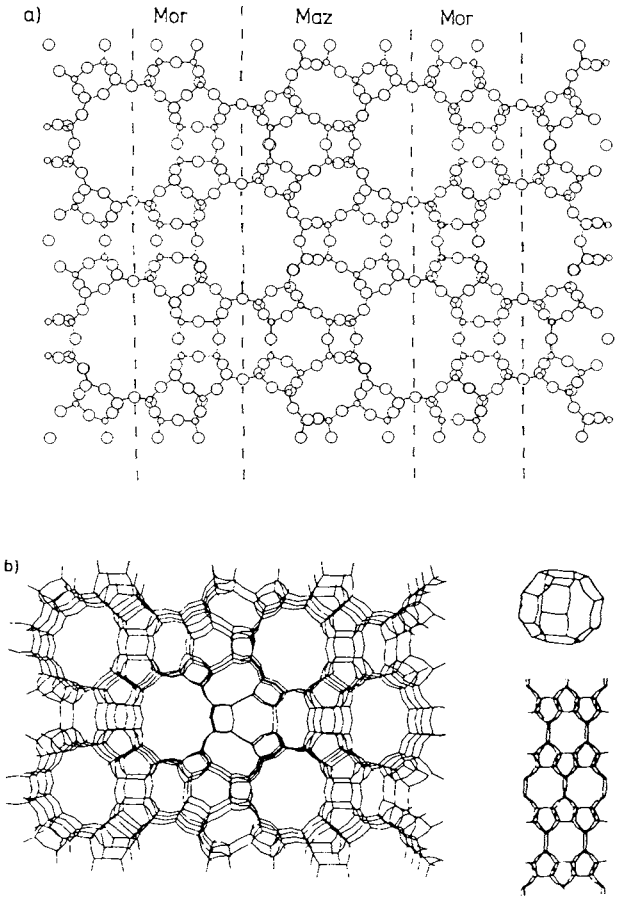

Fig. 11. a) Projection of the ECR-1 zeolite structure along the *a*-axis showing the component sheets of mordenite (Mor) and mazzite (Maz). Large spheres denote oxygen atoms, small ones T-atoms (Si and Al). b) Perspective view of the ECR-1 framework (left). The top right inset shows the gmelinite cage as observed in mazzite, the bottom right inset shows a layer of the mordenite structure.

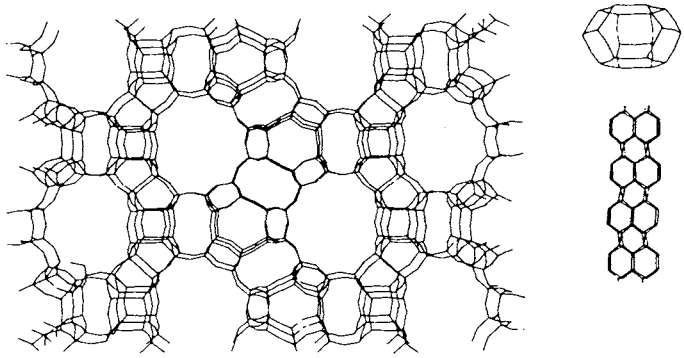

Fig. 12. Left: Perspective view of the framework of the theoretically predicted [62] new zeolite DF-1. The top right inset shows the cancrinite cage and the bottom right inset the layer of four-, five- and six-rings which is found in DF-1.

ZSM-5 catalyst. In this synthesis a distribution of aromatic products, typified by that shown in Figure 14, is observed. In practice, however, product distribution curves of this kind are found to vary quite appreciably from one preparation of ZSM-5 to another. Moreover, with ZSM-11, the carbon number for the peak as well as the distribution curve itself shifts to higher values, compared with the re-

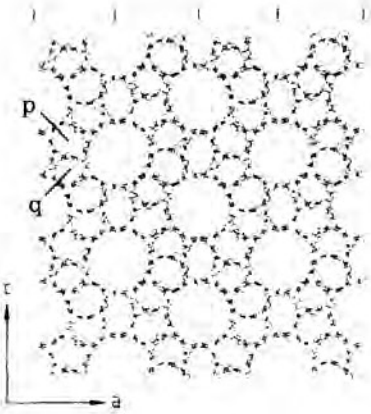

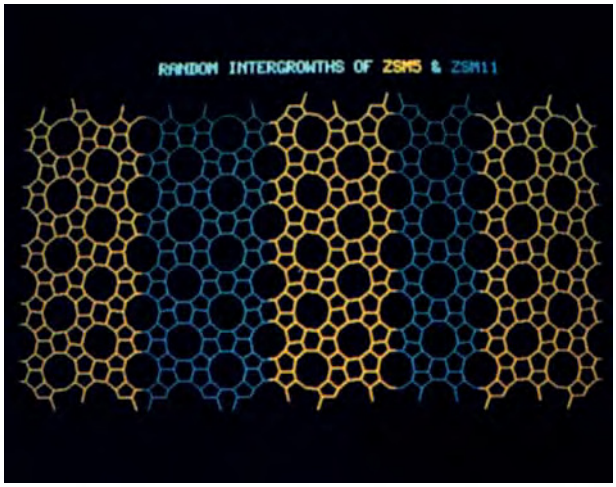

Fig. 13. Top: ZSM-11 is closely related to ZSM-5 (compare with Fig. 5b); bottom: intergrowths, drawn schematically in color here, of the two are known to exist. (The symbol i denotes inversion; p and q refer to the larger and smaller 5-membered rings, respectively.)

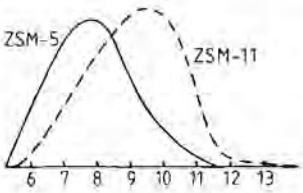

sults for ZSM-5. It is not difficult to appreciate why this is so. There are in ZSM-11 two kinds of cavities created by the intersecting channels. One cavity has a volume about 1.6 times that of the other, the volume and shape of which is exactly the same as the single type of cavity found in ZSM-5. The shape and size of these cavities crucially govern the maximum dimension attainable in the transition-state when the alkylcarbenium ions, formed from methanol, are established inside the zeolite catalysts.[64,65] The shift of the distribution curve to higher values is therefore explicable in terms of the subtleties of the mode of operation of shape-selective catalysts. And the reason why preparations of ZSM-5 exhibit variability in catalytic performance vis-a-vis product distributions is attributable to the fact that intergrowths of ZSM-11 (present to a variable degree) occur within the ZSM-5. Proof of the occurrence of intergrowths has been presented previously and is seen in the high-resolution micrograph that constitutes Figure 15.

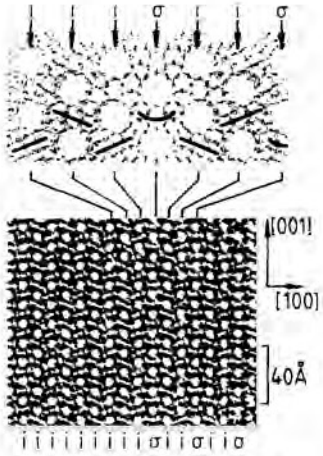

Fig. 15. High-resolution electron micrograph of a typical ZSM-5/ZSM-11 catalyst which contains some intergrowths at the sub-unit-cell level. In perfectly ordered ZSM-11 one sheet (on (100)) is related to its predecessor by a mirror (σ) relation, whereas in ZSM-5 successive sheets are related by inversion (i).

The preparation and characterization of new zeolites has rapidly gained pace in recent years, largely because of the arrival of a range of powerful new techniques for identifying and determining their structures.[42] Moreover, some techniques, notably multinuclear NMR spectroscopy as well as IR, laser Raman and other spectroscopic procedures are applicable to solutions and gels so that information can be gleaned about the role of organic templates in governing the formation of cages and other secondary building units in the evolution of the precursor state prior to crystallization. It is premature, at this stage, to draw too many firm conclusions. But already it has become apparent that many of the originally introduced templates—such as the tetraethylammonium ion (for the preparation of zeolite beta) or bis-(2-hydroxyethyl)-dimethyl-ammonium ion in sodium aluminate-sodium silicate solutions (for the preparation of ECR-1)—tend not to remain intact during the course of synthesis. More work needs to be done to clarify the role of templates, to assess the importance of Ostwald ripening, and other related processes before one can envisage reaching the state of designing a new zeolite, de novo.

One of the most fascinating aspects of crystalline microporous solids, of which zeolites and the aluminum phosphates described below are prominent subsets, is the great variety of framework types that are already known to exist, and the even larger range that is theoretically possible. Much work has been done in the enumeration of possible, as yet hypothetical structures. This follows on from the pioneering studies of *Wells*[66] who was among the first to deal systematically with the analysis of three-dimensional nets and polyhedra in relation to inorganic structures based on four-cornered, three-dimensional topologies.[67]

In such analyses, the tetrahedral junctions (or nodes) of the nets represent the Si (or Al, Ga, B etc.) so-called 'T' atoms of the zeolite, and the linkages between nodes are, in reality, oxygen bridges represented for convenience as straight lines.

2.2. Designing New $AlPO_4$-Based Molecular Sieves

In the last six years, thanks largely to the efforts of *Wilson, Lok, Flanigen* et al., many new types of open framework structures have been brought to light. Most of these have trivalent aluminum and pentavalent phosphorus as the principal occupants of the tetrahedral site, with other elements (such as Li, Be, Mg, B, Si and As) also capable of being incorporated into the tetrahedrally-bonded framework. Aluminum phosphate, either in its pure state (designated ALPO), or as the metal-aluminum phosphate (where the metal (M) can also be Li, Fe, Mn, Co, Zn and Ni) and metal-silicon aluminum phosphates (MAPO and MAPSO respectively) may take up some of the structures previously identified among the zeolitic aluminosilicates (faujasite, chabazite, sodalite, erionite, zeolite rho etc.), but quite often they adopt structures that are novel. These materials are synthesized by the use of organic amines as templates. Typical templates for generating large-pore variants are the tetrapropylammonium ion and tri-*n*-propylamine which favor the production of a hitherto unknown channel structure termed ALPO-5 (Fig. 16 left). The effective pore diameter is ca. 8 Å, comparable to that in the aluminosilicate faujasitic structure (zeolite Y), which also has twelve tetrahedral sites circumscribing the aperture. Recently, *Davis* et al.[68] have described eighteen-numbered rings in a new ALPO structure, termed VPI-5, that is believed to be a reamed out version of ALPO-5 (Fig. 16 right). The pore diameters in VPI-5 are 12 to 13 Å.

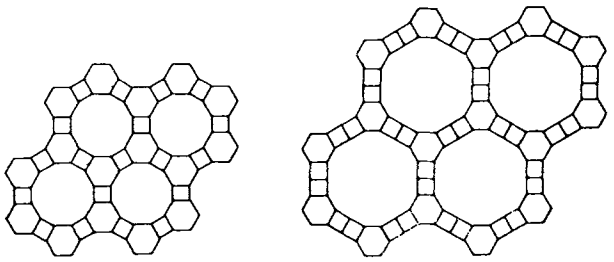

Fig. 16. Schematic structural projection drawing of the new molecular series known as ALPO-5 (left) and VPI-5 (right).

Intermediate-pore-diameter ALPOs, SAPOs, MAPOs and MASPOs (i.e. with apertures of from ca. 6 Å) are favored with amines such as di-*n*-propylamine, and small-pore analogues (diameters of ca. 4 Å) using either isopropylamine, piperidine or quinuclidine. Very small pore ALPOs (ca. 3 Å diameter) tend to be favored using tetramethylammonium ions in the mother liquid from which the ALPO is produced.

As yet, the full potential of these new, crystalline $AlPO_4$-based solids as uniform heterogeneous catalysts has not been adequately explored. The SAPOs are exceptionally good in converting methanol to olefines (with no aromatics);[69] and others are quite promising, as may be assessed from Table 3 which lists the pseudo first-order rate coefficients, for *n*-butane cracking over the corresponding molecular sieve.

Table 3. Typical catalytic performance, expressed as first-order rate coefficients, k_A for the cracking of *n*-butane over $ALPO_4$-based molecular sieves at 400°C [27].

Catalyst	k_A	Catalyst	k_A
AlPO-5	0.05	CoAPO-36	11
CoAPO-5	0.4	CoAPO-34	3.7
MnAPO-5	1.2	MnAPO-34	ca. 4.0
SAPO-5	ca. 0.2	BeAPSO-34	7.6

More will undoubtedly be heard about the variety of other uniform heterogeneous catalysts that may be derived from the $AlPO_4$-based molecular sieves, especially in the light of *Rabo*'s recent work.[69] It is interesting to observe that framework structures (such as ALPO-5) which were not known among the previously reported, and extensively researched (prior to 1988) family of aluminosilicate zeolites, have subsequently been prepared in their all-silica forms. Starting from the all-silica molecular sieve, SSZ-24, recently described by *Van Norstrand* et al.,[70] SAPO-5, in which some substitution of Si by tetrahedral Al and P atoms occurs, has also been prepared. With the aid of the technique of re-alumination,[55] and the recently derived method[50] of introducing Ti into open framework structures, enormous scope now exists for the design and synthesis of both $AlPO_4$- and SiO_2-based uniform catalysts into which delicately minute amounts of Al, Ti and other catalytically potent elements (such as Ga used for dehydrocyclization) may be introduced. Owing to fundamental differences in bonding we cannot expect *all* the SiO_2 structures exhibited to be repeated in the ALPO or SAPO series and vice versa. Geometric arguments take no account of the relative strengths and lengths of T-O bonds or of the magnitude of T-O-T angles. Aluminosilicate zeolites have T-O distances which fall in the range 1.58 to 1.78 Å and most of the T-O-T angles in the range 126 to 170°. The structures of aluminosilicate zeolites with angles close to these limits tend to be rather fragile, and the same arguments, but based on different values for (Al, P, M)-O distances and (Al, P, M)-O-(Al, P, M) angles, apply to new $AlPO_4$-based molecular sieve catalysts. It is interesting to note that, despite strenuous efforts, it seems that no one has yet prepared the ALPO analogues of the pentasils (ZSM-5, ZSM-11 and intergrowths) described by *Kokotailo* and *Meier*.[71]

The report by *Davis* et al.[68] describing VPI-5 which has pore apertures significantly larger than those hitherto found for aluminosilicate zeolites prompts speculation as to which other large-pore structures are feasible. Geometrically, and taking into account known structural patterns (combinations of secondary and tertiary building units), numerous large-pore structures may be proposed, like that shown[72] in Figure 17. Imaginative synthetic inorganic chemistry may lead, via an adroit choice of templates, to

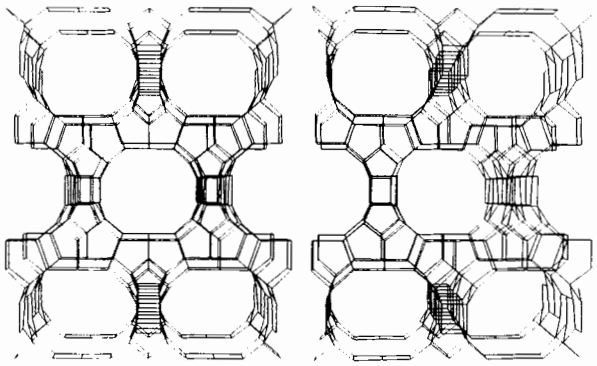

Fig. 17. One of the many possible large-pore crystalline molecular sieve catalysts (after *Akporiaye* [72]). Here there are channels intermediate in diameter between those of zeolite beta and VPI-5.

the synthesis of structures such as these. What would be helpful in this regard is sound theoretical guidance based on estimates of the relative lattice energies. In that fashion[62,73] specific structures with less intrinsic metastability, could be selected as preferred targets for synthesis. It must not be forgotten, however, that kinetic and other means of stabilization which the synthetic chemist routinely harnesses could lead to the preferential isolation of less rather than more stable structures. It must also be emphasized that isolating a new large-pore zeolitic solid is not synonymous with designing a new catalyst. The root cause of Brønsted acidity (see Fig. 5) lies in the immediate environment of the uniformly distributed heteroatom. Quantum-chemical and other arguments[74–77] show that the specific architectural detail plays a critical role in governing the detachability of protons loosely bound to the framework.

3. Uniform Clay Catalysts and their Pillared Variants

Many members of the clay mineral family exhibit powerful catalytic properties, especially after being subjected to slight changes of composition or structure. The catalytically significant centers reside, and are uniformly distributed, in the interlamellar spaces of these two-dimensional aluminosilicates. So far as acid catalysis is concerned, these centers are either the quasi-free protons generated by hydrolysis of cations such as $Al^{3\oplus}$ or $Cr^{3\oplus}$ introduced by ion-exchange, or the weak Brønsted acidic centers that are attached to interlamellar macrocations (such as the Keggin ion $[Al_{13}O_4(OH)_{24}(H_2O)_{12}]^{7\oplus}$), additional functions of which are to enhance the separation of the component sheets, to increase the surface area and to improve the thermal stability of the original clay. When the clay is used as a redox catalyst, transition-metal or other, including organometallic, cations are inserted by various chemical means[78]—either by ion-exchange of the naturally occuring or synthetic clay or during the course of synthesis—into the interlamellar region. Again there is every reason to believe that these ions, which are the catalytically active centers, are arranged in a spatially uniform fashion in the available interlamellar space.

The sheet silicates of principal interest for present purposes (i.e. montmorillonites and hectorites) have edge-sharing octahedral layers ($M(O,OH)_6$ where M is typically Al, Mg, Fe, Na, Li, etc.) flanked on either side by corner-sharing tetrahedral (SiO_4 or occasionally $(Si,Al)O_4$) layers. The octahedral and the tetrahedral layers may be partially substituted by ions of lower valency (e.g. $Mg^{2\oplus}$ or $Li^{\oplus}$ in the former and $Al^{3\oplus}$ or $Fe^{3\oplus}$ in the latter case). This confers a negative charge upon the layers and this charge is balanced by interlamellar, exchangable cations, which are often $Na^{\oplus}$ or $Ca^{2\oplus}$ in naturally occurring clays. The idealized formula of three currently used clay catalysts are:

$(Na, \frac{1}{2}Ca)_x(Si_8)^{IV}(Al_{4-x}, Mg_x)^{VI}O_{20}(OH)_4 \cdot nH_2O$ montmorillonite

$(Na, \frac{1}{2}Ca)_x(Si_8)^{IV}(Mg_{6-x}, Li_x)^{VI}O_{20}(OH)_4 \cdot nH_2O$ hectorite

$(Na, \frac{1}{2}Ca)_x(Si_{8-z}Al_z)^{IV}(Al_4)^{VI}O_{20}(OH)_4 \cdot nH_2O$ beidellite

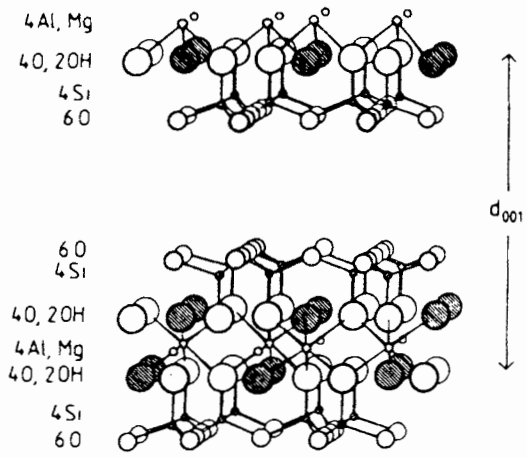

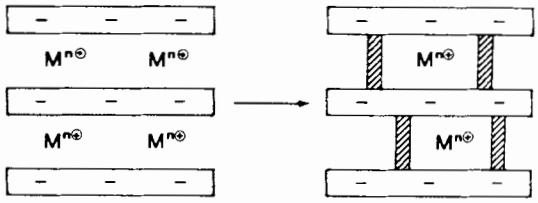

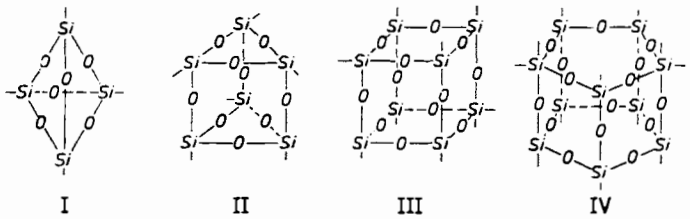

Fig. 18. Top: Schematic illustration of the structure of montmorillonite. Middle: Illustration of how a clay mineral (typically montmorillonite or beidellite) is converted into its pillared form. Bottom: Siliceous pillars (vertical hatched regions of the drawing above can have repeat units such as those shown (I to IV).

where *IV* and *VI* refer to the tetrahedrally and octahedrally cordinated ions. Figure 18 top illustrates the disposition of the constituent atoms in montmorillonite prior to ion-exchange; Figure 18 middle shows schematically, and 18 bottom in atomic detail, what is achieved in the process of pillaring. There is considerable evidence[79] for believing that the pillars are formed from the 'Al_{13}' Keggin ions and composed predominantly of pencils of alumina, the surface of which has more or less uniformly exchanged acid groups. It is possible to introduce totally siliceous (SiO_2) pillars by an ingenious[80] organo-silicon route using sesquisiloxanes. As expected, siliceous pillars possess hardly any Brønsted acidity, but other cations of catalytic significance can be accommodated uniformly elsewhere in the interlamellar space which is enlarged by the presence of the silica pillars. Ammonium ions[81] and transition-metal chelates[82] have also been used as pillaring cations, but the thermal stability of the resulting pillared clay is inadequate for general catalytic purposes. Other polycations include those of zirconium,[83] titanium,[84] iron,[85] chromium[86] as well as various of the ever-popular aluminum.[17,87,88] Alumina-crated silica pillars have also been successfully introduced. The best pillared clays for catalytic purposes have[17,74] surface areas of 200 to 500 $m^2\,g^{-1}$, pore volume of 0.15 to 0.20 mL g^{-1}, and layer spacings of 16 to 20 Å, which is the consequence of an expansion of 6 to 10 Å of the interlamellar distance of the starting material.

Synthetic hectorites, first produced by the LaPorte Company in England and subsequently named laponite, may also be prepared as fluoro derivatives, which are more thermally stable than their hydroxy analogues. Laponites are not sufficiently crystalline to yield precise X-ray structural data. Recently, large crystalline specimens of the sodium tetrasilicic mica (designated TSM) have been produced by Topy Industries, Japan. This material is a fluoro derivative and has the formula $NaMg_{2.5}Si_4O_{10}F_2$. In the as-prepared state it possesses no Brønsted acidity.

A selection of the reactions that are catalyzed by clay-based solids is shown in Table 4. These are acid (proton)-catalyzed reactions of the type illustrated mechanistically in Figure 19. Other non-acid catalyzed reactions which have been explored by *Morikawa* et al.,[78] are represented by the selection shown in Figure 20. Further details about the optimal conditions and mechanistic features of these reactions have been given elsewhere.[4,90,96] Briefly, proton-catalyzed conversions, similar to those that occur with uniform zeolitic catalyst, take place within the interlamellar spaces.

Table 4. A selection of organic reactions catalyzed by clays. [9–12, 95, 96]

Cracking and hydrocracking of hydrocarbons
Dehydration of alkanols, with the formation of ethers, alkenes, and naphthenes
Isomerizations, alkylations, and cyclizations
Conversion of primary amines to secondary ones
Dimerizations, oligomerizations, and polymerizations
Oxidations and reductions
Hydration, alkylation, and acylation of alkenes to form alkanols, ethers, and esters
Hydrogen exchange and hydrodesulfurizations
Decarboxylations and lactonizations
Polycondensations (e.g., peptides from amino acids)

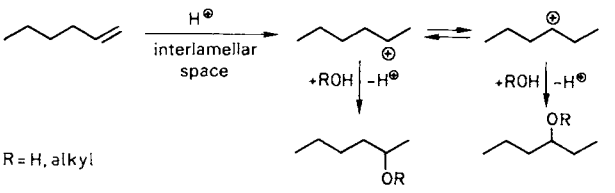

Fig. 19. The interlamellar regions of certain clays function as uniform acidic heterogeneous catalysts for the production of alcohols and ethers from alkenes [9, 96].

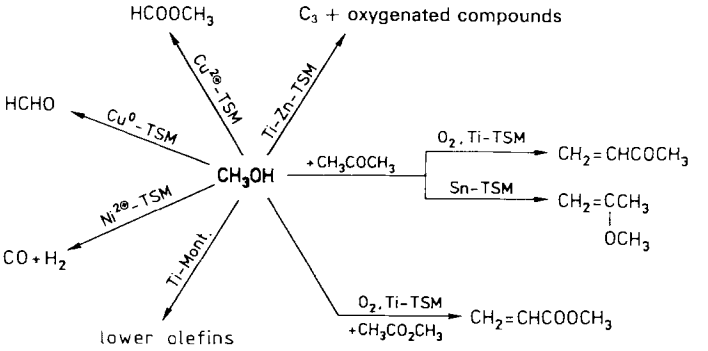

Fig. 20. A selection of non-acid-catalyzed reactions of metal-substituted clays [78].

3.1. Prospects for Designing More Effective Clay Catalysts

We have already seen that synthesizing the fluoro analogues of naturally occurring clays improves their thermal stability (compare fluorohectorite with ordinary hectorite) and that fluorotetrasilicic mica (FTSM) can be prepared in such good states of crystallinity and swellability (after intercalation) that they are amenable to single-crystal X-ray structural analysis. We also note that there are already a number of alternatives for introducing thin pillars into the interlamellar region, thereby enhancing the all-round catalytic performance of the clay.

Further scope exists for designing better clay catalysts. Thus, $Li^{\oplus}$ ions may be diffused into the octahedral sublattice of certain montmorillonite clays, leading to a reduction in the density of negative charge on the individual layers.[97] This in turn reduces the cation-exchange capacity of the clay catalyst and, if it were subsequently pillared, one would expect the pillar separation distance to increase (see Figure 18 middle).

Another strategem for structural variation is suggested by recent Chinese work on rectorite clays, which are interstratified at the unit-cell level and consist of thin sheets of mica in a more or less regularly spaced matrix of a swellable montmorillonite clay. Pillaring of such interstratified material leads to a more thermally resistant product than those derived from other clays. The challenge now is to devise inorganic syntheses so as to generate the best possible combination and sequence of interstratified aluminosilicates. In this connection, beidellite, which bears its surplus negative charge in the tetrahedral rather than the octahedral sub-lattice,[14,15] may have advantages over montmorillonite in view of the ostensible ease of 'keying' Keg-

gin-like cations to the sheets, thereby strengthening the binding of the pillar to the sheet. Further scope also exists in chemically derivatizing the cylindrical surfaces of the pillars with well-defined, accessibly and uniformly arranged 'active sites'.

All these design features, if successful, would lead to two-dimensional analogues of solids but with substantially enlarged pore-apertures (> 15 Å). Amongst other things such hosts, with polyvalent cations capable of hydrolyzing water, such as $La^{3\oplus}$ or $Al^{3\oplus}$, would be suitable for the catalytic cracking and hydrocracking of molecules a good deal larger than those that can be so processed by $La^{3\oplus}$-exchanged faujasitic zeolites.

4. Uniform Oxide Catalysts

Whereas in uniform zeolitic catalysts there are discrete active sites, such as framework $Al^{3\oplus}$ ions in the aluminosilicate framework or extra-framework $La^{3\oplus}$ ions with their associated protons loosely bound to the framework, in the oxide catalysts that concern us here the situation is quite different. In this type of uniform heterogeneous catalyst all the oxygen of the structure is potentially implicated in the catalytic oxidation: the reactant combines with, and removes, the oxygen situated at the surface of the solid, but the sacrificial loss of oxygen is made good by assimilation of gaseous oxygen into the solid allowed by its conversion to oxide ions and the migration of the latter throughout the bulk catalyst. During this kind of catalysis the oxide is rendered non-stoichiometric (oxygen deficient), the extent and nature of which is governed by the prevailing conditions.

Several industrially important processes[98, 100] utilize uniform heterogeneous oxide catalysts, the best known being the ammoxidation of propylene to acrylonitrile and its oxidation to acrolein (over bismuth molybdates). But there are many other laboratory-scale reactions where it has been established that such oxide catalysts function in the sacrificial manner described above. Oxide catalysts of this kind also figure eminently in certain electrocatalytic processes,[101, 102] such as the oxidation of methane, and in autoemission exhaust systems.[103] There are doubtless many other oxidation processes which use oxide catalysts of one kind or another where it has not yet been confirmed that structural oxygen is implicated.

4.1. Fluorites and Perovskites as Uniform Catalysts

What is it that enables some oxides to release their structural oxygen reversibly so as to form grossly non-stoichiometric intermediates and thereby to function as efficient oxidation catalysts? Why, for example, are perovskite-based structures so prominent among this category of catalyst? We do not, as yet, know the answer to these questions; but accumulated chemical experience teaches us to use analogies between different types of perovskite and other structures, so that some progress can be made in the search for more efficient and specific catalysts.

One of the key attributes of a desired new uniform oxide catalyst is its ability to sustain gross non-stoichiometry. The solid-state chemist knows that it is no easy task to predict which oxide structures are favorable in this regard. Thus TiO_2 in the form of rutile, but not in the form of either of the other two principal polymorphs anatase and brookite (which are quite similar to rutile in the coordinates of the $Ti^{4\oplus}$ ion) is easily rendered grossly non-stoichiometric (e.g. TiO_x, $1.5 < x < 2.0$). MgO, which has the rock salt structure, is incapable of housing high concentrations of point defects, whereas in solid solutions of MnO and MgO that also have the rock salt structure, a substantial fraction of the oxygen atoms can be removed without changing the structure. Again, with oxides of the AO_2 type, those that crystallize with the fluorite structure, provided the A cation is capable of variable valency, can often be rendered grossly non-stoichiometric; yttrium-stabilized zirconia, for example, has many anion vacancies, a typical example being $Zr_{0.83}Y_{0.17}O_{1.915}$. For structures such as ABO_3, those that have the pyroxene or wollastonite structure seem incapable of being rendered non-stoichiometric by loss of oxygen, whereas in the perovskite structure (Fig. 21), they can be accommodated in non-stoichiometric forms. In addition to the requirements of valency, it seems that the structure's elastic properties are crucial in governing ease of formation of high concentrations of point defects and especially of planar faults. But the whole question of non-stoichiometry in binary and ternary metal oxides is a complicated one, and even the broad outline of the determinative principles are not yet clear.

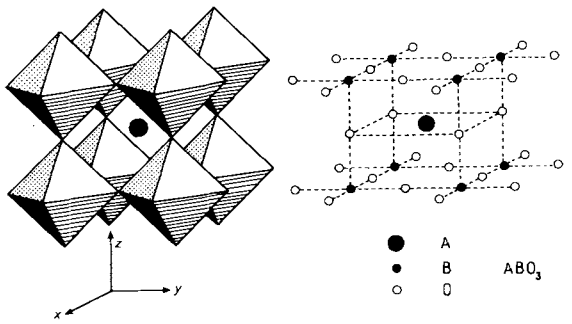

Fig. 21. Two schematic representations of the idealized perovskite ($CaTiO_3$) structure. The B site in ABO_3 is octahedrally coordinated to oxygen.

4.2. Bismuth Molybdates and Calcium Manganates

Experiments that use[22, 104] isotopic labelling as well as secondary ion mass spectrometry (SIMS) point unmistakenly to the participation of bulk oxygen, which migrates to the seat of a reaction at the surface of the oxide catalyst and is made good by dissolution and subsequent compensatory reduction of gaseous oxygen. This is true of the bismuth molybdates,[98–100] of which the α- ($Bi_2Mo_3O_{12}$), β- ($Bi_2Mo_2O_9$) and γ-phases (Bi_2MoO_6) are the best known, in the selective oxidation and ammoxidation of alkenes. The first step in each of these selective oxidations is the abstraction of hydrogen from the alkene at a bismuth center to produce allylic intermediates (π-complex). This intermediate then forms a σ-bonded complex and finally a second hydrogen is abstracted (Fig. 22). Mechanistic details of these conversions are described elsewhere.[98, 99]

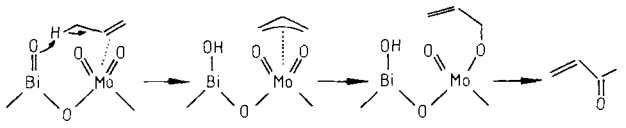

Fig. 22. The selective oxidation of propene over a bismuth molybdate catalyst proceeds via an allylic intermediate complex.

For a long while the broadly similar catalytic performance of the α-, β- and γ-phases was difficult to reconcile with the seemingly quite different crystallographic structures of the respective phases. (The α-phase, $Bi_2Mo_3O_{12}$, has been described as a defect scheelite structure. Scheelite itself ($CaWO_4$) has ABO_4 repeat units in which the A cation is eight-coordinated by oxygen and the B cation is hexavalent and present as discrete BO_4 tetrahedra. The α-phase can be regarded as a structure containing one cation vacancy (□) for every two $Bi^{3\oplus}$ ions and may be written as $Bi_{2/3}\square_{1/3}MoO_4$. The β-phase, $Bi_2Mo_2O_9$, has a defect fluorite structure, the $Bi^{3\oplus}$ being in eight-fold coordination and again there are distorted MoO_4 tetrahedra. Below about 570 °C the structure of the γ-phase, Bi_2MoO_6, is that of the rare mineral koechlinite, where there are alternating sheets of $Bi_2O_2^{2\ominus}$ and $MoO_4^{2\ominus}$, the latter being composed of corner-sharing MoO_6 octahedra.) With such variety in crystal structure, and in particular in the coordination of the hexavalent Mo, it was puzzling that the catalytic performance of all three phases was so similar. Recent work[105] using electron diffraction and high-resolution electron microscopy, has shown that these ostensibly different bismuth molybdates—as well as others—can all be considered as defect fluorites (Fig. 23–25). The α-phase may readily be regarded as a defect fluorite structure if one allows for small displacements of some of the oxygens.

Recognizing that essentially all of the catalytically active bismuth molybdates possess the same kind of fluorite based structure—like δ-Bi_2O_3 itself, which may be written as $Bi_{2/3}O_{3/2}\square_{1/2}$, where ◘ now stands for an oxygen vacancy—it is not surprising in broad terms that the catalytic performance of the respective phases are so comparable. But this conclusion does presuppose that the surfaces of all these catalysts are also comparable structurally. It is not certain how different the surfaces of these solids are, in their active catalytic state, from those of the bulk solids. Compositional changes under operating conditions can certainly be expected.[106]

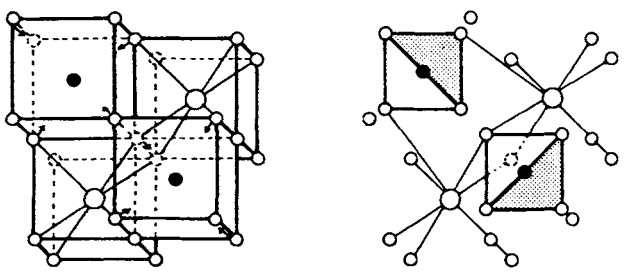

Fig. 23. Modification of a single fluorite-like unit cell, containing two bismuth and two molybdenum atoms (left) to produce two MoO^4 tetrahedra, schematically shown right. Movement of oxygen atoms in the left picture is indicated by arrows [105].

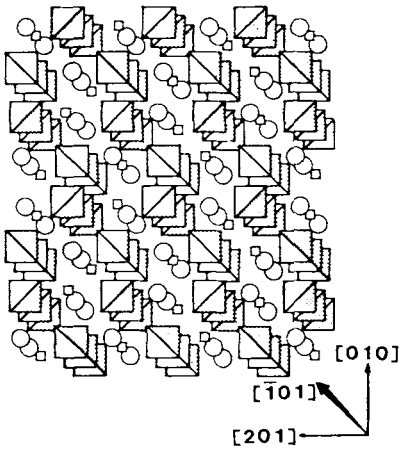

Fig. 24. Schematic clinographic projections of the $Bi_2Mo_3O_{12}$ structure, viewed down [$\bar{1}$01] axis, showing the two fluorite-like axes down which bismuth and molybdenum atoms do not superimpose. Vacant bismuth sites are denoted by □.

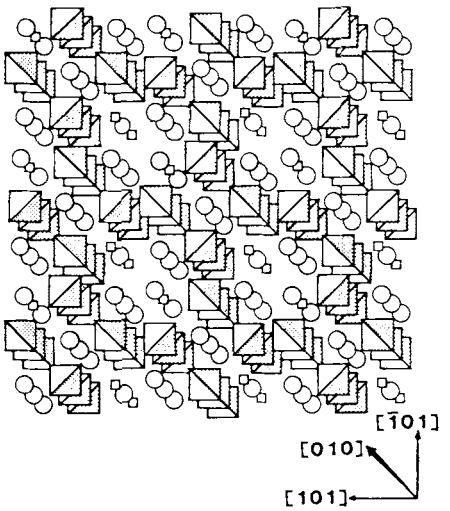

Fig. 25. Clinographic projection of the structure of $Bi_2Mo_2O_9$, viewed down [010] axis.

Bismuth molybdate catalysts are not always based on the defect fluorite structure. When some of the Mo is replaced by hexavalent W, forming a solid of stoichiometry $Bi_2(Mo,W)_{12}O_{35}$ a totally novel structure (established by HREM) is formed[107, 108] (Fig. 26). Here there are interleaved layers of bismuth oxide and mixed Mo-W oxides. In the latter, which are six corner-sharing octahedra in height, there are both corner-sharing and edge-sharing $(Mo,W)O_6$ octahedra parallel to the layers. Along the layers, at regular intervals, are crystallographic shear (CS) planes at which, locally, corner-sharing is replaced by edge-sharing of the $(Mo,W)O_6$ units. The presence of these CS planes modifies the stoichiometry of the six octahedra wide layers from $(Mo,W)O_3$ to $(Mo,W)_2O_5$; and the stoichiometry of the bismuth oxide, cationic layer, from Bi_2O_2 (which is what it is in koechlinite) to Bi_2O_3. It is very likely that numerous other structures of bismuth oxide-based selective oxidation catalysts are built up on these general principles: variable composition can be adapted by varying the thickness of the corner- and edge-sharing of the oxide layers and also by changing the spacing of the shear

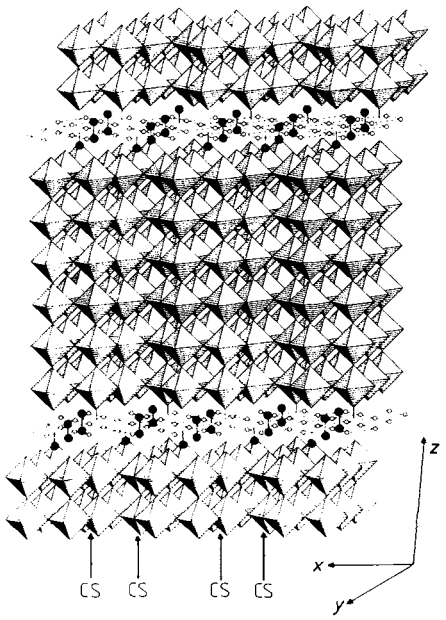

Fig. 26. This hitherto unknown structure for the uniform selective oxidation catalyst $Bi_2(Mo,W)_{12}O_{35}$ was deduced from high-resolution electron microscopic imaging and related techniques [107, 108]. The crystallographic shear (CS) planes (see text) are perpendicular to the sheets of bismuth oxide.

planes. It is possible that, during the course of a particular catalytic reaction, given the lability of compositional oxygen, that the spacings of CS planes, and the accompanying composition of the $Bi_2O_2^{2\oplus}/Bi_2O_3$ layer, may undergo dynamic change.

Many metal oxides ABO_3 possessing the perovskite structure ($CaTiO_3$) have been known to exhibit promising catalytic properties.[103] One such oxide, $CaMnO_3$, selectively oxidizes[24] propene to benzene and 2-methyl propene to *para*-xylene. In so doing the solid itself is converted into more or less grossly non-stoichiometric products, $CaMnO_{3-x}$, where x is, typically, 0.20 or 0.25. Many other perovskites display similar properties; and although not all perovskitic solids of formula ABO_{3-x} are catalytically active, it is well-known that many of them can be converted relatively easily, by progressive removal of oxygen, to the stage $ABO_{2.5}$ without disrupting the structural integrity—apart from creating oxygen vacancies—of the perovskite. $CaFeO_{2.5}$ for example,[109] the product of reduction of the ferrite, $CaFeO_3$, is made up of stacks of alternate layers of FeO_6 octahedra and FeO_4 tetrahedra. This structure corresponds to that of the naturally occurring mineral brownmillerite. Variants of this structure have been reported by *Bando* et al.[110] in $Ca_4YFe_5O_{13}$ and by *Alario-Franco* et al.[111] in $Ca_2LaFe_3O_8$ and $Ca_xLa_{1-x}FeO_{3-y}$.

For intermediate phases between perovskite-like ABO_3 and brownmillerite-like $ABO_{2.5}$, *Grenier* et al.[112] argued that there were $n-1$ perovskite-like layers of BO_6 octahedra alternating with one layer of BO_4 tetrahedra. Such structures undoubtedly exist for certain kinds of transition-metal ions B. For $CaMnO_3$, however, *Reller* and others[24, 113] have shown that square-pyramidal (MnO_5) entities—similar to those in $Na_4Mn_2O_5$ as was first reported by *Brachtil* and *Hoppe*[114]—are produced in ordered states with progressive reduction of the $CaMnO_3$ to its grossly non-stoichiometric forms. The essence of the conversion from $CaMnO_3$ to $CaMnO_{2.5}$ is symbolized in Figure 27.

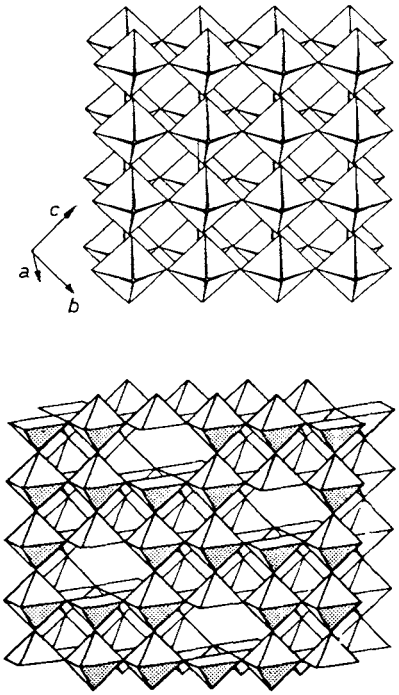

Fig. 27. Top: The ReO_3-type structure shown here has corner-sharing (MO_6) octahedra, which are also present, along with the A atoms at the center of a cube of such octahedra, in the perovskite structure (see Fig. 21). Bottom: When the uniform heterogeneous catalyst $CaMnO_3$ is used in the selective oxidation of propene it can be converted to non-stoichiometric variants, one of which is shown here (for simplicity without the $Ca^{2\oplus}$ ions). Oxygen removal from the solid converts MO_6 octahedra to MO_5 square pyramids [113].

Ideally, the way to explore precisely which ordered, non-stoichiometric phases of ABO_{3-x} are the most catalytically active and selective, and at the same time to test the ease with which oxygen is released and regained by the active catalyst, is to employ an in-situ crystallographic method of study. In principle, transmission electron microscopy is capable of uncovering such information. But it is not easy to perform the necessary experiment in the appropriate microscope hot-stage. Sensible progress can, however, be made by ex situ studies combining selected-area electron diffraction, high-resolution imaging and optical diffractometry. (All of these are essentially 'bulk' methods, but since we are dealing with uniform heterogeneous catalysts they are perfectly valid probes.)

Reller et al.[24] have arrived at the structural character of five distinct, grossly non-stoichiometric solids: $CaMnO_{2.88}$, $CaMnO_{2.75}$, $CaMnO_{2.667}$, $CaMnO_{2.556}$ and $CaMnO_{2.5}$. And although oxygen migration within these solids was not studied, the subtlety of the adapted structure *for a given composition* could be ascertained. For $CaMnO_{2.5}$, for example, five distinct structures were discovered differing in their superlattice character one from the other. Schematic drawings of two of these are shown in Figure 28. (Note the presence of the square-pyramidal MnO_5 units, formed by loss of oxygen from MnO_6 octahedra.)

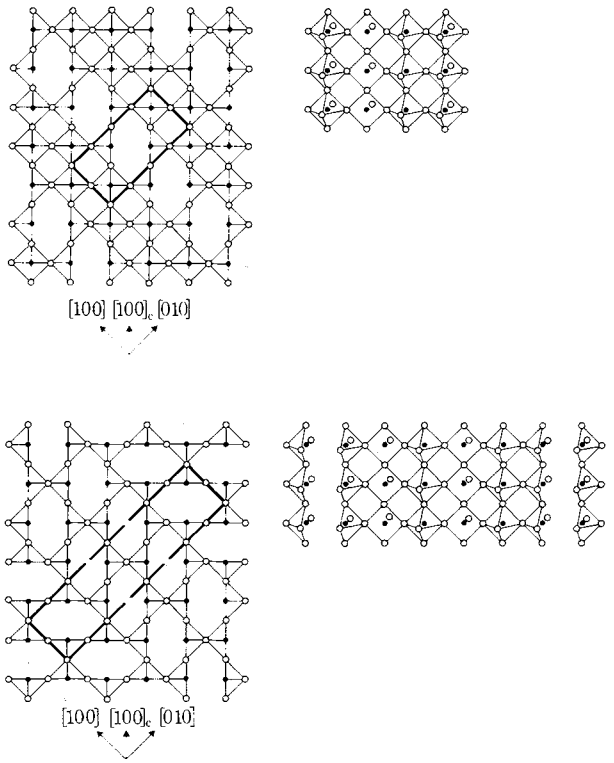

Fig. 28. Top: Schematic drawing of one of the many structures taken up by the uniform oxidation catalyst $CaMnO_{2.5}$. There is a supermesh, shown in thick outline, of $2\sqrt{2} \times \sqrt{2}$ times the parent one and rotated by 45°. Bottom: Another structure found by *Reller* et al. [113] for the $CaMnO_{2.5}$ catalyst. Here the supermesh, also rotated, is $4\sqrt{2} \times \sqrt{2}$. In both drawings small dotted circles denote location of the $Ca^{2\oplus}$ ions in the parent perovskite structure.

There are other perovskites[115, 116] which exhibit catalytic properties (see Table 1) in the oxidation of hydrocarbons. $Ba_2Bi_2LaO_6$ and its non-stoichiometric (oxygen deficient) variants ($Ba_2Bi_{2-x}La_xO_{6-y}$) are one set of examples. The recently discovered high-T_c superconductors $YBa_2Cu_3O_{7-\delta}$ ($0 \leqslant \delta \leqslant 1$) are another. It is not yet established whether, as in the bismuth molybdates, sacrificial loss of oxygen is a cardinal feature of the catalysis. But it is quite clear[117] that there can be facile loss and gain of oxygen into structures such as $YBa_2Cu_3O_{7-\delta}$ at the low temperatures required for catalysis freely to proceed. A new family[118] of related metallic oxides, derived from perovskite by loss of oxygen (e.g. $La_4BaCu_5O_{13}$—see Fig. 29),

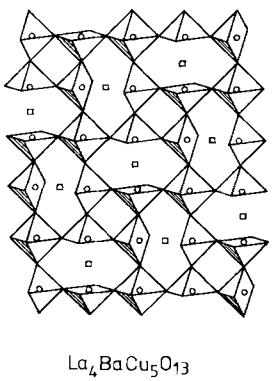

Fig. 29. Schematic representation of the recently reported [118] metallic oxide which is replete with ordered vacancies (compare Fig. 27 bottom).

can also be rendered grossly non-stoichiometric. But little is known as yet of the chemical properties of these fascinating complex oxides. They are, however, likely to function as oxidation catalysts, just as $YBa_2Cu_3O_{7-\delta}$ catalyze the following reactions:

$$CO + \tfrac{1}{2}O_2 \longrightarrow CO_2$$

$$2\,NO \longrightarrow N_2 + O_2$$

$$C_6H_5CH_3 \xrightarrow[O_2]{NH_3} C_6H_5CN$$

On the basis of work done by *Jacobson* et al.[115, 116] who studied the ease of generating non-stoichiometric perovskites as a function of the cation constituents, it is clear that much scope exists to fine-tune the performance of new uniform, selective oxidation catalysts. They studied perovskites of composition $A_2BB'O_6$ in which the initial (stoichiometric) structure shows B-cation order when there were large differences in charges and radii of B and B'. This happens in Ba_2LaBiO_6 for example. They found that on increasing x in the series $Ba_2Bi_{2-x}La_xO_{6-y}$ ($0 \leqslant x \leqslant 1$) more severe reducing conditions were required to reduce the $Bi^{5\oplus}$ ions completely. They concluded that removal of oxygen from this structure is relatively easy from Bi^{V}-O-La^{III} and Bi^{V}-O-Bi^{III} structural units, and that cation disorder increases the probability of occurrence of Bi^{V}-O-Bi^{III} linkages. This family of non-stoichiometric uniform oxides are good heterogeneous catalysts for the oxidation of propene to benzene and 2-methyl propene to *para*-xylene.

4.3. Aurivillius, Sillén and Related Structures

The discovery[105] that at least six of the bismuth molybdate phases are based on the defect fluorite structure prompted *Zhou* et al.[119–121] to re-investigate the structural principles displayed by so-called solid solutions in other systems, notably Bi_2O_3-WO_3, Bi_2O_3-Nb_2O_5, Bi_2O_3-V_2O_5 and Bi_2O_3-Ta_2O_5. The full potential of the catalytic performance of these solids remains to be explored; but at least some of them exhibit catalytic activity, both thermal and photo-induced.[122] Their structures, which have been the subject of systematic investigation by combined electron diffraction and electron microscopy, are quite remarkable, and the salient features are summarized in Figure 30. Depending upon the precise compositional range and the pair of metals involved, the 'solid solutions' are found to take up large superlattices based on fluorite, or pyrochlore, or perovskite, and two other phases. One of these has the well-known Aurivillius structure (which is a regular interleaving of $Bi_2O_2^{2\oplus}$ and anionic perovskitic layers), the other is a unit-cell-level hybrid of pyrochlore and perovskite subunits.

Recently, layered bismuth oxyhalides belonging to the large class of structures first identified by Sillén,[123] such as $MBi_3O_4X_2$ (M = Na, K ..., X = F, Cl, Br) have been found[124] to be promising hydrocarbon oxidation catalysts. Their structures are shown in Figure 31. It is not yet known whether these solids are genuinely uniform heterogeneous oxide catalysts, but they have been shown[125] to lose oxygen rather freely during contact with one or more hydro-

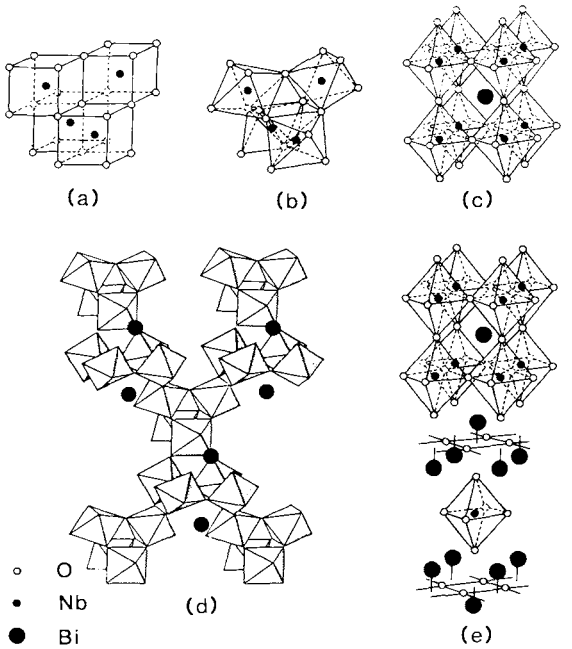

Fig. 30. Depending upon the precise composition, the so-called solid solutions formed between Bi_2O_3 and oxides such as Nb_2O_5, V_2O_5 etc. take up well-defined superstructures based on fluorite (a), pyrochlore (b), perovskite (c), half perovskite-half pyrochlore (d) and the Aurivillius structure (e) (see text) [119, 121].

carbon reactants. Several novel structures, including unit-cell-level intergrowth structures formed from an Aurivillius and Sillén phase end-member (general formula $(Bi_2O_2)^{2\oplus}Cl^{\ominus}(Bi_2O_2)^{2\oplus}(A_{n-1}BO_{3n+1})$ where the A and B cations are two- and six-coordinated respectively as in a perovskite), can be formed[126] and these, as well as others,[127] show some promise as oxidation catalysts.

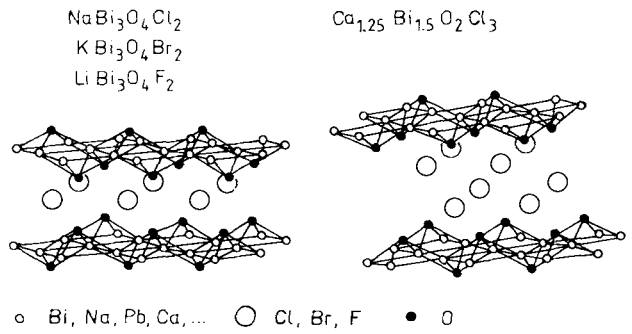

Fig. 31. Examples of the Sillén-type structures taken up by certain layered bismuth oxychlorides which are [124] promising hydrocarbon oxidation catalysts.

5. Epilogue

Many seemingly widely different types of heterogeneous catalysts, encompassing a variety of structures and compositions, are seen to belong to the same family, the key characterizing feature of individual members of which is their spatial uniformity. Apart from its practical convenience, this classification, by uniting a large number of distinct materials, reinforces the role that the design and synthesis of new solids in general can play in formulating and preparing new heterogeneous catalysts in particular. It also demonstrates the applicability of most of the structural techniques of solid-state chemistry to the central problems associated with the characterization of the growing class of inorganic catalysts, many of which already figure eminently in processes conducted on the industrial scale (see Table 1).

As tends to happen with all classifications, distinctions sometimes become blurred. With zeolitic catalysts, for example, there are two situations under which it is no longer true that all the active sites are uniformly distributed throughout their bulk. First, some of the active elements of the framework (e.g. $Al^{3\oplus}$ in the tetrahedral macroanion) may be partially leached out into intra-zeolitic cavities. Such detrital aluminous material may itself be catalytically significant. Often this is quite uniformly distributed but not invariably so. Second, when platinum or other noble metal species are atomically or very finely (ca. 5 Å diameter) distributed inside a zeolite so as to confer upon the catalyst the bifunctional character, it is found that the minute particles of platinum, initially uniformly distributed, tend to accrete, sinter and grow. The resulting catalyst may still retain its uniformity so far as its Brønsted acidity is concerned, but with respect to the platinum it now develops features more akin to category 1 (see Table 1) catalysts. Likewise, with clay and pillared clay catalysts, when they collapse, as sometimes occurs on extended use, they are no longer uniform and only their exterior surfaces are catalytically active, again resembling materials in category 1. With oxides it is occasionally found that, even at the outset, the sacrificial loss of oxygen and its subsequent replenishment is restricted to the exterior surface—the entire bulk of the oxide is not implicated. Additionally, some oxide catalysts which undoubtedly operate via sacrificial loss of structural oxygen, exhibit superior performance when in contact with a second or third solid component, usually an oxide. Under these circumstances it is no longer adequate to talk of uniform heterogeneous catalysts. With selective hydrogenation catalysts like the well known copper chromite system,[128] where uniformly distributed platinum particles serve as gateways for the release of hydrogen held as in a reservoir within the bronze, it may also be profitable to place this type of "reverse spillover"[128, 129] catalyst into category 2. And it may well transpire that very finely divided metallic catalysts of colloidal dimension may also be best regarded as spatially uniform in the sense defined here.

In the main, however, the merits of identifying the existence of uniform heterogeneous catalysts are considerable both on practical and other grounds. One particular advantage of recognizing the importance of the structure of the entire solid catalyst, not merely that of its surface, is that the chemist has at his disposal a wide sweep of new routes for the preparation of new catalysts. Since many of these have to be produced as metastable solids the elegant variations of structure pioneered for metal oxides by *Magneli*,[130] who first prepared the hexagonal tungsten bronze form of WO_3 (Fig. 32 which should be compared with Figure 27 top) may be implemented in the realm of the sacrificial metal oxides just as they have been already in the zeolites and the aluminum phosphates. In this regard, the

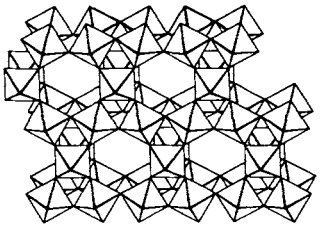

Fig. 32. Structure of hexagonal WO_3 showing one-dimensional tunnels [130].

set of 'soft' chemical principles—termed 'chimie douce' by their French originators, *Rouxel, Livage* and *Figlarz*[131-133] and already widely exploited by others[134-139] in other contexts—have a role to play in the production of new uniform heterogeneous catalysts.

Another important advantage of recognizing the bulk, solid-state chemical essence of uniform catalysts is that new powerful conceptual advances[140,141] in the use of equipotential and minimum potential surfaces for the deeper understanding of chemical properties can be readily applied to this class of heterogeneous catalysts.

Received: August 22, 1988 [A 703 IE]
German version: *Angew. Chem. 100* (1988) 1735

[1] J. A. Rabo, *Catal. Rev. Sci. Eng. 24* (1982) 202.
[2] E. G. Derouane in M. S. Whittingham, A. J. Jacobson (Eds.): *Intercalation Chemistry*, Academic Press, New York 1982, p. 101.
[3] W. O. Haag, R. M. Lago, P. B. Weisz, *Nature (London) 309* (1984) 589.
[4] J. M. Thomas, *Proc. Int. Congr. Catal. 8th 1* (1984) 31.
[5] S. Ramdas, J. M. Thomas, A. K. Cheetham, P. W. Betteridge, E. K. Davies, *Angew. Chem. 96* (1984) 629; *Angew. Chem. Int. Ed. Engl. 23* (1984) 671.
[6] W. Hölderich, M. Hesse, F. Naumann, *Angew. Chem. 100* (1988) 232; *Angew. Chem. Int. Ed. Engl. 27* (1988) 226.
[7] A. Weiss, *Clays Clay Miner. 10* (1963) 191.
[8] A. Weiss, *Angew. Chem. 93* (1981) 843; *Angew. Chem. Int. Ed. Engl. 20* (1981) 850.
[9] J. M. Thomas in [2], p. 55.
[10] T. J. Pinnavaia, *Science (Washington) 220* (1983) 365.
[11] J. A. Ballantine, J. H. Purnell, J. M. Thomas, *J. Mol. Catal. 27* (1984) 157.
[12] R. M. Barrer, *Philos. Trans. R. Soc. London A 311* (1984) 333.
[13] D. E. W. Vaughan, R. J. Lussier, *Proc. Int. Conf. Zeolites 5th 1980*, 94.
[14] P. A. Diddams, J. M. Thomas, W. Jones, J. A. Ballantine, J. H. Purnell, *J. Chem. Soc. Chem. Commun. 1984*, 1340.
[15] D. Plee, F. Borg, L. Gatineau, J. J. Fripiat, *J. Am. Chem. Soc. 107* (1985) 2362.
[16] D. T. B. Tennakoon, W. Jones, J. M. Thomas, *J. Chem. Soc. Faraday Trans. 1 82* (1986) 3081.
[17] J. W. Johnson, J. F. Brody in M. M. J. Treacy, J. M. Thomas, J. M. White (Eds.): *Microstructure and Properties of Catalysts (Mater. Res. Soc. Symp. Proc. 111* (1988) 257).
[18] P. Mars, D. W. van Krevelen, *Chem. Eng. Sci. Suppl. 3* (1954) 41.
[19] A. W. Sleight in J. J. Burton, R. L. Garten (Eds.): *Advanced Materials in Catalysis*, Academic Press, New York 1977, p. 181.
[20] R. K. Grasselli, J. D. Burrington, *Adv. Catal. 30* (1981) 133.
[21] W. M. H. Sachtler, N. H. de Boer, *Proc. Int. Congr. Catal. 3rd 1965*, 252.
[22] C. R. Adams, T. Jennings, *J. Catal. 2* (1963) 63.
[23] J. Haber, *Catal. Sci. Technol. 2* (1981) 13.
[24] A. Reller, J. M. Thomas, D. A. Jefferson, M. K. Uppal, *Proc. R. Soc. London A 394* (1984) 223.
[25] S. T. Wilson, B. M. Lok, C. A. Messina, T. R. Cannon, E. M. Flanigen, *J. Am. Chem. Soc. 104* (1982) 1146.
[26] B. M. Lok, C. A. Messina, R. L. Patton, T. R. Gajeh, T. R. Cannon, E. M. Flanigen, *J. Am. Chem. Soc. 106* (1984) 6092.
[27] E. M. Flanigen, B. M. Lok, R. L. Patton, S. T. Wilson in P. A. Jacobs (Ed.): *New Developments in Zeolite Science and Technology*, Elsevier, Amsterdam 1986, p. 103.
[28] S. I. Zones, *US-Pat. Nr. 4665110*, 1987.
[29] a) P. J. Grobet, J. Martens, P. A. Jacobs (Eds.): *Innovation in Zeolite Materials Science*, Elsevier, Amsterdam 1987; b) J. M. Bennett, B. K. Marcus in [29a], p. 209.
[30] E. A. Mamedov, *Russ. Chem. Rev. Engl. Transl. 50* (1981) 291.
[31] This is not to imply that the solid catalyst is totally free of coherent intergrowths of various kinds [32] or of zoning or other structural defects. Rather, we use the term uniform in the sense that, within a given microregion of the catalyst, the active sites are present uniformly throughout that spatially specified region.
[32] C. N. R. Rao, J. M. Thomas, *Acc. Chem. Res. 18* (1985) 113.
[33] D. C. Phillips, *Proc. Natl. Acad. Sci. USA 57* (1967) 484.
[34] A. R. Fersht: *Enzyme Structure and Mechanism*, Freeman, New York 1977.
[35] A. J. Russell, A. R. Fersht, *Nature (London) 328* (1987) 496; A. R. Fersht, J.-P. Shi, A. J. Wilkinson, D. M. Blow, P. Carter, M. M. Y. Waye, G. P. Winter, *Angew. Chem. 96* (1984) 455; *Angew. Chem. Int. Ed. Engl. 23* (1984) 467; E. T. Kaiser, *ibid. 100* (1988) 945, and *27* (1988) 913, respectively.
[36] *Lehn* gives an excellent overview in his Nobel lecture: J.-M. Lehn *Angew. Chem. 100* (1988) 91; *Angew. Chem. Int. Ed. Engl. 27* (1988) 89.
[37] G. A. Somorjai, *Pure Appl. Chem. 60* (1988) 1499.
[38] G. Ertl, J. Küppers: *Low Energy Electrons and Surface Chemistry*, VCH Verlagsgesellschaft, Weinheim 1985.
[39] a) H. Knözinger, B. G. Gates, H. H. Lamb, *Angew. Chem. 100* (1988) 1162; *Angew. Chem. Int. Ed. Engl. 27* (1988) 1127; b) C. O'Donohae, J. K. A. Clarke, J. J. Rooney, *J. Chem. Soc. Chem. Commun. 1979*, 649; c) E. L. Muetterties, T. N. Rhodin, E. Band, C. F. Bucker, W. R. Pretzer, *Chem. Rev. 79* (1979) 91; d) N. D. S. Canning, R. J. Madix, *J. Phys. Chem. 88* (1984) 2437; e) Y. I. Yermakov in B. N. Kuznetsov, V. A. Zakharov (Eds.): *Catalysis by Supported Complexes*, Elsevier, Amsterdam 1982, p. 1; f) W. H. Weinberg, *J. Am. Chem. Soc. 108* (1986) 1824; g) Chong Zheng, Y. Apeloig, R. Hoffmann, *ibid. 110* (1988) 749.
[40] J. T. Yates, J. N. Russell, S. M. Gates in R. Vanselow, R. F. Howe (Eds.): *Chemistry and Physics of Solid Surfaces, Vol. 6 (Springer Ser. Surf. Sci. 5)*, Springer, Berlin 1986, p. 237.
[41] There are *very* few techniques that are suited to probe transition state characteristics in chemical kinetics. When one talks of a time-resolved experiments it is reckoned to be a great achievement if nanosecond time-scales are reached. But this is still some five orders of magnitude too slow for tracking the fundamental dynamics of chemical change. Only very recently has femtosecond real-time dynamics been reached [M. J. Rosker, T. S. Rose, A. H. Zewail, *Chem. Phys. Lett. 146* (1988) 175; M. J. Rosker, M. Dantus, A. H. Zewail, *Science (Washington) 241* (1988) 1200] in simple, gas-phase reactions. With this temporal discrimination the potential energy surfaces of the transition-state can be explored.
[42] J. M. Thomas, C. R. A. Catlow, *Prog. Inorg. Chem. 35* (1987) 1.
[43] X. D. Zhu, H. Suhr, Y. R. Shen, *Phys. Rev. B 35* (1987) 3047.
[44] I. E. Maxwell, *Adv. Catal. 31* (1982) 1.
[45] W. J. Mortier, R. A. Schoonheydt, *Prog. Solid State Chem. 16* (1985) 1.
[46] G. K. Boreskov, K. M. Minachev (Ed.): *Applications of Zeolites in Catalysis*, Akademiai Kiado, Budapest 1979.
[47] H. Heinemann, *Catal. Sci. Technol. 1* (1981) 1; see also: K. Hedden, J. Weitkamp, *Chem. Ing. Tech. 55* (1983) 907; C. Besoukhanova, D. Barthomeuf, J. Guidot, M. Breysse, J. R. Bernard, *J. Chem. Soc. Faraday Trans. 1 77* (1981) 1595.
[48] M. F. M. Post, T. Huisingia, G. A. Emeis, J. M. Nanne, W. H. T. Stork, personal communication.
[49] J. M. Thomas, J. Klinowski, *Adv. Catal. 33* (1985) 191; G. Engelhardt, D. Michel: *High-Resolution Solid-State NMR of Silicates and Zeolites*, Wiley, Chichester, England 1987.
[50] G. Perego, G. Bellusi, C. Corno, M. Taramasso, F. Bounomo, A. Esposito in K. Murakami, J. W. Ward (Eds.): *New Developments in Zeolite Science and Technology*, Kodanska, Tokyo 1986, p. 129; see also B. Natari in [29a], p. 413; B. Kraushaar, J. H. C. van-Hooff, *Catal. Lett. 1* (1988) 81.
[51] H. M. Rietveld, *J. Appl. Crystallogr. 2* (1969) 65.
[52] A. K. Cheetham, J. C. Taylor, *J. Solid State Chem. 21* (1977) 253.
[53] A. K. Cheetham, M. M. Eddy, J. M. Thomas, *J. Chem. Soc. Chem. Commun. 1984*, 337.
[54] R. S. Brown, B. E. Hingerty, J. C. Dewan, A. Klug, *Nature (London) 303* (1983) 543.
[55] P. Fejes, I. Kiricsi, I. Hannus, A. Kiss, G. Schobel, *React. Kinet. Catal. Lett. 14* (1980) 481; see also X. S. Liu, J. M. Thomas, J. Klinowski, *J. Chem. Soc. Chem. Commun. 1986*, 582.
[56] W. M. Meier, D. H. Olson: *Atlas of Zeolite Structure Types*, 2nd edit., Butterworths, London 1987, p. 221.
[57] J. M. Thomas, G. R. Millward, *J. Chem. Soc. Chem. Commun. 1982*, 1382.

[58] G. R. Millward, S. Ramdas, J. M. Thomas, *Proc. R. Soc. London A 399* (1985) 57; see also M. Audier, J. M. Thomas, G. R. Millward, S. Ramdas, L. A. Bunsill, *J. Phys. Chem. 86* (1982) 581.

[59] J. M. Thomas, *Ultramicroscopy 8* (1982) 13; see also M. M. J. Treacy, J. M. Newsam, D. E. W. Vaughan, R. A. Beyerlein, S. B. Rice, C. B. De Gruyter, *Mater. Res. Soc. Symp. Proc. 111* (1988) 1.

[60] M. M. J. Treacy, J. M. Newsam, *Nature (London) 332* (1988) 249.

[61] M. E. Leonowicz, D. E. W. Vaughan, *Nature (London) 329* (1987) 819.

[62] D. E. Akporiaye, S. D. Pickett, A. K. Nowak, J. M. Thomas, A. K. Cheetham, *Catal. Lett. 1* (1988) 133.

[63] G. R. Millward, J. M. Thomas, S. Ramdas, M. T. Barlow, *J. Chem. Soc. Faraday Trans. 2 79* (1983) 1075.

[64] N. Y. Cheng, W. W. Kaeding, F. S. Dwyer, *J. Am. Chem. Soc. 101* (1979) 6783.

[65] J. R. Anderson, K. Foger, T. Mole, R. A. Rajadyaksha, J. V. Sanders, *J. Catal. 58* (1979) 114.

[66] A. F. Wells: *Three Dimensional Nets and Polyhedra*, Wiley, New York 1977.

[67] Many mathematical crystallographers have given accounts of tesselation theory which has a strong bearing on both inorganic and biological significant structures consisting of continuous nets. See, for example, E. D. T. Atkins, J. K. Sheehan, I. A. Nieduszynski, *J. Mol. Biol. 91* (1975) 153. Valuable surveys of the geometry and inter-relationships within tetrahedral networks in zeolites have been made by J. V. Smith, *Chem. Rev. 88* (1988) 149; F. C. Hawthorne, J. V. Smith, *Can. Mineral. 24* (1986) 643; D. E. Akporiaye, G. D. Price, *Zeolites*, in press.

[68] M. E. Davis, C. Saldorriaga, C. Montes, J. Ganca, C. Crowder, *Nature (London) 331* (1988) 698.

[69] a) J. A. Rabo in H. G. Karge, J. Weitkamp (Hrsg.): *Zeolites as Catalysts, Sorbents and Detergent Builders, Proc. Int. Symp.*, Würzburg, September 1988, im Druck; b) R. J. Pellet, P. K. Coughlin, E. S. Shamshouin, J. A. Rabo, *ACS Symp. Ser. 368* (1988) *(Perspectives in Molecular Sieve Science)* p. 512.

[70] R. A. van Nostrand, W. S. Santelli, S. I. Zones, *ACS Symp. Ser. 368* (1988) 236.

[71] G. T. Kokotailo, W. M. Meier, *Chem. Soc. Spec. Publ. 33* (1980) 133.

[72] D. E. Akporiaye, unpublished.

[73] D. E. Akporiaye, G. D. Price, *Zeolites*, in press.

[74] V. B. Kazansky, V. Yu. Borovkov, L. M. Kustov, *Zeolites 3* (1983) 77.

[75] J. Sauer, W. Schirmer in [29a], p. 323.

[76] R. Vetrivel, C. R. A. Catlow, E. A. Colbourn in [29a], p. 309.

[77] J. Dwyer in [29a], p. 444.

[78] Y. Morikawa, T. Takagi, Y. Moro-oka, T. Ikawa, *Proc. Int. Congr. Cat. 8th, 5* (1984) 679.

[79] D. T. B. Tennakoon, W. Jones, J. M. Thomas, *J. Chem. Soc. Faraday Trans. 1 82* (1986) 545.

[80] R. M. Lewis, K. C. Ott, R. A. van Santen, *US-Pat. No. 4510257*, 1985.

[81] R. M. Barrer: *Zeolites and Clay Minerals as Adsorbents and Molecular Sieves*, Academic Press, New York 1978, p. 407.

[82] R. H. Loeppert, M. M. Mortland, T. J. Pinnavaia, *Clays Clay Miner. 27* (1979) 201.

[83] G. J. Bantley, R. Burch, *Appl. Catal. 19* (1985) 175.

[84] S. Yamanaka, T. Nishihara, M. Hattori, *Mater. Chem. Phys. 17* (1987) 87.

[85] J. M. Oades, *Clays Clay Miner. 32* (1984) 49.

[86] G. W. Brindley, S. Yamanaka, *Am. Mineral. 64* (1979) 830.

[87] D. E. W. Vaughan, *ACS Sym. Ser. 368* (1988) 2711.

[88] M. L. Occelli, *J. Mol. Catal. 35* (1986) 337.

[89] M. L. Occelli, *Proc. Int. Clay Conf., Denver 1985*, Clay Minerals Soc., IN, USA 1987, p. 319.

[90] J. M. Thomas, S. E. Morsi, J. P. Desvergne, *Adv. Phys. Org. Chem. 15* (1977) 63.

[91] J. M. Thomas in J. V. Acrivos, A. D. Yoffe, N. F. Mott (Eds.): *Physics and Chemistry of Electrons and Ions in Condensed Matter*, Reidel, Dordrecht 1984, p. 521.

[92] J. M. Thomas, *Philos. Trans. R. Soc. A 311* (1984) 271.

[93] J. A. Ballantine, J. H. Purnell, J. M. Thomas, D. T. B. Tennakoon, W. Jones, *Chem. lett. 1985*, 763.

[94] W. Jones, D. T. B. Tennakoon, J. M. Thomas, L. J. Williamson, J. A. Ballantine, J. H. Purnell, *Proc. Indian Acad. Sci. Chem. Sci. 92* (1983) 27.

[95] J. A. Ballantine in R. Setton (Ed.): *Chemical Reactions in Organic and Inorganic Constrained Systems*, Reidel, Dordrecht 1986, p. 197.

[96] J. A. Ballantine, J. H. Purnell, J. M. Thomas, *Clay Miner. 18* (1983) 347.

[97] J. H. Purnell, J. M. Thomas, P. A. Diddams, J. A. Ballantine, W. Jones, unpublished.

[98] R. K. Grasselli, J. D. Burrington, *Adv. Catal. 30* (1981) 133.

[99] A. W. Sleight, W. J. Linn, *J. Catal. 41* (1976) 134.

[100] a) J. M. Herrmann, M. J. Pires and M. F. Portella (*J. Chem. Soc. Faraday Trans. 1985*, 81) as well as J. F. Brazdil and R. R. Grasselli (*J. Catal. 79* (1983) 104) describe inter alia the use of $Bi_{2-x}Ce_x(MoO_4)_3$ which is a monophasic, secrificial oxidation catalyst when $x \geq 1$; b) J. Haber, *Proc. Int. Congr. Catal. 8th 1* (1984) 85.

[101] B. C. H. Steele, I. Kelly, H. Middleton, R. Rudkin, *Solid State Ionics*, in press.

[102] B. A. Boukamp, I. C. Vinke, K. J. de Vries, A. J. Burgraaf, *Solid State Ionics*, in press.

[103] R. J. H. Verhoeve in J. J. Burton, R. L. Garten (Eds.): *Advanced Materials in Catalysis*, Academic, New York 1977, p. 129.

[104] V. V. Popovskii, G. K. Boreskov, V. S. Muzykantov, V. A. Sazonov, S. G. Sbukmikov, *Itogi Nauki Tekh. Ser. Kinet. Katal. 10* (1969) 786.

[105] D. J. Buttrey, D. A. Jefferson, J. M. Thomas, *Philos. Mag. 53* (1986) 897.

[106] J. Haber, *Catal. Sci. Technol. 2* (1981) 13.

[107] D. A. Jefferson, J. M. Thomas, R. K. Grasselli, M. K. Uppal, *J. Chem. Soc. Chem. Commun. 1983*, 594.

[108] J. M. Thomas, D. A. Jefferson, G. R. Millward, *JEOL News Ser. Electron Opt. Instrum. 23 E* (1985) 7.

[109] J. Berggren, *Acta Chem. Scand. A 37* (1985) 7.

[110] Y. Bando, Y. Sekikawa, H. Yamanura, Y. Matsui, *Acta Crystallogr. A 37* (1981) 723.

[111] M. Alario-Franco, J.-C. Joubert, J. P. Levy, *Mater. Res. Bull. 17* (1982) 733.

[112] J.-C. Grenier, M. Pouchard, P. Hagenmuller, *Struct. Bonding 47* (1981) 1.

[113] A. Reller, D. A. Jefferson, J. M. Thomas, M. K. Uppal, *J. Phys. Chem. 87* (1983) 913.

[114] G. Brachtil, R. Hoppe, *Z. Anorg. Allg. Chem. 468* (1980) 130.

[115] R. A. Beyerlein, A. J. Jacobson, K. R. Poeppelmeier, *J. Chem. Soc. Chem. Commun. 1988*, 225.

[116] R. A. Beyerlein, K. R. Poeppelmeier, A. J. Jacobson, *US-Pat. Nr. 4503166* (1985).

[117] M. Hervieu, B. Domenges, J. Provost, F. Deslandes, B. Raveau, B. Chevalier, J. Etourneau, *Angew. Chem. 100* (1988) 403; *Angew. Chem. Int. Ed. Engl. 27* (1988) 440.

[118] J. Torrance, T. Tokura, A. Nazzal, S. S. P. Parkin, *Phys. Rev. Lett. 60* (1988) 542.

[119] Zhou Wuzong, D. A. Jefferson, M. Alario-Franco, J. M. Thomas, *J. Phys. Chem. 91* (1987) 512.

[120] Zhou Wuzong, J. M. Thomas, D. A. Jefferson, A. Harriman, *J. Solid State Chem. 72* (1988) 126.

[121] Zhou Wuzong, D. A. Jefferson, J. M. Thomas, *J. Solid State Chem. 70* (1987) 129.

[122] A. Harriman, J. M. Thomas, Zhou Wuzong, D. A. Jefferson, *Mater. Res. Soc. Symp. Proc. 111* (1988) 295.

[123] L. G. Sillén, *Z. Anorg. Allg. Chem. 242* (1939) 41; *ibid. 246* (1941) 115.

[124] W. Ueda, J. M. Thomas, *9th Int. Congr. Catal.*, Calgary, June 1988, paper 123; *J. Chem. Soc. Chem. Commun. 1988*, 1148.

[125] J. Williams, J. M. Thomas, unpublished.

[126] J. F. Ackerman, *Mater. Res. Bull. 17* (1982) 883.

[127] K. D. M. Harris, W. Ueda, J. M. Thomas, G. W. Smith, *Angew. Chem. 100* (1988) 1415; *Angew. Chem. Int. Ed. Engl. 27* (1988) 1364.

[128] M. Daage, J. P. Bonnelle in J. Pojonk (Ed.): *Spillover of Adsorbed Species*, Elsevier, Amsterdam 1983, p. 261.

[129] P. A. Sermon, G. C. Bond, *J. Chem. Soc. Faraday Trans. 1 76* (1980) 889.

[130] A. Magneli, *Acta Chem. Scand. 7* (1983) 315.

[131] M. Figlarz, *Chem. Scr. 28* (1988) 3.

[132] J. Livage, *Chem. Scr. 28* (1988) 9.

[133] J. Rouxel, *Chem. Scr. 28* (1988) 33.

[134] Siehe *Rev. Chim. Miner. 21* (1984) No. 20.

[135] H. Rebbah, G. Desgandin, B. Reaveau, *Mater. Res. Bull. 14* (1979) 1125.

[136] D. W. Murphy, C. Cros, F. J. Di Salvo, J. V. Waszczak, *Inorg. Chem. 16* (1977) 3027.

[137] R. Schöllhorn, *Angew. Chem. 92* (1980) 1015; *Angew. Chem. Int. Ed. Engl. 19* (1980) 983; *100* (1988) 1446 or *27* (1988) 1392.

[138] G. Svensson, L. Kihlborg, *J. React. Solids*, in press.

[139] C. N. R. Rao, J. Gopalakrishnan: *New Directions in Solid State Chemistry*, Cambridge University Press, Cambridge 1986, Chap. 7.

[140] H. G. von Schnering, R. Nesper, *Angew. Chem. 99* (1987) 1087; *Angew. Chem. Int. Ed. Engl. 26* (1987) 1059.

[141] S. T. Hyde, S. Andersson, *Z. Kristallogr. 170* (1985) 225.

When submitting manuscripts, authors of articles intended for publication as "Communications" are requested to read the "Notice to Authors" reproduced in the January issue of the journal following the list of contents; upon request, a copy can be obtained from the editorial office.

1,6-Methano[10]annulene Dianion, a Paratropic 12π-Electron Dianion with a C_{10} Perimeter**

By *Dietmar Schmalz* and *Harald Günther**

Dedicated to Professor Fabian Gerson on the occasion of his 60th birthday

The synthesis of 1,6-methano[10]annulene **1** by *Vogel* and *Roth*,[1] which marked the beginning of the chemistry of bridged annulenes with acene perimeters, is clearly a milestone of modern arene chemistry. Since then, numerous investigations of the physical and chemical properties of **1** have confirmed the interesting bonding situation in this hydrocarbon.[2] However, its reduction to the dianion $\mathbf{1}^{2\ominus}$ has not yet been reported. Only the derivative **2**, modified at the bridge, could be transformed into the ionic system $\mathbf{2}^{2\ominus}$ by reaction with metallic lithium.[3] The ^{1}H NMR spectrum, however, shows only a relatively small upfield shift of 2–3 ppm for the perimeter protons and therefore $\mathbf{2}^{2\ominus}$ is only weakly paratropic.[4]

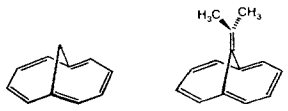

1 **2**

Results recently obtained for dilithium naphthalene $\mathbf{3}^{2\ominus}$[5] suggested that the reduction of **1** might also be possible under identical conditions. Indeed, reaction of **1** and lithium sand in [D$_8$]THF at −80 °C with vigorous vibration afforded the dark brown solution of a species that, according to its NMR spectroscopic data, is unambiguously characterized as the dilithium salt of $\mathbf{1}^{2\ominus}$ (Fig. 1, Table 1).

The reductive transformation of the diamagnetic 10π-electron system of **1**[6] into the paramagnetic 12π-electron system of $\mathbf{1}^{2\ominus}$ results in the expected[4,7] shifts of the ^{1}H NMR signals and in ^{1}H NMR data similar to that observed for bridged [14]annulene dianions[3] and the 12π-electron monoanion bicyclo[5.4.1]dodecapentaenide **4**.[8]

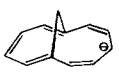

4

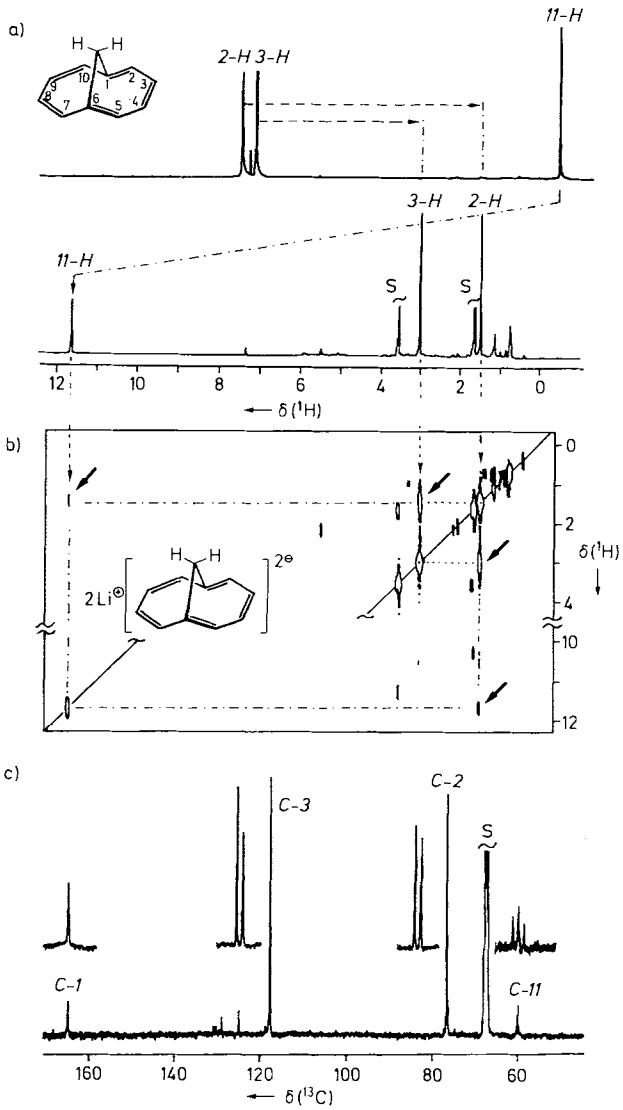

Fig. 1. a) 400-MHz ^{1}H NMR spectra of **1** ($CDCl_3$) and 2 $Li^{\oplus}/\mathbf{1}^{2\ominus}$ ([D$_8$]THF). b) COSY-45 [9b] spectrum of 2 $Li^{\oplus}/\mathbf{1}^{2\ominus}$ (cross signals marked with arrows). c) 100-MHz ^{13}C NMR spectrum of 2 $Li^{\oplus}/\mathbf{1}^{2\ominus}$ with the multiplets of the ^{1}H-coupled spectrum. S = solvent signal, X = unknown product. $T = -80$ °C.

Table 1. ^{1}H and ^{13}C NMR data [δ relative to TMS] for **1**, $\mathbf{1}^{2\ominus}$, and $\mathbf{3}^{2\ominus}$ [a].

	1	$\mathbf{1}^{2\ominus}$	$\mathbf{3}^{2\ominus}$	Δδ [ppm] $\mathbf{1}^{2\ominus}-\mathbf{1}$	Δδ [ppm] $\mathbf{3}^{2\ominus}-\mathbf{3}$
δ(2,5,7,10-H)	7.27	1.59	1.27	− 5.68	− 6.43
δ(3,4,8,9-H)	6.95	3.07	3.09	− 3.88	− 4.25
δ(11-H)	−0.52	11.64	—	+12.16	—
δ(C-2,5,7,10)	128.7	76.5	82.7	−52.2	−45.0
δ(C-3,4,8,9)	126.1	118.0	112.9	− 8.1	−12.7
δ(C-1,6)	114.6	165.0	163.7	+50.4	+30.4
δ(C-11)	34.8	60.0	—	+25.2	—

[a] Naphthalene is numbered unsystematically in accordance with **1**.

The protons in the methano bridge of the dianion $\mathbf{1}^{2\ominus}$ are shifted about 12 ppm downfield compared with those of **1**, whereas the perimeter protons are strongly shielded.

[*] Prof. Dr. H. Günther, Dipl.-Chem. D. Schmalz
Fachbereich 8, Organische Chemie II der
Universität-Gesamthochschule
Postfach 101240, D-5900 Siegen (FRG)

[**] This work was supported by the Fonds der Chemischen Industrie.

Assignment of the signals was only possible by means of a two-dimensional COSY experiment,[9] since cross peaks between scalar-coupled protons appear even when, as in this case, the coupling in the 1D NMR spectrum is not resolved.[10] To determine the long-range coupling between the protons in the bridge and those at C-2,5,7,10, which is crucial for signal assignment, the successful pulse sequence with a fixed time interval (50 ms in this case) before and after the second 90° pulse was employed.[9b] As shown in Figure 1b, there is a cross peak between the 11-H signal and the high-field signal at $\delta = 1.59$, which is therefore assigned to the perimeter protons 2,5,7,10-H in α-positions.

High-field shifts are also observed for the ^{13}C resonances of C-2,5,7,10 and C-3,4,8,9, whereas C-11 and C-1,6 are strongly deshielded. The signal assignment in this case was achieved via a 2D $^{13}C,^{1}H$ shift correlation,[11] the results of which were corroborated by the multiplicities in the ^{1}H-coupled ^{13}C NMR spectrum (Fig. 1c).

Whereas the low-field shift of the C-11 signal can be ascribed in part to a paramagnetic ring-current effect,[12] the strong deshielding of C-1,6 must be due to a partial positive charge at these positions in the dianion. Positive charges at bridgehead positions have also been found for the dianions of bridged [14]annulenes.[3] This finding, along with the other NMR parameters of $\mathbf{1}^{2\ominus}$, shows striking parallels to the data of $\mathbf{3}^{2\ominus}$, so that the two systems presumably have very similar charge distributions. This is also expected in terms of HMO theory, since the lowest unoccupied π molecular orbitals of **1** and **3**, which are essentially responsible for the charge distribution in the dianions, are practically identical.[5, 13]

The $^{1}J(^{13}C,^{1}H)$ coupling at C-11 (136 Hz), which is appreciably smaller than the corresponding coupling in **1** (142 Hz),[6] as well as the low-field position of the C-1,6 resonance, prove, moreover, that $\mathbf{1}^{2\ominus}$ cannot be formulated as the dianion of the bisnorcaradiene **5**.[12, 14] As in

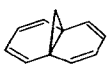

5

the case of naphthalene,[5, 15] reduction of **1** to the dianion should lead to an increase in the distance between the quaternary C atoms. Further, the unresolved $^{3}J(^{1}H,^{1}H)$ coupling between 2-H and 3-H[16] indicates that $\mathbf{1}^{2\ominus}$, like **4**,[8] is strongly distorted from planarity owing to folding of the C2–C5 and C7–C10 fragments.

The chemical structural proof of $\mathbf{1}^{2\ominus}$ is based on the oxidation by air, which affords the hydrocarbon **1** in 88% yield. Dianion $\mathbf{1}^{2\ominus}$ exhibits remarkable thermal stability. At room temperature, the ^{1}H NMR signals disappear only after about 20 h, that is, when the solvent THF undergoes partial decomposition by reaction with residual lithium metal.

Received: July 11, 1988 [Z 2853 IE]
German version: *Angew. Chem. 100* (1988) 1754

[1] E. Vogel, H. D. Roth, *Angew. Chem. 76* (1964) 145; *Angew. Chem. Int. Ed. Engl. 3* (1964) 228.
[2] Cf. reference 13 in E. Vogel, *Israel J. Chem. 20* (1980) 215.
[3] K. Müllen, T. Meul, P. Schade, H. Schmickler, E. Vogel, *J. Am. Chem. Soc. 109* (1987) 4992.
[4] F. Sondheimer, *Acc. Chem. Res. 5* (1972) 81.
[5] R. Benken, H. Günther, *Helv. Chim. Acta 70* (1988) 694.
[6] H. Günther, *Z. Naturforsch. B 20* (1965) 695.
[7] a) J. A. Pople, K. Untch, *J. Am. Chem. Soc. 88* (1966) 4811; b) F. Baer, H. Kuhn, W. Regel, *Z. Naturforsch. A 22* (1967) 103.
[8] S. W. Staley, A. W. Orvedal, *J. Am. Chem. Soc. 95* (1973) 3384.
[9] a) W. P. Aue, E. Bartholdi, R. R. Ernst, *J. Chem. Phys. 64* (1976) 2229; b) A. Bax, R. Freeman, *J. Magn. Reson. 44* (1981) 542; c) reviews: R. Benn, H. Günther, *Angew. Chem. 95* (1983) 381; *Angew. Chem. Int. Ed. Engl. 22* (1983) 350; H. Kessler, M. Gehrke, C. Griesinger, *ibid. 100* (1988) 507 and *27* (1988) 490.
[10] a) W. Peters, M. Fuchs, H. Sicius, W. Kuchen, *Angew. Chem. 97* (1985) 217; *Angew. Chem. Int. Ed. Engl. 24* (1985) 231; b) D. Moskau, H. Günther, *ibid. 99* (1987) 151 and *26* (1987) 156.
[11] A. A. Maudsley, R. R. Ernst, *Chem. Phys. Lett. 50* (1977) 368; cf. also [9c].
[12] H. Günther, W. Schmickler, *Pure Appl. Chem. 70* (1975) 807.
[13] F. Gerson, E. Heilbronner, W. A. Böll, E. Vogel, *Helv. Chim. Acta 48* (1965) 1494; F. Gerson, K. Müllen, C. Wydler, *ibid. 59* (1976) 1371.
[14] a) D. Cremer, B. Dick, *Angew. Chem. 94* (1982) 877; *Angew. Chem. Int. Ed. Engl. 21* (1982) 865; b) E. Vogel, T. Scholl, J. Lex, G. Hohlneicher, *ibid. 94* (1982) 878 and *21* (1982) 869.
[15] J. J. Brooks, W. Rhine, G. D. Stucky, *J. Am. Chem. Soc. 94* (1972) 7346.
[16] An upper limit of 5 Hz may be estimated from the line width of the NMR signals.

Titanium(0) Arene Complexes: Synthesis and X-ray Crystal Structure of $[(\eta^6\text{-}C_{10}H_8)Ti\{t\text{BuSi}(CH_2PMe_2)_3\}]$**

By *Thomas G. Gardner* and *Gregory S. Girolami**

Arene complexes of titanium are exceedingly uncommon, and only two principal classes of such species are known: titanium(II) complexes of stoichiometry $[(arene)TiX_2]$[1–4] and titanium(0) sandwich complexes $[(arene)_2Ti^0]$.[5–8] The sandwich compounds are important examples of molecules that, at present, can best be made by metal-vapor techniques, although it has been postulated that reductive carbonylation of titanium halides by naphthalenesodium yields titanium(0) naphthalene intermediates that subsequently undergo irreversible substitution by carbon monoxide.[9] We wish to report here the isolation, characterization, and X-ray crystal structure of the unique titanium(0) naphthalene complex $[(\eta^6\text{-}C_{10}H_8)Ti(trimpsi)]$ **1**, where trimpsi is the tripod phosphane $t\text{BuSi}(CH_2PMe_2)_3$. This 16-electron species exhibits a folding of the naphthalene ring that is indicative of partial diene–diyl bonding and strong metal-to-ligand δ backbonding.

Reductive carbonylation of $[TiCl_3(trimpsi)(thf)]$ by naphthalenesodium gives the titanium(0) carbonyl $[(trimpsi)Ti(CO)_4]$.[10] In the absence of carbon monoxide, the reduction results in a deep red-purple solution in tetrahydrofuran, from which the naphthalene complex $[(\eta^6\text{-}C_{10}H_8)Ti(trimpsi)]$ **1** may be obtained.

$$[TiCl_3(trimpsi)(thf)] + 3\,C_{10}H_8Na \longrightarrow [(\eta^6\text{-}C_{10}H_8)Ti(trimpsi)] + 3\,NaCl + 2\,C_{10}H_8$$

1

Compound **1** is a deep red-purple crystalline solid which is very air-sensitive, but thermally stable at room temperature in solution or as a solid. Unlike the known

[*] Prof. Dr. G. S. Girolami, T. G. Gardner
School of Chemical Sciences
The University of Illinois at Urbana-Champaign
Urbana, IL 61801 (USA)

[**] We thank Dr. *S. Wilson* and *C. Stern* for the X-ray crystallographic analysis and the National Science Foundation, the Office of Naval Research under their Young Investigator Award Program, and the A. P. Sloan Foundation (Research Fellowship to *G. S. G.*) for financial support.

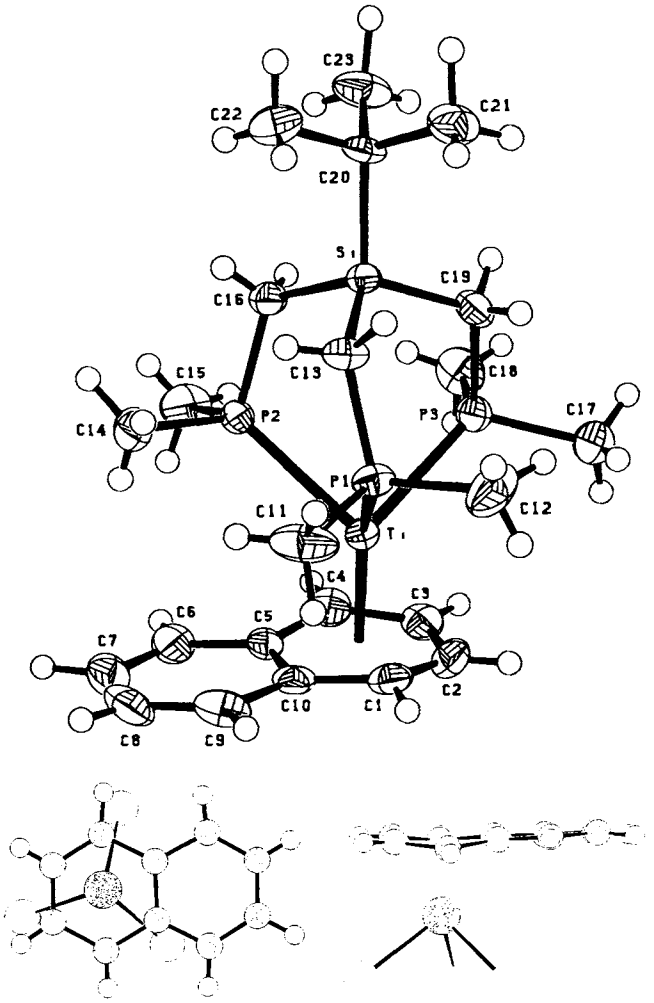

Fig. 1. Top: Molecular structure of $[(\eta^6\text{-}C_{10}H_8)Ti(trimpsi)]$ **1**. Important bond distances [Å] and angles [°]: Ti-P1 2.532(2), Ti-P2 2.552(2), Ti-P3 2.523(2), Ti-C^n 1.833(1), Ti-C1 2.236(7), Ti-C2 2.303(8), Ti-C3 2.296(8), Ti-C4 2.244(7), Ti-C5 2.417(6), Ti-C10 2.390(7), Ti···Si 3.921(2), C1-C2 1.39(1), C2-C3 1.37(1), C3-C4 1.45(1), C4-C5 1.43(1), C5-C10 1.424(9), C5-C6 1.41(1), C6-C7 1.36(1), C7-C8 1.35(1), C8-C9 1.37(1), C9-C10 1.44(1), C10-C1 1.44(1); P1-Ti-P2 86.73(6), P1-Ti-P3 88.03(7), P2-Ti-P3 88.30(6), Si···Ti-C^n 177.73, P1-Ti-C^n 128.98(6), P2-Ti-C^n 124.64(6), P3-Ti-C^n 126.97(7). Bottom left: Relative orientation of the phosphane and naphthalene ligands. Important torsion angles [°]: P1-Ti-C^n-C1 16.1(6), P2-Ti-C^n-C5 13.3(5), P3-Ti-C^n-C3 10.1(6). Bottom right: Edge-on view of the conformation of the naphthalene ligand. The coordinated ring is folded 12.4° from planarity. For clarity, only the phosphorus atoms of the trimpsi ligand have been included.

bis-arene titanium(0) complexes,[5] compound **1** is apparently paramagnetic and no peaks ascribable to coordinated naphthalene or trimpsi were present in ^{1}H NMR spectra in $[D_{14}]$methylcyclohexane or other solvents under a variety of conditions. Treatment of **1** with CO rapidly yields the previously described[10] titanium(0) tetracarbonyl [(trimpsi)Ti(CO)$_4$].

The molecular structure of **1** is shown in Figure 1.[11] The overall geometry can be described as a three-leg piano stool, with the P-Ti-P angles being essentially equal and averaging 87.7°. A view down the Ti···Si vector (Fig. 1, bottom left) shows the orientation of the three phosphane ligands in relation to the naphthalene ring. The mean P-Ti-C^n-C torsion angle (C^n = centroid) is 13(1)°, which is about halfway between an eclipsed and a staggered conformation. Interestingly, a similar twist of 19(1)° is seen in $[(\eta^6\text{-naphthalene})Cr(CO)_3]$,[12] whereas the related complexes $[(\eta^6\text{-anthracene})Cr(CO)_3]$ and $[(\eta^6\text{-phenanthrene})Cr(CO)_3]$ are rigorously staggered with torsion angles of 30°.[13,14]

Figure 1, bottom right, shows an edge-on view of the naphthalene ligand. The coordinated naphthalene ring is folded about the C1-C4 vector with a dihedral angle of 12.4°. The noncomplexed ring, by comparison, is accurately planar. The folding of the π-bound ring causes the Ti-C distances to fall into three groups: C1 and C4 are closest at a mean Ti-C distance of 2.24(1) Å and C2 and C3 are at a medium distance of 2.30(1) Å, while C5 and C10 are most distant at 2.40(1) Å. This contrasts sharply with the structure of $[(C_6H_6)_2Ti]$, which has planar benzene rings and essentially equal Ti-C distances of 2.217-2.247(8) Å.[8] It is not uncommon for fused-ring arene ligands to have unequal M-C distances, with the longest being to the shared C-C bond; examples of this are seen in $[(naphthalene)Cr(CO)_3]$, $[(anthracene)Cr(CO)_3]$, and $[(phenanthrene)Cr(CO)_3]$; however, the π-bound rings in these chromium complexes are not deformed from planarity.[12-14] The bis-arene complex $[(\eta^6\text{-naphthalene})_2Cr]$ also possesses essentially planar naphthalene rings.[15]

The folding of the naphthalene ring can be thought of in terms of partial diene-diyl bonding character. This is consistent with strong metal-to-ligand δ back-bonding[16] from a filled Ti $d_{x^2-y^2}$ orbital into the LUMO of naphthalene, a B_{2g} orbital[17] that has large contributions from C1 and C4, smaller contributions from C2 and C3, and no contribution from C5 or C10. In this context, it is interesting to note that the "σ" Ti-C1 and Ti-C4 distances are comparable to that of 2.217(2) Å in the titanium *alkyl* complex $[TiMe_2(dmpe)_2]$.[18] The strong donor ability of the (trimpsi)Ti unit has been previously established from the low $\tilde{\nu}_{CO}$ IR stretching frequencies and strongly deshielded ^{13}C chemical shifts of $[Ti(CO)_4(trimpsi)]$.[10] The strong metal-to-ligand back-bonding and diene-diyl distortion of the arene ring is similar to the bonding in several electron-rich butadiene complexes of group 4 elements, in which an ene-diyl bonding mode is observed.[19,20] The dihedral angle of 12.4° in **1** is much smaller than the dihedral angles of 25° to 43° in authentic η^4-arene complexes of early-transition-metals, in which hexahapto coordination would exceed an 18-electron configuration.[21,22] Interestingly, a dihedral angle of 14.5° was noted in the X-ray crystal structure of the naphthalene dianion in $[Li(tmeda)]_2C_{10}H_8$ (tmeda = *N,N,N',N'*-tetramethylethylenediamine).[23] The folding of the naphthalene ring in **1** is not the result of steric repulsions with the methyl groups of the phosphane ligand: the closest van der Waals contact between the trimpsi ligand and the free ring of the naphthalene ligand is 3.04 Å (H14b···C7).

The average Ti-P distance of 2.536 Å in **1** is close to the 2.545-2.633-Å range observed for titanium(0) phosphane carbonyls (e.g., $[Ti(CO)_4(trimpsi)]$,[10] $[Ti(CO)_3(dmpe)_2]$,[24] and $[Ti(CO)_2(PF_3)(dmpe)_2]$[25]); in fact, all titanium-phosphane distances fall in the range 2.58 ± 0.07 Å, irrespective of oxidation state, spin state, or coordination number. The Ti-C^n distance of 1.833(1) Å is slightly longer than in $[(C_6H_6)_2Ti]$ (1.736 Å),[8] and the Si···Ti-C^n angle of 177.7° is essentially linear.

The complex $[(\eta^6\text{-}C_{10}H_8)Ti(trimpsi)]$ **1** has been shown to possess unusually strong metal-to-ligand back bonding into a naphthalene δ-acceptor orbital that causes a folding of the naphthalene ring. Additionally, **1** is a useful intermediate in the synthesis of other titanium(0) complexes such as $[Ti(CO)_4(trimpsi)]$.

Experimental Procedure

To a stirred solution of [$TiCl_3$(trimpsi)(thf)] (3.90 g, 7.27 mmol) in tetrahydrofuran (50 mL) at −78 °C was added naphthalenesodium (150 mL, 0.145 M in THF, 21.8 mmol). A red-purple solution formed immediately. The solution was warmed to room temperature slowly, and the solvent was removed in vacuum. The excess naphthalene was removed by sublimation in vacuum at 25 °C. The dark purple residue was extracted with diethyl ether (5 × 200 mL), and the combined extracts were concentrated to 200 mL and cooled to −20 °C to give dark purple crystals of **1**. Yield: 1.4 g (40%); m.p. 196–204 °C. Correct elemental analysis (C,H,Ti).

Received: April 28, 1988;
revised: September 5, 1988 [Z 2728 IE]
German version: *Angew. Chem. 100* (1988) 1755

[1] E. O. Fischer, F. Rohrschied, *J. Organomet. Chem. 6* (1966) 53.
[2] H. Martin, F. Vohwinkel, *Chem. Ber. 94* (1961) 2416.
[3] U. Thewalt, F. Österle, *J. Organomet. Chem. 172* (1979) 317.
[4] U. Thewalt, F. Stöllmaier, *J. Organomet. Chem. 228* (1982) 149.
[5] M. T. Anthony, M. L. H. Green, D. Young, *J. Chem. Soc. Dalton Trans. 1975*, 1419.
[6] P. D. Morand, C. G. Francis, *Inorg. Chem. 24* (1985) 56.
[7] P. N. Hawker, E. P. Kündig, P. L. Timms, *J. Chem. Soc. Chem. Commun. 1978*, 730.
[8] O. N. Krasochka, A. F. Shestakov, G. G. Tairova, Y. A. Shvetsov, E. F. Kvashina, V. I. Ponomarev, L. O. Atovmyan, Y. G. Borod'ko, *Khim. Fiz. 11* (1983) 1459; *Chem. Abstr. 100* (1984) 43387g.
[9] K. M. Chi, S. R. Frerichs, B. K. Stein, D. W. Blackburn, J. E. Ellis, *J. Am. Chem. Soc. 110* (1988) 163.
[10] T. G. Gardner, G. S. Girolami, *Organometallics 6* (1987) 2551.
[11] Crystal data for **1**: $C_{23}H_{41}P_3SiTi$, $M = 486.49$, monoclinic, space group $P2_1/n$, $a = 9.796(6)$, $b = 18.391(8)$, $c = 14.922(5)$ Å, $\beta = 92.52(3)°$, $V = 2686(4)$ Å^3; $Z = 4$, $\rho_{calcd} = 1.203$ g cm^{-3}; $\mu_c(Mo_{K\alpha}) = 5.42$ cm^{-1}, $R = 0.044$, $R_w = 0.048$ for 377 parameters and 2118 unique data with $I > 2.58\sigma(I)$. Further details of the crystal structure investigation may be obtained from the Fachinformationszentrum Energie, Physik, Mathematik GmbH, D-7514 Eggenstein-Leopoldshafen 2 (FRG), on quoting the depository number CSD-53343, the names of the authors, and the journal citation.
[12] V. Kunz, W. Nowacki, *Helv. Chim. Acta 50* (1967) 1052.
[13] F. Hanic, O. S. Mills, *J. Organomet. Chem. 11* (1968) 151.
[14] K. W. Muir, G. Ferguson, G. A. Sim, *J. Chem. Soc. B 1968*, 467.
[15] C. Elschenbroich, R. Möckel, W. Massa, M. Birkhahn, U. Zenneck, *Chem. Ber. 115* (1982) 334.
[16] J. C. Green, M. R. Kelly, P. D. Grebenik, C. E. Briant, N. A. McEvoy, D. M. P. Mingos, *J. Organomet. Chem. 228* (1982) 239.
[17] F. A. Cotton: *Chemical Applications of Group Theory*, Wiley, New York 1971, 161.
[18] J. A. Jensen, S. R. Wilson, A. J. Schultz, G. S. Girolami, *J. Am. Chem. Soc. 109* (1987) 8094.
[19] G. Erker, K. Engel, C. Kruger, A.-P. Chiang, *Chem. Ber. 115* (1982) 3311.
[20] S. S. Wreford, J. F. Whitney, *Inorg. Chem. 20* (1981) 3918.
[21] J. O. Albright, S. Datta, B. Dezube, J. K. Kouba, D. S. Marynick, S. S. Wreford, B. M. Foxman, *J. Am. Chem. Soc. 101* (1979) 611.
[22] H. Yasuda, A. Nakamura, *Angew. Chem. 99* (1987) 745; *Angew. Chem. Int. Ed. Engl. 26* (1987) 723.
[23] J. J. Brooks, W. Rhine, G. Stucky, *J. Am. Chem. Soc. 94* (1972) 7346.
[24] P. J. Domaille, R. L. Harlow, S. S. Wreford, *Organometallics 1* (1982) 935.
[25] S. S. Wreford, M. B. Fischer, J.-S. Lee, E. J. James, S. C. Nyburg, *J. Chem. Soc. Chem. Commun. 1981*, 458.

Metal-Ion-Selective Exchange Resins by Matrix Imprint with Methacrylates

By *Wilhelm Kuchen** and *Jürgen Schram*

Various attempts have been made to increase the ion selectivity of exchange resins by carrying out cross-linking polymerization of monomeric or oligomeric complex-forming compounds in the presence of metal ions. A template effect should lead to preferential binding of the respective ions by the resin.[1] Similar results have already been achieved for the separation of racemates on polymers having chiral cavities.[2]

We have now succeeded in increasing the selectivity by cross-linking copolymerization of well-defined metal complexes containing polymerizable ligands. According to our concept, removal of the metal ions from the resin with suitable eluants should leave the arrangement of binding groups intact, which are thus tailored for subsequent binding of the type of ion used to prepare the resin.[3]

Herein we report on the application of this principle to copper(II) methacrylates $Cu_2L_4 \cdot 2D$, $L = H_2C{=}C(CH_3)CO_2^{\ominus}$ (**1**, $D = H_2O$; **2**, D = pyridine; **3**, D = 4-vinylpyridine (vpy)). The results we obtained with the complexes ML_2 ($M = Zn^{2\oplus}$, $Cd^{2\oplus}$, $Pb^{2\oplus}$) and $[M_4OL_6]$ ($M = Zn^{2\oplus}$, $Pb^{2\oplus}$) are discussed in Ref. [4a] and corresponding experiments with metal acrylates are described in Ref. [4b].

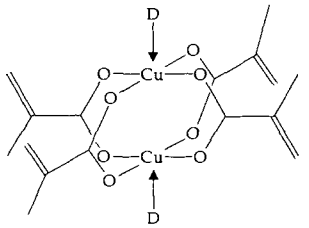

$Cu_2L_4 \cdot 2D$
1-3

The macroporous resins $\mathbf{1}_H$-$\mathbf{3}_H$ (specific surface ca. 400 m^2 g^{-1}), readily wetted by water, were prepared from the copper complexes **1**-**3** by radical polymerization (precipitation polymerization in an ampoule; initiator azodiisobutyronitrile, AIBN) in the presence of an inert solvent (porogen), in this case benzene/methanol, with ethylene glycol dimethacrylate (EGDMA) as cross-linking agent. After polymerization, the resins were ground, a suitable particle size was separated out (0.8–0.2 mm), and the solvent was completely removed by drying in vacuo. Small amounts of nonpolymerized components could be removed by washing with methanol.

For comparison, we similarly prepared the "blind resins" $\mathbf{1}_B$ and $\mathbf{3}_B$, which contain the same number of polymerizable ligands (introduced into the reaction as ammonium salts NH_4L and as a mixture of NH_4L and vpy, respectively), whose distribution in the matrix, however, is purely random.

The electronic excitation spectra (measured in reemission) of the green or blue copper-containing resins do not differ significantly from the spectra of the corresponding complexes **1**-**3**. Therefore, it is safe to assume that the arrangements of the ligands around $Cu^{2\oplus}$ in the starting complexes **1**-**3** and in the resins $\mathbf{1}_H$-$\mathbf{3}_H$ are the same. To investigate the exchange behavior of the resins, they were first converted into the ammonium form by treatment with an NH_3/NH_4Cl solution (1 M in both components); in this way, all metal ions accessible to the eluant were removed from the resin as their ammine complexes (ca. 60–70% of the metal ions used in preparing the resin).

The effective loading capacity—that is, the maximum amount of metal ion that a specified amount of resin can carry under given conditions—was then determined by the batch procedure (shaking the resin with a solution of the metal salt).

Comparison of the values in Table 1 shows that the copper-imprinted resins $\mathbf{1}_H$-$\mathbf{3}_H$ exhibit an increased effective capacity for $Cu^{2\oplus}$. Upon loading, the resins bind ca. 30–40% of the amount of metal ion used in their preparation.

[*] Prof. Dr. W. Kuchen, Dr. J. Schram
Institut für Anorganische Chemie und Strukturchemie der Universität
Universitätsstrasse 1, D-4000 Düsseldorf 1 (FRG)

Table 1. Effective capacity [μmol/g resin] of "copper-imprinted" resins and of the corresponding blind resins with respect to various cations $M^{2\oplus}$. Determined by the batch procedure (25°C, 2.5 h), solution 4.08×10^{-3} M in $M^{2\oplus} \triangleq 200$ μmol $M^{2\oplus}$ per gram of resin, pH 4.7 (acetic acid/acetate buffer).

Resin	$Zn^{2\oplus}$	$Cd^{2\oplus}$	$Pb^{2\oplus}$	$Cu^{2\oplus}$
$\mathbf{1}_H$	10.3	7.4	15.5	45
$\mathbf{2}_H$	9.7	7.8	15.2	49
$\mathbf{1}_B$	4.6	4.6	16.5	12.5
$\mathbf{3}_H$	12.4	5.7	6.7	52
$\mathbf{3}_B$	3.2	4.1	12.6	30

Moreover, their capacity does not change after repeated cycles of loading and elution.

If the resins are simultaneously exposed to two kinds of metal ion in identical concentrations, one binds preferentially to the resin. The selectivity coefficients k[5] can be obtained from the equilibrium (a) according to Equation (b).

$$M1_{resin} + M2_{solution} \rightleftharpoons M2_{resin} + M1_{solution} \quad (a)$$

$$k = \frac{[M2]_{resin}[M1]_{solution}}{[M1]_{resin}[M2]_{solution}} \quad (b)$$

The blind resins $\mathbf{1}_B$ and $\mathbf{3}_B$ also exhibit a certain degree of metal-ion selectivity, owing to the different strengths of interaction of the metal ions with the randomly distributed binding groups, which are not arranged for specific metal binding. Thus, comparison of the k values of the imprinted resins with those of the blind resins allows a rough determination of the effect of imprinting on selectivity. As a measure of the selectivity due to imprinting, a relative selectivity coefficient k' [Eq. (c)] can be defined.

$$k' = \frac{k_{resin,\,imprinted}}{k_{blind\,resin}} \quad (c)$$

As shown in Table 2, $k' \gg 1$ for copper. Thus, the $Cu^{2\oplus}$ selectivity of the imprinted resins is markedly higher than that of the blind resins.

Table 2. Competitive loading of M1 ($Cu^{2\oplus}$) and M2 by copper-imprinted resins and blind resins. Batch procedure (25°C, 2.5 h), solution 2.04×10^{-3} M in M1 and M2 ≙ 100 μmol M1 and M2 per gram of resin, pH 4.7 (acetic acid/acetate buffer).

Resin	$M2^{2\oplus}$	$[M1]_{resin}$ [μmol/g]	$[M2]_{resin}$ [μmol/g]	k	k'
$\mathbf{1}_H$	Zn	46	1.4	58	14
	Cd	49	0.70	136	41
	Pb	45	2.8	28	62
$\mathbf{2}_H$	Zn	47	1.4	62	15
	Cd	50	0.65	153	46
	Pb	46	2.9	29	63
$\mathbf{1}_B$	Zn	11.9	3.1	4.2	—
	Cd	13.2	4.4	3.3	—
	Pb	6.2	12.6	0.46	—
$\mathbf{3}_H$	Zn	52	2.3	46	3.2
	Cd	56	0.20	635	61
	Pb	52	0.22	491	223
$\mathbf{3}_B$	Zn	20	1.7	14	—
	Cd	23	2.8	10.4	—
	Pb	19	9.8	2.2	—

Although the effective capacity of the imprinted resins (not optimized in our experiments!) is still small, these resins are capable of selectively removing $Cu^{2\oplus}$ from very dilute solutions, as shown by the following experiment: With a column (300 mm × 14 mm) containing $\mathbf{3}_H$ (10 g), it was possible to remove ca. 70% of the copper ions from 25 L of a solution containing 2×10^{-5} M each of $Cu^{2\oplus}$, $Pb^{2\oplus}$, $Cd^{2\oplus}$, and $Zn^{2\oplus}$ at pH 4.8 (rate of elution 15 mL min^{-1}), whereas the other ions passed almost completely through the column. Further, this method allowed $Cu^{2\oplus}$ ions to be removed from waste water to below the limits of detection (differential pulse inverse voltammetry). The copper ions remained in a very narrow zone in the upper part of the column as revealed by the intense color of the upper column layer. Since the copper could be eluted from this zone with only a small amount of eluant, highly concentrated solutions could be obtained. The resins described here thus allow the removal and concentration of copper from highly dilute solutions.

Since, in the meantime, we have also succeeded in increasing considerably the selectivity of resins by using other metal complexes, the principle described here offers an interesting alternative procedure for preparing ion-selective exchange resins.

Experimental Procedure

Tetrakis(μ-methacrylato-*O*,*O*')bis[aquacopper(II)] **1** (M = 503.4): A mixture of basic copper carbonate (10.1 g, 45.2 mmol) and methacrylic acid (16.0 g, 186 mmol) in methanol (50 mL) was first stirred for 24 h at room temperature and then heated for 5 h at reflux. After addition of an additional 150 mL of methanol, the reaction mixture was heated for a short period to boiling and then filtered, and the filtrate was allowed to stand for ca. 12 h at −20°C. During this time, blue needles separated out; these were recrystallized from methanol. Yield 11 g (48%); decomposition at ca. 196–198°C; M = 483 (osmometry in methanol); $\mu_{eff} = 1.35\mu_B$ (298 K); λ_{max}(reemission) = 722, 364 nm.

2 and **3**: **1** (10.0 g, 19.9 mmol) in methanol (200 mL) was allowed to react at reflux with pyridine (4.0 g, 50.0 mmol) or with 4-vinylpyridine (5.2 g, 50.0 mmol). The product, which precipitated within ca. 12 h at −20°C, was recrystallized from benzene.

Tetrakis(μ-methacrylato-*O*,*O*')bis[(pyridine)copper(II)] **2** (M = 625.6): 9.6 g green needles (77%); decomposition at ca. 183–184°C; M = 614 (osmometry in benzene); $\mu_{eff} = 1.39\mu_B$ (298 K); λ_{max}(reemission) = 749, 384 nm.

Tetrakis(μ-methacrylato-*O*,*O*')bis[(4-vinylpyridine)copper(II)] **3** (M = 677.7): 9.9 g green needles (73%); decomposition at ca. 187–189°C; M = 689 (osmometry in benzene). $\mu_{eff} = 1.45\mu_B$ (298 K); λ_{max}(reemission) = 746, 386 nm.

A crystal structure analysis of **3** was carried out [6a, b]. The resins were prepared according to the method given in [2b] (see Table 3).

Table 3. Composition of the polymerization mixtures [a].

Resin	Imprinting complex [g]	Solvent [g]	
		MeOH	Benzene
$\mathbf{1}_H$	1.485 **1**	20	20
$\mathbf{2}_H$	1.846 **2**	—	40
$\mathbf{1}_B$	1.217 NH_4L	20	20
$\mathbf{3}_H$	2.000 **3**	—	40
$\mathbf{3}_B$	1.217/0.615 NH_4L/vpy	20	20

[a] In each case, 40 g of EGDMA was used as cross-linking agent and 0.200 g of AIBN as initiator.

Received: July 15, 1988 [Z 2861 IE]
German version: *Angew. Chem. 100* (1988) 1757

[1] a) H. Bernhard, F. Grass, *Monatsh. Chem. 98* (1967) 1050, 1464; b) H. Nishide, E. Tsuchida, *Makromol. Chem. 177* (1976) 2295; c) H. Nishide, J. Deguchi, E. Tsuchida, *J. Polym. Sci. Polym. Chem. Ed. 15* (1977) 3023; d) V. A. Kabanov, A. A. Efendiev, D. D. Orujev, *J. Appl. Polym. Sci. 24* (1979) 259; e) M. Kato, H. Nishide, E. Tsuchida, T. Sasaki, *J. Polym. Sci. Polym. Chem. Ed. 19* (1981) 1803; f) A. A. Efendiev, V. A. Kabanov, *Pure Appl. Chem. 54* (1982) 2077; g) S. N. Gupta, D. C. Neckers, *J. Polym. Sci. Polym. Chem. Ed. 20* (1982) 1609.

[2] a) G. Wulff, A. Sarhan, K. Zabrocki, *Tetrahedron Lett. 1973*, 4329; b) G. Wulff, J. Vietmeier, H.-G. Poll, *Makromol. Chem. 188* (1987) 731; c) G. Wulff in W. T. Ford (Ed.): *Polymeric Reagents and Catalysts (ACS Symp. Ser. 308* (1986)), p. 186.

[3] a) U. Braun, W. Kuchen, E. Lehnert, A. Mundt, *Phosphorus Sulfur 18* (1983) 477; b) U. Braun, *Dissertation*, Universität Düsseldorf 1983; c) U. Braun, W. Kuchen, *Chem. Ztg. 108* (1984) 255.
[4] a) J. Schram, *Dissertation*, Universität Düsseldorf 1988; b) J. Schram, *Diplomarbeit*, Universität Düsseldorf 1984.
[5] See *Pure Appl. Chem. 29* (1972) 619.
[6] a) D. Mootz, A. Deeg, personal communication; b) A. Deeg, *Diplomarbeit*, Universität Düsseldorf 1988.

Protecting-Group-Dependent Stability of Intersaccharide Bonds— Synthesis of a Fucosyl-Chitobiose Glycopeptide**

By *Horst Kunz** and *Carlo Unverzagt*

Tumor cells exhibit an increased metabolism of fucose compared with normal cells and, as a consequence, a higher degree of fucosylation of their cell-membrane glycoproteins.[1] Glycoproteins fucosylated on the oligosaccharide side chains are therefore of interest as potential tumor-associated cell-membrane antigens.[2] A characteristic coupling site for the fucose residue in *N*-glycoproteins is O-6 of the asparagine-linked glucosamine unit of the chitobiose portion of the core region (structure **1**). We report here the synthesis of glycopeptides that contain structural element **1** and are partial sequences of a viral envelope protein.

GlcNAcβ1→4GlcNAcβ1→Asn
6
↑
Fucα1 **1**

To construct the fucosyl-chitobiose trisaccharide unit **1**, the fucosyl donor **3** is linked in an α-glycosidic fashion by the in-situ anomerization procedure,[3] to chitobiosyl azide **2**,[4] containing a free hydroxyl group at position 6. Here, the fucosyl donor **3** must be protected by non-neighboring-group-participating blocking functions (Scheme 1).

The coupling is carried out most easily with the benzyl-protected fucosyl bromide **3a**. The usual hydrogenation on platinum catalysts[5] cannot be used to reduce the azido function of the trisaccharide azide **4a** so obtained, since it would result in cleavage of the benzyl ether bonds. We achieved a selective hydrogenation to give the trisaccharide **5a** by using neutral (!) washed Raney nickel.

To synthesize the protected fucosylated chitobiosylasparagine building block **7a** (see Scheme 2), **5a** was linked, in the presence of ethyl 2-ethoxy-1,2-dihydroquinoline-1-carboxylate (EEDQ),[6] to *N*-allyloxycarbonyl(Aloc)aspartic acid *tert*-butyl ester.[7]

The Aloc group can be removed from the complex trisaccharide-asparagine conjugate in a selective and practically quantitative fashion by palladium(0)-catalyzed allyl group transfer to dimedone as weakly basic acceptor.[7] In this process, all other protecting groups, as well as the *O*- and *N*-glycosidic bonds, remain completely intact. Subsequent condensation of the selectively deprotected trisaccharide-asparagine ester **8a** with the *N*-protected dipeptide **9** affords the fully protected trisaccharide-tripeptide **11a**, a partial structure of turkey ovomucoid.[8] Upon attempted selective cleavage of the *tert*-butyl ester bond of **11a** with

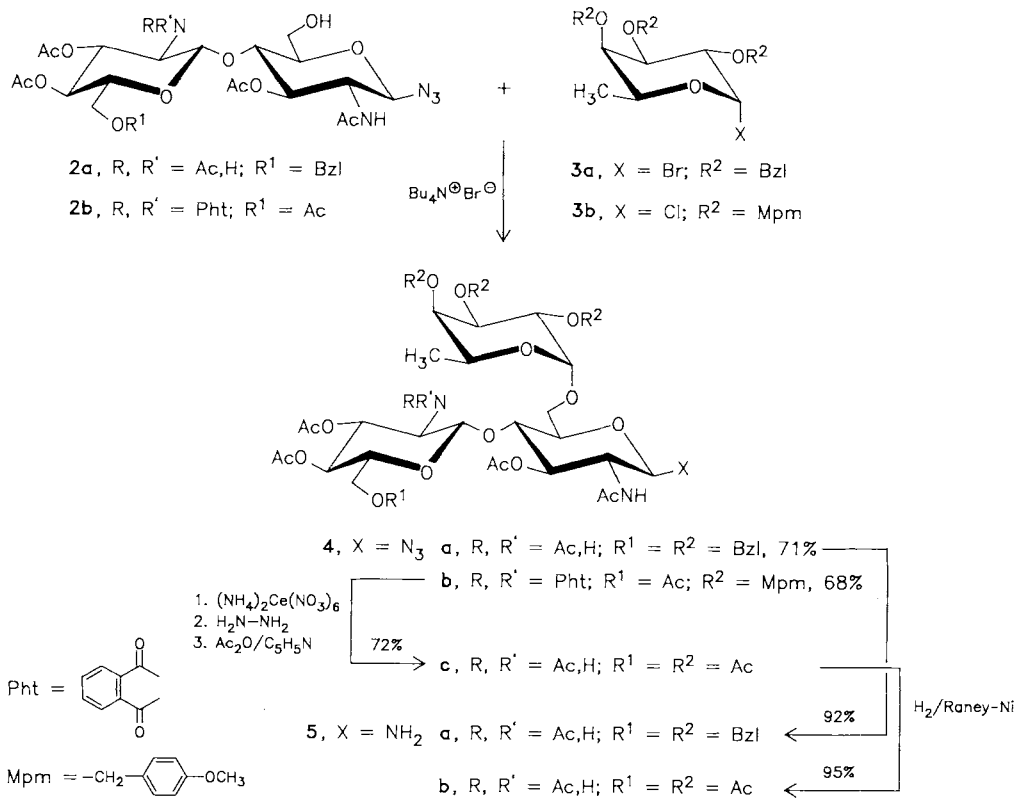

Scheme 1. Synthesis of the fucosyl-chitobiose trisaccharide unit in **1**. Bzl = Ph–CH_2.

trifluoroacetic acid for later immunological evaluation, complete cleavage of the fucoside bond occurred.

This discouraging result, obtained at the end of the multistep synthesis, reveals the inherent sensitivity of complex

[*] Prof. Dr. H. Kunz, Dr. C. Unverzagt
Institut für Organische Chemie der Universität
J.-J.-Becher-Weg 18-20, D-6500 Mainz (FRG)

[**] This work was supported by the Deutsche Forschungsgemeinschaft and the Fonds der Chemischen Industrie.

glycopeptides and shows what problems have to be foreseen and taken into consideration, even at the planning stage, in attempting the synthesis of complex glycoconjugates. We ascribe the sensitivity of the fucoside bond to the ether-type protecting groups in this monosaccharide building block.

We therefore developed a new concept for the synthesis of fucosyl-chitobiose asparagine derivatives of type **1**, which makes accessible compounds containing exclusively acyl (preferentially acyl = acetyl) protecting groups in the saccharide portion. To link the fucose in an α-glycosidic fashion to the chitobiosyl azide **2b**, the (*p*-methoxyphenyl)methyl(Mpm)-protected fucosyl donor **3b**[10] is employed according to the in-situ anomerization principle[4] (see Scheme 1). By oxidation with ammonium ceric nitrate,[9] the Mpm groups can be removed selectively from the trisaccharide azide **4b**. Subsequent hydrazinolysis removes the Pht group. The functional groups liberated in these reactions are then acetylated. The azide **4c** thus obtained in good yields is reduced to the corresponding trisaccharide amine **5b**, as already discussed for **4a**. Condensation with **6** gives the trisaccharide-asparagine conjugate **7b**, which bears exclusively acetyl protecting groups in the carbohydrate portion (Scheme 2).

Pd^0-catalyzed cleavage removes the Aloc group, again in a selective and effective fashion, from the product of this multistep synthesis, **7b**. Reaction of the *N*-deprotected trisaccharide-asparagine ester **8b** with the Aloc-dipeptide **10** gives, in high yield, the trisaccharide tripeptide **11b**. This glycoconjugate, in turn, is treated with trifluoroacetic acid for the subsequent *C*-terminal chain extension or for binding to a carrier. This cleavage of the *tert*-butyl ester bond is complete after 2 h at room temperature, without accompanying cleavage of the α-fucoside bond. The selectively *C*-terminal-deprotected trisaccharide tripeptide **12** is isolated in practically quantitative yield.

The fucoside bond is markedly more labile toward acid than the corresponding galactoside bond.[12] The contrasting behavior of the trisaccharide tripeptides **11a** and **11b** toward trifluoroacetic acid clearly reveals a strong effect of the *O*-protecting groups in the fucose portion on the acid stability of this bond. We ascribe the stabilizing effect of the *O*-acetyl groups in **11b** on the intersaccharide bond to the fact that the carbonyl oxygen atoms of the acyl protecting groups in this and in analogous glycoconjugates are protonated. Coulomb repulsion hinders further protonation of the intersaccharide and the ring oxygen atoms and therefore prevents saccharide cleavage. Thus, the acetyl groups not only protect the hydroxyl functions of the fucose residue but also protect an especially sensitive structural element to which they are not directly bonded: the intersaccharide bond. This effect is of great practical im-

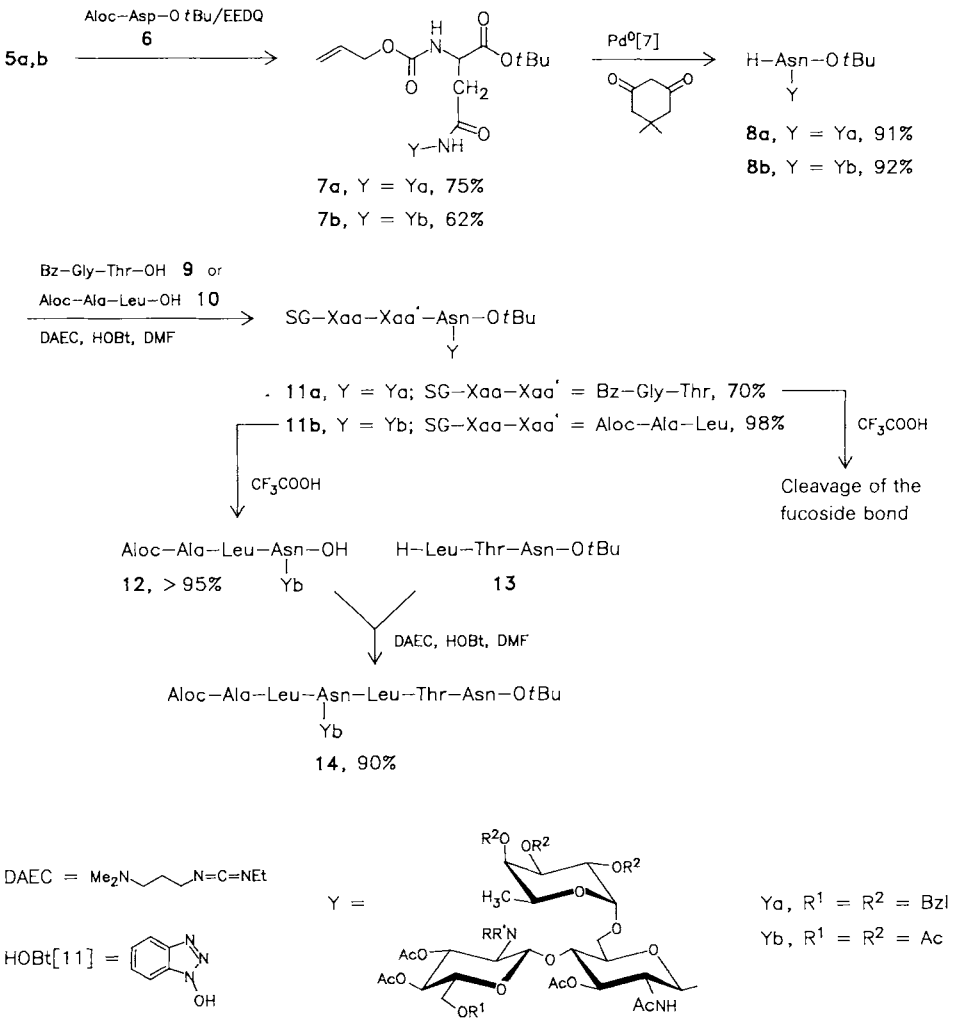

Scheme 2. Synthesis of fucosyl-chitobiose glycopeptide **14**. DMF = dimethylformamide.

portance for developing and carrying out syntheses of such complex, sensitive glycopeptides, since it defines the conditions under which the efficient *tert*-butyl protecting groups can be employed in the synthesis of polyfunctional glycoconjugates. It also explains the observed stability of serine and threonine glycopeptides[13] and the remarkable stability of the intersaccharide bond in chitobiosyl *N*-glycopeptides, even toward strong acids.[14]

The *C*-terminal-deprotected glycopeptide **12** was linked with the tripeptide ester **13** to give the trisaccharide hexapeptide **14**.[15] Compound **14** is the first fucose-containing trisaccharide glycopeptide to be obtained by both *N*- and *C*-terminal deprotection and corresponds to a partial structure of the linking region of the envelope protein of a leukemia virus.[16]

Received: July 29, 1988 [Z 2875 IE]
German version: *Angew. Chem. 100* (1988) 1763

[1] Review: M. C. Glick in E. F. Walborg, Jr. (Ed.): *Glycoproteins and Glycolipids in Disease Processes (ACS Symp. Ser. 80* (1978)), p. 404.
[2] a) A. Kobata, K. Yamashita, *Pure Appl. Chem. 56* (1984) 821; b) K. Yamashita, J. Ueda, M.Kuroki, Y. Matsuoka, A. Kobata, *Proc. 8th Int. Symp. Glycoconjugates* (Houston, Texas, USA 1985).
[3] R. U. Lemieux, K. B. Hendriks, R. V. Stick, K. James, *J. Am. Chem. Soc. 97* (1975) 4056.
[4] C. Unverzagt, *Dissertation*, Universität Mainz 1988; Details of the synthesis will be reported elsewhere.
[5] C. H. Bolton, L. Hough, M. Y. Khan, *Biochem. J. 101* (1966) 184.
[6] B. Belleau, G. Malek, *J. Am. Chem. Soc. 90* (1968) 1651.
[7] a) H. Kunz, C. Unverzagt, *Angew. Chem. 96* (1984) 426; *Angew. Chem. Int. Ed. Engl. 23* (1984) 436; b) H. Kunz, H. Waldmann, C. Unverzagt, *Pept. Proc. Eur. Pept. Symp. 19th 1986* (1987), 615.
[8] E. M. Taga, A. Waheed, R. L. van Etten, *Biochemistry 23* (1984) 815.
[9] R. Johansson, B. Samuelsson, *J. Chem. Soc. Perkin Trans. I 1984*, 2371.
[10] The Mpm group has already been employed in the synthesis of an analogous fucosyl-chitobiose trisaccharide: H. H. Lee, D. A. Schwartz, J. F. Harris, J. P. Carver, J. J. Krepinski, *Can. J. Chem. 64* (1986) 1912.
[11] W. König, R. Geiger, *Chem. Ber. 103* (1970) 788.
[12] W. G. Overend, C. W. Rees, J. S. Sequeira, *J. Chem. Soc. 1962*, 3429.
[13] a) V. Verez, Bencomo, P. Sinaÿ, *Carbohydr. Res. 116* (1983) C9; b) H. Paulsen, M. Schultz, J. D. Klamann, B. Waller, M. Paal, *Liebigs Ann. Chem. 1985*, 2028.
[14] H. Kunz, H. Waldmann, *Angew. Chem. 97* (1985) 885; *Angew. Chem. Int. Ed. Engl. 24* (1985) 883.
[15] **14**: $[\alpha]_D^{22} = -42.3$ (0.1, MeOH); $R_f = 0.60$ ($CHCl_3$/MeOH = 5/1); FAB-MS: *m/z* 1632 (*M*+1), 1654 (*M*+Na); 100-MHz ^{13}C NMR ([D$_6$]DMSO): $\delta = 172.0$–169.0 (C=O), 155.5 (urethane-C), 133.4 (=CH), 116.9 (H_2C=), 99.3 (C-1'), 95.1 (C-1'', Fuc), 80.4 (C_q of *t*Bu), 77.5 (C-1), 66.5 (β-C, Thr), 36.7 (β-C, Asn), 22.5 (NAc), 21.5 (δ-C, Leu), 20.6–20.3 (OAc), 19.3 (γ-CH_3, Thr), 18.0 (CH_3, Ala), 15.3 (CH_3, Fuc). C-1 and C-1' are the anomeric C atoms of the GlcNAc units at the reducing and nonreducing ends of the chitobiose, resp.
[16] M. Schlüter, D. Linder, R. Geyer, *Carbohydr. Res. 138* (1985) 305.

Synthesis and Structure of [MeAlN(2,6-*i*Pr$_2$C$_6$H$_3$)]$_3$: An Aluminum-Nitrogen Analogue of Borazine**

By *Krista M. Waggoner, Håkon Hope* and *Philip P. Power**

The poly(*N*-alkyliminoalanes), $(RAlNR')_n$, constitute an interesting class of aluminum-nitrogen compounds.[1] They are most notable for the variety and novelty of structures that they can adopt. Typically these are of a three-dimensional type involving an Al–N framework wherein both the Al and N atoms are four coordinate. The simplest structure involves a regular Al_4N_4 cubane framework as in $(PhAlNPh)_4$.[2] However, $(RAlNR')_n$ compounds with higher degrees of aggregation, up to n = 16, have been reported and the structures are known for such compounds where n = 4, 6, 7, 8, and R and R' = a variety of alkyl, aryl and hydrogen substituents.[1] To date, however, no aggregates involving n values less than 4 have been described. The lower $(RAlNR')_n$ compounds, where n = 1, 2 or 3 are of interest because they imply the presence of Al–N multiple bonds, as in the monomer RAlNR', or the potentially aromatic ring systems such as $(RAlNR')_3$. We now report the first example of a trimeric iminoalane. This is the title compound [MeAlN(2,6-*i*Pr$_2$C$_6$H$_3$)]$_3$ **1** which has been characterized by X-ray crystallography and ^1H- and ^{27}Al-NMR spectroscopy.

The compound **1** was synthesized, in high yield, as colorless crystals via a two stage elimination reaction between $AlMe_3$ and 2,6-*i*Pr$_2$C$_6$H$_3$NH$_2$ [Eq. (a)].

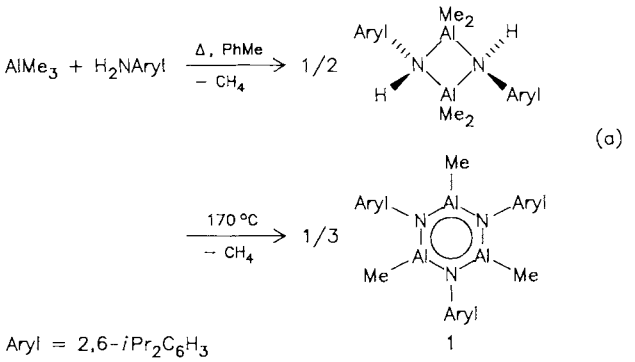

The crystal structure of **1**[3] is illustrated in Figure 1. It consists of a central planar six-membered ring of alternating Al and N atoms with an average Al–N bond length of 1.78 Å. The C atoms bonded to Al or N are coplanar with

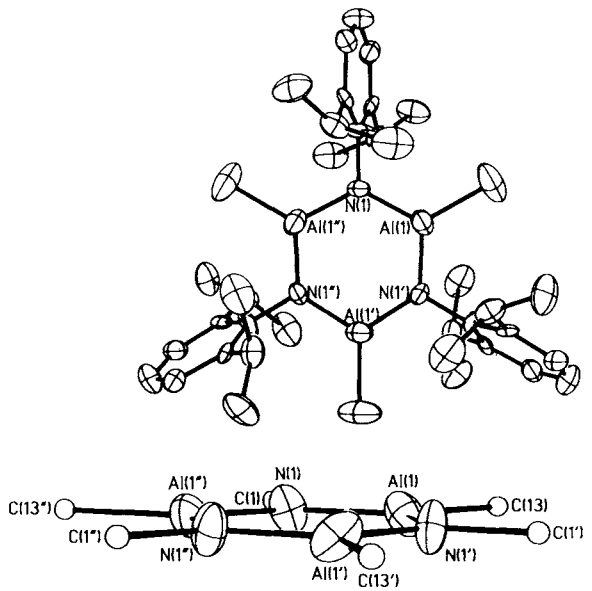

Fig. 1. Two views of the crystal structure of one of the molecules of **1** (H atoms omitted for clarity). Selected bond distances [Å] and angles [°]. Al(1)–N(1) 1.782(4), Al(1)–C(13) 1.978(15), N(1)–C(1) 1.442(14); N(1)–Al(1)–N(1') 115.3(5), Al(1)–N(1)–Al(1') 124.7(5). The dihedral angle between the Al_3N_3 and C(1) rings is 75.2°.

[*] Prof. P. P. Power, K. M. Waggoner, Prof. H. Hope
Department of Chemistry, University of California
Davis, California 95616 (USA)

[**] This work was supported by the National Science Foundation. We also thank *R. A. Bartlett* and Dr. *M. M. Olmstead* for helpful discussions and experimental assistance.

the central ring. The Al–N distance may be compared with the Al–N bond lengths found in the higher polyiminoalanes which generally range from 1.89–1.96 Å.[1] Since the latter distances invariably involve four-coordinate Al and N centers, a bond-shortening is to be expected in the case of **1**. Unfortunately, very few compounds with bonding between three-coordinate aluminum and nitrogen centers are available for comparison. An exception is $Al[N(SiMe_3)_2]_3$,[4] which was reported to have an Al–N bond length of 1.78 Å. Clearly more structural data regarding Al–N bonding will be needed to assess more accurately the amount of bond-shortening in **1**.

The ^{1}H-NMR spectrum of **1** confirms the X-ray crystallographically determined composition, since the ratio of Al–Me groups to aryl groups is 1 : 1. The ^{27}Al-NMR spectrum reveals a broad singlet at $\delta = 168$ ($\nu_{1/2} = 8800$ Hz), which is shifted slightly downfield compared to the signals generally observed for three-dimensional polyiminoalanes.[5] These ^{27}Al-NMR data are consistent with the lower coordination number and the asymmetry of the aluminum center in **1**.

The title compound **1** bears an obvious isoelectronic resemblance to the recently synthesized boraphosphabenzenes $(RBPR')_3$.[6,7] It is notable, however, that the Al–N bonds are considerably shorter than the B–P (1.84 Å) distances. The much greater ionic character of the Al–N pair may account for part of this difference. It is also noteworthy that **1** is an aluminum counterpart of a substituted borazine.[8] However, **1** appears to be much more reactive and is instantly decomposed by traces of air or moisture.

Although the equivalence and shortness of the Al–N bonds support delocalization, the possible aromatic nature of **1** remains an open question. In the case of the related B_3P_3 rings there is some ^{1}H NMR spectroscopic evidence which supports the presence of a ring current.[7] The ^{1}H-NMR spectrum of **1**, however, appears to display no unusual shifts which could be attributed to a ring current. Preliminary calculations[9] on both the B_3P_3 and Al_3N_3 rings indicate extensive delocalization. However, more firm conclusions await the synthesis and characterization of a range of Al_3N_3 ring systems.

Experimental Procedure

A 2.0 M solution of $AlMe_3$ (13 mL, 26 mmol) in toluene was added dropwise, under anaerobic and anhydrous conditions, to a solution of 2,6-diisopropylaniline (4.9 mL, 26 mmol) in toluene (50 mL) at room temperature. The mixture was then heated under reflux for 20 h. Concentration under reduced pressure to ca. 20 mL afforded colorless crystals of $[Me_2AlNH(2,6\text{-}iPr_2C_6H_3)]_2$ (yield: 4.8 g, 10.3 mmol, 79%; m.p. = 135 °C). Heating $[Me_2AlNH(2,6\text{-}iPr_2C_6H_3)]_2$ at 170 °C resulted in frothing due to evolution of CH_4. After ca. 10 minutes gas evolution ceased and the reaction mixture resolidified to give **1** in essentially quantitative yield; m.p. = 272 °C. Crystals for X-ray structural characterization were grown from hexane. 300 MHz ^{1}H-NMR (C_6D_6): $\delta = 6.94$ (m; aryl-H), 3.38 (sept.; CH), 1.18 (d, $J = 9$ Hz; $CH(CH_3)_2$), −0.38 (Al–CH_3).

Received: July 27, 1988 [Z 2888 IE]
German version: *Angew. Chem. 100* (1988) 1765

[1] E. Wiberg, A. May, *Z. Naturforsch. B 10* (1955) 232; S. Amirkhalili, P. B. Hitchcock, J. D. Smith, *J. Chem. Soc. Dalton Trans. 1979*, 1206, and references cited therein. M. Cesari, S. Cucinella in I. Haiduc, D. B. Sowerby (Eds.): *The Chemistry of Inorganic Homo and Heterocycles, Vol. 1*, Academic Press, London 1987, Chapter 6.

[2] T. R. R. McDonald, W. S. McDonald, *Acta Crystallogr. Sect. B 28* (1972) 1619.

[3] Crystal data for **1** (130 K, $Mo_{K\alpha}$ ($\lambda = 0.71069$ Å)): $a = 19.035(6)$ Å, $c = 20.422(7)$ Å, trigonal, $P\bar{3}c1$, $Z = 6$, 1609 unique observed ($I > 3\sigma(I)$) data, $R = 0.10$. Further details of the crystal structure investigation may be obtained from the Fachinformationszentrum Energie, Physik, Mathematik GmbH, D-7514 Eggenstein-Leopoldshafen 2 (FRG), on quoting the depository number CSD-53394, the names of the authors, and the journal citation.

[4] G. M. Sheldrick, W. S. Sheldrick, *J. Chem. Soc. A 1969*, 2279.

[5] H. Nöth, P. Wolfgardt, *Z. Naturforsch. B 31* (1976) 637.

[6] H. V. R. Dias, P. P. Power, *Angew. Chem. 99* (1987) 1320; *Angew. Chem. Int. Ed. Engl. 26* (1987) 1270.

[7] H. V. R. Dias, P. P. Power, *J. Am. Chem. Soc.*, in press.

[8] In this regard the trivial name alumazine may be justified for the $(AlN)_3$ ring.

[9] W. Hehre, private communication.

Novel Anionic Aryl Complexes of Rh^{III}: $[Rh(C_6F_5)_5]^{2\ominus}$ and $[Rh(C_6F_5)_4(CO)_2]^{\ominus}$**

By *María P. García,* Luis A. Oro,* and *Fernando J. Lahoz*

Anionic transition-metal complexes have received considerable attention due to their reactivity towards organic molecules as well as their utility in the preparation of homo- and heteronuclear transition-metal clusters.[1,2] Compounds containing π-acceptor ligands such as PR_3, $P(OR)_3$, and AsR_3 are the most numerous and the most stable of all alkyl and aryl complexes of transition metals. As far as we know, it has been possible to prepare rhodium complexes containing exclusively one, two, or three aryl or alkyl groups by transmetalation reactions (for instance, $[RhMe_3(PMe_3)_3]$[3]). When the starting compounds do not contain ancillary π-acceptor ligands, the arylation can progress even to the formation of anionic transition-metal complexes.[4] Although the pentahaloaryl complexes are more stable than their unsubstituted aryl analogues, complexes with this sort of group are rather scarce.[5]

These considerations prompted us to study the arylation of rhodium compounds without group V ligands by reaction with an excess of LiC_6F_5, in order to obtain anionic aryl derivatives.

Reaction of **1** with an excess of LiC_6F_5 (ratio 1 : 8) leads to a solution containing the arylated anion $[Rh(C_6F_5)_5]^{2\ominus}$, which can be crystallized as **2** by addition of a salt of a bulky cation. Complex **2**, the first anionic homoleptic

$$[RhCl_3(SC_4H_8)_3] + 5\,LiC_6F_5 \xrightarrow[-3\,SC_4H_8]{-3\,LiCl} Li_2[Rh(C_6F_5)_5]$$

1

$$\xrightarrow[-2\,LiCl]{2[P(CH_2Ph)Ph_3]Cl} [P(CH_2Ph)Ph_3]_2[Rh(C_6F_5)_5]$$

2

Rh^{III} complex, does not react with PPh_3, pyridine, or $P(OMe)_3$; it reacts immediately with CO in CH_2Cl_2, at room temperature, giving a pale yellow solution ($\tilde{\nu}(CO) = 2065$ cm^{-1}). The spectroscopic data (IR and ^{19}F NMR) of the solid obtained after workup indicate that it is a mixture of compound **2** and a new product, presumably **3** (^{19}F NMR

$[P(CH_2Ph)Ph_3]_2[Rh(C_6F_5)_5(CO)]$ **3**

spectrum in [D$_6$]acetone, new signals at $\delta = -105.7$ (*o*-F), -167.9 (*m*- and *p*-F)). This compound is probably an intermediate of a carbonylation process, since prolonged treatment of **2** with CO, in CH_2Cl_2 (or THF) at refluxing tem-

[*] Dr. M. P. García, Prof. Dr. L. A. Oro, Dr. F. J. Lahoz
Departamento de Química Inorgánica
Instituto de Ciencia de Materiales de Aragón
Universidad de Zaragoza—C.S.I.C.
E-50009 Zaragoza (Spain)

[**] This work was supported by C.A.I.C.Y.T. (Spain).

perature, leads to a new species with a CO stretching frequency at 2100 cm^{-1}. The solution becomes colorless and the white crystalline solid obtained was identified as **4**. A similar carbonylation reaction has been reported by *Foster* et al.[6] for $[RhBr_5(CO)]^{2\ominus}$.

trans-$[P(CH_2Ph)Ph_3][Rh(C_6F_5)_4(CO)_2]$ **4**

Surprisingly, complex **4** (being a Rh^{III} derivative) can be prepared by arylation of a Rh^{I} compound, $[RhCl(CO)_2]_2$, with LiC_6F_5 in the presence of BrC_6F_5 (see *Experimental Procedure*). If BrC_6F_5 is not present, the reaction gives an oily mixture from which we have not been able to isolate any solid product. Since $[RhCl(CO)_2]_2$ does not react with BrC_6F_5 under the same reaction conditions, the formation of the anion of **4** probably takes place through an intermediate anion *cis*-$[RhR_2(CO)_2]^{\ominus}$[6] followed by oxidative addition of BrC_6F_5 to the Rh^{I} species; finally, by further reaction with LiC_6F_5, the bromine atom is replaced by a C_6F_5 group.

The arylation of $[RhCl(CO)(PPh_3)]_2$ with LiC_6F_5 produces yellow crystals identified as the rhodium(I) complex **5**. The structures of compounds **2** and **4**, determined by

trans-$[Rh(C_6F_5)(CO)(PPh_3)_2]$ **5**

single-crystal X-ray diffraction studies[7] are shown in Figures 1 and 2, respectively. In the solid state, the anion of **2**, $[Rh(C_6F_5)_5]^{2\ominus}$, has a square-pyramidal geometric arrangement with the rhodium atom slightly above (0.222(3) Å) the plane of the four basal C_6F_5 groups, while in solution, at room temperature, the ^{19}F NMR shows that all the C_6F_5 groups are equivalent. The anion $[Rh(C_6F_5)_4(CO)_2]^{\ominus}$ exhibits a clear octahedral structure with the CO groups in mutually *trans* positions. Interestingly, both Rh–CO distances are 1.93(1) Å, slightly longer than those reported in the structurally related complex $[RhI_4(CO)_2]^{\ominus}$.[6]

All the complexes prepared are solids which can be handled in air or in solution for long periods without evident decomposition.

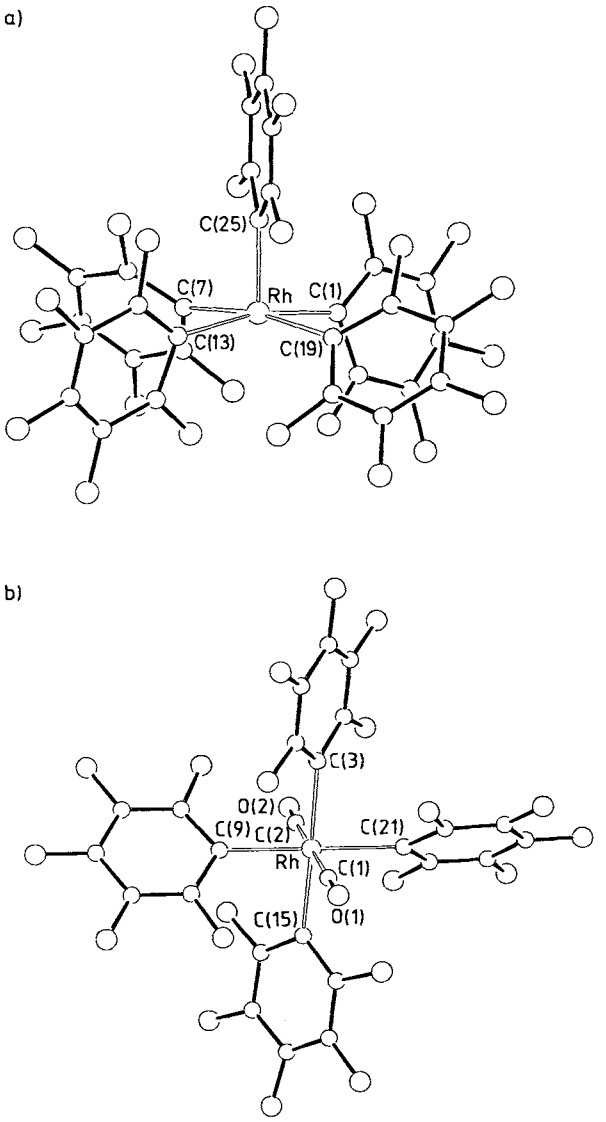

Fig. 1. Molecular structures of the anions of **2** and **4**. Selected bond lengths [Å] and angles [°]: a) **2**: Rh-C(1) 2.13(1), Rh-C(7) 2.12(1), Rh-C(13) 2.09(1), Rh-C(19) 2.12(1), Rh-C(25) 1.97(1); C(1)-Rh-C(7) 95.7(4), C(1)-Rh-C(13) 166.8(4), C(1)-Rh-C(25) 97.3(4). b) **4**: Rh-C(1) 1.93(1), Rh-C(2) 1.93(1), Rh-C(3) 2.12(1), Rh-C(9) 2.13(1), Rh-C(15) 2.13(1), Rh-C(21) 2.12(1); C(1)-Rh-C(2) 179.3(4), C(3)-Rh-C(15) 178.1(4), C(9)-Rh-C(21) 179.3(4).

Experimental Procedure

1: A suspension of commercial $RhCl_3 \cdot x H_2O$ (0.5 g) in $CHCl_3$ (10 mL) was treated with SC_4H_8 (1 mL) and 96% ethanol (20 mL). The mixture was stirred for two days at room temperature. A yellow-orange suspension was formed. Partial evaporation of the solvent and addition of diethyl ether gave a yellow-orange solid in almost quantitative yield. Correct elemental analysis for **1**.

2: To a solution of LiC_6F_5 (1.47 g, 8.44 mmol) in dry diethyl ether (30 mL) at −78 °C was added **1** (0.5 g, 1.06 mmol), and the mixture was stirred for 3 h at room temperature, hydrolyzed with aqueous ether, and then evaporated to dryness. The residue was treated with dichloromethane/acetone (20/30 mL) and filtered through $MgSO_4$-silica. Evaporation of the filtrate to ca. 10 mL and addition of $[P(CH_2Ph)Ph_3]Cl$ (0.9 g, 2.3 mmol) in 2-propanol (30 mL) led, after partial evaporation, to **2** (yellow crystalline solid; 1.40 g, 80% yield). Correct elemental analysis. NMR spectra in [D$_6$]acetone: 188-MHz ^{19}F NMR (standard $CFCl_3$): $\delta = -116.6$ (*o*-F), −168.7 (*m*- and *p*-F); 81-MHz $^{31}P\{^1H\}$ NMR: $\delta = 24.54$.

4: This complex has been prepared by two methods: a) Bubbling CO for 90 min through a solution of complex **2** (0.200 g, 0.12 mmol) in CH_2Cl_2 (or THF) at refluxing temperature gave a colorless solution. Partial evaporation of the solvent and addition of hexane gave 0.11 g of a white solid (75% yield). b) To a mixture of LiC_6F_5 (2.32 g, 12.0 mmol) and BrC_6F_5 (0.3 mL, 2.36 mmol) in diethyl ether (40 mL) at −78 °C, $[RhCl(CO)_2]_2$ (0.45 g, 2.3 mmol) was added. The reaction mixture was allowed to reach room temperature, stirred for 4 h, hydrolyzed with aqueous diethyl ether and then evaporated to dryness. The residue was extracted with dichloromethane/acetone (15/20 mL) and filtered through $MgSO_4$-silica. Evaporation of the filtrate to ca. 10 mL and addition of $[P(CH_2Ph)Ph_3]Cl$ (1 g, 2.58 mmol) in 2-propanol (30 mL) led, after partial evaporation, to a white solid (**4**; 1.9 g, 72% yield). Spectroscopic data: IR (CH_2Cl_2): $\tilde{\nu}(CO) = 2100\ cm^{-1}$; 88 MHz ^{19}F NMR ([D$_6$]acetone): $\delta = -107.1$ (*o*-F), −161.3 (*p*-F), −163.0 (*m*-F).

5: Starting compounds: $[RhCl(CO)(PPh_3)]_2$ and LiC_6F_5, ratio 1 : 4.5. The synthesis was carried out as reported for **2**. Before addition of the salt, a yellow solid separated out with diethyl ether (40% yield). Complex **5** was identified by its spectroscopic (IR, NMR) and analytical data and its molecular weight.

Received: June 6, 1988 [Z 2803 IE]
German version: *Angew. Chem. 100* (1988) 1766

[1] A. A. Del Paggio, R. A. Andersen, E. L. Muetterties, *Organometallics 6* (1987) 1260, and references cited therein.
[2] F. A. Cotton, L. R. Falvello, R. Usón, J. Forniés, M. Tomás, J. M. Casas, I. Ara, *Inorg. Chem. 26* (1987) 1366; R. Usón, J. Forniés, M. Tomás, J. M. Casas, F. A. Cotton, L. R. Falvello, *ibid. 26* (1987) 3482, and references cited therein.
[3] R. A. Anderson, R. A. Jones, G. Wilkinson, *J. Chem. Soc. Dalton Trans. 1978*, 446.
[4] R. Usón, J. Forniés, P. Espinet, R. Navarro, F. Martínez, M. Tomás, *J. Chem. Soc. Chem. Commun. 1977*, 789; R. Usón, J. Forniés, F. Martínez, M. Tomás, *J. Chem. Soc. Dalton Trans. 1980*, 888; R. Usón, A. Laguna, M. Laguna, E. Fernández, P. G. Jones, G. M. Sheldrick, *ibid. 1982*, 1971.

[5] R. S. Nyholm, P. Royo, *Chem. Commun. 1969*, 421; R. L. Bennett, M. I. Bruce, R. C. F. Gardner, *J. Chem. Soc. Dalton Trans. 1973*, 26; G. Tresoldi, F. Faraone, P. Piraino, *ibid. 1979*, 1053; G. B. Deacon, S. J. Faulks, J. M. Miller, *Transition Met. Chem. (Weinheim, Ger.) 5* (1980) 305.
[6] J. J. Daly, F. Sanz, D. Foster, *J. Am. Chem. Soc. 97* (1975) 2551.
[7] Siemens AED diffractometer ($Mo_{K\alpha}$): **2** (diethyl ether solvate): monoclinic, $P2_1/n$, $a=12.250(1)$, $b=42.913(3)$, $c=14.665(1)$ Å, $\beta=91.34(1)°$, $V=7707(1)$ Å^3, $\rho_{calcd}=1.450$ g cm^{-3}, $\mu=3.59$ cm^{-1}, $Z=4$; $3\le 2\theta\le 42°$, total number of reflections 8847, 4967 observed with $I\ge 3\sigma(I)$, $R=0.068$, $R_w=0.070$. **4** (2-propanol solvate): Monoclinic, $C2/c$, $a=32.700(3)$, $b=15.051(3)$, $c=21.312(2)$ Å, $\beta=92.24(1)°$, $V=10460(2)$ Å^3, $\rho_{calcd}=1.537$ g cm^{-3}, $\mu=4.58$ cm^{-1}, $Z=8$; $3\le\theta\le 42°$, total number of reflections 11578, 4115 observed with $F\ge 5\sigma(F)$, $R=0.068$, $R_w=0.075$. Further details of the crystal structure analyses may be obtained from the Cambridge Crystallographic Data Centre, University Chemical Laboratory, Lensfield Road, Cambridge CB2 1EW (UK), on quoting the full journal citation.

Soluble Chromium Selenides and Tellurides: Preparation and Structures of $[(C_6H_5)_4P]_3[Cr_3Te_{24}]$ and $[(C_6H_5)_4P]_3[Cr_3Se_{24}]$**

By *Walter A. Flomer, Samuel C. O'Neal, William T. Pennington, David Jeter, A. Wallace Cordes,* and *Joseph W. Kolis**

We have been interested in synthesizing soluble transition metal clusters containing heavy polychalcogen ligands in the hope that they might be used as reagents for the preparation of new materials, particularly low-dimensional compounds with unique conductive properties.[1] Several soluble binary selenidometalate clusters have been reported previously, such as $[Fe_2Se_{12}]^{2\ominus}$,[2] $[W_2Se_9]^{2\ominus}$,[3] $[W_2Se_{10}]^{2\ominus}$,[3] and $[V_2Se_{13}]^{2\ominus}$,[4] but in general the area is quite neglected compared to metal polysulfide chemistry.[5,6] The solid-state chemistry of metal tellurides has recently been reviewed.[7] We have found that Zintl ions such as $Te_2^{2\ominus}$, $Te_4^{2\ominus}$, and $Se_3^{2\ominus}$ can be extracted from potassium tellurides and selenides with dimethylformamide. They have proven to be convenient reagents for the preparation of a variety of chalcogenidometalates such as $[Cr(CO)_4Te_4]^{2\ominus}$,[8] $[MoSe_4]^{2\ominus}$,[9] and $[NbTe_{10}]^{3\ominus}$.[10] Herein, we report on the reaction of polytelluride and polyselenide solutions with chromium chloride leading to the novel clusters $[Cr_3Te_{24}]^{3\ominus}$ and $[Cr_3Se_{24}]^{3\ominus}$, which we believe to be the first soluble chromium selenides and tellurides.

The reaction of solids of nominal composition K_2Se_3 or K_2Te_2 with $CrCl_3$ in DMF under rigorously anaerobic conditions produces a brown solution in the case of tellurium and a red solution in the case of selenium. Slow addition of THF in the presence of $(C_6H_5)_4PBr$ leads to separation of black crystals [Eq. (a)].[11]

$$Cr^{3\oplus} + 2E_4^{2\ominus} \longrightarrow 1/3[Cr_3E_{24}]^{3\ominus} \qquad (a)$$

X-ray diffraction analyses revealed compounds of the composition $[(C_6H_5)_4P]_3[Cr_3Se_{24}]$ and $[(C_6H_5)_4P]_3[Cr_3Te_{24}]$. The two structures are similar, even though the compounds crystallize in different unit cells.[12] The selenide compound contains two different $[Cr_3Se_{24}]^{3\ominus}$ clusters per asymmetric unit, but the structural features of each are similar. Each compound consists of three well separated $[(C_6H_5)_4P]^{\oplus}$ ions and a cluster of the formula $[Cr_3E_{24}]^{3\ominus}$ (E = Se, Te). The trianion is a linear array of three chromium atoms which are linked by six tetrachalcogenide groups (Fig. 1, top). The two terminal chromium atoms are octahedrally coordinated by three bidentate $E_4^{2\ominus}$ ions. Each of the chalcogenide chains has one terminal atom which is μ-2, bridging one terminal metal atom and the central metal atom. The net result is three face sharing octahedra, if only the coordinated chalcogenides are considered. The overall structure is similar to that of $[(C_6H_5)P_4]_2Na[Cr_3(SCH_2CH_2O)_6]$.[13] Each compound possesses an inversion center at the central chromium atom, making these molecules two of the very few purely inorganic meso compounds. A view down the Cr_3-axis shows the overall S_6 symmetry (Fig. 1, bottom).

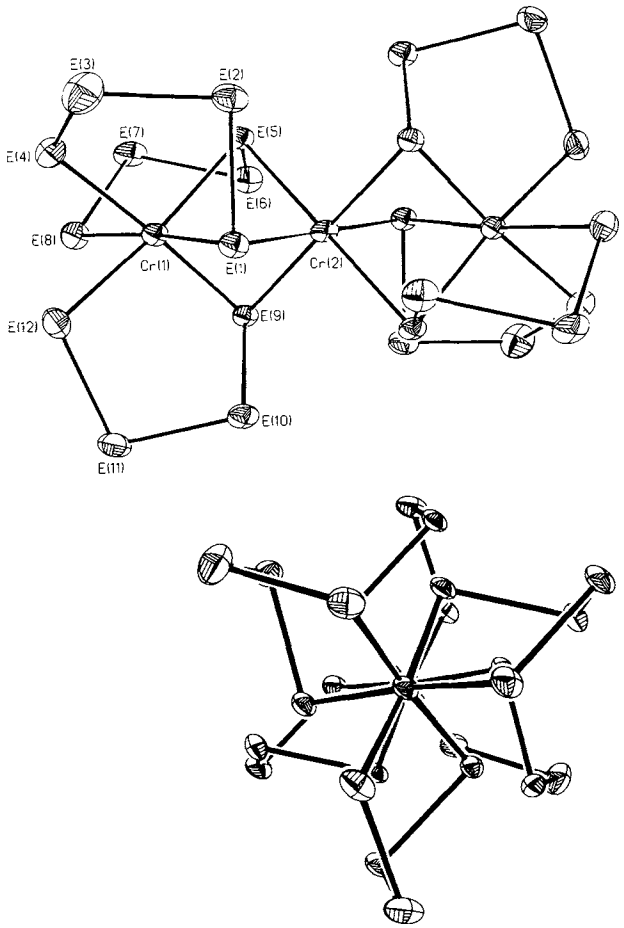

Fig. 1. Top: Side view of the $[Cr_3E_{24}]^{3\ominus}$ ion, where E = Se, Te. Bottom: End view of the $[Cr_3E_{24}]^{3\ominus}$ molecule showing the $S6$ symmetry.—Some important distances [Å] and angles [°] in the $[Cr_3Te_{24}]^{3\ominus}$ ion: Cr1–Cr2 3.41(1), Cr1–Te1 2.737(6), Cr1–Te4 2.688(8), Cr1–Te5 2.753(7), Cr1–Te8 2.684(7), Cr1–Te9 2.741(8), Cr1–Te12 2.696(7), Cr2–Te1 2.746(3), Cr2–Te5 2.735(2), Cr2–Te9 2.722(3), Te1–Te2 2.773(4), Te2–Te3 2.705(5), Te3–Te4 2.823(5), Te5–Te6 2.782(4), Te6–Te7 2.731(5), Te7–Te8 2.813(4), Te9–Te10 2.781(3), Te10–Te11 2.725(5), Te11–Te12 2.792(5); Cr1–Te1–Cr2 77.2(2), Cr1–Te5–Cr2 77.1(1), Cr1–Te9–Cr2 77.5(2), Te1–Cr1–Te4 102.5(2), Te5–Cr1–Te8 102.5(2), Te9–Cr1–Te12 101.5(2).—Some important distances [Å] and angles [°] in the $[Cr_3Se_{24}]^{3\ominus}$ ion: Cr1–Cr2 3.207, Cr1–Se1 2.529(9), Cr1–Se5 2.520(9), Cr1–Se9 2.541(9), Cr2–Se1 2.585(17), Cr2–Se4 2.476(16), Cr2–Se5 2.586(17), Cr2–Se8 s.474(17), Cr2–Se9 2.589(16), Cr2–Se12 2.450(17), Se1–Se2 2.378(13), Se2–Se3 2.317(13), Se3–Se4 2.368(15), Se5–Se6 2.367(15), Se6–Se7 2.342(13), Se7–Se8 2.364(15), Se9–Se10 2.383(14), Se10–Se11 2.332(12), Se11–Se12 2.368(13); Cr1–Se1–Cr2 77.7(4), Cr1–Se5–Cr2 77.8(4), Cr1–Se9–Cr2 77.4(4), Se1–Cr2–Se4 98.1(6), Se5–Cr2–Se8 97.5(6), Se9–Cr2–Se12 97.9(6).

[*] Prof. J. W. Kolis, W. A. Flomer, S. C. O'Neal, W. T. Pennington
Chemistry Department, Clemson University
Clemson, SC 29634 (USA)
Prof. A. W. Cordes, D. Jeter
Chemistry Department, University of Arkansas
Fayetteville, AR 72701 (USA)

[**] Acknowledgment is made to the donors of the Petroleum Research Fund, administered by the ACS, and to the National Science Foundation for support of this research.

The Te–Te distances average 2.767 Å compared to 2.72 Å in PhTe–TePh, while the Se–Se distances average 2.358 Å compared to 2.29 Å in PhSe–SePh.[14] The average Cr–Te distance is 2.719 Å and the average Cr–Se distance is 2.525 Å, with the *bridging* Cr–E distance being longer by about 0.1 Å in each case. They thus resemble the Cr–Te distance of 2.726 Å in $[(CO)_4CrTe_4]^{2\ominus}$[8] and the Cr–Se distance of 2.453 Å in $[\{(C_5H_5)CrNO\}_2(\mu\text{-}SePh)_2]$.[15] The Cr–Cr distances of 3.41 Å in the telluride and 3.20 Å in the two molecules of the selenide compound are substantially longer than a Cr–Cr bond. The effective magnetic moments of the selenido- and tellurido-clusters at 300°K, are 5.25 and 5.74, respectively, indicating a spin = 3/2 system with reasonably strong antiferromagnetic coupling in each case.[16]

Molecular chromium chalcogenides were hitherto unknown; however, several solid-state chromium selenides and chromium tellurides have been reported, but many of these have not been structurally characterized.[17] The binary compounds CrSe and CrTe crystallize with the NiAs-type structure.[18] A chromium telluride of composition $CrTe_3$[19] has a complicated structure consisting of octahedrally coordinated $Cr^{3\oplus}$ atoms and layers containing $Te_2^{2\ominus}$ and $Te_3^{2\ominus}$ as well as $Te^{2\ominus}$ ions. The Cr–Te and Te–Te distances in this compound resemble those in $[Cr_3Te_{24}]^{3\ominus}$.

Received: May 24, 1988 [Z 2776 IE]
German version: *Angew. Chem. 100* (1988) 1768

[1] A. Meerschaut, J. Rouxel in J. Rouxel (Ed.): *Crstal Chemistry and Properties of Materials with Quasi-One Dimensional Structures*, Reidel, Dordrecht 1986, p. 205.
[2] H. Strasdeit, B. Krebs, G. Henkel, *Inorg. Chim. Acta 89* (1984) L11.
[3] R. W. M. Wardle, C.-N. Chau, J. A. Ibers, *J. Am. Chem. Soc. 109* (1987) 1859.
[4] C.-N. Chau, R. W. M. Wardle, J. A. Ibers, *Inorg. Chem. 26* (1987) 2740.
[5] M. Draganjac, T. B. Rauchfuss, *Angew. Chem. 97* (1985) 745; *Angew. Chem. Int. Ed. Engl. 24* (1985) 742.
[6] A. Müller, *Polyhedron 5* (1985) 323.
[7] P. Böttcher, *Angew. Chem. 100* (1988) 781; *Angew. Chem. Int. Ed. Engl. 27* (1988) 759.
[8] W. A. Flomer, S. C. O'Neal, A. W. Cordes, D. Jeter, J. W. Kolis, *Inorg. Chem. 27* (1988) 969.
[9] S. C. O'Neal, J. W. Kolis, *J. Am. Chem. Soc. 110* (1988) 1971.
[10] W. A. Flomer, J. W. Kolis, *J. Am. Chem. Soc. 110* (1988) 3682.
[11] Typical procedure: A mixture of K_2Se_3 (250 mg, 0.790 mmol), $CrCl_3$ (125 mg, 0.790 mmol) and $(C_6H_5)_4PBr$ (660 mg, 1.58 mmol) is treated under argon with 20 mL of DMF. The reaction mixture is than stirred at room temperature for 1 h, filtered and the filtrate (red solution) is covered with a layer of THF (5 mL). After one week, 200 mg of large black crystals can be isolated (25% yield based on chromium). The telluride is prepared in a similar way, but a threefold excess of polytelluride is required; furthermore, a microcrystalline product usually results. It is often easier to obtain single crystals by first dissolving the appropriate amounts of telluride and phosphonium salt in DMF, and then adding $CrCl_3$. The selenide, on the other hand, readily forms large crystals upon slow addition of THF.
[12] Crystal structure data: a) $[(C_6H_5)_4P]_3[Cr_3Se_{24}]$: space group $P\bar{1}$, $a=13.971(5)$, $b=14.208(3)$, $c=25.756(5)$ Å, $\alpha=74.17(2)$, $\beta=86.04(4)$, $\gamma=84.83(2)°$, $V=4893(3)$ Å^3, $Z=2$, $\mu_{MoK\alpha}=92.25$ cm^{-1}, refined, using 2275 reflections ($2\theta\leq45°$) with $F_o^2>3\sigma(F_o^2)$, to $R=0.0833$ and $R_w=0.0967$ for 349 refined parameters, $[w=1/(\sigma^2F+0.001F^2)]$ holding all phenyl rings as rigid groups. b) $[(C_6H_5)_4P]_3[Cr_3Te_{24}]$: space group $P\bar{1}$, $a=10.749(5)$, $b=14.328(5)$, $c=20.395(5)$ Å, $\alpha=72.09(4)$, $\beta=80.87(3)$, $\gamma=73.24(4)°$, $V=2853(3)$ Å^3, $Z=1$, $\mu_{MoK\alpha}=63.65$ cm^{-1}, refined using 2978 reflections ($2\theta\leq45°$), with $F_o^2>3\sigma(F_o^2)$, to $R=0.0636$, $R_w=0.0808$. The solution of the structure of the telluride is hampered by a disordering of one of the three $(C_6H_5)_4P^{\oplus}$ counterions about an inversion center. The final refinement was based on an idealized molecule from the best fit of observed difference map peaks. Variations in the modeling of the disordered counterion, or its removal from the refinement altogether, have no effect on the structural parameters of the anion. The displacement of the phosphorus atom from the inversion center by 3.75 Å indicates that the lattice cavity is much larger than needed. The vacant space remaining may be filled by solvent molecules, however, as no suitable model for the disorder may be resolved, the presence of a solvent molecule could not be determined.—Further details of the crystal structure investigations are available on request from the Fachinformationszentrum Energie, Physik, Mathematik GmbH, D-7514 Eggenstein-Leopoldshafen 2 (FRG), on quoting the depository number CSD-53331, the names of the authors, and the journal citation.
[13] J. R. Nicholson, R.-J. Wang, J. C. Huffman, G. Christou, C.-H. Chang, D. N. Hendrickson, *J. Chem. Soc. Chem. Commun. 1985*, 1781.
[14] A. F. Wells, *Structural Inorganic Chemistry 5th edit.*, Clarendon Press, Oxford 1984, p. 728.
[15] J. Rott, E. Guggolz, A. Rettmeier, M. L. Ziegler, *Z. Naturforsch. B37* (1982) 13.
[16] C. J. O'Connor, J. W. Kolis, unpublished.
[17] F. Hulliger in M. O'Keefe, A. Navrotsky (Eds.): *Structure and Bonding in Crystals, Vol. II*, Academic Press, New York 1981, p. 297.
[18] A. F. Wells: *Structural Inorganic Chemistry*, Clarendon Press, Oxford 1984, p. 1315.
[19] K. O. Klepp, H. Ipser, *Angew. Chem. 94* (1982) 931; *Angew. Chem. Int. Ed. Engl. 21* (1982) 911; *Angew. Chem. Suppl. 1982*, 2004.

Acyl–Alkylidyne Coupling in the Synthesis of Dinuclear Complexes**

By *Ian J. Hart, John C. Jeffery, Rachel M. Lowry,* and *F. Gordon A. Stone**

The two main classes of primary products derived from Fischer-Tropsch synthesis are terminal alkenes and primary alcohols.[1] The carbide–methylene mechanism,[2] which would logically involve methylidyne fragments in an intermediate step, satisfactorily accounts for the production of terminal alkenes. However, a pathway involving incomplete reduction of CO must be responsible for the production of primary alcohols and minor oxygen-containing products such as aldehydes, ketones, carboxylic acids, and esters.[2]

One popular mechanism to account for the oxygenated products is based on 'CO insertion' into a metal–carbon bond.[3] Herein we report the first acyl–alkylidyne coupling reactions in which carbon–carbon bond formation takes place.[4] The acyl ligands are derived from alkyl migration at a mononuclear metal center. The resulting compounds have organic groups displaying unusual ligating properties.

$[W(\equiv CR)(CO)_2(\eta\text{-}C_5H_5)]$ **1**, $(R = p\text{-}C_6H_4Me)$

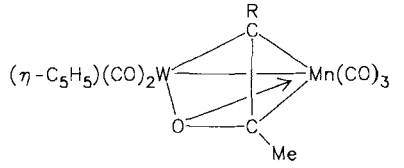

2

The alkylidynetungsten complex **1** reacts with $[Mn(Me)(CO)_5]$ in refluxing toluene to give the MnW-complex **2** identified by its spectroscopic properties[5] and by an X-ray structure analysis (Fig. 1).[6a] The combination of the acyl and alkylidyne moieties occurs via carbon–carbon bond formation giving a bridging C(R)C(O)Me ligand. The most striking aspect of the coordination of this ligand is that it formally donates six electrons to the metal centers. The carbon C10, derived from the alkylidyne unit, bridges the W–Mn bond, whilst the carbon C9 and oxygen O9, de-

[*] Prof. Dr. F. G. A. Stone, I. J. Hart, Dr. J. C. Jeffery, R. M. Lowry
Department of Inorganic Chemistry, University of Bristol
Bristol BS8 1TS (UK)

[**] This work was supported by the U.K. Science and Engineering Research Council.

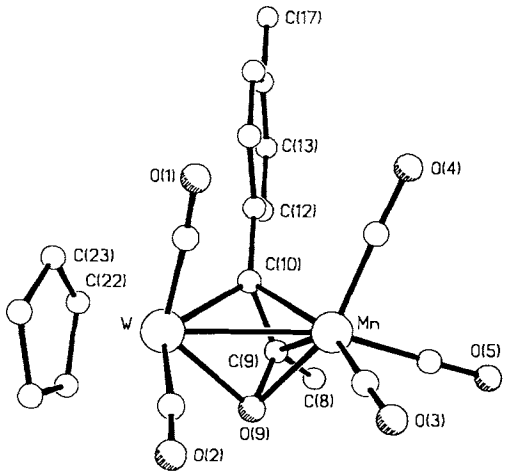

Fig. 1. Crystal structure of **2**. Selected bond lengths [Å] and angles [°]: W-Mn 2.696(1), Mn-C9 2.115(6), Mn-O9 2.043(4), W-O9 2.148(4), C9-O9 1.398(6), O9-C9-C10 105.5(4).

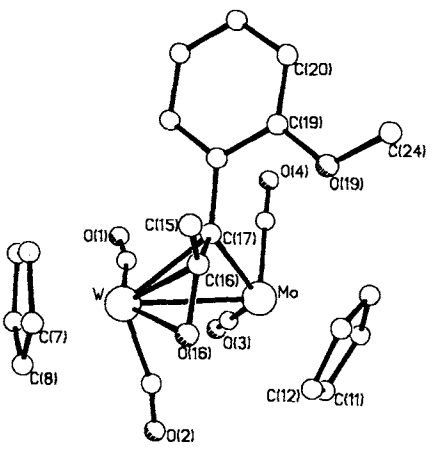

Fig. 2. Crystal structure of **3c**. Selected bond lengths [Å] and angles [°]: Mo-W 2.935(1), W-C16 2.370(4), W-O16 2.157(4), C16-O16 1.321(7), O16-C16-C17 115.9(5).

rived from the inserted CO, are bonded to the manganese and tungsten respectively. The manganese atom is also ligated by a dative bond from the oxygen O9.

This remarkable coordination gives rise to a very short W-Mn separation (2.696(1) Å), being almost 0.3 Å shorter than the only previously determined W-Mn bond length of 2.9939(8) Å.[7] This is also formally a single bond. Evidently the C(R)C(O)Me ligand constrains the two metal atoms, holding them very close indeed. Noteworthy also is the lengthening of the acyl derived C9-O9 bond to 1.398(6) Å. Previously determined uncoordinated manganese-acyl bond lengths fall in the range 1.20-1.22 Å.[8]

The mechanism whereby **2** is formed must involve migration of the manganese-ligated methyl group to a carbonyl ligand to generate a transient unsaturated species $[Mn\{C(O)Me\}(CO)_4]$ to which the W≡C triple bond of **1** can coordinate. Carbon-carbon bond formation followed by loss of CO would then lead to the observed product.

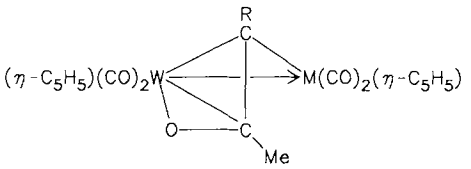

3a, M = Mo, R = p-C_6H_4Me
3b, M = W, R = p-C_6H_4Me
3c, M = Mo, R = o-C_6H_4OMe

The reaction between **1** and the complexes $[M(Me)(CO)_3(\eta\text{-}C_5H_5)]$ (M = Mo or W) under UV irradiation affords the dinuclear complexes **3a**, **b**.[9] Similarly, reaction of $[W(\equiv C\text{-}o\text{-}C_6H_4OMe)(CO)_2(\eta\text{-}C_5H_5)]$ and $[Mo(Me)(CO)_3(\eta\text{-}C_5H_5)]$ furnished **3c**, the structure of which was established by X-ray diffraction (Fig. 2).[6b] This confirmed that acyl and alkylidyne groups had again combined to give μ-C(R)C(O)Me fragments, but the mode of bonding to the dimetal centers was substantially different from that in **2**. In the compounds **3** the alkylidyne derived carbon atom again bridges the metal-metal bond but the acyl derived carbon and oxygen atoms are both bonded to the same metal center. A metal-metal donor bond allows each metal atom to conform to the 18-electron rule.

Previously, we have demonstrated the synthetic utility of the alkylidyne complex **1** in rational metal cluster syntheses.[10] We have now further shown the potential of **1** in the preparation of complexes exhibiting unusual organic ligands.[11]

Experimental Procedure

2: A solution of **1** (0.41 g, 1.0 mmol) and $[Mn(Me)(CO)_5]$ (0.21 g, 1.0 mmol) in toluene (ca. 20 mL) was refluxed under nitrogen for 4 h. The solvent was removed in vacuo, and the residue was dissolved in CH_2Cl_2 (ca. 10 mL) and chromatographed on an alumina column (2 × 10 cm) with CH_2Cl_2-light petroleum (3 : 1) as eluent. A yellow fraction was collected. After removal of solvent in vacuo, the residue was dissolved in CH_2Cl_2 (ca. 5 mL), and light petroleum (ca. 25 mL) was added. After cooling to −78 °C, and removal of supernatant liquid there remained yellow microcrystals of **2** (0.53 g, 90%).

3a: A solution of **1** (0.41 g, 1.0 mmol) and $[Mo(Me)(CO)_3(\eta\text{-}C_5H_5)]$ (0.26 g, 1.0 mmol) in light petroleum was cooled under nitrogen to 0 °C and irradiated with UV light for 12 h. The solvent was removed in vacuo and the residue was dissolved in CH_2Cl_2 (ca. 10 mL) and chromatographed on an alumina column (2 × 15 cm). Elution with CH_2Cl_2-light petroleum (4 : 1) gave a purple band, which was collected and the solvent removed in vacuo. Dissolution of the residue in CH_2Cl_2 (ca. 5 mL), addition of light petroleum (ca. 25 mL), and removal of the supernatant liquid furnished purple microcrystals of **3a** (0.32 g, 48%).

In an analogous way, compound **1** (0.41 g, 1.0 mmol) and $[W(Me)(CO)_3(\eta\text{-}C_5H_5)]$ (0.35 g, 1.0 mmol), and $[W(\equiv C\text{-}o\text{-}C_6H_4OMe)(CO)_2(\eta\text{-}C_5H_5)]$ (0.42 g, 1.0 mmol) and $[Mo(Me)(CO)_3(\eta\text{-}C_5H_5)]$ (0.26 g, 1.0 mmol), gave the complexes **3b** (0.24 g, 32%) and **3c** (0.31 g, 45%), respectively.

Received: August 8, 1988;
supplemented: August 29, 1988 [Z 2915 IE]
German version: *Angew. Chem. 100* (1988) 1769

[1] G. Henrici-Olivé, S. Olivé, *Angew. Chem. 88* (1976) 144; *Angew. Chem. Int. Ed. Engl. 15* (1976) 136.

[2] R. P. A. Sneedon in E. W. Abel, F. G. A. Stone, G. Wilkinson (Eds.): *Comprehensive Organometallic Chemistry*, Pergamon Press, New York 1982, Vol. 8, pp. 40-73; W. A. Herrmann, *Angew. Chem. 94* (1982) 118; *Angew. Chem. Int. Ed. Engl. 21* (1982) 117.

[3] F. Calderazzo, *Angew. Chem. 89* (1977) 305; *Angew. Chem. Int. Ed. Engl. 16* (1977) 299.

[4] Previously acyl-alkylidyne couplings have been reported wherein carbon-oxygen bond formation occurs; see E. O. Fischer, J. Chen, U. Schubert, *Z. Naturforsch. B37* (1982) 1284.

[5] Selected NMR data ($CDCl_3$): ^1H, $\delta = 2.14$, 2.33 (C(O)Me, p-Me); $^{13}C\{^1H\}$, $\delta = 226.4$, 226.0 (WCO), 223.3 (MnCO), 142.0 (*C*(O)Me), 106.4 (CR), 25.1 (C(O)*Me*), and 21.0 (*p*-Me).

[6] a) **2**, $C_{20}H_{15}MnO_6W$, $M = 590.1$, triclinic, space group $P\bar{1}$ (No. 2), $Z = 2$, $a = 8.210(2)$, $b = 8.413(2)$, $c = 14.887(3)$ Å, $\alpha = 97.16(2)$, $\beta = 94.32(2)$, $\gamma = 106.09(2)°$, $V = 973.8(4)$ Å^3, $\rho_{calcd} = 2.01$ g cm^{-3}, $F(000) = 564$, $\mu(Mo_{K\alpha}) = 66.86$ cm^{-1}; $2\theta \leq 50°$ ($Mo_{K\alpha}$, $\bar{\lambda} = 0.71069$ Å, Wyckoff ω-scans, 283 K), 3098 absorption corrected intensities ($F \geq 5\sigma(F)$). Refinement with anisotropic thermal parameters for all non-hydrogen atoms, and hydrogen atoms included in calculated positions, gave $R_1 = 0.028$, $R_2 = 0.029$; b) **3c**, $C_{24}H_{20}MoO_6W \cdot CH_2Cl_2$, $M = 769.1$, triclinic, space

group $P\bar{1}$ (No. 2), $Z=2$, $a=13.344(4)$, $b=9.191(3)$, $c=11.164(3)$ Å, $\alpha=100.51(2)$, $\beta=75.86(2)$, $\gamma=95.07(2)°$, $V=1304.0(6)$, $\rho_{calcd}=1.96$ g cm^{-3}, $F(000)=740$, $\mu(Mo_{K\alpha})=52.16$ cm^{-1}; $4° \le 2\theta \le 50°$, 4206 absorption corrected intensities ($F \ge 2.5\sigma(F)$). Refinement with anisotropic thermal parameters for all non-hydrogen atoms, and hydrogen atoms included in calculated positions, except the two in the poorly resolved CH_2Cl_2 molecules, which were excluded, gave $R_1=0.030$, $R_2=0.033$; c) further details for the crystal structure analyses are available on request from the Cambridge Crystallographic Data Centre, University Chemical Laboratory, Lensfield Road, Cambridge CB2 1EW (UK). Any request should be accompanied by a full literature citation for this communication; d) computations were carried out on a Data General 'Eclipse' Computer with the SHELXTL system of programs.

[7] N. E. Kolobova, L. L. Ivanov, O. S. Zhvanko, A. S. Batsanov, Yu. T. Struchkov, *J. Organomet. Chem. 279* (1985) 419.

[8] C. P. Casey, C. A. Bunnell, *J. Am. Chem. Soc. 98* (1976) 436.

[9] Selected NMR data ($CDCl_3$): **3a**, ^{1}H, $\delta=1.94$, 2.28 (C(O)Me, *p*-Me); $^{13}C\{^1H\}$, $\delta=242.4$, 239.9 (MoCO), 237.5, 212.4 (WCO), 170.7 (*C*(O)Me), 117.3 (*C*R), 21.4, 20.9 (C(O)*Me* and *p*-Me); **3b**: ^{1}H, $\delta=1.96$, 2.35 (C(O)Me, *p*-Me); $^{13}C\{^1H\}$, $\delta=232.6$, 231.6, 229.0, 207.7 (CO), 168.7 (*C*(O)Me), 105.5 (CR), 21.1, 20.8 (C(O)*Me* and *p*-Me); **3c**: ^{1}H, $\delta=1.96$ (C(O)Me), 3.94 (*o*-OMe); $^{13}C\{^1H\}$, $\delta=244.8$, 242.5 (MoCO), 238.4, 215.0 (WCO), 173.8 (*C*(O)Me), 113.5 (*C*-*p*-C_6H_4OMe), 45.0 (*o*-OMe), 21.6 (C(O)*Me*).

[10] F. G. A. Stone, *Angew. Chem. 96* (1984) 85; *Angew. Chem. Int. Ed. Engl. 23* (1984) 89; *Pure Appl. Chem. 58* (1986) 529; G. P. Elliott, J. A. K. Howard, T. Mise, C. M. Nunn, F. G. A. Stone, *J. Chem. Soc. Dalton Trans. 1987*, 2189.

[11] D. B. Barratt, S. J. Davies, G. P. Elliott, J. A. K. Howard, D. B. Lewis, F. G. A. Stone, *J. Organomet. Chem. 325* (1987) 185; I. J. Hart, A. E. Jardin, J. C. Jeffery, F. G. A. Stone, *ibid. 341* (1988) 391.

2,2′,7,7′-Tetrahydroxy-1,1′-binaphthyl: a Versatile Chiral Spacer for Novel Mono- and Ditopic Cyclophane Hosts with Apolar Binding Sites**

By *François Diederich,* Matthew R. Hester,* and *Mike A. Uyeki*

We recently reported on the synthesis of an optically active cyclophane host and described ^{1}H-NMR evidence for the formation of diastereomeric complexes with (*R,S*)-naproxen and its methyl ester in aqueous solution.[1] The rather low stability of these complexes was explained in force-field computational studies by a reduced degree of preorganization[2] of the apolar binding site shaped by a chiral 4-phenyl-1,2,3,4-tetrahydroisoquinoline spacer. According to the calculations, the energetically lowest host conformations did not provide sufficient cavity space for the inclusion of aromatic guests. We subsequently identified the known 2,2′,7,7-tetrahydroxy-1,1′-binaphthyl unit **1**[3] as a potentially more efficient, readily available, and versatile chiral spacer for our cyclophanes. The ditopic component has C_2-symmetry and possesses two distinctive geometric clefts. For a dihedral angle Θ about the chirality axis of 88°, the O···O distance in **1** is ca. 3.60 Å for the minor groove.[4] The minor grooves of binaphthyls shape efficient cation binding sites, as demonstrated by *Cram* et al.[5] in their impressive studies with optically active binaphthyl crown ethers. With an O···O distance of ca. 7.05 Å, the major groove in **1** is almost twice as wide and should be ideal to shape flat binding sites for arenes.[1] In this paper, we describe the synthesis of the racemates of the monotopic host **2** and the ditopic component **3** derived from **1**. Their binding properties clearly demonstrate that **1** is indeed a superior chiral spacer for cyclophanes with apolar binding sites.[6, 7]

[*] Prof. Dr. F. Diederich, M. R. Hester, M. A. Uyeki
Department of Chemistry and Biochemistry
University of California
Los Angeles, CA 90024-1569 (USA)

[**] This work was supported by the National Science Foundation and by the Office of Naval Research.

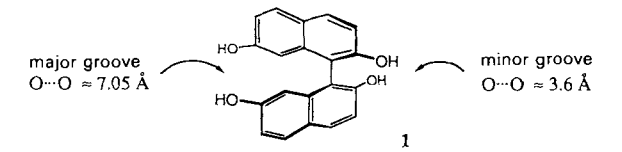

1

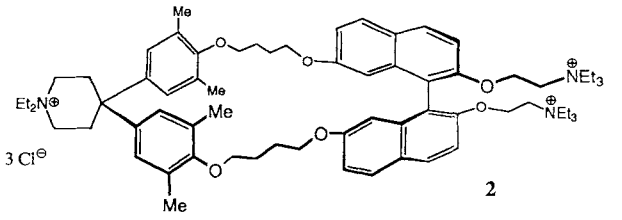

2

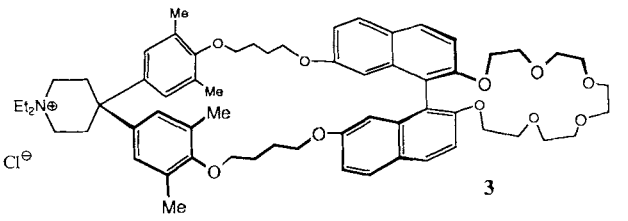

3

For the synthesis of the novel hosts, it was necessary to prepare a regioselectively protected derivative of **1**. In an oxidative coupling reaction of 7-benzyloxy-2-naphthol with $Mn(acac)_3$ (acac = acetylacetonate; CH_3CN, N_2, 45°, 1 d),[8] the binaphthyl unit **4** (m.p. = 104–106 °C), protected at the major groove, was obtained in 43% yield. For the preparation of the cyclization component **7** on the way to host **2**, the binaphthol **4** was converted with α-bromo-*N,N*-diethylacetamide into the diamide **5** (m.p. = 98–100 °C, K_2CO_3, DMF, 80% yield). Deprotection at the major groove (10% Pd/C, $NH_4^{\oplus}HCOO^{\ominus}$, MeOH, N_2, 64% yield) afforded the binaphthol **6** (m.p. = 238–241 °C), which was reacted with 1,4-dichlorobutane to give **7** (m.p. = 120–121 °C, Cs_2CO_3, DMF, 79% yield). The cyclization of **7**

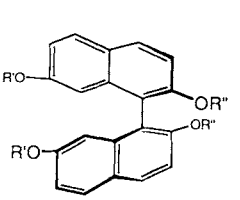

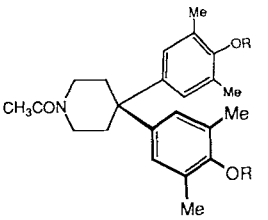

	R'	R"
4	$PhCH_2$	H
5	$PhCH_2$	CH_2CONEt_2
6	H	CH_2CONEt_2
7	Cl-$(CH_2)_4$	CH_2CONEt_2

8, R = H
9, R = $(CH_2)_4$-Cl

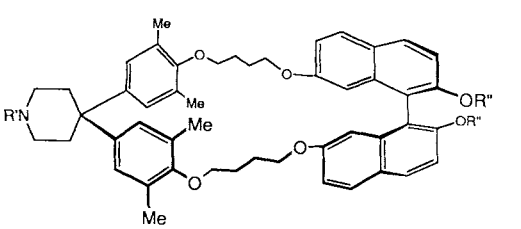

	R'	R"
10,	CH_3CO	CH_2CONEt_2
11,	CH_3CH_2	$CH_2CH_2NEt_2$

with **8**[9] led to the macrocyclic triamide **10** (colorless foam, Cs_2CO_3, DMF, 37% yield), which was reduced with $BH_3 \cdot THF$ to give the triamine **11** (m.p. = 162 °C, 65% yield). Quaternization in pure ethyl iodide followed by anion exchange (Dowex, $Cl^{\ominus}$) and recrystallization from acetone/ether furnished the target host **2** (m.p. = 207–209 °C, 87% yield) as colorless hygroscopic crystals.

For the preparation of the ditopic host **3**, the binaphthol **4** was allowed to react with pentaethyleneglycol di-*p*-toluenesulfonate to give the binaphthyl crown ether **12** (NaH, THF, N_2, 57% yield, colorless foam). The subsequent conversions followed the procedures described above. Deprotection led to the binaphthol **13** (m.p. = 190–192 °C, 69% yield), which was cyclized with the dichloride **9**[9] to give the ditopic macrocycle **14** (m.p. = 188–189 °C, 23% yield). Reduction to **15** (m.p. = 163–165 °C, 43% yield) followed by quaternization, ion exchange, and recrystallization from acetone/ether afforded the target compound **3** as colorless crystals (m.p. = 205–207 °C, dec., 75% yield).

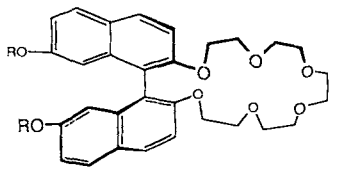

12, R = $PhCH_2$
13, R = H

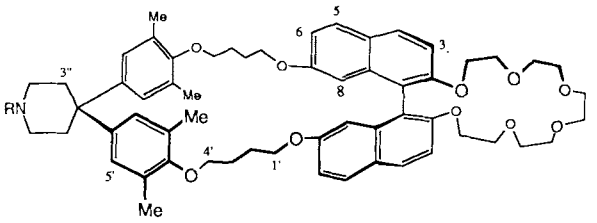

14, R = CH_3CO
15, R = CH_3CH_2

^{1}H-NMR spectroscopic studies showed the efficient inclusion complexation of ten neutral naphthalene derivatives by the hosts **2** and **3** in D_2O/[D_4]methanol (60:40). The observed large and specific complexation-induced shifts of both host and guest resonances indicated that the guests are included pseudo-axially in the apolar binding sites and, in time average, assume a similar orientation as in the cavities of the previously studied bis(diphenylmethane) hosts.[10,11] A direct comparison of the association constants for the 1:1 complexes of 6-methoxy-2-naphthonitrile (**16**), determined from ^{1}H-NMR titrations in D_2O/[D_4]methanol (60:40; T = 293 K), clearly demonstrates that the novel cyclophanes **2** (K_a = 1990 L·mol^{-1}) and **3** (K_a = 4510 L·mol^{-1}) are much better binders than the above-mentioned host shaped by a 4-phenyl-1,2,3,4-tetrahydroisoquinoline unit (K_a = 336 L·mol^{-1}).[1]

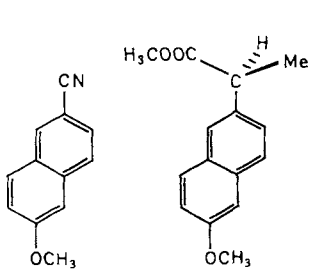

16 **17**

Only a few ditopic hosts are known for which the efficient complexation of two different guests could be unambiguously demonstrated.[12] In most of these studies, the solvent dependency of the two complexation events was very similar. However, a very different solvent dependency could be expected for the complexation of an alkali cation and a neutral naphthalene derivative at the two binding sites of **3**. We investigated the binding of potassium cations and of **16** in various D_2O/[D_4]methanol mixtures. Table 1 shows the association constants determined from

Table 1. Association constants K_a [L·mol^{-1}] and free binding enthalpies $-\Delta G^0$ [kcal·mol^{-1}] for the complexes of host **3** with $K^{\oplus}$ and **16** (T = 293 K) [13].

	Guest	D_2O/[D_4]methanol [Vol.-%] 60 : 40	40 : 60	20 : 80	0 : 100
K_a [a]	$K^{\oplus}$	≈ 13	89	274	1770
$-\Delta G^0$ [b]		≈ 1.5	2.61	3.27	4.35
K_a [a]	**16**	4510	441	142	24
$-\Delta G^0$ [b]		4.90	3.52	2.88	1.85

[a] Accuracy of the K_a values: ±25%. [b] Accuracy of the $-\Delta G^0$ values: ±0.2 kcal·mol^{-1}.

^{1}H-NMR titrations for the 1:1 complexes formed in the various solvent mixtures.[13] As expected, the stability of the complex of **16** markedly decreases with increasing methanol content of the solvent mixture,[7b] whereas the stability of the $K^{\oplus}$-complex markedly increases with increasing methanol content.[14] The opposite solvation characteristics of the two complexation processes are shown in Figure 1. Clearly, the host **3** constitutes a ditopic receptor

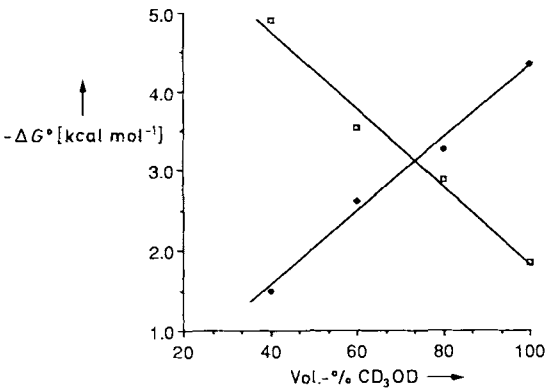

Fig. 1. Complexation of $K^{\oplus}$ (◆) and of **16** (□) by the ditopic host **3** in D_2O/[D_4]methanol mixtures.

which can be switched from an efficient binder of neutral naphthalene derivatives to an efficient binder of potassium cations by simply changing the water content of the water-methanol mixture. The formation of a 1:1:1 ($3 \cdot K^{\oplus} \cdot 16$) complex was observed in all four solvent mixtures shown in Table 1. Although specific shifts in the ^{1}H-NMR spectra[15] indicate a considerable change in the conformation of the binaphthyl unit upon complexation of a potassium cation, the complexation ability of the major groove binding site is only weakly affected by the cation binding at the minor groove. The binding of **16** by host **3** in 0.1 molar solutions of KCl in various D_2O/[D_4]methanol mixtures is only slightly weaker than the binding in the absence of KCl.

Preliminary chiral molecular recognition studies with racemic **2** and **3** show that the preparation and the study of

Advertisement pages 1707–1710

the enantiomerically pure hosts represent extremely worthwhile objectives. The methyl ester of (*S*)-naproxen **17** forms stable inclusion complexes with both hosts, and the ^{1}H-NMR spectra show significant differential shifts of the aromatic host resonances in the resulting diastereomeric complexes. As an example, the ^{1}H-NMR spectrum of a solution with $[\mathbf{17}]=[\mathbf{2}]=1.2\times10^{-3}$ mol·L^{-1} in D_2O/[D_4]methanol at an estimated degree of complexation of approx. 60% contains two signals for the binaphthyl proton 8-H which are shifted by 0.17 and 0.13 ppm, respectively, against the resonance of 8-H in the solution of pure host.

In conclusion, the results of the first binding studies with **2** and **3** show that derivatives of **1** are novel, synthetically readily available chiral spacers for cyclophanes with apolar binding sites. They are comparable in their efficiency and versatility to the diphenylmethane units which we use successfully in our host systems. We are now pursuing the optical resolution of **4** on the preparative scale as well as the preparation of the enantiomerically pure hosts **2** and **3**.

Received: August 10, 1988;
revised: September 26, 1988 [Z 2921 IE]
German version: *Angew. Chem. 100* (1988) 1775

[1] R. Dharanipragada, S. B. Ferguson, F. Diederich, *J. Am. Chem. Soc. 110* (1988) 1679-1690.

[2] a) D. J. Cram, *Angew. Chem. 98* (1986) 1041-1060; *Angew. Chem. Int. Ed. Engl. 25* (1986) 1039-1057.

[3] a) K. Brass, R. Patzelt, *Chem. Ber. 70* (1937) 1349; b) B. Feringa, H. Wynberg, *Tetrahedron Lett. 1977*, 4447; c) W. H. Pirkle, J. L. Schreiner, *J. Org. Chem. 46* (1981) 4988; M. Tisler, *Org. Prep. Proced. Int. 18* (1986) 17.

[4] a) PCMODEL-MMX, Macintosh II version of the MODEL-program by *W. C. Still*, Columbia University; Serena Software, P.O. Box 3076, Bloomington, IN 47402-3076, USA. b) For a conformational analysis of the binaphthyl system, see: W. R. Busing, *J. Am. Chem. Soc. 104* (1982) 4829. In the region between 60° and 120°, changes of the dihedral angle Θ about the chirality axis do not considerably alter the strain energy of the binaphthyl.

[5] a) D. J. Cram, J. Cram, *Acc. Chem. Res. 11* (1978) 8-14; b) C. B. Knobler, F. C. A. Gaeta, D. J. Cram, *J. Chem. Soc. Chem. Commun. 1988*, 330-333.

[6] Chiral cyclophane hosts with apolar binding sites: a) I. Takahashi, K. Odashima, K. Koga, *Tetrahedron Lett. 25* (1984) 973; b) A. Collet, *Tetrahedron 43* (1987) 5725; c) C. S. Wilcox, M. D. Cowart, *Tetrahedron Lett. 27* (1986) 5563; d) T. J. Shepodd, M. A. Petti, D. A. Dougherty, *J. Am. Chem. Soc. 110* (1988) 1983; e) R. E. Sheridan, H. W. Whitlock, Jr., *ibid. 110* (1988) 4071.

[7] a) F. Vögtle, W. M. Müller, U. Werner, H.-W. Losensky, *Angew. Chem. 99* (1987) 930; *Angew. Chem. Int. Ed. Engl. 26* (1987) 901; b) H.-J. Schneider, K. Philippi, J. Pöhlmann, *ibid. 96* (1984) 907 and *23* (1984) 908.

[8] Elemental analyses and spectroscopic data (IR, 500-MHz 1D and 2D COSY-^{1}H-NMR, EI-MS and FAB-MS) corroborate the structures proposed for all the new compounds.

[9] F. Diederich, K. Dick, D. Griebel, *Chem. Ber. 118* (1985) 3588.

[10] Examples for complexation-induced changes in chemical shift $\Delta\delta$ [ppm] of the host resonances in D_2O/[D_4]methanol (40:60) with $[\mathbf{3}]=[\mathbf{16}]=1.1\times10^{-3}$ mol·L^{-1}: $\Delta\delta\approx+0.4$ to $\approx+0.5$ (2′,3′-H); +0.05 (Ph–CH_3); −0.12 (3″-H); $\approx+0.7$ to $\approx+0.8$ (1′,4′-H); −0.17 (8-H); −0.19 (6-H); −0.16 (5′-H); −0.07 (3-H); −0.23 (5-H); −0.16 (4-H). + = upfield shift; for the numbering, see formula **14/15**. For characteristic complexation-induced shifts of the guest protons, see Ref. [13].

[11] F. Diederich, *Angew. Chem. 100* (1988) 372; *Angew. Chem. Int. Ed. Engl. 27* (1988) 362.

[12] a) J. Rebek, Jr., *Acc. Chem. Res. 17* (1984) 258; b) J.-M. Lehn, *Angew. Chem. 100* (1988) 91; *Angew. Chem. Int. Ed. Engl. 27* (1988) 89; c) I. Willner, Z. Goren, *J. Chem. Soc. Chem. Commun. 1983*, 1469; d) F. P. Schmidtchen, *J. Org. Chem. 51* (1986) 5161; e) A. D. Hamilton, P. Kazanjian, *Tetrahedron Lett. 26* (1985) 5735; f) E. Kimura, H. Fujioka, M. Kodama, *J. Chem. Soc. Chem. Commun. 1986*, 1158; g) C. J. van Staveren, D. E. Fenton, D. N. Reinhoudt, J. van Eerden, S. Harkema, *J. Am. Chem. Soc. 109* (1987) 3456; h) J. H. Griffin, P. B. Dervan, *ibid. 109* (1987) 6840; i) P. D. Beer, A. S. Rothin, *J. Chem. Soc. Chem. Commun. 1988*, 52.

[13] The ^{1}H-NMR titrations were evaluated by a non-linear least-squares curve fitting procedure. The concentration ranges were chosen to provide approximately 20-80% complexation of the binding partner present at constant total concentration. For the determination of the stability of the complexes of **2** and **3** with guest **16**, the host concentration was continuously changed, and the resonances of the four guest protons 1-H, 3-H, 5-H, and OCH_3 were evaluated. The binding data in Table 1 are averaged data. *Example*: $[\mathbf{16}]=5\times10^{-4}$ mol·L^{-1} and $[\mathbf{3}]=3\times10^{-4}$–$5\times10^{-3}$ mol·L^{-1} in D_2O/[D_4]methanol (40:60): 1-H: $\Delta\delta_{max/obs}=1.86$, $\Delta\delta_{sat/calcd}=2.67$: $K_a=448$. 3-H: $\Delta\delta_{max/obs}=1.13$, $\Delta\delta_{sat/calcd}=1.61$: $K_a=476$. 5-H: $\Delta\delta_{max/obs}=1.01$, $\Delta\delta_{sat/calcd}=1.47$; $K_a=435$. OCH_3: $\Delta\delta_{max/obs}=0.35$, $\Delta\delta_{sat/calcd}=0.57$; $K_a=406$. $K_{a\,average}=441$ L·mol^{-1}. For the determination of the stability of the $\mathbf{3}\cdot K^{\oplus}$ complexes, the potassium cation concentration was changed and the shifts of the resonances of the host proton 8-H and the diastereotopic protons Naph-O-CH_AH_B-CH_2-O were evaluated. *Example*: $[\mathbf{3}]=5\times10^{-4}$ mol·L^{-1} and [KCl] $=5\times10^{-3}$–8×10^{-2} mol·L^{-1} in D_2O/[D_4]methanol (40:60): 8-H: $\Delta\delta_{max/obs}=0.136$, $\Delta\delta_{sat/calcd}=0.154$; $K_a=88$. CH_A: $\Delta\delta_{max/obs}=0.340$, $\Delta\delta_{sat/calcd}=0.363$; $K_a=100$. CH_B: $\Delta\delta_{max/obs}=0.263$, $\Delta\delta_{sat/calcd}=0.301$; $K_a=80$. $K_{a\,average}=89$ L·mol^{-1}.

[14] R. M. Izatt, R. E. Terry, D. P. Nelson, Y. Chan, D. J. Eatough, J. S. Bradshaw, L. D. Hansen, J. J. Christensen, *J. Am. Chem. Soc. 98* (1976) 7626.

[15] In a solution of $[\mathbf{3}]=5.0\times10^{-4}$ mol·L^{-1} and $[KCl]=8.0\times10^{-2}$ mol·L^{-1} in D_2O/[D_4]methanol (40:60, $T=293$ K) with ≈88% of the total amount of host complexed, the binaphthyl resonances of **3** are specifically shifted against the resonances observed in the solution of pure host: 8-H: $\delta=6.18$ ($\Delta\delta=+0.14$; + = upfield shift); 6-H: 6.689 (−0.06); 3-H: 7.521 (−0.12); 5-H: 7.687 (−0.12); 4-H: 7.983 (−0.14). The specific upfield shift of the signal for 8-H can be explained by a reduction of the dihedral angle Θ as a result of the complexation of a potassium cation. Such a complexation-induced conformational change could be expected on the basis of X-ray crystallographic data for binaphthyl crowns and their cation complexes; see: D. J. Cram, K. N. Trueblood, *Top. Curr. Chem. 98* (1981) 43.

A Donor-Acceptor Substituted Quinoid Pentalene

By *Toyonari Sugimoto, Akihiko Sakai, Toshiki Takahashi, Hiroshi Ando, Tatsushi Okuda, Zen-ichi Yoshida,* Yasushi Kai, Nobuko Kanehisa,* and *Nobutami Kasai**

Antiaromatic systems can be stabilized by the simultaneous presence of electron-donating (Do) and electron-withdrawing (A) substituents,[1] because the antiaromatic destabilization is reduced by participation of a push-pull type of π-electron conjugation. As a typical example, a Do_2/A_2 cyclobutadiene substituted with two diethylamino (Do) and two methoxycarbonyl (or ethoxycarbonyl) (A) groups has been realized.[2] Such a Do/A synergic effect on pentalene, the second smallest antiaromatic system (8π, n = 2 for 4nπ), has not been investigated so far, although some reports have appeared in the literature on the individual effect of Do and A groups.[3] We now wish to report on the synthesis and structure of the pentalene **1**, which is formally substituted in one of the five-membered rings by a 3,4-dicyanocyclopentadienide group ($Do^{\ominus}$) and in the other by a tetramethylamidinium group ($A^{\oplus}$).

The pentalene **1** was synthesized by a novel reaction from the calicene **2**[4] and the fulvene **3**.[5] A mixture of **2**

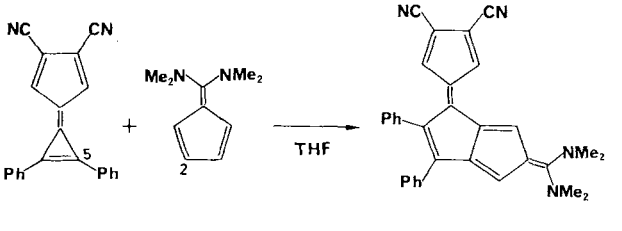

2 3 1

[*] Prof. Dr. Z. Yoshida, Dr. T. Sugimoto, A. Sakai, T. Takahashi, H. Ando, T. Okuda
Department of Synthetic Chemistry, Kyoto University
Yoshida, Kyoto 606 (Japan)
Prof. Dr. N. Kasai, Prof. Dr. Y. Kai, N. Kanehisa
Department of Applied Chemistry, Osaka University
Yamadaoka, Suita 565 (Japan)

(0.1 mmol) and **3** (0.15 mmol) in anhydrous THF (10 mL) was heated under reflux for 3 h under argon. After thin-layer chromatographic separation of the crude product (silica gel, CH_2Cl_2) and recrystallization from chlorobenzene, **1** was isolated as blue-violet crystals (m.p. 220°C (dec.)) in 16% yield. The mass spectrum showed a parent peak at *m/e* 466, which corresponds to the sum of the molecular weights of **2** and **3** minus two H atoms.[6] The 400-MHz ^{1}H-NMR spectrum in CD_2Cl_2 consisted of six signals, at $\delta = 7.38$ (m, 4H), 7.20 (m, 7H), 6.64 (d, $J = 0.85$ Hz, 1H), 5.84 (d, $J = 2.20$ Hz, 1H),), and 3.10 (s, 12H). No signal appeared at about $\delta = 8$, where the proton of the seven-membered ring of 5,6-bis(*tert*-butylthio)-9-[bis(dimethylamino)methylidene]cyclopent[*e*]azulene-1,2-dicarbonitrile is observed.[7] Moreover, the coupled signals at

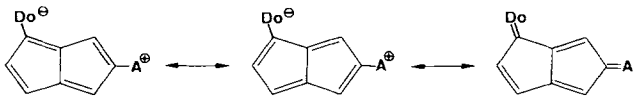

$\delta = 6.64$ and 5.96 appear at similar positions as those of the ring protons of **3**.[8] The presence of the 3,4-dicyanocyclopentadienyl group was inferred from the appearance of one of the two coupled signals at about $\delta = 7.20$, which is hidden by overlapping with signals of the *m*- and *p*-protons of the phenyl ring. On the other hand, the partner signal was unexpectedly observed at a fairly high field ($\delta = 5.84$).[9] There was no indication of coalescence of the two signals, even at a temperature of ca. 100°C, thus indicating a large rotation barrier around the C=C bond. These results are consistent with a quinoid-Do/A pentalene structure rather than a $Do^{\ominus}/A^{\oplus}$-pentalene structure for **1**.

For confirmation, an X-ray structure analysis was carried out (Fig. 1).[10] It follows therefrom that **1** undoubtedly has a quinoid-type pentalene structure. The central pentalene moiety is planar within a deviation of 0.02 Å for each atom. The dicyanocyclopentadienylidene moiety forms a torsional angle of 14.6° with this plane along the C1–C9 bond. The two phenyl groups and the bis(dimethylamino)methylidene moiety also deviate from the pentalene plane, forming torsional angles of 61.2°, 47.5° and 35.2° about the C2–C21, C3–C31, and C5–C14 bonds, respectively. The interatomic distances C2–C3, C4–C8, C6–C7, C1–C9, C10–C11, and C12–C13 must be regarded as equivalent to elongated double bonds, since they are significantly shorter than the other carbon–carbon bonds in **1**.[11] Preferred adoption of the Do/A-quinoid pentalene structure in spite of the presence of comparatively weak $Do^{\ominus}$ and $A^{\oplus}$ groups, clearly reflects a strong tendency to avoid antiaromatic destabilization due to the eight π-electrons. Very interestingly, this result is in marked contrast with that of a Do_2/A_2 cyclobutadiene, in which a quinoid type of structure has not apparently been recognized.[12]

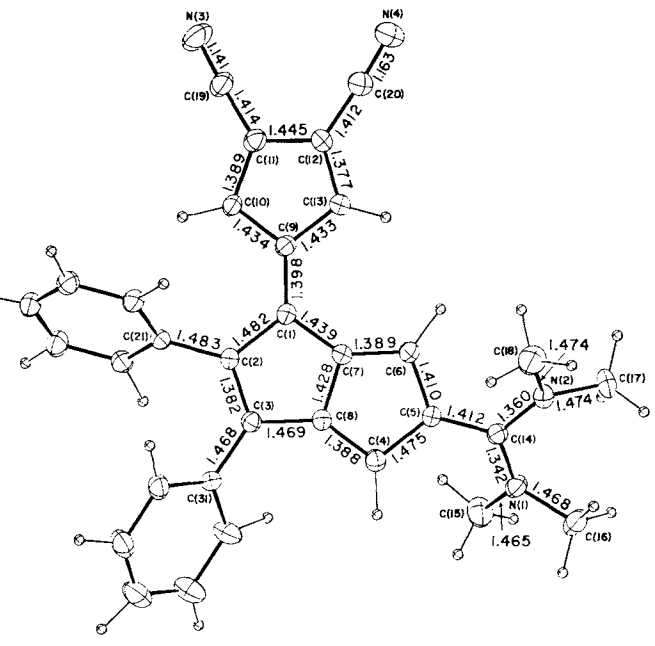

Fig. 1. Molecular Structure of **1** with selected interatomic bond distances. Thermal ellipsoids for non-hydrogen atoms are drawn at the 30% probability level. The hydrogen atoms are shown as spheres with arbitrary temperature factor of 1.0 Å^2. The standard deviations for bond distances lie between 0.007 and 0.010 Å.

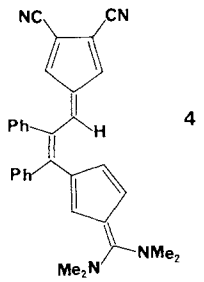

4

On the other hand, when the same reaction of **2** with **3** was carried out at room temperature, an acyclic product (**4**) was obtained in 23% yield as considerably unstable violet crystals (m.p. 140°C, decomp.) together with **1** (2% yield): *m/e* 468. ^{1}H-NMR ($CDCl_3$): $\delta = 7.48$ (s, 1H), 7.4–7.0 (m, 12H), 6.66 (s, 2H), 5.21 (s, 1H), and 3.11 (s, 12H). On exposing the CH_2Cl_2 solution of **4** to air for 4 h, **1** was obtained in 11% yield. This could be indicative of the mode of formation of **1**: possibly C-2 of **3** attacks the 5-position of **2** and then opening of the cyclopropene ring to give **4** followed by ring-closure and dehydrogenating aromatization leads to **1**.

Received: June 28, 1988;
revised: August 22, 1988 [Z 2833 IE]
German version: *Angew. Chem. 100* (1988) 1777

[1] a) J. D. Roberts, *Spec. Publ. (Chem. Soc.) 12* (1958) 111; b) R. Hoffmann, *J. Chem. Soc. Chem. Commun. 1969*, 240.

[2] a) R. Gompper, G. Seybold, *Angew. Chem. 80* (1968) 804; *Angew. Chem. Int. Ed. Engl. 7* (1968) 824; b) M. Neuenschwander, A. Niederhauser, *Chimia 22* (1968) 49.

[3] a) K. Hafner, K. F. Bangert, V. Orfanos, *Angew. Chem. 79* (1967) 414; *Angew. Chem. Int. Ed. Engl. 6* (1967) 451; b) K. Hartke, R. Matusch, *ibid. 84* (1971) 61 and *11* (1972) 50; c) K. Hafner, M. Suda, *ibid. 88* (1976) 341 and *15* (1976) 314; d) K. Hafner, M. Goltz, *ibid. 94* (1982) 771 and *21* (1982) 695.

[4] H. Prinzbach, E. Woischnik, *Helv. Chim. Acta 52* (1969) 2472.

[5] a) K. Hafner, G. Schluz, *Justus Liebigs Ann. Chem. 678* (1964) 39; b) K. Hartke, *Tetrahedron Lett. 1964*, 2737.

[6] A satisfactory elemental analysis was obtained.

[7] Z. Yoshida, M. Shibata, E. Ogino, T. Sugimoto, *Angew. Chem. 97* (1985) 68; *Angew. Chem. Int. Ed. Engl. 24* (1985) 60.

[8] The ^{1}H-NMR spectrum of **3** in $CDCl_3$ showed two doublet signals at $\delta = 6.30$ and 6.12.

[9] The molecular structure obtained by the X-ray crystallographic analysis can also be assumed in solution. Thus, one proton on the five-membered ring is located so closely to the plane of the neighboring phenyl ring as to be susceptible to a magnetic anisotropy effect.

[10] Crystal data of **1** (Rigaku four-circle diffractometer using nickel-filtered $Cu_{K\alpha}$ radioation): $C_{32}H_{26}N_4$, $M_r = 466.6$, triclinic, space group $P\bar{1}$, $a = 12.500(1)$, $b = 11.762(1)$, $c = 9.437(1)$ Å, $\alpha = 101.51(1)$, $\beta = 107.10(1)$,

$\gamma = 89.82(1)°$, $V = 1297.2(3)$ Å^3, $\rho_{calcd} = 1.197$ g cm^{-3}, $Z = 2$, $F(000) = 492$, $\mu(Cu_{K\alpha}) = 5.2$ cm^{-1}. A total of 3253 independent reflections were collected up to $2\theta = 110°$ by the $\theta - 2\theta$ scan technique. The intensity data were corrected for the usual Lorentz and polarization effects, but an absorption correction was not applied. The structure was solved by direct methods (SHELXS-86) (G. M. Sheldrick in G. M. Sheldrick, C. Krüger, R. Goddard (Eds.): *Crystallographic Computing 3*, Oxford University Press, Oxford 1985, pp. 175–189) and refined by the full-matrix least-squares method (XRAY-76) (J. M. Stewart: *XRAY-76: Report TR-446*, University of Maryland, 1976) using 2197 observed reflections [$|F_o| > 3\sigma(F_o)$] to $R = 0.076$ and $R_w = 0.097$, including non-hydrogen atoms with anisotropic thermal parameters and hydrogen atoms with isotropic thermal parameters, where $R = \Sigma(|F_o| - |F_c|)/\Sigma|F_o|$, $R_w = [\Sigma w(|F_o| - |F_c|)^2/\Sigma w|F_o|^2]^{1/2}$, and the weighting scheme used was $w = [\sigma(F_o)^2 + 0.003(F_o)^2]^{-1}$. Further details of the crystal structure investigation can be obtained from the Director of the Crystallographic Data Centre, University Chemical Laboratory, Lensfield Road, Cambridge CB2 1EW (UK), on quoting the journal citation.

[11] The X-ray crystallographically determined lengths of the single and double bonds differ even more in the case of dimethyl-4,6-di-*tert*-butylpentalene-1,2-carboxylate (B. Kitschke, H. J. Lindner, *Tetrahedron Lett. 1977*, 2511), than in the case of **1**, suggesting a partial participation of a $Do^{\oplus}/A^{\ominus}$-pentalene structure for **1**.

[12] The X-ray structure analysis indicates a nearly square-planar geometry for the central four-membered ring; H. J. Lindner, B. V. Gross, *Angew. Chem. 83* (1971) 489; *Angew. Chem. Int. Ed. Engl. 10* (1971) 490.

Synthesis, Structure and Bonding in the Donor-Acceptor Complex [*t*Bu$_2$PSe$_2$]·[PNAryl]: En Route to the P≡N Bond**

By *Edgar Niecke,* Martin Nieger, Franz Reichert,* and *Wolfgang W. Schoeller*

Dedicated to Professor Hans Bock on the occasion of his 60th birthday

The formal replacement of the terminal nitrogen atom in a diazonium ion[1] **A** by a phosphorus atom leads to a species **B** in which phosphorus has coordination number 1; until now phosphaalkynes **C**[2] were the only stable compounds in which phosphorus has this coordination number. We report here the synthesis of a donor-stabilized iminophosphenium ("monophosphadiazonium") ion **B** by reaction of the imino(phosphino)phosphane **1** with selenium.

$[N{\equiv}N{-}R]^{\oplus}$ **A** $[P{\equiv}N{-}R]^{\oplus}$ **B** $P{\equiv}C{-}R$ **C**

It appears likely that selenium is primarily added to the central phosphorus atom to give the selenoxophosphane **2**.[3] Subsequent selenium insertion into the P–P bond yields the imino(seleno)phosphane **3**,[4] which can be isolated in the form of reddish-brown crystals upon reaction of equimolar amounts of the starting materials. Further addition of selenium leads to a red, crystalline 1:1 "adduct" of **3** and selenium; the latter proved to be the donor-stabilized iminophosphenium ion **4** (Scheme 1).

The structures of the compounds **3** and **4** have been determined from their elemental analyses, mass spectra,[5] NMR data,[5] and, in the case of **4**, by an X-ray structure analysis. In the $^{31}P\{^1H\}$-NMR spectrum of **3** the $>P-Se-P=N-$ structural unit gives rise to two groups of signals ($\delta = 324.7$, 84.5 ppm; $J_{PP} = 212$ Hz), the ^{77}Se satellites of which ($J_{PSe} = 366$ and 202 Hz) confirm the coupling of the two phosphorus atoms via a selenium bridge. The drastic changes induced in the phosphorus spectrum by the addition of a second selenium atom ($\delta = 92$, 79 ppm; $J_{PP} = 35$ Hz), and in particular the extreme difference in the ^{31}P-^{77}Se coupling constants ($J_{PSe} = 15$ and 516 Hz), cannot be explained by the presence of classical structures with sp^2-hybridized λ^5- and λ^3-phosphorus atoms such as $>P(=Se)-Se-P=N-$ or $>P-Se-P(=Se)=N-$. These results, as well as the $^{77}Se\{^1H\}$-NMR spectrum, which shows only one set of signals at higher field, indicate a fast exchange process induced by an intramolecular nucleophilic attack of the selenoxo selenium atom at the electrophilic center of the P=N group. At a temperature of $-80°C$ the multiplet structure remains unchanged, though the "iminophosphane" phosphorus signal is shifted upfield by 25 ppm; the energy barrier for such an exchange process must therefore be very low. The solid-state ^{31}P-NMR spectrum of **4** was surprisingly almost unchanged from that in solution ($\delta = 116$ (br), $J_{PSe} = <20$ Hz; 81, $J_{PSe} = 520$ Hz), and can be interpreted in terms of a "frozen transition state" **4'**.

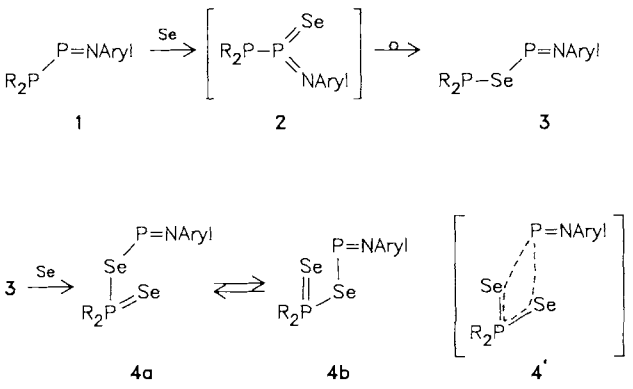

Scheme 1. R = *t*Bu, Aryl = 2,4,6-*t*Bu$_3$C$_6$H$_2$.

This suggested structure is confirmed by the X-ray structural analysis (Fig. 1).[6] The distorted tetrahedral coordination of the P(1) atom and the P(1)–Se(1)/Se(2) bond lengths (216–217 pm) correspond to the typical structural features of a diselenophosphinate. The P–N distance of 150 pm is considerably shorter than that found in iminophosphanes (e.g. Mes*–P=N*t*Bu: 156 pm[7]) and corresponds to that in the PN molecule (149 pm[8]). The N–N bond length in diazonium compounds (109–111 pm[8]) is also comparable with that in the N_2 molecule (110 pm[9]). The valence angle of 169° at the N atom shows it to be sp-hybridized, the deviation from the ideal angle of 180° indicating the presence of an interaction between the donor ligands and the PN bond system: in agreement with this, the P(2)–Se(1)/Se(2) bond lengths (264 and 279 pm respectively) are considerably shorter than the sum of the van der Waals radii. The electron transfer to the P(2) atom also manifests itself in the (*E*)-configuration of the PSe_2PN

[*] Prof. Dr. E. Niecke, M. Nieger, Dipl.-Chem. F. Reichert
Anorganisch-chemisches Institut der Universität
Gerhard-Domagk-Str. 1, D-5300 Bonn 1 (FRG)
Prof. Dr. W. W. Schoeller
Fakultät für Chemie der Universität
Postfach 8640, D-4800 Bielefeld 1 (FRG)

[**] This work was supported by the Deutsche Forschungsgemeinschaft and the Fonds der Chemischen Industrie. We thank Dr. *H. Förster*, Bruker Analytische Messtechnik, Karlsruhe (FRG), for recording the solid-state NMR spectrum. Aryl = 2,4,6-*t*Bu$_3$C$_6$H$_2$.

skeleton (folding angles $\alpha = 160°$, $\beta = 125°$) (Fig. 1, bottom) and the resulting pyramidalization at P(2), which indicates stereochemical activity of the lone pair on this phosphorus atom.

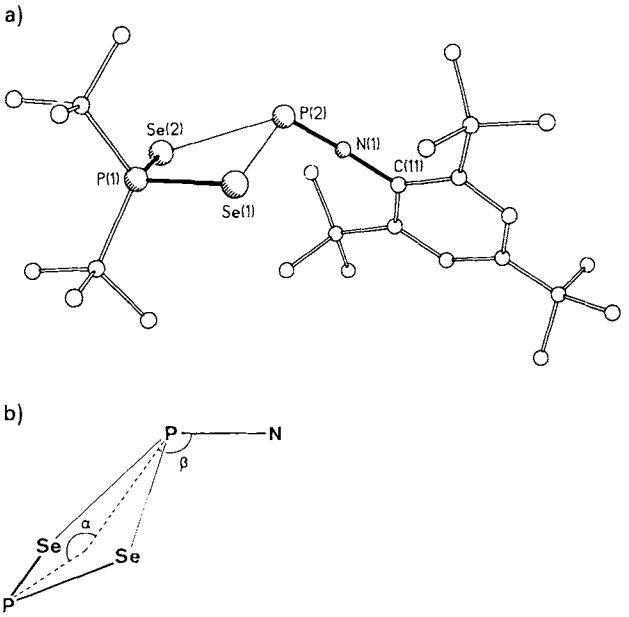

Fig. 1. a) Crystal structure of **4** (H atoms not shown); most important bond lengths [pm] and angles [°]: P(1)-Se(1) 217.0(5), P(1)-Se(2) 215.9(4), P(2)-Se(1) 263.6(5), P(2)-Se(2) 278.8(5), P(2)-N(1) 149.3(12), N(1)-C(11) 139.7(18); Se(1)-P(1)-Se(2) 108.3(2), Se(1)-P(2)-Se(2) 80.6(1), P(1)-Se(1)-P(2) 85.7(2), P(1)-Se(2)-P(2) 82.2(2), Se(1)-P(2)-N(1) 112.6(6), Se(2)-P(2)-N(1) 119.6(5), P(2)-N(1)-C(11) 169.1(11). b) Folding angles of the PSe_2PN skeleton: $\alpha = 159.8°$, $\beta = 125.6°$.

The analysis of the interactions between the frontier orbitals of the anion $[H_2PSe_2]^{\ominus}$ **I** and the cation $[H-N\equiv P]^{\oplus}$ **II** showed that electron density is transferred from the three almost degenerate doubly occupied p-MOs of the selenium atom into the π^*-MOs of the PN bond, thus leading to a weak bond between selenium and P(2). Electron transfer in the opposite direction does not occur because of the considerably greater energy difference between the HOMO of **II** and the LUMO of **I**. **I** and **II** form the donor-acceptor complex **III**. This is in accord with the results

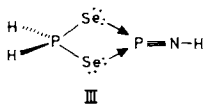

III

of population analyses at various levels (semiempirical, ab initio).[11] The polarity of the PN bonding system in **III** is similar to that in the isolated cation **II**; both the PN molecule and **II** and **III** have a high degree of triple bond character.

Experimental

A mixture of **1** (1.4 g, 3.21 mmol) and grey selenium (253 or 507 mg; 3.21 and 6.42 mmol respectively) in 7 mL of benzene was stirred for 3 h at room temperature. The solution was filtered off and the solvent removed in vacuo. The product was purified by recrystallization from a little hexane or from 9 mL of hexane/toluene (4:3). M.p. = 156–158 °C (**3**), 170–173 °C (**4**). Yields: 1.05 g (64%) and 1.23 g (65%) respectively.

Received: October 5, 1987;
revised: September 7, 1988 [Z 2460 IE]
German version: *Angew. Chem. 100* (1988) 1779

[1] S. Patai: *The Chemistry of Diazonium and Diazo Groups, Part II.* Wiley, New York 1978, p. 511-591.

[2] G. Becker, G. Gresser, W. Uhl, *Z. Naturforsch. B 36* (1981) 16; R. Appel, A. Westerhaus, *Angew. Chem. 93* (1981) 215; *Angew. Chem. Int. Ed. Engl. 20* (1981) 197; review: M. Regitz, P. Binger, *Angew. Chem. 100* (1988) 1541; *Angew. Chem. Int. Ed. Engl. 27* (1988) 1484.

[3] Reported in part at the Int. Congr. Phosphorus Chem., Bonn, September 1986; for a review see: E. Niecke, D. Gudat, M. Leuer, M. Lysek, E. Symalla, *Phosphorus Sulfur 1987,* 467.

[4] Compare the formation of a metallo(thioxo)phosphaalkene: D. Gudat, E. Niecke, W. Malisch, U. Hofmockel, S. Quashie, A. H. Cowley, A. M. Arif, B. Krebs, M. Dartmann, *J. Chem. Soc. Chem. Commun. 1985,* 1687.

[5] **3**: MS (EI, 70 eV): *m/z* 515 ($M^{\oplus}$, 2%), 314 ($M^{\oplus} - C_8H_{18}P - C_4H_8$, 11%), 290 ($C_{18}H_{29}NP^{\oplus}$, 100%); $^{31}P\{^1H\}$ NMR (C_6D_6, 25 °C): $\delta = 324.7$ (d, $J_{PP} = 211.7$ Hz, $J_{PSe} = 365.3$ Hz), 84.5 (d, $J_{PP} = 211.7$ Hz, $J_{PSe} = 201.8$ Hz); $^{77}Se\{^1H\}$ NMR (C_6D_6, 25 °C, standard: Me_2Se, sign positive for low-field shift): $\delta = 762.3$ (dd, $J_{SeP} = 365.3$ Hz, $J_{SeP} = 201.8$ Hz); ^1H NMR (C_6D_6, 25 °C): $\delta = 7.7$ (d, $J_{HP} = 1.8$ Hz, 2H), 1.6 (s, 18H), 1.4 (s, 9H), 1.2 (d, $J_{HP} = 12.0$ Hz, 18H); ^{13}C NMR (C_6D_6, 25 °C): $\delta = 148.2$ (d, $J_{CP} = 32.7$ Hz, PN*C*), 134.8 (d, $J_{CP} = 11.0$ Hz, PNC*C*), 122.2 (d, $J_{CP} = 3.2$ Hz, PNCC*C*), 144.5 (d, $J_{CP} = 4.4$ Hz, PNCCC*C*), 36.4 (d, $J_{CP} = 1.6$ Hz, PNC(*o*-CC_3)), 32.0 (s, PNCC(*o*-CC_3)), 34.9 (d, $J_{CP} = 1.1$ Hz, PNCCCC(*p*-CC_3)), 31.9 (s, PNCCCC(*p*-CC_3)), 34.3 (dd, $J_{CP} = 36.6$ Hz, $J_{CP} = 4.4$ Hz, SePCC_3), 30.6 (d, $J_{CP} = 15.3$ Hz, SePCC_3).—**4**: MS (EI, 70 eV): *m/z* 595 ($M^{\oplus}$, 3%), 370 ($M^{\oplus} - C_8H_{18}PSe$, 1%), 290 ($C_{18}H_{29}NP^{\oplus}$, 100%); $^{31}P\{^1H\}$ NMR (C_6D_6, 25 °C): $\delta = 92.4$ (d, $J_{PP} = 34.9$ Hz, $J_{PSe} < 2$ Hz), 79.2 (d, $J_{PP} = 34.9$, $J_{PSe} = 516.2$ Hz); $^{77}Se\{^1H\}$ NMR (C_6D_6, 25 °C, external standard Me_2Se, sign positive for low-field shift): $\delta = 34.2$ (d, $J_{SeP} = 515.5$ Hz); ^1H NMR (C_6D_6, 25 °C): $\delta = 7.6$ (d, $J_{HP} = 1.5$ Hz, 2H), 1.7 (s, 18H), 1.4 (s, 9H), 1.3 (d, $J_{HP} = 12.9$ Hz, 18H); ^{13}C NMR (C_6D_6, 25 °C): $\delta = 137.3$ (d, $J_{CP} = 51.3$ Hz, PN*C*), 142.5 (d, $J_{CP} = 13.2$ Hz, PNC*C*), 122.0 (d, $J_{CP} = 4.4$ Hz, PNCC*C*), 146.2 (d, $J_{CP} = 7.3$ Hz, PNCCC*C*), 36.4 (d, $J_{CP} = 2.2$ Hz, PNCC(*o*-CC_3)), 31.5 (s, PNCC(*o*-CC_3)), 35.1 (d, $J_{CP} = 1.5$ Hz, PNCCCC(*p*-CC_3)), 31.6 (s, PNCCCC(*p*-CC_3)), 41.2 (d, $J_{CP} = 22.0$ Hz, SePCC_3), 27.1 (d, $J_{CP} = 2.9$ Hz, SePCC_3).

[6] Crystal structure analysis of **4** ($C_{26}H_{47}NP_2Se_2 \cdot 0.5\,C_6H_6$): red crystals (from hexane/benzene). Crystal dimensions $0.3 \times 0.4 \times 0.5$ mm^3, $M_r = 632.5$, monoclinic, space group $P2_1/a$, $a = 11.159(3)$, $b = 17.362(6)$, $c = 17.457(7)$ Å, $\beta = 102.49(3)°$, $V = 3.302$ nm^3, $Z = 4$, $\rho_{calcd} = 1.27$ g cm^{-3}, $\mu = 2.3$ mm^{-1} ($Mo_{K\alpha}$); 5217 measured, 4311 symmetry-independent intensities ($2\theta_{max} = 45°$), 2077 reflections with $|F| > 3\sigma(F)$ used for the structure determination (direct methods) and refinement (292 parameters), empirical absorption correction, non-hydrogen atoms anisotropic, H atoms localized by difference electron density determination and refined with a "riding" model, 0.5 solvent molecules (benzene) in the asymmetric unit, $R = 0.111$ ($R_w = 0.084$, $w^{-1} = \sigma^2(F) + 0.0005F^2$). Further details of the crystal structure analysis are available on request from the Fachinformationszentrum Energie, Physik, Mathematik GmbH, D-7514 Eggenstein-Leopoldshafen 2 (FRG), on quoting the depository number CSD-52737, the names of the authors, and the journal citation.

[7] A. N. Chernega, M. Y. Antipin, Y. T. Struchkov, A. V. Ruban, V. D. Romanenko, *Zh. Strukt. Khim. 28* (1987) 105.

[8] J. Curry, L. Herzberg, G. Herzberg, *Z. Phys. 86* (1933) 348.

[9] S. Patai: *The Chemistry of Diazonium and Diazo Groups, Part I,* Wiley, New York 1978, p. 95-136.

[10] *CRC Handbook of Chemistry and Physics,* 61st Edition, 1980-1981, CRC Press, Boca Raton, FL, USA 1980.

[11] a) Basis sets for the ab-initio SCF calculations: P(10,6,1) [5.5 × 1/4.2 × 1] $\zeta_d = 0.50$; N(8,4,1) [5.3 × 1/3.1] $\zeta_d = 0.95$; H(4,1) [3.1] $\zeta_d = 0.65$. S. Huzinaga: *Approximate Atomic Functions II,* Technical Report, The University of Alberta, Canada 1971. The SCF calculations were carried out using the Cyber Columbus program package, Karlsruhe version; R. Ahlrichs, H.-J. Boehm, C. Ehrhardt, P. Scharf, H. Schiffer, H. Lischka, M. Schindler, *J. Comput. Chem. 6* (1985) 20. b) Equilibrium geometries (distances [pm] and angles [°] [°D: $r_{PN} = 145$ (PN), 143 (HNP$^{\oplus}$), ∢HNP = 180.0. c) Net charges: HNP$^{\oplus}$(PN) = P + 1.12 (+0.46), N −0.36 (−0.46), H +0.24. In comparison, MNDO calculations give the following charge densities for the PN fragment in the complex $[H_2PS_2]\cdot[PNH](PNH^{\oplus})$: P +0.84 (+1.12), N −0.65 (−0.44).—The corresponding donor complex $[tBu_2PS_2]\cdot[PNAryl]$ has a structure comparable with that of **4**: *E. Niecke, M. Nieger, F. Reichert,* unpublished.

Arylimino(halogeno)phosphanes $XP{=}NC_6H_2tBu_3$ (X = Cl, Br, I) and the Iminophosphenium Tetrachloroaluminate $[P{\equiv}NC_6H_2tBu_3]^{\oplus}[AlCl_4]^{\ominus}$: the First Stable Compound with a PN Triple Bond

By *Edgar Niecke,* Martin Nieger,* and *Franz Reichert*

Dedicated to Professor Hans Bock on the occasion of his 60th birthday

The formal replacement of an alkyl group in alkyl(aryl)diazo compounds **I** by a halogen atom leads, as is well known, to the diazonium compounds **II**.[1] There have been several recent reports concerning the iminophosphanes R–P=N–Aryl analogous to **I**[2] and their carbene-like behavior, which has been demonstrated by numerous [n+1]-cycloaddition reactions.[2,3] A PN-analog of **II** was however previously unknown. We report here the synthesis and structure of the first arylimino(halogeno)phosphanes and also of an iminophosphenium ("monophosphadiazonium") ion which is obtainable from them.

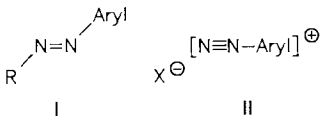

I II

Surprisingly, the stable chloro(imino)phosphane **1** can be readily prepared by reaction of PCl_3 with 2,4,6-tri-*tert*-butylaniline in the presence of triethylamine. The corresponding bromo- and iodo-derivatives **2** and **3** were obtained via halogen exchange with bromo- and iodotrimethylsilane respectively.

$$PCl_3 + H_2N{-}Aryl \xrightarrow[-Et_3NHCl]{Et_3N} \underset{\mathbf{1}}{Cl{-}P{=}N{-}Aryl} \xrightarrow[-Me_3SiCl]{Me_3SiX} \underset{\mathbf{2},\ X=Br;\ \mathbf{3},\ X=I}{X{-}P{=}N{-}Aryl}$$

Aryl = 2,4,6-$tBu_3C_6H_2$

The iminophosphanes **1**–**3** are bright-red (**1**, **2**) or orange (**3**) solids which are stable under inert gas. Their structures have been determined by elemental analysis, mass and NMR spectroscopy, and, in the case of **1**, by an X-ray structural analysis. While in the corresponding *P*-alkylated iminophosphanes R–P=N–Aryl $\delta(^{31}P) = 487$–516 ppm,[2] compounds **1**–**3** show a remarkable high-field shift for the ^{31}P nucleus: $\delta = 139$ (**1**), 153 (**2**), 218 (**3**); this can be interpreted in terms of a high degree of s-character for the PN bond.[4] The molecular structure[5] (Fig. 1) confirms this suggestion: thus the angle of 155° at N(1) is significantly larger than that in the known structures of amino(imino)phosphanes and aryl(imino)phosphanes,[6] while the Cl–N–P–C skeleton has a *cis*-geometry not previously observed for iminophosphanes.[7] Both results are in agreement with the very short P–N bond (149.5 pm) and the long P–Cl bond (214 pm), which indicate a transition to the iminophosphenium ion analogous to **II**. **4** could indeed be prepared by treating **1** with aluminum trichloride, in analogy to the synthesis of aminophosphenium ions from amino(chloro)phosphanes.[8]

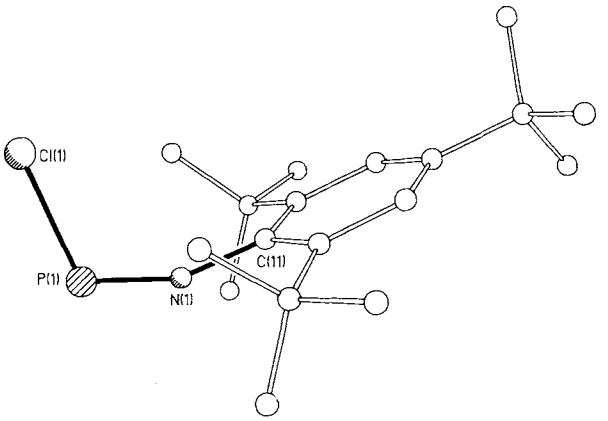

Fig. 1. Crystal structure of **1**. Important bond lengths [pm] and angles [°]: P(1)–Cl(1) 214.2(4), P(1)–N(1) 149.5(4), N(1)–C(11) 140.2(6); Cl(1)–P(1)–N(1) 112.4(2), P(1)–N(1)–C(11) 154.8(4), Cl(1), P(1), N(1) and C(11) are coplanar.

$$\mathbf{1} \xrightarrow[-[AlCl_4]^{\ominus}]{AlCl_3} [PNAryl]^{\oplus}\ \mathbf{4} \qquad Aryl = 2,4,6\text{-}tBu_3C_6H_2$$

The formation of the cation **4** is accompanied by a significant high-field shift of the ^{31}P-NMR signal; the phosphorus nucleus in the isoelectronic phosphaalkyne $P{\equiv}C{-}C_6H_2tBu_3$ is also comparatively strongly shielded.[9] The X-ray structural analysis of **4**[10] (Fig. 2) showed unequivocally that "isolated" molecular ions are present in the crystal. The bond lengths and angles in the anion are typical for tetrachloroaluminates (e.g. $KAlCl_4$: 211–214 pm[11]). With respect to Cl(1), Cl(2) and Cl′ the coordination at the P atom is distorted trigonal bipyramidal with the lone pair in an equatorial position.[12] While in **II** both N atoms are in contact with four Cl atoms,[1] in **4** there is an interaction only for the P atom; this indicates very considerable localization of the positive charge at this atom, the shortest contact (P···Cl(2) 316 pm) demonstrating that the cation originates from the iminophosphane **1**. The bonding situation in the cation, with an almost ideal hybridization of the N atom (177°) and the very short PN

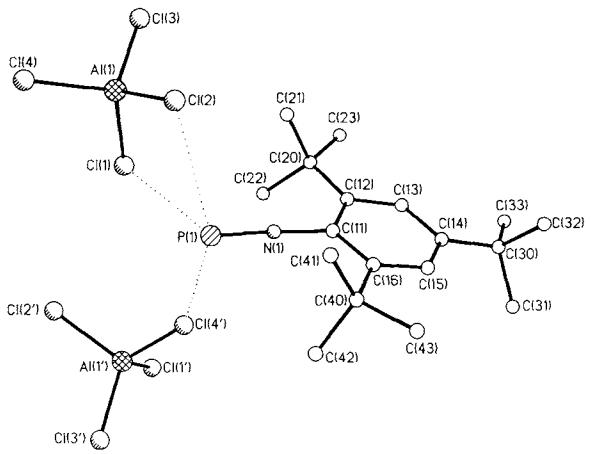

Fig. 2. Crystal structure of **4**. Important bond lengths [pm] and angles [°]: P(1)–N(1) 147.5(8), N(1)–C(11) 140.9(12), Al(1)–Cl(1) 213.2(5), Al(1)–Cl(2) 212.3(5), Al(1)–Cl(3) 210.8(5), Al(1)–Cl(4) 212.0(5), P(1)–Cl(1) 316, P(1)–Cl(2) 327, P(1)–Cl(4′) 352; P(1)–N(1)–C(11) 177.0(7).

[*] Prof. Dr. E. Niecke, M. Nieger, Dipl.-Chem. F. Reichert
Anorganisch-chemisches Institut der Universität
Gerhard-Domagk-Strasse 1, D-5300 Bonn 1 (FRG)

[**] This work was supported by the Deutsche Forschungsgemeinschaft and the Fonds der Chemischen Industrie. We thank Dr. *K. Harms*, Universität Marburg, for carrying out low-temperature X-ray diffraction measurements on the chloroiminophosphane.

bond (147.5 pm; $[P\equiv NH]^{\oplus}$, 147.6 pm[13]), thus corresponds to a formulation in which **4** has a very high degree of triple-bond character in the phosphorus-nitrogen bond ($[:P\equiv N-Aryl]^{\oplus}$); an SiN triple bond is also assumed for the isoelectronic arylsilaisocyanide $:Si\equiv N-Aryl$.[14]

Experimental

1: A solution of 2,4,6-tri-*tert*-butylaniline (3.70 g, 14.2 mmol) in pentane (5 mL) was treated wiith an excess of PCl_3 (113 mmol) and Et_3N (148.5 mmol): the mixture was stirred at room temperature until the reaction was complete (5 d). The amine hydrochloride formed was removed via an inverse sintered glass filter and the filtrate freed in vacuo from all volatile materials. **1** was obtained as a deep-red solid after two recrystallizations from a little *n*-hexane. Yield 3.88 g (72%); m.p. = 93–94 °C, MS: *m/z* 325 ($M^{\oplus}$, 60%), 310 ($M^{\oplus}-CH_3$, 100), 290 ($M^{\oplus}-{}^{35}Cl$, 18) and further ions; ^{31}P NMR (hexane/C_6D_6): $\delta = 138.6$; ^1H NMR (C_6D_6): $\delta = 1.3$ (s, 9H, *p*-*t*Bu), 1.5 (s, 18H, *o*-*t*Bu), 7.6 (d, $J_{HP} = 2.1$ Hz, 2H, Aryl); ^{13}C NMR (C_6D_6): $\delta = 31.0$ (d, $J_{CP} = 2.4$ Hz, *o*-CC_3), 31.6 (d, $J_{CP} = 1.0$ Hz, *p*-CC_3), 35.0 (d, $J_{CP} = 1.3$ Hz, *p*-CC_3), 35.9 (d, $J_{CP} = 1.8$ Hz, *o*-CC_3), 122.1 (d, $J_{CP} = 3.6$ Hz, PNC*C*), 138.7 (d, $J_{CP} = 40.6$ Hz, PN*C*), 139.7 (d, $J_{CP} = 10.6$ Hz, PNC*C*), 147.4 (d, $J_{CP} = 5.8$ Hz, PNCC*C*).

2, **3**: A solution of **1** (0.84 g, 4.2 mmol) in *n*-hexane (10 mL) was treated dropwise at 0 °C with an equimolar amount of Me_3SiBr or Me_3SiI respectively. After stirring for 3 h the solvent was removed in vacuo; the red (**2**) or brown (**3**) solid remaining was purified by recrystallzation from pentane/toluene (5:1). Yield 0.67 g (43%) **2**, m.p. = 79–81 °C; 0.79 g (45%) **3**, m.p. = 87–89 °C.—**2**: MS: *m/z* 369 ($M^{\oplus}$, 11%), 354 ($M^{\oplus}-CH_3$, 8), 290 ($M^{\oplus}-{}^{79}Br$, 86) and further ions; ^{31}P NMR (hexane/C_6D_6): $\delta = 153.3$; ^1H NMR (C_6D_6): $\delta = 1.3$ (s, 9H, *p*-*t*Bu), 1.5 (s, 18H, *o*-*t*Bu), 7.6 (d, $J_{HP} = 2.4$ Hz, 2H, aryl); ^{13}C NMR (C_6D_6): $\delta = 31.2$ (d, $J_{CP} = 2.2$ Hz, *o*-CC_3), 31.5 (d, $J_{CP} = 1.5$ Hz, *p*-CC_3), 35.1 (d, $J_{CP} = 1.5$ Hz, *p*-CC_3), 36.0 (d, $J_{CP} = 2.2$ Hz, *o*-CC_3), 122.2 (d, $J_{CP} = 3.7$ Hz, PNCC*C*), 139.0 (d, $J_{CP} = 42.8$ Hz, PN*C*), 139.7 (d, $J_{CP} = 11.0$ Hz, PNC*C*), 148.2 (d, $J_{CP} = 5.9$ Hz, PNCCC*C*).

3: MS: *m/z* 417 ($M^{\oplus}$, 1%), 290 ($M^{\oplus}-{}^{127}I$, 100), and further ions; ^{31}P NMR (toluene/C_6D_6): $\delta = 217.7$, ^1H NMR (C_6D_6): $\delta = 1.4$ (s, 18H, *p*-*t*Bu), 1.5 (s, 18H, *o*-*t*Bu), 7.5 (d, $J_{HP} = 2.4$ Hz, 2H, aryl); ^{13}C NMR (C_6D_6): $\delta = 31.3$ (d, $J_{CP} = 1.5$ Hz, *p*-CC_3), 31.6 (d, $J_{CP} = 2.2$ Hz, *o*-CC_3), 35.1 (d, $J_{CP} = 1.5$ Hz, *p*-CC_3), 36.2 (d, $J_{CP} = 1.5$ Hz, *o*-CC_3), 122.3 (d, $J_{CP} = 3.7$ Hz, PNCC*C*), 138.3 (d, $J_{CP} = 11.0$ Hz, PNC*C*), 140.4 (d, $J_{CP} = 50.3$ Hz, PN*C*), 148.6 (d, $J_{CP} = 5.9$ Hz, PNCCC*C*).

4: A solution of **1** (1.9 g, 5.83 mmol) in toluene (10 mL) was treated at 0 °C with 0.78 g (5.83 mmol) $AlCl_3$. After stirring for 2 h the solvent was removed. The residue was recrystallized twice from C_6H_6/CH_2Cl_2 (2:1). Yield 1.57 g (59%) pale yellow crystals. M.p. = 132–135 °C (dec.). MS: spectrum not reproducible; ^{31}P NMR (toluene/C_6D_6): $\delta = 79.3$; ^1H NMR (C_6D_6): $\delta = 1.3$ (s, 9H, *p*-*t*Bu), 1.6 (s, 18H, *o*-*t*Bu), 7.5 (d, $J_{HP} = 4.5$ Hz, 2H, aryl); ^{13}C NMR (C_6D_6): $\delta = 29.9$ (d, $J_{CP} = 1.5$ Hz, *o*-CC_3), 30.4 (s, *p*-CC_3), 35.1 (s, *p*-CC_3), 35.9 (s, *o*-CC_3), 123.3 (d, $J_{CP} = 2.9$ Hz, PNCC*C*), 153.3 (d, $J_{CP} = 5.9$, PN*C*), 153.8 (d, $J_{CP} = 5.1$ Hz, PNC*C*), 157.2 (d, $J_{CP} = 8.8$ Hz, PNCCC*C*).

Received: May 19, 1988;
revised: September 7, 1988 [Z 2770 IE]
German version: *Angew. Chem. 100* (1988) 1781

[1] S. Patai: *The Chemistry of Diazonium and Diazo Groups*, Wiley, New York 1978.

[2] a) E. Niecke, R. Rüger, W. W. Schoeller, *Angew. Chem. 93* (1981) 1110; *Angew. Chem. Int. Ed. Engl. 20* (1981) 1034; b) L. N. Markovskii, V. D. Romanenko, A. V. Ruban, A. B. Drapailo, *J. Chem. Soc. Chem. Commun. 1982*, 319; c) M. Yoshifuji, K. Shibayama, K. Toyota, N. Inamoto, S, Nagase, *Chem. Lett. 1985*, 237; d) E. Niecke, M. Lysek, E. Symalla, *Chimia 40* (1986) 202; e) V. D. Romanenko, A. B. Drapailo, a. V. Ruban, L. N. Markovskii, *Zh. Obshch. Khim. 56* (1986) 714; f) D. Barion, *Diplomarbeit*, Universität Bonn 1987.

[3] a) E. Niecke, M. Lysek, *Tetrahedron Lett. 29* (1988) 605; b) V. D. Romanenko, A. B. Drapailo, A. V. Ruban, L. N. Markovskii, *Zh. Obshch. Khim. 57* (1987) 1402; E. Niecke, D. Barion, *Tetrahedron Lett.*, in press.

[4] Compare the donor-acceptor complex $[R_2PSe_2][PNC_6H_2tBu_3]$: E. Niecke, M. Nieger, F. Reichert, W. W. Schoeller, *Angew. Chem. 100* (1988) 1779; *Angew. Chem. Int. Ed. Engl. 27* (1988) 1713.

[5] X-ray structure analysis of **1**: red crystals ($0.5\times0.5\times0.8$ mm^3), $M_r = 325.8$, space group *Pnma*, $a = 25.518(3)$, $b = 12.747(4)$, $c = 5.871(1)$ Å, $V = 1.910$ nm^3, $Z = 4$, $\rho_{calcd} = 1.13$ g cm^{-3}, $\mu(Cu_{K\alpha}) = 2.54$ mm^{-1}, Enraf-Nonius CAD4, $T = 153$ K; 1491 symmetry-independent reflections ($2\theta_{max} = 120°$), 1214 with $|F| > 4\sigma(F)$ used for the structure determination (direct methods) and refinement (119 parameters), non-H atoms anisotropically refined, empirical absorption correction; $R = 0.068$ ($R_w = 0.071$, $w = \sigma^2(F) + 0.0001F^2$) [15].

[6] Review: L. N. Markovskii, V. D. Romanenko, A. V. Ruban, *Zh. Obshch. Khim. 57* (1987) 1433.

[7] According to theoretical calculations the *cis*-conformation of the halogen(imino)phosphanes is energetically more favorable than the *trans*-conformation: W. W. Schoeller, personal communication.

[8] A. H. Cowley, R. A. Kemp, *Chem. Rev. 85* (1985) 367.

[9] G. Märkl, H. Sejpha, *Tetrahedron Lett. 27* (1986) 171.

[10] X-ray structure analysis of **4**·C_7H_8: yellow crystals ($0.2\times0.3\times0.6$ mm^3), $M_r = 551.3$; space groups *Pbca*, $a = 24.915(14)$, $b = 20.354(7)$, $c = 12.139(8)$ Å, $V = 6.156$ nm^3, $Z = 8$, $\rho_{calcd} = 1.19$ g cm^{-3}, $\mu(Mo_{K\alpha}) = 0.48$ mm^{-1}, Nicolet R3m; 4029 symmetry-independent reflections ($2\theta_{max} = 45°$), 1713 with $|F| > 4\sigma(F)$ used for the structure determination (direct methods) and refinement (242 parameters), non-H atoms anisotropic (C atoms of the solvent toluene isotropic with phenyl ring as ideal hexagon: C-C = 1.395 Å, C-C-C = 120°), H atoms refined with a "riding" model; $R = 0.070$ ($R_w = 0.070$, $w^{-1} = \sigma^2(F) + 0.0001F^2$) [15].

[11] G. Mairesse, P. Barbier, J.-P. Wignacourt, *Acta Crystallogr. B 34* (1978) 1328.

[12] The geometry at phosphorus results from the sum of the squares of the deviations of all angles involving phosphorus (with respect to ideal angles). See also: W. S. Sheldrick, *Top. Curr. Chem. 73* (1978) 1.

[13] R. J. Buenker, P. J. Bruna, S. Peyerimhoff, *Isr. J. Chem. 19* (1980) 309.

[14] H. Bock, R. Dammel, *Angew. Chem. 97* (1985) 128; *Angew. Chem. Int. Ed. Engl. 24* (1985) 111, and references cited therein.

[15] Further details of the crystal structure investigations are available on request from the Fachinformationszentrum Energie, Physik, Mathematik GmbH, D-7514 Eggenstein-Leopoldshafen 2 (FRG), on quoting the depository numbers CSD-53316 (**1**) and -53137 (**4**), the names of the authors, and the journal citation.

Electrocatalytic Haloform Reaction: Transformation of Methyl Ketones into Methyl Esters

By *Gennady I. Nikishin,* Michail N. Elinson,* and *Irina V. Makhova*

The haloform reaction is often used for the conversion of methyl ketones into carboxylic acids or esters.[1,2] It has acquired importance primarily because of the fact that the introduction of a carboxyl group as substituent onto an aromatic ring is usually more difficult than the introduction of the acetyl group.

Methyl ketones are generally converted into carboxylic acids by halogen and sodium hydroxide.[1] Recently, sodium bromite has been found to be an effective reagent for the haloform reaction.[3] In the course of our investigations on the synthetic utility of alkali metal halides as mediators in the electrooxidation of organic compounds[4–6] we have now found the electrocatalytic variant of the haloform reaction.

The electrolysis of the methyl ketones **1** in an undivided cell in methanol in the presence of 0.35–3.00 molar equivalents of sodium bromide leads to the corresponding methyl esters **2** (Table 1).

$$\underset{\mathbf{1}}{RC(O)Me} \xrightarrow[NaBr,\ MeOH]{-e^-} \underset{\mathbf{2}}{RCOOMe}$$

Table 1. Electrooxidation of the methyl ketones **1**.

Ketone	R	[NaBr]/[**1**]	Yield [%] of **2**
1a	Ph	3.00	71
1a	Ph	1.50	74
1a	Ph	0.75	63
1a	Ph	0.35	64
1b	1-naphthyl	1.50	88
1c	$Me(CH_2)_5$	1.50	62
1d	*i*Pr	1.50	67 [a]
1e	PhCH=CH	1.50	61

[a] Determined by gas chromatography.

[*] Prof. Dr. G. I. Nikishin, Dr. M. N. Elinson, Dr. I. V. Makhova
N. D. Zelinsky Institute of Organic Chemistry,
USSR Academy of Sciences
Leninsky Prospect 47, Moscow B-334 (USSR)

On completion of the reaction we also detected bromoform, in quantities decreasing from 0.2 to 0.05 equivalents with decreasing amount of sodium bromide used.

The mechanism suggested for the reaction is shown in Scheme 1.

anode: $6\,Br^{\ominus} \longrightarrow 3\,Br_2 + 6\,e^{\ominus}$

cathode: $6\,MeOH + 6\,e^{\ominus} \longrightarrow 6\,MeO^{\ominus} + 3\,H_2$

in solution: $RC(O)Me + 3\,Br_2 \longrightarrow RC(O)CBr_3 + 3\,H^{\oplus} + 3\,Br^{\ominus}$

$RC(O)CBr_3 + MeO^{\ominus} \longrightarrow RCOOMe + CBr_3^{\ominus}$

Scheme 1. Possible reaction mechanism of the electrocatalytic haloform reaction.

The bromoform formed in the last reaction step is further reduced at the cathode or reacts with methoxide ion. Both reactions lead to the regeneration of bromide ions. Thus the reaction proceeds catalytically, but for good yields as shown in Table 1, an excess of bromide is recommended.

Our facile and effective method has, therefore, the great advantage that sodium bromide, which is readily accessible and easy to handle, can be used instead of three molar equivalents of halogen or sodium bromite.

As shown in Table 1, not only aryl and alkyl methyl ketones but also unsaturated methyl ketones (**1e**) are converted into the corresponding methyl esters.

Under the same conditions cyclohexanone **3a** and ethyl phenyl ketone **3b** are oxidized to the α-hydroxy acetals **4a** and **4b** respectively in 75–80% yield; the reaction proceeds similarly to a previously reported reaction.[7]

$$R^1C(O)CH_2R^2 \xrightarrow[NaBr,\ MeOH]{-e^-} R^1C(OMe)_2CHOHR^2$$

3a, b **4a, b**

a, $R^1 + R^2 = -(CH_2)_4-$; **b**, $R^1 = Ph$, $R^2 = Me$

Only benzyl methyl ketone behaved differently under these conditions: it afforded **7** and, by electrochemically induced Favorskii rearrangement, the propionate **6** (yields: 40 and 50% resp.).

$$PhCH_2C(O)Me \xrightarrow[NaBr,\ MeOH]{-e^-}$$

5

$$PhCH_2CH_2COOMe + PhCHOHC(OMe)_2Me$$

6 **7**

5 : 4

Experimental

The experimental procedure is described for the example **2b**: A solution of **1b** (0.02 mol) and NaBr (0.03 mol) in methanol (20 mL) was electrolyzed in an undivided cell equipped with a Pt-anode (4.5 cm^2) and a Cu-Zn (60:40) cathode (4.5 cm^2) at 30 °C under constant current density 220 mA cm^{-2} until 8 F/mol of electricity had been used. The solvent was then removed and the reaction mixture extracted with ether, washed with water, and dried with Na_2SO_4. After distillation 3.3 g (88%) of **2b**, b.p. 93–94 °C (0.1 torr), $n_D^{21} = 1.6079$ was obtained; ^{1}H-NMR ($CDCl_3$): $\delta = 4.01$ (s, 3H, OCH_3), 7.5–8.3 (m, 7H, aryl-H) [8].

Received: May 24, 1988 [Z 2778 IE]
German version: *Angew. Chem. 100* (1988) 1782

[1] R. C. Fuson, B. A. Bull, *Chem. Rev. 15* (1934) 275.
[2] R. T. Arnold, R. Buckles, J. Stoltenberg, *J. Am. Chem. Soc. 66* (1944) 208.
[3] S. Kajigaeshi, T. Nakagawa, N. Nagasaki, S. Fujisaki, *Synthesis 1985*, 674.
[4] G. I. Nikishin, M. N. Elinson, S. K. Feducovich, *Izv. Akad. Nauk SSSR, Ser. Khim. 1984*, 2154.
[5] G. I. Nikishin, M. N. Elinson, S. K. Feducovich, *Izv. Akad. Nauk SSSR, Ser. Khim. 1986*, 1920.
[6] M. N. Elinson, S. K. Feducovich, G. I. Nikishin, *Izv. Akad. Nauk SSSR, Ser. Khim. 1987*, 228.
[7] T. Shono, Y. Matsumura, K. Inoue, F. Iwasaki, *J. Chem. Soc. Perkin Trans. 1, 1986*, 73.
[8] All compounds were characterized by their ^{1}H-NMR spectra (250 MHz).

The First Transition Metal Complex of a Thiepin; Synthesis of the Thermally Labile 1-Benzothiepin 1-Oxide from 1-Benzothiepin(tricarbonyl)iron

By *Keitaro Nishino,* Sumiko Ishigami, Yutaka Tamura, Kazuko Imagawa, Yoshikazu Ikutani,* and *Ichiro Murata**

Unlike thiepin 1,1-dioxide **3**,[1] which has been isolated as a stable crystalline compound, thiepin itself **1** and its 1-oxide **2** are considered to be extremely unstable molecules.[2] On the other hand, 1-benzothiepin **4**[3,4] and its 1,1-dioxide **6**[5–7] are well characterized, but 1-benzothiepin 1-oxide **5** has not yet been synthesized. Hitherto known thiepin 1-oxides, which are confined to heavily substituted 1-benzothiepin 1-oxides such as **7a**–**7d**,[8] are thermally less stable than the corresponding 1-benzothiepins. Therefore, in view of the thermal instability of **4**

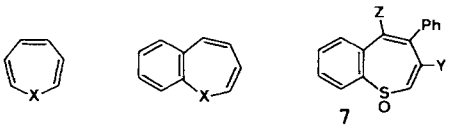

1, X = S **4**, X = S **7**
2, X = SO **5**, X = SO
3, X = SO_2 **6**, X = SO_2

a, Y = $OCOCH_3$, Z = OCH_3
b, Y = Z = OCH_3
c, Y = OCH_3, Z = $OCOCH_3$
d, Y = Z = $OCOCH_3$

($\tau_{1/2}$ at 47 °C = 58 min),[3b] synthesis of unsubstituted **5** has to be done using an appropriate precursor under mild reaction conditions. Lack of success in our previous attempts[6] to synthesize **5** by means of direct oxidation of **4** prompted us to take advantage of a transition-metal complexation strategy.[9] Thus, **4** was converted into iron tricarbonyl complex **8** in 41% yield (Scheme 1). The η^4 complexation at the thiepin ring was confirmed by the ^{1}H NMR spectrum of **8** which exhibits substantially high-field chemical shifts for H-2 and H-5 ($\delta = 3.89$ and 4.29, respectively). Complex **8** provides the first example of a thiepin–metal complex.

On oxidation with *m*-chloroperbenzoic acid (*m*CPBA), complex **8** was smoothly converted into the monoxide **9** in 98% yield as stable yellow needles. The structure of **9** was unambiguously established through its spectral data (Table 1) together with its chemical behavior. Thus, reduction of **9** with lithium aluminum hydride regenerated **8**, whereas further oxidation of **9** with *m*CPBA provided dioxide complex **10**, which was identical in all respects with an authentic sample prepared from the known 1-benzothiepin 1,1-dioxide **6**.[5,6]

[*] K. Nishino, S. Ishigami, Y. Tamura, K. Imagawa, Prof. Y. Ikutani
Department of Chemistry, Osaka Kyoiku University
Minamikawahori-cho, Tennoji, Osaka 543 (Japan)
Prof. Dr. I. Murata
Department of Chemistry, Faculty of Science,
Osaka University
Toyonaka, Osaka 560 (Japan)

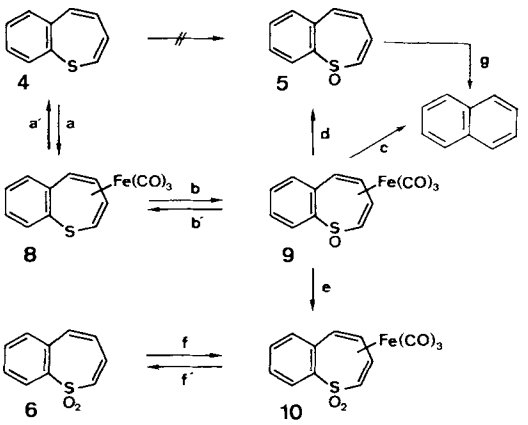

Scheme 1. Synthesis of **5** from **4** and some related reactions. a) $Fe_2(CO)_9$ (large excess) in hexane, $<15°C$, 3 d (41%). a') $Ce(NH_4)_2(NO_2)_6$ (CAN) (2.0 equiv.) in acetone, 0°C, 2 h (73%). b) *m*-chloroperbenzoic acid (*m*CPBA) (1.2 equiv.) in chloroform, −40°C, 1 h (98%). b') $LiAlH_4$ (excess) in ether/THF (1:1), −20°C, 2 h (63%). c) CAN (2.0 equiv.) in acetone, −30°C, 1 h, then −10°C, 3 h (afforded only naphthalene). d) Irradiation (400-W Hg lamp) in THF, −50°C, 1 h (afforded **5** exclusively). e) *m*CPBA (1.2 equiv.) in chloroform, −40°C, 2 h (61%). f) $Fe_2(CO)_9$ (3.0 equiv.) in THF, 40°C, 1 d (58%). f') Irradiation (400-W Hg lamp) in THF, 0°C, 2 h (76%). g) At 13°C (<1 h).

Table 1. Selected physical data for **5**, **8**, **9**, and **10** [10].

5: Pale yellow needles at −40°C; 200-MHz ^1H NMR (CD_2Cl_2) at −30°C: $\delta=6.08$ (d, 1 H, $J=9.8$ Hz, H-2), 6.38 (dd, 1 H, $J=9.8$, 5.4 Hz, H-3), 6.69 (dd, 1 H, $J=12.0$, 5.4 Hz, H-4), 7.38 (d, 1 H, $J=12.0$ Hz, H-5), 7.4–8.0 (m, 4 H, H-6,7,8,9)

8: Yellow needles, m.p. 83.0–83.5°C (from hexane); UV (cyclohexane): $\lambda_{max}(\lg\varepsilon)=276$ (4.06), 310 (sh, 3.94) nm; IR (Nujol): $\tilde{\nu}=2050$, 1982, 1977 cm^{-1}; 90-MHz ^1H NMR ($CDCl_3$): $\delta=3.89$ (dd, 1 H, $J=7.0$, 1.8 Hz, H-2), 4.29 (dd, 1 H, $J=8.1$, 0.8 Hz, H-5), 5.04 (ddd, 1 H, $J=8.1$, 4.7, 1.8 Hz, H-4), 5.24 (ddd, 1 H, $J=7.0$, 4.7, 0.8 Hz, H-3), 6.91–7.04 (m, 3 H, H-6,7,8), 7.18–7.29 (m, 1 H, H-9)

9: Yellow needles, m.p. >300°C (from benzene + hexane); UV (EtOH): $\lambda_{max}(\lg\varepsilon)=210$ (3.43), 225 (sh, 3.42), 312 (2.74) nm; IR (Nujol): $\tilde{\nu}_{CO}=2063$, 2006, 1988, $\tilde{\nu}_{SO}=1017$ cm^{-1}; 500-MHz ^1H NMR ($CDCl_3$): $\delta=3.86$ (d, 1 H, $J=8.4$ Hz, H-5), 4.03 (d, 1 H, $J=6.7$ Hz, H-2), 5.99 (dd, 1 H, $J=8.4$, 5.0 Hz, H-4), 6.10 (dd, 1 H, $J=6.7$, 5.0 Hz, H-3), 7.24–7.36 (m, 3 H, H-6,7,8), 7.48 (m, 1 H, H-9)

10: Yellow needles, m.p. 168.5–169.5°C (from benzene); UV (EtOH): $\lambda_{max}(\lg\varepsilon)=215$ (3.90), 312 (2.17) nm; IR (Nujol): $\tilde{\nu}_{CO}=2088$, 2028, 2006, $\tilde{\nu}_{SO_2}=1275$, 1120 cm^{-1}; 500-MHz ^1H NMR ($CDCl_3$): $\delta=3.84$ (dd, 1 H, $J=7.2$, 1.4 Hz, H-2), 3.95 (bd, 1 H, $J=8.4$ Hz, H-5), 5.87 (ddd, 1 H, $J=8.4$, 5.0, 1.4 Hz, H-4), 5.92 (ddd, 1 H, $J=7.2$, 5.0, 0.8 Hz, H-3), 7.28–7.34 (m, 3 H, H-6,7,8), 7.74 (m, 1 H, H-9)

In order to obtain **5** through oxidative decomplexation, **9** was treated with ceric ammonium nitrate. Monitoring of the reaction by thin layer chromatography reveals that a new polar spot appears, accompanied by a decrease in the less polar spot due to **9**. After 3 h at −10°C, however, the reaction mixture exhibited neither a polar nor a less polar spot on TLC examination. Workup of the reaction mixture afforded only naphthalene quantitatively, suggesting that the species responsible for the new polar spot might be assigned to **5**. The decomplexation can also be performed by photolysis. Irradiation of a dilute THF solution of **9** with a 400-W Hanovia lamp through quartz at −50°C resulted in the formation of **5**, which could be isolated and purified as pale yellow needles (at −40°C) through low-temperature column chromatography on silica gel (hexane) at −40°C.[10]

The first indication of its structure came from the 200-MHz ^1H NMR spectrum[11] measured at −30°C in CD_2Cl_2 which exhibited two doublets at $\delta=6.08$ (H-2) and 7.38 (H-5), two doublets of doublets at $\delta=6.38$ (H-3) and 6.69 (H-4), and an aromatic proton multiplet at $\delta=7.4$–8.0 in the ratio 1:1:1:1.2:5.5, indicating a small contamination with naphthalene. These chemical shifts are quite similar to those of 1-benzothiepin **4**. This implies no appreciable changes in electronic and geometric structures on going from **4** to its *S*-oxide **5**.[12] As expected, **5** was found to be less stable than **4** and the ^1H NMR signals due to **5** were completely replaced by those of naphthalene within 1 h at 13°C.

In view of the fact that the thermal stability of 2,3-diphenylthiirene 1-oxide was reported to be greater than that of the corresponding 1,1-dioxide,[13] it is interesting to note that 1,1-dioxide **6** is markedly more stable than 1-oxide **5**.

It is thus apparent that the thermally labile **4** and **5** can be substantially stabilized by complexation with iron tricarbonyl. Furthermore, the success in decomplexation of **9** by means of irradiation at low temperature suggests, in principle, the possibility of detecting parent thiepin **1** through its transition-metal complex by low-temperature photolysis. Efforts to achieve this goal are in progress.

Received: June 1, 1988 [Z 2797 IE]
German version: *Angew. Chem. 100* (1988) 1785

[1] W. L. Mock, *J. Am. Chem. Soc. 89* (1967) 1281; H. L. Ammon, P. H. Watts, Jr., *ibid. 90* (1968) 4501.
[2] I. Murata, K. Nakasuji, *Top. Curr. Chem. 97* (1983) 33.
[3] a) V. J. Traynelis, Y. Yoshikawa, J. C. Sih, L. J. Miller, *J. Org. Chem. 38* (1973) 3978; b) I. Murata, T. Tatsuoka, Y. Sugihara, *Angew. Chem. 86* (1974) 161; *Angew. Chem. Int. Ed. Engl. 13* (1974) 142.
[4] N. Yasuoka, Y. Kai, N. Kasai, T. Tatsuoka, I. Murata, *Angew. Chem. 88* (1976) 295; *Angew. Chem. Int. Ed. Engl. 15* (1976) 297.
[5] V. J. Traynelis, R. F. Love, *J. Org. Chem. 26* (1961) 2728.
[6] T. Tatsuoka, *Ph. D. Thesis*, Osaka University 1975.
[7] N. Yasuoka, Y. Kai, N. Kasai, *Acta Crystallogr. Sect. B 31* (1975) 2729.
[8] a) H. Hofmann, H. Gaube, *Angew. Chem. 87* (1975) 843; *Angew. Chem. Int. Ed. Engl. 14* (1975) 812; b) *Chem. Ber. 112* (1979) 781; c) H. Hofmann, R. Bohme, E. Wilhelm, *ibid. 111* (1978) 309.
[9] Cf. A. J. Pearson: *Metallo-organic Chemistry*, Wiley, New York 1985, p. 61ff.
[10] All new compounds gave satisfactory elemental analyses (except **5**) and spectroscopic data consistent with the proposed structures.
[11] We thank Dr. *Shoko Yamazaki*, Nara University of Education, for the 200-MHz ^1H-NMR spectrum of **5**.
[12] It has been suggested [13] that thiirene, which is regarded as 4π-electron vinylogue of thiepin, is "doubly unique in being both potentially aromatic, assuming the possibility of d-orbital conjugation effects, and potentially antiaromatic, in view of the presence of an unshared electron pair on the sulfur atom."
[13] L. A. Carpino, H.-W. Chen, *J. Am. Chem. Soc. 93* (1971) 785.

Direct Michael Additions of Silyl Groups to α,β-Unsaturated β-Arylketones and an α-Benzylidenelactone with Mixtures Obtained from Copper(I) Cyanide, Butyllithium and Chlorosilanes

By *Willi Amberg* and *Dieter Seebach**

It is well known that the silyl cuprates generated in the usual way from lithiosilanes undergo 1,4-addition to α,β-unsaturated carbonyl compounds.[1,2] The prerequisite lithiosilanes are prepared from the corresponding disilanes and an alkyllithium compound (HMPA/0°C)[3] or from chlorosilanes and Li metal (THF/−8°C/36 h).[4] It is also known[5] that the primary adduct enolates formed on addi-

[*] Prof. Dr. D. Seebach, Dipl.-Chem. W. Amberg [+]
Laboratorium für organische Chemie,
Eidgenössische Technische Hochschule
ETH-Zentrum, Universitätstr. 16, CH-8092 Zürich (Switzerland)
[+] Part of the projected Ph. D. thesis of W. A., ETH Zürich

tion of organocuprates[5–8] or Grignard reagents doped with Cu^{I} salts[9] to α,β-unsaturated carbonyl compounds can be trapped in situ as silyl enol ethers by carrying out the reactions in the presence of chlorosilanes.

Much to our surprise, we found that a variety of α,β-unsaturated β-arylketones (**3**) and an α-benzylidenelactone (**1**) furnish the β-silylated carbonyl derivatives **4** and **2**, respectively, when a solution of butyllithium and CuCN in THF is treated slowly at −75°C with a mixture of enone and chlorosilane (1:2), followed by low-temperature quenching with aqueous ammonia.[10]

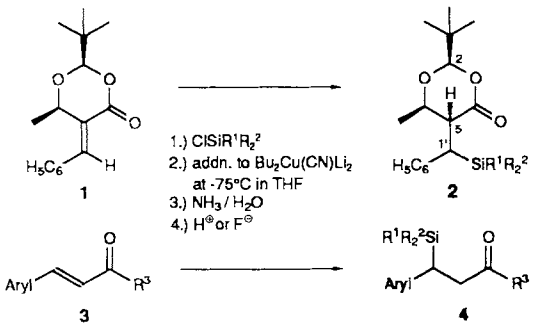

Table 1. Products **2** and **4** obtained from dioxanone **1** [11] and from the enones **3** [4-phenyl-3-buten-2-one, 1,3-diphenyl-2-propen-1-one, 3-(*p*-methoxyphenyl)-1-phenyl-2-propen-1-one] (see typical procedure). The specific rotations $[\alpha]_D^{RT}$ were measured in $CHCl_3$ (c=0.5–1.0). The IR, ^1H and ^{13}C NMR, and MS spectra as well as the elemental analyses are all in agreement with the structures shown.

	Product						
	R_1	R^2	R^3	Aryl	Yield [%]	M.p. [°C]	$[\alpha]_D^{RT}$ [°]
2a	CH_3	CH_3	—	—	81	oil	−61.5
2b	C_2H_5	C_2H_5	—	—	70	oil	−63.0
2c	t-C_4H_9	CH_3	—	—	71 [a]	92–93	−55.5
2d	C_6H_5	CH_3	—	—	52	96–97	−52.0
4a	t-C_4H_9	CH_3	CH_3	C_6H_5	68	oil	
4b	C_6H_5	CH_3	CH_3	C_6H_5	65	40–41	
4c	CH_3	CH_3	C_6H_5	C_6H_5	66	83–84	
4d	C_6H_5	CH_3	C_6H_5	C_6H_5	62	73–74	
4e	CH_3	CH_3	C_6H_5	p-$CH_3OC_6H_4$	59	92–93	
4f	C_6H_5	CH_3	C_6H_5	p-$CH_3OC_6H_4$	72	76–78	

[a] The temperature must be raised to −40°C for addition to be completed in this case.

No concomitant butyl transfer was observed with the dioxanone substrate **1**,[11] but only the reaction **1**→**2**, whereas the open-chain β-silylketones **4** were formed together with the corresponding β-butyl derivatives in the ratio 6:1–10:1 from the enones **3**.[12] The specific products prepared are listed together with some physical data in Table 1; the yields given are those obtained after *O*-desilylation of the initially formed silyl enol ethers[13] and after subsequent flash chromatographic purification.

Of the possible Michael adducts **2**, in each case only a single stereoisomer was formed with a selectivity of 92% (**2d**), 97% (**2c**) and 98% (**2a**, **b**). The chirality sense at C2 and C6 of these products must be (*R*), as in the precursor;[11] following a comparison of the coupling constants H-C5/H-C6 in the ^1H-NMR spectra with those of numerous analogous products we assign an (*R*) configuration to C5 as well.[14] The configuration of the silylated carbon C(1′) was not determined.[15]

Under the conditions described here it is possible to add a variety of silyl groups to certain Michael acceptors in a much simpler way than was possible by previously reported methods.

Typical Procedure

A suspension of 1 equiv. CuCN in dry THF (20–30 mL) was treated with 2 equiv. BuLi (1.4 M in hexane) at −75°C and the mixture warmed to −40°C under argon. To the slightly yellow solution thus obtained was added dropwise at −75°C a solution of 0.5 equiv. **1** or **3** and 1.0–1.5 equiv. $R^1R_2^2SiCl$ in THF (10–15 mL) within 1 h. A temporary dark yellow (with **1**) or deep red color (with **3**) developed. The slightly yellow solutions present after completion of addition of **1** or **3** were stirred at −75°C until the starting material was consumed (tlc analysis of withdrawn samples). Concentrated aq. NH_3 (10–30 mL for 1–10 mmolar runs) was added, and the mixture allowed to warm to +20°C, with the reaction flask open to the air. Subsequent extraction with ether (blue aq. phase), drying over $MgSO_4$ and removal of the solvent by evaporation afforded a crude mixture containing varying ratios of silylated free ketone and silylated silyl enol ether. The latter was treated as mentioned in Ref. [13] to hydrolyze the enol ethers. Flash chromatography and kugelrohr distillation, or crystallization, furnished the pure products (for yields, see Table 1).

Received: June 30, 1988 [Z 2838 IE]
German version: *Angew. Chem. 100* (1988) 1786

[1] D. J. Anger, I. Fleming, S. K. Patel, *J. Chem. Soc. Perkin Trans. 1 1981*, 2521.
[2] I. Fleming, T. W. Newton, *J. Chem. Soc. Perkin Trans. 1 1984*, 1805.
[3] W. C. Still, *J. Org. Chem. 41* (1976) 3063.
[4] E. W. Colvin: *Silicon Reagents in Organic Synthesis*, Academic Press, London 1988, p. 51, and references cited therein.
[5] E. J. Corey, N. W. Boaz, *Tetrahedron Lett. 26* (1985) 6015, 6019.
[6] C. R. Johnson, T. J. Marren, *Tetrahedron Lett. 28* (1987) 27.
[7] A. Alexakis, J. Berlan, Y. Besace, *Tetrahedron Lett. 27* (1986) 1047.
[8] R. J. Lindermann, A. Godfrey, K. Horne, *Tetrahedron Lett. 28* (1987) 3911; N. Rehnberg, T. Freyd, G. Magnusson, *ibid. 28* (1987) 3589; R. J. Lindermann, A. Godfrey, *ibid. 27* (1986) 4553.
[9] Y. Horiguchi, S. Matsuzawa, E. Nakamura, I. Kuwajima, *Tetrahedron Lett. 27* (1986) 4553.
[10] Direct silyl transfer was observed only in one case: the reaction was carried out at −95°C in THF with *cis*-4-phenyl-3-buten-2-one and TMSCl in the presence of naphthalenelithium [5].
[11] The enantiomerically pure (2*R*,6*R*)-(*E*)-5-benzylidene-1,3-dioxan-4-one (**1**) [m.p. 82–83°C, $[\alpha]_D^{RT}$ = −59.0° (c=2.4, $CHCl_3$)] used was prepared from the parent dioxanone and benzaldehyde in an overall yield of 50%; cf. D. Seebach, J. Zimmermann, *Helv. Chim. Acta 69* (1986) 1147; *ibid. 71* (1988), in press.
[12] The two Michael adducts are readily separated by flash chromatography.
[13] Silyl enol ethers of the products **2** which had survived the aqueous workup were desilylated with tetrabutylammonium fluoride (THF/−75°C), while the crude *E*/*Z*-silyl enol ether mixture of the open-chain products **4** was hydrolyzed with 2 N HCl (THF/+20°C).
[14] See References in [11] and Y. Noda, D. Seebach, *Helv. Chim. Acta 70* (1987) 2137; D. Seebach, J. Zimmermann, U. Gysel, R. Ziegler, T.-K. Ha, *J. Am. Chem. Soc. 110* (1988), in press. For stereoselective protonations of enolates of β-silylated carbonyl compounds see: I.Fleming, J. H.-M. Hill, D. Parker, D. Waterson, *J. Chem. Soc. Chem. Commun. 1985*, 318; I. Fleming, J. J. Lewis, *ibid. 1985*, 149.
[15] If the silyl groups were added to **1** from the same diastereotopic face as cuprate-derived carbon nucleophiles, the configuration of C(1′) would be *S*.

$[V_{19}O_{41}(OH)_9]^{8\ominus}$, An Ellipsoid-Shaped Cluster Anion Belonging to the Unusual Family of V^{IV}/V^{V} Oxygen Clusters

By *Achim Müller,* Michael Penk, Erich Krickemeyer, Hartmut Bögge,* and *Heinz-Jürgen Walberg*

Although only one "larger" V^V isopolyanion, namely, $[V_{10}O_{28}]^{6\ominus}$, has been reported so far, the number of V^{IV}/V^V

[*] Prof. Dr. A. Müller, M. Penk, E. Krickemeyer, Dr. H. Bögge, H.-J. Walberg
Fakultät für Chemie der Universität
Postfach 8640, D-4800 Bielefeld 1 (FRG)

oxygen clusters should be far greater according to our hypothesis.[1] We have now obtained the black compound **1**, which belongs to this family of clusters and have characterized it by elemental analysis, manganometric titration of V^{IV}, thermoanalysis, IR spectroscopy, magnetic measurements, and single-crystal X-ray structure analysis.[2]

$(NH_4)_8[V_{19}O_{41}(OH)_9]\cdot 11H_2O$ **1**

The anion $[V_{19}O_{41}(OH)_9]^{8\ominus}$[3] contains a large number of protons: it has the shape of an ellipsoid of approximate C_3 (or, without the central V atom, D_3) symmetry and is generated by joining 12 VO_6 octahedra (V^{IV}) and 6 VO_4 tetrahedra (V^V) as well as a central V^VO_4 unit (Fig. 1). A summation of the exponentially weighted V-O bond lengths for each V atom[4] indicates that, in the anion of **1**, all V^{IV} are in octahedral environments and all V^V are in tetrahedral environments (no example is known for V^{IV} in a tetrahedral environment). The number of V^{IV} atoms so determined is in agreement with the results of manganometric titration of V^{IV} (compare also the significant differences between $V^{IV}V^{IV}$ and $V^{IV}V^V$ separations).

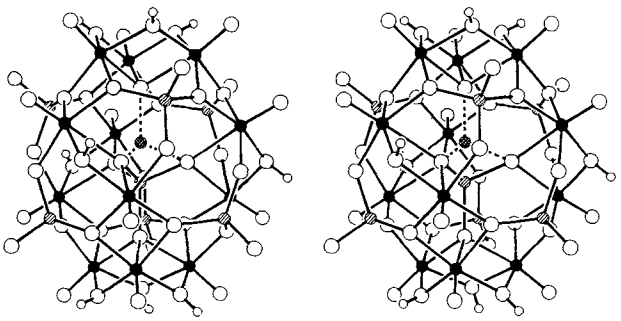

Fig. 1. Stereoprojection of the structure of the $[V_{19}O_{41}(OH)_9]^{8\ominus}$ ion in crystals of **1** (view perpendicular to the near C_3 axis; V^{IV} = black, V^V = hatched, central disordered V hatched in the first position and cross-hatched with V-O bonds drawn with broken lines in the second, O and H = white). Distances [pm] and angles [°] (central VO_4 tetrahedron and μ_3-O atom omitted; cf. text): $V^{IV}\cdots V^{IV}$ 289.6(2)-299.4(2), $V^{IV}\cdots V^V$ 330.1(2)-361.0(2), V-O_{term} 159.2(6)-162.8(6), V^{IV}-(μ_2-O(H)) 195.8(5)-202.5(5), V^{IV}-(μ_2-O) 196.0(5)-199.4(6), V^{IV}-(μ_3-O) 197.2(5)-203.1(5), V^V-(μ_2-O) 165.7(6)-168.7(5), V^V-(μ_3-O) 179.0(5)-181.9(6); O_{term}-V^{IV}-(μ-O) 95.8(2)-103.9(3), O_{term}-V^V-(μ-O) 104.7(3)-109.9(3), (μ-O)-V^{IV}-(μ-O) 82.4(2)-93.9(2), 153.0(2)-164.7(2), (μ-O)-V^V-(μ-O) 108.1(3)-114.5(2), V^{IV}-(μ_2-O)-V^V 129.5(3)-131.6(3), V^{IV}-(μ_2-O(H))-V^{IV} 111.1(3)-116.0(3), V^{IV}-(μ_3-O)-V^V 122.2(3)-143.7(3), V^{IV}-(μ_3-O)-V^{IV} 92.6(2)-96.0(2).

Within the anion are a VO_4 tetrahedron and a μ_3-O atom disordered over two lattice sites in a ratio of 1:1; the disorder could only be solved for the V atom, since the positions of the μ_3-O atoms of the two tetrahedral sites as well as those of the μ_4-O atom and the additional μ_3-O atom do not differ significantly. The 18 outer V atoms are joined by the μ_4-O atom and the 4 μ_3-O atoms in the center of the anion as well as by 12 μ_3-O and 15 μ_2-O atoms in the "outer shell". Of the latter, the nine μ_2-O atoms involved in edge-sharing of two VO_6 octahedra are protonated; the six remaining, unprotonated μ_2-O atoms each join a VO_6 with a VO_4 unit.

The V^{IV} centers are antiferromagnetically coupled ($\mu = 3.2\mu_B$ at room temperature), whereby the magnetic susceptibility continuously decreases with decreasing (measured to 160 K) temperature. Our investigations indicate that an unusually large number of "binary" mixed-valence clusters exist for vanadium; in addition, they may have different electron populations.[1] The low redox potential $V^{IV} \rightleftharpoons V^V$ may be important in this connection. Furthermore, the $V^{IV}/V^V/O$ system is of importance for understanding the technical V_2O_5 catalyst (fluid mixture of V_2O_5 and Na vanadate, in which similar clusters could be present), for which an appreciable proportion of V^{IV} has been detected by ESR spectroscopy.[5]

The class of compounds discussed here does not belong, in our opinion, to the "classical" isopolyanions, since for no other metal do isolated species exist in which the number of metal centers of different oxidation states is comparable.

Experimental Procedure

NH_4VO_3 (8.0 g, 68.4 mmol) was dissolved in H_2O (250 mL) contained in a 300-mL Erlenmeyer flask (narrow neck) at 75°C (pH 5.8). The solution was cooled to 70°C, hydrazinium sulfate (1.37 g, 10.5 mmol) was added (color change from yellow via olive green and blue-violet to dark brown), and the reaction mixture was stirred for 5 min at this temperature (the pH value increased to 7.3). The stirred mixture was then adjusted to pH 5.3-5.4 by addition of 10%-H_2SO_4 and, immediately afterward, the reaction solution (covered with a watch glass) was allowed to stand for 5 h in an oil bath (65-70°C) without stirring. The black crystals of **1** (streak color: dark brown) thereby formed were filtered from the hot solution, washed with 2-propanol and diethyl ether, dried under a stream of argon, and stored under argon. Yield: 5.0 g (2.36 mmol, 65.5%). Main adsorption bands in the IR spectrum (solid/CsI pellet): $\tilde{\nu}$ [cm^{-1}] = 970 (s, ν(V-O_{term})), 860 (s), 810 (s), 720 (s, ν_{as}(V-O-V)), 525 (m, γ(OH)).

Received: December 23, 1987;
revised: September 9, 1988 [Z 2554 IE]
German version: *Angew. Chem. 100* (1988) 1787

[1] A. Müller, E. Krickemeyer, M. Penk, H.-J. Walberg, H. Bögge, *Angew. Chem. 99* (1987) 1060; *Angew. Chem. Int. Ed. Engl. 26* (1987) 1045.

[2] **1**: space group $P\bar{1}$; $a = 1317.3(3)$, $b = 1433.1(3)$, $c = 1602.3(3)$ pm, $\alpha = 91.16(2)$, $\beta = 93.46(2)$, $\gamma = 91.52(2)°$, $V = 3017.7 \times 10^6$ pm^3; $\mu = 28.2$ cm^{-1}; $Z = 2$; $\rho_{calcd} = 2.33$ g cm^{-3}; $R = 0.056$ for 8008 unique reflections ($F_0 > 3.92\sigma(F_0)$; Syntex $P2_1$ diffractometer, $Mo_{K\alpha}$ radiation, graphite monochromator). The water molecules and the ammonium ions are in part disordered, so that their H atoms could not be localized. All nine hydrogen positions of the VOH groups, on the other hand, were determined by high-angle refinement of the non-hydrogen atoms followed by difference Fourier synthesis with internal reflections ($2\theta \leq 40°$). Further hydrogen atoms in the anion were not found. The hydrogen parameters thus obtained were fixed in the final refinement. The powder diffraction diagram calculated from the single-crystal data is in agreement with the measured one. Further details of the crystal structure investigation may be obtained from the Fachinformationszentrum Energie, Physik, Mathematik GmbH, D-7514 Eggenstein-Leopoldshafen 2 (FRG), on quoting the depository number CSD-53333, the names of the authors, and the journal citation.

[3] With respect to the number of protons, the formula is unambiguously established by redundant investigations (very precise N and V^{IV} analysis values), by different coordination of V^{IV} and V^V, by study of the hydrogen bond lengths, and by analysis of the V-O-V distances (cf. the procedure followed in [2]). The V^{IV}-O distances of the nine protonated and the six unprotonated μ_2-O atoms are similar, since the unprotonated μ_2-O atoms are also each involved in a markedly shorter V^V-O bond. V^{IV}-O(H)-V^{IV}: 196-203 pm; V^{IV}-O-V^V: 196-199 and 166-169 pm. Thus, the (μ_2-O)-V^{IV} distance can be lengthened both by protonation of the oxygen atom and by a (μ_2-O)-V^V bond in "close proximity" having an appreciable π-bond component. Eight H atoms display H-O distances of 77-113 pm and a V-O-H angle of 98-135°, a further H position has an "H-O" distance of 55 pm (presumably with significant error owing to the coordination of the H atom to a disordered water molecule). Of these nine H atoms, six form intermolecular hydrogen bonds to (unprotonated) terminal O atoms of other anions, whereby, as expected, the O-O distances of the (μ_2-O)-H$\cdots O_{term}$ groups are short and lie in the range 269-286 pm.

Owing to the higher electron density on the oxygen atom, the protonation of V^{IV}-O-V^{IV} centers is more reasonable than that of V^{IV}-O-V^{V} centers. Furthermore, twelve V^{IV} and six V^{V} centers can be unequivocally localized by an exponentially weighted summation of all V-O bond lengths of each V atom (cf. [4]; the bond lengths for the V^{V} atom of the central VO_4 tetrahedron deviate from those of the other V^{V} centers since they are in error owing to the disorder). The anion $[V^{IV}_{12}V^{V}_{7}O_{41}(OH)_8]^{8\ominus}$ differs from "$[V^{IV}_{6}V^{V}_{13}O_{48}(OH)]^{8\ominus}$" prepared by *Johnson* (but not published), (cf. [6, 7]), above all in the structure, the number of O and H atoms, and the V^{IV}/V^{V} ratio. Here, it is necessary to consider that *Johnson* did not determine unambiguously the number of protons and the V^{IV}/V^{V} ratio in his anion and could not account for additional electron density found in the proximity of the central V atom.

[4] For 50 structurally known compounds, it has been possible to divide the VO_n centers into V^{IV} and V^{V} centers (cf. [6]) by use of the summation $\sum_{i=1}^{n} \exp(-2.7d(V-O_i))$, which was developed based on *Pauling*'s concept of bond strength (L. Pauling, *J. Am. Chem. Soc. 69* (1947) 542).

[5] C. N. Kenney, *Catalysis 3* (1980) 123.

[6] G. K. Johnson, *Dissertation*, University of Columbia-Missouri, Columbia, MO, USA 1977.

[7] M. T. Pope: *Heteropoly and Isopoly Oxometalates* (*Inorg. Chem. Concepts 8*), Springer, Berlin 1983.

A Novel Heterocluster with D_3-Symmetry Containing Twenty-One Core Atoms: $[As^{III}_6V^{IV}_{15}O_{42}(H_2O)]^{6\ominus}$

By *Achim Müller** and *Joachim Döring*

Arsenic-vanadium clusters with arsenic and vanadium in low oxidation states were previously unknown. The novel cluster anion reported here has an interesting structure and symmetry and exhibits cryptand properties. The brown compound $K_6[As^{III}_6V^{IV}_{15}O_{42}(H_2O)]\cdot 8H_2O$ **1** was synthesized by reduction of vanadate with hydrazinium sulfate in the presence of As^{III} and isolated as rhombohedral crystals.[1] Cluster **1** was characterized by elemental analysis (including manganometric titration and thermogravimetric determination of crystal water), vibrational spectroscopy,[2] magnetic measurements,[2] and a single-crystal X-ray structure analysis.[3]

The anion has crystallographic D_3 symmetry. It consists of 15 distorted tetragonal VO_5 pyramids and 6 trigonal AsO_3 pyramids (Fig. 1). It includes at its center a statistically disordered H_2O molecule. The 15 VO_5 pyramids are linked with one another through vertices and edges and with AsO_3 groups only through vertices. Two AsO_3 groups are joined to each other via an oxygen bridge, forming a handlelike As_2O_5 moiety.

The VO_5 pyramids can be divided into three differently linked groups. The first group includes six polyhedrons, each of which is joined through two edges and three vertices with its neighboring pyramids and through one vertex with an AsO_3 group. The second group contains six VO_5 pyramids, which are joined through three edges with other VO_5 pyramids and through two vertices with two AsO_3 groups. Finally, the third group consists of three VO_5 pyramids, which are mutually joined through two vertices and two edges with four VO_5 pyramids and through two vertices with two As_2O_5 moieties.

In the crystal lattice, the anions are joined to one another through "hydrated" potassium ions, which have a distorted octahedral coordination sphere composed of terminal oxygens of the anions and oxygen atoms of the crystal water.

V^{IV} and V^{IV}/V^{V} clusters are cryptands and tend to form spherical structures. This is shown by experience[4] as well as by quantum-chemical calculations (it is important, in this context, that the As_2O_5 groups are separated as far as possible). In the cluster anion of **1**, too, the V centers, which are antiferromagnetically coupled,[2] are localized on a spherical surface ($r = 385 \pm 15$ pm), see Ref. [4]; the As_2O_5 groups give rise to bulges.

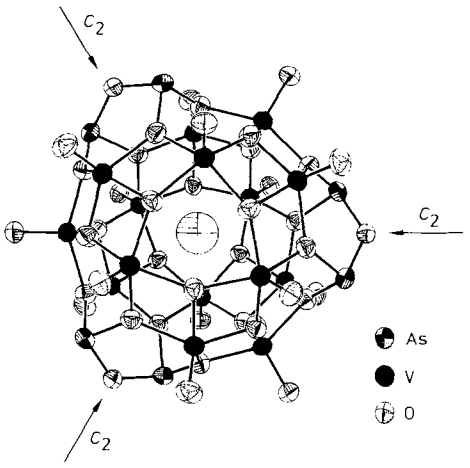

Fig. 1. Structure of the anion $[As^{III}_6V^{IV}_{15}O_{42}]^{6\ominus}$ with an interstitial, disordered H_2O molecule in the crystal of **1**: C_3 axis perpendicular to the plane of the paper. Selected bond lengths [pm]: V···V 287.0(1) to 304.9(1), V-(μ_3-O) 191.2(5) to 200.6(5), As-O 177.0(4) to 179.0(4), V-O_{term} 161.0(5) to 161.8(5); Selected bond angles [°]: O_{term}-V-(μ_3-O) 105.3(2) to 113.8(2), (μ_3-O)-V-(μ_3-O) 76.9(2) to 91.6(2) and 133.1(2) to 149.5(2), As-O-As 130.7(1), As-O-V 123.5(2) to 135.2(2), V-O-V 95.5(2) to 104.5(2) and 147.0(3) to 149.1(3).

The cluster anion of **1** may be regarded as a model for species that are formed during poisoning of the V_2O_5 catalyst (which contains V^{IV} centers) by arsenic.

Received: July 25, 1988 [Z 2885 IE]
German version: *Angew. Chem. 100* (1988) 1789

[*] Prof. Dr. A. Müller, J. Döring
Fakultät für Chemie der Universität
Postfach 8640, D-4800 Bielefeld 1 (FRG)

[1] *Experimental Procedure:* **1**: KVO_3 (4.1 g, 29.7 mmol), As_2O_3 (1.4 g, 7.1 mmol), KSCN (10.0 g, 103 mmol), and KOH (1.0 g, 17.8 mmol) were dissolved in H_2O (100 mL) at 85 °C with stirring (pH value of the solution ca. 8.6). After stepwise addition of solid hydrazine sulfate (2.5 g, 19.2 mmol), the reaction mixture was stirred for 2 min at 85 °C (color change to greenish brown; pH value ca. 6.8). The mixture was then allowed to stand at 20 °C, whereby the pH value increased to ca. 8.4 and large brown crystals formed. The crystals were collected by filtration after 1-2 days. Yield: 1.48 g (55.0%).

[2] IR spectrum (solid/CsI pellet): $\tilde{\nu}$(OH) = 3400 (s), δ(HOH) = 1610 (m), $\tilde{\nu}$(V-O_{term}) = 970 (s), $\tilde{\nu}$(V-O-V) = 720 (s), $\tilde{\nu}$(As-O) = 635 cm^{-1}. Magnetic measurements: μ_{eff}(160 K) = 2.9 B.M., μ_{eff}(290 K) = 4.2 B.M.

[3] $R\bar{3}c$; $a = 1402.9(4)$ pm, $\alpha = 79.26(2)°$, $V = 2632.0 \times 10^6$ pm^3; $\mu = 67.74$ cm^{-1}; $Z = 2$; $R = 0.052$ for 1693 unique reflections ($F_0 > 5.0\sigma(F_0)$; Syntex $P2_1$ diffractometer, $Mo_{K\alpha}$ radiation (graphite monochromator). Further details of the crystal structure investigation may be obtained from the Fachinformationszentrum Energie, Physik, Mathematik GmbH, D-7514 Eggenstein-Leopoldshafen 2 (FRG), on quoting the depository number CSD-53334, the names of the authors, and the journal citation.

[4] Cf. A. Müller, E. Krickemeyer, M. Penk, H. J. Walberg, H. Bögge, *Angew. Chem. 99* (1987) 1060; *Angew. Chem. Int. Ed. Engl. 26* (1987) 1045.

Rapid Detection of Manganese Deficiency in Conifer Needles by Electron Spin Resonance Spectroscopy**

By *Peter Laggner,* Ruth Mandl, Annemarie Schuster, Monika Zechner,* and *Dieter Grill*

Manganese is an ubiquitous and important trace element in green plants[1] and is involved as a specific cofactor in the light-induced water oxidation in photosystem II.[2,3] Furthermore, green leaves and needles contain a Mn^{II} pool which takes part in the action of superoxide dismutases.[4,5] A well-documented correlation exists between manganese deficiency and reduced tree vitality.[6,7] Mn^{II} shows a strong, characteristic six-line ESR spectrum,[8,9] which can be easily distinguished from that of other paramagnetic species involved in photosynthesis. We have used this feature to develop a method for rapid screening of conifer needles for manganese deficiency. The results from a two-year screening test in Austrian forests demonstrate the diagnostic value of the method.

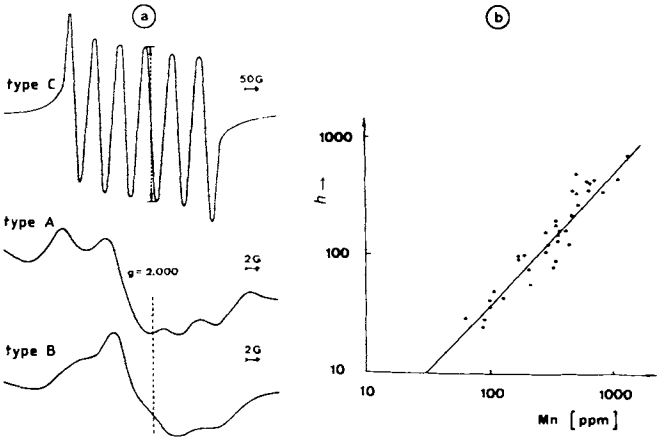

Fig. 1. a) Representative ESR spectra of spruce *(P. abies)* needles. A Varian E104-A X-band spectrometer was used for recording the spectra. The spectra were "smoothed" by hand. Typical instrument settings were: 3400 Gauss field set; scan range/100-kHz field modulation amplitude, 1000/2 Gauss (for the Mn^{II} signal), 40/2 Gauss (for signals A or B); 9.48-GHz microwave frequency; 10-mW microwave power; scan time/time constant, 2 min/0.25 s (for Mn^{II}), 4 min/4 s (for signals A or B). Needles were filled into 0.4-cm inner-diameter quartz sample tubes to a height of 3–4 cm. The net packing density achieved by gentle shaking was 0.4 ± 0.025 g cm^{-3} (mean ± S.D. for $n = 14$). Washing experiments with distilled water and metal complexing agents (EDTA) showed no interference by surface depositions. b) Double-logarithmic plot of the signal height h (arbitrary units) of type-C spectra versus total manganese concentration (of dry weight) measured by atomic absorption spectroscopy in 36 needle samples. The dots represent single determinations for any one sample. The line was determined by linear regression analysis ($r = 0.85$).

In general, the ESR spectra of spruce *(P. abies)* needles can be classified into three distinct types (Fig. 1a). Two of them, referred to by us as types A and B, have relatively weak and narrow lines and therefore require high magnification and resolution. The type-A spectrum was formerly assigned to the plastosemiquinone radical cation in photosystem II[10] but recently shown to originate more probably from a tyrosine radical;[11,12] type B is an altered form of the type-A spectrum and has possible pathological significance, since it appears for samples from visibly diseased trees.[13] Type C, a strong six-line spectrum extending over abut 500 Gauss, with a peak-to-peak separation of 95 Gauss is characteristic of motionally restricted Mn^{II}.[14,15] Figure 1b shows the correlation between the total manganese concentration in the needles and the height of the signals in the type-C spectrum. The linear regression shows an operational relationship that can be used to estimate the total manganese concentration between about 50 and 1000 ppm directly from the signal height. Between 25 and 50 ppm, the type-A spectrum becomes dominant; below about 25 ppm, the line-shape corresponds to type B.

Figure 2 shows the distribution of the spectral types as a function of manganese concentration, together with the relationship between manganese content and tree-vitality status as defined by *Kreutzer*.[6,7] With due account for the overlap between the spectral types on the one hand and between the diagnostic assignments on the other, the spectral types coincide well with the tripartite vitality scale.

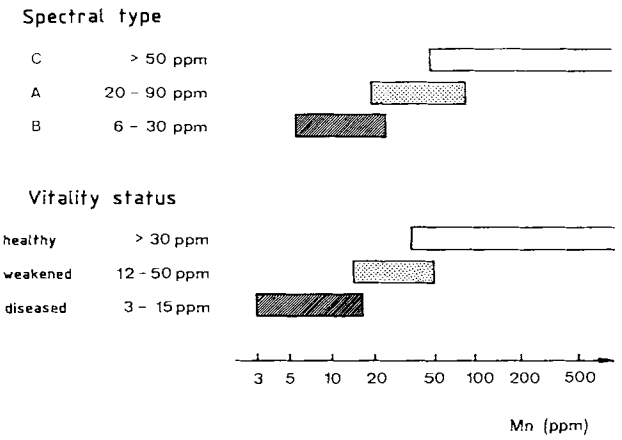

Fig. 2. Manganese concentration ranges (of dry weight) for the spectral types defined in this study (top) and for the vitality status according to *Kreutzer* [6, 7] (bottom).

The Mn^{II} ESR spectrum of photosynthetic organs is known to be light-dependent.[15,16] Since the present analysis is performed in the dark, below the threshold of such effects, they are irrelevant for the above classification. Variations in signal strength of type C do occur with the age of needles and also with the distance to the crown. These are generally in the range of less than 20% and therefore lower than the variations between trees of different vitality status. In no case did we observe a situation where, at the same time, different samples from one tree showed both type-C and type-A or -B spectra.

A representative result of a one-year monthly screening in one observation area is shown in Figure 3a. The distribution of spectral types shows that in this region, where all three vitality groups are present, the proportion of trees with no manganese deficiency (type C) remained stable,

[*] Prof. Dr. P. Laggner, Dr. R. Mandl, A. Schuster, M. Zechner
Institut für Röntgenfeinstrukturforschung der
Österreichischen Akademie der Wissenschaften
und der Forschungsgesellschaft Joanneum
Steyrergasse 17, A-8010 Graz (Austria)
Prof. Dr. D. Grill
Institut für Pflanzenphysiologie der Universität
Schubertstrasse 51, A-8010 Graz (Austria)

[**] We thank Dr. *W. Kosmus,* Institut für Analytische Chemie der Karl-Franzens-Universität, for help with atomic absorption spectroscopy. This work has been supported by a grant from the Styrian Research Foundation (*P. L.*).

while the number of diseased trees (type B) increased at the expense of the weakened ones (type A). At the beginning of the vegetation period, May and June, parallel measurements of the new and one-year-old needles showed generally the same spectral type. However, the new shoots gave weaker signals which can be related to their higher water content. The one-year course for a single tree is shown in Figure 3b.

The results obtained at the four observation sites in the same month of three subsequent years are shown in Figure 3c. Generally, the distributions of spectral types are in good correlation with the documented stress regions defined by the forest authorities. Thus, the high proportion of type C in region "Gruber" corresponds to its low-pollution situation, while the results in region "Au" reflect its physiologically poor environment for spruce, in an immediate urban neighborhood.

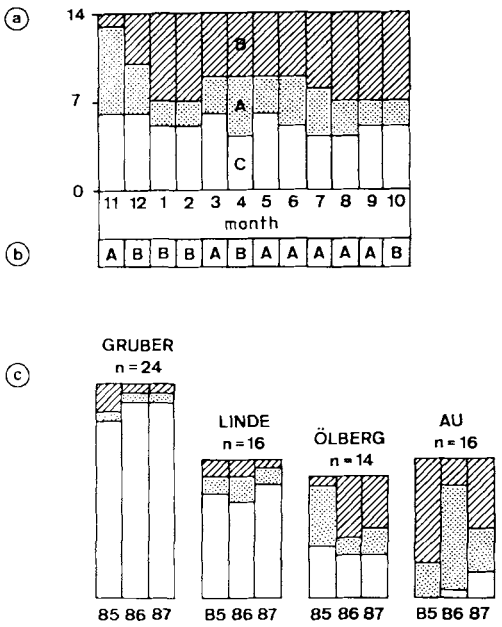

Fig. 3. a) Seasonal dependence of the spectral-type distribution in one observation area (Ölberg, 14 trees). Needles were collected from marked trees at monthly intervals from October 1985 to April 1988. The graph shows the results of a one-year screening (November 1985-October 1986). Samples were brought to the laboratory as twigs and either measured immediately or stored in a dark cold-room (2–4°C) for less than 48 h until measurement. Within this time no significant alterations in the ESR signals could be observed. b) Typical one-year course for a weakened tree, about 15 years old, growing on rock under pressure from neighboring trees in understory, showing signs of crown thinning and red-rot. c) Spectral-type distribution in four observation areas measured in November of three subsequent years (1985-1987).

Independently of the spectroscopic results, all trees in the regular observation areas were classified for risk factors by visual assessment according to established criteria. As an example, Figure 4 shows the correlation between this classification and the spectral types for the area "Ölberg". For all trees where two or more risk factors were diagnosed, severe manganese deficiency was manifest by the spectral type B. On the other hand, type-C trees invariably were of intact vitality. Spectral type A was found to correlate with trees growing in understory without visible decay symptoms. This systematic correlation pattern was also observed in all other areas of sampling. Although we cannot exclude the possibility that there exist diseased trees which do not show manganese deficiency, our present results strongly suggest that manganese deficiency as diagnosed by the absence of spectral type C is indeed a good and general indicator for tree disease.

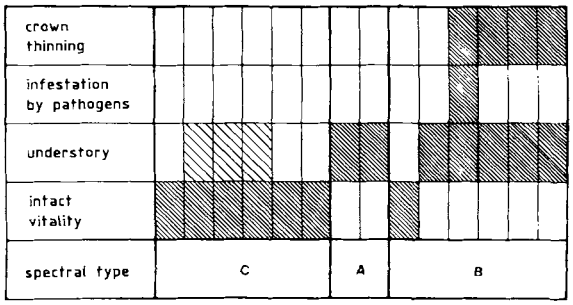

Fig. 4. Correlation between visible risk factors and spectral types for 14 trees in the area "Ölberg".

The remarkable correlation between the threshold for the appearance of a dominant Mn^{II} spectrum (type C) and apparently intact tree vitality is a fact worthy of physiological consideration. In photosystem II, Mn^{III} and Mn^{IV} are functionally involved,[2,3] as revealed by ESR spectroscopy at room temperature. This suggests that the ESR-detectable Mn^{II} is not important to photosynthetic activity. However, it was recently reported[17] that illumination of spruce needles induces changes in intensity of the Mn^{II} signal. Possibly, an excess of Mn^{II} is required to maintain redox balance in photosynthesis. Another possible function for this Mn^{II} pool may be to serve as a radical scavenger in the protection against photooxidation reactions. Of course, these two alternatives are not mutually exclusive and may well be both operative.

In order to be useful for large-scale screening, the method has to be rapid and simple. Therefore, the primary aim of the present work was not to achieve high precision in Mn determination, but to find spectroscopic criteria which can be used in a diagnostic risk assessment.

Notwithstanding the demonstrated correlation between tree vitality and spectroscopically measurable Mn^{II} content, it has to be mentioned that variations in Mn^{II} availability from the soil certainly can affect the manganese content of needles.[18] To further elucidate combined environmental effects, the presently described simple and rapid ESR method offers an attractive analytical tool.

Received: May 31, 1988;
revised: August 24, 1988 [Z 2793 IE]
German version: *Angew. Chem. 100* (1988) 1790

[1] P. J. Kramer, T. T. Kozlowsky: *Physiology of Woody Plants*, Academic Press, London 1979.
[2] B. Kok, R. Radmer, C. F. Fowler, *Annu. Rev. Biochem. 44* (1979) 409.
[3] T. Kambara, Govindjee, *Proc. Natl. Acad. Sci. USA 82* (1985) 6119.
[4] J. Amesz, *Biochim. Biophys. Acta 726* (1983) 1.
[5] D. C. McCain, J. L. Markley, *Biophys. J. 48* (1985) 687.
[6] K. Kreutzer, *Forstwiss. Centralbl. 89* (1970) 275.
[7] K. Kreutzer, *Forstwiss. Centralbl. 91* (1972) 80.
[8] N. M. Atherton: *Electron Spin Resonance. Theory and Applications*, Wiley, New York 1974.
[9] H. M. Swartz, J. R. Bolton, D. C. Borg: *Biological Applications of Electron Spin Resonance*, Wiley-Interscience, New York 1972.

[10] P. J. O'Malley, G. T. Babcock, R. C. Prince, *Biochim. Biophys. Acta 766* (1984) 283.
[11] R. J. Debus, B. A. Barry, G. T. Backcock, L. McIntosh, *Proc. Natl. Acad. Sci. USA 85* (1988) 427.
[12] B. A. Barry, C. T. Babcock, *Proc. Natl. Acad. Sci. USA 84* (1987) 7099.
[13] H. B. Stegmann, H. J. Ruff, K. Scheffler, *Angew. Chem. 97* (1985) 407; *Angew. Chem. Int. Ed. Engl. 24* (1985) 425.
[14] R. E. Blankenship, K. Sauer, *Biochim. Biophys. Acta 357* (1974) 252.
[15] M. Dunach, M. Seigneuret, J. Rigaud, E. Padros, *Biochemistry 26* (1987) 1179.
[16] Y. Siderer, R. Malkin, R. Poupko, Z. Luz, *Arch. Biochem. Biophys. 179* (1977) 174.
[17] H. B. Stegmann, P. Schuler, H. J. Ruff, submitted for publication.
[18] W. Nebe, *Arch. Forstwes. 16* (1967) 109.

Formation of an Oxalate-filled Cavity in a Reduced Cyclic Octanuclear Polyoxomolybdate $[(n\text{-}C_4H_9)_4N]_2[Mo_8O_{16}(OCH_3)_8(C_2O_4)]$ formed from α-$[(n\text{-}C_4H_9)_4N]_4[Mo_8O_{26}]$ and Rhodizonic Acid**

By *Qin Chen, Shuncheng Liu,* and *Jon Zubieta**

Investigations of the interactions between polyoxometalate clusters and substrate organic molecules have been prompted by the structural relationship of polyoxoanions to solid oxides.[1-4] In the specific case of polyoxomolybdate-carbonyl interactions, carbonyl insertion into a molybdenum-oxygen bond provides the common feature of the chemistry.[5-7] The syntheses of organooxomolybdates **1** with acetyl-,[5] **2** with diacetyl-,[6] and **3** with diketal-structures,[7] depending upon the choice of organic substrate, have been discussed in terms of acid-base pair binding sites and models for substrate binding on solid oxide surfaces.[8] However, the products of such molybdate-carbonyl reactions also depend intimately upon the nature of the organic precursor, as demonstrated by the isolation of the oxalatodimolybdate **4** from the reaction of the complex **5** with chloranilic acid **6** in methanol.[7] This observation suggests that ligand dissociation will occur, subsequent to carbonyl insertion, with organic residues capable of stabilizing a cationic leaving group. In order to examine the generality of carbonyl insertion coupled with ligand dissociation in polyoxomolybdate-carbonyl chemistry, we have investigated the reaction of the molybdate **5** with rhodizonic acid **7**.

$[RCHMo_4O_{15}H]^{3\ominus}$ **1**

$[HCCHMo_4O_{15}X]^{3\ominus}$ **2**

$[(C_{14}H_8)Mo_4O_{15}(OH)]^{3\ominus}$

3, $C_{14}H_8$ = phenanthrenediyl

$[(n\text{-}C_4H_9)_4N]_2[Mo_2O_4Cl_4(C_2O_4)]$ **4**

α-$[(\eta\text{-}C_4H_9)_4N]_4[Mo_8O_{26}]$ **5**

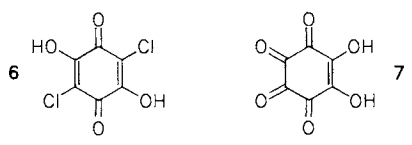

6 7

The product of the reaction of **5** with **7** is a light-green, crystalline, diamagnetic species of analytical composition **8**.[9] The IR spectrum of **8** shows a band at 2930 cm^{-1} associated with the C-H stretching modes of the methoxy groups, and strong bands at 1665 cm^{-1} and 1543 cm^{-1} which are assigned to the carbonyl stretching vibrations ν(C=O) of non-equivalent carbonyl residues. The band at 972 cm^{-1} is assigned to the $\nu(Mo{=}O_t)$ stretching vibration (O_t = terminal oxo group); furthermore, the position of the absorption suggests that the molybdenum centers of the Mo^{VI} starting compound have been reduced. The band at 815 cm^{-1} establishes the presence of bridging oxo groups ($Mo\text{-}O_b\text{-}Mo$).

$[(n\text{-}C_4H_9)_4N]_2[Mo_8O_{16}(OCH_3)_8(C_2O_4)]$ **8**

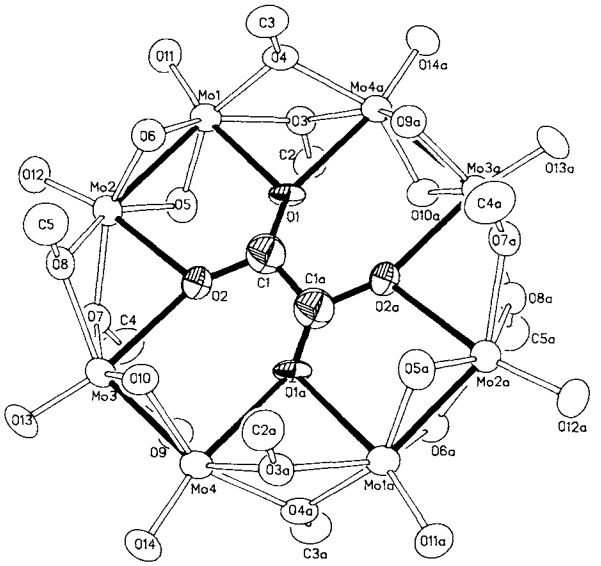

Fig. 1. Structure of the dianion $[Mo_8O_{16}(OCH_3)_8(C_2O_4)]^{2\ominus}$ of **8** in the crystal. Selected bond lengths [Å] and angles [°]: Mo1-O1, 2.367(7); Mo2-O2, 2.377(7); Mo3-O2, 2.385(8); Mo4-O1a, 2.367(7); Mo-O_t, 1.678(11) (av); Mo-O_b, 1.932(12) (av); Mo-O(methoxy), 2.106(11) (av); Mo1-Mo2, 2.582(2); Mo2-Mo3, 3.262(1); Mo3-Mo4, 2.574(2); Mo4-Mo1a, 3.312(1); C1-O1, 1.25(2); C1-O2, 1.37(2); C1-C1a, 1.43(2); O3-Mo1-O4, 71.4(3); O5-Mo1-O6, 94.3(3); O9-Mo3-O10, 94.2(3); O3a-Mo4-O4a, 71.2(3); O9-Mo4-O10, 94.5(3); Mo-O_b-Mo, 83.7(5) (av); Mo-O(methoxy)-Mo, 101.7(6) (av). Abbreviations: O_t, terminal oxo group; O_b, bridging oxo group; O(methoxy), bridging methoxy group oxygen donor.

The complex anion of compound **8** (Fig. 1)[10] consists of an octagonal array of Mo atoms, alternately bridged by two methoxy groups or two oxo groups producing a cyclic "tiara" framework $[Mo_8O_{16}(OCH_3)_8]^0$. The Mo-Mo distances display a short-long alternation around the ring (with average values of 2.578 and 3.287 Å, resp.). Each of the bonding Mo-Mo pairs is bridged by two oxo groups, while two methoxy groups bridge each of the Mo-Mo pairs with non-interacting distances. The methoxy groups

[*] Prof. Dr. J. Zubieta, Q. Chen, S. Liu
Department of Chemistry
State University of New York at Albany
Albany, NY 12222 (USA)

[**] This work was supported by the National Science Foundation (Grant CHE 8514634 to J. Z.).

fold out from the ring, whereas the oxo groups fold into the cavity formed by the ring. The Mo-Mo bonding distance of 2.578 Å is characteristic for Mo^{V} d^1 centers in bridged binuclear systems where a direct Mo-Mo interaction is present[11] and it accounts for the observed diamagnetism of **8** as a consequence of strong magnetic coupling.

A remarkable feature of the structure of **8** is that the cavity of the cyclic $[Mo_8O_{16}(OCH_3)_8]^0$ unit is occupied by an oxalate moiety, $[C_2O_4]^{2\ominus}$. Each oxygen of the oxalate group bridges two Mo centers with non-bonding Mo···Mo distances. The oxalate unit, the eight Mo centers and the eight terminal oxo groups form a planar $[Mo_8O_8(C_2O_4)]^{22\oplus}$ unit (maximum deviation of 0.02 Å from the best plane through all atoms). The C-O distances of the oxalate unit are distinctly non-equivalent (C1-O1, 1.25(2) Å; C1-O2, 1.37(2) Å), suggesting that the multiple bond character is localized in the C1-O1 moieties.

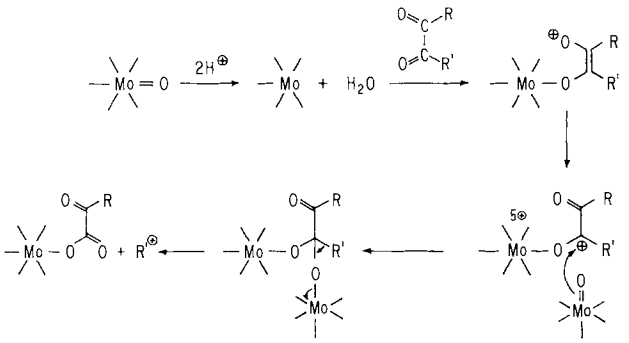

Scheme 1.

The synthesis of a Mo^{V}-oxalate cluster from polyoxomolybdate(VI) and rhodizonic acid precursors implies that in this instance the well-documented carbonyl insertion reaction is coupled with ligand dissociation and redox processes. Although the mechanism of this chemical transformation is not yet known in detail, the process most likely involves a succession of two-electron transfers and cationic intermediates of the type illustrated in Scheme 1. Since multicenter Mo clusters are involved in the chemistry, the formally Mo^{IV} sites produced in this sequence of electron transfer steps are in proximity to oxidized Mo^{VI} sites and rapid disproportionation is to be expected:

$$Mo^{IV}\cdots Mo^{VI} \longrightarrow Mo^{V}-Mo^{V}$$

Since the mechanism requires the formation of organic cations, the isolation of the oxalate derivative is dependent on the stability of the cationic species. Thus, whereas α-glyoxal and phenanthrenequinone yield the simple insertion products **2** and **3**, respectively, chloranilic acid **6** and rhodizonic acid **7** undergo concomitant ligand dissociation to yield the oxalate derivatives **4** and **8**, respectively. As anticipated, effective stabilization of the cationic leaving group promotes the formation of oxalato complexes. For example, di-*tert*-butylglyoxal (2,2,5,5-tetramethyl-3,4-hexanedione) reacts with the molybdate **5** to give the complex **8** in 70% yield. We are currently investigating the structural consequences of variations in the substituents of such α-diketones upon the products of the carbonyl insertion into oxometalate cores.

Received: June 27, 1988 [Z 2828 IE]
German version: *Angew. Chem. 100* (1988) 1792

[1] V. W. Day, W. G. Klemperer, *Science (Washington, DC) 228* (1986) 533.
[2] M. T. Pope: *Heteropoly and Isopoly Oxometalates*, Springer, New York 1983.
[3] E. M. McCarron III, R. L. Harlow, *J. Am. Chem. Soc. 105* (1983) 6179.
[4] T.-C. Hsieh, S. N. Shaikh, J. Zubieta, *Inorg. Chem. 26* (1987) 4079.
[5] R. D. Adams, M. F. Fredrich, W. G.Klemperer, R.-S. Liu, *J. Am. Chem. Soc. 101* (1979) 491; R. D. Adams, W. G. Klemperer, R.-S. Liu, *J. Chem. Soc. Chem. Commun. 1979*, 256.
[6] V. W. Day, M. R. Thompson, W. G. Klemperer, R.-S. Liu, *J. Am. Chem. Soc. 102* (1980) 5973.
[7] S. Liu, S. N. Shaikh, J. Zubieta, *Inorg. Chem.*, in press.
[8] H. Knoziger, *Adv. Catal. 25* (1976) 184.
[9] Rhodizonic acid **7** (0.766 g, 4.63 mmol) was added to a suspension of the complex **5** (2.00 g, 0.93 mmol) in MeOH (50 mL). After stirring at room temperature for six hours, the green solution was filtered and the solvent removed under vacuum. The resultant green oil was dissolved in methanol and carefully covered with a layer of ether. After standing for 8 days, light green crystals of **8** were collected in 25% yield.
[10] Crystal Data: $C_{42}H_{96}N_2O_{28}Mo_8$, triclinic space group, $P\bar{1}$, $a=10.720(2)$, $b=13.450(2)$, $c=13.476(2)$ A°, $\alpha=73.28(1)$, $\beta=80.83(1)$, $\gamma=79.92(1)°$, $V=1819.8(6)$ Å^{-3}, $Z=1$. Structure solution and refinement based on 2215 reflections with $F_o>6\sigma(F_o)$ ($Mo_{K\alpha}$, $\lambda=0.71073$ Å); final discrepancy factor, 0.0486. Further details of the crystal structure investigation are available on request from the Fachinformationszentrum Energie, Physik, Mathematik GmbH, D-7514 Eggenstein-Leopoldshafen 2 (FRG), on quoting the depository number CSD-53330, the names of the authors, and the journal citation.
[11] B. Spivack, Z. Dori, *Coord. Chem. Rev. 17* (1975) 99, and references cited therein.

Reductive Oligomerization of 1,2-Di-*tert*-butyl-1,1,2,2-tetrachlorodisilane: The Tricyclo[2.2.0.$0^{2,5}$]hexasilane and Tetracyclo[3.3.0.$0^{2,7}$.$0^{3,6}$]octasilane Systems**

By *Yoshio Kabe,* Mutsumi Kuroda, Yoshihiro Honda, Osamu Yamashita, Takeshi Kawase,* and *Satoru Masamune**

Numerous recent publications are concerned with both the theoretical and synthetic aspects of strained polycycles,[1,2] for example, the bicyclo[1.1.0]tetrasilane system.[2a-e] The successful construction of this particular ring system suggests that trichlorosilanes ($RSiCl_3$) and 1,1,2,2-tetrachlorodisilanes ($RSiCl_2-SiCl_2R$) could serve, with the judicious selection of R, as precursors of hitherto unknown polycyclic systems including those represented by the molecular formula $(RSi)_{2n}$. Summarizing our initial investigations along this line, we describe below that reductive oligomerization of 1,2-di-*tert*-butyl-1,1,2,2-tetrachlorodisilane (**1**)[3] proceeded in a unique and somewhat unexpected manner to provide tricyclo[2.2.0.$0^{2,5}$]hexasilane and tetracyclo[3.3.0.$0^{2,7}$.$0^{3,6}$]octasilane derivatives.[4] The following communication will then disclose an important aspect of ^{29}Si-NMR spectroscopy displayed by these cyclic compounds.[5]

[*] Dr. Y. Kabe, M. Kuroda, Dr.Y. Honda, Dr. O. Yamashita
Institute for Fundamental Research and
Tochigi Research Laboratory, Kao Corporation
Ichikai-machi Haga-gun, Tochigi 321-34 (Japan)
Prof. Dr. S. Masamune, Dr. T. Kawase
Department of Chemistry, Massachusetts Institute of Technology
Cambridge, MA 02139 (USA)

[**] The part of this work carried out at MIT was supported by the National Science Foundation (USA).

Treatment of **1** with a 1.2 M solution of naphthalenelithium (LiNp) in dimethoxyethane (DME) at −78 °C for 1 h provided sets of products which vary with the LiNp/**1** molar ratio. Typically, use of 2.5 equiv. of LiNp in the reduction followed by the usual workup (using fractional recrystallization for separation) gave rise to compounds **2** (tBu$_4$Si$_4$Cl$_4$, 8–20% yield), **3a** (tBu$_6$Si$_6$Cl$_2$, 4%), **4** (tBu$_6$Si$_6$Cl–tBuSiCl$_2$, 6%) and **5a** (tBu$_8$Si$_8$Cl$_2$, 6%). In contrast, an increase in the amount of reductant to 5 equiv. led, after silica gel chromatography, to the formation of **3b** (tBu$_6$Si$_6$Me$_2$), **5b** (tBu$_8$Si$_8$MeCl) and **5c** (tBu$_8$Si$_8$Me$_2$)[6] in a combined yield of 12%. The molecular formulas and group assignments shown in parenthesis are based on mass and ^{1}H-NMR spectral analyses (see Table 1).

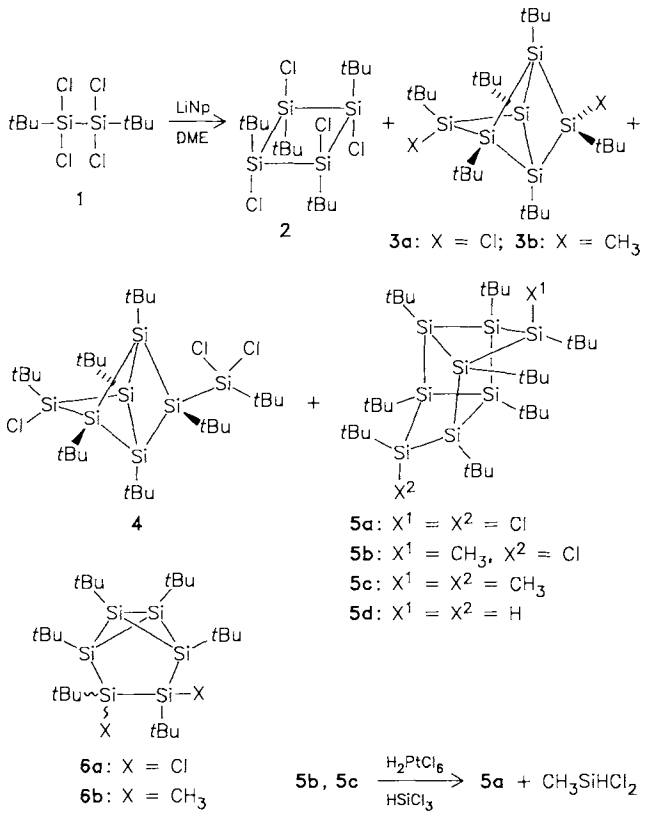

In the case of **5b–d** the steric array is not confirmed.

Analysis of **2** by ^{1}H-, ^{13}C-, and ^{29}Si-NMR spectroscopy shows the presence of four-fold symmetry in the molecule. Furthermore, an X-ray analysis establishes that the *tert*-butyl groups exist in an all-*trans* orientation, as shown in **2**, but not in all-*cis* or *cis-trans-cis*-orientations.[6]

Compounds **3a** and **3b** must be tricyclic from their molecular formulas, since the absence of an SiSi double bond in either **3a** or **3b** is evident from the known spectral and chemical properties of disilenes. Each Si_6 species of **3a** and **3b** exhibits three NMR signals for its ^{29}Si nuclei and *tert*-butyl protons rather than six. This molecular symmetry requires that the structures of these compounds be expressed by those shown for **3a** and **3b** or **6a** and **6b**. The latter two structures **6a** and **6b** are clearly incompatible with the chemical behavior of compounds **3a** and **3b** as compared with the known chemistry of the bicyclo[1.1.0]tetrasilane system.[2a] This leads to the conclusion that **3a** and **3b** possess the tricyclo[2.2.0.0^{2,5}]hexasilane skeleton. Compounds **3a** and **3b** are the dichloro- and dimethyl-derivatives, respectively, **3b** being formed apparently at the expense of **3a** when a larger amount of the reductant is used with the solvent DME. It is known that silyl anions react with DME to form methyl derivatives.[9]

The structure of **4** has been established by X-ray crystallography (see Fig. 1).[10] It is likely that the precursor of **4** is **3a**. The anion derived from **3a** via reduction presumably attacks **1** with concomitant SiSi bond cleavage of **1** and elimination of a silyl anion instead of a chloride ion.

Table 1. Some physical properties of **2**, **3a**, **3b**, **4**, **5a**, **5b**, **5c** and **5d**. ^{1}H NMR (270 MHz, C_6D_6), ^{13}C NMR (67.9 MHz, C_6D_6), ^{29}Si NMR (53.7 MHz, C_6D_6).

2: m.p. (decomp.) 214 °C; ^{1}H NMR: δ = 1.30 (s; 36 H); ^{13}C NMR: δ = 26.59 (s), 28.41 (q); ^{29}Si NMR: δ = 19.20; MS (EI, 20 eV): calcd. *m/z* for $C_{16}H_{36}Si_4Cl_4$ 480.0648, found 480.0654

3a: m.p. > 300 °C; ^{1}H NMR: δ = 1.28 (s; 18 H), 1.39 (s; 18 H), 1.44 (s; 18 H), ^{13}C NMR: δ = 23.46 (s), 23.87 (s), 27.69 (s), 29.34 (q), 33.77 (q), 33.92 (q); ^{29}Si NMR: δ = −58.27, −53.00, 75.74; MS (EI, 70 eV): calcd. *m/z* for $C_{24}H_{54}Si_6Cl_2$ 580.2218, found 580.2242

3b: m.p. (decomp.) 208 °C; ^{1}H NMR: δ = 0.87 (s; 6 H), 1.33 (s; 18 H), 1.34 (s; 36 H); ^{13}C NMR: δ = 1.04 (q), 30.99 (q), 31.03 (s), 33.70 (s), 34.32 (q), 34.41 (q), 34.82 (s); ^{29}Si NMR: δ = −59.21, −39.83, 54.25; MS (EI, 20 eV): calcd. *m/z* for $C_{26}H_{60}Si_6$ 540.3311, found 540.3310

4: m.p. > 300 °C; ^{1}H NMR: δ = 1.23 (s; 9 H), 1.35 (s; 9 H), 1.38 (s; 9 H), 1.41 (s; 9 H), 1.45 (s; 9 H), 1.47 (s; 9 H), 1.51 (s; 9 H); ^{13}C NMR: δ = 22.06 (s), 22.24 (s), 24.12 (s), 25.05 (s), 25.40 (s), 26.38 (s), 27.08 (q), 27.69 (s), 29.89 (q), 33.91 (q), 34.30 (q), 34.32 (q), 34.45 (q), 34.65 (q); ^{29}Si NMR: δ = −61.02, −51.53, −51.09, −32.63, 37.71, 43.39, 75.42; MS (EI, 20 eV): calcd. *m/z* for $C_{28}H_{63}Si_7Cl_3$ 700.2380, found 700.2369

5a: m.p. > 300 °C; ^{1}H NMR: δ = 1.39 (s; 18 H), 1.47 (s; 9 H), 1.48 (s; 9 H), 1.50 (s; 18 H); ^{13}C NMR: δ = 26.15 (s), 26.20 (s), 26.81 (s), 27.18 (s), 29.53 (q), 32.71 (q), 33.79 (q), 34.69 (q); ^{29}Si NMR: δ = −41.99, −20.78, 8.11, 53.06; MS (EI, 70 eV): calcd. *m/z* for $C_{32}H_{72}Si_8Cl_2$ 750.3166, found 750.3184

5b: m.p. (decomp.) 261 °C; ^{1}H NMR: δ = 0.78 (s; 3 H), 1.27 (s; 9 H), 1.37 (s; 9 H), 1.38 (s; 9 H), 1.43 (s; 9 H), 1.44 (s; 9 H), 1.52 (s; 9 H), 1.53 (s; 18 H); ^{13}C NMR: δ = −3.37 (q), 21.78 (s), 25.90 (s), 26.11 (s), 26.16 (s), 26.37 (s), 26.65 (s), 26.94 (s), 27.05 (s), 29.82 (q), 30.78 (q), 32.86 (q), 32.94 (q), 33.85 (q), 34.11 (q), 34.90 (q), 35.00 (q); ^{29}Si NMR: δ = −41.15, −37.42, −21.84, −16.04, 6.30, 10.50, 12.96, 50.68; MS (EI, 20 eV): calcd. *m/z* for $C_{33}H_{75}Si_8Cl$ 730.3731, found 730.3742

5c: m.p. > 300 °C; ^{1}H NMR: δ = 0.83 (s; 6 H), 1.31 (s; 18 H), 1.42 (s; 18 H), 1.44 (s; 18 H), 1.48 (s, 18 H); ^{13}C NMR: δ = −2.95 (q), 21.76 (s), 26.05 (s), 26.27 (s), 26.55 (s), 31.06 (q), 33.10 (q), 34.16 (q), 35.22 (q); ^{29}Si NMR: δ = −36.12, −17.19, 8.09, 8.79; MAS (EI, 20 eV): calcd. *m/z* for $C_{34}H_{78}Si_8$ 710.4258, found 710.4247

5d: m.p. > 300 °C; ^{1}H NMR: δ = 1.34 (s; 18 H), 1.39 (s; 18 H), 1.48 (s; 18 H), 1.52 (s; 18 H), 4.45 (s; 2 H); ^{13}C NMR: δ = 21.28 (s), 24.50 (s), 24.59 (s), 25.28 (s), 31.60 (q), 32.90 (q), 32.96 (q), 33.95 (q); ^{29}Si NMR: δ = −39.71, −25.63, −17.14, 9.90; MS (EI, 70 eV): calcd. *m/z* for $C_{32}H_{74}Si_8$ 682.3945, found 682.3936

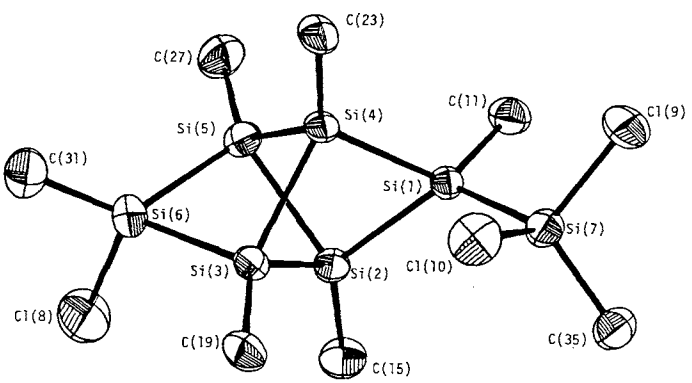

Fig. 1. Perspective ORTEP drawing of **4** showing 50% thermal ellipsoids for non-hydrogen atoms. The carbon atoms of the *tert*-butyl methyl groups have been omitted for clarity. Silicon–silicon bond distances [Å] are given below with their estimated standard deviations: Si1–Si2 2.366(2), Si1–Si4 2.370(2), Si1–Si7 2.384(2), Si2–Si3 2.364(2), Si2–Si5 2.407(2), Si3–Si4 2.392(2), Si3–Si6 2.351(2), Si4–Si5 2.389(2), Si5–Si6 2.345(2).

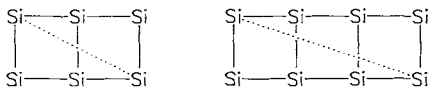

3 5

Compounds **5b** and **5c** are quantitatively converted into **5a** via Benkeser's reaction, a reaction which specifically effects the H_2PtCl_6-catalyzed Me/Cl exchange with $HSiCl_3$.[11] Treatment of **5a** with LiNp in toluene (instead of DME) provides **5d** after protolytic workup. These chemical correlations leave little doubt that compounds **5a–d** share a common Si_8 skeleton, and the molecular structure disclosed by a crystallographic analysis of **5a** (*Fig.* 2)[10] establishes the structures of all of these compounds. These structures are consistent with the symmetry displayed in the NMR spectra of these compounds (Table 1).

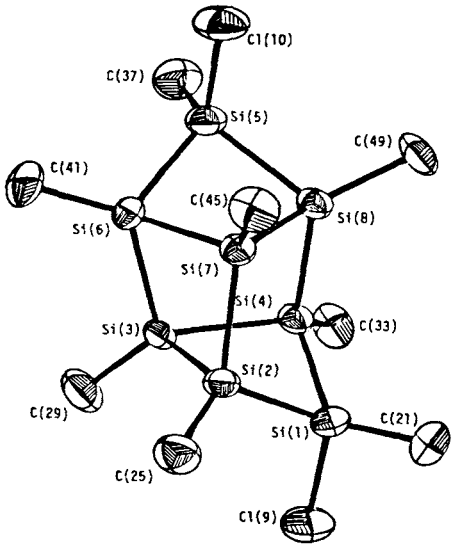

Fig. 2. Perspective ORTEP drawing of **5a** showing 50% thermal ellipsoids for non-hydrogen atoms. The carbon atoms of the *tert*-butyl methyl groups have been omitted for clarity. Since two molecules (enantiomers) are present in the asymmetric unit, two values are given for each bond distance [Å]. Each molecule contains an approximate C_2 axis, and the (approximately) equivalent bonds are paired below: Si1–Si2 2.335(2) and 2.337(2), Si5–Si6 2.335(2) and 2.342(2); Si1–Si4 2.371(2) and 2.383(2), Si5–Si8 2.370(2) and 2.371(2); Si2–Si3 2.376(2) and 2.375(2), Si6–Si7 2.378(2) and 2.377(2); Si2–Si7 2.395(2) and 2.393(2), Si3–Si6 2.393(2) and 2.397(2); Si3–Si4 2.438(2) and 2.452(2), Si7–Si8 2.447(2) and 2.445(2); Si4–Si8 2.362(2) and 2.363(2).

With the structures of the products having been established, the pathways leading to these products appear to be clarified. Of particular interest are the modes of intramolecular ring closure that are involved in the formation of the tri- and tetracyclic systems, as indicated by the dotted lines in the two skeletons **3** and **5** shown below. There was no indication that octasilacubane[12] and hexasilaprismane derivatives were present even in minute quantities among the above reduction products of **1**. It is interesting to note that the tricyclo[2.2.0.$0^{2,5}$]hexane skeleton is often exhibited by inorganic polycycles.[13]

Received: July 5, 1988 [Z 2848 IE]
German version: *Angew. Chem. 100* (1988) 1793

[1] For reviews: S. Masamune in J. Y. Corey, E. R. Corey, P. P. Gaspar (Eds.): *Silicon Chemistry*, Ellis Horwood, New York 1988, p. 257f; R. West in G. Wilkinson, F. G. Stone, E. W. Abel (Eds.): *Comprehensive Organometallic Chemistry*, Pergamon, Oxford 1982, p. 365f.

[2] Bicyclo[1.1.0]tetrasilane system: a) S. Masamune, Y. Kabe, S. Collins, D. Williams, R. Jones, *J. Am. Chem. Soc. 107* (1985) 5552; b) R. Jones, D. J. Williams, Y. Kabe, S. Masamune, *Angew. Chem. 98* (1986) 176; *Angew. Chem. Int. Ed. Engl. 25* (1986) 173; c) T. Dabish, W. W. Schoeller, *J. Chem. Soc. Chem. Commun. 1986*, 896; d) S. Collins, R. Dulter, A. Rauk, *J. Am. Chem. Soc. 109* (1987) 2564; e) P. von R. Schleyer, A. F. Sax, J. Kalcher, R. Jonoscheck, *Angew. Chem. 99* (1987) 374; *Angew. Chem. Int. Ed. Engl. 26* (1987) 364; spiro[2.2]pentasilane system: f) P. Boudjouk, R. Sooriyakumaran, *J. Chem. Soc. Chem. Commun. 1984*, 777; bicyclo[2.2.0]hexasilane system: g) H. Matsumoto, H. Miyamoto, N. Kojima, Y. Nagai, *ibid. 1987*, 1316; for the theoretical treatment of some $(SiH)_{2n}$ systems: h) A. Sax, R. Janoschek, *Angew. Chem. 98* (1986) 634; *Angew. Chem. Int. Ed. Engl. 25* (1986) 651; i) D. A. Clabo, H. F. Schafer III, *J. Am. Chem. Soc. 108* (1986) 4344; j) B. F. Yates, D. A. Clabo, H. F. Schaffer, *Chem. Phys. Lett. 143* (1988) 421; k) S. Nagase, M. Nakano, T. Kudo, *J. Chem. Soc. Chem. Commun. 1987*, 60; l) A. F. Sax, J. Kalcher, *ibid. 1987*, 809.

[3] Compound **1** was prepared by $AlCl_3$-mediated Ph/Cl exchange reaction of 1,2-di-*tert*-butyl-1,1,2,2-tetraphenyldisilane, which was in turn obtained by reductive coupling of commercially available *tert*-butylchlorodiphenylsilane. We were informed that Prof. *R. West* also obtained **1** and **2** (private communication).

[4] Although (carbo)tricyclo[2.2.0.$0^{2,5}$]hexane derivatives are recorded in the literature [J. A. Uliana, *Diss. Abstr. Int. B 37(10)* (1977) 5099], the (carbo)tetracyclo[3.3.0.$0^{2,7}$.$0^{3,6}$]octane system is apparently unknown.

[5] M. Kuroda, Y. Kabe, M. Hashimoto, S. Masamune, *Angew. Chem. 100* (1988) 1795; *Angew. Chem. Int. Ed. Engl. 27* (1988) 1727.

[6] Crystals of **2** suitable for X-ray crystallography were obtained by recrystallization from DME in a glove box. **2**: orthorhombic, space group $P2_12_12_1$, $a=13.057(2)$, $b=14.854(2)$, $c=13.698(2)$ Å, $V=2656$ Å^3, $\rho_{calcd}=1.20$ g/cm^3, $Z=4$. The structure was solved from 1433 collected independent reflections [$2\theta \leq 63°$, $|F_o| > 3\sigma(|F_o|)$] measured on a Rigaku four-circle diffractometer using $Cu_{K\alpha}$ radiation ($\lambda=1.5418$ Å). The structure was solved by direct methods (MULTAN 80) [7]. Strong diffractions of heavy atoms (Si, Cl) produced the satisfactory solution of the Si-framework, but severe disordering of *tert*-butyl groups resulted in a moderate quality of the refinement.

[7] P. Main, S. J. Fiske, S. E. Hull, L. Lessinger, G. Germain, J. P. Declercq, M. M. Woolfson: *MULTAN 80, a system of computer programs for the automatic solution of crystal structures from X-ray diffraction data*, University of York (England) and Louvain-la-Neuve (Belgium) 1980.

[8] Further details of the crystal structure investigations are available on request from the Fachinformationszentrum Energie, Physik, Mathematik GmbH, D-7514 Eggenstein-Leopoldshafen 2 (FRG), on quoting the depository number CSD-53324, the names of the authors, and the journal citation.

[9] D. Wittenberg, D. Aoki, H. Gilman, *J. Am. Chem. Soc. 80* (1958) 5933.

[10] The X-ray analyses of **4** and **5a** were carried out in a similar fashion as cited in reference [6]. **4**: monoclinic, space group $P2_1/a$, $a=22.517(4)$, $b=14.448(2)$, $c=12.485(2)$ Å, $\beta=90.47(1)°$, $V=4061$ Å^3, $\rho_{calcd}=1.15$ g/cm^3, $Z=4$, 4824 collected reflections, $R=0.0633$. **5a**: triclinic, $P\bar{1}$, $a=11.502(2)$, $b=40.484(8)$, $c=11.219(1)$ Å, $\alpha=87.51(3)$, $\beta=119.10(1)$, $\gamma=95.54(3)°$, $V=4543$ Å^3, $\rho_{calcd}=1.10$ g/cm^3, $Z=4$, 10771 collected reflections, $R=0.0741$.

[11] a) K. R. Beck, R. A. Benkeser, *J. Organomet. Chem. 21* (1970) P35; b) R. West, *Abstr. Int. Symp. Organosilicon chem. 5th* (1978) 132; c) E. Hengge, W. Peter, *J. Organomet. Chem. 148* (1978) C22.

[12] Shortly after submission of this paper, a communication reporting the synthesis of an octasilacubane appeared in the literature: H. Masamuto, K. Higuchi, Y. Hoshino, H. Koike, Y. Naoi, Y. Nagai, *J. Chem. Soc. Chem. Commun. 1988*, 1083.

[13] M. Veith, *Angew. Chem. 99* (1987) 1; *Angew. Chem. Int. Ed. Engl. 26* (1987) 1.

^{29}Si-^{29}Si Long Range Couplings in Strained Cyclic Polysilanes**

By *Mutsumi Kuroda, Yoshio Kabe,* Masayuki Hashimoto* and *Satoru Masamune**

^{13}C 2D-INADEQUATE spectroscopy can conveniently disclose the connectivity of each carbon atom embedded

[*] Dr. Y. Kabe, M. Kuroda, Dr. M. Hashimoto
Institute for Fundamental Research and
Tochigi Research Laboratory, Kao Corporation
Ichikai-machi Haga-gun, Tochigi 321-34 (Japan)
Prof. Dr. S. Masamune
Department of Chemistry, Massachusetts Institute of Technology
Cambridge,. Massachusetts 02139 (USA)

[**] The authors are grateful to the staff of JEOL Ltd. for their valuable technical assistance. The part of this work carried out at MIT was supported by the National Science Foundation (USA).

in a molecule and has found widespread use in structural elucidation of organic compounds.[1] This technique is extremely powerful when the size of ^{13}C-^{13}C one-bond coupling (^1J) is much larger than that of long-range couplings (^nJ, $n \geq 2$), which is usually the case in the acyclic and unstrained alicyclic systems thus far investigated.[2] Using the INEPT-INADEQUATE technique specifically modified for ^{29}Si nuclei,[3] we have been examining ^{29}Si-^{29}Si couplings in several cyclic compounds and wish to disclose two general trends: 1) With the decrease in ring size from six to three, $^1J_{Si,Si}$ values become smaller and $^2J_{Si,Si}$ values larger; 2) in strained polycyclic compounds such as tetracyclo[3.3.0.$0^{2,7}$.$0^{3,5}$]octasilane and tricyclo[2.2.0.$0^{2,5}$]hexasilane derivatives (**1a–b** and **2**, respectively),[4] not only are ^1J and ^2J comparable in magnitude but even two nuclei that are three and even four bonds apart and oriented in a stereochemically unique manner display a sizeable interaction.

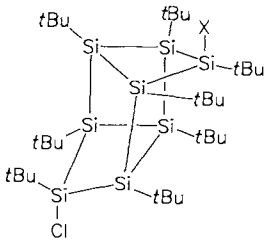

1a, X = CH_3
1b, X = Cl

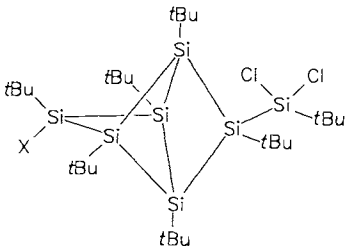

2

Very little information is available concerning the size of ^{29}Si-^{29}Si coupling constants.[5] Tables 1 and 2 list ^1J and ^nJ of several silicon compounds selected from those which have been subjected to spectral analysis (**3–7** and **1a**, **b**, resp. and **2**). The characterizations of polysilanes **3–7** appearing in Table 1 are summarized in Table 3. Compound **3**, respresenting acyclic compounds, shows ^1J values in the range 55–70 Hz, while the ^2J and ^3J values are an order of magnitude smaller (2.5–5.0 Hz). In the (relatively) strain-free six- and five-membered ring compounds **4** and **5** the ^1J values decrease slightly, but a sizeable increase in ^2J is definitely noticeable. This trend becomes pronounced with the strained systems exemplified by **6** and **7**. While ^1J values are still approximately twice as large as ^2J values in **6**, the observed ^1J for **7** is only 24.1 Hz. This increase in the magnitude of ^1J with an increase in ring size is consistent with the view that ^1J is approximately correlated with the amount of s-character of the Si orbitals participating in the ring formation.[6]

The 2D-NMR spectrum of the tetracycle **1a**[4] (Fig. 1) reveals the presence of 15 ^{29}Si-^{29}Si couplings of approximately 20 to 40 Hz. Since this system is constructed by eleven SiSi bonds, four of the 15 couplings must be long-range (^nJ). Through somewhat lengthy but logical arguments,[7] ^{29}Si signals 1–8 are assigned to the Si nuclei of compound **1a** in the manner shown in Table 2. With the completion of the spectral assignment of **1a**, that of **1b** (having a C_2 axis) readily follows. In **1b** there are three pairs of observable, significant long-range couplings of which a pair of couplings is rather small (5.8 Hz). Compound **2** also exhibits two sizeable long-range couplings demonstrated by its spectrum (Fig. 2) as there are eleven observed J's of approximately 15 to 40 Hz while only nine SiSi bonds build the framework of **2**. The most appropriate chemical shift assignments of **2** are tabulated.[7]

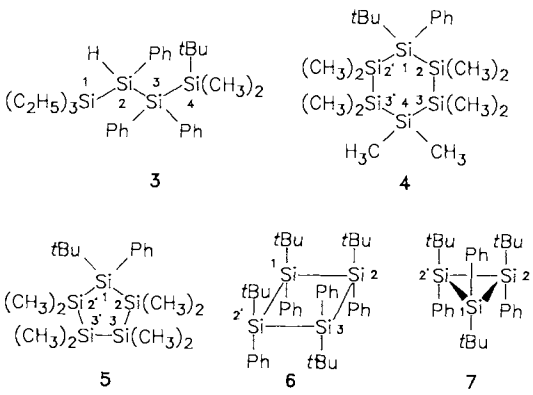

3 4 5 6 7

Table 1. ^{29}Si-^{29}Si coupling constants in various acyclic or monocyclic polysilanes **3–7**.

Cpd.	δ (vs. Me_4Si) [a]	^1J [Hz]	^nJ ($n \geq 2$) [Hz]
3	− 1.55 (1) [b]	68.4 (3–4)	4.9 (2–4)
	− 3.92 (4)	65.4 (1–2)	2.9 (1–3)
	−37.54 (3)	57.6 (2–3)	2.9 (1–4)
	−63.78 (2)		
4	−22.90 (1)	62.1 (3–4 or 3′–4)	9.4 (2–4 or 2′–4)
	−40.33 (3 and 3′)	57.4 (1–2 or 1–2′)	8.2 (1–3 or 1–3′)
	−42.21 (2 and 2′)	[c] (2–3, 2′–3′)	
	−42.59 (4)		
5	−18.50 (1)	57.6 (1–2 or 1–2′)	9.8 (1–3 or 1–3′)
	−41.73 (2 and 2′)	[c] (2–3, 2′–3′)	9.8 (2–3′, 3–2′)
	−43.22 (3 and 3′)		
6	9.11 (1 or 3)	46.9 (1–2 or 1–2′)	27.3 (1–3)
	1.40 (3 or 1)	46.9 (2–3 or 2′–3)	
	− 8.02 (2 and 2′)		
7	−33.42 (2 and 2′)	24.1 (1–2 or 1–2′)	
	−37.33 (1)		

[a] ^{29}Si chemical shifts and coupling constants of **3–7** in C_6D_6 (25 °C) at 53.7 MHz. [b] The numbers in parentheses refer to the silicon atom numbering scheme shown in the structures for **3–7**. [c] The chemical shifts of these ^{29}Si nuclei were too close to permit accurate measurement of the coupling constant between them.

Table 2. ^{29}Si-^{29}Si coupling constants for the polycyclic polysilanes **1a**, **1b** and **2**.

Cpd. [a]	^1J [Hz]		^nJ ($n \geq 2$) [Hz]
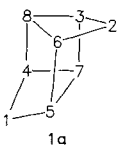 1a	42.2 (2–6)	41.8 (1–5)	24.1 (1–3)
	41.0 (2–3)	33.4 (1–4)	23.1 (4–5)
	30.8 (4–7)	28.9 (3–8)	22.5 (3–6)
	28.3 (3–7)	25.7 (4–8)	19.9 (2–4)
	25.7 (5–6)	18.0 (5–7)	
	17.3 (6–8)		
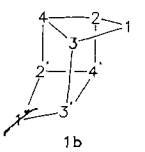 1b	41.0 (1–3, 1′–3′)		23.5 (1–2′, 1′–2)
	35.1 (1–2, 1′–2′)		23.5 (2–3, 2′–3′)
	29.3 (2–4, 2′–4 or 2′–4′)		5.8 (1–4, 1′–4′)
	17.5 (3–4, 3′–4′)		
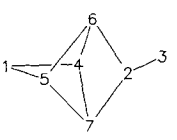 2	43.0 (2–3)	36.1 (1–4)	
	34.1 (2–6)	32.2 (2–7)	13.7 (1–3)
	29.3 (1–5)	27.4 (5–7)	16.6 (3–4)
	24.5 (4–6)	23.4 (4–7)	
	[b] (5–6)		

[a] The silicon nuclei of each molecule are numbered according to the order of their chemical shifts as shown in Figs. 1 and 2. [b] The chemical shifts of these ^{29}Si nuclei were too close to permit accurate measurement of the coupling constant between them.

Table 3. Some physical data of the polysilanes **3**, **4**, **5**, **6** and **7**. ^{1}H NMR (270 MHz, C_6D_6), ^{29}Si NMR (53.7 MHz, C_6D_6).

3: oil; ^{1}H NMR: $\delta = 0.10$ (s; 3H), 0.22 (s; 3H), 0.58 (q, $J = 7$ Hz; 6H), 0.78 (s; 9H), 0.83 (t, $J = 7$ Hz; 9H), 4.73 (s; 1H), 7.11–7.24 (m; 9H), 7.55–7.58 (m; 2H), 7.77–7.85 (m; 4H); ^{29}Si NMR: $\delta = -63.78, -37.54, -3.92, -1.55$; MS (EI, 20 eV): m/z 518 ($M^{\oplus}$), 461 ($M^{\oplus} - t$Bu)

4: glassy solid; ^{1}H NMR: $\delta = -0.03$ (s; 6H), 0.00 (s; 3H), 0.20 (s; 3H), 0.21 (s; 6H), 0.45 (s; 6H), 0.53 (s; 6H), 1.13 (s; 9H), 7.14–7.17 (m; 3H), 7.61–7.64 (m; 2H); ^{29}Si NMR: $\delta = -42.59, -42.21, -40.33, -22.90$; MS (EI, 70 eV): m/z 452 ($M^{\oplus}$), 395 ($M^{\oplus} - t$Bu)

5: glassy solid; ^{1}H NMR: $\delta = 0.01$ (s; 6H), 0.22 (s; 6H), 0.38 (s; 6H), 0.43 (s; 6H), 1.10 (s; 9H), 7.14–7.17 (m; 3H), 7.58–7.62 (m; 2H); ^{29}Si NMR: $\delta = -43.22, -41.73, -18.50$; MS (EI, 70 eV): m/z 394 ($M^{\oplus}$), 337 ($M^{\oplus} - t$Bu)

6: m.p. (decomp.) 176°C; ^{1}H NMR: $\delta = 0.99$ (s; 9H), 1.14 (s; 9H), 1.55 (s; 18H), 6.80–7.27 (m; 12H), 7.05–8.16 (m; 8H); ^{29}Si NMR: $\delta = -8.02, 1.40, 9.11$; MS (EI, 20 eV): m/z 648 ($M^{\oplus}$), 591 ($M^{\oplus} - t$Bu)

7: m.p. (decomp.) 246°C; ^{1}H NMR: $\delta = 1.00$ (s; 9H), 1.21 (s; 18H), 7.04–7.24 (m; 7H), 7.54–7.89 (m; 4H), 8.02–8.06 (m; 4H); ^{29}Si NMR: $\delta = -37.33, -33.42$; MS (EI, 20 eV): m/z 486 ($M^{\oplus}$), 429 ($M^{\oplus} - t$Bu)

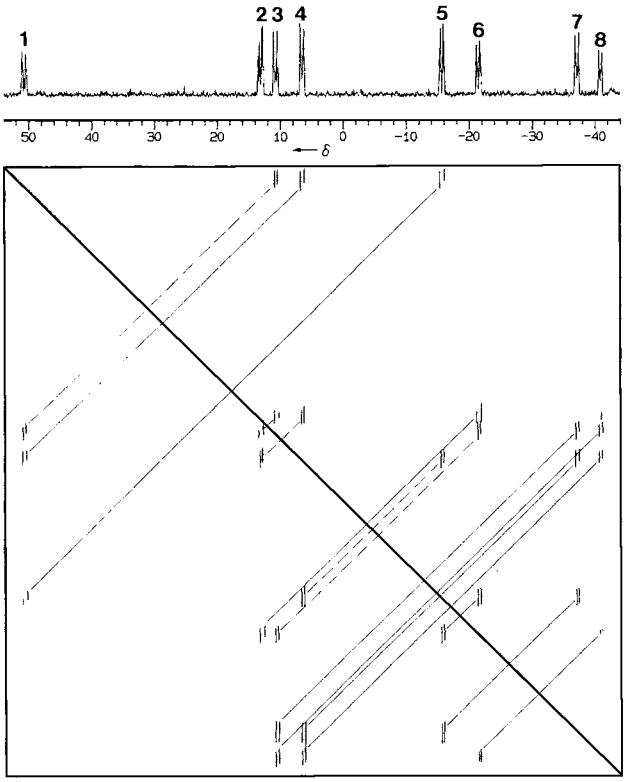

Fig. 1. 53.7-MHz ^{29}Si-^{29}Si 2D-INEPT-INADEQUATE spectrum of the tetracycle **1a** in C_6D_6 and projection of the 2D spectrum on the F_2 axis (top). Signals connected by solid lines correspond to one-bond interactions (^1J); those connected by dotted lines denote long-range couplings (^nJ).

In strained systems such as **1** and **2**, ^1J's cannot be distinguished from ^nJ's merely through the inspection of their magnitudes; in fact some ^1J's are smaller than ^nJ's. A considerable amount of information has been accumulated pertaining to long-range ^{13}C-^{13}C couplings in both unstrained and strained systems.[8,9] In comparison with the data in Tables 1 and 2, long-range ^{13}C-^{13}C and ^{29}Si-^{29}Si interactions show more or less similar trends, but, in general, the magnitude of the latter in strained systems appears more pronounced. The ^4J value in **2** is particularly noteworthy.

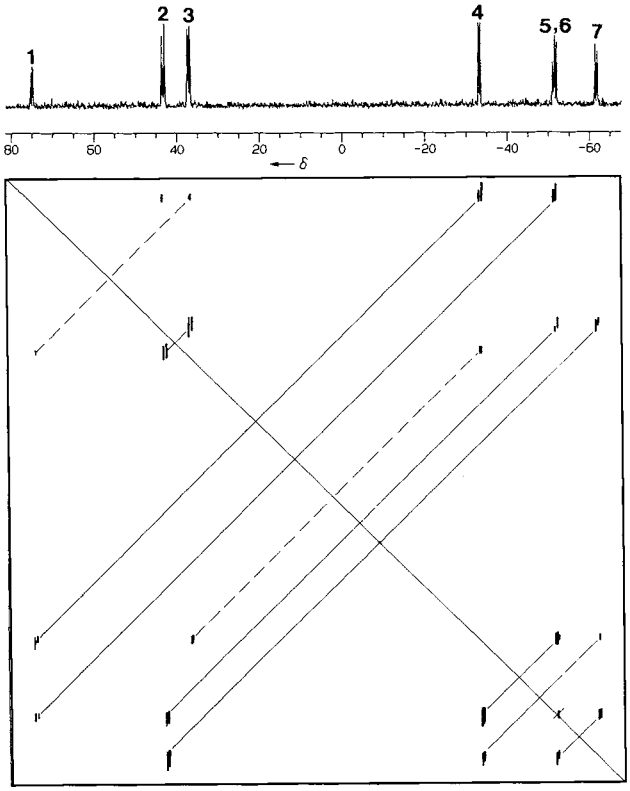

Fig. 2. 53.7-MHz ^{29}Si-^{29}Si 2D-INEPT-INADEQUATE spectrum of the tricycle **2** in $CDCl_3$ (40°C) and projection of the 2D spectrum on the F_2 axis (top). Signals connected by solid lines correspond to one-bond interactions (^1J); those connected by dotted lines denote long-range couplings (^nJ).

Received: July 5, 1988 [Z 2849 IE]
German version: *Angew. Chem. 100* (1988) 1795

[1] a) A. Bax: *Two-Dimensional Nuclear Magnetic Resonance in Liquids*, Delft University Press, Delft 1982, Chap. 5; b) W. E. Hull in W. R. Croasmun, R. M. K. Carlson (Eds.): *Two-Dimensional NMR Spectroscopy. Applications for Chemists and Biochemists*, VCH Publishers, New York 1987, Chap. 2.

[2] For example, a) A. Bax, S. P. Kempsell, R. Freeman, *J. Magn. Reson. 41* (1980) 349; b) M. A. Phillipi, R. J. Wiersema, J. R. Brainard, R. E. London, *J. Am. Chem. Soc. 104* (1982) 7333; c) R. Freeman, T. Frenkiel, M. B. Rubin, *ibid.* (1982) 5545.

[3] All spectra were recorded on a JEOL JNM GX-270 spectrometer using 2D-INEPT-INADEQUATE pulse sequences and complete proton decoupling. Chemical shifts are reported as δ values referred to tetramethylsilane. The pulse sequence is shown below:

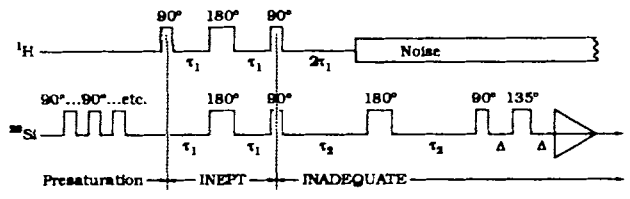

Application of 1D-INEPT-INADEQUATE to ^{13}C: a) O. W. Sorensen, R. Freeman, T. Frenkiel, T. H. Mareci, R. Schuck, *J. Magn. Reson. 46* (1982) 180; Application of INEPT and 1D-INEPT-INADEQUATE to ^{29}Si: b) T. A. Blinka, B. J. Helmer, R. West, *Adv. Organomet. Chem. 23* (1984) 193; c) H. B. Yokelson, J. Maxka, D. A. Siegel, R. West, *J. Am. Chem. Soc. 108* (1986) 4239; d) H. B. Yokelson, A. J. Millevolte, B. R. Adams, R. West, *ibid. 109* (1987) 4116; e) H. B. Yokelson, A. J. Millevolte, G. R. Gillete, R. West, *ibid. 109* (1987) 6865.

[4] Y. Kabe, M. Kuroda, Y. Honda, O. Yamashita, T. Kawase, S. Masamune, *Angew. Chem. 100* (1988) 1793; *Angew. Chem. Int. Ed. Engl. 27* (1988) 1725.

[5] a) H. Marsmann in P. Diehl, E. Flusch, R. Kosteld (Eds.): *NMR Basic Principles and Progress, Vol. 17*, Springer, New York 1981, p. 128; b) J. D.

Kennedy, W. McFarlane in J. Mason (Ed.): *Multinuclear NMR*, Plenum Press, New York 1987, p. 318.
[6] For a general discussion of ^{13}C-^{13}C coupling constants: J. B. Stothers: *Carbon-13 NMR Spectroscopy*, Academic Press, New York 1972, Chap. 10.
[7] The arguments which have been examined by reviewers are available upon request from *S. Masamune*.
[8] For reviews, see a) A. P. Marchand: *Stereo Chemical Application of NMR Studies in Rigid Bicyclic Systems*, Verlag Chemie International, Dearfield Beach 1982, Chap. 4; b) J. L. Marshall: *Carbon-Carbon and Carbon-Proton NMR Couplings*, Verlag Chemie International, Deerfield Beach 1983, Chaps. 3 and 5.
[9] a) F. J. Weigert, J. D. Roberts, *J. Am. Chem. Soc. 94* (1972) 6021; b) J. L. Marshall, d. E. Miller, *ibid. 95* (1973) 8305; c) D. Doddrell, I. Burfitt, J. B. Grutzner, M. Barfield, *ibid. 96* (1974) 1241; d) M. Barfield, I. Burfitt, D. Doddrell, *ibid. 97* (1975) 2631; e) M. Barfield, S. A. Conn, J. L. Marshall, D. E. Miller, *ibid. 98* (1976) 6253; f) M. Stoecker, M. Klessinger, *Org. Magn. Reson. 12* (1979) 107; g) M. Barfield, *ibid. 102* (1980) 1; h) M. Barfield, J. L. Marshall, E. D. Canada, *ibid. 102* (1980) 7; i) S. Berger, *Org. Magn. Reson. 14* (1980) 65; j) M. Klessinger, H. Megen, K. Wilhelm, *Chem. Ber. 115* (1982) 50; k) M. Klessinger, J. Cho, *Angew. Chem. 94* (1982) 782; *Angew. Chem. Int. Ed. Engl. 21* (1982) 764; l) S. R. Walter, J. L. Marshall, C. R. McDaniel, E. D. Canada, M. Barfield, S. R. Walter, *ibid. 105* (1983) 4185; m) M. Barfield, S. R. Walter, *ibid. 105* (1983) 4191; n) E. W. Della, P. E. Pigou, *ibid. 106* (1984) 1085; o) E. W. Della, H. Gangodawila, P. E. Pigou, *J. Org. Chem. 53* (1988) 592.

Linkage of Alkylidyne, Carbonyl, and Alkyne Ligands at a Tungsten Center to Form a Metallacyclopentadienone and an η^3-Oxocyclobutenyl Complex**

By *Andreas Mayr,* Ken S. Lee,* and *Bart Kahr*

The reactivity between metal-carbon triple bonds and carbon-carbon triple bonds is complex. High-valent alkylidyne metal complexes interact with alkynes to give metallacyclobutadienes, which—depending on the system—may be activated towards alkyne metathesis,[1] insertion of a second alkyne to give cyclopentadienyl ligands,[2] or the formation of cyclopropenyl metal complexes.[3] The low-valent carbyne alkyne metal complex **1** was proposed as an intermediate in the formation of a cyclopropenyl metal complex.[4] The low-valent metal carbynes $[M(CR)Br(CO)_4]$[5] were shown to induce the polymerization of acetylenes (M = W)[6] and to give annelated phenols in reactions with α,ω-diynes (M = Cr, W).[7] We have recently described evidence for the existence of low-valent carbyne alkyne tungsten complexes of the type **2** and facile protonation to give the carbene alkyne tungsten complexes **3**.[8] Here we report the reaction of a low-valent carbyne carbonyltungsten complex with alkyne in the absence of proton sources to give a novel metallacyclopentadienone and a metal η^3-oxocyclobutenyl complex.

$[Mo(CMe)(\eta^5\text{-}C_5H_5)(PhC_2Ph)\{P(OMe)_3\}_2]$ **1**

$[W(CPh)Cl(CO)(alkyne)(PMe_3)_2]$ **2**

$[W(CHPh)Cl_2(alkyne)(PMe_3)_2]$ **3**

Reaction of **4**[9] with excess phenylacetylene (15 equiv.) in dichloromethane [Eq. (a)] generates a mixture of products from which purple complex **5** and orange complex **6** were isolated in 26 and 13% yield, respectively.[10] The molecular structure of complex **5** is shown in Figure 1.[11] The tungsten center, the former carbyne and carbonyl ligands,

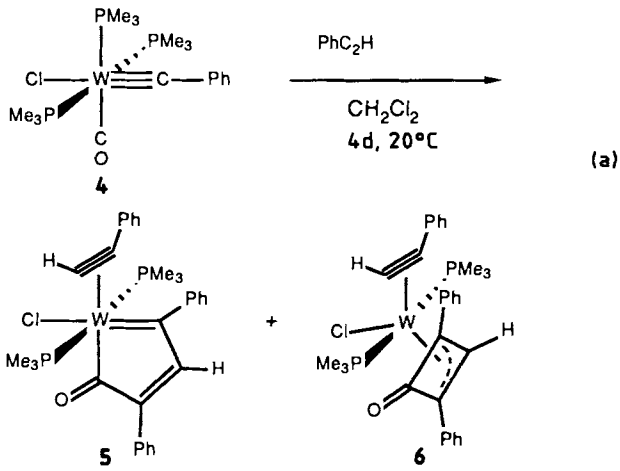

and phenylacetylene combine to form a metallacyclopentadienone ring, a cyclic metal carbene. The intraring distances indicate the presence of fairly localized π bonds. The W–C(1) distance is similar to the value of the tungsten-carbon double bond (1.97(2) Å) in the related alkylidene alkyne tungsten complex **3**, alkyne = Ph_2C_2, and the W–C(8) distance may be compared to the W–CH_2CMe_3 bond length (2.258(9) Å) in **7** (dmpe = bis(dimethylphosphino)ethane).[12] The C(9)–C(30) bond length is close to the accepted value for carbon-carbon double bonds (1.34 Å) and the C(1)–C(30) as well as the C(8)–C(9) distances are in the range of C_{sp^2}–C_{sp^2} single bonds (1.48 Å). Fairly localized double bonds have also been found in the molecular structure of an organic cyclopentadienone,[13] supporting the formal analogy with the metallacyclopentadienone ring in **2**.

$[W(CCMe_3)(CHCMe_3)(CH_2CMe_3)(dmpe)]$ **7**

The η^3-oxocyclobutenyl complex **6** is formally derived from **5** by extrusion of tungsten from the metallacycle. ^{13}C

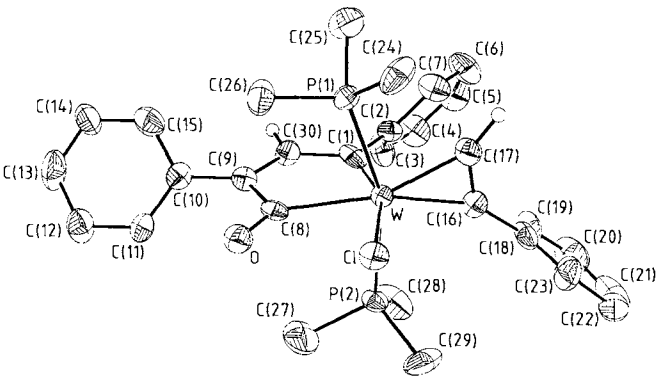

Fig. 1. Molecular structure of **5**. Important distances [Å] and angles [°]: W–C(1) 2.00(1), W–C(8) 2.28(1), W–C(16) 2.05(1), W–C(17) 2.04(1), W–Cl 2.430(1), W–P(1) 2.508(3), W–P(2) 2.522(3), C(1)–C(30) 1.49(2), C(9)–C(30) 1.37(2), C(8)–C(9) 1.52(2), C(8)–O 1.23(1); C(1)–W–C(8) 76.0(4), W–C(1)–C(30) 119.8(7), C(1)–C(30)–C(9) 120(1), C(8)–C(9)–C(30) 110.1(9), W–C(8)–C(9) 113.9(7), C(1)–W–Cl 157.5(3); C(8)–W–centroid[C(16)–C(17)] 174.5; P(1)–W–P(2) 157.8(1); dihedral angle formed by the planes W–C(1)–C(2) and W–C(16)–C(17) 92.2.

[*] Prof. A. Mayr
Department of Chemistry
State University of New York at Stony Brook
Stony Brook, NY 11794 (USA)
K. S. Lee, B. Kahr
Department of Chemistry
Princeton University
Princeton, NJ 08544 (USA)

[**] This work was supported by the National Science Foundation (CHE-8617472).

NMR resonances at $\delta = 181.2$ (CO), 59.4 ($J_{CH} = 195.8$ Hz, CH), 67.2, and 57.3 (CPh) are assigned to the carbon atoms of the oxocyclobutenyl ring. Signals at $\delta = 193.2$ ($J_{CP} = 12.5$ Hz, CPh) and 184.6 ($J_{CH} = 196.8$ Hz, $J_{CP} = 17.0$ Hz, CH) are observed for the phenylacetylene ligand.[10]

When reaction (a) was conducted with $Ph^{13}C{\equiv}CH$, the label was found to be distributed equally between the CPh groups in the metallacyclopentadienone ring of **5** and the oxocyclobutenyl ligand of **6**. Since the two CPh groups in the symmetrically substituted oxocyclobutenyl ligand[14] of **6** may exchange between equivalent sites by simple dynamic processes, we tested whether interconversion of compounds **5** and **6** may provide a mechanism for scrambling the label in complex **5**. Pure samples of **5** and **6** were heated in toluene. Compound **5** underwent conversion to **6** irreversibly. This reaction proceeds at 100 °C in about one hour, but is too slow at room temperature to account for formation of **6** in reaction (a).[15] Consequently, compounds **5** and **6** form independently in reaction (a). To account for these results we propose a mechanism involving the initial coupling of carbyne and alkyne ligands to give metallacyclobutadiene and metal cyclopropenyl intermediates. Insertion of carbon monoxide into the metallacyclobutadiene could generate the metallacyclopentadienone.[16] Insertion of carbon monoxide into a metallacyclobutene to give a metallacyclopentanone was recently reported.[17] Carbonyl insertion of the cyclopropenyl ligand may initiate formation of the oxocyclobutenyl complex. This latter type of reactivity is well established for cyclopropenyl carbonylmetal complexes.[18]

Since metal carbenes are postulated as the active species in acetylene polymerization,[6] the transformation of tungsten carbynes into tungstenacyclopentadienones represents a possible pathway for the formation of acetylene polymerization catalysts from carbonylmetal carbynes. Metallacyclopentadienones may also be considered as intermediates on the way to phenols from carbonylmetal carbynes and α,ω-diynes.[7] Insertion of a second acetylene unit into the metallacycle followed by reductive elimination would generate the organic ring system.

Received: May 30, 1988 [Z 2788 IE]
German version: *Angew. Chem. 100* (1988) 1798

[1] M. R. Churchill, J. W. Ziller, J. H. Freudenberger, R. R. Schrock, *Organometallics 3* (1984) 1554.
[2] J. Okuda, R. C. Murray, J. C. Dewan, R. R. Schrock, *Organometallics 5* (1986) 1681.
[3] R. R. Schrock, S. F. Pedersen, M. R. Churchill, J. W. Ziller, *Organometallics 3* (1984) 1574.
[4] F. J. Feher, M. Green, A. G. Orpen, *J. Chem. Soc. Chem. Commun. 1986*, 291.
[5] E. O. Fischer, G. Kreis, *Chem. Ber. 109* (1976) 1673.
[6] T. J. Katz, T. H. Ho, N.-Y. Shih, Y.-C. Ying, V. I. W. Stuart, *J. Am. Chem. Soc. 106* (1984) 2659.
[7] T. M. Sivavec, T. J. Katz, *Tetrahedron Lett. 26* (1985) 2159.
[8] A. Mayr, K. S. Lee, M. A. Kjelsberg, D. Van Engen, *J. Am. Chem. Soc. 108* (1986) 6079.
[9] A. Mayr, M. F. Asaro, M. A. Kjelsberg, K. S. Lee, D. Van Engen, *Organometallics 6* (1987) 432.
[10] Preparative thin layer chromatography on silica under Ar at 0 °C; eluant, CH_2Cl_2/ethyl acetate 9:1.
5: ^1H NMR (250 MHz, $CDCl_3$): $\delta = 12.00$ (m, 1H; HC≡CPh), 8.33 (t, 1H, $^4J_{PH} = 2.1$ Hz; CH); ^{13}C NMR (62.9 MHz, $CDCl_3$, 233 K): $\delta = 284.5$ (m, W=C), 217.5 (C=O), 200.3 (PhC≡CH), 193.0 ($J_{CH} = 194$ Hz; PhC≡CH), 158.6 ($J_{CH} = 156$ Hz; CH), 157.7 (CPh); ^{31}P NMR (101.2 MHz, $CDCl_3$, 298 K): $\delta = -12.6$ ($J_{WP} = 182$ Hz; PMe_3); IR (CH_2Cl_2): $\tilde{\nu}_{C=O} = 1597$ cm^{-1}.
6: ^1H NMR (250 MHz, $CDCl_3$): $\delta = 10.74$ (m, 1H; HC≡Ph), 4.50 (d, 1H, $J_{PH} = 11.7$ Hz; CH), 1.77 (d, 9H, $J_{PH} = 8.7$ Hz; PMe_3), 1.36 (d, 9H, $J_{PH} = 8.3$ Hz; PMe_3); ^{13}C NMR (62.9 MHz, $CDCl_3$, 233 K): see text; ^{31}P NMR (101.2 MHz, $CDCl_3$): $\delta = -11.1$ (m; $2PMe_3$); IR (CH_2Cl_2): $\tilde{\nu}_{C=O} = 1663$ cm^{-1}; satisfactory C,H analysis.
[11] **5**: Orthorhombic, *Pcab* (standard *Pbca*, No. 61), $a = 13.381(5)$, $b = 20.903(5)$, $c = 21.151(7)$ Å, $V = 5916(3)$ Å^3, $Z = 8$, $\mu(Mo_{K\alpha}) = 43.5$ cm^{-1}, $\rho_{calcd} = 1.56$ g cm^{-3}. All intensity measurements were made at 175 ± 3 K on a Nicolet R3m four-circle diffractometer by applying $Mo_{K\alpha}$ radiation ($\lambda = 0.71069$ Å). Of 5214 unique reflections with $3° \le 2\theta \le 50°$ and $h,k,l \ge 0$, 3702 with $|F_o| \ge 3\sigma(F_o)$ were considered observed after applying Lorentz, polarization, and empirical absorption corrections. The structure was solved by standard heavy-atom techniques and refined by least-squares methods. All hydrogen atoms were located at idealized positions except H(17) and H(30) which were located in the final difference Fourier map and fixed. $R = 0.058$, $R_w = 0.054$, GOF = 1.33. The highest peak in the final difference map (2.5 e Å^{-3}) near W. Further details of the crystal structure investigation can be obtained from the Fachinformationszentrum Energie, Physik, Mathematik GmbH, D-7514 Eggenstein-Leopoldshafen 2 (FRG), by quoting the depository number CSD-53295, the names of the authors, and the journal citation.
[12] M. R. Churchill, W. J. Youngs, *Inorg. Chem. 18* (1979) 2454.
[13] A. Nishinaga, T. Itahara, T. Matsuura, A. Rieker, D. Koch, K. Albert, P. B. Hitchcock, *J. Am. Chem. Soc. 100* (1978) 1826.
[14] The molecular structure of an adduct of **6** with trifluoromethanesulfonic acid has been determined by X-ray diffraction analysis. It features a symmetrically substituted diphenyloxocyclobutenyl ligand: B. Kahr, unpublished results.
[15] Complexes **5** and **6** could also be generated in a 1:2 ratio (as determined by ^1H NMR) by reaction of $[W(CPh)Cl(CO)(PMe_3)_2(py)]$ with excess PhC_2H in CH_2Cl_2 at 0 °C for 1 h.
[16] Formation of **5** by sequential coupling of the carbyne ligand with carbon monoxide and phenylacetylene (via a ketenyl intermediate) would place the label only at C(1).
[17] N. J. Conti, W. M. Jones, *Organometallics 7* (1988) 1666.
[18] W. A. Donaldson, R. P. Hughes, *J. Am. Chem. Soc. 104* (1982) 4846.

Structure, Magnetochemistry and Biological Relevance of $[Mn_4O_3Cl_4(OAc)_3(py)_3]$, a Complex with $S = 9/2$ Ground State**

By *Qiaoying Li, John B. Vincent, Eduardo Libby, Hsiu-Rong Chang, John C. Huffman, Peter D. W. Boyd, George Christou,** and *David N. Hendrickson**

Two to four Mn ions serve as the active site for catalyzing the oxidation of two molecules of H_2O to give one molecule of O_2 during photosynthesis.[1] Two research groups independently reported an EPR signal for the S_2 state of this site near photosystem II (PS II).[2] This signal, comprising a $g \approx 2$ feature structured with 16–19 Mn hyperfine lines and a subsequently identified $g \approx 4$ feature, was shown to be consistent with a tetranuclear $Mn_3^{III}Mn^{IV}$ site.[3] The $g \approx 2$ feature has been assigned to a low-lying $S = 1/2$ excited state, and the $g \approx 4$ feature to either the $S = 3/2$ ground state of the same $Mn_3^{III}Mn^{IV}$ site[4] or to an $S = 3/2$ state of a different conformation of this site.[5] These assignments are still matters of active discussion vis à vis detailed saturation, temperature dependence and sample history studies.

As part of our efforts to model this site, we recently reported the preparation of the first $Mn_3^{III}Mn^{IV}$ complex **1**.[6]

$(H_2Im)_2[Mn_4O_3Cl_6(HIm)(OAc)_3] \cdot 3/2\,MeCN$

1, HIm = imidazole, $H_2Im^{\oplus}$ = imidazolium cation

[*] Prof. Dr. G. Christou, J. B. Vincent, E. Libby, Dr. J. C. Huffman
Department of Chemistry and the Molecular Structure Center
Indiana University
Bloomington, IN 47405 (USA)
Prof. Dr. D. N. Hendrickson, Q. Li, H.-R. Chang,
Dr. P. D. W. Boyd [+]
School of Chemical Sciences, University of Illinois
Urbana, IL 61801 (USA)
[+] On sabbatical leave from the Chemistry Department of the University of Auckland, Auckland (New Zealand).

[**] This work was supported by the U.S. National Institutes of Health (GM 39083 and HL 13652).

The low symmetry of **1** has prevented an accurate theoretical description of its electronic structure; however, we now report the synthesis of **2**, a second complex of this type,

$[Mn_4O_3Cl_4(OAc)_3(py)_3]\cdot 3/2\,MeCN$ **2**

which has crystallographically imposed C_3 symmetry, allowing an accurate quantum mechanical description of its electronic structure to be formulated. Of specific and considerable interest and potential relevance to the S_2-state EPR signal is the finding that complex **2** has an $S=9/2$ ground state with no low-lying excited states.

$[Mn_3O(OAc)_6(py)_3](ClO_4)$ **3**

A stirred brown solution of **3** (1.74 g, 2.0 mmol) in freshly distilled MeCN (80 mL) was treated dropwise with Me_3SiCl (0.60 mL, 4.7 mmol). Overnight storage of the deep red-brown solution gave black crystals of complex **2** which were collected by filtration, washed with MeCN, and dried; yield 15–20%.[7] The complex has imposed C_3 symmetry (Fig. 1). As found for the anion of **1**, the

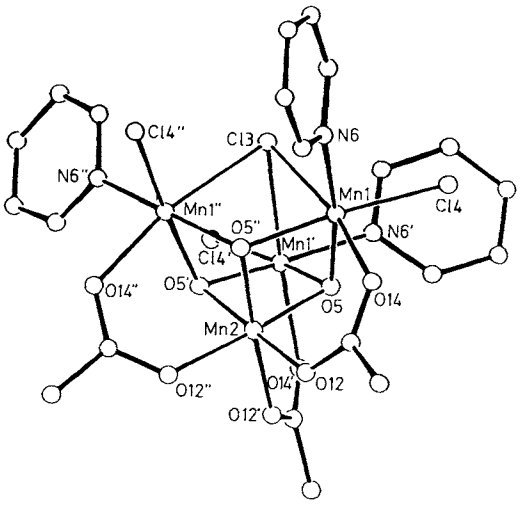

Fig. 1. Structure of complex **2** in the crystal. Selected bond distances [Å]: Mn1···Mn2, 2.815(2); Mn1···Mn1', 3.272(2); Mn1–Cl3 2.672(2); Mn1–Cl4, 2.237(2); Mn1–O5, 1.922(3); Mn1'–O5, 1.966(3); Mn1–O14, 2.146(3); Mn1–N6, 2.045(4); Mn2–O5, 1.865(3); Mn2–O12, 1.950(3). Primed and unprimed atoms are related by the threefold rotation axis.

$[Mn_4(\mu_3\text{-}O)_3(\mu_3\text{-}Cl)]^{6\oplus}$ core is best considered as an Mn_4 pyramid with the Mn^{IV} ion Mn2 at the apex; the μ_3-$Cl^{\ominus}$ ligand Cl3 bridges the basal plane, the μ_3-$O^{2\ominus}$ ions bridge each remaining face. Alternatively, the core can be considered as a severely distorted Mn_4O_3Cl cubane. Three μ-$OAc^{\ominus}$, $Cl^{\ominus}$ and py ligands complete the distorted octahedral geometry at each metal. Bridging Mn–Cl distances are appreciably longer than Mn–Cl terminal distances (2.627(2) vs. 2.237(2) Å), a point of potential relevance to the question of the possible presence of $Cl^{\ominus}$ ligands in any of the S_n states of PS II as addressed by EXAFS studies.[8]

The only available theoretical model[4] to account for the magnetic exchange interactions in a cubic $Mn_3^{III}Mn^{IV}$ model complex for the S_2-state makes the assumption that an $Mn^{III}Mn^{IV}$ pair is strongly antiferromagnetically coupled to give an $S=1/2$ state which is ferromagnetically coupled to the $Mn^{III}Mn^{III}$ pair, the latter being itself weakly antiferromagnetically coupled. The C_3 symmetry of **2** eliminates the need to make these assumptions in interpreting the solid-state magnetochemistry of **2**. As found[6] for **1**, the effective magnetic moment (μ_{eff}) per molecule of **2** increases gradually with decreasing temperature from 8.66 μ_B at 301.9 K to a maximum of 9.27 μ_B at 60.0 K, below which μ_{eff} decreases to 8.28 μ_B at 5.0 K (Fig. 2a).

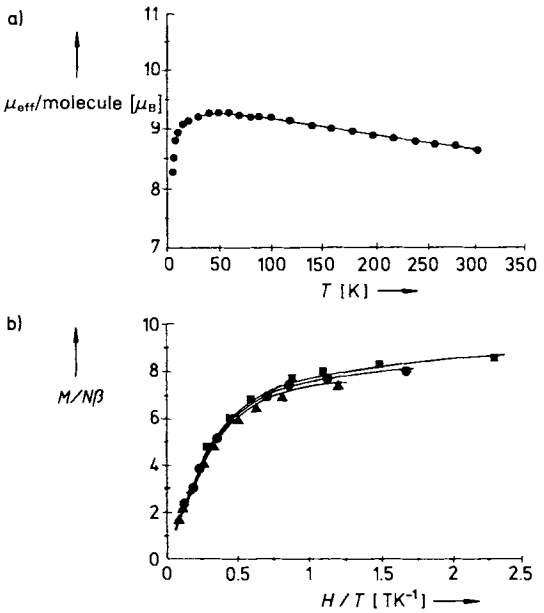

Fig. 2. a) Effective magnetic moment (μ_{eff}) per molecule as a function of the temperature T for $[Mn_4O_3Cl_4(OAc)_3(py)_3]\cdot 3/2\,CH_3CN$ at 1 T. Data are shown as points and the solid line represents the least-squares fit to the theoretical susceptibility equation with $J_1(Mn^{IV}\text{-}Mn^{III}) = -26.8\ cm^{-1}$, $J_2(Mn^{III}\text{-}Mn^{III}) = +12.1\ cm^{-1}$ and $g = 1.86$. (The data were fit only down to 30 K because the decrease in the effective moment at lower temperatures is due to zero-field splitting. To include the effects of zero-field splitting, a full matrix diagonalization procedure needs to be employed where the matrix is 500×500.) b) Plot of the molar magnetization (M) versus H/T for **2**, where H is the magnetic field in T and T is the temperature in K. Data were collected at three field strengths: ▲, 2.48 T; ●, 3.45 T; □, 4.5 T. Three isofield lines are drawn for an $S=9/2$ state with $D=0.32\ cm^{-1}$.

A Kambe vector-coupling model[9] was derived for the C_3-symmetric complex **2** by first coupling together the spin operators for the three Mn^{III} ions and then vectorially adding this to the spin operator for the Mn^{IV} ion. None of the assumptions of the previous model[4] were needed.

Three parameters were employed to least-squares fit the susceptibility data for **2** to the equation resulting from the C_3-symmetry vector-coupling model: J_1 for the three Mn^{IV}–Mn^{III} exchange interactions, J_2 for the Mn^{III}–Mn^{III} interactions, and an average g value. A systematic examination of the total parameter space (different sign combinations of J_1 and J_2, initial parameter values, etc.) showed that three sets of parameters gave reasonable fits. In the format (J_1, J_2, g) these three sets are: ($-376\ cm^{-1}$, $-94.7\ cm^{-1}$, 2.14), ($+7.4\ cm^{-1}$, $-3.6\ cm^{-1}$, 1.86) and ($-26.8\ cm^{-1}$, $+12.1\ cm^{-1}$, 1.86), the estimated standard deviations in these parameters being ±5%. Not only do these three fits deviate considerably from the view of the previous theoretical model, where J_1 is a large negative number and there is an $S=3/2$ ground state with a nearby

$S=1/2$ excited state, the three fits are each quite different. The first gives an $S=7/2$ ground state with an $S=9/2$ excited state only 9 cm^{-1} higher in energy. The second fit has an $S=9/2$ ground state and an $S=7/2$ excited state, separated by only 0.5 cm^{-1} with seven other spin states lying within 50 cm^{-1} of the ground state; whereas, the third fit has an $S=9/2$ ground state with the closest excited state being $S=7/2$ at 226 cm^{-1} above the ground state. This third fit was used for the calculation of the unbroken curve in Figure 2a.

To our surprise, magnetization data for complex **2**, collected over the temperature range 1.8 to 40 K at field values from 2.5 to 4.5 T, conclusively show an isolated $S=9/2$ ground state (Fig. 2b). This is in agreement with the third set of parameters obtained from the susceptibility data. Additional support for the isolation of this $S=9/2$ level is found in the fact that, although there are some changes and loss of resolution at elevated temperatures, the EPR spectrum of **2** (powder or glass) is readily seen at both liquid-helium and liquid-nitrogen temperatures. Such behavior would not be expected from the manifold of spin states found in the second fit.

It is likely that all the features in the glass EPR spectrum of **2** at $g \approx 2$, 6, and 9 (similar to those seen for **1**,[6]) are attributable to transitions between components of the $S=9/2$ ground state, which, as a detailed analysis of the M versus H/T data (Fig. 2b) shows, experiences an axial zero-field splitting ($D\hat{S}_z^2$) with $D=0.25$–0.35 cm^{-1}. Whether the S_2 state of PS II contains a cluster similar to that of **2** is still unclear, but the described work does suggest that the possibility that the S_2-state EPR spectral features might also arise from components of a large-spin ground state should be seriously considered. Interestingly, we have just characterized[10] a dinuclear $Mn^{II}Mn^{III}$ complex which is also ferromagnetically coupled and has an $S=9/2$ ground state (verified by M versus H/T data). The EPR spectrum for this $Mn^{II}Mn^{III}$ complex is similar to those for **1** and **2**.

Received: June 28, 1988 [Z 2832 IE]
German version: *Angew. Chem. 100* (1988) 1799

[1] G. Renger, *Angew. Chem. 99* (1987) 660; *Angew. Chem. Int. Ed. Engl. 26* (1987) 643; G. C. Dismukes, *Photochem. Photobiol. 43* (1986) 99; Govindjee, T. Kambara, W. Coleman, *ibid. 42* (1985) 187; J. Amesz, *Biochim. Biophys. Acta 726* (1983) 1.

[2] G. C. Dismukes, Y. Siderer, *Proc. Natl. Acad. Sci. USA 78* (1981) 274; O. Hansson, L. E. Andreasson, *Biochim. Biophys. Acta 679* (1982) 261.

[3] G. C. Dismukes, K. Ferris, P. Watnick, *Photobiochem. Photobiophys. 3* (1982) 243.

[4] J. C. de Paula, G. W. Brudvig, *J. Am. Chem. Soc. 107* (1985) 2643; J.C. de Paula, W. F. Beck, G. W. Brudvig, *ibid. 108* (1986) 4002; J. C. de Paula, J. B. Innes, G. W. Brudvig, *Biochemistry 24* (1985) 8114.

[5] O. Hansson, R. Aasa, T. Vanngard, *Biophys. J. 51* (1987) 825; J. L. Zimmerman, A. W. Rutherford, *Biochemistry 25* (1986) 4609.

[6] J. S. Bashkin, H.-R. Chang, W. E. Streib, J. C. Huffman, D. N. Hendrickson, G. Christou, *J. Am. Chem. Soc. 109* (1987) 6502.

[7] Correct elemental analysis for $C_{24}H_{28.5}N_{4.5}O_9Cl_4Mn_4$; X-ray structure data: rhombohedral, space group $R\bar{3}$, $T=-155$°C, $a=b=c=13.031(4)$ Å, $\alpha=\beta=\gamma=74.81(2)$°, $Z=2$, data collected $6° \leq 2\theta \leq 45°$, 1458 unique reflections with $F>3.00\sigma(F)$, $R=0.0371$, $R_w=0.0417$. All non-solvent hydrogen atoms were located in a difference Fourier and included in the final refinement cycles with isotropic thermal parameters. Further details of the crystal structure investigation are available on request from the Director of the Cambridge Crystallographic Data Centre, University Chemical Laboratory, Lensfield Road, Cambridge CB2 1EW (UK), on quoting the complete journal citation.

[8] V. K. Yachandra, R. D. Guiles, A. McDermott, R. D. Britt, S. L. Dexheimer, K. Sauer, M. P. Klein, *Biochim. Biophys. Acta 850* (1986) 324.

[9] K. Kambe, *J. Phys. Soc. Jpn. 5* (1950) 48.

[10] J. S. Bashkin, A. R. Schake, J. B. Vincent, H.-R. Chang, Q. Li, J. C. Huffman, G. Christou, D. N. Hendrickson, *J. Chem. Soc. Chem. Commun. 1988*, 700.

Chlorotetain from *Bacillus subtilis*, an Antifungal Dipeptide with an Unusual Chlorine-containing Amino Acid**

By *Claudius Rapp, Günther Jung,* Werner Katzer,* and *Wolfgang Loeffler*

Dedicated to Professor Theodor Wieland on the occasion of his 75th birthday

We have recently isolated new di- and tripeptides (rhizocticins A–D) from cultures of the bacterial strain *Bacillus subtilis* ATCC 6633.[1] These phosphono-containing active substances exhibit, inter alia, fungicidal properties. This inspired us to undertake a systematic search for new hydrophilic antibiotics from the genus *Bacillus subtilis*.

The antifungal activity, which was found in culture filtrates of *B. subtilis* BGSC 1E2, was competitively antagonized by di- and tri-peptides. The active compound was isolated from the culture mixture (after 84 h fermentation at 27 °C, complex culture medium) using methods suitable for the isolation of hydrophilic microbial metabolites. Thus, after removal of proteins by precipitation with alcohol and enrichment by adsorption on active charcoal, purification was carried out by gel chromatography (CM-Sephadex C-25, Sephadex G-10). The final purification of the antibiotic was performed on cellulose (yield 5 mg per liter culture filtrate). This amphoteric compound was identified as chlorotetain **1** [(*S*)-alanyl-(*S*)-3-[(*R*)-3′-chloro-4′-oxo-2′-cyclohexenyl]alanine (Ala-CCAla)], which contains the previously unknown, chlorine-containing amino acid CCAla.

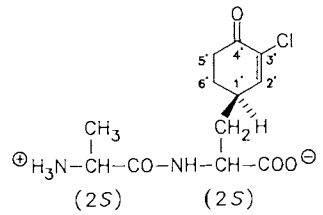

1

An amino acid determination showed the presence of the components L-alanine and L-tyrosine. The determination was carried out as follows: after acid total hydrolysis (6 N HCl, 18 h, 110 °C) the resulting hydrolyzate was esterified with *n*-propanol, acylated with trifluoroacetic anhydride, $(tfa)_2O$, and analyzed by gas chromatography on Chirasil-Val.[2] The FD mass spectrum of **1** showed a peak due to $[M+H]^{\oplus}$ at m/z 289 accompanied by an isotope peak at m/z 291 (Table 1). From this mass difference of 2 and the fragment ion at m/z 253 ($[M-Cl]^{\oplus}$), the presence of chlorine in **1** could be deduced. UV and NMR spectra showed that L-tyrosine is not a natural component of **1**, but rather the decomposition product from the acid-sensitive *C*-terminal amino acid. GC-MS analysis (capillary quartz column SE 52) of the *N*-tfa-dipeptide methyl ester showed (at m/z 363) the peak of highest mass corre-

[*] Prof. Dr. G. Jung, Dipl.-Chem. C. Rapp
Institut für Organische Chemie der Universität
Auf der Morgenstelle 18, D-7400 Tübingen (FRG)
Dipl.-Biol. W. Katzer, Prof. Dr. W. Loeffler
Institut für Biologie, Mikrobiologie I der Universität
Auf der Morgenstelle 28, D-7400 Tübingen (FRG)

[**] This work was supported by the Deutsche Forschungsgemeinschaft and the Fonds der Chemischen Industrie.

sponding to $[M-Cl]^{\oplus}$. The fragment ions at *m/z* 140 and 141 are typical for *N*-terminal alanine,[3] the presence of which was confirmed by dinitrophenylation. To explain the formation of tyrosine a six-membered ring system with a 1,4-arrangement of the peptide group and the keto-functionality is required. That the chloro-substituent occupies position 2 in the 2-cyclohexenone system was shown by the NMR chemical shifts of the olefinic proton ($\delta = 7.3$) and of the carbon atom to which it is bound ($\delta = 156.3$).[4]

The *C*-terminal amino acid contains the cyclohexenone chromophore, with an asymmetric C-atom in the 1'-position, in its side chain. Since, for steric reasons, only an equatorial position for the peptide group need be considered, only one half-chair configuration for each of the two diastereomers is conceivable, in which the 6'-CH_2 group is twisted out of the plane, either downwards [(*R*)-configuration at C-1'] or upwards [(*S*)-configuration]. The configuration at the C-1' atom was determined by measurement of the circular dichroism (Table 1). The reversed octant rule

Table 1. Analytical data for chlorotetain **1**.

^{1}H-NMR [a]:	Alanine: 4.11 (H-2), 1.58 (H-3) CCAla: 4.29 (H-2), 1.99 (H-3), 7.29 (H-2'), 2.60 (H_a-5'), 2.74 (H_e-5'), 1.85 (H_a-6'), 2.22 (H_e-6')
^{13}C-NMR [a]:	Alanine: 172.8 (C-1), 51.6 (C-2), 19.0 (C-3) CCAla: 180.6 (C-1), 55.7 (C-2), 38.1 (C-3), 37.3 (C-1'), 156.3 (C-2'), 132.9 (C-3'), 198.8 (C-4'), 38.8 (C-5'), 29.4 (C-6')
UV (in H_2O, pH 5.7, $c = 10^{-4}$ mol L^{-1}):	$\lambda_{max} = 249$ nm ($\varepsilon = 7050$)
R_f [b]:	0.47 [*n*-propanol/water (70/30)], 0.75 [*n*-propanol/pyridine/acetic acid/water (15/10/3/12)]
FD-MS:	289/291 ($[M+H]^{\oplus}$), 253 ($[M-HCl]^{\oplus}$)
GC-MS for the *N*-tfa-dipeptide methyl ester:	363 ($[M-Cl]^{\oplus}$), 256. 230/232, 224, 214/216, 140/141
CD (in H_2O, pH 5.7, $c = 5 \times 10^{-3}$ mol L^{-1}) [c]:	Maxima at 245 nm ($[\Theta]_M = 23200$), 312 nm ($[\Theta]_M = -1475$)

[a] H-1' signal obscured by H_e-5' signal; Bruker WM400 (in D_2O, pH 5.5, 18 mg/0.5 mL). [b] Silica gel 60 F_{254}. [c] $[\Theta]_M$ in [grad·cm^2·d mol^{-1}].

can be applied to the almost planar cyclohexenone ring system, as for α,β-epoxy- and α,β-cyclopropylketones.[5,6] According to this, the observation of a negative n,π*-Cotton effect, which in this case can be attributed to the negative contribution of the 6'-CH_2 group, requires an (*R*)-configuration.

Chlorotetain **1** is stable in aqueous solution at pH 5 at room temperature. In more strongly acidic solutions and also under alkaline conditions the biological activity rapidly decreases, particularly upon warming. It is known that amino- and amidoenones readily undergo a 1,4-addition to form 6-oxo-octahydroindoles.[7,8] A similar reactivity could well be partly responsible for the instability of **1**.

1 inhibits the growth of various fungi and, in higher concentrations, gram-positive and gram-negative bacteria. The fungi *Aspergillus fumigatus*, *Candida albicans*, and *Paecilomyces variotii* are particularly sensitive (MIC < 1 μg). **1** is the first chlorine-containing peptide to be isolated as a metabolite from *B. subtilis*. Other chlorine-containing amino acids and peptides are known to be metabolites of bacteria, fungi, plants, and sponges.[9]

The bacterial strain produces another antibiotic substance, which is structurally related to **1**. This was identified as the tetain (bacilysin)[10] (*S*)-alanyl-(*S*)-3[(*R*)-2',3'-epoxy-4'-oxocyclohexyl]alanine **2**. The *C*-terminus, which

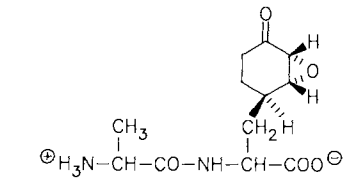

2

was also isolated as anticapsin,[11] irreversibly inhibits the glucosamine-6-phosphate synthetase of bacteria and yeasts after intracellular hydrolysis of the dipeptide.[12,13]

Since **1** and **2** are structurally similar it is conceivable that **1** is formed from **2** during isolation. However, the fact that it was possible, prior to isolation, to correlate the biological activity with the HPLC detection via UV spectroscopy, refutes this suspicion. We were able to show that bacilysin **2** occurs relatively frequently in *Bacillus subtilis* and related species. In contrast, only one of the investigated cultures of *B. subtilis* strains, which produced bacilysin, namely *B. subtilis* BGSC 1E2, was found also to contain chlorotetain **1**. Therefore, **1** represents a new chlorine-containing secondary metabolite, which, like **2** and other oligopeptides, can enter the bacterial cell *via* the dipeptide transport system.[14]

The aromatization, which was found after the acid total hydrolysis of CCAla, is also exhibited by other peptide antibiotics containing a labile six-membered alicyclic ring. Thus aromatization of the 4-aminocyclohexadienyl system of the amiclenomycin peptides[15] with elimination of ammonia leads to the formation of L-homophenylalanine, and aromatization of the epoxide-containing six-membered ring of **2** yields L-tyrosine. Because of this tendency to form stabilized aromatic rings, the ring systems of **1** and **2** are only accessible with difficulty by chemical synthesis.

Received: July 6, 1988 [Z 2850 IE]
German version: *Angew. Chem. 100* (1988) 1801

[1] C. Rapp, G. Jung, M. Kugler, W. Loeffler, *Liebigs Ann. Chem. 1988*, 655.
[2] H. Frank, G. J. Nicholson, E. Bayer, *J. Chromatogr. Sci. 15* (1977) 174.
[3] F. Weygand, A. Prox, H. H. Fessel, K. K. Sun, *Z. Naturforsch. B 20* (1965) 1169.
[4] G. Höfle, *Tetrahedron 32* (1976) 1431.
[5] C. Djerassi, W. Klyne, T. Norin, G. Ohloff, E. Klein, *Tetrahedron 21* (1965) 163.
[6] G. Snatzke: *Optical Rotatory Dispersion and Circular Dichroism in Organic Chemistry*. Heyden, London 1967.
[7] B. C. Laguzza, B. Ganem, *Tetrahedron Lett. 22* (1981) 1483.
[8] M. Souchet, J. Guilhem, F. Le Goffic, *Tetrahedron Lett. 28* (1987) 2371.
[9] S. Hunt in G. C. Barrett (Ed.): *Chemistry and Biochemistry of the Amino Acids*, Chapman, London 1985, p. 55.
[10] J. E. Walker, E. P. Abraham, *Biochem. J. 118* (1970) 563.
[11] N. Neuss, B. B. Molloy, R. Shah, N. de la Higuera, *Biochem. J. 118* (1970) 571.
[12] M. Kenig, E. P. Abraham, *J. Gen. Microbiol. 94* (1976) 37.
[13] H. Chmara, H. Zähner, E. Borowski, S. Milewski, *J. Antibiot. 37* (1984) 652.
[14] H. Diddens, H. Zähner, E. Kraas, W. Göhring, G. Jung, *Eur. J. Biochem. 1976*, 11.
[15] A. Kern, U. Kabatek, G. Jung, R. G. Werner, M. Poetsch, H. Zähner, *Liebigs Ann. Chem. 1985*, 877.

Oxidative Addition of Water to the Ru^{II} Catalyst $K[Ru^{II}(Hedta)(CO)]$: Homogeneous Catalysis of the Water-Gas Shift Reaction under Ambient Conditions

By *Mirza M. Taqui Khan,* Shivappa B. Halligudi,* and *Sumita Shukla*

The reaction of CO with H_2O to form CO_2 and H_2 [Eq. (a)] is a very important reaction[1] and is a principal method for obtaining H_2 for the Haber–Bosch synthesis of NH_3. Reaction (a), commonly referred to as the water-gas shift (WGS) reaction, is virtually the reductive decomposition of water by CO.

$$CO + H_2O \rightleftharpoons CO_2 + H_2 + 42\ kJ\ mol^{-1} \qquad (a)$$

The conventional heterogeneous catalysts for the water-gas shift reaction[2,3] consist of chromium-activated iron oxide (Fe_3O_4/Cr_2O_3) or cobalt-molybdenum oxide catalyst (CoO/MoO_2); the reaction is carried out at 400–460 °C and 200 atm of CO or CO + H_2.

Though the WGS reaction has been carried out under homogeneous catalysis,[4–10] only a few attempts have been made to perform the reaction under milder conditions (180 °C and 35 atm of CO) using metal carbonyls of the type $M(CO)_6$ (M = Fe, Cr, Mo, W, Rh, etc.) in alkaline or acidic medium. The turnover number reported[7] is 83.3 moles of CO_2/H_2 per mole of catalyst per hour.

We report here the catalysis of reaction (a) by $K[Ru^{II}(Hedta)(CO)]$ at 20–80 °C and 1–35 atm of CO. The effect of CO pressure (expressed as concentration of dissolved CO) on the rate of CO conversion into CO_2 and H_2 is shown in Figure 1. The rate v depends linearly on CO

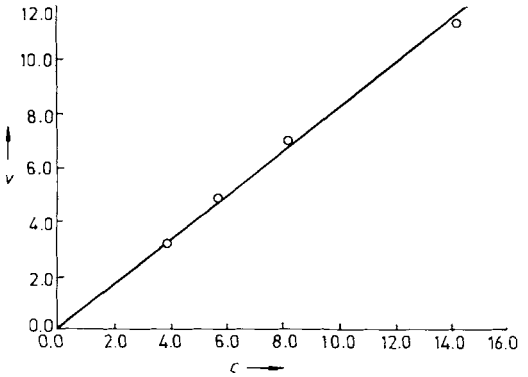

Fig. 1. Effect of concentration c [10^{-4} M] of dissolved CO on the rate v [10^{-3} M min^{-1}] of the water-gas shift reaction (1 mmol catalyst, 30 °C, 100 mL H_2O).

pressure; moreover, the rate observed at 1 atm of CO pressure ($\triangleq$ 0.00012 M concentration of dissolved CO) indicates the feasibility of the reaction even under ambient conditions. The effect of temperature on the rate of CO conversion was studied between 20 and 80 °C, as shown in the plot of $-\ln v$ versus $1/T$ in Figure 2; an activation energy E_a of 6.15 kJ mol^{-1} was found. Since the reaction is exothermic, it is not favored by higher temperatures. In fact, we observed formaldehyde formation at higher temperature (see Scheme 1). The optimum reaction conditions for the water-gas shift reaction are 50 °C and 15 atm of CO, for which the turnover number is 350 moles of CO_2/H_2 per mole of catalyst per hour.

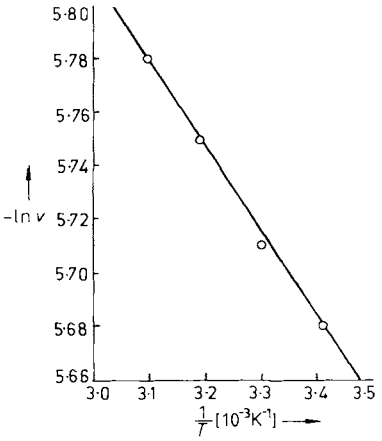

Fig. 2. Effect of temperature on the rate v of the water-gas shift reaction (1 mmol catalyst, 15 atm CO, 100 mL H_2O).

The water-gas shift reaction was also conducted at 1 atm of CO and 20 °C. A 75% conversion of CO into CO_2 and H_2 was determined after a contact time of 4 h with 3×10^{-3} M catalyst concentration. Figure 3 shows that the rate of CO conversion increases with increasing catalyst concentration for the WGS reaction conducted at 1 atm of

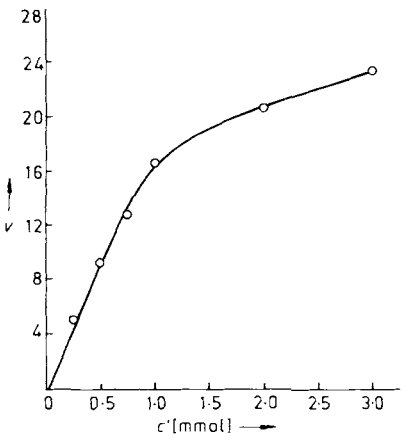

Fig. 3. Effect of catalyst concentration c' on the rate v [10^{-6} M min^{-1}] of the water-gas shift reaction at 20 °C and 1 atm of CO (100 mL H_2O).

CO and 20 °C with a contact time of 4 h. For 0.25–1.0 mmol catalyst, the reaction showed a first-order dependence on catalyst concentration. Beyond a catalyst concentration of 1.0 mmol, saturation kinetics with respect to catalyst concentration was observed. The first-order rate constant calculated in the linear range (0.25–1.0 mmol catalyst) is 1.67×10^{-2} min^{-1}. This is the first quantitative study using soluble metal complexes to catalyze the water-gas shift reaction in which it has been proved beyond doubt that the Ru^{II} catalyst species, $K[Ru^{II}(Hedta)(CO)]$, exhibits a catalytic activity far surpassing that of any known catalyst.

[*] Prof. M. M. Taqui Khan, Dr. S. B. Halligudi, S. Shukla
Discipline of Coordination Chemistry and Homogeneous Catalysis
Central Salt & Marine Chemicals Research Institute
Bhavnagar 364002 (India)

Based on the above observations a proposed mechanism for the water-gas shift reaction catalyzed by [(Ru(Hedta)(CO)]$^{\ominus}$ **1** is shown in Scheme 1.

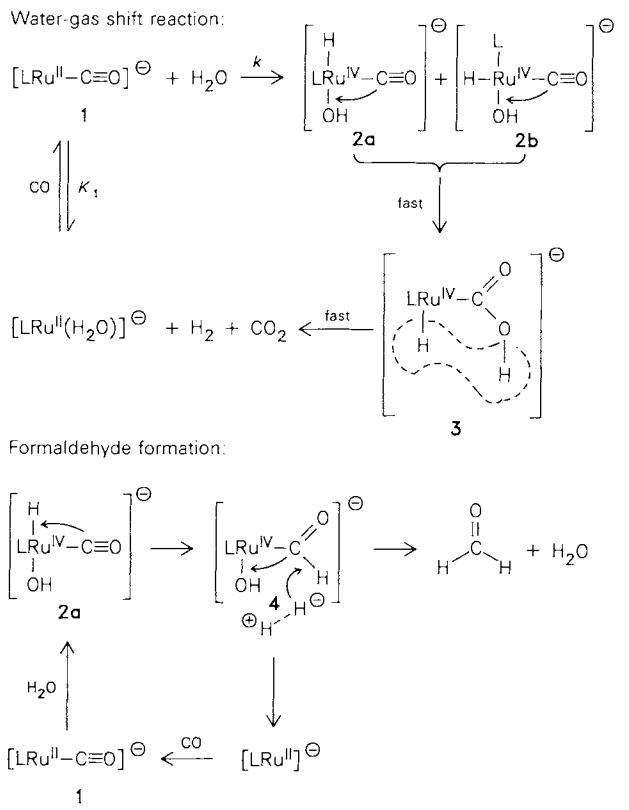

Scheme 1. Possible reaction mechanism for homogeneous catalysis of the water-gas shift reaction by **1**. L = Hedta.

The rate-determining step of the reaction has been suggested to be the oxidative addition of H_2O to **1** to form hydrido carbonyl species **2a** and **2b**. This reaction step is supported by the ^1H NMR spectrum of the reaction solution which shows peaks at $\delta = -20.1$ and -8.1 for hydrides *trans* to OH and CO, respectively. The formation of the hydrido carbonyl complexes **2** is also supported by the UV spectrum, which has a characteristic d–d band of Ru^{IV} in the Ru^{IV} hydrido carbonyl complex at 426 nm ($\varepsilon = 65$). The differential pulse polarogram of the reaction mixture, obtained with a platinum electrode, showed a wave at $+0.4$ V (vs. Pt, $\mu = 0.1$ M $NaClO_4$) which is attributed to the Ru^{IV}/Ru^{II} redox couple. The expected Ru–H stretching frequency at 1980 cm^{-1} was not observed in the IR spectrum since this band falls in the region of the strong ligational peaks of EDTA.

Insertion of CO into the Ru^{IV}–OH bond of **2** in a fast step gives a probable η^1-formato complex **3**, which dissociates in a fast step by reductive elimination of CO_2 and H_2 to form [Ru^{II}(Hedta)(H_2O)]$^{\ominus}$. This intermediate, in turn, gives **1** on reaction with CO, thereby completing the catalytic cycle. The participation of surface hydroxyl groups in the water-gas shift reaction catalyzed by iron–chromium catalyst has recently been proposed.[10] An *O*-coordinated formato species has been suggested[10] as an intermediate, whose formation involves a change in the valence state of iron. An η^1-formato intermediate in our case seems to explain much better the enhanced catalytic activity of **1** in the reaction.

The formation of formaldehyde (Scheme 1) is explained by the insertion of CO into the Ru–H bond of **2a**. A molecule of hydrogen generated in situ attacks the resulting intermediate **4**, leading to the formation of H_2CO, H_2O, and [Ru^{II}(Hedta)]$^{\ominus}$, which is immediately transformed into species **2a** in the presence of CO and H_2O.

The values of the equilibrium constant K_1 and the rate constant k at 50° and 15 atm of CO are 11 M^{-1} and 80.0 min^{-1}, respectively, with a turnover of 350 moles of CO_2/H_2 per mole of catalyst per hour, the highest reported so far in the liquid phase water-gas shift reaction. The activation energy of the reaction was found to be 6.15 kJ mol^{-1}, which amounts to a decrease of about 188.1 kJ mol^{-1}[11] for the proposed dissociation of H_2O into $H^{\oplus}$ and $OH^{\ominus}$ in the rate-determining step. The entropy and enthalpy of activation are 2.45 e.u. and 3.35 kJ mol^{-1}, respectively.

Experimental Procedure

The water-gas shift reaction was conducted in a 300-mL stainless-steel autoclave equipped for automatic control. The reactor was charged with known quantities of catalyst, CO, and H_2O. The catalyst precursor K[Ru(Hedta)Cl]·2H_2O was prepared according to the method described elsewhere [12]. Gaseous samples withdrawn at different time intervals were analyzed by chemical gas analysis apparatus (ORSAT) and gas-liquid chromatographic (GLC) methods for CO, CO_2, and H_2. The CO used was 99.96% pure. The only solvent used was doubly distilled water. The ambient condition experiments were also conducted in a similar manner at 20°C and 1 atm of CO. The gaseous components were withdrawn after a contact time of 4 h, slowly flushed with N_2, and passed through a stirred 0.05 N KOH solution over a period of 0.5 h. The resulting solution was diluted to 100 mL by adding water and titrated against 0.025 N HCl to determine the amount of CO_2 formed during the WGS reaction. The 100-MHz ^1H NMR spectrum of the solution was recorded in D_2O (standard: sodium 3-trimethylsilylpropanesulfonate).

Received: March 11, 1988;
revised: August 30, 1988 [Z 2659 IE]
German version: *Angew. Chem. 100* (1988) 1803

CAS Registry numbers:
H_2O, 7732-18-5; K[Rh(II)(Hedta)(CO)], 117800-19-8; CO, 630-080-0; H, 1333-74-0.

[1] R. M. Laine, E. J. Crawford, *J. Mol. Catal. 44* (1988) 357.
[2] R. P. A. Sneeden in G. Wilkinson, F. G. A. Stone, E. W. Abel (Eds.): *Comprehensive Organometallic Chemistry*, Pergamon, Oxford 1982, p. 9, and references cited therein.
[3] a) R. B. Anderson in P. H. Emmett (Ed.): *Catalysis 1954–1960 4* (19), p. 1; b) P. J. Denny, D. A. Whan, *Catalysis (London) 2* (1978) 46.
[4] R. W. Joyner, *J. Catal. 50* (1977) 176.
[5] G. A. Martin, M. Primet, J. A. Dalmon, *J. Catal. 53* (1978) 321.
[6] M. Primet, *J. Chem. Soc. Faraday Trans. 1 74* (1978) 2570.
[7] A. D. King, Jr., R. B. King, D. B. Yang, *J. Am. Chem. Soc. 102* (1980) 1028; *J. Chem. Soc. Chem. Commun. 1980*, 529.
[8] P. Escaffre, A. Thorez, P. Kalck, *J. Mol. Catal. 33* (1985) 87, and references cited therein.
[9] a) K. I. Zamaraev, *React. Kinet. Catal. Lett. 35* (1987) 469; b) V. A. Likholobov, Yu. I. Yermakov, *Kinet. Katal. 21* (1980) 904.
[10] D. Shopov, A. Andreev, *Kinet. Katal. 28* (1987) 133.
[11] J. A. Kerr, *Chem. Rev. 66* (1966) 465.
[12] M. M. Taqui Khan, A. Kumar, Z. Shirin, *J. Chem. Res. 1986*, 130.

 © VCH Verlagsgesellschaft mbH, D-6940 Weinheim, 1988

The Chemistry and Biochemistry of *N*-Substituted Porphyrins. By *D. K. Lavallee*. VCH Verlagsgesellschaft, Weinheim/VCH Publishers, New York 1987. x, 313 pp., bound, DM 89.00.—ISBN 3-527-266-933/0-89573-147-9

This monograph brings together in book form, for the first time, the considerable knowledge which has been accumulated during the past two decades on the chemistry of *N*-substituted porphinoids and their formation in biological systems. This survey of a particular aspect of porphin derivatives should be of interest to chemists and biochemists concerned with metalloporphyrins, heme proteins and heme biosynthesis. In accordance with the nature of this topic, the book consists of a "chemical" part and a "biochemical" part (containing four and three chapters respectively).

The first, introductory, chapter establishes the reasons for the chemical, biological, and also medical interest in *N*-substituted porphinoids.

The second chapter deals with the structures of some particular series of *N*-substituted porphinoids and compares them with those of the porphyrins. In addition to the detailed discussion of the structural effects of *N*-substitution in metal-free and metal-containing porphinoids (which includes a considerable amount of data in the form of tables, though unfortunately these are not always clearly presented and appropriately titled), an attempt is made at establishing a quantitative relationship between the bonding conditions and fundamental structural parameters such as the *N*-hybridization and π-bond order in the porphyrin ligands. Regrettably several errors in this chapter have escaped unnoticed, and adversely affect the understanding of the material.

In the third chapter, which deals at some length with the spectroscopy of *N*-substituted porphinoids, a large part of the data now available is discussed and listed in numerous (perhaps too many) tables. A strong point of this chapter is again the clear way in which the data for porphinoids are presented alongside those for the *N*-substituted porphinoids. A weakness, though, is that the important UV/VIS absorption spectra (for example) have in most cases been crudely reproduced by hand drawing. The more concise and information-packed sections on reactions and on the preparation of *N*-substituted porphinoids (Chapters 4 and 5) summarize the current state of knowledge in a clear and understandable form, and also include a short but useful collection of recipes for syntheses.

In the second, "biochemical" part of the book, Chapter 6 discusses in a lucid way the functioning of certain *N*-alkylated porphinoids as inhibitors in the enzymic incorporation of iron in the heme biosynthesis. Chapter 7 discusses the important mechanistic and structural aspects of the formation of *N*-substituted heme derivatives in the reactions of pharmacologically active substances, and of a selection of other substances (including especially "suicide" inhibitors), with Cytochrome P-450. For the reader interested in the topics covered, these two chapters provide much well-presented information.

The first part of Chapter 8 describes, as other important routes whereby *N*-substituted porphinoids are formed in biological media, the reaction of hydrazines with heme proteins, and rearrangement reactions of model compounds. The second part of the chapter is essentially a recapitulation of a part of Chapter 5.

This remarkably long work, with a total of over 300 pages, ends with a detailed author index (11 pages), and a subject index which, compared with the latter, is rather lacking in content (less than 3 pages).

The book is a comprehensive source of information on the chemistry and biochemistry of *N*-substituted porphinoids, which is nowadays recognized as an important aspect of porphinoid chemistry. Regrettably, the long-term usefulness of the work is reduced by some conspicuous weaknesses, such as the unsatisfactory layout of the text, a succession of minor errors, and some misleading comments (especially in Chapters 2 and 3). The readability of the book is also marred by a lack of clear explanations in the headings of some of the tables and in figure legends, and by the use of abbreviations that are not explained. Nevertheless, this monograph, which at present has no competitor in the field which it covers, can be well recommended for the readership mentioned at the beginning of this review.

Bernhard Kräutler [NB 911 1E]
Laboratorium für Organische Chemie
der Eidgenössischen Technischen Hochschule
Zürich (Switzerland)

Intermediate Organic Chemistry. By *J. C. Stowell*. Wiley, Chichester 1988. xv, 268 pp., bound, $ 46.50.—ISBN 0-471-09899-X

Many of the experimental and theoretical innovations developed in the last few decades, although eagerly adopted by chemists, have been slow to find a place in the major textbooks and laboratory handbooks. Examples are new spectroscopic methods, the concept of retrosynthesis, and also working methods such as on-line literature searching and molecular modeling.

Although topics such as these are very familiar to the practising chemist, the student of chemistry usually only learns of them at a late stage in his training, and often only in a fragmented way. To set out to give students a systematic description of a few of these topics which have now become so important is therefore a commendable objective. With this aim *J. C. Stowell*, in his book "Intermediate Organic Chemistry", has set out to bring together eight logically interrelated topics so as to give an overall view of organic chemistry. Following an introduction to basic nomenclature the reader is familiarized with the technique of searching the literature and with the principles of stereochemistry. This is followed by a three-part section on methods for introducing and exchanging functional groups, the formation of C—C bonds, and the concept of retrosynthesis. The chapters which follow deal with methods for elucidating reaction mechanisms, possibilities for physically influencing chemical reactions, and interdependent reactions. The book concludes with an introduction to the interpretation of NMR spectra. Exercises at the end of each chapter enable the reader to test what he has learned; unfortunately, though, he must look up the cited papers to discover the answers. Selected literature refer-

ences extending up to 1985 are provided to facilitate more advanced study.

The book is attractively printed and contains hardly any errors (one occurs in the formula for dimethylsulfoxide on page 72), although more elegant methods are available for some of the reactions given (e.g. dehydrogenation using Se, p. 84). The easily comprehensible style makes easy reading.

It is, quite understandably, not possible to treat all these topics with anything approaching completeness in 264 pages of text. Accordingly an attempt is not even made at accounting for all the facts in a logical way, nor at dealing in greater detail with the reaction schemes and rearrangements that are listed. It is perhaps on these grounds that the author has avoided giving mechanistic interpretations in the very long section on syntheses. Nevertheless, this reviewer sees the omission as a significant shortcoming, since it means that the logical conception of the subject which the author obviously sets out to promote is here disregarded, and arbitrarily selected facts and examples are substituted for a proper understanding.

Chemists nowadays are self-taught as regards their working habits. However, the work is neither a textbook nor a course book in the conventional sense: it is, in *Stowell*'s words, a novel experiment. It is an attempt to give beginners in chemistry a view of the whole scene and the interrelationships that exist; according to the introduction it should be regarded as an aid to making progress in practical organic chemistry, a bridge from basic education into the diversity of fields of more advanced chemical research.

Consequently the book is hardly suitable as a means of acquiring a thorough knowledge of the topics that are treated. Perhaps, therefore, it is just this fragmentary manner of presentation that makes the book especially suitable for students who wish to test the knowledge acquired in their studies. It can be thoroughly recommended for this purpose.

Hartmut Laatsch [NB 914 IE]
Institut für Organische Chemie
der Universität Göttingen (FRG)

Biotechnology. A Comprehensive Treatise in 8 Volumes. Series Editors: *H.-J. Rehm* and *G. Reed*. **Vol. 7a. Enzyme Technology.** Volume Editor: *J. F. Kennedy*. VCH Verlagsgesellschaft, Weinheim 1987. xii, 761 pp., bound, DM 495.00/subscription price: DM 425.00.—ISBN 3-527-25769-1

Reactions catalyzed by enzymes collectively form the foundation of biotechnology. This volume on Enzyme Technology is a very welcome addition to the mammoth task undertaken by the editors and the publisher. Incidentally, although the title says the Treatise is to have 8 volumes, the series[*] will really have 10 volumes when all the work is done.

The aim of this volume is to provide for the reader a review of the chemistry and biology of enzymes, and of how enzymes are prepared and used. In this, the authors have generally been very successful. One should not look to this volume to learn about the economics of enzyme production, or for a perspective on the historical trends in the industry or the market, or of the commercial potential of enzymes. Use or potential use of enzymes for hazardous waste treatment also could have received an emphasis. Despite this, the volume will serve as an extremely effective and comprehensive resource for any scientific worker interested in enzymes.

There are 15 chapters in all in this volume, many of them written by people who have made a good name for themselves over the years with admirable research and development contributions. Three of the chapters (numbers 1, 2 and 6) should be seen as providing the fundamentals of enzyme kinetics and molecular biology. These appear to be geared not for the uninitiated but for those who are at least somewhat familiar with the fields.

Another set of three chapters does a very good job of describing how enzymes are made via fermentation and then isolated and purified. The 146-page chapter on enzyme fermentations is in the nature of a scientific review article, as are many of the other chapters in this volume. The chapter has a good list of references spanning some 29 pages and generally has an "industrial" type outlook which helps make up for the lack of such data. Perhaps the coverage of the "fermentation engineering" aspects could have been better.

While there is some repetition in the two chapters on small scale and large scale enzyme recovery, the chapters are generally complementary. The chapters include some excellent comments which will be of great benefit to someone starting work on enzyme recovery. The perspective provided on ion-exchange chromatography is especially good. This reviewer would have liked to see a better coverage of cell separation techniques, of enzyme production economics, and of at least one flow scheme used in making any of the large volume industrial enzymes.

Two highly readable and well written chapters are on immobilized enzymes and immobilized cells. They provide a very good perspective on the types and methods available for immobilization. The authors, who have otherwise done some very good work in the field, could have elucidated why some of the approaches to immobilization have been successful on the industrial scale and why others have not. Synthetic enzymes, or the use of polymers and macrocyclic compounds to achieve "enzyme like" catalysis is the subject of another brief and readable chapter.

A chapter on the engineering aspects of enzyme reactor systems is comprehensive and well written. Here again, repetition of some of the enzyme kinetics already covered in Chapter 1 might have been avoidable.

How enzymes have been or can be used is the subject of a group of four chapters by authors several of whom have outstanding credentials. The chapter by veterans *Reed* and *Peppler* on the use of enzymes as food or animal feed processing aids shows one has to appreciate the terminology of the industry, be it baking or starch processing or brewing or dairy or wine or meat or whatever. The emphasis is on process recipes/procedures rather than on the chemistry involved. A gem here is a listing of some costs of enzyme-based processing; e.g., the cost of isomerizing 100 kg dextrose to fructose by a bacterial isomerase is 33–66 US cents. This reviewer would have liked to see more such perspectives by other authors in the volume.

Enzymes in their "free" (soluble) or immobilized form find many uses in the pharmaceutical and chemical industries and are discussed in two chapters. The use of enzymes in the making of amino acids, organic acids, antiviral compounds, coenzymes, peptides such as insulin and aspar-

[*] Cf. *Angew. Chem. Int. Ed. Engl. 26* (1987) 1057.

tame, alcohols, detergents, and antibiotics is covered in varying details.

Any volume of this type had to have a contribution by the Tanabe Seiyaku Co. team of *Chibata, Tosa* and *Sato* and it does. One of the pioneers and developers of practical scale processes based on immobilized biocatalysts, their survey chapter is most readable. Being as successful as they have been, they could have given their readers the benefit of a discussion of some of the failures; i.e., the reasons why in some of the cases the commercialization efforts did not work out. Some material on the chemical engineering of enzyme reactors, encountered earlier in the reaction engineering chapter, is repeated here, but fortunately it adds to the perspective.

The specificity of enzymes can be exploited for the analysis of scores of compounds, and the last applications chapter surveys the literature on "enzyme sensors". The author has many research achievements to his credit and could have added to the perspective by listing which of the sensors are or can be used in a practical or commercial sense, and indicating those that are commercially available.

Safety and regulatory aspects of using enzymes is the subject of a valuable chapter. Some of these aspects are also covered earlier in the chapter on the use of enzymes in food processing. There is repetition of which microorganisms produce which enzymes and the commercial food uses of enzymes. Nevertheless, the chapter adds a highly needed perspective on enzyme technology.

All in all, this volume does an excellent job of maintaining the spirit of this series. Of the 10 volumes, the first two covered the fundamentals in the field. Volumes 3 through 6b have focused on the applications of biotechnology. This volume is the first of two volumes on the core of biotechnology. We can now look forward to the next volume in the series: Gene Technology.

Bhavender Paul Sharma [NB 910 IE]
Genencor Inc.,
South San Francisco, CA (USA)

The Chemistry of the Semiconductor Industry. By *S. J. Moss* and *A. Ledwith*. Blackie, Glasgow and London 1987. xiv, 426 pp., bound, £ 50.00.—ISBN 0-412-01321-5

This book consists of sixteen chapters in which British and American experts from industrial, government and university laboratories describe the chemical aspects of semiconductor manufacturing and processing. Here for the first time specialists have set out to explain some of the chemistry involved in making integrated circuits, by taking a cross-section through all the relevant stages of production. They are thus able to show to what a great extent, and in how many different ways, semiconductor devices used in micro- and opto-electronics are the products of chemistry, with the background of understanding and optimization provided by solid state physics.

First the book prepares the reader by giving an overview; it is made clear that the semiconductor industry is now in a stage of rapid growth, not only in economic terms but also as regards its science and technology. In the succeeding fifteen chapters, each with its own bibliography, the different topic areas are covered in turn, in the logical sequence of their industrial application.

The first topic discussed is silicon production. The author proceeds from the extraction of raw silicon through its initial refinement to the technique of growing single crystals, and the production and conditioning of wafers. In the two chapters on III/V- and II/IV-type compound semiconductors, techniques for synthesizing these materials and growing single crystals are described; particular attention is given to the growing importance of gallium arsenide and related compounds. Next come two chapters on the deposition of thin films from the gas phase, with and without the use of a plasma, for producing epitaxial, polycrystalline or amorphous silicon films, and also thin metal films and dielectric films; kinetic aspects and technical details are also covered.

Thin epitaxial films of compound semiconductors are the main theme of the next two chapters, which are devoted to vapor phase epitaxy from organometallic compounds and to liquid phase epitaxy. Here there is a certain amount of overlapping with material covered earlier, but the large and growing importance of these techniques justifies treating them in separate chapters. Next there are chapters on photoresists and on resists for electron beam and X-ray lithography. There then comes a detailed treatment of all aspects of the use of wet etching processes in semiconductor production, in lithographic operations and in materials characterization. A short chapter is devoted to polyimides, which are being used increasingly as dielectrics and lacquers.

A chapter entitled "Molecular Electronics" gives a short survey of current research and future prospects in organic semiconductors, Langmuir–Blodgett films, and organic materials for use in integrated optics. On a related theme is a chapter which considers semiconductor junctions from a novel theoretical standpoint, not with the usual semiconductor physics approach but instead by using computer models based on the methods of the quantum chemist; for example, the models are used to describe crystal growth at the atomic level, and the incorporation of dopant atoms into silicon clusters. The final two chapters highlight the recent striking growth in the importance of plasma etching processes. The technology and mechanisms of the etching of structures in semiconductors, dielectrics, silicides and metals, and of polymer films, are described.

In nearly all cases there is a good balance between the chemical fundamentals and the technology. The current scientific and technological situation is well reviewed, and a clear distinction is made between industrial processes and laboratory procedures. Reaction equations and the kinetics and thermodynamics involved are included where these are known and are of importance, whilst those areas in which empirical knowledge does not yet have a solid scientific basis are clearly identified. The authors have consciously omitted a number of topics, such as analysis and the purification of chemicals used in the processes. Since it is often necessary in the semiconductor industry to reduce impurities to sub-ppb levels, it would have been useful to include a separate description of the techniques of purification and analysis which have been developed specially for this purpose.

The material within individual chapters of the book is clearly arranged in sub-sections, and adequately illustrated by diagrams, figures and tables. The literature references extend up to 1985 in most cases, and allow one to study topics in greater depth. Some spot checks did not reveal any incorrect citations.

The book is intended as a survey for use by scientists involved in research and development in the semiconductor and related industries. Nevertheless, it is written in language which should present little difficulty for beginners

in the field and advanced students. Only a few specialist terms are used without explanation, e.g. "latch up". The authors have succeeded in their ambitious aim of showing, by means of a sort of cross-sectional picture, the important role which chemistry plays in this rapidly developing technology. However, the reader who becomes intensively involved with a particular topic will very soon find that he must refer to the original papers or detailed monographs that are cited.

Hermann Fußstetter [NB 908 IE]
Wacker Chemitronic GmbH, Burghausen (FRG)

Electron Transfer Reactions in Organic Chemistry. By *L. Eberson*. Springer, Berlin 1987. xiii, 234 pp., bound, DM 128.00.—ISBN 3-540-17599-7

In recent years electron transfer (ET) has come more and more into the foreground of discussion as a component of organic reaction mechanisms. Even classical reactions such as nucleophilic aliphatic substitution and electrophilic aromatic substitution are being considered from this viewpoint. Whereas the proponents of these ideas view the whole of organic chemistry from this aspect, there are many others who are uncertain about its importance. Thanks to *Lennart Eberson* an attempt has now been made in this monograph to define the situation with regard to electron transfer in organic reactions and the limits of its applicability.

This relatively compact volume of the series "Reactivity and Structure Concepts in Organic Chemistry" begins by introducing electron transfer as a "neglected concept in organic chemistry". After defining and clarifying the concept of electron transfer (Chapter 2), which is here frequently given the unnecessarily extended description of "single electron transfer" (SET), theories of electron transfer are discussed in Chapter 3. Here, as expected, the Marcus theory, still not as well known to organic chemists as it ought to be, plays a central role. The next two chapters contain advice on the practical application of this theory, and on experimental diagnostic methods for investigating reactions thought to involve electron transfer.

I appreciate especially the great emphasis that is placed on the quantitative analysis of experimental data. It is only through careful evaluation of kinetic and thermodynamic data that a clearer view of the situation can be arrived at; for many reactions such data are not yet available. The book makes a valuable contribution by repeatedly emphasizing this point. At the same time it becomes apparent how difficult it is to obtain unambiguous evidence for the involvement of ET.

Chapters 6 to 8 describe reactions of non-metallic organic and inorganic species, reactions of organic compounds with inorganic oxidizing agents, and electron transfer processes involving exclusively organic reactants. Here again it is emphasized that in many cases much further work will be needed to establish an unambiguous picture of the mechanisms.

Chapter 9 deals with electron transfer processes induced by light or by electrodes, and Chapter 10 is concerned with the important area of ET-catalyzed reactions, which has undergone extensive development during the past two decades. Before the relatively brief account in the final chapter of applications of ET to technological synthetic processes, *Eberson*, in Chapter 11, examines the distinction between polar mechanisms and ET mechanisms. From this one recognizes how difficult it can be to draw the line between the two, and how much work still remains to be done in order that ET can be given its proper place in organic chemistry.

Although the book has been written by one of the proponents of the ET concept, care has been taken to always discuss the evidence from a critical standpoint, with a justifiable emphasis on the quantitative side, i.e. on the application of the Marcus theory. It is to be hoped that this monograph will contribute to a wider knowledge of the Marcus theory of electron transfer in organic chemistry, and will give extra impetus to this rapidly developing area of research.

For reasons of space the book does not attempt to cover ET in biological processes and in organometallic chemistry. The literature is thoroughly covered, and in some parts includes references up to 1987. The book is recommended for reading by everyone who wishes to obtain an overview of the current status of ET in organic chemistry.

Reiner Sustmann [NB 916 IE]
Institut für Organische Chemie
der Universität-Gesamthochschule Essen (FRG)

Registered names, trademarks, etc. used in this journal, even when not marked as such, are not to be considered unprotected by law.

© VCH Verlagsgesellschaft mbH, D-6940 Weinheim, 1988. – Printed in the Federal Republic of Germany by Zechnersche Buchdruckerei, Speyer/Rhein.

All rights reserved (including those of translation into foreign languages). No part of this issue may be be reproduced in any form – by photoprint, microfilm, or any other means – nor transmitted or translated into a machine language without written permission from the publishers. Only single copies of contributions, or parts thereof, may be made for personal use. This journal was carefully produced in all its parts. Nevertheless, authors, editors and publisher do not warrant the information contained therein to be free of errors. Readers are advised to keep in mind that statements, data, illustrations, procedural details or other items may inadvertently be inaccurate.

Valid for users in the USA: The appearance of the code at the bottom of the first page of an article in this journal (serial) indicates the copyright owner's consent that copies of the article may be made for personal or internal use, or for the personal or internal use of specific clients. This consent is given on the condition, however, that the copier pay the stated per-copy fee through the Copyright Clearance Center, Inc., for copying beyond that permitted by Sections 107 or 108 of the U.S. Copyright Law. This consent does not extend to other kinds of copying, such as copying for general distribution, for advertising or promotional purposes, for creating new collective works, or for resale. For copying from back volumes of this journal see 'Permissions to Photo-Copy: Publisher's Fee List' of the CCC.

Editorial office: Pappelallee 3, D-6940 Weinheim, Federal Republic of Germany, Telephone (06201) 602315, Telex 465516 vchwh d, Telefax (06201) 602328.

Editor: *P. Gölitz.*

Associate editors: *D. I. Loewus, A. Stimson.* **Editorial assistant:** *E. Schweikart*

Publishers: VCH Verlagsgesellschaft mbH. (Managing Director: *Hans Dirk Köhler*), Pappelallee 3, D-6940 Weinheim, Federal Republic of Germany.
Correspondence concerning advertisements should be addressed to VCH Verlagsgesellschaft mbH. (Advertising Manager *R. J. Roth*), Boschstr. 12. P.O. Box 101161, D-6940 Weinheim, Federal Republic of Germany. Telephone Weinheim (06201) 602-0, Telex 465516 vchwh d, Telefax (06201) 602 328.

Beilagenhinweis: Dieser Ausgabe liegt ein Prospekt der VCH-Verlagsgesellschaft, 6940 Weinheim, bei.

ADVANCED MATERIALS

Editorial Advisors: E. M. Engler (USA), D. Haarer (FRG), N. Ogata (Japan), G. Petzow (FRG), J. M. Thomas (UK), G. Wegner (FRG)

Chemistry of Materials

Editorial Essay

By Leonard V. Interrante*

The association of chemical processes with the preparation and utilization of materials has its roots in the prehistory of materials technology. The fire-hardening of wooden tools and weapons by prehistoric man depended on the same basic chemical process as the current fabrication of carbon fiber by carbonization of an organic polymer fiber. The subsequent bronze and iron ages were similarly dependent on the chemical extraction of copper and iron from their ores, again reflecting the intimate association between chemical processes and materials technology.

Despite the fundamental reliance of materials processing on chemistry, the chemical profession has been slow to take up the challenges of materials technology. Perhaps as a result of this lack of strong input from chemists, the application of chemistry in materials technology has tended to be empirical in nature with an incomplete understanding of the relevant chemical processes involved.

In recent years the increasing demand for advanced materials to meet the needs of current technology has led to a reexamination of this interface between chemisty and materials science as well as an increasing recognition of the need to involve chemistry and chemical engineering more directly in the pursuit of solutions to materials-related problems.[1] The increasing interest in chemistry as a source of new materials, or as a means of processing and using known materials more effectively, is illustrated by the titles of several recent international meetings, e.g., "Better Ceramics Through Chemistry", "Molecular Design of Materials" and "Molecular Chemistry for Solid State Electronics".[2] In the United States this interest has also been reflected in increasing employment opportunities for chemists and chemical engineers in areas which were traditionally the exclusive province of other disciplines, for example, the electronic materials processing and ceramics industries.

Examples of the successful marriage of chemistry and materials science can be found in many areas of current technology. In electronics one can cite the development of chemical and biosensors using surface-modified electrodes[3] and the widespread use of polymers as dielectric materials and as radiation-sensitive resist materials.[4]

Chemistry has also played an important role in the etching and deposition of thin film electronic materials with a rapidly growing interest in plasma- and laser-assisted processing as well as in chemical vapor deposition using designed organometallic precursors.[5] The key role of chemistry in the selective addition and removal of the wide range of materials involved in the construction of a silicon integrated circuit is illustrated by the cross-sectional view of an advanced bipolar device structure in Figure 1.[6] Each of the many steps involved in the construction of this device

Contents

L. V. Interrante
Chemistry of Materials 1741
M. Antonietti
Microgels—Polymers with a Special Molecular Architecture 1743
H. Inokuchi
New Organic Superconductors 1747
Research News
J. M. Thomas
Molecular Electronics: Silicon to Soliton and Other Trends 1751
Conference Reports
W. Faul
Advanced Materials—R & D Efforts in Germany 1754
W. H. Meyer
Speciality Polymers 1757
Conference Calendar 1759

Editor: *P. Gölitz* **Editorial Assistant:** *L. Dominguez*

[*] Prof. Dr. L. V. Interrante
Department of Chemistry, Rensselaer Polytechnic Institute
Troy, NY 12180-3590 (USA)

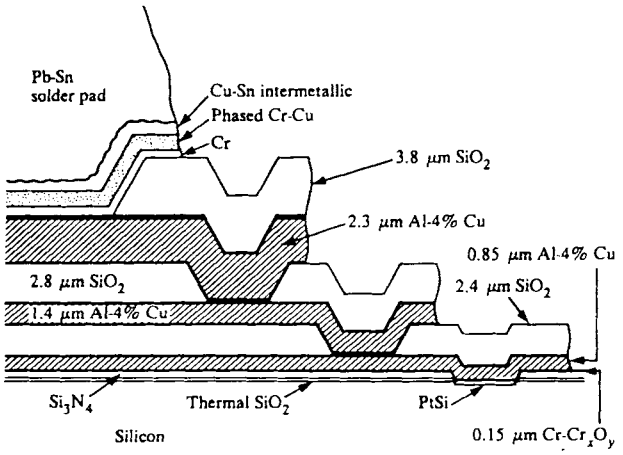

Fig. 1. Cross-section of an integrated circuit chip. [6]

employs one or more chemical processes which bring into play elements of inorganic, organic and polymer chemistry.

In the area of structural and, in particular, composite materials, chemists have been called upon to produce polymeric precursors to materials such as silicon nitride and silicon carbide which can be used to prepare high temperature, high strength ceramic fibers.[7] This work extends to inorganic polymers the growing interest in rod-like organic polymers and carbon fibers as reinforcements for light weight, high strength structural composites.[8]

The current focus on chemistry as a solution to materials-related problems encompasses all of the major chemistry and chemical engineering disciplines and involves both the development of new materials and the processing of known materials. In the context of materials processing there is an increasing demand for improved methods of obtaining known materials in unusual forms such as epitaxial thin films, stable colloidal suspensions, and microporous membranes. The increasing use of sol–gel methods for the processing of ceramic powders, monoliths and films provides an illustration of the opportunities for chemistry in this area.[1,9]

A common theme in materials-related research is the interaction between materials and their environment, for example, in connection with heterogeneous catalysis, corrosion, adhesion, abrasion resistance, the design of biomaterials, chemical sensors and thin film deposition. The full understanding and control of these processes depends to a large extent on the skills of chemists and chemical engineers who are trained in areas such as surface science, analytical chemistry, chemical kinetics and thermodynamics, as well as in the theory and modeling of chemical processes on solid surfaces. On the other hand, it is clear that chemists or chemical engineers working in isolation are not likely to provide the solutions to these and the many other chemistry-related problems in materials science and technology. It is well known in industry that the greatest likelihood of success comes from an interdisciplinary approach to problems, where chemists and chemical engineers combine their knowledge with that of other scientists and engineers.

A prerequisite for effective interaction is effective communication. The scientific and technological questions posed by materials science, and their chemical implications, must be presented and discussed in a manner which is clearly understandable to all of the participants. This will require a better mechanism for communicating the results of forefront research in the area of materials science to chemists and chemical engineers. Similarly, materials scientists and technologists would benefit from increased exposure to the opportunities and advances in materials chemistry. These goals can be attained most effectively through the scientific literature, by the publication of articles which highlight and bring to the attention of the chemical and materials science communities some of the key areas of current interest in materials chemistry as well as examples of forefront research in this area.

The new Advanced Materials section of Angewandte Chemie provides an illustration of how this can be accomplished using a chemistry-related journal. The emphasis on commentary, review papers and meeting highlights in areas of current interest within materials science gives the reader an opportunity to view current work in this area from a chemical perspective.

The American Chemical Society began to explore the prospect of establishing a new primary research journal in materials chemistry in 1985. A major concern throughout this process was whether a new journal was needed, considering the proliferation of journals and the limited resources of our libraries. It was eventually decided that the need for better visibility for materials research within the chemistry community and the lack of an adequate common forum for the broad spectrum of materials chemistry

Prof. Dr. Leonard Interrante received his Ph. D. in inorganic chemistry in 1964 at the University of Illinois, Champaign-Urbana. After postdoctoral study at University College London, and several years as an assistant professor at the University of California at Berkeley, in 1968 he joined the research staff of the General Electric Research and Development Center in Schenectady, N. Y. where he conducted research in inorganic and materials chemistry. He assumed his present position as a Professor of Inorganic Chemisty at Rensselaer Polytechnic Institute in 1985. He has authored and co-authored over 75 publications in coordination chemistry, organometallic and solid state chemistry. His current research interests cover a wide range of materials-related subjects, including the synthesis and investigation of organometallic precursors to ceramic materials, chemical vapor deposition processes, and the preparation of molecular solids with novel electrical and magnetic properties. Dr. Interrante was selected as editor of the new ACS journal, Chemistry of Materials, in January 1988.

research currently in progress throughout the world required a new journal. Such a journal would highlight the role of chemistry as a source of new materials and processes for materials technology and bring together work now widely scattered throughout the literature. The recommendation that a new journal be established was subsequently approved by the ACS and the first issue is scheduled for publication in January, 1989.

From the beginning *Chemistry of Materials* was envisioned as a primary research journal which would emphasize the more chemical and fundamental aspects of materials science which underlie current and future materials technology. This journal seeks to publish the results of forefront research efforts with a molecular-level perspective at the interface of chemistry, chemical engineering and materials science. Preliminary communications and full papers, in addition to selected short reviews highlighting particular topics in materials chemistry, will be featured in its bimonthly issues.

[1] As evidence of this increasing interest in establishing better connections between chemistry, chemical engineering and materials science in the USA, several granting agencies have recently established special initiatives such as the National Science Foundation's "Materials Chemistry" initiative which are specifically directed at encouraging research at the interface between these disciplines.

[2] J. Brinker, D. E. Clark, D. R. Ulrich (Eds.): *Better Ceramics Through Chemistry*, Symposia at Materials Research Society Meetings, 1987 and 1988, published in Volumes 32 and 73 of the MRS; "Molecular Design of Materials", Biennial Inorganic Chemistry Symposium, Inorg. Div., Am. Chem. Soc., Harvard Univ., July 1987; "Molecular Chemistry for Solid State Electronics", Symposium of the Royal Society of Chemistry, London, March 1989.

[3] J. Janda, A. Bezegh, *Anal. Chem. 60* (1988) 62 R ("Chemical Sensors"); G. Rechnitz, *Chem. Eng. News 66* (1988) No. 36, p. 24 ("Biosensors"); M. Wrighton, *Science (Washington) 231* (1986) 32.

[4] Symposium on "Polymeric Materials for Electronic Packaging and Interconnection", *Proc. ACS Div. Polym. Mater. Sci. Eng.58* (1988) No. 2; M. J. Bowden, S. R. Turner (Eds.): *Polymers for Electronic and Photonic Applications (ACS Symp. Ser. 346* (1987)); C. G. Willson (Ed.): *Advances in Resist Technology, Proc. SPIE 469* (1984), Santa Clara, CA, USA 1984.

[5] M. J. Ludowise, *J. Appl. Phys. 58* (1985) R31; S. T. Picraux, L. E. Pope, *Science (Washington) 226* (1984) 615; P. D. Dapkus, *Annu. Rev. Mater. Sci. 12* (1982) 243; R. M. Osgood, Jr., *Annu. Rev. Phys. Chem. 34* (1981) 77.

[6] L. J. Fried et al., *IBM J. Res. Dev. 26* (1982) 362.

[7] G. L. Legrow, T. F. Lim, J. Lipowitz, R. S. Reach, *J. Chim. Phys. 83* (1987) 869; J. Lipowitz, H. A. Freeman, R. T. Chen, E. R. Prack, *Adv. Ceram. Mater. 2* (1987) 121; K. Okamura, *Composites 18* (1987) 107; K. J. Wynne, R. W. Rice, *Annu. Rev. Mater. Sci. 14* (1984) 297.

[8] J. Economy in M. Good (Ed.): *Biotechnology and Materials Science. Chemistry for the Future*, American Chemical Society, Washington D.C., USA 1988, pp. 117-128 ("High Strength Composites"); T.-W. Chou, R. L. McCullough, R. B. Pipes, *Sci. Am. 255* (1986) 192.

[9] J. D. Mackenzie, D. Ulrich (Eds.): *Ultrastructure Processing of Advanced Ceramics*, Wiley, New York 1988 (1010 pages).

Microgels—Polymers with a Special Molecular Architecture

Polymer Networks
Cross-linking
High-impact Polymers

By Markus Antonietti*

1. Introduction

The development of new polymeric systems and the improvement of their physical properties for technological applications can be brought about by two main directions of research. On the one hand, polymer properties can be adjusted by developing new monomer units: the resulting changes in local molecular properties such as rotation barriers, polarity or anisotropy are reflected in bulk polymer properties such as stiffness or flexibility, solubility, or properties associated with crystallinity. However, for obvious reasons, the scope for inventing useful "new" monomers is limited. Consequently this strategy increasingly leads to "low quantity" polymers with very special properties.

On the other hand, the properties of polymeric materials are also determined by the geometrical parameters of their macromolecules. For instance, short and long chain linear polymers have completely different properties; branched and cross-linked systems again show different behavior. Here the microscopic topology of the polymer chains and the resulting geometrical interactions, such as entanglements or even knots, are reflected in the product properties. An understanding of the relationships between these microscopic parameters and macroscopic properties helps to improve existing materials by controlling the topological structure without necessarily changing the chemical composition of the macromolecular system. These types of approaches have just started to yield quantitative relationships in polymer science. Thus, the possibilities for obtaining "new" materials (or better still, old materials with new properties) are most promising. Often small changes in reaction conditions result in different topologies and create or improve the desired property.

[*] Dr. M. Antonietti
Institut für Physikalische Chemie der Universität
Welder Weg 15, D-6500 Mainz (FRG)

This article is concerned with the second approach to improving the properties of polymeric materials; a group of polymers with a very special topology will be discussed: synthetic microgels ("μ-gels") or μ-networks. We will also focus on some of their unconventional properties and potential applications. Defining the term "μ-gel" is not a straightforward matter. It can be illustrated by means of Figure 1.

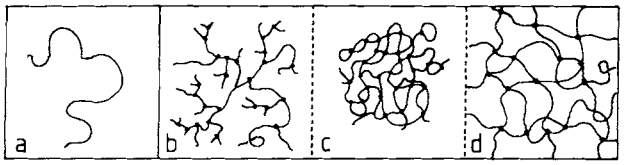

Fig. 1. Sketch showing polymer systems with different topologies: a) linear and b) branched macromolecules, c) μ-gel and d) macroscopic network.

Most commercial polymers, such as polystyrene, polyethylene or polycarbonate, have linear or slightly branched chains. Highly branched structures appear more often in the field of biopolymers, e.g. amylopectins. Networks are the oldest known "synthetic" materials: we are familiar with the properties of vulcanized "natural" rubber in daily life. μ-Gels represent structures that are intermediate between branched and macroscopically cross-linked systems. Their overall dimensions are still comparable with those of high molecular weight linear polymers. However, the internal structure of μ-gels resembles a typical network. Of course, the transition to the neighboring structures is continuous, and the definition is to some extent arbitrary. In the field of synthetic materials, μ-networks have not been extensively studied, but they are well known in biochemistry: most enzymes are linear chains cross-linked to each other by S_2 bridges or by secondary valences. Here again, special properties result from a combination of a particular geometrical arrangement with chemical functionality.

μ-Gels interestingly combine characteristics of both: being molecular structures they dissolve (networks only swell) but their conformation is nearly fixed. They can be processed like linear polymers but the final product still shows characteristic network behavior. Their solubility allows one to use the classical methods of polymer analysis in solution, enabling typical network characteristics to be identified. Therefore the objectives in studying μ-networks are twofold. First, one can study networks by modeling them with μ-gels, taking advantage of the convenience of solution characterization to examine network properties. Second, one hopes to develop a completely new group of materials with special properties. Both aspects will be illustrated in the following sections.

2. Synthesis of μ-Networks

Compared to the natural synthesis of enzymes, the possibilities available to a polymer chemist are limited. Only two routes to μ-networks are known:

1) Type A μ-gels: The addition of cross-linking agents to polymers or of multifunctional monomers to a polymerizing system usually leads to networks. According to the Ziegler dilution law, diluting the systems increases the probability of intramolecular cross-linking. This can be forced up to a threshold where no more macroscopic gelation occurs and only μ-gels are formed.[1-3]

This transition has the character of a phase transition where the critical concentration c_{crit} is given by the Flory argument:[4] internal cyclization reduces the average number of bonds to other chains below the critical value of two. Slightly below the critical concentration, structures with molecular masses $> 10^8$ g mol^{-1} are easily obtained.[1] At concentrations low compared to c_{crit} the μ-gels become smaller, until at very low concentrations only the elementary structures[3] or the "self cross-linked" molecule are formed[2,5] (molecular mass does not change upon cross-linking).

2) Type B μ-gels: μ-Gels are also obtained when the cross-linking reaction is carried out in a restricted volume, for instance in the small micelles of an emulsion,[6] or in μ-emulsion polymerization[7] of lipophilic monomers in water. Although such reaction conditions would result in macroscopic networks, the absolute molecular mass of the μ-networks is determined by the maximum micelle size, which can easily be controlled to be between 10 nm and 500 nm. This corresponds to molecular masses between 10^6 and 10^{11} g mol^{-1}.

3. Static and Dynamic Properties of μ-Gels

Type A and B μ-gels exhibit completely different properties. Cross-linking in dilution produces a lot of small loops, and, under suitable experimental conditions, a controllable proportion of dangling ends.[1,3] At the critical concentration of cross-links, type A μ-networks show an internal structure which is "self-similar". Geometrically this can be described as a "fractal", a geometrical body with a broken dimensionality. It has been proved by small angle neutron scattering measurements that this theoretical treatment fits the experimental data; a spatial dimension of $d_f = 2.5$ in the unperturbed state is obtained.[3] One can visualize a structure where the local fine structure repeats itself on a larger linear scale within the μ-network. Because type A μ-gels are still embedded in the "usual" three-dimensional space, they have a rather dense center and open up continuously towards the outer regions.

In contrast μ-networks of type B exhibit an internal structure comparable to that of macroscopic networks, except that close to the surface of the particles a higher concentration of loops is formed to ensure the molecular character. The characterization of these particles with static and dynamic light scattering reveals that the μ-gels in solution behave like nearly homogeneous swollen spheres, if the amount of cross-linking is moderate or high.[7] Where

ADVANCED MATERIALS

the amount of cross-linking is small, a transition to branched structures is observed, as mentioned above.[8] For these reasons, μ-networks of type B can be used to model the behavior of macroscopic networks. Possible perturbations due to surface contributions can be estimated by changing the absolute size of the μ-networks and thus the surface to volume ratio.

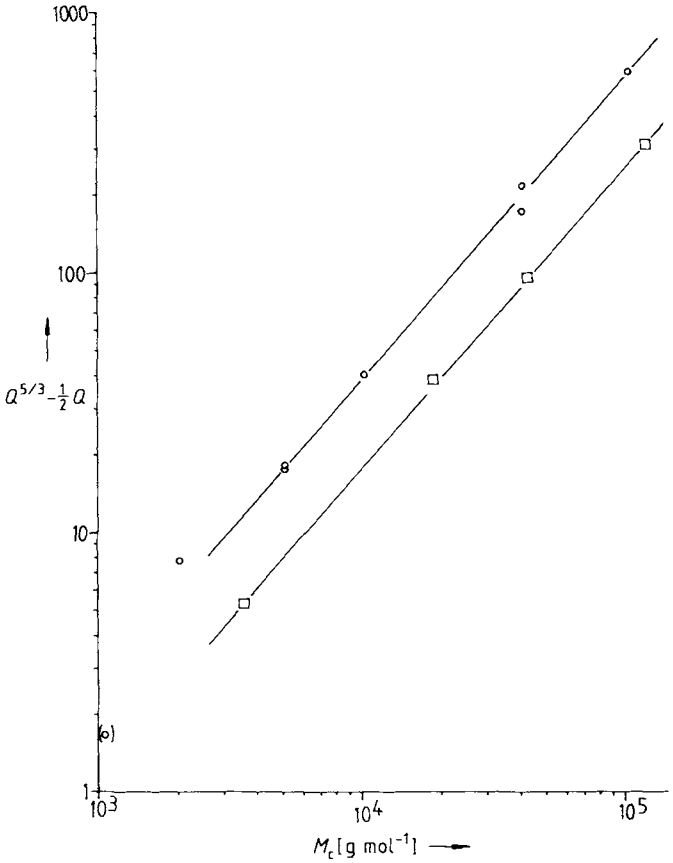

Fig. 2. Flory plot of the swelling ratio Q as a function of the chain length between two cross-links M_c; circles: styrene/*m*-diisopropenylbenzene μ-gels in toluene [7]; squares: styrene/divinylbenzene μ-gels in DMF [6].

The study of networks by substituting experiments on μ-gels is illustrated by the determination of the swelling ratio Q. Here, simple viscosity measurements replace the ambiguous swelling measurements on networks. The intrinsic viscosity $[\eta]$, a typical solution property of polymers, measures the relative increase of the viscosity of a solution per gram added polymer extrapolated to infinitesimally small polymer concentrations. According to *Einstein*, for spherical particles $[\eta]$ yields directly the average density of the swollen polymer within the sphere.[9] Since the degree of swelling of a network depends on the number of cross-links, *Flory* has derived an exact relationship between these two properties using the equations of entropy elasticity.[4] Figure 2 shows data obtained for two different network systems consisting of μ-gels.

The straight lines indicate the theoretical behavior of macroscopic networks for two different types of solvents. These measurements clearly show that type B μ-networks model the situation for all cross-linked systems. Measurements of the swelling ratio as a function of the density of cross-links, determined by intrinsic viscosity measurements, were also performed for the smallest possible μ-gels, the self-cross-linked molecules.[2] Although the treatment of the data is more complicated, the results are qualitatively in good agreement.

The situation in the case of type A μ-gels is more complicated: due to their fractal structure the swelling ratio depends only slightly on the density of cross-links, but is a function of the absolute molecular mass.[3] Although the fractal nature of type A μ-gels is more a matter for academic discussion, there are interesting implications for "real" systems. From these studies it seems likely that one can deduce certain topological knotting rules, which will lead to the understanding of internal cyclization, a typical network defect. Moreover, μ-gels offer a new way of easily determining the topological structures that result from different polymerization techniques, with regard to the degree of internal cyclization.

For characterizing the dynamic behavior of μ-gels, dynamic mechanical experiments provide the most detailed information. Here, information about both the internal, intramolecular modes of mobility and the dynamic quantities relating to the complete molecule can be obtained. In dynamic shear experiments the real and complex parts of the elastic constants (G' and G'') of the polymer are measured as a function of shear stress and frequency ω. G' describes the energy which is stored during the deformation (comparable to a spring constant) whereas G'' accounts for the viscous contribution and the energy which has been lost. From these two quantities, the complex viscosity η^* which describes the flow resistance at a certain frequency can be easily calculated.

Since we observe the response of small chain segments at high frequencies and of larger structures on a longer time scale, the data can also be interpreted as a measure of the molecular visco-elasticity as a function of a correlation

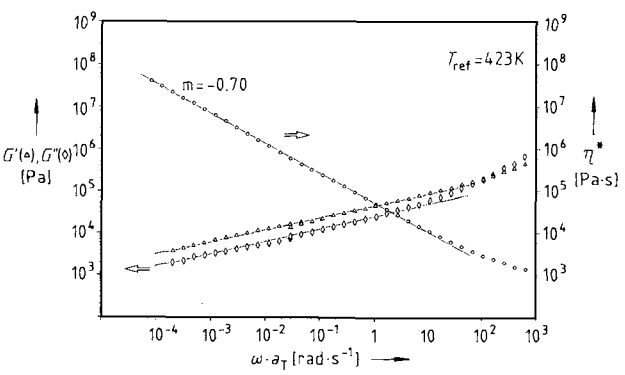

Fig. 3. Dynamic-mechanical spectrum of a type A μ-gel (material: polystyrene).

length. This length is of the same order as typical molecular substructures. For these reasons, the dynamic responses of different parts of the same polymer molecule become separated in the frequency domain.

Figure 3 shows the dynamic mechanical spectrum of a "fractal" type A μ-gel above the glass transition at a reference temperature of 150°C. In this double logarithmic plot, the elasticity varies over three orders of magnitude, while the frequency covers six decades. The resulting plots are strictly linear, with a spring constant which depends on the time scale of the mechanical perturbation.[10] Independently of frequency, a certain amount of energy is always lost (G' parallels G'').

The opposite is observed for type B μ-networks, as seen in Figure 4. Here, G' is nearly independent of frequency, as theoretically expected for an ideal macroscopic network. This is due to the fact that in the ideal case the cross-link density is uniform throughout. The plateau value in this specific sample exceeds that of linear polystyrene by a factor of two, and the mechanical loss at low frequencies is extraordinarily low for polymers. Here 98% of the stored energy can be recovered.[11]

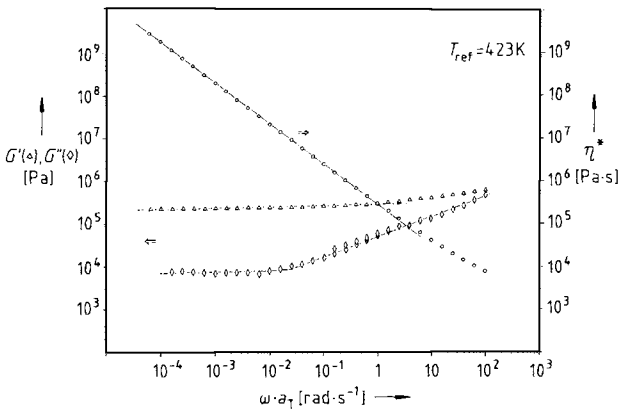

Fig. 4. Dynamic-mechanical spectrum of a type B μ-gel (material: polystyrene).

A potential application for these systems is their use as fillers for optically transparent "high impact" polymers. Here, μ-gels embedded in a matrix of linear polymer chains stabilize the whole structure by distributing the mechanical tension. Similar structuring techniques are already known, although the chemical pathway to them does not involve μ-gels.

In addition to that, one can construct composites consisting of two topologies of the same polymer. This represents a simple method of improving already existing products. Comparing Figures 3 and 4 one clearly recognizes the importance of topology in determining polymer properties: although both systems consists of the same chemical components (even molecular mass and chemical cross-linking density could be the same), a completely different macroscopic behavior can result for different topologies. Therefore, topologically structured μ-gels and networks will play a role of increasing importance since in that way the properties of any polymeric material can be varied over a wide range to fulfil the technological demands for special applications.

4. Complex Structured μ-Gels

Up to this point we have dealt with homogeneous μ-networks made of one kind of monomer and cross-linking agent. More complex molecules with μ-gel structure can easily be synthesized, and these cover a much wider range of properties and applications.

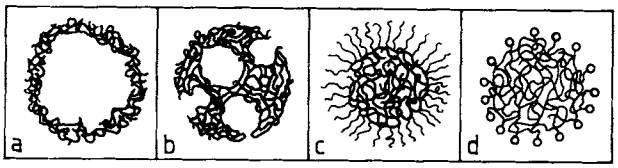

Fig. 5. Sketch showing various more complex μ-networks: a) hollow sphere μ-gel, b) macroporous μ-network, c) core-shell μ-gel, d) functionalized μ-gel where the circles indicate the centers of functionality.

Varying only structural parameters but preserving the molecular chemistry, it is possible to construct special porosities within the μ-networks (Fig. 5). The simplest case is given by the geometry of a hollow sphere, where the surface consists of cross-linked material of a controllable thickness (see Fig. 5a). Although this structure is reminiscent of vesicles prepared from special amphiphilic monomers,[13] fundamental differences exist. The hollow sphere μ-gels can be synthesized from most monomers on a larger scale, but the surface structure and the porosity are certainly far less defined. However, from a technical point of view, hollow sphere μ-gels can be used for some chemical applications which have been extensively discussed in the case of synthetic vesicles.

The second type to be discussed are macroreticular μ-networks. In simple terms, these are μ-gels with pores of different sizes. The polymerization of type B μ-gels in the presence of an ambident non-solvent leads directly to porous structures,[7] in analogy to the already known case of macroreticular networks.[14] The distinctive geometry, which is stabilized by the cross-links, results from the spinodal decomposition of the polymer and the non-solvent during the polymerization process. Materials with a continuum of pore sizes and macroscopic stability are the basis of all size exclusion chromatography techniques.[14] A study of these μ-gels by the techniques developed for simpler systems could help to provide a relationship between reaction conditions during network synthesis and the chromatographic separation properties. Such a relationship would help in designing column packings, which have hitherto been chosen more or less empirically. In this case, the step from research to a final product is small: by increasing the size of the network particles from the

nm-region to approximatey 10 μm, they can immediately be used as column packings.

In addition to these two geometrical strategies for the construction of complex μ-networks, many other possibilities exist based on varying the chemical composition of μ-gels. Just two of the most important should be mentioned. *Burchard* et al. have examined μ-gels made of two incompatible polymers, where a cross-linked core of one polymer is surrounded by a shell of grafted linear chains of the other type.[15] Light scattering techniques can be used to determine the structures of these systems, which model inner surfaces in polymer blends. Another course is being followed by *Obrecht, Seitz* and *Funke,* who have examined[15] different possibilities for synthesizing "reactive" or functionalized μ-gels. For instance, some properties of μ-networks containing vinyl, sulfate or hydroxy groups have been described.

Although the strategies applied for μ-network synthesis are still relatively crude (compared to nature), some possible goals of all these efforts are worth mentioning. The combination of a fixed, soluble structure of nanometer dimensions with a specific functionality is one possible starting point for the construction of tailor-made polymeric catalysts, mediators or phase transfer reagents. The term "artificial enzyme" in the context of this kind of research is certainly presumptuous, but functionalized μ-gels are already used as catalysts in non-aqueous media and as stabilizers in complex coatings, and that is just the beginning. Nature's concepts will increasingly be applied to synthetic materials. The development and examination of structured polymers is just one field where the patterns of nature are imitated; μ-gels are one component within this strategy.

Received: September 5, 1988

[1] W. Burchard, M. Schmidt, *Macromolecules 14* (1981) 370.
[2] W. Arbogast, A. Horvath, B. Vollmert, *Makromol. Chem. 181* (1980) 1513.
[3] M. Antonietti, D. Ehlich, K. J. Fölsch, H. Sillescu, M. Schmidt, P. Lindner, *Macromolecules*, in press.
[4] P. J. Flory: *Principles of Polymer Chemistry*, Cornell University Press, Ithaca, NY 1953.
[5] M. Antonietti, M. Schmidt, H. Schuch, H. Sillescu, *Macromolecules 21* (1988) 736.
[6] M. Hoffmann, *Makromol. Chem. 175* (1974) 613.
[7] M. Antonietti, W. Bremser, M. Schmidt, unpublished results; W. Bremser, *Diplomarbeit*, University of Mainz 1988.
[8] M. Schmidt, D. Nerger, W. Burchard, *Polymer 20* (1979) 582.
[9] $[\eta]=2.5/\rho$ where ρ is the polymer density inside the spherical particle.
[10] M. Antonietti, K. J. Fölsch, H. Sillescu, T. Pakula, *Macromolecules*, in press.
[11] M. Antonietti, K. J. Fölsch, unpublished results; K. J. Fölsch, *Dissertation*, University of Mainz 1988.
[12] G. E. Molau, *J. Polym. Sci. A 3* (1975) 1267.
[13] H. Ringsdorf, B. Schlarb, J. Venzmer, *Angew. Chem. 100* (1988) 118; *Angew. Chem. Int. Ed. Engl. 27* (1988) 117.
[14] J. Seidl, J. Malinsky, K. Dusek, W. Heitz, *Adv. Polym. Sci. 5* (1964) 113.
[15] D. Kunz, W. Burchard, *Coll. Polym. Sci. 264* (1986) 498.
[16] W. Obrecht, U. Seitz, W. Funke, *Makromol. Chem. 179* (1978) 2145 and references cited therein.

New Organic Superconductors

BEDT-TTF Salts
2D (Super)Conductors
Charge-Transfer Complexes

By Hiroo Inokuchi*

1. Introduction

The first report of the discovery of an organic superconductor, $(TMTSF)_2PF_6$, a tetramethyltetraselenafulvalenium cation radical salt, appeared in 1980.[1] Since then, thirty different types of charge transfer complexes have been reported as organic superconductors, as summarized in Table 1.

Of the seven kinds of $(TMTSF)_2X$ superconductors, the so called Bechgaard salts, only the $ClO_4^{\ominus}$ salt becomes superconducting at ambient pressure. Though TMTSF contains selenium atoms, after the discovery of superconductivity in $(BEDT\text{-}TTF)_2ReO_4$, the first sulfur-based organic superconductor, a large part of the research into organic superconductors was devoted to the BEDT-TTF salts. The most important BEDT-TTF superconductor was β-$(BEDT\text{-}TTF)_2I_3$.[23] It was the first ambient-pressure BEDT-TTF superconductor, in addition its T_c could be increased greatly to 8 K by the application of moderate pressure; this value was the highest T_c of organic superconductors before the discovery of $(BEDT\text{-}TTF)_2Cu(NCS)_2$. Following β-$(BEDT\text{-}TTF)_2I_3$, several other BEDT-TTF iodine salts with different crystal structures, designated by the Greek letters β, γ, θ, and κ, were found to be ambient-pressure superconductors. The β-$(BEDT\text{-}TTF)_2I_3$ salt also stimulated research into salts with other linear anions, from which it has been found that $IBr_2^{\ominus}$ and $AuI_2^{\ominus}$ salts[26,27] can become superconducting.

One should also mention the unique $[M(dmit)_2]$ series; these salts are the only acceptor-based organic supercon-

[*] Prof. Dr. H. Inokuchi
Institute for Molecular Science
Myodaiji, Okazaki 444 (Japan)

ductors known so far. The asymmetric donor DMET, which is a hybrid of TMTSF and BEDT-TTF, has been found to generate superconductors. A superconductor based on another asymmetric donor, MDT-TTF, has also been discovered (Table 1).

Table 1. Organic Superconductors.

Compounds	T_c	Ref.
$(TMTSF)_2PF_6$	1.4 K (6.5 kbar)	[1, 16]
$(TMTSF)_2AsF_6$	1.4 K (9.5 kbar)	[17]
$(TMTSF)_2SbF_6$	0.38 K (10.5 kbar)	[18]
$(TMTSF)_2TaF_6$	1.35 K (11 kbar)	[18]
$(TMTSF)_2ClO_4$	1.4 K	[19]
$(TMTSF)_2ReO_4$	1.2 K (9.5 kbar)	[20]
$(TMTSF)_2FSO_3$	2.1 K (6.5 kbar)	[21]
$(BEDT\text{-}TTF)_2ReO_4$	2 K (4 kbar)	[22]
β-$(BEDT\text{-}TTF)_2I_3$	1.5 K	[23]
	8 K (1.3 kbar)	[24, 25]
β-$(BEDT\text{-}TTF)_2IBr_2$	2.5 K	[26]
β-$(BEDT\text{-}TTF)_2AuI_2$	3.8–5 K	[27]
γ-$(BEDT\text{-}TTF)_2(I_3)_{2.5}$	2.5 K	[28]
θ-$(BEDT\text{-}TTF)_2I_3$	3.6 K	[29]
κ-$(BEDT\text{-}TTF)_2I_3$	3.6 K	[30]
$(BEDT\text{-}TTF)_4Hg_3Cl_8$	1.8 K (12 kbar)	[31]
$(BEDT\text{-}TTF)_4Hg_3Br_8$	4.3 K	[32]
$(BEDT\text{-}TTF)_3Cl_2(H_2O)_2$	2 K (16 kbar)	[3]
$(BEDT\text{-}TTF)_2Cu(NCS)_2$	10.4 K	[2]
$TTF[Ni(dmit)_2]_2$ [a]	1.6 K (7 kbar)	[33]
α-$TTF[Pd(dmit)_2]_2$ [a]	6 K (19 kbar)	[34]
$[(CH_3)_4][Ni(dmit)_2]_2$ [b]	5 K (7 kbar)	[35]
$(DMET)_2Au(CN)_2$ [b]	0.8 K (5 kbar)	[36]
$(DMET)_2AuCl_2$ [b]	0.83 K	[37]
$(DMET)_2AuI_2$ [b]	0.55 K (5 kbar)	[37]
$(DMET)_2I_3$ [b]	0.47 K	[38]
$(DMET)_2IBr_2$ [b]	0.59 K	[38]
$(DMET)_2AuBr_2$ [b]	1 K (1.5 kbar)	[39]
$(MDT\text{-}TTF)_2AuI_2$ [c]	3.5 K	[40]

[a] $Ni(dmit)_2$ =

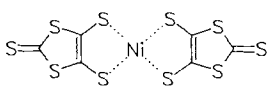

[b] DMET =

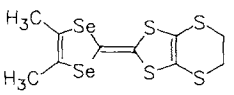

[c] MDT–TTF:

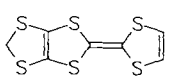

Recently, *Urayama* et al. of the Institute for Solid State Physics, University of Tokyo, discovered an ambient pressure superconductor, $(BEDT\text{-}TTF)_2Cu(NCS)_2$, BEDT-TTF = bis(ethylenedithio)tetrathiafulvalene, with a transition temperature T_c above 10 K.[2] *Mori* and the present author, of the Institute for Molecular Science, Okazaki, have reported a novel organic superconductor, $(BEDT\text{-}TTF)_3Cl_2\cdot 2H_2O$, with an unusual molecular structure,[3] with $T_c = 2$ K at a pressure of 16 kbar.

In this article we shall review these two organic superconductors with their historical background.

2. Historical Background

Between 1925 and 1940, two groups worked on "perylene addition compounds". *Clar* et al. reported on perylene polyhalides under the title of "unpaired halides" or "anomalous halides". Their first paper[4] described the formation of dark brownish black needles by the addition of bromine to a saturated benzene solution of perylene; the needles were found to have the composition of perylene tribromide, $C_{20}H_{12}Br_3$.

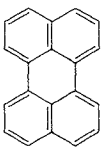

perylene, $C_{20}H_{20}$

Zinke et al. published a large series of papers entitled "Studies on Perylene and its Derivatives". They reported that pulverized perylene absorbed bromine quickly and produced a greenish-black product. This product, with assigned formula $C_{20}H_{12}Br_4$, was not stable and liberated hydrogen bromide.[5]

These results were very interesting in the light of considering perylene as a fragment of graphite, and the reported electrical conductivity of graphite-lamellar compounds, now known to be graphite-intercalation compounds.[6]

In 1954 we prepared a perylene-bromine complex by *Zinke*'s method and measured its magnetic susceptibility and electrical resistivity.[7] The pressed pellets of the complex were found to have a resistivity of 8 Ωcm. The magnetic susceptibility, -61×10^{-6}, was smaller than that estimated by the additivity rule, -286×10^{-6}. This was the first report of the electrical conductivity of charge transfer complexes.

Since this discovery an enormous amount of research has been carried out to obtain novel conducting organic compounds—the so-called "conductive charge transfer complexes"—and the research field of organic semiconductors/conductors has been developed.

3. Two-dimensional conductors: BEDT-TTF complexes

The charge transfer complexes, $(TMTSF)_2X$ (X = PF_6 or AsF_6) have a metal-to-semiconductor transition at 19 and 15 K respectively at ambient pressure, while under moderate pressure these salts remain metallic, with the onset of superconductivity at 0.9 and 1.3 K, respectively. From this consideration it seemed desirable to synthesize organic metals, in which the metal-to-semiconductor transition is suppressed, so as to make new type organic superconductors and to lead to a better understanding of the requirements for them.

ADVANCED MATERIALS

The alkylthio substituted tetrathiafulvalene (TTF), BEDT-TTF **1**, a π donor, was therefore made in the hope that the chemical modification by extending the TTF moiety, with an increased polarizability, would increase the conduction band width and reduce the on-site Coulomb repulsion, resulting in a considerable enhancement of the metallic character.[8]

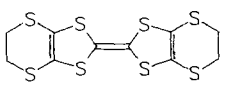

BEDT-TTF, 1

This character was confirmed by resistivity measurements on $(BEDT\text{-}TTF)_2ClO_4 \cdot Cl_2HCCH_2Cl$ in comparison with $(TMTTF)_2ClO_4$ (TMTTF = tetramethyl-TTF), as shown in Figure 1. As listed in Table 1, two-thirds of organic superconductors are BEDT-TTF derivatives; at present, BEDT-TTF is the most appropriate π-donor to produce organic superconductors.

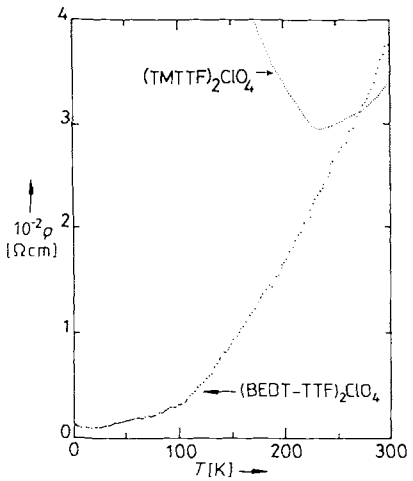

Fig. 1. Electrical resistivity ρ vs. temperature T along the elongated axis of a $(BEDT\text{-}TTF)_2ClO_4 \cdot 0.5$ 1,1,2-trichloroethane single crystal compared with that of $(TMTTF)_2ClO_4$.

4. $(BEDT\text{-}TTF)_2Cu(NCS)_2$[*]

$(BEDT\text{-}TTF)_2Cu(NCS)_2$ is the first organic superconductor with a T_c higher than 10 K under ambient pressure.[2] The preparation and crystal growth of this charge-transfer complex was carried out as follows: 30 mg of highly purified BEDT-TTF and 250 mg of purified K(18-crown-6 ether)$Cu(NCS)_2$ were placed in the anode side of an H-type reaction cell (total volume about 20 mL), and 50 mg of K(18-crown-6 ether)$Cu(NCS)_2$ were placed in the cathode side. The cell was evacuated and then filled with nitrogen. 100 mL of dried 1,1,2-trichloroethane was added, and it was stirred 15 h under inert gas. The electrolysis, using platinum wires (1–2 mm diameter), was carried out at a constant current (1 to 5 μA). Crystal growth (typical dimensions $3 \times 2 \times 0.05$ mm^3) proceeded for 5 to 14 days and the harvested crystals were washed with 1,1,2-trichloroethane, methanol and tetrahydrofuran and dried under vacuum. The crystals were stable against air and moisture.

The crystal structure of $(BEDT\text{-}TTF)_2Cu(NCS)_2$ is analogous to that of κ-$(BEDT\text{-}TTF)_2I_3$. However, the superconducting transition temperature T_c was different. In the crystal two BEDT-TTF molecules form a dimerized pair and the pairs are linked to each other by short S···S contacts almost perpendicularly, forming two-dimensional conducting sheets in the *bc*-plane. Each conducting layer is sandwiched by the insulating layers of anions along the *a*-axis.

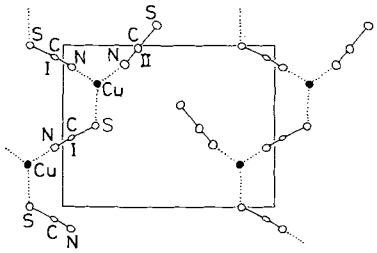

Fig. 2. Packing of $Cu(NCS)_2^{\ominus}$ anions in $(BEDT\text{-}TTF)_2Cu(NCS)_2$.

The anion $Cu(NCS)_2$ is neither symmetric nor linear, but asymmetrically bent like a boomerang. Two crystallographically independent NCS groups (I and II in Fig. 2) are almost linear. The boomerang units are arranged one after the other along the *b*-axis to form a zig-zag one-dimensional flat polymer. Three NCS groups (I, I, II) coordinate to a copper cation ($Cu^{\oplus}$) with two nitrogen atoms and one sulfur atom. Thus the polymer is represented as

$$(SCN(I)\text{–}Cu\text{–})_n$$
$$\quad\quad\quad

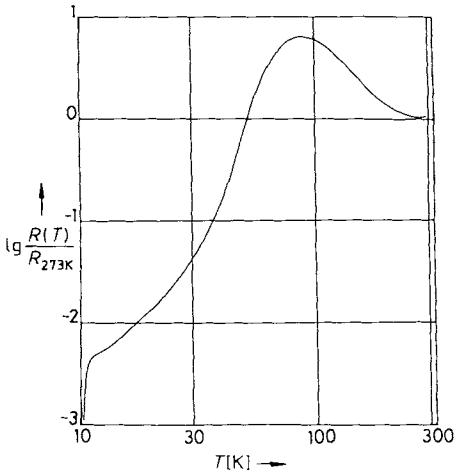

Fig. 3. Temperature dependence of electrical resistivity of (BEDT-TTF)$_2$Cu(NCS)$_2$.

ing transition at 10.4 K. The physicochemical properties, electronic structure,[9] XPS and ESR spectra,[10] thermoelectric power,[10] magnetic resistance,[9] magnetic susceptibility,[12] a.c. magnetic susceptibility, polarized reflectance spectra, anomalous NMR relaxation, tunneling spectroscopy,[13] and other properties, have already been measured. From the tunneling spectroscopy data the observed gap of 4 meV leads to a value of 4.5 for $2\Delta/kT_c$, (where $2\Delta = 4$ meV and $T_c = 10.4$ K), which is of the same order as the BCS ratio of 3.52.

5. (BEDT-TTF)$_3$Cl$_2$·2H$_2$O[*]

The chlorine salt, (BEDT-TTF)$_3$Cl$_2$·2H$_2$O, shows superconduction at 2 K under a pressure of 16 kbar.[3] An enormous number of charge-transfer complexes with halogens as acceptors have been prepared. However, no report of complex formation with chlorine has appeared so far as we know. In the case of graphite intercalation compounds, only the larger size halogens, Br_2, I_2, ICl and IBr can form intercalation compounds, and the fluorine molecule reacts directly with graphite to form insulating compounds involving F-substituted sp^3 carbon atoms.

In the structural chemistry of the BEDT-TTF salts, the discontinuity between iodine and bromine is related to the ability of iodine to form trimer anions such as $I_3^{\ominus}$. The halogen atoms Br and Cl are themselves too small to form charge-transfer complexes with BEDT-TTF, but the clusters solvated by H_2O are included in the BEDT-TTF salts. The 3:2 BEDT-TTF salts occur when the counter-anions are relatively small, e.g. as with $ClO_4^{\ominus}$ and $ReO_4^{\ominus}$. Because the Br and Cl salts have not only the same composition but also a similar donor arrangement to the salts of these tetrahedral anions, these complex anion clusters, $Br_2(H_2O)_2$ and $Cl_4(H_2O)_4$, can be regarded as rather small anions.

[*] With *T. Mori*.

The preparation of this intriguing complex, (BEDT-TTF)$_3$Cl$_2$(H$_2$O)$_2$, was also unusual: the complex was obtained by electrolysis using $[(C_2H_5)_4N]_2CoCl_4$ as electrolyte,[14] and by chlorine abstraction from the solvent CH_2Cl_2.[15] Recently the same complex was obtained by electrolysis in the presence of $[(n\text{-}C_4H_9)_4N]Cl$.

The structure of the anion, $Cl_4(H_2O)_4$, in the salt is illustrated in Figure 4. Two Cl atoms are connected to two O atoms through hydrogen bonds to form a rectangle. This unit has a close resemblance to the $Br_2(H_2O)_2$ unit in (BEDT-TTF)$_3$Br$_2$(H$_2$O)$_2$. However, in the chlorine salts additional Cl and O atoms are attached to this unit by hydrogen bonding.

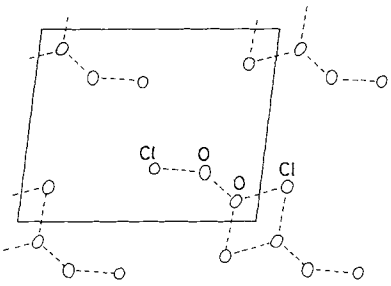

Fig. 4. Packing of $[Cl_4(H_2O)_4]^{\ominus}$ anions.

The bromine salt, (BEDT-TTF)$_3$Br$_2$(H$_2$O)$_2$, exhibits metallic conduction at room temperature, and then undergoes a metal-to-insulator transition at 185 K. On the other hand, the chlorine salt, (BEDT-TTF)$_3$Cl$_2$·2H$_2$O, has a high conductivity as a (BEDT-TTF) complex, 500 S cm^{-1} at room temperature, and is metallic down to 100 K. Although this salt undergoes a metal-to-insulator transition arund 100 K, superconductivity has been found at 2 K under a pressure of 16 kbar as mentioned above.

As can be seen from Table 1, all other organic superconductors except this chlorine salt have the 2:1 composition, irrespective of whether the conducting components are donors or acceptors, and their energy bands are quarter-filled. If the band structure is calculated by the extended Hückel approximation, the BEDT-TTF superconductors usually give comparatively simple two-dimensional metal bands. This chlorine superconductor, on the contrary, gives a semimetallic energy band.[14] This result demonstrates that neither the 2:1 composition nor a simple two-dimensional metal band is a necessary condition for organic superconductivity.

Schweitzer et al. have reviewed their excellent contributions to the field of BEDT-TTF molecular metals and superconductors.[41]

Received: October 17, 1988

[1] D. Jerome, A. Mazaud, M. Ribault, K. Bechgaard, *J. Phys. 41* (1980) L95.

[2] H. Urayama, H. Yamochi, G. Saito, K. Nozawa, T. Sugano, M. Kinoshita, S. Sato, K. Oshima, A. Kawamoto, J. Tanaka, *Chem. Lett. 1988*, 55. H. Urayama, H. Yamochi, G. Saito, S. Sato, A. Kawamoto, J. Tanaka, T. Mori, Y. Maruyama, H. Inokuchi, *ibid. 1988*, 463.

[3] T. Mori, H. Inokuchi, *Solid State Commun. 64* (1987) 335.
[4] K. Brass, E. Clar, *Ber. Dtsch. Chem. Ges. 65* (1932) 1660.
[5] A. Zinke, F. Linner, O. Wolfbauer, *Ber. Dtsch. Chem. Ges. 58* (1925) 323.
[6] F. R. M. McDonnell, R. C. Pink, A. R. Ubbelohde, *J. Chem. Soc. 1951*, 191.
[7] H. Akamatu, H. Inokuchi, Y. Matsunaga, *Nature (London) 173* (1954) 168; *Bull. Chem. Soc. Jpn. 29* (1956) 213.
[8] G. Saito, T. Enoki, K. Toriumi, H. Inokuchi,, *Solid State Commun. 42* (1982) 557.
[9] K. Oshima, T. Mori, H. Inokuchi, H. Urayama, H. Yamochi, G. Saito, *Phys. Rev. B38* (1988) 938.
[10] H. Urayama, H. Yamochi, G. Saito, T. Sugano, M. Kinoshita, T. Inabe, T. Mori, Y. Maruyama, H. Inokuchi, *Chem. Lett. 1988*, 1057.
[11] K. Nozawa, T. Sugano, H. Urayama, H. Yamochi, G. Saito, M. Kinoshita, *Chem. Lett. 1988*, 617.
[12] T. Sugano, K. Terui, S. Mino, K. Nozawa, H. Urayama, H. Yamochi, G. Saito, *Chem. Lett. 1988*, 1171.
[13] Y. Maruyama, T. Inabe, H. Urayama, H. Yamochi, G. Saito, *Solid State Commun. 67* (1988) 35.
[14] T. Mori, H. Inokuchi, *Chem. Lett. 1987*, 1657.
[15] M. J. Rosseinsky, M. Kurmoo, D. R. Talham, P. Day, D. Chasseau, D. Watkin, *J. Chem. Soc. Chem. Commun. 1988*, 270.
[16] K. Andres, F. Wudl, D. B. McWhan, G. A. Thomas, D. Nalewajek, A. L. Stevens, *Phys. Rev. Lett. 45* (1980) 1449.
[17] R. Brusetti, M. Ribault, D. Jerome, K. Bechgaard, *J. Phys. 13* (1982) 801.
[18] S. S. P. Parkin, M. Ribault, D. Jerome, K. Bechgaard, *J. Phys. C14* (1981) L445.
[19] K. Bechgaard, K. Carneiro, M. Olsen, F. B. Rasmussen, C. S. Jacobsen, *Phys. Rev. Lett. 46* (1981) 852.
[20] S. S. P. Parkin, D. Jerome, K. Bechgaard, *Mol. Cryst. Liq. Cryst. 79* (1982) 213.
[21] R. C. Lacoe, S. A. Wolf, P. M. Chaikin, F. Wudl, E. Ahron-Shalon, *Phys. Rev. B27* (1983) 1947.
[22] S. S. P. Parkin, E. M. Engler, R. R. Schumaker, R. Latier, V. Y. Lee, J. C. Scott, R. L. Greene, *Phys. Rev. Lett. 50* (1983) 270.
[23] E. B. Yagubskii, I. F. Shchegolev, V. N. Laukin, P. A. Kononovich, M. V. Kartsovnic, A. V. Zvarykina, L. I. Buravov, *Pis'ma Zh. Eksp. Teor. Fiz. 39* (1984) 12; *JETP Lett. 39* (1984) 12.
[24] K. Murata, M. Tokumoto, H. Anzai, H. Bando, G. Saito, K. Kajimura, T. Ishiguro, *J. Phys. Soc. Jpn. 54* (1985) 1236.
[25] V. N. Laukin, E. E. Kostyuchenko, Y. V. Sushko, T. F. Shchegolev, E. B. Yagubskii, *Pis'ma Zh. Eksp. Teor. Fiz. 41* (1985) 68; *JETP Lett. 41* (1985) 81.
[26] J. M. Williams, H. H. Wang, M. A. Beno, T. J. Emge, L. M. Sowa, P. T. Copps, F. Behroozi, L. N. Hall, K. D. Carlson, G. W. Crabtree, *Inorg. Chem. 23* (1984) 3839.
[27] H. H. Wang, M. A. Beno, U. Geiser, M. A. Firestone, K. S. Webb, L. Nunez, G. W. Crabtree, K. D. Carlson, J. M. Williams, L. J. Azevedo, J. F. Kwak, J. E. Schirber, *Inorg. Chem. 24* (1985) 2465.
[28] R. P. Shibaeva, V. F. Kaminskii, E. B. Yagubskii, *Mol. Cryst. Liq. Cryst. 119* (1985) 361.
[29] H. Kobayashi, R. Kato, A. Kobayashi, Y. Nishio, K. Kajita, W. Sasaki, *Chem. Lett. 1986*, 789.
[30] R. Kato, H. Kobayashi, A. Kobayashi, S. Moriyama, Y. Nishio, K. Kajita, W. Sasaki, *Chem. Lett. 1987*, 507.
[31] R. N. Lyubovskaya, R. B. Lyubovskii, R. P. Shibaeva, M. Z. Aldoshina, L. M. Gol'denberg, L. P. Rozenberg, M. L. Khidekel', Y. F. Shul'pyakov, *Pis'ma Zh. Eksp. Teor. Fiz. 42* (1985) 380; *JETP Lett. 46* (1985) 188.
[32] R. N. Lyubovskaya, E. I. Zhilyaeva, S. I. Pesotskii, R. B. Lyubovskii, L. O. Atovmyan, O. A. D'yachenko, T. G. Takhirov, *Pis'ma Zh. Eksp. Teor. Fiz. 46* (1987) 149; *JETP Lett. 46* (1985) 188.
[33] L. Brossard, M. Ribault, M. Brousseau, L. Valade, P. Cassoux, *C. R. Acad. Sci. Paris, Ser. 2 302* (1986) 205.
[34] L. Brossard, H. Hurdequint, M. Ribault, D. Jerome, J. P. Legros, P. Cassoux, *Proc. Int. Conf. Synth. Metals*, Santa Fe 1988 (*Synth. Metals*, in press).
[35] A. Kobayashi, H. Kim, Y. Sasaki, R. Kato, H. Kobayashi, S. Moriyama, Y. Nishio, K. Kajita, W. Sasaki, *Chem. Lett. 1987*, 1819.
[36] K. Kikuchi, M. Kikuchi, T. Namiki, K. Saito, I. Ikemoto, K. Murata, T. Ishiguro, K. Kobayashi, *Chem. Lett. 1987*, 931.
[37] K. Kikuchi, K. Murata, Y. Honda, T. Namiki, K. Saito, H. Anzai, K. Kobayashi, T. Ishiguro, I. Ikemoto, *J. Phys. Soc. Jpn. 56* (1987) 4241.
[38] K. Kikuchi, K. Murata, Y. Honda, T. Namiki, K. Saito, T. Ishiguro, K. Kobayashi, I. Ikemoto, *J. Phys. Soc. Jpn. 56* (1987) 3436.
[39] K. Kikuchi, K. Murata, Y. Honda, T. Namiki, K. Saito, K. Kobayashi, T. Ishiguro, I. Ikemoto, *J. Phys. Soc. Jpn. 56* (1987) 2627.
[40] G. C. Papavassiliou, G. A. Mousdis, J. S. Zambounis, A. Terzis, A. Hountas, B. Hilti, C. W. Mayer, J. Pferffer, *Proc. Int. Conf. Synth. Metals*, Santa Fe 1988 (*Synth. Metals*, in press).
[41] D. Schweitzer, E. Gogu, I. Hennig, T. Klutz, H. J. Keller, *Ber. Bunsenges. Phys. Chem. 91* (1987) 890.

Research News

Molecular Electronics: Silicon to Soliton and Other Trends

When the British Association for the Advancement of Science (BA) first met in Oxford some one hundred and fifty years ago, only a few scientists, apart from *Faraday*, were then engaged in the new task of assembling electrical circuits. In those days, long before the age of mass production, the diameter of conducting rods was of millimeter dimension. Nowadays, with world-wide interest in the pursuit of the ultramicro-miniature, there is intense activity in the design and construction of molecular electronic devices made up of organic semiconductors, organic metals and conducting polymers which are of either organic or inorganic provenance (such as polysulfur nitride). Into the lexicon of the molecular architect a new word has been recently introduced, a "proconductor" which is the non-conducting form of a molecular entity that can also be made conducting by loss or gain of an electron by partial oxidation or reduction. Present day studies[1] which, inter alia, seek to arrive at favored molecules for memory, logic and amplification—with a view to constructing computers based, not on silicon or gallium arsenide, but on self-assembling molecules of the kind that abound in biology—focus on such problems as whether a π-conjugated molecule, a hundred Ångstrom or so in length, can serve as a proconductor or a conductor when placed between two metallic conductors. It is conceivable that the 'electronic wiring', which, it is thought, will be a characteristic of the

molecular electronic device of the future, will consist of bridges similar to those recently discussed by *Aviram* (see Fig. 1). The diameter of these 'wires' is of nanometer dimension. A diminution in diameter by a factor of 10^6 has therefore been achieved in the interval between the date of the first and most recent (September 1988 at Oxford) BA meeting.

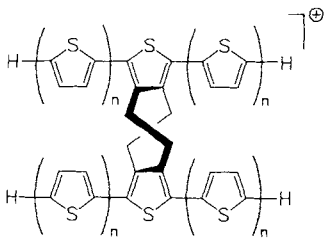

Fig. 1. A proconductor and a conductor chain connected by a σ bridge which forces the two π terminals to be at 90° to each other [1].

One of the numerous minisymposia held at Oxford focussed on some key aspects of molecular electronics. Present day microelectronic and opto-electronic industries rely mainly on inorganic materials. It has been clear for some time, however, that future requirements for more complex system designs predicate a renewed interest in the organic solid-state, the study of the electronic properties of which began in earnest forty years ago.[2,3] By the early seventies, these materials were seen to hold promise as sensors, protonic conductors and other useful devices.[4]

G. G. Roberts (University of Oxford and Thorn EMI plc) targeted his remarks largely on the wide scope and numerous advantages offered by carefully tailored Langmuir–Blodgett (LB) films. He demonstrated the advantages to be gained by capitalizing on the ultra-thinness and controlled, crystalline architecture of these monomolecular assemblies. That LB films may be used to generate dilute radioactive sources, magnetic monolayers and model biological membranes has been recognized quite early in their adoption as physico-chemical curiosities. What was not fully appreciated in the early days, however, was that considerable advantage could be taken of the comparative ease of preparing non-centrosymmetric, crystalline LB films. Materials with non-centrosymmetric structures exhibit pyroelectricity as well as strikingly non-linear optical behavior. *Roberts* referred in particular to work recently published[5,6] in which a novel organo-transition-metal complex had been synthesized specifically for use with the LB deposition procedure. Thus, by coordinating the liquid crystal compound **1** with $[Ru(PPh_3)_2Cp]$ forming **2**, the electron withdrawing nature of the parent molecule is greatly enhanced and, at the same time, multilayer formation, in the LB sense, is facilitated.[5] Optical second-harmonic generation yields a value for the hyperpolarizability much larger than that of most inorganic materials. Films of **2** have a pyroelectric coefficient (3×10^{-6} cm^{-2} K^{-1}) that is thought to be the largest yet reported. It is apparent from

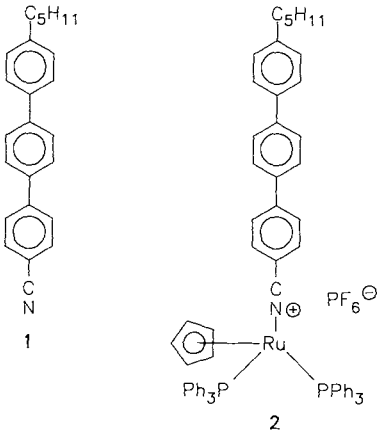

this as well as other work by *Treadgold* et al.[7] (not presented at Oxford) that alternating LB films of polymers and merocyanine monomers (possessing large alkyl chains as quaternizing agents) are very efficient second-harmonic generators, enabling visible radiation to be generated from infrared sources. (Parenthetically, we note that it is of considerable technical and fundamental interest[8,9] that infrared–visible sum-frequency generation[10] can now be used to obtain vibrational spectra of adsorbed monolayers on metal and semiconductor surfaces).

J. White (Thorn EMI plc) dealt with the applications of liquid crystals. Although these fascinating materials have been known since the classic work in Germany in 1888, only after *G. W. Gray*'s pioneering studies at the University of Hull in the early 1970's did it become possible to produce, to order, environmentally stable liquid crystals. In the context of television displays, it is obvious that, for reasons of mass alone, the cathode ray tube cannot be a candidate for very large area (e.g. 3 m × 2 m) viewing screens. This is where it is felt that liquid crystal displays will prove advantageous, just as they have done for the currently available pocket-sized TV sets.

P. Day (Inorganic Chemistry Laboratory, Oxford and I.L.L., Grenoble) summarized the landmarks in the search for new molecular materials and superconductors. In the last few years molecular organic compounds have been discovered that not only conduct electricity like metals, but even become superconducting at low temperatures (see Fig. 2). In contrast to conventional metals, the charge-transfer salts which sometimes exhibit these properties are made from solution at room temperature by electro-crystallization. Again, in contrast to the traditional metals, the properties of 'molecular metals' are extremely sensitive to small changes in their packing arrangements. Minute alterations in the inter-molecular spacings can have profound consequences. And small chemical adjustments to the anions (e.g. the replacement of a $PF_6^\ominus$ for $ClO_4^\ominus$) in the charge-transfer salts transforms them from superconductors to normal metals or even to insulators. This is especially so for the tetrathiafulvalene derivatives. *Day* drew attention to some remarkably interesting charge-transfer

ADVANCED MATERIALS

complexes, prepared in his laboratory at Oxford, that changed from being semi- to superconducting on application of pressure. He also referred to the recent work of *Saito* et al. at the Institute of Solid State Physics, Tokyo, where an organic complex involving copper thiocyanate has a superconducting transition of 10.4 K (see review by *Inokuchi* in this issue). What is apparent from the behavior of such a material is that the rate of rise of the superconducting transition temperature (Fig. 2) is much steeper for molecular organic compounds than for the rare earth-alkaline-earth-copper oxides or their bismuth-based analogues.

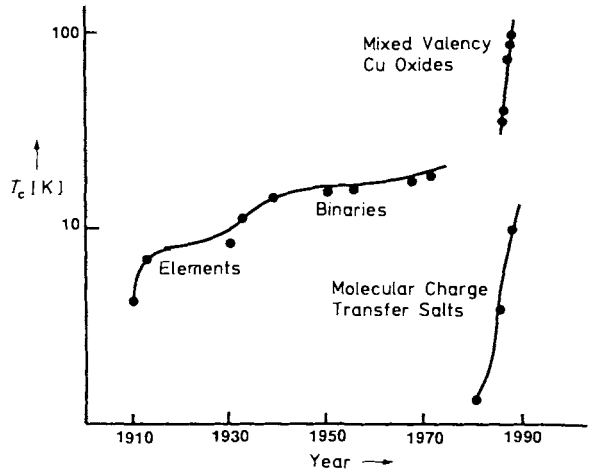

Fig. 2. The T_c history of superconductors.

H. G. Heller's presentation, based on his elegant work over the past decade at the University of Wales (first at Aberystwyth and latterly at Cardiff) was entitled 'Chameleonic chemicals'. Organic compounds that change color reversibly on exposure to light have enormous commercial potential. These thermally stable photochromic compounds can be developed for optical information storage in computers, as well as played on home video and audio equipment. By means of molecular tailoring and design, their properties can be modified so that they change color in direct sunlight and fade rapidly at room temperatures. Such compounds can be incorporated into lightweight plastic lenses which darken in sunlight and clarify under diffuse daylight. Another application lies in the security printing of banknotes, checks and other documents. By and large the chemistry of these chameleonic materials rests on the guidelines offered by the Woodward-Hoffman rules:[11] photo-stimulated, conrotatory reactions ensue freely whereas thermally-stimulated, disrotatory reactions entail overcrowding and, hence, are sluggish and unfavored.

Molecular electronics was also discussed in the Biology section of the BA meeting at Oxford, although the main emphasis was on the fundamentals of molecular recognition rather than molecular engineering. Whereas *C. R. Lowe* (Biotechnology Unit, University of Cambridge) sought to exploit the ease with which biological recognition takes place and to combine it with conventional solid-state electronics—and in so doing demonstrated how this would, inter alia, lead to effective remote sensing (especially under adverse environmental conditions) and continuous, one-line, real-time quantitative chemical or biochemical analysis—his colleague at Cambridge, *R. N. Perham* (Department of Biochemistry) ranged freely, during the course of his address, over topics such as the uncanny kinship in the architecture of the active sites in a dozen or so ostensibly quite unrelated enzymes and the role of an enzyme as an asymmetric unit. He also indicated that moving a 'recognition center' from one antibody into another was already a reality. As his was the presidential lecture of the Biology Section, he also considered other exciting areas of biochemical research: techniques are now available to enable the DNA sequence of a gene to be altered at will, thereby permitting the amino acid sequence of the encoded protein to be correspondingly changed. This testifies to the biochemists' ability directly to design protein molecules for specific, and otherwise inaccessible, purposes. *Perham* outlined how we are just beginning to acquire the ability to intervene in the elaboration of shape and form in multi-subunit, self-assembling systems.

Shortly after these minisymposia ended the 8 September issue of *Nature* appeared. In it *R. H. Friend* and his colleagues at the Cavendish Laboratory, University of Cambridge described new semiconductor devices using organic polymer diodes and transistors.[12] These devices are fashioned from polyacetylene, a conjugated polymeric semiconductor, which can readily be produced in (amorphous) thin film form, as a result of a thermally-stimulated conversion of a precursor developed at the University of Durham by *Feast* et al.[13] The devices constructed by *Friend* et al. operate in a novel way: charge is stored in localized soliton-like excitations of the polymer chain. These excitations are introduced by the presence of an adjustable surface electric charge. This is a fundamentally different method of introducing excitations from that used in devices based on silicon or gallium arsenide, where doping with controllable amounts of deliberately added impurities is the principle employed. The presence of charged solitons changes the optical properties of the hydrocarbon polymer.

The results reported by *Friend* et al. do not yet pose a threat[14] to established semiconductor technology: it must never be forgotten that the mobilities of electrons and holes in two dimensions in materials based on Si or III/V compounds, and their quantum-well variants, are phenomenally good. And, as yet, there is no organic metallic or semiconducting polymer that approaches Si in this regard. It is, therefore, arguable whether transistor devices based on organic polymers are likely to become commercial in the near future. (It is noteworthy that *Roberts* et al.[15] over a decade ago produced a p/n function based on two-dimensional LB films of anthracene. But these did not pre-

sage a growth in organic semiconductor technology). What one can reasonably expect, however, is that the elegant work of *Friend* et al. might soon lead to the development of high-performance sensors utilizing relatively cheap and easily processed organic materials.

John M. Thomas
The Royal Institution of Great Britain
London (UK)

[1] A. Aviram, *J. Am. Chem. Soc. 110* (1988) 5687.
[2] D. D. Ely, *Nature (London) 162* (1948) 819.
[3] H. Akamatu, H. Kuroda, *Solid State Phys. 2* (1959) 1. See also H. Inokuchi: *Electrical Conduction in Solids*, Routledge and Kegan Paul, London 1965.
[4] J. M. Thomas, T. J. Lewis, J. R. N. Evans, *Discuss. Faraday Soc. 51* (1971) 73, and references cited therein.
[5] R. Colbrook, B. Holcroft, G. G. Roberts, M. E. C. Polywka, S. G. Davies, *Proc. Eur. Conf. Non-linear Properties of Polar Mater.* (Zurich, August 1988), to be published in *Ferroelectronics*.
[6] T. Richardson, G. G. Roberts, M. E. C. Polywka, S. G. Davies, *Thin Solid Films 160* (1988) 231.
[7] R. H. Treadgold, M. C. J. Young, R. Jones, P. Hodge, P. Kalinsky, R. J. Jones, *Electron. Lett. 24* (1988) 308.
[8] A. L. Harris, C. E. D. Chidsey, N. J. Levinos, D. N. Loiasono, *Chem. Phys. Lett. 141* (1987) 350.
[9] P. B. Davies, personal communication.
[10] X. D. Zhu, H. Suhr, Y. R. Shen, *Phys. Rev. B35* (1987) 3047.
[11] R. B. Woodward, R. Hoffmann, *Angew. Chem. 81* (1969) 797; *Angew. Chem. Int. Ed. Engl. 8* (1969) 781.
[12] J. H. Burroughs, C. A. Jones, R. H. Friend, *Nature (London) 335* (1988) 137.
[13] J. H. Edwards, W. J. Feast, *Polymer Commun. 21* (1980) 595.
[14] D. Bloor, *Nature (London) 335* (1988) 115.
[15] G. G. Roberts, G. Owen, W. A. Barlow, P. S. Vincett, Br. Pat. No. 1,572,181 (1975).

Conference Reports

Advanced Materials— R & D Efforts in Germany

A good three years after the German Federal Ministry for Research and Technology (Bundesministerium für Forschung und Technologie, BMFT) initiated its Materials Research Program, the first Materials Research Symposium took place in Hamm/Westphalia on September 12–14, 1988. Approximately 600 scientists and engineers discussed, in plenary lectures and review papers. the current state of knowledge and techniques in materials research. Results obtained up to now in various advanced research and development projects were presented in specialist papers and posters.

Following intensive discussions with many experts, five main themes that appeared to offer a high potential for innovation had been chosen for the Materials Research Program: ceramics, powder metallurgy, metallic materials for high temperatures and specialized applications, new polymers, and composite materials. The idea of the program is to stimulate progress by setting up joint interdisciplinary research projects involving academic research institutes and industrial laboratories, with well-matched complementary work plans carefully drawn up and agreed in advance. The industrial partners contribute with about 50% of the cost of such R & D projects. Federal funding up to a total of DM 1.1 billion is to be made available over the ten-year program. The Materials Research program is being supervised on behalf of the BMFT by the Materials Research Project Group of the KFA (Nuclear Research Center), Jülich.

The DM 940 million that has been committed to the Materials Research Program up to the time of this interim review in Hamm is divided between 265 collaborative projects involving 637 research laboratories; Table 1 summarizes the distribution between topics. Of the funding provided by the BMFT, 34% has gone to academic research institutes and 66% to industrial laboratories.

Table 1. Distribution of presently committed research funds between the five main themes of the Materials Research Program (million DM).

	Ceramics	Powder metallurgy	High temperature metals	Polymers	Composites
Total budget	251	94	176	200	220
BMFT contribution	124	58	99	103	116

Ceramics

This part of the program is aimed mainly at research and development on monolithic ceramics, and also includes ceramic films. It is strongly focussed on high performance structural ceramics (engineering ceramics). At present there are very few applications for which the reliability of complex shaped ceramic engineering components under dynamic load is adequate. It should be possible to greatly improve the reliability of ceramic components by quality control during manufacture, or by structural reinforcement, helped by the expected development of more reliable non-destructive testing methods. The powders used as starting materials for the manufacture of ceramic engineering components can be synthesized by reactions in the solid state, by production from melts, or by precipitation from solutions or from gaseous phases. An example of the

many developments in progress is that by Elektroschmelzwerk Kempten (ESK) in collaboration with Kühnle, Kopp & Kausch AG (KKK) of Frankenthal and the Technical University of Braunschweig; this team is working on a new process for manufacturing turbocharger rotors from sintered silicon carbide or silicon nitride materials (SSiC, SSN and SRBSN). In particular, with Si_3N_4 rotors it has already been found that the frictional conditions at 1300 K allow peripheral velocities greater than 500 ms^{-1} to be achieved, and in tests with a SSiC rotor an operating life of 10000 km has been obtained. There are good prospects for achieving peripheral velocities of $>500\ ms^{-1}$ at 1500 K and a failure probability of less than 0.1%. However, considerable further work will be needed to achieve consistent series production with this level of quality, while also paying adequate attention to economic aspects. With the R & D work that is currently under way, ceramics research in the Federal Republic of Germany has taken a considerable step forward. However, there is likely to be an increasing need in the future for R & D work in the field of functional ceramics (including glass-ceramics and glass) with special physical properties, e.g. as regards electrical, electronic, optical or magnetic behavior.

Powder Metallurgy

Some of the topics in the powder metallurgical part of the Materials Research Program are: the reproducible manufacture of rapidly quenched powders for making alloys that are not accessible by melt metallurgy; the development of new process methods for manufacturing engineering components and semi-finished parts with, for example, spatial variations in their properties (graded structures), or with unusually high strength and toughness; the development of economical methods of production for large mechanical components. As an example, work is in progress at the Technical University of Hamburg-Harburg and at the Max Planck Institute for Metals Research, Stuttgart, in collaboration with several industrial partners, to develop high-strength aluminum alloys made by powder metallurgical techniques; with alloys of the type Al-Zn-Mg-Cu-X it was found that yield stresses as high as 750 MPa and a fatigue strength of 300 MPa could be obtained, thus giving strength properties significantly better than those of the corresponding alloys made by melt metallurgy.

Densification of powders by the direct explosive method offers an attractive means of compacting, especially for the newly developed rapidly quenched types of alloys, or for brittle materials such as ceramics or intermetallic phases. The possibilities for industrial applications of this technology are being investigated in a collaborative project between ESI GmbH, Eschborn, and Rheinmetall GmbH, Düsseldorf. The studies are based on a commendable symbiosis of theoretical calculation and experiment. The very rapid densification process, which is characterized by extremely high pressures and material velocities, was simulated using a computer program for finite element calculations. The parameters thus determined were then used in setting up experiments, and this resulted in the production of samples with 99% densification. Following the successful compaction of spherical samples, it is planned that the next stage of the project will investigate explosive densification of powders consisting of plates and of complex mechanical components such as turbine blades.

Metallic Materials for High Temperatures and Special Applications

Metallic materials continue to occupy a preferred position in high performance engineering applications, and are used in many areas of modern technology. They have high strength and toughness with good thermal conductivity, and can be economically produced and worked. The application of new metallurgical knowledge has led to improved properties with regard to strength, toughness, stability at high temperatures, and corrosion resistance, showing that the scope for continued development of metals made by melt metallurgical techniques is still far from exhausted. One factor that limits the potential applications of metallic materials is the maximum service temperature; excessive temperatures result in deterioration of the mechanical properties and corrosion resistance, and a reduction in creep strength. An example of an approach to these problems is the collaboration between the Ruhr University of Bochum and the VAW, Bonn, which is concerned with R & D work on new types of structures in Al-Li based alloys. The demand in airplane construction for materials that are ever lighter but also stronger has led to the development of Al-Li alloys with reduced density and increased tensile modulus. This allows the construction of aircrafts with significantly reduced structural masses. In these research studies the combination of new materials structures and optimized heat treatments has led to materials whose mechanical properties are superior to those of conventional cast and wrought aluminum alloys.

The overall impression is that the work on materials for high temperatures and special applications covers a wide range of topics, including both the further development of conventional high performance materials and basic studies on the potential uses of more novel materials.

New Polymers

This aspect of the program is concerned both with developing high performance polymers for use as engineering materials and with producing functional polymers with entirely novel physical properties, e.g. electrical, electronic, optical or magnetic properties. High mechanical performance in polymers may involve requirements such as stabil-

ity even at very high temperatures, or high strength while retaining good processability. Looked at in terms of theoretically attainable values, only a fraction of the potential strength properties of polymers has been used up to now. It is true that the theoretical values cannot be fully realized in practice, but there is nevertheless an enormous potential for development. Possible approaches include specifically synthesizing or otherwise forming a precisely defined molecular architecture. An example of this is a development at the Max Planck Institute for Polymer Research, Mainz, in which flexible side-chains are attached to rigid main-chains with the aim of reducing the melting temperature so as to facilitate down-stream processing, without a significant deterioration in the good mechanical properties.

Remarkable progress has been achieved in the field of functional polymers. For example, BASF in collaboration with Bayreuth University and the Max Planck Institute for Polymer Research, Mainz, has succeeded in producing polymers with intrinsic electrical conductivity similar to that of metals.

In another research project on "polymeric optical fibers", Hoechst AG, Frankfurt, has scored a notable success. Precursors for making a polymeric light-transmitting fiber have been synthesized; these have better high temperature resistance ($T_g > 130\,^{\circ}C$) and considerably lower light attenuation (20 dB km^{-1}) than conventional polymeric optical fibers made of polymethylmethacrylate (PMMA: 100 dB km^{-1}). This has been achieved by means of a hydrogen/fluorine and hydrogen/deuterium exchange in esters of acrylic and methacrylic acids. These materials make it possible to transmit signals over a distance of 1500 m without intermediate amplification, whereas the plastic optical fibers used previously have needed booster amplifiers every 100 m.

A large market in the field of short-range information technology (transmission distances under 2 km) is predicted for polymeric optical fibers, as they are more flexible than glass fibers, even with large fiber diameters, and they also offer a wider range of choice in refractive index; also the cost of a system is less owing to easier working of the material and lower manufacturing costs.

Functional polymers are likely to become especially important as a result of future advances in research. Efforts are being made to ensure close cooperation between research partners in the electronics and chemical industries.

Composite Materials

This research topic is concerned with high performance materials in which a polymeric, ceramic or metallic matrix is reinforced by the inclusion of fibers, whiskers or particles. Such materials are used in applications requiring high strength, stiffness and heat resistance with low mass.

An example of development work in this area is a project on composites based on polymer matrices, under the overall control of Volkswagen AG. This is concerned with developing economic production methods using winding and tape-laying techniques for producing motor vehicle components. A typical example is the manufacture of transmission shafts for automobiles. Here the rate of production was increased to such an extent that it is now possible to make these components with an operating cycle of less than 30 s.

Another example that may be mentioned is a joint project by the companies Didier and Kolbenschmidt to develop a composite material with a matrix of ceramic and metal. It has previously been shown that ceramic fiber reinforced metallic materials already come very close to meeting the specifications for use as pistons in automobile engines. The idea being investigated in this project is to combine the advantages of the two materials by building into the piston a fiber gradient. According to this concept the piston has a dense ceramic layer on the combustion face, with a continuous gradation of the ceramic fiber fraction along the length of the piston, from 100% at this face down to zero at the other end. The mechanical characteristics thus obtained show an improvement over those for conventional piston materials which is in some cases as much as 100%. Another very important property of materials used for pistons is the resistance to thermal shock. In this case fiber reinforcement gives an improvement of 300 to 400% in the results of temperature cycling tests.

The idea followed at Hamm of organizing the conference program with a strong interdisciplinary emphasis has proved especially successful, bringing together scientists and engineers from all branches of materials science in wide-ranging and stimulating discussions covering different disciplines. The proceedings of the symposium have been published by the Materials Research Project Group of the KFA Jülich. In addition, an overall evaluation of the results achieved compared with international developments will be published by the BMFT late in 1988.

Wolfgang Faul
Kernforschungsanlage Jülich (FRG)

As of January 1989, ADVANCED MATERIALS can be subscribed to separately at the annual rate of DM 178.00. Please order through your bookseller or write to VCH Verlagsgesellschaft mbH, Postfach 101161, D-6940 Weinheim, FRG. Customers in Switzerland, in the UK and in the USA should write to VCH Verlags AG, Hardstrasse 10, Postfach, CH-4020 Basel, Switzerland, VCH Publishers, Wellington Court, 8 Wellington Street, Cambridge CB1 1HW, UK, and VCH Publishers, Suite 909, 220 East 23rd Street, New York, NY 10010-4606, USA, respectively.

ADVANCED MATERIALS

Speciality Polymers

The 3rd International Conference on New Polymeric Materials, "Speciality Polymers '88", was organized by the journal *Polymer* and held from September 13–15, 1988 at Queens' College in the beautiful old university town of Cambridge, UK. About 350 participants attended to hear about the newest developments in the field, which were presented in six plenary lectures and two parallel sessions with 22 papers each, devoted to "High Performance Polymers" and "Electroactive Polymers", respectively.

In the first plenary lecture *D. T. Clark* (ICI, UK) discussed approaches to meet the development goals for high temperature performance polymers for air- and spacecraft applications: The T_g/T_m window of aromatic polyetherketones-co-sulfones can be adjusted by suitably balancing the sulfone and keto group content, with high keto content generally giving rise to high T_m, while increasing the sulfone content lowers the degree of crystallinity. The fine control of properties depends on a number of additional parameters, amongst which the sequence and isomer distribution are of major importance for the crystallization behavior and morphology, with the effective sulfone content of the interlamellar phase controlling the T_g.

From the number of papers devoted to electrically or optically active polymers, and the high innovative content of the presentations, it became clear that the bias of this session was towards polymer systems with highly sophisticated optical and/or electro-optical properties. The rich diversity of structural types of liquid-crystalline (LC) polymers, studies on their structure-property relationships, and various efforts to tailor their optical or electro-optical response for particular applications, were reviewed by *G. M. Gray* (University of Hull, UK). Taking siloxane and acrylate LC polymers as examples, it was stressed that analytically pure materials, with respect to precursor removal, molecular weight and dispersibility, are essential in order to obtain reproducible results on transition temperatures, dielectric properties, elastic constants and electro-optical response. To meet the challenge of the search for LC polymers with non-linear optical (NLO) properties, *Gray* and his coworkers have introduced a new type of LC copolymer with conventionally and laterally attached rod-like mesogens. LC side-chain polymers based on siloxanes or acrylates with birefringent, dichroic, fluorescent and NLO properties were discussed by *H. J. Coles* (University of Manchester, UK). Special consideration was given to nematic and smectic, and also ferroelectric phases, and optical effects as fast as 10^{-9} s with lateral resolution of about 10^{-6} m have been demonstrated in such systems. The kinetics of the alignment process in LC side-chain polymers can be studied by dielectric relaxation spectroscopy, as demonstrated by *G. Williams* (University of Wales, Aberystwyth, UK).

The diacetylenes, which offer a great variety of primary structures, are very promising as NLO materials and, because they can be laid down as ultrathin layers using the Langmuir-Blodgett (LB) technique, as candidates for integrated optics; accordingly they were discussed by several speakers. An alternative to LB films derived from diacetylenes, which have to be post-polymerized, are LB films from preformed polymers based on substituted acrylates with mesogenic side chains, as described by *P. Hodge* (University of Lancaster, UK). Symmetric as well as noncentrosymmetric LB multilayers can be assembled by using two or more different polymers. Second Harmonic Generation (SHG) in spin-coated PMMA films containing azo dyes was discussed by *Le Barny* (Thomson-CSF, France).

The development of "photonic computing" based on optical shutters, logic elements and storage elements requires materials with very fast (10^{-12} s) switching times, as was outlined by *R. S. Potember* (Johns Hopkins University, USA). The only processes in organic molecules that are fast enough for this purpose are electronic level jumps or polarizability changes. As an example the excitation of π-states in ladder type oligomers with an indanthrone type backbone was discussed, with the optical response varying dramatically according to the type of substitution and degree of polymerization. A final link between diacetylenes and LC materials was offered by *M. A. Schen* (National Bureau of Standards, Gaithersburg, USA), who reported on the polymerization of diacetylenes from a smectic c-phase, in which the activation energy for thermal polymerization was considerably lower than that in the crystalline phase.

The common features of electroactive polymers, and the influence of molecular or supermolecular defects on their performance as conducting, charge-storing, piezo- or pyroelectric materials were reviewed by *T. J. Lewis* (University College of North Wales, Bangor, UK). The concepts of charge transport involving localized states, tunneling structures and the influence of interfaces and phase boundaries in the solid state of conducting materials were discussed.

The contribution by *P. Kathirgamanathan* (Cookson, UK), entitled "The Future of Conducting Polymers" was expected by most of the participants to clear up some of the uncertainties in this particular field. Since the review of the present situation in conducting polymers took up all the available time, the speaker unfortunately did not reach the discussion of their future. However, the future of conducting polymers was touched on in a number of contributions, which dealt with the problems of processing such materials: *P. Smith* (University of California, Santa Barbara, USA) reported on the synthesis of polyacetylene (PA) in a polyethylene gel, from which it could be drawn into highly anisotropic fibers. *R. W. Lenz* (University of Massa-

chusetts, Amherst, USA) reported on a new route to poly(arylene-vinylenes) from polyelectrolyte precursors. Since the precursor polymers are easily soluble, they can be processed into films etc. prior to converting them thermally into conducting materials. While the "Durham route" to PA has become acknowledged as the prototype for precursor routes to conducting polymers, no such route is yet working satisfactory for poly(*p*-phenylene). *J. Feast* (University of Durham, UK) introduced a new approach via a Pd-catalyzed polycondensation of boronic acid derivatives of appropriate phenylenes, to yield side-chain substituted poly(*p*-phenylenes), which are soluble. Future prospects for the application of conducting polymers were reviewed by *J. H. Burroughes* (University of Cambridge, UK), who has succeeded in assembling a MIS-FET transistor using polyacetylene made by the Durham route.

Ionic charge transport in polymers was addressed by *S. A. Dobrowsky* (University of Leeds, UK), who has investigated *N*-substituted poly(acrylamides) as a matrix for inorganic salts to form ionically conducting polymer-salt complexes. *A. Gandini* (École Française, Paris) reviewed polymer-salt complexes with polyethyleneoxide or polypropyleneoxide networks as the matrix. In the polymer-salt complexes the glass transition behavior is found to be the dominant feature determining the ion transport properties. This seems not to be the case in polyelectrolyte glasses based on polymeric ammonium salts ("ionenes"), whose molecular dynamics and dielectric properties were compared by *G. Wegner* (Max-Planck-Institute for Polymer Research, Mainz, FRG).

It was due to the exceptionally interesting presentations that "Speciality Polymers '88" became a very successful meeting for materials scientists.

Wolfgang H. Meyer
Max-Planck-Institut für Polymerforschung
Mainz (FRG)

Call for Short Communications · Call for Short Communications · Call for Short Communications

... doesn't melt, won't dissolve, just can't be broken down — let's send it to ADVANCED MATERIALS!

ADVANCED MATERIALS from now on welcomes short communications from all over the world, from academia and from industry, from chemists, physicists and materials scientists, provided they are in keeping with the program outlined in the editorial published in May. Authors who are interested in submitting short communications (up to six pages of double-spaced manuscript together with an appropriate number of figures and/or formulas) should prepare their manuscripts in accordance with the "Notice to Authors" of Angewandte Chemie reproduced in the January issue of the journal following the list of contents; upon request, a copy can be obtained from the editorial office:

ADVANCED MATERIALS/ANGEWANDTE CHEMIE
Postfach 101161
D-6940 Weinheim
Federal Republic of Germany

Call for Short Communications · Call for Short Communications · Call for Short Communications

Conference Calendar

January 1989

15–18 **Composites and Advanced Ceramics,**
13th Annu. Conf.
Cocoa Beach (USA)
Contact: The American Ceramic Soc., 757 Brooksedge Plaza Dr., Westerville, OH 43081-6136, USA

15–20 **Optics, Electro-Optics, and Laser Applications in Sci. and Eng.,**
Symp. and Exhibition
Los Angeles (USA)
Contact: Soc. of Photo-Optical Instrumentation Eng. (SPIE), P.O. Box 10, Bellingham, WA 98227, USA

17–19 **Optical Data Storage**
Top. Mtg.
Los Angeles (USA)
Contact: Optical Soc. of America (OSA), 1816 Jefferson Pl. NW, Washington, DC 20036, USA

19 **Electron Beam Testing of Integrated Circuits**
London (United Kingdom)
Contact: Meetings Officer, Inst. of Physics, 47 Belgrave Sq., London SW1X 8QX, UK

23–24 **Commercial Applications of Superconductivity,**
2nd Annu. Cambridge Conf.
Boston (USA)
Contact: World Tech. Press, 1 Kendall Sq., Suite 2200, Cambridge, MA 02139, USA

31–3 **Polymer,**
17th Australian Symp.
Brisbane (Australien)
Contact: Dr. D. J. T. Hill, Chem. Dept., Univ. of Queensland, Brisbane 4067, Australia

31–3 **Sintering of Multiphase Metal and Ceramic Systems**
Int. Conf.
New Delhi (India)
Contact: G. S. Upadhyaya, Convener ICSMC '89, Dept. of Metallurgical Eng., Indian Inst. of Technol., Kanpur 208 016, India

February 1989

2 **Silicon Molecular Beam Epitaxy**
E-MRS Spring Mtg.
Strasbourg (France)
Contact: E. Kasper, AEG-Forschungszentrum, Sedanstr. 10, D-7900 Ulm, FRG

2–4 **Nonlinear Guided Wave Phenomena: Physics and Applications,**
Top. Mtg.
Houston (USA)
Contact: Optical Soc. of America (OSA), 1816 Jefferson Pl. NW, Washington, DC 20036, USA

5–9 **Biomedical Polymers,**
Int. Symp.
Perth (Australia)
Contact: Secretary, W. A. Polymer Group, Royal Australian Chemical Inst., 125 Hay St., Perth, W. A. 6000, Australia

6–10 **Composites,**
SPI Inst. Annu. Conf.
Dallas (USA)
Contact: Composites Inst., SPI, 355 Lexington Ave., New York, NY 10017, USA

6–9 **Optical Fiber Communication,**
IEEE-LEOS-OSA Conf.
(OFC '89 and IGWO '89)
Houston (USA)
Contact: Optical Soc. of America (OSA), 1816 Jefferson Pl. NW, Washington, DC 20036, USA

7–9 **Physics and Chemistry of Semiconductor Interfaces (PCSI-6)**
Bozeman (USA)
Contact: G. J. Lapeyre, Physics Dept., Montana State Univ., Bozeman, MT 59717, USA

12–15 **High-Resolution Optical FT Spectrometry and Noninvasive Assessment of Visual Systems,**
Top. Mtgs.
Santa Fe (USA)
Contact: Optical Soc. of America (OSA), 1816 Jefferson Pl. NW, Washington, DC 20036, USA

13–17 **Plasma Processing in Semiconductor Materials**
Bristol (United Kingdom)
Contact: Dr. S. Pringle, Dept. of Extramural Studies, The Univ., Queens Rd., Bristol BS8 1HR, UK

19–22 **Adhesion,**
12th. Annu. Mtg.
Hilton Head Island (USA)
Contact: D. Hunston, NBS, Polym. Div., Gaithersburg, MD 20899, USA

21–24 **Recent Advances in Drug Delivery**
Salt Lake City (USA)
Contact: K. Knutson, Univ. of Utath, Dept. of Pharmaceutics, CCCD, 421 Wakara Way, Suite 318, Salt Lake City, UT 84108, USA

21–26 **Optical Fibers and their Applications,**
5th Symp.
Warsaw (Poland)
Contact: R. S. Romaniuk, IPI Warsaw Univ. of Technol., Nowowiepska 15-19, PL-00-665, Warsaw, Poland

26–3 **Microlithography,**
Symp. and Exhibition (Micro '89)
Santa Clara (USA)
Contact: Soc. of Photo-Optical Instrumentation Eng. (SPIE), P.O. Box 10, Bellingham, WA 98227, USA

27–1 **Microphysics of Surfaces, Beams and Adsorbates,**
3rd Top. Mtg.
Salt Lake City (USA)
Contact: R. B. Hall, Exxon Research & Eng., Rt. 22E, Annandale, NJ 08801, USA

27–3 **Superconductivity,**
Gordon Conf.
West Coast (USA)
Contact: A. Sleight, E. I. Du Pont de Nemours, Experimental Station 356/301, Wilmington, DE 19898, USA

27-3 **High-Temperature Superconducting Oxides: Processing & Related Properties,**
TMS Annu. Mtg.
Las Vegas (USA)
Contact: M. Karl, The Metallurgical Soc., 420 Commonwealth Drive, Warrendale, PA 15086, USA

March 1989

1-3 **Technical Ceramics,**
2nd Int. Congr. and Exhibition (Techkeram 2)
Wiesbaden (Fed. Rep. Germany)
Contact: Demat Exposition Managing, P.O. Box 110611, D-6000 Frankfurt, FRG

5-10 **Liquid Crystals,**
6th Eur. Winter Conf.
Schladming (Austria)
Contact: P. Laggner, Inst. für Röntgenfeinstrukturforschung of the Austrian Academy of Sci., Steyrergasse 17, A-8010 Graz, Austria

6-8 **Crystal Structure, Microstructure and Properties of Minerals and Ceramic Materials,**
Int. Colloq.
Bochum (Fed. Rep. Germany)
Contact: Prof. O. W. Flörke, Ruhr-Univ. Bochum, Inst. für Mineralogie, P.O. Box 102148, D-4630 Bochum, FRG

6-8 **Lithium Battery Technology & Applications,**
4th Int. Seminar
Deerfield Beach (USA)
Contact: S. P. Wolsky, Ansum Enterprises Inc., 950 De Soto Rd., Suite 3B, Boca Raton, FL 33432, USA

6-9 **Condensed Matter Division**
9th Gen. Conf.
Nice (France)
Contact: Dr. F. Raymond CNRS-Bât. 3, rue Albert Einstein, F-06560 Valbonne, France

6-9 **Advanced Materials**
MRS Industry-Univ. Conf.
Denver (USA)
Contact: Dr. Fred Smith, Adv. Mater. Inst., Colorado School of Mines, 1500 Illinois, Golden, CO 80401, USA

6-10 **Quantum Wells for Optics and Optoelectronics; Picosecond Electronics and Optoelectronics,**
Top. Mtg.
Salt Lake City (USA)
Contact: Optical Soc. of America (OSA), 1816 Jefferson Pl. NW, Washington, DC 20036, USA

8-9 **Molecular Chemistry of Solid-State Electronics**
London (United Kingdom)
Contact: The Royal Society, 6 Carlton House Terrace, London SW1Y 5AG, UK

9-11 **Makromolekulares Kolloquium**
Freiburg (Fed. Rep. Germany)
Contact: Prof. H. Finkelmann, Inst. für Makromol. Chemie der Univ., Stefan-Meier-Str. 31, D-7800 Freiburg, FRG

11-14 **Surface Finishing '89**
Brighton (United Kingdom)
Contact: Inst. of Metal Finishing, Exeter House, 48 Holloway Head, Birmingham B1 1NQ, UK

12-14 **High-Tech-Materials and Finishing**
Berlin (West)
Contact: Technik + Kommunikation-Verlag GmbH, Ritterfelddamm 82 h + i, D-1000 Berlin 22

12-25 **Diffusion in Materials,**
NATO Adv. Study Inst.
Aussois (France)
Contact: A. L. Laskar, Phys. and Astron. Dept., Clemson Univ., Clemson, SC 29631, USA

13-14 **Regio Macro II**
Basel (Switzerland)
Contact: Prof. M. Mutter, Inst. für Org. Chem., Univ. Basel, St. Johanns-Ring 19, CH-4056 Basel, Switzerland

15-17 **Confocal Microscopy/3-D Image Processing in Microscopy,**
1st Int. Conf./2nd Int. Conf.
Amsterdam (Netherlands)
Contact: Bureau PAOG, Congr. Office, Tafelbergweg 25, NL-1105 BC, Amsterdam, Netherlands

15-17 **Intelligent Materials,**
Int. Workshop
Ibaraki (Japan)
Contact: T. Kurino, The Soc. of Nontraditional Technol., Toranomon Kotohira-Kaikan Bldg. 3F, 1-2-8 Toranomon, Minato-ku, Tokyo 105, Japan

20-22 **Mechanical Properties of Materials at High Rates of Strain,**
4th Int. Conf.
Oxford (United Kingdom)
Contact: J. Harding, Eng. Sci. Dept., Univ. of Oxford, Parks Rd., Oxford OX1 3PJ, UK

20-22 **Refractory Metals and Silicides**
Eur. Workshop
Houthalen (Belgium)
Contact: R. De Keersmaecker, IMBE, Kapeldreef 75, B-3030 Leuven, Belgium

20-23 **Surface Science,**
Interdisciplinary Conf.
Liverpool (United Kingdom)
Contact: P. Weightman, Liverpool Univ., Oliver Lodge Lab., Oxford St., P.O. Box 147, Liverpool L69 3BX, UK

27-31 **Aerospace Sensing,**
Tech. SPIE's Symp.
Orlando (USA)
Contact: Soc. of Photo-Optical Instrumentation Eng. (SPIE), Technical Program Committee, P.O. Box 10, Bellingham, WA 98227, USA

28-31 **Aluminum-Lithium**
5th Int. Conf.
Williamsburg (USA)
Contact: Al-Li-V, School of Eng. and Applied Sci., Thornton Hall, Univ. of Virginia, Charlottesville, VA 22901, USA

29-31 **Neutron and X-Ray Scattering: Complementary Techniques**
Canterbury (United Kingdom)
Contact: Dr. R. J. Newport, Univ. of Kent, Physics Dept., Canterbury, Kent CT2 7NR, UK

30-31 **Colorado Microelectronics**
Colorado Springs (USA)
Contact: CMC '89 Conf. Secretary, Microelectronics Research Lab., Univ. of Colorado, Colorado Springs, CO 80933-7150, USA

30–14 **High-T_c Superconductors,**
Exp. Workshop
Miramare (Italy)
Contact: Int. Ctr. for Theoretical Physics, P.O. Box 586, I-34100 Trieste, Italy

April 1989

1–6 **Superconductivity,**
2nd World Congr.
Houston (USA)
Contact: R. D. Kane, World Congr. on Superconductivity, P.O. Box 27805, Houston, TX 77227-7805, USA

3–5 **Modern Practice in Stress and Vibration Analysis**
Liverpool (United Kingdom)
Contact: Meetings Officer, Inst. of Physics, 47 Belgrave Sq., London SW1X 8QX, UK

3–6 **Low Energy Ion Beams,**
5th Conf.
Guildford (United Kingdom)
Contact: Meetings Officer, Inst. of Physics, 47 Belgrave Sq., London SWIX 8QX, UK

3–7 **Copolymerization and Copolymers in Dispersed Media**
Lyon (France)
Contact: I. Guillot/C. Pichot, Lab. des Materiaux Organiques, BP 24, F-69390 Vernaison, France

3–7 **High Temperature Materials '89**
Gaithersburg (USA)
Contact: J. W. Hastie, National Bureau of Standards, Gaithersburg, MD 20899, USA

4–14 **Phase Transition in Soft Condensed Matter,**
NATO Adv. Study Inst.
Geilo (Norwegen)
Contact: G. Jarret, Inst. for Energy Technol., Dept. of Physics, P.O. Box 40, N-2007 Kjeller, Norwegen

6–7 **Modeling in Crystal Growth from the Melt,**
NATO Workshop
Parma (Italy)
Contact: G. Müller, Inst. für Werkstoffwissenschaften 6, Martensstraße 7, D-8520 Erlangen, FRG

10–12 **Bayreuther Polymer Symp.,**
(BPS '89)
Bayreuth (Fed. Rep. Germany)
Contact: BPS '89, Lehrstuhl Makromolekulare Chemie II, Univ. Bayreuth, Postfach 101251, D-8580 Bayreuth, FRG

10–13 **Microscopy of Semiconducting Materials,**
MRS 6th Oxford Conf.
Oxford (United Kingdom)
Contact: Administrator, Royal Microscopy Soc., 37/38 St. Clements, Oxford OX4 1AJ, UK

11–13 **Catalysis by Well Characterized Materials**
Liverpool (United Kingdom)
Contact: Prof. R. W. Joyner, Leverhulme Ctr. for Innovative Catalysts, Univ. of Liverpool, Grove St., P.O. Box 147, Liverpool L69 3BX, UK

17–26 **Ceramics and Composite Materials,**
Spring College in Mater. Sci.
Trieste (Italy)
Contact: Int. Ctr. for Theoretical Physics, Spring College in Mater. Sci. 1989, P.O. Box 586, I-34100 Trieste, Italy

18–19 **Industrial Water-Soluble and Water-Swellable Polymers**
Manchester (United Kingdom)
Contact: The Registar (Mid-Career Training), UMIST, P.O. Box 88, Manchester M60 1QD, UK

23–28 **Nondestructive Testing,**
12th World Conf.
(WCNDT '89)
Amsterdam (Netherlands)
Contact: B. de Jong, RAI Organisatie Bureau Amsterdam bv, Europaplein 12, 1078 GZ Amsterdam, Netherlands

23–27 **American Ceramic Society,**
91st Annu. Mtg. and Expo.
Indianapolis (USA)
Contact: Dr. K. M. Nair, Electronics Dept., E.I. du Pont de Nemours Co., Inc., 3181 Buffalo Ave., Niagara Falls, NY 14302, USA

24–28 **Optical Science and Engineering,**
2nd Int. Congr.
Paris (France)
Contact: Soc. of Photo-Optical Instrumentation Eng. (SPIE), P.O. Box 10, Bellingham, WA 98227, USA

24–28 **Lasers and Electro-Optics,**
LEOS-IEEE-OSA Conf.
(CLEO '89)
Baltimore (USA)
Contact: Optical Soc. of America (OSA), 1816 Jefferson Pl. NW, Washington, DC 20036, USA

24–28 **MRS-Spring Mtg.**
San Diego (USA)
Contact: J. B. Ballance, MRS, 9800 McKnight Rd., Suite 327, Pittsburgh, PA 15237, USA

25–27 **Hot Isostatic Pressing of Materials**
Antwerpen (Belgium)
Contact: Hot Isostatic Pressing Conf., c/o K. VIV, Jan van Rijswijcklaan 58, B-2018 Antwerpen, Belgium

26–28 **Joining Ceramics, Glass and Metal**
3rd Int. Conf. (CGM '89)
Contact: Dtsch. Gesellsch. Metallkd., Adenauerallee 21, D-6370 Oberursel, FRG

May 1989

1–3 **Tunable Solid State Lasers,**
Top. Mtg.
North Falmouth (USA)
Contact: Optical Soc. of America (OSA), 1816 Jefferson Pl. NW, Washington, DC 20036, USA

1–5 **Scanning Microscopy,**
Salt Lake City (USA)
Contact: O. Johari, Scanning Microscopy Int., P.O. Box 66507, Chicago, IL 60666, USA

4–6 **The Solid State—Dynamics and Kinetics**
Annu. Mtg. Dtsch. Bunsen-Gesellsch. für Phys. Chem.
Siegen (Fed. Rep. Germany)
Contact: Dtsch. Bunsen-Gesellsch., Carl-Bosch-Haus, Varrentrappstr. 40/42, D-6000 Frankfurt am Main 90, FRG

7–12 **High-T_c Superconductor Technologies**
175th Mtg. Electrochem. Soc.
Los Angeles (USA)
Contact: S. Raider, IBM T. J. Watson Research Ctr., P.O. Box 218, York Town Heights, NY 10598, USA

8–12 **High Temperature and Wear Resistant Materials in a World of Changing Technology**
12th Int. Plansee Seminar
Plansee (Austria)
Contact: Metallwerk Plansee, A-6600 Reutte, Austria

9–11 **Coatings and Sensors for Acoustic and Electromagnetic-Optical Applications**
Univ. Park. (USA)
Contact: V. K. Varadan, Dept. of Eng. Sci. and Mechanics, Penn. State Univ., 227 Hammond Bldg., Univ. Park, PA 16802, USA

10–11 **Polyimides**
Montpellier (France)
Contact: Prof. M. Abadie, LEMD/MAO-USTL, F-34060 Montpellier Cedex 1, France

16–19 **Modern Developments in Materials Science and Technology,**
Annu. Mtg. Dtsch. Gesellsch. Metallkd.
Karlsruhe (Fed. Rep. Germany)
Contact: Dtsch. Gesellsch. Metallkd., Adenauerallee 21, D-6370 Oberursel, FRG

22–24 **Werkstoffanalytik,**
Wien (Austria)
Contact: Prof. Dr. M. Grasserbauer, Inst. für Analytische Chem. der Tech. Univ. Wien, Getreidemarkt 9, A-1060 Wien, Austria

22–24 **Glastechnische Tagung**
Stuttgart (Fed. Rep. Germany)
Contact: Dtsch. Glastechn. Gesellsch., Mendelssohnstr. 75–77, D-6000 Frankfurt am Main, FRG

22–25 **Graphite Intercalation Compounds,**
5th Int. Symp. (ISGIC-5)
Berlin (West)
Contact: Dr. F. W. Froben, Fachbereich Physik, Freie Univ. Berlin, Arnimallee 14, D-1000 Berlin 33

24–26 **Advances in the Stabilization and Controlled Degradation of Polymers,**
11th Int. Conf.
Luzern (Switzerland)
Contact: Dr. A. V. Patsis, Inst. in Materials Sci, State Univ. of New York, New Paltz, NY 12561, USA

25–26 **Quantitative Methods in Assessment of Structural Defects**
Kansas City (USA)
Contact: A. P. Berens, Univ. of Dayton, Research Inst., 300 College Park Ave., Dayton, OH 45469, USA

29–31 **Cross-linked Polymers,**
3rd Int. Conf.
Luzern (Switzerland)
Contact: Dr. A. V. Patsis, Inst. in Materials Sci, State Univ. of New York, New Paltz, NY 12561, USA

29–2 **Molecular Beams**
Perugia (Italy)
Contact: V. Aquilanti, Univ. di Perugia, Dipt. di Chimica, I-06100 Perugia, Italy

31–2 **Applied Surface Analysis,**
11th Symp.
Cleveland (USA)
Contact: J. Grant, Research Inst., 300 College Park, Dayton, OH 45469-0001, USA

31–2 **Thermogravimmetry and Thermal Engineering,**
6th Biennial Conf.
Budapest (Hungary)
Contact: I. Benko, MATE, House of Technol. III. 318, P.O. Box 451, H-1372 Budapest, Hungary

June 1989

6–9 **Chemistry of Functional Dyes,**
Int. Symp. (ESTech '89)
Osaka (Japan)
Contact: Prof. T. Kitao, General Secretary of the Symp., Kinki Chem. Soc., Japan
1-8-4, Utsubo honmachi, Nishi-ku, Osaka 550, Japan

12–14 **Rubber,**
Int. Conf. 90 IRC Exhibition
Paris (France)
Contact: Soc. de Chimie Industrielle, 28, rue Saint-Dominique, F-75007 Paris, France

12–15 **Narrow-Gap Semiconductors and Related Materials,**
Int. Conf.
Ogunquit (USA)
Contact: D. G. Seiler, Phys. Dept., Univ. of North Texas, P.O. Box 5368, Denton, TX 76203, USA

18–21 **Colloid & Surface Science,**
63rd ACS Div. of Colloid & Surface Chem. Symp.
Seattle (USA)
Contact: J. Berg, Dept. of Chemical Eng. BF-10, Univ. of Washington, Seattle, WA 98105, USA

19–21 **SAMPE-Electronics,**
3rd Int. Conf.
Los Angeles (USA)
Contact: M. Smith, Business Director, SAMPE, P.O. Box 2459, Covina, CA 91722, USA

21–23 **Chemically Modified Surfaces,**
Midland (USA)
Contact: W. T. Collins, Dow Corning Corp., Mail Stop C41C00, Midland, MI 48686, USA

22–25 **Optics Asia '89**
Singapore (Singapore)
Contact: Asia '89, 994 Bendemeer Rd., N° 04-03, Singapore 1233, Singapore

25–30 **Solid State Sensors and Actuators (Transducers -5)/ Eurosensors III**
Montreux (Switzerland)
Contact: COMST S.A., P.O. Box 415, CH-1001 Lausanne 1, Switzerland

26–28 **Molecular Design of Functional Polymers,**
IUPAC Int. Symp.
Seoul (Korea)
Contact: IUPAC Int. Symp., c/o Polymer Soc. of Korea, Rm. 601, Hyecheon Bldg., 831 Yeoksam-dong, Kangnam-ku, Seoul 135-792, Korea

26–30 **Solid State Chemistry,**
2nd Int. Symp.
Pardubice (Czechoslovakia)
Contact: Dr. L. Koudelka, Inst. of Chem. Technol., Leninovo nam., 565, CS-53210 Pardubice, Czechoslovakia

26–30 **Supermembranes**
Trieste (Italy)
Contact: Int. Ctr. for Theoretical Physics, P.O. Box 586, I-34100 Trieste, Italy

27–28 **Polymer Latex III**
London (United Kingdom)
Contact: Miss M. Peacock, Plastics and Rubber Inst., 11 Hobart Place, London SW1W 0HL, UK

28–30 **Oxide Surfaces**
Midland (USA)
Contact: W. T. Collins, Mail Stop C41C00, Dow Corning Corp., Midland, MI 48686-0994, USA

July 1989

2–7 **Solid State Organic Materials,**
9th Int. Conf.
Como (Italy)
Contact: Centro di Cultura Scientifica, "A. Volta", Villa Olmo, Via Cantoni 1, I-22100 Como, Italy

3–6 **Conduction and Breakdown in Solid Dielectrics**
3rd Int. Conf. (ICSD '89)
Trondheim (Norway)
Contact: Prof. Sletbak, ICSD '89, The Norwegian Inst. of Technol., Sem Sælands V 13, N-7034 Trondheim, Norway

4–7 **Nonlinear and Electro-optics**
Int. Conf.
Cambridge (United Kingdom)
Contact: The Meetings Officer, The Inst. of Physics, 47 Belgrave Square, London SW1X 8QX, UK

9–14 **Zeolites,**
8th Int. Conf.
Amsterdam (Netherlands)
Contact: M. Laboushere, 792 Keizersgracht, 1017 EC, Amsterdam, The Netherlands

10–12 **Applied Organometallic Chemistry: an Entry to the New Technology**
The Pines Resort (Australia)
Contact: Dr. A. F. Masters, School of Chemistry, Univ. of Sydney, Sydney, N. S. W. 2006, Australia

10–13 **Magnetic Resonance in Polymers,**
9th Spec. Colloq. Ampere
Prague (Czechoslovakia)
Contact: P. M. M. Secretariat, c/o. Inst. of Macromol. Chem., Czech. Acad. of Sci., 16206 Prague, Czechoslovakia

10–14 **Electron Spectroscopy,**
4th Int. Conf.
Honolulu (USA)
Contact: G. E. McGuire, Microelectronics Ctr. of North Carolina, P.O. Box 12889, Research Triangle Park, NC 27709, USA

10–14 **Organic Coatings Science and Technology,**
15th Int. Conf.
Athens (Greece)
Contact: Dr. A. V. Patsis, Inst. in Materials Sci, State Univ. of New York, New Paltz, NY 12561, USA

11–14 **Numerical Analysis of Semiconductor Devices and Integrated Circuits,**
6th Int. Conf.
Dublin (Ireland)
Contact: J. J. H. Miller, Nase-Code Conf., INCA, P.O. Box 2, Dún Laoghaire, Ireland

16–21 **Catalysis,**
Eur. Conf.
Berlin (West)
Contact: Prof. G. Ertl, Fritz-Haber-Inst. der Max-Planck-Gesellsch., Faradayweg 4–6, D-1000 Berlin

17–20 **Polymer Blends**
Prague (Czechoslovakia)
Contact: P. M. M. Secretariat, c/o. Inst. of Macromol. Chem., Czech. Acad. of Sci., 16206 Prague, Czechoslovakia

18–20 **Polymer Chemistry: Aspects of Radical Polymerization**
Lancaster (United Kingdom)
Contact: Dr. J. R. Ebdon, Dept. of Chemistry, Univ. of Lancaster, Lancaster LA1 4YA, UK

18–21 **Integrated Optics and Optical Fiber Communications,**
7th Int. Conf. (IOOC-7)
Kobe (Japan)
Contact: P. W. Shumate, Jr., Bell Communications Research, 435 S St., Morristown, NJ 07960, USA

23–28 **Materials and Mechanisms of Superconductivity: High-Temperature Superconductors,**
Int. Conf. (HTSC-M^{2}S)
Stanford (USA)
Contact: Dr. T. H. Geballe, Dept. of Applied Phys., Stanford Univ., Stanford, CA 94305, USA

24–26 **Composite Structures,**
5th Int. Conf.
Paisley (United Kingdom)
Contact: Dr. I. H. Marshall, Dept. of Mechanical and Production Eng., Paisley College of Technol., High St., Paisley PA 12BE, UK

31–2 **Biologically-Engineered Polymers**
Cambridge (United Kingdom)
Contact: Royal Soc. of Chemistry, Burlington House, London W1V 0BN, UK

August 1989

2–7 **Pure and Applied Chemistry,**
32nd IUPAC Congr.
Stockholm (Sweden)
Contact: Stockholm Convention Bureau, P.O. Box 6911, S-10239 Stockholm, Sweden

13–26 **High-T_C Superconductors,**
NATO Adv. Study Inst.
Bad Windsheim (Fed. Rep. Germany)
Contact: R. Kossowsky, Applied Res. Lab., Pennsylvania State Univ., P.O. Box 30, State College, PA 16804, USA

14–17 **Shock Compression of Condensed Matter,**
APS Top. Conf.
Albuquerque (USA)
Contact: A. Roach, MS-P 915, Los Alamos Nat. Lab., Los Alamos, NM 87545, USA

20-24 **Imaging Systems – 150 Years of Photography,**
Int. Symp. (ISIS '89)
Dresden (German Dem. Rep.)
Contact: Conf. Secretary, ISIS '89, Technische Univ. Dresden, Sektion Physik, Wissenschaftsbereich Photophysik, Mommsenstr. 13, DDR-8027 Dresden, GDR

20-25 **Crystal Growth: Progress in Science and Technology,**
9th Int. Conf.
Sendai (Japan)
Contact: Prof. T. Nishinaga, Inter Group Corp., Akasaka Yamakatsu Bldg., 8-5-32, Akasaka Minato-ku, Tokyo 107, Japan

21-26 **Photochemistry,**
Int. Conf.
Beijin (People's Rep. China)
Contact: Prof. S. Wu, Inst. of Photographic Chem., Academia Sinica, Beijing, People's Rep. China

28-31 **Dynamical Processes in Excited States of Solids,**
7th Int. Conf. (DPC '89)
Athens (USA)
Contact: DPC '89, Prof. J. E. Rives, Dept. of Physics and Astronomy, Univ. of Georgia, Athens, GA 30602, USA

28-1 **Ferroelectricity,**
7th Int. Mtg. (IMF-7)
Saarbrücken (Fed. Rep. Germany)
Contact: Dr. J. Albers, Univ. des Saarlandes, Fachbereich Physik, D-6600 Saarbrücken, FRG

28-1 **Sintering,**
7th World Round Table Conf.
Herceg-Novi (Yugoslavia)
Contact: Dr. D. P. Uskoković, Serbian Academy of Sci. and Arts, Knez-Mihailova 35, 11000 Beograd, Yugoslavia

28-1 **X-Ray Optics and Microanalysis,**
12th Int. Congr.
Cracow (Poland)
Contact: S. Jasienska, Academy of Mining and Metallurgy, Inst. of Metallurgy, 30-059 Cracow, Poland

28-2 **Photochemistry for High Technology,**
Int. Summer School
Leuna-Merseburg (German Dem. Rep.)
Contact: Prof. H.-J. Timpe, Sektion Chemie, Technische Hochschule für Chemie, Leuna-Merseburg, Gensaerstr., DDR-42 Merseburg, GDR

29-2 **Innovation and Perspectives in Solid Phase Synthesis,**
Int. Symp.
Oxford (United Kingdom)
Contact: R. Epton, School of Appl. Sci., Wolverhampton Polytech., Wolverhampton WV1 1SB, UK

September 1989

4-8 **Electrically and Optically Active Polymers,**
21st Europhysics Conf.
Lodz (Poland)
Contact: Dr. J. Ulanski, Polymer Inst., Tech. Univ. of Lodz, Zwirki 36, 90-924 Lodz, Poland

4-8 **Macromolecules 89,**
Oxford (United Kingdom)
Contact: Prof. R. Epton, School of Appl. Sciences, The Polytechnic, Wulfruna St., Wolverhampton WV1 1SB, UK

4-8 **Olefin Metathesis and Polymerization,**
8th Int. Symp.
Bayreuth (Fed. Rep. Germany)
Contact: Office ISOM 8, Lab. für Anorg. Chem., Univ. Bayreuth, Postfach 101251, D-8580 Bayreuth, FRG

5-7 **Interfacial Phenomena in Composite Materials,**
Int. Conf.
Sheffield (United Kingdom)
Contact: J. Herriot, Conf. Organizer, Butterworth Scientific Ltd., P.O. Box 63, Westbury House, Bury St., Guildford, Surrey GU2 5BH, UK

5-8 **Optical, Electrical and Acoustic Properties**
Kent (United Kingdom)
Contact: M. D. Shuttleworth, Plastics and Rubber Inst., 11 Hobart Pl., London SW1W 0HL, UK

6-9 **Magnetic Materials and Applications '89**
Rimini (Italy)
Contact: I. Pareti, Local Chairman EMMA '89, Istituto Maspec CNR, Via Chiavari 18/A, 43100 Parma, Italy

10-14 **Optical Communications,**
15th Eur. Conf.
Gothenburg (Sweden)
Contact: P. A. Andrekson, Dept. of Optoelectronics, Chalmers Univ. of Technol., S-41296 Gothenburg, Sweden

11-13 **Charge Transfer in Polymeric Systems,**
RSC, Faraday Div.
Contact: Dr. J. F. Gibson, Royal Soc. of Chemistry, Burlington House, Piccadilly, London W1V 0BN, UK

11-13 **Holographic Systems, Components and Applications,**
2nd Int. Conf.
Bath (United Kingdom)
Contact: Inst. of Electronic and Radio Eng., Conf. Dept., Savoy Hill House, London WC2R 0JD, UK

11-13 **Surface Analysis Techniques and Applications**
Manchester (United Kingdom)
Contact: E. Wellingham, Conf. Secretariat, Field End House, Bude Close, Nailsea, Bristol BS19 2FQ, UK

13-15 **Microscopy,**
150th Anniversary Commemorative Mtg.
Oxford (United Kingdom)
Contact: Microscopical Soc., 37-38 St. Clements, Oxford OX4 1AJ, UK

17-22 **Defect Recognition and Image Processing in Semiconductors,**
3rd Mtg. (DRIP-3)
Yokohama (Japan)
Contact: Prof. T. Ogawa, Gakushuin Univ., Dept. of Physics, 1-5-1 Mejiro, Toshima-ku, Tokyo 171, Japan

17-22 **Optics and Optical Engineering,**
Cambridge Symp.
Cambridge (USA)
Contact: Soc. of Photo-Optical Instrumentation Eng. (SPIE), P.O. Box 10, Bellingham WA 98227, USA

AUTHOR INDEX [*Angew. Chem. Int. Ed. Engl. 27* (1988)]

The page numbers in square brackets refer to the German edition [*Angew. Chem. 100* (1988)] of Angewandte Chemie. In the case of book reviews the names of the authors are given; the corresponding GE reference can be found in the Author Index of the German Edition. AM = Advanced Materials.

ABEL, T. 944 [1006]
Adam, W. 429, 1536 [443, 1594]
Adamek, C. 1059 [1110]
Ahlrichs, R. 421 [418]
Akkerman, O. S. 687, 1084 [735, 1143]
Akpapoglou, S. 280 [288]
Al-Ahmad, S. 1353 [1404]
Albert, M. R. 1198
Albinati, A. 563 [571]
Allwohn, J. 961, 1370 [961, 1421]
Alonso, F. J. G. 1167 [1224]
Alston, D. R. 1184 [1215]
Altmann, E. 858 [855]
Altmann, K.-H. 858 [855]
Amberg, W. 1718 [1786]
Amberger, E. 699 [722]
Anderson, K. R. 1355 [1406]
Andersson, S. 953 [995]
Ando, H. 560, 1711 [597, 1777]
Andres, W. 1182 [1212]
Andrews, D. L. 721
Angermund, K. 833, 1559 [853, 1616]
Annen, U. 713 [725]
Antel, J. 703, 1186 [739, 1200]
Antonietti, M. 1743 AM [1813]
Appel, R. 416, 957 [437, 957]
Appelman, E. H. 392 [425]
Arif, A. M. 1099 [1132]
Asensio, G. 1546 [1604]
Ashton, P. R. 966, 1550 [981, 1608]
Ashworth, D. M. 1089 [1122]
Astruc, D. 643, 1347 [662, 1394]
Attygalle, A. B. 460 [475]
Atwood, J. L. 1361 [1412]
Augart, N. 952, 1368 [956, 1433]
Aumann, R. 1456 [1512]
Aurbach, I. 291 [278]

BACEIREDO, A. 301, 1350 [289, 1397]
Bachmann, J. 971 [983]
Bachstädter, G. 1522 [1580]
Ballardini, R. 692 [712]
Balli, H. 566 [590]
Balsaa, P. 263 [280]
Balzani, V. 692 [712]
Bamfield, P. 445
Bargon, J. 1189 [1225]
Barluenga, J. 1546 [1604]
Barron, A. R. 837 [873]
Bartmann, K. 391 [424]
Basten, J. E. M. 1177 [1217]
Bastian, E. 1066 [1113]
Baudler, M. 280, 561, 1059 [288, 579, 1110]
Bauer, J. 1558 [1618]
Bäuerle, P. 281 [274]
Baum, G. 414, 684, 961 [397, 727, 961]
Baumann, H. 41 [41]
Beattie, I. R. 1161 [1202]
Beck, G. 1344 [1391]
Beck, J. 896 [927]
Becker, W. 574 [604]
Bednorz, J. G. 735 AM [757]
Behr, A. 661 [681]
Behrens, D. 1407
Beifuss, U. 703, 1186 [739, 1200]
Beister, H. J. 1101 [1116]
Belaj, F. 701 [703]
Belluš, D. 797 [820]
Benecke, B. 1194 [1238]
Benken, R. 1182 [1212]
Bennett, M. A. (589), 941 [(610), 1002]
Berger, S. 1196 [1198]
Berndt, A. 960, 961, 1370 [959, 961, 1421]
Berthold, J. 1524 [1581]
Bertrand, G. 301, 1350 [289, 1397]
Betz, P. 1157, 1326 [1219, 1373]
Beuter, G. 1094 [1099]
Bewersdorf, M. 1176 [1232]
Bhardwaj, C. 923 [1000]
Bhardwaj, R. C. 923 [1000]
Bhargava, S. K. (589) [(610)]
Bickelhaupt, F. 687, 936, 1083, 1084 [735, 998, 1100, 1143]
Biedenbach, B. 1157 [1219]
Binder, H. 262, 1174 [270, 1229]
Bingel, C. 1373 [1422]
Binger, P. 1157, 1484, 1559 [1219, 1541, 1616]
Birnbrich, P. 1158 [1197]
Blackburn, D. W. 437 [408]
Blank, N. E. 1064 [1096]
Bläser, D. 294, 304, 553, 579 [292, 293, 592, 572]
Blatter, T. 1163 [1211]
Blechert, S. 558 [596]
Bliefert, C. 1565
Block, E. 1342 [1389]
Blohm, D. 207 [213]
Blum, Z. 953 [995]
Blümel, J. 977 [1011]
Blumen, A. 1210 AM [1252]
Blümich, B. 1655 [1716]
Boche, G. 846, 973, 1522 [868, 965, 1580]
Bock, H. 1067, 1068 [1125, 1127]
Boese, R. 294, 304, 553, 579, 952, 1368, 1537 [292, 293, 592, 572, 956, 1433, 1595]
Bogdanović, B. 1513 [1569]
Bögge, H. 1719 [1787]
Bohle, D. S. 302 [308]
Bollschweiler, C. 207 [213]
Bolm, C. 835 [882]
Bonrath, W. 833 [853]
Borrmann, H. 1339 [1386]
Bosold, F. 973 [965]
Bossek, U. 685 (—) [718 (894)]
Bosum, A. 558 [596]
Bott, S. G. 1361 [1412]
Böttcher, P. 759 [781]
Boudjouk, P. 1355 [1406]
Bovin, J.-O. 555 [580]
Boyd, P. D. W. 1731 [1799]
Boyer, J. H. 985
Brandt, P. 1521 [1578]
Brauer, D. J. 438 [432]
Brauers, F. 404 [413]
Braunstein, P. 927 [972]
Braunwarth, H. 698 [731]
Breker, J. 1562 [1620]
Brellochs, B. 262 [270]
Bremser, W. 247 [252]
Brendelberger, G. 1089 [1122]
Brieden, W. 404 [413]
Brimah, A. K. 1521 [1578]
Brückner, R. 278 [285]
Brudermüller, M. 298 [267]
Brunner, H. 708, 718, 1180 [717, 730, 1231]
Buchholz, E. 580 [603]
Budzikiewicz, H. 280, 1059 [288, 1110]
Bühler, M. 41 [41]
Bühner, M. 1553 [1611]
Bulak, E. 958 [964]
Bungardt, D. 1537 [1595]
Burgemeister, T. 270 [299]
Burger, K. 848 [860]
Buschmann, J. 1534 [1592]
Buss, V. 423 [422]

CAHN, R. W. 1569 AM [1629]
Campos, P. J. 1546 [1604]
Carlson, R. M. K. 1567
Carrano, C. J. 277 [306]
Carrol, P. J. 1097 [1138]
Castanet, Y. 683 [711]
Caulton, K. G. 1165 [1236]
Chan, D. M. T. 442 [436]
Chang, H.-R. 1731 [1799]
Chapman, O. L. 398 [402]
Charrier, C. 950 [997]
Cheetham, A. K. 861
Chemla, D. S. 986
Chen, Q. 1724 [1792]
Chen, Y.-C. J. 333 [342]
Cheung, S. S. 705 (1200) [716, (1242)]
Chevalier, B. 440 [403]
Chi, K. M. 437 [408]
Chiesi-Villa, A. 576 [587]
Chrambach, A. 1109
Chrisciel, J. 1355 [1406]
Christen, D. 294 [292]
Christl, M. 931, 1369 [969, 1427]
Christou, G. 1731 [1799]
Ciriano, M. A. 402 [406]
Closs, F. 842 [875]
Coleman, A. W. 1361 [1412]
Collman, J. P. 984
Colvin, E. 1567
Cordes, A. W. 1702 [1768]
Coucouvanis, D. 1353 [1404]
Couret, C. 828 [885]
Cowley, A. H. 277, 837, 838, 1349 [306, 873, 874, 1396]
Cox, P. A. 719
Cram, D. J. 1009 [1041]
Cremer, D. 427 [431]
Croasmun, W. R. 1567
Crocco, G. 301 [289]
Curtis, A. C. 1530 [1588]

DAMMEL, R. 828 [885]
Dannheim, J. 701 [724]
Darbre, A. 306
Daub, J. 291 [278]

Davis, W. M. 835 [882]
Day, P. 861
de Boer, H. J. R. 687 [735]
Demartin, F. 563 [571]
Deming, S. N. 1565
de Riese-Meyer, L. 561 [579]
Desiraju, G. R. 1003
Deslandes, F. 440 [403]
Detering, J. 695 [714]
Deutscher, J. 1040 [1072]
Devenish, R. 927 [972]
Devore, D. D. 569 [583]
Diederich, F. 362, 1705 [372, 1775]
Dietl, S. 389, 709 [426, 720]
Dietrich, A. 1077 [1119]
Dippel, K. 1074 [1093]
Dirnberger, T. 948 [993]
Ditrich, K. 1176 [1232]
Dockner, T. 679 [699]
Dombo, B. 711 [732]
Domengès, B. 440 [403]
Döring, J. 1721 [1789]
Dötz, K. H. 713 [725]
Drage, J. S. 941 [1002]
Dräger, M. 828 [885]
Dratva, A. 714 [723]
Driess, M. 399 [410]
Duff, D. G. 1530 [1588]
du Mont, W.-W. 431 [434]
Dunham, W. R. 1353 [1404]
Dunitz, J. D. 387, 880 [415, 910]
Dunn, M. J. 1109
Durfee, L. D. 1181 [1218]
Dyrbusch, M. 433 [438]

EBATA, T. 1097 [1138]
Ebel, H. F. 1565
Eberbach, W. 568 [599]
Eberson, L. 1740
Ebert, G. 902 [933]
Edwards, P. P. 1530 [1588]
Effenberger, F. 281, 716 [274, 737]
Egert, E. 433, 1194 [438, 1238]
Ehlen, A. 1189 [1225]
Ehlers, J. 1556 [1614]
El-Essawi, M. 1160 [1194]
Eling, A. 829 [856]
Elinson, M. N. 1716 [1784]
Elkins, T. M. 1349 [1396]
Ellis, J. E. 437 [408]
Elschenbroich, C. 414, 684 [397, 727]
Enders, D. 581, 1522 [594, 1580]
Engelhardt, G. 1410
Enkelmann, V. 1377 [1429]
Epe, B. 429 [443]
Erikson, T. K. G. 1527 [1585]
Erk, P. 267 [286]
Ermer, O. 411, 829 [450, 856]
Ernst, B. 797 [820]
Ernst, R. D. 1099 [1132]
Eschenmoser, A. 5 [5]
Escudié, J. 828 [885]
Esswein, A. 1178 [1234]
Esteruelas, M. A. 1563 [1621]
Etourneau, J. 440 [403]
Ettmayer, P. 1379 [1431]

FALBE, J. 41 [41]
Faleschini, G. 701 [703]
Fanwick, P. E. 1181 [1218]
Farhataziz 861
Faupel, P. 423 [422]
Favre, T. L. F. 856 [884]
Fehlhammer, W. P. 1344 [1391]
Fehlner, T. P. 424 [400]
Feilong, J. 424 [400]
Felixberger, J. K. 394, 946 [420, 975]
Fenske, D. 965, 1067, 1277, 1512 [978, 1125, 1300, 1572]
Fessner, W.-D. 1103 [1140]
Field, L. D. 590
Fietz, H. 1326 [1373]
Finke, R. 984
Finkelmann, H. 987 AM [1019]
Fischer, R. A. 1509 [1566]
Fischer, R. D. 1521 [1578]
Fischer, R. H. 285 [301]
Flomer, W. A. 1702 [1768]
Floriani, C. 576 [587]
Flörke, U. 263 [280]
Fobker, R. 943 [1005]
Fochem, H. 41 [41]
Folting, K. 587, 1165 [585, 1236]
Fontain, E. 1558 [1618]
Forstmeyer, D. 1558 [1618]
Fox, C. F. 1110
Franck, B. 1170 [1203]
Franck, H.-G. 1108
Franke, M. 265 [295]
Franken, S. 976 [987]
Freiermuth, B. 585 [589]
Freist, W. 773 [795]
Frerichs, S. R. 437 [408]
Fritz, H. 568, 1103 [599, 1140]
Fuess, H. 929 [1013]
Fukuda, Y. 1411

GAA, K. 848 [860]
Gabius, H.-J. 1267 [1321]
Gais, H.-J. 1092, 1540 [1108, 1598]
Gallezot, P. 927 [972]
Gandolfi, M. T. 692 [712]
García, M. P. 1700 [1766]
Gardner, T. G. 1693 [1755]
Garratt, P. J. 306
Gasser, R. P. H. 1385
Gates, B. C. 1127 [1162]
Gauss, J. 427 [431]
Geerts, R. L. 277 [306]
Gehrke, M. 490 [507]
Geigert, J. 985
Geith, K. 848 [860]
Gemmecker, G. 564 [600]
Gerhardt, R. 1534 [1592]
Gerischer, H. 63 [63]
Gernon, M. 1342 [1389]
Geuder, W. 1553 [1611]
Gieren, A. 294 [292]
Girolami, G. S. 1693 [1755]
Gleiter, R. 840, 1559 [851, 1616]
Gmahl, E. 270 [299]
Goesmann, H. 1067 [1125]
Gol, F. 956 [1008]
Golightly, D. W. 1387
Gölitz, P. 3 [3]
Gompper, R. 842, 1437 [875, 1492]
González, J. M. 1546 [1604]
Goodgame, D. M. L. 261 (589) [266 (—)]
Goodisman, J. 860
Graf, W. 417 [439]
Granier, M. 1350 [1397]
Graser, G. 1145 [1181]
Gray, G. W. 1002
Grée, R. 1188 [1233]
Grehn, L. 400 [411]
Grelbig, T. 1534 [1592]
Gries, W.-K. 1553 [1611]
Griesinger, C. 490 [507]
Griffiths, K. D. (589), 941 [(610), 1002]
Grill, D. 1722 [1790]
Grob, C. A. 714 [723]
Grohmann, A. 1544 [1602]
Groneberg, R. D. 1097 [1138]
Grotemeyer, J. 447 [461]
Grubb, D. T. 1220
Gründel, M. 714 [723]
Guastini, C. 576 [587]
Gunnarsson, K. 400 [411]
Günther, H. 1182, 1692 [1212, 1754]
Günther, W. 1086 [1118]
Guthmann, W. 275 [268]

HAAG, S. 1101 [1116]
Haarer, D. 1210 AM [1252]
Haas, W. 406, 409 [445, 448]
Haasnoot, J. G. 856 [884]
Hachgenei, J. 1277 [1300]
Haenel, M. W. 1064 [1096]
Hafner, K. 1191 [1213]
Haiduc, I. 1107
Hall, S. W. 837, 838 [873, 874]
Halligudi, S. B. 1735 [1803]
Halterman, R. L. 553, 835 [592, 882]
Hannemann, K. 284, 853 [273, 880]
Hansen, A. 1158 [1197]
Hargittai, I. 720
Hargittai, M. 720
Harms, K. 713, 846, 1522 [725, 868, 1580]
Harris, K. D. M. 1364 [1415]
Hart, I. J. 1703 [1769]
Hartley, F. R. 1110
Hartmann, A. 1091 [1111]
Hartmann, U. 1077 [1119]
Hartweg, M. 574 [604]
Harvey, S. C. 863
Hasemann, L. 1536 [1594]
Hashimoto, M. 1727 [1795]
Haubold, W. 925 [958]
Haupt, E. T. K. 1062 [1091]
Haupt, H.-J. 263 [280]
Heaton, B. T. 927 [972]
Hees, U. 272 [304]
Hegedus, L. G. 984
Hegedus, L. L. 592
Hegedus, L. S. 1113 [1147]
Hegmann, J. 931 [969]
Hehre, W. J. 862
Heikenfeld, G. 414 [397]
Helm, S. 1331 [1378]
Hendrickson, D. N. 1731 [1799]
Henkel, G. 1326 [1373]
Henkelmann, J. 295 [303]
Herberich, G. E. 958 [964]
Herdtweck, E. 394, 946, 1509 [420, 975, 1566]
Herges, R. 1558 [1618]
Herrmann, G. 1417 [1471]
Herrmann, H.-F. 1067 [1125]
Herrmann, R. 1558 [1618]
Herrmann, W. A. 394, 946, 1297, 1509 [420, 975, 1269, 1566]
Hervieu, M. 440 [403]
Hess, Jr., B. A. 938 [1014]
Hesse, M. 226 [232]
Hesse, W. 1341 [1388]
Hessen, B. 1058 [1115]
Hester, M. R. 1705 [1775]
Hettich, B. 574 [604]

Heyns, A. M. 969 [973]
Hierholzer, B. 1069 [1127]
Hill, C. L. 1526 [1583]
Hillen, H. 207 [213]
Hillig, K. W. 1356 [1407]
Hinrichs, W. 856 [884]
Hirsinger, F. 41 [41]
Hoffman, D. M. 587 [585]
Hoffmann, H. 902 [933]
Hoffmann, R. 1593 [1653]
Hoffmann, R. W. 1176 [1232]
Hölderich, W. 226 [232]
Holdt, G. 1358 [1409]
Hollnagel, A. 965 [978]
Hollstein, W. 846 [868]
Honda, Y. 1725 [1793]
Hope, H. 1699 [1765]
Hopf, H. 701 [724]
Horn, E.-M. 579, 1368 [572, 1433]
Hoyle, C. E. 1409
Huber, B. 419, 1542, 1544 [441, 1600, 1602]
Huber, R. 79 [79]
Hübner, T. 294 [292]
Huch, V. 1381 [1418]
Huckett, S. C. 1513 [1569]
Huffman, J. C. 587, 1165, 1731 [585, 1236, 1799]
Humphreys, C. J. 927 [972]
Hünig, S. 267, 1553 [286, 1611]
Hunkler, D. 1103 [1140]
Hunold, R. 961, 1370 [961, 1421]
Hupfeld, B. 433 [438]
Hurley, J. 684 [727]
Huttner, G. 698, 1529 [731, 1586]
Hwang, C.-K. 1362 [1413]
Hyla-Kryspin, I. 1559 [1616]

IKUTANI, Y. 1717 [1785]
Imagawa, K. 1717 [1785]
Inokuchi, H. 1747 AM [1817]
Interrante, L. V. 1741 AM [1811]
Irngartinger, H. 387 [415]
Isaacs, N. S. 966 [981]
Ishigami, S. 1717 [1785]
Iyoda, M. 1080 [1131]

JACOBS, P. A. 1004
Janietz, N. 708 [717]
Janoschek, R. 701 [703]
Jansen, M. 1341 [1388]
Jefferson, D. A. 1530 [1588]
Jeffery, J. C. 1703 [1769]
Jeter, D. 1702 [1768]
Johnson, B. F. G. 1530 [1588]
Jones, P. G. 1562 [1620]
Jones, R. A. 277, 1349 [306, 1396]
Jordanov, J. 1174 [1229]
Jung, G. 1733 [1801]
Jung, M. 404 [413]

KABE, Y. 1725, 1727 [1793, 1795]
Kabuto, C. 434 [428]
Kahr, B. 1730 [1798]
Kai, Y. 1711 [1777]
Kaim, W. 1174 [1229]
Kaiser, E. T. 902 [945]
Kajita, T. 1078 [1129]
Kalyanasundaram, K. 722
Kämpf, G. 574 [604]
Kanehisa, N. 1711 [1777]
Kang, H. 1342 [1389]
Käppler, O. 689 [706]
Karcher, M. 840 [851]
Kasack, V. 1174 [1229]
Kasai, N. 1711 [1777]
Kasi, S. R. 1203 AM [1245]
Kastner, F. 270 [299]
Katz, J. J. 1111
Katzer, W. 1733 [1801]
Kauffmann, T. 943, 944 [1005, 1006]
Kaupp, G. 1511 [1568]
Kawaguchi, S. 1566
Kawase, T. 1725 [1793]
Kaysser, W. A. 989 AM [1021]
Keller, W. 925 [958]
Kervennal, J. 927 [972]
Kessler, H. 490, 564 [507, 600]
Kinoshita, K. 1218
Kirkland, A. I. 1530 [1588]
Kirmse, W. 1538 [1596]
Kiyomine, A. 1061 [1134]
Kläui, W. 580 [603]
Klein, N. 555 [580]
Klenke, K. 1168 [1195]
Kliche, C. 295 [303]
Klinge, M. 1194 [1238]
Klingebiel, U. 1074 [1093]
Klumpp, G. W. 1083 [1100]
Knauf, T. 1373 [1422]
Kniep, R. 1101 [1116]
Knipp, B. 406, 409 [445, 448]
Knoch, F. 691, 1164 [710, 1221]
Knollmüller, M. 1379 [1431]
Knözinger, H. 1127 [1162]
Knübel, G. 1170 [1203]
Knüppel, P. C. 956 [1008]
Koch, M. 1553 [1611]
Kochi, J. K. 1227 [1331]
Köhler, F. H. 977 [1011]
Kohnke, F. H. 692, 966 [712, 981]
Kolis, J. W. 1702 [1768]
Koltzenburg, G. 1066 [1113]
Kompa, K. L. 1314 [1287]
König, W. A. 307, 979, 1556 [—, 989, 1614]
Kowalewski, R. 1374 [1437]
Kraft, A. 1369 [1427]
Krämer, A. 926 [963]
Krampitz, G. 1145 [1181]
Krapf, H. 285 [301]
Kratochvíl, P. 1221
Krebs, B. 1326 [1373]
Kreitmeier, P. 1360 [1411]
Kremer, K. A. M. 1522 [1580]
Krickemeyer, E. 1719 [1787]
Krug, V. 293 [277]
Krüger, C. 387, 833, 1064, 1092, 1157, 1544, 1559 [415, 853, 1096, 1108, 1219, 1602, 1616]
Krüger, M. 1176 [1232]
Kubiniok, S. 431 [434]
Kuchen, W. 1695 [1757]
Kuchler, J. G. 394, 946 [420, 975]
Kuck, D. 1192 [1222]
Kuczkowski, R. L. 1356 [1407]
Kuhn, N. 579, 1368 [572, 1433]
Kumagai, T. 1061 [1134]
Kunz, H. 711, 1086, 1375, 1697 [732, 1118, 1424, 1763]
Kunz, T. 268 [297]
Küper, S. 433 [438]
Kuroda, M. 1725, 1727 [1793, 1795]
Kutschke, D. 1201 AM [1243]

LABARGE, M. S. 1356 [1407]
Laber, N. 568 [599]
Labib, L. 1160 [1194]
Laggner, P. 1722 [1790]
Lahoz, F. J. 402, 1700 [406, 1766]
Lamb, H. H. 1127 [1162]
Lange, C. 980 [967]
Langford, H. D. 754
Lappas, D. 587 [585]
Laszlo, P. 479 [495]
Latscha, H. P. 287 [298]
Lavallee, D. K. 1737
Lazraq, M. 828 [885]
Lebbe, T. 438 [432]
Ledermann, M. 272, 1559 [304, 1616]
Ledwith, A. 1739
Lee, K. S. 1730 [1798]
Lehn, J.-M. 89, 1059 [91, 1121]
Leigh, J. S. 396 [399]
Leitner, W. 1180 [1231]
Lempert, G. 1203 AM [1245]
Lentz, D. 845 [871]
Leumann, C. H. 1172 [1227]
Lex, J. 406, 409, 411 [445, 448, 450]
Li, Q. 1731 [1799]
Libby, E. 1731 [1799]
Lidin, S. 953 [995]
Lifshitz, Y. 1203 AM [1245]
Lindner, H. J. 1540 [1598]
Lingnau, R. 436 [409]
Liotta, D. 444
Lippard, S. J. 344 [353]
Lippold, U. 960 [959]
Lisowsky, R. 1087 [1124]
Liu, S. 1724 [1792]
Löchner, U. 929 [1013]
Loeffler, W. 1733 [1801]
Lohray, B. B. 581 [594]
Lorberth, J. 1160 [1194]
Losensky, H.-W. 1189 [1225]
Lowry, R. M. 1703 [1769]
Lübben, S. 1168 [1195]
Lucas, H. 1177 [1217]
Luger, P. 1534 [1592]
Lukasch, H. 960 [959]
Lundquist, E. G. 1165 [1236]
Lutz, H. D. 404 [413]
Lutz, S. 979, 1556 [989, 1614]

MAAS, G. 591
Maatta, E. A. 569 [583]
Mackay, A. L. 849 [867]
Maercker, A. 404 [413]
Maier, G. 295, 309, 566, 938 [303, 317, 590, 1014]
Maier, J. 980 [967]
Maier, S. 281 [274]
Maigrot, N. 950 [997]
Maisuls, S. 275 [268]
Makhova, I. V. 1716 [1784]
Mallien, M. 1062 [1091]
Malm, J.-O. 555 [580]
Mandl, R. 1722 [1790]
Manners, I. 958 [964]
Mannschreck, A. 270 [299]
Marder, T. B. 442 [436]
Margaretha, P. 1374 [1437]
Marinetti, A. 1382 [1435]
Markies, P. R. 1084 [1143]
Märkl, G. 389, 709, 963, 1360 [426, 720, 1009, 1411]
Marsch, M. 846, 1522 [868, 1580]
Martens, J. A. 1004
Martin, H.-D. 695 [714]
März, J. 1375 [1424]

Masamune, S. 1725, 1727 [1793, 1795]
Mason, J. 1386
Massa, W. 414, 684, 961, 1160, 1370 [397, 727, 961, 1194, 1421]
Mathews, E. A. 1161 [1202]
Mathey, F. 950, 1382 [997, 1435]
Matusch, R. 717 [729]
Maverick, E. F. 387, 880 [415, 910]
Mayer, H. 958 [964]
Mayer, J. M. 1527 [1585]
Mayr, A. 1730 [1798]
Mazzanti, M. 576 [587]
McCammon, J. A. 862
McDermott, S. D. 1161 [1202]
Means, C. M. 1361 [1412]
Meier, W. 708 [717]
Meijer, E. W. 975 [1004]
Meinigke, B. 280 [288]
Melder, J.-P. 1103 [1140]
Meléndez, E. 1099 [1132]
Melloul, S. 683 [711]
Merz, G. 1365 [1425]
Merzweiler, K. 965, 1277, 1512 [978, 1300, 1572]
Metzger, J. O. 1168 [1195]
Meyer, U. 1563 [1621]
Meyer-Zaika, W. 952 [956]
Meyer zu Reckendorf, W. 1075 [1094]
Michael, H. 845 [871]
Michel, D. 1410
Michels, G. 272 [304]
Michl, J. 863
Millington, K. R. 1161 [1202]
Minet, U. 1373 [1422]
Mink, C. 1191 [1213]
Misaki, Y. 1078 [1129]
Mitchell, D. K. 930 [985]
Miyashi, T. 434 [428]
Möhwald, H. 728 AM [750]
Moll, M. 1164 [1221]
Montaser, A. 1387
Mootz, D. 391, 392 [424, 425]
Morgan, E. D. 460 [475]
Morgan, S. L. 1565
Mori, K. 859 [872]
Morley, S. D. 1361 [1412]
Morss, L. R. 1111
Mortreux, A. 683 [711]
Moss, S. J. 1739
Mosset, P. 1188 [1233]
Motz, D. 939 [970]
Moulines, F. 1347 [1394]
Mukai, T. 434, 1061 [428, 1134]
Müllen, K. 288, 1377 [290, 1429]
Müller, A. 1719, 1721 [1787, 1789]
Müller, G. 417, 419, 583, 935, 977, 1071 (—), 1516, 1542 [439, 441, 574, 979, 1011, 1135 (1440), 1574, 1600]
Müller, H. 1103 [1140]
Müller, K. A. 735 AM [757]
Müller, P. 574 [604]
Müller, U. 293 [277]
Müller, W. 572 [577]
Müller-Fahrnow, A. 393 [429]
Mulley, S. 927 [972]
Münster, H. 280 [288]
Murata, I. 1717 [1785]
Murugaraj, P. 980 [967]
Musso, H. 298 [267]
Mutter, M. 858 [855]
Mynott, R. 1157, 1559 [1219, 1616]

NAARMANN, H. 288 [290]
Nachbaur, E. 701 [703]
Nagase, S. 1081 [1097]
Nagatomi, T. 560, 1078 [597, 1129]
Nakajima, T. 1219
Nakano, M. 1081 [1097]
Näumann, F. 226 [232]
Neidlein, R. 294 [292]
Neidleman, S. L. 985
Neubert, W. 287 [298]
Neubold, P. 933 [990]
Neves, A. 685 (—) [718 (894)]
Nickon, A. 1197
Nicolaou, K. C. 1097, 1362 [1138, 1413]
Niecke, E. 1713, 1715 [1779, 1781]
Nieger, M. 416, 957, 976, 1713, 1715 [437, 957, 987, 1779, 1781]
Niemann, B. 957 [957]
Nikishin, G. I. 1716 [1784]
Nishino, K. 1717 [1785]
Nixdorf, M. 387 [415]
Noe, C. R. 1379 [1431]
Noltemeyer, M. 850, 1074, 1194, 1330 [852, 1093, 1238, 1377]
Nomoto, T. 1084 [1143]
Norton, J. R. 984
Nöth, H. 1, 842, 1331, 1603 [1, 875, 1378, 1664]
Nuber, B. 389, 685 (—), 708, 709, 933 [426, 718 (894), 717, 720, 990]
Nugiel, D. A. 1362 [1413]
Nunn, C. M. 277, 837, 838, 1349 [306, 873, 874, 1396]
Nunn, K. 1188 [1233]

ODA, M. 1080 [1131]
Odell, B. 1547, 1550 [1605, 1608]
Ohmer, J. 1277, 1512 [1300, 1572]
Okada, J. 859 [872]
Okuda, T. 1711 [1777]
Olah, G. A. 590
O'Neal, S. C. 1702 [1768]
Opiela, S. 1059 [1110]
Oro, L. A. 402, 1563, 1700 [406, 1621, 1766]
Ostoja Starzewski, K. A. 839 [861]
Otani, H. 1080 [1131]
Ouzounis, D. 280, 1059 [288, 1110]
Oxender, D. L. 1110

PACIELLO, R. A. 946 [975]
Paetzold, P. 958 [964]
Patai, S. 444, 1199
Pauer, F. 1074 [1093]
Paulmier, C. 444
Paulsen, H. 1365 [1425]
Paulus, H. 1540 [1598]
Paust, J. 285 [301]
Pavlovski, V. I. 789 [812]
Pawelke, G. 392 [425]
Pawlenko, S. 446
Payne, K. R. 1385
Pedersen, C. J. 1021 [1053]
Penk, M. 1719 [1787]
Pennington, W. T. 1702 [1768]
Pereyre, M. 445
Peters, E.-M. 931 [969]
Peters, K. 851, 931 [878, 969]
Petford-Long, A. 555 [580]
Petit, F. 683 [711]
Pettig, D. 1194 [1238]
Petzow, G. 989 AM [1021]
Pickardt, J. 1077 [1119]
Pilz, M. 1370 [1421]
Plenio, H. 1330 [1377]
Ploog, K. 593 [611]
Pohl, S. 431 [434]
Poignée, V. 294 [292]
Polborn, K. 699 [722]
Poll, T. 1553 [1611]
Poll, W. 392 [425]
Pople, J. A. 862
Popp, T. 574 [604]
Pörschke, K. R. 833 [853]
Port, H. 281 [274]
Power, J. M. 838 [874]
Power, P. P. 1699 [1765]
Poznyak, A. L. 789 [812]
Prakash, G. K. S. 590
Prechtl, F. 1536 [1594]
Preibsch, W. 1524 [1581]
Priepke, H. 278 [285]
Prigogine, I. 983
Prinzbach, H. 1103 [1140]
Pritzkow, H. 287, 299, 399, 706, 926, 1519 [298, 272, 410, 705, 963, 1577]
Provost, J. 440 [403]
Przybilla, K. J. 976 [987]
Psaras, P. A. 754

QUIN, L. D. 591
Quintard, J.-P. 445

RABALAIS, J. W. 1203 AM [1245]
Rabek, J. F. 1568
Rabenau, A. 980 [967]
Raddatz, P. 426 [414]
Radhakrishnan, T. P. 427 [431]
Radola, B. J. 1109
Radom, L. 862
Radunz, H.-E. 426 [414]
Ragnarsson, U. 400 [411]
Rahm, A. 445
Range, K.-J. 969 [973]
Rapp, C. 1733 [1801]
Rappoport, Z. 444, 1199
Raveau, B. 440 [403]
Ray, M. S. 1001
Razim, C. 726 AM [748]
Reber, G. 1071 (—) [1135 (1440)]
Reddington, M. V. 1547, 1550 [1605, 1608]
Reed, G. 1738
Reedijk, J. 856 [884]
Reetz, M. T. 994 AM, 1373 [1026, 1422]
Regitz, M. 272, 591, 713, 1157, 1484, 1559 [304, —, 725, 1219, 1541, 1616]
Rehm, H.-J. 1738
Reichert, F. 1713, 1715 [1779, 1781]
Reisenauer, H. P. 295, 566 [303, 590]
Reissig, H.-U. 268, 1518 [297, 1576]
Reith, W. 699 [722]
Renneke, R. F. 1526 [1583]
Rétey, J. 1089 [1122]
Reynolds, K. 1089 [1122]
Rheingold, A. L. 424 [400]
Ricard, L. 950 [997]
Rice, S. A. 983
Rickard, C. E. F. 302 [308]
Riede, J. 935, 1516 [979, 1574]
Riera, V. 1167 [1224]
Ries, M. 927 [972]
Rigault, A. 1095 [1121]
Ringsdorf, H. 113 [117]
Roberts, N. K. 941 [1002]
Robertson, G. B. (589), 941 [(610), 1002]
Robinson, J. A. 1089 [1122]
Robinson, K. D. 1361 [1412]

Rodgers, M. A. J. 861
Roesky, H. W. 850, 1330, 1372 [852, 1377, 1417]
Röhrich, J. 1377 [1429]
Röhrig, P. 411 [450]
Roper, W. R. 302 [308]
Rosmus, P. 1329 [1376]
Roth, E. 1174 [1229]
Rothwell, I. P. 1181 [1218]
Rufińska, A. 1513 [1569]
Rühlmann, A. 1186 [1200]
Ruiz, M. A. 1167 [1224]
Ruiz-Pérez, C. 294 [292]
Ruloff, C. 1381 [1418]
Russey, W. E. 1565
Ruther, M. 1186 [1200]

SAAK, W. 431 [434]
Saalfrank, R. W. 851, 1188 [878, 1233]
Saatkamp, K. 1326 [1373]
Saenger, W. 393 [429]
Saier, Jr., M. H. 1040 [1072]
Saito, K. 434 [428]
Sakai, A. 1711 [1777]
Salbeck, J. 291 [278]
Salifoglou, A. 1353 [1404]
Samaraweera, U. 1355 [1406]
Sander, W. 398, 572 [402, 577]
Sands, R. H. 1353 [1404]
Sanz, M. G. 1167 [1224]
Satake, K. 1061 [1134]
Satgé, J. 828 [885]
Saupe, T. 865 [895]
Sauvage, J.-P. 930 [985]
Sawitzki, G. 925 [958]
Sawyer, L. C. 1220
Schaad, L. J. 938 [1014]
Schach, T. 272 [304]
Schäfer, U. 566 [590]
Schäfer, V. 299 [272]
Schäufele, H. 1519 [1577]
Scherbaum, F. 419, 1542, 1544 [441, 1600, 1602]
Scherer, O. J. 405, 694 [423, 738]
Schiffmann, D. 329 [443]
Schlag, E. W. 447 [461]
Schlarb, B. 113 [117]
Schleyer, P. von R. 862
Schlosser, H. 281 [274]
Schlosser, W. 963 [1009]
Schlüter, A.-D. 296 [283]
Schmalz, D. 1692 [1754]
Schmickler, H. 406, 411 [445, 450]
Schmid, G. 555, 952 [580, 956]
Schmid, R. D. 755
Schmidbaur, H. 2, 417, 419, 1071 (—), 1542, 1544 [2, 439, 441, 1135 (1440), 1600, 1602]
Schmidt, G. 717 [729]
Schmidt, R. R. 1178 [1234]
Schmidt, T. 427 [431]
Schmidtchen, F. P. 1516 [1574]
Schmidt-Lukasch, G. 960 [959]
Schmutzler, R. 1562 [1620]
Schneider, G. 426 [414]
Schneider, H.-J. 1163 [1211]
Schnering, H. G. von 574, 851, 931 [604, 878, 969]
Schnöckel, H. 421 [418]
Schobert, R. 855 [869]
Schoeller, W. W. 1713 [1779]
Schoenfeld, R. 1050 [1083]
Schöllhorn, R. 1392 AM [1446]
Schöllkopf, U. 433, 1194 [438, 1238]
Schram, J. 1695 [1757]
Schreer, M. 944 [1006]
Schrobilgen, G. J. 479 [495]
Schröder, S. 973 [965]
Schuhn, W. 416 [437]
Schul, W. 971 [983]
Schultz, N. 1075 [1094]
Schultz, P. G. 1172 [1227]
Schulz, M. 948 [993]
Schulze, E. 1194 [1238]
Schumann, H. 1077 [1119]
Schümann, U. 584 [573]
Schunck, S. 421 [418]
Schurz, K. 935 [979]
Schuster, Andreas 1192 [1222]
Schuster, Annemarie 1722 [1790]
Schütz, J. U. von 267 [286]
Schwartz, H. 426 [414]
Schwarz, H. 1337 (—), 1533 [1384 (1628), 1591]
Schwarz, M. 574 [604]
Seaborg, G. T. 1111
Sebastián, S. 402 [406]
Seebach, D. 1351, 1624, 1718 [1398, 1685, 1786]
Seep, C. 1511 [1568]
Seitz, F. 289 [281]
Sellmann, D. 689, 691, 1164 [706, 710, 1221]
Seppelt, K. 1534 [1592]
Seubert, B. 1164 [1221]
Sharpless, K. B. 835 [882]
Sheldrick, G. M. 703, 850, 1074, 1186, 1330 [739, 852, 1093, 1200, 1377]
Sheldrick, W. S. 956 [1008]
Shimizu, S. 622 [640]
Shinjo, T. 1410
Shokat, K. M. 1172 [1227]
Shukla, S. 1735 [1803]
Sicard, G. 301 [289]
Sicheneder, A. 718 [730]
Sicken, M. 409, 411 [448, 450]
Siebert, W. 299, 399, 926 [272, 410, 963]
Silversmith, E. F. 1197
Simon, A. 159, 1339 [163, 1386]
Sinnwell, V. 270 [299]
Slawin, A. M. Z. 966, 1184, 1547, 1550 [981, 1215, 1605, 1608]
Smeets, W. J. J. 1084 [1143]
Smith, D. J. 555 [580]
Smith, G. W. 1364 [1415]
Sola, E. 1563 [1621]
Sone, K. 1411
Sonnenberg, U. 1537 [1595]
Sooriyakumaran, R. 1355 [1406]
Sowerby, D. B. 1107
Spek, A. L. 1058, 1084 [1115, 1143]
Spelthann, H. 1189 [1225]
Spencer, C. M. 966 [981]
Spencer, N. 1547 [1605]
Spiess, H. W. 1655 [1716]
Staab, H. A. 865 [895]
Stadelhofer, J. W. 1108
Stalke, D. 1562 [1620]
Stark, A. 851 [878]
Steckhan, E. 265 [295]
Steenken, S. 1066 [1113]
Stehling, L. 571 [575]
Stelzer, O. 438, 956 [432, 1008]
Steudel, R. 1358 [1409]
Steuernagel, S. 564 [600]
Stoddart, J. F. 692, 966, 1184, 1547, 1550 [712, 981, 1215, 1605, 1608]
Stone, F. G. A. 1703 [1769]
Stowell, J. C. 1737
Strähle, J. 436, 896, 929, 1094 [409, 927, 1013, 1099]
Straub, A. 716 [737]
Strössner, K. 1101 [1116]
Strube, A. 1529 [1586]
Stucky, G. 1351 [1398]
Stürmer, R. 1176 [1232]
Stylianides, N. A. 1097 [1138]
Suckling, C. J. 537 [555]
Sugasawara, R. 1172 [1227]
Sugimoto, T. 560, 1078, 1573 AM, 1711 [597, 1129, 1633, 1777]
Sülzle, D. 1337 (—), 1533 [1384 (1628), 1591]
Sundermeyer, J. 1372 [1417]
Sünkel, K. 939 [970]
Sustmann, R. 572 [577]
Suzuki, T. 434 [428]
Swarowsky, H. 694 [738]
Swarowsky, M. 405, 694 [423, 738]
Syassen, K. 1101 [1116]

TAKADA, T. 1410
Takahashi, T. 1711 [1777]
Tamura, Y. 1717 [1785]
Tanaka, S. 1061 [1134]
Taqui Khan, M. M. 923, 1735 [1000, 1803]
Teles, J. H. 938 [1014]
Terlouw, J. K. 1533 [1591]
Teuben, J. H. 1058 [1115]
Thiele, G. F. 1191 [1213]
Thomas, J. M. 1364, 1673 [1415, 1735]
Thulstrup, E. W. 863
Tietze, L. F. 703, 971, 1186 [739, 983, 1200]
Tinkham, M. L. 437 [408]
Tiriliomis, A. 713 [725]
Tiripicchio, A. 402, 1167 [406, 1224]
Tiripicchio Camellini, M. 402, 1167 [406, 1224]
Toda, F. 859 [872]
Töllner, F. 1381 [1418]
tom Dieck, H. 1062, 1556 [1091, 1614]
Tonegawa, S. 1028 [1060]
Torkelson, J. M. 1409
Touhara, H. 1219
Trueblood, K. N. 880 [910]
Tsay, Y.-H. 1064 [1096]

UEDA, W. 1364 [1415]
Ugi, I. 1558 [1618]
Unverzagt, C. 1697 [1763]
Uyeki, M. A. 1705 [1775]

VAN AELST, S. F. 1177 [1217]
van Boeckel, C. A. A. 1177 [1217]
van der Does, T. 936 [998]
van Eikema Hommes, N. J. R. 1083 [1100]
Vanhoye, D. 683 [711]
Vargas, F. 429 [443]
Vasuez, L. 706 [705]
Veith, M. 1087, 1381 [1124, 1418]
Venanzi, L. M. 563 [571]
Venzmer, J. 113 [117]
Verhoeven, M. 1533 [1591]
Verkade, J. G. 591, 863
Vincent, J. B. 1731 [1799]
Voelkel, R. 1468 [1525]
Vogel, E. 406, 409, 411 [445, 448, 450]
Vogelbacher, U. J. 272 [304]
Vogt, T. 929 [1013]

Vögtle, F. 976, 1189 [987, 1225]
Vollhardt, J. 1092, 1540 [1108, 1598]
Vollhardt, K. P. C. 553, 1106 [592, —]
Vonholdt, E. 1524 [1581]

WACHTER, J. 708 [717]
Wade, K. 590
Waggoner, K. M. 1699 [1765]
Wagner, H.-U. 842, 1437 [875, 1492]
Wagner, W. 394 [420]
Walberg, H.-J. 1719 [1787]
Waldmann, H. 274 [307]
Wallace, A. S. 1530 [1588]
Walsh, C. T. 333 [342]
Walz, L. 574 [604]
Wang, G. 714 [723]
Wang, Y. 387 [415]
Wasgestian, F. 280 [288]
Watanabe, N. 1219
Weber, L. 1537 [1595]
Weichert, U. 1365 [1425]
Weil, K. G. 1091 [1111]
Weiss, E. 584 [573]
Weiss, J. 685 (—), 933 [718 (894), 990]
Weiss, K. 275 [268]
Wensing, M. 943 [1005]
Wenz, G. 979, 1556 [989, 1614]
Werner, H. 948, 1563 [993, 1621]
Werner, H.-P. 267 [286]
Whitmire, K. H. 396 [399]
Wiberg, N. 935 [979]
Wickramasinghe, W. A. (589), 941 [(610), 1002]
Wieghardt, K. 685 (—), 933 [718 (894), 990]
Wientges, H. 1064 [1096]
Wilczok, U. 1513 [1569]
Wild, D. 429 [443]
Wildenauer, M. 969 [973]
Wilke, G. 185, 571, 833 [189, 575, 853]
Wilkinson, D. L. 583, 977 [574, 1011]
Willenbrock, F. 1089 [1122]
Williams, D. J 261 (589), 966, 1184, 1547, 1550 [266 (—), 981, 1215, 1605, 1608]
Williams, R. E. 90
Willis, A. C. (589) [(610)]
Willson, A. D. 1161 [1202]
Wimmer, T. 1071 (—) [1135 (1440)]
Winpenny, R. E. P. 261 (589) [266 (—)]
Wirz, J. 585, 853 [589, 880]
Witt, M. 850 [852]
Witte, J. 839 [861]
Wolf, H. C. 267, 281 [286, 274]
Wolf, P. 288, 1377 [290, 1429]
Wolfer, M. K. 563 [571]
Wolmershäuser, G. 405, 694 [423, 738]
Wong, H. N. C. 705 (1200) [716 (1242)]
Wong, T. 705 (1200) [716 (1242)]
Wright, J. D. 1003
Wrighton, M. S. 289 [281]
Wronna, C. 691 [710]
Wulff, G. 1158 [1197]
Wünsch, M. 414 [397]
Wüstefeld, C. 929 [1013]
Wynberg, H. 975 [1004]

YAMADA, H. 622 [640]
Yamashita, O. 1725 [1793]
Yamashita, Y. 434 [428]
Yamauchi, J. 1078 [1129]
Yanagida, H. 1389 AM [1443]
Yates, Jr., J. T. 1198
Yoshida, Z. 560, 1078, 1573 AM, 1711 [597, 1129, 1633, 1777]

ZANDER, K. 1538 [1596]
Zangwill, A. 1409
Zarzycki, R. 1184 [1215]
Zauder, E. 579 [572]
Zechner, M. 1722 [1790]
Zenneck, U. 706, 1519 [705, 1577]
Zhang, H. 1361 [1412]
Ziegler, M. L. 389, 708, 709, 1099 [426, 717, 720, 1132]
Ziegler, T. 716 [737]
Zimmer, R. 1518 [1576]
Zoebelein, H. 41 [41]
Zsolnai, L. 698, 1529 [731, 1586]
Zubieta, J. 1342, 1724 [1389, 1792]
Zybill, C. 583 [574]
Zyss, J. 986

SUBJECT INDEX

(page numbers in brackets indicate an erratum to the corresponding article)

(R) = Review Article (C) = Short Communication (B) = Book Review (L) = Correspondence (AM) = Advanced Materials

Ab initio calculations, Formation of dioxirane from carbonyl oxide (C) 427
— Is tetrasilatetrahedrane kinetically stable? (C) 1081
— Is the molecule BOK quasi-linear? (C) 1329
— Structure of molecular PNO, matrix isolation and ab initio calculations (C) 421
— [1,2,4]Triazolo[1,2-*a*][1,2,4]triazole-1,3,5,7(2*H*,6*H*)-tetrone (urazourazole), synthesis and structure (C) 701
γ-Acetoxylation, C_5 building blocks for terpene syntheses: γ-acetoxylation of (*E*)-2-methyl-2-butenals (C) 285
Acetylene polymerization with ylide-nickel catalysts (C) 839
Actinides, The chemistry of the actinide elements (B) 1111
Active site, Catalytic activity of enzymes altered at their active sites (R) 913
Acylations, *N*-Aryl-*O*-acylhydroxylamines: preparation by *O*-acylation or *N*→*O* transacylation and reaction with amines; model reactions for key steps connected with the carcinogenicity of aromatic amines (C) 973
Adamantanediones, Chirality solely due to the presence of an excited state (C) 975
Adamantoid compounds, The first "adamantoid" alkaline earth metal chelate complex: synthesis, structure, and reactivity (C) 851
Advanced materials—a critical view (AM) 726
— Editorial (AM) 723
Air-sensitive compounds, The manipulation of air-sensitive compounds (B) 308
Aldol reactions, Diastereo- and enantioselective aldol reactions via α-silyl ketones, asymmetric synthesis of the aggregation pheromone sitophilure (C) 581
Alkali-metal compounds, A monomeric diboryldilithiomethane with a 1,3-diboratallene structure (C) 1370
— A monomeric potassium salt of bis(trimethylsilyl)methyl phenyl sulfone and the determination of the $^1J(^{13}C,^{29}Si)$ coupling constants of Si-stabilized "carbanions" (C) 1092
— 1,2-Dilithioethane from ethylene and lithium (C) 1083
— From the dilithiooctamethylcyclotetrasilazane to the 1,3,5,7-tetraaza-2,4,6,8,9-pentasilabicyclo[3.3.1]nonane system (C) 1074
— Higher thermostability and selectivity of Köbrich reagents by transmetalation (C) 943
— Isolated, complex Zintl molecules in the gas phase (C) 1091
— Isolation and structure of $[\{fluorenone^{\odot\ominus}\}\{Na^{\oplus}(dme)_2\}]_2$ — a touchstone for radical contact ion pairs? (C) 1067
— 3-Lithio-2-(*o*-lithiophenyl)naphthalenedilithium—a tetralithio compound with σ- and π-bonded lithium atoms (C) 1182
— Novel layer structure of sodium calix[4]arenesulfonate complexes—a class of organic clay mimics? (C) 1361
— Phase transformations of lithium nitride under pressure (C) 1101
— Solid state structure of a lithium triorganostannate (C) 1381
— Structure and reactivity of lithium enolates. From pinacolone to selective *C*-alkylations of peptides. Difficulties and opportunities afforded by complex structures (R) 1624
— Structure of a chiral lithium azaenolate: monomeric, intramolecular chelated lithio-2-acetylnaphthalene-SAMP-hydrazone (C) 1522
— Synthesis and structure of $[NaTi(2,6\text{-}Me_2C_6H_3O)_4(py)]_2$: a dimeric material containing a novel phenoxide bridge (C) 1181
— Synthesis and structure of $[\{Na(tmeda)\}_3][LiPh_4]$, an organometallic complex containing two different alkali metals (C) 584
— X-ray structure investigation of 2,2-diphenyl-1-(phenylsulfonyl)cyclopropyllithium–dimethoxyethane (2/3): a sulfonyl "carbanion" having an α-C atom with a tetrahedral configuration (C) 846
Alkaloids, Synthesis of strictosidine analogues by hetero-Diels-Alder reaction and their biomimetic transformation to indole alkaloids (C) 971
Alkanes, Selective photochemical dehydrogenation of saturated hydrocarbons with quantum yields approaching unity (C) 1526
Alkynes, Acid-catalyzed alkyne/alkene coupling at Re^{III} centers (C) 1509
— Alkyne coordination to organorhenium oxides with rhenium in high oxidation states (C) 946
— Oxidative coupling of racemic and of optically active 3,6-di-*tert*-butylocta-1,4,7-triyne-3,6-diol (C) 859
— Tetrakis[bis(trimethylsilyl)ethyne]diiron (C) 1519
Aluminum compounds, New complex cations of aluminum(III) and gallium(III) (C) 277
— Synthesis and structure of $[MeAlN(2,6\text{-}iPr_2C_6H_3)]_3$: an aluminum-nitrogen analogue of borazole (C) 1699
Amines, "Proton sponges" and the geometry of hydrogen bonds: aromatic nitrogen bases with exceptional basicities (R) 865
Amino acids, Amino acid methyl esters as chiral auxiliaries in aza-Diels-Alder reactions in aqueous solution (C) 274
— A simple access to 2-substituted 3,3,3-trifluoroalanine derivatives (C) 848
— Chlorotetain from *bacillus subtilis*, an antifungal dipeptide with an unusual chlorine-containing amino acid (C) 1733
— Enantio- and diastereoselective synthesis of methyl (2*R*)-2-amino-5-oxocarboxylates from enones and bislactim-ether cuprates (C) 1194
— Enantioselective synthesis of (*R*)-*N*-Boc-1-amino-2-arylcyclopropene-1-carboxylic acid methyl ester (C) 433
— Reduction with yeast cells, the key step of an efficient synthesis of (3*S*, 4*S*)-4-amino-3-hydroxypentanoic acids (C) 426
— Synthesis and properties of N^{α}-Di-*tert*-butoxycarbonyl and N^{α}-benzyloxycarbonyl *tert*-butoxycarbonyl amino acids (C) 400
Amino imino boranes, The chemistry of amino imino boranes (R) 1603
Analytical methods, Atomic motions in molecular crystals from diffraction measurements (R) 880
— Classical light scattering from polymer solutions (B) 1221
— Gas chromatographic separation of enantiomeric olefins (C) 1556
— High-resolution solid-state ^{13}C-NMR spectroscopy of polymers (R) 1468
— Inductively coupled plasmas in analytical atomic spectrometry (B) 1387
— Multiphoton-ionization-mass spectrometry (MUPI-MS) (R) 447
— NOESY-TOCSY, an advantageous 2D NMR technique for the analysis of peptide sequences (C) 564
— Pheromones in nanogram quantities: structure determination by combined microchemical and gas chromatographic methods (R) 460
— Polymer microscopy (B) 1220
— Two-dimensional NMR spectroscopy: background and overview of the experiments (R) 490
Antibodies, An antibody-mediated redox reaction (C) 1172
Antigenes, Somatic generation of immune diversity (Nobel lecture) (R) 1028
Antimony compounds, Synthesis and structure of an azastibacubane (C) 287
— Tris(2,3-di-*tert*-butylcyclotriphosphanyl)stibane—a compound containing three P_3 rings linked by an antimony atom (C) 561
Arene complexes, Alkyne(arene)cobalt, μ-alkynebis(arenecobalt), and μ-benzylidynetris(arenecobalt) from arene/cobalt cocondensates (C) 706
— π Complexes of an amino-9-fluorenylideneborane (C) 1331
— Electron-electron/spin-spin long-range interaction as studied in the diradical dication $[Di\{bis(dimethylphosphino\text{-}\eta^6\text{-}benzene)chromium(I)\}\text{-}nickel(0)]^{++}$ (C) 414
— (Octamethyltetrasila-η^{12}-[2.2]paracyclophane)chromium — synthesis, structure, and characteristics (C) 684
— $2,4,6\text{-}Ph_3C_6H_2M$ (M = Cu, Ag), monomeric Cu^I- and Ag^I-complexes with coordination number 1 (C) 436
— Stabilization of 1,2,4,5-tetradehydrobenzene by complexation at two nickel(0) centers (C) 941
— Titanium(0)-arene complexes. Synthesis and X-ray crystal structure of $[(\eta^6\text{-}C_{10}H_8)Ti\{tBuSi(CH_2PMe_2)_3\}]$ (C) 1693
Arenes, *N*-Aryl-*O*-acylhydroxylamines: preparation by *O*-acylation or *N*→*O* transacylation and reaction with amines; model reactions for key steps connected with the carcinogenicity of aromatic amines (C) 973
— Industrielle Aromatenchemie. Rohstoffe, Verfahren, Produkte (B) 1108
— Isolation and structure of $[\{fluorenone^{\odot\ominus}\}\{Na^{\oplus}(dme)_2\}]_2$ — a touchstone for radical contact ion pairs? (C) 1067
— Methyl 4-hydroxy-5-iodo-2,3-dimethoxy-6-methylbenzoate: the aromatic fragment of calichemicin γ^1_α. Synthesis, X-ray crystallographic analysis, and properties (C) 1097
— "Proton sponges" and the geometry of hydrogen bonds: aromatic nitrogen bases with exceptional basicities (R) 865
— Strongly bent naphthalene units in [2](2,6)naphthalino[2]paracyclophane and [2](2,6)naphthalino[2]paracyclophane-1,11-diene (C) 1064
Aromaticity, A donor-acceptor substituted quinoid pentalene (C) 1711
— Biomimetic synthesis of an octavinylogous porphyrin with an aromatic [34]annulene system (C) 1170
— Bis([1,2,5]thiadiazolo)[3,4-*b*;3′,4′-*e*]pyrazine, a novel 14π-electron heterocycle with high electron affinity (C) 434
— Donor-acceptor-substituted cyclic π-electron systems—probes for theories and building blocks for new materials (R) 1437
— 1,6-Methano[10]annulenedianion, a para-

tropic 12π-electron dianion with a C_{10} perimeter (C) 1692
— Synthesis and structure of 2,7-Di-*tert*-butyldicyclopenta[*a,e*]cyclooctene (C) 1191
— 1,3,4,6-Tetraamino-2,5-diazapentalenes: delocalized antiaromatic compounds (C) 842
— Tetraoxaporphycene dication (C) 411
— Tetraoxaporphyrin dication (C) 406
— Tetraoxaporphyrinogen (tetraoxaquaterene): oxidation to the tetraoxaporphyrin dication (C) 409
— The cyclohepta[*def*]carbazolium ion (C) 585
— Tris(fluoren-9-ylidene)cyclopropane, a novel [3]radialene (C) 1080
— Tris(thioxanthen-9-ylidene)cyclopropane, and its radical cation and dication (C) 1078
Aromaticity (B) 306
Arsenic compounds, A novel heterocluster with D_3-symmetry containing twenty-one core atoms: $[As_6^{III}V_{15}^{IV}O_{42}(H_2O)]^{6\ominus}$ (C) 1721
Artificial elements, Synthesis of the heaviest chemical elements—results and perspectives (R) 1417
Aryl complexes, Novel anionic aryl complexes of Rh^{III}: $[Rh(C_6F_5)_5]^{2\ominus}$ and $[Rh(C_6F_5)_4(CO)_2]^{\ominus}$ (C) 1700
Asymmetric induction, First case of interannular, possibly electronically transmitted, asymmetric induction in an organometallic compound (C) 553
— in the [2,3] Wittig rearrangement by chiral substituents in the allyl moiety (C) 278
— Structure of a chiral lithium azaenolate: monomeric, intramolecular chelated lithio-2-acetylnaphthalene-SAMP-hydrazone (C) 1522
Asymmetric synthesis, Asymmetric induction in the replacement of diastereotopic bromine atoms by lithium atoms (C) 1176
— Diastereo- and enantioselective aldol reactions via α-silyl ketones, asymmetric synthesis of the aggregation pheromone sitophilure (C) 581
Azacyclobutadienes, Reactivity of Tri-*tert*-butylazete (C) 272
Azastibacubanes, Synthesis and structure of an azastibacubane (C) 287
Azatriphosphatetracyclodecadienes, Reaction of 1,3-azaphosphinines with 2-*tert*-butyl-1-phosphaethyne: 9-aza-2,4,6-triphosphatetracyclo[5.3.0.0^{2,4}.0^{3,6}]deca-8,10(1)-diene (C) 389
Azetes, First structure analysis and photoelectron spectroscopic investigation of an azete and an azete-cobalt complex (C) 1559
Azirines, Azirineimine as a structural unit in the side chain of a hexofuranose (C) 1075
Azoles, Nitroazoles. The *C*-nitro derivatives of five-membered *N*- and *N,O*-heterocycles (B) 985

Baeyer-Villiger oxidations, Enzymic Baeyer-Villiger oxidations by flavin-dependent monooxygenases (R) 333
Biochemistry, A synthetic heparin-like compound which still activates antithrombin III although it contains an open chain fragment instead of α-L-idopyranuronate (C) 1177
— Enzymic Baeyer-Villiger oxidations by flavin-dependent monooxygenases (R) 333
— Evidence for a folded conformation of methotrexate in solution (C) 423
— Facile reduction of 1,2-dioxetanes by thiols as potential protective measure against photochemical damage of cellular DNA (C) 429
— Flexibility and rigidity of proteins and protein-pigment complexes (R) 79
— Isoleucyl-tRNA synthetase: an enzyme with several catalytic cycles displaying variation in specificity and energy consumption (R) 773
— Oxo-bridged polyiron centers in biology and chemistry (R) 344
— Protein phosphorylation in bacteria—regulation of gene expression, transport functions, and metabolic processes (R) 1040
— Reduction with yeast cells, the key step of an efficient synthesis of (3*S*, 4*S*)-4-amino-3-hydroxypentanoic acids (C) 426
— Short, highly enantioselective synthesis of a key intermediate for the preparation of leucotriene B_4 and its 14,15-didehydro derivative (C) 1188
— Somatic generation of immune diversity (Nobel lecture) (R) 1028
— The chemistry and biochemistry of *N*-substituted porphyrins (B) 1737
— The cyclopropyl group in studies of enzyme mechanism and inhibition (R) 537
— Tumor lectinology: at the intersection of carbohydrate chemistry, biochemistry, cell biology, and oncology (R) 1267
Biogenesis, 4,6,6-Trimethyl-4-cyclohexene-1,2,3-trione, a contribution to the biogenesis of norcarotinoids (C) 695
Biohalogenation. Principles, basic roles, and applications (B) 985
Bioinorganic chemistry, Oxo-bridged polyiron centers in biology and chemistry (R) 344
Biomembranes, Molecular architecture and function of polymeric oriented systems: models for the study of organization, surface recognition, and dynamics of biomembranes (R) 113
Biomimetic syntheses, Biomimetic synthesis of an octavinylogous porphyrin with an aromatic [34]annulene system (C) 1170
— Synthesis of strictosidine analogues by hetero-Diels-Alder reaction and their biomimetic transformation to indole alkaloids (C) 971
Biomineralization, Molecular mechanisms of biomineralization in the formation of calcified shells (R) 1145
Biosensors, International workshop 1987 (B) 755
Biosynthesis, Vitamin B_{12}: experiments concerning the origin of its molecular structure (R) 5
Biotechnology, Vol. 7a: Enzyme Technology (B) 1738
Bismuth compounds, $[Cp_2Co][Bi\{Co(CO)_4\}_4]$: a paramagnetic, ten-electron, tetrahedral complex of bismuth (C) 396
— $Cs_2Bi_{10}Ca_6Cl_{12}O_{16}$: a new type of catalyst for selective oxidation derived from bismuth oxychloride (C) 1364
Boron compounds, A monomeric diboryldilithiomethane with a 1,3-diborataallene structure (C) 1370
— B_6H_{14}, a dimeric B_3H_7? (C) 262
— π Complexes of an amino-9-fluorenylideneborane (C) 1331
— Compounds with partial boron-carbon triple bonds (C) 961
— Dications based on a hydrotris(phosphonio)borate skeleton (C) 1071
— 1,3-Dihydro-1,3-diborafulvene derivatives (C) 299
— Lewis-base adducts of methyleneboranes (C) 960
— Nitrogen fixation by borabenzene (C) 295
— Novel boron-phosphorus cages with $C_4B_4P_4$ and $C_2B_4P_4$ frameworks (C) 399
— Reversible coupling and opening of a boron-carbon bond (C) 952
— Synthesis and structure of a 1,2,5,6-tetrahydro-1,2,5,6-tetraborocine (C) 926
— Synthesis and structure of $[Cp_2NbH(tBuB{\equiv}NtBu)]$, a compound with side-on coordinated iminoborane (C) 958
— Synthesis of oligomeric and polymeric monosaccharides by aldol group-transfer polymerization (C) 1158
— The chemistry of amino imino boranes (R) 1603
— The first *closo*-diphosphahexaborane $P_2B_4Cl_4$ (C) 925
Butadiene-1,4-diyl as ligand, Triple proton abstraction from a 1-methylallyl ligand on thermolysis: formation of a $Hf_3(C_4H_4)$ cluster (C) 1058
Butadiyne, Mono- and dinuclear nickel(0) complexes of butadiyne (C) 833

Cage compounds, A donor cage with bent tetrathiafulvalene moiety (C) 1377
— Functionalized, enantiomerically pure [2.1.1]-, [2.2.1]-, and [2.2.2]-triblattanes (C) 1103
— Novel boron-phosphorus cages with $C_4B_4P_4$ and $C_2B_4P_4$ frameworks (C) 399
— Reductive oligomerization of 1,2-Di-*tert*-butyl-1,1,2,2-tetrachlorodisilane: the tricyclo[2.2.0.0^{2,5}]hexasilane and tetracyclo[3.3.0.0^{2,7}.0^{3,6}]octasilane systems (C) 1725
— ^{29}Si-^{29}Si long range couplings in strained cyclic polysilanes (C) 1727
— The first *closo*-diphosphahexaborane $P_2B_4Cl_4$ (C) 925
Calcification, Molecular mechanisms of biomineralization in the formation of calcified shells (R) 1145
Calichemicins, Methyl 4-hydroxy-5-iodo-2,3-dimethoxy-6-methylbenzoate: the aromatic fragment of calichemicin $\gamma_{1\alpha}^{I}$. Synthesis, X-ray crystallographic analysis, and properties (C) 1097
Carbanions, A monomeric potassium salt of bis(trimethylsilyl)methyl phenyl sulfone and the determination of the $^{1}J(^{13}C,^{29}Si)$ coupling constants of Si-stabilized "carbanions" (C) 1092
— as intermediates in the synthesis of Grignard reagents (C) 687
— 1,2-Dilithioethane from ethylene and lithium (C) 1083
— Metal-free carbanion salts as initiators for the anionic polymerization of acrylic and methacrylic acid esters (C) 1373
— 1,6-Methano[10]annulenedianion, a paratropic 12π-electron dianion with a C_{10} perimeter (C) 1692
— Synthesis and structure of [*cyclo*-$C_3H_4{-}SO_2Ph]_2Ti[OCH(CH_3)_2]_2$, a *C*-titanated "α-sulfonyl carbanion" (C) 1540
— X-ray structure investigation of 2,2-diphenyl-1-(phenylsulfonyl)cyclopropyllithium-dimethoxyethane (2/3): a sulfonyl "carbanion" having an α-C atom with a tetrahedral configuration (C) 846
Carbene Complexes, Annelation of carbene ligands by λ^3-phosphaalkynes, an entry to functionalized phosphaarenes (C) 713
— Heterogeneous, bimetallic metathesis catalysts by reaction of Fischer-type carbene complexes with reduced Phillips catalyst (C) 275
— Ketenimine complexes from carbene complexes and isocyanides: versatile building blocks for carbocycles and N-heterocycles (R) 1456
Carbenes, Diisocyanogen (C) 936
— Formation of cycloheptatriene/norcaradiene systems in the decomposition of diaryldiazomethanes in benzene (C) 284
— 4-Oxo-2,5-cyclohexadienylidene — a carbene with a stable triplet and metastable singlet state? (C) 572
— Preparative UV-laser photochemistry: a biscarbene intermediate in the synthesis of a 5,6-dihydrodibenzo[*a,e*]cyclooctene containing a *trans*-double bond (C) 853
Carbenium ions, Inductivity and bridging in ammonium and carbenium ions (C) 714
Carbohydrates, A synthetic heparin-like compound which still activates antithrombin III although it contains an open chain fragment instead of α-L-idopyranuronate (C) 1177

— Azirineimine as a structural unit in the side chain of a hexofuranose (C) 1075
— β-Mannosides from β-glucosides by intramolecular nucleophilic substitution with inversion of configuration (C) 1086
— Protecting-group-dependent stability of intersaccharide bonds — synthesis of a fucosyl-chitobiose glycopeptide (C) 1697
— Simple synthesis of KDO α-glycosides by anomerically selective *O*-alkylation (C) 1178
— Synthesis of oligomeric and polymeric monosaccharides by aldol group-transfer polymerization (C) 1158
— Tumor lectinology: at the intersection of carbohydrate chemistry, biochemistry, cell biology, and oncology (R) 1267
Carbon-carbon linkage, Acid-catalyzed alkyne/alkene coupling at Re^{III} centers (C) 1509
— Acyl-alkylidyne coupling in the synthesis of dinuclear complexes (C) 1703
— Carbon dioxide as an alternative C_1 synthetic unit: activation by transition-metal complexes (R) 661
— Conjugated and nonconjugated cyclopentenones by a reaction cascade from methyl 6-oxo-5-phenyl-1,3,4-oxadiazine-2-carboxylate and 1,3-butadienes (C) 931
— First case of interannular, possibly electronically transmitted, asymmetric induction in an organometallic compound (C) 553
— Iodine-induced stereoselective carbocyclizations: a new method for the synthesis of cyclohexane and cyclohexene derivatives (C) 1546
— Linkage of alkylidyne, carbonyl, and alkyne ligands at a tungsten center to form a metallacyclopentadienone and an η^3-oxocyclobutenyl complex (C) 1730
— Pentadienyl, a more reactive and more strongly bound ligand than cyclopentadienyl (C) 1099
— Structure and reactivity of lithium enolates. From pinacolone to selective *C*-alkylations of peptides. Difficulties and opportunities afforded by complex structures (R) 1624
— The influence of polar and steric effects on the selectivity of the β-cleavage of alkyl radicals (C) 1168
— The reagent diphenyldiselane/Iodine: no phenylselenenyl iodide but a charge transfer complex with cyclic moieties (C) 431
Carbon compounds, Carbon—electrochemical and physicochemical properties (B) 1218
— Graphite fluorides (B) 1219
Carbon films, From carbon beams to diamond films (AM) 1203
Carbon oxides, Carbon dioxide as an alternative C_1 synthetic unit: activation by transition-metal complexes (R) 661
— C_5O_2 (1,2,3,4-pentatetraene-1,5-dione), a new oxide of carbon (C) 566
Carbonylation, Rhodium-catalyzed reductive carbonylation of methyl formate to acetaldehyde (C) 683
Carbonyl oxide, Formation of dioxirane from carbonyl oxide (C) 427
Carbonyls, Molecular organometallic chemistry on surfaces: reactivity of metal carbonyls on metal oxides (R) 1127
Carboxime (Isofulminic acid) (C) 938
Carcinogenicity, *N*-Aryl-*O*-acylhydroxylamines: preparation by *O*-acylation or *N*→*O* transacylation and reaction with amines; model reactions for key steps connected with the carcinogenicity of aromatic amines (C) 973
Carotinoids, 4,6,6-Trimethyl-4-cyclohexene-1,2,3-trione, a contribution to the biogenesis of norcarotinoids (C) 695
Catalysis, Acid-catalyzed alkyne/alkene coupling at Re^{III} centers (C) 1509
— An antibody-mediated redox reaction (C) 1172
— An introduction to chemisorption and catalysis by metals (B) 1385
— Catalyst design. Progress and perspectives (B) 592
— Catalytic fixation of nitrogen by the photocatalytic $CdS/Pt/RuO_2$ particulate system in the presence of aqueous $[Ru(Hedta)N_2]^{\ominus}$ complex (C) 923
— Catalytic isomerization of methylated 1,5-cyclooctadienes (C) 1062
— Catalytic syntheses of functionalized nitrogen heterocycles from cyanogen (C) 1372
— Contributions to organo-nickel chemistry (R) 185
— Coordination of H_2 and O_2 to $[OsHCl(CO)(PiPr_3)_2]$: a catalytically active $M(\eta^2\text{-}H_2)$ complex (C) 1563
— $Cs_2Bi_{10}Ca_6Cl_{12}O_{16}$: a new type of catalyst for selective oxidation derived from bismuth oxychloride (C) 1364
— Direct Michael additions of silyl groups to α,β-unsaturated β-arylketones and an α-benzylidenelactone with mixtures obtained from copper(I) cyanide, butyllithium and chlorosilanes (C) 1718
— Electron-transfer chain catalysis in organotransition metal chemistry (R) 643
— Enantioselective catalytic transfer-hydrogenation of α,β-unsaturated carboxylic acids with triethylammonium formate (C) 1180
— High oxidation state organometallic chemistry, a challenge—the example of rhenium (R) 1297
— Linkage of alkylidyne, carbonyl, and alkyne ligands at a tungsten center to form a metallacyclopentadienone and an η^3-oxocyclobutenyl complex (C) 1730
— Molecular organometallic chemistry on surfaces: reactivity of metal carbonyls on metal oxides (R) 1127
— Principles and applications of organotransition metal chemistry (B) 984
— Rhodium-catalyzed reductive carbonylation of methyl formate to acetaldehyde (C) 683
— Selective photochemical dehydrogenation of saturated hydrocarbons with quantum yields approaching unity (C) 1526
— Synthesis, structure and bonding of $[Cl_2Sn\{Rh(PMe_3)_3Cl\}_2]\cdot THF$, an unusual Sn^{II}-Rh^{I} adduct (C) 442
— Tris(2,2′-bipyridyl-5-sulfonic acid)rhodium(III), an improved redox catalyst for the light-induced and the electrochemically initiated enzymatic reduction of carbonyl compounds (C) 265
— Zeolites: catalysts for organic syntheses (R) 226
Catenanes, A topologically chiral [2]catenand (C) 930
Centrohexaindan, the first hydrocarbon with topologically non-planar molecular structure (C) 1192
Ceramics, Advanced materials by powder metallurgy (AM) 989
— Intelligent materials—a new frontier (AM) 1389
C—H Activation, Synthesis of octahedral hydrido(vinyl)iridium(III) complexes by C—H activation: an example of a thermodynamically favored rearrangement $[M(CHR{=}CHX)]\rightarrow[M(H)(CR{=}CHX)]$ (C) 948
Charge transfer, Electron transfer and charge transfer: twin themes in unifying the mechanisms of organic and organometallic reactions (R) 1227
Charge-transfer complexes, A conjugated bis(tetrathiafulvalene) system with tetrathia-*s*-indacene structure (C) 288
— New donors for molecular organic (super)conductors and ferromagnets (AM) 1573
— New organic superconductors (AM) 1747
— The reagent diphenyldiselane/Iodine: no phenylselenenyl iodide but a charge transfer complex with cyclic moieties (C) 431
Chelate ligands, 3- and 3,6-silylated 2-pyridinethiols: new hindered bidentate ligands and their novel silver and copper clusters (C) 1342
— A stable bis(chelate) analogue of the Creutz-Taube ion (C) 1174
— Cu^{II} and Cu^{I} coordination chemistry of a novel *O,O,Cl*-chelate ligand. Formation of a stable carbonylcopper complex (C) 580
— Elementary reactions at metal-sulfur centers: base-induced substitution of PPh_3 in $[Ru(PPh_3)_2(bmae)]$ (C) 689
— Second-sphere photochemistry and photophysics: luminescence of the $[Pt(bpy)(NH_3)_2]^{2\oplus}$-dibenzo[30]crown-10 adduct (C) 692
— The first "adamantoid" alkaline earth metal chelate complex: synthesis, structure, and reactivity (C) 851
— Transformation of open-chain thioether-dithiolato to cyclic thioether ligands by C–S bond cleavage and bond formation at ruthenium centers: synthesis of the trithiobenzo[9]crown-3 complex $[Ru(Bzo\text{-}9S3)(CO)Br_2]$ (C) 691
— Trimethylplatinum–theophylline hexamer: a novel Pt_6 heterocycle containing both Pt–N and Pt–O bonds (C) 1160
Chemical bonding, A pictorial approach to molecular bonding (B) 863
Chemical elements, Synthesis of the heaviest chemical elements—results and perspectives (R) 1417
Chemisorption, An introduction to chemisorption and catalysis by metals (B) 1385
Chemistry and language, Say it in English, please! (R) 1050
— The art of scientific writing. From student reports to professional publications in chemistry and related fields (B) 1565
— Under the surface of the chemical article (R) 1593
Chiral auxiliaries, Amino acid methyl esters as chiral auxiliaries in aza-Diels-Alder reactions in aqueous solution (C) 274
— Paraformaldehyde as possible chirality amplifier (C) 1379
— Reactivity of (*R*)-2-*tert*-butyldihydrooxazole derivatives prepared from serine and threonine: novel, versatile chiral building blocks (C) 1351
Chirality, A topologically chiral [2]catenand (C) 930
— CD spectroelectrochemistry, a method for the characterization of chiral electron transfer reagents and chiral reaction intermediates (C) 291
— Functionalized, enantiomerically pure [2.1.1]-, [2.2.1]-, and [2.2.2]-triblattanes (C) 1103
— Oxidative coupling of racemic and of optically active 3,6-di-*tert*-butylocta-1,4,7-triyne-3,6-diol (C) 859
— solely due to the presence of an excited state (C) 975
— Synthesis and crystal structure of a chiral C_3-symmetric monophosphane (C) 835
— Synthesis of optically active phosphanes via Sharpless epoxidation (C) 718
— 2,2′,7,7′-Tetrahydroxy-1,1′-binaphthyl: a versatile chiral spacer for mono- and ditopic cyclophane hosts with apolar binding sites (C) 1705
Chlorine compounds, The structures of perchloric acid, $HClO_4$, and its anhydride, Cl_2O_7 (C) 1339
Chlorotetain from *bacillus subtilis*, an antifungal dipeptide with an unusual chlorine-containing amino acid (C) 1733
Chromium compounds, Electron-electron/spin-spin long-range interaction as studied in the diradical dication [Di{bis(dime-

thylphosphino-η^6-benzene)chromium(I)}-nickel(0)]$^{++}$ (C) 414
— Heterogeneous, bimetallic metathesis catalysts by reaction of Fischer-type carbene complexes with reduced Phillips catalyst (C) 275
— (Octamethyltetrasila-η^{12}-[2.2]paracyclophane)chromium — synthesis, structure, and characteristics (C) 684
— Reactions of pentacarbonyl(trichloromethyl isocyanide)chromium (C) 1344
Circular dichroism, CD spectroelectrochemistry, a method for the characterization of chiral electron transfer reagents and chiral reaction intermediates (C) 291
— Influence of chromophore orientation on the circular dichroism of isomeric helical molecules (C) 976
— Spectroscopy with polarized light. Solute alignment by photoselection, in liquid crystals, polymers, and membranes (B) 863
Clusters, 3- and 3,6-silylated 2-pyridinethiols: new hindered bidentate ligands and their novel silver and copper clusters (C) 1342
— A new cubane cluster with the $[MoFe_3S_4]^0$ core and possible relevance to the Fe_3-centers in ferredoxins. The synthesis, structure and properties of the $[Fe_3S_4(SEt)_3Mo(CO)_3]^{3\ominus}$ anion (C) 1353
— A new type of unsaturated *triangulo* transition-metal cluster and homogeneous catalyst (C) 263
— A novel heterocluster with D_3-symmetry containing twenty-one core atoms: $[As_6^{III}V_{15}^{IV}O_{42}(H_2O)]^{6\ominus}$ (C) 1721
— A novel tetranuclear copper(I) cluster with alternate bridging halide and triazolopyrimidine ligands (C) 856
— $[Cp_2Co][Bi\{Co(CO)_4\}_4]$: a paramagnetic, ten-electron, tetrahedral complex of bismuth (C) 396
— $[Cu_8(i\text{PrPCH}_2P i\text{Pr})_2Cl_4(py)_5]$, a novel Cu^I cluster containing pentacoordinated phosphorus in μ_3-PRR′ bridges (R = *i*Pr, R′ = $CH_2P i$Pr) (C) 956
— Formation of an oxalate-filled cavity in a reduced cyclic octanuclear polyoxomolybdate $[(n\text{-}C_4H_9)_4N]_2[Mo_8O_{16}(OCH_3)_8(C_2O_4)]$ formed from α-$[(n\text{-}C_4H_9)_4N]_4[Mo_8O_{26}]$ and rhodizonic acid (C) 1724
— Formation of difluoroethyne as a ligand by coupling of two fluoromethylidyne ligands (C) 845
— New transition metal clusters with ligands from main groups five and six (R) 1277
— $[Ni_9(\mu_4\text{-As})_6(PPh_3)_5Cl_3]$, a cubic body-centered Ni_9-cluster (C) 1512
— of valence electron poor metals—structure, bonding, and properties (R) 159
— Photolytic cluster synthesis: synthesis and structure of $[\{(Ph_3P)Au\}_7Mo(CO)_3]OH$ (C) 1094
— Preparation of 2,3,4-tris(η^5-cyclopentadienyl)-1,5-diphenyl-1-phospha-2,3,4-tricobaltapentaborane(5); phenyl group migration from phosphorus to boron (C) 424
— Reaction of [NiCp(PPh$_3$)Cl] with $E(SiMe_3)_2$; the structures of $[Ni_4Se_2Cp_4]$ and $[Ni_4E_2Cp_4(PPh_3)_2]$ (E = Se, Te) (C) 965
— Real-time atomic-resolution imaging of polymorphic changes in ruthenium clusters (C) 555
— Silica-supported Fe-Pd bimetallic particles: formation from mixed-metal clusters and catalytic activity (C) 927
— Soluble chromium selenides and tellurides: preparations and structures of $[(C_6H_5)_4P]_3[Cr_3Te_{24}]$ and $[(C_6H_5)_4P]_3[Cr_3Se_{24}]$ (C) 1702
— Tetranuclear complexes as intermediates in transannular oxidative-addition reactions. Structure of the first tetrairidium linear cluster (C) 402
— Triple proton abstraction from a 1-methylallyl ligand on thermolysis: formation of a $Hf_3(C_4H_4)$ cluster (C) 1058
— $[V_{19}O_{41}(OH)_9]^{8\ominus}$, an ellipsoid-shaped species belonging to the unusual family of V^{IV}/V^V oxygen clusters (C) 1719
Coal, Chemicals from coal: new processes (B) 1385
Cobalt compounds, Alkyne(arene)cobalt, μ-alkynebis(arenecobalt), and μ-benzylidynetris(arenecobalt) from arene/cobalt cocondensates (C) 706
— Cobalt-catalyzed reactions of octamethyl-[4]-radialene and 2,5-dimethyl-2,3,4-hexatriene with ethene (C) 571
— $[Cp_2Co][Bi\{Co(CO)_4\}_4]$: a paramagnetic, ten-electron, tetrahedral complex of bismuth (C) 396
— First case of interannular, possibly electronically transmitted, asymmetric induction in an organometallic compound (C) 553
— $[\{Hg_3Co(C_4H_6NO)_6\}(NO_3)_2]_n$: a macrobicyclic bimetallic chain polymer incorporating deprotonated 2-pyrrolidone bridges (C) 261 (589)
— Photochemical reaction of $[(CO)_4Co(SiEt_3)]$ with ethylene: implications for cobaltcarbonyl-catalyzed hydrosilation of alkenes (C) 289
— Preparation of 2,3,4-tris(η^5-cyclopentadienyl)-1,5-diphenyl-1-phospha-2,3,4-tricobaltapentaborane(5); phenyl group migration from phosphorus to boron (C) 424
Cocondensations, Alkyne(arene)cobalt, μ-alkynebis(arenecobalt), and μ-benzylidynetris(arenecobalt) from arene/cobalt cocondensates (C) 706
Coenzymes, The enzymic interconversion of isobutyryl and *n*-butyrylcarba(dethia)-coenzyme A: a coenzyme-B_{12}-dependent carbon skeleton rearrangement (C) 1089
Coinage Metals, $[Au_2Ag_4L_4]^{2\ominus}$, $[Au_2Cu_4L_4]^{2\ominus}$, $[Au_3Cu_3L_4]^{2\ominus}$, $[Cu_4L_3]^{2\ominus}$, and $[Ag_9L_6]^{3\ominus}$ (L = ethane-1,2-dithiolate)—novel homoleptic complexes of the coinage metals, including the first heteronuclear metal thiolates (C) 1326
Colloidal metals, A morphology-selective copper organosol (C) 1530
Complexes with boron ligands, 1,3-Dihydro-1,3-diborafulvene derivatives (C) 299
— New complex cations of aluminum(III) and gallium(III) (C) 277
— Preparation of 2,3,4-tris(η^5-cyclopentadienyl)-1,5-diphenyl-1-phospha-2,3,4-tricobaltapentaborane(5); phenyl group migration from phosphorus to boron (C) 424
— Synthesis and structure of $[Cp_2NbH(t\text{BuB}{\equiv}N t\text{Bu})]$, a compound with side-on coordinated iminoborane (C) 958
Complexes with chalcogen ligands, New transition metal clusters with ligands from main groups five and six (R) 1277
— Reaction of [NiCp(PPh$_3$)Cl] with $E(SiMe_3)_2$; the structures of $[Ni_4Se_2Cp_4]$ and $[Ni_4E_2Cp_4(PPh_3)_2]$ (E = Se, Te) (C) 965
Complexes with hydrido ligands, Coordination of H_2 and O_2 to $[OsHCl(CO)(P i\text{Pr}_3)_2]$: a catalytically active $M(\eta^2\text{-}H_2)$ complex (C) 1563
— Mechanism of ethylene hydrogenation by the molecular hydrogen complex $[Ir(H)_2(H_2)(PMe_2Ph)_3]^{\oplus}$—characterization of intermediates (C) 1165
— Synthesis of octahedral hydrido(vinyl)iridium(III) complexes by C–H activation: an example of a thermodynamically favored rearrangement $[M(CHR{=}CHX)]{\rightarrow}[M(H)(CR{=}CHX)]$ (C) 948
— Synthesis, structure, and reactivity of $[Mn_2(\mu\text{-}H)_2(CO)_6(\mu\text{-}Ph_2PCH_2PPh_2)]$ (C) 1167
Complexes with nitrogen ligands, A novel tetranuclear copper(I) cluster with alternate bridging halide and triazolopyrimidine ligands (C) 856
— Coupling metal centers with linearly bridging, delocalized, π-bonded ligands: *p*-phenylenediimido dimolybdenum complexes (C) 569
— Helicates: tetra- and pentanuclear double helix complexes of Cu^I and poly(bipyridine) strands (C) 1095
— Stable sandwich complexes with pentamethylpyrrole ligands (C) 579
— The pentazadienide ion as a ligand in metal complexes (R) 896
— Transformation of η^1-nitrosyl to η^2-hydroxylaminyl ligands in the reduction of $[Mo(NO)_2(\text{'}S_4\text{'})]$ to $[Mo(\eta^2\text{-}NH_2O)(NO)(\text{'}S_4\text{'})]$: a model reaction for a partial step in the enzymatic $[NO_3^{\ominus}{\rightarrow}NH_3]$ conversion (C) 1164
Complexes with phosphorus ligands, $[(\eta^5\text{-}C_5Me_4Et)Rh(\mu,\eta^2\text{-}P_2)_2Rh(\eta^5\text{-}C_5Me_4Et)]$, a sandwich complex with a P_4 rectangle (C) 405
— $[Cu_8(i\text{PrPCH}_2P i\text{Pr})_2Cl_4(py)_5]$, a novel Cu^I cluster containing pentacoordinated phosphorus in μ_3-PRR′ bridges (R = *i*Pr, R′ = $CH_2P i$Pr) (C) 956
— $[Os(\eta^2\text{-PHS})(CO)_2(PPh_3)_2]$, a stable η^2-thioxophosphane(H–P=S)-metal complex (C) 302
— $P_4^{2\ominus}$ Isomers as complex ligands (C) 694
— Preparation of 2,3,4-tris(η^5-cyclopentadienyl)-1,5-diphenyl-1-phospha-2,3,4-tricobaltapentaborane(5); phenyl group migration from phosphorus to boron (C) 424
— Synthesis and molecular structure of the diphosphaarsirane $[\{[(\eta^5\text{-}C_5Me_5)(CO)_2Fe]P\}_2AsC_6H_2t\text{Bu}_3]$ (C) 1537
— Template synthesis of macrocyclic multiphosphane ligands with functional groups (C) 438
— The first diphosphaallyl system coordinated to two metal centers (C) 416
Complexes with pnictogen ligands, Linear twofold coordination of arsenic in $[Cp'(CO)_2Mn{=}As{=}Mn(CO)_2Cp']^{\oplus}$ (C) 1529
— New transition metal clusters with ligands from main groups five and six (R) 1277
— $[Ni_9(\mu_4\text{-As})_6(PPh_3)_5Cl_3]$, a cubic body-centered Ni_9-cluster (C) 1512
Complexes with sulfur ligands, A new cubane cluster with the $[MoFe_3S_4]^0$ core and possible relevance to the Fe_3-centers in ferredoxins. The synthesis, structure and properties of the $[Fe_3S_4(SEt)_3Mo(CO)_3]^{3\ominus}$ anion (C) 1353
— $[Au_2Ag_4L_4]^{2\ominus}$, $[Au_2Cu_4L_4]^{2\ominus}$, $[Au_3Cu_3L_4]^{2\ominus}$, $[Cu_4L_3]^{2\ominus}$, and $[Ag_9L_6]^{3\ominus}$ (L = ethane-1,2-dithiolate)—novel homoleptic complexes of the coinage metals, including the first heteronuclear metal thiolates (C) 1326
— $[\{Cp(CO)_2Mn\}_2SPh]^{\oplus}$, the first sulfur analogue of a phosphanediyl ("phosphinidene") complex (C) 698
— Elementary reactions at metal-sulfur centers: base-induced substitution of PPh_3 in $[Ru(PPh_3)_2(bmae)]$ (C) 689
— $[Os(\eta^2\text{-PHS})(CO)_2(PPh_3)_2]$, a stable η^2-thioxophosphane(H–P=S)-metal complex (C) 302
— Stepwise synthesis and crystal structure of tricarbonyl[pentakis(methylthio)cyclopentadienyl]manganese $[\{C_5(SMe)_5\}Mn(CO)_3]$ (C) 939
— Synthesis and structure of $[(C_5Me_5)_2Rh_2S_8]$, a dirhodium complex with unusual polysulfide bridge (C) 708
— $[TiSCl_4]^{2\ominus}$ and $[Ti_3O(S_2)_3Cl_6]^{2\ominus}$, a multinuclear complex with a structure typical for clusters (C) 293
— Transformation of open-chain thioether-

dithiolato to cyclic thioether ligands by C-S bond cleavage and bond formation at ruthenium centers: synthesis of the trithiobenzo[9]crown-3 complex [Ru(Bzo-9S3)(CO)Br_2] (C) 691
Computers, Equipotential surfaces in periodic charge distributions (C) 849
— Reaction of tropone with a homopyrrole. The result of a computer-assisted search for unique chemical reactions (C) 1558
— Structure elucidation and artificial intelligence (R) 247
Conformation, Evidence for a folded conformation of methotrexate in solution (C) 423
Conjugation, Coupling metal centers with linearly bridging, delocalized, π-bonded ligands: *p*-phenylenediimido dimolybdenum complexes (C) 569
— Synthesis and optical properties of terminally substituted conjugated polyenes (C) 281
Coordination, Alkyne coordination to organorhenium oxides with rhenium in high oxidation states (C) 946
— Cu^{II} and Cu^{I} coordination chemistry of a novel *O,O,Cl*-chelate ligand. Formation of a stable carbonylcopper complex (C) 580
— [Cu_8(*i*PrPCH_2P*i*Pr)$_2Cl_4$(py)$_5$], a novel Cu^{I} cluster containing pentacoordinated phosphorus in μ_3-PRR′ bridges (R = *i*Pr, R′ = CH_2P*i*Pr) (C) 956
— Helicates: tetra- and pentanuclear double helix complexes of Cu^{I} and poly(bipyridine) strands (C) 1095
— Hypercarbon chemistry (B) 590
— Intramolecularly stabilized organogallium compounds (C) 1077
— Linear twofold coordination of arsenic in [Cp′$(CO)_2$Mn=As=Mn$(CO)_2$Cp′]$^{\oplus}$ (C) 1529
— Naked molecule chemistry: different bonding modes of CO to FeX_2 (C) 1161
— [{$Hg_3Co(C_4H_6NO)_6$}$(NO_3)_2$]$_n$: a macrobicyclic bimetallic chain polymer incorporating deprotonated 2-pyrrolidone bridges (C) 261 (589)
— of H_2 and O_2 to [OsHCl(CO)(P*i*$Pr_3)_2$]: a catalytically active M(η^2-H_2) complex (C) 1563
— Organobimetallic Mg–Pd complexes as intermediates in the formation of amorphous $MgPdC_xH_y$ from $Mg(C_2H_5)_2$ and [Pd(η^3-$C_3H_5)_2$] (C) 1513
— 2,4,6-$Ph_3C_6H_2M$ (M = Cu, Ag), monomeric Cu^{I}- and Ag^{I}-complexes with coordination number 1 (C) 436
— Phosphane-stabilized Cu^{I} and Ag^{I} silanes (C) 1349
— Photochemical reactions of ligands in transition-metal complexes (R) 789
— Polycyclic silylamides of Ge^{II} and Sn^{II} with different structures — bis(germanediyl) versus distannate (C) 1087
— Second sphere coordination adducts of phosphane-transition metal complexes with β-cyclodextrin and its methylated derivative (C) 1184
— Stepwise synthesis and crystal structure of tricarbonyl[pentakis(methylthio)cyclopentadienyl]manganese [{C_5(SMe)$_5$}Mn$(CO)_3$] (C) 939
— Synthesis and structure of [Cp_2NbH(*t*BuB≡N*t*Bu)], a compound with side-on coordinated iminoborane (C) 958
— Synthesis and structure of [{Na(tmeda)}$_3$][$LiPh_4$], an organometallic complex containing two different alkali metals (C) 584
— The microwave spectrum and structure of the ethylene–sulfur dioxide complex (C) 1356
— The pentazadienide ion as a ligand in metal complexes (R) 896
— The surface scientist's guide to organometallic chemistry (B) 1198
— Variety in coordination modes of ligands in metal complexes (B) 1566
— X-ray structure investigation of 2,2-diphenyl-1-(phenylsulfonyl)cyclopropyllithium–dimethoxyethane (2/3): a sulfonyl "carbanion" having an α-C atom with a tetrahedral configuration (C) 846
Copper compounds, A morphology-selective copper organosol (C) 1530
— 3- and 3,6-silylated 2-pyridinethiols: new hindered bidentate ligands and their novel silver and copper clusters (C) 1342
— A novel tetranuclear copper(I) cluster with alternate bridging halide and triazolopyrimidine ligands (C) 856
— Cu^{II} and Cu^{I} coordination chemistry of a novel *O,O,Cl*-chelate ligand. Formation of a stable carbonylcopper complex (C) 580
— [Cu_8(*i*PrPCH_2P*i*Pr)$_2Cl_4$(py)$_5$], a novel Cu^{I} cluster containing pentacoordinated phosphorus in μ_3-PRR′ bridges (R = *i*Pr, R′ = CH_2P*i*Pr) (C) 956
— Helicates: tetra- and pentanuclear double helix complexes of Cu^{I} and poly(bipyridine) strands (C) 1095
— 2,4,6-$Ph_3C_6H_2M$ (M = Cu, Ag), monomeric Cu^{I}- and Ag^{I}-complexes with coordination number 1 (C) 436
— Phosphane-stabilized Cu^{I} and Ag^{I} silanes (C) 1349
— The copper salt of 2-iodo-5-methyl-*N,N′*-dicyanoquinonediimine—a radical anion salt exhibiting metallic conductivity down to low temperatures (C) 267
Corrosion, DECHEMA corrosion handbook: corrosive agents and their interaction with materials, volume 1 (B) 1407
Crown ethers, The activation of phenylmagnesium compounds by crown ethers (C) 1084
— The discovery of crown ethers (Nobel lecture) (R) 1021
Crystal structure analysis, Atomic motions in molecular crystals from diffraction measurements (R) 880
— Distorted triple-diamond structure of 3,3-bis(carboxymethyl)glutaric acid ("methanetetraacetic acid") (C) 829
— Equilibrium structure, stabilized transition state, or disorder in the crystal? Studies of the antiaromatic systems tetra-*tert*-butyl-*s*-indacene and tetra-*tert*-butylcyclobutadiene by low-temperature crystal structure analysis (C) 387
— The crystal structure of hypofluorous acid: chain formation by O–H···O hydrogen bonds (C) 392
— The fluoronium ions $H_2F^{\oplus}$ and $H_3F_2^{\oplus}$: characterization by crystal structure analysis (C) 391
— X-ray structure investigation of 2,2-diphenyl-1-(phenylsulfonyl)cyclopropyllithium–dimethoxyethane (2/3): a sulfonyl "carbanion" having an α-C atom with a tetrahedral configuration (C) 846
C_1 Synthetic units, Carbon dioxide as an alternative C_1 synthetic unit: activation by transition-metal complexes (R) 661
Cubanes, Synthesis and structure of an azastibacubane (C) 287
Cuprates, Direct Michael additions of silyl groups to α,β-unsaturated β-arylketones and an α-benzylidenelactone with mixtures obtained from copper(I) cyanide, butyllithium and chlorosilanes (C) 1718
Cyclacenes, Towards the making of [12]collarene (C) 966
Cycloadditions, Reaction of tropone with a homopyrrole. The result of a computer-assisted search for unique chemical reactions (C) 1558
— Reactivity of Tri-*tert*-butylazete (C) 272
Cyclobutabenzenes, Structures and deformation electron densities of 1,2-dihydrocyclobutabenzene and 1,2,4,5-tetrahydrodicyclobuta[*a,d*]benzene (C) 304
Cyclobutadienes, Equilibrium structure, stabilized transition state, or disorder in the crystal? Studies of the antiaromatic systems tetra-*tert*-butyl-*s*-indacene and tetra-*tert*-butylcyclobutadiene by low-temperature crystal structure analysis (C) 387
— Tetrahedrane and cyclobutadiene (R) 309
Cyclobutanones and cyclobutenones in nature and in synthesis (R) 797
Cyclobutenones, Cyclobutanones and cyclobutenones in nature and in synthesis (R) 797
Cyclodextrins increase surface tension and critical micelle concentrations of detergent solutions (C) 393
— Modified cyclodextrins—novel, highly enantioselective stationary phases for gas chromatography (C) 979
— Second sphere coordination adducts of phosphane-transition metal complexes with β-cyclodextrin and its methylated derivative (C) 1184
Cyclododecatetraenes, Synthesis of all-*cis*-1,4,7,10-cyclododecatetraene (C) 298
Cyclohepta[*def*]carbazolium ion, (C) 585
Cycloheptatrienes, Formation of cycloheptatriene/norcaradiene systems in the decomposition of diaryldiazomethanes in benzene (C) 284
Cyclohexenetriones, 4,6,6-Trimethyl-4-cyclohexene-1,2,3-trione, a contribution to the biogenesis of norcarotinoids (C) 695
Cyclooctadienes, Catalytic isomerization of methylated 1,5-cyclooctadienes (C) 1062
Cyclopentanes, Induced and non-induced diastereoselective intramolecular ene reaction of 1,6-dienes: the unusual formation of *trans*-1,2-disubstituted cyclopentanes (C) 1186
Cyclopentenones, Conjugated and nonconjugated cyclopentenones by a reaction cascade from methyl 6-oxo-5-phenyl-1,3,4-oxadiazine-2-carboxylate and 1,3-butadienes (C) 931
Cyclophanes, Complexation of neutral molecules by cyclophane hosts (R) 362
— Cyclobis(paraquat-*p*-phenylene). A tetracationic multipurpose receptor (C) 1547
— Influence of chromophore orientation on the circular dichroism of isomeric helical molecules (C) 976
— Isostructural, alternately-charged receptor stacks. The inclusion complexes of hydroquinone and catechol dimethyl ethers with cyclobis(paraquat-*p*-phenylene) (C) 1550
— Multidecker metallocenophanes (C) 701
— (Octamethyltetrasila-η^{12}-[2.2]paracyclophane)chromium — synthesis, structure, and characteristics (C) 684
— Strongly bent naphthalene units in [2](2,6)naphthalino[2]paracyclophane and [2](2,6)naphthalino[2]paracyclophane-1,11-diene (C) 1064
— Synthesis and conformational behavior of dibenzo[2.2]metaparacyclophanediene (C) 705 (1200)
— 2,2′,7,7′-Tetrahydroxy-1,1′-binaphthyl: a versatile chiral spacer for mono- and ditopic cyclophane hosts with apolar binding sites (C) 1705
Cyclophosphazenes, Synthesis and structure of [$ClV(OSiMe_3)N_2PPh_2]_2$, the first cyclodimetallaphosphazene—an eight-membered planar unsaturated heterocycle (C) 850
Cyclopropabenzenes, The structures of 1*H*-cyclopropabenzene and its 1,1-bis(triisopropylsilyl) derivative (C) 294
Cyclopropanes, The chemistry of the cyclopropyl group (B) 1199
— The cyclopropyl group in studies of enzyme mechanism and inhibition (R) 537
Cyclopropyllithium, X-ray structure investigation of 2,2-diphenyl-1-(phenylsulfonyl)cyclopropyllithium–dimethoxyethane (2/3): a sulfonyl "carbanion" having an α-C atom with a tetrahedral configuration (C) 846

Decalins, Stereoselective synthesis of *trans*-

decalins via intramolecular ene reactions; synthesis of the enantiomerically pure cadinane-sesquiterpene veticadinol (C) 703
Dehydrogenation, Selective photochemical dehydrogenation of saturated hydrocarbons with quantum yields approaching unity (C) 1526
Detergents, Cyclodextrins increase surface tension and critical micelle concentrations of detergent solutions (C) 393
— Solubilization of elemental sulfur in water by cationic and anionic surfactants (C) 1358
— Surfactants, micelles and fascinating phenomena (R) 902
Diamond-like networks, Distorted triple-diamond structure of 3,3-bis(carboxymethyl)glutaric acid ("methanetetraacetic acid") (C) 829
Diastereoselectivity, A new route to *trans*-substituted γ-lactones (C) 268
— Asymmetric induction in the replacement of diastereotopic bromine atoms by lithium atoms (C) 1176
— Diastereo- and enantioselective aldol reactions via α-silyl ketones, asymmetric synthesis of the aggregation pheromone sitophilure (C) 581
— Enantio- and diastereoselective synthesis of methyl (2*R*)-2-amino-5-oxocarboxylates from enones and bislactim-ether cuprates (C) 1194
— First case of interannular, possibly electronically transmitted, asymmetric induction in an organometallic compound (C) 553
— Induced and non-induced diastereoselective intramolecular ene reaction of 1,6-dienes: the unusual formation of *trans*-1,2-disubstituted cyclopentanes (C) 1186
— Iodine-induced stereoselective carbocyclizations: a new method for the synthesis of cyclohexane and cyclohexene derivatives (C) 1546
— Simple synthesis of KDO α-glycosides by anomerically selective *O*-alkylation (C) 1178
— Stereoselective synthesis of *trans*-decalins via intramolecular ene reactions; synthesis of the enantiomerically pure cadinane-sesquiterpene veticadinol (C) 703
Diastereospecifity, Diastereospecific gas/solid additions with cholesterol derivatives (C) 1511
1,1'-Diazaferrocene, Does a 1,1'-diazaferrocene exist? (C) 1368
Diazapentalenes, Synthesis and physical properties of 3,6-di-*tert*-butyl-1,4-diazapentalene (C) 1061
Diazocompounds, A new route to nitrile oxides via α-nitrosodiazo derivatives (C) 301
— First direct evidence for nitrile imine-diazo isomerization. Synthesis of Relatively stable *N*-silylated nitrile imines (C) 1350
— Formation of cycloheptatriene/norcaradiene systems in the decomposition of diaryldiazomethanes in benzene (C) 284
— Properties and synthesis (B) 591
Dicyclopentadienes, Blocking of the retro-Diels-Alder reaction by complex formation: [(η^5-cyclopentadienyl)(η^5-dicyclopentadienyl)iron] (C) 977
Diels-Alder reactions, Amino acid methyl esters as chiral auxiliaries in aza-Diels-Alder reactions in aqueous solution (C) 274
— Methoxyallenes as components in Diels-Alder reactions with inverse electron demand: synthesis of 6*H*-1,2-oxazines (C) 1518
Dienes, Competition of endoperoxide and hydroperoxide formation in the reaction of singlet oxygen with cyclic, conjugated dienes (C) 717
Difluoroethyne, Formation of difluoroethyne as a ligand by coupling of two fluoromethylidyne ligands (C) 845
Diheteropentalenes, A simple route to furo[3,4-*b*]furans, compounds with a new diheteropentalene system (C) 568
Dihydrocyclobutabenzenes, Structures and deformation electron densities of 1,2-dihydrocyclobutabenzene and 1,2,4,5-tetrahydrodicyclobuta[*a*,*d*]benzene (C) 304
Diisocyanogen (C) 936
α-Diketones, Tricyclo[3.1.0.$0^{2,6}$]hexanedione (the valene of *o*-benzoquinone), bicyclo[2.1.1]hexane-2,3-dione, and valenes of a quinoxaline, of phenazine, and of a benzophenazine (C) 1369
1,2-Dilithioethane from ethylene and lithium (C) 1083
Dioxetanes, Facile reduction of 1,2-dioxetanes by thiols as potential protective measure against photochemical damage of cellular DNA (C) 429
Dioxirane, Formation of dioxirane from carbonyl oxide (C) 427
1,4-Diphosphabutatriene (C) 1360
closo-Diphosphahexaboranes, The first *closo*-diphosphahexaborane $P_2B_4Cl_4$ (C) 925
Diphosphatricyclopentane, Formation of the diphosphatricyclo[2.1.0.$0^{2,5}$]pentane ring system via phosphaalkyne dimerization and carbon monoxide incorporation (C) 837
2,7-Di-*tert*-butyldicyclopenta[*a*,*e*]cyclooctene, Synthesis and structure of 2,7-Di-*tert*-butyldicyclopenta[*a*,*e*]cyclooctene (C) 1191
Donor-acceptor substitution, Donor-acceptor-substituted cyclic π-electron systems—probes for theories and building blocks for new materials (R) 1437
Dynamics, Flexibility and rigidity of proteins and protein-pigment complexes (R) 79
— of proteins and nucleic acids (B) 862
— Synthesis and conformational behavior of dibenzo[2.2]metaparacyclophanediene (C) 705 (1200)

Ecology, Natural fats and oils—renewable raw materials for the chemical industry (R) 41
Electrochemistry, Carbon—electrochemical and physicochemical properties (B) 1218
— CD spectroelectrochemistry, a method for the characterization of chiral electron transfer reagents and chiral reaction intermediates (C) 291
— Electrocatalytic haloform reaction: transformation of methyl ketones into methyl esters (C) 1716
— Electron-transfer chain catalysis in organotransition metal chemistry (R) 643
— Theoretical foundations, quantum and statistical mechanics, thermodynamics, the solid state (B) 860
— The use of light in the study of interfacial electrochemical reactions (R) 63
Electrochromism, Redox-active thieno[3,2-*b*]-thiophene as a novel, three-color electrochromic system (C) 560
Electronics industry, Fine chemicals for the electronics industry (B) 445
Electronic structure, The electronic structure and chemistry of solids (B) 719
Electron/ion transfer, From electronic/ionic conductors to superconductors: control of materials properties (AM) 1392
Electron microscopy, Real-time atomic-resolution imaging of polymorphic changes in ruthenium clusters (C) 555
Electron transfer and charge transfer: twin themes in unifying the mechanisms of organic and organometallic reactions (R) 1227
— CD spectroelectrochemistry, a method for the characterization of chiral electron transfer reagents and chiral reaction intermediates (C) 291
— Reactions in organic chemistry (B) 1740
Electron-transfer catalysis, Electron-transfer chain catalysis in organotransition metal chemistry (R) 643
Electrophoresis, Advances in electrophoresis (B) 1109
Enantiomer separation, Gas chromatographic separation of enantiomeric olefins (C) 1556
— The practice of enantiomer separation by capillary gas chromatography (B) 307
Enantioselectivity, Diastereo- and enantioselective aldol reactions via α-silyl ketones, asymmetric synthesis of the aggregation pheromone sitophilure (C) 581
— Enantio- and diastereoselective synthesis of methyl (2*R*)-2-amino-5-oxocarboxylates from enones and bislactim-ether cuprates (C) 1194
— Enantioselective catalytic transfer-hydrogenation of α,β-unsaturated carboxylic acids with triethylammonium formate (C) 1180
— Enantioselective synthesis of (*R*)-*N*-Boc-1-amino-2-arylcyclopropene-1-carboxylic acid methyl ester (C) 433
— Modified cyclodextrins—novel, highly enantioselective stationary phases for gas chromatography (C) 979
— Short, highly enantioselective synthesis of a key intermediate for the preparation of leucotriene B_4 and its 14,15-didehydro derivative (C) 1188
Endoperoxides, Competition of endoperoxide and hydroperoxide formation in the reaction of singlet oxygen with cyclic, conjugated dienes (C) 717
ENDOR spectroscopy in water: reductions and oxidations of organic compounds (C) 1069
— Isolation and structure of [(fluorenone$^{\odot\ominus}$){$Na^{\oplus}$(dme)$_2$}]$_2$ — a touchstone for radical contact ion pairs? (C) 1067
Ene reactions, Induced and non-induced diastereoselective intramolecular ene reaction of 1,6-dienes: the unusual formation of *trans*-1,2-disubstituted cyclopentanes (C) 1186
— Stereoselective synthesis of *trans*-decalins via intramolecular ene reactions; synthesis of the enantiomerically pure cadinane-sesquiterpene veticadinol (C) 703
Energy transport, Synthesis and optical properties of terminally substituted conjugated polyenes (C) 281
Environmental chemistry, Rapid detection of manganese deficiency in conifer needles by electron spin resonance spectroscopy (C) 1722
Enzyme catalysis, Catalytic activity of enzymes altered at their active sites (R) 913
— Enzyme-catalyzed synthesis of 1-deoxymannojirimycin, 1-deoxynojirimycin, and 1,4-dideoxy-1,4-imino-D-arabinitol (C) 716
— Enzymic Baeyer-Villiger oxidations by flavin-dependent monooxygenases (R) 333
— Isoleucyl-tRNA synthetase: an enzyme with several catalytic cycles displaying variation in specificity and energy consumption (R) 773
— Microbial and enzymatic processes for the production of biologically and chemically useful compounds (R) 622
— The enzymic interconversion of isobutyryl and *n*-butyrylcarba(dethia)-coenzyme A: a coenzyme-B_{12}-dependent carbon skeleton rearrangement (C) 1089
— Tris(2,2'-bipyridyl-5-sulfonic acid)rhodium(III), an improved redox catalyst for the light-induced and the electrochemically initiated enzymatic reduction of carbonyl compounds (C) 265
Enzyme chemistry, Enzymes and curvature (C) 953
— The cyclopropyl group in studies of enzyme mechanism and inhibition (R) 537
Enzyme inhibitors, Enantioselective synthesis of (*R*)-*N*-Boc-1-amino-2-arylcyclopropene-1-carboxylic acid methyl ester (C) 433

— Enzyme-catalyzed synthesis of 1-deoxymannojirimycin, 1-deoxynojirimycin, and 1,4-dideoxy-1,4-imino-D-arabinitol (C) 716
Equipotential surfaces, Enzymes and curvature (C) 953
— in periodic charge distributions (C) 849
Errata, Dinuclear complexes of gold(I) containing bridging cyclometalated arylphosphane or arylarsane ligands (E) 589
ESR spectroscopy, Rapid detection of manganese deficiency in conifer needles by electron spin resonance spectroscopy (C) 1722
— Structure, magnetochemistry and biological relevance of $[Mn_4O_3Cl_4(OAc)_3(py)_3]$, a complex with $S=9/2$ ground state (C) 1731
Ethylenedithione (C_2S_2): generation and characterization by neutralization-reionization mass spectrometry (C) 1337
Experimantal design: a chemometric approach (B) 1565

Fine chemicals for the electronics industry (B) 445
Fluorescence microscopy, Controlling the microstructure of monomolecular layers (AM) 728
Fluorine compounds, A simple access to 2-substituted 3,3,3-trifluoroalanine derivatives (C) 848
— Formation of difluoroethyne as a ligand by coupling of two fluoromethylidyne ligands (C) 845
— Graphite fluorides (B) 1219
— Novel anionic aryl complexes of Rh^{III}: $[Rh(C_6F_5)_5]^{2\ominus}$ and $[Rh(C_6F_5)_4(CO)_2]^{\ominus}$ (C) 1700
— The crystal structure of hypofluorous acid: chain formation by O—H···O hydrogen bonds (C) 392
— The fluoronium ions $H_2F^{\oplus}$ and $H_3F_2^{\oplus}$: characterization by crystal structure analysis (C) 391
— The SF_5-unit as steric protecting group; synthesis and structure of $F_5S-C\equiv SF_3$ (C) 1534
Fractals, Polymeric photoconductors—new concepts (AM) 1210
Furofurans, A simple route to furo[3,4-*b*]furans, compounds with a new diheteropentalene system (C) 568

Gallium compounds, Intramolecularly stabilized organogallium compounds (C) 1077
— New complex cations of aluminum(III) and gallium(III) (C) 277
Gas chromatography, Modified cyclodextrins—novel, highly enantioselective stationary phases for gas chromatography (C) 979
— Pheromones in nanogram quantities: structure determination by combined microchemical and gas chromatographic methods (R) 460
— The practice of enantiomer separation by capillary gas chromatography (B) 307
Gas/solid additions, Diastereospecific gas/solid additions with cholesterol derivatives (C) 1511
Genetic code, Isoleucyl-tRNA synthetase: an enzyme with several catalytic cycles displaying variation in specificity and energy consumption (R) 773
Genetic engineering, Pharmaceutical proteins (R) 207
Germanium compounds, $(Mesityl)_2Ge$(fluorenylidene)—stabilization of a Ge-C double bond by charge transfer into an aromatic system (C) 828
— Polycyclic silylamides of Ge^{II} and Sn^{II} with different structures—bis(germanediyl) versus distannate (C) 1087
Glycoconjugates, β-Mannosides from β-glucosides by intramolecular nucleophilic substitution with inversion of configuration (C) 1086
Glycopeptides, Protecting-group-dependent stability of intersaccharide bonds—synthesis of a fucosyl-chitobiose glycopeptide (C) 1697
— Solid-phase synthesis of *O*-glycopeptide sequences (C) 1365
— Solid phase synthesis of peptides and glycopeptides on polymeric supports with allylic anchor groups (C) 711
— The *p*-nitrocinnamyloxycarbonyl (noc) moiety—an acid-stable amino-protecting group removable under neutral conditions for peptide and glycopeptide synthesis (C) 1375
Gold compounds, "Aurophilicity" as a consequence of relativistic effects: the hexakis(triphenylphosphaneaurio)methane dication $[(Ph_3PAu)_6C]^{2\oplus}$ (C) 1544
— Dinuclear complexes of gold(I) containing bridging cyclometalated arylphosphane or arylarsane ligands (E) 589
— Photolytic cluster synthesis: synthesis and structure of $[\{(Ph_3P)Au\}_7Mo(CO)_3]OH$ (C) 1094
— Polyauriomethane compounds (C) 419
— Use of the CH acidity of 2,4,4-trimethyl-4,5-dihydrooxazole to synthesize triauriomethanes and novel gold clusters (C) 1542
— Weak intramolecular bonding relationships: the conformation-determining attractive interaction between gold(I) centers (C) 417
Grignard Reactions, Carbanions as intermediates in the synthesis of Grignard reagents (C) 687
— The activation of phenylmagnesium compounds by crown ethers (C) 1084
Grob fragmentation, Carbon as leaving group—stereochemistry of nucleophilic substitution (C) 1538
Guaiacolato complexes, Dinuclear vanadium(II)- and vanadium(III)-guaiacolato complexes related to vanadium-based systems for the reduction of nitrogen (C) 576

Hafnium compounds, $[M(CO)_4\{CH_3C(CH_2PMe_2)_3\}]$, M = Ti, Zr, Hf, complexes of zerovalent titanium, zirconium, and hafnium. First structural characterization of a Zr^0-carbonyl complex (C) 437
— $P_4^{2\ominus}$ Isomers as complex ligands (C) 694
— Triple proton abstraction from a 1-methylallyl ligand on thermolysis: formation of a $Hf_3(C_4H_4)$ cluster (C) 1058
Haloform reactions, Electrocatalytic haloform reaction: transformation of methyl ketones into methyl esters (C) 1716
Halogen-metal exchange, Asymmetric induction in the replacement of diastereotopic bromine atoms by lithium atoms (C) 1176
Helix, Helicates: tetra- and pentanuclear double helix complexes of Cu^I and poly(bipyridine) strands (C) 1095
— Influence of chromophore orientation on the circular dichroism of isomeric helical molecules (C) 976
— Oxidative coupling of racemic and of optically active 3,6-di-*tert*-butylocta-1,4,7-triyne-3,6-diol (C) 859
Helix inversion, How high is the activation barrier to helix inversion of 1,4,5,8-tetrasubstituted phenanthrenes? (C) 270
Heteroallenes, A monomeric diboryldilithiomethane with a 1,3-diborataallene structure (C) 1370
Heteroannulenes, Biomimetic synthesis of an octavinylogous porphyrin with an aromatic [34]annulene system (C) 1170
— Tetraoxaporphycene dication (C) 411
— Tetraoxaporphyrin dication (C) 406
— Tetraoxaporphyrinogen (tetraoxaquaterene): oxidation to the tetraoxaporphyrin dication (C) 409
Heteroarenes, Annelation of carbene ligands by λ^3-phosphaalkynes, an entry to functionalized phosphaarenes (C) 713
— 1,4-Di-*tert*-butyl-2,6-bis(trimethylsilyl)silabenzene, the first silabenzene stable in solution at −100 °C (C) 963
— Phosphaalkynes—syntheses, reactions, coordination behavior (R) 1484
— Reaction of 1,3-azaarsinines with 2-*tert*-butyl-1-phosphaethyne—2,9,10-tri-*tert*-butyl-4,6-diphenyl-1,3,8-triphospha-7-arsatetracyclo[4.4.0.$0^{2,8}$.$0^{3,7}$]deca-4,9-diene (C) 709
— Synthesis and structure of $[MeAlN(2,6\text{-}iPr_2C_6H_3)]_3$: an aluminum-nitrogen analogue of borazole (C) 1699
— Triazatrimetallabenzenes, a new class of inorganic heterocycles; synthesis and structure of $[Cp^*TaN(Cl)]_3$ (C) 1330
— Tris(thioxanthen-9-ylidene)cyclopropane, and its radical cation and dication (C) 1078
Hetero-Claisen rearrangement, Unsaturated hydrindanone derivatives from arenes by hetero-Claisen rearrangement (C) 558
Heterocycles, Addition of a distannene to a phosphaalkyne. Formation of a phosphadistannacyclobutene (C) 838
— Alkali-metal hydrogen tetraphosphides M^IHP_4—the first salts of bicyclo[1.1.0]tetraphosphane (C) 1059
— α-Methylene-β-lactone, a novel heterocyclic ring system via deoxygenation of α-methylene-β-peroxylactones with triphenylphosphane (C) 1536
— A novel tris(azo)macrobicyclic molecule—synthesis, photochemistry, and isomer separation (C) 1189
— A simple route to furo[3,4-*b*]furans, compounds with a new diheteropentalene system (C) 568
— A tetramethylene-1,4-distannacyclohexane from 3,4-dilithio-2,5-dimethyl-2,4-hexadiene and dichlorodimethylstannane: the first dimetalla[6]radialene (C) 404
— Bis([1,2,5]thiadiazolo)[3,4-*b*;3′,4′-*e*]pyrazine, a novel 14π-electron heterocycle with high electron affinity (C) 434
— Catalytic syntheses of functionalized nitrogen heterocycles from cyanogen (C) 1372
— Dications based on a hydrotris(phosphonio)borate skeleton (C) 1071
— 1,4-Diphospha-2-rhodacyclopentadiene—an isolable intermediate in the metal-induced cyclodimerization of *tert*-butylphosphaacetylene (C) 1157
— First structure analysis and photoelectron spectroscopic investigation of an azete and an azete-cobalt complex (C) 1559
— Formation of the diphosphatricyclo[2.1.0.$0^{2,5}$]pentane ring system via phosphaalkyne dimerization and carbon monoxide incorporation (C) 837
— From the dilithiooctamethylcyclotetrasilazane to the 1,3,5,7-tetraaza-2,4,6,8,9-pentasilabicyclo[3.3.1]nonane system (C) 1074
— Intramolecularly stabilized organogallium compounds (C) 1077
— 4-Iodo-1,3,5,7-tetramethyl-1,3,5,7-tetraaza-4λ^5-phosphaspiro[3.3]heptane-2,6-dione: synthesis and crystal structure of the first iodophosphorane (C) 1562
— 5-Isopropyliden-1,2-oxathiole 2-oxide by photoisomerization of 2,2-dimethyl-3(2*H*)-thiophenone 1-oxide (C) 1374
— Ketenimine complexes from carbene complexes and isocyanides: versatile building blocks for carbocycles and N-heterocycles (R) 1456
— Methoxyallenes as components in Diels-Alder reactions with inverse electron demand: synthesis of 6*H*-1,2-oxazines (C) 1518
— Nitroazoles. The *C*-nitro derivatives of five-membered *N*- and *N,O*-heterocycles (B) 985
— Phosphaalkynes—syntheses, reactions, coordination behavior (R) 1484

— Polycyclic silylamides of Ge^{II} and Sn^{II} with different structures — bis(germanediyl) versus distannate (C) 1087
— Reaction of 1,3-azaarsinines with 2-*tert*-butyl-1-phosphaethyne — 2,9,10-tri-*tert*-butyl-4,6-diphenyl-1,3,8-triphospha-7-arsatetracyclo[4.4.0.0^{2,8}.0^{3,7}]deca-4,9-diene (C) 709
— Reaction of 1,3-azaphosphinines with 2-*tert*-butyl-1-phosphaethyne: 9-aza-2,4,6-triphosphatetracyclo[5.3.0.0^{2,4}.0^{3,6}]deca-8,10(1)-diene (C) 389
— Reactivity of (*R*)-2-*tert*-butyldihydrooxazole derivatives prepared from serine and threonine: novel, versatile chiral building blocks (C) 1351
— Redox-active thieno[3,2-*b*]thiophene as a novel, three-color electrochromic system (C) 560
— Reductive oligomerization of 1,2-Di-*tert*-butyl-1,1,2,2-tetrachlorodisilane: the tricyclo[2.2.0.0^{2,5}]hexasilane and tetracyclo[3.3.0.0^{2,7}.0^{3,6}]octasilane systems (C) 1725
— Reversible coupling and opening of a boron-carbon bond (C) 952
— ^{29}Si-^{29}Si long range couplings in strained cyclic polysilanes (C) 1727
— Synthesis and molecular structure of the diphosphaarsirane [{[(η^5-C_5Me_5)(CO)$_2$Fe]P}$_2$As$C_6H_2tBu_3$] (C) 1537
— Synthesis and structure of a 1,2,5,6-tetrahydro-1,2,5,6-tetraborocine (C) 926
— Synthesis and structure of [ClV(OSiMe$_3$)N$_2$PPh$_2$]$_2$, the first cyclodimetallaphosphazene—an eight-membered planar unsaturated heterocycle (C) 850
— The chemistry of inorganic homo- and heterocycles. Vol. 1 and 2 (B) 1107
— The cyclohepta[*def*]carbazolium ion (C) 585
— The first transition metal complex of a thiepin; synthesis of thermally labile 1-benzothiepin 1-oxide from 1-benzothiepin(tricarbonyl)iron (C) 1717
— The first triphosphabicyclobutane—evidence for a 1,2,3-triphosphabutadiene (C) 957
— [1,2,4]Triazolo[1,2-*a*][1,2,4]triazole-1,3,5,7(2*H*,6*H*)-tetrone (urazourazole), synthesis and structure (C) 701
— Trimethylplatinum-theophylline hexamer: a novel Pt_6 heterocycle containing both Pt-N and Pt-O bonds (C) 1160
Hetero-Diels-Alder reactions, Amino acid methyl esters as chiral auxiliaries in aza-Diels-Alder reactions in aqueous solution (C) 274
— Reaction of 1,3-azaarsinines with 2-*tert*-butyl-1-phosphaethyne — 2,9,10-tri-*tert*-butyl-4,6-diphenyl-1,3,8-triphospha-7-arsatetracyclo[4.4.0.0^{2,8}.0^{3,7}]deca-4,9-diene (C) 709
— Synthesis of strictosidine analogues by hetero-Diels-Alder reaction and their biomimetic transformation to indole alkaloids (C) 971
Heterofulvalene, New organic superconductors (AM) 1817
Heterofulvalenes, A conjugated bis(tetrathiafulvalene) system with tetrathia-*s*-indacene structure (C) 288
— A donor cage with bent tetrathiafulvalene moiety (C) 1377
— New organic superconductors (AM) 1747
— Synthesis and structure of (ET)[Ni{SC(CN)=C(CN)S}$_2$], a radical cation salt of bis(ethylenedithio)tetrathiafulvalene (C) 699
— Tetraphosphafulvalenes (C) 950
Heterofulvenes, 1,3-Dihydro-1,3-diborafulvene derivatives (C) 299
Heterogeneous catalysis, Heterogeneous, bimetallic metathesis catalysts by reaction of Fischer-type carbene complexes with reduced Phillips catalyst (C) 275
— Methylrhenium oxides: synthesis from Re_2O_7 and catalytic activity in olefin metathesis (C) 394
— Photochemical reaction of [(CO)$_4$Co(SiEt$_3$)] with ethylene: implications for cobaltcarbonyl-catalyzed hydrosilation of alkenes (C) 289
— Silica-supported Fe-Pd bimetallic particles: formation from mixed-metal clusters and catalytic activity (C) 927
— Uniform heterogeneous catalysts: the role of solid-state chemistry in their development and design (R) 1673
Heterogeneous systems, Photochemistry in microheterogeneous systems (B) 722
Hetero-metal compounds, Silica-supported Fe-Pd bimetallic particles: formation from mixed-metal clusters and catalytic activity (C) 927
Heterometallic clusters, A Pt_2AgH_2 complex (C) 563
Heterometallic compounds, [{$Hg_3Co(C_4H_6NO)_6$}$(NO_3)_2$]$_n$: a macrobicyclic bimetallic chain polymer incorporating deprotonated 2-pyrrolidone bridges (C) 261 (589)
Heteropentalenes, Synthesis and physical properties of 3,6-di-*tert*-butyl-1,4-diazapentalene (C) 1061
— 1,3,4,6-Tetraamino-2,5-diazapentalenes: delocalized antiaromatic compounds (C) 842
Heteropolyanions, A novel heterocluster with D_3-symmetry containing twenty-one core atoms: $[As_6^{III}V_{15}^{IV}O_{42}(H_2O)]^{6\ominus}$ (C) 1721
Hexatrienes, Cobalt-catalyzed reactions of octamethyl-[4]-radialene and 2,5-dimethyl-2,3,4-hexatriene with ethene (C) 571
History of chemistry, One or several pioneers? The discovery of noble-gas compounds (R) 479
Homocycles, Catalytic isomerization of methylated 1,5-cyclooctadienes (C) 1062
— Centrohexaindan, the first hydrocarbon with topologically non-planar molecular structure (C) 1192
— Synthesis and structure of 2,7-Di-*tert*-butyldicyclopenta[*a*,*e*]cyclooctene (C) 1191
— The chemistry of inorganic homo- and heterocycles. Vol. 1 and 2 (B) 1107
— Tricyclo[3.1.0.0^{2,6}]hexanedione (the valene of *o*-benzoquinone), bicyclo[2.1.1]hexane-2,3-dione, and valenes of a quinoxaline, of phenazine, and of a benzophenazine (C) 1369
Homogeneous catalysis, Acetylene polymerization with ylide-nickel catalysts (C) 839
— A new type of unsaturated *triangulo* transition-metal cluster and homogeneous catalyst (C) 263
— Carbon dioxide as an alternative C_1 synthetic unit: activation by transition-metal complexes (R) 661
— Cobalt-catalyzed reactions of octamethyl-[4]-radialene and 2,5-dimethyl-2,3,4-hexatriene with ethene (C) 571
— Contributions to organo-nickel chemistry (R) 185
— Oxidative addition of water to the Ru^{II} catalyst K[Ru^{II}(Hedta)(CO)]: homogeneous catalysis of the water-gas shift reaction under ambient conditions (C) 1735
Host-guest chemistry, A novel type of cationic host molecules with π-acceptor properties (C) 1553
— Complexation of neutral molecules by cyclophane hosts (R) 362
— Cyclobis(paraquat-*p*-phenylene). A tetracationic multipurpose receptor (C) 1547
— Host-guest bonding of oxoanions to guanidinium anchor groups (C) 1516
— Isostructural, alternately-charged receptor stacks. The inclusion complexes of hydroquinone and catechol dimethyl ethers with cyclobis(paraquat-*p*-phenylene) (C) 1550
— Metal-ion-selective exchange resins by matrix imprint with methacrylates (C) 1695
— Modification of hydrophobic and polar interactions by charged groups in synthetic host-guest complexes (C) 1163
— The design of molecular hosts, guests, and their complexes (Nobel lecture) (R) 1009
— 2,2′,7,7′-Tetrahydroxy-1,1′-binaphthyl: a versatile chiral spacer for mono- and ditopic cyclophane hosts with apolar binding sites (C) 1705
Hydrindanones, Unsaturated hydrindanone derivatives from arenes by hetero-Claisen rearrangement (C) 558
Hydrogenation, Enantioselective catalytic transfer-hydrogenation of α,β-unsaturated carboxylic acids with triethylammonium formate (C) 1180
— Mechanism of ethylene hydrogenation by the molecular hydrogen complex [$Ir(H)_2(H_2)(PMe_2Ph)_3$]$^{\oplus}$—characterization of intermediates (C) 1165
— Reduction and hydrogenation with the system hydrocarbon/carbon (R) 679
Hydrogen bonds, On the structure of the cation $N_2H_7^{\oplus}$ with an N−H···N hydrogen bond in the monoammonia adduct of ammonium iodide (C) 1524
— "Proton sponges" and the geometry of hydrogen bonds: aromatic nitrogen bases with exceptional basicities (R) 865
— The fluoronium ions $H_2F^{\oplus}$ and $H_3F_2^{\oplus}$: characterization by crystal structure analysis (C) 391
Hydroperoxides, Competition of endoperoxide and hydroperoxide formation in the reaction of singlet oxygen with cyclic, conjugated dienes (C) 717
Hydrosilation, Photochemical reaction of [(CO)$_4$Co(SiEt$_3$)] with ethylene: implications for cobaltcarbonyl-catalyzed hydrosilation of alkenes (C) 289
Hydroxylamines, *N*-Aryl-*O*-acylhydroxylamines: preparation by *O*-acylation or *N*→*O* transacylation and reaction with amines; model reactions for key steps connected with the carcinogenicity of aromatic amines (C) 973
Hydroxylation, Kinetics and stereochemistry of the $SO_4^{\odot\ominus}$-induced hydroxylation of cyclohexenes in aqueous solution (C) 1066
Hypercarbon chemistry (B) 590
Hypofluorous acid, The crystal structure of hypofluorous acid: chain formation by O−H···O hydrogen bonds (C) 392

Iminoboranes, Synthesis and structure of [$Cp_2NbH(tBuB{\equiv}NtBu)$], a compound with side-on coordinated iminoborane (C) 958
— The chemistry of amino imino boranes (R) 1603
Iminophosphanes, Arylamino(halogeno)-phosphanes XP=N$C_6H_2tBu_3$ (X = Cl, Br, I) and the iminophosphenium tetrachloroaluminate [P≡N$C_6H_2tBu_3$]$^{\oplus}$[$AlCl_4$]$^{\ominus}$: the first stable compound with a PN triple bond (C) 1715
— Synthesis, structure and bonding in the donor-acceptor complex [tBu_2PSe_2]·[PNAryl]: en route to the P≡N bond (C) 1713
Immune system, Somatic generation of immune diversity (Nobel lecture) (R) 1028
s-Indacenes, Equilibrium structure, stabilized transition state, or disorder in the crystal? Studies of the antiaromatic systems tetra-*tert*-butyl-*s*-indacene and tetra-*tert*-butylcyclobutadiene by low-temperature crystal structure analysis (C) 387
Indoles, Transition metals in the synthesis and functionalization of indoles (R) 1113
Intelligent materials—a new frontier (AM) 1389
Intercalation, Partially reversible intercala-

tion of ferrocene in a zeolite-like host lattice consisting of $Fe(CN)_6$ and Me_3Sn units (C) 1521
Iodophosphoranes, 4-Iodo-1,3,5,7-tetramethyl-1,3,5,7-tetraaza-4λ⁵-phosphaspiro[3.3]heptane-2,6-dione: synthesis and structure of the first iodophosphorane (C) 1562
Ion beam epitaxy, From carbon beams to diamond films (AM) 1203
Ion exchange resins, Metal-ion-selective exchange resins by matrix imprint with methacrylates (C) 1695
Iridium compounds, Mechanism of ethylene hydrogenation by the molecular hydrogen complex $[Ir(H)_2(H_2)(PMe_2Ph)_3]^{\oplus}$—characterization of intermediates (C) 1165
— Synthesis of octahedral hydrido(vinyl)iridium(III) complexes by C—H activation: an example of a thermodynamically favored rearrangement $[M(CHR{=}CHX)]\rightarrow[M(H)(CR{=}CHX)]$ (C) 948
— Tetranuclear complexes as intermediates in transannular oxidative-addition reactions. Structure of the first tetrairidium linear cluster (C) 402
Iron compounds, A new cubane cluster with the $[MoFe_3S_4]^0$ core and possible relevance to the Fe_3-centers in ferredoxins. The synthesis, structure and properties of the $[Fe_3S_4(SEt)_3Mo(CO)_3]^{3\ominus}$ anion (C) 1353
— Blocking of the retro-Diels-Alder reaction by complex formation: [(η⁵-cyclopentadienyl)(η⁵-dicyclopentadienyl)iron] (C) 977
— π Complexes of an amino-9-fluorenylideneborane (C) 1331
— Does a 1,1′-diazaferrocene exist? (C) 1368
— Naked molecule chemistry: different bonding modes of CO to FeX_2 (C) 1161
— Oxo-bridged polyiron centers in biology and chemistry (R) 344
— Partially reversible intercalation of ferrocene in a zeolite-like host lattice consisting of $Fe(CN)_6$ and Me_3Sn units (C) 1521
— Short, highly enantioselective synthesis of a key intermediate for the preparation of leucotriene B_4 and its 14,15-didehydro derivative (C) 1188
— Synthesis and structure of $[(OC)_4Fe{=}Si{=}Fe(CO)_4\cdot 2(Me_2N)_3PO]$—a complex of formally zerovalent silicon (C) 583
— Tentacled iron sandwiches (C) 1347
— Tetrakis[bis(trimethylsilyl)ethyne]diiron (C) 1519
Isocyanides, Reactions of pentacarbonyl(trichloromethyl isocyanide)chromium (C) 1344
Isofulminic acid, Carboxime (Isofulminic acid) (C) 938
Isoleucyl-tRNA synthetase: an enzyme with several catalytic cycles displaying variation in specificity and energy consumption (R) 773
Isomerization, Catalytic isomerization of methylated 1,5-cyclooctadienes (C) 1062
— 5-Isopropyliden-1,2-oxathiole 2-oxide by photoisomerization of 2,2-dimethyl-3(2*H*)-thiophenone 1-oxide (C) 1374
Isopolyanions, Formation of an oxalate-filled cavity in a reduced cyclic octanuclear polyoxomolybdate $[(n\text{-}C_4H_9)_4N]_2[Mo_8O_{16}(OCH_3)_8(C_2O_4)]$ formed from α-$[(n\text{-}C_4H_9)_4N]_4[Mo_8O_{26}]$ and rhodizonic acid (C) 1724
— $[V_{19}O_{41}(OH)_9]^{8\ominus}$, an ellipsoid-shaped cluster anion belonging to the unusual family of V^{IV}/V^{V} oxygen clusters (C) 1719

Ketenimines, Ketenimine complexes from carbene complexes and isocyanides: *versatile building blocks for carbocycles* and N-heterocycles (R) 1456
Köbrich reagents, Higher thermostability and selectivity of Köbrich reagents by transmetalation (C) 943
β-Lactones, α-Methylene-β-lactone, a novel heterocyclic ring system via deoxygenation of α-methylene-β-peroxylactones with triphenylphosphane (C) 1536
γ-Lactones, A new route to *trans*-substituted γ-lactones (C) 268
Lasers in chemistry (B) 721
— Laser photochemistry at surfaces—laser-induced chemical vapor deposition and related phenomena (R) 1314
— Preparative UV-laser photochemistry: a biscarbene intermediate in the synthesis of a 5,6-dihydrodibenzo[*a*,*e*]cyclooctene containing a *trans*-double bond (C) 853
Ligand reactions, Pentadienyl, a more reactive and more strongly bound ligand than cyclopentadienyl (C) 1099
— Photochemical reactions of ligands in transition-metal complexes (R) 789
Liquid crystals—state of the art (B) 987
— Thermotropic liquid crystals (AM) 1002
Lithium nitride, Phase transformations of lithium nitride under pressure (C) 1101

Macrocycles, A novel tris(azo)macrobicyclic molecule—synthesis, photochemistry, and isomer separation (C) 1189
— A novel type of cationic host molecules with π-acceptor properties (C) 1553
— A topologically chiral [2]catenand (C) 930
— Cyclobis(paraquat-*p*-phenylene). A tetracationic multipurpose receptor (C) 1547
— $[\{Hg_3Co(C_4H_6NO)_6\}(NO_3)_2]_n$: a macrobicyclic bimetallic chain polymer incorporating deprotonated 2-pyrrolidone bridges (C) 261 (589)
— Isostructural, alternately-charged receptor stacks. The inclusion complexes of hydroquinone and catechol dimethyl ethers with cyclobis(paraquat-*p*-phenylene) (C) 1550
— Modification of hydrophobic and polar interactions by charged groups in synthetic host-guest complexes (C) 1163
— Novel layer structure of sodium calix[4]arenesulfonate complexes—a class of organic clay mimics? (C) 1361
— Supramolecular chemistry—scope and perspectives; molecules, supermolecules, and molecular devices (Nobel lecture) (R) 89
— Template synthesis of macrocyclic multiphosphane ligands with functional groups (C) 438
— The design of molecular hosts, guests, and their complexes (Nobel lecture) (R) 1009
— The discovery of crown ethers (Nobel lecture) (R) 1021
— Towards the making of [12]collarene (C) 966
Macromolecular chemistry, Molecular architecture and function of polymeric oriented systems: models for the study of organization, surface recognition, and dynamics of biomembranes (R) 113
Magnesium compounds, Carbanions as intermediates in the synthesis of Grignard reagents (C) 687
— Organobimetallic Mg-Pd complexes as intermediates in the formation of amorphous $MgPdC_xH_y$ from $Mg(C_2H_5)_2$ and $[Pd(\eta^3\text{-}C_3H_5)_2]$ (C) 1513
— The activation of phenylmagnesium compounds by crown ethers (C) 1084
— The first "adamantoid" alkaline earth metal chelate complex: synthesis, structure, and reactivity (C) 851
Manganese compounds, $[\{Cp(CO)_2Mn\}_2SPh]^{\oplus}$, the first sulfur analogue of a phosphanediyl ("phosphinidene") complex (C) 698
— Linear twofold coordination of arsenic in $[Cp'(CO)_2Mn{=}As{=}Mn(CO)_2Cp']^{\oplus}$ (C) 1529
— Rapid detection of manganese deficiency in conifer needles by electron spin resonance spectroscopy (C) 1722
— Stepwise synthesis and crystal structure of tricarbonyl[pentakis(methylthio)cyclopentadienyl]manganese $[\{C_5(SMe)_5\}Mn(CO)_3]$ (C) 939
— Structure, magnetochemistry and biological relevance of $[Mn_4O_3Cl_4(OAc)_3(py)_3]$, a complex with $S=9/2$ ground state (C) 1731
— Synthesis, structure, and reactivity of $[Mn_2(\mu\text{-}H)_2(CO)_6(\mu\text{-}Ph_2PCH_2PPh_2)]$ (C) 1167
β-Mannosides from β-glucosides by intramolecular nucleophilic substitution with inversion of configuration (C) 1086
Mass spectrometry, Ethylenedithione (C_2S_2): generation and characterization by neutralization-reionization mass spectrometry (C) 1337
— Generation and characterization of sulfurous acid (H_2SO_3) and of its radical cation as stable species in the gas phase (C) 1533
— Isolated, complex Zintl molecules in the gas phase (C) 1091
— Multiphoton-ionization-mass spectrometry (MUPI-MS) (R) 447
Materials science, Advanced materials—a critical view (AM) 726
— Advanced materials by powder metallurgy (AM) 989
— Advanced Materials Editorial (AM) 723
— Advancing materials research (B) 754
— Chemistry of materials (AM) 1741
— Materials federations—the state of play (AM) 1569
— Microscopical structuring of solids by molecular beam epitaxy—spatially resolved materials synthesis (R) 593
— Nonlinear optical properties of organic molecules and crystals (B) 986
— The technology and applications of engineering materials (B) 1001
Matrix isolation, Carboxime (Isofulminic acid) (C) 938
— C_5O_2 (1,2,3,4-pentatetraene-1,5-dione), a new oxide of carbon (C) 566
— 1,4-Di-*tert*-butyl-2,6-bis(trimethylsilyl)silabenzene, the first silabenzene stable in solution at −100°C (C) 963
— Naked molecule chemistry: different bonding modes of CO to FeX_2 (C) 1161
— Nitrogen fixation by borabenzene (C) 295
— 4-Oxo-2,5-cyclohexadienylidene — a carbene with a stable triplet and metastable singlet state? (C) 572
— Structure of molecular PNO, matrix isolation and ab initio calculations (C) 421
— 3,3,6,6-Tetramethylcyclohexyne (C) 398
Membranes, Molecular architecture and function of polymeric oriented systems: models for the study of organization, surface recognition, and dynamics of biomembranes (R) 113
Mercury compounds, $[\{Hg_3Co(C_4H_6NO)_6\}(NO_3)_2]_n$: a macrobicyclic bimetallic chain polymer incorporating deprotonated 2-pyrrolidone bridges (C) 261 (589)
Metal-free polymerization, Metal-free carbanion salts as initiators for the anionic polymerization of acrylic and methacrylic acid esters (C) 1373
— New methods for the anionic polymerization of α-activated olefins (AM) 994
Metallocenophanes, Multidecker metallocenophanes (C) 701
Metal-metal bonds, Clusters of valence electron poor metals—structure, bonding, and properties (R) 159
— μ-Hydroxo- and μ-oxobis(μ-acetato)dirutheniun complexes with weak intramolecular Ru···Ru interactions (C) 933
— Polyauriomethane compounds (C) 419
— Tellurium-rich tellurides (R) 759
— Tetranuclear complexes as intermediates

in transannular oxidative-addition reactions. Structure of the first tetrairidium linear cluster (C) 402
— Weak intramolecular bonding relationships: the conformation-determining attractive interaction between gold(I) centers (C) 417
Metal-metal multiple bonds, Acyl-alkylidyne coupling in the synthesis of dinuclear complexes (C) 1703
— A new type of unsaturated *triangulo* transition-metal cluster and homogeneous catalyst (C) 263
— Base-induced intramolecular formation of a Mo-Mo bond in $[L_2Mo_2^{III}(\mu\text{-}OH)(\mu\text{-}CH_3CO_2)_2]^{3\oplus}$ (L = *N*,*N*′,*N*″-trimethyl-1,4,7-triazacyclononane) (C) 685
— Tetrakis[bis(trimethylsilyl)ethyne]diiron (C) 1519
Metals, Metallic superlattices—artificially structured materials (B) 1410
Metathesis, Heterogeneous, bimetallic metathesis catalysts by reaction of Fischer-type carbene complexes with reduced Phillips catalyst (C) 275
— Methylrhenium oxides: synthesis from Re_2O_7 and catalytic activity in olefin metathesis (C) 394
Methanetetraacetic acid, Distorted triple-diamond structure of 3,3-bis(carboxymethyl)glutaric acid ("methanetetraacetic acid") (C) 829
Methotrexate, Evidence for a folded conformation of methotrexate in solution (C) 423
Methyleneboranes, Lewis-base adducts of methyleneboranes (C) 960
(*S*)-α-Methylserine, Synthesis of peptides containing (*S*)-α-methylserine (C) 858
Micelles, Cyclodextrins increase surface tension and critical micelle concentrations of detergent solutions (C) 393
— Molecular architecture and function of polymeric oriented systems: models for the study of organization, surface recognition, and dynamics of biomembranes (R) 113
— Surfactants, micelles and fascinating phenomena (R) 902
Michael additions, Direct Michael additions of silyl groups to α,β-unsaturated β-arylketones and an α-benzylidenelactone with mixtures obtained from copper(I) cyanide, butyllithium and chlorosilanes (C) 1718
Microanalysis, Pheromones in nanogram quantities: structure determination by combined microchemical and gas chromatographic methods (R) 460
Microbial transformations, Microbial and enzymatic processes for the production of biologically and chemically useful compounds (R) 622
Microgels—polymers with a special molecular architecture (AM) 1743
Molecular beam epitaxy, Microscopical structuring of solids by molecular beam epitaxy—spatially resolved materials synthesis (R) 593
Molecular dynamics, Atomic motions in molecular crystals from diffraction measurements (R) 880
— Equilibrium structure, stabilized transition state, or disorder in the crystal? Studies of the antiaromatic systems tetra-*tert*-butyl-*s*-indacene and tetra-*tert*-butylcyclobutadiene by low-temperature crystal structure analysis (C) 387
— Reversible coupling and opening of a boron-carbon bond (C) 952
Molecular mechanisms of biomineralization in the formation of calcified shells (R) 1145
Molecular recognition, Complexation of neutral molecules by cyclophane hosts (R) 362
— Supramolecular chemistry—scope and perspectives; molecules, supermolecules, and molecular devices (nobel lecture) (R) 90
Molybdenum compounds, A new cubane cluster with the $[MoFe_3S_4]^0$ core and possible relevance to the Fe_3-centers in ferredoxins. The synthesis, structure and properties of the $[Fe_3S_4(SEt)_3Mo(CO)_3]^{3\ominus}$ anion (C) 1353
— Base-induced intramolecular formation of a Mo-Mo bond in $[L_2Mo_2^{III}(\mu\text{-}OH)(\mu\text{-}CH_3CO_2)_2]^{3\oplus}$ (L = *N*,*N*′,*N*″-trimethyl-1,4,7-triazacyclononane) (C) 685
— Coupling metal centers with linearly bridging, delocalized, π-bonded ligands: *p*-phenylenediimido dimolybdenum complexes (C) 569
— Formation of an oxalate-filled cavity in a reduced cyclic octanuclear polyoxomolybdate $[(n\text{-}C_4H_9)_4N]_2[Mo_8O_{16}(OCH_3)_8(C_2O_4)]$ formed from $\alpha\text{-}[(n\text{-}C_4H_9)_4N]_4[Mo_8O_{26}]$ and rhodizonic acid (C) 1724
— Photolytic cluster synthesis: synthesis and structure of $[\{(Ph_3P)Au\}_7Mo(CO)_3]OH$ (C) 1094
— Transformation of η^1-nitrosyl to η^2-hydroxylaminyl ligands in the reduction of $[Mo(NO)_2(\text{'}S_4\text{'})]$ to $[Mo(\eta^2\text{-}NH_2O)(NO)(\text{'}S_4\text{'})]$: a model reaction for a partial step in the enzymatic $[NO_3^{\ominus} \rightarrow NH_3]$ conversion (C) 1164
MO theory, Ab-initio molecular orbital theory (B) 862
Multiphoton-ionization-mass spectrometry (MUPI-MS) (R) 447
Multiple bonds, Arylamino(halogeno)phosphanes $XP{=}NC_6H_2tBu_3$ (X = Cl, Br, I) and the iminophosphenium tetrachloroaluminate $[P{\equiv}NC_6H_2tBu_3]^{\oplus}[AlCl_4]^{\ominus}$: the first stable compound with a PN triple bond (C) 1715
— Compounds with partial boron-carbon triple bonds (C) 961
— Linear twofold coordination of arsenic in $[Cp'(CO)_2Mn{=}As{=}Mn(CO)_2Cp']^{\oplus}$ (C) 1529
— (Mesityl)$_2$Ge(fluorenylidene)—stabilization of a Ge-C double bond by charge transfer into an aromatic system (C) 828
— Synthesis, structure and bonding in the donor-acceptor complex $[tBu_2PSe_2]\cdot[PNAryl]$: en route to the P≡N bond (C) 1713
— "Wittig reactions" of unsaturated silicon compounds >Si=Y: isolation and structure of possible intermediates (C) 935

Natural products, A photolytic entry into oxepane systems (C) 1362
— Cyclobutanones and cyclobutenones in nature and in synthesis (R) 797
— Diastereospecific gas/solid additions with cholesterol derivatives (C) 1511
— Reactivity of (*R*)-2-*tert*-butyldihydrooxazole derivatives prepared from serine and threonine: novel, versatile chiral building blocks (C) 1351
— Structure and reactivity of lithium enolates. From pinacolone to selective *C*-alkylations of peptides. Difficulties and opportunities afforded by complex structures (R) 1624
— Vitamin B_{12}: experiments concerning the origin of its molecular structure (R) 5
New analytical methods, Two-dimensional solid-state NMR spectroscopy: new possibilities for the investigation of the structure and dynamics of solid polymers (R) 1655
Nickel compounds, Acetylene polymerization with ylide-nickel catalysts (C) 839
— Contributions to organo-nickel chemistry (R) 185
— Electron-electron/spin-spin long-range interaction as studied in the diradical dication [Di{bis(dimethylphosphino-η^6-benzene)chromium(I)}-nickel(0)]$^{++}$ (C) 414
— Mono- and dinuclear nickel(0) complexes of butadiyne (C) 833
— $[Ni_9(\mu_4\text{-}As)_6(PPh_3)_5Cl_3]$, a cubic body-centered Ni_9-cluster (C) 1512
— Reaction of $[NiCp(PPh_3)Cl]$ with $E(SiMe_3)_2$; the structures of $[Ni_4Se_2Cp_4]$ and $[Ni_4E_2Cp_4(PPh_3)_2]$ (E = Se, Te) (C) 965
— Stabilization of 1,2,4,5-tetradehydrobenzene by complexation at two nickel(0) centers (C) 941
— Synthesis and structure of (ET)[Ni{SC(CN)=C(CN)S}$_2$], a radical cation salt of bis(ethylenedithio)tetrathiafulvalene (C) 699
Niobium compounds, Extremely short nonbonding oxygen-oxygen distances: the crystal structures of $NbBO_4$, $NaNb_3O_8$, and $NaTa_3O_8$ (C) 969
Nitrile imines, First direct evidence for nitrile imine–diazo isomerization. Synthesis of Relatively stable *N*-silylated nitrile imines (C) 1350
Nitrile oxides, A new route to nitrile oxides via α-nitrosodiazo derivatives (C) 301
Nitrogen compounds, Catalytic syntheses of functionalized nitrogen heterocycles from cyanogen (C) 1372
— Host-guest bonding of oxoanions to guanidinium anchor groups (C) 1516
— On the structure of the cation $N_2H_7^{\oplus}$ with an N–H···N hydrogen bond in the monoammonia adduct of ammonium iodide (C) 1524
— Structure of a chiral lithium azaenolate: monomeric, intramolecular chelated lithio-2-acetylnaphthalene-SAMP-hydrazone (C) 1522
— Synthesis and physical properties of 3,6-di-*tert*-butyl-1,4-diazapentalene (C) 1061
— Synthesis and structure of an azastibacubane (C) 287
— Transition metals in the synthesis and functionalization of indoles (R) 1113
Nitrogen fixation by borabenzene (C) 295
— Catalytic fixation of nitrogen by the photocatalytic CdS/Pt/RuO_2 particulate system in the presence of aqueous $[Ru(Hedta)N_2]^{\ominus}$ complex (C) 923
Nitrogen reduction, Dinuclear vanadium(II)- and vanadium(III)-guaiacolato complexes related to vanadium-based systems for the reduction of nitrogen (C) 576
NMR spectroscopy, A monomeric potassium salt of bis(trimethylsilyl)methyl phenyl sulfone and the determination of the $^1J(^{13}C,^{29}Si)$ coupling constants of Si-stabilized "carbanions" (C) 1092
— Catalytic isomerization of methylated 1,5-cyclooctadienes (C) 1062
— High-resolution solid-state ^{13}C-NMR spectroscopy of polymers (R) 1468
— High-resolution solid-state NMR of silicates and zeolites (B) 1410
— 3-Lithio-2-(*o*-lithiophenyl)naphthalene-dilithium—a tetralithio compound with σ- and π-bonded lithium atoms (C) 1182
— 1,6-Methano[10]annulenedianion, a paratropic 12π-electron dianion with a C_{10} perimeter (C) 1692
— Multinuclear NMR (B) 1386
— NOESY-TOCSY, an advantageous 2D NMR technique for the analysis of peptide sequences (C) 564
— Organobimetallic Mg–Pd complexes as intermediates in the formation of amorphous $MgPdC_xH_y$ from $Mg(C_2H_5)_2$ and $[Pd(\eta^3\text{-}C_3H_5)_2]$ (C) 1513
— Phosphorus-31 NMR spectroscopy in stereochemical analysis (B) 591
— Selective INADEQUATE, a farewell to 2D-NMR? (C) 1196
— ^{29}Si-^{29}Si long range couplings in strained cyclic polysilanes (C) 1727
— Two-dimensional NMR spectroscopy (B) 1567
— Two-dimensional NMR spectroscopy: background and overview of the experiments (R) 490
— Two-dimensional solid-state NMR spec-

troscopy: new possibilities for the investigation of the structure and dynamics of solid polymers (R) 1655
Nobel lecture, Perovskite-type oxides—the new approach to high-T_c superconductivity (AM) 735
— Somatic generation of immune diversity (Nobel lecture) (R) 1028
— Supramolecular chemistry—scope and perspectives; molecules, supermolecules, and molecular devices (Nobel lecture) (R) 89
— The design of molecular hosts, guests, and their complexes (Nobel lecture) (R) 1009
— The discovery of crown ethers (Nobel lecture) (R) 1021
Noble-gas compounds, One or several pioneers? The discovery of noble-gas compounds (R) 479
Noc, The *p*-nitrocinnamyloxycarbonyl (noc) moiety—an acid-stable amino-protecting group removable under neutral conditions for peptide and glycopeptide synthesis (C) 1375
Nonlinear optical properties of organic molecules and crystals (B) 986
Norcaradienes, Formation of cycloheptatriene/norcaradiene systems in the decomposition of diaryldiazomethanes in benzene (C) 284
Norcarotinoids, 4,6,6-Trimethyl-4-cyclohexene-1,2,3-trione, a contribution to the biogenesis of norcarotinoids (C) 695
Nuclear chemistry, Synthesis of the heaviest chemical elements—results and perspectives (R) 1417
Nucleic acids, Dynamics of proteins and nucleic acids (B) 862
Nucleophilic substitution, Carbon as leaving group—stereochemistry of nucleophilic substitution (C) 1538

Onium ions, A novel type of cationic host molecules with π-acceptor properties (C) 1553
— The cyclohepta[*def*]carbazolium ion (C) 585
— The fluoronium ions $H_2F^{\oplus}$ and $H_3F_2^{\oplus}$: characterization by crystal structure analysis (C) 391
Organic chemistry, Intermediate organic chemistry (B) 1737
— Molecular crystals (B) 1003
— Organic solid state chemistry (B) 1003
— The name game. Modern coined terms and their origins (B) 1197
Organic Chemistry (B) 1106
Organic conductors, New organic superconductors (AM) 1747
— The copper salt of 2-iodo-5-methyl-*N,N'*-dicyanoquinonediimine—a radical anion salt exhibiting metallic conductivity down to low temperatures (C) 267
Organic metals, New donors for molecular organic (super)conductors and ferromagnets (AM) 1573
Organic synthesis, Functionalized, enantiomerically pure [2.1.1]-, [2.2.1]-, and [2.2.2]-triblattanes (C) 1103
— Microbial and enzymatic processes for the production of biologically and chemically useful compounds (R) 622
— Organoselenium chemistry (B) 444
— Principles and applications of organotransition metal chemistry (B) 984
— Reduction and hydrogenation with the system hydrocarbon/carbon (R) 679
— Reduction of epoxides, α,β-unsaturated aldehydes, and vicinal diketones with "reactive titanocene" (C) 855
— Selenium reagents and intermediates in organic synthesis (B) 444
— The chemistry of organic selenium and tellurium compounds, Vol. 1 (B) 444
— The chemistry of the metal-carbon bond. Vol. 4: The use of organometallic compounds in organic synthesis (B) 1110
— Tin in organic synthesis (B) 445
Organometallic chemistry, Molecular organometallic chemistry on surfaces: reactivity of metal carbonyls on metal oxides (R) 1127
Osmium compounds, $[Os(\eta^2\text{-PHS})(CO)_2(PPh_3)_2]$, a stable η^2-thioxophosphane(H–P=S)-metal complex (C) 302
Oxazines, Methoxyallenes as components in Diels-Alder reactions with inverse electron demand: synthesis of 6*H*-1,2-oxazines (C) 1518
Oxepanes, A photolytic entry into oxepane systems (C) 1362
Oxidative coupling of racemic and of optically active 3,6-di-*tert*-butylocta-1,4,7-triyne-3,6-diol (C) 859
Oxoanions, Host-guest bonding of oxoanions to guanidinium anchor groups (C) 1516
4-Oxo-2,5-cyclohexadienylidene—a carbene with a stable triplet and metastable singlet state? (C) 572
Oxygen, Competition of endoperoxide and hydroperoxide formation in the reaction of singlet oxygen with cyclic, conjugated dienes (C) 717
Oxygen compounds, A new approach to ionic ozonides (C) 1341
— Coordination of H_2 and O_2 to $[OsHCl(CO)(PiPr_3)_2]$: a catalytically active $M(\eta^2\text{-}H_2)$ complex (C) 1563
Ozonides, A new approach to ionic ozonides (C) 1341

Palladium compounds, Organobimetallic Mg–Pd complexes as intermediates in the formation of amorphous $MgPdC_xH_y$ from $Mg(C_2H_5)_2$ and $[Pd(\eta^3\text{-}C_3H_5)_2]$ (C) 1513
— Transition metals in the synthesis and functionalization of indoles (R) 1113
Paraformaldehyde as possible chirality amplifier (C) 1379
Pentadienes, Pentadienyl, a more reactive and more strongly bound ligand than cyclopentadienyl (C) 1099
Pentalenes, A donor-acceptor substituted quinoid pentalene (C) 1711
Pentatetraene-dione, C_5O_2 (1,2,3,4-pentatetraene-1,5-dione), a new oxide of carbon (C) 566
Pentazadienide, The pentazadienide ion as a ligand in metal complexes (R) 896
Peptides, Catalytic activity of enzymes altered at their active sites (R) 913
— Chlorotetain from *bacillus subtilis*, an antifungal dipeptide with an unusual chlorine-containing amino acid (C) 1733
— NOESY-TOCSY, an advantageous 2D NMR technique for the analysis of peptide sequences (C) 564
— Solid phase synthesis of peptides and glycopeptides on polymeric supports with allylic anchor groups (C) 711
— Synthesis of peptides containing (*S*)-α-methylserine (C) 858
— The *p*-nitrocinnamyloxycarbonyl (noc) moiety—an acid-stable amino-protecting group removable under neutral conditions for peptide and glycopeptide synthesis (C) 1375
Pharmaceutical proteins (R) 207
Phenanthrenes, How high is the activation barrier to helix inversion of 1,4,5,8-tetrasubstituted phenanthrenes? (C) 270
Pheromones, Diastereo- and enantioselective aldol reactions via α-silyl ketones, asymmetric synthesis of the aggregation pheromone sitophilure (C) 581
— in nanogram quantities: structure determination by combined microchemical and gas chromatographic methods (R) 460
Phosphaalkenes, 1,4-diphosphabutatriene (C) 1360
Phosphaalkynes, Annelation of carbene ligands by λ^3-phosphaalkynes, an entry to functionalized phosphaarenes (C) 713
— 1,4-Diphospha-2-rhodacyclopentadiene—an isolable intermediate in the metal-induced cyclodimerization of *tert*-butylphosphaacetylene (C) 1157
— Reaction of 1,3-azaarsinines with 2-*tert*-butyl-1-phosphaethyne — 2,9,10-tri-*tert*-butyl-4,6-diphenyl-1,3,8-triphospha-7-arsatetracyclo[4.4.0.0^{2,8}.0^{3,7}]deca-4,9-diene (C) 709
— Phosphaalkynes—syntheses, reactions, coordination behavior (R) 1484
Phosphadistannacyclobutenes, Addition of a distannene to a phosphaalkyne. Formation of a phosphadistannacyclobutene (C) 838
Phosphorus compounds, Addition of a distannene to a phosphaalkyne. Formation of a phosphadistannacyclobutene (C) 838
— A novel entry to the PC-double bond: the "phospha-Wittig" reaction (C) 1382
— Dications based on a hydrotris(phosphonio)borate skeleton (C) 1071
— Formation of the diphosphatricyclo[2.1.0.0^{2,5}]pentane ring system via phosphaalkyne dimerization and carbon monoxide incorporation (C) 837
— Novel boron-phosphorus cages with $C_4B_4P_4$ and $C_2B_4P_4$ frameworks (C) 399
— Synthesis and crystal structure of a chiral C_3-symmetric monophosphane (C) 835
— Synthesis and molecular structure of the diphosphaarsirane $[\{[(\eta^5\text{-}C_5Me_5)(CO)_2Fe]P\}_2AsC_6H_2tBu_3]$ (C) 1537
— Synthesis of optically active phosphanes via Sharpless epoxidation (C) 718
— Tetraphosphafulvalenes (C) 950
— The first *closo*-diphosphahexaborane $P_2B_4Cl_4$ (C) 925
— The first diphosphaallyl system coordinated to two metal centers (C) 416
— The first triphosphabicyclobutane—evidence for a 1,2,3-triphosphabutadiene (C) 957
Phosphorus homocycles, Alkali-metal hydrogen tetraphosphides M^IHP_4 — the first salts of bicyclo[1.1.0]tetraphosphane (C) 1059
— On the pentaphosphacyclopentadienide ion, $P_5^{\ominus}$ (C) 280
— Tris(2,3-di-*tert*-butylcyclotriphosphanyl)-stibane—a compound containing three P_3 rings linked by an antimony atom (C) 561
Phosphorus-nitrogen compounds, Arylamino(halogeno)phosphanes $XP{=}NC_6H_2tBu_3$ (X = Cl, Br, I) and the iminophosphenium tetrachloroaluminate $[P{\equiv}NC_6H_2tBu_3]^{\oplus}[AlCl_4]^{\ominus}$: the first stable compound with a PN triple bond (C) 1715
— 4-Iodo-1,3,5,7-tetramethyl-1,3,5,7-tetraaza-4λ^5-phosphaspiro[3.3]heptane-2,6-dione: synthesis and crystal structure of the first iodophosphorane (C) 1562
— Reaction of 1,3-azaphosphinines with 2-*tert*-butyl-1-phosphaethyne: 9-aza-2,4,6-triphosphatetracyclo[5.3.0.0^{2,4}.0^{3,6}]deca-8,10(1)-diene (C) 389
— Structure of molecular PNO, matrix isolation and ab initio calculations (C) 421
— Synthesis and structure of $[ClV(OSiMe_3)N_2PPh_2]_2$, the first cyclodimetallaphosphazene—an eight-membered planar unsaturated heterocycle (C) 850
— Synthesis, structure and bonding in the donor-acceptor complex $[tBu_2PSe_2]\cdot[PNAryl]$: en route to the P≡N bond (C) 1713
Phosphorylation, Protein phosphorylation in bacteria — regulation of gene expression, transport functions, and metabolic processes (R) 1040
Photochemistry, A novel tris(azo)macrobicyclic molecule—synthesis, photochemistry, and isomer separation (C) 1189
— A photolytic entry into oxepane systems (C) 1362
— Catalytic fixation of nitrogen by the pho-

tocatalytic CdS/Pt/RuO_2 particulate system in the presence of aqueous $[Ru(Hedta)N_2]^{\ominus}$ complex (C) 923
— Facile reduction of 1,2-dioxetanes by thiols as potential protective measure against photochemical damage of cellular DNA (C) 429
— in microheterogeneous systems (B) 722
— 5-Isopropyliden-1,2-oxathiole 2-oxide by photoisomerization of 2,2-dimethyl-3(2*H*)-thiophenone 1-oxide (C) 1374
— Laser photochemistry at surfaces—laser-induced chemical vapor deposition and related phenomena (R) 1314
— Mechanisms of photophysical processes and photochemical reactions in polymers (B) 1568
— Photochemical reaction of $[(CO)_4Co(SiEt_3)]$ with ethylene: implications for cobaltcarbonyl-catalyzed hydrosilation of alkenes (C) 289
— Photochemical reactions of ligands in transition-metal complexes (R) 789
— Photolytic cluster synthesis: synthesis and structure of $[\{(Ph_3P)Au\}_7Mo(CO)_3]OH$ (C) 1094
— Preparative UV-laser photochemistry: a biscarbene intermediate in the synthesis of a 5,6-dihydrodibenzo[*a,e*]cyclooctene containing a *trans*-double bond (C) 853
— Second-sphere photochemistry and photophysics: luminescence of the $[Pt(bpy)(NH_3)_2]^{2\oplus}$-dibenzo[30]crown-10 adduct (C) 692
— Selective photochemical dehydrogenation of saturated hydrocarbons with quantum yields approaching unity (C) 1526
Photoconductors, Polymeric photoconductors—new concepts (AM) 1210
Photophysics of polymers (B) 1409
Photosynthesis, Structure, magnetochemistry and biological relevance of $[Mn_4O_3Cl_4(OAc)_3(py)_3]$, a complex with $S=9/2$ ground state (C) 1731
Platinum compounds, A Pt_2AgH_2 complex (C) 563
— Trimethylplatinum-theophylline hexamer: a novel Pt_6 heterocycle containing both Pt-N and Pt-O bonds (C) 1160
Polyauriomethanes, "Aurophilicity" as a consequence of relativistic effects: the hexakis(triphenylphosphaneaurio)methane dication $[(Ph_3PAu)_6C]^{2\oplus}$ (C) 1544
— Use of the CH acidity of 2,4,4-trimethyl-4,5-dihydrooxazole to synthesize triauriomethanes and novel gold clusters (C) 1542
Polyenes, Synthesis and optical properties of terminally substituted conjugated polyenes (C) 281
— Synthesis of all-*cis*-1,4,7,10-cyclododecatetraene (C) 298
Polymerization, Acetylene polymerization with ylide-nickel catalysts (C) 839
— Metal-free carbanion salts as initiators for the anionic polymerization of acrylic and methacrylic acid esters (C) 1373
— New methods for the anionic polymerization of α-activated olefins (AM) 994
— Synthesis of oligomeric and polymeric monosaccharides by aldol group-transfer polymerization (C) 1158
— The central propellane bond as polymerizable CC single bond: poly(tricyclo-[4.2.0.0^{2,7}]octane-1,7-diyl) — a "poly([1.1.1]propellane)" (C) 296
Polymers, Classical light scattering from polymer solutions (B) 1221
— High-resolution solid-state ^{13}C-NMR spectroscopy of polymers (R) 1468
— Mechanisms of photophysical processes and photochemical reactions in polymers (B) 1568
— Microgels—polymers with a special molecular architecture (AM) 1743
— Photophysics of polymers (B) 1409
— Polymer microscopy (B) 1220
— Two-dimensional solid-state NMR spectroscopy: new possibilities for the investigation of the structure and dynamics of solid polymers (R) 1655
Porphycenes, Tetraoxaporphycene dication (C) 411
Porphyrins, Biomimetic synthesis of an octavinylogous porphyrin with an aromatic [34]annulene system (C) 1170
— Tetraoxaporphyrin dication (C) 406
— Tetraoxaporphyrinogen (tetraoxaquaterene): oxidation to the tetraoxaporphyrin dication (C) 409
— The chemistry and biochemistry of *N*-substituted porphyrins (B) 1737
Powder metallurgy, Advanced materials by powder metallurgy (AM) 989
Prismanes, Synthesis and properties of a bridged *syn*-tricyclo[4.2.0.0^{2,5}]octa-3,7-diene: formation of propella[3$_4$]prismane (C) 840
Propellanes, The central propellane bond as polymerizable CC single bond: poly(tricyclo[4.2.0.0^{2,7}]octane-1,7-diyl) — a "poly([1.1.1]propellane)" (C) 296
Propella[3$_4$]prismane, Synthesis and properties of a bridged *syn*-tricyclo[4.2.0.0^{2,5}]octa-3,7-diene: formation of propella[3$_4$]prismane (C) 840
Protecting groups, In-situ blocking of an aldehyde function by formation of (α-triphenylphosphoniumalkoxy)-titanium or -niobium complexes (C) 944
— Protecting-group-dependent stability of intersaccharide bonds — synthesis of a fucosyl-chitobiose glycopeptide (C) 1697
— Synthesis and properties of N^{α}-Di-*tert*-butoxycarbonyl and N^{α}-benzyloxycarbonyl *tert*-butoxycarbonyl amino acids (C) 400
— The *p*-nitrocinnamyloxycarbonyl (noc) moiety—an acid-stable amino-protecting group removable under neutral conditions for peptide and glycopeptide synthesis (C) 1375
— The SF_5-unit as steric protecting group; synthesis and structure of $F_5S-C\equiv SF_3$ (C) 1534
Proteins, Controlling the microstructure of monomolecular layers (AM) 728
— Dynamics of proteins and nucleic acids (B) 862
— Flexibility and rigidity of proteins and protein-pigment complexes (R) 79
— Pharmaceutical proteins (R) 207
— Practical protein chemistry—a handbook (B) 306
— Protein engineering (B) 306
— Protein engineering (B) 1110
— Protein phosphorylation in bacteria—regulation of gene expression, transport functions, and metabolic processes (R) 1040
Proton sponges and the geometry of hydrogen bonds: aromatic nitrogen bases with exceptional basicities (R) 865
Publications, The art of scientific writing. From student reports to professional publications in chemistry and related fields (B) 1565
— Under the surface of the chemical article (R) 1593
Pyrazines, Bis([1,2,5]thiadiazolo)[3,4-*b*;3′,4′-*e*]pyrazine, a novel 14π-electron heterocycle with high electron affinity (C) 434
Pyrroles, Stable sandwich complexes with pentamethylpyrrole ligands (C) 579

Quinonediimines, The copper salt of 2-iodo-5-methyl-*N,N*′-dicyanoquinonediimine—a radical anion salt exhibiting metallic conductivity down to low temperatures (C) 267

Racemization, How high is the activation barrier to helix inversion of 1,4,5,8-tetrasubstituted phenanthrenes? (C) 270
Radialenes, Cobalt-catalyzed reactions of octamethyl-[4]-radialene and 2,5-dimethyl-2,3,4-hexatriene with ethene (C) 571
— Tris(fluoren-9-ylidene)cyclopropane, a novel [3]radialene (C) 1080
— Tris(thioxanthen-9-ylidene)cyclopropane, and its radical cation and dication (C) 1078
Radiation chemistry. Principles and applications (B) 861
Radical ions, ENDOR spectroscopy in water: reductions and oxidations of organic compounds (C) 1069
— Generation and characterization of sulfurous acid (H_2SO_3) and of its radical cation as stable species in the gas phase (C) 1533
— Isolation and structure of $[(fluorenone^{\odot\ominus})\{Na^{\oplus}(dme)_2\}]_2$ — a touchstone for radical contact ion pairs? (C) 1067
— Kinetics and stereochemistry of the $SO_4^{\odot\ominus}$-induced hydroxylation of cyclohexenes in aqueous solution (C) 1066
— Synthesis and structure of $(ET)[Ni\{SC(CN)=C(CN)S\}_2]$, a radical cation salt of bis(ethylenedithio)tetrathiafulvalene (C) 699
— The copper salt of 2-iodo-5-methyl-*N,N*′-dicyanoquinonediimine—a radical anion salt exhibiting metallic conductivity down to low temperatures (C) 267
— Tris(fluoren-9-ylidene)cyclopropane, a novel [3]radialene (C) 1080
— Tris(thioxanthen-9-ylidene)cyclopropane, and its radical cation and dication (C) 1078
Radicals, The influence of polar and steric effects on the selectivity of the β-cleavage of alkyl radicals (C) 1168
Radiochemistry, Synthesis of the heaviest chemical elements—results and perspectives (R) 1417
Raw materials, Chemicals from coal: new processes (B) 1385
— Industrielle Aromatenchemie. Rohstoffe, Verfahren, Produkte (B) 1108
— Natural fats and oils—renewable raw materials for the chemical industry (R) 41
Reaction mechanisms, Acyl-alkylidyne coupling in the synthesis of dinuclear complexes (C) 1703
— Carbon as leaving group—stereochemistry of nucleophilic substitution (C) 1538
— Electron transfer and charge transfer: twin themes in unifying the mechanisms of organic and organometallic reactions (R) 1227
— Inductivity and bridging in ammonium and carbenium ions (C) 714
— Kinetics and stereochemistry of the $SO_4^{\odot\ominus}$-induced hydroxylation of cyclohexenes in aqueous solution (C) 1066
— Slow tautomerization in a rhenium-oxo-hydroxide complex (C) 1527
— The influence of polar and steric effects on the selectivity of the β-cleavage of alkyl radicals (C) 1168
Reagents, High oxidation state organometallic chemistry, a challenge—the example of rhenium (R) 1297
— Reactions of pentacarbonyl(trichloromethyl isocyanide)chromium (C) 1344
Rearrangements, The enzymic interconversion of isobutyryl and *n*-butyrylcarba(dethia)-coenzyme A: a coenzyme-B_{12}-dependent carbon skeleton rearrangement (C) 1089
Redox reactions, An antibody-mediated redox reaction (C) 1172
— ENDOR spectroscopy in water: reductions and oxidations of organic compounds (C) 1069
Reductions of epoxides, α,β-unsaturated aldehydes, and vicinal diketones with "reactive titanocene" (C) 855
— Reduction with yeast cells the key step of an efficient synthesis of (3*S*, 4*S*)-4-amino-3-hydroxypentanoic acids (C) 426
— Transformation of η^1-nitrosyl to η^2-hydroxylaminyl ligands in the reduction of $[Mo(NO)_2(S_4)]$ to $[Mo(\eta^2\text{-}NH_2O)$-

(NO)('S_4')]: a model reaction for a partial step in the enzymatic [$NO_2^{\ominus} \rightarrow NH_3$] conversion (C) 1164
Reflectance spectroscopy, The use of light in the study of interfacial electrochemical reactions (R) 63
Regioselectivity, C_5 building blocks for terpene syntheses: γ-acetoxylation of (*E*)-2-methyl-2-butenals (C) 285
Renewable raw materials, Natural fats and oils—renewable raw materials for the chemical industry (R) 41
Retro-Diels-Alder reactions, Blocking of the retro-Diels-Alder reaction by complex formation: [(η^5-cyclopentadienyl)(η^5-dicyclopentadienyl)iron] (C) 977
Rhenium compounds, Acid-catalyzed alkyne/alkene coupling at Re^{III} centers (C) 1509
— Alkyne coordination to organorhenium oxides with rhenium in high oxidation states (C) 946
— A new type of unsaturated *triangulo* transition-metal cluster and homogeneous catalyst (C) 263
— High oxidation state organometallic chemistry, a challenge—the example of rhenium (R) 1297
— Methylrhenium oxides: synthesis from Re_2O_7 and catalytic activity in olefin metathesis (C) 394
— Slow tautomerization in a rhenium-oxo-hydroxide complex (C) 1527
— Synthesis and structure of a resonance stabilized (Trimethylphosphonio)metallapropenide (C) 587
Rhodium compounds, [(η^5-C_5Me_4Et)-Rh(μ,η^2-P_2)$_2$Rh(η^5-C_5Me_4Et)], a sandwich complex with a P_4 rectangle (C) 405
— 1,4-Diphospha-2-rhodacyclopentadiene—an isolable intermediate in the metal-induced cyclodimerization of *tert*-butylphosphaacetylene (C) 1157
— Novel anionic aryl complexes of Rh^{III}: $[Rh(C_6F_5)_5]^{2\ominus}$ and $[Rh(C_6F_5)_4(CO)_2]^{\ominus}$ (C) 1700
— $P_4^{2\ominus}$ Isomers as complex ligands (C) 694
— Rhodium-catalyzed reductive carbonylation of methyl formate to acetaldehyde (C) 683
— Synthesis and structure of [$(C_5Me_5)_2Rh_2S_8$], a dirhodium complex with unusual polysulfide bridge (C) 708
— Synthesis, structure and bonding of [$Cl_2Sn\{Rh(PMe_3)_3Cl\}_2$]·THF, an unusual Sn^{II}-Rh^{I} adduct (C) 442
— Tris(2,2'-bipyridyl-5-sulfonic acid)rhodium(III), an improved redox catalyst for the light-induced and the electrochemically initiated enzymatic reduction of carbonyl compounds (C) 265
Ruthenium compounds, A stable bis(chelate) analogue of the Creutz-Taube ion (C) 1174
— Elementary reactions at metal-sulfur centers: base-induced substitution of PPh_3 in [$Ru(PPh_3)_2$(bmae)] (C) 689
— μ-Hydroxo- and μ-oxobis(μ-acetato)diruthenium complexes with weak intramolecular Ru···Ru interactions (C) 933
— Oxidative addition of water to the Ru^{II} catalyst $K[Ru^{II}$(Hedta)(CO)]: homogeneous catalysis of the water-gas shift reaction under ambient conditions (C) 1735
— Real-time atomic-resolution imaging of polymorphic changes in ruthenium clusters (C) 555
— Transformation of open-chain thioether-dithiolato to cyclic thioether ligands by C–S bond cleavage and bond formation at ruthenium centers: synthesis of the trithiobenzo[9]crown-3 complex [Ru(Bzo-9S3)(CO)Br_2] (C) 691

Sandwich complexes, [(η^5-C_5Me_4Et)Rh(μ,η^2-P_2)$_2$Rh(η^5-C_5Me_4Et)], a sandwich complex with a P_4 rectangle (C) 405
— Does a 1,1'-diazaferrocene exist? (C) 1368
— Electron-electron/spin-spin long-range interaction as studied in the diradical dication [Di{bis(dimethylphosphino-η^6-benzene)chromium(I)}-nickel(0)]$^{++}$ (C) 414
— Multidecker metallocenophanes (C) 701
— (Octamethyltetrasila-η^{12}-[2.2]paracyclophane)chromium—synthesis, structure, and characteristics (C) 684
— Partially reversible intercalation of ferrocene in a zeolite-like host lattice consisting of $Fe(CN)_6$ and Me_3Sn units (C) 1521
— Stable sandwich complexes with pentamethylpyrrole ligands (C) 579
— Tentacled iron sandwiches (C) 1347
Say it in English, please! (R) 1050
Second harmonic generation, Methyl 4-hydroxy-5-iodo-2,3-dimethoxy-6-methylbenzoate: the aromatic fragment of calichemicin γ^1_{α}. Synthesis, X-ray crystallographic analysis, and properties (C) 1097
Selenium compounds, Organoselenium chemistry (B) 444
— Selenium reagents and intermediates in organic synthesis (B) 444
— Soluble chromium selenides and tellurides: preparations and structures of [$(C_6H_5)_4P]_3[Cr_3Te_{24}$] and [$(C_6H_5)_4P]_3$-[$Cr_3Se_{24}$] (C) 1702
— The chemistry of organic selenium and tellurium compounds, Vol. 1 (B) 444
— The reagent diphenyldiselane/iodine: no phenylselenenyl iodide but a charge transfer complex with cyclic moieties (C) 431
Self organization, Helicates: tetra- and pentanuclear double helix complexes of Cu^{I} and poly(bipyridine) strands (C) 1095
— Molecular architecture and function of polymeric oriented systems: models for the study of organization, surface recognition, and dynamics of biomembranes (R) 113
Semiconductors, The chemistry of the semiconductor industry (B) 1739
Sensors, Intelligent materials—a new frontier (AM) 1389
Sesquiterpenes, Stereoselective synthesis of *trans*-decalins via intramolecular ene reactions; synthesis of the enantiomerically pure cadinane-sesquiterpene veticadinol (C) 703
Sharpless epoxidations, Synthesis of optically active phosphanes via Sharpless epoxidation (C) 718
Silanediyls, Convenient routes to Di-*tert*-butylsilanediyl: chemical, thermal and photochemical generation (C) 1355
Silicates, High-resolution solid-state NMR of silicates and zeolites (B) 1410
Silicon chemistry, Organosilicon chemistry (B) 446
Silicon compounds, Convenient routes to Di-*tert*-butylsilanediyl: chemical, thermal and photochemical generation (C) 1355
— 1,4-Di-*tert*-butyl-2,6-bis(trimethylsilyl)silabenzene, the first silabenzene stable in solution at −100 °C (C) 963
— From the dilithiooctamethylcyclotetrasilazane to the 1,3,5,7-tetraaza-2,4,6,8,9-pentasilabicyclo[3.3.1]nonane system (C) 1074
— Is tetrasilatetrahedrane kinetically stable? (C) 1081
— Phosphane-stabilized Cu^{I} and Ag^{I} silanes (C) 1349
— Polycyclic silylamides of Ge^{II} and Sn^{II} with different structures—bis(germanediyl) versus distannate (C) 1087
— Reductive oligomerization of 1,2-Di-*tert*-butyl-1,1,2,2-tetrachlorodisilane: the tricyclo[2.2.0.$0^{2,5}$]hexasilane and tetracyclo[3.3.0.$0^{2,7}$.$0^{3,6}$]octasilane systems (C) 1725
— Silicon reagents in organic synthesis (B) 1567
— ^{29}Si-^{29}Si long range couplings in strained cyclic polysilanes (C) 1727
— Synthesis and structure of $[(OC)_4Fe{=}Si{=}Fe(CO)_4 \cdot 2(Me_2N)_3PO]$—a complex of formally zerovalent silicon (C) 583
— "Wittig reactions" of unsaturated silicon compounds >Si=Y: isolation and structure of possible intermediates (C) 935
Silver compounds, 3- and 3,6-silylated 2-pyridinethiols: new hindered bidentate ligands and their novel silver and copper clusters (C) 1342
— A $Pt_2Ag_2H_2$ complex (C) 563
— 2,4,6-$Ph_3C_6H_2M$ (M = Cu, Ag), monomeric Cu^{I}- and Ag^{I}-complexes with coordination number 1 (C) 436
— Phosphane-stabilized Cu^{I} and Ag^{I} silanes (C) 1349
Singlet oxygen, Competition of endoperoxide and hydroperoxide formation in the reaction of singlet oxygen with cyclic, conjugated dienes (C) 717
Solid-phase syntheses, Solid-phase synthesis of *O*-glycopeptide sequences (C) 1365
— Solid phase synthesis of peptides and glycopeptides on polymeric supports with allylic anchor groups (C) 711
Solid state chemistry, Clusters of valence electron poor metals—structure, bonding, and properties (R) 159
— Microscopical structuring of solids by molecular beam epitaxy—spatially resolved materials synthesis (R) 593
— Phase transformations of lithium nitride under pressure (C) 1101
— Techniques (B) 861
— The chemistry of the semiconductor industry (B) 1739
— The electronic structure and chemistry of solids (B) 719
— Uniform heterogeneous catalysts: the role of solid-state chemistry in their development and design (R) 1673
Spectroscopy, Structure elucidation and artificial intelligence (R) 247
— The use of light in the study of interfacial electrochemical reactions (R) 63
— with polarized light. Solute alignment by photoselection, in liquid crystals, polymers, and membranes (B) 863
Stereochemical analysis, Phosphorus-31 NMR spectroscopy in stereochemical analysis (B) 591
Strained rings, Cyclobutanones and cyclobutenones in nature and in synthesis (R) 797
— Is tetrasilatetrahedrane kinetically stable? (C) 1081
— Preparative UV-laser photochemistry: a biscarbene intermediate in the synthesis of a 5,6-dihydrodibenzo[*a*,*e*]cyclooctene containing a *trans*-double bond (C) 853
— Strongly bent naphthalene units in [2](2,6)naphthalino[2]paracyclophane and [2](2,6)naphthalino[2]paracyclophane-1,11-diene (C) 1064
— Synthesis and properties of a bridged *syn*-tricyclo[4.2.0.$0^{2,5}$]octa-3,7-diene: formation of propella[3_4]prismane (C) 840
— 3,3,6,6-Tetramethylcyclohexyne (C) 398
— The central propellane bond as polymerizable CC single bond: poly(tricyclo-[4.2.0.$0^{2,7}$]octane-1,7-diyl)—a "poly([1.1.1]propellane)" (C) 296
— The cyclopropyl group in studies of enzyme mechanism and inhibition (R) 537
Structural chemistry, Equipotential surfaces in periodic charge distributions (C) 849
Structure elucidation, A morphology-selective copper organosol (C) 1530
— and artificial intelligence (R) 247
— Controlling the microstructure of monomolecular layers (AM) 728
— Dinuclear complexes of gold(I) containing bridging cyclometalated arylphosphane or arylarsane ligands (E) 589

— Extremely short non-bonding oxygen-oxygen distances: the crystal structures of $NbBO_4$, $NaNb_3O_8$, and $NaTa_3O_8$ (C) 969
— First structure analysis and photoelectron spectroscopic investigation of an azete and an azete-cobalt complex (C) 1559
— Novel layer structure of sodium calix[4]arenesulfonate complexes—a class of organic clay mimics? (C) 1361
— On the structure of the cation $N_2H_7^{\oplus}$ with an N–H···N hydrogen bond in the monoammonia adduct of ammonium iodide (C) 1524
— Solid state structure of a lithium triorganostannate (C) 1381
— Synthesis of TiNF and structure determination by powder diffraction using synchrotron radiation (C) 929
— The structures of perchloric acid, $HClO_4$, and its anhydride, Cl_2O_7 (C) 1339
Sulfur, Solubilization of elemental sulfur in water by cationic and anionic surfactants (C) 1358
Sulfur compounds, The first transition metal complex of a thiepin; synthesis of thermally labile 1-benzothiepin 1-oxide from 1-benzothiepin(tricarbonyl)iron (C) 1717
— The microwave spectrum and structure of the ethylene-sulfur dioxide complex (C) 1356
— The SF_5-unit as steric protecting group; synthesis and structure of $F_5S-C\equiv SF_3$ (C) 1534
Sulfurous acid, Generation and characterization of sulfurous acid (H_2SO_3) and of its radical cation as stable species in the gas phase (C) 1533
Superconductivity, Accurate determination of the redox state in high-T_c superconductor oxides (C) 980
— From electronic/ionic conductors to superconductors: control of materials properties (AM) 1392
— New organic superconductors (AM) 1747
— Oriented domains and twins in the "tetragonal" superconductor $LaBa_2Cu_3O_{6.7}$ (C) 440
— Perovskite-type oxides—the new approach to high-T_c superconductivity (AM) 735
— The crystal structures of the superconducting oxides $Bi_2(Sr_{1-x}Ca_x)_2CuO_{8-\delta}$ and $Bi_2(Sr_{1-y}Ca_y)_3Cu_2O_{10-\delta}$ with $0 \le x \le 0.3$ and $0.16 \le y \le 0.33$ (C) 574
Supramolecular chemistry, Helicates: tetra- and pentanuclear double helix complexes of Cu^I and poly(bipyridine) strands (C) 1095
— Scope and perspectives; molecules, supermolecules, and molecular devices (Nobel-lecture) (R) 89
— Second sphere coordination adducts of phosphane-transition metal complexes with β-cyclodextrin and its methylated derivative (C) 1184
— Second-sphere photochemistry and photophysics: luminescence of the $[Pt(bpy)(NH_3)_2]^{2\oplus}$-dibenzo[30]crown-10 adduct (C) 692
— The design of molecular hosts, guests, and their complexes (Nobel lecture) (R) 1009
— Towards the making of [12]collarene (C) 966
Surfaces, From carbon beams to diamond films (AM) 1203
— Laser photochemistry at surfaces—laser-induced chemical vapor deposition and related phenomena (R) 1314
— Metallic superlattices—artificially structured materials (B) 1410
— Molecular organometallic chemistry on surfaces: reactivity of metal carbonyls on metal oxides (R) 1127
— Physics at surfaces (B) 1409
— The surface scientist's guide to organometallic chemistry (B) 1198
— The use of light in the study of interfacial electrochemical reactions (R) 63
Symmetry through the eyes of a chemist (B) 720
Synthetic methods, Cyclobutanones and cyclobutenones in nature and in synthesis (R) 797
— Ketenimine complexes from carbene complexes and isocyanides: versatile building blocks for carbocycles and N-heterocycles (R) 1456
— Microbial and enzymatic processes for the production of biologically and chemically useful compounds (R) 622
— Phosphaalkynes—syntheses, reactions, coordination behavior (R) 1484
— Reduction and hydrogenation with the system hydrocarbon/carbon (R) 679
— Silicon reagents in organic synthesis (B) 1567
— Transition metals in the synthesis and functionalization of indoles (R) 1113
— Zeolites: catalysts for organic syntheses (R) 226

Tantalum compounds, Extremely short non-bonding oxygen-oxygen distances: the crystal structures of $NbBO_4$, $NaNb_3O_8$, and $NaTa_3O_8$ (C) 969
— Triazatrimetallabenzenes, a new class of inorganic heterocycles; synthesis and structure of $[Cp^*TaN(Cl)]_3$ (C) 1330
Tautomerization, Slow tautomerization in a rhenium-oxo-hydroxide complex (C) 1527
Tellurium compounds, Soluble chromium selenides and tellurides: preparations and structures of $[(C_6H_5)_4P]_3[Cr_3Te_{24}]$ and $[(C_6H_5)_4P]_3[Cr_3Se_{24}]$ (C) 1702
— Tellurium-rich tellurides (R) 759
— The chemistry of organic selenium and tellurium compounds, Vol. 1 (B) 444
Terpenes, C_5 building blocks for terpene syntheses: γ-acetoxylation of (*E*)-2-methyl-2-butenals (C) 285
Tetradehydrobenzene, Stabilization of 1,2,4,5-tetradehydrobenzene by complexation at two nickel(0) centers (C) 941
Tetrahedranes, Is tetrasilatetrahedrane kinetically stable? (C) 1081
— Tetrahedrane and cyclobutadiene (R) 309
Tetrahydrodicyclobuta[*a,d*]benzenes, Structures and deformation electron densities of 1,2-dihydrocyclobutabenzene and 1,2,4,5-tetrahydrodicyclobuta[*a,d*]benzene (C) 304
Tetrahydrotetraborocines, Synthesis and structure of a 1,2,5,6-tetrahydro-1,2,5,6-tetraborocine (C) 926
Tetramethylcyclohexyne, 3,3,6,6-Tetramethylcyclohexyne (C) 398
Tetramethylene-1,4-distannacyclohexanes, A tetramethylene-1,4-distannacyclohexane from 3,4-dilithio-2,5-dimethyl-2,4-hexadiene and dichlorodimethylstannane: the first dimetalla[6]radialene (C) 404
Theoretical chemistry, *Ab initio* methods in quantum chemistry, part I and part II (B) 983
— Ab-initio molecular orbital theory (B) 862
— A pictorial approach to molecular bonding (B) 863
— Donor-acceptor-substituted cyclic π-electron systems—probes for theories and building blocks for new materials (R) 1437
— Reaction of tropone with a homopyrrole. The result of a computer-assisted search for unique chemical reactions (C) 1558
Thermochromism, Inorganic thermochromism (B) 1411
Thiadiazoles, Bis([1,2,5]thiadiazolo)[3,4-*b*;3′,4′-*e*]pyrazine, a novel 14π-electron heterocycle with high electron affinity (C) 434
Thienothiophenes, Redox-active thieno[3,2-*b*]thiophene as a novel, three-color electrochromic system (C) 560
Thiepins, The first transition metal complex of a thiepin; synthesis of thermally labile 1-benzothiepin 1-oxide from 1-benzothiepin(tricarbonyl)iron (C) 1717
Thioxophosphanes, $[Os(\eta^2\text{-}PHS)(CO)_2(PPh_3)_2]$, a stable η^2-thioxophosphane (H–P=S)-metal complex (C) 302
Tin compounds, Addition of a distannene to a phosphaalkyne. Formation of a phosphadistannacyclobutene (C) 838
— A tetramethylene-1,4-distannacyclohexane from 3,4-dilithio-2,5-dimethyl-2,4-hexadiene and dichlorodimethylstannane: the first dimetalla[6]radialene (C) 404
— Polycyclic silylamides of Ge^{II} and Sn^{II} with different structures—bis(germanediyl) versus distannate (C) 1087
— Solid state structure of a lithium triorganostannate (C) 1381
— Synthesis, structure and bonding of $[Cl_2Sn\{Rh(PMe_3)_3Cl\}_2]\cdot THF$, an unusual Sn^{II}-Rh^I adduct (C) 442
— Tin in organic synthesis (B) 445
Titanium compounds, π Complexes of an amino-9-fluorenylideneborane (C) 1331
— In-situ blocking of an aldehyde function by formation of (α-triphenylphosphoniumalkoxy)-titanium or -niobium complexes (C) 944
— $[M(CO)_4\{CH_3C(CH_2PMe_2)_3\}]$, M = Ti, Zr, Hf, complexes of zerovalent titanium, zirconium, and hafnium. First structural characterization of a Zr^0-carbonyl complex (C) 437
— Pentadienyl, a more reactive and more strongly bound ligand than cyclopentadienyl (C) 1099
— Reduction of epoxides, α,β-unsaturated aldehydes, and vicinal diketones with "reactive titanocene" (C) 855
— Synthesis and structure of $[cyclo\text{-}C_3H_4\text{–}SO_2Ph]_2Ti[OCH(CH_3)_2]_2$, a *C*-titanated "α-sulfonyl carbanion" (C) 1540
— Synthesis and structure of $[NaTi(2,6\text{-}Me_2C_6H_3O)_4(py)]_2$: a dimeric material containing a novel phenoxide bridge (C) 1181
— Synthesis of TiNF and structure determination by powder diffraction using synchrotron radiation (C) 929
— $[TiSCl_4]^{2\ominus}$ and $[Ti_3O(S_2)_3Cl_6]^{2\ominus}$, a multinuclear complex with a structure typical for clusters (C) 293
— Titanium(0)-arene complexes. Synthesis and X-ray crystal structure of $[(\eta^6\text{-}C_{10}H_8)Ti\{t\text{BuSi}(CH_2PMe_2)_3\}]$ (C) 1693
Topotactic reactions, From electronic/ionic conductors to superconductors: control of materials properties (AM) 1392
Transannular oxidative-addition reactions, Tetranuclear complexes as intermediates in transannular oxidative-addition reactions. Structure of the first tetrairidium linear cluster (C) 402
Transmetalation, Higher thermostability and selectivity of Köbrich reagents by transmetalation (C) 943
Triblattanes, Functionalized, enantiomerically pure [2.1.1]-, [2.2.1]-, and [2.2.2]-triblattanes (C) 1103
Trifluoroalanines, A simple access to 2-substituted 3,3,3-trifluoroalanine derivatives (C) 848
Triketones, 4,6,6-Trimethyl-4-cyclohexene-1,2,3-trione, a contribution to the biogenesis of norcarotinoids (C) 695
Tumor lectinology: at the intersection of carbohydrate chemistry, biochemistry, cell biology, and oncology (R) 1267
Tungsten compounds, Linkage of alkylidyne, carbonyl, and alkyne ligands at a tungsten center to form a metallacyclopentadienone and an η^3-oxocyclobutenyl complex (C) 1730

Ultrathin organic films, Controlling the microstructure of monomolecular layers (AM) 728
Urazoles, [1,2,4]Triazolo[1,2-*a*][1,2,4]triazole-1,3,5,7(2*H*,6*H*)-tetrone (urazourazole), synthesis and structure (C) 701

Valenes, Tricyclo[3.1.0.0^{2,6}]hexanedione (the valene of *o*-benzoquinone), bicyclo[2.1.1]hexane-2,3-dione, and valenes of a quinoxaline, of phenazine, and of a benzophenazine (C) 1369
Vanadium compounds, A novel heterocluster with D_3-symmetry containing twenty-one core atoms: $[As_6^{III}V_{15}^{IV}O_{42}(H_2O)]^{6\ominus}$ (C) 1721
— Dinuclear vanadium(II)- and vanadium(III)-guaiacolato complexes related to vanadium-based systems for the reduction of nitrogen (C) 576
— Synthesis and structure of $[ClV(OSiMe_3)N_2PPh_2]_2$, the first cyclodimetallaphosphazene—an eight-membered planar unsaturated heterocycle (C) 850
— $[V_{19}O_{41}(OH)_9]^{8\ominus}$, an ellipsoid-shaped cluster anion belonging to the unusual family of V^{IV}/V^{V} oxygen clusters (C) 1719
Veticadinol, Stereoselective synthesis of *trans*-decalins via intramolecular ene reactions; synthesis of the enantiomerically pure cadinane-sesquiterpene veticadinol (C) 703
Viscoelasticity, Surfactants, micelles and fascinating phenomena (R) 902
Vitamin B_{12}: experiments concerning the origin of its molecular structure (R) 5

Water-gas shift reaction, Oxidative addition of water to the Ru^{II} catalyst $K[Ru^{II}(Hedta)(CO)]$: homogeneous catalysis of the water-gas shift reaction under ambient conditions (C) 1735
"Wittig reactions", A novel entry to the PC-double bond: the "phospha-Wittig" reaction (C) 1382
— Wittig reactions of unsaturated silicon compounds $\geq Si{=}Y$: isolation and structure of possible intermediates (C) 935
Wittig rearrangements, Asymmetric induction in the [2,3] Wittig rearrangement by chiral substituents in the allyl moiety (C) 278

Ylides, Acetylene polymerization with ylide-nickel catalysts (C) 839
— Synthesis and structure of a resonance stabilized (Trimethylphosphonio)metallapropenide (C) 587

Zeolites: catalysts for organic syntheses (R) 226
— High-resolution solid-state NMR of silicates and zeolites (B) 1410
— Synthesis of high-silica aluminosilicate zeolites (B) 1004
Zintl compounds, Isolated, complex Zintl molecules in the gas phase (C) 1091
— Tellurium-rich tellurides (R) 759
Zirconium compounds, $[M(CO)_4\{CH_3C(CH_2PMe_2)_3\}]$, M = Ti, Zr, Hf, complexes of zerovalent titanium, zirconium, and hafnium. First structural characterization of a Zr^0-carbonyl complex (C) 437
— $P_4^{2\ominus}$ Isomers as complex ligands (C) 694